AACR Annual Meeting 2024 Regular Abstracts

This PDF contains all regular abstracts (submitted for the November 16, 2023 deadline) that were scheduled for presentation as of Monday, April 1, 2024, with the exception of abstracts that are embargoed as part of the AACR Annual Meeting Press Program.

Abstracts are sorted in presentation number order. Session categories and titles are included.

Sunday, April 7, 2024

IMMUNOLOGY: Adoptive Cell Therapies 1: Tumor Antigen-Specific T-cells and TCR-T
Poster Session

#0001 Biomarkers of response and acquired resistance to TIL-ACT in solid tumors.

W. Robinson[1], A. Castro[1], M. Al-Bakir[1], J. J. Gartner[2], C. A. Chamberlain[1], A. H. Kverneland[3], T. H. Borch[3], I. Svane[3], M. Donia[3], P. Robbins[2], K. Litchfield[1]; [1]University College London, London, United Kingdom, [2]National Institutes of Health, Rockville, MD, [3]National Center for Cancer Immune Therapy (CCIT-DK), Copenhagen, Denmark

Background: Cancer immunotherapy has revolutionized cancer treatment in the last decade. However, most patients either do not respond to immunotherapy or eventually relapse so there is a need to identify biomarkers of response and understand mechanisms of resistance. Most biomarker studies have analyzed patients treated with immune checkpoint inhibitors (CPI) therapy while the few studies of adoptive cell transfer of tumor infiltrating lymphocytes (TIL-ACT) have analyzed relatively small patient cohorts.
Methods: To systematically identify biomarkers of response and resistance to TIL-ACT, we collected published and unpublished whole-exome and transcriptomic data for tumors from 400 patients treated with TIL-ACT from five tumor types across four institutions and processed these datasets using a standardized bioinformatic pipeline.
Results: To identify biomarkers of response in pre-treatment tumors, we analyzed previously reported biomarkers and performed biomarker discovery in our cohorts. For the subset of 200 patients with T cell reactivities identified from the infusion products and fresh tumor, we refined our biomarkers to include neo-antigen reactivities in addition to identifying both mutational processes and transcriptional signatures associated with neo-antigens reactivity. To identify mechanisms of acquired resistance to TIL-ACT, we analyzed 15 patients with paired pre- and post-treatment tumors and found multiple mechanisms of immune evasion specific to infused reactive T cells including loss of heterozygosity of the HLA allele presenting the neo-antigen, genomic loss of the neo-antigen and inactivation of interferon-gamma signaling pathway.
Conclusions: In summary, we will present the biomarkers landscape of TIL-ACT therapy including differences between histology and across treatment modalities to improve our understanding of the mechanisms of treatment response.

#0002 T cells selected from lymph node acquisition for adoptive cell therapyin NSCLC.

Tatiana Delgado Cruz[1], Yanping Yang[2], Rachel Honigsberg[3], Geoffrey Markowitz[4], Nasser K Altorki[5], Vivek Mittal[4], Moonsoo M. Jin[6], Jonathan Villena-Vargas[4]

[1]Weill Cornell Medicine/Sandra and Edward Meyer Cancer Center, New York, NY,[2]Radiology, Houston Methodist, Houston, TX,[3]Meinig School of Biomedical Engineering, Weill Cornell, ithaca, NY,[4]Cardiothoracic Surgery, Weill Cornell Medicine/Sandra and Edward Meyer Cancer Center, New York, NY,[5]Cardiothoracic surgery, Weill Cornell Medicine/Sandra and Edward Meyer Cancer Center, New York, NY,[6]Radiology, Houston Methodist Research Institute, New York, NY

Background: A primary limitation of PD-1 inhibitors in non-small cell lung cancer (NSCLC) arises from their inability to act on 'cold' tumors without tumor-reactive T cells, necessitating alternative approaches. Adoptive cell therapy (ACT) using (CAR)-engineered cells, strives to enhance antitumor immunity but faces several challenges such as identifying safe antigens, tumor heterogeneity, antigen escape, cell trafficking, and T cell persistence. To address these issues, we explored a new source of T cells from the benign tumor draining lymph nodes (tdLNs) of NSCLC patients. Our initial results have shown that tdLNs is a reservoir for of tumor-relevant 'stem-like' T cells. We posit that employing these pluripotent T cells for ACT could achieve significant tumor rejection in NSCLC.
Methods: Resected tumors, tdLN, non-draining (ndLN), and blood from NSCLC patients, as well as a syngeneic murine lung cancer model (344SQ), underwent analysis. T cells were profiled using flow cytometry, cytotoxicity and proliferation assays. TCR and single cell (sc)RNA sequencing assessed clonal expansion, diversity, and transcriptional profiles of tumor-relevant T cells. T cells were then transduced with an ICAM-1 targeting CAR, in vivo efficacy was evaluated in an A549 murine lung cancer model.
Results: T cell subsets with stem-cell memory characteristics, as indicated by PD-1+, TCF1hi, CXCR5+, and CD8+ expression, which were not significantly found in the tumor or PB. These T cells exhibited progenitor-like transcriptional signatures, enhanced SELL and TCF-1 expression, fewer exhaustion markers, and superior in vitro proliferation compared to TILs from both a murine lung cancer model and patient-derived tissues. scRNA sequencing, coupled with TCR "tumor matching" (TM) techniques, exposed a rich clonal diversity of tumor-relevant clones within tdLNs, which showcased a broader transcriptional memory profile and distinct CD4+ and CD8+ phenotypes. Upon analyzing the top 100 expanded (n>3) TM clones, 47 featured the presence of tdLN-derived T cells, covering progenitor, stem cell-like, and central memory clusters. T cell subsets were then transduced with a CAR targeting ICAM-1—a cell surface protein frequently overexpressed in NSCLC tumors. Manufacturing protocol yielded high transduction efficiency and T cell expansion within two weeks in 6/6 patients, consistent with PB-derived CAR T cells and on par with the optimal dosing requirements of an ICAM-1 CAR Phase I trial (NCT04420754). tdLN-CAR T cells showed potent antitumor efficacy compared to the control in an aggressive NSCLC murine model (Median survival 103d vs 66d; respectively; p=0.006).
Conclusions: This represents the first reported use of T cells from tdLN for genetically engineered ACT. The data indicate that modifying antigen-experienced, stem-like T cells from tdLN with CAR is a promising and efficient method in a NSCLC murine model, warranting further research.

#0003 Multiomics analyses reveal functional DNA, methylation pattern changes in clinical transgenic T-cell receptor cell therapy products.

G. Protti, C. Peters, M. Kawakami, C. Kidd, V. Subramanyam, A. Lechien, A. Dinh, A. Ribas, M. Pellegrini, **T. S. Nowicki**;
UCLA - University of California Los Angeles, Los Angeles, CA

Background: Transgenic T-cell receptor T-cells (TCR-T) directed against tumor-specific antigens are associated with robust initial clinical responses. However, these responses are often not durable, and patients relapse frequently. Therefore, there is a significant need to understand how these cells change at the epigenomic level over time following infusion into the patient.
Methods: We analyzed MART-1 TCR-T products from 8 patients treated under a clinical trial at UCLA (NCT00910650). Samples from the baseline infusion product and samples from day +30 recovered from peripheral circulation were sorted for TCR+ cells via flow cytometry, and were then subjected to whole genome bisulfite sequencing (WGBS), ATACseq, and RNAseq in parallel. Differential chromatin accessibility and gene expression by the ATACseq and RNAseq datasets, respectively, were analyzed via DESeq2, with P adjusted less than 0.1. WGBS datasets were analyzed via Metilene, and differentially methylated regions (DMRs) were defined as those regions with CpG loci containing a methylation difference >= 10% and a P adjusted < 0.05. Functional DMRs were defined as those repressed over time (increased DNA methylation with decreased chromatin accessibility/gene expression relative to infusion product), or activated over time (decreased DNA methylation with increased chromatin accessibility/gene expression relative to infusion product). Functional DMRs were then analyzed via EnrichR to evaluate gene ontology and pathways significantly enriched in gene lists.
Results: We collectively identified three genes with repressed DMR activity and 49 genes with activated DMR activity compared to baseline infusion products. Our findings revealed that genes associated with repressed DMRs included IL2RA, FBLN7, and ZNRF1. These genes were collectively associated with a decrease in T-cell activation, cytokine signaling, and migration activity, potentially impacting the functional capabilities of T-cells in the post-infusion environment. Conversely, genes associated with activated DMRs included PDCD1 (PD1), FGR, KIR3DL1, KIR2DL4, and KLF3, with pathway enrichment analysis indicating a significant shift in the T-cell landscape towards reduced anti-tumor activity, decreased T-cell proliferation, T-cell aging, and the promotion of immune escape tumor phenotypes.
Conclusions: This comprehensive multi-omics approach showcases an atlas of genes in clinical TCR-T cell therapeutics which are subject to functional changes in DNA methylation over time *in vivo.* These findings shed light on the complex interplay between DNA methylation, chromatin accessibility, and gene expression in the context of TCR-T cell therapy, with implications for the development of more effective immunotherapeutic strategies.

#0004 Identifying novel patient-derived T cell receptors targeting TP53 public neoantigens.

Michael V. Gormally, Smita S. Chandran, Inaki Etxebarria, Christopher Klebanoff

Memorial Sloan Kettering Cancer Center, New York, NY

Adoptive cell transfer (ACT) is a promising immunotherapeutic strategy to bolster reactivity against immunologically cold tumors through infusion of T cells that can recognize and eliminate cancer cells bearing mutation-derived neoantigens (NeoAgs). T cell receptors (TCRs) that confer recognition of public NeoAgs--an elite subset of Human leukocyte antigen (HLA)-restricted epitopes arising from recurrent hotspot mutations in driver genes that enhance cancer cell fitness and are clonally conserved--are highly desirable and would be effective against many tumors sharing the common hotspot mutation. Tumor suppressor *TP53* is a supreme target for this approach: it is the most frequently mutated gene in cancer yet remains untargetable with FDA-approved therapies. The most common *TP53* alteration (R175H) generates a public NeoAg in the context of *HLA-A*02*, an allele expressed by ~40% of the North American and Western European populations. Earlier work established the immunogenicity of this public NeoAg by isolating a *TP53*(R175H)-specific clone from a colorectal cancer patient. ACT of this TCR in a single patient produced an objective anti-tumor response, but also resulted in multisystem organ failure indicating this receptor might possess off-target reactivity to unrelated proteins in healthy tissue. To discover safe and effective *TP53*(R175H)-specific TCRs, we assembled a unique biorepository of peripheral blood mononuclear cells (PBMCs) from *n=26* cancer patients with diverse tumors that co-express *HLA-A*02*/*TP53*(R175H) and applied a novel high-throughput screening technique to retrieve candidate TCRs. These efforts resulted in a panel of *n=9* genetically distinct and functionally validated receptors, each with NeoAg-specific anti-tumor activity against a panel of cancer cell lines. To define the cross-reactivity profile of these novel TCRs and the benchmark TCR that caused toxicity, we performed amino acid scanning mutagenesis (X-Scan) to identify potential off-targets. Importantly, we identified significant off-target reactivity to normal human proteins for the benchmark TCR, which may explain the lung and kidney toxicities observed in the trial patient. By contrast, a subset of the novel TCRs exhibited exquisite specificity for the *TP53* public NeoAg with no predicted off-targets. Finally, we performed ACT of all TCRs in a mouse xenograft model and identified several novel TCRs that potently eliminated *TP53*(R175H)$^{+}$/*HLA*A02*$^{+}$ tumors in vivo. Based on these data, we are now proceeding with the clinical development of a best-in-class TCR. This work is poised to bring an important new class of precision immunotherapeutics to patients with *TP53*-mutant tumors that presently lack effective molecularly targeted agents.

#0005 Cytosine base editor ameliorates the safety profile of TCR edited T cells for the adoptive cell therapy of gastrointestinal tumors.

M. Spiga[1], A. Potenza[1], S. Beretta[2], A. Airaghi[1], C. Iozzi[1], M. Fiumara[2], S. Ferrari[2], N. Mohammadi[1], O. Botrugno[1], M. Reichert[3], M. Protti[1], S. Crippa[4], M. Falconi[4], L. Naldini[2], E. Ruggiero[1], C. Bonini[1];

[1]Universita Vita-Salute San Raffaele, Milan, Italy, [2]San Raffaele Telethon Institute for Gene Therapy (SR-TIGET), Milan, Italy, [3]Technical University of Munich, Munich, Germany, [4]Ospedale San Raffaele, Milan, Italy

Among gastrointestinal tumors, colorectal cancer (CRC) and pancreatic ductal adenocarcinoma (PDAC) are major unmet medical needs, with a high mortality rate mainly related to the onset of metastases, hindering the therapeutic efficacy of conventional treatments. Adoptive Cell Therapy (ACT) with TCR-edited T cells is a promising therapeutic strategy for patients with late-stage tumors, but its applicability is limited by the paucity of TCRs targeting relevant tumor antigens and the presence of an immunosuppressive tumor microenvironment. Moreover, the safety of the therapeutic cellular products, generated by genome editing tools, is fundamental for an effective and rapid clinical translation. With the aim of improving the safety profile of T-cell based therapeutic products manufactured by genome editing, we evaluated the efficacy and safety of cytosine base editor (CBE). We disrupted the endogenous TCR to redirect T cells specificity toward tumor cells, and TIGIT, a major inhibitory molecule in gastrointestinal tumors to enhancing T cell ability to counteract immunosuppression. Beyond the high efficiency of CBE in simultaneously disrupting the target genes, we observed only marginal sgRNA-dependent and -independent off-target events as measured by targeted sequencing of the top predicted off-target loci and by ultra-deep whole exome sequencing, respectively. In addition, unlike CRISPR/Cas9-treated cells, we could not detect translocations in CBE edited T cells. To select the antigens to target by engineered T cells, we investigated published datasets and identified 19 relevant tumor-associated antigens. By clonal tracking of the TCR repertoire of T cells stimulated with autologous APCs loaded with the selected antigens, we isolated 5 different TCRs specificities, including mesothelin. Importantly, these antigens are expressed in our cohort of primary and metastatic PDAC and CRC patients. TCR-edited T cells displayed anti-tumor activity against PDAC cell lines, CRC and PDAC patient-derived organoids while sparing HLA-unrelated and antigen-negative controls. To boost the efficacy of anti-tumor T cells, we coupled TIGIT disruption with TCR editing. By challenging TCR-edited $TIGIT_{KO}$ T cells *in vitro* and in an orthotopic model of CRC liver metastases, we observed that TIGIT disruption can ameliorate the ability of tumor-specific T cells to control tumor growth. Our findings suggest that base editors can generate cellular products with a better safety profile and a promising therapeutic efficacy in gastrointestinal tumors.

#0006 Defining and therapeutically targeting a fusion-derived public neoantigen in desmoplastic small round cell tumor using T cell receptor gene therapy.

L. Banks[1], H. Arkin[1], S. Chandran[1], E. Slotkin[1], M. Espinosa-Cotton[1], N. Shukla[1], L. Morris[1], M. Ladanyi[1], A. Kung[1], M. Klatt[2], C. Klebanoff[1];
[1]Memorial Sloan Kettering Cancer Center, New York, NY, [2]Charité University Medicine, Berlin, Germany

Sarcomas are a heterogenous group of mesenchymal cell malignancies that are difficult to treat and often respond poorly to current immunotherapies. Approximately 30% of sarcomas are associated with oncogenic driver fusion proteins. Desmoplastic small round cell tumor (DSRCT) is a prototypical fusion-driven sarcoma defined by a pathognomonic *EWSR1-WT1* fusion event. The resultant EWSR1-WT1 fusion protein contains a shared junctional amino acid sequence that is clonally conserved and significantly divergent from normal human proteins. Consequently, the EWSR1-WT1 fusion might yield a highly immunogenic shared, or public, neoantigen (NeoAg) that may serve as a target for novel immunotherapeutic approaches.Using a functional HLA-immunoprecipitation/mass spectrometry (HLA-IP/MS) screen, we identified a 9-amino acid peptide sequence derived from the junction of the most common EWSR1-WT1 fusion protein that is presented in the context of the prevalent HLA-A*03 and -A*11 alleles. We confirmed that HLA-A*03$^+$ DSRCT cells physiologically present the same peptide sequence. Using fluorophore-conjugated HLA-multimers loaded with the HLA-IP/MS-derived fusion NeoAg, we identified a rare population of circulating NeoAg-specific CD8$^+$ T cells in HLA$^+$ DSRCT patients. Through antigen-directed clonal expansion, we discovered n=3 HLA-A*03-restricted and n=1 HLA-A*11-restricted fusion NeoAg-specific T cell clones and retrieved the paired TCRαβ gene sequences of their T cell receptors (TCRs) using 10x single-cell sequencing. Polyclonal CD8+ T cells transduced with candidate TCRαβ gene sequences robustly upregulated TNFα after coculture with HLA$^+$/Fusion$^+$ target cells but not HLA$^-$/Fusion$^+$ or HLA$^+$/Fusion$^-$ control cells. Further, T cells expressing candidate TCRs, but not viral-protein-specific TCRs, lysed HLA$^+$ DSRCT cells *in vitro* and controlled established DSRCT tumors *in vivo*. Finally, we discovered that one TCR was capable of cross HLA allele fusion NeoAg recognition and could lyse both HLA-A*03$^+$ and -A*11$^+$ DSRCT cells. These findings imply that a single TCR therapeutic could cover >36% of North American DSRCT patients.Collectively, our data establish for the first time that DSRCT cells present a junction-spanning fusion-derived neoantigen in the context of two prevalent HLA alleles that may be therapeutically targeted using TCR gene therapy. These data lay the foundation for first-in-human clinical translation of a T-cell based therapy targeting EWSR1-WT1. More broadly, these findings establish proof-of-principle that recurrent fusion proteins are an actionable source of immunogenic public NeoAgs, providing a framework for developing targeted immunotherapies for other fusion-driven malignancies.

#0007 Ginsenoside Rb1 delays the senescence of $CD8^+$ T cells to expand T cells with superior antitumor immunity.

C. Ma, X. Sheng, C. Li;
Shandong University, Jinan, China

Background and Objective: Immunosenescence represents a distinct state of T cell dysfunction in the TME, and plays crucial role in many age-related diseases including tumor. Senescent cell removal by senolytic agents or therapies that inhibit the SASP have demonstrated benefit in both preclinical and clinical models of geriatric decline and chronic diseases. Here, we aimed to screen anti-aging compounds to delay T-cell senescence in TME, and explore novel strategies of reversing tumor induced T-cell senescence to restore antitumor immunity.
Methods and Results: Using in vitro senescence inducing system, we screened ginsenoside Rb1 from 22 anti-aging compounds as the compound that had the most effective activity to reduce CD8+ T cell senescence, displayed as decreased β-gal, p16, and p21. Further analysis showed that ginsenoside Rb1 promoted anti-CD3/CD28-induced TCR signaling and the secretion of effector cytokines IFN-γ, TNF-α and IL -2 in OTI T cells. Intriguingly, ginsenoside Rb1 treatment significantly increased TCF-1 in $CD8^+$ T cells, and ginsenoside Rb1 treated OT-I T cells significantly inhibited tumor growth. Moreover, ginsenoside Rb1 greatly enhanced the efficiency of CD19-CART cells to kill Namalwa tumor cells.
Conclusion: Ginsenoside Rb1 delays T cell senescence and enhances T cell antitumor activity. This data provides a new insight into T cell based antitumor therapy.

#0008 Deep Immunomics pipeline for discovery and validation of novel cancer-specific T cell receptors.

H. Fields[1], J. Velez Lujan[1], K. Wu[2], N. Epstein[1], N. Beevi[1], F. Chioh[2], N. Tan[2], N. Kulkarni[2], N. Mukobo[2], S. R[2], Y. Purwanti[2], E. Newell[3], A. Nardin[2], M. Fehlings[1], K. Fink[2], D. MacLeod[1];

[1]ImmunoScape, San Diego, CA, [2]ImmunoScape, Singapore, Singapore, [3]Fred Hutchinson Cancer Center, Seattle, WA

Background: T cell receptor-engineered T cell (TCR-T) therapy has been studied as a high potential approach for cancer treatment. Beyond cell-surface tumor antigens, TCR-Ts can recognize HLA-presented intracellular epitopes which allows them to address a wide range of cancer-specific targets. Existing TCR-T therapies focus on a limited number of epitopes, many of which are restricted to HLA allele HLA-A*02:01. Identification of novel anti-tumor TCRs covering a broad range of HLA alleles is necessary to address unmet clinical needs. Natural T cells undergo thymic selection and present a favorable safety profile for mining such anti-tumor TCRs for therapeutic development. However, discovery of natural anti-tumor TCRs has been challenging due to i) the absence of high-throughput methods for identifying tumor-reactive TCRs in limited quantity human samples and ii) lack of sensitivity in detecting low frequency, naturally occurring tumor-reactive T cells.

Methods: We developed TargetScape® as a part of our Deep Immunomics platform for efficient discovery of natural tumor-specific TCRs in healthy donors and cancer patients. Cells from blood and tissue samples were stained with metal-barcoded peptide-MHC tetramers, containing 500+ tumor-specific antigens, alongside metal-conjugated antibodies, allowing rapid identification and high dimensional phenotypic analysis of CD8+ T cells at the millions of cells scale. Single-cell sequencing revealed paired TCR sequences. Selected TCRs were introduced into luminescent Jurkat reporter cells for validation screening with peptide-pulsed targets and the relevant HLA restriction. TCRs of interest were further integrated into primary T cells and evaluated for their effector function.

Results: We utilize our sensitive, high-throughput TargetScape® platform to detect and characterize putative cancer-specific TCRs from blood and tissue samples in frequencies as low as ~0.003% of total CD8+ cells. We have functionally validated over 100 TargetScape® derived TCRs with luminescent Jurkat reporters. Validated TCRs cover high prevalence HLA alleles and target a broad range of cancer antigen classes, including tumor associated antigens (TAA), Human endogenous retroviruses (HERVs), shared splice variants, and frameshift mutations. Several natural TCRs demonstrate recognition of low concentrations of peptide, indicating high functional avidity. Further evaluations of specificity and activity of TCRs of interest transduced into primary T cells are currently in progress.

Conclusions: Our Deep Immunomics platform allows us to identify and confirm activity of novel, naturally-derived TCR candidates against therapeutically relevant cancer antigens presented on six common HLA alleles. These findings validate our discovery workflow leading to a portfolio of potential clinically relevant candidates that are currently under preclinical development.

#0009 AFNT-212: A *TRAC*-knocked-in KRAS^{G12D}-specific TCR-T cell product enhanced with CD8αβ and a chimeric cytokine receptor for treatment of solid cancers.

A. Drain[1], N. Rouillard[1], N. Swanson[1], M. Canestraro[1], S. Narayan[1], T. Warner[1], N. Danek[1], K. Gareau[1], J. Liang[1], L. Shen[1], T. Tetrault[1], I. Priyata[1], S. Vidyasagar[1], T. Riggins-Walker[1], H.-W. Liu[1], K. Pechhold[1], L. Brown[1], J. Francis[1], X. He[1], P. Browne[2], R. Lamothe[2], M. Storlie[2], G. Cost[2], T. M. Schmitt[3], P. D. Greenberg[3], S. S. Chandran[4], C. A. Klebanoff[4], H. Lam[1], A. Gupta[1], D. Hallet[1], G. Shapiro[1], K. Nguyen[1], **L. Vincent**[1];
[1]Affini-T Therapeutics, Inc., Watertown, MA, [2]Metagenomi, Emeryville, CA, [3]Fred Hutchinson Cancer Research Center, Seattle, WA, [4]Memorial Sloan Kettering Cancer Center (MSKCC), New York, NY

The KRAS^{G12D} mutation is an ideal target for anti-cancer therapies as its expression is typically clonal, restricted to cancer tissue, and is among the most common oncogenic drivers in solid tumors. TCR-T cell therapies have demonstrated clinical activity in some solid cancers but have been limited by heterogeneous antigen expression and unfavorable tumor microenvironments. By targeting the KRAS^{G12D} mutation for which the cancer has established genetic dependency, AFNT-212 is designed to selectively target all cancer cells while avoiding on-target/off-tumor toxicities. AFNT-212 is non-virally engineered to knock-in a 5-transgene cassette expressing a high-avidity TCR specific for the KRAS^{G12D} mutation, a CD8α/β coreceptor, and a chimeric cytokine receptor. Transgene insertion at the *TRAC* locus disrupts expression of the endogenous TCRα, further enhancing the expression/activity of the transgenic KRAS^{G12D} TCR.

Primary human CD8$^+$ and CD4$^+$ T cells were genetically engineered by a novel CRISPR-Cas nuclease system to integrate AFNT-212 transgenes within the *TRAC* locus. A cGMP compatible scale-up process for non-viral knock-in was established to support AFNT-212 clinical manufacturing. The activity of AFNT-212 was assessed against a panel of human KRAS^{G12D} tumor cell lines *in vitro* and established mouse xenograft models *in vivo*. The preclinical safety profile of AFNT-212 was evaluated by X-scan and crossreactivity assessment, alloreactivity studies, and cytokine independent growth studies. The specificity of gene-editing (GE) was assessed by an unbiased oligo-capture method followed by targeted sequencing.

AFNT-212 TCR-T cells demonstrated potent *in vitro* anti-tumor activity against endogenously expressing HLA-A*11:01 KRAS^{G12D} tumor cells, including during chronic exposure to viable tumor cells. AFNT-212 TCR-T cells showed robust antitumor activity in established xenograft mouse models *in vivo*. No cross-reactivity was identified for the KRAS^{G12D} TCR against potential self-peptides even at supraphysiological levels, demonstrating high specificity of the TCR. No alloreactivity or cytokine-independent proliferation was observed. GE safety evaluations did not reveal any off-target activity using high sensitivity (~0.1%) NGS-based analyses or any GE-associated chromosomal rearrangements. The manufacturing of AFNT-212 consistently delivered >50-fold expansion of engineered TCR-T cells to meet expected clinical dose levels and exhibit memory/stemness phenotypes and negligible markers of immunologic exhaustion.

AFNT-212, a novel TCR T cell therapy targeting KRAS^{G12D} mutant tumors, demonstrates robust activity against KRAS^{G12D} mutant tumors *in vitro* and *in vivo*. The robust manufacturing process developed using non-viral gene editing in the *TRAC* locus will support future clinical development of AFNT-212.

#0010 Non-viral engineered T cell therapy specific for the hotspot mutation p53 R175H that integrates signal 1 (TCR), signal 2 (co-stimulation) and signal 3 (cytokine) and co-opts FasL-dependent apoptosis to achieve a coordinated antitumor CD4/8 T cell response.

S. Narayan[1], K. Gareau[1], A. Gupta[1], J. Ferrell[1], N. Rouillard[1], T. Warner[1], J. Liang[1], L. Shen[1], T. Tetrault[1], J. Francis[1], X. He[1], P. J. Browne[2], R. Lamothe[2], M. D. Storlie[2], G. J. Cost[2], T. M. Schmitt[3], P. D. Greenberg[3], S. S. Chandran[4], D. Hallet[1], M. Gormally[4], C. A. Klebanoff[4], **G. Shapiro**[1], K. Nguyen[1], L. Vincent[1]; [1]Affini-T Therapeutics, Inc., Watertown, MA, [2]Metagenomi, Inc., Emeryville, CA, [3]Fred Hutchinson Cancer Research Center, Seattle, WA, [4]Memorial Sloan Kettering Cancer Center, New York, NY

Adoptive T cell therapy (ACT) has demonstrated antitumor efficacy in patients with solid cancers but requires further optimization to become a reproducibly effective treatment. T cell receptor (TCR)-engineered T cells recognize peptides derived from intracellular and surface proteins presented in the context of MHC class I. Targeting mutated oncogenic drivers addresses many of the major obstacles of this modality, in that the antigenic epitope is: 1) tumor-specific, 2) essential for tumor survival, and 3) derived from a stably expressed protein. However, the immune-suppressive tumor microenvironment makes further optimization of engineered T cells necessary to bring long-term clinical benefit to patients. For an optimal anti-tumor response, T cells require three signals: TCR, co-stimulation, and cytokine signaling. The tumor suppressor *TP53* is the most frequently mutated gene across human cancers, with a highly recurrent arginine to histidine hotspot alteration in codon 175 leading to novel tumor-dependent functions. Here we report the use of a novel CRISPR-Cas nuclease system to knock-in a six-parameter multi-cistronic cassette into the *TRAC* locus with high efficiency. We employed several strategies to maximize the potency and durability of a TCR-T cell product targeting the p53 R175H oncogenic driver, including: 1) A high-affinity TCR (α and β chains) specific for the p53 R175H mutation presented by HLA-A*02:01 permits the recognition of tumor cells expressing even low levels of the epitope (Signal 1), 2) Inclusion of the CD8αβ co-receptor drives stimulation of CD4+ T cells with the MHC class I restricted TCR, allowing for a physiologic coordinated immune response required for maximal efficacy, 3) A FAS-41BB switch receptor acts as a dominant negative to the FASL-inducing apoptotic signal in the tumor microenvironment and drives stimulation and persistence of the T cell product via 41BB co-stimulatory signaling (Signal 2), 4) A chimeric cytokine receptor (constitutive Interleukin Receptor) promotes expansion and survival while avoiding immunologic exhaustion (Signal 3). Together, these strategies deliver the three signals required for maximal T cell function: antigen-driven activation, co-stimulation, and growth/survival-promoting cytokine signaling. The non-viral *TRAC*-knocked-in T cells demonstrate robust and specific cytotoxicity against endogenously expressing HLA-A*02:01 and p53 R175H cell lines *in vitro* and effective anti-tumor activity *in vivo* while maintaining a favorable preclinical safety profile. These data support the planned clinical development of a novel non-viral *TRAC*-knocked-in T cell therapy for the treatment of p53 R175H-mutant solid tumors.

#0011 Development of innovative off-the-shelf cancer immunotherapies with iPSC-derived CD8-positive T-cells.

R. Tawo[1], M. Mirenda[2], O. Cypris[1], P. Hublitz[1], N. Wagner[1], M. Epstein[3], M. Esquerre[2], A. Holtzinger[1], M. Braun[1], **M. Dangl**[1], R. Grandy[3], D. Sommermeyer[1];
[1]Evotec International GmbH, Goettingen, Germany, [2]Evotec France SAS, Toulouse, France, [3]Evotec (UK) Ltd., Abingdon, United Kingdom

Chimeric antigen receptor (CAR) based T-cell immunotherapies have transformed the oncology landscape and evolved as part of the standard of care for several hematological malignancies. To generate CAR-T-cell products, autologous patient-derived αβT-cells are engineered with a CAR for tumor cell targeting. However, generating autologous T-cell products fails in a significant number of cases due to the poor quality and quantity of blood-derived T-cells and is associated with manufacturing and logistical complexity as well as high product costs. Therefore, it is crucial to develop strategies for off-the-shelf T-cell products as otherwise many patients are left without this treatment option. Manufacturing allogeneic T-cells from induced pluripotent stem cells (iPSCs) has a great potential to generate cell products with consistently high quality and scalable quantities. In addition, high fidelity gene-editing can be performed in iPSCs to address tumor resistance mechanisms and to prevent exhaustion of the T-cells. We have established a feeder-free differentiation protocol that enables robust production of iPSC-derived αβT-cells (iαβT). Flow cytometry and single cell transcriptome analysis ensure stringent monitoring of all process stages. To demonstrate functional activity of iαβT, cytotoxicity and cytokine release assays were performed. We compared the differentiation potential of iPSC lines derived from T-cells (t-iPSCs) to a hematopoietic stem cell-derived iPSC line with an αβTCR knock-in. Hematopoietic progenitor cells were induced from the different iPSC lines and differentiated into iαβT. During the differentiation process, surface markers CD45, CD5 and CD7 were displayed, and cells started to express αβTCRs. Importantly, iαβT derived from the different iPSC lines expressed CD8α and CD8β which is crucial for the function of cytotoxic T-cells. The CD4/CD8 double positive stage is an important step in T-cell development and was observed only when T-cells were generated from t-iPSC, but not from the TCR knock-in cells. Functional analysis of iαβT-cells confirmed their cytotoxic activity and potential to release cytokines after activation. Our scalable process for iαβT differentiation generates CD8-positive T-cells that secrete cytokines and show cytotoxic activity against tumor cells, demonstrating their potential as a promising cell source for TCR-T or CAR-T cancer immunotherapies.

#0012 TCR-gated control of costimulatory switch protein (CSP) activation in rTCR-T cells expressing PD1-41BB.

M. Buerdek, P. U. Prinz, K. Mutze, **A. Coluccio**, S. Tippmer, M. Bosch, G. Longinotti, M. Catarinella, K. Davari, C. Geiger, B. Loesch, K. Crame, D. J. Schendel; Medigene Immunotherapies GmbH, a subsidiary of Medigene AG, Planegg-Martinsried, Germany

Chimeric antigen receptor (CAR-)/T cell receptor (TCR-)T-based immunotherapies have shown promising results in the treatment of patients suffering from hematological malignancies. However, targeting solid cancer patients with CAR-T/TCR-T cells represents a more challenging approach, due to various factors present within the hostile tumor micro-environment (TME), inhibiting T cell functionality and leading to T cell exhaustion. Programmed cell death ligand-1 (PD-L1) is expressed on tumor cells as well as various cell types within the TME and binds to programmed cell death protein 1 (PD-1) expressed on the surface of activated T cells, thereby inducing T cell exhaustion and mediating tumor immune escape. To impair this inhibitory mechanism and improve TCR-T cell efficacy for the treatment of solid tumors, we use the chimeric costimulatory switch protein (CSP) PD1-41BB that turns the inhibitory signal mediated via the PD-1-PD-L1 axis into a costimulatory one. The CSP-mediated costimulatory signal is TCR-gated, whereby costimulation can only occur if a specific peptide-HLA complex present on a target cell interacts with a recombinant TCR expressed in T cells. *In vitro* co-cultures of rTCR-T cells expressing the CSP (CSP rTCR-T cells) and antigen-negative or -positive cell lines carrying or lacking PD-L1 demonstrated that CSP rTCR-T cells display functionality only if the respective target antigen is expressed in target cells, but not in the absence of target antigen. PD-L1-positive, antigen-negative tumor cells are not lysed by CSP rTCR-T cells, not even in the presence of antigen-positive tumor cells, showing gated functionality and a favorable safety profile of CSP-armored TCR-T cells. CSP rTCR-T cells displayed enhanced cytokine release and killing after encounter of PD-L1-positive tumor cell lines, compared to tumor cells lacking PD-L1, and showed the capacity to recognize and lyse a large panel of tumor cell lines expressing various levels of HLA-A*02, target antigen and PD-L1 *in vitro*. 3D spheroids derived from PD-L1-positive, target antigen-positive tumor cell lines mimicking cell-cell interactions within a solid tumor mass efficiently triggered CSP rTCR-T cells, leading to specific IFN-γ release and lysis of tumor spheroids. Furthermore, CSP rTCR-T cells showed enhanced proliferative capacity and expansion in co-cultures with PD-L1-positive tumor cells, compared to tumor cells lacking PD-L1 expression. Importantly, various target antigen-negative healthy cell types expressing or lacking PD-L1 and representing different vital organs were not cross-recognized by CSP rTCR-T cells *in vitro*. Our preclinical *in vitro* assessments of CSP rTCR-T cell functionality and safety proved their superior and gated functionality as well as favorable safety profile, showing the great potential for the treatment of cancer patients suffering from advanced solid tumor malignancies.

#0013 Discovery and development of T cell receptors targeting MAGE family antigens for adoptive T cell therapy against solid tumors.

J. Velez Lujan[1], H. Fields[1], K. Wu[2], Y. Purwanti[2], E. Xin Zi Tang[1], M. Cordeau[1], K. Mendez[1], M. Wirawan[2], M. Fehlings[1], K. Fink[2], Z. Liu[1], D. MacLeod[1]; [1]ImmunoScape, San Diego, CA, [2]ImmunoScape, Singapore, Singapore

Background: T cell receptors (TCRs) recognize epitopes from intracellular and cell surface antigens, enabling targeting of diverse tumor antigen classes including overexpressed, differentiation, cancer-testis antigens, as well as those from driver mutations, frameshift mutations, splice variants, and human endogenous retroviral elements (HERV). Melanoma-associated antigens (MAGE) are highly expressed in various solid tumor types, including melanoma, non-small cell lung cancers (NSCLC), bladder, and head and neck cancers, representing promising targets for TCR-T therapy. However, discovering robust and specific MAGE-reactive TCRs remains challenging due to limited throughput of TCR screening methodologies, and the inherently low frequency of tumor-reactive T cells in tumor samples and peripheral blood.

Methods: We employ a proprietary mass-cytometry-based multiplexed tetramer staining approach, TargetScape®, to screen and characterize CD8+ T cells in healthy donors and patients' samples. Our screening panels contain multiple peptides for MAGE family antigens including A1, C2, and A10. Subsequent single cell sequencing or single cell PCR (scPCR) of identified tumor antigen-specific T cells with high sensitivity enables comprehensive analysis of T cell phenotype, transcriptome, TCR specificity, and paired TCR sequence. TCRs identified through this method are transduced for expression in Jurkat reporter cell lines and their reactivity to corresponding peptides is assessed. Selected TCR candidates are then transduced into primary T cells and evaluated for activation and effector function using a variety of cancer cell lines expressing the corresponding endogenous antigens. Specificity assessment is performed through alanine scans and identification of potential off-target peptides and screening for reactivity.

Results: We utilized this approach to discover natural TCRs that target several MAGE family antigens. Through Jurkat reporter screening, we observed specific activation of multiple TCRs in the presence of antigen presenting cells and the peptide initially employed to identify the TCRs. Primary T-cells expressing promising TCR candidates exhibited killing activities and cytokine release when confronted with multiple solid tumor cell lines expressing endogenous levels of the MAGE antigen. Specificity assessment is currently in progress, with preliminary data indicating overall favorable specificity profiles for selected TCRs.

Conclusions: Our Deep Immunomics platform enables us to detect, characterize, and validate TCR candidates against highly clinically relevant shared cancer antigens. Leveraging this platform, we identified various natural tumor specific TCRs exhibiting activities against a range of solid tumor cell lines expressing MAGE antigens. Promising candidates are currently undergoing in vivo efficacy studies.

#0014 Identification of tumor-reactive T cell receptors through functional single cell interaction analyses for personalized T cell therapy.

T. R. Wagner[1], N. Kehl[1], S. Steiger[1], M. Kilian[1], B. Schonfelder[1], T. Boschert[1], K. Lindner[1], P. Schmidt[2], K. Rippe[1], H. Goldschmidt[3], M.-S. Raab[3], M. Platten[1], M. Friedrich[4], S. B. Eichmuller[1];

[1]DKFZ German Cancer Research Center, Heidelberg, Germany, [2]National Center for Tumor Diseases (NCT), Heidelberg, Germany, [3]University Hospital Heidelberg, Heidelberg, Germany, [4]Broad Institute of MIT and Harvard, Boston, Germany

Innovative immunotherapy approaches such as adoptive transfer of chimeric antigen receptor (CAR) T cells or tumor infiltrating lymphocytes (TILs) have shown great success in the treatment of solid tumors and hematological malignancies. Although treatment of multiple myeloma with CAR T cells can induce deep responses, relapses frequently occur due to antigen escape and limited CAR T cell persistence. TCR-engineered T cells may show prolonged persistence *in vivo* and could mediate sustained antitumor effects. A further benefit of TCR transgenic T cells is the ability to target intracellular antigens that are inaccessible to CAR T cells, expanding the range of potential targets for immunotherapy. In our project, we propose to identify T cell receptors (TCRs) specifically targeting autologous myeloma cells. Tumor-reactive T cells were identified using the Bruker Cellular Analysis Lightning® platform, allowing simultaneous functional analysis of up to 1500 individual T cell/target cell interactions on a chip. Reactive T cells were identified upon detection of secreted cytokines (IFNγ, TNFα, IL2) and measurement of 4-1BB (CD137) surface expression. Tumor-reactive T cells showing various cytokine secretion patterns and 4-1BB expression profiles were detected in each myeloma patient (on average 11.9 T cells out of 1243 cells tested per assay run). Individual tumor-reactive T cells have been isolated and their TCRs were sequenced. TCR sequences of tumor-reactive T cells were mapped to single-cell RNA sequencing data of T cells from the same patiens to reveal a gene expression signature of myeloma-reactive T cells. TCR genes of reactive T cells were cloned and overexpressed in autologous T cells for functional validation and analysis of tumor derived neoepitope specificity. In summary, we present a pipeline allowing identification of myeloma-recognizing T cells and recovery of *bona fide* tumor-reactive TCRs eligible for patient-individualized T cell therapy.

#0015 Massively parallel base-editing screens to map variant effects on anti-tumor hallmarks of primary human T cells and improve cell-based cancer immunotherapies.

Z. H. Walsh, P. Shah, N. Kothapalli, G. Nikolenyi, S. Shah, G. Leuzzi, N. Vasan, M. AlQuarishi, A. Ciccia, J. Melms, B. Izar;
Columbia University Irving Medical Center, New York, NY

Base editing enables precise generation of single nucleotide variants, but large-scale screening in primary human T cells has been limited by low editing efficiency. Here, we developed a high-throughput approach for highly efficient, massively parallel adenine and cytosine base-editor screening in primary human T cells. We performed multiple large-scale pooled screens editing 108 genes with central functions in T cells and whole-gene tiling mutagenesis of selected genes. All screens were functionally read out to capture the effect of variants on hallmarks of T cell anti-tumor immunity, including activation, proliferation, long-term persistence, and cytokine production. We discovered a broad landscape of gain-of-function and loss-of-function mutations and characterized their impact across multiple axes of T cell functions. Among others, we identified gain-of-function mutations in *PIK3CD* and its regulatory subunit *PIK3R1, LCK, AKT1,* and loss-of-function mutants of *CTLA-4,* driving increased T cell polyfunctionality. We validated several of these mutations by probing downstream signaling and functional outputs. To demonstrate the feasibility of using such screen results for improving cell-based cancer immunotherapies, we used human T cells with engineered T cell receptors recognizing specific epitopes in melanoma models. We base-edited these T cells with mutations identified in our screens and demonstrate that these mutations indeed significantly enhance cytotoxic cytokine production and tumor-lytic capacity with minimal off-target activity. Lastly, we also provide proof-of-feasibility for high-efficiency combinatorial base-editing in T cells. This study presents a framework for large-scale base editing screens with multi-dimensional functional readouts in cells that are typically difficult to molecularly engineer in a precise manner. This work also has important therapeutic implications: T cells are the substrate for clinically active cell-based therapies, such as adoptive transfer of tumor-infiltrating lymphocytes (TILs) or chimeric-receptor antigen T (CAR-T) cells. Our screen-informed base editing to achieve an improved T cell product against melanoma exemplifies the therapeutic power of generating synthetic protein variants that improve a wide range of existing and future T cell-based cancer immunotherapies.

#0016 CD4+ and CD8+ TCRαβ-deficient bioluminescent reporter T cells for screening and characterization of neoantigen-specific TCRs.

M. Cong, J. Grailer, M. Slater, P. Stecha, J. Hartnett;
Promega, Madison, WI

Adoptive antigen-specific T cell therapy is currently comprised of chimeric antigen receptor (CAR) and T cell receptor (TCR) engineered T cells. Clinical results from CAR-T cells have demonstrated promising results in treating leukemias, while TCR-engineered T cells, which have the advantage of recognizing intracellular tumor antigens, is still in early development. Here, we report the development of CD4+ or CD8+ TCRαβ-KO reporter T cell lines for the screening and characterization of transgenic TCRs. A TCRαβ-KO reporter T cell line was first developed by knocking out the endogenous TCR α and β chains in the reporter T cell line using CRISPR/Cas9. Successful knockout was confirmed by phenotypic assays and TCR v chain locus sequencing. We demonstrated that re-introduction of influenza hemagglutinin (HA) peptide-specific TCR (HA1.7) α and β chains into TCRαβ-KO reporter T cell lines results in HA peptide-dependent TCR activation and luciferase reporter expression when HA peptide is presented by a MHCII+ cell line. Similarly, re-introduction of MART-1-specific TCR (DMF5) resulted in MART-1-dependent activation in the presence of MHCI+ cells. The select expression of CD4- or CD8-expressing variants of the TCRαβ-KO reporter T cell line enables the development of transgenic TCRs for both MHCI- and MHCII-restricted tumor antigen targets. Further development of CD4/CD8 double-positive and double-negative cell lines enables screening of low and high affinity TCRs without MHC bias. Together, this TCRαβ-KO platform represents a powerful tool for the screening and characterization of neoantigen-specific TCRs.

#0017 Metabolic screening of T cells guides the enrichment of stem cell memory phenotype.

A. Lauer, N. Karassina, K. Sylvester, J. Vidugiriene;
Promega Corporation, Madison, WI

The efficacy of T cell-mediated immunotherapy is improved by the proliferation of T cells with a stem cell memory phenotype (Tscm). These cells are capable of long-term persistence, self-renewal, multipotency, and robust engagement with cancer cells. This study focuses on refining T cell activation protocols to bolster the presence of Tscm within the therapeutic arsenal against cancer. Through a series of cell health and metabolic assays, we traced the activation-induced metabolic reprogramming that results from Tscm enrichment. *Ex vivo* activation was characterized by a rapid 2.5-3 fold increase in ATP production and a 2 fold shift in intracellular reducing potential, paralleling the metabolic demands of Tscm in the cancer microenvironment. Progression of activation intensified the metabolic flux through catabolic and anabolic pathways, with significant fluctuations in metabolites such as glucose, lactate, glutamine, glutamate, branched chain amino acids, and pyruvate. These metabolic alterations were accompanied by a 2 fold increase in the prevalence of Tscm cells, and demonstrated a dependency on media composition. Our findings reveal that metabolic profiling during T cell activation provides early and actionable insights into the enrichment of Tscm, and may serve as a strategic guideline for the enhancement of cancer immunotherapies.

#0018 The polyamine-hypusine axis is a promising avenue to improve T-cell metabolism and persistence for adoptive cell therapy.

M. Kehinde-Ige, O. Okoko, G. Zhou, H. Shi;
Augusta University, Augusta, GA

There are significant barriers to the application of Adoptive Cell Therapy (ACT) to many cancer types. One of these barriers is a result of poor metabolic fitness of T cells, leading to poor proliferation, persistence, and dampened anti-tumor function. Leveraging T-cell metabolism to improve their function is becoming increasingly important to make significant strides in immunotherapy. Stat5a has been shown to be a master regulator of energy and metabolism in T cells, highlighting it as a promising avenue to improve T-cell metabolism for ACT. We have established that the expression of Constitutively Active Signal Transducer and Activator of Transcription 5A (CASTAT5) on tumor-specific $CD4^+$ T cells improves their persistence, polyfunctionality, and anti-tumor effects in a mouse model. This study further examines Stat5a and its downstream metabolic targets in the context of ACT. We carried out scRNAseq analysis and found that Stat5a directly interacts with genes involved in polyamine metabolism. More specifically, Stat5a activation increases the expression of ornithine decarboxylase (Odc1), spermidine synthase (Srm), deoxyhypusine synthase (Dhps), and deoxyhypusine hydroxylase (Dohh) in a subset of $CD4^+$ T cells expressing CASTAT5. Cleavage Under Targets and Tagmentation (Cut&Tag) analysis of histone H3K27ac also demonstrated increased H3K27ac at promoter and enhancer regions of polyamine pathway genes in CASTAT5 compared to control $CD4^+$ T cells. To further examine the function of Stat5a, the murine pro-B cell line, Ba/F3, is being used as a model to study Stat5a-mediated signaling. We have found that upon withdrawal of IL-3 from Ba/F3 cells, Stat5a activation is significantly downregulated. Our scRNA-seq-based metabolic flux estimation showed a significant reduction in metabolic fluxes and related genes, including polyamines, following IL-3 withdrawal. Correspondingly, Stat5a ChIP-Seq and Cut&Tag analyses of H3K27ac revealed Stat5a binding to active enhancer regions in the presence of IL-3 that are lost following its withdrawal. Untargeted metabolomics confirmed the marked Stat5a-mediated reduction in metabolite abundance after IL-3 deprivation, in a time-dependent manner. The polyamine-hypusine axis revealed in our studies is a promising avenue to improve T-cell function. This axis has been shown to regulate T-cell function, and potentially modulate mitochondrial respiration and T-cell activation. Hence, our studies have identified polyamine supplementation and gene modulation as promising strategies to improve the metabolism of Adoptive T cells in a Stat5a-mediated manner. Further studies will evaluate the effectiveness of this avenue in improving T-cell function, improving their efficacy for ACT, and improving patient outcomes.

#0019 Patient derived tumor-on-a-chip platform potentiates adaptive immune response against primary tumor cells.

C. R. Schaaf[1], T. Liu[1], D. Hutchins[1], M. Kooshki[1], **C. Wagner**[1], N. Edenhoffer[1], S. Forsythe[2], R. Greissinger[1], L. Miller[1], P. Triozzi[1], E. Levine[1], S. Soker[1], A. R. Hall[1], K. I. Votanopoulos[1];

[1]Wake Forest University School of Medicine, Winston-Salem, NC, [2]National Institute of Health, Bethesda, MD

Background: Adoptive cellular therapy (ACT) is a promising antitumor immunotherapy showing success in select trials/patients. However, major challenges limit ACT in all tumors including insufficient cell numbers and failure to target heterogeneous tumors. To improve ACT, we developed a novel biomimetic device where patient-derived tumor organoids, enriched with antigen presenting cells, are cocultured with autologous peripheral blood mononuclear cells (PBMCs) in a microfluidic tumor-on-a-chip system (TOC). As PBMCs circulate through the device, they are exposed to dispersed tumor polyclonal neoantigens, leading to formation of patient- and tumor-specific organoid interacting lymphocytes (OILs).

Objectives: Demonstrate that a 3D tumor-on-a-chip (TOC) platform generates organoid interacting lymphocytes (OILs) with enhanced antitumor reactivity.

Methods: Specimens were collected from 15 surgical patients: melanoma (2), mesothelioma (6), and metastatic appendiceal adenocarcinoma (9). Tumor cells were combined with autologous antigen presenting cells (healthy spleen/lymph node) in a 3D matrix to generate immune-enhanced tumor organoids in the TOC system. Autologous PBMCs circulated through the system to produce OILs (7 days). Uncirculated PBMCs and tumor infiltrating lymphocytes (TILs) were cultured as controls. Resultant CD8+ controls and OILs were examined by single cell proteomics to compare cytokine secretion polyfunctionality. To assess anti-tumor reactivity, OILs and controls were reintroduced to tumor cells via coculture. Secreted bulk cytokine profiles were compared by Isoplexis CodePlex and confirmed by ELISA. NanoString Geomx spatial proteomic analysis of coculture PTOs identified key lymphocyte activity and phenotypes during anti-tumor reactivity. Coculture cytotoxic lymphocyte activation and tumor cell death was confirmed by flow cytometry. Data were analyzed using student *t*-test and differential expression from linear mixed-effect model.

Results: Compared to controls, CD8+ OILs showed increased polyfunctionality within single cells immediately after training, particularly in effector T-cell associated cytokine profiles (INF-γ, Granzyme B, Perforin). Upon re-introduction to PTOs, OILs excreted significantly increased inflammatory-associated proteins IFN-γ, MCP-1, and Granzyme A ($p<0.05$). Furthermore, OIL re-exposure to tumor led to cytotoxic lymphocyte activation (CD8+CD69+) and significantly increased tumor cell death compared to control ($p<0.05$).

Conclusion: Compared to controls, OILs produced in the TOC system show enhanced cytotoxic lymphocyte polyfunctionality and induce tumor cytotoxicity, independent of tumor type. With further validation of the OILs' increased tumor-targeting efficacy, we propose a new potential ACT modality to target a broad array of tumors previously untreatable by current therapies.

#0020 KSQ-001EX: An engineered TIL therapy manufactured from a clinical-scale, feeder-free process for the treatment of solid tumor indications.

S. Lin[1], G. Martinez[1], M.-A. Forget[2], K. Adlerz[2], M. Ghose[1], L. Williams[1], P. Dunbar[1], F. Thompson[1], F. Sharp[1], H. Gannon[1], C. Calnan[1], A. Yeri[1], D. Sangurdekar[1], D. Sakellariou-Thompson[2], S. Fix[1], T. Griffith[2], E. Jafari[2], J. Zulovich[2], P. Balasubramanian[2], E. Willert[2], M. Benson[1], C. Bernatchez[2], **K. K. Wong**[1];

[1]KSQ Therapeutics, Lexington, MA, [2]CTMC, Houston, TX

Tumor Infiltrating Lymphocyte (TIL) therapy is an autologous adoptive cell therapy involving the isolation, ex vivo expansion and infusion of tumor infiltrating lymphocytes (TIL) into late-stage cancer patients for therapeutic benefit. While clinical responses to TIL therapy have been observed in metastatic melanoma, efficacy in other tumor types including non-small cell lung cancer (NSCLC), and head and neck squamous cell carcinoma (HNSCC) [SM1] is limited by the intrinsic functionality and persistence of transferred T cells and the immunosuppressive tumor microenvironment. To improve the clinical outcome of TIL therapy, we have developed KSQ-001EX, an engineered TIL therapy using CRISPR/Cas9 technology to knockout the SOCS1 gene, for the treatment of solid tumors. SOCS1 is a negative regulator of cytokine signaling in T cells that we previously identified as a top target restraining T cell anti-tumor function and persistence using genome-wide in vivo CRISPR screens. To streamline and shorten TIL manufacture, we established a next-generation manufacturing process with resected tumors or core biopsies as starting materials that eliminates the use of feeder cells and REP, shortening the length of manufacture to 22 days. We demonstrated robust manufacture of cryopreserved KSQ-001EX at clinical scale from NSCLC, HNSCC, checkpoint refractory melanoma, and heavily pre-treated colorectal carcinoma (CRC). KSQ-001EX manufactured from clinical-scale runs were highly viable (>90%) following cryopreservation and thaw, with > 90% SOCS1 on-target editing and complete knockdown of SOCS1 at the protein level. Importantly, KSQ-001EX across all indications assessed showed high frequency of CD8 (median ~80%), an attribute associated with TIL clinical responses. KSQ-001EX also retained high diversity of TCR repertoire. Consistent with the biology of SOCS1 editing, KSQ-001EX exhibited greater cytotoxicity and higher IFNγ production against tumor spheroids in comparison to TIL and enhanced induction of pSTAT4 upon IL-12 stimulation, demonstrating heightened sensitivity of KSQ-001EX to cytokines. In conclusion, KSQ-001EX, an engineered TIL therapy with CRISPR/Cas9 mediated inactivation of SOCS1, can be manufactured at clinical doses from surgical resections or core biopsies within 22 days using a simplified feeder-free manufacturing process from multiple indications. KSQ-001EX exhibits heightened anti-tumor activity in preclinical models, with therapeutic benefit to be evaluated in a planned clinical trial in patients with treatment-refractory melanoma, NSCLC, and HNSCC. [SM1]Spell out these at first instance?

#0021 Discovery of ALK-specific TCR clonotypes for the development of TCR-T cell therapies against ALK-positive cancers.

C. Mecca[1], A. Azambuja[1], L. Alessandri[1], E. Bergaggio[1], S. Piane[1], M. Simoes-Costa[1], E. L. Reinherz[2], R. Blasco-Patino[1], R. Chiarle[1];
[1]Boston Children's Hospital, Boston, MA, [2]Dana-Farber Cancer Institute, Boston, MA

Introduction: Anaplastic Lymphoma Kinase (ALK) tyrosine kinase inhibitors (TKIs) have extended the survival of patients with ALK-rearranged cancers, including non-small cell lung cancer (NSCLC). Unfortunately, acquired resistance develops within 2-3 years, highlighting the urgent need for novel and effective therapeutic strategies for these patients. Here, we aimed to identify T cell receptor (TCR) clonotypes against two human ALK immunogenic peptides we previously identified by mass spectrometry in biopsies from patients with ALK-rearranged NSCLC (PMID:37430060) and to develop TCR-T cell therapies for ALK-positive NSCLCs.
Methods: BALB/c mice were vaccinated with the murine ALK peptide PGPGRVAKI and transgenic mice expressing human HLA-B*07:02 were vaccinated with human ALK peptides RPRPSQPSSL and IVRCIGVSL. All mice received two priming injections (days 1 and 14) followed by two boosters, and activated $CD8^+$ T cells were sorted and subjected to single-cell sequencing.
Results: As proof of concept, we first vaccinated BALB/c mice with the ALK peptide PGPGRVAKI and identified 381 unique ALK-specific clonotypes. Among these, we cloned the most expanded 5 clonotypes and confirmed that these clonotypes were functional as evidenced by the release of significant amounts of IFN-γ and IL2, and potent *in vitro* killing activity following co-culture with murine ALK-positive lung cancer cells. To identify TCR clonotypes for the development of TCR-T therapy in patients with ALK-positive cancers, we next vaccinated transgenic mice expressing human HLA-B*07:02 with human ALK peptides RPRPSQPSSL and IVRCIGVSL. We again identified multiple unique ALK-specific TCR clonotypes among $CD8^+/CD137^+$ cells from these transgenic mice vaccinated with RPRPSQPSSL peptide (N=353 TCR clonotypes) and IVRCIGVSL peptide (N=742 TCR clonotypes). Single-cell RNA sequencing of the expanded clonotypes (TCR clonotype frequency ≥4) versus non-expanded clonotypes (TCR clonotype frequency <4) revealed significant upregulation of *Ccl3, Ccl4, Ccl1, Ifng, Xcl1, and Il13* across mice vaccinated with RPRPSQPSSL and IVRCIGVSL ($p < 0.05$). Gene set enrichment analysis (GSEA) confirmed significant upregulation of multiple pathways of adaptive immune response, including T cell activation, IFN-γ signaling and production, cytokine release, and T cell proliferation (adjusted $p < 0.05$), suggesting functional activity of these TCR clonotypes against ALK.
Conclusion: Here, we first demonstrated the feasibility of isolating ALK-specific TCR clonotypes by mice vaccination that exerted anti-tumor activity. Additionally, we identified ALK-specific TCR clonotypes from transgenic mice expressing human HLA-B*07:02 vaccinated with two human ALK peptides. This discovery lays the basis for the successful development of TCR-T cell therapies for ALK-positive NSCLCs, and possibly other ALK-positive cancers.

#0022 Development and characterization of human tumor specific cytotoxic lymphocytes for preclinical drug development.

I. Rohleff, L. Grone, K. Lashuk, **J. B. Schueler**;
Charles River Laboratories, Inc., Freiburg, Germany

Heterogeneity within a tumor allows it to better adapt to changing conditions and can have therefore a negative impact on a patient's prognosis, response to treatment and overall health. Breast cancer is a highly heterogeneous disease caused by distinct genetic mutations in mammary epithelial cells, resulting in significantly different forms of the disease and a need for highly personalized treatment schemes for patients. Hence, it is important to develop and improve (immuno)therapies for breast cancer patients. Adoptive T-cell therapy with autologous CD8+ cytotoxic T cell lymphocytes (CTL) is a promising method that has already shown promising effects in melanoma patients. Unfortunately, there is almost no information about the use in breast cancer patients. We developed an in vitro protocol to generate tumor-specific CTLs by priming on HER2+ breast cancer cell lines JIMT-1 and SKBR-3. Subsequently, these primed CTLs were tested in 2D and 3D immune cell killing assays in a life cell imaging device in combination with an endpoint viability assay. The activity was compared with unspecific CD8+T cells activated by phytohemagglutinin (PHA) or αCD2/αCD3/αCD28, HER2-peptide specific T cells and HER2-CAR T cells serving as a positive control. We investigated the feasibility to freeze CTLs for use in subsequent studies and validated the relevance of HER2 as the main druggable target in the tumor lines using an siRNA approach. The CTLs were most effective on JIMT-1 in a 3D setting, whereas the SKBR-3 CTLs displayed similar activity in 2D and in 3D. The respective CTLs were tumor line specific, as SKBR-3 CTLs did not kill efficiently the JIMT-1 cells and vice versa. The same CTLs displayed the same efficacy pattern after thawing but less pronounced. Thus, within one experimental set-up it is recommended to use either one. The Her2 knockdown in the target cells reduced the killing activity of the CTLs slightly. However, this effect was not statistically significant proving the importance of CTLs as treatment option as well as neoantigens as targets in drug development. In summary, the CTLs proved to capture the respective tumor heterogeneity showing high killing rates in both SK-BR3 and JIMT-1 being more active than HER2-peptide specific T cells. The availability of CTLs in a preclinical setting facilitates screening approaches for combinational studies. Beyond that they can serve as starting material to develop cancer vaccines and identify highly immunogenic neoantigens.

#0023 The use of baboon envelope pseudotyped lentiviral (BaLV) vector allows high-efficiency transduction of CD8+ T cells.

I. Kaplan, M. Sheffer, Y. Abdulhamid, E. Bobilev, R. Romee;
Dana-Farber Cancer Institute, Boston, MA

CAR-T (chimeric antigen receptors T) cell therapy has been proven to be effective in treating various types of cancers. To prevent graft vs. host disease, CAR-T cells are mostly produced from the patient's own T-cells and transduced using pseudotyped vesicular stomatitis virus glycoprotein (VSV-G) lentivirus system. Typically, CD8+ effector T cells have relatively low transduction rates, compared with CD4+ T cells, and yet it is the CD8+ T cells that are the dominant effector immune cells in a CAR product. To achieve high efficacy of the CAR-positive effector T cells, a higher number of the patient's CD8+ T cells are needed for transduction. However, cancer patients may not have enough T cells by the time they are eligible for CAR-T therapy due to multiple treatment cycles. One potential way to overcome this problem is to achieve a much higher transduction rate of the CD8+ T cells.

Recently, our lab published the use of pseudotyping CAR lentivirus with baboon endogenous retroviral envelope (BaEV) for the generation of CAR transduced natural killer (NK) cells, exhibiting high transduction rates of above 50%. BaEV lentivirus targets the amino acid transporter, SLC1A5 (ASCT2), to enter the cell. SLC1A5 is highly expressed on activated NK and T cells. Therefore, we hypothesized that CAR-T transduced with BaEV lentivirus will have increased transduction rates compared with VSV-G.

To assess transduction, we used anti-mesothelin (MSLN) CAR construct which consists of the mesothelin single chain variable fragment (scFv), CD8α hinge and transmembrane domain, 4-1BB costimulatory domain, and a CD3ζ activation domain, followed with GFP linked by self-cleavage P2A. The concentrated virus was titrated in Jurkat cells, resulting in 90% transduction efficiency with VSV-G and 50% with BaEV, for the same amount of virus.

Primary CD8+ T cells were isolated from the peripheral blood of 3 healthy donors and activated with CD3/CD28 beads for three days prior to transduction. Then, the cells were transduced with either VSV-G or BaEV meso-CAR pseudotyped lentiviruses. Transduction rates were measured by flow cytometry, 3 days post-transduction. In addition, the CAR-T cells were expanded *in vitro* to evaluate their cytotoxicity against the mesothelin-positive cell line OVCAR-8, for 24 hours. VSV-G led to 10-20% transduction rates, while BaEV exhibited much higher transduction rates (55-70%), leading to improved cytotoxicity against the tumor cells.

The successful increase of transduction rates for CD8+ CAR-T using our BaEV lentiviral system can be utilized in the clinic to treat patients that previously didn't qualify for adoptive therapy, due to low lymphocyte counts. In addition, higher numbers of CD8+ CAR-T cells may result in better tumor control in both blood and solid tumor settings, compared with the traditional approach for CAR-T production.

#0024 Utilizing T cell receptor-based therapy to treat anaplastic thyroid cancer.

S.-H. Hung, Y. C. Henderson, P. Ke, Y. Chiu, S. Singh, Y. Chen, S. Y. Lai, C. Yee;
UT MD Anderson Cancer Ctr., Houston, TX

Anaplastic thyroid cancer (ATC) is one of the most aggressive solid tumor in thyroid tissue, with a 6-month medium overall survival. The effectiveness of conventional treatments in extending the survival of patients is limited. Therefore, there is an urgent need to develop novel systemic therapeutic interventions. Adoptive cell therapy has revolutionized cancer immunotherapy by successfully treating B-cell malignancies through chimeric antigen receptor-based approaches. For solid tumors, there is a need to identify a broader spectrum of tumor target antigens, and the field has now shifted towards leveraging T cell receptors (TCRs) which can recognize both intracellular and extracellular antigen-derived epitopes. Our team has established an immunogenic epitope discovery pipeline, followed by a specialized protocol for empiric validation of candidate epitopes. We characterized immunogenic epitopes by coupling tandem mass spectrometry of MHC-eluted peptides with tumor proteome and MHC-peptide binding prediction databases. By integrating multi-omics data (genomics, transcriptomics, and immunopeptidomics) from both in-house and publicly available ATC databases, we find that ATC exhibits significant upregulation of pathways associated with microtubule-based movement, chromosome segregation, and kinetochore complex components. We have identified several HLA-A2- and A24-restricted immunogenic peptides representing these pathway-associated proteins that covered more than 60% of the patient population. These immunogenic peptides were subsequently utilized to isolate antigen-specific T cells from peripheral blood and identify cognate TCR. These peptide-specific T lymphocytes elicit cytotoxicity toward multiple HLA-matched ATC cell lines and tumor samples *in vitro* and *in vivo*. In conclusion, our studies contribute to the development of a new treatment paradigm for treating ATC.

#0025 Multimodal single-cell analysis of lifileucel tumor-infiltrating lymphocyte (TIL) product identifies additional high-resolution potential features.

J. Dean, J. Yglesias, H. Yin, R. Qi;
Iovance Biotherapeutics, San Carlos, CA

Introduction: Autologous TIL cell therapies such as lifileucel have demonstrated durable responses in patients (pts) with various solid tumors including melanoma and lung cancer. The TIL drug product (DP) phenotype was previously assessed and extensively characterized based on the bulk population. The current research further characterizes the TIL DP at a single-cell level using high-dimension multimodal sequencing and explores features that have a potential to inform future development of TIL therapies.

Methods: Manufactured lifileucel TIL DP from 20 pts (best overall response [BOR]: 6 complete response [CR], 4 partial response, 5 stable disease, 5 progressive disease [PD]) from the registrational melanoma C144-1 trial were analyzed using single-cell RNA and T-cell receptor (TCR) sequencing, resulting in 153K single-cell transcriptomes. To aid with cell-type annotation, 130 surface proteins on TIL DP samples from a subset of 4 pts (BOR: 2 CR, 2 PD) were detected via Cellular Indexing of Transcriptomes and Epitopes by sequencing. Multimodal weighted nearest-neighbor analysis combined with manual cluster annotation (via known marker genes and proteins), cell-type-specific gene signatures, and automated annotation were used to develop a single-cell TIL (scTIL) reference map, resulting in high-resolution subsets of cells. TCR clonotypes from lifileucel TIL DP were compared to those from respective pretreatment tumors previously identified by bulk TCR sequencing.

Results: Mapping of the full dataset to the novel scTIL reference revealed a $CD8^+$ TIL-dominant composition of responder TIL DP. TIL from pts with BOR PD exhibited reduced $CD8^+$ effector memory (Tem)-like and resident memory (Trm)-like T cells. Differential expression analysis showed that responder $CD8^+$ TIL had increased expression of TCR signaling genes while responder $CD4^+$ TIL exhibited gene expression consistent with a more cytotoxic-like phenotype. Relative to responders, $CD8^+$ TIL of pts with BOR PD had lower expression of the $CD39^-CD69^-$ (stem-like) gene signature and higher expression of the $CD39^+CD69^+$ (terminal differentiation) gene signature. Pseudotime trajectory analysis found that both $CD8^+$ and $CD4^+$ TIL of pts with BOR PD were more terminally differentiated. Single-cell TCR sequencing revealed that $CD8^+$ T-cell clusters had greater clonal overlap than $CD4^+$ T-cell clusters. Expanded clonotypes in pretreatment tumor tissues were more prevalent in TIL TCR repertoires of responders and were more likely to be expressed by $CD8^+$ (specifically $CD8^+$ Tem- and Trm-like TIL) than $CD4^+$ T cells.

Conclusions: Collectively, these results shed additional light on the cellular and molecular characteristics of ex vivo expanded lifileucel TIL DP and signal additional features with a potential to guide future TIL product development.

#0026 An HLA-class II restricted HPV18 E7 specific TCR cloned from a long-term surviving cervical cancer patient.

J. Long[1], X. Chen[2], S. Ou[2], M. Ma[2], J. Chu[2], **Y. Han**[2];
[1]Department of Oncology, Cancer Center, the First Affiliated Hospital, Sun Yat-sen University, Guangzhou, China, [2]HRYZ BIOTECH Co., Ltd., Shanghai, China

T cell receptor (TCR)-engineered T cell therapy is a promising approach for the treatment of solid malignancy, with multiple clinical trials reporting impressive responses using affinity-matured TCRs. However, artificially mutated TCRs can increase the risk of off-target toxicities due to unexpected cross-reactions, which limits the overall safety of this approach. To tackle this challenge, we have developed a novel strategy for cloning tumor-specific endogenous therapeutic TCRs from long-term surviving patients who have responded to immunotherapy. Specifically, we have identified a TCR (10F04) that is specific to human papillomavirus type 18 (HPV18) $E7_{84-98}$ and restricted to human leukocyte antigen (HLA) class II molecular DRA/DRB1*09:01 from the peripheral blood of a patient with HPV-positive metastatic cervical cancer who received multiple antigens stimulating cellular therapy (MASCT) and exhibited sustained T-cell immunological responses. Upon transduction into human T cells, the 10F04 TCR demonstrated robust antitumor activity in both *in vitro* and *in vivo* models. Notably, the TCR effectively redirected both CD4 and CD8 T cells to specifically recognize tumor cells and induced multiple cytokine secretion along with durable antitumor activity. Importantly, no cross-reactivity was detected in toxicity studies. As a result, this TCR is currently being investigated in a phase I clinical trial for treating HPV18-positive cancers (NCT05787535). The first-in-human infusion had been just completed. No severe adverse event had been observed, while an early proliferation of TCR-T was detected several days after infusion. Our approach of cloning tumor-specific and safe endogenous therapeutic TCRs from long-term surviving patients offers a promising strategy for developing safe and effective TCR-engineered T-cell therapies for solid tumors. These findings provide important insights into the potential of HLA class II-restricted TCR-T therapy as a novel cancer treatment modality.

#0027 A single amino acid mutated AFP specific T cell receptor uniting synergistic functionalities of CD4 and CD8 T Cells with no cross-activity.

Chen-Song Huang[1], shudan Ou[2], Jun Li[2], Junjun Chu[2], **Yanyan Han**[2]

[1]Department of Pancreato-Biliary Surgery, the First Affiliated Hospital, Sun Yat-sen University, Guangzhou, China,[2]HRYZ BIOTECH Co., Ltd., Shanghai, China

Background: Genetically engineered T cells with T cell receptor (TCR-T) cell therapy have shown great potential for cancer treatment by targeting tumor-associated antigens. Despite its success in treating various tumor types, such as synovial sarcoma, head and neck tumors, and cervical cancer, its application in liver cancer is limited. Alpha-fetoprotein (AFP), a highly expressed tumor-associated antigen in liver cancer, is an ideal target for TCR-T cell therapy. Although early human trials have confirmed the safety of AFP-targeting TCR-T products, their efficacy is still modest, highlighting the need for further research and development.

Methods: We developed a robust strategy combining ex vivo stimulation and single-cell paired TCR sequencing to identify AFP-recognizing TCRs in liver cancer patients. To optimize TCR expression and minimize mispairing, we employed codon optimization and replaced the constant regions with murine counterparts. Furthermore, structural analysis guided the affinity optimization of the CDR3 region to enhance the antitumor function of the selected TCR. The anti-tumor efficacy of TCR-T cells was rigorously evaluated through in vitro cytotoxicity assays using the Real-Time Cell Analyzer (RTCA) system and in vivo antitumor assessment in immunodeficient mouse xenograft models. Antigen specificity, HLA restriction, and other potential toxicity were carefully evaluated in both *in vitro* and *in vivo* models.

Results: We successfully cloned a highly effective TCR that recognizes the $AFP_{158-166}$ epitope presented by HLA-A*0203. After sequence optimization, we further changed a single amino acid on the TCR vβ chain based on AI prediction. The expression and functionality of this TCR was significantly improved. When introduced into human T cells, the single amino acid mutated TCR demonstrated robust and specific anti-tumor activity in various models, including cultured tumor cells, patient-derived organoids, and mouse xenografts models. Notably, this TCR also redirected CD4 T cells to recognize tumor cells, induced the secretion of multiple cytokines, and maintained long-lasting anti-tumor effects. Our rigorous screening assays confirmed that the TCR showed no cross-reactivity with the human proteome or major HLA subtypes. Additionally, extensive preclinical safety assessments in tumor-bearing animals treated with ST08A01-AM14 TCR-T cells showed no significant safety concerns.

Conclusion: In this study, we have developed an HLA-A*0203 restrict $AFP_{158-166}$ specific TCR-T therapy, which exhibits exceptional anti-tumor effects while ensuring a favorable safety profile. The promising results support the further investigation against AFP-positive solid tumors in clinic.

#0028 A CRISPR/Cas9 screening platform ImmuT Finder® enables in vivo T cell functional screening and identification of potent immunoregulatory targets for next-generation T cell therapy.

J. Sun, J. Jin, J. Wang, Y. Sheng, F. Li, L. Chen, Y. Tan, Z. Xu, Y. Liu, K. Liu, Y. Liu;
Grit Biotechnology, Shanghai, China

Insufficient tumor infiltration and the presence of various immunosuppressive mechanisms in tumor microenvironment (TME) are two major challenges compromising the anti-tumor efficacy of T cell therapy post infusion. PD-1/PD-L1 blockade has been proven to benefit a portion of late-stage solid tumor patients, however KO of PD-1 may impact the long-term persistence of CAR-T cells, indicating target selection strategies for gene editing of cell therapy products may differ from antibody drugs. To discover potent and/or novel immunoregulatory targets that could maximize the function of T cell therapy, we established an *in vivo* CRISPR/Cas9 screening platform, ImmuT Finder®, to identify functional gene targets in primary mouse T cells. Notably, T cells carrying sgRNA library have been collected at different harvest time points post transfer based on different screening purposes; library size has been rationally designed to ensure good coverage of the whole library in harvest samples. We selected top targets from *in vivo* screening and quickly validated their function in primary human T cells in a 96-well array. Then, the top targets that showed significant enhancement in proliferation and function of human T cells were further selected, and their combinational effects on human peripheral T cells and TIL were tested both *in vitro* and *in vivo*. Finally, GT307 stands out as the most potent KO combination, which significantly improves serial tumor killing of TCR-T and CAR-T as well as autologous tumor cytotoxicity of TIL *in vitro*. Furthermore, GT307 KO TCR-T and TIL demonstrated significantly improved tumor control in mouse models than their unedited counterparts and promoted long-term persistence with low support of IL-2. In summary, these data demonstrated that our ImmuT Finder® platform enables discovery of potent and/or novel targets for the development of T cell product and supports the clinical assessment of GT307 as a next-generation T cell therapy.

#0029 A genetically modified tumor-infiltrating lymphocytes product (GT216) enhanced anti-tumor efficacy against solid tumor by fine-tuning multiple negative immune regulators.

J. Sun, Y. Tan, J. Jin, J. Wang, L. Chen, F. Guo, Y. Tan, Z. Xu, Y. Liu;
Grit Biotechnology, Shanghai, China

Adoptive cell therapy by tumor-infiltrating lymphocytes (TILs) has demonstrated promising clinical benefits for patients with solid tumors. However, the large-scale expansion during manufacture may drive hypofunction or exhaustion status of the final TIL product, leading to impaired anti-tumor efficacy and persistence post infusion. Grit Biotechnology designed a genetically engineered TIL product (GT216) to overexpress an intracellular protein that is induced by antigen-specific T cell response and mediates the degradation of multiple immunoregulatory molecules, which releases the therapeutic potential of TIL with enhanced cytotoxicity as well as persistence *in vitro* and *in vivo*. Multiple vector construct designs of GT216 were compared and the best design was selected based on stable and efficient expression of surrogate marker in TILs. GT216 could be successfully manufactured by Grit's StemTexp® and StaViral® platforms with good memory phenotype and no signs of overactivation or exhaustion. In vitro functional analysis showed that GT216 demonstrated significantly increased cytotoxicity and cytokine production when cocultured with tumor cells and better tumor control ability during a serial killing assay than conventional TILs. Notably, GT216 TILs eradicated tumor growth with low IL-2 support in NOG mice inoculated with HLA-matched tumor cells while conventional TILs showed limited tumor control with high IL-2, corelated with their better infiltration and persistence in tumor and periphery. In summary, GT216 demonstrated enhanced anti-tumor efficacy and persistence as well as reduced IL-2 dependency *in vitro* and *in vivo*, supporting the clinical evaluation of GT216 as a next-generation TIL therapy in treatment of refractory solid tumors.

IMMUNOLOGY: Adoptive Cell Therapies 2: CAR-T Cells
Poster Session

#0033 Revitalizing CAR-T cells for TNBC: Targeting phosphorylation of TCF7 to overcome T cell exhaustion.

Z. Jiang[1], Y.-Y. Chu[1], H.-H. Lee[1], M.-C. Hung[2], L. Yang[1], C. Lin[1];
[1]UT MD Anderson Cancer Center, Houston, TX, [2]China Medical University, Tai Chung, Taiwan

Breast cancer stands as the second leading cause of cancer-related deaths among women in the United States, with triple-negative breast cancer (TNBC) representing the most aggressive subtype. Although immune checkpoint inhibitors (ICI) demonstrated durable response in some TNBC patients, the added benefit of current FDA-approved ICI in combination with chemotherapy is estimated to be only around 10%. Fortunately, TNBC displays the highest number of tumor-infiltrating lymphocytes (TILs), compared to other BC subtypes, indicating an optimal context for the survival of T cells. Therefore, CAR-T therapy emerges as a promising therapeutic option for TNBC patients. Expanding the application of CAR-T therapies to solid tumors, including breast cancer, remains challenging. One of the key hurdles lies in the immunosuppressive tumor microenvironment, where the T cell receptor experiences long-term exposure to tumor antigens, leading to T cell exhaustion. This state impedes the T cells' capacity to efficiently target and eliminate cancer cells. Identifying key regulatory mechanisms downstream of the T cell receptor holds the potential to revolutionize existing immunotherapeutic strategies.

In our study, we discovered that the presence of the master transcriptional factor of T cell stemness, TCF1, in $CD8^+$ T cells, is essential for controlling TNBC tumors. TCF1 undergoes phosphorylation by LCK, a crucial component of initiating T cell receptor signaling, upon T cell activation. We found this phosphorylation site is indispensable for TCF1's transcriptional activities, inhibiting the downstream program of T-cell persistence and causing T-cell exhaustion. Reversing this process, either through LCK inhibition or introducing a non-phosphorylated form of TCF1, results in a more sustained CAR-T cell-mediated anti-tumor response. Our findings reveal the significance of TCF1 post-translational modification in the development and longevity of stem-like $CD8^+$ T cells, bridging the gap between TCR signaling and transcriptional and epigenetic programs of stem-like CD8+ T cells. This insight contributes to a potential cure for TNBC by maintaining T cell persistence.

#0034 Improving CAR T cell efficacy in pancreatic cancer using an *in vivo* CRISPR Cas9 screen.

T. Kienka[1], F. Korell[1], N. Knudsen[2], K. Yates[2], A. Cheng[2], D. Sen[1], M. Maus[1], R. Manguso[2];
[1]Massachusetts General Hospital, Boston, MA, [2]Broad Institute of MIT and Harvard, Cambridge, MA

Introduction

Chimeric antigen receptor (CAR) T cell therapy has demonstrated remarkable success in the treatment of certain hematologic malignancies. However, efficacy against solid tumors has remained limited and is associated with relatively low T cell persistence. Here, we perform an *in vivo* CAR T cell CRISPR screen in pancreatic adenocarcinoma using a curated guide library to identify genes that enhance CAR T cell persistence *in vivo*.

Material and Methods

The Mario library consists of 1180 total guide RNAs targeting 135 genes that have been shown to modulate T cell functions in other models. To generate Mario-CART cells, primary human T cells were transduced with two lentiviral vectors, the first encoding an anti-mesothelin CAR and the second containing a fixed guide targeting the TCR alpha gene constant region (TRAC) as well as the Mario library. Mario-CART cells were transduced at low MOI, expanded in vitro and selected for loss of CD3 expression using magnetic selection, to enrich for cells that had a successful gene-edited event. Purified Mario-CART cells were intravenously injected into NSG mice bearing subcutaneous pancreatic adenocarcinoma (ASPC1). Tumor and spleen were harvested 2 or 4 weeks after Mario-CART injection, and engrafted T cells were isolated by CD45 positive selection. Genomic DNA was prepared from retrieved cells and illumina sequencing was used to evaluate guide abundance to identify gene knockouts that had been enriched after tumor exposure *in vivo*.

Results

The transcription factor, GATA3, was consistently identified as the most enriched hit across two donor T cells when Mario-CART was recovered at the 2-week timepoint. When compared to control or a depleted hit, GATA3 KO CAR showed early improvements in tumor clearance *in vivo.* However, relapse occurred at similar timepoints across groups. At the 4-week timepoint, the most enriched guides comprised a different set, including genes involved in transforming growth factor beta and JAK-STAT signaling pathways as well as T cell trafficking. In vivo anti-tumor control data are being collected.

Conclusions

Our findings highlight the dynamic nature of CART-tumor interactions. Gene knockouts that confer enhancements may change over time with varying context (such as in vitro vs in vivo conditions). It may be difficult to identify single gene knockouts that enhance CAR-T cell functions across different conditions and over time, but rather it may be necessary to exert more dynamic functional control of CAR T cells to enhance their function in different settings.

#0035 *In situ* CAR T cell engineering using lipid nanoparticles for B cell lymphoma therapy.

N. Zhang, E. Robinson, A. Rivera-Rodriguez, J. Wang, Y. Guo, B. Wu, S. K. Tumbale, M. Raie, M. Inayathullah, D. K. Czerwinski, R. Levy, K. W. Ferrara; Stanford University School of Medicine, Palo Alto, CA

Chimeric antigen receptor (CAR)-T cell therapy represents a breakthrough in immunotherapy, offering promising outcomes in the management of hematological malignancies. Current CAR-T cell *in vitro* manufacturing routes involve T cell isolation, purification, activation, gene transduction and cell expansion. The process duration and the costs present significant barriers. Therefore, there is a need for innovative strategies to address these concerns. Herein, we developed lipid nanoparticles (LNPs) to deliver CAR-mRNA efficiently and safely to T cells *in vivo*, thereby enabling *in situ* CAR-T cell engineering. By optimizing their composition and introducing anti-CD5 as the targeting ligand, we were able to enhance mRNA delivery and T cell transfection efficiency while maintaining T cell function. Furthermore, to augment T cell responsiveness to exogenous genetic elements, we investigated the pretreatment of T cells with interleukin (IL-7), thereby modulating T cell homeostasis by enhancing survival and proliferation, and rendering the cells more receptive to exogenous genetic modifications. We tracked firefly luciferase (FLuc) in naïve Balb/c mice using *in vivo* and *ex vivo* bioluminescence imaging after intravenous injection of anti-CD5 FLuc-mRNA LNPs. We observed positive mRNA expression in lymphoid organs, particularly in the spleen. Additionally, we harvested the lymphoid organs, and performed immunophenotyping analysis using flow cytometry after the administration of anti-CD5 LNPs encapsulating mRNA encoded CD19-CAR with a flag tag. We showed enhanced LNP binding in 65.2% of T cells and CAR expression in 11.64% of T cells as compared with non-treated controls, anti-CD5 FLuc-mRNA LNPs, or IgG CAR-mRNA LNPs. In a $CD19^+$ A20 tumor-bearing mouse model, treatment with CAR-LNPs resulted in a significant increase in chemoattractants (CCL2, CCL4, CCL5, CCL7 and CXCL10) and pro-inflammatory cytokines (TNF-α, IFN-γ, IL6, IL8 and IL15) in blood, and infiltration of T cells and other immune cells in tumors, compared to the non-treated control group over 48 hours post treatment. *In vivo* engineering allows simultaneous CAR T cell engineering and delivery, reducing the time between manufacturing and treatment, minimizing contamination risks, eliminating complex *ex vivo* processes, and reducing the need for high-dose preconditioning chemotherapy. In conclusion, the adoption of *in situ* CAR-T cell production holds promise for improving this therapeutic approach.
The authors acknowledge the funding support from NIHR01CA253316 and Leukemia and Lymphoma Society (LLS, Grant ID: 8022-20)

#0036 The discovery of a novel CD19xCD22 dual-targeting CAR for the development of an IPSC-derived cell therapy.

J. M. Carton, **J. Wheeler**, C. Dower, L. Campion, H. J. Millar, M. Beqiri, B. Morse, B. Gurung, R. Genovese, S. DeLuca, C. Dominick, M. Naso, H. Levitsky; Century Therapeutics LLC, Philadelphia, PA

Dual-targeting cell therapies to address CD19 antigen loss in heme malignancies are being explored by Century Therapeutics and others for unmet clinical need in hematological malignancies. CD22 chimeric antigen receptor (CAR) T-cell therapies have shown promising efficacy in relapsed or refractory B-lineage acute lymphoblastic leukemia (B-ALL) alone and in combination with CD19 CAR-T cell therapies (1,2). CD22 is a multi-domain glycoprotein expressed on B-cells. Natural splice variants of CD22 can exclude domains near the N-terminus, allowing for therapeutic resistance when these domains are targeted. We identified novel single domain antibodies (VHH) to CD22 that bind to multiple epitopes on different domains of CD22, including membrane proximal binders. The VHHs were affinity matured to enhance cell-based binding and formatted as CARs in monovalent and tandem, bivalent formats. Our data demonstrates the best efficacy against CD22+ tumor cells with a biparatopic, tandem VHH CAR format. Through additional engineering, bispecific CARs that combined three CD22-binding VHH and the anti-CD19 scFv, FMC63, in a loop CAR configuration were designed and tested. This CD19xCD22 bispecific, CD22 biparatopic CAR was engineered into primary T-cells and demonstrated cytotoxicity activity against CD19 and CD22 positive tumor cells as well as CD19 knockout and CD22 knockout cell lines. CD19xCD22 bispecific primary CAR-T cells were efficacious in controlling tumors in mouse xenograft models. This novel CAR is being tested in IPSC-derived iT and iNK cells for off-the-shelf allogeneic cell therapy to expand patient access beyond CD19 CAR-T cell therapies. Ref: 1. Nat Med. 2018;24(1):20-28. doi: 10.1038/nm.4441. 2. Blood. 2018;132(suppl 1). Abstract 27

#0037 IL-4 drives CART cell exhaustion in a CD4 independent manner.

C. M. Stewart[1], E. L. Siegler[1], T. N. Huynh[1], R. Sakemura[1], B. Kimball[1], L. Mai[1], K. Yun[1], J. H. Girsch[1], J. Feigin[1], O. Gutierrez Ruiz[1], M. Rodriguez[1], E. Ogbodo[1], I. Can[1], C. Manriquez Roman[1], O. Sirpilla[1], H. Xia[1], J. Kim[2], J. Budka[2], M. Mattie[2], N. Scholler[2], S. Filosto[2], S. S. Kenderian[1];
[1]Mayo Clinic, Rochester, MN, [2]Gilead Sciences Inc., Foster City, CA

While chimeric antigen receptor T (CART) cell therapy has shown remarkable success, the development of exhaustion limits durable response. We identified a role for interleukin (IL)-4 in the development of CART cell exhaustion through three independent approaches including: 1) a genome-wide CRISPR knockout screen using healthy donor CART cells in an *in vitro* model for exhaustion, 2) RNA and ATAC sequencing on freshly produced and chronically stimulated healthy donor CART cells, and 3) RNA and ATAC sequencing on pre-infusion CART cell products from responders and non-responders in the Zuma-1 clinical trial that led to the FDA approval of axi-cel. Further, *in vitro* validation studies revealed that CD19 directed CART (CART19) cells chronically stimulated in the presence of human recombinant IL-4 (hrIL-4) displayed signs of exhaustion such as 1) decreased proliferation ($p = 0.01$), 2) increased coexpression of inhibitory receptors ($p = 0.01$), and 3) decreased production of IL-2 and interferon (IFN)-γ ($p= 0.02$, $p = 0.002$). Encouragingly, CART19 cells combined with an IL-4 monoclonal antibody improved antitumor activity ($p = 0.045$) and expansion ($p = 0.01$) while also decreasing the co-expression of inhibitory receptors ($p = 0.02$) in a mantle cell lymphoma xenograft mouse model. Building on these results, we asked if IL-4 driven exhaustion results from a direct impact of IL-4 on CART cells. To test this, we used a tumor-free assay where CART19 cells were chronically stimulated with CD19 beads in the presence of hrIL-4 or diluent. CART cells treated with hrIL-4 displayed an exhausted phenotype characterized by increased co-expression of inhibitory receptors ($p = 0.04$) and decreased production of IL-2 ($p = 0.01$). Next, we asked if IL-4 driven CART cell exhaustion is dependent on the costimulatory domain. We tested the impact of IL-4 on both CD28ζ and 41BBζ costimulated CART19 cells. Similar to our previous studies with CART19-28ζ cells, chronic stimulation of CART19-BBζ cells in the presence of hrIL-4 enhanced the exhausted phenotype as seen by increased co-expression of inhibitory receptors ($p = 0.04$) and decreased production of IL-2 and IFN-γ ($p = 0.08$ and $p = 0.007$). Finally, we asked if IL-4 induces exhaustion independently of its classic role in Th2 polarization of CD4 CART cells. Following CART production, we isolated CD8 cells and chronically stimulated them in the presence of hrIL-4 or diluent. CD8 CART cells treated with hrIL-4 displayed an enhanced exhausted profile as seen by 1) decreased proliferative ability ($p < 0.0001$), 2) increased co-expression of inhibitory receptors ($p = 0.01$), and 3) decreased production of IL-2 and IFN-γ ($p < 0.0001$, $p = 0.004$). Together, our data indicates a novel role for IL-4 in the development of CART cell exhaustion that is independent of tumor cells, costimulatory domain, and CD4 cells. As such, we believe IL-4 neutralization may be a widely applicable and actionable approach to improve the durable response to CART cell therapy.

#0038 AB-2100, a PSMA-inducible CA9-specific CAR T cell product for the treatment of ccRCC provides long-term tumor responses in preclinical mouse model.

S. Mohanty, J. Chen, A. Gomez, A. Boroughs, I. Scarfo, L. Lim, K. Dang, M. Chew, R. Sudhakah, M. Nguyen, T. J. Gardner, B. Millare, J. Zhang, D. Moskowitz, S. Zhou, N. H. Xie, N. Attanasio, A. Fearon, I. Chan, V. Sail, V. Thomas, J. Smith, J. McDevitt, L. Gray-Rupp, **A. Gonzalez**, C. Murriel, W. Haining;
Arsenal Biosciences, South San Francisco, CA

Common challenges of CAR-T cell therapies in solid tumors, such as clear cell renal cell carcinoma (ccRCC), include insufficient therapeutic potency and lack of tumor specificity. We have developed AB-2100, an autologous integrated circuit T (ICT) cell product, generated via CRISPR-mediated knock-in of a single transgene into a safe-harbor locus. AB-2100 encodes a transcriptionally regulated sequential AND gate that comprises a priming receptor (PrimeR) specific for PSMA and an inducible CAR targeting CA9 antigen, which is widely expressed on local and metastatic lesions. AB-2100's sequential AND logic-gate confers tumor-specific activity by priming off of PSMA-expressing tumor vasculature to induce CA9 CAR expression. This unique feature of the logic gate is intended to increase the safety profile of AB-2100 given that PSMA and CA9 are predicted to have limited co-expression in normal tissues. Additional functionality includes short-hairpin RNAs (shRNA) against Fas and TGFBR designed to prevent tumor-mediated resistance, and a synthetic pathway activator (SPA) that drives constitutive STAT3 signaling and enhanced T cell cytotoxicity and expansion. Mechanism of action studies demonstrate that AB-2100 can prime off of PSMA-expressing endothelial cells and induce tumor-specific killing of CA9 tumor cells, leading to the eradication of ccRCC targets in vitro. AB-2100 also exhibited selective killing of dual antigen expressing tumors in vivo using a dual-flank subcutaneous xenograft model. Preclinical xenograft studies also demonstrated that TGFBR shRNA and SPA modules enhanced antitumor activity of ICTs. When AB-2100 potency was evaluated in the subcutaneous A498 xenograft model, treatment with AB-2100 resulted in complete and durable anti-tumor responses. In summary, preclinical data demonstrate that AB-2100 selectively targets tumors co-expressing PSMA and CA9, and can overcome multiple suppressive mechanisms in the tumor microenvironment. These results support the evaluation of AB-2100 in the clinic for the treatment of advanced or metastatic ccRCC.

#0039 Preclinical *in vitro* and *in vivo* evaluation of CD8αβ+ CD19 CAR iPSCs T cells generated in a TCR signal-independent manner using DLL4/VCAM-coupled microbeads.

M. S. Belew[1], R. Carpenedo[1], A. Pallaoro[1], H. Hoi[1], A. Deyati[2], D. C. Kirouac[2], S. Chandrasekaran[2], V. Wall[2], L. Abraham[2], S. Apelu[2], M. H. Cadell[2], A. AuYeung[1], O. Subedar[1], E. Martinez[1], S. Joshi[1], E. Csaszar[1], S. Woodside[1], E. Titus[1], C. Bond[2];
[1]Notch Therapeutics, Inc., Toronto, ON, Canada, [2]Notch Therapeutics, Inc., Seattle, WA

The use of clonally-derived, induced pluripotent stem cells (iPSCs) as starting material for therapeutic T cell manufacturing would overcome many limitations of autologous Chimeric Antigen Receptor T cell (CAR-T) therapies. Complex, multi-stage genome engineering, large batch production and rigorous lot testing could provide a consistent source of off-the-shelf, functionally enhanced T cell products. However, this vision cannot be realized using existing T cell differentiation platforms, which fail to present Notch ligands with the precision and intensity required to control T cell differentiation in scalable, suspension culture.

We have previously shown that VCAM1 synergizes with DLL4 to enhance Notch signaling and progenitor T cell differentiation. We have extended the utility of this discovery through the creation of DLL4/VCAM1-coated magnetic microbeads, enabling precise and temporal control of Notch signaling in suspension culture. iPSC-derived CD34+ cells cultured with DLL4/VCAM1 beads demonstrate dose-responsive activation of Notch gene expression (e.g., Notch1, DTX1, TCF7), resultant T lineage commitment (e.g. CD5, CD7 expression) and maturation to CD4-CD8+ (single positive) cells in a TCR signal-independent manner. Removal of the endogenous TCR is necessary to prevent graft-versus-host-disease. Therefore, differentiation and maturation in a TCR-independent process presents substantial advantage in the development of safe, off the shelf iPSC T cell products.

Using a clonal iPSC line with a CD19 CAR knocked in at the *TRAC* locus, we apply this approach to generate CAR-expressing, CD8αβ+ functional T cells, capable of multiple rounds of *in vitro* tumor cell lysis and sustained tumor growth inhibition *in vivo* comparable to primary T cells. This advancement demonstrates proof-of-concept for generation of highly efficacious, off-the-shelf CAR-T cells using novel, small-footprint manufacturing in order to broaden the applicability and accessibility of T cell therapies for cancer patients.

#0040 Persistence but not antitumor efficacy of CAR-engineered lymphocytes is governed by a FAS/FAS ligand auto-regulatory circuit.

Fei Yi[1], Tal Cohen[1], Paul Zumbo[2], Razan Eltilib[1], Hannah Arkin[1], Michael Gormally[3], Christopher S. Hackett[4], Korbinian Kropp[1], Smita Chandran[1], Jae H. Park[5], Doron Betel[2], Christopher A. Klebanoff[1]

[1]Human Oncology and Pathogenesis Program, Memorial Sloan Kettering Cancer Center, New York, NY,[2]Applied Bioinformatics Core, Weill Cornell Medicine, New York, NY,[3]Memorial Sloan Kettering Cancer Center, New York, NY,[4]Weill Cornell Medical College, New York, NY,[5]Cell Therapy Service, Memorial Sloan Kettering Cancer Center, New York, NY

Adoptive cell transfer of chimeric antigen receptor (CAR) engineered T and NK cells has revolutionized the treatment of many B-lymphoid malignancies; however, limited persistence of infused lymphocytes can restrain the full potential of this approach. Apoptosis induction through the FAS ligand/FAS pathway is a key negative regulator of lymphocyte survival. To define which cellular subsets express *FASLG*, the gene encoding FAS ligand, we generated a single-cell transcriptomic atlas from 37 patients with diverse cancer types. We discovered that *FASLG* expression is highly constrained and limited primarily to T and NK cells while stromal and tumor cells express minimal to no *FASLG*. Multiplex RNA *in situ* hybridization of clinical samples from patients treated with anti-CD19 CAR-T cells confirmed these results and revealed significantly higher *FASLG* content in CAR-expressing compared with non-CAR expressing T cells. Based on these findings, we hypothesized that FAS ligand expression by CAR^+ T and NK cells will engage FAS^+CAR^+ cells to induce apoptosis and limit cellular persistence. To test this hypothesis, we performed competitive fitness assays using two phenotypically discernable populations of human CAR-T and CAK-NK cells that are either responsive or unresponsive to FAS-signaling through expression of a FAS dominant negative receptor (ΔFAS). ΔFAS^+ and ΔFAS^- CAR-expressing cells were co-infused 1:1 into tumor bearing hosts and persistence of each population was quantified. For both CAR-T and CAR-NK, we measured significant enrichment in ΔFAS-expressing cells across multiple tissues, demonstrating that FAS-signaling regulates CAR^+ cell survival in a cell-intrinsic manner. Knock out (KO) of *FASLG* using CRISPR/Cas9 prevented population skewing while KO of the *AAVS1* control locus had no effect, indicating that CAR-derived *FASLG* is sufficient to restrain the persistence of transferred cells. By contrast, we discovered that *FASLG* was dispensable for CAR-T and CAR-NK mediated tumor killing both *in vitro* and *in vivo*. Finally, using two different tumor models, we found that adoptive transfer of CAR-T or CAR-NK cells that co-express ΔFAS resulted in superior antitumor efficacy compared with control cells that express the CAR alone. Taken together, these findings reveal that CAR-engineered lymphocyte persistence is governed by a FAS/FAS ligand auto-regulatory circuit. Further, they indicate that the therapeutic benefit of a FAS-dominant negative receptor is broadly applicable and agnostic of whether *FASLG* is expressed by cells in the tumor microenvironment.

#0041 Mitigating on-target off-tumor toxicity of mesothelin-targeting CAR T cells by affinity-tuning.

Y. Yang[1], Y. Vedvyas[1], Y. Alcaina[2], J. Y. Son[2], N. Salehi[2], I. M. Min[1], M. M. Jin[1];
[1]Houston Methodist Research Institute, Houston, TX, [2]Weill Cornell Medicine, New York, NY

Purpose: Mesothelin (MSLN) is a surface antigen associated with tumor invasion and is overexpressed in mesothelioma and lung, pancreatic, ovarian, and other cancers. Chimeric antigen receptor (CAR) T cells targeting MSLN have been tested in patients with MSLN-positive solid tumors. Despite reported patient fatalities in trials sponsored by PENN, Memorial Sloan Kettering/Atara Bio, and MD Anderson/TCR[2], the design approach for MSLN CAR remains constructing high affinity CARs to maximize target cell killing. In this study, we designed MSLN CARs with two different antibodies: one targeting human MSLN specifically and another binding both human and mouse MLSN with comparable affinities. The objectives are to 1) elucidate the risk of fatal on-target off-tumor toxicity associated with high affinity MSLN CAR, and 2) demonstrate how optimizing the affinity of CARs can render CAR T cells to spare normal tissues while retaining cytotoxicity against tumors.
Methods: To asses on-target off-tumor toxicity in animal models, we developed a CAR using a nanobody isolated from an immune alpaca library with nanomolar affinity for both human and mouse MSLN (labeled as hmMSLN CAR). For comparison, we constructed a CAR using a scFv specific only to human MSLN, designated hMSLN CAR. Each CAR is designed to co-express somatostatin receptor 2 to enable PET/CT imaging of CAR T cells with ^{18}F-NOTA-Octreotide. Anti-tumor activities and toxicities were assessed in NSG mice using MSTO-211H cell line expressing human MSLN.
Results: In NSG mice bearing subcutaneous MSTO-211H tumors, hMSLN CAR T cells eliminated tumors rapidly without inducing any overt toxicity. In contrast, hmMSLN CAR T cells not only failed to control tumor growth but also caused severe toxicity, resulting in significant body weight loss and necessitating euthanasia. PET/CT imaging revealed while hMSLN CAR T cells expanded exclusively within the tumor and subsequently contracted after tumor elimination, hmMSLN CAR T cells exhibited extensive infiltration and expansion in the lungs, liver, and bone marrow, indicating off-tumor, normal tissue-driven proliferation of CAR T cells. To test if affinity-tuned hmMSLN CAR T cells can selectively target tumors, we used a yeast display system to screen for affinity variants of the hmMSLN CAR. We identified one micromolar affinity CAR that binds approximately 1,000 times weaker to MSLN than the parental CAR. In stark contrast to the onset of severe toxicity soon after the administration of the parental hmMSLN CAR T cells, animals treated with micromolar affinity hmMSLN CAR T cells exhibited tumor regression without overt toxicity.
Conclusions: Our findings underscore the risks of using high affinity CAR against MSLN, which may cause unpredictable on-target, off-tumor toxicities. Fine tuning the affinity of MSLN CAR offers a promising strategy for developing a potent and safe CAR for the treatment of MSLN-expressing solid tumors.

#0042 Tunneling CARs: Gene modifications to enhance CAR-T infiltration into solid tumors.

S. N. Van Pelt[1], B. Omer[1], L. Talbot[2], C. Rooney[1], R. Fernandes[3], C. Tat[4], M. White[1];
[1]Baylor College of Medicine, Houston, TX, [2]St. Jude, Memphis, TN, [3]The George Washington University, Washignton, DC, [4]Texas Childrens Hospital, Houston, TX

Background: CAR-T therapy has been largely ineffective in solid tumors because the dense, rigid, extracellular matrices (ECMs) and basement membranes (BMs) that encapsulate these tumors exclude T cells. Tumor-specific ECMs and BMs, made of type I and type IV collagen respectively, are heavily cross-linked and characterized by small pores. T cell infiltration into tumors relies upon the enzymatic degradation of these matrix fibers, and adhesion molecule-mediated movement. Gene expression analysis of tumor infiltrating leukocytes from patient samples showed that MMP-7, an enzyme that degrades type IV collagen, and osteopontin (OPN), a molecule that interacts with adhesion molecules to mediate movement, were highly upregulated in infiltrating cells compared to those that were tumor adjacent, suggesting they may be important in navigating tumor-specific environments. *We hypothesized that overexpressing MMP-7 and/or OPN in CAR-T cells will enhance their infiltration into solid tumors.*
Methods: We overexpressed MMP-7 and OPN in second-generation CAR-Ts (GD2-28Z and HER2-28Z) and evaluated their infiltration *in vitro* using Halo invasion assays. T cell movement out of type IV collagen and into tumor droplets, composed of tumor targets polymerized in type I collagen, was visualized over time to characterize T cell movement through the tumor-specific BM and ECM, respectively. The expansion, phenotype, and cytotoxicity of OPN and MMP-7-modified GD2-28Z CAR-Ts was compared to unmodified GD2 CAR-Ts by counting, flow cytometry and chromium release, respectively. We then used a xenograft model of neuroblastoma to determine if increases in GD2 CAR-T infiltration led to reduced tumor burden.
Results: *In vitro*, MMP-7 overexpression increased GD2-28Z (2.05-fold, $p<0.0001$) and HER2-28Z (3.16-fold, $p<0.0001$) CAR-T infiltration, and OPN overexpression increased GD2-28Z (1.20-fold, $p=0.0496$) and HER2-28Z (1.49-fold, $p=0.002$) CAR-T infiltration. *In vivo*, 52 days after CAR-T infusions, mice treated with OPN-modified GD2-28Z CAR-Ts had reduced tumor burden (0.206 cm, ±0.21) compared to GD2-28Z CAR-Ts (0.903 cm, ±0.33, $p=0.0449$).
Conclusions: The overexpression of MMP-7 or OPN in second-generation CAR-Ts enhances CAR-T infiltration *in vitro*, and the expression of these genes does not impair CAR-T expansion, phenotype or cytotoxicity. The overexpression of OPN in GD2-28Z CAR-T enhances tumor clearance in a xenograft model of neuroblastoma, and may increase overall survival.

#0043 Targeting trogocytosis through cathepsin B inhibition enhances CAR T cell persistence.

K. A. Dietze[1], M. L. Olson[2], E. Gebru[1], D. Atanackovic[1], A. P. Rapoport[1], T. Luetkens[1];
[1]University of Maryland, Baltimore, Baltimore, MD, [2]Dana Farber Cancer Institute, Boston, MA

Chimeric Antigen Receptor (CAR) T cell therapy is an effective treatment for cancer patients. While CAR T cells have shown remarkable efficacy, most patients receiving CAR T cell therapy eventually relapse. CAR-mediated trogocytosis (CMT) is a potential tumor escape mechanism involving the transfer of cell surface proteins from tumor cells to CAR T cells. CMT results in antigen-negative tumor cells and correlates with reduced CAR T cell persistence, possibly due to increased CAR T cell fratricide or exhaustion. To date it has not been conclusively demonstrated that antigens transferred by CMT are the cause of fratricide or exhaustion. To answer this question, we developed a system to rapidly degrade trogocytosed protein in CAR T cells. Using this system, we show that the transfer of CD19 to CAR T cells directly causes CAR T cell fratricide and exhaustion. We hypothesize that reducing CMT will increase CAR T cell persistence. To identify molecular mechanisms driving CMT as potential therapeutic targets, we inhibited various proteins essential for cell adhesion, endocytosis, actin polymerization, or antigen processing using small molecule inhibitors. We found that inhibition of the cysteine protease Cathepsin B (CTSB), with a membrane-permeable (Ca-074) or membrane-impermeable (Ca-074-Me) inhibitor, significantly reduced CMT without affecting CAR T cell cytotoxicity. We hypothesize that CTSB inhibition could be a potential therapeutic approach to limit CMT.CTSB activity is regulated by the protein Cystatin A (CSTA). Both Ca-074-Me and CSTA sterically block access to the active site cysteine of CTSB. We found that overexpression of CSTA in CAR T cells significantly reduced CTSB activity and reduced antigen transfer. CSTA overexpression minimized antigen loss on tumor cells, indicating that CTSB inhibition blocks CMT early during the trogocytic process. CSTA overexpression reduced CAR T cell exhaustion but did not alter their expansion, tumor cell killing, or phenotype, indicating that this approach selectively inhibits CMT. Next, we assessed the effect of CSTA overexpression on CAR T cell persistence in vivo. NALM6 tumor-bearing NSG mice were injected with conventional or CSTA-overexpressing CD19 CAR T cells. Four weeks after CAR T cell injection, we observed substantially increased CAR T cell numbers in the blood (10.6x, p=0.0317), bone marrow (7.3x, p=0.0159), and spleens (5.6x, p=0.0556) of mice treated with CSTA-overexpressing CAR T cells. Taken together, we provide the first experimental evidence that CMT directly causes fratricide and exhaustion, reducing CAR T cell persistence. We demonstrate that CMT can be targeted efficiently by overexpressing the CTSB inhibitor CSTA in CAR T cells, resulting in substantially increased CAR T cell persistence. This represents a promising approach to improve CAR T cell efficacy and limit the occurrence of relapse in patients receiving CAR T cell therapy.

#0044 A novel, codon-based method to modulate off-tumor toxicity of chimeric antigen receptor (CAR) T cells.

R. A. Vedia, S. Lu, A. V. Philips, A. Sergeeva, L. S. St John, K. Clise-Dwyer, G. Alatrash, J. J. Molldrem;
UT MD Anderson Cancer Center, Houston, TX

Chimeric antigen receptor (CAR) T cell therapies for hematologic malignancies, while promising and efficacious, can also result in a variety of adverse effects. Of note, on-target, off-tumor toxicity is one adverse effect that continues to limit the safety and efficacy of CAR-T cells and has even led to life-threatening or fatal outcomes in patients (Morgan et al. 2010.). To address this, we have developed a unique, codon-based approach by replacing strategically selected codons within CAR non-antigen binding domains with their rare synonymous isoforms. Hoekema et al. (1987) reported the ability of synonymous rare codons to alter gene and protein expression in other model systems. In CAR-T cells, we aim to use this novel, codon-based approach to fine tune and modulate CAR-T cell expression and function to elicit full on-tumor activity while lessening off-tumor toxicity.

In our approach, we replaced specific endogenous codons within the non-antigen binding domains of Hu8F4-CAR, a TCR-like 2nd generation CAR developed by our group which targets the leukemia-associated antigen PR1/HLA-A2 (Ma et al. 2016.). Briefly, we created variants of Hu8F4-CAR containing rare codon substitutions in two subtypes: intracellular-based (type 1) and combined extracellular- and intracellular-based (type 2). Each variant subtype (type 1 or 2) had either between 6 and 30 or 27 and 57 rare codons introduced, respectively. Expression profiling and functional assessment of the Hu8F4-CAR variants was assessed in the Jurkat mutant cell line (J.RT3-T3.5) or human primary healthy peripheral blood mononuclear cells (PBMCs) that were enriched for T cells, respectively. Expression profiling results show that surface expression is reduced in J.RT3-T3.5 cells when assessed by flow cytometry by 1-1.5-fold compared to unmodified Hu8F4-CAR. When evaluated by immunoblotting, novel lower molecular weight bands emerge only in rare codon-modified variants, suggesting that rare codons may have altered translational or post-translational processing leading to truncated CAR protein isoforms (30, 45, or 60kDa vs 73kDa for unmodified Hu8F4-CAR), which may contribute to reduced cell surface CAR expression. Furthermore, we have conducted *in vitro* functional testing of the rare codon-modified variants and show reduced activity against non-malignant off-tumor targets that express PR1 and/or HLA-A2 including healthy donor PBMCs, mobilized hematopoietic cells, and bone marrow. Importantly, in addition to reduced off-tumor activity against healthy myeloid cells, rare codon-modified variants preserve their activity against on-tumor target cells, including the U937-A2+ cell line and primary acute myeloid leukemia. Altogether, these results suggest that our approach can modulate CAR expression and functionality creating a novel methodology to reduce the likelihood of off-tumor adverse effects typically associated with CAR therapies.

#0045 Driving AMPK signaling in CD4+ CART cells enhances metabolic capacity, memory formation, and anti-leukemia activity.

E. Braverman[1], H. Schuler[1], M. Qin[2], C. Byersdorfer[1];
[1]University of Pittsburgh, Pittsburgh, PA, [2]Tsinghua University, Beijing, China

Background: While Chimeric Antigen Receptor (CAR)T cell therapy has seen great success in pediatric and young adult acute lymphoblastic leukemia, up to 50% of patients will relapse following treatment. Increased memory formation and mitochondrial capacity, particularly in the CD4+ subset, have been linked to improved CART cell function and enhanced *in vivo* persistence, leading to long-term relapse-free survival. AMP-activated protein kinase (AMPK) is a cellular energy sensor responsible for promoting metabolic efficiency and T cell memory formation. We have previously demonstrated AMPK activity can be increased in human T cells via overexpression of the AMPKγ2 domain. We hypothesized that overexpression of AMPKγ2 in CART cells would enhance their metabolic capacity and improve their anti-leukemia function.

Methods: Human CART cells bearing a CD19-CAR utilizing a 41BB costimulatory domain were generated from healthy human donors via lentiviral transduction and co-transduced with AMPKγ2 (AMPK) or an empty vector (EV) control. Flow sorting for the co-transduced populations yielded >95% CD4+ CART cells. CARTs were expanded in IL-2 for approximately 2 weeks, followed by overnight stimulation and subsequent metabolic analysis using the Seahorse Metabolic Analyzer. Memory status was assessed by CD62L and CCR7 co-expression. *In vitro* CART function was assessed using Zs-green+ NALM6 targets, with loss of green fluorescence over time measured on the Incucyte analyzer. Where indicated, tumor conditioned media was harvested from 72-hour NALM6 cultures. For *in vivo* experiments, immunodeficient NOD-scid IL2Rγ^{null} (NSG) mice were injected with luciferase+ NALM6 targets, followed one week later by AMPK- or EV-CARTs. Leukemia burden, via IVIS imaging, and survival were followed over time.

Results: CD4+ CARTs co-transduced with AMPKγ2 (AMPK-CARTs) increased oxygen consumption, maximal respiration, and spare respiratory capacity following overnight stimulation by ~20% compared to CARTs co-transduced with the EV (EV-CARTs) ($p<0.05$). Following expansion, CD62L+CCR7+ central memory cells were 4.5-fold more abundant in the AMPK-CART group (2.4-6.2-fold, $p<0.01$). *In vitro*, while AMPK-CARTs demonstrated similar cytotoxicity against NALM6 targets as EV-CARTs in standard media, they mediated faster killing of NALM6 targets when challenged in tumor conditioned media ($p<0.001$). *In vivo*, recipients of AMPK-CARTs showed a consistent decrease in tumor burden as measured by median radiance values, translating to a significant survival advantage ($p<0.05$).

Conclusions: Increasing AMPK signaling in CD4+ CARTs via overexpression of AMPKγ2 improved metabolic profile, increased memory generation, and enhanced toxicity against leukemia targets both *in vitro* and *in vivo*. Together, these features make elevating AMPK signaling an attractive method to increase the efficacy of CART therapy.

#0046 Mechanisms and impact of bystander killing by CAR T cells.

J. Chorazeczewski, L. Xie, X. Chen, S. Wang, J. Kline;
University of Chicago, Chicago, IL

While CD19-directed chimeric antigen receptor (CAR) T cell therapy has improved outcomes of patients with relapsed/refractory diffuse large B cell lymphoma (r/r DLBCL), a majority will suffer disease relapse following CAR T cell infusion. Therefore, understanding mechanisms of CAR T cell killing is critical to enhance therapeutic efficacy. Cytolysis of CAR T cell targets presumably involves recognition of CD19 antigen by the CAR followed by activation of the granzyme/perforin axis. However, bystander elimination of CD19-negative lymphoma cells by CAR T cells has been reported, indicating that an alternative pathway may be required for optimal killing. Through in-depth phenotyping of a large panel of human DLBCLs and *in vitro* killing assays, we observed that CD19 expression levels on DLBCL cells and vulnerability to CAR T cell killing were weakly correlated. Conversely, cell surface expression of the death receptor, FAS, on DLBCL cells was strongly associated with susceptibility to CAR T cell killing. Although FAS expression across DLBCL cell lines varied, it could be broadly enhanced following exposure to IFNγ. Potent CAR T cell-mediated cytolysis of CD19-negative, Fas-positive murine DLBCL cells required the presence of CD19-positive lymphoma cells in the culture. CRISPR/Cas9 targeting was employed to delete *FAS* and/or *CD19* in isogenic human DLBCL cells to generate $CD19^{+}FAS^{+}$, $CD19^{+}FAS^{-}$, $CD19^{-}FAS^{+}$, and $CD19^{-}FAS^{-}$ subsets, which enabled us to define the extent to which CD19 engagement by the CAR was required to affect killing via FAS. When CAR T cells were co-cultured with equal numbers of the four gene-modified DLBCL cells described above, $CD19^{+}FAS^{+}$ DLBCL cells were killed most effectively, followed by $CD19^{+}FAS^{-}$ DLBCL cells, and $CD19^{-}FAS^{+}$ DLBCL cells. Double-negative DLBCL cells were poorly killed. This result suggested that CD19 engagement by the CAR was required for optimal DLBCL cell killing via FAS, and that CD19 and FAS need not necessarily be engaged on the same target cell. Future studies will determine if Fas/FasL interactions can be exploited by overexpression of FasL in CAR T cells and examination of DLBCL killing *in vitro* and *in vivo*.

#0047 Stabilization of long CAR T cells is crucial for in vivo antitumor efficacy.

H. Paavilainen[1], J. Koski[2], V. Nikoskelainen[1], M. Elmadani[2], E. Elbasani[1], C. Hekim[1], E.-L. Ihantola[1], V. Kergourlay[1], P. Vehmaan-kreula[1], M. Nyman[1], K. Kalke[1], M. Nurmi[1], H. Monzo[3], P. Ojala[3], A. Autio[1], M. Korhonen[2], **A. Thotakura**[1];

[1]Orion Corporation, Turku, Finland, [2]R&D, Finnish Red Cross Blood Service, Helsinki, Finland, Helsinki, Finland, [3]Translational Cancer Medicine Research Program, University of Helsinki, Helsinki, Finland

Introduction: Genetically engineered T cells expressing chimeric antigen receptors (CARs) have shown substantial anti-tumor efficacy in hematological malignancies during recent years. As the field evolves to novel target epitopes, longer CAR structures are needed to reach membrane proximal epitopes for improved efficacy. Our approach to reach such epitopes is to have (non-functional) SIRPalpha based extracellular extension, spacer, to our CAR structure. We have shown, in this proof-of-concept study, that stability of the extracellular spacer of a CAR plays a pivotal role to improve in vivo anti-tumor efficacy. Various SIRPalpha-based CARs, FiCARs, targeting CD19 was studied for their function. Protein stability of the CD19 CAR structures were characterized and subsequently the killing efficacy of target cells and cytokine release in in vitro as well as in vivo anti-tumor efficacy was evaluated.

Methods & Results: In vitro co-culture assays with primary CD19 CAR T and CD19 positive cancer cells had shown no significant differences between the different spacer containing FiCAR structures. A dose dependent killing efficacy was observed in all the tested structures with up to >90% killing of NALM6 and Raji cells. Comparable results for IL-2, IFN-gamma, TNF-alpha, IL-4, IL-13 and granzyme B response were seen in co-cultured assay. In the protein stability studies, modifications in the extracellular part of the CAR structure led to an increase in thermal stability (over 2 °C) and reduced/halted multimer formation. To study the FiCAR T cell function in an in vivo tumor model, NSG mice were injected i.v with Raji cells and few days later mice were injected i.v with FiCAR T cells. Anti-tumor efficacy and overall survival were studied at the end of the study (60 days), the enhanced stability of FiCAR T structure translated into improved anti-tumor efficacy and survival. Interestingly, none of the mice survived in the least stable structure, 40% survival with intermediate stability structures and over 70% survival was observed in most stable structures.

Conclusion: A stabilized SIRPalpha-based CD19 FiCARs dramatically enhance anti-tumor efficacy and survival in Raji tumor model. The stabilization is critical for improved efficacy, especially in the in vivo setting. This data suggests that, in addition to the length of the CARs stability of the CAR structure appear to play a crucial role in the efficacy of the CAR T cells. The modifications presented here enhanced CD19-targeting CAR T cell efficacy. This approach requires further investigation to improve the efficacy of currently approved CAR T cells, especially CD19-CAR T cells.

#0048 T cell-specific *in vivo* transduction with preclinical candidate KLN-1010 generates BCMA directed CAR T cells with potent anti-multiple myeloma activity.

E. T. Beura, H. J. Latimer, D. Wong, J. Obrigewitch, A. J. Warr, S. Dong, M. Ariel, J. Figueroa, J. Figueroa, C. S. Dobson, S. K. Janaka, **A. J. Najibi**, M. Lau, S. Contrastano, K. Friedman;
Kelonia Therapeutics, Inc., Boston, MA

Introduction: Multiple Myeloma (MM) is the second most diagnosed hematologic malignancy and remains an incurable disease. KLN-1010 is a novel treatment for MM currently in preclinical development that uses our iGPS^{TM} platform, an envelope-modified lentiviral vector particle engineered for specific and efficient in vivo gene delivery, to transduce T cells. T cells modified in vivo by KLN-1010 express a fully human anti-BCMA CAR following a single IV injection without the need for additional treatments or conditioning chemotherapy.
Results: Human T cells exposed to KLN-1010 in vitro resulted in transduction and expansion of anti-BCMA CAR T cells in a concentration dependent manner. The resulting CAR T cells were highly avid and specific to BCMA-expressing cell lines. KLN-1010 treatment of preclinical mouse models resulted in T cell-specific CAR expression with no evidence of off-target modification including in the lung and liver, except phagocytes. A varied CAR T cell lineage composition was observed that included effector and memory CD4 and CD8 T cells. A single dose of KLN-1010 caused potent anti-tumor efficacy and complete tumor regression in a stringent model that requires high dose levels of ex vivo-cultured CAR T cells similar to those commercially available. When the anti-BCMA CAR molecules used in KLN-1010 are compared in preclinical models to other clinically relevant CARs, we observed superior tumor control by the KLN-1010 anti-BCMA CAR molecules. Clinical application of iGPS technology was modeled in non-human primates (NHP) using an NHP T cell-targeting particle that expresses an anti-CD20 CAR. CAR T cell activity, assessed by B cell depletion, and tolerability were evaluated without prior lymphodepleting chemotherapy across a 10x dose range. Rapid clearance of the iGPS particles from the blood was observed at all dose levels. Even at a low dose of 1.3e8 IU/kg, potent and durable CAR T cell activity was observed as evidenced by complete B cell depletion lasting over two months. Multiple CAR T cell expansions and contractions were observed during this period. The treatment at all dose levels was highly tolerable with no observed toxicities, cytokine release syndrome, or neurotoxicity.
Conclusions: These data demonstrate that KLN-1010 is safe and efficacious in preclinical models and may offer greater accessibility than other therapeutic modalities to address an unmet medical need in MM. Without requirements of ex vivo manufacturing, lymphodepletion and inpatient treatment that restrict patient access to therapy, the iGPS technology is well poised to provide significant clinical benefit for a multitude of indications as an off-the-shelf, single dose treatment.

#0049 LYL119, an investigational ROR1-targeted CAR T-cell product incorporating four novel reprogramming technologies designed for effective cell therapy for solid tumors.

V. C. Lam[1], A. Li[1], M. Galindo Casas[2], J. Barragan[1], **C. Cheung**[1], J. Briones[1], E. Afreen[2], G. Vavra[2], J. Lu[1], P. Sundar[1], R. Martinez[1], C. Sims[1], S. Potluri[1], O. Ali[1], A. S. Cheung[1], R. C. Lynn[1];

[1]Lyell Immunopharma, Inc., South San Francisco, CA, [2]Lyell Immunopharma, Inc., Seattle, WA

Effective solid tumor cell therapy requires new strategies to improve T-cell activation, persistence, and durable function. We developed four complementary T-cell reprogramming technologies to enhance chimeric antigen receptor (CAR) T-cell therapy in solid tumors: 1) overexpression of the activator protein 1 (AP-1) family transcription factor c-Jun to delay T-cell exhaustion and improve antitumor activity; 2) nuclear receptor subfamily 4A member 3 (NR4A3) gene knockout (KO) to further delay exhaustion and enhance functionality; 3) Epi-R^{TM} manufacturing protocols to preserve stem-like characteristics; and 4) Stim-R^{TM} technology, a novel activating reagent to improve product potency compared with standard reagents. LYL119 is an investigational ROR1-targeted CAR T-cell product that combines these technologies to create potent and durable CAR T cells. Healthy or NSCLC patient donor T cells were manufactured with the Epi-R protocols, activated with Stim-R or a standard reagent, and transduced with a vector encoding a ROR1 CAR and c-Jun. The *NR4A3* gene or a control gene was edited using SpyFi^{TM} Cas9 nuclease (Aldevron®). Cytotoxicity, cytokine production, phenotype, and single-cell transcriptomic and epigenetic profiles were evaluated in vitro after antigen restimulation assays designed to promote exhaustion. CAR T cell activity was evaluated in vivo using a ROR1^{+} NSCLC xenograft mouse model. Research and clinical scale LYL119 products achieved ~90% genome editing efficiency at the *NR4A3* target gene resulting in a 13-fold protein reduction compared to non-edited CAR T cells. LYL119 exhibited superior cytotoxicity and cytokine production upon antigen restimulation across 7 different ROR1^{+} solid tumor cell lines compared to CAR T cells that lacked one or more reprogramming technologies. After repeated rounds of tumor cell killing, LYL119 displayed reduced surface expression of exhaustion-related receptors (e.g. TIM-3) and higher expression of stemness-related markers (e.g. CD127) compared to non-edited CAR T cells. Furthermore, transcriptomic analysis revealed global downregulation of exhaustion-related gene signatures and retention of unique cell subsets characterized by upregulation of memory and effector-associated gene signatures. LYL119 exhibited robust antitumor efficacy in vivo across a 10-fold dose range, including a very low dose of $1x10^5$ CAR T cells. Lastly, LYL119 derived from NSCLC patient donor T cells also demonstrated enhanced cytotoxicity in vitro compared to control CAR T cells. These nonclinical data suggest LYL119, which combines c-Jun overexpression, *NR4A3* KO, Epi-R protocols, and Stim-R technology, can limit exhaustion, maintain stem-like features, and has the potential to provide effective and durable CAR T-cell antitumor activity in patients with ROR1^{+} solid tumors.

#0050 ALK inhibitors increase ALK expression and sensitize neuroblastoma cells to ALK.CAR-T cells.

E. Bergaggio[1], W.-T. Tai[1], A. Aroldi[2], C. Mecca[1], E. Landoni[3], M. Nuesch[1], I. Mota[1], J. Metovic[4], L. Molinaro[4], L. Ma[5], D. Alvarado[6], C. Ambrogio[4], C. Voena[4], R. B. Blasco[1], T. Li[7], D. Klein[7], D. J. Irvine[5], M. Papotti[4], B. Savolodo[3], G. Dotti[3], R. Chiarle[1];

[1]Boston Children's Hospital, Boston, MA, [2]University of Milano-Bicocca, Monza, Italy, [3]University of North Carolina at Chapel Hill, Chapel Hill, NC, [4]University of Torino, Torino, Italy, [5]Koch Institute and MIT, Cambridge, MA, [6]Celldex Therapeutics, New Haven, CT, [7]Yale University School of Medicine, New Haven, CT

Neuroblastoma is the most common extracranial solid tumor of childhood, with limited success in treating refractory or relapsed cases using current therapies. Chimeric antigen receptor (CAR) T cell therapy targeting GD2 has shown promise in neuroblastoma treatment, but relapses are associated with loss of antigen expression. The selection of the best tumor antigen is critical for the therapeutic success of CAR-T cells in hematologic malignancies and solid tumors. The Anaplastic Lymphoma Kinase (ALK) receptor is expressed by most neuroblastomas while virtually absent in most normal tissues. ALK is an oncogenic driver in neuroblastoma and ALK inhibitors show promising clinical activity. All these features make ALK an attractive target for CAR-T cell therapy. We developed ALK.CAR-T cells that show potent efficacy in monotherapy against neuroblastoma with high ALK expression without toxicity. For neuroblastoma with low ALK expression, combination with ALK inhibitors specifically potentiates ALK.CAR-T cells but not GD2.CAR-T cells. In neuroblastoma cell lines and in a patient-derived xenograft (PDX), the combination of ALK inhibitors and ALK.CAR-T cells significantly reduced tumor growth and extended mice survival. Mechanistically, ALK inhibitors impair tumor growth and upregulate the expression of ALK, thereby facilitating the activity of ALK.CAR-T cells against neuroblastoma. Thus, while neither ALK inhibitors nor ALK.CAR-T cells will likely be sufficient as monotherapy in neuroblastoma with low ALK density, their combination specifically enhances therapeutic efficacy. These findings provide insights into the potential of ALK.CAR-T cells as a novel therapeutic strategy for neuroblastoma. A Phase I clinical trial to test ALK.CAR-T cells in combination with ALK TKIs in children with refractory/relapsed neuroblastoma is being implemented based on these results.

#0051 OPB-101: An optimized mesothelin-specific CAR T cell product expressing CD8-targeted IL-2/15 and engineered to resist T cell exhaustion.

R. Amin, H. Moffett, K. Haworth, J. Chen, J. Yokoyama, A. Wang, L. Tait, M. Steele, J. Crowl, T. Davenport, J. DeSautelle, J. Hammer, W. Obenza, V. Montoya, R. Kirkpatrick, L. Baker, T. Tan, K. Shirley, B. Hammerson, R. Langan, D. Clausen, P. Sample, B. Weitzner, S. Yuan, M. Lajoie, S. Boyken, A. Foster; Outpace Bio, Inc., Seattle, WA

T cell therapies have had modest efficacy in solid tumors due to their failure to proliferate following infusion. We have designed a mesothelin (MSLN) CAR T product (OPB-101) which includes a novel promoter (OP1), an optimized CAR, a safety switch, and a CD8α-targeted IL-2/15 designed cytokine to promote T cell expansion and improve efficacy in solid tumors. Human anti-MSLN binders were optimized for the target using our OUTSPACER^{TM} library. CAR evaluation was conducted using *in vitro* coculture assays and validated NSG tumor xenograft models. OUTSMART^{TM} IL-2/15 was designed to avoid regulatory T cell activation by ablating IL-2Rα binding and re-targeted to CD8α to enhance CD8^{+} T cell and NK stimulation. EGFRopt^{TM} was engineered for improved sensitivity to EGFR-targeted immunotherapies. Using 2A polypeptides, all transgenes were expressed with an antigen-dependent, inducible “stim-on” promoter (OP1) to regulate CAR expression, cytokine production, and resistance to exhaustion. The efficacy of the OPB-101 construct was tested in stringent exhaustion assays. *In vivo* efficacy was assessed with mice engrafted with s.c. H1650 tumors that were treated by i.v. injection of mock, CAR only or OPB-101 T cells at doses ranging from 0.25 x 10^6 to 2 x 10^6 cells. Tumor volume and weight were measured for 80 days. T cell levels and phenotype were measured by peripheral blood (PB) draws and intratumoral analysis (IT; day 14). OPB-101 efficiently killed MSLN^{+} tumor cell lines in repeat challenge and spheroid assays, and inducibly produced the IL-2/15 cytokine. IL-2/15 expression did not result in antigen-independent CAR T cell proliferation but extended survival in conditions without exogenous cytokine support. *In vivo* efficacy studies showed tumor control at 2 x 10^6 cells in the CAR only condition and modest anti-tumor efficacy at the 1 x 10^6 dose. In contrast, OPB-101 demonstrated complete and durable tumor elimination at the lowest dose of 0.25 x 10^6 cells (OPB-101 versus CAR only at 1 x 10^6 cells, $p < 0.0001$ and $p < 0.0005$ for donor 1 and 2, respectively). OPB-101 efficacy was associated with robust expansion in the PB (>100-fold) within IT (>5-fold) compared to the CAR only condition. OPB-101 PB and IT T cells showed reduced levels of PD-1, TIGIT and CD39 compared to CAR only suggesting resistance to exhaustion. Finally, studies conducted in tumor-free mice showed that OPB-101 expansion *in vivo* was dependent on the presence of tumor. In summary, OPB-101 using a regulated promoter (OP1) to dynamically express an optimized MSLN CAR, EGFRopt^{TM}, and a CD8-targeted IL-2/15 cytokine enhances anti-tumor efficacy against solid tumors by promoting CAR expansion and persistence while limiting T cell exhaustion. These technologies allow for complete elimination of solid tumors at a low treatment dose (i.e., <250K cells) and may pave the way to more effective CAR T cell therapies for solid tumors.

#0052 CRISPR-mediated knock-out of A20 lowers the activation threshold and induces metabolic rewiring of CAR-T cells.

N. J. Chu[1], C. Nava-Barbero[2], A. Merlino[1], P.-H. Lee[1], D. Baker[2], B. Taylor[2], G. Moody[1], L. Giardino[2];
[1]AstraZeneca US, Gaithersburg, MD, [2]AstraZeneca, Cambridge, United Kingdom

Background: Common failures of chimeric antigen receptor (CAR)-T cell therapy regimens stem from immune escape of target antigen low tumors. Strategies to improve CAR-T cell therapy efficacy include enhancing intrinsic effector function while preventing T cell exhaustion. The ubiquitin-modifying enzyme A20, is a key negative regulator of the NF-kB pathway downstream of T cell receptor activation in T cells. Dysfunctional CD8 T cells in tumors have high expression of A20, and deletion of A20 enhances antitumor activity of CD8 T cells in murine tumor models. We tested whether CRISPR-mediated knock-out (KO) of tumor necrosis factor α-induced protein 3 (TNFAIP3), the gene for A20, increases the effector function and alters the metabolic state of CAR-T cells.
Results: A20 deletion led to upregulation of NF-κB target genes and resulted in higher levels of activation marker expression and effector cytokine secretion compared to unarmored CAR-T upon incubation with target cells. In addition, A20 KO CAR-T cells maintained prolonged expression of activation markers upon antigen clearance in the absence of enhanced differentiation, and were more resistant to dysfunction in a repeat challenge serial kill assay. *In vivo*, A20 deficient CAR-T exhibited increased anti-tumor efficacy against low, medium, and high target expressing tumor models. Consistent with NF-κB upregulation, A20 KO cells significantly upregulated key glycolytic intermediates suggesting that amino acid anabolism was fueled by glycolysis and the pentose phosphate pathway. Moreover, the preferential increase of glycolysis over oxidative phosphorylation confirmed that A20 KO CAR-T cells were skewed towards an effector-like phenotype. Notably, glutathione and its cysteine-glycine bi-products were upregulated upon activation to a higher level in A20 KO CAR-T suggesting enhanced resistance to oxidative stress, in line with their prolonged persistence.
Conclusions: CRISPR-mediated knock-out of A20 lowers the activation threshold of CAR-T cells producing enhanced *in vitro* and *in vivo* anti-tumor efficacy particularly against tumors with very low levels of target expression. A20 KO induces metabolic rewiring of CAR-T cells by promoting glycolysis and amino acid anabolism to sustain their superior effector functions. This intrinsic armoring strategy can be applied to any CAR-T in any indication to increase tumor control and reduce immune escape.

#0053 T-cell receptor repertoire changes associated with clinical response in patients with B-cell non-Hodgkin's lymphoma receiving CD19 CAR-T therapy.

A. J. Faruqi[1], P. Wang[2], R. Bansal[2], A. De Menezes Silva Corraes[2], H. Zhang[2], Z. Shao[2], K. Regan[2], E. Moreno Cortes[2], A. Khurana[2], N. Bennani[2], Y. Wang[2], P. Hampel[2], J. Paludo[2], P. Johnston[2], H. Murthy[2], M. Iqbal[2], S. Ansell[2], J. Munoz[2], A. Rosenthal[2], M. Kharfan Dabaja[2], J. E. Castro[2], S. Kenderian[2], H. Dong[2], Y. Li[2], Y. Lin[2];

[1]Mayo Clinic College of Medicine and Science, Rochester, MN, [2]Mayo Clinic, Rochester, MN

Background: Although CAR T-cell therapy has achieved remarkable response rates in adult patients (pts) with relapsed and refractory B-cell non-Hodgkin's lymphoma (NHL), 20-30% of pts still have primary refractory disease, and 30-40% of pts relapse, often within 6 months of therapy. Given that durable clinical response can be achieved without CAR T cell persistence, we hypothesized that durable remission is correlated with the expansion of tumor-reactive T-cell receptor (TCR) clones following CAR T-cell infusion. To assess this, we examined the TCR repertoire of adult pts with B-NHL who received CD19 CAR T-cell (axi-cel) therapy to identify correlates of clinical response.

Methods: Single-cell (sc) RNA sequencing (seq) and scTCR-seq were performed on peripheral blood mononuclear cells from B-NHL pts before lymphodepletion chemotherapy (pre), at peak CAR-T expansion (peak), and one month following CAR-T (M1). scRNAseq and scTCR-seq data were processed using CellRanger v7.0.1, which were then analyzed using Immunarch (v0.9.0) for TCR clonality and sample diversity. Diversity was assessed using the Gini coefficient to indicate clone size inequality (0 = maximum diversity). TCR diversity and phenotype of expanded and emerged TCR clones post CAR-T were compared across clinical response categories: CR (complete remission for at least 6 months), PD1 (primary refractory), and PD2 (relapsed after partial or complete response).

Results: We analyzed 107,035 T cells from 77 serial samples of 32 pts (16 CR, 4 PD1, 12 PD2) and 5 healthy controls. Compared to pts with PD1 and PD2, pts with CR had a larger Gini coefficient for TCR clones at M1 relative to Pre and Peak. The Gini coefficient was the largest for tumor recirculating CD8 T effector memory (Tem) and activated CD8 peripheral memory (Tpm) cells at M1 for pts with CR. Examining the repertoire of emerged and expanded TCR clones at Peak and M1 from Pre, pts with PD2, compared to pts with CR, had a higher percentage of activated CD8 T peripheral memory (Tpm) and T regulatory cells (Treg) among the emerged clones and activated CD8 Tpm among the expanded clones. Patients with PD1, relative to patients with CR, had more proliferating and non-activated CD8 Tpm among the expanded and emerged clones.

Conclusion: NHL pts with CR after CAR-T had more robust clonal expansion of T cells, particularly tumor recirculating CD8 Tem and activated CD8 Tpm, compared to pts with relapsed or refractory disease. In contrast, pts with relapsed or refractory disease had an expansion of TCR clones with a larger proportion of CD8 Tpm and Tregs. Endogenous tumor-reactive TCR expansion may help predict favorable clinical response following CAR T-cell therapy.

#0054 Engineering chimeric antigen receptor (CAR) T cells using autoantigen binding domains for treatment of B cell malignancies with increased specificity.

Abiagil Cheever, Hunter Lindsay, MacKenzie Hansen, Chloe Kang, K. Scott Weber, Kim O'Neill

Microbiology and Molecular Biology, Brigham Young University, Provo, UT

Introduction: Chronic inflammation often leads to cancer, and many autoimmune diseases lead to a significantly increased risk of developing cancer. Though many autoimmune diseases, like Graves' Disease (GD), don't have treatments that address this risk. Chimeric antigen receptor (CAR) T cells are an effective treatment for hematological cancers by eliminating all B cells, but a more targeted form of CAR T cells could eliminate specific B cell populations in B cell malignancies, including GD.
Methods: To allow our CAR T cells to target specific B cell populations that cause GD, we engineered chimeric autoantigen receptors (CAAR) with epitopes of thyroid stimulating hormone receptor (TSHR) as the binding domain. This acts as bait for the anti-TSHR B cells. Jurkat T cells were lentivirally transduced with these CAAR plasmids. Anti-TSHR B cell lines were engineered by transducing Nalm6 cells with lentivirus for anti-TSHR B cell receptors. Cytotoxicity assays were performed on primary human TSHR CAAR T cells incubated with the anti-TSHR B cell lines. Cytokine production, proliferation, and cytotoxicity assays were performed on these coincubated cells to determine the efficacy of our TSHR CAAR T cells.
Results: Two of the three Jurkat TSHR CAAR T cells showed significant binding to anti-TSHR antibodies (TRAbs). They also showed significant activation, measured by CD69 expression, when incubated with plate bound TRAbs, but not soluble TRAbs. The B cell lines were validated by binding to TSHR. The primary TSHR CAAR T cells showed significantly increased proliferation and production of TNF, IFN-γ, and IL-2, when compared with controls. The TSHR CAAR T cells also had significant cytotoxic action against the anti-TSHR B cell lines, but not Nalm6 B cells. The cytotoxic function was comparable to our CD19 CAR T cell with the same activation domains, though it demonstrated specificity to only anti-TSHR B cells.
Conclusion: TSHR CAAR T cells are a potentially curative treatment for GD that will stop chronic inflammation and could reduce GD patient's risk of developing thyroid cancer. This is also an important development in CAR T cell therapies that allows for specific targeting of certain B cell populations.

#0055 CD70-specific CAR-T cell therapy for the treatment of glioblastoma.

Alexandros Kourtesakis[1], Hiu Nam Hannah Chow[1], Dennis Alexander Agardy[2], Eileen Bailey[1], Sandra Horschitz[3], Ammar Jabali[3], Rainer Will[4], Denise Reibold[1], Sonja Pusch[1], Christoph Schifflers[5], Manuel Fischer[6], Ling Hai[1], Dirk C. Hoffmann[1], Yu-Chan Chih[2], Robin Wagener[7], Leon Kaulen[7], Philipp Koch[3], Michael Breckwoldt[2], Michael Schmitt[8], Wolfgang Wick[7], Tim Sauer[8], Tobias Kessler[7]

[1]Clinical Cooperation Unit Neurooncology, German Cancer Research Center, Heidelberg, Germany,[2]Clinical Cooperation Unit Neuroimmunology and Brain Tumor Immunology, German Cancer Research Center, Heidelberg, Germany,[3]Hector Institute for Translational Brain Research, Mannheim, Germany,[4]Core Facility Cellular Tools, German Cancer Research Center, Heidelberg, Germany,[5]Department of Immunotherapy and Immunoprevention, German Cancer Research Center, Heidelberg, Germany,[6]Department of Neuroradiology, University Hospital Heidelberg, Heidelberg, Germany,[7]Department of Neurology, University Hospital Heidelberg, Heidelberg, Germany,[8]Department of Hematology, Oncology and Rheumatology, University Hospital Heidelberg, Heidelberg, Germany

Despite the remarkable success of chimeric antigen receptor (CAR)-T cell treatment for patients with hematologic malignancies, this method has yet failed to confer meaningful survival benefits to patients suffering from glioblastoma (GB), the most lethal type of brain tumor. This highlights the need to develop novel CAR-T cell approaches for this disease. CD70 is a member of the tumor necrosis factor receptor (TNFR) superfamily. Although absent on normal brain tissue, it is ectopically expressed in a substantial fraction of GB patients, indicating its suitability as a CAR-T cell therapy candidate. In this study, we generated CD70-targeting CAR-T cells and tested their cytotoxicity *in vitro* and *in vivo*. First, we detected CD70 in a panel of primary GB cell lines and to investigate its role, it was overexpressed in human and murine GB cells. In a syngeneic glioma model, C57BL/6J mice injected with CD70-overexpressing GL261 cells developed significantly larger tumors compared to the control counterparts. Additionally, RNA-sequencing revealed that CD70-overexpression in the same cells led to higher expression levels of immunosuppressive marker *CD200* and lower levels of tumor inhibition genes *Prkg2* and *Sh3bgrl2*, suggesting a tumor-promoting role in GB. For our immunotherapeutic intervention, we designed CD70-targeting CAR-T cell constructs featuring different co-stimulatory domains (CD27, CD28 or 4-1BB) and successfully transduced primary T-Cells from healthy donors. In an *in vitro* co-culture, all CAR-T cells recognized and eliminated primary cancer cells in a target-dependent and donor-independent manner, while secreting high levels of Granzyme B. The killing capacity of these cells was further highlighted in a 3D system in which *in vitro*-generated cortical organoids were treated with CAR-T cells after being infiltrated by CD70-expressing or control cells. Immunofluorescence (IF) staining and enzyme-linked immunosorbent assay (ELISA) revealed increased levels of Granzyme B and IFN-γ in all treated organoids previously infiltrated by $CD70^+$ tumor cells. Importantly, generated CAR-T cells showed high specificity and efficiency in killing $CD70^+$ tumors *in vivo* in the brains of immunodeficient mice. Namely, 80% of NSG mice orthotopically implanted with $CD70^+$ GB cells and subsequently treated by CARs but not mock-transduced T-Cells showed complete tumor remission by the end of the experimental endpoint, determined by bioluminescence imaging (BLI). IF analysis of these brains showed high levels of apoptotic marker cleaved caspase-3, enhanced effector cell presence and significantly lower tumor cell occupancy compared to control-treated animals. In conclusion, we provide evidence in favor of utilization of CAR-T cells against CD70-expressing gliomas. Based on these findings, a phase-I clinical trial to assess the safety and efficacy of autologous CD70-specific CAR-T cells for relapsed $CD70^+$ GB is being planned.

#0056 Preclinical *in vivo* characterization underpinning LGR5-targeting CAR-T cells as a cancer immunotherapy.

J. Foeng[1], T. Tyllis[1], C. Abbott[1], D. McPeake[1], E. Thompson[2], V. Bandara[1], B. Gundsambuu[1], S. Napoli[1], C. Bonder[1], I. Comerford[1], T. Sadlon[1], S. Barry[1], S. McColl[1];

[1]University of Adelaide, Adelaide, Australia, [2]Centre for Cancer Biology, Adelaide, Australia

Incidences of early-onset colorectal cancer (CRC) have been accelerating worldwide. To begin to address the lack of therapeutic options for CRC, we have developed a CAR-T cell therapy specific for leucine-rich repeat-containing G-protein coupled receptor 5 (LGR5). LGR5 is known to potentiate Wnt/B-catenin signaling and mark cells-of-origin in intestinal cancers. Extensive screening has demonstrated elevated expression of LGR5 in CRC, which is correlated with reduced patient survival. In CRC, LGR5 has been intimately linked with metastasis, cell survival and perturbation of chemotherapeutic interventions. We have developed a 9-day preclinical manufacturing method to generate LGR5-targeting CAR-T cells with a minimally differentiated T cell phenotype, which was concomitant with significant cytotoxic and activation marker expression. In human CRC xenograft mouse models, LGR5-targeting CAR-T cells eradicated tumors at doses as low as 800,000 CAR^+ cells, and were capable of significantly inhibiting advanced tumor growth following delayed administration. Robust CAR-T cell-mediated immunological protection was observed in rechallenge experiments, in which secondary tumor growth was undetectable in mice which had tumors rejected following previous CAR-T cell administration. LGR5 protein and mRNA expression was also detected in a diverse range of cancer families, including ovarian, brain, liver and stomach, expanding upon the clinical indications with which LGR5-targeting CAR-T cells may be harnessed. These results contribute to a preclinical body of work that culminated in a Phase I/IIa clinical trial in metastatic colorectal cancer patients, which was approved for initiation by the FDA and commenced in 2023 (NCT05759728).

#0057 Ibrutinib improves chimeric antigen receptor T cell control of leukemia by inhibiting myeloid-derived suppressor cells.

B. F. Frost[1], O. Shestova[2], F. Shen[2], C. Sharpe[3], J. C. Byrd[3], S. I. Gill[2];
[1]Perelman School of Medicine, University of Pennsylvania, Philadelphia, PA, [2]Department of Medicine, University of Pennsylvania, Philadelphia, PA, [3]Department of Medicine, University of Cincinnati, Cincinnati, OH

Background: In patients with chronic lymphocytic leukemia (CLL), we and others have shown that the addition of the BTK inhibitor ibrutinib to CART cells increases the rates of durable complete responses. The mechanism for this remains unknown. Lymphodepletion (LD) is considered critical for CART cell therapy success, yet emergency myelopoiesis during recovery from LD may induce a surge of myeloid-derived suppressor cells (MDSC), particularly in patients with advanced cancer. BTK inhibition has been shown to inhibit MDSC function in vitro. We therefore hypothesized that administration of ibrutinib during and following LD could reduce MDSC-mediated suppression of CART cells and thereby improve CART cell outcomes.
Methods: To explore the effects of ibrutinib on human MDSCs, we engineered suppressive monocytes through *in vitro* culture of CD14+ cells in the presence of IL-6 and GM-CSF. We added ibrutinib to the culture on Days 0-4 and compared the ability of the monocytes to inhibit proliferation of human CAR-T cells. To model CLL treatment with CART in immunocompetent mice, we used the Em-*TCL1* adaptive transfer model of CLL. Mice were treated with ibrutinib (I), cyclophosphamide and fludarabine (FC), or ibrutinib + FC (FC+I). MDSCs were isolated from these mice for *in vitro* function studies. In subsequent experiments mice were also treated with syngeneic CART19 with or without FC or FC+I.
Results: *In vitro* generated human MDSC suppressed CART19 function, and this was prevented by pre-treatment of MDSC with ibrutinib. Myeloid cells from the spleens of CLL-bearing mice inhibited syngeneic CART19 function *ex vivo* regardless of treatment with FC or I alone, but myeloid cells harvested from CLL-bearing mice treated with FC+I lost suppressive function. Finally, mice treated with CART19 after a LD regimen resembling that in our recently reported clinical trial (FC+I) showed a survival advantage over all other groups.
Conclusions: BTK inhibition with ibrutinib prevents myeloid cell suppression of CART cells *in vitro* in human and murine systems. When combined with lymphodepleting chemotherapy (FC), ibrutinib enhances CART cell control of CLL *in vivo*, possibly by preventing MDSC-mediated suppression of CART cells.

#0058 Immunocytokines with specificity for invariant region of CAR molecules enhance effector function of multiple CAR T cell therapies.

J. T. Keane, O. K. Dagher, F. Liu, **A. D. Posey, Jr.**;
University of Pennsylvania, Philadelphia, PA

The effector functions of CAR T cells can be enhanced through delivery of immunostimulatory cytokines, such as IL-12, IL-18, or IL-23. However, systemic delivery of recombinant cytokines or paracrine secretion by CAR T cells can elicit toxicities due to non-specific targeting of the cytokines. Here, we designed immunocytokines with antibodies specific for the invariant linker peptides that join variable domains in the CAR scFv and immunostimulatory cytokines. The immunocytokines were capable of targeting CAR molecules agnostic of target antigen, demonstrating broad applicability without the need for further genetic engineering of CAR therapies, such as co-expression of a surrogate molecule (tEGFR, etc.). The addition of immunocytokines enhanced CAR T cell cytolytic activity and secretion of type I cytokines, even at low concentrations of immunocytokine. In a stringent Nalm6 xenograft model, the addition of immunocytokines delivering IL-12 enhanced the anti-tumor activity of anti-CD19 CAR T cells and overall survival compared to controls of antibody alone or PBS. This technological development presents the opportunity to specifically enhance the activity of multiple CAR T cell therapies in the absence of non-specific toxicities.

#0059 Triple negative breast cancer (TNBC) targeting CAR-T cell constructs with phage display-derived peptides.

M. G. Khodary[1], A. W. Yirsaw[1], Y. A. Elsobky[2], R. Gurung[1], J. Jaynes[1], T. Samuel[1], M. Sandey[3], D. Bedi[1];
[1]Tuskegee University, Tuskegee, AL, [2]University of Sadat City, Sadat City, Egypt, [3]Auburn University, Auburn, AL

Introduction: Triple Negative Breast Cancer (TNBC) poses treatment challenges due to the absence of effective targeted therapies. CAR-T cell therapy, successful in hematological cancers, is now being investigated for solid tumors. Finding new CAR-T targets is vital to overcome TNBC's therapeutic constraints.
Methods: In this study, a Biopanning phage display strategy employing a library of random peptides was utilized to identify potential targets for CAR-T cell therapy against TNBC. Through this approach, Heat Shock Protein 60 (HSP60) emerged as a promising candidate due to its binding affinity to the selected phage clones. Subsequent validation of HSP60 surface expression on TNBC cell lines in comparison to normal cells was conducted using flow cytometry. Concurrently, patient survival data were gathered and analyzed to evaluate the clinical significance of HSP60 expression in TNBC. The identified peptides demonstrating high specificity and affinity for HSP60 on the surface of TNBC cells were chosen for the development of a third-generation CAR-T model, incorporating various optimizations and innovations.
Results: The Biopanning strategy successfully identified HSP60 as a prominent target for CAR-T cell therapy in TNBC. Flow cytometry analysis confirmed significantly elevated surface expression of HSP60 on TNBC cell lines compared to their normal counterparts, substantiating its potential as an accessible antigen for targeted therapy. Patient survival analysis linked elevated HSP60 levels with poorer prognosis in TNBC, highlighting the protein's clinical relevance. Peptides showing high specificity and binding to TNBC's HSP60 were integrated into a meticulously engineered third-gen CAR-T cell model. This design aimed to boost the CAR-T's precision in targeting and eliminating HSP60-expressing TNBC cells. Iterative optimizations ensured the construct's accuracy, laying the groundwork for a potent, tailored TNBC immunotherapy.
Discussion: The discovery of HSP60 as a prime target for CAR-T cell therapy in TNBC is a pivotal advancement. Its distinct presence on TNBC cell surfaces, confirmed via flow cytometry, highlights its suitability for targeted immunotherapy. The correlation between elevated HSP60 levels and poorer prognosis in TNBC patients underscores its value as both a biomarker and a therapeutic focus. The peptides' exceptional specificity and strong binding to HSP60 validate their use in crafting a third-generation CAR-T cell model. Their integration and careful refinements in CAR-T design aim to optimize efficacy while reducing off-target effects, laying a robust foundation for tailored TNBC immunotherapy. Preclinical evaluations are imperative to thoroughly assess the safety and effectiveness of this innovative CAR-T approach.

#0060 Functional mapping of glioblastoma recurrence reveals targetable dependencies in an axonal guidance pathway in highly invasive brain cancers.

S. K. Singh[1], C. Chokshi[1], V. Shaikh[1], B. Brakel[1], A. Anand[1], C. Venugopal[1], T. Kislinger[2], K. Henry[3], M. Rossotti[3], K. Brown[4], J. Lazo[5], J. Moffat[4]; [1]Centre for Discovery in Cancer Research, McMaster University, Hamilton, ON, Canada, [2]University of Toronto, Toronto, ON, Canada, [3]NRC, Ottawa, ON, Canada, [4]Hospital for Sick Children Research Institute, Toronto, ON, Canada, [5]University of Virginia, Charlottesville, VA

Resistance to genotoxic therapies and tumor recurrence are hallmarks of glioblastoma (GBM), an aggressive brain tumor. Here, we explore the functional drivers of post-treatment recurrent GBM. By conducting genome-wide CRISPR-Cas9 screens in patient-derived GBM models, we uncover distinct genetic dependencies in recurrent tumor cells that were absent in their patient-matched primary predecessors, accompanied by increased mutational burden and differential transcript and protein expression. These analyses map a multilayered genetic response to drive tumor recurrence, identifying protein tyrosine phosphatase 4A2 (*PTP4A2)* as a novel modulator of self-renewal, proliferation and tumorigenicity at GBM recurrence. Genetic perturbation or small molecule inhibition of PTP4A2 represses axon guidance activity through a dephosphorylation axis with roundabout guidance receptor 1 (ROBO1), exploiting a functional dependency on ROBO signaling. Importantly, engineered anti-ROBO1 single-domain antibodies also mimic effects of PTP4A2 inhibition. Since a pan-PTP4A inhibitor was limited by poor penetrance across the blood brain barrier (BBB) *in vivo*, a second-generation chimeric antigen receptor (CAR)-T cell therapy was engineered against ROBO1 that elicits specific and potent anti-tumor responses *in vivo*. A single dose of anti-ROBO1 CAR-T cells doubles median survival in patient-derived xenograft (PDX) models of recurrent glioblastoma, and also eradicates tumors in around 50% of mice engrafted with PDX models of lung-to-brain metastases and pediatric relapsed medulloblastoma. We conclude that functional reprogramming drives tumorigenicity and dependence on a multi-targetable PTP4A-ROBO1 signaling axis at GBM recurrence, with potential in other malignant brain tumors.

#0061 A novel immunotherapy for metastatic prostate cancer: A monoclonal antibody that can bind both STEAP1 and STEAP2.

M. Sheng[1], G. Thillainadesan[2], A. Sparkes[2], B. Su[1], E. Matus[1], J. Wright[1], S. Liu[2], J. Gariepy[2], H. S. Leong[2];
[1]University of Toronto, Toronto, ON, Canada, [2]Sunnybrook Research Institute, Toronto, ON, Canada

Prostate cancer (PCa) is the second most prevalent cancer among males, and the 5-year survival rate for patients with metastatic PCa (mPCa) is ~30%. Although significant progress has been made in improving survival in mPCa patients, many of these patients experience relapse or systemic toxicities. Protein expression of prostate-specific membrane antigen (PSMA), a common PCa antigen often targeted in PCa therapy, is unfortunately lost in the later stages of mPCa. In contrast, six transmembrane epithelial antigen of the prostate 1 and 2 (STEAP1 and STEAP2) are both overexpressed in most PCa compared to normal and vital organs and has emerged as a next-generation target in mPCa.
We hypothesize that an antibody that binds to both STEAP1 and STEAP2 via their second extracellular domain (60% homology) could be useful therapeutically. Using an immunogen of this second extracellular domain, we raised several antibody clones that appear to have an affinity towards both STEAP1 and STEAP2 (STEAP1/2). The specificity and affinity of these antibody clones were successfully determined by immunofluorescence, flow cytometry and ELISA. Immunofluorescence results in PCa cell lines and those that overexpress STEAP1 and STEAP2 demonstrate the potential specificity of one clone for human STEAP1 and STEAP2. In addition, ELISA data revealed that the binding affinity of this clone to STEAP1 and STEAP2 is in the low nanomolar and low micromolar range, respectively. This monoclonal STEAP1/2 antibody has been sequenced and will become the basis for future development of immunotherapies thus expanding the therapeutic armamentarium for mPCa.

#0062 Intra-tumor persistence of activated anti-mesothelin hYP218 CAR T cells is associated with increased efficacy in gastric and colorectal cancers.

S. A. Mir, A. Venugopalan, J. Zhang, M. Khanal, C. Stathopoulou, M. Sengupta, Q. Jiang, R. Hassan;
National Institutes of Health (NIH), Bethesda, MD

Purpose: Patients with gastric and colorectal cancers that have progressed after standard therapies have poor prognosis. Given the high expression of mesothelin in these tumor types, we examined the potential utility of the anti-mesothelin hYP218 CAR T cells to treat these cancers.
Experimental Design: Cell surface mesothelin expression in a panel of gastric and colorectal cancer cell-lines was analyzed using flow cytometry. *In vitro* efficacy of hYP218 CAR T cells against these cell lines was evaluated using cytotoxicity and cytokine release assays. *In vivo* efficacy of hYP218 CAR T cells was studied using gastric (HGC27) and colorectal (SW48) tumor xenografts in NSG mice. NSG mice were injected with 1×10^6 cancer cells and the tumors were allowed to grow until they reached a volume of 80-100mm³, after which the mice were treated with either 5×10^6 hYP218 CAR T cells, 5×10^6 untransduced T cells, or saline and monitored over time. Persistence of CAR T cells in the tumor was evaluated over time and expression of activation and exhaustion markers were studied.
Results: hYP218 CAR T cells demonstrated strong cytotoxic activity against mesothelin positive gastric and colorectal cancer cell lines and exhibited increased pro-inflammatory cytokine production. In both the HGC27 and SW48 tumor models hYP218 CAR T cells demonstrated significant reduction in tumor volume and overall survival compared to mice treated with untransduced T cells or saline. CAR T cells isolated from tumors of both the xenograft models, at day 40 after treatment, displayed higher expression levels of activation markers CD39 and CD69 when compared to the infused product. Furthermore, a concomitant elevation in the levels of effector cytokines, TNF-α and IFN-γ, was detected in the blood of treated mice demonstrating the functional capacity of the CAR T cells to not only persist but also to maintain an activated state.
Conclusions: hYP218 CAR T cells show anti-tumor efficacy against gastric and colorectal tumor xenografts due to increased accumulation of activated CAR T cells in the tumor and warrants further investigation for treatment of patients with these cancers.

IMMUNOLOGY: Biomarkers, Immune Monitoring, and Immune Assays
Poster Session

#0065 Differential impacts of PD-L1 expression in tumor vs. stroma on survival in esophageal squamous cell carcinoma.

Tomohiro Murakami[1], Satoru Furuhashi[1], Yuuki Sakai[1], Kenichi Sekimori[1], Ryoma Haneda[1], Eisuke Booka[1], Tomohiro Matsumoto[1], Hirotoshi Kikuchi[1], Yoshihiro Hiramatsu[2], Hiroya Takeuchi[1]

[1]Department of Surgery, Hamamatsu University School of Medicine, Hamamatsu, Shizuoka, Japan,[2]Department of Surgery, Perioperative Functioning Care & Support, Hamamatsu University School of Medicine, Hamamatsu, Shizuoka, Japan

Background: Esophageal squamous cell carcinoma (ESCC) has high incidence and recurrence rates, particularly in advanced stages. While the combined positive score (CPS) and tumor proportional score (TPS) are standard benchmarks for PD-L1 assessment in ESCCs, they face challenges such as reliance on subjective human interpretation and the uncertain clinical significance of strong staining intensities. Our study utilizes H-scores for PD-L1 expression and separates analysis of tumor and stroma, providing additional layers of information that complement current methods and contribute to a more comprehensive understanding of the role of PD-L1 in ESCC.
Methods: This retrospective single-center cohort analysis involved 194 cases of ESCC who underwent surgical resection. We performed a comprehensive evaluation of PD-L1 expression within the tumor and stroma using whole slide images (WSI). QuPath image analysis software was used to classify regions as tumor or stroma and quantify the PD-L1 expression H-score.
Results: Using optimal H-score cutoffs determined from the minimum P-value method, the Kaplan-Meier survival analysis showed that higher PD-L1 expression was significantly linked with better post-operative survival across all compartments. This correlation was most pronounced in the stroma ($P<0.001$). However, in multivariate Cox regression analysis, only high tumoral PD-L1 expression emerged as an independent predictor of favorable prognosis (HR=0.47, 95% CI: 0.27-0.81, $P=0.007$). The non-significant contribution of stromal PD-L1 in this model could be attributed to its association with advanced pT and pN stages, and the presence of lymphatic and venous invasion ($P<0.001$, respectively). Interestingly, stromal PD-L1 expression was associated with a longer duration of cytotoxic chemotherapy (cutoff 8 months, Median H-score 98.28 vs 55.24, $P=0.026$), but no significant correlation was observed with the duration of immune checkpoint inhibitor treatment.
Conclusions: The study underscores the complex role of PD-L1 in ESCC, with tumoral PD-L1 expression emerging as an independent prognostic factor, and stromal PD-L1 expression found to be related with tumor progression and the duration of cytotoxic chemotherapy response.

#0066 A new mechanism of tumor immune escape: TCF19 promotes the development of novel terminally exhausted T cells through E2F and MYC transcription family.

F. Wang, N. Dong, C. Zhang;
The Seventh Affiliated Hospital of Sun Yat-sen University, Shen Zhen, China

Introduction: ICB (immune checkpoint blocking) has been a promising therapy in cancer treatment, but there are still some patients do not response to this therapy. And it is well known that the majority cells reactivated to ICB are TCF1+ precursor exhausted T cells. Thus, studying the formation and heterogeneity of exhausted T cells are very necessary for improving the efficacy of ICB therapy. In this research, we identified a new population as TCF19+PD1+TIM3+ exhausted CD8+ T cells, which blocked the responds to ICB therapy.
Methods: We collected single cell sequencing data, including colorectal cancer, gastric cancer, melanoma, and lung cancer, and drew tumor immune cells map through cluster analysis. Then using bioinformatics tools CytoTRACE. T and CCAT. A to calculate the differentiation of exhausted T cell populations, which discovered a new subset of highly proliferative and poorly differentiated terminal exhausted T cells. Subsequently, the existence of this group of cells was verified through in vitro experiments, and their formation mechanism and correlation with immunotherapy were further studied.
Results: We utilized CytoTRACE.T and CCAT.A to predict differentiation states of terminally exhausted T cells. Then GEO and KEGG pathway gene set enrichment analysis were used. After analyzing, we found out that there was a subset of cells in terminally exhausted T cells defined as TCF19+PD1+TIM3+ Tex cells, which presented low differentiated and high proliferative potential.Then we performed multiple immunofluorescence staining and flow cytometry to verified the existence of TCF19+PD1+TIM3+ Tex cells in vitro. Clarifing the generation of these cell subset through regulating the expression of E2F and MYC transcription factor families.By collecting pathological sections of patients with immunotherapy information, we found that the amount of TCF19+PD1+TIM3+ Tex cells was inversely proportional to the efficacy of ICB, through immunofluorescence staining and immunohistochemical analysis as well as organoid models cocultured with T cells.
Conclusion: In this research, we found a new subpopulation of terminal Tex cells, which showed high proliferation and low differentiation. For cells, TCF19 mediated the generation of stemness terminal Tex cells may through regulating the expression of E2F and MYC. Finally, we discovered that the existence of TCF19+PD1+TIM3+ Tex cells can predict the efficacy of ICB, that the more TCF19+PD1+TIM3+ Tex cells contained, the less efficacy of ICB in patients.This finding may provide a new research direction for immunotherapy. Thus, more attention should be paid to this new cell subset.

#0067 Predicting colorectal patient prognoses by functional characterisation of heterogeneous cell types and their spatial interaction using a new technique: Whole slide imaging mass cytometry.

R. M. Costello[1], S. Fenton[1], H. McGuire[2], L. Lim[3], D. Howell[3], Q. Raza[3], J. Chwee[4], R. Kemp[1];
[1]University of Otago, Dunedin, New Zealand, [2]University of Sydney, Sydney, Australia, [3]Standard BioTools Canada Inc., Toronto, ON, Canada, [4]Standard Biotools Canada Inc., Markham, ON, Canada

Immunotherapies stimulate T cell function in the tumor microenvironment (TME). CD3+ and CD8+ T cell infiltration can predict disease recurrence in colorectal cancer (CRC) patients and has been validated as Immunoscore® (IS). The TME comprises multiple heterogeneous populations of immune cells, including T cells and cancer-associated fibroblasts (CAFs); CRC tumors are also morphologically diverse. Standard BioTools™ (SBI) has developed a novel whole slide Imaging Mass Cytometry™ technique that allows complete analysis of cell population heterogeneity in the TME using >40 markers.
We hypothesised there are multiple heterogeneous subtypes of CAFs within CRC tumors and that they modulate T cell infiltration and patient outcome. In collaboration with SBI, we studied a cohort of CRC patients stratified based on T cell infiltrate and disease recurrence. We identified multiple CAF populations that interact with tumor-infiltrating T cell populations.
Slides from 10 CRC patients with high or low CD3+CD8+ T cell infiltrate (IS) were stained with a panel encompassing markers for CAF and T cell heterogeneity, function, and metabolism. Slides were imaged using the Hyperion XTi™ Imaging System at SBI. Using a scan mode called Preview Mode, the whole slide was imaged in minutes to identify CAF and T cell phenotypic regions of interest. Next, the same slide was imaged at 1 µm resolution using Cell Mode (CM). Finally, for each sample, an additional serial section was imaged using a slightly lower resolution called Tissue Mode (TM). TM allowed us to image the samples in several hours instead of days while capturing the full heterogeneity of the entire tissue sample. We used clustering to identify phenotype clusters and neighbourhood analysis to study spatial enrichment. We also compared results between CM and TM.
We report: Identification of heterogeneous CAF subtypes in CRC patients with high or low IS; determination of CAF populations that spatially interact with T cells in patients with high or low IS; and examination of consistent spatial interactions between CAF and T cells in CRC, and whether these interactions differ in patients with high or low IS. TM revealed several heterogeneous cellular populations that differed between patients with high or low IS; importantly, low IS tumors had more podoplanin+αSMA+ CAF populations and fewer podoplanin+αSMA- cell populations compared with high IS tumors. High IS tumors had more PD-1+CD8+ T cells compared with low IS tumors; these PD-1+CD8+ T cells spatially interacted with podoplanin+αSMA- CAF populations in high IS tumors. CAF-PD-1+CD8+ T cell interactions were absent from low IS tumors. Thus, CAF-PD-1+CD8+ T cell interactions are important in CRC patients with high IS, and these cellular interactions require further investigation.

#0068 Imaging Endothelial PD-L1 expression with ultrasound molecular imaging to stratify immune checkpoint inhibitor responders.

A. Natarajan, F. Tabesh, M. Bataghva, R. Paulmurugan, A. N. El Kaffas;
Stanford University School of Medicine, Palo Alto, CA

Immune checkpoint blockade therapies (ICTs) have revolutionized oncology through substantial and lasting treatment outcomes, but only in 15-20% of patients. Non-invasive diagnostic tools to select patients that are most likely to respond to ICT and guide treatment regimens, and thus minimize toxicities to non-responder patients, are in high demand. Program death-1 ligand (PD-L1) marker evaluation in the tumor vasculature and tumor microenvironment is an essential criterion for identifying a suitable patient for PD-L1 based ICT, and it also serves as a prognostic marker in tumor response evaluation. Ultrasound molecular imaging (USMI) is an up-and-coming non-invasive imaging modality that enables longitudinal characterization of endothelial-specific markers. We are developing USMI methods to image immune markers expressed specifically on endothelial cells (EC) of tumors as a decision-support tool for guiding ICT strategies. In this work, we demonstrate for the first time the potential of imaging EC-specific immunosuppressive markers such as PD-L1 and investigate whether it can act as a marker for predicting ICT response. Target-ready microbubble (MB) was used (Trust Bio-sonics, Taiwan) to generate PD-L1 antibody (Ab) linked MBs (TMBs). DSPE-PEG was functionalized to anti-PD-L1 Ab or isotype-Ab (control) to generate stable TMBs (~5×10^7 MBs/mL) to target PD-L1 expressing ECs *in vivo*. We studied the treatment effect of anti-PD-L1-Ab and isotype-Ab using a syngeneic CT-26 tumor in mice and demonstrated the targeting potency of TMB or iso-Ab-MB (NMB). US imaging was performed using Vevo 2100 high-frequency US system with M250 transducer to evaluate and quantify the differentially targeted enhancement parameter (dTE). We observed that TMBs bound PD-L1 expressing ECs in vivo, with high and low enhancement for TMB and NMB, respectively, in tumors validated by dTE quantification through characterization of the slower washout kinetics. Furthermore, TMBs exhibited increased tumor retention and prolonged binding with average differential targeted enhancement values (dTE) (+/- SD) of 5.2 ± 7.4 for TMBs compared to 2.4 ± 3.9 for NMBs (p=0.14). Preliminary results of USMI (dTE values of TMBs) indicate that PD-L1-treated mice showed a higher response (4.5 ± 5.2; n=9) to the treatment group than control mice that did not receive Ab (1.4 ± 0.8; n=4). The tumor growth rate for the treated mice group was 5.4 -fold retarded compared to the control group which correlated with USMI dTE values. The USMI signals correlated with IHC performed on tumor tissue ex vivo from the respective mouse used for US imaging. Overall, our pre-clinical study suggests that USMI using TMBs may contribute to non-invasive assessment of IC expression on tumor ECs, and that it may serve as a predictive biomarker of ICT response. This novel TMB agent could be a game changer for CE USMI-based cancer prognosis in ICB therapy.

#0069 Versican proteolysis signature as a potential immune infiltration biomarker for colorectal cancer.

D. Buckalew, S. Kraus, K. Johnson, C. A. Pasch, D. A. Deming;
University of Wisconsin - Madison, Madison, WI

Background: A subset of patients with mismatch repair proficient colorectal cancers (CRCs) benefit from immunotherapies, though currently no markers predict which cancers are likely to respond. Our group demonstrated that versican (VCAN), an immunoregulatory tumor matrix proteoglycan, when proteolyzed to an immunostimulatory fragment called versikine (Vkine) results in enhanced CD8+ T cell infiltration across multiple cancers. Here we evaluate if a RNA expression signature of VCAN proteolysis can identify CRCs with an immune cell infiltrated phenotype.
Methods: The TCGA PanCancer Atlas colorectal adenocarcinoma dataset (594 patients (pts)) was divided into cohorts based on RNA expression Z-scores for VCAN, TIMP3, and ADAMTS4. The VCAN proteolytic predominant (VPP) cohort (Z-score VCAN >0, TIMP3 <0.5, ADAMST4 >0) was compared to the VCAN proteolytic weak (VPW) cohort (Z-score VCAN >0, TIMP3 >0.5, ADAMST4 >0). Differences in clinical characteristics, mutation profile, differential gene expression, and gene set enrichment analysis (GSEA) were evaluated.
Results: The VPP group consisted of 42 pts (20:22 female: male, median age: 68.5 years old). The VPW group consisted of 29 pts (12:17 female: male, median age: 64 years old). The two groups had no significant difference between stages of disease. There was a significant increase in the mutation count in the VPP cohort (VPP median=115.5, VPW median=91, p=0.045). The MSI MANTIS scores were not different between the cohorts (VPP median=0.35, VPW median=0.37, p=0.325). The VPP cohort was enriched for gene sets associated with immune cell infiltration (interferon gamma response (FDR q<0.001), inflammatory response (FDR q<0.001), complement (FDR q<0.001), TNFA signaling via NKFB (FDR q<0.001), IL2 STAT5 signaling (FDR q<0.001), and IL6 JAK STAT3 signaling (FDR q<0.001). The VPW cohort was enriched for gene sets involving cell proliferation (WNT beta catenin signaling (FDR q<0.214), hedgehog signaling (FDR q<0.190), and KRAS signaling DN (q<0.159). Specifically, the VPP group demonstrated enhanced expression of CD274 (PD-L1; log2FC=1.41, p<0.001), LAG3(log2FC=1.41, p<0.001), PDF1(log2FC=1.34, p<0.001), CD8A(log2FC=1.25, p<0.001), CXCL9(log2FC=1.19, p=0.001), CXCL10(log2FC=1.44, p=0.001), IL6(log2FC=2.23, p<0.001), and CD19(log2FC=1.26, p<0.001).
Conclusion: VPP expression signature correlates with immune infiltration based on RNA expression and deserves further investigation to predict response to immunotherapies in CRC as well as other cancer types.

#0070 Unlocking the potential of the T-cell receptor in prostate cancer.

E. N. Glud[1], J. H. Fredsoe[1], I. K. Nordentoft[1], A. Kjar[1], M. Rusan[1], B. E. Laursen[2], B. G. Pedersen[1], N. J. Birkbark[1], L. Dyrskjot[1], M. Borre[1], K. D. Sorensen[1]; [1]Aarhus University Hospital, Aarhus, Denmark, [2]Aarhus University, Aarhus, Denmark

Introduction: Prostate cancer (PC) is the most commonly diagnosed cancer among western men, with its diagnosis and subsequent monitoring still heavily dependent on the prostate specific antigen (PSA) test. However, the prognostic accuracy remains poor, leading to overtreatment of patients with non-aggressive cancer and undertreatment of those with aggressive cancer in need of intervention. Malignant cells are subject to constant monitoring and elimination by T-cell lymphocytes recognizing cancer-specific antigens through the T-cell receptor (TCR). Consequently, to establish itself and progress, cancer must evade or modulate the surveillance mechanisms of the immune system. As cancer growth accelerates, immune evasion becomes more difficult, resulting in a more pronounced impact on the immune system. Recently, our research group documented the clinical value of tumor-infiltrating T-cells as markers of aggressive PC. Here, we hypothesize that this signal can also be found in circulating T-cells isolated from the blood and used as proxy for the antitumoral immune response in tissue.

Methods: This study utilizes a diverse and well-characterized cohort, encompassing 220 castration resistant PC patients (CRPC) with blood samples taken at the time of CRPC diagnosis, 30 newly diagnosed hormone-naïve PC patients, and 30 healthy male donors. For a deeper understanding of the mechanisms underlying the antitumoral immune response and its impact on disease progression, a subset of CRPC patients (n = 25) are TCR sequenced throughout their disease course and uniquely, the TCR repertoire of their metastatic biopsies is characterized.

Results: In an initial comparison of 8 CRPC patients and 8 age-matched healthy males, we observed that cancer patients had a higher proportion of hyper-expanded T-cell clones (P = 0.003; Fisher's exact test) and a less diverse TCR repertoire in blood. Furthermore, 86.5 % of hyper-expanded clones found in peripheral blood samples could also be found in malignant prostate tissue from matched CRPC patients, while overlap between patients was virtually non-existent

Conclusion: Our pilot study detected differences in the TCR repertoire between cancer patients and matched controls. The clones contributing most to this difference were concurrently found in malignant tissue indicating that the antitumoral immune response can indeed be detected in the periphery. Given these promising results, we are currently running the larger study described above to obtain a better understanding of the TCR repertoire and establish its prognostic potential in PC. While the findings showcased in this abstract exclusively stem from the pilot study, results for the full cohort will be presented at the conference.

#0071 Differential infiltration of key immune cell populations across malignancies varying by immunogenic potential and likelihood of response to immunotherapy.

A. A. Tarhini[1], I. Eljilany[1], S. Coleman[2], D. J. Hedges[3], M. McCarter[4], J. Carpten[5], H. Colman[2], A. Naqash[6], I. Puzanov[7], S. Arnold[8], M. Churchman[3], P. Hwu[1], W. S. Dalton[3], G. J. Weiner[9], A. Tan[2], J. R. Conejo-Garcia[10], P. C. Rodriguez[1];

[1]H. Lee Moffitt Cancer Center, Tampa, FL, [2]Huntsman Cancer Institute, Salt Lake City, UT, [3]Aster Insights, Tampa, FL, [4]University of Colorado Cancer Center, Denver, CO, [5]USC Norris Comprehensive Cancer Center, Los Angeles, CA, [6]Stephenson Cancer Center, Oklahoma City, OK, [7]Roswell Park Comprehensive Cancer Center, Buffalo, NY, [8]Markey Cancer Center, Lexington, KY, [9]University of Iowa Holden Comprehensive Cancer Center, Iowa City, IA, [10]Duke Cancer Institute, Durham, NC

Background: Emerging literature has identified key immune cell populations that appear to significantly impact immune activation or suppression in patients with cancer. We investigated candidate populations and their differential infiltration within tumors as estimated from mRNA co-expression levels of corresponding cellular markers.

Methods: We utilized clinical and transcriptomic data from patients with melanoma, urothelial, ovarian, and pancreatic carcinomas enrolled in the Total Cancer Care Protocol (NCT03977402) to which patients provided a written informed consent. We analyzed mRNA co-expression levels of biomarkers defining stem-like tumor-infiltrating lymphocytes (TILs) (TCF7, IL7R, CXCR5, CD28, and CD27), tissue-resident memory (TRM) T cells (CD69 and CD103), early dysfunctional T cells (PD1+, CCR5+, TCF7+, TIM3-), late dysfunctional T cells (PD1+, CD38+, CD39+, CD101+, TIM3+), activated-potentially anti-tumor (APA) T cells (PD1+, CD27+, CD28+, CD137+, GITR+), and Butyrophilin 3 A (BTN3A) isoforms (BTN3A1, BTN3A2, BTN3A3). Mann-Whitney U or Kruskal-Wallis H tests were used to compare median gene expression signature scores between immunotherapy (IO) responders (> 2 years survival) and non-responders (< 2 years survival). Cox regression was used to assess 2-year survival outcomes following immunotherapy.

Results: We found a significant difference in the estimated infiltration of APA T-cells in melanoma ($P = 4.67 \times 10^{-12}$ and $P = 5.80 \times 10^{-12}$) and in urothelial carcinoma ($P = 1.86 \times 10^{-09}$ and $P = 1.38 \times 10^{-09}$) as compared to ovarian and pancreatic tumors, respectively. There was less TRM T-cell infiltration in ovarian compared to melanoma ($P = 2.23 \times 10^{-8}$), urothelial ($P = 3.86 \times 10^{-28}$) and pancreatic ($P = 7.85 \times 10^{-9}$). A similar trend was seen with stem-like T-cells, early dysfunctional T cells, and late dysfunctional T cells. Differences in the expression of BTN3A isoforms were less apparent between the different tumors, with a trend towards higher expression in melanoma. In melanoma, a higher density of stem-like TIL, TRM, early dysfunctional T cells, late dysfunctional T cells, activated-potentially anti-tumor T cells, and BTN3A isoforms were associated with improved survival ($P = 0.0075$, 0.00059, 0.013, 0.005, 0.0016 and 0.041, respectively). A higher density of stem-like TIL was associated with improved survival in the urothelial cohort ($P = 0.028$). TRM gene signature had the best AUCROC as a moderate predictor of survival in our melanoma cohort (AUROC = 0.65); Examining the 6 signatures in public datasets of IO treated melanoma patients, they were similarly predictive of survival (AUROC of 0.61 - 0.64).

Conclusions: Our results support a higher infiltration of key cellular elements related to immune activation within immunogenic versus non-immunogenic tumors supporting a central role in anti-tumor immune response.

#0072 A spatial interactomics approach reveals interplay between the tumor microenvironment and T cell activation.

D. Eden, J. Vennberg, T. Busgen, **D. Raykova**, A. Zieba-Wicher;
Navinci Diagnostics AB, Uppsala, Sweden

Background: T cells play a fundamental role in immune response to tumors. However, the tumor microenvironment (TME) - a complex network of cells, signaling molecules, and extracellular matrix components - employs various strategies to evade immune surveillance and suppress T cell activity. Among the many molecular interactions taking place in the TME, the role of CD8/MHC I, LAG3/MHC II and PD1/PDL1 is pivotal in modulating anti-cancer response and the escape routes that cancer in turn uses to withstand immune defense. LAG3/MHC II and PD1/PDL1 interactions are inhibitory, causing T cell dysfunction and exhaustion, while the CD8/MHC I interaction is essential for initiating an effective anti-tumor response. Here, we used a cutting-edge *in situ* proximity ligation strategy combined with immunofluorescence (IF) to reveal these key interactions and TME biomarkers in hepatocellular carcinoma and Hodgkin lymphoma. Since the method does not compromise the structural integrity of tissues, communication between proteins can be studied in their native milieu.
Method: Protein-protein interactions (PPIs) were detected with the NaveniFlex Tissue Atto647N kit in human FFPE tissues according to the manufacturer's protocol. This technique can detect proteins located within interaction range (<40 nm) via oligonucleotide-antibody conjugates that create amplified fluorescent signal. Parallel IF co-staining for α-fetoprotein, Ki67, CD30 and CD3 was performed during the Naveni® detection step. Slides were mounted and imaged on the Olympus V200 automated scanner.
Results: Tumor cells were identified by α-fetoprotein/Ki67 (hepatocellular carcinoma) or CD30 (Reed-Sternberg in Hodgkin lymphoma) IF staining, and tumor-infiltrating lymphocytes were visualized by CD3 staining. With the help of the Naveni® assay, we observed abundant interaction between CD8/ MHC I in hepatocellular carcinoma and Hodgkin lymphoma. Suppressive immune checkpoint interactions such as LAG3/MHC II and PD1/PDL1 were also detected. In the case of Hodgkin lymphoma, the CD8/MHC I, LAG3/MHC II and PD1/PDL1 interactions were largely seen in the same areas, and specifically between T cells and Reed-Sternberg cells, indicating a crosstalk between the TME and the immune landscape in the cancer tissues.
Conclusion: The interactomics approach, employing *in situ* proximity ligation for observing protein function as opposed to mere expression, allows the detection of key PPIs in the TME. Understanding the intricate crosstalk between them is crucial in developing effective immunotherapies. Targeting these pathways simultaneously or in combination, such as using immune checkpoint inhibitors against PD1/PDL1 while exploring strategies to modulate LAG3/MHC II and CD8/MHC I interactions, holds promise in reinvigorating T cell responses against cancer and improving the efficacy of immunotherapies within the complex landscape of the TME.

#0074 Exploring the expression of cancer-intrinsic PD1 in osteosarcoma cells: A comprehensive proteomic analysis of its functional landscape.

K. J. Dziubek[1], J. Faktor[1], T. Hupp[2], M. Parys[2], S. Kote[1];
[1]University of Gdansk, Gdansk, Poland, [2]University of Edinburgh, Edinburgh, United Kingdom

Cancer treatment was revolutionized by immune checkpoint inhibitors (ICIs) targeting the PD1/PDL1 axis - a brake to the immune system. Despite remarkable success, some patients do not respond to therapy or rapidly deteriorate due to an unclear mechanism. As reported for several types of tumors, PD1 receptor is not solely expressed on immune cells but also on cancer cells. Depending on the tumor type, it may act either as a suppressor or a tumor promoter. The limited response to ICIs was also reported in osteosarcoma (OSA), the most common type of bone cancer, mostly affecting children and young adults. With no significant improvement in therapy over the past 30 years, there is an urgent need for therapeutic advancement. This study aimed to determine if PD1 protein is expressed in OSA and whether it has a functional role, potentially affecting the response to ICIs. Strikingly, our results revealed both surface and intracellular PD1 expression in U2OS osteosarcoma cells, confirmed by Western Blot, flow cytometry and immunofluorescence analyses. siRNA-mediated *PDCD1* gene silencing significantly increased cell migration and viability in scratch and viability assays. LC-MS-based global proteomics showed that *PDCD1* knockdown markedly affects U2OS cells' proteomic landscape compared to the control. To dissect PD1 receptor downstream signaling effects, we subjected the identified proteins to GO and GSEA large-scale data interpretation tools. The results strongly suggested that *PDCD1* silencing leads to the enrichment of proteins involved in cell growth, migration and motility, corresponding to the cellular effects we initially observed. Importantly, the analysis clearly indicated positive regulation of MAPK cascade in cells with perturbed PD1 expression, aligning with PD1 mediated MAPK regulation in T cells. To reveal the mechanism underlying PD1 signaling, we focused on proteins with significantly changed expression in response to the knockdown. Using the STRING database, we created their interacting network, revealing that numerous proteins are closely related, and the majority of them are phosphoproteins, indicating significance in cellular signaling. Remarkably, many of the STRING-analyzed proteins belong to intersecting pathways, such as AKT1S1 and LAMTOR proteins, the critical components for mTORC1 signaling, or selected members of the Src family kinases along with their negative regulator CSK. In summary, we report previously undiscovered functional expression of PD1 in OSA cells, providing insights into the landscape of PD1 downstream signaling. Our studies indicate the role of PD1 in regulating cell growth, proliferation, and motility, suggesting osteosarcoma-expressed PD1 as a tumor suppressor. Further studies are urgently needed to investigate its therapeutic significance and explore if we could make ICIs more effective to treat osteosarcoma.

#0075 Luciferase reporter cell lines allow simultaneous incorporation of tumor cells, innate immune cells, and adaptive immune cells for in-depth immune checkpoint studies.

H. Chang, A. C. Walker, J. G. Foulke, L. Chen, F. Tian, Z. Gu;
American Type Culture Collection (ATCC), Manassas, VA

Despite the considerable success of immune checkpoint therapies targeting T cells, a sizable proportion of patients experience resistance or relapse due to the immunosuppressive nature of the tumor microenvironment. Myeloid cells, a major component that suppresses effector lymphocytes, have emerged as an alternative and promising therapeutic target. However, there is a deep lack of widely accessible immunological models capable of representing the intricate three-way interaction between tumor cells, T cells, and myeloid cells. To address this need, we conducted a comprehensive protein profiling of human tumor and immune cell lines available at ATCC for various established and novel immune checkpoint molecules. Cell lines with high endogenous expression of the immune checkpoint proteins, such as programmed death-ligand 1 and 2 (PD-L1 and PD-L2), cluster of differentiation 155 (CD155), B7 homolog 3 (B7-H3), sialic acid-binding Ig-like lectin 10 (Siglec-10), or signal-regulatory protein alpha (SIRPα), were selected and constructed into luciferase reporter cell lines. For tumor reporter cell lines, a gamma interferon activation site (GAS) response element was placed upstream of the luciferase gene in the lentiviral vector, enabling the activation of the JAK-STAT signaling pathway within tumor cells to induce luciferase expression. In myeloid reporter cell lines, a nuclear factor kappa B (NF-κB) response element replaced GAS to monitor the activation of the NF-κB signaling pathway. In the presence of corresponding immune checkpoint inhibitors that enhance T cell-mediated anti-tumor activity, these reporter cell lines produce a bioluminescent signal based on luciferase expression. This signal can be easily detected and quantified to assess the efficacy of the inhibitor. Our data revealed that bioluminescence intensity in the tumor and myeloid reporter cell lines increased by >100-fold in a dose-dependent manner in response to interferon gamma (IFN-γ) and tumor necrosis factor alpha (TNF-α) stimulation, respectively, and by >50-fold in response to the conditioned media collected from activated primary T cells. Furthermore, in co-culture assays involving various combinations of immune cell and tumor cell types with corresponding immune checkpoint inhibitors, these reporter cell lines demonstrated a significant increase in bioluminescence intensity. In conclusion, these newly established luciferase reporter cell lines offer an excellent ex vivo model for cancer immunotherapy. These cell lines naturally express immune checkpoint proteins, enabling the sensitive and reproducible monitoring of combinatorial responses from various immune cell types.

#0076 Correlated multi-scale 3D optical microscopy of tumor tissues.

J. Zheng, S.-Y. Lee;
University of Illinois at Chicago, Chicago, IL

Three-dimensional (3D) optical microscopy in combination with advanced tissue clearing methods permits the interrogation of intact large-sized tumor tissues. There are many optical microscopy methods (e.g. light-sheet and confocal microscopy) offering 3D tumor images at varying levels of spatial resolution (e.g. organ, tissue, cell, and molecule level). However, it is a challenge to correlatively integrate various resolution 3D images obtained by different optical microscopy of tumor tissue. In this project, we developed a correlated multi-scale 3D optical microscopy method that enables the acquisition of macroscopic to microscopic spatial information from a single tumor tissue in 3D. Firstly, we used light sheet microscopy to image a whole large-sized, cleared tumor tissue and analyzed the results to identify regions of interests (ROIs). After defining ROIs in the 3D whole tumor image, we added a UV-activatable visible dye, spiropyran, in the agarose gel surrounding the cleared tumor and exposed the sample to a UV light sheet horizontally at the height (z-axis) of the tumor where the ROIs present. The activated dye showed ‘purple’ colored lines in the agarose gel and we physically marked the gel along the visible colored lines. We further sectioned the tumor at the ROI positions using a vibratome after reversing tissue clearing process. After immunofluorescence staining and aqueous-based tissue clearing, confocal microscopy allowed the localization of various cell types in the ROIs of tumor macrosections. To validate the method for multi-scale evaluation of cancer immunotherapy, we tested it with control and DMXAA-treated mouse mammary tumor tissues. We successfully acquired the 3D images of whole tumors by capturing autofluorescence signals with a 633 nm excitation laser and its matched emission filter. Based on the autofluorescence tumor images, we defined two ROIs for each control and treated tumor and performed optical marking and physical sectioning of the tumors as described above. Next, we stained the macrosections (400 µm thick) with DAPI, CK8-DL488, CD45-DL550, and ER-TR7-DL680 to visualize cancer, immune, and stromal cells in the ROIs at cellular resolution. We quantitatively analyzed the correlated multi-scale 3D image data for assessment of the effects of DMXAA treatment on the tumor microenvironment including eradiation of cancer cells, immune infiltration, and remodeling of tumor stroma. In summary, this new microscopy method will provide comprehensive spatial information of tumor tissues and benefit a broad cancer research field such as the discovery of new tumor biomarkers and the development of effective cancer therapies.

#0077 Real-time multiparametric assessment of immune cell-mediated cytotoxicity.

G. Yang, Y. Lu, T. Wang, P. Ye, **X. Zhang**;
Agilent Technologies, Inc., San Diego, CA

A hallmark of effective immunotherapy is the reliance on the cytotoxic effects of immune cells, such as T-cells and natural killer (NK) cells, on tumor lesions. Cell cluster formation is an important sign of activation, and proliferation, as well as an indication of the killing capability of immune cells. Understanding and modulating the mechanisms underlying the activation, proliferation, and clustering of immune cells is essential for the development of innovative approaches to promote immune cell-induced cytotoxicity and address tumor progression. Here, we report a novel kinetic immuno-oncology assay using the Agilent xCELLigence RTCA eSight, which can simultaneously and quantitatively assess effector/immune cell clustering and proliferation through brightfield live cell time-lapse imaging and immune cell-mediated cytotoxicity of target/cancer cells through real-time monitoring cancer cell viability over a chronic treatment. In this study, we validated the assay using 2 cell models, including CD19 CAR T-cells against Raji cells and NK-92 cells against A549 cells, in a 96-well plate format. The activation, clustering, and proliferation of CD19 CAR T-cells and NK-92 at different Effector: Target (E: T) ratios, as well as the sequential killing of the target cancer cells, were plotted using imaging and cellular-impedance-based readouts throughout the entire assay, respectively. Our results showed 1) the clustering and proliferation of the effector cells could be accurately assessed by brightfield without the facilitation of fluorescent label using the image analysis module of the system; 2) the killing efficacy of the effector cells quantified by the impedance readout highly correlated to their clustering and proliferation assessed by the live-cell imaging; 3) cellular impedance provided a sensitive readout CAR-T killing of immobilized Raji cell count, independent of fluorescent labeling; 4) the kinetics of cluster formation/proliferation and killing efficacy of CD19 CAR T-cells were different from NK cells. The capability of multiparametric assessment of immune cell-medicated cytotoxicity from both effector and target cell perspectives of the assay provides a simple and real-time workflow to understand the correlation and interaction between effector and target cells, which could be an addition of immense value to the development of innovative immunotherapies.

#0078 Superior resolution of intracellular markers with CyTOF reveals greater functional diversity of human T cells.

E. L. Smith-Mahoney[1], M. J. Cohen[2], A. C. Belkina[1], T. Selvanantham[2], D. King[2], C. Loh[2], A. J. Cappione III[2], J. E. Snyder-Cappione[1];
[1]Boston University Chobanian and Avedisian School of Medicine, Boston, MA, [2]Standard Biotools, Markham, ON, Canada

Measuring functional signatures of immune cells in a comprehensive manner, spanning the inflammatory (Th1/Th17) and immunosuppressive (Th2/Treg) lineages, would provide key insights into several facets of cancer research and therapy. Determining mechanisms underlying success/failure of checkpoint blockade, defining immunosuppressive activity of the tumor-resident cell subsets, and identifying immunological biomarkers that predict clinical outcomes, could all be achievable if detection of cytokines spanning many lineages among individual cells was in reach. To achieve this goal, powerful cytometric research tools are required. Cell phenotyping panels are expanding and often now include measurement of intracellular markers of functional potential, such as cytokines, phosphorylation events, and transcription factors. Many of these readouts, including cytokines of the Th2/Treg lineages (IL-5, IL-10, and IL-13), have been notoriously difficult to detect in human cells using fluorescence-based cytometry. Large panels with multiplex intracellular markers are subject to challenges with autofluorescence and spillover spread, thus limiting fluorochrome capacity and reducing resolving power for rare subsets even with full spectrum flow cytometers. For such applications, mass cytometry may overcome such limitations and enable better signal resolution. To address this, we evaluated three small (13-plex) panels using a full spectrum flow cytometer and the CyTOF XT™ mass cytometer. Each panel was comprised of surface and intracellular analytes (cytokines, phospho-epitopes, or transcription factors) and designed to minimize potential impact of spectral overlap on the resolution of spectral flow data. PBMCs were stimulated, split, and stained with either fluorochrome- (Cytek® Aurora) or metal-conjugated antibodies (CyTOF XT). Data sets were analyzed by PhenoGraph clustering and visualized with opt-SNE to determine cellular functional diversity. Overall, data collected on the CyTOF XT demonstrated superior resolution for many intracellular readouts, including cytokines IL-5, IL-10, and IL-13. Also, when better signal/noise enabled accurate clustering, a higher number of immune cell clusters possessing distinct functional signatures resulted from mass cytometry datasets as compared with fluorescent counterparts. In summary, the CyTOF XT mass cytometry platform offers superior signal resolution compared to spectral flow for a range of intracellular targets. Use of mass cytometry translates to the identification of more diverse functional subsets and thus a clearer understanding of the immune signatures present in a sample in the context of unbiased analysis. Our findings indicate that the CyTOF XT platform could serve as a catalyst for seminal discoveries in immune profiling to drive therapeutic design and advanced disease monitoring in cancer.

#0079 Enabling fast and convenient immune profiling of fresh and long-term stabilized human whole blood samples with CyTOF.

M. Cohen, S. Hasan, S. Li, C. Loh;
Standard BioTools, Markham, ON, Canada

Accurate phenotyping of immune cells in whole blood (WB) from patients with cancer is critical for making disease prognoses and monitoring clinical efficacy of immunotherapies. Fresh WB must be analyzed within 24 hours of collection to minimize changes in cellular composition. However, WB collection and cytometric analysis are often performed at different sites, which can result in sample processing delays. Several WB preservation reagents have been developed to address this challenge, including PROT1 (Smart Tube Inc.) and Cytodelics Whole Blood Cell Stabilizer (Cytodelics). However, not all antibody panels are compatible with these reagents. A CyTOF® panel was developed to be compatible with these commercial WB stabilizers and for use in pharmaceutical and clinical research. CyTOF flow cytometry uses metal-tagged antibodies to identify cellular and functional phenotypes. Advantages and features of CyTOF technology enable rapid design and application of 50-plus-marker panels and convenient workflows in which samples can be stained and acquired in a single tube. Compensation is not required since CyTOF flow cytometry has low signal spillover and no autofluorescence. Moreover, antibody cocktails and stained samples can be frozen for later use and acquisition. Thus, CyTOF technology overcomes major hurdles of fluorescence-based cytometry and provides a streamlined and flexible workflow in clinical research. The CyTOF panel contains 20 antibodies to identify over 30 immune cell populations. For easy customization, there are more than 30 additional open channels to analyze markers of interest. The panel works with fresh and stabilized WB samples and is amenable to different staining and acquisition workflows. To show the flexibility of sample staining and stabilization, WB from three healthy donors was assessed using two stabilization workflows. First, fresh WB samples were stained with the antibody panel, followed by PROT1 or Cytodelics stabilization and storage at -80 °C. The second workflow involved immediate stabilization/fixation of WB with PROT1 or Cytodelics and storage at -80 °C. Subsequently, the samples for the second workflow were thawed, surface stained, and acquired. To reduce technical variability from staining, the antibodies were pooled together and frozen at -80 °C as single-use aliquots. Furthermore, all samples were barcoded and acquired as a single tube to reduce variability from sample acquisition. The CyTOF panel developed for broad immune profiling is compatible with WB stabilizers, which overcomes traditional and logistical challenges with WB processing and acquisition. Furthermore, freezing antibody cocktails is a unique feature of CyTOF flow cytometry, ensuring batch-to-batch consistency in clinical research. Thus, CyTOF workflows enable swift and convenient analysis of WB samples. For Research Use Only. Not for use in diagnostic procedures.

#0080 Toward best practices for B-cell receptor repertoire profiling.

W. Xiao, BCR-SEQC consortium;
Food & Drug Administration, Silver Spring, MD

FDA anticipates that immune cell receptor profiling will become crucial to the Agency's evaluation of the efficacy and safety of emerging cancer immunotherapies and immunomodulatory drugs by advancing precision medicine and providing orthogonal, functional evidence. High-throughput sequencing of B-cell receptor sequencing (BCR) gene rearrangements and downstream analysis empowers researchers to define the B-cell clonal landscape, as well as identify biomarkers for minimal residual disease (MRD). Although this field has made vast strides over the last decade, it lacks standardized assay controls, adequate sensitivity and specificity in gene mapping/alignment, and appropriately qualified reference data sets, materials, and validation methods. Moreover, detailed comparisons of wet-bench analytical methods or bioinformatic procedures have not appeared. The FDA led B-cell receptor sequencing quality control (BCR-SEQC) consortium is establishing protocols for the development of reference materials and data sets for the evaluation of NGS-based BCR repertoire reconstruction. The consortium is also developing materials for performance bench-marking studies. To this end, we performed whole-genome sequencing, RNAseq, and BCR-seq on 50 B-cell lines to determine the clonotype, full-length transcripts, and expression abundance of BCR genes in each cell line. Two batches of reference materials (DNA, RNA, and cells) were generated from each of nine cell lines that were determined unambiguously to be monoclonal in BCR expression of both heavy and light chains. These materials were distributed to ten companies to test up to 15 BCR-seq products. Our benchmarking studies include six widely-used sequencing technologies. The overarching objectives of this research were to elucidate current capabilities and limitations, address fundamental technical needs, provide reference materials and data sets, and establish actionable best practices for reconstructing B cell receptor repertoires from NGS data.

#0081 High-resolution monitoring of B cell isotype switching for biomarker analysis of adenosine pathway inhibition immunotherapy.

R. Prathapam[1], K. Champion[1], A. Burkhardt[2], C. L. Smith[2], R. Singh[2], **T. J. Looney**[3];
[1]Quest Diagnostics, Lewisville, TX, [2]Quest Diagnostics, Chantilly, VA, [3]Quest Diagnostics, Austin, TX

Background B cell isotype switching gives rise to IgG-, IgA-, and IgE-expressing B cells and is an essential step in generating effective humoral responses to antigen challenge. Within the tumor microenvironment, extracellular adenosine may contribute to cancer immune evasion by inhibiting isotype switching through interaction with A2aR, a possibility that has driven investigation of adenosine pathway inhibition as an immunotherapeutic modality. In this context, methods to quantify isotype switching may provide insight into the pharmacodynamics of candidate agent activity and serve as a source of predictive biomarkers of response. We recently clinically validated the Oncomine IGH-LR assay for the measurement of CLL somatic hypermutation (SHM). Given that this assay also detects isotype switching events, we retrospectively analyzed our validation dataset to determine the suitability of the assay as a potential tool for biomarker analysis of adenosine pathway inhibition immunotherapy.
Methods The Oncomine IGH-LR assay determines B cell SHM and isotype through targeted next-generation sequencing of IGH chains from RNA. The assay software organizes detected IGH chains into B cell clonal lineages, of which a subset may comprise multi-isotype lineages indicative of isotype switching events. The software further reports secondary repertoire features such as clonality/evenness. Total RNA was extracted from peripheral blood mononuclear cells or bone marrow aspirates from patients identified as having >10% monoclonal B-cell population by flow cytometry. Intra-assay precision was evaluated by processing RNA from 7 samples in triplicate and sequencing in the same run. Inter-assay precision was evaluated by having different operators process 10 samples on different days with different sequencing barcodes. Dominant clone isotype and clonal lineage assignment, total isotype abundance, and repertoire clonality were evaluated across replicates.
Results Overall, 100% concordance was achieved for dominant clone isotype and clonal lineage calls for both intra- and inter-assay studies. Intra-assay and inter-assay median coefficient of variation (CV) for reported isotype frequencies ranged from 0.10-0.16 and 0.15-0.28, respectively. Intra-assay and inter-assay median CV for clonality (1 - Normalized Shannon Entropy) was 0.06 and 0.04, respectively.
Conclusions We observe high reproducibility and repeatability of the IGH-LR assay for B cell isotyping, clonal lineage analysis, and clonality assessment. Multi-isotype clonal lineages are automatically reported by the software and provide a means to directly monitor isotype switching events in the context of antigen challenge or immunomodulation. Taken together, we anticipate this assay to be a useful tool for biomarker analysis of adenosine pathway inhibition immunotherapy.

#0082 Single-cell cytokine secretion kinetics probed by Time-lapse flow (TM) cytometry.

M. Fahlberg[1], S. Forward[1], E. Assita[1], T. Brown[1], P. Chattopadhyay[2], S. Kwok[1];
[1]LASE Innovation, Woburn, MA, [2]Talon Biomarkers, Whippany, NJ

Cytokine secretion from immune cells is a central element of the immune response and a major determinant of immunotherapy efficacy. Several methods, including bulk in-solution assays and flow cytometry, have been used to measure cytokine secretion. Population-level analyses have shown that different cytokines can have different rates of secretion, depending upon their differentiation state or the stimulus itself. However, no current method can interrogate cytokine secretion from individual cells over time.

Here, we describe a novel flow cytometry-based assay for measuring single-cell cytokine secretion kinetics. Our approach, called "Time-lapse flow TM" uses semiconductor probes called laser particles (LPs) to optically barcode individual cells, providing a means to track single cells across a series of measurements over time. We applied this approach to measure T-cell cytokine secretion kinetics using stimulated primary human T cells.

Isolated T cells from cryopreserved human PBMCs were barcoded with LPs and stained with a bispecific antibody that binds to the cell surface on one end and "catches" secreted cytokines (IFNy and IL-2) on the other end. This permits analysis of cytokines from live cells. Next, T cells underwent three sequential stimulations over the course of 3 hours with PMA/Ionomycin. After the first stimulation, cells were stained with a surface marker panel that defined T cell memory phenotypes (CD3, CD4, CD8, CD45RA, CCR7, CD57, CD27, and CD95) and "detection" antibodies that recognized IFNy and IL-2 bound to the cell surface. The detection antibodies were re-added after each stimulation to quantify the accumulating cytokine on the cell surface. In total, kinetic profiles from over 100,000 CD3+ cells were measured.

We discovered massive heterogeneity of responding cells, identifying at least three distinct groups of cells defined by their initial time of cytokine secretion (early, middle, and late responders) and varying intensities of cytokine accumulation over time. Cells peaking in cytokine expression at the middle time points were mainly memory types with higher intensity, while later responders skewered towards naïve cells with less cytokine. However, IFNy variation wasn't solely due to these markers, as diverse kinetics occurred across all subsets. For IL-2, we found that most responses initiated later than those of IFNy, and there was a reduced heterogeneity of both intensity and kinetics at these time points. These results were consistent across multiple donors and replicates (n=3).

Laser particle barcoding enables measurement of single-cell function over time. This novel time-lapse data allows interrogation of functional heterogeneity of immune cells at scale, enabling discovery of new relationships between T cell responses, diseases, and immunotherapies.

#0083 NK cell ADCC assays: Leveraging flow cytometry and reporter cell lines for enhanced biological relevance and throughput.

D. W. Draper, Y. Xing, S. Wise;
Labcorp, Ann Arbor, MI

Amid the growing arsenal of cancer treatments, antibody-dependent cellular cytotoxicity (ADCC) assays have emerged as a significant contributor to the quest for more effective therapies. The ADCC-based antibody therapy often exploits Natural Killer (NK) cells as effectors. This immunotherapeutic approach harnesses the innate cytotoxic potential of NK cells, offering a promising solution for the precision targeting of malignant cells. In this study, we employed two methods that can be used to measure ADCC potency and specificity during preclinical drug discovery. The first was a flow cytometry-based approach that focused on enhancing biological relevance by utilizing primary human peripheral blood mononuclear cells (PBMCs) as a source for NK effector cells. To this end, target cells were fluorescently labeled with CFSE and cultured with freshly isolated PBMCs at 3 effector to target (E:T) ratios, in the presence of ADCC antibody. After 16h incubation, a viability dye was added, and percent cytotoxicity was measured in CFSE+ targets cells by flow cytometry. The second method offered a high-throughput plate reader-based approach (ADCC Reporter Bioassay; Promega), that utilized an ADCC reporter effector cell line harboring a luciferase cassette driven by an NFAT promoter, which is activated when effector and targets cells are bridged by a therapeutic antibody. Cytotoxicity was read out by measuring light output on a Cytation 3 plate imaging reader (Agilent Technologies) after a 6h cell culture incubation using the recommended 6:1 E:T ratio. Preclinical application for both assays was demonstrated using an anti-HER2 therapeutic antibody (trastuzumab) against BT-474, which is a HER2 positive cell line. To demonstrate specificity, an anti-VEGF antibody (bevacizumab) and Hs 578T cells (HER2 low) were used as controls. Our results revealed trastuzumab induced a strong dose-dependent increase in cytotoxicity in the BT-474 cells but not the Hs 578T cell line (range: 40-70%) while bevacizumab failed to induce any cytotoxicity above background levels at any concentration. Furthermore, the flow cytometry and plate reader methodologies produced similar trends. In summary, both applications can be used to produce reliable ADCC drug screening assessments. Additional considerations include investigational needs surrounding high throughput capability versus biological relevance. Unlike traditional models using immortalized cell lines, primary human PBMCs more faithfully recapitulate the physiological interactions between effector cells and target cells. On the other hand, the more streamlined reporter cell line approach not only accelerates assay throughput but also ensures consistent and reliable results in an attractive option for large-scale screening and drug development efforts.

#0084 StarBright Dyes: Fluorophores with superior performance for multiplexing in flow cytometry and Western blotting.

S. Sanderson, **O. Rosenwasser**, M. Blundell;
Bio-Rad Laboratories, Kidlington, United Kingdom

New StarBright^{TM} Dyes from Bio-Rad are bright fluorescent fluorophores ideal for many antibody-based applications, for example, western blotting and flow cytometry. Traditional fluorophores can be dim, have high cross laser excitation, or don't work with all protocols, leading to poor data. StarBright Dyes have been designed to address these pain points.

Western blotting secondary antibodies are available conjugated to StarBright Blue 700 and StarBright Blue 520 Dyes. Their brightness, the short exposure time required, and low background make them ideal for detection of a single target, or as shown here for multiplex detection of several proteins in combination with other common fluorophores.

For flow cytometry, we have a full range of 32 StarBright Dyes excited by the most common laser lines: 355 nm, 405 nm, 488 nm, 561 nm, or 640 nm. They are available conjugated to highly cited clones against common immunophenotyping targets. Data shown here on the ZE5 Cell Analyser demonstrates how the features of StarBright Dyes can improve multiplexing immunophenotyping data. They have narrow excitation and emission spectral profiles, which reduce compensation and spread. This, combined with their exceptional brightness, enables high resolution of cell populations. They work in all buffers and fixatives, so including them in existing panels does not require a change in protocol. They can also be premixed in a master mix for over six months with no loss in performance. Premixes are ideal when using the same panel over an extended period, such as in clinical and longitudinal studies, to ensure reproducible results, also saving time and money.

StarBright Dyes are ideal for multiplexing assays in both western blotting and flow cytometry.

#0085 Immunomics of immune-deficient mouse models before and after CD34 humanization.

H. Luche, L. Hadjem, M. Mello, P. Canavese, F. Angelis, A. Joachim, S. Bouilly, F. Guinut, F. Fiore, B. Malissen, A. Zarubica, E. Corcuff;
Janvier Group, Le Genest Saint Isle, France

Preclinical tumor oncology research relies historically on the analysis of mouse or human tumor cell lines implanted onto severely immune-deficient mouse models carrying nude, SCID or Rag mutations on different genetical background (C57Bl/6N, BalbC, NMRI, CB17 or NOD). These lines harbor defects in several leukocyte lineages among which Tc, Bc and NKc might be affected. Humanized mice are emerging models that have been transplanted with human cells or tissues (and/or equipped with human transgenes). Currently, the most advanced strains are the nonobese diabetic, severe combined immunodeficiency (NOD-SCID) mouse with complete disruptions in the interleukin-2 (IL-2) common γ-chain (IL2R γ null) receptor (NSG) and BALB/c $Rag2^{-/-}$ IL2R γ null $Sirpa^{NOD}$ mice (BRGS).[1] Neonate or juvenile chimera are reconstituted in NSG, BRGS or B6 RGS with CD34+ hematopoietic progenitor cell (HPCs) from human cord blood yielding robust engraftment of a human immune system (HIS).. We genetically modified the mouse genome introducing mutations involved in Tc, Bc and NKc development. We then immuno-phenotyped over 23 lines of mouse mutants produced from the same animal house to minimize the impact of microbiota on innate immune cell populations. High content cytometry analysis of several organs was performed in a standardized manner before and after humanization. The resource obtained of these immunotypes was used to highlight similarities and differences among these lines across several genetical background and will help in selecting the most appropriate model to use for tumor implantation and CD34 or PBMC humanization.

#0086 Deep immuno-profiling of syngeneic tumor mouse models for preclinical studies.

A. Joachim, E. Maturin, M. Mello, L. Hadjem, M. Grange, O. Deas, A. Zarubica, B. Malissen, H. Luche, F. Romagne, S. Blanchin;
Janvier Group, Le Genest Saint Isle, France

The identification of the major cellular players involved in the progression of a type of cancer is a key step for the success of new immunotherapies for personalized medicine. Immune cells play critical functions in cancer, and mice with intact immune systems are vital to understanding tumor immunology. It is however a daunting challenge as complex relationships interplay between tumor cells and the immune system. Each component of innate immunity or adaptive immunity, such as T lymphocytes, macrophages or neutrophils, may be directed to a pro- or anti-tumor function. In order to cope with the complexity of the tumor microenvironment, it is necessary to use an experimental approach capable of characterizing the heterogeneity of the cell types present in the tumor, the evolution of their relative proportion and their fine-tuned functional specificity. This approach leads to the identification of new cellular biomarkers of different stages of tumor progression in order to identify new targets for therapeutic time-window of and improve cancer diagnosis
To decipher the impact of immunotherapy treatments involved in the anti-tumor response, cellular phenotyping of leukocytes infiltrating a tumor but also those present in peripheral organs is necessary. Essentially based on extracellular labeling, this primary screen aims to quantify the different cell populations present in a syngenic tumor models on B6/N or BalbC genetical backgrounds. In order to increase our understanding in the precise mode of action of anti-PD1 treatment at the cellular level in sensitive and unsensitive models, we investigated immunophenotypes and responses to immune checkpoint inhibitor (ICI) of several hallmark syngeneic tumor models (MC38, CT26, B16F10, B16-OVA, RENCA, EMT6) in immunocompetent mouse models by flow and mass cytometry. We compared growth kinetics and profiled the immune cell composition of tumor microenvironment (TME), draining lymph node (dLN) and blood in order to establish immune-phenotypic cell signatures that correlates with treatment efficacy. Supervised, unsupervised and integrative data analysis as well as visualization tools are used to identify significant changes across different experimental settings. Our results indicate that each model possesses a unique tumor-immune infiltrate profile that can be modulated with immunotherapies.
Overall, these studies provide an important resource of highly-characterized syngeneic tumor model and highlight the importance of tumor immune landscape variance across models that will drive selecting the most appropriate model to test novel immunotherapeutic agents and enhance our translation of knowledge from syngeneic models to human tumors.

#0087 Integrated pipeline for immuno-oncology drug testing: from patient-derived organoid assays with reconstituted TME to fresh ex vivo patient tissue cultures.

E. Kaya Aksoy, S. Chavez Abiega, T. Stessuk, S. De Man, **M. Putker**, S. Basten, N. Meesters, E. Spanjaard, L. S. Price, G. Goverse, N. Beztsinna;
Crown Bioscience Netherlands B.V., Leiden, Netherlands

Introduction: Successful pre-clinical evaluation of immuno-oncology drugs requires complex models to accurately represent all components of the human tumor microenvironment (TME). Patient-derived organoids (PDO) are known to reflect genetic and morphological profiles of the original patient's tumors. In our immuno-oncology in vitro assays, PDOs can be combined with immune cells and fibroblasts to re-constitute the TME and study drug efficacy and mechanism of action. Alternatively, we have developed assays with fresh tumor material containing native TME in the 3D Ex Vivo Patient Tissue (EVPT) platform. Both types of assays have advantages and limitations. Here, we will present a case study displaying both capabilities and benchmarking the technologies against each other.
Methods: Patient tumor tissues were obtained from tissue providers and processed within 24 hours to preserve the TME. Freshly isolated ex vivo tumor clusters were embedded in a protein-rich hydrogel and exposed to drug panels in a 384-well format for 5-7 days. Phenotypic effects of therapies on morphological features were measured using our proprietary automated high content imaging (HCI) analysis platform. IHC, FACS, or sequencing, were used for in-depth sample characterization. In parallel, PDOs were generated, biobanked and characterized from same ex vivo samples. Allogenic or autologous PBMCs were isolated from blood. PDOs and PBMCs were then co-cultured together in presence of immuno-oncology drugs, and drug effects were analyzed by the same automated HCI analysis platform.
Results: Samples from ovarian, head and neck, breast, prostate, lung cancer, and melanoma were used in the pipeline. Fresh ex vivo culture of a melanoma sample presented here has shown mild responses (tumoroid size reduction) to immunomodulatory treatments (SEA and Pembrolizumab) and strong responses to targeted therapy treatment (Dabrafenib and Trametinib). Genetic characterization of the sample identified heterozygous BRAF V600E mutation and IHC analysis showed a large proportion of immune cells (CD3, CD4, CD8, CD80 and CD68 positive cells) present, confirming the observed ex vivo drug responses. Part of the melanoma sample was allocated for PDO generation and biobanking. Established PDOs were used in co-culture with allogeneic and autologous PBMCs and treatment responses to SEA stimulation and CD3/CD28 beads as well as increased PBMC infiltration rates were observed.
Conclusion: Choice of the pre-clinical model for immuno-oncology studies relies on multiple factors such as biological relevance, replicability, TME representation, and scalability. Here we present a spectrum of assays ranging from complex ex vivo systems (EVPT) for 'close to the clinic' scenarios to more scalable PDOs co-cultured with allogeneic and/or autologous PBMCs for high-throughput mechanistic drug screenings.

#0088 Novel cell-based bioassays enable preclinical animal studies during immuno-oncology drug development.

J. Wang, D. Garvin, A. Paguio, E. Perrin, J. Hartnett, M. Cong, J. Grailer;
Promega, Fitchburg, WI

Translation of immuno-oncology research into novel therapies relies on animal models to advise target selection and portray mechanism of action (MoA) and pharmacokinetics of lead candidates. Mouse, monkey, and more recently, canine models of human cancers are being utilized to this end. However, one major challenge in developing and utilizing these models is the lack of technology to characterize non-human analogs of therapeutic antibodies. Herein, we report the development of novel cell-based bioassays for mouse, monkey, and canine targets to enable immuno-oncology preclinical studies. Antibody-dependent cellular cytotoxicity (ADCC) and antibody-dependent cellular phagocytosis (ADCP) are important MoAs for antibody-based cancer immunotherapies. We have developed a suite of cell-based bioassays, each expressing a corresponding animal Fcγ receptor (FcγR) and a luciferase reporter that responds to FcγR activation. These assays exhibit sensitive and quantitative luciferase readouts of FcγR activation. Animal models are further used to provide insight into the potential efficacy of immune checkpoint (IC) inhibitors. Programmed cell death protein 1 (PD-1) is an IC receptor that negatively regulates T cell function. Blockade of PD-1 has demonstrated clinical efficacy, but there remains a significant fraction of patients unresponsive to this therapy. Combination of PD-1 inhibitors with other interventions has been a significant focus for many programs. However, tools for functional validation of non-human PD-1 inhibitors are lacking. We report here the development of two new bioassays for functional characterization of PD-1/PD-L1 inhibitors for mouse and canine targets. Each of these assays consists of two engineered cell lines: a T effector cell line that express a luciferase reporter driven by specific promoter/response elements responding to the intracellular signals mediated by the T cell receptor (TCR), with modulation from PD-1, and an artificial antigen presenting cell line (aAPC). The bioassays are sensitive, quantitative, and have demonstrated characteristics required for potency assays for validation of antibodies in preclinical combination studies.

#0089 Comprehensive cell based bioassay approaches for characterization, and clinical development of therapeutic agonistic antibodies for cancer immunotherapy and autoimmune diseases.

V. Chari, J. Lin-Jones, L. Yang, J. E. Lamerdin, **G. Agrawal**;
Eurofins DiscoverX, Fremont, CA

Agonistic antibodies are emerging as promising therapeutics for targeting immune checkpoints, particularly those within the TNF Receptor Superfamily, as they play a crucial role in regulating immune cell function, especially in the context of cancer treatment. In addition, there is also a growing focus on the potential of agonistic antibodies to selectively activate co-inhibitory checkpoint receptors. This offers a promising avenue for suppressing inflammation in autoimmune diseases and restoring tolerance in graft-vs-host disease (GvHD) while avoiding the complications of global immunosuppression.
While a substantial number of clinical trials are currently underway for oncology and autoimmune indications, there is a notable scarcity of commercially available assays to support the clinical development of this class of therapeutics, impacting their time-to-clinic. Existing assays frequently fail to accurately assess the agonistic activity of antibodies as they are unable to replicate the necessary physiologically relevant conditions.
In this context, we present several case studies that highlight the pivotal role of cell-based bioassay approaches developed by Eurofins DiscoverX in driving the characterization and clinical development of agonistic antibody therapeutics targeting various checkpoint receptors. Additionally, we discuss our data demonstrating the indispensable role of FcyR-mediated antibody clustering in establishing the otherwise elusive agonistic activity of antibodies.

#0090 *In vitro* functional evaluation of immuno-oncology drug candidates in customized bioassays.

Martijn Vlaming, Emmanuelle Sidot, Jezabel Lefevre, Ellen Boelen, Sofie Pattyn

ImmunXperts SA, a Q2 Solutions Company, Charleroi, Belgium

Increased understanding of the complex tumor microenvironment and its interactors has boosted therapeutic interest and highlighted the importance of the development of innovative *in vitro* bioassays to represent all the players of the cancer immune response and thereby potentially provide pivotal information on the functional dynamics of candidate therapeutics. Regulatory T cells play an important role by downregulating the anti-tumor response. Their regulation mechanisms constitute an important target for new therapeutics. To study these mechanisms in a human model, suppressive Treg bioassays, mimicking the suppressive action of these cells, were developed and optimized. We further highlight the study of neutrophil function *in vitro* using flow-cytometry or the Incucyte® live imaging system to monitor neutrophil functions such as antibody-dependent cell-mediated cytotoxicity (ADCC), Neutrophil Extracellular Traps (NETs) formation and the release of Reactive Oxygen Species (ROS). Additionally, multiplex cytokine and peroxidase enzyme analysis after activation and stimulation of neutrophils can be evaluated using ELISA or Luminex technology. Moreover, to refine/reduce non-human primate (NHP) usage, we aimed to develop cost-effective NHP *in vitro* assays with predictive value for *in vivo* studies. We isolated Cynomolgus Macaque monocytes and successfully differentiated/polarized them into M0- and M2-like macrophages with a cell surface phenotype comparable to that of their human counterparts. We further developed a Cynomolgus Macaque PBMC x human dendritic cell (DC) mixed lymphocyte reaction (MLR) assay for functional evaluation of test compounds, effectively generated Cynomolgus Macaque immature DCs and implemented Cynomolgus Macaque cytokine release assays.Using high quality primary human immune cells from our own biobank, *in vitro* bioassays have been developed with superior robustness and reproducibility to screen candidate Immuno-Oncology therapeutics.

#0091 Comprehensive 27-marker standard panel for immune monitoring of pre-clinical tumor mouse models using spectral analyzer technology.

J. F. Hummel, **P. Metzger**, R. Sonntag, D. Borrero-Wolff, C. Obodozie, H. Weber;
Reaction Biology Europe GmbH, Freiburg, Germany

Within the last decade, major technological advances in flow cytometry and (single cell) RNA-sequencing have deepened our understanding of complex anti-tumoral immune responses. This allows a comprehensive immune monitoring of novel therapies in pre-clinical models.
Conventional flow cytometry is reaching its technical limitation. The emitted fluorescence signal of the target population stained with antibodies is evaluated with simple bandpass filters, which leads to spectral overlap and thus the number of parameters that can be analyzed simultaneously is limited. The spectral analyzer technology combines both methods, providing great flexibility in evaluating different immune cell populations. This provides the opportunity to obtain target information by measuring the entire fluorescence spectrum measuring each wavelength individually and thus evaluating the true signal of each fluorochrome unaffected by autofluorescence or spillover.
Our standard all-in-one flow cytometry panel uses the full capacity of a conventional BD Fortessa flow cytometer and enables the differentiation of important immune cell populations in tumors, such as T cells (CD4+, CD8+, regulatory T cells), B and NK cells as well as macrophages (M1/M2), MDSCs (granulocytes and monocytes) and dendritic cells. However, it would be of great advantage to gain further insights into activation and effector functions of the immune cells using markers like CD44 & CD62L, CD69, PD-1, Lag-3, Tim-3 and PDL-1, CD80, CD86, CD40 and Ki-67. The Sony ID7000 spectral analyzer enables the simultaneous assessment of 27 markers to evaluate immune phenotypes, with the ability to include up to 4 individual target antibodies.
Flow cytometry data from various tumor models are presented, demonstrating the enormous utility and potential of the spectral analyzer, especially with limited and precious tumor sample material, by evaluating different immune cell populations simultaneously without reaching its technical limits. The spectral analyzer technology enables us to mechanistically investigate differences in tumor therapies such as PD-1 treatment or other immune cell modulators not only phenotypically but also with regard to activation and differentiation of immune cell populations.

#0092 Assessment of an in vitro potency assay for evaluation of immune cell-mediated cytotoxicity using the Omni Pro 12 automated imaging platform.

D. Sullivan[1], L. Stemkens[2], I. Thijssen,[2], **S. Meiler**[2], D. Califano[1], S. Chvatal[1], D. Millard[1];
[1]Axion BioSystems, Atlanta, GA, [2]Axion BioSystems, Eindhoven, Netherlands

The development of immunotherapies relies on the use of *in vitro* potency assays—which are key for understanding complex interactions between immune cells and cancer cells. Immune effector T-cells are a promising cancer therapy due to their innate cytotoxicity. In particular, CAR T-cell therapy uses genetically engineered T-cells that express a chimeric antigen receptor that binds to a specific antigen on tumor cells. Assessing the efficacy and potency of CAR T-cell therapies *in vitro* and at high throughputs is vital for the preclinical development of these promising therapies. Here, we describe an *in vitro* potency assay that uses an automated imaging platform to quantify immune cell-mediated cytotoxicity of cancer target cells by immune effector cells. A GFP fluorescent and HER-2 expressing lung cancer cell line, A549, was seeded into a 96-well cell culture plate. Then, HER-2 CAR T-cells were added at 24 hours post target cell seeding at various E:T ratios (1:10, 1:5, 1:2, 1:1, and 5:1). Fluorescent images of the target cells were captured every 6 hours by the Omni Pro 12, an automated, high-throughput, live-cell analysis platform designed for continuous multi-well imaging inside an incubator. Automated image analysis was performed using the Confluency Module in the Axion Portal to view attachment and proliferation and quantify cytolysis of fluorescent A549 target cells. Percent cytolysis of the target cells was calculated by comparing the green fluorescent confluency of treated wells to no treatment control wells. A549-GFP cells showed a dose-dependent decrease in confluency over time that correlated with increasing amounts of CAR T-cells. At 92 hours post HER-2 CAR T-cell addition, the 5:1 ET group demonstrated approximately 91.8% +/- 2.0% cytolysis of A549-GFP cells, while the 1:10 group demonstrated approximately 69.2% +/- 3.0% cytolysis. Future work will evaluate differences in CAR T-cell potency when co-cultured with target cells that express different levels of HER-2. Overall, the Omni Pro 12 platform enables continuous quantification of the potency and kinetics of immune cell-mediated cytolysis.

#0093 Validation of an impedance-based *in vitro* potency assay for repeatability and precision.

D. Califano[1], J. Jiang[2], D. Windgassen[2], C. De La Flor[2], S. Chvatal[1], D. Sullivan[1], D. Millard[1];
[1]Axion BioSystems, Atlanta, GA, [2]Miltenyi Biotec, Inc, San Jose, CA

Cell-based immunotherapies, such as CAR T cells, are emerging as a promising approach to therapeutic intervention against cancer. Developing cell and gene therapy products requires reliable and reproducible methods of quantifying critical quality attributes, such as potency, to ensure product strength and consistency. A variety of assays can be used to assess potency; however, it is crucial that these tests are qualified for assay performance to ensure intra- and inter-assay precision. Although inherently variable, biological assays are often the best methods to investigate a product's mechanism of action and predict clinical outcomes. Previous work has shown that impedance-based potency assays provide a non-invasive, real-time measure of effector cell-mediated cytotoxicity, thus reducing cell manipulation that impacts data reliability. Here, we describe an *in vitro* potency assay that demonstrates low variability and high precision across replicates, analysts, and days. Effector cell-mediated cytotoxicity was performed using a CD19-positive liquid tumor cell line (Raji) tethered to the well surface using an anti-CD40 antibody. CD19-specific CAR T effector cells were added 24 hours after the target cells and co-cultured with the target cells across a range of E: T ratios, and cytolysis was monitored for three days. Real-time measurement of cell-mediated cytotoxicity also allowed for the calculation of kill time 50 (KT50), defined as the time required for 50% cytolysis of the target cells. Repeatability was calculated across three replicates per E:T ratio. The co-culture experiment was performed in duplicate by a second analyst and on two subsequent days for a comparison of f three plates as well as two operators to evaluate inter-assay precision. In addition to this, CAR T-mediated cell killing in a multiplate impedance system was also investigated for plate-to-plate variability. The percent coefficient of variation (% CV), a statistical measure that describes the precision and repeatability of an assay, was calculated to assess variability between assay replicates, operators, and plate replicates. In all conditions tested, the percent CV for all E:T ratios was below 20%, illustrating the repeatability and precision of the assay. These data support the use of an impedance-based potency assay for evaluating and characterizing immunotherapy products.

#0094 Interrogation of STING induced cytokines in the tumor microenvironment using an Integrated MultiOmyx-RNAscope panel for spatial and quantitative profiling.

S. Lam, **C. Todorov**, J. Fei, H. Nunns, E. Leones, M. Thio, F. Sahafi, E. Parnell, Q. Au;
NeoGenomics, Aliso Viejo, CA

The STING (Stimulator of Interferon Genes) pathway is a pivotal player in the innate immune response, responsible for detecting cytosolic accumulation of endogenous DNA and initiating a cascade of events leading to the production of pro-inflammatory type I interferons, which promote an antitumor environment through activation of T cells, dendritic cells, and natural killer cells. Therefore, STING agonists are currently being explored as a potential therapeutic for cancer treatment, often in combination with immune checkpoint inhibitors. While the STING pathway can be stimulated in multiple cell types, activation in antigen presenting cells, such as dendritic cells (DC), is crucial for antitumor activity in the tumor microenvironment (TME). Additionally, the type 1 interferon family consists of multiple subtypes, including IFNb and IFNa, which can produce differential biological responses. Although the STING pathway is known to induce expression of multiple cytokines, combined spatial characterization of STING and type I interferons in the TME has not been performed. To characterize STING-interferon expression in the TME, we use the Integrated MultiOmyx-RNAscope platform. MultiOmyx^{TM} (NeoGenomics Laboratories, Inc) is a proprietary multiplex immunofluorescence (mIF) platform for the visualization and characterization of up to 60 protein biomarkers in a single formalin-fixed paraffin-embedded (FFPE) section and offers high-resolution spatial and quantitative analysis of protein expression in tissue samples. RNAscope^{TM} (Bio-Techne) Multiplex is a highly sensitive fluorescent in-situ hybridization (ISH) assay that can detect up to 3 RNA markers in a single FFPE section. The Integrated MultiOmyx-RNAscope assay allows for simultaneous detection of both protein and RNA markers in a single sample. Herein we report the design and use of a novel panel of commercially-available antibodies and ISH probes broad enough to characterize various immune subpopulations and cytokine expressing cells, including DCs and interferons, in the TME of a variety of tumor indications including melanoma and head and neck squamous cell carcinoma. Quantification and analysis will be performed using NeoLYTX^{TM}, the proprietary MultiOmyx Analytics pipeline, to examine the spatial distribution and expression levels of key STING pathway induced cytokines to elucidate the dynamic communication of signaling molecules and their localization within specific cell populations. Understanding of the variety and phenotype of STING/cytokine expressing cells in the TME is crucial to define the populations being targeted by therapies for cancer treatment.

IMMUNOLOGY: Tumor-Induced Immune Suppression 1: Extrinsic Factors
Poster Session

#0097 A E2F6 ceRNA network suppresses dendritic cell function, via PBX1/IL-10 signaling, in ovarian cancer.

M. W. Chan[1], Y.-C. Chen[1], C.-W. Lin[1], F. Cheng[1], C.-C. Yan[2], C.-P. Hsu[2], Y.-M. Chuang[1], J.-T. Low[1], X. Ma[3], Y.-T. Huang[1], C.-B. Chang[1], C. Li[1], H.-C. Lai[4], S.-F. Wu[1], S.-H. Hung[5], J.-C. Tsai[5];

[1]National Chung Cheng University, Chia Yi, Taiwan, [2]Academia Sinica, Taipei, Taiwan, [3]Weill Medical College of Cornell University, New York, NY, [4]Taipei Medical University, Taipei, Taiwan, [5]National Tsing Hua University, Hsinchu, Taiwan

It is reported that long-term use of estrogen could increase the risk of ovarian cancer. However, the role of estrogen in immunoevasion is not fully explored. We have previously demonstrated that estrogen-mediated upregulation of E2F6, and, c-Kit, by epigenetic silencing of miR-193a, and a competing endogenous (ceRNA) mechanism. In this study, we found that PBX1, a transcriptional activator of the immunosuppressive cytokine, IL-10, is also a target of miR-193a. Importantly, overexpression of the E2F6 3'UTR upregulates both E2F6 and, PBX1, as well as IL10 in ovarian cancer cell lines, suggesting that ceRNA mechanism exists between E2F6 and PBX1. These phenomena are further supported by our stochastic simulation of the estrogen-mediated E2F6 ceRNA network on the distribution of E2F6 and PBX1 mRNA in cancer cells, which is consistent with the TCGA ovarian cancer RNA-Seq dataset. Importantly, monocyte-derived dendritic cell activation of T-cell function was inhibited by pretreatment of conditioned media derived from ovarian cancer cells overexpressing E2F6 3'UTR; such inhibition was rescueable by an anti-IL-10 antibody. Clinically, IL10 level was higher in ovarian cancer patients with higher E2F6 and PBX1, and in ovarian cancer cell lines overexpressed with E2F6 3'UTR. Taken together, these results showed that E2F6 could suppress anti-tumor immune response of dendritic cell, E2F6 ceRNA network. Epigenetic intervention in restoring the expression of miR-193a may be able to enhance anti-tumor immune response against ovarian cancer.

#0098 SETDB1 promotes tumorigenesis in endometrial cancer through suppressing anti-tumor immune response and increasing proliferation.

K. Salari[1], J. Hao[1], M. Wells[2], E. Johnson[1], R. Jilek[1], J. Gilbert[1], R. Mclerran[1], D. Meyerholz[1], M. Yates[3], B. Li[1], S. Yang[1];
[1]University of Iowa, Iowa City, IA, [2]Rosalind Franklin University, North Chicago, IL, [3]University of North Carolina, Chapel Hill, NC

Background: An H3K9 methyltransferase and cancer driver gene, SETDB1, promotes tumorigenesis in many cancer types, such as melanoma, and breast cancer. SETDB1 is often overexpressed and correlates with worse survival. Multiple mechanisms have been reported for its oncogenesis from promoting tumorigenesis and regulating immune evasion. The roles of SETDB1 in driving endometrial cancer (EC) progression is not well-studied.
Methods: EC cell lines were used for knockout SETDB1 using CRISPR-Cas9 system, RNA-seq was conducted to discover SETDB1 regulated genes. ChIP-qPCR was performed to identify SETDB1 direct targets. Immunocompromised NSG and immunocompetent C57BL/6 mice were utilized to investigate SETDB1 promoted tumor growth, immune evasion, and mice survival. IHC and flow cytometry was conducted to evaluate macrophage infiltration. Cytokines were screened by qPCR for potential macrophage chemoattractant.
Results: *In vitro*, knockout SETDB1 decreased cell proliferation and enhanced G1/S cell cycle arrest. RNA-seq data revealed that in SETDB1$^{-/-}$ clones, many important oncogenes such as POLR2A, MUC5AC, and MKI67 were downregulated, while tumor suppressors such as PGR, RERG, and ZNF582 were upregulated. ChIP assay discovered that SETDB1 directly binds and represses ZNF582, ZNF266, ZNF841 expression via depositing H3K9me^3 at promoter region. *In vivo*, SETDB1$^{-/-}$ significantly reduced tumor growth and prolonged NSG mice survival up to 100 days. SETDB1 promoted tumor growth via 1. Intrinsic: increasing mitotic figure, pH3-S10 and Ki67 level, 2. Extrinsic: blocking macrophage infiltration and chemokine secretion. Our *in vitro* functionality assay confirmed that bone-marrow derived M1-polarized macrophages promoted greater killing for SETDB1$^{-/-}$ cells. We surveyed 17 cytokines and found CCL5, CXCL9, and IL6 mRNA expression were enhanced in SETDB1$^{-/-}$ tumors suggesting active immune response. Consistent with the elevated CCL5 mRNA expression, CCL5 protein level was also upregulated in macrophages and cancer cells in SETDB1$^{-/-}$ tumors. To prove SETDB1 directly regulates CCL5 expression, we re-expressed SETDB1 in SETDB1$^{-/-}$ cells, and indeed, the SETDB1 re-expression did suppress CCL5 expression. Using immunocompetent C57BL/6 mice, we further confirmed that SETDB1 promotes tumor growth of MSH2-369 mice cells and blocks macrophage infiltration. To understand SETDB1 regulated pathways in EC patients' samples, using EC-TCGA data, we discovered that high SETDB1 expression correlated with higher level of active transcription genes and reduced immune response genes. Our findings provide the mechanisms behind these observations.
Conclusion: SETDB1 drives EC tumorigenesis by both intrinsically upregulating cell proliferation genes and promoting immune escape extrinsically. Our novel findings suggest SETDB1 is a promising anticancer target for EC patients.

#0099 Versican regulates T cell abundance within the colorectal cancer microenvironment.

S. Kraus, P. Emmerich, M. Hayes, K. Matkowskyj, W. Zhang, C. Pasch, F. Asimakopoulos, D. A. Deming;
University of Wisconsin-Madison, Madison, WI

Background: Clinical benefit from immunotherapy is seen in a minority of patients with metastatic colorectal cancer (CRC). Identifying how the tumor microenvironment (TME) influences immune infiltration and treatment response is an unmet need. Versican (VCAN), a chondroitin sulfate proteoglycan, common in the CRC TME has immunoregulatory properties and can be cleaved releasing an immunostimulatory product, versikine (Vkine). Here we evaluate the impact of the abundance of VCAN and Vkine on CD8+ T cell infiltration in CRC.
Methods: Samples include 306 primary colon tumors, an additional 176 primary CRCs with matched liver metastases (175 samples), and 328 normal samples (238 colon and 90 liver). Samples were stained via immunohistochemistry (IHC) for VCAN, Vkine, and CD8. CD8+ tumor infiltrating lymphocytes (TILs) were counted per high powered field (HPF, 400X magnification) and presented as averages. Intensity of VCAN and Vkine expression were scored from 0-3+. Samples designated a 0/1 were considered low accumulation and samples scored as a 2/3+ were designated high. Samples scored low for VCAN but high for Vkine were designated VCAN proteolytic predominant (VPP) and all other combinations considered VCAN proteolytic weak (VPW). To create an *in vitro* model, the mouse MC38 cell line was CRISPR engineered to over-express VCAN. Conditioned media was then concentrated and added to a collagen matrix in a transwell with activated T cells. The number of cells and their subtype that migrated through the matrix were evaluated with flow cytometry.
Results: VCAN accumulation was highest in cancerous stroma with 58% of cancers being VCAN high and only 14% of adjacent normal tissues ($p<0.001$). Vkine accumulation was similar between groups, with 67% of tumors and 54% of adjacent normal samples scored as Vkine high. The VPP phenotype was least common in tumor tissues with only 27% of tumor samples designated VPP versus 43% of adjacent normal samples ($p<0.001$). VCAN high tumors had significantly fewer TILs with 4 TILs/HPF vs 13 in the VCAN low tumors ($p<0.001$). High levels of Vkine correlated with greater TIL abundance (Vkine high: 10 TILs/HPF, Vkine low: 5 TILs/HPF; $p=0.02$). Versican proteolysis had the strongest correlation with TIL abundance in cancers (VPP: 18 TILs/HPF, VPW: 5 TILS/HPF; $p<0.001$). In vitro, the addition of VCAN containing media into transwell matrices reduced both CD4+ and CD8+ T cell migration through the matrix (Control: 4277 CD8+ T cells, VCAN: 2603 CD8+ T cells; $p<0.001$ and Control: 7770 CD4+ T cells, VCAN: 5340 CD4+ T cells; $p=0.007$).
Conclusions: VCAN accumulation in human CRCs is common and correlates with reduced TIL abundance, whereas VCAN proteolysis correlates with increased TILs. *In vitro,* VCAN demonstrated the ability to reduce T cell migration. Future studies will explore the mechanism by which VCAN abundance leads to decreased T cell infiltration and the importance of this as an immunotherapy biomarker.

#0100 Blockade of CCL5 and CXCL10 signaling as a novel immunotherapy for epithelial ovarian cancer.

A. C. Lin, J. Moscarelli, **Z. Lin**, E. S. Ratner;
Yale University School of Medicine, New Haven, CT

Background: Cancer immune evasion remains a major barrier in developing enduring therapies for epithelial ovarian cancer (EOC). Expression of programmed death-ligand 1 (PD-L1) is known for its immunosuppressive role in cancer, thus interferences to PD-L1 have shown marked efficacy against many advanced cancers. However, the mechanisms by which PD-L1-negative cancers evade immune response remain unelucidated. We have found chemokine (C-C motif) ligand 5 (CCL5) and (C-X-C motif) ligand 10 (CXCL10) to up-regulate in PD-L1-negative EOC. Therefore, the present study aims to investigate blockade of CCL5/CXCL10 signaling to overcome immune evasion of EOC.
Methods: Isogenic BRCA2-mutated PEO1 and BRCA2-wild type PEO4 EOC cells were treated with IFNγ, olaparib, or both in combination for western blot and flow cytometric analyses of PD-L1 expression. The conditioned medium of PEO1 and PEO4 cells was analyzed for immune array analysis to determine and compare the levels of 36 cytokines. PEO1 and PEO4 cells were co-cultured with CD3/CD28 antibodies-activated human peripheral blood mononuclear cells (PBMCs). Then, PBMCs were stained with anti-CD8 or CD4 and CD25 antibodies for flow cytometric analyses of cytotoxic or helper T cells, respectively. PEO1 and PEO4 cells were co-cultured with activated PBMCs in the presence and absence of TAK-779 or AMG-487. Thereafter, PBMCs were stained with anti-CD4, CD25, and FOXP3 antibodies for flow cytometric analyses of regulatory T cells (Tregs). PEO1 and PEO4 cells were transfected with CCL5- or CXCL10-siRNA and subsequently co-cultured with activated SUPT1 cells or PBMCs. The conditioned medium was collected and analyzed for the levels of IFNγ by ELISA.
Results: PEO1 cells exhibited an up-regulation of basal and IFNγ-induced PD-L1 compared with PEO4 cells. PEO4 cells displayed a pronounced increase in the CCL5 and IFNγ-induced CXCL10 compared with PEO1 cells. Co-culture of PBMCs with PEO1 and PEO4 cells led to a significant decrease in activated CD8+ effector T and CD4+ helper T cells. However, co-culture of PBMCs with PEO4 cells caused a significant increase in activated CD4+ helper T cells. Co-culture of PBMCs with PEO4 cells caused a significant increase in FOXP3+CD4+CD25+ Tregs. This increase in Tregs was significantly reduced by the treatment with the CCL5/CCR5 antagonist TAK-779 or the CXCL10/CXCR3 antagonist AMG-487. Silencing of CCL5 or CXCL10 in PEO4 cells by siRNA significantly increased IFNγ production by SUPT1 cells and PBMCs.
Conclusions: PEO4 cells secrete CCL5 and IFNγ-induced CXCL10 to activate Tregs, enabling tumor cells to evade host immune response by dysregulating their microenvironment. PEO4 cells-induced Tregs are reduced by CCL5/CXCL10 signaling blockade with TAG-779 or AMG-487. Furthermore, silencing of CCL5 or CXCL10 in PEO4 cells with siRNA abolishes Treg-mediated immunosuppression and restores the antitumor activity of effector T cells.

#0101 A novel humanized mouse model recapitulates the unique TME found in patients with HIV-associated NSCLC.

M. Juric[1], G. Kaufmann[1], L. Zhu[1], K. Ranjan[1], K. Agrawal[1], B. Rajendran[1], J. K. Rajashekar[1], H. Zhao[2], Y. Kluger[1], B. Emu[1], K. A. Schalper[1], P. Kumar[1], R. A. Flavell[1], **M. Chiorazzi**[1];

[1]Yale School of Medicine, New Haven, CT, [2]Yale School of Public Health, New Haven, CT

Among people with HIV (PWH), non-small cell lung cancer (NSCLC) is increasing in incidence, presents with more advanced disease, and portends a worse prognosis compared to the general NSCLC population. Despite effective control of viral replication with antiretroviral therapy (ART), PWH have evidence of immune dysfunction, and it is unknown whether these immune perturbations impact the tumor microenvironment (TME) to influence disease disparities.Here we preclinically model HIV-associated NSCLC using MISTRG6-A2, a humanized mouse system that is highly optimized for development of functional innate and adaptive immune cells. We compare tumor growth and immune features of HIV-infected, ART-suppressed MISTRG6-A2 hosts to uninfected hosts, with parameters informed by parallel analyses of human tissue samples obtained from PWH with NSCLC, and non-HIV controls.MISTRG6-A2 mice were engrafted with human CD34+ HSPCs from HLA-A*02-expressing donors on post-natal day 2 and intravenously infected with HIV-1 at 6 weeks of age. When HIV viral titers were $>10^6$ copies of viral RNA/ml plasma and hCD4 T cells were depleted, ART was initiated (RAL/FTC/TDF). When plasma viral RNA was undetectable and CD4 T cells recovered, NSCLC PDX tissue from HLA-A*02-expressing tumor was implanted into these HIV-infected, ART-suppressed MISTRG6-A2 mice as well as non-infected littermate controls which had received HSPCs from the same donor. HIV-infected mice displayed enhanced growth of PDX tissue (mean tumor size 206.7 mm^3 vs 110.2 mm^3; $p < 0.05$).Quantitative immunofluorescence of the TME from these hosts revealed significantly increased infiltration of CD4 and CD8 T cells in tumors of HIV-NSCLC mice ($p<0.01$ and 0.05, respectively); of note, enhanced T cell infiltration was restricted to tumors, with similar frequency of CD4 and CD8 T cells detected in spleen, lung and liver tissues of HIV-infected vs uninfected hosts. Staining of tumor epitopes revealed increased expression of B2M and EGFR in tumors from HIV-NSCLC mice (mean qIF scores in NSCLC vs HIV-NSCLC $3.8x10^6$ vs $1.2x10^7$ for B2M, $p<0.001$; 440 vs 1,971 for EGFR, $p<0.01$), consistent with our findings in samples from HIV-NSCLC tumor tissues vs NSCLC tumor tissues. Of note, elevated EGFR staining was only present in tumor tissue, not found in stromal cells or other tissues. Single cell transcriptomic analyses of the TME revealed prominent interferon and antigen presentation signatures in HIV-NSCLC tumors, as well as differential expression of immunoregulatory molecules.These results demonstrate the fidelity of the HIV-NSCLC MISTRG6-A2 system as a model for HIV-associated NSCLC and suggest EGFR-directed therapies as potentially relevant in this neglected disease.

#0102 LMP1-mediated recruitment of ALIX directs exosomal PD-L1 sorting and contributes to immunosuppression in EBV$^+$ nasopharyngeal carcinoma.

F. He, Y. Gong, Y. Zhou, C. Xie;
Wuhan University, Wuhan, China

Epstein-Barr virus (EBV) is known to cause multiple cancers and plays a pivotal role in tumor immune evasion. Latent membrane protein 1 (LMP1) is a key viral oncoprotein expressed in most EBV-associated cancers and contributes to tumor microenvironment remodeling. However, the exact role of LMP1 in modulating tumor immunity remains unclear. In this study, we elucidate how LMP1 interacts with PD-L1 and ALIX to form a trimolecular complex, facilitating the selective sorting of PD-L1 into exosomes and consequently impairing $CD8^+$ T cell function in nasopharyngeal carcinoma (NPC). Specifically, the transmembrane domain of LMP1 interacts with and stabilizes PD-L1, while the intracellular domain of LMP1 binds to ALIX, thus enabling access to the exosomal secretory pathway. This interaction leads to the formation of a trimolecular complex comprising LMP1, PD-L1, and ALIX, which is indispensable for the exosomal trafficking of PD-L1. Importantly, disrupting ALIX significantly diminishes LMP1-induced exosomal PD-L1 secretion, thereby restoring $CD8^+$ T cell functionality. Furthermore, we found that elevated levels of LMP1/ALIX expression are positively associated with immunosuppressive characteristics and poorer outcomes in human NPC. Our findings highlight the crucial role of the LMP1/ALIX axis in exosomal PD-L1 sorting and EBV-mediated immune evasion, presenting a novel and promising target for cancer immunotherapy.

#0103 Prostate cancer bone metastasis: Therapeutic targeting of tumor associated macrophages.

H. Zhang, S. Mei, N. E. Jeffries, D. M. Dahl, C.-L. Wu, P. J. Saylor, **D. B. Sykes**;
Massachusetts General Hospital, Boston, MA

Introduction: Castration-resistant bone metastatic prostate cancer is a morbid and deadly disease with an exceedingly low response rates to available immunotherapies. Understanding the mechanisms behind immune evasion and tumor progression is critical to improving therapy. Historically, bone metastases have been challenging to model in the laboratory. Our foundational work was built upon fresh patient samples taken directly from the operating room for analysis across multiple platforms: IHC, single cell expression profiling, and spatial transcriptomics. We compared tumors from patients with bone metastatic disease to tumors from patients with disease localized to the prostate. Our work (*Cancer Cell*, 2021 and *Nature Communications*, 2023) has consistently pointed towards dysregulated myeloid populations within the tumor microenvironment, particularly TREM2+ tumor associated macrophages (TAMs), as key drivers of disease progression.
Methods: Our patient samples and murine pre-clinical models of prostate cancer highlighted several specifically upregulated molecules and pathways in TAMs. Here we focus on TAMs *in vitro* and *in vivo* using a new and genetically tractable myeloid model to interrogate the mechanistic role of key pathways, and how they may contribute to T-cell immune suppression. The ER-Hoxb8 system of conditional myeloid differentiation permitted the generation of isogenic cell lines to interrogate the roles of key molecules TREM2, MSR1, APOE, and MERTK through overexpression or CRISPR/Cas9 knockout.
Results: Using a system of co-culture *in vitro*, we quantified the role of these proteins in suppressing T-cell proliferation and cytokine production, as well as their role in TAM differentiation and function. *In vivo*, these lines were co-injected subcutaneously with syngeneic RM1-BM3 tumor cells to quantify their effect on tumor growth and T-cell suppression *in vivo*. In addition to localized subcutaneous tumors, bone metastatic disease was established by intracardiac injection. Furthermore, established tumors were treated with TAM-directed small molecule therapy (e.g., MERTK inhibition) as well as immune checkpoint inhibition (anti-PD1) alone, and in combination.
Conclusions: TAMs are immune suppressive myeloid cells that are not found in normal tissues. They are specifically recruited to tumors and highly enriched in bone metastatic disease. Transcriptomic analyses highlighted signaling pathways potentially amenable to productive therapeutic targeting. The ER-Hoxb8 system was highly effective in generating a genetically tractable model of TAM for study *in vitro* and *in vivo*. Our work supports the hypothesis that the specific targeting of TAMs, by focusing on critical signaling pathways, can be effective in the treatment of pre-clinical models of prostate cancer. This new approach merits further study as a potential strategy for the treatment of patients with bone metastases.

#0104 Profiling peripheral blood to predict response to targeted androgen receptor axis therapy in mice.

Marco A. De Velasco, Yurie Kura, Kazuko Sakai, Yoshitaka Saito, Takafumi Minami, Kazuhiro Yoshimura, Kazutoshi Fujita, Kazuto Nishio, Hirotsugu Uemura

Kindai University Faculty of Medicine, Osaka-Sayama, Japan

Background: Targeting the androgen receptor (AR) signaling axis (ARAT) continues to be the mainstay treatment for advanced-stage prostate cancer. Using second-generation antiandrogens like abiraterone acetate (Abi) and apalutamide (Apa) has contributed to the survival of prostate cancer patients. However, resistance to these therapies remains a problem and most of these patients progress to castration-resistant prostate cancer (CRPC). Myeloid-derived suppressor cells (MDSCs) have been shown to drive CRPC. We previously showed that unfavorable responses to androgen deprivation therapy (ADT) or ADT plus Apa were associated with polymorphonuclear MDSCs (PMN-MDSCs) cells enriched in prostate tumors from conditional *Pten/Trp53*-double knockout (DKO) mice. Here, we explore the association between pre-treatment immune cell subsets blood and antitumor to ARAT therapy DKO mice.
Methods: Twenty-eight-week-old DKO mice were surgically castrated and after four weeks were randomized to treatments with vehicle, Apa or Abi for an additional four weeks (*n*=20). Individual treatment responses were assessed and classified according to tumor burden as follows: high tumor burden (HTB), ≥20% of median; moderate tumor burden (MTB), -20% to 20% of median; or low tumor burden (LTB), ≤-20% of median. Peripheral blood was collected both before and after treatment and analyzed by multi-color flow cytometry panels for lymphoid and myeloid subsets. Blood samples from healthy wildtype and untreated DKO mice with castration-naïve prostate tumors were collected as reference samples. Subsets of PMN-MDSCs and monocytic-MDCSs (m-MDSCs) were represented as % of total abundance and 5 of parental population. revealed a signature that was correlated with treatment responses. Profiles were constructed and the data was used to train supervised learning models to predict treatment responses. Shapely additive explanations (ShAP) were used to determine feature importance. The model was tested and validated on an independent cohort of 20 DKO mice treated with ADT and ADT plus Abi.
Results: Moderate prediction from baseline blood could be identified for tumor burden following ARAT using a Naïve Bayes classifier. Model evaluation, using an independent cohort, yielded favorable performance with area under the curve (AUC) mean, 0.707; HTB, 0.627; MTB, 0.750; and LTB, 0.745. The most important features for prediction were identified.
Conclusion: Our study revealed that MDSC subsets present in blood were associated with treatment responses to ARAT.

#0105 Understanding the role of β2-adrenergic receptor signaling on type II innate lymphoid cells in cancer.

J. Choi, C. R. MacDonald, S. Daneshmandi, J. Wang, N. T. Roberts, C. M. James, P. L. McCarthy, H. Mohammadpour, E. A. Repasky;
Roswell Park Comprehensive Cancer Center, Buffalo, NY

Increased norepinephrine (NE) due to chronic stress can activate adrenergic receptors, specifically β2-adrenergic receptors (β2AR), to produce an immunosuppressive tumor microenvironment (TME). Previous work by our lab demonstrated that tumor burden can be reduced by blocking β2AR signaling. Immune cells express β2AR and we have shown that the increased β2AR signaling leads to increased T cell exhaustion and increased inhibitory activity of myeloid-derived suppressor cells (MDSCs). In general, the resulting immunosuppression leads to a modest but significant reduction in tumor growth. However, the lack of a dramatic reduction in tumor growth reveals the complex nature of adrenergic signaling dependent regulation of the cancer immune response. Recent literature revealed that innate lymphoid cells (ILCs), especially type II ILCs (ILC2s), express high levels of β2AR. Therefore, we evaluated whether β2AR regulates ILC2s within the TME and how that affects tumor prognosis. We generated a genetic conditional knockout murine model where β2AR expression in ILC2s was deleted by crossing $IL5^{cre}$ expressing mice to $\beta2AR^{flox/flox}$ mice ($IL5^{cre}\beta2AR^{f/f}$). AT3 breast cancer cell line was injected into the 4^{th} mammary fat pad and tumor volume was measured every 2-3 days. Tumor infiltrating ILC2s ($CD45^{+}Lineage^{-}CD90.2^{+}CD127^{+}ST2^{+}$) were analyzed by flow cytometry at D36 post-tumor implantation. Notably, $IL5^{cre}\beta2AR^{f/f}$ mice had increased AT3 breast cancer tumor growth compared to control mice. Flow cytometric analysis of the tumor revealed an increased frequency of $GATA3^{+}$ ILC2s within the TME. These $GATA3^{+}$ ILC2s lacking β2AR expressed higher levels of the IL33 receptor, ST2, and a higher percentage of $IL13^{+}$ cells compared to WT $GATA3^{+}$ ILC2 cells. We also observe a trend toward increased MDSC population within the TME of mice lacking β2AR in ILC2s. These results reveal an anti-tumor function of β2AR signaling through the suppression of ILC2 activity within the TME that warrants further investigation. This work has been in part supported by NIH Grants F30 CA284763 (to J.C.), K99 HL155792 (to H.M.), and RO1 CA205246 (to E.R.)

#0106 Selective elimination of CD169^{+} macrophages in lymph nodes invaded by breast cancers.

Y. Maeshima[1], T. R. Kataoka[2], A. Vandenbon[3], M. Hirata[3], Y. Takeuchi[3], Y. Suzuki[4], Y. Fukui[1], Y. Ibi[5], H. Haga[3], S. Morita[5], M. Toi[1], S. Kawaoka[6], K. Kawaguchi[1];

[1]Kyoto University Hospital, Graduate School of Medicine, Kyoto, Japan, [2]Iwate Medical University, Iwate, Japan, [3]Kyoto University, Kyoto, Japan, [4]The University of Tokyo, Tokyo, Japan, [5]Kyoto University Graduate School of Medicine, Kyoto, Japan, [6]Tohoku University, Sendai, Japan

Background: Lymph node metastasis is known as one of the strongest prognostic factors in breast cancer. The invasion mechanism of metastasized cancer cells in such immune cell-rich organs remains clear. Here, we aimed to elucidate the impact of metastasized cancer cells on the lymph node immune cell landscape.

Methods: Multiscale transcriptomic analyses were performed on both metastatic and nonmetastatic lymph node samples from breast cancer patients with lymph node metastasis. As cancer cells interact with lymphocytes in lymph nodes in direct, proximal, and distant manners, we tried to capture the direct and proximal impact on immune cells in invaded lymph nodes by comparing paired metastatic and non-metastatic lymph node samples. Laser-micro-dissected sections were obtained from 17 lymph nodes across six breast cancer patients at stages II–III, with each patient contributing both types of lymph nodes for direct comparison. We performed bulk transcriptome, spatial transcriptome, and imaging mass cytometry to analyze the obtained lymph nodes. Furthermore, we conducted immunohistochemistry analyses against a larger patient cohort (574 lymph nodes from 58 patients).

Results: Comparing the transcriptomes of paired lymph nodes with and without metastasis from the same patients revealed selective downregulation of CD169+ macrophage-related genes in metastatic lymph nodes. The spatial transcriptome indicated a potential depletion of CD169+macrophages, initiators of anticancer immunity, from their residence in metastatic lymph nodes, while other principal immune cell types were unaltered. Mass cytometry imaging revealed that the numbers of CD169+ macrophages were smaller in the metastatic lymph nodes than in the nonmetastatic lymph nodes. Conversely, the number of B cells, CD4+ T cells, CD8+T cells, Treg cells, and CD11c+ cells remained comparable in both lymph node types. Additional immunohistochemistry analysis of 315 nonmetastatic lymph nodes and 159 metastatic lymph nodes from 58 patients with breast cancer showed that a reduced CD169+ macrophage population was prevalent in all breast cancer subtypes. CD169+ macrophages gradually decreased in correlation with pathological lymph node metastasis status, while no correlation was identified with pathological tumor size classification or metastasized cancer volume in invaded lymph nodes.

Discussion: CD169+ macrophages are a unique type of resident macrophages in the lymphoid organs that present cancer-derived antigens to CD8+ T cells. The antigen-presenting role of CD169+ macrophages to T cells is a pivotal step in adaptive immunity. The elimination of CD169+ macrophage implies the disruption of the first step of the initial immune response. This study uncovered CD169+ macrophage suppression as a pronounced pathological phenotype in lymph nodes with breast cancer metastasis, thereby establishing it as a critical future therapeutic target.

#0107 Application of MSD on the lung cancer associated idiopathic pulmonary fibrosis.

Wei Bao, Ying-Ji Li, Jin-Fan Gu, Cong-Lin Yang, Yi-Da Wang, Tie-Jun Bing, **Wen-Jen Yu**

ICE Bioscience, Inc., Beijing, China

Idiopathic pulmonary fibrosis (IPF) is a progressive and irreversible chronic disease that kill ten thousand of people in China every year. The risk of IPF is highly correlated with smoke, air pollution, dust, virus infection and aging. Average survival period of patients diagnosed as IPF is around 2.8 years which is less than several types of cancers, therefore, IPF is also thought to be a lung cancer-like disease. In the past few decades, many animal models were created to mimic human IPF, however, induction materials, animal species and strain differences, sex, physiology structure and progress of disease make the choice of IPF animal models selection more difficult. In addition, lack of strong evidence of cytokines biomarker detection hampered the discovery of anti-IPF drugs. Meso Scale Discovery (MSD) instrument is an efficient tool to high throughput analyze the lowest level of several cytokines and other biomarkers in the same time and was used to detect the bleomycin (BLM) induced mouse lung fibrosis. Meanwhile, animal sex and dose effects of BLM were also tested to define the proper mouse model for anti-IPF drugs development. Our results indicated that 0.6-0.8 mg/kg of intratracheal injection of single dose BLM is sufficient to create the IPF model without sex differences by examining the lung weight, lung ratio, soluble hydroxyproline, HE staining and mason staining. However, male mice were more resistant to the lethal effect of BLM due to the larger size or bodyweight. Using MSD detection, several mouse cytokines were measured simultaneously and showed that IFN-γ, IL-5, TNF-α, and IL-10 were increased in the IPF mouse model and were recovered after pirfenidone treatment at day 14 which mimics the cytokines profile in IPF patients. In summary, the MSD detection and pathological evaluation prove that male mouse treated with 0.8 mg/kg BLM through intratracheal injection is a suitable mouse model for the development of anti-IPF dugs.

#0108 Tumor-derived complement C3 is overexpressed in STK11 mutant non-small cell lung cancer and contributes to an immunosuppressive tumor microenvironment in a syngeneic mouse model.

S. Suzuki, C. Ting, B. Kandar, T.-A. Chen, A. Khan, T. Giridharan, B. Segal, **E. H. Yau**;
Roswell Park Comprehensive Cancer Center, Buffalo, NY

Mutations in *STK11* that lead to loss of its protein LKB1 occur in 15-20% of non-squamous non-small cell lung cancer (NSCLC) and are frequently co-mutated with oncogenic *KRAS* mutations. *KRAS* and *STK11* co-mutant NSCLC is associated with poor prognosis, low PD-L1 expression, low T-cell infiltration, and poor response to immune-checkpoint inhibitors (ICI). Loss of LKB1 leads to altered transcriptional programs with the activation of CREB-dependent gene transcription and changes in the tumor microenvironment including recruitment of suppressive myeloid cells. We used the syngeneic *Kras* mutant murine CMT167 tumor cell line that is wild-type for *Tp53* and *Stk11* and sensitive to ICI and generated isogeneic *Stk11* knockout cell lines (CMT167-Stk11-KO) by CRISPR/Cas-9 deletion. Loss of *Stk11* recapitulated LKB1-loss transcriptional signatures and rendered CMT167 tumors resistant to ICI. Single-cell RNA sequencing (10x) of implanted tumors demonstrated significantly less CD8 T-cells and increased neutrophils (PMN) in *Stk11*-KO versus *Stk11*-WT tumors. Analysis of differentially expressed genes in the tumor compartment identified increased expression of complement pathway genes including the central mediator *C3* in CMT-167-Stk11-KO tumors. Examination of a well characterized clinical cohort of human *KRAS*-mutant NSCLC patient samples with and without *STK11* mutation confirmed the increased expression of complement *C3* in *STK11*-mutant tumors. Analysis of a human NSCLC cell line panel demonstrated that *C3* expression was modulated by LKB1. Knockout of *C3* in CMT167-Stk11-KO tumor resulted in dramatic inhibition of tumor growth and re-sensitized CMT167-Stk11-KO tumors to ICI treatment in WT mice. Using *C3*-/- knockout mice, this effect was determined to be reliant on tumor-derived *C3* and dependent on adaptive immunity as no difference in growth of CMT167-Stk11-KO tumors occurred in nude mice or in WT mice after CD8 T-cell depletion. We then compared the transcriptome of Stk11-KO tumor cells with and without *C3* deletion, and observed that *C3* upregulates the expression of *Cxcl1*, *Cxcl2* and *Cxcl3* which mediate PMN recruitment and activation. Since these chemokines ligate Cxcr2, we asked whether Cxcr2 mediated tumor growth and ICI resistance in Stk11-KO tumors. While treatment with single-agent Cxcr2 inhibitor and anti-PD-1 therapy had no effect on tumor growth, the combination resulted in significant suppression of tumor growth *in vivo*. These results support a role for tumor-derived *C3* suppressing CD8 T-cell immunity, potentially indirectly through recruitment of PMN or inducing PMN suppressor function. Our results also provide rationale for targeting tumor-derived complement and inhibiting Cxcr2 to enhance ICI efficacy as novel therapeutic approaches in patients with *STK11*-mutant NSCLC.

#0109 Identification of tumor-intrinsic and extrinsic mechanisms of T cell exclusion in estrogen receptor-positive (ER+) breast cancer through integration of bulk and single-cell transcriptome and spatial analysis.

K. Shimada[1], Y. X. Cui[2], D. Michaud[2], K. F. Zheng[3], J. Goldberg[2], R. Pastorello[4], L. Kania[3], S. S. McAllister[5], S. M. Tolaney[2], A. Waks[2], R. Jeselsohn[2], P. K. Sorger[1], J. Agudo[2], J. L. Guerriero[1], E. A. Mittendorf[1];

[1]Harvard Medical School, Boston, MA, [2]Dana-Farber Cancer Institute, Boston, MA, [3]Brigham and Women's Hospital, Boston, MA, [4]Hospital Sirio Libanes, Sao Paulo, Brazil, [5]Brigham and Women's Hospital, Boston, MA

T cells are generally present in low numbers in estrogen receptor-positive (ER+) breast cancer (BC) potentially due to limited antigens or impaired antigen presentation, however defined mechanisms are not fully understood. This study explores the interplay between estrogen receptor signaling (ERS), antigen presentation machinery (APM), and T cell signaling (TC) using diverse datasets, including BC cell lines, TCGA, METABRIC, and clinical trial bulk transcriptomes, single-cell RNA-sequencing of ER+ primary BC, and single-cell spatial multi-plex cyclic immunofluorescence (CyCIF) of primary BC patients. Co-expression analysis of both computationally and manually curated genes in TCGA and METABRIC data unveiled distinct 29-gene ERS and 225-gene combined APM/TC modules with strong inverse correlations in ER+ BC. This inverse correlation was confirmed in independent cohorts. ERS and APM/TC modules were down- and up-regulated, respectively, in response to aromatase inhibitor therapy in ER+ BC patients from the ACOSOG Z1301B trial who demonstrated clinical benefit. Analysis of published single-cell RNA-sequencing data of 20 primary ER+ BC was performed to elucidate cell types that express individual genes in the modules. It confirmed that high ERS activity is associated with reduced T cells, and identified distinct cell types contributing to each module, showing higher ERS activity in tumor cells and higher APM/TC activity in stromal and immune cells. At the cell type level, we found distinct contributions and precise insights of individual genes. The prevalence of ERS activity in tumor cells prompted investigation to determine if the ERS and APM/TC modules were preserved as tumor-intrinsic signaling. Analysis of 54 BC cell lines indicated partially preserved module correlations in cancer cell lines and revealed that the APM/TC module is a contribution of both tumor-intrinsic (e.g., complement and type-I IFN-response), and tumor-extrinsic (e.g., lymphocyte activation) factors. CyCIF analysis of 29 ER+ BC samples was performed to bridge gene signatures with spatial biology and validated that higher ERS activity correlates with lower T cell infiltration. The spatial pattern of T cells varied from immune desert to stromally bound to fully inflamed tumors. Neighborhood analysis revealed increased frequency of CD8 T cells around a tumor cell is associated with elevated MHC I and II in broad immune cells and macrophage subsets, respectively. pTBK1+ macrophages inversely correlated with CD8 T cell frequency and MHC expression in neighboring cells, suggesting an immunosuppressive role. This study uncovers robust and tightly regulated ERS and APM/TC signaling in ER+ patients, unraveling molecular intricacies and offering potential insights for targeted therapeutic interventions.

#0110 Adoptive transfer of tumor antigen-specific T cells alters the renal tumor microenvironment in the presence and absence of immunotherapy.
H. Stephens, E. Elkins, F. Dempsey, Z. Swalley, J. Li, J. Zhang, R. Kirkman, B.-R. Chen, Z. Roberts, S. Sudarshan, B. Sleckman, H. Tse, D. L. Smith, Jr., L. A. Norian;
University Of Alabama At Birmingham, Birmingham, AL

Immunotherapies are the standard of care for patients with renal cancer, yet their effects on renal tumor antigen-specific CD8 T cell responses and their subsequent ability to modulate the renal tumor microenvironment remain difficult to evaluate. In order to address this gap in the field, we developed a novel murine model to examine tumor-antigen specific CD8 T cell immune responses in orthotopic renal cancer utilizing a new cell line, Renca-tERK-LUC. Parental Renca cells were transduced with a lentivirus expressing the naturally-occurring, mutated tERK peptide found in CMS5 fibrosarcoma cells to create Renca-tERK-LUC tumor cells. The tERK mutation consists of a one base pair change that creates an Sfc1 site, so it can be detected by RT-PCR followed by restriction enzyme digestion. Our data show that Renca-tERK-LUC cells express tERK at high levels and grow progressively in control BALB/c mice, but are rejected in DUC Thy1.1 mice, which contain endogenous TCR transgenic CD8+ T cells specific for tERK peptide / MHC I complexes. We then performed adoptive transfers of 5×10^5 DUC Thy1.1 T cells into mice with established, orthotopic Renca-tERK-LUC tumors to evaluate: 1) the effects of immunotherapy on tumor-antigen-specific T cell responses; and 2) the effects of tumor-antigen-specific T cells on the broader renal tumor microenvironment. Our data indicate that the transfer of relatively low numbers of tumor antigen-specific CD8+ T cells induces transcriptomic and cellular changes in the tumor microenvironment in both the presence and absence of immunotherapy. Defining the parameters surrounding tumor-antigen-specific T cell responses and their ability to modulate the renal tumor microenvironment under the influence of clinically relevant immunotherapeutic intervention has the potential to increase the understanding of immunity to renal tumors, which could ultimately prove beneficial for renal cancer patients.

#0111 Establishing orthotopic renal cell carcinoma xenograft in PBMC-humanized immunodeficient NSG-MHC I/II double knock-out mice.

W. Kang[1], Y. Wang[2], Y. N. Laimon[3], O. Pham[1], B. Matran[1], L. Bottoms[1], S. Khang[1], H.-C. Yuan[2], N. Murugan[2], A. B. Sheshdeh[3], L.-c. Yao[1], J. Yang[1], M. Cheng[1], S. Signoretti[3], W. A. Marasco[2], J. G. Keck[1];

[1]The Jackson Laboratory, Sacramento, CA, [2]Dana Farber Cancer Institute, Boston, MA, [3]Brigham and Women's Hospital, Boston, MA

Clear cell renal cell carcinoma (ccRCC), the predominant histological subtype of RCC, is highly correlated with immune cells, an association that is linked to a worse prognosis. Our study aimed to establish an orthotopic ccRCC mouse model reconstituted with human peripheral blood mononuclear cells (PBMCs) and implanted with human ccRCC SKRC-59 cells under the kidney capsule in immunodeficient NSG-MHC I/II double knock-out (DKO) mice. The study was conducted using two experimental designs to optimize humanization and tumor formation. In the first experimental design, the mice were engrafted with SKRC-59 cells under the left kidney capsule 24 hours post-irradiation on study day 0. The PBMCs were then injected intravenously on study day 9. The second experimental design involved irradiating mice on study day -1, followed by engraftment with PBMCs either perfectly (6/6) or partially (3/6) matched human leukocyte antigens (HLA) with the tumors. Subsequently, SKRC-59 cells were placed under the kidney capsule on study day 0. Daily post-operative observations were conducted for six days following surgery to ensure the well-being of the mice. Tumor burden was assessed twice weekly using an *in vivo* imaging system, along with monitoring body weights and clinical signs. The humanization rates were evaluated 7, 14, and 21 days post-PBMC engraftment, as well as at the end of the study, using peripheral blood. Approximately 5 to 6 weeks post-tumor implantation, the mice were euthanized, and both left and right kidneys were collected and weighed for further analysis. The humanization rates were significantly higher when the PBMCs were engrafted on the same day as irradiation compared to 10 days post-irradiation. The PBMC humanization, and HLA-type PBMC donors did not affect tumor burden. Additionally, we found that distant metastasis in the lungs developed in several mice. Using flow cytometry and immunohistochemistry (IHC) to analyze tumor infiltrating leukocytes (TILs), a predominant number of CD3+ T cells were found in human CD45+ TILs, indicating that this model could be useful for evaluating T cell-mediated immunotherapies. Moreover, lympho-myeloid aggression (LMA) was observed in this peripheral blood leukocytes (PBL) mouse model, showing early stage tertiary lymphoid structures (TLS), which potentially provides a powerful tool to recapitulate TLS formation and study associated mechanisms and therapies. Our study demonstrated the growth of ccRCC SKRC-59 tumors under the renal capsule and observed TILs and metastatic patterns in PBMC humanized DKO mice. This PBMC-humanized orthotopic ccRCC xenograft model can recapitulate tumor microenvironment (TME), and be potentially used to assess the safety and efficacy of various immunotherapeutics.

#0112 The NSG-Flt3KO; Tg(hFLT3LG); hIL15 mouse strain improves engraftment of innate immune cells post-CD34+ humanization.

S. Boreddy, S. Hu, B. Soper;
The Jackson Laboratory-West, Sacramento, CA

Human immune system mouse models play critical roles in numerous preclinical drug development pipelines, including immunology, infectious diseases, and immuno-oncology. These models are constantly evolving, with addition of human cytokines to sustain engraftment of human immune cells. To date, most humanized models have primarily focused on T lymphocyte cell biology, leaving room for improvement in developing models that effectively represent NK cells and the myeloid lineage. Previously, we demonstrated that the introduction of human IL-15 (NSG-IL-15) or FLT3L (NSG-FLT3L) to NOD-scid IL2rγ^{null} (NSG) mice enhanced engraftment of innate immune cells, including human CD56^{+} NK cells, CD141^{+} and CD1c^{+} DC subsets, CD123^{+} pDCs, and CD14^{+} monocytes. In this study, we describe a new NSG mouse variant (NSG-Flt3KO; Tg(hFLT3LG); hIL15) that expresses physiological levels of both human IL-15 and FLT3L and detail the immune cell diversity following HSC engraftment. NSG-Flt3KO; Tg(hFLT3LG); hIL15 mice, along with control strains NSG, NSG-IL15, and NSG-FLT3L, were engrafted with human umbilical cord blood derived CD34^{+} hematopoietic stem cells from three different donors, and blood samples were collected until Week 20 post-transplantation. Blood samples were analyzed via flow cytometry to assess the engraftment of innate and adaptive immune cells. Spleen and bone marrow samples were collected at Week 12 post-transplantation and analyzed for lymphoid and myeloid immune cell populations via flow cytometry. To compare the differences among the strains in terms of immune cell sub-populations across weeks, a Two-Way ANOVA (mixed-model) was conducted, with $p<0.05$ considered statistically significant. Overall, the results demonstrate that NSG-Flt3KO; Tg(hFLT3LG); hIL15 mice have enhanced CD56$^{+/dim}$ CD16^{+} NK cells compared to NSG-FTL3L strain (20.5±12.8% vs 7.0±3.5% at Week 12), but comparable to NSG-IL15. Furthermore, myeloid sub-lineage cells in NSG-IL15-FLT3L mice, such as monocytes, macrophages (M1), granulocytes, dendritic cells, and neutrophils, were greater than in NSG or NSG-IL15 strains, but comparable to NSG-FLT3L mice. Overall levels of hCD45+ and T cell sub-populations (CD3^{+} or CD4^{+} or CD8^{+}) were comparable across all strains tested. In sum, our NSG-Flt3KO; Tg(hFLT3LG); hIL15 engraftment data suggest an improved model that supports drug development targeting human myeloid and NK cell populations.

#0113 Generation and validation of a novel humanized IL-31/IL-31RA/OSM/OSMR mouse model.

L. Wang[1], L. Zhao[1], M. Zhang[1], Z. Zhang[1], Z. Chen[1], **M. Kuraguchi**[2], J. Lian[1], J. Zhang[1];
[1]Biocytogen Pharmaceuticals (Beijing) Co., Ltd., Beijing, China, [2]Biocytogen Boston Corp, Waltham, MA

Oncostatin M (OSM) and interleukin-31 (IL-31) are two pleiotropic cytokines that share a common signaling receptor subunit, the OSM receptor beta (OSMR). Both cytokines are released by monocytes, macrophages, dendritic cells and T lymphocytes in inflammatory situations, and upon binding to their respective receptors, induce the production of inflammatory cytokines (such as IL-6), chemokines, and other cellular growth factors during tissue repair, mainly via the JAK/STAT signal pathway. As OSM and IL-31 are reported to be involved in a variety of physiological and pathological processes, targeting IL-31 or OSM signaling is of therapeutic interest. To provide a novel preclinical platform for testing novel modulators of these signaling axes, a humanized IL-31/IL-31RA/OSM/OSMR mouse model was generated. First, single gene knock-in mice were constructed by gene editing technology; multigenic knock-in mice were then obtained by breeding, yielding a quadruple humanized model in which the murine cytokine sequences were replaced by full-length human cytokine sequences *in situ*, while the murine receptor sequences were replaced by chimeric sequences comprised of the human extracellular region and murine intracellular regions *in situ*. mRNA expression confirmed expression of IL-31, IL-31RA, and OSMR in this model, while ELISA confirmed expression of human OSM protein in the model without evidence of murine OSM expression. Next, the signaling capacity of the humanized OSMR receptor was confirmed: mouse embryonic fibroblasts (MEFs) isolated from humanized B-hOSM/hOSMR mice were capable of responding to human OSM to release IL-6, while wild-type MEFs could only respond to murine OSM. Subsequently, the ability of IL-31RA antibodies to alleviate scratching was tested in a chemically induced model of atopic dermatitis. Compared to mice receiving control antibodies, scratching frequency in humanized B-hIL31/hIL31RA/hOSMR mice treated with nemolizumab was attenuated (analog antibody was generated in-house). Finally, blood counts and flow cytometric profiling indicates that the humanized mice have a normal frequency of leukocytes and lymphocytes. Taken together, this quadruple humanized IL-31/IL-31RA/OSM/OSMR mouse model is a promising preclinical tool that can be used to evaluate novel modulators of this signaling pathway prior to clinical development.

#0114 Identification of the actionable target, LILRB4, through genetic linkage analysis of Diversity Outbred (DO) F1 mice expressing HER2(neu).

J. B. Jacob[1], W.-Z. Wei[1], B. L. Kidder[1], T. Adeyelu[2], A. Elliott[2], G. Bepler[1], J. D. Reyes[1];
[1]Wayne State University School of Medicine, Detroit, MI, [2]Caris Life Sciences, Irving, TX

Our goal is to identify, *in situ*, the regulatory genes that dictate the onset age and growth rate of spontaneously arising tumors to implement new intervention strategies. For genetic linkage analysis, we crossed HER2(neu) Tg mice with Diversity Outbred (DO) mice, an outbred population comprised of 8 founding strains (A/J, C57BL/6J, 129S1/SvlmJ, NOD/ShiLtJ, NZO/HILtJ, CAST/EiJ, PWK/PhJ, WSB/EiJ) maintained by non-sibling crossing to ensure each mouse is genetically unique. Using R/QTL package, we linked Quantitative Trait Loci (QTL) in Chr 1 and X with tumor onset age, and a Chr 10 QTL with tumor growth rate. The Chr1 (=human Chr2) QTL was linked to human breast cancer diagnosis in 11 Genome-Wide Association Studies (GWAS; the human GWAS catalog, https://www.ebi.ac.uk/gwas/). Because human GWAS data is deficient in Chr X mapping and also does not assess tumor growth rate as a trait, the QTL loci identified in mouse Chr X and 10 were discoveries beyond the capacity of human GWAS. In total, we identified 26 candidate genes across the 3 QTL. For clinical validation, the genes were analyzed with CodeAI (Caris LS) which associated cancer patient clinical data with candidate gene expression. We found 21/26 genes significantly associated with the survival of patients with primary (n=3,533) and/or metastatic (n=4,870) breast cancers and 17/26 were associated with lung cancer (n=11,334) survival, with 13 overlapping genes between lung and breast cancer, indicating broad applicability of these candidate genes.
We interrogated the immune status in BALB NeuT and (BALBxPWK)F1 NeuT mice because the F1 mice developed tumors around 9 wk, much earlier than the 14 wk observed in BALB NeuT mice. Surprisingly, (BALBxPWK)F1 mice responded to cancer vaccines more vigorously. Single cell RNA (scRNA) libraries from (BALBxPWK)F1 NeuT tumors showed an expanded lymphocyte cluster (12%), compared with BALB NeuT (2%) and an enrichment of T cell activation genes. These findings may reflect a deficiency in tumor cell recognition by the activated anti-tumor effectors and a window of opportunity for correction.
Of the 21 candidate genes, LILRB4, a myeloid cell checkpoint molecule, was of particular interest. Expression of LILRB4 is predictive of patient survival in both breast and lung cancer. Using scRNA
sequencing, we found this transmembrane receptor expressed primarily by tumor infiltrating myeloid cells. In a reported scRNA sequencing dataset (GSE161529), LILRB4 was expressed by infiltrating macrophages in human breast cancers, and is also correlated with reduced survival. In a PAN Cancer ATACseq dataset (Corces et al., 2018), promoter accessibility of LILRB4 was associated with reduced survival. Taken together, there are multiple immune regulatory mechanisms of tumor progression and LILRB4 is an important new actionable target. CA76340 (WZW), KCI TBM program (JBJ) and CCSG P30 CA022453 (GB).

#0115 Developing uPAR CAR T Cells for High-Grade Serous Ovarian Cancer.

Zeda Zhang[1], Xin Fang[1], Yu-jui Ho[1], Sascha Haubner[1], Friederike Kogel[1], Clemens Hinterleitner[1], Stella Paffenholz[1], Kevin Chen[1], Wei Luan[1], Amanda Kulick[1], Gertrude Gunset[1], Andreina Garcia Angus[1], Jing Zhang[1], Zijian Xu[1], Adam Wang[2], Qingwen Jiang[1], Elisa de Stanchina[1], Britta Weigelt[1], Dmitriy Zamarin[3], Aveline Filliol[1], Judith Feucht[1], Jorge Mansilla-Soto[4], Corina Amor[1], Michel Sadelain[1], Scott Lowe[1]

[1]Memorial Sloan Kettering Cancer Center, New York, NY,[2]Rockefeller University, New York, NY,[3]Icahn School of Medicine at Mount Sinai, New York, NY,[4]Moffitt Cancer Center, Tampa, FL

Chimeric Antigen Receptor (CAR) T cells are a modality of immunotherapy that act to eliminate cancer cells by redirecting the cytolytic activity through targeting a protein overexpressed on the surface of the cancer cell. In contrast to move conventional cancer therapies, their anti-cancer activity does not depend on a cancer-specific molecular vulnerability but rather the differential expression of the target antigen on tumor cells compared to normal tissues. We have developed CAR T cells targeting the urokinase plasminogen activator receptor (uPAR), which is overexpressed on senescent cells but not expressed highly in vital organs, to selectively target senescent cells in a range of tissue damage pathologies where they are known to be pathogenic. uPAR is also highly overexpressed in a wide range of cancer types, including pancreatic, kidney, bladder, brain and ovarian carcinomas, respectively, raising the possibility that CAR T cells targeting uPAR may also be effective against cancer. Indeed, leveraging an electroporation-based genetically-engineered mouse model of ovarian cancer, we demonstrate the robust anti-tumor efficacy of murine uPAR CAR T cells in immunocompetent syngeneic mice. Moreover, through an exhaustive functional screening of 37 distinct human uPAR single-chain fragment variants (scFVs), we have successfully identified lead scFVs exhibiting subnanomolar affinity to membrane-anchored uPAR. Significantly, these human uPAR CAR T cells exhibit the capability to eliminate both orthotopic and metastatic human HGSOC xenograft tumors without inducing severe adverse effects. Ongoing efforts encompass the assessment of the long-term safety and toxicity profiles of uPAR CAR T cells utilizing a humanized mouse model platform. Our results provide a strong rationale for developing uPAR CAR T cells as an anticancer strategy relevant to a broad range of tumor types, and provide an avenue for safety profiling of uPAR CAR T cells prior to clinical testing in non-cancer patients harboring senescence-related pathologies.

#0116 Generation of humanized PD-1/PD-L1/CD94/NKG2A mice for evaluating novel combination therapies.

F. He[1], J. Yuan[1], Y. Shan[1], H. Bahetiyaer[1], Q. Xu[1], **J. Frame**[2], Q. Lin[2], X. Zhou[1], C. Shang[1];
[1]Biocytogen Pharmaceuticals (Beijing) Co., Ltd., Beijing, China, [2]Biocytogen Boston Corp, Waltham, MA

NKG2A and its co-receptor, CD94, are expressed on the surface of NK cells, and function to send inhibitory signals to NK cells upon recognition of the HLA-E complex on adjacent cells. Blockade of the NKG2A/CD94 complex is a promising strategy for cancer immunotherapy, due to the potential to trigger NK-mediated tumor killing. Previously, we generated humanized NKG2A/CD94 mice for testing novel therapeutics targeting human NKG2A/CD94. To explore the potential that this complex could be targeted as part of a novel combination therapy, we crossed humanized NKG2A/CD94 mice with humanized PD-1/PD-L1 mice, which were previously engineered to express the extracellular regions of human PD-1/PD-L1. Flow cytometric data from splenocytes isolated from the quadruple humanized mice confirmed expression of human NKG2A and CD94 in NK cells and activated CD8 T cells, as well as PD-1/PD-L1 on the surface of T cells. To test the efficacy of antibodies targeting these checkpoints *in vivo*, B-hHLA-E plus/hPD-L1 MC38 colon cancer cells were subcutaneously implanted into the quadruple humanized mice and treated with antibodies targeting human NKG2A, human PD-L1, or both antibodies. Results indicate that the combination therapy significantly reduced tumor growth when compared to NKG2A single antibody treatment. Together, these data suggest that humanized PD-1/PD-L1/CD94/NKG2A mice are a validated model for further evaluation of novel combination therapies.

#0117 Improved PBMC humanized mouse models for immuno-oncology drugs evaluation.

B. Xie, X. Hou, P. Yang, Y. Zhou, **D. Wen**;
Shanghai LIDE Biotech Co., Ltd., Shanghai, China

It has been demonstrated that anti-PD(L)1 therapy could significantly improve survival outcomes for patients with metastatic solid cancers, such as melanoma, non-small cell lung cancer and MSI-H colorectal cancer. However, more than half of these patients (NCT02563002, NCT02142738, NCT02563002) do not respond to immune checkpoint blockade (ICB) therapy, and 90% of colorectal cancer patients have MSS/pMMR characteristics and almost no response at all, which drives scientists to design novel drug candidates urgently and integrate tumor and tumor microenvironment (TME) signals systemically to rejuvenate exhausted immune system and overcome ICB resistance. LIDE has developed both traditional PBMC humanized mice model, and human immune cells and cancer co-inoculated model for IO drugs functional evaluation in the last 5-years by using unique PBMC donor selection and standard cancer biobank (PDX patient-derived xenografts, CDX cell derived xenograft) establishment. Cancer biopsies with MDM2 amplification or DNMT3A alternation have been shown resistant to PD1-Ab therapy but sensitive to chemical combo-therapy, and pMMR cancer PDX models seem responsible well to EGFR targeted, CD39-CD73-Adenosine targeted therapy. Human IL15 transgenic mice are used as one useful tool to investigate in vivo function of NK cells, NK engagers/modulators as well as drugs with ADCC (Antibody dependent cell-mediated cytotoxicity) effect. The activated immune cells and cancer co-transfer model, can significantly delay the graft-versus-host-reaction for another month compared with traditional PBMC humanized model, and archives maximal therapeutic effect of the testing drugs by pre-activating T cells with specific tumor antigens. Dendritic cells or macrophages could be successfully introduced into this co-inoculated system to work together with T cells, mimic human tumor tissue complexity, to help determine the overall effect induced by integrated signals. It seems CD40 agonist or CD47 antagonist could well synergies with anti-PD(L)1 to control melanoma and triple negative breast cancer development, respectively. This optimized PBMC humanized cancer-bearing mice models have been tested for various cancer targets, e.g. PD(L)1, Tim3, Lag3, Tigit, PVRIG, TGFβ1, CD73/CD39, CD47/Sirpa, DLL3/CD3, Claudin18.2/4-1BB, B7-H3, GITR, to better understand the interaction between cancer cells and immune cells.

#0118 Development of a novel murine model, NCG-M/hIL15, for enhanced post-HSC transplantation immunoreconstruction.

H. Wang, J. Xing, J. Fan, Y. Fan, J. Zhao, X. Gao, C. Ju;
Gempharmatech Co., Ltd., Nanjing, China

Advances in the field of immunology and hematopoietic stem cell (HSC) transplantation have prompted the development of murine models that faithfully recapitulate human immune responses. We present the NCG-M/hIL15 model, an innovative advancement in the realm of preclinical research, addressing two key challenges associated with existing models: the limited capacity for human natural killer (NK) cell regeneration in NCG-M and the suboptimal reconstitution of T cells, myeloid lineage cells in NCG-hIL15 mice.

Compared to the conventional NCG-M model, the NCG-M/hIL15 model demonstrates a significant improvement in its ability to regenerate human NK cells post-HSC transplantation. This advancement offers a valuable tool for studying NK cell biology, immune surveillance, and antitumor responses.

Furthermore, when compared to the NCG-hIL15 model, the NCG-M/hIL15 model outperforms in the reconstitution of human T cells and myeloid lineage cells, contributing to a more comprehensive simulation of human immune responses. The overall survival of mice in this model is notably stable, further enhancing its utility for long-term immunological studies.

The NCG-M/hIL15 model not only advances our understanding of human immune responses but also has significant implications for the development of novel immunotherapies and the preclinical evaluation of HSC transplantation strategies. This novel murine model offers a more accurate representation of the human immune system, with the potential to expedite the development of innovative therapeutic interventions. We present this model as a valuable addition to the preclinical research toolkit, promising a deeper understanding of immunology and a brighter future for clinical applications.

#0119 A non-surgical method for developing a pre-clinical orthotopic mouse model for colorectal cancer.

N. Singh[1], S. Sharma[1], K. Jeught[2], Z. Zhou[1], X. Zhang[1], X. Lu[1];
[1]Indiana University School of Medicine, Indianapolis, IN, [2]University of Miami Miller School of Medicine, Miami, FL

Recapitulating physiologically relevant tumor microenvironment is important yet a significant challenge in modeling colorectal cancer (CRC) for basic and translational studies. Among the different methods, using the cecal-wall injection technique is the most common way to create animal models of colorectal cancer (CRC). However, this approach requires complex surgery, and its unnatural placement creates a significant obstacle for developing treatments. Here, we report a non-surgical procedure for establishing orthotopic CRC mouse models, reflecting the appropriate tumor microenvironment to better model the disease development and facilitate translational studies including drug identification and validation. In this procedure, anesthesia is induced in overnight fasted study immunocompetent or immunodeficient mice while placed on a thermostat-controlled heating blanket. A specialized catheter is inserted and distended into the mouse colon to gently block the colon and ensure the localization for tumor development. Hereafter, the colonic epithelium is treated with proteases and mechanical abrasion to cause mild disruption. Following the local gut inflammation, the targeted colon region is incubated with tumor cells, leading to the adhesion of tumor cells to the colonic epithelium. Based on the animal background and the cell line used, the tumor developed within 3-4 weeks. The stages of tumor development at different time points were successfully confirmed using hematoxylin and eosin stain. Tumor microenvironment data revealed a significant increase in the immune cell infiltration specifically $CD4^+$ T-cells and tumor-associated macrophages in the non-surgical procedure as compared to the cecal-wall injection. Furthermore, a significant increase in the PD-1 expression of the $CD8^+$ T-cells in the cecal-wall injection as compared to the non-surgical procedure, suggests that the precise location of the tumor site may exert a substantial influence on pre-clinical therapeutic outcomes of immune-checkpoint inhibitors, thereby potentially hampering the clinical efficacy of drug treatments. Additional adaptations of this procedure may include: i) tumor development in different mouse strains, ii) local delivery of adeno-Cre in transgenic mice for CRC, and iii) delivering tumor organoids and patient-derived xenografts in immuno-deficient mice. Overall, our non-surgical procedure overcomes the technical difficulties of surgery and offers several advantages like ease of handling, cost-effectiveness, pain-free with nearly no procedure-associated mortality and adaptability to several strains. In conclusion, this procedure provides novel and promising alternative to conventional surgical orthotopic CRC mouse models for therapeutic interventions.

#0120 A closer Look at colorectal cancer risk: Insights from the complex relationship of HIV, helminths, and immune responses.

B. P. Damane[1], T. V. Mulaudzi[2], S. S. Kader[1], R. E. Ogunsakin[2], P. Naidoo[1], Z. Dlamini[2], Z. L. Mkhize-Kwitshana[1];
[1]University of KwaZulu-Natal-Natal, Durban, South Africa, [2]University of Pretoria, Pretoria, South Africa

The advent of antiretroviral therapy has markedly increased the survival rates of individuals with human immunodeficiency virus (HIV). However, this demographic, particularly in low-middle-income countries (LMICs) where HIV-helminth co-infections are prevalent, remains susceptible to infections. The intricate interplay between helminth infections and HIV susceptibility, often inducing immunological phenotypes that heighten vulnerability, remains poorly understood. Studies have shown the association between HIV-helminth co-infections and elevated susceptibility to colorectal cancer (CRC), introducing an additional layer of health concerns for this already vulnerable population.

This retrospective observational study delves into the profound effects of HIV-helminth co-infections on immune responses, with a specific focus on type 2 T helper (Th2) cell immunomodulation and susceptibility to CRC. Utilizing samples from a master project (n=414), 80 systematically randomized individuals were categorized into uninfected control, HIV-infected only, helminth-infected only, and HIV-helminth co-infected groups. Parasite detection employed the Kato-Katz technique, and serum testing was conducted for helminth-specific antibodies. Serological HIV testing, viral load categorization, white blood cell counts, and differential analyses were performed. Human ProcartaPlex Panel 1 was used for cytokine profiling of immune stimulatory and inhibitory soluble proteins.

A significant reduction in B and T lymphocyte attenuator (BTLA) (p=0.049) in helminth infections compared to the control. The association of BTLA with its ligand, herpesvirus entry
mediator (HVEM), establishes a direct link between the CD28 and tumor necrosis factor receptor (TNFR) families, triggering wide-ranging and robust immune responses. Subsequently, a notable reduction in CD28 was observed in HIV-infected subjects (p=0.003), followed by helminth-infected and HIV-helminth co-infected individuals (p=0.03) compared to the control. Furthermore, programmed death ligand-2 (PD-L2) expression, a major contributor to alternatively activated macrophage polarization during helminth infections, was significantly increased in the HIV-helminth co-infected group (p = 0.05), favoring a shift towards Th2 immune responses.

These observed alterations underscore the complexity of the immunological interplay in co-infected individuals, emphasizing an additional risk factor for colorectal cancer development. This necessitates a comprehensive understanding, providing valuable insights for the development of therapeutic strategies in LMICs and similar settings, addressing the heightened risk of CRC within this population.

#0121 Gut microbiome association with dietary habits and abemaciclib-induced diarrhea:A multicenter, prospective study.

Y. Fujimoto[1], K. Kawaguchi[2], Y. Maeshima[1], H. Ishiguro[3], K. Yamagami[4], S. Takahara[5], H. Suwa[6], M. Torii[7], S. Nagai[8], Y. Sagara[9], W. Tsuji[10], H. Yamashiro[11], T. Kotake[11], S. Fukuda[12], K. Saito[13], Y. Yamamoto[13], M. Kataoka[2], Y. Himoto[7], A. Yonezawa[2], Y. Fukui[1], Y. Nakamura[1], W. Li[1], S. Tanaka[2], M. Takada[1], S. Morita[1], M. Toi[1];

[1]Kyoto University Graduate School of Medicine, Kyoto, Japan, [2]Kyoto University Hospital, Kyoto, Japan, [3]Saitama Medical University International Medical Center, Hidaka, Japan, [4]Shinko Hospital, Kobe, Japan, [5]Kitano Hospital, Tazuke Kofukai Medical Research Institute, Osaka, Japan, [6]Hyogo Prefectural Amagasaki General Medical CenterKyoto University Graduate School of Medicine, Amagasaki, Japan, [7]Japanese Red Cross Wakayama Medical Center, Wakayama, Japan, [8]Saitama Prefectural Cancer Center, Kitaadachi, Japan, [9]Sagara Hospital, Kagoshima, Japan, [10]Shiga General Hospital, Moriyama, Japan, [11]Tenri Hospital, Tenri, Japan, [12]Keio University, Tsuruoka, Japan, [13]Fujita Health University, Toyoake, Japan

Background: Abemaciclib, a leading treatment used for HR-positive, HER2-negative metastatic and primary breast cancer patients, often causes diarrhea. Understanding the reasons machinery behind this adverse event leads to reduce the toxicity and improve the quality of life. This study explores a hypothesis that specific gut microbiota profiles are engaged in gastrointestinal toxicities caused by abemaciclib and may be influenced by patients' dietary habits. We assessed it using the Brief Diet History Questionnaire (BDHQ).

Materials and Methods: Our research involved collecting blood and stool samples, as well as dietary data through the BDHQ from 39 patients diagnosed with HR-positive, HER2-negative metastatic breast cancer. These were obtained prior to the start of abemaciclib treatment, at the first imaging evaluation, and at either disease progression or treatment discontinuation due to adverse effects. Incidence and severity of diarrhea were evaluated by the Bristol stool scale at baseline, from day 1 to day 14, and at day 90 of treatment. Stool samples were collected at baseline and at day 90 after the start of abemaciclib treatment. We conducted 16S metagenomic sequencing for gut microbiome analysis and used mass cytometry along with RNA-sequencing to profile immune cells.

Results: Our findings indicate a significant association between the gut microbiota composition and abemaciclib-induced diarrhea, which also appears to be modulated by dietary patterns. An increase in Dorea was observed with higher Bristol Stool Scale scores, while Bifidobacterium and Sellimonas abundances were inversely related to changes in stool characteristics. The presence of Dorea was also positively associated with the consumption of specific food items such as tea, root vegetables, and dietary minerals. In contrast, Collinsella abundance decreased as the frequency of diarrhea increased and it was associated with the consumption of fried foods and certain fats.

Conclusion: The prevalence of diarrhea as a side effect of abemaciclib treatment highlights the need for better management strategies. Our study indicates that gut microbiota, altered by dietary habits, is linked to this adverse effect. The data suggest a possibility of using specific gut bacteria as probiotics to alleviate this condition, pointing towards personalized dietary interventions as a potential avenue for improving treatment tolerance.

#0122 *Fusobacterium nucleatum* in saliva of oral cancer patients induces tumor stemness defense phenotype in cancer stem cells.

Partha Jyoti Saikia[1], Bidisha Pal[2], Lekhika Pathak[3], Shirsajit Mitra[4], Tutumoni Baishya[5], Rupam Das[5], Bikul Das[1]

[1]Department of Cancer and Stem Cell Biology,Department of Stem Cell and Infectious Diseases, KaviKrishna Laboratory, Guwahati, India,[2]Department of Experimental Therapeutics, Thoreau Laboratory for Global Health, M2D2 University of Massachusetts, Lowell, MA,[3]Department of Cancer and Stem Cell Biology, Department of Stem Cell and Infectious Diseases, KaviKrishna Laboratory, Guwahati, India,[4]Department of Cancer and Stem Cell Biology, KaviKrishna Laboratory, Guwahati, India,[5]KaviKrishna Telemedicine Care, Sualkuchi, Assam, India

Background: Oral squamous cell carcinoma (OSCC) is a highly aggressive cancer. Cancer Stem Cells (CSCs) having cell surface markers CD44, ALDH, and EpCAM+ have been identified in OSCC. However, the host pathogen interaction between CSCs and oral microbiome has not yet been studied. A number of studies have recently demonstrated the presence of specific oral bacteria populations and their lipopolysaccharides (LPS) in the tumor microenvironment (1). We previously reported pathogenic bacterial internalization in the CSCs (2). Based on the findings, we have developed an in-vitro model to investigate how oral microbiota may integrate into the tumor microenvironment's CSC population and control its activity. Here, we investigated the host/pathogen interaction between CSCs and FN.
Methods: Oral bacteria FN was selectively isolated using FEA agar plates from oral saliva of oral cancer patients (n=10) at stage 3 or 4. The isolated bacteria was co cultured with SCC 25 cells at MOI of 1:50. After co culturing the stemness genes such as SOX 2, OCT 4, Nanog ,LPS and ABCG2+ cancer stem cell markers were analysed. ABCG2+ CSCs and ABCG2- cells were immunomagnetically sorted and lysed followed by RNA extraction and RT QPCR was performed to observe if FN has selectively internalised in the CSCs. Also ABCG2+ and ABCG 2- cells were used to perform clonogenic assay.
Results: Coculture of FN with SCC 25 cell line induced high expression of stemness genes SOX, OCT 4 and Nanog along with CSC markers ABCG2+. Moreover high expression of LPS was observed indicating the presence of FN in the coculture. Importantly live bacteria was found internalized in ABCG2+ cells but not in ABCG2- cells. High clonogenicity was observed in ABCG2+ CSCs compared to ABCG2- cells. Notably, we found that live bacteria and their LPS, mostly *Fusobacterium nucleatum* isolated (FN) from clinical subjects, were capable of invading CSCs in the in-vitro setting. Post the host-pathogen interaction; it enabled the activation of a niche modulatory tumor stemness defense (TSD) phenotype in the CSCs. These aggressive CSCs with the TSD phenotype have been found to have a critical role in the progression and relapse of oral cancer.
Conclusion: Expression of stemness genes infers the niche defence mechanism of the CSCs of the tumour microenvironment due to infection of FN. Importantly presence of live bacteria in ABCG2+ CSCs indicates that FN selectively infects ABCG2+ CSCs but not ABCG2- cells. High clonogenicity of ABCG2+ CSCs confirms the TSD phenotypic attributes of the CSCs .
References:1. doi: 10.3389/fimmu.2023.1198269. 2. doi: 10.3389/fimmu.2022.933329.

#0123 Establishment of humanized CD3EDG/4-1BB mice for testing novel T cell engagers.

C. Shang[1], C. Li[1], L. Zhao[1], Q. Xu[1], **J. Jin**[2], M. Ren[1];
[1]Biocytogen Pharmaceuticals (Beijing) Co., Ltd., Beijing, China, [2]Biocytogen Boston Corp, Waltham, MA

Agonism of the 4-1BB receptor is an attractive therapeutic strategy for tumor cell therapy, due to the ability of this receptor to stimulate activity of T and NK cells for tumor cell killing. Many classes of biologics targeting 4-1BB have been generated to date, including bispecific or multispecific engagers designed to stimulate 4-1BB and CD3 activity on the T cell surface. To provide a preclinical platform to test such therapies, Biocytogen generated a humanized B-hCD3EDG/h4-1BB mouse model. This was achieved by crossing humanized mice expressing chimeric CD3E, CD3D and CD3G with mice expressing the human extracellular region of 4-1BB. Previously, we showed that these humanized CD3EDG mice and humanized 4-1BB mice can be used for validating efficacy of anti-human CD3 and 4-1BB antibody-based therapies, respectively. Here, we confirmed expression of human CD3 and 4-1BB on splenocytes in homozygous humanized B-hCD3EDG/h4-1BB mice by flow cytometry, which also demonstrated lack of murine CD3 and 4-1BB expression. Assessment of leukocyte subpopulations in the spleen and peripheral blood confirmed that humanization of the mice did not significantly alter the development or frequency of blood cell populations. Further evaluation of lymphocyte frequency was also performed, which demonstrates no significant alterations in the CD4/CD8 T cell ratio in spleen, lymph node, or peripheral blood of the animals. Presence of T_{reg} and NK cells was also confirmed. Taken together, these data indicate that the humanized B-hCD3EDG/h4-1BB model is a novel, robust tool for testing novel T cell engagers.

#0124 Validation of humanized TL1A mice for advancing preclinical research.

C. Li[1], S. Zhang[1], Z. Zhang[1], J. Feng[1], **J. Jin**[2], Y. Du[1];
[1]Biocytogen Pharmaceuticals (Beijing) Co., Ltd., Beijing, China, [2]Biocytogen Boston Corp, Waltham, MA

TL1A, or Tumor Necrosis Factor-Like Ligand 1A, plays a pivotal role in regulating the immune system and has garnered considerable attention in the field of cancer research. Studies have shown that TL1A can impact the tumor microenvironment via inflammatory signaling, immunosuppression, and tumor growth and survival. Targeting TL1A or its downstream effects could offer new avenues for cancer treatment and immunotherapy. To this end, we generated a human *TL1A* knock-in (B-hTL1A) mouse model. Human *TL1A* gene expression in B-hTL1A mice was confirmed by RT-PCR. TL1A protein expression was not altered following TL1A humanization in B-hTL1A mice as shown by flow cytometry. Lastly, soluble human TL1A was detected in B-hTL1A mice by ELISA. Due to the purported role of TL1A in mucosal immunity, efforts to induce inflammatory bowel disease in this humanized model are currently underway. Taken together, we established a preclinical B-hTL1A mouse model for the evaluation of TL1A-targeted immunotherapy.

#0125 Development of humanized VEGFA models to assess preclinical efficacy of novel therapeutics *in vivo*.

S. Zhang[1], C. Liu[1], J. Guo[1], Z. Shen[1], **J. Jin**[2], B. Huwatibieke[1], Y. Shen[1];
[1]Biocytogen Pharmaceuticals (Beijing) Co., Ltd., Bejing, China, [2]Biocytogen Boston Corp, Waltham, MA

VEGFA is an essential growth factor required for angiogenesis in the context of normal wound healing as well as malignant tissue growth, ultimately facilitating the delivery of oxygen and nutrients to fuel cellular survival, expansion, and repair. VEGFA signaling has also been reported to exert effects on cancer cells and immune cells directly, with evidence suggesting that the pathway can both support tumor growth and inhibit immune surveillance. Thus, targeting VEGFA has been intensely explored as a therapeutic strategy for several cancer indications. Here, we generated a novel humanized VEGFA model (B-hVEGFA mice) to explore the ability of novel VEGFA-targeting therapeutics to curb cancer cell growth and angiogenesis *in vivo*. This was achieved by replacing the murine *Vegfa* gene with the corresponding human *VEGFA* coding region. We confirmed exclusive expression of human VEGF in lung homogenates of the humanized model at levels comparable to murine VEGF quantified in wild-type C57BL/6 mice. Immunohistochemical analysis at 8 weeks of age demonstrates no significant difference in the CD31+ area in several organs of the humanized mice when compared to wild-type C57BL/6 mice, including kidney, heart, liver, and eye. To assess the functional utility of this model in evaluating VEGFA modulators, tumor studies were conducted: murine colon cancer MC38 cells that were also engineered to express VEGFA in a similar manner (B-hVEGFA MC38 cells) were subcutaneously implanted into homozygous B-hVEGFA mice. Treatment with bevacizumab analog essentially abolished tumor growth in the humanized mice, while control tumors continued to expand over the 3 week study. To further evaluate the role of novel combination therapies or bispecific antibodies targeting VEGFA and PD-1, we also generated a triple humanized model expressing human VEGF, PD-1, and PD-L1 (B-hPD-1/hPD-L1/hVEGFA mice) by crossing B-hVEGFA mice with our B-hPD-1/hPD-L1 mice model, which expresses the extracellular domains of human PD-1 and PD-L1. Flow cytometric analysis of this model is currently underway to validate the model for further efficacy testing. Together, these humanized VEGF models provide robust *in vivo* platforms to evaluate novel VEGFA therapeutic candidates.

#0126 Effect of active cytomegalovirus infection on symptoms of fatigue, cancer-related cognitive impairment, and peripheral neuropathy in ovarian cancer survivors.

X. Li, K. Brown, K. Honeyfield, D. Hunter-Schlichting, M. Gruner, D. Teoh, M. Geller, H. Nelson, R. I. Vogel;
University of Minnesota, Minneapolis, MN

Background: Fatigue, cancer-related cognitive impairment (CRCI) and neuropathy are among the most common and distressing side effects reported by individuals treated with chemotherapy for ovarian cancer. Cytomegalovirus (CMV) is a highly prevalent herpes virus infection worldwide, affects inflammation and immune function, and can reactivate with treatment for cancer. This study aimed to explore the associations between active CMV infection and patient-reported symptoms among ovarian cancer survivors who have completed front-line chemotherapy.
Methods: We conducted a cross-sectional study among individuals with a history of a diagnosis of ovarian cancer, primary peritoneal cancer, or fallopian tube cancer from academic and community cancer clinics in Minnesota at any time point after completion of front-line chemotherapy. Participants completed a one-time survey and provided a blood sample. The exposure of interest was plasma CMV DNA level measured using digital PCR, with ≥100 copies/mL of plasma considered active infection (CMV+). We measured symptoms of fatigue (Fatigue Symptom Inventory), CRCI (PROMIS Cognitive Function 8a) and peripheral neuropathy (Functional Assessment of Cancer Therapy/Gynecologic Oncology Group - Neurotoxicity) using validated self-reported measures. Data were analyzed using descriptive statistics and compared by active CMV infection status (CMV+ vs. CMV-) in the full group and by treatment status (receipt of chemotherapy within 30 days prior to data collection) using t-tests.
Results: A total of 160 participants were analyzed. Participants were median of 64.0 years old and 2.3 years from initial diagnosis. Most (75.2%) had advanced stage disease, 43.8% had experienced at least one recurrence, and 40.0% received chemotherapy within 30 days prior to participation. Overall, 40.0% were CMV+, with 40.6% CMV+ among those who received chemotherapy within 30 days and 39.6% CMV+ among those who had not. Participants who were CMV+, compared to those who were CMV-, had overall worse symptoms, with greater symptoms of neuropathy in the full group (11.9±9.2 vs. 9.1±7.8, p=0.04) and particularly greater symptoms of CRCI among those who had recently received chemotherapy (29.2±7.4 vs. 33.2±6.7, p=0.03).
Conclusion: We identified that active CMV infection is common in this survivor population and found that worse symptoms of neuropathy and CRCI are associated with CMV+ status. These results are consistent with studies among other immune-compromised populations, and with further validation, provide a potential therapeutic path for reducing these symptoms.

TUMOR BIOLOGY: Developmental Origins and Drivers of Pediatric Cancer
Poster Session

#0129 Understanding the molecular drivers that regulate Ewing sarcoma cell fate.
D. Truong, D. McCall, C. Agyemang, S. Krishnan, A. Lazar, J. Ludwig;
UT MD Anderson Cancer Center, Houston, TX

Like other translocation-positive sarcomas, Ewing sarcoma (ES) harbors a pathognomonic fusion protein (FP) capable of widespread epigenetic reprogramming that can lead cells to acquire a high-grade, undifferentiated phenotypic state. To better understand how this might occur, we employed a CRISPR knockout (CRISPR-KO) model of A673, targeting exon 4 of the N-terminus EWSR1 portion of the FP and generated a clonal pool (EWSR1 CRISPR KO). We used single-cell RNA and ATAC sequencing (scMultiome) to identify the transcriptional and chromatin changes after the FP knockout (FP KO). We identified several clusters of ES cell heterogeneity. Since the EWSR1-KO is a pooled population, we used known FP-regulated genes to delineate cells bearing the FP KO from wild-type (FP WT) cells. We observed robust expression of FP-activated genes, *PRKCB,* and *LIPI,* in many clusters suggesting regular FP function (FP WT). Conversely, FP-repressed genes, *LOX,* and *IGFBP3* were elevated in a single cluster containing only EWSR1-KO cells. This suggests the FP was successfully knocked out in this cluster (FP KO). That FP KO cluster also lost transcriptional resemblance to ES. A granular identification with cell lines confirmed that all clusters except FP KO were identified as A673 cells. However, the FP KO resembled cell lines with a fibroblastic phenotype. We analyzed enriched motifs and observed no significant difference between the FP KO and FP WT for EWSR1::FLI1. However, the FP KO cells were enriched for motifs in the Fos/Jun family and Smad2/3, which have roles in EMT and mesenchymal differentiation. The FP-KO cells significantly expressed the Fos/Jun family of proteins. Next, we identified peak-gene associations within a ± 500 kb window around the TSS. When we analyzed peaks linked to genes expressed in FP-WT, we found enrichment of the Fos/Jun protein family ($p < 1e-34$), Ets family, and GGAA-microsatellites. However, the FP-KO were strongly enriched for Fos/Jun protein family ($p < 1e-540$) with no change in Ets family motif. Knocking out the FP in the A673 cell line significantly shifted the ES lineage. We observed peaks linked to genes positively associated or regulated by the FP were enriched for Fos/Jun family, Ets family, and GGAA-microsatellites. There may be a cooperative interaction between these TFs that affects the genes linked to the FP. The fact that FP loss enriched the Fos/Jun family motifs, but not Ets family or GGAA-microsatellites, suggests that FP loss activates FP-repressed genes and enables chromatin remodeling to open previously inaccessible DNA binding sites.

#0130 Multi-omic analysis of desmoplastic small sound cell tumors reveal distinct epithelial and neuroendocrine lineages.

D. Truong[1], E. Arslan[1], V. Kochat[1], S. Krishnan[1], C. Agyemang[1], M. Divenko[1], D. Ingram[1], R. Lascano[1], A. Basi[1], J. Gomez[1], H. Beird[1], C.-C. Wu[1], J. Burks[1], P. Futreal[1], A. Lazar[1], R. Ratan[1], N. Daw[1], A. Hayes[2], K. Rai[1], J. Ludwig[1];

[1]UT MD Anderson Cancer Center, Houston, TX, [2]Howard University, Washington, DC

Desmoplastic small round cell tumor (DSRCT) is a rare and aggressive sarcoma subtype that is usually uncurable. All malignant cells harbor a pathognomonic EWSR1::WT1 fusion protein (FP), but FP-targeted agents are nonexistent, and less than 20% of patients survive beyond five years. Lacking the availability of FP-targeted drugs, we seek to understand how the FP regulates tumor cells to promote the characteristic multilineage phenotypes of epithelial and neuroendocrine (NE) cell fates to discover a therapeutic opportunity. Herein, we share the results of gene expression and chromatin accessibility analyses to explore fundamental mechanisms explaining epithelial and NE biology in DSRCT. We profiled 85,640 nuclei from fresh-frozen tissue of nine DSRCT patients post-chemotherapy using single-nucleus RNA-sequencing (snRNA-seq) and ATAC-sequencing (snATAC-seq). A subset of DSRCT patients with low or negative expression of AR expressed partial NE reprogramming, akin to NE prostate cancer (NEPC), exhibiting NE markers (SYP, ENO2, CHG, FOXA2, ASCL1, and SOX2). Another patient subset expressed epithelial markers (MUC1, MUC6, KRT18, KRT23, CDH1). One specimen appeared to exhibit both markers - implying a hybrid or a poorly differentiated phenotype. This suggests that DSRCT could be classified into three subtypes: 1) Epithelial/AR-positive, 2) NE-positive, and 3) hybrid AR/NE. We used CytoTRACE to predict differentiation states. As expected, normal cells (i.e., fibroblasts and immune cells) were the most differentiated. Neoplastic cells, identified by EWSR1::WT1 gene targets and copy number variations, had lower differentiation scores, indicative of a less differentiated phenotype. The NE subtype had the lowest differentiation score indicative of open chromatin and greater plastic capacity, previously implicated in NEPC. SnATAC-seq revealed that the WT1 motif was enriched in malignant cells. Epithelial/AR-positive subtypes were enriched in DNA-response elements for nuclear receptors (ARE, GRE, and PGR) and the forkhead box family of transcription factors (FOXA1, a known pioneer factor for AR). The NE subtype lacked the ARE, GRE, and PGR motifs but was enriched with FOXA1 and neural-specific motifs, including NEUROD1, ATOH1, OLIG2, and NANOG.We show significant heterogeneity in DSRCT phenotypes, where we observe both epithelial and NE lineages. Initially, we detected the Epithelial/AR-positive and NE-positive lineages by gene expression, but the snATAC-seq data also supports this. Although the emergence of the NE subtype in prostate cancer is generally in response to therapy, how it emerges in DSRCT is yet unknown. The CytoTRACE analysis suggests that NE dedifferentiated from the more differentiated Epithelial/AR-positive subtype, but this remains an active area of investigation. Finally, we are working to understand the Epithelial/AR and NE in DSRCT dimorphic states.

#0131 Utilizing human induced pluripotent stem cells (hiPSCs) as a model to study the genetic drivers of rhabdomyosarcoma.

Celeste Romero, Yanbin Zheng, Lin Xu, Stephen Skapek

UT Southwestern Medical Center, Dallas, TX

Rhabdomyosarcoma (RMS) is a childhood soft tissue sarcoma composed of skeletal myoblast-like cells that lack the capacity to differentiate despite their high expression of terminal differentiation markers like myogenin. There are two main types of RMS: fusion-positive RMS (FP-RMS), which is associated with a chromosomal translocation resulting in an oncogenic fusion protein (PAX3-FOXO1), and the more common form, fusion-negative RMS (FN-RMS) which lacks this translocation and is instead thought to be driven by numerous other oncogenes. Our lab used a Bayesian-based computational algorithm to analyze NGS sequencing data from 290 RMS samples and identified 25 potential genetic drivers of RMS. We aim to use induced pluripotent stem cells as a new model to study how these drivers, including the PAX3-FOXO1 fusion gene, influence RMS formation and progression. To this aim, we have successfully made a doxycycline inducible lentiviral vector containing the full-length sequence of human PAX3-FOXO1 which we used to ectopically express PAX3-FOXO1 in two well-characterized iPSC lines. We subcutaneously injected these iPSCs into NOD/SCID mice and treated them with doxycycline to form teratomas, non-malignant tumors containing tissue from all three germ layers. We hypothesized that PAX3-FOXO1 induction in these differentiating teratomas, may have transforming capabilities and may deregulate transcriptional programs to form FP-RMS-like tumors. We have found that PAX3-FOXO1 overexpressing teratomas grew faster and histologically look more “immature” than their control counterparts but do not seem to give rise to rhabdo-like tumors. We want to further understand what other critical factors are necessary to drive RMS formation by focusing on one of our drivers of interest EZH2, a histone methyltransferase implicated as either an oncogene or a tumor suppressor in certain forms of cancer. We have data suggesting that EZH2-dependent histone methylation activity may act as a proto-oncogene with PAX3-FOXO1 to silence the expression of key tumor suppressor genes CDKN2A and CDKN2B in RMS. To this aim, we reasoned that iPSCs differentiated into myogenic progenitors, one of the potential cells of origin of RMS, will be a novel way to study the role of oncogenes like PAX3-FOXO1 and EZH2 in RMS. We have derived myogenic progenitors from iPSCs (iPSC-MPCs) that express key myogenic factors like PAX7 and MYOD and differentiate and fuse to form mature myofibers. We plan to next explore how ectopic expression of EZH2 and/or PAX3-FOXO1 alters gene expression and histone methylation and whether these alterations can drive RMS formation in these iPSC-MPCs. Using this model system of iPSC-MPCs to drive expression of these oncogenes has the potential to offer new and exciting ways to identify the most important genes in driving cancer formation hopefully providing insight into better targets for treatment of RMS.

#0132 DNA-PK inhibition to enhance etoposide therapy in neuroblastoma.

M. Norouzi, B. Zhu, T. Izumi, E. J. Rellinger, B. Evers, P. G. Rychahou;
University of Kentucky, Lexington, KY

Introduction. Neuroblastoma is the most common extracranial solid tumor in children and accounts for ~15% of all pediatric cancer deaths. DNA-PK, a key regulator of repair responses to double-strand DNA breakages induced by radiation or induction chemotherapy is used in the treatment of high-risk neuroblastomas. Here, we have demonstrated that high DNA-PK expression is associated with poor overall survival in a patient population, DNA-PK is highly activated in neuroblastoma cell lines, and inhibition of DNA-PK enhances therapeutic effects of DNA damaging therapies.
Methods. DNA double-strand break damage was induced with etoposide, a topoisomerase II inhibitor. DNA-PK activity was inhibited with peposertib or DNA-PK siRNA. DNA-PK Ser2056 phosphorylation was analyzed in *MYCN* amplified (SK-NDZ, BE(2)-C, LAN-1) and *MYCN* non-amplified (SK-N-AS, SK-N-SH) cell lines. Clonogenic and proliferation assays were used to evaluate the efficacy of peposertib in combination with etoposide in BE-2-C and SK-N-DZ neuroblastoma cell lines. DSB-induced DNA repair was visualized with confocal laser scanning microscopy using γ-H2AX immunofluorescence. Western blot was used to confirm inhibition of DNA-PKcs (pDNA-PKcs S2056) and analyze cleaved PARP expression in combination groups.
Results. DNA-PK inhibition resulted in enhancement of etoposide cytotoxic therapy (BE-2-C IC50 ET = 2.77 ± 0.2, ET+Pep 0.76 ± 0.04; SK-N-DZ IC50 ET = 0.55 ± 0.06, IC50 ET+Pep = 0.11 ± 0.02) in both BE-2-C and SK-N-DZ cell lines. Immunofluorescence analysis detected γH2AX foci increase in the etoposide and peposertib combination group. DNA-PK inhibition in combination with etoposide treatment significantly increased PARP cleavage in BE-2-C and SK-N-DZ cell lines. The effect of DNA-PK knockdown on neuroblastoma cell survival was even more pronounced compared to DNA-PK inhibition with peposertib. DNA-PK knockdown by siRNA alone increased PARP cleavage to the levels comparable to 2 μM etoposide treatment. The combination of etoposide and DNA-PK knockdown enhanced PARP cleavage even further in neuroblastoma cells.
Conclusions. High DNA repair activity is commonly associated with cancer drug resistance. We have shown that DNA-PK activation is continuously supported in both *MYCN* amplified and *MYCN* non-amplified neuroblastoma cell lines. The importance of DNA-PK activity in neuroblastoma cell lines is confirmed with DNA-PK knockdown that leads to apoptosis in MYCN amplifiedneuroblastoma cell lines. In addition, the combination of DNA-PK inhibition or DNA-PK knockdown with DNA-damaging therapies stalled DNA damage response and enhanced neuroblastoma cell apoptosis. These findings demonstrate the significance of high DNA-PK activity in neuroblastoma cells and provide a potent therapeutic strategy to enhance neuroblastoma cell apoptosis with selective DNA-PK inhibition.

#0133 GMDS is a key driver of *MYCN*-amplified neuroblastoma core fucosylation and tumorigenesis.

B. Zhu[1], M. Pitts[1], M. Buoncristiani[1], L. Bryant[1], O. Lopez-Nunez[2], J. Gurria[2], C. Shedlock[3], R. Ribas[3], S. Keohane[3], J. Liu[1], C. Wang[1], M. Gentry[3], N. Shelman[1], D. Allison[1], B. Evers[1], R. Sun[3], **E. J. Rellinger**[1];

[1]University of Kentucky, Lexington, KY, [2]Cincinnati Children's Hospital Medical Center, Cincinnati, OH, [3]University of Florida, Gainesville, FL

Introduction: *MYCN*-amplification (*MYCN*-amp) is a genetic hallmark of ~40% of high-risk neuroblastomas (NBs). N-MYC is an oncogenic transcription factor and master regulator of metabolism. Glycosylation is a major post-translational modification that is critical for cancer progression, spread, and immune evasion. How genetic signatures such as *MYCN*-amp alter glycosylation profiles is unknown. Herein, we utilized matrix-assisted laser desorption/ionization mass spectrometry imaging (MALDI-MSI) to define the N-linked glycome of *MYCN*-amp NBs *in situ* identifying enrichment of core fucosylated glycans. GDP-mannose 4,6-dehydratase (*GMDS*) is the first enzyme responsible for *de novo* GDP-fucose synthesis. We hypothesized that GMDS is a key mediator of NB core fucosylation and tumorigenesis.

Methods: MALDI-MSI was performed on five *MYCN*-amp primary NBs and six *MYCN* non-amplified primary NBs using a timsTOF fleX mass spectrometry imager. Significance analysis of metabolites (SAM) was performed with a q-value <0.05 used to define significance. Kaplan-Meier analysis was performed to determine whether *GMDS* expression correlated with overall survival using the R2 Platform. GMDS blockade was performed using genetic knockdown and chemical inhibition with 2-fluorofucose (2-FF). Core fucosylated glycan abundance was measured by western blotting, ELISA, and flow cytometry using *Aleuria aurantia* lectin. *MYCN* tet-inducible NB cells were used to investigate the interplay of N-MYC and *GMDS* expression. Chromatin immunoprecipitation (ChIP) and luciferase promoter assay were performed to investigate the direct interplay of N-MYC and the *GMDS* promoter. Subcutaneous tumor formation was our measure of *in vivo* tumorigenesis.

Results: MALDI-MSI revealed increased expression of eleven N-linked glycans within *MYCN*-amp NBs, and six of these glycans feature core fucosylation. High *GMDS* expression is associated with poor overall patient survival ($p=3.5x10^{-22}$) and correlates with *MYCN*-amp in human NB tumors ($p=7.4x10^{-27}$). Genetic and chemical inhibition of GMDS blocks core fucosylated glycan abundance and secretion, while impeding NB cell growth and adhesion *in vitro*. Induction and blockade of N-MYC directly correlates with GMDS expression. ChIP and promoter luciferase reporter assay demonstrates direct binding and activation of the *GMDS* promoter by N-MYC. Importantly, GMDS knockdown blocks NB tumor formation ($p<0.01$), and 2-FF impedes established tumor progression ($p<0.05$).

Conclusions: This multi-institutional study utilized MALDI-MSI to reveal that core fucosylated glycans are enriched in *MYCN*-amp NBs. GMDS is a key regulator of NB core fucosylation that is driven by N-MYC. GMDS blockade impairs NB growth *in vitro* and *in vivo*. These critical findings identify *de novo* GDP-fucose production as a metabolic vulnerability that may be exploited in designing novel treatment paradigms for high-risk NBs.

#0134 ZEB2 as a therapeutic target in fusion-positive rhabdomyosarcoma.

A. Fahs, A. Munshi, L. Barbar, S. Zimmerman, C. Counter, C. Linardic;
Duke University, Durham, NC

Rhabdomyosarcoma (RMS) is a highly aggressive childhood soft tissue cancer with skeletal muscle histogenesis. It is classified at the molecular level into fusion-negative (FN) and fusion-positive (FP) subtypes, with FP subtypes being defined by their signature oncofusions between the transcription factors PAX3 (or PAX7) and a variety of 3' partners. Patients with FP-RMS have a five-year survival of &lt30%, and current treatments remain ineffective against the driving oncofusions. To address this challenge, we are interested in identifying proteins that interact with the oncofusions as alternate therapeutic targets, and conducted an unbiased proximity labeling screen for seven of the known RMS oncofusions. This approach revealed that ZEB2 is a common member of the interactome for all seven FP-RMS subtypes. ZEB2 is a DNA-binding transcriptional repressor that interacts with SMAD proteins and is known to be important for coordinating muscle and nerve development during embryogenesis. ZEB2 has been identified as an oncogene in various cancer types such as leukemia, glioblastoma, lung, and breast cancers. Further analysis of ZEB2's expression in FP-RMS cell lines, compared to skeletal muscle and other cancer cell lines, showed significantly higher levels of expression. In silico analyses of genomic CRISPR and RNAi screens in DepMap suggested a strong dependency of FP-RMS on ZEB2, with ZEB2 being one of the top four differential CRISPR dependencies in RMS cell lines compared to all other cancer cell lines. To investigate the functional consequences of ZEB2 suppression, we employed a loss-of-function approach using RNAi (siRNA and shRNA) in human FP-RMS cells. Our experiments confirmed the knockdown of ZEB2 through qRT-PCR and immunoblotting. Interestingly, the extent of ZEB2 knockdown determined whether FP-RMS cells underwent apoptosis or differentiation, potentially towards a neurodifferentiation pathway. We hypothesize that ZEB2 holds potential as a therapeutic target for FP-RMS patients. We aim to elucidate ZEB2's phenotypic role and mechanism of action in FP-RMS tumorigenesis, and assess its value as a therapeutic target *in vivo*. Our long-term goals for this project are to contribute to the development of innovative therapies that can mitigate the oncogenic activity driven by oncofusions in FP-RMS.

#0135 Resolving the tumorigenesis continuum of DICER1 syndrome with novel lineage-trackable genetically engineered mouse model.

J. Zhang[1], S. Chen[1], Y. Moscovitz[1], B. Lynch[1], M. Douglas[1], J. Senz[1], W. Scott[2], M. Underhill[3], Y. Wang[1], D. Huntsman[1];
[1]BC Cancer Research Centre, Vancouver, BC, Canada, [2]Sunnybrook Health Sciences Centre, Toronto, ON, Canada, [3]University of British Columbia, Vancouver, BC, Canada

Background: DICER1 syndrome is a rare cancer predisposition syndrome associated with germline *DICER1* mutations, which develops pulmonary or extra-pulmonary manifestations mostly in pediatric patients. Unlike classic tumor suppressors, the 2nd hit in *DICER1* gene is a missense mutation that renders the RNase IIIb domain defective; therefore, this mutant form of DICER1 is the only protein expressed in these cancer cells, leading to a biased 5p-miRNA production deficiency. Many DICER1 cancers are sarcomas; we therefore postulate the cell of origin is mesenchymal. We recently developed a RNase IIIb-mutant mouse strain and embryonic activation of this mutant along with silencing of the other Dicer1 allele in Mullerian mesenchymal progenitor cells led to the development of tumors resembling sarcomas in human patients. To expand the model and enable lineage tracking, we developed a tamoxifen inducible, tdTomato-trackable, Hypermethylated in Cancer 1 (HIC1)-creERT2 driven transgenic mouse strain. Hic1 marks mesenchymal progenitors. With this strain, we created a model that histologically recapitulates the 3 renal tumors in DICER1 syndrome: cystic nephromas, Wilms tumors, and anaplastic sarcomas. **Objective:** to identify oncogenic events underlying *Dicer1* mutation-driven murine kidney tumor development with single cell RNA-sequencing (scRNA-seq).
Method: To build the tumorigenesis continuum, we harvested kidneys from *Dicer1*$^{+/fl\text{-}D1693N}$ and *Dicer1*$^{fl/fl\text{-}D1693N}$ mice at 1, 3, 6, months post tamoxifen injection, sorted out tdTomato+/CD45-/Epcam- cells, and performed scRNA-seq. Five endpoint tumors were included for analyses. Single cell transcriptomic profiles were integrated and clustered using Seurat to identify cell populations that emerge and expand along the tumor development continuum. Differential gene expression, pathway analysis were conducted to identify genes/oncogenic pathways that are activated along the course of tumor development. Cell differentiation trajectory analysis will be performed using Monocle.
Results: Integration of 5 tumors revealed diverse cell populations: epithelial, mesenchymal, endothelial cells, lymphocytes, and macrophages. We further clustered the mesenchymal population and identified sub-populations such as highly proliferative cells, muscle satellite cells, and terminally differentiated muscle cells. These mesenchymal cells show high expression of blastema markers (Ncam1, Sox11) - a histological component in Wilms tumors. Temporal trajectory of tumorigenesis with time point samples is currently being analyzed.
Conclusion: With scRNA-seq, we begin to unravel heterogeneity of these murine tumors and will identify critical oncogenic events driving the development of DICER1 syndrome-associated cancer, enabling us to utilize this model to develop therapeutic approaches to improve patient management.

#0136 Determining the genomic basis of PAX3-FOXO1 mediated transformation in rhabdomyosarcoma.

B. T. Stevens, Y. Zhang, R. K. Larsen IV, G. E. Adkins, J. D. Hopkins, D. W. Kimbrough, M. R. Garcia, B. J. Abraham, M. E. Hatley;
St. Jude Children's Research Hospital, Memphis, TN

Rhabdomyosarcoma (RMS) is the most common pediatric soft tissue sarcoma. Despite rigorous scientific advances and clinical trials, the survival rate for high-risk RMS has not increased above 20% in the last three decades. A deeper understanding of the basic biology driving RMS tumorigenesis is needed to discover novel therapeutic targets. RMS can be divided into two major histologic subtypes: embryonal RMS (ERMS) and alveolar RMS (ARMS). ARMS accounts for 20% of pediatric cases and has poorer survival. The majority of ARMS tumors harbor t(2;13)(q35;q14) or t(1;13)(p36;q14) chromosomal translocations resulting in the PAX3-FOXO1 (P3F) and PAX7-FOXO1 (P7F) fusion oncoproteins, respectively. ARMS tumors that lack oncofusions more closely resemble ERMS. Classifying on fusion status more accurately describes the disease and highlights the significance of P3/7F. ARMS tumor genomes only contain an average of 6.4 somatic mutations suggesting the oncofusion protein is the key oncogenic driver and a potential candidate for therapeutic intervention. RMS is commonly thought to arise from skeletal muscle progenitor cells that fail to terminally differentiate. However, RMS occurs throughout the body in sites devoid of skeletal muscle, underscoring the potential for alternative cells of origin. Our lab established that endothelial progenitors are indeed a cell of origin for ARMS by generating a genetically engineered mouse model with endothelial cell specific P3F expression coupled with *Cdkn2a* loss. We further generated a human model system derived from *TP53*-null human induced pluripotent stem cells (iPSCs), in which we direct differentiation to endothelial cell fate and then force P3F expression. P3F expression during endothelial cell directed differentiation blocked endothelial maturation and instead reprogrammed cells shifting cell fate to skeletal muscle-like cells that form ARMS tumors in mice. Generation of iPSC-derived ARMS (iARMS) occurs over 15 days and provides a unique model to determine the kinetics and specific genomic contributions facilitated by P3F during RMS transformation. To investigate the genomic changes occurring during iARMS transformation I utilized CUT&RUN for P3F and H3K27ac to assess P3F occupancy and enhancer landscape, ATAC-seq to assess chromatin accessibility, and RNA-seq to assess gene expression changes at timepoints throughout the transformation event. These results define the fundamental genomic changes needed for transformation into FP-RMS by P3F and uncovers the key determinants of ARMS cell identity. The iARMS system provides a unique platform to uncover how P3F establishes and maintains RMS cell state and to dissect the specific dependencies required to maintain the ARMS cell state. Understanding the fundamental mechanism of P3F-driven tumorigenesis could provide greater resolution into the key disease determinants to focus pre-clinical efforts on pivotal targets.

#0137 Increased activity of protein kinase A is sufficient to cause fibrolamellar carcinoma.

M. Shirani, M. Tomasini, S. Levin, s. heissel, H. Molina, Y. De Jong, c. Rice, P. Coffino, B. Lyons, S. Simon;
The Rockefeller University, New York, NY

Tumor cells of almost all patients with fibrolamellar carcinoma (FLC) have a somatic mutation, a ~400 kB deletion on one copy of chromosome 19 that results in a fusion transcript of DNAJB1 to PRKACA, the catalytic subunit of protein kinase A. The resulting fusion oncoprotein, DNAJB1::PRKACA, has kinase activity, and is required and sufficient for transformation. To understand the oncogenesis of this tumor and to help identify potential therapeutic targets, we explored the pathways of pathogenesis mediated by the aberrant kinase. We explored three mechanisms that might explain transformation by the oncogenic kinase:

- A difference in the substrate specificity of DNAJB1::PRKACA kinase versus native PRKACA kinase.
- A difference in the interactome of DNAJB1::PRKACA kinase versus native PRKACA kinase.
- An increase of total catalytic kinase activity (DNAJB1::PRKACA + PRKACA) versus the native PRKACA condition.

We found, comparing cytosolic extracts of tumor and normal liver cells, that there are differences in the substrate specificity of the DNAJB1::PRKACA kinase. Additionally, such comparisons revealed differences in the interactions between the catalytic subunit of the kinase and cytosolic components. We also demonstrated a consistent increase in total PRKACA catalytic subunit in the FLC tumor, relative to the adjacent nontransformed tissue. Further, there is an increase in free, unregulated catalytic activity in the tumor cells and a change in the localization of the catalytic subunit in the tumor cells. Additionally, we have found that this increase in free catalytic activity is sufficient to account for the changes in the transcriptome in tumor cells of FLC patients. Importantly, enhanced expression in hepatocytes of either DNAJB1::PRKACA kinase or native PRKACA kinase caused very similar changes in the transcriptome, and the resultant transcriptomes closely resembled that of tumor cells from FLC patients. This suggests that the DNAJB1 domain is dispensable and not critical for transformation. In our investigation of patient tumors we found two rare and different subclasses of FLC that are indistinguishable from “classic” FLC, based on their transcriptome and based on their drug response profiles. Importantly, both subclasses are associated with changes of PRKACA, but neither involves the DNAJB1 domain. Thus, the DNAJB1 domain is not a critical component of transformation, and the significant driver is an increase of the cellular catalytic activity.

#0138 UCHL5 and PAX3-FOXO1 resolve replication stress in rhabdomyosarcoma.

A. J. Sabnis, P. K. Sahu, Y. Pan;
UCSF - University of California San Francisco, San Francisco, CA

PAX3-FOXO1 positive rhabdomyosarcoma (RMS) is an aggressive pediatric sarcoma with a terrible prognosis. The resultant fusion acts as a chimeric transcription factor, in part remodeling chromatin to inhibit terminal differentiation and maintain cancer cell proliferation. As this oncoprotein is not directly druggable, we have used genetic screens to identify dependencies downstream of *PAX3-FOXO1* to improve our understanding of pathogenesis and develop new therapeutic targets. We performed pooled CRISPRi screening in an isogenic system of a patient-derived RMS cell line with or without knockdown of *PAX3-FOXO1.* Loss of the ubiquitin hydroxylase *UCHL5* led to selective depletion of *PAX3-FOXO1* positive Rh30 cells compared to *PAX3-FOXO1* knockdown cells, suggesting that the fusion creates *UCHL5* dependence. We validated this finding in competition growth assays in additional fusion positive (FP) and fusion negative (FN) RMS cell lines, and observed *UCHL5* dependency only in the former. By contrast, *UCHL5* was dispensable for cell growth and survival in FN RMS cell lines. These data were recapitulated in the large DepMap dataset, which also identified the top genetic co-dependencies of *UCHL5* as INO80-complex (INO80c) members. We therefore investigated whether the fusion selective effects of *UCHL5* were mediated by the INO80c, of which UCHL5 is an N-terminal member. We observed that knockdown of another N-terminal component of INO80c, *NFRKB*, phenocopies the fusion-selective effects of UCHL5 loss. Conversely, the catalytic ATPase *INO80* was pan-essential, suggesting that only N-terminal subunits of INO80c regulate PAX3-FOXO1 specific functions. INO80c plays an essential role in mitigating DNA replication stress. Indeed, loss of *UCHL5* led to DNA damage as measured by γH2AX and slowing of replication forks as measured by fiber assays in FP, but not FN RMS. Unexpectedly, acute degradation of *PAX3-FOXO1* also slowed DNA replication fork speed, suggesting a genetic model in which *UCHL5* and *PAX3-FOXO1* cooperate to resolve replication stress in FP RMS. Finally, *in vivo* experiments using cell line xenografts confirms that loss of *UCHL5* slows the growth of FP RMS, but not FN RMS. These findings suggest that loss of UCHL5 induces replication stress in a fusion-specific manner, and offers both an opportunity to study the mechanisms by which the PAX3-FOXO1 oncoprotein mitigates replication stress, and to develop UCHL5 inhibitors as precision therapies for FP RMS patients.

#0139 Modeling and genomic profiling of osteosarcoma development in murine chondrocyte-origin models.

X. Zhou, H. Beird, Y. Yi, Z. Xu, Z. Zhang, H. Singh, W. Zhang, Y. Wang, S. Jusu, M. Roth, J. Gill, R. Gorlick;
The University of Texas MD Anderson Cancer Center, Houston, TX

Osteosarcoma (OS) manifests during puberty, coinciding with rapid bone growth, a feature requiring exploration. We selectively deleted *p53* or both *p53* and *Rb1* alleles in growth-dependent chondrocyte-origin models, utilizing Col10a1-Cre or Agc-CreERT2, incorporating with ROSA-Tomato for tracing and isolating the mutant cell collection.

Col10p53^{flfl}(tm) and Col10p53^{flfl}Rb^{fl+}(tm) mutants exhibited 100% penetrance in osteoblastic OS, with the latter displaying shortened latencies (mean: 335 vs 265 days) and increased metastases. Tamoxifen-induced AgcCreERT2 models highlighted growth stage-dependent OS development, correlating penetrance inversely and latencies positively with mouse age at tamoxifen treatment. Tumors exclusively occurred in endochondral bones, near growth plates.

Whole-genome profiling of tm$^+$ tumor cells revealed genetic variations, including SNPs, Indels, CNVs, and SVs. CNVs involved genes altered in human OS, emphasizing losses in *Dmd* and gains in *Myc*, *Vegfa*, *Foxm1*, *Akt1*, *Aurkb*, and *Ccen1*. A common CNV (losses, Chr. 10: 34,158,531-34,443,999, Log ratio <-0.05) occurred in all sequenced primary and metastatic samples, with male specimens sharing a loss in the Y chr. p region (approximately 725,200-799,409).

Orthotopic transplantation of tm$^+$ p53$^-$ stromal cells from 4-month-old Col10p53^{flfl}tm mice gave rise to bone tumors and lung migration in wild-type recipients, explicitly establishing the transplanted cells as the direct origin of the cancer precursors within early tm$^+$ p53$^-$ stromal populations. Whole-genome sequencing unveiled a discernible progression of genomic alterations from 1 to 4-month-old tm$^+$ p53$^-$ stromal cells, culminating in donor-derived tumors. Notably, only these specific donor-derived tumors, and not the early tm$^+$ p53$^-$ stromal cells, exhibited the Chr. 10 CNV observed in autochthonous malignancies.

Micro-metastases, identified by fluorescence imaging, were prevalent, alongside macro-metastases (~10% in Col10p53^{flfl}Rb^{fl+}tm and ~25% in AgcCreERT2p53^{flfl}Rb^{fl+}tm cohorts). Notably, amputation of primary OS sites in mice surviving longer revealed larger and more abundant tm+ cell clusters. Some micro-metastases not only expressed signature genes typical of macro-lung metastases but also shared genomic variations with corresponding primaries, including the prevalent loss in Chr. 10. Enhanced immune cell infiltration was evident in lungs hosting micro-metastases, suggesting a potential immune response triggered by pre-tumor early seeding cells.

Murine OS models faithfully replicate human OS features, underscoring chondrocytes as significant contributors to OS cell sources. The inclusion of a tomato reporter enables precise tracking, rendering these models invaluable for studying OS etiology, particularly in unraveling pre-tumor molecular events in both primary and metastatic settings.

#0140 Distinct pathways regulated by activated β-Catenin and YAP in hepatoblastoma pathogenesis.

W. Liao[1], X. Chen[2];
[1]West China Hospital of Sichuan University, Chengdu, China, [2]Hawaii University Cancer Center, Honolulu, HI

Hepatoblastoma (HB) is a rare, yet the most common primary malignant hepatic liver in children. A significantly portion of children with HB have tumors that are not resected at diagnosis, leading to the dismal prognosis in these patients. Concomitant YAP and β-catenin activation could be seen 80% of HB. The signaling pathways regulated by YAP and β-catenin in HB pathogenesis remain unclear. Here, we engineered a inducible HB murine model using hydrodynamic injection to deliver transposon plasmids encoding constitutive YAP and doxycycline (Dox) inducible ΔN90-β-Catenin (*Yap/TRE-β-Catenin*). When fed with Dox, HB formed rapidly in the mice. Upon Dox withdraw, HB regressed over the long term. We analyzed gene expression patterns in mouse HB lesions upon short term Dox withdrawal, i.e, tumors still existed yet ΔN90-β-Catenin was turned off. This approach assisted to identify genes regulated by the activated β-Catenin in HB tumors. We compared these genes with the previously identified YAP regulated genes and found the distinct gene expression programs regulated by YAP and β-Catenin in HB. Specifically, YAP off down-regulated Hippo pathway and up-regulated metabolism-related pathways, whereas β-Catenin off down-regulated protein export, DNA replication pathway and up-regulated immune-related pathways. Finally, we identified ONECUT1 as a gene down-regulated by activated β-Catenin in HB. ONECUT1 expression was down-regulated in human HBs, and co-expression of ONECUT1 strongly suppressed Yap/β-Catenin HB formation in mice. Mechanically, ONECUT1 could regulate proliferation-related downstream signaling. Altogether our studies demonstrated that suppression of activated *CTNNB1* mutations could repress HB progression *in vivo*, and we identified distinct pathways regulated by activated β-catenin and YAP in HB. Suppression of ONECUT1 expression by β-catenin is a key genetic event leading to HB formation.

#0141 A human induced pluripotent stem cell model of KMT2A rearranged leukemia.

E. Guest, M. Vacek, J. Nemechek, I. Pushel, B. T. Thornton, M. Leyda, M. S. Farooqi, J. M. Perry, J. L. Vivian;
Children's Mercy Kansas City, Kansas City, MO

Acute lymphoblastic leukemia in infants (iALL) is a high-risk subtype of childhood leukemia with poor survival outcomes despite intensive therapies. Rearrangement of *KMT2A* (*KMT2A*-r) occurs in 70% of cases and is associated with refractoriness to therapy, early relapse, and rapid leukemia progression. *KMT2A*-r generates a driver fusion oncogene, most commonly *KMT2A::AFF1* in iALL, which leads to epigenetic dysregulation of target gene transcription. iALL with *KMT2A::AFF1* is an unusual cancer in that other somatic mutations are uncommon, there are no known genetic risk factors, and phenotypic switch from lymphoid to myeloid, mixed, or undifferentiated phenotype is common during treatment and particularly resistant to therapies. The cell of origin is thought to be a very early hematopoietic precursor, with transcriptomic studies of iALL blasts showing similarities to hematopoietic stem and progenitor cells (HSPCs), multipotent progenitors and early lymphoid progenitors (ELPs). Unfortunately, research into this rare but devastating disease has been hindered by a lack of appropriate, representative models. Interestingly, *KMT2A*-r originates in HSPCs *in utero* and the age of onset of iALL is a strong prognostic factor, with age younger than six months associated with the highest risk of relapse. However, little is known regarding how *KMT2A*-r subverts early hematopoiesis or drives the severe disease phenotype. In an effort to understand the role of the developmental state of the cell of origin in iALL, we have created a highly controlled induced pluripotent stem (iPS) cell model system of *KMT2A::AFF1* leukemia. Specifically, we engineered human iPS cell lines with doxycycline regulatable expression of *KMT2A::AFF1* fusion and we are employing CRISPR gene editing technology to introduce clinically identified variants of interest. Utilizing directed differentiation, we have produced functional HSPCs from iPS cells. Notably, this model recapitulates hematopoietic ontogeny, with the ability to control iALL induction at specific developmental stages. Following doxycycline treatment, we demonstrate that the cells express *KMT2A::AFF1* fusion transcripts. We are utilizing single cell genomics to investigate transcriptomic changes during hematopoietic differentiation of our *KMT2A::AFF1* iPS cells. We will compare these results to published data sets of single cell RNA sequencing data from healthy fetal HSPCs and to our existing iALL and pediatric *KMT2A*-r ALL single cell sequencing data sets. Our iPS cell based iALL model system provides the opportunity to investigate a range of critical and outstanding questions of iALL disease initiation, progression, and treatment.

#0142 HDAC3 is required for pathognomonic features of Langerhans cell histiocytes.

P. Dimitrion[1], J. Toor[1], J. Ge[1], Q. Wang[1], C. Allen[2], L. Zhou[1], Q.-S. Mi[1];
[1]Henry Ford Health System, Detroit, MI, [2]Baylor College of Medicine, Houston, TX

Langerhans cell histiocytosis (LCH) is an inflammatory myeloid neoplasm that develops due to dysregulated dendritic cell (DC) development and most commonly affects the children with an incidence of 2.6 to 8.9 cases per million individuals per year. $BRAF^{V600E}$, the most common disease-driving mutation, activates the mitogen-activated protein kinase (MAPK) pathway causing pathognomonic features that lead to the accumulation of LCH cells and formation of granulomatous lesions. These features include enhanced myelopoiesis, reduced tissue-egress and acquisition of an oncogene induced senescence-associated secretory phenotype (SASP) (marked by increased expression of anti-apoptotic proteins and inflammatory cytokines). Accumulation of LCH cells can occur in any organ causing a wide range of clinical sequelae, which is directly related to the originating cell bearing the oncogenic mutation. Frontline therapy for LCH involves combination chemotherapy and steroidal anti-inflammatories, or MAPK inhibitors, which have significant toxicity and fail to eliminate disease causing precursors. We have found that HDAC3 is required for epidermal LC homeostasis and hypothesized that LCH cells rely on similar epigenetic factors to LCs. *$CD11c^{Cre}$ LSL-BRAFV600E* (*$BRAFV600E^{CD11c}$*) mice develop severe multifocal LCH with pronounced lesion development in their livers and lungs, hepatosplenomegaly, and a reduced lifespan due to the accumulation of LCH cells. To test our hypothesis, we generated *$BRAFV600E^{CD11c}$ $HDAC3^{fl/fl}$* (*$BRAFV600E^{HD3KO}$*) mice, which produce LCH cells that harbor a conditional deletion in the deacetylase domain of HDAC3. Compared to *$BRAFV600E^{CD11c}$* mice, *$BRAFV600E^{HD3KO}$* mice exhibited significantly less hepatosplenomegaly, reduced lesional burden, and improved survival indicating reduced LCH disease burden. Compared to *$BRAFV600E^{CD11c}$*, flow cytometry showed *$BRAFV600E^{HD3KO}$* had reduced numbers of LCH cells in lungs and livers, which were more apoptotic. We also found decreased frequencies of circulating LCH cells and LCH precursors, indicating that a lack of HDAC3 activity prevents the development of LCH cells. Bone-marrow derived LCH-like cells provide a valuable drug screening tool. We treated Bone-marrow derived LCH-like cells with RGFP966, an HDAC3-specific inhibitor, increased apoptosis indicated by annexin-V and DAPI staining, reduced expression of Bcl-2, increased CCR7 expression, and decreased S6 phosphorylation (an indication of a loss of the SASP), thus inhibition of HDAC3 may prove therapeutically efficacious by abrogating pathognomonic features of LCH cells. Together, our findings identify HDAC3 as a critical epigenetic regulator LCH cell pathophysiology and HDAC3 blockade would address a great need in treatment of patients with LCH. Furthermore, our results indicate that LCH cells rely on similar epigenetic regulators as epidermal LCs despite coming from a different myeloid lineage.

#0143 Molecular profiling of tumor-initiation events in rhabdomyosarcoma uncovers mitochondrial vulnerabilities.

B. Kalita[1], G. Martinez-Cebrian[2], J. McEvoy[3], B. Gordon[3], K. Blankenship[3], A. Karlstorm[3], E. Stewart[3], M. Dyer[3], B. Dynlacht[1];
[1]NYU Langone Health Perlmutter Cancer Ctr., New York, NY, [2]Josep Carreras Leukaemia Research Institute, Barcelona, Spain, [3]St. Jude Children's Research Hospital, Memphis, TN

Background: Alveolar Rhabdomyosarcoma (ARMS) is a very aggressive soft tissue tumor affecting children and adolescents. It is found that pediatric patients with RMS harboring chimeric PAX fusion transcription factors (TFs) exhibit a greater incidence of tumor relapse, metastasis, and poor survival outcome, thereby underscoring the urgent need to develop effective therapies to treat this subtype of childhood cancer.
Methods: We generated a novel ARMS model by stable transduction of myogenic progenitor cells with a cassette encoding the exact PAX3/7-FOXO1 fusion protein found in ARMS tumors. We analyzed genome-wide expression levels with RNA-seq and utilized Cut&Run to map the binding sites of PAX3/7-FOXO1, active histone marks, enhancers, and super-enhancers in our novel model. Hi-C and promoter capture HiC (pCHiC) were also performed to generate 3D chromatin conformation maps in cells expressing the oncogenic TFs. We compared these data with analogous datasets from orthotopic patient-derived xenografts (O-PDXs) of PAX3/7-FOXO1 fusion-positive ARMS tumors from St. Jude and established ARMS cell lines to validate whether our model system recapitulates ARMS tumors. CRISPRi was performed to silence key targets in two representative ARMS cell lines and proliferation was scored after silencing. Next, we found that ARMS tumors displayed anomalies in mitochondrial mass and numbers, metabolic parameters, and membrane potential by performing TEM, Seahorse assays, and FACS-based TMRM and mitotracker Red dye uptake in a panel of ARMS cells and PDX samples. We performed cell viability and colony forming assays in ARMS cells treated with single drugs and combinations of drugs targeting FGFR4 and mitochondrial metabolism.
Results: Our data provide evidence to support muscle progenitors as potential cells-of-origin for ARMS. We showed that rewiring of chromatin architecture mediated by PAX3/7-FOXO1 TFs is evident across established cell lines, primary tumors as well as O-PDXs. By integrating PAX3/7-FOXO1 binding, RNA-seq, and pCHiC data, we identified key promoter-enhancer (P-En) interactions that are erased or established de novo at multiple loci of master TFs like *MYOD*, *MYOG* and *MYCN*. We also identified key regulators of proliferation, including FGFR4, and mitochondrial function that are essential for tumor growth and invasiveness. Our data indicated aberrant and enhanced mitochondrial metabolism in ARMS as well as selective sensitivity to mitochondrial inhibitors in RMS cells. Administration of these inhibitors preferentially inhibited cell viability and clonogenicity in ARMS, and prompted a pre-clinical phase II study to test these inhibitors at St. Jude Research Hospital.
Conclusion: We present a novel treatment strategy leveraging the mitochondrial dependencies of fusion positive PAX-driven tumors which can be exploited for precision therapy in high-risk ARMS.

#0144 Sex bias in neuroblastoma: Worse outcomes for female patients are associated with dysregulation of *DLK1* and *H19*.

Mariya Raleigh[1], Vishwa Patel[1], Lorraine R. Benhamou[2], Xin Shen[1], Dennis A. Sheeter[2], Erika C. Espinosa[2], Niharika Reddy Badi[2], Chase Calvert[2], Garrett Bourne[2], John T. Powers[2]

[1]Division of Pharmacology and Toxicology, College of Pharmacy, University of Texas at Austin, Austin, TX, [2]Department of Pediatrics, Dell Medical School at the University of Texas at Austin, Austin, TX

Neuroblastoma (NB) is a devastating neural crest-derived tumor primarily affects children under five. Forty percent of NB patients are classified as high-risk (HR), and less than half of them survive. HR disease is split into two equally sized groups: one exhibiting genetic amplification of the *MYCN* proto-oncogene (*MA*), and another where *MYCN* is non-amplified (*MNon*). Overall survival (OS) studies are often either poorly annotated or focused on outcomes across the entire patient group, which may mask differential outcomes or biases among NB subgroups. Here we report our assessment of OS among several genetic, histopathological, and sex-based subgroups in three different well annotated NB patient datasets. Our analysis reveals a previously unseen sex-bias in HR *MNon* patients, where female patients have significantly worse OS than males. This disparity carries into stage 4s NB, defined by high survival in infants despite the presence of broadly disseminated disease. In stage 4s patients across two studies, we observe no deaths among males (n=66) and 6 among females (n=48), again marking significantly worse OS in females. Expression analysis comparing male and female HR *MNon* patients identifies *DLK1* and *H19*, two imprinted genes implicated in multiple malignancies, as frequently overexpressed in females. A similar pattern is seen in RNA seq analysis of human *MA* (n=4) and *MNon* (n=4) cell lines. In addition, both *DLK1* and *H19* are associated with worse prognosis in female but not male patients. We also report that depletion of either gene results in reduced growth *in vitro*. Moreover, the NB-related *ATRX* tumor suppressor has been shown to inhibit *H19* via insertion of histone variant *H3.3*. We observe an inverse correlation between *H3.3B* and *H19* expression in female HR *MNon* patients. Further, *H19* levels increase upon *ATRX* depletion in human NB cells, suggesting that *ATRX* indeed regulates *H19* in NB. These findings provide the first evidence of female-biased outcomes in NB and suggest functional involvement of *DLK1*, *H19* and *ATRX*.

#0145 Unraveling SMARCB1 depletion in hiPSC-derived neural crest cells: Implications for ATRT cell of origin.

C. Wang, F. Furnari;
University of California San Diego - UCSD, La Jolla, CA

Atypical teratoid rhabdoid tumors (ATRTs) are highly aggressive pediatric brain cancers that lack standardized treatment regimens and are associated with poor prognoses. Despite being driven by biallelic inactivation of a single gene, *SMARCB1*, ATRTs exhibit three epigenetic subgroups (SHH, TYR, and MYC), each with different clinical outcomes. Like many pediatric brain tumors, ATRTs share the fundamental underlying mechanism of stalled differentiation, suggesting that it may arise from neural progenitor cells that fail to terminally differentiate. However, unlike other brain tumors, ATRTs share molecular similarities with malignancies found outside of the CNS, especially in the kidney and soft tissues. This unique feature implies a putative cell of origin that is not restricted to the CNS: neural crest cells, a transient embryonic cell population that emerges from the neuroectoderm but then migrates throughout the embryo during development. To study SMARCB1 loss in a genetically defined neural progenitor cellular context with isogenic controls, the Furnari lab engineered a doxycycline inducible *SMARCB1* knockdown system into human induced pluripotent stem cells (hiPSCs). After simultaneous *SMARCB1* knockdown with directed neural differentiation, the resulting SMARCB1-depleted neural progenitor cells exhibited transcriptomic profiles that were similar to ATRTs, particularly to the SHH subgroup. Building upon these findings, the engineered hiPSCs were differentiated into neural crest cells using a modified version of a published protocol. Via RT-qPCR, these hiPSC-derived neural crest cells were confirmed to express typical neural crest marker genes and lose expression of *SMARCB1* in the presence of doxycycline. Remarkably, ATP assays demonstrated that neural crest cells that were differentiated without SMARCB1 acquired enhanced proliferation in comparison to those differentiated with SMARCB1 intact. Further work aims to tease apart this proliferative phenotype in the neural crest cellular context via RNAseq, evaluate the impact of cell identity upon subgroup status, and to determine whether SMARCB1 depletion post-differentiation also enhances proliferation. Together, these findings feature the utility of hiPSC-derived models for investigating mechanisms underlying ATRTs to hopefully identify novel subgroup-specific targets.

#0146 Development of a novel pediatric patient-derived xenograft model with THPO and NDUFB3 mutations.

J. Shilyansky, C. J. Chan, K. L. Coleman, M. Leidinger, S. Bhagavathi, A. Sharathkumar, P. Ear;
University of Iowa, Iowa City, IA

Familial myeloproliferative neoplasms (MPN) of childhood are extremely rare and have propensity towards malignant transformation such as leukemia and lymphoma. Due to the rarity of these cases, few cellular and mouse models are available for understanding the tumor biology. Therefore, the molecular mechanisms of malignant transformation remain poorly understood limiting the therapeutic progress to treat these conditions. Here, we report the development of a novel pediatric patient-derived xenograft (PDX) mouse model harboring mutations in the THPO and mitochondrial subunit NDUFB3 genes and characterization of their functions . THPO is a regulator of hematopoiesis and induces trilineage hematopoiesis through HSPC proliferation while NDUFB3 is a subunit of the mitochondrial complex 1. We isolated malignant cells from an enlarged spleen sample and blood sample from a pediatric patient with TPO mediated MPN and established a PDX model (PDX-2333) that recapitulates the patient's disease. Short tandem repeat analyses confirmed an exact match between the PDX-2333 tumors and patient samples. Exome and Sanger sequencing analyses were performed to identify mutations. Immunohistochemistry staining was used for tumor characterization. Wildtype (WT) and mutant forms of NDUFB3 genes were cloned into expression plasmids with a puromycin selection marker and stably transfected in HEK-293 cells. Stable clones of HEK-293 overexpressing WT and NDUFB3 mutants were tested for growth and sensitivity to anti-cancer therapies. We established a novel PDX model of lymphomagenesis harboring unique mutations in *THPO* and *NDUFB3* genes. The *THPO (c.-52C>T)* mutation in upstream open reading frame causes loss of inhibition of THPO mRNA expression. The NDUFB3 (c.23 A>G) mutation results in a change of amino acid from glutamine 8 (E8) to glycine 8 (G8) (Ndufb3_E8) and is highly conserved in many vertebrate species. HEK-293 cell lines stably overexpressing WT or NDUFB3 mutants were tested for growth and their sensitivity to ruxolitinib, a Jak2 inhibitor and doxorubicin, an FDA-approved treatment for leukemia and lymphoma. Our data showed that cells overexpressing Ndufb3_E8 have increased proliferation and are highly resistant to ruxolitinib and doxorubicin in comparison to the WT NDUFB3. Developing a novel pediatric PDX model and exome sequencing allow us to identify novel genes involved in malignant transformation leading to lymphoma development. Our data demonstrated that mutations in the THPO (c.-52C>T) and NDUFB3 (c.23 A>G) genes play a key role in the pathogenesis of a lymphoma and in regulating drug sensitivity.

#0147 Identification of cell sub-populations in Neuroblastoma cell lines with single-cell-sequencing analysis.

Michele Tomanelli[1], Davide Ceresa[1], Adriana Bajetto[2], Paola Modesto[3], Paolo Malatesta[1], Tullio Florio[2], Aldo Pagano[1]

[1]Department of Experimental Medicine, University of Genoa, Italy, Genova, Italy,[2]Department of Internal Medicine, University of Genoa, Italy, Genova, Italy,[3]Istituto Zooprofilattico Sperimentale del Piemonte, Liguria E Valle D'aosta, Turin, Italy

Neuroblastoma is the most frequent extracranial tumor in neonatal patients. Engineering SKNBE2 Myc-N amplified Neuroblastoma cell lines we generated individual clones expressing NDM29 non-coding-RNA at different levels. Using these cell models we documented a specific role of NDM29 in tumor cell differentiation leading to the identification of novel genes to be pharmacologically targeted for an efficient control of tumor malignancy (CA9 and MCM2 genes). Further studies taking advantage of the same models suggested the possible co-existence of different cell sub-populations in the apparently homogeneous cell culture with possible different roles in tumor maintenance and growth. Here we test this hypothesis by performing single-cell sequencing analysis and identified different sub-populations on the base of their gene expression patterns. The characterization of their specific profiles of membrane markers allowed an efficient separation of the individual populations by FACS analysis. Our preliminary results show the co-existance of cells with a marked neural phenotype with other two populations one VEGF secreting and the other VEGF recipient/responder. These preliminary findings suggest further detailed investigations of possible paracrine loops that might be at the base of tumor cell nodule growth and maintenance.

#0148 Multiomic sequencing reveals diversity in clonal landscape and genomic alterations in a lung metastatic PDX osteosarcoma model.

S. Jusu, W. Zhang, Z. Zhang, X. Zhaohui, S. Kannan, Y. Wang, Z. Xin, Y. Yanhua, M. Roth, J. Gill, R. Gorlick;
The University of Texas MD Anderson Cancer Center, Houston, TX

Introduction: Osteosarcoma is a primary malignant bone tumor characterized by the production of spindle cells resulting in immature bone formation. The lung is the most frequent site of metastatic disease and relapse occurs in more than 30 % of patients. Recent results show that relapse is due to a subset of cells with different phenotypic and genetic signatures conferring advantage to drive progression and drug resistance within the intra-tumorally heterogeneous population. Thus, developing a defined in vivo model that can identify the rare genetic subpopulation and recapitulate clonal evolution is crucial. In this study, we used whole exome, barcode and RNA sequencing to characterize the landscape of genomic alterations and also track and identify the clonal subpopulations, clonal and genetic drivers of lungs metastasis.
Methods: We injected barcoded PDX (OS17) cells intravenously in ten SCID mice to track the clonal subpopulation of cells that metastasize to the lungs. Metastasized lung nodules were collected following death or euthanasia. All samples collected were snap frozen in liquid nitrogen and stored at -80^{0}C. DNA and RNA was extracted and analyzed by PCR, NGS, WES and RNA sequencing to map clonality, mutational and evolutionary profiles.
Results: Four (40%) of the mice developed lung metastases with three mice having multiple metastatic lung nodules. Surgery to remove the metastatic nodules was performed 216 ± 55.5 days following tumor cell injection. Nine metastatic lung nodules from three mice were used for sequencing and analysis. A Shannon-Weaver and Jaccard similarity index show a diversity in clonal architecture between the lung nodules. A total of 15,394 somatic variants was identified including 12,547 single nucleotide variants (SNV), 4054 synonymous, 2662 missense, 28 nonsense mutations and 1639 somatic indels. The SNVs accounted for 81% of all variants followed by CNV 11 % and indels 8% respectively. Synonymous and missense mutations were the most frequently observed in all samples. Copy number loss was two-fold compared to copy number gain across all tumors. Furthermore, the deletions span longer genomic distances compared to amplifications. The mutational spectrum showed that the highest substitutions were C>T/G>A followed by T>C/A>G; the least substitutions were T>A/A>T. Also, we identified a large set of genes with genomic aberrations. These include amplifications in VEGF, RB1, RUNX, PARP4, ICAM3, EGFR, BRCA2, COLA6A1, COLA6A2, CCND3, CDKN2D etc.
Conclusions: In the current model, we identified multiple tumorigenic seeding clones and the diverse set of genes mutated in osteosarcoma. Further analysis of the mutational signature resulted in the identification of potential genes that act as drivers in the lung metastatic process. Acknowledgments: Swim Across America, the Foster Foundation and the Barbara Epstein Foundation.

#0149 Modeling patient-specific *CHEK2* genetic variants associated with high-risk neuroblastoma.

X. Xiong[1], S. Cohen-Gogo[2], A. Villani[2], A. Shlien[2], M. S. Irwin[2], M. Hayes[2];
[1]University of Toronto, Toronto, ON, Canada, [2]The Hospital for Sick Children, Toronto, ON, Canada

Background: Neuroblastoma (NB) is the most common extra-cranial solid tumor in children and accounts for approximately 10% of childhood cancer deaths. Recently, next-generation sequencing of patients enrolled in the SickKids Cancer Sequencing (KiCS) program revealed somatic and germline alterations in genes involved in the DNA damage response (DDR). Multiple germline and somatic pathogenic variants in *CHEK2* were detected in patients with NB.
Aims and Methods: To better understand potential roles for *CHEK2* in NB pathogenesis, we are modeling patient-derived *CHEK2* variants in an established transgenic zebrafish model of MYCN-driven NB. Using a CRISPR/Cas9 “knock-in” approach, we have generated stable zebrafish lines that are homozygous and heterozygous for variants of interest with either null, heterozygous, or wild-type *tp53* functional status. We aim to assess tumor incidence, growth, and metastasis using direct visualization of disseminated EGFP+ tumor cells, as compared to MYCN over-expression only control fish. Given potential drug sensitivities, we also plan to assess the efficacy of various DDR pathway inhibitors in combination with frontline chemotherapies, which are effective in the treatment of DDR-deficient adult cancers.
Results: Targeting *chek2* in a *tp53* null background had no significant effect on tumor incidence and growth compared to *tp53* mutant control animals ($p=0.1570$ log-rank test). This contrasts with other patient-specific DDR models including gene targeting *brca2* ($p=0.0235$, log-rank test), *atm* ($p<0.001$, log-rank test), and *bard1* ($p<0.001$, log-rank test), potentially highlighting Tp53-dependent roles for Chek2 in NB formation *in vivo*. Through functional characterization of patient-specific *CHEK2* variants in NB progression, our work will provide important preclinical information that will inform future diagnostics and therapeutic strategies for patients with high-risk NB.

#0150 Transcriptional rewiring of BET inhibitor treated Ewing sarcoma cells augments their dependency on focal adhesion kinase.

S. S. Ganapathi[1], E. Wrenn[1], N. Garcia[1], N. Katiyar[1], A. Miyaki[1], Y. Kang[2], M. Chan[2], T. S. Gujral[2], E. R. Lawlor[1];
[1]Seattle Children's Research Institute, Seattle, WA, [2]Fred Hutchinson Cancer Center, Seattle, WA

Outcomes for patients with recurrent and metastatic Ewing sarcoma (EwS) are dismal and novel therapies are needed. As EwS are initiated and maintained by the EWS::FLI1 transcription factor, agents that target aberrant gene transcription are of interest and bromodomain inhibitors (BETi) have shown promise in preclinical models. Nevertheless, despite initial efficacy, BETi tolerance emerges across tumor types, often via transcriptional rewiring. We reasoned that the therapeutic potential of BETi in EwS could be augmented by identifying and targeting mechanisms of drug resistance. To investigate this, we performed transcriptional and phenotypic profiling of BETi-naïve, responsive, and drug-tolerant (DT) EwS cells and used these data to nominate biologically-informed drug combinations. EwS cells (A673, CHLA10, TC32) were exposed for 72 hrs or 20 days to BMS-986158, a clinical grade BETi being tested in a phase I pediatric clinical trial (NCT0393465). A profound cytostatic effect was observed at 72 hrs but in all cell lines proliferation was restored by 20 days. RNA-seq confirmed reversion of the EWS::FLI1-dependent gene signature at 72 hrs and this was maintained at 20 days, demonstrating continued on-target effects despite restored growth of DT cells. Interrogation of differentially expressed genes between drug naïve, cytostatic, and DT cells indicated that that DT cells had been transcriptionally rewired to more mesenchymal states, with notable upregulation of genes involved in integrin signaling. In support of this, DT populations displayed more fibroblastic morphologies, increased F-actin filaments, and enhanced invasion in collagen-rich 3D culture. In parallel, an unbiased kinase inhibitor screen that exploits mathematical modeling revealed that, while BETi-treated cells were overall more resistant than parent cells to kinase inhibitors, their viability depended on focal adhesion kinase (FAK) activity. Western blot confirmed increased phospho-FAK in DT cells. We next tested BMS-986158 and the FAK-inhibitor Defactinib singly or in combination *in vitro* and *in vivo*. Defactinib induced cell death in 2D cultures and blocked invasion of 3D spheroids in collagen. Conversely, BMS-986158 enhanced invasive potential in 3D. The combination of Defactinib and BMS-986158 in naïve and DT populations was highly synergistic in 2D assays. In 3D collagen assays, viability and invasion of DT tumor spheroids were significantly reduced by the combination. Finally, ongoing studies show that the combination of FAK and BET inhibition prolongs survival of mice with EwS tumor xenografts. Thus, our studies reveal that exposure of EwS cells to BETi induces transcriptional rewiring that activates integrin and FAK signaling, restoring proliferation. This work supports further investigation of FAKi as agents that could prevent or reverse the BETi tolerant state in EwS.

#0151 BMP signaling determines neuroblastoma cell fate and sensitivity to retinoic acid.

M. Pan, Y. Zhang, W. C. Wright, H.-M. Lee, R. H. Chapple, X. Liu, J. Low, D. Currier, A. J. Loughran, D. A. Dyer, S. M. Pruett, B. Freeman, T. Chen, B. J. Abraham, E. Stewart, J. Easton, P. Geeleher;
St. Jude Children's Research Hospital, Memphis, TN

While retinoic acid (RA) has been successfully used for leukemia treatment for decades, the attempt to treat solid tumors with RA remains challenging, with less than 10% of neuroblastoma (NB) patients achieving complete remission when treated with RA alone. It has been believed the anti-cancer activity of retinoids is due to retinoid-induced terminal differentiation, however, what determines cell response or whether differentiation is the main effect of RA has never been fully understood. To better understand RA's activity, we conducted genome-wide CRISPR modifier screens in RA-treated hyper-sensitive NB cell lines. Surprisingly, we found that, in these cells, RA primarily decreased cell viability via apoptosis or senescence, rather than differentiation—activities in which the CRISPR screens strongly implicated bone morphogenetic protein (BMP) signaling. BMP activation promoted apoptosis/senescence and sensitized cells to RA. Conversely, BMP inhibitors and *SMAD9* (a critical transcription factor of the BMP pathway) knockout enhanced RA's ability to induce differentiation but reduced cell sensitivity to RA. Our ChIP-seq and RNA-seq data showed these behaviors were mediated by the coordinated gene regulatory actions of *RARA* and BMP-family SMAD transcription factors. Furthermore, in a panel of 19 cell lines we screened with RA, we assessed the correlations between RA IC50 and the expression of all (~20,000) genes (publicly available data from the GDSC and Depmap). Remarkably, *SMAD9* was the number 1 and number 10 most correlated gene, respectively, with RA IC50 (ranked by Pearson correlation coefficient; GDSC R = -0.92, $P = 4.2 \times 10^{-6}$; Depmap R = -0.81, $P = 4.8 \times 10^{-4}$). We also performed comprehensive large-scale drug screens in these cell lines with combinations of RA and a BMP activator FK506. RA exhibited a synergistic effect with FK506 in all the NB cell lines, very strikingly in some cell lines. All these data suggest BMP signaling is generally required for RA sensitivity and BMP activators are promising candidates in combination with RA to treat NB. Using published bulk and single cell RNA-seq data from NB patient samples, we found BMP signaling activity is relatively low in primary tumors, but well maintained in disseminated NB cells derived from bone marrow. This explains why RA is clinically used as a maintenance therapy and can only successfully treat the minimal residual disease and suggests that tumor microenvironment is a critical factor in determining cell response to RA. Overall, our study revealed that BMP controls NB cell fate and sensitivity in RA treatment. Notably, interactions between BMP signaling and RA are well established in developmental biology, where BMP signaling can tip cell fate decisions between differentiation, apoptosis, and senescence upon exposure to endogenous RA. Our data suggest that this developmental process can be maintained in NB cells, unveiling a novel mode of anti-neoplastic action.

#0152 Exploring the impact of heat shock protein 90 on the antitumor efficacy and stemness in medulloblastoma cells.

S.-M. Chen[1], H.-Y. Huang[1], C.-K. Wang[1], Y.-Y. Yang[1], S.-J. Leu[1], Y.-Y. Li[2];
[1]Taipei Medical University, Taipei, Taiwan, [2]Department of Veterans Affairs, Miami VA Healthcare System, Floria, United States, Miami, FL

Background: Medulloblastoma (MB) is the most common children's malignant brain tumor. Although MB can be treated with conventional chemotherapies, chemoresistance has been frequently developed and thereby hampers their therapeutic effectiveness. The preliminary reports of our research showed that some heat shock proteins have higher levels in MB cells. Among these heat shock proteins, HSP70 and HSP90 expressions are particularly high in MB CD133+ cancer stem cells (CSCs), which arouses our attention and interest. Numerous studies demonstrated that heat shock proteins are prominent in some chemotherapy-resistant cancer cells and CSCs. As known HSP90 and its client proteins are required for the maintenance of self-renewal/stemness and regulation of cell cycle, synergistic killing of cancer cells by simultaneous inhibition of HSP90 expression and activity may be a considerable good therapeutic strategy for treating MB. The purpose of this study is to verify the regulatory function of HSP90 in chemoresistance and stemness of MB.
Materials and Methods: The levels of HSP90, its client proteins (P13K/pAKT, Erk, NFκB, and c-Myc), and stemness makers were detected using immunoblotting and immunoprecipitation after the treatment of HSP90 inhibitor (17-AAG) or knockdown of HSP90 by siRNA in MB and MB CSCs. The antitumor effects of HSPs inhibitors or knockdown of HSPs on these cells were evaluated by MTT assay, Annexin V/PI analysis and cell cycle analysis.
Results: Our findings revealed elevated expression of HSP90 and its target client proteins in MB cells compared to normal astrocytes. Silencing or inhibiting HSP90 expression induced cell cycle arrest in MB cells. Notably, CD133+ MB CSCs exhibited higher HSP90 levels than parental MB cells. Inhibition of HSP90 led to reduced sphere formation and expression of stemness markers in CD133+ MB CSCs. Treatment with 17-AAG demonstrated antitumor activity in CD133+ MB CSCs, and a synergistic effect was observed when combining conventional chemotherapeutic agents with 17-AAG in MB cells
Conclusion: These results illustrated that inhibition of HSP90 could eliminate CSCs, and thereby overcome resistance to chemotherapeutic agents in MB. Chemotherapies in combination with HSP90 blockade may be an emerging MB therapy in the future.

#0153 Noncoding elements of *MYCN* mRNA are powerful drivers on oncogenicity in neuroblastoma.

V. Patel[1], L. Benhamou[2], D. T. Powers[2];
[1]The University of Texas At Austin, Austin, TX, [2]Dell Medical School at The University of Texas at Austin, Austin, TX

Precision in genetic modeling of oncogene-driven cancer is crucial for comprehending disease pathology. Traditionally, models focused on protein expression through open-reading-frame (ORF) transgenes. This approach overlooks post-transcriptional regulation in endogenous mRNAs, which include noncoding elements like 5' and 3' UTRs and introns. All patient oncogene mRNAs encompass these elements, and grasping the collective impact of noncoding and protein coding components may revolutionize our comprehension of cancer origins.Neuroblastoma (NB) is the most common extracranial solid tumor in children. Genetic amplification of *MYCN* (*MA*) in NB results in very high mRNA levels and drives poor prognosis. *MYCN* mRNA is targeted by multiple microRNAs, including *let-7*. We previously demonstrated that in *MA* disease the 3' UTR of *MYCN* can sequester *let-7*, inhibiting its function. *MYCN* mRNA thus also influences genetic patterning in NB by relieving the selective pressure to lose chromosome arms harboring *let-7* loci, an event frequent in *MYCN* non-amplified NB but exceedingly rare in *MA* disease. This work established for the first time that noncoding mRNA elements within an oncogenic mRNA can itself contribute to disease pathology. To further understand the roles of noncoding elements within *MYCN* mRNA, we generated BALB/c 3T3 fibroblasts and murine Neuro-2a cells that express the following transgenes:
1.*MYCN*-ORF: expresses only *MYCN* open reading frame sequence.2.*MYCN*-GL: intact genetic locus of *MYCN*, expresses full length *MYCN* mRNA.3.*M/GFP*-GL: variant of #2 where *MYCN* protein coding sequences are replaced by *EGFP*.
All three constructs demonstrated significantly enhanced *in vitro* proliferation compared to GFP control cells. Notably, cells expressing *MYCN*-GL exhibited best growth in both cell types, despite possessing an intact 3'UTR. Unexpectedly, *M/GFP*-GL cells demonstrated comparable growth to *MYCN*-ORF in 3T3s and significantly outperformed *MYCN*-ORF in Neuro-2a cells. This observation not only validates our prior research on the oncogenic role of the *MYCN* 3' UTR but also extends it by revealing direct contributions to growth advantages, occasionally surpassing even MYCN protein. Syngeneic animal studies mirrored these trends, with *MYCN*-GL and *M/GFP*-GL inducing nearly 100% tumor incidence, surpassing the 57% incidence associated with *MYCN*-ORF. Tumors induced by *MYCN*-GL and *M/GFP*-GL were more than twice the size of those induced by *MYCN*-ORF. These observations underscore that full-length *MYCN* mRNA, encompassing all noncoding elements, serves as a more potent driver of cellular growth and oncogenicity than only MYCN protein expression. These findings have exciting implications for understating neuroblastoma pathology and genetic patterns, with broader implications for other oncogene-driven cancers. We are currently generating transgenic mouse models based on the above three constructs.

#0154 Diffuse midline glioma invasion and metastasis rely on cell-autonomous signaling through a phenotypic switch controlled by BMP7.

M. Bruschi[1], L. Midjek[1], Y. Ajlil[1], S. Vairy[1], M. Lancien[1], S. Ghermaoui[1], T. Kergrohen[1], M. Verreault[2], A. Idbaih[2], C. de Biagi, Jr.[3], I. Liu[3], M. G. Filbin[3], K. Beccaria[4], T. Blauwblomme[4], S. Puget[4], A. Tauziede-Espariat[5], P. Varlet[5], V. Dangouloff-Ros[4], N. Boddaert[6], G. Le Teuff[7], J. Grill[1], G. Montagnac[8], N. Elkathib[8], M.-A. Debily[1], **D. Castel**[1];

[1]Inserm U981, Gustave Roussy, Villejuif, France, [2]Institut du Cerveau, ICM, Paris, France, [3]Dana-Farber Cancer Institute, Boston, MA, [4]Necker Enfants Malades Hospital, Paris, France, [5]GHU Paris Psychiatrie & Neurosciences, Paris, France, [6]Necker Enfants Malades Hospital, Villejuif, France, [7]Gustave Roussy, Villejuif, France, [8]Inserm U1279, Gustave Roussy, Villejuif, France

Diffuse midline gliomas (DMG) are pediatric tumors with negligible two-year survival after diagnosis characterized by their ability to infiltrate the central nervous system. In the hope of controlling the local growth and slowing the disease all patients receive radiotherapy. However, distant progression occurs frequently in DMG patients. Current clues as to what causes tumor infiltration circle mainly around the tumor microenvironment, but there are currently no known determinants to predict the degree of invasiveness. We use patient-derived glioma stem cells (GSCs) to create patient-specific 3D avatars to model interindividual invasion and elucidate the cellular supporting mechanisms. We show that 3D models mirror the invasive behavior of the parental tumors, thus proving the ability of DMG to infiltrate as an autonomous characteristic of tumor cells. Furthermore, we distinguished two modes of migration, mesenchymal and amoeboid-like, and associated the amoeboid-like modality with GSCs derived from the most invasive tumors. Using transcriptomics of both organoids and primary tumors, we further characterized the invasive amoeboid-like tumors as oligodendrocyte progenitor-like, with highly contractile cytoskeleton and reduced adhesion ability. Moreover, we identified the cell-autonomous BMP7-related signaling as a major regulator of DMG motility and invasion, controlling a switch between two migration modalities. Finally, we deciphered MEK, ERK and Rho/ROCK kinases activated downstream of the BMP7 stimulation as actionable targets controlling tumor cell motility. Our findings identify two new therapeutic avenues. First, patient-derived GSCs represent a predictive tool for stratification of patient with increased risk of metastatic progression in order to adapt their irradiation strategies within weeks after diagnosis. Second, autocrine and short-range BMP7-related signaling becomes a druggable target to prevent DMG spread and metastasis.

#0155 Clinico-radiological and histomolecular analyses identify of a new subtype of diffuse midline glioma, H3 K27 and BRAF/FGFR1 co-altered.

L. Auffret[1], Y. Ajlil[1], A. Tauziede-Espariat[2], T. Kergrohen[1], C. Puiseux[3], L. Riffaud[4], P. Blouin[5], A.-I. Bertozzi[6], P. Leblond[7], K. Blomgren[8], S. Froelich[9], A. Picca[10], M. Touat[10], M. Sanson[10], K. Beccaria[11], T. Blauwblomme[11], V. Dangouloff-Ros[11], N. Boddaert[11], P. Varlet[2], M.-A. Debily[1], J. Grill[1], **D. Castel**[1];
[1]INSERM U981, Gustave Roussy, Villejuif, France, [2]GHU Paris psychiatrie & neurosciences, Paris, France, [3]Rennes University Hospital, Rennes, France, [4]Rennes University Hospital, Villejuif, France, [5]CHRU de Tours, Tours, France, [6]Hopital des Enfants, Toulouse, Toulouse, France, [7]Centre Leon Berard, Lyon, France, [8]Karolinska University Hospital, Stockholm, Sweden, [9]Hopital Lariboisiere AP-HP, Paris, France, [10]Institut du Cerveau, ICM, Paris, France, [11]Necker Enfants Malades Hospital, Paris, France

Diffuse midline gliomas (DMG) H3 K27-altered are incurable grade 4 gliomas and represent a major challenge in neuro-oncology. This tumor type is now classified in four subtypes by the 2021 edition of the WHO Classification of the Central Nervous System (CNS) tumors. However, the H3.3-K27M subgroup still appears clinically and molecularly heterogenous. Recent publications reported that rare patients presenting a co-occurrence of H3.3K27M with *BRAF* or *FGFR1* alterations tended to have a better prognosis. To better study the role of these co-driver alterations, we assembled a large pediatric and adult cohort of 29 tumors H3K27-altered with co-occurring activating mutation in *BRAF* or *FGFR1* as well as 31 previous cases from the literature. We performed a comprehensive histological, radiological, genomic, transcriptomic and DNA methylation analysis. Interestingly, unsupervised t-distributed Stochastic Neighbor Embedding (tSNE) analysis of DNA methylation profiles regrouped $BRAF^{V600E}$ and all but one $FGFR1^{MUT}$ DMG in a unique methylation cluster, distinct from the other DMG subgroups and also from ganglioglioma (GG) or high-grade astrocytoma with piloid features (HGAP). This new DMG subtype harbors atypical radiological and histopathological profiles with calcification and/or a solid tumor component both for $BRAF^{V600E}$ and $FGFR1^{MUT}$ cases. Contrary to other DMG, these tumors occur more frequently in the thalamus (70% for $BRAF^{V600E}$ and 58% for $FGFR1^{MUT}$) and patients have a longer overall survival with a median above three years. The analyses of a H3.3-K27M $BRAF^{V600E}$ tumor at diagnosis and corresponding *in vitro* cellular model showed that mutation in *H3-3A* was the first event in the oncogenesis, indicating a distinct oncogenesis from classical DMG despite an identical founder H3K27 alteration, and possible subclonal evolution.In conclusion, *DMG, H3 K27 and BRAF/FGFR1 co-altered* represent a new subtype of DMG with distinct genotype-phenotype characteristics, which deserve further attention with respect to trial interpretation and patient management. Our work also lays the foundations for therapeutic development highly-needed against this deadly disease.

TUMOR BIOLOGY: Macrophages, Neutrophils, and NK Cells in Cancer
Poster Session

#0159 LYVE-1-expressing macrophages modulate the hyaluronan-containing extracellular matrix in the mammary stroma and contribute to mammary tumor growth.

A. K. Elfstrum, A. H. Rumahorbo, B. M. McCluskey, K. L. Schwertfeger;
University of Minnesota, Minneapolis, MN

Macrophages represent a heterogeneous myeloid population with diverse functions in normal tissues and tumors. While macrophages expressing the cell surface marker lymphatic vessel endothelial hyaluronan receptor 1 (LYVE-1) have been identified in stromal regions of the normal mammary gland and in the peri-tumoral stroma, their functions within these regions are not well-understood. Using a genetic LYVE-1^+ macrophage deletion mouse model, we demonstrate that loss of LYVE-1^+ macrophages is associated with altered extracellular matrix remodeling in the normal mammary gland and reduced mammary tumor growth in vivo. In further studies focused on investigating the functions of LYVE-1^+ macrophages in the tumor microenvironment, we demonstrate that LYVE-1 expression correlates with an increased ability of macrophages to bind, internalize, and degrade hyaluronan. Consistent with this, we show that deletion of LYVE-1^+ macrophages correlates with increased hyaluronan accumulation in both the normal mammary gland and in mammary tumors. Analysis of single cell RNA sequencing of macrophages isolated from these tumors reveals that deletion of LYVE-1^+ macrophages in tumors drives a shift in the majority of the remaining macrophages towards a pro-inflammatory phenotype, as well as an increase in $CD8^+$ T cell infiltration. Together, these findings demonstrate that LYVE-1^+ macrophages represent a tumor-promoting anti-inflammatory subset of macrophages that contributes to hyaluronan remodeling in the tumor microenvironment.

#0160 FGFR1+ cancer associated fibroblasts (CAFs) produce an extracellular matrix (ECM) that curbs infiltration of phagocytic tumor-associated macrophages (TAMs)..

N. Di Siervi, M. Revuelta, N. Zamponi, G. Inghirami, L. Cerchietti;
Weill Cornell Medicine, New York, NY

About 40% of diffuse large B-cell lymphoma (DLBCL) pts do not respond to immunochemotherapy. In human and murine models, we and others have shown that the lymphoma microenvironment (LME) changes with disease progression and treatment resistance. This lymphoma cell-LME co-evolutionary process results in expansion of treatment-resistant lymphoma cells as well as reduced infiltration of T cells and reprogramming of CAFs and TAMs into immune suppressive entities. Our analysis of relapse or refractory (RR)-DLBCLs showed not only an immune depleted LME but also an enrichment of CAFs harboring activation of fibroblast growth factor receptor (FGFR1+). Since FGFR1 inhibitors (FGFR1i) are clinically available, we sought to determine its anti-neoplastic effect on DLBCL. We first confirmed that lymphoma cells, including murine and human, and primary and RR-DLBCLs, did not express FGFR1. Accordingly, no anti-tumoral effect was detected when the selective FGFR1i SSR128129E was administered in vitro to a lymphoma cell panel. However, oral administration of FGFR1i to pre-clinical lymphoma models including two RR-DLBCL patient-derived xenografts (PDX) and four syngeneic murine models representing distinct DLBCL genetic subtypes produced a significant anti-lymphoma effect in all cases. In addition to decreased lymphoma cells, we observed increase in the ECM and TAM infiltration, even in the murine models, suggesting that FGFR1i reprogrammed the CAFs. We thus conducted matrisome analysis (i.e., ECM proteomics) in a murine model (p53 mutant) and found a significant up-regulation of proteoglycans and the immune active glycoproteins decorin, lumican and byglican (q-value <0.05 vs. vehicle). To determine whether these ECM changes affect lymphoma cells, we performed 3D co-cultures of lymphoma cells embedded into de-celularized ECM obtained from FGFR1i vs. vehicle mice. We found that FGFR1i-ECM (vs. vehicle-ECM) modifies the secretome of lymphoma cells by upregulating several cytokines including IL6, IL16 and TNF-alpha. To further characterize the functional state of CAFs and TAMs, we conducted single cell RNA-seq in the two RR-DLBCL PDXs treated as before. We found that FGFR1-CAFs in the LME of FGFR1i tumors (vs. vehicle) were reprogrammed into inflammatory-like CAFs characterized by the expression of several monocyte/macrophage chemotactic factors including CCL2, CCL7, CXCL3, and CXCL12. Consequent with these findings we not only observed an increase infiltration of TAMs in the LME of FGFR1i tumors but also that they were reprogrammed in phagocytic phenotypes. In sum, our results suggest that CAF-FGFR1+ produce an immune “silent” ECM that characterizes RR-DLBCL while FGFR1i reverses this ECM phenotype ultimately resulting in the infiltration of antitumoral TAMs, delineating a novel ECM-directed therapeutic approach for this disease.

#0161 Aged mice decelerate bone metastasis of prostate cancer by decreasing infiltration of M2 macrophages.

X. Zhang, W. Yu, X. Huang, Y. Lu, J. Zhang;
Southern University of Science and Technology, Shenzhen, China

Bone metastasis is a major contributor to the mortality of patients with prostate cancer and results in the development of an immunosuppressive microenvironment in the bone marrow. While advanced age increases the risk of bone metastasis, effects of age-related changes on immune microenvironmental homeostasis are not yet clearly understood. To investigate interactions between cancer cells and the immune microenvironment in elderly individuals, we utilized murine-derived specific bone metastatic prostate cancer cells (RM1-BM), which we had previously isolated from bone metastatic mice and transfected with a luciferase-based reporter gene. We then injected the cells into the left ventricle of both 3–6 months and 22–24 months, male, wild-type mice to induce bone metastasis, using age-matched mice injected with PBS as a control. We employed *in vivo* imaging to compare the metastatic levels in both groups of mice every other day. On day 14, we extracted bone marrow cells for CyTOF analysis and femurs and tibias for Hematoxylin and Eosin staining. Interestingly, our preliminary results demonstrated that healthy aged mice exhibited a lower susceptibility to develop bone metastasis when compared to their younger counterparts. A further investigation of the immune subtypes revealed an increase in the percentage of macrophages in $CD45^+$ immune cells in young mice that developed bone metastasis as opposed to age-matched controls. However, the percentage decreased in aged mice, going from 12.20% to 9.92% (p = 0.001). Lastly, macrophages were isolated from the bone marrow of 3–6 months and 22–24 months old mice and were co-cultured with ovalbumin-transfected RM1-BM cells (RM1-BM-ova) *in vitro* for 24 hours. The flow cytometry results indicated that both groups consist mainly of $CD206^+$ (M2) macrophages. Nonetheless, those obtained from aged mice exhibited reduced ovalbumin presentation capability while maintaining a steady level of type I major histocompatibility complex (MHC-I). These findings suggested that increased infiltration of pro-inflammatory M2 macrophages within the tumor microenvironment may contribute to the bone metastasis of prostate cancer. Therefore, inhibiting M2 macrophages recruitment to the bone marrow microenvironment may prove a useful approach for treating patients with prostate cancer bone metastasis. This study was supported by the NSFC projects (81972420, 81972766, 82173336), and grants from the Shenzhen Science and Technology Innovation Commission (JCYJ20190809161811237, JCYJ20210324104214040).

#0162 Fatty acid synthesis blockade synergizes with immune checkpoint blockade by repolarizing macrophages and enhancing anti-tumor cytotoxicity in gastric cancer.

H. Wang, T. Shi, Y. Wang, Y. Luo, Y. Pan, X. Zhou, Y. Zhang, B. Liu, J. Wei;
The Comprehensive Cancer Centre of Drum Tower Hospital, Medical School of Nanjing University & Clinical Cancer Institute of Nanjing University, Nanjing, China

Background: Immune checkpoint blockade (ICB), which unleashes potent $CD8^+$ T cell-based anti-tumor responses, has emerged as a promising therapeutic option for several cancer types. However, response rates stay limited in gastric cancer (GC) patients, indicating the necessity of combinational strategies to overcome other immunosuppressive factors. Fatty acid synthesis (FAS) is an indispensable metabolic pathway proven to support cancer cell survival. The rate-limiting enzyme of FAS, FASN, is upregulated in several cancers and could contribute to cancer immune escape. Though some investigations propose that specific gene alterations can cause FASN upregulation under the GC setting, the immunoregulatory role and therapeutic value of FASN in the tumor microenvironment (TME) of GC have not been fully elucidated.
Methods: FASN expression was measured by Western Blotting and flow cytometry. Bioinformatic analysis was conducted via an online website (www.camoip.net). The syngeneic GC mouse model was established by subcutaneous inoculation of MFC cells in 615-line mice, treated by vehicles, FASN inhibitor (FASNi), anti-PD-1 antibodies, or FASNi+anti-PD-1 antibodies. TAM and $CD8^+$ T cell depletion was implemented by anti-CSF1R and anti-CD8α antibodies. Bone marrow-derived macrophages (BMDMs) were extracted from the femurs of 615-line mice, induced by M-CSF and stimulated by LPS or IL-4. The proportions and functional status of immune cells were identified by flow cytometry.
Results: FASN was upregulated in GC tissues and GC human cell lines. Bioinformatic analyses demonstrated that FASN expression was related to poor infiltration of cytotoxic lymphocytes, as well as the downregulation of pathways related to anti-cancer immune responses. FASNi inhibited tumor growth in a syngeneic GC mouse model, with elevated PD-1 and IFN-γ expression in $CD8^+$ T cells and increased NK cell infiltration, suggesting the enhancement in anti-cancer cytotoxicity. Meanwhile, FASNi induced a shift from M2-like to M1-like in tumor-associated macrophages (TAM). We detected that M2-like TAM and $CD8^+$ T cells harbored higher FASN expression than other immune cells in GC mouse tissues, and tumor-suppressing effects of FASN inhibition could be reversed by TAM and $CD8^+$ T cell depletion, which corroborated the key role of TAM and $CD8^+$ T cells in shaping FASN-mediated tumor regulation. FASNi could also repolarize BMDMs from M1-like to M2-like *in vitro*. Finally, FASNi exhibited synergistic tumor control with anti-PD-1 therapy in GC and melanoma mouse models.
Conclusion: This work sheds light on the impact of FASN on TME modulation of GC. We proved that FASNi could repolarize M2-like TAM to M1 phenotypes and promote cytotoxic lymphocyte-mediated anti-tumor immunity. Our results propose FASN inhibition as a potential therapeutic strategy to sensitize ICB therapy in GC.

#0163 Role of macrophages in the development of ovarian cancer stem-like cells during chemotherapy.

L. S. Cruz, D. Stevenson, M. Robinson, S. Mathew, I. Amador, G. Jordan, C. D. House;
San Diego State University, San Diego, CA

Ovarian cancer is a poorly understood disease with 75% death rate when identified after metastasis. Drug resistance and tumor recurrence are likely due to cancer stem-like cells (CSCs) that evade chemotherapy and induce relapse with phenotypes that are distinct from bulk tumor cells. It remains unclear how CSCs facilitate relapse and what role the tumor microenvironment (TME) plays in this process. Our preliminary data show that a secreted cytokine, tumor necrosis factor-like weak inducer of apoptosis (TWEAK), and its receptor Fn14 are overexpressed in ovarian tumors and increase after chemotherapy. TWEAK is a strong inducer of stem cell features and enhances survival of CSCs during chemotherapy exposure. The source of TWEAK has not been clarified, although clinical data from human ovarian tumors show that TWEAK mRNA was primarily observed in a subset of infiltrating immune cells known as tumor associated macrophages (TAMs). When we evaluated TWEAK expression in cells found in the ovarian TME, including PBMC and THP-1-derived macrophages, IMR-90 activated fibroblasts, and ovarian cancer cell lines, we found that PBMC macrophages were the primary source of TWEAK production. Since cytotoxic chemotherapy can enrich for different TAM populations, we propose that TWEAK producing TAMs support CSC survival and expansion and contribute to the high rate of relapse in ovarian cancer patients. We further found that treatment with a small molecule inhibitor of TAM polarization leads to decreased TWEAK production, fewer CSCs, and prolonged remission in mouse models of ovarian cancer relapse as compared to vehicle. Currently we are testing whether knockout of Fn14 in ovarian cancer cells co-cultured with TAMs reduces stem cell features dependent on TWEAK-Fn14 signaling. Identification of immune populations responsible for TWEAK production could lead to new therapeutic strategies for patients with high rates of relapse.

#0164 Genetic elimination of β-catenin using a doxycycline-regulated GEM model fails to restore checkpoint blockade efficacy due to persistent M2-like macrophages.

A. Cabanov, R. Tonea, J. Shapiro, A. Martinez, Y. Zha, T. F. Gajewski;
University of Chicago, Chicago, IL

Response to checkpoint blockade immunotherapy (CBI) is not universal, partly due to a wide variation in baseline immune cell infiltration in the tumor microenvironment (TME). One mechanism contributing to this variability is tumor cell-intrinsic activation of the β-catenin signaling pathway, which has previously been shown to result in a non-T cell-inflamed TME. Constitutive β-catenin signaling resulted in reduced Batf3-lineage dendritic cell (cDC1) recruitment, leading to reduced T cell activation and infiltration and loss of anti-CTLA-4+anti-PD-L1 therapeutic efficacy. Efforts to target the Wnt/β-catenin pathway to enhance immune responses in β-catenin-active tumors have seen limited success. A genetic experiment eliminating β-catenin expression after establishment of a non-T cell-inflamed TME might illustrate the maximal biologic effect that could be expected with blockade of the pathway. We developed a genetically engineered mouse (GEM) model that allows for dynamic regulation of β-catenin on and off. This model employs tyrosinase-driven tamoxifen-regulated Cre-recombinase to activate the BRAF V600E oncogene and delete the tumor suppressor gene PTEN, along with a transactivator for doxycycline-regulated expression of a non-degradable β-catenin. Topical application of 4-hydroxytamoxifen resulted in melanoma formation, and administration of doxycycline resulted in robust nuclear expression of melanocyte-specific β-catenin compared to non-treated controls. This was accompanied by a significant reduction in $CD3^+$ T cell infiltration within the TME, confirming the link between active β-catenin signaling and T cell exclusion. Discontinuing doxycycline treatment led to complete reduction of nuclear β-catenin expression in the tumor cells within seven days and a substantial return of $CD3^+$ T cells into the TME. However, despite the re-infiltration of $CD3^+$ T cells, the tumors previously expressing β-catenin (ex-β-catenin tumors) did not regain therapeutic responsiveness to anti-CTLA-4+anti-PD-L1. Single cell RNA sequencing of the ex-β-catenin tumors indicated the presence of an immunosuppressive-like macrophage population, characterized by the expression of Ccl8, Gas6 and Cd163. This finding suggests that the prior presence of β-catenin may induce long-lasting changes in the TME that suppress the immune response even after β-catenin levels are reduced. These data corroborate previous findings on the role of β-catenin in modulating the immunological landscape of melanoma and extend it by demonstrating the long-term persistence of immune evasion by suppressive myeloid cells even after β-catenin signaling is eliminated. These insights have implications for clinical strategies aiming to block Wnt/β-catenin signaling, which may additionally require myeloid cell modulation to restore immunotherapy efficacy.

#0165 PVRL2 upregulation by tumor-associated macrophages confers a regulatory phenotype and is associated with poor prognosis in high-grade serous ovarian cancer.

K. Murakami, H. Ando, M. Doucet, D. Ding, W. Huang, S. Ganguly;
Johns Hopkins University School of Medicine, Baltimore, MD

Advanced or recurrent high-grade serous ovarian cancer (HGSOC) are associated with poor prognosis. While HGSOC is moderately immunogenic, anti-PD-1/L1 therapy has fared poorly in trials. PVRL2 (Nectin2) is both a cell-adhesion molecule as well as a ligand for PVRIG, a novel co-inhibitory receptor. While PVRL2 is constitutively expressed by epithelial/tumor cells, it can also be upregulated by macrophages. Whether macrophage-expressed PVRL2 functions exclusively as an immunoregulatory ligand in HGSOC is not known. $CD45^+$ tumor infiltrate from 6 treatment-naïve and 3 neoadjuvant chemotherapy-treated patients with HGSOC was evaluated by CITE-seq. Multiplex immunofluorescence (mIF) of PanCK, CD68 and PVRL2 was performed on 28 FFPE sections. *In vivo*, we monitored survival of wild-type and $PVRL2^{-/-}$ mice as well as corresponding bone marrow chimeras orthotopically implanted with ID8-Vegf-Defb29 ovarian tumors. CITE-seq was run on $CD45^+$ cells sorted from wild-type vs $PVRL2^{-/-}$ tumors and ascites. In tumor-bearing mice, macrophages, CD8 or NK cells were depleted and differences in survival assessed. *In vitro*, M1 and M2 macrophages were differentiated from steady-state bone marrow progenitors and myeloid gene profiles were analyzed. CITE-seq of patient-derived immune cells revealed that PVRL2 expression was restricted to macrophage clusters. Macrophages with low PVRL2 expression showed M1 polarity and abundant expression of inflammatory cytokines and chemokines. Overall macrophage counts and PVRL2 expression were lower in post-chemotherapy cases. In mIF, PVRL2 staining was observed on CD68-positive cells as well as tumor cells. In addition, PVRL2-expressing macrophages accumulated in tumor areas, especially in residual tumor areas after chemotherapy. $PVRL2^{-/-}$ mice and PVRL2 bone marrow chimeras had significantly improved survival compared to their respective control cohorts. Macrophage depletion significantly shortened the prognosis of $PVRL2^{-/-}$ mice compared to wild-type mice. In contrast, depletion of CD8 T cells or NK cells had no effect on survival of wild-type and $PVRL2^{-/-}$ mice. M1 macrophages from $PVRL2^{-/-}$ mice expressed higher levels of inflammatory cytokines and chemokines compared to their wild-type counterparts. Furthermore, CITE-seq showed that tumor-infiltrating macrophages in $PVRL2^{-/-}$ mice exhibited M1 polarization compared to those from wild-type tumors. However, the inflammatory phenotype appeared to be linked more with the tumor-infiltrating macrophages than with ascites macrophages. In conclusion, our research suggests that PVRL2 upregulation by tumor-infiltrating macrophages polarizes towards a pro-tumor phenotype and affects prognosis of HGSOC. PVRL2-deficient macrophages exert their antitumor effects via inflammatory tumor killing and not via antigen-presentation to effector T cells.

#0167 Modulation of PD-1/PD-L1 by simvastatin in TNBC and macrophages and its impact on the efficacy of immunotherapy.

S. Lee[1], J. Kim[2], A. Park[1], J. Baik[1], J.-J. Jung[3], H.-B. Lee[2], W. Han[1];

[1]Seoul National University Graduate School, Seoul, Korea, Republic of, [2]Seoul National University Hospital, Seoul, Korea, Republic of, [3]Seoul National University College of Medicine, Seoul, Korea, Republic of

Introduction: Statins, known as inhibitors of HMG-CoA, not only reduce cholesterol but also exhibit pleiotropic effects which include anti-tumor activities by targeting tumor microenvironments. They inhibit the synthesis of FPP and GGPP, which is important for prenylation of signaling proteins. Although PD-1/PD-L1 inhibitors has been approved for treatment for TNBC patients with PD-L1 positive, the response remains unsatisfactory. Also, it has been reported that statins affect PD-L1 expression in other tumors, but it is still uncertain in TNBC. Therefore, we aimed to identify the effect of statins on the expression of PD-L1 in TNBC and to verify the efficacy of combination therapy with statins and immune checkpoint inhibitors.

Methods: Human and mouse TNBC cell lines, mouse macrophage cell line (RAW 264.7), and clinically approved simvastatin were used. Flow cytometry, western blot, proliferation assay, qRT-PCR, immune phenotyping and immunohistochemistry were conducted. A co-culture of macrophages and cancer cells was performed. An orthotopic syngeneic mouse model by injection of EMT6 cells into mammary gland fat pad were produced. Mice were treated with simvastatin(20mg/kg) by oral gavage daily and anti-PD-1(200μg) by intraperitoneal injection two times per week.

Results: Among thirteen human TNBC cell lines, we confirmed that TNBC cell lines showed various PD-L1 expression, and especially MDA-MB-231 and HCC38 highly expressed endogenous/constitutive PD-L1. Statins reduced PD-L1 expression and exerted anti-proliferative effects in MDA-MB-231, HCC38, and EMT6 in a dose- and time-dependent manner. Phosphorylation of AKT and STAT3 was reduced when simvastatin was treated. Mice with combination therapy of anti-PD-1 and simvastatin had less effective inhibitory effect on tumor growth than mice with anti-PD-1 monotherapy, which showed the highest tumor suppression effect. In immune phenotyping, tumor-infiltrated T cells did not have significant differences among groups. However, M1:M2 macrophage ratio was highest in anti-PD-1 group but decreased in combination therapy group with simvastatin. To determine the effect of simvastatin on macrophages, RAW264.7 cells were stimulated with MDA-MB-231 conditioned medium, revealing an upregulation of PD-1 expression.

Conclusions: Our findings show that simvastatin has an anti-tumor effect, which reduces Pd-L1 expression and kills breast cancer cells, reducing phosphorylation of STAT3 and AKT. However, when combined with PD-1 checkpoint inhibitor, it reduces the anti-tumor effect by increasing PD-1 expression in macrophages and promoting M1 to M2 polarization. Further study is needed to demonstrate the mechanism by which simvastatin regulate polarization of macrophages and to confirm the polarization of macrophages in samples of TNBC patients who had been taking simvastatin.

#0169 Prevalence, immune checkpoint expression and spatial interplay of intraepithelial lymphocytes, macrophages, and dendritic cells in 4740 human carcinomas.

Z. Huang[1], T. Mandelkow[1], J. H. Muller[1], A. H. Marx[2], T. Krech[3], G. Sauter[1], J. Ebner[1], M. Lennartz[1], R. Simon[1], M. Kluth[1], C. Hube-Magg[1], S. Minner[1], E. Bady[1], N. C. Blessin[1];

[1]University Medical Center Hamburg-Eppendorf, Hamburg, Germany, [2]Academic Hospital Fuerth, Fuerth, Germany, [3]Clinical Center Osnabruck, Osnabruck, Germany

Background: Although there is raising evidence that the density and the level of immune checkpoint expression of immune cell subpopulations that are in direct contact to the tumor cells (intraepithelial) can predict response to immune checkpoint therapy and patient's outcome, a comprehensive assessment of intraepithelial immune cell subpopulations and their spatial interplay is lacking.

Material and methods: To comprehensively assess the density, level of immune checkpoint expression, and spatial interplay of 48 immune checkpoint expressing intraepithelial leukocyte subpopulations in 46 carcinoma entities, 4740 tumor samples in a tissue microarray format were stained with 21 antibodies using our BLEACH&STAIN mfIHC approach. A deep learning-based framework comprising 18 different convolutional neuronal networks (U-Net and DeepLabv3+) were used for image analysis.

Results: The mean intraepithelial immune cell density of $CD8^+$ cytotoxic T-cells, $CD4^+$ T-helper cells, $FOXP3^+$ Tregs, $CD20^+$ B-cells, M1/ M2 macrophages and $CD11c^+$ dendritic cells varied markedly between tumor entities and individual tumors. For example, 88 (±90) cells/ mm^2 were found in tubular breast cancer, 661 (±729) cells/ mm^2 in colorectal cancer, and 1280 (±1334) to 2325 (±2131) cells/ mm^2 in squamous cell cancers from various origins. The abundance of T-cell subpopulations, M2 macrophages, and dendritic cells was highly concordant (range r=0.49 to 0.92) across all tumor entities, while the density of M1 macrophages was unrelated (r=0.1, p<0.001). Unsupervised hierarchical clustering across all tumor entities revealed a cluster A of 634 patients from almost all different tumor entities with an exceptionally high density of intraepithelial immune cells, thus a highly inflamed tumor microenvironment that was characterized by the strongest interaction between intraepithelial $CD8^+$ T-cell and $CD4^+$ T-helper cells, M2 macrophages, as well as dendritic cells (DC, p<0.002 each) along with the highest expression level of TIM3, PD-1, CLTA-4 and PD-L1. In contrast, a cluster C of 2245 patients with the lowest intraepithelial immune cell infiltration was characterized by a significantly increased M1 proportion (p<0.001) and an enriched proportion of regulatory T-cells (p<0.001). Across all analyzed tumor entities, the intraepithelial highly inflamed cluster A was significantly linked to low pT (p<0.001).

Conclusion: The data from this study provide a comprehensive characterization of intraepithelial immune cells across 46 different human carcinomas and identify an inflamed phenotype defined by strong interactions of intraepithelial $CD8^+$ cytotoxic T-cells, $CD4^+$ T-cells, dendritic cells, and M2 macrophages along with highest levels of TIM3, PD-1, PD-L1, and CTLA-4 expression that is linked to a favorable tumor phenotype.

#0170 Targeting of macrophage PI3Kyin prostate cancer using Eganelisib (IPI-549) reprograms immune-suppressive infiltrating macrophages to enhance anti-tumor immune responses and promote immunologically mediated tumor growth.

K. M. Adusei[1], T. R. Nirschl[1], A. J. Lee[1], F. Shen[1], X. Wang[1], M. Praharaj[1], J. Alvarez[1], I. Gross[1], K. A. Lombardo[1], T. L. Lotan[1], J. A. Varner[2], J. C. Zarif[1]; [1]Johns Hopkins University School of Medicine, Baltimore, MD, [2]University of California, San Diego, La Jolla, CA

Background: Prostate cancer (PCa) is traditionally considered an immunologically 'cold' indication, as evidenced in part by significant infiltration of immunosuppressive tumor associated macrophages (TAMs) and few activated effector $CD8^+$ T cells. Attempts to (re)invigorate an anti-prostate cancer immune response with immune checkpoint blockade (ICB) such as anti-CTLA-4 and anti-PD-1 have been largely ineffective clinically, despite promising results in other cancers. This is likely due to a multitude of immunosuppressive cell types and secreted factors within the tumor microenvironment (TME) that diminish T cell activation and trafficking. Reducing the immunosuppressive burden intratumorally by targeting TAMs is a clinically attractive approach and offers opportunity to sensitize PCa to immune checkpoint blockade. While PI3K signaling is ubiquitous in most cell types, specific catalytic isoforms and regulatory elements are differentially expressed depending on cell type, with PI3Kγ being significantly enriched in myeloid cells and therefore offering a unique therapeutic opportunity for specific targeting.
Methods: Utilizing novel syngeneic prostate cancer tumors, PI3Kγ deletion and antagonism using Eganelisib (a small molecule inhibitor for PI3Kγ), we tested our hypothesis that targeting PI3Kγ signaling in PCa TAMs would lead to tumor growth inhibition and anti-tumor immune responses.
Results: We show here that PCa tumor cells do not express the PI3Kγ isoform and, therapeutic inhibition of PI3Kγ with Eganelisib reduces the TAM suppressive phenotype. We also show PI3Kγ signaling is essential to monocyte anti-apoptotic signaling, and inhibition of PI3Kγ can enhance anti-tumor immune responses in preclinical models of PCa. Specifically, inhibition of PI3Kγ alone is sufficient to enhance anti-tumor immune responses in the less aggressive B6CaP PCa model, but insufficient in the more aggressive RM-1 PCa model. However, treatment of RM-1 tumors with Eganelisib produces improved tumor control when combined with anti-PD-1 therapy, relative to Eganelisib or anti-PD1 as a monotherapy.
Conclusions: Altogether, these data highlight the integral role of PI3Kγ signaling in TAMs and the potential for therapeutic targeting with Eganelisib to sensitize PCa to ICB.

#0171 Chemotherapeutic agent, cisplatin, influences the proportion of TREM2 (+) M2 macrophages in the TME of LUAD.

Y. Cha, M. Park, Y. Chang;
Yonsei University College of Medicine, Seoul, Korea, Republic of

Background: Triggering receptor expressed on myeloid cells (TREM2) serves as an immune signaling hub that senses and interacts with a wide range of ligands arising from damaged tissues in pathologic conditions. Despite TREM2's diverse role in casting immune suppressive environment, the effects of chemotherapy on tumor microenvironment (TME), TREM2 and their interactions are not well established. In this study, we aimed to investigate the characteristics of TREM2 (+) Mφ within the lung TME (Tu), focusing on the impact of chemotherapy on the immune dynamics of lung adenocarcinoma (LUAD).
Method: Changes in the number and distribution of Mφ subclusters in normal appearing lung tissue (NL) and Tu were examined using open-source single cell RNA sequencing (scRNA-seq) datasets and immunofluorescent staining of lung cancer-induced Kras-G12D mouse tissue. Clinical measures affecting the expression of TREM2 were explored using the TCGA-LUAD and -LUSC datasets, and the effects of anticancer drugs and the apoptotic cells on Mφ were observed by differentiating THP1 cells into M0, M1, and M2.
Results: scRNA-seq analysis on LUAD datasets showed that Mφ were the second most abundant cell population that constitutes the lung TME, and the proportion of Mφ in the Tu decreases compared to NL. Among the Mφ subclusters in Tu, a subcluster which specifically increased in Tu shows enrichment of apoptotic cell clearance gene sets, including TREM2. In lung cancer induced Kras-G12D mouse, compared to NL the Tu has an increase in M2 proportion, showing the characteristics of interstitial Mφ in addition with overexpression of TREM2 and enrichment of monocyte chemotaxis gene set enrichment. Among TCGA-LUAD, the high TMB group has low TREM2 expression, and the proportion of TREM2 (+) M2 in the Tu decreases in cisplatin-treated Kras-G12D mouse Tu, suggesting the expression of TREM2 in M2 is suppressed by either cisplatin treatment itself or active immunity in Tu. Additionally, we are going to observe the effect on TREM2 expression by adding cisplatin treated A549-GFP cells or cisplatin alone, to the THP-1 cells that were differentiated into M0, M1, or M2 state.
Conclusion: In addition to changes in the lung immune environment due to the tumor, anticancer treatment changes in the characteristics of M2 in TME, in terms of decrease in TREM2 (+) Mφ fraction. Considering that TREM2 plays a central inhibitory role in the tumor immune environment, the effect of anticancer chemotherapeutic agents should be considered in the development TREM2 targeting agents.

#0172 Targeting the poliovirus receptor to activate T cells and induce myeloid-derived suppressor cells to differentiate to M1-like macrophages via the IFNγ-pSTAT1-IRF8 axis in cancer therapy.

M. Feng, S. Tan, Q. Ma, B. Zhang, Y. Chen, Q. Li, Y. Wang;
West China Hospital of Sichuan University, Chengdu City, China

T cell immunoglobulin and ITIM domain (TIGIT) is one of the most important immune checkpoints expressed on lymphocytes, and poliovirus receptor (PVR, also CD155) serves as the most crucial ligand for TIGIT, harboring an important function in cancer cells and influencing the tumor microenvironment (TME). While it's well-established that TIGIT blockade could reverse immunosuppression, the question of whether direct inhibition of PVR yields comparable results remains to be fully elucidated. In this study, we generated a mouse gene Pvr knock out (KO) Lewis lung cancer (LLC) cell line and found that the Pvr-KO tumors tended to develop a pro-inflammatory TME, as reflected by a downregulation of monocytic-myeloid derived suppressor cells (M-MDSCs) and an upregulation of CD8+ central memory T cells. Through bulk RNA-seq and multi-cytokines measurement, we quantified the transcription and protein levels of immunostimulatory cytokines and chemokines and found they were significantly upregulated in Pvr-KO TME, including GM-CSF, IFN-γ, TNF-α, IL-2/4/6/10, CCLs (including CCL2/3/4/5) and CXCLs (including CXCL1/2/5). We further employed single-cell RNA sequencing (scRNA-seq) on 20,026 intra-tumoral CD45+ immune cells. Using a conserved MDSCs gene set and the 'AddModuleScore' function of Seurat package, we identified the clusters of MDSCs and found the differentiation ability of M-MDSCs in Pvr-KO TME was enhanced. Through pseudo-temporal ordering, we found the M-MDSCs in the Pvr-KO TME have a trend to differentiate towards M1-like macrophages, which could play an essential positive role in anti-tumor immunity. We further focused on the scRNA-seq of T cell subsets and found the enhanced function of cytotoxic CD8+ T cells, leading to increased production of IFN-γ. In the intercellular communications analysis, a significant upregulation of the IFNG-IFNR signal between T cells: MDSCs in the Pvr-KO group was observed. Moreover, we found that Irf8, a key factor in myeloid cell differentiation, was significantly upregulated in the M-MDSCs of Pvr-KO tumor. We then employed CUT & Tag sequencing and confirmed that IFN-γ induces phosphate Stat1, which then binds on the promoter of Irf8. These findings suggest that the IFN-γ-Stat1-Irf8 axis plays a crucial role in MDSCs differentiation and may be a potential target for therapeutic intervention in cancer. Next, an anti-PVR nanobody was synthesized and its efficacy was evaluated in the context of LLC and 4T1 tumor grafts. When in combination with anti-PD-1 therapy, anti-PVR exhibited a remarkable capacity to reduce tumor size in both tumor models with no notable indications of toxicity observed. Our findings provide new insights into the role of PVR in modulating the TME and offer potential strategies for enhancing the effectiveness of immunotherapy.

#0173 Studying the interaction between macrophages and solid stress in novel models of the tumor immune microenvironment.

A. Burchett, S. Siri, H. Chen, S. Howard, M. Datta;
University of Notre Dame, Notre Dame, IN

Glioblastoma (GBM) is one of the most aggressive forms of cancer, resisting conventional and immune-based therapies and typically killing patients within two years of diagnosis. This is largely due to the immunosuppressive GBM tumor microenvironment (TME), mediated in large part by tumor-resident macrophages. Macrophages' role as immune regulators, as well as their sheer quantity in brain tumors, makes them attractive therapeutic targets. The GBM TME also features mechanical abnormalities. As a tumor grows, it expands into the surrounding brain, generating compressive solid stress. Macrophages can contribute to up to half of tumor mass and are known to respond to mechanical cues, allowing them to both contribute to and respond to solid stress, but this relationship has not yet been explored experimentally. To isolate the contribution of macrophages on solid stress, we incorporated RAW264.7 murine macrophages into agarose gels with varying stiffnesses. Over time, spheroids form as the cells proliferate. Because cells cannot alter agarose, cell aggregates must generate stress as they grow and displace the surrounding gel matrix. The resulting agarose-embedded spheroids were stained with calcein AM to observe spheroid viability and morphology. Using confocal microscopy and image processing, we obtained the final spheroid geometry and imported it into COMSOL to model the solid stress resulting from spheroid formation. Our initial experiments show that macrophages have distinct growth patterns dependent on the stiffness of their surrounding gel. At larger sizes, the spheroids adopt an ellipsoid shape and generate a distinct stress field compared to spheroidal shapes. To stimulate the solid stress that macrophages experience within a growing mass, we applied a custom weight to macrophages grown on a porous membrane. This applies 0.15 kPa of compressive solid stress, corresponding to the stress measured in murine glioma models. After 24 hours of compression, macrophages upregulate expression of both nitric oxide synthase and arginase-1, canonical M1 and M2 markers, respectively. This indicates that compression causes a more complex phenotype than can be described by the traditional M1/M2 axis, something that has been observed in tumor-associated macrophages. We also found an apparent difference in the fluorescence lifetime of compressed and uncompressed macrophages, indicating that compression alters macrophage metabolism. Both the spheroid and compression culture models are unique in the context of macrophages. This work will elucidate key pathways involved in myeloid "immunomechanics" and inform strategies to target the innate immune system in cancers such as GBM, as well as other immunological diseases.

#0174 Cholesterol efflux protein ABCA1 skews macrophages towards an anti-tumor phenotype and consequently impacts breast cancer progression.

S. V. Bendre[1], N. Krawczynska[1], S. Bhogale[1], E. Weisser[1], S. Han[1], B. Hajyousif[1], A. Singh[1], R. K C[1], Y. Wang[1], C. P. Schane[1], A. T. Nelczyk[1], A. DasGupta[1], H. E. V. Gamage[1], K. T. VanBortle[1], E. Tajkhorshid[1], S. Sinha[2], W. Cho[3], E. R. Nelson[1];

[1]University of Illinois at Urbana-Champaign, Urbana, IL, [2]Georgia Institue of Technology, Atlanta, GA, [3]University of Illinois Chicago, Chicago, IL

With a lifetime risk of approximately 1 in 8, breast cancer maintains in its position as the most prevalent form of cancer and ranks second in terms of cancer-related fatalities in women. The primary cause of mortality is often attributed to the recurrence of metastatic breast cancer. While immune therapy shows some effectiveness, many patients do not exhibit meaningful responses, likely due to immune-suppressive factors present within the tumor microenvironment. These factors include myeloid cells such as Macrophages(MΦ), therefore, there is a strong need to devise strategies to shift (MΦ) from a pro-tumor to an anti-tumor phenotype. Our previous research has uncovered the susceptibility of MΦs to disruptions in cholesterol metabolic balance. Considering these findings, coupled with epidemiological evidence linking elevated plasma cholesterol to unfavorable prognosis, the impact of cholesterol homeostasis in tumor associated MΦs on breast cancer becomes evident. An in-depth computational screen helped us identify ABCA1—a cholesterol efflux protein with elevated mRNA expression associated with increased survival. Beyond cholesterol efflux, ABCA1 also facilitates the movement of cholesterol from the inner membrane layer to the outer layer. Previous work has shown that cholesterol within the inner membrane layer can directly interact with and activate various receptors on the membrane's surface, initiating downstream signaling events. Consequently, the activities of ABCA1 in cholesterol efflux and translocation likely hold substantial regulatory implications. Underscoring the clinical significance of ABCA1 are our findings that heightened ABCA1 expression within breast tumors correlates with augmented levels of cytotoxic T cells, T cell effector enzymes (Prf-1 and Gzmb), and improved survival rates. Crucially, our in vitro investigations indicate that ABCA1 modulates multiple functions of MΦs to adopt an anti-cancer phenotype, encompassing: (1) the ability to infiltrate tumor spheroids, (2) angiogenesis, (3) efferocytosis—an immune-suppressive phagocytic process devoid of antigen presentation, and (4) the expansion, migration, and activity of cytotoxic T cells. ABCA1 transports cholesterol from macrophages to a lipid poor ApoA1 protein and facilitates the formation of nascent HDL via reverse cholesterol transport. We leveraged this mechanism to therapeutically target ABCA1 using ApoA1 mimetics 5A and 4F. Our data so far indicates that these ApoA1 phenocopy ABCA1 overexpression in MΦs. Together, our data provides compelling evidence for the involvement of ABCA1 in the pathophysiology of breast tumors. The anticipated outcomes of this research will establish the basis for the future utilization of ABCA1 and its downstream effects for therapeutic purposes.

#0175 Tumor-associated monocytes and neutrophils: Targets for immunotherapy?.

K. Jung;
Seoul National University, Seoul, Korea, Republic of

Cancer is the leading cause of deaths worldwide. However, current anti-VEGF therapies for solid cancers provide limited survival benefit as tumors rapidly develop resistance to these agents.We have uncovered an immunosuppressive role for non-classical Ly6C^{low} monocytes that mediates resistance to anti-VEGFR2 treatment. We found that the chemokine CX3CL1 was upregulated in both human and murine tumors following the VEGF signaling blockade, resulting in recruitment of CX3CR1^{+} Ly6C^{low} monocytes into the tumor. We also found that treatment with VEGF-A reduced expression of CX3CL1 in endothelial cells. Intravital microscopy revealed that CX3CR1 is critical for Ly6C^{low} monocyte transmigration across the endothelium in tumors. Moreover, Ly6C^{low} monocytes recruit Ly6G^{+} neutrophils via CXCL5 and produce IL-10, which inhibits adaptive immunity. Preventing Ly6C^{low}monocyte or Ly6G^{+} neutrophil infiltration into tumors enhanced inhibition of tumor growth with anti-VEGFR2 therapy. Furthermore, we developed a gene therapy using a nanoparticle formulated with a siRNA against CX3CL1, which reduced Ly6C^{low} monocyte recruitment and improved outcome of anti-VEGFR2 therapy.Taken together, we identified immunosuppressive non-classical Ly6C^{low} monocytes as key players in tumor resistance to anti-angiogenic therapy in cancers. We also revealed molecular mechanisms underlying anti-angiogenic treatment resistance, suggesting potential immunomodulatory strategies to enhance the long-term clinical outcome of anti-VEGF therapies, proven by state-of-the-art *in vivo* imaging modalities.

#0176 Stearic acid induces pro-inflammatory macrophage response important for lung cancer development.

A. Roy[1], M. Davis[1], S. Weinberg[2], A. Mallisetty[1], A. Hulbert[1], F. D. Weinberg[1];
[1]University of Illinois Chicago, Chicago, IL, [2]Northwestern University, Chicago, IL

Background Survival is improved with early detection and treatment initiation in patients with lung cancer (LC) emphasizing the importance of tumor initiation and biomarker development in individuals at high risk for developing LC and those with early-stage LC. Recent studies suggest that immunologic and metabolic changes within the microenvironment are pivotal for tumor formation. We recently demonstrated that in patients with resectable, early-stage LC, elevated levels of stearic acid (SA), a long chain fatty acid, and macrophage inflammatory protein 1β (MIP-1β/CCL4) were predictive of tumor affected lung lobes. Therefore, we hypothesize that SA promotes LC initiation through the activation of macrophages (MΦ) and production of proinflammatory cytokines like CCL4.
Methods and Results: We performed untargeted metabolomics utilizing LC-MS from the plasma of patients with various stages of LC and found elevated levels of SA in patients with early-stage LC. To further study the mechanistic role of SA in tumorigenesis, cell lines including immortalized lung epithelial , LC cells, and immune (MΦ and T) cells were treated with SA. We found that physiological concentrations of SA did not affect cellular viability. However, in MΦ, SA induced expression of inflammatory (IL6, iNOS), and immunomodulatory (Arg1, CD206) genes suggesting a role for SA in promoting a pro-tumorigenic immunologic state. Additionally, analysis of the secretome from SA stimulated MΦ using single cell proteomic analysis (Isolight, Bruker Cellular Analysis, Inc), indicated a significant enrichment of polyfunctional MΦs with enhanced secretion of enriched effector and stimulatory cytokines. Furthermore, conditioned media derived from SA stimulated MΦ led to increased proliferation, as well as anchorage independent growth, of BEAS2B immortalized lung epithelial cells.
Conclusion: Our data demonstrates plasma levels of SA are increased in early-stage compared to late-stage patients with LC. This observation corresponds to our prior data demonstrating enrichment of SA in the tumor affected lobes of patients with early-stage LC. Recent studies demonstrating the induction of inflammatory responses through MΦ activation in obese patients by circulating SA in blood corroborates our observations as well. Our data suggests that the SA effect on MΦ, is critical in LC initiation not only increasing proliferation but also induction of neoplastic transformation of immortalized lung epithelial cells. Furthermore, our data indicates that blood plasma levels of SA, a fatty acid understudied in tumor biology, could also be exploited as a potential biomarker for LC development in individuals at high-risk for LC development as well as those patients with early-stage disease.

#0177 Targeting murine or human KLRG1 exerts potent anti-tumor efficacy involving both CD8T cells and NK cells.

T. A. Jones[1], S. Sinicrope[1], K. Yasuda[2], J. Pinkas[2], T. F. Gajewski[1];
[1]University of Chicago, Chicago, IL, [2]Pyxis Oncology, Boston, MA

Clinical response to anti-PD-1 immunotherapy is correlated with patients who have a T cell-inflamed tumor microenvironment. Some patients with immune cell infiltration fail to respond, and some patients experiencing an initial clinical response develop acquired resistance. It is likely that additional immune-regulatory pathways need to be targeted to expand the efficacy of immunotherapies. To identify a broader array of therapeutic relevant immunotherapy molecules in T cell-inflamed tumors, our lab utilized gene expression profiling to characterize tumor antigen-specific dysfunctional $CD8^+$ T cells in the tumor microenvironment. One molecule that was found to be overexpressed on these $CD8^+$ T cells was C-type lectin inhibitory receptor, KLRG1. KLRG1 is an ITIM domain-containing receptor mostly explored on NK cells, and the known ligands are N- and E- cadherins which are broadly expressed in solid cancers. Analysis of single cell RNA-Seq data from tumor biopsies of melanoma patients classified as responders or non-responders to anti-PD-1 therapy revealed significantly higher expression of KLRG1 expression on tumor-infiltrating T cell subsets in non-responders, suggesting a possible salvage immune suppressive role. To determine the potential functional relevance of KLRG1 on tumor control, we generated KLRG1 knockout (KO) mice, then implanted tumors and assessed tumor growth rate *in vivo*. KLRG1 KO mice showed markedly slowed B16 melanoma tumor growth compared to WT mice, arguing it is a critical negative regulator of anti-tumor immunity. Both antigen-specific $CD8^+$ T cells and NK cells were expanded in these tumors, and depletion of $CD8^+$ T cells or NK cells eliminated this tumor control. Genetic deletion of N-cadherin from B16 cells also resulted in slowed tumor growth, suggesting that tumor cells are providing the functionally relevant ligand.
To assess the degree of inhibitory function of human KLRG1, we generated a humanized KLRG1 knock-in mouse model. We confirmed that human KLRG1 can biochemically interact with murine cadherins. Knock-in mice with the humanized KLRG1 protein had significantly increased tumor growth compared to both WT and KLRG1 KO mice, indicating a stronger immunosuppressive effect of human KLRG1 compared to murine KLRG1. An antagonistic antibody blocking interaction of human KLRG1 with its ligands was generated, which potentiated human T cell activation *in vitro*. Administration of anti-human KLRG1 Ab to tumor-bearing humanized KLRG1 mice led to markedly reduced tumor growth.
In summary, our data support KLRG1 as a functionally critical negative regulator of the anti-tumor immune response and that blocking KLRG1-cadherin interactions has potential as a therapeutic candidate.

#0178 Adipose tissue upregulates expression of RANKL in B-cell acute lymphoblastic leukemia through prostaglandin E2 signaling.

M. Cohen[1], J. Tan[1], T. Kuk[1], B. Nadeak[1], I. Ahn[1], X. Yang[1], E. Orgel[2], S. D. Mittelman[1];
[1]UCLA Mattel Childrens Hospital, Los Angeles, CA, [2]Children's Hospital Los Angeles, Los Angeles, CA

Obesity increases the risk of developing cancer and worsens treatment outcome. Our lab has shown that adipose tissue contributes to B-cell acute lymphoblastic leukemia (B-ALL) resistance to chemotherapy both *in vitro* and *in vivo*. However, the mechanisms by which adipose tissue causes ALL cell resistance are complex and not completely understood. We therefore implanted obese mice (n=3) with syngeneic BCR/ABL B-ALL cells and performed single-cell RNA sequencing (scRNAseq) of ALL collected from epididymal adipose tissue vs. bone marrow. Our data uncovered a strong adipose microenvironment effect on the ALL transcriptome, identifying 577 differentially expressed genes using a $\log_2$ fold threshold of 0.25 and Bonferroni corrected p-values <0.05. Notably, we found that ALL cells in adipose tissue upregulate expression of *Tnfsf11*, the gene that encodes receptor activator of nuclear factor kappa beta ligand (RANKL). 93% of ALL cells in adipose tissue express RANKL compared to 33% in marrow, along with a $\log_2$ fold expression increase of 2.12 ($p<1x10^{-100}$, Wilcoxon test). Because ALL expression of RANKL has been linked to bone resorption and CNS invasion, both of which have increased incidence in obese patients, we elected to explore this further. *Ex vivo* culture with human visceral adipose tissue validated ALL cell RANKL upregulation, demonstrating a 1.63 and 17.5-fold increase in gene expression after 48 hours in BV173 and RS4;11 B-ALL cell lines, respectively (n=4-6, both $p<0.01$, paired t test). Soluble RANKL was not detected in media from ALL cells cultured alone, detectable in media conditioned by human adipose tissue (0.018 pM), but increased in media from adipose-ALL cocultures (RS4;11: 0.065 pM, BV173: 0.317 pM, n=1). One potential candidate signal to stimulate ALL cell RANKL expression is the inflammatory mediator prostaglandin E2 (PGE2), which is known to be released by adipose tissue. Physiological concentrations of PGE2 (200 ng/mL) caused a similar increase in ALL cell RANKL gene expression as adipose tissue in both cell lines (n=6). PGE2 treatment also caused a mild resistance of ALL cells to daunorubicin chemotherapy *in vitro*, increasing the EC_{50} from 27±4 to 53±12 nM in RS4;11 (n=6, $p<0.05$), and from 39±11 to 62±19 nM in BV173 (n=6, $p=0.06$). Adipose tissue induction of RANKL expression was partially blocked by the addition of PGE2 receptor EP2 and EP4 blockers. Taken together, our results suggest that PGE2 produced by the adipose microenvironment activates ALL cell RANKL expression, which could potentially contribute to CNS invasion, bone breakdown, and chemoresistance.

#0179 Identification of a novel crosstalk between MDSC and NKregs in immunotherapy resistant triple negative breast cancer.

M. Das[1], S. Henry[2], S. Singh[1], C. D. Santos[2], R. Chakrabarti[1];
[1]University of Miami Sylvester Centr.-I, Miami, FL, [2]Cold Spring Harbor Laboratory, Cold Spring Harbor, NY

Triple-negative breast cancer (TNBC) is one of the most aggressive forms of breast cancer and lacks standard treatment options. Although immunotherapy shows some response in these patients along with chemotherapy, heterogeneity of tumor cells and immune cells results in significant low response to immunotherapy treatment. Based on single cell sequencing which enables identity of heterogenous population at single cell level and functional studies involving preclinical mouse models, our laboratory recently identified distinct $CD56^{bright}SOCS3^{high}CD11b^{-}CD27^{-}$ immature NK cells subpopulations, with diminished cytotoxic granzyme signatures that promote TNBC tumor progression. However, the precise characterization and functionality of these rogue tumor promoting NK cells remains unclear in clinical samples. Here, we aimed to illustrate mechanistic insight of these novel immature NK subpopulation in context of immunotherapy resistant TNBC patient samples. The scRNA seq analysis of TNBC patient samples identified four specific subclusters of NK cells in TNBC. We further found that NK2 and NK3 subclusters are $CD56^{dim}$ $Granzyme^{high}$ cytotoxic NK cells and the other two subclusters (NK0 and NK1) are $CD56^{bright}$ immature NKs. Interestingly, the NK0 and NK1 subcluster specifically exhibit distinctive characteristics and functions. Notably, $CD56^{bright}$ immature NK1 cells, identified as tissue-resident NK cells, were engaged in direct communication with myeloid-derived suppressor cells (MDSCs). The $CD56^{bright}$ NK0 possesses moderate to low SOCS3 expression and moderate to high granzyme expression with elevated early NK activation markers and inhibitory receptor expressions, suggesting its regulatory property (NKregs). scRNA seq and flow cytometry analysis showed higher NKregs and immunosuppressive MDSC population, specifically with high monocytic-MDSCs (mMDSCs) in non-responder TNBC (to adjuvant combinational treatment of chemo and immunotherapy) patient samples rather than responder patients' tissue. Based on *in silico* analysis, we further found a potential crosstalk between these mMDSC & NKreg within the tumors of non-responsiveness of TNBC patients. Overall, our studies show a connection of MDSCs and NKregs in TNBC patients, who do not respond to immunotherapy, highlighting a possible mechanism for immunotherapy resistance, which could be targeted in near future for better treatment options in TNBC.

#0180 *LINC00261* is functionally linked to tumor DNA mutational burden and tumor immune microenvironment composition in lung adenocarcinoma.

J. Castillo, T. Xue, M. Norwood, S. Joseph, A. L. Epstein, W. D. Wallace, A. W. Kim, C. N. Marconett;
University of Southern California, Los Angeles, CA

Immunotherapy has emerged as a breakthrough in the improvement of survival outcomes for lung adenocarcinoma (LUAD), however effective response requires the combination of blocking inhibitory signals on the tumor surface and antigen presentation to the tumor surface for proper immune recognition. Several commercially available and robust methods exist for identification of tumors displaying immune-inhibitory surface receptors, such as PD-L1, however it is currently difficult to predict effectiveness of antigen presentation on the cell surface. To address this, we utilized clinical and next-generation sequencing data from The Cancer Genome Atlas (TCGA) to identify gene signatures that are correlated to tumor mutational burden (TMB) within cancers of epithelial origins as a surrogate for neoantigen signatures. We identified *LINC00261* as a top gene correlated to TMB, whose expression activates DNA damage response pathways *in vitro* along with resistance to cisplatin. *LINC00261* expression was also significantly correlated to MHC class I and II genes involved in endogenous neoantigen presentation expression within the TCGA-LUAD cohort. This relationship was confirmed *in vitro* through ectopic reintroduction of *LINC00261* for key MHC class II presentation genes. Interferon gamma-induced MHC gene activation *in vitro* was also able to induce endogenous expression of *LINC00261*. Staining of primary human lung cancer sections suggested that loss of *LINC00261* is associated with an immunosuppressive tumor microenvironment. Taken together, our results suggest there is a mechanistic relationship in the silencing of *LINC00261* in LUAD and compromised DNA repair, accumulation of mutations, and reduced antitumor immune response.

#0182 Cyclooxygenase-2 blockade is crucial to restore natural killer cell activity before anti-CTLA-4 therapy against high-grade serous ovarian cancer.

F. Gomez-Valenzuela[1], I. Wichmann[2], F. Suarez[1], S. Kato[1], E. Ossandon[1], M. Hermoso[3], E. Fernandez[4], M. A. Cuello[1];
[1]Pontificia Universidad Catolica de Chile, Santiago, Chile, [2]Stanford University School of Medicine, Santiago, CA, [3]University of Chile, Santiago, Chile, [4]Fundacion para el Progreso de la Medicina (CONICET), Facultad de Ciencias Exactas, Fisicas y Naturales, Universidad Nacional de Cordoba, Cordoba, Cordoba, Argentina

Objective: Here our goal was to evaluate the impact of the immunosuppressive enzyme cyclooxygenase-2 (COX-2) expression on the immune effector capacity against high-grade serous ovarian cancer (HGSOC) tumor cells through bioinformatic tools and *in vitro* validation.
Methods: We performed an integrated bioinformatics analysis from transcriptomic data based on RNAseq (TCGA-OV, n=368; Australian cohort AOCS, n=80) and RNA microarrays (GSE26193, n=62; GSE30161, n=45). We estimated the proportion and characteristics of immune cells employing Gene Set Variation Analysis (GSVA), MIXTURE and Ecotyper cell deconvolution algorithms. Survival curves and Cox-regression models were built up according to known risk factors and immune scores predicted by *in-silico* analysis. Afterward, we validated these results using flow cytometry and cytotoxicity assays on circulating NK cells collected from advanced HGSOC patients treated at our institution (n=5). After three days of incubation, isolated NK cell cultures were stimulated with three pulses of a selective COX-2 inhibitor (celecoxib) or MOCK, daily. An anti-CTLA-4 monoclonal antibody (ipilimumab) or MOCK was added at the third pulse. Two ovarian cancer cell lines (SKOV3 and HeyA8) were treated similarly. Next, NK cells were co-cultured with SKOV3 or HeyA8 and cytotoxicity on these cells was examined using lactate dehydrogenase (LDH) cell viability assay.
Results: Transcriptomic data evidenced a non-linear relationship between COX-2 gene, *PTGS2*, and *CTLA4* in advanced stages of HGSOC. Hence, *PTGS2*/*CTLA4* ratio allows us to investigate how COX-2 influences changes in the immune profile of these patients. Based on bioinformatics, a high *PTGS2*/*CTLA4* ratio determines particularly dysfunctional NK cell states, along with the reduction of NK gene score associated with infiltration, cytotoxicity, and survival in HGSOC. Additionally, selective COX-2 blockade improves NK cell cytotoxicity against HGSOC cell lines independently of the CTLA-4 signaling. In fact, ipilimumab effect was almost absent in those cases with high COX2 activity. Interestingly, previous treatment with celecoxib on NK cells mainly explains the difference in cytotoxicity ($p= 0.0253$, two-way ANOVA test with Tukey's multiple comparisons).
Conclusions: This work represents the first evidence of the influence of COX-2 on NK cell function as a crucial factor for the efficacy of anti-CTLA-4 therapy in HGSOC patients who exhibited high tumoral levels of CTLA-4. HGSOC patients present dysfunctional circulating NK cells preferentially due to the strong CO-2 expression. Last, we emphasize the modulation of chronic inflammation to direct an immune pattern with greater antitumor capacity in HGSOC. (Funding: Fondecyt 1201083 and FONDAP 152220002 [MAC], CONICYT/Doctorado Nacional 2019-Folio 21190421 [FGV], CONICYT FONDAP 15130011 [MAC, IW]).

#0183 A novel bispecific antibody macrophage engager (BiME) designed for the treatment of solid tumors.

D. Sun, H. Jiang, Y. Geng, Y. Wu, R. Gao, Y. Lu, Q. Qiu, Y. Hu, Y. Liu, X. Guo, X. Niu, H. Lu;
Elpiscience Biopharma, Shanghai, China

Background: Anti-CD3-based bispecific T cell engagers (BiTE) showed limited clinical efficacy in solid tumors and caused significant cytokine storm. Similar to BiTE where T cells are activated by CD3 antibody, we constructed a novel bi-specific macrophage engager (BiME) platform where macrophage is activated by anti-SIRPa that is directed to a particular tumor via the targeting of the tumor-associated antigen (TAA), resulting in phagocytosis of the tumor cells. This BiME does not lead to cytokine storm and is particularly applicable for the treatment of solid tumors whose microenvironment contains plenty of macrophages. Tumor-associated macrophages are major component of immune cells in the tumor micro-environment (TME) that express an array of effector molecules leading to the inhibition of anti-tumor immune responses. Signal regulatory protein α (SIRPα) is a myeloid-lineage inhibitory receptor that restricts phagocytosis through engagement of its ligand CD47 expressed on tumors and normal tissues. Compared to anti-CD47 therapeutics, targeting myeloid-restricted SIRPα provides a differential pharmacokinetic, safety, and efficacy profile. Here, we report the construction of a SIRPα antagonist-based bispecific macrophage engager (BiME) platform, a potent tumor-killing bi-specific antibody platform.
Methods: We have generated a panel of single domain antibody (sdAb), scFv or Fab antibodies targeting different TAAs and SIRPa. We constructed BiME antibodies using different orientations, ratios, and IgG isotypes of anti-TAA arm and anti-SIRPα arm. These bispecific antibodies were evaluated for homologue binding, and CD47-SIRPα blocking properties by ELISA and FACS. In vitro function activity was determined by phagocytosis assay using human monocyte derived macrophage and mouse bone marrow derived macrophage. In vivo anti-tumor efficacy was tested in a syngeneic tumor model with hSIRPα knock-in mice. The pharmacokinetic (PK) and safety profile were assessed in hSIRPα knock-in mice or cynomolgus monkeys.
Results: Through Elpiscience proprietary BiME platform, we have generated a panel of TAA/SIRPα bispecific antibodies with TAA being Claudin18.2, EGFR, PDL1 and DLL-3. The BiME treatment demonstrated strong anti-tumor efficacy in multiple mouse syngeneic tumor models. Mechanistically, both myeloid and T cells were activated and contributed to antitumor activity of BiME bispecific antibody. the BiME bispecific antibodies were well tolerated in non-human primates (NHPs) and there is no hematotoxicity or cytokine release syndrome (CRS) observed after treatment of BiME antibodies.
Conclusions: These findings provide novel mechanistic insights into how myeloid and T cells can be uniquely modulated by the bispecific macrophage engagers (BiMEs) and demonstrate the potential and advantage of BiME in future clinical development for solid tumor treatment as compared to BiTE approach.

#0184 M1-like macrophage infiltration, CD8+ T cell activation, and increased cancer cell apoptosis in immunologically cold Lewis lung carcinoma treated with tumor-trophic Salmonella Typhimurium expressing anticancer proteins in immunocompetent C57BL/6 mice.

Q. He, L. R. Brncick, B. Gong, J. L. Flowers;
Purdue University, West Lafayette, IN

Immunotherapy has revolutionized cancer treatment with immune checkpoint inhibitors (ICIs) and genetically engineered T-Cells expressing chimeric antigen receptors (CARs). CAR-T treatment of hematologic malignancies has achieved outstanding patient response rate. CAR-T cell therapy, however, is thwarted in solid tumor treatment due to two major factors: the immune-suppressive tumor microenvironment that inhibits T-cell infiltration and T-cell function. In addition, T-cell dysfunction also renders ICIs ineffective in solid tumor treatment. This research aims to activate proinflammatory anticancer immune responses in immunologically cold solid tumors using the genetically engineered Salmonella typhimurium VNP20009 strains that express anticancer proteins. Previously, we have shown that the Salmonella Typhimurium VNP20009 strains expressing recombinant methioninase (rMETase) and/or Tumor Necrosis Factor (TNFα) caused rapid tumor destruction of cold Lewis Lung Carcinoma (LLC) grown on immunocompetent C57BL/6 mice. In this investigation, several mechanisms of this tumor tropic anti-cancer bacteria were studied including the innate and adaptive immune system responses and cancer cell apoptosis. In a pilot study, we selected eight tumor tissues treated with several different bacteria strains and performed histological analysis to observe the effectiveness of each. We found that in the tumor tissues treated with VNP20009_rMETase_TNFα, there was infiltration and activation of CD8+ T cells coupled with reduced amounts of T regulatory cells, as well as an increased ratio of M1-like to M2-like macrophages. We also observed increased tumor apoptosis associated with an elevated detection of an apoptosis biomarker and a suppressed amount of the Ki67 tumor growth signal. These findings indicate that VNP20009_rMETase_TNFα anticancer bacteria can disrupt the tumor microenvironment in the cold LLC tumors and active innate and adaptive anti-cancer immune responses in immunocompetent mice. Further, we are investigating additional cold solid mouse tumor models to validate our findings and how this can apply to bacteria-based immunotherapy.

#0186 Tumor exosome-macrophage interactions: The role of tumor-associated glycans and scavenger receptor class A.

F. Jousheghany[1], E. S. Blitz[1], S. V. Jenkins[1], S. R. Post[1], V. Raj[2], R. A. Kore[1], A. Jamshidi-Parsian[1], R. J. Griffin[1], T. J. Kelly[1], B. Monzavi-Karbassi[1];
[1]University of Arkansas for Medical Sciences, Little Rock, AR, [2]University of Arkansas at Pine Bluff, Pine Bluff, AR

Introduction: Increased macrophage infiltration and polarization towards a breast tumor-supportive phenotype have been linked to therapy resistance, immune suppression, and poor patient prognosis. Despite their importance, the specific interactions that drive tumor-associated macrophage (TAM) polarization remain poorly understood. The class A scavenger receptor (SR-A) is a pattern-recognition receptor expressed by macrophages, and the accumulation of SR-A-expressing TAMs has been correlated with poor patient outcomes. Our preliminary data show that SR-A binds to tumor-associated glycans (TAGs) on the surface of breast cancer cells. However, how macrophages bind tumor cell ligands in the tumor microenvironment (TME) is not clear. Tumor-derived exosomes (TDEs) are secreted extracellular vesicles that resemble the tumor cell membrane, carrying cargo that may mediate an immune response within the TME. In this study, we investigated whether TDE glycans represent tumor cell-surface TAGs and whether TDEs interact with macrophages through SR-A.
Methods: TDEs were isolated from the murine breast cancer cell line (E0771) by ultracentrifugation of the cell culture medium and then sized and counted using nanoparticle tracking analysis and electron microscopy. The glycans present on the tumor cell surface and TDEs were characterized using plant lectins in flow cytometry and sandwich ELISAs. The isolated TDEs were then fluorescently labeled, and their binding to the murine macrophage cell line Raw 264.7 was assayed by flow cytometry and fluorescence microscopy.
Results: SR-A binds strongly to breast cancer cell lines, and a significant portion of the binding depends on the presence of cell surface N-linked glycans. Lectins reactive with sialylated and fucosylated terminal structures showed differential binding to tumor cells and TDEs. We observed that the glycan profiles of E0771 cells and exosomes isolated from E0771 cultures were similar. Our results indicate that TDEs interact with Raw 264.7 cells, and the interaction is mediated by SR-A.
Conclusions: TDEs released in the TME can potentially interact with TAMs through SR-A. The glycan profile of TDEs is representative of host cells and may contribute to SR-A-mediated interaction with TAMs.

#0187 Macrophage instead of leukemia cell expressed PD-L1 drives T cell exhaustion and immune evasion of BCRABL1 chronic myeloid leukemia.

X. Lu, H. Fang, X. Fang, A. Matsunaga, K. Liu, J. Cortes, J. K. Cowell, T. Hu;
Medical College of Georgia, Augusta, GA

BCR-ABL1 fusion gene is the hall marker of chronic myeloid leukemia (CML). Currently, the immune microenvironment of BCRABL1 CML remains largely unexplored. Our recent investigation in a transgenic mouse model of BCRABL1 CML revealed a continuous increase in CD11b+Ly6C^{int} PMN-MDSC with the progression of the disease. Concurrently, there was an increase in CD11b+Ly6C^{high} M-MDSC and F4/80+ macrophages. However, The levels of CD4+ T cells, CD8+ T cells, CD19+ B cells, and CD49b+ NK cells, which are essential for tumor-killing significantly decreased. This immune phenotype was consistently observed in both primary leukemia induction and following serial transplantation of cells from primary leukemic mice. Intriguingly, only recipient mice subjected to sublethal irradiation developed the disease, while mice with intact immune system remained disease-free, which underscores the vital role of the immune system in the development of CML. The predominant presence of CD11b+Ly6C^{int} PMN-MDSC in the peripheral blood, bone marrow and spleen implies these cells may be at least partially consisted of CML leukemia cells. To examine the hypothesis, qRT-PCR and immunofluorescence (IF) staining were conducted. In both assays, Ly6G+ cells from BCRABL1 mice coexpressed the BCRABL1 oncogene. Furthermore, when co-cultured with CD4 T cells, the division of T cells was significantly inhibited, implying immune suppression by the Ly6G+ PMN-MDSCs and/or CML leukemia cells. In addition, the immuosuppressive pathway genes including Arg1, Hif1a, Enptd1, TGFβ were significantly upregulated. To investigate the possible role of the PD1/PDL1 axis in the BCRABL1 model, flow cytometry analysis was conducted. Unexpectedly, PDL1 was barely expressed in CML leukemia cells, whereas the expression of PDL1 in M-MDSCs and macrophages significantly increased, accompanied by remarkable upregulation of PD1 expression on CD4 T cells and CD8 T cells during leukemia progression. In other words, PDL1 expression on macrophages, rather than leukemia cells, was found to induce T cell exhaustion. For translational purpose, mice transplanted with the primary CML leukemia cells were treated with chemotherapy drugs ponatinib alone or in combination with the anti-PD1 antibody. Compared with the chemotherapy alone group, the mice in the combinational therapy group exhibited rapid remission and better disease control. Most importantly, the disease relapse occurred at a slower rate after treatment discontinuation, suggesting the value of combinational therapy in achieving treatment free remission. In summary, our study not only revealed the dynamic changes of immune microenvironment in the BCRABL1 CML mouse model, but also revealed the different mechanisms underlying immune evasion of BCR-ABL1 CML leukemia cells, which sheds light on a combinational treatment for achieving the treatment free remission of CML.

#0188 Investigating the macrophage and microglia response to ferroptosis in glioblastoma.

S. Y. Chih[1], M. Tang[1], S. Kim[1], T. Lu[1], R. Harter[2], J. Thorpe[1], W. Li[1];
[1]Penn State College of Medicine, Hershey, PA, [2]Penn State University, University Park, PA

Glioblastoma (GBM) is the most common malignant primary brain tumor. The median survival is less than two years. The mesenchymal (MES) subtype of GBM is particularly associated with treatment resistance, poor prognosis, and enriched infiltration of immune cells, including tumor-associated microglia and/or macrophages (TAMs). Despite promising results in preclinical studies, clinical trials targeting TAMs have been unsuccessful. Necrosis is a hallmark of GBM and correlates with unfavorable outcomes, but how necrosis results in poor prognosis is not well understood. We previously showed that neutrophils promote tumor necrosis and GBM progression by inducing ferroptosis, a form of regulated cell death due to iron-dependent lipid peroxidation. Understanding the effects of GBM ferroptosis on TAMs can provide further insights into how tumor necrosis ultimately leads to poor prognosis in GBM. We developed an orthotopic xenograft GBM mouse model harboring a constitutively active mutant of the Hippo pathway transcriptional coactivator with PDZ-binding motif (TAZ). Tumors of this model displayed MES characteristics and developed necrosis to an extent similar to patients with GBM. Using this model, confocal microscopy and flow cytometry studies revealed the presence of immune cells positive for markers of neutrophils and macrophages/microglia in the necrotic region of the tumor. Although we have yet to establish an in vitro model to study these cells, we found that conditioned media (CM) derived from ferroptotic GBM cells induced more macrophage differentiation from bone marrow cells when compared to live GBM CM. This led us to hypothesize that ferroptosis in GBM is immunogenic and orchestrates the immune response mounted by TAMs. We conducted an RNA sequencing (RNA-seq) study of bone marrow cells cultured in ferroptotic CM. Compared to live CM, ferroptotic CM upregulated several pro-inflammatory cytokine signaling pathways. We validated the mRNA expression levels of the identified cytokines by RT-qPCR. RNA-seq analysis also revealed the activation of phagosome formation pathway. Through phagocytosis assay, we showed that macrophages preferentially engulfed ferroptotic GBM cells over necrotic or live cells. To identify transcriptional changes in GBM cells undergoing ferroptosis, we carried out an RNA-seq study showing that ferroptotic GBM cells also upregulated several pro-inflammatory cytokine signaling pathways, which were validated by RT-qPCR. We also found that ferroptotic GBM cells released ATP extracellularly, where such release temporally coincided with the increase in pro-inflammatory cytokines. Our results suggest that ferroptosis in GBM is immunogenic and induces a pro-inflammatory response in macrophages/microglia. We are conducting further in vitro and in vivo studies to better understand how these macrophages/microglia modulate other immune cells and play a role in GBM progression.

TUMOR BIOLOGY: Membrane, Biophysical, and EMT Aspects of Motility/Metastasis
Poster Session

#0192 Orchestrating CDC42 turnover to regulate membrane protrusion and tumor metastasis.
S.-Y. Hsieh;
Chang Gung Memorial Hospital - Taoyuan Branch, Taoyuan, Taiwan

F-actin cytoskeleton remodeling is essential for cell migration, organ development, and immune responses. CDC42, a factor orchestrating F-actin remodeling for membrane dynamics, switches between its inactive GDP- and active GTP-bound forms. However, the biological and clinical significance of the mechanisms regulating CDC42 protein turnover remains unclear. Here we show that KLHL23-mediated CDC42·GTP polyubiquitylation for degradation and RhoGDI-mediated CDC42·GDP sequestration away from the plasma membrane co-inactivate CDC42 in a spatiotemporal context, influencing membrane dynamics and homeostasis during migration. Via a functional genomic screen, we identified KLHL23 as a suppressor of tumor invasion. Decreased KLHL23 level was associated with tumor metastasis and poor clinical outcomes in patients with liver and pancreas cancers. KLHL23 functions as the E3 ligase responsible for CDC42 polyubiquitylation and degradation. KLHL23 shares with RhoGDI the switch II region of CDC42 for binding, enhancing selective targeting of CDC42·GTP and CDC42·GDP, respectively. KLHL23 depletion in cells leads to F-actin and membrane over-protrusion, as well as epithelial-mesenchymal transition and tumor metastasis. Fluorescence resonance energy transfer assays reveal that the KLHL23—CDC42·GTP interaction plays a primary role in quenching CDC42 activity during membrane protrusion-retraction, while the RhoGDI—CDC42·GDP interaction occurs lately. Our results demonstrate the spatiotemporal interplay between RhoGDI and KLHL23 in regulating CDC42 turnover for membrane dynamics. As KLHL23/RhoGDI—CDC42 axis dysregulation causes tumor metastasis, our findings open avenues for exploring novel therapeutics.

#0193 Melanoma cytoskeletal dynamics, membrane remodeling, and motility are regulated by TRIM9.

Kimberly Lukasik, Jordan Brooks, Sam Redinbo, James Bear, Stephanie Gupton

University of North Carolina at Chapel Hill, Chapel Hill, NC

Cell shape change and motility are essential in metastasis and involve remodeling of the actin cytoskeleton, cell adhesions, and plasma membrane. How these cytoskeletal and membrane remodeling are regulated and coordinated remains largely unknown. We previously identified TRIM9 as a regulator of actin dynamics and exocytosis in developing neurons. Deletion of murine *Trim9* impairs neuronal migration, netrin-induced axon turning, and axonal and dendritic branching, and increased exocytosis and filopodial stability. In addition, we have shown TRIM9 alters dynamics of the actin polymerase VASP at filopodia tips via non-degrative mono-ubiquitination. TRIM9 is expressed in other motile cells, but the non-neuronal role of TRIM9 remains unknown. TRIM9 was identified as a possible prognostic biomarker in melanoma and high expression correlates with low patient survival. Melanomas undergo phenotype switching, where three distinct phenotypes exist that are associated with differences in gene expression. The three phenotypes consist of a melanocytic proliferative state, a neural crest-like invasive state, an intermediate state. Single cell RNAseq (scRNASeq) data from patient-derived melanoma indicate TRIM9 is highly expressed in the proliferative melanocytic state, which correlates with poor prognosis. *We hypothesize that TRIM9 coordinates actin dynamics, adhesion, and exocytosis in melanoma.* We show that TRIM9 protein is enriched in several human melanoma lines. Here we examine the role of TRIM9 in regulation of focal adhesions, exocytosis, migration, and invasion in two of these lines. Genetic loss of TRIM9 increased random migration velocity but reduced directional persistence. Interestingly, we find that TRIM9 plays a role in promoting bleb-like morphology and inhibits the ability to durotax on shallow gradients on soft substrate. Fluorescence recovery after photobleaching (FRAP), Total internal reflection fluorescence microscopy (TIRF), and widefield microscopy revealed that loss of TRIM9 results in increased focal adhesions, cell size, and altered dynamics of focal adhesion proteins VASP, zyxin, and paxillin dynamics. In addition, TRIM9 knockout cells exhibit reduced filopodial length and density and altered filopodial localization of VASP. In-gel zymography indicates that TRIM9 knockout cells also display an increased degradative capacity. Current studies are investigating how loss of TRIM9 alters parameters of cell contractility, lamellipodia, invadopodia, and exocytosis to define the role of TRIM9 in melanoma motility. Together these findings suggest TRIM9 reduces adhesion and migration, increases proliferation and blebbing and may be an important regulator of phenotype switching in melanoma.

#0194 Single-cell mechanical analysis reveals that astrocytes and glioblastoma cells have similar viscoelastic properties.

J. Najera, K. Onwudiwe, L. Holen, A. A. Burchett, D. Rodriguez, M. Zarodniuk, S. Siri, M. Datta;
University of Notre Dame, Notre Dame, IN

Despite recent advances in treatment, the survival rate of glioblastoma (GBM) patients remains low due to the cancer's resistance to current treatment modalities. Solid tumors like GBM are known to harbor physical abnormalities at the tissue and cell level. An understanding of GBM cell mechanics may therefore lead to the identification of novel disease mechanisms, biomarkers, and therapeutic strategies to improve treatment outcomes. In this study, we aimed to compare the mechanics of human GBM cells and their normal counterpart, immortalized human astrocytes (IHAs). To accomplish this, we used a parallel-plate flow system to expose single cells to physiological fluid shear stress and recorded the resulting deformation using a camera-coupled microscope. We then utilized digital image correlation analysis to create strain-time profiles of individual cells and fit the profiles with a three-parameter generalized Maxwell model to characterize their nuclear and cytoplasmic viscoelastic properties. We also used fluorescence microscopy and atomic force microscopy to quantify actin density and alignment and adhesion energy in both cell types, respectively. Our results showed that, contrary to extracranial cancer cells, the viscoelastic properties of GBM cells are similar to their normal counterpart. This may explain why metastasis in GBM patients is rare and conventional treatment options are unsuccessful. We also found that actin organization and localization and adhesion energy is different between GBM cells and IHAs. Thus, future research which links the genetic and microenvironmental factors that modulate these unique mechanical features may lead to the development of rational and novel clinical strategies against GBM.

#0196 *In vitro* modeling of pediatric solid tumor lung metastases.

M. Zylka[1], C. Hafemeister[1], L. Watzke[2], U. Mann[2], D. Surdez[3], E. Sweet-Cordero[4], B. Liegl-Atzwanger[5], M. Dettmer[6], M. Farlik[2], F. Halbritter[1], M. Metzelder[2], H. Kovar[1], B. Radic-Sarikas[1];

[1]St. Anna Children's Cancer Research Institute, Vienna, Austria, [2]Medical University of Vienna, Vienna, Austria, [3]Universitatsklinik Balgrist, Balgrist, Switzerland, [4]University of California, San Francisco, San Francisco, CA, [5]Medical University Graz, Graz, Austria, [6]Klinikum Stuttgart, Stuttgart, Germany

Metastasis remains the main cause of death in pediatric cancer patients with the lung being one of the most common affected organs. Our inability to cure these patients is largely due to insufficient knowledge about tumor and metastatic niche plasticity, while existing models are not fully effective in mirroring the response seen in clinical setting. Our goal is to overcome these limitations by establishing *in vitro* lung metastasis models using tumor/lung organoid co-cultures to study lung infiltration of pediatric solid tumors. We successfully established patient-derived lung organoids from pediatric lung tissue and characterized them according to the presence and the localization of the respective lung epithelial cell types. Co-culture conditions of lung organoids with PDX-derived Ewing sarcoma and osteosarcoma cells were optimized and models established, while the establishment of models for other pediatric solid tumor entities is ongoing. We have observed infiltration of the lung organoids by tumor cells, and our preliminary findings suggest distinct patterns of infiltration among different tumor entities. Furthermore, we have performed single-cell RNA sequencing analysis on these co-cultures in comparison to the parental lung organoids and tumor cells, aiming to uncover the specific signaling pathways activated in the lung metastatic niche in response to tumor cell invasion. Additionally, experiments using conditioned medium suggest that the lung organoid secretome is sufficient to induce homing of osteosarcoma and Ewing sarcoma cells to the organoids, with the CXCL12/CXCR4 signaling axis as a prime candidate driver. To ascertain the extent to which our *in vitro* model recapitulates the *in vivo* lung metastatic niche, we performed spatial transcriptomics (using VISIUM/10X Genomics) on formalin-fixed paraffin-embedded (FFPE) tissue blocks of paired primary tumors and lung metastasis samples for Ewing sarcoma and osteosarcoma. Comprehensive data analysis is currently ongoing, which will instruct a stepwise incorporation of additional factors into our modular organoid co-culture model, resulting in a better representation of the lung metastatic niche. Further, the analysis of patient-derived material will elucidate the spatial organization of solid tumor lung metastases and contribute to the identification of signaling pathways implicated in lung infiltration. In conclusion, our study not only unravels the complexities of pediatric solid tumor metastasis, but also lays the foundation for exploring the anti-metastatic potential of pathway-specific compounds targeting tumor/lung interactions using the established *in vitro* lung metastasis models. This study is supported by grant 35353-B of the Austrian Science Fund.

#0197 The GPR52-MCAM axis as a novel regulatory mechanism of breast cancer cell clustering and metastatic potential.

S. Z. Hanif[1], C. C. Au[1], I. Torregroza[1], B. Bhinder[1], L. Dow[1], O. Elemento[1], T. Evans[1], **K. A. Brown**[2];
[1]Weill Cornell Medicine, New York, NY, [2]University of Kansas Medical Center, Lawrence, KS

Background: Breast cancer is the most diagnosed cancer worldwide and is the second leading cause of cancer death among women in the United States. Despite breakthroughs in targeted therapies for breast cancer, the 5-year survival rate for women with metastatic breast cancer is 30%. There is a strong rationale to explore the therapeutic potential of G-protein coupled receptors (GPCRs), which comprise the largest class of proteins successfully targeted by FDA-approved drugs. Importantly, at least one-third of GPCRs are “orphans” and remain largely uncharacterized. One of these orphan GPCRs is GPR52. To date, there is no literature on the role of GPR52 in any cancer type, but we find from publicly available clinical data that low mRNA expression of GPR52 in breast tumors correlates with reduced overall survival (hazard ratio=0.67 [0.53-0.83], logrank P= 0.00035) and that GPR52 mRNA levels tend to be lower in tumor metastases compared to primary tumor (n>80, p=4.45e-17). Therefore, we hypothesize that loss of GPR52 may support breast cancer metastasis.
Results: We used CRISPR-Cas9 to knockout (KO) GPR52 in triple-negative breast cancer cell lines MDA-MB-468 and MDA-MB-231, and in the non-cancerous breast epithelial cell line MCF10A, and confirmed the generation of frameshift mutations by Sanger sequencing. Interestingly, we observed that GPR52 KO cells clustered together *in vitro* in 2D and hypothesized that this characteristic may allow GPR52 KO breast cancer cells to increase their metastatic potential. We conducted invasion assays though Matrigel and found that GPR52 KO cells were more likely to invade as sheets or clusters. To determine the *in vivo* impact of GPR52 loss, we injected MDA-MB-468 GPR52 KO cells in zebrafish (*Danio rerio*) two days post-fertilization and observed that GPR52 loss led to increased metastatic foci and total cancer surface area thirty hours post-injection ($n \geq 12$, $p<0.05$). We determined from RNA-sequencing (n=3, p<.0001) and confirmed with western blotting that the melanoma cell adhesion molecule (MCAM) is upregulated in the MCF10A and MDA-MB-468 GPR52 KO cells. Increased mRNA expression of MCAM has been associated with reduced overall survival in breast cancer patients (hazard ratio=1.33 [1.05-1.62], logrank P= 0.02)
Conclusion: Knockout of GPR52 from breast cancer cells promotes increased cell clustering *in vitro* and metastasis in zebrafish. These data support the investigation of GPR52 as a biomarker of cancer aggression and a potential therapeutic target for breast cancer patients whose tumors express GPR52.

#0198 Selective targeting of endothelial mTORC1 reduces transendothelial fatty acid delivery to improve anti-tumor immunity and suppress metastatic outgrowth.

D. N. Edwards[1], S. Wang[1], W. Song[1], L. C. Kim[2], Y. Hwang[1], J. Chen[1];
[1]Vanderbilt University Medical Center, Nashville, TN, [2]Vanderbilt University, Nashville, TN

Tumor metastasis requires sufficient nutrients to support outgrowth of disseminated tumor cells. Cancer cells utilize fatty acids as a key source of energy and biomass, but these nutrients impair the cytotoxic activities of T cells, serving to support metastatic progression. Blood is a rich source of fatty acids, but the vascular endothelium serves as a barrier to limit access to the surrounding tumor tissue. However, it is unclear how long-chain fatty acid delivery to early metastatic tumors is regulated. Here, we report that endothelial mTORC1 promotes transport of fatty acids into developing metastatic tumors, leading to reduced anti-tumor immune responses and improved outgrowth. Using a murine model of metastatic outgrowth in the lung, tumor burden was significantly reduced upon targeted deletion of Raptor, an essential component of the mTORC1 complex, in endothelial cells ($Rptor^{ECKO}$). We employed a multifaceted approach using metabolomics, transcriptomics, and molecular assays to identify a Raptor/mTORC1-mediated mechanism of transendothelial fatty acid transport via RAB and CLSTN1 cargo trafficking. In vivo uptake of a fluorescent palmitic acid analog in tumor cells and T cells was reduced in $Rptor^{ECKO}$ lung metastatic tumors, which correlated with improved markers of cytotoxicity. Combination of low-dose RAD001/everolimus, which selectively inhibits mTORC1 in endothelial cells, with anti-PD1 reduces metastatic disease and impairs long-chain fatty acid uptake in T cells, corresponding to improved anti-tumor immunity. These findings describe a novel mechanism of transendothelial fatty acid transportation during metastatic outgrowth, supporting future development of therapeutic strategies to target endothelial mTORC1 activity.

#0199 Fluid shear stress enhances metastatic potential and rapidly alters metabolism of circulating tumor cells.

D. L. Moose, **A. N. Pope**, M. Dykstra, E. B. Taylor, P. Breheny, M. D. Henry;
Carver College of Medicine, University of Iowa, Iowa City, IA

Background and Purpose: Circulating tumor cells (CTCs) are exposed to mechanical and biochemical stresses including fluid shear stress (FSS) and oxidative distress. Recently we have shown that viable CTCs actively resist destruction when exposed to FSS by a mechano-adaptive mechanism that depends on RhoA-actomyosin activity [PMID: 32187555]. Since the RhoA-actomyosin axis is implicated in other cellular behaviors that might contribute to metastasis; herein, we explored the hypothesis that exposure to FSS alters the biology of viable CTCs to promote metastatic colonization.
Methodology: To determine if exposure to FSS alters metastatic potential, we exposed PC-3 prostate and MDA-MB-231 breast cancer cells to FSS prior to injection into the tail-vein of NCG mice. We then monitored metastatic colonization by weekly bioluminescence imaging. Further, we examined if FSS exposure altered the invasive potential of PC-3 and MDA-MB-231 cells, as well as their ability to survive/proliferate under anchorage-independent conditions. We conducted GC/LC-MS metabolomic profiling and measured lactate production following FSS exposure. To investigate oxidative burden on FSS exposed cells, we used dihydroethidium to measure general ROS production and a lipid peroxide sensor.
Results: We found that FSS exposure shortens the time for metastatic colonization for both cell lines. We found that FSS exposure leads to approximately two-fold increase in invasion through collagen matrix, which, for PC-3 cells, is RhoA dependent. Moreover, FSS exposure resulted in increased proliferation (~25%) under anchorage independent conditions in both cell lines. Metabolomic profiling revealed that FSS exposure resulted increased glycolysis, reduced entry into the TCA cycle, and increased lactate levels. We blocked glycolysis in PC-3 and MDA-MB-231 cells with 2-deoxyglucose and found that this increased the fraction of cells destroyed by FSS ~20-30%. We also investigated redox stress and found that compared to cells held in suspension, those exposed to FSS demonstrate lower ROS burden. Interestingly, cells exposed to FSS exhibit lower levels of lipid peroxides in a manner that depends on RhoA.
Conclusion: Our findings demonstrate that brief pulses of FSS exposure can enhance metastatic potential, increase invasive and anchorage-independent proliferative capacity and rapidly alter metabolism. The phenotypic changes driven by exposure to FSS depend in part on RhoA activation but may also reflect other mechanisms by which cancer cells sense and respond to FSS. The rapid changes in metabolism may act to reduce oxidative distress while CTCs are in suspension. In summary, our data indicate that FSS exposure in the circulation not only represents a physical force that CTCs must overcome to survive, but it also provides instructive cues that may enhance the metastatic behavior of some CTCs.

#0200 OA inhibits the development of breast cancer through K1108 acetylation of Zeb1.

M. Guo, Y. Wang, Y. Shi, S. Yang;
Nankai University, Tianjin, China

Background: Olive oil has long been considered a healthier edible oil, rich in 75% oleic acid (OA) as its main component. OA is a monounsaturated fatty acid, and recent studies have shown that it is no longer limited to protecting cardiovascular and cerebrovascular systems, but can also reduce the risk of cancer. However, there is limited research on the specific mechanism. After fatty acid is ingested into the body, through fatty acids β-oxidation produces acetyl-CoA, which is a donor of protein acetylation. EMT is an important process to regulate tumor metastasis, and Zeb1 is one of the important EMT transcription factors. Therefore, we explored whether OA could inhibit the progress of breast cancer by affecting the acetylation modification of Zeb1.
Methods: Western blotting, CCK8 assay, and Transwell were used to test the impact of gradient doses of OA on breast cancer cells. Immunoprecipitation and Immunoprecipitation mass spectrum were used to determine the acetylation modification sites of Zeb1. Coimmunoprecipitation, IF, and pull-down were used to test and verify the acetylase and deacetylase of Zeb1. Knockdown endogenous *ZEB1* and then reconstructed stable cell lines of Zeb1 wild-type ($Zeb1^{K1108WT}$), acetylation activated ($Zeb1^{K1108Q}$), and inactivated mutants ($Zeb1^{K1108R}$) by lentivirus. Detection of Zeb1 acetylation in patient tissue samples and mouse models under OA treatment using Zeb1-specific acetylation-modified antibodies.
Results: OA inhibits the proliferation and migration of breast cancer cells in a concentration gradient-dependent manner, and inhibits the expression of Zeb1, N Cadherin, and upregulates E Cadherin. Among numerous fatty acids, only OA can promote the acetylation of Zeb1 by adjusting the ratio of acetyl-CoA and NAD+/NADH. K1108 is a biologically functional acetylation site of Zeb1, $Zeb1^{K1108R}$ exerts the cancer promoting function of Zeb1, while $Zeb1^{K1108Q}$ does not. OA can promote acetylation of $Zeb1^{K1108WT}$, but cannot promote acetylation of $Zeb1^{K1108R}$.
Conclusions: OA inhibits the development of breast cancer through K1108 acetylation of Zeb1. These results suggest that breast cancer may be ameliorated through dietary interventions.

#0201 Morphological changes to the vulvar squamous carcinoma cell line, A431, resulting from clobetasol-induced upregulation of vimentin.

J. E. Lewis, K. Haering, K. Yokoyama;
SUNY Geneseo, Geneseo, NY

Vimentin is recognized as an important marker in the epithelial-mesenchymal transition (EMT) of several cancer cell types. The overexpression of vimentin appears to coincide with increased tumor growth, migration, and poor prognosis. The vulvar cancer cell line, A431, is of squamous cell origin and displays hallmarks of a squamous cell including expression of cytokeratins 8 and 18 as well as E- and P-cadherin. We have found that treatment of A431 cells with the glucocorticoid, clobetasol, results in upregulation of vimentin which is accompanied by change to a more mesenchymal-like morphology. Despite this change in morphology, the cells continue to express cytokeratins 8 and 18. This suggests that the vimentin has a greater impact on cell morphology than does cytokeratins 8 and 18. However, we previously reported that the analogous glucocorticoid, dexamethasone, also downregulates E- and P-cadherin in these cells which may account for the observed change in morphology. Here we examine more closely the impact of vimentin on cellular morphology in the clobetasol treated A431 cells by both immunofluorescence microscopy and Raman imaging.

#0202 Spry1 targeting enhances E-cadherin expression in cutaneous melanoma.

Barbara Montico[1], Giorgio Giurato[2], Roberto Guerrieri[1], Annamaria Salvati[2], Francesca Colizzi[1], Lorena Baboci[1], Luca Sigalotti[1], Alessia Covre[3], Michele Maio[3], Agostino Steffan[1], Tuula Anneli Nyman[4], Alessandro Weisz[2], Maurizio Mongiat[1], Eva Andreuzzi[5], Elisabetta Fratta[1]

[1]Centro di Riferimento Oncologico IRCCS, Aviano, Italy,[2]'Scuola Medica Salernitana', University of Salerno, Salerno, Italy,[3]Center for Immuno-Oncology, University Hospital of Siena, Siena, Italy,[4]Institute of Clinical Medicine, University of Oslo, Oslo, Norway,[5]Institute for Maternal and Child Health IRCCS Burlo Garofolo, Trieste, Italy

Background: Cutaneous melanoma (CM) is a very aggressive malignancy that still represents the deadliest form of skin cancer. About 50% of CM harbors the activating $BRAF^{V600}$ mutation which exerts most of the oncogenic effects through the MAPK signaling pathway. In the last years, a number of MAPK modulators have been identified, including Spry1. In this context, we have recently reported that Spry1 knockdown ($Spry1^{KO}$) reduced the expression of several markers of epithelial-mesenchymal transition (EMT) both *in vitro* and *in vivo*. Loss of E-cadherin is a hallmark of EMT in CM, and the presence of aberrant E-cadherin expression in CM is usually associated with a significantly worse overall survival. Based on these premises, in this study we wondered to explore whether Spry1 influences EMT through the modulation of E-cadherin expression.

Material and Methods: SPRY1 gene was knocked-out using the CRISPR strategy in BRAF wild-type (wt) and in BRAF-mutant CM cell lines. By using *in vitro* and *in vivo* models, the effects of $Spry1^{KO}$ on E-cadherin expression and localization was investigated through RNA-sequencing (RNA-seq), quantitative real-time PCR, western blot, and immunofluorescence analyses. To gain insight into Spry1 interactome, immunoprecipitation coupled to mass spectrometry (IP-MS) was performed.

Results and Discussion: E-cadherin mRNA and protein levels were significantly increased both *in vitro* and *in vivo* in $Spry1^{KO}$ clones. In addition, immunofluorescence analysis revealed a sustained redistribution of E-cadherin to the plasma membrane following Spry1 loss, thus confirming that Spry1 plays a role in EMT in CM. E-cadherin requires p120-catenin (p120) to maintain cell adhesion and functional adherens junctions. Indeed, p120 dysregulation results in the rapid turnover of E-cadherin complexes. Intriguingly, IP-MS analyses identified several Spry1 protein partners, including p120. Although a number of functional studies are still ongoing, preliminary western blot analysis of cytosolic and mitochondrial proteins indicated that Spry1 and p120 were mostly located in mitochondria.

Conclusion: Spry1 reduced E-cadherin expression *in vitro* and *in vivo*. Starting from preliminary data, we hypothesized that Spry1-p120 interaction might influence E-cadherin distribution over the plasma membrane.

#0203 Promotion of metastasis of ERBB2-positive breast cancer by mesenchymal stem cells via exosomes-mediated activation of ERBB2/ERBB3→PI3K/Akt singaling pathway.

Y. Wu[1], L. Chen[1], Y. Cao[2], Q. Huang[1], H. Niu[1], X. Lai[1], M. Zhao[1], H. Yan[1], H. Lyu[3], B. Liu[4], S. Zhang[1], **S. Wang**[1];
[1]Affiliated Dongfang Hospital of School of Medicine (the 900th Hospital), Xiamen University, Fuzhou, China, [2]Fuzhou General Clinical Medical School, Fujian Medical University, Fuzhou, China, [3]Stanley S. Scott Cancer Center, School of Medicine, Louisiana State University (LSU) Health Sciences Center, New Orleans, LA, [4]Stanley S. Scott Cancer Center, School of Medicine, Louisiana State University (LSU) Health Sciences Center, Fuzhou, LA

Elevated expression of ERBB3 receptor correlates with increased distant metastasis of breast cancers with amplification and/or overexpression of *ERBB2* (*HER2/neu*), which the underlying molecular mechanism remains unclear. In recent years, cumulative studies have demonstrated that mesenchymal stem cells (MSCs), one of the important cellular components in tumor microenvironment, play important roles in multiple hallmarks of cancer including invasion and metastasis. However, its role in metastasis of ERBB2-positive breast cancer as well as the precise mechanisms are largely unrevealed. In our current study, we found that co-culture with MSCs or treatment with exosomes derived from MSCs can significantly promote the epithelial-mesenchymal transition (EMT), migration and invasion of ERBB2-positive breast cancer cells. MSCs exhibited significantly higher expression of NRG-1, a known ligand of ERBB3, as compared with ERBB2-positive breast cancer cells. The presence of NRG-1 in exosomes derived from MSCs was also evidenced. Mechanistically, co-culture with MSCs or treatment with exosomes derived from MSCs induced upregulation of ZEB1 and Slug via activation of downstream PI3K/Akt singaling to promote EMT of ERBB2-positive breast cancer cells. In addition, the expression of MMP2 was also upregulated by treatment with MSCs-derived exosomes, which enhanced the migration and invasion of ERBB2-positive breast cancer cells simultaneously. Interestingly, our study further demonstrated that treatment with MSCs-derived exosomes could significantly downregulate the expression of PTEN, the key negative regulator of PI3K/Akt singaling, via transferring three PTEN-targeting miRNAs (miR-21-5p, miR-23a-3p, and miR-148a-3p). Taken together, we presented here that MSCs may, on the one hand, directly activate the ERBB2/ERBB3→PI3K/Akt signaling pathway in ERBB2-positive breast cancer cells through the expression and secretion of NRG-1 via exosomes. Meanwhile, miR-21-5p, miR-23a-3p, and miR-148a-3p targeted delivery by exosomes specifically downregulated the expression of PETN, thus reliefs the negative regulation of PI3K/Akt signaling in ERBB2-positive breast cancer cells. These effects of MSCs act in concert to promote the metastasis of ERBB2-positive breast cancer. Our study lays a theoretical foundation and preliminary experimental basis for the development of novel combined therapies for patient with ERBB2-positive breast cancer through co-targeting MSC-derived NRG-1 and miR-21-5p, miR23a-3p, miR148a-3p/PTEN axis in tumor microenvironment in the future.

#0204 Quantitative evaluation of biomarkers for TGF-β-induced epithelial-mesenchymal transition in biochemical, cellular, and 3D spheroid model systems.

A. W. Wood[1], E. Heimsath[2];
[1]Cell Signaling Technology, Inc., Danvers, MA, [2]Agilent Technologies, Inc., Winooski, VT

Epithelial-mesenchymal transition (EMT) is a cellular differentiation process whereby epithelial cells lose epithelial features and acquire mesenchymal, fibroblast-like properties, leading to reduced cell-cell contacts and increased motility. EMT is a fundamental biological process required for normal embryonic development, but may be co-opted by malignant epithelial tumors to facilitate metastatic spread. A known driver of EMT is the TGF-β superfamily of growth factor ligands, which elicit receptor-mediated responses in cells, primarily via TGF-β/SMAD signaling pathways. In these pathways, receptor-mediated SMAD (R-SMAD) proteins serve as the primary downstream effector molecules, the activities of which are regulated through receptor-mediated phosphorylation. The magnitude and duration of ligand-induced receptor activation influences the level of SMAD phosphorylation, which in turn influences the magnitude of the downstream cellular response(s). In this study, we describe high-throughput methods to quantitatively evaluate the biochemical and cellular responses to TGF-β/SMAD pathway activation in a cellular model of TGF-β-induced EMT. Effects of pathway activation are examined at different levels of biological complexity (biochemical, cellular, and multicellular), using 2D and 3D (spheroid) models. Collectively, these approaches enable a comprehensive evaluation of TGF-β/SMAD pathway activation that is amenable to high-throughput analysis platforms.

#0205 Adaptive membrane trafficking activated by epithelial-to-mesenchymal transition drives lung adenocarcinoma progression.

O. E. Obaleye, K. L. Fulp, G.-Y. Xiao;
University of Kentucky, Lexington, KY

Cancer cells can become metastatic and develop resistance to targeted therapies through epithelial-to-mesenchymal transition (EMT), which is regulated by epigenetic factors. Our ultimate objective is to understand the molecular mechanisms behind EMT-driven cancer progression and identify potential targets for preventing cancer metastasis. Recently, we made groundbreaking discoveries indicating that EMT can modify membrane trafficking machinery to coordinate cancer cell invasion and immunosuppression in the tumor microenvironment (TME) of lung adenocarcinoma (LUAD). To dissect the “adaptive” membrane trafficking program, we initiated a CRISPRi *in vivo* screen to assess more than 2000 trafficking-related genes in syngeneic mouse LUAD models for their requirements for tumorigenesis both with and without immune selective pressure. We identified a panel of membrane trafficking regulators that specifically “dropped out” in immunocompetent mice, suggesting their essential roles in the immunosuppressive TME. Of particular interest is REEP2. REEPs are an evolutionarily conserved protein family that is critical to the endoplasmic reticulum (ER) function and potentially regulates secretory trafficking. We discovered that REEP2 is specifically linked to poor prognosis in LUAD patients and is highly correlated with a z-normalized, 16-gene EMT score (P = 1.32e-27) that was previously reported. Our previous studies demonstrated that the EMT activator, ZEB1, accelerates membrane trafficking dynamics by silencing a microRNA network that targets multiple membrane trafficking components. Analysis of REEP2 3’-untranslated regions (3’-UTRs) identified predicted binding sites for several microRNAs, which are silenced by ZEB1. Thus, we hypothesize that ZEB1 coordinates a microRNA network to activate REEP2-driven ER trafficking. We show that REEP2 depletion significantly reduces the invasion of cancer cells but does not affect their migration and proliferation. These findings suggest that REEP2 plays a significant role in extracellular matrix (ECM) modification to enhance the invasion of metastatic cells, conferring a vulnerability in EMT-driven LUAD metastasis.

#0206 Intratumoral accumulation of CD38 enhances immune evasion and metastasis in models of breast cancer with EMT plasticity.

T. Visal;
The University of Texas MD Anderson Cancer Center, Houston, TX

Background- Triple-negative breast cancer (TNBC) is challenging to treat due to fewer clinically detectable targets and its propensity to metastasize. Epithelial to mesenchymal transition (EMT) is a key feature of the metastatic cascade. Recent data highlights the enhanced metastatic potential of hybrid epithelial-mesenchymal (EM) phenotypes from partial activation of EMT. However, mechanistic insights and targetable vulnerabilities within hybrid EM remain elusive. We identified that hybrid EM tumors are enriched in CD38, an immunesuppressive molecule associated with worse clinical outcomes in liquid malignancies. Hence, we sought to investigate role of CD38 in hybrid EM-driven metastasis. We hypothesize that hybrid EM tumors drive metastasis via intratumoral accumulation of CD38, promoting an immunosuppressive tumor microenvironment (TME).
Methods- Reverse Phase Protein Array, cell migration/invasion assays, flowcytometry and immunohistochemistry were used to evaluate phenotype, immune cell populations and molecular mechanisms upon CD38 knockdown (KD) and overexpression (OE) *in vivo*.
Results- CD38 KD weakened the process of EMT and reduced cell migration and invasion. Tumors lacking CD38 showed increased infiltration of CD8 T cells and M1-like (anti-tumor) macrophages coupled with a decrease in immunosuppressive regulatory T cells (T_{regs}) and M2-like (pro-tumor) macrophages. In contrast, cancer cells with CD38 OE maintained a hybrid phenotype through co-expression of epithelial and mesenchymal markers and also showed significant increase in cell migration and invasion. Tumors arising from CD38 OE cells displayed a significant increase in T_{regs}. Most strikingly, hybrid EM tumors that no longer express CD38 show reduction in lung metastases and circulating tumor cell colonies. Taken together, these findings suggest that CD38 is important for the metastatic and immune evasive potential of hybrid EM breast cancers.
Conclusion- Our data exposes CD38 as a survival strategy in hybrid EM tumors to suppress immune cells and sustain metastasis with strong implications in other carcinomas which have hybrid EM properties.

#0207 Tumor suppressive role of NKX2-1 in advanced thyroid cancer progression.

Y.-T. Shirai, S. Kimura;
National Institutes of Health, National Cancer Institute, Bethesda, MD

NKX2-1 is a homeodomain transcription factor, known as a master regulator of thyroid development. NKX2-1 is also crucial for lung epithelium differentiation, and the involvement of NKX2-1 in lung carcinogenesis and cancer progression has been intensely investigated. However, the role of NKX2-1 in thyroid cancer progression remains elusive. The Cancer Genome Atlas (TCGA) dataset analysis demonstrated that papillary thyroid cancer (PTC) patients with low *NKX2-1* mRNA expression had significantly poorer prognosis than those with a combination of intermediate and high mRNA expression of *NKX2-1.* Lentivirus-transduced tetracycline (Tet)-inducible system was used to achieve NKX2-1 overexpression in advanced follicular thyroid cancer (FTC) cell lines, FTC-238 and WRO, and an anaplastic thyroid cancer (ATC) cell line 8305C, in which NKX2-1 expression is barely/not detected. All these thyroid cancer cell lines showed significant suppression of cell proliferation with NKX2-1 overexpression. In addition, NKX2-1 overexpression inhibited migration of FTC-238 cells. The levels of mRNA and protein expression of mesenchymal markers, matrix metalloproteinase-2 (MMP-2) and fibronectin, were decreased by NKX2-1 overexpression in FTC-238 cells, suggesting a possibility that NKX2-1 partially inhibits epithelial-mesenchymal transition (EMT). SNAIL and SLUG are essential EMT transcription factors involved in metastasis in cancer progression. *NKX2-1* mRNA expression was significantly lower in high *SNAI1* (encoding SNAIL) expressing PTC in TCGA database. Indeed, suppression of SNAIL protein expression was found upon overexpression of NKX2-1 in FTC-238 cells which naturally express high level of SNAIL. These findings suggest that NKX2-1 may inhibit the migration of advanced thyroid cancer cells through SNAIL-induced EMT. Similarly, suppression of SLUG protein expression by overexpression of NKX2-1 was observed in WRO and 8305C cells which express high level of SLUG protein. Whether NKX2-1 overexpression inhibits migration and invasion of WRO and 8305C cells through SLUG-induced EMT is currently under examination. The Tet-inducible NKX2-1 expressing thyroid cancer cells will be used for *in vivo* evaluation of their metastatic ability using an immunocompromised mouse model. The findings so far suggest that NKX2-1 exerts a tumor suppressive activity in advanced thyroid cancers through suppression of cell proliferation, and cell migration presumably via suppression of EMT transcription factors.

#0208 FGFR2 splice variant as a cell fate adjudicator determines clinical outcomes in non-small cell lung cancer.

H. Yu[1], M. Horie[2], A. Lindberg[1], M. Backman[1], N. Hekmati[1], J. Mattsson[1], N. Miyashita[3], H. Brunnstrom[4], F. Ponten[1], A. Saito[5], C. Strell[1], P. Micke[1]; [1]Uppsala University, Uppsala, Sweden, [2]Kanazawa University, Kanazawa, Japan, [3]Duke University School of Medicine, Durham, NC, [4]Lund University, Lund, Sweden, [5]The University of Tokyo, Tokyo, Japan

The splice variants specific protein expression in tumor cells presents promising targets for cancer therapy. The concept is supported by the recent introduction of the splice variant-specific antibody against FGFR2 IIIb (FGFR2b) in gastric cancer. Indeed, signaling of the two FGFR2 splice variants FGFR2b and FGFR2 IIIc (FGFR2c), whose expression is mutually exclusive on a cellular level, is mediated by different ligands and distinct downstream responses that can contribute to many aspects of tumorigenesis. Our study aimed to characterize the expression FGFR2b and 2c in non-malignant lung and non-small cell lung cancer (NSCLC) tissue and relate splice variant-specific expression to the histological and molecular background of cancer and its clinical impact.FGFR2b/FGFR2c isoforms expression was determined in RNA-seq data from 180 NSCLC patients and 19 tissues from normal lung (patient-matched). Cell-type specific expression and pan-cancer analysis of FGFR2 were explored using a public database, including DBTSS (NSCLC: 26, normal lung epithelium: 1, normal lung fibroblast 1) and CCLE (Total: 1019, NSCLC: 131), GTEx (normal lung tissue: 578) and HPA (scRNAseq for lung).Our results confirm a cell-specific expression in normal cells with dominance of FGFR2b in epithelial cells and FGFR2c in mesenchymal cells. In normal lung tissue, the FGFR2b variant showed high abundance. Pan-cancer analysis revealed FGFR2c dominant cancers (e.g., CNS tumors, kidney, liver) as well as FGFR2b dominant cancer types (e.g., breast, colon, lung cancer). The RNAseq data from our NSCLC cohort showed a chief expression of FGFR2b in 116 cases (64%), FGFR2c in 31 cases (17%), and a mixed FGFR2c/FGFR2b transcriptomics (18%). The ratio of FGFR2b/FGFR2c as a metric for splice variant dominance was associated with squamous histology, higher stage, and KRAS mutations. Differential gene expression analysis of cancer tissue and cell lines revealed an association of the splice variant FGFR2c to epithelial-mesenchymal transition (EMT) and the regulation of genes (ZEP1, ERSP1, CDH1) involved in the TGF-beta signal pathway. Finally, the ratio of FGFR2b /FGFR2c demonstrated a strong association with overall survival in NSCLC patients with the FGFR2c variant as unfavorable predictors (High vs low ratio, $p = 0.01$). Our study indicates cell-specific splice variant expression in non-malignant and malignant cells. The prognostic unfavorable impact of the FGFR2c variant on NSCLC patient survival might be explained by its association with TGF signaling and EMT. The observed clinical and biological difference between FGFR2b and FGFR2c dominated cancers gives further rationale to exploit splice variants as therapeutical targets.

#0210 Carcinogenic influence of e-cigarette aerosols on breast and lung cancer models.

R. Begum, S. Thota, N. Chintala, B. Sapkota, A. Pandit, J. Francis;
Louisiana State University, Baton Rouge, LA

Background and Purpose: With the rising popularity of E-cigarettes among the youth, there is an urgent need to understand their long-term health implications, particularly the potential for carcinogenesis. Although tobacco smoking is established as a major cancer risk factor, the carcinogenic potential of E-cigarettes remains underexplored. Given that metastatic cancer accounts for most cancer-related deaths in the United States, elucidating the biological impacts of E-cigarette aerosols on cancer progression is critical for developing effective interventions. This study aims to address this critical gap by exploring the effects of E-cigarette aerosols on cellular models pertinent to breast and lung cancer.
Methods: Mouse breast epithelial cells (HC11), triple-negative breast cancer cells (4T1), and human lung adenocarcinoma cells (Calu-3) were exposed to E-cigarette aerosol at the air-liquid interface for one hour, followed by a 24-hour recovery period.
Results: Our study revealed that E-cigarette aerosols with mint flavor induce epithelial-to-mesenchymal transition (EMT) in both normal mammary epithelial and breast cancer cells. Furthermore, we also observed activation of the TGF pathway and an increased expression of stemness-related markers (OCT4, SOX2, NANOG, KLF4, and c-MYC) in 4T1 cells exposed to mint and menthol-flavored E-cigarette aerosols in both 2D and 3D cell culture environments. Microscopic examination at a 10X magnification level revealed that 4T1 and Calu-3 cells exposed to menthol-flavored E-cigarette aerosols exhibited signs of cellular disassociation and detachment whereas the control cells maintained discoidal aggregate morphology.
Conclusion: The data presented here illuminate a potential link between E-cigarette use and carcinogenic processes, challenging the notion of E-cigarettes as a safe smoking alternative. This research is of paramount importance to cancer research as it unveils possible new avenues for tumor progression, emphasizing the necessity for a critical evaluation of E-cigarette products.

#0211 Applying cellular thermal shift assays to uncover novel regulators of epithelial to mesenchymal transition in triple negative breast cancer.

Jessica A. Lidster[1], Ser Yue Loo[2], Zhengwei Wu[2], Lingyun Dai[3], Seow Qi Ng[2], Nayana Prabhu[4], Dennis Kappei[1], Wai Leong Tam[2]

[1]Cancer Science Institute of Singapore, Singapore, Singapore,[2]Genome Institute of Singapore, Singapore, Singapore,[3]Nanyang Technological University, Singapore, Singapore,[4]Institute of Molecular and Cell Biology (IMCB), Singapore, Singapore

Metastatic Breast Cancer is accountable for over half a million deaths worldwide each year, the majority of which are from the triple negative breast cancer (TNBC) subtype, known to be highly aggressive, metastatic and resistant to targeted therapy. Metastasis is driven by the ability of cancer cells to undergo epithelial to mesenchymal transition (EMT), a cell state transition involving a gain of stemness, cell motility and chemoresistance. EMT has been well characterized using a range of techniques based upon quantitative proteomics and transcription profiling, yet targeting EMT to prevent tumor metastasis and chemoresistance is an obstacle that remains to be fully overcome. Using a cellular thermal shift assay coupled with mass spectrometry (CETSA-MS), we have measured changes in protein stability upon induction of EMT and have uncovered key enzymes in the citric acid (TCA) cycle that are stabilized during EMT of human mammary epithelial cells. Such enzymes are responsible for the conversion of TCA cycle intermediates required for a recently discovered post-translational modification. In TNBC cells, we find that loss of these enzymes causes not only global changes to crucial post-translational modification of mitochondrial proteins, but very specific alterations in several cytoskeletal proteins, leading to altered EMT status as well as reduced tumor growth and initiation both *in vitro* and *in vivo*. This demonstrates the importance of TCA cycle-controlled post-translational modification of cytoskeletal proteins in tumorigenesis and establishes basis for further investigation into their role in EMT and metastasis of breast cancer. Through pharmacological inhibition and immunofluorescence imaging, we discovered regulators of post-translational modifications that may be viable drug targets to overcome chemoresistance and relapse in TNBC patients with limited and inefficacious options.

#0212 Repression of NKX2-1 promote epithelial-mesenchymal transition and tumor neutrophil recruitment in lung cancer progression.

S.-H. Chiou, P.-H. Tsai, M.-L. Wang;
National Yang-Ming University, Taipei, Taiwan

Background: Malignant transformation is associated with tumor aggressiveness and poor patient outcome. This cellular alteration is due to either activation of oncogenes or the silencing of tumor suppressor genes. NKX2-1 was identified as a lineage-specific gene downregulated in poorly differentiated lung adenocarcinoma (LUAD). However, the molecular mechanism and functional role of infiltrated immune cells in NKX2-1-negative tumors are not clearly understood.

Methods: Clinical relevance of NKX2-1 expression and disease status were evaluated by immunohistochemical analysis of LUAD tissue arrays and the overall survival analysis of TCGA databases. *In vitro* and *in vivo* experiments were applied to confirm the role and mechanisms of NKX2-1 actions in transformed cells. The secretion of chemokines was evaluated by using chemokine array. Flow cytometry and single-cell RNA sequencing analysis of mouse tumor tissue were used to demonstrate the infiltration of neutrophils in mouse models.

Results: Low expression of NKX2-1 was observed in high-grade LUAD tumors. LUAD patients who express a pattern of NKX2-1^{high}/TGF-β^{low} had better survival outcomes than those with NKX2-1^{low}/TGF-β^{high}. Mechanistically, TGF-β induced the downregulation of NKX2-1 which led to enhanced epithelial-mesenchymal transition (EMT), cell motility, and CXC chemokine expression. The high release of these chemoattractants promoted the recruitment of neutrophils. Meanwhile, NKX2-1-dependent suppression of CXC chemokines gene expression may be via repressive histone methylation at the promoter region of CXC chemokines in lung cancer cells. In the *in vivo* syngeneic LUAD models, exacerbated neutrophil infiltration was noted. Single-cell RNA sequencing and flow cytometry both revealed that neutrophils were recruited via CXCLs/CXCR2 activation in LUAD tumors with NKX2-1 knockdown.

Conclusion: Our data showed that NKX2-1 represses tumor growth, metastasis, and neutrophil recruitment via the CXCLs/CXCR2-dependent mechanisms. Notably, targeting CXCR2 in NKX2-1-negative tumors may improve LUAD patient outcomes.

#0213 NEK1-mediated phosphorylation of YAP1 is key to prostate cancer progression.

D. M. Olatunde, I. Ghosh, A. De Benedetti;
Louisiana State University Health Sciences Center, Shreveport, LA

The key to preventing metastatic castration-resistant prostate cancer (mCRPC) progression is understanding how androgen-sensitive (AS) PCa cells progress to independence and modify accordingly their transcriptional repertoire. We recently identified a novel axis of the Hippo pathway characterized by the sequential kinase cascade induced by androgen deprivation, AR⁻>mTOR>TLK1B>NEK1>pYAP1-Y407, leading to CRPC adaptation. Phosphorylation of YAP1-Y407 increases upon androgen deprivation therapy (ADT), correlated with increased NEK1 activity, and this is suppressed in a YAP-Y407F mutant. Overexpression of wt-GFP-YAP but not the Y407F SDM resulted in dramatic morphologic changes. In fact, LNCaP expressing wt-YAP were AI whereas the Y407F mutant were AS, and LNCaP expressing wt-GFP-YAP underwent EMT transformation. This, largely reflecting transcriptional differences in both AR-dependent genes (FKBP5, PSA) and some involved in EMT (ZEB1, TWIST, E-CAD); all of which could be effectively reversed with J54-mediated inhibition of TLK1>NEK!>YAP signaling. We found that J54, a pharmacological inhibitor of the TLK1>NEK1>YAP1 nexus led to degradation of YAP1, suggesting that the Y407 phosphorylation is critical for transcriptional activation and stabilization of YAP. Specifically, Nek1-mediated phosphorylation of YAP-Y407 increases its productive interaction with transcriptional activators like TEAD or AR, resulting in its nuclear retention and stabilization. This was later demonstrated by coIP of TEAD4 or the AR with GFP-YAP antiserum, as well as via LUC expression transfections using ARE and Hippo reporter plasmids in LNCaP expressing wt-GFP-YAP or Y407F proteins, as well as by ChIP for key AR-responsive gene promoters. Further, in NEK1 haploinsufficient TRAMP mice we determined reduced YAP1 expression, a key transcriptional activator of CRPC progression, and, if castrated at 12 weeks, the mice failed to show to overt prostate carcinomas, even while displaying reduced E-Cadherin (E-Cad) expression in hyperplastic ductules. Finally, IHC examination of prostate cancer biopsies revealed that pYAP1-Y407 nuclear signal is low in samples of low-grade cancer but elevated in high GS specimens.

TUMOR BIOLOGY: Organoid Models of Cancer 1
Poster Session

#0217 Establishment of a spatially defined co-culture model of non-small cell lung cancer organoids and cancer-associated fibroblasts to investigate phenotypic heterogeneity.

C.-K. Park, R. Navab, E. D'Arcangelo, Q. Li, H. Ogawa, N. Radulovich, N.-A. Pham, M.-S. Tsao;
Princess Margaret Cancer Centre, Toronto, ON, Canada

Background: Cancer-associated fibroblasts (CAFs) are heterogeneous, with CAF subtypes being localized in spatially defined areas of tumors. However, it remains unclear which CAF subsets specifically play a role in fundamental processes such as tumor growth, invasion, and response to therapy. This study aims to establish a novel *in vitro* model that recapitulates the *in vivo* tumor-stroma spatial relationship to investigate CAF heterogeneity and its impact on tumor cell growth in non-small cell lung cancer (NSCLC).
Methods: The *in vitro* model was established using NSCLC patient-derived CAFs and tumor organoids as a 6:1 ratio. Tumor cells originating from xenograft-derived organoids (XDOs) were embedded in a hydrogel containing CAFs (Day 0) and co-cultured for 5 days. Confocal microscopy was utilized to characterize and measure the proliferation of the XDO tumor cells in the co-culture setup, and the proliferation rate was defined as differences in tumor spheroid area between Day 1 and 5. Single-cell RNA-sequencing (scRNAseq) and gene set enrichment analysis (GSEA) were then used to assess the gene expression and signaling pathways dominant in mono- and co-culture to characterize CAF heterogeneity in this model.
Results: Initially, the culture media formulations and the matrix for the growth of both CAFs and tumor cells were screened to assess the compatibility of different culture elements. Both CAFs and XDO tumor cells proliferated well in reduced organoid media (M27RD). This reduced medium and the novel matrix composition (50% Matrigel/50% Rat Tail type I collagen) also allowed for maintaining CAF contractility and XDO proliferation. Utilizing these harmonized media and matrix conditions, a spatially defined co-culture model, which incorporated XDOs as a central cluster surrounded by CAFs, was generated. In confocal microscopy, the proliferation rate of tumor cells was significantly higher in co-cultures with CAFs (adjusted p-value < 0.01), while not significant in mono-culture of tumor cells. The GSEA using the Hallmark gene sets on scRNAseq data generated in three co-cultures identified the heterogeneity among CAFs: two CAFs showed significantly higher effect on tumor cell proliferation with the most highly differential expressed genes (DEGs) enriched with inflammation and mitosis and the top high DEGs associated with epithelial-mesenchymal transition, while the other CAF has no effect.
Conclusion: The harmonized co-culture conditions for NSCLC organoids and CAFs enabled the characterization of both cell phenotypes and the building of an informed model architecture to study tumor-stroma communication. The presence of CAFs increased tumor cell growth with enrichment in secreted proteins involved in epithelial-mesenchymal transition.

#0218 Deciphering tumoroid-CAF interactions through a spatially segregated coculture model.

S. Kim[1], Y. Ko[1], H. Park[1], S. Jang[2];

[1]AMIST, Asan Medical Center, University of Ulsan College of Medicine, Seoul, Korea, Republic of, [2]Asan Medical Center, University of Ulsan College of Medicine, Seoul, Korea, Republic of

In the context of lung cancers, cancer-associated fibroblast (CAF) plays a pivotal role as a key component of the tumor microenvironment (TME), affecting tumor growth, invasion, metastasis, immune modulation, and drug resistance. Despite the recognized impact of CAFs, the precise interaction between the CAF and tumor cell remains elusive. Previous studies have reported that CAFs stimulate tumor cell growth both *in vitro* and *in vivo*. However, our tumoroid models reveal an intriguing phenomenon where CAFs inhibit tumoroids growth within Matrigel. This led us to hypothesize that paracrine signaling might be the primary mode of interaction between CAFs and tumor cells. To unravel the intricacies of this interaction, we developed an innovative coculture method. Using hydrophobic barrier, we segregated the coculture of nine sets of CAFs and tumoroids within a single well, preventing CAFs from infiltrating the tumoroid culture area. This setup enabled interaction solely through paracrine signaling. Surprisingly, cocultured tumoroids exhibited no significant differences compared to individually cultured tumoroids. Conversely, cocultured CAFs displayed a remarkable increase in growth compared to their individually cultured counterparts. This suggests that tumoroids influence CAF growth, while CAFs do not significantly impact tumoroid growth. Furthermore, in three coculture sets, tumor cells within the Matrigel migrated towards the CAF culture area, indicating that CAFs induce tumor cell metastasis. Immunofluorescence staining confirmed this metastatic phenomenon. To identify the paracrine factors influencing CAFs and tumoroids, we employed RNA-sequencing, single-cell RNA-sequencing, and proteomic analysis of culture soup. Proteomic analysis revealed a substantial increase in proteins and signaling pathways related to the extracellular matrix in cocultures compared to single cultures. Our findings suggest that tumor cells recruit CAFs, promoting CAF growth to establish and fortify their TME, ultimately leading to drug resistance, metastasis, and immune modulation

#0219 Molecular and therapeutic characterization of a large-scale collection of metastatic colorectal cancer patient-derived xenografts and matched organoids for translational oncology.

S. M. Leto, E. Grassi, M. Avolio, V. Vurchio, F. Cottino, M. Ferri, E. R. Zanella, L. Di Blasio, A. Puliafito, L. Primo, A. Bertotti, L. Trusolino;
Candiolo Cancer Institute - IRCCS, Candiolo, Italy

Strong evidence supports the use of patient-derived xenografts (PDXs) as faithful models reflecting patient outcomes. Since not all research can support the use of animals, exploiting patient-derived *in vitro* models such as organoids (also know as tumoroids) is essential. However, current biobanks of metastatic colorectal cancer (mCRC) tumoroids have important limitations, such as small sample size and a lack of systematic *in vivo* validation with paired xenografts, which decreases the translational value of tumoroid-based pipelines. Here we describe XENTURION, a unique open-science resource of XENografts and Tumoroids for Research In ONcology that encompasses 129 sibling pairs of mCRC PDXs and PDX-derived tumoroids (PDXTs) with accompanying molecular and therapeutic characterization.The vast majority of XENTURION models were analyzed for mutations (targeted next-generation sequencing of 116 relevant CRC genes), gene copy number architecture (DNA shallow sequencing) and global transcriptomics (RNAseq) and benchmarked against large patient datasets (TCGA and MSK-IMPACT). Results showed that the PDX-PDXT collection proved to be representative of the genetic heterogeneity of mCRCs and displayed high genetic and transcriptional similarity between matched pairs. A PDXT-based population trial with the clinically approved anti-EGFR antibody cetuximab was performed in 116 PDXTs, revealing variable sensitivities that were consistent with clinical response biomarkers and with tumor growth changes in 79 matched PDXs. Cetuximab response profiles also recapitulated the outcome of EGFR knock-out by CRISPR-Casp9 technology in 13 representative PDXTs. Adaptive signals upregulated by EGFR blockade both in tumoroids and PDXs were computationally and functionally prioritized. Top candidates were screened in PDXTs and 3 surviving compounds were identified as actionable co-extinction targets with cetuximab in 12 PDXT models. Results were finally validated in PDXs.To our knowledge, this is the first large-scale study in which a systematic comparison of molecular and therapeutic profiles between PDXT-PDX pairs was attempted. As a publicly available resource, XENTURION will offer a knowledge base of disseminatable methods, resources and information to streamline preclinical studies and accelerate new treatments for patients with mCRC.

#0220 Thresholding response assessment in biliary tract cancer organoids to inform sensitivity to chemotherapy across molecular subtypes.
E. Riedl, A. Stram, M. Hossan, E. Lin, J. Warner, L. Koeppel, J. D. Kratz;
University of Wisconsin - Madison, Madison, WI

Background: Cholangiocarcinoma (CCA) remains a highly morbid cancer for which accurate models. Patient-derived cancer organoid (PCOs) have been generated in CCA, however their utility in clinical prediction has not been validated. Z' factoring often fails in assessing CCA organoid response. Prior analysis for organoid response has shown an effect size by Glass's Delta (GΔ) of ≥1.25 in growth inhibition is predictive of clinical response. Here, we present subclonal organoid response across a diverse set of CCA models in response to therapy by growth and organoid level viability response.
Methods: PCOs were expanded from the NCI's Patient-Derived Model Repository (PDMR), tissue biopsy, and rapid autopsy. Organoid response was tracked from growth using Z-stacked high content imaging (Cytation5) with endpoint at 144h and stained using established viability markers, Caspase-3/7 (C3/7) and ToPro3. Treatment groups included media control, positive control of cycloheximide 200uM continuous, gemcitabine (gem) 10uM 24h, cisplatin (cis) 5uM 48h, combination gem+cis, and FGFR2 inhibitor futibatinib (futi) 300nM continuous.
Results: Across models, PCO growth directly correlated with Z' factor thresholding (R= 0.868). NCI PDMR organoids, CK11523 and CK10519 are *IDH1*mutant *(*mt), and both showed superior response to gem when compared to cis by growth (gem GΔ 1.18 and 0.44 v. cis GΔ 0.11 and 0.23) and C3/7 (gem GΔ 3.25 and 2.34 v. cis GΔ 1.46 and 0.33). *BRCA1*mt CCA was found to achieve modest growth inhibition with gem and gem+cis (GΔ 1.09 and 1.17) and yet significant increase in C3/7 (gem GΔ 1.68 and gem+cis GΔ 1.36) and ToPro3 (gem GΔ 1.65 and gem+cis GΔ 1.82). Despite this result, the patient developed early clinical recurrence after neoadjuvant gem+cis chemotherapy (<3 months). *FGFR2-HPGDS* fusion CCA achieved no meaningful difference in growth response with gem+cis (GΔ 0.94) or futi (GΔ 0.36). These findings were consistent with the clinical outcome of primary chemotherapy resistance and progression on futi. However, we observed increase in C3/7 positivity with both gem+cis (GΔ 2.11) and futi (GΔ 1.37).
Conclusions: Primary resistance to both targeted and chemotherapy remains a formidable barrier to therapeutic development in CCA. While growth inhibition remains a validated marker of clinical response, further work is needed to understand thresholds for C3/7 and ToPro3 across physiologic drug dosing. This is the first report of modeling the novel *FGFR2-HPGDS* fusion CCA in organoids. Ongoing work is evaluating therapeutic sensitivity across prospective specimens of CCA in support of establishing thresholding for response to apoptosis (C3/7) and necrosis (ToPro3).

#0221 Novel organotypic patient derived primary tumor tissues for oncology drug safety and efficacy studies.

S. Ayehunie[1], M. Groves[2], B. Bryda[1], A. Armento[1], A. Tolcher[2];
[1]MatTek Corporation, Ashland, MA, [2]Next Oncology, San Antonio, TX

Organotypic, three-dimensional (3D) cancer tissue models (OCTM) have enabled investigators to develop predictive markers that can be used in preclinical cancer drug development. However, a drawback of the existing models is that they are mostly based on cell lines based are not physiological. In vitro development of 3D tumoroids using patient derived primary tumors (PDPT) in tumor microenvironment (TME) will have clinical significant and can predict human responses to cancer therapeutics. Here, we describe the generation of OCTM from patient-derived metastatic colorectal cancer, the second most deadly cancer. PDPT were grown in Matrigel for 5 passages and for biobanking purposes tumoroids were further expanded in faCellitate 384 well plates or Sun Bioscience plates to harvest large amounts of well-defined tumoroids cultured for over 21 days. Expanded tumoroids were collected and cryopreserved or gently mixed several times using a pipet tip to break up tumoroids into smaller fragments. These tumor fragments were mixed with endothelial cells, dendritic cells, fibroblasts and embedded in a collagen matrix to simulate TME. The collagen-cell mixture was then added to Transwells and induced to gel to form a collagen gel matrix that simulates TME. The tumoroids were cultured with a specialized medium that supports the growth of complex cell types. The tumor development was monitored daily using bright field microscopy and image analysis was used to monitor tumor size. To evaluate the utility of the OCTM, treatment was initiated at day 10 of the culture period by exposing tissues with the chemotherapeutic drug Cisplatin on days 0, 2, 4, 7, 9, and 11. After each treatment, OCTM tissues (N=2) were fixed for H&E and live/dead staining. Overall, the results of the study showed that: 1) PDPT can be expanded for 5 passages (this low passage number is not expected to change the phenotype of the tumor) and further expanded in high throughput format, 384 well plates, 2) the PDPT could be cultured with multiple cell types in a collagen-gel matrix to recreate the TME, 3) histological evaluation of the OCTM showed a glandular-like tumoroid, 4) immunohistochemical staining revealed that the PDPT in the in vivo-like microenvironment were positive for CK20, and 5) the PDPT shrank following 3 treatment cycles with Cisplatin (day 4). Conclusion: The data shows metastatic colorectal PDPT can be expanded in vitro and cultured in a complex tumor microenvironment on tissue culture inserts. These OCTMs can be used to screen drug safety and efficacy. This study opens new avenues for high-throughput cancer drug screening format using PDPT embedded in a in vivo like TME. This model can be used as a tool for personalized oncology drug testing and for translational assays tailored to other cancer types from our patient derived primary tumor pool.

#0222 Establishment of patient-derived tumor organoids from head and neck cancers for predicting response to treatments.

M. Perreard[1], V. Bastit[1], L. Lecouflet[2], G. Desmartin[2], R. Florent[2], C. Jeanne[3], J. Thariat[2], E. Babin[1], L. Poulain[2], L.-B. Weiswald[2];
[1]Universite de Caen Normandie / CHU de Caen / Centre Francois Baclesse, Caen, France, [2]Universite de Caen Normandie / Centre Francois Baclesse, Caen, France, [3]Centre Francois Baclesse, Caen, France

The risk of relapse or recurrence of Head and Neck Squamous Cell Carcinoma (HNSCC) is high despite the combination of surgery and radiochemotherapy, responsible for high toxicity. It is crucial to develop new therapeutic strategies and to identify patients likely to benefit from these treatments. Patient-Derived Tumor Organoids (PDTO) are three-dimensional multicellular structures derived from patient tumor samples and faithfully reproduce the histological and molecular characteristics of the original tumor. A growing body of research indicates that PDTO may predict the clinical response, representing a major opportunity for the development of new therapeutic strategies and precision medicine. The purpose of this translational study is to generate PDTO from HNSCC patients to evaluate their predictive value. PDTO were obtained after dissociation of tumor specimen of HNSCC patients through the setup of the clinical study ORGAVADS (NCT04261192). Tumor cells were embedded in extracellular matrix and cultured in specific medium. Histological and immunohistochemical characterizations were performed to validate the resemblance between PDTO and their original tumor. Response of PDTO to chemotherapy, radiotherapy and innovative therapies were evaluated by live-cell imaging and viability assays. The culture conditions were optimized to improve the success rate of PDTO establishment which now exceeded 50%. Twenty-one PDTO lines have been established and showed histological characteristics close to the original tumor. Expression of immunohistochemical tumor markers p53, p40, p63, and p16 were similar in tumors and paired PDTO. Functional assays were performed on 15 PDTO to analyze the response to treatments (cisplatin, olaparib, X-Rays) and heterogeneity of response was observed between the models. When clinical response was available, PDTO derived from good responders showed high sensitivity to treatments while PDTO from bad responders showed low sensitivity to treatments. Interestingly, two PDTO lines derived from HPV+ oropharyngeal tumors displayed very high sensitivity to cisplatin, matching with the patient's profile and response. Our results showed feasibility to derive PDTO from HNSCC and to perform functional assay to assess their response to different treatments. The first studies of correlation between PDTO and patient responses are promising and will be further investigated in more patients. This will allow to demonstrate the predictive value of PDTO from HNSCC with the purpose to develop a clinically compatible predictive functional assay.

#0223 Precision medicine-based platform to guide the treatment of EML4-ALK fusion lung cancers and other NSCLC.

Nathan M. Merrill[1], Aaron Udager[1], Angel Qin[1], Kiran Lagisetty[1], Liwei Bao[1], Xu Cheng[1], Hamadi Madhi[1], Ananya Banerjee[1], Ananya Banerjee[1], Marziyeh Salehi Jahromi[1], Laura Goo[1], Varun Kathawate[1], Bryce Vandenburg[1], Marisa Aikins[1], Mark Slayton[1], Peter Ulintz[1], Zhaoping Qin[1], Chia-jen Liu[1], Habib Serhan[1], John Jefferies[2], Muhammad Sajawal Ali[3], Vishal Navani[4], Michael Monument[4], Johannes Kratz[5], Amber Smith[6], Andrew Chang[1], Gregory Kalemkerian[1], Sunitha Nagrath[1], Peggy Hsu[1], Matthew B. Soellner[1], Sofia D. Merajver[1]

[1]University of Michigan, Ann Arbor, MI,[2]University of Tennessee Health Science Center, Memphis, TN,[3]Weill Cornell Medicine, New York, NY,[4]Tom Baker Cancer Centre, Calgary, AB, Canada,[5]University of California San Francisco, San Francisco, CA,[6]The Rare Cancer Research Foundation, Durham, NC

Background: Lung cancer (LC) remains the top cause of cancer-associated mortality worldwide, with a 10-year overall survival rate of only 5%. While most LCs are smoking related, in the US, 25% of non-small cell LC (NSCLC) are diagnosed in patients with little or no smoking history. Fusions involving anaplastic lymphoma kinase (ALK) are the oncogenic driver in ~3-7% of NSCLC. While inhibitors targeting the kinase domain of ALK (TKIs) have proven extremely effective, inevitably, resistance develops with limited effective treatment options. Additionally, NSCLCs without identified molecular alterations have limited treatment options beyond radiation, immunotherapy, chemotherapy, and resection.
Methods: We developed a precision medicine-based platform (PMP) to screen patient-derived material (PDM) directly from the operating room with curated panels of drugs. PDM collected during clinically indicated procedures is plated in 3D-culture to generate patient-derived organoids (PDOs) and screened with drugs curated to each tumor type. PDOs are screened at therapeutically relevant doses, drawing from pharmacokinetic data for each drug. We have optimized an assay to rapidly screen for EML4-ALK fusions and can perform next-generation sequencing in real time (~7 days) to integrate with drug screening results.
Results: To date, we have screened 83 cases, including 8 EML4-ALK NSCLC. We have demonstrated an ability to produce high quality data from low input samples (biopsies). In one EML4-ALK NSCLC we were able to collect PDM from two distinct anatomic spaces (pleural effusion and peritoneal fluid) and screen with the same panel of drugs, with nearly identical results, highlighting the reproducibility and consistency of our assay. Screening of EML4-ALK tumors which have progressed to second or higher line TKIs, demonstrate sensitivity to earlier generation ALK TKIs, a known phenomenon. Characterization of tumors with unknown clinical drivers identifies ~1/3 tumors with no prioritized variants and particularly poor response to chemotherapies. Our results recapitulate known resistance/progression in samples previously exposed to therapy, demonstrating a strong negative predictive value. Longitudinal assessment will be required to robustly assess positive predictive value (PPV).
Conclusions: Our PMP captures robust and reproducible results that are consistent with known clinical pathogenesis. Moving forward, we are collecting longitudinal data from enrolled patients in parallel with clinical trials to demonstrate the PPV of our PMP. We additionally strive to demonstrate reproducibility to obtain Clinical Laboratory Improvement Amendments approval and to deliver results to patients and physicians to help guide clinical care.

#0224 Combining functional precision medicine and radiotherapy with bio-printed organoids in head and neck squamous cell carcinoma.

L. Lin, K. K. Bommakanti, A. V. Sannajust, Y. Alhiyari, B. Mo, L. Evans, P. Tebon, M. St. John, A. Soragni;
UCLA - University of California Los Angeles, Los Angeles, CA

The study aims to establish a high throughput *ex vivo* organoid-based drug screening platform for head and neck squamous cell carcinoma (HNSCC) to investigate interactions between radiotherapy and different chemotherapies or targeted therapy agents and ultimately provide functional precision medicine therapeutic suggestions. HNSCC is the sixth most common cancer worldwide. Both HPV+ and HPV- cancers can be treated with surgery, radiotherapy, chemotherapy, or a combination of these. Cetuximab is currently the only FDA-approved targeted agent for HNSCC. Few clinical trials to date have shown an improved clinical outcome when combining targeted agents with radiotherapy, thus there is a need to identify new therapeutic combinations to improve outcomes.

In order to characterize HNSCC tumor behavior and sensitivity to therapy, we have leveraged our high throughput 3D tumor organoid screening platform. Our approach entails seeding tumor cells in extracellular matrix around the perimeter of tissue culture wells in ring-like structures, which we have successfully deployed in other cancer types (Phan et al, 2019; Al Shihabi et al, 2022; Nguyen et al, 2022; Al Shihabi et al 2023). To optimize a chemoradiation platform, we used the HN30, HN31, and SCC154 cell lines representing HPV- primary, HPV- metastatic, and HPV+ head and neck tumors. The cell-line-derived 3D models are exposed to both radiotherapy and various chemotherapy or targeted therapy drugs. We measured cell responses by ATP-release assays and by applying our machine learning-based brightfield image analysis pipeline (Al Shihabi et al, 2022).

Our results showed that the HPV+ SCC154 was the most sensitive line to radiotherapy while HPV- metastatic HN31 was the most resistant. HN31 was resistant to most drug treatments except for gemcitabine, docetaxel, and mitomycin c, while HN30 and SCC154 were sensitive to a broader set of agents. We have investigated combinatorial efficacy of radiation and chemotherapy as well as targeted agents and extended this platform to HNSCC patient-derived tumor organoids. Our proof-of-concept study highlights how our organoid-based drug screening platform can be used to test chemoradiation approaches that are more effective and personalized.

#0225 Integration of patient-derived tumor organoids and patient clinical multimodal data to investigate the role of organoids in predicting treatment response.

K. A. Burke[1], B. Larsen[1], Y.-H. C. Tan[1], J. Barbeau[1], C. Brinkman[1], E. Moore[1], N. Callamaras[1], J. R. Dry[1], I. Huerga[1], K. Sasser[1], J. A. Borgia[2]; [1]Tempus Labs, Inc., Chicago, IL, [2]Rush University, Chicago, IL

Introduction: Patient-derived organoids (PDOs) enable the ex vivo study of tumor heterogeneity and its effect on response to treatment. Our previous work demonstrated that our robust pan-cancer organoid platform shows genetic and transcriptomic concordance with clinical tumor samples and can be deployed for high-throughput drug response screening. Here, we ran a standard of care (SOC) panel on PDOs with paired de-identified clinically curated data to enable a comparison of patient response to the same drugs ex vivo and exploration of potentially more effective treatment alternatives.
Methods: Patient tumor samples were cultivated into tumor PDOs in extracellular matrix + chemically defined media. PDOs underwent pathological review to ensure development of malignant tissue. PDOs were identified by clusters of Hoechst-positive cells and live and dead cell counts for each PDO were determined using fluorescent stains. The median number of cells per PDO in the well was calculated, excluding PDOs with <3 cells and the top 1% of PDOs by area. Drug screens were run with 6 doses of the compound and the inverse area under the curve of ToPro3 live cell measurements was calculated to quantify response. Tempus xT DNA-seq and xR whole-transcriptome assays were used to perform NGS on organoids and patient samples where available. Data was processed through our standard pipeline to identify targetable mutations, neoantigens, copy number variants (CNVs) and fusions.
Results: We analyzed 38 PDOs with paired patient data across 9 different cancer types comprising mostly lung (n=14) and colorectal (n=12); 17 PDOs had responses associated with treatment given close to the biopsy collection date. Across the full PDO cohort, we observed a range of responses to SOC compounds, providing a platform to better understand biomarkers and mechanisms of response. Treatment response in PDOs correlated with patient response in many cases. In the 3 patients with progression-free survival >1 year and outcomes of either complete response or stable disease, all showed strong responses to the corresponding drugs in the SOC panel. For most patients with progressive disease recorded after treatment the corresponding PDO cluster showed limited response to treatment. The SOC panel includes several targeted therapies that provide insight into how patients respond to treatment beyond chemotherapy. For two patients with limited response to treatment in both patient and PDO, we identified targeted therapies relevant to their clinico-genomic landscape. One patient showed improved clinical outcomes to a later line of therapy with a similar mechanism of action to the drug that showed response in the organoid.
Conclusion: These results suggest that PDOs may serve as a powerful tool for predicting patient response to treatment and aid the development of new therapies.

#0226 Effect of MCL-1 inhibitor on organoids derived from cholangiocarcinoma patients with IDH1 mutation.

S. Suzuki[1], J. Matsuzaki[1], T. Muramatsu[1], Y. Kanai[2], Y. Saito[1];
[1]Keio University Faculty of Pharmacy, Tokyo, Japan, [2]Keio University School of Medicine, Tokyo, Japan

Cholangiocarcinomas are highly aggressive malignancies with a poor prognosis. The global incidence of cholangiocarcinoma patients appears to be on the rise. While surgical resection remains the curative option for cholangiocarcinoma patients, the majority of cases are diagnosed at an advanced stage, resulting in poor outcomes. Patients with inoperable cholangiocarcinomas typically undergo chemotherapy regimens, including Gemcitabine, but their efficacy is limited, leading to low 5-year survival rates. Recent advancements in organoid culture technology allow for the in vitro replication of tissue structures by culturing tissue stem cells in three dimensions, offering great promise for personalized medicine. Utilizing patient-derived organoids has proven effective in predicting the outcomes of therapeutic drugs. We have successfully established organoids using cancer tissue derived from cholangiocarcinoma patients, and stably culturing and maintaining them, promoting their application to personalized medicine (Saito Y et al. Cell Rep. 27, 1265, 2019, Saito Y et al. Cancer Cell 40, 226, 2022). IDH1 mutations have been identified in approximately 15% of intrahepatic cholangiocarcinomas and are known to convert α-ketoglutarate (α-KG) in the TCA cycle to produce 2-hydroxyglutarate (2-HG), which is observed in gliomas and acute myeloid leukemia. 2-HG acts as an antagonist to α-KG-dependent dioxygenases, promoting cancer development. This study aims to develop a novel treatment for cholangiocarcinomas with IDH1 mutations. Metabolomic analysis of patient-derived cholangiocarcinoma organoids revealed 2-HG accumulation and reduced ATP production in IDH1-mutated cholangiocarcinoma organoids compared to IDH1 wild-type cholangiocarcinoma organoids. This may suppress the protein synthesis of MCL-1 and mTOR signaling through the activation of AMPK kinase, suggesting that further inhibition of MCL-1 could be lethal in IDH1-mutated cholangiocarcinoma organoids. Indeed, exposure to S63845, an MCL-1 inhibitor, significantly inhibited cell proliferation in IDH1-mutated cholangiocarcinoma organoids, unlike in IDH1 wild-type cholangiocarcinoma organoids. Furthermore, the combination of MCL-1 inhibitor and BCL-XL inhibitor demonstrated a synergistic and potent growth inhibitory effect on cholangiocarcinoma organoids. These findings indicate that the MCL-1 inhibitor holds promise as a new therapeutic agent for cholangiocarcinoma patients with IDH1 mutations.

#0227 Novel and easy-to-use approach to triple-negative breast cancer tumoroid culture.

B. Balhouse, C. Yankaskas, C. Paul, S. Salen, S. Beam, P. Shahi Thakuri, M. Dallas, D. Kuninger;
Thermo Fisher Scientific, Frederick, MD

Triple-negative breast cancer (TNBC) accounts for 15-20% of all breast cancer diagnoses in the United States. Patients with metastatic TNBC have a low survival rate, driven in part by limited treatment options for the disease. Tumoroids, also known as cancer organoids, have been shown to better maintain tumor-specific mutational and gene expression profiles over long-term culture, and evidence is growing that the functional response of tumoroids to therapeutics better recapitulates in vivo response. These improved preclinical models of TNBC may facilitate the development of new therapies, but tumoroids are yet to be widely adopted due to challenging culture methods. In this study, we show that two TNBC tumoroid models publicly available through the National Cancer Institute Patient-Derived Models Repository can be expanded in suspension culture using Gibco™ OncoPro™ Tumoroid Culture Medium supplemented with FGF10 and beta-estradiol. We compared the bulk tumoroid morphologies, growth rates, maintenance of mutational and gene expression profiles, and molecular phenotypes of cells grown in the NCI-recommended medium in embedded culture, and the OncoPro medium in embedded culture and suspension culture. We saw comparable morphologies and growth rates in all culture conditions. A multivariate analysis of the allelic frequencies of single nucleotide variants and ploidy values of copy number variants for cells expanded in all experimental conditions revealed >95% and >88% correlation, respectively, with the initial material. Interestingly, despite the change in the medium formulation, gene expression was also highly correlated between the initial material and the OncoPro medium conditions for >20,000 RefSeq genes (Pearson r>0.94) and for a cancer-gene specific panel of 1,423 genes (r>0.87). Further analysis showed unchanged expression levels in 97% of total genes analyzed and the basal molecular subtype was maintained for both lines in all conditions. The OncoPro media system was also used to derive a new TNBC tumoroid line, which demonstrates consistent growth rate and maintains the patient-specific mutational profile of the original breast tumor. Differential gene expression analysis revealed that changes in the gene expression profile were largely due to the loss of non-malignant cell populations from the original tumor. Finally, we utilized this new tumoroid line to examine donor-specific killing efficiencies of primary natural killer cells in a co-culture experiment. The discrepancy in the dynamics of killing a tumoroid line versus the standard K562 cell line indicates that tumoroids may offer an improved approach for screening new cell therapies. In summary, the easy-to-adopt OncoPro medium and culture method does not change the characteristics of existing models and may be used to derive new tumoroid lines, both of which can be leveraged for preclinical studies to develop critical new therapies for TNBC.

#0228 Patient-derived gbm organoids reflect tumour heterogeneity and treatment sensitivity in patients..

M. A. Vooijs[1], L. Hoosemans[1], J. Piepers[1], M. Verduin[1], M. Vanmechelen[2], M. Van Heumen[1], F. De Smet[2], A. Hoeben[1];
[1]Maastricht UMC+, Maastricht, Netherlands, [2]KU Leuven, Leuven, Belgium

Glioblastoma (GBM) is the most common and incurable adult primary brain tumour. Treatment resistance and relapse is the primary cause of death in GBM. Tumour heterogeneity is one of the significant determinants of treatment failure. Patient-derived cancer organoids have been shown to maintain genetic and phenotypic tumour features and recapitulate intratumoral heterogeneity. Here, we report the development and molecular characterisation of patient-derived GBM organoid (PGO) models to study treatment response to existing and new treatment combinations. GBM biopsies were dissociated, suspended in Cultrex, and cultured in a brain stem cell medium. PGOs were characterised by whole-exome (WES) single-cell karyotype (scKaryoSeq) and RNA sequencing. The IC-50 and viability of PGO upon temozolomide (TMZ) and small molecule inhibitors were determined. Gene expression profiling was performed before and after TMZ treatment. Single-cell spatial heterogeneity was determined using Multiplex Immunostaining of PGO and matched patient samples. PGOs were established with a success rate of 80% (n=31). WES analysis between PGOs from the same patient at multiple time points (1-3 months) showed high maintenance of Single Nucleotide Variants (92.3%-97.7%). In PGOs key somatic oncogene variants and copy number variations were retained compared to the primary tumour (58%-90%). scKaryoseq (N=7) of different clinical GBM subtypes showed a high degree of genetic heterogeneity, with some PGO having up to 10 subclones. Single-cell phenotypic landscaping of patient biopsies showed mixed cellular states maintained after long-term culture in the matched PGO. PGOs showed a differential response to TMZ, corresponding with MGMT methylation and patient mutation status. RNAseq of PGO revealed TMZ-responsive genes, including upregulation of the prognostic JUN kinase pathway. Combination treatment of a JUN kinase inhibitor and TMZ showed a synergistic effect. In addition, PGOs were screened for their sensitivity to clinically approved brain-penetrable small molecule inhibitors targeting key GBM driver pathways. Combining small molecular inhibitors of MEK/PI-3/CDK4/EGFR kinase strongly reduced cell viability and activation of cell death pathways. phosphoKinome screens detected compensatory pathway activation upon kinase inhibition (MEK/CDK4 inhibitor) in several PGO. Data will show novel kinase interaction pathways that increase drug sensitivity in PGO. These data show that PGOs can be used as a stable phenotypic and genetic representative of the patient's tumour and have the potential to function as patient avatars for adaptive treatment selection and actionable drug target discovery.

#0229 Molecular-genomic characterization of metastatic gastric cancer organoids and establishment of organoid-immune cell co-culture model.

H. Mun[1], j. Park[2], J. Jang[3], J. Che[3], T. Kim[3], W. Kwon[3], H. Chung[4], S. Rha[4];

[1]Brain Korea 21 PLUS Project for Medical Science, Yonsei University College of Medicine, Seoul, Korea, Republic of, [2]Yonsei University College of Medicine, Seoul, Korea, Republic of, [3]Song-Dang Institute for Cancer Research, Yonsei University College of Medicine, Seoul, Korea, Republic of, [4]Division of Medical Oncology, Department of Internal Medicine, Yonsei Cancer Center, Yonsei University Health System., Seoul, Korea, Republic of

Advanced gastric cancer (AGC) showed marked molecular heterogeneity with aggressive behavior and treatment resistance, especially AGC with ascites from peritoneal metastasis. Tumor organoids are valuable *in vitro* model for mimicking organ characteristics and are used for developing therapeutic strategies. Therefore, we aimed to understand the characteristics of organoids established from AGC patient-derived fluids. Also, we are in progress of setting up an organoid-immune cell co-culture model for drug screening of immune checkpoint inhibitors (ICI) for AGC. All established organoids from peritoneal and pleural fluid of AGC patients were authenticated through short tandem repeat (STR) profiling, comparing with their matched PBMCs. We compared the morphological characteristics using Operetta High Content Imaging (Perkin Elmer). Also, the *in house* targeted sequencing and RNA sequencing data were obtained from the genome database of the Song-Dang Institute for Cancer Research and it was verified using molecular methods. Then, we co-cultured organoids with healthy donor PBMCs that were pre-activated using anti-human CD3/CD28 Dynabeads (Gibco). 3D spheroids, rather than single cells, and the PBMCs were co-cultured in matrigel (Corning Inc.) for more than 3 days. The overall success rate of the organoid establishment was 53.8% (78/145), with different sources of peritoneal (54%, 61/113) and pleural fluids (53.1%, 17/32). The organoid success rate was various as in EBV positive (66.7%, 2/3) and dMMR (0%, 0/4). Based on the analysis of 91 patients eligible for histopathology, the success rate of HER2-negative (57.5%, 46/80) is higher than that of HER2-positive (36.4%, 4/11). The organoids were observed in a variety of morphologies categorized in 3 groups such as grape-like, compact and glandular structure. Based on genomic data of 31 organoids, we could subgrouping for TCGA subtypes and EMT subtype. RTKs were amplified in 10 organoids, including the amplification of ERBB2 (n=2), MET (n=4) and FGFR (n=4). And KRAS alterations including amplification (n=2) and G12A/D (n=2) mutation were also detected. Then, we established the condition for organoid-immune co-culture model with PBMCs with Dynabead activation for 3-10 days. We confirmed that higher dose of PBMCs killed the tumor cells with reduction of organoid size and partial disintegration. We established the proper PBMC dose and characterization to maintain the organoids co-culture for further drug (ICI) sensitivity testing. In conclusion, we evaluated phenotypic and molecular characteristics of gastric cancer organoids established from malignant peritoneal and pleural effusion. The established organoid-immune cell co-culture models can be utilized to evaluate a variety of drug screenings, including ICI and various combinations, helping in the selection of drugs for individual patient.

#0230 Deep learning embedding-based segmentation for morphological analysis in organoids.

A. Sureshkumar[1], S. Bisht[2], H. Easwaran[2];
[1]Johns Hopkins University, Baltimore, MD, [2]Johns Hopkins University School of Medicine, Baltimore, MD

Background: The organoid model is a useful tool for modeling the cellular microenvironment of the organ from which they are derived. Organoids recapitulate the self-organization of heterogenous cell types and the microenvironment. Quantifying the morphological features of organoids can provide valuable insights into cellular organizational defects and growth characteristics, which can facilitate drug discovery. Measurement of these characteristics in live organoids can be performed quickly and easily directly in culture using widefield microscopy. The current state-of-the-art method to detect and identify the shape of individual organoids in brightfield images uses the U-Net Convolutional Neural Network (CNN) with a watershed transform to label pixels. However, this method yields jagged shape proposals and cannot detect overlapping regions. We propose the use of an embedding-based segmentation network based on the Branched ERF-Net to solve these issues.

Methods: Organoids were established from the proximal colon of $Braf^{V600E}$ heterozygous mice, and 50 phase-contrast images of the organoids were acquired at 2.5x and 4x magnification. Organoids present in acquired images were labeled manually. The network was trained on this collection of manually labeled images and validated on a separate validation dataset.

Results: The network accurately labels organoids. Overlapping organoids are segmented correctly and shape proposals are smoother. Detection of overlapping organoids with the Branched ERF-Net architecture yields an accurate organoid count, verified against manual counting. Smoother shape proposals also enable the use of convexity defects to measure organoid budding.

Conclusions: Deep-learning analysis of widefield images enables the rapid assessment of morphological characteristics, such as size, count, and budding, which are key to understanding proliferation and differentiation changes. The modified Branched ERF-Net architecture we propose for organoid segmentation is a robust and versatile method to quantify organoid morphology.

#0231 Live cell painting of drug responses in high grade serous cancer organoids.

D. W. Andrews, B. Li, W. Schormann, A. Buzina, L. Gien, H. MacKay;
Sunnybrook Health Sciences Centre, Toronto, ON, Canada

While most patients with high grade serous ovarian cancer (HGSC) respond to platinum-based chemotherapy, the response is rarely durable and recurrence almost inevitable. A characteristic of HGSC is defective DNA repair. A class of drugs called PARP inhibitors (PARPi) exploit this vulnerability and have proven useful in delaying recurrence. However, resistance is inevitable. In models of HGSC a protein that frequently confers resistance is called Bcl-xL, a member of the Bcl-2 family of proteins that prevent apoptosis. If treating the patients with a PARPi makes cancer cells dependent on Bcl-xL then adding an inhibitor of Bcl-xL to their treatment would be sufficient to cause the cancer cells to die. To test this, we have initiated companion studies for a clinical trial in which patients that have had a recurrence after receiving platinum-based therapy will first be treated with the PARPi Olaparib and then, an inhibitor of Bcl-xL, Navitoclax, will be added to their course of treatment. The idea is that for some women this will provide the one-two-punch needed to eliminate the cancer or at least dramatically prolong response. However, Bcl-xL is only one of the five known inhibitors of apoptosis. To identify which women will benefit most from adding Navitoclax to their treatment we need a biomarker(s). An ideal biomarker would also let us determine for other women which inhibitor of Bcl-2 proteins would be best combined with a PARPi.

Our hypothesis is that patient derived organoids can be used as a pragmatic way to identify for individual patients which Bcl-2 protein inhibitor will synergize with a PARPi to optimize treatment.

We are using organoids to develop biomarkers for High Grade Serous Cancer (HGSC) treatment response. Organoids generated from biopsy samples acquired prior to treatment for HGSC promise to be efficient and reliable experimental models that recapitulate in vitro patient tumors faithfully enough to facilitate translation to therapeutic decisions for patients. By adapting the relatively new technique of conditional reprogramming and combining it with novel methods for cell aggregation and hydrogel based synthetic ECM supports we can reproducibly generate HGSC patient-specific tumor organoids models in weeks with greater than 90% success. Organoids grown 384 well format are stained with novel non-toxic dyes enabling live cell painting of chemoresponses to drugs alone and in combination with drugs targeting anti-apoptotic proteins. Our data suggest that this approach captures the inherent heterogeneity of the disease, albeit local to the sampled site. We are now employing deep learning AI algorithms to enable automated analyses of 3D confocal image stacks of organoids to infer drug responses that will be compared to patient responses in ongoing clinical trials.

#0232 Multi-dimensional patient-derived organoid analysis highly correlates with progression-free survival of pancreatic cancer patients in a retrospective clinical trial.

A. Lin[1], M. Le Compte[1], T. Gilcrest[2], E. Cardenas De La Hoz[1], G. Roeyen[3], F. Lardon[1], C. Deben[1];
[1]University of Antwerp, Antwerp, Belgium, [2]Orbits Oncology, San Francisco, CA, [3]University Hospital Antwerp, Antwerp, Belgium

Patient-derived tumor organoids (PDOs) are promising cancer models, since they preserve the clonal heterogeneity, mutational landscape, and histological architecture of the originating patient tumor[1-2]. Recent studies have even provided first evidence that PDOs responded similarly to the corresponding patient when treated with the same standard of care therapy, but these studies were only able to predict clinical responses in a subset of patients[3,4]. This restriction was largely due to the limitation of current analysis methods. The gold-standard analysis method for PDO-based research, CellTiter-Glo 3D,[5,6] fails to account for the heterogeneity of PDOs by relying on a bulk lysis approach, and thus only extracts a fraction of the clinically-relevant information that PDOs could provide[7]. Therefore, we hypothesized that using higher-dimensional analysis methods, will further unlock the predictive performance of PDOs and facilitate translation of research. In this study, we developed an artificial intelligence-driven analysis platform for live-PDO imaging. By combining drug screening metrics with dynamic quantification of organoids on a single-organoid resolution, we unraveled patient-specific tumor heterogeneity and PDAC aggressiveness in response to therapies[8]. Using a fully characterized a PDAC organoid panel (n=8) we matched our PDO analysis with retrospective clinical patient response to standard of care therapies (gemcitabine-paclitaxel and FOLFIRINOX). Our results demonstrated that our PDO analysis method identified patient-specific sensitives to therapy that were in-line with clinical outcomes. Moreover, our PDO readouts highly correlated with progression-free survival of matched patients (R=0.97), which was a significant improvement to the current, conventional drug response readouts. Taken together, our approach increased the clinical translatability of PDOs by more accurately recapitulating and measuring the complexity of human tumors. This work highlights the potential applications (extendable to other tumor types) and clinical translatability of our approach in drug discovery and clinical care, in the emerging era of personalized medicine. References: 1. Seppala, T.T., et al. *Ann Surg* 272 (2020) 2. Hadj Bachir, E., et al. *Biol Cell* 114 (2021) 3. Ooft, S.N., et al. *Sci Transl Med* 11(2019). 4. Driehuis, E., et al. *Proc Natl Acad Sci* 116 (2019) 5. Sachs, N., et al. *Cell* 172 (2018) 6. Kijima, T., et al. *Cell Mol Gastroenterol Hepatol* 7 (2019) 7. Phan, N., et al. *Commun Biol* 2 (2019) 8. Le Compte, M., et al. *npj Precis Oncol* (2023)

#0234 Microfluidic chip for drug response studies in non-small cell lung carcinoma patient-derived organoids.

Q. Luan, I. Pulido, A. Isagirre, **J. Zhou**, T. Shimamura, I. Papautsky;
University of Illinois Chicago, Chicago, IL

Background. Organoids have been widely accepted as 3D tumor models for patient-specific drug response. However, research involving non-small cell lung cancer (NSCLC) organoids is hampered by the lack of appropriate platforms. Although dome cultures show promising results, the relatively large size variability of patient-derived organoids (PDOs) hinders their application in drug response studies. Here, we report a microfluidic chip for maintaining high uniformity and requiring miniscule sample volume for PDO drug screening.
Methods. The microfluidic chip includes a bottom microwell layer and a top microchannel layer. Each chip has 5 channels for parallel treatment conditions, with 30 U-shaped microwells (400μm dia x 250μm deep) per channel. PDOs were loaded from side channels and trapped by filters adjacent to microwells. NSCLC PDOs F231/F671 (NCI PDMR) were cultured and treated by $KRAS^{G12C}$ inhibitor adagrasib (0-2000nM, 72h). PDO drug response was assessed via viability using fluorescent dyes.
Results. On-chip PDO size after one-week incubation exhibited the coefficient of variation (CV) of 28% for F231 and 36% for F671, which was notably lower than measurements obtained using Matrigel dome (126%, n=3) and low attachment plate (80%, n=4). The F231/F671 showed viability >81% after 1wk (n=20). On-chip cytotoxicity results showed that both $KRAS^{G12C}$ PDOs exhibited sensitivity to adagrasib, matching the clinical response, with IC_{50} values of 830 nM (F231) and 1324nM (F671). When cultured with fibroblast (WI-38) supernatant, the cytotoxic effect was mitigated due to the fibroblast-induced resistance, with IC_{50} increasing ≥2×. No statistical difference was observed for the fibroblast effect in the open-format microwells and our microfluidic chip (69.6±16.9% to 80.2±9.0% vs. 69.0±12.2% to 82.2±4.1%, respectively, following 500nM adagrasib for 72h), further underscoring the reliability of our chip for PDOs' drug response studies. Application of continuous perfusion at 70nL/min yielded no statistical difference in viability from static conditions.
Conclusions. Our microfluidic chip offers uniform PDO growth with perfusion allowing drug screening in almost real time. The on-chip response to adagrasib was clinically relevant. Resistance due to tumor microenvironment (TME) can be readily assessed using fibroblast supernatant, and could be expanded to other TME components in future studies to investigate their impact on treatment resistance.

#0235 Application of high-grade serous ovarian cancer organoids in functional precision medicine.

Wojciech Senkowski[1], Laura Gall-Mas[1], Matias M. Falco[2], Yilin Li[2], Kari Lavikka[2], Aura Crispino[1], Jaana Oikkonen[2], Daria Bulanova[1], Yan-Jun Chen[1], Elena M. Doncel[1], Karolin Vo?grone[1], Erdogan P. Erkan[2], Jun Dai[2], Anastasia Lundgren[2], Jutta Huvila[3], Kaisa Huhtinen[2], Johanna Hynninen[4], Sampsa Hautaniemi[2], Anna Vaharautio[2], Krister Wennerberg[1]

[1]University of Copenhagen, Copenhagen, Denmark,[2]University of Helsinki, Helsinki, Finland,[3]University of Turku, Turku, Finland,[4]Turku University Hospital, Turku, Finland

High-grade serous ovarian cancer (HGSC) is the most frequent and lethal ovarian cancer type. Despite responding favorably to first-line therapy, most HGSC patients eventually relapse. HGSC is characterized by high interpatient genomic heterogeneity and few recurrent mutations that could be used as therapeutic biomarkers. Thus, except the introduction of PARP inhibitors for BRCA1/2-mutated patients, there has been little progress with personalizing HGSC treatment. Functional precision medicine - tailoring personalized therapies based on functional assays on patient-derived cells - has been applied in cancer clinical trials to address this issue. Organoids - three-dimensional cell cultures, recapitulating aspects of original tumors' structure and function - have often been used as models in these efforts. However, inefficient and time-consuming organoid derivation protocols have been hindering the application of HGSC organoids in functional precision medicine clinical trials, due to the short time during which the therapy must be selected.

To address this, we here aimed to establish whether we could predict second-line therapy drug sensitivities in relapsed HGSC using organoids from tumor material from first-line therapy. We have previously derived a collection of 23 organoid models from 16 patients, sampled sequentially at different times of their treatment (1). Here, for several organoid primary-relapse pairs, we performed drug screens using a library of 370 compounds (approved, in clinical development or tool compounds). We found that 90% of the hit compounds in the primary organoids also were hits in the matched relapse-derived organoid models. In several patients, we observed a pronounced cytotoxicity of several cyclin-dependent kinase (CDK) inhibitors, all of which potently inhibit CDK9, including two selective inhibitors (AZD4573 and VIP152) in clinical development. Screening of CDK9 inhibitors in an extended panel of organoid models revealed that most organoids are sensitive to CDK9 inhibition in nanomolar range. CDK9 inhibitors also prevented organoid outgrowth in long-term culture (>1.5 month) in drug-free medium.

Taken together, we demonstrate that HGSC organoids from material sampled during first-line treatment predict most drug sensitivities of relapse-derived organoids. This suggests a feasibility of functional precision approach for selection of second-line therapy using only primary tumor material, circumventing the problem of limited time available for the therapy choice after tumor sampling. This work also highlights that CDK9 inhibitors, currently in clinical development for hematological malignancies, are worthwhile to be explored in HGSC.

1. Senkowski et al. A platform for efficient establishment and drug-response profiling of high-grade serous ovarian cancer organoids. Developmental Cell (2023)

#0236 Modeling multi-step retinoblastoma genesis with cone reporter retinal organoids.

J. Bai[1], D. S. Koos[1], K. Stepanian[1], K. Stachelek[1], B. Bhat[1], S. Fraser[2], R. Moats[1], D. Cobrinik[1];
[1]Children's Hospital Los Angeles, Los Angeles, CA, [2]University of Southern California, Los Angeles, CA

Purpose: This study aims to develop a human retinoblastoma organoid (RBRO) model that recapitulates the cell-of-origin and multi-step retinoblastoma genesis.
Background: Retinoblastomas originate from maturing cone photoreceptor precursors with biallelic *RB1* inactivation. *Rb1* mutant animal models fail to recapitulate retinoblastomagenesis with a cone precursor cell-of-origin, likely due to human-specific cone development features. In explanted fetal retina, pRB-depleted post-mitotic cone precursors proliferate, followed by a 3-5 month premalignant indolence phase before retinoblastoma-like masses emerge at tissue ages similar to retinoblastomas *in vivo*. However, tissue availability limits research with this disease model. *RB1*$^{-/-}$ retinal organoids (ROs) provide a potential alternative, as they demonstrate cone proliferation, but they deteriorate before forming indolent premalignant lesions or malignant retinoblastoma foci. Here, we developed methods with which to examine the effects of cone precursor pRB loss in otherwise healthy retinal tissue.
Methods: We generated cone-reporter GNAT2-EGFP iPSC lines through CRISPR knock-in of EGFP-P2A at the N-terminus of *GNAT2* in WTC11-mTagRFPT-LMNB1. A second round of CRISPR editing produced homozygous *RB1* knockout. Chimeric *RB1* WT ROs and *RB1*-null RBROs were generated from cone reporter iPSCs mixed with unedited parental iPSCs. ROs and RBROs were embedded in hydrogel and live-imaged episodically to track EGFP+ cone proliferation dynamics. scRNA-seq was carried out on FACS isolated EGFP+ *RB1*-null cones at various ages.
Results: In *RB1* WT ROs, EGFP+ cone precursors appeared at d34 and adopted cone morphology at ~d120, with rapid inner segment growth between ~d120 and ~d150. Immunohistochemistry confirmed cone-specific EGFP expression. In *RB1*-null RBROs, bi-weekly live confocal imaging revealed initial EGFP+ *RB1*$^{-/-}$ cone proliferation followed by a pre-malignant indolence phase starting at ~d150. The majority of the initially proliferating cones were Ki67-negative with some adopting mature cone photoreceptor morphology. Nascent retinoblastoma-like foci co-expressing EGFP, cone markers, and Ki67 formed in five of six RBROs after d281, a tissue age that equates to the first post-natal month when early retinoblastomas typically emerge. scRNA-seq of EGFP+ *RB1*$^{-/-}$ cones from the initial proliferation, indolence, and retinoblastoma-like stages revealed distinct molecular signatures.
Conclusions: We generated a human retinoblastoma organoid model that recapitulates the cell-of-origin and timing of multi-step retinoblastomagenesis, with each tumorigenesis stage harboring distinct molecular signatures. This model may enable the identification of epigenetic and transcriptomic changes underlying malignant progression and screening for compounds that efficiently block this process.

#0237 Establishment of an *ex vivo* tissue culture model as a potential preclinical drug testing platform for hepatocellular carcinoma.

H. Feng[1], M. Cieri[2], C. Esposito[3], K. Guja-Jarosz[3], D. Liberati[3], L. Bubendorf[1], S. D. Soysal[1], M. Coto-Llerena[1], L. M. Terracciano[2], O. Kollmar[1], S. Piscuoglio[3]; [1]University Hospital Basel, Basel, Switzerland, [2]Humanitas Clinical and Research Center,IRCCS, Milan, Italy, [3]Department of Biomedicine, University of Basel, Basel, Switzerland

Background: Hepatocellular carcinoma (HCC) is a leading cause of cancer-related deaths worldwide, and there is a critical need for more effective treatments. The development of new therapies, especially those aiming to modulate the tumor microenvironment (TME), is limited by the lack of *in vitro* and *in vivo* models that recapitulate the complexity of the TME and spatial architecture of HCC. Here, we aimed to establish an HCC model to assess the treatment response and hepatotoxicity of selected drugs by *ex vivo* culturing fresh human liver tumor tissue and adjacent normal tissue, respectively.
Materials and Methods: Fresh human liver tissues, including 5 malignant and 20 adjacent-normal, were obtained from surgical resections. PDX tumors were generated from patient-derived organoids. Tissue resections were cut into ultra-thin slices (from 150µm to 350µm) using a vibratome. Related culture conditions such as high oxygen partial pressure, air-liquid interface (ALI) culture, artificial extracellular matrix (AEM), and delay duration were evaluated to optimize the protocol. As a readout, cell viability was quantified by an expert pathologist using Hematoxylin/Eosin staining. The preservation and complexity of the TME were evaluated by immunohistochemistry or flow cytometry using specific antibodies for each cell population (T cells, anti-CD3; stroma cells, a-SMA; endothelial cells, CD34; Kupffer cells, CD68). Liver cell function was tested by measuring ALT/AST activity, albumin release, and CYP340 activity.
Results: The highest tissue viability was observed in normal and tumor tissue with a thickness of 150µm and 250µm, respectively. Compared to standard conditions, the combination of ALI and high-oxygen partial pressure conditions dramatically improved tissue viability, with most of the samples having 70% and 50% cell viability at days 3 and 5 of *ex vivo* culture, respectively ($p<0.05$). AEM could prevent the efflux of cellular components ($p=0.016$). The impact of the time delay between the liver resection and the start of slicing was minimal when the slicing occurred within two hours after hepatectomy ($p<0.05$). Key cellular components including hepatocytes, T cells, fibroblasts, and Kupffer cells also remained better preserved throughout the 5-day culture period in optimized conditions.
Conclusion: Our study has successfully optimized the *ex vivo* tissue culture model of liver tissue, capable of maintaining the tissue for several days while preserving the unique TME. These results highlight the potential of using the *ex vivo* tissue culture model in the preclinical setting to further investigate and evaluate TME-related treatments and their hepatotoxicity in HCC tissues.

#0238 Investigating size-dependent invasion behaviors and therapeutic responses of the 42MGBA glioblastoma spheroids.

S. Fok, Y. Ivanova, V. Kriuchkovskaia, B. Harley;
University of Illinois at Urbana-Champaign, Champaign, IL

Introduction: Glioblastoma (GBM) is one of the most aggressive malignant brain tumors. Many studies have reported that the tumor microenvironment (TME) contributes greatly to invasion and drug resistance of GBM. Our lab has previously described a tri-culture model using methacrylamide-functionalized gelatin (GelMA) with brain microvascular endothelial cells (BMVEC), human normal astrocytes (NHA), and human brain vascular pericyte (HBVP) recapitulated the *in vivo* brain microenvironment. However, phenotypic drug response was only observed under supraphysiological dosage. To evaluate therapeutic response more precisely, we decided to combine the Tri-culture system with the IdenTx3 microfluidic device (AIM Biotech). By separating the immature perivascular network from the GBM spheroids, we are hoping to generate a model that can more realistically mimic the TME. While many studies have used cancer spheroid in GBM studies, little is known about the impact of spheroids size. Since spheroid size correlates with nutrient and oxygen gradients, we are also curious to find out whether an increase in spheroid size increases the necrotic population and affects drug response and invasion.

Materials: Wild-type (WT) and TMZ resistant 42MGBA cell lines were seeded at different cell numbers to generate spheroids of different sizes. Spheroids were dissociated for flow analysis to quantify the necrotic population. In the invasion assay, spheroids were encapsulated in GelMA hydrogel with or without the addition of perivascular cells including BMVECs, HBVP, and NHA (3:1:1). Vasculature formation inside the chip was initiated 5 days prior to the introduction of GBM spheroids.

Results: 42MGBA-WT and 42MGBA-TMZres spheroids demonstrated phenotypical and proliferative differences. Spheroids sizes showed a direct relationship with necrotic cell numbers. Small spheroids (1000 cells) and large spheroids (10,000 cells) were encapsulated inside the hydrogel and subjected to different treatments of temozolomide. A difference in invasion area and proliferation was found when subjected to bulk or metronomic dosages. The two 42MGBA cell lines displayed an increase in invading area when co-cultured with perivascular cells. This result coincided with our previous finding that perivascular network increases GBM proliferation and invasion in GBM6 spheroid (Ngo et al, 2022). In addition, a different invasion behavior was observed between the 42MGBA-WT and 42MGBA-TMZres spheroids when introduced inside the microfluidic device. Surprisingly, the wildtype showed a larger invading area compared to the TMZ resistant.

Conclusion: We demonstrated a direct relationship between size and necrotic population in the 42MGBA spheroids. We also showed that bulk or metronomic treatment exert different effects on the cancer spheroids. Finally, we have verified that TME is critical to invasion and drug resistance.

#0239 Establishing a murine intratumoral bacterial model.

Ryan A. Hannon, Dongqing Xu, Fengyi Wan

Johns Hopkins Bloomberg School of Public Health, Baltimore, MD

Background: Long thought to be sterile spaces, current evidence now suggests that host microbiota can be found within cancerous tissue. Emerging data has illuminated that microbes are integral components of tumor tissue itself, which may correlate with tumor progression, treatment responsiveness, and disease prognosis. A recent *Cell* article from *Fu et al.* demonstrated that tumor-resident intracellular microbiota can promote metastatic colonization in breast cancer. Others within this research landscape see therapeutic opportunity - harnessing the tropism of these microbes to deliver TME modifying payloads directly to cancerous lesions.
Purpose: Before studying the mechanism underlying their tropism to solid tumors, it is necessary to first establish a murine model that would allow for an oncotropic bacteria to be detected and quantified within tissues of interest. My research entailed the design and execution of pilot experiments developing xenograft melanoma and genetic colorectal models for future research projects.
Methods: In all mouse studies, an *E. coli* Nissle 1917 strain called "*NisLux*" was used, who's integration with a *luxCDABE* cassette allowed it to be selectively identified via luminescence using traditional exposure photography or endpoint luminescence detection using a 96-well plate reader. A xenograft melanoma model was developed using C57BL/6J mice and a B16-F10 murine melanoma line. A genetics model was developed using C57BL/6J-*Apc*^{min} mice which spontaneously develop colorectal adenomas as they age. Tumors, spleens, and healthy tissue were harvested and processed following tail vein injections of either *NisLux* or PBS solution. Harvested tissue was normalized by weight and concentration of resident *NisLux* was calculated from serially diluted samples plated on LB agar.
Results: In both the xenograft and genetics murine models, *NisLux* exhibited tropism to tumor sites, enriching at a concentration above that of healthy background tissue. *NisLux* dosing correlated with splenomegaly without changes to the mass of the primary lesion compared to control.
Conclusions: *NisLux* exhibits tropism to tumor sites in our xenograft and genetics murine models. Both models should undergo further procedural and control optimization. Two possible modifications to future melanoma xenograft experiments include the collection of non-cancerous skin negative control samples and a further delayed takedown day for tissue processing. In future C57BL/6J-*Apc*^{min} mice experiments, healthy colon sections from *NisLux* dosed C57BL/6J mice should be used as negative controls. Overall, the results from both models were promising and encourage future exploration of the mechanism underlying *NisLux*'s tropism to solid tumors. Subsequent experiments could involve comparing the tropism of engineered KO strains to WT *NisLux* or performing comparative sequencing of isolated tumor resident *NisLux* to the initial dosing population.

#0240 Mix and match - A comprehensive pipeline for matched patient-derived PDX and PD3D® modelsfor cancer research and preclinical drug development.

J. Loskutov[1], E. Oswald[2], **L. Wedeken**[1], C. J. Reinhard[1], J. Schueler[2], C. R. A. Regenbrecht[1];
[1]CELLphenomics GmbH, Berlin, Germany, [2]Charles River Laboratories, Freiburg, Germany

Relevant *in vivo* and *in vitro* cancer models have been invaluable for our current understanding of cancer biology, as well as for therapy development. Using appropriate models in the drug development process significantly supports reliable and swift decision making in proceeding along the value chain. In parallel, animal experiments can be designed more specific to the scientific and regulatory needs, resulting in shorter development cycles and eventually the availability of better therapies for cancer patients. Patient-derived xenografts (PDX) are generated by implantation of cancerous tissue from a patient's tumor either under the skin (ectopic) or into the organ of tumor origin (orthotopic) of an immunocompromised mouse and are the most used *in vivo* model for preclinical drug development. Patient-derived 3D cell culture models (PD3D®) are gaining increasing significance as relevant *in vitro* cancer models that recapitulate the original tumor tissue's biology and are suitable for high-throughput drug screening. The combination of both platform's increases the translational relevance of the development pipeline and offers the possibility to enlarge the respective panels of tumor models. Tackling an unmet medical need, we initially created matched mesothelioma PD3D® and PDX models. Mesothelioma is an aggressive cancer with poor prognosis and limited treatment options. Development of new therapies is hampered by shortage of available relevant tumor models. We created PD3D® models from PDX mesothelioma models and vice versa and generated drug sensitivity profiles with standard of care such as Gemcitabine, platinum derivates and a number of targeted agents to confirm their suitability as matched models for future projects. We were able to prove that models express stable histological, phenotypic features and drug sensitivity profiles across the two platforms. With this proof-of-concept study, the feasibility to combine the PD3D® biobank comprising more than 500 models from CELLphenomics with the PDX bank from CRL including 700 PDX models, has gained momentum. In consideration of the changing regulatory landscape, the combination of *in vitro* and *in vivo* platforms is a crucial step towards a drug development pipeline that incorporates the principles of 3R and increases its translational value due to fully human technologies being the corner stones of the drug development process.

#0241 Patient-derived organoids as a reliable screening platform for assessing ADC efficacy and specificity.

D. Mori, V. Adegbenro, F. Morales, R. Overmeer, S. Lukovac, S. Boj, M. Derksen;
HUB Organoids, Utrecht, Netherlands

Antibody-drug conjugates (ADCs) are a new class of pharmaceutical drugs designed to deliver cytotoxic agents to cells expressing specific antigens selectively. Based on Paul Ehrlich's "magic bullet" concept, ADCs are designed to target cancer cells, minimizing systemic toxicity typical of conventional chemotherapy. ADCs structurally consist of a particular monoclonal antibody linked to a cytotoxic agent.
Patient-derived Organoids (PDOs) provide a new tool for studying cancer biology and patient stratification. PDOs are adult stem cell-based culture systems maintaining the patient-specific genetic and phenotypic characteristics, including surface marker expression. HUB Organoids has generated a large biobank of PDOs characterized on the genomic and transcriptomic level.
The work presented here shows the suitability of the organoid platform for performing ADC screening. Organoids were selected based on their target-antigen (TA) expression, assessed by flow cytometry and RPKM. Organoid killing was assessed with a viability readout (CellTiter Glo) after six days of treatment. Results of viability screening show a correlation between TA-targeting ADC-induced organoid killing and TA expression in the organoids.
These results reveal that PDOs hold value for the preclinical development of ADCs and for evaluating their tumor specificity. Moreover, PDOs have the potential to predict patient specific response to ADCs.

#0242 Development of organoids-bacteria co-cultures for medium-to-high throughput screening.

E. Valle-Encinas[1], M. Doorn[1], F. Pourfarzad[1], L. San Mateo[2], P. Gokare[2], D. Pocalyko[2], S. F. Boj[1], **C. S. Verissimo**[1];
[1]HUB Organoids, Utrecht, Netherlands, [2]Janssen Research & Development LLC, Philadelphia, PA

HUB patient derived organoids, (HUB-Organoids™ or PDOs) are self-organized epithelial cell structures with near-physiological features, extensively used to model aspects of cancer initiation and progression. Microinjection of colibactin-producing pks+ *E. coli* into the lumen of PDOs resulted in the appearance of two co-occurring mutational signatures identified in a subset of colorectal cancer (CRC) patients, demonstrating that pks+ *E. coli* plays a causative role in CRC development. The scalability of PDO bacteria microinjection is, however, limited and represent a bottleneck in the screening of preventive therapies for these patients. Here we develop a bacteria-PDO co-culture system (PDO-fragment exposure model), alternative to PDO microinjection, that is compatible with medium-to-high throughput screening methods. We validated the genotoxicity of colibactin-producing bacteria and showed the potential of the PDO fragment exposure model for the screening of drugs targeting colibactin-dependent genotoxicity.

#0243 Organoid co-cultures with allogenic T cells to assess toxicity and efficacy of bispecific antibodies.

C. Oyarce, V. Bruno, L. Spagnuolo, C. Beaurivage, J. Frias Aldeguer, F. Pourfarzad, R. G. J. Vries, **S. F. Boj**;
HUB Organoids B.V., Utrecht, Netherlands

Recent advances in cancer immunotherapy positively impacted the life expectancy of patients for an extensive range of clinical indications. With new treatment strategies, druggable targets and biomarkers being identified at an increasing pace, the number of patients eligible for cancer immunotherapy is expected to expand steadily. For example, the emerging Bispecific T cell Engagers (BiTEs) designed to simultaneously target CD3 and tumor-specific antigens and promote T cell cytotoxicity have seen recent clinical success. While BiTEs have been approved for the treatment of hematologic malignancies, promising therapeutic developments for solid tumors face hurdles in translating preclinical findings into therapy since conventional two-dimensional cancer models fail to recapitulate the immune cell interactions in the tumor microenvironment and therefore hold low clinical predictive value. We developed an innovative alternative, building on the discovery that adult stem cells proliferate and organize into three-dimensional organotypic structures that maintain complex characteristics of the original parental tissue, including molecular heterogeneity and morphological and functional traits.
Here, we show the development of a patient-relevant preclinical platform for immunotherapy development in which colorectal (CRC) and non-small cell lung cancer (NSCLC) organoids are co-cultured with allogenic or autologous T cells to evaluate the activity and assess the cytotoxic potential of a BiTEs. The expression of tumor-specific BiTE target antigens is determined in patient-derived organoids (PDOs) by flow cytometry. Following this assessment, T cell-induced organoid death is quantified and characterized in real-time by image-based analysis of fluorescent live/dead dyes. Additionally, we measure cytokine secretion as a read-out of T cell activation and function. In our co-cultures, T cell-induced PDO death was increased upon BiTEs treatment. Similarly, IFNγ secretion correlated with expression levels of the targeted tumor antigen. In addition, PDO apoptosis and IFNγ secretion increased in a dose-dependent fashion in the presence of the TA-targeting TCB.
In summary, our organoids and T cell co-cultures offer a powerful platform for developing and validating immunotherapies such as T cell-bispecific antibodies and will significantly contribute to our understanding of the critical factors determining successful immunotherapies.

#0244 Patient-derived organoids: A pre-clinical model to assess infection and killing capacity of viral vectors for cancer therapy.

F. Morales-Rodriguez[1], M. Sasso[2], T. Bezhaeva[1], S. Bailey-Bucktrout[2], K. Lai[1], F. Gkogkou[1], **S. Boj**[1];
[1]HUB Organoids, Utrecht, Netherlands, [2]Akamis Bio Limited, Abingdon, United Kingdom

HUB's patient-derived organoids (PDOs) are *in vitro* models that preserve tissue morphology and original cellular complexity. Additionally, PDOs are compatible with (high) throughput screening methods, enabling informed decision-making early in the drug development pipeline and significantly improving the odds of positive outcomes in clinical trials. Akamis Bio has developed experimental viral vector-based tumour gene therapies that have the potential to treat a variety of solid tumours by driving the expression of immunologically active biomolecules and therapeutic proteins hampering tumour immune evasion. These vectors are based on a replication competent, chimeric group B adenovirus backbone that selectively replicates and expresses transgene payloads in tumor cells, and additionally exerts oncolytic activity. To evaluate the efficacy of such a virus-based gene delivery strategy, HUB set up a proof-of-concept study to assess the propagation capability of Akamis Bio's viral vectors in tumour PDOs. Intact PDOs from primary pancreatic tumours were infected with several viral loads, ranging from 0.1 viral particles per cell (PPC) to 100 PPC. The viral vector encoded a GFP reporter gene to identify infected cells using fluorescence imaging. The cultures were imaged daily for 14 days, allowing the assessment of cytotoxicity and infection efficiency and dynamics. Independently of PPC, infections always started in the exterior of PDOs in a few GFP-positive cells. The gradual increase over time in GFP-signal toward the interior of PDOs suggests the high likelihood of secondary infection events. Crucially, GFP intensity was correlated with cell death in PDOs, as evidenced by morphological features detected in brightfield images. Moreover, the infection dynamics were dose-dependent, as the GFP intensity peak arose later with decreasing PPC. These results show the capacity of HUB PDOs to study the infection dynamics of Akamis viral vectors . This pre-clinical platform permits rapid and efficient screening and dose evaluation for oncolytic virotherapies. Unique access to extensive tumour PDO biobanks with characterized genomic landscapes allows best-in-class stratification of treatment response based on tumour type and genetic heterogeneity.

TUMOR BIOLOGY: Stem Cells in Tumor Initiation and Progression
Poster Session

#0248 HSPA9/mortalin regulates erythroid maturation through a TP53-dependent mechanism in human CD34+ hematopoietic progenitor cells.

T. Liu[1], C. Butler[1], M. Dunmire[1], G. Szalai[2], A. Johnson[2], J. Choi[3], M. Walter[3];
[1]West Virginia School of Osteopathic Medicine, Lewisburg, WV, [2]Burrell College of Osteopathic Medicine, Las Cruces, NM, [3]Washington University in St. Louis, St. Louis, MO

Mortalin, encoded by the HSPA9 gene, is a highly conserved heat-shock chaperone belonging to the HSP70 family. It is predominantly presented in the mitochondria, and is critical in regulating a variety of cell physiological functions such as response to cell stress, control of cell proliferation, and inhibition/prevention of apoptosis. Myelodysplastic syndromes (MDS) are a group of hematopoietic stem cell malignancies characterized by ineffective hematopoiesis, increased apoptosis of bone marrow cells, and anemia. Up to 25% of MDS patients harbor an interstitial deletion on the long arm of chromosome 5, also known as del(5q), creating haploinsufficiency for multiple genes including HSPA9. Our prior study showed that knockdown of HSPA9 induces TP53-dependent apoptosis in human CD34+ hematopoietic progenitor cells, consistent with cytopenia observed in MDS patients. Since anemia is another featured symptom of MDS, we hypothesize that HSPA9 plays a role in regulating erythroid maturation. To test our hypothesis, we inhibited the expression of HSPA9 using various methods and measured the erythroid maturation in human CD34+ cells. We used siRNA targeting HSPA9 and found that HSPA9 siRNA significantly inhibited the cell growth, increased cell apoptosis, inhibited erythroid maturation (using CD71 as a surrogate marker), and increased p53 expression ($p<0.01$) compared to control siRNA in human CD34+ cells. Pharmacologic inhibition of HSPA9 by the chemical MKT-077, an inhibitor of HSP70 protein family members including mortalin, also increased p53 expression and inhibited erythroid maturation in human CD34+ cells. In addition, knockdown of HSPA9 by shRNA showed significant inhibition of erythroid maturation in human CD34+ cells compared to control shRNA. In order to test whether the regulation of erythroid maturation by HSPA9 is TP53-dependent or not, we constructed shRNAs targeting TP53 genes and simultaneously transduced lentivirus containing shRNAs targeting HSPA9 and TP53 respectively in human CD34+ cells using double antibiotics selection (puromycin for shRNA targeting HSPA9 and hygromycin for shRNA targeting TP53). We found that TP53 knockdown partially rescued the erythroid maturation defect caused by HSPA9 inhibition, suggesting that erythroid maturation inhibition by HSPA9 knockdown is partly mediated through a TP53 mechanism. Collectively, our results suggest that the increased apoptosis and reduced erythroid maturation observed in del(5a)-associated MDS is TP53-dependent. HSPA9/mortalin may be a potential target to treat anemia in del(5q) MDS patients, although simultaneous loss of multiple genes on del(5q) likely contributes to the complex phenotypes observed in MDS. Thus, our study not only uncovers some underlying mechanisms of del(5q) MDS, but also provides potential therapeutic indications through gene targeting in clinical MDS treatment.

#0249 Deciphering the impact of TRIB3-ELF4 interaction in regulating CDK6 on cancer stem cell activity in endometrial cancer.

W.-L. Wang, W.-W. Chang;
Chung Shan Medical University, Taichung, Taiwan

Background: Endometrial cancer (EC) is the most common gynecological tumor among women worldwide, posing a serious threat to women's health. ELF4 (E74 like ETS transcription factor 4), a member of the ETS family, plays a role in facilitating cancer progression. Our previous work demonstrated the role of direct binding between ELF4 and tribbles pseudokinase 3 (TRIB3) in promoting β-catenin expression. In this study, we further explore ELF4's involvement in the maintenance of cancer stem cells (CSCs) in EC.
Methods: The vital role of ELF4 in EC was determined through gain- and loss-of-function assays. ELF4 was silenced in two EC cell lines, AN3CA and HEC-1A, and primary EC cells from a Taiwanese patient (EMC6), using RNA interference techniques. The expression of ELF4, TRIB3, and CDK6 in human EC samples was assessed using immunohistochemistry. Tumorsphere formation assays, quantitative real-time PCR, and immunoblotting quantified CSC activity and the involvement of related signaling pathways. Transcriptional regulation associated with ELF4 was investigated using luciferase reporter assays and chromatin immunoprecipitation.
Results: Analysis of the TCGA database via the TISIDB web tool revealed that elevated ELF4 levels correlated with higher histological grades, advanced clinical stages, and poorer overall survival in EC patients. A grade-dependent increase in ELF4 expression was observed using tissue microarrays. Knockdown of ELF4 in EC cell lines and patient-derived EC cells significantly reduced cell proliferation, cell cycle progression, migration, invasion, and CSC activity. RNA-seq data analysis of ELF4-knockdown EC cells identified CDK6 as a potential downstream target of the ELF4/TRIB3 interaction. Knockdown of ELF4 and TRIB3 significantly downregulated CDK6 expression. Co-expression of TRIB3 and ELF4 enhanced CDK6 expression, and their expression was positively associated with CDK6 in EC specimens. We also demonstrated that CDK6 facilitates EC-CSC activity. Knockdown of CDK6 significantly attenuated tumorsphere formation and reduced the levels of cancer stemness-related proteins, including OCT4, NANOG, and c-MYC.
Conclusion: Our study demonstrates the essential roles of ELF4 and TRIB3 in regulating CDK6 expression, contributing to the maintenance of EC-CSCs.

#0250 Sex differences in cancer stemness among individuals with early onset colorectal cancer.

O. Aladelokun[1], K. Sumigray[2], S. A. Khan[2], C. Johnson[1];
[1]Yale School of Public Health, New Haven, CT, [2]Yale University, New Haven, CT

Since 1990, the overall incidence and mortality rates of late onset colorectal cancer (LOCRC ≥50 years) have been decreasing due to improvements in access to screening and available treatment options. However, the rates for early onset CRC (EOCRC ≤ 49 years) have steadily increased in men and women. Less than 30% of LOCRC patients present with late-stage tumors (clinical stages III or IV) at the time of diagnosis compared to 70% of EOCRC patients. Despite this, the cellular and molecular mechanisms underlying the incidence and stage are unclear, as are appropriate strategies for prevention of recurrence in men and women with EOCRC. Effective prognostic markers are therefore urgently needed. To address this issue, we performed a detailed bioinformatics analysis based on Gene Expression Omnibus database (GSE39582; n=585 patients), wherein we identified 7 prognostic biomarkers for EOCRC: *KRAS, LGR5, CTNNB1, MYC*, *BMI1, CD44* and *ASNS*. Importantly, Kaplan Meier analysis revealed tumor onset at a younger age was significantly (p = 0.0082) associated with poorer 5-year survival in men with EOCRC only, after adjusting for KRAS status. *CTNBB1* and *CD44* transcript levels were higher in men with EOCRC versus men with LOCRC. Conversely, female EOCRC had a higher frequency of *KRAS* mutations (52.6%) compared to their LOCRC counterpart (38.8%), and an increased expression of markers of tumor stem cell and metabolic reprogramming including *LGR5, MYC, BMI*, and *ASNS.* A single CRISPR-Cas9 deletion of *ASNS* in HCT116 cell lines, a pre-clinical model of EOCRC, caused an inhibition of 3D spheroid formation compared to HCT116 *ASNS* wild type cells. In vivo study using a cell line derived R2G2 mouse xenograft model showed that ASNS disruption caused a reduction in tumor burden that was accompanied by low *Lgr5* and *Myc* transcripts compared to the *ASNS* wild type group, indicating that ASNS may regulate cancer stemness. Together, this data suggests a unique molecular fingerprint for EOCRC and highlights sex-specific influences on cellular metabolism during EOCRC progression.

#0251 MCAM controls mammary cell state in luminal progenitor-derived breast cancer and alveologenesis.

B. L. Gates[1], O. Balcioglu[1], D. W. Freeman[1], B. M. Hagos[2], B. T. Spike[1];
[1]University of Utah Huntsman Cancer Institute, Salt Lake City, UT, [2]Oregon Health and Science University, Portland, OR

To establish and maintain functional and properly formed tissues, cells must integrate cues from their environment into fate decisions. External cues—from other cells and the extracellular matrix for instance—must be met with appropriate responses to ensure cell fate decisions that control lineage plasticity and favor proper development, maintenance, or regeneration of tissues while suppressing neoplastic transformation. MCAM (CD146; MUC18; S-endo-1; and Gicerin) is an integral membrane glycoprotein whose misexpression is associated with a variety of epithelial cancers, including breast cancer. However, the mechanisms by which MCAM conveys extracellular cues into malignant cellular outputs is not well understood. Our observation that MCAM is normally expressed in transplantable fetal and adult mammary stem cells (MaSCs) with multilineage potential, suggested it could control mammary cell state plasticity in both neoplastic and normal mammary tissue. Using a plastic, mouse mammary tumor cell line derived from the MMTV-PyMT mouse (Py230) that has been reported to exhibit mammary stem cell and luminal progenitor features, we tested the role of Mcam in controlling the tumorigenicity and lineage/cell-state relationships of mammary tumor cells. We found that Mcam knockdown in Py230 cells increases STAT3 expression, activation, and downstream target transcription, leading to a shift in the predominant cell state away from a luminal progenitor state toward more differentiated alveolar and basal phenotypes. Mechanistically, these changes involve altered activity of casein kinase II (CK2) against multiple substrates including STAT3 and PTEN. This effect may be mediated by direct coupling and sequestration of CK2 to various substrates via the cytoplasmic tail of MCAM. We have also found that inhibition of Ck2 or Stat3 reversed the transcriptional state change elicited by *Mcam* knockdown. In grafted tumors *in vivo*, this state switch correlates with reduced overall tumorigenicity and attenuated expression of Sox10, a gatekeeper of neural crest-like invasive features. In the normal gland, we hypothesize that this activity regulates multilineage stem cell potential upon transplantation and multilineage regenerative potential across lactation/involution cycles as we found reciprocal expression patterns for MCAM and STAT3 in alveolar mammary epithelial cells. These data point to an integral role for MCAM in lineage plasticity of normal mammary epithelial cells that is co-opted during transformation to potentiate tumor cell plasticity, progression, and evasion of targeted cancer therapies.

#0252 Functional and lineage atlas of salivary gland regeneration charted by rapid in vivo gene targeting.

Q. Gan, Z. Ying;
Icahn School of Medicine at Mount Sinai, New York, NY

The crucial function of the salivary gland of keeping the oral cavity lubricated to facilitate breathing, swallowing, and lingual communication is often compromised following cancer radiotherapies. Due to the ultra-high radiosensitivity and low regeneration potential of the salivary epithelium, radiation-induced damage is largely permanent, representing a major clinical challenge. To solve this problem, we have developed a scalable rapid gene targeting system in the murine salivary gland using in-utero injection of lentiviruses. This allows us to transduce ectodermal progenitors of salivary glands with high efficiency and full randomness. Barcoded lentiviral lineage tracing suggests that every major salivary gland originated from a defined number of progenitors, each progenitor-derived clone has relatively equal expansion potential during development and equally contributes to regeneration post radiation challenge. This observation indicates that the major salivary glands of a single mouse can be used as a platform to study lineage dynamics or test up to ~2600 different genetic conditions during regeneration. With this robust approach in hand, we identified major barriers to salivary gland regeneration from among hundreds of differentially regulated signaling pathways and genes post-irradiation. Based on these discoveries, we are currently in the process of 1) Understanding the molecular mechanisms underlying the top regeneration barriers; 2) Dissecting the cell fate dynamics of salivary gland regeneration with or without regeneration barriers; and 3) Testing if we can restore the salivary gland in situ via combinatorial removal of regeneration barriers. Our work will provide unbiased functional and lineage roadmaps of post-irradiation salivary gland regeneration and potentially serve as the cornerstones of future therapeutic interventions.

#0253 Investigating key molecular players in putative stem cell subpopulations of prostate cancer.

W. Cheng[1], M. D. Menna[1], F. Bonollo[1], P. Chouvardas[1], G. N. Thalmann[2], S. Karkampouna[1], M. K. d. Julio[1];
[1]University of Bern, Bern, Switzerland, [2]Inselspital Hospital, Bern, Switzerland

Background: Androgen deprivation therapy is the standard treatment for prostate cancer (PCa). Nevertheless, despite initial effectiveness, pre-existing cancer stem cell (CSC) populations invariably lead to incurable castration-resistant prostate cancer. CSCs are a subset of cancer cells possessing self-renewal properties, driving tumor progression and regrowth. CD44+ PCa cells exhibit more stemness features and are enriched in tumorigenic and metastatic progenitor cells. Here, we aim to explore different subpopulations in tumors based on levels of CD44 expression and investigate whether they have distinct molecular properties and functional characteristics.
Material and Method: The number of CD44+ cells was evaluated in a tissue microarray from primary prostate cancer patient samples (EMPACT cohort) with clinical follow-up. Flow cytometry sorted the CRPC model LAPC9 tumor into CD44 high (CD44-H) and CD44 low (CD44-L) cells. RNA sequencing was performed on these subpopulations to explore their transcriptomic profiles. CD44 expression was validated at the cDNA and protein levels using qPCR and Western blot (WB) analysis. Sorted cells were maintained as organoids in vitro. To trace the dynamics of CD44-H and CD44-L subpopulations in vivo, LAPC9 tumor was labeled by fluorescent and luciferent markers. The CD44 status was determined by flow cytometry when tumor growth.
Results: Patients with elevated expression of CD44 (higher number of CD44+ cells) at the time of surgery exhibited a greater propensity for clinic progression (5-year progression-free survival: 75% vs 95%, P=0.03). Furthermore, CD44-H cell ratio increased in the LAPC9 after castration, indicating that CD44-H cells can survive after treatment. Subsequent WB analysis confirmed that CD44 was highly expressed in sorted CD44-H cells, validating the flow cytometry results. Analysis of the CD44 RNA-seq data showed CD44 transcript variants CD44v10 (CD44-201) and CD44v7-10 (CD44-209) were notably upregulated in CD44-H cells. In organoid culture, sorted CD44-H cells displayed enhanced formation, indicating they possessed higher proliferative capacity and clonogenicity than CD44-L cells. Furthermore, when GFP-labeled CD44-H cells and RFP-labeled CD44-L cells were recombined in vivo, CD44-H cells exhibited robust proliferation, while CD44-L cells transitioned to a CD44hi state to facilitate tumor growth. Moreover, those GFP and RFP subpopulations displayed the same CD44hi cell ratio at the endpoint.
Conclusion: Elevated CD44 expression is related to an increased risk in primary PCa. In addition, CD44-H cells exhibit high tumorigenicity in vitro and in vivo and can convert to each other. Moreover, the ratio of CD44-H cells in tumor at endpoint is consistent despite the starting CD44 expression status. Furthermore, the upregulation of CD44v10 and v7-10 in the CD44-H subpopulation may promote tumor formation and metastasis.

#0254 Triggering head and neck cancer cell cornification leads to mucosa-like differentiation, chromatin remodeling, and loss of cell malignancy.

F. Oppel[1], S. Gendreizig[1], L. Martinez-Ruiz[2], J. Florido[2], A. Lopez-Rodriguez[2], H. Pabla[1], L. Loganathan[1], L. Hose[1], P. Kuhnel[1], P. Schmidt[1], M. Schurmann[1], J. M. Neumann[3], F. Viyof Ful[1], L. Scholtz[1], I. Todt[1], L. Dina[4], F. Brasch[4], N. Karsten[3], G. Escames[2], T. Busche[1], J. Kalinowski[1], P. Goon[5], H. Sudhoff[1];
[1]University Hospital OWL of Bielefeld University, Bielefeld, Germany, [2]Institute of Biotechnology, Biomedical Research Center, Health Sciences Technology Park, University of Granada, Granada, Spain, [3]Bielefeld University, Bielefeld, Germany, [4]Klinikum Bielefeld, Bielefeld, Germany, [5]National of University of Singapore and National University Health System, Bielefeld, Singapore

Head and neck squamous cell carcinoma (HNSCC) is the 6th most common tumor disease worldwide with a death rate of about 50%. As mortality and morbidity of affected patients were not substantially improved in recent decades, new treatment options are urgently needed. HNSCCs that are negative for the human papillomavirus are characterized by areas of differentiated keratinized tissue. Dissecting the mechanisms regulating this terminal differentiation of HNSCC cells may unravel targets with high potential for anti-tumor therapy. Using primary tumor-initiating spheroid cells, we established a model of HNSCC cell differentiation by cornification and observed a deprivation of cell malignancy leading to the adhesion of spheroid cells, loss of single-cell cloning capacity, and diminished tumor-initiating potential in immunodeficient mice. Analysis of our differentiation model employing ATAC-seq, RNA-seq, and proteomics showed an increased accessibility of small promoter regions despite overall genome closure, activation of a wound healing-associated signaling program, and upregulation of the stress keratin 17 (KRT17) as well as cornification markers including SPRR3. These results suggest that the differentiation of HNSCC cells resembles the differentiation process in other stem cell-maintained tissue systems. Multi-marker immunofluorescence analysis of human tissue revealed a reversion of the role of KRT17 from a basal stem-cell marker in normal mucosa to an early differentiation marker in HNSCC tissue and dysplastic mucosa preceding cornification. This proposes KRT17 as potential biomarker for HNSCC prevention screening. Human tissue analysis identified distinct cell differentiation states shared between HNSCC tissue and normal mucosa that were detected in higher and lower differentiated tumor tissue of distinct anatomical sub-locations. Cornification was observed to be induced at the interface between vital tumor tissue and necrotic, immune-infiltrated areas in human HNSCCs, suggesting a promoting influence of pro-inflammatory stimuli on cell differentiation. Treatment of tumor spheroids with inflammatory mediators resulted in cell attachment and cornification, indicating a potential strategy to stop the self-renewal of HNSCC cells. Our study thus reveals that the targeted differentiation of HNSCC tumor-initiating cells could be used as a future therapy approach against squamous cell carcinomas of the head and neck and other tissues.

#0255 Redefining SOX2 as a bifunctional mediator of transcription and adjusted translation control.

N. Mittal[1], M. Ataman[1], H. Wang[2], S. Candido[1], J. Lotscher[1], S. Velychko[3], L. Tintignac[1], T. Bock[1], A. Borsch[1], J. Ba?ler[4], T. Nageswara Rao[5], J. Zmajkovic[6], S. Roffeis[1], J. Loliger[1], F. Jacob[1], A. Dumlin[1], C. Schurch[1], A. Schmidt[1], R. C. Skoda[1], C. Hess[7], H. R. Scholer[8], H. Zaehres[9], E. Hurt[4], M. Zavolan[1], C. Lengerke[10], **T. Schaefer**[1];

[1]University of Basel, Basel, Switzerland, [2]Shanghai University of Medicine and Health Sciences, Shanghai, China, [3]Harvard Medical School, Boston, MA, [4]University of Heidelberg, Heidelberg, Germany, [5]Cantonal Hospital St. Gallen, St. Gallen, Switzerland, [6]IMP, Vienna, Austria, [7]University of Cambridge, Cambridge, United Kingdom, [8]Max Planck Institute for Molecular Biomedicine, Munster, Germany, [9]Ruhr University Bochum, Bochum, Germany, [10]University Hospital Tubingen, Tubingen, Germany

The vertebrate transcription factor SOX2 (SRY Homology Box 2) is essential for stem cell maintenance, a prominent (co)inductor of pluripotency in reprogramming technology, and an oncogenic driver of transformation, therapy resistance, and disease relapse in cancer. These cell fate discriminatory events are currently understood as SOX2-imposed changes in DNA activity and the resultant co-transcriptional rewiring inside the cell's nucleus. Cytoplasmic forms of SOX2, on the other hand, receive comparatively little scientific attention and are typically marginalized as a molecular reservoir for nuclear entry. We now challenge this notion as we identify further cell fate discriminatory significance selectively within the cytoplasmic pool of SOX2.

Specifically, we find extra-nuclear forms of SOX2 in physical association with the ribosome where they modulate the translation rate of selected, SOX2-imposed mRNAs in the cytosol. These translational adaptations occur independent of nuclear structures or DNA and involve protein segments that have no DNA-binding capacity on their own. Very intriguingly, whereas transcriptional SOX2 targets impose stemness and pluripotency phenotypes, the newly identified co-translational targets predominantly relate to morphogenesis and differentiation events. This matches natural expression patterns in early ontogenesis, where SOX2 stains the nuclei of the inner cell mass (i.e., embryonic stem cells, ESCs), but the cytosol of the surrounding trophectoderm (i.e., differentiating non-stem cells). Most importantly though, we find the ribosome modulatory activity of SOX2 functionally abolished by a disease-linked human polymorphism, indicating a (patho)physiological relevance of our discovery.

Taken together, we present experimental evidence that redefines SOX2 as a bifunctional modulator of transcription and translation control, which may pave the way for further refinements in reprogramming technology and the fight against cancer.

#0256 A novel transcriptional complex of OLIG2-STAT5 mediates glioma stem cell self renewal and invasion.

A. Miller[1], C. Lo Cascio[2], M. Blomquist[1], J. B. McNamara[2], K. Orndorff[2], M. Dufault[2], C. Sereduk[1], J. Loftus[1], S. Mehta[2], N. L. Tran[1];
[1]Mayo Clinic College of Medicine and Science, Scottsdale, AZ, [2]Barrow Neurological Institute, Phoenix, AZ

Glioblastoma (GBM) is the most common and lethal primary brain tumor in adults, despite current treatment options. One of the major contributing factors to this dismal outcome is a subset of cells called glioma stem cells (GSCs) that are highly tumorigenic, invasive, and resistant to conventional treatments. Thus, studies that focus on the properties of GSC biology are needed to develop novel therapies to improve overall survival. Here we report a novel role of STAT5 in GSC stemness and survival. In GBM tumors, STAT5 has been shown to be active in the infiltrative, residual population of cells remaining post-surgery. Knockdown of STAT5 results in the decrease in GSC stemness and therapeutic resistance. Interestingly, we find that expression of OLIG2, a key cell fate factor important for the tumorigenic potential of GSCs, affects STAT5 activation with a positive correlation between OLIG2 and STAT5 mRNA expression in GBM tumors. Furthermore, we find that in GSCs expressing EGFRvIII, STAT5 interacts with OLIG2 and pharmacological inhibition of STAT5 activation or knockdown of STAT5 expression results in decrease of OLIG2-mediated GSC invasion. Together, these data suggest a novel transcriptional complex, STAT5-OLIG2, in the potential role for GSC survival, maintenance, and invasion.

#0257 Plasticity of preneoplastic cells drives esophageal squamous cell cancer initiation.

K. Ko, J. Zhang, S. Jun, J.-I. Park;
UT MD Anderson Cancer Center, Houston, TX

Esophageal squamous cell carcinoma (ESCC) accounts for over 80% of esophageal cancer, with a poor prognosis mainly due to a lack of early-stage symptoms. Early detection of ESCC is challenging due to its origin in the basal cell layer and invasion into the lamina propria upon becoming neoplastic. Thus, understanding the transition mechanism from preneoplasia to neoplasia is crucial for early-stage detection of ESCC before dissemination. To dissect the mechanisms of ESCC preneoplasia and neoplasia, we utilized both spatial and temporal datasets of ESCC in conjunction with a genetically engineered organoid model. For spatial datasets, we conducted comparative analyses of single-cell transcriptomes from healthy esophageal tissues, normal tissue adjacent to cancer (NAC), and paired ESCC tumors to identify distinguishable preneoplastic cells. Notably, unlike normal or ESCC, NAC harbors a distinct preneoplastic cell cluster characterized by the exclusive expression of the *CELF2* (CUGBP Elav-Like Family Member 2) gene, high gene copy number variations, cell hyperproliferation, and apoptosis, reminiscent of a 'crisis state'. Consistently, we detected a significant presence of CELF2 positive (+) cells at the stage of inflammation, a very early lesion preceding neoplasia in a temporal model of ESCC development. Copy number variations were also already abundant from the inflammation stage, as we observed in the NAC dataset. Interestingly, both spatial and temporal preneoplastic cells showed decreased scores of *TP53* and *CDKN2A* signaling pathways, of which mutations are observed in 68% of ESCC patients. To recapitulate this phenotype, we employed genetically engineered esophageal organoids and found that the loss of *Trp53* and *Cdkn2a* (PC) generated preneoplastic CELF2$^+$ cells. Intriguingly, these preneoplastic CELF2$^+$ cells exhibited remarkable cellular plasticity in two ways. Firstly, CELF2$^+$ cells of PC display increased stemness mediated by SOX2-driven reprogramming with disrupted normal esophageal cell lineage. Second, CELF2$^+$ cells of PC undergo epithelial-mesenchymal plasticity to generate fibroblast-like cells, releasing cytokines involved in immune remodeling. Consequently, preneoplastic CELF2$^+$ cells developed significant tumors compared to CELF2-negative cells in transplantation assays. Our study identified preneoplastic CELF2$^+$ cells driven by *TP53* and *CDKN2A* loss as pivotal drivers in ESCC initiation via cell-autonomous (cellular reprogramming) as well as non-cell autonomous (immune niche remodeling) processes, proposing CELF2$^+$ cells and their molecular signatures as potential biomarkers and therapeutic targets for early-stage ESCC.

#0258 An organoid model for investigating Lynch syndrome tumorigenesis.

Caroline Guild, Christopher Heinen, Samantha Nadeau

Center for Molecular Oncology, University of Connecticut Health Center, Farmington, CT

Lynch syndrome (LS) is the most common inherited predisposition for developing colon cancer and is caused by germline variants in mismatch repair (MMR) genes. Still, the mechanism of tumorigenesis in these patients is unknown. An LS patient inherits one defective copy of an MMR gene. At some point in their lifetime, the remaining wild-type allele is lost in a cell rendering it entirely MMR deficient. MMR deficiency increases mutational rate and the chance of acquiring mutations in an oncogene or tumor suppressor that drive tumor initiation. However, loss of MMR in cells also leads to increased resistance to certain forms of DNA damage. Thus, our question is whether this phenotype imparts a selective advantage in colonic cells that may lead to clonal expansion of MMR-deficient cells as a first step towards tumorigenesis in LS patients.

To test this, we are using stem cell-derived human colonic organoids and CRISPR gene editing to examine competition between MMR-deficient (MMRd) and MMR-proficient (MMRp) colonic cells over time. We have initially observed that MMRd stem cells are much more efficient at generating colonic organoids that grow larger and survive longer, consistent with our hypothesis of a selective advantage. To mimic the spontaneous loss of heterozygosity that occurs in LS patients' colonic crypts, we are forming organoids from differentially labeled MMRd and MMRp stem cells. Live fluorescent imaging of individual organoids is used to quantify changes in cell population over time. Preliminary data indicate that MMRd cells can outgrow MMRp cells resulting in a shift in the ratio of green to red cells over a two-week time period while challenged with a DNA-damaging agent. These results suggest that loss of MMR function imparts an immediate selective advantage in colonic cells in response to DNA damage.

#0259 Zebrafish empowered large-scale drug screen to uncover novel targets of self-renewal in T-cell acute lymphoblastic leukemia initiating cells.

M. Al-Hamaly[1], Y. Chernyavskaya[1], E. Arvin[1], L. Turner[1], M. Haney[2], J. Blackburn[1];
[1]University of Kentucky, Lexington, KY, [2]Cincinnati Children's Hospital Medical Center, Cincinnati, OH

T-cell Acute Lymphoblastic Leukemia (T-ALL) patients who experience relapse have a dismal prognosis, with 5-year overall survival rates of 10% for adults and 36% for children. Relapse is attributed to cytotoxic chemotherapy's inability to target Leukemia Initiating Cells (LICs) that have the potential to re-populate the cancer. There is a need for novel therapeutic strategies to target LIC self-renewal in T-ALL with improved safety profiles and better chances of transition to clinical development. This project utilized a transgenic zebrafish model that accurately recapitulates the most aggressive form of the human T-ALL. This model offered several advantages, including a high frequency of LICs and suitability for drug testing. Over 770 FDA-approved drugs were screened, *in vivo* using >2,500 syngeneic CG1 zebrafish. Further secondary screening in human T-ALL cells narrowed down the potential hits into 4 compounds that specifically interfere with self-renewal. Finally, the hit drug Amiloride was confirmed by a limiting dilation assay (LDA), resulting in a more than 4-fold decrease in the LIC frequency (p=0.0026). The top hit, Amiloride, which reduced the frequency of LICs in zebrafish and human T-ALL cells, is an inhibitor of the Sodium Hydrogen Exachanger-1 (NHE1). NHE1 has been previously linked to the proliferation, migration, and drug resistance of different cancers. In addition, Amiloride treatment was found to impair mitochondrial function in cancer cells, offering a possible mechanism for the inhibition of LICs. Research has not yet investigated how NHE1, and the altered mitochondrial dynamics related to its inhibition affect the development and persistence of LICs in T-ALL. In our human T-ALL cells, we found that Amiloride significantly reduced mitochondrial basal respiration (p=0.0074), ATP production (p=0.0008) and increased the expression of genes associated with mitochondrial stress such as *TFAM*, *PINK1*, *PARKIN* and *MT-CO1.* Experiments using shRNA mediated knock down of the NHE1 in human T-ALL cells are underway and will be followed by investigating the impact of NHE1 inhibition on primary patient-derived T-ALL cells in a mouse model. Overall, this project showcases of the power of the zebrafish in cancer research in an efficient and accurate large-scale screen for drugs that impact LIC self-renewal. We have identified Amiloride as a top hit that reduces the frequency of LIC *in vivo* and *in vitro*. Finally, we are continuing to investigate the role of the NHE1 in self-renewal in human T-ALL and the associated mitochondrial alterations.

#0260 Depletion of *Ezh2* in the intestinal adenoma induced by *JAK2V617F* mutation leads to the malignant neoplasm.

Nardana Esmaeili[1], Ahmed Bakheet[1], Wen Gao[1], Haifeng Li[2], Dan Cai[1], **Xiaonan Han**[1]

[1]Department of Medicine, MetroHealth Medical Center, Case Western Reserve University School of Medicine, Cleveland, OH,[2]Chinese Academy Institute of Medical Sciences (CAMS) and Peking Union Medical College (PUMC), Beijing, China

Background The increased JAK2 and EZH2 plays a critical role in the colorectal or colon cancer (CRC) progression. Targeting aberrant JAK2 expression caused by JAK2 gain-of-function (GOF) mutation, *JAK2V617F* and deregulated EZH2 kinase activity, JAK2 and/or EZH2 inhibitors have been used to treat the advanced CRCs. However, it is unclear whether the aberrant JAK2 can directly induce CRC or intestinal epithelial (IEC) malignancy.
We **hypothesize** that the overexpressed JAK2 driven by *JAK2V617F* GOF mutation increases IEC neoplasia in which depletion of EZH2 can lead to IEC malignant neoplasm.
Materials and Methods Colorectal samples were collected from 20 cases of CRC patients. Immunohistochemistry staining (IH), confocal immunofluorescence staining (IF) and bulk RNAseq were used to determine LGR5, Ki67, JAK2, EZH2, mutant β-catenin and *JAK2V617F* GOF mutation. Crypt-derived organoids or tumoroids were used to determine the JAK2 and EZH2 in the proliferative LGR5 cells ($Ki67^{hi}LGR5^{+}$) and were treated with JAK2 and/or EZH2 inhibitors. The mice with JAK2 and/or EZH2 deficiency in IECs were generated by crossing *VilCre*ER mice, floxed-*Jak2* and/or floxed-*Ezh2* mice to determine the intestinal and colonic neoplasia. Lgr5, Ki67, Cdx2 Jak2, Ezh2, and mutant β-catenin IH or IF, organoids culture and peritoneal xenograft were used to determine the malignant neoplasm. The *JAK2V617F*-transfected HT29 or Caco-2 cells were used to determine the migration induced by *JAK2V617F* GOF mutation, then treated with EZH2 inhibitors to determine the effects of EZH2 inhibition on *JAK2V617F* GOF mutation-induced migration. The spheres were formed with Caco-cells with *JAK2V617F* GOF mutation and were used to observe the effects of *JAK2V617F* GOF mutation on IEC neoplasia formation.
Results JAK2 and/or EZH2 overexpression are positively correlated with the probability of CRC initiation. JAK2 and EZH2 are highly expressed in the CRC tumoroids. Inhibition of EZH2 increases the CRC tumoroids growth and spheroid formation, and reduces budding numbers while reducing the proliferation of organoids from healthy crypts. *Jak2* over-expression in IECs increases intestinal microadenoma, and depletion of EZH2 in the adenoma increases mutant β-catenin and severity of intestinal adenoma, suggesting that depletion of EZH2 enhances the malignancy of overexpressed *Jak2*-derived IEC neoplasia. Consistently, J*AK2V617F* GOF mutation increases HT29 or Caco-2 cell migration.
Conclusion *JAK2V617F* GOF mutation can drive IEC neoplastic proliferation and adenoma, depletion of EZH2 in the adenoma leads to IEC malignant neoplasm. Our research suggests that loss of *Ezh2* may synergistically cooperate with the *Jak2V617F* mutation in the pathogenesis of IEC malignant neoplasm.

#0261 Akt1 and Cyclin D1 govern polarity of self-renewing divisions in breast cancer stem cells.

X. Jiao[1], X. Sun[2], Z. Li[1], X. Ju[2], D. Li[1], R. Harish[1], G. Robertson[3], A. W. Ashton[4], **R. G. Pestell**[1];
[1]Baruch S. Blumberg Institute, Wynnewood, PA, [2]Thomas Jefferson University, Philadelphia, PA, [3]Dxige Research Inc., Courtenay, BC, Canada, [4]Lankenau Institute for Medical Research, Wynnewood, PA

Background. Stem-like cells contribute to the development and progression of human cancers. Genes that control symmetric cell divisions have an evolutionarily conserved role in the regulation of cell polarity and in tumorigenesis. Two cells generated by asymmetric divisions have reduced proliferative potential compared with symmetric divisions. The cell survival oncoprotein Akt (Protein Kinase B) is encoded by three isoforms that are altered in human cancers. The Akt isoform-specific impact on breast cancer stem cell function and polarity is controversial, with Akt1 either reducing (1) or promoting (2) cell polarity and migration in tissue culture. Deletion of *Akt1* reduced mammary tumor progression and metastasis in transgenic mice (2,3).
Methods. Analysis of *Akt1*, cyclin D1 and Notch signaling was conducted from public databases, and human as well as murine breast cancer samples. Cells derived from *Akt1* gene deletion MMTV-ErbB2 breast oncomice (MMTV-ErbB2/Akt1$^{+/+}$ and MMTV-ErbB2/Akt1$^{-/-}$) and from the human MCF-7 breast cancer cell line with regulated expression of cyclin D1 and p53 were analyzed for the symmetry of cell division, stem cell function, and signaling pathways.
Results. In breast tumors derived from MMTV-ErbB2 transgenics, associated with reduced metastasis, Akt1 genetic deletion reduced the frequency of symmetric cell divisions and the production of mammospheres. *Akt1* deletion increased p53 and reduced cyclin D1. Pharmacological reactivation of p53 with Nutlin correlated with the reinduction of asymmetric cellular divisions and reduction in mammospheres in murine and human BCa cells. *Akt1* deletion abrogated Nutlin-mediated induction of asymmetric cell divisions. Cyclin D1 induced symmetrical cell divisions, mammosphere formation and reduced p53 and Numb.
Conclusions. Akt1 promoted symmetrical cell division at least in part via cyclin D1 suppression of Numb, and induction of γ secretase activity and thereby Notch signaling.

Reference.

(1) Irie HY, Pearline RV, Grueneberg D, Hsia M, Ravichandran P, Kothari N*, et al.* Distinct roles of Akt1 and Akt2 in regulating cell migration and epithelial-mesenchymal transition. J Cell Biol **2005**;171:1023-34.
(2) Ju X, Katiyar S, Wang C, Liu M, Jiao X, Li S*, et al.* Akt1 governs breast cancer progression in vivo. Proc Natl Acad Sci U S A **2007**;104:7438-43.
(3) Chen X, Ariss MM, Ramakrishnan G, Nogueira V, Blaha C, Putzbach W*, et al.* Cell-Autonomous versus Systemic Akt Isoform Deletions Uncovered New Roles for Akt1 and Akt2 in Breast Cancer. Mol Cell **2020**;80:87-101 e5

#0262 Gastrin-dependent suppression of CCK2R+ antrum stem cells inhibits gastric atrophy and cancer initiation in C57BL/6 mice.

B. Zheng, G. Lian, E. Malagola, H. Kobayashi, R. Tu, F. Wu, J. Qian, Q. Waterbury, Y. Ochiai, L. Zamechek, T. Wang;
Columbia University Medical Center, New York, NY

Background The cholecystokin-2/gastrin receptor (CCK2R) is expressed by rare epithelial cells in the gastric antrum that are bone fide +4 gastric stem cells. CCK2R+ antral stem cells are relatively quiescent, divide asymmetrically, and lineage trace entire antral glands. Their stemness is sustained over time through gastrin/CCK2R signaling (Cell Stem Cell 26, 739-754, May 7, 2020). However, the role of gastrin/CCK2R signaling in antral stem cells during mucosal injury and regeneration has not been explored.
Methods We generated CCK2R-CreERT2; Gastrin-BAC-DTR-P2A-TdTomato; Rosa26-ZsGreen mice in a C57BL/6 background. Hypogastrinemia was induced through diphtheria toxin-dependent ablation of antral G cells, while hypergastrinemia was achieved via Alzet pump gastrin infusion. Lineage tracing from antrum CCK2R+ stem cells was assessed quantitatively during homeostasis and also during injury in chronic H. pylori infection and MNU injury models.
Results Our findings revealed that G cell ablation increased lineage tracing of CCK2R+ antral stem cells at day 14 and increased proliferation of antral epithelial cells (Ki67+ cells) ($P<0.05$). Moreover, sorted antrum CCK2R+ cells (24 hours post-tamoxifen induction) from DT-treated mice had increased organoids forming capacity and in vitro cell growth, consistent with an increase in active progenitors, while hypergastrinemia reduced their growth ($P<0.05$). Numb staining showed that G cell ablation led to increased symmetric division of CCK2R+ stem cells, while gastrin infusion maintained asymmetric division ($P<0.05$). In the chronic H. pylori infection model, after 3 months of infection, the G cell ablation group exhibited more severe gastric antral atrophy compared to controls. In the MNU injury model, after 18 weeks of injury, the G cell ablation group had a higher dysplasia score, with dysplastic lesions largely derived from CCK2R+ cells ($P<0.05$). In our ongoing studies of MNU injury, the G cell ablation group at 36 weeks showed significantly greater tumor number and size than the control groups. Single-cell RNA-seq data showed that G cell ablation led to the proliferation and expansion of CCK2R+ antral stem/progenitor cells.
Conclusions In conclusion, while gastrin maintains long-term antral stem cell quiescence and self-renewal, hypogastrinemia over the short-term leads to expansion and proliferation of CCK2R+ antral stem cells, thus predisposing over the long-term to antral atrophy and cancer initiation. In C57BL/6 mice, hypergastrinemia appears to be a protective factor against antral cancer development.

#0263 RNA Editing ADAR1 Deaminase Activation Responsive (READAR) platforms for dynamic detection of clonal myeloproliferative neoplasm stem cell fitness.

I. van der Werf[1], L. Balaian[1], J. Pham[1], W. Ma[1], A. Mohebbi[1], E. Klacking[1], A. Ruiz[1], K. Mack[1], J. Mascarenhas[2], T. Whisenant[3], L. Alexandrov[3], S. Morris[1], C. Jamieson[1];

[1]Sanford Stem Cell Institute, Division of Regenerative Medicine, Department of Medicine, Moores Cancer Center, University of California, San Diego, La Jolla, CA, [2]Icahn School of Medicine, Mount Sinai, New York, NY, [3]University of California, San Diego, La Jolla, CA

Introduction Myeloproliferative neoplasms (MPNs) are clonal hematopoietic stem cell (HSC) derived disorders that can progress to acute myeloid leukemia (AML) at variable rates depending on macroenvironmental stressors and microenvironmental inflammatory cytokines. The total symptom score (TSS) and variant allele frequency (VAF) of mutations have proven valuable predictors of therapeutic response. Recently, we discovered inflammatory-cytokine-responsive ADAR1 RNA editing enzyme overexpression during MPN progression. However, dynamic prediction of clonal MPN stem cell fitness and progression to AML remains challenging.

Methods We performed longitudinal 150-gene next-generation sequencing (NGS) analyses for 129 MPN patients. We developed single-cell RNA Editing ADAR1 Deaminase Activation Responsive (READAR) platforms to quantify ADAR1 activity with a novel ADAR1 nanoluc-GFP reporter assay, whole transcriptome RNA editome analyses, and MPN stem cell replating assays. To identify novel RNA editing sites, we performed whole genome sequencing on $CD34^+$ cells from 43 MPN patients and whole transcriptome sequencing on FACS-purified HSC and progenitor cells from 32 MPN patients and 24 non-MPN controls.

Results Sequential NGS analysis was performed with a median follow-up of 958 days (range 0-4214; interquartile range (IQR) 314-1350). On average, 6 NGS analyses (range 1-19; IQR 3-9) were performed for each patient. In our cohort, 58.9% of patients were JAK2 V617F+, while mutations in CALR and ASXL1 were observed in 11.6% and 14.0% of cases, respectively. In total, 44.2% (N=57) of patients in our cohort received Inrebic, with 56% reaching the maximum dose of 400mg. Notably, most patients on Inrebic were JAK2 V617F+ (N=38, 67.7%). In JAK2 V617F+ patients on Inrebic, 50% (n=19) experienced a reduction in the JAK2 V617F VAF from their peak value with a median drop of 16% (range 4-57). Our analyses using READAR platforms revealed increased RNA editing levels in JAK2 V617F+ patients from whole transcriptome sequencing analyses compared with JAK2 wild-type patients. Transduction of our ADAR1 nanoluc-GFP reporter into $CD34^+$ cells from MPN patients (N=7), enabled us to quantify ADAR1 activity in an ex vivo setting. Moreover, $CD34^+$ cells from MPN patient samples (n=7) treated in stromal co-cultures with ADAR1 inhibitor, Rebecsinib, demonstrated inhibition of self-renewal in replating assays. A significant reduction in ADAR1-GFP reporter activity was observed in MPN $CD34^+$ cells following Rebecsinib treatment of stromal co-cultures. Also, humanized ADAR1-GFP-luciferase reporter AML mouse models showed a significant reduction in ADAR1 activity and leukemia stem cell self-renewal following Rebecsinib treatment.

Conclusion These READAR platform results suggest that ADAR1 activity can be utilized to predict clonal MPN stem cell fitness and progression.

#0264 Differentiation therapy: Esculetin as a potent agent to alter cellular plasticity of leukemic & solid tumor stem cells.

A. Mathur, D. Saluja;
University of Delhi, Delhi, India

Background The “Differentiation therapy” has been emerging as a promising and more effective strategy against acute leukemia relapses.
Objective In extension to the revolutionising therapeutic outcomes of All Trans Retinoic Acid (ATRA) to induce terminal differentiation of Acute Promyelocytic Leukemic (APL) blast cells, we decipher the potential effect of a natural compound “Esculetin” to serve as a differentiating agent in Acute Myeloid Leukemia (AML) as well as solid tumour cells. Underlaying role of Wnt signaling pathways in esculetin mediated blast cell differentiation was also evaluated.
Methods Human acute myeloid leukemic cells (Kasumi-1) with t(8;21/AML-ETO) translocation were used as a model system. Growth inhibitory and cytotoxic activity of esculetin were analysed using growth kinetics and MTT assay. Morphological alterations, cell scatter characteristics, NBT reduction assay and cell surface marker expression pat- terns were analysed to detect terminally differentiated phenotypes. We employed RT2profiler PCR array system for the analysis of transcriptome profile of Wnt signaling components. Calcium inhibitors (TMB8 and Amlodipine) and Transforming growth factor beta (TGF-β) were used to modulate the Wnt signaling axes. To investigate whether esculetin exerts the similar effects on the invasive solid tumour cancer stem cells subset, we used a cellular model system of colon carcinoma HCT116 cells reflecting EMT phenotype.
Results We illustrate cytotoxic as well as blast cell differentiation potential of esculetin on Kasumi-1 cells. Morphological alterations akin to neutrophilic differentiation as well as the corresponding acquisition of myeloid lineage markers indicate terminal differentiation potential of esculetin in leukemic blast cells. Exposure to esculetin also resulted in downregulation of canonical Wnt axis while upto ~ 21 fold upregulation of non-canonical axis associated genes. Esculetin also showed potential to revert the CSC marker expressions and concurrent EMT consistent with reduced functional aggressiveness in colon cancer cells.
Conclusions Our study highlights the importance of selective use of calcium pools as well as “axis shift” of the canonical to non-canonical Wnt signaling upon esculetin treatment which might abrogate the inherent proliferation to release maturation arrest and induce the differentiation in leukemic blast cells as well as CSC stem cells. The current findings provide further therapeutic interventions to consider esculetin as a potent differentiating agent to counteract relapses.

#0265 Reconstructing the early steps of breast tumor initiation.

Anais Grandon, Shuheng Lin, Martin Castagne, Julien Wicinski, Olivier Rosnet, Christophe Ginestier, Emmanuelle Charafe-Jauffret

Cancer Research Center of Marseille, Marseille, France

Breast cancer screening programs, detect not only the early stages of the disease but also various preneoplastic lesions which are very difficult to predict if and when they may develop into cancer. This uncertainty can lead to over-diagnosis, over-treatment and stress for millions of screened women. As consequence, discovering reliable biomarkers of this evolution could make it possible to monitor these patients appropriately and propose an effective prevention strategy. To meet this challenge, we urgently need to better understand the mechanisms that regulate human mammary homeostasis during early steps of tumor initiation. The hierarchy and the composition of human mammary epithelium, composed of stem, myoepithelial, luminal progenitors and mature luminal cells, are complex. This complexity raises the question of whether a given mammary epithelial cell is equally likely to be the cell-of-origin of breast cancer. Interestingly, increasing evidences show that disruption of lineage integrity can be a precursor of breast tumor initiation, and the basal and the luminal lineages respond differently to a given oncogenic stress and may each follow their own rule towards malignant transformation. These results strongly suggest that each lineage may have its own pliancy to be transformed by a given oncogene, hijacking the inter-tumoral heterogeneity observed in breast cancers. The objectives of this study are to develop a model to reconstruct the early steps of breast tumor initiation and understand the interplay between the initiating oncogenic event and the cell-of-origin. To answer these questions, we used a human mammary epithelial cell lines (HME) that maintains a cellular hierarchy with mammary stem cells (MaSC) and luminal cells (LC). Upon oncogenic expression of $HRAS^{G12V}$ or c-Myc, we observed different modifications of cell homeostasis, with altered proportions of the lineages populations in the cell line. Depending on the oncogenic stress induced, we also demonstrated a modification in the morphology and the cellular composition of HME organoids, as well as in the capacity to form tumors. $HRAS^{G12V}$ induces increase of MaSC compartment, formation of more branched organoids and generate aggressive basal-like tumors. Conversely, c-MYC leads to an almost loss of MaSC and formation of more proliferative unbranched organoid and generate tumors with limited growth. To address more precisely how cell-of-origin and lineage plasticity influence malignant transformation, we are developing for the first time a lineage tracing model in human mammary epithelium with HME. Moreover, a single cell RNA-seq was performed at different early time points during HME cellular differentiation in homeostasis and upon oncogenic stress to decipher the molecular mechanisms that underpin the very earliest steps of breast tumor initiation.

#0266 The effects of retinoid agents and retinoic acid receptor genotype on proliferation, differentiation, and stem cells in colorectal cancer.

V. O. Hunsu, C. O. B. Facey, B. M. Boman;
Helen F. Graham Cancer Center & Research Institute, Newark, DE

Understanding how to therapeutically target colonic stem cells (SCs) is important because SC overpopulation drives CRC growth and development. Our *goal* is to therapeutically sensitize cancer SCs (CSCs) to the differentiation-inducing effects of retinoid agents. We previously found that ALDH specifically marks normal and malignant colonic SCs. We also found that retinoic acid (RA) receptors and other RA signaling components are selectively expressed in ALDH+ SCs, indicating that RA signaling occurs through ALDH+ SCs. Because all-trans retinoic acid (ATRA) is a highly effective treatment for acute promyelocytic leukemia, which is caused by a genetic translocation involving retinoic acid receptor alpha (RARA), we conjecture that the response of RA agents may be effective against solid tumors depending on their pathway genotype. Our bioinformatics analysis on mutations and overexpression of RA signaling component genes in CRC showed that most of the RA pathway genes are altered in human CRCs. Therefore, we *hypothesize* that the ability of retinoid agents and retinoid metabolism blocking agents to induce differentiation of CSCs depends on the RA pathway genotype of CRC cells.Testing the effect of various retinoid drugs on cell proliferation shows that RA pathway genotype affects the response of RA agents in CRC cell lines. HCT116 and SW480 CRC cell lines, which have RA receptor mutations, displayed resistance to ATRA. In contrast, HT29 CRC cells that have wild-type RA receptors are sensitive to ATRA. All three cell lines however showed similar dose responses to the ATRA metabolizing enzyme, CYP26A1 inhibitor Liarozole. This finding indicates that regardless of RA receptor mutations, inhibition of ATRA metabolism can increase intracellular RA levels in a similar manner on all three cell lines to induce anti-proliferative effects. We used CRISPR-Cas9 gene editing to knock out the *RARA* gene in HT29 cells and evaluated its response to ATRA compared to HT29 cells. The *RARA* knockout derived lines showed reduced sensitivity to ATRA treatment and a slower rate of cell division compared to HT29 control cells. Additionally, Nanostring mRNA profiling analysis shows that ATRA treatment of HT29 cells increases expression of *RARA*, *CYP26A1*, and *KRT20* (differentiation marker); and decreased decreases expression of CSC markers *LGR5* and *ALDH1A1*. Altogether, these findings indicate that upregulated RA signaling can reduce cell proliferation, increase differentiation, and decrease CSC numbers in CRCs. Overall, our findings indicate that colon SCs are regulated by RA signaling mechanisms and dysregulation of RA signaling contributes to the SC overpopulation that drives CRC growth. Thus, therapeutically sensitizing CSCs to differentiation-inducing effects of retinoid agents should provide insight into designing new SC-targeted therapies for CRC.

TUMOR BIOLOGY: Stroma Interactions
Poster Session

#0270 Dissecting the effects of p53 mutation and p53 loss on pancreatic tumor microenvironment.
Y. Chen;
UT MD Anderson Cancer Center, Houston, TX

Pancreatic ductal adenocarcinoma (PDAC) is a devastating malignant disease with a dismal prognosis. In the past decades, a plethora of genetically engineered mouse models (GEMMs) with autochthonous pancreatic tumor development have greatly facilitated the studies of pancreatic cancer. Commonly used GEMMs of PDAC often harbor the oncogenic KRAS driver mutation (*Kras*^{G12D}), in combination with either p53 mutation by knock-in strategy (*Trp53*^{R172H}) or p53 loss by conditional knockout (*Trp53*^{cKO}) strategy, in pancreatic cell lineages. However, the systematic comparison of the tumor microenvironment between *Kras*$^{G12D;}$ *Trp53*^{R172H} (KP^{mut}) mouse models and *Kras*$^{G12D;}$ *Trp53*^{cKO} (KP^{loss}) mouse models is still lacking. In this study, we conducted cross-dataset single-cell RNA-sequencing (scRNA-seq) analyses to compare the pancreatic tumor microenvironment from KP^{mut} mouse models and KP^{loss} mouse models, especially focusing on the cell compositions and transcriptomic phenotypes of major cell types including cancer cells, B cells, T cells, granulocytes, myeloid cells, cancer-associated fibroblasts, and endothelial cells. We identified the similarities and differences between KP^{mut} and KP^{loss} mouse models, revealing the effects of p53 mutation and p53 loss on oncogenic KRAS-driven pancreatic tumor progression.

#0271 The effects of B-cell acute lymphoblastic leukemia cells on the adipose tissue microenvironment.

J. Tan, M. Cohen, J. Ding, I. Ahn, X. Yang, S. D. Mittelman;
UCLA Mattel Childrens Hospital, Los Angeles, CA

Obesity increases the risk of developing many cancers, including breast, colon, kidney, and acute lymphoblastic leukemia (ALL). We have previously shown that ALL cells are recruited to migrate into adipose tissue, where they are protected from chemotherapy. In vitro, ALL cells induce significant changes in adipocytes which may contribute to these protective effects. However, how ALL cells affect the complex cell populations found in adipose tissue in vivo remains unknown. We therefore conducted single-cell RNA sequencing (scRNAseq) of the non-adipocyte stromal vascular fraction (SVF) from adipose tissue in obese mice with and without implanted syngeneic BCR-ABL positive ALL. Differential expression analysis was performed on individual SVF cell types to compare ALL vs. control adipose tissue and pathway enrichment analysis was used in identifying altered molecular processes between conditions. SVF from leukemic mice showed substantial differences in gene expression compared to control mice, suggesting that the ALL potentially induces changes in the microenvironment. Some of the largest differences were found in adipose tissue macrophages, and pathway enrichment analysis identified neutrophil recruitment and regulation as one of the top ten pathways upregulated in adipose macrophages from leukemic mice (4.10 fold enrichment, p<1x10-17 by Fisher's exact test). Selected macrophage genes of interest in this pathway included CYBB (Cytochrome B-245 Beta), a neutrophil interaction gene that has been associated with macrophage infiltration in gastric cancer, was expressed 2.28 log2-fold higher in macrophages from leukemic compared to nonleukemic mice ($p<1x10^{-99}$ by Wilcoxon test). ITGAL (Integrin subunit alpha L), which has been shown to be involved in neutrophil recruitment and implicated in cancer cell growth and transformation was expressed 2.85 log2-fold higher in macrophages from leukemic mice ($p<1x10^{-99}$). Interestingly, adipose from leukemic mice showed a population of neutrophils (1.9% of SVF cells), while neutrophils were largely absent in adipose from nonleukemic mice (<0.1% of SVF cells), which is consistent with macrophage involvement in neutrophil recruitment. Our findings highlight the importance of adipose tissue in the leukemia microenvironment and show that ALL cells can influence this microenvironment in complex ways. Further work will confirm and investigate these cell-cell interactions, potentially improving our understanding of how adipose tissue contributes to cancer mortality.

#0272 Novel role for eIF4E in homing of acute myeloid leukemia cells.

L. M. Martinez[1], E. Caldas Lopes[1], M. Sugita[1], J. Gasiorek[2], K. Alilovic[1], K. L. B. Borden[2], M. L. Guzman[1];
[1]Weill Cornell Medicine, New York, NY, [2]Institute for Research in Immunology and Cancer, Universite de Montreal, Montreal, QC, Canada

Acute myeloid leukemia (AML) remains with dismal outcomes, mostly attributed to the inability of therapies to eliminate leukemia stem cells (LSCs) leading to relapse. LSCs home to the bone marrow (BM) niche where they maintain their quiescence state once in contact with mesenchymal stromal cells (MSCs). Therefore, understanding what controls AML-niche interactions could lead to therapeutic approaches that can prevent relapse.
First, we implemented a novel 3D in vitro system to mimic human AML-niche interactions. This 3D structure consists of a spheroid formed with BM-MSCs (HS5 cell line), recreating a hypoxic microenvironment. When AML cells (MM6 cell line) are added to the spheroid in a 1:1 proportion, AML cells migrate to the spheroid. After 24 hours, 0.18% of the AML cells home/colonize the spheroid (n=8). Next, we assessed the cell cycle status of AML cells in co-culture with the spheroid and compare to those in liquid culture or placed on a MSC monolayer (2D). We found that cells upon contact with MSCs increased their quiescence, 18.63% G0 in 2D and significantly higher in 3D conditions (25.03%; p=0.0048). It is also important to point out that colonizing cells have a lower proliferate capacity than non-colonizing cells after 7 days of co-culture (p=0.0286). This quiescence feature suggests a stem-like behavior of cells homing to the spheroid.
Eukaryotic translation initiation factor 4E (eIF4E) has been found altered in AML. While the capacity of eIF4E to increase cell migration and growth has been shown in solid cancers, the mechanism of eIF4E to accelerate AML progression remains unknown. Thus, we hypothesized that eIF4E may play a role in homing of AML cells to the niche. To this end, we used CRISPR to deplete eIF4E in MM6 cells and found that CRISPR 4E cells have significantly decreased homing capacity to the spheroid compared with control cells (p=0.0065). Importantly, we found a lower percentage of CRISPR 4E cells underwent quiescence after co-culture with MSCs (2D or 3D) (p<0.0001). We corroborated observations using xenograft mice. After 20 hours of intravenous injection, we observed a higher percentage of AML cells in the blood of the mice injected with CRISPR 4E cells compared with control cells (p=0.0286), suggesting that CRISPR 4E cells are not able to effectively exit from peripheral blood to home to their niche.
Altogether, we stablished a novel in vitro 3D model that mimics stem cell features of the AML-BM niche. We demonstrated that the depletion of eIF4E in AML cells decreases their homing and prevents them from acquiring niche-induced quiescence.

#0273 Extrinsic photoaging vs intrinsic aging in dermal fibroblasts: Its impact on the microenvironment and melanoma progression.

V. Wang[1], Y. Chhabra[2], L. Hueser[2], A. Weeraratna[1];
[1]Johns Hopkins University School of Medicine, Baltimore, MD, [2]Johns Hopkins University School of Public Health, Baltimore, MD

Melanoma is the deadliest form of skin cancer, with chronological aging as a major negative prognostic factor due to the influence of intrinsic aging on the tumor microenvironment (TME) to promote tumor initiation and progression. Ultraviolet radiation (UVR) exposure, which is a major risk factor for melanoma, also can cause a physical premature aging phenotype, known as extrinsic photoaging, from chronic UVA irradiation of the underlying dermis. Photoaging of the skin often occurs in tandem with chronological aging, and contributes to similar physical alterations in normal skin structure. However, the molecular mechanisms of how photoaging compares to chronological aging in changing the TME and on tumor progression is still lacking. Here we found that extrinsically photoaged fibroblasts have a higher level of secretion of lysosomal proteases, Cathepsins, which have been shown to be secreted via lysosomal exocytosis and play a functional role in extracellular matrix (ECM) remodeling at neutral PH levels. We found that Cathepsins B and D are secreted at higher levels in both extrinsically photoaged young fibroblasts and in intrinsically aged fibroblasts and upregulated at the endogenous protein level. Cathepsin B has been shown to be highly expressed in metastatic but not primary melanoma patient samples, and cleaves ECM proteins such as fibronectin and tenascin. Immunofluorescent staining of *in-vitro* fibroblast derived matrices (CDMs) confirmed that photoaging disrupts subsequent deposited extracellular matrix proteins similarly to that of intrinsically aged healthy fibroblasts and these matrix changes influences the growth pattern of melanoma lines plated on these CDMs. Mass spectrometry analysis of secreted proteomics confirmed that aged fibroblasts secrete more cathepsins than intrinsically young fibroblasts, and Cathepsins B and D were also detected in extracellular vesicle (EV) cargo proteomics. Single-Particle Interferometric Reflectance Imaging (SP-IRIS) of EVs showed that UVA irradiation induced a significant increase in the total number of secreted of exosomes and in expression of tetraspanin protein CD63 , which plays a role in cargo sorting and has been detected in high levels in the plasma of melanoma patients. We hypothesize that extrinsic photoaging of fibroblasts induces the secretion of exosomes packaged with Cathepsins that play an integral role in ECM remodeling and matrix degradation in a beneficial manner for melanoma invasion. Further studies will assess the influence on secreted cathepsins on melanomagenesis and melanoma invasion through both mechanical and biochemical changes in the TME with *in-vitro* and *in-vivo* studies.

#0274 Cancer-associated fibroblasts exhibit increased motility under hypoxic conditions via interaction with cancer cells.

J. Park[1], S. Lee[1], J. M. Kurie[2], Y.-H. Ahn[1];
[1]Ewha Womans University, Seoul, Korea, Republic of, [2]University of Texas MD Anderson Cancer Center, Houston, TX

Cancer-associated fibroblasts (CAFs) are key components of the tumor microenvironment, playing various roles through interactions with cancer cells and other stromal cell types. In a 3D co-culture system of CAFs and lung cancer cells, a specific subgroup of CAFs exhibited increased motility, while another subgroup of CAFs remained stationary. Using the photoconvertible fluorescent protein Dendra2, we isolated these distinct CAF subgroups and conducted RNA sequencing. Gene set enrichment and gene ontology analysis revealed that upregulated genes in motile CAFs are associated with hypoxia and glycolysis. Conditioned medium from mesenchymal-like cancer cells enhanced the expression of genes related to hypoxia and glycolysis in CAFs. Among these genes, Aldoa and Ldha were chosen for knockdown in CAFs, resulting in a reduction in CAF motility. We confirmed that mesenchymal-like cancer cells promoted CAF motility and intensified hypoxic conditions within the co-culture system, which was monitored using a hypoxia reporter. Ceruloplasmin (CP) was identified as a secretory protein from mesenchymal-like cancer cells through mass spectrometry. Knockdown of CP led to the inhibition of CAF motility. In conclusion, the motility of CAFs is enhanced under hypoxic conditions facilitated by the secretion of CP from mesenchymal-like cancer cells in the lung tumor microenvironment.

#0275 Deciphering biphasic responses to Sonic Hedgehog pathway inhibition in breast cancer: Insights from a tumor-fibroblast spheroid model and PDXs.

H. M. Rosado-Galindo[1], M. Acevedo-Esquillin[1], W. Torres-Garcia[1], A. M. Reyes-Ramos[1], G. Ortiz-Soto[2], M. M. Martinez-Montemayor[2], **M. Domenech**[1]; [1]University of Puerto Rico - Mayaguez, Mayaguez, PR, [2]Universidad Central del Caribe, Bayamon, PR

A significant subset (30-40%) of triple-negative breast cancer (TNBC) cases exhibit hyperactivation of the sonic hedgehog (SHH) pathway, correlating with poor clinical outcomes. However, the therapeutic efficacy of SHH inhibitors in TNBC has yielded inconsistent results, showcasing biphasic tumor responses going from complete remission in some patients to faster disease progression in others. Such tumor response discrepancies underscore the need for more relevant culture models to elucidate how stromal cells respond to SHH signals and impact tumor cell reprogramming.We have developed a tumor-fibroblast spheroid model of robust paracrine SHH signaling to examine alterations in aggressive tumor cell phenotypes resulting from altered SHH pathway activity levels to understand better how SHH therapy leads to biphasic effects in tumor tissues. Specifically, tumor stemness alterations were examined as a function of SHH signal strength altered by tumor-fibroblast proximity, and findings were confirmed in two PDX models of TNBC of divergent sensitivity to pharmacological SHH pathway inhibition. In vitro, results show that tumor stemness potency is enriched by tumor-fibroblast proximity and inversely correlates with SHH pathway activity levels. Tumor stemness potency was determined via a mammosphere forming assay and resistance to chemotherapy using docetaxel as treatment. CD44+ sorted tumor cells derived from adjacent fibroblast cultures showed higher mammosphere forming efficiency and docetaxel sensitivity than those from mixed cultures. These effects correlated with differences in SHH pathway activity strengths and were reverted by pharmacological inhibition of SHH confirming pathway activity involvement. In two PDX models, both exhibiting high SHH pathway activity and similar tumor vascularization, we observed variable response to pharmacological SHH inhibition. PDX2 displayed favorable responses with minimal alpha-smooth muscle actin-positive (SMA+) fibroblast infiltration, while PDX1 exhibited no benefit from SHH therapy, accompanied by a high level of SMA+ fibroblasts. Spatial transcriptomic analysis confirmed stemness enrichments in the PDX1 model treated with SHH inhibitor- a scenario our mixed co-culture model resembled. Stemness-enriched tumor regions were positive for the Ki67 proliferation marker and confined to areas of high SMA+ cell abundance. Plotting Ki67 vs SMA+ cell levels revealed a positive correlation, suggesting that SMA levels may predict tumor response to SHH pathway inhibition.In summary, our studies demonstrate that pharmacological SHH inhibition can induce altered tumor plasticity by favoring stemness phenotypes. Strategies targeting tumor stemness may mitigate biphasic effects in response to SHH inhibitors, offering insights for optimizing TNBC therapeutic approaches.

#0276 Artificial intelligence-powered analysis of tumor-stroma ratio and fibroblast density as prognostic indicators in colorectal cancer.

M. Jung[1], J. Kim[1], M. Kang[2], J. Lee[2], S. Song[2], T. Lee[2], W. Jung[2], S. Cho[2];
[1]Yonsei University College of Medicine, Seoul, Korea, Republic of, [2]Lunit, Seoul, Korea, Republic of

Introduction: The tumor microenvironment (TME) plays a critical role in cancer prognosis. In colorectal cancer (CRC), the tumor-stroma ratio (TSR) and cancer-associated fibroblast (CAF) density are emerging as prognostic markers. However, accurately quantifying them remains challenging. Recent studies have shown that artificial intelligence (AI)-powered analyzers can quantify features in the TME including these.
Methods: Lunit SCOPE IO, an AI-powered H&E whole-slide image analyzer that detects fibroblasts and segments cancer area and stromal area, was applied to evaluate TSR and CAF density in treatment-naive, stage II or III CRC surgical specimens (N = 207) from Severance Hospital. TSR was calculated as the ratio of the area of the cancer area (CA) to the sum of the CA and the cancer stromal area (CS) within a slide. CAF density was evaluated as the fibroblast density within the CA or CS, or the ratio between them. Cox survival analysis determined the hazard ratios (HRs) in progression-free survival (PFS) between the high/low TSR/CAF groups, defining high/low groups based on optimized hazard ratio (HR) cutoffs.
Results: The study found a mean TSR of 0.481±0.126 and CAF densities of 69.96±37.53/mm² (cancer area) and 1844.29±440.31/mm² (stromal area). Higher TSR, lower CAF density in CA, and higher CAF density in CS were linked to better prognosis (Table 1). The mean CAF ratio (CAF density of CS divided by CAF density of CA) was 33.92±25.35, and a group with high values showed a favorable prognosis. Dividing patients based on TSR and CAF ratio, we found that high levels in either or both metrics predicted better outcomes compared to low levels in both.
Conclusions: In this study, we found a favorable prognosis in the group with higher TSR or higher density of CAF in CS compared to CA. This result suggests that AI-enhanced analysis of TSR and CAF can effectively predict prognosis in CRC, highlighting the potential roles of these markers in cancer prognosis.

Table 1. Prognosis by tumor-stroma ratio (TSR) and cancer-associated fibroblast (CAF) density

Factor	Group	Hazard ratio (95% confidence interval)	Mean progression-free survival (months)	p-value
TSR (cutoff: 0.351)	Low (N = 34)	Reference	43.7	<0.001
	High (N = 173)	0.32 (0.19 - 0.56)	67.2	
CAF density of cancer area (CA) (cutoff: 46.8)	Low (N = 62)	Reference	69.3	0.056
	High (N = 145)	1.86 (0.98 - 3.50)	60.7	
CAF density of cancer stromal area (CS) (cutoff:1,901)	Low (N = 116)	Reference	58.2	0.015
	High (N = 91)	0.50 (0.29 - 0.88)	69.9	
The ratio of CAF density of CS to CA (CAF ratio) (cutoff: 53.1)	Low (N = 187)	Reference	61.5	0.043
	High (N = 20)	0.13 (0.02 - 0.94)	80.9	
Combination of TSR and CAF ratio	Both low (N = 32)	Reference	41.2	<0.001
	TSR high, CAF ratio low (N = 155)	0.32 (0.19 - 0.56)	65.8	
	TSR low, CAF ratio high (N = 2)	0.00 (0.00 - ∞)	83.4	
	Both high (N = 18)	0.06 (0.01 - 0.45)	80.2	

#0277 Cancer-associated fibroblasts, educated by tumor cells, differentially facilitate cancer cell invasion in cell-line based human gastric tumoroids.

H. Hwang, S.-B. Lee, **H.-J. Kuh**;
Catholic University of Korea, Seoul, Korea, Republic of

Purposes: Gastric cancer can be categorized into two subtypes: intestinal and diffuse. The latter is notorious for frequent peritoneal metastasis, resulting in a poorer prognosis. Cancer-associated fibroblasts (CAFs) in the tumor microenvironment play crucial roles in tumor invasion and metastasis. However, little is known about whether CAFs are associated with the differential progression between the two subtypes of gastric tumors. This study investigated whether differential cancer invasion may be attributed to tumor-specific CAF activation, using a cell-line-based human gastric tumoroid model.
Methods: Heterotypic tumor spheroids (TS) were prepared with human gastric cancer lines of intestinal (MKN28, MKN74) and diffuse type (MKN45, KATO III) mixed with human gastric fibroblasts (HGFs) using a minipillar-array chip previously developed. Invasion phenotype and expression of epithelial-mesenchymal transition (EMT)-related proteins were evaluated in heterotypic TSs. mRNA expression in HGFs isolated from heterotypic TSs was analyzed and compared between the two subtypes.
Results: While both heterotypic TSs displayed increased invasion by HGFs, the diffuse type TS showed a higher level of invasion with individual or amoeboid migration and loose binding of cancer cells with HGF. In contrast, the intestinal type TS showed collective migration and tight binding between cancer cells and HGFs. HGFs in each heterotypic TS exhibited differential morphology, matrix remodeling patterns, and gene expression in a tumor subtype-specific manner. Compared to normal HGFs, HGFs isolated from diffuse heterotypic TS showed enriched expression of cytoskeleton-associated genes and several integrins, whereas those of intestinal heterotypic TS exhibited increased expression levels of inflammatory cytokines.
Conclusions: This study established tumoroid models for human gastric cancer subtypes, intestinal and diffuse, using heterotypic TS culture. Our results suggest that the subtype-specific invasion ability of tumor cells is driven by CAFs that are differentially educated by tumor cells in the tumor microenvironment. Our model not only advances our understanding of CAFs' role in tumor progression but also offers an *in vitro* model for assessing potential therapeutic targets and drug candidates for human gastric cancers.

#0278 Investigating the functional role of cancer-associated fibroblasts in the emergence of drug-tolerant persisters in ovarian cancer.

A. S. N. Ng[1], N. Bui[2], L. Ailles[1];
[1]University of Toronto, Toronto, ON, Canada, [2]Princess Margaret Cancer Centre, Toronto, ON, Canada

Chemoresistance remains a major clinical challenge for the treatment of high-grade serous ovarian cancer (HGSC), the most lethal gynecologic malignancy. The majority of patients who initially respond to first-line platinum/taxane-based chemotherapy eventually relapse with chemoresistant disease, leading to poor survival outcomes. It is increasingly recognized that cancer cells can enter a reversible drug-tolerant persister (DTP) state through non-genetic mechanisms to evade chemotherapy-induced cytotoxicity prior to the development of chemoresistance. However, how environmental signals and extracellular factors from the tumor microenvironment drive the process remains poorly understood. Cancer-associated fibroblasts (CAFs) are a functionally heterogeneous population of activated fibroblasts. CAFs play a critical role in shaping the tumor microenvironment and tumor behaviors, including promoting tumor growth and mediating therapy resistance. Here, we demonstrated that HGSC cell lines co-cultured with patient-derived FAP-high CAFs, a subpopulation of CAFs previously identified in our lab to be tumor-promoting, significantly increase the formation of DTPs upon prolonged carboplatin treatment compared to the mono-cultured condition. Interestingly, the extracellular matrix (ECM) organization signature is enriched in FAP-high CAFs compared to their FAP-low counterparts, and we found that ECM deposited by FAP-high CAFs also facilitates the emergence of DTPs in HGSC cells. Future work will focus on elucidating the mechanisms by which FAP-high CAFs and the associated ECM promote DTP formation in HGSC cells through transcriptomic and proteomic profiling. This will aid the identification of potential therapeutic vulnerabilities to target cancer cells in the DTP state in FAP-high HGSC patients.

#0279 Iatrogenic immunosuppression emplaces tacrolimus to drive squamous skin cancer progression and influence the microenvironment.

E. Kumah[1], Y. Chhabra[2], V. Wang[2], A. Dixit[2], A. Weeraratna[2], K. Bibee[1];
[1]Johns Hopkins Medicine, Baltimore, MD, [2]Johns Hopkins School of Public Health, Baltimore, MD

One in thirteen organ transplant recipients (OTRs) develop post-transplant cutaneous squamous cell carcinoma (cSCC), leading to significant morbidity upon disease progression. Although chronic ultraviolet (UV) exposure primarily underlies keratinocyte carcinogenesis, long-term immunosuppression is a critical etiologic risk factor due to reduced systemic surveillance of dysplasia. Calcineurin inhibitors such as tacrolimus are commonly administered to suppress the immune system by blocking T-cell proliferation and preventing donor organ rejection. Contrarily, studies have evinced the off-target effects of immunosuppressives, namely azathioprine and cyclosporine, but not tacrolimus — the most widely used in all immunosuppression. In addition, the preclinical research literature has overlooked the contribution of stromal fibroblasts in the cSCC tumor microenvironment (TME). Hence, we hypothesize that tacrolimus exerts direct carcinogenic effects on keratinocytes and fibroblasts in the skin. We further postulate that tacrolimus enables a tumor-permissive microenvironment by activating dermal fibroblasts to cause aggressive and invasive keratinocyte carcinoma in OTRs. To examine this cellular crosstalk phenomenon, we used human keratinocytes, primary dermal fibroblasts and cSCC cells in mono- and co-cultures to mimic cutaneous and tumor complexities. Next, we assessed the molecular mechanisms utilized by tacrolimus to potentiate tumorigenesis pertinent to cell survival, proliferation and invasion. Herein, we show that tacrolimus promotes cell survival dose-dependently in cSCC cells. We also found that a fibroblast-cSCC spheroid co-culture significantly enhances cell invasion. In a wound-healing migration assay, tacrolimus increased the migratory capacity of normal keratinocytes and cSCC cells. However, cell proliferation remains nebulous due to cyclical dose-response effects in vitro. We then queried whether cell proliferation is affected in vivo using immunodeficient mice, and similar results were observed. We confirmed via immunoblotting that tacrolimus induced elevated expression of proliferation markers at distinct drug concentrations. Altogether, our findings illuminate keratinocyte-stroma interactions and particularly isolate the contributory role of tacrolimus in non-immune mediated cSCC pathogenesis. This knowledge suggests newer immunosuppressives that do not inhibit calcineurin activity may help relieve cutaneous malignancies in transplant recipients.

#0280 Aberrant β-catenin signaling from the bone marrow niche leads to transformation of *IDH1/2*-mutant hematopoietic stem cells and compromises response to IDH1/2 inhibitors.

P. Vgenopoulou[1], L. Flores[1], I. Mosialou[1], J. Zhao[1], X. Liu[1], P. Sung[2], V. Penard-Lacronique[3], M. Carroll[4], S. Kousteni[1];
[1]Columbia University Irving Medical Center, New York, NY, [2]Roswell Park Comprehensive Cancer Center, Buffalo, NY, [3]Institut Gustave Roussy, Villejuif, France, [4]University of Pennsylvania, Philadelphia, PA

Our purpose is to identify stromal-derived signals required for *IDH1/2*-mut hematopoietic stem cells (HSCs) to become leukemogenic. Mutations in *IDH* genes are found in 20% of acute myeloid leukemia (AML) patients and are not transformative. They produce the oncometabolite 2HG which inhibits key epigenetic regulators. We explored whether epigenetic changes in the bone marrow (BM) niche could provide cooperative signals to IDH-mut HSCs leading to their transformation and disease development. We found that 2HG is elevated in the BM plasma of MDS/AML patients with *IDH1/2* mutations as compared to *IDH*-wt patients. Interestingly, 2HG is taken up by BM stromal cells (BMSCs) suggesting it may induce aberrant methylation patterns in them. Indeed, methylome analysis showed hypermethylation in BMSCs of AML patients with *IDH1/2* mutations compared to wt. Among the most hypermethylated genes in the *IDH*-mut stroma are *AXIN1*, *AXIN2* and *NDK2,* all negative regulators of β-catenin; this pathway activation was previously shown to cause MDS/AML in mice and present in 38% of patients. In agreement with these findings βcat activation in the stroma of *IDH*-mut vs *IDH*-wt AML patients showed a strong positive correlation as 50% of *IDH*-mut patients had activated βcat in their BMSCs. Inquiring whether stroma methylation precedes HSC transformation, we analyzed samples from healthy individuals with *IDH*-mut clonal hematopoiesis. They exhibited increased global and *AXIN1* promoter methylation compared to samples without such clones, but not active βcat in osteoblasts, indicating this might be a later step along with disease development. In fact, transplantation of HSCs from *Idh2*-mut mice to recipients expressing active βcat in osteoblasts led to increase in blasts and shortened survival compared to wt mice transplanted with *Idh2*-mut HSCs. As many patients relapse following treatment with IDH inhibitors, we investigated a potential role for βcat signaling in treatment outcome. *IDH*-mut AML patients who do not respond to treatment with the IDHi present more frequently with activated βcat in osteoblasts compared to responders. Analyzing samples from the same patient pre- and post-treatment with IDHi, we found before treatment most patients were positive for βcat stromal activation, whereas after treatment, all patients with complete response were negative, while patients with progressive disease remained positive. Our model suggests *IDH*-mut HSCs secrete 2HG inducing epigenetic alterations in the niche, some of which cause activation of the βcat pathway. In turn, this additional signal leads to the transformation of HSCs to dysplastic cells and MDS/AML development. This work uncovers a new mechanism for transformation to MDS/AML and resistance to IDHi treatment. Thus, targeting βcat activation in the stroma, in combination with IDHi, could improve treatment outcome.

#0281 The function of FGFR2+ cancer-associated fibroblasts on cancer stem cell expansion of esophageal squamous cell carcinoma.

Y. Wang, P. Feng, T.-c. Jiang, X.-y. Guan, Y.-f. Xia;
Sun Yat-sen University Cancer Center (SYSUCC), Guangdong, China

Aims: FGFR2+ fibroblasts were reported to promote tumor progression, but the mechanisms remained unexplored in esophageal squamous cell carcinoma (ESCC).Methods: Multiplex immunohistochemistry (mIHC) displayed the distributions of FGFR2+ fibroblasts and cancer stem cells (CSCs). After FGFR2+ fibroblast isolation, tumor cells were stimulated with fibroblasts supernatant to assess radioresistance and CSC properties. RNA-seq analysis identified the downstream BMP5 expression.Results: In our preliminary study, the immunohistochemistry results showed that FGFR2+ fibroblasts were always represented in the area near cancer stem cells (CSCs), and FGFR2+ fibroblasts infiltration was associated with poor outcomes. When we cocultured FGFR2+ fibroblasts with tumor cells, we found the proportion of CSCs were upregulated. The results of RNA sequencing and ELISA showed that FGFR2+ fibroblasts overexpressed BMP5. Using FGFR2+ fibroblasts or BMP5 to stimulate cancer cells, the proportion of cancer stem cells was increased, the capabilities of sphere formation and survival after radiation were enhanced. Both RNA sequencing and immunoblotting results indicated that BMP5 affected H2AX phosphorylation in DNA repair pathway and activated its potential upstream pathway MAPK signaling pathway. In vivo experiments also showed that FGFR2+ fibroblasts could upregulate CSCs proportions.Conclusions: Our findings suggested that BMP5 derived from FGFR2+ fibroblasts might induce CSCs expansion and led to poor prognosis in the ESCC.

#0282 *SFRP4+* cancer associated fibroblasts activate epithelial to mesenchymal transitions in malignant cells and dictate adverse clinical outcomes in stomach cancer.

Seungho Lee[1], Austin Cho[2], Hyoung-Il Kim[3], Hoon Hur[4], Jae-Ho Cheong[5], Tae-Min Kim[6]

[1]Department of Surgery, Seoul National University Hospital, Jongro-gu, Korea, Republic of,[2]Department of Genetics, University of Minnesota, Minnesota, MN,[3]Department of Surgery, Yonsei University Health System, Jongro-gu, Korea, Republic of,[4]Department of Surgery, Ajou University School of Meedicine, Soowon, Korea, Republic of,[5]Department of Surgery, Yonsei University Health System, Seodaemoon-gu, Korea, Republic of,[6]The Catholic University of Korea, Seocho-gu, Korea, Republic of

Cancer-associated fibroblasts (CAFs), a pivotal component in the tumor microenvironment (TME) of gastric cancer (GC), play a crucial role in tumor progression and resistance to treatment. In this study, we performed analyses to build a comprehensive cellular landscape of fibroblasts in GC EMT using three single-cell RNA cohorts including ours (GSE183904, GSE134520 and GSE167297). We observed distinct fibroblast subtypes (CXCL14+/POSTN+, CXCL14+/APOE+, SFRP4+, and SFRP2+ fibroblasts). Among the subtypes, we observed that SFRP4+ fibroblasts sharing cellular origins with normal tissue-residing SFRP2+ myofibroblasts. Notably, SFRP4+ fibroblasts showed a regional prediction for tumor and deep tumor layers compared to normal and superficial tumor layers, respectively. To further understand the role of these fibroblasts, we employed spatial transcriptome data. Spatially resolving the cellular interactions within the TME, the adjacency of SFRP4+ CAFs to malignant cells undergoing epithelial-to-mesenchymal transition (EMT), was observed. Ligand-receptor analyses demonstrated SFRP4+CAFs regulate key genes of EMT in malignant cells (TGFBI, COL1A1, SPARC, COL3A1, COL1A2, and BGN). The regulatory roles of SFRP4+ CAFs in driving the epithelial-mesenchymal transition (EMT) of malignant cells were further validated in vitro. Clinical relevance was also demonstrated with the correlation between the abundance of SFRP4+ CAF and clinical outcomes, i.e., high SFRP4+CAF abundance was consistently associated with shorter survival of GC patients across cohorts. Thus, we present SFRP4+ CAFs as major fibroblast subtypes in GC TME. Spatial cellular architectures and in vitro evidence support that SFRP4+fibroblasts activate the EMT of malignant cells along with their association with patient prognosis. This study advances our understanding into the mechanistic roles of SFRP4+ fibroblasts in GC pathogenesis and progression, paving the way for potential targeted therapeutic strategies.

#0283 Fibroblast diversity and immune microenvironment in pseudoangiomatous stromal hyperplasia (PASH): Associations with breast cancer risk.

N. Cruz-Reyes[1], M. Rossi[1], M. Stallings Mann[1], B. McCauley[2], T. Hoskin[2], R. Vierkant[2], S. Winham[2], A. Degnim[2], M. E. Sherman[1], D. C. Radisky[1];
[1]Mayo Clinic College of Medicine and Science, Jacksonville, FL, [2]Mayo Clinic College of Medicine and Science, Rochester, MN

Benign breast disease (BBD) affects over one million women annually in the United States and is diagnosed in nearly half of all women during their lifetime. Pseudoangiomatous stromal hyperplasia (PASH), a common BBD subtype, is characterized by an overaccumulation of tissue fibroblasts. Current research suggests a pivotal role of the immune microenvironment in progression of BBD to breast cancer, suggesting its composition as a determinant of breast cancer risk. Our study evaluates whether fibroblast variations and immune microenvironment differences in BBD biopsies containing PASH lesions are associated with subsequent breast cancer development. We evaluated BBD biopsies from women who subsequently developed breast cancer (cases, N=5) or remained cancer-free (controls, N=5). Using Opal-based multiplex immunofluorescence (mIF) assays, we mapped expression of fibroblast markers linked to breast cancer associated fibroblasts (CAFs), including vimentin (VIM), smooth muscle actin (ACTA2), fibroblast specific protein-1 (S100A4/FSP1), fibroblast associated protein (FAP), integrin beta-1 (CD29/ITGB1), and platelet derived growth factor receptor beta (PDGFRβ) and markers of key immune cells (T cells: CD4, CD8; dendritic cells: CD11c; B cells: CD20; and macrophages: CD68) along with MKI67 as a proliferation marker. Our results revealed marked differences in fibroblast marker expression and immune cell populations between these groups in the normal lobules in the BBD biopsies. PASH cases showed elevated PDGFRβ and CD29/ITGB1 expression in VIM-positive fibroblasts, markers characteristic of CAF subtypes known to accumulate in more aggressive tumor microenvironments. Conversely, a higher percentage of FSP1+/VIM+ cells, similar to that of a different CAF subtype, was noted in the lobules of PASH controls. This difference in biomarker expression, along with corresponding variations in immune cell counts, suggests a complex interplay between fibroblast composition and immune response that ultimately modulate cancer risk in PASH-containing BBD tissues. Additionally, increased MKI67 expression in PASH cases potentially signals the higher likelihood of cancer development. This work advances our understanding of fibroblast heterogeneity in BBD and its implications for breast cancer risk and progression, and paves the way for innovative strategies to improve clinical outcomes for BBD patients to reduce their incidence of breast cancer.

#0284 Crosstalk with postmenopausal obese mammary adipocytes impacts breast cancer cell metabolism and promotes tumorigenesis.

R. Roy[1], R. Aldakhlallah[2], S. Cobbs[2], E. Man[2], C. Hallinan[2], K. Lee[1], M. Lotz-Bousvaros[3], S. Pories[4], M. A. Moses[1];
[1]Boston Children's Hospital, Harvard Medical School, Boston, MA, [2]Boston Children's Hospital, Boston, MA, [3]Mount Aurburn Hospital, Cambridge, MA, [4]Mount Auburn Hospital, Harvard Medical School, Cambridge, MA

Introduction: Obesity is associated with an increased risk and a poor prognosis of breast cancer (BC) in postmenopausal (PM) women. The mechanism(s) underlying obesity-related PM BC are not clearly understood. We hypothesized that the increased local presence of 'obese' mammary adipocytes within the breast tumor microenvironment (TME) promotes the acquisition of an invasive BC cell phenotype and markedly accelerates tumor proliferation and progression.
Methods: We asked whether cancer-associated mammary adipocytes (CA-MAd) differ from normal mammary adipocytes (N-MAd) in their ability to promote tumorigenesis of dormant BC cells and if so, what the underlying mechanism(s) might be. Using a 2D transwell model, BC cells (ER- and ER+), were cocultured with obese PM CA-MAd isolated from breast cancer patients or obese mammary N-MAds from PM disease-free women and analyzed for migration, proliferation, phenotypic, signaling and metabolic alterations.
Results: Compared to monoculture (MC) conditions, BC cells cocultured (CC) with CA-MAd displayed significantly increased migration and proliferation. Quantitative phase imaging indicated that CA-MAd secretome-treated BC cells displayed increased motility, speed, distance covered and cell size/area compared to N-MAd. Consistent with these results, mesenchymal markers such as fibronectin, vimentin and SNAIL were upregulated whereas the epithelial marker E-cadherin was downregulated in CC *vs*. MC conditions suggesting that Ads in the TME promote EMT in BC cells. Interestingly, mature Ads CC with BC cells underwent delipidation and dedifferentiation as indicated by reduced Oil Red staining, decreased lipid content and reduced expression of Ad maturation markers such as *FABP4*, *ADIPOQ* and *PLIN1*. Consistently, we determined that CC BC cells exhibited increased lipid uptake and BODIPY staining and upregulated pAMPK, pACC and CPT1A signaling when compared to MC BC cells. Short term treatment of BC cells with both N-MAd and CA-MAd secretomes resulted in increased oxygen consumption rate (OCR), basal respiration, ATP-linked respiration and proton-linked respiration compared to control and as determined by the Seahorse extracellular flux assay. CC with MAds significantly downregulated OCR and all respiration parameters in BC cells suggesting decreased glucose uptake and glycolytic flux.
Conclusions: Compared to MC, CC with obese M-Ads promoted functional, phenotypic and metabolic changes in BC cells. Taken together, our results indicate that crosstalk between BC cells and obese MAds promotes delipidation of MAds and a concomitant lipid uptake in BC cells and a switch to lipid metabolism signaling pathways that may, in turn, drive a metabolic shift in BC cells and promote tumor growth. [Supported by NIH RO1CA185530, the Breast Cancer Research Foundation, the Karp Family Foundation and the Nile Albright Research Foundation]

#0285 Targeting TXNDC5 in stromal fibroblasts resolves desmoplasia and resistance to immune checkpoint blockade in mesenchymal-type colorectal cancer.

Kai-Lin Cheng[1], Chih-I Chen[2], Shu-Han Yu[3], Huai-Wen Liang[4], Yi-Wei Tsai[1], Chen-Ting Hung[1], Yu-Shan Lin[1], Yi-Shiuan Tzeng[5], Sung-Jan Lin[6], Yueh-Feng Wu[6], Jen-Kuang Lee[7], Chia-Hui Yu[8], Shuei-Liong Lin[8], Shih-Yu Chen[5], Tzu-Tang Wei[1], Yun-Ju Huang[9], Ruey-Hwa Chen[10], Ching-Chow Chen[1], Kai-Chien Yang[1]

[1]Department and Graduate Institute of Pharmacology, National Taiwan University College of Medicine, Taipei City, Taiwan,[2]Division of Colon and Rectal Surgery, Department of Surgery, E-Da Hospital, I-Shou University, Kaohsiung, Taiwan,[3]Institute of Biotechnology, National Taiwan University, Taipei City, Taiwan,[4]Division of Cardiology, Department of Internal Medicine, E-Da Hospital, I-Shou University, Kaohsiung, Taiwan,[5]Institute of Biomedical Sciences, Academia Sinica, Taipei City, Taiwan,[6]Department of Biomedical Engineering, National Taiwan University, Taipei City, Taiwan,[7]Division of Cardiology, Department of Internal Medicine, National Taiwan University Hospital, Taipei City, Taiwan,[8]Graduate Institute of Physiology, National Taiwan University College of Medicine, Taipei City, Taiwan,[9]Graduate Institute of Oncology, National Taiwan University College of Medicine, Taipei City, Taiwan,[10]Institute of Biological Chemistry, Academia Sinica, Taipei City, Taiwan

Objectives: Mesenchymal-type colorectal cancer (CRC), characterized by strong stromal infiltration and immune tolerance, resists immune checkpoint blockade and has poor outcomes. Cancer-associated fibroblasts (CAFs), abundant in tumor stroma, actively remodel the extracellular matrix (ECM), modulate immune evasion, and drive tumor progression. We have recently identified thioredoxin domain-containing protein 5 (TXNDC5), a protein disulfide isomerase (PDI), as a critical mediator of fibroblast activation and ECM remodeling in organ fibrosis. We hypothesized that TXNDC5 could contribute to fibroblast activation, stroma formation and disease progression in cancer, especially in the stroma-enriched fibrogenic mesenchymal-type CRC.
Methods: Transcriptome databases of CRC were re-analyzed to determine the clinical relevance of TXNDC5. Experimentally, CRC was induced in mouse lines by azoxymethane (AOM) and dextran sulfate sodium (DSS) stimuli, a model sharing multiple characteristics with human mesenchymal-type CRC. Human colonic fibroblast line CCD-18co was used to investigate the molecular mechanisms by which TXNDC5 regulates colonic fibroblast activities. Fibroblast-specific TXNDC5 knockout (*Col1a2-Cre/ERT2*TXNDC5*$^{fl/fl}$) mice were generated, combining with single-cell RNA sequencing analyses on AOM/DSS-induced CRC tumors in these animals, to clarify how fibroblast TXNDC5 impact tumor microenvironment, CRC progression and response to immune checkpoint blockade.
Findings: TXNDC5 was predominantly expressed in stromal fibroblasts of human and mouse CRC. Fibroblast-specific deletion of *Txndc5* lessened CAF activation, attenuated tumor fibrosis and reduced tumor burden in AOM/DSS-induced CRC. Mechanistically, increased TXNDC5 levels augments TGFβ signaling in CAF by post-translational stabilization of TGFBR1 through its PDI activity. In addition, deletion of *Txndc5* in CAFs led to less tumor desmoplasia, decompressed tumor vessels and attenuated intra-tumoral hypoxia, thereby easing immune tolerance and increasing cytotoxic T cell infiltration in CRC. Single-cell transcriptome analysis revealed a marked change of intra-tumoral immune cell populations upon fibroblast-specific deletion of TXNDC5, shifting from myeloid-derived suppressive cells to cytotoxic tumor-infiltrating lymphocytes. Importantly, depletion of TXNDC5 in CAFs potentiated the anti-tumor effects of immune checkpoint blockade with anti-PD1 therapy in CRC.
Conclusions: Our data suggest an important yet previously unrecognized role of fibroblast TXNDC5 in CRC progression, through enhancing CAF activation, stroma formation and immune escape. Combining immune checkpoint blockade with TXNDC5 deletion synergistically improved anti-tumor effects in CRC. Targeting TXNDC5, therefore, can be a novel therapeutic approach for CRC patients.

#0286 Multiplex imaging of human pancreatic tumors reveal novel dynamics of dysplastic stem cells, remodeling of associated fibroblasts and cell-to-cell spatial dependencies.

M. Batardiere[1], S. Ayman[1], C. Beaussier[1], J. Baig[1], Z. Ghanmeh[2], M. Farias-Gonzalez[1], J. Wong[1], A. Archambault-Marsan[1], L. Rousseau[3], S. Turcotte[1], A. Means[4], M. Tan[4], K. DelGiorno[5], E. Dianati[1], V.-H. Trinh[1];

[1]University of Montreal, Montreal, QC, Canada, [2]Concordia University, Montreal, QC, Canada, [3]Centre Hospitalier Universite de Montreal, Montreal, QC, Canada, [4]Vanderbilt University Medical Center, Nashville, TN, [5]Vanderbilt University, Nashville, TN

This study aims to investigate human normal pancreatic tissue, pancreatic precursor lesions, and invasive pancreatic ductal adenocarcinoma to provide the most extensive spatial characterization as disease progress by mapping dysplastic stem cells (DSCs) - a reservoir of cancer cells - and fibroblast populations which modulate the tumor microenvironment and participate in disease progression. We performed 12 cycles of multiplex immunofluorescence using 26 validated antibodies covering fibroblasts [CXCL12, αSMA, FAP, CD74, CD105, PDGFRA, COL1A1], DSCs diversity [CD44v9, CD133, CD166, SPP1, S100P], and immune populations, onto tissue samples from 75 patients screened for normal, low grade, high grade dysplasia, and invasive cancer. We used our codes in Python, R, and QuPath 0.4.3. The pipeline includes shading correction, whole slide image registration (at subcellular level), region of interest and stromal mask annotations by a pathologist [normal duct, acinar to ductal metaplasia (ADM), low grade, high grade, invasive], automatic cell detection, and signal extraction. We developed a novel Python code for cell-to-cell spatial dependency analysis by using the x,y centroid positions of one cell from the tumor to other cells from the stroma mask based on pre-defined distances.

For this abstract, we interrogated 264,732 cells and observed SPP1+, S100P+ DSCs expansion from low grade to high grade dysplasia, whereas CD133+ and CD166+ populations contract ($p<0.0001$). S100P+ DSCs gradually expand as disease progress reaching 74.13% of invasive cells being positive. CD44v9 follows dynamic changes variations, being expressed in 59.6% of cells undergoing ADM, dropping to 5.4% in dysplasia, and re-increasing to 25.4% in invasive cancer (all $p<0.0001$). Focusing on stromal composition, CXCL12+, CD105+, αSMA+, CD74+ fibroblasts expand whereas FAP+ fibroblasts contract from low- to high grade (p-values <0.0001). COL1A1 expression increases at each step of the normal duct - ADM - low grade - high grade - invasive cancer sequence (all $p<0.0001$). The pattern of CD44v9 tumor population showed dynamic alterations with the CD105 fibroblast population, as CD44v9 and CD105 are highly expressed in coordination during ADM. However, in dysplastic lesions and invasive cancer, mutual exclusivity between the tumor CD44v9 populations and the underlying CD105 fibroblast populations is observed, confirmed by our spatial algorithm within 50 µm of cell-to-cells distance ($p<0.0001$). In tumors, when CD44v9 tumor cell populations are expressed, the adjacent fibroblasts were CD105 negative.

Multiplex imaging reveals dysplastic stem cells and fibroblasts dynamics in low- to high grade transition. The high-throughput capabilities of this method lead to the discovery of the CD44v9 tumor and CD105 fibroblast dependencies in pancreatic tumors.

#0287 Analysis for the role of antigen-presenting cancer-associated fibroblasts in tumor microenvironment of colorectal cancer.

Yasuhiro Fukui[1], Hiroaki Kasashima[1], Zizhou Wang[1], Ken Yonemitsu[1], Kishu Kitayama[1], Yuichiro Miki[1], Mami Yoshii[1], Tatsunari Fukuoka[2], Tatsuro Tamura[1], Masatsune Shibutani[1], Takahiro Toyokawa[1], Hiroaki Tanaka[3], Shigeru Lee[1], Masakazu Yashiro[2], Kiyoshi Maeda[1]

[1]Gastroenterological Surgery, Osaka Metropolitan University Graduate School of Medicine, Osaka, Japan,[2]Molecular Oncology and Therapeutics, Osaka Metropolitan University Graduate School of Medicine, Osaka, Japan,[3]Surgery, Fuchu hospital, Osaka, Japan

A new subset of cancer associated fibroblasts (CAFs) called antigen presenting CAF (apCAF) was recently identified, and modulation of the tumor immunity might be associated with tumor progression. We examined the markers of apCAF, such as IRF5, HLA-DRA and HLA-DQA1 by bioinformatics analyses of human colorectal cancer (CRC) datasets. The expression of apCAF markers were upregulated in CAFs isolated from human CRCs and liver metastases compared with their normal counterparts. Kaplan-Meir analysis of 172 human CRC samples clarified that the patients with apCAF marker positive expression in the tumor stroma had worse prognosis than that with negative expression. In addition, the origin of apCAFs was reported to be mesothelial cells, therefore, we established cancer-associated mesothelial cells (CAmes) from ascites of human CRC patients with peritoneal dissemination. Consistently, the expression of antigen-presentation markers was highly upregulated in CAmes, however, allo-mixed lymphocyte reaction analysis demonstrated that their stimulating activity of $CD4^+$ T lymphocytes was diminished. In an in vivo study, we applied a rectal orthotopic transplant model with mouse tumor organoid (MTO) to investigate the effect of apCAF on tumor progressions. Using fluorescence-activated cell sorting (FACS), we examined the ratios of apCAF, myCAF, and iCAF in orthotopic rectal tumors. The percentage of apCAF was highest in the 6-week-tumors and the percentage of myCAF was highest in the 9-week-tumors. Interestingly, the percentage of apCAF was higher in liver metastases than in primary tumor, consistent with bioinformatics analysis. The apCAF increased during the stage of tumor growth, and the percentage of myCAF increase in the later stage of tumor progression with fibrosis. In summary, apCAF might be associated with tumor progression in CRC.

#0288 Middle-aged murine models of triple negative breast cancer (TNBC) show significant differences in tumor immune and stromal environments when compared to classic 6-8 week old models; Challenges and opportunities for preclinical efficacy studies.

P. Falvo[1], S. Gruener[2], S. Orecchioni[1], G. Talarico[1], G. Bravetti[1], G. Mitola[1], F. Pisati[3], I. Barozzi[2], **F. Bertolini**[1];
[1]IEO - European Institute of Oncology, Milan, Italy, [2]University of Vienna, Vienna, Austria, [3]Cogentech, Milan, Italy

The immune system orchestra suffer a deficit of function during aging, and the incidence of the large majority of cancer types is significantly increased in elderly humans. Although BC can occur in young women, it is way more common in middle-age and elderly women. There is evidence that a tonic immune system is pivotal for the success of therapies aimed at awakening a dormant or exhausted immunological response against cancer cells by mean of checkpoint inhibitors (CI). However, rodent models of cancers are currently using very young mice of a few weeks of age, which have a fully functional and tonic immune system and thymus and thus might be poorly representative of adult human cancer patients. We have recently reported that that a triple therapy (TT) involving antigen-presenting cell activation by vinca alkaloids and the generation of new TCF1+ stem cell-like T cell (scT) clones by an alkylating agent can significantly improve the efficacy of the CI anti-PD-1 in models of cancer known to be otherwise CI-resistant such as TNBC and lymphoma (Falvo et al, Cancer Res 2021; Orecchioni et al, JCM 2023). TT effect was due to T cells, as it was abrogated by their in vivo depletion. In the present study we investigated differences in TNBC growth kinetics, TT preclinical activity and tumor microenvironment (TME, including intratumoral immune and stroma cells) in young (6-8w, representative of a 6y old human) versus adult (12m, representative of 40y humans) mice. Models included 4T1 and EMT6 TNBC cells, the former generating a mostly lymphoid TME and the latter generating a mostly myeloid TME. In both models, TT efficacy was similar in young and in adult mice, as the treatment abrogated TNBC local and metastatic growth. CD8+ (but not CD4+) scTs, likely crucial players in TT efficacy, were only slightly reduced in adult mice in spite of age-related thymus involution. This notwithstanding, single cell RNA (10x), IHC and flow cytometry analyses of immune (CD45+EPCAM-) and stroma (CD45-EPCAM-) cell populations indicated major differences in the TME of young vs adult mice. Adults had significantly less CD4+ scTs, B naïve and NK cells and significantly increased memory B cells. TME matrix CAF were skewed in young, while pro-inflammatory stromal populations and myofibroblasts were skewed in adults. Matrix CAFs down regulated a signature involved in different ECM-remodeling abilities, and up regulated metabolic and hypoxic pathways. Expression of genes encoding for glycoproteins, basement membrane components, and collagens were also upregulated. Our data indicate profound differences between young and adult mice immune and stromal TMEs that should be taken into consideration when selecting the age of mice to be used in preclinical efficacy studies in orthotopic immune competent mice.

#0289 Temporal and spatial dynamics of glial cells apolipoprotein E expression in astrocytoma microenvironment.

T.-Y. Chien, C.-S. Chiang;
National Tsing Hua University, Hsinchu City, Taiwan

Introduction: Brain tumors have proven challenging to treat due to the complex and sensitive architecture of the brain. Previous research has shown that GBM cells depend highly on cholesterol uptake, and apolipoprotein E (APOE) is required to transport cholesterol among tissues or cells. APOE is primarily synthesized by astrocytes and has been extensively studied in neurodegenerative diseases. While extensively studied in neurodegenerative diseases, limited studies are focusing on their roles in brain tumor development. Here, we analyzed the temporal and spatial expression of APOE during brain tumor progression in a murine astrocytoma tumor model.

Material and method: ALTS1C1 astrocytoma cells were intracranially injected into the mouse brain. The animal was sacrificed, and the left hemisphere, right hemisphere, and tumor tissue were collected for flow cytometry analysis. CD45, CD11b, and GFAP were used to recognize macrophages, microglia, and astrocytes. CD68, TMEM119, and GFAP were used for tissue immunostaining to label macrophages, microglia, and astrocytes, respectively.

Results and Discussion: Flow cytometry analysis revealed upregulated APOE in tumor-infiltrating microglia, macrophages, and lymphocytes. $GFAP^{high}$ astrocytes displayed lower APOE levels than $GFAP^{low}$ astrocytes. IHC analysis showed that CD68+ macrophages exhibited higher APOE expression at the tumor edge than normal tissue. On the contrary, GFAP+ astrocytes at the tumor edge displayed a lower APOE signal than the normal tissue. Previous studies have shown the participation of APOE in regulating immune response in various cancers. Further studies to analyze the dynamic change of APOE on the gene expression level with *in situ* hybridization and the quantification of cholesterol levels in the microenvironment may help uncover their roles in the glioma microenvironment.

Conclusion: This study demonstrated that APOE was temporal and spatial differentially expressed in macrophages and astrocytes in the brain tumor microenvironment. Tumor-infiltrating cells showed an elevated APOE expression, while $GFAP^{+}$ astrocytes expressed reduced APOE levels. Although the mechanism of these alterations remains unclear, this study provides a basis for future studies about the roles of APOE in the brain tumor microenvironment.

#0290 The role of tumor stromal topography-regulated genes in modulating the cellular landscape of tumor stroma in breast cancer.

C.-Y. Su;
National Yang Ming Chiao Tung University, Taipei City, Taiwan

The tumor remodels the surrounding extracellular matrix fibers to become topographically aligned at the tumor front, further facilitating cancer cell migration. Our recent studies show that aligned tumor stromal topography promotes the detachment of breast cancer cells from the main tumor, then, in the following cell migration, upregulating genes such as genes encoding the cytochrome P450 family 1 subfamily A member 1 (CYP1) and inhibitor of DNA binding (ID) proteins. In this study, we further explored the role of topography-regulated genes in modulating the cellular landscape of tumor stroma. By analyzing the correlation of topography-regulated genes with stromal cell infiltration in bioinformatics databases, we found significant positive correlations between the RNA expression levels of most topography-regulated genes and the infiltration levels of cancer-associated fibroblasts and endothelial cells. Notably, the strongest correlation was between the expression level of ID3 and the infiltration levels of cancer-associated fibroblasts ($r = 0.509$) and endothelial cells ($r = 0.506$). Additionally, ID3 remained highly expressed in circulating tumor cells but exhibited low expression at distant metastatic sites. These findings suggest that genes regulated by tumor stromal topography, especially ID3, may play a role in neovascularization and fibrosis of the tumor microenvironment and the survival adaptation of cancer cells in circulation, thereby promoting metastasis.

#0291 Unveiling heterogeneity of cancer-associated fibroblasts (CAFs) across multiple solid cancer types.

A. Kravets, B. Shpak, A. Zotova, M. Savchenko, S. Kust, O. Golubeva, M. Abdou, F. Grigoryev, I. Bulusheva, B. Sargsyan, P. Pavlovich, V. Maximov, V. Kushnarev, M. Goldberg, N. Kotlov, A. Bagaev;
BostonGene, Corp., Waltham, MA

Background: Stromal cells, including CAFs, are a heterogeneous group of cells in the tumor microenvironment. Many models describe their heterogeneity like the classification into 3 main subtypes in breast cancer: myCAF (myofibroblasts), iCAF (inflammatory CAF), and PVL (perivascular-like) cells. However, a pan-cancer model has not been established to exhaustively characterize stromal cell heterogeneity, undermining efforts in targeting CAFs with anti-tumor therapies. We investigated the heterogeneity of stromal cells in diverse diagnoses with single-cell RNA sequencing (scRNA-seq) data and bulk RNA-seq of sorted stromal cells to define consistent subtypes.
Design: First, a meta-cohort of 11 scRNA-seq open-source datasets (>500,000 cells, >100 patients, 6 diagnoses) was analyzed. We also generated a scRNA-seq dataset of CD90+ cells derived from tumor tissue of an ovarian cancer patient. Additionally, bulk RNA-seq of 6 PVL, 2 iCAF, and 4 myCAF sorted cell samples across four solid cancers was performed. scRNA-seq data was analyzed with the SCANPY Python package.
Results: Stromal cell clusters were defined as positive for PDGFRB, THY1 (CD90), and COL1A1 expression, and negative for the expression of known non-stromal and endothelial cell markers, by separately analyzing the open-source scRNA-seq datasets. Analysis of stromal cell heterogeneity revealed that the CAFs were consistently classified into 3 subtypes across all datasets: myCAF (high expression: FAP and ACTA2), PVL (high expression: MCAM (CD146) and ACTA2), and iCAF (high expression: APOD and cytokines IL6, CXCL12, CXCL2). Differential gene expression analysis of the scRNA-seq meta-cohort allowed us to develop functional gene expression signatures to define each subtype. All scRNA-sequenced CD90+ cells from ovarian cancer tissue were classified into the CAF subtypes. The myCAF and PVL signatures were specifically upregulated in the corresponding cell types ($p<0.01$, Mann-Whitney U test). While the iCAF signature was enriched in both iCAFs and myCAFs, myCAF and PVL signatures were downregulated in iCAFs. Finally, we developed a fluorescence-activated cell sorting (FACS) panel to separate CAF subtypes, using negative markers (CD45, CD31, EPCAM), a positive marker for stromal cells (CD90) and cell-type surface markers (CD146, FAP, CD91, CD44) for myCAF, iCAF and PVL cells. The high expression of CAF-specific genes in the sorted CAF populations denoted high sample purity. Importantly, the 3 CAF subpopulations separated by gating based on different levels of cell-type surface markers showed expression patterns congruent with the developed signatures across diagnoses.
Summary: Altogether, the consistent classification of stromal cells with our cell-specific expression profiles demonstrated that the 3 CAF subtypes are conserved in many cancer types, offering groundwork for a pan-cancer model of stromal cell heterogeneity.

#0292 Cell non-autonomous downregulation of the tumor suppressor DAB2IP in the cancer microenvironment: Molecular mechanism and biological implications.

A. Bellazzo[1], R. De Florian Fania[2], C. Agostinis[3], R. Bulla[2], I. Segatto[1], B. Belletti[1], V. G. D'Agostino[4], I. M. Bonapace[5], L. Collavin[2];
[1]Centro di Riferimento Oncologico di Aviano (CRO) IRCCS, Aviano, Italy, [2]University of Trieste, Trieste, Italy, [3]Institute for Maternal and Child Health, IRCCS Burlo Garofolo, Trieste, Italy, [4]University of Trento, Trento, Italy, [5]University of Insubria, Busto Arsizio, Italy

Background and Purpose: The tumor suppressor DAB2IP is a cytoplasmic Ras-GAP and an adaptor protein that restrains oncogenic signaling by extracellular inputs, contributing to modulate the dynamic crosstalk established between tumor cells and their stromal compartment. In human malignancies, DAB2IP is frequently disabled by epigenetic and post-transcriptional means. DAB2IP loss-of-function in cancer cells promotes their aberrant proliferation, dissemination, and tumor-promoting inflammation, potentially favor progression of tumors. Intriguingly, endothelial-specific DAB2IP depletion in mouse models fosters the formation of a pro-metastatic niche, implicating that also the loss-of-function of DAB2IP in stromal cells might dramatically impact cancer progression. We previously found that the secretome of prostate cancer cells reduced DAB2IP levels in non-transformed prostate epithelial cell lines, and in primary endothelial cells, thereby fostering their proliferation, migration and expression of angiogenesis markers. Accordingly, cell non-autonomous DAB2IP inactivation in the stromal compartment may reprogram the response to paracrine and autocrine signals, thus supporting a tumor-promoting behavior; however, molecular basis and clinical implication of this phenomenon await clarification. Materials and
Methods: We used conditioned medium (CM) from prostate (PCa) and breast (BCa) cancer cell lines, to study its effects in mediating DAB2IP downregulation and in inducing tumor-associated phenotypes in endothelial cell and fibroblasts. Through multiple approaches, we isolated extracellular vesicles from PCa and BCa conditioned media, to test their involvement in mediating DAB2IP downregulation in recipient cells. Finally, we used cancer cells'CM or specific siRNAs to study the consequence of DAB2IP loss in fibroblasts.
Results: The treatment with CM from PCa and BCa cells induces DAB2IP downregulation in immortalized and in primary fibroblasts, and in endothelial cells. Analysis of DAB2IP levels in primary fibroblasts from PCa and BCa surgical samples confirmed differential expression of DAB2IP protein in normal vs. tumor-associated fibroblasts. Exploring the biochemical nature of extracellular signals involved in DAB2IP downregulation by cancer cells' CM, we found that DAB2IP inhibition in recipient cells is partially mediated by miR-149-3p contained in extracellular vesicles. Finally, we found that DAB2IP reduction potentiates fibroblasts proliferation and invasion, facilitates gel contraction and extracellular matrix remodeling, and fosters expression of markers of activated fibroblasts.
Conclusions: Together, these data support the hypothesis that cancer cells can modulate DAB2IP levels in nearby stromal cells, pushing them to acquire a metastasis-supporting phenotypes.

#0293 Distinctive roles of mammary adipomes in breast cancer progression: Insights from functional analysis and differential gene expression.

H. Thangavel[1], K. Lizardo[1], R. I. Glazer[2], J. F. Nagajyothi[1];
[1]Center for Discovery and Innovation (Hackensack Meridian Health), Nutley, NJ, [2]Georgetown University, Washington, WA

Breast Cancer (BC) is a heterogeneous disease that impacts treatment response. This is due in part to the tumor microenvironment (TME), which contributes significantly to BC pathogenesis, including metastasis. Women with higher breast density and reduced breast fat face an increased BC risk across multiple tumor subtypes. This is exemplified by the correlation between increased tumor progression, the appearance of fibrosis and the loss of mature adipocytes. While the role of adipokines in this process has been studied extensively, the contribution of adipocyte-derived extracellular vesicles (EV) or "adipomes" in tumorigenesis and metastasis remains poorly understood. To address this question, we developed a novel technique for isolating intact adipomes from normal mammary fat (MF) obtained from wild-type C57BL/6 mice as well as from tumor-associated MF (TAMF) obtained from mice inoculated orthotopically with EO771 mammary tumor cells. Adipome isolation involved high-speed centrifugation to separate macro- and micro-vesicles, purification using the ExoQuick EV isolation system, and immunomagnetic capture of adipomes. Characterization of adipomes by transmission electron microscopy revealed two adipome populations, large L-adipomes of ~350 nm, and small S-adipomes of ~40 nm. Notably, the quantity of L-adipomes in tumor-associated mammary fat (TAMF) was 10-fold greater than the amount of L-adipomes in the MF of non-tumor-bearing mice. To identify possible functional roles of L-adipomes in the pathogenesis of BC, lipidomic profiling was undertaken. L-Adipomes from TAMF showed significantly altered lipid species in comparison to MF-derived L-adipomes. Adipomes were further characterized by treating EO771 cells for 72 hr with TAMF- or MF-derived adipomes at a cell to adipome ratio of 1:10, followed by RNAseq analysis. Differentially upregulated genes in TAMF-derived L-adipomes included Esr1, Erbb2, Tgfb1, Bcl2, MMP2, and Notch associated with fibrosis, EMT, angiogenesis and invasion and downregulation of genes linked to tumor suppression, apoptosis, and mitochondrial metabolism. Overall, our study illustrates the importance of tumor-associated adipomes in regulating gene expression in tumor cells, which emphasizes the specificity of adipome content relating to the cell-of-origin and the host's pathologic and metabolic state and in modulating signaling pathways involved in BC progression.

#0294 The HOXB7 protein promotes breast cancer cell growth through activation of the CCL5/CCR5 pathway in the crosstalk of adipocyte.

A. G. Akume, **K. Jin**;
Albany College of Pharmacy & Health Sciences, Albany, NY

Homeobox genes are regulatory genes that encode nuclear proteins acting as transcription factors during normal development and differentiation. One such gene, HOXB7, plays a role in various developmental processes, including hematopoietic differentiation, lymphoid development, and mammary gland development. However, the role of HOX genes in breast cancer development remains largely unexplored. Our previous studies revealed that HOXB7 expression was significantly elevated in primary cancer and distant metastasis. HOXB7 overexpression promoted cell proliferation in SKBR3 breast cancer cells, leading to robustly vascularized xenografts in immunodeficient mice. Furthermore, HOXB7 enhanced tumor growth through TGF beta signaling and recruitment of macrophages, indicating the role of HOXB7 in the crosstalk of stromal components. We found evidence that HOXB7 overexpression in ER+ breast cancer cells promotes tumor cell growth through increased expression and signaling of CCL5/CCR5 in crosstalk with adipocytes. By screening secreted factors in adipocytes induced by TCM of MCF-7-HOXB7 cells, it was also found that CCL5 is highly expressed in HOXB7-overexpressing MCF-7 cells. The CCR5 inhibitor, maraviroc, sensitized MCF-7-HOXB7 cells compared to control cells. These findings suggest that blocking the interaction between CCL5 and CCR5 signaling significantly inhibits ER+ breast cancer with HOXB7 overexpression. We aim to further investigate if HOXB7 overexpression in ER+ breast cancer cells promotes tumor cell growth through increased expression and signaling of CCL5/CCR5 in crosstalk with adipocytes and the role of CCL5 in breast cancer cell growth and migration.

#0295 Fibroblast-specific endoglin deletion alters colonic immune infiltrate in premalignant colorectal lesions.

Subinuer Abudukelimu, Mark J. A. Schoonderwoerd, Madelon Paauwe, Eveline S. M. de Jonge-Muller, Stef G. T. Janson, Nadine van Montfoort, Lukas JAC Hawinkels

Gastroenterology and Hepatology, Leiden University Medical Center (LUMC), Leiden, Netherlands

Background: Endoglin expression on cancer-associated fibroblasts has been reported to promote tumor growth and metastasis, especially in colorectal cancer (CRC). However, little research has been done on the function of endoglin-expressing fibroblasts in the early stages of CRC and how it interacts with the host immune system. Here, we investigated the role of endoglin expression on fibroblasts during intestinal inflammation and tumorigenesis in a chemically induced colitis-associated CRC model.

Methods: We generated two inducible fibroblast-specific endoglin (ENG) knockout mice Collagen1a1 CreERT2.ENGfl/fl ($ENG^{Col1a1-/-}$) and Collagen1a2-CreERT.ENGfl/fl ($ENG^{Col1a2-/-}$). Cre-mediated recombination in mice was induced by oral administration of tamoxifen for three consecutive days. Polyp formation was induced by a single injection of azoxymethane (AOM), followed by three cycles of dextran sodium sulphate (DSS). Analysis of the immune cell composition in the colons and polyps was done using flow cytometry. Hematoxylin and eosin (H&E) staining was performed to evaluate intestinal inflammation.

Results: $ENG^{Col1a1-/-}$ mice showed a considerably higher number of colonic lesions than non-induced controls, whereas in the $ENG^{Col1a2-/-}$, surprisingly no significant difference in the number of lesions was observed. Flow cytometry analysis revealed, compared to controls, the lesions of $ENG^{Col1a1-/-}$ mice had a significant increase in $F4/80^{+}$ $Ly6C^{-}$ macrophages and $Ly6G^{+}$ neutrophils, while those of $ENG^{Col1a2-/-}$ mice had a marked decrease in $CD11C^{+}$ dendritic cells. Given the changes in immune cell infiltration, we also assessed acute inflammation, using a short-term DSS experiment. Interestingly, $ENG^{Col1a1-/-}$ mice lost significantly more weight compared to controls, indicating increased inflammation. Although weight loss did not differ in Col1a2 mice between the two groups, $ENG^{Col1a2-/-}$ mice had a much lower H&E staining score, indicating less colonic damage and inflammation. Furthermore, a decrease in $F4/80^{+}$ $Ly6C^{-}$ macrophages was observed in the colons of both $ENG^{Col1a1-/-}$ and $ENG^{Col1a2-/-}$ mice, despite no change in the overall $CD45^{+}$ immune cell population. Notably, the number of $Ly6G^{+}$ neutrophils was decreased in the colons of $ENG^{Col1a1-/-}$ mice but increased in $ENG^{Col1a2-/-}$ mice. In addition, a decrease in $CD11C^{+}$ dendritic cells was seen in the colons $ENG^{Col1a2-/-}$ mice.

Conclusion: Our results suggest that AOM/DSS-induced polyp formation and infiltrating immune cells differ in $ENG^{Col1a1-/-}$ and $ENG^{Col1a2-/-}$ mice. Fibroblast-specific deletion of endoglin can reduce macrophage and dendritic cell infiltration, colonic damage, and protect mice from DSS colitis.

#0296 BRAFi-induced ROCK-mediated non-canonical nuclear β-catenin shuttling drives a phenotypic switch in cancer-associated fibroblasts..

B. da Silva Soley[1], R. Athalye[1], R. Zhang[1], T. Andl[2], Y. Zhang[1];
[1]University of Cincinnati, Cincinnati, OH, [2]University of Central Florida, Orlando, FL

The discovery of BRAF mutations in around 60% of melanoma patients and the subsequent development of targeted inhibitors to counter the hyperactive BRAF-driven pro-tumorigenic signaling pathway have marked a significant milestone in melanoma therapy. However, despite this progress, the long-term outcomes remain unsatisfactory for many patients due to the occurrence of drug resistance. We previously reported that cancer-associated fibroblasts (CAFs) are stimulated by BRAF inhibitors (BRAFi) to drive matrix remodeling and therapeutic escape pathways in melanoma cells. However, the underlying mechanism by which CAFs are reprogrammed by BRAFi to obtain enhanced phenotypes remains elusive. Here, we present compelling evidence showing that BRAFi (PLX4032), but not CRAF inhibitor (GW5074) or pan-RAF inhibitor (RAF709), induces the accumulation of nuclear β-catenin in CAFs harboring wild-type BRAF, a process mediated by BRAF and CRAF but not ARAF isoform. BRAFi binding to BRAF and CRAF leads to robust RAF kinase dimerization, including BRAF and CRAF homodimer and BRAF: CRAF heterodimer. RAF dimers are subsequently recruited to the plasma membrane, where BRAF and CRAF are phosphorylated on residues Thr599 and Ser338, respectively, and activated in a RAS-GTP-dependent manner. RAF activation stimulates the downstream Rho kinase (ROCK) and MEK/ERK signaling pathways simultaneously. Notably, ablating RAS and RAF isoforms effectively suppressed BRAFi-induced activation of ROCK1/2 signaling in CAFs, further confirming that the ROCK pathway is a downstream effector of BRAFi-driven RAF activation and is intricately linked to increased nuclear β-catenin in CAFs. The pharmacological blockade of ROCK activity, using HA-1077, diminished BRAFi-induced nuclear β-catenin accumulation in CAFs, suggesting BRAFi-driven cytoskeletal remodeling plays a pivotal role in the nuclear shuttling of β-catenin. Using a mouse model that mimics human BRAF-mutant melanoma, we found that elevated level of nuclear β-catenin drives the conversion of fibroblasts into α-SMA-positive CAFs, leading to elevated collagen deposition and contributing to melanoma progression *in vivo*. In summary, BRAFi reprograms the transcriptional activity in CAFs by driving increased nuclear β-catenin to increase their ability to remodel the tumor ECM and promote melanoma cell proliferation. Collectively, the data offer new insights into the molecular mechanisms that underlie the paradoxical reprogramming of CAFs by BRAFi in melanoma therapy through the non-canonical β-catenin pathway.

#0297 Role of purine metabolism in CLL cell pathobiology and CLL disease progression.

S. Sinha[1], W. Han[1], Z. Wang[1], K. G. Rabe[1], S. L. Slager[1], C. E. McCabe[1], D. R. O'Brien[1], S. A. Parikh[1], E. Braggio[2], Y. Chen[3], F. Tan[4], S. P. Anthony[3], Y. Chen[3], B. Dai[3], Y. Shen[4], N. E. Kay[1];

[1]Mayo Clinic, Rochester, MN, [2]Mayo Clinic, Phoenix, AZ, [3]Newave, Pleasanton, CA, [4]Lupeng Bio, Guangzhou, Guangdong, China

The treatment of Chronic lymphocytic leukemia (CLL) has been revolutionized in recent years, however CLL is still incurable, and the leukemic cells often develop drug resistance. Previous studies show that the interaction of CLL cells with the bone marrow (BM) microenvironment promotes spontaneous and drug induced survival. But the nature of this interaction is still in need of a full understanding. To pursue this we discerned RNA profiles using RNA-seq in paired CLL cells isolated from untreated blood and BM (n=6) and in untreated patients CLL cells (n=4) cultured alone or cocultured with BM stromal cells (BMSCs). CLL cells from blood/BM and CLL cells cultured alone or with BMSCs were examined by Western blot (WB), untargeted metabolomics (LCMS+GCMS) and preclinical drug sensitivity assays. We found upregulation of 232 genes in CLL cells from BM vs the paired blood and 917 genes in cocultured CLL cells compared to CLL cells cultured alone (p&lt0.05, fold change &gt1.5). Here we detected only 13 genes that overlap between BM and cocultured CLL cells. When we analyzed the expression of these 13 genes in blood CLL cells from a cohort of 162 untreated patients by RNA-seq we found a positive relationship between 4 (*PNP*, *C16orf54*, *MOB3A*, *CDK2AP2*) with CLL patient clinical outcome including overall survival (OS), progression free survival (PFS), and time to first treatment (TTFT) [multivariable Cox proportional hazards models, p&lt0.05]. Out of the 4 genes, purine nucleoside phosphorylase (*PNP*), an enzyme in the purine salvage pathway, showed the most significant association for patient's OS, PFS, and TTFT. Metabolomic profiling indicated an increased level of purine salvage pathway metabolites adenosine, inosine, and hypoxanthine in cocultured CLL cells. WB analysis using blood CLL cells from untreated patients showed a variable PNP protein expression (high, low /no PNP) and induction in PNP protein levels were found in blood CLL cells expressing low/no PNP only when in contact with BM/BMSCs**.** But PNP inhibitor forodesine did not show any significant killing in high vs low/no PNP group. When we treated CLL cells from untreated patients with Bcl2 inhibitors venetoclax, S55746 and LP-118 (Bcl-2/Bcl-xl inhibitor, Newave), CLL cells showed increasing sensitivity to the Bcl2 inhibitors associated with their PNP expression (high&gtlow&gtno PNP). But a covalent and non-covalent BTKi LP-168 (Newave) cultured with CLL cells showed no difference in drug sensitivity associated with CLL PNP levels. In contrast CLL cells when treated with both venetoclax and LP-168, showed more drug sensitivity in the high PNP expressing CLL cells vs low/no PNP. These results indicate that active purine metabolism in CLL cells can contribute to differential novel agent drug responses of CLL patients. Future studies to understand the exact mechanism of how PNP relates to this differential drug sensitivity should be instructive in regard to alternate maneuvers to treat CLL.

#0298 Contribution of cancer associated fibroblasts to treatment response and resistance in high-risk multifocal prostate cancer.

N. Lupsa[1], E. Heninger[1], A. Ding[1], S. R. Reese[1], X. T. Hazelberg[1], A. M. LeBeau[1], B. P. Johnson[1], P. P. Geiger[1], D. J. Beebe[1], D. A. Quigley[2], J. M. Lang[1]; [1]UW-Madison, Madison, WI, [2]UCSF, San Francisco, CA

Patients with multifocal, locally advanced prostate cancer are at the highest risk of recurrence and death. Neoadjuvant therapies have limited response rates in this patient cohort and there remains a critical need to develop curative treatments. Prostate cancer (PC) shows marked heterogeneity, which is not limited to tumor cells but extends across immune and stromal compartments and has been linked to metastatic disease and therapeutic resistance. Cancer associated fibroblasts (CAFs) have been proposed to play a critical role in PC progression and invasion, but it is still unclear how CAFs interact with tumor cells. We evaluated CAFs from prostatectomy specimens as drivers of resistance to neoadjuvant androgen receptor signaling inhibitor (ARSi) and chemotherapy and assessed treatment response in co-culture systems in the context of CAF presence.

We have utilized a novel radio-pathology tool that integrates PSMA PET/MRI scans to identify regions of interest that associate with heterogenous treatment response. MRI scans were utilized to print patient-specific 3D molds to micro dissect live tissue for subsequent cell sorting and molecular analyses. We have established a multi-parameter flow cytometry panel to characterize primary prostate fibroblasts from tumor foci and adjacent normal prostate tissue. In addition, co-culture assays were performed including immortalized CAF (hPrCSC-44) and MSC-derived fibroblast. To examine the tumor-promoting role of CAFs, fibroblasts were co-cultured with androgen-sensitive 3D tumor PC spheroids (LNCaP, C42B and LAPC4) in the integrated microfluidic STACKs platform that allows for the assessment of spatio-temporal interaction in a variety of culture microenvironments to model complex interactions. Cytotoxicity in 3D PC spheroids was assessed after Apalutamide, Darolutamide, or Docetaxel treatment by confocal microscopy.

Integrated DNA, RNA, and radiology analysis of tumor biopsies have identified gene signatures associated with early biochemical recurrence. Most biopsies had low tumor purity, evidence of the cytotoxic impact of chemohormonal therapy while high tumor purity predicted high tumor expression. Poor clinical outcome was significantly associated with elevated stromal scores while epithelial and stromal enrichment were inversely correlated (rho= -0.80, $p< 5x10^{-16}$). The presence of CAFs significantly decreased Docetaxel (C42B only vs C42B+CAF, 86.07% vs. 44.57%, respectively, $p<0.001$; LAPC4 only vs LAPC4+CAF, 70.98% vs 26.64%, respectively, $p<0.001$) and Darolutamide-induced (C42B only vs C42B+CAF, 52.59% vs 37.87%, respectively, $p=0.0407$).

In conclusion, recurrent PC is linked to increased stromal content and the presence of CAFs supported tumor survival in response to ARSi and Docetaxel treatment. The molecular drivers of this phenomenon are currently being investigated.

#0299 FAP/αSMA association with tumor visibility and progression in prostate cancer.

Jenni Saila[1], Timo-Pekka Lehto[2], Annabrita Schoonenberg[3], Katja Valimaki[3], Andrew Erickson[2], Antti Rannikko[2], Olli Kallioniemi[3], Tuomas Mirtti[2], Teijo Pellinen[3]

[1]Research Program in Systems Oncology (ONCOSYS), Faculty of Medicine; FIMM, University of Helsinki, Helsinki, Finland,[2]Research Program in Systems Oncology (ONCOSYS), Faculty of Medicine, University of Helsinki, Helsinki, Finland,[3]FIMM, University of Helsinki, Helsinki, Finland

Introduction Prostate cancer (PCa) ranks as the second most frequently diagnosed cancer in the male population worldwide. The challenge in effectively managing PCa is the absence of well-established biological markers, which often leads to both over and under treatment. To address this issue, a deeper understanding of the molecular alterations within PCa is essential for more accurate patient stratification. In this research, we embark on a comprehensive examination of how the presence of fibroblast activation protein (FAP) and alpha smooth muscle actin (αSMA) in PCa tissue associates with the visibility of the disease in Magnetic Resonance Imaging (MRI) and their impact on cancer progression. The objective of this study is to analyze cell compartmental expression of FAP and aSMA using an AI based image analysis method. We also study the role of FAP and αSMA expression in predicting disease progression and mortality.

Materials and Methods We applied FAP (ab207178, Abcam)/αSMA (M0851, DAKO) double chromogen immunohistochemical (IHC) staining to three independent cohorts of formalin-fixed paraffin-embedded (FFPE) prostate cancer tissue microarrays. All together, we analyzed 835 patients' samples. First cohort consists of 387 patients with preoperative multiparametric MRI and robot-assisted laparoscopic prostatectomy (RALP) as primary treatment. Second cohort was case vs control cohort of Grade group 2-4 localized PCa at radical prostatectomy (RP) with 168 patients. Third cohort consists PCa patents from continuous, population-based collection of radical prostatectomies of 319 patients. Image analysis was performed with Aiforia Create, which is cloud-based deep-learning artificial intelligence software that provides platform for training and validating automated image analysis pipelines using convolutional neural networks. Analysis algorithm in this project was based on semantic, pixel-level area segmentation.

Results FAP expression was higher and αSMA lower in MRI-visible tumors compared with MRI-invisible tumors. Stromal and epithelial FAP expression associate with tumor progression. We could also see statistically significant differences in FAP positivity between clinically significant (GS ≥7) and insignificant (GS ≤6) tumors. Hazard ratios imply that FAP and αSMA have significant impact on risk of biochemical recurrence in patients with MRI-visible tumors.

Conclusions FAP is closely linked to tumor MRI visibility, cancer progression, and Gleason scores, marking it as a valuable biomarker in PCa assessment. High stromal αSMA is primarily associated with MRI visibility. Our automated AI-based image analysis method has demonstrated reliability, aligning with our previous findings. This advances the potential for more accurate and efficient prostate cancer diagnosis and prognosis, offering a potential benefit to future patient care.

TUMOR BIOLOGY: Tumor Adhesion
Poster Session

#0303 Revealing molecular mechanism of G protein-coupled receptor kinase 2 (GRK2)-mediated extracellular matrix remodeling in ovarian cancer.

W. Lei[1], S. Yu[2], C. Lei[1], Z. Zhang[1], T. Liu[1], W. Chang[1], L. Lee[1];
[1]University of Macau, Macao, Macao, [2]Second Affiliated Hospital of Harbin Medical University, Harbin, China

G protein-independent pathway (β-arrestin dependent signaling cascade) is initiated by activated GPCRs phosphorylated by G protein-coupled receptor kinases (GRKs), triggering multiple signaling pathways. The purpose of this research is to reveal the role of GRK2 on the tumor microenvironment (TME). Through *in vitro* assays, we showed that GRK2 overexpression led to loss of cell-matrix and cell-cell adhesion. The cell spreading assay further indicated that the loss of focal adhesion (FA) assembly and cell size decreased in GRK2-overexpressing cells. *In vivo* experiments demonstrated that tumor formation and metastasis were suppressed in xenograft mouse models implanted with GRK2-overexpressing ovarian cancer cells. In addition, label-free imaging detection of the collagen pattern suggested that GRK2 overexpression caused bundle loss but the formation of thicker, twisted collagen fibers in xenograft tumor samples. Together with the transcriptome and proteomic data, we hypothesize that GRK2 suppresses cell motility and metastasis by reducing FA and extracellular matrix (ECM) remodeling in ovarian cancer. This research revised the mechanisms underlying GRK2-mediated ovarian cancer metastasis and suggested the potential to target the GRK2-meditated pathway for cancer suppression.

#0304 The role of DDR1 mediated E-cadherin stability in collective colon cancer cell migration.

H.-C. Chen, Y.-C. Wang, Y.-C. Ching, C.-P. Cheng, C.-E. Ku, S.-R. Lee, W.-T. Chao;
Tunghai University, Taichung City, Taiwan

In cancer metastasis, the mechanism of single cell migration and collective cell migration are investigated. The dynamics of E-cadherin is critical in collective cell migration as the important mechanism of metastasis. DDR1 (Discoidin Domain Receptor 1) has been shown to promote E-cadherin stability at adherens junction in epithelial cells by regulating endocytosis of E-cadherin. However, in the growth of epithelial cell cluster and collective cell migration, the role of DDR1 in the cell-cell contacts is not clear. In this study, HT-29 colon cancer cells with epithelial phenotype were used in the experiments. Cells were treated with epidermal growth factor to stimulate E-cadherin turnover or applied with lysosome inhibitor chloroquine to interfere cellular vesicle transport. DDR1 and E-cadherin were revealed by immuno-confocal microscopy. The immunostaining results showed DDR1 was localized at cell-cell contacts and co-localized with E-cadherin. When cells were treated with epidermal growth factor, the phosphor MAPK activity was increased and DDR1 was localized at cell-cell contacts intensively. When lysosome activity was blocked by chloroquine treatment. The cellular vesicle transport and collective cell migration was reduced and furthermore inhibited DDR1 translocation to the cell-cell contacts. This study demonstrated DDR1 co-localized with E-cadherin is responsible for epidermal growth factor stimulation in cell cohort. Lysosome activity is required for E-cadherin turnover and affected DDR1 translocation. Chloroquine maybe the potential drug to suppress tumor nest growth and collective cell migration by interfere DDR1 mediated E-cadherin stability.

#0305 Bioinspired synthetic hydrogel in pancreatic cancer organoid matrix modeling.

M. Hossan[1], A. Stram[1], E. Lin[1], S. McIlwain[1], C. Lebakken[2], W. Richards[2], J. D. Kratz[1];
[1]University of Wisconsin-Madison, Madison, WI, [2]Stem Pharm, Inc., Madison, WI

Background: Pancreatic ductal adenocarcinoma (PDAC) is a leading cause of cancer mortality with a primary hallmark, including dense collagen matrix in the desmoplastic stroma. Organoid technologies often rely on commercially available EHS mouse sarcoma matrix materials, and it remains uncertain how batch-to-batch variability of this matrix impacts the consistency of cancer signaling. Here, we present a novel photo-activated hydrogel tuned to the properties of the desmoplastic stroma in PDAC organoid cultures.
Method: We designed multiple synthetic hydrogel materials with tunable mechanical properties, including SP-139 (Stem Pharm, Inc), a polyethylene glycol-based hydrogel functionalized with norbornene and formed with both degradable and non-degradable crosslinking peptides and a cell adhesion peptide (CRGDS). We used rheometry to measure the elastic modulus of the polymerized hydrogel after visible light photoactivation (395 nm) and expanded multiple cancer organoid cultures. RNAseq was performed from patient-derived xenografts to expanded organoids across matrix designs (Cultrex® v. SP-139) and analyzed by GSVA pathway analyses.
Result: We optimized the ratio of non-degradable v. degradable crosslinking peptide to support culture expansion and enzymatic digestion with dispase II (125 µg/mL) and collagenase II (1 mg/mL). Using rheometry, SP-139 at 75% v/v had increased elastic modulus versus Cultrex RGF BME matrix Type 2 at 100% v/v (4992±76.3 v. 68.4±5.6 Pa, $p<0.0001$). Phenotypic growth was confirmed across serial passages (>8) and a diversity of gastrointestinal cancer types (n=5). Baseline growth rates were identical over 48h between SP-139 (75% v/v) and Cultrex (50% v/v) (+13.4% v. +13.0, $p=0.75$). Growth remained consistent for SP-139 yet increased with Cultrex at interval of 48-96h (+12.9% SP-139 v +22.4% Cultrex, $p<0.005$) and interval of 96-144h (+13.6% SP-139 v +24.0% Cultrex®, $p<0.0001$). Therapeutic response was assessed using 3D CellTiter-Glo® using gemcitabine 100 µM (24h) with comparable inhibition of normalized cell viability in SP-139 v. Cultrex® (35.4±1.9% v. 52.3±6.5%, n.s.) and qualitatively with viability staining using calcein AM and Caspase 3/7 ^{FITC}. RNAseq revealed Cultrex, when compared to SP-139, yielded down regulation of epoxygenase p450 pathways ($p_{adj}<0.012$) and negative regulation of the p38 MAP kinase cascade ($p_{adj}<0.048$).
Conclusions: Functionalized PEG-based synthetic hydrogel matrix materials can be tuned for physical properties to mimic cancer tissue microenvironments more accurately. SP-139, designed to mimic the desmoplastic stroma of the pancreatic cancer microenvironment, has favorable properties including controlled growth rates and compatibility with high content imaging by luminescence and fluorescence. RNAseq pathway analysis shows SP-139 maintains pathways of p450 and MAP kinase signaling of importance with therapeutic resistance.

#0306 The role of exosomal UBE2R2 in colorectal cancer drug resistance.

C. Maeng[1], M. Choi[2];
[1]Kyung Hee University, Seoul, Korea, Republic of, [2]Kyung Hee University Hospital, Seoul, Korea, Republic of

Background: Ctherapy resistance has been a major barrier against successful theratment. Exosome (EV), an important intercellular communication mediator, participates in a highly and complex network that drug resistance of cancer cells. EV has been reported to be able to transfer drug resistance from drug-resistant tumor cells to adjacent drug-sensitive cells. We identified a novel target, UBE2R2, based on our previous exosome proteomics analysis of resistant colorectal cancer cell lines. The main goal of this study is to validate the underlying mechanisms leading to chemotherapy resistance.
Methods: We isolated EV from drug resistant cancer cell lines including coloractal cancer cell lines (HCT116-OXAR, DLD-1 OXA-R, DLD-1-OXA-R/SN38) its parental cell lines (HCT116, DLD-1) using the ExoLutE isolation kits based on a combination of multiple isolation techniques. Based on the existing data (proteomic analysis), we conducted experiments to elucidate the functions and mechanisms involved in cancer resistance of the identified UBE2R2. Cell viability assay and invasion asaay were performed to assess the effects of EVs drived from drug resistance colorectal cells on oxaliplatin and irinotecan resistance. In addition, cells transfected with siControl and siUBE2R2 were treated with oxaliplatin to access the relative UBE2R2 drug resistance effect. To explore the related mechanisms, we performed real time PCR and western blot to identify the UBE2R2-SMYD3-P53 pathway, and FACS analysis to confirm apoptosis. Additionally, TMA samples were utilized to confirm resistance according to patient stage, and UBE2R2 expression was validated by immunohistological methods.
Results: UBE2R2, which is involved in ubiquitination, was most prominently expressed in resistant cell lines compared to controls in our previous proteomic analysis. Based on these results, we found that cell lines treated with exosomes which were derived from resistant cell lines showed lower sensitivity to the drug. Notably, treatment of resistant cell lines with siUBE2R2 resulted in increased sensitivity, confirming the involvement of UBE2R2 in resistance. As a possible mechanism in which UBE2R2 may be involved, western analysis targeting the SMYD-P53 mechanism showed that the combination of UBE2R2-SMYD3-p53 promoted the ubiquitination and degradation of p53. Analyzed using TMA patient samples, we found that the expression of UBE2R2 increased towards more advenced stage.
Conclusion: Our results suggest a novel mechanism of chemotherapy resistance may be associated with UBE2R2. Exosome (including UBE2R2) which was drived from drug resistance cells may induce oxaliplatin and irinotecan resistance in parental colorectal cells via regulation of SMYD3-UBE2R2-P53 signaling pathway, which will be useful for investigating a potential clinical target in prediction drug resistance.

#0307 Generation and characterization of a glioblastoma stem cell model with acquired resistance to LSD1 inhibition.

K. H. Patel, L. Stitzlein, D. Nam, F. Lang, J. Gumin, J. Chandra;
MD Anderson Cancer Center, Houston, TX

Epigenetic modifications play an important role in the initiation of various cancer types, including glioblastoma (GBM), and in the development of therapeutic resistance. Patients with GBM, a common malignant brain tumor, have an average survival of 12-15 months after first-line therapy. Lysine-specific demethylase 1 (LSD1) is a histone demethylase that is overexpressed in glioblastoma stem cells (GSCs) and functions to promote proliferation, inhibit differentiation, and enhance motility. Previous work from our group has investigated LSD1 as a therapeutic target in glioblastoma and identified genes that may predict resistance to pharmacological LSD1 inhibitors using RNA-seq. Five upregulated genes, HKDC1, RAB3IL1, RAB39B, FTH1, and FAM213A, were associated with LSD1 inhibitor (LSD1i) resistance and were validated in brain tissue of a GBM model treated with GSK-LSD1 after succumbing to tumor burden. In order to determine whether selection pressure from LSD1 inhibitor treatment caused upregulation of these genes, we created a model of acquired resistance in GSC lines in vitro. Isogenic resistant lines were generated by treating MDA-GSC17 cells with increasing concentrations of LSD1i or diluent (DMSO), as tolerated starting at 50 uM (which was five fold below the IC50 for these lines). In parallel, MDA-GSC17 controls were exposed to DMSO. The resistant line was created over 4 weeks and monitored by cell number and viability to reach 90%. To assess the change in gene expression, we conducted quantitative PCR for the five genes in the parental and resistant MDA-GSC17 line and saw upregulation in 3 of the 5 genes. Two genes, HKDC1 and RAB3IL1, were unable to be assessed due to low basal expression. However, 3 genes were upregulated which are RAB39B, FTH1, and FAM213A. RAB39B is a Ras-analog in brain (RAB) small GTPase and a member of the RAS oncogene family, involved in vesicular trafficking. High expression of ferritin heavy chain 1 (FTH1) is correlated with high-grade gliomas and poor prognosis in glioblastoma. Lastly, the redox regulatory protein, FAM213A, can activate antioxidant proteins and elevated expression is associated with worse outcomes for AML patients. This suggests that modulating the RAS signaling pathways and specific redox pathways may overcome LSD1 resistance. Understanding the changes in gene expression as the cells acquire resistance to LSD1 inhibitors will help us understand the mechanism of resistance to LSD1 inhibitors in glioblastoma and to design new treatment strategies.

#0309 AHNAK nucleoprotein 2 tune oxidative stress and resistance to chemotherapy in triple negative breast cancer.

N. Hao;
The First Affiliated Hospital of Xi'an Jiaotong University, Xi'an, China

Background: Resistance to chemotherapy is a major reason for the poorerprognosis in patients with triple negative breast cancer (TNBC). Growing evidence suggests that oxidative stress induced by reactive oxygen species (ROS) is an important factor in both tumourprogression and responses to chemotherapies, however, many signalling pathways and key molecular underlying the regulation of cancer cells to the ROS metabolism remains unclear.
Aim: (i) To investigate the mechanistic role of AHNAK nucleoprotein 2 (AHNAK2) in TNBC and its links with breast cancer mortality, particularly caused by chemotherapeutic resistance; and (ii) to test a hypothesis that AHNAK2 facilitates the abnormal activation of ROSscavenging system, result in the resistance to chemotherapy in TNBC.
Methods: The expression level of AHNAK2 was determined by immunohistochemical staining and analysed the mRNA expression profiles from The Cancer Genome Atlas of triple negative breast tumors. Roles of AHNAK2 in cancer cell growth, metastasis, chemotherapeutic resistanceand activation of oxygen scavenging systemwere determined by molecular and cell biology methods. A jetPEI nanocarrier was used as the vehicle for anti-AHNAK2 siRNAs in mouse models of cancer therapeutics.
Results: AHNAK2 is a novel triple negative breast cancer target, which is overexpressed in TNBC tissues and significantly associated with clinical pathology of chemotherapeutic resistance and poor prognosis of tumour patients. Mechanistically, AHNAK2 antagonizes the ROS accumulation induced by epirubicinvia activating JAK-STAT signaling pathway and transportingphosphorylated STAT1 & STAT4 to the nucleus to promote the expression of SOD2, a key gene in ROS metabolism.And epirubicin enhanced AHNAK2 expression by induced the accumulation of ROS,which hence the Sp1-driven transcription of AHNAK2,result inde novo resistance. Furthermore, AHNAK2-specific siRNAs encapsulated by jetPEI nanocarriers prominently inhibit tumor growth and epirubicin-induced resistance in vivo.
Conclusions: AHNAK2 plays a key role in resistance to chemotherapyby regulating the oxidative stressand ROS metabolism,representing a future biomarker and therapeutic target of TNBC.

#0310 Cadherin-dependent modulation of chemosensitivity in oral tumor progression.

A. Mody, C. Decker, K. R. Lawson;
Midwestern University - Glendale Campus, Glendale, AZ

The progression of healthy oral epithelia to an oral carcinoma often involves aberrant expression of a group of calcium-dependent transmembrane proteins called cadherins. Histological studies of human tumors have demonstrated increased expression of the epithelial-resident placental (P-cadherin) and ectopic expression of the mesenchymal neuronal (N-cadherin) cadherin in oral dysplasia. We hypothesized that these changes in cadherin expression during early oral tumor development could facilitate increases in survival signaling. We genetically modified dysplastic oral keratinocytes to overexpress P-cadherin or suppress endogenous expression of N-cadherin. P-cadherin overexpression and N-cadherin suppression independently elicited a 3-6-fold decrease in apoptosis levels in response to docetaxel treatment compared to similarly treated controls. We found that in untreated dysplastic cells, P- and N-cadherin expression had positive and negative correlations, respectively, with the activation of the survival-associated enzymes focal adhesion kinase (FAK), mitogen-activated protein kinase (MAPK), and AKT kinase. The total levels of nuclear factor kappa B (NFkb) were positively correlated with P-cadherin overexpression and reciprocally correlated with levels of N-cadherin. In docetaxel-treated dysplastic cells, we observed the reverse effect compared to untreated cells: the increased level of N-cadherin was positively correlated with FAK activity whereas FAK activity was suppressed by P-cadherin. P-cadherin expression in docetaxel-treated cells also increased activation of both MAPK and AKT, whereas alteration of N-cadherin levels had no effect. Because N-cadherin levels are known to increase in late-stage oral tumors, we extended these signaling studies to oral squamous carcinoma cells (OSCCs) expressing low or high levels of N-cadherin. In contrast to its suppression of survival pathways in docetaxel-treated dysplastic cells, in docetaxel-treated OSCCs, N-cadherin expression strongly enhanced phosphorylation of MAPK and AKT, and increased expression of NFkb. N-cadherin overexpression during this treatment also increased expression of the antiapoptotic proteins Mcl-1 and suppressed phosphorylation of the apoptotic regulator signal transducer and activator of transcription 3 (pSTAT3). Increase cadherin expression in all untreated cell lines increased expression of an inducer of epithelial to mesenchymal transition, the transmembrane protein mucin-1 (MUC1). N-cadherin overexpression also increased motility in both cell lines. Taken together, our data demonstrate antiapoptotic signaling directed by increased levels of P-cadherin in oral dysplasia and N-cadherin in OSCC, whereas increased levels of N-cadherin in dysplastic cells directed cellular signaling that were associated with a proapoptotic phenotype.

MOLECULAR/CELLULAR BIOLOGY AND GENETICS: Advances in Genomic Sequencing Platforms, Methodologies, and Interpretation 1
Poster Session

#0313 Benchmarking immune repertoire sequencing technologies.
S. Maheshwari, C. Morrison, S. Taylor, BCR-SEQC consortium;
10X Genomics, Pleasanton, CA

In the past decade, single cell gene expression technologies have transformed basic and translational research and are more frequently found in the toolbox of immunologists alongside the standard bulk B-cell receptor (BCR) sequencing and transcriptome profiling assays. While conventional bulk BCR assays capture the frequency of single chains, single-cell immune profiling reveals the frequency of *paired* heavy and light chains along with the cells transcriptional profile. Here we present the results of a single-blind benchmarking experiment conducted in collaboration with the U.S. Food and Drug Administration (FDA) that compares the performance of standard bulk DNA and RNA BCR repertoire sequencing assays, with the 10x Genomics Single Cell Immune Profiling solution. The FDA selected nine unambiguously monoclonal BCR-expressing cell lines to generate a reference mixture that was shared with each study participant, without revealing the input proportions. This reference cell line mixture was also diluted to 10% and 1% with B-cells sorted from peripheral blood mononuclear cells (PBMC) to further test the limits of clonotype detection.
For each experiment, we targeted ~10,000 cells and in aggregate generated a paired gene expression and V(D)J dataset from ~100,000 cells. BCR clonotypes were detected in 78% of the captured cells across all samples profiled. Each of the 9 top unique clonotypes observed in our dataset corresponded to a cell line in the reference mixture, allowing us to decode the mixing percentages of each BCR-expression cell line. In addition, we were able to identify rare cell line clonotypes to as low as 0.01% in the dilution experiments. Furthermore, the multimodal nature of the single cell data also resolved the transcriptional profile of each cell line into its own cluster thus enabling independent verification of clonotype proportions.
In summary, we have generated a resource for the immunology community to evaluate and compare data generated with different repertoire sequencing technologies.

#0314 Fixative eXchange (FX)-seq reveals single nucleus transcriptional landscapes of archived clinical cancer FFPE specimens.

H.-E. Park, Y. Lee, J. Lee, J. Lee, H. Ji, Y.-L. Song, Y. Han, H. Kim, C. Sohn;
Yonsei University, Seoul, Korea, Republic of

The wide availability of FFPE tissues stored in hospitals and biobanks could potentially be an invaluable resource to gain insights for improved medical treatment towards precision medicine by combining genomic and transcriptomic data with pathological annotations and medical records. Nevertheless, the majority of current single-cell sequencing methods depend on fresh or fresh-frozen samples to generate high-quality transcriptome data due to the limited reverse transcription (RT) yields in FFPE samples. Consequently, single-cell level transcriptomic studies of FFPE samples have been a longstanding challenge. Here, we present Fixative-eXchange (FX)-seq, a highly scalable snRNA-seq method for heavily paraformaldehyde (PFA)-fixed and/or FFPE samples. We successfully analyzed a total of nearly 320k nuclei from various samples, including PFA-fixed tissue, FFPE blocks, FFPE and hematoxylin and eosin (H&E)-stained sections from mouse brain and human clinical cancer specimens. In a human gastrointestinal stromal tumor (GIST) FFPE sample, we observed rare transcriptomic transitions toward increased epigenetic modifications affected by acquired resistance in response to prolonged imatinib treatment. Furthermore, in an archived human colorectal cancer (CRC) FFPE sample, spatially-contextualized FX-seq with pathologist annotation distinguishes tumor cells from epithelial progenitors along with identification of the tumor microenvironment (TME) such as cancer-associated fibroblasts (CAFs). We then proceeded to investigate transcriptional programs associated with drug resistance and lack of response in immunotherapy observed in CRC patients. With a hypothesis-driven curation, we compared transcription profiles at the single-nucleus level observed in MSS and MSI-H CRC patients from archived FFPE blocks and found distinctive transcriptional profiles from each group. Overall, FX-seq holds promise for clinical research, precision medicine, biomarker discovery, and molecular diagnosis using archived clinical FFPE specimens.

#0315 Cost-effective, comprehensive detection of gene fusions from DNA and RNA using the UG100 sequencer.

G. Lithwick-Yanai[1], S. Pollock[1], D. Lebanony[1], K. Ben Simhon[1], S. Benjamin[1], D. Bogumil[1], N. Iremadze[1], M. Sexton[1], P. Winer[1], M. Levy[1], S. Gilad[1], J. Haimes[2], G. Corbet[2], J. Pavlica[2], D. Lipson[1];

[1]Ultima Genomics, Fremont, CA, [2]Watchmaker Genomics, Inc., Boulder, CO

Background: Gene fusions, resulting from chromosomal rearrangements, play a critical role in the oncogenesis of various cancers, often acting as diagnostic markers and therapeutic targets. Their detection is important for understanding tumor biology and guiding personalized treatment strategies. With the evolution of economical sequencing technologies, hypothesis-free gene fusion detection in cancer genomics is becoming more accessible. This study demonstrates the use of the cost-effective Ultima Genomics UG100 platform for a comprehensive analysis of gene fusions, uniquely integrating Whole Genome Sequencing (WGS) and Whole Transcriptome Sequencing (WTS). This integration capitalizes on the strengths of both methods: WGS, which enables a broad analysis of structural variations including extragenic events, and WTS for more functional characterization of expressed gene fusions and abnormal isoforms, offering a synergistic approach that enhances the detection and characterization of genomic rearrangements.

Methods: Five cancer cell lines (K562, THP-1, NCI-H660, Kasumi-1, MV4-11) with 29 previously detected gene fusions were sequenced, using both WTS and WGS, in addition to a standard fusion reference sample (Seraseq Fusion RNA Mix, with 16 RNA fusions). The libraries were sequenced on a UG100 sequencer using single ended reads of length ~250bp and analyzed with publicly available software: STAR-Fusion, combined with FusionInspector were used to detect RNA fusions; Manta and GridSS were used to detect DNA structural variations, including translocations.

Results: 93% of the documented fusion events were detected in DNA and in RNA, in addition to the 16 evaluated just in RNA (100% detected). Sequence data from both WTS and WGS on the UG100 platform successfully identified a spectrum of gene fusions in both DNA and RNA, thereby confirming the platform's detection capabilities in both types of assays. The structural variation events detected in the WGS were comprised mainly of translocations, but also deletions and duplications.

Conclusions: The Ultima Genomics UG100 sequencer has proven to be a cost-effective and efficient tool for the genome-wide discovery and validation of gene fusions, which can be impactful in clinical oncology settings. This study underscores the potential of using an integrated WTS and WGS approach on a single platform to advance our understanding of the genomic complexity of cancer, paving the way for more effective diagnostic and therapeutic strategies.

#0316 A novel, high-throughput full-length scRNA-seq workflow for improved biomarker discovery.

P. Xu[1], J. Liu[1], Y. Ryan[1], K. Tori[1], X. Li[1], H. Anbunathan[1], M. Covington[1], T. Uchiyama[1], M. Fallahi[1], X. Qu[2], X. Xing[2], T. Wang[2], B. Bell[1], **S. Chen**[1], Y. Yun[1], A. Farmer[1];

[1]Takara Bio USA, San Jose, CA, [2]Washington University in St. Louis, St. Louis, MO

Objective: Single-cell RNA-seq (scRNA-seq) analysis has been widely applied in oncology research for biomarker discovery. Although droplet-based methods are commonly used for such studies owing to their high throughput, they still miss important insights due to their lack of full-length transcript coverage. While full-length methods are available, to date, they have not been able to meet the throughput demands of many researchers. Moreover, both droplet and full-length scRNA-seq methods do not currently provide adequate readouts for non-coding genes, thereby limiting investigation of gene regulatory networks to protein coding genes. To close these gaps, we have developed a new high-throughput full-length scRNA-seq workflow that comprehensively profiles both protein-coding and non-coding genes in up to 60,000 cells within two days.

Methods: Our new high-throughput workflow uses two rounds of combinatorial indexing, starting with a 96-well plate format for the first barcoding step followed by an automated second barcoding step in a 5,184-nanowell chip using an automated nanodispensing system. Initial testing demonstrated that our method could handle up to 60,000 cells without generating significant levels of doublets due to barcode collisions. To further illustrate the capacity of the new scRNA-seq approach, we profiled a total of approximately 11,000 isogenic A549 cells that either express WT TP53 or are TP53 null. In addition, both isogenic cell lines were treated with epigenetic therapy or mock treatment. Libraries were generated and sequenced using an Illumina® NextSeq®2000 sequencer. The sequencing data was then analyzed to define differential gene expression for both protein-coding and non-coding transcripts as a function of TP53 genotype and treatment condition, using Cogent™ NGS software.

Results: Preliminary analysis showed that, on average, approximately 11,000 genes and 40,000 transcripts were detected per single cell at a read depth of 100,000 reads per cell. UMAP-based clustering confidently separated the cells according to their genotypes and treatment conditions using either protein-coding genes or non-coding genes. Furthermore, differential expression analysis identified both protein-coding and non-coding transcripts with significant expression differences, underscoring biological significance.

Conclusion: Our new high-throughput full-length scRNA workflow enables preparation of high-quality full-length RNA-seq libraries for up to 60,000 cells with only two rounds of barcoding and shows high sensitivity and specificity in gene/transcript detection and quantification. The technology significantly improves the ability to identify new biomarkers by enabling comprehensive profiling of both protein-coding and non-coding full length transcripts.

#0317 Using the Biomek NGeniuS Next Generation Library Prep System to automate the Illumina TruSight Oncology 500 assay.

Z. Smith;
Beckman Coulter Life Science, Indianapolis, IN

Cancer researchers using next generation sequencing (NGS) need reliable sample preparation methodologies that generate high-quality, sequence-ready libraries from often-challenging samples. This process can be aided using automated liquid handling systems.

The Biomek NGeniuS Next Generation Library Prep System from Beckman Coulter Life Sciences is a reliable, easy-to-use, purpose-built liquid handler for NGS library preparation ideal for laboratories requiring more flexibility and less hands-on time. The user-friendly software requires no programming skills, making it easy to set up and run. Biomek NGeniuS Next Generation Library Prep System's hardware features include an on-deck thermal cycler, gripper, temperature-controlled reagent storage, and high-density tip storage which reduces user interventions and enables more walkaway time. An extensive and growing library of complimentary demonstrated NGS sample prep protocols allows the user to select from a variety of applications for NGS workflows. One such workflow is Illumina TruSight Oncology 500 assay, which represents a comprehensive NGS assay targeting the full coding regions of 523 genes implicated in the pathogenesis of solid tumors. Using enrichment-based library preparation techniques for use with formalin-fixed, paraffin-embedded (FFPE) samples, the Illumina TruSight Oncology 500 assay, when running the DNA Only workflow, can detect single nucleotide variants (SNVs), indels, amplifications, and multinucleotide variants (MNVs) in a single sequencing run. The Illumina TruSight Oncology 500 assay also detects immunotherapy biomarkers for tumor mutational burden (TMB) and microsatellite instability (MSI) in DNA samples. The Illumina TruSight Oncology 500 assay also offers a combined RNA/DNA workflow that also allows for the assessment of fusion events.

In this poster, we show the utility of the Biomek NGeniuS Next Generation Library Prep System to perform the Illumina TruSight Oncology 500 assay, which saves researchers valuable hands-on time and offers a highly streamlined setup process for users new to liquid handling automation.

#0318 Demystifying tumor heterogeneity with a fully automated, high-throughput single-cell DNA-Seq (scDNA-seq) workflow.

X. Li, R. Mendoza, S. Leong, H. Anbunathan, M. Covington, M. Fallahi, B. Bell, S. Chen, Y. Yun, A. Farmer;
Takara Bio USA, San Jose, CA

Objective: Genetic heterogeneity is a key factor underlying tumor drug resistance and metastatic potential. Understanding this heterogeneity is therefore vital to improving both prognosis and treatment. Next-generation sequencing is a valuable tool for analyzing the genetic makeup of tumors. However, bulk sequencing methods lack the sensitivity to fully resolve tumor heterogeneity. While single cell methods provide a powerful approach to dissect such heterogeneity, to date, these methods have been limited in their throughput. To address this bottleneck, we have developed a fully automated workflow for generating scDNA-seq libraries based on PicoPLEX® whole genome amplification (WGA) technology. This high-throughput method, which has been optimized on our ICELL8® cx Single-Cell System, enables the generation of WGA libraries for >1,000 single cells within one day.
Methods: We first sought to demonstrate the ability of this new high-throughput method to generate WGA libraries of comparable quality to the standard PicoPLEX workflow in terms of genome coverage, GC bias, and other typical quality metrics. We additionally assessed copy number variant (CNV) detection sensitivity using two cell lines with well-characterized small segmental CNVs: GM22601 (~25Mb deletion on chromosome 4) and GM05067 (~45Mb gain on chromosome 9). We also analyzed a lymphoblastoid line (K562) that carries a range of chromosomal aneuploidies. A total of 1,288 single-cell WGA libraries were generated and sequenced to a depth of 250K paired-end reads per cell. Data analysis was done using the Ginkgo CNV pipeline with an average bin size of 500 kb. As a final proof of principal, we also generated single cell data using tumor and adjacent normal tissue from two clear cell renal cell carcinoma (ccRCC) samples.
Results: Libraries generated using our high-throughput workflow had a high mapping rate, with 94.1% of the reads being uniquely mapped. Additionally, the libraries were comparable to those generated with the standard PicoPLEX workflow in terms of coverage uniformity, GC bias and other metrics. Moreover, the segmental aneuploidies in both GM22601 and GM05067 were reliably detected in >90% of cells at a read depth as low as 250,000 reads per cell. Analysis of the ccRCC samples revealed subclonal heterogeneity with various CNVs common to ccRCC, including deletion of chr. 3p, amplification of chr. 5q, and duplication of chr. 2.
Conclusion: By adapting PicoPLEX technology to high throughput using the ICELL8 cx Single-Cell System, we have obtained single-cell WGA libraries from up to 1,200 cells at once and enabled the reliable detection of CNVs and tumor subclones at a shallow sequencing depth. In addition, by leveraging the automated nanoliter-dispensing capabilities of ICELL8 cx system this method provides a significant reduction in reagent use and labor compared to plate-based methods.

#0319 Demonstrating the use of Archer VARIANT*Plex*™and FUSION*Plex*™assays in observing variants at sub-0.1% allele frequencies and low transcript number fusions in acute myeloid leukemia relevant genes.

L. A. Johnson, M. Washburn, P. Kalavakur, D. Legare;
IDT, Boulder, CO

The presence of acute myeloid leukemia (AML) residual disease is valuable for understanding cancer progression. Studies have shown that variants detected at allele frequencies as low as 0.01% are useful for stratifying acute myeloid leukemias [1]. Both low limits of detection and high specificity are required for an assay to be useful in this context. Therefore, labs must choose an assay that has inherently low levels of background noise and that employs robust error suppression techniques.

Here we demonstrate the use of IDT's Archer Next Generation Sequencing-based VARIANT*Plex* and FUSION*Plex* assays (RUO) and accompanying software, Archer Analysis, for the application of detecting low allele frequency and low transcript number fusions with high levels of sensitivity and specificity. Currently available Archer assays and software solutions target AML-relevant variants and are compatible with multiple sequencing platforms. Using Archer technology, key AML-related mutations were detected at allele frequencies less than 0.1%, and low transcript numbers of myeloid relevant fusions were identified. In addition, greater than 95% of the bases in the targeted region of interest were powered to detect variants at allele frequencies of less than 0.1% in the VARIANT*Plex* libraries. Finally, error correction and noise filtering techniques remove many false positive variants in order to reduce the false positive variant calling rate.

To generate the input material, 1,000 ng total gDNA or 200 ng total RNA from commercially available cell lines containing myeloid relevant variants was diluted into a background of wild type gDNA at a mass ratio of 1:100 or RNA at a mass ratio of 1:20 to assess analytical sensitivity. Libraries were prepared using the catalog panels VARIANT*Plex* AML Focus or the FUSION*Plex* Pan Heme assay. Libraries were sequenced on Illumina and Element Biosciences sequencing platforms. Data were analyzed with Archer Analysis using a pipeline which includes read cleaning, deduplication, error correction, variant calling, and reporting steps.

In conclusion, the VARIANT*Plex* AML Focus assay used with Illumina or Element sequencers demonstrated the ability to detect variants down to allele frequencies of 0.05%, and the FUSION*Plex* Pan Heme assay was used to detect low transcript number fusions which may be useful for AML minimal residual disease research.

1. Dillon et. al. JAMA. 2023;329(9):745-755.

#0320 Development and automation of a streamlined targeted enrichment method for cancer mutation detection.

Z. Wu[1], M. Baird[1], C. Mechlen[2], P. Hahn[2], J. M. Shaffer[1];
[1]QIAGEN, Inc., Frederick, MD, [2]QIAGEN GmbH, Hilden, Germany

Next Generation Sequencing (NGS) of DNA is a powerful tool for the detection of genetic variations, including single nucleotide polymorphisms, copy number variation, and small insertions/deletions. Target enrichment technologies enhance DNA sequencing by enabling users to analyze specific regions of interest only, which helps to effectively increase sequencing depth and sample throughput while minimizing cost. However, many targeted DNA library construction workflows are not optimal for routine genetic testing needs due to inconsistent, lengthy workflow. This poses significant challenge to application like cancer mutation profiling that requires detection sensitivity down to 1% or below due to heterogeneous nature of tumor tissue. In addition, high throughput testing with minimal hands on time is desirable with the rapid advance of precision medicine. Magnetic bead separations are commonly used between the individual reactions of targeted DNA library preparation workflows for cleanup and size selection. These bead clean up reactions are not only labor-intensive and tedious procedures but can also greatly contribute to sample-to sample variation especially when employing automated library preparation procedures. With the sophisticated QIAseq Targeted DNA Pro, we developed a novel streamlined targeted DNA workflow that greatly reduces handling variation by replacing the majority of bead clean up steps with enzymatic reactions, which now can be finished in as little as six hours. In combination with the newly developed QIAseq Normalizer kit, the protocol has been successfully implemented on the Hamilton NGS Star liquid handling platform resulting in up to 96 highly uniform, complex and ready-to-sequence libraries that can be effortless generated in one run. This complete automated solution saves researcher up to four hours of hands-on time. When using commercial reference samples, cancer mutations down to 1% were consistently detected with this automated workflow. The presented data demonstrate that this integrated and streamlined workflow does not only provide an automation friendly workflow but also allows to reliably identify low frequent cancer mutations. The applications presented here are for research use only. Not for use in diagnostic procedures.

#0321 Optimized RNA Seq library preparation for fusion calling from FFPE samples.

G. Corbet, J. Haimes, T. Sanders, M. Ranik, T. Harrison, E. Casas, K. Reed, D. Wendel, K. Giorda, A. Hanek, J. Pavlica, B. Kudlow;
Watchmaker Genomics, Boulder, CO

Gene fusions due to chromosomal rearrangement, duplication, or deletion can be important drivers of cancer. Detection of gene fusions plays a valuable role in selecting targeted therapies. A widely used method for detecting fusion transcripts is targeted RNA sequencing, which focuses sequencing reads on known fusions but does not allow for the detection of novel fusions. Whole transcriptome analysis (WTA), where the entire transcriptome is interrogated, offers an opportunity to detect both known and novel fusions.

Herein we examine the effect of sample quality, input mass, increased reverse transcriptase (RT) and insert size on fusion calling. Libraries are prepared using the Watchmaker RNA Library Preparation Kit with or without Polaris Depletion and, for target enrichment, the Twist Exome 2.0 panel prior to paired end 2x150 Illumina sequencing. First, control samples, specifically Seraseq Fusion RNA v4 high quality and FFPE samples, are used to determine if any of the parameters interrogated increase the number of breakpoint spanning reads both in a WTA and targeted sequencing context. Once established, the optimized workflow is applied to real FFPE samples.

Targeted sequencing results in a higher number of breakpoint spanning reads, compared to WTA, when controlling for sequencing depth, resulting in a higher number of reads supporting each fusion call. Longer insert sizes, achieved by modified SPRI ratios, maintain library complexity and may enhance fusion calling. Taken together, these data demonstrate an optimized protocol for fusion calling from FFPE and demonstrate the utility of both WTA and targeted sequencing for fusion detection.

#0322 Ultraplex genome and exome sequencing of rare single cells.

I. Andreou[1], **S. Rulli, Jr.**[2], K. Heitz[1], S. Huebner[1], C. Meerschiff[1], E. Lader[2];
[1]QIAGEN GmbH, Hilden, Germany, [2]QIAGEN Sciences, Frederick, MD

Single-cell genome analysis enables researchers to gain novel insights into tumor heterogeneity. Conducting single-cell genomic analysis using next-generation sequencing (NGS) methods has traditionally been challenging since the amount of genomic DNA present in a single cell is limited. PCR-based amplification methods normally have high error rates, low coverage uniformity, and extensive allelic drop-outs making interpretation of SNVs and CNVs challenging.Here we introduce a new whole-genome amplification method which utilizes an optimized isothermal DNA amplification reaction with a Hi-fidelity, error correcting polymerase and downstream library preparation protocol to allow pooling of amplified DNA. The key DNA amplification steps use multiple displacement amplification (MDA) technology to amplify gDNA directly from single cells, nuclei or previously isolated genomic DNA. During the MDA reaction, sample-barcodes are incorporated into the newly synthetized DNA, allowing the amplified DNA to be pooled and processed in to one ultraplex library. This method saves library preparation time, reduces DNA library costs and limits plastic consumable usage.Our current workflow allows 24 samples to be multiplexed in one library and 24 libraries to be produced for a total of 576 samples per sequencing flow cell. This method can be used to investigate chromosomal instability with low pass sequencing or SNV and CNV analysis following whole genome, exome-capture workflows.

#0323 Optimization of a liquid biopsy assay to accommodate low cfDNA samples and increase throughput.

M. Salmans[1], D. Kim[2], A. Carson[1], M. Wang[1], B. Lee[1], B. Leatham[1];
[1]Genece Health, Inc., San Diego, CA, [2]GC Genome, Yongin-si, Korea, Democratic People's Republic of

Molecular testing that interrogates cell free DNA (cfDNA) from plasma has significant potential value across the cancer care continuum, including early cancer detection, driver mutation identification, and disease recurrence monitoring. To achieve this potential, liquid biopsy assays must be optimized to address multiple challenges. For one, cfDNA quantity in the blood is highly variable, with different amounts present depending on malignancy and stage of progression. This requires optimization to detect low concentrations of circulating tumor DNA (ctDNA) and to accommodate variable tumor fractions. In addition, minimizing assay costs will improve test accessibility and adoption. To address these issues, Genece Health is optimizing their lung cancer liquid biopsy assay to accommodate minimal cfDNA input into library preparation. Furthermore, Genece is testing algorithms that tolerate reduced read depths from low-pass whole genome sequencing (LP-WGS) while maintaining high performance. The Genece lung cancer liquid biopsy assay profiles fragment end-motif and size (FEMS) and fragment coverage signals using LP-WGS (Illumina) and proprietary machine learning algorithms. This study first tested the frequency of end motifs in pooled ctDNA after modifying library preparation (IDT) to reduce reagent volumes from 1X down to 0.5X, 0.25X, and 0.1X of manufacturer specification. A range of cfDNA input from 0.25 ng to 6 ng was tested with each library preparation volume. In addition, LP-WGS read coverage from 5X to 1X was evaluated to assess impact on end motif frequency and assay sensitivity. Performance characterization was further evaluated with a cohort of 50 clinical lung cancer and 100 healthy donor plasma samples tested at 1X and 0.25X library reagent volume. We observed an expected increase in library complexity at higher cfDNA input and library reagent volume. Assay performance was minimally impacted by variable cfDNA input and library reagent volume. However, reducing sequencing read depth is tolerated down to 1.25X depth before increasing the variability of end motif frequencies. These observations are corroborated in the 150 clinical sample cohort. This data shows that by altering standard library preparation conditions and reducing unique read depth, liquid biopsy assays can accommodate a wider range of cfDNA, while concurrently decreasing overall costs.

#0324 Comparison of xGen Exome Hyb Panel v2 (IDT) kit and Twist Exome 2.0 (TWIST) kit for whole exome sequencing optimization from low input and degraded FFPE samples.

R. Rock, N. Prasad, M. Robinson, D. Wildman, O. Montoya, M. Sykes, B. Umylyn, T. Halsey;
Discovery Life Sciences, Huntsville, AL

FFPE is the most common method used to store precious clinical samples at room temperature for extended periods (sometimes>15 years). FFPE samples are therefore one of the most commonly available samples that can be used for discovery and diagnosis. Whole Exome Sequencing (WES) is one of the most used NGS assays that is used for profiling somatic and tumor mutations. With future clinical trials moving towards less invasive collection methodology, core needle biopsy samples are becoming a method of choice. The FFPE fixation process leads to the degradation of nucleic acids due to cross-linkage and the availability of sufficient nucleic acid from CNB fixed samples for downstream NGS assays is becoming limited. Here we report a comparison of two Whole Exome capture kits from several degraded FFPE samples, NA12878, OncoSpan gDNA HD827 and SeraSeq Breast CNV mix gDNA samples using the xGen Exome Hyb Panel v2 (IDT) Kit and the Twist Exome 2.0 (TWIST) Kit. Libraries were prepared in triplicate at 50ng, and 10ng using the Ultra™ II DNA Library Prep (NEB) kit. Pre-capture libraries were evaluated to determine the total DNA library available for capture using the KAPA Library Quantification Kit (Roche) kit. The recommendations for input amount vary between the kits, with IDT recommending 500ng, and TWIST recommending 200ng per library. KAPA Library Quantification Kit kit was used to assess the nanomolar amounts of ligated libraries. Final libraries were pooled equimolar and then sequenced as 2x100bp Paired-end sequencing on the NovaSeq 6000 instrument to achieve a target of 150-300X overall coverage. The performance of each capture kit was evaluated on the number of libraries eligible for capture, percent duplication rate, median insert size, and mean target coverage. IDT capture had 49% of libraries eligible at recommended input of 500ng, with 34% of libraries generating between 100-499ng input and the remaining 17% failing to generate 100ng input for hybridization. TWIST capture had 83% of libraries eligible at recommended input of 200ng, with 4% of libraries generating between 50-199ng input and the remaining 13% failing to generate 50ng input for hybridization. Most notably, 96% of libraries at 50ng DNA input were eligible for TWIST capture, while only 46% of libraries at 50 ng DNA input were eligible for IDT capture. The average Q30 for IDT and TWIST capture were 93-94% respectively. Both IDT and TWIST capture kits produced similar duplication rates and average mean target coverage was comparable. Taken together, our testing shows that TWIST and IDT kits generated comparable sequencing metrics. However, the TWIST Kit outperforms the IDT Kit in percent eligible libraries qualifying for hybridization capture. TWIST Kit is a great qualifier for highly degraded FFPE samples, especially those with limited input DNA material.

#0325 Validation of Aventa FusionPlus: An LDT NGS assay for comprehensive cancer genomic profiling.

S. Melnyk, J. Belton, S. Nomikou, K. Powell, D. Heiney, R. Khalife, D. Jones, A. Schmitt, C. Wilson, M. Won, A. Magliocco, C. Roberts;
Aventa Genomics, Orlando, FL

Next-generation sequencing (NGS) assays play a pivotal role in illuminating the genomic landscape of cancer by providing insights into gene regulation and biomarker detection for the purpose of guiding therapeutic decisions to advance personalized medicine. We validated the Aventa FusionPlus Test, a Laboratory-Developed Test (LDT) that integrates HiC technology to enhance detection of actionable gene fusions and rearrangements in solid tumors, including those that are missed by current standard of care tests. This is a DNA-based test that is robust to DNA degradation in FFPE specimens, in contrast with RNA-seq and long-read technologies. The test utilizes the Element Biosciences AVITI sequencing platform to achieve high quality sequencing data at low cost per sample. The Aventa FusionPlus test enables gene-level detection of structural variants near or within 361 medically actionable or diagnostically relevant cancer genes. The 3D structure and long-range linkages captured by the test amplify the signal counts for each rearrangement. The test integrates the Arima-HiC+ FFPE sample prep and the Arima Library Prep Kit workflow. After dewaxing and rehydrating the FFPE tissue, the chromatinized DNA is fragmented and the fragmented ends are filled in with a biotinylated nucleotide. Next, spatially proximal fragmented ends of DNA are ligated, capturing the 3D structure of the genome. The proximally-ligated DNA is then purified and further fragmented, and the biotinylated ligation fragments are enriched. DNA libraries are prepared from these enriched fragments and sequenced in “paired-end” mode. Genes involved in genomic rearrangements were detected using the Arima-SV pipeline along with manual curation.

The test achieved robust detection of structural variants, with accuracy of 98.8% relative to reference methods. FFPE tumor specimens from 10 different tissue types and a wide range of tumor content (20%-100%) were included. No correlation between tumor cellularity and sensitivity was observed, suggesting that samples with as low as 20% tumor cellularity can be tested. When comparing to RNA-based and other targeted reference methods, we found additional fusions nearby oncogenes missed by these reference methods. As an example, in a breast cancer case, a fusion of genomic regions neighboring BRAF and MYC oncogenes on chromosomes 7 and 8 respectively, was missed by the reference method but was successfully detected by the Aventa FusionPlus test.

The Aventa FusionPlus test is a highly sensitive, specific, and accurate method for comprehensive cancer genomic profiling. The enhanced understanding of gene fusions and rearrangements positions the test as a valuable tool for clinical decision-making in oncology.

#0326 Matched fresh frozen and FFPE patient tissues reveal the enhanced sensitivity and data quality of a novel DNA library prep method.

M. R. Heider, J. Sun, B. Sexton, B. W. Langhorst, L. Blum, P. Liu;
New England Biolabs, Inc., Ipswich, MA

In cancer genomics, a common source of DNA is formalin-fixed, paraffin-embedded (FFPE) tissue from patient surgical samples, where in most cases high quality fresh or frozen tissue samples are not available. FFPE DNA poses many notable challenges for preparing NGS libraries, including low input amounts and highly variable damage from fixation, storage, and extraction methods. It is difficult to obtain libraries with sufficient coverage and the sequencing artifacts arising from damaged DNA bases confound somatic variant detection. Additionally, many laboratories process FFPE tumor samples alongside matched, high quality, normal DNA and many library prep workflows are not readily compatible with both sample types.

We developed a novel NGS library prep method compatible with both high quality and very low quality FFPE DNA samples, employing a novel enzymatic DNA repair mix, enzymatic fragmentation mix, and PCR master mix. To validate this workflow on real patient sample sets, we obtained DNA extracted from matched tumor and normal tissue of various tissue types preserved by both fresh frozen and FFPE methods. The FFPE DNA samples ranged in quality from DNA integrity number (DIN) 1.5 to 6.8, including samples stored for nearly 3 decades. We prepared libraries using this method compared against other library prep workflows and sequenced them by WGS and target capture. We assessed the performance of these workflows by library yield, library quality metrics, depth and evenness of coverage, and somatic variant calling with fresh frozen-extracted DNA providing the gold standard for library quality and mutation content.

This new enzymatic fragmentation-based library prep workflow not only reduced the false positive rate in somatic variant detection by repairing damage-derived mutations in FFPE DNA samples but also improved the library yield, library quality metrics (including mapping, chimeras, and properly-paired reads), library complexity, coverage depth and uniformity, and hybrid capture library quality metrics. Comparing the variant calls from matched FFPE and frozen tissues revealed an improved sensitivity and accuracy of variant calling using this library prep method compared to mechanical shearing and other enzymatic fragmentation library prep approaches.

This new suite of enzyme mixes allows even highly damaged FFPE samples to achieve high quality libraries with a greater sensitivity for somatic variant identification. The workflow is robust and flexible, compatible with both FFPE DNA and matched high quality DNA samples as well as automation-friendly for convenience in sample processing.

#0327 A comparison of Illumina and Element Biosciences sequencing platforms.

S. Johnson, **K. Lee**, N. Riccitelli;
Navigate BioPharma Services, Carlsbad, CA

Introduction: Advancements in sequencing technologies have revolutionized the field of genomics, enabling scientists to study the genetic information of organisms at unprecedented scale and speed. Next Generation Sequencing (NGS) has been utilized in clinical oncology from discovering and characterizing oncogenic driver mutations to providing personalized treatment of cancer. Among sequencing technologies, Illumina has emerged as the market leader, however, in recent years several alternatives have emerged. Herein, we evaluate the performance of NextSeq2000 and NextSeq550Dx platforms by Illumina to the Aviti platform from Element Biosciences.

Method: Eight (8) Archer Core Myeloid Panel libraries previously sequenced on NextSeq550Dx as part of a validated workflow were selected, normalized to 100 nanomolar (nM), pooled and sequenced on NextSeq2000 and Aviti sequencers with 2x150 paired-end sequencing. Samples included the HD829 myeloid DNA control from Horizon Discovery, a well-characterized HAPMAP sample, and a mixture of HD829 in HAPMAP. Prior to sequencing on the Aviti system, libraries were circularized with the Elements Adept chemistry. Fastq files from both Aviti and NextSeq2000 sequencing were uploaded to Archer Analysis Software, standardized filtering was applied to all generated datasets, and results compared across platforms.

Result: Aviti and NextSeq2000 platforms exhibited comparable sequencing reads, with an average total reads per sample of 76,205,719 and 74,201,570 from Aviti and NextSeq2000, respectively, while the lower throughput NextSeq550 platform yielded an average 17,619,350 reads per sample. Standardized filtering across all platforms provided 100% detection of true positives, however additional false positives (FP) were present in all samples and platforms that mapped to regions requiring normal dataset correction as part of the validated NextSeq550 workflow. The lowest numbers of FPs were detected on the Aviti platform, while both NextSeq550 and NextSeq2000 derived results contained several FP calls at elevated (>10%) variant allele frequency (VAF).

Conclusion: The three platforms compared in this study were able to detect all true positives of the tested samples using the same filtering criteria. The performance metrics of NextSeq2000 and Aviti were comparable and higher than NextSeq550Dx, in line with expectations due to the higher sequencing capacity. Although the Aviti platform required additional hands-on time, it in-turn generated cleaner data with less FP variants in comparison to Illumina's sequencing platforms. Overall, these results indicate robust sequencing throughout all three platforms.

#0328 A comprehensive genomic profiling of myeloid malignancies demonstrates mutational spectrum of DNA variants, FLT3-ITDs, and gene fusions.

J. Huang[1], H. Gu[2], J. Orton[2], M. Sedova[1], S. Rozenzhak[3], F. Hyland[1], G. Liu[2];
[1]Thermo Fisher Scientific, South San Francisco, CA, [2]Sonora Quest Laboratories, Phoenix, AZ, [3]Thermo Fisher Scientific, Carlsbad, CA

Introduction: Myeloid malignancies encompass diverse hematopoietic disorders, including acute myeloid leukemia (AML), myeloproliferative neoplasms (MPN), myelodysplastic syndromes (MDS), chronic myeloid leukemia (CML), chronic myelomonocytic leukemia (CMML), and juvenile myelomonocytic leukemia (JMML). We developed two assays to address the genetic complexity of myeloid malignancies, Oncomine™ Myeloid Assay and Oncomine™ Myeloid Assay GX v2, detecting mutations in 45 DNA genes and >30 fusion driver genes, including >700 fusion isoforms. Our panel includes genetic alterations such as *FLT3*-Internal Tandem Duplications (ITDs), *IDH1/2*, *CEBPA*, *CALR*, and *TP53*.
Methods: Here we describe the genomic profiles of 8503 clinical research samples (including AML, MPN, MDS, CML, CMML, or JMML). A total of 4723 samples were run on the Ion GeneStudio™ S5 System and analyzed using the Oncomine™ Myeloid Research workflow on Ion Reporter™ 5.18. A total of 3780 samples were run on the Ion Torrent™ Genexus Software 6.6 and analyzed using the Oncomine™ Myeloid Assay GX v2.
Results: On Genexus, the turnaround time (the time between starting the run and NGS data report) was 23-25 hours and the hands-on time was around 1 hour. The success rate of the samples was 100%.
Frequency of relevant mutations and variant allele frequency by gene: Genes like *TET2* (detected in 12.6% of samples), *ASXL1* (9.3%), *DNMT3A* (7.8%), *TP53* (7.5%) exhibited high mutation rates. 56.4% of samples had mutations, averaging 2.3 mutations per sample. Common co-occurring mutations included *ASXL1-TET2* and *SRSF2-TET2*. Variant allele frequency varied greatly, e.g., *ANKRD26* had a median VAF of 66%, while *MYD88* had only 7%.
Mutation spectrum of FLT3ITD variants: *FLT3*-ITD was observed in 3% of samples, with an average VAF of 0.32, featuring a multi-modal length with the highest peak at around 34 bp and maximum length at 151 bp.
Mutation spectrums of fusions: 710 (8.4%) samples were fusion-positive with read counts ranging 21-113,000. *ABL1* was the most common driver and *BCR-ABL1* was the most common gene pair. Other common drivers included *KMT2A*, *MYH11*, *RARA*, and *RUNX1*. 17 distinct driver genes, 49 gene pairs, and 110 gene isoforms were observed, including rare fusions like *ZMYM2-FGFR1* and *KAT6A-CREBBP* that are not detectable by traditional methods like qPCR (quantitative polymerase chain reaction) or FISH (fluorescence in-situ hybridization).
Conclusions: The Oncomine Myeloid Assay is a fast, robust, and reproducible solution for comprehensive genomic profiling of myeloid malignancies. We describe the mutational spectrum of DNA variants and RNA fusions in a range of clinical research samples. (For research use only. Not for use in diagnostic procedures.

#0329 NanoTelo: A workflow for detecting telomere absolute length based on nanopore sequencing technology.

J. Lang, Y. Chen, Z. Yang, B. Huo;
Qitan Technology (Beijing) Co., Ltd., Beijing, China

Background: Telomeres are specialized nucleoprotein structures located at the end of linear chromosomes in eukaryotic cells, and protect the ends of chromosomal DNA from degradation, end-to-end fusion and abnormal recombination. Changes in telomere length have become an important biomarker, which is closely related to cellular aging, all-cause mortality and a variety of diseases. However, there are still challenges in quantifying telomere absolute length, due to repeats of nucleotide sequence (5'-TTAGGG-3')n in single-stranded G-rich telomeric region, and lack of a method for nucleotide separation and enrichment of individual telomeres.
Methods: We developed NanoTelo, a workflow for detecting telomere absolute length based on nanopore sequencing technology. For experimental steps, a self-designed telomere adapter was first connected to the C-rich strand at the end of the chromosome by utilizing the 3' end overhang. And the 5' end of the telomere adapter was complementary to the sequencing adapter, allowing the antisense telomere chain to perform single-strand extension sequencing in the 5' to 3' direction, thus into the sub-telomeric region from the telomere end. The sequencing library was nanopore-sequenced on the QPursue-6k according to the manufacturer's instructions. For data analysis, reads were strictly extracted (dataset B) with the telomere adapter and library structure in raw sequencing data (dataset A). The reads of dataset A and dataset B were corrected, aligned to the human reference genome (T2T-CHM13v2.0), and calculated the telomere length distribution of each chromosomal (autosomes and sex chromosomes) p/q-arm, respectively. Defined the mean telomere length of all chromosomes represented the overall telomere length, the estimated results of dataset A and dataset B were weighted to obtain the final telomere absolute length.
Results: We selected 5 cell lines, which was HCT116, 293T, T24, IMR90 and WI38, and performed 2 experimental replicates for each one. We found that the estimated telomere lengths for each cell line were 3,528/3,512 bp, 4,298/4,311 bp, 2,745/2,685 bp, 4,926/4,915 bp and 4,143/4,096 bp, respectively. A comparative analysis with results from the Pacbio sequencing platform for each cell line in the *Tham et al.*'s paper, showed that there was no significant statistical difference (two-tailed T-test: *p-value*=0.98), and the mean absolute difference for estimated telomere length between the two platforms was 7.7 bp (95% CI: 5.4-10.0 bp).
Conclusions: NanoTelo demonstrated the possibility of measuring telomere absolute length with a single chromosomal p/q-arm at nucleotide-level resolution. We hope that NanoTelo can not only be used as an important tool for estimating telomere length to dynamically monitor aging, but also provide strong technical support for scientific research and/or clinical application related to human anti-aging and disease intervention.

#0330 FusionPlex™-HT and VariantPlex™-HT: Automation ready solutions for anchored multiplex PCR.

David Knupp, Christine Troutman, Allison Hadjis, Dhruti Legare, Paula Kalavakur, Michael Washburn

Integrated DNA Technologies, Inc., Boulder, CO

Introduction: Anchored Multiplex PCR (AMP™) assays, VariantPlex and FusionPlex are amplicon-based, next generation sequencing (NGS) workflows that identify genomic variations present in DNA or RNA input, respectively. AMP reagents are available in a lyophilized format which are user-friendly and convenient to store. However, lyophilized reagents are not suitable for liquid handlers or high-throughput environments. Thus, we developed AMP reagents in liquid format to satisfy the need for a platform-agnostic method of high-throughput (-HT) AMP library preparation.
Methods: The performance of our liquid reagent-based VariantPlex-HT and FusionPlex-HT workflows were evaluated relative to legacy lyophilized reagents using several input of varying quantity, quality and type. In addition, we examined liquid reagent performance across multiple AMP panels, which target solid tumor and blood cancers variants. Prepared libraries were then sequenced and analyzed using Archer™ Analysis v7.0 software.
Results: When using 50ng SeraSeq® Myeloid DNA input (LGC Clinical Diagnostics, Inc.) and the VariantPlex Core Myeloid panel (37 gene targets), both the lyophilized VariantPlex and VariantPlex-HT detected 100% (22/22) known variants ranging from 3.8% to 20.4% allele frequency (AF). When using low-quality FFPE and the VariantPlex Complete Solid Tumor panel (430 gene targets), both workflows captured 28/28 (AF: 1.4%-20.2%) and 11/11 (AF:1.2%-18.9%) single nucleotide variants (SNVs) and Insertion and Deletions (InDels) when 50ng of SeraSeq compromised FFPE or 200ng Horizon Severe FFPE was used as input, respectively. The FusionPlex-HT workflow consistently showed increased library complexity using the FusionPlex Lung V2 panel with 20ng or 50ng of Seraseq RNA Fusion Mix v4 input. This, coupled with greater on-target percentage resulted in an average increase in fusion supporting reads of 1.95x ± 0.53 and 2.2x ± 0.41 for 20ng and 50ng input, respectively. Next, we prepared a dilution series of SeraSeq RNA Fusion Mix v4 FFPE material at 100%, 25%, 10% and 5% dilutions. We utilized our FusionPlex Pan Solid Tumor panel (137 gene targets) which covers all expected fusions in this input material. At 100% and 25% dilutions, all expected fusions were detected by lyophilized FusionPlex and FusionPlex-HT workflows. However, at 10% and 5% dilutions FusionPlex-HT detected 100% and 91% of expected fusions, respectively, while legacy lyophilized reagents detected 80% and 60% of expected fusions.

#0331 Ion Torrent™ NGS sequencing of the TERT promoter hotspots with Ion AmpliSeq™ HD technology.

A. Sharma[1], G. Luo[1], N. Li[1], G. Pea[2], F. Hyland[3];
[1]Thermo Fisher Scientific, Carlsbad, CA, [2]Thermo Fisher Scientific, Milan, Italy, [3]Thermo Fisher Scientific, South San Francisco, CA

Introduction: Recurrent mutations C228T and C250T in the *TERT* gene promoter are prevalent in cancer and serve as important biomarkers for aggressive disease. Ion Torrent™ NGS sequencing, combined with Ion AmpliSeq™ HD technology, enables comprehensive genomic profiling with ultra-high sensitivity for low-frequency variants in cell-free DNA (cf-DNA) and highly heterogeneous solid tumor samples. However, the high GC content (>80%) and the presence of G repeats that are known to adopt a compact stacked three-G-quadruplex conformation in the *TERT* gene promoter region pose sequencing challenges such as low read depth and strand-bias, i.e. prematurely truncated reads on one strand.
Methods: We designed nine AmpliSeq™ HD panels with amplicon sizes of 70 to 104 bp, ideal for cf-DNA and FFPE samples, to target the recurrent *TERT* promoter hotspots. The designs were tested alone and combined with a larger Ion AmpliSeq™ HD DNA research panel resulting in highly multiplexed libraries. The libraries were used for Ion 540™ chip template preparation on the Ion Chef™ instrument and subsequently sequenced using the Ion GeneStudio™ S5 System. Sequencing data was used to evaluate coverage of the target hotspots by each design for each condition, and additional panels were designed to test single amplicons covering both *TERT* promoter hotspots.
Results: Through performance evaluation, we selected two overlapping amplicons, each effectively amplifying one of the two hotspots. Individually tested, these amplicons yielded approximately 3000 families each from a 10ng gDNA input and when combined into the larger Ion AmpliSeq™ HD DNA research panel, they produced several thousand reads across various libraries, providing molecular coverage of around 200 functional molecules. While capture efficiency was lower compared to *TERT* amplicon-only libraries, these improved amplicons allow downstream analysis of variants. A single-pool solution (single amplicon/s covering both hotspots) will be explored further using the second batch of amplicons/primers.
Conclusions: The optimized amplicons in two pools developed in this study enable the detection of challenging yet clinically significant *TERT* promoter hotspot mutations using the ultra-sensitive Ion AmpliSeq™ HD technology.

#0332 Improved high-throughput genomic analysis of urine samples using pixelated-ultrasound to enable personalized genomic profiling and therapeutic developments in cancer.

M. Evans-Holm[1], N. Lumbres[1], **R. Sen**[2], P. Montilla-Perez[2], M. A. Paradise[2], P. Lentz[1];
[1]Convergent Genomics, South San Francisco, CA, [2]Active Motif, Carlsbad, CA

Here we address some of the existing challenges in liquid biopsy workflows which can potentially benefit urine analysis from bladder cancer patients because approximately 1/4th of all human cancers are urological tumors. Globally, bladder cancer is the 10th most prevalent, and the 9th cause of mortality due to malignancy. The challenge addressed here is an improvement to sample preparation for sequencing. Among genders and disease states, urine samples vary in terms of cell count and hence, in DNA concentration. Therefore, it is critical to obtain consistent DNA fragments from variable samples across large cohorts of patients so that the sequencing leads to accurate identification of biomarkers of disease risk, progression, and treatment-response. In this direction, we present the advantages of a novel pixelated ultrasound technology which significantly improves sample-preparation in a very fast, economical, and high-throughput manner. Here, DNA is extracted from human urine samples and subjected to sonication to generate fragment sizes. Extracted DNA was loaded onto a regular 96-well round-bottom plate, which is sealed and placed inside the system where 12 columns of the 96-well plate are individually programmed and run simultaneously, hence enabling quick optimization. The system does not require time- and labor-intensive processing of the samples before or after the sonication which is required for other similar technology. Overall, the DNA samples were processed with significant improvement over other similar technology in terms of consistency, speed, and economy. Subsequently, the fragment sizes were analyzed. Analysis of results, as presented in the figures, show that the DNA fragment had the average size as predicted, uniform shearing, and very consistent across the 96-well plate containing different samples with no cross-contamination. The time, labour, expense, and risk turned out to be very low compared to other similar technology. The sizes were appropriate for library preparation and sequencing. The technology works consistently for both low and high cell numbers which is a critical factor for heterogenous samples from patients. In conclusion, the study presents improvements to library preparation for sequencing which fit into the larger workflow of non-invasive liquid biopsy using urine samples. The ability to obtain consistent DNA fragments in a quick and economical manner will greatly enable unique fingerprinting of an individual's cancer or cancer risk across large cohorts, with the potential for integration in automation workflows.

#0333 Stability and performance of a partially used 8-lane microwell cartridge on single-cell capture and immune response profiling.

H.-W. Song[1], R. A. Acob[2], Z. Hlathu[2], X. Zhao[2], J. Moskwa[2], L. Wang[2], A. Ayer[2];
[1]BD Biosciences, San diego, CA, [2]BD Biosciences, San Jose, CA

In this study, we introduce an innovative microwell-based approach, offering the capability to capture up to 500,000 single cells and show stability of a partially used 8-lane microwell cartridge up to 6 months after first use. Stability of microwell cartridges used for single-cell capture and the integrity of the individual lanes are crucial factors in genomics research to ensure the accuracy and reliability of generated data. Stability is paramount to ensure consistent results over multiple experiments. High-quality materials and manufacturing processes are essential to prevent wear and tear, ensuring that the microwell cartridges function optimally for an extended period. Integrity between the individual lanes must also be intact to prevent cross-contamination between samples. To demonstrate partial use stability of the 8-lane microwell cartridge, multiple assay combinations were performed on different lanes of the cartridge, collected at different time points. Whole transcriptome amplification (WTA) together with AbSeq antibody-oligonucleotide conjugates for cellular indexing of transcriptomes and epitopes (CITE-Seq) was performed on peripheral blood mononuclear cells (PBMCs), loaded and captured in Lanes 1 and 2, on Day 1; sample multiplexing was used with targeted mRNA assay on Jurkat and Ramos cells, loaded and captured in Lanes 3 and 4, after four months; and WTA together with the AbSeq Assay was performed on PBMCs, loaded and captured in Lanes 5 and 6, after six months. The different time points collected were compared to a single-lane microwell cartridge. Our data showed that assay performance was not compromised with the storage of a partially used cartridge, and there was no contamination detected between the lanes. High-throughput cell load and capture using WTA and the AbSeq Assay also showed that each lane of the 8-lane microwell cartridge was able to process up to 65,000 cells with no limit of detection on assay sensitivity. By maintaining cartridge stability and stringent measures to prevent contamination, researchers can ensure the reliability and accuracy of their data. This is vital for various applications such as developing targeted immunotherapies and precision medicine approaches, ultimately enhancing our capacity to combat a wide range of diseases.

#0334 Flexible and high-throughput microwell-based single-cell capture for multiomic ATAC-seq and RNA-seq profiling.

R. Nguyen[1], H. Huang[1], Q. Bao[1], P. Narayan[1], H.-W. Song[2], E. Hatami[2], Z. Zhang[2], T. McCarthy[1], Y. Kim[1], R. Li[1], C. Gordon[1], L. Wang[1], A. Ayer[1];
[1]BD Biosciences, San Jose, CA, [2]BD Biosciences, San Diego, CA

The simultaneous profiling of chromatin accessibility and gene expression is an active area of interest for researchers studying how epigenetic changes regulate gene expression at the single-cell level. Here, we demonstrate the feasibility of single nuclei assay for transposase-accessible chromatin (snATAC) seq either with or without simultaneous gene expression profiling using the microwell-based BD Rhapsody™ HT Xpress System. Taking advantage of an eight-lane microwell cartridge, the BD Rhapsody™ HT Xpress System can support the snATAC seq assay with nuclei input ranging from 1,000 to 400,000 nuclei in a single experiment. To demonstrate the flexible throughput capabilities, 1,000 to 50,000 nuclei from cryopreserved peripheral blood mononuclear cells (PBMCs) were tagmented and loaded onto a single lane of the BD Rhapsody™ HT Xpress System. The snATAC assay libraries were prepared and sequenced, revealing multiple high-quality ATAC-seq metrics: high counts of unique ATAC fragments, high fraction of reads in peak regions (FRiP), and high transcriptional start site (TSS) enrichment score. The data were obtained consistently across the wide range of input nuclei with use of the gentle and robust nuclei loading capabilities of the BD Rhapsody™ HT Xpress System. Moreover, after capturing ATAC fragments, the BD Rhapsody™ Enhanced Cell Capture Beads are stable and can be stored at 4 °C for up to 3 months, allowing researchers the flexibility in sequencing subsets of nuclei or lanes for QC purposes before sequencing the entire library and returning to samples for complete sequencing. Furthermore, to demonstrate the consistency of both open chromatin profiling and mRNA gene expression as a combination (multiomic snATAC + snRNAseq), firstly, we compared snRNAseq data from a whole transcriptome assay (WTA) with snRNAseq from an ATAC+mRNA multiomic assay using the same sample. This strategy enabled us to show that there is negligible gene expression differences between snRNAseq from the BD whole transcriptome assay and snRNAseq from the multiomic scATAC and scRNA assay. Likewise, the snATACseq assay and snATACseq assay with simultaneous whole transcriptome profiling shows that chromatin accessibility profiling is equivalent with and without gene expression profiling. Enabling this new scATAC assay on the BD Rhapsody™ HT Xpress System can advance the study of epigenetic regulation of gene expression with a robust and flexible workflow. This will allow researchers to analyze both open chromatin and mRNA at varying nuclei inputs with single-cell resolution to understand the underlying molecular mechanisms in gene expression regulatory pathways. This assay can be readily extended to broader samples to gain greater understanding of disease states in immunology and immuno-oncology studies. For Research Use Only. Not for use in diagnostic or therapeutic procedures.

#0335 BD®OMICS-Guard Sample Preservation Buffer preserves mRNA and cell surface epitopes for single-cell sequencing applications.

S. X. Shi[1], C. Sakofsky[2], Z. Zhang[1], S. Vadrevu[2], X. Shi[2], H.-W. Song[1], A. Ayer[2];
[1]BD Biosciences, San Diego, CA, [2]BD Biosciences, San Jose, CA

Multiomics has emerged as a powerful tool to derive insights on the transcriptomic and proteomic data of human cancer samples and preclinical models of blood and tumor malignancies. Due to the sensitivity of sequencing techniques, sample quality and stability can potentially interfere with results. BD® OMICS-Guard Sample Preservation Buffer (SPB), a novel preservation solution, allows cells and bulk tissues to be stored for up to 72h at 4 °C, while reliably capturing the true biology of cells. This reagent gently preserves mRNA and protein integrity without the traditional cross-linking and harsh fixatives, increasing flexibility and expanding options for study designs. Here, we showcase the preservation properties ofthis reagent for multiomic readouts in human cells and mouse tissue across three different timepoints.BD® OMICS-Guard SPB's preservation of mRNA from human PBMC and bulk mouse spleen tissues wasevidenced by WTA for differentially expressed genes in samples preserved for 24, 48 and 72h comparedto fresh/unpreserved controls. Protein epitope preservation was demonstrated via CITE-Seq assay withthe BD® AbSeq Human Immune Discovery Panel (human PBMC) or a 30-plex panel of anti-mouse BD®AbSeq Antibody-Conjugated Oligonucleotides (mouse splenocytes) and confirmed with multicolor flowcytometry. For both sample types, high correlation R^2 values (>0.87) were calculated for the preservation time points versus fresh controls. Concomitant flow cytometry analysis of major cell types and surface protein expression was consistent with sequencing data for all samples. Specificity and sensitivity of major cell type markers and cell surface proteins across cell types and time is visualized in the BD®AbSeq Antibody-generated heatmap for each sample. Additionally, BD® OMICS-Guard SPB maintains mRNA integrity in targeted gene assays and VDJ full-length assays, suggesting robust preservation of select transcripts readily interrogated in single-cell profiling. Batch effect across time and technical replicates for both sample types was limited with the BD Rhapsody™ HT Xpress System and delineated by donor/sample specific tSNEs across time. We demonstrate that the BD® OMICS-Guard Sample Preservation Buffer effectively preserves both mRNA and surface proteins for single-cell experiments. BD® OMICS-Guard SPB allows the convenient preservation of samples such as tumor biopsies to be collected and stored for up to 72h at 4 °C while maintaining mRNA and protein integrity, allowing the flexibility for precious samples to be potentially shipped to a central sequencing site to ensure standardized sequencing workflows. For Research Use Only. Not for use in diagnostic or therapeutic procedures.BD and BD Rhapsody are trademarks of Becton, Dickinson and Company or its affiliates.

#0336 Genome integrity assessment by optical genome mapping for cell manufacturing/bioprocessing applications.

A. Hastie, **A. W. C. Pang**, A. Chaubey;
Bionano, San Diego, CA

Cells and cell lines are used for multiple applications such as bioprocessing, therapy, and research. To ensure quality of cells and downstream applications, appropriate quality control (QC) methods are critical. Historically, karyotyping has been employed, but it is limited by its very low resolution and tedious laboratory workflow. Other methods such as PCR and targeted sequencing can characterize only small genomic variants at specific loci. Whole genome sequencing can detect small variants genome-wide but has limited sensitivity in detecting structural variants (SVs). Optical genome mapping (OGM) is a novel genome analysis technique that can fill many of the gaps in current capabilities for assessing genome integrity. To find clonal variants, 400 Gbp of data is collected from the parental/control and test samples. For both samples, a *de novo* assembly is constructed, and homozygous or heterozygous SVs are assessed. Subsequently, the dual variant annotation pipeline identifies unique SVs in the test sample compared to the parental sample. To discover subclonal SVs down to 5% variant allele fraction (VAF), the workflow leverages the generation of 1.5 Tbp of data, requiring a simple adjustment to longer data collection time. Comparison of test sample to parental sample enables easy determination of acquired variants. Finally, generation of ~5 Tbp of data, requiring 2-3 flowcells to be run, enables the detection of SVs at ultra-low VAF down to ~1%. In this study, several dilutions and simulations were performed to examine OGM's limit of detection. Targeting a coverage of 5 Tbp and analysis using the somatic SV-analysis workflow revealed that OGM has the sensitivity to detect deletions >50kbp, insertions >20kbp, duplications >100 kbp, and translocations at ~1% VAF. We have applied the clonal and somatic workflows to verify genomes' integrity after cell immortalization, induced pluripotency, transgene-integration, and gene-editing. The data using the robust and sensitive workflows demonstrate that the OGM platform is a cost-effective solution for cell manufacturing/bioprocessing QC applications.

#0337 Balanced-strand sequencing for highly efficient duplex variant calling in circulating tumor DNA.

A. Widman[1], A. P. Cheng[2], A. Sossin[2], S. Rajagopalan[3], M. Al Assaad[3], S. Deochand[2], Z. Steinsnyder[2], D. Manaa[2], M. Marton[2], C. Reeves[2], I. Rusinek[4], E. Meiri[4], O. Barad[4], Z. Shipony[4], S. Gilad[4], A. Jaimovich[4], M. Sigouros[3], J. Manohar[3], A. King[3], D. Wilkes[3], J. Otilano[3], O. Elemento[3], B. M. Faltas[3], J. M. Mosquera[3], D. A. Landau[3];

[1]Memorial Sloan Kettering Cancer Center, New York, NY, [2]New York Genome Center, New York, NY, [3]Weill Cornell Medicine, New York, NY, [4]Ultima Genomics, Newark, CA

Several approaches for the detection of circulating tumor DNA (ctDNA) are anchored in the accurate identification of cancer-specific single nucleotide variants (SNVs) in plasma. Such approaches are limited in ultra-low tumor fraction (TF) contexts, such as early cancer detection or the identification of postoperative minimal residual disease, where ctDNA SNVs are difficult to distinguish against background sequencing error. ctDNA detection in these critical low TF contexts is further limited by the sparse amount of cell free DNA (cfDNA) in plasma (Zviran et al., 2020). To reduce single-stranded artifact and base calling errors, duplex sequencing can be used to jointly analyze corresponding Watson and Crick strands to detect true, double-stranded variants. Recent work has demonstrated that duplex sequencing can decrease error rates to 10^{-7} (Hoang et al., 2016) and can be deployed in the whole-genome sequencing (WGS) setting (Cheng et al., 2023). A significant limitation for existing duplex techniques is the need to analytically pair matching DNA strands through exhaustive sequencing, resulting in inefficient use of scarce input material, particularly in plasma cfDNA. These techniques typically capture 1-5% of sequenced molecules, restricting duplex coverage depth. We present balanced-strand sequencing, a PCR-free approach that leverages the hydrogen bonds of complementary DNA to carry matched native strands directly into sequencing, enabling massively scalable duplex sequencing. The approach relies on Ultima Genomics sequencing, where DNA denaturation is not required prior to clonal amplification. In balanced strand sequencing, double-stranded DNA is partitioned and clonally amplified on sequencing beads through emulsion-PCR. Each double-stranded DNA molecule contributes to a single sequencing read, allowing for a linear increase in duplex recovery with increasing sequencing depth. The approach does not require redundant sequencing and therefore maximizes unique molecule throughput. We applied balanced strand sequencing to cfDNA, input as low as 5 ng, and achieved 7-35x whole-genome duplex coverage, roughly 20-fold higher than our prior duplex WGS. We further developed a machine-learning guided single read mutation calling framework, which when combined with duplex error suppression, reduced error rates to 10^{-7} and enabled accurate ctDNA detection at concentrations $<10^{-5}$. Use of our analysis framework in APOBEC-mutant bladder cancer plasma samples allowed us to identify APOBEC signatures in plasma and platinum exposure signatures indicative of prior chemotherapy treatment. Altogether, balanced strand sequencing radically enhanced duplex efficiency and has broad applications across cancer. In cfDNA applications, balanced strand sequencing enhances error-correction in tumor-informed ctDNA detection and paves the way for non-tumor informed WGS ctDNA detection.

#0338 Unraveling layers of proteogenomic complexity in cancer through multiomic exploration of archived FFPE tissue.

A. J. O'Hara, Y. Han, I. DeVito, L. Turner, H. Latif;
GENEWIZ from Azenta Life Sciences, South Plainfield, NJ

Formalin Fixed Paraffin Embedded (FFPE) tissues are a staple in clinical diagnostics associated with solid tumor. The preserved tumor tissue can be interrogated using classical histopathology and complemented with molecular approaches to elucidate cancerous SNPs, indels, structural variants, repeat expansion, copy number expansions, and mutational burden. Increasingly, approaches are being deployed to interrogate tissue not only through individual datasets but through integrated approaches that provide spatial information that defines the tumor microenvironment. Here, we illustrate using FFPE blocks from various tissues a multiomic workflow that allows for deep exploration of the molecular underpinnings of cancerous tissue. FFPE blocks were serially sliced into various FFPE slides with a single slide H&E stained. Individual slides were then utilized to explore the genome, epigenome, single cell RNA-seq, and digital spatial profiling. Genome information was captured using hybrid capture based approaches (whole exome sequencing and targeted cancer panel) followed by deep NGS on an Illumina platform and analyzed for a variety of variants and tumor mutational burden. DNA methylation was detailed using target capture probes targeting DNA methylation sites. Single cell approaches were applied to explore the transcriptome using 10X Genomics scRNAseq Flex kit. Digital spatial profiling was done using the NanoString for both transcriptomics and proteomics, with the GeoMx Whole Transcriptome Atlas and Human Core and Pan-Tumor protein panels. Aggregating these data illustrates the expanding landscape of information that can be extracted from FFPE derived tissue and the potential for novel discovery and diagnostic power integrating these complex data types holds.

#0339 Universal synthetic TCR/BCR spike-in controls to evaluate immune receptor profiling assay and next-generation sequencing performance.

A. Chenchik, **T. Liu**, M. Makhanov, D. Hu, K. Ghias, P. Diehl;
Cellecta, Inc., Mountain View, CA

Adaptive immune receptor (AIR) repertoire diversity assays are susceptible to biases arising from variations in conditions in the RT-PCR and next-generation sequencing (NGS) steps. We designed synthetic TCR and BCR spike-in controls to mitigate these biases and to serve as universal standards for any PCR-based immune receptor profiling assay. We synthesized 48 BCR constructs representing different IGH, IGK, and IGL genes and 39 TCR constructs for TRB, TRA, TRG, and TRD genes. The spike-in controls were tested as (16x3) BCR constructs and (13x3) TCR Triplex isoform pools added to multiple samples in the same batch to detect cross-contamination across samples. We successfully discriminated between controls and background sequences by combining a unique molecular identifier (UMI)-based correction strategy with spike-in controls at the data analysis step. We also tested 48 BCR and 39 TCR Premixed Controls by spiking into peripheral blood mononuclear cells (PBMC) RNA samples before reverse transcription using Cellecta's DriverMap™ Adaptive Immune Receptor Profiling Assay that uses a multiplex RT-PCR approach with gene-specific primers and UMIs. We successfully used it to evaluate assay performance by adding premixed controls at different concentrations. Results showed a linear trend as the number of spike-in molecules increased. Our analysis revealed an average sequencing error rate of 0.4%-0.8% per base, aligning with the reported error rate range of Illumina sequencing. This suggests the reliability of our spike-in controls, which can be used to rectify biases in the AIR protocol and accurately estimate error and mutation rates for the DriverMap AIR assay or any other sequencing-based immune receptor profiling assay. This innovative approach enhances the robustness of immune receptor profiling technology, facilitating more accurate assessments of repertoire diversity.

#0340 Validation of TSO500 NGS panel for comprehensive genomic profiling from FFPE tumor samples.

J. Li[1], Z. Yan[1], W. Liu[1], L. Shi[1], C. Spittle[1], C. Galderisi[2];
[1]ICON Clinical Research, Inc., Cambridge, MA, [2]ICON Clinical Research, Inc., Portland, OR

Comprehensive genomic profiling (CGP) of tumor sample using large targeted NGS panels (e.g. MSK-IMPACT) has been shown to allow the detection of biomarkers from hundreds of cancer relevant genes involved in targeted and immunotherapy. Illumina TruSight Oncology 500 (TSO500), a commercial CGP assay, allows concurrent analysis of DNA and RNA to simultaneously detect multiple types of variants across 523 genes. The assay is intended to detect single nucleotide variants (SNV), insertions and deletions (indel), and multinucleotide variants (MNV), copy number gain (CNV), tumor mutational burden (TMB) and microsatellite instability (MSI) in DNA, and fusions and splicing variants (exon skipping) in RNA. Here we aimed to validate TSO500 assay for its analytical performance on FFPE tumor samples. The validation samples include commercial controls, cell lines, clinical FFPE from NSCLC, CRC, Uterus and GIST (tumor content ≥20%). Library preparation was performed from minimum of 40 ng DNA and 40ng RNA. The data analysis is performed using TruSight Oncology 500 Local App software (LRM v2.2). A custom script (v1.0) was used to add SNP annotation for small variants and combine data output into cumulative format. For SNV and indel detection QC, 61 of 64 DNA libraries (95%) passed the QC for library size (median insert size ≥70bp) and coverage (median exon coverage ≥150). The percentage of DNA libraries passing QC for CNV and MSI are 95% and 88%, respectively. All 64 RNA libraries passed QC. The analytical performance of TSO500 was summarized in the Table below. In summary, the results showed that all the acceptance criteria were met and the TSO500 assay can be utilized for genomic profiling of FFPE tumor samples. The study also identified a few limitations of the Illumina LRM software e.g. potential false positive SNV within a indel background, potential false negative of complex indel, and the challenge of long indel detection.

Summary of analytical performance of TSO500

	Sensitivity and specificity	Assay LoD	Accuracy by concordance	Inter-run reproducibility
SNV/Small indel	Sensitivity for SNV and indel detection are 99.24% and 99.36%. Specificity for SNV and small indel detection are 99.9998% and 100.00%, respectively.	The LoD for SNV is 3-5%, for DEL is 5-10% and for INS is 3-5%.	PPA for SNV detections is 96.64% (115/119; 95% CI: 91.68%, 98.69%) and for small indel is 92.86% (13/14; 95% CI: 68.53%, 98.73%) between TSO500 and comparator assays.	The positive call rate across all SNV and small indel variants is 98.7% (42842/43419).
MSI	Sensitivity and Specificity for MSI detection are both 100%.	NA	MSI status for all samples were detected with 100% of concordance by three assays; PPA is 100% (95% CI: 51.01%, 100%) and NPA is 100% (95% CI: 34.24%, 100%).	MSI concordance for MSI-H is 100% (95% CI: 60.97%, 100.0%) and for MSS is 100% (87.13%, 100.0%).
TMB	NA	NA	TSO500 reported TMB is well correlated and comparable to exome determined TMB.	The CV values for samples are acceptable.
CNV	NA	NA	All positive CNVs detected by the comparator assay were detected by the TSO500 assay with similar fold changes; PPA between TSO500 and OCAV3 assays is 100% (95% CI: 51.01%, 100%).	The overall reproducible call rate is 91.5% (43/47).
Fusion	Sensitivity and specificity for fusion detection is 91.94% and 100%, respectively.	NA	All TSO500 assay detected fusions were confirmed by other assays;PPA is 100% (95% CI: 60.97%, 100%) and NPA is 100% (95% CI: 75.75%, 100%)	The reproducibility of fusion call is 92.59% (25/27; 95% CI: 76.63%, 97.94%).
Splicing	Sensitivity and Specificity for splicing variant detection are 91.67% and 100.00%, respectively.	NA	The splicing variant detections were confirmed by OCAV3, OFA and Archer assays; PPA is 100% (95%% CI: 20.65%, 100%) and NPA is 100% (95% CI: 83.18%, 100%)	The overall reproducibility of positive call is 100% with 95% CI (43.85%, 100%) and negative call reproducibility is 100% with 95% CI (87.13%, 100%).

#0341 Co-detection of BCR::ABL1 common and atypical fusion and mutation using a novel NGS assay, Dup-Seq BCR-ABL1.

J. Li[1], Z. Yan[1], L. Shi[1], W. Li[1], W. Liu[1], C. Spittle[1], C. Galderisi[2];
[1]ICON Clinical Research, Inc., Cambridge, MA, [2]ICON Clinical Research, Inc., Portland, OR

The clinical management of CML and Ph+ ALL patients requires the identification of BCR::ABL1 transcript variants and drug resistance mutations. Currently these assessments need to be performed using separate assays resulting in higher sample requirements, longer turnaround times and higher costs. In this study a custom NGS assay (Dup-Seq BCR-ABL1) was developed and validated that enables co-detection and identification of transcript variants (common and atypical) and resistance mutations. The assay design covers BCR exon 1 to ABL1 exon 10 and employs duplicate PCR amplification of BCR-ABL1 from a single source of the 1st strand cDNA initiated by ABL1 specific priming. The custom data analysis pipeline enables overlapped mutation calling from duplicates as well as transcript determination. The assay minimizes the low-level artifacts that can be seen with other NGS-based BCR::ABL1 assays. This study demonstrates that the Dup-Seq BCR-ABL1 assay achieves high accuracy (PPA for fusion: 0.985; PPA and NPA for mutation at 0.978 and 0.9999, respectively) and sensitivity (LoD for mutation detection at 3% from 10,000 copies of BCR-ABL1 input). The use of the Dup-Seq BCR-ABL1 assay for both transcript variant identification and mutation detection provides comprehensive and accurate results for the clinical management of CML and Ph+ ALL patients while reducing sample requirements, testing costs and turnaround time.

MOLECULAR/CELLULAR BIOLOGY AND GENETICS: Apoptosis and Ferroptosis
Poster Session

#0346 Trop-2 induces apoptosis via transcriptional activation of TRAIL, FAS-FASL, CD40-TNFRSF5.

S. Alberti[1], E. Guerra[2], A. Moschella[1], M. Ceci[2], L. Pantalone[2], R. Di Pietro[2], M. Trerotola[2];
[1]University of Messina, Messina, Italy, [2]University of Chieti-Pescara, Chieti, Italy

Trop-2 is a transmembrane signal transducer that activates cancer growth and metastatic diffusion (1). However, this does not occur in all tumor types, as Trop-2 is associated to better disease outcome in some cancers, e.g. breast and lung tumors. A prototypic pattern of Trop-2 expression in normal multistratified epithelia, e.g. epidermis, esophagus, is that of preferential expression in non-proliferating, terminally differentiated cells. The corresponding expression gradient parallels that of induction of programmed cell death, e.g. in the corneum layer of skin keratinocytes. This led us to explore Trop-2 function as a trigger of apoptosis. We thus assessed NS-0 myeloma Trop-2 transfectants for apoptosis induction by dynamic cell morphometry and quantification of membrane blebbing and cell fragmentation. This was shown to be preceded by phosphatidyl-serine membrane exposure, and was followed by nuclear pyknosis and karyorrhexis. DNA fragmentation was shown by TUNEL and DNA laddering, and was accompanied by a dramatic increase of apoptotic death of Trop-2-expressing cells. Transcriptomic analysis at early time points of apoptosis induction indicated overexpression of TRAIL, FAS/FASL and CD40/TNFRSF5 transmembrane death receptors. This paralleled upregulation of downstream death-inducing signaling complex components and of executioner Caspases 8 and 3, suggesting Trop-2 as a trigger of extrinsic apoptosis pathways. Apoptosis induction translated into diminished tumor growth in vivo, which was shown to be proportional to Trop-2 expression levels. However, apoptosis induction was found to parallel stimulation of NS-0 cell growth and of defence mechanisms from apoptosis, as increased levels of inhibitory transcription factors, Rb-binding protein, survivin, Myd-118. These findings suggest a previously unappreciated balance between stimulation of cell growth and triggering of cell death by Trop-2, and may pave the way for selective anticancer therapy approaches in Trop-2-expressing cancers.(1) Trerotola M. *et al.*, Neoplasia 23: 415-428 (2021).

#0347 Tumor necrosis factor related apoptosis inducing ligand (TRAIL)-induced cytokine production in TNBC promotes neutrophil chemotaxis and immune suppression.

M. Kundu[1], Y. E. Greer[1], L. A. Ridnour[2], D. Wink, Jr.[2], Y. S. Ng[1], R. Weigert[1], S. Lipkowitz[1];
[1]National Institute of Health, Bethesda, MD, [2]National Institute of Health, Frederick, MD

Background: TRAIL induces apoptosis in many preclinical cancer models including breast cancers and has been extensively studied as a potential cancer therapeutic. However, its efficacy in clinical trials is limited, suggesting an unknown modulatory mechanism responsible for lack of TRAIL activity *in vivo*. Here, we describe that TRAIL treatment elicits transcriptional changes in TNBC cells that alter the immune milieu.
Method: We performed RNAseq of MDA-MB-231 cells treated with TRAIL for different time points, followed by validation with RT-PCR in various TNBC cells. RNAi, silencing key differentially regulated genes, along with RT-PCR, ELISA and CHIP assays, were used to validate RNAseq findings. Elucidation of the functional relevance of the outcome was supported both *in vitro* and *in vivo* by chemotaxis assay, cytotoxicity assay, RNAseq analysis of donor isolated neutrophils and intravital microscopy, CODEX analysis in TNBC xenografts from mice treated with the TRAIL respectively.
Results: TRAIL treatment of the TNBC significantly induced expression of several cytokines, such as CXCLs 1, 2, 3, 8,11 and IL6, both *in vitro and in vivo* which are known to affect neutrophil function. Mechanistically, induction of these cytokines was predominantly mediated by death receptor 5 and caspase-8 protein, but not caspase-8 enzymatic activity. GSEA of the RNAseq data indicated that NFKB pathway was significantly enriched. Concordantly, we confirmed that both canonical NFKB1 and non-canonical NFKB2 pathways were activated by TRAIL in *vitro and in vivo*. However, the induction of the cytokine mRNAs was primarily dependent on the NFKB2 pathway. Neutrophils isolated from healthy human donors incubated with supernatants from TNBC cells *in vitro* indicated that TRAIL-induced CXCLs and IL6 significantly increased neutrophil chemotaxis. Additionally, CODEX analysis as well as intravital imaging confirmed that TRAIL treatment increases the number of neutrophils in the tumor. Preincubation of neutrophils with supernatants from TRAIL-treated TNBC significantly inhibited their cytotoxic effect against TNBCs. Further, transcriptome analysis of neutrophils incubated with either TRAIL or supernatant of TRAIL treated TNBC revealed significant enrichment of expression of inflammatory cytokine genes, immune modulating and immune checkpoint genes like PDL1. Functional studies with these neutrophils confirmed their suppressive effect on T cell function as well as the effect of TRAIL on decreased neutrophil apoptosis.
Conclusion: Collectively, our study suggests the novel role of TRAIL-induced NFKB2-dependent cytokine production promoting neutrophil chemotaxis and immune suppression. This study implies that alterations in the innate immune system may modulate the effects of TRAIL on TNBC tumors.

#0349 The role of RELTfms and FLNA in human cancer and cellular apoptosis.

E. Chou[1], E. Chang[1], I. Abed[1], A. Christensen[1], K. Nguyen[1], A. Yanumula[1], Y. Shyu[1], A. Abram[1], J. Alcaide[1], G. Cusick[1], M. Batiste[1], Y. Shi[2], E. Mohammed[1], J. Cusick[1];

[1]California Northstate University, Elk Grove, CA, [2]California Pacific Medical Center Research Institute, San Francisco, CA

Receptor Expressed in Lymphoid Tissues (RELT) is a Tumor Necrosis Factor Receptor family member implicated in several cancers. RELL1 and RELL2 (RELT-Like 1 and 2) are RELT homologs that bind RELT; the three proteins are collectively referred to as RELT family members (RELTfms). We sought to evaluate the role of the OXSR1 kinase and actin-binding protein Filamin A (FLNA) in modulating RELT-induced apoptosis of cancer cells. We also assessed RELTfm expression in human breast and lung cancer biopsies and their ability to sensitize breast cancer cells to chemotherapeutic agents.

Methods: Empty vector or expression plasmids for RELTfms were transiently transfected into MDA-MB-231 (231) breast cancer cells with TransfeX reagent. Cell death was assessed by morphology assays and ATP luciferase assays. Apoptosis of 231 cells was assessed by Annexin V/PI staining using Flow cytometry (FC). Immunohistochemistry (IHC) was used to assess RELT expression in human breast and lung cancer biopsies. IHC and western blotting were utilized to determine RELT cellular localization.

Results: All three RELLfms were co-immunoprecipitated by a C-terminal fragment of FLNA. RELT overexpression induced death in 231 cells, and this effect was increased with co-transfection of a FLNA S215A mutant, an important phosphorylation site that protects FLNA from cleavage. 231s transfected with RELT and RELL2 demonstrated increased Annexin V/PI signal in comparison to vector control, demonstrating that these RELTfms induce death via an apoptotic pathway. Co-transfection of a mutated plasmid for the OXSR1 kinase did not abrogate RELT-induced apoptosis. A RELT construct with a mutated binding site for the OXSR1 kinase induced apoptosis to a similar extent as wild-type RELT. An increase in doxorubicin-induced apoptosis was observed when 231 cells were transfected with RELL2 versus vector control. IHC results showed increased RELT expression in malignant breast cancer biopsies compared to patient-matched benign tissue. Interestingly, RELT was localized in the nucleus of some malignant lung cancer biopsies, and western blot analysis indicates that RELT translocates to the nucleus and interacts with chromatin in 231 cells.

Conclusions: Collectively, these results demonstrate that RELTfms induce apoptosis of breast cancer cells, and potentially increase the sensitivity of breast cancer cells to chemotherapeutic agents. Furthermore, this work enhances our understanding of the interaction between RELT and FLN, a protein that is implicated in many cancers, including breast cancer. Phosphorylation by OXSR1 was previously shown to be required for RELT to activate the p38 pathway, yet the OXSR1 kinase is not required for RELT-induced death. RELT expression is enhanced in breast cancer biopsies, and interestingly, RELT can localize to the nucleus in cancerous cells. Collectively, these findings significantly enhance our understanding of RELTfms and cancer.

#0350 Targeting prohibitins by fluorizoline leads to the activation of ISR and apoptosis through DELE1 and HRI by an impairment of the mitochondrial protein import machinery.

I. Sanchez-Vera[1], N. Maritorena-Hualde[1], M.-H. Schuler[2], A.-. Cosialls[1], R. Lavilla[1], G. Pons[1], L. Jae[2], D. Iglesias-Serret[1], **J. Gil**[1];
[1]Universitat de Barcelona, Barcelona, Spain, [2]Ludwig-Maximilians-Universitat Munchen, Munchen, Germany

Prohibitins are ubiquitously expressed within the cell, but they are mainly located at the inner mitochondrial membrane. These proteins are closely associated with tumour progression, invasion, and apoptotic resistance, being overexpressed in various primary tumours such as lymphoma and endometrial cancer. Notably, we have developed a novel synthetic molecule, fluorizoline, which induces apoptosis by selectively targeting PHBs in different cancer cell lines and primary samples from various haematological neoplasias. We have previously described that fluorizoline-induced apoptosis is mediated through the activation of the pro-apoptotic branch of the integrated stress response (ISR) pathway in HeLa and HAP1 cells, concretely, by the ATF4-CHOP-NOXA axis. In a recent study, we identified compensatory mechanisms for four ISR-related kinases. Importantly, HRI emerged as the primary kinase responsible for activating this pathway and promoting apoptosis, suggesting that mitochondrial stress could lead to this activation of the ISR.Here, we investigate the OMA1-DELE1-HRI molecular pathway responsible for sensing mitochondrial stress and activating the ISR cancer cell lines. Firstly, we demonstrate that fluorizoline treatment triggers the cleavage of large DELE1 (L-DELE1) to its cleaved form (S-DELE1) through western blot analysis, and its subsequent sorting to the cytosol as confirmed by confocal analysis. Using DELE1 KO lines generated by CRISPR/Cas9 technology, we demonstrate that DELE1 is involved in the activation of the ISR and apoptosis induced by fluorizoline. However, although we cannot rule out OMA1 involvement, fluorizoline-induced ISR activation does not strongly depend on OMA1. Interestingly, our data suggests that targeting PHBs, either by fluorizoline or by their downregulation, could result in mitochondrial protein import machinery impairment. This impairment may potentially be the cause of DELE1 accumulation in the cytosol, leading to the subsequent activation of the ISR by HRI upon fluorizoline treatment.

#0351 Quaratusugene ozeplasmid mediated TUSC2 upregulation in EML4-ALK bearing non-small cell lung carcinoma can induce cellular apoptosis.

A. Banerjee[1], N. Busette[1], M. S. Berger[2], M. B. Soellner[1], A. Qin[1], S. D. Merajver[1], N. M. Merrill[1];
[1]University of Michigan, Ann Arbor, MI, [2]Genprex, Inc., Austin, TX

Anaplastic Lymphoma Kinase (ALK), a potent oncogenic driver in Non-Small Cell Lung Carcinoma (NSCLC), is found to be rearranged and fused to Echinoderm microtubule-associated protein-like 4 (EML4), contributing to approximately 5% of NSCLC as a distinct clinicopathological subset. Tumors bearing the EML4-ALK fusion are sensitive to ALK Tyrosine Kinase Inhibitors (TKIs), that form the first and second line of treatment for these patients. However, ALK+ lung cancers develop resistance to ALK inhibitors, creating the need for newer treatment strategies in ALK+ NSCLC. Tumor Suppressor Candidate 2 (TUSC2) is a tumor suppressor gene that is known to have low endogenous expression in NSCLC in general but data on TUSC2 in ALK+ lung cancers are not available. Quaratusugene ozeplasmid, developed by Genprex, is an immunogene therapy that upregulates TUSC2 expression in cancer cells by delivering the functional TUSC2 gene. It consists of the TUSC2 gene expressing plasmid encapsulated in non viral lipid nanoparticles. We evaluated TUSC2 expression in 3 ALK+ cell lines, both before and after exposure to quaratusugene ozeplasmid and to a TUSC2-containing plasmid. Controls were non-ALK+ cell lines and transfection with a plasmid containing no insert. Our studies in ALK+ lung cancer reveal that overexpressing TUSC2 using quaratusugene ozeplasmid treatment of ALK+ lung cancer cell lines is able to suppress colony formation by 50%, the effect being more significant than using a TUSC2-containing plasmid. Furthermore, we have observed a robust pro-apoptotic response to TUSC2 expression in ALK+ NSCLC, as both quaratusugene ozeplasmid and TUSC2-containing plasmid induced an increase in caspase 3/7 activity in the cancer cells, accompanied by an increase in cleaved PARP expression. Taken together, our data indicate that overexpression of TUSC2 in ALK+ NSCLC cell lines with quaratusugene ozeplasmid or with TUSC2-containing plasmid is effective in decreasing growth and proliferation through the activation of apoptotic pathways and warrants further investigation as an anti-ALK NSCLC strategy.

#0353 Investigate the role of homoharringtonine in treating B-cell acute lymphoblastic leukemia.

Emilie An An Jiao, Kei Ching Yuen, Bai Lin Li, Chun Fung Sin

Pathology, University of Hong Kong, The - Li Ka Shing Faculty of Medicine, Pok Fu Lam, Hong Kong

B lymphoblastic leukemia (B-ALL) is an aggressive and highly lethal hematolymphoid malignancy and it is the most common cancer in children. Although the incidence of B-ALL in adult is lower than that in children, adult patients with B-ALL have a poor prognosis. Relapse/refractory disease is still the main cause of death in B-ALL patients. Homoharringtonine (HHT) is a plant alkaloid that was approved to treat chronic myeloid leukemia (CML) by FDA. Herein, we aimed to investigate the anti-leukemic activity of HHT in B-ALL. Cell viability was reduced in a time and dose-dependent manner upon treatment with HHT. Moreover, HHT was able to induce apoptosis in B-ALL cell lines by downregulating the MCL-1 protein level after 24 hours of treatment. Cell cycle analysis indicated G1 phase arrest, and western blot analysis demonstrated downregulation of CDK-4 and CDK-6. A proteomics study using label-free protein quantitation revealed enrichment of proteins involved in fatty acid oxidation, and further analysis showed downregulation of acyl-CoA desaturase after HHT treatment. Additionally, HHT significantly reduced the leukemic burden and prolonged survival in NSG mice injected with the PALL-2 cell line. Overall, the findings suggest that HHT is effective in treating B-ALL by inducing cell cycle arrest, with a potential inhibitory effect on fatty acid oxidation. Further studies will be conducted to evaluate the mechanism of modulation of fatty acid oxidation.

#0355 BCLxL inhibition enhances copanlisib response in colorectal cancer.

A. E. Schmitz, R. A. DeStefanis, A. K. DeZeeuw, A. M. Olson, A. L. Lippert, K. J. Maduscha, K. A. Johnson, S. Kraus, C. A. Pasch, D. A. Deming;
University of Wisconsin - Madison, Madison, WI

Background: Anti-apoptotic signaling, including through BCLxL, is a potential mechanism of resistance to PI3K inhibition in *PIK3CA* mutant cancers. We have previously demonstrated enhanced activity of PI3K inhibition in combination with BCLxL inhibition in *PIK3CA* mutated colorectal cancer (CRC) models. Here we examine the potential impact of BCLxL expression in *PIK3CA* mutant CRCs and the mechanism of treatment response with the combination of copanlisib and navitoclax.

Methods: *PIK3CA* mutant CRCs were identified within TCGA colorectal adenocarcinoma data set and two cohorts were generated based on *BCL2L1* (gene that encodes protein BCLxL) expression. Differentially expressed genes and gene set enrichment analysis were performed. CRC cell lines SW48 and SW48PK (Horizon Discovery, SW48 with a *PIK3CA*$^{H1047R/+}$ mutation) were treated with copanlisib (copan) (1-100 nM) and navitoclax (250 nM). Immunoblotting was performed quantified using ImageJ to evaluate PI3K and apoptotic signaling. Flow cytometry using annexin V and propidium iodide (PI) was performed as a measure of apoptosis. Immunohistochemistry (IHC) using Ki67 was performed as a measure of cell proliferation on SW48PK xenografts and quantified as percent positive nuclei at 40x field of view (FOV).

Results: Two datasets comprised of *PIK3CA* mutant CRC patients with either high or low *BCL2L1* expression containing 39 and 47 patients, respectively, were used in the TGCA analysis. There was no difference in age, gender, or staging between these two datasets. An increase in DNA repair (false discovery rate q-value= 0.034) and interferon alpha signaling pathways (q= 0.022) was seen in *PIK3CA* mutant and high *BCL2L1* expression compared to *PIK3CA* mutant and low *BCL2L1* expression patients. *PIK3CA* mutant patients with low expression of *BCL2L1* had a greater disease-free and overall survival (p= 0.037 and p= 0.042, respectively). Combination of copan and navitoclax treatment of the SW48 and SW48PK cell lines resulted in a reduction in activated ribosomal protein S6 (pRPS6) as compared with control or navitoclax alone at both 6 and 24. Cleaved PARP increased in SW48PK cells treated with 100 nM copan plus navitoclax versus control at both 6 and 24 hour timepoints (p= 0.03, p= 0.049). SW48 and SW48PK cells that were treated with copan and navitoclax for 24 hours had an increase in annexin v, a marker for apoptosis, compared to cells treated with control or single agents. In SW48PK xenografts, a significant reduction in Ki67 percent positive nuclei was seen in combination compared to control (median percent positive nuclei: 20.5, control: 33.2, p<0.001).

Conclusions: High BCLxL expression is a sign of poor prognosis for *PIK3CA* mutant CRC. Inhibiting BCLxL can enhance the sensitivity of PI3K inhibition in *PIK3CA* mutant cancers and deserves further investigation clinically.

#0356 Developing a multiplex assay to monitor apoptosis and necrosis using the Cellaca® PLX Image Cytometer.

J. Mukherjee, M. Pierce, Y. Huang, A. Lin, L. L. Chan;
Revvity Health Sciences, Inc., Lawrence, MA

Apoptosis is a critical pathway for programmed cell death that cancer cells can evade to ensure survival. For pharmaceutical drug discovery, it is important to characterize and compare cancer therapeutics (i.e., small molecules, antibody drugs, cell therapies) that can initiate the process of apoptosis, allowing for the identification of potential therapeutic candidates. In this work, we developed and demonstrated a multiplex detection method for monitoring apoptosis and necrosis with Annexin V, Caspase 3/7, and Propidium Iodide (PI) using the Cellaca® PLX Image Cytometer. First, apoptosis was induced in Jurkat and K562 cell lines with staurosporine over the course of 24 h, and were monitored at 0, 1, 1.5, 2, 4, 20, and 24 h timepoints. Samples were stained with Hoechst 33342 (total dye), Annexin V-APC (early-stage apoptosis), Caspase-3 488 (late-stage apoptosis), and PI (necrosis) at each timepoint and evaluated using the Cellaca® PLX. Results showed that apoptotic factors and cascades were successfully detected along the pathway from early to late-stage apoptosis, and ultimately necrosis. A clear trend was observed during the first 2 h showing differences of up to 25% between the single Annexin V+ and Caspase-3+ populations in treated Jurkat cells, however, a significant increase in double positive apoptotic/necrotic cells for Annexin V+PI+ and Capase-3+PI+ was not observed until 20 h. Upon further analysis amongst apoptotic populations, Annexin V+ only populations were higher than Caspase-3+ only populations by up to 30% between 0-2 hours. Conversely, K562 cells did not exhibit a notable change in apoptotic and necrotic populations due to low sensitivity to staurosporine. The proposed image-based detection method using the Cellaca® PLX may provide an effective and efficient tool for rapid and reliable simultaneous detection of early, late-stage apoptosis, and necrosis. This may allow researchers to better characterize and screen potential cancer therapeutic drug candidates in a high-throughput manner to determine their treatment efficacy.

#0357 Reducing reagent-resistant transferrin receptor 1 dimer is a specific marker for ferroptosis.

J. He[1], M. Kelleher[1], L. Reynolds[1], H. Tanczos[1], Z. Huang[1], B. McLaughlin[1], W. Huang[2], L. Pope[3], G. Veeckmans[4], T. Vanden Berghe[4], S. J. Dixon[3], Y. Shah[2], Z. T. Schafer[1];

[1]University of Notre Dame, Notre Dame, IN, [2]University of Michigan, Ann Arbor, MI, [3]Stanford University, Stanford, CA, [4]University of Antwerp, Antwerp, Belgium

Ferroptosis is an iron-dependent cell death caused by the catastrophic accumulation of lipid peroxidation. Despite the burgeoning ferroptosis research, there remains a void for an intrinsic and comprehensive ferroptosis indicator. Here we reported a simple and cost-effective way to detect ferroptotic cell death using reducing reagent-resistant (RRR) transferrin receptor 1 (TfR1). The TfR1 RRR dimer strongly correlates with ferroptosis induced by various ferroptosis-inducing conditions and relies on lipid peroxidation, which is not observed in other types of cell death. Through iron-overloading and tumor xenograft mouse models, we validate the in vivo ferroptosis detection using this technique. Furthermore, we identify the presence of TfR1 RRR dimers in extracellular vesicles isolated from the plasma of mice with ferroptosis-related diseases. Since TfR1 is a ubiquitously expressed protein, the increase of TfR1 RRR dimer can be used as a specific and endogenous ferroptosis marker with potential clinical applications.

#0358 Ferroptosis modulates melanoma progression in an age-specific manner through changes in the tumor microenvironment.

M. R. Rocha, Y. Chhabra, L. Huser, E. I. Harper, A. Dixit, V. Wang, A. E. Carey, C. Palm, F. Huang, A. T. Weeraratna;
Johns Hopkins Bloomberg School of Public Health, Baltimore, MD

Aging is an independent prognostic factor for melanoma, the most aggressive form of skin cancer. Although immune therapy has shown a dramatic improvement in melanoma treatment, resistance to it still occurs in some patients. Higher oxidative damage in tumor cells as well as lipid and iron accumulation are singular characteristics of the aged tumor microenvironment (TME). Here, we investigate the impact of these characteristics of the aged TME in the promotion of ferroptosis, a caspase independent iron mediated type of cell death, and as possible modulators of the response to checkpoint blockade therapy. Lipid peroxidation levels were assessed through immunohistochemical staining for the marker 4-HNE in tumors of young and aged mice injected intradermally with Yumm1.7 cells.Correlation analysis between transcriptomic data (TCGA-SKCM) was performed to identify common denominators among proteins associated with the aged TME, ferroptosis pathway and IFN-y signaling. Our in vitro experiments consisted of viability assays with combinations of IFN-y, young and aged skin fibroblast conditioned media (CM), arachidonic acid (AA) or ferroptosis inducers such as RSL-3. Protein levels of ferroptosis related markers in melanoma cells treated with fibroblast conditioned media, and in Wnt5a high/low cell lines were analyzed through western blot (WB). Tumors from aged mice showed stronger staining with 4-HNE antibody when compared to young. Wnt5a (present in the aged TME) showed a strong correlation with several ferroptosis related transcripts. WB analysis of Wnt5a high/low lines indicate differences in GPX4, FTL1, SLC3A2, GCH1 and DHODH. Wnt5a levels show an inverse correlation with ferroptosis resistance and anti-ferroptotic proteins. Our data indicate that aged TME favors ferroptosis death in melanoma cells. To understand how ferroptosis impacts tumor growth in young and aged mice, we used a syngeneic tumor model injecting Yumm1.7 cells intra-dermally in mice and treated with a lipid peroxidation inhibitor, Liproxstatin, or an ferroptosis inducer, IKE. Liproxstatin lead to reduced tumor growth only in young mice followed by changes in immune cell populations such as monocytes and macrophages. IFNy induction of these events might be associated with changes in proteins of the pathway or alterations in fatty acid uptake as suggested by lipid accumulation and AA potentiation of its cytotoxic effects. Further exploration of ferroptosis will impact our understanding on how aged TME modulates immune cell killing and provide evidence to target or revert resistance to checkpoint blockade therapy associated with an IFN-y signature and new strategies for treatment of older patients.

#0359 The Hippo pathway on breast tumor recurrence <and> collateral vulnerability to ferroptosis.

C.-C. Lin, J.-T. Chi;
Duke University, Durham, NC

Comparing with primary breast tumors, recurrent breast cancers are generally considered more aggressive and incurable. Therefore, novel molecular strategies are urgently needed to target these type of cancers. Here, we report that murine recurrent breast tumor cells are highly susceptible to ferroptosis, a novel form of cell death. Discoidin Domain Receptor Tyrosine Kinase 2 (DDR2), the receptor for collagen I, is upregulated in ferroptosis-sensitive recurrent tumor cells. Ferroptosis inducer, erastin treatment leads to DDR2 upregulation and phosphorylation, independent of collagen I. Furthermore, DDR2 silencing not only prevent ferroptosis but also abolished the robust cell proliferation of murine recurrent tumor cells. Both the ferroptosis protection and reduction of active cell growth may be compatible with the compromised YAP/TAZ upon DDR2 inhibition. Collectively, these findings suggest the role of DDR2 in recurrent breast tumors to drive aggressive cell growth but at the same time reveals its weakness to YAP/TAZ-mediated ferroptosis, providing potential molecular mechanism to target recurrent breast cancers.

#0360 Dissecting the role of oncogenic KRAS and ferroptosis within colorectal cancer.

A. Rosa-Vazquez[1], V. Bernard-Pagan[2], J. Chen[2], C. Taniguchi[2];
[1]Universidad Central del Caribe School of Medicine, Bayamon, PR, [2]The University of Texas MD Anderson Cancer Center, Houston, TX

Introduction: Ferroptosis is a novel iron-dependent regulated cell death mechanism triggered by a toxic accumulation of membrane lipid peroxidation. This mechanism is counteracted by ferroptosis defense systems, such as the GPX4/GSH system, which function as antioxidants that limit lipid peroxidation. Oncogenic KRAS ($KRAS^{mut}$) is a key driver for many aggressive cancers, including colorectal cancer (CRC). Previous studies have suggested that oncogenic KRAS plays a pleiotropic role in the ferroptosis pathway. Yet, the interplay between oncogenic KRAS and ferroptosis has not been fully elucidated in CRC. Here, we aimed to dissect the role of oncogenic KRAS in ferroptosis using CRC as a cancer model.
Methods: Cells from a KRAS-inducible model (iKAP) were seeded and treated with ferroptosis-inducing drugs (e.g., Erastin and RSL3) and/or a KRAS inhibitor (MRTX1133). Lipid peroxidation was then measured by BODIPY assay followed by flow cytometry to detect the quantity of BODIPY-stained cells. Protein expression of known ferroptosis defense mechanisms was also profiled (e.g., SLC7A11 [xCT] and GPX4).
Results: Results from this study demonstrate that $KRAS^{mut}$ activation leads to a reduction in mean fluorescence intensity when compared to $KRAS^{WT}$ of BODIPY-stained cells. This decreased mean fluorescence intensity is indicative of lower levels of lipid peroxidation and, consequently, ferroptosis. $KRAS^{mut}$ cells were also found to be resistant to ferroptosis following treatment with ferroptosis inducers. To replicate a pharmacologically induced $KRAS^{WT}$ phenotype, iKAP cells were treated with MRTX1133, which led to a significant decrease in viability when combined with RSL3. We observed a decreased protein expression of the membrane antiporter xCT following treatment with MRTX1133, which we believe works synergistically with the GPX4 inhibition of RSL3.
Conclusion: We observed that $KRAS^{mut}$ may induce resistance to ferroptosis *in* vitro in CRC cells. Genetic and pharmacological inhibition of KRAS resulted in sensitization to ferroptosis inducers. Future work will uncover mechanisms through which oncogenic KRAS leads to ferroptosis resistance in CRC. More importantly, understanding the interaction between ferroptosis, oncogenic KRAS, and its antagonist systems has significant therapeutic potential in oncology.

#0361 Targeting the suppressor of ferroptosis to improve the treament effeciency of glioblastoma.

J. Wang;
Sun Yat-sen University Cancer Center (SYSUCC), Guagnzhou, China

Glioma is the most frequent tumor in central nervous system (CNS), which makes up about 30% of CNS tumors. The current standard strategy for glioma treatment is surgery plus adjuvant chemotherapy and concurrent radiotherapy. Even though, the prognosis of glioma is still poor. It's encouraging that temozolomide (TMZ) prolongs the overall survival of glioma patients, but the following TMZ resistance is really frustrating. It's urgent to figure out efficient ways to improve the long term prognosis of patients, such as antagonizing the TMZ resistance. Ferroptosis was a newly discovered type of regulated cell death characterized by iron-dependent aberrant lipid peroxidation and membrane damage in the last decade. Ferroptosis-associated iron transport proteins modulate the process precisely through controlling the iron content. ZIP14, also known as SLC39A14, is an eight-transmembrane protein which could transport divalent metal ion like Mn^{2+}, Zn^{2+} and Fe^{2+}. Our preliminary data showed that the expression level of ZIP14 was higher in tumor tissues than paired normal tissue, which was corelated with poor prognosis of glioma. Knock down ZIP14 could induce cell death, and which could be rescued by inhibitors for ferroptosis but not for apoptosis or necrosis. Knock down ZIP14 decreased the ferroptosis inhibition by Ferroptosis suppress protein 1 (FSP1) which through reduction of lipid peroxidation, and sensitized cells to TMZ. Furthermore, we found that ZIP14 formed a complex with Ubiquinone. And it was known that FSP1 is critical in the switch of ubiquinone to ubiquinol. Therefore, we propose that ZIP14 suppress lipid peroxidation through blockage of the transition of ubiquinone to ubiquinol. While ZIP14 was knocked down, the complex with Ubiquinone wad damaged, and could not further change to Ubiquinol, so the suppression to lipid peroxidation was released, and then, ferroptosis was upregulated. In this study, we are going to figure out the molecular mechanism about how ZIP14 suppress ferroptosis and find out efficient small molecule inhibitors to activate ferroptosis by abolishing ZIP14 and improve the prognosis of glioma patients.

#0362 Arsenic sulfide triggers ferroptosis in hepatocellular carcinoma cells via TRPC6/GPX4 signaling.

S. Lu, Y. Cai, C. Zhu, Z. Feng, S. Chen, S. Chen;
Xin Hua Hospital, School of Medicine, Shanghai Jiao Tong University, Shanghai, China

Background: Ferroptosis is critically involved in the pathological process of various human diseases, including cancer. Due to this, ferroptosis-inducing drugs are gaining more attention for the clinical treatment of tumors.
Methods: The cell counting kit-8 (CCK-8) assay was conducted to observe cell viability of hepatocellular carcinoma (HCC) cell lines. Ferroptosis was determined by levels of Fe^{2+}, lipid reactive oxygen species (ROS), malondialdehyde (MDA) and transmission electron microscopy. Enzyme-linked immunosorbent assay (ELISA), western blot, quantitative polymerase chain reaction and immunofluorescence staining were utilized to evaluate glutathione peroxidase 4 (GPX4) and transient receptor potential channel 6 (TRPC6). Co-immunoprecipitation assay was conducted to determine the binding between GPX4 and TRPC6.
Results: Arsenic sulfide initiated ferroptotic cell death in HCC cells, which was concomitant with ROS accumulation, lipid peroxidation, and GSH depletion. Arsenic sulfide -mediated cell death in HCC cells was blocked by ferroptosis inhibitors ferrostatin-1 (Fer-1), but not Z-VAD-FMK, necrosulfonamide, or chloroquine, suggesting that ferroptosis contributed to arsenic sulfide -induced cell death. Furthermore, TRPC6 expression was notably inhibited under arsenic sulfide intervention and the overexpression of TRPC6 rescued the effects of arsenic sulfide on cell viability and ferroptosis of HCC cells. Furthermore, GPX4 was identified to interact with TRPC6 through confocal microscopy images and co-immunoprecipitation assay.
Conclusion: Our findings led us to conclude that arsenic sulfide could be considered as a prospective drug for liver cancer treatment.

#0363 Genetic or pharmacological inactivation of CREBBP sensitizes B-cell acute lymphoblastic leukemia to ferroptotic cell death upon BCL2 inhibition.

A. Garcia Gimenez, J. Ditcham, D. M. A. Azazi, E. Meduri, R. Asby, N. Sakakini, C. K. Lopez, N. Narayan, J. Bagri, T. Beinortas, S. Agrawal Singh, G. Giotopoulos, M. P. Murphy, S. J. Horton, B. J. P. Huntly, S. E. Richardson;
University of Cambridge UK, Cambridge, United Kingdom

B-cell acute lymphoblastic leukemia (B-ALL) is an aggressive hematological malignancy of B lineage progenitors. It remains a leading cause of death in childhood, while outcomes in adults are dismal. There is therefore a need to better understand drivers of high-risk B-ALL and to develop novel therapeutic approaches targeting these challenging patient cohorts. Loss-of-function mutations affecting *CREBBP* are recurrent second-hit mutations across multiple genetic subtypes of B-ALL and are associated with adverse features, including high-risk genetic subtypes and persistent measurable residual disease. In addition, they have been mechanistically associated with chemoresistance and are more frequently found in relapse. We sought to identify novel treatment options for *CREBBP*-mutated high-risk B-ALL. *CREBBP*-mutated isogenic human B-ALL cell lines were genome-engineered to provide a platform for synthetic lethal drug screening. We subjected these cell lines to a targeted drug screen focused on clinically-actionable drugs in classes that have either been implicated or hypothesized to show differential sensitivity patterns in published models of B cell lymphoma and other *CREBBP*-mutated malignancies. Unexpectedly, *CREBBP*-mutated cells were not differentially sensitive to traditional cytotoxic chemotherapy, and paradoxically showed a degree of sensitization to the glucocorticoid Dexamethasone, used in current ALL induction regimens. As anticipated, and validating our screen design, inhibitors of the *CREBBP* paralogue *EP300* (the CREBBP/EP300-specific bromodomain inhibitor Inobrodib and the CREBBP/EP300 acetylase inhibitor A485) exhibited synthetic lethality, consistent with previous reports in B-cell lymphoma. The most potent hit was the BCL2 inhibitor Venetoclax, which we show acts through a non-canonical, but BCL2-dependent mechanism resulting in ferroptotic programmed cell death. *CREBBP*-mutated cell lines were transcriptionally and functionally characterized, revealing underlying differences in cell-cycle, metabolism and response to oxidative stress. Acquisition of resistance to Venetoclax further dysregulated these pathways and resulted in a transcriptionally-convergent state. Lastly, we demonstrate that small-molecule inhibition of CREBBP sensitizes B-ALL cells, regardless of genotype, to Venetoclax-induced ferroptosis *in vitro* and *in vivo*, providing a potential novel drug combination for broader clinical translation in B-ALL. In summary, we have identified a number of actionable compounds that specifically target *CREBBP*-mutated high-risk B-ALL, demonstrate a novel mechanism-of-action for the BCL2 inhibitor Venetoclax in B-ALL and propose CREBBP-inhibitors and Venetoclax as a novel treatment combination for B-ALL across genotypes.

#0364 Targeting LILRB1 to sensitize human myeloma to ferroptosis through disrupting cholesterol homeostasis.

M. Xian, Q. Yi, Q. Wang, L. Xiao, L. Zhong, c. zhang, y. Li, J. Qian;
Houston Methodist Hospital, Houston, TX

Multiple myeloma (MM) is a hematologic malignancy characterized by the uncontrolled clonal proliferation of plasma cells in the bone marrow (BM). Despite the demonstrated benefits of novel therapies, relapses are frequent, and acquired resistance to MM treatment eventually emerges in most, if not all, patients. MM patients who suffer more aggressive progression usually result in poorer survival. The genes driving such unfavored outcomes in MM have not been fully understood. Therefore, there is an urgent need to identify the genes and mechanisms that contribute to the aggressive behaviors of MM in order to develop improved therapeutic strategies for the disease. To discover new potential therapeutic targets for MM patients, we analyzed gene-profiling data of MM patients and identified leukocyte immunoglobulin-like receptor B1 (LILRB1), a transmembrane receptor conducting negative immune response, as one of the top-ranked genes associated with poor prognosis. LILRB1 on immune cells was reported to bind to its ligand, b2-microglobulin, on tumor cells. This interaction leads to immune suppression responses in various immune cells. However, the function of tumor-derived LILRB1 in tumor biology remains unclear and the role of LILRB1 in MM has been poorly studied. Our further analysis of the patient data demonstrated that MM patients with high expression of LILRB1 are closely related to higher MM recurrence rates, advanced stages, and lower survival rates, indicating that LILRB1 is an important player in MM pathogenesis and thus a promising target for MM therapy. Interestingly, RNA-seq data of human MM cells from the BM of MM-bearing mice showed that knockdown (KD) of LILRB1 activated cholesterol metabolism- and ferroptosis-related pathways in murine BM. Moreover, KD of LILRB1 significantly impaired tumor progression in murine models. Consistently, in vitro experiments also demonstrated that LILRB1 protected MM cells from ferroptosis inducer-caused lipid ROS and ferroptotic cell death, indicating that LILRB1 promotes the progression of MM cells by protecting them from ferroptosis. Further study were then conducted to reveal the underlying mechanism. LC-MS/MS analysis followed by co-IP demonstrated that LDLRAP1, an adaptor protein that interacts with LDLR, bound with LILRB1 and formed a complex together with LDLR. KD of LILRB1 inhibited LDL uptake by disrupting the interaction between LDLR and LDLRAP1 and triggering the compensatory cholesterol synthesis by upregulating the expression of SQLE that converted squalene to (S)-2,3-epoxysqualene. With less squalene to protect MM cells from lipid peroxidation, MM cells were more susceptible to the induction of ferroptosis. Thus, this study uncovers a novel function of LILRB1 in regulating cholesterol metabolism and protecting MM cells from ferroptosis during MM progression and implicates LILRB1 as a promising therapeutic target for MM patients.

#0365 Proteomic analysis of cytoplasmic lipid droplets and whole cell lysates reveal ferroptosis regulation by fatty acid synthase-derived lipid droplets in metastatic breast cancer.

C. Andolino[1], K. K. Buhman[1], M. F. Coleman[2], S. D. Hursting[2], M. Layosa[1], M. K. Wendt[1], D. Teegarden[1];
[1]Purdue University, West Lafayette, IN, [2]University of North Carolina, Chapel Hill, NC

Breast cancer remains a serious public health concern, where metastasis accounts for the majority of patient mortality. Lipid accumulation in metastases is associated with reduced treatment response and poorer patient outcomes, although the mechanisms linking lipid accumulation and metastasis are not clear. We previously demonstrated that metastatic MCF10CA1a breast cancer cells have higher *de novo* lipogenesis and cytoplasmic lipid droplets (CLDs) compared to non-metastatic MCF10A-*ras* cells. Additionally, fatty acid synthase (FASN)-derived TAG stores sustained key metastatic processes in the MCF10CA1a cells. The proteome of CLDs is diverse and plastic, reflecting differing CLD functions; therefore, we sought to identify proteins differentially abundant on CLDs from vehicle-treated and FASN-inhibited MCF10CA1a breast cancer cells. We performed untargeted, global proteomics analysis on whole cell lysates (WCLs) and CLDs from vehicle-treated and FASN-inhibited (TVB-3166) MCF10CA1a cells to determine protein pathways differentially enriched on CLDs. Together, 2,416 and 3,539 proteins were identified within CLD fractions and WCLs, respectively. Of the proteins identified in CLD fractions, ~30% (717) were commonly identified within both conditions. Interestingly, 1,571 proteins were unique to the CLD fraction from vehicle-treated cells, whereas only 19 proteins were unique to the CLD fraction from FASN-inhibited cells. Proteins unique to CLDs from vehicle-treated cells include those known to reduce cancer cell survival and progression, such as proteins involved in cadherin-binding and cell cycle regulation. Proteins known to reduce cancer progression that associate with CLDs may prevent them from functioning at their normal site of action. Interestingly, an inhibitor of ferroptosis, glutathione peroxidase 4 (GPX4), was only detected in the vehicle-treated CLD and WCL samples, whereas proteins that promote ferroptosis were more abundant on CLDs of the more migratory cells, although their levels between WCLs were similar. Taken together, these data suggested that the machinery for ferroptosis may be mislocalized in TAG-rich cells, thereby protecting them from ferroptosis. Indeed, FASN-inhibited cells had nearly 30% more intracellular iron compared to the vehicle-treated cells, an important prerequisite for ferroptosis, thus indicating higher levels of ferroptotic stress. Functionally, the vehicle-treated cells were 25% more readily rescued by N-acetylcysteine from ferroptosis induced by erastin than were FASN-inhibited cells, despite comparable sensitivity to erastin. These preliminary findings suggest that FASN-derived CLDs in metastatic cells may aid in protecting against ferroptosis to promote breast cancer progression.

MOLECULAR/CELLULAR BIOLOGY AND GENETICS: Cellular Stress Responses 1
Poster Session

#0369 In silico investigation of hypoxia and its association with disease outcome and ecDNA detection in TRACERx.

N. Sharma[1], C. Bailey[2], C. Richard[1], J. Kittel[1], W. K. Liu[1], A. M. Frankell[3], G. Satvrou[1], D. Moore[1], M. Sivakumar[1], M. J. Hanjani[1], C. Swanton[2], N. Kanu[1]; [1]UCL Cancer Institute, University College London (UCL), London, United Kingdom, [2]The Francis Crick, London, United Kingdom, [3]University of Cambridge, Cambridge, United Kingdom

Tumors exhibit dynamic gradients of oxygen diffusion and consumption leading to regions of hypoxia. The presence of hypoxia is associated with poor clinical prognosis and elevated genomic instability. Genes can be amplified extrachromosomally as ecDNA, which are acentric circular structures that can rapidly generate large genomic copy number amplifications. The amplification of oncogenes on ecDNA is unstable thus providing cells with an advantage to adjust and survive the changing environment. Here, we have analysed the effect of hypoxia on disease outcome and ecDNA formation in the multiregional longitudinal NSCLC TRACERx (TRAcking Cancer Evolution through therapy (Rx)) cohort. We have analysed next generation sequencing, clinical and histopathological data available from the tumours that were harvested at the time of surgery from patients recruited into the lung TRACERx study. Hypoxia was first quantified using the mRNA-based Buffa hypoxia gene signature. Complexheatmap from R-Bioconductor package was used for clustering based on mRNA expression of gene signature. Moreover, hypoxia scores for each region were established using the Gene Set Variation Analysis (GSVA) from R- Bioconductor package. The impact of hypoxia on overall and disease-free survival was performed using the survminer package. Histopathological data was used to study the association between hypoxia and necrosis. The genetic instability was analyzed using whole exome sequencing. The amplicon architect tool was used to study the association of hypoxia with ecDNA detection. Our preliminary results demonstrate that the extent of hypoxia varies widely both within and between primary tumours, suggestive of the presence of inter and intratumour hypoxia heterogeneity. High hypoxia status is associated with worse overall and disease-free survival in adenocarcinoma but not in squamous-cell carcinoma. The presence of necrosis in the primary tumour was associated with higher hypoxia. Moreover, higher hypoxia scores correlate with circulating tumour DNA (ctDNA) shedding in pre-surgery plasma samples (p value< 0.05). Higher hypoxia was significantly associated with increased wGII scores, indicative of genomic instability. Also, hypoxia resulted in increased detection of ecDNA in both lung adenocarcinoma and squamous cell carcinoma. In conclusion, there is inter and intratumoral heterogeneity in hypoxia levels in lung TRACERx. Moreover, the presence of hypoxia is associated with the detection of necrosis and ctDNA shedding. The increased genomic instability and detection of ecDNA in this study could be associated with the poor prognosis that is observed with hypoxic tumours and could merit further investigation.

#0370 BACH1 metastatic activity is regulated by oxygen-dependent proline hydroxylation in triple-negative breast cancer.

Thomas Li[1], Long Chi Nguyen[1], Christopher Dann[1], Madeline Henn[1], Dongbo Yang[1], Emily Shi[1], Lydia Robinson-Mailman[1], Kazuhiko Igarashi[2], Marsha R. Rosner[1]

[1]Ben May Department for Cancer Research, University of Chicago, Chicago, IL,[2]Tohoku University School of Medicine, Sendai, Japan

Hypoxia, low oxygen availability at the tissue level, is a key driver of metastasis in solid tumors. Oxygen-sensitive activation of hypoxia-induced transcription factors is in part regulated by prolyl hydroxylase domain proteins (PHDs). We and others previously showed that the BTB and CNC homolog 1 (BACH1) transcription factor promotes metastasis in various cancer types. In accompanying work, we show that BACH1 is prolyl-hydroxylated and degraded in an oxygen-dependent manner in triple-negative breast cancer (TNBC). Here we show that BACH1 lacking its hydroxylated proline sites (i.e., mutant BACH1) expressed in TNBC cells exhibits increased DNA binding to a canonical BACH1 binding site as well as greater transcriptional output of metastasis and hypoxia-response-related genes relative to wild-type BACH1. Furthermore, *in vivo* assays showed that mutant BACH1 promotes greater tumor metastasis of TNBC cells than wild-type BACH1. Our findings suggest that the proline hydroxylation of BACH1 directly regulates BACH1's transcriptional activity by modulating its DNA-binding activity. Together, these results reveal a mechanism underlying oxygen-sensitive regulation of BACH1 that could potentially contribute to BACH1-mediated pro-metastatic signaling and therapeutic resistance under hypoxia in TNBC.

#0371 Hypoxia-induced centrosome loss as a driver of chromosomal instability in prostate cancer.

J. M. Ryniawec, G. C. Rogers, A. E. Cress;
University of Arizona, Tucson, AZ

PURPOSE: This study aims to identify a causal mechanism of centrosome loss previously observed in primary prostate cancer. Prostate cancer progression is accompanied by bursts of chromosomal instability (CIN), including chromosomal translocations, oncogene amplifications, and chromothripsis. While high CIN correlates with most metrics of aggressive disease, we lack a mechanistic understanding of how CIN originates in prostate cancer. Recently, we discovered that cells in primary prostate tumors lack centrosomes, cytoplasmic organelles that ensure the fidelity of chromosome segregation by organizing the shape of the mitotic spindle. Experimental elimination of centrosomes in immortalized, non-tumorigenic prostate cell lines was sufficient to generate extensive CIN, resulting in oncogenic transformation of these lines when sub-cutaneously injected into NSG mice. Because we identified centrosome loss as a potential driver of CIN, we sought to understand mechanisms that can trigger centrosome loss in the prostate. Although centrosome loss naturally occurs during the development of some tissues, for example centrosome elimination during oogenesis, the mechanisms that trigger loss are not known. Therefore, we first investigated microenvironmental changes in early prostate cancer as a potential cause. Hypoxia, pathologically low oxygen concentration, is common in the aging prostate due to loss of vasculature and is associated with poor prostate cancer prognosis and high CIN. Therefore, we hypothesized that hypoxic exposure induces centrosome loss in prostate cells. Indeed, we found that exposure to 1% oxygen concentrations leads to progressive centrosome loss in non-tumorigenic, immortalized prostate epithelial cell lines. Using immunofluorescence of centrosomes in cultured cells, we found that hypoxia-induced centrosome loss is independent of HIF transcription but requires activation of the confluence-dependent Hippo signaling pathway. Mechanistically, we found that centrosome disassembly begins with the removal of the pericentriolar material (PCM), the outer shell of the centrosome that nucleates microtubules. We were able to block centrosome disassembly by over-expressing a constitutively-active mutant of Polo-like Kinase 1, which normally strengthens the PCM during mitosis to promote centrosome maturation. Furthermore, centrosome loss was prevented by treatment with the Protein Phosphatase 2A (PP2A) inhibitor Okadaic Acid. Using RNAseq, we have identified potential PP2A regulatory subunits that are up-regulated in cells undergoing hypoxia-induced centrosome loss. Our model is that hypoxia induces dephosphorylation of the PCM, mechanically weakening the centrosome and leaving it vulnerable to disassembly. Together with previous findings, we conclude that hypoxia-induced centrosome disassembly is a plausible driver of CIN in early prostate cancer.

#0372 Cell polarity proteins as novel regulators of macropinocytosis in pancreatic cancer.

G. Lambies Barjau[1], S.-W. Lee[2], C. Commisso[1];
[1]Sanford Burnham Prebys Med. Discovery Inst., San Diego, CA, [2]Crinetics Pharmaceuticals, San Diego, CA

Pancreatic ductal adenocarcinoma (PDAC) is considered one of the deadliest cancers. This is likely because it is detected at a very late stage and the therapeutic approaches that have been used for its treatment have proven to be quite ineffective. Therefore, new therapeutic strategies are needed for a better prognosis in patients suffering of pancreatic cancer. PDAC cells often rewire their metabolism to survive and progress. This metabolic rewiring permits the acquisition of nutrients by the cells when these are exposed to a poor nutrient microenvironment. One of the most used processes in nutrient stress conditions is the “cell-drinking” pathway macropinocytosis, an endocytic pathway that cancer cells exploit to support cancer metabolism in such unfavorable conditions. Macropinocytosis inhibition has shown to suppress PDAC growth in mice and thus, it has become a promising therapeutic target for PDAC treatment. Here, we describe that atypical Protein Kinase C (aPKC) isoforms Protein Kinase C zeta (PKCζ) and Protein Kinase C iota (PKCι) regulate PDAC macropinocytosis in the context of glutamine stress. Genetic depletion and pharmacological inhibition of aPKC impair macropinocytosis promotion in PDAC cells exposed to a glutamine-deprived environment and in cells treated with DON, a glutamine analog that blocks glutamine metabolism. In epithelial cells, aPKCs are known to regulate the establishment of cell polarity in association with the scaffold proteins Par3 and Par6, constituting the cell polarity complex, which controls the function of different targets such as Par1 kinases. Loss of Par3, Par6 and Par-1a affects glutamine stress associated macropinocytosis in a similar extent than aPKC depletion, presenting a novel role of the cell polarity protein network in the modulation of macropinocytic uptake.

#0373 Transcriptional and post-transcriptional positive regulatory loops between HIF-1a and the RNA-Binding protein hnRNPA18.

E. Solano-Gonzalez, **F. Carrier**;
Univ. of Maryland Marlene & Stewart Greenebaum Cancer Ctr., Baltimore, MD

Hypoxia, the scarcity of oxygen, is a hallmark of solid tumors to which they adapt by activating the hypoxia-inducible transcription factor 1 (HIF-1). HIF activates the transcription of genes bearing hypoxia responsive elements (RE) in their promoter regions including genes related to angiogenesis, glucose metabolism, cell proliferation, survival, invasion, and metastasis. The HIF-1 pathway is thus an attractive target to prevent cancer aggressiveness and improve the effectiveness of cancer therapy. HIF-1α activity is known to be mainly regulated through post-translational modification by prolyl hydroxylase domain (PHD) enzymes, but accumulating evidence indicate that it is also regulated by other mechanisms such as transcriptional initiation, translational initiation, protein-protein interaction, post-translational modifications and post-transcriptionally, primarily through the action of trans-acting factors (noncoding RNAs and RNA-binding proteins) that interact with the HIF-1α mRNA to regulate its decay and translational rates. We recently identified the RNA binding protein hnRNP A18 as a regulator of HIF-1α translation under hypoxic conditions. hnRNP A18 is a nuclear stress responsive protein that translocates to the cytosol in response to cellular stress including hypoxia to bind to a recognition motif in the 3'UTR of its targeted transcripts including HIF-1α to stabilize the transcripts and increase their translation. Using a bicistronic reporter plasmid containing a HIF-1α internal ribosome entry site (IRES) we now show that hnRNP A18 can also regulate HIF-1α through its IRES in the 5'UTR. In fact, cells expressing hnRNP A18 significantly increase translation of a reporter CAT protein under the control of HIF-1α IRES in the presence of the hypoxia mimetic agent $CoCl_2$. On the other hand, deletion of hnRNP A18 prevents the translation of the CAT reporter protein even in the presence of $CoCl_2$. Moreover, we also identified several HIF-1α REs in hnRNP A18 promoter. Two of the predicted HIF-1α REs, located at -57 and -226 upstream of the hnRNP A18 start codon were validated as bonafide HIF-1α binding sites by Electromobility Shift Assay with recombinant HIF-1α protein and by Chromatin Immunoprecipitation assay in human pancreatic cancer cells Panc 01. These data thus indicate that a positive regulatory loop between hnRNP A18 and HIF1-1α exist to amplify HIF-1α expression under cellular stress. hnRNP A18 can upregulate HIF1α protein expression by stabilizing its transcript at the 3'UTR and by binding to its IRES. On the other hand, HIF-1α can upregulate hnRNP A18 by binding to its proximal promoter. Targeting hnRNP A18 could thus provide a new mechanism to regulate HIF-1α expression and sensitize cancer cells to therapies.

#0374 Hypoxia-induced mitochondrial glutathione transporter expression causes drug resistance in colorectal cancer.

C.-C. Lin;
National Cheng Kung University, New Taipei City, Taiwan

Colorectal cancer (CRC) is the third most common type of cancer worldwide, with higher incidence and mortality rates. In order to adapt stress conditions during cancer progression, the cancer cells will be subject to metabolism reprogramming to increase energy production and remove hazardous substances. One of the important organelles, mitochondria is responsible for cellular ATP production, ion homeostasis, and several metabolic pathways. Therefore, mitochondria require a series of transporters called solute carrier family 25 (SLC25) to transport metabolites crossing the mitochondrial inner membrane, and dysregulation of those transporters causes abnormal cell morphology and diseases. In this study, members of the SLC25 family were analyzed in CRC via bioinformatics analysis, and a mitochondrial glutathione transporter was identified to overexpress in several public datasets of CRC and our own clinical specimens. In addition, its role has not been reported in any disease, including cancer. To systemically analyze the underlying mechanism causing overexpression of glutathione transporter during CRC progression, several stress conditions had been applied to colon cancer cells. However, only hypoxia was identified to induce its protein expression but not mRNA expression. Since a previous study reported that glutathione deprivation induced its protein expression, hypoxia didn't alter the abundance of glutathione level suggesting that another glutathione-independent regulatory mechanism might be involve it. Interestingly, our findings revealed that hypoxia-induced glutathione transporter protein expression was mediated through the activation of internal ribosome binding site-mediated translation under hypoxia. To identify the potential role of glutathione transporter during colon cancer progression, its mitochondrial metabolite profiles from knockout cells of previous studies were further analyzed and identified that the changes of metabolites were associated with the urea cycle which had been reported to be associated with the sensitivity of oxaliplatin and 5-fluorouracil (5-FU) in cancer treatment. Importantly, our results showed that hypoxia-attenuated those chemotherapeutic effects were abolished by loss of glutathione transporter in colon cancer cells, indicating its crucial role in hypoxia-induced drug resistance. In conclusion, our study shows that glutathione transporter increased by hypoxia might lead to drug resistance of cancer therapy in colon cancer.

#0375 Lipogenic phenotype is an adaptation to nutrient stress in the tumor microenvironment.

C. Griffith, D. Abrahams, A. Ortiz, A. Tassielli, J. Johnson, R. Gatenby, **S. Pillai**;
Moffitt Cancer Center, Tampa, FL

The nutrient and oxygen poor microenvironment combined with acidosis arising from fermentative metabolism imparts strong selection pressure on cancer cells that promotes evolution of more aggressive cancer types. Poor nutrient availability in the tumor microenvironment forces cancer cells to adapt to alternate routes of metabolism, nutrient scavenging and autophagy leading to a shift in their metabolic phenotype. These adaptations promote evolution of invasive and aggressive phenotypes. To test this hypothesis and to characterize the evolution of cancer cells under nutrient stress, we generated nutrient stress adapted cells from MCF7-GFP cells by subjecting them to multiple cycles of nutrient starvation and repletion. Distinct clones that outgrew were selected as nutrient stress adapted cells (NSA). Here we show that MCF7-NSA cells that are adapted to grow in low nutrient conditions exhibited robust accumulation of lipid droplets compared to parental MCF7-GFP cells as shown by confocal microscopy after neutral lipid staining as well as immunofluorescence staining for PLIN2 (Perilipin 2), a lipid droplet coat protein. In addition, MCF7-NSA cells showed elevated expression of the nuclear receptor PPARγ and the adipokine FABP4 indicating an adipogenic/lipogenic signature. Strikingly, these nutrient stress adapted cells were capable of nutrient scavenging by macropinocytosis compared to control cells even under nutrient replete conditions. Macropinocytosis was assessed by DQ-BSA processing and TMR-Dextran uptake. NHE inhibitor EIPA (ethyl isopropyl amiloride), that blocks macropinocytosis, but not receptor mediated endocytosis confirmed dextran uptake through macropinocytosis. Similarly, macropinocytosis inhibitor KH7 blocked dextran uptake in these adapted cells. Furthermore, MCF7-NSA cells showed high expression of TFEB and TFE3, master regulators of autophagy and lysosomogenesis suggesting that the necrotic cell debris scavenged through macropinocytosis and processed through autolysosome machinery might be contributing to *de novo* lipogenesis. Although control and adapted cells exhibited similar growth kinetics *in vitro*, when implanted in mammary fat pads (MFP) of NSG mice, NSA cells formed significantly smaller and slow growing primary tumors. Interestingly, 80% of these mice showed metastasis to other organs (lung, liver, kidney) whereas control mice did not develop metastasis as parental MCF7 is not an aggressive cell line in xenograft models. MCF7-NSA cells were more migratory *in vitro* in wound healing assays and were capable of developing lung metastases in a mouse model where primary tumor from mammary fat pad was resected to allow for metastases to develop. Taken together, our data suggest that lipogenic phenotype confers survival advantage in the harsh tumor microenvironment and selects for more invasive and aggressive phenotypes.

#0376 Targeting the convergence on HIF-1α of CDK4/6 and MAPK pathway: Implications for enhanced anticancer strategies.

S. Zhao, L. Zhou, S. Zhang, W. S. El-Deiry;
Brown University, Providence, RI

Hypoxia-inducible factor 1-alpha (HIF-1α) plays a pivotal role in orchestrating cellular responses to hypoxia, influencing cancer cell survival and progression. Our previous work identified a non-canonical mechanism wherein Smurf2 mediates HIF-1α degradation under CDK4/6 inhibition. Through proteomic analysis, we discovered that serine 451 phosphorylation occurs on HIF-1α but not in palbociclib-treated samples. Point mutations at this site, substituting serine with alanine, resulted in decreased HIF-1α levels and enhanced interaction with Smurf2. Intriguingly, under palbociclib treatment, we observed phosphorylation at the serine 643 site. This site has been previously associated with MAPK-dependent regulation of HIF-1α localization and activity (Ilias Mylonis, *et al*., 2006), particularly relevant given the reported MAPK reliance in acquired CDK4/6 inhibitor-resistant scenarios (Renée de Leeuw, *et al*., 2018). To explore therapeutic implications, we investigated the impact of combined CDK4/6 (palbociclib) and MEK1/2 inhibition (trametinib, selumetinib, PD98059, U0126). Dual inhibition robustly reduced HIF-1α expression in colorectal cancer cells (HCT116, SW480) and suppressed HIF-1α activity in luciferase reporter assays. This effect extended to synergistic inhibition of cell viability under both normoxia and hypoxia in HCT116 and SW480 cells. Such effect is also applicable to other cancer types and cell lines (*e.g.* U251). In summary, our findings unveil a phosphorylation site on HIF-1α associated with CDK4/6 activity, influencing its protein stabilization. This discovery supports the rationale for combining CDK4/6 and MEK1/2 inhibition as a promising strategy in the treatment of solid tumors.

#0377 Saturation mutagenesis of KEAP1 to identify pathogenic mutations in lung cancer patients and gain insight into KEAP1 molecular function.

N. Kastelowitz, S. Shrishrimal, S. Jun, A. M. Y. Zhang, R. Wang, I. Ilerten, M. Diehn;
Stanford University School of Medicine, Stanford, CA

Introduction: KEAP1 and NFE2L2 (NFR2) mutations occur in roughly 20% of non-small cell lung cancer (NSCLC) patients and are associated with resistance to a broad range of therapies including radiotherapy, chemotherapy, targeted therapies, and immunotherapy. In prior work, we demonstrated that not all KEAP1 mutations observed in NSCLC patients are pathogenic. These benign mutations have a wild-type phenotype that does not impart therapy resistance. However, only roughly 100 of ~13,000 (<1%) possible KEAP1 single amino acid substitution mutations have been characterized. Here, we performed saturation mutagenesis of KEAP1 to comprehensively evaluate all possible point mutation phenotypes *in vitro*.

Methods: Saturation mutagenesis was accomplished using the High-throughput Mutagenesis by Integrated TilEs (MITE) method. In brief, the KEAP1 sequence was divided into 21 tiles each containing a 90 bp variable region flanked by a 30 bp constant region. At each codon position, mutations representing the 20 possible natural amino acids and a stop codon were included for a total of 13,076 KEAP1 variants. The tiles were assembled such that each full length KEAP1 construct contained a single desired mutation. The KEAP1 MITE lentivirus library was transduced into H1299-KEAP1^{NULL} cells that were then treated with vehicle or H_2O_2 for 24 days. The KEAP1 ORF was amplified from gDNA and mutations were quantified by next generation sequencing. Mutation enrichment analysis was used to derive functional annotations.

Results: Oxidative stress resulted in a bimodal distribution of KEAP1 mutations. Cells with KEAP1 nonsense mutations were enriched while cells with silent mutations were depleted. Using a threshold of 95% specificity for silent mutations to distinguish benign from pathogenic mutations, 94% of nonsense mutations and 88% of previously characterized pathogenic mutations were identified as pathogenic. While the majority of KEAP1 mutations were benign (64%), analysis of mutations found in TCGA NSCLC patients showed an enrichment of pathogenic mutations (72%). Overlaying mutation calls onto the KEAP1 structure showed enrichment of pathogenic mutations in the BTB homodimerization interface, hydrophobic core of the oxidative stress sensing IVR domain, and NRF2 binding pocket of the Kelch domain.

Conclusions: Saturation mutagenesis of KEAP1 generated a comprehensive list of pathogenic KEAP1 single amino acid substitutions. Assignments strongly agreed with biologic function and prior literature. The assessment of KEAP1 mutation phenotypes is important as benign mutations occur in a significant subset of NSCLC patients and are not expected to impart therapy resistance. Our results will allow identification of benign and pathogenic KEAP1 mutations in clinical studies, which will enable testing of personalized therapeutic strategies for patients with KEAP1 mutations.

#0378 PHD3 dependent stabilization of β3-adrenoceptor induces HIF-1αactivation in Ewing sarcoma.

A. Pasha, L. Zocca, F. Carrozzo, C. Banella, R. Amato, A. Tondo, C. Favre, M. Calvani;
Meyer Children's Hospital - IRCCS, Firenze, Italy

Hypoxia is a condition of oxygen deficiency which occurs in most growing solid tumors and stimulates a cascade of cell signals through a family of transcription factors named as hypoxia inducible factors (HIFs) that transactivate several regulatory genes involved in tumor proliferation. β3-adrenoceptors (β3-ARs) are involved in several hypoxic scenarios and in pathological conditions where hypoxia leads to important steps for cancer progression. Studies showed that β-AR blockade of mice suppressed hypoxia induction of renal HIF-1α accumulation, erythropoietin production, and erythropoiesis in vivo. In this work we assumed that through PHD3 activity, β3-AR mediates hypoxia sensing needed for HIF-1α stabilization, thus we investigated a putative correlation between β3-AR/HIF-1α and PHD3. Data showed a similar outcome of β3-ARs and HIF-1α at short time of hypoxia, and that β3-AR antagonist, SR59230A reduced HIF-1α protein expression under hypoxia. β3-AR silencing under hypoxia revealed an evident reduction of HIF-1α protein expression that confirmed the β3-AR modulation of HIF-1α expression. SR59230A treatment strongly reduced the HIF-1α target genes as GLUT1, HK-2 and HIF-1α expression at long time treatment confirming the β3-AR modulation of HIF-1α transcriptional activity. Conversely, the HIF-1α-transcriptional inhibitor Topotecan did not affect β3-AR expression confirming that β3-AR mediates HIF-1α activation. Immunofluorescence and nuclear-cytoplasmic fragmentation showed that β3-AR co-localized with the nucleus under hypoxia, more than normoxia, and presence of both β3-AR and HIF-1α in the nucleus. Co-immunoprecipitation of β3-AR/HIF-1α revealed that under hypoxia, HIF-1α dissociates from β3-AR binding, but this process was abrogated by SR59230A. HIF-1α, released under hypoxia from the link with β3-AR, can play its transcriptional activity in the nucleus, while the binding with β3-AR blocks its transcriptional activity. Moreover, the β3-AR upregulation under hypoxia occurs trough an early inhibition of PHD3 activity that did not influence HIF-1α expression. Hypoxic PHD2 inhibition results after PHD3 leading to HIF-1α upregulation. Moreover, the blockade β3-AR by SR59230A, inhibited HIF-1α upregulation by increasing PHD2 activity.

#0379 Landscape of HIF-1α expression across 24,186 solid tumors using comprehensive immune profiling.

H. I. Parikh[1], S. Pabla[1], M.-F. Senosain[1], R. Seager[1], E. Vanroey[1], S. Gao[1], Y. Pulivendula[1], P. DePietro[1], M. Nesline[1], D. Dash[1], J. Conroy[1], S. Hastings[2], H. Ko[2], K. Strickland[2], R. Previs[2], E. Severson[2], T. Jensen[2], S. Ramkissoon[2], M. Eisenberg[3], B. Caveney[3];
[1]OmniSeq Inc. (Labcorp Oncology), Buffalo, NY, [2]Labcorp Oncology, Durham, NC, [3]Labcorp, Durham, NC

Background: Transcription factor Hypoxia Inducible Factor-1α (HIF-1α) is a key regulator of various cellular and systemic responses to hypoxia, with HIF-1α mediated pathways playing an important role in tumor progression and metastasis. Recent studies have highlighted the correlation between *HIF-1α* expression with tumor cell survival, angiogenesis, and invasion. In this study, we explore the landscape of *HIF-1α* expression across 35 solid tumor histologies, its co-expression with immune checkpoint and angiogenesis-related genes, as well as its association with outcomes from a retrospective cohort of patients with non-small cell lung cancer (NSCLC) treated with pembrolizumab.
Methods: A discovery cohort of 24,186 solid tumors across 35 types were evaluated by comprehensive immune profiling assay. *HIF-1α* gene expression was normalized and ranked against a reference population of 735 samples yielding a percentile rank values [0-100], with rank classified as high (≥75), moderate (≥25 and <75) and low (<25). We investigated the distribution of *HIF-1α* expression, cellular proliferation signature, and co-expression with other immunotherapy targets using Spearman correlations (r_s). Additionally, Kaplan-Meier analysis and Chi-squared tests were utilized for overall survival (OS), progression free survival (PFS) and objective response rate (ORR) differences in a retrospective cohort of 72 patients with NSCLC, treated with pembrolizumab.
Results: Pan-cancer analysis confirmed a broad distribution of *HIF-1α* expression, with highest median expression levels observed in brain and central nervous system (CNS) (median=64), thyroid (median=49) and uterine (median=42) cancers. Significant associations ($p<0.001$) were observed between PD-L1 positivity (TPS≥1%, CPS≥1) and HIF-1α expression, with 60% of HIF-1α high cases (n=1,314/2,193) being PD-L1 positive, whereas 53% of HIF-1α low cases (n=4,834/9,135) were PD-L1 negative. Significant correlations ($p<0.05$) of ranked expression of HIF-1α with immune checkpoint blockage targets like PD-1 and CTLA-4, as well as angiogenesis-related genes like *VEGFA* and *PTEN* were observed. Within our pembrolizumab-treated retrospective cohort, there were no significant differences in OS and PFS between HIF-1α high and HIF-1α low tumors. However, the response to pembrolizumab was significantly higher in HIF-1α low tumors (ORR=58.82%, $p<0.01$) compared to HIF-1α high tumors.
Conclusion: In clinically tested solid tumors, *HIF-1α* showed a dynamic expression range, with highest levels observed in brain, thyroid and uterine cancers. Significant co-expression of *HIF-1α* with various downstream genes, especially angiogenesis-related genes, enabled identification of gene signatures that characterize the hypoxic tumor microenvironment and may aid in the development of novel combination therapy strategies.

#0380 Co-downregulation of GRP78 and ATR enhances apoptosis in pancreatic ductal adenocarcinoma.

S. Lee[1], A.-R. Nam[1], K.-S. Oh[1], J.-M. Kim[1], J.-H. Bang[1], Y. Jeong[1], S. Choo[1], H. Kim[1], J. Yoon[2], T.-Y. Kim[2], D.-Y. Oh[2];
[1]Seoul National University, Seoul, Korea, Republic of, [2]Seoul National University Hospital, Seoul, Korea, Republic of

Background: Targeting endoplasmic reticulum (ER) stress is a potential therapeutic strategy in preclinical models of pancreatic duct adenocarcinoma (PDAC). GRP78 is known as the master regulator of the unfolded protein response (UPR) pathway, regulating ER stress by activating the UPR pathway to avoid cell apoptosis and regulates the activation of UPR pathway signals by binding PERK. Overexpression of GRP78 in PDAC results in the retention of misfolded and unassembled proteins, as well as the accumulation of ROS, leading to the promotion of genomic instability. However, there has been limited research on targeting GRP78 as a therapeutic strategy in PDAC. In this study, we aimed to investigate the anticancer effects of BOLD-100, an inhibitor of GRP78, in PDAC.
Methods: We used 9 PDAC cell lines (Capan-1, AsPC-1, HPAFII, MIA-PaCa2, Panc-1, Capan-2, SNU-213, SNU-324, SNU-2918). The mouse xenograft model of Capan-1 was established for in vivo study. BOLD-100 (GRP78 inhibitor), AZD6738 (ATR inhibitor), NAC (N-Acetylcysteine; ROS scavenger) and TUDCA (Tauroursodeoxycholic acid; ER stress inhibitor) were used. MTT assay, CFA assay, cell cycle analysis, RT-PCR, western blot, immunoprecipitation, DCF-DA staining and Annexin V assay were used to elucidate the action of BOLD-100. The combination of BOLD-100 with AZD6738 has been evaluated in both *in vitro* and *in vivo* model.
Results: BOLD-100 suppressed the proliferation of PDAC cells and decreased the mRNA level of GRP78, which in turn disrupted the interaction between GRP78 and PERK. BOLD-100 increased ER stress and ROS, leading to activation of PERK, eIF2a, and CHOP. Activation of UPR pathway induced CHOP-dependent apoptosis and inhibited PDAC cell growth. Moreover, TUDCA reversed the ROS accumulation induced by BOLD-100, confirming that ER stress regulates ROS levels. The accumulation of ROS upregulated the active forms of ATR and CHK1, suggesting the activation of the DNA damage repair pathway. Notably, the treatment of NAC abrogated the activation of ATR-CHK1 axis by BOLD-100-induced ROS accumulation. AZD6738 synergized with BOLD-100 in *in vitro* and *in vivo*, by suppressing BOLD-100-induced ATR phosphorylation.
Conclusion: GRP78 could serve as one of the potential therapeutic targets in PDAC. The combination of BOLD-100 and AZD6738 demonstrates a synergistic effect suggesting GRP78/ATR dual targeting as a promising therapeutic option for patients with PDAC.

#0381 DUSP12 in glioblastoma: Insights into nucleolar stress and DNA damage response.

V. K. Boell, F. L. Forti;
IQ USP, Sao Paulo, Brazil

Glioblastoma (GBM), an extremely aggressive brain tumor, presents molecular complexities that require enormous challenges for its better understanding. The relatively unexplored dual-specificity phosphatase 12 (DUSP12) is an attractive target due to its zinc finger-like domain suggesting potential interactions with nucleic acids and ribonucleoproteins. This highly conserved enzyme plays a pivotal role in ribosome biogenesis across eukaryotes. Importantly, cell cycle arrest induced by DNA damage often coincides with alterations in ribosome biogenesis, a phenomenon termed nucleolar stress, linked to changes in the localization and activity of nucleophosmin (NPM) and p53 proteins. Bioinformatic analysis of public databases revealed elevated DUSP12 expression in glioblastoma samples compared to normal tissue, displaying strong positive correlations with p53 and NPM. While DUSP12 expression did not impact tumor progression in wild-type p53 patients, its lower expression was associated with increased tumor progression in p53-mutant cases, emphasizing the significance of p53 status in understanding DUSP12's roles in GBM. Gene ontology analysis of DUSP12-correlated genes in glioblastoma patients showed robust enrichment in biological processes like ribosome biogenesis, chromosome organization, cell cycle, and DNA repair, with a substantial number of nucleoplasmic and nucleolar proteins being recently identified by our group through mass spectrometry as DUSP12 partners in other tumor models. A substantial difference in DUSP12 protein levels between the GBM cell lines U87MG (wild-type p53) and U138MG (mutant p53) was observed, with the latter presenting higher levels of this phosphatase. Some biological responses of these cell lines were assessed after exposure to the topoisomerase inhibitors doxorubicin (DX) and camptothecin (CPT) through viability assays in adherent and spheroid cultures, γH2AX foci formation, and ATM/Chk2 activation, showing marginal differences between the cell lines. Notably, DX treatment displayed strong nucleolar stress features, such as alterations in the number and size of nucleoli observed by NPM subcellular distribution changes in both cell lines, and induction of p21 expression only in the p53-profficient U87MG. These alterations were accompanied by nuclear accumulation of DUSP12, underlining its potential regulatory role in this process. The knockdown of DUSP12 with specific siRNA led to a substantial decrease of the treatment responsiveness in U138MG, consistent with the lower levels of this phosphatase associated with a more aggressive phenotype in mutant p53 patients. In summary, DUSP12 emerges as a pivotal player in glioblastoma, influencing nucleolar stress dynamics and tumor aggressiveness, particularly in the context of p53 mutations.

#0382 Pancreatic cancer-derived organoids alter muscle fiber type and increased energy consumption leading to cachexia.

B. Han[1], S. Zhao[1], z. Yang[1], J. Trevino[2], S. Grossman[1], H.-J. Lenz[1], B. X. Hoang[1];
[1]Keck School of Medicine of USC, Los Angeles, CA, [2]Virginia Commonwealth University, Richmond, VA

Cachexia, marked by continuous skeletal muscle mass loss and severe metabolic disturbances, presents a substantial challenge for pancreatic ductal adenocarcinoma (PDAC) patients. Despite its prevalence and the adverse impact on quality of life and survival rates, effective clinical treatments for cachexia remain elusive. This study aims to bridge this gap by employing innovative in vitro models to investigate the underlying mechanisms of cachexia and identify potential therapeutic targets. To enhance the relevance of cell culture models, modifications were introduced to replicate in vivo conditions, where the muscle is exposed to the ongoing kinetics of constant tumor secretion of active factors. Patient-derived PDAC cells were cultured in a dense 3D stiffness extracellular matrix (ECM) to mimic the hypoxic desmoplastic tumor microenvironment. The conditioned medium from prolonged cultured patient-derived organoids (PDOs) was then used to supplement C2C12-derived myotubes. The investigation focuses on dynamic adaptations in muscle fiber type and metabolism when exposed to tumor paracrine factors. Metabolomic investigations of PDO-conditioned medium (PDO CM) on myotubes revealed distinct metabolic differences compared to non-treatment controls. Discriminatory metabolites included those associated with glycolysis, lipid, amino acid, and fatty acid metabolism. PDO CM induced a significant shift in muscle fiber type from slow-twitch to fast-twitch phenotypes, accompanied by de novel expression of embryonic and neonatal Myosin Heavy Chain (MyHC) isoforms. Fast fiber (F59) staining also confirmed the protein expression. Concurrently, PGC-1a, a master regulator of mitochondrial biogenesis and oxidative metabolism, significantly decreased, along with reduced ATP and Mito tracker staining, indicating a metabolic switch under the influence of tumor paracrine factors. Metabolome results on C2C12 myotubes treated with PDO CM also revealed significantly changed ABC transporter-related pathways, an adaptive process required to optimize substrate use under the influence of tumor secretome. However, the genes involved in the proteasome degradation process, such as MAFbx and MuRF1, did not show altered expression. The establishment of an in vitro cachexia model, focusing on changes in energy metabolism and utilizing muscle fiber type alterations as markers, will deepen our understanding of the mechanisms of cancer-associated cachexia. The insights gained may pave the way for identifying potential therapeutic targets to mitigate muscle wasting in PDAC patients and improve overall outcomes.

#0383 Mic19 regulates mitophagy in non-small cell lung cancer under hypoxic microenvironment.

H. Huang[1], C. Ding[1], Z. Zhang[1], D. Wu[1], C. Chen[2], Y. Li[2], H. Liu[2], **J. Chen**[1];

[1]Department of Lung Cancer Surgery, Tianjin Medical University General Hospital, Tianjin 300052, People's Republic of China, Tianjin, China, [2]Tianjin Lung Cancer Institute, Tianjin Key Laboratory of Lung Cancer Metastasis and Tumor Microenvironment, Tianjin Medical University General Hospital, Tianjin 300052, People's Republic of China, Tianjin, China

Background: Mitophagy is a pivotal cellular process crucial for maintaining homeostasis in hypoxic conditions, selectively eliminating dysfunctional mitochondria through autophagy. This process is implicated in various diseases, including cancer. Non-Small Cell Lung Cancer (NSCLC), known for its prevalence and aggressiveness, often encounters hypoxic microenvironments. Mic19, a core protein of the mitochondrial cristae membrane, plays vital roles in maintaining mitochondrial architecture and function. However, its involvement in mitophagy in hypoxic NSCLC and the underlying molecular mechanisms remain inadequately explored.

Methods: NSCLC cells were cultured under conditions with 1% O2 oxygen concentration to simulate a hypoxic microenvironment. Protein expression levels of Mic19 were analyzed using Western Blot and immunofluorescence (IF). Cellular proliferation and metastasis capability were assessed through CCK8 and transwell experiments. Immunoprecipitation experiments were conducted to validate the interaction between Mic19 and key mitophagy regulatory proteins. IF, confocal microscopy, ATP measurement, oxygen consumption rate (OCR), mitochondrial membrane potential, and transmission electron microscopy were employed to assess the formation of mitochondrial cristae and the level of mitophagy.

Results: In hypoxic conditions, Mic19 exhibited up-regulation in NSCLC cells. Subsequent in vitro experiments confirmed Mic19's pivotal role in promoting the growth and metastasis of lung cancer cell lines. Through clinical data analysis, Mic19 emerged as an independent prognostic indicator for NSCLC. Inhibition of Mic19 expression exacerbated the disruption of mitochondrial morphology and structure in lung cancer cells, accompanied by the loss of mitochondrial cristae. Notably, Mic19 expression closely correlated with ATP and OCR production in tumor cells. Assessment of mitochondrial membrane potential and transmission electron microscopy revealed Mic19 as a critical downstream target of hypoxia, mediating mitophagy. Overall, these findings not only underscore the significance of Mic19 in regulating mitochondrial dynamics but also highlight its multifaceted role in tumor progression, positioning Mic19 as a promising therapeutic target and prognostic biomarker for NSCLC.

Conclusion: This study provides novel insights into the mechanistic understanding of hypoxia-induced mitophagy in NSCLC, emphasizing the regulatory role of Mic19. Mic19 emerges as a potential therapeutic target for future interventions in NSCLC patients.

#0384 SLC7A11 modulates sensitivity to the first-in-class mitochondrial peroxiredoxin 3 inhibitor thiostrepton (RSO-021) via a ferroptosis independent pathway.

T. Messier[1], V. Gibson[1], A. Bzura[2], J. Dzialo[2], C. Poile[2], S. Stead[1], A. Saaman[1], G. N. Naumov[3], D. A. Fennell[2], **B. Cunniff**[1];
[1]Larner College of Medicine at The University of Vermont, Burlington, VT, [2]University of Leicester and University Hospitals of Leicester, Leicester, United Kingdom, [3]RS Oncology, Cambridge, MA

Mitochondrial peroxiredoxin 3 (PRX3) has been identified as an actionable cancer vulnerability that is currently being investigated in the first-in-human phase 1 clinical trial, MITOPE (NCT05278975). RSO-021 (thiostrepton or TS) is a redox-active drug that inhibits PRX3's peroxidase activity via covalent adduction of its active site peroxidatic and resolving cysteine residues, forming an irreversible crosslink across the protein dimer. Covalent inhibition of PRX3 results in tumor cell death due to a diminished ability to remove high levels of mitochondrial reactive oxygen species (ROS) in cancer cells. To better understand the mechanism underpinning sensitivity and resistance, TS-tolerant human mesothelioma cell lines were generated under constant TS pressure and subjected to a drug-screen comprising chemotherapeutic agents, metabolic inhibitors, ROS modulating agents and ferroptosis-inducing compounds, to identify synergistic interactions compared with TS- sensitive cell lines. Erastin, an SLC7A11 inhibitor exhibited the greatest synergy when combined with TS, potentiated PRX3 covalent crosslinking and cellular ROS levels. Synergy with TS was enhanced by cystine depletion and could be phenocopied by siRNA knockdown of SLC7A11. SLC7A11 was up-regulated in TS-tolerant cells and resistance could be overcome with erastin. TS-tolerant cell lines have significantly reduced glutathione levels and slowed proliferation. Ferroptosis inhibitors ferrostatin-1 and liproxstatin-1 did not inhibit TS or TS in combination with erastin. In summary, SLC7A11 up-regulation confers tolerance to TS through a mechanism involving a cysteine-dependent modulation of the redox state independent of canonical ferroptosis, that can be overcome by the addition of an SLC7A11 inhibitor. The correlation between SLC7A11 with response to TS in a 33-patient primary mesothelioma explant co-clinical trial, and patients enrolled into the MITOPE phase 1/2 trial will be presented.

#0385 Stress-induced pentraxin 3 enhances anoikis resistant-associated metastasis and post-chemotherapeutic recurrence in head and neck cancer.

T.-W. Chang[1], W.-C. Chang[2], B.-K. Chen[1];
[1]National Cheng Kung University, Tainan, Taiwan, [2]Taipei Medical University, Taipei, Taiwan

Head and neck squamous cell carcinoma (HNSCC) is one of the most aggressive cancer with the properties of local recurrence and lymphatic metastasis. During metastatic process in blood circulation, cancer cells lose the interaction with extracellular matrix and encounter the anoikis stress, resulting in successfully extravasate and form micrometastasis in distal organs. However, most patients develop chemo-drug resistance during the metastatic recurrence which leading to poor prognosis. Thus, it is a pressing matter to elucidate the molecular mechanisms involved in cancer metastasis and the behaviors of the post-chemotherapy treated HNSCC cells. Our previous studies suggest that growth factor signaling stimulated HNSCC cells metastasis by the expression of pentraxin 3 (PTX3). Moreover, recent findings also reveal that chemotherapy mediated oxidative stress induce PTX3 expression and poor progression. Here, we raise the hypothesis that the expression of PTX3 through stress signal may promote cancer cells against from anoikis and promote the post-chemotherapeutic survival. The first, we identified that the secondary messenger-reactive oxygen species (ROS) dominate the gene activation of PTX3 by spheroid culture and platium-based agents' treatment. The ROS scavenger, NAC, inhibited cisplatin (CDDP)-induced PTX3 expression and rescue the cell viability by decreasing the ROS level. The oxidative stress inducer-H2O2 treatment also verify the PTX3 expression through AKT and NF-κB pathways. In addition, both the spheroid selection and CDDP-induced PTX3 regulated the EMT phenotype and further strengthen the growth factor signaling. In addition, we found that PTX3 also regulate the survival during spheroid selection and drug treatment. The post-selected cells also exhibit the unique glycosylated modification on PTX3. Disrupted the PTM modification of PTX3 could inhibit the spheroid survival and cell invasion. The animal studies revealed that both spheroid selection and CDDP-treated HNSCC cells had stronger extravasation ability than parental cells in NOD-SCID mice. Depletion of PTX3 also repressed the HNSCC cells extravasation ability. The results indicate that PTX3 were essential for oxidative stress-induced tumor metastasis and recurrence. It also speculates that the combination of antioxidants and PTX3 antibody may prevent tumor metastatic recurrence after chemotherapy in HNSCC.

#0386 BACH1 is a key regulator of the tumor hypoxia response.

L. C. Nguyen[1], C. Dann[1], D. Yang[1], M. Henn[1], E. Shi[1], T. Li[1], L. Stock[1], W. Liu[1], M. Matossian[1], A. Valdespino[1], Y. J. Han[1], J. Zhang[1], G. Yerradoddi[1], Y. Li[1], M. Matsumoto[2], O. I. Olopade[1], K. Igarashi[2], M. R. Rosner[1];

[1]University of Chicago, Chicago, IL, [2]Tohoku University, Sendai, Japan

Hypoxia is an important hallmark of aggressive solid tumors and a key driver of metastasis and resistance to therapy. Hypoxic stress induces the activation of various factors, such as hypoxia-inducible factors (HIFs), which facilitate cellular adaptation and promote tumorigenesis. Given the complexity of this mechanism, identifying novel targets that sensitize hypoxic tumors to therapy could have significant clinical impact. Here we show that the pro-metastatic BTB and CNC homology 1 (BACH1) transcription factor is prolyl-hydroxylated by the HIF Prolyl Hydroxylase (PHD), similar to HIFs, in an oxygen-dependent manner. We describe two major prolyl hydroxylation sites in BACH1 and demonstrate that prolyl hydroxylation increases protein turnover and decreases DNA binding in normoxia. We further demonstrate HIF-independent induction of BACH1 within multiple TNBC (Triple-Negative Breast Cancer) cell lines and patient-derived organoids under hypoxic conditions. Utilizing ChIP-seq, bulk, single-cell and spatial transcriptomics across diverse BACH1 knockout tumor models, our study revealed that BACH1 selectively and directly modulates the transcriptional response associated with hypoxia and stress in TNBC. Our findings identify BACH1 as a clinically relevant target for attenuating hypoxia induced, pro-metastatic signaling and therapeutic resistance in cancers.

#0387 Ionizing radiation induces lipid metabolism-associated vulnerabilities in glioblastoma multiforme.

A. R. Izawa-Ishiguro, S. Nandakumar, N. Carbone, A. V. Ferrotta, R. Raziuddin, K. C. Vogt, D. A. Heller, I. K. Mellinghoff;
Memorial Sloan Kettering Cancer Center, New York, NY

Introduction: Glioblastoma multiforme (GBM) is the most common primary malignant brain tumor in adults. It is highly resistant to its current standard-of-care regimen, which includes surgical resection followed by adjuvant ionizing radiation and temozolomide. Therapy resistance can be attributed to the abundance of genomic alterations in GBM tumors that evolve over time, which contribute to intra-and inter-tumoral heterogeneities that render targeted therapies as inadequate treatment options. Thus, there is an urgent unmet need for effective therapies targeting primary and recurrent GBM. Here, we investigated the impact of ionizing radiation on the transcriptome of patient derived GBM tumor spheres to identify key alterations and biological pathways involved in therapy resistance.

Materials and methods: We acquired four independent human GBM tumor sphere cell lines, which were derived from patients and cultured in serum-free media. Tumor spheres were treated with either a sham radiation or a single dose of 10Gy. Using poly-A enrichment whole transcriptome sequencing, we evaluated transcriptional alterations occurring in GBM tumors spheres at 96h post-radiation. To do so, we performed differential expression analysis and gene set enrichment analysis (GSEA) to identify top differentially expressed genes and significant changes in biological phenomena. Additionally, we evaluated the cell viability response of these GBM tumor spheres to radiation.

Results and discussion: PCA analysis of the four human GBM tumor sphere cell lines demonstrates that cell type has a substantial impact on variation among samples compared to non-irradiated and irradiated treatment conditions. Upon analysis of genes in common that are either upregulated or downregulated followed by GSEA, we identified enrichment of genes associated with inflammatory responses and ferroptosis repression (e.g., NUPR1, PTGS1, AOX1), and depletion of genes involved in fatty acid metabolism (e.g., INSIG1, PLA2G3, ACAT2). Furthermore, the GBM tumor sphere cell viability responses allowed us to stratify our models into radiosensitive and radioresistant subgroups.

Conclusion: Radiosensitive human GBM tumor spheres exhibit transcriptional alterations in genes linked to inflammation and fatty acid metabolism to a greater extent compared to radioresistant tumor spheres. Our study characterizes the radiation response of patient derived GBM models, which is to be leveraged for combating therapeutic resistance.

#0388 Identifying synthetic lethalities in GCN2 KO tumors using an *in vivo* targeted CRISPRi screen.

N. R. Sommers, R. A. Cordova, A. J. Klunk, R. C. Wek, K. A. Staschke;
Indiana University School of Medicine, Indianapolis, IN

The integrated stress response (ISR) is an intracellular signaling pathway that fosters cell adaptation to diverse stresses. The ISR is mediated by a family of four eIF2 kinases that each sense distinct cellular stresses. Activation of the eIF2 kinases results in reprogrammed gene expression through translational and transcriptional mechanisms that help prevent stress damage. Previously, we reported that prostate cancer (PCa) cells rely on GCN2 eIF2 kinase for maintenance of amino acid (AA) homeostasis to sustain growth (Cordova et al., 2022 *eLife* 11:e81083). GCN2 inhibition through pharmacological or genetic means results in decreased expression of AA transporters, depletion of intracellular AAs, and reduced growth of PCa cells in culture and mouse xenograft models. Although loss of GCN2 results in a significant reduction in PCa cell growth, minimal cell death is observed. We hypothesize that loss of GCN2 in PCa cells results in vulnerabilities that can be exploited and targeted to induce cell death. To optimize GCN2-targeted therapies for PCa, we utilized a targeted CRISPR-interference (CRISPRi) screen in castration-resistant 22Rv1 cells with functional wild type (WT) GCN2 or those with it deleted (GCN2 KO). The CRISPRi screen was performed in cells grown in culture or grown as tumor xenografts in mice and featured a guide library targeting genes that encode druggable targets, including kinases, phosphatases, and metabolic enzymes. While reduced expression of 152 genes was synthetically lethal with loss of GCN2 in the *in vitro* screen, more genes (202) were synthetically lethal with loss of GCN2 *in vivo*. Of note, reduced expression of many metabolic enzymes was synthetically lethal with GCN2 ablation only in the *in vivo* screen, potentially due to the abundance of nutrients in standard culture media. A group of six metabolism-related genes, identified as hits in the *in vivo* screen and targets of FDA-approved drugs, were selected for follow-up studies. One of these metabolic enzymes was GART, a trifunctional enzyme that carries out 3 of the 10 enzymatic steps in *de novo* purine biosynthesis. Based on our findings showing that GCN2 maintains AA levels to support nucleotide pools in PCa cells, we initially focused on this critical enzyme. Inhibition of GART using antifolates, including the FDA-approved Pemetrexed, resulted in minimal cell death of parental and GCN2 KO PCa cells cultured in standard culture media. However, when cultured in reduced nutrient media that better mimicked reduced nutrient availability *in* vivo, GART inhibition resulted in selective death of GCN2 KO cells. Our CRISPRi screening strategy uncovers new vulnerabilities in GCN2-inhibited PCa cells and reveals a general strategy to identify actionable targets with the potential to combine with GCN2 inhibitors for the treatment of PCa.

#0389 The role of endoplasmic reticulum stress in immune surveillance and effectiveness of immunotherapy in renal and ovarian carcinoma.

M. Svoboda[1], L. Moran[1], B. Vavrusakova[1], L. Krejci[1], K. Souckova[2], K. Vasickova[1], M. Holanek[1];
[1]Masaryk Memorial Cancer Institute (MMCI), Brno, Czech Republic, [2]CEITEC - Central European Institute of Technology, Brno, Czech Republic

In complex tumor-host interactions, the immune response has a dual role, with the capacity to both promote and suppress tumor growth, requiring complex interactions of regulatory molecules within the cellular network of the tumor-immune microenvironment (TIME). Various factors in TIME, such as low pH and hypoxia, cause Endoplasmic Reticulum Stress (ERS). Immune cells exposed to ERS lack antigen presentation, exhibit a suppressor phenotype, and can initiate apoptosis. Therefore, relieving ERS can benefit immune surveillance and response to immunotherapy. Our research is focused on tumor-immune cells interaction, specifically in ovarian and renal cancers. We conducted in vitro co-cultures of these cancer cells with peripheral blood mononuclear cells (PBMC) and manipulated ERS using a well-established ERS inducer tunicamycin and a chemical chaperone tauroursodeoxycholic acid (TUDCA). We then employed various techniques such as MTT, RT-qPCR, western blotting, immunofluorescence staining, scratch wound assay, and 3D co-cultures to analyze cellular viability, gene expression, protein levels of ERS markers (e.g., BiP, CHOP, PERK), immune cell activity (e.g., IL-2, INFγ, FoxP3, PD-1), migration, invasiveness, interaction, spheroid formation, and immune cell infiltration. Furthermore, we examined ERS and immune profiles in tumor samples from patients with ovarian and renal cancer who underwent conventional therapy or immunotherapy.Relieving ERS increased the infiltration of PBMC into tumor spheroids and reduced the expression of BiP and PERK in PBMC. In vitro, the viability of ovarian and renal cancer cells increased when cultured alone after ERS alleviation. However, when co-cultured with PBMC, their viability decreased, indicating enhanced immune cell response. Additionally, the growth and migration of ovarian and renal cancer cells were limited in these co-cultures, along with increased expression of BiP and CHOP and an elevated CHOP/BiP ratio. We connected these findings to the molecular background of ERS in patient samples and observed a positive correlation between a favorable clinical outcome, higher lymphocyte infiltration at the tumor site, and increased levels of BiP and CHOP in cancer cells. We further applied these results to OC and RCC in vivo syngeneic mouse models, currently with very promising outcomes.Based on these results we expect ERS alleviation as a suitable approach to improving the survival and effectiveness of immune cell populations within hostile tumor-induced microenvironment with positive effects on anticancer immunotherapy. *Supported by Ministry of Health of the Czech Republic, grant nr. NU21-03-00539, and by the Johannes Amos Comenius Programme, project SALVAGE nr. CZ.02.01.01/00/22_008/0004644.*

#0390 Direct interaction of Pin1 with HIF-prolyl hydroxylase 2: Implications for breast cancer cell growth and survival.

Y. N. Guillen Quispe[1], S.-J. Kim[1], S. Saeidi[1], G.-J. Choi[1], C. Chelakkot[1], T. Zhou[2], S.-B. Bang[1], T.-W. Kim[1], Y.-K. Shin[1], Y.-J. Surh[1];
[1]Seoul National University, Seoul, Korea, Republic of, [2]The University of Edinburgh, Edinburgh, United Kingdom

Prolyl hydroxylase domain 2 (PHD2) is the main hypoxia-inducible factor (HIF)-prolyl hydroxylase. PHD2 in normoxia hydroxylates specific proline residues in HIF-1α and HIF-2α, which facilitates their ubiquitination and proteasomal degradation. Although the activity of PHD2 is reduced in hypoxia, significant levels of residual activity of this monooxygenase are still detected under hypoxic conditions. However, its role under hypoxia is poorly understood. Peptidyl-prolyl isomerase (Pin1) binds to target proteins containing phosphorylated serine or threonine residues followed by proline (pS/T-P). As PHD2 harbors several pS/T-P motifs, it may be a potential substrate of Pin1. We found for the first time interaction between Pin1 and PHD2 in human breast cancer MDA-MB-231 cells in normoxic and hypoxic conditions. Additionally, the breast cancer tissue array showed elevated expression of PHD2 as well as Pin1 in tumors compared to adjacent normal tissues. LC-MS/MS spectrometry identified three amino acid residues (S125, T168, and S174) of PHD2 undergoing phosphorylation. Among these, serine 125 was found to be the principal site required for Pin1 binding. As a novel binding partner of Pin1, oncogenic PHD2 can be explored as a therapeutic target for the treatment of breast cancer.

#0391 Role of NRF2 in HIF-2α-mediated cancer stem cell phenotype.

M.-K. Kwak, S. P. Hallis;
The Catholic Univ. of Korea College of Pharmacy, Bucheon, Korea, Republic of

The acquisition of cancer stem cell (CSC) properties is influenced by the microenvironment, with tumor hypoxia playing a pivotal role. Elevated levels of nuclear factor erythroid 2-like 2 (NRF2), a redox balance-maintaining transcription factor, have been linked to enhanced tumor growth and therapy resistance. This study investigates the potential role of NRF2 in hypoxia-inducible factor-2α (HIF-2α) regulation in cancers. First, in a model of a 72-hour hypoxic incubation, chronic hypoxia led to CSC characteristics, including increased expression of KLF4 and OCT4, heightened cancer migration, and spheroid growth, which are associated with HIF-2α accumulation. NRF2 inhibition mitigated these effects, while NRF2 activation enhanced chronic hypoxia-induced CSC traits. Mechanistically, NRF2/miR181a-2 signaling emerged as a regulator of HIF-2α-mediated CSC phenotypes in chronic hypoxic conditions. Second, in clear cell renal cell carcinoma (ccRCC), characterized by pVHL gene mutation and constitutive HIF-2α elevation, the role of NRF2 in aggressive cancer phenotypes was explored. Silencing of *NRF2* impaired aggressive phenotypes in multiple ccRCC cell lines with a reduction in HIF-2α expression. Promoter analysis elucidated that NRF2 directly upregulates HIF-2α expression through antioxidant response elements in the human *HIF-2α* gene. Collectively, our study suggests the involvement of NRF2/miR181a-2 signaling in the development of HIF-2α-mediated CSC phenotypes in sustained hypoxic environments and also proposes NRF2 as a promising target for mitigating HIF-2α-mediated CSC traits in ccRCC.

#0392 MYB regulates a specific subset of hypoxia-induced genes and exhibits altered genomic occupancy under hypoxia.

S. Anand, M. Khan, K. Vikramdeo, S. Singh, A. Singh;
USA Health Mitchell Cancer Institute, Mobile, AL

Hypoxia, an unavoidable microenvironmental stress, greatly influences the tumor cell behavior and therapeutic outcomes. Under low oxygen condition, tumor cells undergo transcriptional reprogramming, largely mediated through hypoxia-inducible factors (HIFs), triggering adaptive response pathways. We recently demonstrated a significant role of MYB in hypoxic survival of pancreatic cancer cells by facilitating adaptive changes in cellular metabolism in collaboration with HIF1α. Here, we employed genome-wide deep sequencing approaches to study the impact of hypoxia on transcriptional reprogramming of pancreatic cancer cells and investigate the role of MYB in the hypoxia-dependent processes. A large number of differentially expressed genes (DEGs) were identified in pancreatic cancer cells subjected to hypoxia (1% O_2) and associated with multiple adaptive response pathways. Specifically, we found that pathways related to autophagy, cell migration, epithelial-to-mesenchymal transition, endocytosis, cytoskeleton reorganization were induced, while those associated with RNA processing, ribosome biogenesis, DNA replication and cell cycle were suppressed. To analyze the role of MYB in these adaptive responses, we compared the relative abundance of transcripts in MYB-overexpressing control and MYB knockout (KO) pancreatic cancer cells when cultured under normoxic or hypoxic conditions. We observed that the transcriptional output of MYB was drastically changed under hypoxia with a vast majority of genes being distinctly altered in response to the loss of MYB expression under normoxia and hypoxia. To examine if it resulted from altered genomic occupancy of MYB under normoxia and hypoxia, we compared MYB ChIP-seq peaks under these conditions. We observed a decrease in overall MYB-bound genomic regions under hypoxia despite the fact that we did not observe a decrease in nuclear MYB expression. More interestingly, the genomic occupancy of MYB shifted substantially from regions proximal to transcription start site to distal intergenic or intronic regions under hypoxia. Studies are currently underway to examine the mechanisms underlying the altered MYB genomic occupancy and its impact on adaptive physiological response of pancreatic cancer cells under hypoxia. Together, our findings bring unprecedented insight into the mechanistic role of MYB in hypoxia adaptation and pancreatic cancer pathobiology.

#0393 RAS and PI3K activation promote glioblastoma progression and ischemia-associated tumor cell death.

S. Kim, M. Tang, S. Chih, J. Thorpe, T. Lu, H.-G. Wang, W. Li;
Penn State College of Medicine, Hershey, PA

Glioblastoma multiforme (GBM) is the most common and aggressive brain tumor in adults. Despite the association of tumor necrosis and a poor prognosis in GBM, the mechanisms underlying tumor necrosis formation remain unclear, likely due to the lack of appropriate experimental models to examine the development of tumor necrosis. In our study, we developed mouse models with tumor necrosis by intracranially injecting human GBM cells expressing KRAS or PI3K active mutants into immunodeficient mice. Surprisingly, despite all tumors displayed similar sizes, the control tumors expressing an empty vector (EV) did not exhibit tumor necrosis. This intriguing observation led us to explore the potential role of KRAS and PI3K in promoting cell death within the tumor microenvironment. Ischemia, which is characterized by insufficient nutrients and hypoxia, is often found in GBM. Under an in vitro ischemia mimetic condition, we found that the KRAS or PI3K activated GBM cells showed more cell death compared to EV cells. Mechanistically, ischemia activates the p38 MAPK-MK2 pathway to induce cell death, a process further enhanced by KRAS or PI3K. Notably, we observed elevated expression of p-MK2 in the peri-necrotic areas of GBMs harboring KRAS or PI3K mutants compared to the cellular tumor zones. Moreover, we revealed that ischemia induces the unfolded protein response (UPR) pathway. Among UPR-related molecules, KRAS and PI3K upregulate ERN1, which encodes the transmembrane protein kinase IRE1, in ischemic conditions. Inhibition of ERN1 not only prevented ischemia-induced cell death but also inhibited the p38 MAPK-MK2 pathway. Furthermore, we observed an increase in the expression of pro-inflammatory cytokine IL-8 under ischemic conditions, a response that was prevented by inhibitors of p38 MAPK or MK2. Lastly, we found that ischemia induces ATP release and calreticulin exposure, indicating the cell death possessing certain immunogenic cell death features. In summary, our findings revealed a pivotal role of KRAS and PI3K in inducing cell death in the ischemic GBM tumor microenvironment through activating the IRE1-p38 MAPK-MK2 pathway. The cell death under this circumstance displays pro-inflammatory and immunogenic properties. Therefore, the IRE1-p38 MAPK-MK2 pathway may be exploited for the treatment of GBM in which RAS or PI3K is activated.

#0394 Preclinical evaluation of ERX-208, a potent inducer of ER stress for the treatment of ovarian cancer.

S. Viswanadhapalli[1], T.-K. Lee[2], S. Elmore[2], G. Sharma[3], R. Gopalam[1], K. Parra[3], T. Reese[3], M. Hsieh[3], U. P. Pratap[1], X. Yang[1], B. Ebrahimi[1], H. Neal[2], C.-Y. Chen[2], K. Kassees[2], C. Cervantes[1], Z. Xu[1], E. Kost[1], G. R. Sareddy[1], R. R. Tekmal[1], J.-M. Ahn[2], G. V. Raj[3], R. K. Vadlamudi[1];
[1]UT Health Science Center at San Antonio, San Antonio, TX, [2]UT Dallas, Richardson, TX, [3]UT Southwestern Medical Center at Dallas, Dallas, TX

Background: Ovarian cancer (OCa) is the deadliest kind of gynecologic cancer in the United States. The long-term survival rate for OCa is less than 20% after five years. Intra-tumoral and inter-tumoral heterogeneity is implicated in tumor resistance to conventional therapies and the unsatisfactory clinical outcomes. Addressing these issues necessitates innovative therapies that target intrinsic common vulnerabilities within OCa. Recent studies have highlighted that high basal level of endoplasmic reticulum stress (ERS) in OCa as a critical vulnerability. We have identified a promising compound, ERX-208 that potently induces ERS in cancer cells. The objective of this study is to characterize the mechanisms and activity of ERX-208 using preclinical models.
Methods: The biological activity of ERX-208 was examined across 17 distinct OCa cells, representing 5 diverse OCa subtypes. Mechanistic studies utilized Western blotting, immunohistochemistry (IHC), RNA-Seq analysis, and CRISPR/Cas9 knockouts (KO). Pharmacokinetics (PK) and toxicity studies were performed on C57BL/6 mice. Comprehensive preclinical assessments were carried out through cell line-derived xenografts (CDXs), patient-derived xenografts (PDXs), organoids (PDOs) and explants (PDEs).
Results: ERX-208 demonstrated an IC_{50} of approximately 50-100 nM inducing ERS and reducing cell viability in OCa cells. Conversely, normal ovarian surface epithelial cells exhibited minimal effects from ERX-208. *In vitro* experiments revealed strong ERX-208-induced apoptosis in OCa cell lines. Mechanistic studies employing RNA sequencing, Western blotting, and RT-qPCR, confirmed activation of ERS pathways observed as early as 5 hours post-ERX-208 treatment. Our studies identified LIPA as a potential target, and KO of LIPA significantly diminished ERX-208 activity. Moreover, LIPA KO substantially impeded *in vivo* OCa tumor growth. ERX-208 up to a dose of 25 mg/kg showed no observable organ toxicity and had no effect on the mice's body weight. Dose range studies identified 10 mg/kg intraperitoneal as the minimal effective dose, achieving more than 50% tumor reduction. In preclinical models, ERX-208 inhibited the growth of OCa CDXs, PDXs, and ex vivo PDEs and PDO's. IHC analyses indicated reduced proliferation (Ki-67) and increased activation of ERS markers, such as GRP78 and p-PERK.
Conclusions: Collectively, our findings underscore the preclinical promise of ERX-208 as a potential therapeutic agent for treating OCa. Conflict: The patents surrounding ERX-208 are licensed to EtiraRx.

#0395 An alternating magnetic field suppresses tumor growth.

Masanari Umemura[1], Taisuke Akimoto[2], Rafikul Islam[3], Kazuhito Kishi[4], Akane Nagasako[5], Rina Nakakaji[1], Takashi Yamaguchi[4], Yuto Mizuno[5], Soichiro Ishikawa[6], Tetsuya Yamamoto[2], Yoshihiro Ishikawa[7]

[1]Yokohama City Univ. Graduate School of Med., Yokohama, Japan,[2]Neurosurgery, Yokohama City Univ. Graduate School of Med., Yokohama, Japan,[3]Biochemistry and Molecular Biology, University of Arkansas for Medical Sciences (UAMS), Little Rock, AR,[4]Ricoh Company, Ltd., Yokohama, Japan,[5]Cardiovascular Research Institute (CVRI), Yokohama City Univ. Graduate School of Med., Yokohama, Japan,[6]Department of Oral and Maxillofacial Surgery, Yokohama City Univ. Graduate School of Med., Yokohama, Japan,[7]CVRI, Yokohama City Univ. Graduate School of Med., Yokohama, Japan

Application of physical forces, ranging from ultrasound to electric field, is recommended in various clinical practice guidelines, including those for bone fracture or cancer treatment. However, mechanistic information for such treatments has been poorly provided, due to the lack of comprehensive study model. Here, we show an alternating magnetic field (AMF) per se exhibits direct anti-cancer effect through enhancing oxidative phosphorylation (OXPOHS) and thus metabolic reprograming. Proliferation of human glioblastoma cells (U87 and LN229), but not normal human astrocytes (NHA), was inhibited upon exposure to AMF within the narrow frequency range. Extracellular acidification rate was decreased while oxygen consumption was increased. These data indicated that AMF induced metabolic reprograming. This was accompanied by increased reactive oxygen species (ROS) production. Mouse models grafted with human glioblastoma cells showed that AMF exposure, 30 minutes per day for two weeks, suppressed the tumor growth and prolonged the overall survival. Our results suggest that the AMF exposure may be a simple strategy to inhibit cancer cell growth by utilizing oxidative stress via metabolic reprograming.

#0396 Effects of hypoxia on cell proliferation and lipidome profile in treatment-resistant prostate cancer cells.

A. Siltari[1], K. Valitalo[1], T. Laamanen[2], K. Tornberg[1], A. Saarinen[1], J. Kreuzer[3], H. Syvala[1], T. L. J. Tammela[4], P. Ilmonen[2], P. Kallio[4], T. J. Murtola[4];
[1]Tampere University, Tampere, Finland, [2]Aalto University School of Science, Espoo, Finland, [3]BioGenium Microsystems Ltd, Tampere, Finland, [4]Tampere University Hospital, Tampere, Finland

Background: Low tissue content of oxygen i.e. hypoxia is typical in prostate cancer (PCa) tumor microenvironment. Hypoxia is also associated with PCa progression and treatment resistance. Modulation of lipid and cholesterol metabolism seems to be one way how tumor cells adapt to hypoxia. However, not much is known about lipidomic profiles in hypoxic condition in advanced PCa and treatment resistance. Aim: The aim of this study was to evaluate the impact of hypoxia on treatment-resistant PCa cells and investigate alterations in the lipidome under hypoxic conditions.
Material and Methods: Testosterone (T)-sensitive, T-independent (castration-resistant), and enzalutamide (enza)-resistant VCaP PCa cells were cultured for three days under hypoxia (1% O_2) and compared with cells grown under normoxia (21% O_2). Additionally, cells were treated with the drugs SREBP-inhibitor fatostatin and mevalonate-pathway inhibitor simvastatin to examine the effects of modulating lipid and cholesterol production on hypoxia responses. Relative cell growth by crystal violet staining and live/dead cell ratio were evaluated after each treatment. Intracellular lipidome was measured using liquid chromatography coupled with MS/MS method. Random forest classification was used of the selection of the lipids. Based on the classification, concentration differences between the groups were calculated.
Results: Growth of the T-sensitive and castration-resistant cells was decreased under hypoxia compared to normoxia. However, enza-resistant cells tolerated hypoxic conditions. Lipid-modifying drugs exhibited similar inhibitory effects on cell growth in both normoxia and hypoxia. Based on live/dead cell ratio, hypoxia induced cell death. Lipidome profiles varied markedly by oxygen content and cellular treatment resistance profile. Simvastatin treatment also influenced lipidome profiles.
Conclusions: Enza-resistant advanced PCa cells tolerated hypoxic conditions better compared to T-sensitive and T-independent cells. Lipidome was different between cell lines but also in hypoxia compared to normoxia, supporting its importance for PCa cells under varying conditions. Interference with lipid metabolism leads to growth inhibition regardless of hypoxia. These findings could be used in identifying potential markers for predicting or delaying disease progression in advanced PCa. Future studies should explore the efficacy of various lipidome-modulating drugs in delaying disease progression in PCa.

#0397 Exploring the role of MDM2-TP53 pathway and ATM in regulation of ferroptosis in dedifferentiated liposarcoma.

C.-C. Yen, S.-C. Chen, C.-H. Chen, J.-Y. Wang, C.-M. Chen, P.-K. Wu, M.-H. Yang, W.-M. Chen;
Taipei Veterans General Hospital, Taipei, Taiwan

Background: Ferroptosis, a process involved in accumulation of lipid-based reactive oxygen species (ROS), is a form of cell death with unique morphologic features and regulatory mechanism. Tumor suppressor p53 (TP53) is a key factor in regulation of ferroptosis through multiple pathways. Mouse double minute 2 homolog (MDM2), a key oncogene of dedifferentiated LPS (DDLPS), is one of the negative regulators of the TP53. In our previous study, we had showed that nutlin-3, a MDM2 inhibitor, could exert synergistic cytotoxicity with ferroptosis-inducing agent (erastin and RSL3) on DDLPS in a sequential manner, possibly through upregulation of SLC3A2 with altered cystine/glutamate exchange (AACR Annual Meeting 2023 abstract#4777). Mutated in Ataxia-Telangiectasia gene (ATM) is a critical gene in DNA damage response. ATM could regulate ferroptosis either directly through altered iron pool, or indirectly through activating TP53 by phosphorylation of MDM2. In this study, we explored the role of ATM and MDM2-TP53 pathway, as well as interaction between them, in regulation of ferroptosis of DDLPS. We also studied the potential role of combination of DNA damaging agent (DDA), such as cisplatin, with ferroptosis-inducing agents in the treatment of DDLPS.
Methods: We explored the possible synergistically cytotoxic effect of cisplatin and ferroptosis-inducing agents in DDLPS cell lines. We also investigated the role of ATM in this synergistic effect by using siRNA or ATM inhibitor. In addition, we used cystine uptake assay (measurement of altered cystine/glutamate exchange) and iron level assay (measurement of labile iron pool) to study the functional change responsible to ferroptosis-inducing effect of cisplatin. Finally, we used immunoblotting study to reveal the potential molecular mechanism responsible for synergistic effect of cisplatin and ferroptosis-inducing agent.
Results: Cisplatin and erastin showed synergistic cytotoxicity in DDLPS cell line, most likely through ferroptosis-inducing effect. Cisplatin could activate ATM, with resultant dissociation of TP53 and MDM2. Cisplatin could exert ferroptosis-inducing effect through down-regulation SLC7A11A with resultant decrease cystine uptake, as well as increase labile iron pool. ATM inhibition could offset the ferroptosis-inducing effect of cisplatin by reversing both effects.
Conclusion: Modulation of ferroptosis is a potential treatment strategy in DDLPS. MDM2-TP53 pathway and ATM as well as interaction of both may play an important role in regulation of ferroptosis in DDLPS. Combination of DDA, such as cisplatin, and ferroptosis-inducing agents is a potential strategy in DDLPS treatment.

MOLECULAR/CELLULAR BIOLOGY AND GENETICS: DNA Damage and Repair 1
Poster Session

#0401 The impact of DNA structural variants on *PRKN* gene function and colorectal cancer pathogenesis.

E. J. van Bree[1], S. Lakbir[2], C. Rubio-Alarcon[1], R. de Wit[3], A. Bolijn[1], P. Delis-van Diemen[1], M. Tijssen[1], E. Stelloo[4], H. Feitsma[4], G. A. Meijer[1], B. Carvalho[1], S. Abeln[5], R. J. A. Fijneman[1];

[1]The Netherlands Cancer Institute, Amsterdam, Netherlands, [2]Vrije Universiteit Amsterdam, VU Bioinformatics, Department of Computer Science; Netherlands Cancer Institute, Department of Pathology, Amsterdam, Netherlands, [3]The Netherlands Cancer Institute, Department of Pathology, Amsterdam; Utrecht University, AI Technology for Life Group, Department of Information and Computing Sciences and Department of Biology, Utrecht, Netherlands, [4]Cergentis B.V., a Solvias company, Utrecht, Netherlands, [5]Vrije Universiteit Amsterdam, VU Bioinformatics, Department of Computer Science, Amsterdam, The Netherlands; Utrecht University, AI Technology for Life Group, Department of Information and Computing Sciences and Department of Biology, Utrecht, Netherlands

Background: Cancer is caused by somatic DNA alterations, such as single nucleotide variants, somatic copy number alterations and structural variants (SVs). PRKN is among the genes most frequently affected by SVs in colorectal cancer (CRC), with 37% of primary cancers and 56% of metastatic lesions having focal deletions in PRKN. PRKN encodes the E3 ubiquitin ligase Parkin, which regulates the biological activity and degradation of substrates via post-translational modifications. The genomic location of PRKN is within a common fragile site. Therefore, it remains unclear whether the high frequency of SVs in PRKN are passenger events due to genomic instability or driver events of CRC pathogenesis.
Aim: Our study aims to investigate the impact of SVs on the functionality of Parkin in CRC pathogenesis.
Methods: We used publicly available DNA deep whole genome sequencing (WGS) and tumor-matched RNA sequencing data (n=394) to estimate the impact of SVs in PRKN on tumor biology. For this, the transcriptome-wide p-value distribution generated by differential expression analysis was used as a measure of biological impact. The HCT116-MLH1-repaired cell line and patient-derived adenoma organoids were genetically modified using CRISPR/Cas9 to mimic the SVs observed in patient material and analyze their impact. RNA-sequencing, whole proteome and ubiquitin remnant-specific proteomics were used to assess the effect of SVs on gene function and identify altered biological processes.
Results: Analysis of WGS and RNA sequencing of patient material showed that SVs in PRKN have a large impact on CRC biology, comparable to the impact of mutations in TP53 (impact score 0.379 vs 0.332). The most pronounced effects are seen in the ubiquitin-like, RING0 and RING1 domains. These domains are important for recognition and/or binding to ubiquitin, E2 ubiquitin-conjugating enzymes and substrates. In the HCT116-MLH1-repaired CRC cell line, hemizygous introduction of an SV in PRKN had minimal effects on genome-wide gene expression. In contrast, homozygous deletion altered the expression of nearly 2000 genes. Analyses of ubiquitin motif remnants showed differential ubiquitination of proteins involved in DNA repair following the introduction of an SV in PRKN in the CRC cell line. These proteins include TOP2A (Log_2 fold change (L_2FC) = -3.69, P = 5.71^{-5}), RAD18 (L_2FC = -4.55, P = 1.35^{-4}) and Spartan (SPRTN; L_2FC = -2.57, P = 7.43^{-4}).
Conclusion: SVs in *PRKN* have a high impact on tumor biology and result in aberrant gene expression and post-translational modifications of proteins related to DNA repair. Further research will expand to the patient-derived adenoma organoids and focus on understanding if these recurrent somatic alterations contribute to genomic instability and the development of CRC pathogenesis.

#0402 Aneuploidy-associated *SQLE* gain promotes prostate cancer aggressiveness by altering lipid metabolism.

Thomas Walter Janas[1], Xiaofeng A. Su[1], Konrad H. Stopsack[2], Daniel R. Schmidt[3], Duanduan Ma[3], Zhe Li[4], Kathryn L. Penny[2], Tamara L. Lotan[5], Lorelei A. Mucci[3], Matthew G. Vander Heiden[3], Elise DeArment[1], Angelika Amon[3], Paul A. Scheet[6]

[1]Center for Prostate Disease Research, Uniformed Services University, Bethesda, MD,[2]Department of Epidemiology, Harvard T.H. Chan School of Public Health, Boston, MA,[3]David H. Koch Institute for Integrative Cancer Research, Massachusetts Institute of Technology, Cambridge, MA,[4]Harvard Medical School, Boston, MA,[5]Department of Pathology, Johns Hopkins University School of Medicine, Baltimore, MD,[6]Department of Epidemiology, The University of Texas MD Anderson Cancer Center, Houston, TX

Prostate cancer (PCa) is the second leading cause of cancer-related death in men in the US. Epidemiology studies on primary PCa cohorts in Physicians' Health Study and Health Professionals Follow-up Study (PHS and HPFS) have shown that high levels of whole-genome aneuploidy, featured by imbalanced chromosome numbers, correlate with lethal progression in PCa. However, details of the mechanisms of how aneuploidy drives PCa aggressiveness are still unclear. Here, we used the case of chromosome 8q (chr 8q, the long arm of chr 8) gain to study aneuploidy-associated prostatic malignancies. Chr 8q gains are the most frequent gain events that occur in approximately 23% of PCa cases. By using the PHS and HPFS cohorts, we modeled the increased expression of each gene located on chr 8q, for predicting the risks for lethal progression, and obtained each corresponding gene's odds ratio (OR). By ranking the ORs, we revealed that a cholesterol biosynthesis gene, squalene monooxygenase (*SQLE)*, is one of the top associators with lethal progression, amongst all chr 8q genes. SQLE plays a pivotal role in cholesterol synthesis. Previous lymphoma studies have shown that loss of SQLE contributes to cholesterol auxotrophy, and squalene build-up protects against oxidative cell death. In our experimental study, we have used normal and cancerous *TMPRSS2-ERG*-driven organoid models and found that over-expression of SQLE promotes formation of invasive structures and proliferation in cancer organoids. Interestingly, overexpression of SQLE decreased the protein levels of TMPRSS2-ERG, which appeared to be independent of androgen receptor levels. We also utilized the TMPRSS2-ERG positive VCaP cell line, which harbors gains of *SQLE* gene copies. We found that knocking down SQLE expression significantly upregulated ERG protein levels. Our recent study has shown that ERG (or other ETS) positive prostate cancers have a strong correlation with downregulation of fatty acid metabolism signature. We speculate that gain of SQLE can drive aggressiveness of prostate cancer by modulating lipid metabolism for growth and migration. Inhibition of SQLE could translate to better clinical outcomes regarding prostate cancer lethality.

#0403 APOBEC3 enzymes induce chromosomal translocations in solid cancer.

T.-C. Cheong, Q. Wang, A. Jang, E. Karaca-Atabay, R. Chiarle;
Children's Hospital Boston and Harvard Medical School, Boston, MA

Introduction: Chromosomal translocations are common oncogenic drivers in human cancers, and an increasing number of translocations are being considered as crucial diagnostic and prognostic markers in clinics. In B-cell lymphoma, a number of chromosomal translocations are directed by the off-target activity of the activation-induced cytidine deaminase (AID; a B-cell specific apolipoprotein B mRNA-editing enzyme, catalytic polypeptode-like (APOBEC) family enzyme). However, in solid tumors, no such enzymes capable of directing chromosomal translocations have been identified. Given recent findings on APOBEC-mediated mutagenesis in solid cancers, APOBECs may be involved in the formation of chromosomal translocations in solid tumors, like AID does in B cells. In human, the APOBEC3 (A3) family consists of seven members (A3A-A3H) and is associated with C
<t or="" c<g="" substitutions.="" recent="" evidence="" shows="" that="" a3a="" might="" be="" involved="" in="" chromosomal="" instability="" leading="" to="" drug="" resistance="" lung="" cancer.="" however,="" it="" has="" not="" been="" explored="" whether="" a3s="" generate="" dna="" dsbs,="" eventually="" translocations.="" this="" study,="" we="" investigated="" the="" role="" of="" and="" their="" mechanisms="" translocations="" solid="" cancer.Methods: We applied high-throughput genome-wide translocation sequencing (HTGTS) approach to map genome-wide chromosomal translocations induced by human A3s in mouse fibroblast and human epithelial cells. We correlated patterns of translocations induced by A3s with several other cellular features including transcription, DNA accessibility, DNA replication timing, and mutational signatures. We validated the contribution of A3 to the generation of oncogenic translocations in lung cancer.

Results: Ectopic expression of A3s significantly increased chromosomal translocations in mouse fibroblasts and human epithelial cells. A3s and AID preferentially induced translocations in different parts of the genome, but some of the translocation hotspots were shared among them. Hierarchical clustering of hotspots showed that A3-mediated translocations were distinguished from AID-mediated translocations. Notably, the junction distribution of breakpoint clusters showed three distinct translocation patterns based on the locations of breakpoint clusters: (1) AID-preferred; (2) A3-preferred; and (3) AID/A3-mixed. AID-mediated translocations were heavily enriched near the transcription start site, whereas A3-mediated translocations were dispersed across the gene body and transcription end site. Furthermore, DNA replication timing and genomic architectures were linked to the formation of A3-mediated chromosomal translocations in solid cancer. Finally, A3 contributed to the formation of oncogenic rearrangements in lung cancer.

Conclusions: A3 enzymes induced chromosomal translocations with distinct patterns compared to AID and facilitated chromosomal translocation formation in solid cancers.

#0404 LINE-1 retrotransposition promotes chromosomal translocations through RNA-templated DNA repair in human cancers.

J. Tao[1], L. Alessandri[1], C. Mendez-Dorantes[2], K. H. Burns[2], Q. Wang[1], R. Chiarle[1];
[1]Harvard Medical School and Boston Children's Hospital, Boston, MA, [2]Harvard Medical School and Dana-Farber Cancer Institute, Boston, MA

Introduction: Approximately 50% of human cancers have somatic integrations of long interspersed element-1 (LINE-1; also known as L1). L1 is a retrotransposon that copies itself through RNA and integrates into new genomic loci. Although L1 sequences comprise approximately 17% of the human genome, only 100-150 L1 loci have retained the ability to retrotranspose. These full-length, retrotransposition-competent L1s are typically repressed in human somatic cells, but there is evidence of their significant reactivation in human cancers. Therefore, L1 overexpression is a hallmark of many human cancers, particularly in highly malignant tumor types such as breast, ovarian, pancreatic, esophageal, lung, head-and-neck, colon, prostate, and liver cancers.
Results: In many cancers, chromosomal translocations are fundamental pathogenetic events initiated by the generation of DNA double-strand breaks (DSBs). Although LINE-1 (L1) retrotransposition events have been implicated in chromosomal rearrangements associated with most human cancers, the frequency and mechanisms by which L1 is involved in these rearrangements, including chromosomal translocations, remain poorly characterized. By combining high-throughput genome-wide translocation sequencing (HTGTS) and two sequencing techniques to detect L1 insertion sites (PolyA-seq and CELTICS-seq), we demonstrated that the presence of an active human L1 retrotransposition significantly increases the frequency of chromosomal translocations. By identifying L1-dependent translocation hotspots in HEK293T cells we highlight the requirement for the L1 reverse transcriptase (RT) activity and the crucial role of pre-existing DNA DSBs in promoting L1-mediated chromosomal translocations. L1-dependent translocation hotspots showed a marked preference for transcription end sites (TES) of active genes, early replication timing regions, and accessible chromatin regions. Therefore, while cancer genome analysis provides a static view of chromosomal rearrangements based on canonical L1 integrations, our functional studies reveal an unanticipated predominance of chromosomal translocations facilitated by non-canonical L1 retrotransposition via RNA-templated repair of existing DSBs, largely expanding our knowledge on the mechanism by which L1 retrotransposition induces genomic instability in human cancers.

#0405 Translocation detection in cancer using low-pass pore-c sequencing.

S. Hickey, X. Dai, S. Aganezov, J. Beaulaurier, E. Harrington, S. Juul;
Oxford Nanopore Technologies, New York, NY

Complex chromosomal rearrangements, including translocations, play a critical role in oncogenesis and are often identified as recurrent genetic aberrations in hematologic malignancies and solid tumors[1]. Translocation detection by karyotyping of an individual's metaphase chromosomes remains challenging for detection of balanced rearrangements, which have no gain or loss of genetic material. Rearrangement detection using whole-genome sequencing is a viable alternative, but it relies on breakpoint-spanning reads and requires high sequencing depth (30-60x) with long reads to achieve high sensitivity, especially in repetitive regions of the genome[2]. Here, we describe a workflow for translocation detection at low sequencing depth with Oxford Nanopore's long read chromatin conformation capture technique, Pore-C[3]. Importantly, for translocation calling, Pore-C does not rely on breakpoint-spanning reads but rather the high intrachromosomal interaction frequency of genomic regions around the breakpoint, thus largely lowering sequencing depth requirements and reducing mapping issues in low complexity regions. We prepared, barcoded, and sequenced Pore-C libraries of 3 cancer cell lines including lung cancer (A549), Acute Monocytic Leukemia (THP-1), melanoma (COLO 829) and its matching normal (COLO 829 BL) on a single Q20+ MinION flow cell (FLO-MIN114). Genome-wide contact maps of low-pass data (<1.5 Gbps per sample) were compared against higher depth (>30 Gbps per sample) Hi-C maps [4], revealing that low-pass Pore-C successfully captured large-scale genomic rearrangement. For example, chromosomal pairs chr8-chr11 and chr15-chr19 in A549, chr9-chr11 and chr1-chr20 in THP1, and chr7-chr15 in Colo829 were detected at <0.5X depth of sequencing coverage. These translocation events were further validated by breakpoint analysis using adaptive sampling, where targeted regions were previously confirmed by independent studies[4],[5]. Low-pass Pore-C detects translocations in an unbiased manner and does not require prior knowledge of the translocation structure. Combined with its simple sample-preparation workflow and the capability to provide genome-wide copy-number information in a single experiment, it can serve as a cost-effective and comprehensive tool for cancer genomic studies. [1] Chromosomal translocations in human cancer, Nature, 372, 143 (1994) [2] Hi-C as a tool for precise detection and characterisation of chromosomal rearrangements and copy number variation in human tumors, Genome Biology, 18, 125 (2017) [3] Identifying synergistic high-order 3D chromatin conformations from genome-scale nanopore concatemer sequencing, Nature Biotechnology, 40, 1488(2022) [4] Chromosomal translocations detection in cancer cells using chromosomal conformation capture data, Genes (Basel), 13, 7 (2022) [5] A multi-platform reference for somatic structural variation detection, Cell Genomics, 2, 6 (2022)

#0406 Characterization of whole genome duplication in a genomic cohort of over 14000 cell free DNA samples.

A. Gross, H. Wang, D. Tolkunov, C. Jenkins, S. Wienke, C. Barbacioru, H.-Y. Chuang;
Guardant Health, Palo Alto, CA

Background: Wide-scale rates of whole genome duplication (WGD) have previously been demonstrated in studies performed in tissue among genomically characterized tumors. Such studies report varied rates of WGD depending on tumor type and stage. Hallmarks of WGD include widespread loss-of-heterozygosity as well as associations with tumor proliferation and specific oncogenic driver events such as loss of function TP53 mutations. It has been proposed that presence of WGD could be a poor prognostic biomarker, leading to interest in profiling this genomic landmark in large retrospective cohorts to inform future clinical studies.
Methods: Samples that were run through the GuardantOMNI high content genomic profiling assay using cfDNA extracted from blood were analyzed. Only samples originating from individuals with primary breast, colorectal, or prostate cancer were considered due to limited sample size in other indications. We deployed a likelihood-based copy-number variant caller, which jointly selects tumor purity and ploidy while fitting normalized coverage and germline variant allele frequencies across genome-wide data. Only samples where we predicted to have greater than 10% tumor fraction from copy number variant (CNV) profiles were considered for statistical analysis. The presence of whole genome duplication was assessed by counting the median major chromosomal copy number. Presence of SNV/InDels were annotated, assessed for pathogenicity, and filtered to those with a pathogenic allele frequency greater than 10%.
Results: A total of 14,076 samples were analyzed, with 5362 passing the 10% observed tumor fraction cutoff. WGD was annotated in 2195 (41%) samples with varying rates across sub-cohorts (31%, 36%, and 54% of breast, colorectal, and prostate cancer, respectively). Mutation in TP53 was associated with a large increase in rate of WGD (odds ratio 6.9, 95% CI 6.1-7.8) which is consistent but higher in magnitude to similar studies in tissue samples. Amplification of CCNE1 and homozygous deletion of genes including WRN and RB1 were also associated with WGD, independent of TP53 mutation status and overall rates of aneuploidy.
Conclusion: WGD was detected in 41% of samples with greater than 10% tumor fraction in cell-free DNA across three cancer types. While this represents a substantial percentage of advanced cancers, more research needs to be done regarding the impact of these events on clinical outcomes and treatment response. Additionally, co-occurrence of these events with other advanced cancer biomarkers such as microsatellite instability or homologous recombination deficiency was not reported. Given the high rates of these events, future retrospective studies are warranted to correlate presence of WGD with patient outcomes and response.

#0407 RNA:DNA hybrid/R-loop determinants variation in distinct basal-like breast cancer cells.

O. Kapali, V. Kuznetsov;
SUNY Upstate Medical University, Syracuse, NY

Introduction: Despite progress in treatment methods and diagnosis, breast cancer remains one of the world's leading cancers causes of death. Among the various subtypes, basal-like breast cancer (BLBC) is highly diverse, low differentiated, most aggressive form with poor prognosis. Co-translational R-loops are created by combining G-rich RNA with complementary C-rich DNA (RNA: DNA hybrid), which creates a three-stranded nucleic acid structure. R-loops are often associated with genome instability and aggressiveness of cancers. However, their role in the diversity of BLBC remains controversial and poorly understood. This study aims to characterize RNA: DNA hybrid variations in BLBC from a cellular, genetic, and biochemical perspective.
Methods: This study investigates the variation of RNA: DNA hybrid formation in stable BLBC cells. We utilize a panel of stable basal-like cell lines (MDAMB231, MDAMB436, SUM149PT) and proliferative non-cancer cells (MCF10A). They represent different genetic and cell lineages in BLBC development which allows us to study R-loop distribution in different basal lineage cells . Luminal breast cancer cells (MCF7) were used in comparative analysis. To detect RNA: DNA hybrids, we optimized Immunofluorescence (IF) specificity using RNase III and H enzymes. Predictions from Quantitative Model of R-loop Forming Sequences (QmRLFS) identify RLFS in specific gene regulatory regions. This design allows us to define R-loop position and boundaries, and optimize primers for the DRIP-qPCR which quantifies RNA: DNA hybrid enrichment in transcription regulatory sites for several breast cancer-associated genes such as BRCA1, TP53, PTEN, and AURKA. The expression of these genes was detected using RTqPCR.
Results: Our IF and computational image analyses demonstrated that RNA: DNA hybrids are present not only luminal cells (as found by others), but also in the studied BLBC cells. The non-cancer proliferative cells (MCF10A) show low RNA: DNA hybrid signals bolstering our experimental technique. Variation of the RNA: DNA hybrid signals were distinct in various BLBC cells which was supported by the DRIP-qPCR and RTqPCR findings. The R-loop formation data variations was referred to the cell line contexts and the studied genes responsible for tumor suppression, DNA damage/repair signaling and impair apoptosis in breast cancer.
Conclusion: Our study suggests that RNA: DNA hybrids are formed and distributed heterogeneously in the genomes and gene regions of stable BLBC cell lines, while in basal proliferative (non-cancer) cells hybrid signals are weak. A subset of the RNA: DNA hybrids might be particularly significant at certain gene loci contributing to tumor progression, indicating their significance in BLBC pathogenesis. This study provides insights into the cellular and molecular basis of the BLBC heterogeneity and implicates the RNA:DNA hybrid as a potential diagnostic and therapeutic markers.

#0408 NEK1 phosphorylation modulates ERCC6 in transcription coupled nucleotide excision repair with implications for prostate cancer.

Oluwatobi M. Ogundepo, Arrigo De Benedetti

Biochemistry and Molecular Biology, Louisiana State University Health Sciences Center, Shreveport, Shreveport, LA

NER operates through two distinct pathways: global genome repair (GGR) and transcription-coupled repair (TC-NER). TC-NER, as its name suggests, is specifically dedicated to rectifying lesions that obstruct the progression of RNA polymerase during active transcription . This process is imperative for the maintenance of cellular homeostasis, as lesions encountered by the transcription machinery can lead to stalling, erroneous transcription, and ultimately, deleterious cellular outcomes. At the heart of the TC-NER pathway lies ERCC6, a helicase orchestrating the repair of DNA lesions within transcribed regions of the genome. ERCC6 (AKA CS-B) plays a pivotal role in detecting and coordinating the repair of transcription-blocking lesions and has been implicated in a plethora of cellular processes underscoring its multifaceted nature and its broader impact on genome stability and cellular health, as exemplified by the severity of syndromes in individuals with loss-of-function mutations. In the US, compared to Caucasians (CC), AA are at higher risk for developing PCa and have more aggressive disease that is refractory to treatment, to some extent explained by genetic differences in some cases attributed to alterations of their “Repairome”. GWAS revealed that, unlike CC, 89% of AA-PCa have at least one mutation in NER pathway genes. A defect in ERCC6 activity, either through reduced expression or mutation (e.g., M1097V found frequently in AA) may result in impaired TC-NER. This may be compounded by aging or obesity-related oxidative stress, resulting in progressive accumulation of damaged bases (e.g., 8-OG) and consequent (cancer-propensity) mutations, the correction of which involves BER or NER. This was investigated in part with PCa cell lines engineered via CRISPR-SDM to carry that particular genomic mutation, by studying their sensitivity to UV and the efficiency of removal of CPDs in vivo. In addition, we have begun investigation of its function in the variants (engineered and naturally found in PCa. Lines) in vitro, after IP from cells, by studying its intrinsic ATPase activity. We have also identified the kinase NEK1 as an important novel interactor and regulator of ERCC6. We previously identified NEK1 as being an early regulator of the adaptive response of PCa cells to ADT.

#0409 Deciphering chromosomal instability in consensus molecular subtypes (CMS) in CRC: Insights from an integrative multi-omics approach.

J. Bischof[1], J. Woodsmith[1], D. Church[2];
[1]Indivumed GmbH, Hamburg, Germany, [2]University of Oxford, Oxford, United Kingdom

CRC is a heterogeneous disease with different molecular subtypes, which can have a profound impact on treatment response and patient outcomes. CMS classification based on gene expression profiles has been shown to differentiate patients into clinically relevant sub-groups. However, deep multi-omics characterization of the CMS classes based on high quality patient data is lacking. Through the integration of multi-omics data, we aim to enhance our understanding of CRC's molecular heterogeneity and thereby facilitate the development of personalized therapeutic strategies.
We performed a multi-omics analysis of CRC patients to identify potential new features of CMS groups. 890 fresh-frozen, surgically resected CRC tumor and adjacent normal samples were used to analyze whole genome and RNA sequencing data. DNA and RNA was prepared using Qiagen AllPrep Universal and KAPA Hyper Prep kit (DNA), as well as TruSeq Stranded Total mRNA kits and sequenced on a NovaSeq6000 system. We identified CMS subtypes based on RNA-Seq data and performed all statistical analyses using R.
Our analysis revealed distinct molecular characteristics across the four CMS subtypes, including unique driver mutations, signaling cascades, and immune cell infiltration profiles. The poor prognosis associated with CMS4 patients was corroborated by our clinical data. Notably, we observed high global chromosomal instability (CIN) profiles for both CMS2 and CMS4 and identified recurrent global aneuploidy patterns within these subtypes that link alterations of known cancer genes to these large-scale structural events. We found higher levels of CIN in CMS2 compared to CMS4, which appears to be predominantly driven by numerical, rather than structural CIN. Specifically, in CMS2, SMAD2/4 is commonly impacted by deletion on chromosome arm 18q, while PLCG1 is more influenced by amplifications on 20q respectively, suggesting potential values as CRC CMS biomarkers.
In conclusion, our integrative multi-omics analysis offers a comprehensive understanding of CRC molecular subtypes, which can inform personalized treatment strategies. Our findings underscore the importance of considering not only specific driver mutations but also large-scale structural rearrangements in the context of CMS subtypes.

#0410 ASXL3 is a potential biomarker of response of SCLC to targeted therapies.

R. Wang, H. Wang, X. Wu, K. Mishra, S. Shiffka, F. Hernandez, M. Zhang, U. T. Tolunay, S. Gara, S. Xi, S. R. Carr, C. D. Hoang, D. S. Schrump;
National Cancer Institute, Bethesda, MD

Small Cell Lung Cancer (SCLC) has been designated a recalcitrant cancer and a priority by National Cancer Institute. Despite recent insights regarding mechanisms mediating stemness, heterogeneity, and metastatic potential, these advances have yet to be fully translated to effective regimens for the treatment of SCLC. Previously, we identified Additional Sex Combs Like-3 (ASXL3) as a novel mediator of pluripotency in human respiratory epithelia and potential therapeutic target in SCLC. ASXL3 is one of three members of the ASXL family, whereas the functions of ASXL1 and ASXL2 as components of the PR-DUB complex have been extensively studied, the functions and significance of ASXL3 during malignant transformation remain elusive. To further investigate the relevance of ASXL3 activation in SCLC, we initially studied ASXL3 expression levels in various SCLC subtypes by qRT-PCR, digital RT-PCR, RNA-seq, and western blotting analysis. These studies demonstrated that ASCL (A) and ASCL and NeuroD1 (A+N) subtypes of SCLC cells contain thousand-folds more ASXL3 ($ASXL3^{high}$) than Pou2f3 (P) and YAP1 (Y) SCLC subtypes ($ASXL3^{low}$). ASXL3 levels were elevated when cancer cells were cultured under stemness-enriched conditions. Under normal culture conditions, $ASXL3^{high}$ SCLC cells showed higher intrinsic DNA damage, evidenced by a high percentage of γ-H2AX positive cells compared to $ASXL3^{low}$ SCLC cells. Additionally, $ASXL3^{high}$ SCLC cells displayed 38% γ-H2AX positive metaphase cells, and 42% of abnormal chromosome segregations during mitosis, including lagging chromosomes, DNA bridges, and unequal chromosome segregation indicative of profound genome instability. One reason for this extensive genomic instability is that ATM pathway activation in response to DNA replication stress is impaired in $ASXL3^{high}$ SCLC cells. Following exposures to 1mM hydroxyurea (HU) for 4, 8, and 24 hours, ATM autophosphorylation levels in $ASXL3^{high}$ SCLC cells were much lower than in $ASXL3^{low}$ SCLC cells. This insufficiency significantly affected the activation of downstream cascade targets including CHK2, KAP-1 and EZH2. Consistent with these findings, $ASXL3^{high}$ SCLC cells showed reduced sensitivities to ATM inhibitors. However, $ASXL3^{high}$ SCLC cells exhibited higher activity of PLK1 and were more sensitive to hydroxyurea. Importantly, low dose HU reduced the IC50 values of the PLK1 inhibitors, BI2536 or NMS-P937 by 80-100-fold in $ASXL3^{high}$ but not $ASXL3^{low}$ SCLC cells, suggesting a strong synergy between these two drugs in $ASXL3^{high}$ SCLC cells. Collectively, these findings suggest that ASXL3 functions to protect cells from lethality induced by genomic instability through monitoring ATM activation. Experiments are underway using SCLC PDX models to demonstrate the efficacy of this combined treatment in-vivo as a prelude to possible evaluation of this drug combination in SCLC patients.

#0411 PI3K-AKT-mTOR signaling pathways play important roles in chromosomal instability-induced innate immune response in cancer cells.

R. Kamata[1], H. Saito[1], Y. Hakozaki[1], Y. Kashima[2], G. Yamamoto[1], T. Y. Morita[1], P. Lu[3], **A. Ohashi**[1];
[1]National Cancer Center Japan, Chiba, Japan, [2]The University of Tokyo, Chiba, Japan, [3]Frederick National Laboratory for Cancer Research, Frederick, MD

Background: Chromosomal instability (CIN) frequently exerts innate immune response, being expected to sensitize immunotherapy. cGAS-STING pathway is a hub to regulate CIN-mediated innate immune activation. We previously demonstrated that small-molecule inhibitors targeting Centromere-associated Protein-E (CENP-E) profoundly accumulated CIN in cancer cells, leading to activation of cGAS-STING and its related innate immune pathways. In this study, aiming to deeply understand molecular mechanisms of CENP-E inhibitor (CENP-Ei)-induced CIN and innate immune activation, we conducted large-scale chemical screening with ~1,400 kinase inhibitors in CENP-Ei-treated reporter cells for NF-κB and IRF. We also experimentally validated the effects of hit compounds on CENP-Ei-induced innate immune activation.
Material and Methods: GSK923295 and Cmpd-A were used as CENP-E inhibitors. HeLa, A549, A549 dual reporter cells were treated with the CENP-Ei at the indicated concentrations, subjected to immunofluorescent, transcriptome, FACS, reporter activity, or gene expression analyses. High-throughput screening (HTS) with ~1,400 kinase library was conducted in A549 dual reporter cells in combinational treatment with GSK923295. Combination effects of the representative hit compounds were confirmed in matrix-combination studies with the CENP-Ei.
Results: Treatment with the CENP-Ei, Cmpd-A and GSK923295, induced CIN (e.g., multinucleation) in both A549 and A549 dual reporter cells, which elevated NFkB and IRF reporter activities as well as gene expressions of inflammatory cytokines and chemokines in innate immune pathways. Transcriptome analyses also confirmed that gene ontologies (GO) for innate immune response, such as cytosolic DNA sensing pathway and cytokine-cytokine receptor interaction pathway, were significantly enriched in CENP-Ei-treated CIN cells. Next, we conducted HTS of IRF-reporter activity with ~1,400 kinase library in combination with GSK923295 in A549 dual reporter cells. The HTS revealed that a series of inhibitors targeting PI3K-AKT-mTOR signaling pathways intensively suppressed CENP-Ei-induced IRF activation, which occupied ~40% of hit compounds. The matrix-combination studies confirmed that sapanisertib (TORC1/2 inhibitor) significantly attenuated CENP-Ei-induced IRF activity.
Conclusions: CENP-Ei-induced CIN potently activates innate immune response pathways in cancer cells, in which PI3K-AKT-mTOR signaling pathway appears to be involved. We are initiating AI-based drug discovery to develop novel CENP-E inhibitors.

#0412 Discovery and preclinical characterization of ISM9342A, a novel, potent, and orally bioavailable WRN inhibitor that suppresses MSI-H tumor growth.

P. Zhao[1], W. Zhu[1], X. Ding[1], J. Wan[1], X. Chen[1], M. Zhang[1], X. Ding[1], S. Bavadekar[2], **S. Rao**[2], F. Ren[1], A. Zhavoronkov[1];
[1]Insilico Medicine, Shanghai, China, [2]Insilico Medicine, New York, NY

Loss of function mutations in DNA mismatch repair genes can result in microsatellite instabilities (MSI) and high levels of MSI (MSI-H) contributes to tumorigenesis and is frequently observed in endometrial carcinoma, gastric cancer, and colorectal cancer. Although immune checkpoint inhibitors have been approved for the treatment of MSI-H tumors, there is still a large proportion of patients with MSI-H tumors who fail to respond to these therapies. Recently, two independent genome-wide loss of function screens have identified Werner syndrome helicase (WRN) as the top dependency for MSI-H cancer cell viability. WRN plays important roles in DNA repair and in the maintenance of genome integrity. Given that WRN deficiency selectively impairs the viability of MSI-H but not microsatellite stable cancer cells, WRN is a synthetic lethal target for MSI-H tumors.
ISM9342A is a novel and potent WRN inhibitor exhibiting single digit nanomolar IC_{50} values in both ATPase and helicase assays. ISM9342A suppressed the proliferation and increased double strand break markers in MSI-H cancer cells. Moreover, ISM9342A demonstrated promising *in vivo* anti-tumor efficacy in an MSI-H xenograft model along with tumor regression. ISM9342A demonstrated good drug-like properties, including excellent *in vitro* ADMET profiles and good *in vivo* exposure, including low clearance and optimal oral bioavailability across multiple preclinical species. Collectively, these findings highlight the potential of ISM9342A as a highly potent WRN inhibitor for the treatment of MSI-H tumors

#0413 Aneuploid cells depend on the RAF/MEK/ERK pathway and on RNA degradation for overcoming DNA damage and transcriptional burden.

M. Ippolito[1], J. Zerbib[2], Y. Eliezer[2], E. Reuveni[2], S. Vigano[1], G. De Feudis[1], A. Kadmon[2], A. Ratti[1], S. Martin[1], K. Laue[2], Y. Cohen-Sharir[2], S. Scorzoni[1], F. Vazquez[3], U. Ben-David[2], S. Santaguida[1];

[1]IEO - European Institute of Oncology, Milano, Italy, [2]Department of Human Molecular Genetics and Biochemistry, Faculty of Medicine, Tel Aviv University, Tel Aviv, Israel, [3]Broad Institute of MIT and Harvard, Cambridge, MA

Aneuploidy, a state of karyotype imbalance, is a hallmark of cancer. Understanding the broad implications of aneuploidy at molecular, cellular, and physiological levels is crucial for effectively targeting aneuploid cancer cells. Aneuploidy often results in specific stress responses within cells, which must adapt to for survival and growth. Exploring these adaptive mechanisms to aneuploidy open avenues for targeted cancer therapies. Here, we induced aneuploidy in non-transformed RPE1-hTERT cells, generating multiple stable clones each exhibiting varying degrees of chromosomal imbalances. Employing a comprehensive genomic profiling strategy, we analyzed six isogenic clones using whole-exome and RNA sequencing. We uncovered a complex landscape, where each degree of aneuploidy brought its own set of changes and challenges. Additionally, we explored their cellular dependency landscapes, performing genome-wide CRISPR/Cas9 screenings along with extensive drug screens. As previously reported, we observed and confirmed increased DNA damage and p53 pathway activation in the aneuploid cells. We also found that the aneuploid clones triggered the DNA damage response (DDR), leading to an increased resistance to further DNA damage. Interestingly, we observed that aneuploid cells showed increased activity in the RAF/MEK/ERK pathway. Moreover, these cells demonstrated a heightened sensitivity to a range of clinically significant drugs that target this pathway, in particular in response to both genetic and chemical inhibition of CRAF. The activity of CRAF was found to be functionally connected to the resistance against DNA damage induction, and the inhibition of CRAF making aneuploid cells more susceptible to chemotherapies that induce DNA damage. Next, we observed increased of RNA synthesis and degradation in the aneuploid cells, along with heightened activity in both the nonsense-mediated decay (NMD) and the microRNA-mediated mRNA silencing processes. As a result, aneuploid cells displayed increased sensitivity to the perturbation of several key components of RNA degradation pathways. Furthermore, the dependencies of aneuploid cells on RAF/MEK/ERK activity and on intact RNA degradation were confirmed through examining a broad range of human cancer cell lines, emphasizing their significance in human cancer. Altogether, our results provide a comprehensive resource of karyotypically stable cells representing a range of aneuploidy states, and they reveal previously unidentified weaknesses in aneuploid cells that may be crucial for therapeutic developments.

#0414 Accelerating DDR related drug discovery through a customized cell panel.

Cong Huang, Xiaoqing Li, Zhengtai Li, Yan Tan, Huawei Pan, Lizhen Zhou, Kejun Mao, Yanyan Qin, Zhida An, Wanxiao Song, Yifan Li, Shuyu Jin, **Tiejun Bing**

ICE Bioscience, Inc., Beijing, China

DNA damage is a major threat to cell survival. Not properly repaired DNA damage can lead to cell senescence, apoptosis or tumor development. DDR (DNA Damage Repair) is a collection of bioprocesses which cells utilize in order to identify and correct the DNA damage of the genome. The usage of various compounds for targeting DNA damage responses as well as attenuating DNA repair is also an approach for cancer therapy that has been widely studied in recent years. Despite the success of drug discovery of DDR related inhibitor, drug resistance has become an emerging issue of the field. Here we have constructed multiple cancer cell lines which are either DDR gene, such as XRCC1 and FANCD2, knock-out or resistant to certain DDR inhibitors. Together with the corresponding parental cell lines, we have generated a DDR cell panel which covers 11 different cancer types. We have first validated those DDR inhibitor sensitive or resistant cell lines with functional cell proliferation assays. Additionally, RNAseq has been performed for all constructed resistant cell lines. In combination with a thorough bioinformatic analysis using our in-house generated algorithms, we can provide the genetic background information of the resistant cell lines and top features that potentially contribute to the resistance mechanism. The representative data in this study has shown that LINC02709, BDKRB1, and PRKCQ are the top featured genes in A375 Vemurafenib resistant cell. Meanwhile, cell cycle, ECM-receptor interaction, and DNA replication are the most enriched KEGG terms. Lastly, we have validated this cell panel against multiple inhibitors targeting different DDR vital proteins such as ATM, PARP, POLQ etc. The result has shown that our unique DDR cell panel is capable of providing fast and comprehensive evaluation of DDR related inhibitors, thus facilitate faster and more efficient discovery of DDR inhibitors in the cancer therapy field.

#0415 Keratin-fusion mutation promotes tumor aggressiveness via genomic instability induction.

H.-H. Chuang, B. Y. Kuo, K. Sriramadasu, Y.-C. Chen, J. J. Sheu;
National Sun Yat-sen University, Kaohsiung, Taiwan

Keratin intermediate filament is one critical component of cellular architectures, which provides necessary mechanical support to vanquish environmental stresses. Our previous study shows that keratin fusion mutation promotes tumor aggressiveness via enhancing cancer stemness in oral squamous cell carcinoma. It implies proper functions of keratins play a critical role in maintain cell integrity and fate determination. In the present study, keratin fusion mutation functions as a driver to promote genomic instability via centrosome overduplication and trigger the formation of polyaneuploid cancer cell (PACC). Interestingly, genes involved in DNA damage repair were found upregulated in keratin fusion expressing cells, an important feature for mitotic slippage during cancer progression. In addition, PACCs caused by keratin fusion render cancer cells insensitive to cisplatin treatment, which coupled with lower levels of γH2AX induction and higher survival rates. Transcriptome analyses revealed enhanced activity for Regulation_of_Actin_Cytoskeleton in the PACCs, leading to increased actin filament network and higher invasiveness. In summary, keratin fusion mutation promote cancer aggressiveness through genomic instability-mediated PACC formation and cytoskeleton remodeling, which lead to enhanced drug resistance and metastasis.

#0416 Development of substituted oxindole derivatives as a Ku-targeted DNA-PK inhibitors for cancer therapy.

D. Chauhan[1], P. L. Mendoza-Munoz[2], N. Kushwaha[1], H. Aruri[1], J. J. Turchi[2], **N. S. Gavande**[1];
[1]Wayne State University, Detroit, MI, [2]Indiana University School of Medicine, Indianapolis, IN

DNA double strand breaks (DSBs) are the most cytotoxic type of DNA damage. DSB repair pathway deficiency, often observed in cancer cells, results in translocations and genetic mutations that contribute to genomic instability. The generation of DNA DSBs is the primary mechanism of numerous chemo- and radio-therapeutic strategies used to treat various cancers. Modulating DSB repair pathways can have a profound impact on the clinical efficacy of DNA damaging therapies. DNA-dependent protein kinase (DNA-PK), which is composed of a DNA-PK catalytic subunit (DNA-PKcs) and Ku80-Ku70 heterodimer, acts as the molecular sensor for DSB and plays a prime role in DSB repair through non-homologous end joining (NHEJ). DNA-PK inhibitors become an attractive therapeutic target for cancer in combination with DSB-inducing radiotherapy and chemotherapy. There are at least 6-7 DNA-PK inhibitors in the preclinical and clinical stages which exhibit potential as treatment for various cancers. However, we have taken a unique and innovative approach to inhibiting DNA-PK via blocking the Ku70/80 heterodimer interaction with DNA, an essential step in DNA-PK activation and phosphorylation activity. Exploiting this unique mechanism of kinase activation, we have expanded our structure-activity relationships of pyrrolone derivatives. Modified synthetic schemes have been developed to allow a series of modifications to the X80 core structure. We have prepared furan, thiophene and pyrrole derivatives that enabled the identification of pharmacophores that impact in vitro potency and cellular off-target toxicity. Towards addressing cellular uptake and bioavailability, we identified substituted oxindole derivatives as potent Ku and DNA-PK inhibitors. These oxindole derivatives exhibited a better cellular uptake while retaining potent Ku inhibitory activity. Our data demonstrate that the cellular effects observed are a function of Ku inhibition and that this novel class of DNA-PK inhibitors can be further developed as anti-cancer therapeutics that can be used as an adjuvant to, or concomitant with radiotherapy and other cancer therapies that induce DNA damage.

#0417 Chromosomal instability leads to durable tumor suppression upon macrophage-checkpoint disruption, with induction of anti-tumor IgG.
D. E. Discher;
University of Pennsylvania, Philadelphia, PA

Solid tumors generally exhibit chromosome copy number variation caused by chromosomal instability (CIN) in mitosis, and the resulting aneuploidy associates with poor prognosis in various cancer types and poor Tcell checkpoint blockade response in melanoma. In such contexts, however, macrophages and the SIRPa-CD47 checkpoint are understudied. Here, CIN is induced pharmacologically in poorly immunogenic B16F10 mouse melanoma cells, generating micronuclei plus diverse aneuploidy and skewing macrophages towards an anti-cancer phenotype based on markers and short-term tumor studies. Mice bearing CIN-afflicted tumors with wild-type CD47 levels survive only slightly longer compared to chromosomally stable controls, but long-term survival can be maximized when anti-tumor IgG opsonization is combined with adoptive transfer of macrophages with SIRPa blockade or with CD47 knockout of the B16F10. Multi-epitope, *de novo* anti-cancer IgG in survivors promote phagocytosis of CD47 knockout B16F10 cells by macrophages and suppress tumoroids *in vitro* and growth of tumors *in vivo*. An unexpected benefit of pairing CIN with maximal macrophage anti-cancer activity is thus an anti-cancer vaccination-like response that can lead to durable cures and potentiate cell-mediated acquired immunity.

#0418 BLM helicase unwinds lagging strand substrates to assemble the ALT telomere damage response.

A. M. Krishnan[1], H. Jiang[1], T. Zhang[1], H. Kaur[2], T. Shi[1], Y. Kwon[2], P. Sung[2], R. A. Greenberg[1];
[1]University of Pennsylvania, Philadelphia, PA, [2]The University of Texas Health Science Center at San Antonio, San Antonio, TX

The Bloom Syndrome helicase (BLM) is critical for Alternative Lengthening of Telomeres (ALT), a homology directed repair mediated telomere maintenance mechanism that is prevalent in cancers of mesenchymal origin. The DNA substrates that BLM engages to direct telomere recombination during ALT remain unknown. Here, we determine that BLM helicase acts on lagging strand telomere intermediates that occur specifically in ALT positive cells to assemble a replication stress associated DNA damage response. Loss of ATRX was permissive for BLM localization to ALT telomeres in S and G2 commensurate with the appearance of telomere C-strand specific single-stranded DNA. Moreover, DNA2 nuclease deficiency increased 5'-lagging strand flap formation and ALT in a BLM dependent manner, and BLM promoted ALT in response to telomere C-strand, but not G-strand, single-stranded nicks. These findings define the seminal events in the ALT DNA damage response, linking aberrant lagging strand DNA replication with a BLM directed HDR mechanism that sustains telomere length in a subset of human cancers.

#0419 Evolutionary trajectories of complex genome rearrangements in osteosarcoma.

I. Cortes Ciriano[1], J. Espejo Valle-Inclan[1], S. de Noon[2], K. Trevers[2], H. Elrick[1], A. M. Flanagan[2];
[1]European Bioinformatics Institute, Cambridge, United Kingdom, [2]University College London, London, United Kingdom

Whole-genome sequencing (WGS) studies have revealed that osteosarcoma genomes are riddled by remarkably intricate forms of structural variants (SV), collectively known as complex genomic rearrangements (CGR). Yet, most CGR detected in osteosarcoma remain unexplained, hinting at the possibility of undiscovered mechanisms that might lead to novel therapeutic strategies. To elucidate the mechanisms underpinning cancer genome complexity in osteosarcomas and the downstream consequences of CGR during tumor evolution, we uniformly processed exiting osteosarcoma WGS data sets and performed high-depth (>120x) multi-regional short- and long-read WGS for hundreds of osteosarcomas. We found that whole genome doubling and diverse types of CGR are frequent clonal events in most osteosarcomas. Through the integration of multi-regional WGS data, we discovered that in tumors with whole-genome doubling, cancer genome evolution and oncogene amplification are the consequence of multi-generational CGR triggered by whole-genome doubling and involving multiple mechanisms, especially chromothripsis and breakage-fusion-bridge cycles. By contrast, in tumors without whole-genome doubling, biallelic inactivation of TP53 and oncogene amplification frequently occur as part of a cascade of genomic instability initiated by a single double-strand break upstream of the TP53 locus. This process results in clonal diversification and rapid tumor growth suggestive of punctuated evolution. In addition, we found that subclonal CGRs are also frequent events. Indeed, clonal expansions triggered by the acquisition of subclonal CGR often colonize distant tumor regions, suggesting that CGR act as subclonal driver events. Finally, we show that some recurrent genomic alterations are prognostic of poor survival, which we validate in independent cohorts.
In sum, using WGS data, we have elucidated the mechanisms underpinning the complexity and evolution of osteosarcoma genomes. Our results indicate that diverse types of CGR, such as chromothripsis, are triggered by whole genome doubling and occur throughout tumor evolution, which primes the cancer genome for ongoing genomic instability, rapid karyotype evolution and clonal diversification. These results have implications for our understanding of the molecular basis of intra-tumor heterogeneity and drug resistance in osteosarcomas and other cancers driven by genomic instability.

#7119 Clinic-ready Polθ inhibitor SYX1097 suppresses solid tumors in vivo.

Y. Zhang, K. Jiang, X. Xu, L. Wu, C. Ge, Y. Xie, H. He, S. Liu, **X. Tang**, S. Shi;
SynRx Therapeutics, Hangzhou, China

A large fraction of tumors with BRCA1 or BRCA2 mutations only have weak responses to PARP inhibitor (PARPi) treatment, and often develop PARPi resistance. To address these challenges, we have developed SYX1097, a selective and potent oral Polθ inhibitor as a single agent or in combination with PARPi for treating tumors with BRCA mutations. Both Polθ and PARP1 play key roles in microhomology-mediated end joining for DNA double-strand repair and in single-strand DNA gap filling during DNA replication.

Using in vitro cellular assays and in vivo animal models, we show that SYX1097 alone or combined with PARPi without obvious side effects. SYX1097 dramatically inhibited proliferation in BRCA -/- isogenic cells with IC_{50} <20 nM, while only had very weak effect on their parental cells (>10000nM). SYX1097 also enhanced tumor cell sensitivity to Olaparib 5 to 15 times. SYX1097 *in vivo* efficacious started at 50mg/kg mono-therapy, and generate >50% tumor regression at 5mg/kg when combined with Olaparib. In a 20-day repeated dosing study, SYX1097 200mg/kg BID was fully tolerated by mice. When considering additive hematological toxicity, comparing with “ATRi + PARPi”, “SYX1097 + PARPi” manifested deep and durable tumor regression without significant body weight loss or reticulocytes decrease. Moreover, SYX1097 is found synthetic lethal with defect of genes **not** involved in homologous recombination repair and able to suppress tumors with specific gene defect in vivo, which indicated SYX1097 can be used as single agent guided by specific biomarker.SYX1097 has a clean safety profile tested with Safety-Screen 44^{TM} Panel, and is well tolerated in mice, rats and dogs. It possesses remarkable pharmacokinetic properties in various species, with no hematological toxicity observed during the preclinical toxicity studies. SYX1097 is advancing towards IND filing in 2024.Collectively, SYX1097 is a promising small molecule that may be utilized as a single agent or in combination with PARPi for cancer treatment not only limited by HR deficiency.

MOLECULAR/CELLULAR BIOLOGY AND GENETICS: Metabolic Pathways 1
Poster Session

#0423 Cell state-specific genomics to define plasticity along the epithelial-mesenchymal transitioncontinuum.
D. K. Williams, N. Hou;
Columbia University, New York, NY

The epithelial-to-mesenchymal transition (EMT) is a biological process that allows epithelial cells to convert into a mesenchymal phenotype, acquiring increased mobility and the capacity to migrate. EMT has historically been represented as binary states; however, a growing consensus supports an EMT continuum involving multiple intermediate stable states. While we lack a comprehensive understanding of the EMT continuum, several reports indicate that the late stable states lead to optimal stem cell traits for cancer. In addition, it has been suggested that EMT heterogeneity within tumor cell populations is associated with poor patient prognosis. Hence, there is a clear need to define the genetic drivers of EM plasticity in heterogeneous cell populations along the EMT continuum. To fulfill this need, we will collect and analyze single cell RNA sequencing (scRNA-seq) data from EMT-cell-state specific genetic CRISPR screens on EMT-heterogeneous cell populations. Here, we apply a series of cloning techniques including polymerase chain reaction and Gibson ligation to engineer an adeno-associated virus (AAV) plasmid containing the avian TVA receptor gene under control of the N-cadherin promoter. Since N-cadherin is predominantly expressed in mesenchymal cells, this AAV enables us to generate cell lines that will exclusively express the TVA receptor when in a mesenchymal state. Consequently, we will be able to deliver mesenchymal-specific CRISPR gene edits via an avian retrovirus-derived RCAS system.

#0424 FDX2-KO induces global down-regulation of iron-sulfur cluster-containing proteins and senescence-like growth arrest or death in ovarian cancer cells.

S. Miyahara[1], M. Ohuchi[2], M. Nomura[2], K. Hayashi[2], M. Shimada[1], N. Yaegashi[1], N. Tanuma[2];
[1]Tohoku University Graduate School of Medicine, Sendai, Japan, [2]Miyagi Cancer Center Research Institute, Natori, Japan

Iron-Sulfur clusters (Fe-S) are synthetized in mainly mitochondria and binds to various proteins (Fe-S proteins). Fe-S proteins play important roles in various cellular functions including energy metabolism, nucleic acid synthesis or redox homeostasis. However, roles of Fe-S clusters in cancer cells are not fully understood. Here, we report that loss of Fe-S biosynthesis causes proliferation arrest with DNA-damage response or cell death depend on TP53 status in ovarian cancer (OVC) cells. CRISPR-screening of all metabolism-related genes identified that Fe-S biosynthesis is essential for OVC proliferation. We chose one of the Fe-S biosynthesis factors, FDX2, and developed a cell line that can maintain FDX2 expression doxycycline (Dox) -dependently. In these cells, FDX2-loss induced irreversible growth arrest. FDX2-KO cells also showed enlarged and flatten morphology, up-regulation of SASP factors, and DNA damage through p53/p21 pathway activation. These were all senescence like phenotypes. To know these mechanisms, we performed proteome analysis and found that FDX2-loss caused global but differential post-transcriptional down-regulation of Fe-S proteins, in turn perturbing mitochondrial respiration, iron-regulation and redox homeostasis. These results all associated with DNA damage. Furthermore, we found that FDX2-KO induced caspase dependent cell death in TP53-KO condition instead of growth arrests. These results suggest that Fe-S cluster biosynthesis is significant in OVC proliferation and fate of FDX2-KO cells depends on TP53 status (senescence or cell death). FDX2 or Fe-S biosynthesis may be a new therapeutic target of OVC.

#0425 GPD1L participates in glycerol-3-phosphate biogenesis and promotes tumor initiation and invasion in hepatocellular carcinoma.

T.-Y. Yu, L. Zhao, L. Tian, C. Kam, J.-F. Lee, D.-H. Ho, L.-K. Chan, Y.-M. Tsui, K.-F. Sze, I.-L. Ng;
Li Ka Shing Faculty of Medicine, The University of Hong Kong, Hong Kong, Hong Kong

Background: Metabolic reprogramming in hepatocellular carcinoma (HCC) has received rising interest. However, current studies often focus on fatty acid *de novo* synthesis or oxidation, but less on glycerolipids metabolism. Interestingly, in HCC, we observed frequent dysregulation in enzymes responsible for glycerol-3-phosphate shuttle, which potentially links glycolysis and glycerolipids metabolism. Hence, we aimed to identify the functional significance of glycerol-3-phosphate dehydrogenase 1 like (GPD1L), an enzyme for the shuttle, and its regulation of expression in HCC.
Methods: We utilized transcriptomic analysis of clinical HCC samples to validate the frequent overexpression of GPD1L in tumor cells and examined its association with clinicopathological features. *In vitro* and *in vivo* assays were performed to explore the functional significance of GPD1L in HCC initiation and progression. Furthermore, with targeted metabolomics analysis, we investigated the role of GPD1L in glycerol-3-phosphate shuttle in HCC. We also performed promoter study to understand the transcriptional regulation on GPD1L expression.
Results: Among GPD family members, GPD1L was consistently upregulated at mRNA level in clinical HCC samples in The Cancer Genome Atlas-Liver Hepatocellular Carcinoma (TCGA-LIHC) (N=50) and our in-house RNA-sequencing cohorts (N=41), and in a separate independent in-house cohort as examined by RT-qPCR (N=80). GPD1L overexpression was associated with increased tumor invasiveness (p=0.008) and poorer overall survival (p=0.0017) in HCC patients. Functionally, knockdown of GPD1L suppressed HCC migration (fold change ≤ 0.43) and invasion (fold change ≤ 0.40). GPD1L knockdown also inhibited tumor initiation abilities, as shown by reduced colony (fold change ≤ 0.37) and sphere formation (fold change ≤ 0.41) *in vitro*, and lower stem cell frequency (p=1.96e-9) *in vivo*. Furthermore, GPD1L knockdown enhanced sensitivity of HCC cells to chemotherapeutic drugs, sorafenib and doxorubicin. Metabolically, GPD1L facilitated synthesis of glycerolipids precursor, glycerol-3-phosphate (G3P) from glycolysis intermediate dihydroxyacetone phosphate (DHAP) in HCC. Lastly, with chromatin-immunoprecipitation and Luciferase reporter assays, we demonstrated ELF1 bound to GPD1L promoter directly to enhance the gene transcription, while knockdown of ELF1 suppressed GPD1L mRNA and protein expression.
Conclusion: Our study demonstrated the overexpression of the glycolysis-related gene, GPD1L, in HCC. GPD1L promoted tumor initiation, invasion and chemoresistance, and in turn might lead to worse clinical outcome. Metabolically, it was responsible for DHAP-to-G3P conversion in HCC and might serve as a linkage between glycolysis and glycerolipid metabolism. Our results also identified the novel role of ELF1 as the transcriptional activator of GPD1L in HCC.

#0427 A molecular signature for the G6PC3 / SLC37A2 / SLC37A4 interactors in glioblastoma disease progression and in the acquisition of a brain cancer stem cell phenotype.

S. Torabidastgerdooei, **B. Annabi**;
Universite du Quebec a Montreal (UQAM), Montreal, QC, Canada

Background: Glycogen plays an important role in glucose homeostasis and contributes to key functions related to brain cancer cell survival in glioblastoma multiforme (GBM) disease progression. Such adaptive molecular mechanism is dependent on the glycogenolytic pathway and intracellular glucose-6-phosphate (G6P) sensing by brain cancer cells residing within those highly hypoxic tumors. The involvement of components of the glucose-6-phosphatase (G6Pase) system remains however elusive.
Objective: We questioned the gene expression levels of components of the G6Pase system in GBM tissues and their functional impact in the control of the invasive and brain cancer stem cells (CSC) phenotypes.
Methods: In silico analysis of transcript levels in GBM tumor tissues was done by GEPIA. Total RNA was extracted and gene expression of G6PC1-3 as well as of SLC37A1-4 members analyzed by qPCR in four human brain cancer cell lines and from clinically annotated brain tumor cDNA arrays. Transient siRNA-mediated gene silencing was used to assess the impact of TGF-β-induced epithelial-to-mesenchymal transition (EMT) and cell chemotaxis. Three-dimensional (3D) neurosphere cultures were generated to recapitulate the brain CSC phenotype.
Results: Higher expression in G6PC3, SLC37A2, and SLC37A4 was found in GBM tumor tissues in comparison to low-grade glioma and healthy tissue. The expression of these genes was also found elevated in established human U87, U251, U118, and U138 GBM cell models compared to human HepG2 hepatoma cells. SLC37A4/G6PC3, but not SLC37A2, levels were induced in 3D CD133/SOX2-positive U87 neurospheres when compared to 2D monolayers. Silencing of SLC37A4/G6PC3 altered TGF-β-induced EMT biomarker SNAIL and cell chemotaxis.
Conclusion: Two members of the G6Pase system, G6PC3 and SLC37A4, associate with GBM disease progression and regulate the metabolic reprogramming of an invasive and CSC phenotype. Such molecular signature may support their role in cancer cell survival and chemoresistance and become future therapeutic targets.

#0429 A novel regulatory role of FLT3/ITD mutation in lipid metabolism of leukemia cells: The mechanism and therapeutic implications.

Y. Hu, F. Yin, M. Zhao, W. Lu, T. Yu;
Sun Yat-sen University Cancer Center, Guangzhou, China

Internal tandem duplication in FMS-like tyrosine kinase 3 (FLT3/ITD), is a common type of activating mutation and frequently detected in AML. FLT3/ITD is associated with poor prognosis of AML. In this study, we investigated the regulation of FLT3/ITD mutation on sterol regulatory element-binding protein (SREBP) and the therapeutic vulnerabilities of lipid metabolism in FLT3/ITD leukemia. With the transcriptomics analysis we found that FLT3/ITD controlled lipid metabolism via the transcription factor SREBP. The analysis of TCGA_LAML dataset revealed that a gene signature involved in fatty acid and cholesterol metabolism, which is regulated by SREBP, was upregulated in FLT3/ITD patients compared with FLT3/wild-type patients. The upregulation of SREBP protein expression in FLT3/ITD leukemia was confirmed using a genetically engineered mouse model. We further demonstrated that FLT3/ITD regulates the protein degradation of SREBP through the PI3K/AKT-GSK3β axis. The metabolomics analysis further showed that FLT3/ITD primarily regulates glycerophospholipid synthesis, which contribute to the key structure lipid in the membrane, specifically, the cardiolipin. Moreover, pharmacologic inhibition of SREBP activation and its downstream enzyme fatty acid synthase (FASN) sensitized FLT3-ITD AMLs to the treatment of FLT3 inhibitor quizartinib. Collectively, our findings reveal a novel regulation of FLT3-ITD in metabolic reprogramming and indicate a targetable vulnerability in a subset of refractory leukemia.

#0430 Precision diet and lipid modulating agents to induce lipid oxidation in breast cancer.

M. Yavari[1], J. Torpey[1], M. Sabatier[1], A. Carmona[1], K. Szylo[1], M. Flores[1], M. Palma[1], C. Fraser[1], Y. Liang[1], S. Hui[1], O. Zeleznik[2], H. Eliassen[1], J. Ubellacker[1]; [1]Harvard School of Public Health, Boston, MA, [2]Brigham and Women's Hospital, Boston, MA

Metastasis is the primary cause of breast cancer-related mortality, and understanding the intricate relationship between the tumor microenvironment, lipid metabolism, and metastasis is crucial for preventing cancer progression. Previous work from our group demonstrated that high exogenous levels of oleic acid, a monounsaturated fatty acid (MUFA), in the lymph node environment protects melanoma cells from ferroptosis. Ferroptosis is an iron-dependent form of cell death induced by accumulation of lipid peroxides, which are commonly formed from polyunsaturated fatty acids (PUFAs), but not MUFAs. Here, we hypothesized that increasing dietary PUFAs would alter the exogeneous lipid content of the lymph node environment, thus rendering breast cancer cells more sensitive to ferroptosis. To test this, we determined the in vitro sensitivity of 4T1 triple negative breast cancer cells to ferroptosis when treated with various PUFAs and MUFAs. We also assessed the impact of various PUFA and MUFA fatty acid-enriched diets on breast cancer metastasis and ferroptosis resistance in the lymph nodes in vivo. In concordance with previously published work, our results demonstrated that pharmacological induction of ferroptosis in vitro increased lipid oxidation and was mitigated by fatty acid treatments with higher MUFA compared to PUFA content. In vivo, cancer cells in lymph nodes of mice on palm oil diets had lower lipid oxidation compared to cancer cells from tumors in the mammary fat pad. These findings support the hypothesis that dietary lipids can alter ferroptosis response and the extent of lipid oxidation in breast cancer cells within lymph nodes. Our research has the potential to further reveal mechanistic connections between dietary lipids, the lymphatic microenvironment, and breast cancer progression.

#0431 Malic enzyme 2 inhibition reveals metabolic vulnerability in serine-dependent triple-negative breast cancer.

M. D. Slayton[1], Z. A. Farah[1], J. Jeon[2], A. Achreja[2], B. Krinkel[3], B. Nilaj[1], Y.-H. Eu[1], J. Sung[1], A. Rosenfeld[1], A. Lui[1], M. Collard[1], L. Bao[1], X. Cheng[1], C. Kleer[1], K. Loomes[3], D. Nagrath[2], S. D. Merajver[1];

[1]University of Michigan, Michigan Medicine, Ann Arbor, MI, [2]University of Michigan, Ann Arbor, MI, [3]University of Auckland, Auckland, New Zealand

Background & Hypothesis: Treatments for triple-negative breast cancer (TNBC) are limited to chemotherapy, PARP inhibitors and immunotherapies. Tumor metabolism seeks to identify metabolic pathways preferentially utilized by cancer. Malic enzyme 2 (ME2) has a role in the malate-aspartate shuttle and pyruvate and NADPH production, contributing to the redox balance and metabolite synthesis. We demonstrated that ME2 knockdown inhibits growth of TNBC cells with upregulated serine biosynthesis pathway. We hypothesized that ME2 knock-down (kd) would be growth inhibitory *in vivo*.

Methods: We used a non-tumorigenic control (MCF10a) and TNBC lines (BT20, MDA-MB-468, HCC1806, HCC70, Hs578T, SUM149). Nude mice received mammary fat pad xenografts of MDA-MB-468, to assess the impact of ME2-shRNA on growth. ME2 relevant metabolite profiling was achieved through the Promega Metabolite-Glo assay, measuring NAD, NADH, NADP, NADPH, Malate, and Glutamate. Cellular proliferation was quantified via the BioTek BioSpa 8 system and Promega CellTiter Glo. Comprehensive profiling of metabolic genes was achieved with the Nanostring nCounter across all cell lines. The potential therapeutic efficacy of NPD-389, MDSA, disodium embonate and doxorubicin was evaluated, alone or in combination, through targeted drug assays. Metabolic flux analyses, specifically mitochondrial and glycolytic function, were conducted using the Seahorse XF96, contrasting ME2-shRNA modified and control cells.

Results: ME2 kd resulted in reduced proliferation in several TNBC cell lines to varying degrees, in contrast to control MCF10a, and to Hs578T. In response to the loss of ME2, several cell lines upregulated serine biosynthesis genes, including PSAT1. MDA-MB-468 ME2 kd cells developed significantly smaller tumors in a nude mouse xenograft model. Increased malate levels, but reduced NADH and NADPH, were detected in TNBC cells with inhibited growth post-ME2 kd, but not in MCF10a or Hs578T cells. Among the tested ME2 inhibitors, NPD-389 had superior efficacy vs. MDSA and disodium embonate. Metabolic flux analysis showed compromised mitochondrial and glycolytic processes in the TNBC cell lines exhibiting growth inhibition upon ME2 kd.

Conclusions: ME2 knockdown selectively impairs cell proliferation and tumor growth in TNBC cell lines, validating its potential as a therapeutic target. The differential metabolic response, including altered malate and NADH/NADPH levels, confirms ME2's importance in TNBC metabolism. NPD-389 effectively reduced growth in ME2-sensitive lines, meriting further investigation. These findings support targeting ME2 in as a novel treatment strategy.

#0432 The noncanonical mechanism of metabolic enzyme LDHA in cancer progression.

J. Liu, W. Hu, Z. Feng;
Rutgers Cancer Institute of New Jersey, New Brunswick, NJ

Metabolic reprogramming is a hallmark of cancer cells and a key contributor to cancer progression, which is a promising target for cancer therapies. The enhanced glycolysis, also known as the Warburg effect, represents the most widely recognized metabolic alteration in cancer, wherein the majority of cancer cells undergoes reprogramming to heavily rely on glycolysis for their accelerated growth and proliferation. The glycolytic enzyme lactate dehydrogenase A (LDHA) catalyzes the conversion of pyruvate to lactate in the final stage of glycolysis. LDHA is frequently overexpressed in cancers, which plays a critical role in promoting glycolysis and cancer progression. To deepen our understanding of the oncogenic mechanism of LDHA, we screened for LDHA-interacting proteins in human breast cancer cells by liquid chromatography mass spectrometry (LC/MS) analysis. Through this strategy, small GTPase Rac1 was identified as an LDHA-interacting protein. LDHA interacted with the active form of Rac1, Rac1-GTP, and impaired the interaction of Rac1-GTP with its negative regulators, GTPase-activating proteins, leading to Rac1 activation independently of the glycolytic enzyme activity of LDHA. In addition, LDHA overexpression was significantly associated with increased Rac1 activity in clinical breast cancer specimens. Inhibiting Rac1 significantly attenuated the oncogenic effect of LDHA. Combining small-molecule inhibitors targeting LDHA enzyme activity and Rac1 activity displayed a synergistic inhibitory effect on breast cancers with LDHA overexpression in mouse models. Thus, our results revealed a novel and critical noncanonical mechanism of LDHA in promoting cancer progression through its direct interaction and activation of Rac1. Given that LDHA is frequently overexpressed in cancer, LDHA overexpression constitutes an important mechanism contributing to aberrant Rac1 activation in cancer. Importantly, our findings also suggest that pharmacologically targeting LDHA enzyme activity and Rac1 activity simultaneously is a promising strategy to treat breast cancers with LDHA overexpression.

#0433 BCAT1 promotes HCC metabolic reprogramming and survival through HIF-1α stabilization.

Misty Shuo Zhang[1], **Kenneth Kin-Leung Kwan**[1], Weixing Li[2], Adonia E. Papathanassiu[2], Irene Oi-Lin Ng[1], Carmen Chak-Lui Wong[1]

[1]Department of Pathology, The University of Hong Kong, Pok Fu Lam, Hong Kong,[2]Ergon Pharmaceuticals, Silver Spring, MD

Hepatocellular carcinoma (HCC) is a highly lethal primary liver malignancy characterized by hypoxia, a common feature of solid tumors, particularly in HCC. Hypoxia-inducible factors (HIFs) play a pivotal role in mediating various cellular processes, such as metabolic adaptation, to support the survival of hypoxic cells. The cytosolic form of branched-chain amino transferase (BCAT1) is responsible for the reversible transamination reaction between branched-chain keto-amino acids (BCKAs) and branched-chain amino acids (BCAAs), facilitating the interconversion between α-ketoglutarate (α-KG) and glutamate. Interestingly, we found that in the context of HCC, BCAT1 consumes α-KG, thereby favoring the stabilization of HIF-1α through suppressing the α-KG-dependent prolyl hydroxylase (PHD). Knockdown (KD) or knockout (KO) of BCAT or BCAT inhibitor (ERG245) suppressed HIF-1 stability, as well as HIF-1 dependent transcriptomic and metabolic changes. Mass spectrometry (MS)-based isotopic carbon tracing showed that KD/KO or ERG 245 suppressed hypoxia/HIF-1-induced glycolytic flux. Interestingly, ERG245 effectively inhibited the proliferative output of hypoxic HCC cells and suppressed HCC growth. ERG245 also profoundly inhibited HCC growth *in vitro* and *in vivo* together with Sorafenib, a tyrosine kinase inhibitor (TKI) used in HCC by increasing the apoptotic cell death. Furthermore, we confirmed that the expressions of BCAT1 and the HIF-1α-targeted metabolic genes are positively correlated in human HCCs. Our findings unequivocally demonstrate
that BCAT1 confers a growth advantage to HCC cells by stabilizing HIF-1α and orchestrating HIF-1α-mediated metabolic reprogramming. Consequently, targeting BCAT1 emerges as a promising therapeutic strategy for HCC patients.

Funding Support: This work was supported by the Centre for Oncology and Immunology under the Health@InnoHK initiative funded by the Innovation and Technology Commission, The Government of Hong Kong SAR, China and National Natural Science Foundation of China (NSFC) (82173123, C.C.-L.W.)

#0434 Understanding metabolic heterogeneity of estrogen receptor positive metastatic breast tumors using spatial transcriptomics and geographic information systems approaches.

J. Yoo[1], S. Akter[1], N. Varma[1], A. Jain[2], A. Soliman[2], Z. Madak Erdogan[1];
[1]University of Illinois Urbana-Champaign, Urbana, IL, [2]National Center for Supercomputing Applications, Urbana, IL

The tumor microenvironment consists of numerous cell populations showing diverse metabolic preferences, causing metabolic heterogeneity and therapy resistance. Fulvestrant, a clinically approved selective estrogen receptor (ER) degrader, is the standard of care for ER-positive breast cancer, yet resistance has been reported among metastatic breast cancer patients. In our previous studies, we showed such resistance is attributable to metabolic heterogeneity in the tumor microenvironment. Despite metabolic heterogeneity posing a common challenge in cancer research, current methods, such as histology and Magnetic Resonance Imaging, cannot explore nutrient uptake at transcript-level resolution with spatial context, making it difficult to understand the heterogeneity that affects cellular growth and metabolism. Visium Spatial Transcriptomics, a method that shows regional gene expression, is emerging as a powerful spatial analysis tool, and we integrated this method with geographic information systems to investigate the tumor microenvironment heterogeneity and highlight the importance of cell-microenvironment interactions. We developed a computational pipeline to visualize hotspots of spatially relevant genes using breast cancer metastatic samples from xenograft models and human patients. This pipeline integrates Visium tools and geospatial methods for processing transcriptome profiling data. We analyzed the degree of local spatial association based on Local Moran's I to estimate regions with significant co-localization of single and multiple gene expressions within a tumor. We then leveraged the co-localized areas in the process of biomarker identification and revealing biological pathways. We also used unsupervised clustering of the complete transcriptome profiles to test the resemblance between identified clusters and hotspots as well as any disruption in the spatial structure of clusters in response to therapy or metastasis. Gene set enrichment analysis of these clusters revealed several glucose or lipid metabolism pathways, and mapping of the genes corresponding to each pathway showed mutually exclusive gene expression patterns in the sample. We also observed minimal co-localization of two metabolic pathways but extensive co-localization between metabolic genes and ER target genes, suggesting distinct metabolic preferences and spatial distributions of endocrine therapy resistant cell populations. Altogether, our analysis pipeline established a computational framework for characterizing the link between tumor microenvironment, local metabolism, and changes in transcriptional response to external stimuli. Our findings support the development of strategies to target different endocrine resistant regions using a combination of ER and metabolic signaling inhibitors.

#0435 A key regulatory role of the translation initiation factor DAP5 in the metabolic reprogramming of metastatic breast cancer.

E. Mitaishvili[1], G. H. Souza Bomfim[2], A. Zou[2], M. Sauane[3], R. Lacruz[2], C. de la Parra[3];
[1]The Graduate Center, CUNY, New York, NY, [2]New York University College of Dentistry, New York, NY, [3]Herbert H. Lehman College, CUNY, New York, NY

Triple negative breast cancer (TNBC) is one of the most aggressive subtypes of breast cancer, accounting for 10-15% of all breast cancers in women. The frequency of metastasis in TNBC is disproportionally high compared to other subtypes of breast cancer and is the primary cause of patient mortality. At the cellular level, TNBC's aggressive nature demands rapid adaptation of the tumor cells to navigate cellular stressors for survival and metastatic transformation. These survival adaptations include a cancer cell's ability to reprogram its metabolism and regulate mRNA translation control, coordinating alternative pathways to retain a selective proteome and metabolites that will aid in survival, proliferation, and migration. Advanced cancers, including TNBC, are generally highly glycolytic, and have lower rates of mitochondrial respiration (OXPHOS), a phenomenon known as the Warburg effect. This metabolic shift prioritizes the generation of essential metabolic intermediates, to facilitate the production of cellular biomass and fuel proliferation. Another notable alternative pathway is mediated by the ubiquitously expressed translation initiation factor, Death Associated Protein 5 (DAP5). DAP5 is a homolog of eIF4G and mediates translation independently of the canonical mTORC1/eIF4E pathway. Our findings suggest that this alternative translation initiation plays a crucial role in regulating the metabolic reprogramming of metastatic breast cancer. This non-canonical pathway via DAP5 facilitates the selective translation of 20-30% cap-dependent mRNAs, many of which are essential in cancer cell survival, migration, and metabolism. Importantly, it has recently been shown that DAP5 is critical for breast cancer metastasis but not in primary tumor development. Furthermore, TNBC patient data shows that elevated levels of DAP5 mRNA are correlated with poor survival and metastasis. Our data, using the highly metastatic TNBC cell line, MDA-MB-231, demonstrated that silencing DAP5 significantly reduced glycolytic rate and glycolytic capacity. Consistent with these findings, translatome profiling, showed that DAP5 silencing reduced numerous metabolic targets including glycolytic enzymes and metabolite transporters. Calcium (Ca^{2+}) signaling, which has an important role in cancer progression, migration, and cellular bioenergetics is also affected by DAP5 in TNBC cells. Collectively, our findings indicate that breast cancer cells utilize the translation initiation factor DAP5 to selectively translate mRNAs that support metabolic reprogramming and cell migration, suggesting that DAP5 has a key regulatory role in the cancer's transformation.

#0436 Extracellular glutathione catabolism as an alternative cyst(e)ine source in cancer.

F. Hecht[1], M. Zocchi[1], E. Tuttle[1], G. Asantewaa[1], T. Scales[1], F. Alimohammadi[1], N. Ward[2], G. DeNicola[2], I. Harris[1];
[1]University of Rochester, Rochester, NY, [2]Moffitt Cancer Center, Tampa, FL

Glutathione (GSH) is the most abundant antioxidant in the human body and plays essential roles in physiology and disease. Unchecked oxidative stress is involved in tumor initiation and progression. Paradoxically, clinical and laboratory data show that ROS-scavenging molecules such as glutathione not only fail to impede tumor growth but, in many cases, accelerate it. Still, preliminary data from our lab show that genetically ablating tumors' ability to synthesize GSH does not affect their growth. This finding suggests that the favorable influence of glutathione on tumor growth may arise from external sources. Yet, the mechanism cancer cells employ to take advantage of extracellular glutathione in this context is unknown. Here, we show that γ-glutamyl-transpeptidase 1 (GGT1), an enzyme that localizes on the outer side of the cell's membrane, can break down extracellular GSH, yielding glutamate and the dipeptide cysteinylglycine. Cysteinylglycine can be further metabolized, generating cysteine and glycine to the cells. We found that the addition of exogenous GSH, as well as cysteinylglycine, can mitigate cell death, proliferation arrest, and oxidative stress caused by cystine depletion. The overexpression of human GGT1 in cancer cells significantly reduces the amount of glutathione needed to rescue cell fitness. Accordingly, pharmacologic inhibition of GGT1 activity prevented GSH's ability to rescue cell proliferation. Moreover, an unbiased pharmacological screening revealed that GGT1-mediated cysteine acquisition renders cancer cells resistant to inhibitors of cystine uptake and utilization, supporting the role of GGT1 as a source of cyst(e)ine. Our findings reveal that cancer cells can access cysteine, a vital yet scarce amino acid, through GGT1's ability to break down glutathione, which is present in remarkably high concentrations within the tumor microenvironment. Although the downstream proteins involved in the transport and utilization of GSH breakdown products are yet to be identified, we anticipate this pathway has the potential to uncover novel therapeutic avenues for cancer treatment by targeting alternative pathways of nutrient acquisition that are potentially implicated in cancer progression and therapy resistance.

#0437 Hydrogen sulfide switches the glucose metabolism through sulfhydration on pyruvate kinase M2.

P.-C. Chien[1], R.-H. Wang[1], P.-R. Chen[1], Y.-T. Chen[1], Y.-C. Chen[1], Y.-H. Chu[1], C.-C. Chien[1], S.-Y. Lo[1], Z.-L. Wang[1], M.-C. Tsou[1], S.-Y. Chen[1], G.-S. Chiu[1], W.-L. Chen[2], Y.-H. Wu[1], H.-C. Wang[1], S.-Y. Lin[2], W.-C. Wang[1], H.-J. Kung[3], L.-H. Wang[4], H.-C. Cheng[1], K.-T. Lin[1];

[1]National Tsing Hua University, Hsinchu, Taiwan, [2]National Health Research Institutes, Taiwan, Miaoli, Taiwan, [3]Taipei Medical University, Taupei, Taiwan, [4]China Medical University, Taiwan, Taichung, Taiwan

Cancer cells reprogram their glucose metabolism from oxidative phosphorylation to aerobic glycolysis. This metabolic transformation is partly based on the activity alterations of a rate limiting enzyme known as the pyruvate kinase M2 (PKM2), which is responsible for the conversion of phosphoenolpyruvate (PEP) into pyruvate. Attributed to its critical regulatory role. PKM2 is recognized as the pivotal enzyme in cancer glucose metabolism By reducing the enzyme activity of PKM2, cancer cells attain a greater fraction of glycolytic metabolites for macromolecule synthesis needed for rapid proliferation. Hydrogen sulfide (H_2S), an endogenously produced gasotransmitter that acts as a critical mediator in multiple physiological processes, modifies proteins mainly through the persulfide (-SSH) bond formation, which is called sulfhydration. Our preliminary study demonstrates that H_2S stimulates PKM2 sulfhydration at multiple cysteine residues, including cysteine 326, leading to the destabilization of active tetrameric PKM2 form into dimers or monomers. The PKM2 dimer/monomer further translocates into the nucleus to simulate the activation of glycolytic related genes. Blocking PKM2 sulfhydration at cysteine 326 through amino acid mutation stabilizes PKM2 tetramer and crystal structure further indicates that the tetramer organization of $PKM2^{C326S}$ is different from the currently known T or R states, revealing $PKM2^{C326S}$ as a newly identified intermediate form. Blocking PKM2 sulfhydration at cysteine 326 inhibited cell proliferation and tumor growth in xenograft mouse model. In summary, our current study illustrates that H_2S-mediated sulfhydration induces the dissociation of the PKM2 tetramer, resulting in the reduced PKM2 activity and subsequently inhibits breast cancer cell proliferation and tumor growth. Targeting the sulfhydration site of PKM2 emerges as a promising therapeutic target specific for cancer metabolism.

#0438 Inhibition of *de novo* lipogenesis with PUFA supplementation induces ferroptosis in advanced prostate cancer.

S. D. Rodrigues, I. Ferrari Teixeira, P. Vitale Nuzzo, H. Pakula, D. Nanus, M. Loda;
Weill Cornell Medicine, New York, NY

Background: Metabolic alterations are recognized as a hallmark of cancer progression. In prostate cancer (PCa), in particular, a notable lipid reprogramming occurs with increased expression levels of multiple enzymes involved in the fatty acid synthesis pathway to fulfill the metabolic and structural demands of cancer cells. Fatty acids are vital for membrane building, ATP production through B-oxidation, and storage in lipid droplets for high-energy demands. In castration-resistant prostate cancer (CRPC), the aberrant overexpression of Fatty Acid Synthase (FASN), the rate-limiting enzyme in *de novo* lipogenesis (DNL), results in synthesis of saturated (palmitate) and monounsaturated fatty acids (SFA and MUFA). If DNL is inhibited, polyunsaturated fatty acids (PUFAs) are taken up from the environment. These could undergo lipid peroxidation generating reactive oxygen species (ROS) and contribute to ferroptosis. We hypothesize that combining the inhibition of DNL with the addition of exogenous PUFAs could increase cell death by ferroptosis.
Methods: PCa cells (LNCaP, 22Rv1 and C4-2) and human organoids were exposed to pharmacologic FASN inhibition and PUFAs for 6 days. Cell viability, lipid peroxidation, superoxide production and, protein carbonylation as a measure of intracellular ROS as well as lipidomic profiling, were assessed.
Results: FASN inhibition significantly increased lipid peroxidation and intracellular ROS, with subsequent membrane potential hyperpolarization in prostate cancer cells. These effects were partially rescued by palmitate, while FASNi supplemented with PUFA potentiated protein carbonylation. Expression levels of GPX4, the main regulator of ferroptosis, were reduced after DNL inhibition and rescued with palmitate addition. Suppression of DNL combined with supplemental addition of PUFAs resulted in significant cell growth inhibition in prostate cancer cells and organoids. Finally, lipid profiling demonstrated that the suppression of DNL triggers increased acyl chain length in phospholipid and several other lipid classes. Again, this effect was significantly potentiated when combining FASN inhibition with PUFA supplementation.
Conclusion: FASN inhibition produces a cascade of intracellular events, including lipid remodeling, increased ROS production and ferroptosis, all potentiated by PUFAs. These findings provide compelling evidence for the use a combined approach involving DNL inhibition and PUFA supplementation as a novel therapeutic avenue to treat advanced prostate cancer.

#0439 Tackling oxidative phosphorylation of glioblastoma stem cells through the specific impairment of transmembrane chloride intracellular channel 1.

Francesca Cianci[1], Ivan Verduci[1], Riccardo Cazzoli[2], Saverio Minucci[2], Michele Mazzanti[1]

[1]University of Milan, Milan, Italy,[2]European Institute of Oncology, Milan, Italy

Solid cancer cells show higher energy and biomolecules requirements compared with healthy cells, making the targeting of cancer metabolic dysfunctions an appealing therapeutic approach. Tackling the tumor metabolism is a daunting task, due to the ability of cancer cells to re-organize their metabolism switching between glycolysis and oxidative phosphorylation. Cancer metabolic plasticity and re-programming is partially supported by altered ionic channels expression and activity. Our laboratory has described the chronic presence transmembrane form of Chloride Intracellular Channel 1 (tmCLIC1) as a marker of malignancy in tumor cells and a possible therapeutic target since it is mainly absent in healthy cells. CLIC1 is described as a metamorphic protein able to shuttle between the cytoplasmic form to a transmembrane conformation. In the present investigation, we show that tmCLIC1 acts as a privileged metformin target in glioblastoma stem-like cells. Metformin is the first-line drug for type 2 diabetes and has been proposed as an antineoplastic drug, but no direct evidence of its' membrane permeability nor of a specific membrane receptor in cancer cells has been found yet. Here we demonstrate that metformin impairs tmCLIC1 activity by direct and specific binding coordinated by arginine 29. This residue mutation prevents metformin from tmCLIC1 binding and abolishes the drug's effect on glioblastoma cells in 2D and 3D models and its actions on mitochondrial respiration. *In vivo* experiments in zebrafish embryos and mice orthotopically engrafted with glioblastoma cells and treated with metformin have shown that metformin binding to tmCLIC1 is crucial for its anti-neoplastic effect.

#0440 BAP1 deubiquitinates ACLY to promote lipogenesis yet predisposing cholangiocarcinoma to iron overload and ferroptosis.

P. Classon[1], S. Jaramillo[1], D. Carlson[1], I. Yan[2], T. Patel[2], S. I. Ilyas[1], R. L. Smoot[1], G. J. Gores[1], **D. Povero**[1];
[1]Mayo Clinic, Rochester, MN, [2]Mayo Clinic, Jacksonville, FL

Background: Cholangiocarcinoma (CCA) is a highly lethal and aggressive epithelial cell malignancy of the liver and biliary tract. CCA survival remains poor and response to chemotherapy or immunotherapy is limited. We AIM to identify metabolic vulnerabilities that render CCA susceptible to ferroptosis, an iron-dependent and caspase-independent cell death driven by lipid peroxidation.
Materials and Methods: We treated human and mouse CCA cell lines with ferroptosis inducers (RSL3, Erastin), inhibitors (Fer-1, Lip-1), necroptosis inhibitor and a pan-caspase inhibitor. Cell viability, intracellular and mitochondrial iron, lipid peroxidation, mitochondrial structure, and function by cell-based and biochemical assays. Gain- and loss-of-function strategies, TURBO proximity-dependent biotin identification, and metabolic techniques were used for mechanistic studies. *In vivo*, orthotopically implanted C57B/6 mice were treated with RSL3 or vehicle intraperitoneally, followed by assessment of tumor burden and immunophenotyping analysis. Epcam-aptamer coated nanoparticles (tMNPs) packaged with siRNA against GPX4 were used for selective ferroptosis induction.
Results: We identified ferroptosis-sensitive and -resistant human and mouse CCA cells. Ferroptosis-sensitive cells, rescued by ferroptosis inhibitors but not by necroptosis or pan-caspase inhibitors, exhibited elevated intracellular free iron and mitochondrial iron overload. This led to significant mitochondrial dysfunction and structural changes associated with ferroptosis. Mitochondrial free iron triggered reactive oxygen species generation and lipid peroxidation. We identified BRCA-associated protein 1 (BAP1) as a potential driver of ferroptosis sensitivity. BAP1, mutated in 22-25% of human CCAs, is a tumor suppressor and deubiquitinase (DUB). BAP1 knockdown by siRNA protected cells from ferroptosis, while re-expression of BAP1 sensitized cells to ferroptosis. Subcellular fractionation identified BAP1 in extranuclear compartments, including mitochondria and cytosol. We found that BAP1 interacts and deubiquitinates ATP citrate lyase (ACLY), which converts iron chelator citrate to oxaloacetate and acetyl-CoA. Inhibition of mitochondrial citrate export, protected cells from iron overload and ferroptosis. *In vivo*, RSL3-induced ferroptosis significantly reduced tumor burden, as compared to vehicle-treated mice. RSL3-induced ferroptosis promoted an immunogenic tumor immune microenvironment. Lastly, tMNPs with siGPX4 induced marked ferroptosis of mouse CCA cells and showed maximal enrichment in liver orthotopic tumors *in vivo*.
Conclusions: Our findings indicate that BAP1 deubiquitination of ACLY predisposes CCA cells to iron overload by exhausting citrate to support lipogenesis. CCA vulnerability to ferroptosis opens up novel therapeutic opportunities for CCA.

#0441 Bioluminescent dehydrogenase assays: A novel approach for metabolic profiling and inhibitor screening in cancer biology.

K. Haupt, N. Karassina, A. Lauer, K. Sylvester, J. Vidugiriene;
Promega Corporation, Madison, WI

Dehydrogenases play a pivotal role in cellular metabolism, acting as gatekeepers in key metabolic pathways. Their activity reflects the metabolic state of the cell, which is particularly relevant in the context of cancer and the immune response, where metabolic reprogramming is a hallmark of tumor progression and differentiation stages. Here, we present the development and application of novel bioluminescent dehydrogenase assays for direct measurement of metabolic activity in cell lysates. Our assays are highly sensitive, requiring as few as 100-500 cells, and have been successfully miniaturized to a 384-well plate format conducive to high-throughput screening. This technological advance allows for the precise monitoring of dehydrogenase activity across the pentose phosphate pathway, glycolysis, and the mitochondrial tricarboxylic acid (TCA) cycle. We demonstrate how shifts in dehydrogenase activity can serve as indicators of the metabolic status of cells, and their modulation during differentiation. Moreover, our bioluminescent assays provide a rapid screening platform for pathway-specific metabolic inhibitors, with potential applications in identifying new therapeutic targets within cancer metabolism. Our data reveal a dynamic landscape of metabolic activity during T cell maturation, underscoring the potential of dehydrogenase activity profiling in cancer immunobiology and the development of targeted cancer therapies.

#0442 Exploring targetable pathways: Unveiling changes in tumor physiology through dietary modification by a ketogenic diet.

O. Hajihassani, M. Zarei, S. Tahhan, P. Gallagher, W. Beegan, J. Choi, S. Lei, A. Murray, A. Loftus, K. Lebo, H. Cheng, A. Mudigonda, S. Alibeckoff, K. Ji, J. Hue, H. Graor, J. Winter;
Case Western Reserve University School of Medicine, Cleveland, OH

Background: A ketogenic diet, with high fat (90% kCal) and low carbohydrate (5% kCal) intake, induces ketosis [2], altering cancer cell carbon utilization toward the tricarboxylic acid cycle (TCA) [3]. While the overall impact on cancer growth is unclear, most literature suggests an anti-cancer effect. Our hypothesis aims to uncover pancreatic cancer cell adaptations to the ketogenic diet, revealing metabolic vulnerabilities for informed therapeutic strategies.
Methods: Mice on a ketogenic or normal diet (control) underwent pancreatic cancer xenograft observation. Tumor metabolites were analyzed with LC/GC-MS, oxidative stress with NAD(P)+/NAD(P)H, and Lipid Peroxidation assays. Western blot assessed enzyme expression. In vitro studies used Seahorse FX Analyzer for mitochondrial function and PicoGreen for cell growth quantification. Ivosidenib and CB839 were used for combination therapies.
Result: A ketogenic diet induces a metabolic shift in pancreatic cancer, altering nutrient and metabolite levels in diverse in vivo models. Besides the expected increase in TCA metabolites, heightened amino acid anaplerosis, particularly with glutamine and glutamate, was observed. Examination of the diet's impact on oxidative phosphorylation enzymes revealed increased BDH1 expression, aiding ketone body utilization, and upregulation of cytosolic IDH1 for antioxidant defense. Enzymes involved in glutamine uptake and conversion, like ASCT2 and GLS, showed altered expression.
Simultaneously, we explored tumor microenvironment vulnerabilities, detecting a significant increase in reactive oxygen species (ROS) levels, specifically lipid peroxidation, in mice on the ketogenic diet.
Given these pancreatic cancer adaptations, we hypothesized that combining therapeutics to elevate ROS levels and target the glutamine pathway would substantially impede tumor growth. To test this, we combined a ketogenic diet with an IDH1 inhibitor for antioxidant defense hindrance and a glutaminase inhibitor to impair mitochondrial function, resulting in a marked reduction in tumor proliferation compared to individual treatments.
Conclusion: A ketogenic diet demonstrates a robust anti-tumor effect in various pancreatic cancer mouse models, likely arising from the diminished glucose and increased fatty acid load inherent in the diet. Metabolic adaptation towards an oxidative phosphorylation (OXPHOS) phenotype makes pancreatic cancer especially susceptible to antioxidant and mitochondrial inhibitors, as well as inhibitors of glutamine-metabolizing enzymes.

#0443 Unsaturated fatty acids promote cell cycle progression and proliferation of platinum resistant ovarian cancer cells.

A. Isac, G. Zhao, H. Cardenas, D. Matei;
Robert H. Lurie Comp. Cancer Ctr. of Northwestern Univ., Chicago, IL

Introduction: Ovarian cancer (OC) depends on fat as fuel for metastasis and growth. We have previously demonstrated that cisplatin resistant (Pt-R) OC cells uptake higher amounts of fatty acids (FAs) compared to sensitive (Pt-S) cells- a process which facilitates cancer cell survival under cisplatin-induced oxidative stress. Here we aimed to determine which class of FAs promotes the Pt-R phenotype and to identify the mechanism through which FAs support cancer survival.
Materials and methods: We used two isogenic OC cell lines pairs, sensitive and resistant to cisplatin: OVCAR5 Pt-S (IC50 = 2.881μM) vs Pt-R (IC50 = 6.831 μM) and PEO1 (IC50 = 4.901 μM) vs PEO4 (IC50 = 8.285 μM). Cells were cultured under low serum conditions, supplemented with 50 μM oleic (OA) or 50 μM palmitic acid (PA), and used for viability assays, RNA-Seq, and cell cycle analysis. Quantitative RT-PCR measured expression of key FAs transporters in Pt-S and Pt-R cells.
Results: A viability assay showed that Pt-R cells were less viable under serum depletion compared to Pt-S OC cells. OA (unsaturated), but not PA (saturated), promoted proliferation of both OC cell lines, and rescued Pt-R vs Pt-S cells; 268.4% vs 91.6% for OVCAR-5 and 38.1% for PEO4 vs 12.1% for PEO1, suggesting that Pt-R cells depend more on unsaturated FAs compared to Pt-S cells. Quantification of key FAs transporters demonstrated that Pt-R cell expressed higher levels of FABP4, FABP5 and CD36 compared to Pt-S cells. Treatment with an FABP inhibitor reduced the Pt IC50 in Pt-R cells (from 11.893 μM to 5.0415 μM in OVCAR5 and from 8.285 μM to 6.968 μM in PEO4). RNA-Seq analysis analysed transcriptomic changes induced by 24 hour treatment with OA in OVCAR5 cells. There were 923 differentially expressed protein-coding genes, with 300 upregulated and 623 downregulated transcripts (FDR<0.05). Pathway analysis revealed cell cycle related pathways like: *cell cycle mitotic*, *cell cycle checkpoints*, *G2/M checkpoints* among the top 10 most significantly upregulated pathways and E2F1 was identified as the main effector. Cell cycle analysis confirmed that OA induced increased percentages of cells in S- and G2/M phases - from 6.95% to 11.6% ($p<0.05$), and 13.6 to 17.6% ($P<0.05$), respectively. Treatment with an E2F1 inhibitor significantly reduced the OA-induced cell proliferation.
Conclusion: Pt-R OC cells are dependent on unsaturated FAs compared to Pt-S cells and upregulate key transporters to allow increased uptake of FAs. OA supports proliferation of Pt-R cells and cell cycle progression from G1 to S- and G2/M phases. Ongoing experiments focus on key mechanisms activated by unsaturated FAs in Pt-R cells.

#0444 Lipid exposure re-wires cellular metabolism away from glycolysis toward the serine pathway conferring oncogenic properties to non-transformed breast cells.

Mariana Bustamante Eduardo[1], Gannon Cottone[1], Shiyu Liu[2], Flavio R. Palma[1], Maria Paula Zappia[3], Abul B.M.M.K. Islam[3], Elizaveta V. Benevolenskaya[3], Maxim V. Frolov[3], Jason Locasale[2], Marcelo G. Bonini[1], Navdeep S. Chandel[1], Seema Khan[1], Susan Clare[1]

[1]Northwestern Univ. Feinberg School of Medicine, Chicago, IL,[2]Duke University, Durham, NC,[3]University of Illinois at Chicago, Chicago, IL

Introduction. A lipid metabolism gene signature is associated with the risk of estrogen negative breast cancer (ER-BC). In vitro, lipid exposure alters histone methylation affecting gene expression and increases flux through various metabolic reactions including those involved in serine, one-carbon, glycine (SOG) and methionine. We hypothesized that the metabolism of lipids in preference to glucose and glutamine results in a metabolic shift toward the serine pathway increasing S-adenosylmethionine (SAM) leading to histone methylation increases and changes in gene expression.
Methods. MCF-10A cells exposed to octanoic acid (OA) were utilized for U13C-glucose tracing. SAM, glutathione (GSH) and 2-hydroxyglutarate (2-HG) concentrations were measured following treatment with OA ± the PHGDH inhibitor CBR-5884. ROS-induced redox changes were monitored live in cells transduced with ORP1-roGFP2 vectors. CUT&RUN was performed for H3K4me3. Expression of OA-induced genes was measured by rt-qPCR upon exposure to OA ± CBR-5884 or OA ± the histone methyltransferase (HMT) inhibitor Piribedil. Alkaline comet assay was done to detect DNA breaks. Single-cell RNA-seq (scRNAseq) was performed on tissue-derived breast microstructures exposed to ± OA.
Results. Upon OA treatment, the Cancer index increased and 1C-THF was redirected to the methionine cycle increasing flux to methylation. OA significantly increased the production of SAM, GSH and 2-HG after 15 min. Blocking the first enzyme in the serine pathway, PHGDH, prevented these increases. After 5 min OA exposure, mitochondrial and nuclear ROS increased significantly ($p < 0.0001$), peaking at 15 min. H3K4me3 CUT&RUN revealed 661 differential peaks (FDR < 0.05) comparing OA to control. 73% of H3K4me3 OA-associated peaks were in regulatory regions of OA-induced genes (FDR < 0.01) including neural, EMT and ER- BC related genes. Motif analysis revealed an overrepresentation of binding sites for serine pathway transcriptional activators ATF3/4 ($p < 0.05$). Blocking PHGDH or HMT prevented OA-induced gene expression changes. Alkaline comet assay showed that OA significantly increased comet tails. scRNAseq revealed OA increased the numbers of cells within all cell clusters expressing ATF3 and PHGDH. Also observed was an increase in the percentage of basal BSL1, luminal progenitor LP3 and hormone sensing HS1 cells.
Conclusions. Metabolism of OA results in a metabolic shift toward the SOG and methionine increasing the production of SAM, GSH and 2-HG which have implications for oncogenesis. The increased SAM fosters epigenetic phenotypic plasticity via altered histone methylation. The increased proportion of specific cell types likely reflects the survival of cells able to mitigate oxidative stress. Increased 2-HG may produce metabolic BRCAness by inhibiting 2-oxoglutarate-dependent dioxygenases.

#0445 Determining the molecular and biologic effects of HER3 and IDH1 antagonism on liver endothelium-PDAC crosstalk.

C. S. Boutros[1], A. W. Loftus[1], M. Rathore[2], M. Zarei[2], K. Curry[2], J. M. Winter[1], R. Wang[2];
[1]Univ. Hospitals Case Medical Ctr., Cleveland, OH, [2]Case Western Reserve University, Cleveland, OH

INTRODUCTION: Pancreatic ductal adenocarcinoma (PDAC) is a highly aggressive malignancy due to the lack of early diagnosis and limited response to treatments. Austere and nutrient-deprived conditions typically present in the PDAC tumor microenvironment (TME) induce chemotherapy resistance. Therefore, novel therapeutic strategies are needed. We have previously demonstrated the primary tumor expresses IDH1 which supports the pro-survival oxidative phosphorylation (OXPHOS) metabolism, and has been successfully targeted by ivosidenib, an IDH1 inhibitor, in preclinical studies. Meanwhile, endothelial cells (ECs) from the liver, the most common site of PDAC metastases, secrete soluble factors in the conditioned medium (CM) that activate HER3, a receptor tyrosine kinase, involved in cell proliferation and metabolism.
OBJECTIVES: We sought to (1) uncover the mechanisms involved in driving the metabolic differences between primary and metastatic tumors through the utilization of ECs from the liver (2) conduct metabolic analyses to determine metabolic effects of HER3 activation, and (3) examine potential synergism of combination therapy against HER3 and IDH1 in primary and metastatic niches. METHODS: The effect of CM on PDAC cell growth was determined by PICO Green Assay. The effects of ECs HER3/IDH1 inhibitions on cellular metabolism were measured by multiple metabolic assays including Seahorse, CellTiter-Glo, lactate ELISA, and TMRE assays. HER3-specific antibody Seribantumab, HER3 inhibitor Sapitanib, and IDH1 inhibitor ivosidenib were used to block HER3 and/or IDH1. Moreover. A cell viability-based synergy study was performed to assess the effects of HER3-IDH1 combination. Effects of HER3 and IDH1 inhibitions on PDAC tumor growth and mouse survival in vivo were determined in syngeneic, orthotopic models with PDAC primary tumors and liver metastases. RESULTS: CM from liver ECs significantly increased cell growth in PDAC cells in vitro and increased glycolytic tropism in multiple HER3 positive PDAC cell lines measured by metabolic assays mentioned above. HER3 antibody and HER3 inhibitor both increased oxidative consumption rate (OCR), an indirect measure of OXPHOS, and decreased extracellular acidification rate (ECAR), a measure of glycolysis measured by Seahorse. Combination therapy utilizing HER3 and IDH1 inhibitors revealed synergy. In our in vivo tumor model, mice treated with combination therapy had significantly longer overall survival than those given either monotherapy or no treatment.
CONCLUSIONS: Our results demonstrated a paracrine role of liver ECs in promoting cell growth via activating HER3 in PDAC cells as well as reprograming cellular metabolism from OXPHOS towards glycolysis. Identification of the metabolic shift that takes place in metastatic PDAC to the liver due to HER3 activation gives way for the development of a potentially lethal drug combination.

#0446 Integrated spatial transcriptomics and lipidomics analyses of intraductal papillary mucinous neoplasm identifies enrichment of long chain sulfatide as an early metabolic alteration.

Y. Chen[1], M. Sans[1], F. Thege[1], R. Dou[1], J. Min[1], M. Yip-Schneider[2], J. Zhang[3], R. Wu[1], E. Irajizad[1], Y. Makino[1], K. Rajapakshe[1], M. Hurd[1], R. Leon-Letelier[1], J. Vykoukal[1], J. Dennison[1], K.-A. Do[1], R. Wolff[1], P. Guerrero[1], M. Kim[1], M. Schmidt[2], A. Maitra[1], S. Hanash[1], J. Fahrmann[1];
[1]UT MD Anderson Cancer Center, Houston, TX, [2]Indiana University-Purdue University Indianapolis, Indianapolis, IN, [3]Indiana University, Bloomington, IN

Purpose: To define the metabolic alterations associated with malignant progression of intraductal papillary mucinous neoplasm (IPMN).
Experimental Procedures: Matrix-assisted laser desorption/ionization (MALDI)-mass spectrometry (MS) was conducted for spatial characterization of lipid profiles on frozen tissue sections from resected human IPMN patients. The specimen set consisted of either low-grade dysplasia (LG) (n=15), high-grade (HG) dysplasia (n=4), or with an associated pancreatic ductal adenocarcinoma (PDAC) (n=4) as well as 15 PDAC tissues. Utilizing serial sections to the same human IPMN cases analyzed with MALDI-MS imaging, we used the Visium Spatial Gene Expression technology platform to characterize the spatiomolecular underpinnings of LG and HG IPMN. H&E images of the same tissue section used for the Visium workflow, were used to annotate the spots in the dataset covering the epithelial lining of the IPMN lesions ("epilesional" areas) and the spots covering the adjacent microenvironment surrounding the lesion ("perilesiopecific" area). Findings were compared with lipidomic analyses of cystic fluid from 89 IPMN patients. The anti-cancer efficacy of UGT8-IN-1, a selective small molecule inhibitor of ceramide galactosyltransferase (CGT, also known as UGT8), was assessed in vitro and in mutant Kras;Gnas allografts.
Results: MALDI/MS-based spatial imaging of human resected IPMN tissues and pancreata from a mutant Kras;Gnas mouse model of IPMN revealed long-chain hydroxylated sulfatides, particularly the C24:0(OH) and C24:1(OH) species, to be selectively enriched in the IPMN and PDAC neoplastic epithelium. Visium spatial transcriptomics data confirmed that the cognate transcripts engaged in sulfatide biosynthesis, including UGT8, Gal3St1, and FA2H, were co-localized with areas of sulfatide enrichment. Lipidomic analyses of cystic fluid from 89 patients with IPMN identified several sulfatide species to be significantly elevated in patients with IPMN/PDAC compared to those with low-grade IPMN. Inhibition of sulfatide metabolism via UGT8-IN-1 reduced viability of Kras;Gnas murine cell lines in vitro and attenuated tumor growth in an allograft IPMN model. UGT8-IN-1 treatment resulted in reduced levels of several sulfatide species, accompanied by a concomitant increase in a subset of quantified sulfatides precursor ceramides, accumulation of mitochondrial mass and reactive oxygen species and time-dependent increases in autophagy/mitophagy markers p62/SQSTM1 and LC-3B, suggesting impaired mitophagy.
Conclusion: Enhanced sulfatide metabolism is an early alteration in cystic pre-cancerous lesions of the pancreas that persists through invasive neoplasia. Targeting sulfatide biosynthesis might represent an actionable vulnerability for cancer interception.

#0447 Anti-tumor efficacy of ompenaclid, a creatine transporter inhibitor, in KRAS mutant tumors, including NSCLC.

P. Lo, V. Sanz Chavez, S. Takeda, M. Tavazoie, **I. Kurth**;
Inspirna, Inc., New York, NY

Background: Pre-clinical studies identified creatine metabolism to be activated in KRAS mutant metastatic colorectal cancer (CRC) as a mechanism to fuel the increased energy demands of RAS mutant tumors. Metastatic colon cancer cells overexpress and subsequently release creatine kinase-B (CKB) into the extracellular space, where it phosphorylates creatine to generate the high energy metabolite phosphocreatine. Ompenaclid is a small molecule inhibitor of the creatine transporter SLC6A8. Inhibition of SLC6A8 by ompenaclid prevents import of phosphocreatine/creatine, resulting in depletion of intracellular creatine, phosphocreatine and ATP levels. This results in tumor apoptosis and robust anti-tumor efficacy in CRC models with a wide range of KRAS mutant alleles. Ompenaclid is currently in a Phase 2 trial, in combination with FOLFIRI and bevacizumab, in patients with RAS-mutated second-line advanced/metastatic colorectal cancer. Here, we assessed efficacy of ompenaclid in tumors beyond CRC, including KRAS WT and KRAS mutant NSCLC.

Methods: Athymic mice were inoculated with CRC, pancreatic, gastric or NSCLC cancer cell lines and treated with ompenaclid once tumors reached ~150 mm^3, until termination. Plasma metabolites were quantified by LC-MS/MS and tumoral expression of CKB and SLC6A8 in NSCLC and CRC tumors was measured by qPCR after treatment with a control or ompenaclid-supplemented diet for ~10 days. Combination treatment with MRTX849, a KRAS G12C inhibitor, was conducted in a pancreatic MiaPaca xenograft model.

Results: Our studies demonstrate ompenaclid anti-tumor efficacy in NSCLC and pancreatic xenografts. Notably, and consistent with findings in CRC, efficacy in NSCLC was more robust in RAS mutant cancer models, relative to those bearing KRAS WT tumors. Metabolite analysis of the plasma of tumor-bearing mice at baseline revealed that mice harboring RAS mutant tumors had higher levels of p-creatine and lower levels of ATP, indicating that RAS mutant tumors utilize higher amounts of ATP, which may be converted to phosphocreatine by tumoral CKB, as confirmed by qPCR analysis. This finding is consistent with metastatic RAS mutant CRC tumors utilizing extracellular ATP to generate phosphocreatine and thus exhibiting greater dependency on creatine metabolism relative to RAS WT tumors. Treatment with ompenaclid also demonstrated additive efficacy in combination with KRAS G12C inhibitors. In summary, these data support development of ompenaclid in indications beyond CRC, including NSCLC, as well as in combination with KRAS G12C inhibitors.

#0448 Alterations in glycolytic pathway enzymes and metabolic plasticity in prostate cancer progression.

C. Sprenger, M. Munari, S. Sun, K. Soriano Epilepsia, S. Plymate;
University of Washington, Seattle, WA

Background: Although oxidative phosphorylation (OXPHOS) is the main ATP source in primary prostate cancer, as the tumor progresses to castration resistance and/or metastatic disease, glycolysis becomes increasingly prevalent. Dependence on glycolysis can further increase under hypoxic conditions found in advanced cancers. We previously demonstrated that a novel small molecule, BKIDC-1553, inhibits proliferation and tumor growth of prostate cancer cell lines and xenografts through a hexokinase-2 (HK2) dependent inhibition of glycolysis. HK2 is a glucose 6-phosphorylating enzyme that works in conjunction with glucose transporter-1 (GLUT1) to drive glycolysis in cells. While our previous work suggests that BKIDC-1553 works primarily through a HK2 dependent mechanism, the objective of this current project is to further examine how expression and function of HK2 and GLUT1 are altered in response to BKIDC-1553 treatment.
Methods: Hypoxic conditions are common in late-stage prostate cancer. Effects of hypoxia on cell proliferation and expression levels of HK1, HK2, and GLUT1 were examined with and without BKIDC-1553 treatment. To examine role of HK1, HK2, and GLUT1 in response to BKIDC-1553 treatment, we created CRISPR knockouts and shRNA knockdowns of HK1 and HK2 in the LNCaP prostate cancer cell line. GLUT1 was inhibited using a commercially available inhibitor, BAY-876. PCR and Western blots were used to confirm expression levels of HK1, HK2, and GLUT1. MTS proliferation assays were used to examine effect of KO and KD on response to BKIDC-1553 and BAY-876.
Results: GLUT1 levels, but not HK1 or 2, increased at 72 hrs under hypoxic conditions. HK1, HK2, and GLUT1 levels all increased in cells in response to 144 hrs of BKIDC-1553 compared with 72 hrs treatment in both normoxic and hypoxic conditions. The KO and KD studies were all conducted in normoxic conditions. Westerns blots demonstrated that HK2 KO, but not HK1 KO, results in increased levels of GLUT1. HK1 or HK2 KD, however, did not alter GLUT1 levels. HK2 KD cells, with GLUT1 levels remaining the same, displayed less growth inhibition than control cells in response to BKIDC-1553 treatment, while HK2 KO cells, with increased levels of GLUT1, remained sensitive to BKIDC-1553. Because GLUT1 levels increase in response to HK2 KO, we wanted to see if inhibiting GLUT1 in these cells could decrease their proliferation. We found that KO cells were indeed more sensitive to growth inhibition of BAY-876.
Conclusion/Summary: These studies indicate that KO of HK2 increases levels of GLUT1. These cells remain sensitive to BKIDC-1553 treatment, which could in part be due to the cells' continued reliance on glycolysis through increased GLUT1. A continued reliance on glycolysis allows BKIDC-1553 to continue to inhibit cell growth. Future studies examining how combination treatment with BKIDC-1553 and BAY-876 affects growth of advanced prostate cancer cells is underway.

#0449 Catabolism of GSH by GGT supports cancer cell survival.

M. Zocchi, F. Hecht Castro Medeiros, F. Alimohammadi, E. Tuttle, G. Asantewaa, T. Scales, I. S. Harris;
University of Rochester Medical Center, Rochester, NY

Cancer metabolism depends on amino acid sources to fuel tumor growth and drug resistance. Using amino acid restriction to treat tumors can enhance existing therapeutic techniques. The tripeptide Glutathione (GSH), which contains cysteine, glutamate, and glycine, is often considered an antioxidant, and its potential as an amino acid pool has been overlooked. GSH is ubiquitous in the tumor microenvironment and could provide a ready source of amino acids to tumor cells through its catabolism by the enzyme γ-Glutamyl transpeptidase (GGT), which has been shown to cleave GSH and its' conjugates in the extracellular space. It is unclear if the cleavage of GSH by GGT supports cancers in vivo. We find that inhibiting GGT with the pharmacologic agent GGsTop blocks GSH catabolism and decreases tumor growth. We show that cultured cells can be rescued from a lethal depletion of cystine upon supplementation with GSH or its catabolic product cysteinylglycine, but not under the conditions of GGT inhibition. Through pharmacokinetic methods, we identify a usable systemic dose of GGsTop and show GGT inhibition in tumor tissue. Further, we demonstrate that systemic GGT inhibition in vivo decreases tumor mass and volume. These findings support the hypothesis that GSH catabolism by GGT1 is a non-canonical source of amino acids for tumor metabolism. Understanding GSH catabolism by GGT could elucidate new metabolic pathways in tumors. Inhibiting GSH catabolism could provide new therapeutic approaches to inhibit tumor growth.

#0450 GCN2 protects cancer cells from hypertranslation and metabolic crisis.

M. Roman-Trufero[1], I. T. Kleijn[2], K. Blighe[3], P. Saavedra-Garcia[2], J. Zhou[2], A. Gaffar[2], M. Christoforou[2], M. Yuneva[4], A. M. Michel[5], G. R. Masson[6], V. Shahrezaei[2], H. W. Auner[1];

[1]CHUV Lausanne University Hospital, Lausanne, Switzerland, [2]Imperial College London, London, United Kingdom, [3]Clinical Bioinformatics Research, London, United Kingdom, [4]The Francis Crick Institute, London, United Kingdom, [5]EIRNABio Ltd, Cork, Ireland, [6]University of Dundee, Dundee, United Kingdom

It is widely assumed that cancer cells rely on high levels of protein synthesis to support growth and proliferation. However, protein synthesis, including ribosome biogenesis, is a highly resource- and energy-demanding process that needs to be coordinated with protein degradation and metabolic programs. GCN2 is an evolutionarily conserved kinase that is primarily activated by uncharged tRNAs when amino acid levels drop and activates the Integrated Stress Response (ISR), which encompasses a global reduction in translation and increased amino acid uptake and generation. GCN2 has been shown to support cancer cell survival under conditions of nutrient scarcity. Here, we used an integrated systems biology approach to delineate the multifaceted role of GCN2 in cancer cells that do not suffer from nutrient shortages.

We carried out a broad array of multiomic analyses (RNA-seq, TMT-labelling based proteomics, Ribo-seq, LC-MS metabolomics) of melanoma cells in which GCN2 was inhibited (GCN2iB) or genetically depleted (constitutive and inducible shRNA) in cell culture and *in vivo* in murine xenografts, supplemented by puromycinylation-based quantification of global protein synthesis.

GCN2 inhibition in A375 cells triggered a transcriptome and proteome response that was dominated by the induction of processes linked to protein and ribosome synthesis while suppressing metabolic pathways such as glycolysis and the proteasome. We confirmed these observations *in vivo* via RNA-seq of tumor samples from mice xenografted with A375 cells in which GCN2 was knocked down by induced shRNA expression and from xenografted mice that were treated orally with GCN2iB. Ribo-seq further demonstrated that, upon GCN2 inhibition, A375 cells expand their translational machinery. Notably, we identified 50 ribosomal genes that were translated at higher rate in GCN2-inhibited cells and whose expression was regulated exclusively at the translational level. GCN2 inhibition/depletion also resulted in an approximately 1.8-fold increase in global protein synthesis and altered the druggable proteome. Moreover, metabolite profiling of GCN2iB-treated cells revealed a loss of metabolic homeostasis including substantial alterations in glycolysis and both amino acid and lipid metabolism. In addition, we observed a significant decrease in ATP levels despite increased translation of mitochondrial ETC complex proteins. Proteomic and translatomic analyses revealed a failure of cells to increase proteasomal subunits and to maintain the production of ECM proteins. Last, but not least, we did not observe a role of GCN2 in preventing or resolving ribosome collisions.

Taken together, our findings reveal GCN2 as a master regulator of translation in cancer cells that do not suffer from nutrient scarcity that keeps protein synthesis in check to maintain metabolic homeostasis.

MOLECULAR/CELLULAR BIOLOGY AND GENETICS: microRNAs and Other Non-coding RNAs as Cancer Genes 1
Poster Session

#0454 microRNAs role in innate immunosenescence during anti-PD1 immunotherapy.
Z. Zhu, T. M. Rana;
UC San Diego, San Diego, CA

Checkpoint inhibitors have achieved durable responses and long-lasting immunologic memory in cancer patients. However, the initial and acquired resistance remains an unsolved problem. It's urgent to learn the molecular mechanisms causing resistance. microRNAs (miRNAs) are short transcripts that regulate many pathophysiological processes. Here, we investigated the miRNAs expression changes after GVAX combined with monoclonal PD-1 antibody treatment in the murine melanoma B16F10 tumors and identified microRNAs down-regulated in responsive tumors. Deletion of this family member in three different syngeneic mouse tumors did not affect their in vitro nor in vivo proliferation but sensitized anti-PD1 immunotherapy. The miRNA deletion with anti-PD1 therapy increased total CD45+ leukocyte infiltration with all types of hematopoietic cells except macrophages. Both tumor bulk RNA sequencing and single-cell RNA sequencing revealed activated innate sensing genes especially for pathogen recognition and phagosome formation. Importantly, we found specific miRNA-deletion effects rely on tumor resident macrophage, IFN-γ release in the tumor microenvironment (TME) and the miRNA regulating machinery protein Argonaut2 (Ago2). Notably, the miRNA expression status of melanoma patients correlates with the survival and innate immune sensing gene expression. Our results suggest that this family of miRNAs participate in initial resistance by escaping innate immunosurveillance. Deletion of the miRNA may turn immune "cold" tumors to "hot" tumors, providing potential therapeutic targets to overcome resistance in melanoma, colorectal, triple-negative breast cancer and possibly other cancers.

#0455 Identification of hsa-miR-6794-3p as a key regulatory factor in human pancreatic cancer metastasis.

H. Kim[1], E.-T. Oh[1], Y. Cho[2], H. Park[1];
[1]Inha University College of Medicine, Incheon, Korea, Republic of, [2]Inha University, Incheon, Korea, Republic of

Metastasis is a major factor in treatment failure in patients with pancreatic cancer, but the underlying mechanisms remain unclear, and new, effective treatment strategies are needed. Here, we sought to identify novel microRNAs (miRNAs) with a key role in pancreatic cancer metastasis. Using a microarray analysis to evaluate miRNA expression in metastatic and non-metastatic pancreatic cancer, we found that expression of the miRNA, hsa-miR-6794-3p, was significantly lower in metastatic pancreatic cancer tissues than in non-metastatic pancreatic cancer tissues. Methylation-specific polymerase chain reaction analyses revealed that hsa-miR-6794-3p expression was downregulated in metastatic pancreatic cancer cells by hypermethylation of CpG islands within the hsa-miR-6794-3p promoter. Gain- and loss-of-function approaches using the human pancreatic cancer cell lines, MIA-PaCa-2 and HPAF-II, expressing low and high levels of hsa-miR-6794-3p, respectively, suggested a role for hsa-miR-6794-3p in decreasing cell invasion, migration, and epithelial-mesenchymal transition (EMT) signaling. Notably, we found that hsa-miR-6794-3p exerts its effects by inhibiting expression of the chromatin remodeling factor, RBBP4, through direct binding to the 3'-untranslated region of its mRNA. The resulting suppression of RBBP4 expression increases levels of the transcription factor GRHL2, which is involved in regulating invasion, migration, and EMT signaling in metastatic pancreatic cancer cells. Thus, lower levels of hsa-miR-6794-3p disrupt GRHL2-mediated regulation of these pathways by disinhibiting expression of the GRHL2 negative regulator, RBBP4. Consistent with these findings, an investigation of the relationship between hsa-miR-6794-3p and clinicopathological features in pancreatic cancer patients using publicly available datasets and immunohistochemistry showed that low levels of hsa-miR-6794-3p are correlated with a poorer prognosis in pancreatic cancer patients. Additional preclinical experiments in nude mice clearly demonstrated that hsa-miR-6794-3p is capable of suppressing pancreatic cancer cell metastasis. Taken together, these results suggest that hsa-miR-6794-3p suppresses tumor metastasis and thus represents a promising prognostic biomarker and therapeutic target in pancreatic cancer.

#0456 A first comprehensive analysis of transcribed ultra conserved regions uncovers important regulatory functions of novel non-coding transcripts in gliomas.

M. K. Gibert, Jr., R. Abounader;
University of Virginia, Charlottesville, VA

Transcribed Ultra-Conserved Regions (TUCRs) represent a severely understudied class of putative non-coding RNAs (ncRNAs) that are 100% conserved across multiple species. We performed the first-ever analysis of TUCRs in glioblastoma (GBM) and low-grade gliomas (LGG). We leveraged large human datasets to identify the genomic locations, chromatin accessibility, transcription, differential expression, correlation with survival, and predicted functions of all 481 TUCRs, and identified TUCRs that are relevant to glioma biology. Of these, we investigated the expression, function, and mechanism of action of the most highly upregulated intergenic TUCR, uc.110, identifying it as a new oncogene. Uc.110 was highly overexpressed in GBM and LGG, where it promoted malignancy and tumor growth. Uc.110 activated the WNT pathway by upregulating the expression of membrane frizzled-related protein, by sponging the tumor suppressor miR-544. This pioneering study shows important roles for TUCRs in gliomas and provides an extensive database and novel methods for future TUCR research.

#0457 Persister cell state-associated lncRNA signatures in non-small cell lung cancer.

J. Gencel-Augusto, W. Wu, T. G. Bivona;
UCSF - University of California San Francisco, San Francisco, CA

Non-small cell lung cancer (NSCLC) is the leading cause of cancer-related mortality worldwide, largely due to late-stage diagnosis and a 5-year survival rate of 9%. Targeted therapies for oncogene-dependent tumors like tyrosine kinase inhibitors (TKIs) improve outcomes yet their clinical efficacy is often limited by occult drug-tolerant persister cells (DTPCs), causing recurrence. Long non-coding RNAs (lncRNAs) are transcripts over 200 nucleotides and typically non-protein coding. They regulate cellular functions by interacting with substrates through their complex secondary structures. Their deregulation is linked to oncogenesis and therapy resistance. While their role in lung cancer has been documented, their involvement in the DTPC state remains unexplored. Our study aims to investigate the role of lncRNAs in mechanisms that drive failure to targeted therapy in NSCLC. We comprehensively analyzed single-cell RNA-seq data from 49 NSCLC biopsies, pre- and during TKI therapy (residual disease, RD). We identified several lncRNAs that were significantly, differentially expressed in RD when compared to treatment naïve (TN) tumors. We orthogonally validated these findings in a minimum of 2 lung cancer cell lines in TN or DTPCs (9-15 days upon TKI exposure in culture) [$p<0.05$, absolute log2 fold change > 0.3]. We found that *MALAT1, HCG11*, and *EPB41L4A-AS1* (lncRNA-UP signature) displayed significantly increased expression in RD relative to TN tumors and parental cell lines. We also found significant downregulation of *LUCAT1* and *LINC00152* (lncRNA-DOWN signature) in RD samples. We further performed Kaplan-Meier survival analysis in an independent set of RD samples stratified by differential expression of our lncRNA signatures (n=18/group). The analysis showed improved overall survival in patients whose DTPCs expressed a high level of the lncRNA-UP signature (hazard ratio, HR=0.56; log-rank test p=0.0331). We did not observe significant differences in survival for the lncRNA-DOWN signature. We additionally performed survival analysis using the GEPIA database for lung adenocarcinoma (primarily TN, n= 239/group). Consistently, the analysis showed improved overall survival for high levels of the lncRNA-UP signature (HR=0.71; p=0.029), whereas high levels of the lncRNA-DOWN signature were indicative of inferior outcomes (HR=1.4, p=0.046). We systematically identified DTPC-associated lncRNA signatures from our unique DTPC cohort, indicating that deregulation of lncRNA expression may play a role in acquired drug resistance in lung cancer. DTPC-associated lncRNA expression patterns are linked to differential overall survival, suggesting a possible tumor-suppressive or promoting role and highlighting their potential as predictive biomarkers and therapeutic targets. Further investigation into the functional roles of these lncRNAs and their interplay with coding molecules is warranted.

#0458 Nanoparticle-mediated delivery of miR-590-3p decreases recurrent GBM tumor growth by inhibits multiple oncogenic nodes.

H. Lopez-Bertoni[1], S. Sall[2], H. Khela[2], J. Korleski[1], K. Luly[1], M. Johnson[2], B. Lal[2], A. Johnson[1], S. Tzeng[1], J. Green[1], J. Laterra[1];
[1]Johns Hopkins School of Medicine, Baltimore, MD, [2]Hugo W Moser Institute at Kennedy Krieger, Baltimore, MD

Glioblastoma (GBM) is the most lethal and aggressive form of brain cancer. Despite aggressive therapy consisting of surgery followed by radio/chemotherapy GBM recurs in almost all patients and, currently, there are no proven therapies to treat recurrent GBM (rGBM). Recent developments in nanomedicine provide new and promising opportunities to develop new targeted therapeutics to treat brain tumors. We have recently developed PBAE nanoparticle formulations optimized for in vivo miRNA delivery to brain tumor stem cells, or GSCs. Carefully selecting one miRNA to target several mRNAs dysregulated within a pathway can allow the targeting of multiple nodes using a single agent, mimicking combinatorial therapies. To test this hypothesis, we performed bioinformatic analysis of RNA sequencing from GSCs and clinical rGBM specimens combined with gene set enrichment analysis (GSEA) and identified TGFBR2 signaling as a targetable pathway in rGBM. We show that SMAD2 signaling, a downstream effector of TGFBR2, is enriched in rGBM and that patients with elevated TGFBR2 transcripts respond poorly to current standard of care. Utilizing patient-derived xenograft lines from rGBM, we show that blocking TGFBR2 signaling using siRNAs or ITD1, a selective TGFBR2 inhibitor, decreases the stem cell capacity, cell viability and re-sensitizes clinical rGBM cells to temozolomide (TMZ) in-vitro. In vivo, we show that ITD1 is modestly effective in subcutaneous and ineffective in orthotopic rGBM models. Not surprisingly, these tumors exhibited classical growth patterns associated with acquisition of resistance. To overcome this obstacle, we performed a miRNA-based network analysis in rGBM and identified miR-590-3p as a putative tumor suppressor that targets SMAD2 signaling at multiple nodes in rGBM. In-vitro, transgenic miR-590-3p robustly decreased the expression of 37 putative oncogenes simultaneously concurrent with decreasing stem cell capacity, cell viability and re-sensitizing rGBM PDX cells to TMZ. In vivo delivery of miR-590-3p to established PDX-derived rGBM orthotopic tumors using novel PBAE nanocarriers robustly decreased tumor sizes and increased tumor necrosis. These results show that the promiscuous nature of miRNAs, in combination with cutting-edge nucleic acid delivery vehicles, can be leveraged as advanced targeted therapeutics for rGBM bypasses the resistance that is developed to standard of care and available small molecules.

#0459 Exosomal miRNA 16-5p/29a-3p secreted from pancreatic cancer induce adipose atrophy by inhibiting adipogenesis and promoting lipolysis.

S.-C. Tien[1], C.-C. Chang[1], I.-C. Chen[2], C.-H. Huang[1], H.-Y. Peng[3], Y.-T. Chang[3], M.-C. Chang[3], C.-M. Hu[1], W.-H. Lee[4];
[1]Genomics Research Center, Academia Sinica, Taipei, Taiwan, [2]Institute of Biochemistry and Molecular Biology, National Yan Ming Chiao Tung University, Taipei, Taiwan, [3]Department of Internal Medicine, National Taiwan University College of Medicine, Taipei, Taiwan, [4]Department of Biological Chemistry, University of California, Irvine, CA

Over 80% of the patients with pancreatic ductal adenocarcinoma (PDAC) have cachexia, which is associated with reduced survival, decreased quality of life, and higher rates of metastatic disease. To date, the diagnostic and therapeutic options of PDAC-associated cachexia remain limited due to the lack of a complete understanding of the underlying pathological mechanism. Here, we demonstrate that fat loss is the earliest feature of cachexia induced by PDAC through its secreted exosomes. By analyzing exosomal components of normal and cancer-derived exosomes through small RNA-seq, we identify miR-16-5p, miR-21-5p, miR-29a-3p and miR-125b-5p enriched in pancreatic cancer-derived exosomes and in the exosomes from sera of mice or patients with pancreatic tumor. Among these, miR-16-5p and miR-29a-3p play a key role in fat loss by inhibiting adipogenesis through decreasing Erlin2 and CMPK1 expression leading to C/EBPβ and PPARγ downregulation. Synergistically, miR-29a-3p increases ATGL expression to facilitate lipolysis by suppressing MCT1 expression. Furthermore, PDAC-derived exosomes deprived of miR-16-5p and miR-29a-3p fail to induce fat loss, suggesting that these two exosomal miRs are required for PDAC-induced fat loss. These findings unravel a precise mechanism of how PDAC causes adipose atrophy via exosomal miRs and may provide new diagnostic and therapeutic strategies for PDAC-induced cachexia.

#0460 Fecal microRNA and microbiome profiles in colorectal cancer patients: Are they predictor of survival and how do behave in longitudinal samples?.

B. Pardini[1], N. Keles[2], G. Ferrero[3], S. Tarallo[1], G. Francescato[3], A. Gagliardi[3], V. Alberini[3], C. Di Battista[4], V. Vymetalkova[5], F. Turkoglu[6], O. Duzgun[6], O. Ozkan[6], B. Tuna[2], P. Vodicka[5], S. Dogan[2], A. Naccarati[1];

[1]Italian Institute for Genomic Medicine (IIGM), Candiolo, Italy, [2]Yeditepe University, Istambul, Turkey, [3]University of Turin, Turin, Italy, [4]Fundacio de Recerca Clinic Barcelona-Institut d`investigacions Biomediques August Pi i Sunyer (FRCB-IDIBAPS), Barcelona, Spain, [5]Institute of Experimental Medicine of the Czech Academy of Sciences, Prague, Czech Republic, [6]University of Health Sciences, Umraniye Training and Research Hospital, Istambul, Turkey

Background: Colorectal cancer (CRC) is characterized by a high complexity that significantly influences treatment response and survival. There is still a lack of prognostic factors after surgery that could help predict postoperative survival. Currently, lymph node metastases are the single most important prognostic factor but it gives no clue on tumor aggressiveness and recurrence. Our group recently contributed to the identification of a fecal microRNA (miRNA) signature that accurately discriminates sporadic CRC and aimed at improving non-invasive diagnosis (Pardini et al, Gastroenterology 2023) as well as altered gut microbiome species associated with CRC (Thomas et al, Nat. Medicine 2019), but there are scanty evidence on the potentiality of such markers for prognosis.
Aims: In the same cohort, we investigated if the fecal miRNome and gut microbiome at diagnosis are associated with CRC patients' prognosis. Moreover, we assessed fecal miRNA in a new set of CRC patients collected longitudinally before and after the surgery to investigate whether such associations reflect miRNA profiles over time. Methods. We performed small RNA and shotgun metagenomic sequencing in stool samples in 3 cohorts from: Italy (IT, 128 CRC), Czech Republic (CZ, 69 CRC), and Turkey (TU, 34 CRC, 40 controls). Stool samples from TU CRC subjects were collected before surgery and after 6 months.
Preliminary Results: In the IT and CZ cohorts, an average of 479 fecal miRNAs were detected with 209 differentially expressed (DE) miRNAs significantly associated with survival, including miR-1246 which was present in the CRC-associated signature identified by us. Two miRNAs (miR-197-5p and miR-6081-5p) were significantly down-regulated in patients with the worst prognosis (adj.p<0.01, HR<0.50) in both cohorts. In TU cohort, 494 miRNAs were DE in CRC (pre-surgery) vs controls. Among them, the 25 DE miRNAs detected in our previous work were also significantly altered, including the 5-miRNA CRC signature (miR-149-3p, miR-607-5p, miR-1246, miR-4488, and miR-6777-5p) identified by machine learning. Notably, after 6 months from surgery, levels of such miRNAs reverted to those measured in controls (for miR-1246 p<0.001 in both controls vs pre- and vs post-surgery comparisons). More analyses on the longitudinal fecal miRNA data are ongoing as well as for the metagenome data assessing the abundancies of CRC-associated microbial species before and after tumor resection and their possible association with survival.
Conclusions: Fecal miRNAs may serve as biomarkers for CRC prognosis. Following tumor resection, CRC levels of altered miRNAs return in a range comparable with those of healthy controls in a time-dependent manner. These data further support the use of fecal miRNAs as accurate diagnostic CRC biomarkers and provide preliminary information on their possible translation as a prognostic tool.

#0461 Dual-kinase targeted miRNA nanotherapy for the treatment of triple-negative breast cancer.

G. Kara[1], P. Atalay Dundar[1], N. Kahraman[1], E. B. Denkbas[2], B. Ozpolat[1];
[1]Houston Methodist Research Institute, Houston, TX, [2]Baskent University, Ankara, Turkey

Triple-negative breast cancer (TNBC) represents 20% of breast cancer (BC) patients (51,000 cases/year in the US). It is associated with a highly aggressive course, early metastasis and relapses, and drug-resistant phenotype. About 40% of the patients die within 5 years despite available therapies. If the disease is metastatic, patients survive only 13 months. Since TNBC does not express targetable receptors such as ER, PR, and HER2, and it is a highly heterogeneous cancer with six genetically defined sub-types, currently, there are no common actionable molecular targets and no effective targeted therapies for TNBC. microRNAs (miRNAs) are 18-20 nt long non-coding RNAs and are often dysregulated in cancer cells. Tumor-suppressive miRNAs specifically silence their protooncogenic target genes (mRNAs) by binding specifically to their 3'-UTRs located in their target mRNAs, leading to inhibition of oncogenes that play critical roles in cell proliferation, cell cycle, migration, invasion, angiogenesis, drug resistance, tumor growth, and progression. We have previously demonstrated that Eukaryotic Elongation factor-2 kinase (eEF2K) and AXL are oncogenic kinases, and their higher expression is associated with poor survival in patients with TNBC. However, currently, there is no FDA-approved eEF2K and AXL-targeted therapeutics. To effectively co-target these kinases, we extensively analyzed miRNA databases using miRNA target prediction algorithms and recently, we discovered that miR-329-3p has a specific binding site at both 3'-UTRs of eEF2K and AXL mRNAs. Analyzing the TCGA TNBC database, we found that low expression of miR-329-3p is correlated with shorter overall survival in TNBC patients, and the expression of miR-329-3p is commonly reduced or lost in TNBC patient tumors. Since the successful clinical application of miRNA-based therapeutics requires safe and effective nano-delivery systems, we have developed magnetic iron-oxide-based nanoparticles (MNPs) for the delivery of miR-329-3p. We showed that miR-329-3p significantly suppresses cell proliferation, invasion, and migration by targeting both eEF2K and AXL and their downstream mediators such as SRC/FAK and Cyclin D1 in TNBC cell lines. In vivo systemic treatment with MNPs-miR-329 completely blocks tumor growth in orthotopic MDA-MB-231 and MDA-MB-436 TNBC xenograft models in mice. Analysis of tumors shows remarkable inhibition in eEF2K and AXL expression, and clinically significant downstream targets including SRC, FAK, and Cyclin D1. We also demonstrated that miR-329 nanotherapy induces apoptosis and inhibits intratumoral proliferation in TNBC tumors in mice. Toxicity markers in mouse blood samples show that miR-329 nanotherapy is safe and not toxic to mice. Taken together, our study suggests that miR-329-3p nanotherapy may be used as a novel potential therapeutic approach in TNBC patients.

#0462 Developing the miR-888 cluster as a therapeutic target for prostate cancer.

K. Routon[1], T. Fachko[1], V. Kasina[2], R. Bahal[2], **A. E. Kerscher**[1];
[1]Eastern Virginia Medical School, Norfolk, VA, [2]University of Connecticut, Storrs, CT

Prostate Cancer (PCa) is a serious health crisis in the United States. 20% of men diagnosed with PCa will progress to fast-growing, advanced disease. There are no curative treatment options for PCa that has spread to distant sites and the 5-year survival rate for metastatic disease remains 30%. Recognizing the need for better PCa therapeutics, we are developing novel anti-microRNA delivery reagents targeted against the noncoding RNA miR-888 cluster to block prostate tumor progression. Our lab identified these oncomiRs in a biomarker discovery screen as elevated in human metastatic PCa cell lines and prostatic fluids from patients with high-grade PCa. We noted that over-expression of miR-888 cluster members (miR-888, miR-891a) promoted prostate cell growth and induced invasiveness *in vitro*. miR-888 and miR-891a also accelerated xenograft tumor growth in mice. Treatment of aggressive PCa cells in culture with synthetic antisense inhibitors against individual cluster members reversed these growth and invasion phenotypes, highlighting their clinical potential. We are testing pH Low Insertion Peptide (pHLIP)-Peptide Nucleic Acid (PNA)-based antimiR conjugates against miR-888 and miR-891a. The delivery vehicle pHLIP is a 36-amino acid peptide that at low pH (< pH 6.5) adopts an alpha-helical conformational change and facilitates the insertion of its C-terminus across lipid bilayers to transport conjugated anti-miRNA cargo into cells. When administered systemically, pHLIP effectively targets solid tumors with acidic microenvironments. We found that these reagents are readily internalized by human PCa cells cultured at pH 6.0 and in prostate xenograft tumors when delivered systemically in mice. Treatment significantly repressed miR-888 and miR-891a and acted to slow prostate cell growth *in vitro.* We are currently moving these studies into mouse prostate models. Furthermore, we are investigating the downstream signaling pathways for the miR-888 cluster. Our work indicates that the miR-888 cluster network coordinates the repression of the Tissue Inhibitors of Metalloproteinase (TIMP) and SMAD4 anti-metastatic pathways to drive extracellular matrix degradation and prostate cell invasion, and as a consequence, induces matrix metalloproteinase (MMP) activity. Expression profiling arrays and luciferase reporter assays indicated that multiple members of the miR-888 cluster co-suppress TIMPs in the prostate and similarly elevate multiple MMPs as well as cadherins, fibronectin and heparinase, and co-modulated several immune response genes. We are currently studying the consequence of various CRISPR-mediated miR-888 cluster deletions to understand how this non-coding RNA cluster functionally overlaps to promote aggressive PCa. This work will establish new clinical tools for aggressive PCa and optimize patient treatment management.

#0463 The small nucleolar RNA SNORD46 and SNORD72 have tumor suppressor activity in diffuse large B cell lymphoma.

E. Y. Chung, F. Spriano, S. Napoli, G. Sartori, L. Cascione, **F. Bertoni**;
IOR - Institute of Oncology Research, Bellinzona, Switzerland

Background. Following the identification of an 11q24.3 gain upregulating the ETS factors ETS1 and FLI1 in diffuse large B cell lymphoma (DLBCL) (Bonetti et al. Blood 2013), we observed the anti-lymphoma activity of blocking the protein-protein interaction of ETS factors with RNA helicases, using YK-4-279 and its clinical derivative TK-216 (Spriano, Chung et al. CCR 2019). DLBCL cells exposed to the two small molecule inhibitors presented a significant upregulation of small nucleolar RNAs (snoRNAs). Besides their primary functions in rRNA processing, snoRNAs are often deregulated in cancers, with microRNA-like actions and direct interaction with proteins. Here, we characterized SNORD46 and SNORD72, the two snoRNAs most upregulated cells after YK-4-279 and TK-216 and mapped to the 1p34.1 locus recurrently lost in DLBCL.
Methods. Real-time PCR, immunoblotting, and shRNA silencing were conducted based on established protocols. RNA-Protein Interaction Prediction (RPISeq) was used to calculate the interaction probabilities of snoRNAs with proteins of interest. The prediction was made using both the Random Forest (RF) and the Support Vector Machine (SVM) classifiers, using a stringent threshold of >0.6.
Results. The time-dependent changes of SNORD46 and 74 were validated with real-time PCR in the U2932 activated B cell-like (ABC) DLBCL cell line exposed to YK- 4-279 for 4 or 8 h. Upregulation of SNORD46 and 74 were significantly upregulated compared to their host genes upon YK-4-279 treatment, suggesting these snoRNAs have different functions from the genes in which they are encoded. Across 48 lymphoma cell lines, SNORD74 was more expressed in ABC DLBCL than in the remaining cell lines (P 0.03) or GCB DLBCL (P 0.05), while SNORD46 did not differ. Stable lentiviral-based overexpression of SNORD46 and 74, U2932 ABC DLBCL demonstrated that both SNORD46 and SNORD74 overexpression impaired growth while SNORD92, the control did not SNORD74 overexpression inhibited pAKT-Ser473, suggesting it could exert its anti-tumor effect by negatively impacting BCR signaling. Since constitutive BCR is the main driver for the pathogenesis in ABC DLBCL, we studied the impact of BCR signaling on SNORD46 and 74 expressions. IgM stimulation downregulated the snoRNAs in U2932 and TMD8 ABC DLBCL cell lines at 1 and 2.5 h poststimulation, with a more substantial effect for SNORD74. Furthermore, the snoRNAs were upregulated in four ABCs and four GCB DLBCLs cell lines exposed to the PI3K/mTOR inhibitor bimiralisib. Bioinformatic analysis indicated the possible binding of SNORD46 and especially of SNORD74 to BCR signaling molecules (SYK, LYN, BTK, PI3Kδ, IRAK4, IRAK1, CARD11), RNA helicases (RHA, DDX21, DDX5) and essential DLBCL proteins (BCL6, IRF4).
Conclusions. SNORD46 and SNORD74 exert tumor suppressor activity in DLBCL cells, possibly as negative regulators of the BCR signaling.

#0464 Chromatin associated long non-coding RNAs involved in dormancy for late recurrence of ER-positive breast cancer.

N. Saitoh, M. Palihati, H. Tachiwana;
The Cancer Institute of JFCR, Koto-ku, Tokyo, Japan

Late recurrence is one of the major problems for hormone receptor-positive breast cancer patients. It is suggested that the risk of recurrence may be maintained by cancer cells that have been already disseminated in the body at surgery. They enter long-term dormancy, thus evade immune surveillance and become resistant to therapies. The detailed molecular mechanism for this process is largely unknown.Nuclear long noncoding RNAs, which are not translated to proteins, often function as epigenetic regulators and determine the phenotype of cells and individuals. We found that a cluster of long noncoding RNAs, ELEANORS, is specifically expressed in ER (estrogen receptor)-positive recurrent breast cancer cells, forms a molecular condensate (RNA cloud) in the nucleus, and activates the *ESR1* gene that encodes ER. ELEANORS define a large chromatin domain, the 0.7 Mb topologically associated domain (TAD), which contains the *ESR1* and three other breast-cancer-associated genes. ELEANORS also regulates the three-dimensional genome architecture. They mediate a long-range chromatin interaction of ESR1 and *FOXO3* genes, which are 42.9 Mb apart, and contribute to their cooperatively activate transcription, equilibrating cell proliferation (*ESR1*) and apoptosis (*FOXO3*). Upon ELEANOR knockdown, the ELEANOR clouds are disappeared, and *ESR1* gene transcription is repressed. Further, the two genes are dissociated and only the *FOXO3* gene remains transcriptionally active, resulting in the induction of apoptosis.Further analysis of clinical specimens revealed that ELEANOR expression in primary tumors correlates with recurrences over 5 years after surgeries, suggesting that ELEANORs are involved in late recurrence. We also found that ELEANOR activates transcription of *CD44,* a breast cancer stem cell marker gene. Cancer stem cell maintenance and equilibration of proliferation and apoptosis by ELEANOR may be involved in long-term tumor dormancy in late recurrence. This study suggests the possibility of ELEANORS as a biomarker to predict late recurrence, as well as a therapeutic target for ER-positive breast cancer.

(References)Abdalla, MOA. et al., *Nat. Commun*, 10, 3778 (2019) Tomita, S. et al., *Nat. Commun*, 6, 6966 (2015)

#0465 Effect of Epstein-Barr virus *lnc-BARTs* on EBV genome maintenance in EBV-associated tumors.

J. Liu, B.-Y. Mok, H. Chen;
The University of Hong Kong, Hong Kong, Hong Kong

Most humans infected with Epstein-Barr virus (EBV) remain asymptomatic throughout the whole life. However, EBV is linked to several human cancers, including Burkitt's lymphoma, Hodgkin's disease, post-transplant lymphoproliferative disorder (PTLD), nasopharyngeal carcinoma (NPC), and gastric carcinoma. Among these EBV-associated tumors, EBV genome is present in 100% of NPC tumor cells. In NPC cells, EBV establishes a latent infection, expressing limited number of viral proteins but elevated levels of non-coding RNAs transcribed from the BamHI-A region of the EBV genome, also known as BamHI-A rightward transcripts (BARTs). The family of EBV BART RNAs includes BART-microRNAs (miRNAs) and long non-coding RNAs (lnc-BARTs). Although various functions of BART miRNAs have been identified, the role of EBV lnc-BARTs remains largely unknown. In this study, we provide evidence demonstrating that lnc-BARTs functions as a regulatory long non-coding RNA, referred to as lnc-BARTs. These lnc-BARTs play keys role in modulating the core networks that maintains EBV latency and promotes NPC oncogenesis through epigenetic mechanisms. Our study found that the apoptosis rate of NPC cells is significantly increased following the knockdown of EBV lnc-BARTs, indicating their anti-apoptotic role in EBV-associated tumors. Mass spectrometry analysis identified several host factors, including transcriptional regulators BRD4 and SC35' interact with EBV lnc-BARTs in NPC cells. RNA-FISH assays showed lnc-BARTs co-localized with BRD4 and SC35 complexes in nuclear s peckles and such interaction were disrupted by JQ1, a BRD4 competitive inhibitor. Binding of lnc-BARTs to BRD4 RNA was confirmed using immunoprecipitation and pulldown assays. ATAC sequencing and transcriptome analyses showed that BART knockdown in EBV-harboring NPC cell line C666-1 led to reduced chromatin accessibility, downregulation of oncogenes, and decreased EBV episome replication and maintenance. Quantitative qPCR and DNA FISH analyses of cell samples treated with shRNA targeting lnc-BARTs or BRD4 reduced EBV copy numbers and EBNA1 RNA expression levels in EBV-infected NPC cells. Finally, ChIP sequencing analysis revealed that lnc-BARTs is critical for BRD4 binding to the oriP region of the EBV genome. These findings support a mechanism by which EBV lnc-BARTs epigenetically regulate host gene expression through functional interactions with elongation regulatory machinery and contribute to the maintenance of EBV latent genome by interaction with BRD4 complex.

#0466 microRNA regulators of neuroendocrine differentiation in metastatic castration-resistant prostate cancer.

D. Asante, S. Nathani, T. J. Lee, A. Sharma, S. Saini;
Augusta University, Augusta, GA

Therapy-induced neuroendocrine prostate cancer (NEPC), an extremely aggressive variant of castration-resistant prostate cancer (CRPC), is increasing in incidence with the widespread use of highly potent androgen receptor (AR)-pathway inhibitors (APIs) via a reversible trans-differentiation process, referred to as neuroendocrine differentiation (NED). The molecular basis of NED is not completely understood leading to a lack of effective molecular markers for its diagnosis. We hypothesized that alterations in key miRNAs drive NED, leading to lineage switching and emergence of NEPC. The aims of our study are: (i) identify key miRNA alterations that occur as PCa cells undergo neuroendocrine differentiation; (ii) develop a miRNA-based classifier for predicting/diagnosing NEPC; (iii) understand the functional role of key miRNA alterations. To systematically investigate the key miRNAs alterations driving therapy induced NED, we performed small RNA-NGS in a retrospective cohort of human metastatic CRPC clinical samples + PDX models with adenocarcinoma features (CRPC-adeno) vs those with neuroendocrine features (CRPC-NE). Further, with the application of machine learning algorithms to sequencing data, we trained a ‘miRNA classifier’ that could robustly classify ‘CRPC-NE’ from ‘CRPC-Adeno’ cases. The performance of classifier was validated in additional cohorts of mCRPC patients acquired from independent sites by employing single model prediction algorithm. We further sought to understand the functional role of these miRNAs by overexpessing in PCa cell lines followed by functional assays. *In vivo* xenograft studies were performed using PC3 cells overexpressing miR-28/control miRNA. We demonstrate for the first time, that lineage switching to NE states is accompanied by key miRNA alterations. Our analysis, measured using receiver operating characteristic (ROC) curves, demonstrated an area under the curve (AUC) value of 0.8318, confirming the robustness of our classifier in distinguishing CRPC-NE from CRPC-Adeno. Furthermore, we identified a select group of 5 miRNAs that were pivotal in distinguishing between these two prostate cancer subtypes. We focused on miR-28-3p, little studied miRNA in prostate cancer. Our *in vitro* and *in vivo* data with prostate cancer cell lines and xenograft model suggests that miR-28-3p acts as a tumor suppressor miRNA in advanced stage prostate cancer. We further found mesenchymal gene Vimentin to be a direct miR-28-3p target. We propose that loss of miR-28-3p promotes epithelial-to-mesenchymal transition (EMT), thereby favoring NED. Our study has important clinical implications and transformative potential as our 'miRNA classifier' can be used as a molecular tool to stratify mCRPC patients into those with/without NED and guide treatment decisions. Further, we identify novel miRNA NED drivers that can be exploited for NEPC therapeutic targeting.

#0467 Genetic ablation of microRNA-10b improves treatment outcomes in mouse models of pancreatic cancer.

K. Kempinska, S. Samuel, S. Rajesh, C. Mallett, L. Sempere;
Michigan State University, East Lansing, MI

Pancreatic ductal adenocarcinoma (PDAC) is a recalcitrant and lethal disease with an overall 5-year survival rate of less than 12%. PDAC is a heterogeneous disease characterized by highly aggressive cancer cells, extensive desmoplastic reaction, and hypovascularity. These unique features endow PDAC tumors with an array of innate resistance mechanisms against standard-of-care (SOC) chemotherapy: gemcitabine/nab-paclitaxel or FOLFIRINOX. Thus, there is clinical need to develop novel targets that enhance treatment efficacy of SOC chemotherapy. microRNA-10b (miR-10b) expression is frequently upregulated in PDAC and correlates with poor outcome. High levels of miR-10b expression within cancer cells correlates with poor treatment response to gemcitabine-containing neoadjuvant chemotherapy and poor overall clinical outcome. We and others reported that miR-10b exerts cancer cell-intrinsic pro-survival, anti-apoptotic, and pro-metastatic functions via downregulation of key target genes (i.e., BIM, PTEN, TIAM1). We hypothesize that upregulation of miR-10b expression is a chemoresistance mechanism to increase cell survival and inhibit apoptosis in PDAC. To test this hypothesis, we generated a KPC model ($Kras^{G12D}$-driven, p53-deleted by Pdx1-Cre) with global *Mir-10b* gene knockout (Mir-10bKO). Animals were recruited when their tumor volume reached 200 mm^3 by multi-mouse MR imaging and were randomly assigned to control or treatment groups (100 mg/kg of gemcitabine q4d). Tumor growth was monitored by weekly MR imaging sessions throughout the duration of the treatment. Untreated KPC;Mir-10bKO animals survived several weeks longer than untreated KPC animals (21.7 vs. 18 weeks, $p = 0.056$), suggesting a weak but detectable tumor promoting role of miR-10b. Remarkably, loss of miR-10b activity enhances treatment response to gemcitabine and significantly prolongs survival in this KPC model. Treated KPC animals lived only 5 weeks longer than untreated KPC (23 vs 18 weeks, $p = 0.015$), whereas KPC;Mir-10bKO lived 9 weeks longer (27 vs 18 weeks, $p = 0.002$). Notably, we observed a more durable response in treated female KPC;Mir-10bKO animals ($n = 4$) compared to any other experimental group ($n > 5$). We are currently performing tissue and molecular analyses to identify direct target genes involved in chemoresistance and sex-specific modulation of treatment response.

#0468 Associations of circulating miRNAs with pancreatic cancer risk differ by years between blood collection & and cancer diagnosis.

H. Cai[1], V. Setiawan[2], X. Guo[1], J. Wu[1], R. Stolzenberg-Solomon[3], C. Zhu[4], Y.-T. Gao[5], J. Berlin[1], F. Ye[1], Q. Cai[1], W. Zheng[1], X.-o. Shu[1];
[1]Vanderbilt University Medical Center, Nashville, TN, [2]University of Southern California, Los Angeles, CA, [3]NIH, Bethesda, MD, [4]NCI, Bethesda, MD, [5]Shanghai Jiao Tong University, Shanghai, China

Pancreatic adenocarcinoma (PDAC) is one of the most fatal cancers and currently used biomarkers for PDAC diagnosis are not adequate for early detection. Therefore, new biomarkers for PDAC early detection are urgently needed. We conducted a large-scale study to prospectively evaluate the association of circulating miRNAs with PDAC risk. Specially, we aimed to examine whether the associations of miRNAs expression levels and changes of those levels from blood collection to cancer diagnosis (BCCD) with PDAC risk. We used pre-diagnostic plasma samples of 1307 PDAC cases from 5 cohort studies (290 from the Prostate, Lung, Colorectal, and Ovarian Cancer Screening Trial, 395 from the Shanghai Women's and Men's Health Studies, 154 from the Southern Community Cohort Study, and 468 from the Multiethnic Cohort). Cancer free controls (n=1307) were selected and individually matched to index cases in each cohort. All miRNAs were measured by the NanoString nCounter Analysis System using the Human v3 miRNA Expression panel (798 miRNAs total). Data were pooled and quantile normalized prior to analysis. Associations of circulating miRNAs with PDAC risk were assessed by odds ratio per decile change in miRNA levels using conditional logistic regression. Fold-change of miRNA for cases versus controls by BCCD was analyzed via linear regression. Median time of BCCD was 7.13 years (range: 0.03-19.61 years). We first conducted the association analysis stratified by BCCD: < 5 years, 5-10 years, and >10 years. We found 20 miRNAs were significantly associated with PDAC risk in the <5 years after FDR correction. In the analysis of regressing fold-change of these 20 miRNAs on BCCD, we found the fold change of miR-155-5p was inversely associated with BCCD (β=-0.04, P<0.01), i.e., the case-control difference was larger when blood was drawn closer to PDAC diagnosis, suggesting its potential utility as disease biomarkers for early detection. Conversely, the fold-change of miR-93-5p (β=0.04, P=0.01), miR-223-3p (β=0.03, P=0.02), let-7i-5p (β=0.03, P<0.01), and miR-191-5p (β=0.05, P<0.01) were positively associated with BCCD, i.e., the case-control difference increased with an increasing the time interval of BCCD, indicating they are more likely biomarkers for PDAC risk. Ingenuity pathway analyses of these five significant miRNAs revealed that they were significantly enriched in ribonucleotide reductase signaling pathways at p<0.05. Notably, the silencing of ribonucleotide reductase M2 subunit suppresses tumorigenesis in pancreatic cancer by deactivating the PI3K/AKT/mTOR pathway, further supporting our findings.
Findings of this large-scale multiethnic study suggest that changes in circulating levels of let-7i-5p, miR-155-5p, miR-93-5p, miR-191-5p, and miR-223-3p may help identify individuals at an elevated risk of developing PDAC, allowing for screening tests and close surveillance.

#0469 PIWI-interacting RNA 50485 (piRNA-50485) is a novel lung tumor suppressor.

M. E. Reeves, Y. G. Amaar;
Loma Linda University and VA Loma Linda Healthcare System, Loma Linda, CA

Introduction: It is crucial to identify new driver genes and associated downstream pathways to facilitate the development of targeted therapies to effectively treat late-stage and metastatic lung cancer. One pathway involves the Ras association domain family 1 (*RASSF1*) gene which encodes multiple isoforms. Our laboratory has discovered that the RASSF1C isoform exhibits functional characteristics of an oncogene. We discovered that RASSF1C modulates the expression of PIWI-(Drosophila)-like 1 *(*PIWIL1, a stem cell renewal gene), as well as novel PIWI-interacting RNAs (piRNAs), which are regulators of the stem cell phenotype and have been linked to oncogenesis. While studying this pathway, we have identified novel piRNAs that are modulated by RASSF1C in non-small cell lung cancer (NSCLC) cells that appear to act as oncogenes or tumor suppressors.
Methods: We conducted a global microarray screen to identify RASSF1C PIWI-interacting RNA (piRNA) gene targets. Several piRNA genes that are up- and down-regulated by RASSF1C were identified and the expression of selected up-regulated and down-regulated target genes were confirmed by RT-PCR. We evaluated the impact of selected piRNAs on lung cancer cell proliferation and migration *in vitro*. We also assessed the expression of the validated piRNA target genes in lung tumor and matched normal tissues. Host and target genes for specific piRNAs were identified using a piRNA database (piRNAdb.org).
Results: Among the down-regulated piRNAs, we found that restoring piR-50485 expression drastically decreased lung cancer cell proliferation and invasion, suggesting that piR-50485 could be a potent inhibitor of lung cancer cell growth and progression. Consistent with this, we found that piR-50485 expression is significantly down-regulated in about 60% of human lung cancers. We also identified that the *ZHX3* gene (a transcription repressor), which is down-regulated in human lung cancers, is the host gene for piR-50485. In addition, we identified the *ZNF618* gene (a transcription co-regulator) that is up-regulated in lung tumor tissue, is a piR-50485 target gene. Consistent with this, treatment of lung cancer cells with piR-50485 mimics resulted in a significant decrease of ZNF618 protein levels, cell proliferation, and migration. Further, increased expression levels of ZHX3 are associated with higher lung cancer patient survival, while increased ZNF618 levels are associated with lower survival. Our novel findings suggest the hypothesis that the *piR-50485-ZHX3-ZNF618* gene axis could negatively impact lung cancer cell growth and progression.
Conclusion: Exploring the impact of the *piR-50485-ZHX3-ZNF618* gene axis on lung cancer growth is a novel concept about which nothing is currently known. We are studying piR-50485 to determine if it can be an effective therapy for lung cancer metastasis, and whether it provides important prognostic information about lung cancer outcomes.

#0470 AR-induced miRNA124-3p.2 suppresses the metastasis-promoting factor CCL2.

S. Aoyama, K. Izumi, A. Mizokami;
Department of Integrative Cancer Therapy and Urology, Kanazawa University Graduate School of Medical Science, Kanazawa-shi, Japan

Objective: The standard treatment for advanced prostate cancer is androgen deprivation therapy that blocks androgen receptor (AR) signaling, but this therapy becomes ineffective within a few years, resulting in castration-resistant prostate cancer. We have previously shown that blockade of AR signaling induces CCL2 and activates cancer cells through an autocrine mechanism, but why AR blockade induces CCL2 secretion has not been elucidated. Micro RNAs (miRs) are endogenous non-coding RNAs that regulate the translation of various proteins. In this study, we investigated whether miRs are involved in CCL2 induction.
Subjects and Methods: We used miRNA PCR Plate Array and Target Scan (https://www.targetscan.org) to search for miRs that are controlled by AR and bind to and repress the CCL2 gene. We knocked down the AR of human prostate cancer cell lines LNCaP and C4-2B with siRNA (siAR) and examined the expression of target miRs and CCL2. siAR-transfected LNCaP and C4-2B were transfected with target miR mimic and CCL2 expression was examined. siAR-transfected LNCaP, C4-2B, and C4-2B were transfected with target miR mimic and CCL2 expression was examined. siAR-transfected LNCaP and C4-2B were transfected with target miR mimic and CCL2 expression was examined. The target miR mimic was introduced into them, and the changes in migration ability were evaluated.
Results: miR-124-3p.2 was extracted as a candidate from miRNA PCR Plate Array and Target Scan. miR-124-3p.2 expression was upregulated in both LNCaP and C4-2B when DHT was added and downregulated when CCL2 was added. In siAR LNCaP and C4-2B, the expression of CCL2 was decreased when miR-124-3p.2 mimic was introduced. Furthermore, in siAR-transfected LNCaP, C4-2B, the introduction of miR-124-3p.2 mimic suppressed the migration.
Conclusion: AR suppresses CCL2 via miR124-3p.2. miR124-3p.2-mediated regulation of CCL2 may be a new therapeutic target for advanced prostate cancer.

#0471 Attenuation of circulating miR-17-5p, miR-20b-5p, and miR-106a-5p in low-risk prostate cancer patients following proton therapy.

J. Velasquez[1], C. Bryant[2], N. Mendenhall[2], L. Ricks-Santi[1];
[1]University of Florida, Gainesville, FL, [2]University of Florida Health Proton Therapy Institute, Jacksonville, FL

Introduction: Liquid biopsies offer a novel approach to diagnose, predict cancer outcomes, and monitor treatment response by analyzing tumor-derived substances. Circulating cell-free microRNAs (miRNAs) show clinical promise as biomarkers within prostate cancer (PCa) and have been implicated with PCa prognosis and outcomes. However, their potential for monitoring and assessing radiotherapy (RT) treatment response remains understudied. Understanding miRNA expression changes during RT is crucial, as they impact RT efficacy by directly affecting genes and proteins within RT-response pathways.
Aim: This study aimed to profile the expression of three oncogenes, miR-17-5p, miR-20b-5p, and miR-106a-5p and to determine their association with PCa risk groups in patients receiving proton therapy (PT).
Patients and Methods: Plasma was obtained from the University of Florida Health Proton Therapy Institute Outcomes Tracking Protocol biobank. Plasma was collected from men diagnosed with localized PCa without metastatic disease at three time points: prior to PT (PRE-PT), at 4 weeks following the start of PT (4WKSPD1), and at 8 weeks following the start of PT (8WKSPD1). The pilot study consisted of 38 patients, with 23 categorized as low-risk and 15 categorized as high-risk for PCa. MiRNA expression levels were evaluated using reverse transcription-polymerase chain reaction and quantified using the Livak method.
Results: The study revealed a downregulation of miR-17-5p in response to PT, with median gene expression levels decreasing from 0.73 at PRE-PT to 0.587 at 8WKSPD1. Low-risk PCa patients also showed distinct miRNA expression changes with all three miRNAs (miR-17-5p, miR-20b-5p, and miR-106a-5p) downregulated from 0.953, 1.037, and 1.010 at PRE-PT to 0.398, 0.216, and 0.298 at 8WKSPD1, respectively. Statistical analysis using a Kruskal-Wallis test followed by a Dunn's post-hoc test identified significant differences ($p=0.035$) specifically between PRE-PT and 8WKSPD1 for miR-17-5p.
Conclusion: The study revealed that PT led to a time-dependent reduction in miRNA levels, indicating a higher responsiveness in low-risk compared to high-risk PCa patients. This differential response highlights miR-17-5p, miR-20b-5p, and miR-106a-5p as potential PT response biomarkers, with clinical implications for personalizing PCa treatment. These results underscore the necessity for further validation of these miRNAs to maximize their clinical utility.

#0472 Long non-coding RNA MIR31HG-derived circRNA enhances the oncogenicity of oral carcinoma.

C.-H. Chou, H.-F. Tu, K.-W. Chang, S.-C. Lin;
National Yang-Ming University, Taipei, Taiwan

Introduction: Oral carcinoma (OC) represents a significant health challenge, with the role of non-coding RNAs, particularly microRNAs and long non-coding RNAs (LncRNAs), being well-established in its progression. However, the implications of circular RNAs (circRNAs) in this context are less well understood, presenting a notable gap in current research. Our study focuses on the MIR31HG LncRNA, identified as crucial in OC, particularly its role in producing circRNA, as evidenced by sequencing. This specific MIR31HG-derived circRNA, designated 31HGcircR, which contains a potential open reading frame (ORF), and may demonstrate phenotypic significances. Alterations to 31HGcircR, either through knockout or ORF mutation, result in remarkable phenotypic changes, highlighting its potential importance in the pathogenesis of OC.
Methods: We implemented 31HGcircR overexpression in OC cell lines, utilizing the TetOff system for gene expression control. CRISPR/Cas9 was employed for gene knockout, and siRNA for gene knockdown. Gene expression was quantified using qPCR. Additionally, the BaseScope assay was used to label and detect the spatial expression of overexpressed 31HGcircR within the cells. Assays to assess cell proliferation, invasion, migration, anchorage-independent growth (AIG), and clonogenicity were conducted.
Results: The findings revealed specific junctions of 31HGcircR and varied expression levels across different OC cell lines. There was a significant correlation among the expression of 31HGcircR, MIR31HG and miR-31-5p. Notably, the knockdown of 31HGcircR led to pronounced inhibition of cell growth, migration, invasion, AIG, and clonogenic activity. Conversely, overexpression of 31HGcircR or its ORFs augmented invasion and clonogenic potential in certain cell lines. The TetOff system demonstrated that minimal concentrations of Doxycycline effectively suppressed 31HGcircR expression, with reversible effects upon removal. Knocking out 31HGcircR resulted in reduced invasion and clonogenic capabilities.
Conclusion: This study provides clues demonstrating the oncogenic roles of 31HGcircR in OC, which simulate the functions of MIR31HG or miR-31-5p. The changes in cell phenotypes following 31HGcircR manipulation suggest its potential as a therapeutic target or biomarker in OC. These findings offer valuable insights, contributing to the evolving understanding of circRNAs in cancer research and potential treatment avenues.

#0473 PVT1 exon 9 overexpression induces AR null phenotype and cellular reprogramming in prostate cancer.

R. E. Sexton-Bonacci, C. Udekwu, B. Boylu, O. O. Ogunwobi;
Michigan State University, East Lansing, MI

Plasmacytoma variant translocation 1 (PVT1) is an oncogenic long-noncoding RNA (lncRNA) gene located directly downstream of MYC on chromosome 8q24. PVT1 is an oncogene overexpressed in prostate cancer (PCa) and can promote oncogenesis by altering gene expression directly or acting as a noncoding RNA sponge. Beyond functioning as a lncRNA, PVT1 gene encodes six microRNAs that each have independent functions. Our group identified overexpression of PVT1 exon 9 in PCa samples derived from men of African Ancestry and overexpression may explain why this population group experiences more aggressive disease. We overexpressed PVT1 exon 9 in RWPE1 prostate epithelial cells (RWPE1_ex9) and found enhanced migration and invasion compared to empty vector (RWPE1_ev). Implantation of RWPE1_ex9 cells into mice led to the formation of tumors with the neuroendocrine PCa (NEPC) phenotype that was histopathologically confirmed. RNA-sequencing analysis of PVT1 exon 9 overexpression showed significant (p-value < 0.05) upregulation of 141 genes. The majority of pathways impacted by PVT1 exon 9 overexpression were interferon type 1 signaling (*RSAD2, CMPK2)*, developmental NOTCH signaling (*HES7)*, cargo-transport (*STX16*) and tumor microenvironment promoting factors (*HS3ST3A1*). We found loss of androgen receptor (AR) expression at mRNA and protein levels in RWPE1_ex9 cells, a hallmark of NEPC, which further supports our hypothesis that PVT1 exon 9 overexpression plays a role in NEPC development. Validation of RNA-sequencing confirmed upregulation of *RSAD2, CMPK2, STX16, HES7* and *HS3ST3A1* within RWPE1_ex9 cells compared to RWPE1_ev and RWPE1 wild-type, suggestive of cellular reprogramming of prostate epithelial cells. We further analyzed expression profile in a novel circulating tumor cell model of castration-resistant 22RV1 cells (C22OH) and found enhanced expression of PVT1 exon 9, suppression of AR, phosphorylation of AR serine residue 308 and enhanced CDK11 activity compared to the primary 22RV1 cell line T22OH suggestive of a cell-cycle mediated regulatory mechanism. We further found enhanced expression of chromogramin A in the C22OH cell line, a marker of NEPC. These results suggest PVT1 exon 9 overexpression may play a critical role in NEPC development from normal epithelial cells via cellular reprogramming as well as facilitating a transition to NEPC from a castration resistant phenotype. PVT1 exon 9 may be a useful predictive biomarker that can identify populations which are likely to have disease progression from castration resistance to NEPC and further highlights the need to identify therapeutic strategies to target PVT1 exon 9 overexpression.

CHEMISTRY: Basic and Applied Nanotechnology and Therapeutics
Poster Session

#0477 Tumor treating fields (TTFields) targeted self assembling nanoparticles for pancreatic cancer treatment: *In vitro* and *in vivo* assessment.
P. P. Desai, S. Prabhu;
Western University of Health Sciences, Rancho Cucamonga, CA

Tumor Treating Fields (TTFields) is a novel, non-invasive and safe treatment modality, which is prescribed to be used in conjunction with classical anticancer chemotherapeutic drugs. TTFields when used alone are safe, but their use in combination with classical chemotherapy continues to offer drug related adverse reactions which ultimately impacts the patient compliance. To address this challenge, we earlier reported meticulously optimized self-assembling cationic-anionic polymer nanoparticles (S-CAP NPs) with average particle size of about 200 nM, encapsulation efficiency of 55-65 % and sustained drug release over 60 h. We also reported that, TTFields were capable of destabilizing the S-CAP NPs leading to targeted drug release. The results were also corroborated with in vitro cytotoxicity and colony formation studies in presence of TTFields using multiple pancreatic cancer cell lines. After establishing the proof-of-concept, the objective was to assess the in vitro cellular uptake of S-CAP NPs. For this, fluorescent dye loaded S-CAP NPs were developed and subjected to cellular uptake analysis. The in vitro cellular uptake studies confirmed the enhanced uptake of S-Cap NPs by passive diffusion in the pancreatic cancer cell lines compared to normal pancreatic epithelial cell line. The studies corroborated preferential cellular uptake of S-Cap NPs by the pancreatic tumor. Among all the formulations, the chitosan- bovine serum albumin S-CAP NPs was most optimum and was used for in vivo safety studies. For this, in vivo acute and repeated dose 28-day toxicity of the optimum placebo S-CAP NPs was conducted in Sprague Dawley rats (Western University of Health Sciences Protocol #R20IACUC031) and OECD guidelines. The in vivo studies showed a LD50 value above 2000 mg/kg and NOAEL value of 1000 mg/kg. These high doses safety of S-CAP NPs confirmed the potential of this approach for future preclinical efficacy studies followed by clinical translation. Lastly, the in vitro stability studies were conducted as per the ICH guidelines for a period of 36 months and the formulations were concluded to be stable. The tumor targeting potential, in vivo safety and stability of S-CAP NPs, establish their translational potential for TTFields triggered targeted drug release in cancer treatment. This approach will not only reduce the adverse effect associated with combination of TTFields and chemotherapy but can also be explored as a platform technology for management of other cancers. This study is supported by AACR-Novocure tumor treating fields research fellowship.

#0479 Enhanced payload delivery for acute myeloid leukemia treatment through CD37-targeting DNA nanobots.

N. Vantangoli[1], **P. D. Halley**[2], J. R. Spitzner[2], J. C. Byrd[3], K. T. Larkin[4], C. E. Castro[1], C. R. Lucas[2];
[1]The Ohio State University, Columbus, OH, [2]DNA Nanobots, LLC, Columbus, OH, [3]University of Cincinnati, Cincinnati, OH, [4]The Ohio State University Comprehensive Cancer Center, Columbus, OH

Acute Myeloid Leukemia (AML) treatment faces considerable challenges, in particular the delivery of therapeutics with sufficient potency and specificity. Traditional Antibody-Drug Conjugates (ADCs) offer a strategic approach to cancer therapy by combining the targeting capabilities of monoclonal antibodies with the cell-killing effect of cytotoxic drugs. However, the limitations in drug-to-antibody ratio (DAR) and the challenges in controlling the release kinetics have often hindered their therapeutic window suggesting novel approaches are necessary. Our approach integrates DNA nanobot technology to facilitate targeted delivery of anthracycline agents directly to CD37-expressing leukemic cells. CD37, a tetraspanin superfamily antigen, has shown promise as a target for AML due to its selective expression on immune cells and favorable internalization properties. By harnessing DNA origami assembly techniques, we developed a customizable platform capable of accommodating a significantly higher payload of chemotherapeutic agents than traditional ADCs. This increased payload potential, paired with the precision targeting of CD37, presents a potent therapeutic strategy with the possibility of reduced systemic toxicity. Here we present preclinical evidence demonstrating targeted delivery of our DNA nanobot drug delivery device and anthracycline payload to $CD37^+$ AML target cells *in vitro*. In addition, we show targeted efficacy *in vitro* and *in vivo* of our anthracycline-loaded DNA nanobot-enabled delivery system, which significantly outperformed free anthracycline in AML target cells. Collectively, our findings suggest an improvement in the therapeutic index of anthracycline and antimitotic agents as well as the ability to combine multiple drug pathways in a single delivery device. The implications of this work extend beyond AML, offering a versatile platform that could revolutionize ADC chemistry and targeted drug delivery. We propose that our DNA nanobot delivery system signifies a pivotal advancement in the field of targeted cancer therapy, with the potential to overcome longstanding barriers in the treatment of AML and potentially other malignancies.

#0480 Nanotherapeutic strategies to improve targeted radionuclide therapy.

D. Pal, M. T. Gonzaleza, A. N. Bibleb, B. Sanders, A. Plechaty, O. Kirpekar, M. Podar, S. M. Davern;
Oak Ridge National Laboratory, Oak Ridge, TN

Cancer is a leading cause of death worldwide. Several multidisciplinary approaches exist for cancer treatment, including radiotherapy and chemotherapy. Radiotherapy uses high-energy radiation to kill cancer cells; chemotherapy inhibits cancer cell proliferation and often kills cells by targeting the cell cycle. Resistance to radiotherapy and chemotherapy is a key determining factor in the outcome of therapeutic efficacy. Conventional nontargeted radiotherapy also affects distant nonirradiated cells, leading to DNA damage and changes in the cell cycle that are often linked to secondary carcinogenesis in patients. In recent years, targeted radionuclide therapy (TRT) has emerged as a promising personalized treatment strategy that delivers cytotoxic levels of radiation directly and specifically to cancer cells. Among radioisotopes,^{225}Ac exhibits desirable properties for TRT: multiple α-particle emission and high cytotoxicity. One of the challenges with ^{225}Ac is the nonspecific toxicity caused by the release and relocation of its decay daughters. Different approaches have been proposed to prevent the relocation of decay daughters, including nanoparticles. Nanoparticles have been pursued as a promising delivery vehicle of α-emitting radioisotopes to the tumor site. Here, we show specific targeting of Her2-positive breast cancer cells with ^{225}Ac-radiolabeled lanthanum orthovanadate (LaVO4) nanoparticles. Nanoparticles' surfaces were functionalized to improve biocompatibility and conjugated to target cancer cells, respectively. Cellular uptake and localization of these engineered nanoparticles were analyzed by a Confocal microscope and IncuCyte live cell analysis system. Results confirm its localization in the nucleus following the endolysosomal path, enhancing the nanoparticles' effectiveness as a delivery vehicle for α-emitting radioisotopes with the potential of increased treatment efficacy. Upon addition of cancer-targeting ligands, these nanoparticles can achieve higher efficiency by delivering the radioisotope to the tumor cells with a potential of safe encapsulation of all α-emitters in the decay chain. The anticancer efficiency of ^{225}Ac-radiolabeled nanoparticles was demonstrated by a dose-dependent effective killing of 3D breast cancer spheroids using both IncuCyte live imaging and the cell survival assays. Ultimately, the results of this study will be crucial in determining the future use of targeted radiolabeled nanoparticle-based delivery systems as an approach for more efficacious cancer treatment.

#0481 Proteomimetic polymers limit tumor growth in multiple models via potent antigen-specific T cell activation.

M. Wang[1], M. Choi[2], B. Zhang[2], N. Gianneschi[1];
[1]Northwestern University, Evanston, IL, [2]Northwestern University, Chicago, IL

Background: Patient-specific cancer vaccines derived from tumor antigen have been explored as a promising therapeutic strategy, however, challenges delivering vaccine components in a coordinated fashion to elicit antitumor responses remain. To overcome these, we utilize a novel nanoplatform called the Protein-Like Polymer (PLP), which allows for sustained and targeted delivery of tumor antigens in conjunction with adjuvants.
Methods: PLPs containing peptide antigens were synthesized via ring-opening metathesis polymerization (ROMP) and characterized. A library of compounds with different sidechain linkage chemistries, degrees of polymerization (DP), and inclusion/exclusion of Oligo-ethylene glycol (OEG) were made to determine design rules for immune activation. Cell uptake and functional assays using payload-specific T Cells were conducted. Immunization in three independent tumor models was done to show generalizability. Ability of PLPs to co-deliver adjuvants was tested by electrostatically coupling small molecule STING agonist, 2'3' cGAMP.
Results: Conjugating peptide antigens to the polymer via a cleavable disulfide linkage, which reduces intracellularly in APCs, resulted in increased endosomal localization, higher levels of induced T cell proliferation, cytokine production, and expression of activation markers in CTLs and APCs. Incorporating a diluent amount of OEG side chains reduced enzymatic degradation while increasing immunogenicity and uptake. Additionally, increasing the DP, and therefore the density of antigen side chains, further improved vaccine efficacy and resistance to proteolysis. Antigen-PLP conjugates enhanced dendritic cell activation and T-cell response only when paired with cells from their cognate system, with no activity in immune cells not expressing receptors for the payload demonstrating antigen-specificity. Mice bearing established B16F10, MC38, or TC-1 tumors treated with PLPs containing gp100, adpgk, or E7 respectively all showed increased survival times, reduced tumor burden with corresponding changes in immune cell profiles, and immunological memory upon rechallenge. Impressively, mice treated with STING-PLP complexes had significantly smaller tumors vs control at day 14 (0.038g vs 0.76g; $p < 0.0001$) and allowed for subcutaneous administration of 2'3' cGAMP, which traditionally requires intratumoral injection. Studies on the effects of vaccinating with pools of neoantigens multiplexed onto one PLP are ongoing.
Conclusion: This work validates the ability of PLPs to overcome major limitations in cancer vaccine development. The modularity of the platform allows for complex nano-architectures including systems capable of delivering challenging compounds, ie small molecule STING agonists, subcutaneously through electrostatic coupling, highlighting its potential to revolutionize cancer vaccinology.

#0482 Advancing treatment for metastatic triple negative breast cancer: Liposomal oncolytic adenovirus as a novel neoadjuvant therapy.

J. R. Shah, T. Dong, A. Phung, S. L. Blair, O. Aisagbonhi, W. C. Trogler, A. C. Kummel;
University of California San Diego, La Jolla, CA

Introduction: Adenovirus type-5 (Ad) is considered a prominent viral vector in cancer therapy due to its modifiability for the selective lysis of cancer cells. However, challenges are posed in Ad delivery to cancers lacking coxsackievirus and adenovirus receptors (CARs). In response to this limitation, Ad-encapsulated DOTAP-folate liposomes were developed, which improved Ad delivery and heightened therapeutic efficacy through membrane fusion and folate receptor-mediated endocytosis.
Methods: The 4T1 mammary carcinoma model, a CAR-negative triple-negative breast cancer (TNBC) cell line (ER-, PR-, HER2-), resistant to adenoviral infection, was utilized for studying the comparative in vitro transduction of green fluorescent protein (GFP)-expressing Ad (Ad-GFP). The study assessed Ad-GFP with and without DOTAP-folate liposomal encapsulation at a multiplicity of infection (MOI) of 50. Additionally, an oncolytic adenovirus, Ad-hTERT, with a human telomerase promoter, underwent liposomal encapsulation. CAR-negative 4T1 GFP-expressing cells and CAR-positive MDA-MB-231-GFP human breast adenocarcinoma TNBC cells were transduced in vitro at MOI 100 with Ad-hTERT, both with and without DOTAP-folate liposomal encapsulation.
Results: CAR-negative 4T1 cells exhibited superior Ad-GFP transduction when encapsulated in DOTAP-folate liposomes, compared to the unencapsulated form ($p < 0.001$). For oncolytic adenovirus Ad-hTERT, encapsulation resulted in 100% cell lysis within 24 hours in 4T1-GFP cells, contrasting with 13% with unencapsulated Ad-hTERT ($P < 0.0001$). In CAR-positive MDA-MB-231-GFP TNBC cells, encapsulated Ad-hTERT showed enhanced efficacy, resulting in 100% cell lysis within 24 hours compared to 75% with unencapsulated Ad-hTERT ($P < 0.001$).
Discussion: DOTAP-folate liposomal encapsulation enhances the efficacy of oncolytic Ad-hTERT in both CAR-negative and CAR-positive TNBC cells, establishing it as an optimal therapy for tumors with CAR heterogeneity. Ongoing in vivo studies with Balb/C immune-competent mice and the 4T1 tumor model will assess the effectiveness of encapsulation through intratumoral administration. This approach may extend the recurrence-free period post-surgical tumor removal.

#0483 Unraveling the impact of cancer cell derived membrane and cytosolic proteins using synthetic small extracellular vesicles.

Y. Chen[1], R. R. Lopez[1], T. Tsering[1], C. Zouggari Ben El Khyat[2], V. Nerguizian[2], J. V. Burnier[1];

[1]Research Institute of the McGill University Health Centre, Montreal, QC, Canada, [2]Ecole de technologie superieure, Montreal, QC, Canada

Background: Extracellular vesicles (EVs) are couriers in cell-cell communication. Evidence suggests that EV biology, from cargo packing, biodistribution, to cell uptake is a non-random and well-orchestrated process. Substantial efforts have been devoted to studying the pathological roles and therapeutic potential of EVs. It is speculated that surface properties, such as membrane proteins, mediate the interaction between EVs and recipient cells, while the enclosed "messages" exert downstream effects. This concept is exemplified in cancer metastasis, where cancer cell-derived EVs were shown to establish pre-metastatic niches and guide cancer organotropism. We propose selectively loading cancer cell membrane and cytosolic proteins into synthetic vesicles (SVs) like liposomes. This approach allows for the isolated study of individual factors, in contrast to the complexity of naturally occurring EVs.

Methods: Cellular membrane and cytosolic proteins were extracted separately from a cancer cell line (MP41) (Mem-PER^{TM} Plus kit). Empty-SV, Mem-SV (with membrane proteins), Cyto-SV (with cytosolic proteins), and Complete-SV (with both) were synthesized in a 3D-printed microfluidic chip and subsequently dialyzed (1000 KDa) overnight. The volume of protein buffer was controlled in all SV syntheses. EVs were isolated from the conditioned medium by ultrafiltration (Amicon) followed by ultracentrifugation. The size (Nanosight), zeta potential (ZetaView), and morphology (Transmission Electron Microscopy) of SVs and EVs were analyzed. Proteins incorporated into SVs were validated by stain-free gel, western blot, and CytoFLEX. SVs and EVs were stained by sp-DiIC18 fluorescent dye. The number of fluorescent particles was quantified (CytoFLEX) and controlled in cell uptake analysis on hepatocytes (IHH) and fibroblasts (BJ) (Incucyte).

Results: All SVs were successfully synthesized with a mean size of ~100 nm. The zeta potential of both Mem-SV (-27.03 mV) and Complete-SV (-24.78 mV) is close to MP41 EVs (-26.01 mV) ($P > 0.05$) and are more negative than Empty-SV (-11.30 mV) and Cargo-SV (-13.38 mV) ($P < 0.05$). Total protein incorporation efficiency was estimated to be ~30%. The relative level of specific proteins (e.g. integrin av, TSG101) in Mem-SV and Cyto-SV matched the level in the raw membrane and cytosolic proteins by western blot. Integrin avb5 was detected on the surface of Mem-SV. Membrane and cytosolic protein incorporation increased the uptake efficiency of SVs compared to Empty-SVs, and the efficiency varied with cell type and protein content.

Conclusion: In this study, we demonstrate that membrane and cytosolic proteins differentially impact the physical (zeta potential) and functional (cellular uptake) properties of SVs. Investigating these distinct roles could further our understanding of cancer EV biology, as well as advance drug delivery systems.

#0484 Enhancing therapeutic responses in NSCLC using iron-oxide nanoparticles combined with pharmacological ascorbate.

M. Singhania, M. S. Petronek, C. F. Pulliam, K. A. Mapuskar, A. Zaher, D. R. Spitz;
University of Iowa Holden Comprehensive Cancer Center, Iowa City, IA

High dose Vitamin C (pharmacological ascorbate; P-AscH$^-$ > 20 mM plasma levels) given intravenously (I.V.), has made a remarkable re-emergence as an adjuvant to combined modality approaches in cancer therapy. P-AscH$^-$ can be readily oxidized in the presence of redox active metals (i.e., P-AscH$^-$ serves as an iron reducing agent), which can result in increased fluxes of H_2O_2. This chemical phenomenon allows for the tumor-selective enhancement of chemo-radiation in NSCLC. We hypothesized that enhancing labile Fe^{2+} in cancer cells using iron-oxide nanoparticles (ferumoxytol, FMX) can increase the effectiveness of P-AscH$^-$ in enhancing cancer cell sensitivity to chemo-radiation in NSCLC by increasing H_2O_2 production. To test this hypothesis, we performed clonogenic cell survival assays in-vitro. To test the role of H_2O_2 in the combined effect of P-AscH$^-$ and FMX, we developed lentiviral-based doxycycline-inducible overexpression models for catalase, and to determine the changes in Fe, we used fluorescent probes that specifically detect changes in labile Fe^{2+}. Results from these experiments showed FMX enhanced clonogenic cell killing in NSCLC. Furthermore, catalase overexpression inhibited this effect, suggesting that enhanced H_2O_2 production plays a central role in the additive effect of P-AscH- and FMX. Finally, staining the cells with the fluorescent iron probes showed that FMX enhanced labile Fe^{2+} in cells treated with P-AscH$^-$. These studies continue to support the hypothesis that H_2O_2 plays a significant role in P-AscH$^-$ toxicity in cancer cells that can be exacerbated using iron oxide nanoparticles. Future studies will test these findings in-vivo using preclinical xenograft models.
(supported by P01 CA217797, P30 CA086862, T32 CA078586, and P01 CA244091).

#0485 Cancer killing effect of ultrasound-responsive mechanophore nanoparticles.

J. Wang, S. Zhao, J. Yi, Y. Sun, M. Agrawal, K. Li, J. S. Moore, M. Oelze, **Y.-S. Chen**;
University of Illinois at Urbana-Champaign, Urbana, IL

Radiotherapy, a mainstay in cancer treatment, often inadvertently damages healthy tissues while targeting malignancies with free radicals. As an alternative, Photodynamic Therapy (PDT) employs non-ionizing photons to generate reactive oxygen species (ROS) in tumors, offering precise targeting with minimal long-term effects. However, its efficacy is constrained to superficial tumors due to the limited penetration of light. Sonodynamic Therapy (SDT), an evolution of PDT, uses ultrasound to enhance tissue penetration while maintaining its non-invasive nature. Initial SDT studies suggest that ultrasound can activate PDT's photosensitizers to produce ROS, offering a potential pathway for tumor eradication. Nevertheless, the principal mechanisms of ROS generation in SDT, namely pyrolysis and sonoluminescence, raise concerns about potential tissue injury. In our research, we introduce an innovative approach employing mechanophores into nanoparticles. Mechanophores, molecular units within polymers sensitive to mechanical stress, undergo transformations under such conditions, including the release of small molecules or free radicals. We have developed injectable nano-sized mechanophore nanoparticles, designed to respond to high-frequency ultrasound (>100 kHz) more efficiently and with reduced energy requirements. This study focuses on nano-engineering the echogenicity of these mechanophore nanoparticles to enhance ROS generation. When agitated with focused ultrasound (FUS), these nanoparticles successfully induced ROS, leading to significant cell death, a result not observed with FUS alone in the absence of nanoparticles. In vivo experiments using mouse orthotopic cancer models demonstrated these nanoparticles' ability to inhibit tumor growth effectively. Under biocompatible ultrasound conditions, the nanoparticles cause effective cancer cell eradication with minimal impact on surrounding healthy tissues. Our findings not only introduce a novel approach to cancer treatment but also pave the way for broader applications of mechanophore nanoparticles in biomedicine. This study underscores the potential of ultrasound-activatable mechanophore nanoparticles as a versatile, effective, and safe option for cancer therapy.

#0486 Paclitaxel nanoformulation attenuates pancreatic tumor desmoplasia and alter tumor immune responses.

V. K. Kashyap, G. P. Darkwah, N. Chauhan, M. Sikander, E. N. H. Ghali, M. Kolli, B. B. Hafeez, M. M. Yallapu, S. C. Chauhan;
University of Texas Rio Grande Valley, McAllen, TX

Pancreatic ductal adenocarcinoma (PDAC) is one of the most lethal types of cancer with a 5-year survival rate of less than 13% due to the lack of effective diagnostic/therapeutic modalities. Paclitaxel (PTX) has been tested in pancreatic cancer (PanCa) therapy with marginally better clinical outcomes, but remains limited by its poor hemocompatibility, biodistribution, and intracellular accumulation in tumor cells. Gemcitabine (GEM) is the most effective therapy for PanCa. However, it shows only a marginal survival benefit of 6 months. The poor therapy response is attributed to high desmoplasia, unfavorable tumor microenvironment (TME), and excessive recruitment of immune suppressive cells. We have recently engineered a multi-layered Pluronic F127 and polyvinyl alcohol stabilized and poly-L-lysine coated paclitaxel loaded poly(lactic-co-glycolic acid) nanoparticle formulation (PPNPs), which effectively inhibits pancreatic tumor. In this study, we demonstrate that PPNPs effectively sensitize tumor cells to GEM *via* attenuation of tumor desmoplasia. Our findings also show that PPNPs synergize GEM therapy response in cell lines and in vivo mouse models. Mechanistically, PPNPs target the TME via inhibition of the sonic hedgehog (SHH) pathway and other oncogenic signaling axis that inhibits bidirectional tumor-stromal cell interaction as determined by qPCR and Western blot analyses. In addition, PPNPs effectively target tumor-associated macrophages (TAM) by repolarizing M2 into M1 phenotype *via* inhibiting expression of M2 markers and an increase in M1 markers in mouse macrophage cell line RAW264.7. M2 polarization of RAW264.7 cells were induced by culture with IL-4 (20 ng/mL) in the presence of PPNPs or vehicle control. Furthermore, PPNPs effectively increase phagocytic capacity in murine macrophages as determined by phagocytosis assay (Vybrant Phagocytosis Assay Kit). In conclusion, we observed that our novel PPNP nano formulation effectively targets TME, and facilitates GEM uptake by inhibiting the activation of SHH signaling and reprograming the tumor immune surveillance mechanisms. This study suggests that PPNPs have great potential for future clinical use in management of pancreatic cancer.

#0487 Peptide amphiphiles hitchhike on endogenous biomolecules for enhanced drug delivery.

J. M. Fischer, M. Stewart, M. Dai, S. Drennan, S. Sabuncu, B. Kingston, I. Dengos, L. Xiang, K. Bonic, X. Yi, S. Ranganathan, B. Branchaud, **A. Yildirim**; Oregon Health & Science University, Portland, OR

Peptide amphiphiles (PAs) have been applied as building blocks for self-assembled nanostructures with various morphologies. These self-assembled nanostructures are promising drug delivery platforms as they are naturally biodegradable and biocompatible with low immunogenicity. One primary focus in drug delivery using the PA nanostructures has been to develop strongly assembled structures to avoid disassembly in the blood and allow them to carry payloads to their intended targets. In this work, rather than developing stable self-assembled PA structures, we focused on weakly assembled PA nanostructures to investigate their interactions with blood components and to understand how these interactions affect their biodistribution. We found that weakly assembled PA nanostructures (SA-E) quickly disassembled in plasma and reassembled with lipoproteins (LPs), which significantly prolonged the blood circulation of SA-E in mice. We showed that SA-E crossed the endothelial barriers through transcytosis only when they were assembled with LPs. Cellular uptake studies showed that SA-E accumulated in cancer cells through lipid-raft-mediated uptake. Interestingly, their cellular internalization was independent of LP receptors, suggesting that SA-E assembles with different endogenous biomolecules in vivo. By exploiting these endogenous interactions, SA-E demonstrated high tumor accumulation in a myriad of small animal tumor models of breast, colon, pancreatic, brain, skin, prostate, or lung cancers. SA-E demonstrated large tumor-to-background signal ratios in live animals (>5), extended retention (>2 weeks), and excellent tissue distribution (tumor to liver signal >3) in these tumor models. Encouraged by the excellent tumor accumulation of SA-E, we prepared SA-E drug conjugate using a highly potent and toxic chemotherapeutic agent, Monomethyl auristatin E (MMAE). SA-E-MMAE conjugate demonstrated strong antitumor efficacy in aggressive breast and glioma models in mice with reduced side effects. With its simple and modular design and universal tumor accumulation mechanism, SA-E represents a promising platform for broad applications in cancer therapy.

#0488 Modulation of ENPP1 activity and 2'3'-cGAMP degradation in ovarian cancer cell lines via loadable pre-formed lipid nanoparticles.

David Taylor, Jiajia Ji, Phillip Rzeczycki, Margaret L. Collins, Lauren Clements, Aileen R. Ariosa

Cayman Chemical Company, Ann Arbor, MI

Ovarian cancer is a complex heterogeneous disease with various subtypes and diverse molecular mechanisms of pathogenesis. Among different forms, epithelial ovarian cancer is the most common, representing up to 90% of total reported cases. Due to the lack of early diagnostic tools, the prognosis is mainly poor, as most cases are typically identified in advanced stages. Thus, a more thorough understanding of the inherent complexities of the disease, in terms of its biochemical etiology, will allow for identification of specific molecular and genetic profiles that could lead to more effective treatment plans. Recent studies have shown that ENPP1 may play a role in cancer cell proliferation, migration, and invasion in ovarian and other types of cancer. ENPP1 is a glycosylated type II transmembrane protein acting as a pyrophosphatase and phosphodiesterase with broad specificity. ENPP1 substrates include mononucleotides and cyclic dinucleotides such as the second messenger, 2'3'-cGAMP, which binds to and activates STING. 2'3'-cGAMP is exported extracellularly by cancerous cells into the tumor microenvironment where uptake into neighboring cells can activate their STING-dependent type 1 interferon pathway and promote antitumoral immune responses. ENPP1 can hydrolyze extracellular 2'3'-cGAMP however, allowing cancer cells to evade such an immune response. In this study, we assessed the activity of ENPP1 in CaOV-3, SK-OV-3, and PA-1 ovarian cancer cell lines using a fluorometric cell-based assay. The effects of ENPP1 inhibition via a chemical inhibitor on extracellular 2'3'-cGAMP levels were characterized and compared with siRNA-mediated knockdown of ENPP1 via loadable pre-formed lipid nanoparticles, which enable small-scale encapsulation and transfection of nucleic acid cargo. In addition, we explored whether uptake of exogenous 2'3'-cGAMP into THP-1 and RAW immune cell lines can be enhanced through delivery via preformed loadable lipid nanoparticles. Corresponding immune cell activation was also assessed using immunoblotting and RT-PCR. Our results demonstrate how modulation of ENPP1 activity and 2'3'-cGAMP levels in ovarian cancer cell lines using unconventional, pre-formed loadable lipid nanoparticle transfection reagent can aid in elucidating mechanisms of immune evasion in cancer cells.

#0489 Unlocking immune resistance and metastasis of PDAC via dual acting circularized nanodisc.

Ahmed Elzoghby, **Hagar Emam**, Seungbin Yim, Cuiyan Xin, Mahmoud Nasr

Engineering in Medicine, Brigham and Women's Hospital, Boston, MA

Pancreatic ductal adenocarcinoma (PDAC) is one of the most aggressive and deadliest forms of cancer. While major progress in immunotherapy has been made in recent years, it remains poorly effective in this malignancy. Two key players stand behind immune resistance of PDAC and inadequate efficacy of immunotherapy to suppress its metastasis. First, the immune-resistant pancreatic cancer stem cells (CSCs) evade immune surveillance acting as a source for tumor relapse and metastasis. This immune resistance stems from low immunogenicity of PDAC cells as well as the inaccessible CSCs that reside deep in the tumor core. Second, pancreatic cancer associated fibroblasts (CAFs) fuel metastasis of PDAC cells by suppressing their immune recognition and establishing pre-metastatic niche at distant organs to help their colonization. Our hypothesis is to overcome immune resistance of PDAC and inhibit early steps of its metastasis via simultaneous immunogenic eradication of immune resistant CSCs and switching immunosuppressive and pro-metastatic CAFs into quiescent ones. Therefore, we engineered ultrasmall circularized nanodiscs (cND) that encapsulate oncolytic peptide LTX-315 and fibroblast remodeling Notch signaling inhibitor. The engineered oncolytic LTX-315 loaded cND successfully induced immunogenic cell death (ICD) of both bulk PANC1 and pancreatic CSCs. Compared to non-treated and free LTX-315 treated cells, LTX-315 cND resulted in enhanced release of DAMPs including ATP and HMGB-1 as well as surface translocation of calreticulin. The ultrasmall size (9 nm) of cND enabled its deep tumor penetration to eradicate resistant CSCs, as revealed using 3D PDAC heterospheroids. In parallel, the Notch blocking cND promoted quiescence of the activated pancreatic stellate cells as denoted by downregulation of SMA, FAP and collagen. In KPC syngeneic PDAC mouse model, the dual oncolytic/Notch blocking cND combined with aPD-L1 therapy significantly suppressed tumor growth and prevented its metastasis to liver compared to vehicle-treated mice. Immunophenotyping study showed marked reduction in the abundance of CSCs and CAFs in the tumor treated with the cNDs. Moreover, the tumor infiltration of CD86+ MHCII+ dendritic cells and cytotoxic CD8+ T cells was enhanced after treatment with the cND. Overall, our dual strategy of targeting pancreatic CSCs and CAFs via oncolytic/Notch blocking cND boosted the anti-tumor and anti-metastatic efficacy of aPD-L1 therapy to eliminate primary PDAC tumor and suppress its metastasis.

#0490 Significant anti-proliferative effects of targeted magnetoelectric nanoparticles as potential theragnostic tools.

Max Shotbolt[1], Elric Zhang[1], Emily Zhu[1], Wael El-Rifai[1], John Bryant[2], Ping Liang[3], Sakhrat Khizroev[1]

[1]University of Miami, Miami, FL,[2]Moffitt Cancer Center, Tampa, FL,[3]UC Riverside, riverside, CA

Although current electroporation therapies have been demonstrated to be effective not only in ablating tumor tissue, but also in eliciting an anti-tumor immune response, they are limited in their application due to the strong risk factors associated with the high voltages required. Current methods of interacting with the body's electrical currents are limited to traditional electrodes, which cause damage to surrounding tissue upon insertion, and require high voltages to create responses at the cellular level. Recent efforts at non-invasive interaction with the body's electric fields have led to the fabrication of magnetoelectric nanoparticles (MENPs), a novel technology which has the ability to convert harmless magnetic fields into strong local electric fields, all while maintaining a diameter of ~70nm. These particles have been demonstrated to trigger neuronal firing under magnetic stimulation both in vitro and in vivo, and have been able to release chemotherapeutic agents on command in vitro and in vivo. This demonstrates the ability for MENPs to wirelessly generate electric fields within the body on demand with high temporal and spatial resolution. This suggests the potential for non-invasive electroporation therapy which could be triggered by external magnetic fields. Given the particles are themselves magnetic, this could show potential as a theragnostic tool as their magnetic properties suggest they may act simultaneously as an MRI contrast and an ablative therapy. To explore this possibility, we fabricated MENPs consisting of a magnetostrictive $CoFe_2O_4$ spinel core coupled with a piezoelectric $BaTiO_3$ perovskite shell. These particles were then PEGylated to reduce agglomeration which is typical of magnetic nanoparticles. 50ul of a 1mg/ml PEG-MENP dispersion was deposited into a cell culture of SKOV-3 ovarian cancer cells. These cells were then stimulated by 120 10ms pulses of a 2kOe magnetic field over the course of 30 minutes. An cell-titre glo ATP assay was performed to indicate viability 24 hours after treatment. Treatment wells were compared to controls of no intervention, magnetic stimulation with no particles, and particles with no stimulation. The combination of particles and magnetic stimulation was the only group which showed significant decreases in viability, with a 32% reduction in viability. Particles on their own showed no effect on cell viability, neither did magnetic-only stimulation. This preliminary investigation into the use of MENPs as a non-invasive cancer treatment has shown some potential. The ability to wirelessly activate the particles provides an inherent targeting mechanism not found in traditional chemotherapeutics, while the nanometer diameter provides a non-invasive method to generate strong electric fields within the body.

#0491 Aerosol delivery of immunotherapy and hesperetin nanoparticles in murine lung cancer model.

S. Yasmin-Karim[1], G. Richard[1], A. Fam[2], A.-M. Ogurek[3], G. Makrigiorgos[4];
[1]Brigham and Women's Hospital, Dana-Farber Cancer Institute and Harvard Medical School, Boston, MA, [2]Northeastern University, Boston, Massachusetts, USA, Boston, MA, [3]Northeastern University, Boston, MA, [4]Brigham and Women's Hospital and Dana-Farber Cancer Institute, and Harvard Medical School, Boston, MA

Purpose: Radiation is the most common modality for lung cancer treatment method. Radiationinduces apoptosis, causing cancer cells to be fragmented and expose the cancer-associatedantigens to the tumor microenvironment. These can be recognized by antigen-presenting cells(APC) to induce the antineoplastic effect by activating cytotoxic T cells. Our prior studies showadding immunoadjuvant like AntiCD40 with radiation can further activate the APCs in its anti-tumor (M1) format. Recent studies have shown that flavonoids like Hesperetin, an ACE2receptor agonist also can induce apoptosis in cancer cells whereas ACE2 receptors are abundant in lung cancer cells.This project aims to develop a novel treatment for non-small cell lung cancer (NSCLC) using nanotechnology for inhalation drug delivery Hesperetin, a flavonoid with antioxidant and pro-apoptotic activity; bound to PLGA-coated nanoparticles (Hesperetin Nanoparticles, HNPs) andAntiCD40 aiming for localized targeted dosing to reduce the treatment-related systemic toxicity.We plan to test the efficacy and safety of this aerosol spray.
Methods: *In-vitro* studies were performed in human A549 (ATCC) and murine LLC1 (ATCC)lung cancer cell lines for growth (MTT) and clonogenic survival assays to demonstrate the anti-cancer cell activity of Hesperetin (Sigma). Next, HNP was prepared using NanoFabTx™ nano-formulation reagent kits (Millipore-Sigma). A syngeneic orthotopic murine model of Lungadenoma was generated in wild (+/+) C57/BL6 background mice with similar background LLC1cell lines. We developed syngeneic orthotopic murine lung tumors with luciferase genetransfected LL/2-Luc2 (ATCC) Lewis Lung Cancer cell line in wild-type C57BL/6 mice(Techonic). Lung tumor-bearing mice were treated with HNP, antiCD40, or both with aerosolspray with a control group treated with the solvent (dH2O) only. To assess the drug delivery withaerosol treatment ex-vivo lung tissue was analyzed for Fluorescence tagged antiCD40 andnanoparticle uptakes. A survival assay was performed to analyze the efficacy of aerosoltreatment of HNPs with or without AntiCD40. All cohorts were also analyzed for body score, body weight, and liver and kidney functions.
Results: We were able to successfully develop an aerosol drug delivery model to administer bothAnti-CD40 and HNP in a murine lung cancer model. In our analysis of an orthotopic murinelung cancer model, we demonstrate a high intake of the HNP and AntiCD40 by the cancer cellssparing the normal lung tissue. Moreover, the highest percentage of survival rate was observed with the combination aerosol treatment with HNP+AntiCD40 ($p<0.001$), compared to CD40alone ($p<0.01$) or HNP ($p<0.01$) alone.
Comments: This treatment model will allow us to make the lung cancer treatment method easilyavailable for the mass population without having hazardous radiation treatment in the lungcancer model.

#0492 Investigating solute carrier SLC46A3 to enhance nanotherapeutic delivery for cancer.

Julianna Kenny-Serrano[1], **Elizabeth B. Nelson**[1], Gil Covarrubias[1], Namita Nabar[2], Joelle Straehla[3], Aanchal Gupta[4], Natalie Boehnke[4], Paula Hammond[2]

[1]Koch Institute for Integrative Cancer Research at MIT, Cambridge, MA,[2]Department of Chemical Engineering, MIT, Cambridge, MA,[3]Pediatric Oncology, Dana Farber Cancer Institute, Boston, MA,[4]Department of Chemical Engineering and Material Science, University of Minnesota, Minneapolis, MN

BACKGROUND: Nanoparticle therapeutics have multifaceted potential to improve efficacy and decrease toxicity of cancer treatments. Nanotherapeutics can encapsulate a range of cargos and have tunable surface chemistry that can enhance drug delivery to tumors. Cellular features also play a role in successful drug delivery, and predictive biomarkers may improve patient selection for clinical trials. In previous work, we identified SLC46A3, a poorly characterized lysosomal solute carrier, as a strong negative regulator of lipid-based nanoparticle uptake across many cancer models. We hypothesize that the expression of SLC46A3 will act as a predictive biomarker for therapeutic nanoparticles.
METHODS: To test this hypothesis, we used two engineered model systems to probe the relationship between SLC46A3 expression and therapeutic response: lentiviral overexpression in a natively low-expressing melanoma model and genetic deactivation in a natively high-expressing breast cancer model. A library of FDA-approved and experimental therapeutic nanoparticles were screened in both models under a range of conditions. Liposomal formulations of chemotherapeutics were included with high and low surface functionalization of polyethylene glycol to investigate the impact of this ubiquitous ‘stealth’ polymer on our biomarker of interest. Solid lipid nanoparticles with nucleic acid cargo were also included. Orthogonal methods were used to probe these interactions and the therapeutic efficacy of nanotherapeutics, including pulsed dosing viability assays and label-free live-cell imaging.
RESULTS: We found that SLC46A3 expression is a class-specific biomarker of lipid-based nanoparticle uptake and is predictive of distinctive patterns of response to therapy-loaded nanoparticles in both formulation and time-dependent manners. Additionally, we present a new technology for long-term, live cell imaging of nanoparticle uptake and trafficking that can discriminate mechanisms of cytotoxicity, accelerating the study of nano-bio interactions. These findings highlight a promising approach for the functional validation of nanoparticle-specific biomarkers using clinically relevant formulations that have the potential for rapid repurposing.

#0493 Unlocking solid tumors to nano-immunotherapy.

B. Carreira[1], R. C. Acurcio[1], A. I. Matos[1], L. M. Moura[1], A. C. Santos[1], R. Gouveia[1], J. Cordeiro[1], C. Peres[1], D. Vaskovich-Koubi[2], R. Kleiner[2], S. Pozzi[2], R. Satchi-Fainaro[2], **H. F. Florindo**[1];

[1]Universidade de Lisboa, Lisboa, Portugal, [2]Tel Aviv University, Tel Aviv, Israel

Despite the remarkable efficiency of cancer immunotherapies, only a low percentage of patients achieve long-lasting clinical responses. Non-tumor cells within the tumor microenvironment (TME), including tumor vasculature and immune stromal cells, dictate therapeutic efficacy. The presence of germinal centers (GC) within the TME of cancer patients, including infiltrating T follicular helper (Tfh) cells and B cells, has been considered predictive of response to immunotherapies. We are developing nano-immunotherapies to induce immunological memory to control tumor relapse without any follow-up treatment.Nanomaterials co-incorporated tumor-associated antigens, clinically relevant toll-like receptor ligands, and regulators of tumor progression, namely the PD-L1/PD-1 expression and the secretion of TGF-β. Nanoparticle (NP) physicochemical properties were fully addressed. The immunotherapeutic potential of this nano-immunotherapy was addressed in melanoma, colorectal cancer (CRC), pancreatic cancer, and triple-negative breast cancer (TNBC) 3D models. These were created using patient-derived tumor cells, cancer-associated fibroblasts, and endothelial cells, to which paired patients' peripheral blood mononuclear cells were added to assess T-cell infiltration and tumor sprouting to identify the best nano-immunotherapy dosage/schedule. Our in vivo studies evaluated tumor volume, and animals' survival, and characterized the tumor-infiltrating immune cells within TME, including the differentiation of Tfh cells and primary GC by flow cytometry.Our nano-immunotherapy remodeled the TME of B16F10 melanoma, MC38 CRC, 4T1 and E0771 TNBC, and KPC PDAC. Different TME subpopulations were identified as major blockers of anti-tumor immunity, and this knowledge guided the selection of combination approaches using modulators of those tumor immune evasion-related pathways (e.g., PD-L1, FAK). Our combination nano-immunotherapies tailored to address the tumor immune suppression profile found in vaccinated animals, significantly delayed tumor development, and increased disease-free survival rates. We found that the adjuvants delivered by our NP led to a ~4-fold increase in antibody production, being far more effective in generating GC responses. Thus, the effectiveness of combinational immunotherapy is at least partially related to the modulation of Tfh cells driving the formation of GC responses.Our nano-immunotherapy is a promising clinically translatable approach to defeating solid tumors.

Acknowledgments: This work was supported by PTDC/BTM-SAL/4350/2021 and LCF/PR/HR22/52420016.

#0494 Fluorescent carbon dots: A novel bioimaging tool to reveal the mechanism of action of anticancer drugs in cells.

A. Clermont-Paquette;
Concordia University, Montreal, QC, Canada

The mechanism of action of many cancer drugs at the subcellular level remains unknown. Yet, this knowledge could be critical in driving structure-activity-relationship studies to improve their efficacy and selectivity. To gain a deeper understanding of the mechanisms governing the action of anticancer drugs within cells, we are developing an innovative methodology to visualize drug interactions. Carbon dots (CDs) are carbon-based nanoparticles, distinguished not only by their remarkable optical properties but also by their minimal cytotoxicity, rendering them highly suitable for bioimaging applications. We recently found that amine-passivated CDs with a negative surface charge and amphiphilic properties were enriched in the cytosol of cultured human cells. These CDs emit fluorescence in the blue spectra with high quantum yields and are not cytotoxic. Importantly, their surface is decorated with amine functional groups that can be used for coupling to polyethylene glycol to create a linker that can be covalently attached to drugs of interest. First, we are covalently linking amine-passivated CDs to Doxorubicin (Dox), a well-known anti-cancer drug that intercalates DNA and also has fluorescence properties that differ from the CDs. This will permit us to monitor and validate the conjugation of Dox to CDs, their cellular uptake and localization. The next step will be to use this approach to reveal the cellular mechanism of action of novel anticancer drugs. Specifically, our group has rationally designed thienoisoquinoline compounds with selectivity and high efficacy for triple negative breast cancer cells. In vitro they disrupt microtubule polymerization in the nanomolar range. However, in cells they cause mitotic arrest and spindle phenotypes that are distinct from colchicine, another microtubule-targeting drug. Our approach will reveal if these compounds target the centrosomes and/or microtubules and if this varies with cell types. This innovative approach could yield profound insights into the intracellular mechanisms of anticancer drugs to facilitate structure-activity-relationship studies, to improve their efficacy and selectivity for drug development.

#0495 Targeting undruggable transcription factor HOXB13 in metastatic prostate cancer by CRISPR/Cas13d-based nanoparticle therapy.

Z. Cui[1], F. Huang[1], K. Fang[2], J. Yan[3], Y. Zhou[2], J. Everitt[1], Y. Zhao[4], W. Hankey[1], Z. Chen[1], H. Wang[1], V. X. Jin[2], Y. Dong[3], Q. Wang[1];
[1]Department of Pathology, Duke University School of Medicine, Durham, NC, [2]Medical College of Wisconsin Cancer Center, Medical College of Wisconsin, Milwaukee, WI, [3]Icahn Genomics Institute, Precision Immunology Institute, Department of Oncological Sciences, Tisch Cancer Institute, Friedman Brain Institute, Icahn School of Medicine at Mount Sinai, New York, NY, [4]Department of Pathology College of Basic Medical Sciences and The First Hospital of China Medical University, Shenyang, China

Background: The oncogenic transcription factor HOXB13, which is highly expressed in castration-resistant prostate cancer (CRPC), has been shown to promote CRPC growth and metastasis. However, HOXB13 is considered untargetable by traditional small-molecule-based drug design. Gene therapy is critical alternative strategy with potential to directly target such traditionally undruggable genes.
Methods: Selective cell in organ targeting (SCORT) nanoparticles for precise delivery of nanoparticles to metastatic cancer cells in an organ were constructed and characterized by the NanoAssemblr Spark, Zetasizer Nano ZS, and transmission electron microscopy (TEM); Cas13d mRNA with pseudouridine modification was synthesized using *in vitro* transcription; Hemi-spleen injection of CRPC cells was performed to build CRPC liver metastatic models; RNA-seq was employed to evaluate off-target effects of Cas13d targeting.
Results: By incorporating a prostate cancer-specific E3 aptamer to functionalized lipid-like nanoparticles (FTT5 LNP-E3), we have successfully constructed SCORT nanoparticles that enable preferential delivery of mRNAs to metastatic CRPC cells in the liver, as opposed to various normal cells in the surrounding liver tissue. We demonstrated that Cas13d-pre-g*HOXB13* mediates highly effective and specific *HOXB13* mRNA knockdown in CRPC cells. Significantly, systemic treatment of SCORT nanoparticles carrying Cas13d-pre-g*HOXB13* mRNA decreased HOXB13 expression in the metastatic tumors, inhibited metastasis, and prolonged survival of mice bearing androgen receptor (AR)-positive (AR+) or negative (AR-) tumors. Notably, long term (6 and a half weeks) administration of SCORT nanoparticle-Cas13d-pre-g*HOXB13* did not significant alter body weight, hepatic and renal function, chemokines and cytokines, and other factors, effectively highlighting its safety.
Conclusions: This study is the first to demonstrate that undruggable oncogenic transcription factors can be targeted using nanoparticle-delivered gene therapy based on CRISPR/Cas13 RNA-targeting. The SCORT-CRISPR/Cas13d system is a highly flexible technology that would impact the larger field of translational science by allowing the design of Cas13d-based, cancer cell-specific delivered nanoparticles targeting other previously-undruggable oncogenic transcription factors in metastatic prostate cancer and other solid tumors.

#0496 Insights into correlation between nanomechanical properties and cytokines expression during gold nanoparticle endocytosis.

T. Kulkarni, E. Wang, R. Angom, D. Mukhopadhyay, **S. Bhattacharya**;
Mayo Clinic Florida, Jacksonville, FL

Gold nanoparticles for therapeutic interventions have become a widely popular source due to the ease in surface chemistry available for modification. Several studies undertaken focusses on the size, shape of nanoparticles as well as the signaling mechanisms and yet, knowledge regarding the alteration in membrane dynamics such as nanomechanical properties and cytokines involved during their uptake has not been studies before. To overcome the knowledge deficit, we employed atomic force microscopy and qRT-PCR techniques to acquire nanomechanical attributes and cytokines expressions respectively, in Panc-1 and AsPC-1 cell lines treated with surface modified gold nanoparticles for 1- and 24-hours' time point. In nanomechanics paradigm, impetus was given on both linear attributes such as membrane stiffness, deformation, and adhesion as well as non-linear attributes such as drained Poisson's ratio, diffusion coefficient and pore size. On the other hand, qRT-PCR technique yielded alterations in relative mRNA expressions of pro-tumorigenic cytokines such as CCL2, CXCL1, CXCL2, CXCL3, IL8, IL11, IL18 and TGFβ-1. Further, using Pearson's correlation, we deduced the dependency between nanomechanical properties and cytokines expressions. We evaluated several criteria such as receptor dependent vs independent, PEGylated vs non-PEGylated and 1 hr vs 24hrs, to deduce correlations between cytokines and nanomechanical attributes. In Panc-1 cell line, we observed that PEGylation vs non-PEGylation of gold nanoparticles demonstrated most significant correlations, whereas in AsPC-1 cell line, receptor independent mechanism played a pivotal role in establishing significant correlations. For instance, D_C and P_D were highly correlated with CXCL1, CXCL2 and TGFβ-1 when non-PEGylated gold nanoparticles were up taken by Panc-1 cells. Similarly, D_C and P_D were highly correlated consistently with our cytokine panel except for TGFβ-1. In AsPC-1 cell line, deformation was significantly correlated with CCL2, CXCL2, CXCL3 and IL-8 whereas, D_C and P_D were significantly correlated with CCL2, CXCL1, CXCL3, IL-18 and TGFβ-1 in receptor independent scenario. This study demonstrated that during the uptake of gold nanoparticles, non-linear nanomechanical attributes are detrimental over linear attributes. Moreover, Surface modified gold nanoparticles induce varying levels of alteration in pro-tumorigenic cytokines. Taken together, this study boosts our insights into correlations describing cytokines regulating nanomechanical attributes in endocytosis paradigm.

#0497 Plant viruses against cancer.

N. F. Steinmetz, Y. Chung, M. Moreno-Gonzalez, Z. Zhao;
UC San Diego, La Jolla, CA

Immunotherapy has significantly transformed the landscape of cancer treatment; however, concerns about safety, efficacy, and long-term outcomes across various tumor types persist. We have developed an intratumoral immunotherapy strategy with an engineered plant virus nanotechnology and demonstrated efficacy in tumor mouse models and canine cancer patients. This method is designed to elicit a systemic (abscopal effect), safe, and enduring anti-tumor immune response that is not limited by tumor type. The power of immunotherapy lies in synergistic combination treatments and toward this goal, we are engineering the next-generation plant virus nanotechnologies. We demonstrate synergistic combination with chemotherapy and immunization strategies the hone in on tumor-associated antigens and key players of inflammation. The combinatorial immunotherapy strategies prevent recurrence post-surgery in mice and canine patients. We will discuss the engineering design principles leading toward synergetic combination immunotherapies to treat and prevent cancer; efficacy studies and underlying mechanism is elucidated through immunomics studies.

Selected references: Steinmetz N.F. et al (2023) Viral nanoparticle vaccines against S100A9 reduce lung tumor seeding and metastasis. Proc. Natl. Acad. Sci. U.S.A. 120 (43) e2221859120. Wang C. and Steinmetz N.F. (2020) A Combination of Cowpea mosaic virus and Immune Checkpoint Therapy Synergistically Improves Therapeutic Efficacy in Three Tumor Models. Advanced Functional Materials, 2002299.

#0499 Enhancing neoantigen cancer vaccine efficacy with a self-assembling peptide conjugates nanoparticle platform.

Y. Wu, J.-D. Huang;
University of Hong Kong, The - Li Ka Shing Faculty of Medicine, Hong Kong, Hong Kong

Tumor neoantigens, arising from genomic mutations during cancer cell proliferation, are absent in normal tissues, making them ideal immunotherapy targets. Predicting neoantigen peptide sequences using artificial neural networks (ANNs) like NetMHCpan offers a promising approach to developing personalized peptide cancer vaccines. However, limitations such as low affinity, short half-life, and weak immunogenicity hinder their efficacy. To address these challenges, we propose loading neoantigens into nanoparticles for protection and slow release within the body. We used ANN prediction to determine neoantigen peptide sequences for various cancer cell lines and engineered these peptides by conjugating them with Toll-like receptor 7 agonist (TLR7a) adjuvants, forming a self-assembling peptide conjugates nanoparticle (SPCN) platform. To assess the immunogenicity of the SPCN platform, we conducted enzyme-linked ELISpot assays and evaluated the activation of antigen-presenting cells (APCs) in draining lymph nodes using flow cytometry analysis. The therapeutic efficacy of the SPCN platform was determined by monitoring tumor growth curves in mouse models. The SPCN platform demonstrated broad applicability, carrying different neoantigens *in vivo*, resulting in robust and safe systemic anti-tumor responses. The SPCN enhanced immunogenicity, stimulating splenocytes to produce more interferon gamma and facilitating efficient absorption by antigen-presenting cells (APCs). Moreover, SPCNs loaded with neoantigens targeted different cancer models, including B16OVA, MB49, and RIL175. In conclusion, our self-assembling peptide conjugates nanoparticle platform enhances APC activation and neoantigen immunogenicity, leading to improved anti-tumor efficacy, offering valuable insights for developing synthetic peptide cancer vaccines.

#0500 Liposomal two-tailed topotecan (L-2TT) induces more apoptosis than topotecan hydrochloride on neuroblastoma xenografts.

S. L. Hernandez[1], I. Iwanicki[1], P. Viza-Gomes[1], L. Wu[1], M. Marquez[2], F. Flores-Guzman[1], R. Sundland[1], M. Tartis[2];
[1]University of Chicago, Chicago, IL, [2]New Mexico Tech, Socorro, NM

Background: Neuroblastoma (NB) is the second most common malignancy diagnosed in infants, accounting for 15% of pediatric tumor deaths. High risk NB have a <50% 5-year survival and often resist treatment, with acute and long-term toxicities. Topotecan, part of the standard of care in NB is a Topoisomerase1 inhibitor with a short half-life in circulation (30 minutes). We esterified phospholipid to topotecan at the phenolic hydroxyl group, producing the prodrug 2T-T. 2T-T was loaded onto liposome membranes (termed L-2TT); thus preventing drug leakage. We hypothesized L-2TT would be more efficient at inducing apoptosis than topotecan in NB models (in vitro and in vivo) in part due to its extended circulation time and endocytic uptake.
Methods: IC50 was determined on 8 NB cell lines using a WST assay, comparing equal dosages of L-2TT to topotecan (empty liposomes were assessed as controls). NB cells were imaged with DiD-tagged liposomes together with lysotracker green, under confocal microscopy 24 hrs. Non-tumor bearing mice received increasing L-2TT doses, assessing weight, body score over five days. Drug circulation time was estimated by following DiR-liposomes in vivo (IVIS) over 72 hrs. Nude mice received 1x10^6 NGP cells (NB cells) intrarenally. When tumors reached 1 gram, xenografts received 10mg/kg L-2TT (containing 3.33mg/kg topotecan) via retroorbital injection, 3.33 mg/kg topotecan-hcl or no drug. Tumors were harvested 24 hrs. later, immunohistochemical analysis (apoptosis marker TUNEL), counting the % of positive cells of total tumor area. Some mice received DiR-liposomes together with L-2TT, fixed in PFA and 50mm sections captured total DiR under confocal microscopy. Finally, we interrogated L-2TT vs. Topotecan-HCl tumors via RNAseq for chemoresistance pathways.
Results: IC50 values of L-2TT were lower than topotecan-HCl by almost 3-fold in 7/8 cell lines (empty liposomes at equal concentrations had no effect). DiD-tagged liposomes formed a punctate pattern and colocalized with lysotracker green, confirming liposomes are endocytosed by NB cells in vitro. L-2TT caused no changes adverse effects on mice. Drug circulation time remained stable over 48 hours and was still detectable at 72hrs after liposomal delivery. L-2TT resulted in 3-fold higher tumor apoptosis than Topotecan-hcl ($p<0.0001$), and itself 3-fold higher than controls ($p<0.001$, $n=5$). Mice receiving L-2TT+L-DiR resulted in 2-fold higher DiR signal than L-DiR only ($p<0.05$, $n=3$. Finally, RNAseq suggests L-2TT elicits less chemoresistance pathways than topotecan.
Conclusions: L-2TT is more potent than topotecan in vitro and in vivo. Mechanisms for these effects could be longer circulation times, different tumor cell uptake, as well as changes in tumor vascular permeability. These drug modifications could provide potent alternative for NB treatment as well as other solid tumor treatment.

EXPERIMENTAL AND MOLECULAR THERAPEUTICS: Cell Cycle, Transcription Regulation, and Anticancer Drug Action
Poster Session

#0504 Anticancer effects of kaempferol through cell cycle arrest and the inhibition of proliferation in genetically distinct triple-negative breast cancer cells.

S. Kaur, P. Mendonca, K. F. Soliman;
Florida A&M University, Tallahassee, FL

Triple-negative breast cancer (TNBC) is one of the most known aggressive subtypes of breast cancer, affecting 1 in 3 newly diagnosed cancers in women. TNBC affects African-American women disproportionally in comparison to Caucasian women. Due to the lack of estrogen receptors (ER), progesterone receptors (PR), and human epidermal growth factor receptors (HER-2), it poses direct challenges to the efficacy of standard hormonal therapies. The current TNBC treatments present higher toxicity and multiple side effects. An alternative would be using natural compounds that have emerged as potential anticancer agents. Kaempferol is a major flavonoid aglycone found in many fruits, vegetables, and herbs, including grapes, tomatoes, broccoli, tea, and ginkgo biloba leaves. In this study, we investigated the differential effect of kaempferol on cell toxicity, cell growth, and underlying mechanisms in inducing cell cycle arrest in genetically different TNBC cells from Caucasian (MDA-MB-231) and African American (MDA-MB- 468) women. Kaempferol significantly inhibited cell growth in both the cell lines with a more profound effect against MDA-MB-231 (IC50: 43.86 µM) compared to MDA-MB-468 cells (IC50: 53.47 µM). Also, kaempferol treatment induced cell cycle arrest at S-phase in both cancer cell subtypes. The MDA-MB-231 cells showed a kaempferol effect at lower concentrations (6.25µM and 12.5µM), while MDA-MB-468 cells showed the same effect at higher concentrations (25µM and 50µM). Kaempferol also modulated CDK gene expression associated with cell cycle progression in breast cancer cells. The inhibition at S-phase is important in cancer treatment because it targets the highly proliferative nature of cancer cells characterized by uncontrolled cell division. This study indicates that, by inducing cell cycle arrest at the S-phase, kaempferol may interfere with cancer cell growth and proliferation by inhibiting DNA replication, offering potential therapeutic benefits. This approach could reduce side effects and increase treatment efficacy, providing hope for more effective interventions in the fight against TNBC.

#0506 TRIP13 is a promising therapeutic target for bladder cancer.

S. P. Singh, K. Goswami, A. S. Asch, C. V. Rao, V. Madka;
OU Health Stephenson Cancer Center, Oklahoma city, OK

Bladder cancer (BCa) is the second most common genitourinary cancer. High recurrence rate, progression to MIBC and poor prognosis in metastatic disease are major challenges for this disease management. Therapeutic options for advanced stage BCa are very limited, hence developing agents to treat this disease progression are highly needed. Thyroid receptor-interacting protein 13 (TRIP13), a member of the AAA-ATPase family, regulates various cellular processes such as DNA repair and spindle assembly. TCGA data analysis showed significant overexpression of TRIP13 that correlates with disease stage and mortality. Recent studies have shown that TRIP13 amplification occurs in several types of human cancers, including BCa, and it regulates cell proliferation, tumor growth, and drug resistance. However, the role of TRIP13 in BCa and its potential as a therapeutic target remain elusive. Therefore, in the present study we performed a preclinical investigation of the TRIP13 role in BCa progression, underlying molecular mechanisms, and develop promising therapeutics against BCa. Initially we profiled TRIP13 expression in 10 different bladder cancer cell lines from a panel of human and rodent origin and found elevated protein expression in multiple BCa cell lines. TRIP13 levels were also significantly elevated in the BBN induced rat- and SV40T driven mouse- bladder tumor tissues compared to normal bladder tissues. Pharmacological inhibition of TRIP13 with a potent drug DCZ0415 significantly suppressed cell proliferation (IC_{50} ~7μM) in J82, NBT-II and MB49 cell lines and induced cell death. DCZ0415 treatment led to cell cycle arrest at G1 phase ($P<0.001$) in BCa cells. In mechanistic investigations on its effect on cell cycle progression by DCZ0415 treatment decreased the expression of CDK4, CDK6, Cyclin D1, and PCNA protein expression. TRIP13 inhibition also suppressed the migration and invasion potential of BCa cells. Annexin V and γ-H2AX staining suggested that DCZ0415 induced apoptosis in BCa cells and increased DNA damage. These findings were also complemented by an increase in cleaved caspase-3 and PARP proteins. We also observed modulation of cGAS-STING signaling pathway in BCa cells with DCZ0415 treatment, indicating potential for its combination with cGAS-STING stimulators. Importantly, we found that TRIP13 inhibition with DCZ0415 significantly suppressed the growth of 3D BCa models as well BBN-induced rat BCa tumoroids and spheroids. Overall, these results suggest that TRIP13 could be a potential therapeutic target for prevention of bladder cancer and warrants further validation in *in vivo* models (Funding supported by P30CA225520 and ACS-IRG grant).

#0507 HLS-22001 induces G2/M cell cycle arrest and apoptotic cell death via tubulin depolymerization in colon cancer.

C.-h. Ahn, **G.-b. Jang**, C. Kim, J. Lee, T. Kim, Y. Yang, E. Cho, M. Kim, Y.-t. Kim, Y.-H. Han, H. Kang;
HLB Life Science R&D Co., Ltd., Gyeonggi-do, Korea, Republic of

Colorectal cancer (CRC) is one of the main malignant tumors and among the leading cause of death in cancer patients worldwide considering that recurrence and chemotherapeutic drug resistance are highly common in the advanced stage of CRC. Mutations in KRAS and BRAF occur frequently in colorectal cancers, and abnormal cell cycles caused by these mutations affect tumor progression and metastasis. Accordingly, inhibition of cell cycle has been a potential target for colorectal cancers and therefore, we have developed a new lead compound, HLS-22001.
Our studies confirmed that HLS-22001 inhibited the proliferation of several cancer cells and significantly induced G2/M arrest and apoptosis of colon cancer cells and chemotherapy resistant colon cancer cells. The docking model studies showed that HLS-22001 was expected to bind to the colchicine binding site of beta-tubulin, and in fact, as a tubulin inhibitor, it had the effect of inhibiting tubulin dimerization and polymerization in the microtubule dynamics. Consistently, in xenograft mouse model, oral administration of HLS-22001 significantly suppressed tumor weight and volume without acute toxicity in mice.
Collectively, these results suggest further development of HLS-22001 as a novel and promising oral drug for colorectal cancer.

#0508 Determining the nuclear and cytoplasmic function of BMI-1 in diffuse intrinsic pontine glioma during M phase.

H.-H. Pang, B. Umaru, S. Senthil Kumar, **R. Drissi**;
Nationwide Children's Hospital, Columbus, OH

Diffuse Intrinsic Pontine Glioma (DIPG) represents one of the most aggressive malignancies of the central nervous system, predominantly affecting children. DIPG is a particularly poor prognosis brain tumor with a median overall survival of less than 1 year. Hence, there is an urgent need to develop novel therapies that not only improve outcome but mitigate long-term complications in children with DIPG. The protein BMI-1, a critical component of the Polycomb Repressive Complex 1 (PRC1), is a proto-oncogene implicated in development, stemness of normal and malignant cells, and self-renewal. BMI-1 has emerged as a potential therapeutic target in DIPG; however, its role in DIPG tumorigenesis and progression remains elusive. We have previously shown that PTC596, a potent BMI-1 modulator, induces chromosome scattering, M phase cell-cycle arrest, BMI-1 phosphorylation and translocation to the cytoplasm leading to the inhibition of its PRC1 canonical function and cell death. These findings imply the induction of the spindle assembly checkpoint (SAC), thereby preventing mitotic exit followed by BMI-1 phosphorylation, probably at multiple sites, suggesting a survival role of BMI-1 in M phase in DIPG. The objective of the present study is to delineate the molecular pathways governing BMI-1 function during M phase and to establish the temporal sequence of these biochemical events related to BMI-1. Our data demonstrated that following PTC596 treatment, BMI-1 is actively transported from the nucleus to the cytoplasm. Furthermore, we observed colocalization of BMI-1 with COX4 in the mitochondria during M phase. Moreover, using Alphafold prediction model, BMI-1 could interact with CRM1 transporter. These findings suggest a potential PRC1-independent role of BMI-1 during early M phase required for DIPG proliferation. We are currently investigating potential pathways involved in BMI-1 nuclear-cytosol translocation through bioinformatic analyses, protein-protein interaction simulations, and pharmacological inhibitor assays. Collectively, these studies aim to elucidate the molecular mechanisms underlying BMI-1 functions in DIPG, thereby potentially paving the way for the development of targeted therapeutic strategies related to M phase progression.

#0509 The MPS1/TTK inhibitor, NMS-01940153, synergizes with tisotumab vedotin in colorectal cancer.

G. Texido[1], F. Gasparri[1], A. Ciavolella[1], L. Gianellini[1], A. E. Pedersen[1], A. Ocana[1], R. Colombo[1], D. Roberti[1], L. Mahnke[2], **C. Perrera**[1];
[1]Nerviano Medical Sciences S.r.l., Nerviano (MI), Italy, [2]Nerviano Medical Sciences Inc., Boston, MA

Background: MPS1 kinase plays a crucial role in maintaining genomic integrity by controlling the spindle assembly checkpoint (SAC). MPS1 is highly expressed in tumors of different origins and overexpression is associated with poor prognosis. By inhibiting MPS1, cancer cells are forced to enter anaphase before chromosomes are aligned, leading to mitotic catastrophe and apoptosis. NMS-01940153 (NMS-153) is a potent and selective MPS1 inhibitor, with antitumor activity *in vitro* and *in vivo*. NMS-153, under investigation in a clinical trial, shows early signs of clinical activity, an acceptable safety profile, with manageable and reversible neutropenia as the main adverse effect (EudraCT 2020-001002-26; Reig et al, Eur J Cancer 174S1, 2022).
Microtubule targeting agents (MTAs), such as taxanes and vinca alkaloids, cause mitotic arrest and activate the SAC. Concomitant SAC disruption by MPS1 inhibition synergizes with MTAs, but the combination is limited by neutropenia in the clinic.
Purpose and Methods: The goal is to show synergism between NMS-153 and MTA and to find a strategy to overcome the limiting neutropenia of this combination. For this, Tisotumab vedotin (TV), an anti-Tissue Factor (TF) with Monomethyl auristatine E (MMAE) payload, was used. TF is aberrantly expressed in a variety of tumors compared to normal tissue counterpart. In colorectal cancer (CRC), TF is overexpressed in patients with distinct molecular features including BRAF mutation, a colon cancer population that hardly responds to chemotherapy or BRAF inhibitors. At therapeutic doses, TV induces low rate of grade ≥3 neutropenia. The combination of NMS-153 and TV is expected to synergize and have an acceptable safety profile. LS411N CRC model expressing TF and harboring a BRAFV600E mutation was selected for testing NMS-153 and TV in combination. *In vivo*, NMS-153 was tested at 13 or 20 mpk every 4 days for 7 doses. TV was tested at 1 or 4 mpk weekly for 2 doses. The 2 therapeutic doses of both agents were tested in combination.
Results: *In vitro*, synergism of NMS-153 with TV in LS411N cells was observed. *In vivo*, NMS-153 and TV as single agents were efficacious in LS411N xenograft with TGIs up to 53% and 89%, respectively. The median survival time (MST) for the vehicle group was 35.5 days. NMS 153 and TV single agents prolonged survival with MSTs up to 53 and 73.3 days, respectively. When combined, a dose-dependent therapeutic benefit was observed, with an MST of >137 days, and 6 out of 10 mice profiting of long-term tumor regressions at the highest doses tested. The combination benefit was statistically significantly different from single agents and more than additive. Treatments were well tolerated.
Conclusions: The combination of NMS-153 with TV is synergistic in the LS411N CRC model. These data strongly suggest the potential for clinical efficacy of NMS-153 with TV and the combinability of NMS-153 with TV and other MMAE-based ADCs in different tumor contexts.

#0510 Flow cytometry evaluation of cell cycle arrest in A549 human non-small cell lung cancer cells and tumors following treatment with cell cycle inhibitors: A multifaceted approach to targeting cancer.

E. E. Trachet, E. Cluff, A. Lemos de Matos, D. Diaz, C. Holmquist, P. Gonzales;
Translational Drug Development (TD2), Scottsdale, AZ

The contemporary landscape of cancer treatment has witnessed significant progress with FDA-approved targeted drugs. The FDA's Project Optimus has underscored the growing need for innovative pharmacodynamic endpoints to determine the optimal biological dose in clinical development. Flow cytometry, a potent analytical tool in clinical and preclinical labs, now plays a leading role in cancer research, enabling the evaluation of new drug effects on cell cycle regulation and consideration of rational drug combinations with approved drugs. At TD2, we strive to enhance the translatability of in vitro induced cell cycle arrest studies to in vivo biomarker proof of concept and efficacy. We employ a comprehensive approach, utilizing flow cytometry to assess cell cycle dynamics in cultured cells and in vivo tumor models after treatment with approved and novel drugs. This abstract focuses on the translational relevance of combined in vitro and in vivo testing of well-known drugs that disrupt the cell cycle, laying the foundation for optimized treatment strategies and potentially personalized cancer therapies. Human A549 non-small cell lung carcinoma cells were treated with either thymidine (2.0mM) or the microtubule-depolymerizing drug nocodazole (100ng/ml) for 18 hours, then examined by flow cytometry. Thymidine induced a greater than 85% S-phase arrest, while nocodazole induced a greater than 88% G2/M-phase arrest. A549 cells ($5x10^6$ cells/mouse) were subcutaneously implanted in SCID mice, followed by treatment with an FDA-approved cell cycle inhibitor, Palbociclib, or cisplatin chemotherapy. Palbociclib, a CDK4/6 inhibitor, and low-dose cisplatin treatment resulted in an increased accumulation of cells in the G0/G1 phase, greater than 80% for each. Both treatments exhibited promising anti-cancer activity, with tumor growth inhibition (TGI) of 69% and 87%, respectively. Our findings highlight flow cytometry's multifaceted utility in assessing cell cycle arrest, providing a comprehensive view of agent effects on cancer cells in culture and within the complex in vivo tumor microenvironment. Determining the impact of any new drug on specific cell cycle checkpoints could allow for a more strategic plan for combination therapy. Integrating flow cytometry could enable early biomarker monitoring of tumor cell cycle changes, offering insights into the therapeutic potential of new agents alone or in combination. This multidimensional evaluation contributes to understanding cancer biology and has the potential to guide the development of novel therapeutic strategies, optimize treatment regimens to identify optimal biological doses, and improve patient outcomes in the era of precision medicine.

#0511 Cell cycle inhibitors exhibit anti-tumor immunomodulatory roles through the HIF-1-DDX41 cytosolic DNA sensing pathway in HCC.

C. Chan, P. Wong, H. Xue, C. Goh, J. Cheu, A. Tse, M. Zhang, C. Wong;
The University of Hong Kong, Hong Kong, Hong Kong

Cell cycle inhibitors have a long history as anti-cancer therapeutics in clinical applications. Uncontrolled and infinite cell cycles are hallmarks of cancer, which enable them to proliferate rapidly and survive. To target these key features of cancer cells, cell cycle inhibitors are used to arrest their active cell cycle and induce cell death. In this study, beyond the known primary effect on cell cycle control, we identified that an expected and a secondary effect in immune modulation by the cell cycle inhibitors. Anti-mitotic agents including Paclitaxel (microtubule stabilizer), Palbociclib (CDK4/6 inhibitor) and AZD1152 and GSK1070916 (Aurora Kinase B inhibitors) can also eliminate cancer cells via an alternative mechanism - the activation of STING signaling. Our results demonstrated that these anti-mitotic agents caused DNA damage and cytosolic DNA accumulation. The cytosolic DNA was captured by a cytosolic DNA sensor DDX41,which triggered STING-TBK1-IRF3/7 pathway to upregulate secretion of pro-inflammatory senescence-associated secretory phenotype (SASP) factors in cancer cells. In addition, we revealed that transcription of DDX41 was mediated by the transcription factor known ashypoxia-inducible factor (HIF). In HCC, hypoxia induced DDX41 expression through HIF-1,thus hypoxic HCC cells were more prone to STING activation and SASP production under mitotic stress induced by cell cycle inhibitors. In the tumor microenvironment, the SASP enhanced infiltration of immune cells into the tumor core to eliminate cancer cells. We also observed the additive effects of cell cycles inhibitors (Paclitaxel, Palbociclib, and AZD1152)with anti-PD-1 mAb to arrest growth of HCC in mouse models. In summary, this study exhibited the novel immune-mediated aspect of cell cycle inhibitors in suppressing tumor growth. Our data suggested the potential combination regimen of cell cycle inhibitors and currently available immunotherapy with promising result.

#0512 Cell-cycle inhibition may influence differences in 2D vs 3D tumor sensitivity profiles.

J. Kumar, C. Maestri, R. Nitiyanandan, I. Trus, R. J. Parker, B. Apfel, C. Apfel;
Sage Medic Corp., Redwood City, CA

Background: Traditional cell culture methods involve growing cells on flat surfaces, which do not fully replicate the human physiological conditions. In contrast, 3D cell cultures accurately reproduce aspects of the *in-vitro* malignant and non-malignant cell behavior. However, differences in tumor sensitivity platforms between 2D vs. 3D models might be relevant for some, but not for other drugs.
Methods: The colorectal cancer cell line HCT-116 was cultured and plated in flat bottom well plates for the 2D condition and in Ultra Low Attachment round-bottom plates for the 3D condition. After plating, cells were treated with chemotherapies and targeted therapies for four days; cellular sensitivity was assessed through a viability assay. Four-parameter logistic (4PL) dose response curves were generated and IC_{50}s were quantified to understand the differences in responses between 2D and 3D cellular environments.
Results: HCT-116 exhibited similar responses to platinum drugs, taxanes, and several other tested drugs in both platforms, with the exception of gemcitabine (2D IC_{50} 0.04 mcM; 3D IC_{50} 12.8 mcM), lapatinib (2D IC_{50} 23; 3D IC_{50} 418), tucatinib (2D IC_{50} 23.3; 3D IC_{50} 79.3), and palbociclib (2D IC_{50} 7.0; 3D IC_{50} 24.0). Interestingly, these drugs share a common mechanism of action, which is the inhibition of cell cycle progression from G1 to S phase. Hence, we hypothesize that this shared mechanism may account for the observed differences in drug efficacy between the two environments.
Conclusions: Similar dose responses have been observed with various drugs on both platforms, yet drugs that inhibit cell cycle progression from G1 to S phase, revealed higher sensitivity in 2D and more resistance in the 3D platform. Confirmatory cell-cycle results analyses are in progress. Further research is needed to understand if this applies to patient samples.

#0513 Intra-tubular damage is targeted by maytansinoids and rescued by NF1: Revisiting mechanism and biomarkers of an established ADC payload.

E. Messuti[1], B. Achutti Duso[1], A. Castiglioni[1], G. Tini[1], E. Bonetti[1], G. Ciossani[1], S. Monzani[1], D. Khuntsariya[2], Z. Lansky[2], M. Braun[2], L. Scietti[1], **L. Mazzarella**[1];

[1]IEO - European Institute of Oncology, Milan, Italy, [2]Institute of Biotechnology CAS - BIOCEV, Vestec, Czech Republic

There is great interest in the identification of biomarkers to guide development of antibody-drug conjugates (ADC). We previously showed that loss of Neurofibromatosis 1 (NF1), a gene frequently mutated across cancers, enhances the activity of DM1, the maytansinoid payload of T-DM1, through a novel function in regulating microtubule (MT) dynamics. Maytansinoids are puzzlingly more effective in cells (in the nanomolar range) vs in vitro (in the micromolar range). Since maytansinoids bind at the interface between tubulin dimers, they are thought to only bind soluble tubulin dimers or MT ends, which would suggest very few binding sites available for pharmacological interaction in vivo, at odds with data. Here we investigated the interaction of DM1 with NF1 and MTs, using cellular and reductionist in vitro systems. To measure in vivo MT dynamics, we transiently transfected the MT end-binding protein EB3-GFP and reconstructed MT trajectories by live-cell imaging. Upon DM1 treatment, KO cells showed a highly significant reduction in MT speed, demonstrating a direct role for NF1 on MT dynamics in cells. In turbidity-based tubulin polymerization assays, recombinant NF1 greatly accelerated polymerization, and completely rescued DM1-induced inhibition. Visual inspection of fluorescent MTs showed that NF1 induced significant MT bundling, a defining feature of many MT-associated proteins, which generates signal indistinguishable from true MT polymerization in turbidity assays. To follow the dynamics of individual microtubules, we applied Total Internal Reflection (TIRF) microscopy on glass-immobilized MTs. As expected, polymerization in the presence of NF1 led to a significant increase in MT dynamics (elongation speed, rescue and catastrophe rate). Expectedly, DM1 led to significant reduction in the fraction of elongating MTs and speed, but these defects were completely or partially rescued by NF1. Importantly, DM1 did not only lead to MT shortening (as proposed by the current model), but also to clear and frequent MT fracturing, indicating that the drug is not only engaging MT ends but also intra-tubular binding sites. This is consistent with recent models of MT formation which incorporate the frequent presence of areas of discontinuity or damage induced by mechanical stress, exposing intra-tubular DM1 binding sites. Interestingly, adding NF1 to DM1-treated MTs generated areas of de novo intra-tubular tubulin insertion, coincident with damaged sites, suggesting an entirely novel role for NF1 in MT repair.In conclusion, we provide evidence for a model in which maytansinoids bind not only to soluble tubulin dimers and MT ends, but also to intra-tubular damaged sites. Thus, the number of binding sites in cells would be proportional to MT damage, suggesting a mechanism for differential efficacy across tumor types and a potential avenue for combinatorial drug development.

#0514 Salt-inducible kinase inhibitor OMX-0407 drives cell-cycle arrest *in vitro* and *in vivo:* An in-depth MoA analysis by phospho-proteomics.

I.-P. Maser[1], M. Stebegg-Wagner[1], B. Bauer[1], F. Konstantinidis[1], A. Schirmer[1], M. Zulley[1], S. Lacher[1], B. Kracher[2], P. Kohvaei[2], M. Yule[1], H. Loferer[1], S. Bissinger[1];

[1]iOmx Therapeutics AG, Munich, Germany, [2]Evotec Munich GmbH, Munich, Germany

Based on iOmx' proprietary iOTarg™ genetic screening platform, salt-inducible kinase (SIK) 3 was identified as a novel cell signaling modulator in cancer biology. OMX-0407, an orally available, spectrum-selective kinase inhibitor targets several members of the SIK family and is known to prevent tumor-promoting function of the SIK-family through repolarization of the tumor microenvironment by enhancing caspase-mediated apoptosis upon death-receptor signaling. In addition, OMX-0407 inhibits individual key members of the tyrosine and tyrosine-like kinase family that are involved in cancer cell proliferation and cell cycle regulation. Via this dual mode of action, OMX-0407 has the potential to effectively fight solid tumors as exemplified by its striking single-agent efficacy in multiple pre-clinical tumor models.

A comprehensive anti-tumor viability screen of >200 human cancer cell lines revealed striking effects of OMX-0407 on cancer cell viability across various cancer indications, resulting in a distinct sensitivity profile across various tumor indications with particularly strong effects on renal cell carcinoma (RCC) and squamous non-small cell lung cancer (sqNSCLC). Phospho-proteomics screening demonstrated pharmacodynamic activity of OMX-0407 in sensitive tumor cell lines via inhibition of key cellular processes such as cell motility, proliferation, and cell cycle regulation across different indications. Orthogonal functional *in vitro* assays confirmed the association of the OMX-0407-mediated anti-tumor efficacy with the arrest of G1/S transition and corresponding downregulation of cell cycle associated proteins PAK1/2 and ARHGAP35.

The profound impact of OMX-0407 on fundamental regulatory mechanisms of cell division and cancer cell apoptosis translates into dose-dependent single-agent, anti-tumor efficacy in various pre-clinical tumor models of selected indications. Combination with Axitinib, a selective orally available inhibitor of vascular endothelial growth factor receptor 2, significantly enhanced anti-tumor efficacy and pharmacodynamic inhibition of cell growth as well as angiogenesis. These data further strengthen the potential of OMX-0407 in the treatment of RCC as well as other indications.

In summary, OMX-0407 is a novel spectrum selective kinase inhibitor, currently under evaluation in a clinical Phase I trial (NCT05826600). OMX-0407 demonstrates strong anti-tumor efficacy in monotherapy in selected sensitive indications through a dual-pronged MoA, by modulating the tumor microenvironment and exerting direct anti-tumor activity in solid tumor indications with high unmet medical need.

#0515 Endocycling cancer cells undergo multiple S phases while repressing myc activity.

M. A. Loycano, K. J. Pienta, S. R. Amend;
Johns Hopkins University School of Medicine, Baltimore, MD

Chemotherapy resistance remains a major challenge when treating patients with metastatic cancer. While intrinsic resistance to therapy has been well studied, phenotypic plasticity that drives entry and exit of resistant cell states is poorly understood. One of these plastic cell states used by cancer cells under chemotherapy treatment is characterized by the reprogramming of the mitotic cell cycle to enter a non-proliferative endocycle. Cells in this endocycling state decouple DNA synthesis from cell division by actively progressing through G1, S, and G2 phases of the cell cycle while repeatedly skipping mitosis. After a dormant period, cells can switch back to a mitotic cell cycle to repopulate a tumor. The underlying mechanisms that drive this cell cycle reprogramming remain unknown. C-myc is an oncogenic transcription factor that is dysregulated in ~70% of human cancers. C-myc is responsible for the activation of several cell cycle drivers, including cyclins and CDKs, and represses cell cycle inhibitors, such as CDK inhibitors. High levels of myc activity allow cells to move through the cell cycle quickly with a rapid doubling time. Documented endocycles in polyploid cells rely on high c-myc activity; however, our data shows that endocycling cancer cells have repressed levels of c-myc protein and transcriptional activity. Transcriptomic data shows that myc target genes are expressed at very low levels compared to the mitotic parental cells, and complementary data shows low protein levels. While myc downregulation is expected in non-proliferative cells, the compensatory mechanisms mediating the G1/S transition in the cancer endocycle remain unknown. Recent data has shown that myc suppression alone is not sufficient to induce a sustained endocycle at a population level, despite premature APC^{Cdh1} activation during G2 in a subset of cells. We hypothesize that restoring myc activity to the levels of mitotic parental cells will drive endocycling cells to resume a proliferative mitotic cell cycle and produce mitotic progeny cells. Understanding the mechanisms that govern this transition is crucial to generate next-generation cancer therapeutics to disrupt endocycling cells, blocking acquired resistance and disease recurrence.

#0516 The role of clathrin-mediated endocytosis of EGFR in glioblastoma cell viability and cell cycle progression.

A. Deter, A. J. Tsung, M. R. Guda, S. Asuthkar, K. Velpula;
University of Illinois College of Medicine (Peoria), Peoria, IL

Glioblastoma (GBM) is characterized by poor prognosis and overexpression of epidermal growth factor receptor (EGFR). EGFR signaling is regulated through endocytosis, including clathrin-mediated endocytosis. We hypothesized that clathrin-mediated EGFR endocytosis promotes GBM cell viability and proliferation. Analysis of patient data from the Gliovis database revealed decreased overall survival in GBM patients with above-median clathrin expression (n=262) compared to below-median expression (n=263, $p<0.05$). Immunocytochemistry and Western blot analysis confirmed increased clathrin levels in GBM patient samples compared to normal brain tissue (n=15, $p<0.01$). To determine the functional effect of inhibiting clathrin-mediated endocytosis, U87 and U251 GBM cells were treated with 15 μM Pitstop-2, a clathrin inhibitor, for 24 hours. Pitstop-2 significantly reduced clathrin levels and cell viability by 40% compared to control ($p<0.001$, n=3). Cell cycle analysis by flow cytometry revealed Pitstop-2 treatment led to G2/M arrest in both cell lines versus control ($p<0.01$, n=3). Together, these findings indicate clathrin-mediated endocytosis of EGFR may promote GBM cell viability and proliferation. Further studies on the effects of clathrin inhibition on EGFR signaling and tumor growth in vivo will elucidate the therapeutic potential of targeting this pathway.

#0517 2OHOA-mediated furin inhibition: Disrupting Notch via processing, transcription, and ADAM downregulation.

R. Rodriguez-Lorca[1], R. Beteta-Gobel[1], R. Roman[1], V. Llado[2], P. Escriba[1], P. Fernandez-Garcia[1];
[1]Laminar Pharma, Inc., Palma de Mallorca, Spain, [2]Laminar Pharma, Inc., Boston, MA

Purpose Glioblastomas (GBMs) are highly treatment-resistant and aggressive brain tumors. Herewe assessed the potential of melitherapy to treat GBM, a strategy based on regulating themembrane's structure and organization to modify aspects of intracellular signaling. In thiscontext, we have evaluated the effects of 2-hydroxyoleic acid (2OHOA) on GBM cells, acompound currently under study in a phase IIB/III clinical trial for newly diagnosed GBMpatients. The current study aims to determine whether 2OHOA modulates the Notch pathway aspart of its antitumoral mechanism, as seen its relevance driving the pathogenesis of GBM.
Methods The effect of 2OHOA was evaluated on different components of the pathway usingseveral methods: W-blot, Q-PCR, and confocal microscopy. The relevance of *HES1* in itsmechanism of action was evaluated by its overexpression and pathway activation assays byJagged1. To analyze Notch receptor processing, we performed subcellular fractionation andcolocalization studies. Furin activity was assessed by fluorescence assays measuring its substratecleavage and its binding affinity to 2OHOA was determined by surface plasmon resonance.
Results 2OHOA suppresses both the Notch3 and Notch2 signaling pathways in GBM cell linesusing a two-fold mechanism. Notch3 signaling is abolished by repressing its transcription.Instead, Notch2 pathway is hindered by blocking its first cleavage through the inactivation offurin activity by physical association. Consequently, the Notch2 receptor is retained in the Golgicomplex, preventing its trafficking to the plasma membrane to initiate the signaling cascade.Moreover, overexpression of its target gene, *HES1*, partially dampened the drug's antiproliferative effect showing the relevance of this pathway in the 2OHOA pharmacologicalefficacy. In addition, considering the levels of Notch intracellular domain (NICD) obtained inJagged1 assays in conjunction with 2OHOA, we evaluated the second cleavage of the Notchprocessing, being also downregulated, as ADAM10 constitutes a furin substrate.
Conclusions These findings elucidate that the antitumoral activity of 2OHOA involves theinhibition of Notch signaling, potentially driven by the direct inhibition of furin. This reveals anovel molecular target for this bioactive lipid in the therapeutic approach to treating GBM.

#0518 The CDK2/9 inhibitor fadraciclib is active in Richter transformation and lymphoma cell lines by targeting both cell survival and proliferation.

R. Chen, Y. Chen, P. Xiong, W. Plunkett;
UT MD Anderson Cancer Center, Houston, TX

Richter transformation (RT), characterized by the transformation of chronic lymphocytic leukemia (CLL) to an aggressive large-cell lymphoma, remains a challenge for the therapy. Genetic aberrations, such as Myc activation, TP53 abnormality, NOTCH1 gene mutation or loss of CDKN2A are associated with uncontrolled RT cell proliferation and escaping of apoptosis. Among those changes, gain of Myc activity, found in around 70% of RT, plays a nexus role in the pathogenesis of RT. As a transcription factor, Myc activation has a profound effect on cell survival, proliferation, adhesion and metabolism. Because of its essential role in lymphoma transformation and aggressiveness, Myc is a vital target for therapy toward RT. Fadraciclib (CYC065) is a second-generation CDK inhibitor with selective potency toward CDK2 and CDK9. We have shown previously that by inhibiting CDK9-mediated transcription, fadraciclib reduced expression of the short-lived anti-apoptotic protein Mcl-1 to initiate apoptosis in primary CLL cells. Like Mcl-1, Myc is a quintessential example of an oncogene with rapid turnover in both its mRNA and protein, therefore a promising target of CDK9 inhibition. Thus, we proposed that fadraciclib would target both the survival and proliferation pathways of RT pathogenesis through collaborative inhibition of Mcl-1, Myc and CDK2. First, our data showed that fadraciclib effectively induced apoptosis in the RT cell line HPRT1, as well as the lymphoma cell lines with Myc amplification, including Raji, Ramos and SU-DHL-2. The IC_{50} for apoptosis was 0.3 μM at 24h in the HPRT1 cells, which is less than the average IC_{50} for the primary CLL cells (0.8 μM). The IC_{50} for the lymphoma lines ranged from 0.8 μM to 1.3 μM. Immunoblots showed reduction of RNA Pol2 phosphorylation by fadraciclib, consistent with the inhibition of CDK9. As a result of loss of RNA Pol2 activity and pausing of transcription, there was a clear reduction of both Mcl-1 and Myc mRNA, measured by real-time RT-PCR, that was associated with the reduction of their protein levels. CDK2 was also inhibited by fadraciclib, shown by the reduction of the phosphorylation of both RB and NPM. Second, Fadraciclib inhibited cell proliferation of the HPRT1 cells at an IC_{50} of 0.25 μM measured by the CellTiter-Glo assay. The IC_{50} for growth inhibition in the lymphoma lines ranged from 0.5 to 0.7 μM. CFSE tracing demonstrated halting of cell division upon fadraciclib incubation. Cell cycle analysis by Click-iT EdU showed reduction of S-phase population and arresting of cells in both G1 and G2. We are currently working on dissecting the contributions of inhibiting Myc, Mcl-1 and CDK2 individually and together, in apoptosis induction and proliferation blockade. Taken together, these data suggest that fadraciclib is active in RT cells and Myc-dependent lymphoma cell lines and support expansion of its clinical testing in patients with RT.

#0519 Targeting MYC as a novel therapeutic strategy for an epigenetic-driven cancer: NUT Carcinoma.

C. Escudero-Iriarte[1], J. Castro[1], I. Beniavides-Puy[1], N. Tissera[1], J. Querol-Panos[1], I. Agusti[1], J. Whitfield[1], M. Vieito[2], L. Nonell[1], T. Macarulla[2], I. Brana[2], L. Soucek[3], T. Tian[1];

[1]VHIO Vall D'Hebron Institute of Oncology, Barcelona, Spain, [2]VHIO Vall D'Hebron Institute of Oncology, Universitary Hospital Vall d'Hebron, Barcelona, Spain, [3]VHIO Vall D'Hebron Institute of Oncology; Peptomyc S.L.; Department of Biochemistry and Molecular Biology, Universitat Autonoma de Barcelona; Institucio Catalana de Recerca I Estudis Avancats (ICREA)., Barcelona, Spain

Epigenetic dysregulation is widespread in cancer, playing a pivotal role in shaping cell function and contributing to the process of oncogenic transformation. NUT Carcinoma (NC) is an exceptionally rare and aggressive cancer lacking effective treatment, with a dismal prognosis - NC patients typically survive less than seven months after the initial diagnosis. NC is characterized by the presence of chromosomal rearrangements involving the gene encoding for the testis-specific NUT protein and a ubiquitous gene encoding an epigenetic regulator, BRD4 in most cases. Previous studies have demonstrated the role of the BRD4-NUT fusion protein in generating clusters of acetylated histones, namely “megadomains,” throughout NC cell chromatin. These NUT-containing fusion proteins are involved in NC oncogenesis by altering the epigenetic and transcriptional landscapes, promoting cell proliferation while impeding cell differentiation. Indeed, several downstream targets, including *P63*, *SOX2*, and *MYC*, have been identified to be modulated by NUT fusion proteins, independently of the fusion partners. This study focuses on a novel therapeutic approach targeting MYC for NC treatment. We conducted a comprehensive preclinical study of OMO-103, a MYC inhibitor currently undergoing clinical evaluation, using various NC patient-derived cell lines. Through cell viability assays, cell cytometry, western blotting, RNA-seq data analysis *in vitro,* as well as *in vivo* drug efficacy evaluation in NC xenografts, we delved into the effects of OMO-103 on NC cells. Our findings reveal that OMO-103 effectively inhibits NC cell growth both *in vitro* and *in vivo*. It induces cell apoptosis, differentiation, and cell cycle arrest *in vitro*, and when tested in xenografts *in vivo*, OMO-103 reduces tumor growth and enhances mouse survival, particularly when combined with a chemotherapy regimen. This study presents a promising therapeutic strategy for an incurable and aggressive cancer type.

#0520 circBRIP1 RNA as a non-invasive target engagement pharmacodynamic biomarker for DHX9 inhibition.

D. Brennan, J. Castro, M. H. Daniels, M. Laidlaw, C. Lu, S. J. Blakemore, S. J. Silver, P. Boriack-Sjodin, K. W. Duncan, J. A. Sager, R. A. Copeland; Accent Therapeutics, Lexington, MA

DHX9 is a multifunctional DEAH-box ATP-independent RNA helicase which has been reported to play important roles in replication, transcription, translation, RNA splicing and RNA processing which contribute to DHX9's role in maintenance of genomic stability. DHX9 can bind specifically to inverted repeat *Alu* elements, preventing back-splicing events that lead to circular RNA and exon skipping of the linear transcript. Upon DHX9 inhibition, a robust induction of *Alu*-mediated circular RNA is observed. For example, circBRIP1 is an *Alu*-mediated circular RNA that is robustly elevated upon DHX9 loss, with no observed change to levels of linear BRIP1. Here we describe data demonstrating circBRIP1 as a DHX9 specific target engagement pharmacodynamic (PD) biomarker and its potential utility as a non-invasive clinical PD biomarker. We have previously demonstrated that DHX9 inhibition by novel small molecule inhibitors is efficacious in microsatellite instable (MSI) colorectal cancer (CRC) with defective mismatch repair (dMMR), both *in vitro* and *in vivo.* DHX9 inhibition in the HCT116 dMMR CRC cell line results in a robust dose dependent induction of the *Alu*-mediated circular RNA, circBRIP1, as early as 6 hours after compound treatment. The development of lead series DHX9 inhibitors exhibited a positive correlation between circBRIP1 EC50 and DHX9 biochemical activity, as well as proliferation inhibition in a dMMR CRC cell line. However, dose dependent induction of circBRIP1 following DHX9 inhibition occurs with similar potencies across DHX9i sensitive and insensitive CRC cell lines. This suggests that elevation of circBRIP1 is a unique proximal target engagement PD biomarker of DHX9 inhibition, but not a predictor of DHX9 sensitivity. Importantly, induction of circBRIP1 is observed intratumorally in human xenograft *in vivo* efficacy studies in mice. Induction in each individual tumor correlates with observed tool compound exposure, providing evidence of a predictable PK/PD relationship. We also observe dose dependent circBRIP1 induction in mouse peripheral blood mononuclear cells (PBMC). We have extended these studies to primary human whole blood, where we see robust dose dependent induction of circBRIP1 after ex vivo treatment with DHX9 inhibitor for 24 hours. Altogether, these studies show evidence for the utility of circBRIP1 as a non-invasive target engagement biomarker for DHX9 inhibitors in the clinic.

#0521 Anticancer mechanisms of epigallocatechin gallate revealed via cellular and molecular profiling.

A. Panchal[1], J. H. Law[1], C. Lo[2], **K. W. Yip**[3];
[1]University of Toronto, Toronto, ON, Canada, [2]Anticancer.ca, Toronto, ON, Canada, [3]University of Toronto, Anticancer.ca, Toronto, ON, Canada

Introduction: Epigallocatechin gallate (EGCG) is a polyphenol present in green tea that is known for its anti-oxidant, anti-inflammatory, anti-angiogenic, pro-apoptotic, and anti-cancer properties. However, EGCG has not been systematically evaluated on a large panel of cancer cell lines. We hypothesized that EGCG exhibits varying effects on specific cancer cell genetic backgrounds and types. This study aimed to provide a comprehensive analysis of EGCG on both cell viability and gene expression profiles.

Methods: 750 cancer cell lines were cultured and seeded in 1536-well plates for cell viability studies (by the CTD^2 Center at the Broad Institute). After 24 h, cells were treated with 16 two-fold serial dilutions of EGCG. After 72 h, cell viability was assayed using CellTiter-Glo. For gene expression profiling (with the Broad Institute and NIH), 8 cell lines were treated with 10 µM EGCG for 6 and 24 h, and transcriptomes were assessed using Affymetrix GeneChip Human Genome U133 Plus 2.0 Arrays. The CMap large-scale transcriptome dataset was used for comparisons.

Results: EGCG had the highest potency in the non-Hodgkins B-cell lymphoma cell line DoHH2 (IC_{50}=0.42 µM), the myeloid leukemia cell line Ku812 (IC_{50}=3.76 µM), and the multiple myeloma cell line KMS-28BM (IC_{50}=4.57 µM). Tissue-of-origin analysis showed that EGCG was most potent against lymphoid cancers, and least potent against prostate cancers. Bioinformatics-based analyses found that EGCG-treated cells resembled cells overexpressing CHEK2, DDP4, CBLC, ZNF350, and TRAF6, and cells underexpressing TRIM16. EGCG-induced gene expression resembled lapatinib and sulfasalazine treatment.

Conclusions: This study provides a comprehensive examination of the differential impact of EGCG treatment on cancer cells. Subsequent research on the timing and duration of the changes, along with pathway enrichment analyses, will potentially guide the translational potential of EGCG and its chemical analogs in personalized cancer treatment approaches.

#0522 *TP53*mutations promote death of breast cancer cells following Kif11 inhibition.

A. L. Lanier, W. Tahaney, J. Qian, C. Moyer, Y. Ma, B. Arun, A. Mazumdar, P. H. Brown;
UT MD Anderson Cancer Center, Houston, TX

Background: Triple-Negative Breast Cancer (TNBC) comprises 15-20% of breast cancer diagnoses. These aggressive breast cancers are characterized by their lack of expression of the estrogen receptor (ER), human epidermal growth factor receptor 2 (HER2), and progesterone receptor (PR), resulting in few targeted therapy options for TNBC patients. While 85-90% of TNBCs contain mutations in *TP53,* mutant p53 is challenging to target directly. Instead, we aim to identify other survival pathways critical for the growth and survival of *TP53* mutant cells. Through a combined *in vitro* and *in silico* drug screen, we identified the Kif11 inhibitor SB-743921 as more effective in *TP53* mutant compared to wild-type breast cancer cells.
Hypothesis: We hypothesized that Kif11 inhibition causes *TP53* mutant cells to undergo cell death due to failure of activation of p53-mediated cell cycle checkpoints.
Methods: Clinical data from the TCGA and METABRIC cohorts was obtained from cBioPortal. Expression and survival analyses were performed using GraphPad Prism. Cell growth assays were conducted by seeding cells, treating under designated conditions, then staining with Hoechst 33342 for cell counting on the ImageXpress Pico. Cell death was determined by staining with Annexin V and PI or DAPI Staining followed by flow cytometry analysis. Cell cycle analysis was conducted following synchronization with Lovastatin and Mevalonate release followed by imaging analysis of cell lines expressing the Fast FUCCI reporter or PI staining and flow cytometry analysis. Immunofluorescence imaging was conducted by staining with anti-alpha-tubulin-AlexaFluor488 and DAPI and imaging on the Nikon TI2 or ImageXPress PICO. *In vitro* expression experiments were carried out through qPCR and western blotting.
Results: KIF11 is most highly expressed in *TP53* mutant and triple-negative tumors and high expression of KIF11 is associated with poorer overall survival. In breast cancer cell lines, Kif11 inhibition leads to a cell cycle block in both *TP53* mutant and wild-type cells, but *TP53* mutant cells then die following this cell cycle block. Furthermore, Kif11 inhibition causes mitotic dysfunction, including monopolar spindle formation and multinucleated cells in *TP53* mutants. Introduction of a *TP53* mutation into *TP53* wild-type cells also induces cell death following Kif11 inhibition.
Conclusions: KIF11 is highly expressed in aggressive breast cancers and is associated with poorer prognosis. Using the small molecule inhibitor SB-74321 that has been tested in phase I/II clinical trials with favorable tolerability, we found that Kif11 inhibition results in mitotic dysfunction and death of TP53 mutant breast cancer cells due to mitotic catastrophe. These results suggest that Kif11 is a promising target for the treatment of *TP53* mutant TNBCs.

#0523 Aronia berry and oligomeric proanthocyanidins synergistically exhibit anticancer effects in colorectal cancer by inhibiting LMNB1.

Y. Li[1], C. Xu[2], A. Goel[2];

[1]Beckman Research Institute of The City of Hope, Duarte, CA, [2]Beckman Research Institute of The City of Hope, Monrovia, CA

Background: Colorectal cancer (CRC) is one of the most common and recurrent diseases globally, ranking as the second leading cause of mortality. The high mortality rates associated with this disease are largely due to the ineffectiveness of current treatments and the development of chemotherapeutic resistance to conventional therapies. In recent years, several natural agents, such as Aronia berry extract (ABE) and oligomeric proanthocyanidins (OPCs), have shown promise in providing a safe, cost-effective, and synergistically multi-targeted treatment approach across various cancers. Herein, we hypothesized that the combined treatment with ABE and OPCs may synergistically regulate multiple oncogenic pathways, thereby presenting a more potent anti-cancer activity, particularly targeting CRC. Methods: We performed a series of cell culture experiments to evaluate the synergistic anticancer effect of the combination of ABE and OPCs in CRC cell lines. By performing genome-wide transcriptomic profiling, we identified specific growth-signaling pathways targeted by the combined treatment and subsequently validated these findings in cell lines and patient-derived 3D organoids. Results: The combined treatment with ABE and OPCs exhibited superior synergistic anti-tumor potential, affecting cell viability, proliferation, migration, and invasion in CRC cells. The transcriptomic analysis identified that LMNB1, associated with the cell apoptosis pathway Fold enrichment [FC]: 4.29, P =0.005), plays a crucial role in the anti-tumorigenic effects of these two natural products. Moreover, the combination of ABE and OPCs significantly altered the expression of key proteins involved in cell apoptosis and suppressed the expression level of LMNB1 in HCT116 (Combination vs. ABE, FC= 0.28; Combination vs. OPCs, FC= 0.24) and SW480 (Combination vs. ABE, FC= 0.65; Combination vs. OPCs, FC= 0.47), thereby inhibiting downstream Akt phosphorylation. Finally, we successfully demonstrated that the combined treatment displayed a superior anti-cancer activity in 3D organoids, significantly reducing both their number and size ($P < 0.05$). Conclusion: We present novel evidence for the synergistic anticancer effects of ABE and OPCs in CRC cells, which are in part achieved by regulating cellular apoptosis and the oncogene LMNB1 within the Akt signaling pathway.

#0524 Using acquired resistance to explore the mechanism of action of the integrated stress response/GCN2 activator NXP800 - A new developmental agent for platinum-resistant ARID1A mutant ovarian cancer.

M. V. Powers[1], R. Hodgson[2], S. Y. Sharp[1], T. Roe[1], K. E. Allen[2], S. Campbell[2], R. te Poele[1], M. Cheeseman[1], K. Jones[1], P. A. Clarke[1], P. Workman[1];
[1]The Institute of Cancer Research, London, United Kingdom, [2]Sheffield Hallam University, Sheffield, United Kingdom

Background: NXP800 is a potent, oral activator of the Integrated Stress response (ISR), inhibitor of heat shock factor 1 (HSF1) activation and tumor cell proliferation, which is in early clinical studies in ARID1A-mutated, platinum resistant, clear cell ovarian cancer (NCT05226507). We discovered NXP800 using multiparameter medicinal chemistry optimization of a hit identified from a cell-based phenotypic screen. Owing to the unbiased nature of phenotypic screening, target identification is crucial to understand the biological and therapeutic activity of hit compounds.
Methods and Results:: By RNAseq profiling human cancer cells treated with NXP800 we identified changes in expression of genes regulated by HSF1 or ATF4 - effects accompanied by eIF2alpha (eIF2a) phosphorylation and resulting activation of the ISR. To further understand this response, we explored whether NXP800 resistance models could inform on its mechanism of action (MoA). We used ARID1A mutant SK-OV-3 human ovarian carcinoma cells that are 1) highly sensitive to NXP800, 2) model the target patient population and 3) MSI-high so likely to have an elevated mutation rate contributing to acquisition of resistance. We generated two independent NXP800-resistant SK-OV-3 cell lines in which NXP800-mediated ATF4 induction and concomitant inhibition of global translation were abolished. By whole exome sequencing, we identified a heterozygous L99P mutation in the alpha subunit of eIF2B (eIF2Ba), the nucleotide exchange factor for eIF2a. Expression of eIF2Ba^{L99P}, but not wild-type, in parental SK-OV-3 cells reduced sensitivity to NXP800 to the same level as cells with NXP800-induced resistance. Using fluorescence recovery after photobleaching to monitor the dynamic association of the eIF2B:eIF2a complex, we elucidated that the eIF2Ba^{L99P} mutation reduces NXP800-mediated inhibition of eIF2a-GFP recycling through eIF2B bodies. Phosphorylation of eIF2a is regulated by four stress-controlled kinases GCN2, HRI, PKR and PERK. Using systematic siRNA knockdown or small-molecule inhibitors, we showed that GCN2 alone is required for ISR activation by NXP800 and that ISR induction inhibited HSF1 activation. Furthermore, inactivation of GCN2 reduced the antiproliferative activity of NXP800 to the same extent observed in NXP800-resistant SK-OV-3 cells. In contrast, exposure of resistant or parental SK-OV-3 cells expressing eIF2Ba^{L99P} to GCN2 inhibitors did not cause further reduction in NXP800 sensitivity - confirming the importance of the eIF2Ba^{L99P} mutation in the resistance mechanism.
Conclusions: We have used acquired resistance to understand the MoA of NXP800 as a potent activator of GCN2 and the ISR pathway. Further studies are underway to determine the exact proximal molecular target of NXP800 and the mechanism of GCN2/ISR activation.

#0525 A comprehensive approach: Copper chelation therapy modulates epigenetic, kinase signaling and metabolic pathways in diffuse midline gliomas (DMG).

F. Michniewicz[1], R. Cazzoli[2], J. Bell[2], F. Saletta[2], E. Poursani[2], J. R. C. Rouaen[2], T. Shai-Hee[2], V. Pham[2], T. Jue[2], M. Biery[3], L. Bramberger[4], T. Lim[4], A. Khan[2], F. M. Giorgi[5], D. Mercatelli[5], C. Mayoh[2], G. Cirillo[6], A. Macmillan[1], R. Whan[1], C. T. Barlow[4], M. Tsoli[2], N. Vitanza[3], S. Berry[1], P. Faridi[4], D. Ziegler[2], O. Vittorio[1];

[1]UNSW Sydney, Kensington, Australia, [2]Children's Cancer Institute, Kensington, Australia, [3]Seattle Children's Research Institute, Seattle, WA, [4]Monash University, Clayton, Australia, [5]University of Bologna, Bologna, Italy, [6]University of Calabria, Calabria, Italy

Diffuse Midline Gliomas (DMG) are incurable pediatric brain tumors driven by histone mutation H3K27M, globally reducing H3K27 trimethylation altering the epigenome and deregulating gene expression. These mutations often partner with and are strongly integrated into kinase signaling and metabolic alterations, driving aggressive tumor growth with many mechanisms which can compensate for one another and therefore evade traditional single agent therapies. Copper over-accumulation has been linked to epigenetic, kinase and metabolic dysregulation in various cancers and neurological disorders. Copper chelators are clinically approved for use in pediatric Wilson's Disease patients, improve neurological symptoms and are under clinical investigation for several cancers. We propose copper chelators may simultaneously target these mechanisms in DMG. We performed transcriptomic interrogation of patient datasets, *in vitro* investigations in a panel of DMG cell lines and an *in vivo* investigation using an orthotopic xenograft model of DIPG (SU-DIPGVI-*Luc*). Copper chelator tetraethylenepentamine-pentachloride (TEPA) was used to treat DMG cells. Transcriptomic (RNA-Seq), proteomic, phospho-proteomic and metabolomic (Mass Spectrometry) investigations, western blots and immunofluorescent microscopy determined efficacy and mechanism. *In vivo* investigation consisted of survival study with concurrent luminescence imaging, histology, and copper assay. We demonstrate copper chaperone transcript expression is increased in DMG patient samples compared to non-DMG samples. *In vitro*, apoptosis and growth assays demonstrated H3K27M DMG were more sensitive to TEPA than H3-WT DMG. In H3K27M DMG, TEPA downregulated ATP, GTP and SAM metabolism which corresponded with downregulated kinase signaling and altered H3K27 trimethylation and DNA methylation patterns around cell cycle genes. Affected genes included those regulating centrosome segregation and ATP synthesis. Further transcriptomic and proteomic investigations highlighted TEPA downregulated G2-M phase kinase pathways, with immunofluorescence demonstrating TEPA reduced expression of mitotic marker p-H3S10 and epigenetic methylators EZH2 and DNMT1. *In vivo,* TEPA reduced brain copper accumulation, eliminated tumors and increased survival in an orthotopic patient-derived xenograft DMG model. Collectively, our data indicates TEPA induced multi-modal targeting of M-phase cell cycle progression through epigenetic, kinase signaling and metabolic mechanisms. Efficacy was observed both *in vitro* and *in vivo*, providing a promising basis for future investigation of copper chelators in DMG. We propose copper-chelation is a viable therapeutic strategy for DMG patients warranting clinical investigation.

#0526 Identification of CDK6 binding proteins by proximity labeling reveals novel mechanisms for CDK4/6 inhibitor resistance in breast cancer.

Chung Wei Ting[1], Yong-Ji Zhuang[1], Chih-Yi Lin[2], Chung-Jen Yu[1], Ta-Chung Chao[2], Ling-Ming Tseng[2], Chun-Yu Liu[1], Yi-Fang Tsai[2], Chi-Cheng Huang[2], **Jiun-I Lai**[1]

[1]National Yang Ming Chiao Tung University, Taipei, Taiwan,[2]Taipei Veterans General Hospital, Taipei, Taiwan

Breast cancer is one of the most prevalent cancer type in human, and the majority (~70%) is the hormone positive (HR+) subtype. The current frontline treatment of choice in metastatic HR(+) breast cancer is CDK4/6 inhibitors (CDK4/6i) combined with endocrine therapy. Current guidelines recommend CDK4/6i treatment as 1st or 2nd line, as CDK4/6i provides survival benefit and good quality of life. However, resistance eventually emerges, leading to discontinuation of CDK4/6i and switching to subsequent treatment. Investigation of mechanisms to CDK4/6i resistance is an active area of intense research. CDK6 overexpression has been reported as an important mechanism for CDK4/6i resistance by several independent groups. We incidentally discovered a point mutation in the CDK6 protein that abolishes the CDK4/6i resistance conferred by CDK6 overexpression. When treated with CDK4/6i, overexpression of wild type CDK6 did not suppress G1/S, while both non-transfected and overexpression of mutant CDK6 both had similar suppression of G1/S. We hypothesized that a binding partner to CDK6 demonstrated differential binding activity to the mutant which abolished the resistance by CDK6 overexpression. To assess this hypothesis, we performed proximity labeling (PL) by APEX2. Both wild type and mutant CDK6 were cloned into APEX-Flag/V5 vectors with either cytoplasm (NES) or nuclear (NLS) signals. Mass spectrometry following treatment by H2O2 induced biotinylation produced candidate peptides that bound with overexpressed CDK6. We identified leading candidates of differentially binding partners that bound to mutant CDK6. Further experimental validation was performed to confirm physical proximity between CDK6 and the candidate protein. Our research uncovered novel insights to how CDK6 conferred resistance towards CDK4/6i and expands knowledge into further therapeutic development.

#0527 Cancer cells in the resistant, endocycling cell state exhibit centrosome amplification.

M. Purkerson, S. Amend, K. J. Pienta;
Johns Hopkins University School of Medicine, Baltimore, MD

Therapy resistance is one of the most common underlying causes of poor prognosis in cancer patients, ultimately driving fatal outcome. We have previous demonstrated that following chemotherapeutic stress, a subset of cancer cells undergo a mitotic skip and enter an endocycle, causing whole-genome duplication without division. This endocycling cell state is resistant to cytotoxic therapies and thus is an actuator of therapy resistance. Cells in the endocycling state eventually undergo depolyploidization and repopulate the tumor, observed clinically as a recurrence. We also demonstrated that the minus-end directed motor protein KIFC1, a mediator of centrosome clustering, has higher expression in cells following treatment. Centrosome amplification (CA) involves aberrations in centrosome number, where cells have 3 centrosomes. Cells with extra centrosomes create a multi-polar spindle during mitosis, which presents high risk for cell death and arrest, but cancer cells with CA avoid this by clustering extra centrosomes to create a pseudo-bipolar spindle. Based upon this data, we hypothesize that studying centrosome dynamics and abnormalities presents a window into better understanding endocycle biology and this novel mechanism of therapy resistance. Cancer cells were treated with LD50 dose of cisplatin and released from treatment for varying lengths of time. CA in endocycling cells increased from 59.2% to 100% during the treatment recovery period while maintaining identical levels of clustering. Endocycling cancer cells have a nearly 5-fold increase in declustered centrosomes compared to proliferative cells. Centrosomes in endocycling cells are displaced from the perinuclear region and toward the cell periphery. We hypothesize that centrosome number may indicate the number of times a cell has endocycled and provide insight into the timing and mechanism of mitotic bypass. Centrosomes play a major role in microtubule nucleation, affecting cell motility and polarity, and act as signaling platforms, enhancing signaling activation and specificity. Because of this, we hypothesize that CA may be a critical mechanism for endocycling cancer cells to survive and maintain this resistant cell state.

#0528 CDK9 inhibition activates innate immune response in prostate cancer cells.

S. Yalala[1], A. Gondane[1], N. Poulose[2], J. Liang[1], I. G. Mills[2], **H. M. Itkonen**[1];
[1]University of Helsinki, Helsinki, Finland, [2]University of Oxford, Oxford, United Kingdom

Hyper-activation of transcription is frequent in cancer, which often leads to increased sensitivity to compounds targeting the transcriptional kinases, in particular cyclin-dependent kinase 9 (CDK9). However, mechanistic details as to why CDK9 inhibition selectively kills cancer cells remain largely unknown. Here, we report that CDK9 inhibition activates innate immune response through viral mimicry. In MYC over-expressing prostate cancer cells, CDK9 inhibition leads to excessive accumulation of mis-spliced RNA. Double-stranded RNA (dsRNA)-activated kinase can recognize these mis-spliced RNAs, and we show that this kinase is required for the CDK9 inhibitor-induced anti-proliferative effects. Using time-resolved transcriptional profiling (SLAM-seq), targeted proteomics and ChIP-seq, we show that, similar to viral infection, CDK9 inhibition significantly suppresses transcription of most genes but allows selective transcription and translation of certain genes. In particular, CDK9 inhibition activates NFκB-driven cytokine-signaling at the transcriptional- and secretome-levels. Transcriptional signature induced by CDK9 inhibition identifies prostate cancers with high level of genome instability, and we propose that it is possible to induce similar effects using CDK9 inhibitors. In summary, here we show that inhibition of CDK9 activates innate immune response through viral mimicry. In the future, it is important to establish if CDK9 inhibitors can potentiate the effects of immunotherapy against the late-stage prostate cancer, a currently lethal disease.

#0529 Investigating the synergistic effect of milciclib and PD0325901 in colorectal cancer therapy.

X. Pei[1], A. Nguyen[2], H. Neiger[2], W. Wang[2], W. Bautista[2], L. Wang[3], A. Cai[2], V. A. Gerriets[2], J. K. Cusick[2], **Y. Shi**[4];
[1]City of Hope, Duarte, CA, [2]California Northstate University, Elk Grove, CA, [3]University of California, Berkeley, CA, [4]California Pacific Medical Center Research Institute, San Francisco, CA

Milciclib, characterized as a potent nanomolar inhibitor of multiple cyclin-dependent kinases, has recently emerged as a promising therapeutic agent in cancer treatment, particularly with its additional role as a spliceosome modulator. Our recent studies employing RNA sequencing technology revealed a comprehensive profile of Milciclib-induced transcriptional changes in colorectal cancer cells, identifying several key regulated pathways. In light of these findings, we explored a novel therapeutic strategy: combining Milciclib with specific inhibitors targeting pathways upregulated by Milciclib treatment. This hypothesis is based on the rationale that such a combination could exert a synergistic effect. We have assessed the efficacy of this combinational therapy and found that the combination of Milciclib and PD0325901 greatly potentiates the killing of colorectal cancer cells versus either treatment alone. PD0325901 has been extensively studied for its efficacy in targeting the MEK/ERK signaling pathway, a critical pathway in many cancers, including colorectal cancer. To further characterize the underlying molecular mechanisms contributing to the observed synergistic effect, we applied quantitative proteomic analysis of 8107 proteins in human colorectal cancer cells with the treatment of different doses of Milciclib and PD0325901 administered alone, or in combination. Our results demonstrate 49 proteins were significantly decreased in a dose-dependent manner, and that many of these proteins are key players regulating pathways associated with the cell cycle, apoptosis, gene expression, metabolism, WNT signaling, and the MEK/ERK signaling pathway. The discovery of the down-regulation of these proteins and pathways after treatment provides a molecular basis to elucidate the synergistic mechanism underlying Milciclib and PD0325901 combination therapy. In conclusion, our study establishes the combinatorial use of Milciclib and PD0325901 as a potential breakthrough in the treatment of colorectal cancer, offering a promising prospect for enhancing future patient outcomes.

#0530 The effect of cardamonin on PD-L1 expression in triple-negative breast cancer cells.

P. Mendonca, B. Kirpal, S. Kaur, K. F. Soliman;
Florida A&M University, Tallahassee, FL

Triple-negative breast cancer (TNBC) accounts for about 10% of all breast cancers and does not express estrogen, progesterone, or HER2 receptors. It has an aggressive nature, it is highly metastatic, and because of the lack of therapies, it continues to be a challenge. These cancer cells employ mechanisms to escape the immune system that induce the upregulation of PD-L1 expression, a ligand encoded by the CD274 gene. Because cancer cells tend to produce higher levels of PD-L1 compared to normal cells, therapies that inhibit PD-L1 may be helpful. Evidence also shows that high levels of oxidative stress and inflammation may participate in both the initiation and progression of cancer. Cardamonin, an aromatic enone flavonoid, has displayed an array of pharmacological activities, including modulation of different signaling molecules involved in the development and progression of cancer. This work investigated the cardamonin's ability to modulate PD-L1 expression and NF-KB in genetically distinct MDA-MB-231 (Caucasian) and MDA-MB-468 (African American) TNBC cell lines. The methodology included cytotoxic assays, ELISA, Real Time-Polymerase Chain Reaction (RT-PCR) assays, and Wes analysis. The results showed that cardamonin treatment caused a dose-dependent decrease in cell viability in both cell lines, ranging from 3.12 μM to 200 μM. The RT-PCR and ELISA data showed that even though IFN-γ stimulated MDA-MB-231 cells showed a higher expression of PD-L1, cardamonin reduced mRNA and protein expression of PD-L1 in both cell lines. As a possible molecular mechanism for PD-L1 inhibition, cardamonin modulated MUC-1, STAT3, and JAK, which are genes that activate the PD1/PD-L1 mechanism. Moreover, data also show that cardamonin modulated NF-KB1 and NF-KB2 genes involved in activating NF-KB signaling. NF-KB is a transcription factor of inflammation and immunity, emerging as a key positive regulator of PD-L1 expression in cancer. Therefore, cardamonin may have the potential utilization as a checkpoint inhibitor that acts by blocking PD-L1 protein, allowing the immune system to recognize and attack the TNBC cancer cells, providing a novel cancer therapy. (Supported by a grant from NIH-NIMHD U54 MD 007582)

EXPERIMENTAL AND MOLECULAR THERAPEUTICS: Drug Resistance 1: Models
Poster Session

#0533 Attenuating EZH2-mediated metastasis and tumor growth by pharmacological-based approaches using three-dimensional in vitro culture models.

x. Rima[1], G. Sarathy[1], C. Hu[2], D. S. Patel[2], D. Ramsey[3], L. Rizotto[1], D. Palmeri[4], G. Fewell[3], B. Ramaswamy[1], E. Reategu[2], **E. Shankar**[1];
[1]The Ohio State University Wexner Medical Ctr., Columbus, OH, [2]The Ohio State University, Columbus, OH, [3]SynVivo Inc, Huntsville, AL, [4]The Ohio State University school of Medicine, Columbus, OH

Triple Negative breast cancer (TNBC) accounts for 10-15% of all breast cancers where patients encounter poor clinical outcomes. Treatment modalities for TNBC are conventional cytotoxic chemotherapy and radiation leads to 35%-40% relapse within 5 years of diagnosis. There is a growing need for more effective targeted therapeutics to inhibit TNBC growth. The role of EZH2 in maintaining tumor growth and metastasis in TNBC is well documented. EZH2 promotes breast tumor-initiating cell expansion (BITC) and cancer progression by impairing the DNA damage repair process favoring activation of oncogenes. Despite the advancement in the discovery of inhibitors for EZH2 that attenuate its catalytic activity, resistance to these small molecules limits their use in solid tumors. The neurotransmitter dopamine via its D1 receptor activation in TNBC cell lines induces apoptosis and autophagy, as well as inhibits the invasion and regress in mammary tumors in vivo. Here we hypothesize that the presence of dopamine D1 receptor agonist (A77636) enhances the efficacy of EZH2 inhibitors (GSK126) to inhibit in vitro TNBC tumor growth and metastasis. To test the efficacy of the combination we employed a 3D culture system of MDA-MB-231 cells encapsulated in calcium-alginate microgels seeded from a microfluidic droplet generator. We also employed a 3D organ-on-chip-based microphysiological (MPS) platform (SynTumor) to study the effect of the drug combination on metastasis in vitro. The SynTumor MPS devices replicate the pathophysiological architecture of native vascularized breast tumors. The combination treatment enhanced a significant reduction of tumor spheroid diameter compared to the vehicle and indicated spheroid regression over treatment. Furthermore, the combination therapy induced necrosis and caused complete inhibition of EZH2 expression. The knockdown of EZH2 inhibited tumor spheroid formation and displayed cytoskeleton de-arrangement. In the microfluidic SynTumor model, circulating tumor cell numbers were reduced by half at 96 hrs after EZH2 combination treatment. Our data indicate that the combinatorial effect of DRD1 agonist and EZH2 inhibitor efficiently attenuates the EZH2-mediated in vitro tumor growth and metastasis (This work is supported by DOD: W81XWH2010065, for Eswar Shankar).

#0534 Novel marginal zone lymphoma models of resistance to the dual inhibition of PI3K and BCL2.

A. J. Arribas[1], L. Cascione[1], E. Cannas[1], H. Bellerjeau[1], F. Fuzio[1], A. Noguera[2], A. Rinaldi[1], M. Esteller[2], E. Zucca[3], A. Alimonti[1], D. Rossi[1], A. Stathis[3], F. Bertoni[1];

[1]IOR - Institute of Oncology Research, Bellinzona, Switzerland, [2]Josep Carreras Leukaemia Research Institute (IJC), Barcelona, Spain, [3]Oncology Institute of Southern Switzerland, Bellinzona, Switzerland

Background: Copanlisib is a PI3K inhibitor with selectivity against PI3Kδ and PI3Kα and is approved for treating patients with follicular lymphoma and marginal zone lymphoma (MZL). Preclinical studies have demonstrated strong synergism of copanlisib and BCL2 inhibitor venetoclax in different lymphoma models, and the combination is under clinical evaluation. Understanding the resistance mechanisms could help the design of improved therapies. Hence, we generated MZL cell lines resistant to the copanlisib/venetoclax combination.

Methods: All cells were tested for cell identity and Mycoplasma status. Resistance was confirmed stable after 3-weeks of drug-free culture. Multi-drug resistance phenotype was ruled out by confirming sensitivity to vincristine. Targeted agents already in the clinics were combined with copanlisib/venetoclax. Cells underwent transcriptome and methylation profiling, targeted DNA sequencing, and immunophenotypic and immunoblotting analyses.

Results: We developed SSK41-derived models with resistance to copanlisib (n.=1) or venetoclax (n.=1) as single agents and to copanlisib/venetoclax (n.=2) by long IC50 or by upfront IC90 exposure. The single-drug-resistant cells showed only partial resistance to copanlisib/venetoclax. In contrast, the cells that developed exposing cells to copanlisib/venetoclax IC90 exhibited a more substantial decrease in sensitivity to the combination. Copanlisib/venetoclax induced apoptosis and cell cycle arrest in PAR but not in resistant cells. Sensitivity to other PI3K, BCL2, and BTK inhibitors was decreased in all resistant lines. The response to MCL1-i, mTOR-i, and epigenetic agents (decitabine, HDAC, BET, and EZH2 inhibitors) was maintained. Triple combinations of copanlisib/venetoclax with the AURKA inhibitor alisertib, PLK inhibitor rigosertib, or the multikinase inhibitor amcasertib were active in both parental and resistant cells. No acquired mutations were observed via targeted DNA sequencing designed to cover various coding genomic regions known to be recurrently mutated in mature B-cell neoplasms, including BCL2, nor via RNA-Seq for PIK3CA/B/G/D genes. Integration of RNA and methylation profiles showed deregulation of genes involved in type-I IFN, chemokines (CCL25, CXCL13), apoptosis regulation, and JAK-STAT signaling. Resistant cells upregulated CD19 expression compared to parental cells. Immunoblotting showed the inability of copanlisib/venetoclax to block BCR signaling in resistant cells.

Conclusions: We created four novel MZL-derived models of secondary resistance to PI3K and BCL2 inhibitors, which will help clarify possible modalities to overcome resistance. Novel potential targets were already identified, such as AURKA or PLK, to be further exploited.

#0535 Resistant PDO models: Unraveling drug resistance mechanisms for discovering new drug targets.

Y. Abouleila, M. Doorn, R. Verkerk, J. Maas, C. Verissimo, S. Boj;
HUB Organoids, Utrecht, Netherlands

Resistance to cancer treatment remains a significant obstacle in curing patients with cancer. Despite recent advancements in novel drug targets for cancer therapeutics, patients often develop treatment resistance even after initial disease remission, leading to tumor relapse. To investigate the mechanisms responsible for developing resistance to standard-of-care therapies, it is essential to gain insights into the stepwise progression leading to complete resistance. Recent research has revealed that cancer cells can evade the effects of chemotherapy and targeted therapy by entering a reversible and slow proliferation state known as the drug-tolerant persister (DTP) state. This DTP state allows cancer cells to survive drug therapy long enough for additional mechanisms of acquired drug resistance to develop. HUB Organoids® or patient-derived organoid (PDO) models are derived from patient tissues, making them more physiologically relevant than traditional cell lines. Thus, studying drug persistence and resistance in PDO models is more likely to reflect in vivo conditions. This study demonstrates the successful development of persistent and resistant CRC PDO models to standard-of-care therapies. All models were characterized using whole exome sequencing and RNA sequencing to confirm their persistent or resistant state and to identify possible pathways involved in developing therapy resistance, as well as potential new drug targets. In conclusion, developing persistent and resistant PDO models is crucial for understanding drug resistance mechanisms, enabling the development of more effective and personalized cancer treatments, and advancing our overall knowledge of how resistance develops in cancer patients.

#0536 Breaking through ADCs resistance: Constructing preclinical enhertu-induced resistant model.

Y. Fang, H. Wang, J. Xing, L. Yang, J. Zhao, X. Gao, C. Ju;
Gempharmatech Co., Ltd., Nanjing, China

Antibody-drug conjugates (ADCs) are compounds that combine the specificity of monoclonal antibodies (mAbs) with the cytotoxic payload of toxic substances. In recent years, ADCs have rapidly developed in the field of cancer therapy, particularly in the treatment of HER2-positive breast cancer. One representative example is Trastuzumab deruxtecan (Enhertu), which has become a new benchmark for anti-HER2 ADCs due to its excellent performance in clinical trials. Despite the impressive clinical outcomes of ADCs, some tumors in patients may still develop resistance to these drugs. Therefore, it is crucial to understand the mechanisms of resistance and develop strategies to overcome ADCs resistance. To achieve these goals, it is essential to establish and utilize preclinical models to study these resistance mechanisms. Preclinical models of resistance to ADCs have mainly been generated using human cultured cell lines. JIMT-1 is a HER2-positive breast cancer cell line that exhibits primary resistance to the anti-HER2 antibody trastuzumab and also shows resistance to trastuzumab-derived ADC T-DM1. However, we found that Enhertu significantly inhibited tumor growth in JIMT-1 xenograft models. We subjected JIMT-1 tumor tissues to continuous passage in mice and administered long-term drug induction. The tumor growth rate gradually increased, and the drug sensitivity decreased, resulting in the acquisition of an Enhertu-resistant tumor model. The obtained resistant tumor tissues not only include tumor cells themselves but also comprise fibroblasts, extracellular matrix, and other cellular components, enabling a more comprehensive investigation into the interactions between different cells within the tumor microenvironment (TME). We believe that the establishment of preclinical Enhertu-resistant models helps predict resistance that has not yet emerged clinically and provides references for future drug development.

#0537 Preclinical PD-1 resistance models: Crucial tools for unveiling PD-1 resistance mechanisms and advancing novel treatment strategies.

Y. Zhu, Y. Fang, H. Wang, J. Xing, L. Yang, J. Zhao, X. Gao, C. Ju;
Gempharmatech Co., Ltd., Nanjing, China

In the cancer-immunity cycle, the immune checkpoint PD-1 and its ligand PD-L1 collaborate to facilitate tumor immune evasion and promote tumor progression by thwarting immunity-induced apoptosis. Immune checkpoint inhibitors disrupt this alliance by preventing PD-1 from binding to PD-L1, thereby reactivating the patient's immune system. While anti-PD-1/PD-L1 therapy has demonstrated remarkable efficacy in treating solid tumors, durable responses are observed in only a minority of patients. The majority of patients do not experience the full benefits of anti-PD-1/PD-L1 therapy, and a significant proportion of initial responders eventually develop acquired resistance. Thus, the establishment of reliable preclinical PD-1 resistance models is of paramount importance for uncovering resistance mechanisms and devising novel treatment strategies.

Common mechanisms contributing to PD-1/PD-L1 resistance include the absence of appropriate tumor antigens, inactivation of tumor surface MHC molecules, aberrant IFNγ signaling pathways, and the presence of an immunosuppressive tumor microenvironment. We have successfully generated multiple drug resistance models at both cellular and animal levels, offering valuable tools for the investigation of diverse drug resistance mechanisms. For instance, our animal model of drug resistance, induced by long-term treatment with the PD-1 antibody (Keytruda), simulates the clinical scenario of acquired resistance due to prolonged medication. Through gene editing techniques, we have created a drug-resistant cell line (CT26-B2M KO) by disrupting the B2M gene in the CT26 cell line, thereby mimicking a tumor model with B2M functional deficiency in mice. Additionally, we have compiled efficacy data from various naturally occurring resistant models, which serve as valuable resources for studying primary resistance or intricate resistance mechanisms.

In summary, preclinical PD-1 resistance models serve as crucial tools for researchers to dissect the intricacies of PD-1 resistance mechanisms and offer essential guidance for the development of innovative treatment strategies.

#0538 Establishment of PARP inhibitor-induced resistant patient-derived ovarian cancer xenograft models.

L. Hua, S. Li, C. Nie, X. Chen, G. Sheng, L. Bourre, **J. Wang**;
Crown Bioscience, Inc., San Diego, CA

Introduction: Poly (ADP-ribose) polymerases (PARPs) can recruit DNA repair effectors and cope with DNA single-strand breaks. For DNA double-strand breaks (DSB), there are two main repair mechanisms: non-homologous end joining repair (NHEJ) which is prone to error due to infidelity events, and BRCA1/2 mediated homologous recombination repair (HR) restoring the original sequence. Therefore, inhibition of PARPs may cause both single stranded break repair deficiency and HR deficiency in BRCA1/2 deficient patients, leading to cell death. The concept of “synthetic lethality” has led to the development of PARP inhibitors, including Olaparib, Niraparib and Rucaparib in clinical practice. Despite encouraging efficacy of these PARP inhibitors, acquired resistance, such as HR repair restoration, drug efflux pump upregulation and replication fork protection, has limited their clinical benefits. Therefore, to investigate novel therapeutic strategies which can overcome the acquired resistance, we established patient-derived xenograft (PDX) ovarian cancer models with PARP inhibitor-induced resistance.

Methods: OV9402, an ovarian cancer PDX model with BRCA 1 c.3155del, was implanted subcutaneously and treated with Niraparib at 35 mg/kg, daily, for 129 days. Relapse tumors (tumor #1 and tumor #2) were isolated and inoculated into naïve mice. Then the 2nd round of treatment (Niraparib, 35 mg/kg, daily) was given when the mean tumor volume reached 140 mm^3. The tumors showing no significant response to Niraparib were collected on either day 32 (#1 derived tumor model) and day 22 (#2 derived tumor model) after randomization and their gene changes were analyzed by RNA sequencing (RNA-seq).

Results: Niraparib significantly inhibited OV9402 tumor growth, with complete regression observed in nine out of ten mice on day 54 after the 1st round of treatment. However, tumor regrowth was observed in two out of the nine mice from day 68 onwards. The relapsed tumors (tumor #1 and tumor #2) from these two mice were collected and re-inoculated into 5 naïve mice to establish tumor models for the 2nd round of Niraparib treatment, separately. For #1 derived tumor model, all the tumors presented complete resistance to the Niraparib treatment. RNA-seq data showed that the gene expression of ABCB1, which encodes for efflux pumps, was upregulated. In parallel, complete resistance to Niraparib was observed in all the tumors derived from 2# tumor bearing mice. The RNA-seq data demonstrated that an acquired secondary genetic deletion on BRCA1 genes, which restored the functional protein expression loss in the parental line and restored HR repair, was found in the tumors.

Conclusion: Ovarian cancer PDX models that have effectively developed resistance to PARP inhibitors have the potential to serve as valuable preclinical tools to evaluate potential next-generation PARP inhibitors and innovative combination strategies.

#0539 LN18-MRTX1719R cell line, a useful cell model for the discovery of the new PRMT5 inhibitors..

Y. Tang, L. Wang, G. Wang, J. Ning, **F. Hao**;
Kyinno Biotechnology Co., Ltd, Beijing, China

In recent years, the PRMT5-MTA complex has emerged as a "synthetic lethal" novel target for the treatment of MTAP (methylthioadenosine phosphorylase)-deficient cancers. Kryukov et al. first reported the "synthetic lethal" effect of inhibiting PRMT5 in MTAP-deficient tumors, and they identified MTAP as the synthetic lethal partner of PRMT5 in 2016. MTAP is a tumor suppressor gene frequently lost in various cancers, including pancreatic cancer, non-small cell lung cancer, and mesothelioma. Furthermore, the loss of MTAP leads to the accumulation of MTA in cancer cells, which competes with PRMT5's co-factor SAM for binding and forms the PRMT5-MTA complex. Cancer cells lacking MTAP show enhanced sensitivity to PRMT5 loss. Therefore, this complex has emerged as a potential therapeutic target, particularly for the treatment of MTAP-deficient cancers. MRTX1719 is a highly effective selective inhibitor of the PRMT5-MTA complex, capable of selectively inhibiting PRMT5 activity in MTAP-deficient cells. As the most promising candidate drug, MRTX1719 is undergoing Phase I/II clinical evaluation for patients with MTAP-deficient cancers. Drug resistance is an inevitable problem with small molecule inhibitors. Currently, the mechanism of resistance to MRTX1719 is not clear, as MTAP/CDKN2A loss is an early driver event in most cancers. To further explore the resistance mechanism of MRTX1719, our group used the MTAP-deficient LN-18 cell line and induced mutagenesis using the mutagen ENU. We then used a drug low-concentration gradient method to establish the LN-18-MRTX1719R-resistant cell line. Specifically, LN-18 cells were treated with increasing doses of MRTX1719 for 6 months, and mixed clones that tolerated MRTX1719 were selected. Subsequently, single clones were selected, and a stable MRTX1719-resistant clone was obtained, named LN-18-MRTX1719R. Cell proliferation inhibition assay showed that the IC50 of LN-18-MRTX1719R was over 1000nM, which is 100-fold more resistant than the parental LN-18 cells (9.87 nM). We explored the resistance mechanisms using RNA-Seq and WES methods. The resistance to MRTX1719 of the LN-18-MRTX1719R cell line was highly stable after 20 cell passages. The LN-18-MRTX1719R cell line can be a useful cell line mode in the development of future PRMT5·MTA inhibitors.

#0540 Identification of therapy resistance mediating extracellular vesicles in single-cell level via a novel microfluidic co-culture device development.
C.-J. Kim, S. Amend, K. Pienta;
Johns Hopkins University School of Medicine, Baltimore, MD

Once cancer has metastasized, it is incurable because tumors evolve resistance to all systemically administered anti-cancer therapies. Resistance to therapy has classically been attributed to the presence of a cancer stem cell or genetic tumor cell heterogeneity. Extracellular vesicles (EVs) are nano-sized (40-1000 nm) vesicles that are released by all cells into the extracellular space. EVs carry diverse cargo dependent on the cell of origin and have been studied as a source of novel cancer-specific liquid biopsy biomarkers and contributors to tumor progression and metastasis. However, the paracrine function of EVs in promoting therapy resistance is under-studied, and the impact of EVs released from therapy-resistant cancer cells on surrounding therapy-sensitive cancer cells is unknown. In this study, we develop an innovative microfluidic device, TREVCo, to enable simultaneous single-cell trap, EV detection, and co-culture modules to evaluate EVs-mediated transfer of cellular information between therapy-resistant cancer cells and adjacent cells, and to characterize EVs released from resistant cells and determine their impact on the resistance phenotype of adjacent therapy-sensitive cancer cells. We utilize resistant cells from multiple prostate (PCa) cell lines that have been selected for therapy resistance by culture with increasing dosages of cancer drugs such as cisplatin, docetaxel. We use the matched untreated therapy-sensitive parental cell lines as the sensitive cells. We hypothesize a novel model of therapy resistance in lethal PCa: EVs released from resistant cells contain pro-resistance factors that are transferred to adjacent sensitive cells upon EV uptake, thus directly enabling therapeutic resistance. We will assess the impact of resistant cell-EVs at a single cell level via a novel device, TREVCo, that enables comprehensive downstream analysis. This single-cell approach enables dissection of critical EV-associated therapy-resistant factors within the large heterogeneity of resistant PCa. Co-culture of a single resistant cell and a hundred adjacent sensitive cells mimicking intra-tumoral interactions is also critical to demonstrate evidence of resistant cell secreting factors inducing a pro-resistance phenotype. These studies will be the first-in-field to assess the impact of resistant PCa cell-derived EVs at single-cell resolution. An understanding of resistant cell-derived EVs and the impact of that EV cargo on adjacent sensitive cells will provide critical insight into the acquisition of therapy resistance in lethal PCa. The novel approach to apply resistant cell-derived EVs in co-culture assay with sensitive cells will enable the screening of transmittable resistance-associated factors and provides critical opportunities for accelerating precision medicine for advanced PCa patients.

#0541 Establishment of Inotuzumab ozogamicin resistant leukemia cell lines; Focusing on p-gp and DNA damage repair for overcoming drug resistance.

N. Ida[1], M. Okura[2], N. Hosono[1], T. Yamauchi[1];
[1]University of Fukui Hospital, Fukui, Japan, [2]DMU Saitama Medical Center, Saitama, Japan

Introduction: Inotuzumab Ozogamicin (IO) is a humanized anti-CD22 monoclonal antibody conjugated with chalicheamicin, which causes single- and double-strand DNA breaks. Although IO shows a high CR/CRi rate in relapsed/refractory CD22-positive B-cell acute lymphoblastic leukemia (ALL), the duration of remission is short due to early acquisition of resistance. Therefore, the present study attempted to enhance the cytotoxicity of IO by focusing on polyadenosine diphosphate-ribose polymerase (PARP) inhibition. Furthermore, IO-resistant cell lines were newly established to investigate the mechanism of IO resistance.
Methods: Reh cell line derived from Ph-negative B-ALL cells was used. To establish IO-resistant cell lines, Reh cells were long-term exposed to IO, followed by limiting dilution. FACS analysis evaluated the CD22 positivity and the induction of apoptosis. WTS assay determined the cell growth inhibition effects. The Comet assay quantitatively assessed DNA damage. Gene expression profiles were determined by using DNA microarray.
Results: The 50%-inhibitory concentration (IC_{50}) of IO was 2.1 ng/mL in Reh cells. Reh cells were synergistically sensitized to IO by the addition of non-toxic concentrations of PARP inhibitors, olaparib or talazoparib, with the Combination Index of 0.19 and 0.42, respectively. Moreover, these combinations augmented the induction of apoptosis (23.5% in IO alone, 51.7% in IO + olaparib, 66.1% in IO + talazoparib). The Comet assay demonstrated that DNA strand breaks observed 1h after IO administration were repaired 6h later. In the combination of IO with olaparib or talazoparib, DNA damage remained even at 6h, suggesting the inhibition of DNA repair by PARP inhibitors. Next, six IO-resistant cell lines were established with IC_{50} more than 60-fold that of parental cells. All these cell lines kept CD22 expression. These cell lines were also resistant to apoptosis induced by IO. In addition of olaparib or talazoparib to IO, the IC_{50} of IO decreased by 40% to 70% in 6 IO-resistant cells. These combinations also augmented the induction of apoptosis (24.2% in IO alone, 45.3% in IO+olaparib, and 56.8% in IO+talazoparib). DNA microarray was performed to compare gene expression profiles between parental and IO-resistant cell lines. ABCB1 (p-gp), a drug efflux pump that causes multi-drug resistance, was overexpressed in resistant cell lines. Moreover, the addition of p-gp inhibitor, PSC-833, to IO enhanced the cell growth inhibition and induction of apoptosis due to more DNA strand break.
Conclusion: The present study demonstrated that the combination of IO with PARP inhibitors exerted synergistic cytotoxicity via the inhibition of DNA repair. In addition, it was suggested that overexpression of p-gp caused IO resistance, which was partially reversed with the combination of PARP inhibitors or a p-gp inhibitor.

#0542 Development of novel syngeneic tumor models with intrinsic or extrinsic resistance mechanisms to PD-1 blockade.

X. Wang[1], Z. Zhang[2], L. Liu[3], X. Zhang[3], D. Wang[1], N. Xu[2], X. Qiang[1], Q. Gu[1], J. Xiang[2], Z. Zhang[1];
[1]WuXi AppTec, Shanghai, China, [2]WuXi AppTec, Suzhou, China, [3]WuXi AppTec, Nantong, China

Programmed cell death-1 (PD-1) blockade has demonstrated remarkable clinical efficacy across various tumor types. However, the current PD-1 blockade monotherapy benefits only a small proportion of patients, and primary or acquired resistance can ultimately lead to cancer progression in clinical settings. Understanding the underlying mechanisms of resistance is both necessary and urgent to enhance clinical outcomes. Increasing evidence suggests that resistance to PD-1 therapy can arise from both tumor-cell-intrinsic and tumor-cell-extrinsic factors. Loss-of-function mutations in the antigen presentation pathway and downstream elements represent intrinsic mechanisms, while tumor-infiltrating immunosuppressive cells such as regulatory T cells (Tregs), myeloid-derived suppressor cells (MDSCs), and tumor-associated macrophages (TAMs) contribute to immune tolerance as extrinsic factors. Currently, the rational design of combination therapies based on these resistance mechanisms remains to be achieved.

In this study, we developed two types of anti-PD-1 antibody-resistant models based on the intrinsic anti-PD-1 treatment-sensitive MC38 models. These models include genetically engineered resistant models with B2M or STK11 knockout (KO) and induced resistant models through *in vivo* progressive drug selection. STK11 KO mutations resulted in reduced expression of PD-L1 on tumor cells and a lower infiltration of $CD8^+$ cytotoxic T lymphocytes in the tumor microenvironment, while B2M KO led to a lack of antigen presentation on the tumor cell surface, blocking the binding of the anti-PD-1 antibody. In terms of the induced anti-PD-1 resistant models, a higher proportion of immunosuppressive cells, including Tregs, MDSCs, and TAMs, were observed in the tumor microenvironment compared to the parental counterparts, contributing to immune escape from PD-1 blockade. These models simulate extrinsic and intrinsic mechanism-based anti-PD-1 resistance, allowing for the identification of combination therapies to overcome resistance to anti-PD-1.

Our study enhances our understanding of the biological basis of anti-PD-1 resistance and supports the discovery of mechanistically-designed combination therapies to overcome resistance to anti-PD-1 therapy, potentially broadening its clinical applicability.

#0543 Identifying drivers of chemoresistance in SQLC using forward and reverse genetic approaches.

M. Haarmann[1], D. Gadalla[2], J. Bragelmann[1];
[1]University Hospital of Cologne, Koln, Germany, [2]University of Cologne, Koln, Germany

Non-small cell lung cancer, mainly lung adenocarcinoma (LUAD) and lung squamous cell carcinoma (SQLC), accounts for about 85 % of all lung cancers. While LUAD treatment options have greatly improved, SQLC remains challenging, as targetable mutations are rare. Immunotherapy provides benefits, nevertheless, chemotherapy remains a backbone of systemic treatment strategies for SQLC patients. Accordingly, a major challenge for SQLC treatment is the development of chemoresistant tumors, oftentimes leading to cross-resistance to multiple drugs and limiting patient survival. Currently, the causal pathways enabling tumor cells to survive therapeutic stress and drivers of chemotherapy resistance are insufficiently known, which impedes the development of novel therapeutic strategies. We therefore leverage forward and reverse genetic approaches including large-scale chemo-genetic perturbations to systematically map the landscape of molecular drivers involved in chemotherapy resistance in SQLC. By integrating the resulting data we derive specific knowledge of the underlying processes, in order to identify druggable targets in chemoresistant tumors and contribute to improved patient care.
To assess genes causally mediating chemotherapy resistance upon overexpression, we performed genome-wide CRISPR activation screens utilizing clinically used cisplatin and taxol. Additionally, we performed CRISPRa screens against four further drugs currently in clinical trials in order to distinguish genes causing cross-resistance to multiple drugs versus drug-specific mechanisms.
In parallel, we generated chemoresistant clones by prolonged low-dose treatment, to analyze transcriptomic adaptions to chemoresistance and validate the CRISPRa screening hits.
Initial findings show a large selection of unique and shared gene sets that were significantly enriched or reduced after treatment in the CRISPRa screen, indicating their involvement in the development of chemoresistance.
Of note, transcriptomic analysis of chemoresistant cells shows an overlap with the CRISPRa screen specifically for the unfolded protein response (UPR) that is transcriptionally enriched in chemoresistant cells and a positive hit in the CRISPRa screen. Chemoresistant clones show increased resistance to tunicamycine induced ER-stress, indicating an increased ability to overcome the accumulation of misfolded protein under cytotoxic treatment through the UPR. Specific inhibition of the UPR during cytotoxic treatment shows promising results in chemoresistant cells.
By combining our CRISPR activation screen and systematic analysis of chemoresistant cells we were able to identify the UPR as a driver and a druggable synthetically lethal dependency of chemoresistance in SQLC. This opens the possibility of studying the UPR as a potential target in the treatment of patients with chemoresistant tumors, improving patient outcome.

#0544 Reverse engineering strategy for new targets identification.

B. Xie[1], T. Zhang[1], L. Li[1], H. Chen[1], Y. Liu[1], L. Bi[2], **D. Wen**[1];
[1]Shanghai LIDE Biotech Co., Ltd., Shanghai, China, [2]China-Japan Union Hospital, Jilin University, Changchun, China

The issue of drug resistance in cancer is very similar to the field of infectious disease, either existing before treatment (intrinsic) or generated during therapy (acquired), highly affected by cell endogenous factors and/or the surrounding environment. Acquired resistance can be occurred several months after targeted therapy via alternations of drug targets due to the genomic mutations of the targets, epigenetic transcriptional or translational changes, for example the C797S mutation impairs AZ9291 binding to the EGFR kinase domain. To overcome this, novel well-designed chemical compounds targeting new mutations would be urgently needed, as well as the potential new oncogenes/susceptible genes driving the resistance. Considering about the heterogeneity of primary tumor tissues, LIDE has established one functional cost-effective *in vitro* and *in vivo* screening method, named reverse engineering strategy for targets identification by using patients-derived conditional reprogramed cancer cell lines (CRs) and IO-FIVE (Immuno-Oncology drugs Five In Vivo Efficacy test). Basically, pro-siRNA library or CRISPR/sgRNA library is carried out in CRs for candidates hunting, alternatively drug-response evaluation among multiple clinical biopsies in mice cancer trials, after filtered with bioinformatic scanning from large groups of patients, and finally it is validated *in vivo* by CRISPR, shRNA silence or targeted compounds. In addition to these known factors (EGFR C797S, Her2/Met amplification, Ras and MAPK activation), we have discovered that epigenetic factors for DNA modification, protein translation kinases, mitochondrial/ peroxisomal transporters and cell membrane lectins may contribute to AZ92921 resistance *in vivo*. And one previously unknown acyltransferase member has been identified as key driver gene for pan-cancer development by IO-FIVE, and patients with high expression level of this enzyme have had poor survival outcomes, accompany with uncontrolled tumor growth and immunotherapy resistance, which is becoming a promising therapeutic target.

EXPERIMENTAL AND MOLECULAR THERAPEUTICS: Identification of Molecular Targets
Poster Session

#0548 Exploiting pronounced selection pressure from therapeutic bottlenecks to identify orthogonal immunotherapy targets.

J. Fisk[1], J. P. Townsend[2];
[1]University of Rhode Island, Kingston, RI, [2]Yale University, New Haven, CT

Evolutionary processes play a crucial role in the development of cancer, where tumor cells continuously adapt, leading to the dominance of cell populations over their non-tumor counterparts, evading treatment and ultimately resulting in death. Effective cancer therapies induce significant and targeted selection pressures. During and in response to the induced bottleneck by therapy, the heterogeneous cancer cell population either diminishes or evolves, causing a subsequent selective sweep and the emergence of cells with resistance traits. However, this bottleneck phase presents a unique opportunity to predictably reduce the diversity of tumor cells. In this context, we propose a framework to quantify the selection on variants before, during, and after the therapeutic bottleneck, enhancing our understanding of the mechanisms underlying the acquisition of therapeutic resistance. Furthermore, we combine measures of selection intensity with the prediction of neoantigens in a patient cohort to identify potential alternative targets for immunotherapy. The outcome is a strategy that exploits the predictability introduced by the primary therapeutic bottleneck to eliminate the remaining tumor cell population. Finally, we illustrate the efficacy of this strategy in the context of several cancer types and empirically identify potential cancer type specific and pan-cancer immunotherapy targets orthogonal to primary, first-line therapies.

#0549 PDZK1 sensitizes TNBC cells to erlotinib via promoting c-Cbl-mediated EGFR degradation and inhibiting EGFR phosphorylation.

J. Zheng, Y. Ma, Z. Fang, Y. Qi;
Capital Medical University, Beijing, China

Background: Triple-negative breast cancer (TNBC) is lack of effective targeted therapies. Epidermal growth factor receptor (EGFR) is a potential therapeutic target for TNBC. However, TNBC is resistant to EGFR-targeted drugs in clinical trials, and the tolerance mechanism remains unclear. This study aimed to elucidate the possible resistance mechanism for TNBC to EGFR-targeted therapy and how sensitize TNBC cells to erlotinib.
Methods: PDZ domain containing 1 (PDZK1) correlated with TNBC development was screened out by bioinformatics analysis and its correlation with resistance to erlotinib was identified by western blotting (WB). Its interaction with EGFR and structural basis were determined by GST-Pull down and coimmunoprecipitation. Its regulation on EGFR signaling activation and expression level were detected by WB in PDZK1 overexpression and knockdown TNBC cells, xenograft tissues and correlation analyses. Correlation was performed by gene set enrichment analysis (GSEA) and immunohistochemistry of tissue microarray followed by Pearson analysis. TNBC-suppressing effects of PDZK1 and its sensitizing effects on erlotinib were investigated using cell viability assay, colony-forming assay, wound healing assay, Matrigel invasion assay and xenograft model in combination with PDZK1 wild type/mutant transfection and rescue experiment.
Results: Here we found that PDZK1 was correlated with TNBC development and its level was downregulated in erlotinib-resistant TNBC cells, suggesting that PDZK1 downregulation was related to erlotinib resistance in TNBC. PDZK1 bound with EGFR. Through the interaction, PDZK1 promoted EGFR degradation by enhancing the binding of EGFR with c-Cbl and inhibited EGFR phosphorylation by hindering EGFR dimerization. PDZK1 was specifically downregulated in TNBC tissues and was correlated with poor prognosis of TNBC. Functional assays *in vitro* and *in vivo* showed that PDZK1 suppressed TNBC development. Restoring EGFR expression and kinase inhibitor treatment reversed the malignancy caused by PDZK1 overexpression and knockdown, respectively. PDZK1 wild type, but not mutant overexpression enhanced the inhibitory effect of erlotinib on EGFR signaling and TNBC malignancy *in vitro* and *in vivo*.
Conclusion: PDZK1 is a significant prognostic factor for TNBC and a potential molecular therapeutic target for TNBC to reverse the tolerance of TNBC cells to erlotinib.

#0550 Identification of isoform switching events linked with esophageal adenocarcinoma patient survival informs novel prognostic and therapeutic targets.

Y. Zhang[1], R. Israel[1], B. Vandenburg[1], S. Barnett[1], J.-J. Riethoven[2], J. L. Clarke[2], M. P. Lee[1], K. Lagisetty[1], J. Lin[1], R. Reddy[1], A. Chang[1], L. A. Kresty[1]; [1]University of Michigan, Ann Arbor, MI, [2]University of Nebraska, Lincoln, NE

Esophageal adenocarcinoma (EAC) represents a growing health problem characterized by rising incidence and poor prognosis. Although it is a cancer with a high mutational burden, it lacks highly prevalent oncogenic drivers that can be therapeutically targeted. Recently, our group characterized isoform switching events, defined by the changing of dominant gene isoforms between conditions, associated with EAC progression and identified 75 switching events comparing Barrett's low-grade dysplasia (BE.LGD) and Barrett's high-grade dysplasia (BE.HGD) patient samples. Herein, we further investigated whether isoform-switching events may offer prognostic or therapeutic value in EAC. Isoform switching analysis was performed using RNA-seq data derived from patient samples between BE.LGD and BE.HGD combined with EAC (BE.HGD + EAC) alone or in combination with *TP53* mutations. Patients were further stratified into tertiles based on isoform expression level followed by survival analysis. Thirty isoforms were significantly ($P \leq 0.05$) linked with all-cause mortality, comparing BE.LGD with BE.HGD + EAC, whereas 20 isoforms were identified when *TP53* mutation status was included. In terms of cancer-specific mortality, 10 isoforms were significantly linked with survival comparing BE.LGD with BE.HGD+EAC. With the inclusion of *TP53* mutation, 16 isoforms were also significantly linked with cancer-specific mortality. Isoform-specific genetic knockdown experiments were designed targeting the top isoforms identified in the analysis, including *TTLL12* and *HM13* isoforms. Knockdown of *TTLL12* and *HM13* isoforms led to significant inhibition of cell viability and migration in two EAC cell lines (OE19 and OE33). Chemotherapeutic agents (Paclitaxel + Carboplatin) further decreased cell viability with synergistic effects observed in both siRNA-treated cell lines suggesting a role for specific isoform switches in therapeutic sensitization. Protein-interaction prediction using STRING and immunoblot analysis suggest different mechanisms leading to the inhibition of cell viability and migration. *TTLL12* is linked with the activation of chaperon-medicated autophagy (LAMP2A and HSC70) and protein translation, whereas *HM13* is linked with unfolded protein response (IRE1α, PERK, and ATF6) and may be linked with immunotherapy outcome. An antigen-dependent cell-mediated cytotoxicity assay is currently underway to investigate whether the knockdown of *HM13* isoforms can sensitize EAC cells to PD-1/PD-L1 immunotherapy agents. Future direction includes using FDA-approved agents to target the two major pathways identified above. In conclusion, isoform switching may provide fresh insight for the identification of prognostic markers and inform new potential therapeutic targets for EAC treatment or prevention.

#0551 Investigation of the antipoliferative effect of the *Xylopia Aethiopica*extract in triple-negative breast cancer cells.

S. Soni, S. Modi, T. Andey;
Massachusetts Col. of Pharmacy & Health Sci., Worcester, MA

Triple-negative breast cancer (TNBC) is the most aggressive subtype of breast cancer and has very limited treatment options. *Xylopia Aethiopica* (XA) is a common spice that is widely used in the regions of central and western Africa. It is known to have various pharmacological properties, one of which is anti-inflammatory activity. The anti-inflammatory effect may portend antiproliferative activity. We hypothesized that the extract of XA will exert antiproliferative activity against TNBC cells. The study aimed to establish the molecular mechanism underlying the antiproliferative activity of XA extract (XAE) against TNBC. The dried fruits of XA were crushed in a mixer and macerated using diethyl ether for 72 h. The macerate was subjected to vacuum and rotary evaporation to remove the organic solvent, and a stock solution was prepared in dimethyl sulfoxide (DMSO). Assessment of the efficacy of XAE was performed using serial dilutions (100 µg/ml, 50 µg/ml, 10 µg/ml, 5 µg/ml, and 1µg/ml) of the XAE stock solution, followed by *in vitro* testing against two TNBC cell lines (MDA-MB-231, and MDA-MB-468 cells). The cytotoxic effect of the XAE was then measured using the resazurin dye assay. XAE resulted in a concentration-dependent cell death in both cell lines. At the highest concentration (100 µg/ml), XAE induced cytotoxic cell death of 89% and 91% in MDAMB231 and MDAMB468 cells, respectively. This was consistent with IC50 values of 32.95 ± 1.32 µg/ml (MDAMB231) and 20.83 ± 1.05 µg/ml (MDAMB468). At the molecular level, western blot analysis of mitogenic markers associated with MAPK oncogenic signaling pathway demonstrated the inhibition of EGFR and AKT protein levels after a 48-h treatment. Acridine orange-ethidium bromide (AO/EB) staining showed a concentration-dependent induction of apoptosis in both cell lines. Flow cytometric analysis was performed to quantify the apoptotic cells. A significant increase of apoptotic cells was observed in treatment groups as compared to control after 72 h. Apoptotic induction was associated with increased p53 protein levels after 48 h treatment compared to control. The study results underscore the anticancer effects of XAE in TNBC cells mediated through induction of apoptosis.

#0552 Non-canonical disulfide isomerases are strongly selective, understudied targets for cancer therapy.

M. E. Law[1], Z. M. Dulloo[1], E. Yaaghubi[2], G. M. Alexandrow[1], B. Forsyth[1], H. Su[3], R. K. Castellano[1], **B. K. Law**[1];
[1]University of Florida, Gainesville, FL, [2]Pacific University, Hillsboro, OR, [3]Smith College, Northampton, MA

A major challenge in cancer therapy is the identification of drug targets that are essential for cancer cells but not non-transformed cells. The Broad Institute's Dependency Map (DepMap) evaluates whether knocking down or knocking out expression of specific genes is "strongly selective" against subsets of cancer cells, in contrast with genes that are "common essential." Of the 22 human Protein Disulfide Isomerases (PDIs), only four, ERp44, TMX1, AGR2, and AGR3, were identified as strongly selective in the DepMap. Importantly, our team previously identified ERp44, AGR2, and AGR3 as targets of bicyclic thiosulfonate compounds termed Disulfide bond Disrupting Agents (DDAs). DDAs exhibit striking anti-cancer activity in xenograft tumor studies. DDA treatment of cancer cells blocks ERp44, AGR2, and AGR3 active site Cys residues, ablating their catalytic activity and binding to client proteins. Evaluation of cancer cell lines predicted to be sensitive to DDAs, based on their AGR2, AGR3, or ERp44 dependence, accurately predicts DDA sensitivity. Cell lines from a variety of tumor types exhibit AGR2, AGR3, or ERp44 dependencies. Our previous work identified HER-family members (i.e., EGFR, HER2, and HER3) and TRAIL receptors (Death Receptors 4 and 5) as important clients of DDA-sensitive PDIs in breast cancer cells, but it was unknown if these observations extend to other tumor types. Initial studies indicate that AGR2 DepMap dependencies are a strong predictor of sensitivity of cancer cells to DDAs, irrespective of their site of origin. It will be important in future studies to determine what the key client proteins for these DDA-sensitive PDIs are and whether they vary across tumor types.

#0553 Assessment of CNTN4 expression and its association with PD-L1 across 18 various cancers using an artificial intelligence-powered immunohistochemistry analyzer.

S. Shin[1], J. Moon[1], S. Cho[1], C.-Y. Ock[1], B.-N. Jeon[2], G. Kim[2], H. Yu[2], M. Cha[2];
[1]Lunit, Seoul, Korea, Republic of, [2]Genome & Company, Sungnam-si, Korea, Republic of

Background: Contactin-4 (CNTN4) has been identified as an inhibitory immune checkpoint protein and mainly expressed on tumor cells. It interacts with APP present in T cells, leading to a reduction in T cell proliferation, activation, and responsiveness to tumors. In this study, we applied artificial intelligence (AI)-powered analyzers to examine the expression of CNTN4 and its association with PD-L1 in various solid tumors.
Methods: The AI-powered immunohistochemistry (IHC) analyzers were developed using pan-cancer whole slide images (WSIs) stained with 18 different IHC types. Pathologists annotated cells and tissues on the WSIs. The universal model was trained by annotations from IHC WSI, which could detect tumor cells with four grade intensities (strong, moderate, weak, and negative) and segment invasive cancer area. Finally, the AI analyzer can count the tumor cells in an invasive cancer area and calculate the ratio based on intensity. The AI analyzer was applied to the pan-cancer tissue microarray dataset (n=795) consisting of 18 cancers to validate the analyzer. The dataset was stained with rabbit monoclonal antibody (clone EPR 8735) and PD-L1 22C3 antibody, respectively. The expression levels of CNTN4 and PD-L1 were calculated with H-score (range 0 to 300) or tumor proportion score (TPS).
Results: When positivity was defined as moderate-to-strong staining intensity in ≥ 30%, 50%, 75%, and 90%, 42.4% (337/795), 25.5% (203/795), 11.4% (91/795), and 5.2% (41/795) of samples were CNTN4 positive, respectively. In case of moderate-to-strong staining in ≥ 50% tumor cells, CNTN4 expression were most frequently observed in hepatocellular carcinoma (63.9%), endometrial carcinoma (50.0%), stomach cancer (43.9%), pancreatic cancer (40.0%), and prostate cancer (35.4%). Notably, 10% of cases with an H-score < 200 (75/757) showed a range of PD-L1 expression (PD-L1 TPS ≥ 1%), while all of the samples with an H-score ≥ 200 (n=38) were PD-L1 TPS <1%.
Conclusions: This study describes the CNTN4 expression levels in various tumors using an AI-powered IHC analyzer. CNTN4 tends to be expressed in opposition to PD-L1, making it a viable immune therapeutic target in cancers that do not conventionally express PD-L1.

#0554 Determining the role of *PROX1* in prostate cancer neuroendocrine trans-differentiation.

S. Raj[1], B. Capaldo[1], J. Bowman[1], M. White[1], X. Moore[1], B. Gryder[2], A. N. Alilin[1], D. Takeda[1], K. Kelly[1];
[1]National Cancer Institute, Bethesda, MD, [2]Case Western Reserve University, Cleveland, OH

Nonbiased mutational screening to identify essential genes and pathways in cancer is a powerful approach for understanding underlying biology as well as the identification of potential therapeutic targets. Epigenetic (EPI) and transcriptional factors (TF) play an important role in the change of phenotype and lineage plasticity from adenocarcinoma to castration resistant prostate cancer (CRPC), double negative (DN) or treatment-induced neuroendocrine prostate cancer (NEPC). When *RB1* loss occurs in combination with *TP53* alterations, stemness and lineage plasticity increase with one consequence being differentiation to a neuroendocrine (NE) lineage. Here, we are identifying and testing the functional role of epigenetic and transcription factors required for the viability of CRPC, DN and NEPC relative to a matrix of genotypic and phenotypic characteristics. We applied CRISPR-CAS9 dropout screens in prostate organoids and cell lines to identify gene/s associated with CRPC, DN and NEPC viability. We successfully CRISPR-engineered LNCaP clones of single (LNCaP-TP53-SKO, LNCaP-RB1-SKO) and double (LNCaP-TP53-RB1-DKO) gene knockouts, which were subsequently characterized for immuno-phenotype and transcriptome. Our dropout screens, targeting all TFs and EPIs, identified 117 TF and 40 EPI genes responsible for the viability of DN, NEPC and LNCaP models. We found known genes such as *FOXA1* and *ASCL1,* as well as novel genes including *PROX1* and *KLF3*, which were validated through guide RNA competition assays. Our results showed PROX1 is essential for cell viability in a DN organoid model, and its expression is associated with increased aggressiveness, indicating *PROX1* has role in stemness/lineage plasticity in treatment resistant adenocarcinoma. RNA-seq analysis following overexpression of *PROX1* in the LNCaP-TP53-RB1 null adenocarcinoma model, with and without enzalutamide, identified pathways enriched for cell proliferation, differentiation, neuronal development, and prostate gland development. In summary, our study has suggested an important role for *PROX1* in the growth and differentiation of poorly differentiated prostate cancer, which may lead to the identification of potential therapeutic targets.

#0555 Role of TRIM31 in the pathogenesis of esophageal adenocarcinoma.

M. Hassan[1], J. Mast[1], A. Ritter[2], S. Ponna[2], N. Awasthi[1], U. von Holzen[1];
[1]Indiana University School of Medicine-South Bend, South Bend, IN, [2]University of Notre Dame, South Bend, IN

Background: Esophageal adenocarcinoma (EAC) is one the deadliest cancers in United States (US) and the only major cancer in the US with increasing incidence. Gastroesophageal reflux disease (GERD) can cause Barrett's esophagus (BE), a columnar metaplasia of the esophagus strongly associated with the development of EAC. GERD leading to BE is a common pre-occurrence in EAC patients, but the mechanism remains obscure. To explore the mechanism and its components, we compared gene expression in BE and EAC cells with normal esophageal cells and found high expression of tripartite motif-containing protein 31 (TRIM31) in BE and EAC compared to normal esophagus (NE) by transcriptomic profiling of RNA extracted from human esophageal tissues. E3 ubiquitin ligase TRIM 31 is a new member of TRIM family and it has been reported to have oncogenic potentials in some cancers. However, its role in EAC pathogenesis is yet to be understood.
Methods: RNA sequencing and transcriptomic profiling were performed on human NE, BE, and EAC epithelial tissue samples. TRIM31 expression in NE cell line (Het-1A) and EAC cell lines (OE19, Flo-1, OE33, SK-GT-2, and OACM5.1C) were identified by Western blot analysis. The Het-1A cell line, after exposure to acidic pH and bile acids, was assessed for variable TRIM31 expression. Cell morphology and viability analyses of NE and EAC cell lines after exposure to acidic pH and bile acids either alone or in combinations were observed by microscopy and WST-1 assay respectively.
Results: Transcriptomic analysis showed that BE and EAC are similar in their differential gene expression with upregulation of the TRIM31 compared to that in NE. Concordant with their columnar phenotype, BE and EAC groups displayed a multitude of differentially expressed genes relative to NE samples; however, less differentially expressed genes were found comparing BE and EAC groups. Western blot demonstrated frequent overexpression of TRIM31 in EAC cell lines with very low expression of TRIM31 in NE epithelial cell line. When NE epithelial cell line Het-1A was exposed to acidic pH as well as bile acids in acidic pH, we saw a change in cell morphology that may correlate with the metaplasia of these cells to more resilient forms, as seen in human BE and EAC. Interestingly, bile acids in acidic pH increased TRIM31 expression in NE cell line Het-1A. Bile acids had a greater effect on decreasing cell viability at high concentrations and that effect is enhanced when bile acids were added in acidic pH. WST-1 cell viability assay revealed that EAC cells were more resistant to bile acids as well as bile acids in acidic pH induced decreased in cell viability compared to that in NE cell line Het-1A. The sustained cell viability of EAC cell lines under these harsh conditions correlates with the upregulation of TRIM31.
Conclusions: Thus, TRIM31 may be an important oncogenic factor in GERD-induced EAC development and may be an innovative therapeutic target and marker for EAC.

#0556 The Idylla™ IDH1-2 Mutation Assay Kit: A tool for mutation detection in *IDH1* and *IDH2* genes.

Bram De Craene[1], Katrien Trappeniers[1], **Ana Marcelino**[1], Lee Robertson[2], Phillippe Taniere[2], Jo Van Dorpe[3], Malaika Van der Linden[3], Maria Arcila[4], Khedoudja Nafa[4], Jochen K. Lennerz[5], Richard Craig Carson[6], Richard D. Ledding[6], Sofie Metsu[1]

[1]Development, Biocartis, Mechelen, Belgium,[2]Molecular pathology diagnostic service, University Hospitals Birmingham, Birmingham, United Kingdom,[3]Department of Pathology, Ghent University Hospital, Ghent, Belgium,[4]Department of Pathology, Memorial Sloan Kettering Cancer Center, New York, NY,[5]Department of Pathology, Center for Integrated Diagnostics, Massachusetts General Hospital/Harvard Medical School, Boston, MA,[6]Histology Laboratory, Benefis Health System, Great Falls, MT

Background: Mutations in the genes encoding isocitrate dehydrogenase *(IDH1* and *IDH2*) are frequently detected in various cancers, including acute myeloid leukemia (~20%) and glioma (up to ~80%). They commonly involve a single amino acid substitution at codon R132 in IDH1, and R140 or R172 in IDH2 and are important for diagnosis and prognosis as well as therapeutic decisions. With advancements in molecular diagnostics and precision therapy, IDH inhibitors such as ivosidenib, vorasidenib and enasidenib are now mainstay in management of patients with a susceptible mutation.
Methods: The Idylla™ IDH1-2 Mutation Assay Kit (RUO) is a fully automated qPCR assay for the qualitative detection of 15 common mutations in IDH1 (R132C/H/G/S/L) and IDH2 (R140Q/L/G/W, R172K/M/G/W/S) at codon level. The assay consists of a ready-for-use Idylla™ DNA Cartridge and an assay specific Idylla™ Vial. It runs on the Idylla™ Platform and covers the entire process from sample to result including specimen processing, real-time PCR amplification, detection, data analysis, and result reporting, within 100 minutes.Five clinical sites in US and Europe participated in an early access program to evaluate performance of the assay and establish a final classification algorithm by testing a total of 241 specimens, including FFPE, human whole blood and bone marrow samples, and extracted DNA from these sample types. Reference results were obtained using a range of established methods with different mutations in scope, such as Sanger sequencing, immunohistochemistry, NGS and qPCR.
Results: Of 241 Cartridges, one invalid result was obtained, while 13 results were flagged as having low DNA input. Compared to available reference methods, overall concordance was 98.3% (235/239), 100% (140/140) and 99.6% (230/231) for IDH1 R132, IDH2 R140 and R172, respectively (see table).
Conclusion: The Idylla™ IDH1-2 Mutation Assay Kit demonstrates a high concordance with established reference methods across a range of different specimen types.

		Reference method(s)			**PPA (%)**	**NPA (%)**	**OPA (%)**
		MUT	**WT**	**Total**			
Idylla™ IDH1-2 Mutation Assay Kit	**IDH1_R132x**	111	3	114	99.1	97.6	98.3
	WT	1	124	125			
	Total	112	127	239			
	IDH2_R140x	10	0	10	100.0	100.0	100.0
	WT	0	130	130			
	Total	10	130	140			
	IDH2_R172x	25	0	25	96.2	100.0	99.6
	WT	1	205	206			
	Total	26	205	231			
Total		148	462	**610**			

#0557 Clofarabine inhibits U87MG glioblastoma cell line proliferation through CD99 signaling pathway.

C. C. W. de Souza[1], R. d. Soares[1], A. M. Lerario[2], S. K. N. Marie[1], **S. M. Oba-Shinjo**[1];
[1]University of Sao Paulo, School of Medicine, Sao Paulo, Brazil, [2]University of Michigan, Ann Arbor, MI

The present work aimed to test the efficacy of clofarabine in glioblastoma (GBM) cells that express high levels of CD99. GBMs are the most malignant with the poorest prognosis among tumors of the central nervous system. Patients have a median survival of 12 to 15 months despite surgical, radio, and chemotherapy. CD99 is a cell surface receptor overexpressed in several types of tumors, including GBMs, justifying the interest of studies in CD99 as a possible therapeutic target. Our group has previously demonstrated that knockout of CD99 in the U87MG GBM cell line promoted a decrease in cell adhesion, migration, and invasion. Clofarabine is a third-line drug used in the treatment of refractory/relapsed childhood acute lymphoblastic leukemia. It is a purine analog that is transported into intracellular space, phosphorylated, and incorporated into DNA chain, inhibiting DNA synthesis and ultimately inducing cell death by apoptosis. The clofarabine effect has also been demonstrated in cells from solid tumors, such as breast, gastric, and bladder. Clofarabine action on the proliferation of Ewing sarcoma cells *in vitro* and *in vivo* was proved to be by direct binding to CD99 and independent of the drug internalization. In addition, clofarabine also had an effect on cells from other tumor types that express CD99. The present work demonstrated the significant action of clofarabine on the high CD99-expressing U87MG cells by inhibiting cell proliferation, adhesion, and migration, and by inducing cell cycle arrest and apoptosis. U87MG cells knocked out for CD99 expression were more resistant to clofarabine action on proliferation. RNAseq analysis of U87MG cells treated with clofarabine and compared to control showed downregulated genes involved in cell cycle regulation and mitosis, while upregulated genes were enriched in extracellular proteins, cell adhesion, locomotion, p53 signaling pathway, and apoptosis. Our data indicates clofarabine as a potential CD99 inhibitor to treat GBM patients.

#0558 Stearoyl-CoA desaturase is a synthetic lethal target in SMAD4-deficient cancers.

A. Lu, S. Fenoglio, H.-J. Wu, M. Zhang, A. Tsai, M. L. D. Ferdinez, L. Grove, S. Liu, E. Wu, A. Choi, S. Throner, S. Meier, Y. Yu, W. Zhang, J. Maxwell, J. N. Andersen, T. Teng, B. B. Haines, Y. P. Chen;
Tango Therapeutics, Boston, MA

Mothers against decapentaplegic homolog 4, or SMAD4, is a member of the SMAD family of transcription factors that mediate TGF-β signal transduction. SMAD4 loss of function mutation or deletion is found in about 30% of PDAC and 15% of COAD and EAC patients, and it is associated with their poor prognosis. Over the past two decades, its tumor suppressor role has been elucidated, and the loss of SMAD4 is sufficient to promote tumorigenesis in multiple GEM models. To identify novel therapeutic vulnerabilities for SMAD4-deficient cancers, a CRISPR dropout screening approach was employed in SMAD4 isogenic PDAC models. We identified stearoyl-CoA desaturase, SCD, as a synthetic lethal target in SMAD4-deficient context. SCD is critical for de novo lipid biogenesis and catalyzes the rate-limiting step in the production of monounsaturated fatty acid. Genetic and pharmacologic studies in vitro confirmed this synthetic lethal relationship. Additionally, drug-anchored CRISPR dropout screening and RNA expression profiling demonstrated that accumulation of saturated fatty acid in response to SCD inhibition drives cytotoxicity in SMAD4-deficient cells. Mouse studies with CRISPR-based knockout of SCD and a well-characterized SCD inhibitor (A939572) demonstrated anti-tumor efficacy in SMAD4-mutant xenograft models. However, compared to genetic KO of SCD the pharmacological inhibitor was less effective at inhibiting tumor proliferation in vivo. Together, these data identify SCD as a selective vulnerability in SMAD4-mutant cancers.

#0559 Investigating DDX3X as a target to improve outcomes in Black and Native American endometrial cancer patients.

J. D. Lausen, D. M. Benbrook;
University of Oklahoma Health Sciences Center, Oklahoma City, OK

Introduction: The goal of this project was to identify and test a new molecular target that will help reduce the worse outcomes of endometrial cancer, especially in Black and Native American patients. Endometrial cancer is rapidly on the rise in the developed world. It has overtaken many other types of cancer in both incidence and mortality. Black populations are disproportionately impacted by endometrial cancer, both in Oklahoma and across the United States. In Oklahoma specifically, Native Americans are the most heavily impacted group.
Methods: Machine learning techniques were used to analyze comprehensive metabolic panel (CMP) data from electronic medical record of patients in the University of Oklahoma (OU) network of hospitals and clinics. This data was broken down by endometrial cancer status, race, and age. Plasma samples of endometrial cancer patients were collected from the OU Health Sciences Center Biobank. These samples were analyzed by mass spectrometry. Endometrial cancer cell lines Ishikawa (low-grade) and ARK-1 and ARK-4 (high grade) were cultured in EMEM. For treating the cells, we used RK-33, a small molecule inhibitor of DDX3X. MTT assays were performed in 96-well plates at increasing concentrations of RK-33 for 48 hours. Western blots were used to determine effect of the drug on cellular DDX3X and yH2AX protein levels.
Results: Machine learning analysis EMR data revealed a difference between races in albumin levels of women with endometrial cancer. Black and Native American patients had lower albumin, which is known to correlate to worse outcomes. IPA analysis of plasma proteomics revealed several proteins that were differentially expressed between races. Among these was DDX3X, the X-linked form of DDX3, a DEAD-box RNA helicase which is involved in DNA damage repair. Patient data indicated that patients with high DDX3X expression tended to have lower survival rates. MTT analysis determined that Ishikawa has a lower IC_{50} than the high-grade cell lines, but all responded. Western blotting confirmed that treatment with RK-33 reduced the amount of DDX3X in the cells and increased y-H2AX, indicating more DNA damage.
Conclusions: This study demonstrates that DDX3X is a valid molecular target in endometrial cancer. The differential expression across race groups indicates that Black and Native Americans may stand to benefit the most from a novel drug targeting this difference. Because DDX3X is involved in DNA damage repair, combining the treatment with a DNA-damaging drug may increase response to the drug as well.

#0560 IGF1 induces the expression of CYR61 in metastatic prostate cancer.

G. L. Ortiz Hernandez[1], M. Walker[1], L. Woods-Burnham[2], R. A. Kittles[2], C. A. Casiano[3], S. Neuhausen[1];
[1]City of Hope National Medical Center, Duarte, CA, [2]Morehouse School of Medicine, Atlanta, GA, [3]Loma Linda University School of Medicine, Loma Linda, CA

The cysteine-rich angiogenic inducer 61 (CYR61) is a member of the cellular communication network (CCN) protein family that can be induced by growth factors. CYR61-specific functions are dependent on cellular context. In prostate cancer (PCa), CYR61 contributes to cell growth and survival through its interactions with extracellular ligands, such as integrins avb3 and a6b4, in the extracellular matrix space. Interestingly, CYR61 contains an insulin-like growth factor-binding protein domain suggesting that it may interact with insulin-like growth factor-I (IGF1). High serum levels of IGF1 are directly linked to PCa development and recently have been studied as a predictor of metastatic disease. Given the important roles that IGF1 and CYR61 play in PCa and their potential interaction, it is critical to investigate their molecular interplay. The correlation between PCa aggressiveness and circulating levels of CYR61 and IGF1 is poorly studied. Our goal was to assess the contribution of CYR61-IGF1 interaction to PCa cell proliferation. Their combined role may explain a proportion of aggressive PCa. This study was designed to characterize the role of IGF1-induced expression of CYR61 in metastatic PCa cellular models and to determine if this interaction contributes to aggressive tumor properties (e.g., proliferation, migration, tumorsphere formation). Using immunoblotting, we demonstrated that CYR61 is upregulated in the metastatic cell line PC3. Furthermore, optimized knockdown of CYR61 using siRNA significantly reduced PC3 cell proliferation, viability, and prostasphere formation. To examine the underlying mechanisms associated with IGF1 signaling, we assessed the activation of either the PI3/Akt and MAPK pathways in PC3 cells with CYR61 silencing. CYR61 siRNA-mediated knockdown decreased activation of the PI3/Akt pathway but did not affect the MAPK pathway. In addition, we found that IGF1 induces protein expression of CYR61 in a time-dependent manner, validated by both immunoblotting and confocal microscopy. In conclusion, these data provided evidence that CYR61 expression is induced by IGF1, and its inhibition decreased the capacity of metastatic PCa cells to proliferate, indicating a potential utilization of CYR61 inhibition in the therapy of metastatic PCa.

#0561 Targeting Y box binding protein 1 (YBX1) in *MYC*-amplified medulloblastoma.

S. Carney[1], J. Hemenway[1], A. Rajendran[1], M. Hathaway[1], E. Nealy[1], C. Bonatto[1], D. Tailor[2], S. Malhotra[2], M. Evans II[1];
[1]Seattle Children's Research Institute, Seattle, WA, [2]Oregon Health & Science University, Portland, OR

Medulloblastoma is the most common malignant pediatric brain tumor. Patients diagnosed with *MYC*-amplified group 3 medulloblastoma (G3 MB) have a devastating prognosis with a 5-year survival rate of <50%. Standard of care (SOC) consists of maximal resection surgery followed by chemoradiotherapy, but these extensive treatments leave patients with neurocognitive and developmental deficits. Therefore, the identification of novel targets that can be used alone or in combination with SOC is of utmost importance. Using a batch-normalized bulk RNA-seq dataset (GSE124814) comprised of 1350 MB samples and 291 normal cerebella, we reveal upregulation of Y-box binding protein 1 (YBX1) in MB compared to normal cerebellum. Further analysis of this dataset and others demonstrates G3 tumors that display high MYC levels also have the highest YBX1 expression. Analysis of ChIP-seq data shows strong binding of MYC to the *YBX1* promoter in G3 MB, concurrent with H3K27ac and H3K4me3 histone modifications. Using a well-established ex vivo model, we demonstrate increased YBX1 expression as normal cerebellar progenitor cells transition to tumorigenic G3 MB stem-like cells. Recent work in leukemia reveals a reciprocal regulation of MYC by YBX1, however, this mechanism is not well established in G3 MB. We utilized an orthogonal pharmacogenetic approach to inhibit YBX1 function and determine its effects on G3 MB tumor biology. Suppression of YBX1 significantly reduced the proliferation and decreased MYC protein expression of G3 MB cells *in vitro*. These findings support a reciprocal MYC-YBX1 axis, which could influence tumor growth *in vivo.* Orthotopic implantation of YBX1 KO G3 MB cells leads to increased animal survival. We next evaluated the therapeutic potential of two recently characterized YBX1 inhibitors which display single agent efficacy *in vitro and in vivo.* YBX1 inhibitors synergized with SOC *in vitro* lowering the IC50 for both chemo and radiotherapy, which could reduce adverse effects experienced by patients. *In silico* molecular docking using PyMOL predicts YBX1 inhibitors interact with amino acids within the cold shock domain of YBX1, likely impairing its ability to bind RNA. We performed formaldehyde RNA immunoprecipitation (fRIP)-sequencing to identify changes in RNA transcript levels following YBX1 pharmacological inhibition. Disruption of YBX1-RNA binding impacts the stability of known oncogenic transcripts which may be required for tumorigenesis. Our findings impart an alluring prospect of targeting YBX1 in combination with standard-of-care, and possibly other compounds to improve patients' outcomes.

#0562 Frequent copy number gain of *MCL1* is a therapeutic target for osteosarcoma.

S. Takagi, R. Katayama;
Japanese Foundation for Cancer Research, Tokyo, Japan

Osteosarcoma (OS) is the most common primary malignant bone tumor that predominantly occurs in children, adolescents, and young adults. The treatment for OS that combines surgery with chemotherapy, which consists of a four-drug combination of adriamycin (DOX), cisplatin (CDDP), high-dose methotrexate (MTX), and ifosfamide, was established in 1970s, and it is still used as a standard therapy. Oncogenic driver mutations and fusion genes common to OS have not been identified, which is one of the reasons for the lack of success in drug development for OS. Herein, to explore the characteristic vulnerability in OS, molecular targeted drugs were screened against OS cell lines and patient-derived cells; obatoclax, a pan-BH3 mimetic, and a concomitant drug that enhances obatoclax-induced apoptosis, OSI906, a dual inhibitor of IGF1R and IR, were found. Fluorescence in situ hybridization (FISH) analysis revealed that copy number gains of *MCL1*, an antiapoptotic Bcl-2 family protein, were observed in 46.3% of formalin-fixed paraffin-embedded (FFPE) specimens from patients with OS (*N* = 41) and in 45.5% of OS cell lines (*N* = 11), thereby causing vulnerability to BH3 mimetics. IHC staining also revealed high expression of Mcl-1 protein in specimens with *MCL1*-amplification in FISH analysis. Pharmacological or genetic inhibition of Mcl-1 induced potent apoptosis in *MCL1*-amplified OS cells, which was enhanced by the co-inhibition with Bcl-xL. Moreover, chromosome 1q21.2-3, where *MCL1* is located, contains several IGF1R/PI3K pathway-related genes, including *PIP5K1A*, *TARS2, OUTD7B*, and *ENSA*, whose copy numbers were also increased in *MCL1*-amplified OS cells, suggesting that 1q21.2-3-amplified OS cells readily activate downstream pathways via IGF1R. IGF signaling activation in 1q21.2-3-amplified OS cells negated the obatoclax-induced apoptosis, which was overcome by OSI906 treatment. Combined obatoclax and OSI906 administration remarkably suppressed *MCL1*-amplified OS tumor growth in the xenograft mouse model and resulted in tumor regression; however, none of the treatments reduced tumor growth of OS without *MCL1* amplification. These results suggest that combining obatoclax with OSI906 could be a potential therapeutic intervention for 1q21.2-3-amplified OS, and that prior stratification of OS based on the 1q21.2-3 amplification status would be important for the success of this combination therapy. Thus, we elucidated the mechanism of action of drugs and their potential as a novel therapeutic strategy for approximately 50% of patients with OS. Moreover, a FISH analysis that can detect copy number gains of *MCL1* in FFPE specimens from patients with OS was established to stratify patients eligible for this therapy.

#0563 Targeting PDE4D reinstates toxic PARP trapping via cAMP-ROS-DNA damage axis and restores the efficacy of standard of care in treatment-refractory ER+ breast cancer.

O. Saatci[1], M. Cetin[1], M. Uner[2], U. M. Tokat[3], I. Chatzistamou[4], E. Montaudon[5], A. Akyol[2], S. Aksoy[6], A. Uner[2], E. Marangoni[5], M. Sajish[4], **O. Sahin**[1];
[1]The Medical University of South Carolina (MUSC), Charleston, SC, [2]Hacettepe University, Ankara, Turkey, [3]Bilkent University, Ankara, Turkey, [4]University of South Carolina, Columbia, SC, [5]Institut Curie, Paris, France, [6]Hacettepe University Cancer Institute, Ankara, Turkey

Endocrine therapies, modulating ER level and/or activity, and the CDK4/6 inhibitors are among the standard-of-care (SOC) therapies used in estrogen receptor-positive (ER+) breast cancer. However, most ER+ breast cancer patients eventually develop resistance to SOC, representing a major clinical challenge that reduces clinical outcome. Therefore, elucidating the common mechanisms of sensitivity and resistance to SOC therapies, and identifying novel actionable targets are urgently needed. Here, we demonstrated that cell death induced by endocrine therapies and CDK4/6 inhibitors involves toxic PARP1 trapping and generation of a functional BRCAness (i.e., *BRCA1/2* deficiency) phenotype, leading to transcriptional blockage. We showed that this is achieved by activation of the cAMP/reactive oxygen species (ROS)/DNA damage axis upon downregulation of phosphodiesterase 4D (PDE4D). Importantly, we identified PDE4D as a novel ER target gene that in turn stimulates ER activity in a feedforward loop in endocrine-responsive models. However, during SOC resistance, an ER-to-EGFR switch induces PDE4D overexpression via c-Jun. Inhibition of PDE4D using BPN14770, the first-in-class PDE4D allosteric inhibitor that has successfully completed Phase II trials in Fragile X syndrome, reinstates PARP1 trapping and BRCAness, leading to drug sensitization in vitro and in vivo. Furthermore, inhibition of EGFR or PARP1 recapitulates the effects of PDE4D targeting and overcomes SOC resistance irrespective of the BRCA1/2 status in cell line models, primary cultures and organoids of endocrine resistant ER+ PDXs. Notably, we demonstrated that high PDE4D mRNA and protein expression is associated with dramatically worse disease-free survival and overall survival in endocrine therapy-treated ER+ breast cancer. Given the availability of potent and non-toxic PDE4D inhibitors, and clinically approved EGFR and PARP1 inhibitors, our findings have great translational potential to improve the clinical outcome of refractory ER+ breast cancers.

#0564 Therapeutic targeting of JAK/STAT signaling and histone acetyltransferase activity in post-myeloproliferative neoplasm secondary AML.

K. Bertulfo[1], K. Debackere[1], H. Miller[1], C. Ma[1], R. Najac[1], A. Ferrando[2], T. Palomero[1];
[1]Columbia University Irving Medical Center, New York, NY, [2]Regeneron Pharmaceuticals Inc., Tarrytown, NY

Post-myeloproliferative neoplasm secondary Acute Myeloid Leukemia (Post-MPN sAML) is an aggressive and lethal hematologic malignancy arising from myeloproliferative neoplasms (MPN). Hyperactivation of JAK/STAT signaling was identified in 50-90% of MPNs - underscoring its role in driving MPN pathogenesis and transformation to post-MPN sAML. Ruxolitinib, a Type-I JAK2 inhibitor approved for the treatment of myelofibrosis, was tested in a Phase II clinical trial in post-MPN sAML. The trial revealed that ruxolitinib improved the quality of life in patients but was not disease-modifying. Thus, there is an urgent need to find synergistic drug combinations capable of complementing the therapeutic activity of JAK2 inhibitors in post-MPN sAML. Here, we demonstrate that combination treatment of ruxolitinib and CBP30, a bromodomain inhibitor of histone acetyltransferases (HAT) CBP and p300, enhances the therapeutic activity of ruxolitinib in post-MPN sAML. Genome-wide CRISPR loss-of-function screens in JAK2-mutated HEL cells determined that knockout of CBP sensitizes leukemic cells to JAK2 inhibitors. Consistently, functional validation through CRISPR/Cas9 demonstrated that genetic deletion of CBP but not of p300 renders HEL cells sensitive to ruxolitinib treatment. Pharmacologic inhibition of JAK/STAT signaling and HAT activity through ruxolitinib and CBP30 treatment in post-MPN sAML lines HEL and SET2 decreases proliferation and induces apoptosis and cell cycle arrest. Mechanistically, the synergism between ruxolitinib and CBP30 elicits a unique transcriptome profile in HEL with significant downregulation of E2F and MYC targets. In addition, epigenetic profiling revealed that the synergism induces global changes in H3K27ac signals with downregulation and upregulation of H3K27ac signals in predicted STAT5/BCL3 and GATA-bounded regions, respectively. Remarkably, combination treatment of ruxolitinib and CBP30 in HEL luciferase NSG mouse xenografts showed significant leukemia regression and decrease in spleen size compared to mice treated with vehicle or single agents. Overall, these results substantiate the potential of targeting JAK/STAT signaling and histone acetyltransferase activity in the treatment of post-MPN sAML.

#0565 PDE7 modulates EMT, cells morphology and mitochondrial cristae in high grade serous ovarian cancer.

L. B. Rangel[1], N. G. Tessarollo[1], I. d. Guimaraes[2], D. Z. dos Santos[1], T. B. Henriques[1], M. L. M. de Souza[1], L. F. Maciel[3], J. A. Almeida[3], T. M. Pimenta[1], J. C. de Souza[1], R. B. Wanzeler[1], B. S. Martins[1], S. S. Butzene[1], J. S. Padilha[1];

[1]Federal Univ. of Espirito Santo, Vitoria, Brazil, [2]National Cancer Institute, Rio de Janeiro, Brazil, [3]State University of the North Fluminense, Campos dos Goytacazes, Brazil

Background: Due to the acquisition of chemoresistant phenotype by epithelial ovarian cancer (EOC) cells and, consequently, disease relapse, the identification of novel therapeutic strategies is urgent. Herein, we targeted phosphodiesterase 7A (PDE7A) in EOC cells, based on data derived from RNA-sequencing assays comparing high-grade serous ovarian carcinoma (HGSOC) and fallopian tube samples.

Methods: To understand the role of PDE inhibition, we evaluated the effects of its inhibitor BRL50481 alone or in combination with paclitaxel (PTX) on untreated A2780 EOC cells and multi-resistant high grade serous ovarian cancer (HGSOC) OVCAR3 cells. To do so, we pursued with the: validation of data obtained by high throughput RNA sequencing assays using qRT-PCR; evaluation of PDE7 expression in normal and EOC cells, as well as in normal Fallopian tube cells by qRT-PCR; immunoblotting; metabolic cell viability (MCV) by MTT assays; cytokine dosage by qRT-PCR and ELISA; scanning electron microscopy; transmission electron microscopy; statistical analysis (GraphPad software).

Results: Drug-sensitive A2780 cells, but not OVCAR3 cells, exhibited lower MCV when treated with the PDE7 inhibitor; however, the combinatory therapy decreased MCV in both cell lines. Of clinical relevance, pre-treatment of A2780 and OVCAR3 with the PDE7 inhibitor BRL50481 followed by PTX lowered its IC_{50} by 10^3- and 625-fold, respectively. While the phosphatidylinositol 3-kinase (PI3K)/protein kinase B(AKT)/mammalian target of rapamycin (mTOR) pathway was inhibited in both cell lines, the pro-apoptotic protein Bcl-2 Associated X-protein (BAX) was overexpressed in A2780 cells only. Analysis of mRNA and protein expression in OVCAR3 pretreated with BRL50481 showed a 2-fold increase in IL-6 cytokine expression. Pre-treatment of OVCAR3 with BRL50481 followed by the combination of BRL50481 and PTX inhibited the expression of vimentin and Octamer-binding transcription factor 4 (OCT4) by 2-fold. BRL50481 promoted changes in EOC cells morphology and mitochondrial cristae.

Conclusions: Altogether, our data led us to postulate that inhibition of PDE7 in EOC cells, specifically in those presenting the chemoresistant phenotype, is a promising strategy to fight this yet highly lethal disease.

#0566 The anticancer effects of polyisoprenylated cysteinyl amide inhibitors involves interaction with the KRAS chaperone calmodulin.

K. Ofosu-Asante, J. M. Lazarte, A. Burra, N. S. Lamango;
Florida A&M University College of Pharmacy & Pharmaceutical Sciences, Tallahassee, FL

Pancreatic cancer is the third leading cause of cancer-related deaths with a 5-year survival rate of less than 10%. Approximately 90% of reported cases are driven by *KRAS* mutations. The mutant *KRAS* acquires its functional localization through interactions with chaperone proteins via its polybasic polyisoprenylated tail. Polyisoprenylated cysteinyl amide inhibitors (PCAIs) mimic this region possibly disrupting the polyisoprenylation-dependent interactions with chaperone proteins. Here, we determine the effect of newly developed PCAIs that were designed to be more water-soluble on cell viability, 3D spheroid invasion, spheroid degeneration and F-actin filaments on MIA PaCa-2 and PANC-1 cells. Of the seven new PCAIs analogs tested, NSL-AB-51 and NSL-AB-45 were the most potent, with EC_{50} values of 2.5 and 5.6 µM against MIA PaCa-2, and 1.7 and 4.5 µM against PANC-1 cells, respectively. At 5 and 10 µM, NSL-AB-51 decreased the invasion area of 3D spheroids by 98 and 99%, respectively. MIA PaCa-2 spheroids degenerated by 61% after 72 h treatment with 10 µM NSL-AB-51. Treatment with 1.0 µM NSL-AB-51 caused cell rounding and reduction of mean cell areas by 69% and F-actin filaments by 96%. Moreover, to identify the pharmacological target of the PCAIs, NSL-AB-45 was coupled to an epoxy-activated Sepharose resin for affinity trapping of PCAIs-interacting proteins. Affinity-analysis of supernatants and detergent membrane extracts from MIA PaCa-2 and PANC-1 cells revealed single Coomassie band of about 17 kDa that was identified as calmodulin by western blotting analysis. The calmodulin-PCAIs affinity interaction was found to be strongest in the presence of calcium and weakest in the presence of EDTA. These findings reveal that calmodulin is the likely target of PCAIs. Since calmodulin is the chaperone protein responsible for KRAS trafficking and localization to the inner surface of the plasma membrane, this finding strongly suggests, at least in part, an anticancer role for the PCAIs that involve disruption of KRAS functions.

#0567 Fisetin sensitizes triple negative breast cancer cells to radiation.

S. Khozooei, S. Veerappan, **M. Toulany**;
University Hospital and Medical Faculty Tubingen, Tubingen, Germany

Triple negative breast cancer (TNBC) represents a highly aggressive subtype, constituting approximately 20% of all breast cancer cases. Y-box binding protein-1 (YB-1) is often overexpressed in various tumor types and has been implicated in conferring resistance to cell death induced by radiotherapy. Fisetin, a flavonoid compound with demonstrated anti-cancer properties, operates in part through inhibiting phosphorylation of YB-1 by p90 ribosomal S6 kinase (RSK). In this study, we investigated the potential synergistic effects of combining fisetin with radiotherapy in TNBC. The activation status of the RSK signaling pathway was assessed in both total cell lysate and subcellular fractions using Western blotting. A standard clonogenic assay was employed to evaluate post-irradiation cell survival. To investigate the frequency of double-strand breaks (DSBs) and chromosomal aberrations, γH2AX foci assay and 3-color fluorescence in situ hybridization analyses were conducted, respectively. The DSB repair pathways targeted by fisetin were examined in cells expressing genomically integrated reporter constructs by quantifying green fluorescence protein expression through flow cytometry. Apoptosis and autophagy were measured using flow cytometric quantification of sub-G1 cells and the assessment of LC3-II protein expression, respectively. Kinase array and phosphoproteomics analyses were carried out to study the potential impact of fisetin on the signaling involved in the DNA damage response (DDR) after irradiation. We demonstrated that fisetin mimics the effects of RSK pharmacological inhibitors in terms of effect on YB-1 phosphorylation. Treatment with fisetin increased frequency of DSB in non-irradiated cells and impaired repair of DSB after irradiation. Fisetin attenuated DSB repair by suppressing the classical non-homologous end-joining and homologous recombination repair pathways. The frequency of chromosomal aberration was enhanced by fisetin treatment. The effect of fisetin on inhibiting DSB repair was partially YB-1 dependent. Phosphoproteomic analysis revealed that fisetin inhibits DDR signaling, which leads to radiosensitization in TNBC cells, as shown in combination with single dose or fractionated doses irradiation. Fisetin neither inhibited DSB repair nor radiosensitized normal human fibroblast HSF7 cells. The radiosensitizing effect of fisetin was not attributed to enhancing apoptosis or modulating autophagy. In summary, combining fisetin with radiotherapy may enhance TNBC radiotherapy outcomes.

-This research was supported by a grant from the German Research Council (DFG,TO 685/2-3).

#0568 Modulation of HER4 isoforms expression in estrogen-stimulated *in vitro* models.

M. Valenti[1], G. F. Bischof[2], J. P. Crown[3], D. M. Collins[1];
[1]Dublin City University, Dublin, Ireland, [2]Puma Biotechnology, Inc.,10880 Wilshire Blvd., Suite 2150, Los Angeles, 90024, CA, [3]St. Vincent's University Hospital, Elm Park, Dublin, Ireland

Introduction HER4, a tyrosine kinase receptor belonging to the Human Epidermal Growth Factor/HER/ErbB-family, has a complex biology that includes four isoforms (JMa-CYT1/2, and JMb-CYT1/2) and tissue specific oncogenic or tumour suppressor roles. In estrogen receptor positive (ER+) breast cancer (BC), HER4 isoforms can either act as a co-regulator of ESR1-mediated gene expression by localising to the nucleus, or activate apoptosis by localising to mitochondria. There is very little known about HER4 function in cutaneous melanoma, despite cutaneous melanoma showing the highest HER4 genomic alteration frequency (17.34%) across different cancers (cBioPortal). Due to the interplay between estrogen signalling and HER4 isoforms in ER+BC, this study investigates the RNA expression of HER4 isoforms along with hormone and nuclear receptors associated with 17β-estradiol stimulation in ER+BC and cutaneous melanoma *in vitro* models.
Material and Methods CAMA1 (ER+BC) and SKMEL24 (cutaneous melanoma) cell lines were serum starved for 4h prior to stimulation with 17β-estradiol (0.5nM, 1nM, 5nM and 10nM). RNA was extracted from cells after 24h using TRIzol, followed by qRT-PCR to assess the expression of HER4 isoforms, the hormone receptors estrogen receptor 1 (ESR1/ER-alpha), estrogen receptor 2 (ESR2/ER-beta), progesterone receptor (PGR/PR), G protein-coupled estrogen receptor 1 (GPER1) and the nuclear receptors retinoic acid receptor alpha (RARA) and retinoid X receptor alpha (RXRA). Cell proliferation and caspase3/7 apoptosis analysis were performed at 24/48/72h in the 17β-estradiol stimulated cells by using the IncuCyte Live Cell Analysis Instrument (Sartorius). SN-38 (150nM) was used as positive control for apoptosis induction. Two-way ANOVA was used for the statistical analysis, $p<0.05$ was significant.
Results The qRT-PCR analysis showed that upon stimulation of CAMA1 with 1nM of 17β-estradiol there is a numerical shift in the CYT-1/CYT-2 ratio towards CYT-2 (not statistically significant, $p>0.05$) and a significant increase in PGR ($p= 0.0027$) and RAR-A ($p= 0.0248$) expression compared to control. CAMA1 stimulated with any concentration of 17β-estradiol showed an increase in proliferation compared to the control. The stimulation of SKMEL24 with 5nM of 17β-estradiol showed an increase in JM-a ($p=0.0075$) and CYT-1 ($p=0.0271$) HER4 isoforms, GPER1 ($p= 0.0286$), and a dose-dependent increase in RARA ($p=0.0011$) compared to control, even in the absence of ESR1, ESR2 and PGR. SKMEL24 stimulated with 17β-estradiol showed a decrease in proliferation compared to control, but no apoptosis induction was found.
Conclusion These findings suggest potential interplay between 17β-estradiol and HER4 isoforms leading to the activation of intracellular pathways that could influence tumour progression/suppression in melanoma. Further studies are needed to clarify the specific receptor interactions and pathways involved.

#0569 Targeting UHRF1's proteasomal destruction as a novel approach for small cell lung cancer treatment.

Yijun Gu, Claudia A. Benavente

University of California, Irvine, Irvine, CA

Small cell lung cancer (SCLC) is an aggressive lung cancer subtype with a five-year survival rate of less than 8% due to rapid tumor growth, early metastasis, and a "cold" immune environment. Genetic alteration at the RB transcriptional corepressor 1 (RB1) is nearly universally present in SCLC patients. However, the therapeutic development was impeded by a lack of druggable oncogenic mutations. Studies in our laboratory identified ubiquitin-like, containing PHD and RING Finger domains 1 (UHRF1) as a critical protein overexpressed in many cancers with RB-pathway inactivation, including SCLC. Despite UHRF1 overexpression correlates with poor survival in SCLC patients, the roles of UHRF1 in SCLC progression remain to be elucidated. We hypothesized that UHRF1 overexpression is essential for SCLC tumor progression and can be targeted through endogenous proteasomal degradation. To define the role of UHRF1 in SCLC, we generated UHRF1 knockout and knockdown human SCLC cell lines. Using these mutants, we assessed changes in proliferation, clonogenicity, migration, and invasion capabilities. We report that UHRF1 overexpression present in human SCLC cell lines contributes to a more aggressive tumor presentation, affecting both tumor growth and metastasis. Besides human cell line models, we also generated genetically engineered mouse models of SCLC to study the role of Uhrf1 in tumor development, especially in an immune environment. Our results indicate that Uhrf1 overexpression promotes SCLC proliferation, angiogenesis, and pro-tumoral macrophage polarization, overall conditioning a tumor microenvironment that supports a more aggressive phenotype. Loss of Uhrf1 in this system results in a robust increase in overall survival. These results strongly support a critical role of UHRF1 in SCLC tumor progression and provide guidance for future SCLC therapeutics targeting UHRF1 or its key downstream effectors. One approach we apply is to utilize UHRF1's endogenous degradative machinery by inhibiting its deubiquitinase USP7. In normal cells, UHRF1 abundance oscillates through cell cycle due to the regulation of ubiquitin machinery. USP7 cleaves ubiquitin marks on UHRF1, antagonizing UHRF1 degradation. We report that same as UHRF1, knocking out USP7 leads to decreased clonogenicity, migration, and invasion in human SCLC cell lines. Highly specific USP7 chemical inhibitors, XL-177A and FT671, were also tested and the same effects as USP7 knockout were observed. Collectively, our findings describe the oncogenic role of UHRF1 in SCLC proliferation, metastasis, and immune recognition and provide a therapeutic strategy of inhibiting USP7 for UHRF1 destruction.

#0570 The role of CD5L in chronic liver disease.

Handan Hong[1], Taojian Tu[1], Lina He[1], Meisam Razaviyayn[2], Sze-Chuan Suan[3], Liyun Yuan[4], Bangyan L. Stiles[1]

[1]Pharmacology and Pharmaceutical Sciences, USC - University of Southern California, Los Angeles, CA,[2]Electrical and Computer Engineering, USC - University of Southern California, Los Angeles, CA,[3]Industrial and Systems Engineering, USC - University of Southern California, Los Angeles, CA,[4]Medicine, USC - University of Southern California, Los Angeles, CA

Macrophage migration inhibitory factor (MIF) is a CD5 molecule like glycoprotein synthesized and secreted by macrophages, also termed CD5L. In liver cancer, serum levels of CD5L has been reported to be higher in steatohepatitis and hepatocellular carcinoma (HCC) patients and proposed to be a serum marker for these conditions. In the liver, steatosis and steatohepatitis is a major comorbid factor for HCC development and associated with poor response to therapy, particularly immune-checkpoint therapy. Here, we assessed the levels of CD5L in plasma samples from 50 advanced HCC patients obtained at baseline prior to initiation of systemic immunotherapy and compared them with that of healthy controls. The data demonstrated a 50% higher plasma CD5L levels in HCC patients vs. healthy donors. Furthermore, CD5L concentrations are higher in patients with higher Child Pugh score. In patients treated with immune checkpoint single or combination therapy, serum CD5L was found to correlate with clinical benefit. To address the role of CD5L and CD5L secreting macrophage in HCC development, we performed in-silico analysis of single cell RNA-seq data and identified Cd5l as a unique gene expressed on liver resident macrophages, the Kupffer cells (KCs). This finding was validated with additional datasets and using two steatosis mouse models representing ALD and NAFLD. Furthermore, our immunofluorescent staining and flow cytometry further confirmed the main source of Cd5l is KCs. In HFD fed mice, we showed that the expression and serum levels of CD5L became more significant with the severity of liver injury, particularly steatotic liver injury. We hypothesize that CD5L may be involved in establish the tumor microenvironment established by steatohepatitis, we performed a free fatty acid (FFA) uptake assay and found that CD5L increased the uptake of FFA in hepatic stellate cells. This ability of CD5L may have contributed to therapy resistance observed in the CD5L high patients who showed reduced clinical benefit.

#0571 CRISPR/Cas9 screening identifies the proteasome subunit PSMC6 as key for the survival of cisplatin-resistant ovarian carcinoma cells.

M. Costantino[1], P. D'arcy[2], L. Mirra[1], C. Corno[1], G. L. Beretta[1], J. Gubat[2], P. Pratesi[1], C. M. Ciniselli[1], P. Verderio[1], S. Linder[3], **P. Perego**[1];
[1]Fondazione IRCCS Istituto Nazionale dei Tumori, Milan, Italy, [2]University of Linkoping, Linkoping, Sweden, [3]Karolinska Institutet, Stockholm, Sweden

Ovarian carcinoma is a disease with poor prognosis, due to delays in diagnosis and the development of drug resistance. Since deregulation of the ubiquitin proteasome system may contribute to the development of drug resistance, the aim of this study was to investigate the interplay between expression of proteasome subunits and cisplatin resistance by utilizing a CRISPR/Cas9 dropout screen. Paired cisplatin-sensitive and -resistant cells (IGROV-1 and IGROV-1/Pt1) were transfected with Cas9 and transduced with gRNAs against proteasome components. Cells were collected at early (day 4) and late (day 21) time exposure and sequenced to identify genes necessary for survival. Various proteasome subunits were found to be essential for the survival of cisplatin-resistant ovarian carcinoma cells, including PSMA5, PSMC6, PSMD7, PSMD12 and PSMD14. Since PSMC6 knockout produced the greatest growth inhibitory effects, it was selected for functional studies utilizing conventional RNA interference. When IGROV-1 and IGROV-1/Pt1 cells were transfected with small interfering RNAs (siRNAs) targeting PSMC6, efficient down-regulation on the mRNA and protein level was observed. Phenotypic analyses of PSMC6 knockdown cells indicated reduced clonogenicity using both 2D and soft agar assays in parental and resistant cells associated with down-regulation of the canonical MAPK pathway. A slight but not significant increase in sensitivity to cisplatin was observed upon PSMC6 silencing in resistant cells using clonogenic assays. Finally, we carried out a pilot study using ovarian carcinoma specimens (n = 134) obtained through the institutional biobank. The samples were representative of the frequency occurrence of the various histological ovarian carcinoma subtypes. We found that PSMC6 expression, evaluated by qRT-PCR, was associated with tumor stage. These findings suggest that PSMC6 is linked to ovarian carcinoma aggressiveness and that PSMC6 targeting may be an interesting therapeutic strategy.

#0572 Identifying potential therapeutic targets through gene expression analysis of peritoneal cavity cells in gastric cancer with peritoneal dissemination.

Y. Hiroshima[1], W. Kawase[1], I. Hashimoto[2], S. Onuma[2], H. Watanabe[2], M. Furuta[2], T. Oshima[2], Y. Miyagi[1];
[1]Kanagawa Cancer Centre Research Institute, Yokohama City, Japan, [2]Kanagawa Cancer Centre, Yokohama City, Japan

Background: Peritoneal dissemination (PD) is the primary mode of metastasis in gastric cancer (GC) and is strongly associated with a poor prognosis. However, the mechanisms underlying PD formation in GC remain largely unknown.Methods and Results: In this study, we collected peritoneal washings from three cytology-positive (CY1) and five cytology-negative (CY0) gastric cancer patients undergoing laparotomy. We performed RNA sequencing on cell components in the peritoneal washings and identified 13 genes that were differentially expressed and upregulated in the CY1 group. Among these genes, we focused on thrombospondin 1 (THBS1) and 2 (THBS2). We evaluated their expression levels in 317 patients with gastric or gastroesophageal junction cancer who underwent primary curative resection at the Kanagawa Cancer Center between January 2002 and December 2012. Patients were stratified into two groups based on the median expression values of these genes, and Kaplan-Meier analysis was conducted. THBS2 expression was found to be inversely associated with disease-free survival (DFS) ($p = 0.041$), peritoneal dissemination-specific DFS ($p = 0.041$), and overall survival (OS) ($p = 0.041$) in the study cohort. In contrast, THBS1 expression did not exhibit a significant association with any of the aforementioned outcomes.Conclusion: Our results suggest that THBS2 expression in gastric cancer tissues may serve as a useful independent prognostic factor for patients, potentially playing a crucial role in the formation of PD.

#0573 SLC22A17 as a promising target for triple-negative breast cancer.

Ajaikumar B. Kunnumakkara, Krishan Kumar Thakur

Biosciences and Bioengineering, Indian Institute of Technology Guwahati, Guwahati, India

Introduction: Triple-negative breast cancer (TNBC) represents a highly aggressive subtype of breast cancer, accounting for approximately 15% of all cases of invasive breast cancer globally. The absence of a well-defined cell membrane receptor has significantly limited the therapeutic options available for treating this malignancy. Consequently, there is a compelling need to explore novel receptors that could potentially revolutionize the treatment strategies employed for TNBC. Recent scientific research has unveiled SLC22A17, a cell surface receptor known for its involvement in iron transport, as a substantial contributor to the development of various cancer types. Thus, the primary objective of this study is to comprehensively evaluate the significance of SLC22A17 and its potential as a therapeutic target in TNBC.
Experimental Procedures: In this study, we meticulously examined the expression patterns of SLC22A17 across distinct subtypes of breast cancer utilizing immunohistochemistry. Computational tools were employed to delve into the role of SLC22A17 within TNBC datasets. To assess the impact of SLC22A17 on TNBC, we employed various methods, including siRNA-mediated silencing, to investigate its role in cell proliferation, apoptosis, epithelial-mesenchymal transition (EMT), and migration. Additionally, we conducted western blot analyses to assess the expression levels of SLC22A17 and cellular signaling molecules, such as Akt/mTOR and JAK/STAT, within the context of TNBC cells.
Results: Our analysis revealed a significant upregulation of SLC22A17 in both TNBC tissues and cell lines, establishing a direct correlation with patient survival outcomes. Silencing the expression of SLC22A17 resulted in reduced cell proliferation, migration, EMT, increased apoptosis, and enhanced autophagy. These effects were accompanied by the inhibition of Akt/mTOR and STAT3 signaling pathways. Moreover, we observed the involvement of the inflammatory cytokine TNF-α, which induced the expression of SLC22A17 in TNBC cell lines and governed various hallmark features of TNBC. Notably, the suppression of SLC22A17 mitigated these processes.
Conclusion: In conclusion, this investigation suggests the pivotal role played by SLC22A17 in TNBC and posits its potential as a novel and promising therapeutic target for the management of this formidable disease.

#0574 Adipocyte-derived FABP4 promotes non-alcoholic fatty liver disease (NAFLD)-induced hepatocellular carcinoma by driving ITGB1-mediated β-catenin activation.

C. O. Leung, S. Gurung, K. Chung, S. Chan, T. Lee;
The Hong Kong Polytechnic University, Hong Kong, Hong Kong

Nonalcoholic fatty liver disease (NAFLD)-induced hepatocellular carcinoma (HCC) is an emerging malignancy in the developed countries. However, the mechanisms contributing to its formation remain largely unknown. Given the role of cancer stem cells (CSCs) in tumor initiation and therapeutic resistance, we hypothesize that adipocytes, one of the key cellular factors within the tumor microenvironment of NAFLD-induced HCC, may play a critical role in HCC development and drug resistance by regulating liver CSCs. Using a co-culture system in which differentiated adipocytes were grown with HCC cells, we found that adipocytes enhanced the self-renewal ability of HCC cells through indirect paracrine secretion. HCC cells pre-incubated with conditioned medium from adipocytes showed enhanced liver CSC properties including self-renewal, tumorgenicity, invasiveness and chemo-resistance to doxorubicin and sorafenib. Secretome profiles showed that FABP4 was preferentially secreted by adipocytes and its level was further augmented when co-cultured with HCC cells. Concurrently, recombinant FABP4 enhanced CSC properties of HCC cells. Drastic delay in the onset of tumor development in FABP4$^{-/-}$ mice upon DEN-injected and high fat diet-induced mouse models of NAFLD-HCC. Mass spectrometry analysis revealed ITGB1 as a direct binding partner of FABP4 for the first time. This data, together with the observation of significant downregulation of the Wnt/β-catenin pathway in tumors of FABP4$^{-/-}$ mice, revealed the role of adipocyte-derived FABP4 promotes liver CSC function by activating the PI3K/Akt/β-catenin signaling pathway via ITGB1. Overexpression of ITGB1 led to poorer survival of HCC patients with NAFLD as a risk factor. The development of a monoclonal neutralizing antibody against FABP4 successfully blocked FABP4-driven CSC functions, implicating the targetability of FABP4 for the treatment of NAFLD-induced HCC.

#0575 Identification of SORL1 as a key regulator of chemoresistance in ovarian cancer.

M. Mansolf, Z. Jian, F. Bi, T. M. P. Hartwich, Y. Yang-Hartwich;
Yale School of Medicine, New Haven, CT

This study aimed to understand the molecular mechanism of platinum chemoresistance in recurrent ovarian tumors with a focus on the SORL1-regulated pathways. SORL1 is an intracellular sorting receptor that binds to HER2 in breast cancer; this promotes HER2 recycling to the cell surface, which ultimately impacts the progression and treatment of breast cancer. The role of SORL1 in ovarian cancer has not been extensively studied.
Method: RNA was extracted from 15 pairs of matched primary and recurrent high grade serous ovarian tumors collected from patients. Human transcriptomic microarray was used to identify the differentially expressed genes. The identified genes were validated by RT-QPCR and western blot in five ovarian cancer cell lines that were treated or untreated with carboplatin. To study the effects of identified target gene SORL1, overexpression and knockdown in ovarian cancer cell lines were established using SORL1 plasmid and shRNA. Proliferation and response to carboplatin were analyzed using celltiter Glo and caspase-3/7 activity assays respectively. EGFR and FGFR4 were identified as the interacting proteins of SORL1 in ovarian cancer cells through FGF1 and EGF1 treatment and co-immunoprecipitation. A proximity ligation assay was performed to validate their interactions. Finally, a xenograft mouse model was used to compare the tumor forming abilities and the response to carboplatin of SORL1-knockdown ovarian cancer cells and the control cancer cells *in vivo*. Protein expression of SORL1, EGFR, and FGFR4 in the collected tumors was determined via western blot.
Result: Transcriptomic analysis of matched human primary and recurrent ovarian tumors identified SORL1 as an upregulated gene in recurrent tumors compared to primary samples. SORL1 expression was also upregulated in ovarian cancer cells surviving carboplatin treatment. Proliferation assays demonstrated that SORL1-overexpressing and knockdown cell lines had increased and inhibited proliferative capabilities respectively. Caspase-3 activity assays showed that SORL1-overexpressing and knockdown cell lines had reduced and increased sensitivity to carboplatin treatment respectively. SORL1 was found to bind to and promote the expression of EGFR and FGFR4. When injected subcutaneously into nude mice, SORL1-knockdown cells had reduced tumor forming capabilities and increased sensitivity to carboplatin. SORL1-knockdown caused the tumors to express lower levels of SORL1, EGFR, and FGFR4 proteins in comparison with the control tumors.
Conclusion: This study demonstrates that SORL1 regulates the EGFR and FGF4 pathways to promote the growth and carboplatin resistance of ovarian cancer cells. Targeting this pathway has potential to aid in the treatment of platinum-resistant ovarian cancer.

#0576 The pan-quadruplex drug QN-302 selectively down-regulates key pathway targets in pancreatic cancer cells that are up-regulated in human pancreatic cancer.

Stephen Neidle[1], Ahmed A. Ahmed[1], Tariq Arshad[2], Tariq Arshad[2]

[1]University College London (UCL), London, United Kingdom,[2]Qualigen Therapeutics Inc, Carlsbad, CA

We have previously disclosed (Ahmed et al, ACS Med Chem Lett, 2020) a novel small molecule G-quadruplex binding compound, QN-302, that is highly potent in pancreatic ductal adenocarcinoma (PDAC) cells and in several in vivo models for this disease. QN-302 was invented at University College London UK and has been subsequently developed by Qualigen Therapeutics Inc. It was cleared by the FDA in August 2023 for Phase 1a clinical trials in USA and is currently under clinical evaluation. RNA-seq whole-genome transcriptome analysis revealed that QN-302 selectively targets G-quadruplexes in cancer-related genes, notably by forming stable G-quadruplex complexes with appropriate promoter sequences. This results in the transcriptional down regulation of affected genes, which map to for example, the hedgehog, axon guidance, WNT/β-catenin and P38 signal transduction pathways. In many instances individual expression changes are modest, though statistically significant: cumulatively, they affect whole pathways. We have revisited the RNA-seq data for QN-302 in PDAC MIA-PACA2 cells (GSE151741 at https://www.ncbi.nlm.nih.gov/geo/) in detail and now identify a small group of eleven down-regulated genes, all with >3-fold expression changes. Interestingly all these genes and their genes products have been previously identified as playing a role in human PDAC (they also have varying roles in other cancer types). Some have been validated as anticancer targets. 10/11 of these genes (https://www.proteinatlas.org/) have been previously reported as being over-expressed in significant fractions of large (>150) groups of human cancer patients from The Cancer Genome Atlas (TCGA) project. Cellular transcriptome data on these eleven genes is presented here, which together with earlier reports on them, supports the designation of QN-302 as a pan-G-quadruplex agent targeting a group of major genes involved in PDAC maintenance and metastasis. Data from a xenograft model for pancreatic cancer is also available for four of these genes, which concurs with the cellular data. We suggest that the identification of these 11 genes may also provide a basis for biomarker selection and possible patient stratification based on transcriptome data.

#0577 Deciphering the mechanism of the menin-MLL complex dependency in HCC.

M. M. Dzama, P. C. Kuhlers, J. R. Raab;
UNC Chapel Hill, Chapel Hill, NC

Liver cancer is the third leading cause of cancer-related death worldwide, with hepatocellular carcinoma (HCC) being the most common primary liver cancer (~90%). The 5-year survival rate of patients with advanced HCC is ~18% due to the late prognosis and the moderate clinical benefit of available systemic therapy options. Mutations in chromatin regulators were detected in ~50% of liver cancer. Since many chromatin regulators have been shown a dependency in various cancer types and can modulate therapy response, we focused on identifying new therapeutic targets of HCC among epigenetic modifiers and evaluating them as potential targets for future drug development. We constructed a CRISPR library of 6000 gRNAs targeting 737 genes involved in chromatin-mediated gene regulation. Using the epigenome-focused CRISPR/Cas9 screening in two-dimensional and three-dimensional settings in multiple liver cancer cell lines (HepG2, HLF, PLC/PRF5), we identified a list of epigenetic regulators as potential new targets in HCC. Two of them, *MEN1* and *ASH2L*, are core subunits of the menin-MLL complex mediating H3K4 trimethylation (me3). We validated dependencies of HCC on *MEN1* and *ASH2L* by performing a negative selection CRISPR/Cas9 competitive growth assay in HLF and PLC/PRF5 cell lines. Moreover, treatment of HCC cell lines (HLF, PLC/PRF5, HepG2) with recently developed menin inhibitor SNDX-5613 (revumenib) revealed a dose-dependent reduction in cell proliferation. To determine transcriptional changes associated with disruption of the menin-MLL complex, we performed RNA sequencing of HLF and PLC/PRF5 cells following either inhibition with 5μM SNDX-5613 for 4 days or knockout of the *MEN1* or *ASH2L* gene. We observed the upregulation of KRAS and the oncogenic signature of TGFβ signaling pathways in all menin-MLL complex disrupting conditions. We did not detect global changes in H3K4me3 levels upon the menin inhibition or *MEN1* or *ASH2L* knockouts assessed by immunoblotting. To explore the mechanism of the antiproliferative effect of the menin inhibition on HCC further, we evaluated changes in the binding of menin to chromatin and H3K4me3 levels in HCC cells by performing CUT&RUN following treatment of HLF cells with 5μM SNDX-5613 for 4 days. Menin inhibition led to a drastic removal of menin from the chromatin, while H3K4me3 levels were only mildly decreased. We identified 8765 genes near promoter regions with menin binding and H3K4me3 mark, of which 1952 genes were near regions with simultaneous loss of menin and decreased H3K4me3 levels upon menin inhibition. Integration of our genomics data revealed a list of 30 genes, which are downregulated upon menin inhibition in both HLF and PLC/PRF5 cells (FC≥1.5) and the direct targets of the menin-MLL complex in HLF cells, suggesting their potential role in HCC cell survival. Altogether, we anticipate that menin and ASH2L serve as promising targets and represent an appealing therapeutic strategy for HCC treatment.

EXPERIMENTAL AND MOLECULAR THERAPEUTICS: Immunotherapy
Poster Session

#0578 Prediction of PD-1 treatment outcome in mismatch repair deficient metastatic colorectal cancer using a multi-omic approach.

B. Saberzadeh-Ardestani[1], O. E. Emiloju[1], R. P. Graham[1], J. T. Lewis[1], C. W. Abbott[2], S. M. Boyle[2], F. A. Sinicrope[1];
[1]Mayo Clinic, Rochester, MN, [2]Personalis, Inc., Fremont, CA

Background: Immune checkpoint inhibitors (ICIs) have revolutionized the treatment of patients with deficient DNA mismatch repair (d-MMR) cancers, yet less than half of patients with metastatic colorectal cancer (mCRC) receive clinical benefit. We analyzed heterogeneity within d-MMR tumors using a multi-omics approach inclusive of percent unstable microsatellite loci (MS).
Methods: We studied consecutive patients with d-MMR mCRC with available primary tumors (N=32) that were treated with an anti-PD-1 antibody at Mayo Clinic (2015-2022). Tumors were profiled using a whole exome and transcriptome platform (ImmunoID NeXT®). MSIsensor was used to calculate percent unstable microsatellite loci from whole exome sequencing data. CIBERSORT and ssGSEA were used to analyze immune gene expression in relationship to percent unstable microsatellite loci. An immune checkpoint gene expression signature was calculated as the mean expression of CD274, CTLA-4, HAVCR2, LAG-3, PDCD1, PDCD1LG2, TIGIT. Aforementioned variables were analyzed in relationship to objective tumor response (RECIST version 1.1). A Cox proportional hazards model was fit to predict progression-free survival (PFS).
Results: Among 32 patients with d-MMR mCRC treated with PD-1 blockade, 16 (50%) received first-line anti-PD-1 therapy; others had $\geq$ 1 prior chemotherapy regimen. Eighteen (56.3%) tumors harbored *BRAF*^{V600E}, 4 (12.5%) had mutant *KRAS*, and median PFS was 24.6 months (95% CI: 8.4, NR) with 18 events. Neither tumor mutation burden (TMB) nor PD-L1 mRNA expression predicted PFS. Median percent unstable MS loci was 14.38 (IQR: 2.6-23.2). Patients whose tumors had higher percent unstable MS loci had significantly better PFS (Q2-4 vs Q1; HR: 0.22, 95%CI: 0.06, 0.62; P=0.003), and were associated with increased objective response (P=0.049). Tumors with higher unstable loci also had higher neoantigen clonality (R= 0.64; P= 0.0003) and increased M0 (resting) macrophages (P=0.02). Nonresponders (vs responders) to PD-1 blockade had an increased immune checkpoint expression signature (P= 0.005).
Conclusion: A higher percentage of unstable microsatellite loci, associated with higher neoantigen clonality and resting macrophages, was predictive of anti-PD-1 efficacy. Furthermore, an immune checkpoint gene expression signature was associated with objective response.

#0579 Assessing the longitudinal efficacy of anti-PD-1 therapy in a murine non-small cell lung cancer model using single-cell and spatial transcriptomics.

N. F. Leon, O. A. Davalos, D. Baliu-Rodriguez, D. K. Murugesh, A. Sebastian, N. R. Hum;
Lawrence Livermore National Laboratory, Livermore, CA

Lung cancer has a high incidence rate and is the main cause of cancer-related deaths with 127,070 fatalities expected in the U.S. this year. Non-small cell lung cancer (NSCLC) accounts for an estimated 85% of all lung cancer cases and is typically diagnosed at an advanced disease stage, where outcomes are often poor and treatment options are limited. Targeted therapies are only available to a minority of NSCLC patients with identifiable tumor-driving mutations. Anti-programmed cell death protein 1 (anti-PD-1) immunotherapy has become a first-line treatment strategy for patients without tumor-driving gene mutations. However, only 15-20% of NSCLC patients exhibit a positive response to anti-PD-1 therapy. Moreover, patients who initially respond to anti-PD-1 therapy still face the risk of primary or acquired resistance, potentially leading to cancer progression. This study leverages a murine lung cancer cell line representative of NSCLC isolated from a genetically engineered mouse model expressing $Kras^{G12D}$ and $P53^{-/flox}$ oncogenic mutations in club cells, employing a cell type-specific promoter (Scgb1a1). After successfully establishing the oncogenic cell line, the cells were subcutaneously injected into immunocompetent C57BL/6 mice and subjected to anti-PD-1 therapy for 3 weeks post-injection. Tumor growth curves revealed a significant size reduction in anti-PD-1-treated tumors when compared to the IgG isotype control group, as confirmed by a paired t-test analysis ($p < 0.045$). To evaluate the longitudinal dynamics of the tumor microenvironment, single-cell sequencing, and spatial transcriptomics were performed throughout effective anti-PD-1 treatment and following tumor relapse. Samples were collected at 2 time points during anti-PD-1 treatment, specifically at 1 and 3 weeks, as well as 3 weeks after the completion of the anti-PD-1 treatment. Subsequently, these samples underwent single-cell RNA sequencing and spatial transcriptomics using the 10x Genomics platform. Single-cell sequencing revealed modulations in immune recruitment throughout the treatment while relapsed tumors display elevated levels of myeloid gene expression and a shift to a highly fibrotic tumor phenotype post-anti-PD-1 therapy. These findings suggest that the established oncogenic cell line exhibits initial responsiveness to anti-PD-1 therapy *in vivo* before undergoing major changes within the tumor microenvironment. This study highlights the relevance and translational potential of our oncogenic cell line in advancing our understanding of NSCLC and its response to anti-PD-1 therapy. *This work was performed under the auspices of the U.S. Department of Energy by Lawrence Livermore National Laboratory under Contract DE-AC52-07NA27344. LLNL-ABS-857319.

#0580 APP as a novel immune checkpoint: Expression in T cells and its clinical implications for immuno-oncology drug refractory.

M. Cha, **B.-N. Jeon**, G. Kim, A. Jeong, S.-M. Park, K. Park, H. Park;
Genome & Company, Sungnam-si, Gyeonggi-do, Korea, Republic of

Amyloid precursor protein (APP) is a type I transmembrane protein expressed in various cell types and tissues. We previously confirmed that APP expressed in T cells is a binding partner protein of a novel immune checkpoint contactin 4 (CNTN4), and APP is a central molecule for conveying the immunosuppressive signal of CNTN4 to T cells. We further profiled an expression of APP in tumor-infiltrating T cells from tumors of NSCLC patients who received anti-PD-1 as a neoadjuvant treatment combined with chemotherapy using single-cell RNA analysis. As a result, the proportion of APP-expressing $CD4^+$ T_{eff} or $CD8^+$ T_{eff} cells was higher in stable disease (SD) patients than in partial response (PR) patients. In contrast, we observed higher PDCD1-expressing $CD4^+$ $T_{naïve}$ and $CD4^+$ T_{eff} cell proportions in PR patients than in SD patients. When we performed a Differential Expression Gene analysis between the PR and SD patients within T_{eff} cells, we observed that the PR patients' $CD8^+$ T_{eff} cells manifested a higher *IFNG* and *PDCD1,* while the SD patients' $CD8^+$ T_{eff} cells predominantly exhibited elevated APP levels. Subsequent pathway analysis also suggested a negative relationship between immune-related pathways and APP expression in $CD8^+$ T_{eff} cells. Such findings imply that the predominant presence of APP in T cells is associated with I/O refractory. From a biological view, we demonstrated increased APP expression in T cells by stimulation with an anti-CD3 antibody or antigen-presenting cell. We also identified that upon stimulation with an anti-CD3 antibody, transcription factors for T-cell activation bind to the proximal promoter of *APP* and increase its expression. Furthermore, it was confirmed that APP in T cells not only increases its expression upon anti-CD3 antibody stimulation but also translocates from the cytoplasm to the membrane through the Golgi apparatus. When anti-CD3 antibody stimulation of T cells persists, the membrane expression of APP increases for 14 to 24 h, then gradually decreases when the stimulation disappears and becomes the same as before stimulation at 48 h. T cells differentiate into various subsets and play an essential role in adaptive immunological responses to foreign substances. In particular, $CD4^+$ (helper) T cells differentiate into different T-cell subsets, such as Th1, Th2, Th17, Th19, Th22, Tfh, and Treg, to govern the overall immune response by producing cytokines that can recruit other cells of the immune system. So, we investigated whether APP is expressed on T cell subsets including naïve, effector, memory, and exhausted T-cells. We identified that APP is expressed in various $CD4^+$ and $CD8^+$ T cell subsets upon stimulation with anti-CD3 antibody. Taken together, our results suggest that APP is expressed on multiple functional T cells and that increased expression of APP on T cells in TIL may increase resistance to immunotherapy.

#0581 Identification of potential biomarkers of response to RASMULTI(ON) plus anti-PD-1 combination in preclinical PDAC models.

L. Seu, M. Menard, J. Lee, C. Chow, C. Blaj, M. Moreno Ayala, N. Shifrin, A. Salmon, S. Ganesh, P. Wig, A. Kumamoto, P. Soto-Perez, T. Taavili, V. Morton, J. W. Evans, J. A. M. Smith, E. Quintana;
Revolution Medicines, Inc., Redwood City, CA

Mutant KRAS is present in more than 80% pancreatic cancer, promotes cancer cell survival, and protects cancer cells from immune recognition and attack. We have shown that inhibitors of the active state of RAS (RAS(ON)) promote cancer neoantigen recognition and synergize with immunotherapy in preclinical immunogenic models. [1] We evaluated the impact of RMC-6236, an investigational RAS^{MULTI}(ON) inhibitor on anti-tumor activity and tumor microenvironment (TME) remodeling in two congenic $KRAS^{G12D/+}$ GEMM-derived PDAC models resistant to anti-PD-1 therapy - KPCY clone 2 (6694c2) and clone 3 (2838c3), developed by Ben Stanger at UPenn. [2] Daily oral administration of RMC-6236 drove tumor regressions in KPCY clone 3, leading to 10% durable complete responses (CRs). In combination with anti-PD-1, 40% of durable CRs were achieved. However, RMC-6236 only drove tumor growth inhibition in KPCY clone 2, and no combination benefit with anti-PD-1. We conducted preclinical biomarker analyses in the TME and periphery to explore differences in response to RMC-6236 alone and in combination with anti-PD-1 in these models. Assessment of baseline predictive biomarkers in tumors elucidated that the KPCY clone 3 cells developed tumors with lower suppressive myeloid cells (gMDSCs) and higher CD8+ T cell infiltration compared to those derived from KPCY clone 2 cells. IHC analyses showed that T cells in clone 3 were in the tumor core, while CD8+ T cells in clone 2 were at the tumor border (the latter frequently observed in PDAC patients). RMC-6236 induced transformation of the TME in favor of anti-tumor immunity in only the KPCY clone 3 - with decreased immunosuppressive gMDSCs, and increased T cells. Limited modulation of the TME was observed in the KPCY clone 2 cells-derived tumors, and gMDSC levels significantly higher than those in baseline tumors of KPCY clone 3. Peripheral immunophenotyping analyses revealed that baseline peripheral suppressive myeloid cells (mMDSCs) were significantly higher in mice harboring tumors originated from KPCY clone 2 cells, suggestive of a more systemic immunosuppressive status. Studies are ongoing to assess additional peripheral immune signatures of preclinical activity of RMC-6236 in combination with anti-PD-1. Taken together, baseline tumor levels of suppressive myeloid cells (gMDSCs) were shown to be a negative predictive biomarker for treatment outcome to RMC-6236 +/- anti-PD-1 in KRAS mutant preclinical PDAC models. Peripheral mMDSCs were shown to be higher in the mice with tumors from the PDAC model not sensitive to the combination of RMC-6236 with anti-PD-1, suggesting that it could be predictive of poor outcome for this combination. These studies in immune-competent models of RAS mutant PDAC allow us to generate tumor and blood-based biomarkers that may predict outcomes to RAS(ON) inhibitor combinations in the clinic. 1 Menard et al. AACR 2023 2 Li et al. Immunity 2018

#0582 Oncogenic *PIK3CA* fortifies immune determinants in vascular cancers.

D. Lee[1], E. Kozurek[2], M. Abdullah[1], R. Li[1], E. B. Dickerson[2], **J. Kim**[1];
[1]University of Florida, Gainesville, FL, [2]University of Minnesota, St Paul, MN

Angiosarcomas are a group of vascular cancers that form malignant blood vessels. These malignancies are seemingly inflamed primarily due to their pathognomonic nature, which consists of irregular endothelium and tortuous blood channels. The malignant vascular spaces host a variety of blood and immune components, where a controlled scavenging system is necessary for tumor maintenance. Oncogenes may convey molecular signals to foster the tumor immune niche, and *PIK3CA* mutations that induce continuous activation of the PI3K pathway occur in a subset of angiosarcomas. Despite the undoubtedly oncogenic properties of *PIK3CA* mutations, the mechanistic role of these mutations - particularly the potential for controlling the hemato-endothelial system in angiosarcomas - remains undetermined. In this study, we demonstrate the functional consequences of oncogenic *PIK3CA* and its molecular properties in angiosarcoma cells. We created isogenic cell clones from two angiosarcoma cell lines engineered to harbor hotspot mutations in *PIK3CA* using CRISPR/Cas9: two homozygous *PIK3CA* H1047R cell clones (C8 and C35) and one wild-type (WT) clone were generated from DHSA-1426 angiosarcoma cells; and one homozygous mutant clone was created from COSB cells. We found that *PIK3CA* mutant cells constitutively activated the PI3K/AKT/mTOR pathway at a greater level than that of WT cells. Bulk- and single cell(sc)-RNA-seq data revealed that mutant cells enriched gene sets associated with PI3K signaling and other oncogenic pathways including KRAS, MAPK, and TGF-beta. Also, mutant cells significantly increased cytokines regulating immune cell migration and chemotaxis such as IL-8 and MCP-1. In addition to the common features, we identified functional and molecular divergence between mutant clones. Noticeable changes in cellular morphology, growth kinetics, and tube-forming capacity were observed between two mutant clones. C35 mutant cells were more sensitive to both pan-PI3K and PI3K-alpha specific inhibitor, and DNA damage was greater than in the C8 clone. C35 cells enhanced activation of IL-6/STAT3 signaling compared to C8, despite the increment of the aforementioned immune cytokines in both mutants. Moreover, our comprehensive analysis of bulk- and sc-RNA-seq, ATAC-seq, and metabolomics data identified molecular signatures associated with metabolic vulnerabilities of C35 cells. In summary, we demonstrate that oncogenic *PIK3CA* perpetuates PI3K signaling activation and reinforces a supply for immune signaling. Furthermore, our data suggest that *PIK3CA* mutations contribute to establishing cellular heterogeneity that reveals a spectrum of vascular, immunogenic, and metabolic activities. Our ongoing work involves developing an experimental model of angiosarcoma using induced pluripotent stem cells to examine if oncogenic *PIK3CA* controls immune determinants during malignant endothelial transformation.

#0583 Spatiotemporal analyses of longitudinal specimens reveal mechanisms of response and resistance to immune checkpoint blockade in metastatic melanoma.

G. Zhang[1], L. Coussens[2], M. Herlyn[3], K. T. Flaherty[4], G. Boland[4], G. Mills[2];
[1]The University of Hong Kong, Hong Kong, China, [2]Knight Cancer Institute, Portland, OR, [3]The Wistar Institute, Philadelphia, PA, [4]Massachusetts General Hospital, Boston, MA

Although durable responses to immune checkpoint blockade (ICB) therapies exhibit by a subgroup of patients with metastatic melanoma, most of patients have no response or develop to acquired resistance to ICB therapies within few years. Molecular mechanisms of primary and acquired resistance to ICB therapies are still elusive, which warrants further elucidation. Here, we used a holistic approach to profile 35 longitudinal tumor specimens at pre-, on-, and post-treatment time points which were derived from 7 patients (3 responders and 4 non-responders) with metastatic melanoma who progressed on sequential ICB therapies, including anti-PD-1 and anti-CTLA-4 therapies. We integrated analyses of RNA sequencing, Whole-exome Sequencing (WES), NanoString nCounter vantage 3D, Cyclic Immunofluorescence (Cyc-IF), NanoString Digital Spatial Profiling (DSP) and Multiplex Immunohistochemistry (mIHC) data of these longitudinal tumor specimens to elucidate evolutionary trajectories that occurred in both the tumor and the tumor immune microenvironment (TiME) that may have orchestrated response and resistance to ICB therapies. Simultaneous analyses of genomic, transcriptomic and proteomic data identified the re-activation of MAPK-RAS as well as PI3K pathway upon or after ICB therapies, which may elucidate the mechanism of resistance to ICB therapies. Spatially-resolved, image-based immune monitoring analysis at single cell resolution revealed that the activation status of T cell markers and T-cell checkpoint is conversely associated with potential mechanism of resistance to ICB therapies. In summary, integrated analyses of muti-oics and spatially image-based data from longitudinal tumor specimens allow us not only to reveal the dynamic co-revolution of both tumor and immune cells in TiME following sequential ICB therapies but also to provide a comprehensive perspective to molecular mechanisms of response and resistance to ICB therapies in patients with metastatic melanoma.

#0584 Synergistic action of ATF6 and EZH2 in sensing metabolic stress to boost anti-tumor immunity.

J. L. Edmondson, M. R. Reed, D. Fil, B. Heflin, B. Koss, A. J. Tackett;
University of Arkansas for Medical Sciences, Little Rock, AR

Although immune checkpoint blockade (ICB) marked a breakthrough in melanoma treatment, half of patients fail to respond, underscoring the crucial need for complementary adjuvant and neo-adjuvant therapies. Due to the low overall response rate and the stark contrast in outcomes between patients that respond and those that fail to respond, identifying the defining characteristics of immune checkpoint blockade (ICB) response is essential for enhancing the efficacy of melanoma treatments. To recapitulate and investigate the ICB-responsive phenotype *in vitro,* melanoma cells were metabolically adapted to an environment lacking glucose which successfully drove the dependence on oxidative metabolism and restored MHC-I expression, two established characteristics of ICB responsive tumors. Further, metabolic adaptations significantly enhance the tumor sensitivity to T-cell killing. Surprisingly even in JAK1 and IFNAR1 deficient cells, metabolic adaptation restored MHC I antigen presentation, indicating an interferon-independent mechanism of MHC-I regulation. Proteomic analysis of three metabolically conditioned melanoma cells lines (human and mouse) identified downregulation of the histone methyltransferase EZH2 and the activating transcription factor ATF6 as key corollaries of MHC-I expression. Interestingly, EZH2 and ATF6 activity were found to be inversely related in metabolically adapted cells and patient tumor samples. These studies mechanistically explore the epigenomic control of antigen presentation machinery and the transcriptional targets of ATF6 controlling sensitivity T cell killing. Here, through *in vitro* and *in vivo* studies, we demonstrate that constitutive activation of ATF6, and thereby activation of the adaptive unfolded protein response (UPR), sensitizes melanoma to immune control. These data suggest that EZH2 and ATF6 act synergistically to balance immune mediated killing during metabolic stress whereby loss of EZH2 increases MHC-I antigen presentation and activation of ATF6 sensitizes tumor cells to T cell-mediated control. Ongoing therapeutic studies combining EZH2 inhibition, ATF6 activation, and ICB in pre-clinical models further suggest targeting the synergy between EZH2 and ATF6 is a putative adjuvant or neo-adjuvant target to improve the clinical response of ICB.

#0585 Regorafenib antitumor immune response is enhanced by a novel drug combination in CRC syngeneic model.

P. Bajpai[1], F. Afaq[1], S. Al Diffalha[1], S. Agarwal[1], H. G. Kim[1], D. Otali[1], S. Varambally[1], A. Manne[2], R. Paluri[3], M. Khushman[4], U. Manne[5];
[1]Department of Pathology, University of Alabama at Birmingham, Birmingham, AL, [2]Department of Internal Medicine, Division of Medical Oncology, the Ohio State University Comprehensive Cancer Center, Columbus, OH, [3]Department of Hematology and Oncology, Wake Forest School of Medicine, Winston-Salem, NC, [4]Department of Medicine, Division of Oncology, Washington University in St. Louis/Siteman Cancer Center, St. Louis, MO, [5]Department of Pathology, O'Neal Comprehensive Cancer Center, University of Alabama at Birmingham, Birmingham, AL

Purpose: In the United States, colorectal cancer (CRC) is the second leading cause of cancer mortality. Metastatic CRC (mCRC) refractory to traditional chemotherapy is managed with regorafenib, a multiple-kinase inhibitor. However, patients show only a modest improvement in overall survival but experience high drug toxicity, adverse side effects, and poor tolerability. Thus, to reduce regorafenib-induced toxicity and to enhance antitumor activity, we combined it with a hybrid/dual JAK/HDAC small-molecule inhibitor (JAK/HDACi) to leverage the advantages of both JAK and HDAC inhibition in a single agent. With syngeneic mice, the efficacy and impact on immunomodulation of this drug combination was assessed.
Methods: To assess effects of the agents, C57BL/6 immunocompetent mice were injected with MC38 murine CRC cells and treated with regorafenib (6mg/kg body wt) or JAK/HDACi (30mg/kg body wt), and their combination every third day for 21 days. Upon completion of the experiment, the tumors were harvested and processed for RNA and protein expression profiles. The effect of drug treatment on immune response was analyzed by nCounter Gene Expression assays (NanoString Technologies). Cytokines were measured in serum using the MesoScale Discovery mouse V-Plex Proinflammatory Panel kit. For pharmacokinetic studies, plasma samples were assayed from C57BL/6 treated with drugs after 1, 7, 21, and 48 hrs of treatment.
Results: The combination treatment significantly reduced tumor growth (volume and weight),relative to the vehicle control or single treatments. Gene expression showed higher CD45 abundance score in the combination treatment. This is an exciting observation, as CD45 has phosphatase activity and dephosphorylates key targets of the drugs used in the study. Additionally, after treatment with the combination, there was higher expression of Gzmb and Gzme and lower expression of Cx3cr1, indicating enhanced immuno modulation relative to regorafenib alone. We confirmed these findings by immunoprofiling of tumors. Higher CD45 staining, noted in tumors of mice treated with the combination, corroborated the gene expression results. Pronounced CD8 T lymphocytes infiltration was observed in combination, compared to regorafenib alone. Reduction of proinflammatory cytokine, TNF-α was noted in the combination group. This is an interesting observation as CD45 negatively regulates TNF, and combination treated mice had highest number of CD45 positive cells. Pharmacokinetic studies showed that the bioavailability of regorafenib was elevated after combination treatment relative to single-agent treatment.
Conclusions: Relative to the single agents, the combination of regorafenib with JAK/HDACi was more effective, with an elevated antitumor immune response and with sustained inhibition of tumor growth. A clinical trial to evaluate this combination for the treatment of mCRCs is warranted.

#0586 Tumor cell-intrinsic PD-1 activation drives therapeutic resistance in colorectal cancer cells.

H. Mok[1], D. Yapp[2], I. Tai[1];
[1]University of British Columbia, Vancouver, BC, Canada, [2]Canada's Michael Smith Genome Sciences Centre, Vancouver, BC, Canada

Background/Aim: Despite advancements in diagnosis and treatment, advanced CRC remains a formidable treatment challenge with limited therapeutic options because these tumors are resistant to chemo-, radio- and targeted-therapies. Emerging research shows that the presence of tumor cell-intrinsic PD-1 (ciPD-1) in various tumor types is involved in tumorigenicity and therapy-refractory disease. For example, ciPD-1 promotes tumor growth in melanoma and liver cancer, but in lung cancer, ciPD-1 exhibits tumor-suppressive behavior. These findings highlight the intriguing possibility that ciPD-1 may exert context specific functions within the tumor, beyond its well-known role in immune response suppression. Consequently, the present study addressed the pressing need to explore the effects of immune checkpoint inhibitors within broader tumor context and tumor microenvironment. We have established drug-resistant CRC cells and found that ciPD-1 was upregulated in these cells. This, together with an observation that ciPD-1-mediated survival signaling pathways was activated in CRC patient populations, prompted us to investigate the role of ciPD-1 in regulation of therapeutic resistance in CRC in the absence of immune cells.
Methods: We evaluated the clinicopathological relevance of ciPD-1 and its correlation with disease progression in CRC samples from clinical cohorts. Monoclonal antibody inhibition and siRNA interference methods were used to characterize the functional roles of ciPD-1 in regulating therapeutic resistance in CRC. The gene expression profiles of PD-1-High and PD-1-Low patient groups retrieved from clinical cohorts were compared to identify ciPD-1-medatied survival pathways in CRC patients.
Results: We found that ciPD-1 had a critical role in regulating CRC tumorigenicity and survival outcomes. Tumors with high expression levels of ciPD-1 also showed higher mutation rate and levels of microsatellite instability. Exposing CRC cells to chemotherapy, radiation, and nutrient deprivation increased ciPD-1 levels. In line with these observations, drug-resistant CRC cells also expressed higher levels of ciPD-1. The inhibition of ciPD-1 in CRC cells by monoclonal antibody or siRNA interference decreased cell proliferation and self-renewal rates, while enhancing treatment efficacy.
Conclusion: Our studies reveal that CRC cells increase ciPD-1 expressions in response to drug treatment and targeting ciPD-1-mediated survival pathways can delay the onset of drug resistance and promote therapeutic sensitiveness in CRC cells.

#0587 Tumor treating fields induce the integrated stress response, alter the transcriptional signatures of cellular metabolism, and modulate immune-related cytokines dependent and independent of p53.

P. R. Srinivasan[1], A. George[1], C. Chou[2], M. Pinho-Schwermann[1], M. Ghandali[1], V. Tajiknia[1], Y. Porat[3], M. Giladi[3], A. Armstead[3], A. Uzun[1], E. T. Wong[4], W. S. El-Deiry[1];

[1]Legorreta Cancer Center at Brown University, Providence, RI, [2]Rhode Island Hospital, Providence, RI, [3]Novocure, Haifa, Israel, [4]Lifespan Cancer Institute, Providence, RI

Tumor treating fields (TTFields) are an FDA-approved therapy for the treatment of glioblastoma and pleural mesothelioma. TTFields employ alternating electric fields delivered by cutaneous transducer arrays to induce cytostatic and cytotoxic effects on solid tumors. Additionally, recent studies suggest that TTFields may enhance anti-tumor immunity. We performed RNA-seq and multiplexed cytokine profiling in HCT116 wild-type and HCT116 p53-/- human colorectal cancer cells to elucidate TTFields' effects on the transcriptome and secretome. TTFields lead to profound changes in the transcriptome related to metabolism, including downregulation of transcripts coding for multiple enzymes involved in the Krebs cycle, fatty acid synthesis, and glycolysis. Furthermore, though only HCT116 p53-wild type cells strongly induced the p53 pathway, both cell types' transcriptomes showed strong downregulation of cell cycle progression. Our cytokine data showed that key tumor-promoting cytokine IL-8 was downregulated independently of p53. We identified upregulation of immunomodulatory cytokines MIF and MICB independently of p53. While MICB promotes NK cell activation, MIF drives tumor progression. Therefore, MICB may be one way in which TTFields enhance anti-tumor immunity; targeting MIF during TTFields treatment may lead to synergy by abolishing its pro-tumor effects. We also identified a p53-dependent decrease in the TRAIL decoy receptor DcR3, which normally protects tumor cells from TRAIL-induced apoptosis. Further mechanistic work showed that TTFields induce EIF2-alpha phosphorylation, the central protein involved in activating the integrated stress response (ISR), across multiple cancer types, leading to suppression of global protein translation. TTFields treatment also resulted in increased expression of surface calreticulin, an endoplasmic reticulum stress marker, which activates the ISR. Future mechanistic work will explore the impact of identified cytokines and the ISR on anti-tumor immunity both *in vitro* and *in vivo*, as well as metabolic alterations induced by TTFields. This work identifies potential biomarkers and rationales for therapeutic combinations exploiting TTFields-induced molecular alterations.

#0588 Preclinical evaluation of novel chimeric vesiculovirus mediated expression of proteolytic enzymes targeting two major stromal components of pancreatic ductal adenocarcinoma.

Khandoker Usran Ferdous, Mulu Z. Tesfay, Camila C. Simoes, Aleksandra Cios, Bolni Marius Nagalo

Department of Pathology, University of Arkansas for Medical Sciences, Little Rock, AR

The vesiculovirus genus has recently garnered interest as an oncolytic virotherapy for pancreatic ductal adenocarcinoma (PDAC). A new synthetic chimeric vesiculovirus, VMG, demonstrated efficacy and safety against PDAC both *in vitro* and *in vivo*. The therapeutic effectiveness of virotherapies against PDAC is often hindered by immunosuppressive factors in the tumor environment, as well as the presence of hyaluronic acid (HA) and collagen (CN), which increase tumor stiffness and interstitial fluid pressure, leading to reduced drug/oncolytic virus and immune cell penetration into tumor. To address this, we engineered VMG viruses incorporating enzymes PH20, collagenase (CNase), and novel proteolytic enzyme SMC, the latter exhibits both PH20 and CNase-like activity. We characterized these modified viruses for their cytotoxicity and performance *in vitro*. Various PDAC cell lines displayed varied sensitivity to VMG vectors, yet they showed consistent oncolytic effects relative to the parent VMG-GFP virus. Our results revealed no compromise in viral replication or apoptosis-inducing ability after transgene insertion, which is evident as infectious viral progenies were produced to approximately similar level of magnitude of around 10^8 $TCID_{50}$/ml in all the cell line tested. Additionally, the VMG-SMC and VMG-hPH20-CNase variants demonstrated notable enzyme activity. To enhance clinical relevance, we utilized an *ex vivo* live tumor platform, which indicated around 20% tumor cell death using VMG vectors compared to that of the control, signifying tumor viability and virus replicability 72 hours post-infection. Fluorescent imagery highlighted the viruses' ability to spread and express functional enzymes within tumors. In summary, VMG vectors expressing stroma-degrading proteolytic enzymes can effectively express PH20, CNase and SMC enzymes that degrade stromal barrier of HA and CN without interrupting the replicability, performance, and oncolytic characteristics of the VMG vectors. Future research should prioritize the safety of these vectors and their potential to augment neoantigen expression and immune cell infiltration *in vivo*, which are the hallmarks of antitumor efficacy.

EXPERIMENTAL AND MOLECULAR THERAPEUTICS: Kinase and Phosphatase Inhibitors 1
Poster Session

#0591 Discovery of ZM-2322, a highly selective, potent inhibitor of membrane-associated tyrosine- and threonine-specific cdc2-inhibitory kinase (PKMYT1).

F. Zhou[1], L. Liu[2], L. Jiang[2], B. Cheng[2], Z. Li[1], D. Zhu[2], J. Xue[2], L. Xue[1], R. Tang[1];
[1]State Key Laboratory of Neurology and Oncology Drug Development, Simcere Zaiming Pharmaceutical Co, Ltd., Shanghai, China, [2]Simcere Zaiming Pharmaceutical Co, Ltd., Shanghai, China

The genome DNA is consistently threatened by a variety of intrinsic and exogenous DNA damage factors. Cell cycle checkpoint is one important mechanism in response to DNA damage and maintaining genome stability. In tumor cells, gene alterations, such as *CCNE1* amplification (encoding for Cyclin E1), result in G1/S checkpoint loss and replication stress, leading to high dependency on the G2/M checkpoint. PKMYT1 inhibits crucial checkpoint protein CDK1 activity by phosphorylating CDK1 at the residues of Thr-14 and Tyr-15 in the G2/M phase. In *CCNE1* amplification cells, the inhibition of PKMYT1 leads to the reduction of pCDK1 and loss of G2/M checkpoint, consequently results in premature mitosis and the accumulation of DNA damage, then finally induces cell death. Here we identify a novel small molecular ZM-2322, which displays robust intracellular binding to PKMYT1 and inhibits the specific downstream phosphorylation of CDK1 Thr-14 with IC_{50} values of 14 nM and 29 nM, respectively. ZM-2322 strongly inhibits the proliferation of the HCC1569 cell line with *CCNE1* high-level amplification and shows a >400× selectivity folds over a *CCNE1* wildtype cell line SKOV3. ZM-2322 also shows significant inhibition of tumor growth in a dose-dependent manner in the HCC1569 xenograft model, and the efficacy correlates well with PK and target inhibition. There is evidence showing that loss-of-function mutations of FBXW7, a cyclin E E3 ligase, lead to cyclin E accumulation and are synthetic-lethal with PKMYT1 inhibition. Consistently, a potent anti-proliferation of ZM-2322 is observed in DLD-1 FBXW7 -/- cells, but not DLD-1 parental cells. These data suggest a high potency of ZM-2322 on PKMYT1 inhibition and a potential good kinase selectivity which is further confirmed by using a kinase panel biochemical assay. As expected, when compared head-to-head with another clinical PKMYT1 inhibitor RP-6306 which shows inhibitory effect on 27 of 217 human kinases with inhibition rates >90% at 1 μM, ZM-2322 is found to be a much more PKMYT1-selective inhibitor and hits only several individual kinases under the same assay condition, suggesting a potentiality in better safety profile and higher dose tolerance. Furthermore, our data illustrates that in combination with gemcitabine, ZM-2322 elicits strong synergetic anti-proliferation activities on HCC1569 cells *in vitro* and results in tumor regression with a minor effect on body weight *in vivo*. Besides, a strong synergy effect is also observed in the combo of ZM-2322 and ATR inhibitor in HCC1569 *in vitro*. These data indicate that ZM-2322 has the potential of application expansion and good tolerance under continuous administration. Taken together, our data suggest that ZM-2322 is a potent and highly selective PKMYT1 inhibitor.

#0592 A novel pMEK inhibitor ABM-4095 for the treatment of pancreatic cancer.

M. Xu, Y. Hu, L. Zhao, X. Chen, Y. Chen, C. Yang, J. Li, C. Chen, X. Lv;
ABM Therapeutics, San Diego, CA

The MEK-ERK pathway is often activated in tumors by mutations of upstream BRAF- or RAS-proteins. The RAS is frequently mutated in several cancers, especially in pancreatic cancer with an about 95% rate. Pancreatic cancer has the highest mortality rate with a 5-year survival rate of 8% and a median survival of 6 months. Targeted therapies have been extensively evaluated in pancreatic cancer, however, survival improvement of this aggressive disease using a targeted strategy has been minimal. The only currently approved targeted therapy is erlotinib in combination with the chemotherapy drug gemcitabine. To date, four MEK inhibitors that block RAF-activation have been approved by the FDA, but their ability to inhibit ERK signal activated by RAS-mutations is limited due to the induction of MEK phosphorylation by relief of ERK-dependent feedback inhibition of RAF. Here, we report a novel small molecule, ATP-uncompetitive, pMEK inhibitor ABM-4095 that potently prevents phosphorylation of MEK by RAF with moderate inhibition of MEK kinase activity. Most of MEK inhibitors approved by FDA or in clinical trials increase pMEK levels instead. ABM-4095 has a good cell permeability. Its anti-cancer efficacy has been demonstrated both in the in vitro cancer cell line proliferation assay and in vivo xenograft models. ABM-4095 showed a synergy effect with erlotinib in pancreatic cancer cells. In a Miapaca-2 xenograft model, ABM-4095 showed good dose-dependent tumor inhibition as a single agent or combining with the KRAS G12C inhibitor AMG-510, and tumor regressions were observed. In summary, ABM-4095 is a potent pMEK inhibitor with a high activity against the RAS-mutant pancreatic cancer in vitro and in vivo. Detailed preclinical results will be presented.

#0593 DCC-3084, a brain penetrant RAF dimer inhibitor, broadly inhibits BRAF class I, II, and III alterations leading to growth inhibition of intracranially implanted tumors in preclinical models.

G. Al-Ani, S. L. Bulfer, J. D. Zwicker, C. K. Crawley, K. M. Elliot, S. Javed, Q. Groer, M. M. Hood, J. W. Large, K. Luther, Y. K. Romero, F. A. Stanley, D. C. Tanner, H. Telikepalli, B. Le Bourdonnec, B. D. Smith, D. L. Flynn;
Deciphera Pharmaceuticals, LLC, Lawrence, KS

Background: Mutations in the RAS/MAPK pathway are a frequent driver of cancer, with oncogenic RAS or RAF mutations occurring in >30% of all cancers. First generation BRAF inhibitors are approved for use for tumors with Class I BRAF mutations (V600X). However, these drugs are not efficacious in RAF dimer mutant and RAS mutant cancers due to paradoxical activation of RAF dimers. Herein, we describe DCC-3084, a brain penetrant, potent and selective investigational switch-control inhibitor of BRAF and CRAF kinases, shown preclinically to target all relevant aberrant signaling mechanisms (monomers, heterodimers and homodimers) and inhibits growth of subcutaneously and intracranially implanted tumors in preclinical models.
Methods: Inhibition of RAF kinases was measured using recombinant enzymes. Cellular proliferation was measured using resazurin to monitor cell viability. Inhibition of ERK or RSK phosphorylation was measured by AlphaLISA or ELISA. Pharmacokinetics (PK) in the plasma, brain and CSF compartments were measured following oral dosing in Wistar rats. Subcutaneous or intracranial BRAF mutant mouse xenograft models were used to assess PK, pharmacodynamics (PD), and efficacy.
Results: DCC-3084 treatment resulted in potent single-agent inhibition of MAPK pathway signaling, and cellular proliferation in a wide range of Class I, II, III BRAF and BRAF fusion altered cell lines. DCC-3084 was demonstrated to be CNS penetrable and exhibited dose dependent oral exposure with robust inhibition of the MAPK pathway in PK/PD models. Oral treatment of DCC-3084 as a single agent resulted in tumor regression in subcutaneously implanted BRAF Class I and BRAF fusion xenograft models. Additionally, DCC-3084 resulted in tumor regression or growth inhibition in intracranially implanted BRAF Class I and BRAF fusion tumor models.
Conclusions: The switch-control inhibitor DCC-3084 broadly inhibits Class I, II and III BRAF mutations, BRAF fusions, and BRAF/CRAF heterodimers leading to tumor regression in preclinical models. DCC-3084 CNS penetration enables potential for further research in brain metastases or primary brain cancer.

#0594 ORIC-613, a potential first- and best-in-class, orally bioavailable, potent and selective PLK4 inhibitor with synthetic lethality in TRIM37 high cancer models.

K. A. Edgar, S. McRee, G. Andretta, C. Chen, C. Colas, W. Fang, W. Kong, J. Long, F. Liu, J. Moore, A. Pankov, D. Shore, J. Tan, R. Warne, L. Ulicna, R. Vekariya, A. Daemen, F. A. Romero, M. R. Junttila, L. S. Friedman;
ORIC Pharmaceuticals, South San Francisco, CA

A synthetic lethal interaction between polo-like kinase 4 (PLK4) and elevated TRIM37 was discovered in breast cancer and neuroblastoma (Meitinger et al. 2020; Yeow et al. 2020). High TRIM37 renders cells dependent on PLK4, a kinase that controls centriole duplication. Amplification and copy number gains of the 17q23 amplicon, where TRIM37 resides, are common in breast cancer and neuroblastoma and associated with early relapse and poor prognosis, making PLK4 a promising new synthetic lethal target for these patients. The development candidate ORIC-613 is an orally bioavailable, potent and exquisitely selective small molecule inhibitor of PLK4, which is synthetic lethal in TRIM37 high cells. ORIC-613 is highly selective against the kinome, including against the closely related aurora and PLK families. ORIC-613 ADME/PK profile includes high cell permeability and low potential for drug-drug interactions based on CYP profiling. ORIC-613 blocked PLK4 trans-autophosphorylation of phosphodegrons, leading to stabilization of PLK4, thus directly demonstrating target engagement in cells. PLK4 protein stabilization correlated with cell viability for ORIC-613, providing a quantifiable pharmacodynamic (PD) association with antitumor activity. Cell viability assessment in cancer cell lines revealed that ORIC-613 showed greater potency in TRIM37 high versus TRIM37 low cell lines. Importantly, ORIC-613 induced significantly greater apoptosis in TRIM37 high versus low cancer cell lines as measured by caspase 3/7 assay. We confirmed that ORIC-613 activity is on-target using an engineered cell line system of PLK4 G95L, in which the leucine mutation maintains enzymatic function but blocks compound binding. In cell viability assays, ORIC-613 was potent in the parental cells and lost activity in G95L cells. Analysis of genomic data from tumors indicates that TRIM37 copy number amplification and gain is prevalent across numerous cancers. Oral dosing of ORIC-613 resulted in tumor growth inhibition and regressions in TRIM37 high xenograft breast tumors with no body weight loss. In summary, ORIC-613 is a potential first- and best-in-class development candidate, with exquisite selectivity for PLK4, which demonstrates synthetic lethality in TRIM37 high tumors and has the potential to benefit these patients.

#0595 Preclinical development of the CDK4 selective inhibitor PF-07220060: Increased CDK4 versus CDK6 inhibition leads to improved anti-tumor efficacy at therapeutic concentrations.

L. Anders, B. Pascual, B. Boras, J. Cianfrogna, S. Garza, N. Li, J. Yuan, M. Moen, N. Huser, G. Gallego, M. Jalaie, S. Ninkovic, S. Cho-Schultz, H. Shen, J. Kath, K. Dress, W. Diehl, S. Nair, R. Jones, J. Lafontaine, A. Murtaza, A. Sacaan, S. Chintharlapalli, T. VanArsdale;
Pfizer Oncology, San Diego, CA

PF-07220060 is a selective inhibitor of CDK4, displaying ~20-fold and ~4-fold increased selectivity for CDK4 versus CDK6 when compared to palbociclib and abemaciclib/ribociclib, respectively. This translates to less PF-07220060 associated neutropenia in beagle dogs and humans when compared to dual CDK4/6 inhibitors. Because neutropenia is the primary culprit necessitating limited and often interrupted clinical dosing of dual CDK4/6 inhibitors, the advantage of PF-07220060 lies in the flexibility to escalate the drug's exposure in patients and thus realize near-complete target coverage of the CDK4 oncogene in tumors that are dependent on this kinase. Here we select tumor types/indications that show dependency on CDK4 but not CDK6 and includes cells derived from luminal breast cancer and androgen-receptor positive metastatic prostate cancer. Additionally, we investigate certain drugs with which PF-07220060 may be combined to maximize its efficacy in these tumor indications. PF-07220060 sensitizes HR+ HER2- breast cancer to the estrogen inhibitor, fulvestrant and the degrader, ARV-471 (vepdegestrant). PF-07220060 + vepdegestrant showed significantly longer tumor regrowth delay vs monotherapy groups and vs Palbo + vepdegestrant and vs PF-07220060 + fulvestrant*. Similarly, PF-07220060 sensitizes prostate cancer to the androgen receptor antagonist, enzalutamide. In HR+ HER2- breast cancer cells, the senescent cell fraction was markedly increased by co-treatment with PF-07220060 and fulvestrant versus either drug alone, albeit the combination did not trigger tumor cell death. Further addition of the PI3K inhibitor alpelisib was sufficient to enforce tumor shrinkage in vivo. Alternatively, inhibition of CDK4 plus CDK2 also led to tumor shrinkage in xenograft models of HR+, HER2- breast cancer. Finally, our preclinical data indicate that the propensity of CDK6 to compensate for CDK4 inhibition in these tumor types is limited. Compensation by CDK6 was seen in only a fraction of the evaluated in vitro and in vivo models. Even so, in these instances, PF-07220060's efficacy remained comparable to palbociclib's when both drugs were used at their therapeutic doses. We conclude that PF-07220060's anti-tumor efficacy is broadly superior to currently approved dual CDK4/6 inhibitors.

#0597 Vebreltinib: A novel brain-penetrating MET kinase inhibitor demonstrates the mechanism of action and pharmacological anti-tumor activity in diverse patient-derived MET-dysregulated tumor models at clinically relevant drug levels.

X. Zhang[1], E. Liu[2], Y. Song[1], P. Yu[1], S. Redkar[1], G.-L. Yu[1];
[1]Apollomics, Inc., Foster City, CA, [2]Zhejiang Apollomics Biotech Co., Ltd., Hangzhou, China

Background: Dysregulation of the MET signaling pathway drives oncogenesis in many human cancers, the majority of which have not been addressed by a MET targeted therapy albeit the emerging therapies for *MET* exon 14 skipping (*MET* ex14) NSCLC. We have developed a novel highly selective MET kinase inhibitor vebreltinib (APL-101, PLB1001, bozitinib) to address unmet medical need. Vebreltinib is being jointly investigated in ongoing pivotal Phase 2 and 2/3 studies in *MET*-dysregulated NSCLC, primary CNS cancers and basket solid tumors in China (as PLB-1001) and globally ex-China (as APL-101). The Phase 1 portion of both studies have been concluded with the same RP2D (200 mg BID by oral administration). Vebreltinib demonstrated blood-brain barrier permeability in PLB-1001 Phase 1 glioblastoma study as previously reported.
Methods: MET enzyme kinetics and vebreltinib intrinsic potency were studied by a radiometric MET kinase assay. Selectivity was profiled by *in vitro* KINOME. Vebreltinib cellular activity on MET signaling and *in vivo* anti-tumor activity were assessed in tumor cell lines and patient-derived tumors (PDX) carrying *MET* alterations.
Results: Vebreltinib is an ATP-competitive inhibitor with Ki of approximately 2.2 nM for recombinant MET kinase and inhibited the native form of activated MET with 0.52 nM IC50. Vebreltinib demonstrated exquisite selectivity in KINOMEscan selectivity panel. Vebreltinib inhibited HGF-dependent and -independent MET signaling in KP4 tumor cell lines with nanomolar concentrations. Vebreltinib inhibited IL-3 independent Ba/F3 cell lines carrying exogenous *MET* ex14 or with secondary mutations induced by other MET TKIs. Vebreltinib inhibited MKN45 gastric tumor xenograft *in vivo* with ED90 of 6 mg/kg PO/QD. Furthermore, Vebreltinib demonstrated strong anti-tumor activity in a variety of PDX tumor types carrying *MET* ex14, *MET* fusions, and *MET* amplification. In these preclinical studies, the total and unbound vebreltinib plasma concentration observed at steady state trough of RP2D was used as a clinically relevant drug level to interpret Vebreltinib efficacy in blocking oncogenic MET signaling, proliferation of Ba/F3 cell lines with a broad spectrum of *MET* mutations and *in vivo* tumor growth in PDXs carrying diverse *MET* alterations. We demonstrated the rationale for Vebreltinib to be an efficacious single-agent MET inhibitor in treating tumors carrying *MET* driver alterations beyond *MET* ex14 NSCLC.
Conclusion: Vebreltinib is a novel potent MET kinase inhibitor showing promising preclinical activity against PDXs from diverse organs sites and genomic alterations such as *MET* ex14, *MET* fusion, *MET* amplification, or *HGF* over-expression at clinically relevant drug levels, providing proof-of-concepts for continued clinical development.

#0598 HSK42360: A potent, brain permeable, BRAF paradox breaker for the treatment of BRAF-driven cancers.

S. Gao[1], Y. Li[2], **J. Wang**[2], P. Tang[1], Z. Shi[1], Y. Li[1], P. Yan[1];
[1]Haisco Pharmaceutical Group Co., Ltd., Chengdu, China, [2]Haisco Pharmaceutical Group Co., Ltd., Shanghai, China

Mutations in the BRAF gene are among the most common identified in human cancers approximately 7% of all cancers evaluated, including 70% of melanomas, 50% of thyroid-like cancers, 10% to 20% of colorectal cancers, 13% of serous ovarian cancers, 3-7% of non-small-cell lung cancers, and most recently, hairy cell leukemia. Approved BRAF inhibitors (or +MEKi) against BRAFV600E/K improved initial clinical efficacy. However intrinsic and acquired resistance often arise through BRAF paradoxical activation, limiting durable responses to current BRAF inhibitors. In addition, Approved BRAFi responds poorly to patients with BRAF mutant gliomas or brain metastases, mainly due to limited brain permeability. More effective therapeutic options are therefore needed. To address this clinical challenge, we developed a potent, brain-penetrating paradox breaker HSK42360, as a promising therapy for patients with BRAFV600E mutation, progression or brain metastases following treatment with approved BRAFi or BRAFi/MEKi therapies. HSK42360 is a potent BRAFV600E inhibitor with IC_{50} value of 5 nM at enzymatic level. Further characterization showed that HSK42360 did not induce homodimer or heterodimer of CRAF with CRAF or BRAF and thereby blocked reactivation of the MAPK pathway in HCT116 cells, whereas Dabrafenib significantly induced RAF dimerization and MAPK reactivation. HSK42360 exhibited significant anti-proliferation activity against multiple tumor cell lines with BRAFV600E, including A375 (melanoma), DU4475 (breast cancer), and COLO205 (colon cancer), but was highly selective for BRAF wild-type cells. HSK42360 was administered orally once daily and showed broad-spectrum antitumor activity in the COLO205 and A375 CDX models. Immunohistochemistry showed a close correlation between the inhibition of tumor growth and ERK1/2 phosphorylation in A375 CDX tumor tissues. To explored the impact of HSK42360 in a brain micro-metastasis model aimed at mimicking early CNS metastatic spread, tumor progression was monitored through BLI (full name) imaging, which revealed that HSK42360 was highly brain penetrant with Kp,uu greater than 1 and triggered potent antitumor activity and prolonged survival in brain metastatic models of melanoma. We next tested the hypothesis that HSK42360 could retain activity in models presenting RAF dimer-driven resistance. Surprisingly, HSK42360 demonstrated promising antitumor effects in the first gen-resistant NRASmA375($NRAS_{Q61K}$, $BRAF_{V600E}$) CDX model, supporting its use as a follow-on therapy for current BRAFi resistance. Collectively, these preclinical studies validated that HSK42360 is a novel brain-permeable BRAF paradox breaker that exhibits outstanding antitumor activity in brain metastasis and RAF dimer-driven resistance.

#0599 Combination of CDK4/6 inhibitors with biguanides for treatment of triple negative breast cancer.

M. Morales Martinez, E. Mauricio Gonzalez, G. Deng, G. Ma, H. Kim, L. Stiles, N. Hamilton, M. E. Jung, R. J. Pietras, D. C. Marquez-Garban;
UCLA David Geffen School of Medicine, Los Angeles, CA

Triple negative breast cancer (TNBC) is the most aggressive subtype of breast cancer (BC) and is associated with early relapse and high frequency of metastasis. This has been attributed in part to the lack of targeted therapies. TNBC occurs more frequently in younger women of African and Hispanic ancestry and with a higher risk of mortality than women of European ancestry. Emerging data shows activation of the AKT/mTOR pathway by insulin may occur in aggressive TNBC and inhibition of mTOR signaling by rapamycin, a potent mTOR inhibitor, induces cell cycle arrest and downregulation of cyclin D1 in TNBC cells. CDK4/6 inhibitors have demonstrated to be an effective therapeutic for estrogen receptor positive BC and although their use in TNBC patients remains uncertain their use in combination with other targeted therapies may be promising. We have developed a set of newly designed biguanides with potent anticancer action and safety doses in vivo that in combination with CDK4/6 inhibitors block TNBC cell growth in vitro and in vivo. Using TNBC cell proliferation in vitro assays, new biguanides show dose-dependent inhibition of cell proliferation ($P<0.01$). Further, combination of biguanides with ribocliclib, an orally bioavailable CDK4/6 inhibitor, produced additive and synergistic effects in TNBC cell lines in vitro ($P<0.01$). Biguanides are known to activate de LKB1-AMPK pathway. Western immunoblots showed our biguanide analogues also induce AMPK phosphorylation and significantly reduce phosphorylation of downstream mTOR signaling pathway components including S6 ribosomal protein and 4E-BP1, an effect that is potentiated by combination treatment with ribociblib. Further, cyclin D1 is known to be overexpressed in about 50% of BCs and binding to CDK 4/6 induces phosphorylation of Rb and cell cycle progression. Treatment with biguanides downregulated cyclin D1 expression in TNBC cells and combination treatment of ribociclib with biguanide JD006 was more effective at decreasing Rb phosphorylation than each drug alone. In addition, seahorse analysis evaluated mitochondrial respiratory function. Treatment with biguanides inhibited oxidative phosphorylation in a dose dependent manner, an important metabolic pathway that can drive drug resistance to therapy in cancer cells. In vivo, combination treatment of ribociclib with biguanide JD006 was more effective than each agent alone in stopping human TNBC xenograft progression in nude mouse models ($P<0.05$). Our preliminary data offer evidence that human TNBC are highly vulnerable to metabolic reprogramming by new biguanides. This work can yield insight on unanticipated mechanisms of biguanide action and rationale for new combination therapies with CDK 4/6 inhibitors as a new option for treatment of TNBC. Funding: CBCRP B27IB3869, JCCC Breast Cancer Award, Hickey Family Foundation, NCI U54 CA143930, Team Research Grant, UCLA TDG.

#0602 Targeting CDK9 with a novel potent and selective inhibitor, YX0798, in CAR-T-relapsed mantle cell lymphoma models.

V. Jiang[1], Y. Xue[2], H. Kim[1], J. McIntosh[1], H. Chen[3], T. Zhang[1], Y. Liu[1], J. Zhou[3], M. Wang[1];
[1]UT MD Anderson Cancer Center, Houston, TX, [2]University of Texas Medical Branc, Galveston, TX, [3]University of Texas Medical Branch, Galveston, TX

Introduction

Cyclin-dependent kinase (CDK) family members play critical roles in multiple cellular processes. CDK9 is a central regulator at several stages of PolII transcription, including initiation, elongation, and termination. CDK9 dysfunction resulted in transcriptomic reprogramming and promotion of the development of cancers, including lymphoma and leukemia. We and others reported that transcriptomic reprogramming is associated with disease progression and therapeutic resistance in mantle cell lymphoma (MCL). Targeting CDK9 with its inhibitors AZD4573 and enitociclib is safe and effective for treatment in preclinical MCL models, and they are currently under clinical investigation to assess their efficacy and safety. The data demonstrated that CDK9 is a promising therapeutic target. In this study, we developed a novel CDK9 inhibitor, YX0798, and assessed its potency and safety in preclinical MCL models.

Method

Cell viability assays were conducted in a time- and dose-dependent manner to assess the *in vitro* efficacy of YX0798 as well as AZD4573. Apoptosis assays and western blots were used to determine the mechanism of action in MCL cells. Patient-derived xenograft models from primary MCL patient samples were established in immunodeficient mice and used to determine the therapeutic potential YX0798.

Results Next generation sequencing showed that CDK9 was upregulated and cancer hallmarks MYC-TARGETS-v1 and -v2 were highly enriched in CAR-T-relapsed MCL patients compared to CAR-T-naïve patients. We hypothesized that CDK9 overexpression and activity may greatly contribute to the enrichment of MYC-TARGETS-v1 and -v2 in patients with CAR-T resistance, so targeting CDK9 may overcome that resistance. YX0798 was developed to be a potent and selective CDK9 inhibitor. It markedly inhibited cell viability and induced robust apoptosis in MCL cell lines. As expected, it inhibited CDK9 kinase activity and suppressed the expression of short-lived proteins like c-MYC and MCL-1 that are critical for MCL cell survival and growth. YX0798 at 2 mg/kg for continuous 7 days via pump or at 5 mg/kg daily by oral administration potently inhibited the tumor growth of xenografts derived from a patient with therapeutic relapse to the CAR-T therapy *in vivo* ($P<0.0001$). This treatment efficacy was found to be similar at that of AZD4573 but at a higher dosage (15+15 mg/kg, 2 hours split, QW, IP). No adverse effects in mice were observed for any of treatments.

Conclusion

These data show that our novel CDK9 inhibitor YX0798 is potent and efficacious in treating aggressive MCL models and overcame CAR-T resistance at a lower dosage than AZD4573.

#0603 BB5523, a multiple kinase inhibitor with HPK1, VEGFR2 and TNIK inhibition, enhanced antitumor immunity in tumor models.

Gongping Duan, Min Li, Puyong Zhang, Wei Hua, Enlun Hao, Shipeng Wang, Xiaoyi Ma, Junheng Wang, Lijie Wei, **Xingmin Zhang**

BroadenBio Co., Ltd, Beijing, China

Introduction: Immuno-suppressive micro-environment and abnormal signaling pathways are crucial for the proliferation of tumor cells. Hematopoietic progenitor kinase 1 (HPK1) inhibitor plays important roles in activation of exhausted T cells and enhancement of anti-tumor immune responses. VEGF/VEGFR2 pathway is the central therapeutic target in anti-angiogenic treatment in multiple cancers. Traf2- and Nck-interacting kinase (TNIK) is a member of the germinal center kinase family, and is reported to be essential for Wnt signaling and colorectal cancer (CRC) proliferation and progression. Blockade of critical kinases in multiple signaling pathways inhibits the proliferation, invasion and metastasis of cancer cells. Therefore, intergradation of these functions in a small molecule serves as the next generation of immune-oncology small molecules for cancer therapy. Methods: BB5523 was developed through structure-based drug design, and optimized by SAR analysis and medicinal chemistry iteration. Biochemical assays and cell-base functional assays were applied in compound evaluation. Pharmacokinetic (PK) and preliminary toxicity studies were performed with mice. CDX and syngeneic tumor models in mice were conducted to evaluate the *in vivo* efficacy of BB5523 as a single agent. Results: BB5523 shows high inhibition potency on HPK1 with good selectivity against other TCR signaling-related kinases, such as FYN and ZAP70. Inhibition of HPK1 kinase activity (IC50 = 3.3 nM) by BB5523 strongly suppresses the phosphorylation of the downstream biomarker protein SLP-76 (IC50 = 30 nM); and boosts the IL-2 secretion in purified human T cells and human peripheral blood mononuclear cells. BB5523 also shows good activities on VEGFR2 (IC50 = 1.6 nM) and TNIK (IC50 = 0.7 nM) which are crucial for the proliferation of cancer cells. In *in vitro* experiments, BB5523 significantly inhibits the proliferation of various tumor cell lines at sub-micromolar concentrations. PK profile of BB5523 shows good oral bioavailability (F > 80%). In preliminary safety evaluation, no abnormal symptoms were observed in mice dosed up to 100 mpk for 14 days. BB5523 showed significant tumor-growth inhibition efficacy in TE-8, JIMT-1, B16-F10 and MC38 tumor models. Conclusion: As a potent and oral available small molecule kinase inhibitor, BB5523 boosts anti-tumor immunity through HPK1 inhibition, while also blocking crucial signaling pathways in tumor micro-environment. BB5523 shows promising *in vitro* and *in vivo* efficacy with a well-tolerated safety profile. The preclinical study of BB5523 is in progress.

#0604 Targeting casein kinase 1 alpha (CK1 alpha) and transcriptional CDKs (CDK7/9) in human liposarcomas.

R. Liu[1], N. L. Solimini[1], P. Bhola[1], T. B. Branigan[1], J. Hao[1], X. Wang[1], R. Alharthi[1], M. Yorsz[1], S. Soni[1], C.-s. Hu[1], I. Snir-Alkalay[2], P. Gokhale[1], A. Letai[1], Y. Yinon Ben-Neriah[2], G. D. Demetri[1], G. I. Shapiro[1];

[1]Dana-Farber Cancer Institute, Boston, MA, [2]Hebrew University-Hadassah Medical School, Jerusalem, Israel

Introduction: Liposarcomas (LPS) are rare mesenchymal cell malignancies of adipocytic origin that are diagnosed in more than 3500 patients in the US each year. The two most common subtypes, well-differentiated LPS (WDLPS) and dedifferentiated LPS (DDLPS), are characterized by extrachromosomal DNA amplifications harboring the *MDM2* (100%) and *CDK4* (90+%) genes, generally with wild type *TP53*. Management of metastatic or surgically unresectable LPS remains purely palliative. Recent clinical trials targeting MDM2 or CDK4/6 with small-molecule inhibitors have shown promise but have been hampered by dose-limiting toxicities. The development of new therapeutics is greatly needed to improve outcomes for patients with LPS.

Results: To identify unique liposarcoma-specific vulnerabilities, we screened multiple human LPS cell lines for transcriptional CDK expression and found high levels of CDK7 and CDK9. We demonstrate that CDK9 inhibitors suppress LPS cell growth and induce apoptosis by decreasing MDM2 levels while inducing expression of p53. To enhance p53 activation in these cells, we screened for expression of known regulators of p53, including CK1α, whose inhibition has previously been shown to activate p53. We demonstrate that LPS cells express CK1α and that the cytotoxic effects of CDK9 inhibitors are enhanced upon CK1α depletion. These data led us to examine combined targeting of CK1α and CDK9 in LPS with the novel agent BTX-A51, which has previously been shown to inhibit CK1α, CDK9, as well as CDK7 with nanomolar efficacy in AML models. BTX-A51 potently reduces expression of MDM2 with marked induction of p53, resulting in profound apoptosis of LPS cells. Through CRISPR/Cas9-mediated p53 knockout, we establish that BTX-A51-mediated apoptosis is primarily p53-dependent. However, BTX-A51 also reduces expression of MCL1 and primes LPS cell lines and primary LPS cells for BIM-induced apoptosis, as demonstrated by BH3 profiling. Importantly, preliminary *in vivo* data in an LPS patient-derived xenograft model reveal that BTX-A51 is well-tolerated with tumor growth inhibition.

Conclusions: Our results suggest that BTX-A51 has potent preclinical efficacy in treating LPS, primarily through inhibition of CK1α and CDK9. Future mechanistic studies will further clarify mechanisms of BTX-A51-mediated apoptosis, as well as the contribution of CDK7 inhibition to anti-tumor activity. Our data justify a planned clinical trial that will evaluate the efficacy of BTX-A51 in patients with advanced WDLPS or DDLPS.

#0605 ABBV-101, a highly potent and selective clinical stage Bruton tyrosine kinase degrader, overcomes BTK mutation-induced resistance to BTK inhibitors.

C. Pan, J. Riehm, T. L. Gururaja, H. Li, H. Nguyen, Y. Zhai, X. Xie, R.-X. Ding, R. Matthew, H. Y. Hoh, Z. J. Jia, B. Liu, C. P. Shu, C. A. Stevenson, C. Will, F. Innocenti, W. Assaily, **L. T. Lam**, A. Rivkin;
AbbVie Inc., North Chicago, IL

Bruton tyrosine kinase (BTK), a clinically validated target for various B-cell malignancies, plays a critical role in regulating cell growth, adhesion, and homing to lymphoid tissues that provide a microenvironment favorable to cancer cells. Despite the success of approved covalent BTK inhibitors in diseases such as CLL, most patients do not achieve complete response with monotherapy and eventually relapse, often via the emergence of the BTK-C481S mutation. Although second-generation reversible BTK inhibitors may temporarily overcome the C481S mutation, novel BTK mutations associated with resistance emerged in the clinic recently. Additionally, covalent BTK inhibitors have not shown sufficient differentiation from standard-of-care (SoC) in B-cell malignancies, such as diffuse large B cell lymphoma (DLBCL) to warrant approval to date. To address these unmet needs, a next-generation orally bioavailable BTK degrader ABBV-101 has been developed. Unlike BTK inhibitors that solely bind to and impede the catalytic domain of BTK, ABBV-101 eliminates the protein in a highly selective fashion. This degradation mechanism targets both the catalytic and scaffolding functions of BTK, and thus may enable deeper and more durable responses in patients with B-cell malignancies. Cellular activity of ABBV-101 was determined in a panel of DLBCL cell lines. We show that most non-germinal center B cell DLBCL (non-GCB-DLBCL) cell lines are sensitive to ABBV-101. To determine whether ABBV-101 could overcome BTK mutations-induced resistance, we engineered human DLBCL cell line TMD8 using CRISPR technology to express these BTK mutations and tested for sensitivity to ABBV-101 and BTK inhibitors. We show that ABBV-101 demonstrates similar potent activity against all BTK mutations associated with resistance to both covalent and reversible BTK inhibitors. The modulation of downstream pathway by ABBV-101 and how it differentiates from other BTK inhibitors will be presented. Further, ABBV-101 induces complete tumor regression in the BTK-C481S TMD8 DLBCL xenograft model. A spontaneous mouse CLL model carrying BTK-C481S mutation was developed through crossing BTK-C481S knock-in mice with the Emu-TCL1 transgenic mice in the C57BL/6 background. ABBV-101 completely inhibits BTK-C481S Emu-TCL1 CLL burden increase in the blood compartment and reduces CLL burden in the spleen and lymph nodes, whereas covalent BTK inhibitors show no activity. Finally, combination with a BCL-2 inhibitor enhances the efficacy of ABBV-101 in CLL and DLBCL models. Taken together, our results suggest that ABBV-101 has potent *in vitro* and *in vivo* efficacy. ABBV-101 is currently in phase 1 clinical trial for a variety of B-cell malignancies. ClinicalTrials.gov identifier: NCT05753501

#0606 The PLK1 inhibitor, onvansertib, synergizes with paclitaxel in small cell lung cancer.

J. C. Schmitz[1], G. Zhang[1], A. Pannucci[1], T. Smeal[2], C.-C. Wu[2], M. Ridinger[2], T. K. Owonikoko[1];
[1]University of Pittsburgh, Pittsburgh, PA, [2]Cardiff Oncology, San Diego, CA

Background: Small cell lung cancer (SCLC) is an aggressive neuroendocrine tumor with rapid disease progression and poor patient survival. Therapeutic options for SCLC remain a challenge due to limited understanding of both the biology of the disease and the major determinants of treatment response. Key transcription factors associated with unique biological phenotypes of SCLC include ASCL1, NEUROD1, YAP1, and POU2F3. Previously, we demonstrated that onvansertib, a highly specific inhibitor of the PLK1 Ser/Thr kinase, was effective in SCLC preclinical models, leading to its ongoing clinical development for relapsed/refractory SCLC patients (NCT05450965). Here we further explored potential strategies to enhance onvansertib activity by assessing its *in vitro* and *in vivo* activity in combination treatments.
Methods: Human SCLC cell lines were treated for 72 hr with onvansertib in combination with paclitaxel, lurbinectedin or the ATR inhibitors BAY1895344 and AZD6738. Effect on cell proliferation was analyzed by WST1 and CellTiterGlo assays. In vivo activity of onvansertib in combination with paclitaxel was tested in 3 SCLC patient-derived xenograft (PDX) models either cisplatin-sensitive (TKO5- ASCL1 subtype) or cisplatin-resistant (TKO2-ASCL1 subtype, TKO8-NEUROD1 subtype). Tumor-bearing nude mice were treated with vehicle, onvansertib (50 mg/kg, oral, 4 times/week), paclitaxel (15 mg/kg, IP, once a week) or the combination for 5 weeks. Mice were followed for tumor growth and survival (defined as time to reach tumor volume greater than 2000 mm^3).
Results: The combination of onvansertib and paclitaxel inhibited cell proliferation synergistically in cell lines from 3 SCLC subtypes (ASCL1, NEUROD1, and YAP1), while the combinations with lurbinectedin or ATR inhibitors were not synergistic. We further examined the combination of onvansertib and paclitaxel in SCLC PDXs. The combination exhibited potent anti-tumor activity, resulting in significantly greater tumor growth inhibition and increase in survival compared to the monotherapies in all 3 PDXs. The combination was well tolerated with no observed body weight loss. While onvansertib and paclitaxel had negligible single agent activity in cisplatin-resistant TK02 PDX and TKO8 PDX models, the combination induced durable complete responses in 25% and 100% of treated mice respectively.
Conclusion: The PLK1 inhibitor onvansertib in combination with paclitaxel showed synergy in multiple SCLC cell lines *in vitro* and potent anti-tumor activity in cisplatin-sensitive and -resistant SCLC PDX models *in vivo*. Tumor tissue analysis is underway to detail the mechanisms of this interaction.

#0607 Development of a novel, selective, and potent inhibitor of RON kinase.

M. Kaadige[1], T. Thode[1], J. Fornetti[2], A. Weston[1], S. Ng[1], T. Ghosh-Halder[1], T. Bargenquast[1], B. Durbin[1], S. Kasibhatla[1], R. Soldi[1], A. Welm[2], S. Sharma[1]; [1]TGen (The Translational Genomics Research Institute), Phoenix, AZ, [2]Huntsman Cancer Institute, SLC, UT

Purpose: Receptor d'origine nantais (RON) is a highly conserved transmembrane protein expressed at low levels in healthy adult tissues of epithelial origin and at various levels in immune cells such as macrophages. Aberrant activation of RON has been described in many solid tumors, and it contributes to tumorigenesis by modulating the immune tumor microenvironment, activating numerous oncogenic signaling pathways, and protecting tumor cells under stress. The overexpression of RON protein and the subsequent generation of oncogenic variants are mainly responsible for the persistent activation of downstream signaling pathways. In breast cancer, more than 80% of primary cancer samples are positive for RON expression, with overexpression reported in approximately 50% of cases. Importantly, tumoral RON expression correlates with increased breast cancer progression, metastasis, and poor prognosis independent of molecular subtype. We hypothesize that a small molecule inhibitor of RON that can target both full-length and truncated isoforms will promote anti-tumor immunity within the tumor microenvironment and block pro-metastatic signaling pathways. Herein, we report the development of a novel, orally bioavailable, selective, and potent inhibitor of RON kinase.

Methods: With structure-guided and iterative medicinal chemistry approaches, we identified a novel chemical entity that potently inhibited RON kinase activity. Further optimization resulted in the identification of ZB-60 with improved potency, selectivity, and desirable drug-like properties. *In vitro* kinase assays were performed using ADP-Glo RON kinase assay kit (Promega). Changes in phosphorylation of RON was demonstrated by Western blotting. Plasma pharmacokinetics (PK) was conducted in mice to measure exposures and to determine the oral bioavailability of ZB-60. *In vivo* efficacy of ZB-60 was evaluated in syngeneic mouse models of breast (EMT6) and colorectal (CT26) cancer.

Results: ZB-60 inhibited RON kinase activity with an IC_{50} of 56 nM and showed greater than 40-fold selectivity against MET and other closest members of the tyrosine kinase family. In ZB-60 treated breast cancer cells, there was a dose dependent reduction of RON phosphorylation and downstream signaling. PK analysis showed a high oral bioavailability with low clearance. *In vivo* evaluation of ZB-60 showed inhibition of tumor growth in EMT6 and CT26 models. Ongoing studies are focused on testing ZB-60 in combination with checkpoint inhibitors. The results from these studies along with ADME-TOX and pharmacokinetics will be presented.

Conclusion: ZB-60 has target specific activity and exhibits favorable drug-like properties.

#0608 NEOS-223 is a small molecule kinase inhibitor which induces apoptosis in selected cancer models.

H. Potu, S. A. Little, S. Fedorchak, S. Chittamuru, T. Murphy, R. Wexler, S. Croce, M. George, L. S. Desai;
NeoSome Life Sciences, Billerica, MA

Due to their critical role in cancer signaling pathways, members of the kinase family have emerged as one of the most comprehensively pursued targets in pharmacological cancer research. Deregulation of kinase activities leads to a variety of upstream and downstream signaling pathway changes in cancer cell. The Ras/Raf/MEK/ERK and PI3K/Akt/mTOR cascades are activated by genetic alterations in selected upstream signaling molecules such as receptor tyrosine kinases. Recently developed therapies which target such kinases (EGFR, BRAF, MEK) with kinase inhibitors have notably improved the prognosis within various cancer patient groups. However, patients with different mutations of EGFR, RAS, and BRAF do not respond completely. In this study the potential of NEOS-223 as a new kinase-targeted therapy in selected cancer models was investigated. Multiple cancer cell lines were assessed for cell growth as well as the direct inhibitory effects of NEOS-223 alone and in combination with other clinically approved kinase inhibitors. NEOS-223 treatment caused cell growth inhibition, blocked colony growth, and induced apoptosis in lung, pancreatic, melanoma, and colon cancer cell lines in vitro and demonstrated potent antitumor activity in *in vivo* xenograft models of colon and lung cancer. We were particularly interested in examining different components of the ERK and PI3K signaling pathways in selected sensitive cell lines, it was identified that NEOS-223 treatment led to downregulation of the expression of pERK and pAKT signaling. Blockage of the PI3K/mTOR pathways showed inhibitory synergy with NEOS-223 in lung cancer in vitro. Most importantly, *in vivo* data showed that while administration of NEOS-223 alone decreased tumor growth, the addition of PI3K/Akt/mTOR inhibitor onatasertib significantly enhanced anticancer effect in a lung cancer model. In lung and pancreatic cancer models, inhibition of EGFR by the small molecule drug gefitinib strongly showed synergistic effect with NEOS-223 both in vitro and *in vivo.* This may be because EGFR potentially activates both the mitogen activated protein kinase (MAPK/ERK) and the PI3K/mTOR signaling cascades in different mutant cancer models. These studies reveal that NEOS-223 inhibits cell proliferation and induces apoptosis via suppressing the PI3K/Akt/mTOR pathway and further suggest that the combination of PI3K/Akt/mTOR and EGFR inhibitors and that NEOS-223 would be a strong potential chemotherapeutic strategy against lung and pancreatic cancers.

#0610 ClpP-dependent and -independent activation of HRI kinase by small molecules.

X. Tian, P. Srinivasan, W. S. El-Deiry;
Brown University, Providence, RI

HRI was initially identified as a kinase essential for maintaining heme-globin balance within red blood cells as well as for controlling the ISR in response to oxidative stress. HRI also responds to a broad range of stresses such as osmotic stress, heat shock, proteasome inhibition. The recently discovered unexpected functions of HRI include innate immunity, translational control of immune evasion in cancer by upregulating PD-L1, proteostasis, mitochondrial stress, inhibition of histone H3 lysine 27 (H3K27) demethylase (KDM6A) and iron deficiency. Importantly, recent evaluation of patient data uncovered high expression of HRI mRNA in a subset of epithelial tumors versus normal tissues. Elevated expression of HRI protein in these tumor cells lead to cell death when BIRC6 ubiquitin complex is inhibited, which mediates degradation of HRI and is required for the survival of the tumors. These further broaden the importance of this member of the eIF2α kinase family as a cancer therapeutic strategy. Dordaviprone (ONC201), an imipridone small molecule, binds to and activates mitochondrial protease ClpP leading to integrated stress response (ISR) and ATF4 transcription factor activation. PG3, a prodigiosin analog, induces ATF4 and pro-apoptotic PUMA. Our data indicate that PG3 activates ATF4 through ISR via eIF2α kinase HRI. ALAS1 (5'-aminolevulinate synthase 1) catalyzes the first rate-limiting step in heme (Iron-protoporphyrin) biosynthesis. ONC201 treatment leads to potent downregulation and inhibition of ALAS1, indicating that ONC201 inhibits heme biosynthesis. It is well known that reduced heme results in activation of the HRI kinase. We show that an inhibitor of heme biosynthesis or knockdown of ALAS1 results in HRI activation, while silencing of HRI or knockout of *HRI* gene potently inhibit the eIF2α phosphorylation and upregulation of ATF4, CHOP and PUMA by PG3 and imipridones. Knockdown of ClpP rescues ONC201-induced downregulation of ALAS1 which blocks ONC201-induced upregulation of CHOP. Also, silencing of ClpP significantly reduced PARP cleavage in HCT116 $p53^{-/-}$ and MDA-MB-468 cancer cells. Our studies identify a novel link between ClpP activation induced by ONC201 treatment and ATF4 upregulation, via the ClpP/ALAS1/HRI/ATF4 pathway. However, PG3 treatment did not lead to degradation of ALAS1, indicating that PG3 does not activate ClpP. PG3 potently induced cell apoptosis through ISR via HRI/ATF4/PUMA pathway independent of ClpP. We are further investigating the targets of PG3 and the signaling pathway that leads to PG3-induced activation of HRI. Our results suggest that different small molecule inducers of the ISR such as ONC201 and PG3 can achieve an anti-tumor effect through different pathways converging on kinase HRI ultimately leading to ATF4 activation and tumor cell death.

#0611 Discovery of LNX231, a multi-kinase inhibitor mainly target FLT3 with robust *in vivo* efficacy in FLT3 mutant AML models.

L. Zhao[1], G. Hao[1], R. Deng[1], N. Zhang[2], J. Yao[1], A. Zhu[2], G. Li[2], E. Wang[2], Z. Li[1], Z. Liu[1], G. Zhang[1];
[1]Lunan Pharmaceutical Group Co. Ltd., Linyi City, China, [2]Shandong New Time Pharmaceutical Co., LTD, Linyi City, China

LNX231 is a multi-kinase inhibitor mainly target FLT3, which could both directly kill cancer cells and promote tumor immunity. LNX231 potently inhibits FLT3 activity in biochemical assay, with a 50% inhibitory concentration (IC_{50}) of 3.5 nM, significantly inhibits FLT3-D835Y and FLT3 ITD, the values of IC_{50} are 20 nM and 4.4 nM. LNX231 inhibits the proliferation of FLT3 mutant AML cell lines via RAS-MARK and JAK-STAT pathway. LNX231 significantly decreases the phosphorylation of STAT5 and ERK in MV-4-11 cells at the high concentration, but has no effect on the phosphorylation of FLT3 and AKT. LNX231 significantly decreases the phosphorylation of FLT3, STAT5 and ERK in MOLM-13 cells at the high concentration, but has no effect on the phosphorylation of AKT. In FLT3 mutated AML models, LNX231 induced sustained tumor shrinkage as a single agent and was well tolerated. At the same dose, LNX231 was more potent than the FDA-approved drug Gilteritinib. In the MC38 tumor-bearing model, the efficacy of LNX231 was better than Sunitinib and Lenvatinib. LNX231 has good oral bioavailability in different species, such as mouse, rat, dog and monkey. DMPK data predicted oral QD dosing in human. It also showed excellent ADMET profile as a pre-clinical candidate. Safety tolerability studies were conducted in mice and dogs. LNX231 has low cardiotoxicity (IC_{50} of hERG is 25.84 μM) and 5-6 times safety window. In conclusion, we discovered LNX231 as a multi-kinase inhibitor for FLT3 mutated AML.

#0613 Oral CHK1 inhibitor BBI-355 allows flexibility of dose and schedule with demonstration of monotherapy and combinational antitumor activity in extrachromosomal DNA (ecDNA) driven preclinical models.

R. J. Hansen, A. Steffy, J. Plum, A. Ardeshiri, E. Tse, S. Garcia, B. Norman, J. Moininazeri, A. Pferdekamper, E. Holmes, D. Liao, R. Elsdon, J. Lange, A. Pinkerton, J. Apuy, S. Chowdhry, C. Hassig, S. Kasibhatla;
Boundless Bio, San Diego, CA

Focal, high copy number amplifications of prevalent oncogenes (e.g., *MYC, EGFR*) frequently occur on extrachromosomal DNA (ecDNA), highly transcribed units of circular, non-chromosomal DNA. While use of targeted therapies is associated with improved survival in patients with cancers that have activating oncogene mutations or fusions, they have demonstrated limited activity for patients whose tumors harbor oncogene amplifications, including those mediated by ecDNA. We have previously identified Checkpoint Kinase 1 (CHK1) as a target essential for ecDNA function in cancer, as tumor cells with oncogene amplification on ecDNA exhibit increased DNA replication stress (RS) and are hypersensitive to inactivation of CHK1, cells' master regulator of RS. Thus, we have developed BBI-355, a novel, orally bioavailable, and selective small molecule inhibitor of CHK1, which is currently being studied in the first-in-human Phase 1/2 POTENTIATE clinical trial for patients with cancer harboring oncogene amplifications, including on ecDNA (NCT05827614).

In vitro antiproliferation activity of BBI-355 was observed in a panel of ecDNA+ oncogene amplified tumor lines and non-amplified lines, with heightened sensitivity and induction of RS observed in ecDNA+ cells. Oral administration of BBI-355 resulted in dose dependent on-target activity, with induced p-CHK1-S345 protein expression, in agreement with measured plasma and tumor concentrations. Subsequent pharmacokinetic/pharmacodynamic (PK/PD) modeling guided continuous and intermittent dose/schedules of single agent BBI-355 that demonstrated durable antitumor activity, including tumor regressions, in multiple ecDNA+ tumor models. Single agent targeted therapy treatment of cancers with oncogene amplification on ecDNA can result in acquired resistance via ecDNA-based mechanisms, further increasing reliance on CHK1. Enhanced antitumor activity of BBI-355 in combination with agents targeting the protein products of amplified oncogenes was demonstrated in multiple in vivo tumor models; these included combination with a pan-FGFR inhibitor in *FGFR2* ecDNA+ amplified gastric cancer and combination with CDK4/6 inhibitors in *CDK4* ecDNA+ amplified sarcoma models.

The first ecDNA-directed therapy (ecDTx) in development, BBI-355 demonstrated significant antitumor activity as a single agent and in combination with targeted therapies in multiple ecDNA+ oncogene amplified tumor models. Oral dosing of BBI-355 provides dose/schedule flexibility to attempt to optimize antitumor activity with a tolerable safety profile in patients with highly aggressive cancers and significant unmet need. The POTENTIATE clinical trial is open and currently enrolling.

#0614 Src family kinase inhibition demonstrates antitumor activity in vitro and in patient-derived xenograft models of human cholangiocarcinoma.

H. Kuipers, J. L. Tomlinson, D. M. Carlson, A. M. Abdelrahman, E. Jessen, J. W. Sample, N. W. Werneburg, H. E. Stumpf, M. J. Truty, S. I. Ilyas, G. J. Gores, R. L. Smoot;
Mayo Clinic, Rochester, MN

Background: Cholangiocarcinoma (CCA) is a lethal and heterogenous malignancy of the biliary tree characterized by perineural invasion. About 85% of CCA show activation of YAP signaling, which promotes proliferation, anti-apoptosis, and therapeutic resistance. YAP signaling is mediated by Src family kinases (SFK) by phosphorylation of YAP ($pYAP^{y357}$). NXP900 is a first-in-class, highly selective, SFK inhibitor with a novel mechanism of action which locks SFK in its closed and inhibited conformation, in contrast to other Src inhibitors such as dasatinib. A phase 1a study of NXP900 in patients with advanced solid tumors was recently initiated. Here, we examined treatment responses of CCA to NXP900 *in vitro* and *in vivo*.
Methods: Cell viability was determined in seven CCA cell lines by CellTiter-Glo. Cell death and apoptosis were assayed by PI/Hoechst and Caspase-Glo 3/7 assay. CalcuSyn software was used to determine synergistic drug effects. Immunoblot analysis, RT-PCR, and IF staining of YAP localization were used to evaluate YAP knockdown. Clones of human CCA cell lines resistant to NXP900 were generated through escalating exposure to NXP900 over 6 months. Five patient-derived xenograft (PDX) tumors were expanded into flanks of NOD/SCID mice. Tumor bearing mice were randomized 1:1 with 5 mice per arm and treated with vehicle or NXP900 (40 mg/kg) once daily for up to 4 weeks. To determine drivers of sensitivity and resistance, predicted sensitivity scores based on tumor growth were linked to multi-omics (RNA seq and [phospho-]proteomics) of our PDX models.
Results: All cell lines were sensitive to NXP900 with IC_{50} values between 7nM-15μM; IC_{50}'s of resistant clones were 1000 times higher. NXP900 induced more cell death compared to vehicle, which appeared to be through apoptosis. NXP900 inhibited pSrc, decreased $pYAP^{y357}$, and upregulated inactive $pYAP^{s127}$. Correspondingly, decreased YAP target gene (Cyr61, NUAK, and CTGF) levels and a nuclear-to-cytoplasmic translocation were observed. NXP900/GemCis combination therapy increased cell death demonstrated a synergistic effect (Combination Indices <1) at all concentrations. In our PDX models, treatment was associated with a significant decrease in tumor growth in 3 models (mean fold change 3.1 vs. 14.2; 1.0 vs. 7.6; 1.4 vs. 2.6). The major resistant signature was the TRK signaling network, involved in nerve growth factor binding activity, while drivers of sensitivity included the SRC network.
Conclusion: NXP900 demonstrated therapeutic activity in vitro and in human PDX models. We are currently performing multi-omic approaches in NXP900 sensitive and resistant cell lines to unravel determinants of activity and resistance. Additional *in vivo* studies will be performed to determine effects of NXP900/GemCis and NXP900/anti-PDL-1 combination therapy.

#0615 NXP900, a novel YES1/SRC kinase inhibitor in phase 1, demonstrates potent inhibition of proliferation in cell lines resistant to ALK and EGFR inhibitors.

N. O. Carragher[1], E. Poradosu[2], B. King[1], A. F. Munro[1], J. C. Dawson[1], A. Unciti-Broceta[1];
[1]University of Edinburgh, Edinburgh, United Kingdom, [2]Nuvectis Pharma Inc., Fort Lee, NJ

Background: NXP900 (eCF506) is a novel potent and selective SRC family kinase (SFK) inhibitor, (IC50 of 0.47 nM against YES1). NXP900 locks its target into its native “closed” conformation (type 1.5), thereby inhibiting both kinase activity and complex formation with protein partners (Temps et al. Cancer Res. 2021, 81, 5438). In contrast, multi-kinase inhibitors, including dasatinib and bosutinib, block SRC in the active “open” conformation (type 1) promoting the association of SFK and signaling partners via allosteric facilitation (Higuchi et al. Cell Rep. 2021, 34, 108876). Activation of SFK suggests that NXP900 may have therapeutic potential in cancers with acquired resistance to EGFR and ALK inhibitors.
Methods: Cell lines: Alectinib sensitive (NCI-H2228, ATCC) and osimertinib sensitive (PC9, RIKEN). Alectinib resistant (H2228-ALR1, H2228-ALR2, H2228-ALR3, H2228-ALR4) and osimertinib resistant (PC9-OR1, PC9-OR3) cell lines were generated by treatment of NCI-H2228 or PC9 with increasing concentrations of, respectively, alectinib or osimertinib. Cell proliferation assay: Intracellular ATP (Oncolines B.V.); cells were treated with inhibitors for 120 hours. Reverse Phase Protein Array (RPPA): Protein extracts were prepared from cell lines at sequential timepoints following treatment with NXP900 or a combination of NXP900 and osimertinib. Extracts were printed as a concentration series onto nitrocellulose coated slides across multiple sub-arrays using an Aushon2470 arrayer, each sub-array was addressed with individual mono-specific antibodies to quantify the abundance of SRC, EGFR and other canonical cancer signaling pathway phosphorylation events.
Results: NXP900 single agent potently inhibited cell proliferation of ALK sensitive (GI50=83nM) and all ALK resistant cell lines (GI50=5.8-16nM). GI50 for EGFR sensitive and EGFR resistant cells were 605 nM and 826-4665 nM, respectively. In combination with a fixed concentration of osimertinib (160nM), NXP900 potently reversed osimertinib resistance in both EGFR resistant cell lines (GI50= 43-121 nM).
Conclusions: Despite high response rates to osimertinib and alectinib, acquired resistance almost universally arises. Here we demonstrate that NXP900 can potently inhibit cell proliferation of ALK resistant cell lines as a single agent and EGFR resistant cell lines in combination with osimertinib. Activation of SFK and YAP1 has been shown to be important in the development of resistance to ALK and EGFR treatment. We have previously demonstrated that NXP900 potently inhibits YAP1 nuclear localization and induces tumor regressions in squamous models in vivo providing additional proof of concept for targeting solid tumors with YES1/SRC and Hippo pathway alterations. A FIH, Phase1 dose escalation study for NXP900 has been initiated.

#0616 Integrating organotypic tissue slices and polypharmacology-based screening to map the toxicity landscape of kinase inhibitors.

Y. Kang, M. Chan, S. Zhu, T. S. Gujral;
Fred Hutchinson Cancer Center, Seattle, WA

Protein kinases play important role in the regulation of various biological processes, and their malfunction and dysregulation are intricately linked to the initiation and progression of cancer. The effectiveness of small-molecule kinase inhibitors (KIs) has been well-established in the therapeutic landscape, with the FDA approving over 70 KIs for the treatment of cancer and other diseases. However, the widespread utilization of KIs has been accompanied by reported adverse events, prominently featuring cardiac complications, alongside hepatic and renal function. While many studies have indicated on-target and off-target kinase specificity associated with organ damage, there is an urgent need for building predictive models that can pinpoint which specific kinases might be involved in different types of organ injuries. Such a model would not only facilitate mechanistic elucidation but also serve as a valuable tool for preemptively identifying potential adverse events associated with KI treatment. In this study, we performed polypharmacology-based screening of kinase inhibitors in organotypic tissue slices prepared from the normal heart, liver, and kidney of three distinct species—human, canine, and rodents. These tissue samples were treated individually using a curated selection of 32 KIs that are representative of a larger set of KIs and collectively target most of the 'kinome.' Subsequently, we developed Elastic Net Regularization models by utilizing the kinase inhibition profiles of ~300 kinases. These models were used to predict changes in tissue viability, measured as a percentage change, following the treatment with the respective kinase inhibitors. Using these models, we predicted the toxicity of 428 kinase inhibitors, both as single agents and in pairwise combinations, against three organs—heart, liver, and kidney—in humans, rodents, or canines. Our data show that the models accurately predicted the renal and cardiac toxicity of many FDA-approved KIs that were previously known. For example, the inhibition of RET kinase was identified to be linked with renal toxicity. Further, we compared the toxicity landscape of kinase KIs among different species and identified distinct sets of kinases that were recognized as essential indicators of toxicity within the same organ across species. These disparities underscore the potential distinctions in organ metabolism. In summary, our data provide a comprehensive landscape of kinase inhibitor toxicity. Our models could serve as a valuable resource for predicting kinase inhibitor toxicity across species by leveraging inhibitor profile data.

#0617 BH-30236, a novel macrocyclic CLK inhibitor modulating RNA splicing, demonstrates potent inhibition of cancer cell growth in a broad panel of cancer cell lines.

P. Jiang, D. Li, N. Ling, D. Zhai, W. Deng, E. Rui, J. Cui;
BlossomHill Therapeutics, Inc., San Diego, CA

Alternative splicing (AS) is a primary mechanism for mRNA transcript diversification and protein expression regulation. In cancer, altered mRNA splicing promotes oncogenic transformation, induces metastasis, and confers resistance to cancer treatment. Mutations or imbalanced expression/activity of splicing factors (SF), such as serine-arginine-rich SFs (SRSFs), often result in deregulation of RNA splicing and tumor progression. CDC2-like kinases (CLK) and dual-specificity tyrosine-regulated kinase (DYRK) are key regulators of AS *via* phosphorylation of SRSFs. BH-30236 is a novel macrocyclic ATP-competitive inhibitor of CLK1/2/4. It also inhibits DYRK1/2, provirus integration site for moloney leukemia virus 3 (PIM3) and FMS-like tyrosine kinase 3 (FLT3) at clinically relevant concentrations. The inhibitory activity of BH-30236 against CLK, DYRK, PIM3 and FLT3 in cancer cells was investigated *via* the phosphorylation inhibition of SRSFs, Tau, 4EBP1 and FLT3, respectively. A panel of 119 hematological and solid tumor cell lines were used to investigate the spectrum of BH-30236 against cancer cell growth. To understand the mechanism of anti-cancer cell growth, the effect of BH-30236 on AS and protein expression of key tumor related biomarkers were examined. In conclusion, BH-30236 effectively inhibited pSRSF (IC_{50} 40-60 nM in IMR-32 cells), pTau (IC_{50} ~50 nM in SH-SY5Y cells), p4EBP1 (IC_{50} ~80 nM in MM1S cells) and pFLT3-ITD (IC_{50} 0.16 nM in MV-4-11 cells). BH-30236 demonstrated broad inhibition of cancer cell growth with a median IC_{50} of 85.2 nM (range 0.55-393 nM) across 12 tumor types. BH-30236 showed great efficacy against cell lines derived from hematological malignancy (median IC_{50} 23.34 nM), neuroblastoma (median IC_{50} 25.73 nM), breast cancer (median IC_{50} 83.80 nM), colon cancer (median IC_{50} 85.17 nM), and lung cancer (median IC_{50} 102.65 nM). Furthermore, BH-30236 demonstrated synergy with KRAS inhibitors in KRAS mutant cell lines, with EGFR inhibitors in RBM10 mutant H1975 cells, and with BCL2 inhibitor Venetoclax in MOLM-13 cells. Mechanistically, BH-30236 modulated AS by increasing pro-apoptotic and anti-proliferative splicing variants of key factors, such as BCL2L1, S6K, and BCLAF1. Meanwhile, BH-30236 downregulated RNA expression of SRSFs and modulated BCL2 family to increase apoptosis. These results strongly support the clinical applications of the novel multikinase CLK inhibitor BH-30236 in hematological malignancies and solid tumors as a single agent or in combination with other therapies.

#0618 Preclinical assessment of APL-030, a selective and orally bioavailable inhibitor of the integrated stress response regulator GCN2 with activity against acute myeloid leukemia.

M. Roman-Trufero[1], G. Whitlock[2], M. Fuchter[3], M. Jeyakumar[3], P. Chaida[4], S. Herzog[4], A. Zebisch[4], R. Butt[5], H. W. Auner[1], N. Clemo[5];
[1]CHUV Lausanne University Hospital, Lausanne, Switzerland, [2]Sandexis Medicine Chemistry Ltd, Sandwich, United Kingdom, [3]Imperial College London, London, United Kingdom, [4]Medical University of Graz, Graz, Austria, [5]Apollo Therapeutics, Cambridge, United Kingdom

GCN2 (EIF2AK4) is an evolutionarily conserved kinase and a pivotal regulator of the Integrated Stress Response (ISR), an adaptive cellular program triggered primarily by amino acid scarcity. Active GCN2 phosphorylates the translation initiation factor eIF2α, resulting in the attenuation of global protein synthesis and a largely ATF4-driven program of resource enhancement. GCN2 promotes cancer cell survival under conditions of microenvironmental or drug-induced intracellular nutrient scarcity. Here, we describe the preclinical development of APL-030, a novel and selective ATP-competitive inhibitor of GCN2. APL-030 was confirmed as a potent inhibitor of GCN2 in an on-target biochemical kinase assay with a Ki of 4.4nM. In a cell-based assay APL-030 decreased eIF2α phosphorylation in a dose-dependent manner via direct GCN2 inhibition with an IC_{50} of 50.8nM. In acute myeloid leukemia (AML) cell lines GCN2 inhibition resulted in a decrease in gene expression of effector genes CHAC1 and DDIT3. Moreover, treatment with APL-030 dose-dependently decreased cell viability in multiple AML cell lines, which was accompanied by an increase in caspase 3/7 activity. Bulk mRNA sequencing of MOLM-13 AML cells showed that APL-030 inhibited the extensive transcriptome changes triggered by glutamine depletion, in line with a high degree of selectivity of APL-030 for GCN2-mediated ISR signaling. In cells grown in rich medium, APL-030 triggered a largely ISR-independent transcriptome response that was dominated by the enrichment of pathways related to cell cycle as well as RNA and protein metabolism. In vivo, APL-030 treatment of an AML xenograft animal model completely inhibited tumor growth and prolonged survival time. Inhibition of AML tumor growth was shown to be a consequence of decreased cell viability and induction of caspase-dependent apoptosis. APL-030 was also tested on primary diagnostic AML cells, which were assessed for cell death by flow cytometry following staining for Annexin-V, 7-AAD, CD45, CD34, and CD38. Treatment with APL-030 caused a statistically significant increase in AML cell death in all six samples studied. Three samples exhibited a measurable CD34+/CD38- compartment, enabling evaluation of this leukemic stem cell-enriched population. APL-030 caused a statistically significant increase in cell death in the leukemic stem cell-enriched population in all three samples studied. APL-030 is a novel GCN2 inhibitor that that has shown encouraging efficacy in preclinical studies using both AML cell lines and patient-derived AML samples. Based on these preclinical results, a phase 1/2 study is planned in hematological tumors.

#0619 Comprehensive cell line profiling of monomer- and dimer-selective small molecule RAF inhibitors uncovers determinants of cellular responses.

J. J. Kooijman, A. Al Koerdi, S. B. van der Leeuw, D. J. F. Kluitmans, E. van den Bossche, J. Dylus, J. A. D. de Roos, J. J. T. Melis, N. Willemsen-Seegers, G. J. R. Zaman;
Oncolines B.V., Oss, Netherlands

Dysregulation of the Mitogen-Activated Protein Kinase (MAPK) pathway is a frequent event in many cancers. The RAF family of kinases, which includes ARAF, BRAF, and CRAF (*RAF1*), plays a key role in MAPK signaling. Of the three isoforms, only BRAF is currently targeted by approved RAF inhibitors. These inhibitors were designed to target BRAF-mutant variants that act as oncogenic monomers. However, BRAF-monomer inhibitors can induce activation of wild-type RAF by the formation of dimers, resulting in hyperproliferative lesions of *BRAF* wild-type cells. Additionally, BRAF-monomer inhibitors do not target RAF-dimers, although this is a potential vulnerability of many MAPK-driven cancers. Novel inhibitors are in development to circumvent these limitations. Further insights into the precise targeting and mechanism of action of RAF inhibitors can help in determining the most promising avenues for drug development. We performed extensive cellular profiling experiments with three approved and five clinical stage inhibitors of RAF to gain more insight into the differences and cellular targeting of these agents. The inhibitors were tested in cell viability assays on a panel of 130 human cancer cell lines from diverse tissue origins. Cell lines were exposed to dose ranges of each inhibitor spanning four logarithmic orders, and viability was determined by measurement of intracellular ATP. Effects of compound on cell viability were related to genomic, transcriptomic, and proteomic status using bioinformatics, with the aim to identify predictive biomarkers for drug response, and to determine selective targeting of MAPK-driven cell lines. Additionally, the primary mechanism of cellular inhibitor activity was determined by relating cell line responses to gene dependency data from large CRISPR knockout screens.
Our results showed striking similarity in the overall inhibitory profile of BRAF-monomer inhibitors and the vemurafenib-derivative and paradox breaker plixorafenib, which all selectively targeted *BRAF*-mutant cell lines. However, whereas vemurafenib increased cell viability in *RAS*-mutant cell lines at high drug concentrations, this effect was greatly reduced for plixorafenib. Western blot analysis of phosphorylated MEK and ERK levels in *RAS*-mutant cell lines treated with BRAF-monomer inhibitors confirmed MAPK pathway activation as cause of the increased cell viability. In addition, RAF-dimer inhibitors potently targeted *BRAF*-mutant cell lines, as well as several *KRAS*- and *NRAS*-mutant cell lines. Lastly, correlation analyses of cell line profiling data with CRISPR knockout data revealed the preferential targeting of *RAF1*-dependent cell lines by the dual RAF/MEK inhibitor avutometinib. The results of our analyses shed light on the intricacies of cellular targeting by RAF inhibitors and provide insights to guide the development of new RAF inhibitors.

#0620 Screening of small-molecule MAPK pathway inhibitors on a panel of 130 human cancer cell lines identifies determinants of response in *RAS*-mutant subgroups.

J. J. Kooijman, A. Al Koerdi, D. J. F. Kluitmans, E. van den Bossche, J. Dylus, J. A. D. de Roos, J. J. T. Melis, G. J. R. Zaman;
Oncolines B.V., Oss, Netherlands

Oncogenic mutations in members of the RAS family, HRAS, NRAS, and KRAS, are frequently identified in various cancers and often lead to increased signaling of the mitogen-activated protein kinase (MAPK) pathway. KRAS is the most frequently mutated RAS isoform, with a mutation incidence of >10% across all cancers, and up to 70% and 20% in pancreatic and non-small cell lung cancer (NSCLC), respectively. RAS has long been considered to be undruggable, and direct inhibition of RAS with small molecule inhibitors has only recently been achieved, with the approval of the KRAS G12C-mutant selective inhibitors sotorasib and adagrasib for treatment of NSCLC. Indirect targeting of *RAS*-mutated cancers by inhibitors of downstream components such as MEK and ERK has shown variable responses. Novel insights into MAPK signaling have renewed interest into targeting the MAPK pathway in *RAS*-mutant cancer, with pan-RAF dimer inhibitors and dual RAF/MEK inhibitors reaching clinical trials. To improve the chances of success, it is important to determine which patient populations are most likely to respond to these inhibitors. To gain more insight into the cellular targeting of MAPK pathway inhibitors, eighteen inhibitors of the MAPK components KRAS, RAF, MEK, and ERK were profiled on a panel of 130 cell lines in cell viability assays (the Oncolines® panel). The cell lines represented a diverse range of tumor tissues and had different genomic backgrounds. Many of the cell lines had mutations in *KRAS*, *NRAS,* or *BRAF*. Drug responses were determined by exposing the cell lines to nine-point duplicate dose ranges of the inhibitors. Using bioinformatics, cell line responses to the inhibitors were related to genomic and transcriptomic features, to identify determinants of drug response in both tissue-agnostic and tissue-specific contexts.
The results of our analyses revealed variable responses of *KRAS*-mutant cell lines to the inhibitors, reflecting clinical responses. Tissue-focused analyses showed that the different responses could be traced back to the different KRAS amino acid substitutions. For instance, in pancreatic cancer cell lines, the KRAS Q61H mutation predicted increased sensitivity to MAPK pathway inhibitors compared to other KRAS amino acid substitutions. Additionally, in tissue groups with a more heterogenous mutation profile, co-mutations explained the decreased effectivity of MAPK pathway inhibitors in *KRAS*-mutant cell lines, such as *PIK3CA* mutations in colorectal cancer cell lines. Lastly, a gene expression-based signature of MAPK activity predicted response to MAPK pathway inhibitors, independent of mutation status. Our findings have uncovered determinants of response to MAPK pathway inhibitors in *RAS*-mutant cell lines. These determinants can serve as markers to select patients who are most likely to benefit from MAPK inhibitors.

EXPERIMENTAL AND MOLECULAR THERAPEUTICS: Mechanisms of Drug Action
Poster Session

#0624 Ptpn1 deficiency collaborates with a NUP98::HOXD13 fusion gene to generate B cell precursor acute lymphoblastic leukemia.

N. Nigam[1], T. Matsukawa[1], R. Bertoli[1], M. L. Tremblay[2], M. Yin[1], P. D. Aplan[1];
[1]NIH-NCI, Bethesda, MD, [2]McGill University, Montreal, QC, Canada

Background: Acute lymphoid leukemia is characterized by inherited or acquired mutations that effect critical differentiation and proliferation pathways. We have shown that Mcm2 deficient mice developed T cell acute lymphoblastic leukemia, due to copy number variations, most commonly interstitial deletions throughout the genome. When crossed with mice that expressed a NUP98::HOXD13 (NHD13) fusion gene, $Mcm2^{-/-}$NHD13 mice developed B cell precursor ALL (BCP-ALL). A majority of these BCP-ALL had acquired homozygous deletions of Ptpn1, a protein tyrosine phosphatase, leading to the hypothesis that Ptpn1 deficiency combined with NHD13 expression leads to BCP ALL.
Objective: To investigate the role of Ptpn1 deletion in BCP-ALL development using mouse models.
Methods: Mice expressing an NHD13 fusion gene were crossed with Ptpn1 knockout mice, generating 6 possible genotypes. Mice were followed for 18 months. Mice with signs of leukemia were characterized by clinical evaluation, CBC, flow cytometry, and IHC. Primary BCP-ALL and derived BCP-ALL cell lines were also evaluated with RNA-seq and molecular pathway analysis.
Results: NHD13+Ptpn1-/- mice developed BCP-ALL with 65% penetrance, characterized by hyperleukocytosis, anemia, thrombocytopenia, and invasion of non-hematopoietic tissues. Similar to human BCP-ALL, NHD13+Ptpn1-/- BCP-ALL had clonal IGH as well as clonal Tcrd gene rearrangements. Flow cytometry revealed CD19 and/or B220 expression. NHD13+Ptpn1+/- mice with BCP-ALL frequently lost the wild-type (WT) Ptpn1 allele in leukemic cells, reinforcing the hypothesis that Ptpn1 can function as a classic tumor suppressor gene in this context. Whole exome sequencing revealed acquired mutations in B-cell differentiation genes (Pax5 or Bcor) and activating mutations in tyrosine kinase genes (Jak1/3 and Flt3). Transcription signature analysis showed significant upregulation of Hoxa/b gene clusters, RNase12 and LncRNAs subsets.
Conclusion: This study demonstrates that Ptpn1 loss combined with expression of NHD13 fusion gene leads to highly penetrant BCP-ALL in mice, suggesting a role for Ptpn1 in preventing malignant transformation. These findings present a collaborative model for BCP-ALL in which the NHD13 transgene leads to increased stem cell self-renewal, somatic Bcor or Pax5 mutations block normal B cell differentiation, and somatic signaling mutations (Jak1/3,Flt3) lead to hyperproliferation, which is potentiated by Ptpn1 deficiency.

#0625 Remodeling of the tumor microenvironment in esophageal squamous cell carcinoma by neoadjuvant immunochemotherapy and its impact on therapeutic efficacy.

R. Aizemaiti[1], H. Zhang[2], C. Zhu[3], K. Zhou[1], T. Hu[3], S. Lin[1], X. Teng[1], J. Wang[3], X. Li[3], P. Ye[1];
[1]Department of Thoracic Surgery, The First Affiliated Hospital, Zhejiang University School of Medicine, Hangzhou, China, [2]Department of Pathology, The First Affiliated Hospital, Zhejiang University School of Medicine, Hangzhou, China, [3]Department of Translational Medicine, Amoy Diagnostics Co., Ltd., Xiamen, China

Background: Patients with local advanced esophageal squamous cell carcinoma (ESCC) benefited from neoadjuvant immunochemotherapy (NAI) with 22%-55% of complete pathological responses (pCR). While unpredicted therapeutic resistance hampered prognosis of these patients. Thus, this study aimed to investigate tumor microenvironment (TME) remodeling pre- and post-NAI identifying predictive biomarkers and potential targets for patients with resistance to NAI.
Methods: 65 patients with locally advanced ESCC, who were treated with neoadjuvant anti-PD-1 antibody and platinum-based chemotherapy at the First Affiliated Hospital of Zhejiang University School of Medicine between November 2019 and June 2020, were included in this study. Genomic DNA and RNA from paired pre-and post-treatment FFPE samples were harvested and subjected to targeted DNA and RNA sequencing. Pre- and post- therapeutic microenvironment and immune cell infiltration were dynamically assessed based on RNA sequencing data.
Results: 37 of 65 patients responded to NAI(TRG0-1), while 28 of 65 patients displayed unfavored response (TRG2-3). Comparative analysis of TME characteristics before and after NAI revealed that, in the TRG2-3 group, LRRC15+ CAFs, and fibroblasts were significantly upregulated, while CD4 T cells and endothelium cells exhibited downregulation. Especially, TIGIT tended to be upregulated after NAI in the TRG 2-3 group. In the TRG0-1 group, significant upregulation of activated B cells, T-cells, myeloid dendritic cells, together with notable downregulations of immune suppressive features like Type 2 T helper cells, Tregs and LRRC15+ CAFs were observed in post-treatment samples.
Conclusions: Our study indicates the dynamic remodeling of TME during-NAI treatment might influence therapeutic efficacy and disclose potentially targetable resistant mechanisms. These preliminary findings pave the way for further validation through prospective clinical studies.

#0626 EGFL6 induced HER2-HER3 signaling controls accurate centrosome deposition of activated ERK and mitotic spindle formation in ovarian cancer cells.

S. Bai, N. Gupta, **Q. Jiang**, R. J. Buckanovich;
Magee-Womens Research Inst. & Foundation, Pittsburgh, PA

Epidermal growth factor EGF-like domain multiple-6 (EGFL6) is highly expressed in high grade serous ovarian cancer (HGSOC) cells and ovarian tumor vasculature. EGFL6 acts on tumor cells to drive tumor cell proliferation and migration. To better understand EGFL6 signaling and develop therapeutic strategies to target EGFL6 signaling in HGSOC, we evaluated phosphorylation of putative EGFL6 receptors and their downstream signaling. We demonstrated that EGFL6 induced phosphorylation and activation of ERBB/HER family of receptors; EGFL6 treatment of ovarian cancer cells led to rapid and transient phosphorylation of EGFR while inducing prolonged activation of both HER2 and HER3, with subsequent phosphorylation of ERK. Interestingly, we found that in EGFL6 stimulated ovarian cancer cells undergoing mitosis, pERK localized to the centrosome and the contractile ring. EGFL6 neutralizing antibodies reduce ERK phosphorylation and resulted in pERK being aberrantly localized. This resulted in altered mitotic spindle alignment and an increased number of cells undergoing mitotic catastrophe. Furthermore, combination anti-EGFL6 therapy with the pan-EGFR receptor inhibitor neratinib, compared to either therapy alone, led to an increase in aberrant pERK localization and cancer cell death in vitro. Consistent with these findings, dual anti-EGFL6 and neratinib therapy significantly restricted tumor growth in vivo, resulting in increased tumor cell death and a reduction in angiogenesis. Combined our data identify an unexplored role for pERK at the centrosome and suggest that dual targeting of the EGFL6/HER signaling axis maybe an effective therapeutic strategy in ovarian cancer.

#0627 IL-6 signaling via JAK/STAT axis influences PIM1 expression in renal cell carcinoma.

K. S. Meza, K. Seymour, S. L. Holder;
Brown University, Providence, RI

Renal cell carcinoma (RCC) is a top ten malignancy in the U.S. Overexpression of the proviral integration site for moloney murine leukemia virus 1 (PIM1) kinase is associated with poor clinical outcomes in RCC patients. PIM1 is a constitutively active serine/threonine kinase promoting cell proliferation, apoptosis resistance, invasion, and migration. The mechanisms underlying PIM1 expression and its function in RCC are not fully delineated. IL-6 is a pleiotropic cytokine that activates the JAK/STAT signaling cascade. High serum IL-6 levels are associated with the poor prognosis of RCC patients and may contribute to RCC invasion and metastasis. STAT3/5 binds directly to the PIM1 promoter inducing PIM1 expression. An IL-6/STAT3/PIM1 axis exists in pancreatic and breast cancer. We previously reported that PIM1 is overexpressed in a panel of human RCC cell lines relative to normal and immortalized renal proximal tubule epithelial cells. We also identified that RCC cells secrete IL-6. Our prior studies suggest that differential expression of PIM1 may be linked to autocrine IL-6 signaling. We thus hypothesize that an IL-6/JAK/STAT pathway regulates the expression of PIM1 in RCC. To understand how IL-6 signaling through the JAK/STAT pathway may regulate PIM1 expression in RCC cells, we examined whether IL-6 blockade using anti-IL-6 antibody or tocilizumab, would modulate PIM1 expression. Similarly, we assessed whether ruxolitinib, and LLL12, a STAT3 inhibitor could regulate PIM1 expression. We then evaluated the effect of ruxolitinib treatment on cell viability. In RCC cell lines, IL-6 blockade through either anti-IL-6 antibody or tocilizumab was sufficient to decrease PIM1 protein levels. Treatment with ruxolitinib leads to a dose and time-dependent decrease in PIM1 levels. Incubation with a STAT3 inhibitor also resulted in decreased PIM1 levels in RCC cells. Treatment with ruxolitinib also appears to decrease cell viability in a dose-dependent manner. These results suggest that differential expression of PIM1 in RCC may be linked to autocrine IL-6 signaling via a JAK/STAT/PIM1 axis. Multiple FDA-approved agents are available that target this pathway. Further investigation is required to determine the efficacy of these agents in pre-clinical models and even clinical trials.

#0628 RNA binding protein Matrin3 acts as a tumor suppressor by inhibiting microtubule nucleation.

P. Subbarayalu[1], S. Rajamanickam[1], S. Timilsina[1], S. Nirzhor[1], D. Medina[1], S. Abdulsahib[1], P. Prabhakar[1], D. Singh[1], F.-Y. Li[1], P. Yadav[1], E. Reddy[2], K. Evani[3], V. Eedunuri[1], T. Do[1], B. C. Onyeagucha[4], T. A. Mohammad[1], J.-H. Ji[1], Y. Chen[1], N. Abdelfattah[5], N. Dybdal-Hargreaves[6], L.-J. Wang[7], Y.-C. Chiu[7], S. Viswanadhapalli[6], R. K. Vadlamudi[6], M. K. Rao[1];

[1]UT Health San Antonio Greehey Children's Cancer Res. Inst., San Antonio, TX, [2]Southern Methodist University, Dallas, TX, [3]UT San Antonio, San Antonio, TX, [4]Mississippi University for Women, Columbus, MS, [5]Houston Methodist Research Institute, Houston, TX, [6]UT Health San Antonio, San Antonio, TX, [7]University of Pittsburgh School of Medicine, Pittsburgh, PA

Introduction: Microtubule-associated proteins (MAPs) regulate microtubule dynamics, which is critical for controlling cell division, proliferation, migration, and intracellular transport. Due to their critical role in maintaining cellular integrity, microtubules have served as potent therapeutic targets for cancer treatment. Here, we report “Matrin 3 (MATR3)” as a novel MAP that interacts with β- tubulin and γ-tubulin, which constitutes microtubule organizing center (MTOC) essential for proper spindle formation and chromosomal segregation.

Methods: Breast cancer cell lines (MDA-MB-231, MDA-MB-468, SKBR3, MCF7, BT549, HMEC, and MCF10A) were purchased from the American Type Culture Collection and cultured in standard medium. Breast cancer cells were transfected either with MATR3 overexpression plasmid or siRNA specific to MATR3. These overexpression/knockdown breast cancer cells were analyzed for cell viability, migration, invasion, colony formation, cell cycle, apoptosis assays, RNA sequencing, RT-qPCR, western blotting, RNA immunoprecipitation, and *in vivo* tumor xenograft study.

Results: Our findings show that MATR3 binds to RNA encoding MAPs including β-tubulin and γ-tubulin, and regulate their stabilization. MATR3 also interacted with β-tubulin protein. Our data demonstrate that MATR3 functions as a tumor suppressor, as its overexpression inhibits cancer growth, while its depletion increased tumor growth *in vivo*. Mechanistic studies confirmed that MATR3 mediates its tumor suppressor role by regulating the expression of the MTOC-associated protein-encoding gene MZT2B (Mitotic Spindle Organizing Protein 2B), which is overexpressed in cancers and promotes cancer growth. Further, loss of MATR3 expression or function results in dysregulated microtubule dynamics and uncontrolled expression of the oncogenic proteins including MZT2B.

Conclusions: In conclusion, our data strongly suggests that MATR3 serves as a novel RNA-binding protein with tumor suppressor properties. This discovery holds significant importance as MATR3 becomes the second protein, following Adenomatous Polyposis Coli (APC), to be identified for its binding to both MAP RNA and protein.

#0629 Activity of VIP943 on AML patient-derived leukemic blasts and healthy donor-derived bone marrow hematopoietic stem cells.

B. Stelte-Ludwig[1], T. Schomber[1], M. M. Frigault[2], J. Birkett[1], A. J. Johnson[2], A.-S. Rebstock[1], S. Ludwig[1], R. Izumi[2], A. Hamdy[2];
[1]Vincerx Pharma, Monheim, Germany, [2]Vincerx Pharma, Palo Alto, CA

Introduction: In patients with acute myeloid leukemia (AML), CD123 has been shown to have high expression on blast cells and leukemic stem cells (LSC) compared with normal hematopoietic stem cells (HSCs) and other more mature CD34+ subsets (Zhou J, World J Stem Cells 2014). LSCs are inherently resistant to standard of care chemotherapeutics and LSC persistence after chemotherapy is associated with disease relapse. VIP943 is an ADC consisting of an anti-CD123 antibody, a unique linker cleaved intracellularly by legumain which is required for release, and activation of a novel kinesin spindle protein inhibitor (KSPi) payload that accumulates inside the cell. Herein, we evaluated the potential of VIP943 to target LSC and progenitor cells.
Methods: Cytotoxicity assay: Bone marrow aspirates (BMA) and peripheral blood from previously untreated patients with primary or transformed from myelodysplastic syndrome AML were used in this experiment. Cells were treated with VIP943 (66 nM or 330 nM). After the end of the 48 h or 72 h incubation, the CD123+ cells and the CD34+CD38- LSC were detected by flow cytometry. Characterization of progenitor cell population: Fresh BM samples from healthy volunteers (HVBM) were stained with specific monoclonal antibodies to identify progenitor cell populations. Depletion assay: The effect of VIP943 on HVBM was evaluated by measuring the depletion of CD34+ progenitor cell populations in comparison to the anti-CD33-ADC, gemtuzumab ozogamicin (gem-oz). At the end of the incubation time, red blood cells were lysed; the remaining cells were stained with a cocktail of antibodies to discriminate between progenitor cells and analyzed by flow cytometry.
Results: Treatment of patient-derived CD123+ leukemic blasts with VIP943 resulted in a 50% reduction after 48 h and up to 80% at 72 h. A reduction of >70% of CD123+CD34+CD38- LSCs derived from BM aspirates of untreated patients with AML was achieved after incubation with VIP943 up to 72h. In addition, HVBM samples derived from five healthy volunteers were treated with VIP943 or gem-oz in a depletion assay, where gem-oz was toxic to CD34+ cells with an EC50 of 0.16 µM in contrast to VIP943 with an EC50 value of 8.83 µM.
Conclusions: In this in vitro analysis of primary samples from patients with AML, activity of VIP943 is observed in AML patient-derived CD123+ blasts as well as chemoresistant LSCs. At anticipated pharmacologic levels, VIP943 shows no adverse effects on HSCs unlike gem-oz suggesting an improved therapeutic index. In the ongoing first-in-human dose-escalation study in subjects with advanced CD123+ hematologic malignancies, VIP943 demonstrates a promising safety profile (NCT06034275).

#0630 The role of AKT pathway in β-catenin mutated hepatocellular carcinoma.

X. Wang, X. Chen;
University of Hawai'i Cancer Center, Honolulu, HI

The Wnt/β-catenin and PI3K/AKT pathways are pivotal contributors to the development of the malignant phenotype in cancer. The activated Wnt/β-catenin pathway synergizes with various signaling cascades to propel HCC formation, operating through its downstream effectors. It has been well-established that the mammalian target of rapamycin complex 2 (mTORC2) serves as an upstream regulator of AKT, orchestrating the phosphorylation and activation of AKT. Once activated, AKT phosphorylates and inhibits canonical downstream targets like forkhead box O protein (FOXO) and tuberous sclerosis complex 2 (TSC2). Studies indicated that AKT-mediated phosphorylation of TSC2 activates mTORC1, subsequently suppressing autophagy. However, there are limited data exist on the interplay between Wnt/β-catenin and AKT pathways in HCC. In this study, we sought to explore the role of the AKT pathway in β-catenin activated HCC tumors. Sleeping beauty-mediated hydrodynamic transfection was used to overexpress constitutively active forms of β-catenin (N90-β-catenin) and c-MET in the livers of mice to establish the HCC model (c-Met/β-catenin model). Notably, the knockout of Rictor, a component of the mTORC2 complex, significantly impeded tumor growth, underscoring the pivotal role of AKT in c-Met/β-catenin tumor development. AKT1 and AKT2 are the two main isoforms expressed in the liver. We determined that both AKT1 and AKT2 isoforms are critical for c-Met/β-catenin tumor growth. Intriguingly, simultaneous knockout of Rictor and activation of mTORC1 in the c-Met/β-catenin model resulted in delayed tumor growth, indicating that mTORC1 is not the sole downstream determinant of AKT signaling during c-Met/β-Catenin tumor development. Furthermore, overexpression of the activated FOXO1 (FOXO1AAA) significantly delayed the tumor growth, which highlighted the importance of FOXO1. Given the limited understanding of FOXO1 in HCC, we extended our investigation on FOXO1 to human HCC cell lines. Overexpression of FOXO1AAA notably delayed tumor growth *in vitro*. RNAseq analysis of FOXO1AAA-overexpressed human HCC cell lines revealed a significant upregulation of "metabolic pathways", suggesting metabolic reprogramming post FOXO1 activation. This study, for the first time, unveils the role of the AKT pathway in β-catenin-mutated HCC growth and highlights the potential therapeutic value of targeting the AKT pathway in patients with β-catenin-mutated HCC.

#0631 Functional genetics of APR-246 rescuable TP53 mutants.

Anais Saunders[1], Caili Tong[1], Anthony N. Karnezis[2], Gary S. Leiserowitz[3], Jeremy R. Chein[1]

[1]Biochemistry and Molecular Medicine, UC Davis School of Medicine, Sacramento, CA,[2]Pathology, UC Davis School of Medicine, Sacramento, CA,[3]Obstetrics and Gynecology, UC Davis School of Medicine, Sacramento, CA

TP53, often referred to as the guardian of the genome, encodes for the p53 tumor suppressor protein, and is one of the most frequently mutated genes in human cancers. Some cancer sub-types, such as non-small cell lung carcinoma (NSCLC) and high grade serous carcinoma (HGSC), have high *TP53* mutation rates reaching up to 56% and 96%, respectively. Given its multi-faceted role in human cancers, there have been several emerging therapeutic approaches targeting mutant p53. APR-246 is a small molecule drug currently in clinical trials for the functional rescue of p53 missense mutants, the most common type of p53 mutant protein, across various cancer types. APR-246 is proposed to bind mutant p53 and promote thermodynamic stabilization of the protein allowing it to regain wild-type-like conformation and consequentially regain WT-like functionality. However, there has yet to be a functional genomic screening of p53 mutants to systematically catalog which mutants are rescuable by APR-246. To address this critical gap, we have performed functional genetic screenings using a *TP53* mutagenesis library. This pooled lentiviral library contains ~8,000 amino acid variants, spanning the entirety of the *TP53* gene. Following stable transduction of this library into p53-null NSCLC and HGSOC cell lines, we performed functional screenings against sublethal doses of APR-246. Next-generation sequencing of the untreated and treated cell population allows for comparison of variant representation and determination of APR-246-sensitivity of p53 mutants. Preliminary statistical analysis of our screens has identified a pool of 117 “hit” mutants which are significantly depleted following treatment, indicative of APR-246-sensitivity. Two of these mutants, C242F and G266V, are non-functional, damaging mutations which occur in patients. Identifying p53 mutants that can be rescued by APR-246 will help identify which patients may benefit most from treatment with the drug.

#0632 AKT supports cancer cell survival through modulation of cholesterol homeostasis.

I. Vivanco[1], K. N. Myint[1], S. Wallace[1], G. Lazaro[2], E. Kostaras[2], N. Palaskas[3];

[1]King's College London, London, United Kingdom, [2]Institute of Cancer Research, London, United Kingdom, [3]University of California, Los Angeles, CA

AKT is a critical effector kinase downstream of PI3K activation. It has been shown to regulate a variety of cellular processes important for homeostasis, many of which are altered during oncogenesis. Not surprisingly, AKT is constitutively activated in a large number of human cancers, and has consequently been pursued as a therapeutic target for many years. Some of these functions are directly involved in establishing one or more hallmarks of cancer including sustained proliferative signaling, resisting cell death, and reprogrammed cellular metabolism. Although AKT inhibitors have demonstrated clinical benefit (most recently in a phase III trial) in combination with other therapies, single agent activity has been limited to a few cases with relatively infrequent activating AKT1 mutations. We have previously proposed that the clear disconnect between the high frequency of AKT activation in cancer and the lack of broad clinical activity of AKT inhibitors is due, at least in part, to the inability of existing compounds to block non-catalytic functions. We have found that while allosteric AKT inhibitors are partial suppressors of these functions, ATP-competitive inhibitors fail to suppress these functions to any significant extent. We now provide evidence that one important non-catalytic function of AKT that impinges on its oncogenic function is the regulation of cholesterol metabolism. We show that AKT represses the activation of LXRβ, thereby maintaining a level of intracellular cholesterol that is compatible with cancer cell viability, and that this repression does not require catalytic activity. Consistently, we find that allosteric AKT inhibitors induce LXRβ activation, and that genetic or pharmacological suppression of LXRβ function limit the growth inhibiting effects of these drugs. Our findings suggest that through a kinase-independent activity, AKT may play a significant role in the regulation of cholesterol homeostasis, and that the therapeutic potential of AKT inhibitors could be broaden by optimizing their ability to interfere with these functions.

#0633 Integrin αVβ3 activation by thyroid hormones triggers JAK/STAT oncogenic pathways that promote T cell lymphoma dissemination.

M. M. Debernardi[1], M. V. Revuelta[2], H. Sterle[1], G. Gonzalez[1], I. L. Souza[3], A. Correa[3], L. Cerchietti[2], G. Cremaschi[1], F. Cayrol[1];
[1]Instituto de Investigaciones Biomedicas (BIOMED-UCA-CONICET), Buenos Aires, Argentina, [2]Weill Cornell Medicine, New York, NY, [3]Instituto Carlos Chagas, Curitiba, Brazil

T cell lymphomas (TCL) are a heterogeneous group of lymphoproliferative disorders with poor prognosis. Aberrant activation of JAK/STAT pathway is associated with lymphoma dissemination in TCL patients. Although the FDA approved the use of inhibitors to target this pathway (Ruxolitinib), significant toxic effects have been reported and their use is limited. Thus making an excellent opportunity to study biological factors that regulate the activation of these pathways. In this sense, we recently showed that thyroid hormones (THs) acting through integrin αVβ3 induced TCL proliferation, which is reduced *in vitro* and *in vivo* in the presence of integrin αVβ3 pharmacological inhibitor. Our aim is to evaluate the impact of THs on JAK/STAT pathway activation and their implications on anti-lymphoma therapy. For the *in vitro* assays we used human and murine TCL cell lines. We used EL4 cells and c57bl/6 syngeneic mice for *in vivo* analysis. Proteomic profiles were evaluated by LC-MS-MS analysis. The GSE58445 database was used for *in silico* analysis. We found that THs induced STAT1, 3 and 5 phosphorylation in TCL cells and that the integrin αVβ3 inhibitor, Cilengitide (Cile) blunted these effects ($p<0.05$). Interestingly, we found that high mRNA expression levels of integrin β3 significantly correlate with worse overall survival in a cohort of TCL patients ($p<0.05$). Additionally, Ruxolitinib (Ruxo) diminished THs-induced STATs phosphorylation ($p<0.05$). As Ruxo reported toxic effects we aim to study alternative therapies such as Bexarotene (Bex), a synthetic retinoid used for cutaneous LCT treatment. We found that Bex significantly reduced cell viability *in vitro* of all TCL subtypes analyzed and combination with Cile resulted in improved anti-lymphoma activity ($p<0.01$). Also, Ruxo significantly decreased TCL cell viability but to a lesser extent than Bex+Cile ($p<0.05$). We previously found that BexT4+Cile (T4+, thyroxine supplementation) significantly decreases the *in vivo* growth of TCL tumors. To understand the mechanisms under this effects we analyzed tumor proteomics profiles and metalloprotease activity after 12 days of treatment. We found that BexT4+Cile regulates proteomic profiles related not only to lymphoma progression (JAK/STAT and PI3K-Akt signaling) but also pathways that impact the tumor microenvironment (TNF and angiogenic factors secretion and Th1/Th2 T cell differentiation). Regarding metalloprotease activity, we found that BexT+Cile inhibited MMP2 and MMP9 activity ($p<0.05$). Finally, we evaluated the dissemination of TCL in an *in vivo* model (by vain tail) and found that BexT4+Cile reduced EL4 cell implantation into the liver and kidneys ($p<0.05$). These results described the mechanisms by which THs induce the activation of JAK/STAT oncogenic pathway and showed how the inhibition of integrin αvβ3 in combination with bexarotene has therapeutic potential for TCL.

#0634 Tuba-seq and CRISPR/Cas9 analysis of TBX2 subfamily genes: Exploring contextual tumor suppression in lung adenocarcinoma.

A. Khalil, J. Maltas, M. Rahm, Z. Faber, M. Bedrock, X. Wei, B. Patel, C. McFarland;
Case Western Reserve University School of Medicine, Cleveland Heights, OH

Lung adenocarcinoma (LUAD) is a multifaceted and genetically diverse cancer, shaped by a myriad of oncogenic and tumor suppressive events. Through recent clinical and *in vitro* investigations, we have discovered that the TBX2 subfamily of genes, encompassing TBX2, TBX3, TBX4, and TBX5, are linked to LUAD progression. Specifically, we have observed marked downregulation of their expression in clinical LUAD specimens, and reduced growth in LUAD cell lines when the subfamily is re-activated- hinting at a potential tumor suppressive function. Paradoxically, the role of TBX2 subfamily genes in other cancer types remains enigmatic, with varying reports of both oncogenic and tumor suppressive effects. In this study, we harnessed the power of Tumor Barcoding with Ultradeep Barcode Sequencing technology (Tuba-seq) and CRISPR/Cas9-mediated genome editing to systematically investigate the effects of knocking-out Tbx genes and associated partners EGR1, CHD2, A20 and ATF3 in LUAD preclinical models. We investigated their effects in both normal lung epithelium and Ras-driven lung tumors via *in situ* gene editing and assessed tumor burden via histology and targeted DNA sequencing of tumor barcodes. TBX2 subfamily gene losses appear to have a profound effect on tumor initiation and early growth, which somewhat attenuates with progression. In Ras-driven tumors, we found that these genes are moderately tumor suppressive when measuring mean growth rate, although these effects (sans Egr1 loss) are more pronounced at 6 weeks of growth than at 20 weeks. Strikingly, however, we observed an unprecedented increase in total tumor burden when deleting these genes in genomically-normal (Kras w.t.) cells, including 4-20+ fold increase in Tbx2, Tbx3, Tbx4, and Tnfaip3-deficient cell lineages 20-week following transduction. Increases in total lineage burden of this magnitude are typically only seen for frequently-deleted hallmark tumor suppressor genes such as Tp53, Stk11, or Pten. This increased burden, however, seems to primarily affect early-stage progression, as no appreciable increases in mean lineage size relative to w.t. lineages are observed after 40 weeks of growth. Our study reveals the context-specific functions of the TBX2 subfamily while introducing the first *in vivo* model for TBX2-driven LUADs. This model facilitates the development of targeted therapeutic strategies and encourages accurate tumor modeling across various progression stages and diverse genetic backgrounds.

#0635 Osteoclasts mediate chemotherapy resistance in a fully humanized microphysiologic system of prostate cancer bone metastases.

A. B. Ding[1], E. Heninger[1], S. R. Reese[1], C. Sanchez-de-Diego[1], R. C. Yada[1], N. Sethakorn[2], S. C. Kerr[1], X. T. Hazelberg[1], M. N. Sharifi[1], D. J. Beebe[1], J. M. Lang[1];

[1]University of Wisconsin - Madison, Madison, WI, [2]Loyola University Chicago, Chicago, IL

Bone metastases (BM) are the most common sites of metastases in prostate cancer, occurring in ~85% of patients. Overall survival of men with castrate resistant prostate cancer with BM is less than 24 months. Docetaxel is the most commonly used therapy for patients with prostate cancer, but the response rate is only 30-40% and median duration of response is less than 9 months. Non-tumor components of the Tumor Microenvironment (TME) have been proposed to mediate treatment resistance, but few pre-clinical models capture the complex physiology of the human bone TME. We report the development of a bone TME using a humanized microphysiologic system to address this need. The LumeNEXT platform is a microphysiologic system that allows the 3-dimensional (3D) reconstitution and integrated analysis of a bone-specific TME microenvironment with functional microvasculature that traverses the chip and can be used to mimic drug delivery in patients. Primary human osteoclasts (OC) were differentiated from patient peripheral blood monocytes. LNCaP prostate cancer spheroids were grown in hanging droplets. We performed co-culture of OCs with 3D LNCaP spheroids and evaluated the efficacy of docetaxel-induced tumor cell killing in the presence of bone cells. OCs and PC spheroids were seeded into LumeNEXT devices in a collagen-based matrix and treated with 20 nM Docetaxel or DMSO vehicle for 48 hours. Docetaxel response was assessed using confocal microscopy for single spheroid diameter and cytotoxicity was measured using fluorescent cell death markers. Docetaxel-mediated killing of tumor spheroids was found to be significantly attenuated in the presence of OCs. In LNCaP only conditions, average Docetaxel-mediated cell death was 68.82%, compared to 53.86% in the LNCaP and OC co-culture condition ($p<0.0001$). Furthermore, Docetaxel treatment resulted in reduced tumor spheroid diameter compared to DMSO control when prostate cancer spheroids were cultured alone ($p=0.0118$). Additionally, the presence of OCs attenuated Docetaxel-induced morphological changes. Our data suggest that osteoclasts play a significant role in mediating chemotherapy response in prostate cancer. Future studies will examine transcriptional changes in prostate cancer cells that may be associated with Docetaxel resistance in the bone microenvironment and identify mechanisms of BM microenvironment-mediated drug resistance. Bioinformatic analysis of patient sequencing datasets is ongoing to identify osteoclast-associated signatures of treatment resistance.

#0636 Coculture model for investigating cellular interactions between colorectal tumor organoids and cancer-associated fibroblasts.

Y. Zhou[1], Y.-K. Huang[1], E. J. Fong[1], E. Elton[1], E. McManus[2], B. Choi[2], S. Kim[1], S. M. Mumenthaler[2];
[1]Ellison Institute, LLC, Los Angeles, CA, [2]University of Southern California, Los Angeles, CA

The tumor microenvironment (TME) is well recognized for its role in tumor progression, chemoresistance, and recurrence. The TME consists of various components, such as extracellular matrix (ECM), chemical and mechanical cues, as well as stromal cells and their interactions. As the most abundant cells in tumor stroma, cancer-associated fibroblasts (CAFs) have drawn a lot of attention. It has been reported that CAFs not only directly interact with cancer cells via surface proteins and cytokines, but also influence their behaviors by remodeling the ECM. However, due to their heterogenous characteristics and diverse functions, the influence of tumor-CAF interactions on drug response is not fully understood. Here, we present a coculture model for investigating CAF effects on patient-derived colorectal tumor organoids (CTOs) growth, differentiation, and drug response. It consists of normal colon fibroblasts, CCD18-Co, or patient-derived CAFs seeded with CTOs in a mixed hydrogel containing 90% basement membrane extract (BME) and 10% collagen type I. Media conditions were optimized (1:1 mix of CTO culture media plus reduced media excluding growth factors and inhibitors) to achieve similar organoid sizes in the monoculture and coculture conditions at the onset of drug testing. To support higher throughput investigations, our workflow incorporates a liquid handler for automated CTO seeding, media and drug exchange, and an automated microscope with a robotic arm for multi-plate imaging. Briefly, single cell CTOs and fibroblasts were seeded at a 1:1 ratio (3000 total cells/well) in 96-well plates. After 4 days in culture, anti-cancer drugs were administrated in reduced media to the samples. Brightfield images were acquired on days 0, 3, and 5 after drug administration. The collected images were analyzed with a neural network (NN) to dynamically monitor the growth and viability of individual organoids. The CellTiter-Glo assay was performed on day 5 to quantify the total CTO cell viability. The normalized drug response (NDR) was calculated from the NN processed images to determine the drug response. An immunostaining panel, which includes protein markers such as CK20, Ki67, α-SMA, Vimentin, and FAP, was used to evaluate the fibroblast phenotypes and CTO differentiation. Additionally, the cultures were subjected to fluorescent lifetime imaging microscopy (FLIM), a label-free imaging technique, to measure the metabolic adaptations of each cell population. Preliminary studies revealed a CAF-dependent increase in CTO growth and glycolytic signatures in the co-culture setting; however, minimal effects on drug response to common chemotherapy agents such as 5-fluorouracil and irinotecan were observed. In the future, we will use this integrated pipeline as a screening method to identify new treatment strategies aimed at targeting the stromal microenvironment in colorectal cancer.

#0638 FGFR4 mediates nuclear accumulation of NRF2 by binding to P62 in gastric cancer.

N. S. Bhat[1], M. Soutto[1], X. Zhang[2], Z. Chen[1], S. Zhu[1], S. Maacha[1], M. Genoula[1], D. Peng[1], H. Lu[1], O. McDonald[1], X. Chen[1], L. Cao[1], Z. Xu[1], W. El-Rifai[1]; [1]University of Miami, Miami, FL, [2]The First Affiliated Hospital of Nanjing Medical University, Nanjing, China

Background: Helicobacter pylori (H. pylori) is the major cause of gastric cancer. Fibroblast growth factor receptor 4 (FGFR4) is a member of the highly conserved tyrosine kinase family known to be activated in cancer. Nuclear Factor Erythroid 2-Related Factor 2 (NRF2), a transcription factor, is essential for the antioxidant response and exhibits cytoprotective properties against cellular stress and oxidative damage. This study investigates the novel functions of FGFR4 and its role in regulating the antioxidant response in gastric tumorigenesis.

Methods: We used public datasets, gastric tissues from mice and human, and gastric cancer cell lines. In vitro and in vivo H. pylori infections were performed. Western blot, RT-qPCR, Immunofluorescence, flow cytometry, Immunohistochemistry, Immunoprecipitation, Proximity ligation assay and Luciferase reporter assays were performed.

Results: The analysis of a public dataset revealed that overexpression of FGFR4 is associated with an oxidative stress signature and poor survival. Gene set enrichment analysis (GSEA) showed that tissue samples with high FGFR4 levels had an enrichment of NRF2 signature genes. In vitro cell models infected with H. pylori showed an increase in reactive oxygen species (ROS). Knockdown of FGFR4 resulted in significant reductions in NRF2 protein and transcriptional activity, leading to increased ROS levels and DNA damage. Immunofluorescence analysis using various models confirmed that FGFR4 knockdown reversed the accumulation of NRF2 in the nucleus. Dysplastic and neoplastic gastric lesions in the TFF1-KO mouse model exhibited high levels of both FGFR4 and NRF2. Pharmacologic inhibition or knockdown of FGFR4 significantly decreased NRF2 levels, as well as the size and number of gastric cancer spheroids. Mechanistically, elevated levels of P62 protein were associated with FGFR4 expression. Binding between FGFR4 and P62 proteins, which competes with NRF2-KEAP1 interaction, was detected using immunoprecipitation and proximity ligation assay. Immunohistochemistry analysis on a tissue microarray showed increased FGFR4 immunostaining in HGD/Cancer samples compared to adjacent normal samples, and this increase correlated with an increase in NRF2 and P62 levels.

Conclusion: These findings revealed that FGFR4 has a distinct functional role in promoting gastric carcinogenesis. FGFR4 binds to P62 to inhibit the interaction between NRF2 and KEAP1, allowing NRF2 to avoid degradation facilitating its translocation and accumulation in the nucleus. The use of FGFR4 inhibitors is a viable treatment option that warrants further research in patients with gastric cancer.

#0639 Evaluation of individual drug response in tumor microenvironment to cisplatin treatment in precision-cut tumor slices of ovarian cancer.

J. Thiel[1], A. Kneer[2], W. Yu[3], B. Winkler[2], G. Sauer[2], G. Ott[2], W. Aulitzky[2], T. Murdter[1], M. Schwab[1], C. Liang[3], M. Dong[1];
[1]Dr. Margarete Fischer-Bosch Institute of Clinical Pharmacology, Stuttgart, Germany, [2]Robert Bosch Hospital, Stuttgart, Germany, [3]University of Wurzburg, Wurzburg, Germany

Ovarian cancer is a complex and heterogeneous disease and the major cause of death among women with gynecological cancers. While patients usually respond well to the platinum-based first-line chemotherapy, the disease often becomes increasingly resistant to the treatment. The tumor microenvironment (TME) plays an important role in tumor development and drug resistance. Characterizing the TME of ovarian cancer after drug treatment is essential to identify molecular mechanisms that allow residual tumor cells to survive chemotherapy in ovarian cancer. We have established a preclinical model using precision-cut tumor slices (PCTS) with 250 µm thickness which preserves the TME of solid tumors with their heterogeneous cell composition during cultivation. The tumor morphology, viability and heterogeneity in terms of tumor and stromal cells as well as the immune compartment are preserved within the system. Based on the PCTS model, we also established a method to perform single-cell RNA sequencing (scRNA-seq) of the PCTS after cultivation and drug treatment to characterize the cellular features and dynamic relationships of different cell populations in the TME after drug treatment. Over 20 cell subtypes including different clusters of epithelial cells, immune cells and fibroblasts can be identified in PCTS after cisplatin treatment through the scRNA-seq analysis. This enables further deeper analysis of each cell subgroup in the TME after drug treatment. In response to cisplatin treatment, patients PCTS showed an individual induction of PD-L1 in different cell types. Additionally, multiplex immunofluorescence (mIF) stainings of the PCTS were performed to spatially trace the response of the TME to drug treatment. The mIF staining allows the simultaneous detection of up to 6 different markers on one FFPE tissue section. Images were analyzed using a machine-learning based workflow, which allows the comparison of biomarker expression and immune cell spatial distribution in the PCTS stromal and tumor areas before and after treatment. Combining the PCTS as a preclinical model with scRNA-seq and mIF staining analysis allows us to bridge the cellular characteristics and cellular spatial distribution with treatment response in the TME of solid tumors. It enables the systematic analysis of residual cancer populations after cisplatin treatment within the complex TME and further identification of predictive markers and targets for an individualized combination of chemotherapy with compounds targeting these mechanisms. The individual drug response of patients can be deeply evaluated and efficacious therapies can be further developed.

#0640 *In vivo* rescue of p53 tumor suppressor function with ADGN-531 across Pan-p53 alterations.

G. Divita[1], A. Grunenberger[2], E. Czuba[2], V. Josserand[3], M. Guidetti[3], N. Desai[1];
[1]AADIGEN, Pacific Palisades, CA, [2]DIVINCELL, Nimes, France, [3]IAB, Grenoble, France

p53 tumor suppressor mutations result in loss of function of p53 in approximately 50% of all human cancers.TP53 missense, nonsense mutations and p53 deletion are present in about 50%, 12% and 5% of all p53 driven cancers, respectively. To date there is no effective treatment for rescuing p53 function in cancers using a pan-p53 approach. The use of ADGN-531 is a new potent strategy combining mRNA with a tumor selective peptide nanocarrier to rescue of p53 tumor suppressor function.

ADGN-531 contains proprietary p53-mRNA complexed with proprietary short amphipathic peptides in the form of nanoparticles. ADGN-531 was evaluated on 20 different cancer cell lines harboring various p53 mutations. In-vivo efficacy of IV-administered ADGN-531 nanoparticles was evaluated on colorectal SW403 (p53 nonsense/KRAS^{G12V}), osteosarcoma SaOs2 (p53 null) and NSCLC NCI-H358 (p53 null/KRAS^{G12C}) mouse xenografts at a dose of 0.25-1.0 mg/kg weekly. ADGN-531/sotorasib synergy was evaluated *in vitro* on NCI-H358 (p53 null/KRAS^{G12C}) and Mia-PACA (p53^{R48W}/KRAS^{G12C}) cells and in vivo on NCI-H358 mouse xenograft. ADGN-531 markedly inhibits the growth of a large panel of cancer cells harboring p53-missense or nonsense mutations or p53-deletion, by rescuing p53 transcriptional activity and subsequent expression of its target proteins.

ADGN-531 induces cell cycle arrest in G1 due to p21 upregulation and apoptosis following BAX and PUMA activation. IV-administration of ADGN-531 resulted in dose responsive tumor growth inhibition in SaOs2, SW403 and H358 xenografts independent of KRAS status. We demonstrated a strong synergy in a NSCLC H358 xenograft (tumor regression 80%) when restoring P53 function with ADGN-531 (0.5mg/kg, weekly) along with inhibition of KRAS^{G12C} mutant using sotorasib (10mg/kg, daily). ADGN-531 potentiated the effect of sotorasib on sotorasib resistant cells harboring high level of KRAS^{G12C} in permanent active state. ADGN-531 treatments are well tolerated, no sign of clinical toxicity was detected after single or repeated administrations.

ADGN-531 is effective in rescuing p53 function both in vitro and in vivo across a wide range of p53 alterations. Our study provides a proof-of-concept that restoration of tumor suppressor function by ADGN-531 could be used as a single agent therapy in P53 altered tumors independent of other driver mutations e.g., KRAS, or with other therapies for potent combinatorial cancer treatment.

#0641 *SCD1* upregulation due to *STK11/KEAP1* loss upregulates *SLC7A11* and causes deregulation of fatty acid metabolism leading to ferroptosis evasion.

U. Sen, C. Coleman, D. Hasson, T. Sen;
Icahn School of Medicine at Mount Sinai, New York, NY

Introduction: Non-small cell lung cancer (NSCLC) with co-occurring loss-of-function (LOF) mutations in serine/threonine kinase 11 (*STK11*) and Kelch-like ECH-associated protein1 (*KEAP1*) (*SK*) are notably aggressive and unresponsive to chemo and immunotherapy, in current care standards. Novel therapeutic strategies are in demand to improve the outcomes for *SK* co-mutant NSCLC patients. We reported earlier that *SK* LOF mutations enhance cell proliferation and tumor growth in xenograft lung cancer models. We also found the ferroptosis evasion genes are enriched, and targeting ferroptosis regulators is a therapeutic opportunity in *SK* co-mutant NSCLC.

Methods: We used CRISPR/Cas9 gene editing to create stable knockouts of *STK11* (S^{KO}), *KEAP1* (K^{KO}) or both (DKO), non-targeting control (NTC) in two NSCLC lines. We performed an *in vitro* druggable genome library CRISPR screening in the same NSCLC lines. We performed kinase profiling and RNA-seq in the cell lines to depict the transcriptomic and proteomic landscape, followed by western blotting and qRT-PCR validation. We also performed BODIPY/C11 assay and lipidomics to explore the ferroptosis and metabolic landscape of *SK* co-mutant NSCLC models.

Results: Stearoyl CoA desaturase-1 (*SCD1*) was the top CRISPR screen hit, a critical modulator of fatty acid metabolism and ferroptosis evasion. *SCD1* expression is significantly higher in NSCLC tissue than adjacent normal tissue ($p<0.0001$), and high *SCD1* expression correlates with poorer prognosis in patients with NSCLC ($p=0.027$). GSEA from the bulk RNA sequencing in *SK* co-mutant cells pre-and post-*SCD1* inhibitor treatment showed *SCD1* inhibition leads to upregulation of the glutathione and glutamic acid pathways compared to NTC cells. Moreover, *SK* co-mutant cells have a significantly higher expression of *SLC7A11, enabling* cystine uptake and subsequent conversion to cysteine, essential for maintaining redox balance and cell survival. Hence, *SK* co-mutant cells are more resistant to cysteine depletion than NTC cells. *SCD1* inhibition causes a decrease in *SLC7A11* expression exclusively in DKO cells. Eventually, *SCD1* inhibition leads to global metabolomic changes in *SK* co-mutant cells, including key pathways involved in lipid and glucose metabolism. Finally, genetic and pharmacological inhibition of *SCD1* prevents tumor growth and sensitizes DKO cells to ferroptosis inducers like erastin.

Conclusions: Our findings highlight the importance of the *SCD1-SLC7A11* axis in regulating ferroptosis in *SK* co-mutant models. Current data impact our understanding of ferroptosis in NSCLC and its ability to target *SCD1* or ferroptosis in cancer treatment. Compounds such as inhibitors of *SLC7A11* (Erastin/IKE) are safe to use with acceptable toxicity and established doses. Hence, our study will facilitate the translation of ferroptosis inducers or *SCD1* inhibitors in clinical trials.

#0642 Flavopiridol inhibits cell proliferation, migration, and invasion via downregulation of FOXM1 in triple negative breast cancer.

S. Dilmac[1], N. Kahraman[1], F. Onder[2], Z. Hamurcu[3], B. Ozpolat[1];

[1]Houston Methodist Research Institute, Houston, TX, [2]Canakkale Onsekiz Mart University, Faculty of Medicine, Canakkale, Turkey, [3]Erciyes University, Faculty of Medicine, Kayseri, Turkey

Triple-negative breast cancer (TNBC) represent 15-20% of all breast cancers and is the subtype of breast cancer that is not responsive to targeted breast cancer treatments such as anti-estrogens (tamoxifen) or HER2 targeted antibodies due to the lack of ER, PR, and HER2 receptors. TNBC is associated with poor prognosis, early relapse, and distant metastasis and drug resistance. With the use of standard chemotherapeutics in the neoadjuvant setting, unfortunately the majority of patients (~60%) with TNBC do not achieve complete remission and 40% of the patients with regional (Stage II) and 90% of the patients with distant metastasis (Stage IV) die within 5-years. Currently, there is no effective targeted therapy for TNBC patients for targeting oncogenic pathways. Although recently the FDA approved sacituzumab (govitecan), a Trop-2-receptor directed antibody conjugated with chemotherapeutic agent topoisomerase inhibitor in metastatic TNBC, and response rate was 30% and the median duration of response is 7.7 months, and the majority of patients did not maintain response longer than 12 months. Therefore, identifying novel molecular targets and developing alternative therapeutic strategies are urgently needed. FOXM1 is a protooncogenic transcription factor suppressed by p53 and drives expression of genes, which play a crucial role in promoting cancer cell proliferation, metastasis, progression, tumorigenesis of TNBC. We previously demonstrated for the first time that *in vivo* targeting of FOXM1 suppresses TNBC tumor growth in mice. Here, analyzing TCGA patient database we found that FOXM1 expression correlates with shorter patient survival and prognosis in TNBC patients. Overall data suggest that FOXM1 is a potential molecular target. However, currently, there is no FDA approved inhibitor of FOXM1. To identify potential inhibitors, utilizing silico docking and molecular dynamics studies we screened the FDA-approved compounds found that flavopiridol interacts with FOXM1. Flavopiridol is a small molecule inhibitor for CDKs and is approved by the FDA for the treatment of Acute Myeloid Leukemia. We demonstrated that flavodilol inhibits FOXM1 expression at nanomolar concentration and cell proliferation, migration, invasion, and induces apoptosis in TNBC cells. We are currently testing favopridol in MDA-MB-231 (human) and 4T1 mouse mammary) TNBC tumor models. In conclusion, our studies suggest that flavopiridol is a highly potent FOXM1 inhibitor and is a promising agent for repurposing to target FOXM1 and for the treatment of TNBC.

#0643 Analysis of the effect of FGFR inhibitor and cannabidiol in colorectal cancer.

Y. Ju[1], W. Kim[1], B. Kim[2], J. Kim[1], J. Bong[1], C. Cheong[1], S. Kang[1], B. Min[1], S. Oh[2], S. Lee[1];

[1]Division Of Colon And Rectal Surgery, Department of Surgery, Korea University Guro Hospital, Korea University College of Medicine, Seoul, Korea, Republic of, [2]Division of Oncology, Department of Internal Medicine, Korea University Guro Hospital, Korea University College of Medicinel, Seoul, Korea, Republic of

Introduction: Colorectal cancer (CRC) remains a serious health problem worldwide. In particular, in the case of stage 4 metastatic cancer, a cure can be expected as multidisciplinary treatment is possible by combining surgery, chemotherapy, and the development of targeted anticancer drugs, but there is still no type of treatment available. It is limited. FGFR (Fibroblast Growth Factor Receptor) has emerged as an important anticancer target in various malignant tumors, and small molecule-based targeted treatments have been developed and clinical trials are underway, and some colon cancer patients are known to have FGFR genetic alterations. Cannabidiol (CBD), a non-psychoactive cannabinoid, has recently been reported to be associated with the ability to induce cell death through various signaling systems in colon cancer, and has anticancer effects and mechanisms related to overcoming anticancer drug resistance. has been identified. Therefore, we sought to analyze the effect of FGFR inhibitors on colon cancer, explore the possibility of developing them as new target substances, and find ways to increase anticancer effects by confirming the effects of combination with cannabidiol (CBD) and related mechanisms.
Method: Cell survival was confirmed through the WST-1 assay, an assay for measuring cell viability. The signaling pathway was identified through western blot. Data were compared using two-tailed Student's t-test or one-way analysis of variance and Tukey's post hoc test.
Result: The FGFR expression pattern was confirmed in various cancer cell lines, and NCI-H716 was confirmed to have high FGFR2 expression in the colorectal cancer cell line. (Figure 1) As a result of treating CBD 4uM and AZD 10nM (Cell proliferation, apoptosis, western blot), cell death occurred more clearly when treated together than when treated alone, confirming the effectiveness of the combination. (Figure 2) An increase in apoptosis of NCI-H716 cells was confirmed when CBD and AZD 4547 were combined. (Figure 3)
Through a heatmap of differentially expressed genes in RNA sequencing, it was estimated that ER stress may be related to the combination effect. (Figure 4)
The relationship between ER stress and the combination of CBD and AZD 4547 on apoptosis of NCI-H716 cells was confirmed. (Figure 5)
Conclusion: It was confirmed that the combined effect of FGFR inhibitor and cannabidiol was effective in colorectal cancer cells, and it was assumed to be related to the ER stress pathway.

#0644 PKC-iota specific inhibitor ICA-1S causes the degradation of mutant p53 in ovarian cancer cell lines.

M. Marzan, N. Oishee, **A. Olatunji**, M. Acevedo-Duncan;
University of South Florida, Tampa, FL

Ovarian cancer is the most lethal malignant disease of female. Treatment options for ovarian cancer are mostly the use of chemotherapeutics, surgery, or radiotherapy. However, due to resistance to drugs, relapse occurs and thus 5 years survival rate is only 47%. The tumor suppressor protein p53 works as a transcription factor to transcribe several proteins such as p21, p16 and PUMA that lead to halt cell cycle and also induce apoptosis when there is a damage in DNA. Mutation in several regions of p53 (mutp53) is quite common in cancers and can lead to the accumulation of p53 with loss of functions or sometimes gain of oncogenic functions. Thus there is a search for drugs that can degrade the mut53 and can restore the functions of normal p53. In this research, it was observed that the treatment of ovarian cancer cell lines (ES-2, HEY and OVCAR3) with atypical protein kinase C-iota (aPKCι) specific inhibitors ICA-1S can cause the degradation of mutp53 (53.6%, N=6 trials). Treatment with ICA-1S also lowered the level of phosphorylated p53 (ser15, 87%, N=3 trials). However, the level of MDM2 protein (murine double minute 2), a known p53 E3 ligase was not significantly (98%, N=2 trials) affected by ICA-1S in ES-2 cell line with mut p53 as well as p21 was also not affected. However level of PUMA was decreased both in ES-2 and HEY cell lines. Immunoprecipitation (IP) with aPKCι specific beads showed the aPKCι is associated with p53, though reverse IP with p53 beads was not able to show the association. Application of proteasome inhibitor MG-132 at a single dose of 0.5μM could not completely inhibit the degradation of mut53 and WTp53 in ICA-1S treated ES-2 cell line and HEY cell line, respectively, indicating the drug may be affecting the transcription of p53 as well. It is therefore postulated that aPKCι can phosphorylate p53, stabilizing it and may be affecting the transcription of p53 as well in those cell lines. Further research (kinase activity assay, immunoprecipitation, immunofluorescence) is going on to reveal the mode of this degradation.

#0645 A systems biology approach uncovers the anticancer mechanisms of curcumin.

A. Aggarwal[1], J. H. Law[2], C. Lo[3], **K. W. Yip**[1];
[1]University of Toronto, Anticancer.ca, Toronto, ON, Canada, [2]University of Toronto, Toronto, ON, Canada, [3]Anticancer.ca, Toronto, ON, Canada

Introduction: Curcumin, the active ingredient of turmeric, generates reactive oxygen species, increases p53 expression, inhibits NF□B signaling, and can induce apoptosis. Despite these potential anticancer effects, there has not yet been a systematic analysis of the effects of curcumin on a large panel of cancer cell lines. We hypothesized that curcumin has differential effects based on the specific cell line and its tissue of origin. This study assessed curcumin's anticancer properties via cell survival assays and gene expression analyses.

Methods: Cell survival assays were performed by the CTD[2] Centre at the Broad Institute. 860 human cancer cell lines were seeded into 1536-well plates, and 24 hours after plating, either DMSO control or curcumin was added to the wells at 16 different concentrations by serial dilution. 72 hours later, cellular ATP levels were measured with CellTiter-Glo as an indication of cell survival. For gene expression analysis, the L1000 assay from the Broad Institute was used. 9 core cell lines were treated with 10 μM of curcumin in 384-well plates. After 6 and 24 hours of incubation, a gene expression signature was identified with the Affymetrix GeneChip HG-U133 Plus 2.0 Array. This signature was compared against signatures from other small molecule and genetic perturbations contained in the CMap database. Afterwards, connectivity scores (incorporating an enrichment score, nominal p-value, and false discovery rate) were used to rank the L1000 signatures by similarity to the signature induced by curcumin.

Results: Curcumin was most potent against SEM (IC_{50} = 1.00 μM; B-acute lymphoblastic leukemia), RPMI-8226 (IC_{50}= 1.62 μM; myeloma), and SCC-4 (IC_{50} = 1.81 μM; squamous cell carcinoma) cell lines. Lymphoid and peripheral nervous system cancers were generally the most sensitive to curcumin, whereas prostate cancers were the least sensitive. Curcumin-induced gene expression changes resembled GPR87 and PRKRA knockdowns, which are associated with reductions in cancer cell survival, chemoresistance, and proliferation in various cancer cell lines. However, these transcriptomic changes also resembled CERS2 downregulation, which is associated with increased cell migration. *In vitro*, curcumin treatment mimicked 2',5'-dideoxyadenosine, BMS-299897, and eudesmic acid administration.

Conclusion: Curcumin induces changes in cell survival and gene expression that support its anticancer properties in a variety of cancer cell lines. However, separating these effects from CERS2 downregulation may be an important component of future translational research for curcumin and its analogs.

#0646 Proteome wide target deconvolution of pharmacologically active natural products by CETSA® coupled to mass spectrometry.

Tomas Friman, Tuomas Tolvanen, Erin Gilson, Alexey Chernobrovkin, Stina Lundgren, Victoria Brehmer, Daniel Martinez Molina

Pelago Bioscience AB, Solna, Sweden

Nature has provided a large plethora of different molecules that in the hands of man has been ascribed to a vast range of pharmacological actions. In some cases, pharmacology is clearly connected to a phenotype e.g., Golgi apparatus dissolution by Brefeldin A, whereas in other cases the proposed phenotypes are many and disparate e.g., Quercetin. Many claims are made around natural compounds as having various positive therapeutic effects on cancer e.g., curcumin and quercetin. Intriguingly, claims about therapeutic effects of various natural compounds keep on surfacing, and we wanted to address this issue by performing target deconvolution of a selection of natural compounds in Hepatic cancer cells: HepG2. We took advantage of the CETSA® (CEllular Thermal Shift Assay) method coupled to Mass spectrometry detection in order to deconvolute the mode of action of seven highly cited natural compounds that comprised both well annotated compounds with an established mode of action: Brefeldin A and Wortmannin; and compounds with a less well established mode of action: Carnosol, Curcumin, Resveratrol, Rhoifolin, and Quercetin. CETSA is a method that allows detection of compound-induced thermal shifts of proteins in intact living cells as well as in cell lysates. Subsequently, a thermal shift of a protein in the presence of a compound then implicates a direct or in the case of intact cells, also an indirect interaction between the protein in question and compound. As CETSA can be performed in intact living cells we could detect proteins that were potential direct binders as well as proteins that were part of the downstream signaling events or part of the phenotypic response. The Natural compounds were assessed in a screening format in which three bio-replicates were analyzed at a single concentration, 30 µM. Good proteome coverage was obtained in the HepG2 cells and all compounds tested induced thermal shifts of proteins at 30 µM. Most of the compounds displayed many protein shifts of both suggested direct targets and proteins presumed to be part of a phenotypic response, as well as novel targets/off-targets. Curcumin and Rhoifolin were the exceptions, which only had a few shifted proteins. Brefeldin A, Quercetin, and Wortmannin engaged proteins associated to their annotated mode of action pathways, whereas Carnosol, Curcumin, and Resveratrol was less specific in their responses with regards to shifted proteins i.e., no clear signaling pathway was determined. In this study we use CETSA coupled to MS detection to delineate mode of action of natural compounds, which shed light on why they could be implicated to have a role in tumor biology. We also found that compounds with a well-established mode of action give a clearer target engagement profile compared to less annotated compounds.

#0647 FDA approved library screen revealed Ewing and clear cell sarcomas have increased sensitivity to filanesib over other cancer types.

H. L. Walker-Mimms, N. Londono, Y. Liao, N. Chaudhary, D. Pena Gomez, Y. Zhang, M. Teng, U. Rix, D. R. Duckett;
Moffitt Cancer Center, Tampa, FL

There is a compelling need for the development of more effective and less toxic therapies for patients with Ewing Sarcoma (ES) and Clear Cell Sarcoma (CCS). ES and CCS are characterized by chromosomal translocations which result in two distinct fusion proteins: EWS-ATF1 (t(12;22)(q13;q12)) in CCS and EWS-FLI1 (t(11;22)(q24;q12)) in ES. There is a strong premise that targeting the fusion proteins or their key downstream signaling pathways will be disease modifying and improve outcomes for patients. Preliminary high throughput screening studies using an FDA approved small molecule compound library identified filanesib, a kinesin spindle protein (KIF11) inhibitor, as having potent anti-proliferative activity in ES and CCS cells over other cancer subtypes. The mechanism linking the fusion proteins with KIF11 and the tumorigenic role of KIF11 in ES and CCS has yet to be described. Previous studies have shown that the EWS-ATF1 fusion protein forms a heterodimer with transcription factors to target the promoters of its downstream genes. In breast cancer, the knockdown of KIF11 has been shown to significantly reduce the phosphorylation of these transcription factors. Additionally, KIF11 has been shown to directly interact with p300/CBP-associated factor (PCAF), a histone acetyltransferase (HAT). HATs are necessary for EWS-FLI1-induced chromatin remodeling. We hypothesize that the fusion proteins, EWS-FLI1 and EWS-ATF1, form a complex with KIF11 that regulates the activity of co-transcription factors during chromatin remodeling. The target of filanesib, KIF11, has essential roles in maintaining cell cycle progression through mitosis and its inhibition results in mitotic arrest and subsequent cell death. We used ImageStream to assess the effects of filanesib on the cell cycle. ImageStream allows both a quantitative and qualitative analysis of the cell cycle by measuring the population of cells that are positive for a given marker as well as imaging each cell by microscopy. Results demonstrate that filanesib promotes an increase in cells arrested in prophase with dramatically altered spindle formation. We are currently addressing the role of KIF11 in regulating the expression levels of the fusion proteins' associated transcriptional coactivators and downstream target genes. By completing these studies, we aim to, i) outline the mechanism underpinning the relationship between KIF11 and the oncogenic fusion proteins in ES and CCS cells, and ii) gain an understanding of why ES and CCS cells are particularly vulnerable to KIF11 inhibition.

This work has been supported in part by the Flow Cytometry and the Molecular Genomics Cores at the H. Lee Moffitt Cancer Center & Research Institute, a comprehensive cancer center designated by the National Cancer Institute and funded in part by Moffitt's Cancer Center Support Grant (P30-CA076292)

#0648 Relevance of substrate selection for the results of biochemical WEE1 in-vitro kinase activity inhibition assays.

D. G. Mueller, **A. Gericke**, F. Totzke, C. Heidemann-Dinger, C. Ketterer, D. Kraemer, T. Weber, M. H. G. Kubbutat;
Reaction Biology Europe GmbH, Freiburg im Breisgau, Germany

Essential biological signaling pathways affecting e.g., proliferation, differentiation, migration, and apoptosis are regulated by protein kinases. Deregulation of protein kinases is observed in many tumor cells and frequently the development and progression of human cancers and other diseases is found to be causally connected to altered activity of specific protein kinases.
Therefore, protein kinases have become a prime molecular target for therapeutic intervention. Multiple small molecule inhibitors targeting different kinases are currently in clinical use for treatment of various types of cancer and other diseases.
A first step in preclinical development of new compounds is testing candidate substances in biochemical in-vitro assays, either based on binding of the compounds to their target or based on alterations of the in-vitro activity of the target kinase monitored in biochemical activity assays.
Depending on the actual mode of action of a compound, the relevance of the results of such in-vitro assays may depend on the actual setup of the assay.
Mainly for reasons of cost and technical feasibility, the use of generic substrates for in-vitro kinase activity assays is well established. While many of those substrates are highly artificial and can only be considered as generic phosphate-group acceptors, they have been successfully used in the past in the development of many approved small molecule kinase inhibitors currently in clinical use.
However, even while many kinases may show activity with generic substrates, for some physiological substrates are required. Members of e.g. the RAF family and other members of the MAPK pathway are highly substrate specific and will not show kinase activity with generic substrates.
Such kinases which have been established with generic substrates are rarely switched to more physiological substrates as most often this will result in increased complexity and associated cost of preclinical compound development.
We have compared the in-vitro activity of WEE1 using different in-vitro activity assay readouts like autophosphorylation, phosphorylation of generic substrates and phosphorylation of its physiological substrate CDK1. In addition, we examined the substrate specificity of WEE1 towards CDK1 alone and in complex with Cyclin B1.
We compared the potency of a selection of WEE1 inhibitors when different substrates were used.
While in early preclinical development the use of rather artificial biochemical assays has been successfully been applied in the past, it should be taken into consideration that at least for the kinase target in focus, the identification, establishment and use of a more physiologically relevant substrate may increase the value of early-stage compound screening results significantly.

#0649 SOX11 regulates BCR signaling via the PAX5/CD19 axis in MCL.

R. Dutta[1], H.-H. Lee[2], V. Leshchenko[1], R. Shukla[1], Y. Liu[2], J. Jin[3], M. Wang[2], S. Parekh[1];

[1]Tisch Cancer Institute, Icahn School of Medicine at Mount Sinai, The Precision Immunology Institute at Mount Sinai, New York, NY, [2]The University of Texas MD Anderson Cancer Center, Houston, TX, [3]Tisch Cancer Institute, Icahn School of Medicine at Mount Sinai, New York, NY

Background: Mantle cell lymphoma (MCL) is an incurable lymphoid neoplasm, comprising about 6% of all non-Hodgkin lymphoma (NHL). The transcription factor SOX11 is overexpressed in the majority of MCL patients and linked to a more aggressive disease course and poorer clinical outcomes. In MCL, naïve B cells experience continuous proliferation because of the dysregulation of the B-cell receptor (BCR) pathway. Our previously published data (Kuo et. al., Blood 2018) identified that SOX11 aberrantly upregulated BCR signaling in transgenic mouse models. The current study describes the exact mechanism by which SOX11 regulates the BCR pathway using a combination of functional and pharmacological approaches.

Methods: To investigate the alterations in signaling pathways regulated by SOX11, we utilized a small molecule SOX11 inhibitor (Jatiani et. al., CCR 2021), performed CRISPR/CAS9 knockout of SOX11, 3X FLAG TAG overexpression, as well as conducted western blot and flow-cytometry experiments.

Results: Our prior published results (Kuo et. al., Oncogene 2015), as well as others (Vegliante et. al., Blood 2013), have shown that PAX5 is a direct target of SOX11. We confirmed PAX5 downregulation after SOX11 depletion in three human MCL cell lines (JEKO, MINO, Z138) using CRISPR-CAS9. Decrease of PAX5 expression was associated with reduction in CD19 expression and a concurrent reduction in phospho-BTK (Bruton tyrosine kinase). Conversely, overexpression of SOX11 could rescue PAX5/CD19 expression and restore p-BTK levels. Furthermore, the treatment of SOX11 expressing cells with small molecule SOX11-specific inhibitors resulted in a reduction in PAX5, CD19 and BCR activation (p-BTK).

Conclusion: Taken together, these findings delineate PAX5 as the direct target and PAX5/CD19 axis as the downstream pathway by which SOX11 regulates B-cell receptor (BCR) signaling in MCL. Notably, our treatment using a SOX11 inhibitor successfully replicated the effects observed with genetic knockdown. In conclusion, our findings provide valuable insights into the molecular mechanisms by which SOX11 contributes to MCL pathogenesis. The further development of pharmacological inhibitors targeting SOX11 holds promise as a beneficial therapeutic strategy for MCL patients, as these will block signaling upstream of current resistance mechanisms.

#0650 Pim3 kinase is a poor prognostic marker and novel molecular target for triple negative breast cancer.

P. Atalay, G. Kara, R. Ozyurt, N. Kahraman, B. Ozpolat;
Houston Methodist Research Institute, Houston, TX

Triple-negative Breast cancer (TNBC) is characterized by the absence of ER, PR, and HER-2 receptors and is associated with poor prognosis, early relapse, and distant metastasis. In neoadjuvant setting, most patients (~50-70%) with TNBC do not achieve complete remission. Currently, there is no effective targeted therapy for TNBC patients. Therefore, identifying novel molecular targets and developing alternative therapeutic strategies are urgently needed. PIM3 is a serine/ threonine kinase and is upregulated in leukemia and various solid cancers. Although PIM1 has been shown to play a critical role in cell proliferation in cMyc-enriched TNBC tumors, the role of PIM3 in TNBC is not known. To determine the clinical significance of PIM3 in TNBC patient prognosis and progression, we performed a Kaplan-Meier analysis in the TCGA TNBC patient database. We found that PIM3 expression is significantly associated with shorter patient survival in TNBC patients (n=77, p=0.0088). PIM3 protein is highly expressed in TNBC cells compared to normal breast epithelium and other ER+ and HER2+ breast cancer subtypes. Inhibition of PIM3 by siRNA significantly suppressed TNBC cell proliferation, migration, and invasion of TNBC cells including MDA-MB-231, MDA-MB-436, and BT20 cells. Lenti-based PIM3 overexpression induced TNBC cell proliferation, invasion, and migration. Non-biased reverse phase protein array (RPPA) assay and Western blot analysis showed that PIM3 inhibition markedly reduced the expression of EF2 Kinase protein, and we found it to be associated with shorter patient survival and poor prognosis. Immunoprecipitation of PIM3 indicated that it forms a heterodimer with EF2K whose inhibition by siRNA also suppressed TNBC cell proliferation, migration, invasion, and tumor growth. Furthermore, PIM3 inhibition by siRNA significantly enhanced the antiproliferative effect of Doxorubicin, which is one of the first-line chemotherapeutics used in patients. Moreover, *in vivo* therapeutic delivery of PIM3 siRNA loaded albumin nanoparticles (ALNPs-PIM3 siRNA) markedly delayed tumor growth of two different TNBC tumor xenograft models (MDA-MB-231 and MDA-MB-436) in mice. Analysis of tumors by IHC after 4 weeks of treatment demonstrated that ALNP-PIM3 siRNA treatment led to inhibition of intra-tumoral proliferation and induction of apoptosis. Currently, we are conducting an in vivo study in TNBC tumor models by combining ALNP-PIM3 siRNA therapy with doxorubicin. Overall, our studies suggest that PIM3 is a marker for poor patient survival that drives TNBC tumor growth and progression and a novel potential molecular target in TNBC.

#0651 3D-bioprinted cancer models for target discovery, drug development, and personalized therapy.

R. Satchi-Fainaro[1], A. Krinsky[1], A. Katyal[1], O. Avramoff[1], E. Yeini[1], L. Neufeld[1], S. Halparin[2], R. Frommer-Shapira[2];
[1]Tel Aviv University, Tel Aviv, Israel, [2]Sheba Medical Center, Ramat Gan, Israel

Many drugs show promising results in laboratory research, but eventually fail in clinical trials. We hypothesize that one main reason for this translational gap is that the cancer models used are inadequate. Most models lack the complex tumor-stromal cell interactions with their microenvironment which are required for tumor progression. Conventional 2D cultures, where cells grow on rigid plastic plates mainly as mono-cultures of a single type of cells, are not able to recapitulate the complex settings of such interactions. Therefore, there is a need to develop a 3D model that better mimics the tumor microenvironment. Hence, we developed a vascularized, hydrogel-based 3D-bioprinted tumor model consisting of patient-derived tumor and microenvironmental cells. Our 3D-bioprinted models are based on a library of hydrogels that we developed as scaffolds for different tumor types, designed according to the mechanical properties of the tissue/organ of origin. The patient-derived models consist of cells from a biopsy, constructed based on CT/MRI scans, and include functional vessels that allow serum and peripheral blood mononuclear cells (PBMC) to flow when connected to a pump. Using this unique model platform, we identified P-selectin as a novel immune checkpoint in the brain regulating cancer-microglia-tumor-associated macrophages (TAMs) interactions. Moreover, we are currently validating our 3D platform for its ability to mimic patient-specific tumors and their microenvironment in order to predict patient response to different treatments (such as chemotherapy, immunotherapy, and targeted therapies). Hence, we are currently conducting an 80-patient “basket” clinical trial testing different treatments on patient samples to validate the ability of our model to predict patient outcomes covering 7 different cancer types. These unique 3D-bioprinted models have the potential to facilitate target discovery and drug development, as well as to serve as a reliable system for precision medicine.

EXPERIMENTAL AND MOLECULAR THERAPEUTICS: Novel Antitumor Agents 2
Poster Session

#0655 Fungal extract screening reveals malformin C to preferentially kill glioblastoma stem-like cells via concerted induction of proteotoxic stress and autophagic flux blockade.

E. L. Phillips[1], S. van Enk[1], S. Kildgaard[2], S. Schlue[1], M. Gottmann[1], V. Jennings[1], F. Bethke[1], G. Muller[1], C. Herold-Mende[3], D. Pastor-Flores[1], M. Schneider[1], D. Helm[1], T. Ostenfeld Larsen[2], V. Goidts[1];

[1]German Cancer Research Center, Heidelberg, Germany, [2]Technical University of Denmark, Copenhagen, Denmark, [3]University Hospital Heidelberg, Heidelberg, Germany

Glioblastoma is a highly aggressive brain tumor for which there is no cure. The dire prognosis of this disease is largely attributable to a high level of heterogeneity, including the presence of a sub-population of tumor initiating glioblastoma stem-like cells (GSCs), which are refractory to chemo- and radiotherapy. Here, in an unbiased marine-derived fungal extract screen, together with bioguided dereplication based on high resolution mass spectrometry, we identified malformin C to preferentially induce cell death in patient-derived GSCs, and explore the potential of this cyclic peptide as a therapeutic agent for glioblastoma. Malformin C significantly reduced tumor growth in an *in vivo* xenograft model of glioblastoma. Using transcriptomics and chemoproteomics, we found that malformin C binds to many proteins leading to aggregation, and rapidly induces unfolded protein response, including autophagy, in GSCs. Malformin C also appears to accumulate in lysosomes, disrupting autophagic flux and driving cells to death. Supporting this, malformin C synergizes with chloroquine, an inhibitor of autophagy. Strikingly, we observed that autophagic flux is differentially regulated in GSCs compared with normal astrocytes. The sensitivity of GSCs to malformin C highlights the relevance of proteostasis and autophagy as a therapeutic vulnerability in glioblastoma.

#0656 A novel dual-targeting peptide HS1002 enhances anti-tumor activity via GnRH/human telomerase reverse transcriptase (hTERT) interaction in human prostate cancer cells.

J. Park, J. Kim, H. Cha, H. Kim;
Sungkyunkwan University College of Pharmacy, Suwon, Korea, Republic of

Human telomerase reverse transcriptase (hTERT) is overexpressed in most human cancers. hTERT is considered as an important target for cancer therapy. In the present study, a new peptide HS1002 were synthesized with sequence of pGlu-His-Trp-Ser-Tyr-Arg-Leu-Arg-Phe-Ile-Pro-NHEt based on the GnRH agonist and hTERT. The aim of this study was to evaluate HS1002 for its anticancer activity by dual-targeting to GnRH/hTERT in prostate cancer cells. Upon comparison with different prostate cancer cell lines, HS1002 exhibited highest cytotoxicity against LNCaP cells. The hTERT expression correlated with telomerase activity in LNCaP cells, was significantly inhibited by HS1002, resulting in reduction of proliferation, metastasis and increase in apoptosis. Additionally, HS1002 suppressed c-Myc and AKT/ERK pathway in LNCaP cells. In the tumor-bearing nude mice model, HS1002 significantly inhibited tumor growth and downregulated the expression of hTERT and Ki-67 in tumor tissue as evidenced by western blot and immunohistochemistry analysis, respectively. Moreover, repeated subcutaneous injection of HS1002 resulted in the reduction of both serum testosterone levels and seminal vesicle weight. HS1002 also increased cytosolic calcium influx and CRE-luciferase activity in GnRHR-overexpressing HEK293 cells compared to mock-transfected transfected cells. Furthermore, a potent cytotoxicity in LNCaP cells was exhibited by HS1002-activated peripheral blood mononuclear cell (PBMC) with interleukin (IL)-2 using LDH release assay. In addition, a flow-cytometric analysis confirmed an elevation in the production of granzyme B and IFN-γ in $CD8^+$ T cells in the MC38 syngeneic mouse model by HS1002. These data indicate that the inhibition of hTERT expression by HS1002 suppresses prostate cancer cell growth and induced anti-cancer immunity. Therefore, HS1002 might be used as a novel therapeutic drug for prostate cancer.

#0657 Discovery of a novel brain penetrant SHP2 allosteric inhibitor with anti-tumor effects.

M. Kim[1], D. Kim[1], Y. Jeon[1], K. Yoon[1], A. Jang[1], M. Lee[2], D. Jeon[2], S. Jang[2], J. Kim[2], E. Kim[2], J. Park[3], V. Hong[3], H. Jung[1], S. Choi[1];
[1]KANAPH Therapeutics, Seoul, Korea, Republic of, [2]Yungjin Pharm, Suwon, Korea, Republic of, [3]Keimyung University, Daegu, Korea, Republic of

KRAS is the most frequently dysregulated oncogene with high prevalence in non-small cell lung cancer (NSCLC), colorectal cancer (CRC), and pancreatic ductal adenocarcinoma (PDAC). Currently, FDA-approved sotorasib and adagrasib provide ground breaking through therapies for cancer patients harboring KRAS G12C mutation. However, there is still high unmet medical needs for inhibitors targeting broader KRAS-driven tumor, especially a substantial unmet medical need for agents that can penetrate BBB to control the brain metastases. SHP2, a key activator of KRAS located in the upstream of RAS pathway, facilitates the conversion of GDP-bound KRAS (off) state to GTP-bound KRAS (on) state serving as a key mechanism of KRAS activation. Therefore, SHP2 could be a promising therapeutic target to shut down the oncogenic RAS pathway as a broad combination partner with RAS/RAF/MEK/ERK pathway inhibitors. Here we report a highly potent and selective brain penetrant SHP2 inhibitor that is designed to target solid tumors metastazied to brain. KT-01766 showed excellent potency against SHP2 protein in various biochemical and cellular assays and showed the robust synergistic effect with RAS pathway inhibitors. KT-01766 as a mono therapy and in combination with KRAS G12C inhibitors demonstrated great anti-tumor efficacy with no apparent toxicity in mouse xenograft models harboring KRAS mutations. Furthermore, robust anti-tumor acitivty was confirmed in intracranial brain tumor model, supporting its potential to control brain-metastasized tumors. The present data suggest that KT-01766 is a potential candidate for combination therapy with agents targeting RAS pathway, as it is able to effectively suppress tumor growth both systemically and within the brain in KRAS mutated cancers.

#0658 Small molecule allosteric regulators of eIF4E activity target proteomic dysregulation and demonstrate potent antiproliferative activity in multiple myeloma models whilst sparing normal immune cells.

L.-M. Sturla, X. Zhang, Y. Kan, R. Gedrich, K. Bowdish, C. VanDeusen;
PIC Therapeutics, Natick, MA

Multiple myeloma is characterized by significant dysregulation of protein translation. The eukaryotic translation initiation factor 4E (eIF4E), a rate determining element of oncogene translation, is highly expressed in multiple myeloma cells compared to normal plasma cells and is associated with enhanced levels of key oncogenic drivers such as MYC. We have developed potent small molecule allosteric regulators of eIF4E activity by aligning medicinal chemistry tools with patient directed pharmacology to optimize and identify orally bioavailable, potent compounds with *in vivo* activity. To identify sensitive cancer models and markers associated with response to PIC eIF4E regulators, we screened the 302-cell line Eurofins OncoPanel™, followed by gene expression profiling comparing the most and least sensitive cell lines and QIAGEN Ingenuity Pathway Analysis. Consistent with the role of eIF4E, we identified proteomic dysregulation as a marker of sensitivity to PIC eIF4E regulators. In addition, the multiple myeloma cell line MM.1R was amongst the most sensitive cell lines. Proteomic analysis of PIC eIF4E regulator treated MM.1R cells identified significant changes, both increases and decreases, in approximately 8% of the 7800 proteins detected by label free mass spectrometry. QIAGEN Ingenuity Pathway Analysis of significantly altered proteins identified enrichment of proteins involved in the G2/M checkpoint, cell cycle control of chromosomal replication, and DNA repair as well as protein translation, EIF4E regulation and mTOR signaling. PIC eIF4E regulators significantly decreased cell viability of both the steroid sensitive MM.1S and steroid resistant MM.1R multiple myeloma cell lines, which was associated with significantly reduced MYC protein levels. Consistent with earlier reported findings and the mechanistic impacts of PIC eIF4E regulators, reduced MYC expression was associated with a significant decrease in hyper-phosphorylated 4EBP1. In contrast to cancer cells, PIC eIF4E regulator treatment did not affect viability of B, T, NK and plasma cell populations in freshly isolated peripheral blood mononuclear cells (PBMCs) at exposures that cause significant cell death in multiple myeloma cells. Furthermore, CD4+ T-cells isolated from fresh PBMCs demonstrated proliferative responses following stimulation (ImmunoCult™) in the presence of PIC eIF4E regulators. The impact on key oncogenic drivers and potent antiproliferative activity in multiple myeloma models with minimal effects on normal immune cell populations suggests that targeting eIF4E activity with PIC allosteric eIF4E regulators could offer an attractive therapeutic strategy in multiple myeloma.

#0659 TR-107 and erastin produce synergistic inhibition of colorectal cancer cell viability *in vitro*.

M. Giarrizzo[1], J. F. LaComb[1], H. R. Patel[1], A. B. Bialkowska[1], R. Reddy[1], L. M. Graves[2], E. J. Iwanowicz[3];
[1]Renaissance School of Medicine at Stony Brook University, Stony Brook, NY, [2]The University of North Carolina at Chapel Hill, Chapel Hill, NC, [3]Madera Therapeutics LLC, Cary, NC

Introduction: Ferroptosis is an emerging potential target for the treatment of colorectal cancer (CRC) and has been shown to sensitize cancer cells to combinatory chemotherapy. Our studies show that the TR-107 compound, an agonist of ClpP - the proteolytic subunit of mitochondrial maintenance complex - can synergize with Erastin, an inducer of ferroptosis cell death. TR-107 potently disrupts mitochondrial proteostasis and attenuates oxidative phosphorylation, resulting in excessive oxidative stress. Here, we show that Erastin synergizes with TR-107 activity by downregulating the cofactor of GPX4, a major intracellular antioxidant defense resulting in CRC cell apoptosis.
Methods: We first evaluated the efficacy of TR-107 against eight CRC cell lines belonging to four established consensus molecular subtypes. Cells were treated with control (DMSO) or TR-107 (10 nM, 50 nM, 1 μM) for 24, 48, and 72 hours. We determined IC_{50} values with Cell Titer-Glo, cell proliferation with the Beckman Coulter cell counter, cell cycle with flow cytometry, OXPHOS activity with Seahorse Real-Time ATP Rate assay, mitochondrial protein levels with western blot and proteomics, and differential gene expression using RNA sequencing and RT-PCR. Subsequently, we assessed the efficacy of TR-107 and Erastin co-treatment. Cells were treated with DMSO, TR-107 (10, 50 nM), Erastin (1, 10 μM), or combinations of the abovementioned concentrations. Cell viability was measured 72 hours post-treatment with Cell Titer-Glo. Synergy scores (HSA) were calculated with Synergyfinder on RStudio. Ferroptosis-related protein expression 24 hours after co-treatment was assessed with western blot and densitometry.
Results: TR-107 IC_{50} values ranged from 2-70 nM, producing a dose- and time-dependent inhibitory effect in cell proliferation. Western blot showed that 50 nM TR-107 abolished the expression of critical mitochondrial proteins ClpX, TFAM, and TUFM. Seahorse data showed a significant reduction in OXPHOS activity. Multi-omics revealed downregulation of respiratory chain complex subunits, mtDNA transcription/translation factors, and upregulation of mitophagy and ferroptosis-related pathways in treated cells. Co-treatment with Erastin produced synergistic HSA scores in 63% (5/8) of assessed CRC cell lines. RKO and NCI-H508 were highly sensitive to Erastin treatment, suggesting that lower Erastin concentrations may synergize with TR-107 and thus reduce dose toxicity. Western blot analysis 24 hours post-treatment showed a loss of GPX4 protein levels in co-treated cells compared to 50 nM TR-107 treatment. This suggests a rapid downregulation of intracellular antioxidant defense that may induce ferroptosis sooner and more effectively than single-agent treatment.
Conclusion: *In vitro* results suggest that co-treating with TR-107 and Erastin produces a significant, synergistic reduction in CRC cell viability.

#0660 OPN-6602, a potent dual EP300/CBP bromodomain inhibitor, targets multiple myeloma through concomitant suppression of IRF4 and c-MYC.

B. Matusow[1], W. Spevak[2], C. Zhang[2], Y. Ma[2], R. Shellooe[1], J. Tsai[2], P. Li[2], P. Chen[1], G. Habets[1], C. Nichols[1], P. Singh[1], K. Inokuchi[1], J. Walling[1], J. Halladay[2], G. Bollag[1];

[1]Opna Bio LLC, South San Francisco, CA, [2]Plexxikon Inc., South San Francisco, CA

Multiple myeloma (MM) is an aggressive hematological cancer derived from malignant plasma cells in the bone marrow. E1A-binding protein (EP300) and CREB-binding protein (CBP) are transcription coactivators that contain both epigenetic writer histone acetyltransferase (HAT) and reader bromo- (BRD) domains that regulate transcription of genes via chromatin remodeling. EP300/CBP inhibition causes cell cycle arrest and apoptosis in MM through suppression of interferon regulatory factor (IRF4) and concomitant repression of c-MYC, rendering EP300/CBP as a novel target for MM. OPN-6602 is a potent, selective, and orally active small molecule dual EP300/CBP inhibitor discovered through structure guided drug design. Its binding interaction exhibits low nM activity on EP300 (Kd= 1.5 nM) and CREBBP (Kd= 1 nM), with > 200-fold less activity against BRD4. OPN-6602 binding to EP300 is particularly potent by Surface Plasmon Resonance analysis, displaying a Kd of 0.87 nM, with a fast association rate (1.5 E+06/Ms) and a slow dissociation rate (1.3 E-03/s) with a residence time of 13 min. It potently inhibits cell growth in MM cell lines OPM-2 (IC50 ~ 4 nM) and MM.1S (IC50 ~ 47 nM) as well as histone acetylation (IC50 ~ 2 nM) via BRD intramolecular modulation of HAT activity. OPN-6602 demonstrated potent inhibition of H3K27Ac in both LK2 (CBP-deficient lung cancer cells, IC50 = 11 nM) and in OPM-2 (IC50 = 1.6 nM). OPN-6602 also potently inhibited H3K27ac expression in PBMCs with IC50s of 0.75 and 1.4 nM, respectively. The effects of OPN-6602 with dexamethasone (dex) or lenalidomide (len) on the growth of OPM-2 and MM1.S cells were evaluated in a matrix combination study. As single agents, maximal growth inhibition reached 60-75% following dex treatment and only 30-40% following len treatment. *In vitro* combination studies utilizing a systematic assessment of a broad range of OPN-6602 concentrations in combination with dex or len demonstrated strong synergy. Synergy was observed between OPN-6602 at 3.7 nM and len through a concentration range from 0.027 to 20 µM. Synergy was observed with 1.2 or 3.7 nM of OPN-6602 in combo with dex concentrations from 0.055 to 40 µM. In the OPM-2 xenograft model, OPN-6602 inhibits tumor growth by 30-111% at doses from 2.5-60 mg/kg QD. This growth inhibition correlated with downregulation of IRF4 and cMYC in tumor samples analyzed by QPCR analysis. The pharmacokinetic profile is favorable for oral QD dose administration due to a high Cmax (19 µg/mL at 24 mg/kg) and short half-life ($T_{1/2}$ = 1.5 hr). A first-in-human study of OPN-6602 in patients with MM is planned for 2024.

#0661 An oral Cbl-b inhibitor with sustained T cell activation demonstrated robust anti-tumor efficacy along with enhanced infiltration and activation of functional T cells.

F. Zhou[1], G. Yang[1], Y. Liu[2], L. Xue[1], W. Chen[2], Z. Li[1], X. Liu[2], J. Li[2], R. Tang[1];

[1]State Key Laboratory of Neurology and Oncology Drug Development, Simcere Zaiming Pharmaceutical Co, Ltd., Shanghai, China, [2]Simcere Zaiming Pharmaceutical Co, Ltd., Shanghai, China

The E3 ubiquitin ligase Casitas B-lineage lymphoma b (Cbl-b) is a member of the highly conserved family of Cbl (casitas b-lineage lymphoma) proteins, which associates with multi-immune response regulations including Teff and NK activation, Treg differentiation. *Cbl-b* KO mice showed enhanced immune responses and resistance to tumor transplantation. Previously, we reported a novel Cbl-b inhibitor, ZM-8026, which robustly activated T cells and efficiently inhibited tumor growth as monotherapy or in combination with anti-PD-1. Here, we further demonstrated that Cbl-b inhibition restores the Teff cells' function in immune suppression conditions, such as in the presence of PGE2, A2AR agonist, and TGF-β. $CD8^+$T proliferation and cytokines induction were maintained in the presence of MDSC. Furthermore, $CD8^+$T function was reversed from an exhausting status induced by a continuous anti-CD3/CD28 activation for a long period. To investigate whether continuous target occupancy was necessary for sustained TCR activation, the dynamic impacts of Cbl-b inhibition on $CD8^+$T cell activation were explored using a washout assay. The results showed that the high-level activated T cells lasted for 48 h after more than 4hs preincubation with 1 μM Cbl-b inhibitor followed by a washout, however, short and weak activation states were found with less than 4hs preincubation or low inhibitor concentration treatment (< 0.1 uM). This finding revealed sufficient inhibitor concentration and treatment time ensure high T-cell activation. Further, *in vivo* efficacy studies demonstrated less anti-tumor growth efficacy for intermittent dosing (Q2D, Q3D) compared with QD dosing. *In vitro* and *in vivo* pharmacokinetics studies exhibited favorable ADME profiles and bioavailability of our Cbl-b inhibitor for oral administration in mice, rats, and dogs. At least in two syngeneic models, our Cbl-b inhibitor exhibited efficient anti-tumor growth with more than 70% TGI (tumor growth inhibition). In a CT26 syngeneic model, complete tumor growth inhibition in 6 of 8 mice was found in the Cbl-b inhibitor combined with an anti-PD1 antibody. The complete regression mice were re-challenged with the same tumor cells, and no measurable tumors were found for up to 30 days, suggesting the treatment-induced immune memory. Tumor samples in mice were collected, RNAseq showed that activated functions of tumor-infiltrated T, NK, DC, and macrophage were dramatically increased in the Cbl-b inhibitor treatment group, and the T and NK activation signature genes such as Gzmb, Ifng were significantly upregulated by RT-PCR. In conclusion, our Cbl-b inhibitor exhibited a favorable PK profile in multi-preclinical animals. The sustained T cell activation *in vitro* was identified and robust anti-tumor growth *in vivo* was demonstrated with optimized dosing frequency.

#0662 Vitamin B1 derivative, fursultiamine, prevents lung cancer cells growth.

N. Boekweg, R. Powers, K. Ramana;
Noorda College of Osteopathic Medicine, LLC, Provo, UT

Lung cancer is the leading cause of cancer death in men and the second leading cause of cancer death in women worldwide. Cigarette smoke-induced oxidative and inflammatory responses are the major risk factors for the development of lung cancer. Several compounds have been tested for their efficacy in preventing lung cancer. However, very few compounds have gone through clinical studies. We hypothesize that with its potent anti-oxidative and anti-inflammatory actions, fursultiamine, a disulfide lipid-soluble derivative of vitamin B1 (thiamine), could prevent lung cancer growth and spread. Our results indicate that treatment of non-small cell lung cancer cells (A549 cells) with fursultiamine prevents A549 cells death in a dose-dependent manner. Similarly, live and dead cell staining assay also confirms that fursultiamine prevents proliferation of A549 cells. Further, fursultiamine prevents A549 cell proliferation by inducing the apoptotic cell death. It also promoted the activation of caspase-3 and cleavage of PARP protein. Fursultiamine also prevented reactive oxygen species in A549 cells. Further, fursultiamine regulated the expression of various anti-apoptotic (Bcl-2, Bcl-x) and pro-apoptotic (Cleaved Caspase-3), survival (Survivin) and anti-survival factors (Clusterin, p-Rad17) in A549 cells. We next planned to examine the effect of fursultiamine on lung cancer growth in vivo using athymic nude mice injected with A549 cells subcutaneously without or with a diet containing fursultiamine. In conclusion, our in vitro results suggest that vitamin B1 derivative, fursultiamine, by promoting the apoptotic pathways prevents lung cancer growth and has potential for further development as a chemoprevention drug.

#0663 Irreversible covalent azetidine-based small molecule inhibitors of Stat3 activity block growth of human pancreatic tumors.

Y. Chen[1], N. Zhai[1], P. Yue[1], C. Brotherton-Pleiss[2], W. Fu[2], K. Nakamura[2], W. Chen[2], M. Tius[2], F. Lopez-Tapia[1], **J. Turkson**[1];
[1]Cedars-Sinai Medical Center, Los Angeles, CA, [2]University of Hawaii, Manoa, Honolulu, HI

The incidence and death rates for pancreatic adenocarcinoma in the US have been increasing by about 1% per year and the death rate has increased by approximately 0.2% yearly. The five-year survival rate has remained below 10% for many years. With surgery, radiation, and chemotherapy being the main treatment options to extend survival or for symptom relief, there is an urgent unmet need for effective new treatment options. Signal Transducer and Activator of Transcription (Stat) 3, one of the Stat family members, is aberrantly activated in human pancreatic and many other cancers. Aberrantly-active Stat3 promotes abnormal tumor-cell intrinsic and extrinsic mechanisms, including dysregulation of gene expression and mitochondria energy metabolism in the tumor cells, and suppression of immune cell functions in the tumor microenvironment. Stat3 is therefore an important target for therapeutic development. Herein we present two small molecules, H182 and H333, which are covalent inhibitors of Stat3 and that potently block Stat3 DNA-binding activity *in vitro*, with IC_{50} 0.66-0.98 μM. H182 and its structural analog, H333 bind Stat3 via irreversible covalent interactions with key cysteine residues in the Stat3 DNA-binding domain to induce a time-dependent inhibition of Stat3 activity. Both compounds inhibit intracellular constitutive Stat3 tyrosine phosphorylation and induce loss of viable cells and apoptosis *in vitro* of human pancreatic Panc-1 and Mia-Paca2 cells. H333 is 13-fold more specific and H182 is 4-fold more specific against tumor cells over normal cells. Furthermore, MiaPaca-2 cells treated with H182 and analyzed by Seahorse showed dramatically decreased mitochondria respiration. Notably, xenograft models of MiaPaca2 treated with H182 or H333 via i.p. every other day for 27 days showed dramatic growth inhibition. Collectively, our results identify H182 and H333 as therapeutically-viable small molecules with unique irreversible mechanism of Stat3 inhibition which accounts for their strong antitumor effects against human pancreatic tumor xenografts.

#0664 GSC000190, a highly potent inhibitor of KIF18A, for tumors with chromosome instability.

P. Tu, C. Zhang, B. Lu, **Y. Xia**, F. Yang;
Changchun Genescience Pharmaceuticals Co., Ltd., Shanghai, China

Chromosome instability (CIN) and Genetic instability is a common feature of malignant tumor cells, which may contribute to tumor progression and lead to drug resistance and tumor metastasis. KIF18A, a member of the kinesin-8 family, is an ATP dependent plus end microtubule motor protein. Studies have found that genetic depletion of KIF18A greatly impacts the chromosome alignment, elongation of mitotic spindles, activation spindle assembly checkpoint of CIN+ tumor cell and leads to cell death, while have little impact towards the survival of normal cells, making KIF18A an attractive therapeutic target for targeting the vulnerability of CIN related tumors. Here we report the pharmacology characterization of a “best in class” potential KIF18A inhibitor for CIN+ tumors. *In vitro*, GSC000190 inhibited KIF18A ATPase activity with a single nM potency and has great potency inhibiting growth of a wide range of TP53 mutant/CIN+ tumor cells. *In vivo*, GSC000190, at approximately one tenth of systematic exposure comparing to that of AMG650, the leading clinical KIF18A inhibitor, causes tumor shrinkage in multiple CDX models including ovarian, colon and lung cancers. In an HGSOC PDX model which is resistant to platinum and olaparib, GSC000190 induced strong tumor regression both as single agent and through combination without significant body weight reduction. PD study confirms a more elevated mitotic phosphorylated histone 3 (PH3) staining in GSC000190 treated tumor tissues, correlating with a better *in vivo* efficacy than that of AMG650. GSC000190 has a favorable ADME profile in rodents, dogs and NHPs, as well as a much better safety profile. GSC000190 is now under IND-enabling study and P1 study is planned in the second quarter of 2024.

Legal entity responsible for the study: The authors.
Disclosure: All authors have declared no conflicts of interest.

#0665 MEN1703/SEL24 exhibits promising antitumoral activity in preclinical models of myelofibrosis both as single agent and combined with ruxolitinib.

M. Iannitto, D. Bisignano, S. Zicari, F. Belli, A. Fiascarelli, S. Talucci, G. Merlino, V. Nicolis di Robilant, C. Irrissuto, M. Bigioni, A. Bressan, D. Bellarosa, M. Binaschi;
Menarini Group, Pomezia, Italy

Myelofibrosis (MF) is a pathological chronic bone marrow (BM) condition characterized by abnormal growth of erythroid and megakaryocytic precursors and deposition of fibrotic tissue. The JAK/STAT pathway plays an important role in MF (Cardoso 2015), and multiple JAK1/2 inhibitors (JAKis) are approved for MF treatment. Despite initially limiting disease symptoms, JAKis often fail due to persistent JAK2 activation and survival of MF-driving cells, hence new treatment strategies are highly needed. PIM kinases also contribute to MF pathogenesis. PIM1 is highly overexpressed in granulocytes, peripheral blood mononuclear cells (PBMCs), and BM of patients with MF. PIM1/2 expression is dependent upon JAK2 signaling in myeloproliferative neoplasms (MPNs). Hence, PIM inhibitors represent potential therapeutic targets for MPNs and have been evaluated in several preclinical and clinical studies (Rampal 2021). MEN1703/SEL24 (MEN) is an oral, first-in-class, dual PIM/FLT3 kinase inhibitor in development for hematologic malignancies.

This study aims to investigate the efficacy of MEN alone and in combination with the JAKi ruxolitinib (RUX) in preclinical MF models and to elucidate the underlying signaling pathways.

MF cell lines ($JAK2^{V617F}$ and JAK2 wild type) were used in MTS assays to assess the *in vitro* cytotoxicity of MEN alone and in combination with RUX, compared with the PIM inhibitor TP-3654 (Dutta 2022). Cell cycle distribution and signaling pathways were analyzed via propidium iodide/FACS analysis and immunocapillary electrophoresis, respectively, upon treatment with the single agents and MEN + RUX. *In vivo* efficacy was assessed in a murine xenograft model treated with MEN +/- RUX.

In vitro studies showed single agent MEN activity with an IC_{50} ranging from 0.3 to 2.3 µM. Moreover, a synergistic drug interaction was found with MEN + RUX in all tested cell lines (Combination Index [CI] range 0.41-0.80). MEN presented cytotoxic and cytostatic capacity, inducing apoptosis and arresting a proportion of cells in G2/M phase. This effect was maintained in combination with RUX. Signaling pathway analysis showed that MEN inhibits phosphorylation of STAT proteins and decreases Mcl1 protein expression. These effects were enhanced with MEN + RUX. Compared with TP-3654, MEN was more effective both as a single agent (IC_{50} 2-3 fold lower than TP-3654) and in combination with RUX (mean CI of 0.77-0.80 compared to 0.79-0.98 with TP-3654).

MEN showed anti-tumoral efficacy in MF preclinical models, moderately higher than TP-3654, exhibiting *in vitro* activity at clinically relevant concentrations. Importantly, MEN combined with the standard of care RUX was synergistic, and molecular analyses confirmed the role of PIM downstream target inhibition. Our results support the therapeutic potential and relevance of MEN in MF treatment strategies.

#0666 ASTX295 engages p53-mediated apoptosis and an inflammatory response in patient derived mesothelioma explants.

D. A. Fennell[1], J. Dzialo[1], J. Rogel[1], D. Faulkner[1], N. Nusrat[1], A. Bzura[1], K. Kutywayo[1], P. Wells-Jordan[1], C. Poile[1], A. Biondo[2], M. Sims[2], A. Nakas[3], J.-L. Luo[1], M. Zhang[4], M. Ahn[2];

[1]University of Leicester, Leicester, United Kingdom, [2]Astex Pharmaceuticals, Cambridge, United Kingdom, [3]Glenfield Hospital, Leicester, United Kingdom, [4]Novogene, Beijing, China

Mesothelioma is a universally lethal, rare cancer caused by asbestos that is lacking effective targeted treatments, particularly in the relapsed setting. P53 is predominantly wildtype (WT 83%) but is likely restrained by MDM2 particularly in the context of 9p21 deletion, a common, clonal somatic event affecting around half of all mesotheliomas that results in deletion of the MDM2 suppressor ARF. 9p21 deletion is also associated with a cold, immunosuppressed microenvironment. Unleashing $p53^{WT}$ by inhibiting its interaction with MDM2 has therapeutic potential in mesothelioma. To test this hypothesis, we employed live *patient derived explants* (PDEs) as a model that reflects the genomic inter-patient heterogeneity of mesotheliomas, and harbours an intact tumour microenvironment. Between August 2017 and April 2021 a total of 71 patients were consented prior to extended pleurectomy decortication, and PDEs were harvested at the time of surgery. PDEs were then cultured and treated with ASTX295, an inhibitor of p53-MDM2 interaction, using two concentrations (0.5 and 1 micromolar) and two timepoints (48 and 72 hours). PDEs passing quality control were subjected to spatial profiling using multiplex immunofluorescence microscopy. PDEs harbouring $p53^{WT}$ showed ASTX295-induced p21 (CDK1A) upregulation, which correlated with induction of apoptosis ($p=0.04$). PDE rank-order sensitivity was conserved across different doses and exposure-times. Transcriptome analysis confirmed ASTX295 induced p53 pathway activation in conjunction with a pro-inflammatory phenotype; both of which were absent in one PDE harbouring an inactivating p53 single nucleotide variant. Constitutive epithelial mesenchymal transition (EMT) was enriched in responding PDEs, as well as MDM2 inhibitor sensitive mesothelioma cell lines. 9p21 deletion (revealed by exome sequencing) was detected in both responding and non-responding PDEs. In summary, inhibition of MDM2-P53 interaction triggers robust p53 activation and a pro-inflammatory phenotype, which is potentiated in EMT enriched mesothelioma PDEs. ASTX295 is currently under clinical investigation (NCT03975387).

#0667 Identification of biomarkers of response to MDM2 inhibition in solid tumours using computational, multi-omics approaches.

H. K. Saini, M. Ahn, G. Ward, J. Kucia-Tran, C. Gewinner, N. Ferrari, J. Brothwood, L. Bevan, **M. Davis**, L. Fazal, M. Sims, M. O'Reilly, G. Chessari, R. Ferraldeschi, J. Lyons, N. Wallis, N. Thompson;
Astex Pharmaceuticals, Inc., Cambridge, United Kingdom

Background High-throughput drug screening and computational methods to associate genomic features of cell lines to drug sensitivity are valuable tools for predicting biomarkers of sensitivity. In addition, integrating genomic features to expression-based patterns could improve biomarker prediction and patient stratification. Particularly weighted gene co-expression networks represent an effective approach to identify key modules and possible biological mechanisms of sensitivity. Using a combination of cell panel screening and gene co-expression networks, we predicted markers of sensitivity to ASTX295 (MDM2i) in cancer cell lines and confirmed expression-based signatures in publicly available clinical datasets.
Method ASTX295 was screened in a panel of 210 p53 wild-type cancer cell lines derived from a range of tumor tissues. ANOVA was used to identify significant associations of genomics features of cell lines to drug response. Transcriptomics profiling of apoptotic and non-apoptotic patient-derived cell lines was performed and significant differentially expressed genes were identified. Further, pathway enrichment and expression-based signatures identified in cell lines were further confirmed in TCGA patient data using weighted gene co-expression network analysis (WGCNA). Expression modules identified by WGCNA were correlated to genomic features and clinical parameters to identify potentially clinically relevant biomarkers.
Results Analysis of the cell panel data identified CDKN2A loss as a statistically significant biomarker predictive of sensitivity to ASTX295. As mesothelioma is one of the indications with high prevalence of loss of CDKN2A, the anti-proliferative activity of ASTX295 was further confirmed in an independent panel of p53 wild-type, patient-derived mesothelioma cell lines. Further, pathway and transcriptional regulator analysis identified the Interferon signalling as significantly enriched in apoptotic cell lines and was confirmed in a TCGA mesothelioma patient data set and the module was found to be significantly correlated with a subgroup of P53 wild-type patients with CDKN2A loss. In conclusion, combining cell panel drug screening with co-expression networks helped to identify biomarkers associated with ASTX295 sensitivity, and provided new insights into the underlying mechanism of ASTX295 response.

#0668 Enhancing chemosensitivity of lung adenocarcinoma via Y-box binding protein 1 (YB-1) inhibition.

J. Lee[1], D. Tailor[1], F. J. Garcia-Marques[2], A. Bermudez[2], S. Pitteri[2], S. V. Malhotra[1];
[1]Oregon Health & Science University, Portland, OR, [2]Stanford University School of Medicine, Palo Alto, CA

Background: Y-box binding protein 1 (YB-1, *YBX1*) is a multifunctional nucleic acid binding protein that regulates the expression of various genes by binding to their mRNA and stabilizing them. In over 20 cancer types, including lung adenocarcinoma (LUAD), *YBX1* expression is significantly elevated in tumor samples compared to normal tissue. Within cancer cells, YB-1 promotes the expression of genes involved in tumorigenesis and chemoresistance. Consequently, elevated *YBX1* expression in tumor is associated with poor clinical outcomes and significantly reduced overall survival in LUAD patients. Therefore, YB-1 emerges as a promising therapeutic target for LUAD treatment. Utilizing a small molecule YB-1 inhibitor, CET056, we performed a series of *in vitro* and *in vivo* analyses to assess the therapeutic efficacy of YB-1 inhibition and unravel YB-1's role in tumorigenesis and disease progression in LUAD.
Methods: Four human and one mouse LUAD cell lines were treated with CET056 and/or chemotherapeutic drugs and analyzed for the *in vitro* therapeutic activity of CET056. Using xenograft and syngeneic LUAD mouse models, the preclinical therapeutic efficacy of CET056 on disease progression of LUAD was also tested.
Results: CET056 was shown to effectively decrease YB-1 expression in both human and mouse LUAD cell lines and exert inhibitory effects on LUAD *in vitro* and *in vivo*. This treatment delayed tumor progression and metastasis in CMT-64 syngeneic mouse model. Proteomics analysis revealed that translational machinery-associated pathways were down-regulated in LUAD cells after CET056 treatment whereas apoptosis and cell death-associated pathways were up-regulated. In alignment with this finding, CET056 treatment in combination with cisplatin showed chemo-sensitizing effect on LUAD *in vitro* and *in vivo*.
Conclusion: Our studies suggest that YB-1 could be a promising target for combating chemoresistance in LUAD. Inhibition of YB-1 with a small molecule drug as a monotherapy or combination therapy could an effective strategy to treat LUAD.

#0669 Interrogating circadian clock compounds as an adjuvant to chemoradiation against GBM.

P. Chan[1], Q. Wu[2], A. Hovsepyan[3], S. Mkhitaryan[3], G. Karapetyan[3], K. Shah[4], H. Wakimoto[5], T. Kamenecka[6], L. A. Solt[6], J. Cope[7], T. Hirota[8], R. A. Moats[3], J. N. Rich[2], S. A. Kay[1];

[1]University of Southern California, Los Angeles, CA, [2]School of Medicine UPMC, University of Pittsburgh, Pittsburgh, PA, [3]Children's Hospital of Los Angeles, Los Angeles, CA, [4]Brigham and Women's Hospital, Harvard Medical School, Boston, MA, [5]Massachusetts General Hospital, Harvard Medical School, Boston, MA, [6]UF Scripps, University of Florida, Jupiter, FL, [7]Synchronicity Pharma, San Jose, CA, [8]Nagoya University, Nagoya, Japan

Despite the extensive efforts of researchers and physicians over the past two decades, glioblastoma (GBM) remains the most prevalent brain tumor type with a grim average survival time of 8 months following diagnosis irrespective of treatment. Additionally, the current standard-of-care has not changed from maximal surgical resection followed by concurrent chemoradiation from its establishment in 2005. One of the major challenges that limits progress in treating GBM is the presence of GBM stem cells (GSCs) that are highly invasive, reaching far past the tumor margins, are resistant to both chemotherapy and radiation, and can recapitulate the primary tumor following resection. Recent studies have found that GSCs, however, are highly sensitive to targeting of core circadian clock components, particularly positive regulators of the clock Brain and Muscle ARNTL-Like 1 (BMAL1) and Circadian Locomoter Output Cycles Protein Kaput (CLOCK). Here we employ the use of small molecule compounds that upregulate the activity of the negative regulators of the clock in order to suppress BMAL1::CLOCK transcriptional activity or repress *BMAL1* transcription. We find that these compounds not only have a much more potent effect against GSCs compared to temozolomide (TMZ) chemotherapy but also, they display combination effect against both GSCs and differentiated GSCs (DGCs) when combined with TMZ. These results suggest that the blood brain barrier (BBB) penetrant circadian clock compounds can be utilized as an adjuvant to current GBM therapies as they can effectively target both the primary tumor cells and GSCs.

#0670 Preclinical candidate LAE120, a novel selective USP1 inhibitor shows effective anticancer and combination activity with PARP inhibitor.

J. Wang, Y. Chen, J. Chen, L. Jiang, X. Lin, C. Cai, M. Zhang, M. Li, J. Gu;
Laekna Therapeutics Shanghai Co., Ltd., Shanghai, China

The Fanconi anemia (FA) and translesion synthesis (TLS) are DNA damage tolerance and repair pathways that have been found to be regulated by reversible ubiquitination in which ubiquitin-specific protease 1 (USP1) plays a key role. Numerous studies have indicated that USP1 inhibitors have therapeutic effects on tumors with homologous recombination deficiency (HRD), including mutations in BRCA1/2. Due to the emergence of resistance to PARP inhibitors in clinical applications, new strategies are needed to address this issue. Here we present LAE120, a novel, allosteric and highly potent USP1 inhibitor, displayed monotherapy potency and combination activity with PARP inhibitor in HRD cancers. LAE120 has a unique tail group distinct from all the published USP1 inhibitors and is predicted to induce a different conformational change at the USP1 allosteric site. In the biochemical assay, LAE120 strongly inhibited USP1 enzymatic activity with IC_{50} of 5.6 nM. LAE120 potently inhibited proliferation of BRCA-mutated MDA-MB-436 breast cancer cell (IC_{50}:19 nM) and exhibited anti-proliferative activity in NCI-H1792 (IC_{50}: 69 nM) and K562 (IC_{50}: 38 nM) cell lines. In the xenograft model of MDA-MB-436 cells with BRCA mutations, LAE120 demonstrated robust single-agent tumor inhibitory activity (TGI: 88%, 10 mg/kg BID) and a favorable dose-dependent response (TGI: 106%, 25 mg/kg BID). We also observed strong tumor-inhibition efficacy of LAE120 as a single agent in the K562 xenograft model with Bcr-Abl expression (TGI: 86%, 10 mg/kg BID). Current research indicates that USP1 inhibitors exhibit synergistic activity in combination with PARP inhibitors and re-sensitizes PARP refractory tumors. Similar results have been confirmed in the xenograft model of BRCA-mutated MDA-MB-436 cells. The combination of LAE120 and Olaparib (PARP inhibitor) yielded a more robust and durable anti-tumor efficacy at low dose (TGI: 110%, LAE120, 5 mg/kg BID + Olaparib, 50 mg/kg QD). LAE120 also displayed favorable ADME properties and PK profiles. Preclinical-tox studies indicated the molecule was well tolerated without significant toxicities and hematological observations. Both in vitro and in vivo data strongly support further investigation of LAE120, whether as a single agent or in combination therapy.

#0671 G-protein coupled receptor (GPCR) screening library identifies sertindole, an antipsychotic, as potential therapeutic option to target GNAQ mutation Q209L in uveal melanoma.

S. Rheinschmidt[1], **T. Bargenquast**[2], S. Adamson[1], T. Thode[1], A. Weston[1], T. Ghosh Halder[1], S. Ng[1], H. Tulasi[1], B. Durbin[1], J. Moser[2], M. Kaadige[1], R. Soldi[1], S. Sharma[1];

[1]TGen (Translational Genomics Research Institute), Phoenix, AZ, [2]HonorHealth Research Institute, Scottsdale, AZ

Background: Uveal melanoma is a rare but aggressive intraocular malignancy with limited therapeutic options. A hallmark genetic alteration associated with uveal melanoma is the mutation of the GNAQ gene, particularly the Q209L substitution in the Gαq protein, which contributes to oncogenic signaling and tumor progression. The GNAQ gene encodes for a Gαq protein that plays a critical role in signal transduction pathways involving G protein-coupled receptors (GPCRs). The Q209L substitution results in a gain-of-function mutation, leading to the chronic activation of downstream signaling pathways. This persistent signaling activity contributes to the uncontrolled growth of uveal melanoma cells. As G protein-coupled receptors (GPCRs) play a crucial role in this process, screening libraries of GPCR inhibitors has been explored as a potential therapeutic avenue. These libraries comprise a vast array of compounds with the potential to block or modulate GPCR activity. Identifying specific inhibitors that can effectively interfere with the oncogenic signaling cascades triggered by the mutated Gαq protein is a critical step in developing targeted therapies for uveal melanoma.
Methods: GPCR library high throughput screening employed isogenic cell lines expressing wild type or mutant (Q209L) GNAQ. This process utilized IP-One assays to identify compounds affecting Gq-coupled receptors by detecting inositol monophosphate accumulation. Subsequently, promising hits were evaluated for their impact on inhibiting the growth and proliferation of uveal melanoma cells. Further analysis involved Western blotting to assess their potential in promoting autophagy and apoptosis, inhibiting downstream signaling pathways, and a migration assay. Finally, ROS generation was assessed using flow cytometry.
Results: Using isogenic cell lines expressing GNAQ gene wild type and the Q209L mutant, a high-throughput screening of GPCR libraries identified sertindole among 5 hits. Sertindole showed a dose-dependent inhibition of Q209L-mutated uveal melanoma cells, significantly reducing cell viability, proliferation, and migration. It also suppressed key signaling pathways, including the critical MAPK pathway, and activated autophagy and apoptosis, likely via ROS generation. These findings suggest sertindole's multifaceted approach in suppressing cancer in uveal melanoma.
Conclusion: Our study highlights the potential therapeutic value of sertindole in GNAQ Q209L-mutated uveal melanoma. Further research is needed to evaluate the efficacy of sertindole in preclinical mouse models of uveal melanoma.

#0672 Small molecule NSC59984 stimulates mitochondria-dependent ferroptosis and overcomes integrated stress response pro-survival signaling in pre-clinical pancreatic and colorectal cancer models.

P. R. Srinivasan, A. J. De La Cruz, M. Pinho-Schwermann, A. George, W. J. MacDonald, S. Zhang, W. S. El-Deiry;
Legorreta Cancer Center at Brown University, Providence, RI

Pancreatic and colorectal cancer are leading causes of cancer deaths worldwide. Resistance to current therapeutics is a significant challenge in treating these cancers. Ferroptosis, a non-apoptotic iron-dependent form of cell death characterized by overwhelming lipid peroxidation, has emerged as a potential strategy to overcome drug resistance. Our lab previously identified the small-molecule NSC59984 as a p53 pathway restoring compound that induces reactive oxygen species, requires p73, and targets mutant p53 for ubiquitin-mediated proteolysis involving MDM2 and HSP90. In pre-clinical models of pancreatic and colorectal cancer, we now show that the small-molecule NSC59984 induces lipid peroxidation and causes reactive oxygen species-dependent apoptosis as monotherapy. However, when combined with ferroptosis inducers or cystine deprivation, NSC59984 potently induces ferroptosis in a mitochondrial complex III-dependent manner. Using CRISPR/Cas9 in pancreatic cancer cells, we further show that HRI, an EIF2-alpha kinase responsible for the cellular response to mitochondrial stress, induces the integrated stress response (ISR) upon treatment with NSC59984 or ferroptosis inducers. The ISR serves as a mechanism for resistance to cell death induced by NSC59984 or ferroptosis inducers, causing upregulation of key anti-oxidative stress and anti-ferroptosis proteins, including the cystine importer SLC7A11 and the GPX4-stabilizing protein HSPA5/BIP/GRP78. The combination therapy overcomes the ISR to induce potent cell death. Our work demonstrates the importance of the interplay between mitochondria and the ISR during ferroptosis induction in pancreatic and colorectal cancer cells.

#0673 Mechanisms of drugs in ovarian cancer and prevention of invasion and metastasis.

L. F. Mortan, D. Benbrook;
University of Oklahoma Health Sciences Center, Oklahoma City, OK

Introduction: Ovarian cancer patients are typically diagnosed late stage after the cancer has left the primary site, this is the major factor contributing to the 70% 5-year mortality rate. Standard of care is Platinum therapies or debulking surgery followed by maintenance therapies to keep cancer from coming back. The limitation to these therapies is overall toxicity to the patient forcing them to stop treatments or eventual resistance to the therapy. The objective of this study is to evaluate the mechanisms in which the novel drug, SHetA2, alone compares to the competitor, Olaparib. Additionally, discover the genetic differences between attached tumor and floating tumor in ascites.Objective: Our objective was to evaluate the mechanisms in which the novel drug, SHetA2, alone compares to the front-line competitor, Olaparib, in affecting Filamin A and cyclin d1 levels in ovarian cancer. Methods: Individual and combination drug treatments were preformed on two ovarian cancer cell lines and patient samples for cell viability assays. Immunocytochemistry was performed to visualize colocalization of proteins. RNA isolation was performed for Nanostring analysis.
Results: Ovarian cancer cells treated with SHetA2 or olaparib demonstrate a decrease of cyclin D1 on the membrane colocalized with filamin A, a structural protein that facilitates movement by acting as a signaling molecule for downstream effects. Nanostring analysis of attached tumor and spheroids form ascites shows significant differential gene expression in tumor versus ascites.
Conclusions: These results suggest the decrease of cyclin D1 with filamin A upon treatment with SHetA2 or olaparib could be one of the primary factors leading to each drug’s efficacy and additivity with each other. The differential gene expression of tumor versus ascites begins to elucidate the fundamental differences between attached and floating tumors and spheroids.

#0674 Novel anti-cancer small molecule targeting the protein regulator of cytokinesis pathway.

A. Peled[1], M. Abraham[2], H. Wald[2], R. Rosenfeld[2], O. Eizenberg[2], A. Aharon[2];
[1]Hadassah Hebrew University Hospital, Jerusalem, Israel, [2]Alonbio ltd, Ness Ziona, Israel

Aberrant migration and proliferation of cancer cells are the hallmark of metastatic tumors. Protein Regulator of Cytokinesis 1 (PRC1) is a scaffold protein that regulates metabolic pathways of cancer cell proliferation, survival, and metastasis. BKT300 is a small molecule (MW 399.33, C22H25NO6), that selectively inhibits the migration and survival of hematological and solid cancer cells. BKT300 inhibits, at high affinity, both actin and microtubule formation and organization leading to G2/M cell cycle arrest, mitotic catastrophe, and apoptosis through the caspase 3 pathway. These effects are selective to cancer cells and were not observed on normal cells. BKT300 was found to arrest PRC1 in a phosphorylated form at position T481, down regulates the expression of CDC25C and up regulate p21. Suppression of PRC1 using SiRNA ablation inhibited BKT300 induced apoptosis on several tumor cell lines and inhibited the effect of BKT300 on G2M cell cycle arrest. Furthermore, using Biacore SPR, microscale thermophoresis (MST), and ELISA assays we were able to demonstrate the direct binding of BKT300 to PRC1. Beyond its single agent activity, BKT300 was shown to synergize with standard of care (SoC) treatments, including anti PD-1 immunotherapy, BCL-2 inhibitor (Ventoclax), topoisomerase I inhibitor (Irinotecan) topoisomerase II inhibitor (Doxorubicin), anti-metabolite Fluorouracil (5-FU) and alkylating agent (Temozolomide). BKT300 has a remarkable safety profile when administered at high doses to mice rats, minipigs and non-human primates. Treatment with BKT300 showed almost no effects on hematopoiesis and biochemistry in doses far higher than the affective ones. The in-vivo activity of BKT300 was demonstrated in multiple Xenograft, Syngeneic and PDX models in mice. In-vivo treatment with BKT300 resulted in preventive (small tumors) as well as therapeutic (large tumors) activity in triple negative breast cancer (TNBC) xenograft, MDA-MB-453 and MDA-MB-468 models leading to over then 70%-90% reduction in tumor size following one to two treatments cycles. Similar results were obtained using PDX models derived from patients with Colon, Ovarian and Pancreatic cancer. BKT300 is a novel, first in class, targeted anti-cancer treatment that inhibits the activity of the scaffold protein PRC1. BKT300 is expected to provide a new treatment option to, the high unmet medical need of, advanced difficult to treat cancers, specifically ones that overexpress PRC1 and CDC25C.

#0675 Targeting Bcl-2/Bcl-xl for small cell lung cancer treatment with LP-118.

L.-L. Lee[1], H. Chen[2], C. Zhu[3], Y. Chen[4], B. Feldmeier[5], Y. Shen[3], Y. Chen[1], S. P. Anthony[1], F. Tan[6], Y. Chen[1], **B. Dai**[1];
[1]Newave Pharmaceutical Inc., Pleasanton, CA, [2]University of Toronto Scarborough, internship at Newave Pharmaceutical Inc., Toronto, ON, Canada, [3]Guangzhou Lupeng Pharmaceutical Co. Ltd., Guangzhou, China, [4]The Quarry Lane School, internship at Newave Pharmaceutical Inc, Pleasanton, CA, [5]Amador Valley High School, internship at Newave Pharmaceutical Inc, Pleasanton, CA, [6]Guangzhou Lupeng Pharmaceutical Co. Ltd., Guanghzou, China

Small cell lung cancer (SCLC) is an aggressive form neuroendocrine carcinoma with limited treatment options and poor prognosis, and novel approaches are urgently needed for the treatment of this disease. Bcl-2 and Bcl-xl are aberrantly expressed in 60-70% SCLC and have been considered as promising therapeutic targets for SCLC. However, navitoclax (ABT-263), a Bcl-2/Bcl-xl dual inhibitor, demonstrated limited efficacy in SCLC while induced sever adverse events, such as thrombocytopenia due to the platelet toxicity mediated by Bcl-xl inhibition. Therefore, agents with novel mechanisms of action and safety profile are to be developed for the treatment of SCLC with Bcl-2/Bcl-xl dependency. LP-118 is a new generation and super potent Bcl-2 inhibitor with moderate Bcl-xl activity, and it is being evaluated in Phase1 clinical trials in solid tumors and hematological cancers (NCT05025358, NCT04771572). In this preclinical study, we aimed to evaluate the single agent activity of LP-118 in a panel of 9 SCLC cell lines and to further determine if LP-118 can enhance the efficacies of Standard of Cares (SOC) *in vitro* and *in vivo*. The results show that LP-118 has high *in vitro* activity in a subset of SCLC cell lines, and it is particularly potent in Bcl-2-depended cell lines, such as NCI-H889, with the IC_{50} of 0.15 nM. LP-118 is also very potent in NCI-H1963, a Bcl-xl dependent cell line (IC50: 5nM), and NCI-H526, a Bcl-2/Bcl-xl co-dependent cell line (IC50: 4-5.1 nM). Overall, LP-118 is more potent than ABT-263 in Bcl-2 or Bcl-2/Bcl-xl co-dependent cell lines, and it is relatively less active in Bcl-2/Bcl-xl/Mcl-1 co-dependent cell lines, such as NCI-H69 (IC50: 169.7 nM). In addition, combinations of LP-118 and SN-38 (the active metabolite of irinotecan), topotecan, or etoposide, induced strong synergist effects in both NCI-H69 and NCI-H146 cell lines, suggesting that LP-118 could enhance the cytotoxicity of these drugs. Consistent with the *in vitro* data, treatment with LP-118 alone induced complete tumor remissions in NCI-H889-derived xenograft models (10/10), whereas no complete tumor remission was observed in the ABT-263-treated group. Moreover, LP-118 plus carboplatin or topotecan dramatically inhibited tumor growth of NCI-H526 xenograft models and has significantly better efficacy than either carboplatin or topotecan alone. Importantly, no significant body weight loss was observed in mice treated with LP-118 single agent or the combinations, indicating such regimens were well tolerated. In summary, LP-118, a new generation Bcl-2/Bcl-xl dual inhibitor, is highly active, as single agent or in combination with SOCs, in a large subset of SCLC cell lines. Clinical trials are ongoing to further evaluate the safety and efficacy of LP-118 in hematological cancers and solid tumors, including SCLC. Additional studies are also underway to develop predictive biomarkers for facilitating patient stratification in the clinic.

#0676 The integrated stress activator BTM-3566 overcomes therapeutic resistance in mantle cell lymphoma.

Y. Liu[1], H.-H. Lee[1], J. McIntosh[1], Y. Li[1], T. Zhang[1], W. Wang[1], M. J. Kostura[2], M. Wang[1];
[1]The University of Texas MD Anderson Cancer Center, Houston, TX, [2]Bantam Pharmaceutical, 8 Davis Dr. Suite 220, Research Triangle Park, NC

Successive generations of BTK inhibitors and CAR T-cell therapy have transformed the treatment of mantle cell lymphoma (MCL). However, treatment resistance has inevitably emerged, creating significant medical need. Recently a novel, clinical stage small molecule, BTM-3566, has been described that targets a mitochondrial process essential for Diffuse Large B-cell lymphoma (DLBCL) survival. BTM-3566 activates the mitochondrial protease OMA1, triggering the ATF4 integrated stress response (ISR). BTM-3566 has robust *in vitro* efficacy in DLBCL cell lines irrespective of genomic background and elicits complete tumor regression in multiple CDX and PDX mouse models of DLBCL. Based on the activity observed in DLBCL, we further explored the effectiveness of BTM-3566 in MCL models *in vitro* and in xenograft mouse models *in vivo*. BTM-3566 inhibited cell proliferation across a panel of MCL cell lines, irrespective of resistance status to ibrutinib and venetoclax (IC_{50}s of 142.5-687.6 nM). Following a 24-hour treatment with BTM-3566, a dose-dependent increase in apoptosis was observed in four tested MCL cell lines—JeKo-1, JeKo-IBN-R, Mino, and Mino-VEN-R, as determined by increased caspase-3 activation and PARP cleavage. Similarly, western blot analysis revealed dose-dependent reductions in MCL-1 and c-MYC, accompanied by an increase in the transcription factor ATF4, indicative of activation of the stress response. We evaluated the *in vivo* efficacy of BTM-3566 in the JeKo-CDX mouse model. Daily oral administration of BTM-3566 at 10, 20 and 30 mg/kg ($n = 5$ for each group) in a 5-day on and 2-day off schedule resulted in tumor regression at all three doses (Treatment vs. Vehicle, $p < 0.01$). We expanded our investigation to PDX mouse models, including those derived from patients resistant to multiple therapies. Four PDX models encompassing naive, rituximab-resistant, BTKi-CAR T dual-resistant and BTKi-VEN-CAR T triple-resistant models were evaluated. BTM-3566 treatment results in nearly complete tumor growth inhibition associated with robust reductions in tumor burden in treated mice across all four PDX models (reduction in tumor weight at the study endpoint, $p < 0.001$). Notably, no toxicity was observed during the treatment period. In summary, BTM-3566 is effective in treating MCL *in vitro* and *in vivo* in preclinical studies.

#0677 Discovery of a first-in-class allosteric inhibitor of the small GTPase Rac1.

Robert Silverman[1], Alan Cooper[1], Ronodip Kar[2], Mayuri V. Raman[2], Ramu Ravirala[2], Mubarak Hasan Shah[2], Sandeep Mahankali[2], **Erik T. Goka**[1]

[1]Revere Pharmaceuticals, Arlington, MA,[2]Aurigene Pharmaceutical Services Limited, Telangana, India

The Rac1 signaling pathway is known to be hyperactivated in numerous solid tumors. We developed a Rac1 AlphaLISA assay that is amenable to high-throughput screening (HTS) to screen large libraries of small molecules. Based on molecular modeling of a putative allosteric binding site for several of the hits, we optimized a series of compounds that lead to RP-102124. RP-102124 engages with Rac1 in both biochemical and cellular target engagement assays. RP-102124 has greater potency than previously reported Rac1 inhibitors in biochemical assays, with potent inhibition of phenotypic characteristics of Rac signaling such as cell migration and cytoskeletal rearrangements. RP-102124 is a Rac^{multi} inhibitor with activity against oncogenic Rac1b. RP-102124 is orally bioavailable and shows dose dependent inhibition of tumor growth in xenograft models at doses that are well-tolerated. RP-102124 is a first-in-class allosteric Rac^{multi} inhibitor that shows promising therapeutic potential.

#0678 Experimental therapy of triple negative breast cancer with next-generation of MDM2 inhibitors.

W. Wang[1], H. Chen[2], Y. Xie[2], S. Datta[1], W. Li[2], R. Zhang[1];
[1]University of Houston, College of Pharmacy, Houston, TX, [2]University of Tennessee Health Science Center, Memphis, TN

Patients with triple-negative breast cancer (TNBC) typically experience minimal benefits from the existing hormonal or trastuzumab-based therapies, necessitating reliance on chemotherapy as the predominant treatment approach, which, unfortunately, is limited by insufficient efficacy, significant side effects, and the development of drug resistance. These issues highlight an urgent demand for the discovery and development of more effective and safer therapeutics for TNBC. Overexpression and amplification of the MDM2 oncogene frequently occur in TNBC, which is associated with invasive and high-grade/late-stage tumors, metastasis, and recurrence, and is an independent negative prognostic factor for TNBC patients. Extensive studies have indicated that MDM2 represents a novel molecular target for TNBC. Thus far, multiple strategies aiming at MDM2 inhibition have not succeeded in Phase II-III clinical trials, largely due to factors like inadequate efficacy, significant drug toxicity, and emergence of resistance. In addition, TNBC tumors commonly harbor mutant p53, and the existing MDM2 inhibitors that block p53-MDM2 binding and depend on wild-type p53 expression in the tumor to exert anticancer effects would have little or no clinical responses or even induce resistant clones by increasing MDM2 expression and its oncogenic activity. Therefore, there is a need for developing new-generation MDM2 inhibitors that are p53-independent. We recently discovered a novel class of MDM2 degraders, representing a paradigm shift in the strategy of targeting MDM2. One of these analogs, WW68, was identified as a potent and selective MDM2 inhibitor. Its *in vitro* and *in vivo* anti-breast cancer activities and underlying mechanisms of action were evaluated in breast cancer cell lines with various p53 backgrounds. Our results demonstrate that WW68 effectively induces MDM2 protein degradation. It selectively inhibits breast cancer cell growth, decreases cell proliferation, and induces G2/M phase arrest and apoptosis in breast cancer cells, regardless of p53 status. Notably, in clinically relevant TNBC PDX models, WW68 inhibited MDM2 and suppressed tumor growth without causing host toxicity. In conclusion, WW68 represents a new class of MDM2 inhibitor that exerts its anticancer activity through directly down-regulating MDM2, and may be developed as a novel anti-TNBC therapeutic agent. (Supported by NIH R01CA214019 and R01CA240447; and DoD W81XWH2010011)

#0679 TXB-001 is an upgraded conjugated anthracycline that targets tumors with reduced risk of cardiotoxicity, hand-foot syndrome and alopecia.

K. Oshida[1], M. Hirakata[1], E. Tomikawa[1], C. Sakai[1], M. Uchida[1], R. Shimozono[1], A. Izawa[1], Y. Koga[1], T. Okano[1], H. Narumi[1], L. Munakata[2], R. Suzuki[2], M. Nonaka[3], Y. Uezono[3];

[1]Toray Industries, Inc., Kamakura, Japan, [2]Teikyo University, Tokyo, Japan, [3]The Jikei University School of Medicine, Tokyo, Japan

TXB-001 is a well-optimized N-(2-hydroxypropyl)methacrylamide copolymer-based conjugated pirarubicin (THP) and a novel candidate for developing anticancer drugs. It exhibits tumor-specific accumulation due to the enhanced permeability and retention effects and prolonged circulation time compared with free THP. Its hydrazone bond is dissociated under lower pH conditions, providing selective and rapid release of THP in acidic tumor environments. Therefore, TXB-001 is expected to have high efficacy and low toxicity. Anthracycline anticancer drugs have been widely used for the treatment of several cancers, but their use is limited by several adverse effects (AEs), including cardiotoxicity, which is a life-threatening AE. Furthermore, the maximum lifetime cumulative dose is decided for each anthracycline in clinical use, which leads to discontinuation of the medication. Hand-foot syndrome (HFS) is a dose-limiting AE of DOXIL®, a liposomal formulation of doxorubicin (DOX), and although it is not a life-threatening condition, it significantly deteriorates quality of life (QOL). Alopecia is another common AE, which is relatively noninvasive but adversely affects mental health and reduces QOL. In this study, we confirmed the efficacy of TXB-001 in a mice triple-negative breast cancer (TNBC) model and evaluated the cardiotoxicity-, HFS- and alopecia-inducing effects of TXB-001 in mice and rats to compare the severity with existing anthracycline anticancer drugs, including DOXIL®. The pharmacokinetic (PK) analysis in several tissues, including plasma, tumor, heart, skin of the chest, and palmar and plantar areas, was also performed after a single intravenous administration in rodents. As a result, TXB-001 showed an equivalent or greater antitumor effects than other anthracyclines in the TNBC model, and the AEs were scarcely observed. TXB-001 did not decrease left ventricular ejection fraction, with no or little HFS-like changes compared with DOXIL®, which showed significant histopathological changes. TXB-001 also showed weaker alopecia-inducing effects than DOX, DOXIL®, and THP. In the PK analysis, TXB-001 was distributed in the tumor at a higher concentration than in other tissues, except for plasma. Hence, most of the THP, the active ingredient, was released in the tumor. The exposure of the heart in the TXB-001-treated group was one-tenth of that in the DOXIL®-treated group. Moreover, accumulation in the skin, especially in palmar and plantar areas, was observed for DOXIL®, but no accumulation in the skin was observed for TXB-001. This PK profile consistently demonstrated the antitumor activity of TXB-001, without AEs. TXB-001 reduces the chance of dose-limiting and QOL-threatening AEs, and thus, cancer patients can continue treatment, making it a more convenient anticancer drug in clinical use with a wide safety margin.

#0680 Leveraging an RNA-targeting platform for the discovery of cell-active c-MYC mRNA-binding small molecules.

M. J. Smola, K. Marran, S. E. G. Thompson, B. Patterson, R. K. Pavana, C. Sutherland, J. A. Sorrentino, **K. D. Warner**;
Ribometrix, Durham, NC

The MYC gene, with its oncogenic potential, has long been a formidable challenge in conventional drug discovery efforts, and its critical role in cancer progression and resistance has underscored the need for innovative therapeutic strategies. Here we demonstrate the capabilities of the Ribometrix RNA-targeting platform to modulate the c-MYC mRNA with small molecules with the aim of reducing c-MYC protein levels.

Using our comprehensive platform of RNA-targeting drug discovery tools and analyses including chemical probing, structure modeling, high-purity RNA production, high-throughput screening, and biophysical characterization, we evaluated the potential to directly target c-MYC mRNA using small molecules. Our analysis revealed six high-confidence structured elements throughout the c-MYC mRNA expected to harbor tertiary structures amenable to drug-like ligand binding. Leveraging the multifaceted chemical probing and structure modeling components of our platform, we confirmed that our *in vitro*-transcribed RNA screening constructs adopt the same structures found in endogenous cellular c-MYC transcripts. After large-scale *in vitro* RNA preparation, we subjected four of these RNA elements to high-throughput screens of chemically diverse drug-like libraries using mass spectrometry affinity-selection that identified multiple chemical series with sub-micromolar affinity. We validated binding affinity using orthogonal methods including isothermal titration calorimetry and NMR. To eliminate pan-binding ligands, we evaluated of selectivity against a panel of non-target mRNA structures. Importantly, these compounds lead to rapid (4 hr) reduction of MYC protein levels in a small cell lung cancer cell line, DMS-273, with no cellular toxicity at 72 hr suggesting an on-target effect. Employing our suite of chemical probing tools, we confirmed that compounds from multiple series engage the c-MYC mRNA in cells. Medicinal chemistry efforts are ongoing to increase potency and define the precise mechanism of action in clinically relevant models.

The discovery of these c-MYC mRNA-binding small molecules not only validates the utility of the Ribometrix RNA-targeted small molecule discovery platform but also showcases its potential in tackling traditionally 'undruggable' targets and provides a promising avenue for developing novel anti-cancer therapies. As we learn more about the intricacies of c-MYC mRNA biology and further refine effective small molecules, our results provide practical insights into previously-unknown vulnerabilities of MYC and present tangible opportunities for advancing targeted cancer therapies.

#0681 Rewiring collagen architecture using a highly potent bi-thiazole inhibitor of LOX mediates chemosensitization in triple-negative breast cancer.

Metin Cetin[1], Ozge Saatci[1], Abdol-Hossein Rezaeian[2], Chintada N. Rao[2], Chad Beneker[2], Harrison Taylor[1], Breanna Pederson[2], Ioulia Chatzistamou[2], Brian Buckley[3], Susan Lessner[2], Peggi Angel[1], Campbell McInnes[2], **Ozgur Sahin**[1]

[1]The Medical University of South Carolina (MUSC), Charleston, SC,[2]University of South Carolina, Columbia, SC,[3]Roswell Park Comprehensive Cancer Center, Buffalo, NY

Lysyl oxidase (LOX) is the founding member of the LOX family proteins and mediates the conversion of lysine residues in collagen I and elastin precursors into highly reactive aldehydes, leading to crosslinking of extracellular matrix (ECM). LOX is upregulated in aggressive tumors with high stiffness, and its higher expression correlates with metastasis, therapy resistance, and worse clinical outcome; however, relatively LOX-specific, orally bioavailable inhibitors are still lacking. Here we discovered bi-thiazole derivatives as potent LOX inhibitors by combining a robust screening platform for drug-like molecules, cell- and recombinant protein-based assays. Structure-activity relationship analysis further identified a potent and relatively LOX-specific lead compound (LXG6403) that reduces collagen content and crosslinking, and fibronectin assembly, leading to increased chemoresponse in triple-negative breast cancer (TNBC) cell lines and PDX organoids in 3D collagen. LXG6403 shows favorable pharmacokinetic properties, reduces collagen content and crosslinking, as demonstrated by the state-of-the-art MALDI-MSI and MP-SHG analyses, respectively. This leads to better drug penetration, inhibition of FAK signaling, and induction of ROS generation/DNA damage, leading to G1 arrest and apoptosis in chemoresistant TNBC PDXs. Overall, our novel, potent, tolerable bi-thiazole LOX inhibitor enhances chemoresponse in TNBC, the deadliest breast cancer subtype.

#0682 Development of novel eIF4E inhibitors to potently and selectively suppress tumor growth across multiple indications.

M. B. Friedersdorf, D. R. Blake, S. E. G. Thompson, R. Pavana, R. V. S. Changalvala, A. S. Truong, K. Marran, A. Bias, J. A. Sorrentino;
Ribometrix, Durham, NC

Despite considerable progress in treating cancer, drug resistance remains the primary hurdle to achieving cures in patients. Tumors often develop resistance through reactivation of the drug-targeted pathway, or activation of alternative parallel pathways, thereby maintaining the original downstream signaling effects. One of the furthest downstream effectors and critical nodes for many oncogenic signaling pathways is eukaryotic translation initiation factor 4E (eIF4E); the main regulator and rate limiting factor for protein synthesis. eIF4E is reactivated by many resistance mechanisms to promote translation of multiple pro-oncogenic factors including Cyclin D1/3, making it an attractive target to potentiate the anti-cancer activity of targeted therapies and to overcome drug resistance. Here, we present the development of novel, potent, and selective eIF4E inhibitors for use in both treatment-naïve and resistance settings across multiple tumor indications.

To capitalize on the potential of targeting eIF4E, we developed a series of compounds with unique properties that maintain anti-tumor efficacy while minimizing toxicity. Our novel, selective, and potent oral eIF4E inhibitors (RBX-eIF4Ei) elicit a reversible, dose-dependent cell cycle arrest. Unlike targeting eIF4A, eIF4E inhibition selectively regulates translation of cancer-dependent pathway proteins instead of global protein synthesis, thus reducing on-target toxicity and increasing tolerability. Cellular profiling demonstrates RBX-eIF4Ei are highly selective, nanomolar inhibitors across many tumor types including, NSCLC, CRC, breast, and melanoma. Additionally, RBX-eIF4Ei demonstrate consistent efficacy across both sensitive and resistant cell lines, including intrinsic and acquired resistance models. Combining RBX-eIF4Ei with standard of care targeted therapies produces additive responses in both settings, suggesting its potential anti-neoplastic benefits post progression.

In vivo, daily oral monotherapy treatment with RBX-EIF4Ei causes significant tumor growth inhibition across a variety of indications including BRAFmut CRC, BRAFmut melanoma and ER+ breast cancer, with minimal signs of toxicity. Intratumoral concentration of RBX-eIF4Ei correlate with significant tumor cell growth inhibition, as well as reductions in eIF4E target proteins, ODC1 and Cyclin D1. Combination studies with standard of care in both the treatment naïve and resistant settings are ongoing.

Collectively, these data support the addition of RBX-eIF4Ei to standard of care in both the naïve and treatment resistance settings across a variety of indications including NSCLC, breast, CRC, and melanoma. IND enabling studies are planned, marking a significant step toward advancing these promising eIF4E inhibitors into clinical development.

#0684 DT-9045, a novel PAR2 inhibitor with best-in-class properties that reduces resistance to both EGFR-targeting therapies and immunotherapy in oncology models.

T. Brugat[1], M. Kadiri[2], S. Aouad[2], A.-L. Blayo[1], B. Rugeri[1], A. Mousson[1], A. Janvier[1], E. Steinberg[1], L. Baron[1], M. Recolet[1], X. Wirth[1], M. Garcia-Leon[1], Q. Ruet[1], M. Semache[3], L. Sabbagh[3], O. Blanchard[1], C. Franchet[1], S. Mayer[1], J. Stagg[2], N. Lenne[1], S. Schann[1];

[1]Domain Therapeutics, Illkirch, France, [2]Universite de Montreal, Montreal, QC, Canada, [3]Domain Therapeutics NA, St-Laurent, QC, Canada

Protease-activated receptor 2 (PAR2) is a promising therapeutic target in oncology and immuno-oncology. It is upregulated and associated with poor prognosis in several cancer types. A pan-cancer meta-analysis showed that PAR2 is one of the genes most significantly associated with resistance to immune checkpoint blockade (ICB) and T cells dysfunction in cancer patients. Mechanistically, being expressed by various cells of the tumor microenvironment, PAR2 promotes both survival and proliferation of cancer cells and dampens the anti-cancer immune response. Domain Therapeutics has developed a novel PAR2 inhibitor, DT-9045, with best-in-class properties. Indeed, compared to its most advanced competitors, DT-9045 is a small molecule, orally bioavailable, insurmountable, biased, and active in tumor-like conditions (i.e. acidic pH and high level of activating proteases). This compound is also highly potent and selective on PAR2. Pharmacokinetic properties are suitable with a once-a-day oral administration. In vitro, DT-9045 completely prevented PAR2-mediated resistance to EGFR-targeting drugs. In vivo, its combination with anti-PD1 therapy showed a significant increase in efficacy over monotherapies in preclinical syngeneic mouse cancer models. This result was similar to the one observed in PAR2 knockout mice, indicating that oral administration of DT-9045 induces a complete inhibition of the receptor. We have further demonstrated that treatment with a PAR2 inhibitor enhances dendritic cell-mediated T cell activation and intratumoral infiltration of CD4+ and CD8+ T cells as well as a decrease in M2 macrophage infiltration. In conclusion, Domain Therapeutic has identified a novel PAR2 inhibitor, DT-9045, with clear competitive advantages. This preclinical candidate has shown strong potency in alleviating the resistance to both EGFR-targeting therapies and immunotherapy in preclinical cancer models. IND-enabling studies are currently ongoing to bring this new hope for cancer patients to the clinic.

EXPERIMENTAL AND MOLECULAR THERAPEUTICS: Radiotherapeutic Combinations, Modifiers, Protectors, Sensitizers, and Molecular Targets Poster Session

#0688 Radium-223 in combination with darolutamide exhibits synergistic antitumor efficacy in LNCaP prostate cancer models.

C. A. Schatz[1], M. I. Suominen[2], A. Schlicker[1], M. Knuuttila[3], E. Alhoniemi[4], S.-M. Kakonen[3], B. Haendler[1], U. B. Hagemann[1], **A. Scholz**[1];
[1]Bayer AG, Berlin, Germany, [2]Pharmatest Services Ltd., Turku, Finland, [3]Aurexel Life Sciences Ltd., Askainen, Finland, [4]Inoi Oy, Turku, Finland

Radium-223 dichloride (radium-223) is a targeted alpha therapy that binds to newly formed abnormal bone in bone metastases and induces DNA double-strand breaks (DSBs) in cancer cells, osteoblasts and osteoclasts. Radium-223 is used for the treatment of patients with metastatic castration-resistant prostate cancer (mCRPC). Darolutamide is an androgen receptor inhibitor indicated for patients with metastatic hormone-sensitive prostate cancer or non-metastatic CRPC. We studied the antitumor effects of radium-223 in combination with darolutamide using LNCaP human prostate cancer cells *in vitro* and an intratibial LNCaP model mimicking prostate cancer metastasized to bone.
The *in vitro* antiproliferative effects of radium-223 and darolutamide were determined using LNCaP cells. Gene set enrichment analysis (GSEA) was conducted on RNA sequencing data from LNCaP cells treated with the synthetic androgen R1881 alone or in combination with darolutamide. LNCaP cells were inoculated into the right tibia of male NOD.scid mice. The mice (n=7-9/group) were randomized based on serum prostate-specific antigen (PSA) and treated with vehicle, radium-223 (330 kBq/kg, Q4Wx2, i.v.), darolutamide (100 mg/kg, BID, p.o.), or with a combination of radium-223 and darolutamide, for 41 days. PSA and the bone turnover markers PINP and CTX-I were measured every second week in serum. Tumor-induced abnormal bone area, bone formation rate and radium-223 uptake in tumor-bearing tibiae were determined by X-ray, histomorphometry and gamma counter, respectively.
The combination of radium-223 and darolutamide showed synergistic antiproliferative effects with combination indexes between 0.69-0.75 *in vitro*. GSEA demonstrated a prominent darolutamide-induced downregulation of DNA damage response (DDR) signaling pathways. *In vivo,* the combination treatment showed synergistic antitumor efficacy (p=0.04) as demonstrated by lower PSA concentrations when compared with the vehicle, radium-223 or darolutamide monotherapies (p=0.004, p=0.011 and p=0.002, respectively). In the vehicle and combination treatment groups, the mean serum PSA was 541% and 95.9% of the pre-treatment level, respectively. Furthermore, radium-223 alone or in combination with darolutamide inhibited increased bone turnover, tumor-induced abnormal bone growth and trabecular bone formation when compared to vehicle. Concurrent administration of darolutamide did not affect radium-223 uptake in tibiae.
Radium-223 in combination with darolutamide exhibited synergistic antitumor efficacy both *in vitro* and *in vivo*. The synergistic effects could be due to the radiosensitization of cancer cells by darolutamide-induced downregulation of DDR pathways. Our results suggest that the combination of targeted alpha therapy with an androgen receptor inhibitor is a promising treatment strategy for mCRPC.

#0689 BUB1 interferes with the repair of radiation-induced DNA damage to radiosensitize triple-negative breast cancer.

S. Sriramulu[1], S. Thoidingjam[1], P. Li[1], S. L. Brown[1], F. Siddiqui[1], B. Movsas[1], M. Green[2], C. Speers[3], S. Nyati[1];
[1]Henry Ford Health, Detroit, MI, [2]University of Michigan, Ann Arbor, MI, [3]UH Seidman Cancer Center, University Hospitals Case Medical Center, Case Western Reserve University, Cleveland, OH

Triple-negative breast cancer (TNBC) is associated with locoregional recurrence and low survival rates. Novel molecular targets are expected to improve the efficacy of radiation therapy (RT) in TNBC. BUB1, a mitotic checkpoint Serine/Threonine-protein kinase is known to impact chromosomal segregation during mitosis. However, its precise role in DNA damage repair in response to RT remains largely unknown. We demonstrated that BUB1 is overexpressed in BC (vs. normal breast) and considerably raised in TNBC with poor survival outcomes using differential gene expression analysis. In multiple TNBC cell lines, cell proliferation assays revealed that pharmacological (BAY1816032) or genomic (CRISPR) ablation of BUB1 was cytotoxic. Using clonogenic survival assays, we observed that BUB1 ablation radiosensitized TNBC cell lines (SUM159, MDA-MB-231, MDA-MB-468, BT-549) while its ablation did not radiosensitized breast epithelial cells (MCF10A). Furthermore, by depleting endogenous BUB1 (siRNAs and CRISPR) and reintroducing wild-type (WT) or kinase-dead (KD) BUB1, we demonstrated that inhibition of BUB1 kinase function is responsible for the radiosensitization phenotype. BUB1 ablation increased tumor doubling time in SUM159 xenografts when combined with radiation. Ki67 levels were also reduced in these tumors, confirming the efficacy of the combined treatment. BUB1 ablation led to persistent radiation-induced DNA DSB (gH2AX foci) indicating decreased DNA-DSB repair. BLRR assays confirmed that BUB1 impacts the non-homologous end joining (NHEJ) pathway. Biochemical analyses showed that BUB1 ablation stabilized total- and phospho- DNAPKcs (S2056) following RT such that half-lives could not be estimated. In contrast, RT alone caused BUB1 stabilization, but pre-treatment with BUB1i and DNAPKi prevented stabilization. To evaluate the recruitment of DDR proteins to the chromatin following RT, soluble nuclear and chromatin-enriched fractionations were performed which illustrated an increase in recruitment of phospho- and total-DNAPK, KAP1, and ATM to chromatin indicating that BUB1 is important in the activation and recruitment of critical NHEJ proteins to DSBs. In addition, BUB1 staining of TNBC TMAs demonstrated significant correlation between BUB1 protein expression with tumor grade and stage in TNBC patients. Our findings demonstrate that ablation of BUB1 sensitizes TNBC cell lines and xenograft to RT and BUB1 mediated radiosensitization may occur through NHEJ. Our results suggest that BUB1 may serve as a novel molecular target for radiosensitization in women with TNBC.

#0690 Investigation of BH-3 mimetics as radiosensitizing agents in glioblastoma.

L. R. Dutton[1], C. Mullen[2], A. L. Koessinger[1], M. Jackson[1], K. Stevenson[1], A. J. Chalmers[1], S. Tait[1], K. J. Campbell[2], J. L. Birch[1];
[1]University of Glasgow - Institute of Cancer Sciences, Glasgow, United Kingdom, [2]CRUK Scotland Institute, Glasgow, United Kingdom

Glioblastoma (GBM) is a highly aggressive primary brain tumor. Treatment consists of maximal safe tumor resection, chemotherapy (temozolomide) and radiotherapy; however, this aggressive treatment offers only a modest improvement in outcomes, with average life expectancy of approximately 12 months. Consequently, novel, effective and easily translatable therapies are urgently required. While radiotherapy is an effective treatment for many solid tumors, GBM displays an innate radio-resistance that contributes to treatment failure. Therefore, there is a need to identify chemotherapeutics that can be used as radiosensitizers to increase efficacy. Notably, a key pathway involved in therapeutic resistance is apoptotic evasion, which is driven by upregulation of pro-survival BCL-2 proteins that inhibit the pro-apoptotic proteins necessary for the apoptotic response. Recent advances in drug development have produced a range of BH3 mimetics - novel chemotherapeutics with potential to reinstate apoptosis by targeting specific pro-survival molecules. We hypothesized that the radiation sensitivity of GBM cells would be enhanced by using BH3 mimetics to inhibit pro-survival molecules and release the apoptotic block. A panel of BH3 mimetics was tested in combination with radiotherapy across three patient-derived GBM cell lines (G7, E2 and R15), using a 3D clonogenic culture system that recapitulates *in vivo* growth patterns and responses. We found that the BCL-XL inhibitor, A1331852, significantly radiosensitized all 3 GBM lines. In addition, Western blot analysis revealed A1331852 to induce PARP1 cleavage in G7 cells when used as a single agent. Subsequent *in vivo* studies were conducted in our well characterized orthotopic G7 xenograft murine model of GBM. Immunohistochemical studies showed that the pro-survival proteins MCL-1 and BCL-XL were upregulated in irradiated tumors. Furthermore, a pharmacokinetic study in the same orthotopic murine model, allowing for drug delivery evaluation, and optimized treatment scheduling. Importantly, A1331852 was found to be blood brain barrier penetrant at 25 mg/kg, with increased drug detected in tumor vs normal brain tissue. From these data, a survival study investigating A1331852 as a radiosensitizing agent was carried out in the same G7 GBM orthotopic xenograft model. Kaplan-Meier analysis showed an increase in survival of mice treated with A133852 plus radiotherapy compared with the radiotherapy only group (p = 0.0309). Overall, we have demonstrated that dependence on BCL-2 family proteins is a vulnerability that can be targeted to improve radiotherapy response in GBM. Furthermore, we have identified a promising BH3 mimetic, A1331852, to use in combination with RT and have completed a proof-of-concept *in vivo* study that confirms the potential of BH3 mimetics to improve outcomes for patients with GBM.

#0691 Preclinical evaluation of valproic acid in combination with radiation in orthotopic models of glioblastoma.

M. Stavnichuk, Z. Opachich, D. Huttenlocher, J. McNamara, J. Molloy, X. He, S. Patel, N. Sanai, A.-C. Tien, S. Mehta;
Barrow Neurological Institute, Phoenix, AZ

Background: Valproic acid (VPA) is an FDA-approved anti-seizure medication that has been demonstrated to have an anti-tumor and radiosensitization effect on multiple cancer cells including aggressive brain cancer, glioblastoma (GBM). VPA is thought to exert its anti-tumor effects in part through inhibition of histone deacetylases (HDACs), upregulation of apoptosis and autophagy, and disruption of DNA repair mechanisms. Overall survival of patients treated with VPA in combination with TMZ and radiation therapy (RT) was significantly improved compared to historical controls (mOS 29.6 months). Hence, to establish a preclinical benchmark, we investigated the effectiveness of VPA alone and in combination with the radiotherapy in patient-derived xenograft (PDX) models of GBM *in vitro* and *in vivo*.
Methods: Anti-proliferative effect of VPA in combination with radiation was assessed across multiple GBM cells lines (long-term cultures and PDX lines). Athymic mice were implanted with PDX GBM cells orthotopically and were randomized into four cohorts: vehicle, VPA, IR (6 gy), VPA + IR (6 gy). Animals were treated with 300mg/kg/day of VPA alone or in combination with 6Gy of radiation. Treatments were performed either via intraperitoneal route for 3 consecutive days or via a gastric gavage 5 days on/2 days off for the duration of the study. For pharmacodynamics (PD), animals were sacrificed after 3 days of drug treatment at 2hr, 24hr and 4 days post last dose and processed for immunohistochemical (IHC) analysis for acetylated H3K9/14, KI67, pH2AX, and cleaved caspase 3.
Results: VPA treatment demonstrated a dose-dependent decrease in GBM cell viability and enhancement of radiation sensitivity. Pharmacodynamic analysis of tumor-bearing mice demonstrated a significant increase in acetylated H3K9/14 levels upon treatment with combination of VPA and irradiation. Elevation of acetylated H3K9/14 levels was present 2 hours after the administration of the last dose of VPA and it persisted for 4 days. Treatment of mice with irradiation upregulated levels of the apoptosis marker, cleaved caspase 3, which was further enhanced upon VPA and irradiation combination treatment. No reduction in tumor volume or survival benefit was seen in VPA alone or combination cohorts.
Conclusion: Consistent with previous reports, treatment of PDX GBM line with VPA reduced cell viability *in vitro*, increased histone acetylation, and cell death. However, these changes were not sufficient to provide survival benefit in the intracranial model and warrants further investigation into the genetic requirements for radiation sensitization by VPA.

#0692 Uncoupling protein 2 (Ucp2) loss of function enhances mitochondrial ROS and sensitizes PDAC to radiation therapy.

E. G. Caggiano, M. Yu, A. Acevedo-Diaz, C. M. Taniguchi;
UT MD Anderson Cancer Center, Houston, TX

Introduction: Pancreatic ductal adenocarcinoma (PDAC) is a lethal cancer with a dependence on highly active mitochondria to grow and metastasize. Normally mitochondria exist in long networks due to mitochondrial fusion but in PDAC mitochondria are fragmented due to excessive fission. We previously found that forcing PDAC cells to increase mitochondrial fusion suppressed tumor growth and metastasis, leading to improved survival in multiple preclinical models. The tumor suppressive mechanisms of mitochondrial fusion remain unclear, and thus we explored the role of redox homeostasis through uncoupling protein 2 (UCP2), a metabolic protein normally upregulated in PDAC that was downregulated upon forced mitochondrial fusion. We hypothesize that UCP2 mediates the oncogenic effects of mitochondrial fragmentation in PDAC.

Methods: We explored if Ucp2 is necessary and sufficient for inducing tumor suppression upon mitochondrial fusion. The effects of Ucp2 loss or overexpression were characterized by metabolic flux assays, proliferation, mitochondrial ROS (mROS), membrane potential, and morphology measurements. We also examined if Ucp2 recapitulates mitochondrial fusion-induced tumor suppression via pharmacological inhibition and genetic ablation and assessed the impact on mitochondrial health and cell growth. We utilized the *LSL-KRAS*^{G12D}; *Trp53*$^{R172H/+}$; *Ptf1α Cre* (KPC) cell line as our parental line for all genetic manipulations, with a nontargeting (sgGFP) KPC cell line as a control.

Results: Murine PDAC cells with enhanced mitochondrial fusion reduced Ucp2 transcript levels by 70% and was correlated with 3.5-fold increase in mROS, 50% reduction in OXPHOS via oxygen consumption rate assay, and a 4-fold increase in membrane potential compared to controls. Ucp2 re-expression did not rescue these phenotypes, suggesting that Ucp2 alone may not be sufficient for tumor suppression. However, inhibition of Ucp2 in PDAC cells reduced proliferation by 70%, while inducing a 3-fold increase in mROS levels, which was recapitulated with Ucp2 abrogation, thus Ucp2 may be necessary for tumor suppression. Enhanced mROS via Ucp2 inhibition significantly increased radiosensitivity (p-value < 0.0001), suggesting that although it does not recapitulate the mitochondrial fusion phenotype, UCP2 may be a novel target for radiosensitization in PDAC.

Conclusions: Mitochondrial fusion may not suppress tumor growth by altering redox homeostasis via UCP2, but forcing mitochondria to fuse elucidated the impacts of UCP2 downregulation on cell metabolism. Thus, we uncovered that UCP2 may be a novel target for radiosensitization. Further insight into UCP2's role in redox balance, and how it is disrupted with UCP2 modulation enables development of novel therapeutic combinations with UCP2 inhibition that complement and potentially synergize with existing therapeutic strategies such as radiation.

#0693 The effect of butyrophilin 1A1 blockade in combination with radiation treatment in tumor models.

N. Li[1], C. Braun[1], Y.-S. Kim[2], A. Park[2], S. Yoo[2], S. Lin[1];
[1]UT MD Anderson Cancer Center, Houston, TX, [2]STCube Pharmaceuticals, Inc., Gaithersburg, MD

Expression of radiation-induced immune escape molecules, including PD-L1, contributes to the efficacy of cancer immunotherapy. We used an unbiased in vivo gene knockdown screen in naïve T-cells and introduced them into irradiated host tumors to identify novel immunosuppressive genes activated during radiation. From the screen, we found that butyrophilin 1A1 (BTN1A1) knockdown causes T-cell expansion in irradiated tumors. This points to the potential immune checkpoint role of BTN1A1. We validated that BTN1A1 expression is inducible in activated T-cells and that blocking BTN1A1 contributes to T-cell activation. We tested an anti-mouse BTN1A1 antibody (STC109) in mouse colon tumor models (CT26 tumors), we observed partial anti-tumor efficacy using single agent STC109, which was enhanced by the combination of STC109 with radiation. We also got similar result in in mouse lung tumor models (LLC tumors) using anti-mouse BTN1A1 antibody, and the combination treatment showed an improved suppression of tumor growth and lung metastasis compared to single agent. Moreover, our data shown that knockout of BTN1A1 in 4T1 tumor models shown dramatic defect of tumor growth, and the BTN1A1 ko tumors are more sensitive to radiotherapy. These findings indicate the role of BTN1A1 in tumor immune response from radiation stress, and that anti-BTN1A1 has strong potential to enhance efficacy of radiotherapy for cancer treatment.

#0694 Evaluation of a synergistic drug combination with ^{177}Lu-rhPSMA-10.1 for prostate cancer: Results of an *in vitro* screen and *in vivo* proof of concept study.

C. Foxton[1], B. Cornelissen[2], E. O'Neill[2], B. Waldron[3], F. Pretzmann[4], R. Veggerby Gronlund[4], M. Wikke Hallund[4], D. J. Stevens[3];
[1]Blue Earth Diagnostics, Oxford, United Kingdom, [2]University of Oxford, Oxford, United Kingdom, [3]Blue Earth Therapeutics, Oxford, United Kingdom, [4]Minerva Imaging, Olstykke, Denmark

Purpose: Prostate-specific membrane antigen (PSMA)-targeted radioligand therapy (RLT) has been shown to extend survival in men with advanced prostate cancer (PCa). Novel radiohybrid (rh) PSMA-targeted ^{177}Lu-rhPSMA-10.1 has shown promising preclinical efficacy and advantageous radiation dosimetry in humans. We conducted an *in vitro* screen to identify known anticancer drugs with potential for synergistic interaction with ^{177}Lu-rhPSMA-10.1. Here we present key screening data and a subsequent *in vivo* efficacy analysis of the lead novel drug combination in PSMA-expressing 22Rv1 PCa xenografts.
Methods: Over 150 FDA-approved anticancer drugs were screened in a clonogenic survival assay of 22Rv1 cells using the test drug alone, at a range of concentrations <20 μM to determine the IC_{50}, and results compared to incubations of the drug + 15 MBq/mL ^{177}Lu-rhPSMA-10.1 after 10 d. A focused screen of 5 lead candidates was then conducted to determine the impact of ^{177}Lu-rhPSMA-10.1 (0-25 MBq/mL) on the drug IC_{50}. A synergy score was determined using the zero interaction potency (ZIP) reference model and the multi-dimensional synergy of combinations (MuSyc) platform.
Subsequently, to evaluate the efficacy of the lead combination, ^{177}Lu-rhPSMA-10.1 (single 30 MBq iv dose) and Cobimetinib (0.25 mg orally per day for 21 d) alone and in combination were administered to 22Rv1 tumor-bearing NMRI nude mice (n = 8 per group plus untreated controls). Tumor volume was measured 2x week for 69 d. Two-way ANOVA and Tukey's multiple comparisons test (data analyzed until n = 3 remained per group) and Kaplan-Meier Log-rank survival analyses were performed.
Results: The *in vitro* screen identified MEK inhibitor Cobimetinib as a lead candidate for synergistic combination with ^{177}Lu-rhPSMA-10.1 across a wide concentration range, with a ZIP synergy score of 13.25% (95% CI ± 2.17) and promising results on MuSyc analysis. The ^{177}Lu-rhPSMA-10.1 + Cobimetinib combination significantly suppressed tumor growth *in vivo* vs untreated controls (from day 13-30; $p<0.01$) and ^{177}Lu-rhPSMA-10.1 alone (from day 17-30; $p<0.001$). The median survival in the combination group (49 d) was significantly longer vs the untreated group (23 d; $p=0.001$) and the group treated with ^{177}Lu-rhPSMA-10.1 alone (36 d; $p=0.002$).
Conclusions: Through an extensive *in vitro* screen, we identified Cobimetinib to have potential for a synergistic anti-tumor effect in combination with ^{177}Lu-rhPSMA-10.1. This may be due to inhibition of the MEK-MAPK pathway by Cobimetinib during DNA damage response, resulting in radiosensitization of cancer cells to ^{177}Lu-labeled RLT agents such as ^{177}Lu-rhPSMA-10.1. This novel combination showed an enhanced therapeutic efficacy vs the single agents in 22Rv1 xenografts and the lack of overlapping monotherapy toxicity reported in the clinic supports clinical investigation in men with PCa.

#0695 Enhancing radiotherapy with lenvatinib by targeting the CXCL13/CXCR5/NF-KB axis.

T.-L. Liao[1], I.-T. Chiang[2], B.-H. Huang[1], F.-T. Hsu[3], M.-H. Chan[1];
[1]National Yang Ming Chiao Tung University, Taipei, Taiwan, [2]Show Chwan Memorial Hospital, Taipei, Taiwan, [3]China Medical University, Taipei, Taiwan

Lung cancer is the leading cause of cancer death worldwide, with non-small cell lung cancer (NSCLC) accounting for approximately 85% of all lung cancers. At the time of diagnosis, it is often already advanced or metastatic, resulting in poor treatment outcomes. Treatment of NSCLC mainly relies on surgery, radiation and chemotherapy, but the survival rate has not increased significantly in the past decade. Therefore, finding appropriate treatment methods is necessary and crucial. Radiotherapy (RT) is a frequently employed approach for tumor treatment and serves as the primary local treatment for NSCLC. However, it often results in a poor prognosis and severe side effects when administered at high-dose irradiation. Existing literature suggests that RT may trigger the expression of nuclear factor kappa B (NF-KB), potentially compromising its therapeutic efficacy. Consequently, the question remains: Can targeting NF-KB signaling enhance the sensitivity of RT in NSCLC Furthermore, studies have indicated that elevated levels of CXCR5 in NSCLC contribute to tumor growth. CXCR5 is situated upstream of the NF-KB pathway. As a result, it becomes imperative and indispensable to develop strategies targeting the CXCL13/CXCR5/NF-KB signaling axis to counteract NSCLC growth. Lenvatinib is a multi-kinase inhibitor targeted drug. It has been proven to inhibit VEGFR1-3, FGFR1-4 and PDGFR, inhibiting tumor growth. Lenvatinib has received clinical approval from the US FDA for the treatment of advanced hepatocellular carcinoma (HCC) and has been shown to inhibit NF-KB expression in HCC. However, the potential radiation-sensitizing mechanism of Lenvatinib in lung cancer remains unexplored. This study is dedicated to investigating the effects and molecular mechanisms of combining Lenvatinib with radiotherapy in NSCLC. Our results suggest that lenvatinib may enhance the sensitivity of NSCLC to RT. Furthermore, evidence from both the intrinsic and extrinsic apoptosis pathways (Caspase-3/Caspase-8/Caspase-9) and TUNEL experiments supports the idea that the combined treatment of lenvatinib with RT induces a more pronounced apoptotic response compared to individual treatments. Additionally, silencing CXCR5 in NSCLC also appears to enhance its responsiveness to RT. In our western blot (p-ATM, p-CHK2), flow cytometry (p-ATM), we showed that the combination of lenvatinib and RT may effective induce DNA damage. Our *in vivo* data demonstrates that the combination of Lenvatinib and RT exhibits superior tumor growth inhibition. Immunohistochemistry (IHC) staining of tumor tissue also revealed an upregulation of apoptosis-related proteins and the downregulation of CXCL13/CXCR5/NF-KB related proteins. In conclusion, our findings suggest that Lenvatinib can serve as a radiosensitizer, enhancing the sensitivity of NSCLC patients to radiotherapy by targeting the CXCL13/CXCR5/NF-KB signaling pathway.

#0696 Proton radiation and Seco-Duocarmycin SA: A synergistic strategy unveiling new frontiers in glioblastoma multiforme therapy.

A. Morcos, A. Bertucci, R. N. Fuller, N. R. Wall, M. E. Vazquez;
Loma Linda University, Loma Linda, CA

Glioblastoma multiforme (GBM) is one of the most aggressive brain cancers with a 6.9% five-year survival rate. More effective therapies are needed as standard treatments, which include surgery, radiation, and chemotherapy are inefficient due to radio-chemo-resistance and relapse. The goal of this project is to investigate the efficacy of seco-duocarmycin SA (sDSA) as an anticancer drug, alone and the potential synergy of combining proton radiation and sDSA in human GBM cell lines. Proton therapy offers numerous advantages in treating cancers because of its superior dose distribution and biological effects. sDSA is an exceptionally potent agent that selectively alkylates DNA at the N3 position of adenine, making it of great interest as a therapeutic drug. We hypothesize that by pairing sDSA with proton radiation, a more dynamic effect will result, which will amplify their collective power, unleashing an enhanced cytotoxicity against human GBM cells. GBM cell lines (T98G and LN18) were exposed to graded doses and concentrations of protons and sDSA respectively in order to evaluate cellular changes in proliferation, survival, cell cycle, apoptosis/necrosis induction, and DNA damage. Results show that proton radiation and sDSA when used alone induce a dose-dependent decrease of cell proliferation, an increase in foci formation, and an increase in G2/M phase arrest in LN18 and T98G cells. The data also illustrates that the combination of proton radiation and sDSA synergistically enhances these effects. The utilization of proton radiation in conjunction with sDSA against GBM represents an innovative and previously unexplored approach. Currently, the cellular mechanisms of sDSA cytotoxicity are not well understood or studied, and even less is known regarding the effects when combined with proton radiation. This study serves as a vital cornerstone in unraveling the biological response of GBM cells when confronted with proton radiation and sDSA, paving the way for the future development of a more precise and potent combination therapy.
.

#0697 Enhanced tumor control and survival in solid tumor models following combined low dose radiotherapy and T cell therapy.

N. Puebla[1], G. Srivastava[2], S. Nizzero[3], N. W. Fowlkes[1], H. Barsoumian[1], Y. Hu[1], C. Leuschner[1], T. Riad[1], M. Loparic[2], M. Plodinec[2], J. Welsh[1];
[1]MD Anderson Cancer Center, Houston, TX, [2]ARTIDIS AG, Basel, Switzerland, [3]ARTIDIS AG, Houston, TX

Background: Solid tumors remain a significant challenge in cancer therapy due to their resistance to conventional treatments. Chimeric antigen receptor (CAR)-T cell therapy has emerged as a promising approach for treating solid tumors, but its effectiveness is often limited by the poor infiltration of CAR-T cells into the tumor microenvironment. Thus, enhancing a robust infiltration of chimeric antigen receptor T cells into solid tumors is essential for an effective antitumor response and therapeutic success.
Methods: In this study, we investigated the combined effects of multiple doses of low-dose radiotherapy (LD-RT) and CAR T-cell therapy on tumor growth and survival using two models of NSG mice implanted with gastric carcinoma (GSU) or pancreatic adenocarcinoma (CAPAN-2) cells. The engineered CAR-T cells were designed to target guanyl cyclase-C (GCC) or mesothelin, respectively. Furthermore, our study employed atomic force microscopy (AFM) in a small cohort to investigate the impact of LD-RT and CAR-T cell therapy on tumor stiffness and plasticity.
Results: The synergistic effect of combining low-dose radiotherapy (LD-RT) with T-cell therapy resulted in enhanced tumor control and prolonged survival in mice with tumors, surpassing the outcomes observed with either monotherapy alone. This combined treatment holds promise for improving responses in patients with solid tumors by leveraging LD-RT to enhance the intratumoral infiltration of effector T cells. Our findings suggest that the nanomechanical signature may be a potential biomarker for LD-RT combined CAR T cell therapy in solid tumors.
Conclusions: Our findings substantially contribute to treating solid tumors using cell therapies, highlighting the potential for improved infiltration of adoptively transferred T cells following radiotherapy (RT), which can transform existing therapeutic strategies for solid tumors while minimizing toxicity.

#0699 Targeting radiation-driven invasion and metastasis in pancreatic cancer.

K. Mclay[1], M. Tesson[2], D. Gilmour[1], J. P. Morton[2], J. L. Birch[1];
[1]University of Glasgow - Institute of Cancer Sciences, Glasgow, United Kingdom, [2]Cancer Research UK Scotland Institute, Glasgow, United Kingdom

Pancreatic ductal adenocarcinoma (PDAC) is an aggressive cancer with a dismal prognosis. Standard of care includes chemotherapy and radiotherapy (RT) for locally advanced, unresectable disease. Despite radiotherapy being an effective and sometimes curative option for many cancer types, radio-resistance is common, and pre-clinical research in recent years has found that RT can initiate a more aggressive, pro-invasive phenotype in the remaining cells post treatment (1,2). Little is known about the molecular mechanisms responsible for this phenomenon.There is accumulating evidence highlighting a role for the RhoGTPase family in mediating radioresistance and enhanced invasion (2, 3). Understanding their role in PDAC progression may aid the identification of novel chemotherapeutics that could be used alongside RT in the future. We present *in vitro* data that confirms the pro-migratory effect of RT and importantly indicates a significant increase in metastases formed in a clinically relevant model of PDAC (KPC Pdx1-Cre; $Kras^{G12D/+}$; $Trp53^{R172H/+}$) after treatment using a small animal radiation research platform (*n=31, p<0.0001*). In concurrence with previous literature, we found that PDAC cell motility was dependent on the RhoGTPase pathway, RhoA/ROCK1 (p=0.004). However, post-RT, this dependency was switched to an alternative pathway, CDC42/Rac1/MRCK, indicating a clear change in the balance of RhoGTPase signaling (p=0.002). This switch was confirmed via high-throughput immunofluorescence analysis. To widen this investigation further, we performed an siRNA screen targeting all members of the RhoGTPase family. Preliminary results indicate signaling dependency on Rac2, Rac3 and CDC42 post-RT. Additionally, we have performed RNAseq to investigate pro-invasive gene signatures arising from the acute irradiation of pancreatic cancer cells. This was done at sufficient depth to identify splice variants, with differential transcript expression (DTE) analysis identifying 236 differentially expressed transcripts and the differential transcript usage (DTU) analysis identifying 28 transcripts and 23 genes. Initial functional enrichment analysis found gene signatures relating to cell migration and adhesion, which may be indicative of an invasive phenotype. In conclusion, we present in vitro and in vivo data suggesting RT may promote a more invasive phenotype in PDAC at least in part due to a switch in RhoGTPase signaling.

1. Mueller, A.C., et al., *Induction of ADAM10 by Radiation Therapy Drives Fibrosis, Resistance, and Epithelial-to-Mesenchyal Transition in Pancreatic Cancer.* Cancer Res, 2021. **81**(12): p. 3255-3269. 2. Birch, J.L., et al., *A Novel Small-Molecule Inhibitor of MRCK Prevents Radiation-Driven Invasion in Glioblastoma.* Cancer Res, 2018. **78**(22): p. 6509-6522.

#0700 Impact of heterogeneity for mismatch repair activity on colon tumor development and therapeutic response.

S. M. Snow, D. Albrecht, P. A. Clark, C. P. Kerr, J. J. Grudzinski, J. J. Jeffery, H. Comas Rojas, R. Hernandez, K. A. Matkowskyj, J. P. Weichert, Z. S. Morris, R. B. Halberg;
University of Wisconsin-Madison, Madison, WI

Background: Colorectal cancers (CRC) that are deficient for DNA mismatch repair (dMMR) proteins have high levels of genetic instability and consequently high mutational burden, creating numerous neoantigens that can elicit an immune response. Therefore, dMMR CRC are the best candidates for immune checkpoint inhibition (ICI) compared to proficient DNA mismatch repair (pMMR) CRC. Early clinical trials revealed that only 30-55% metastatic dMMR CRC responded to ICI. Recent studies utilizing allograft models have demonstrated that tumor immune landscape can be primed with radiopharmaceutical therapy (RPT). Although early results have been quite promising, allograft models often fail to accurately predict efficacy for many reasons, but most often are due to a lack of heterogeneity.
Methods: To better understand how heterogenous MMR expression impacts tumor development and response to ICI alone or in combination with RPT, we developed a new mouse model that develops three tumor types: (1) homotypic dMMR tumors that express green fluorescent protein, (2) homotypic pMMR tumors that express red fluorescent protein, and (3) heterotypic tumors with a mixture of dMMR and pMMR cells. Surveillance bright field and fluorescent colonoscopies allow us to assess treatment response by measuring tumor size and proportion of dMMR and pMMR tumor cells in real-time. These outcomes are verified through *ex vivo* imaging and histological analysis.
Results: Tumor response to anti-PD-L1 ICI was dependent on MMR status. Homotypic dMMR tumors exhibited the strongest response: significantly smaller in treated mice than controls, exhibited areas of vascular congestion and increased CD8+ cytotoxic T-cells infiltration. Response of heterotypic MMR tumors varied depending on percentage of dMMR cells; tumors with a high percentage of dMMR cells remained small, whereas tumors with a low percentage of dMMR had an outgrowth of pMMR cells. Treated and untreated homotypic pMMR tumors were indistinguishable. To enhance the response of all three tumor types, mice were treated with dual ICI treatment, anti-PD-L1 and anti-CTLA-4, or RPT. Animals administered the tri-therapy (dual ICI + RPT) survived significantly longer with fewer tumors than animals treated with either dual ICI or RPT alone.
Conclusions: Our innovative mouse model allows for the highly detailed characterization of tumor response to therapies. Simplistic allograft models may not adequately account for the dynamic effects that neighboring cell death may have on radio-resistant cells, on tumor vascular perfusion and oxygenation, or on tumor immune infiltration and adaptive immune recognition of remaining cells. We begin to fill these critical gaps in knowledge and therefore the results from our studies will help guide the translation and integrated use of ICIs and RPTs in clinic.

#0701 Preclinical data of a novel DNA-PK inhibitor in combination with radiation therapy shows promise in the treatment of established GBM and lung carcinoma cell lines.

A. C. Mladek[1], D. L. Burgenske[1], W. F. Elmquist[2], W. Zhong[3], J. N. Sarkaria[1];
[1]Mayo Clinic, Rochester, MN, [2]University of Minnesota, Minneapolis, MN, [3]Waynola Biopharm, Inc, Corona, CA

Radiation therapy (RT) is a cornerstone of oncologic therapy for the majority of solid malignancies, and unrepaired DNA double-strand breaks are responsible for radiation-induced cytotoxicity. RT-induced DNA lesions can be repaired by multiple mechanisms including homologous recombination (HR) and non-homologous end joining (NHEJ), and disruption of either of these pathways can enhance cytotoxicity. A key component of the NHEJ pathway is the catalytic subunit of DNA-dependent protein kinase (DNA-PKcs), and loss of kinase activity can significantly increase radiosensitivity. Herein we describe the results of our medicinal chemistry campaign to develop a potent and selective DNA-PKcs inhibitor, WNC0901. WNC0901 inhibits DNA-PKcs kinase activity in a cell free system with an IC_{50} of 0.071 nM and demonstrated at least 30-fold higher sensitivity than other family members (ATM, ATR, mTOR, PI3K). WNC0901 has limited aldehyde oxidase (AO) liability with a $T_{1/2}$ >2000 min in liver cytosol and is stable for over 120 minutes in the presence and absence of an AO inhibitor. A preliminary pharmacokinetic analysis in wista han rat (IV=2mg/kg, PO=20mg/kg) demonstrated 116% apparent absolute oral bioavailability, 2.6 hour terminal half-life, 33.0 mL/min/kg clearance, and a 2.6% unbound brain-to-plasma partition coefficient (Kpuu). WNC0901 also had favorable pharmacokinetic properties in beagle dog (IV=2mg/kg, PO=20mg/kg) with moderate clearance (8.5 mL/min/kg), high apparent absolute oral bioavailability (131%) with good exposure (AUC=36092 h*ng/mL), moderate half-life (4.28 h), and low protein binding (74.3% fraction unbound). The volume of distribution was moderate in both species (Vss = 1.32 L/kg in wistar han rat and 1.87 L/kg in beagle dog). In cell culture, WNC0901 inhibited autophosphorylation of DNA-PKcs in HT29 cells irradiated with 10 Gy with an IC_{50} of 32.7 nM and robustly inhibited autophosphorylation in both U251 glioma and A549 lung cancer cell lines at 300 nM in combination with 5Gy. In a clonogenic assay, 5Gy irradiation (10% survival) combined with 100nM WNC0901 demonstrated modestly enhanced cell killing (1.5% survival), and maximal effects were seen at 300nM (0.04% survival, $p<0.01$). Similar radiosensitizing effects with 300 nM WNC0901 were seen in the A549 cell line (0.2% survival with combination compared to 19% with 5Gy alone, $p<0.01$).
In summary, WNC0901 inhibits DNA-PK kinase activity and provides potent radiosensitization in a GBM and lung cancer cell line. Future studies will assess the combination of WNC0901 and RT in GBM patient-derived xenograft models *in vivo*.

#0702 Development of a radioresistant PDX prostate cancer model to evaluate potential radiosensitizing compounds.

M. Z. Alfsen[1], M. Thaysen[2], N. Nielsen[1], M. Wick[3], L. Piggott[4], S. Gnosa[1], C. H. Nielsen[1];
[1]Minerva Imaging, Oelstykke, Denmark, [2]University of Copenhagen, Copenhagen, Denmark, [3]XenoSTART, San Antonio, TX, [4]Debiopharm International SA, Lausanne, Switzerland

Prostate cancer is the second most common cancer diagnosis worldwide and the fifth leading cause of cancer related death among men. Several treatment strategies are used including the FDA approved ^{177}Lu-vipivotide tetraxetan (^{177}Lu-PSMA-617) for the treatment of prostate-specific membrane antigen (PSMA)-positive metastatic castration-resistant prostate cancer. However, not all patients respond to treatment due to tumor intrinsic resistance mechanisms. Therefore, the combination of targeted radionuclide therapy with inhibitors against e.g. DNA damage response, cell cycle progression or cell survival pathways are investigated to enhance the radiosensitivity of the tumor. Current models to study radioresistance in prostate cancer are based on cancer cell lines or cell-line derived xenograft models, but these models do not account for the heterogenous and complex biology of the disease. To overcome this issue, we have developed a radioresistant patient-derived xenograft (PDX) prostate cancer model (ST1273, XenoSTART), that is positive for PSMA. Resistance to radiation was initially established by sequential irradiation of the tumors with external beam radiation. Moreover, the model has proven to be resistant towards treatment with 30 MBq ^{177}Lu-PSMA-617. Utilizing this radioresistant model we are now able to investigate the treatment response of ^{177}Lu-PSMA-617 in combination with different drug inhibitor classes to evaluate their potential radiosensitizing effect. The PARP inhibitor, Olaparib, was administered at 50 mg/kg QDx48 alone or in combination with a single dose of ^{177}Lu-PSMA-617 in radioresistant ST1273 tumor bearing NMRI nude mice. First results showed a prolonging treatment effect of Olaparib given in combination with ^{177}Lu-PSMA-617 compared to ^{177}Lu-PSMA-617 alone. Tumor relapse was observed 29 days after treatment with ^{177}Lu-PSMA-617 alone, whereas it was observed 49 days after combination treatment. Olaparib given alone did not influence tumor growth. To further investigate the mechanism of resistance we are currently investigating the radiosensitizing potential of additional compounds and evaluating the tumors by RNA- and whole-exome- sequencing. Altogether, we successfully established a PSMA positive prostate cancer model resistant to PSMA targeted radionuclide therapy. With this model we are able to investigate the radiosensitizing effect of different drug classes.

#0703 GABA(A) receptor activation drives GABARAP-Nix mediated autophagy to radiosensitize primary and metastatic lung adenocarcinoma tumors.

D. Bhattacharya[1], R. Barrile[2], D. Kamdem Toukam[1], V. S. Gawali[1], L. Kallay[1], T. Ahmed[3], H. Brown[4], S. Rezvanian[3], A. Karve[5], P. B. Desai[5], M. Medvedovic[2], K. Wang[1], D. Ionascu[1], N. Harun[6], C. Wang[1], A. M. Baschnagel[7], J. A. Kritzer[4], J. Cook[3], D. A. Pomeranz Krummel[8], S. Sengupta[9]; [1]University of Cincinnati College of Medicine, Cincinnati, OH, [2]University of Cincinnati, Cincinnati, OH, [3]University of Wisconsin-Milwaukee, Milwaukee, WI, [4]Tufts University, Medford, MA, [5]University of Cincinnati College of Pharmacy, Cincinnati, OH, [6]Cincinnati Children's Hospital, Cincinnati, OH, [7]University of Wisconsin School of Medicine and Public Health, Madison, WI, [8]University of North Carolina at Chapel Hill, Chapel Hill, NC, [9]University of North Carolina at Chapel Hill, Lineberger Comprehensive Cancer Center, University of North Carolina, Chapel Hill, NC

In non-small cell lung cancer (NSCLC) treatment, targeted therapies help a subset of patients, and radiotherapy responses are not durable and toxicity limits therapy. Most advanced-stage NSCLC patients have brain metastases that render an abysmal prognosis. Standard-of-care radiation therapy for NSCLC brain metastasis includes stereotactic radiosurgery (SRS) if the number of lesions is less than ten, otherwise whole brain radiation therapy (WBRT) is administered. Challenges in applying radiotherapy include overcoming radiation resistance and reducing significant associated co-morbidities. Cancer neuroscience is an evolving area, and the purpose of this study is to determine if activation of GABA(A) receptors intrinsic to NSCLC cells can improve radiation efficacy in primary NSCLC and its brain metastasis. We find that a GABA(A) receptor activator, AM-101, impairs the viability and clonogenicity of NSCLC primary and brain metastatic cells. Employing a human-relevant *ex vivo* ‘chip’, AM-101 is as efficacious as docetaxel, a chemotherapeutic used with radiotherapy for advanced-stage NSCLC. *In vivo*, AM-101 potentiates radiation, including conferring a significant survival benefit to mice bearing NSCLC intracranial tumors generated using a patient-derived metastatic line. GABA(A) receptor activation stimulates a selective-autophagic response via multimerization of GABA(A) Receptor-Associated Protein (GABARAP), stabilization of mitochondrial receptor Nix, utilization of ubiquitin-binding protein p62, and upregulation of Beclin-1. A high-affinity peptide disrupting Nix binding to GABARAP inhibits the cytotoxicity of AM-101. This supports a model of GABA(A) receptor activation driving a GABARAP-Nix multimerization axis that triggers autophagy. In NSCLC brain metastases patients, GABA(A) receptor activation may improve radiation efficacy and tumor control while allowing radiation dose de-intensification to reduce toxicity.

#0704 Targeting hypoxic survival pathways to overcome radiotherapy-related treatment resistance.

C. Beckers, L. Vasilikos, A. Sanchez-Fernandez, L. Moor, M. Pruschy;
University of Zurich, Zurich, Switzerland

Tumor cells undergo biological adaptations in order to survive stress conditions, such as hypoxia and nutrient deprivation. These biological adaptations include the activation of hypoxic survival pathways that play an important role in acquiring radioresistance which becomes most challenging with treatment regimens using high doses of radiation/fraction (e.g., hypofractionated radiotherapy). Therefore, inhibiting key regulators within these pathways and thereby exploiting these survival mechanisms, gives rise to new potential drug targets for combined treatment modalities. This novel strategy investigated in our laboratory relies on the concept of biological cooperation: while ionizing radiation kills primarily well-oxygenated cells, such inhibitors of survival kinases will drive quiescent tumor cells under hypoxia and/or nutrient deprivation either directly into cell death or into re-entry into a proliferative and thereby more ionizing radiation-sensitive state. One of the survival kinases we are investigating in combination with ionizing radiation (IR) is DYRK1B (dual-specificity tyrosine regulated kinase 1B). We demonstrated that the expression of DYRK1B was upregulated under serum-starvation and hypoxia, but not in response to IR. The small molecule DYRK1B inhibitor AZ191 and shRNA-mediated DYRK1B knockdown significantly reduced proliferative activity and clonogenicity of SW620 tumor cells alone and in combination with IR under serum-starved conditions, which correlated with increased ROS levels and DNA damage. Furthermore, AZ191 successfully targeted the hypoxic core of tumor spheroids while IR preferentially targeted normoxic cells in the rim of the spheroids. A combined treatment effect was also observed in patient-derived colorectal carcinoma organoids but not in healthy tissue organoids. This data shows that inhibition of DYRK1B in quiescent tumor cells could drive tumor cells on their own into crisis or into a more radiosensitive cell cycle phase and thus supports our strategy of biological cooperation. In the continuation of this project, we have performed a drug-screen with approx. 3’000 clinically relevant compounds in colorectal tumor cells lines under normoxic and hypoxic conditions in order to explore additional hypoxia-mediated survival pathways contributing to radioresistance. Thereby we aim to identify novel combined treatment modalities to overcome radiotherapy-induced hypoxia and hypoxia-related resistance mechanisms.

#0705 *miR-21-5p* induces radioresistance through reinforced DNA damage response in oral squamous cell carcinoma.

Q. Liu, W. Hu, X. Li, Y. Deng, L. Ma;
Shenzhen University, Shenzhen, China

Cancers arising from oral cavity and oropharynx are commonly treated with radiotherapy, whereas tumor radioresistance results in poor outcome. The prerequisite for developing more effective interventions for these patients is that the molecular mechanisms leading to a radioresistant phenotype in these tumors are clear to researchers. Unfortunately, the radioresistant mechanisms remain elusive to date. We recently identified that a highly conserved and cancer-related microRNA, i.e. *miR-21-5p*, plays an important role in radioresistance of oral squamous cell carcinoma (OSCC). We analyzed the RNA-sequencing data of 290 tissue samples from TCGA database, and found the expression of *miR-21-5p* was significantly upregulated in many OSCC samples (N=271) when comparing to adjacent normal tissues (N=19). The difference was further confirmed on our freshly collected OSCC tissues from patients in operation room. We performed RNA-sequencing analysis in 11 OSCC samples and their adjacent normal tissues. Among the 2106 differentially expressed genes between OSCC and normal control groups, we found that several important DNA repair genes (RAD50 double strand break repair protein gene, *RAD50*; DNA Polymerase Theta, *POLQ*; Ataxia Telangiectasia and Rad3-related, *ATR*) were significantly overexpressed in OSCC samples ($P<0.05$), while positive correlations between *miR-21-5p* expression and DNA repair genes *RAD51* and *XRCC4* were identified in the OSCC cohort. Notably, *ATR* is an important DNA damage response gene, while *XRCC4*, *RAD51*, and *POLQ* are involved in DNA double strand break (DSB) repair through non-homologous end joining, homologous recombination, and microhomology-mediated end joining, respectively. OSCC cell lines were further recruited to study the relations of *miR-21-5p* with radiation-induced DSB repair. By analyzing kinetics of 53BP1 foci, a biomarker for detecting DSBs, we found that anti-*miR-21-5p* transfected cells showed more residual foci, indicating of unfinished repair of DSBs, at 5 hours and 18 hours post irradiation. The deficient DSB repair resulted from anti-*miR-21-5p* transfection were further confirmed by single cell gel electrophoresis with comet assay. Consistently, the same treatment resulted in fewer clonogenic survivors in colony formation assay, demonstrating increased radiosensitivity of OSCC cells when *miR-21-5p* was antagonized. This work provided novel insights about the mechanism of *miR-21-5p*-induced radioresistance in OSCC, which may give rise to novel therapeutic strategy for improved treatment of OSCC patients.

#0706 Advancing radiotherapy strategies for high-risk rhabdomyosarcoma: Unveiling BCL-xL inhibition as a potent sensitizer to radiotherapy.

S. Park[1], N. Struyf[1], T. Erkers[1], S. Lehmann[2], M. T. Meister[3], J. Drost[3], F. C. P. Holstege[3], N. Herold[1], P. Ostling[1], J. Stenman[1], O. Kallioniemi[1], J.-I. Henter[1], B. Seashore-Ludlow[1], K. Karlsson[1];

[1]Karolinska Institute, Stockholm, Sweden, [2]Uppsala University, Uppsala, Sweden, [3]Princess Maxima Center for Pediatric Oncology, Utrecht, Netherlands

Pediatric soft-tissue sarcomas are a group of solid tumors that account for about 7% of childhood cancer cases. Rhabdomyosarcoma (RMS), the most common subtype, further stratifies into PAX3 or PAX7 and FOXO1 fusion-negative (FN) or fusion-positive (FP) RMS. FP RMS is the higher risk subtype and is more aggressive, metastatic, and less responsive to treatment. Front-line treatments for RMS FP patients have had limited progress in the recent years and existing treatments such as radiotherapy lacks tumor cell selectivity, resulting in toxic side effects.

To address this, we conducted a high-throughput drug screen to identify radiosensitizers to enhance efficacy of RMS radiotherapy. Using three patient-derived FP RMS tumoroids, we screened a comprehensive drug library with and without radiation, comprising 528 drugs at varying stages of pre-clinical and clinical trials. A validation screen of the top 29 drugs was conducted on a larger cohort of samples including eight patient-derived FP RMS tumoroids and three non-cancer models. The screening revealed that drugs targeting the anti-apoptotic protein B-cell lymphoma-extra-large (BCL-xL) exhibited both potent radiosensitization and cytotoxicity selectively for FP RMS. Notably, the sensitivity to BCL-xL inhibitors correlated with elevated *BCL2L1* expression and PAX3 fusion status. Additionally, drugs targeting polo-like kinase 1 (PLK1) and other cell cycle-related genes exhibited robust radioprotective effects across both RMS and non-cancer models.

Our findings propose the therapeutic potential of BCL-xL inhibition, either as a standalone treatment or in combination with radiotherapy. In parallel, we show the protective potential of PLK1 inhibition to mitigate radiation toxicity. In the long term, we aspire to integrate the identified radiosensitizing and radioprotecting compounds with existing treatment regiments for RMS, maximizing precision and efficacy in RMS radiotherapy.

#0707 Calorie restriction to augment radiation response in models of Black women with breast cancer.

N. B. Francois[1], A. A. Shastri[1], S. Harding[2], T. DeAngelis[1], A. Adekeye[1], N. Simone[1];
[1]Thomas Jefferson University, Philadelphia, PA, [2]Sidney Kimmel Medical College, Philadelphia, PA

Introduction: Black women have higher mortality from breast cancer (BrCa) than other populations. While several factors contribute to this disparity, insulin-like growth factor 1 receptor (IGF-1R), is notably overexpressed in tumors originating in Black women compared to White women, which is associated with tumor progression and resistance to radiation therapy (RT). Caloric restriction (CR) is noted to reduce the expression of members of the IGF-1R pathway. We hypothesize that CR increases the efficacy of RT, in Black women, by downregulating the IGF-1R pathway to decrease tumor growth.
Methods: To understand the feasibility of implementing CR in Black women with BrCa, patients received a CR diet during adjuvant breast RT on an IRB approved investigator-initiated clinical trial and pre- and post- measures were evaluated. BrCa cell lines originating from Black (MD-MBA-468 and MD-MBA-157) or White patients (MDA-MB-231 and MDA-MB-436) were exposed to RT in the presence and absence of CR medium, IGF-1 to upregulate the pathway, and PPP, an IGF-1R inhibitor to evaluate the role of dietary interventions and IGF-1R pathway modulation in altering the RT response. Finally, human BrCa tissue was collected and ex vivo explants were used to evaluate the role of diet to augment the RT response.
Results: In the pilot clinical trial, 32 patients were enrolled, 50% of whom were Black (16B/16W). Black patients had more adverse baseline physiologic parameters and corresponding higher insulin and systemic inflammation as measured by ESR, IFNγ, Il-1β, and TNFα at baseline. Adherence to CR was 87.3% for the Black patients who had an average weight loss of 7.33 lbs, and decreased insulin and cholesterol levels after CR+RT. In intro, in Black originating cells, cell viability experiments showed that CR+RT decreased cell viability by 53% & 46% while RT alone reduced viability by 32 & 41%. In White originating cells, CR+RT decreased cell viability by 52% and 53% while RT alone reduced viability by 42% and 26%. IGF-1R inhibition with PPP caused a more significant decrease in viability when given with RT than CR+RT did. The opposite effect was noted when IGF-1 was added to the cell lines and that increase was prevented by treatment with IGF-1+RT+CR. This was confirmed in vivo. Explants revealed CR helped decrease proliferation and increase apoptosis for all cancer patients.
Conclusion: Taken together, these data demonstrate that Black patients can adhere to dietary interventions during RT therapy for breast cancer which may help achieve better tumor control via downregulation of the IGF-1R pathway which is often notably upregulated in this population. This benefit is widely applicable with equivalent efficacy between patients of both races and all breast cancer subtypes. Future studies should investigate the role of downregulating IGF-1R via dietary interventions to narrow disparities in breast cancer outcomes in our black patient population.

#0708 Targeting aurora kinase B (AURKB) as a radiosensitizing strategy in syngeneic models of triple negative breast cancer (TNBC).

K. M. Jungles[1], Z. Wang[1], C. Bishop[1], C. Wilson[1], M. Liu[1], J. James[1], M. Green[1], J. M. Rae[1], C. W. Speers[2], L. J. Pierce[1];
[1]University of Michigan, Ann Arbor, MI, [2]Case Western Reserve, Cleveland, OH

Purpose: Triple negative breast cancer (TNBC) is an aggressive breast cancer (BC) subtype with few treatment options. Radiation therapy (RT) is a mainstay therapy for the treatment of BC, but local recurrence following RT therapy is common. Consequently, decreasing local recurrence in patients with TNBC is a critical clinical need. Prior work demonstrated that AURKB is overexpressed in TNBC, and over-expression correlates with poor prognosis. Here, we examined the effects of AURKB inhibition as a novel radiosensitizing strategy in syngeneic TNBC models.
Methods: Cell viability assays were used to determine the half-maximal inhibitory concentrations (IC50) of the AURKB inhibitors Barasertib-HQPA and SP-96 72 hours post treatment. Clonogenic survival assays were used to assess the radiosensitivity of TNBC murine cell lines to AURKB inhibition. In these assays, AURKB inhibitors were delivered at sub-IC50 concentrations 24 hours prior to RT, and radiation enhancement ratios (rERs) were calculated. Immunofluorescent microscopy using DAPI stain assessed micronuclei. Propidium iodide staining to assess aneuploidy was completed via flow cytometry. To assess the radiosensitizing effects of AURKB inhibition *in vivo*, the 4T1 syngeneic TNBC cell line was injected bilaterally into Balb/c mice and treated with Barasertib and RT. Tumor volume was recorded twice weekly throughout the study.
Results: Aurora kinase B inhibitors (500-750 nM Barasertib-HQPA, 100-200 nM SP-96) delivered 24 hours prior to radiation therapy induced radiosensitization in the murine TNBC cells 4T1 (rER: 1.24-1.56) and Py8119 (rER: 1.51-1.72). Mechanistically, combined AURKB inhibition and RT significantly increased micronuclei formation in 4T1 cells 24 hours after RT compared to vehicle control ($p<0.0001$). Furthermore, combined AURKB inhibition and RT induced aneuploidy in murine TNBC cell lines 24 hours after radiation therapy compared to vehicle control. Combined AURKB inhibition (Barasertib 25 mg/kg, IP) and RT (8 Gy RT in 1 fraction) significantly decreased tumor volume compared to mice that had received vehicle control (777 ± 61 mm^3 vs 1623 ± 126 mm^3; $p < 0.0001$).
Conclusion: AURKB inhibition induces radiosensitization in syngeneic models of TNBC and leads to increased micronuclei and aneuploidy, suggesting a mechanism of sensitization. These results suggest that AURKB is a potential radiosensitizing strategy for the treatment of triple negative disease. Ongoing studies are further refining the underlying mechanisms of AURKB inhibition and RT on the antitumoral immune response.

#0709 Enhancing prostate cancer treatment: Synergistic effects of mechano-thermal focused ultrasound and radiation therapy.

S. Chatterjee[1], S. Singh[1], S. Barry[2], C. Guha[2];
[1]Albert Einstein College of Medicine, The Bronx, NY, [2]Montefiore Medical Center, The Bronx, NY

Current treatments for prostate cancer primarily rely on radiation and hormone deprivation therapy, yet they often lack effective immunotherapeutic effects. Furthermore, long-term hormone ablation has side effects, such as, impotency and osteoporosis. Addressing this gap, we introduce an innovative dual-frequency focused ultrasound (FUS) platform for non-ablative focal therapy, which induces protein unfolding, ER stress, and increases heat-shock protein expression along with translocation of endoplasmic reticular chaperone proteins (e.g., calreticulin) on the tumor cell surface, thereby sensitizing them for phagocytosis by dendritic cells for efficient antigen presentation and cross priming. We hypothesized that FUS-mediated acoustic immune priming can be combined with ablative therapies, such as, hormone ablation and/or radiation therapy (RT) for induction of tumor-specific adaptive immune response and better tumor control than monotherapy in murine prostate cancer models. Utilizing murine prostate cancer cell lines, MyC-CaP and RM1, we explored the cellular responses to androgen deprivation, observing distinct sensitivities. Twenty-four hours after FUS treatment tumor cells experienced mechano-thermal stress response with 15-fold increase in Hspa1a expression. Transmission Electron Microscopy studies showed formation of myelin figures, nuclear membrane deformation, and lipid droplet formation. In vivo, the combination of FUS (220w/cm^2 intensity for 3 sec at focal point) and RT (8-10 Gy daily x two fractions) markedly delayed tumor growth and achieved complete cure in 14-17% of animals. Through multicolor flow cytometry, we detected significant alterations in the immune microenvironment, including increased CD8+ T cell infiltration and reduced tumor-associated macrophages in the tumor bed. However, we also observed a compensatory rise in pro-tumor immune cells such as PMN-MDSCs and Tregs with significant suppression of eosinophils ($p<0.05$). Interestingly, there was suppression of splenic PMN-MDSCs, Mo-MDSCs, and tumor draining lymph node macrophages, suggesting systemic immune modulation in peripheral lymphoid organs of FUS+RT-treated tumor-bearing animals. Our findings reveal that the combination therapy of FUS and RT improves tumor control in murine prostate cancer and significantly modulates the systemic and tumor immune microenvironment. This approach offers new avenues for immunotherapy, potentially transforming the treatment landscape for prostate cancer, typically resistant to conventional immunotherapeutic strategies.

#0710 Post-exposure suppression of radiation pneumonitis suggests non-redundant independent effects of TGF-beta and TRAIL/DR5.

J. Strandberg[1], A. Louie[1], W. MacDonald[1], P. Srinivasan[1], L. Zhang[1], L. Zhou[1], S. Lee[2], W. El-Deiry[1];
[1]Legorreta Cancer Center at Brown University, Providence, RI, [2]D&D Pharmatech, Gaithersburg, MD

Radiation pneumonitis is one of the most common but challenging toxicities seen in patients that are receiving ionizing radiotherapy for thoracic malignancies. While radiation effectively eliminates cancer cells, the damage it causes to surrounding healthy lung tissue leads to an immune response that can impact treatment regimen and lead to long term fibrotic tissue formation. The mechanism of radiation pneumonitis and the inflammatory response in the lungs is poorly understood. However, it is known that the TRAIL pathway plays an important role in inflammatory and fibrotic response. Through our previous work, it was discovered that modulating the TRAIL pathway via pegylated recombinant long-acting TRAIL (TLY012) in both WT and TRAIL-/- C57Bl/6 could suppress radiation pneumonitis in mice that were exposed to 20 Gy of thoracic radiation with shielding of other organs as early two weeks post exposure. In addition to the TRAIL pathway, transforming growth factor-beta (TGF-β) is a cytokine that is known to play a key role in fibrosis. Broad spectrum integrin inhibitor GLPG0187 is known to inhibit the activation of TGF-β via binding to specific integrin receptors. In order to determine if the inhibition of TGF-β could suppress radiation pneumonitis without stimulation of the TRAIL pathway, DR5 null mice were utilized for the experiment. Male DR5-/- C57Bl/6 mice received a single 20 Gy thoracic radiation dose with shielding of other organs and were treated with 100 mg/kg of GLPG-0187 or control twice a week via IP injection with the first dose being administered 1 hour before radiation (n = 4/treatment/group). 13 days post-irradiation, lungs, sternal bone marrow, and peripheral serum were collected. Upon histological analysis, it was observed that there were thinner alveolar borders and lessened inflammation compared to the control mice. Mice were weighed every three days, and it was discovered that mice treated with GLPG-0187 maintained steady weight compared to the control group. Additional analysis including immunohistochemistry, cytokine profiling, and quantification needs to be conducted. As the TRAIL pathway could not be modulated in the DR5 null mice, these findings suggest that GLPG-0187 was able to suppress radiation pneumonitis via inhibition of TGF-β. While some rescue from radiation pneumonitis was observed via GLPG0187, it was to a lesser extent compared to treatment of WT and TRAIL-/- C57Bl/6 mice with TLY012. Future directions include investigating the synergistic effects between TLY012 and GLPG0187 in suppressing radiation pneumonitis and decreasing fibrotic response to radiation.

#0711 HDAC3 sustains resistance to hypofractionated radiotherapy in fusion positve rhabdomyosarcoma cells.

M. Cassandri[1], A. Porrazzo[2], **S. Pomella**[1], S. Camero[2], F. A. Aiello[1], L. D'Archivio[1], C. Zwergel[2], B. Noce[2], M. Tomaciello[2], F. Vulcano[3], L. Milazzo[3], F. Pedini[3], M. Signore[3], A. Fanzani[4], C. Marchese[2], G. Minniti[2], S. Valente[2], A. Mai[2], F. Megiorni[2], R. Rota[1], F. Marampon[2];
[1]Bambino Gesu Children's Hospital, Rome, Italy, [2]Sapienza University of Rome, Rome, Italy, [3]Istituto Superiore di Sanita, Rome, Italy, Rome, Italy, [4]University of Brescia, Brescia, Italy

Rhabdomyosarcoma (RMS) is the most common soft tissue sarcoma of childhood. The fusion-positive (FP)-RMS variant expressing chimeric oncoproteins such as PAX3-FOXO1 and PAX7-FOXO1 shows a dismal prognosis with 5-year survival of less than 30% compared to non-metastatic fusion-negative (FN)-RMS variant. In the last years, a lot of interest has focused on new targets identification to improve the radiotherapy (RT) efficacy. HDAC inhibitors (HDACi) radio-sensitize different cancer cell types including RMS. Recently, we reported that MS-275, a Class I and IV HDACi, in combination with RT affected cell survival, reduced colony formation ability, increased DNA damage repair inhibition and reactive oxygen species formation in FP-RMS cells. However, despite promising preclinical studies , HDAC inhibitors (HDACi) achieved only modest success in human clinical trials for solid tumors, frequently showing several toxicities, probably because of the limited specificity of many HDACi. Thus, a major effort is being directed toward identification of HDACi which are selective for HDAC isoforms often uniquely implicated in the radioresistance of specific cancers. In order to identify the class I HDAC responsible of radioresistance in RMS we knocked-down HDAC1, HDAC2, HDAC3, and HDAC8 expression in combination with RT. Interestingly, we observed an increased radiosensitivity only in HDAC3-depleted FP-RMS cells. Thus, we focused on HDAC3 to understand the mechanisms by which it promotes radioresistance in RMS. We observed that HDAC3 is overexpressed in RMS patients and cell lines compared to the normal counterpart. Furthermore, RMS cells are strongly dependent by HDAC3 expression while slight dependency has been observed with other class I HDACs in DepMap portal. We demonstrated that HDAC3 depletion by CRISPR in combination with RT in FP-RMS cells increases apoptosis, reduces colony formation ability, cancer stem cells population and anchorage independent growth and reduces cell growth *in vivo* and *in vitro*. Accordingly, HDAC3 depleted cells in combination with RT reduces levels and activation of key player of FP-RMS biology such as MYCN, ERK and AKT. Moreover, HDAC3 KD increases radiotherapy-induced DNA double strand break and impairs DNA repair mechanisms reducing levels and activation of both homologous recombination (HR) and non-homologous end joining (NHEJ) factors such as ATM, RAD51 and DNA-PKcs. Thus, we developed a new potent and highly specific HDAC3 inhibitor (HDAC3i). The new HDAC3i is highly specific in targeting FP-RMS cell growth *in vitro* while no effects have been observed in normal cells such as myoblasts and lung fibroblast. Moreover, the drug treatment in combination with radiotherapy phenotypically and molecularly recapitulated what observed in HDAC3 depleted cells.The study has been founded by Italian Association for Cancer Research (AIRC) to FM.

EXPERIMENTAL AND MOLECULAR THERAPEUTICS: Tumor Microenvironment
Poster Session

#0715 Nanomedicines loaded with TLR agonists and inhibitors of immunosuppression to reprogram the tumor microenvironment.

F. Torres Andon, Sr.[1], A. Pensado-Lopez[1], C. Anfray[2], A. Ummarino[2], I. Fernandez-Marino[3], L. Sanjurjo[3], J. Crecente-Campo[3], E. Fernandez-Megia[4], F. Castro[5], M. Oliveira[5], A. Calvo[6], R. Garcia Campelo[1], A. Mantovani[2], M. Alonso[3], P. Allavena[2];
[1]Oncology Unit, Complexo Hospitalario Universitario de A Coruna (CHUAC) Instituto de Investigacion Biomedica de A Coruna (INIBIC), A Coruna, Spain, [2]Clinical and Research Hospital Humanitas, Istituto di Ricovero e Cura a Carattere Scientifico (IRCCS), Milan, Italy, [3]Centre for Research in Molecular Medicine and Chronic Diseases (CIMUS), Universidade de Santiago de Compostela, Santiago de Compostela, Spain, [4]Centre for Research in Biological Chemistry and Molecular Materials (CIQUS), Department of Organic Chemistry, Universidade de Santiago de Compostela, Santiago de Compostela, Spain, [5]i3S-Instituto de Investigacao e Inovacao em Saude, Universidade do Porto, Rua Alfredo Allen, Porto, Portugal, [6]School of Medicine, IDISNA and Program in Solid Tumors and Biomarkers, Center for Applied Medical Research (CIMA), CIBERONC, ISC-III, University of Navarra, Pamplona, Spain

The stroma of solid tumors is populated by myeloid cells, which mostly represent macrophages. Tumor-associated macrophages (TAMs), strongly influenced by cancer cell-derived factors, are key drivers of immunosuppression and support tumor growth and spread to distant sites. Increasing evidence demonstrates their ability to hamper cancer patients' response to most treatments currently applied in the clinic, including immunotherapy. Therefore, strategies to counteract negative effects of TAMs are nowadays gaining momentum at preclinical, translational, and clinical levels.
Here, we present the development and evaluation of nanoparticles (NPs) loaded with TLR agonists and/or inhibitors of immunosuppressive pathways to reprogram TAMs and the tumor microenvironment (TME) to unleash an effective immune response to fight against the tumor. Firstly, we have evaluated *in vitro* the ability of poly(I:C) and/or R848, agonists of TLR3 and TLR7/8 respectively, to reprogram TAMs into antitumor effector cells, and also the efficacy of Stattic and/or Galunisertib, inhibitors of STAT3 and TGF-β pathways respectively, to inhibit immunosuppression by cancer cells and/or TAMs. The best combinations of these drugs were encapsulated in nanoemulsions or polymeric nanocapsules for improved TAM-targeting and pharmacokinetics *in vivo*. These NPs were characterized for their physicochemical properties and also tested *in vitro* using primary human macrophages. For *in vivo* evaluation, subcutaneous and orthotopic murine models of lung cancer (CMT167) were used, showing antitumoral efficacy and TME reprogramming as evaluated by FACS, RNA analysis and multiplex immunofluorescence. Protamine-NCs-loaded with poly(I:C)+R848 and coated with an additional layer of hyaluronic acid functionalized with mannose were used to target the CD206 receptors, showing antitumoral efficacy mediated by TAM reprogramming, evaluated as higher CD86 while lower CD206 and Arg1 expression. Nanoemulsions with a PEGylated surfactant, encapsulating Stattic+Galunisertib+R848 showed faster antitumoral activity *versus* the free drugs. Experiments performed in IFN-γ KO mice and immune deficient mice (NSG and Balb/c nude) revealed that a fully functional immune system is crucial for the response to the treatment.
In conclusion, our work demonstrates the antitumoral efficacy and reprogramming of the tumor microenvironment by combinations of TLR agonists and/or inhibitors of immunosuppression, which can be improved by nanotechnological approaches. Further investigations are ongoing to assess their antitumoral efficacy in other tumor models (i.e. breast and pancreatic cancer), with the final aim of clinical translation.

#0716 Depletion of stromal cells remodels tumor microenvironment and potentiates immune checkpoint blockade in pancreatic cancer.

J. Rupert[1], A. Daquinag[1], L. Cai[2], Y. Dai[1], Z. Zhao[1], D. Anastassiou[2], M. Kolonin[1];
[1]University of Texas at Houston, Houston, TX, [2]Columbia University, New York, NY

During carcinoma progression, mesenchymal stromal cells (MSCs) become recruited to tumors and contribute to the pool of cancer-associated fibroblasts (CAFs). Sub-populations of CAFs, have diverse and incompletely understood effects on disease progression and resistance to therapy. Adipose stromal cells (ASCs), the MSCs from fat tissue increasingly recruited by carcinomas in the context of obesity, have been shown to support cancer progression. Here, the roles of perivascular CAFs expressing platelet-derived growth factor receptor beta (*Pdgfrb)* and of CAFs expressing non-glycanated decorin (ngDCN), a marker of ASCs, were analyzed. We used mice orthotopically grafted with pancreatic ductal adenocarcinoma (KPC) cells. Ablation of cells expressing thymidine kinase under the control of *Pdgfrb* promoter with ganciclovir resulted in suppression of primary pancreatic tumor growth. However, ablation *Pdgfrb*+ cells induced spontaneous metastases to the liver. For depletion of ngDCN+ cells, we used a hunter-killer peptide D-CAN, which has been previously reported to induce apoptosis of ASCs and CAFs in mouse models. Here, D-CAN also had a negative effect on pancreatic tumor growth, however, there was no significant effect on metastatic dissemination. Single cell RNA sequencing of tumors demonstrated that targeting of *Pdgfrb*+ and ngDCN+ stromal cells had distinct effects on sub-populations of CAFs. Endothelial cell and cancer cell survival was decreased by depletion of either *Pdgfrb*+ or ngDCN+ stroma. However, pathway analysis revealed that depletion of *Pdgfrb*+ and ngDCN+ stromal cells has different effects on the markers of cancer cell aggressiveness. D-CAN treatment, and to a less extent *Pdgfrb*+ cell ablation, suppressed macrophage M2 polarization and increased infiltration of cytotoxic T-lymphocytes. This observation, confirmed in the MyCap graft model of prostate cancer, suggested that ablation of ngDCN+ stroma should synergize with immune checkpoint inhibitors. We tested the effect of D-CAN on the efficacy of anti-PDL1 antibody in the orthotopic KPC model. Compared to D-CAN and anti-PDL1 antibody alone, combination treatment had a synergistic effect on tumor growth. Importantly, liver metastases were suppressed by the D-CAN / anti-PDL1 antibody combination, but not by individual agents. We conclude that improved approaches to target mesenchymal stroma in tumors may be effective in combination with immunotherapy.

#0718 CCR8 antibody drug conjugates: Targeting regulatory T cells for tumor sensitization.

L. J. Stafford[1], H. Roth[1], S. Campbell[1], S. Brady[1], V. Fiers[1], F. Yu[2], A. Tsourkas[2], R. Payne[1], M. Pitts[1], K. Guldner[1], T. Phillips[1], B. Tyrell[1], C. Ulke[1], A. Snyder[1], M. Assogba[1], H. Ohl[1], I. Sanchez[1], B. Doranz[1], J. Rucker[1], R. Chambers[1];
[1]Integral Molecular, Philadelphia, PA, [2]AlphaThera, Philadelphia, PA

Background: Regulatory T (Treg) cells in the tumor microenvironment have an immune suppressive function, and their presence is associated with poor prognosis. Depletion of Treg cells may be a mechanism to sensitize tumors and represents a novel strategy for cancer immunotherapy. High expression of chemokine receptor CCR8 has been found in Treg cells in microenvironments of numerous tumors but not on Treg cells in systemic lymphoid tissues. The ability to selectively kill Treg cells in tumor environments may provide an opportunity for therapy that leaves Treg function intact elsewhere in the body where they normally mediate tolerance to self-antigen.
Methods: We sought to identify CCR8 antibodies for therapeutics and designed an antibody discovery strategy to address the challenges of this target. CCR8 is a member of the G protein-coupled receptor (GPCR) family. Like many GPCRs, CCR8 is a valuable therapeutic antibody target but challenging to access due to its poor expression, membrane-dependent structure, and poor immunogenicity due to sequence conservation. We developed an antibody discovery platform (MPS) that specifically addresses each of these challenges through use of advanced immunization techniques and evolutionarily divergent host species (chickens) for robust immune responses against conserved targets. We extensively engineered CCR8 antigen to enable high expression for immunization. When sufficient antibody diversity was not obtained using our standard immunization techniques, we developed mRNA immunization techniques for this program. Antibody binding was measured using flow cytometry on transfected cells and human Treg cells. The ability of antibodies to inhibit CCR8 function was measured using intracellular calcium influx assays. Antibody internalization was measured using dye uptake assays and flow cytometry. Antibodies were conjugated with cytotoxic payloads and tested for the ability to mediate killing.
Results: Using these approaches, we identified a panel of high-affinity antibodies that bound in the nanomolar or subnanomolar range with high specificity, and we selected a lead molecule to progress. We will present data from our antibody discovery campaign including mRNA immunization, binding profiles, GPCR functional data, receptor-mediated internalization, and the ability of antibody-drug conjugates (ADC) to kill CCR8+ cells, including human Treg cells, *in vitro*.
Conclusion: Treg cells are a primary driver of the immunosuppressive microenvironment in many solid tumors. Targeting immune-suppressive CCR8+ Treg cells using ADC has potential to expand the treatment of solid tumors

#0719 A tumor-activated PD1/IL2 bispecific molecule, designed to overcome IL-2 receptor-mediated clearance, improve tolerability and stimulate antigen-experienced $CD8^+$ T cells in the tumor microenvironment of murine models.

E. Eryilmaz, W. Guzman, S. Hsiao, P. Johnson, L. Quinn, J. Lakhani, B. Whalen, R. Quiroz, K. Jenkins, B. Lanter, O. Yerov, W. Scott, J. Greene, Z. Liu, J. Hedges, M. McLaughlin, S. Vu, C. Turcotte, J. Taylor, C. O'Toole, M. Pederzoli-Ribeil, H. Duprey, N. Malkova, D. Fantini, D. Crowe, K. Smith, J. Card, J. Lee, K. Smith, B. Nicholson, J. O'Neil, C. U. Bialucha;
Xilio Therapeutics, Waltham, MA

PD-1/PD-L1 therapies have shown significant activity across a range of tumor types, however, 70-90% of patients do not derive durable benefit. In preclinical settings, delivery of PD-1 blockade and IL-2 agonism in cis via a bispecific molecule, comprising a PD-1 antibody fused to IL-2, has demonstrated superior activity compared to delivery of individual components or their combination. Targeting of IL-2 to $PD\text{-}1^+$ cells in cis has been shown to drive a unique differentiation path endowing $CD8^+$ T cells with enhanced functionality. However, we show that the IL-2 component in an unmasked PD1/IL2 bispecific molecule dominates its pharmacology, driving marked peripheral activation of immune cells, rapid IL-2 receptor-mediated clearance and systemic toxicity. To address these challenges and enable tumor-specific activity, we designed a PD1/IL2 bispecific molecule that incorporates a single domain antibody-based mask to bind to the IL-2 component and maintain it in a quiescent state until activated by prevalent and dysregulated proteases in the tumor microenvironment (TME). In preclinical models, the affinity-optimized mask prevented peripheral IL-2 receptor binding, associated toxicity and receptor-mediated clearance. Improved pharmacokinetics of our tumor-activated PD1/IL2 enabled PD1 antibody-like exposures and is projected to achieve complete blockade of PD1 signaling. Tumor-activated PD1/IL2 significantly inhibited tumor growth compared to anti-PD-1 alone or vehicle and demonstrated improved tolerability compared to an unmasked PD1/IL2 bispecific in mouse models. In addition, pharmacodynamic activity of tumor-activated PD1/IL2 was restricted to the TME. Consistent with the masked design, we observed no significant change in $CD8^+$ T cells in the periphery and significant increases in antigen specific $CD8^+$ T cells, memory $CD8^+$ T cells and $TCF1^+$ stem-like $CD8^+$ T cells in the TME. Ex vivo protease cleavage assays performed in human samples demonstrated efficient activation of tumor-activated PD1/IL2 by multiple tumor types and minimal activation in human plasma. In non-human primates, tumor-activated PD1/IL2 achieved tolerable exposures that were comparable to those of existing PD-1 blocking immunotherapies. Taken together, these preclinical data suggest that tumor-activated PD1/IL2 has the potential to improve upon existing PD-1/PD-L1 immunotherapies by inhibiting PD-1/PD-L1 axis and simultaneously directing immunostimulatory IL-2 to antigen-experienced effector cell populations in the TME.

#0720 Combining zelasudil, a small molecule ROCK2 inhibitor, with chemotherapy or immunotherapy improves response in preclinical models of pancreatic cancer.

M. Pajic[1], B. McLean[1], D. Chacon Fajardo[1], S. Porazinski[1], D. H. Upton[1], D. Schuhmacher[1], A. Istadi[1], T. Cox[1], P. Timpson[1], D. J. Wilcock[2], K. J. Anderson[2], H. Mason[2], N. E. S. Guisot[2], C. D. Jones[2], C. Phillips[2], R. Armer[2];

[1]Garvan Institute of Medical Research, Sydney, Australia, [2]Redx Pharma Plc, Greater Manchester, United Kingdom

Zelasudil (RXC007) is an orally available, highly selective small molecule inhibitor of Rho-associated coiled-coil containing protein kinase 2 (ROCK2), which has demonstrated pre-clinical anti-fibrotic efficacy and is currently being tested in a Phase 2a clinical trial for the treatment of idiopathic pulmonary fibrosis (IPF) (NCT05570058). Pancreatic ductal adenocarcinoma (PDAC) is an aggressive and therapeutically challenging disease with a dense and highly fibrotic tumor microenvironment which may limit efficacy of conventional therapies. Here, we investigate the benefit of combining an anti-fibrotic, RXC007, with either standard of care chemotherapy or immunotherapy in mouse models of PDAC.In a fibrotic patient-derived metastatic PDAC orthotopic model, RXC007 (10mg/kg, 50mg/kg and 100mg/kg BID 5d on/2d off PO) in combination with SoC chemotherapy Gemcitabine (100mg/kg IP QW)/Abraxane (30 mg/kg IP QW) improved survival in a dose-dependent manner (all P<0.0001) compared to Gemcitabine/Abraxane alone.In the immunocompetent orthotopic LSL-KrasG12D/+; LSL-Trp53R172H/+; Pdx1-Cre (KPC) model of metastatic PDAC, survival was significantly increased (P<0.0001) upon treatment with a combination of RXC007 (50 mg/kg BID 5d on/2d off PO) and anti-PD1 (200 ug BIW) compared to anti-PD1 alone. ROCK2 inhibition elicited positive immunomodulatory effects in KPC pancreatic tumors, with increase of CD8+ (P=0.0031) and CD4+ (P=0.008) T cell infiltrate into the tumor cortex and reduction in immunosuppressive FOXP3+ regulatory T cells at the tumor border. Furthermore, RXC007 monotherapy exhibited anti-fibrotic effects, via a decrease in collagen content and organization, effects associated with CAF reprogramming and reduced intra-tumoral aSMA+ PDPN+ myofibroblast-like CAFs (myCAFs; P=0.0406).This data highlights the potential for treating highly fibrotic tumours with RXC007 in combination with SoC chemotherapy or immunotherapy in order to improve patient outcomes in this aggressive and treatment-refractory cancer.

#0721 Novel and distinctive anti-HLA-G antibody, IMB-201, inhibits tumor progression by breaking immune escape mechanism and enhancing cytotoxicity.

H. Kang, S. Baek, I. Lee, M. Ju, S. Han, E. Han, S. Kang, J. Koo, Y. Kim, S. Park, E. Cho, C. Lee, G. Ha;
IMBiologics Corp., Suwon, Korea, Republic of

Human leukocyte antigen-G (HLA-G), a type of MHC class I, is known to be expressed only in the placenta and acts as an immune suppressor to protect the fetus from maternal immunity. Recent studies have revealed that HLA-G suppresses various tumor-infiltrated immune cells, such as T cells, NK cells, and macrophages, through interaction with inhibitory receptors Ig-like transcript 2 (ILT2). HLA-G has recently emerged as an attractive anticancer target because HLA-G is a highly specific tumor antigen and has a role in immune evasion of cancer cells. Additionally, the expression pattern of ILT2 differs from that of PD-1 in tumor-infiltrated CD8+ T cells. Therefore, an HLA-G targeting strategy is expected to be an alternative to address unmet medical needs for those not responding to anti-PD(L)1 therapies. In this study, we screened the novel anti-HLA-G antibody, IMB-201, using phage display technique and confirmed that IMB-201 selectively bound to the membrane HLA-G of cancer cells. It exhibited superior activities in ILT2 blockade, NK cell activation, and antibody-dependent cellular cytotoxicity (ADCC) compared to the reference antibody. Furthermore, IMB-201 demonstrated more efficient suppression of tumor growth compared to the reference antibody in subcutaneous gastric cancer xenograft model. Notably, the group administered IMB-201 with NK92MI cells (CD16-negative NK cells) in the ovarian cancer xenograft model showed stronger tumor growth inhibition compared to the group treated only IMB-201, indicating that NK92MI cells were activated by IMB-201. This result indicates that one of the mechanisms of action (MoA) of IMB-201 worked effectively *in vivo*. In addition, to maximize the efficacy of IMB-201 and differentiate it from competitors, various efficacy enhancing modality could be applicable. We aim to develop biopharmaceuticals by selecting the optimized modality. Based on these results, IMB-201 could overcome the limitations of existing cancer immunotherapy, potentially becoming highly influential in cancer treatment as a novel immune checkpoint inhibitor. It is also expected to exhibit higher anticancer efficacy in combination therapy with immune checkpoint inhibitors.

#0722 A cancer-associated fibroblast model to discover mechanisms of growth, survival, and treatment sensitivity in PAX3/7-FKHR fusion-positive alveolar rhabdomyosarcoma.

Patrick Sipila[1], Son Tran[1], Chunfen Zhang[1], Anne-Marie Langevin[2], Aru Narendran[1]

[1]Department of Oncology, University of Calgary, Calgary, AB, Canada,[2]Pediatric Hematology/Oncology, UT Health San Antonio, San Antonio, TX

Introduction: Rhabdomyosarcoma (RMS) is the most common pediatric soft tissue sarcoma. Among various subtypes, alveolar RMS (ARMS) is generally more aggressive and usually carries the fusion transcription factor, PAX3/7-FKHR. High-risk ARMS has an extremely poor prognosis, with ~25% five-year survival. Hence, novel therapeutic approaches are urgently needed. However, potential therapies are often hindered by the immunosuppressive tumor microenvironment (TME) associated with sarcomas. The TME is highly dynamic and includes fibroblasts, immune cells, and extracellular matrix. Cancer-associated fibroblasts (CAFs) may promote tumor growth and survival by secreting distinct factors to regulate proliferation, metastasis, and resistance to therapy. In this study, we investigated mechanisms involved in this phenomenon and identified a novel therapeutic strategy targeting the TME of ARMS.

Methods: Cells were isolated from a PAX3-FKHR fusion-positive ARMS tumor specimen, following ethics approval and informed consent. The PAX3-FKHR fusion status and mesenchymal biomarkers were analyzed by immunoblotting. The patient's CAFs (designated KCCF14), RMS lines (RD, RH30, RH41), and control fibroblasts (BJ, HS68, WI-38) were cultured in vitro and their respective supernatant media was harvested for subsequent experiments. Cell proliferation and viability were determined by hemocytometer and alamar blue assay, respectively. The scratch wound healing assay was used to assess cell migration. Cytokine analysis was performed with a 96-plex array. For drug screening, cells were treated with a panel of CXCR4 antagonists to generate dose-response curves.

Results: KCCF14 CAFs isolated from an ARMS tumor exhibit elongated spindle morphology and are positive for mesenchymal biomarkers, including PDGFR-β and smooth muscle α-actin. As expected, these cells lack characteristics of the patient's tumor, notably the expression of PAX3-FKHR fusion and N-myc. KCCF14-conditioned media significantly enhances ARMS cell proliferation and migration in a concentration-dependent manner. Analysis of the conditioned media revealed upregulation of key growth factors and cytokines, including PDGF-AA, VEGF-A, MCP-1, and IL-11, that promote tumor aggressiveness through proliferative signaling, angiogenesis, activation of migration, and immune evasion. Because SDF-1 (CXCR4 ligand) was also increased, we tested targeted inhibition of CXCR4, which induced cytotoxicity with increased sensitivity (IC_{50} = 0.5 μM) in KCCF14 cells compared to control fibroblasts.

Conclusions: This study provides, for the first time, findings from a continuously growing CAF model system for RMS. Our data describes key tumor growth and survival mechanisms supported by the TME and establishes a method to identify treatments with novel therapeutic strategies.

#0723 Reduction of immunosuppressive function of regulatory T cells enhances antigen-specific T cell mediated cytotoxicity against tumor cells.

A. A. Khan[1], J. Park[1], N. LaVoy[1], C. Tompkins[1], J. Bellinder[2], T. San Miguel[2], N. Lawrence[2], B. Schoen[2];
[1]Charles River Laboratories, Inc., Bothell, WA, [2]Charles River Laboratories, Inc., Northridge, CA

Regulatory T cells (Tregs) maintain immune homeostasis by suppressing abnormal immune response to self and non-self-antigens. Tregs are also involved in tumor development and progression by inhibiting anti-tumor immunity. Infiltration of Tregs in the tumor microenvironment (TME) inhibit anti-tumor immunity by suppressing tumor antigen-specific T cell responses. This results in tumor progression and poor prognosis in patients with various types of cancers. Therefore, depletion of Tregs could be a promising immunotherapy target to augment the anti-tumor immune response. Molecules highly expressed by Tregs such as CD25, immune checkpoint molecules, and chemokine receptors have been targeted by antibodies or small molecules to deplete Tregs and its immunosuppressive function has been tested in the clinic. However, a thin line exists between augmenting effective immunity and inducing autoimmunity, posing difficulties in harnessing Tregs modulation in cancer treatment. Thus, additional strategies to selectively control Tregs are urgently needed for the effective treatment of cancer. In this study we evaluated the role of Tregs in suppressing the effector function of antigen-specific T cells and targeted killing of cancer cells *in vitro*. We observed Tregs mediated suppression of antigen-specific cytotoxicity against cancer cells. When Tregs were treated with cyclophosphamide, CD25 depleting antibody and anti-CTLA4 antibody alone or in combination, we observed enhanced killing of cancer cells *in vitro* as a result of potentiated effector function of antigen-specific T cells. This study provides a path forward to fine-tune and optimize strategies to target various molecules that are highly expressed on Tregs and augment anti-tumor immunity by antigen-specific T cells to achieve therapeutic outcome.

#0724 MPSA-AB5000: A high-throughput membrane proteins screening array for therapeutic biologics specificity profiling.

L. Li, J. Xiong, J. Ning, **F. Hao**;
Kyinno Biotechnology Co., Ltd, Beijing, China

The development of novel antibody drugs is a lengthy journey. Many factors can lead to failures during clinical development. According to reports, off-target binding of antibodies could also be a significant cause. It has been stated that about 25% of preclinical candidates might have off-target issues. With the emergence of new modalities like CD3 bispecific antibodies, ADCs, and CAR-T therapies, early-stage off-target screening of antibodies has become even more crucial. Although techniques such as immunohistochemistry, ELISA, and flow cytometry (FACS) have been used for off-target testing of antibodies, these methods still lack sensitivity and specificity, and their throughput is limited. To address the need for antibody target deconvolution and receptor identification, we developed a novel membrane protein screening array-AB5000 (MPSA-AB5000). MPSA-AB5000 is a high-throughput cell-based platform for identifying the targets of antibodies and other ligands that bind to membrane proteins. MPSA-AB5000 is an excellent solution for antibody specificity screening, which enables early off-target screening and can de-risk the antibody drug development program. The MPSA-AB5000 makes use of the full coverage of unique human membrane proteins, including receptors, transporters, enzymes, miscellaneous, and others. Each membrane protein is expressed in live cells to ensure native conformation. In addition, the same membrane protein clones with a C-terminal epitope tag were constructed, allowing confirmation of protein expression and cellular location. To provide the highest level of sensitivity, MPSA-AB5000 uses luciferase reporter cell line detection. The wash-free strategy reduces false negatives, and signal amplification makes remarkable discrimination. Compared to similar technologies, we possess significant advantages in the following aspects: a. High sensitivity and sigh throughput: our technology platform offers not only high sensitivity, capable of detecting subtle interactions but also supports high-throughput screening, allowing for the evaluation of a large number of samples in a short timeframe. b. Avoidance of false negative signals: by eliminating washing steps, our method reduces the risk of false negative signals, ensuring reliable detection of non-specific binding. c. Comprehensive validation approaches: We employ various validation methods such as FACS and ELISA to eliminate false positive signals and enhance the accuracy and credibility of our results. All the advantages ensure that MPSA-AB5000 is more rapid, simple, and highly sensitive than traditional assays.

#0725 Listeria-inspired phagosome escape drives STING responses to CD47 blockade.

B. R. Schrank, Y. Wang, A. Antony, W. Jiang;
UT MD Anderson Cancer Center, Houston, TX

Purpose: Through phagocytosis, antigen-presenting cells (APCs) engulf and neutralize malignant cells. However, engulfed tumor cells are destroyed in phagolysosomes leaving few peptides to enter cytosol, where cross-presentation of antigens and immune activation occurs. *Listeria (L.) monocytogenes* escape phagolysosomes by secreting a pore-forming protein Listeriolysin O (LLO). Our breakthrough centers on harnessing LLO to create LLO-CD47, a novel protein-antibody conjugate that fuses the myeloid checkpoint anti-CD47 to LLO. By promoting tumor cell-phagocytosis and the release of tumor peptides and DNA from phagolysosomes, we hypothesize that LLO-CD47 enhances the immune functionalities of APCs.
Procedures: Anti-CD47 was conjugated to LLO using a water-soluble SPDP crosslinker and purified by affinity chromatography. Transmission electron microscopy (TEM) was used to visualize the integrity of macrophage phagolysosomes following treatment. C57BL/6 mouse bone marrow-derived macrophages (BMDMs) were used to study M2-to-Ml polarization, tumor cell phagocytosis, STING activation, and antigen presentation. Mice bearing orthotopically implanted spontaneously metastatic murine triple-negative 4T1 tumors and E0771 tumors received intratumoral (IT) or intraperitoneal (IP) injection. CD8+ T cells or tumor-associated macrophages (TAMs) were depleted from tumor-bearing mice using an anti-CD8 antibody or anti-CSF-1R antibody prior to treatment.
Results: 1. LLO-CD47 skews BMDMs from M2-to-M1 inflammatory phenotypes and enhances the phagocytosis of E0771 tumor cells. 2. BMDMs visualized by TEM show breaches in phagosome membranes following LLO-CD47, but not anti-CD47, treatment. 3. LLO-CD47 increases levels of phosphorylated STING, IFN, and TNFa in BMDMs in vitro and TAMs in vivo, relative to anti-CD47. 4. IT delivery of LLO-CD47 inhibits the growth and metastasis of orthotopically implanted murine breast tumors relative to anti-CD47. Harvested tumors show increased M1 polarized macrophages and CD8+ T cells, which express high levels of PD-1. 5. Co-administration of IP anti-PD-1 and LLO-CD47 delays the progression of breast tumor metastasis and prolongs animal survival relative to animals treated with anti-PD-1 and anti-CD47. 6. The elimination of CD8+ T cells or TAMs abrogates the antitumor effect of LLO-CD47. 7. IP administration of LLO-CD47 showed acceptable toxicity with stable body weight gain and no long-term hematological, renal, or hepatic toxicities.
Conclusion: Conjugation of LLO to anti-CD47 enhances macrophage STING activation, antigen presentation, and tumor cell phagocytosis. Our work represents the first antibody-drug conjugate specifically designed to enhance immune activation against cancer.

#0726 The retinoid X receptor agonist MSU42011 enhances efficacy of anti-PD1 therapy in a HER2+ breast cancer model through a CD4-IL12 axis.
A. S. Leal, K. T. Liby;
Indiana University School of Medicine, Indianopolis, IN

Immunotherapy is rarely effective in breast cancer and most current therapeutic options fail to target the stromal compartment. We have developed a new small molecule, MSU42011, that induces tumor regression in experimental models of Kras-driven lung cancer and HER2+ breast cancer. This tumor regression is dependent on a functional immune system. Here, we dissected the tumor stroma, revealing a CD4 and IL12a dependency for the anti-tumor activity of MSU42011. Cancer immunotherapy responses are mostly driven by CD8 T cells. Using a murine HER2+ tumor model, anti-CD8 antibodies (200ug/mouse) were injected 24 hours before treatment with MSU42011 (100MG/KG in power diet) was started. Mice were maintained on diet for 10 days. Anti-CD8 antibodies were also administered on days 3, 7 and 10. The combination did not affect the inhibition of tumor growth by MSU42011, suggesting that its anti-tumor efficacy is not dependent on CD8 T cells. In contrast, tumors treated with MSU42011 and anti-CD4 antibodies grew ($p=0.0016$ versus MSU42011 alone) at the same rate as tumors treated with control diet ($p=0.0139$ versus MS42011). Furthermore, anti-CD4 reversed inhibition of tumor growth by MSU42011 in a carcinogen-induced lung tumor model. Interestingly, MSU42011 increased the levels of IL12 by 4x ($p=0.01$) and IFN by 8x ($p=0.03$) compared to the controls. These data suggest that MSU42011 increased Th1 CD4 T cell polarization; the increase in IL12 was lost following CD4 T cell depletion. Following depletion of IL12a with antibodies (loading dose of 1 mg, followed by 0.5mg per mouse IP), tumors treated with the combination of MSU42011 and anti-IL12a antibodies grew at the same rate as the controls. T cell engagement with MSU42011 suggests that this small molecule is a good candidate for combination with immunotherapy. HER2+ MMTV-Neu mice with established tumors were treated with the combination of MSU42011 and anti-PD1 antibodies. Treatment with MSU42011 at 100mg/Kg of diet for 10 days, followed by anti-PD1 antibodies (200ug) twice weekly failed to increase survival. In contrast, 2 doses of anti-PD1 antibodies (300ug), followed by treatment with MSU42011 increased survival by 10 days compared to controls. The tumors in the MSU42011+anti-PD1 group initially grew rapidly, with increased redness and heat, suggesting an enhanced inflammatory response. When anti-PD1 antibodies were given at a lower loading dose (200ug and then 100ug twice weekly) followed by a higher dose of MSU42011 (300 mg/Kg of diet), survival markedly increased ($p=0.052$). These findings demonstrate that activation of RXR in the stroma can be used to increase the effectiveness of immunotherapy.

#0727 FGFR4 promotes colon cancer progression through CAF activation via the CXCL10-CXCR3 axis.

S.-H. Cho, H. Bang, E.-G. Sun, J.-N. Choi, M.-R. Park, H.-J. Shim, J.-E. Hwang, W.-K. Bae, I. Chung;
Chonnam National Univ. Hwasun Hospital, Hwasun-Gun, Korea, Republic of

Cancer-associated fibroblasts (CAFs) contribute to cancer progression via crosstalk with cancer and immune cells in the tumor microenvironment (TME). Despite the significant role of CAF, the understanding of the trigger mechanisms of cancer-mediated CAF activation remains unclear. We previously reported the mechanism by which FGFR4 in colon cancer secretes amphiregulin (AREG), resulting in anti-EGFR chemoresistance. It motivated us to investigate whether FGFR4 overexpressing tumors may change the TME, so we explored the mechanism of CAF activation under the FGFR4 signaling pathway. CAF was isolated from BALB/C mice after injecting 1×10^6 CT-26/EV or FGFR4 cells using microbeads and conditioned media (CM) was prepared by filtering after 48h cancer cell culture with serum-free medium In mice model, CT-26/FGFR4 showed more significant tumor progression and CAF abundance (α-SMA, FAP, PDGFR, and vimentin) than CT-26/EV. Additionally, CT26/FGFR4-derived CAFs showed significantly increased invasiveness and contractility, indicating the highly activated status of CAFs. In order to verify the effect of cancer secretome from FGFR4 in cancer cells , normal fibroblast (NIH/3T3) were co-cultured with either stable cancer cells or CM. As a result, CT-26/FGFR4 cells robustly induced the expression of CAF markers in NIH/3T3 cells, indicating the promotion of CAF differentiation from resting fibroblasts. Also, CT-26/FGFR4-derived CM significantly promoted further activation of CAFs compared to CT-26/EV-derived CM. Taken together, FGFR4 contributes not only to CAF differentiation but also to CAF activation via secretome. Next, we performed RNA seq of CT-26/EV and CT-26/FGFR4 cells and identified the upregulated genes related with the interferon (IFN) signaling. Among these genes, we identified IFNβ and CXCL10 as targetable molecules via the activation of TLR3-TBK-IRF and IFN-STAT-CXCL10 signaling pathways. These results were confirmed by RT-PCR and western blot assay. Secreted CXCL10 induced gene expression of CAF markers in fibroblast and increased CAF functions such as migration, invasion and contractibility, reflecting CAF activation. Blocking antibodies and knocking down of CXCL10 inhibited the cancer secretome-mediated CAF markers. The blockade of CXCR3, which is the CXCL10 cognate receptor, also showed an inhibitory effect on the FGFR4-overexpressing cancer-educated CAF. In human colon cancer specimens, the expression of FGFR4, CXCL10, and CAF markers showed a positive correlation with each other. Finally, dual inhibition of FGFR4 and CXCR3 in tumor mouse model suppressed the tumor growth, accompanied by CAF suppression. Our findings reveal the novel mechanism of FGFR4 leading CAF differentiation/activation in TME via the CXCL10-CXCR3 axis. This suggests that FGFR4/CXCR3 inhibitor could be used as a potential therapeutic strategy to attenuate CAF in stromal dominant tumors.

#0728 Oral TGF-beta receptor1 inhibitor vactosertib promotes osteosarcoma regression by targeting tumor proliferation and enhancing anti-tumor immunity.

S. Choi[1], J. Myers[1], S. Tomchuck[1], M. Bonner[1], S. Eid[1], D. Kingsley[1], K. VanHeyst[1], S.-J. Kim[2], B.-G. Kim[1], A. Huang[1];
[1]Case Western Reserve University School of Medicine, Cleveland, OH, [2]MedPacto Inc, Seoul, Korea, Republic of

Osteosarcoma (OS) is an aggressive malignant bone cancer, with the lung as the most frequent site of metastasis. Unresectable pulmonary metastasis remains a significant challenge with a survival rate of less than 20%. Identification of novel therapeutic strategies are desperately needed. Transforming growth factor-β1 (TGF-β) is a potent immune suppressive cytokine in OS tumor microenvironment (TME). TGF-β1 expression is increased in the sera and tumor tissues of OS patients and this increase is associated with high-grade OS and lung metastases. Therefore, blocking TGF-β1 signaling may be a novel therapy for OS treatment. In this study, we show that blocking TGF-β1 signaling using the orally bioavailable small molecule TGF-βR1 inhibitor, Vactosertib, significantly inhibited OS proliferation *in vitro and in vivo*. Notably, Vactosertib inhibits c-Myc expression in the OS cells and oral administration of Vactosertib significantly reduces OS growth *in vivo*. Vactosertib increased immune effectors (e.g., $IFN\gamma^{+}CD8^{+}$ cells and NK cells) and inhibited immune suppressors (e.g., M2-like TAM, MDSC) in the OS TME. Our results suggest that inhibition of TGF-β1 signaling is an effective therapeutic strategy against OS through a multi-pronged approach that targets tumor intrinsic and extrinsic factors to achieve optimal immune-effector functions and maximal clinical response.

#0729 IDO1 inhibition enables IFNγ-elicited responsiveness of pulmonary breast cancer metastases to hypoxia-directed tumoricidal agents.

S.-C. Shen[1], S. Dey[2], J. B. DuHadaway[3], E. Sutanto-Ward[3], G. C. Prendergast[3], A. J. Muller[3];
[1]Drexel University College of Medicine, Philadelphia, PA, [2]Wuxi Advanced Therapeutics, Inc., Philadelphia, PA, [3]Lankenau Institute of Medical Research, Wynnewood, PA

In mouse models of lung carcinoma and pulmonary breast cancer metastasis, genetic ablation of the tryptophan catabolizing enzyme IDO1 (indoleamine 2,3-dioxygenase 1) resulted in restricted tumor outgrowth associated with attenuated induction of the inflammatory cytokine IL6 (interleukin 6). Utilizing the 4T1 breast cancer metastasis model to further elucidate the mechanistic basis underlying IDO1's pro-tumor activity in the lungs established that IDO1 acts as an integral determinant of a tumor-promoting inflammatory state that supports neovascular retention. *Ido1*$^{-/-}$ (nullizygous) mice exhibited impaired pulmonary metastases neovascularization and outgrowth that was driven by IFNγ (interferon gamma) in the absence of IDO1-dependent IL6 production. Hypoxia was likewise elevated, and these stress conditions increased the susceptibility of the metastatic tumor cells to cytotoxicity associated with administration of GSK2656157, an inhibitor of PERK (protein kinase RNA-like ER kinase), which acts as a primary sensor for activating the UPR (unfolded protein response) survival pathway. In WT (wild type) mice with established 4T1 lung metastases, administration of the IDO1 inhibitors epacadostat, navoximod or indoximod each similarly resulted in rapid collapse of the metastatic tumor neovasculature and concomitantly increased intratumoral hypoxia and sensitivity to PERK inhibition. Therefore, while IDO1 inhibition does not directly promote effective tumor cell killing in this context, the disruption of blood supply due to IFNγ-mediated neovascular regression subjects the tumor cells to hypoxic environmental stress, raising the possibility for therapeutic intervention with selectively targeted agents. Combining chemotherapy with immune checkpoint blockade (ICB) is recognized as an effective strategy for treating lung cancer, with first-line therapy for some patients including the alkylating agent carboplatin in conjunction with pembrolizumab. The challenge remains, however, that chemotherapy causes systemic side effects that can negatively impact quality of life and limit efficacy. Evofosfamide is an alkylating prodrug that was designed to be selectively activated in regions of hypoxia, thereby limiting systemic exposure. We report that enhanced metastatic tumor cell killing with evofosfamide can be achieved by co-administration of an IDO1 inhibitor. Elevated intratumoral hypoxia has also previously been linked to increased expression levels of PDL1, a favorable indicator of ICB responsiveness, and we have confirmed the upregulation of PDL1 in 4T1 lung metastases following IDO1 inhibitor administration. Our data in the lung metastasis model support future studies to evaluate whether IDO1 inhibition can be effectively combined with evofosfamide and anti-PD1 treatment to improve therapeutic outcomes.

#0730 Leveraging microdissection for proteogenomic analysis of histological sections to advance drug development.

I. Shin[1], M. Tangrea[2], M. R. Emmert-Buck[3], **D. J. Johann, Jr.**[1];
[1]UAMS Winthrop P. Rockefeller Cancer Institute, Little Rock, AR, [2]Loyola University Maryland, Baltimore, MD, [3]Avoneaux Medical Institute, Baltimore, MD

Background: Combining proteogenomics with laser capture microdissection (LCM) in cancer research offers a targeted way to explore the intricate interactions between tumor cells and the tumor microenvironment. This is especially important for immuno-oncology (IO) research where improvements in the predictability of patient response to IO-based drugs is sorely needed. An improved understanding of the spatial relationships involving tumor cells proper, stromal cells, blood supply and immune cell interactions may help to inform drug development and improve the indicators of success for IO-based drug regimens.
Methods: LCM is used to isolate and obtain distinct histological cell types from fresh frozen tissue. Once cells have been captured, nucleic acids and proteins are extracted for in-depth multi-modality molecular profiling assays involving multiple genomic modalities and a customized solution-based mass spectrometry proteomics approach for samples or specimens with a limited amount of tissue.
Results: Optimizing analysis of minute tissue quantities from LCM captured cells is challenging. Following the isolation of nucleic acids, RNA-seq may be performed for gene expression and DNA sequencing performed for the discovery and analysis of actionable mutations, copy number variation, and methylation profiles. Regarding genomic-based studies, commercial kits are often utilized for these steps due to their general availability, rapid innovation, and the robust performance of these products. However, this kit-based adaptive approach is not true for proteomics. There remains a need for highly sensitive proteomic methods targeting small-sized samples. A significant part of our proteogenomics approach is focused around an enhanced liquid chromatography mass spectrometry (LC-MS) analysis of micro-scale and/or nano-scale tissue sections. This is achieved with a silver-stained one-dimensional sodium dodecyl sulfate polyacrylamide gel electrophoresis (1D-SDS-PAGE) approach developed for LC-MS analysis of fresh-frozen tissue specimens obtained via LCM. This includes an in-gel digestion method adjusted and specifically designed to maximize the proteome coverage from amount-limited LCM samples to better facilitate in-depth molecular profiling.
Conclusions: Reported here is a proteogenomic approach that is leveraging from microdissected fresh frozen tissue. The methodology may also be applicable to other types of specimens having limited nucleic acids, protein quantity, and/or sample volume.

#0731 pHLIP targeted intracellular delivery of calicheamicin.

M. DuPont[1], C. Klumpp[1], M. Iraca[1], D. Allababidi[1], H. Visca[1], D. Engelman[2], O. Andreev[1], A. Moshnikova[1], Y. Reshetnyak[1];
[1]University of Rhode Island, Kingston, RI, [2]Yale, New Haven, CT

Calicheamicin is a potent, cell-cycle independent enediyne antibiotic that binds and cleaves DNA. Toxicity has led to its approved use in a targeted form as antibody-drug conjugates (ADC) for the treatment of liquid tumors. Mylotarg, one of the first such ADCs, was voluntarily withdrawn from the market due to safety concerns. However, Mylotarg was recently reapproved for acute myeloid leukemia based on new data that demonstrated efficacy with an acceptable safety profile. Besponsa, a related ADC, was approved for acute lymphocytic leukemia in 2017. In both agents, Mylotag and Besponsa, calicheamicin is conjugated to antibodies via an acid-labile hydrazone linker. We used a reduced calicheamicin to conjugate it to a single cysteine residue at the membrane-inserting end of a pH Low Insertion Peptide (pHLIP) via a disulfide bond to generate a linkerless cytoplasmic release. The cytoplasmic reduction of the disulfide releases the calicheamicin, which leads to its activation, DNA binding, and strand scission. pHLIP is a tumor-targeting agent now in clinical trials with imaging and therapeutic payloads. We studied the interaction of pHLIP-calicheamicin with liposomal and cellular membranes and demonstrated that the agent exhibits cytotoxic activity both in highly proliferative cancer cells and in non-proliferative immune cells, such as polarized M2 macrophages. In mice, treatment led to the growth inhibition of immuno-suppressive CT26 tumors with no signs of toxicity. Biodistribution studies confirmed tumor targeting with no accumulation of the agent in organs and tissues. The fluorescent version of the agent was observed within the tumor mass and tumor-stroma interface, where CD206+ M2 tumor-associated macrophages (M2-TAMs) reside. Treatment of tumors led to the depletion of M2-TAMs within the tumor core. Thus, pHLIP-calicheamicin could be developed into an effective therapeutic for the treatment of solid tumors with abundant immuno-suppressive M2-TAMs.

#0732 Toward optimizing CXCR4 inhibition with beta adrenergic blockade to enhance chemotherapy response in acute myeloid leukemia.

B. Loera[1], C. Zhang[2], P. M. Cardarelli[3], N. G. Caculitan[3], S. Chien[4], J. Dai[4], V. G. Oehler[5], J. Zhang[1], G. Marcucci[1], **P. S. Becker**[1];
[1]City of Hope National Medical Center, Duarte, CA, [2]Amgen, Thousand Oaks, CA, [3]GPCR Therapeutics, Redwood City, CA, [4]University of Washington, Seattle, WA, [5]Fred Hutchinson Cancer Center, Seattle, WA

Introduction: CXCR4 is a chemokine receptor for CXCL12 that plays a critical role in homing of hematopoietic stem cells (HSCs) to the bone marrow microenvironment. The CXCR4 inhibitor plerixafor is used to increase mobilization of peripheral blood stem cells in combination with filgrastim. This pathway has also been investigated for applications in hematologic malignancies such as acute myeloid leukemia (AML), including clinical trials, with the goal of disrupting AML from the protective marrow environment. These have included use of plerixafor with 7+3 or MEC, BL-8040 with cytarabine, and ulocuplumab with MEC. For the ulocuplumab trial, at the study site of the authors, CR/CRi correlated with >10% CXCR4 expression (Becker et al. ASH 2014). The objective of this preclinical study is to identify the AML patient population most likely to respond to CXCR4 inhibition, and the role of combined beta-adrenergic blockade, as the latter has been shown pre-clinically to augment mobilization of HSCs when combined with a CXCR4 inhibitor, GPC-100 (Sukhtankar et al. PLoS One, 2023).
Procedures: AML patient samples (N=124 including 90 blood and 34 bone marrow samples, and 21 with both) were obtained with informed consent on an IRB approved protocol. Multicolor flow cytometry was performed with sequential gating on blasts (by FSC/SSC, CD45/SSC, CD34 or phenotype), and leukemia stem cells (LSCs:$CD34^{+}CD38^{-}$,$CD123^{+}$), then analysis for CXCR4 and beta-2 adrenergic receptor (ADRB2) surface expression. Correlations between CXCR4 expression and clinical characteristics including age, gender, new diagnosis vs. relapse, ELN2022 risk, cytogenetics, FLT3/NPM1 mutation status, CR1 duration, and overall survival were performed. GraphPad Prism9 was used for statistical analysis, and Mann Whitney test (two groups) and ordinary one-way ANOVA (>2 groups) were used for comparisons.
Results: The range of CXCR4 expression by AML blasts is 0.05 to 99.7% (median 13.1%; mean 16.2%), and by AML LSCs 0 to 99% (median 2%, mean 15.7%). The expression by blasts and LSCs for each patient exhibited tight correlation, R^2=0.88 p=1.23 X10e-25). There was higher % expression of CXCR4 by both blasts and LSCs for new diagnosis, as compared to relapsed, patient samples (p=0.002). There was no correlation between level of CXCR4 expression and the other clinical features. For a subset of 20 patient samples analyzed for both CXCR4 and ADBR2 expression by AML blasts, ADBR2 expression ranged from 0.4 to 20.1%. For the samples that express ADBR2, there was high level expression of CXCR4, range 35.9 to 98.7% (median 78.4%, mean 76%).
Conclusion: These studies support further investigation of whether simultaneous blockade of CXCR4 and ADBR2 may potentiate chemotherapy response in AML by limiting microenvironment mediated chemotherapy protection and reveal that patients with new diagnosis may be more susceptible to this approach.

#0734 Inhibition of equilibrative nucleoside transporter 1 relieves intracellular adenosine-mediated immune suppression.

T. J. Sanders[1], C. S. Nabel[2], M. Brouwer[1], A. L. Hermant[1], L. Chaible[1], J.-P. Deglasse[1], A. Pabois[1], W. Cathou[1], A. Smets[1], M. Deligny[1], J. Marchante[1], Q. Dubray[1], M.-C. Lettelier[1], C. Martinoli[1], R. Marillier[1], O. De Henau[1], Y. McGrath[1], M. G. Vander Heiden[2], **E. Houthuys**[1];
[1]iTeos Therapeutics, Gosselies, Belgium, [2]Koch Institute for Integrative Cancer Research at MIT, Cambridge, MA

The profound benefit of immune checkpoint blockade for cancer therapy is restricted to limited subsets of patients with specific cancers. Many factors contribute to primary and acquired resistance to immune checkpoint blockade, including local accumulation of immunosuppressive metabolites such as the nucleoside adenosine and downstream adenosine receptor signaling. Pharmacological inhibition of adenosine generation and signaling are active areas of clinical investigation. Here we report a novel mechanism whereby adenosine suppresses anti-cancer immune responses by intracellular accumulation. We show that human T cells readily take up adenosine via equilibrative nucleoside transporter 1 (ENT1), suppressing proliferation and effector function by inhibition of *de novo* pyrimidine nucleotide synthesis in T cells. ENT1 expression increases upon T cell activation, suggesting uptake of extracellular adenosine is a mechanism to limit T cell responses in high adenosine environments. Quantitative mass spectrometry imaging reveals adenosine concentrations in human tumors up to the range of 100 µM - levels significantly greater than previously demonstrated and consistent with suppression of T cell responses. Deletion of ENT1 leads to potent control of tumor growth in syngeneic mouse models including KPC, a poorly immunogenic model of pancreatic ductal adenocarcinoma, and is associated with increased CD8+ T cell frequency, proliferation and cytokine production within tumors. Furthermore, ENT1 expression was observed by flow cytometry on human tumor-infiltrating $CD8^+$ T cells. We have discovered and characterized EOS301984, a potent ENT1 antagonist that is currently being evaluated in patients with advanced solid tumors. EOS301984 blocks intracellular adenosine transport and restores pyrimidine levels in T cells activated in the presence of adenosine, resulting in enhanced tumor cell killing by memory T cells and increased *ex vivo* expansion of functional human tumor-infiltrating lymphocytes in adenosine-rich environments. Finally, in a humanized mouse model of triple negative breast cancer resistant to anti-PD-1 blockade (MDA-MB-231), combination of EOS301984 with nivolumab synergistically led to control of tumor growth. Thus, ENT1 inhibition represents a novel approach to augment anti-cancer immune responses through restoring pyrimidine nucleotide synthesis in T cells suppressed by adenosine.

#0735 Mitigation of liver toxicity effects of bispecific T cell engagers in immune-competent liver-tumor co-culturing high-throughput platform.

M. Rudnik[1], L. Holting[1], T. Hafeli[1], O. Yavaş Grining[1], F. Greve[1], D. Ortiz Franyuti[2], R. Matheis[2], **L.-A. Ligeon**[1], E. Breous-Nystrom[3], O. Frey[1];
[1]InSphero AG, Schlieren, Switzerland, [2]Roche Pharma Research & Early Development, Roche Innovation Center, Basel, Switzerland, [3]Roche Pharma Research & Early Development Roche Innovation Center, Basel, Switzerland

The remarkable clinical therapeutic effects and wide-ranging applications of bispecific T cell engagers (BiTEs) have revolutionized the treatment approaches in the field of oncology. While the advantages of these innovative immunotherapies are undeniable, it is imperative to thoroughly investigate their safety aspects. With increasing use of biologics for treatment of various cancers, the incidence of immune-related adverse events (irAEs) will undoubtedly increase. Therefore, there is a compelling need to develop measures to effectively prevent or manage irARs already on the stage of the development of new clinical candidates. To address this need, we have created a high-throughput, automation friendly, 384-well-format platform in which 3D spheroid models are co-cultured in units interconnected by microfluidic channel. The tissue-tissue interaction was facilitated by a gravity-driven, tubeless flow system. The design allows for the simultaneous evaluation of the anti-tumor efficacy and liver safety of immunotherapeutics. In our system, we employed 3D spheroids comprised of primary human hepatocytes and Kupffer cells to model the liver, ensuring the preservation of their metabolic and inflammatory functions. Additionally, we established a solid tumor model using human cancer cell lines (HCT116-GFP) and primary cancer-associated fibroblasts, effectively mimicking the complex tumor microenvironment We treated 3D spheroid models with runimotamab (HER2xCD3 BiTE), catumaxomab (EPCAMxCD3), nivatrotamab (GD2xCD3) and control bispecific antibodies in the presence of peripheral blood mononuclear cells (PBMCs). Tumor viability and growth was assessed by fluorescence measurements, while liver toxicity and function were monitored by release of liver aminotransferases ALT and microscopy. To mitigate potential liver toxicity, we co-treated spheroid co-cultures with adalimumab (anti-TNF), tocilizumab (anti-IL-6R), raleukin (IL-1R antagonist) (each 100ug/ml), desatanib, dexamethasone or ruxolitinib (each 100nM). The treatment with all bispecific antibodies resulted in a significant decrease of fluorescence and size of tumor spheroids in comparison to control antibody. At the same time increased ALT concentrations were observed after the treatment with BiTEs. The application of small molecular drugs protected against liver damage, but also severely disrupted tumor killing. Interestingly, adalimumab revealed liver protective actions without affecting tumor killing, suggesting TNF-mediated mechanism of toxicity. In summary, we have developed a relevant, high-throughput platform for the evaluation of novel immunotherapies closely reflecting clinical scenarios. High throughput of the assay represents a powerful screening tool for clinical candidate development.

#0736 ACTM-838 safely and comprehensively re-activates the immunosuppressive TME by exploiting myeloid biology intrinsic in many cancers.

W. Lu, K. Cron, J. Janes, L. Berryman, G. Singh, C. Thanos, A. Udyavar;
Actym Therapeutics, Berkeley, CA

ACTM-838 is a genetically modified bacterial vehicle encoding a DNA plasmid with two engineered payloads, IL-15plex and constitutively active eSTING. The bacterial vehicle is a highly attenuated S. typhimurium, engineered to facilitate safe IV administration. ACTM-838 is designed to specifically enrich in the TME via auxotrophic dependency on extracellular adenosine and purine metabolites. ACTM-838 is then selectively internalized by tumor-resident myeloid cells achieving tumor-specific payload delivery.

Previously, we showed ACTM-838 exhibited significant and durable anti-tumor efficacy across syngeneic tumor mouse models (EMT6 breast, MC38 colon) and MMTV-PyMT GEMM.

To elucidate TME changes induced by ACTM-838, EMT6 tumors were analyzed post-treatment by scRNA-seq, which demonstrated that ACTM-838 induced significant transcriptional changes in several cell populations in the TME. Cytolytic pathways were upregulated in T and NK cells, while type I IFN and PDL1 were upregulated in myeloid populations consistent with previous bulk RNAseq analyses.

To understand the tolerability and safety of ACTM-838, a GLP toxicology study was performed on naïve cynomolgus monkeys (NHP). No ACTM-838-related clinical or veterinary observations were reported at any dose level. Acute dose-dependent increases in serum cytokines were observed at 4 hours which reverted to baseline by 24 hours. ACTM-838 was cleared from blood by 24 hours post-dose with no significant shedding in urine or feces. ACTM-838 was only detected in the spleen in 2 and 1 animals at 22- and 49-days post treatment, respectively. Pre-existing ADA was observed in some animals with subsequent increases in ADA upon dosing in most animals. However, no correlation of serum ADA and blood PK levels suggested that the presence of ADA does not impact drug stability.

The ACTM-838 mechanism of action requires high levels of adenosine or purine metabolites to enrich and colonize the TME as well as phagocytic internalization by tumor-intrinsic myeloid cells to achieve tumor-specific payload delivery. Myeloid cells comprise roughly half of all cells in the TME in human tumors. Bioinformatics analyses of the public patient datasets identified key tumor indications enriched in both adenosine and myeloid pathways. To further understand the spatial heterogeneity in the TME across tumors, we performed multiplex immunofluorescence on patient tumor microarrays to validate tumor types with a high prevalence of myeloid populations coupled with an active adenosine pathway, which will help guide future clinical study design.

In summary, we demonstrate that ACTM-838 modulates the TME and is stable and safe in animal models. Additionally, our studies recommend the prioritization of certain tumor indications for treatment with ACTM-838 in the clinic.

#0737 Arrays of 3D ECM-embedded fibroblast clusters for characterization of ECM remodeling by primary cancer associated fibroblasts and for evaluation of drugs attenuating fibrotic ECM remodeling.

E. H. Danen;
Leiden Univ., Leiden, Netherlands

Chronic fibrosis can lead to organ failure and is also associated with cancer, where the tumor is interpreted as a chronic wound, and the fibrotic tumor environment drives disease progression. Fibrosis occurs in an inflammatory environment where macrophages are activated, and fibroblasts transdifferentiate into myofibroblasts. Activated macrophages stimulate the myofibroblasts to produce excessive amounts of collagen-rich ECM. Changes in proteolytic activity and high contractile forces that myofibroblasts apply onto their tissue environment, further lead to extensive remodeling of the healthy tissue matrix into a scar matrix. Similar activity is displayed by cancer-associated fibroblasts (CAFs) in tumors. Intervening with the excessive ECM remodeling by activated fibroblasts represents a candidate therapeutic strategy to normalize the architecture of fibrotic and malignant tissues. We developed a screening platform using an assay based on automated image guided injection of clusters of fibroblasts in wells of multi-well plates preloaded with a collagen-rich ECM network. The identical x-y-z position, spacing, and size of the ECM-embedded fibroblast clusters in each well facilitates automated real time confocal microscopy and quantitative image analysis algorithms. We use this setup for automated quantitative analysis of ECM remodeling activity of CAFs obtained from early-stage colorectal cancer patients. We find that CAFs from these early-stage lesions display increased ECM remodeling capacity as compared to patient matched normal fibroblasts. We then use the same setup to screen a series of compounds for their ability to attenuate ECM remodeling triggered by TGFb-activated primary human fibroblasts. We detect known and novel pathways, and we identify small molecule inhibitors with a promising efficacy versus toxicity profile. Lastly, we detect a previously unknown concentration-dependent side effect of ALK5 inhibitors that leads to the identification of a novel profibrotic pathway and indicates that caution is warranted for the clinical application of ALK5 inhibitors.

#0738 MBRC-101: a novel antibody-drug conjugate (ADC) targeting the tyrosine kinase receptor EphA5.

F. I. Staquicini[1], F. H. F. Tang[2], V. de Oliveira[1], D. I. Staquicini[2], Y. Wu[1], K. F. Barnhart[1], J. Parsons[1], W. Arap[3], I. Chen[1], R. Pasqualini[3];
[1]MBrace Therapeutics, San Diego, CA, [2]Rutgers University, Newark, NJ, [3]Rutgers University and Cancer Institute of New Jersey, Newark, NJ

Introduction: The receptor tyrosine kinase EphA5 has the classical receptor kinase topology with an extracellular-binding domain, a single-pass transmembrane domain, and a cytoplasmic kinase domain. Previously, EphA5 has been shown to contribute to DNA-damage repair and radiation therapy resistance in lung cancer. We investigated EphA5 expression in lung cancer as well as breast, pancreatic, gastric, and colorectal cancer and assessed its potential as a therapeutic target using a novel ADC, MBRC-101.
Methods: MBRC-101 is composed of a humanized anti-EphA5 IgG1 monoclonal antibody conjugated to monomethyl auristatin E (MMAE) via a cleavable valine-citrulline linker using site-specific ThioBridge™ technology. The specificity profile of the anti-EphA5 antibody was characterized using a membrane proteome array. Receptor-mediated antibody internalization was determined by real-time live-cell analysis, and cell killing assays were performed using analysis of cell confluence and luminescent-based viability. Expression of EphA5 in archival human tissue sections was evaluated by immunohistochemistry (IHC) using a commercial antibody. Efficacy studies used patient-derived xenograft (PDX) models of lung adenocarcinoma, squamous cell carcinoma of both lung and head and neck, and breast cancer.
Results: IHC demonstrated selective EphA5 membrane expression in 78% (18/23) of triple negative and 88% (23/26) of hormone receptor-positive breast cancer tumors tested. EphA5 membrane expression was also detected in 85% (29/34), 73% (16/22), 70% (7/10), 70% (15/22), and 50% (6/12) of lung squamous cell carcinoma, lung adenocarcinoma, gastric, colorectal, and pancreatic patient tumors tested, respectively. EphA5 expression was not detected in adjacent, non-malignant tissue in any of the tumors examined. The anti-EphA5 antibody bound exclusively to EphA5 and did not cross-react with other members of the Eph receptor/ephrin ligand family. Binding of the anti-EphA5 antibody on the cell surface triggered rapid internalization and processing through the endosomal-lysosomal system. MBRC-101 was cytotoxic to EphA5-expressing cells and its activity was concentration-dependent and commensurate to levels of EphA5 on the cell surface. In PDX models, once weekly administrations of intravenous MBRC-101 showed dose-dependent, robust, and reproducible anti-tumor activity. Partial tumor responses were observed at doses of 2.5 mg/Kg and complete tumor responses starting at 5 mg/Kg. Toxicologic findings in Sprague-Dawley rats and cynomolgus monkeys were attributed to the MMAE payload and not target-related. Based on an HNSTD of 10 mg/kg in monkeys, the starting human dose was 0.5 mg/kg with ~15-fold safety margin.
Conclusions: EphA5 is a new and promising molecular target for the development of ADC-based therapies against many human cancers. A Phase 1/1b study of MBRC-101 is currently recruiting (NCT06014658).

#0739 AMT-253, a first-in-class MUC18-targeting antibody-drug conjugate, for the treatment of MUC18-positive solid tumors.

Jing Shi[1], Jiaqing Yan[1], Yaling Huang[1], Jun Guo[2], Yan Kong[2], Xun Meng[1], **Shu-Hui Liu**[3]

[1]Multitude Therapeutics, Shanghai, China,[2]Peking University Cancer Hospital and Institute, Beijing, China,[3]Multitude Therapeutics, Redwood City, CA

MUC18, also known as MCAM (melanoma cell adhesion molecule) or CD146, is a type I transmembrane glycoprotein originally identified as a cell adhesion molecule of melanoma that plays important roles in tumor growth and progression including tumor angiogenesis, epithelial-mesenchymal transition (EMT), and metastasis. MUC18 is overexpressed in a variety of solid tumors including (but not limited to) melanoma, osteosarcoma, head and neck, lung, esophagus, breast, ovarian, and cervical cancer and hepatocellular carcinoma, with restricted presence on normal healthy tissues, mainly on blood vessels and a minor subset of T helper cells. Limited expression in normal tissues and high expression in tumors makes MUC18 a promising target for the development of antibody drug conjugate (ADC). AMT-253 is a novel ADC targeting MUC18. It is composed of a humanized MUC18-targeting IgG1 antibody conjugated with Exatecan, a topoisomerase I inhibitor, attached to a proprietary self immolative T moiety linker through reduced interchain disulfide bonds with a drug-to-antibody ratio (DAR) of 8. AMT-253 was stable *in vitro* with less than 0.5% of payload releasing when incubated with human, monkey, mouse or rat plasma for 21 days at 37℃. AMT-253 selectively bound to cell surface MUC18 and was efficiently internalized into MUC18-positive cancer cells. AMT-253 exhibited antiproliferative activity against several MUC18-positive cancer cell lines and demonstrated potent bystander killing effect *in vitro*. Treatment with AMT-253 resulted in tumor growth inhibition or regression in a panel of MUC18 positive cell line derived xenograft (CDX) or patient derived xenograft (PDX) models. In addition, AMT-253 was well tolerated in a GLP compliant toxicity study in cynomolgus monkeys at dose levels ≤45 mg/kg. Taken together, our preclinical *in vivo* efficacy and toxicity studies demonstrated that AMT-253 has a wide therapeutic window and could potentially provide benefits for cancer patients with highly unmet medical needs. AMT-253 is currently being evaluated in a Phase I first-in-human clinical trial (NCT05906862).

#0740 CNTN4 as a novel target for solid cancer with antibody-drug conjugate.

M. Cha, **H. Kim**, S. Byun, Y. Ha, K. Park, H. Yu, B.-N. Jeon, M. Kim, S. Moon, K. Park, H. Park;
Genome & Company, Sungnam-si, Gyeonggi-do, Korea, Republic of

As a novel immune checkpoint, we previously confirmed that contactin 4 (CNTN4) regulates T cell activity negatively by binding to amyloid precursor protein (APP) on T cells. CNTN4 is highly expressed in various types of tumors, including gallbladder, pancreas, stomach, endometrium, liver, prostate, bladder cancer, melanoma, and other tumors, with positive rates over 70% through immunohistochemistry analysis in contrast to low-level expression in normal tissues. Based on the tumor-specific expression profile of CNTN4, we evaluated the potential of CNTN4 as a novel target for antibody-drug conjugate (ADC). First, the internalization of the anti-CNTN4 antibody in the IND submission stage, GENA-104A16, into CNTN4-positive cancer cells was confirmed. For investigation of the potential of targeting CNTN4 using ADC, clinically validated various linker-payloads (MMAE, MMAF, SN-38, and exatecan derivate) were conjugated to GENA-104A16 using thiol maleimide conjugation with average drug-to-antibody ratio (DAR) in the range of 4.0 to 4.8. After preparing ADCs, we confirmed the binding affinity for CNTN4 was maintained as high even after the payload conjugation through an ELISA. *In vitro* studies have demonstrated the highly cytotoxic effect of MMAF conjugate among the conjugates of GENA-104A16 on CNTN4-positive cancer cells compared to negative cancer cells. And there was no cytotoxic effect on normal cells. Furthermore, treating MMAF conjugate of GENA-104A16 showed promising efficacy in the Pan02 pancreatic orthotopic mouse model and the patient-derived xenograft model. These results suggest that CNTN4 could be a highly potential ADC target that could expand the options for cancer treatment strategies.

#0741 Distinct functional effects of ILT family members in mediating the activity of an ILT2/ILT4/ILT5 cross-reactive monoclonal antibody in releasing the suppression on innate and adaptive anti-tumor immunity.

S. Ye[1], D. Zhang[1], B. Singh[1], J. Bankoti[1], D. Cohen[1], S. Tan[1], D. Choi[1], J. Hickson[2], M.-Z. Wu[1], U. Kolhatkar[1], M. Binnewies[1], W. Jin[1], J. Hall[1], J. Engelhardt[1], A. Shoemaker[2];

[1]AbbVie Bay Area, South San Francisco, CA, [2]AbbVie Inc., North Chicago, IL

The expression of ILT (LILRB) family members and their major ligand HLA-G within solid tumors are associated with immune suppression and poor patient survival. Blocking multiple ILT family members might be more potent than targeting individual members by overcoming compensatory resistances within tumor microenvironment. Based on this hypothesis, we developed a monoclonal antibody (mAb) LITCHI 7 which reacts to three major ILT family members, ILT2, ILT4 and ILT5, and blocks ligand binding to these receptors. LITCHI 7 exhibits a broad binding capability to a wide range of human myeloid and T cell subsets that express ILT2, ILT4, and/or ILT5. Binding to monocyte-derived dendritic cells (moDC), LITCHI 7 released the inhibition on activating Fcγ receptor. On LPS-treated macrophages, LITCHI 7 enhanced inflammatory macrophage differentiation. The effect is primarily mediated by blocking ILT4 since ILT4 mono-specific mAb is as potent as cross-reactive LITHI 7 in modulating myeloid differentiation although both ILT2 and ILT5 are highly expressed by different myeloid subsets. The result was further confirmed by CRISPR Cas9 knock down of ILT2 or ILT5. In the absence of either ILT2 or ILT5, the accumulation of $CD14^+$ monocytes and inflammatory macrophages were not changed during differentiation. While different ILT family members are generally enriched on myeloid cells, ILT2 is also expressed on NK cells and effector memory $CD45RA^+$ T cells (Temra). Blocking ILT2 by LITCHI 7 enhanced TCR signaling when co-culturing the MART-1 specific T cell reporter line with MART-1/HLA-G positive melanoma cells. The effect of LITCHI 7 is mediated by ILT2 blockade since knocking out ILT2, but not ILT4 and ILT5, reduced accumulation of Temra in activated PBMC. To assess whether immune modulation of LITCHI 7 can be translated into anti-tumor activity by blocking different ILT family members, tumor killing assays were performed using innate and adaptive immune effector cells. LITCHI7 enhanced NK cell-mediated cytotoxicity on HLA-G^+ tumor cells by blocking ILT2. Both ILT2 and ILT4 blockade play a role in macrophage phagocytosis on lymphoma cells since LITCHI 7 as well as individual anti-ILT2 or ILT-4 mAbs increased macrophage phagocytosis to a similar level. Finally, LITCHI 7 could boost *in vitro* T cell-mediated killing of $CD19^+$ lymphoma by CD19 specific CAR-T cells in the presence of $CD33^+$ myeloid cells. In summary, LITCHI 7 can enhance both innate and adaptive anti-tumor immunity through ILT2 or ILT4 blockade directly on effector cells or indirectly through myeloid cell reprogramming. As clinical trials are ongoing by targeting ILT2 and ILT4, blocking multiple ILT family members through a single cross-reactive mAb may provide broad anti-tumor effects and advantages when combining with additional oncology treatments.

#0742 PYX-201, a stroma-targeting ADC composed of an anti-EDB+FN antibody conjugated to Auristatin0101, demonstrates strong anti-tumor efficacy across multiple human cancer indications in pre-clinical PDX tumor models.

N. Severe, A. Facklam, L. McMichael, B. Das, S. Lewandowski, J. Trickett, L. Diao, C. Merriman, C. Shen, J. Feng, S. Harriman, M. Crochiere, P. Steiner, J. Pinkas;
Pyxis Oncology, Boston, MA

Stroma is crucial to support solid tumor growth, metastasis and resistance to treatment. While most antibody-drug conjugates (ADCs) directly bind to cancer cells, PYX-201, an investigational drug, is designed to target tumor stroma by binding to the extra-domain B splice variant of fibronectin (EDB+FN), a matrix protein abundantly expressed in the tumor microenvironment of many solid tumors with absent or low expression in normal adult tissues. *In vitro* studies demonstrated PYX-201 was strongly cytotoxic to EDB+FN positive Caki2 cells, but not to EDB+FN negative HT29 cells. In addition, PYX-201 was 30-times more potent than a non-targeted ADC control, demonstrating PYX-201 cytotoxic effects were EDB+FN dependent. Furthermore, when Caki2 and HT29-luciferase cancer cells were co-cultured, the luciferase activity was used to quantify the amount of EDB+FN negative HT29 cells only. Interestingly, PYX-201 was able to kill EDB+FN negative cancer cells in a co-culture assay as shown by a decrease in luciferase activity, demonstrating PYX-201 bystander activity. Pre-clinical mouse model studies were conducted to evaluate PYX-201 anti-tumor efficacy and pharmacokinetic (PK) properties. First, a comprehensive patient-derived xenograft (PDX) mouse model trial was designed to evaluate the anti-tumor efficacy of PYX-201. To fully represent the diversity and characteristics of human tumors, PDX models were pre-selected from ten solid tumor indications based on different levels of EDB+FN protein expression and stromal density. PYX-201 (Q4D×4 at 3mg/kg) was well tolerated, and strong anti-tumor responses (% Tumor Growth Inhibition [TGI] >90%) were observed in PDX models across various cancer indications. Potential correlations between EDB+FN protein expression with anti-tumor activity will be evaluated. Remarkably, long-term anti-tumor efficacy of PYX-201 was observed as tumors did not relapse even after >100 days in a breast cancer PDX model. Additionally, plasma samples were analyzed from a cell line derived xenograft mouse model after a single dose of PYX-201 to determine its PK profile. At 3 mg/kg, the maximum concentration (Cmax) was 28.1 µg/mL, area under the curve (AUC) was 1,732.7 h*µg/mL, with a low clearance of 1.5 mL/h/kg, and the half-life of the mAb from PYX-201 was calculated at 81.2 h. These PK parameters were associated with strong PYX-201 anti-tumor efficacy (% TGI >90%) in the H1975 xenograft model. Altogether, PYX-201 was well tolerated and demonstrated strong anti-tumor efficacy in a variety of pre-clinical human PDX models. PYX-201 is a promising and innovative ADC which is currently under investigation in a Phase I clinical trial (NCT05720117).

#0743 Using a novel NextGen linker system to generate a conditionally active biologic (CAB) anti-nectin4-ADC demonstrates improved efficacy in pancreatic PDX cancer models and improved tolerability and toxicity profile in non-human primates.

J. Wang, J. Chen, G. Frey, H. Liu, C. Xing, K. Woodard, H. Chang, W. J. Boyle, **J. M. Short**;
BioAtla, San Diego, CA

Antibody-drug conjugates (ADCs) are a promising treatment for various forms of cancer. The treatment efficacy is often limited by on-target/off-tumor toxicity caused by the antigen expression in healthy tissue and by unwanted payload release outside the tumor caused by cleavage of the linker via circulating proteases. Our conditionally active biologics (CAB) technology addresses the on-target/off-tumor toxicity and assists in reducing the off-target/off-tumor toxicity by reducing binding to the target under normal physiological conditions (1). To eliminate the remaining off-target/off-tumor toxicity, we developed a novel linker with superior serum stability, solubility, and tumor-specific payload release. Conjugation can be accomplished using regular IgG backbones without the need for sequence modification. Here we report the *in vitro* and *in vivo* characterization of a NextGen linker system to generate a CAB anti-Nectin4-ADC that combines the advantages of CAB antibody pH selectivity with the new linker technology. *In vivo* efficacy data demonstrated complete tumor regression in several cell line derived xenograft models as well as superior efficacy to an enfortumab vedotin analogue in a patient derived pancreatic cancer model. PK and tox data from a toxicology study in non-human primates will be presented. In addition, data demonstrating the influence of linker technology on specific cancer models will also be presented. In conclusion, the NextGen Nectin4 CAB ADC represents a potentially more effective treatment with increased safety in the clinic.

(1) Chang HW, Frey G, Liu H, Xing C, Steinman L, Boyle WJ,*and Short JM* Generating tumor-selective conditionally active biologic anti-CTLA4 antibodies via protein-associated chemical switches. Proc Natl Acad Sci U S A 2021;118

#0744 Novel conditionally active biologic (CAB) tetravalent T-cell engagers targeting solid tumors.

A. Cugnetti, H. Liu, P. McNeeley, C. Xing, K. Woodard, H. Chang, G. Frey, W. J. Boyle, **J. M. Short**;
BioAtla, San Diego, CA

The use of T-cell engagers (TCEs) has great therapeutic potential in oncology. This potential, however, is diminished due to severe toxicity (cytokine release effects, as well as on-target off-tumor toxicities). We leveraged BioAtla's Conditionally Active Biologic (CAB) technology (1) to develop bispecific antibodies which have no or very little binding to CD3 and to the tumor target antigen (TAA) in healthy tissue (normal physiological conditions), yet have strong binding in diseased tissues (*i.e.* tumor microenvironment, TME) derived from glycolytic tumor metabolism, which supports tumor growth (Warburg effect). The conditional activity in the TME is achieved by optimizing the sequences of the binding domains and does not require masking and subsequent activation of the binding domain as used in pro-drugs. We have developed dual-CAB T-cell engagers targeting serval well-established tumor associated antigens. Data demonstrating superior potency with reduced off-target binding through *in vitro* and *in vivo* characterization of three new DualCAB TCEs, targeting PSMA, Trop2, and Tissue Factor (TF) will be presented.(1) Chang HW, Frey G, Liu H, Xing C, Steinman L, Boyle WJ and Short, JM Generating tumor-selective conditionally active biologic anti-CTLA4 antibodies via protein-associated chemical switches. Proc Natl Acad Sci U S A 2021;118.

PREVENTION / EARLY DETECTION / INTERCEPTION: Cancer Prevention
Poster Session

#0748 Impact of oral supplementation of sulforaphane for 12 months on lung cancer-related gene expression in former smokers at high risk for lung cancer: Results from a randomized placebo-controlled phase II clinical trial.

K. Demanelis[1], A. Spira[2], Y. Kefella[2], R. Wang[3], J. Adams-Haduch[3], T. W. Kensler[4], J. E. Beane[2], D. O. Wilson[1], J.-M. Yuan[1];
[1]University of Pittsburgh, Pittsburgh, PA, [2]Boston University, Boston, MA, [3]UPMC Hillman Cancer Center, Pittsburgh, PA, [4]Fred Hutchinson Cancer Center, Seattle, WA

Introduction: Higher consumption of dietary sulforaphane (SFN), a phytochemical found in many cruciferous vegetables, has been shown to be associated with lower risk of lung cancer (LC). SF activates the NRF2-pathway, which initiates cellular detoxification, antioxidant, and anti-inflammatory responses. To date, no chemoprevention trial for LC has examined the impact of SFN on LC-related gene expression (GE) as an endpoint in nasal and bronchial tissue. The objective of our study was to examine whether oral intake of SF for 12 months impacts the GE of previously identified LC- and premalignant lesions (PML)-related genes in bronchial and nasal brushing samples.
Methods: A randomized, placebo-controlled clinical trial (NCT03232138) was conducted in former smokers with ≥ 30 pack-years and quitting smoking for 1-10 years in Western Pennsylvania, USA. Forty-three subjects were randomly assigned to the SFN treatment (n = 21) or placebo group (n = 22) in 2018-2022. Each participant was instructed to take 4 Avmacol® or identical placebo capsules BID for 12 months. Each Avmacol® capsule contained 15 mg of glucoraphanin, which yielded a daily internal dose of 120 µmol SFN. Nasal swabs and bronchial brushings were obtained at baseline and after 12 months. Among the 37 participants who completed the study, RNA was extracted from their nasal swabs and bronchial brushings. We constructed single sample gene signature scores (GSS) using the GSVA algorithm for the following: 1) the NRF2-pathway, 2) genes associated with LC risk in bronchial biopsies, and 3) genes associated with PML. The genes in these sets were stratified by their up- or down-regulation in LC or PML. We evaluated the association between the interaction of SFN supplementation over time (pre-/post-treatment) on GSS using linear mixed models, adjusted for the fixed effects of age at baseline, RNA integrity number (RIN), packyears of smoking, and random effect of participant.
Results: GE data was available for 31 participant pairs with bronchial and/or nasal samples. Within nasal tissue, SFN treatment increased both the GSSs of the NRF2-pathway (p=0.0089) and the downregulated LC-risk genes (p=0.0047), and decreased the upregulated LC-risk genes (p=0.012) over time, whereas SFN had no significant impact on GSSs of the NRF2-pathway and LC-risk genes in the bronchial tissue. No association between SFN treatment over time and the PML-related GSS was observed in nasal or bronchial tissue.
Conclusion: Our initial analysis indicates that SFN treatment over 12 months impacted LC-associated GE in nasal tissue but not in bronchial tissue from former smokers. The discrepancy results may be due to small sample size and additional studies are warranted to confirm if SFN has direct impact on LC-risk related genes in bronchial tissue (NIH grant No. R01CA213123).

#0749 Randomized placebo-controlled phase II clinical trial on oral supplementation of sulforaphane for 12 months that reduced bronchial Ki-67 index in former smokers at high risk for lung cancer.

J.-M. Yuan[1], T. W. Kensler[1], S. Dacic[1], D. J. Harman[1], R. Wang[1], P. Balogh[1], L. Seigh[1], Y. T. Pham[1], J. Adams-Haduch[1], S. Singh[1], J. G. Herman[1], A. Spira[2], D. O. Wilson[1];

[1]University of Pittsburgh, Pittsburgh, PA, [2]Boston University, Boston, MA

Background: Epidemiological studies showed higher intake of cruciferous vegetables or their active compounds, isothiocyanates (ITCs), with lower risk of lung cancer. ITCs inhibited tobacco-carcinogen induced lung adenocarcinoma in animal models, along with reduced cellular proliferative marker Ki-67 and increased apoptotic markers Caspase-3 and TUNEL. However, human data lack. The aim of our study was to assess if oral intake of sulforaphane (SFN) for 12 months would stop/reverse the progression of bronchial histopathology, reduce Ki-67 index and/or increase Caspase-3 and TUNEL indices.

Methods: A randomized clinical trial (NCT03232138) was conducted in former smokers with ≥ 30 pack-years and quitting smoking for 1-10 years in USA. Forty-three subjects were randomly assigned to the SFN (n = 21) or placebo group (n = 22) in 2018-2022. Each participant was instructed to take 4 Avmacol® or identical placebo capsules BID for 12 months. Each Avmacol® capsule contained 15 mg of glucoraphanin, which yielded a daily internal dose of 120 µmol SFN. Biopsies were collected from 6 predetermined bronchial sites at baseline and the end of treatment, respectively. The primary outcomes were the average changes of histopathology scores, Ki-67, Caspase-3 and TUNEL indices in post- *vs*. pre-treatment biopsies.

Results: Thirty-seven participants completed the study. In the SFN group (n = 17) at baseline, 13 were men, all white, mean age 64.1 (SD 5.3) years, body mass index (BMI) 30.6 (6.1) kg/m^2, years of smoking 39.5 (8.2), cigarettes per day (CPD) 23.8 (10.7), and years of quitting smoking 4.3 (2.9). The corresponding figures in the placebo group (n=20) were 9 men, 19 white, age 68.0 (3.2), BMI 28.6 (4.2), years of smoking 42.2 (4.5), CPD 25.5 (8.4), and years of quitting smoking 6.8 (3.2). The baseline medians of total Ki-67 positive nuclei were 22.3 nuclei/mm^2 in the SFN group and 22.9/mm^2 in the placebo group (p = 0.96). After treatment, the number of positive Ki-67 nuclei decreased by 5.3/mm^2 (-24%) in the SFN group and increased by 18.0/mm^2 (+79%) in the placebo group (p = 0.014) with adjustment for baseline Ki-67 and other covariates. The post- and pre-treatment difference was even greater in high-density (3+) positive Ki-67, with -46% decrease in the SFN group *vs.* +99% increase in the placebo group (p = 0.004). There was a dose-response effect of higher compliance with SFN intake on reducing Ki-67 index (p_{trend} = 0.01). SFN treatment had no impact on Caspase-3, TUNEL, or bronchial histopathology. No severe adverse event was observed in the SFN group.

***Conclusion*:** Daily intake of 120 µmol SFN for 12 months significantly reduced Ki-67 index in bronchial tissue. The findings support the potential chemopreventive effect of SFN against lung cancer development in high-risk former smokers (Grant # R01CA213123).

#0750 Specific oral bacterial profile associated with oral HPV status in Puerto Rican People with HIV.

Y. N. Ortiz-Maldonado[1], G. Borges-Velez[1], J. Torres-Reyes[1], A. A. Peralta-Betanncourt[1], J. L. Salgado-Montilla[1], J. Viera-Vera[1], M. M. Sanchez-Vazquez[1], M. Martinez-Ferrer[2], A. P. Ortiz-Martinez[1], R. F. Gonzalez-Garcia[3], **J. Perez-Santiago**[1];

[1]University of Puerto Rico Comprehensive Cancer Center, San Juan, PR, [2]University of Puerto Rico Medical Sciences Campus, San Juan, PR, [3]University of Puerto Rico Medical Science Campus, San Juan, PR

Human papillomavirus (HPV) accounts for more than 70% of oropharyngeal cancers and people with HIV (PWH) are disproportionately affected by HPV infection even with successful antiretroviral therapy. Puerto Rico (PR) is in the top ten in terms of HIV prevalence in the US, and also has disparities in HPV-related malignancies. The oral microbiome can increase the risk of HPV infection and persistence; however, it has not been investigated in the context of HIV in PR. Therefore, we evaluated diversity and composition of the oral bacteriome of 48 virologically suppressed PWH (men and women ≥21 and <64 years old) living in PR in relation to HPV status (HPV+: n=18 vs. HPV-: n=30). We collected saliva (16S rDNA sequencing), oral rinse (HPV genotyping) as well as sociodemographic, lifestyle and behavioral characteristics. Short chain fatty acids (SCFA, acetate, butyrate and propionate) were quantified using gas chromatography and mass spectrometry. Periodontal disease was assessed by a clinical full-mouth periodontal assessment using the CDC/AAP guidelines. All analyses were performed using QIIME2 and R-statistical software. There were no significant differences in alpha diversity (Shannon, observed OTUs, and Faith) between HPV+ and HPV- groups. Absolute CD4 count was not significantly different between HPV+ and HPV- participants (794 cells/µL vs. 735 cells/µL), and did not correlate with either microbial richness or diversity. Higher microbial richness was associated with lower levels of acetate ($r=-0.35$, $p<0.05$) and propionate ($r=-0.31$, $p<0.05$,). Additionally, higher phylogenetic diversity was also associated with lower levels of acetate ($r=-0.38$, $p<0.05$) and propionate ($r=-0.35$, $p<0.05$) irrespective of the HPV status. On the other hand, higher levels of butyrate was significantly associated with higher microbial diversity (Shannon index; $r=0.33$, $p< 0.05$). Taxonomic analyses showed significantly higher abundance of *Dialister* and *Nanosynbacter* genera in HPV+ participants and higher abundance of *Rothia* genus and *Capnocytophaga sputigena* in HPV- participants. Overall, we found specific prokaryotic profile and associated metabolites associated with HPV infection, which may suggest that the oral microbiome could influence the natural history of HPV infection via SCFA signaling. Members of the *Dialister* genus have been found to be prevalent in Hispanic and Black women cervicovaginal microbiota, and as well as in HPV infection and oral cancer. Understanding the underpinning mechanisms of how the oral microbiome can facilitate HPV infection and persistence in PWH is essential to establish targets for early identification and personalized treatment approaches for oral HPV-related malignancies.

#0751 Gut microbiome and breast cancer: Report from a case-control study in Vietnam.

Sang Minh Nguyen[1], Huong T. T. Tran[2], Jirong Long[1], Martha J. Shrubsole[1], Hui Cai[1], Yaohua Yang[3], Thuan V. Tran[4], Wei Zheng[1], Xiao-Ou Shu[1]

[1]Vanderbilt University Medical Center, Nashville, TN,[2]Vietnam National Cancer Institute, National Cancer Hospital, Hanoi, Viet Nam,[3]Department of Public Health Sciences, School of Medicine, Center for Public Health Genomics, UVA Comprehensive Cancer Center, University of Virginia, Charlottesville, VA,[4]Hanoi Medical University, Ministry of Health, Hanoi, Viet Nam

The importance of gut microbiome on human health is being increasingly recognized. The gut microbiota may play a critical role in breast cancer etiology, likely through the roles of the gut microbiota in estrogen and nutrient metabolism as well as in immune regulation. However, evidence on associations between breast cancer and gut microbiota is limited and inconsistent. Using resources from the Vietnamese Breast Cancer Case-Control Study (VBCS), we evaluated differences in gut microbiome profiles between women with breast cancer and healthy women. Pre-treatment tool samples of 162 incident breast cancer cases (age: 50.0±9.5) and stool samples of 370 age-matched controls (age: 49.7±9.0) were included in the study. The gut microbiome was measured using shotgun metagenomic sequencing. Differences in gut microbiome α-diversity and β-diversity between breast cancer patients and healthy controls were evaluated via linear regression models and PERMANOVA testing, respectively. Case-control differences in gut microbial taxa abundance were assessed through the differential abundance analysis with adjustment for potential confounders, including age, income levels, residence, menopausal status, reproductive factors, body mass index, comorbidity, dietary intake, and physical activity. An association with a false discovery rate (FDR) <0.1 was considered statistically significant. No significant difference between breast cancer patients and healthy controls was observed for α- and β-diversities. A total of 2,905 gut microbial taxa were evaluated. Among them, significant case-control differences were found in the abundance of one phylum, two classes, four orders, three families, four gena, and 67 species (all p<0.05 and FDR <0.1). Compared to healthy controls, breast cancer patients had a decreased abundance of species *Pauljensenia keddieii*, *Bifidobacterium bifidum* (phylum *Actinobacteriota*), *Clostridium Q symbiosum, Faecalicatena fissicatena, Massilioclostridium methylpentosum, Parvimonas micra* (phylum *Firmicutes A*), *Leptotrichia wadei* (phylum *Fusobacteriota*)*, Enterococcus D gallinarum, Lactobacillus H fermentum, Gemella haemolysans B,* genus *Streptococcus* and its 24 species such as *S. anginosus C, S. constellatus, S. equinus, S. infantis I, S. mitis, S. oralis, S. pseudopneumoniae O* (phylum *Firmicutes*) (all p<0.05 and FDR <0.1). The species *Clostridium Q symbiosum* showed the strongest association, with a log2 fold-change (SE) of -2.02 (0.45), $p=7.35x10^{-6}$; FDR=0.006. Additionally, breast cancer patients had an increased abundance of three species belonging to the phylum *Firmicutes A* including MGYG-HGUT-03165, MGYG-HGUT-04111, and MGYG-HGUT-00903, compared to healthy controls (p<0.05 and FDR <0.1). These results suggest that the gut microbiome of breast cancer differs from that of control women. Additional analyses are ongoing to reveal the biological underpinning of the observed associations.

#0752 Association of gut bacterial toxins with colorectal neoplasia in Lynch syndrome patients in Puerto Rico.

I. Montes-Rodriguez[1], D. Rodriguez-Santiago[2], N. Marquez-Andino[2], G. Montalvo-Noguera[3], S. Colon-Serrano[4], L. R. Llanos[1], O. Diaz-Miranda[1], H. Centeno-Girona[1], M. Gonzalez-Pons[1], M. Cruz-Correa[1];

[1]University of Puerto Rico Comprehensive Cancer Center, San Juan, PR, [2]University of Medicine and Health Sciences, KN, Saint Kitts and Nevis, [3]University of Puerto Rico-Medical Sciences Campus, San Juan, PR, [4]University of Puerto Rico- Rio Piedras Campus, San Juan, PR

Lynch syndrome (LS) is an autosomal dominant condition caused by germline mutations in DNA mismatch repair pathway genes that predispose individuals to develop colorectal cancer (CRC) and other malignancies. Not all LS patients develop CRC, and age at diagnosis varies significantly, even among individuals with identical mutations. Although several prospective genetic modifiers have been reported, the contribution of environmental exposures to colorectal carcinogenesis and age of onset is unknown. The gut microbiota composition, influenced by environmental factors, may have a role in CRC development. Dysbiosis, or abnormalities in host-bacteria interactions, can lead to inflammatory bowel disorders and CRC. Certain strains of bacteria, like *Escherichia coli* and *Enterococcus sp.*, harbor pro-inflammatory/genotoxic genes that promote sustained inflammation in the host- *pks, tcpc, gelE, cnf-1, usp,* and *murB*. The association between inflammation and carcinogenesis is well established, yet the contribution of bacteria-induced inflammation and genotoxicity to CRN is not fully understood. This study aims to investigate if changes in the prevalence of the genotoxic/pro-inflammatory bacterial genes are associated with CRN in LS patients. Stool samples were collected from 32 LS subjects and 94 age/gender-matched control subjects without a history of CRC. Qualitative data regarding the six genes in these samples were assessed using RT-PCR with SYBR green. Among LS subjects, 68.8% had two or more of the six genes in their stool samples, whereas controls only had 27.7%. Furthermore, LS subjects had 4.06 times the odds of having ≥2 gut bacterial toxin genes in their stool (95% CI: 1.48-11.12) when compared to controls after adjusting by age. The most prevalent gene in LS patients was *murB*, detected in 62.5% of the individuals. The presence of *gelE* and *murB* genes was significantly higher among LS patients (p-value <0.001 and 0.02, respectively). Interestingly, the *usp* gene was absent in any LS patients. Additionally, LS subjects had 4.52 times the odds of having the *gel-E* gene (95% CI: 1.69-12.14) compared to controls after age adjustment. Given the documented evidence about the impact of CRC on the composition of gut microbiota, we performed analysis to assess the prevalence of these genes in LS subjects without a history of CRC, as well as in control subjects. After adjusting by age, LS subjects had higher odds of having ≥2 gut bacterial toxin genes in their stool (OR= 2.94, 95%: CI 0.52-16.50) than controls. This study shows that LS patients have a higher prevalence of the genotoxic/pro-inflammatory bacterial genes. However, further studies are necessary to validate these associations and provide a more comprehensive understanding of the role of gut bacterial genes in colorectal neoplasia among LS patients.

#0753 CEACAM1 induces microbiome and metabolite driven diversion of TGF-β signaling to promote colon cancer.

K. Bhowmick[1], K. Ohshiro[1], X. Xiang[1], S. John[1], X. Yang[1], K. Idicula[1], N. Beauchemin[2], R. Mazumder[3], K. A. Crandall[4], M. I. Hassan[5], T. Mohammad[5], **L. Mishra**[1];

[1]Feinstein Institutes for Medical Research, & Cold Spring Harbor Laboratory, New York, NY, [2]The Rosalind and Morris Goodman Cancer Institute, Montreal, QC, Canada, [3]The George Washington University, Washington, DC, [4]Milken Institute School of Public Health, Washington, DC, [5]Jamia Millia Islamia, New Delhi, India

Background: Colon cancer is rising in younger individuals in the United States. Potential causal factors are altered diets and gut microbiomes. Yet key signaling pathways, host-microbe interactions, and metabolites such as ammonia in cancer remain unclear. CEACAM1 responds to pathogenic microbes, interacts with the TGF-β/SPTBN1 and levels are raised in invasive colon cancer. Alterations in the TGF-β pathway occur ~40% of human GI cancers, and mouse models with disrupted TGF-β signaling (*Tgfbr2*$^{-/-}$, *Smad4*$^{+/-}$*Sptbn1*$^{+/-}$, *and Tgfb1*$^{-/-}$) develop colorectal cancer (CRC) that is dependent upon an altered gut microbiome. Our previous studies indicate the lipid metabolites (reactive aldehydes) form toxic adducts with cleaved SPTBN1 and divert TGF-β signaling to pro-oncogenic process. Poor prognosis CRC is associated with raised levels of microbial metabolites, such as ammonia. Thus, we hypothesized that "*the intricate relationships among pathogen-binding CEACAM1, the gut microbiome, metabolites such as ammonia, and βII-Spectrin drive colon cancer development".*

Methods: We examined gut microbiota composition, immune cell population, inflammation, and cancers in *Smad4*$^{+/-}$*Sptbn1*$^{+/-}$ and *Sptbn1*^{LSKO} mice fed a normal chow diet or a high-fat diet (HFD). We evaluated CEACAM1 and TGF-β member alterations in in CRCs using TCGA datasets. Alphafold-based molecular modeling predicted interaction sites between βII-Spectrin and CEACAM1 was followed by functional studies.

Results: Increased CEACAM1 levels with alterations in TGF-β members were associated with lower survival (TCGA). Mice with disrupted TGF-β signaling (*Smad4*$^{+/-}$*Sptbn1*$^{+/-}$) develop CRC, have high CEACAM1 levels, and an altered gut microbiome signature. CEACAM1 interacts with βII-Spectrin, and levels are restored to normal in βII-Spectrin LSKO which restores the gut microbiome and blocks inflammation and cancer. Ammonia induces CASPASE-3 mediated cleavage of βII-Spectrin, forms toxic adducts and divert TGF-β signaling to pathological pro-oncogenic signaling, triggering CRC.

Conclusion: We have found a critical role for CEACAMs in CRC cancer development, through diverting the TGF-β signaling pathway to a pro-oncogenic phenotype. CEACAM1 and βII-Spectrin are attractive therapeutic targets for CRC.

#0754 Exploring the association among pain, gut microbiota, and dietary intake of macronutrients.

E. Samami[1], F. Yi[2], M. Weaver[1], A. Starkweather[1], D. Lyon[1], D. L. Kelly[1];
[1]University of Florida, Gainesville, FL, [2]University of Idaho, Moscow, ID

Hematopoietic cell transplantation (HCT) is a potentially curative treatment for individuals diagnosed with hematological malignancies. As survival gains increase, symptom management is also being considered as an endpoint for treatment success yet there is paucity in the literature regarding biological correlates of symptoms. Pain is a major concern for patients undergoing HCT. Underlying inflammation has been suspected in the pathogenesis of symptoms including pain. Emerging evidence supports the gut microbiota (GM) as a potential pathway for the initiation of inflammation. Diet is a potentially modifiable factor demonstrating a significant impact on GM diversity and amenable to intervention. Understanding the interplay among pain, GM, and diet, particularly macronutrients, may inform the development of a targeted, dietary self-management intervention to mitigate pain symptoms in HCT patients. This investigation uses baseline data from a longitudinal descriptive study to explore associations among pain, GM composition (richness and evenness) using Shannon and Chao beta diversity indices, and macronutrients (protein, carbohydrates and fat), in 47 adults (> 18 years of age) receiving HCT for hematologic cancer. Pain was measured using the Brief Pain Inventory, GM was assessed using 16S ribosomal gene (V4 region) amplicons using Illumina MiSeq, and dietary information was collected using the Automated Self-Assessment 24-hour Dietary Assessment Tool (ASA-24). Data analysis was performed with the R ‘correlation’ package using Bayesian estimation of robust correlations and production of 95% Credibility Intervals (CI) and Bayes Factors (BF).The mean age of participants was 56.21 years + 14.67 years. Participants were diagnosed with myeloma (40%), lymphoma (29%) and leukemia (13%). The majority received autologous HCT (n=30). Macronutrient fat {r=-0.25, BF=1.72} had an inverse association with pain interference. Results provided at least anecdotal (BF > 1) support for a positive correlation between Healthy Eating Index (HEI) {r=0.21, BF=1.08}, total fat {r=0.32, BF=4.50}, carbohydrate {r=0.28, BF=2.47} and fat {r=0.32, BF=4.50}, and GM composition. Also, there was a positive association between the amount of protein {r=0.21, BF=1.03}, carbohydrate {r=0.27, BF=2.22}, and Chao Index. There was an inverse association between total HEI {r=-0.27, BF=1.87} and CRP levels. Taxonomic units {r=-0.41, BF=21.44}, Chao Index {r=-0.41, BF=20.28} and Shannon Index {r=-0.25, BF=1.47} had an inverse association with CRP level. This study associate pain, GM, and dietary macronutrients, suggesting potential GM targeted interventions. More research with larger sample size is needed to understand underlying dietary macronutrients' role in pain through GM diversity after HCT, aiming to ease symptoms and enhance survivorship.

#0755 Fecal microbial dysbiosis is associated with colorectal cancer risk.

J. Kim[1], **M. Gunathilake**[1], H. Yeo[1], J. Oh[1], B. Kim[1], N. Han[1], B. Kim[1], H. Pyun[1], M. Lim[2], Y.-D. Nam[2], H. Chang[1];
[1]National Cancer Center - Korea, Seoul, Korea, Republic of, [2]Korea Food Research Institute - Korea, Jeollabuk-do, Korea, Republic of

Although there is evidence of an association between the fecal microbiota and colorectal cancer (CRC) risk in epidemiologic studies, there is a lack of data from large-scale population-based studies. To address this gap, we assessed the dysbiosis of the fecal microbiome in a large-scale study in Korea. We recruited 287 CRC patients from the Center for Colorectal Cancer, National Cancer Center Hospital, Korea to perform 16S rRNA gene sequencing of fecal samples. A total of 287 age- and sex-matched healthy participants were selected from 890 cohort of healthy Koreans that are publicly available (PRJEB33905). The microbial dysbiosis index (MDI) was calculated based on the differentially abundant species. The association between MDI and CRC risk was observed using conditional logistic regression. Alpha-diversity indices were not significantly different between CRC cases and controls. The first three principal coordinates derived by a principal coordinate analysis (PCoA) based on weighted UniFrac distance explained 41.24% of the overall microbial diversity, with a significant divergence of the microbial composition between CRC patients and controls (PERMANOVA p=0.001). Three enterotypes were found based on CRC patients' microbial composition. Those who were in the third tertile of the MDI showed a significantly increased risk of CRC in the total population (OR: 6.59, 95% CI: 3.83-11.33, p-trend<0.001) compared to those in the lowest tertile. Similar results were found for men (OR: 6.58, 95% CI: 3.17-13.63, p-trend<0.001) and women (OR: 6.69, 95% CI: 2.91-15.37, p-trend<0.001). Dysbiosis in the fecal microbiota may be associated with an increased risk of CRC. Due to the potentially modifiable nature of the gut microbiota, our findings may have implications for CRC prevention among Koreans.
Key words: Fecal microbiome, 16S rRNA gene sequencing, Microbial dysbiosis, Colorectal cancer

#0756 Differences in composition, diversity, and function of the fecal microbiota of post-menopausal breast cancer patients compared to healthy, age-matched controls.

N. Kabbej, F. Ashby, E. Atencio, E. Rosenkrantz, D. Day, K. Dang, J. Gauthier, R. Newsome, J. Sommerville, T. Naas, R. Gharaibeh, C. Jobin, A. Quevedo, C. D. Heldermon;
University of Florida College of Medicine, Gainesville, FL

Gut microbiota are a community of organisms that colonize the intestinal tract with essential roles in immune function, gut epithelial integrity, and metabolite production. Dysbiosis occurs when the gut microbiota environment is negatively altered causing detrimental changes to these functions, which may predispose an individual to breast cancer development. To understand the relationship between dysbiosis and breast cancer development, fecal microbiota samples were collected from 27 post-menopausal breast cancer patients of varying hormone receptor statuses (ER+HER2-, ER+Her2+, ER-HER2+, or ER-Her2-) prior to starting chemotherapeutic treatment. Samples were compared to 25 healthy controls, and all samples underwent 16srRNA sequencing. Samples from breast cancer patients and control groups were compared for significant differences ($P<.05$) in alpha (within sample) and beta (between sample) diversity. Using the Shannon Index and Generalized Least Squares Model, significant differences in alpha diversity were identified between all breast cancer types vs. controls ($P=.0104$), and between ER+HER2- breast cancer vs. controls ($P=.00153$). Healthy controls exhibited a higher mean Shannon Index than breast cancer patients, thus higher within sample diversity. Using principal coordinate analyses, significant differences in beta diversity were identified between all breast cancer types vs. controls ($P = .01199$), and ER+HER2- breast cancer vs. control ($P = .008991$). Further analyses identified significant taxa of microbiota with functions related to breast cancer development and progression. Of note, *Lachnoclostridium*, a genus of bacteria that can produce β-glucuronidase, which can deconjugate estrogen, was increased in all breast cancer types and ER+HER2- breast cancer when compared to controls. Deconjugation of estrogen can cause elevated blood estrogen levels, potentially increasing Estrogen Receptor binding in hormone-receptor-positive breast cancer. Additionally, *Akkermansia*, a genus implicated in gut barrier dysfunction, was decreased in ER+HER2- patients, while *Parvimonas*, a tumorigenic cell-cycle regulator, was increased. Elucidating if these effects are causative or reactionary may have important implications for understanding breast cancer etiology. Samples are currently undergoing additional metagenomic analyses using long-read sequencing to identify specific bacteria, viruses, fungi, parasites, and phages that may be contributing to dysbiosis. Overall, this study is the first, to our knowledge, to employ short and long-read sequencing to the fecal samples of untreated postmenopausal breast cancer patients. We provide mechanistic insight into the relationship between microbiota and breast cancer development, with the intent of informing future patient screening and prevention.

#0757 Integrating microbiome analysis and multi-modal data to identify high-risk population for esophageal adenocarcinoma.

D. Altinok Dindar[1], M. Krieger[1], A. Palma[1], J. Cheney[1], F. Otaki[2], J. Yu[2], S. Wood[3], T. J. Sharpton[4], J. McGann[1], L. Karstens[2], G. G. Yardimci[1], Z. Zhang[1]; [1]OHSU Knight Cancer Institute, Portland, OR, [2]OHSU, Portland, OR, [3]OHSU School of Medicine, Portland, OR, [4]Oregon State University, Portland, OR

INTRODUCTION: Esophageal Adenocarcinoma (EAC) represents a pressing public health concern with a rising incidence and a staggering 5-year survival rate of less than 20%, emphasizing the critical need for early detection. Barrett's Esophagus (BE) serves as a well-established precursor to EAC, presenting an opportunity for proactive screening. The salivary microbiome provides a novel opportunity to identify a high-risk population with early-stage esophageal diseases. Here, we assessed whether the oral microbiome, in combination with lifestyle and clinical data, is associated with esophageal disease progression.
METHODS: The study included n=23 esophageal adenocarcinoma patients, n=51 with Barrett's Esophagus, and n=32 healthy controls. Saliva samples were collected along with comprehensive lifestyle, dietary intake, and clinical data. Shotgun Metagenomics Sequencing was employed to investigate the microbiome composition of participants. Comprehensive microbiome analyses were performed to evaluate taxonomic profiles, including microbial abundance, microbiome diversity, and functional/metabolic insights. A multi-modal data integration strategy was used to incorporate data from the Diet Health Questionnaire (DHQ) and lifestyle and health records, aiming to utilize these multimodal features to predict esophageal disease formation and progression.
RESULTS: A significant difference was observed in the salivary microbiome beta diversity between healthy controls and esophagus disease groups (p= 0.03). Clustering by microbiome taxonomic composition using the Dirichlet Multinomial Mixtures (DMM) framework indicates that some microbial signatures are associated with esophageal diseases (p=0.03). Healthy Eating Index Scores, total score (p=0.01); vegetables (p=0.003); greens, and beans score (p=0.009) were significantly different between study groups. Microbial pathways associated with diet, microbial taxa linked to lifestyle and medications, and supervised classification results reveal group characteristics and diversity variations based on key covariates such as B12 and sugar uptakes.
CONCLUSION: The study presents an innovative analytic approach to identify high-risk populations for esophageal diseases by integrating microbiome analysis and multi-modal data, providing insights into early detection and prevention. The potential of this research lies in its ability to revolutionize screening strategies, offering a non-invasive and cost-effective means to identify individuals at risk of EAC at earlier, more treatable stages.

#0758 Comparative Microbiome Analysis of Paired Mucosal and Fecal Samples in Korean Colorectal Cancer Patients.

S. Lee;
Dankook Univ., Yongin-Si, Korea, Republic of

Background Beyond the known risk factors such as age over 50, unhealthy diet, ethnicity, and smoking, emerging evidence suggests that gut microbial dysbiosis plays a crucial role in the early stages of colorectal cancer (CRC) by contributing to chronic inflammation and various intestinal dysfunctions. Even though various bacterial species have been studied, the gut microbiome profile as a representative biomarker in CRC patients remains largely unreported. This study presents a comparative analysis of the microbiome profiles of fecal and mucosal samples from CRC patients, followed by metagenomic profiling investigation to validate dominant bacteria in each sample type of CRC patients.
Methods The study involved 12 patients receiving CRC resection at Myongji Hospital in South Korea, recruited from May 2020 to June 2021. Fecal samples were collected pre-surgery, and mucosal samples during surgery. Paired-end sequencing was performed using Illumina MiSeq (Illumina, San Diego, USA) platform. 16s rRNA gene-based microbiome profiling was analyzed using QIIME2 (V.2020.11), a plugin-based platform for microbiome analysis. Sequencing reads were filtered, denoised, and clustered into amplicon sequence variants (ASVs) using DADA2 included in QIIME2. Taxonomic classification was assigned in the QIIME2 pipeline using a pre-trained classifier based on the Silva 138.1 reference sequence. Linear discriminant analysis (LDA) effect size (LEfSe) analysis was performed with LDA score ≥3.0 and *p*-value of 0.05.
Results The study subjects included 12 Korean patients, with an average age of 71 ± 10 years. The gender distribution included 3 men and 9 women whose body mass index was 24.6 ± 2.4 (mean ± SD). There was significant difference observed in UniFrac beta-diversity between the two groups (p=0.001). The relative taxonomic patterns of the microbiota between CRC stool and tissue showed that *Bacteroides* and *Fusobacterium* were more dominant in tissue than stool at both phylum and genus levels. Further taxonomic differences between the samples revealed that *Firmicutes*, *Bacilli*, and *Lactobacillacease* were over-represented in CRC patient stool, while *Pseudomonadales* (p<0.001) and *Pseudomonas* (p<0.001) were identified in the mucosal tissue.
Conclusion Our findings revealed that notable distinction was observed in the beta-diversity, indicating a unique microbial composition in tissue. Specifically, higher prevalence of *Bacteroides* and *Fusobacterium* at the genus level were identified in tissue. Additionally, our analysis highlighted *Pseudomonadales* and *Pseudomonas* emerged in CRC mucosal tissues. Furthermore, by comparing with a healthy control group, we aim to further elucidate potential markers unique to CRC patients.

#0759 Soy protein diet changes metabolic profile in liver of 7,12-dimethylbenz(*α*)anthracene (DMBA)-induced mammary tumors in obese zucker rats.

R. Hakkak[1], S. Melnyk[2];

[1]University of Arkansas for Medical Sciences, Little Rock, AR, [2]Arkansas Children Research Institue, Little Rock, AR

Obesity is associated with the risk of certain types of cancers development including breast cancer. Previously, we reported that obesity increased mammary tumor development using obese Zucker rat model. Several studies have shown the health benefit of soy protein consumption. However, the effects of soy protein diet on liver of mammary tumor for oxidative stress and DNA reaction is less known. We used DMBA induced-mammary tumor model to investigate the effects of soy protein diet on pro-oxidative environment and oxidative DNA modification in liver of obese DMBA mammary tumors rats. Female obese zucker rats (n=45) were either fed casein as control (OC; n=20) or soy protein isolate (OS; n=25), received DMBA (65mg/kg BW) at the age 50 days and sacrificed 20 weeks later. We used HPLC-ECD, HPLC-UV and LC-MS techniques for liver metabolic analysis. Comparing liver of OS vs. OC, soy protein 1) decreased the level of Methionine ($P<0.02$), increased 2) free reduced Homocysteine ($P<0.02$), 3) S-Adenosylmethionine (SAM, $P<0.03$), 4) S-Adenosyhomocysteine (SAH, $P<0.001$) and 5) 5methyl-Cytosine (5mC, $P<0.03$). Also, soy protein decreased ($P<0.003$) level of free oxidized Glutathione (GSSG), increased ($P<0.02$) GSH/GSSG oxidative stress ratio, without any changes a level of free reduced Glutathione (GSH), followed decrease ($P<0.04$) in liver DNA level of 8-OH-Guanosine (8-OH-G) and level ($P<0.02$) of 5hmethyl-Cytosine (5hmC). Our results shows soy protein diet capable change liver metabolism: a. Modify a methylation status by increasing levels of SAM (universal methyl group donor) following global liver DNA hypermethylation (5mC), and SAH (methylases inhibitor); b. Alleviate level of oxidative stress in liver by decreasing level of GSSG (not active glutathione), increasing GSH/GSSG ratio (antioxidative capacities), following lower ROS liver DNA damages by decrease levels of 8-OH-G and 5hmC. In conclusion, using obese DMBA-induced mammary tumor Zucker rat model, soy diet making a complex and significantly modification of metabolic conditions in liver affecting both methionine cycle and transsulfuration metabolic pathways.

#0760 Alteration to transcriptional rhythmicity in mammary glands from pubertal MMTV-PyMT mice fed a high-fat diet.

L. Yan, D. G. Palmer, H. Zeng;
USDA-ARS (Agricultural Research Service), Grand Forks, ND

Biological clocks, existing in all human organ systems, cycle every 24 hours in a diurnal pattern and control the daily rhythms of human life (e.g., eating vs. fasting, sleep vs. wakefulness), which is essential for health and wellbeing. Disruption of the biological clocks, either by genetic or environmental alteration, disturbs circadian rhythms, which may lead to chronic diseases. Childhood obesity is a risk factor for breast cancer in adult women. Lifestyle changes in the modern world (e.g., energy-dense diets) serve as environmental factors that contribute to alterations in biological clocks and obesity. The present study examined transcriptional rhythmic changes in mammary glands from pubertal MMTV-PyMT mice fed a high-fat diet (HFD). Three-week-old female mice (FVB background) were randomly assigned into three groups - wild-type (WT) mice fed the AIN93G diet and MMTV-PyMT mice fed the AIN93G diet or an HFD for three weeks. At the end of the study, mammary glands were collected every 4 hours over a period of 24 hours (Zeitgeber time 0-24 hours) for RNA-sequencing analysis. The mammary weight was 0.45±0.02, 0.59±0.02, and 0.67±0.02 g for WT mice fed the AIN93G diet and MMTV-PyMT mice fed the AIN93G and HFD, respectively (means ± SEM, all *p*<0.05 when three groups were compared each other). The rhythmicity analysis using R showed that greater than 1,000 transcripts were classified as “loss of rhythm” when MMTV-PyMT mice (both AIN93G-fed and HFD-fed groups) were compared to WT mice fed the AIN93G diet. Eighteen transcripts were classified as “loss of rhythm” in MMTV-PyMT mice when the HFD was compared to AIN93G diet. Hierarchical clustering analysis showed differentially expressed genes that were significantly altered and KEGG enrichment analysis showed the most upregulated and downregulated metabolic pathways in treatment groups than in the control group at each time point over the 24-hour period. These findings indicates that genetic alterations may have a greater effect than dietary effects on transcriptional rhythmicity in mammary glands from pubertal mice.

#0761 The relationship between ANGPTL4 and epidermal malignant transformation.

N. A. Yawson[1], J. D. Diedrich[1], K. T. Liby[2], J. Veenstra[3], J. J. Bernard[1];

[1]Michigan State University, East Lansing, MI, [2]Indiana University School of Medicine, Indianapolis, IN, [3]Henry Ford Health, Detroit, MI

High body mass index (BMI) is a risk factor for several types of cancers. Although epidemiology suggests obesity is negatively associated with non-melanoma skin cancer (NMSC), bariatric surgery has been shown to reduce the risk, suggesting a possible role of adipose tissue in the initiation and promotion of skin cancer. To gain mechanistic insight into how adipose tissue drives cutaneous carcinogenesis, we cultured non-tumorigenic mouse keratinocytes (JB6 P^+ cells) with or without factors released from murine visceral adipose tissue (mFTF) and performed RNA-Sequencing. Published work demonstrated mFTF induces anchorage-independent cell growth, a surrogate marker for malignant transformation. Transcriptomic analysis demonstrated a significant induction of *Angptl4* mRNA in JB6 P^+ cells cultured with mFTF for 3 and 8 hours compared to the vehicle-treated cells. ANGPTL4 is an endogenous inhibitor of lipoprotein lipase that modulates free fatty acid delivery to adipose tissue and oxidative tissues such as muscle and liver. The C-terminal protein demonstrates tumor-associated activities such as angiogenesis, metastasis, protection against anoikis, and enhancement of cell survival. Therefore, we hypothesized that the induction of this gene promotes malignant transformation. RNA-seq data was validated in multiple cell models, including primary keratinocytes with human adipose tissue. Immunohistochemistry was used to assess ANGPTL4 expression in 37 actinic keratosis (pre-malignant) and cutaneous squamous cell carcinoma (cSCC) from patients with different BMIs (18.6 - 49.5). Notably, ANGPTL4 was only observed in the suprabasal epidermal layers in normal skin. For samples containing both lesional and perilesional skin, there was an increase in ANGPTL4 expression in the lesional epidermis relative to the normal perilesional skin. Furthermore, ANGPTL4 expression increased from transition to actinic keratosis to cSCC *in situ*, suggesting that ANGTL4 is induced during malignant transformation as observed in our pre-clinical models. Interestingly, once cSCC developed an invasive component, ANGTPL4 expression was lost in the invasive keratinocytes but persisted in the *in situ* component. There was no association between ANGPTL4 expression and BMI in lesional tissue. These data suggest that targeting ANTPLT4 may be a novel therapy for the prevention of skin cancer and that ANGPTL4-high patients or cancer patients with obesity may be a critical demographic for potential risk assessment or therapeutic intervention. Future studies will determine the impact of knocking out ANGTPL4 in our models of malignant transformation.

#0762 The combination of EPA and naproxen suppresses colon tumorigenesis via altering the TME, and promoting epithelial maturation in cancerous crypts.

R. Beach[1], M. Martinez[1], V. Gunasekharan[2], D. W. Rosenberg[1];
[1]UConn Health, Farmington, CT, [2]NIH/NCI, Bethesda, MD

Introduction: Colorectal cancer (CRC) is a leading cause of cancer-associated mortality. Our recent study in Pirc rats revealed that the combination of eicosapentaenoic acid and sodium naproxen exhibited additive tumor protection. While the results from this preclinical study were impressive, showing tumor suppression in excess of 95%, potential mechanisms underlying this tumor protection remain unclear. The purpose of this study was to determine the transcriptomic changes resulting in the tumor suppression afforded by the combination of EPA and naproxen supplementation in the diet.
Methods: Six week-old Pirc rats were fed either a control AIN-93G diet, or AIN-93G diet supplemented with 2% EPA combined with 200 ppm naproxen, for a total of 20 weeks. Global transcriptomic analysis was performed using RNA sequencing (RNA-Seq) of colon tumors and tumor-adjacent normal tissue from 26-week-old Pirc rats. 100-bp paired-end sequencing was performed on an Illumina NovaSeq to a depth of 25 million reads per sample. Reads were trimmed with Trimmomatic-v0.39, and reads were mapped to the mRatBN7.2.105 rat reference genome using HISAT2. Differentially expressed genes were calculated using DESeq2, and gene set enrichment analysis (GSEA) were performed using Rstudio.
Results: DESeq2 identified 809 differentially expressed genes (DEGs, 2-fold change > 1, FDR < 0.05) between large tumors from AIN-93G fed rats versus suppressed tumors from rats fed the combination of EPA and naproxen (490 up-regulated, 319 down-regulated). GSEA analysis revealed activation of inflammatory pathways including IL-17 signaling, JAK-STAT signaling, complement activation, cytokine signaling, ribosome biogenesis, and cell cycle were enriched in untreated control. In contrast, suppressed tumors from animals supplemented with EPA and naproxen were enriched in pathways including negative regulation of *Wnt* signaling, cell fate specification, ion channel complexes, and nutrient absorption. Furthermore, suppressed tumors shared significant GSEA pathway overlap with normal tissue, leading us to believe the combination of EPA and naproxen may be preventing tumorigenesis in part by maintaining cells in a differentiated state.
Conclusion and Future directions: Inflammation plays a key role in tumorigenesis and promoting cancer stem cell niches in tumors. According to our analysis, the combination of EPA and naproxen attenuated cancer-associated inflammation and reduced proliferation in part by augmenting tumor differentiation. Future studies will utilize single-nuclei RNA-Seq (snRNA-Seq) to determine at a single cell resolution the transcriptomic changes of epithelial and stromal populations within the TME. This work was supported by National Cancer Institute task order 75N91019F00132.

PREVENTION / EARLY DETECTION / INTERCEPTION: Epidemiology
Poster Session

#0765 Tobacco smoke exposure, hormonal history, and estrogen metabolism in women with EGFR-mutant non-small cell lung cancer (NSCLC).

A. Raza[1], J. Treat[2], D. D. Krzizike[2], L. Vanderveer[2], M. Cheung[2], C. Zawislak[2], L. Etkins[2], E. Ross[2], D. B. Flieder[2], M. J. Edelman[2], M. L. Clapper[2], J. N. Bodor[2];

[1]Temple Univ. Lewis Katz School of Medicine, Philadelphia, PA, [2]Fox Chase Cancer Center, Philadelphia, PA

Introduction: The factors responsible for NSCLC development in never-smokers remain unclear, thus hindering prevention efforts. Our group is one of the first in the U.S. to build a registry of never-smokers with NSCLC to facilitate research to address this global problem. Given the high prevalence of women among cases, we are investigating the contribution of estrogen metabolism to this disease. CYP1B1 converts parent estrogens to the putative carcinogen 4-hydroxyestrogen (4-OHE), a process further accelerated by tobacco smoke exposure. In contrast, CYP1A1 generates 2-hydroxyestrogen (2-OHE), which may be converted to anti-proliferative derivatives. We determined previously that women with EGFR-mutant NSCLC enrolled in the registry have a 2-fold higher ratio of 4-OHEs to 2-OHEs, as compared to cancer-free controls. While EGFR-mutant NSCLCs are typically thought to be diagnosed in never-smokers, prior data indicate that a fraction of patients report some smoking history. The goal of this current study is to determine the smoking prevalence among women with EGFR-mutant NSCLC in our registry and explore the impact of smoking and hormonal history on estrogen metabolism.
Methods: The Lung Cancer in Never-Smokers Risk Registry (LCNS-RR) is recruiting patients with NSCLC who are never-smokers (<100 cigarettes/lifetime) and/or have tumors with oncogenes characteristically present in never-smokers (e.g., EGFR, ALK). In addition to donating biospecimens (e.g., blood, urine), participants complete a survey on tobacco and environmental exposures, hormonal history, and other factors. Using UPLC-MS/MS, profiles of urinary estrogens (E_1, E_2, E_3, 4-OHE_1, 4-OHE_2, 2-OHE_1, 2-OHE_2) were determined for 32 women with EGFR-mutant NSCLC in the LCNS-RR. The proportion of each estrogen species over total estrogen and the ratio of 4-OHEs to 2-OHEs were calculated. Medians were compared using the Wilcoxon rank-sum test.
Results: Among women in this EGFR-mutant cohort, none were current smokers, 16 were former smokers, and 16 were never-smokers. Among the former smokers, median pack-years was 11.6. The ratio of 4-OHEs to 2-OHEs was comparable in former- vs. never-smokers (0.51 vs. 0.49, p-value = 0.956). Twenty-three women (71.8%) had a history of oral contraception use, and 5 (15.6%) reported early menarche (<12 years of age). However, neither of these factors correlated with 4-OHE production. Among 28 post-menopausal women, 7 (25%) reported estrogen use since menopause, an exposure that was not associated with 4-OHE levels.
Conclusion: This preliminary analysis suggests that smoking history, use of hormones, or early menarche do not enhance the production of 4-OHEs in women with EGFR-mutant NSCLC. Recruitment to the LCNS-RR is ongoing and will facilitate future analyses in a larger cohort. (Supported by a Ride Hard Breathe Easy Innovation Award)

#0766 Effects of supplemental calcium and vitamin D on circulating biomarkers of gut barrier function in colorectal adenoma patients: A randomized controlled trial.

Sangji Lee[1], Veronika Fedirko[2], Roberd M. Bostick[3], Bradley Pearce[3], Elizabeth L. Barry[4], Robin E. Rutherford[3], March E. Seabrook[5]

[1]Texas A&M University, College Station, TX,[2]MD Anderson Cancer Center, Houston, TX,[3]Emory University, Atlanta, GA,[4]Dartmouth College, Hanover, NH,[5]Consultants in Gastroenterology, West Columbia, SC

Introduction: Recent experimental evidence shows that intestinal barrier disruption initiates colon inflammation, which may promote colorectal carcinogenesis. In experimental models, vitamin D and calcium improved gut barrier function; however, this has not been assessed in humans.
Method: To test the effects of supplemental calcium and vitamin D_3 on circulating biomarkers of intestinal mucosal damage (intestinal fatty-acid binding protein, IFABP) and exposure to bacterial products due to impaired gut barrier (lipopolysaccharide-binding protein, LBP), we conducted an “adjunct biomarker study” to a larger 11-center, randomized, placebo-controlled, partial 2x2 factorial chemoprevention clinical trial, the Vitamin D/Calcium Polyp Prevention Study. Participants were randomized into four different treatment groups: placebo, 1,200 mg/day calcium, 1,000 IU/day vitamin D_3, and 1,200 mg/day calcium plus 1,000 IU/day vitamin D_3. Circulating concentrations of LBP and IFABP were measured at baseline and 1-year follow-up using the Meso Scale Discovery electrochemiluminescence assays in a subset of 118 participants included in the adjunct biomarker study.
Result: Following one year of vitamin D_3 treatment, in the vitamin D_3 plus calcium and vitamin D_3 groups *versus* placebo and calcium groups, LBP decreased 10% (316 ng/ml; *P=0.23*) and IFABP 18% (77 ng/ml; *P=0.06*). A similar decrease of 20% (*P=0.10*) was observed for IFABP, but not LBP, in the vitamin D_3 plus calcium *versus* the calcium group. There were no appreciable biomarker changes with calcium treatment. In stratified analyses, we found possible effect modifications by baseline serum 25-OH-vitamin D, total calcium intake, body mass index, and interleukin 6 (IL-6) concentration on estimated vitamin D_3 treatment effects on LBP and/or IFABP.
Conclusion: These preliminary results are consistent with vitamin D’s potential protective effects on intestinal mucosal barrier and support further research of vitamin D against gut barrier disruption and colorectal neoplasms.

#0767 The role of abdominal obesity in the association between obesity and prostate cancer: A U.S. population-based cross-sectional study NHANES 2001-2020.

A. E. Ahmed[1], C. B. . Martin[1], B. Dahman[2], S. Q. Kern[1], G. T. Chesnut[1];
[1]Uniformed Services University of the Health Sciences, Bethesda, MD, [2]Virginia Commonwealth University, Richmond, VA

Background: Research suggests inconsistent evidence regarding the association between general obesity and prostate cancer among men in the United States. This study aimed to examine whether the association between general obesity and prostate cancer is influenced by abdominal obesity.
Methods: This study utilized data from the National Health and Nutrition Examination Survey (NHANES), 2001-2020, a nationally representative survey. The analysis was restricted to 16,703 non-Hispanic men (10,683 White and 6,020 Black). General obesity was defined by a body mass index of 30 kg/m^2 or greater and abdominal obesity was defined by a waist circumference of 102 cm or greater. Respondents were classified into four mutually exclusive groups according to the body fat indicators: 1) presence of both general and abdominal obesity, 2) abdominal obesity without general obesity, 3) general obesity without abdominal obesity, and 4) none of the two (the reference group).
Results: The overall prevalence of prostate cancer was 2.25% (95% CI: 2.0-2.5%). Men with abdominal obesity without general obesity have significantly higher prevalence of prostate cancer (4.28%) compared to men with both abdominal obesity and general obesity (2.23%), men with neither abdominal obesity or general obesity (1.70%), and men with general obesity without abdominal obesity (0.18%), P <.0001. Black men with abdominal obesity without general obesity have the highest prevalence of prostate cancer (7.21%), followed by White men with abdominal obesity without general obesity (4.10%). With and without adjusting for age and education, men with abdominal obesity without general obesity had significantly higher odds of prostate cancer, regardless of ethnicity. Black men with both abdominal obesity and general obesity had significantly higher odds of prostate cancer. General obesity without abdominal obesity was inversely associated with prostate cancer in White men but not in Black men.
Conclusions: This study illustrates that waist circumference is a potential classifier of prostate cancer as it shows variation in prevalence of prostate cancer by general obesity within the same and different racial and ethnic groups.

#0768 Awareness and use of genetic testing among cancer survivors in the United States: A HINTS-SEER study.

K. Ramalingam[1], A. Scheffler[1], E. Van Blarigan[1], S. Li[1], R. C. Vanderpool[2], S. H. Nash[3], S. Shariff-Marco[1], S. Gomez[1], M. Hebert-DeRouen[1];
[1]University of California San Francisco, San Francisco, CA, [2]National Cancer Institute, Rockville, MD, [3]University of Iowa, Iowa City, IA

Background: Germline genetic testing is a valuable tool for cancer treatment and family cancer risk assessment, but its uptake among cancer survivors remains low. Understanding the factors that influence awareness and use of genetic testing among survivors is crucial for improving access to this important tool.
Methods: We analyzed HINTS-SEER data, a pilot project conducted by the National Cancer Institute (NCI) in 2021, that oversampled cancer survivors diagnosed prior to 2018 using three registries from the Surveillance, Epidemiology, and End Results (SEER) Program (Iowa, New Mexico, Greater Bay Area). We examined sociodemographic factors in relation to awareness and use of genetic testing using survey-weighted multivariable logistic regression models. We also examined associations among breast and prostate cancer survivors, separately, as these cancer types have guidelines for genetic testing and had sufficient observations (>100) for stratified analyses.
Results: Of 1232 survivors included in the analysis, 277 (23%) had a history of breast cancer, 285 (23%) had prostate cancer, 82 (6.7%) had colorectal cancer, 25 (2%) had ovarian cancer, and 563 (45.7%) had other cancers. Overall, 76.5% of survivors were aware of genetic testing and 23.5% had used it. Among breast and prostate cancer survivors: 40.0% of breast and 20.6% of prostate cancer survivors were aware of genetic testing, and 21.0% and 2.4% had used it, respectively.
In multivariable models, female gender (vs. male; OR=3.1, 95% CI: 2.3, 4.2), higher education (high school or less education vs. greater than high school; OR=2.4, 95% CI: 1.4, 3.9), higher income ($100,000 or more vs. <$20,000; OR=3.2, 95% CI: 1.8,5.7), and family history (OR=2.0, 95% CI: 1.4,3.0) were significantly associated with higher odds of awareness of genetic testing. Older age (≥65 vs. <40 years; OR=0.4, 95% CI: 0.2,0.6), Asian American race (vs. non-Hispanic white; OR= 0.3, 95% CI: 0.3-0.9), and Hispanic ethnicity (vs. non-Hispanic white ; OR= 0.5, 95% CI: 0.3-0.9) were associated with lower odds of awareness of genetic testing.
Female gender (vs. male; OR=5.3, 95% CI: 3.3,8.5) was significantly associated with higher odds of use of genetic testing. Older age (>65 years vs. <40 years; OR=0.4, 95% CI: 0.2,0.7) and unemployed status (OR=0.4, 95% CI: 0.3-0.6) were significantly associated with lower odds of use of genetic testing. In stratified analyses, only older age among breast cancer survivors (≥65 vs. <40 years; OR=0.2, 95% CI: 0.0,0.9) was associated with lower odds of use of genetic testing.
Conclusion: Our study provides valuable insights into genetic testing awareness and utilization among a large sample of cancer survivors in the United States. The identified factors associated with awareness and utilization can be used by healthcare providers to target interventions aimed at improving genetic testing awareness and utilization among cancer survivors.

#0769 Incorporating a cross-ancestry polygenic risk score into a clinical model improved breast cancer risk prediction in women with pathogenic variants.

P. Tshiaba[1], M. Sun[1], D. Ratman[1], J. N. Weitzel[2], P. Shah[1], M. Rabinowitz[1], A. Kumar[1], K. Im[1];
[1]MyOme, Menlo Park, CA, [2]Precision Prevention, The University of Kansas Comprehensive Cancer Center, Kansas City, KS

Introduction. We previously developed and validated a cross-ancestry polygenic risk score (caPRS) to predict risk of developing breast cancer (BC) in women who do not carry pathogenic variants (PVs) in BC susceptibility genes. Here we aimed to expand upon that study by integrating the caPRS with the Breast and Ovarian Analysis of Disease Incidence and Carrier Estimation Algorithm (BOADICEA) model to combine the effects of genetic and clinical factors in carriers of PVs in BRCA1, BRCA2, PALB2, CHEK2 and ATM.

Methods. We explored the association of caPRS among 12,525 women from the UK Biobank and the Consortium of Investigators of Modifiers of BRCA1/2. The effect size of the caPRS was evaluated separately for individuals carrying PVs in BRCA1, BRCA2, CHEK2, ATM and PALB2. We used a logistic regression model adjusted for age, first-degree BC family history (FHx) and cohort for BRCA1 and BRCA2 to examine the association of the caPRS with BC. The effect sizes were expressed as standardized odds ratios (ORs) with 95% confidence intervals (CIs). The estimated absolute risks to age 80 of developing BC were calculated for unaffected women by combining the caPRS-based risk with gene-specific clinical risk estimates from the BOADICEA model based on U.S. incidences.

Results. The caPRS was significantly associated with BC risk across all PV carrier groups. Using BOADICEA alone, the estimated absolute BC risk by age 80 for an average unaffected 20-year-old female in the U.S. with an unknown FHx ranged from 23.8% for CHEK2 carriers to 79.4% for BRCA2 carriers. Integration of caPRS into BOADICEA, yielded the distribution of risk for each gene. (Table)

Gene	N	OR per SD (95% CI)	Absolute risk by BOADICEA	Median absolute risk by BOADICEA + caPRS (Range)
ATM	2,037	1.46 (1.25 - 1.71)	24.9%	27.1% (0.1 - 70.5)
BRCA1	5,794	1.24 (1.18 - 1.31)	76.1%	75.6% (55.6 - 87.7)
BRCA2	4,018	1.40 (1.31 - 1.49)	79.4%	78.7% (45.2 - 92.1)
CHEK2	372	1.88 (1.41 - 2.55)	23.8%	28.2% (0.0 - 78.4)
PALB2	304	1.81 (1.37 - 2.43)	53.9%	56.3% (2.9 - 90.9)

Conclusions. The caPRS significantly modified BC risk for carriers of PVs and could help tailor guidelines for women with PVs, particularly in moderate penetrance genes. More data is needed to increase the precision and reach of risk assessment in diverse populations.

#0770 The innate immune system response to malignancy- under the radar?.

M. Tobi[1], H. Talwar[1], B. McVicker[2];
[1]Saginaw VA Medical Center, Southfield, MI, [2]Omaha VA Medical Center, Omaha, NE

It has become clear that many cancers evade detection by, for example, silencing of immune checkpoints. Re-activation of the immune armamentarium by checkpoint inhibitors has improved survival in many types of cancer. However, we still are unable to gauge the response of the innate immune system (InImS) to incipient malignancy. The InImS is likely both a sentient early warning system and an immediately deployed cancer combatant. We describe a potential marker that quantifies the innate immune system response to multiple deadly tumors. Methods: We obtained a database of patients at high risk of colorectal neoplasia and prospectively noted those who contracted cancer on follow up. We contrasted the historic, premorbid biomarker response from the time of enrolment, primarily using the FERAD ratio. This was obtained by dividing the ferritin blood concentration by the denominator of fecal shedding of a Paneth cell marker, p87. We also compared the FERAD response to the absolute neutrophil:lymphocyte ratio (NLR), a known prognostic biomarker, and also the available, known PDL-1 response for each group of cancers. Results: We found that certain groups of cancers historically had very low FERAD ratios while others were high. Using FERAD ratios for lung, gastric, non-Hodgkin's lymphoma, melanoma, thyroid, renal, and head and neck cancers, there is a significant inverse correlation between survival and FERAD ($r=-0.8;p<0.025$) which is similar to that of NLR ($r=-0.7;p<0.035$). For prostate cancer, breast, colorectal cancer (CRC), leukemia/MDS, there is a direct correlation between survival and FERAD ($r=0.99;p<0.002$). There is also an inverse relationship between NLR and PDL-1 response rates ($r=-0.8;p<0.04$). An observed mild positive trend for FERAD PDL-1 response rates may bode well for melanoma, lung, head and neck and renal cancers. Conclusions: Since p87 could be manipulated by dietary means to affect the FERAD ratio favorably, this could be incorporated into more effective chemotherapy regimens and result in better cancer treatment outcomes. Hepatocellular cancer (HCC) and CRC-liver metastasis appear to be immunological outliers. This will need an additional unique approach such as TIGIT intervention therapy (Zheng et al.. Immune checkpoint targeting TIGIT in HCC. Am J Transl Res. 2020). This may allow modulation of the immune response based on FERAD, NLR ratios, and other considerations of mutational burden and genetic mutations, in patients with selected cancers.

#0771 A TGF-β superfamily member, myostatin contributes to MASH and HCC via muscle atrophy by disrupting TGF-β signaling, and is a potential marker with PKM2 for human HCC.

K. Ohshiro[1], K. Bhowmick[1], X. Xiang[1], S. Kapoor[1], R. Amdur[1], S. Dasarathy[2], A. R. Krainer[3], **L. Mishra**[1];
[1]Feinstein Institutes for Medical Research & Cold Spring Harbor Laboratory, New York, NY, [2]Cleveland Clinic, Cleveland, OH, [3]Cold Spring Harbor Laboratory, New York, NY

Background: In patients with cirrhosis and hepatocellular carcinoma (HCC), sarcopenia or skeletal muscle loss, as well as metabolic alterations are frequent and progressive comorbidities. Myostatin, a TGF-β superfamily member is expressed primarily in skeletal muscle, inhibits muscle growth, and causes sarcopenia in cirrhosis. Previously, we had observed liver-specific knockout of the SMAD3 adaptor, βII-spectrin -*Sptbn1* (βS-LSKO) or siRNA targeting βII-spectrin blocks sarcopenia, fatty liver disease-MASH and HCC (Sci TM 2021), suggesting that βII-spectrin may be a viable strategy to identify mechanisms, as well as new biomarkers of MASH and HCC.
Methods: 1. SPTBN1^{Flox} (control) and liver-specific βII-spectrin knockout (SPTBN1^{LSKO}) mice were fed Western diet (WD) and treated with Diethylnitrosamine (DEN) for obesity-associated HCC. Muscle mass, body weight and multiple enzymes involved in glycolysis as well as sarcopenia were measured in mutant mice. 2. In tumors, a rate-limiting enzyme in glycolysis, pyruvate kinase isozyme M2 (PKM2) that mediates inflammation and aerobic glycolysis in Warburg effect. Therefore, we further examined TGF-β pathway-enriched biomarkers such as Myostatin and PKM2 for markers of HCC and whether these could stratify risk in patients with cirrhosis for HCC, in a four-institution cohort, (n=157) compared to cirrhosis patients (n=380).
Results: 1. Like human fatty liver disease, obese mutant mice show marked sarcopenia with increased PKM2 and Myostatin levels with decreased p-RPS6/total-RPS6 ratio (indicating mTOR signaling inhibition) in striated muscle tissue. In contrast, levels are restored to normal in the liver specific knockout of SPTBN1. 2. Using the 108 markers as well as PKM2 and myostatin (MSTN), we found 31 markers with false discovery rate (FDR) p values < 0.10 from univariable Kruskal-Wallis tests for the associations of markers with HCC vs. cirrhosis.
Conclusions: Our results reveal that SMAD3 adaptor, βII-spectrin liver-specific knockout decreases Myostatin and PKM2 expression, providing new insight into molecular mechanisms in MASH and HCC. These studies reflect that these are biologically functional circuits that could provide new serum markers, such as Myostatin and PKM2 for risk stratification of HCC.

#0772 Investigation of gender disparity in liver tumor formation using a hydrodynamic tail vein injection mouse model.

A. Bernal, M. McLaughlin, A. Tiwari, F. Cigarroa, L. Sun;
The University of Texas Health Science Center At San Antonio, San Antonio, TX

The incidence of hepatocellular carcinoma (HCC), the major form of liver cancer, is 4 times higher in men than in women. This gender disparity is difficult to study since it is believed to be multifactorial, due in part to differences in risk factors, behaviors, and hormones. The liver is a sexually dimorphic organ that is extremely susceptible to interactions with estrogens and androgens. Estrogen has been proven to have a protective effect against HCC with a demonstrable gender-related hormonal effect on the growth of HCC, though the underlying mechanisms are not fully understood. The hydrodynamic tail vein injection (HTVI) mouse model allows for the induction of liver tumors in the host. Eliminating the social and behavioral aspects of the gender disparity will allow us to determine what role estrogen plays in tumor development. In our study, a gender disparity in tumor development was observed between 6-week-old male and female FVB/NJ mice injected via HTVI of plasmids expressing c-MET, a mutated beta-catenin (b-Cat) and Sleeping Beauty transposon. HTVI of a Luciferase and Sleeping Beauty transposon expressing plasmid showed no significant difference in photon flux by bioluminescence imaging between male and female mice 24 hours after injection. When imaging was repeated one week after injection, the photon flux reduced by an order of magnitude in both male and female mice with the female mice showing more uniform reduction than the male mice. Similar luciferase gene copy number was detected in the liver tissue of male and female mice. These data suggest that there appears to be no gender difference in the transient expression and stable integration of the transfected plasmid. Plasma alpha-fetoprotein (AFP) was used to monitor tumor formation in the mice that were injected with c-MET and b-Cat without luciferase as luciferase is immunogenic. The male mice had significantly higher AFP levels at 3.5 weeks, 8 weeks, and 12 weeks post-injection than the female mice. At termination, the liver weight confirmed that female mice had much lower tumor burden than the males. We are currently using quantitative PCR to confirm similar copy number of exogenous c-MET and b-Cat inserted in the tumor cell genome and using RT-qPCR and Western blotting to determine whether the transgene expression is different in tumors from male and female mice. To determine whether estrogen played a role in preventing tumor development and progression in female mice, six-week-old male and ovariectomized female mice have been injected with the same oncogene plasmid combination plus the sleeping beauty. Interestingly, AFP levels between male and ovariectomized female mice were comparable when measured at 3 weeks. We will present our findings at the meeting.

#0773 Overexpression of phosphoserine phosphatase (PSPH) in prostate cancer and in tumor microenvironment promotes tumor cell proliferation.

Liankun Song[1], Noriko Yokoyama[1], Jun Xie[1], Yunjie Hu[1], Zhenyu (Arthur) Jia[2], Beverly Wang[1], Dan Mercola[1], Edward Uchio[1], Thomas Ahlering[1], Michael Lilly[3], Xiaolin Zi[1]

[1]University of California, Irvine, Orange, CA,[2]University of California, Riverside, Riverside, CA,[3]Medical university of south Carolina, Charleston, SC

Reprogrammed cellular metabolism is one of the key features of cancer and tumor microenvironment. L-3-phosphoserine phosphatase (PSPH) is one of the five rate-limiting enzymes in the biosynthesis of serine from glucose that supports cell proliferation. Here, we aim to study the role of PSPH in prostate cancer (PCa) and its tumor microenvironment. We find that PSPH not only is overexpressed in prostate cancer cell lines compared to normal prostate epithelial cells (PrEC) and benign prostate epithelial cells (BPH-1), but also exhibits a higher level in patient-derived carcinoma-associated fibroblasts (CAFs) compared to the matched benign associated fibroblasts (BAFs), which are derived from fresh radical prostatectomy specimens of African American (AA) and European American (EA) men. Notably, MDAPCa2b cells derived from an AA prostate cancer patient and AA CAFs have even higher expression of PSPH protein. The mRNA levels of PSPH are also significantly elevated in prostate cancer tissues in AA men compared to EA men and predict poor survival in PCa patients. Knock-down of PSPH expression significantly inhibits the proliferation and colony formation of prostate cancer cells. Growth of xenograft tumors derived from PSPH knockdown MDAPCa2b cells has also been suppressed markedly. Gene expression profiling revealed that suppression of PSPH expression by shRNAs in LNCaP and MDAPCa2b cells is associated with the regulation of gene expression related to metabolism, immunity, extracellular matrix remodeling, and Ion channels. Similarly, analysis of publicly available PCa RNA seq databases also demonstrates that PSPH amplification or over-expression is associated with alterations of gene expression related to metabolism and immunity. Our results suggest that PSPH is upregulated in prostate cancer cells and their surrounding fibroblasts to support tumor growth via reprogramming metabolic pathways and transcriptomes.

#0774 Genetic architecture, evolutionary genomics, and genomic risk of prostate cancer in sub-Saharan Africa.

T. R. Rebbeck[1], R. Janivara[2], W. C. Chen[3], U. Hazra[2], M. Network[1], J. Lachance[4];

[1]Dana-Farber Cancer Institute, Boston, MA, [2]Georgia Institute of Technology, Atlanta, GA, [3]Wits Health Consortium, Johannesburg, South Africa, [4]Georgia Institute of Technology, Atlanta, GA

Men of African descent have the highest prostate cancer (CaP) incidence and mortality rates, yet the genetic basis of CaP in African men has been understudied. We performed the first large-scale genomic analysis of CaP across sub-Saharan Africa (SSA). We evaluated the evolutionary history of CaP-associated loci, generated a novel genomic risk score, inferred ancestry-specific genetic architectures, and fine-mapped disease associations using in 3,963 CaP cases and 3,509 controls recruited in Ghana, Nigeria, Senegal, South Africa, and Uganda through the Men of African Descent and Carcinoma of the Prostate (MADCaP) Network. Fifteen independent associations at 8q24.21, 6q22.1, and 11q13.3 reached genome-wide significance, including four novel associations. Multiple lead SNPs were private alleles in SSA, a pattern arising from recent mutations and the out-of-Africa bottleneck. These SSA-specific alleles contribute to haplotypes with odds ratios for CaP above 2.4. The genetic architecture of CaP differs across SSA, with effect size differences contributing more to this heterogeneity than allele frequency differences. Population genetic analyses reveal that SSA CaP associations are largely governed by neutral evolution, as opposed to natural selection. This finding is consistent with the late onset of this disease. Focusing on 2,502 age-matched cases and 2,222 non-cancer controls, we generated a novel genomic predictor of CaP. We then assessed the extent to which this polygenic risk score was correlated with age of onset, PSA levels, genetic ancestry, and family history of study participants. The performance of this novel polygenic risk score was tested on other populations of African descent, as well as populations with non-African ancestry. Our findings emphasize the utility of conducting genetic studies in diverse populations.

#0775 Underlying germline genetic architecture of pediatric sarcomas: Evaluating the role of common and rare variants in 4,160 patients.

L. Mirabello[1], L. E. Egolf[1], B. Zhu[1], D. Gianferante[1], K. Wang[2], S. A. Li[2], M. J. Machiela[1], L. G. Spector[3], J. D. Schiffman[4], A. Sabo[5], A. Renwick[5], B. Martin-Giacalone[6], M. E. Scheurer[5], S. Plon[5], D. Hawkins[7], R. Venkatramani[5], D. Stewart[1], L. M. Morton[1], M. M. Hudson[8], G. T. Armstrong[4], S. Bhatia[9], M. Dean[1], K. A. Janeway[10], A. Patino-Garcia[11], F. Lecanda[12], M. Serra[13], C. Hattinger[13], K. Scotlandi[13], A. M. Flanagan[14], F. Amary[14], I. L. Andrulis[15], J. S. Wunder[15], M. L. Ballinger[16], D. M. Thomas[16], O. Delattre[17], A. K. Hubbard[1], J. Liu[2], W. Luo[2], B. D. Hicks[2], M. Yeager[2], M. Rafati[1], W.-Y. Huang[1], M. T. Landi[1], A. Lori[18], R. Diver[18], S. A. Savage[1], S. J. Chanock[1], P. J. Lupo[5];

[1]National Cancer Institute, NIH, Bethesda, MD, [2]Frederick National Laboratory for Cancer Research, Frederick, MD, [3]Department of Pediatrics, University of Minnesota, Minneapolis, MN, [4]Huntsman Cancer Institute, University of Utah School of Medicine, Salt Lake City, UT, [5]Human Genome Sequencing Center, Baylor College of Medicine, Houston, TX, [6]Division of Public Health Sciences, Washington University in St. Louis School of Medicine, St. Louis, MO, [7]Department of Pediatrics, Seattle Children's Hospital, Seattle, WA, [8]Department of Oncology, St. Jude Children's Research Hospital, Memphis, TN, [9]Institute for Cancer Outcomes and Survivorship, University of Alabama at Birmingham, Birmingham, AL, [10]Dana-Farber/Boston Children's Cancer and Blood Disorders Center, Harvard Medical School, Boston, MA, [11]Department of Pediatrics/Medical Genomics Unit and Program in Solid Tumors, Cima-Universidad de Navarra, Cancer Center Clinica Universidad de Navarra (CCUN), Pamplona, Spain, [12]Center for Applied Medical Research (CIMA)-University of Navarra, IdiSNA, and CIBERONC, Pamplona, Spain, [13]IRCCS Istituto Ortopedico Rizzoli, Osteoncology, Bone and Soft Tissue Sarcomas and Innovative Therapies, Pharmacogenomics and Pharmacogenetics Research Unit, Bologna, Italy, [14]Royal National Orthopaedic Hospital NHS Trust, Stanmore, United Kingdom, [15]Lunenfeld-Tanenbaum Research Institute, Sinai Health System, University of Toronto, Toronto, ON, Canada, [16]Garvan Institute of Medical Research, Darlinghurst, Australia, [17]SIREDO Oncology Centre, Institut Curie, Paris, France, [18]Department of Population Science, American Cancer Society, Kennesaw, GA

Some evidence suggests that pediatric sarcomas have both shared and distinct genetic profiles; however, large-scale efforts to characterize germline genetic susceptibility across these malignancies are limited by their rarity. We evaluated the role of common and rare variants in the genetic etiology of the more frequent pediatric sarcomas: osteosarcoma (OS); Ewing sarcoma (ES); and rhabdomyosarcoma (RMS), subcategorized into embryonal (ERMS) and alveolar (ARMS).

METHODS: We evaluated 4,161 European-ancestry cases with genotype data (1,843 OS, 733 ES, 1,585 RMS, and ~61,000 cancer-free adult controls) and 2,474 cases with exome or genome sequencing (1,002 OS, 579 ES, 893 RMS, and 1,057 controls; jointly called with the same QC). Analyses included: 1) estimating disease heritability for both common SNPs (MAF>3%; genome-wide) and rare loss-of-function variants (MAF<1%; exome-wide); and 2) determining the frequency of rare predicted pathogenic (P) or likely pathogenic (LP; ACMG-AMP) variants in cancer susceptibility genes (CSG).

RESULTS: For OS, we conducted a new GWAS and determined that common variants explained 2.7% (SE 1.1%) of disease heritability, while rare LOF variants explained 12.7% (SE 1.5%; compared to 0.4% for synonymous variants). A similar pattern was observed for ERMS, where rare LOF variants explained a greater proportion of disease heritability (RMS 8.6%, SE 1.2%; ERMS 12.6%, SE 1.7%; ARMS n/a due to small sample size) compared to common variants from our new GWAS (0.9%, SE 1.6%). Conversely, common variants explained a greater proportion of ES heritability (5.4%, SE 0.5%) and of ARMS heritability (15.5%, SE 6.4%). For 113 established CSGs, and for the 60 moderate-to-high penetrant autosomal dominant (AD) genes, OS and ERMS had significantly (P_{exact}<0.01) more rare P/LP variants overall compared to controls; whereas ARMS and ES had significantly fewer P/LP variants than ERMS and OS, similar to the controls. We confirmed previously reported AD genes, and identified new genes, with an enrichment of P/LP variants in ERMS and OS compared to controls. For both ARMS and ES, the only AD gene significantly enriched for P/LP variants was *CHEK2*. For all cases, patients with a P/LP variant were significantly younger and had significantly more poor outcomes (ie, metastasis, stage 4 disease, and/or death) than those without. For 49 autosomal recessive CSGs, heterozygous P/LP carrier frequencies were similar among all sarcomas (8-11%), and several specific genes had similar P/LP variant enrichment across sarcomas, and for ES and ARMS only, compared to controls.

CONCLUSION: In the largest set of pediatric sarcoma cases assembled to date, genetic susceptibility was largely driven by rare P/LP AD gene variants in tumor types not characterized by canonical somatic fusions (OS and ERMS). In contrast, fusion-driven tumor types (ES and ARMS) were driven more by common variants.

#0776 Change in background contrast enhancement category on abbreviated breast MRI with administration of 6 months of bazedoxifene and conjugated estrogen vs wait list control.

C. J. Fabian, O. Winblad, A. L. Kreutzjans, K. Pittman, C. Altman, K. R. Powers, M. McCarthy, L. Nye, **B. F. Kimler**;
University of Kansas Medical Center, Kansas City, KS

Background MRI background contrast enhancement (BPE) has found to be a marker of breast cancer risk providing information beyond that provided by assessment of breast density. BPE is qualitatively classified into categories that correspond to BPE estimates as minimal, <25% BPE; mild, 25-50% BPE; moderate, 50-75% BPE; and marked, >75% BPE. We divided minimal into minimal and almost none (≤5%). We conducted a feasibility study of change in BPE after 6 months of the selective estrogen receptor modulator bazedoxifene (BZA) 20 mg + conjugated estrogen (CE) 0.45 mg marketed commercially as Duavee™ for relief of hot flashes and prevention of osteoporosis in postmenopausal women.
Methods STUDY00145121 started 5-27-2020 with randomization to 6 months of Duavee™ vs waitlist control but was stopped after 11 entrants because participants were unable to receive follow-up breast MRIs due to COVID and Duavee™ became unavailable. STUDY0014761 was opened in early 2022 when a source of BZA was found. Doses of BZA and CE were the same as Duavee™ but given as two pills instead of one. 16 women have been randomized to 6 months of BZA/CE vs a wait list control between 2-14-2022 and 9-19-2023. Inclusion criteria are postmenopausal women ages 45-65 at increased risk for breast cancer, BMI < 36 kg/m^2 and having current vasomotor symptoms. Participants had a blood draw, 3D mammogram, and abbreviated breast MRI at baseline and the studies were repeated at 6 months. Volumetric density was assessed by Volpara™ fully automated software. Research evaluation of abbreviated MRI background parenchymal contrast enhancement (BPE) was assessed by 5 categories as almost none, minimal, mild, moderate, and marked. BPE was evaluated by a single radiologist blinded to treatment assignment and compared to the 4-category clinical assessment.
Results A total of 27 women have been entered in these studies. Six were not evaluable from STUDY00145121 because of the inability to perform 6-month MRI. Two women on STUDY0014761 are not endpoint evaluable due to early drop out and 3 have not yet completed study. A total of 16 women have completed the 6-month portion of the study and abbreviated MRI, with median age 55 (range 47-62) and median BMI 26 kg/m^2 (20-33 kg/m^2). At baseline, BPE were 3 almost none, 4 minimal, 8 mild, 1 moderate, and 0 marked. There was little correlation between absolute baseline mammographic fibroglandular volume and baseline BPE. A shift in BPE category using the 5-category assessment was noted in 6/11 women (all but one decreased) randomized to BZA +CE and 2/5 women (both decreased) on waitlist. The one increase and four categorical decreases would not have been detected without expansion of BPE to a 5-category system.
Conclusion Using the 5-category classification, abbreviated MRI BPE may have promise as a response biomarker in prevention trials for postmenopausal high-risk women.

#0777 Notch signaling dependent chemoresistance in racial disparity in ER$^+$ breast cancer.

S. Singh, M. Das, R. Chakrabarti;
University of Miami Miller School of Medicine, Miami, FL

Breast cancer (BCa) is the leading cause of cancer related death in women worldwide. The most common BCa subtype is the Estrogen/Progesterone receptor (ER$^+$/PR$^+$) luminal subtype, comprising up to 75% of all newly diagnosed BCa. Although these patients show initial benefit with chemotherapy and endocrine therapy, however, 40-50% of them eventually don't respond to treatment due to resistance. Thus, the need for additional targeted therapies for this large subset of ER$^+$ BCa patients is critical. Based on recent studies, it is observed that Afro-American (AA) patients experience substantially higher BCa mortality (40% more) than White American (WA) women in ER$^+$ breast cancer. Unfortunately, the cause behind this difference in mortality in AA patients is not well understood. Notch signaling is a highly conserved intercellular communication mechanism critical for many cellular processes and is composed of several receptors and ligands. Recent data show that Notch receptors are overexpressed in hormone treatment refractory ER$^-$ patients of (Afro-American) AA origin, hinting connection of Notch signaling to racial disparity in breast cancer. Notch signaling is also identified in several metabolic disorders involving fatty acids and other lipids. However, function of Notch signaling in context of chemoresistance in AA ER$^+$ breast cancer is still unknown. Using single cell sequencing, we found that chemo-resistant AA ER$^+$ breast cancer patient samples have a distinct Notch signature enriched subpopulations in tumor cells, which was missing in WA patients. Notch signaling happens through juxtacrine signaling of ligand/receptor signaling. Further analysis in tumor microenvironment shows lipid enriched tumor associated macrophages, which are Notch dependent, suggesting potential crosstalk between lipid heavy tumor-macrophages and tumor cells, which may drive the chemoresistance in AA patients. Further analysis using patient derived explants, an attractive new tool for drug efficacy testing in ex vivo, we found that chemotherapy itself increases Notch signaling in the tumors. Ongoing studies involving scRNAseq, untargeted lipidomics and chemo-resistant PDE will delineate the precise mechanism of action between tumor cells and tumor associated lipid heavy macrophages in context of Notch signaling in chemo-resistant AA ER$^+$ breast cancer.

#0778 Atorvastatin modulates serum biomarkers in women at increased risk for breast cancer.

A. L. Lanier, J. Fahrmann, F. N. A. Mustafayev, A. Gutierrez Barrera, P. H. Brown, B. Arun;
UT MD Anderson Cancer Center, Houston, TX

Background Tamoxifen and Aromatase inhibitors have been shown to be highly effective at reducing the incidence of ER-positive breast cancers in women at increased risk, but there are no approved agents for the risk reduction of ER-negative cancers. Evidence from observational and preclinical studies supports the study of statins for breast cancer risk reduction.
Objective This study aimed to investigate the effects of Atorvastatin treatment on serum and tissue biomarkers in women at increased risk for breast cancer.
Methods Women at increased risk for breast cancer were accrued prospectively at UTMDACC, Breast Medical Oncology High-Risk Clinic. The study was approved by the IRB and all participants signed informed consent. High risk was defined as having a previous history of DCIS, LCIS, or atypical hyperplasia, 5-year projected Gail risk >1.67 %, or lifetime risk >20 % calculated by clinical models. Patients were randomized to no treatment (n=15) or daily 10mg (n=15), 20mg (n=14), or 40mg (n=16) Atorvastatin for 3 months. Fasting blood and breast tissue samples via fine needle aspiration (FNA) were collected at baseline and at study completion. Serum biomarkers were analyzed with ELISA (R&D Systems). The IGF1/IGFBP3 molar ratio was calculated using [IGF1 (ng/mL) x 0.13] / [IGFBP-3 (ng/mL) x 0.035]. The Wilcoxon matched-pairs signed rank test was used to determine significance.
Results Tissue biomarker evaluation was previously reported. Serum biomarker levels of IGF1 and its main binding proteins IGFBP1 and IGFBP3 were compared in baseline and post-intervention samples by ELISA analysis. The average change in serum IGF1 (ng/mL) levels between pre- and post-treatment samples (represented as average difference with interquartile range) was +3.5 (-16.8 to 8.7) p=0.98, -0.6 (-23.6 to 15.4) p=0.64, -1.76 (-27.7 to 28.6) p=0.81, and +2.6 (-14.5 to 32.2) p=0.67 in the 0, 10, 20, and 40mg groups respectively. The average change in serum IGFBP1 (pg/mL) was -23.2 (-2372 to 4487) p=0.33, -480 (-4567 to 3008) p=0.72, 429 (-1259 to 3039) p=0.54, and -250 (-3581 to 2492) p=0.94 in the 0, 10, 20, and 40mg groups. The average change in serum IGFBP3 (ng/mL) was -24 (-193 to 98) p=0.72, -119 (-353 to 111) p=0.17, -190 (-433 to 14) p=0.07, and -234 (-369 to -79) p=0.002 in the 0, 10, 20, and 40mg groups. Serum IGF1/IGFBP3 molar ratio was +0.012 (-0.018 to 0.026) p=,0.76, +0.0065 (-0.013, to 0.047) p=0.53, +.0073 (-0.036 to 0.045) p=0.86, and +.027 (-.011 to .062) p=0.058 in the 0, 10, 20, and 40mg groups.
Conclusions Serum IGFBP3, which has been associated with breast cancer risk, was decreased in a dose-dependent manner in patients treated with Atorvastatin. The IGF1/IGFBP3 molar ratio was increased in the 40mg group, although not statistically significant (p=.0577). This shows that treatment with Atorvastatin induced changes in circulating biomarkers and that Atorvastatin could be further studied in larger prospective breast cancer prevention trials.

#0779 Functional role of TGF-beta receptor type-2 in breast cancer progression and survival.

M. Srivastava[1], A. Bera[1], H. B. Pollard[1], H. Hu[2], C. D. Shriver[3];
[1]Uniformed Services University, Potomac, MD, [2]Chan Soon-Shiong Institute of Molecular Medicine, Windber, PA, [3]Murtha Cancer Center Walter Reed National Military Medical Center,, Bethesda, MD

Background and Rational: Transforming growth factor β (TGFβ) signaling is pivotal in cellular proliferation and can exhibit either tumor-suppressive or promoting effects depending on cellular context and genetic alterations. TGFβ receptor type-2 (TGFβR2), the ligand-binding receptor, is implicated in various cancers. This study explores the functional role of TGFβR2 in breast cancer (BrCa) progression. Materials and
Method: Genomic alterations in TGFβR2 were assessed in TCGA samples. TGFβR2 mRNA and protein expression were examined in a panel of BrCa cell lines, including MCF7, MCF12A, MDA-MB-231, and MDA-MB-468. Additionally, serum samples from BrCa patients, meticulously categorized into subtypes such as triple-negative (TN), human epidermal growth factor receptor 2-positive (Her2+), Luminal A (LA), Luminal B1 (LB1), and Luminal B2 (LB2), were analyzed. BrCa cell lines were treated with TGFβ ligand to investigate receptor expression modulation.
Results: Analysis of genomic alterations in TGFβR2 from The Cancer Genome Atlas (TCGA, n=1084, BrCa samples) revealed TGFβ copy number amplification in 25% of samples, while less than 1% showed TGFβR2 amplification. Elevated TGFβR2 levels were identified in aggressive triple-negative MDA-MB-231 cells compared to other tested cell lines. Serum samples from BrCa patients (n=240) demonstrated higher TGFβR2 levels, particularly in Luminal B1 subtype and African American patients. Treatment of BrCa cell lines with TGFβ ligand induced TGFβR2 expression, suggesting ligand-induced receptor upregulation.
Discussion: The findings suggest TGFβR2 as a potential biomarker for BrCa, with higher levels associated with aggressiveness and racial disparities. Ligand-induced receptor upregulation implies a potential oncogenic role. These results contribute to understanding TGFβR2's functional significance and its implications in breast cancer progression, offering insights into potential biomarkers and therapeutic targets.

#0780 Normal breast tissues harbor rare populations of aneuploid epithelial cells.

Y. Lin*[1], J. Wang*[1], K. Wang[1], S. Bai[1], A. Thennavan[1], R. Wei[1], Y. Yan[1], J. Li[1], H. Elgamal[1], E. Sei[1], A. Casasent[1], M. Rao[1], C. Tang[1], J. Montalvan[2], C. Nagi[2], S. Winocour[2], B. Lim[2], A. Thompson[2], N. Navin[1];

[1]UT MD Anderson Cancer Center, Houston, TX, [2]Baylor Medical College, Houston, TX

Although aneuploidy is a hallmark of invasive breast cancers, the presence of aneuploid cells in breast tissues of disease-free women is poorly understood. Furthermore, the expansion of aneuploid cells and the specific copy number events that they harbor, as well as their relationship to invasive breast cancers has not been characterized in large cohorts of women. In this study, we obtained viable cell suspensions from 31 disease-free women that underwent reduction mammoplasty surgeries and fresh tissue collection in the HBCA project along with the collection of clinical metadata. The viable cell suspensions from 31 women were enriched for epithelial cells and used to perform high-thoughput nanowell scDNA-seq. In total, 55,321 cells were analyzed. The normal breast tissue samples were also embedded into OCT and frozen to perform Spatial Transcriptomics (Visium 10X Genomics) profiling and embedded into FFPE to perform histopathological analysis. Our data shows that all women harbored rare populations of aneuploid epithelial cells (mean 4.3%) that increased in frequency and their number of copy number aberrations with age. Many aneuploid epithelial cells (mean 79%) in normal breast tissues underwent clonal expansions of their genomes and harbored chromosomal aberrations detected in invasive breast cancers (gain of 1q and loss of 7q, 10q, 16q). Spatial mapping showed that aneuploid cells are localized in focal regions of ductal and lobular epithelial structures with normal histopathological features. Collectively, these data show that aneuploid epithelial cells exist in the normal breast tissues of disease-free women and increase with age. In many women, the aneuploid cells expand and harbor CNA events associated with invasive breast cancer.

#0781 Impact of vitamin D and pyruvate carboxylase on hypoxia inducible lipid droplet associated (HILPDA) protein in metastatic breast cancer cells.
Y. Song, C. Andolino, D. Teegarden;
Purdue University, West Lafayette, IN

Metastatic breast cancer, a critical health issue for women globally, is closely linked to aberrant lipid metabolism. One feature of this dysregulated metabolism is the increase in lipid storage in the form of cytoplasmic lipid droplets (CLDs), although what drives their accumulation or their role in metastasis is not clear. In prior studies, we demonstrated that the active form of vitamin D (1,25-dihydroxyvitamin D, $1,25(OH)_2D$) downregulates pyruvate carboxylase (PC), a key metabolic enzyme, thereby reducing lipid accumulation in metastatic breast cancer cells (MCF10CA1a). Additionally, we have demonstrated that both $1,25(OH)_2D$ treatment and PC-inhibition reduce breast cancer cell migration. Therefore, the goal of the current research is to identify the proteins associated with CLDs in metastatic MCF10CA1a breast cancer cells following $1,25(OH)_2D$ treatment or reduction in PC expression (shPC). Proteins from CLDs and whole cell lysates (WCL) were processed for untargeted proteomic analysis. In the CLD fractions, 1562 identified enriched proteins were common to both MCF10CA1a and $1,25(OH)_2D$ treated cells, while 160 proteins were higher in the MCF10CA1a cells, and 550 proteins were higher in the $1,25(OH)_2D$-treated cells compared to MCF10CA1a CLD fraction. In the CLD fractions, MCF10CA1a and shPC cells had a similar level of 380 enriched proteins, although 65 were higher in the shPC compared with MCF10CA1a, whereas 1268 were more enriched in the MCF10CA1a CLD fraction. Hypoxia Inducible Lipid Droplet Associated (HILPDA, known to inhibit triacylglycerol lipolysis) was only enriched in the CLD fraction of the metastatic MCF10CA1a cells. HILPDA was not identified in the CLDs of the $1,25(OH)_2D$ treated or the shPC cells, nor in any WCL fraction. Further investigation of HILPDA is important to determine if HILPDA plays a role in dysregulated cellular metabolism, including CLD accumulation, or migration, and may potentially be a target for future therapies to prevent breast cancer progression.

#0782 Correlation between collagen peptides and physical features of fibrosis in breast tissue from women at increased risk of cancer.

D. Rujchanarong[1], A. T. Stopeck[2], C. Preece[1], R. Sun[1], P. Chalasani[3], S. Brown[4], J. D. K. Bai[5], H. Jensen Smith[6], S. You[1], P. M. Angel[4], P. Thompson[1]; [1]Cedars-Sinai Medical Center, Los Angeles, CA, [2]Stony Brook Cancer Center, New York, NY, [3]George Washington University, Foggy Bottom, DC, [4]Medical University of South Carolina, Charleston, SC, [5]Stony Brook University, Stony Brook, NY, [6]University of Nebraska Medical Center, Omaha, NE

Breast cancer risk increases significantly in women who maintain higher radiologically dense breast tissue as they age. However, the mechanisms that underlie this association remain poorly understood, especially in postmenopausal women. A predominant contributor to dense breasts and differences between women is the relative amount of fibrillar collagens. Experimental models suggest that changes in collagen properties such as fiber alignment and stiffness promote local stromal fibrosis, which we hypothesize may contribute to the relationship between breast density, aging, and tumorigenesis. Normal breast biopsy samples from the contralateral, healthy breast of 32 postmenopausal breast cancer patients participating in a clinical trial for drug effect on breast density were examined and scored for areas of fibrosis and analyzed using second harmonic generation microscopy (SHG) and mass spectrometry proteomics. Our aim was to identify areas of fibrosis and relate the severity of focal fibrosis to the physical properties and peptide composition of collagen fibers. Using GraphPad Prism, we conducted one-way ANOVA and Kruskal-Wallis tests and post-hoc multiple comparison tests. H&E-stained breast tissue samples were scored according to percent fibrosis. The minimum and maximum percent fibrosis were 5% and 100%, respectively, with a median of 60% (95% CI: 97.06%). Out of 31 people, 16 had a higher fibrosis score than the median. Consistent with pathologic scoring of the presence and extent of fibrosis, fiber counts were significantly lower in tissue with lower fibrosis scores than samples with more highly scored fibrosis (p-value <0.001). Distance to the nearest fiber was greater in samples with < 20% fibrosis, whereas greater alignment to the nearest fiber was observed in higher fibrosis percentages. At the molecular level, 22 peptides demonstrated a strong correlation with percent fibrosis (spearman r ≥ 60), of which 13 peptides were statistically significant (p-value <0.0001). The putatively identified peptides belong to type I, III, IV and VI collagens. Fiber length and straightness, but not fiber width, were higher in tissues with greater percent fibrosis. Significant correlations were identified between collagen physical features and peptides: two distinct peptides correlated with collagen fiber length and straightness while 20 peptides correlated with fiber width. These putative peptides belong to types I, III, IV and V collagens with ~70% of the peptides containing at least one hydroxyproline modification. This study is the first to explore the link between focal fibrosis and collagen-associated peptides in healthy breast tissue of high-risk postmenopausal women. These findings provide novel insights on stromal collagens associated with fibrotic changes in normal at-risk breast tissue that may act in tissue susceptibility to tumor formation.

#0783 Early impact assessment of in-house EGFR testing for NSCLC in Kenya.

A. Njau, S. Nguku, J. Abuodha;
Aga Khan University Hospital, Nairobi, Kenya

Introduction: Quality of life and survival among non-small cell lung cancer (NSCLC) patients have improved in the last two decades owing mainly to use of tyrosine kinase inhibitors (TKIs) and other targeted therapies. Low and middle-income countries (LMICs) especially in Africa, are lagging in realizing these benefits largely due to hurdles in molecular testing. In addition, quality histology and molecular data from LMICs is deficient. The aim of this study is to assess the immediate impact of improved access to epidermal growth factor receptor (EGFR) testing in Kenya, and to establish a long term-lung cancer data base.
Methods: Staring mid-June 2023, an in-house PCR-based method was adopted for EGFR testing of NSCLC in order to side step the challenges of out-of-country send outs which was until then, the only option for EGFR testing. Further, a sponsored access program was created. From prospectively accrued samples, we performed a before-and-after assessment of the number of NSCLC cases intercepted, cost and turnaround times (TAT) as measures of impact. Demographic, histopathology, and EGFR mutation profiles were analyzed in comparison to Asia, USA and European data. Whole slide histology scanned images are made to compliment the database.
Results: Over the four-month period, 62 NSCLC cases were accrued, median age at diagnosis was 63 with a range of 24 - 93. The male to female ratio was 1: 1.5. Adenocarcinomas comprised 89%, squamous cell carcinoma 5% and 3% were not classifiable. Metastatic disease was reported in 14 (22%) with the brain being the commonest site. EGFR mutations were identified in 16 (25%) with exon 19 deletions and L858R mutations constituting 94% of them. Monthly requisitions for EGFR have increased 3-fold, and the average TAT has been halved to 7 days.
Conclusion: Similarities between our data and global patterns are noted; median age is in the seventh decade, NSCLC is more common in women, and so are the rates of EGFR mutations, adenocarcinomas are the predominant type, and there are high rates of brain metastasis at diagnosis. EGFR mutation rates appear to be higher than USA and European data but lower than Asian data. In-house and sponsored testing has had an immediate impact in reduction of costs and TAT and increased requisitions. Assessment of access to targeted therapy, clinical outcome, survival, expansion of molecular profiling beyond EGFR, and build-up of the database including virtual histology images for exploring artificial intelligence algorithms are our next steps.

#0784 Proteome-wide mendelian randomization identifies causal association between plasma proteins and lung cancer.

G. Si, W. Li, Y. Zhang, Z. Lyu, F. Song, **K. Chen**;
Tianjin Medical Univ. Cancer Inst. & Hospital, Tianjin, China

Background: Lung cancer is one of the world's main health issues, and the exploration of novel protein markers can help to understand the mechanisms of lung cancer development and the discovery of therapeutic targets. Based on this, we used proteome-wide Mendelian Randomization to determine causal associations between plasma protein levels and the risk of developing lung cancer and subtypes. Methods: We performed a two-sample Mendelian Randomization analysis using genome-wide association data for 4907 proteins from the deCODE genetics study and five lung cancer and its subtypes from the FinnGen database. Causal effects were estimated using the Wald-ratio method or the inverse variance weighted (IVW) method, with additional analyses using the other four common methods when the number of SNPs was more than one. The Steiger filter method was used to test the correct direction of the causal effect. Multiple corrections were utilized by the Benjamini-Hochberg method. Results: After filtering, we finally analyzed 4645 proteins for the causal association with lung cancer, and the F-statistic of the instrumental variable for each protein was more than 10. After multiple tests, the levels of four genetically predictive proteins were found to be associated with the risk of lung cancer, and one protein was associated with the risk of small-cell lung cancer. In detail, elevated levels of three genetically predicted proteins were significantly associated with increased risk of lung cancer, namely, SYSC (OR:4.75, 95%CI: 2.47-9.16, FDR=0.007), TM11D (OR: 1.34, 95%CI: 1.17-1.53, FDR=0.02), and PDC6I (OR: 2.35, 95%CI: 1.58-3.49, FDR=0.03). Elevated levels of FASLG (OR: 0.87, 95%CI: 0.82-0.92, FDR=0.007) were associated with a reduced risk of lung cancer. In addition, genetically predicted elevated levels of GRP (OR: 0.05, 95%CI: 0.01-0.17, FDR=0.02) were associated with an increased risk of small-cell lung cancer. The Steiger filter test showed that all directions were from proteins to lung cancer. Conclusion: In this study, we found that five proteins may have effects on the risk of lung cancer, in which genetically predicted SYSC, TM11D, and PDC6I were significantly associated with an increased risk of lung cancer, whereas FASLG and GRP were associated with a decreased risk of lung cancer and small-cell lung cancer, respectively. The above may help to explore the pathogenesis of lung cancer, but further comprehensive studies are still needed.

#0786 Genomic distinctions of HIV- and EBV-associated DLBCL in a diverse African cohort.

K. Antel[1], A. Nesmelov[2], M.-X. Wu[1], C. Slome[3], D. Chetty[3], R. Kriel[3], E. Postovalova[2], R. Redd[1], M. Aryee[1], D. Armand[1], L. McGrath[1], N. Xiong[1], J. Oosthuizen[3], K. Brown[3], A. Tyshevich[2], S. Podsvirova[2], F. Frenkel[2], N. Kuzkina[2], J. Scher[2], C. Tazearslan[2], K. Zornikova[2], N. Kotlov[2], A. Bagaev[2], N. Fowler[2], A. Freedman[1], S. Rodig[4], E. Verburgh[3], M. A. Murakami[1];

[1]Dana-Farber Cancer Institute, Boston, MA, [2]BostonGene, Waltham, MA, [3]University of Cape Town, Cape Town, South Africa, [4]Brigham & Women's Hospital, Boston, MA

Lymphoma, a leading cancer cause of death among people living with HIV (PLHIV) globally, poses a pressing public health challenge in Sub-Saharan Africa (SSA), the epicentre of the HIV epidemic. Despite its prevalence, the genetic underpinnings of lymphoma in Black Africans and PLHIV remain poorly defined, contributing to regional disparities. This study aims to elucidate the impact of HIV status and EBV on the genetic landscape, molecular subtypes and survival outcomes of diffuse large B-cell lymphoma (DLBCL) in ethnically diverse SSA patients.

We established a cohort of 117 newly diagnosed DBLCL cases (55 HIV+, 21 EBV+, 62 Black Africans), with histopathologic and clinical annotation from a public teaching hospital in Cape Town, South Africa (2010-22). Tumor specimens underwent histologic review, whole exome sequencing (WES) and bulk whole transcriptome sequencing. Germline variants were filtered by paired normal WES (when available) and normal references augmented by supervised machine learning in tumor-only specimens. Aberrant somatic hypermutation (ASHM) was assessed in curated genes within paired samples. Microsatellite instability (MSI) was assessed via MSI-sensor.

Canonical genetic aberrations reproduced in this cohort included recurrent SNVs in *TP53*, *CARD11*, *TET2*, *SOCS1*, *MYD88*, and *KMT2D* with differences in relative proportion compared to the NCI consortium cohort being more attributable to HIV or EBV status than ethnicity. HIV+ cases harbored frequent mutations in *TET2*, *BRAF*, and *KRAS*, with fewer in NFKB pathway genes including *CARD11*, *IKBK*, and *BTK*. ABC-type HIV+ cases manifested higher expression of genes in the JAK-STAT pathway. EBV+ cases exhibited distinct genomic features including amplifications in *NOTCH1*, *CARD11*, *NFKBIE*, *MYC*, *CD274*, and *JAK2*, as well as frequent gain-of-function (GOF) mutations in the *NOTCH1* PEST domain (40% vs 3.8% q=0.04). Tumor mutation burden was consistent across ethnic and virological strata (median mutations 139-167, p>0.05). Notably, ASHM was not identified as a predominant mutational signature in either HIV-positive or negative cases, and 4 HIV+ DLBCL cases exhibited MSI, corroborated by protein-affecting mutations in mismatch repair genes. The 2-year overall survival (OS) was less than 40%, markedly inferior to published Western cohorts, even when controlled for clinical prognostic factors and treatment regimen.

This study highlights genetic and biological distinctions in DLBCL due to HIV and EBV. Key findings include the absence of ASHM correlates of pathogenic driver mutations, challenging a prevailing hypothesis of HIV-associated lymphomagenesis, and the identification of MSI in HIV+DLBCL. The dismal survival of this cohort and distinct genomic features, especially in EBV+DLBCL, highlight the urgency of further biological interrogation and inclusive clinical trials for these demonstrably underserved populations.

#0787 SARS-COV-2 P.1 strain infection in lung, breast and colon tumoral patient-derived organoids.

T. F. Sassaro[1], A. Viana[1], M. Zalis[2], C. Ferreira[2], J. Canedo[2], D. Ferreira[3], A. S. Moreira[1], E. Mello[1], F. Rondao[2], B. I. S. Ferreira[1], O. C. Moreira[1], D. A. Moreira[1], B. B. Souza[4], M. C. Waghabi[1], **T. M. Tilli**[1];

[1]Oswaldo Cruz Foundation, Rio de Janeiro, Brazil, [2]Oncoclinicas, Rio de Janeiro, Brazil, [3]Invitrocue Brazil, Rio de Janeiro, Brazil, [4]Oncoclinicas, Sao Paulo, Brazil

Coronavirus 2019 disease (COVID-19), caused by the newly identified strain of the coronavirus family capable of inducing acute respiratory syndrome, rapidly escalated into a pandemic, triggering a public health emergency. Throughout this period, it became evident that increased attention should be addressed towards at-risk groups, particularly individuals with chronic illnesses, including cancer. World widely, lung, breast, and colon cancer stand as the most prevalent types of cancer exhibiting high mortality rates in both men and women. Epidemiological data demonstrate that cancer patients, particularly those with lung, breast, and colon cancer, face elevated risk and severity when infected by SARS-CoV-2, resulting in even higher mortality rates. However, there is a knowledge gap concerning the interaction between COVID-19 and cancer patients, and thus, the current proposal evaluated SARS-CoV-2 infection in biopsy cells extracted from lung, breast, and colon cancer patients, cultivated as a patient-derived organoid (PDOs). Additionally, we also evaluated SARS-CoV-2 infection in a 3D model of spheroids in LC319, CALU-3, A549, H460, MRC-5, MDA-MB-231, MCF-10A and CACO-2 cell lines. Both PDOs and spheroids were infected with the SARS-Cov-2 P.1 strain with a multiplicity of infection (MOI) of 0.01 for 24 hours. We observed that PDOs and tumoral and non-tumoral spheroids were equally permissive to SARS-CoV-2 infection showing similar viral load levels. However, we observed a cytopathic effect after SARS-CoV-2 P.1 strain infection only in tumoral cells in comparison to non-tumoral cells from the same tissue. Furthermore, we explored the cytopathic effects caused by SARS-CoV-2 infection in PDOs and in tumoral and non-tumoral spheroids by scanning electron microscopy (SEM). Interestingly, we observed morphological alterations on the surface of SARS-CoV-2 P.1 strain -tumoral infected cells, with the occurrence of surface projections after 1 hour infection. Finally, we performed an exome sequencing analysis of PDOs and
tumoral and non-tumoral cells which preliminarily indicated an intriguing and informative crosstalk between cancer-related genes and SARS-CoV-2 infection pathways. Here we have identified missense and nonsense mutations in genes involved in PI3K pathway, immune function, and cell cycle regulation. In summary, our study showed that SARS-CoV-2 P.1 strain can infect and directly induce cytopathic effects in lung, breast, and colon tumors.

#0788 Leveraging multi omics approach to examine the potential role of causative viruses in glioblastoma..

Bavani Gunasegaran[1], Aziz Abdullah A Alnakli[1], Gilles J. Guillemin4[2], Seong Beom Ahn[1], Benjamin Heng[1]

[1]Macquarie University, Sydney, Australia,[2]ICTRYM Pty Ltd, Sydney, Australia

Glioblastoma (GB), a grade IV brain cancer, has the lowest survival rate. Despite aggressive and targeted therapies, patients remain to have the worst prognosis. More than 16% of cancer incidence worldwide has been attributed to infectious agents, raising uncertainties about the role of infections in the development of brain cancer. While numerous studies have suggested potential viral involvement in GB pathogenesis, a common limitation is the reliance on a singular technology, such as DNA/RNA sequencing or immunohistochemistry, within each study. This approach may restrict the comprehensive exploration of viral contributions, as different technologies offer distinct insights into the complex mechanisms underlying GB development. Utilizing a combination of techniques could provide a more holistic understanding, enhancing the robustness of findings and potentially uncovering nuanced aspects of viral influence that a single technology might overlook. To clarify the role of viruses in GB pathology, our study employs a comprehensive approach integrating three distinct research methods. We screened 178 publicly accessible raw mass spectrometry (MS) data of GB tumors from three independent publications (PMID: 31331834, 31154438, 36720864) by employing our internally developed data identification pipeline. The pipeline transforms raw MS data for downstream analysis, conducts database searches against the latest viral protein databases and undergoes peptide validation for enhanced robustness. Subsequent analysis filters duplicate hits and consolidates nested peptides. The final protein list includes only those identified with two or more peptides of over eight amino acids. The pipeline concludes by inferring and listing the corresponding viruses, ensuring a comprehensive and refined approach to the identification and analysis of viral proteins in the context of MS data. To enhance this dataset, we incorporated whole-genome metagenomics and MS-based proteomics, examining a preliminary cohort of15 GB tumor tissues. This approach explored a wide range of viral encoded proteins. Our comprehensive analysis, integrating bioinformatics, genomics, and proteomics, identified multiple herpesvirus species across our cohorts. This potential identification of viruses within GB has the capacity to redefine the stratification of tumor types in GB patients, signaling a significant development in our understanding of the disease.

#0789 GrafGen: Distance-Based Inference of Population Ancestry for *Helicobacter pylori* Genomes.

W. Wheeler[1], D. Wang[2], I. Zhao[3], Y. Jin[4], **C. S. Rabkin**[2];
[1]Information Management Services, Rockville, MD, [2]National Cancer Institute, Bethesda, MD, [3]Axle Informatics, Rockville, MD, [4]National Center for Biotechnology Information, Bethesda, MD

BACKGROUND: The 1.67 megabase *H. pylori* genome contains ~143,000 biallelic single-nucleotide polymorphisms (SNP) with minor allele frequency > 1%. Confounding by population stratification is a major source of bias requiring adjustment in genome-wide association studies (GWAS). Previous model- and distance-based methods for bacterial genomes yield varying results depending upon which strains are included for comparison in analyses. We therefore developed a robust classification of *H. pylori* ancestry to facilitate generalizable inferences about disease associations. **METHODS:** GrafGen is an R software package adapted from the GrafPop tool for human ancestry (Jin et al., 2017; Jin et al., 2019). The underlying classification algorithm compares SNPs of an individual genome with frequencies in reference populations to estimate subject ancestry and ancestral proportions based on calculated genetic distances. Outputs incorporate visualization tools that provide natural geometric interpretation of population structure. **RESULTS:** Training data were obtained from the *H. pylori* Genome Project (*Hp*GP), a global survey of 1011 *H. pylori* genomes collected across 51 countries (Thorell et al., 2023). Based on genetic distances, *Hp*GP sequences clustered into nine mutually exclusive populations designated by their predominant geographic source. Previously published population assignments for a test set of 255 sequences obtained from GenBank mapped to specific GrafGen classifications (Table). GrafGen assignments based on randomly selected sets of 14,300 and 1430 SNPs were >97% and >90% identical, respectively, to those based on all 143,000 SNPs. **CONCLUSIONS:** GrafGen's universal categorization of *H. pylori* ancestry has utility for bacterial GWAS. The software code is publicly available for research on this important pathogen. Theoretically, the same algorithm can be implemented to infer ancestry of any single chromosome haploid species that has sufficient sequence data for references.

#0790 Sex and race-dependent variations in the mutational landscape of clonal hematopoiesis.

Kanaka Dhuri, Houda Alachkar

USC - University of Southern California, Los Angeles, CA

Introduction: Clonal hematopoiesis of indeterminate potential (CHIP) has emerged as a significant precursor to hematological malignancies and is associated with several age-related diseases. Recent studies in relatively small disease specific cohorts have suggested that CHIP may exhibit variations among different races and between males and females raising intriguing questions about potential genetic and environmental influences. Understanding the differences in CHIP across races and between males and females may have implications for personalized cancer risk assessment and targeted therapeutic strategies.
Methods: Patient's data were obtained from the Cancer Therapy and Clonal hematopoiesis via cBioportal. The original study was designed to examine clonal hematopoiesis mutations that were found in blood samples obtained from 24,146 patients with non-hematological cancers and their tumor-blood pairs were analyzed using targeting sequencing data MSK-IMPACT (Memorial Sloan Kettering-IMPACT). The cohort consisted of 45.7% males and 54.3% females; including 6.8% Asians, 6.2% Blacks, and 76.3% Whites. We examined mutation frequencies among these racial groups and between genders, employing the two-sided Fisher's exact test and adjusting p-values for multiple comparisons. Differences were considered significant when both P value and Q values are less than 0.05.
Results: *DNMT3A* mutations were substantially more prevalent in females than in males (38.94% vs 31.37%, p-value: $<10^{-10}$, q-value: $6.19e^{-09}$), While *ASXL1* mutations were more frequent in males than females (5.82% vs 2.69%, p-value: $<10^{-10}$, q-value: $6.19e^{-09}$). In the racial cohorts with sufficient sample sizes, *STAT5B* and *CSF1R* mutations were most frequent in Asian (1.40% and 0.84%), followed by Black (0.98% and 0.24%) and White populations (0.29% and 0.09%), (p-value: $8.099e^{-04}$ and $7.490e^{-04}$, q-value: 0.0234 and 0.0232). Several other CHIP mutations were enriched in Black: *RARA*, *SMAD2*, *CDKN1B*, *CENPA*, *CTLA4*, *EIF1AX*, *ELF3*, *MSI1*, *MYC*, *SOX17*, *AURKA*. On the other hand, *H3C1*, *H3C4*, *MYCL* were enriched in the Asian cohort.
Conclusion: Our analysis provides insights into the complex interplay of sex and racial factors in shaping CHIP mutation frequencies. As CHIP continues to gain recognition as a critical precursor to malignancies, understanding these variations contributes to refining our understanding of its underlying mechanisms and clinical implications.

#0791 Evaluation of BCR spike-in controls using DriverMap adaptive immune receptor (AIR) profiling technology.

A. Chenchik, T. Liu, M. Makhanov, D. Hu, K. Ghias, P. Diehl;
Cellecta, Inc., Mountain View, CA

The DriverMap™ Adaptive Immune Receptor (AIR) repertoire profiling assay employs multiplex RT-PCR for comprehensive profiling of CDR3 or full-length receptor profiling of all variable heavy and light chains of T-cell receptors (TCR) and B-cell receptors (BCR) from either RNA or DNA. In this study, initiated by a U.S. Food and Drug Administration (FDA) consortium to compare performance of different BCR repertoire profiling technologies, we tested spike-ins in peripheral blood mononuclear cell (PBMC) RNA and DNA control mixtures prepared from nine different B-cell lines. We measured the sensitivity, linearity and accuracy of AIR RNA and DNA BCR profiling for the IGH, IGK and IGL chains of the spike-in controls. Our comprehensive analysis, encompassing CDR3 profiling and full-length receptor profiling (CDR1, CDR2, and CDR3) sequencing, revealed a 100X increase in sensitivity of detection of spike-in controls in RNA compared to the DNA assay. The high sensitivity of the full-length DriverMap AIR RNA assay allowed the detection of controls from all nine cell lines, with 8 out of 9 cell lines detected in the DNA assay, which demonstrates the robustness of the DriverMap AIR profiling technology.
This study highlights the remarkable sensitivity of the AIR RNA assay in quantifying transcripts. This approach enables the detection of low-frequency BCR clonotypes, which is particularly advantageous when working with samples containing low numbers of B cells. Furthermore, our AIR DNA assay in combination with spike-in controls offers a quantitative tool for minimal residual disease (MRD) applications, providing accurate insight into cell numbers, which then facilitates tracking clonal expansion of immune cells.

#0792 Continuous, probabilistic variant interpretation with Bayesian graphical models.

W. M. Korn, Y. Kobayashi, F. M. Facio, A. Nampally, K. Nykamp, R. Nussbaum, A. Colavin, B. Johnson, T. Manders;
Invitae, San Francisco, CA

Introduction: Current variant classification (VC) frameworks rely on rules-based approaches that use heuristic weighting of various types of evidence, resulting in > 50% of variants being classified as variants of uncertain significance (VUS), and leaving many patients with uncertainty about their disease risk or diagnosis. We propose a probabilistic and scalable Bayesian approach to model the causal relationships between various types of evidence. A fully quantitative system maximizes the utility and integration of various evidence types, empowering clinicians to make more nuanced management decisions.
Methods: Probabilistic graphical models (PGMs) are uniquely suited to the needs of clinical VC. Two different component PGMs were developed to model two of the evidence categories that will ultimately be used in a comprehensive VC system: population allele frequency (Population PGM) and reported phenotype observations (Reported Phenotype PGM).
Results: The Population PGM treats population allele frequency observations as a binomial process. By conditioning the model on partial observations, the probabilistic relationships between pathogenicity and allele frequencies can be estimated while stochastic variational inference allows uncertainty to be efficiently propagated. The resulting model performs well across a large number of genes at inferring pathogenicity of a variant from its allele frequency, with an average precision of >99% for benign variants.
In the Reported Phenotype PGM, phenotypic features characteristic of a disorder are learned from patients expected to be affected based on genotype. Patient-level predictions are in turn combined at the variant level to derive variant pathogenicity likelihoods. To date, models representing at least 102 inherited conditions and 259 genes have demonstrated high predictive performance (>0.8 AUROC) for both patient-level and variant-level predictions.
Finally, as a proof-of-concept, we demonstrate how each component PGM can be combined into a probabilistic Bayesian VC framework that also includes protein structure and stability, evolutionary conservation, and sequence context. This framework has high concordance with known, well-accepted pathogenic and benign variants classified with rules-based systems, and could make high-confidence predictions for many variants currently classified as VUS.
Conclusion: We present a Bayesian approach that can integrate diverse types of evidence to achieve high VC accuracy while quantifying uncertainty. Future expansion of this Bayesian framework to all evidence types relevant to VC may allow for more accurate risk management guidelines and further inform medical and genetic counseling recommendations.

POPULATION SCIENCES: Cancer Disparities 1: Emerging Trends in Cancer Disparities Research
Poster Session

#0796 Exploring the impact of masculine beliefs on colorectal cancer screening participation among Hispanic/Latino men in Florida, New York, and Texas.

A. E. Sedani[1], J. Y. Islam[2], D. M. Griffith[3], K. K. Rifelj[1], C. L. McCall[1], O. Garcia-Rodriguez[2], M. Camacho-Rivera[4], C. R. Rogers[1];
[1]Medical College of Wisconsin, Milwaukee, WI, [2]H. Lee Moffitt Cancer and Research Institute, Tampa, FL, [3]Georgetown University, Washington, DC, [4]SUNY Downstate Health Sciences University, Brooklyn, NY

Introduction: The existing literature on colorectal cancer-related inequities among Hispanic/Latino men may be poorly descried as most outcome data to date for this ethnic group are reported in aggregate. This study explored how masculine beliefs may influence colorectal cancer screening participation among ethnic subgroups of Hispanic/Latino men aged 45-75 years.
Methods: Utilizing a consumer panel, self-identified Hispanic/Latino men that were age-eligible for colorectal cancer screening and fluent in either English or Spanish were recruited from Florida, New York, and Texas (February-March 2022). The Masculinity Barriers to Medical Care (MBMC) scale, comprising six theoretically derived subscales, was assessed masculinity. Multivariable logistic regression was employed to estimate the association between MBMC and colorectal cancer screening participation, adjusting for Hispanic/Latino subgroup, marital status, survey language, age, and health insurance status. Next, to explore differences by Hispanic/Latino subgroups (Mexican/Mexican American/Chicano; Puerto Rican; Cuban; Other Hispanic/Latino), results were stratified by subgroup and adjusted for confounding.
Results: There were 611 male participants, with roughly 31% identifying as Puerto Rican, 30% a different Hispanic ethnic background ("Other Hispanic/Latino"), 26% Mexican, and 14% Cuban. More than half (63%) of whom had ever been screened for colorectal cancer. No variations in screening rates were observed across Hispanic/Latino subgroups. Stool-based tests were more commonly used for screening compared to exam-based tests (60% vs. 49%). After adjusting for confounding, masculinity barriers reduced the odds of the screening participation. Differences were observed by Hispanic/Latino subgroup for a few MBMC scale items. Specifically, Cuban men were most likely to report trust in healthcare professionals, but least likely to report receiving quality medical care. Latino men of other Hispanic ethnicity were more likely to report taking risks with their own health if it benefits their family. Among Puerto Rican men, higher scores on the restrictive emotionality subscale were associated with a lower likelihood of screening participation. Conversely, higher scores on the health-related self-reliance subscale were associated with a greater likelihood of screening participation among men of other Hispanic/Latino ethnicity.
Conclusion: Differences in colorectal cancer screening participation by Hispanic/Latino ethnicity were not observed, suggesting barriers to screening may be similar among subgroups. Masculinity barriers to colorectal cancer screening may exist among Latino men, particularly among Puerto Rican men. Intervening on these masculinity-related barriers masculinity may improve colorectal cancer screening uptake among Latino men.

#0797 Area deprivation, rurality, healthcare utilization, quality of life, and health status among cancer patients.

H. Lee[1], D. Lee[1], D. Ng[2], D. Wiese[1], A. Jemal[1], F. Islami[1];

[1]American Cancer Society, Atlanta, GA, [2]University of California Irvine, Irvine, CA

Background: Living in deprived or rural neighborhoods can negatively influence individual health through various mechanisms, including limited access to care due to scarce resources, medical facilities, or health professionals. Prior ecological studies have shown an association between living in rural or disadvantaged areas and higher cancer morbidity or mortality, but research on the association between neighborhood of residence and cancer patients' healthcare utilization, health status, or quality of life has been limited.

Method: We used survey and electronic health records data on cancer patients aged ≥18 years (N=16,606) from All of US Controlled Tier Dataset v7 (summer 2017-July 1, 2022). Area deprivation index (ADI) was based on six items, including 3-digit zip code-level median household income, proportions of high school graduation, vacant housing, recipients of public assistance income, and individual without health insurance or with incomes below the poverty level. Rural-urban status was defined at the 3-digit zip code-level as urban (100% urban), mostly urban (≥50%-<100% urban), and rural (>50% rural). Logistic regression models were used to estimate the association between ADI or rurality and health care utilization (general doctor, specialist, mental health, or nurse practitioner/physical assistant [NP/PA] visits) or health outcome (fair/poor physical and mental health status, quality of life), controlling for various covariates.

Results: Cancer patients living in the most deprived areas (ADI 5th quintile) were less likely to have general doctor visits (OR=0.73; 95% CI=0.54-0.85), NA/PA visits (OR=0.87; 95% CI=0.77-0.99), or mental health professional visits (OR=0.85; 95% CI=0.74-0.98), and more likely to have fair or poor quality of life (OR=1.31; 95% CI=1.06-1.62), compared to those living in the least deprived areas (ADI 1st quintile), controlling for all covariates. Similarly, rural cancer patients were less likely to have general doctor visits (OR=0.58; 95% CI=0.42-0.79) or mental health professional visits (OR=0.53; 95% CI=0.41-0.67), and more likely to have fair/poor physical health (OR=1.27; 95% CI=1.03-1.57), compared with urban cancer patients. However, rural cancer patients were more likely to have NA/PA visits (OR=1.29; 95% CI=1.04-1.58) and less likely to have fair/poor mental health (OR=0.66; 95% CI=0.48-0.92). Cancer patients in mostly urban areas showed similar patterns to those in rural areas but the magnitudes of associations were smaller.

Conclusions: In this study, cancer patients living in deprived or rural areas were less likely to have general doctor or mental health professional visits and more likely to have poor physical health compared to patients in the least deprived or urban area. Community-level interventions in deprived or rural areas are required to mitigate disparities in healthcare and health among cancer patients.

#0798 Increasing breast cancer incidence across generation status in Mexican American women: The Multiethnic Cohort.

X. Zhang[1], I. Cheng[2], A. Paik[1], B. Huang[1], **V. W. Setiawan**[1];
[1]University of Southern California, Los Angeles, CA, [2]UCSF, San Francisco, CA

Background: Breast cancer (BC) is the most commonly diagnosed cancer among Latino women in the US. Compared to foreign-born Latino women, US-born Latino women have a higher incidence of BC. While prior studies have suggested this difference in incidence may be explained by risk factors such as unhealthy lifestyle behaviors, reproductive history, and neighborhood socioeconomic status, it is unclear how the risk of BC has changed over generations among Latinos women. In this study, we investigated the association between generational status and BC incidence among Mexican American women within the Multiethnic Cohort (MEC).

Methods: The study population included 15,303 self-reported Mexican Americans from the MEC. Generational status was categorized as: 1st generation (Mexico-born, n = 6,347), 2nd generation (US-born with one or two parents born in Mexico, n = 6,390), or 3rd generation (US-born with both parents born in the US, n = 2,566). Multivariable Cox models were used to calculate the hazard ratios (HR) and 95% confidence intervals (CI) of BC incidence by generational status. All models were adjusted for relevant risk factors including age, physical activity, smoking, alcohol intake, education, body mass index, diet, family history of BC, menopausal status, age at menarche, parity, mammography history, hormone use, neighborhood socioeconomic status, and Hispanic ethnic enclave.

Results: During an average 21.5-year follow-up, 815 incident BC cases were identified. The age-adjusted incidence rate (per 100,000) of BC increased by generation (1st: 191.9; 2nd: 265.3; 3rd: 284.0). Third (70.4%) and 2nd (66.5%) generations had a larger proportion of localized disease at diagnosis compared to 1st generation women (59.7%). Compared to 1st generation Mexican Americans, 2nd (HR = 1.24; 95% CI: 1.03-1.49) and 3rd generation (HR = 1.28; 95% CI: 1.02-1.60) had elevated risks of BC (p-trend: 0.02) The positive association with generational status remained significant when restricting to women who reported mammogram use (HR 2nd vs. 1st = 1.27, 95% CI: 1.04-1.55; HR 3rd vs. 1st = 1.34, 95% CI: 1.06-1.70) (p-trend: 0.01).

Conclusions: Our findings suggest that generational status among Mexican American women is associated with risk of BC, after adjusting for sociodemographic, lifestyle, neighborhood, and reproductive risk factors. Further studies are warranted to discover the potential factors that contribute to this increased risk and elucidate the underlying etiology.

#0799 Area-level socioeconomic deprivation is associated with inadequate access to quality preoperative care and increased readmission after surgery for early-stage lung cancer.

S. Tohmasi[1], D. B. Eaton, Jr.[2], B. T. Heiden[1], N. E. Rossetti[1], M. W. Schoen[3], S.-H. Chang[1], Y. Yan[1], M. R. Patel[2], B. F. Meyers[1], B. D. Kozower[1], V. Puri[1]; [1]Washington University in St. Louis School of Medicine, St. Louis, MO, [2]Veterans Affairs St. Louis Health Care System, St. Louis, MO, [3]Saint Louis University School of Medicine, St. Louis, MO

Objective: Socioeconomic deprivation (SED) has been associated with higher lung cancer risk and mortality. However, the effects of SED on lung cancer outcomes in an integrated, single-payer healthcare system, such as the Veterans Health Administration (VHA), remains unknown. We sought to examine the impact of area-level SED on access to care and outcomes in veterans with early-stage non-small cell lung cancer (NSCLC).
Methods: We conducted a retrospective cohort study of patients with clinical stage I NSCLC receiving definitive surgical treatment in the VHA from 2006-2016. Patients were assigned an area deprivation index (ADI) score, a ZIP code-level measure of SED incorporating multiple poverty, education, housing, and employment indicators from the United States Census. Using multivariable analysis, we evaluated the relationship between ADI and guideline-concordant quality metrics (QMs) that stage I NSCLC patients should routinely meet in the preoperative (positron emission tomography [PET] imaging, smoking cessation support [SCS], pulmonary function testing [PFT], and timely surgery) and postoperative (cancer surveillance imaging, SCS, and appropriate oncology referral) periods. We also assessed the association between ADI and various cancer-specific outcomes including overall survival (OS).
Results: The study included 9,704 patients. High ADI was associated with lower likelihood of receiving PET imaging (ADI ≥76 vs. ≤50: adjusted odds ratio [aOR] 0.592, 95% CI 0.502-0.698) and PFT (ADI ≥76 vs. ≤50: aOR 0.816, 95% CI 0.694-0.959) before surgery. High ADI was also associated with delayed surgery (>12 weeks after diagnosis; ADI ≥76 vs. ≤50: aOR 1.202, 95% CI 1.058-1.366). ADI was associated with 30-day readmission after surgery (ADI ≥76 vs. ≤50: aOR 1.380, 95% CI 1.103-1.726) but not with 30-day mortality (ADI ≥76 vs. ≤50: aOR 1.221, 95% CI 0.816-1.826), major complications (ADI ≥76 vs. ≤50: aOR 0.927, 95% CI 0.780-1.101), prolonged hospital length of stay (≥14 days; ADI ≥76 vs. ≤50: aOR 0.893, 95% CI 0.755-1.056), or 90-day mortality (ADI ≥76 vs. ≤50: aOR 0.876, 95% CI 0.645-1.190). ADI was not associated with adherence to postoperative QMs (ADI ≥76 vs. ≤50: aOR 0.888, 95% CI 0.764-1.032), OS (ADI ≥76 vs. ≤50: aHR 0.984, 95% CI 0.911-1.062), or cumulative incidence of cancer recurrence (ADI ≥76 vs. ≤50: aHR 1.047, 95% CI 0.930-1.179).
Conclusions: Area-level SED is associated with inadequate adherence to preoperative QMs and increased readmission after surgery for stage I NSCLC. Our data suggests that veterans with high SED experience inadequate access to quality preoperative care for early-stage NSCLC but do not have inferior long-term outcomes after resection. Future VHA policies should focus on providing more equitable guideline-concordant preoperative care and preventing postoperative readmission for stage I NSCLC.

#0800 Spatial accessibility of gynecologic oncologists and time to surgery in a diverse cohort of women with ovarian cancer in Northern California.

E. Chirikova[1], P. P. Inamdar[1], V. McGuire[1], S. Shariff-Marco[1], V. S. Lee[2], L. J. Collin[3], C. T. Sanchez-Diaz[4], J. Kavecansky[5], C. B. Powell[1], J. A. Doherty[3], L. H. Kushi[2], E. V. Bandera[4], S. L. Gomez[1];

[1]UCSF - University of California San Francisco, San Francisco, CA, [2]Kaiser Permanente Northern California, Oakland, CA, [3]University of Utah, Salt Lake City, UT, [4]Rutgers Cancer Institute, New Brunswick, NJ, [5]Kaiser Permanente Northern California, Antioch, CA

Introduction: To expand our understanding of factors contributing to racial and ethnic disparities in ovarian cancer outcomes, we examined the association between spatial accessibility of gynecologic oncologists and time from cancer diagnosis to surgery in the KPROCS Study, a diverse cohort of women diagnosed with ovarian cancer between 2000-2018 at Kaiser Permanente Northern California (KPNC). Spatial medical accessibility is a component of healthcare access that captures the proximity and availability of healthcare resources in the area.

Methods: Ovarian cancer cases were identified through the KPNC Cancer Registry. Demographic and clinical information was extracted from KPNC databases. Neighborhood characteristics from the California Neighborhoods Data System were linked to the residential addresses of cases at the time of diagnosis. Spatial medical accessibility was measured using the 2-step floating catchment area method based on the location of the infusion centers where KPNC gynecologic oncologists practice and the residence location of cohort members. We used generalized estimating equations with independent correlation structure and robust standard errors to examine the association between spatial accessibility of gynecologic oncologists and time to ovarian cancer surgery, adjusting for year and age at diagnosis, stage, histotype, race, ethnicity, neighborhood socioeconomic status (nSES), and receipt of neoadjuvant chemotherapy.

Results: The cohort comprised 4,910 women with ovarian cancer, of whom 3,304 had surgery at KPNC. Of this group, 13% were Hispanic, 14% were non-Hispanic (NH) Asian American women, 5% NH Black women, and 67% NH White women. The proportion of women residing in areas of the lowest spatial accessibility of gynecologic oncologists was highest among NH White women (26%) and women residing in the highest quintile of nSES (29%). The median time from diagnosis to surgery was 4 days (interquartile range 22 days). In adjusted analyses, not including the information on spatial accessibility, the time from diagnosis to surgery was 5.1 days longer (95% CI 1.5, 8.7) for NH Black women than NH White women. After adding information on spatial accessibility, this time did not considerably change, resulting in a 5.3-day (95% CI 1.7, 8.9) difference. In this model, the lowest quintile of spatial accessibility of gynecologic oncologists was associated with a longer time from diagnosis to surgery, but this association was not statistically significant (0.4 days difference, 95% CI -1.3, 2.0).

Summary: In our preliminary analyses, spatial accessibility of gynecologic oncologists was not found to be a contributing factor to the disparity in time from diagnosis to surgery between NH Black and NH White women. Further analyses will examine time from diagnosis to chemotherapy overall and stratified by racial and ethnic groups.

#0801 Severe housing cost burden and premature cancer mortality by state Medicaid expansion status.

W. R. Lawrence[1], N. D. Freedman[1], J. K. McGee-Avila[1], L. Mason[1], Y. Chen[1], A. P. Ewing[2], M. S. Shiels[1];
[1]National Cancer Institute, Bethesda, MD, [2]The Ohio State University, Columbus, MS

Introduction: The fraction of people living in unaffordable housing in the U.S. has grown, and prior studies have documented a relationship between housing cost burden and worsening health. Medicaid expansion has been suggested to improve housing financial stability by reducing health care costs and improving access to preventative care. However, the role of expanded access to Medicaid on the relationship between housing cost burden and cancer mortality remains poorly understood. We investigated the relationship between county-level severe housing cost burden and premature cancer mortality by state Medicaid expansion status for all cancers and leading sites.
Methods: This ecological study used county-level data from 2016-2020 American Community Survey linked with county-level mortality data. Severe housing cost burden measured by percentage of households within a county that spend ≥50% of their income on housing categorized into quintiles (1=lowest, 5=highest) and state Medicaid expansion status (expanded and non-expanded). Age-adjusted cancer mortality rates and adjusted-mortality rate ratio (aRR) were estimated by sex.
Results: Across quintiles of county-level severe housing cost burden, age-adjusted cancer mortality rates were largely greater in non-Medicaid expanded states than Medicaid expanded states among women and men. Among counties in the lowest quintile of severe housing cost burden, rates for overall cancer mortality in women were 9% (aRR=1.09; 95%CI 1.05-1.14) higher in non-Medicaid expanded states compared with expanded states. Additionally, among the third quintile of severe housing cost burden, colorectal cancer mortality rate was 8% higher (aRR=1.08; 95%CI 1.02-1.14) in non-Medicaid expanded states. Among men in the lowest quintile of severe housing cost burden, overall cancer mortality rates were 5% (aRR=1.05; 95%CI 1.02-1.09) higher in non-Medicaid expanded states than Medicaid expanded states. Further, among men in counties in the highest quintile of severe housing cost burden, colorectal cancer mortality rate was 8% higher (aRR=1.08; 95%CI 1.05-1.12) and lung cancer mortality was 13% higher (aRR=1.13; 95%CI 1.10-1.15) in non-Medicaid expanded states compared with expanded states.
Conclusions: Counties with a lower fraction of households experiencing severe housing cost burden had greater premature cancer death rates within non-Medicaid expanded states than Medicaid expanded states. However, among men rates were also elevated in non-Medicaid expanded states in counties with the greatest severe housing cost burden.

#0802 Molecular profile of gastric cancer in Hispanics living in Puerto Rico.

I. Montes-Rodriguez, H. Centeno-Girona, N. Rivera, M. Cruz-Correa;
University of Puerto Rico Comprehensive Cancer Center, San Juan, PR

Gastric cancer (GC) is the 4th leading cause of cancer death globally. The incidence and mortality rates of GC differ dramatically between racial/ethnic groupings. In the United States (U.S.), Hispanics, non-Hispanic Blacks, and Asian or Pacific Islanders are more likely to be diagnosed with GC and have a higher mortality rate than non-Hispanic Whites. Among the Hispanic population living in Puerto Rico (PRH), GC ranks among the top ten leading causes of cancer death, whereas this malignancy is not a major cause of cancer mortality in the mainland U.S. Tumor profiling approaches have resulted in the discovery of actionable gene alterations, which serve as a guide for treatment strategies and ultimately enhance the overall survival rates of individuals diagnosed with cancer. However, descriptive information regarding the genetic mutational landscape of GC tumors from PRH is limited. This study aims to describe the genomic profile of GC tumors in PRH and to identify the most prevalent genetic mutations. We retrospectively examined GC tumor mutational profiles from 106 PRH that underwent NGS testing from 2015 to 2022 (provided by CARIS Life Sciences and the Precision Oncology Alliance). We compared PRH GC tumor somatic mutation prevalence to TCGA and the AACR Project Genomics Evidence Neoplasia Information Exchange (GENIE), both available through the cBioPortal for Cancer Genomics. Descriptive statistics were performed to characterize the database. Among the top mutated genes for GC tumors in PRH were *TP53* (54.1%, n=85), *ARID1A* (34.2%, n=73), *KMT2D* (30.5%, n=82), *CDH1* (29.4%, n=85) and *ZFHX3* (27.3%, n=55). The most frequent gene amplifications were *ERBB2* (7.1%, n=84), *KRAS* (6.0%, n=84), and *CCNE1* (4.9%, n=81). Compared to other datasets, PRH had significantly different mutational frequencies of GC driver genes like *TP53, ARID1A, CDH1*, and *KMT2D*. This study is the first to report PRH GC tumor mutational profiles and compare the mutational frequencies to other non-Hispanic and U.S. mainland Hispanic populations using TCGA and GENIE data sets. Furthermore, our study provides data on the specific mutational landscape for Hispanics with GC and the implications on therapeutic options and clinical outcomes. Developing new treatments for genomically diverse populations requires understanding the most common carcinogenic molecular pathways that affect Hispanics with GC.

#0803 Disparities unveiled: A comprehensive analysis of evolving trends in lung cancer risk factors in the ten most populous countries.

C. T. Jani[1], S. A. Kareff[1], H. Singh[2], A. Salazar Zetina[1], G. Lopes[1];
[1]University of Miami Miller School of Medicine, Miami, FL, [2]Medical College of Wisconsin, Milwaukee, WA

Introduction: Evolving Lung cancer (LC) trends necessitate a continual reassessment of associated risk factors.
Methods: We utilized the Global Burden of Disease database to extract Age-Standardized Mortality Rates (ASMR) and risk factor-associated ASMR for Tracheal, Bronchial, and Lung cancer (TBLC) from 1990-2019. The aim was to analyze overall trends along with two pivotal LC risk factors associated trends—tobacco use and air pollution—across ten most populous nations as of 2023 population census. Joinpoint analysis was employed to analyze trends.
Results: Globally, TBLC mortality has decreased by 8%, with reductions observed in both tobacco and air pollution-associated mortality. Despite a decrease in male mortality (-17%) and increase in female mortality (+15%), males have exhibited higher mortality for past three decades with M:F ratio of 2.5 in 2019. Similarly, male mortality was higher across all countries. Globally, although tobacco and air pollution-associated mortality has decreased for males and increased for females, both risk factors are linked to significantly higher mortality in males, with M:F ratios of 4.4 and 2.6 for tobacco and air pollution, respectively, in 2019. For tobacco-associated ASMR, China and Indonesia have shown an increase, while China, India, Pakistan, and Nigeria have shown an increase for Air pollution-associated ASMR. On evaluating proportional ASMR, tobacco and air pollution have overall shown a reduction, indicating an increase in other or non-risk factor-related mortality.
Conclusion: The fluctuating trends in tobacco-associated and the concerning rise in air pollution-associated in specific countries underscore the complex interplay of societal and environmental factors in LC mortality. The decline in ASMR associated with established risk factors emphasizes the necessity for focused interventions to tackle the changing molecular characteristics of lung cancer and its associated risk factors.

Comparison of risk factor-associated Lung Cancer ASMR (1990 vs 2019)

Country(ASMR per 100,000 population)	1990 overall ASMR (N)	1990 Tobacco associated ASMR N (%)	1990 Air Pollution Associated N (%)	2019 overall ASMR(N)	2019 Tobacco associated ASMR N (%)	2019 Air Pollution Associated ASMR N (%)
Global	27.3	19.8 (72)	5.6 (20)	25.2	16.7 (66)	4.8 (19)
India	7.0	4.2 (60)	2.5 (35)	8.1	4.0 (50)	2.6 (33)
China	31.2	20.2 (65)	10.3 (33)	38.7	26.3 (68)	10.7 (28)
US	49.4	40 (81)	4.5 (9)	36.1	26.1 (72)	1.5 (4)
Indonesia	18.0	10.6 (59)	5.4 (30)	24.4	14.7 (60)	4.6 (19)
Pakistan	14.7	10.9 (74)	5.4 (36)	17.2	10.7 (63)	5.5 (32)
Nigeria	6.8	2 (29)	2.6 (38)	8.3	1.9 (23)	2.7 (32)
Brazil	18.0	13.9 (77)	3.2 (18)	15.8	9.7 (61)	1.5 (10)
Bangladesh	9.7	6.9 (71)	3.6 (37)	7.8	4.7 (59)	2.6 (33)
Russia	32.4	23.2 (72)	4.4 (13)	22.8	16.6 (73)	1.8 (8)
Mexico	15.1	9.6 (63)	3.4 (22)	9.7	4.4 (45)	1.5 (16)

#0804 Temporal trends and disparities by race and ethnicity in treatment of women diagnosed with advanced hormone receptor-positive breast cancer: A SEER-Medicare analysis.

K. Zhu[1], E. Bandera[2], F. Khosrow-Khavar[1];
[1]Rutgers Institute for Health, Healthcare Policy and Aging Research, New Brunswick, NJ, [2]Rutgers Cancer Institute of New Jersey, New Brunswick, NJ

Background: The clinical guidelines for management of advanced hormone receptor-positive (HR+) breast cancer (BC) have changed in the past decade with the addition of novel drug classes. We assessed temporal patterns of treatment initiation among women diagnosed with advanced HR+ BC and examined disparities in treatment initiation by race and ethnicity.
Methods: Women aged ≥65 years diagnosed with stage IV or metastatic HR+ BC between 2010-2019 were identified in SEER-Medicare. Poisson models were used to estimate age-adjusted annual incidence rates (IR) and 95% confidence intervals (CIs) for treatment initiation within 12 months of BC diagnosis independently by human epidermal growth factor receptor 2 (HER2) status. Age-adjusted incidence rate ratios (IRR) and 95% CIs were estimated to compare rates of initiation among non-Hispanic Black (NHB) and Hispanic patients with non-Hispanic White (NHW) patients.
Results: Among 3,476 eligible patients with a mean age of 76.7 (SD: 7.5) years at diagnosis, 79.6% were NHW, 9.5% were NHB, and 6.0% were Hispanic. Among 2,668 women with HR+/HER2- BC, most initiated on aromatase inhibitors (AIs) alone (56.7%), followed by AIs with palbociclib (12.6%). There was a temporal increase in rates of initiation of AIs with palbociclib (IR [95% CI] per 1000 person-years: 252.8 [240.8, 265.4] in 2015 and 343.9 [330.8, 357.7] in 2019. We did not observe significant differences in rates of initiation of AIs alone or with palbociclib by race and ethnicity. Among 537 HR+/HER2+ patients, 25.0% initiated on AIs alone, 24.6% on pertuzumab and trastuzumab with chemotherapy, 14.3% on trastuzumab with chemotherapy, and 9.1% on AIs and trastuzumab with chemotherapy. IRs (95% CI) for initiation of pertuzumab and trastuzumab with chemotherapy increased from 175.6 (146.3, 210.9) in 2013 to 756.5 (698.3, 819.5) in 2019, while rates for trastuzumab with chemotherapy declined from 963.1 (809.4, 1146.0) in 2010 to 88.4 (72.6, 107.5) in 2019. Rates of initiation of AIs and trastuzumab with chemotherapy remained constant over time. Compared to NHW, NHB and Hispanic women were less likely to initiate pertuzumab and trastuzumab with chemotherapy (IRR [95% CI]: 0.52 [0.27, 1.00] and 0.54 [0.24, 1.23] respectively) and more likely to initiate AIs alone (IRR [95% CI]: 2.23 [1.39, 3.55] and 2.98 [1.69, 5.24] respectively).
Conclusions: We observed a temporal increase in the initiation of AIs with palbociclib among patients with advanced HR+/HER2- BC. Among patients with HR+/HER2+ BC, rates of initiating pertuzumab and trastuzumab with chemotherapy increased while rates of trastuzumab with chemotherapy declined. The observed differential management of NHB and Hispanic compared with NHW patients with HR+/HER2+ BC using pertuzumab and trastuzumab with chemotherapy and AIs alone requires further investigation.

#0805 Employment characteristics and work ability differences by race and income before undergoing curative treatment for prostate cancer (PCW WF-1802).

Joanne C. Sandberg[1], Emily V. Dressler[1], Louis S. Krane[2], Karen M. Winkfield[3], Lingyi Lu[1], Andrew M. Mayfield[1], Drew C. Monitto[4], J. Daniel Pennington[5], Deimante M. Tamkus[6], Glenn J. Lesser[1]

[1]Wake Forest University School of Medicine, Winston-Salem, NC,[2]Southeastern Louisiana Veterans Care Health System, New Orleans, LA,[3]Meharry-Vanderbilt Alliance, Nashville, TN,[4]Spartanburg Regional Healthcare System, Spartanburg, SC,[5]Virginia Urology, Richmond, VA,[6]John H. Stroger, Jr. Hospital of Cook County, Chicago, IL

Background: African American (AA) men are, on average, diagnosed with prostate cancer at younger ages and more advanced stages than white men and therefore may be at greater risk of having cancer treatment negatively impact their work ability and job opportunities. This longitudinal, observational study aims to better identify whether race, household income (< or ≥ 300% the U.S. poverty line), or work-related factors may place some men with prostate cancer at greater risk for experiencing negative employment impacts from cancer treatment and its side effects. Here we report on individual and employment-related factors by race and income prior to treatment initiation.

Methods: AA and white men who were expected to undergo primary curative treatment (prostatectomy or radiation therapy) in the near future for prostate cancer were recruited through the Wake Forest NCORP Research Base (UG1CA189824, NCT03963739) between 2019 and 2023. Participants were AA or white, recently employed, expecting to be working in 6 months, and willing to disclose income status. Participants answered questions prior to treatment initiation related to employment and working conditions, work ability, and demographic characteristics. Differences in outcomes by race and income were analyzed with Fisher's exact test or t-test.

Results: The baseline questionnaire was completed by 244 men; 48% AA/52% white and 64% higher/36% lower Income. Most planned treatments included radiation therapy (60%) and/or prostatectomy (41%), with no statistical differences by income or race. Higher income men were significantly more likely than lower income men to be married, have attained higher education, have a management or professional job, work full-time, be a permanent employee, salaried, eligible to retain their job under FMLA, work in an office/home, have a psychologically demanding job, and less likely to hold a physically demanding job. AA men were significantly less likely than white men to be married, have attained higher education, have a management or professional job, or work in an office/home. AA men were more continuously hopeful about the future (69%) compared to white men (52%; p=0.0079). There were no significant differences across categories in age, perceived current work ability in relation to physical (69% very good) or mental (71% very good) demands, or number of jobs held. Prior to treatment, participants reported almost optimal current work ability (mean 9.0, SD 1.2) with a range of 0 to 10 with 10 as best possible work ability.

Conclusion: In this study, income category is a greater predictor than race of job characteristics that may impact employment following definitive prostate cancer treatment.

#0806 Rural residence as a protective factor in melanoma mortality: Insights from a comprehensive analysis of 3,979 New Mexico cases (2010-2017).

Y. Park[1], A. Segura[2], L. Midani[1], B. Gutierrez[2], L. I. Rodriguez[3], C. Wiggins[2], V. S. Pankratz[2], J. R. Durkin[1];

[1]University of New Mexico School of Medicine, Albuquerque, NM, [2]University of New Mexico Hospital, Albuquerque, NM, [3]University of Miami Miller School of Medicine at Holy Cross Hospital, Miami, FL

Purpose

Cutaneous melanoma is a significant public health concern with increasing incidence rates over the past three decades. While survival rates have improved, disparities exist among racial/ethnic groups and socioeconomic factors. Our objective was to explore the connection between survival rates of cutaneous melanoma and demographic/socioeconomic factors in New Mexico's varied population, particularly in rural vs. urban settings.

Methods

This retrospective study utilized data from the New Mexico Tumor Registry (NMTR) within the National Cancer Institute's Surveillance, Epidemiology, and End Results (SEER) Program. A total of 3,979 cases of cutaneous melanoma diagnosed between 2010 and 2017 among New Mexico residents were analyzed based on specific ICDO-3 criteria. The impact of demographic characteristics, socioeconomic factors, and stage at diagnosis on melanoma-specific mortality was investigated. Cases with incomplete data or where melanoma was not the primary cancer were excluded. Survival differences were assessed using Kaplan-Meier methods and the Cox Proportional Hazards Model, with analyses conducted with a significance threshold set at P=0.05. Only histologically confirmed melanoma cases were included in the study.

Results

In our analysis of 3,979 melanoma cases spanning 2010 to 2017, non-Hispanic whites (NHW) displayed the highest incidence (n = 3,617, $P < 0.001$). Conversely, Hispanic Whites (HW) and American Indians (AI) exhibited a higher likelihood of later-stage diagnoses, with 19.2% of American Indians diagnosed at stage 3, in contrast to 3.9% of NHW and 10.3% of Hispanic Whites ($P < 0.001$). Rural areas showed a propensity for advanced-stage diagnoses ($P < 0.001$), and diagnosis stage exhibited an inverse relationship with per capita income ($P < 0.001$). Increased mortality was observed among males, individuals over 50, and American Indians (all $P <0.05$). Rural American Indian or Hispanic patients had a hazard ratio of mortality at 0.37 (95% CI, 0.15-0.89). An overall decline in melanoma mortality post-2012, with a notable reduction after mid-2015 ($P < 0.001$), despite a slight increase in diagnoses from 529 in 2010 to 569 in 2017 ($P = 0.034$) was observed. Sensitivity analyses revealed that rural residence among AI/Hispanic individuals was associated with a lower risk of melanoma-specific mortality (HR 0.37, $p = 0.026$ in the inclusive analysis; HR 0.36, $p = 0.025$ in the exclusion of in-situ cases).

Conclusions

Our study indicates rural residency is associated with more advanced melanoma diagnoses and lower income correlates with later-stage diagnoses. However, rural living may offer a protective effect against mortality for American Indian/Hispanic populations. Overall mortality has declined since 2012, contrasting with a slight rise in diagnoses.

#0807 An ethno-phenomenology based approach to study breast cancer disparity in rural India.

D. Dutta[1], R. Das[2], C. Das[3], T. Sarma[3], S. Das[4], A. Dutta[1], T. Baishya[3], L. Pathak[1], **B. Das**[3];
[1]KaviKrishna Laboratory, Research park, Indian Institute of Technology, Guwahati, India, [2]KaviKrishna center of Indian Knowledge System, Sualkuchi, India, [3]KaviKrishna Telemedicine Care, Sualkuchi, India, [4]Thoreau Laboratory for Global Health, Lowell, MA

There are fundamental lack of right methodologies to study the breast cancer disparity in rural India. Here, we have used an ethnographic-phenomenology approach to study the disparity in breast cancer care in Assam by using retrospective database of a rural cancer care non-profit clinic, the KaviKrishna Telemedicine Care (KTC), set up 1994 to develop a CBPR based cancer care (Abstract 3342, AACR 2019). Methodology: For one and half years, the doctors, researchers, nurses, caregivers, and physician assistants of KaviKrishna Laboratory and KaviKrishna Telemedicine Care were interviewed (total number: 15), and plus literature of the lab and the clinic were studied. Then, the breast cancer patients (n=10) and the families were subjected to ethnographies-phenomenology study to find their experiences of treatment and suffering. Next, thematic analysis and grounded theory were applied to come up with novel approaches to reduce breast cancer disparity. For comparison, 5 patients from rich urban families were interviewed. Results: We found that 10/10 patients found it extremely difficult to navigate the complexity of care in urban hospitals, but found the KTC approachable and comfortable. Importantly, these 10 breast cancer patients were positively responding to our KTC based care services/focussed group discussion (https://zenodo.org/records/8062404). They revealed positive experiences in emotionally and psychologically dealing with diagnostic, surgery, and chemotherapy processes. Next, our analysis of the last 25 years of the care data at KTC showed that in rural population, the loweconomic status, inadequate access to breast cancer detection clinics, lack of awareness,indecisive treatment protocols and social stigma are the main reasons for breast cancer disparity. Grounded theory-based analysis indicates that cancer biomarker study in rural populations can be a suitable method for early detection. Whole genome sequencing of cancer tissue frombiopsy samples shall provide landscape of mutation in the entire coding as well as noncodingregions. Mutation profiling along with correlation studies from patients can lead to discoveryof novel marker(s). Primary health care clinics in rural areas can be trained to collect patientsamples, isolate genomic DNA and perform PCR for the markers (a similar model asfollowed during Covid-19). The PCR samples can be sent to non-profit advanced diagnostic center such as KaviKrishna Lab to perform sequencing to study mutation markers. The method is also cost effective to both thecare givers and the patients as compared to setting up advanced diagnostic lab in every part ofrural area. Conclusion: The community based participatory research based model developed by KTC can be an effective strategy to reduce breast cancer disparity in the rural population since the primary health clinics shall act as a bridge between geologically isolated areas and modern technology.

#0808 iCCaRE engagement of faith-based organizations to co-create and co-disseminate infographics addressing disparities in prostate cancer literacy and clinical and biospecimen studies.

J. C. Morrison[1], K. T. Ashing[1], G. Song[1], T. J. Bonner[2], C. Ngufor[2], G. Dagne[3], A. Merriweather[4], J. McCall[5], E. Cobran[6], C. N. Moore,[7], F. Bedell[8], R. Oladapo[9], F. B. Willis[10], R. Chidebe[9], N. A. Stephenson,[11], J. S. Oliver[12], V. Gordon[10], F. Odedina[11];

[1]City of Hope National Medical Center, Duarte, CA, [2]Mayo Clinic, Rochester, MN, [3]University of South Florida, Tampa, FL, [4]American Legion Post 197, Jacksonville, FL, [5]iCCaRE Consortium Community PI, Bethel Baptist Church, CA, Duarte, CA, [6]Mayo Clinic, Phoenix, AZ, CA, [7]Mayo Clinic, Phoenix, AZ, [8]City of Hope National Medical Center, Lancaster, CA, [9]Covenant University, Nigeria, Nigeria, [10]Mayo Clinic, Jacksonville, CA, [11]Mayo Clinic, Jacksonville, FL, [12]University of Alabama, Tuscaloosa, AL

Black men hold the highest prostate cancer burden among all ethnicities; thus, there is an urgent need for research to inform the development and implementation of a culturally tailored intervention to reduce disparities and improve outcomes. In response, the Inclusive Cancer Care Research Equity (iCCaRE) Consortium was created to advance health equity and reduce disparities in prostate cancer. Addressing the unique needs of Black men require a genuine bidirectional relationship between scientist and the community. In the Black community, faith-based organizations are respected institutions advocating for health equity and justice. Given their vital role as community health gatekeepers, the iCCaRE Consortium partners with faith-based organizations. Rooted in community engaged research (CER), we conducted an environmental scan through stakeholder meetings to discuss the prevailing challenges and opportunities to meet the needs of the Black community along the prostate cancer care continuum. iCCaRE investigators including Partnership Engagement Services (PES) core partnered with faith-based organizations to ensure and advance community responsive cancer prevention. Together, with our faith-based leaders (N=18), we identified gaps including issues associated with the care continuum from screening to diagnosis and from treatment to survivorship; disparities according to health coverage and social determinants of health, and best practices to assist patients including care coordination, patient navigation, digital innovations, and programs offered by patient advocacy organizations. In response to the needs of the community and the strengths of faith-based organization, we prioritized our initial focus on increasing community prostate cancer literacy and activation using co-design educational infographics for both traditional and technology-based communication platforms. The infographics provided evidence-based facts about prostate cancer burden in the Black community; and using a call to action approach, we emphasized the importance of taking action for life saving screening, prevention and healthy lifestyle. Taking action in prostate cancer symptom recognition, survivorship care, and quality care. Also, co-designed infographics were created for clinical studies and biospecimen awareness and participation and the importance of advocacy and equitable care. Another component incorporated face to face trainings and presentations to enhance their knowledge of cancer screening tools, epidemiology of prostate cancer, and pathways to care. This presentation highlighted the first step towards community based intervention development, implementation and dissemination towards equity and justice for prostate cancer prevention and patient/survivor improvements for Black men.

#0809 Neighborhood disadvantage and prostate tumor aggressiveness among African American and European American men.

J. Boyle[1], J. Yau[2], J. L. Slade[3], D. A. Butts[4], J. Wimbush[5], J. Y. Park[6], A. Hussain[2], E. Onukwugha[7], C. L. Knott[8], D. C. Wheeler[1], K. H. Barry[2]; [1]Virginia Commonwealth University, Richmond, VA, [2]University of Maryland School of Medicine, Baltimore, MD, [3]Maryland Community Health Engagement Partnership, Upper Marlboro, MD, [4]Prostate Cancer Awareness Alliance of DC, MD, and VA, New York, NY, [5]University of Maryland Greenebaum Comprehensive Cancer Center Tumor Registry, Baltimore, MD, [6]H. Lee Moffitt Cancer Center, Tampa, FL, [7]University of Maryland School of Pharmacy, Baltimore, MD, [8]University of Maryland, College Park, College Park, MD

Introduction: African American (AA) men experience greater prostate cancer (PC) incidence and mortality compared to European American (EA) men, but the reasons are not fully understood. Some literature has identified connections between neighborhood disadvantage and aggressive PC, and AA men may be more likely to experience these factors than EA men. However, it is unclear if these associations may vary by race. We tested associations of two neighborhood disadvantage measures (neighborhood socioeconomic deprivation and racial segregation) with prostate tumor aggressiveness, overall and separately by race. We hypothesized that they would be positively associated and that associations would be stronger among AA men.
Methods: We leveraged data from the University of Maryland Greenebaum Comprehensive Cancer Center Tumor Registry for AA and EA men who were diagnosed with PC from 2004-2021. We geocoded participants' addresses at diagnosis to determine census tract-based Area Deprivation Index (ADI) and Racial Isolation Index (RI) values. ADI analyses included men diagnosed in 2005 or later (778 AA men and 687 EA men), and RI analyses included men diagnosed in 2009 or later (606 AA men and 454 EA men) based on data availability. We used logistic regression to model the odds of aggressive PC, defined as a Gleason pattern of 4+3 or a total Gleason score >=8, overall and by race. We fit models with scaled ADI or RI as the exposure variable, adjusting for race, age at diagnosis, and year of diagnosis. We also assessed an interaction between each neighborhood measure and race.
Results: Median (interquartile range) ADI scores were 118 (101-137) for AA men and 92 (83-102) for EA men, and RI scores were 0.68 (0.35-0.87) for AA men and 0.11 (0.06-0.20) for EA men, indicating greater neighborhood deprivation and AA residential segregation among AA participants. The greatest values for these scores were concentrated in central and west Baltimore. A one-standard deviation (SD) increase in ADI was associated with significantly greater odds of aggressive tumors for AA men (OR=1.28, 95% CI: 1.10, 1.49; p<0.01), but not for EA men (OR=0.85, 95% CI: 0.67, 1.08; p=0.19), and the p-value for interaction (p<0.01) was statistically significant. Similarly, a one-SD increase in RI was significantly associated with aggressive tumors for AA men (OR=1.24, 95% CI: 1.03, 1.49; p=0.03), but not for EA men (OR=1.23, 95% CI: 0.84, 1.80; p=0.29), although the p-value for interaction was not statistically significant.
Conclusions: Neighborhood disadvantage was significantly associated with higher odds of aggressive PC. The association of neighborhood deprivation and tumor aggressiveness was stronger among AA men. Additional analyses will consider other measures, including historical redlining, to further evaluate the relationship of neighborhood disadvantage with prostate tumor aggressiveness.

#0810 Assessing human papillomavirus (HPV) awareness and intentions to participate in HPV vaccination and clinical trials (CT) among Latinos/as in Los Angeles (LA) County: A multicomponent intervention.

Alejandra Ramos, Carolina Aristizabal, **Lourdes A. Baezconde-Garbanati**

Keck School of Medicine of USC, Los Angeles, CA

Background: The incidence of HPV-related cancers continues to disproportionately affect women and men of Latino origin. In LA, a total of 20,868 individuals have been diagnosed with HPV-related cancers from 2009 to 2019. HPV infection knowledge and interpersonal barriers contribute to HPV vaccine delay and refusal. Similarly, Latinos/as continue to also have low participation in clinical trials research. To address the low knowledge, attitudes, and intentions towards HPV vaccination and participation in clinical trials (CT), we have adopted the NCI National Outreach Network framework and have used community health educators to deliver bilingual-culturally appropriate workshops on HPV and CT.
Methods: Individuals, 18 and over and parents with eligible age children (in respect to the HPV initiative) were recruited through community outreach and local community partnerships to participate in the bilingual (English and Spanish) health education workshops. A baseline assessment was administered before each educational workshop and a follow-up assessment was administered after to evaluate change in HPV and CT knowledge, intentions to vaccinate, and likelihood to participate in CT. Descriptive statistics were calculated to assess distribution of demographic variables of interest and a paired T-test was used to explore matched pre-post differences in knowledge scores and intentions.
Results: 290 (HPV) 272 (CT) individuals participated in the workshops. The mean age of participants was 41.13yrs with a (SD=11.63). More than half of participants were women 453 (81.7%), men 94 (16.9%) and other 7 (1.26%). Comparing HPV knowledge scores of matched pre-and post-surveys, showed that for baseline (n=182) (M=72.9%, SD=13.3) was statistically different from post-scores (n=182) (M=81%, SD=9.85) where $p<0.05$. Intentions were measured using a Likert scale, baseline (M=4.1), agree to get HPV vaccine, post (M=4.5) strongly agree to get HPV vaccine. In respect to CT baseline knowledge (n=174) (M=75.3%, SD=0.15), following a Likert scale response of (M=3.4), unsure to join a clinic trial. In assessing post-CT scores (N=174) (M=78%, SD:0.14), mean scores were significant where $p<0.05$ and an increase to (M=3.7) agree to join a clinical trial. After workshops attendance, not only was knowledge increased, but intentions to vaccinate against HPV and to participate in a clinical trial was strengthen.
Conclusions: Strengthening community-based education and providing the necessary tools, can help reframe misconceptions about HPV and HPV vaccination and promote willingness to vaccinate and participate in clinical trials.

#0811 Impact of Medicaid eligibility expansion to adults regardless of immigration status on health insurance access among Latina patients.

N. Huguet[1], J. Kaufmann[1], H. Holderness[1], M. Vieira[1], G. Mertes[2], J. Shannon[1], J. Heintzman[1];
[1]OHSU, Portland, OR, [2]OCHIN, Portland, OR

Background: Disparities in the receipt of cancer screening and preventive services are strongly associated with health insurance status. Even after federal- and state-wide initiatives to boost access to health insurance such as the Patient Protection and Affordable Care Act (ACA) Medicaid Expansion to all individuals earning ≤138% of the federal poverty level (FPL) and nationwide individual health insurance marketplaces, Latino populations continue to have the highest uninsured rate of any racial or ethnic group in the US, with 17% of Latinos remaining uninsured compared to 5% of non-Hispanic white peers. In 2021, California and Oregon states amended their respective Medicaid program to expand eligibility to adults regardless of immigration status; which could reduce access disparities for patients from Latino communities. This study shows preliminary results of changes in health insurance status among Latina patients (who have multiple cancer prevention services recommended in middle age) receiving care in community health centers.
Methods: A retrospective cohort study of Latina, non-Hispanic Black, and non-Hispanic white women ages 50-64 years receiving primary care from 382 community health clinics in California and Oregon. Using 2018, 2019, 2021, and 2022 electronic health record data, we estimated monthly rates of insured-type visits per 100 visits. We compared rates pre- and post-Medicaid eligibility expansion, both within and between race and ethnicity groups. Reported estimates were derived from generalized estimating equations Poisson regression, clustered on clinic, and adjusted for clinic-level demographics.
Results: Of 41,960 patients, over half (53%) were Latina, most of whom (83%) preferred Spanish language communication. Latina patients had more uninsured visits pre-Medicaid eligibility expansion than did non-Hispanic Black and white patients (Rate: 27% versus 5% and 4%, respectively). All racial and ethnic groups experienced a decrease in uninsured visit rates, and this change was similar for all groups [Difference-in-difference Latina versus Black patients: 0.77 (95% CI 0.55, 10.7) and versus white patients: 1.02 (95% CI 0.89, 1.17)]. Overall rates of Medicaid-insured visits increased only for Latina patients [pre-to-post Relative Rate=1.06 (95% CI: 1.03-1.10)]. Both non-Hispanic Black and white patients experienced a drop in Medicaid-insured visits. Only Black patients experienced a significant decline in private-insured visits [pre-to-post RR=0.79 (95% CI: 0.70-0.89)].
Conclusion: These early results suggest an uptake of Medicaid-paid visits among Latina patients. This increase in healthcare coverage for Latina patients could significantly reduce disparities in access to primary care and especially in cancer preventive care.

#0812 Association of obesity with the early onset and diagnosis of triple negative breast cancer in black women.

S. Sudan[1], A. Sharma[1], K. Vikramdeo[1], W. Davis[2], C. Nelson[1], K. Singh[3], A. Singh[1], S. Singh[1];
[1]USA Health Mitchell Cancer Institute, Mobile, AL, [2]University of South Alabama, Mobile, AL, [3]University of Texas Tyler, Mobile, AL

Breast cancer (BC) continues to be the most common cancer and the second leading cause of cancer-related death in American women. Furthermore, it affects Black women more adversely than their White counterparts, who experience an early disease onset, diagnosed more often with aggressive triple-negative breast cancer (TNBC) molecular subtype, and face greater mortality. The reasons for these disparities; however, are largely unknown. Here, using a retrospective dataset, we examined the association of body mass index (BMI) with BC early onset and diagnosis with specific molecular subtype in race-based distributions. Study cohort included 1085 BC patients, who visited University of South Alabama Health clinics between October, 2017 and March, 2022. Patients were divided into three BMI [(normal weight, NW (<24.9), overweight, OW (25-29.9), and obese, Ob (>30.0)], three age (<45 years, 45-65 years, >65 years), and four molecular subtypes [Luminal A (HR+, HER2-), Luminal B (HR+, HER2+), HER2 enriched (HR-, HER2+), and TNBC (HR-, HER2-) categories. The data show a higher prevalence of BC in Ob women (46%) than OW (27%) and NW (27%) women of all age groups and its incidence was much greater in Ob Black women (61%) than Ob White women (39%). Further, Black women had nearly twice higher diagnosis at an early age than White women. Moreover, Ob Black women had over 7- and 1.5-folds higher incidence of early onset BC than NW and OW Black women, respectively, whereas, early onset BC did not exhibit a correlative pattern in White women. Luminal A and TNBC subtypes were the most common in women with early onset BC and Black women exhibited more than twice incidence of TNBC (32%) compared to the White women (14%) of all ages. In contrast, incidence of luminal A subtype was less prevalent in Black (57.4%) than in White (72.6%) women. Interestingly, both luminal A and TNBC subtypes were also more prevalent in Ob women; however, the risk of being diagnosed with TNBC increased dramatically in Ob Black women compared to Ob White women. Together, these findings establish obesity as a major underlying cause of early onset BC and TNBC diagnosis in Black women, which could be targeted to diminish the BC disparity gaps.

#0813 Primary cutaneous gamma-delta T-Cell lymphoma in the United States: A nationwide analysis of demographics and survival outcomes among the Hispanic population.

K. Thiel, R. White, Q. Liu, J. Michalek, A. Diaz Duque;
UT Health Science Center at San Antonio, San Antonio, TX

BACKGROUND: Primary Cutaneous Gamma-Delta T-Cell Lymphoma (PCGDTCL) is a rare subtype of cutaneous T-cell lymphoma (CTCL) that, despite comprising <1% of cutaneous lymphomas, has gained recognition in recent years as an entity separate from other rare CTCLs. (*LeukemiaPMID 35732829)* A 5 year survival of 11% demonstrates a low response to current available therapies. (*BloodPMID 30635287*, *Clin Hematol Int.PMID 35950208)* Due to lack of consistency in behavior between CTCLs, there exists a need for studies of demographic, clinical, and survival disparities, including between Hispanics (HI) vs. non-Hispanics (NH).
METHODS: Data were analyzed on PCGDTCL patients in the United States reported to the National Cancer Database (NCDB) between 2004-2019. Demographic and treatment characteristics were compared between ethnic groups. Kaplan-Meier and Cox regression analyses were used to compare OS between populations. Multivariate analysis and propensity score matching was performed with adjustment for age, stage, co-morbidity score, and insurance status, type of facility and great circle distance.
RESULTS: Among 132 PCGDTCL patients studied (5% HI, 92% NH), the HI group was younger at diagnosis than NH (49.5y vs. 60y) (p=0.384); The majority of HI (50%) was diagnosed between 2010-2012 vs 2017-2019 for NH (45%) (p=0.673). Most of HI and NH were white (67% vs 79%).
Private insurance was the most prevalent type in HI (67%) vs government sponsored for NH (49%). The most non-Insured group was NH (3%) vs HI (0%).
The most prevalent bracket for Census Median Income (2008-2012) was $63,000+ for both HI (50%) and NH (31%). 17% HI vs 13%. NH had median income <$38,000.
For Charlson-Deyo Score (comorbidities score), HI had 0% =/> 2 score, vs NH 6%. NCI-designated comprehensive cancer centers were the most prevalent type of facility providing care for HI (100%) and NH (56%)
Survival probability (OS) at 2, 5 and 10y (HI vs NH) were (80% vs 48%), (80% vs 44%), and (80% vs 26%), respectively. Median survival time (MS) was not reached for HI vs 1.9 years for NH. Overall survival (OS) difference favored HI (p=0.13)
On multivariate analysis, there was no independent variable associated with better or worse OS. Interestingly, the propensity matched analysis demonstrated significant MS difference between HI vs NH (median not reached vs. 1.35 years).
CONCLUSION: There was no significant difference in OS between groups; however, the weighed MS favored the HI cohort, likely in part due to the difference in numbers between cohorts. The drastically low survival in all demographics is consistent with prior studies. These results demonstrate an unmet need for more comprehensive studies with the potential inclusion of correlatives looking at intrinsic biologic characteristics that may offer insight into druggable targets, aiming for improvement in survival outcomes for this rare lymphoma.

#0814 Bridging the gap: Informal caregivers' access to information on genetic testing for cancer risk.

E. Adjei Boakye[1], P. G. Patel[2], C. S. Dagli[2], S. Wagoner[3], M. Nair[1], N. Osazuwa-Peters[4], V. Bernacchi[5], S. H. Tam[1];
[1]Henry Ford Health System, Detroit, MI, [2]University of Alabama at Birmingham, Birmingham, AL, [3]University of Kansas Medical Center, Kansas City, KS, [4]Duke University School of Medicine, Durham, NC, [5]Michigan State University, East Lansing, MI

Introduction: Cancer risk genetic testing (referred to as genetic testing thereafter) benefits patients by allowing them to make informed behavioral and medical decisions to reduce cancer risk and by facilitating surveillance and earlier detection. Informal caregivers, who often serve as primary advocates for those at risk, play a pivotal role in supporting behavioral and medical decisions based on genetic testing information. Assessing caregivers' knowledge of genetic testing can guide future interventions supporting informed decision-making to ensure that all groups benefit equally from advances in genetic testing. We examined the association between caregiving and knowledge of genetic testing as well as other individual and socioeconomic factors.
Methods: Secondary data analysis was conducted using the 2020 Health Information National Trends Survey (HINTS 5 Cycle 4). HINTS is a nationally representative survey of adults in the civilian non-institutionalized US population. Exposure variable was caregiving (yes/no) assessed with the question "Are you currently caring for or making health care decisions for someone with a medical, behavioral, disability, or other condition?". The outcome variable was genetic testing knowledge (yes/no) assessed with the question "have you heard of high-risk cancer genetic testing - e.g., BRCA 1/2". Weighted, multivariable logistic regression was used to estimate the association between caregiving and genetic testing knowledge adjusting for age, gender, race/ethnicity, marital status, education level, having a regular provider, rural-urban residence, and self-reported general health status.
Results: A total of 3,136 participants aged ≥18 were included in the study, of whom 16.4% were caregivers and 35.9% had heard of genetic testing. In the adjusted analysis, there was no statistically significant difference between caregivers and non-caregivers in relation to genetic testing knowledge (P=0.7881). However, respondents who were ≥65 years old (aOR=0.54, 95% CI: 0.40-0.72) were less likely to have heard about genetic testing compared to those aged 18-49, as were respondents who had no regular provider (aOR=0.71, 95% CI: 0.53-0.95) compared to those with a regular provider. Compared to non-Hispanic White respondents, non-Hispanic Black (aOR=0.45, 95% CI: 0.31-0.66) or Hispanic respondents (aOR=0.44, 95% CI: 0.29-0.68) were less likely to have heard about genetic testing. Female respondents (aOR=2.02, 95% CI: 1.55-2.61) were twice as likely to have heard about genetic testing than their male counterparts.
Conclusions: We found that about a third of Americans had heard about genetic testing; patients who were younger, female, White, and those who had access to a regular provider were more likely to be aware of testing. Interventions targeting under-resourced caregivers are urgently needed to promote equity in genetic testing and its benefits.

#0815 Leveraging clinical workflow for rapid integration of social needs assessment in a urologic oncology clinical practice.

Samuel L. Washington[1], Kim F. Rhoads[2], Peter R. Carroll[2], Salma Shariff-Marco[2], June M. Chan[2]

[1]UCSF - University of California San Francisco, Daly City, CA,[2]UCSF - University of California San Francisco, San Francisco, CA

Introduction: Social determinants of health and resulting social needs are known to impact cancer care, yet characterization of social needs within a specific clinic's population remains in its infancy. We aim to characterize early findings from social needs screening in patients seen in a tertiary urologic oncology clinic.
Methods: Screening was conducted using survey questions about specific domains of social needs (e.g., financial strain, unmet transportation needs, and food insecurity) that were integrated into new patient and annual follow-up questionnaires for all patients seen within a urologic oncology faculty clinic, starting in January 2023. Screening items were rapidly implemented into workflow by taking advantage of existing processes. Clinical and demographic data and screening responses were abstracted from the electronic medical record. Summary statistics were calculated. P value<0.05 was deemed statistically significant.
Results: A total of 2305 patients were included (4% Non-Hispanic Black, 11% Asian American, 8% Latinx, and 63% Non-Hispanic White). Responses increased from 30 in January to 399 in October. Respondent mean age was 67 years [standard deviation (SD) 12.3] with 87.8% identifying as male. Roughly 13% screened positive for at least one social need (one positive 8.1%, two positive 3.4%, three positive 1.2%) with variations by domain [transportation 3.6%, food insecurity 5.4%, 10.2%] and race and ethnicity (Figure 1, p<0.001 for all).
Conclusions: By leveraging the existing clinical workflow, rapid uptake of social needs screening demonstrates variations by social needs domains and race and ethnicity within a urologic oncology patient population. These efforts represent institutional action towards characterizing the burdens faced by our patient population and inform the design of interventions to address social needs within the catchment area, to improve clinical care and clinical trial participation.

#0816 Implementation of a community-based multi-component cancer screening intervention supported by a cross-sector community coalition.

R. Rechis, M. Aquino, H. Gardiner, B. Puga, M. T. Walsh, Jr.;
The University of Texas MD Anderson Cancer Center, Houston, TX

It is widely agreed that screening and early detection of cancer saves lives. However, disparities exist in those who received routine screenings and variability in clinic screening protocol. Working with community-based clinics on quality improvement as well as systematically screening all eligible patients can result in increased equity in screening and thus early detection. Be Well Communities™ is MD Anderson's place-based approach for cancer prevention and control, working with communities to promote wellness and address modifiable risk factors for cancer. The first several years of the initiative in Baytown focused on healthy eating and active living interventions for cancer prevention, over time the community's trust and appetite increased which allowed for additional and more traditional cancer prevention interventions (e.g., human papilloma virus vaccination, screening). In this project, three evidence-based interventions for cancer screening were implemented in collaboration with Chambers Health, a local FQHC in Baytown, Texas, to work toward addressing the disparities in screening outcomes experienced by community residents. Chambers Health compliance rates have increased since the beginning of the Cancer Screening Navigation program, supported by Be Well Communities. Two full-time patient navigators are supported to facilitate increased screening through patient education, increased clinic compliance and development of standard operating procedures for navigation related operations. In addition, one full-time Outreach Coordinator is supported to engage with patients and provide education on cancer screenings. Compared to 2022, there was a 39% increase in colon cancer screening compliance rates, a 25% increase in cervical cancer screening compliance rates, and a 47% increase in breast cancer screening compliance rates. Compliance refers to any patient who is up-to-date in their cancer screenings. The Be Well Communities team supported Chambers Health through funding, technical assistance, and capacity building. They were then able to provide culturally relevant and high-quality care to enhance community capacity to address low rates of cancer screening in Baytown. Furthermore, Chambers Health has since integrated the patient navigators and Outreach Coordinator into their operational budget, a notable systems change for the organization and demonstration of commitment to the project and continued clinic quality improvement and more so dedication to the patients served.

#0817 Establishing a niche to improve Africa's contribution to cancer research.

U. A. Malami[1], S. A. Malami[1], U. E. Nwokwu[1], U. W. Mohammed[2], F. Mohammed[2];
[1]National Institute for Cancer Research and Treatment (NICRAT), Abuja, Nigeria, [2]Ahmadu Bello University, Zaria, Nigeria

Africa has been a key source of scientific discoveries to the global community, especially in areas of scientific experiments and implementation. However, Africans are underrepresented in their contribution to global science and within the African countries, access to adequate funding and infrastructure to do high quality science is limited. These inequities contribute to the 10/90 gap in which only an estimated 10% of global health research funding is used to address health problems in Africa. Thus, it is not surprising that today, Africa contributes just about 2 percent of world research output, 1.3 percent of research spending, and 0.1 percent of all patents. To bridge the aforementioned gaps, mitigate the effect of brain drain and structural constraints and improve support for the next generation scientists, the Nigerian Government recently established the National Institute for Cancer Research and Treatment (NICRAT). It is worthy to note that cancer incidence and mortality rates in Africa are increasing 1.1 million new cases, with 711,000 deaths reported in 2020. This indicate a mortality-to-incidence ratio (MIR) of 0.64. These cancer challenges in Africa necessitates a concerted approach towards effective cancer control and management. Here, we show in detail how the NICRAT support improving science while integrating with Nigerian national development plans and strategies. We also show how the NICRAT is establishing a mechanism for domestic funding, while fostering national and international collaborations for African scientists and encouraging women into careers in cancer research. Currently, the NICRAT's key task also includes centralizing cancer control efforts, mobilizing funding from different sources for cancer research, and coordinating cancer treatment activities across Nigeria. In addition, the institute facilitates collaboration between researchers, healthcare providers, and patients, and provides guidance for cancer policy formulation and implementation. The establishment of NICRAT by Nigeria's government as well as similar centers elsewhere in Africa may improve active participation of African scientists in scientific practice, discourse, and decision making and spotlight their intellectual contributions towards solving science-associated global problems.

#0818 Fighting prostate cancer with a multimedia approach.

V. Gordon[1], F. Odedina[1], K. Ashing[2], A. Merriweather[3], R. Dronca[1], C. Ngufor[4], S. Rotimi[5], E. Kaninjing[6], A. Odedina[7], J. McCall[2], A. Hill[8], A. Yahaya[1], E. Agboola[8];

[1]Mayo Clinic Jacksonville, Jacksonville, FL, [2]City of Hope, Duarte, CA, [3]American Legion Post 197, Jacksonville, FL, [4]Mayo Clinic Rochester, Rochester, MN, [5]Covenant University, Logos, Nigeria, [6]Georgia College, Milledgeville, GA, [7]NA, NA, FL, [8]NA, Jacksonville, FL

Introduction: Black men have the highest prostate cancer (CaP) mortality rates. The reason for this disparity is multifaceted, including the barriers that they face at the individual, provider, and health system levels. To address these challenges the iCCaRE for Black Men Consortium uses a multi-level approach to disseminating CaP information. This approach is rooted in research which shows that Black men prefer to receive information through multi-media channels tailored to their needs. In addition, studies have reported that CaP survivors were viewed as credible sources of information. This presentation reports on how iCCaRE Consortium is bridging the digital divide in minoritized communities to disseminate CaP information in a way that is meaningful to the community.
Methodology: iCCaRE uses a multimedia method to reach Black men. This includes twitter post, Facebook, YouTube, ecancer and community lunch and learns. In addition to social media, we have partnered with LitTV Network, a locally owned digital TV platform, on which we have iCCaRE TV. On Lit TV network we have the ability to reach 11,000 homes in our catchment area. Furthermore, the consortium has produced informational flyers that are disseminated at outreach events and at the American Legion Post 197. On the twitter page the consortium post: (1) 2 scientific publications per day authored by members of the consortium, (2) 2 weekly “Did You Know” facts about prostate cancer with sources attached, (3) 2 weekly url post sharing a link to a video from the iCCaRE consortium YouTube page and (4) clips of CaP survivors sharing their experiences. On the YouTube page we currently have: videos series of a CaP survivor who is also a physician scientist, interview series with MPIs and members of the consortium, CaP survivor series including a barbershop interview with a survivor.
Results: The iCCaRE Consortium multimedia efforts have a global reach, in less than a year we have gained 102 twitter followers. On average the twitter page receives 8,700 impressions during the CaP awareness month in September the twitter page garnered over 14,000 impressions. Our videos on the ecancer platform have a combined global view of 341 representing countries such as the United States, Nigeria, Cameroon, United Kingdom, Macedonia, and Mexico. The American Legion Post 197 in North Jacksonville has served a cumulative of 229 people through outreach and educational event called lunch and learns. Our YouTube channel has had almost 100 views in its first month of being active.
Conclusion: Using a multi-level approach to reduce the burden of CaP for Black men is vitally important; without such efforts the disparate thread in mortality will continue to persist. Meeting Black men through the mediums they use for gathering health information removes barriers, increases access and will aid in the fight against CaP for Black Men.

#0819 Feasibility of patient-centered home care (PCHC) to reduce disparities in high-risk black men with advanced prostate cancer.

R. S. Dronca[1], F. Odedina[1], C. Ngufor[1], K. Ashing[2], E. Kaninjing[3], S. Rotimi[4];
[1]Mayo Clinic College of Medicine and Science, Jacksonville, FL, [2]City of Hope Medical Center, Duarte, CA, [3]Georgia College & State University, Tallahassee, FL, [4]Covenant University, Ota, Nigeria

The objective of our study is to evaluate the feasibility, acceptance, and impact of patient-centered home care (PCHC) on patient reported outcomes (PROs) and health-related quality of life (HQoL) of black men with advanced prostate cancer (CaP). Meeting patients where they are and offering treatment in or closer to their homes reduce psychological distress and increase treatment compliance, especially for disadvantaged patients in rural areas, those on low incomes, with poor access to transport, elderly and people with disabilities. In 2023, Mayo Clinic has developed the Cancer Care Beyond Walls (CCBW) program, a cancer care delivery model that integrates virtual with in facility treatment and provides a package of care to support administration of cancer-directed therapy (chemotherapy, immunotherapy, hormonal therapy) and/or supportive care in the patients' homes. Our study will assess if patients and families are comfortable with cancer therapy at home, what factors influences their decision, and use this data to inform our understanding of the proportion of the black men with advanced CaP who would be willing to receive and would benefit from this level of care at home. Patients with advanced CaP from our practice requiring active anti-cancer therapy are administered a brief questionnaire regarding preference for location of therapy at the infusion center or in the home, with perceived difficulties and advantages of each approach. A focus group session with prostate cancer survivor advocates is also conducted to capture patients' thoughts, feelings, attitudes, and questions towards cancer treatments being administered at home versus a hospital setting. In addition, we are conducting an observational study of 20 patients with advanced prostate cancer receiving supportive care/symptom management and/or anti-cancer therapy in the home as part of the Mayo Clinic CCBW Program to assess the safety of cancer directed therapy when administered at home by a home health provider with remote patient monitoring and command center support, and establish the impact of home cancer treatment administration on patient-reported function and global health/quality of life, patient-reported symptoms, clinical outcomes, and cost of care. Successful completion of the project will deliver data on patient understanding and acceptability of cancer care at home, strategies for overcoming barriers to care for underserved communities, and the foundation from which we discover, translate and apply new knowledge in administering personalized care to vulnerable populations.

#0820 Decolonizing data: Diversifying cancer registries to include SWANA.

Guleer Shahab, Michael Preston

Health Behavior and Policy, Virginia Commonwealth University - VCU, Richmond, VA

Southwest Asian/North African communities (SWANA) make up over 3-4% of immigrants in the U.S. and yet their health status is largely unknown because these ethnic groups are misclassified within the U.S. racial schema as White, deeming them ‘invisible minorities’. Administrative forms specify that White includes Middle-Eastern but SWANA persons may also self-identify as Black, Asian, and Other. With the rise of Islamophobia and increased US intervention in the Middle Eastern region, SWANA Americans face unique challenges that require a deeper understanding of their health status.One methodology to obtain cancer statistics on SWANA is using naming algorithms. Similar to SWANA, the Latine population was invisible in administrative data prior to the 1970’s. Grassroots efforts and advocacy from the Latine community led to the development of validated Latine surname algorithms which have been implemented by the National Cancer Institute. Similarly, SWANA activists have advocated for the creation of a federal identification category for over 50 years arguing that SWANA communities are not perceived as White due, in large part, to a long-standing history of political racism in the United States.The purpose of this study was to develop a SWANA Surname Algorithm (SSA) to inclusively identify SWANA in cancer health data. We used surnames by country of descent to leverage interpretable decision trees to effectively distinguish SWANA from non-SWANA individuals by iteratively selecting the best surname roots at which to split the data to maximize the separation of SWANA individuals from others based on their surname. We integrated these patterns into our SSA so that when presented with a new surname, the algorithm simply follows the decision patterns down to the leaf nodes, otherwise known as the predicted class (SWANA vs non-SWANA).We developed a preliminary SWANA Surname List (SSL) using publicly available naming databases by country of origin (N=71,300). We cross-referenced the SSL against the VCU Massey Cancer Center data repository and found 4.9% of all cancer patients from 2016 to 2020 matched as SWANA. Notably, the prevalence of SWANA patients has been increasing over the last few decades, 3.8% in 1991-1995, to 4.2% in 2001-2005, and then most recently 4.9% in 2016-2020. We will use our SSA to validate these findings. These preliminary findings underscore the valuable insights that naming algorithms can provide in elucidating the true demographic composition of cancer patients. Lack of racial/ethnic disaggregation perpetuates existing inequities in access to essential health resources among SWANA communities. The inclusion of SWANA in cancer disparities research would allow researchers to better examine the cancer health status of this underrepresented but growing community while also aligning with the true racialization of SWANA in the United States.

#0821 Uptake of cervical cancer screening services by women living with HIV in Kajiado County Kenya.

C. Kamau[1], A. Njoroge[1], **F. Makokha**[1], K. T. Ashing[2];
[1]Mount Kenya University, Thika, Kenya, [2]City of Hope National Medical Center, Duarte, CA

Background: This project is an African Caribbean Cancer Consortium (AC3) facilitated study: Women living with HIV (WLHIV) are more susceptible to cancer due to their immune-compromised status. The Kenya Ministry of Health recommends that women diagnosed with HIV should be screened for cervical cancer annually by either visual inspection with acetic acid (VIA) or visual inspection with Lugol's iodine (VILI), cytology and testing for HPV once every two years.
Objective: We determined the uptake of cervical cancer screening and HPV testing by women living with HIV (WLHIV) in Kajiado County in 2022.
Methodology: The electronic health information system was used to abstract data for WLHIV in Kajiado county. Kajiado county has 57 antiretroviral (ART) facilities. However, our analysis accessed data from 38 facilities whose data is captured in the health information system. Authorized health care workers from the county were requested to abstract redacted data from the health information system. No personal identifiers were collected from the system as a means of protecting the privacy of individuals and abiding with the Kenya's data protection law. Authorization to access the county was obtained from the county's department of health while ethical approval was obtained from Mount Kenya University's Institutional Scientific and Ethics Review Committee.
Results: A total of 16,827 people living with HIV were enrolled for care at the 38 ART selected sites in 2022. Out on the total population that was enrolled for care, 11,785 (70%) were women with an age range of 15 to 49 years. A total of 3342 WLHIV, representing 28.36% of the target population, were screened by using visual inspection with acetic acid (VIA). Data for other methods of screening and HPV testing was not available in the health information systems. Of those screened, 3240 (97%) tested negative, 78 (2.3%) had positive results while 24 (0.7%) had suspicious lesions.
Conclusion: Our analysis shows low uptake of cervical cancer screening services with only 28.36% of the targeted women being screened in 2022. The only available testing method (VIA) is less robust as compared to cytology and HPV testing. We also found a gap in reporting of HPV testing in the county. We thus recommend implementation science research examining the systemic barriers to HPV testing and reporting to better inform best practice HPV-related cancer prevention and control policy and practice to reduce cancer-related morbidity and mortality among WLHIV.

#0822 A retrospective study on the disparities of hepatocellular carcinoma.

X. Zhou[1], B. Aldridge[1], N. Rahmanov[1], Z. Liu[2], J. Mao[3], N. Varshney[1];

[1]University of Mississippi Medical Center, Jackson, MS, [2]Shanxi Medical University, Taiyuan, China, [3]Tougaloo College, Jackson, MS

Background: Hepatocellular carcinoma (HCC) is the most common type of primary liver cancer in adults and the third leading cause of cancer-related deaths worldwide. Studies report that the incidence of, and mortality from HCC vary significantly by age, sex, and race/ethnicity; however, disparities in the expression level of tumor biomarkers, liver functions, lipid profiles, and comorbidities have not been thoroughly investigated among subpopulations of patient with HCC.
Methods: A retrospective study was conducted to review 247 serial HCC cases enrolled in the University of Mississippi Medical Center during June 2000 to May 2023. The entire HCC population was stratified into subpopulations by race, gender, age and BMI. Then comparisons were performed between two corresponding subpopulations in the expression level of HCC-related biomarkers including Alpha-FP, liver functions including albumin, ALT, AST, and ALP, plasma lipid profiles including cholesterol, and comorbidity conditions including cirrhosis in benign liver tissues, smoking, alcohol using, and illness with viral hepatitis. Two-tailed Student's T-test was used to calculate the difference in mean values, and Chi-Square Test was used to compare the difference in rates or percentages. The significant p value was set at $p<0.05$.
Results: In total 247 HCC cases, males were 178 (72.1%) and females were 69 (27.9%) with a male to female ratio of 2.6:1; black patients were 108 (43.7%), white patients were 127 (51.4%), and others were 4.9%. The mean age was 59.6 years and mean BMI was 27.04. AFP was the only one of detected tumor biomarkers showing disparities: it was significantly higher in patients of male ($p=0.026$), younger age ($p<0.0001$), lower BMI ($p=0.039$), smokers ($p=0.0325$) and illness with viral hepatitis ($p=0.0007$). Disparities in liver functions included: 1) AST was significantly higher in Black HCC patients ($p=0.027$); 2) no statistical difference of liver functions in gender; 3) younger HCC patients had significantly lower level of Albumin ($p=0.006$), and higher levels of ALT ($p=0.014$) and AST ($p=0.0032$); 4) HCC patients with lower BMI also had lower level of Albumin ($p=0.015$), and higher levels of AST ($p=0.0480$ and ALP ($p=0.0057$). There was no statistical difference of plasma lipid profiles between subpopulations, Black HCC patients except that Black HCC patients had significantly higher levels of cholesterol ($p=0.0006$) and HDL ($p=0.048$). In comorbidity, Black HCC patients had higher rates of alcohol using and existence of cirrhosis; and male HCC patients had higher rates of smoking, alcohol usage and viral hepatitis.
Conclusions: HCC patients are greatly disparate in the expression level of tumor biomarkers, liver functions, plasma lipid profiles and comorbidity conditions between subpopulations stratified by race, gender, age and BMI. These results could provide useful information for clinical management and prognosis of patients with HCC.

#0823 Parent-endorsed potential interventions to improve language disparities in pediatric cancer.

M. Stall[1], N. Winick[1], E. Kaye[2];
[1]University of Texas Southwestern Medical Center, Dallas, TX, [2]St Jude Children's Research Hospital, Memphis, TN

Introduction: Children with cancer whose parents speak languages other than English (LOE) experience disparities including underrepresentation on clinical trials, decreased access to resources and inadequate interpretative services. Few studies in pediatric oncology have investigated the communication experiences of families who speak LOE, and rarely have studies sought parental recommendations for improvement. In this study, we aimed to characterize the experiences of parents of children with cancer who speak LOE and identify stakeholder-driven interventions to improve deficiencies.
Methods: We enrolled parents of children with cancer who spoke any LOE and conducted semi-structured interviews about perceptions of medical care, communication and support from the medical team within 3 months of a new cancer diagnosis and 6-12 months post-diagnosis. Inductive content analysis was performed, with iterative transcript review and memo-writing informing the development of codes. Code frequency, temporal duration and distribution across language subtype were calculated and reported as descriptive statistics. Analysis was organized in MAXQDA, a mixed-methods data analysis software.
Results: Twenty-eight parents, representing 7 different languages, were enrolled. All parents completed first interviews and 14 have completed second interviews to date. Parents described frequent problems with interpretation and felt their child's care would be improved if they spoke English. Parents made suggestions on how to improve their experience and understanding of their child's medical care (Table 1).
Conclusion: Challenges related to language interpretation are pervasive and parents who speak LOE believe their child's cancer care would be improved if they spoke English. Parents identified preferred communication practices and specific interventions that may be useful in promoting understanding of their child's medical care and overall enhance supportive resources.

Parent-endorsed communication practices and potential interventions to improve language disparities

Preferred communication practices	Use simple terms	Limit conversations between providers when no interpreter present	Speak to English and non-English speakers equally	Always automatically use professional interpreters	Take your time
	Repeat	Demonstrate	Rephrase	Use drawings	Point
	Ask for preferred language	Be specific and detailed	Speak slowly	Use short phrases	Allow time for interpretation
Requested resources in preferred language	Educational videos	Written educational materials	Translated hospital documents	List of supportive resources	List of financial resources
	List of reliable websites	Language matched parent buddy support system		Side by side instructions in English and preferred language	
System-level changes	Increased in-person interpreter staffing	Staff education on approach to LOE encounters	Patient advocate to review medications and check labels	Interpreter use at all points of contact	Provision of language concordant providers

#0824 Comparing experiences of Spanish and non-English/non-Spanish speaking parents of children with cancer.

M. Stall[1], N. Winick[1], E. Kaye[2];
[1]University of Texas Southwestern Medical Center, Dallas, TX, [2]St Jude Children's Research Hospital, Memphis, TN

Introduction: Children with cancer whose parents speak languages other than English (LOE) experience disparities including underrepresentation on clinical trials and decreased access to resources. Few studies in pediatric oncology have investigated the communication experiences of families who speak LOE, particularly for languages other than Spanish. The primary objective of this study was to characterize the experiences of parents of children with cancer who speak LOE.
Methods: Parents of children recently diagnosed with cancer who spoke LOE were enrolled concurrently in two cohorts, Spanish speaking and non-English/non-Spanish speaking. Semi-structured interviews were conducted about parent perceptions of medical care, communication and support from the medical team within 3 months of a new cancer diagnosis and 6-12 months post-diagnosis. Inductive content analysis was performed, with iterative transcript review and memo-writing informing the development of codes. Code frequency, temporal duration and distribution across language subtype were calculated and reported as descriptive statistics. Analysis was organized in MAXQDA, a mixed-methods data analysis software.
Results: Of the 28 parents enrolled, 20 spoke Spanish and 8 spoke other languages including Dari, Nepali, Karan, Cantonese, Chuukese and French. All parents completed first interviews and 14 have completed second interviews to date. All parents described challenges with interpretation, but difficulties were reported more often by non-Spanish speakers: 67% of non-Spanish speakers encountered interpreters who spoke a different dialect (vs. 35% of Spanish speakers), 33% had interactions where no interpreter was available via any modality (vs. 0%), and 75% of their children were asked to interpret by the medical team (vs. 12%). Additionally, non-Spanish speakers lacked access to written educational materials or hospital documents in their language and they were unable to build rapport with interpreters, whereas Spanish speakers described regular access to these resources. Spanish speakers also frequently reported incorrect interpretation that was recognized by providers who understood some Spanish. This was never reported by non-Spanish speakers as no medical team members spoke their languages.
Conclusion: Nearly 40% of the United States population speaks a language other than English or Spanish at home, yet their needs are significantly underrecognized and understudied. Our findings demonstrated that challenges related to interpretation are pervasive, and non-English/non-Spanish speakers may face greater difficulties. Overall, parents who speak LOE report receiving disparate care and deficient resources. An urgent need exists to provide equitable communication and resources, particularly for non-Spanish speakers who report significant obstacles in receipt of high-quality pediatric cancer care.

#0825 Adverse childhood experiences and history of depression among cancer survivors.

O. A. Babatunde[1], V. Collucielli[2], M. S. Jefferson[3], S. A. Adams[4], C. Hughes Halbert[5], J. Obeysekare[1], F. Clark[1], A. Nagar[1], N. Osazuwa-Peters[6], E. Adjei Boakye[7];

[1]Prisma Health, Greenville, SC, [2]University of South Carolina School of Medicine, Greenville, SC, [3]Medical University of South Carolina, Charleston, SC, [4]University of South Carolina, Columbia, SC, [5]University of Southern California, Los Angeles, CA, [6]Duke University School of Medicine, Durham, NC, [7]Henry Ford Health System, Detroit, MI

Introduction: Adverse Childhood Experiences (ACEs) are stressful life events that are associated with an increased risk of depression. Depression is experienced by 25% of cancer survivors in the US. While previous studies have examined the associations between ACEs and depression in the general population, studies on cancer survivors are lacking. We aimed to examine the predictors of depression with a primary focus on ACEs among cancer survivors.
Methods: Using a cross-sectional data from the 2020 Behavioral Risk Factor Surveillance System for 19,241 cancer survivors aged 18 and above, we categorized ACEs based on severity. The ACE categories (zero, one, two-three, ≥four) included questions assessing exposure to eight types of ACEs before age 18 years. The outcome is self-reported history of depression diagnosis (yes/no). Weighted multivariable logistic regression models estimated odds of depression by ACEs as the primary variable and covariates were age, gender, smoking status, income, education, marital status, body mass index, health status and race.
Results: In this sample of cancer survivors, 41%, 22%, 21% and 16% reported having experienced zero, one, two-three, and ≥4 ACEs respectively. Personal history of depression was reported by 21% of survey respondents. In the adjusted model, survivors with 1 ACE (aOR: 1.6, 95% CI. 1.2- 2.0), 2-3 ACEs (aOR: 1.7, 95% CI. 1.3- 2.1), or >=4 ACES (aOR: 4.4, 95% CI. 3.4- 5.7) had higher odds of depression compared with those with zero ACEs. Additional notable predictors of higher odds of depression are younger age, 18-39 (aOR: 2.7, 95% CI. 1.8- 4.0), middle age, 40-64 (aOR: 1.6, 95% CI. 1.3- 1.9) compared with those aged 65 and older; females (aOR: 2.1, 95% CI. 1.7- 2.5) compared with males; obese respondents (aOR: 1.5, 95% CI. 1.2- 1.9) compared with respondents with normal body mass index; current smokers (aOR: 1.5, 95% CI. 1.2- 2.0) compared with respondents who never smoked; and poor or fair health status (aOR: 3.2, 95% CI. 2.6- 3.9) compared with respondents with excellent/good health status.
Conclusion: Adult cancer survivors who experience ACEs as children represent an important targeted prevention group to reduce risk of depression. Variation by age, obesity, female gender, current smoking status, and poor health associated factors that may reduce the risk of depression warrants additional studies regarding potential for identification of resilient factors; and this may inform future selective prevention strategies, as well as identify a pathway between ACE and depression among cancer survivors.

POPULATION SCIENCES: Environmental and Occupational Risk Factors, Infection, and Aging
Poster Session

#0828 Associations of perfluoroalkyl substances with breast cancer incidence risk and mediation role of mitochondrial DNA copy number: A prospective case-cohort study.

Y. Feng, H. Guo;
Department of Occupational and Environmental Health, State Key Laboratory of Environmental Health (Incubating), School of Public Health, Tongji Medical College, Huazhong University of Science and Technology, Wuhan, China

Background: Perfluorinated carboxylic acids (PFCAs) and perfluorinated sulfonic acids (PFSAs), notable representatives of perfluoroalkyl substances (PFASs), are synthetic persistent chemicals widely accumulated and detected in humans. Short-chain PFASs [PFCAs with carbon number <8 and PFSAs <6, e.g. perfluoroheptanoic acid (PFHpA)] are considered less bioaccumulative and increasingly used in commercial products, yet their health impacts are rarely investigated. Perfluorooctanoic acid (PFOA) has been categorized as a possible human carcinogen (group 2B) and a potential mammary toxicant. However, few population studies explored the prospective associations of PFOA and other common PFASs with breast cancer risk nor the underlying mechanisms.
Methods: Hence, we conducted a case-cohort study within the DongFeng-Tongji Cohort, compromising 226 incident breast cancer cases and a random sub-cohort of 990 individuals. Plasma concentrations of four PFCAs [PFOA, perfluorononanoic acid (PFNA), perfluorodecanoic acid (PFDA), and PFHpA] and two PFSAs [perfluorooctane sulfonic acid (PFOS) and perfluorohexane sulfonic acid (PFHxS)], as well as peripheral blood mitochondrial DNA copy number (mtDNAcn) levels, were measured at baseline.
Results: Using Barlow-weighted Cox regression, we found 35% and 20% increased incident risk of breast cancer for each 1-unit ln-transformed increase in PFOA and PFHpA, respectively [HR (95% CI) = 1.35 (1.03, 1.78) and 1.20 (1.02, 1.40)]. Quantile g-computation analysis revealed a 19% increased incident risk of breast cancer along with each simultaneous quartile increase in all ln-transformed PFCA concentrations [HR (95% CI) = 1.19 (1.01, 1.41)], driven mainly by contributions from PFOA (56%), PFNA (24%), and PFHpA (20%). Besides, mtDNAcn was positively associated with PFHpA levels [β (95% CI) =0.027 (0.005, 0.048)], but not with PFOA or PFNA (P>0.05). We also found significantly higher breast cancer risk in participants with the highest mtDNAcn (Q4, ≥1.52) than those with the lowest (Q1, <0.87) [HR (95% CI) =2.92 (1.69, 5.04)], and that mtDNAcn mediated 12.77% of PFHpA-breast cancer association [Indirect effect, HR (95% CI) =1.02 (1.00, 1.04)]. No significant mediation effect of mtDNAcn was observed in associations of PFOA and PFNA with breast cancer (P>0.05).
Conclusions: Our work unveiled the relationship of short-chain PFHpA with increased incident risk of breast cancer for the first time and highlighted the intermediate role of mtDNAcn in this association, providing a research clue for exploring the potential mechanisms of PFAS-induced breast cancer. Moreover, co-exposure to PFASs was observed as a risk factor for breast cancer, shedding light on breast cancer prevention by regulating PFASs as a chemical class.

#0829 Phthalate exposure results in circadian rhythm-induced BBB dysfunction increasing the risk for breast cancer brain metastasis.

D. Tiburcio, S. Adolphe, I. B. Akpu, T. Teglas, O. Naranjo, S. H. L. George, M. J. Toborek;
University of Miami Miller School of Medicine, Miami, FL

Phthalates, classified as plasticizers, represent a group of chemicals pervasive in the general U.S. population, with notably higher levels in non-Hispanic Blacks compared to non-Hispanic Whites. These persistent organic pollutants (POPs) have been identified for their impact on the circadian rhythms of the brain and vascular system. Several studies indicate that phthalates can elevate neuroinflammation and reduce levels of the junctional protein ZO-1 in the hypothalamus, home to the master circadian clock known as the suprachiasmatic nucleus (SCN). The SCN regulates cellular and tissue circadian rhythms, including tight junction proteins essential for the blood-brain barrier's (BBB) main barrier function. Interestingly, experimental studies reveal that prolonged chronic circadian rhythm disruption (CRD) in mice leads to increased breast cancer metastasis. However, the effects of phthalates on CRD concerning brain cancer and metastasis remain poorly understood. Given their significant prevalence and biological impact, we hypothesize that phthalate exposure induces CRD through hypothalamic dysregulation, resulting in BBB dysfunction and an elevated risk of brain metastasis.
Results. We developed an in vitro BBB model using endothelial cells and exposed them to an environmentally relevant mixture of five phthalates simulating chronic low-grade exposure. Analysis showed dysregulation of critical clock genes (Bmal1 and Clock), along with a substantial decrease in BBB tight junction proteins (claudin-5 and occludin) at the protein and mRNA levels. The tumor trans-endothelial migration assay using breast adenocarcinoma cells along with endothelial cells demonstrated an increased metastatic potential following phthalate exposure.
Conclusion. These findings offer crucial insights into the molecular mechanisms underlying phthalate exposure, suggesting potential targets for future brain metastasis treatments. Additionally, they hold implications for the future regulation and management of phthalate usage and policy. This work was supported by the University of Miami U-LINK Resilience Challenge grant.

#0830 Michigan cancer and research on the environment study (MI-CARES) cohort: Baseline methods and participant characteristics.

Lilah Khoja[1], Maxwell Salvatore[1], Minh Tung Phung[1], Isabella De Sa[1], Heatherlun Uphold[2], Justin Colacino[1], Alison M. Mondul[1], Bhramar Mukherjee[1], Dana Dolinoy[1], Celeste Leigh Pearce[1]

[1]University of Michigan, Ann Arbor, MI,[2]Michigan State University, East Lansing, MI

Michigan has a long history of adverse environmental exposures, many of which are still ongoing, like the Flint water crisis, extreme air pollution burden, and widespread PFAS exposure. Michigan is also home to a diverse population of Latinx, Black, White, and Middle Eastern/North African (MENA) Americans. Because minority populations are underrepresented in environment and cancer research despite being at greater risk of being exposed to environmental hazards and having worse cancer outcomes, Michigan is uniquely positioned for studying the associations between environmental exposures and cancer risk. In June 2022, the Michigan Cancer and Research on the Environment Study (MI-CARES) began recruitment with a goal of establishing a cohort of over 100,000 Michiganders to examine these associations. Any Michigander aged 18-49 is eligible to enroll in MI-CARES. By focusing on this age range, we will capture exposures during important windows of susceptibility prior to the onset of most cancers.While recruitment is open to all state-wide, efforts are focused on six environmental injustice hotspots, identified using the MiEJScreen tool, a relative summary score capturing pollution burden and population vulnerability: the metro areas of Kalamazoo, Grand Rapids, Flint, Lansing, Detroit, and Bay City-Saginaw.MI-CARES will enroll equal numbers of Black, Latinx, MENA, and White participants. To support participation in diverse communities, study materials are available in Arabic, English, and Spanish. MI-CARES has employed a multifaceted community engagement strategy and is recruiting from these communities directly and with the help of community partners. An incentive of $10 is also provided to participants who successfully complete the questionnaire.To democratize participation, MI-CARES enrollment can be completely remote, but in-person and paper-based enrollment is available. Enrollment includes a baseline questionnaire, consent for data linkage, and annual follow-up surveys. Participants are also asked to provide saliva and blood spot samples via a mailed at-home biospecimen collection kit. Biospecimens will be analyzed for environmental exposures like heavy metals and for intermediate cancer markers including inflammation, cellular aging, immune function, and altered metabolism. Participant data will be linked to neighborhood-level exposure databases, administrative databases like cancer registries and death indices, and to the Michigan Neonatal Biobank. More than 4,000 Michiganders have enrolled in MI-CARES. Data on initial cohort members including environmental exposure history and demographic characteristics will be presented. MI-CARES is part of the Cohorts for Environmental Exposures and Cancer Risk (CEECR) consortium, which is funded by the National Cancer Institute and the National Institute for Environmental Health Sciences.

#0831 Occupational-related exposure to benzene and risk of breast cancer: Systematic review and meta-analysis.

V. DeStefano[1], D. Shah[1], V. Shah[2], M. Sadat Seyyedsalehi[3], M. Bonetti[3], P. Boffetta[1];
[1]Stony Brook University, Renaissance School of Medicine, Stony Brook, NY, [2]Northeastern University, Boston, MA, [3]University of Bologna, Bologna, Italy

Purpose: Benzene is a recognized carcinogen as evidenced by its association with leukemia; however, its association with breast cancer is not well established. Hence, a meta-analysis of cohort and case-control studies was performed to determine the association between benzene exposure and the risk of breast cancer.
Methods: A systematic literature review was conducted and 7221 publications were identified, from which 21 cohort and case-control studies were retained, and evaluated using meta-analyses (fixed effects model). PECOS criteria and STROBE guidelines were followed, and the study protocol was registered in the PROSPERO database (Registration No. 379720). Study quality was assessed using a modified Newcastle-Ottawa scale (NOS).
Results: The summary relative risk (RR) for ever-benzene exposure was 1.08 (95% CI=1.02-1.14, I^2=43.6%, n=21); corresponding RR for cancer incidence and mortality were 1.08 (95% CI=1.02-1.14, I^2=58.6%, n=15) and 1.09 (95% CI=0.87-1.38, I^2<0.001%, n=9), respectively. These main results were confirmed in sub-analyses by geographical region, industry type, publication year, and levels of exposure. No heterogeneity was detected amongst geographical regions (p-het=0.19), industry of employment (p-het=0.05) or and duration of the dose (low, high; p-het=0.64). Studies published before 2003 reported a summary RR of 1.24 (95% CI=1.13-1.37), compared to a summary RR of 1.02 (95% CI=0.95-1.08) for studies published later (p-het=0.001). Heterogeneity was observed when evaluating studies at and above, or below the NOS mean (p-het=0.00), with a summary RR of 1.25 (95% CI=1.13-1.28, I^2<0.001%, n=9) for studies below the median NOS score. Sub-group analysis of study design demonstrated heterogeneous results (p-het=0.001) with a summary RR of 1.19 (95% CI=1.10-1.29, I^2<0.001%, n=16) for cohort studies while compared to the findings of case-control studies. Publication bias was detected (p=0.04).
Conclusions: Our meta-analysis identified an association between occupational benzene exposure and risk of breast cancer. The association was restricted to studies published before 2003, below the median NOS score, and cohort studies. Residual confounding variables cannot be excluded, which, together with potential bias, prevents conclusions of causality.

#0832 Gender differences in urinary tract cancer susceptibility associated with radon in water: A population based study from Finland.

P. Y. Li;
Max Planck Institute for Demographic Research (MPIDR), Rostock, Germany

Background: Radon as a common source of environmental radiation, while its carcinogenic effect on urinary tract cancer has not been fully investigated.
Methods: Men and women who have continuously lived in Finland from year 1987 onward and reached 40+ years old at the beginning of 2017 were followed up for urinary tract cancer, including bladder cancer (ICD-O 3 code C67) and kidney cancer (C64-C66 and C68) for 5 years until the end of 2021. The residential location and type of buildings of the cohort members were traced from year 1987 until 2016 annually and linked to the average cumulative exposure of radon concentration in well water on municipality level. Newly diagnosed UTC cases were identified based on the Finnish cancer register. Pre-existing health conditions, such as hypertension, diabetes, chronic kidney disease, calculus of kidney and lower urinary tract, family history of cancer, as well as socioeconomic factors were ascertained from multiple registry databases. Data were analyzed with Cox proportional hazards model conditional on birth cohorts and adjusted with available covariates.
Findings: Among 1,019,331 men and 1,192,960 women with 30-years average radon exposure, 4206 and 2226 urinary tract cancer cases were diagnosed during follow-up period from 2017 until correspondingly. Men with higher radon exposure (>500 Bq/m^3) had about 14% higher risks of UTC in total (HR 1.14, 95% CI 1.07-1.21), 19% higher risks of bladder cancer (HR 1.19, 95%CI 1.09-1.32), 10% higher risks of kidney cancer (HR 1.10, 95%CI 1.02-1.20) comparing with lower exposed samples. Women with higher radon exposure had about 1% higher risks of UTC in total (HR 1.01, 95%CI 0.93-1.10), 3% higher risks of bladder cancer (HR 1.03, 95%CI 0.88-1.22), 1% higher risks of kidney cancer (HR 1.01, 95%CI 0.92-1.11). In the sub-population who only lived in houses during the 30-years exposure period, men with higher radon exposure had about 24% higher risks of UTC (HR 1.24, 95% CI 1.12- 1.36), 30% higher risks of bladder cancer (HR 1.30, 95%CI 1.12-1.51), 20% higher risks of kidney cancer (HR 1.20, 95%CI 1.06-1.36). No significant association was observed in women who only lived in houses during exposure period.
Conclusions: For men, higher radon exposure was significantly associated with elevated risks of UTC. No significant association was observed in women. Further investigates were needed to explore the mechanisms of gender differences in UTC susceptibility associated with radon exposure.
Keywords: Radon, Radiation, Cancer, Urinary tract cancer, Kidney cancer, Bladder cancer

#0833 No association between air pollution and lung cancer incidence in a 2 million South Korean cohort.

S.-Y. Kim[1], J. Park[2], O.-J. Kim[3], M. Shin[1], S. Kang[4], S.-s. Hwang[4], Y. Kim[1], Y.-J. Cho[5];

[1]National Cancer Center - Korea, Goyang, Korea, Republic of, [2]Yonsei University, Seoul, Korea, Republic of, [3]National Institute of Environmental Research, Incheon, Korea, Republic of, [4]Seoul National University, Seoul, Korea, Republic of, [5]Seoul National University Bundang Hospital, Seoul, Korea, Republic of

Background: Accumulating evidence has consistently suggested long-term exposure to air pollution as a risk factor of lung cancer incidence. Our previous study of long-term exposure to particulate matter air pollution and lung cancer incidence in a South Korean cohort showed no association with hazard ratios greater than one. This inconsistent finding with those from previous cohort studies could be due to limited exposure assessment relying on district averages and a relatively small sample size of 80 thousand people. The present study aimed to overcome the two major limitations and re-analyzed the association for long-term exposure to particulate matter ≤ 10 μm and 2.5 μm in diameter (PM10 and PM2.5), nitrogen dioxide (NO2), and ozone. Specifically, we improved our exposure assessment for individual exposure using 100-meter grid addresses, and increased the population size to 2 million people based on the National Health Insurance Database (NHID) composed of the entire South Korean population.

Methods: Our study population included 1,976,265 people who aged 30 years or older, had no history of cancer for 2002-2006, underwent health screening for 2005-2007, and resided in the Seoul Metropolitan Area. We defined lung cancer incidence as the first diagnosis based on the International Classification of Diseases 10th revision code and identified the incidence for 10 years of follow-up from 2007 through 2016. We estimated individual long-term exposure to PM10, PM2.5, NO2, and ozone as five-year average concentrations on each year at 100-meter grid addresses of participants' homes by using previously-validated exposure prediction models. Finally, we applied time-varying Cox proportional hazard model to estimate hazard ratios (HRs) and 95% confidence intervals (CIs) for a 10 μg/m3 or 10 ppb increase of each of the four pollutants after adjusting for individual- and area-level characteristics.

Results: Out of 1,976,265 people, 15,707 people (0.79%) developed new cases of lung cancer for 10 years of follow-up. In all analyses for long-term exposure to four pollutants and lung cancer incidence, we did not find an association (PM10: HR= 0.999 [95% CI=0.956 - 1.044]; PM2.5: 0.890 [0.787 - 1.006]; NO2: 1.002 [0.967 - 1.037]; ozone: 1.027 [0.978 - 1.077]). Our stratified analyses by individual and area-level characteristics as well as 79 districts showed that the null findings in the total population were not derived by specific subpopulations.

Conclusion: Despites the considerable improvement in exposure assessment and population size, our findings are contradictory to previous evidence. In addition to the possibility of no association, our null findings could be due to a relatively short period of exposure, the lack of histological information, and exposure measurement error resulting from indoor-outdoor difference and time activity. Future studies should overcome these limitations and re-examine the association.

#0834 Farm animal exposures and the oral microbiome in the Agricultural Health Study.

V. C. Chang[1], V. Purandare[1], R. Sinha[1], G. Andreotti[1], S. Li[2], X. Hua[3], Y. Yano[1], K. R. Dalton[4], M. Lee[4], C. G. Parks[4], S. J. London[4], D. P. Sandler[4], M. H. Gail[1], J. Shi[1], J. N. Hofmann[1], C. C. Abnet[1], E. Vogtmann[1], L. E. Beane Freeman[1];

[1]National Cancer Institute, Bethesda, MD, [2]Johns Hopkins Bloomberg School of Public Health, Baltimore, MD, [3]Fred Hutchinson Cancer Center, Seattle, WA, [4]National Institute of Environmental Health Sciences, Research Triangle Park, NC

Raising farm animals involves a variety of exposures, including microbes, antimicrobial agents, bioaerosols, and pesticides that may influence the human microbiome. Exposure to farm animals has also been associated with some cancers including lower risk of lung cancer and elevated risks of certain hematologic malignancies, with heterogeneity by animal species. Increasing epidemiologic evidence suggests that changes in the oral microbiome contribute to cancer development. Few human studies have investigated the potential influence of farm animal exposures on the oral microbiome. We investigated associations between farm animal exposures and the oral microbiome in 1245 Iowa and North Carolina farmers and spouses from the Agricultural Health Study. Participants provided information on types and numbers of farm animals raised in telephone interviews close to the time of oral wash sample collection. DNA was extracted from oral wash specimens and analyzed using 16S rRNA gene (V4 region) sequencing. We evaluated associations between farm animal exposures and alpha diversity metrics [e.g., observed amplicon sequence variants (ASVs)] using linear regression and assessed differences in beta diversity metrics (e.g., weighted Unifrac) using permutational multivariate analysis of variance. In addition, we evaluated associations with the presence and relative abundance of specific genera using zero-inflated negative binomial regression. All analyses adjusted for potential confounders (e.g., sex, age, state of residence, smoking). Overall, 63% of participants reported raising any animals, most commonly cattle (46%) and hogs (20%). Raising sheep/goats was associated with lower alpha diversity [e.g., 18 (95% confidence interval: 3-33) fewer observed ASVs compared to not raising sheep/goats], with an exposure-response trend for increasing number of sheep/goats (13 and 24 fewer observed ASVs for 1-29 and ≥30 sheep/goats vs. none, respectively; P_{trend} = 0.048). Increasing numbers of hogs and poultry were associated with higher and lower alpha diversity, respectively. Associations were similar after mutual adjustment for other farm animal types. Based on beta diversity analyses, we did not observe statistically significant differences in microbial compositions between participants with and without farm animals. After adjusting for multiple testing, having any farm animal was associated with an increased relative abundance of *Porphyromonas*, and several genera were more likely to be absent with specific animal exposures (e.g., *Capnocytophaga* for cattle and sheep/goats; *Corynebacterium* and *Abiotrophia* for sheep/goats). To our knowledge, this was the largest investigation of farm animal exposures and the human microbiome to date. Our preliminary findings suggest that animal farming may alter the oral microbiome and provide new insights into the potential role of animal exposures in cancer etiology.

#0835 Occupational-related exposure to benzene and risk of female genital cancers: Systematic review and meta-analysis.

D. Shah[1], V. DeStefano[1], V. Shah[2], M. S. Seyyedsalehi[3], M. Bonetti[3], P. Boffetta[1];
[1]Renaissance School of Medicine at Stony Brook University, Stony Brook, NY, [2]Northeastern University, Boston, MA, [3]University of Bologna, Bologna, Italy

Purpose: The IARC monograph has classified benzene as a class I carcinogen, as evidenced by its association with hematological malignancies. However, its association with female genital cancers (ovarian, uterine, cervical) has not been characterized. Therefore, a meta-analysis of cohort studies was performed to determine the possible correlation between occupational benzene exposure and the risk of female genital cancers.
Methods: A systematic literature review was conducted that identified 7221 relevant publications. A total of 9 cohort studies detailing occupational exposure to benzene and correlated risk of ovarian, uterine, and cervical cancers were retained, and a meta-analysis (using fixed effects model) was performed. PECOS criteria and STROBE guidelines were followed, and the study protocol was registered in the PROSPERO database (Reg. No. 379720). Study quality was assessed using a modified Newcastle-Ottawa scale (NOS).
Results: The summary relative risk (RR) for ever-benzene exposure was 1.22 (95% CI=1.03-1.44, I^2<0.001%, n=19); corresponding RR results for female genital cancers incidence and mortality were 1.09 (95% CI=0.92-1.29, I^2=5.0%, n=17) and 1.69 (95% CI=1.18-2.4, I^2<0.001%, n=9), respectively. These findings were confirmed in sub-analyses by geographical area, industry type, publication year, and levels of benzene exposure. Heterogeneity was detected amongst industries of employment (p-het=0.012) which included petroleum, chemical, printing, and mixed industries categories. Notably, the printing industry (compositors, press operators, and bookbinders) had a summary RR of 2.56 (95% CI=1.45-4.52, I^2=35.0%, n=2). However, no heterogeneity was observed for geographical regions (p-het=0.77), duration of benzene exposure (p-het=0.73), publication year (p-het=0.89), or among varying study quality (< or ≥ median NOS score; p-het=0.14). No publication bias was detected (p=0.43).
Conclusions: Our meta-analysis identified an association between occupational benzene exposure and the risk of female genital cancers. The association was restricted to the industry of employment. Effects of residual confounding variables cannot be excluded, however, given the present association, there is a potential for causality, especially in workers employed in the printing industry.

#0836 Long-term particulate matter and mortality in cancer patients and survivors compared to general population.

M. Shin[1], O.-J. Kim[2], S.-A. Choe[3], Y.-J. Choi[1], H. Kim[4], W. Lee[4], H. Lee[1], S.-Y. Kim[1];

[1]Graduate School of Cancer Science and Policy, National Cancer Center, Goyang, Korea, Republic of, [2]National Institute of Environment Research, Incheon, Korea, Republic of, [3]College of Medicine, Korea University, Seoul, Korea, Republic of, [4]Graduate School of Public Health, Seoul National University, Seoul, Korea, Republic of

Background and Aim Exposure to particulate matter (PM) has been reported as a major environmental hazard to human health. Although many studies found the associations with mortality and its susceptibility in patients with diabetes and heart diseases, few studies paid attention to cancer. In addition, there were no studies that compared these associations in cancer patients and survivors with those in healthy people from the same population. The aim of this study is to compare the association between long-term exposure to PM with all-cause and cause-specific mortality between the general population and cancer patients and survivors both of which were selected from the same cohort in the Seoul Metropolitan Area (SMA), South Korea.

Methods Using the National Health Insurance Services-National Sample cohort, we selected the subjects who received health screening during 2005-2007, had full address information, and were aged 30-80 without severe disability. We defined cause-specific mortality based on the International Classification of Disease, 10^{th} reversion from 2007 to 2015. Using a previously-validated prediction model, we estimated annual-average PM concentrations at participants' district-level addresses and assessed individual long-term exposure as the average concentrations in the previous 5 years on each year during the follow-up. Then, we performed time-varying Cox proportional hazards model to estimate hazard ratios (HRs) and 95% confidence intervals (95%CI) per 10 ug/m^3 increase in $PM_{2.5}$ and PM_{10} adjusting for sociodemographic characteristics, family history of cancer, and health behaviors.

Results Our study population of 98,493 adults include 94,494 (95.9%) general population and 3,999 (4.1%) cancer patients and survivors in the SMA at baseline. In the general population, we observed the associations with deaths from all causes ($PM_{2.5}$: HR=1.31, 95% CI: 1.10-1.55; PM_{10}: 1.07, 1.00-1.15), non-accidental causes ($PM_{2.5}$: 1.51, 1.24-1.84; PM_{10}: 1.10, 1.02-1.20), and cardiopulmonary diseases ($PM_{2.5}$: 1.57, 1.07-2.31); PM_{10}: 1.22, 1.04-1.43). In contrast, although all HRs of all-cause and cause-specific mortality were not statistically significant, cancer patients and survivors showed much higher HRs for all-cancer and lung-cancer mortality ($PM_{2.5}$: 1.57 and 1.99; PM_{10}: 1.01 and 1.33) than those for all or other cause-specific mortality as well as those of cancer-related mortality in the general population.

Conclusions Our findings provided suggestive evidence of the different causes of deaths associated with long-term exposure to air pollution between the general population and cancer patients and survivors. While PM could behave as a risk factor of cardiopulmonary deaths in the general population, after diagnosed with cancer, exposure to PM may increase the risk of dying of cancer.

#0837 Carbaryl use and cancer incidence in the agricultural health study - An updated analysis.

P. A. Erickson[1], G. Andreotti[1], R. Remigio[1], C. G. Parks[2], D. P. Sandler[2], P. S. Albert[1], K. H. Barry[3], J. N. Hofmann[1], L. E. Beane Freeman[1];
[1]National Cancer Institute, Rockville, MD, [2]National Institute of Environmental Health Sciences, Durham, NC, [3]University of Maryland School of Medicine, Baltimore, MD

Background: Carbaryl is a carbamate insecticide with widespread residential and agricultural uses. Previous epidemiologic investigations, including in the Agricultural Health Study (AHS), have suggested potential associations between carbaryl use and cancer risk. In this analysis, we updated a previous AHS evaluation of carbaryl and cancer risk by incorporating additional exposure information and follow-up time.
Methods: The AHS is a prospective cohort study of licensed pesticide applicators in North Carolina (NC) and Iowa (IA). Information on lifetime pesticide use, including carbaryl, was reported on questionnaires at enrollment (1993-1997) and follow-up (1999-2005). We evaluated cancer risks associated with ever-use and intensity-weighted lifetime days (IWLD) of carbaryl use, comparing those who reported use to those who did not. For IWLD, carbaryl exposure was categorized (quartiles, tertiles, or the median) among users, depending on the number of cases. Among 52,625 applicators, 8,713 incident cancers were identified from linkages with state cancer registries through 2014 (NC) or 2017 (IA). We used Poisson regression to estimate risk ratios (RR) and 95% confidence intervals (CI), controlling for confounders, and evaluated lagged exposures.
Results: Approximately 50% of applicators reported use of carbaryl. Among cancer cases, 53% reported carbaryl use. Increasing IWLD of carbaryl use was associated with stomach cancer (RR_{T3}=2.15, 95% CI: 1.11-4.15, *p*-trend=0.02), which persisted across lags up to 15 years. Carbaryl users in the highest quartile of IWLD had an increased risk of leukemia (RR_{Q4}=2.12, 95% CI: 1.05-4.29, *p*-trend=0.08); this risk remained elevated, though attenuated, when exposure was lagged by 5-years (RR_{Q4}=1.86, 95% CI: 0.91-3.81, *p*-trend=0.14). Ever-use of carbaryl was also suggestively associated with both esophageal (RR=1.45, 95% CI: 0.98-2.14) and tongue (RR=1.87, 95% CI: 0.93-3.74) cancers.
Conclusion: This study provides novel evidence of associations between carbaryl use, leukemia, and stomach cancer, as well as suggestive evidence of elevated risks of esophageal and tongue cancers. With more than 7,000 added cancer cases and up to 14 additional years of follow-up time as compared to a previous analysis in the AHS, we were able evaluate cancer sites not previously examined, making this the largest prospective study of carbaryl and cancer risk to date. Our findings highlight the need for additional studies of this widely used insecticide.

#0838 Population attributable fraction of occupational carcinogens for cancer incidence among Korean adults in 2020.

E. Kim[1], D.-H. Koh[2], S. Park[3], Y.-J. Choi[4], H. Seo[4], I. Kim[5], J.-S. Im[4];

[1]National Health Insurance Service, Wonju, Korea, Republic of, [2]International St. Mary's Hospital, Incheon, Korea, Republic of, [3]Seoul National University College of Medicine, Seoul, Korea, Republic of, [4]National Cancer Center, Goyang, Korea, Republic of, [5]Hanyang University College of Medicine, Seoul, Korea, Republic of

Assessing the level and scope of exposure to occupational carcinogens on a country-specific basis presents challenges, and as a result, it has been appraised as uncertain when compared with other factors in the estimation of the burden of cancer. The Korean CARcinogen Exposure (K-CAREX) developed in 2021 is utilized to estimate the population at risk in industrial work environments in Korea (Koh et al., 2021). Our goal is to estimate preventable cancer incidence attributable to occupational carcinogens in Korea, utilizing the K-CAREX program and employing appropriate methodology. Among the exposures classified as Group 1 factors by IARC, considering the possibility of occupational exposure. Population attributable fractions (PAFs) were computed using Levin's Formula (1953), considering a latency period of 15 years between exposure and cancer in our assessment. The prevalence of exposure was calculated using K-CAREX program and census data. The relative risk (RR) for incidence was derived from a meta-analysis of literature. It was possible to calculate PAFs for 11 occupational factors linked with 8 cancer types. This estimation was chosen based on a combination of exposure and sufficient evidence of human carcinogenicity. As a result, Population attributable fractions (PAFs) for cancer incidence associated with occupational carcinogens was estimated at 1% in 2020. Lung cancer (approximately 90%) was found to be the most prevalent type of cancer attributable to occupational factors, as widely acknowledged. The prevalence of exposure to occupational carcinogens was 22%, with Diesel engine exhaust being the most significant source for both genders. Since the early 2000s, the exposure levels of asbestos, subject to usage prohibition and restriction measures, were estimated to be at a lower level compared to other countries. It is evident that these estimates reflect the characteristics of the Korean industry. This is anticipated to provide a foundation for the development of methodologies and indicators essential for measuring the burden of occupational cancer in the country.

#0839 Interaction between solvent exposure and genetic susceptibility and risk for bladder cancer.

D. Tadesse[1], N. Rothman[1], S. Xie[1], L. Hurwitz[1], M. C. Friesen[1], D. Baris[1], M. Schwenn[2], A. Johnson[3], M. Karagas[4], D. T. Silverman[1], S. Koutros[1];
[1]National Cancer Institute, Rockville, MD, [2]Formerly Maine Cancer Registry, Augusta, ME, [3]Formerly Vermont Department of Health, Burlington, VT, [4]Giesel School of Medicine at Dartmouth, Hanover, NH

Introduction: Recent studies have reported an increased bladder cancer risk with occupational exposure to organic solvents, including exposure to benzene, toluene, and xylene (BTX). The metabolism of solvents is known to be influenced by genetic susceptibility. Here, we evaluated the association between BTX and bladder cancer, stratified by genotype in known bladder cancer susceptibility loci and in variants shown to impact the metabolism of solvents.
Methods: We evaluated if single-nucleotide polymorphisms (SNPs) modified the association between BTX exposure and bladder cancer risk in 1182 cases and 1408 controls from a population-based case-control study in New England. Ever and cumulative lifetime exposure to BTX was assessed using occupational histories obtained by personal interviews and exposure-oriented modules in conjunction with a job-exposure matrix. Genotyping was conducted using Illumina arrays and *GSTM1* and *GSTT1* deletion were determined using melt curve/copy number assays. We used multivariate logistic regression to calculate odds ratios (ORs) and 95% confidence intervals (CIs) for the association between BTX exposure and bladder cancer, stratified by genotype and to calculate p-values for multiplicative interaction.
Results: Ever exposure to BTX was more strongly associated with bladder cancer risk among individuals with the *GSTT1* null (deletion) genotype (OR 3.53, 95% CI 1.26-9.89), while exposed individuals with the *GSTT1* active genotype had a diminished risk (OR 1.40, 95% CI 0.93-2.10, P-interaction = 0.06). The association between benzene exposure and bladder cancer was similarly modified by *GSTT1* genotype (carriers of the deletion: OR 5.19, 95% CI 1.91, 14.13; carriers of one or two copies: OR 1.22, 95% CI 0.79, 1.89, p-interaction=0.008).
Conclusion: *GSTT1* genotype has been shown to impair the metabolism of solvents, particularly for benzene**.** Here we show that bladder cancer risk is higher among those exposed to solvents who also harbor a common deletion in *GSTT1,* adding to the evidence of a plausible link between BTX exposures and bladder cancer risk.

#0840 Serum concentrations of per- and polyfluorinated substances and risk of non-Hodgkin lymphoma.

J. Rhee[1], J. Koponen[2], J. N. Sampson[1], A. P. Keil[1], M. H. Ward[1], J. N. Hofmann[1], W.-Y. Huang[1], D. T. Silverman[1], P. Rantakokko[2], M. P. Purdue[1];
[1]National Cancer Institute, Rockville, MD, [2]Finnish National Institute of Health and Welfare, Helsinki, Finland

Per- and polyfluoroalkyl substances (PFAS) are persistent organic pollutants, some immunotoxic, that are detectable in the serum of most U.S. adults. Some studies of highly-exposed individuals have suggested positive associations between PFAS and non-Hodgkin lymphoma (NHL); however, it is unknown whether associations exist at lower exposure levels that are more common in the general population. To address this knowledge gap, we conducted a nested case-control study investigating serum PFAS concentrations and NHL within the Prostate, Lung, Colorectal and Ovarian Cancer Screening Trial. We measured pre-diagnostic serum concentrations (collected between 1993-2001) of five PFAS among 706 cases and 706 controls individually matched on the basis of age at baseline, sex, self-reported race and ethnicity, study center, calendar year of blood collection, and number of prior serum thaws. We estimated odds ratios (ORs) and 95% confidence intervals (CIs) for PFAS concentrations in relation to NHL, both overall and for selected histologic subtypes [diffuse large B cell lymphoma (DLBCL), follicular lymphoma (FL), lymphoplasmacytic lymphoma (LPL), and marginal zone lymphoma (MZL)] using conditional logistic regression. We found no evidence of a positive association with NHL for any of the five PFAS in analyses adjusting for all measured PFAS. In analyses of histologic subtypes, we observed a positive association between perfluorohexane sulfonate (PFHxS) and DLBCL (OR per doubling in concentration=1.27, 95% CI=1.07, 1.50) which remained for cases diagnosed ≥10 years after blood collection (OR=1.34, 95% CI=1.09, 1.64). We also observed inverse associations with PFNA for all subtypes (DLBCL, OR=0.84, 95% CI=0.72, 0.98; FL, OR=0.86, 95% CI=0.69, 1.08; LPL/MZL, OR=0.86, 95% CI=0.66, 1.12), although these associations were null among participants with blood drawn prior to 1997 (DLBCL: $OR_{<1997}$=0.95, $OR_{\geq 1997}$=0.67, $P_{interaction}$=0.001; FL: $OR_{<1997}$=1.01, $OR_{\geq 1997}$=0.77, $P_{interaction}$ =0.08; LPL/MZL: $OR_{<1997}$=1.26, $OR_{\geq 1997}$=0.88, $P_{interaction}$ =0.03). In conclusion, our findings from a cohort study with PFAS serum concentrations comparable to that of the general population do not support an association with increased risk of NHL overall. The suggestive evidence of a positive association between PFHxS and DLBCL warrants further investigation.

#0841 Fine particulate matter exposure during breast cancer treatment among older women associated with increased mortality.

B. Bates[1], R. Nethery[2], M. Rua[1], H. Iyer[3], E. Bandera[3], S. Setoguchi[1];

[1]Rutgers Institute for Health, Health Care Policy, and Aging Research, New Brunswick, NJ, [2]Harvard T.H. Chan School of Public Health, Boston, MA, [3]Rutgers Cancer Institute of New Jersey, New Brunswick, NJ

Background: Fine Particulate Matter ($PM_{2.5}$) is associated with higher mortality among people with chronic conditions. Breast cancer (BC) survivors may be particularly vulnerable during cancer treatment. We assessed the association between $PM_{2.5}$ during 9-months following BC diagnosis and all-cause and BC-mortality using policy relevant $PM_{2.5}$ cut-offs.

Methods: Using SEER-Medicare linked with a high-resolution model-based $PM_{2.5}$ by residential zipcode (2007-2016), we assembled a cohort of women ≥66 years with incident stage I-IV BC. We assessed $PM_{2.5}$ exposure, categorized as <8 μg/m^3 (low), 8-12 μg/m^3 (moderate) and >12 μg/m^3 (high—above air quality standard), and types of cancer treatments (surgery [SX], chemotherapy [CTX], radiation therapy [RTX]) during a 9-month landmark period. We identified all-cause and BC death within 5 years of diagnosis. We fit multivariable Cox proportional hazard models to assess associations with $PM_{2.5}$ exposure adjusting for individual-level characteristics (demographics, tumor characteristics, comorbidities), neighborhood SES, SEER state, and long-term $PM_{2.5}$ exposure. We also evaluated the association between $PM_{2.5}$ exposure and mortality by treatment types (SX, SX + RTX, SX + CTX, SX + RTX + CTX, and RTX and/or CTX). We used multiple imputation to account for missing variables (race, ER status, HER2 status, grade).

Results: Among 72,798 women (mean age 75 years, 83% white, 56% stage I, 32% II, 9.2% III, 2.9% IV), 41%, 32%, 13%, 8.4%, and 5.1% received SX + RTX, SX only, SX + Chemo + RTX, SX + Chemo, and CTX and/or RTX. The mean $PM_{2.5}$ level was 8.8 μg/m^3 [36%, 52% and 11% were exposed to <8, 8-12, and >12, respectively]. We observed 12,163 all-cause and 4,729 BC deaths during follow-up. Compared to those exposed to low levels, higher levels of $PM_{2.5}$ exposure were associated with increased all-cause mortality for both moderate $PM_{2.5}$ [HR 1.03 (95%CI:1.00-1.05)] and high $PM_{2.5}$ [HR 1.09 (95%CI: 1.06-1.14)] but not BC-specific mortality. Among treatment subgroups, $PM_{2.5}$ was associated with higher all-cause mortality in SX+RTX for moderate [HR 1.24 (95%CI:1.18-1.32)] and high $PM_{2.5}$ [HR 1.36 (95%CI: 1.25-1.48)] and SX+RTX+CTX for high $PM_{2.5}$ [HR 1.33 (95%CI: 1.17-1.51)]. There were no association between moderate/high $PM_{2.5}$ with all-cause mortality in SX only and SX+CTX. Among the SX+RTX subgroup, BC-specific mortality was elevated for both moderate [HR 1.50 (95%CI:1.35-1.66)] and high $PM_{2.5}$ [HR 1.81 (95%CI: 1.55-2.12)].

Conclusion: Even below EPA regulatory thresholds ($PM_{2.5}$ <12 μg/m^3), we observed increased risk of death in BC survivors who had high $PM_{2.5}$ exposure during treatment period. The elevated mortality primarily occurred among women who received RTX and was present for all-cause and BC-specific mortality. The potential interaction between RTX and $PM_{2.5}$ exposure, even after adjusting for tumor subtype and stage, warrants further evaluation.

#0842 Maize consumption and circulating aflatoxin B_1 levels in Mexican adults.

M. Lajous[1], O. Solis-Martinez[2], A. Monge[1], J. Groopman[3], K. A. McGlynn[4], M. Romero[1], C. Batis[1], H. Lamadrid-Figeuroa[2], H. Riojas-Rodriguez[2];
[1]Instituto Nacional de Salud Publica, Ciudad de Mexico, Mexico, [2]Instituto Nacional de Salud Publica, Cuernavaca, Mexico, [3]Johns Hopkins Bloomberg School of Public Health, Baltimore, MD, [4]National Cancer Institute, Rockville, MD

Objective: To estimate the impact of maize consumption on aflatoxin B_1 [AFB_1] levels, a potent carcinogen, in Mexican adults living in south and eastern Mexico.
Methods: Study participants were women and men ≥40 years of age living in five high hepatocellular carcinoma burden states who participated in Mexico's 2018 National Health and Nutrition Survey, a stratified, multi-stage, and cluster survey probability sampling household survey that is representative of the Mexican population. We estimated the consumption of maize intake in grams per day using a previously validated semi-quantitative food frequency questionnaire with a time reference of the previous seven days. We determined circulating AFB_1-albumin lysine adduct [AFB_1-lys] levels in serum using liquid chromatography. Guided by subject-matter knowledge we fit multivariable linear regression models that considered the survey design and included age, sex, residence, ethnicity, education, socioeconomic status, and foods known to be contaminated with aflatoxins including peanuts, rice, dried chili, milk, and cheese.
Results: Among the 915 participants, median maize consumption was 307 grams per day [Q1-Q3: 165 - 554]. Maize *tortillas* contributed 80% of the total maize consumption. The median maize *tortillas* consumption was 252 grams per day [Q1-Q3: 120 - 462], approximately 8 tortillas per day. Prevalence of AFB_1-lys detection was 92% and median levels were 0.127 pg/µL [Q1-Q3: 0.052 - 0.449]. After adjusting for factors that may affect aflatoxin levels, for every 100 grams of maize consumption AFB_1-lys levels were 7.4% [β: 0.071, 95% CI: 0.030 - 0.112] higher. And for every tortilla consumed [30 g of maize], we observed a 2.0% [β: 0.020, 95% CI: 0.006 - 0.034] higher level of circulating AFB_1-lys.
Conclusion: These findings indicate that maize and maize *tortillas* may be an important source of AFB_1 exposure in the Mexican population. Mexico requires effective public health interventions to mitigate exposure to AFB_1.

#0843 The burden of Merkel cell carcinoma attributable to immunosuppression, ultraviolet radiation, and Merkel cell polyomavirus in the United States.

J. T. Tribble[1], K. Volesky-Avellaneda[1], Q. Luo[1], M. R. Sargen[1], I. Brownell[2], E. K. Cahoon[1], M. Shiels[1], R. Pfeiffer[1], A. Moreno[3], B. Y. Hernandez[4], E. Engels[1]; [1]National Cancer Institute, Rockville, MD, [2]National Institute of Arthritis and Musculoskeletal and Skin Diseases, Bethesda, MD, [3]Texas Department of State Health Services, Austin, TX, [4]University of Hawai'i Cancer Center, Honolulu, HI

Background: Merkel cell carcinoma (MCC) is a rare, aggressive skin cancer. No published study has estimated the contribution of the major potentially modifiable risk factors, such as immunosuppression, ultraviolet radiation (UVR) and infection with Merkel cell polyomavirus (MCPyV), to the burden of MCC in the US. We estimated the population attributable fractions (PAFs) for MCC associated with immunosuppression (HIV and organ transplantation), MCPyV, and UVR in the US during 2001-2020.

Methods: We calculated PAFs for immunosuppression and UVR using the formula: prevalence in cases (Pc)*[(Relative risk, RR-1)/RR]. The proportion of MCC cases among organ recipients and people with HIV (Pc) were derived from US cancer registries in the HIV/AIDS Cancer Match Study, Transplant Cancer Match Study, and the Surveillance Epidemiology and End Results (SEER) Program data. To approximate the RRs, we calculated standardized incidence ratios (SIRs) comparing MCC incidence in people with HIV and organ recipients to the general population. We merged SEER data on MCC cases by county with data on ambient UVR levels in order to create population quintiles of UVR exposure. Since only non-Hispanic White individuals showed elevated IRRs for increased ambient UVR exposure, we estimated the PAF of UVR by calculating incidence rate ratios (IRR ≈ RR) comparing MCC incidence in non-Hispanic White individuals to all other races/ethnicities (at any UVR level) as the reference; here, Pc was the proportion of non-Hispanic White patients in each quintile. To estimate the PAF of MCPyV, we meta-analyzed US studies reporting on MCPyV prevalence in MCC tissues (here PAF ≈ Pc).

Results: Over the study period (2001-2020), 40,571 MCCs were diagnosed in the US. Compared to the general population, organ recipients had 13 times higher (SIR=12.7, CI: 11.3-14.2) and people with HIV had three times higher (SIR=2.78, CI: 2.01-3.75) risk of MCC. Due to the rarity of these exposures (HIV Pc = 0.4%; Transplant Pc = 1.9%), only 0.2% of MCC cases were attributable to HIV and 1.7% were attributable to organ transplantation. Compared with people in other racial/ethnic groups, the IRRs of non-Hispanic White individuals at the various levels of ambient UVR for MCC arising on the head and neck ranged from 4.24 to 5.03 and for other primary sites ranged from 2.81 to 3.36. After combining the PAFs for these sites, the overall PAF for UVR was 65.8%. Meta-analyzing 20 studies with 984 MCC cases combined, we found that 66.1% (CI: 58.0-72.2%) of MCCs were attributable to MCPyV.

Conclusions: While a small proportion of MCCs were due to immunosuppression from HIV infection and organ transplantation, UVR and MCPyV played a major role in MCC burden. Future research is required to assess the combined impact of these risk factors on MCC incidence.

#0844 DNA methylation-derived immune cell profiles and risk of cancers in Black participants in the ARIC Study.

C. S. Semancik[1], N. Zhao[1], D. Koestler[2], E. Boerwinkle[3], J. Bressler[4], K. Kelsey[5], E. A. Platz[6], D. S. Michaud[1];
[1]Tufts University School of Medicine, Boston, MA, [2]University of Kanas Medical Center; University of Kansas Cancer Center, Kansas City, KS, [3]Human Genetics Center, School of Public Health, University of Texas Health Science Center at Houston; Human Genome Sequencing Center, Baylor College of Medicine, Houston, TX, [4]Human Genetics Center, School of Public Health, University of Texas Health Science Center at Houston, Houston, TX, [5]Brown University, Providence, RI, [6]Johns Hopkins Bloomberg School of Public Health; The Sidney Kimmel Comprehensive Cancer Center at Johns Hopkins, Baltimore, MD

Background: Prior cohort studies assessing cancer risk based on immune cell subtype profiles have predominantly focused on White populations. This limitation can obscure vital insights into how cancer risks vary across races, ethnicities, or exposures. This study was designed with the purpose of examining associations between pre-diagnostic immune cell profiles and cancer risk in Black participants.
Methods: In this study, DNA methylation was measured in blood samples collected between 1993 and 1995 from a subset of 2,467 Black participants in the Atherosclerosis Risk in Communities (ARIC) prospective cohort study. Immune cell subtype proportions were estimated using deconvolution based on leukocyte DNA methylation markers. The analysis included 668 incident cancers ascertained between time of blood draw and 2015. Cox proportional hazards regression models were used to analyze the association between immune cell subtype proportions and cancer incidence (all cancers; lung, breast, and prostate cancers). Models controlled for age, sex, BMI, self-reported smoking status, self-reported and methylation-derived smoking pack-years, postmenopausal hormone use, and batch effect, along with other cancer-specific factors.
Results: Increased T regulatory cell (Treg) proportions were associated with significantly higher risk of lung cancer (HR: 1.22, 95% CI = 1.06, 1.41 per percent increase; n = 84 cases) and suggestively higher risk of all cancers. Increased B memory cell proportions were associated with significantly higher risk of prostate cancer (HR: 1.17, 95% CI = 1.04, 1.33; n = 173 cases), all cancers (HR: 1.13, 95% CI = 1.05, 1.22), and suggestively higher risk of lung cancer. Increased CD8+ naïve cell proportions were associated with suggestively lower risk of lung cancer and all cancers, and significantly lower risk of all cancers in participants over the median age of 55 years (HR: 0.91, 95% CI = 0.83, 0.98). Cancer risks for other immune cell subtypes were null.
Conclusions: These results in Black participants align closely with prior findings in largely White populations. Deconvolution allowed for the extension of work on cancer immunity (which has largely focused on major immune cell types) to immune cell subtypes like B memory cells and CD8+ naïve cells. The results are consistent with Tregs initiating and accelerating cancer development by impeding the usual protective immune response. A large reservoir of CD8+ naïve cells may allow for a more targeted and efficient elimination of malignant clones. Further studies should assess these relationships in other cancer types and better elucidate the interplay of B cells in theorized mechanistic processes. This study provides insight into the role of immune cell subtypes in cancer risk among Black men and women.
Funding: NHLBI, NCR, NPCR

#0845 Population attributable fraction of cancer incidence due to infectious agents in 2020 in the Republic of Korea.

K.-S. Lee[1], H. Lee[2], Y.-J. Choi[1], M. Ki[1], A. Shin[3], J.-H. Kim[4], S.-K. Park[3], S.-S. Sung[3], S. Moon[3], H. Seo[1], J.-K. Oh[1], J.-S. Im[1];
[1]National Cancer Center - Korea, Goyang-si, Gyeonggi-do, Korea, Republic of, [2]National Medical Center - Korea, Seoul, Korea, Republic of, [3]Seoul National University College of Medicine - Korea, Seoul, Korea, Republic of, [4]Sungkyunkwan University School of Medicine- Korea, Suwon, Korea, Republic of

Purpose: Earlier in 2009, National Cancer Center Korea estimated population attributable fraction (PAF) of cancer incidence due to infectious agents as 24.5% in men and 15.4% in women. This study aimed to investigate the proportion of cancer incidence attributable to infectious agents in the Korean population as of 2020.
Materials and Methods: We organized the Consensus Committee to establish strategy and methodology of PAF estimation. Based on the consensus, infectious agents and cancer sites for PAF estimation were selected according to the IARC List of classification with sufficient evidence in human. As a result, infectious agents included hepatitis B and C virus (HBV and HCV), *Helicobacter pylori* (*H. pylori*), human papilloma virus (HPV), *Clonorchis sinensis* (*C.sinensis*), Epstein Barr virus, and human immunodeficiency virus, and cancer sites included hepatocellular carcinoma (HCC), cholangiocarcinoma (CCC), gastric cancer, pancreatic cancer, cervical cancer, and non-Hodgkin lymphoma. The PAF was calculated by using Levin's formula including exposure prevalence and relative risks (RRs). Exposure prevalence data were collected from literature review of studies in Korean population in 2005 or earlier, assuming at least 15 years of latent period from risk exposure to cancer development. We performed systematic review for cohort studies and case-control studies which investigated RRs or ORs of cancer due to infectious agents in Korean population. Pooled RRs were estimated by meta-analysis of RRs or ORs by using random-effects model.
Results: The fractions of all cancer incidence attributable to infectious agents were estimated to be 13.5% and 7.1% in men and women, respectively. The reduction in PAFs of cancer incidence due to infection in 2020 compared to 2009 is considered due to decrease in exposure prevalence. The major findings regarding infectious agents with large PAFs are as the following. We found that the fractions of HCC cases attributable to HBV infection were 47.7% and 38.4% for cancer incidence in men and women, respectively. The estimated PAFs of gastric cancer due to *H. pylori* were 40.4% in men and 38.2% in women. *C. sinensis* was related to 9.8% of CCC cases in men and 5.2% in women. A total of 77.7% of cervical cancer incidence was attributed to HPV infection.
Conclusion: Although the total PAF due to infection has decreased over the last decade, infection still contributes a substantial fraction to cancer incidence in Korea. These recent estimates of cancer burden due to infection are important for planning and evaluating the national cancer prevention programs.Funding Sources: This work was supported by the National Cancer Center Grant (NCC-2210840).

#0847 Association of methylation-based stem cell divisions with lifetime cancer risk and cancer progression.

Y. Wu[1], C. Thompson[2], F. Schumacher[1];

[1]Case Western Reserve University School of Medicine, Cleveland Heights, OH, [2]Penn State College of Medicine, Hershey, PA

Cancer initiation arises from the accumulation of somatic mutations acquired during stem cell mitotic events mediated by carcinogenic risk factors. On an ecological level, Tomasetti and Vogelstein (2015) demonstrated that lifetime risk of solid tumor cancer types were strongly correlated with total number of stem cell divisions estimated from tissue-specific cell lines. Recently, several mitotic clocks (MC) have been developed to estimate stem cell division rates (SCDR) based on whole-genome methylation arrays. Here, we compare estimated SCDR for several tissue types with tissue-specific cancer incidence and lifetime risk estimates. Furthermore, we assess the link between SCDR with cancer progression and survival.

Array-based methylation data derived from normal adjacent tissue in TCGA was used to estimate SCDR for 15 cancer types. A Pearson correlation test was performed to assess the association between SCDR and cancer-specific incidence and lifetime risk for each cancer type overall and stratified by self-reported race (*e.g.* White and Black). SCDR was estimated in tumors from TCGA for 4 common cancers and subtypes: breast (BRCA), prostate (PRAD), lung adenocarcinoma (LUAD), and lung squamous cell carcinoma (LUSC). A Spearman correlation test was used to identify potential trends between SCDR and pathological stage. Cox proportional hazard (PH) models adjusted for age at diagnosis and treatment status (*e.g.* surgery, radiation, *etc.*) were used to evaluate the association of time to death with SCDR terciles across different cancer stages.

We observed a similar trend between SCDR and overall incidence (cor=0.61, p=0.01), aligning with earlier findings. Stratified-specific trends between cancer incidence and SCDR was consistent for both Black and White populations (cor=0.62 vs 0.66). Tumor analysis revealed a significant correlation between SCDR and pathological stage (*e.g.* stage 1, 2, and 3/4) for BRCA ($p<0.001$) and pathological stage (*e.g.* stage 2, 3 and 4) for PRAD ($p<0.001$), suggesting its potential as a marker of cancer progression. However, the correlation between LUAD, LUSC and pathological stage was insignificant. Based on Cox PH model, within stage III BRCA, SCDR significantly contributed to explaining variability in survival (p=0.04), emphasizing its potential prognostic value beyond cancer stage.

Our study supports earlier findings applying methylation based SCDR estimates and shows that this association is consistent across racial groups. This implies that SCDR may act as a biological marker of a combination of various genetic and environmental risk factors underlying disease etiology. Further analyses will be extended to all cancers in TCGA. Lastly, we demonstrate that MC-based SCDR estimation has the potential to serve as a clinical tool to identify individuals at elevated risk of cancer initiation, track progression, and complement cancer stage for predicting survival.

#0848 Influence of young age at diagnosis on the clinical presentation of disease and survival among patients with multiple myeloma.

K. L. Ong, K. D. Arnold, G. Ravi, L. J. Costa, E. E. Brown;
University of Alabama at Birmingham, Birmingham, AL

Background: Age is an important prognostic factor for multiple myeloma (MM). We evaluated the influence of age on the clinical presentation and outcomes among newly diagnosed patients with MM to optimize risk stratification.
Methods: In 850 patients with first primary confirmed MM prospectively enrolled in the Integrative Molecular And Genetic Epidemiology (IMAGE) study (2009-2020), we evaluated the presence of diagnostic myeloma-defining events (MDE), progression free survival (PFS) and overall survival (OS) by young age at diagnosis (≤50 years). We evaluated the association of young age with the prevalence of diagnostic MDE, clinical features and chromosomal abnormalities using the prevalence odds ratio (OR) and corresponding 95% confidence interval (CI) calculated from multivariable logistic regression. Median PFS and OS were graphically examined using Kaplan-Meier survival curves with log-rank tests used to compare survival by diagnostic age group. Risks of disease progression and all-cause mortality were estimated using hazard ratios (HR) and corresponding 95% CI calculated from multivariable Cox proportional hazard models.
Results.: Of the 850 patients, 15.4% were diagnosed at ≤50 years of age, 54% were male and 40% self-identified as Black. Compared to patients diagnosed with MM over the age of 50, young patients were more likely to self-identify as Black (59.5% vs 40.5%; P<0.0001) and to report a negative smoking history (66.2% v 56.4%; P=0.01), and less likely to present with age-dependent comorbidities including hypertension, hyperlipidemia and diabetes mellitus type II (P≤0.0001). In multivariable analyses, young patients, compared to older patients, were more likely to present at diagnosis with higher median percent bone marrow plasma cells (70% v 55%; P=0.02) and to undergo autologous stem cell transplant (ASCT) as part of their first-line treatment (82.0% v 67.6%; P=0.01) after controlling for sex, race, body mass index, smoking status and comorbidities. We did not observe significant associations of young age with the prevalence of any other MDE, clinical feature or chromosomal abnormality evaluated. The median OS was 106.9 months (range, 0.23-356.1). OS was significantly longer in young patients with MM compared to patients aged greater than 50 years (159 v 99 months, respectively; P<0.001) leading to a suggestive 1.5-fold decreased risk of mortality among younger newly diagnosed patients (HR=0.67, 95% CI 0.39-1.14; P=0.14) after adjusting for sex, International Staging System-stage, adverse cytogenetic abnormalities, and ASCT. We did not observe associations with age and PFS (P=0.81).
Conclusions: Findings suggest that newly diagnosed younger patients with MM are more likely to self-identify as Black, present with more bone marrow plasma cells, have less age-dependent comorbidities, and undergo ASCT leading to a suggestive survival advantage.

#0849 Deciphering the link between aging, lobular involution, and breast cancer risk: The role of LIFR/pSTAT3 signaling.

J. C. Lue[1], D. Radisky[2], M. Stallings-Mann[2], M. Sherman[3], A. Degnim[3], B. McCauley[3], T. Hoskin[3];

[1]Mayo Clinic Graduate School of Biomedical Sciences, Jacksonville, FL, [2]Mayo Clinic, Jacksonville, MN, [3]Mayo Clinic, Rochester, MN

Background: Age-related lobular involution (ARLI), characterized by regression of breast epithelial tissue during the peri-and post-menopausal period, plays a crucial role in breast cancer risk. Delayed or incomplete ARLI is linked with increased postmenopausal breast cancer susceptibility.This study focuses on unraveling the molecular mechanisms of ARLI, drawing parallels with the well-characterized postpartum involution (PPI). Our aim was to discover biomarkers differentiating women who progressed through ARLI from those with stagnant ARLI.

Methods: We utilized the Mayo Clinic Benign Breast Disease (BBD) cohort, analyzing 108 perimenopausal women aged 45-55 who had a subsequent benign biopsy between 2-15 years later. We assessed Lobular Involution (LI) status by comparing the number and size of lobules in initial and subsequent biopsies. RNA profiling of initial biopsies was performed using NanoString 10360 and BC360, identifying differentially expressed genes between ARLI progression and stagnation. Immunohistochemistry (IHC) mapped the expression of these biomarkers in epithelial lobules.

Results: We identified 37 genes with significant differential expression, highlighting Leukemia Inhibitory Factor Receptor (LIFR) as upregulated in ARLI stagnant samples. LIFR, part of the IL-6 cytokine signaling pathway, is known for its role in the induction of apoptosis during PPI via pSTAT3 activation. Our IHC analyses of initial biopsies of women who differentially progress through ARLI confirmed differential expression of LIFR that is coordinately regulated with pSTAT3.

Conclusion: Our findings reveal significant parallels between ARLI and PPI. Future research will assess how LIFR/pSTAT3 signaling is linked to induction of apoptotic markers in perimenopausal women and will investigate how anomalies in the LIFR/pSTAT3 pathway might contribute to heightened breast cancer risk in women with delayed or incomplete ARLI. This study not only sheds light on the complex biological processes of aging in breast tissue but also opens new avenues for breast cancer risk assessment and prevention strategies.

#0850 Androgenic alopecia and risks of overall and aggressive prostate cancer: An updated meta-analysis.

S. Amar[1], D. Hanelin[2], **I. Agalliu**[2];
[1]Yeshiva University, New York, NY, [2]Albert Einstein College of Medicine, Bronx, NY

Background: Androgenic alopecia, known as male pattern baldness (MPB), is a common hair loss disorder among men. MPB has similar risk factors with prostate cancer (PrCa) including advancing age, family history, and sex hormones. Several studies have examined the associations between MPB and PrCa but the evidence remains unclear. We carried out a meta-analysis of epidemiological studies that examined the relationship between patterns of baldness: frontal, vertex, or both and PrCa risk.
Methods: A literature search was performed in October 2022 using PubMed and Web of Science databases for epidemiological studies published between 1/1/2000 and 10/31/2022, which examined the above hypothesis. From each eligible study, relevant data were extracted on study design, population, sample size, prevalence of MPB at various ages, and corresponding associations with risks of total and aggressive PrCa. Pooled relative risks (RR) and corresponding 95% confidence intervals (CI) were calculated using the DerSimonian and Laird random-effects models. Heterogeneity across studies was assessed by I^2 statistic.
Results: A total of 14 studies: 14,573 cases and 132,434 controls/non-cases were included. The prevalence of MPB increased from 5% to 70% with aging and varied across studies. Vertex MPB at ages 40 years or older was associated with a pooled RR of 1.08 (95%CI 1.00-1.17) of total PrCa, but there was no association with frontal MPB. The onset of MBP at younger ages was also associated with RR=1.10 (95% CI 0.93 - 1.29) of PrCa, although results were not statistically significant. Results were similar when data were stratified by clinical features of PrCa, although there was large heterogeneity in the definition of aggressive PrCa across studies.
Conclusions: Men with vertex MPB may have modest increased risk of PrCa. However, the majority of studies were conducted in Caucasian men and they did not evaluate effect modifications by genetic variations in androgen metabolism pathway genes or changes in serum levels of androgens. Further, large well-designed prospective cohort studies are needed to better understand the complex relationship between genetic susceptibility, endogenous hormones, MBP and risk of PrCa.

#0851 Uncovering a novel role of succinate metabolism in tregulatory cells of aged epithelial ovarian cancer mice.

M. Udumula, H. Singh, F. Rashid, M. Hijaz, S. Giri, R. Rattan;
Henry Ford Health System, Detroit, MI

Epithelial Ovarian Cancer (EOC), the most fatal gynecologic cancer is a disease of older women, with median age of 63 years at diagnosis. Reduced naive T cell generation and a rise in immunosuppressive regulatory T (Treg) cells are hallmarks of aging, which are strongly correlated with advanced cancer stage. Aging also alters host and cellular metabolism, which can influence Treg number and function. Although metabolic alterations are known to impact ant-tumor immune response, the relationship between age-related metabolic dysfunction and immune cells is not fully understood. We utilized young (2 months) and old (18 months) female C57/B6 mice, and were injected intraperitoneally with $5x10^6$ mouse epithelial ovarian cancer $ID8^{p53-/-}$ cells. Old mice with EOC showed decreased survival compared to young mice (median survival 49 vs 65 days). Old mice with EOC presented with decreased $CD4^+$ and $CD8^+$ T cells, but a significant increase in $CD4^+CD25+FoxP3^+$ Treg cells in tumor micro environment (TME) and in blood. The Tregs from old mice displayed enhanced expression of IL10 and TGFβ, which corelated with their increased suppression of CD4 and CD8 T cells compared to Tregs isolated from young EOC mice. The CD4+ and CD8+ T cells also displayed decreased effector makers including CD4+IFNγ, CD8+IFNγ and CD8+ Granzyme B, compared to young EOC mice in TME and in blood. The tumor promoting role of Treg was validated by depleting Tregs using anti-CD25 antibody which resulted in decreased tumor burden and improved overall survival, of both young and old mice, more significantly in old EOC mice. Tregs from old mice with EOC displayed enhanced metabolic activity, reflected in increased oxidative phosphorylation (OXPHOS) compared to young EOC mice. Further, on inhibition of OXPHOS, the Tregs from old mice showed decreased expression of immunosuppressive markers Foxp3 and IL10. Targeted metabolomics of TCA cycle in the Tregs, revealed a 5-fold increase in succinate levels in old EOC Tregs compared to young. Succinate treatment enhanced the immunosuppressive Treg function along with an increase in levels of IL10 and TGFβ, while inhibition of succinate synthesis reversed the increase in FOXP3, IL10 and TGFβ. We identified fibroblast growth factor 21 (FGF-21), a hormone essential for T cell development, to be significantly decreased in ascites and plasma, of old mice. Supplementing FGF21 decreased Treg survival, number, and suppressive ability, resulting in increased $CD4^+$ and $CD8^+$ cells in aged EOC mice. FGF21 treatment decreased OXPHOS and succinate levels in aged Tregs. Overall, our observations indicate Tregs to be vital in driving aggressive EOC in old mice. The hyper-suppressive Tregs in old mice reprogram succinate metabolism to drive their suppressive ability which may be negatively regulated by FGF21. Thus, Treg-succinate-FGF21 may be a potential actionable pathway in precision targeting of EOC in the older population.

#0852 Measuring the level of knowledge and awareness about radon in Northeast Tennessee.

K. Al ksir[1], S. Stanifer[2], M. Quinn[1], H. Mamudu[1], D. Slawson[1];
[1]East Tennessee State University, Johnson City, TN, [2]University of Kentucky, Lexington, KY

Introduction: Radon, a radioactive gas found in soil and rocks, is the second leading cause of lung cancer in the United States (1). Despite its significant health risks, radon awareness and knowledge remain low (2). In Tennessee, where geological factors contribute to elevated radon levels, understanding the levels of awareness and knowledge about radon is crucial (3). This study focuses on Northeast Tennessee, an area known for its high radon concentrations.
Methods: This cross-sectional study, conducted from September to November 2023, aims to assess radon awareness and knowledge among participants from seven Northeast Tennessee health councils. These councils play a critical role in public health initiatives and provide access to individuals actively involved in health-related discussions. A convenience sample of 150 participants was chosen from an email listserv of 650 health council members. Participants, aged 18 or older, affiliated with the health councils in the study area, and physically present in the US, were eligible to participate. Demographic data, radon knowledge and awareness were assessed. Additional questions evaluated information sources, concern levels, and willingness to inform the community about radon.
Conclusion: This research addresses a significant knowledge gap regarding radon awareness and knowledge in Northeast Tennessee, an area with unique geological factors that elevate radon exposure risks. The study's findings will contribute to the development of targeted educational campaigns and interventions, ultimately promoting awareness and proactive measures to mitigate radon exposure in the region. With the potential to inform policy and public health efforts, this study holds the promise of reducing the health risks associated with radon in Northeast Tennessee.

#0853 Assessment of racial and ethnic disparities in environmental exposure-related cancer burden.

J. R. Bobbitt[1], F. Liu[1], J. Cullen[1], R. A. Keri[2];

[1]Case Western Reserve University School of Medicine, Cleveland, OH, [2]Lerner Research Institute, Cleveland Clinic Foundation, Cleveland, OH

The United States Environmental Protection Agency designates superfund sites as regions contaminated with hazardous waste. These sites have previously been associated with adverse health outcomes, including an increased incidence of cancer. Historically, communities with racial and ethnic minorities and people of low socioeconomic status have served as prime locations for these sites, as these communities have lacked the ability to advocate against this land use. Here, we ask whether racial and ethnic minorities are disproportionately exposed to these sites or other regions of hazardous waste in our catchment area at the Case Comprehensive Cancer Center, and in the state of Ohio. Further, we are examining whether areas of high exposure are associated with adverse health outcomes including higher cancer incidence and mortality. We utilized the Environmental Justice Index (EJI) database from the Centers for Disease Control and Prevention to assess, on a census tract level, the percent of racial and ethnic minorities in a region, defined as all persons except white, non-Hispanic individuals. We also queried hazardous and toxic waste sites including regions with a national priority list site, a toxic release inventory site, treatment, storage, and disposal sites, risk management plan sites, coal mines, and lead mines. We intersected these data and found that census tracts with a higher percentage of minority persons were more likely to be exposed to hazardous and toxic sites. Our current studies are assessing whether this high environmental burden is contributing to disproportionately worse cancer burden for these individuals. We will test this by comparing EJI data with data from the Ohio Cancer Incidence Surveillance System database to assess cancer incidence and mortality in Ohio. This will also provide an avenue for identifying specific exposures that may contribute to different cancer types. Further, we plan to assess if persons with low socioeconomic status or those living with disabilities are disproportionately affected by environmental burden. Overall, understanding environmental burden and health outcomes will facilitate the prioritization of communities at greatest need, contributing to greater health equity.

BIOINFORMATICS / COMPUTATIONAL BIOLOGY / SYSTEMS BIOLOGY / CONVERGENT SCIENCE: Application of Bioinformatics to Cancer Biology 1 Poster Session

#0857 Identify ROR1 expression in healthy human tissues using single-cell RNA sequencing.

Mingyang Feng[1], Sirui Tan[1], Yue Chen[1], Qiu Li[1], Yongsheng Wang[2]

[1]Department of Medical Oncology, Cancer Center, and State Key Laboratory of Biotherapy, West China Hospital of Sichuan University, Chengdu City, China,[2]Thoracic Oncology Ward, Cancer Center, and State Key Laboratory of Biotherapy, West China Hospital of Sichuan University, Chengdu City, China

Introduction: The Receptor Tyrosine Kinase-like Orphan Receptor 1 (ROR1) is a receptor for Wnt5a and is considered a tumor-specific antigen. Researchers are actively exploring the development of antibodies and adoptive cell therapies targeting ROR1, while the potential "on-target, off-tumor" toxicity is still a major concern. Previous studies have provided inconsistent results regarding the expression of ROR1 in normal tissues, highlighting the complexity of its expression profile. Therefore, we are conducting this study to address this challenge through the detection of ROR1 mRNA expression via single-cell RNA sequencing (scRNA-seq) and the evaluation of ROR1 protein levels by immunohistochemistry (IHC).
Methods: We retrieved the Gene Expression Omnibus (GEO) database and downloaded the scRNA-seq data of each organ. We used the Seurat package to normalize data, perform dimensionality reduction and conduct clustering. The differentially expressed genes of each cell cluster were identified, and the cell clusters were then manually annotated. We further conducted the IHC on the tissue microarray (TMA), and evaluated the ROR1 immunostaining.
Results: We analyzed the scRNA-seq data of 908,941 cells from 14 types of healthy human organs, and 132,837 (14.61%) of cells expressed ROR1. Cell clusters in which the organ's ROR1 positive rate was >1% included the human Heart (Overall 25.99%, Ventricular cardiomyocyte 70%, Atrial cardiomyocyte 50%, Mesothelial 37% and Adipocytes 27%), Pancreas (Overall 9.36%, Beta cell 12.4%, Alpha cell 9.1%, Duct cell 7.3%, Acinar cell 7.2% and Delta cell 7.2%), Colon and small intestine (Overall 6.09%, Paneth 14.9%, Intermediate absorptive enterocyte 14.4%, Transit amplifying 13.8% and Enteroendocrine cell 12.5%), Lung (Overall 3.86%, Alveolar type I 23%, Ciliated cells 5.8% and Alveolar type II 5.4%), Bladder (Overall 2.73%, Fibroblasts 6.8% and Myofibroblast 6.4%), Esophagus (Overall 1.93%, Epithelial suprabasal 5% and Epithelial basal 4.4%) and Stomach (Overall 1.31%, Gland mucous cell 3% and Pit mucous cell 1.9%). The ROR1 expression was found relatively low (<1%) on Adipose, Kidney, Ileum, Liver, Spleen, Bone marrow and PBMC. For the IHC, ninety normal tissues were prepared and used. Consistent with the scRNA-seq results, we found relatively high ROR1 protein on the Heart, Lung, Stomach, Duodenum and Colon and low ROR1 protein on Liver and Ileum. However, ROR1 protein was not detected on Bladder, Pancreas or Esophagus during the IHC process.
Conclusion: Our findings suggest that some healthy human tissues may be at risk of "on-target, off-tumor" toxicity when utilizing ROR1-targeted therapies, including Heart, Colon and small intestine, Lung and Stomach. Close monitoring of possible toxicities related to the high ROR1 expressing organs should be considered in future clinical trials.

#0858 A functional atlas of cancer mutation-rewired protein interactome networks.

A. Agrawal[1], D. McGrail[2], N. Sahni[3], S. Yi[1];
[1]University of Texas at Austin, Austin, TX, [2]Cleveland Clinic, Cleveland, OH, [3]University of Texas MD Anderson Cancer Center, Houston, TX

Somatic mutations in cancer can exert effects on protein-protein interactions (PPIs), leaving some wild-type (WT) interactions perturbed while others unperturbed. The type of PPI perturbations can be used to link the mutation to its phenotypic effects. Here, we apply a technique known as functional variomics to characterize PPI profile changes for around 1,000 cancer missense mutations. Remarkably, our results reveal 5 distinct classes (edgotypes) of mutations: mutations losing PPIs compared to WT (edgetic), gaining PPIs (gain), gaining & losing PPIs (gain/loss), losing all PPIs (quasi-null), and those that do not perturb PPIs (quasi-WT). Notably, gastroenterological cancers have a greater proportion of edgetic mutations, whereas reproductive cancers have a greater proportion of gain edgotype mutations, demonstrating the link between edgotype and cancer type. We further show that more severe cancer stages are associated with interaction-perturbing mutation edgotypes, and the gain/loss edgotype is the most deleterious of all. In addition, pathway enrichment analysis suggests that the edgotypes are predictive of biological effects. For example, mutation edgotypes with loss of interactions are involved in apoptotic process and DNA damage repair, consistent with the expected loss of such functions in cancer. Meanwhile, gain edgotype is linked with cell division and G2/M transition. To our knowledge, this represents the first attempt to perform systematic interactome profiling for cancer mutations. As our results can reveal specific phenotypic attributes and biological functions that are altered for different PPI profiles, our functional platform is important for cancer precision medicine. Our study strengthens the link between genotypes and phenotypes while illustrating the significance of edgotypes in complex disease modeling.

#0859 Development of non-smoking lung cancers by indoor carcinogenic aerosols through epigenetic reprogramming of lung stem cells: Bioinformatics and artificial intelligence analysis..

J. Anderson[1], M. Delgado[1], M. Lovett[1], M. Saunders[1], G. Lake[1], S. Darko[1], R. M. Stiffin[1], A. Huisso[1], M. Sherman[1], L. Appleton[1], A. Mihnea[1], S. Das[2], M. M. Algahtani[3], R. Vadapalli[4], B. Basu[5], A. Biswas[6], N. Neha[7], M. Das[7], M. A. Ruiz[8], M. Doke[9], **J. K. Das**[1];
[1]Florida Memorial University, Miami Gardens, FL, [2]Miami Coral Park Senior High School, Miami, FL, [3]King Saud University, Riyadh, Saudi Arabia, [4]University of Miami, Coral Gables, FL, [5]Chittaranjan National Cancer Institute, Kolkata, India, [6]University of Kalyani, Kalyani, India, [7]Palm Beach Sate College Lake Worth Campus, Lake Worth, FL, [8]Baptist Health Miami Cancer Institute, Miami, FL, [9]University of Miami, Miami, FL

Several scientific studies discovered the toxic effects of indoor aerosols on different organs' adult stem cells of the human body. The most importantly, the indoor toxic aerosols comprised of numerous carcinogens namely, sodium dodecyl sulfate, phthalic acids from floor cleaners, formaldehyde, acetaldehyde, benzene, toluene, ethyl benzene, xylenes, from air fresheners, Hydramethylnon, Pyrethrins, imiprothrin, cypermethrin, tetramethrin, prallethrin and permethrin from ant and roach Killer. However, there was a lack of analysis revealing the mechanism of toxic effects and epigenetic reprogramming of human lung stem cells and development of non-smoking lung cancers. In this study, we analyzed the toxic effects of these chemicals and the mechanism of epigenetic reprograming on lung epithelial cells using Comparative Toxico-genomics Database (CTD), database of Environmental Health Perspectives (EHP), National Institute of Environmental Health Sciences (NIEHS), Google search browser with generative artificial intelligence (AI) and other biological informatics methods (Reactome, Cytoscape PSICQUIC services, and ChEMBL database). We observed from CTD analysis that the chemical gene interactions as risk factors from indoor aerosols showed transcriptionally highly expressed of 31 common genes, by phthalic acids, sodium dodecyl sulfate, from the total of 1347 genes, 107 common genes by formaldehyde, acetaldehyde from the total of 4193 genes and all other toxic ingredients of indoor aerosols. The epigenetic mechanism of histone modifications (H3K4me3, H3K9me3, H3K27me3, H3K27ac, H3K36me3, H3K4me1, Hsa-mir-1301 of lung epithelial, and miRNAs have been revealed by NIH Roadmap Epigenomics Mapping Consortium and the lung tissue arrays were analyzed with AI and matplotlib program. The heterogenic adult stem cell reprogramming is regulated by epigenetic bivalent histone modifications at transcript starts sequences (TSS) of target genes and our current study revealed that CD44, CD80, ALDH2, ALDH3A1, ALDH3B2 are epigenetically reprogrammed with close interaction of other genes by these toxic ingredients of indoor aerosols. Therefore, our results are significant for the carcinogenic effects of indoor aerosols causing for development of lung cancer epigenetically, which may give a clue for the prevention and treatment of nonsmoking lung cancer.

#0860 Pan-tissue master regulator inference reveals mechanisms of MHC alterations in cancers.

M. N. Gondal, R. Mannan, Y. Bao, J. Hu, M. Cieslik, A. M. Chinnaiyan;
University of Michigan, Ann Arbor, MI

Introduction: Major histocompatibility complex (MHC) genes are an integral part of the adaptive immune system. The T-cells can detect and kill cancer cells through the recognition of mutant peptides on the cell surface via the MHC. As a result, many cancers evade the immune system by altering their MHC regulation which can also lead to resistance to immune checkpoint blockade (ICB). Therefore, understanding MHC regulation in both baseline (normal state) and cancer is critical for uncovering mechanisms behind MHC alterations. Here, we have undertaken a pan-tissue evaluation to comprehensively decode MHC transcriptional regulation in healthy tissues and various cancers using a large compendium of single-cell RNA-seq (scRNA-seq) datasets.
Methods: To study MHC class I (MHC-I) and MHC class II (MHC-II) transcriptional regulation at baseline we leveraged a large-scale scRNA-seq dataset encompassing 18 tissues and 124 epithelial cell types. Upon re-clustering and annotation, we investigated MHC expression across cell types and tissues and quantified its heterogeneity using the Gini coefficient. Next, we sought to identify transcription factors (TF) predictive of MHC-I and MHC-II expression, for that, we employed a master regulator inference that utilizes uni- and multi- regression models. Further, to investigate MHC and nominated TFs dysregulation in cancer, we curated a compendium of scRNA-seq datasets comprising 43 datasets, 20 cancer types, across 538 patients.
Results: In normal epithelial cell types, we observed a large range (~8 fold) in MHC-I expression. We also detected MHC-II expression in unexpected cell types such as club cells in the prostate. We found that lung epithelial cells showed elevated MHC-II expression. Immunohistochemistry was performed to validate these findings. Using master regulator inference, we nominated 104 and 107 TFs which predict MHC-I and MHC-II expression, respectively. The nominated TFs showed significant enrichment ($p < 0.001$) for known TFs, alongside putative novel transcriptional regulators such as YBX1 (MHC-I $p < 2e-16$, MHC-II $p = 8e-07$) and XBP1 (MHC-I $p < 2e-16$, MHC-II $p = 7e-04$). Using our single-cell compendium of 20 cancer types we also observed a pan-cancer repression in MHC genes ($p < 0.001$). Next, we utilized an ICB cohort to identify specific TFs that could predict therapeutic benefits. Interestingly, XBP1 ($p < 1e-16$) and SP100 ($p < 2.2e-08$) were strong predictors of patients' survival. We also observed a large heterogeneity in MHC-II expression among colon cancer patients. Upon investigation, we found that patients with high MHC-II expression were mismatch repair deficient, this implicates MHC-II upregulation as an immune evasion mechanism.
Conclusion: In conclusion, we have comprehensively evaluated MHC expression in 124 epithelial cell types and across 20 cancers identifying TFs predictive of MHC-I and MHC-II expression and their effects on patient outcomes.

#0861 Integrative multi-omics analysis enables a comprehensive characterization of prostate cancer and unveils metastasis-associated candidate biomarkers.

M. Villa[1], G. Cazzaniga[1], M. Bolognesi[1], V. Crippa[1], F. Malighetti[1], A. Aroldi[1], G. Bozzini[2], F. Pagni[1], R. Piazza[1], L. Mologni[1], D. Ramazzotti[1];
[1]University of Milano-Bicocca, Monza, Italy, [2]Hospital ASST Lariana, Como, Italy

Prostate cancer (PCa), a common malignancy in men, presents a complex and variable disease landscape, requiring precise evaluation for personalized treatment decisions. Urologists employ a range of assessments, including clinical staging, PSA levels, imaging, Gleason scores, and emerging biomarkers. Nevertheless, the need for additional biomarkers to enhance precision medicine continues. This study utilizes extensive omics datasets to thoroughly profile PCa. We conducted an in-depth analysis of primary PCa data from the multi-omics dataset from The Cancer Genome Atlas studies to identify molecular subtypes showing significant prognostic differences. We conducted integrative clustering analysis on a dataset comprising 341 primary prostate adenocarcinomas with comprehensive multi-omics data, including substitutions, small insertions/deletions, copy number alterations, DNA methylation, gene expression profiles, micro-RNA expression, reverse-phase protein arrays, and microbiome data. The analysis revealed seven distinct clusters (C1 to C7) based on multi-omics features. At the genomic level, recurrent copy number losses and DNA methylation/demethylation were the most prominent alterations across clusters. When looking at survival curves, the 7 clusters could be clearly partitioned into two groups. Therefore, to further investigate multi-omics features specifically linked to prognosis, we grouped clusters with similar prognoses into two macro-clusters. Clusters C1 to C4 formed MC1 (favorable prognosis), while C5 to C7 constituted MC2 (poor prognosis). A comprehensive comparison between MC1 and MC2 revealed molecular differences associated with survival. We performed computational validation of candidate prognostic biomarkers using two external datasets. By utilizing these selected features, we could stratify patients in both the validation datasets into groups with significant differences in survival. The analysis identified six features consistently associated with prognosis across both datasets, including CCNB1, PCNA, RAD51, FOXM1, miR-503-5p (positively associated with risk), and miR-7704 (negatively associated with risk). The practical applicability of these biomarkers was explored through immunohistochemical analysis on biopsy samples obtained at diagnosis and from metastatic sites. Based on their potential relevance according to the literature, we investigated three candidate biomarkers derived from the multi-omics analysis: FOXM1, CCNB1 and RAD51. The expression of these proteins was found to correlate with PCa progression and mark the metastatic stage. In summary, this study highlights the potential of translating comprehensive multi-omics bioinformatic analyses into practical approaches for understanding the molecular mechanisms of tumors and identifying prognostic markers.

#0862 Multi-omic analysis of allelic expression patterns of imprinted and non-imprinted genes in cancer and their association with drug response.

J. Krushkal[1], T. L. Jensen[2], G. Wright[1], Y. Zhao[1];
[1]National Cancer Institute, Rockville, MD, [2]The Emmes Company, LLC, Rockville, MD

Malignant cells undergo a broad array of epigenetic changes, including changes in imprinting patterns. In normal cells, imprinted genes have parent of origin-specific monoallelic expression, which is controlled via epigenetic mechanisms. Imprinted gene loci are often complex and frequently include multiple isoforms, which have different individual patterns of parent-of-origin monoallelic or biallelic expression in the normal tissues. Many imprinted genes promote cell proliferation and body growth, and their expression is important during embryonic and postnatal development. Dysregulation of imprinting in tumors has been suggested to contribute to growth and proliferation of cancer cells. Previously we reported that chemotherapy responses of cancer cell lines from a variety of tumors and of patient-derived acute myeloid leukemia samples were associated with copy number, expression, or DNA methylation of selected imprinted genes. In the current project, we examined allele-specific patterns of expression (monoallelic vs. biallelic) of imprinted genes and isoforms in tumors and studied their potential effect on response of cancer cells to drug treatment. We analyzed expression patterns at the whole gene, isoform, and exon levels of 59,283 autosomal protein-coding genes and ncRNA genes, with a special focus on 94 imprinted genes and their isoforms. We developed a computational pipeline to evaluate monoallelic and biallelic expression patterns of each gene in cancer cell lines and in tumor samples based on available matched RNA-seq expression data, whole exome sequencing information, and copy number data. Our initial analysis included 108 cell lines from the Cancer Cell Line Encyclopedia (CCLE), which had been derived from 9 pediatric and adult tumor histologies. We observed variation of allelic expression patterns of imprinted genes and their isoforms in tumor cell lines, including differences across and within cancer histologies. We also observed predominantly monoallelic expression of multiple additional genes. Some of them (*PRIM2, BCLAF1, MAP2K3,* and *SEC22B*) had been previously reported as potentially imprinted. Monoallelic expression of other genes identified in our analysis (e.g., *GRK2, CBX4,* and additional genes) was likely caused by molecular mechanisms other than imprinting. Allelic expression patterns and overall expression levels of isoforms of multiple imprinted and non-imprinted monoallelically expressed genes (e.g., *CPA4, MAP2K3,* and other genes) were associated with *in vitro* drug response. We also report our ongoing validation of allelic expression patterns of imprinted and non-imprinted genes, isoforms, and exons in primary bladder and breast tumors and in matched solid normal tissue samples using patient data from the Cancer Genome Atlas (TCGA). These results provide new knowledge about epigenetic dysregulation in cancer.

#0863 Scratch: A highly modular pipeline for single-cell cancer research.

Andre F. Fonseca[1], Guangchun Han[1], Marcel Ribeiro-Dantas[2], Enyu Dai[1], Diljot Grewal[3], Matthew Zatzman[3], Eliyahu Havasov[3], Andrew McPherson[3], Break Through Cancer, Data Science TeamLab, Michael N. Noble[4], Rameen Beroukhim[5], Rachel Karchin[6], Sohrab P. Shah[3], Linghua Wang[1]

[1]Genomic Medicine, UT MD Anderson Cancer Center, Houston, TX,[2]Graduate Program in Biotechnology, Potiguar University, Natal, Brazil,[3]Epidemiology and Biostatistics, Memorial Sloan Kettering Cancer Center, New York, NY,[4]Break Through Cancer, Boston, MA,[5]Cancer Biology, Dana-Farber Cancer Institute, Boston, MA,[6]Genomic Medicine, Johns Hopkins Medical Institutions, Baltimore, MD

Background: Single-cell RNA sequencing (scRNA-seq) is a robust approach to facilitate cancer research, revealing insights into tumor heterogeneity, microenvironment, and treatment response. However, scRNA-seq results frequently encounter reproducibility challenges due to i) high data complexity, intensified by human intervention, and ii) insufficient methods standardization, leading to inconsistent findings.
Methods: Here, we introduce SCRATCH (Single-Cell RnA-seq Toolkit and Pipeline for Cancer researcH), a Nextflow-based pipeline designed to improve reproducibility through a layered and modular architecture. SCRATCH follows FAIR principles and guidelines provided by the nf-core community.
Result/Discussion: The pipeline provides three execution modes: end-to-end, iterative, and custom. In the end-to-end mode, the pipeline processes data from raw input to downstream analyses automatically. This mode employs ranking- and aggregation-based approaches. For instance, the ranking approach leverages benchmark metrics to select the most suitable method in distinct steps, e.g., batch correction. Therefore, ensuring a consistent and data-driven selection. On another hand, the aggregation approach uses multiple predictions to increase confidence levels, such as on CNV inference and malignant cell identification. These strategies minimize human intervention, ideal for beginner users, enabling rapid access to preliminary results and biological insights. Alternatively, the iterative mode allows intermediate users to define workflow breakpoints in a layered-based fashion. Users can pause, review results, and adjust decisions at stages (e.g., TME annotation), facilitating a "semi-supervised" approach for a more tailored analysis while retaining the SCRATCH framework. Thirdly, the custom mode enables precise executions based on modules for similar tasks (e.g., trajectory analysis and cell-cell communication), allowing experienced users to bypass the SCRATCH workflow and use it as an on-demand toolkit. This mode leverages pipeline parallelism for efficient processing, perfect for ongoing single-cell projects. SCRATCH produces HTML reports to ensure traceability and reproducibility.
Conclusion: SCRATCH, an evolving project, comprises 05 subworkflows, 18 modules, and 25 tools. We envisage SCRATCH as an open-source tool and invite developers to leverage its modules for their pipelines. For more information, please visit https://break-through-cancer.github.io/btc-scrna-training.

#0864 Pan-cancer analysis of lactic acid metabolism landscape across the Cancer Genome Atlas.

X. Wei[1], L. Cai[2], Q. He[1];

[1]Department of Hepatobiliary Surgery, Shenzhen University General Hospital, Shenzhen, China, [2]Institute of Hepatopancreatobiliary Surgery, Chongqing General Hospital, Chongqing, China

Introduction: Metabolic reprogramming plays an important role in tumor occurrence and progression. Our studies confirmed the survival state of patients with different metabolic systems was heterogeneous and glycolytic metabolism may cause tumor progression. Based on these findings, lactic acid metabolism in glycolysis aroused our interest. This study evaluated the potential association between lactate metabolism gene and tumor clinical process in hepatocellular carcinoma, and proved that it can be used as an effective tool for survival prediction and treatment guidance of 32 kinds of tumor patients by establishing lactate score prognosis model.

Methods: We used the expression profile, proteomics and epigenetics of HCC lactate gene set in the Cancer Genome Atlas Database to systematically describe the changes of lactate related genes. The differentially expressed genes were then verified in 32 clinical tumor data sets. A prognostic model of tumor lactic acid infiltration was constructed to evaluate its correlation with the prognosis of patients. Finally, we analyzed the effects of lame score, immunotherapy and drug response on the clinical process of tumor.

Results: Firstly, we analyzed the differential expression of lactate metabolism genes in HCC and found that the prognosis of patients with high lactate infiltration was significantly lower than that of mild infiltration. AF angiogenesis factor and EMT factor in high infiltration may be the main reason for their differential expression. We constructed a tumor lactic acid prognosis model through six significantly different lactic acid genes, and found that lame score can be used as a predictor of immunotherapy. In addition, we proved the role of lame score in Pan cancer. PGA was positively correlated with lame score in most tumors. The prognosis of 16 tumors with high lame score group was significantly lower than that of low lame score group. There were significant differences in lame score between metastatic and non metastatic cancer groups of Cesc, kirc and kirp. The high and low risk groups of some tumors showed different dryness indices and dampness. At the same time, methylation gene modification has a significant impact on the Lame score of pan cancer, and the Lame score is used to link the drug tolerance and specific pathway enrichment of pan cancer tumor cell lines, confirming the targeted effect of Lame score on tumor treatment. Finally, we used the clinical characteristics and immunohistochemical analysis of a cohort study of real patients with breast cancer endocrine therapy (Tamoxifen) and hepatocellular carcinoma targeted therapy (Lenvartinib) to verify the clinical treatment prediction ability of lame score.

Conclusions: Our study provides a comprehensive analysis of lactate metabolic across cancers and highlights the potential treatment of lactate targeted therapies for cancers.

#0865 Single-cell sequencing identification of malignant cell subpopulations linked to recurrence in hepatocellular carcinoma.

Y. Dong[1], X. Guo[1], X. Wang[1], F. Yang[2], Y. Zheng[2], Y. Chen[1];
[1]Peking Union Medical College, Beijing, China, [2]Peking Union Medical College Hospital, Beijing, China

Introduction: Hepatocellular Carcinoma (HCC) is a highly malignant and challenging-to-treat tumor, with early recurrence affecting up to 35-50% of patients within two years after surgery, significantly impacting prognosis. Identifying high-risk patients for recurrence is critical for guiding postoperative adjuvant therapy. The rapidly advancing field of single-cell RNA sequencing technology offers an unprecedented opportunity to discover clinically relevant cell subpopulations. Here, we harnessed single-cell techniques to unveil a cell subpopulation closely linked with HCC recurrence, highlighting its clinical significance.
Methods and Results: We conducted single-cell RNA sequencing on four HCC samples and harmonized data from three public datasets (GSE112271, GSE125449, CNP0000650) to elucidate the heterogeneity of malignant cells in HCC. Our investigation revealed a distinctive HCC subpopulation enriched in patients with early recurrence (11.4% vs. 3.8%, *P*=0.02). This subpopulation exhibited up-regulated *STMN1* and *EZH2*, signifying high proliferative potential and a propensity for epithelial-mesenchymal transition (EMT). Applying the CIBERSORTx algorithm to the TCGA-LIHC dataset (N=323 patients), we inferred the proportion of this recurrence subpopulation among all malignant cells. Notably, patients with a higher proportion of this subpopulation (N=160) demonstrated significantly shorter recurrence-free survival (31.2 vs. 42.9 months, *P*=0.002), reduced median survival (45.9 vs 55.7 months, *P*=0.03) and a higher rate of microvascular invasion (35% vs. 23%, *P*=0.01). To validate this recurrence-related subpopulation in clinical samples, we conducted multiplex immunohistochemistry staining on paraffin-embedded (FFPE) HCC samples (including CD45, CD31, ARG1, STMN1, EZH2) and used machine learning for its identification. Our findings revealed that patients with a higher proportion of this recurrence subpopulation (N=40) experienced significantly shorter median survival (38.5 vs. 51.0 months, *P*<0.005) and progression-free survival (25.1 vs. 33.4 months, *P*=0.01) compared to a lower proportion (N=40). Multivariate Cox regression analysis confirmed that the proportion of this recurrence subpopulation is an independent predictor of worse prognosis (*P*=0.003).
Conclusion: Through the power of single-cell RNA sequencing technology, we have unearthed and characterized a malignant cell subpopulation intricately connected with HCC recurrence. Importantly, this subpopulation can be identified in FFPE tissue samples and correlates robustly with patient prognosis. Our study underscores the transformative possibility of single-cell techniques in developing cell subpopulation-based biomarkers, emphasizing their clinical relevance and potential utility in guiding postoperative adjuvant therapy for HCC patients.

#0866 Identification of survival-associated epithelial cell markers linked to TROP2 through single-cell and bulk sequencing analysis.

N. N. Al-Bzour[1], A. N. Al-Bzour[1], A. Qasaymeh[1], **A. Saeed**[2], L. Chen[3], A. Saeed[4];

[1]Jordan University of Science and Technology, Irbid, Jordan, [2]University of Vermont Medical Center, Burlington, VT, [3]University of Pittsburgh, School of Medicine \ UPMC Hillman Cancer Center, Pittsburgh, PA, [4]University of Pittsburgh Medical Center (UPMC) \ UPMC Hillman Cancer Center, Pittsburgh, PA

Introduction: Colorectal Cancer (CRC) is known for its aggressiveness and drug resistance. This has increased the interest in antibody-drug conjugates (ADCs) as a possible therapy. In this study, we aim to investigate the effects of the ADC target TROP2, on the level of epithelial cells and its correlation with survival outcomes in CRC patients.

Methods: Single-cell RNA (scRNA) data was downloaded from Gene Expression Omnibus (GEO) for CRC patients and evaluated for TROP2 expression. Patients were grouped into low and high-TROP2 based on median TROP2 expression, and pseudo-bulk analysis was used to find the differentially expressed genes (DEGs). The DEGs were used to find the survival association in the TCGA-CRC cohort. A risk score was built using principal component analysis (PCA) on the TROP2-DEGs and cutoff point was chosen based on survival. Kaplan-Meier curve was used to compare overall survival (OS), progression-free survival (PFS), and disease-free survival (DFS) risk groups. Gene Set Variation Analysis (GSVA) was used to identify the enriched pathways between low- and high-TROP2 in GSE using pseudo-bulk by pooling epithelial cells of individual patients.

Results: Of the 10424 cells of 15 different types for 9 CRC patients retrieved from GSE146771, TROP2 was significantly expressed by epithelial cells (n = 766) with mean expression of 1.64 (SD: 1.96, P-value: 0.003) using pseudo-bulk analysis. Three significant DEGs were obtained which are: KIF13B, UCHL3, and PLAC8. These were evaluated for survival association in resectable stages (I-III) CRC patients (n = 419) using PCA to group the patients into low-risk (n = 88) and high-risk (n = 331), using -1.4 as the cutoff point. High risk group showed a better survival with a 1-year survival probability of 94% compared to 90% in the low group and a 5-year survival probability of 74% vs. 46% in the low group. The Kaplan-Meier curve showed that OS, PFS & DFS were significantly better in the high-risk group (p-value = 0.004, 0, 04, and 0.024 respectively). TROP2 and PLAC8 were significantly associated with worse prognosis, whereas UCHL3 was associated with better prognosis (p-value = <0.001), however, KIF3B did not significantly affect the prognosis. APC gene mutation and TP53 were higher in the low-risk group (p-value = 0.004, 0.007 respectively). KRAS-signaling, IL-18-signaling, MET activation of PTK2-signaling were upregulated in high-TROP2 group, while MYC targets, MTORC1 signaling, DNA repair, reactive-oxygen-species signaling, and TCR-signaling were upregulated in low-TROP2.

Conclusion: In this study we developed a TROP2-associated risk score that significantly predicted OS, PFS, and DFS in patients with resectable CRC by combining single-cell and bulk-RNA-seq datasets and showing predominant expression of TROP2 in epithelial cells. These findings support the development of TROP2 targeting therapeutics in this space.

#0867 Molecular and functional characterization of melanocyte subpopulations in human epidermis based on single-cell RNA sequencing.

Peinan Zhao*[1], Fumihito Noguchi*[1], Christopher Chew[1], Gamze Kuser Abali[1], Pacman Szeto[1], Youfang Zhang[1], Malaka Ameratunga[1], Isobel Leece[1], Jen G. Cheung[1], Miles Andrews[1], Nicholas C. Wong[1], Anthony T. Papenfuss[2], Mark Shackleton[1]

[1]Monash University, Melbourne VIC, Australia,[2]The Walter and Eliza Hall Institute, Melbourne VIC, Australia

The biological and molecular mechanisms that underpin the malignant transformation of normal melanocytes to melanomas are largely unknown. In part, this is due to the limited understanding of normal human melanocyte homeostasis and how melanocytes respond to oncogenic insults such as ultraviolet radiation (UVR). This is particularly true for interfollicular epidermal melanocytes, which have the highest levels of UVR exposure and from whence most melanomas are thought to arise. These knowledge gaps impede the development of strategies for active, targeted prevention of melanoma formation.
We thus evaluated epidermal melanocytes transcriptionally, phenotypically and functionally after isolating them from human skin. Using single-cell RNA sequencing (scRNA-seq), we identified multiple transcriptionally distinct subpopulations within human epidermal melanocytes. RNA velocity analysis revealed subpopulations in different states of melanocytic differentiation, and immunohistochemistry staining demonstrated their distinct anatomical distribution throughout follicular and interfollicular epidermal compartments. Notably, one melanocyte subgroup, marked by increased expression of neurotrophic receptor tyrosine kinase 2 (*NTRK2*) and genes associated with ribosome biogenesis, exhibited molecular characteristics of progenitor cells. This subpopulation displayed human embryonic stem cell (hESC)-derived melanoblast markers, and their anatomical localization corresponded to that of intermediate melanocyte progenitors.
NTRK2+ melanocytes demonstrated enhanced clonogenicity after UVR exposure in primary cell cultures and in ex vivo whole skin explants. In contrast, NTRK2- melanocytes were suppressed by UVR. Furthermore, scRNA-seq data of ex vivo melanocytes after UVR exposure revealed the upregulation of genes associated with cell proliferation within NTRK2-expressing melanocytes. In mouse back skin, the ratio of Ntrk2+ melanocytes increased within 24 hours of UVB irradiation, suggesting a proliferative response in these cells in vivo following UVR.
We thus report the discovery in human epidermis of a putative melanocytic cell hierarchy, and of a candidate melanocyte progenitor subpopulation that responds proliferatively to UVR and is thus a candidate cell of origin of melanoma.

#0868 A novel unsupervised machine learning model applied to neuroblastoma single-cell RNA-seq data reveals a drug-induced mesenchymal-like gene expression program.

R. Chapple[1], **X. Liu**[1], S. Natarajan[1], M. I. M. Alexander[1], Y. Kim[1], A. Patel[1], C. W. LaFlamme[1], M. Pan[1], W. C. Wright[1], H.-M. Lee[1], Y. Zhang[1], M. Lu[1], S. C. Koo[1], C. Long[1], J. Harper[1], C. Savage[1], M. D. Johnson[1], T. Confer[1], W. J. Akers[2], M. A. Dyer[1], H. Sheppard[1], J. Easton[1], P. Geeleher[1];
[1]St. Jude Children's Research Hospital, Memphis, TN, [2]University of Texas Southwestern Medical School, Dallas, TX

High-risk neuroblastoma is one of the most difficult to treat pediatric cancers, with a survival rate of only about 50% and significant long-term consequences from current chemotherapy. Preclinical models such as cell lines and mice are the backbone of drug development and experimental-mechanistic oncology, but the development of new treatments is hampered in part by a lack of understanding of the direct clinical relevance of such data collected in preclinical models. Despite this, few formal methods have been developed to determine how these various models represent/resemble primary patient tumors. Here, we present the first comprehensive single-cell RNA-seq analysis of neuroblastoma across an extensive cohort of patient tumors and a variety of preclinical model systems (n = 126 total samples assembled - the largest cohort of its kind). By building an innovative unsupervised machine learning method, which we term “automatic consensus nonnegative matrix factorization” (acNMF), we have integrated and contrasted the transcriptional landscapes of patient tumors with those of cell lines, patient-derived xenografts (PDX), and genetic mouse models (GEMM).Using these tools, we discovered the dominant adrenergic gene expression programs found in neuroblastoma patient tumors were preserved across all preclinical models. However, the presumptive chemo-resistant mesenchymal-like programs, while identifiable in cell lines, were primarily restricted to subpopulations of cancer-associated fibroblasts and Schwann-like cells in vivo. Surprisingly, a mesenchymal-like program could be acutely chemotherapy-induced in GEMM and was evident in pre-treated patient and PDX samples, suggesting a previously uncharacterized mechanism of therapy escape. In addition to these core findings, our computational tools were able to further delineate the classical neuroblastoma adrenergic and mesenchymal gene expression programs, discovering for example, novel subpopulations of cancer associated fibroblasts. These behaviors were conserved across tumors and most preclinical models, which we validated by RNA in situ hybridization, which is a high resolution ultra sensitive spatial transcriptomics technology. Our work cautions against overreliance on traditional preclinical models without recognizing their limitations and we offer a nuanced, high-resolution view of neuroblastoma pre-clinical systems for advancing therapeutic development. We have launched an open-source web resource, featuring this integrated map to aid the scientific community in further exploration of these data and hypothesis generation (available at http://pscb.stjude.org).

#0869 Single-cell DNA replication dynamics in genomically unstable cancers.

Adam C. Weiner, Marc J. Williams, Hongyu Shi, Ignacio Vazquez-Garcia, Sohrab Salehi, Nicole Rusk, Sohrab P. Shah, Andrew McPherson

Memorial Sloan Kettering Cancer Center, New York, NY

Background: DNA replication and cell cycle regulation are frequently disrupted as part of a cancer's progression toward uncontrolled proliferation, generating somatic copy number alterations (CNAs) and producing intratumoral heterogeneity that drives subsequent evolution. Structural variation and CNAs have been shown to impact epigenetic and chromatin states, but our ability to assess their impact on DNA replication timing (RT) and cell proliferation rates remains limited. Single-cell whole genome sequencing (scWGS) is a powerful method for studying clonal heterogeneity and CNAs, and has the potential to provide greater insight into DNA replication dynamics in aneuploid populations. However, computational identification of S-phase cells and distinguishing inherited somatic CNAs from transient DNA replication changes remain challenging.
Methods: We present a new method, PERT, which uses a Bayesian framework to model read depth as a combination of somatic copy number, replication, and sequencing bias, enabling estimation of DNA replication profiles and cell cycle phase from scWGS data. Unlike previous approaches, PERT provides unbiased estimates of RT and cell cycle phase which allows for analysis of previously uncharacterized cell types using any scWGS platform. These unique properties enable PERT to perform novel analysis such as estimating clone-specific proliferation rates and studying the interplay between RT and somatic CNAs during tumor evolution. We applied PERT to a cohort of >50,000 scWGS cells obtained from a collection of genomically unstable breast and ovarian cell lines, xenografts and primary cancer tissues.
Results: Clone RT profiles correlated with future copy number changes in serially passaged cell lines. Cell type was the strongest determinant of RT heterogeneity, while whole genome doubling (WGD) and mutational signature had weaker RT associations but were associated with accumulation of late S-phase cells. Recurrent CNAs affecting chromosome X had striking impact on RT, with loss of the inactive X allele shifting replication earlier, and loss of inactive Xq resulting in reactivation of Xp. Analysis of time series xenografts illustrated that cell cycle distributions approximate clone proliferation. This relationship enabled us to observe that highly proliferative clones were the most chemosensitive in cisplatin-treated xenografts and, separately, present novel evidence that WGD leads to slower proliferation.
Conclusions: Our analysis implicates cell type as the strongest determinant of RT with chrX being the locus of highest RT variation due to X-inactivation. Separately, quantification of S-phase cells enables interrogation of the on- and off-treatment fitness of genetically distinct subclones. This work leads to better understanding of how DNA replication dynamics drive and are further modulated by genomic instability.

#0871 Unveiling the potential of bispecific antibodies: A comprehensive analysis of efficiency, toxicity, and repurposing in cancer treatment.

B. Wang, S. Madan, A. Schaffer, E. Ruppin;
NIH-NCI, Bethesda, MD

Bispecific antibodies have emerged as promising candidates for cancer treatment, prompting the necessity for a comprehensive understanding of their potential efficacy and toxicity across various cancer types. Leveraging single cell sequencing data, we systematically evaluated the efficacy and toxicity of all cell surface gene pairs across multiple cancers. First, we found that gene pairs involved in successful bispecific antibodies phase I/II clinical trials exhibited significantly higher efficacy scores and lower toxicity scores than gene pairs in those that failed, underscoring the utility of our method in selecting high-quality bispecific pairs. Second, to facilitate the identification of new pairs, we established baseline efficacy and toxicity scores based on successful phase I/II clinical trials, employing these scores to assess the potential of novel combinations. We systematically identified both cancer type-specific and pan-cancer candidate new bispecific antibody pairs. This extensive analysis not only provides valuable insights into the potential of bispecific antibodies to broaden the spectrum of cancer treatments, but also yields a highly confident list of candidate gene pairs capable of constructing effective bispecific antibodies.

#0872 Development of a nomogram and prognostic model based on immune-related genes in kidney renal papillary cell carcinoma.

Adrian Lim, Mouad Edderkaoui, Yi Zhang, Stephen J. Pandol, Yan Ou

Medicine, Cedars-Sinai Medical Center, Los Angeles, CA

Background: Kidney renal papillary cell carcinoma (KIRP) is frequently associated with an unfavorable prognosis for affected individuals. Unfortunately, there has been insufficient exploration in search for a reliable prognosis signature and predictive indicators to forecast outcomes for KIRP patients. Thus, we have used bioinformatics of existing transcriptomic and health data to identify survival-related and prognostic immune genes.
Methods: Processed RNA-seq FPKM data of 289 KIRP and 32 adjacent normal KIRP tissues were downloaded from the TCGA data portal. We downloaded 2499 immune-related genes via the Immunology Database and Analysis portal database and used the Cistrome database to identify and extract 318 total transcription factors (TFs). The differentially expressed immune-related genes and TFs were detected using the Wilcoxon test method. R was used to generate heatmaps and volcano plots. R was also used to perform Gene Ontology (GO) and Kyoto Encyclopedia of Genes and Genomes (KEGG) pathway enrichment analysis. Multivariate Cox regression analysis was implemented to investigate the prognostic value of differentially expressed immune-related genes used to construct the predictive model and nomogram. Kaplan-Meier analysis was performed to compare overall survival. We used Tumor Immune Estimation Resource (TIMER) and the Human Protein Atlas database (HPA) to validate expression and explore associations between a prognostic model and immune cell infiltration. Statistical analyses were performed using R; a p-value < 0.05 was considered to be significant.
Results: A total of 368 immune-related genes and 60 TFs were identified as differentially expressed in KIRP tissues compared with normal tissues. Of the 368, 23 were found to be related to overall survival. GO and KEGG analysis suggested that these prognostic immune-related genes mainly participated in the ERK1 and ERK2 cascades, Rap1 signaling pathway, and the PI3K-Akt signaling pathway - pathways shown to be significantly correlated with the development of cancer. Of these 23 genes, 9 (GRN, PDGFRB, APOH, BIRC5, CCL19, RETN, HTR3A, PTGER1, TRAV39) were identified from Cox regression to be statistically significant prognostic-related genes. Survival analysis showed that a model based on these 9 prognostic-related genes has high predictive performance. Our constructed nomogram has good predictive power and clinical practicability. Immunohistochemistry results show that APOH, BIRC5, CCL19 and GRN were significantly increased in kidney cancer. B cells and CD4+ T cells were positively correlated with risk score model.
Conclusion: We were able to create a prognostic model based on 9 immune-related genes correlated with overall survival in KIRP. We hope that this work helps to provide some insight into therapeutic approaches and prognostic predictors of KIRP.

#0873 Elucidating immune-related gene transcriptional programs via factorization of large-scale RNA profiles.

Shan He, Vakul Mohanty, Matthew Gubin, Hind Rafei, Rafet Basar, Merve Dede, Xianli Jiang, Yukun Tan, Maura Gillison, Katayoun Rezvani, Weiyi Peng, Ken Chen

UT MD Anderson Cancer Center, Houston, TX

Background: Despite the recent success in Immune checkpoint blockade (ICB) therapy, limited patients benefit due to immune-related adverse events or treatment resistance, especially in solid tumors. To overcome these hurdles, understanding the molecular mechanisms behind treatment response is essential. However, the current lack of immune gene transcriptional programs (GTPs) hampers data-driven immunological discovery. Constructing immunity-specific knowledgebases with rigorously curated gene sets (irGSs) and rich immunological language can unlock new insights, enabling interpretation of high-throughput immune microenvironment profiling studies and fostering personalized, effective cancer treatments.
Methods: We collected 83 BulkRNAseq datasets from the ImmuneSigDB. These datasets contain 1826 samples challenged with infections, cytokines or immunological perturbations of different kinds and magnitude, possessing yet-to-be discovered immune functions that lie beneath the transcriptomic profiles. Using non-negative matrix factorization (NMF), we identified gene sets with coordinated expression. We used CITE-seq and selected scRNAseq to annotate the immunological functions of each gene set and validated the clinical utilities of these gene sets from different aspects using data from Cancer Genome Atlas Program (TCGA) pan-cancer, ICB cohorts and a 10X Genomics Visium FFPE Human Breast Cancer spatial slide.
Results: We presented 19 lymphoid-data derived and 9 myeloid-data derived gene sets (irGSs), encompassing a diverse array of immune functions. Through extensive validation using BulkRNAseq, scRNAseq and spatial transcriptomics data, we revealed six irGSs-defined pan-cancer microenvironment subtypes in TCGA with significantly distinct survival patterns regardless of cancer types. Moreover, irGSs are associated with T cell exhaustion phenotypes, which in turn well predicted (classification accuracy of 72%) Nivolumab response using 104 treatment-naïve melanoma patients. Lastly, irGSs simultaneously isolated out tumor regions and highlighted immune infiltration with high specificity in breast cancer spatial transcriptomics H&E image.
Conclusions: These pioneering gene sets, originally derived from non-cancerous experiments, hold tremendous promise for cancer research across diverse contexts. Similarities between cancerous and sepsis immune microenvironments underscore their wide applicability. By studying gene set activities, immunologists can gain profound insights into cancer survival drivers, unravel the intricacies of ICB treatment mechanisms, and potentially conquer therapeutic resistance. These translational utilities herald a transformative era in cancer immunotherapy and open new frontiers in the fight against cancer.

#0874 Expanded detection of *BAP1* alterations in cancer and comparison of tumor type-specific gene expression scores.

Ian R. Sturgill, Jesse R. Raab, Katherine A. Hoadley

UNC Chapel Hill, Chapel Hill, NC

BAP1 is a tumor suppressor gene that was originally studied in uveal melanoma (UVM), kidney renal cell clear cell carcinoma (KIRC), and malignant mesothelioma (MESO). Early analyses focused on single-nucleotide variants, but other alteration types such as larger indels and gene-level copy number (CN) loss can also lead to loss of *BAP1* expression. By incorporating these, we can improve our assessment of cancer type-specific consequences of *BAP1* loss and broaden our findings beyond the initial small subset of cancer types which were studied in the context of mutations alone. We performed integrated multi-omic analyses using data from The Cancer Genome Atlas (TCGA), for 33 cancer types and more than 10,000 individuals. By combining and manually reviewing existing variant calls and new calls derived from a de novo local realignment pipeline across multiple independent variant callers including indel callers, we increased detection of high-quality somatic variant calls by 30% from 85 to 111, including 14 indels ≥5bp. Including CN loss alterations, we found a total of 1561 samples from 32 cancer types to be *BAP1*-altered, with alterations being predominantly CN-driven. We confirmed that expression of *BAP1* was lower in altered versus unaltered tumors ($p<0.001$). Alteration frequencies across cancer types were highly variable, ranging from 0% in thyroid cancer to >30% in KIRC, cholangiocarcinoma (CHOL), UVM, MESO, lung squamous carcinoma (LUSC), and head-neck squamous cell carcinoma (HNSC). Tumor types such as CHOL, UVM, MESO, and liver hepatocellular carcinoma (LIHC) were relatively more mutation-driven whereas other tumor types like KIRC, LUSC, and HNSC were almost entirely CN-driven. To better understand the tissue and context-specific consequences of *BAP1* alteration, we performed differential expression analyses across *BAP1*-altered and -unaltered samples. For each cancer type, we separately computed per-sample *BAP1* alteration signature z-scores summarizing expression of the set of differentially expressed genes. In UVM, we observed distinct patterns of RNA expression, consistent with established literature on *BAP1* loss and serving as a baseline for comparison for the biological effects of *BAP1* loss in other less-studied cancer types. The *BAP1* altered scores for 66% of cancer types were positively correlated with the UVM *BAP1* altered signature, suggesting shared biological responses and affected pathways including immune responses, epithelial-mesenchymal transition, oxidative phosphorylation, and proliferation – all known roles of *BAP1*. In LIHC, we noted enrichment of bile duct gene expression in *BAP1*-altered tumors, suggesting a possible role for *BAP1* in maintaining cell identity distinguishing hepatocytes and cholangiocytes. Our findings broadly emphasize the improvements that are gained by using new computational approaches in large cancer-genome studies such as TCGA.

#0875 Quantitative systems pharmacology modeling of loncastuximab tesirine combined with mosunetuzumab and glofitamab helps guide dosing for patients with DLBCL.

Y. Li[1], **A. K. Wilkins**[1], T. Knab[1], J. P. Boni[2];
[1]Metrum Research Group, Tariffville, CT, [2]ADC Therapeutics America, Murray Hill, NJ

Introduction: CD19 and CD20, B-lymphocyte surface antigens, are clinically validated therapeutic targets for the treatment of B-cell malignancies. Loncastuximab tesirine (loncastuximab tesirine-lpyl [Lonca]) is an antibody-drug conjugate comprising an anti-CD19 antibody conjugated to a pyrrolobenzodiazepine dimer cytotoxin. Mosunetuzumab (Mosun) and glofitamab (Glofit) are CD20 × CD3 T-cell-engaging bispecific antibodies (bsAbs) that redirect T cells to eliminate malignant B cells. These agents target a different B-cell surface antigen than Lonca; hence, combining Lonca with either one of these bsAbs is expected to have additive or even synergistic efficacy. Previously, a novel physiologically-based pharmacokinetic (PBPK)-quantitative systems pharmacology (QSP) model was developed (Utsey K, et al. *Clin Pharmacol Drug Dev*. 2023;12:123-125) and validated with Lonca monotherapy clinical observations in R/R DLBCL (Caimi P, et al. *Blood*. 2022;140:9548-9550). Modeling results of Lonca in combination with Mosun or Glofit in R/R DLBCL are described herein.

Methods: The model was based on the previously validated and published Lonca PBPK-QSP model. This model was reduced in physiological complexity to be compatible with a published minimal PBPK model of Mosun (Hosseini I, et al. *NPJ Syst Biol Appl*. 2020;6:28) while maintaining the core functionality of predicting tumor dynamics during Lonca monotherapy. The following assumptions were made: (1) Lonca or Mosun/Glofit induce healthy and malignant B-cell killing; (2) the tumor comprises malignant B cells and T cells; (3) tumor volume is calculated using malignant B-cell number; and (4) T cells can enter or leave the tumor as they enter or leave other tissues.

Results: Improved tumor growth inhibition (TGI) should result from Lonca + bsAb combination therapy compared with any of the agents as monotherapy. While TGI was predicted to plateau by Cycle (C) 2 with Mosun and Glofit monotherapies, maximum activity of Lonca + bsAb combination therapies may not be observed until C4 or later. Additionally, predicted TGI increased with additional treatment cycles.

Conclusions: Results indicate that treatment by the end of C3 for Lonca + Mosun and by the end of C4 for Lonca + Glofit would promote substantially more TGI compared with any of these agents alone. Increased doses of Lonca in combinations were predicted to have limited additional therapeutic benefit; however, additional cycles of combination treatment were predicted to increase TGI. This model suggests that Lonca doses could be reduced to allow for improved tolerability for longer periods of time, up to the point of maximal benefit, although clinical testing is needed to explore these results. The ongoing LOTIS-7 clinical trial (NCT04970901) evaluates the safety and anticancer activity of Lonca in combination with both Glofit and Mosun.

#0876 *spatialGE*: Empowering researchers to study the tumor microenvironment leveraging spatial transcriptomics.

O. Ospina, R. Manjarres-Betancur, G. Gonzalez-Calderon, A. C. Soupir, I. Smalley, K. Tsai, J. Markowitz, A. Berglund, X. Yu, B. L. Fridley;
Moffitt Cancer Center, Tampa, FL

The use of single-cell RNA-seq (scRNA-seq) to understand the complexity of the tumor microenvironment (TME) has been pivotal in advancing cancer research and treatment strategies. Nevertheless, locating the individual TME components in their spatial contexts is essential to understanding the complexity of the TME, tumorigenesis, metastasis, and drug response. The recent popularity of spatially resolved transcriptomics (SRT) allows researchers to describe the TME and their spatial neighborhoods; however, SRT data analysis can be challenging for non-data scientists. Thus, we have developed *spatialGE*, a point-and-click web application designed to empower researchers in the analysis of SRT data. Our application offers a suite of functionalities, including the visualization of spatial gene expression activity maps, quantification of the spatial heterogeneity, testing of pathway-level spatial aggregation, tissue domain/niche detection, detection of spatial gradients in expression patterns, and differential expression analysis. Furthermore, *spatialGE* allows direct comparative analysis of gene expression with the morphology in tissue images, as well as methods for cell/domain phenotyping. Data input has been streamlined and made flexible to receive outputs from multiple SRT platforms. Analyses and results are stored within user-defined projects to facilitate accessibility at any time. We demonstrate the usefulness of *spatialGE* through its application to leptomeningeal metastatic melanoma (LMM) tissues assayed with the Visium platform. The gene expression tissue domain detection and gradient analysis in *spatialGE* indicated that *SERPINA3* expression is higher in tumor regions closer to stroma. This finding led to cell culture experiments indicating that knocking down *SERPINA3* results in the sensitization of tumors to MAPK-targeting therapy. These results highlight the utility of *spatialGE* for exploring SRT data and the empowerment of cancer researchers to explore the spatial architecture of the TME.

#0877 Molecular and radiographic profiling of lung cancer in never-smokers.

M. Lee[1], A. Yadav[2], G. Liu[1], S. Dubinett[3], J. Beane[1], W. Hsu[3], A. Prosper[3], D. Aberle[3], M. Lenburg[1];
[1]Boston University Chobanian & Avedisian School of Medicine, Boston, MA, [2]University of California, Los Angeles, Los Angeles, CA, [3]David Geffen School of Medicine at UCLA, Los Angeles, CA

Gene expression changes in nasal and bronchial epithelium, and quantitative features from chest CT reflect the presence of lung cancer in current and former smokers and can serve as biomarkers. Between 10-20% of lung cancer cases are diagnosed in patients who have never smoked (<100 lifetime cigarettes) and biomarkers could assist the diagnosis of pulmonary nodules discovered incidentally in this population. We compared lung cancer-associated gene expression and radiomic features in never-smokers and ever-smokers. Nasal epithelial RNA was isolated and sequenced from brushings collected at UCLA from 73 patients presenting to interventional radiology for biopsy for suspected lung cancer. *Limma* was used to identify genes with lung cancer-associated expression in never-smokers by comparing 13 patients with benign nodules with 14 patients diagnosed with lung cancer. Similarities between cancer-associated genes in never-smokers and those previously identified in ever-smokers were assessed by gene set enrichment analysis (GSEA). Next, using all 73 samples, genes whose lung cancer-associated expression is modified by smoking status were identified via an interaction term. Radiomic features for 46 patients (31 ever-smokers, 15 never-smokers) were extracted using *PyRadiomics*, including features from the interior of the nodule and perinodular features generated 10, 15, and 20 mm away from the boundary of the nodule. A binomial model was used to identify features with a significant interaction effect between cancer and smoking status. We identified 74 genes decreased and 84 genes increased in cancer in never-smokers ($p < 0.005$), controlling for age and median TIN. Genes changed in ever-smoker lung cancer patients were significantly enriched among the genes most associated with lung cancer in never smokers (GSEA; $p = 0.0059$ and $p = 4.38e\text{-}15$). Next, there were 51 genes with a p-value < 0.01 for the cancer*smoking interaction term. Lastly, four radiomic features were associated with the perinodular term for cancer and smoking status (FDR< 0.2), including two nodular and two boundary features. These results suggest that lung cancer-associated gene expression differences in ever-smokers are preserved in never-smokers, suggesting the potential relevance of previously derived biomarkers for this population. There may also be never-smoker-specific gene expression patterns associated with lung cancer. Our radiomic findings suggest that both nodular and perinodular characteristics may be important predictors of malignancy.

#0878 Enhancing single-cell RNA sequencing analysis in cancer research: A machine learning framework based on LightGBM for automated cell type annotation.

T. Chuang[1], L.-C. Lai[2], T.-P. Lu[3], M.-H. Tsai[4], H.-H. Chen[5], E. Chuang[1];
[1]Graduate Institute of Biomedical Electronics and Bioinformatics, National Taiwan University, Taipei, Taiwan, [2]Graduate Institute of Physiology, College of Medicine, National Taiwan University, Taipei, Taiwan, [3]Institute of Health Data Analytics and Statistics, National Taiwan University, Taipei, Taiwan, [4]Institute of Biotechnology, National Taiwan University, Taipei, Taiwan, [5]Institute of Computer Science and Information Engineering, National Taiwan Normal University, Taipei, Taiwan

Single-cell RNA sequencing (scRNA-seq) has been widely used in cancer research to understand the complex gene expression diversity and cancer heterogeneity. However, manual annotation of cell types in the scRNA-seq pipeline is time-consuming and depends on the expertise of analyzers, which can significantly influence the results of downstream analyses. To address this problem, we proposed a novel machine learning framework utilizing the LightGBM model for automated and efficient cell-type annotation of scRNA-seq.
Two independent scRNA-seq datasets of non-small cell lung cancer (NSCLC) downloaded from the Gene Expression Omnibus (GEO) were used to train and test our model. A standard procedure is applied to both scRNA-seq datasets for quality control and preprocessing, in which poor-quality cells with low gene expressions or high scores for cellular stress/death were excluded. In addition, Harmony is applied to mitigate batch effects in scRNA-seq that could cause variability due to non-biological factors in experiments. Nine different cell types, including endothelial, epithelial, fibroblast, macrophages, mast, plasma, pulmonary alveolar, B, and T cells, were manually labeled in the two datasets by the providers, which were also examined using gene markers corresponding to different cell types from PanglaoDB and DAVID. These manually labeled cell types were used as the ground truth for training and testing our model. In the training stage, the training dataset (containing 85,000 cells from 44 NSCLC samples) of scRNA-seq was used to train the LightGBM model with its high-variable genes. Then, the model would be evaluated using an independent test dataset (containing 8,000 cells from 18 NSCLC samples) by comparing the automatically predicted and manually labeled cell types.
The training result showed that our model could successfully specify the nine different cell types, achieving an overall average accuracy, F1 score, and precision of 0.86 each respectively. In the independent dataset test, the model demonstrated good generalization, showing high predictive performance across all cell types, with an average accuracy, F1 score, and precision of 0.8, 0.78, and 0.8, respectively. Specific to the predictions in the test dataset, we found that some epithelial cells were mistakenly identified as other cell types. This might be because of the complex gene expression patterns exhibited by tumor epithelial cells, making accurate predictions challenging.
The proposed machine learning framework facilitates cell labeling and unravels the intricate heterogeneity within lung cancer datasets. The combination of LightGBM and standardized preprocessing establishes a benchmark for high-throughput, accurate single-cell analysis, paving the way for discoveries that are more targeted and have significant clinical impact.

#0879 The AVERON Notebook to discover druggable cancer dependencies through the mutant-directed protein-protein interactions.

H. Chen, S. Yeung, B. Revennaugh, H. Fu, A. A. Ivanov;
Emory University, Atlanta, GA

Cancer is a devastating disease that takes more than 10 million lives every year. The genomic alterations, such as mutations in cancer driver genes, can disrupt the essential networks of protein-protein interactions (PPIs), dysregulating major oncogenic pathways and inducing the transformation. While some mutations can disrupt existing PPIs, others can create neomorph PPIs (neoPPIs), which are unnatural for wild-type counterparts. Discovery of such mutant-created neoPPIs is vital for understanding the molecular mechanisms of mutant-driven tumorigenesis and developing new personalized clinical strategies in cancer. However, systematic experimental interrogation of the clinical significance and biological functions of neoPPIs is highly challenging. To address this critical challenge, we develop a novel computational platform called AVERON Notebook for identifying new Actionable Vulnerabilities Enabled by Rewired Oncogenic Networks. The AVERON employs specially designed algorithms and statistical techniques to i) Assess and compare the levels of neoPPIs in cancer patients; ii) Examine their impact on clinical outcomes; iii) Identify distinctive sets of signature genes and oncogenic pathways regulated by individual neomorph PPIs; and iv) Discover clinically significant neoPPI-regulated genes with available clinical compounds and approved drugs. Together, the AVERON Notebook provides a powerful tool for exploring the functional consequences of tumor-driving mutations mediated through the neoPPI networks and sheds new light on previously unexplored clinically actionable dependencies enabled by neomorph PPIs in cancer patients. The AVERON Notebook is freely available onGitHub: https://github.com/aivanovlab/averon_notebook and Code Ocean: https://doi.org/10.24433/CO.7986101.v1

Acknowledgments: This work was supported in part by NCI's Informatics Technology for Cancer Research (ITCR) Program (R21CA274620, A.A.I.), Mary Kay Foundation Grant for Cancer Research (A.A.I), NCI Emory Lung Cancer SPORE (P50CA217691, H.F.), NCI P01CA257906 (H.F.), Career Enhancement Program (A.A.I., P50CA217691), Winship Cancer Institute (NIH 5P30CA138292).

#0880 Identifying ANKRD22 and fostamatinib as a theragnostic target and drug candidate for metastatic pancreatic cancer through in silico analysis.
H. T. Huynh, H. G. Lim, Y.-C. G. Lee, C.-H. Chen, A. T. Wu;
Taipei Medical University, Taipei, Taiwan

Introduction: Pancreatic cancer (PC) presents significant clinical challenges, marked by a low 5-year survival rate and frequent distant metastasis. When PC metastasizes to other organs, it leads to a notable decrease in the 5-year survival rate for PC in metastasis, dropping from 11% to 3%. Despite the effectiveness demonstrated by advanced anti-cancer therapies targeting these mutated genes, the improvement in survival rates remains modest. Another critical consideration is the rising resistance to Gemcitabine, a standard drug used for treating PC. Hence, it is imperative to gain a more profound understanding of the comprehensive mechanisms underlying metastatic pancreatic cancer (mPC) and actively explore novel drugs for its treatment. Methods: First, we reanalyzed the RNA-seq of three of PC's most common metastatic sites, including liver, lung, and peritoneum. Using the Galaxy platform, we identified DEGs (differentially expressed genes) between metastatic sites. After that, we further utilized other web-based tools and databases, such as GEPIA, TIMER 2.0, Alphafold, PubChem, Drugbank, and Chembl, to identify ANKRD22 and perform molecular docking of Fostamatinib binds to this gene. Results: Our research focused on exploring the role of ANKRD22, which contains four copies of L-shaped ankyrin motifs, an emerging oncogenic molecule associated with various cancers. In the current study, we identified that ANKRD22 exhibited significant expression in the pancreatic adenocarcinoma (PAAD) cohort, correlating with deteriorating OS rates in PC patients. Moreover, it displayed distinct expression patterns in advanced stages of the disease compared to early stages, Furthermore, we uncovered a noteworthy correlation between ANKRD22 and the Kras, TP53, CDKN2A, and SMAD4 genetic anomaly, linked to diminished survival rates, as widely recognized, in the initiation and progression of PC, these four genes stand out as the most frequently mutated. Mechanistically, ANKRD22 exhibited associations with KRAS dependency signature, U12 type spliceosome assembly, multivesicular body routing, cell invasion, tumor cell line invasion, and tumor cell line migration, all indicative of PC progression and dissemination. Expanding our investigation through the DrugBank and ChEMBL databases, we delved into fostamatinib, an FDA-approved drug known as a spleen tyrosine kinase (SYK) inhibitor. Molecular docking experiments revealed the potential interaction between ANKRD22 and fostamatinib, suggesting its candidacy to treat mPC. Conclusion: Our findings identify ANKRD22 as a pivotal oncogenic factor promoting metastasis in PC and propose fostamatinib as a potential inhibitory treatment.

#0881 Cell-type-specific gene programs suggest immune and stromal drivers of relapse in colorectal cancer.

Nicholas J. Hornstein[1], Mingshuang Wang[2], Abdelrahman Yousef[2], Saikat Chowdhury[2], Fadl Zeineddine[2], Mohammad Zeineddine[2], Mahmoud Yousef[2], Shuangjie You[2], Betul Gunes[2], David Menter[2], Scott Kopetz[2], John Paul Shen[2]

[1]Medical Oncology Fellowship, UT MD Anderson Cancer Center, Houston, TX,[2]GI Medical Oncology, UT MD Anderson Cancer Center, Houston, TX

Background: Molecular profiling of colorectal cancer (CRC) has demonstrated marked heterogeneity between tumors that appear histologically similar. Although existing classification systems such as the Consensus Molecular Subtypes (CMS) have shown clinical utility, these bulk sequencing-based methods fail to adequately address the intra-tumoral heterogeneity of CRC. To disentangle the complex landscape and identify clinically-relevant properties of CRC we generated a single cell sequencing (scRNASeq) database from 225 tumor samples derived from resection of primary colon or liver metastases. Our analysis defines cell-type-specific gene programs significantly associated with relapse and survival and suggests interventions which may abrogate their effect.
Methods: Utilizing a bio-repository of CRC specimens with an average of 5 years of clinical follow-up, we performed scRNASeq on 225 patient samples comprising ~ 1,000,000 total cells and 2.4 billion gene expression measurements. Following traditional clustering approaches, we then inferred gene expression programs through consensus non-negative matrix factorization (cNMF) to characterize cell activities. Gene program activity was explored on a cell-type-specific level and associated with clinical outcomes such as relapse. Treatment effects were additionally explored.
Results: We identified 56 cell-type specific gene programs significantly associated with relapse in adult CRC patients. Interestingly these programs spanned all cellular compartments with the majority found in stromal or immune, as opposed to tumor cells. Program activity such as the non-canonical Granulocyte Chemotaxis program in B Cells was protective of relapse (relapse median expression 0% activity vs non-relapse activity 40% pAdj $<.05x10^{50}$) whereas the Epithelial Mesenchymal Transition (EMT) program in Cancer Associated Fibroblasts (CAF) was strongly associated with relapse (relapse median expression 16% activity vs non-relapse activity 0% pAdj $<.05x10^{10}$). Cumulative program usage enabled stratification on a patient level to provide an estimate of comparative disease free survival (DFS) and overall survival (OS); gene-programs were significantly associated with outcomes such as the CAF-EMT program which was associated with a DFS HR of 3 (pAdj <.0005). Responses to chemotherapy and treatment effect were also explored; prior treatment with Bevacizumab was associated with a significant reduction in the CAF-EMT program (11% activity in non-exposed patients versus 0% activity in exposed patients pAdj $<.05x10^{10}$).
Conclusions: Analysis of the largest CRC scRNASeq cohort to date identifies a number of previously undescribed cell-type specific gene programs significantly associate with relapse after surgery. These programs provide insights into the underlying mechanisms and suggest that the TME plays an important role in relapse.

#0882 Harnessing single cell multi-omics data to identify predictors of clinical outcome in CD19 CAR T cell therapy.

R. Y. Louie[1], J. Samir[1], C. Cai[1], H. McGuire[2], T. Amos[3], J. Fergsuson[3], I. Deveson[3], T. Adikari[1], M. Bonomi[4], D. Bishop[5], C. E. Mason[6], R. Balderas[7], M. Ruella[8], M. Singh[3], D. Gottlieb[2], E. Blyth[2], K. Micklethwaite[1], **F. Luciani**[1];

[1]UNSW Sydney, Sydney, Australia, [2]University of Sydney, Sydney, Australia, [3]Garvan Institute, Sydney, Australia, [4]University of Bologna, Bologna, Italy, [5]University Sydney, Sydney, Australia, [6]Weill Cornell Medicine, New York City, NY, [7]Beckman Dickinson, San Francisco, CA, [8]UPenn, Philadelphia, PA

Background: Chimeric antigen receptor (CAR) T cell therapy is effective in treating B-cell malignancies, but factors influencing the persistence of functional CAR^+ T cells, such as product composition, patients' lymphodepletion, and immune reconstitution, are not well understood. To shed light on this issue, we conducted single-cell multi-omics analysis of transcriptional, clonal, and phenotypic profiles from pre- to 1-month post-infusion of CAR^+ and CAR^- T cells from patients who received a donor-derived 4-1BB CAR product targeting CD19.

Methods: Longitudinal blood samples and infusion products were obtained from 10 individuals with large B cell lymphoma or B-cell acute lymphoblastic leukemia (CARTELL cohort in Sydney Australia[1]). $CD45^+$ cells and enriched CAR+ T cells were single cell sorted for simultaneous scRNA-seq, 41 barcoded proteins (N=41) and T cell receptors, n= 115,000 cells across 21 samples. Machine learning methods were used to identify subsets of immune cells associated with clinically relevant parameters.

Results: Following infusion, CAR^+ and CAR^- T cells showed similar differentiation profiles with clonally expanded populations across heterogeneous phenotypes, demonstrating clonal lineages and phenotypic plasticity. These findings were validated by performing the same analysis on two publicly available scRNA-seq data sets from two cohorts [2, 3] of paediatric (N=18) and adult (N=32) individual with large B cell lymphoma who received CAR19 T cells. Analysis of mass-cytometry data from our cohort and from 28 patients with B cell lymphoma treated with commercial CAR19 T cells (axi-cel)[4], identified an association of CAR^- and also CAR^+ T cells, both expressing an $2B4^- CD11b^+ CD8^+$ phenotype, with complete remission or progressive disease at 3 and 6 months post-infusion. Finally, we report additional analysis on the immunogenomics of circulating CAR T cells in two patients who developed CAR T cell induced lymphoma and compared it with ascites and CAR-Lymphoma cells.

Discussion:These results suggest that CAR^+ and $CAR^- CD8^+$ T cells share a differentiation trajectory terminating in an NK-like phenotype that is associated with clinical outcome, and that non-CAR-derived signals may influence patients' immune recovery and outcomes.References

1.Bishop, D.C. *et al.* Development of CAR T-cell lymphoma in 2 of 10 patients effectively treated with piggyBac-modified CD19 CAR T cells. *Blood* 138, 1504-1509 (2021).2.Haradhvala, N.J. *et al.* Distinct cellular dynamics associated with response to CAR-T therapy for refractory B cell lymphoma. *Nat Med* 28, 1848-1859 (2022).3.Wilson, T.L. *et al.* Common Trajectories of Highly Effective CD19-Specific CAR T Cells Identified by Endogenous T-cell Receptor Lineages. *Cancer Discov* 12, 2098-2119 (2022).4.Good, Z. *et al.* Post-infusion CAR T(Reg) cells identify patients resistant to CD19-CAR therapy. *Nat Med* 28, 1860-1871 (2022).

#0883 Genetic characteristics between males and females with urothelial bladder cancer.

R. Nair[1], R. Khalife[2], A. Magliocco[2];
[1]University of Central Florida, Orlando, FL, [2]Protean BioDiagnostics, Orlando, FL

Urothelial bladder cancer (UBC) affects the epithelial cells of the urinary tract and is the most common type of bladder cancer worldwide. Statistically, males are four times more likely to develop UBC than females. It is known that decreased expression of the KDM6A gene, coded on the X chromosome, corresponds with a higher incidence of UBC. KDM6A mutations are known to be more prevalent in females with non-muscle-invasive UBC. These mutations are targetable by inhibiting EZH2, an enzyme coded by its namesake gene. On the environmental side, males are at a higher risk of developing carcinogenic complications due to smoking and environmental toxins. However, this discrepancy fails to exist when comparing males and females who smoke similar levels. Though environmental factors may play a role in influencing behavior and altering levels of risk to develop UBC, research suggests that they do not single-handedly explain sex-based disparities in UBC. In this study, we characterize the molecular mechanisms associated with altered overall survival by uncovering previously unreported data on the expression of KDM6A and FGFR3, a commonly altered oncogene, in UBC patients. Our in silico approach consisted of broad survival data analysis through cBioPortal (n=1486), sequencing-based gene expression data through ICGC Portal (n=295), and single nucleotide polymorphism identification with the PLCO Atlas (n=69,429). The 5-year overall survival (OS) curves of 13 therapeutic and/or significantly altered genes between males and females were analyzed. BRCA2 was the only gene associated with worse survival for females with alterations. Interestingly, males with alterations to the following genes had significantly better OS outcomes: ERCC2, KDM6A, BRCA2, FGFR3. However, there was no gene whose alterations were associated with significantly better OS outcomes for females. KDM6A and FGFR3, two genes whose alterations are typically associated with worse OS outcomes in males, exhibit the opposite effect. Additionally, males exhibited significantly worse OS outcomes when presenting with CDKN2A and CDKN2B alterations, while females exhibited significantly worse OS outcomes when presenting with CDKN2A and NTRK1. A majority of European males had SNPs on the following genes: CDKN2B, ERBB2, CREBBP, while a majority of European females had SNPs on BRCA2. Differential expression also revealed 714 genes that were significantly expressed in one sex when compared to the other. Therefore, we suggest that there are unique molecular differences between sex that conflict with previous analyses; further research should be conducted to explore the effect of sex via the tumor-suppressive characteristics of KDM6A as well as oncogenic properties of FGFR3.

BIOINFORMATICS / COMPUTATIONAL BIOLOGY / SYSTEMS BIOLOGY / CONVERGENT SCIENCE: Artificial Intelligence and Machine/Deep Learning 1
Poster Session

#0886 Integrated deep learning model for predicting DNA methylation and tumor types from histopathology in central nervous system tumors.

E. D. Shulman[1], D.-T. Hoang[2], R. Turakulov[1], Z. Abdullaev[1], O. Singh[1], E. M. Campagnolo[1], E. A. Stone[2], M. P. Nasrallah[3], E. Ruppin[1], K. Aldape[1]; [1]NIH-NCI, Bethesda, MD, [2]Australian National University, Canberra, Australia, [3]Perelman School of Medicine at the University of Pennsylvania, Philadelphia, PA

Precision in diagnosis of diverse central nervous system (CNS) tumor types is crucial for optimal patient treatment. DNA methylation profiles, which capture the methylation status of thousands of individual CpG sites, are data-driven means to enhance diagnostic accuracy, but this technique is expensive, time-consuming, and not yet routinely available. To address this, we developed DEPLOY, a deep-learning model that predicts 10 major categories of CNS tumors from histopathology. DEPLOY integrates three distinct components: the first classifies CNS tumors directly from histopathology slide images (‘direct model’); the second initially generates predictions for DNA methylation beta values, which are subsequently used for tumor classification (‘indirect model’); and the third classifies tumor types directly from routinely available patient demographics. First, we find that DEPLOY accurately predicted beta values from histopathology images, suggesting that application of inferred methylation data is a promising approach for deep learning histopathology-based classifiers. Using a 10-class model trained on an internal dataset, we apply this model on two independent external test datasets of 1,522 and 348 cases, achieving top-1 accuracies of 96% and 94%, respectively on samples which are predicted with high confidence. Taken together, DEPLOY could assist pathologists in diagnosing CNS tumors, in an equitable very low-cost manner, within a clinically relevant short time frame.

#0887 Fast, interactive, AI-assisted 3D lung tumour segmentation.

M. Patwari[1], Y. Wei[1], M. Xu[1], Z. Zhang[2], K. Sidiropoulos[1], B. Selvaraj[3], G. Hughes[1], N. Garibli[1], K. Ojiako[1], M. Lella[1], L. Fedden[1], J. Parkin[1], M. Parker[1], S. Patel[1], Q. Li[4], K. Patwardhan[4];

[1]ASTRAZENECA UK LIMITED, Cambridge, United Kingdom, [2]ASTRAZENECA, Gaithersburg, MD, [3]ASTRAZENECA AB, Gothenburg, Sweden, [4]ASTRAZENECA, Waltham, MA

Segmentation of lung tumors is an important step in the planning of clinical treatment and operative procedures. Automatic segmentation of advanced lung tumors is challenging due to local invasion and heterogeneous metastasis. Fully automatic deep learning models often fail to accurately delineate advanced disease boundaries and do not allow the user to provide hints to improve segmentation performance. In contrast, interactive segmentation accepts user inputs and is an efficient way to segment lesions while reducing radiologist effort.

This paper describes an interactive segmentation approach for lung lesion segmentation in CT scans. Our pipeline is built atop the SwinUNETR neural network architecture and can be expanded to support alternate models. The backbone model accepts radiologists' hints in the form of mouse clicks that indicate whether a location on the scan corresponds to a lesion. Our approach has the following novel contributions: (1) Context-aware encoding of guidance clicks by combining geodesic and Gaussian smoothing, resulting in improved segmentation of lesion boundaries. (2) An iterative prompting strategy to achieve higher accuracy with fewer clicks at inference time. (3) Guidance-aware Conditional Random Fields to refine the produced segmentation masks. (4) Volume cropping around guidance clicks at inference to improve segmentation precision and inference speed. (5) Linearly scaling our approach on multiple GPUs, to improve inference speed.

On a public non-small cell lung cancer dataset predominantly containing advanced stage cancers (68\% stage III, and 27\% stage IV), our interactive approach delivers a Dice score of 0.74 with a single click, a 21\% improvement from the fully automatic approach (Dice Score = 0.61), and a Dice score of 0.81 with 5 clicks, which is a 33\% improvement. Inference speed is an important metric for an interactive pipeline. On a typical 350 $\times$ 350 $\times$ 150 voxel chest CT scan volume, our interactive approach infers 5 times faster than the original fully automated approach on a single GPU. After scaling to 4 GPUs, we infer in only 0.5 seconds; 20 times faster than the original approach. Qualitative evaluation from three independent radiologists indicates that our interactive pipeline significantly improved their standard clinical segmentation experience.

#0888 Uncovering clinically relevant omics signatures from pan-cancer imaging and multi-omics data integration.

J. Wang, R. Hong, J. Tan, W. Liu, D. Fenyò;
NYU Grossman School of Medicine, New York, NY

Despite advancements in deep learning for histopathology, integrating these insights with multi-omics data to uncover clinically relevant omics pathway-level signatures remains a challenge. Our study addresses this gap by applying unsupervised learning techniques on pan-cancer multi-omics data, leveraging 3,080 Hematoxylin and Eosin (H&E) images from 1,010 patients in Clinical Proteomic Tumor Analysis Consortium (CPTAC) to uncover omics pathway-level signatures that drive discernable morphology phenotypes at the tissue level. First, imaging models were trained to predict clinical and mutation outcomes, and thereafter, integrated with transcriptomic and proteomic expression data using sparse canonical correlation analysis. Our findings reveal that images of TP53 mutated samples exhibited increased nuclear size and dense lymphoplasmacytic infiltration. These morphological changes correlated with neutrophil and macrophage signaling at the proteomic level, and IL-1 mediated signaling at the transcriptomic level, highlighting the complementary perspectives different omics can provide. To further elucidate immune interactions, we applied multi-omics deconvolution to identify 7 immune subtypes, characterizing each with gene set enrichment, germline DNA variations, and kinase activations. We show that imaging models trained to predict these subtypes differentiate tissue morphologies corresponding to immune enrichment (AUROC: 0.84). To further confirm the robustness of our approach, we trained models to predict co-regulated proteomic modules clustered by independent component analysis. We demonstrate a signature in pan-squamous tumors, consisting of T cell markers and interferon-gamma response proteins like CD4, CD48, and GBP5, which imaging models can successfully predict from histopathology. Manual review from pathologists confirmed lymphocytic T-cell density as a differentiator in samples with the highest and lowest T-cell signaling.
Together, these approaches demonstrate that genomic characteristics discovered via unbiased mining of pan-cancer multi-omics data manifest as quantitative imaging phenotypes. These results underscore the potential of multi-omics and digital pathology to integratively uncover and confirm new cancer biology. Our ongoing work will explore predicting drug response and survival from morphology patterns related to multi-omics signatures.

#0889 Machine learning-enhanced targeted versus whole-exome sequencing as a guide to cancer care.

H. Woo, S. S. Chavan, A. J. Hanrahan, A. L. Richards, A. Noronha, A. Zehir, A. Drilon, M. F. Berger, D. B. Solit, M. T. A. Donoghue;
Memorial Sloan Kettering Cancer Center, New York, NY

Targeted DNA sequencing of cancer-associated genes has been widely adopted clinically. In addition, the increasing availability of targeted and whole-exome/genome sequencing (WES/WGS)-derived big data suggests avenues of computationally enhancing power of targeted assays via machine learning. We directly compared targeted (MSK-IMPACT) and WES in a cohort of 1,483 cancer patients using the same DNA libraries. We found high sensitivity and specificity of mutation detection by WES for overlapping genes. Comparatively higher estimates of tumor mutation burden by MSK-IMPACT arose from enrichment of oncogenic mutations in the targeted gene set. WES had minimal value in identifying actionable alterations beyond those from MSK-IMPACT, whereas RNA-sequencing identified additional targetable fusions that led to durable responses. We developed a deep learning-based algorithm (DeepSig) that enhances power of mutational signature detection, enabling detection of a select group of signatures with mutation counts of ~5 or less. Hypermutation-associated signatures, including POLE, temozolomide, and mismatch repair deficiency could be detected robustly using targeted sequencing data. In summary, WES had limited clinical value over targeted sequencing panels and future clinical diagnostic development should focus on transcriptome and WGS that can detect additional signatures and gene fusions.

#0890 Multimodal modeling of digitized histopathology slides improves risk stratification in hormone receptor-positive breast cancer patients.

K. M. Boehm, A. Marra, J. S. Reis-Filho, S. Chandarlapaty, F. Pareja, S. P. Shah;
Memorial Sloan Kettering Cancer Center, New York, NY

In early-stage hormone receptor-positive breast cancer, genomic risk scores identify patients who stand to benefit from up-front chemotherapy but introduce financial and logistical hurdles to care. We assembled a cohort of 5,244 patients with 11,671 corresponding whole-side images of breast tumors stained with hematoxylin and eosin. We developed a multimodal machine learning model to infer risk of distal metastatic recurrence from routine clinical data. Specifically, the model interprets text from the pathologist's report using a large language model and uses self-supervised vision transformers to interpret the corresponding whole-slide image. Tensor fusion joins the modalities to infer Genomic Health's Oncotype DX recurrence score. Inferred recurrence score from the multimodal model correlated with measured score with a concordance correlation coefficient of 0.64 (95% C.I. 0.59 - 0.69) in the withheld test set, compared to 0.55 (95% C.I. 0.49 - 0.61) and 0.56 (95% C.I. 0.52 - 0.60) for the linguistic and visual unimodal models, respectively. The multimodal model attains an area under the precision-recall curve (AUPRC) of 0.69 (AUROC=0.88) for identifying high-risk disease in the full-information setting (when images and pathology reports with quantitative hormone receptor status and grade are available) in a withheld test set, compared to AUPRC of 0.61 and 0.66 for the linguistic and visual models, respectively. By comparison, in the same full-information setting, the clinical nomogram introduced by Orucevic et al. in 2019 achieves an AUPRC of 0.48. We suggest the operating point at which precision is 94.4% and recall is 33.3%. Digitized whole-slide images of routine breast biopsies and their associated synoptic pathology reports contain much of the information necessary to stratify patients by risk of distal metastatic recurrence, when modeled appropriately. Our model could enable hospitals to rapidly triage the need for genomic risk testing, possibly precluding one third of orders without loss of accuracy. This helps allocate scarce resources for genomic tests and valuable weeks prior to beginning therapy while maintaining the standard of precision oncology.

#0891 Turning data into information: Using PD3D® models to guide colorectal cancer therapy by Optim.AI™.

Ulrike Pfohl[1], Masturah Mohd Abdul Rashid[2], **Jhin Jieh Lim**[2], Juergen Loskutov[1], Lena Wedeken[1], Edward Kai-Hua Chow[3], Hugo Saavedra[2], Christoph Reinhard[1], Christian R. A. Regenbrecht[4]

[1]CELLphenomics GmbH, Berlin, Germany,[2]KYAN Therapeutics, Singapore, Singapore,[3]Cancer Science Institute of Singapore, Singapore, Singapore,[4]ASC Oncology GmbH, Berlin, Germany

Colorectal cancer (CRC) is one of the most prevalent and lethal malignancies globally with up to 50 % of patients eventually progressing to metastatic disease. The mitogen-activated-protein kinase (MAPK) pathway emerges as a key player, being one of the most frequently mutated signaling pathways in the oncogenesis of CRC. However, given the numerous genomic aberrations and tumor heterogeneity in CRC, patients may benefit from combinatorial therapies, particularly those who have inoperable or metastatic tumors. In the present study, we investigated the feasibility of combining two platforms, patient-derived 3D (PD3D®) models with Optim.AI™, to identify more effective cancer therapies. PD3D® models can robustly retain the genotypic and histopathologic features of the primary patient tumor, model tumor heterogeneity and were shown to predict a patient's drug response. Optim.AI™ is a hybrid computational-experimental platform that uses small data sets to rationally converge to optimal drug combinations within a defined drug search space. By mapping experimental data points to a second-order quadratic function, Optim.AI™ can predict every possible 531k data points and thus the cell-killing efficacy for all other possible combinations without testing each individual drug-dose combination. Two CRC PD3D® models with different mutation profiles were tested with 155 different combinations of 12 drugs at variant concentrations. The post-treatment cell viability was measured and used for Optim.AI™ analysis to evaluate and compare the best therapies. Optim.AI™ analysis revealed differential drug sensitivity between tested CRC PD3Ds®. The top-ranked drug combinations included SN-38, active compound of commonly used chemotherapeutic irinotecan, paired with MEK-inhibitors trametinib or cobimetinib which we could confirm with both platforms. With this study, we successfully demonstrated the feasibility, the robustness, and the efficiency of combining PD3Ds® and Optim.AI™ in identifying effective drug combination therapies, here for CRC, within one month. This combined technology provides precise insights into tumor treatability and its functional causes of treatment outcomes, leading to new treatment combinations and accelerating the development of new cancer drugs in a time- and cost-effective manner.

#0892 Pan-cancer tumor microenvironment profiling with multiplexed immunofluorescence microscopy and self-supervised learning.

Gantugs Atarsaikhan[1], Isabel Mogollon[1], Katja Valimaki[1], Tuomas Mirtti[2], Teijo Pellinen[1], **Lassi Paavolainen**[1]

[1]Institute for Molecular Medicine Finland (FIMM), University of Helsinki, Helsinki, Finland,[2]University of Helsinki, Helsinki, Finland

Multiplexed immunofluorescence (mIF) microscopy reveals the spatial architecture of cancer tissue and its microenvironment that is not being fully explored with existing analysis methods. Most analysis approaches for mIF microscopy data focus on single-cell or region classification and rely on supervised machine learning. In this work, we present a self-supervised spatial profiling method for mIF images that takes local and global associations into account, and apply this method to profile cancer-associated fibroblasts (CAFs) in a pan-cancer dataset.

We studied a 2-stage self-supervised training scheme to learn the representations of mIF tissue microarray (TMA) images in local and global scales (cellular and long-range associations). During the 1st self-supervised training stage, a Vision Transformer learns the local-scale representations by using small patches from TMA images. Then, the local representations are used as input to the 2nd stage where a similar self-supervised learning strategy is used to learn global patterns in the TMA images.

We applied the method to profile multiple cohorts from three different solid tumors: prostate, renal, and lung cancer. In total, these cohorts include more than 5,000 TMA cores from over 1,750 patients extracted from the tumor center, tumor edge, and adjacent benign areas. The samples were stained with a CAF panel including FAP, aSMA, PDGFRB, pSTAT3/PDGFRA, nuclear and epithelial markers, and imaged with cyclic mIF microscopy.

Samples were studied at the patch-level and TMA core-level. Small patches enable further analysis of associations in the local environment, whereas the core-level enables associations with patient clinical information. Clustering of patch-level (1st stage) and core-level (2nd stage) representations showed independently that self-supervised learning is capable of learning the representations of the mIF images. We were able to identify regions and cases with high pTNM staging from the prostate cancer samples and similar histological subtypes from renal cancer samples. We further validated the clustering using k-NN classification that showed high classification accuracy in all cohorts. Moreover, we developed a stopping criteria for the final model selection that balances between the similarities of samples and patches inside of samples to prevent overfitting.

Our study shows that self-supervised learning enables unbiased discoveries from large-scale mIF microscopy imaging datasets. The developed method uncovers associations between imaging data and clinical information and highlights directly the patterns that are most meaningful for these associations.

#0893 Studying the impact of CNVs on expression at single-cell resolution in HGSOC using autoencoders.

M. Marin Falco[1], T. Narhi[1], E. P. Erkan[2], J. Hynninen[3], A. Vaharautio[1];
[1]University of Helsinki, Helsinki, Finland, [2]Tampere University, Tampere, Finland, [3]University of Turku and Turku University Hospital, Turku, Finland

High-grade serous ovarian cancer (HGSOC) is one of the most lethal gynecological malignancies. Lack of common targetable oncogenic mutations has complicated the development of directed therapies to combat emerging resistance. This malignancy is mainly characterized by the mutation of gene TP53, which promotes genome instability for the emergence of extensive copy number variations (CNVs). However its impact on gene expression at the single-cell level is not well understood. In this study, we aim to investigate the effect of CNVs on transcriptomic signatures by taking advantage of variational autoencoders (VAE) ability for dimensionality reduction, unsupervised learning and feature extraction. The use of VAEs is becoming more popular for the analysis of scRNAseq data, and scVI is one of the most versatile VAE applications performing wide variety of tasks. Here, we used single-cell RNA sequencing (scRNA-seq) data from 90 longitudinal samples of 64 HGSOC patients and inferred CNVs in each cell using inferCNV, an established computational pipeline. Then, we modified scVI algorithm to allow the VAE to reconstruct CNVs from a latent space originated from gene expression profiles and viceversa. Our models were capable of reconstructing CNV profiles accurately from expression data and also remove batch effect. From these models we could observe how, after the integration of genomic information, the latent clusters produced from the transcriptomic space were influenced by the amplifications or deletions of certain genomic regions. Moreover, some of these clusters were characterized by the alteration of important oncogenes in HGSOC, such as KRAS and CCNE1, and allowed us to focus on the transcriptomic consequences of their amplifications. With the results from the approach presented here, we gained a more comprehensive picture of the impact of genomic alterations on HGSOC. As future work, we plan to validate of this results on external cohorts and link the identified signatures to clinically relevant features such as prognosis or chemotherapy response.

#0894 Radiomics at baseline MRI are associated with tumor shrinkage in patients with unresectable renal cell carcinoma treated with neo-adjuvant Cabozantinib.

L. LI[1], E. Nicaise[2], B. Schmeusser[2], A. Midya[1], A. Davarpanahfakhr[1], A. Madabhushi[1], M. Bilen[1], V. Master[2], **R. Shiradkar**[1];
[1]Emory University, Atlanta, GA, [2]Emory University School of Medicine, Atlanta, GA

Background: Neoadjuvant Cabozantinib targeted therapy (nCabo) has been shown to facilitate tumor size reduction in patients with renal cell carcinoma (RCC). However, there is unmet clinical need to identify pre-treatment markers predictive of response to nCabo to limit financial, dose-related toxicity. We investigated computationally derived radiomic signatures from baseline magnetic resonance imaging (MRI) for their association with response to tumor shrinkage following nCabo.**Methods** Seventeen patients with non-metastatic, clinical stage ≥T3, biopsy-confirmed clear cell RCC were enrolled in a phase II clinical trial (NCT04022343) examining primary tumor response to nCabo. Patients underwent 3 Tesla MRI at baseline, 6 and 12 weeks. Partial response (PR) or stable disease (SD) was determined per Response Evaluation Criteria in Solid Tumors at 12 weeks. Tumor regions of interest (ROI) were delineated on axial, arterial phase T1-weighted (T1W) series under the guidance of expert radiologist. T1W were normalized with respect to enhancement in cortex region of kidney. 75 radiomic features quantifying texture heterogeneity were derived from tumor ROI on a per-voxel basis at baseline. Wilcoxon ranksum test was used to evaluate significant differences in radiomics between patient groups PR and SD. **Results**: Following nCabo, 6/17 patients experienced PR. 22 radiomic features from T1W quantifying intensity based heterogeneity showed significant differences between patients with SD and PR after nCabo ($p<0.05$; top 3 in **Table**). None of the clinical variables showed significant differences between SD and PR. **Conclusion**: In this proof-of-concept preliminary study, we observed that radiomics at baseline MRI may allow for identifying RCC patients who would favorably respond to nCabo in terms of tumor shrinkage. Future studies will include analysis on longitudinal data, correlation against survival on large-scale datasets.

Association between tumor shrinkage following nCabo and radiomic features, clinical variables

			Stable Disease (N=6)		**Partial Response (N=11)**	
Category	**Feature**	**P-value**	**median**	**IQR**	**median**	**IQR**
Radiomic	Haralick	**0.01**	1.50	0.51	2.31	0.51
	Gradient Filter	**0.02**	88.06	107.28	289.58	107.28
	CoLlAGe	**0.03**	224.28	10.73	210.50	10.73
Clinical	Age	0.12	56.00	14.00	52.50	14.00
	BMI	0.48	29.90	8.50	27.30	8.50
	modified Glasgow Prognostic Score	0.21	1.00	1.00	0.00	1.00
	Baseline Tumor Size (cm)	0.48	9.50	5.15	9.50	5.15
	ECOG PS at presentation	0.23	0.00	1.00	0.00	1.00
	Charlson Comorbidity Index	0.72	6.00	6.00	4.00	6.00

#0896 Predicting metastatic transcriptomes of patient tumors with deep learning.

G. Li[1], E. Beal[1], D. Sumner[1], G. G. Galli[1], V. Cremasco[2], J. M. Korn[2], F. Dondelinger[1], **D. Ruddy**[2], A. Kauffmann[1], S. Dimitrieva[1];
[1]Novartis, Basel, Switzerland, [2]Novartis, Cambridge, MA

Metastases are the primary cause of cancer-related death, and improving the means of predicting and targeting their development is one of the major goals in cancer research. While surgical resection and neo-adjuvant therapy can cure well-confined primary tumors, our ability to effectively treat cancer is largely dependent on our capacity to interdict the process of metastasis. The recent accumulation of ‘omics data from metastatic tumors provides an unprecedented opportunity to develop machine learning models to predict the molecular changes during metastasis and explore the patterns of metastasis formation. With this in mind, we developed *MetMapper*, a deep learning model trained on primary and metastatic tumors from > 13 000 patients integrating data from 11 published data resources. MetMapper can predict the transcriptomic changes of a primary tumor when it metastasizes to different distant organs. The results were extensively validated using transcriptomics data from matched primary and metastatic tumor biopsies extracted from the same patients. Furthermore, MetMapper’s predictions revealed that the non-random patterns of cancer metastases can be partly explained by the degree of transcriptome reprogramming needed during metastasis: primary tumors tend to metastasize to organs that require minimal changes to their transcriptomes. Using MetMapper, we derived a metastatic potential score for patient tumors and demonstrate that this score can be used to stratify patients into high and low survival groups across different indications. The predicted metastatic potential of patient tumors significantly correlates with experimentally characterized metastatic potential of cancer cell lines. Additionally, by performing *in-silico* perturbations of genes and oncogenic pathways that can alter the metastatic potential of patient tumors, we identified genomic features that are highly associated with metastases to specific organs, some of which were reported by existing pan-cancer clinical sequencing studies. Our results demonstrate the utility of MetMapper as a novel AI-powered methodology for investigating mechanisms and patterns of metastatic dissemination, as well as forecasting metastatic outcomes of patient tumors.

#0897 Synthetic lethality screening with Recursive Feature Machines.

Adityanarayanan Radhakrishnan[1], Cathy Cai[2], Barbara A. Weir[3], Christopher Moy[4], Caroline Uhler[2]

[1]Harvard University / Broad Institute of MIT and Harvard, Cambridge, MA,[2]Massachusetts Institute of Technology / Broad Institute of MIT and Harvard, Cambridge, MA,[3]Johnson and Johnson Innovative Medicine, Cambridge, MA,[4]Johnson and Johnson Innovative Medicine, Spring House, PA

Synthetic lethality refers to the concept that simultaneous perturbation of gene pairs leads to cell death but individual perturbation does not. Synthetically lethal gene pairs (SL pairs) provide a potential avenue for selective targeting of cancer cells based on underlying genetic vulnerabilities. The rise of large scale gene perturbation screens such as the Cancer Dependency Map (DepMap) offers the opportunity to identify SL pairs automatically using machine learning. Yet, a key difficulty in using machine learning models for this task is the lack of labeled data in the form of known SL pairs. Thus, prior approaches framed SL pair identification as a feature learning problem where the goal is to identify the genomic features most influential for predicting low cellular viability under a gene knockout. These prior approaches have primarily utilized random forests since these machine learning models are one of the only nonlinear models for which feature importances are provided explicitly. On the other hand, if we could identify features learned by state-of-the-art models on screening tasks such as kernel machines, we would be better powered in finding SL pairs. In this work, we present a computationally efficient and effective pipeline for SL pair screening built on a recently developed class of feature learning kernel machines known as Recursive Feature Machines (RFMs). We show that our pipeline more accurately recovers experimentally verified SL pairs than prior work including the best model from the DepMap portal and previous random forest based approaches (see the table below). Moreover, our pipeline identifies several new candidate SL pairs for further analysis, opening new avenues for targeting genetic vulnerabilities in cancer.

Rank of verified SL pairs across unsupervised methods (lower is better with a minimum value of 1).

Experimentally Verified SL Pairs	Pearson Correlation	PARIS	DepMap	RFMs (Ours)
SMARCA2/SMARCA4	1	1	1	1
ARID1A/ARID1B	1	1	1	1
STAG1/STAG2	1	1	1	1
CREBBP/EP300	1	1	1	1
VPS4A/VPS4B	7	> 10	5	1
DDX17/DDX5	4	1	1	1
ENO1/ENO2	> 10	1	1	1
SMARCC1/SMARCC2	> 10	1	1	1
UBB/UBC	> 10	1	> 10	1
MAGOH/MAGOHB	1	1	1	1
FAM50A/FAM50B	1	1	1	1

#0898 Deep learning-based cell types scores in tumor microenvironment estimated by H&E images associated with PD-L1 status in lung adenocarcinoma.

S. Cook[1], H. Shin[1], J. Koh[2], H. Choi[3], K. Na[4];

[1]Portrai, Inc., Seoul, Korea, Republic of, [2]Department of Pathology, Seoul National University Hospital, Seoul, Korea, Republic of, [3]Department of Nuclear Medicine, Seoul National University Hospital, Seoul, Korea, Republic of, [4]Department of Thoracic and Cardiovascular Surgery, Seoul National University Hospital, Seoul, Korea, Republic of

Purpose: The spatial distribution of cell types in the tumor microenvironment (TME) is associated with functional status of tumor immunology and eventually affects the response to immuno-oncology treatment. We have developed a deep learning model that was trained by integrating H&E images of lung adenocarcinoma with spatial transcriptomic data. We applied this model to predict various cell types within the TME using only hematoxylin and eosin (H&E) images to correlate with the PD-L1 status.

Methods: A deep learning model to predict five cell types enrichment score maps from H&E images was trained by spatial transcriptomics data combined with matched H&E images. The five cell types of TME included B cells, T/NK cells, myeloid cells, fibroblasts, and epithelial cells. wAnother dataset based on tissue microarray (TMA) data of H&E images of lung cancer patients (n = 94) was used to predict cell type enrichment scores associated with PD-L1 status estimated by TPS score. The cell type scores derived from the H&E-stained lung cancer images were correlated with the PD-L1 status.

Results: The cell types predicted by the model using H&E image patches showed a significant correlation with those determined through spatial transcriptomic data, serving as an internal validation. All cell types (B cells, T/NK cells, myeloid cells, fibroblasts, and epithelial cells) from TMA cores showed significant differences according to the PD-L1 expression groups. The enrichment scores of B cells, T/NK cells, myeloid cells and fibroblasts were significantly higher in the PD-L1 high group.

Conclusions: Our research introduces a deep learning model for precise cell type mapping within the tumor microenvironment and applied to H&E-stained TMA cores. The relationship between PD-L1 status and the cell type enrichment scores within the tumor microenvironment, as predicted by the deep learning model analyzing H&E images, demonstrates the potential for using H&E-based characterization of the tumor microenvironment as a biomarker in immuno-oncology treatments.

#0899 Development of a deep learning model for cell type mapping in colorectal cancer using H&E images leveraging image-based spatial transcriptomics data.

S. Cook[1], D. Lee[1], M. Lim[1], J. Lee[1], D. Lee[1], H.-J. Im[2], J.-S. Pyo[3], K. Na[4], H. Choi[5];
[1]Portrai, Inc., Seoul, Korea, Republic of, [2]Department of Molecular Medicine and Biopharmaceutical Sciences, Graduate School of Convergence Science and Technology, Seoul National University, Seoul, Korea, Republic of, [3]Department of Pathology, Uijeongbu Eulji Medical Center, Eulji University School of Medicine, Gyeonggi-do, Korea, Republic of, [4]Department of Thoracic and Cardiovascular Surgery, Seoul National University Hospital, Seoul, Korea, Republic of, [5]Department of Nuclear Medicine, Seoul National University Hospital, Seoul, Korea, Republic of

Purpose The tumor microenvironment (TME) is crucial in colorectal cancer as it influences disease progression, treatment response, and patient outcomes, providing valuable insights for personalized therapies and prognostic assessments. Here, we have developed a deep learning model by integrating hematoxylin and eosin (H&E) stained images of colorectal cancer and image-based spatial transcriptomics (Xenium) to infer spatial mapping of cell types in TME only using H&E images.
Methods A total of 30 H&E images of colorectal cancer obtained by tissue microarray were registered with image-based spatial transcriptomics data (Xenium). Utilizing a Variational Autoencoder (VAE) based model and leveraging reference single-cell data enables the acquisition of cell types for individual cells in image-based spatial transcriptomics. A convolutional neural network (CNN) model was developed using H&E image as inputs to predict cell types in H&E-stained tissue image patches of colorectal cancer collected from various patients. The model also estimated the cell types from H&E-stained whole slide tissue image of colorectal cancer of The Cancer Genome Atlas (TCGA-COAD).
Results The accuracy of the model's predictions for cell types using H&E image patches was notably high and exhibited a significant concordance with the results obtained through the validation. The Intersection over Union (IoU) metric for image segmentation indicated a value of 0.66 for epithelial cells and 0.44 for TNK cells. The output of deep learning model for epithelial cells and T/NK cells from TCGA-COAD tissue images showed a correlation with human-labeled regions of cancer epithelium and immune cells.
Conclusions Leveraging image-based spatial transcriptomics, we developed a deep learning model capable of discerning various cell types within the tumor microenvironment solely from H&E images. This clinically translatable approach is valuable for investigating tumor microenvironment to develop biomarkers associated with various cancer therapeutics particularly immuno-oncology drugs. This approach can yield objective deep learning-based models without human labels for characterizing the tumor microenvironment in single-cell resolution, particularly regarding spatial immune distribution.

#0900 Development and validation of an artificial-intelligence-based pathomics biomarker to predict resistance to first-line treatment in metastatic colorectal cancer.

L. Lazzari[1], G. Mauri[2], V. Giannini[3], D. Cafaro[4], G. Nicoletti[5], C. Marchio[6], A. Sartore-Bianchi[7], F. Marmorino[8], M. Munoz[9], N. Saoudi Gonzalez[10], A. Puccini[11], C. Cremolini[8], C. Montagut[12], E. Elez[13], S. Sciallero[11], E. Berrino[14], M. Carullo[8], P. Vitiello[15], M. Aquilano[16], M. Di Como[16], E. Bonoldi[16], S. Siena[17], A. Bardelli[18], D. Regge[19], S. Marsoni[1];

[1]IFOM ETS - The AIRC Institute of Molecular Oncology, Milano, Italy, [2]Universita degli Studi di Milano, Milano, Italy; IFOM ETS - The AIRC Institute of Molecular Oncology, Milan, Italy, Milano, Italy, [3]University of Turin, Turin, Italy; Radiology Unit, Candiolo Cancer Institute, FPO - IRCCS, Candiolo (TO), Italy, Torino, Italy, [4]Candiolo Cancer Institute, FPO - IRCCS, Candiolo (TO), Italy, Candiolo (TO), Italy, [5]University of Turin, Turin, Italy; Department of Electronics and Telecommunications, Polytechnic of Turin, Turin, Italy, Turin (IT), Italy, [6]Candiolo Cancer Institute, FPO-IRCCS, Candiolo (TO), Italy; Department of Medical Sciences, University of Turin, Turin, Italy, Milano, Italy, [7]Universita degli Studi di Milano, Milano, Italy; Division of Clinical Research and Innovation, Grande Ospedale Metropolitano Niguarda, Milan, Italy, Milano, Italy, [8]University Hospital of Pisa, Pisa, Italy; Department of Translational Research, University of Pisa, Pisa, Italy, Pisa, Italy, [9]Hospital del Mar, Barcelona, Spain, Barcelona, Spain, [10]Vall d'Hebron University Hospital, Barcelona, Spain, Barcelona, Spain, [11]IRCCS Ospedale Policlinico San Martino, Genoa, Italy, Genova, Italy, [12]Hospital del Mar, Barcelona, Spain, Barcelona, Italy, [13]Vall d'Hebron University Hospital, Barcelona, Spain, Barcelona, Italy, [14]Candiolo Cancer Institute, FPO-IRCCS, Candiolo (TO), Italy, Turin, Italy, [15]IFOM ETS - The AIRC Institute of Molecular Oncology; University of Turin, Turin, Italy, Milano, Italy, [16]Grande Ospedale Metropolitan Niguarda, Milano, Italy, Milano, Italy, [17]Universita degli Studi di Milano, Milano, Italy; Department of Hematology Oncology, and Molecular Medicine, Grande Ospedale Metropolitan Niguarda, Milano, Italy, Milano, Italy, [18]University of Torino, Torino, Italy; IFOM ETS - The AIRC Institute of Molecular Oncology, Milan, Italy, Milano, Italy, [19]University of Pisa, Pisa, Italy; Radiology Unit, Candiolo Cancer Institute, FPO - IRCCS, Candiolo (TO), Italy, Pisa, Italy

Background: The backbone chemotherapy of first-line standard of care (SOC) for microsatellite stable (MSS) metastatic colorectal cancer (mCRC) combines 5-Fluorouracil to oxaliplatin and/or irinotecan. There are no biomarkers to predict response, which is complete or long-lasting (CR/LLR) in 20-25% of patients, while 10-15% are primary refractory. The aim of this work is to develop a predictive biomarker, based on digital pathology images, that can help stratify patients according to their risk of resistance.

Methods: We trained a supervised bag-of-words artificial intelligence (AI)-based model on a cohort of response outliers mCRC patients classified as “really sensitive” (RS) if they achieved CR or LLR >10 months to any SOC, or “really resistant” (RR) if progression occurred at first disease reassessment. Whole-slide Imaging (WSI) of the resected primary tumors were tiled into patches of 224x224 pixel (0.5µm/pixel). First-order and texture features were subsequently extracted from all tumoral tiles and grouped into homogenous clusters through a k-means algorithm (k=6). For each patient, the percentage of tiles belonging to each tiles’ cluster was computed to represent new features (called bag of words) with whom different machine learning classifiers were trained. Main clinicopathological features were matched to treatment response by Fisher’s exact test.

Results: To date, we analyzed 82 response outlier patients, of whom 35 were classified as RS and 46 RR. Of them, patients identified at Italian centers were used as construction cohort (N=47; 27 RR and 20 RS) and those identified at Spanish centers were used a validation cohort (N=35; 19 RR and 16 RS). The best result was obtained using a stepwise logistic regression, reaching a negative predictive value (NPV) of 90% (18/20; 95% CI=70-97%) and 71% (10/14; 95% CI=49-87%), in the construction and validation sets. No standard clinicopathological features (including stage, *RAS/BRAF* status, histology and sidedness) was associated with the chance of being RR.

Conclusions: We demonstrated that a pathomics signature has the potential to predict resistance to SOC in MSS mCRC. Further validation of these preliminary findings on a larger cohort of response outlier patients is ongoing.

#0901 BATCHIE: An active learning platform for scalable combination drug screens.

C. Tosh[1], M. Tec[2], J. White[1], J. F. Quinn[1], G. Ibanez Sanchez[1], P. Calder[1], A. L. Kung[1], F. S. Dela Cruz[1], W. Tansey[1];
[1]Memorial Sloan Kettering Cancer Center, New York, NY, [2]Harvard University, Cambridge, MA

Large-scale combination drug screens are largely considered intractable due to the immense number of possible combinations. Existing approaches use ad hoc fixed experimental designs then train machine learning models to impute novel combinations. We introduce BATCHIE, an orthogonal approach that adaptively conducts experiments in batches. BATCHIE uses information theory and probabilistic modeling to design each batch to be maximally informative based on the results of previous experiments. BATCHIE is fully modular, allowing any Bayesian probabilistic model to be used and any study constraints to be incorporated while maintaining optimality guarantees.

Results: In retrospective simulations on public combination screens, BATCHIE saved 10s of thousands to 100s of thousands of experiments relative to non-adaptive baselines. We conducted a prospective study focusing on pediatric sarcomas with BATCHIE. Our study covered 16 cell lines spanning Ewing sarcoma (EWS), osteosarcoma, rhabdomyosarcoma, as well as non-sarcoma cancers and non-cancer lines. We used a drug library of 206 drugs at two doses. After 15 rounds of BATCHIE-driven data collection, we observed 54K unique combinations, covering 4% of the experimental landscape. On unobserved validation data, the BATCHIE model predictions were highly accurate (Pearson's rho=0.91, p<10-30) and detected the rare (0.004%) combinations with significant synergy (AUC of ROC=0.85, p<10-5). We further investigated 10 combinations that BATCHIE predicted to have high therapeutic index (TI) for a broad selection of EWS lines, meaning a large differential effect between the predicted viabilities of the control lines and the target lines. We found that the TI scores for the top hits were significantly larger than the rest of the screen ($p<10^{-}50$), with the median top hit TI score lying in the 98th percentile of observed TI scores. We further validated 6 of the top hits in an ex vivo study on 2 patient-derived EWS samples, again finding significantly large TI values (p<10-13), with the median ex vivo TI score lying in the 96th percentile of observed TI scores. The top hits also exhibited biologically plausible rationales including combining PARP inhibitors with topoisomerase 1 inhibitors and alkylating agents, despite our model utilizing no prior knowledge on the molecular targets of our drug library. Combining PARP inhibitors with topoisomerase 1 inhibitors comprise 3 of the 6 currently open phase II clinical combination trials for EWS.

#0902 Explainable AI: Graph machine learning for response prediction and biomarker discovery.

J. Cohen-Setton[1], K. Bulusu[1], J. Dry[2], B. Sidders[1];
[1]AstraZeneca UK, Cambridge, United Kingdom, [2]Tempus AI, Boston, MA

Accurately predicting drug sensitivity and understanding what is driving it are major challenges in drug discovery. Graphs are a natural framework for capturing diverse pharmacological data for efficacy predictions, thanks to their ability to integrate multimodal data and represent relationships such as gene-gene or drug-target interactions as edges. They have also had proven success across a range of other drug discovery tasks including repositioning and target identification. In this study, we sought to address the explainability challenges of drug response predictions. Recent developments in the field of Graph AI have led to improvements in interpretability mechanisms that highlight parts of a graph which are driving predictions. We have conducted a comprehensive review of multiple major approaches for tackling drug efficacy prediction using graph methods, benchmarking the performance and interpretability of these algorithms across indications.

Methods: We assembled a combined dataset of GDSC1 and GDSC2 drug response data in cell lines, with multiomic cell line data and drug target and chemical structure data. We then applied graph-based approaches for the prediction of binarized IC50 on an indication-by-indication basis. Approach 1 involved the creation of a ‘GDSC knowledge graph’, where drug response and cell line ‘omic information is represented in an unweighted knowledge graph: cell lines are connected to genes expressed in them, drugs are connected to genes they target, and so on. We then used state-of-the-art graph embedding techniques to predict IC50 using paired drug and cell line embeddings. In Approach 2 we used a weighted knowledge graph instead, and generated embeddings using heterogeneous graph neural networks (HGNNs). In Approach 3, we modelled response prediction as a graph classification task, where one single graph captures one drug-cell line interaction. The graph classifier and HGNN models both have in-built interpretability mechanisms, including graph attention, that can signify the genes in the cell line which were most important for the eventual prediction. We can also integrate biomedical prior knowledge with all these models by capturing gene-pathway and gene-gene data in the graphs.

Results: Our models outperformed benchmark models including DNNs and GBMs, and identified both established and novel response biomarkers in NSCLC cell lines (AUC = 0.94, Accuracy = 89%). We have also applied our models to Breast Cancer, Pancreatic Cancer, Colorectal Cancer and Haematological malignancies with similar predictive performance and explainability.

Conclusions:Our graph analytical framework for response predictions showed better performance than benchmarking models and provided insights from explainability. This framework is easily extendable to response and ‘omic data from any disease model and patient studies.

#0903 AURIGIN: A comprehensive single-cell OMICs atlas of human development and an AI/ML framework to classify and identify the drivers of tumor plasticity and altered cellular state.

J. DeBartolo III, H. Wilson, K. S. Straley, M. Bhatta, S. Sharma, S. Sinicropi-Yao, J. Neef, B. Chan, A. McRiner, M. Bittinger, L. Antipov, K. E. Yen, T. G. Graeber, D. S. Millan;
Auron Therapeutics, Newton, MA

Altered cellular state and plasticity have been increasingly identified as drivers of poor prognosis and treatment-resistance in cancer. Identifying therapeutics that correct altered cellular state and plasticity meets a broad need in the field of oncology, particularly in tumors resistant to standard-of-care therapy. Tumor plasticity and altered cellular states encompass many potential configurations, including dedifferentiated and transdifferentiated tumors, so classifying tumors based on their specific cell state profile is critical to identifying the gene drivers that are specific to that altered state. For that reason, we have developed AURIGIN - a platform that combines a comprehensive single-cell OMICs atlas of human development with an AI/ML framework that can classify cell state plasticity and identify the genes and pathways that drive those specific altered cellular states. AURIGIN is more comprehensive than previously disclosed single cell atlases in that it focuses and enriches the diverse stem, progenitor, and developmental states commonly involved in plastic cell states of cancer. The platform standardizes and integrates these states with multiple atlases of differentiated adult tissues to create a unified atlas of human development. In addition, the AI/ML paradigm of AURIGIN is embedded with developmental biology models that enable it to deconvolute state heterogeneity within tumor indications for precise identification of the most relevant gene targets for novel therapies. AURIGIN also unifies classified plasticity across tissue types by identifying altered cellular states that span multiple indications. Furthermore, we present the implementation of AURIGINDRIVE ML models that integrate pathway information, physical interaction datasets, and regulatory annotations to accurately predict the gene targets at the top of hierarchy of control of tumor plasticity. AURIGIN also enables and accelerates target validation by identifying models that map to the relevant classified plastic states. Similarly, AURIGIN defines clinically relevant patient selection and treatment efficacy biomarkers that are specifically defined from the classified plastic cellular state. We demonstrate the success of AURIGIN for therapeutic discovery. In sum, AURIGIN amplifies the value of multiOMIC tumor data in cellular state and plasticity target discovery by mapping the data into a developmental biology-informed ML framework.

#0904 AI platform provides an EDGE and enables state-of-the-art identification of peptide-HLAs for the development of T cell inducing vaccines.

J. Klein, D. Sprague, M. Lane, M. Hart, O. Petrillo, I. do Valle, M. Davis, A. Ferguson, A. Allen, K. Jooss, **A. Dhanik**;
Gritstone bio, Inc., Emeryville, CA

T cell inducing vaccines are key for the development of effective therapies against cancer and infectious diseases. Peptides, presented by Human Leukocyte Antigens (HLAs), are the targets of T cells, and their identification is therefore critical to the development of such vaccines. Here, we present the latest improvement in our EDGE^{TM} (Epitope Discovery for GEnomes) platform to address this critical need. EDGE is comprised of AI models that can predict peptide presentation by HLA class I and class II. Although the models are trained primarily using immunopeptidomics data, EDGE scores are predictive of peptide-HLA immunogenicity. There are three class I presentation models in EDGE: an allele-specific model, a pan-specific model, and a model specific for infectious diseases. The allele-specific model is applicable to a large but pre-defined set of HLA alleles. On a large test dataset, the allele-specific model achieved an average precision (AP) of 63% (PPV40=79%) compared to the AP of a standard best-available public model of 21% (PPV40=28%). A Ph1/2 clinical study of personalized cancer vaccines encoding neoantigens predicted from the allele-specific model demonstrated a ~50% molecular response (defined as >=30% reduction in circulating tumor DNA relative to baseline) rate with associated extended overall survival (vs non-responders) in metastatic, microsatellite stable colorectal cancer patients. We observed that ≥50% of the mutations were able to elicit T cell responses. The pan-specific class I model uses HLA sequences as input feature when training and, therefore, is applicable to any HLA. On the same test dataset as above, it achieved an AP of 65% (PPV40=81%) and performed better on average for ~40 less-common HLA alleles. Prediction of viral peptide presentation by HLA class I is challenging due to the lack of immunopeptidomics data. The class I model for infectious diseases was specifically optimized to predict for viral peptides and, therefore, performed better than available class I models on published HIV and Influenza A datasets. Prediction of peptide presentation by HLA class II is challenging due to the flexibility in how the longer peptides interact with open HLA grooves as well as the lack of immunopeptidomics data as compared to the class I peptides. The class II model in EDGE, EDGE-II, uses the latest developments in protein large language models, a novel learned HLA allele-deconvolution strategy, and in-house immunopeptidomics data, resulting in improved prediction of peptide presentation by HLA class II and immunogenicity driven by $CD4^+$ T cells. On a benchmark validation dataset, EDGE-II achieved an AP of 71% as compared to AP of 62% of a leading published model. In summary, EDGE^{TM} provides a comprehensive state-of-the-art platform for the development of vaccines that can induce both $CD8^+$ and $CD4^+$ T cell responses to provide durable benefit to patients.

#0905 ML quantification of tumor-Infiltrating lymphocytes distinguishes immune-phenotypes and reveals phenotypic heterogeneity.

N. Le[1], B. Rahsepar[1], J. Hipp[1], J. Conway[1], Y. Gerardin[1], E. Krause[1], C. Shen[1], R. Biju[1], M. Nercessian[1], N. Indorf[1], S. Degryse[1], M. Markey[1], V. Mountain[1], P. Vaidya[2], W. Wijaya[2], A. Shrotre[2], P. Caplazi[2], D. Inzunza[2], J. Palma[2], E. Huntzicker[2], C. Tribouley[2], D. Chen[2], R. Prediou[2], F. Chen[2], K. Kolahi[2];
[1]PathAI, Inc., Boston, MA, [2]AbbVie, Chicago, IL

Immune phenotypes (IP), defined by the tumor-infiltrating lymphocyte (TIL) distribution within the tumor microenvironment (TME), is prognostic and predictive of treatment response. Here, machine learning (ML) models that characterize the TME were deployed in non-small cell lung cancer (NSCLC) and head and neck squamous cell carcinoma (HNSCC) to exhaustively label TILs directly from hematoxylin and eosin (H&E)-stained whole slide images (WSI), compute IP and quantify TIL distribution, tasks which are manually untenable.

ML-powered TME models (PathAI, Boston, MA; commercially available as PathExplore™) for NSCLC and HNSCC that quantify tissue regions (e.g. tumor, epithelium, and stroma) and cells (e.g. lymphocytes) in H&E-stained WSI were deployed on 126 NSCLC and 103 HNSCC commercial samples. Ground truth CD3 and CD8 scores were obtained from paired immunohistochemically-stained WSI (HALO, Indica Labs, Albuquerque, NM). Inflamed, desert, or excluded IPs (based on data-driven cutoffs) were inferred from the mean TIL density in epithelium and stroma (slide-level IP, sIP), and from the fraction of “hot” patches in all 100um x 100um patches tiling the tumor and stroma areas (patch-level IP, pIP). TIL spatial distribution was measured by the Morisita-Horn index that computes the patch-wise overlap between TILs and cancer cells (MHI, ranging from 0 to 1), and epithelial-stromal interface distance index (EDI) indicating the hot stromal patch bias toward the epithelium (-EDI) or stroma (+EDI).

ML-predicted TIL densities highly correlated with ground truth CD3+ and CD8+ cell densities (NSCLC/HNSCC CD3, CD8: tumor Pearson r= 0.88/0.85, 0.74/0.74; epithelium r= 0.76/0.71, 0.88/0.62; stroma r= 0.74/0.87, 0.61/0.76). High s- and pIP agreement was seen (NSCLC 93% and HNSCC 83%); 6/26 discordant cases were driven by TIL hotspots with high density (116%-310% of the cutoff) but few (median = 26%) hot patches in the epithelium. MHI was higher for the inflamed vs excluded IP ($p < 0.0001$ for NSCLC and HNSCC) and intra-group variability was high (NSCLC/HNSCC inflamed: 0.66±0.11/0.31±0.14, excluded: 0.51±0.12/0.26±0.17, desert: 0.48±0.09/0.28±0.17; mean±std). EDI was lowest and negative in inflamed IP but near zero in desert and excluded IP (NSCLC/HNSCC inflamed: -43±4um/-184±19um, excluded: 1.6±4um/-41±13um, desert: 18±4um/-14±13; mean±sem). Excluded and desert IPs had roughly equal + and - EDI cases (NSCLC +/-: 57/46; HNSCC +/-: 39/29).

ML-powered IP prediction using TIL distribution enables accurate and rapid profiling of the TME using routine histopathology. pIPs were concordant with sIPs and highlight TIL heterogeneity. Spatial markers (MHI and EDI) reveal differences between IP classes and intra-group heterogeneity relevant for drug discovery and patient stratification. Investigating prognostic associations of these markers is a promising direction for future studies.

#0906 Large-scale surface protein abundance prediction from single-cell transcriptomes with a zero-shot model and its applications to cancer research.

R. Chen, B. Chen, J. Zhou;
Michigan State University, East Lansing, MI

We develop SPIDER, a zero-shot model which can predict the abundance for a large scale (>2,000) of surface proteins from single-cell transcriptomes in various contexts. This is to overcome the challenges in current single-cell protein abundance quantification tools (e.g., flow cytometry, CITE-seq) and computational models (e.g., totalVI, Seurat, cTPnet), where routinely only <300 surface proteins can be quantified or predicted. Comprehensive benchmarking on four external validation sets shows that the prediction accuracy of SPIDER outperforms other state-of-the-art methods including Seurat, totalVI, and cTPnet, with a prediction accuracy elevated as much as 42.5% in new contexts. We further conduct case studies in cancers by applying SPIDER to predict the abundance of >2,500 surface proteins on scRNA-seq datasets of hepatocellular carcinoma (HCC) and colorectal cancer liver metastasis (RCRLM), where the predicted surface protein abundance data is analyzed to demonstrate the broad downstream applications of SPIDER including facilitating cell type annotation, disease biomarker/target identification, and cell-cell interaction (CCI) inference. For instance, in these datasets we find that SPIDER can reveal (novel) disease biomarkers that are overlooked by solely observing transcript expression, such as CD44/PIK3IP1 in hepatocytes/ γδ2 T cells as a positive/negative HCC biomarker, demonstrating the capability of SPIDER to compensate for the limitations in the RNA modality. In conclusion, we propose the SPIDER model which can provide valuable information on the abundance of a large scale of surfaceomes in single cells, and can be further used to gain new insights into cancers via promoting cell type annotation, disease biomarker/target identification, and CCI inference.

#0907 ScreenDL: A transfer learning framework integrating tumor omics and functional drug screening for personalized clinical drug response prediction.

C. Sederman, T. Di Sera, Y. Qiao, X. Huang, B. E. Welm, A. L. Welm, G. Marth;
University of Utah, Salt Lake City, UT

Precision oncology hinges on accurate prediction of patient-specific treatment response from tumor molecular inputs. While deep learning (DL) models achieve state-of-the-art response prediction in cell lines, existing methods do not readily translate to the clinic where training data is limited. Here, we have developed and validated ScreenDL, a novel DL framework designed explicitly for use in clinical precision oncology applications. The underlying architecture of ScreenDL consists of two fully connected branches dedicated to learning rich embeddings of a drug's chemical structure and a tumor's transcriptomic profile respectively. These tumor omic and drug molecular embeddings are fed into a shared response prediction subnetwork which outputs predicted ln(IC50) values. The ScreenDL training schema incorporates three phases, each designed to improve clinical response prediction: (1) an initial pretraining phase leverages large-scale cell line pharmacogenomic datasets to extract patterns/relationships linking tumor omics and drug response; (2) subsequent transfer learning integrates pharmacogenomic data from patient-derived models of cancer, adapting the pretrained model to a more patient-relevant context; (3) patient-level omics and drug screening data (e.g., from matched patient-derived organoid (PDO) models) is integrated through patient-specific fine-tuning, generating a patient-specific response prediction model. Importantly, biomaterial from surgical tumor resection is often available for organoid establishment and patient-specific drug screening in practical clinical scenarios. To assess the utility of our ScreenDL framework for clinical response prediction, we applied ScreenDL to predict treatment response in 50 advanced/metastatic triple negative breast cancer (TNBC) patient-derived xenograft models (PDX). We leveraged tumor omics profiles for each PDX and drug screening data from matched PDX-derived organoids (PDxOs), mirroring the combination of patient-level tumor omic characterization and functional drug screening in matched PDOs, a protocol currently being piloted in Functional Precision Oncology trials at the University of Utah Huntsman Cancer Institute. After cell line pretraining, ScreenDL achieves a modest median Pearson correlation per drug of 0.15 relative to 0.03 for the leading compared model. However, transfer learning and subsequent PDX-specific fine-tuning significantly improve performance, producing median Pearson correlations per drug of 0.39 and 0.51, respectively. These results demonstrate the ability of our ScreenDL framework to dramatically improve response prediction in clinically relevant domains, bringing DL-based precision treatment selection closer to clinical application.

#0908 SeNMo: A self-normalizing deep learning model for enhanced multi-omics data analysis in oncology.

A. Waqas[1], **A. Tripathi**[1], S. Ahmed[1], A. Mukund[1], P. Stewart[1], M. Naeini[2], H. Farooq[3], G. Rasool[1];
[1]Moffitt Cancer Center, Tampa, FL, [2]University of South Florida, Tampa, FL, [3]University of Minnesota, Minneapolis, MN

Multi-omics research has enhanced our understanding of cancer heterogeneity and progression. Investigating molecular data through multi-omics approaches is crucial for unraveling the complex biological mechanisms underlying cancer, thereby enabling more effective diagnosis, treatment, and prevention strategies. However, predicting patient outcomes through integration of all available multi-omics data is still an under-study research direction. Here, we present SeNMo (Self-normalizing Network for Multi-omics), a deep neural network that ensures the zero mean and unit variance of activations across network layers using the self-normalizing technique. Such normalizing techniques are critical in stable and robust learning of deep learning models. SeNMo is particularly efficient in handling multi-omics data characterized by high-width (many features) and low-length (fewer samples) attributes. We trained SeNMo for the task of overall survival of patients using pan-cancer multi-omics data involving 28 cancer sites from the Genomic Data Commons (GDC). The training multi-omics data includes gene expression, DNA methylation, miRNA expression, and protein expression modalities. We tested the model's performance on the Moffitt Cancer Center's internal data involving RNA expression and protein expression data. We evaluated the model's performance in predicting patient's overall survival using the concordance index (C-Index), which provides a robust measure of the model's predictive capability. SeNMo performed consistently well in the training regime, reflected by the validation C-Index≥0.6 on GDC's public data. In the testing regime on Moffitt's private data, SeNMo performed with a C-Index of 0.68. The model's performance increased when tested on low-dimensional data or when tested on single omic data such as RNA or protein expression data with a C-Index of 0.7. SeNMo proved to be a mini-foundation model for multi-omics oncology data because it demonstrated robust performance, adaptability across molecular data types, and universal approximator capabilities for the scale of molecular data it was trained on. SeNMo can be further scaled to any cancer site and molecular data type. It can also be fine-tuned for other downstream tasks such as treatment response prediction, risk stratification, patient subgroup identification, and others. Its ability to accurately predict patient outcomes and adapt to various downstream tasks indicates a new era in cancer research and treatment. For future research, SeNMo offers a powerful tool for uncovering deeper insights into the complex nature of cancer and sets a precedent for how artificial intelligence can be leveraged to handle the vast and intricate data in the biomedical field. We believe SeNMo and similar models are poised to transform the oncology landscape, offering hope for more effective, efficient, and patient-centric cancer care.

#0909 Enhancing genomic analysis in cancer diagnostics: A machine learning approach for removing artifacts in FFPE specimens.

J. Lim[1], S. Park[1], W.-C. Lee[2], R. Kim[1], S. Lee[2], J. Lee[1], B.-L. Oh[1], Y. Ju[1];
[1]Genome Insight Technology, Inc., Daejeon, Korea, Republic of, [2]Genome Insight, Inc., San Diego, CA

Formalin-Fixed Paraffin-Embedded (FFPE) specimens, widely utilized in clinical cancer diagnostics, present significant challenges by introducing artifacts into genomic data. This study aimed to profile these FFPE-induced genomic alterations, with a particular focus on single-nucleotide variants (SNVs), small insertions and deletions (indels), and copy-number variations (CNVs), and to develop computational methods for filtering out such artifacts. Our primary focus was twofold: first, to comprehensively characterize the unique error profile of FFPE specimens observed through whole-genome sequencing (WGS), and second, to construct artifact classifiers and noise filters for SNV/indels and CNVs. We utilized machine learning (ML) and signal-processing techniques on a dataset of FFPE and matched fresh-frozen (FF) samples. The dataset of 52 FFPE-FF pairs were obtained from four different medical institutes and from various cancers including liver, breast, colon, stomach, and lung cancer, with varied FFPE archiving times. We also analyzed additional FFPE-only samples to refine our methods. Our methodology incorporated advanced computational approaches, including stacking ensemble, transfer learning, and wavelet transform, to enhance robustness and accuracy. The method's design was centered around the notion of not only achieving high performance in distinguishing true signals from FFPE-induced artifacts but also addressing the real-world challenges posed by the varying quality and conditions of clinical FFPE samples. In the analysis, we found peculiar patterns of FFPE-specific error profile, including well-known cytosine deamination and novel mutational signatures. The classifier, building on our findings, effectively differentiated true genomic variants from FFPE-induced artifacts for both SNVs and indels, demonstrating a sensitivity of 0.97, specificity of 0.87, and an F1 score of 0.94 for SNVs. For indels, it achieved a sensitivity of 0.91, specificity of 0.91, and an F1 score of 0.91. The CNV filter notably enhanced the signal-to-noise ratio (SNR) of CNV depth profiles, increasing it from 13dB to 17.5dB on average. Furthermore, we conducted evaluations on two critical measures in cancer and clinical genomics: homologous recombination deficiency (HRD) and tumor mutational burden (TMB), achieving post-filtering concordance rates of 0.99 for HRD—correctly identifying all 8 HRD-positive patients in our dataset—and 0.96 for SNV-based TMB and 0.87 for indel-based TMB. Additionally, a post hoc procedure for sensitive detection of cancer driver mutations resulted in concordance rates of 0.94 for SNVs, 0.91 for indels, and 0.95 for oncogene amplification. Taken together, our study advances FFPE WGS analysis in cancer diagnostics by effectively filtering artifacts and addressing challenges with older, degraded samples, enhancing clinical applicability.

#0910 Clinical inference and biological dissection of tumor ploidy and heterogeneity in cutaneous melanoma for immunotherapy response using deep learning.

M. Glettig, G. Tarantino, T. Aprati, H. Elmarakeby, D. Liu;
Dana-Farber Cancer Institute, Boston, MA

Background: Tumor ploidy and heterogeneity demonstrated to be pivotal in predicting immunotherapy response in cutaneous melanoma in several independent cohorts (Liu NatMed2019, Tarantino BioRXiv2022). Their estimation can guide more personalized and rational utilization of these immunotherapies. However, 1) the biology underpinning ploidy and heterogeneity is unknown; and 2) these findings were derived in patients using retrospective research tumor-normal paired whole exome sequencing which is not performed for clinical management.
Methods: This study addresses this gap by employing deep learning models to predict these crucial markers using routinely available clinical assays, including H&E images. Attention-based computer vision models enable the identification of key morphological features in H&E slides. Segmentation of tumor tissue to perform automated masking, enhances ploidy inference.Moreover, biologically informed neural networks (P-Net, Elmarakeby Nature2021) uncover transcriptional and genomic features linked to ploidy and tumor heterogeneity. Our models are trained on publicly available data (e.g., Liu et al Nature Medicine 2019; TCGA SKCM) from melanoma cohorts and further validated in independent cohorts to ensure robustness.
Results: We developed and validated automated tumor tissue masking, enabling the prediction of Whole Genome Doubling (WGD) from H&E Slides with an AUC > 0.75. Attention-based models identify distinct Tumor Microenvironment (TME) structures predictive of high tumor heterogeneity. P-Net application revealed the Calmodulin pathway, previously associated with regulating proliferation in cancer and targeted with chemotherapy, as intricately linked to high tumor heterogeneity, providing valuable insights into underlying mechanisms.
Conclusion: In conclusion, our study strategically harnesses and integrates existing datasets to rigorously test, refine, and validate hypotheses concerning the biological and therapeutic implications of genomic heterogeneity and ploidy. Notably, our predictive models with automated tumor masking demonstrate a remarkable AUC >0.75 for biomarkers traditionally challenging to derive from clinical assays. This breakthrough opens avenues for novel therapeutic strategies targeting genomic heterogeneity and ploidy, providing a transformative potential to enhance patient care and outcomes.

#0911 Automatic identification of subjective appetite or weight loss in clinician notes empowers studies of cachexia.

T. Park, K. Pichotta, C. J. Fong, N. Schultz, P. Iyengar, J. Jee, E. Reznik;
Memorial Sloan Kettering Cancer Center, New York, NY

Cachexia is a debilitating syndrome characterized by loss of skeletal muscle tissue that affects over 50% of cancer patients. Defining cachexia for the purposes of epidemiologic analyses has historically been determined by specific weight loss over specific time, and more recently relied on technically challenging interpretation of imaging studies. Subjective appetite or weight loss (AWL) as documented from clinician notes may offer another method of defining a similar phenotype. Although annotation of free-text notes at scale is challenging, we hypothesized that natural language processing (NLP) might successfully annotate AWL from cancer diagnosis medical notes and that such annotations would follow patterns expected from classic cachexia studies.

We created a gold-standard dataset for NLP training and validation by manually labeling AWL in a cohort of 762 free-text initial consultation notes that were extracted from lung and pancreatic adenocarcinoma electronic health records. Using these labels, we fine-tuned a pre-trained neural Longformer model to classify whether a patient has symptoms of cachexia.

The AWL model was evaluated on a cohort of 391 pan-cancer notes independent of the training cohort and achieved an AUC of 0.92, precision of 0.88, recall of 0.95, and accuracy of 0.94. To test whether the labels generated by this model behaved as expected from classic cachexia studies, we applied the model to 46,980 initial consultation notes from a pan-cancer cohort of patients with tumor genomic profiling from MSK-IMPACT, an FDA-authorized tumor sequencing assay. Overall, AWL was present in 28% of the patients and it was associated with gastrointestinal cancers, which is expected from previous studies of cachexia. Our analysis revealed that esophagogastric and pancreatic cancer patients had the highest rates of cachexia at around 67%. We also observed that patients with cachexia symptoms have a reduced overall survival compared to patients without (HR=1.80, 95% CI=[1.75, 1.85]), which held in several specific cancers including NSCLC (HR=1.79, 95% CI=[1.66, 1.94]), pancreatic cancer (HR=1.34, 95% CI=[1.22, 1.47]), and colorectal cancer (HR=1.71, 95% CI=[1.55, 1.89]). Cachexia symptoms were more prevalent in male patients than in female patients. Underweight patients by BMI at presentation were most likely to have cachexia symptoms.

These results reciprocate well-established information about cancer cachexia, demonstrating that our text classification NLP model can be reliably used to predict AWL from free-text medical notes. AWL may thus be a viable means of studying correlates of cachexia at scale in real-world cohorts.

#0912 CheckpointPx, an interpretable radiology AI tool, predicts checkpoint blockade benefit independent of PDL1 status in non-small cell lung cancers (NSCLC): A multi-institutional validation study.

A. Hiremath[1], S. Lee[2], J. Lee[2], P. Kim[3], K. Zhang[1], S. Lee[4], M. Yadav[5], M. Chuchuca[5], T. Um[5], M. Nam[6], L.-Y. Chung[5], H. Kim[5], J. Yu[7], T. Djunadi[8], L. Kim[9], Y. Oh[10], S. Yoon[5], Z. Shah[11], Y. Kim[5], I. Hong[12], G. Kang[12], J. Jang[12], A. Cho[12], S. Lee[13], C. Nam[12], T. Hong[12], Y. S. Velichko[5], A. Gupta[14], V. Velcheti[15], A. Madabhushi[1], N. Braman[1], Y. Chae[5];

[1]Picture Health, Cleveland, OH, [2]Kyungpook National Univeristy, Daegu, Korea, Republic of, [3]The University of Texas at Austin, Austin, TX, [4]School of Medicine at UCI, Irvine, CA, [5]Feinberg School Of Medicine, Northwestern University, Chicago, IL, [6]Lincoln Medical Center, Bronx, NY, USA, New York, NY, [7]Dignity Health - St. Rose Dominican Hospital, Henderson, NV, [8]Richmond University Medical Center, Staten Island, NY, [9]Ascension Saint Francis, Evanston, IL, [10]John H. Stroger, Jr. Hospital of Cook County, Chicago, IL, [11]Roswell Park Comprehensive Cancer Center, Buffalo, NY, [12]Northwestern University, Chicago, IL, [13]Johns Hopkins Bloomberg School of Public Health, Baltimore, MD, [14]University Hospitals Cleveland Medical Center, Cleveland, OH, [15]Laura and Isaac, New York, NY

Background: Immune Checkpoint Inhibitors (ICIs) are a cornerstone in the treatment of cancers such as Non-Small Cell Lung Cancer (NSCLC). Despite the standard use of biomarkers such as PD-L1 expression for selecting ICI regimens, recent studies suggest missed opportunities for benefit in PD-L1 low/negative patients. Therefore, there is an urgent need for new biomarker strategies capable of guiding the use of ICIs in NSCLC. We introduce and validate an AI-powered radiology tool for ICI patient selection that provides interpretable predictions by quantifying aspects of tumor biology on baseline CT scans directly associated with ICI efficacy, such as tumor heterogeneity and twistedness of the tumor-associated vasculature.

Methods: We analyzed CT scans of 439 patients treated with ICI at 4 institutions (D1-D4) using the Picture Health Px platform. Experienced radiologists and physicians across institutions delineated target lesions on baseline CT scans. A deep learning model was used to segment pulmonary vessels. CheckpointPx v1.11, an interpretable neural network incorporating quantitative features extracted from within the tumor and its vasculature, was trained to predict ICI response (defined as disease control per RECIST best overall response) on n=247 patients (D1-D3). It was assessed with respect to response and progression free-survival (PFS) on 192 patients (D2-D4), with D4 (n=105) being an external validation set. CheckpointPx was also evaluated within PDL1 subsets among testing set patients where available (n=138).

Results: The cohort was predominantly late stage (Stage 3/4) (>85%) and was mixed with respect to ICI line of treatment (1st-4th). 122 of 247 (49%) and 119 of 192 (62%) were responders in training and test cohorts respectively. CheckpointPx included 16 features, such as entropy-based heterogeneity and quantitative vessel tortuosity (twistedness). The model predicted response to ICI with an AUC=0.65 on the test set. The CheckpointPx High Risk group significantly stratified patients by PFS (HR=1.67 [1.22-2.28], p=0.001). This separation remained significant within the subset of PDL1-negative (HR=2.71 [1.35-5.44], p=0.005) and PDL1-positive patients (HR=2.05 [1.22-3.46], p=0.007).

Conclusions: From baseline radiology, CheckpointPx was shown to strongly predict ICI outcomes across multiple institutions, NSCLC stages, and lines of ICI. Furthermore, the tool stratified patients by ICI benefit within both PDL1-positive and negative subsets - suggesting the potential of CheckpointPx to address critical gaps in the NSCLC biomarker landscape. CheckpointPx is driven by interpretable imaging biomarkers, and thus its predictions are tied to specific and quantifiable phenotypic attributes of the tumor and its microenvironment.

#0913 Automated reasoning artificial intelligence (AI) to model the cell-cell biochemical and cellular interactions in the tumor microenvironment (TME) of oral cancer (OC).

K. Mahtouk[1], M. Vincent[2], Y. Le Meitour[1], B. Vanbervliet-Defrance[1], S. Canjura[1], C. Degletagne[1], L. Tonon[3], L. Michon[1], J. Bouaoud[1], A. Excoffier[3], P. Zrounba[3], R. Boutonnet[2], A. Amara[2], **P. Saintigny**[3];

[1]Cancer Research Center of Lyon, Lyon, France, [2]Turing Biosystems, Lyon, France, [3]Center Leon Berard, Lyon, France

Our goal was to study the spatial complexity of HPV negative OC by integrating scRNAseq and spatial transcriptomics from 11 samples including 5 from never smokers never drinkers (NSND). We used Turing Biosystems proprietary graph database engine and automated reasoning AI to analyze and model the cell-cell biochemical and cellular interactions in the TME. The tumors H&E images, Visium 10X, and single cell 10X data were pre-processed using standard methods. QC-based genes and cells filtering, gene expression normalization, dimensionality reduction, clustering of Visium spots, and identification of spatially variable genes were performed. We generated multiple networks from tumor data and prior biological knowledge to integrate different layers of information: single-cell and spatial transcriptomics data, cell-cell interactions networks, cell neighboring, spatial correlation networks. We first used a novel network-based technique to identify the spatial distribution of any cell subtypes (e.g. CAF, T cells), by integrating differentially expressed genes from scRNAseq, prior knowledge and prior data (e.g. TCGA). We used a multilayer network approach to integrate the different networks of data and an automated reasoning AI analysis which allows to interpret the results based on a reasoning on biological and clinical knowledge in opposition to machine learning methods based on statistical patterns. We identified CAFs/T cells/IFN-g to be strongly correlated within the tumor islets interacting with the stroma in NSND while they were more correlated within the stromal regions in smokers. We also identified 2 or 3 subtypes of tumor islets areas based on their functional states (e.g., immune pathways activated or metabolic differences), allowing us to unravel a more detailed map of the intratumoral heterogeneity when compared to histopathology annotations. In order to get some insights into the functional impact of the spatial distribution of cells, the tumors were then represented as multilayer networks to identify all possible cell-cell interactions in the TME. This was followed by a spatial simulation of these interactions using logic (e.g., inhibition, activation) and correlative (e.g., gene expression, imaging features correlations) interactions in the networks to identify spatial interactions. From that we analysed all the possible known protein-protein and metabolite-protein interactions between the cell types analysed and mapped the tumors with the gene expressions corresponding to the pairs of interacting proteins (or enzymes linked to metabolites). We found an interaction between CAF and Tregs via CXCL12 (CAFs) and CXCR4 (Tregs). In conclusion, automated reasoning AI integrating scRNAseq and spatial transcriptomics allows an in-depth analysis of cells spatial distribution and its functional impact in OC.

#0914 Combination analysis of tumor-associated collagen frameworks and tumor immune phenotype of lung carcinomas using virtual staining.
S. Alexanian, Y. Rivenson, N. Xuan, B. Cone, Z. Fang, S. Meyering, L. A. V. Carvalho, D. Palacios, R. Kozikowski;
Pictor Labs, Inc., Los Angeles, CA

An emerging predictive parameter of immunotherapy response is the patient's tumor immune status, generally classified as "inflamed", "immune excluded" and "desert". Historically, classification was performed semi-quantitatively with somewhat subjective parameters as evidenced by the recent Delphi Workshop consensus. There are a variety of approaches to classifying immune status, most based upon analysis of H&E images (counting tumor infiltrating lymphocytes, TILs), or counting subpopulations of immune cells using immunologic staining. However, use of multiplexed or multiple stains has recently been explored to better quantify the counts and types of immune cells in individual tissue compartments. While the immune microenvironment represents an important parameter in predicting patient response, other regions such as the extracellular matrix (ECM) may yield complementary information, as collagen-rich ECMs may present a barrier to drug diffusion and the orientation of fibers may direct the migration of malignant cells.
Here we present a proof of concept virtual staining enhanced image analysis pipeline, which converts autofluorescence signals from a single tissue section into virtual H&E and Masson's Trichrome along with virtual detection of pan cytokeratin (AE1/AE3/PCK26) and CD45 (LCA) positive cells. We apply image analysis to the panel of virtual stains to study the spatial and case-by-case heterogeneity of tumor collagen frameworks and immune phenotype.
Using a standard slide scanner (Axio Scan Z1, Zeiss), multiple autofluorescence images were captured from unstained sections (4-6um thick) of lung tissue. The virtual staining was performed by four deep neural networks trained in a supervised learning fashion. Select chemical stains were performed on previously scanned tissues and reviewed by pathologists side-by-side with virtual stains to ensure consistency and quality control. Four perfectly registered WSI virtual stain images were generated from each tissue section. The multi-stain results were rendered from a variety of lung cancers, including tissue microarray slides. Image analysis was performed using HALO (Indica Labs) and custom python scripts. We identified unique areas of tumor and adjacent stroma with heterogeneous immune phenotype and collagen characteristics, suggesting that an interplay might exist that could be utilized to improve patient selection or prognosis when deploying advanced AI tools. Future work includes applying this virtual stain technique retrospectively to cases with known immunotherapy treatment responses to determine the prognostic significance of the combined immune/ECM phenotype.

#0919 Veterans Health Administration: Decentralized clinical trials.

A. Press[1], J. Ordman[1], J. Boreland[1], Z. Burningham[2], S. Schoenborn[1], T. Stewart[1], B. Oberg[1], P. Pepperman[1], H. Morris[1], S. Bloemers[1], N. Kutub[1], S. Elam[1], M. J. Kelley[1], D. Friedman[1];

[1]Durham VAMC, Durham, NC, [2]Salt Lake City VAMC, Salt Lake City, UT

Purpose: The Veterans Health Administration (VA) created National TeleOncology (NTO) service in 2019 to provide telehealth cancer care to Veterans and to augment care provided at VA facilities through a hub and spoke model. More recently, VA established a Decentralized Clinical Trials (DCTs) infrastructure to support clinical trials (CTs) that rely on telehealth, where research staff are at different locations, and/or where a single IRB provides oversight even when subjects are at different locations.

Brief Description: Research support and infrastructure is variable across VA facilities resulting in uneven access to cancer CTs in the VA system. Veterans often live in rural areas or have transportation challenges, which are barriers to participate in CTs. The COVID-19 pandemic resulted in increased telehealth use in clinical care and in CTs, providing the rationale for a focused effort in DCTs. DCTs have the potential to reduce barriers to CT involvement at the facility- and patient-level and may be more representative of real-world clinical scenarios.

Summary of Data: Since its inception, NTO has provided hematology and oncology telehealth care to over 10,000 Veterans, of which 47.5% live in rural or highly rural areas, 76.5% are white and 13.2% are black or African American. Because the NTO program provides clinical care via telehealth modalities, patients who receive care through NTO may be more comfortable with participating in CTs that use telehealth, and thus are part of a pool of potentially eligible subjects.Since creation of the DCT program, three cancer DCTs have been conducted in the VA (1) BNT001 Digital Therapeutic Feasibility Pilot Study, (2) Cemiplimab Survivorship Epidemiology (CASE) Study, and (3) Proof-Of-ConcepT DEcentralized CliNical TrIAL (POTENTIAL) study. The BNT study enrolled 24 Veterans, 19 were male, 22 were white, 13 lived in rural areas, and the median age at enrollment was 68 years, including numerous cancer diagnoses. Veterans enrolled in the BNT study received cancer care at seven VA facilities. The CASE study has enrolled 24 male Veterans, 23 were white, 5 lived in rural areas, and the median age at enrollment was 74 years. The POTENTIAL study enrolled 4 male Veterans, 3 were white, 2 lived in rural areas, and the median age at enrollment was 72 years. Upcoming DCTs will focus on the following disease types: metastatic non-small cell lung cancer, multiple myeloma, and relapsed/refractory diffuse large B-cell lymphoma.

Conclusions: The VA provides clinical cancer care to Veterans through the NTO program. The DCT program builds upon the existing clinical infrastructure to conduct CTs on a national scale. The NOP DCT team is a component of the VA's Enhance Equity and Access to Clinical Trials (ENACT) initiative, which is part of Cancer Moonshot. The DCT program intends to expand CT opportunities to Veterans with cancer, minimize barriers to CT activation and enrollment, and improve access to cancer CTs for all Veterans.

#0920 Insights from the National Cancer Institute's request for information on existing data sharing processes for NIH-funded research.

M. Ghosh, N. Boyd, S. Jagu;
National Cancer Institute, Rockville, MD

Data sharing plays a crucial role in accelerating biomedical research discoveries, promoting rigorous and reproducible research, enabling research data reuse, and fostering public trust. To facilitate data sharing, a coordinated, sustainable, and streamlined infrastructure is required to store, preserve, retrieve, and make data findable, accessible, interoperable, and reusable. Starting January 25, 2023, researchers funded by the National Institutes of Health (NIH) are required to comply with the NIH Data Management and Sharing Policy (https://sharing.nih.gov/data-management-and-sharing-policy/about-data-management-and-sharing-policies/data-management-and-sharing-policy-overview) and indicate how research data funded by the NIH will be managed and broadly shared. As institutions prepare to meet these requirements, the National Cancer Institute (NCI) is looking to understand the existing processes of data storage, preservation, and sharing including what infrastructure and services are available to facilitate data sharing. To carry out this goal, the NCI's Office of Data Sharing (ODS), dedicated to promoting responsible and efficient sharing of cancer research data, issued a Request for Information (RFI) to understand the existing data sharing processes for NIH-Funded Research. The RFI was designed to collect information on services (e.g. guidance on data standards and file formats), technologies (e.g. storage, compression, retrieval, archival, analysis tools, workbenches), and processes (e.g. governance, communication, education, outreach) that promote data sharing. ODS utilized the RFI to gather input from stakeholders involved in facilitating data sharing. This included personnel from various fields such as research laboratories, scientific instrumentation core facilities, offices of research and/or sponsored programs, provost offices or other research administration, libraries, information technology, and institutional review boards. We also engaged with bioinformaticians and data scientists who are actively contributing to data curation, formatting, and analysis. Here, we present analysis of the responses received, including insights relating to gaps and challenges in data sharing, and proposed next steps and recommendations.

#0921 The value of cancer genomic data sharing.

S. Nelson, C. Caga Anan, E. Gillanders;
National Cancer Institute, Rockville, MD

Our understanding of and ability to combat cancer relies on the generation, analysis, and sharing of data. The Epidemiology and Genomics Research Program in the National Cancer Institute's Division of Cancer Control and Population Sciences (DCCPS) has supported generation of large genomic data sets and advocated for and/or required broad sharing of this data. One of DCCPS's scientific priorities is focused on data strategies namely, "the use, enhancement, expansion, and accessibility of new and existing DCCPS-supported data resources to accelerate cancer control research" (https://cancercontrol.cancer.gov/overview-highlights/2022/future_directions.html).EGRP funded the Genetic Associations and Mechanisms in Oncology (GAME-ON) Initiative, a multidisciplinary collaboration of researchers focused on understanding the genetic architecture, biology, and clinical and epidemiologic utility of common cancer risk variants. This program focused on 5 common cancer types - breast, colorectal, lung, ovarian, and prostate - and required research that incorporated multiple research domains and sharing of any data generated. A major accomplishment of this program was development of the OncoArray genotyping chip, which used information from genetic epidemiology studies, biological/functional analyses, and clinical and epidemiologic insights to create a comprehensive, high-density genotyping array for pan-cancer studies that has led to the discovery of hundreds of new cancer predisposition variants. This chip was used in a massive, coordinated genotyping effort that culminated in the generation of 7 datasets comprising genotyping data for nearly 500,000 individuals. All the data were deposited in dbGaP between 2014 and 2021 and are available (via controlled access) to any investigators. To understand the secondary use of these data, we determined the number of times the data had been downloaded, who downloaded the data, and types of research for which it was used. We also identified publications using OncoArray data and characterized the publications by research type, cancer type, and other details. Through this analysis, we explore how well the GAME-ON initiative and the OncoArray projects promote the DCCPS scientific priority of optimizing secondary research by making the data findable, accessible, interoperable, and reusable (FAIR).

#0922 Comparison of adverse effects of different combination therapies of immune checkpoint inhibitors and radiotherapy: A systematic review and meta-analysis.

H. Zhou[1], Z. Guo[2], T. Wang[2], L. Cai[2], P. You[3], **Z. Jiang**[4];

[1]Guangdong Provincial People's Hospital (Guangdong Academy of Medical Sciences), Southern Medical University, Guangzhou, China, [2]The First Affiliated Hospital of Guangdong Pharmaceutical University, Guangzhou, China, [3]Nanchang University, Nanchang, China, [4]University of California, Berkeley, Berkeley, CA

Background: Numerous ongoing trials are investigating cancer treatment combinations based on the combination of radiotherapy and immune checkpoint inhibitors. Understanding the toxicity profile of treatment-related adverse events is crucial. The purpose of this study is to comprehensively investigate the incidence and overview of treatment-related adverse events in different combination therapies involving radiotherapy and immune checkpoint inhibitors.
Methods: We conducted a systematic review and meta-analysis of different combination therapies involving radiotherapy and immune checkpoint inhibitors. We searched English-language articles published between January 1, 2000, and May 31, 2023, in Pubmed, Embase, and the Cochrane database, investigating globally approved therapies based on PD-1, PD-L1 inhibitors, or CTA-4. Only prospective trials reporting overall incidence rates or lists of treatment-related adverse events data were included, and studies recruiting fewer than 10 patients were excluded. Retrospective studies were also excluded to minimize the risk of bias. The primary outcomes were the overall incidence and overview of treatment-related adverse events of all grades and grade 3 or higher. Heterogeneity among studies was assessed using the I^2 statistic. The summary measure for primary outcomes was incidence rate (95% CI). This protocol is registered in PROSPERO (CRD42023390147).
Results: We identified 1300 records, of which 50 studies (1655 patients) met the inclusion criteria. The incidence of treatment-related adverse reactions in the concurrent group was 76.0% (95% CI 73.5-78.4), and the incidence of grade 3 or higher adverse events was 23.5% (21.1-25.9). In the sequential group, the incidence of treatment-related adverse reactions was 75.9% (70.8-80.6), and the incidence of grade 3 or higher adverse events was 22.5% (18.0-27.5). In the induction group, the incidence of treatment-related adverse reactions was 72.8% (65.0-79.8), and the incidence of grade 3 or higher adverse events was 37.1% (29.4-45.3). The most common specific adverse event in the concurrent group was Fatigue (27.8% [25.2-30.6]); in the sequential group, it was Fatigue (43.3% [33.3-53.7]); in the induction group, it was Fatigue (71.4% [56.7-83.4]). Grade 3 or higher adverse events in the concurrent group was Lymphocyte Count Decreased (7.2% [5.4-9.4]); in the sequential group, it was Pneumonitis (11.1% [5.7-19.0]); in the induction group, it was Fatigue (10.5% [5.6-17.7]).
Conclusion: Our study provides comprehensive data on treatment-related adverse events in different combination therapies involving radiotherapy and immune checkpoint inhibitors. Our results provide an essential reference of toxicity profiles of radiotherapy combined with immune checkpoint inhibitors for clinicians in routine practice of cancer care.

#0923 Biomarker use in oncology approvals in the US.

Y. Dou[1], C. Grimstein[2], J. Wang[2], J. Mascaro[2];
[1]AstraZeneca, Mississauga, ON, Canada, [2]AstraZeneca, Gaithersburg, MD

Introduction: Precision medicine through the use of biomarkers has revolutionized the way we understand and combat cancer. We are summarizing the current state and challenges of biomarker use in the context of cancer therapeutic products approved by the United States Food and Drug Administration (FDA).
Methods: We curated a dataset of oncology therapeutic products approved by the FDA through the regular and accelerated pathways from 2011 to 2022, based on publicly available FDA database, approval letters and reviews, prescribing information, publications, and clinicaltrial.gov.
Results: During the period of 2011 to 2022, the FDA granted 132 accelerated and 331 regular approvals for 80 and 144 oncology therapeutic products with 133 and 340 new indications, respectively. The percentage of approvals for a biomarker-defined population was higher in accelerated approvals in comparison to regular approvals (i.e., 51% vs. 39%). The five disease sites with the highest number of approved indications were leukemia, lung, non-Hodgkin lymphoma, breast, and skin. The vast majority of lung and breast cancer indications were approved in a biomarker-defined population through a range of different biomarkers. Overall, HER2-, EGFR-, BRAF-, HR-, and ALK-defined populations received the highest numbers of approvals. The most common biomarkers linked to the approval of a specific cancer type include Philadelphia chromosome for leukemia, EGFR/ALK for lung cancer, HER2/HR for breast cancer, BRAF for skin cancer, and BRCA for ovarian cancer. Multiple myeloma, kidney cancer, and Hodgkin lymphoma did not have any approval with a biomarker-defined population. Non-Hodgkin lymphoma had a large number of approvals, but the percentage approved for a biomarker-defined population was small. dMMR, MSI-H or dMMR, BRAF mutation, NTRK fusions, TMB H, and RET fusions are biomarkers linked to tissue-agnostic indications approved for solid tumors only through the accelerated pathway.
Conclusion: To the best our knowledge, the analysis represents the most comprehensive overview of the current landscape on integration of biomarker in oncology therapeutic products approved by the FDA through both the accelerated and regular pathways. Our analysis shows that the FDA has increasingly approved indications based on biomarkers, particularly through the accelerated approval pathway. Biomarkers are reshaping cancer therapy under an evolving regulatory landscape with a growing emphasis on precision medicine that promises continued progress in personalized cancer care.

#0924 Patterns of specialty referral in cancer patients treated with immunotherapy regimens.

A. Chen, S. Dusza, D. Faleck, N. Shah, M. E. Lacouture;
Memorial Sloan Kettering Cancer Center, New York, NY

Background: Specialty referral rates have been steadily increasing, as much as 94% within a 10-year period (1). Previous studies have shown the benefits of specialty referral in oncology management in specific populations such as lung cancer patients (2). However, there have yet to be larger-scale studies on general trends in specialty referral in oncology. In particular, patients on immune checkpoint inhibitors frequently develop immune-related adverse events (irAEs) affecting a variety of organ systems and may benefit from specialty care (3).
Objectives: To evaluate the patterns of specialty referral in patients treated with immune checkpoint inhibitors and identify referral patterns that affect patient outcomes.
Methods: This was a retrospective study of all specialty referral for patients on an immunotherapy regimen from 6/1/2022-6/1/2023 at a single-institution cancer center. The specialties consulted included cardiology, dermatology, endocrinology, gastroenterology, infectious disease, neurology, pulmonology, and nephrology.
Results: In total, there were 5,602 patients on an immunotherapy regimen, of whom 3,519 patients (62.8%) were referred to a specialist. Of these patients, 2,017 (57.3%) attended a specialist appointment. A majority of the patients were male (n=1038, 51.5%), had a mean age of 64.1 years (SD=13.8) at initial consult, and were White/non-Hispanic (n=1414, 70.1%). The mean and median number of consults per patient were 1.7 (SD=1.3) and 1 (IQR=1), respectively. The maximum number of consultations for a patient was 17. Dermatology was the most commonly consulted service (n=841, 25.9%), followed by neurology (n=781, 24.0%), and endocrinology (n=446, 13.7%). For dermatology, the most common reason for consultation was evaluation of a rash (n=500, 59.5%). Dermatology also had the highest ratio of outpatient to inpatient consultations at 10.4 to 1. The next closest service was endocrinology at 3.0 to 1. The pulmonary service had the shortest time between consult request and patient visit (10 days), followed by dermatology (13 days), and gastroenterology (15 days). Prior to their initial consultation, the vast majority of patients (82.6%) were on a single therapy, and the most common single therapy was pembrolizumab (n=1589, 59.2%). The most common combination therapy was ipilimumab plus nivolumab, accounting for 59.3% of combinations. Fifty percent of patients (n=1008) who saw a specialist were able to continue their immunotherapy regimen.
Conclusions: There is a range of specialty and multidisciplinary care that is necessary for the management of patients on immunotherapy regimens.

#0925 Continuing anti-EGFR treatment prolonged survival in mCRC patients receiving conversion liver resection.

Y.-Y. Hsieh[1], C.-W. Tsai[2], T-CARE Group, **Y.-H. Liang**[3];
[1]Taipei Medical University Shuang Ho Hospital, Ministry of Health and Weldare, New Taipei City, Taiwan, [2]Taipei Medical University, Taipei City, Taiwan, [3]National Taiwan University Hospital, Taipei City, Taiwan

Introduction: Anti-EGFR monoclonal antibody plus doublet chemotherapy is the mainstay of first-line treatment of RAS/BRAF wild-type metastatic colorectal cancer (mCRC) patients. Some of these patients might undergo secondary resection. However, there is no standardized suggestion on whether colorectal cancer liver metastasis patients should keep target therapy after secondary resection. NCCN guidelines suggest chemotherapy only in patients receiving primary liver resection. Whether we could spare the use of target therapy after secondary resection is the main aim of our study.
Methods: Using Taiwan's National Health Insurance Research Database, we established a cohort of KRAS wild-type mCRC patients treated with first-line anti-EGFR therapy plus doublet chemotherapy between 2013 and 2018. Secondary surgery was defined as either resection of liver metastases or radiofrequency ablation.
Results: 5694 stage IV mCRC patients received anti-EGFR MAb plus doublet chemotherapy as a first-line treatment between 2013 and 2018. 174 patients were enrolled in the final analysis, with 153 continuing anti-EGFR MAb after secondary resection and 21 patients without anti-EGFR MAb. Compared with those who without anti-EGFR therapy after secondary resection, patients who continued anti-EGFR MAb exhibited significantly longer overall survival (OS; median, 43.8 vs. 31.9 months, $p = 0.031$) but not in time to treatment failure (TTF; median, 22.2 vs. 26.6 months, $p = 0.841$). The OS benefits of continuing anti-EGFR MAb remained regardless of left-sided or right-sided primary tumors (40.9 vs. 43.0 months, $p = 0.980$). The patient cohort from 2016 to 2018 showed more prolonged survival than from 2012 to 2015 (not reached vs. 40.450, $p = 0.0305$). TTF has no statistical difference when considering patient cohort or primary tumor location. In multivariate analyses, continuing first-line anti-EGFR MAb therapy after secondary resection remained an independent predictor of longer OS.
Conclusion: For mCRC patients who received secondary resection after first-line anti-EGFR and doublet chemotherapy, continuing anti-EGFR MAb after resection was associated with significantly longer OS regardless of primary tumor sidedness.

#0926 Adaptive universal platform for real-world observational studies (AUPROS): An emerging model for clinical, epidemiologic, and precision oncology research.

S. H. Barghout, S. Raptis, L. J. Zhan, F. Al-Agha, M. C. Brown, D. Patel, G. Liu;
Princess Margaret Cancer Centre, University Health Network, Toronto, ON, Canada

Background: Adaptive Universal Platform for Real-world Observational Studies (AUPROS) is an emerging study design and platform for the generation of real-world evidence (RWE) particularly in malignancies with rare molecular aberrations. Here, we evaluate the efficiency of AUPROS as an innovative model for real-world observational studies in oncology.
Methods: We conducted a mixed-methods study to evaluate three AUPROS studies at Princess Margaret Cancer Centre either locally or as a part of national and international collaborations: 1) METAL (Molecular Epidemiology of ThorAcic Lesions; n=11,378), 2) THANKS (Translational Head And NecK Study; n=3,506), and 3) CARMA (Canadian Cancers with Rare Molecular Alterations; NCT04151342; n=3,879). Specifically, we reviewed data collected, study elements, protocol language, coordination, institutional review boards (IRBs), and contracts. We also performed stakeholder-directed survey and discussions, analysis of funding, research output, and collaborations, as well as a Strengths-Weaknesses-Opportunities-Threats (SWOT) analysis.
Results: AUPROS is an innovative study design that borrows design elements from master protocol trials, adaptive trials, and master observational trials as well as retrospective and ambispective designs, enabling comprehensive data collection. The universality of AUPROS allowed for multi-purpose analyses of various real-world data (RWD) including epidemiological, clinical, patient-reported outcomes, biospecimens, and imaging data. The adaptive nature created opportunities for multi-source funding (e.g., academic, pharmaceutical, philanthropic, among others), as well as national/international collaborations and involvement in consortia (e.g., ILCCO, TCGA, BEACON, and INHANCE). Additionally, AUPROS has allowed the development of an expanding national RWE platform that involves collaborations among medical and radiation oncologists and surgeons across different tumor sites. As assessed by research output analyses, AUPROS provided a platform for enhanced research productivity in different areas and utilizing various data sources (METAL=130; THANKS=31; CARMA=5 publications). Our survey and SWOT analysis identified several cost and operational benefits of AUPROS over conventional observational studies, as well as several challenges pertinent to ethics approvals, sustainability, complex coordination, and data quality.
Conclusions: AUPROS is an innovative model for real-world observational studies with significant logistical and methodological benefits over conventional RWD study designs. Our findings may help broaden the use of AUPROS to address emerging needs in the scope of precision oncology and clinico-epidemiological research.

#0927 Real-world (RW) biomarker characteristics and clinical outcomes in pre-treated non-MSI-H/dMMR metastatic colorectal cancer (mCRC) patients.

M. M. Amonkar[1], S. Sura[2], K. Desai[1], R. Jain[1], Z. Liu[3], N. Niehoff[2], T. W. Wilson[2], G. Patton[2], D. Cosgrove[4];
[1]Merck & Co., Inc., Rahway, NJ, [2]Ontada, Irving, TX, [3]Eisai Inc., Nutley, NJ, [4]Compass Oncology, Vancouver, WA

Introduction: Given sparse RW evidence, we assessed biomarker characteristics & clinical outcomes in community oncology practices among pre-treated non-MSI-H/dMMR mCRC patients.
Methods: This retrospective cohort study used structured & chart review data from iKnowMed, The US Oncology Network electronic health record data & included non-MSI-H/dMMR adult mCRC patients pre-treated with standard of care (SoC) chemo who initiated subsequent systemic anticancer treatment (SACT), best supportive care (BSC) or neither from 1/1/2016 - 12/31/2021. Index date for SACT users was the regimen start date post SoC chemo & for patients on BSC & no SACT/BSC, it was last chemo administration date. Patients were followed from index date until 8/31/2022 for overall survival (OS) & real-world progression-free survival (rwPFS). KM analyses assessed outcomes, overall & stratified by treatment, RAS status & metastasis sites.
Results: Of mCRC patients with ≥2 visits, 70.9% received MSI/MMR testing. In 292 eligible chart review patients, 69.5% received SACT in pre-treated setting (regorafenib 14.8%, trifluridine/tipiracil (TAS-102) 12.3%, other 72.9%), 28.8% received BSC & 1.7% neither. 76.7% reported KRAS/NRAS testing with 60.7% wild-type & 39.3% mutant. Common metastasis sites were liver-only (44.2%), liver & lung (10.3%) & lung-only (8.9%). Median (range) duration of follow-up was 5.2 (2.7, 10.0) months for regorafenib, 5.3 (2.5, 8.6) for TAS-102 & 10.7 (5.3, 18.0) for the other treatments group. Median OS was 7.4 (95% CI: 5.8, 8.8) months & median rwPFS was 3.5 (95% CI: 3.2, 4.3) months (outcomes data in Table).
Conclusions: 29.1% pre-treated, mCRC patients did not receive guideline recommended MSI/MMR testing, highlighting the need to improve testing. Outcomes varied by treatment, RAS status, & metastatic sites. The modest RW clinical benefit for SoC regorafenib & TAS-102, was consistent with trials & other RW studies; all highlighting an unmet need.

Cohorts	**Median (95% CI) OS (months)**	**Median (95% CI) rwPFS[1] (months)**
Overall	7.4 (5.8, 8.8)	3.5 (3.2, 4.3)
Regorafenib	5.6 (3.1, 9.7)	2.4 (1.8, 3.0)
TAS-102	5.9 (3.4, 8.6)	3.0 (2.1, 3.4)
Other SACT[2]	12.8 (9.8, 17.2)	4.9 (3.7, 5.8)
BSC	2.4 (1.8, 3.2)	-
RAS mutation		
Wild-type	8.6 (6.6, 11.5)	4.0 (3.3, 4.9)
Mutant	5.4 (3.4, 9.5)	3.2 (2.1, 4.6)
Metastatic sites		
Liver only	8.0 (5.7, 11.7)	3.9 (3.0, 4.9)
Lung only	17.0 (7.8, 35.6)	7.9 (3.3, 10.5)
Liver & lung only	5.4 (2.4, 7.2)	3.5 (2.1, 5.4)
Other	6.7 (4.1, 9.4)	3.2 (2.7, 3.9)

Abbreviation: CI: confidence interval, TAS-102: trifluridine/tipiracil, OS: overall survival, rwPFS: real-world progression-free survival, SACT: systemic anticancer treatment [1]Overall rwPFS was calculated among patients receiving subsequent SACT only (n = 203) [2]Top 2 “other SACT” included irinotecan- or oxaliplatin-based treatment

#0928 Real-world comparison of first-line treatments for metastatic clear cell renal cell carcinoma (mccRCC).

O. Yazdanpanah, S. Dwabe, G. Harada, S. Seyedin, N. Mar;
University of California, Irvine, Irvine, CA

Multiple regimens are available for management of mccRCC including either immuno-oncology doublet (IO/IO) or combinations of IO and tyrosine kinase inhibitors (TKI). Clinical trials have compared these regimens to sunitinib, with no direct comparison between them. As such, there is ambiguity among physicians about preferred first-line for mccRCC. We performed a single-institution retrospective study of adults treated in first-line for mccRCC between 1/1/2017 and 1/1/2023. Regimens included IO/IO (ipilimumab/nivolumab [I/N]) or IO/TKI (pembrolizumab/axitinib [P/A], nivolumab/cabozantinib [N/C], or pembrolizumab/lenvatinib [P/L]). We compared efficacy and toxicity endpoints, using Kruskal-Wallis test for medians and Chi-square for categorical variables. 42 patients with median age of 61 (range: 36-95) were included. Patient distribution in IO/IO vs IO/TKI group was 20.0% vs 30.8% in International Metastatic Database Consortium (IMDC) favorable risk, 46.7% vs 38.5% in intermediate-risk, and 33.3% vs 30.8% in poor-risk group. 78.6% vs 66.6% of patients had WHO grade 3/4 ccRCC, 18.8% vs 15.4% had sarcomatoid features in the IO/IO vs IO/TKI, respectively. 38% (16/42) received I/N, 7% (3/42) N/C, 52% (22/42) P/A, and 2% (1/42) P/L. Median follow-up was 109 weeks. Table-1 compares the efficacy of IO/IO vs IO/TKI. IO-related toxicity, TKI-related toxicity, treatment interruptions, dose reductions, and need for steroids were not significantly different between IO/IO and IO/TKI (p= 0.240, p=0.372, p=0.923, p=1.00, and p=0.248, respectively). Genomic characteristics will be reported in poster.

Variable	**IO/IO**	**IO/TKI**	***p*-value**
Median treatment duration (weeks)	8.3	59.4	<0.001
Disease control rate (complete response + partial response + stable disease) (%)	50.0	91.7	0.024
Time from 1st line to 2nd line therapy (weeks)	14.6	57.1	0.001
Median overall survival (weeks)	63.6	Not reached	0.001

Despite small sample size, our real-world data showed that patients treated with IO/IO had significantly worse outcomes compared to those treated with IO/TKI. While this difference may stem from a more aggressive disease in IO/IO group but further insights needs to be obtained through future prospective studies comparing IO/IO and IO/TKI regimens.

#0929 Characterizing first- & second-generation follow on drugs: Clinical trial & development timelines of Bruton tyrosine kinase (BTK) inhibitors.

A. Varma[1], W. B. Feldman[2], A. S. Kesselheim[2], E. R. S. Cliff[2];

[1]University of Texas Health Science Center, San Antonio, TX, [2]Program on Regulation, Therapeutics and Law, Brigham and Women's Hospital, Harvard Medical School, Boston, MA

Once a promising new cancer therapy emerges, other manufacturers often develop drugs with the same molecular target. Some follow on drugs offer meaningful benefit via improved efficacy or reduced toxicity, but others offer minimal benefit. We hypothesized there are two cohorts of follow on drugs: those developed concurrently before efficacy & safety of the therapy is established (first generation) & those developed as follow ons after that point (second generation). We analyzed BTK inhibitor (BTKi) development to evaluate patterns of concurrent & follow on development.

Methods BTKis from 1996-2023 were identified in Pharmaprojects (Citeline, NY). We collected drug development information including indications pursued, development phase reached, & outcome (ongoing development, discontinued development, or completed development with FDA approval). We constructed timelines including the first publicized report of the drug, Phase 2 initiation & date of development discontinuation or FDA approval.

Results We identified 19 BTKis targeting CLL, of which 6 (32%) were concurrent and 13 (68%) were follow-ons relative to ibrutinib's 2014 approval. A cluster of new agents began development immediately after ibrutinib approval, suggesting two distinct groups in this case. We identified 10 BTKis for MCL, of which only 2 (20%) were concurrently developed drugs, and 8 (80%) were follow on, based on ibrutinib's 2013 approval for MCL, with similar clustering to CLL.

Conclusions Among BTKis, market entry progressed in two phases. In a first phase, a smaller group of sponsors attempted to demonstrate safety & efficacy of the novel class. After proof of safety & efficacy, lowering risks for later competitors, a follow on phase of development began in which multiple sponsors sought to enter the market. Knowledge of which drugs belong to which class can aid with evaluation of trial design as part of regulatory approval decisions & with drug price negotiation.

Bruton Tyrosine Kinase inhibitors in Clinical Stage Development in Chronic Lymphocytic Leukemia

Drug	Sponsor	Entry Date	Date of approval/ discontinuation	Outcome
Ibrutinib	AbbVie / J&J	12/12/2007	02/13/2014	Approved (first in class)
Spebrutinib	Bristol Myers Squibb	12/12/2008	01/16/2014	Discontinued
Vecabrutinib	Biogen/ Viracta	04/07/2011	03/23/2016	Discontinued
Tirabrutinib	Gilead/Ono	01/14/2012	09/19/2023	Discontinued
Fenebrutinib	Roche	11/26/2013	Unknown	Discontinued
Pirtobrutinib	Eli Lilly	12/27/2013	08/08/2023	Approved
Acalabrutinib	Acerta/AstraZeneca	01/01/2014	06/11/2019	Approved
Luxeptinib	Apstose Biosciences	08/19/2014	-	Ongoing
Zanubrutinib	BeiGene	08/27/2014	01/14/2022	Approved
Nemtabrutinib	Merck	05/06/2016	-	Ongoing
Orelabrutinib	Biogen, Beijing Innocare	06/20/2017	-	Ongoing
AS-1763	Carna Biosciences	11/24/2017	-	Ongoing
JNJ-624264681	J&J	08/03/2018	-	Ongoing
HMPL-760	Hutchmed	06/10/2020	-	Ongoing

CLINICAL RESEARCH: Application of Precision Medicine for Cancer Care
Poster Session

#0933 Single-cell inference and validation of heterogeneous drug sensitivity in cholangiocarcinoma reveals dacinostat as novel therapeutic candidate.

A. Obradovic[1], L. Tomassoni[1], D. Yu[2], C. G. Drake[1], F. D. Cruz[2], A. Kung[2], A. Califano[1];
[1]Columbia University Irving Medical Center, New York, NY, [2]Memorial Sloane Kettering, New York, NY

Cholangiocarcinoma is a rare, aggressive malignancy with limited treatment options, due to a paucity of actionable mutations and low response to immune checkpoint inhibitors. Furthermore, its extreme heterogeneity prevents identification of actionable dependencies from bulk-tissue profiles, such that transformed cells themselves represent as little as 10% of cells comprising the complex micro-environment of these tumors. To address these challenges, we introduce a highly generalizable, single-cell framework for the mechanism-based prioritization of drugs to treat rare, heterogeneous tumors. Analysis of tumor cells isolated by single-cell RNA-Sequencing across six patients and two independent data sources using protein activity inference has revealed three molecularly distinct subphenotypes of cholangiocarcinoma cells, present to varying degrees across patients but with highly conserved proteomic signatures, and predicted to be sensitive to four drugs by regulatory network analysis. A seventh independent patient recapitulated these phenotypes, and drug sensitivity predictions at single-cell level for this patient were validated in low-passage, patient-derived xenografts from the same patient, which confirmed tumor growth rate control by two of these drugs (plicamycin and dacinostat) and further validated predicted subpopulation-specific effects, such that dacinostat alone inhibited tumor growth across all three tumor subphenotypes, while plicamycin preferentially inhibited some but not all, allowing the remaining phenotypes to reconstitute a treatment-resistant tumor. This approach suggests dacinostat as a promising candidate for follow-up clinical trials in cholangiocarcinoma, either alone or in combination with current standard-of-care chemotherapies, and is highly generalizable to elucidate complementary dependencies of other aggressive, heterogeneous tumors.

#0934 RNA-based precision medicine predicts sensitivity to selinexor in select pancreatic ductal adenocarcinoma patients.

A. Curiel-Garcia, L. Tomassoni, T. C. Dalton, A. R. Decker-Farrell, C. F. Palermo, D. R. Ross, S. A. Sastra, U. N. Wasko, I. M. Goncalves, P. S. Mundi, B. S. Bakir, R. A. Safyan, H. Hibshoosh, G. A. Manji, A. Califano, K. P. Olive;
Columbia University Irving Medical Center, New York, NY

Sensitivity to therapeutic agents is impacted both by genetic heterogeneity between patients or among clones within a tumor and by heterogeneity of epigenetic cell states. Prior work demonstrates that human pancreatic tumors comprise malignant cells in a mixture of multiple cell states with distinct genetic dependencies, leading to a reservoir of chemoresistance across the tumor; targeting just one or two malignant cell states is insufficient to achieve durable therapeutic responses. One approach to overcome this challenge is to identify agents with efficacy against malignant cells in multiple cell states. However, in the absence of genetic distinctions between cell states, identifying therapeutic vulnerabilities for each malignant cell state present in a patient's tumor in real time remains a challenge. OncoTreat is a CLIA certified algorithm that matches drugs to patients based on tumor gene expression profiles. The approach utilizes regulatory network analysis, a systems biology framework that transforms gene expression data into regulatory protein activity profiles, in a manner that facilitates the identification of master transcriptional regulators of cell state. We carried out a Phase 1 clinical trial of the OncoTreat framework to examine feasibility for implementing RNA-based precision medicine in patients with metastatic pancreatic ductal adenocarcinoma (2^{nd} line and beyond). Patient-derived xenografts were established from subjects prior to 1^{st} line therapy, and selected agents matched by OncoTreat were assessed co-clinically while subjects received standard of care regimens, with the potential for subsequent treatment with successful agents upon progression. Two subjects in the study matched to selenexor, an XPO1 inhibitor that is FDA approved for multiple myeloma. Co-clinical studies of selinexor in patient-derived xenograft models generated from the matched subjects showed prolonged survival compared to control regimens. Single-cell RNA sequencing analysis of these tumors found that the activity of master regulators confirmed that the activity of selinexor-responsive master regulators were inverted in response to treatment *in vivo*, reducing the fraction of malignant cells in the tumors. Strikingly, selenexor treatment was associated with significant inhibition of RAS/MAPK signaling, suggesting a potential novel role for selinexor targeting Ras. Together, these data indicate a potential therapeutic vulnerability for a subset of PDAC patients that can be predicted by a CLIA-certified RNA-based precision medicine platform.

#0935 Co-clinical endometrial cancer (EC) patient-derived organoids (PDO) to assess functional effects of replication stress (RS)-targeting agents.

E. Ivanova[1], A. L. Saldanha[1], S. Roychoudhury[1], B. Kochupurakkal[1], A. P. Zlota[1], C. E. Padrick[1], H. V. Vo[1], E. K. Greenberg[1], H. Sawyer[1], C. Feeney[1], C. H. Qi[1], S. Narayan[1], J. D. Curtis[1], N. Tayob[1], M. R. Nucci[2], P. Konstantinopoulos[1], D. Chowdhury[1], G. Shapiro[1], C. P. Paweletz[1], U. A. Matulonis[1], J. F. Liu[1]; [1]Dana-Farber Cancer Institute, Boston, MA, [2]Brigham and Women's Hospital, Boston, MA

Background: EC is the most commonly diagnosed gynecologic cancer in the US and has both rising incidence and mortality. Uterine serous cancer (USC) and uterine carcinosarcoma (UCS) are high grade ECs characterized by *TP53* mutation and molecular alterations suggesting high replication stress (RS) and cell cycle dysregulation. These molecular alterations could engender sensitivity to RS-targeting strategies such as WEE1 inhibition. In a single arm phase 2 of 35 patients, the WEE1 inhibitor adavosertib demonstrated clinical activity in recurrent USC, with an overall response rate of 29.4%. To support the development of predictive biomarkers of sensitivity to RS targeting agents, we report on the establishment of co-clinical EC PDOs from pre- and on-treatment biopsies from patients with USC or UCS enrolled to a translational trial of adavosertib.

Methods: Patients with USC or UCS consented for trial participation underwent pre- and on-treatment biopsies while receiving adavosertib monotherapy. Biopsies were dissociated and passaged as 3D organoid cultures in Matrigel in an optimized media. Established PDOs were seeded in 3D microfluidic devices, treated with adavosertib in a dose-dependent manner and assessed for viability after 6 days of treatment by dual labeling live/dead imaging. IC50 values were calculated using log(inhibitor) vs response - variable slope (four parameters) model in GraphPad Prism. To assess the effect of adavosertib on replication fork speed, DNA fiber assays were conducted with PDOs treated with adavosertib for 72 hours. Finally, FFPE blocks were created from PDOs for assessment of DNA damage repair biomarkers by IHC.

Results: 19 biopsies were obtained from 11 participating patients. 6 biopsies did not yield sufficient tumor cells for PDO generation. From the remaining 13 samples, 5 PDOs were successfully established (3 USC and 2 UCS), with a higher success rate when 3 biopsy cores were received (3 of 4; 75%) compared to when 2 biopsy cores were received (2 of 9; 22 %). Dual labeling live/dead imaging of PDOs treated with adavosertib resulted in IC50 values ranging from 113nM to 856nM. DNA fiber assays revealed consistent decrease in fork speed with adavosertib exposure, consistent with the hypothesized effect of adavosertib in increasing RS in these cells. A dose dependent effect on replication fork speed was observed, with greater decreases in fork speed with increasing concentrations of adavosertib. Due to the limited number of samples and the number of PDOs generated from on-treatment as opposed to pre-treatment biopsies, clinical correlation between PDO adavosertib sensitivity and clinical activity was not formally assessed. IHC analysis of potential DNA damage biomarkers is ongoing.

Conclusions: We describe the successful establishment of co-clinical EC PDOs for functional evaluation of sensitivity to RS targeting agents.

#0936 Targeted proteomics and next-generation sequencing (NGS) for biomarker discovery in metastatic colorectal cancer (mCRC).

William J. Kelly[1], Barrett Nuttall[1], Marlon Rebelatto[2], Marcus Schick[3], Armin Meier[3], Steve Sweet[4], Beom-Jun Kim[2], David Chain[4], Yeoun Jin Kim[4], Zhongwu Lai[5], Ying Wang[6], Todd H. Creasy[7], Ramya Gurrapu[8], Sakshi Gulati[9], Alice Barkell[10], Brian Dougherty[1], Danielle Carroll[10], Fabiola Cecchi[2]

[1]Translational Medicine, AstraZeneca, Waltham, MA,[2]Translational Medicine, AstraZeneca, Gaithersburg, MD,[3]Computational Pathology, AstraZeneca, Munich, Germany,[4]Diagnostic Proteomics, AstraZeneca, Gaithersburg, MD,[5]Bioinformatics, AstraZeneca, Waltham, MA,[6]Oncology Data Science, AstraZeneca, Waltham, MA,[7]Oncology Data Science, AstraZeneca, Gaithersburg, MD,[8]R&D IT, AstraZeneca, Chennai, India,[9]Oncology Data Science, AstraZeneca, Cambridge, United Kingdom,[10]Translational Medicine, AstraZeneca, Cambridge, United Kingdom

Background: Multi-omics analysis is widely used in cancer diagnosis, prognosis and prediction of treatment response. Here we introduce the use of targeted proteomics coupled with NGS as tools to assess oncogenic alterations along with quantitative protein expression in patients with mCRC. Our proteomics panel included proteins that are antibody drug conjugates (ADCs) targets (ERBB 1-4, TROP2, CEACAM5 etc.) as well as proteins involved in sensitivity to ADC payload (SLFN11, drug efflux pump, TOP1 etc.).
Methods: The HORIZON III trial (NCT00384176) evaluated FOLFOX + bevacizumab or cediranib as first-line treatment in patients with mCRC (Schmoll *J Clin Oncol* 2012). In the current analysis, a subset of samples from the HORIZON III trial were assessed for molecular alterations using NGS and proteomics. Pre-existing HER2 IHC scores were used as previously referenced (Cecchi *J Clin Oncol* 2023). Samples were processed (n=135) with an automated extraction and library preparation method, then sequenced with both a Whole Exome and targeted-custom gene panel. NGS analysis had a success rate of 116/135 samples (87.3%). Absolute quantitation of protein targets was performed using parallel reaction monitoring (PRM) mass spectrometry after collecting tumor epithelial cells by laser microdissection and punch biopsies (n=60) followed by trypsin digestion.
Results: The NGS analysis showed that patients had mutated *RAS* (50%), *BRAF* (10%), *PIK3CA* (16%), and TMB-H (18%) and MSI-H (5%) status. A distinguished pattern of mutual exclusivity among *KRAS*, *NRAS*, and *BRAF* mutations is evident. The HER2-positive patients were wildtype *RAS*, *BRAF*, and *PIK3CA*, MSS and TMB-L. Samples that were IHC HER2-positive matched those with NGS *ERBB2* amplification. Using PRM, nearly all the evaluable samples had detectable HER2. HER2 IHC 3+ sample showed the highest protein expression at 30,000 amol/ug (equivalent to 1M receptors/cell). Within the HER2-negative patients, HER2 protein expression showed broad dynamic range. CEACAM5 and HER2 are the only ADC targets that reached the level of 1M receptors/cell. Highest TROP2 protein expression is 5 times lower than the highest HER2 value.
Conclusions: Our preliminary findings for this cohort indicate the benefit of the use of multi-modal methodologies to inform better strategies for patient stratification and precision medicine, though further assessment of proteogenomic characteristics is needed. This data may inform future clinical development and guide patient eligibility to clinical trials and possible treatment sequencing for ADCs.

#0937 Prioritizing treatment targets for an adolescent with metastatic processive malignancy using proteomics and personalized xenograft models within an actionable timeframe.

G. D. Barnabas[1], T. A. Bhat[1], V. Goebeler[1], P. Leclair[1], N. Azzam[2], N. Melong[2], J. N. Berman[3], J. A. Chan[4], D. L. Senger[5], S. Parker[1], C. A. Maxwell[1], G. S. Reid[1], J. Bush[1], C. Strahlendorf[1], R. Deyell[1], C. Lim[1], **P. F. Lange**[1];

[1]University of British Columbia, Vancouver, BC, Canada, [2]Children's Hospital of Easern Ontario, Ottawa, ON, Canada, [3]Children's Hospital of Eastern Ontario, Ottawa, ON, Canada, [4]Universtiy of Calgary, Calgary, AB, Canada, [5]Lady Davis Institute for Medical Research, Montreal, QC, Canada

Translation of precision oncology data into feasible precision therapies for hard-to-cure childhood, adolescent and young adult malignancies remains a significant challenge. Identifying therapeutic targets at the protein and pathway level and demonstrating treatment response in personalized models hold great promise, particularly for combination therapies, but may be considered complex and time consuming. Here, we present the case of an adolescent with metastatic, progressive spindle epithelial tumor with thymus-like differentiation (SETTLE) and evaluate how proteomics combined with rapid patient-derived models can identify treatment options not apparent at the genome or transcript level.

Mass spectrometric proteome analysis of macro-dissected tumor and adjacent normal from formalin fixed paraffin embedded sections was completed within two weeks of biopsy and identified key proteins involved in one-carbon metabolism, including SHMT2 and DHFR as possible targets for single or combination therapy. Elevated SHMT2 levels were validated by immunohistochemistry and compared to levels across AYA tumors. Based on the suitability for an innovative therapy trial, we prioritized single-agent sertraline, a commercially available anti-depressant medication that inhibits SHMT2, and confirmed a positive drug response in both chicken chorioallantoic membrane (CAM) and larval zebrafish xenografts generated from the patient. Retrospective expansion in a murine xenograft enabled metabolic tracing on isolated SETTLE- patient-derived xenograft cells using $^{13}C_6$-glucose confirming SHMT2 activity and response to *in vitro* treatment. Following failure of cytotoxic chemotherapy and second-line sorafenib treatment, a monotherapy trial of sertraline was initiated by the patient but stopped after 8 weeks after evidence of progressive disease. Possible combination therapies were evaluated further in the patient-derived models. Combining sertraline with the common antibiotic trimethoprim, resulted in enhanced growth inhibition of SETTLE cells in the larval zebrafish xenografts.

Significance: Overall, we demonstrate that proteomics and personalized xenograft models may provide supportive pre-clinical data in a clinically meaningful timeframe to support medical decision-making and impact clinical practice.

#0938 Screening the entire kinase-directed, FDA-approved pharmacopeia against the largest collection of wild-type and mutant kinases reveals many opportunities for drug repurposing and targeted therapy.

C. M. Loch, S. Liang, J. Wu, M. Eason, A. Goupil, A. Acinapura, J. Purcell, M. Dominguez;
Reaction Biology Corporation, Malvern, PA

We sought to screen all FDA approved, cancer-indicated, kinase targeting drugs using the gold standard radiometric biochemical activity assay (HotSpot) against the largest collection of kinases in the world (>100 drugs against 735 total kinases including 395 wild type and 340 mutants). Virtually every drug examined exhibits polypharmacology inhibiting many kinases. Rarely does the intended target represent the greatest inhibition observed from a drug. Furthermore, most drugs inhibit a select group of mutant kinases, including especially mutants of kinases distinct from the intended target. Within a given kinase, each cancer-identified mutation is often as distinct as the different wild-type kinases are from each other, in terms of inhibition profile. Considering mutants, then, the cancer-relevant druggable kinome is many thousand distinct targets, not 518 “plus a few”. Exposing this reality is a first step towards developing all the therapeutic tools necessary to ultimately defeat cancer. Here, we reveal vast and specific repurposing opportunities among the existing pharmacopeia for tumors that are driven by kinases not previously recognized as targets for certain drugs, and for tumors that have become chemotherapy-resistant through mutation of specific kinases. The most exciting and clinically relevant opportunities were confirmed in cell-based assays, results of which will also be presented.

#0939 Comprehensive genomic and transcriptomic analysis to guide therapy for patients with metastatic solid tumors.

B. Uzunparmak[1], F. Su[1], A. M. Johnson[1], K. Nomie[2], N. Fowler[2], L. Kontselidze[2], A. Bagaev[2], A. Butusova[2], E. E. Dumbrava[1], J. Rodon-Ahnert[1], S. Fu[1], D. S. Hong[1], T. A. Yap[1], A. Naing[1], S. A. Piha-Paul[1], D. D. Karp[1], P. R. Pohlmann[1], A. M. Tsimberidou[1], K. P. Patel[1], F. Meric-Bernstam[1];
[1]UT MD Anderson Cancer Center, Houston, TX, [2]BostonGene, Waltham, MA

Introduction: Precision oncology, which aims to profile tumors for identifying actionable alterations to guide therapy has become mainstream in cancer clinics. While most approaches focus on DNA aberrancies on targeted panels, not all patients' tumors show targetable genomic alterations in these limited gene sets, indicating a need for more comprehensive methodologies combining whole exome (WES) and transcriptome sequencing (RNAseq) to direct a larger fraction of patients to therapies. Here, we aimed to compare the feasibility and utility of BostonGene's (BG) analytical platform with WES and RNAseq to two targeted exome panels in identifying actionable alterations and therapy selection for patients with metastatic solid tumors.
Methods: Study enrolled patients with solid tumors who have had next-generation-sequencing (NGS) testing with one of two tissue-based targeted exome sequencing panels, Oncomine (ThermoFisher, 148 genes), or MDA-MAPP (615 genes) with identification of no College of American Pathologists Tier-1 actionable DNA alterations between August 2022 and November 2023. Patients' tissue and blood/saliva samples were subjected to BG's NGS platform. An alteration-level actionability analysis was done upon receipt of WES results to inform treatment decision making, based on functional and therapeutic effects of the alterations detected.
Results: A total of 64 patients were enrolled; testing was cancelled for 7 patients (10.9%) with samples showing <10% tumor content, while 5 patients' reports were pending at the time of data analysis. Median turn-around time from consent to sample acquisition (SA) and from SA to available genomic profile were 8 and 15.5 days, respectively. 52 patients had NGS results representing a diverse group of tumor types, including sarcoma (*n*=11, 21.2%), head and neck (*n*=*9*, 17.3%) and mesothelioma (*n*=*5*, 9.6%). BG reported DNA alterations (mean: 3.75; median: 4) not shown by prior testing for 94.2% (49/52) of patients, whereby the most common alteration types included SNVs (43.1%), deletions (23.6%) and amplifications (11.8%). BG identified additional actionable DNA alterations (referred to as "AAs"; mean: 1.9, median: 2) in 32 (61.5%) patients, whereby majority of AAs were deletions (59.7%) and amplifications (27.4%). BG detected AAs in 58.8% (10/17) vs 62.9% (22/35) of patients for whom the same vs different samples were used across different tests compared (*P*=0.8). Of 32 patients with AAs, 7 (21.9%) were directed to DNA-informed treatments within 6 months based upon the new genomic findings reported by BG, 14 (43.8%) are being followed for treatment matching, while 11 (34.4%) were deceased.
Discussion: Our results show the feasibility and utility of comprehensive molecular testing to match patients to WES-informed treatments within a clinically relevant time frame. Assessment of the additional benefit of RNA expression analysis is forthcoming.

#0940 Integrated analysis of cfDNA fragmentomics, DNA methylation and cfRNA transcription in metastatic castration-resistant prostate cancer (mCRPC).

C. Dai, L. Zhu, Y. Huang, G. Bonora, K. Zhou, S. Jia, P. Du;
Predicine, Newark, CA

Background Liquid biopsies based on cell-free DNA (cfDNA) analysis provide non-invasive clinical diagnostic insights. Recently, cfDNA fragmentomics has emerged as a tool for inferring epigenomic and transcriptional information from tumor-derived cfDNA. We conducted a comprehensive profiling of cfDNA fragmentomics, whole transcriptome sequencing (WTS), and genome-wide DNA methylation on two metastatic castration-resistant prostate cancer (mCRPC) samples to systematically investigate molecular aberrations in mCRPC.
Methods Two mCRPC patient plasma samples were extensively profiled using high-depth 150x whole-genome sequencing (WGS), 30x whole-genome methylation, and cfRNA WTS. CfDNA fragmentomics analysis was performed to assess androgen receptor (AR) transcriptional activity. We calculated fragment coverage around AR binding sites (ARBS) and quantified ARBS nucleosome profiling abnormality scores (ARBS scores) by comparing centric fragment coverage with normal plasma background. Additionally, we calculated fragment size entropy around AR promoter and enhancer regions to reflect AR gene expression activity. Fragmentomics-inferred gene activity was validated through promoter-targeted panels and WTS profiling of matched mCRPC samples.
Results Both mCRPC plasma samples exhibited significant ARBS nucleosome depletion. Sample A showed a higher ARBS score compared to Sample B. Interestingly, AR enhancer activity inferred from high-depth WGS and targeted panels was high in both samples, while AR promoter activity was high only in Sample A. Genome-wide DNA methylation revealed hypo-methylation in AR enhancer and ARBS regions in both samples, with Sample A showing more pronounced hypo-methylation. Copy number variation analysis indicated AR amplification in Sample A and RB1 loss in Sample B. Collectively, these findings suggest that Sample A may represent androgen receptor-dependent prostate cancer (ARPC), while Sample B may have developed resistance to androgen therapy, possibly indicating neuroendocrine prostate cancer (NEPC).
Conclusions This study, to our knowledge, is the first to combine high-depth WGS, promoter-targeted panels, WTS, and genome-wide DNA methylation to systematically study epigenomic and transcriptional dysregulation in mCRPC. The integration of mutation, copy number variation, fragmentomics, and DNA methylation profiling holds potential clinical utility for inferring prostate cancer subtypes, facilitating patient stratification, and guiding treatment selection.

#0941 Patient-derived model systems of endometrial cancers for disease modeling and drug sensitivity testing.

T. Li[1], X. Huang[2], R. Rosenmeyer[1], S. Robinson[1], K. Salsabil[3], Y. Xiong[1], X. Meng[1], S. Yang[1];
[1]The University of Iowa, Iowa City, IA, [2]Nanjing Medical University, Nanjing, China, [3]California State University, Los Angeles, CA

Background: Endometrial cancer (EC) is the most common gynecological cancer in the US, with increasing incidence and mortality rates. The survival rate lags behind four decades ago (81% vs 87%), underscoring the critical need for more effective treatment strategies. The heterogeneous nature of EC contributes to varied outcomes with current treatments. This project aims to establish reliable EC models for characterizing each individual tumor, distinguish optimal drug treatment, and determine specific drug effect mechanisms for personalized therapy.
Methods: Freshly collected tumors were used for patient-derived xenograft models (PDXs) and patient-derived primary cancer cells (PDCs). Immunohistochemistry (IHC) staining was used to confirm the tumors grown in mice faithfully replicate the characteristics of patient tumor tissues. FDA-approved anticancer drugs were used to screen the optimal drugs to inhibit tumor cell proliferation and further utilized to inhibit tumor growth using PDXs.
Results: We have collected 26 EC tumors and characterize them by DNA mutation and RNA-seq analysis. We implanted them in NSG mice, and 16 tumor samples have successfully grown in mice with a success rate of 61%. Most PDXs can be faithfully passaged to three generations. From the 16 PDXs, we created six novel PDCs. Using 2D and 3D spheroid cell culture, we screened 133 FDA-approved oncology drugs in the EC-PDC models. The drug screening results clearly highlighted several standout drugs, including CUDC-907 (a dual PI3K/HDAC inhibitor), two histone deacetylase (HDAC) inhibitors including romidepsin and panobinostat, four topoisomerase II (TOP II) inhibitors including mitoxantrone, daunorubicin, doxorubicin, and epirubicin, two proteasome inhibitors including carfilzomib and bortezomib, 2 DNA-directed RNA synthesis inhibitor dactinomycin and plicamycin, omacetaxine mepesuccinate (protein synthesis inhibitor), and valrubicin (DNA synthesis inhibitor). These drugs have demonstrated a significant capacity to inhibit tumor cell proliferation. Our pilot studies using single drugs, CUDC-907, romidepsin and mitoxantrone, achieved moderate drug effects. Combine mitoxantrone with romidepsin or CUDC-907 show surprisingly synergistic effects in multiple PDC models. The combination strategy will be tested in PDXs in the near future.
Conclusion: Our unique PDXs and PDCs are excellent models for representing various characteristics of EC and testing novel therapeutics. This current study presents a promising direction for developing personalized therapy options for EC patients and provides a platform for further investigation of drug mechanisms and tumor development. Future studies will also involve etiology, such as chronic psychological stress, DNAm age and intratumoral microbiome. This information will help with endometrial cancer prevention, diagnosis, and prognosis.

#0942 Response to systemic therapies in patient-derived cell lines from primary and recurrent adult granulosa cell tumors.

G. Brink[1], N. Hami[1], S. Mertens[1], W. Hofhuis[2], J. Piek[3], C. de Kroon[4], C. Lok[5], E. Roes[6], L. van Lonkhuijzen[7], H. Nijman[8], H. Snippert[1], J. Groeneweg[1], P. Witteveen[1], R. Zweemer[1];

[1]University Medical Center Utrecht, Utrecht, Netherlands, [2]Franciscus Gasthuis & Vlietland, Rotterdam, Netherlands, [3]Catharina Hospital, Eindhoven, Netherlands, [4]Leiden University Medical Center, Leiden, Netherlands, [5]Antoni van Leeuwenhoek Hospital, Amsterdam, Netherlands, [6]Erasmus MC Cancer Institute, Rotterdam, Netherlands, [7]Amsterdam University Medical Center, Amsterdam, Netherlands, [8]University Medical Center Groningen, Groningen, Netherlands

Introduction: In patients with adult-type granulosa cell tumor (aGCT), a rare subtype of ovarian cancer, surgery is the preferred treatment for both primary and recurrent disease. However, the probability of complete resection decreases after multiple recurrences, in which case systemic treatment is an alternative option. Response rates of systemic therapy are variable, resistance is a problem and it is difficult to predict which therapy will work in which patient. Drug screen testing on patient-derived aGCT cell lines may offer a solution.

Methods: In a national prospective study on aGCT, fresh tissue was collected immediately after surgery. Tumor tissue was cultured and developed into 2D cell lines. Both clinically applicable and experimental drugs were tested on the patient-derived cell lines and two control cell lines. Dose-response curves and synergy were calculated using GraphPad Prism and Compusyn software.

Results: We cultured 34 patient-derived cell lines from tissue of seven patients with primary aGCT and from 13 patients with recurrence. In eight patients multiple sites were cultured. A total of 27 drugs were tested, including 10 monotherapies and 17 combinations. Carboplatin/gemcitabine showed efficacy and synergy 33 of 34 patient-derived cell lines (97%), in contrast to the regular carboplatin/paclitaxel and carboplatin/etoposide combinations (50% and 74%, respectively). The experimental combinations alpelisib/fulvestrant and alpelisib/gemcitabine showed efficacy of more than 75%. Testing of anti-hormonal therapy was not sufficiently reliable with this technique.

Conclusion: Drug screening on patient-derived tumor cell lines adequately reflects the reality of the variable response to systemic therapy in aGCT. In future research, this technique could be used to personalize the systemic treatment of aGCT patients. The response to carboplatin/gemcitabine in our patient-derived cell lines is striking.

#0943 Identification and validation of unusual drug combinations identified from combination databases.

R. Grant[1], **M. Pinheiro**[2], R. Weller Roska[1], R. Felix[2];
[1]Bio-Techne Corporation, Minneapolis, MN, [2]Bio-Techne Corporation, Bristol, United Kingdom

There is a noted trend in the identification and subsequent approval of rational drug combinations to treat various diseases, particularly cancer. When applied in a clinical setting, synergistic combinations can have significant benefits including improved patient response and avoiding or overcoming drug resistance. Although multiple strategies have been successfully implemented to identify rational drug combinations, extensive validation is initially required to confirm a combination as synergistic. The existence and growing use of web-based repositories containing comprehensive drug combination data is a key resource and can be a valuable starting point for identifying synergistic combinations. However, are synergistic combinations from these datasets expected or rational and can they be validated experimentally? By mining available drug combinations from the DrugCombo database, we wanted to identify unusual drug combinations reported as synergistic and experimentally validate these with dose-response assays. In addition, we set out to establish if cytokines could be used as an inhibition biomarker to easily assess synergy. We found multiple unexpected synergies including a predicted synergy between the JAK1/2 inhibitor Ruxolitinib with Maraviroc, a CCR5 antagonist, or Levetiracetam, an SV2A binding anti-epileptic reported in the lymphoma cell line, L-1236. Experimentally, these predicted synergies could not be validated. In the context of synergistic drug combinations, this work shows that experimental validation is crucial, particularly for combinations with uncertain biological mechanisms.

#0944 Pre-clinical activity of the Wnt pathway inhibitor RXC004 in combination with MAPK pathway inhibitors in GI cancer models.

S. A. Woodcock, D. Keppel, C. Eagle, J. Kelly, E. Flanagan, E. Bishop, I. Bhamra, C. D. Jones, R. Armer, J. Robertson, C. Phillips;
Redx Pharma Plc, Manchester, United Kingdom

Background: Gastrointestinal (GI) cancers cause more cancer deaths than any other body system, with 3.4 million related deaths in 2018. Wnt pathway activation is common in GI cancers, with the pathogenic upstream Wnt pathway variant sub-population (RNF43 loss of function / RSPO gain of function) showing a combined prevalence of 4.7% in GI cancer patients; pre-clinically this sub-population shows exquisite sensitivity to RXC004, a small molecule Porcupine inhibitor. A striking co-occurrence of upstream Wnt pathway variants with MAPK pathway driver mutations (KRAS, BRAF, NRAS) was detected in 77% of Microsatellite stable (MSS) GI cancers, suggesting co-inhibiting these pathways could enhance clinical activity in these patients.
Methods: *In vitro* proliferation assays were performed in pre-clinical models of upstream Wnt pathway mutated MSS GI cancer (SNU-1411, HPAF-II and AsPC-1) using Wnt (RXC004) or MAPK (Trametinib) pathway inhibitors at multiple concentrations as single agents or in combination. Control cells with downstream Wnt pathway mutations (WiDr and HCT116) were also tested. Synergistic combination effects were detected by BLISS scores. RXC004 (1.5mg/kg QD) and Trametinib (0.3mg/kg QD) were evaluated in an RSPO-fusion xenograft model (SNU-1411) as single agents or in combination. Efficacy was measured by tumour volume and weight; PD markers were assessed in end of study tumour samples. Relative *AXIN2* and *DUSP6* gene expression changes were determined upon inhibitor treatment by quantitative Polymerase Chain Reaction (qPCR).
Results: RXC004 in combination with Trametinib demonstrated strong anti-proliferative synergy in SNU-1411 cells and moderate synergy/additivity in HPAF-II and AsPC-1 cells; no synergy was observed in control cells. *In vivo*, RXC004 and Trametinib monotherapy led to significant moderate tumour growth control ($p<0.05$) at the doses tested, whereas their combination led to significantly enhanced efficacy ($p<0.05$). Gene expression analysis demonstrated a reciprocal Wnt/MAPK signaling mechanism; RXC004 strongly suppressed Wnt signaling (AXIN2) but increased MAPK signaling (DUSP6), whilst Trametinib strongly suppressed MAPK signaling (DUSP6) but increased Wnt signaling (AXIN2). Combination of RXC004 and Trametinib sustained inhibition of both Wnt and MAPK signalling. Similar effects were observed with inhibitors of other MAPK pathway components.
Conclusion: Wnt and MAPK pathways are frequently co-activated in GI cancers, particularly in the upstream Wnt pathway mutated sub-population. Pre-clinically we show that Wnt and MAPK pathways act as potential reciprocal resistance mechanisms following single agent inhibition of either pathway; co-inhibition of these pathways leads to synergistic effects *in vitro* and enhanced efficacy *in vivo.* This provides a clear rationale to assess this combination approach in the clinic.

#0945 *In vivo* anti-tumor activity of onvansertib, a PLK1 inhibitor, combined with gemcitabine or carboplatin in platinum- resistant ovarian carcinoma patient-derived xenograft models.

M. Chiappa[1], F. Guffanti[1], I. Mengoli[1], M. Ridinger[2], G. Damia[1];
[1]Istituto di Ricerche Farmacologiche Mario Negri IRCCS, Milan, Italy, [2]Cardiff Oncology, San Diego, CA

Background: The standard treatment for high grade ovarian carcinoma (HGOC) is cytoreductive surgery followed by a platinum based therapy. Despite an initial high rate of complete remission, most of the patients relapse with a platinum resistant disease. Patients with resistant tumors have few options, including monotherapy with gemcitabine, and new effective therapeutic alternatives are needed. The Polo-like kinase 1 (PLK1) is a master regulator of mitosis and recent evidences suggest its role in interfering with several DNA repair mechanisms. We investigated the effect of onvansertib (ONVA), a highly selective ATP-competitor PLK1 inhibitor, in combination with carboplatin (CARBO) and gemcitabine (GEM) in platinum-resistant HGOC patient-derived xenografts (PDXs).
Methods: The combination of ONVA with either CARBO or GEM was investigated in two platinum-resistant HGOC PDXs, one intrinsically resistant to platinum (MNHOC#315), the other made resistant after repeated *in vivo* treatments with cisplatin (MNHOC#266R). Tumors were subcutaneously (s.c.; MNHOC#315) or orthotopically (i.p.; MNHOC#266R) transplanted in nude mice, mice were treated for 4 weeks with vehicle, single agents or drug combinations and followed for tumor growth (s.c. model) and survival.
Results: CARBO- and GEM-ONVA combinations were well tolerated, with a maximum body weight loss of 6.6%. Both combinations showed strong anti-tumor activities in the two tested models. In MNHOC#315 PDX, CARBO- and GEM-ONVA combinations caused a tumor stabilization that extended beyond the dosing period and resulted in a higher tumor growth inhibition as compared to vehicle and single agents treated mice. In i.p. MNHOC#266R PDX, single agents were inactive, while a statistically significant increase in survival was observed in CARBO/ONVA and in GEM/ONVA treated mice as compared to vehicle treated mice, with a 6.6- and 7-fold increase in mean survival time, respectively. Pharmacodynamic studies are ongoing to decipher the mechanisms underlying the synergic effects of both combinations.
Conclusions: The combinations of ONVA with either CARBO or GEM showed potent anti-tumor activities in two platinum-resistant HGOC PDXs. Additional studies in other HGOC platinum-resistant models, both *in vivo* and *in vitro*, as well pharmacodynamic studies are ongoing to validate these results and to get insights in the mechanisms underlying their efficacy.

#0946 Landscape of HRD aberration in EGFR mutated lung cancer and the role of PARP-inhibitor in EGFR mutated lung cancer with HRD aberration.

J. Kim[1], H. Choi[2], L.-Y. Chung[3], Y. Chae[3];

[1]University of Vermont, Larner School of Medicine, Burlington, VT, [2]The Queen's Medical Center, Honolulu, HI, [3]Northwestern University, Feinberg School of Medicine, Chicago, IL

Introduction: Olaparib, an oral poly polymerase (PARP) inhibitor has received approval for treating malignancies displaying homologous recombination deficiency (HRD). Current data is insufficient in establishing the role of PARP inhibitors in non-small cell lung cancer (NSCLC) in the setting of third generation EGFR tyrosine kinase inhibitor (TKI) use. Preclinical investigation suggests heightened PARP inhibitor sensitivity of TKI-resistant EGFR mutant NSCLC cells compared to TKI-sensitive cells.

Methods: We utilized The Cancer Genome Atlas (TCGA) to investigate the prevalence of HRD gene mutations in patients with NSCLC harboring EGFR mutations. We also present a case demonstrating a favorable response to the dual therapy of olaparib and osimertinib in NSCLC harboring EGFR, RAD50, and ARID1A mutations that progressed on osimertinib.

Results: There were 2298 patients in the NSCLC cohort (MSKCC database). Among 687 patients with EGFR mutations, 24 patients (3.5%) exhibited ARID1A mutations, 8 patients (1.2%) had BRCA1 mutations, 11 patients (1.6%) had BRCA2 mutations, and 5 (0.7%) had RAD50 mutations. A 71-year-old female presented with stage IV adenocarcinoma of the lung. She had recurrent malignant pericardial effusion requiring pericardiocentesis for previous cardiac tamponade. Computed tomography (CT) of the chest revealed a 3cm irregular left hilar mass with bilateral mediastinal and hilar lymph nodes. Tissue next generation sequencing (NGS) at baseline identified EGFR exon19 deletion along with RAD50 R726H which is a HRD pathway gene. Circulating tumor DNA (ct-DNA) NGS (Guardant360) showed EGFR E746_A750del 4.8%. The patient achieved partial response to osimertinib for 28 months. Follow-up CT showed disease progression. Olaparib 200mg twice daily was added to osimertinib based on repeat ct-DNA NGS indicating a new ARID1A alteration (splice site SNV) along with the known BRCA1 mutation. Follow up scans currently have consistently demonstrated ongoing partial response for 19 months. Combining olaparib with osimertinib can be effective in an osimertinib-resistant NSCLC patient with EGFR mutation and HRD aberration. The favorable response could be attributed not only to pre-existing RAD50 mutation but also to acquired mutations in ARID1A HRD genes.

Conclusion: HRD aberrations are uncommon in EGFR mutated lung cancer patients. Further investigation on the role of PARP inhibitor in EGFR mutated lung cancer is warranted.

#0947 A nanodroplet cell processing platform for identifying synergistic drug combinations for neuroblastoma treatment in TH-MYCN transgenic mice.

Y.-T. Liao[1], Z.-K. Yu[1], C.-T. Kuo[2], W.-M. Hsu[3], Y.-X. Huang[1], H. Lee[1];
[1]Department of Life Science, National Taiwan University, Taipei City, Taiwan, [2]Department of Mechanical and Electro-Mechanical Engineering, National Sun Yat-sen University, Kaohsiung Cty, Taiwan, [3]Pediatric Surgery, National Taiwan University Hospital, National Taiwan University, Taipei City, Taiwan

Neuroblastoma is the most common pediatric extracranial solid tumor and contributes to more than 15% of child mortality. It is characterized by extreme heterogeneity and high-risk tumors often resulting in poor prognosis. Currently, chemotherapy is a prevailing standard treatment for neuroblastoma. However, it is plagued by multiple challenges such as drug resistance and debilitating side effects. Synergistic drug combination is proposed as an innovative approach to potentially improve clinical outcomes of single-agent chemotherapy. We propose a novel approach to screen for effective chemo-synergistic drug combinations using Bioinspired nanodroplet processing (BioNDP) screening platform. This platform overcomes the limitations of conventional drug screening approaches, including the requirement for large cell numbers and the low translation rate from bench to bedside. In this study, we utilize TH-MYCN transgenic mice, a well-known genetically engineered mouse model of neuroblastoma that recapitulates critical genetic and clinical aspects of high-risk MYCN-amplified neuroblastoma. With its genetically homogeneous background and spontaneous tumor development, TH-MYCN mice offer a valuable comparison to traditional xenograft mouse models. We have also developed an optimal procedure of primary murine tumor isolation using both negative and positive selection approaches. The purity of the isolated cells was verified with GD2 expression, one of well-known marker of neuroblastoma. In addition, we have successfully identified an effective drug combination of cyclophosphamide, doxorubicin, and vincristine, using primary neuroblastoma tumor samples derived from TH-MYCN transgenic mice as a target. The *in vitro* synergistic effect of primary mouse tumor cell cytotoxicity was confirmed by using luminescent cell viability assay. Further *in vivo* experiments have demonstrated the therapeutic efficacy of this selected drug combination in suppressing tumor growth and improving survival rate in all TH-MYCN transgenic mice treated. To sum up, we aim to establish a future patient-centric paradigm by which minimal primary cell samples from a personalized biopsy of patients may undergo drug screening, leading to the identification of a tailored drug combination. The BioNDP platform we developed may become a pivotal resource for personalized therapy to ensure a faster and more efficient treatment strategy for patients.

#0948 A novel combinatorial therapy for lethal neuroendocrine prostate cancer.

M.-E. Wang[1], W.-L. Tu[1], Y. Lu[1], J. Wu[1], A. Bawcom[1], A. J. Armstrong[1], Q. Wang[1], Y. Wang[2], J. Huang[1], M. Chen[1];
[1]Duke University School of Medicine, Durham, NC, [2]University of British Columbia, Vancouver, BC, Canada

Background: Neuroendocrine prostate cancer (NEPC) is a highly aggressive subtype of prostate cancer that can arise *de novo*, but more commonly develops after hormone therapies for advanced prostate adenocarcinoma. Current treatment options for NEPC are only palliative, and most patients die within several months. Additionally, single-agent clinical trials targeting NEPC so far have only produced disappointing results, highlighting the clear need to develop effective combinatorial therapies for NEPC. *RB1* loss, a pivotal event in the development of NEPC, can sensitize cancer cells to ferroptosis in multiple cancer cell types, including prostate cancer. Here, we aim to identify an optimal combinatorial therapy for NEPC based on targeting ferroptosis.
Methods: We determined the cell-killing efficacy of ferroptosis inducers and several current and emerging treatment regimens for NEPC as single agents, then performed drug synergism analyses of the above two potent treatments. Lastly, we investigated the molecular mechanisms of drug synergism by examining the major types of cell death induced by combinatorial treatment through molecular and biochemical assays.
Results: Our results demonstrated that both ferroptosis inducers and BCL2 inhibitors as single agents led to robust cell death in NEPC cell lines tested. In contrast, cisplatin, the standard of care for NEPC, and Aurora kinase A inhibitor showed modest to no cell-killing effect. Furthermore, suboptimal doses of ferroptosis inducers and BCL-2 inhibitors synergistically induced cell death in NEPC cell lines. Unexpectedly, we found that low-dose ferroptosis inducer led to increased production of mitochondria ROS, which in turn exacerbated BCL-2 suppression-induced apoptosis.
Conclusions: Our findings reveal a novel combinatorial therapy for NEPC. Based on our in vitro data, we will further test the *in vivo* therapeutic efficacy of ferroptosis inducers combined with BCL-2 inhibitors against NEPC growth.

#0949 A single stranded DNA library preparation workflow used for hybridization capture based WES assay showed superior uniformity.

J. Chu, R. Schell, F. Wu, M. Krawczyk, D. Whang, S. Jung, H. Nam, K. B. Thomas, F. J. Lopez-Diaz, V. Funari, J. A. Mayer, S. Kulkarni, J. Guo, S. P. Lau-Rivera;
NeoGenomics, Aliso Viejo, CA

Introduction: In many instances in Precision Oncology Medicine fragmented DNA from formalin-fixed paraffin-embedded (FFPE) samples is the only option. The majority of such degradedsamples need to be sequenced using next generation sequencing (NGS) [1]. Standardizedguidelines highlight that a minimum of 500× coverage depth is required for tissue analyses [2].However, coverage isn't the only metric required for a successful NGS analysis. Highly uniformDNA libraries allow clinical labs to generate more hits from their screens, saving both time andmoney across the course of diagnosis therefore ultimately benefits patient care. The commerciallyavailable single stranded DNA library prep kit tested in this study renders all input moleculessingle-stranded before ligation therefore it recovers template molecules containing DNA nicks andlabile lesions thus maximizing library complexity.
Method: 10 solid tumor FFPE derived DNA samples went through three different NGS workflows:100ng of DNA input in an amplicon-based assay 325 gene panel (Assay A), 60ng input for a 500gene mechanical sheared-based double strand DNA library preparation with hybridization captureassay (~500 gene panel, Assay B), 50ng and 10ng input for a enzymatic shear-based singlestranded DNA library preparation with hybridization capture assay (WES with 1000+ enhancedgene content, Assay C). Data from assays A and C was processed with in-house bioinformaticpipeline, while Assay B's data was processed with a commercially available bioinformatic pipelinethat was bundled with the assay. NGS QC metrics were compared across the three datasets.
Results: This novel single stranded DNA library preparation with hybridization capture workflowshowed superior QC metrics compared to the other two workflows, especially on coverageuniformity and percent target above 100X, with as low as 10ng input.
Conclusion: Employing a novel commercially available DNA library preparation workflow in anNGS assay, NeoGenomics was able to rescue poor quality samples that had previously failed tomeet our internal uniformity metric on other NGS assays and generate robust and reportableresults with as low as 10ng DNA input.[1] Nagahashi et al., *J Surg Res*. 2017 Dec; 220: 125-132.[2] Cappello et al., J Pers Med. 2022 May; 12(5): 750.

#0950 Functional characterization of atypical somatic variants in the Gundersen Precision Oncology Cohort.

P. Feiszt, **P. A. Kenny**;
Gundersen Medical Foundation, La Crosse, WI

The generation and widespread sharing of large somatic mutation datasets has revolutionized our understanding of genetic mechanisms driving cancer initiation and progression. For well-understood mutations, this has created the opportunity for individualized therapeutic intervention in a wide range of malignancies. Beyond these well-characterized mutations, there exists a wide range of alterations that remain poorly understood and which require some kind of functional genomics analysis to determine whether such patients are eligible for the targeted therapy used for more typical mutations in that gene, whether these alterations are passenger mutations that don't affect throughput on the associated signaling pathway, or reflect another more nuanced phenomenon. Whether using ectopic overexpression in cell lines or generation of genetically modified mice, addressing this problem at scale using functional genomics approaches is challenging. A key limitation is the absence of the original tissue context in which that variant co-evolved with other genetic alterations as well as data on the clinical response of the patient to successive lines of therapy. This can be addressed, in part, by the banking of tissue from patient cohorts who have had comprehensive genomic profiling as part of their routine clinical care.

The Gundersen Precision Oncology Cohort is a growing dataset of FFPE specimens and longitudinal clinical data from more than 750 patients who have had comprehensive cancer genome profiling using assays from a wide range of diagnostic companies. We use this resource for biomarker discovery and functional classification of many atypical cancer variants. Current subgroups include atypical point mutations in BRAF, ERBB2 and ERBB3, as well as fusions affecting BRAF, PIK3CA and ROS1. We present examples illustrating the value of this approach for classification of variants detected in a range of tumor types.

#0951 3D-PREDICT - An *ex vivo* precision oncology and clinical trial enrichment platform by Nilogen Oncosystems.

J. Ehrhart, S. Currlin, M. Ataya, A. Humphrey, R. Chakraborty;
Nilogen Oncosystems, Tampa, FL

Background: Immuno-oncology (IO) therapy with checkpoint inhibitors has demonstrated a higher response rate, duration of response, and overall survival than chemotherapy. However, predicting which FDA approved IO therapies or pharmaceutical agents, as well as best combinations and delivery sequence, will have optimal patient response remains a significant challenge for personalized medicine. Nilogen Oncosystem's 3D-PREDICT is a novel *ex vivo* therapeutic investigative platform that provides a functional model of a patient's tumor to investigate susceptibility to different therapeutic approaches directly. Derived from core biopsies, the 3D-PREDICT model captures the tumor heterogeneity while preserving the tumor microenvironment by retaining stromal components and cell-cell and cell-extracellular matrix interactions. Here, we employed the 3D-PREDICT platform to compare the efficacy of different immunotherapeutic approaches in various solid tumor indications *ex vivo*.
Methods: Tumoroids from 18-gauge core biopsies from solid tumors were generated using Nilogen Oncosystems's proprietary mechanical process forgoing any enzymatic digestion or propagation while keeping the spatial contexture of stroma intact. Pooled tumoroids were treated *ex vivo* for 72 hours with various standard-of-care mono or combo therapy (carboplatin, anti-programmed death-ligand 1 (PD-L1) antibody atezolizumab, anti-CD47 antibody magrolimab, anti-programmed cell death receptor-1 (PD-1) antibody nivolumab, or a combination of magrolimab and atezolizumab). Treatment-mediated immune modulation in tumor microenvironment were analyzed to predict patient response to subjected therapies.
Results: Treatment-mediated tumor cell killing activity was evaluated using 3D high throughput confocal imaging and Nilogen Oncosystems's proprietary algorithm for data analysis. The *ex vivo* response to checkpoint inhibitors was correlated with retrospective patient clinical information. Tumoroid samples treated with atezolizumab and magrolimab demonstrated enhanced tumor cell killing. Approximately 20% of tumors showed increased CD8 T-cell activation upon *ex vivo* treatment, correlating with proinflammatory cytokine release in conditioned media.
Conclusions: The 3D-PREDICT *ex vivo* tumoroid platform provides a unique resource to predict patients' response to treatment, potentially serving as a clinical diagnostic to guide clinical care and stratifying patient procurement into clinical trials. This would allow prospective assessment of therapeutic efficacy *ex vivo* to match each patient to the most effective and least toxic, to improving outcomes, reducing costs, and assigning therapeutics on a more rational basis.

#0952 *Ex vivo* drug testing identifies a potentially effective drug in 94% of cases for 403 patients in 42 tumor types.

R. Rosati[1], A. C. Rajevski[1], P. Chatterjee[1], L. R. Appleyard[1], A. Cordero Schmidt[1], S. Pereira[1], R. L. Diaz[1], B. Bernard[1], B. Bernard[2], C. Grandori[1], C. J. Kemp[3];

[1]SEngine Precision Medicine, Seattle, WA, [2]Earle A. Chiles Research Institute, Providence Cancer Institute, Portland, WA, [3]Fred Hutchinson Cancer Research Center, Seattle, WA

Objective: To determine whether patient derived tumor cells (PDTC) could be derived from a variety of solid tumors and used to select effective therapies, we developed a CLIA certified assay, the PARIS® test, to quantify drug sensitivities using PDTCs.

Methods: Oncologists referred patients for the PARIS® test and patients had the option to consent to SEngine Precision Medicine's IRB protocol. Samples were obtained from multiple cancer centers across the US and abroad. Patients were at all stages in their clinical journey ranging from treatment naïve to late stage, recurrent/refractory disease settings. Fresh specimens obtained from surgical resections, core biopsies, or body fluids arrived at our CLIA laboratory within 48 hrs from collection. Tumor origin and driver mutations were confirmed by IHC or DNA sequence in 88% of the cases.

Results: PDTCs derived from 403 patients diagnosed with 42 different solid tumor types, including both common and rare tumors, were subjected to the PARIS® assay. An average of 67 oncology drugs (ranging from 6-307), including chemotherapies and targeted agents, were tested for each patient sample. A report ranking drug sensitivities was provided to the oncologist with an average turnaround time of less than 3 weeks. Drug sensitivity was classified as exceptional/good, moderate/low and no responses. Remarkably, 94.2% of the PDTCs exhibited selective exceptional/good responses to at least one, and typically several drugs, despite the majority of PDTCs being derived from patients with drug resistant, metastatic disease. The drug sensitivity profiles showed highly individualized responses as well as tumor type specificity. While known biomarkers/drug sensitivity associations were confirmed, many samples exhibited sensitivity to targeted agents in the absence of known biomarkers. For example, HER2+ breast cancers demonstrated sensitivity to HER2/EGFR inhibitor and a subset of luminal B and triple negative breast cancers demonstrated HER2/EGFRi responses without underlying genetic alterations. Functional testing was also useful in the rare tumor types. For example, low grade serous ovarian cancer (LGSOC) cells, differentiated from high grade by their response to specific receptor tyrosine kinase inhibitors and estrogen antagonists, but a poor response to standard of care, as is observed in the clinic. Three patients with LGSOC that were treated with the PARIS test top scoring drugs had a positive clinical response and cases from other tumor types will be presented.

Conclusions: Functional testing of PDTCs from both common and rare tumor types is feasible, even for those that have failed standard of care. We provide an unprecedented view of patient-specific, actionable vulnerabilities to current oncology drugs. Personalization of cancer care will require improved access to off-label drugs.

#0953 Integration of functional precision medicine assay for high grade glioma management: A single institution experience.

G. Guzman[1], S. Bettadapura[1], W. J. Shelton-Correa[1], T. Brooks[2], M. Rayner[2], C. Wardell[1], A. Rodriguez[1];
[1]University of Arkansas for Medical Sciences, Little Rock, AR, [2]Kiyatec, Inc., Greenville, SC

Despite the advances in precision oncology, genomic approaches have not significantly improved outcomes for high grade gliomas (HGGs) as once was anticipated. Recurrent HGG pose even greater therapeutic challenge. The integration of functional precision medicine (FPM), in which drugs screens are performed on live tissue, into clinical routine practice presents a promising alternative by offering personalized treatments based on the unique characteristics of the patient's tumor. Here, we present our institutional experience of integrating a spheroid-based drug screening assay (3D Predict^{TM} Glioma) in the treatment management of HGG patients to evaluate its feasibility and efficacy as a therapeutic tool in a clinical setting. We also sought to determine factors that related to assay success. Tissue from intracranial lesions of patients with presumed HGG and planned surgical resection at our institution were collected for ex vivo 3D cell culture and challenged with 12 drug agents to determine patient-specific response parameters. The impact of potential variables, such as ki67, tumor pathology, and shipment timing, on the assay's success was evaluated. Clinical correlation was established between ex vivo response and clinical response in HGG patients. 57 samples, including 24 upfront HGGs, 32 recurrent HGGs, and one medulloblastoma, were sent for spheroid formation and drug testing. In total, 57.9% (33/57) or 23% (13/57) of the assays were successful and resulted in complete or partial functional profiling data, respectively. We conducted a multivariable analysis of our cohort to determine which variables (i.e. tumor volume sent, ki-67 proliferation index, tumor percentage determined by DNA sequencing by Tempus Lab, recurrent status, sample shipment time) were predictive of assay success. The only variable significantly associated with assay success was tumor percentage with samples comprised of >70% tumor leading to assay success, 40%-70% leading to 60% chance of success, and <40% having 0% success. Among 46 patients with partial or complete assay success, 26 patients (56.5%) had a targetable mutation and 17/26 yielded a moderate or full response to one or more of their corresponding targeted drugs in the assay. Treatments were newly administered or altered from prior treatments in 40/57 patients (70%) based on FPM results. Our study demonstrates the technical feasibility of incorporating FPM approaches in the development of treatment regimens for patients with HGG. Success was correlated to tumor percentage present in the sample which indicates intraoperative communication between surgeon and pathologist can lead to improved assay results. Our institutional protocol demonstrates that Integrating FPM into routine clinical practice is possible and can serve as a valuable guide in the refinement of therapeutic recommendations for HGG patients.

#0954 An evaluation of the combination of metformin and Y15 for the treatment of platinum-resistant ovarian cancer.

M. A. Duarte[1], K. Garcia[1], M. A. Arriaga[1], S. Chew[1], A. S. Levy[2], I. Mendez[1];
[1]University of Texas Rio Grande Valley, Brownsville, TX, [2]Nova Southeastern University, Fort Lauderdale, FL

Ovarian cancer is the fifth leading cause of cancer mortality among women. This high mortality rate is linked to the development of resistance to first-line chemotherapy with platinum compounds which has been attributed in part to increased activity of focal adhesion kinase (FAK). The anti-diabetic drug Metformin was previously shown to inhibit the proliferation and migration of ovarian cancer cells and thus, the combination of a FAK inhibitor, Y15, and Metformin may be a promising treatment for platinum-resistant ovarian cancer (PROC). The objective of this study was to evaluate the combination of Y15 and Metformin on PROC cell viability and the mechanism of cell death. An MTT assay was used to analyze cell viability in PROC OVCAR3 cells after 48 h of treatment by measuring the absorbance at 570 nm with a microplate reader. Western blot was used to determine the protein levels of the apoptosis marker cleaved PARP and the autophagy marker LC3B-II. The exposure of OVCAR3 platinum-resistant ovarian cancer cells to Metformin (4.5 mM) + Y15 (5.5 μM) resulted in a significantly enhanced cytotoxicity (32.6 ± 1.8%) compared to single drug treatment with either Metformin (4.5 mM) (65.0 ± 4.2%) or Y15 (5.5 μM) (66.0 ± 4.8%). A combination of Metformin (7.8 mM) + Y15 (5.5 μM) also resulted in a significantly enhanced cytotoxicity (22.8 ± 1.5%) compared to single drug treatment with either Metformin (7.8 mM) (50.7 ± 3.7%) or Y15 (5.5 μM) (66.0 ± 4.8%). Cells treated with the combination of Metformin and Y15 for 24, 48, and 72-hours showed an increase in cleaved PARP compared to the control, Metformin alone and Y15 alone. For Metformin alone, there was an increase in cleaved PARP compared to the control at all timepoints and increased from 24 hours to 72 hours. For Y15 alone, the amount of cleaved PARP was also higher compared to the control at all time points, however, decreased over time from 24 hours to 72 hours. Cells treated with Metformin, Y15, and a combination of Metformin and Y15 showed no conversion of LC3B-I to LC3B-II, which occurs during autophagy. Thus, it is concluded that the mechanism of cell death for both Metformin and Y15 is through apoptosis and not autophagy and apoptosis is enhanced with the combination of the drugs. The delivery of Metformin and Y15 can result in an additive effect on cell viability through apoptosis and can be further explored as a promising approach for the treatment of PROC.

#0955 Double-targeting of pancreatic ductal adenocarcinoma (PDAC): Unveiling the potent combination of NMS-873 and BAY-876.

E. R. Eppinger, C. Schneeweis, D. Saur;
TranslaTUM, Munchen, Germany

Pancreatic ductal adenocarcinoma (PDAC) stands out as one of the most aggressive and challenging-to-treat cancers known. Consequently, the development of effective therapeutic strategies holds significant importance in enhancing patient outcomes. In contrast to single-drug treatments, combination therapies offer the potential for improved results by addressing multiple pathways. This approach not only reduces the likelihood of drug resistance but also encourages synergistic effects, all while permitting the use of lower individual drug doses, thus minimizing potential side effects. In this study, we subjected a panel of PDAC cell lines with varying degrees of sensitivity to a high-throughput combinatorial drug screen. Mitochondrial complex 1/p97 inhibitor NMS-873 was tested in combination with 95 other compounds, revealing remarkable synergy when paired with Glut1 inhibitor BAY-876. In order to affirm the validity of these findings, we conducted further experiments involving multi-dose drug combinations within long-term clonogenic assays. These supplementary investigations also demonstrated significant synergistic effects between BAY-876 and NMS-873, as quantified through the calculation of Bliss and Zip scores. Notably, this combination exhibited superior efficacy when confronting PDAC cell lines that are more resistant to NMS-873, highlighting the potential of this combination to overcome therapy resistance. To gain insights into the underlying mechanisms behind these outcomes, we performed a gene enrichment analysis which revealed that the more sensitive cell lines exhibited elevated rates of cell division, while the more resistant ones demonstrated heightened cRNA processing and increased metabolic activity, particularly in protein, phospholipid, and lipid synthesis. The combination of BAY-876 and NMS-873 presents a promising avenue for the targeted treatment of PDAC. This study underscores the remarkable synergy observed in mouse PDAC cell lines with a particular emphasis on the heightened efficacy against cell populations that are more resistant to NMS-873. These results warrant further investigation to elucidate the underlying molecular mechanisms and validate these findings in clinical settings.

#0956 NCX 4040 and napabucasin synergistically inhibits stemness in human prostate cancer (PCa) cellular models and potently targets transgenic murine PCa cells via inducing oxidative stress.

S. Shah, G. Munirathinam;
University of Illinois College of Medicine (Rockford), Rockford, IL

Prostate cancer (PCa) continues to have a substantial impact on men's wellbeing and quality of life regardless of recent progress in diagnosis and treatments and it continues to have the second highest occurrence rate following lung cancer. The strategy of combination drug therapy has gradually become a valuable choice for treating various cancer types, addressing the heterogeneity within tumors, and surpassing the constraints of existing treatment methods. In our previous work, when we combined two drugs NCX 4040 (an oxidative stress inducer) and napabucasin (a STAT3 signaling inhibitor), we discovered that the combination treatment synergistically works to inhibit the malignant characteristics of human PCa cells. Also, the combination upregulated the cGAS-STING immunogenic pathway in PCa cells which could potentially activate the cancer-targeting cytotoxic T-cells. In the current study, we aimed at investigating the anti-stemness properties of the drug duo which can not only inhibit cancer cell differentiation but also can be effective in preventing cancer relapse. We used two cell lines i.e., BPH-Cd which served as a model of cadmium induced PCa and DU145 as a model of advanced PCa to examine the anti-stemness properties of the drug combination. Based on western-blot analysis, we found the downregulation of transcription factors such as Oct4, Sox2, Nanog, β-catenin and cell surface markers like CD44, CD133 and ALDHA1, which are responsible for stem-cell like properties. In addition, we have tested the combinatory anticancer effects in transgenic mouse derived PCa cell line (Myc-Cap) as a prelude to conduct future studies in FVB mouse syngeneic model to evaluate the tumor suppressive and the antitumor immunogenic responses of combination treatment as it activated cGAS-STING pathway. By performing the cell viability assay, we found that the IC_{50} value of NCX 4040 is ~10μM and that of napabucasin is ~1μM, however when used in combination, ~90% inhibition is seen at 10μM of NCX and 250nM of napabucasin dual treatment. The drug combination also showed synergy in inhibiting tumorigenicity in clonogenic assay and migratory potential in wound-healing assay. By investigating the ROS production, cell death and cell cycle mechanism using flow cytometric analysis, it was observed that the combination therapy synergistically induces cellular oxidative stress which causes cancer cells to undergo late apoptosis and halts the growth of Myc-Cap cells in G2M phase of cell cycle. In conclusion, our data suggests that combination therapy of NCX 4040 and napabucasin can be potential treatment strategy for PCa warranting further evaluation in *in vivo* models.

CLINICAL RESEARCH: Circulating Nucleic Acids 1
Poster Session

#0960 Improved cfDNA methylation profiling through correction of misrepaired jagged-ends.
R. Wang, E. G. Hamilton, D. Almanza, A. Hui, M. Diehn, A. A. Alizadeh;
Stanford University School of Medicine, Palo Alto, CA

Background: Profiling cfDNA methylation enables early cancer detection and classification, but challenges arise from "jagged ends" (JEs) for ~90% of cfDNA molecules, as well as for FFPE samples and partially degraded genomic DNA. Repair of these jagged ends introduces erroneous methylation signals, especially in shorter cfDNA fragments enriched for tumor derived molecules. Separately, DNA conversions during 5mC profiling hamper accurate simultaneous ctDNA genotyping of somatic mutations. To meet these needs, we developed a method preserving double-stranded cfDNA molecules without error-prone end-repair at jagged ends. This enables superior methylation profiling including hemimethylation detection, and simultaneous ctDNA SNV genotyping.
Methods: We present JEEPERS (Jagged-End Error Polishing of Enzymatically misRepaired Sequences), a novel method for correcting errors in double-stranded library preparation for methylation profiling. JEEPERS detects and quantifies enzymatic repair errors at JEs, correcting them in silico. Leveraging duplex UMIs, it utilizes complementary strands and sibling reads from cfDNA families without jagged ends. The method exploits the 5' to 3' polarity of ER-associated errors and JE length profiles for correction. JEEPERS introduces anchor CpGs for precise correction of rare signals and enables accurate SNV calling at non CpG sites, addressing the challenge of differentiating true SNVs from conversion artifacts leading to C>T/G>A changes in sequencing data.
Results: Analyzing 248 cfDNA samples (139 NSCLC patients, 109 healthy controls) by methylation profiling (EM-Seq) and ctDNA mutation genotyping (CAPP-Seq), JEEPERS correction efficiently addressed distortions, even at low tumor concentrations. Limiting dilution experiments demonstrated JEEPERS achieving a LOD95 of ~0.2% with 95% specificity (n=300). Despite ~50% lower molecular depth, JEEPERS-corrected cfDNA EM-Seq enabled accurate simultaneous methylation profiling and ctDNA genotyping, correlating strongly with CAPP-Seq genotypes ($R=0.998$, $n=30$). As expected, mutant ctDNA molecules were shorter than wild-type in both CAPP-Seq and EM-Seq data. cfDNA methylation patterns varied by oncogene vs. tumor suppressor status; EGFR mutants showed increased methylation ($p<0.01$), while TP53 mutants had lower methylation levels ($p<0.05$).
Conclusions: Our method effectively corrects cfDNA methylation data, even at low tumor concentration, ensuring enhanced methylation signal accuracy and proficient SNV calling capabilities. This integrated approach offers a powerful means for investigating the link between SNVs and DNA methylation, significantly enhancing the accuracy of cancer detection using cfDNA, especially for early-stage tumors. This paves the way for a deeper understanding of the molecular mechanisms driving cancer initiation and progression.

#0961 Detection of minimal residual disease in lymph predicts recurrence in HPV-negative head and neck cancer patients.

W. Winckler[1], Z. Gu[1], D. Whitfield[1], N. Earland[2], A. Harmon[1], M. Long[1], P. Harris[2], Z. Xu[3], R. Ramirez[2], S. Gerndt[2], M. Pacula[1], M. S. Francis[1], J. P. Zevallos[3], A. A. Chaudhuri[2];

[1]Droplet Biosciences, Inc., Cambridge, MA, [2]Washington University School of Medicine, St. Louis, MO, [3]University of Pittsburgh Medical Center, Pittsburgh, PA

Background: Locoregional cancer relapse remains a major cause of failure in head and neck squamous cell carcinoma (HNSCC), particularly for HPV-negative patients whose 2-year locoregional failure rate is up to 50%. There is unmet need for an accurate diagnostic test that predicts risk of recurrence prior to adjuvant therapy selection. We present a novel proximal assay for minimal residual disease (MRD) profiled in lymphatic exudate collected via surgical drains (“lymph”).
Methods: Lymph, plasma, and blood were collected from 46 HPV-negative HNSCC patients postoperatively at 24 hours along with resected tumor. Cell-free DNA was extracted from lymph and plasma and sequenced using the TruSeq Oncology 500 panel to a depth of >100 million reads. Somatic mutations were identified by exome sequencing (200x) tumor and blood. Five patients had <2 mutations in tumor and were excluded. Two patients were censored due to lack of clinical data, yielding 18 patients with disease recurrence (REC) and 21 with no evidence of disease (NED) with >1 year of follow-up. Tumor-specific variants were force-called in lymph and plasma using a custom pipeline. Patients were considered MRD positive if the mean variant allele fraction (mVAF) was greater than 0.015% (the estimated limit of detection). The Kaplan-Meier (KM) estimator with log-rank test and Cox proportional-hazards model were used for survival analyses. Logistic regression model was performed with 5-fold cross-validation.
Results: KM survival analyses showed lymph accurately predicts recurrence (sensitivity (SN) = 78%, specificity (SP) = 67%; p = 0.003, Hazard ratio (HR) = 4.7), while plasma was not significant (p = 0.92) at this postoperative timepoint. Performance was enhanced for locoregional relapse (SN = 92%, SP = 67%; p = 0.001, HR = 13.9. N=33). We also observed accurate recurrence prediction (SN = 83%, SP = 69%, p = 0.03, HR = 7.7) in the 19 N0 patients (node-negative by pathology). Lymph MRD outperformed individual pathology features (extranodal extension, perineural invasion, lymphovascular invasion, and nodal disease status) for recurrence prediction (HR = 3.4, 0.88, 2.5, 2.4, respectively). A logistic regression model combining lymph MRD with these 4 high-risk pathologic features showed superior performance over lymph alone or pathology alone (SN = 89%, SP = 67%; p = 0.0007, HR = 8.6).
Conclusions: ctDNA analysis of lymph from surgical drains represents a novel proximal MRD approach in HPV-negative HNSCC. Postoperative lymph significantly outperforms plasma for prediction of recurrence, particularly in patients with locoregional relapse. Accurate MRD identification in patients with lower risk pathologic features suggests that lymph MRD testing has potential to augment traditional pathology and provide more personalized adjuvant treatment decision-making in patients with HPV-negative HNSCC.

#0962 Monitoring on-treatment tumor molecular dynamics using plasma whole genome sequencing (pWGS) and whole exome sequencing (pWES) of circulating tumor DNA (ctDNA) in advanced esophageal cancer: An exploratory analysis of KEYNOTE-590.

M. Shah, E. Dettman, A. Albright, C. Chen, J. Kobie, S. Shah, C. Pena, R. Cristescu, Z. Cao;
Merck & Co., Inc., Rahway, NJ

Background: We evaluated on-treatment tumor molecular dynamics using ctDNA-based pWGS and pWES in patients (pts) with locally advanced or metastatic esophageal cancer that responded to pembro + chemo or chemo alone and later experienced PD in KEYNOTE-590 (NCT03189719). **Methods:** Pts with locally advanced, unresectable, or metastatic esophageal or Siewert type 1 gastroesophageal junction cancer were randomized 1:1 to first-line pembro 200 mg or placebo + chemo (5-fluorouracil + cisplatin) Q3W for ≤35 cycles. Cell-free DNA (cfDNA) was isolated and sequenced from plasma samples collected at baseline (BL), during on-treatment response (cycle 5 [C5]), and at PD (discontinuation [D]) from pts with response and subsequent PD. ctDNA burden (tumor fraction [TF]) was estimated using low-pass pWGS by quantifying tumor aneuploidy in cfDNA. All samples with TF >1.5% underwent high-depth pWES. ctDNA burden from pWES was estimated as maximum somatic allele frequency (MSAF). Associations of TF with MSAF were assessed using Spearman correlation coefficient *r*. For each subject, Jaccard index (JI) was calculated to evaluate the overlap of variants between BL and D. Variant allele frequency (VAF) and normalized VAF (nVAF) were used to determine variant clonality. **Results:** 108 pts (pembro + chemo, 59; chemo, 49) with initial response and subsequent PD had plasma samples available from BL, C5, and D. Samples from 94 pts had TF >1.5% by pWGS and underwent pWES. MSAF correlated with TF at BL (r = 0.84), C5 (0.56), and D (0.86). ctDNA TF was lower at C5 than at BL and D, with a mean of 4.4% (C5) vs 20.9% (BL) and 14.0% (D) with pembro + chemo and 4.0% (C5) vs 15.8% (BL) and 15.5% (D) with chemo. In variant-level analyses of pWES data from samples with high TF (≥2.5%) at BL and D (n = 65), 39.2% and 44.2% of variants were shared between BL and D with pembro + chemo and chemo, respectively. Higher overlap was observed for variants between BL and D for the chemo arm (JI: median, 0.54; range, 0.04-0.91) vs pembro + chemo (0.37; 0.01-0.92). Shared variants between BL and D had higher clonality compared with variants at BL-only or D-only with pembro + chemo (BL and D mean nVAF = 0.50 vs BL-only = 0.39, and D-only = 0.38) and chemo (0.49 vs 0.38 and 0.38). In pooled variant analyses, *TP53* was the most commonly observed mutation and was rarely lost or acquired at D. **Conclusions:** Comprehensive pWES was feasible with sufficient ctDNA burden (TF ≥2.5%). ctDNA burden dynamics followed high disease burden at BL and D, consistent with radiographic determination of response/PD. Tumor variants at BL and D generally had a common clonal trunk and a higher overlap of variants was observed at D in the chemo arm. These results provide preliminary molecular evidence of immune editing in pts receiving immunotherapy that warrants further study.

#0963 Comprehensive epigenomic profiling from plasma to inform therapy selection: A proof-of-concept study in cancer.

T. Clark[1], J.-H. Seo[2], A. D'Ippolito[1], A. Gorthi[1], J. Beagan[1], J. Guess[1], A. Donahue[1], M. Greene[1], A. Lau[1], F. Ramirez[1], K. Cibulskis[1], H.-H. Jeong[1], M. Davidsohn[2], G. Lakshminarayanam[2], M. Coyne[1], B. Tran[1], T. Tamakloe[1], H. Sawaengsri[1], M. Eid[2], K. Semaan[2], B. Fortunato[2], C. A. Painter[1], **J. Chmielecki**[1], T. K. Choueiri[2], J. Barrett[1], G. Otto[1], M. L. Freedman[2], M. L. Eaton[1], S. C. Baca[2];

[1]Precede Biosciences, Inc., Boston, MA, [2]Dana-Farber Cancer Institute, Boston, MA

BACKGROUND: Analysis of genomic alterations in circulating tumor DNA is gaining traction in clinical oncology and can provide insights into tumor biology without the need for invasive tissue sampling. In addition to genetic alterations, epigenomic reprogramming leads to transcriptional dysregulation and drives cancer phenotypes including molecular subtypes, histologic subtypes, and mechanisms resistance. As current liquid biopsy assays fail to effectively capture transcriptional biology, new approaches are needed to examine the transcriptional status of therapeutic gene targets and pathways including those relevant to rapidly emerging classes such as antibody-drug conjugates (ADC) and radio-conjugates.

METHODS: We developed a novel multimodal assay that reveals genome-wide transcriptional activity of promoters, enhancers from chromatin and surveys the DNA methylome using 1ml of patient plasma. We applied this assay to patient plasma samples from across 15 tumor types generating 7000 genome-wide transcriptional profiles.

RESULTS: We confirmed a significant correlation between epigenomic signals of transcriptional activation and gene expression from RNA-seq (Promoter vs RNA-seq: ρ =0.95, $p<0.05$; DNA methylation vs RNA-seq: ρ=-0.16, $p<0.05$). We identified transcriptional activation in cancer patient plasma of well-established cancer-associated biomarkers (e.g. MET, DLL3, PSMA) in a tumor-specific manner. Epigenomic profiling simultaneously inferred the expression of multiple pertinent ADC targets currently under investigation (MET, HER2, HER3, TROP2, B7H4 in breast cancer), and SLFN11, a known biomarker for sensitivity to these agents. Unlike targeted panels, the platform assesses transcriptional regulation genome-wide, enabling the assessment of transcriptional activity of select genes as well as related pathways. For example, a multimodal classifier robustly predicted HER2 status across metastatic breast cancer plasma samples based on features both within the *HER2* amplicon as well as *HER2*-distal genes that are activated in HER2+ cancers (AUC = 0.93, 0.84-1.0 95% CI). The multimodal classifier out-performed individual analyte-based classifiers ($AUC_{Promoter+Enhancer}$ = 0.85, 0.72-0.98 95% CI; $AUC_{DNA\text{-}methylation}$ = 0.69, 0.48-0.90 95% CI). Epigenomic signatures were also used to delineate multiple mechanisms of resistance to androgen receptor signaling inhibition in prostate cancer, including reactivation of the androgen receptor, glucocorticoid signaling bypass, and histological transformation to a neuroendocrine subtype.

CONCLUSION: This comprehensive epigenomic liquid biopsy assay provides a platform for simultaneous genome-wide transcriptional assessment of disease and therapy relevant genes and pathways, representing a paradigm shift in our ability to longitudinally monitor cancer in individual patients.

#0964 Updated results of a prospective observational multicenter study on resistance mechanisms to osimertinib using circulating tumor DNA analyses in EGFR-mutated non-small cell lung cancer patients (ELUCIDATOR study).

M. Osuga[1], A. Tamiya[2], D. Harada[3], Y. Mizumori[4], S.-i. Isa[2], Y. Taniguchi[2], K. Nakamura[5], T. Shinohara[6], H. Yanai[7], K. Nakatomi[8], M. Oki[9], M. Mori[10], T. Kuwako[11], K. Yamazaki[12], A. Tamura[13], M. Ando[14], Y. Koh[1];

[1]Wakayama Medical University, Wakayama, Japan, [2]National Hospital Organization Kinki-Chuo Chest Medical Center, Sakai, Japan, [3]National Hospital Organization Shikoku Cancer Center, Matsuyama, Japan, [4]National Hospital Organization Himeji Medical Center, Himeji, Japan, [5]National Hospital Organization Asahikawa Medical Center, Asahikawa, Japan, [6]National Hospital Organization Kochi Hospital, Kochi, Japan, [7]National Hospital Organization Mito Medical Center, Higashiibaraki, Japan, [8]National Hospital Organization Ureshino Medical Center, Ureshino, Japan, [9]National Hospital Organization Nagoya Medical Center, Nagoya, Japan, [10]National Hospital Organization Osaka Toneyama Medical Center, Toyonaka, Japan, [11]National Hospital Organization Shibukawa Medical Center, Shibukawa, Japan, [12]National Hospital Organization Kyushu Medical Center, Fukuoka, Japan, [13]National Hospital Organization Tokyo National Hospital, Kiyose, Japan, [14]Nagoya University Hospital, Nagoya, Japan

Background: Although osimertinib (Osi) is the key standard therapy for patients (pts) with advanced non-small cell lung cancer (NSCLC) harboring sensitizing epidermal growth factor receptor (EGFR) mutations, most of cases experience the progressive disease (PD) after initial response to the treatment. Therefore, understanding the Osi resistance mechanisms and identifying the poor responders are essential to develop better treatment strategies. Thus, we conducted a prospective observational multicenter study and analyzed serially collected circulating tumor DNA (ctDNA). Here we report the results from updated analyses focusing on the association between genetic information from ctDNA and clinical outcome.

Methods: Patient eligibility criteria were as follows: a definitive diagnosis of non-squamous NSCLC confirmed through biopsy or cytology, EGFR exon 19 deletion (19del) or L858R mutation, Osi planned as first-line treatment, and pts who could provide blood specimens. Paired plasma DNA samples were collected before starting Osi as baseline (BL) and at PD and analyzed to investigate Osi resistance by next-generation sequencing (NGS). Correlations between genetic information obtained from ctDNA and clinical outcome such as progression free survival (PFS) and overall survival (OS) were evaluated. The median follow-up time was 33.1 months.

Results: One hundred eighty-eight pts were enrolled between May 2019 and January 2021, and 125 (66%) were female, 96 (51%) were EGFR 19del mutation, and 109 (58%) were never smoker. Among those, 178 pts were included in the analyses, and 111 experienced PD. In consistent with previous reports, median PFS (mPFS) and median OS (mOS) were 19.1 months and 36.0 months, respectively. The efficacy of Osi differed between 19del and L858R in both PFS and OS, with 19del being longer outcome [mPFS, 23.3 months vs. 17.2 months, HR: 1.56 (95%CI: 1.08-2.26), mOS, 40.3 months vs. 30.4 months, HR: 1.54 (95%CI: 0.98-2.45)]. Univariate analysis revealed that the presence of TP53 mutations and MET amplification (amp) at BL was a predictive factor of shorter PFS and OS. Multivariate analysis also revealed that the TP53 mutations at BL was a predictive factor of shorter PFS and OS. Plasma samples from 85 pts were available for ctDNA analysis. New adaptive mutations or amp at PD were detected in genes such as PIK3CA in 3 cases, MET amp in 4, TP53 in 4, BRIMP3 in 2, APC in 1, and BRAF in 2. Secondary EGFR C797S resistance mutation was detected in 1 case.

Conclusions: TP53 mutation at BL could be predictive of poor response to Osi. MET amp and PIK3CA mutations were detected as the most common resistance mechanisms, and secondary EGFR resistance mutations were observed less frequently than previous reports.

#0965 Urine cell-free DNA multi-omics combining copy number analysis with fragmentomics to detect minimal residual disease in bladder cancer patients.

Arpit Panda[1], Irfan Alahi[2], Pradeep S. Chauhan[2], John Sheng[2], Nathan Colon[2], Cayce Nawaf[2], Alexander Shiang[3], Peter K. Harris[2], Faridi Qaium[2], Eric H. Kim[2], Melissa A. Reimers[2], Woodson Smelser[2], Zachary L. Smith[2], Aadel A. Chaudhuri[2]

[1]University of Chicago, Chicago, IL,[2]Washington University in St. Louis, St. Louis, MO,[3]Cedars-Sinai Medical Center, Los Angeles, CA

Background: Standard-of-care for patients with localized muscle-invasive bladder cancer (BC) is neoadjuvant chemotherapy followed by radical cystectomy (RC). Bladder-sparing treatments are limited by our current inability to sensitively detect minimal residual disease (MRD). Here, we analyzed urine, a noninvasive and proximal biofluid, from patients with bladder cancer and utilized an approach that incorporates copy number-derived tumor fraction as well as fragmentomics to sensitively detect MRD and predict pathologic complete response (pCR).
Methods: We acquired urine preoperatively from 51 BC patients (80% muscle-invasive) on the day of standard-of-care RC, and after neoadjuvant chemotherapy in 57% of patients. We performed whole genome sequencing (WGS) of urine cfDNA (median depth: 10X) from all 51 BC patients and 13 healthy adults. Tumor fraction level based on genome-wide copy number alterations was estimated using ichorCNA. We inferred fragment size and genomic coverage of urine cfDNA using Picard Tools. Then, we computed the short-to-long (S/L) fragment ratio for genomic bins in each sample. The S/L ratio per bin was derived by partitioning the genome into 100 kb bins and evaluating the ratio of GC-corrected short fragments (50-150 bp) to long fragments (151-250 bp) within each bin. A normalized genome-wide S/L score was calculated by averaging across all bins.
Results: In our cohort of 51 BC patients, 45% of patients achieved pCR (n = 23) while 55% had residual disease detected in their surgical sample (no pCR; n = 28). Patients with no pCR had significantly higher copy number-derived tumor fractions in urine compared to patients with pCR (median 10.6% vs 1.9%, p = 0.0002) and healthy adults (n = 12) (median 10.6% vs 1.8%, p = 0.003). Tumor fraction achieved an AUC of 0.89 for classification of No pCR from pCR with sensitivity of 82% and specificity of 92%. Presumed cancer-free patients (healthy and pCR) had significantly longer urine cfDNA median fragment sizes than patients with no pCR (median 177 bp vs 156 bp, p = 0.002). Presumed cancer-free patients (healthy and pCR) also had significantly lower S/L ratio scores than no pCR patients (mean .98 vs 1.5, p = 0.007). The top 100 bins with maximally differential S/L ratio between these two patient groups were enriched for genes involved in KEGG pathways implicated in cancer and immune signaling (autophagy, transcriptional misregulation in cancer, Th1 differentiation) indicating biological relevance.
Conclusion: Copy number alteration-derived tumor fraction inference combined with fragmentomic analysis of urine cell-free DNA can enable sensitive detection of MRD to predict pCR and reveal potentially onco-relevant pathways.

#0966 Longitudinal comparative analysis of circulating tumor DNA and matched tumor tissue DNA in patients with metastatic colorectal cancer receiving palliative first-line systemic anti-cancer therapy.

J.-W. Kim[1], S.-b. Lee[2], H.-G. Kim[2], S.-H. Hwang[1], K.-J. Kim[1], J. Lee[3], J. Seo[1], M. Kang[1], E. Jung[1], K. Suh[1], S. Kim[1], J. Kim[1], Y. Kim[1], J. Kim[1], N.-J. Kwon[2], K.-W. Lee[1];

[1]Seoul National University Bundang Hospital, Seongnam, Korea, Republic of, [2]Macrogen, Inc., Seoul, Korea, Republic of, [3]Hankuk University of Foreign Studies, Yongin, Korea, Republic of

Background: Plasma circulating tumor DNA (ctDNA) analysis has become an attractive method for precision oncology. This study compared mutational landscapes of ctDNA with matched tumor tissue DNA (ttDNA) to explore clinical applicability and to better understand clonal evolution in patients with metastatic colorectal cancer receiving palliative first-line systemic anti-cancer therapy (SACT).

Methods: We performed unique molecular identifier-based targeted sequencing of 88 cancer-associated genes using the following samples: ttDNA, germline DNA, ctDNA at baseline (baseline-ctDNA), and ctDNA at progressive disease (PD-ctDNA).

Results: Of the 208 consecutively enrolled patients, 84 were selected (41 males; median age 59, ranging from 35 to 90) with access to all four samples. Excluding duplicated mutations, a total of 202 driver mutations were discovered in 34 genes. ttDNA exhibited the highest occurrence of mutations (N=232), followed by baseline-ctDNA (N=155) and PD-ctDNA (N=117). Genotype concordance for the ten most mutated genes was highest between baseline-ctDNA and PD-ctDNA, at 94.3%, while the concordance rates for ttDNA were 85.5% with baseline-ctDNA and 83.6% with PD-ctDNA. Overall, 40 of the 84 patients (47.6%) benefited from sequencing ctDNA in addition to ttDNA as it identified additional mutations. Compared to ttDNA and baseline-ctDNA, PD-ctDNA identified 13 novel mutations in ten patients (11.9%). Notably, 7 mutations in five patients (6.0%) were missense or nonsense mutations in *APC*, *TP53*, *SMAD4*, and *CDH1* genes. In baseline-ctDNA, patients with maximal variant allele frequency (VAF) values of >0.059 showed significantly worse progression-free survival (median 10.5 vs. 17.1 months, P=0.036) and overall survival (median 18.1 vs. 40.3 months, P=0.010). Moreover, overall survival was significantly worse in those with higher VAF values of *APC* (median 18.1 vs. 36.8 months, P=0.012), *TP53* (median 24.7 vs. 40.3 months, P=0.012), and *KRAS* (median 13.7 vs. 27.6 months, P=0.005) mutations.

Conclusions: While ttDNA remains more sensitive than ctDNA, our unique molecular identifier-based ctDNA platform demonstrated the validity and potential value when ttDNA was unavailable. Furthermore, post-SACT analysis of PD-ctDNA revealed new pathogenic mutations, indicating the clonal evolution of cancer. In addition, the VAF values of baseline-ctDNA predicted prognosis after SACT.

#0967 Clinical applicability of targeted panel sequencing in liquid biopsies for disease diagnosis and monitoring of patients with pediatric solid tumors.

E. Christodoulou, V. Yellapantula, K. O'Halloran, L. Xu, J. L. Berry, F. Navid, D. Ostrow, J. A. Biegel;
Children's Hospital Los Angeles, Los Angeles, CA

Liquid biopsy assays based on sequence analysis of cell-free DNA (cfDNA) have the potential to transform patient care. We recently validated a liquid biopsy platform, LBSeq4Kids, for patients with retinoblastoma, brain tumors and solid tumors using low pass whole genome sequencing (LP-WGS) of cfDNA from aqueous humor (AH), cerebrospinal fluid (CSF), and plasma (PL) to detect Copy Number Alterations (CNAs) in circulating tumor DNA (ctDNA). Herein, we present phase 2, a high-depth comprehensive Next-Generation Sequencing (NGS) panel using cfDNA that allows us to detect SNV's, indels and gene fusions in clinically relevant genes for pediatric solid and brain tumors. Seventy-four cfDNA specimens have been analyzed to date, using plasma from 43 patients with solid tumors, CSF from 25 patients with brain tumors and AH from six patients with ocular tumors including retinoblastoma. cfDNA was extracted at diagnosis, during therapy, at remission and/or relapse. Sequencing libraries were constructed with the xGen Prism DNA Library Prep Kit using 5ng of cfDNA. For the detection of recurrent mutations and fusions we designed a custom panel using a hybridization-based capture method (Twist Bioscience) that included full coverage of the exons of 136 genes harboring recurrent mutations and selected introns for five genes with recurrent rearrangement breakpoints including *BRAF, EWSR1, SYT, FOXO1* and *NTRK1*. Hybridized libraries were paired-end sequenced (Illumina NextSeq 500) at an average 1000x collapsed coverage. Mutations identified in cfDNA were compared with those in the primary or metastatic tumors profiled with our OncoKids® NGS panel. A total of 35/43 (81%) plasma specimens were positive for either an SNV, deletion or fusion with the most common events being a somatic missense variant in *TP53* (13/35, 37%) or translocation involving *EWSR1* (9/35, 26%). A total of 16/25 (64%) CSF specimens were positive for SNVs and fusions, most often involving *KIAA1549::BRAF* (7/25, 28%) in low grade gliomas. A germline variant in *RB1* was detectable in two AH specimens from the left and right eye of a patient with bilateral retinoblastoma while plasma from a patient with metastatic retinoblastoma demonstrated clinically relevant variants in *RB1* and *DICER1*. Serial cfDNA profiling revealed a clinically reported *TP53* c.746G>C missense variant in the plasma of a patient with osteosarcoma at multiple timepoints through the disease course, with evidence for relapse prior to standard imaging. These data suggest that clinical implementation of a second version of LBSeq4Kids that combines CNA and mutation analysis allows for diagnosis, residual disease detection and risk stratification for pediatric patients with diverse tumor types, regardless of histologic grade, with a variety of pediatric solid and brain tumors.

#0969 Tumor-agnostic ctDNA monitoring in patients with metastatic HR+/HER2- breast cancer receiving first-line CDK4/6 inhibitor and endocrine therapy.

M. J. Elliott[1], J. Fuentes-Antrás[2], A. Dou[1], N. Gregorio[1], E. Shah[3], E. Van de Laar[3], G. Yalamanchili[4], L. M. Drusbosky[4], E. Amir[1], M. B. Nadler[1], C. Yu[3], H. K. Berman[5], L. L. Siu[1], P. L. Bedard[1], D. W. Cescon[1];

[1]UHN Princess Margaret Cancer Centre, Toronto, ON, Canada, [2]NEXT Oncology, Hospital Universitario Quironsalud Madrid, Madrid, Spain, [3]Cancer Genomics Program, Princess Margaret Cancer Centre, Toronto, ON, Canada, [4]Guardant Health, Inc., Redwood City, CA, [5]Department of Pathology and Laboratory Medicine, University Health Network, Toronto, ON, Canada

Introduction: CDK4/6-inhibitors (-i) in combination with endocrine therapy are first-line treatment for metastatic HR+/HER2- breast cancer (mBC). Baseline circulating tumor DNA (ctDNA) burden and changes on therapy are prognostic in mBC. GuardantINFINITY is a tumor-agnostic platform which measures aggregated epigenomic methylation signals that can distinguish ctDNA from non-tumor derived signals and permits the detection of somatic alterations in a 753 NGS panel. Longitudinal measurement of ctDNA quantity and characterization of emerging mutations may permit early identification of resistance and allow for intervention prior to clinical/radiographic progression.

Methods: Patients with HR+/HER2- mBC receiving CDK4/6i were enrolled in a prospective cohort study from 2018 onwards. Plasma samples were collected at baseline (prior to initiation of CDK4/6i) and regularly in clinical follow up. Samples were analyzed using the GuardantINFINITY platform. Clinical information, pathologic characteristics, and dates of clinical progression were collected.

Results: 57 patients with 350 clinical timepoints (median of 5 per patient, range 2-15) were evaluated. Median follow up was 28.6m (range: 0.9-64.3m). Median age at diagnosis of mBC was 59 (range: 38-88). CDK4/6i received included 42/57 (73%) palbociclib, 14/57 (25%) ribociclib and 1/57 (2%) abemaciclib; 40/57 (70%) were in combination with an aromatase inhibitor and 17/57 (30%) with fulvestrant. 5/350 (1.4%) of samples failed analysis related to low cfDNA input. ctDNA was detected (by methylation) in 49/57 (86%) at baseline (1 fail, 7 not detected), and 208/345 (60%) of all samples. Median methylation-based tumour fraction (TF) at baseline was 0.0132 (range: 0.000875-0.433); a higher baseline methylation TF (≥1%) was associated with worse CDK4/6i-PFS (14.7m vs. 26.7m; HR: 2.27, 95%CI: 1.12-4.62, p=0.023). 19/49 patients had ctDNA clearance, which was associated with improved CDK4/6i-PFS (34.4m vs. 13.9m; p<0.0001). In longitudinal sampling, methylation TF rose prior to clinical progression and genomic alterations associated with CDK4/6i-resistance were detected, including copy-number loss in *RB1*.

Conclusion: Baseline methylation TF and ctDNA clearance as measured by GuardantINFINITY were prognostic in this cohort. Longitudinal sampling permitted genomic characterization and detection of alterations conferring acquired-resistance prior to clinical progression. Clinical correlates of ctDNA detection, clearance, and further serial genomic analyses will be presented.

#0970 Liquid biopsy-informed precision oncology clinical trial to evaluate the utility of ctDNA comprehensive genomic profiling.

M. Fatteh[1], M. Conroy[1], T. Wanchoo[1], S. Shiqing Teh[1], J. Wehr[1], A. Balan[1], R. Karchin[1], E. Verner[2], K. Karaindrou[1], R. Xian[1], C. Gocke[1], M.-T. Lin[1], P. Fitzpatrick[1], C. L. Hann[1], J. C. Murray[1], V. K. Lam[1], J. L. Feliciano[1], J. R. Brahmer[1], K. A. Marrone[1], P. M. Forde[1], K. Fiallos[1], D. Petry[1], T. Botsis[1], M. Sausen[2], t. Molecular Tumor Board Investigators[1], J. Canzoniero[1], J. Tao[1], V. Anagnostou[1];

[1]Johns Hopkins School of Medicine, Baltimore, MD, [2]Personal Genome Diagnostics/Labcorp, Baltimore, MD

Background: The expanding role of next-generation sequencing (NGS) in precision oncology has led to a paradigm shift towards genotype-targeted therapies, with liquid biopsies (LBs) offering a minimally invasive means of comprehensive genomic profiling.
Methods: This is an observational LB-informed precision oncology clinical trial with primary endpoints to assess feasibility and determine the prevalence of actionable mutations in LB informing genotype-targeted therapeutic recommendations by the Johns Hopkins Molecular Tumor Board (JH MTB; NCT05585684). Secondary endpoints are progression-free and overall survival, ctDNA dynamics assessment, and concordance between plasma and tumor NGS. Target enrollment is 150 patients with advanced solid tumors who have progressed on at least one line of systemic therapy. Serial LB-derived genotypes are obtained at baseline, early on therapy, and upon progression using a CLIA ultra-sensitive 33-gene panel NGS assay (Elio Plasma Resolve, Personal Genome Diagnostics/Labcorp). Variant actionability is assessed by an ensemble knowledgebase, registry, and computational characterization approach, and results are reviewed by the JH MTB, followed by treatment recommendations.
Results: The trial's pre-specified interim analysis included 30 enrolled patients with evaluable LBs; 30 baseline, 13 on-therapy, and 6 progression LBs were analyzed. Twenty-five patients had non-small cell lung cancer among which 9 were EGFR-mutated, 1 patient had small cell lung cancer, 3 patients had gastro-esophageal cancer, and 1 patient had a neuroendocrine tumor. In total, 74 variants were identified across all time points; these were cross-referenced in somatic and germline registries, variant knowledgebases, and the biomedical literature, together with computational characterization of functional consequence to assign mutation actionability. Tumor-confirmed variants comprised 36% of baseline and 42% of both on-therapy and progression variants. At baseline, 20% of the variants were putatively clonal hematopoiesis-derived with similar findings at the on-therapy timepoint. Thirty percent of baseline variants and 33% of variants at progression were deemed actionable. Upon JH MTB review, 29% of patients received a genotype-matched therapeutic recommendation based on LB results, with MTB recommendations followed in 38% of the patients. In analyzing ctDNA dynamics, of the 13 patients with on-therapy samples, 23% showed ctDNA clearance, 31% showed persistence, while 46% had undetectable ctDNA at both time points. Among patients with LBs at the time of progression, a third showed ctDNA emergence, a third had ctDNA persistence, and the remainder had undetectable ctDNA throughout the follow-up period.
Conclusion: Our findings highlight the clinical relevance of liquid biopsies in guiding treatment selection and monitoring.

#0971 Validation of a tumor-naïve circulating tumor DNA (ctDNA) response monitoring panel in advanced non-small cell lung cancer (aNSCLC).

A. C. Chiang[1], R. W. Madison[2], Y. Huang[2], A. Fine[2], D. X. Jin[2], G. R. Oxnard[3], J. Hughes[2], Z. J. Assaf[4], Y. Cao[4], V. Antic[5], O. Gjoerup[2], A. Young[2], D. Fabrizio[2], S. Lakhanpal[6], R. Zuniga[7], K. Schulze[4], L. W. Pasquina[2];

[1]Yale School of Medicine, Dept of Medicine, New Haven, CT, [2]Foundation Medicine, Inc., Cambridge, MA, [3]Boston Medical Center, Boston, MA, [4]Roche/Genentech, South San Francisco, CA, [5]F. Hoffmann-La Roche, Basel, Switzerland, [6]Alabama Oncology, Birmingham, AL, [7]New York Cancer & Blood Specialists, New York, NY

Introduction: Monitoring of ctDNA can be a minimally invasive complement to tumor imaging for assessing treatment effect. Technical limitations require methods to distinguish tumor signal from clonal hematopoiesis (CH), often including non-tumor sequencing. We developed a tumor-naïve panel (FoundationOne® Monitor) to quantify ctDNA tumor fraction (TF). TF analytical validation used peripheral blood mononuclear cell (PBMC) sequencing. We then leveraged plasma collected serially from patients with aNSCLC in the real-world (rw) Prospective Clinico-Genomic (PCG; NCT04180176) study to investigate the utility of TF for monitoring therapy (tx) response.

Methods: TF was quantified using a combination of aneuploidy and variant allele frequencies of genomic alterations (GAs), while excluding CH mutations and aneuploidy using fragmentomic signal from cfDNA. In the PCG study, data from consenting patients were collected from electronic health records from 23 participating Flatiron Health Research Network sites. We analyzed plasma collected 6-15 weeks after start of tx in exploratory and validation cohorts per prespecified criteria. We defined molecular response (MR) as undetectable TF on tx regardless of baseline TF. Hazard ratios (HR) and 95% confidence Interval (CI) were calculated with univariate Cox proportional hazard regression.

Results: For TF validation, 1135 samples separate from the PCG study with paired PBMC results were included. Overall, 24/4274 (0.56%) CH derived non-aneuploidy GAs detected in 1134 samples were falsely classified as somatic. Of these, 4 were detected among 317 samples with no tumor signal, resulting in a false positive TF value (specificity = 98.7%). CH derived aneuploidy was observed in 27 PBMCs and was appropriately filtered during TF estimation in all cases. Assessing the impact of CH aneuploidy filtering on sensitivity, we only identified 1/320 (0.31%) samples where non-CH derived aneuploidy was omitted. To assess clinical validity, 222 patients were analyzed from the PCG study. MR was assessed after a median of 10.8 weeks of tx (IQR 8.9-12.0). In a subset of 152 patients treated with physicians' choice, MR was associated with favorable rw progression free survival (rwPFS: 9.4 v 2.8 months [mo]; HR = 0.30; 95% CI: [0.21-0.44]) and rw overall survival (rwOS: 22.0 v 7.5 mo; HR = 0.33 [0.22-0.49]). We validated this finding on 70 patients receiving immunotherapy (50 with chemo). Again, MR was associated with favorable rwPFS (9.0 v 2.8 mo; HR = 0.28 [0.16-0.51]) and rwOS (20.2 v 9.4 mo; HR = 0.42 [0.23-0.78]).

Conclusions: We describe a highly specific tumor naïve algorithmic filtration of non-tumor signal to enable high confidence ctDNA quantification and MR assessment. On tx MR is associated with favorable outcomes. These findings may enable personalized tx approaches tailored to a patient's risk of progression and downstream cancer morbidity.

#0972 Non-invasive detection of homologous recombination deficiency in metastatic prostate cancer patients.

G. Vlachos, T. Moser, A. Eberhard, L. Glaswitch, J. Blatterer, E. Bauernhofer, N. Monsberger, K. Kashofer, J. Geigl, T. Bauernhofer, E. Heitzer;
Medical University of Graz, Graz, Austria

Background: The recent endorsement of poly ADP ribose polymerase inhibitors (PARPi) has been a breakthrough in managing prostate cancer (PCa) with homologous recombination deficiency (HRD). However, due to its propensity to metastasize to the bone, HRD assessment in tissue biopsy poses a challenge in advanced PCa. Circulating tumor DNA (ctDNA) as a tumor surrogate may be a promising substitute for pinpointing patients who may benefit from PARPi treatment.
Methods: To test whether causes and consequences of HRD can be detected non-invasively in plasma, we pre-selected 139 plasma samples from PCa patients based on aneuploidy screening (mFAST-SeqS). We then applied targeted sequencing using a QIAseq panel including homologous recombination repair (HRR)-related genes as well as genes involved in cell cycle regulation (*TP53, RB1, PTEN*). Putative, pathogenic germline variants were sequencing in constitutional DNA using Sanger sequencing. Moreover, we performed low pass whole genome sequencing to determine the levels of genomic instability using the shallow HRD (sHRD) algorithm.
Results: In our cohort, at least one pathogenic mutation was detected in 68/139 (48.9%) of the patients, of which the majority consisted of alterations in *PTEN*, *TP53* or *RB1* (44/139, 31.7%). Pathogenic *BRCA1*/2 mutations were detected in 13/139 patients (9.4%), the majority of which originated from the germline. In 8/139 patients (5.6%) a pathogenic variant in other HRR genes could be observed and in 3/139 patients (2.2%) *CKD12* mutations were detected. As expected, samples with pathogenic HRR mutations and elevated tumor fraction, presented high sHRD scores (<20) in plasma DNA. In contrast, the majority of high ctDNA samples with mutations in *PTEN*, *TP53* or *RB1* had sHRD score below the cut-off of 20. However, the detection of genomic instability was clearly depending on tumor fractions. Conclusion: Our study indicates that a non-invasive assessment of root causes and subsequent effects of the HRD phenotype in prostate cancer is feasible, and that mutations in HRR correlate with a high genomic instability. However, to detect and quantify genomic instability in plasma, elevated ctDNA levels are required. Based on in-house data from mFAST-SeqS aneuploidy screening of over 900 plasma samples from advanced prostate cancer, approximately 30% of cfDNA samples would have sufficiently high ctDNA fractions for a combined assessment of causes and consequences of HRD, which might be most informative to direct PARPi treatment in PCa.

#0973 Plasma a*ndrogen receptor (AR)* copy number gain at progression in patients randomized in the STAMPEDE phase 3 abiraterone acetate, prednisolone (AAP) and enzalutamide (ENZ) trial: An ancillary biomarker study.

G. Leone[1], F. Orlando[2], S. Thakali[1], S. Lall[1], D. Wetterskog[1], A. Wingate[1], N. W. Clarke[3], N. D. James[4], F. Demichelis[2], G. Attard[1];
[1]University College London (UCL) Cancer Institute, London, United Kingdom, [2]Department of Cellular, Computational and Integrative Biology, University of Trento, Trento, Italy, [3]Christie and Salford Royal NHS Foundation Trusts, Manchester, United Kingdom, [4]Institute of Cancer Research, London, United Kingdom

Addition of ENZ or AAP to androgen deprivation therapy (ADT) as first-line treatment for advanced prostate cancer improves survival compared to ADT alone. Genomic alterations in *AR* associate with resistance to ENZ/AAP when started for castration-resistant prostate cancer (CRPC). We aimed to test whether early use of AAP/ENZ altered the incidence of *AR* alterations at progression. Between July 2014 and March 2016, 1976 patients with metastatic or high-risk locally advanced prostate cancer were randomized to ADT or ADT+ENZ+AAP in the STAMPEDE trial (NCT00268476). Consenting patients were given the option to donate blood for the ancillary biomarker study at trial-defined progression and prior to start of the next line of treatment. We focused on patients who progressed within 4 years from the end of recruitment (early progressors), as these patients represent the greatest unmet need. We obtained plasma DNA at emergence of CRPC from 115 early progressors (ADT n=63, ADT+ENZ+AAP n=52). We performed liquid biopsy-focused, custom, high-coverage targeted enrichment sequencing (PCF-SELECT, Orlando et al, NAR Cancer 2022). We used a bespoke computational pipeline, leveraging allelic imbalance and fragmentome analysis, to detect circulating tumor DNA (ctDNA) in plasma samples and copy number changes. Of 108 samples that passed quality control, 94 were positive for tumor (ADT n=52, ADT+AAP+ENZ n=42). The detection rate and ctDNA fractions were similar between the two treatment groups [ADT: 86.7% (52/60), mean ctDNA fraction 0.18; ADT+ENZ+AAP: 87.5% (42/48), mean ctDNA fraction 0.21; p=0.34]. The proportion of plasma with detectable ctDNA and *AR* gain was significantly higher with ADT+AAP+ENZ vs ADT alone (15/42, 35.7% vs 8/52, 15.4%, p=0.03). We then implemented the same approach on plasma collected from patients progressing on ENZ started for metastatic CRPC in a prospective Phase 3b trial (PRESIDE, NCT02288247): we confirmed a high prevalence of *AR* gain in plasma samples with detectable ctDNA (47.7%, 95% CI 38.8-54.9) in the CRPC setting. Significant copy number aberrations in relevant prostate cancer-related genes/pathways (deletions of *TP53*, *RB1*, *PTEN* or DNA repair genes, or gain of *PI3K*/*AKT1*) were identified in 9 out of 42 evaluable samples in the ADT group and 18 out of 38 evaluable samples in the ADT+ENZ+AAP group (21.4% vs 47.4%, p=0.014). Treatment with ADT+ENZ+AAP increases detection of plasma *AR* gain at emergences of CRPC in early progressors compared to ADT alone. Detection of plasma *AR* gain increases at progression on ADT+ENZ regardless of the treatment setting. The impact of early use of ENZ/AAP on the detection of copy number aberrations, especially homozygous deletions, in other prostate cancer-related genes in plasma requires further investigation.

#0974 DNA methylation and gene expression as determinants of genome-wide cell-free DNA fragmentation.

M. Noe, A. V. Annapragada, Z. H. Foda, J. E. Medina, D. Mathios, S. Cristiano, C. Cherry, D. C. Bruhm, N. Niknafs, V. Adleff, L. Ferreira, H. Easwaran, S. Baylin, J. Phallen, R. B. Scharpf, V. E. Velculescu;
Johns Hopkins University, Baltimore, MD

Cell-free DNA (cfDNA) in the bloodstream is increasingly gaining attention as a diagnostic tool for the early detection of cancer. Nevertheless, the characteristics and sources of cfDNA fragmentation in the blood remain poorly understood. In this study, we sought to unravel the impact of DNA methylation and gene expression on the naturally occurring genome-wide fragmentation of cfDNA. We performed a comprehensive analysis of plasma samples from 969 individuals, including 182 individuals diagnosed with cancer (pancreatic, colorectal, ovarian, lung and breast cancer). In healthy individual cfDNA fragmentation patterns like DNA motifs at cfDNA fraqgments ends, recurrent cfDNA fragment start sites, cfDNA coverage and cfDNA fragment size were compared to publicly available data on cfDNA methylation and gene expression from myeloid cells. We discovered that the ends of cfDNA fragments, particularly those containing CGs or CCGs, displayed a distinct pattern of enrichment or depletion, respectively, at methylated CpG positions throughout the genome. This phenomenon is consistent with structural models suggesting an increased interaction of CG fragment ends with nucleosomes. cfDNA fragments were more prevalent (up to 3.7 fold) and of larger sizes (up to 4-5 base larger) when derived from regions of methylated CpGs or transcriptional start sites of genes that were not actively expressed. Differences in cfDNA fragmentation reflected specific biological pathways associated with their tissue of origin (like E2f transcription factors and blood cell metabolism genes in cfDNA from healthy individuals). Through analyses of cfDNA from patients with cancer, we identified a connection between tumor-related hypomethylation, increased gene expression, and a global reduction in cfDNA fragment size. This connection may offer an explanation for the generally smaller cfDNA fragments found in individuals with cancer. We found that cancer-specific methylation at CpG sites from pancreatic cancers were associated with widespread changes in cfDNA fragment ends, particularly for patients with pancreatic (test statistic = Welch two sample t-test; $p<2.2e-16$) and other cancers. These findings establish a direct link between epigenetic modifications and cfDNA fragmentation that may have implications for non-invasive detection of cancer.

#0975 Genomic landscape of circulating tumor DNA in cervical cancer in Asia: NCCH1905/A-TRAIN trial.

Prathepamalar Yehgambaram[1], Yuki Kojima[2], Kazuki Sudo[2], Shu Yazaki[2], Momoko Tokura[2], Munehiro Ito[2], Mai Hoshino[2], Wong Yoke Fui[3], Pei Jye Voon[4], David SP Tan[5], Arb-aroon Lertkhachonsuk[6], Anh Tuan Pham[7], Thinh Dang Huy Quoc[8], Wan Zamaniah Wan Ishak[9], Hiroshi Yoshida[2], Shinji Kohsaka[10], Yukari Nagasaka[2], Ryunosuke Machida[2], Tomomi Hata[2], Kenichi Nakamura[2], Kan Yonemori[2]

[1]Hospital Kuala Lumpur, Kuala Lumpur, Malaysia,[2]National Cancer Center Hospital, Tokyo, Japan,[3]National Cancer Institute, Putrajaya, Malaysia,[4]Sarawak General Hospital, Sarawak, Malaysia,[5]National University Hospital, Singapore, Singapore,[6]Ramathibodi Hospital, Bangkok, Thailand,[7]National Cancer Hospital, Hanoi, Viet Nam,[8]Ho Chi Minh City Oncology Hospital, Ho Chi Minh, Viet Nam,[9]University Malaya, Kuala Lumpur, Malaysia,[10]National Cancer Center Research Institute, Tokyo, Japan

Background: Cervical cancer is the second most common cancer among women worldwide, with over 500,000 new cases diagnosed annually and a 50% mortality rate in Asia. The incidence and prevalence of cervical cancer is high in Asia due to limited screening, awareness of HPV infection, and access to vaccines. The purpose of this study is to evaluate the comprehensive genomic profiles of circulating tumor DNA (ctDNA) in Asian cervical cancer patients with different histological subtypes and their association with clinicopathological features.
Methods: This is an Asian multicenter prospective observational study conducted by nine institutions in Japan, Singapore, Malaysia, Thailand, and Vietnam (NCT05099978, ClinicalTrials.gov). Eligible patients had histological diagnosis of cervical cancer with metastatic or recurrent disease. Patients on chemotherapy or radiotherapy were excluded. ctDNA was analyzed in blood samples collected at newly initial diagnosis of metastatic disease and/or at disease progression. Genomic profiling was conducted by Guardant360 (Guardant Health).
Results: Ninety-nine samples from 101 cervical cancer patients were analyzed. ctDNA was detected in 70 (70.7%) samples; median time to test results was 11 days. The median number of genomic abnormalities was 1 (range, 0-22). The most frequently altered genes were *PIK3CA* (n=28. 28.3%), *TP53* (n=18, 18.2%), *KRAS* (n=12, 12.1%) and *STK11* (n=6, 6.1%). Clinical trial-related genomic abnormalities were detected in 59 patients (59.6%) with 40 associated with approved drugs in other indication, including those targeting *PIK3CA* mutation (n=28), homologous recombination deficiency (*BRCA1/2*, *ATM* and *CDK12* mutation) (n=5), *ERBB2* amplification (n=4) and *FGFR3*alterations (n=3). In squamous cell carcinoma (n=59), commonly altered genes were *PIK3CA* (n=21, 35.6%), *TP53*(n=12, 20.3%), *ERBB2* (n=5, 8.5%), *NOTCH1* (n=5, 8.5%) and *ARID1A* (n=5, 8.5%). In adenocarcinoma (n=36), commonly altered genes were *KRAS* (n=7, 19.4%), *PIK3CA* (n=6, 16.7%) and *TP53* (n=5, 13.9%). The number of patients with genomic alterations relevant for clinical trials was 39 (66.1%) and 19 (52.8%) for squamous cell carcinoma and adenocarcinoma, respectively. There were no differences in the number of genomic alterations according to prior chemotherapy or radiation therapy.
Conclusion: Comprehensive genomic profiling using liquid biopsy can rapidly identify potential candidates for targeted therapy in cervical cancer patients, regardless of histopathology. Clinical studies of precision medicines in Asia are encouraged for such patients.

#0976 Detection of circulating tumor DNA predicts survival in advanced HCC patients treated with personalized therapeutic DNA cancer vaccine in combination with immune checkpoint blockade.

J. Yan[1], B. Li[2], J. Northcott[2], C. W. Abbott[2], R. M. Pyke[2], R. Perales-Linares[1], N. Cooch[1], S. Rochestie[1], J. Peters[1], E. J. Gane[3], M. Yarchoan[4], T. U. Marron[5], S. M. Boyle[2], I. Csiki[1], R. Chen[2], N. Y. Sardesai[1];

[1]Geneos Therapeutics, Inc., Philadelphia, PA, [2]Personalis, Inc., Fremont, CA, [3]University of Auckland, Auckland, New Zealand, [4]Sidney Kimmel Comprehensive Cancer Center, Johns Hopkins University School of Medicine, Baltimore, MD, [5]Tisch Cancer Institute, Icahn School of Medicine at Mount Sinai, New York, NY

Circulating tumor DNA (ctDNA) has enabled the non-invasive monitoring of molecular residual disease (MRD) which reflects therapeutic response/resistance prior to conventional imaging approaches. However, little is known about the applications of ctDNA in the neoantigen-targeted personalized cancer vaccine setting, potentially due to the limited sensitivity of current ctDNA assays. NeXT Personal®, an ultra-sensitive tumor-informed ctDNA assay was used to longitudinally track ctDNA in advanced hepatocellular carcinoma (HCC) patients treated with GNOS-PV02 (a personalized therapeutic DNA cancer vaccine) in combination with pembrolizumab.

Advanced unresectable or metastatic HCC patients that progressed on, or were intolerant to, first-line TKI therapy were enrolled into the Phase 1b/2a GT-30 study [NCT04251117]. Whole exome/transcriptome tumor sequencing was used for the design of GNOS-PV02. Patients were treated with GNOS-PV02 (1mg; Q3W x 4, Q9W) and plasmid-encoded IL-12 (0.3mg; Q3W x 4, Q9W) in combination with pembrolizumab (200mg; Q3W). Clinical Response was evaluated by RECIST 1.1 at baseline and Q9W. The ctDNA analysis and tracking for progression was performed as an exploratory objective.

Over 200 prospective baseline and on-treatment plasma samples from 31 patients were collected and analyzed using NeXT Personal. WGS was performed to identify up to ~1,800 selected tumor variants to create a personalized panel for MRD detection. NeXT Personal has been analytically validated to detection thresholds down to 1-3 parts per million (PPM) of ctDNA with >99.95% specificity.

ctDNA was detected in 152 of 207 plasma samples with a dynamic range of 1.76 - 166,968 PPM. The limit of ctDNA detection ranged down to 1.05 PPM. 96% (24/25) of patients were baseline ctDNA+. The percentage change of ctDNA relative to baseline at week 9 (C4D1) significantly correlated with best overall response (CR/PR/SD vs. PD: p = 0.0076). The ctDNA change from baseline to week 9 was predictive of OS (P=0.008), with 31.2% 2-yr OS (95% CI: 13.2 - 73.7%) for molecular non-responders vs 100% 2-yr OS (95%CI: 100 - 100%) for molecular responders. In addition, the ctDNA levels at week 9 were predictive of best overall response (P = 0.017). ctDNA burden at week 9 was significantly correlated with overall survival (HR = 5.46, 95%CI: 1.79 - 16.65; P=0.003; C-index = 0.886). ctDNA clearance was observed in all 3 CR patients with a lead time of 483, 126 and 105 days compared with MRI.

This ultra-sensitive ctDNA assay shows significant association between ctDNA change and clinical response and survival, and can be used to accurately predict clinical outcome. The convenience of non-invasive liquid biopsy and rapid availability of data could enable the use of ctDNA to allow real-time monitoring of personalized cancer immunotherapy.

#0977 Germline BRCA1/2 mutations detected by circulating tumor DNA testing in breast cancer patients: A retrospective mutiinstitutional analysis.

Letizia Pontolillo[1], Carolina Reduzzi[1], Andrew A. Davis[2], Arielle J. Medford[3], Annika Putur[3], Lorenzo Gerratana[4], Katherine Clifton[2], Whitney L. Hensing[2], Marko Velimirovic[5], Surbhi Warrior[6], Mara S. Serafini[1], Eleonora Nicolo[1], Laura Munoz-Arcos[1], Jeannine Donahue[1], Charles S. Dai[3], Jennifer C. Keenan[3], Amir Behdad[7], William J. Gradishar[6], Diana Giannarelli[8], Emilio Bria[9], Cynthia X. Ma[2], Aditya Bardia[3], Massimo Cristofanilli[1]

[1]Department of Medicine, Division of Hematology-Oncology, Weill Cornell Medicine, New York, NY,[2]Department of Medicine, Washington University in St Louis School of Medicine, Saint Louis, MO,[3]Massachusetts General Hospital Cancer Center / Harvard Medical School, Boston, MA,[4]CRO Aviano, National Cancer Institute, IRCCS,, Aviano, Italy,[5]Cleveland Clinic, Cleveland, OH,[6]Department of Hematology, Oncology, Robert H. Lurie Comprehensive Cancer Center, Northwestern University, Chicago, IL,[7]Pathology and Laboratory medicine,, Cleveland Clinic, Cleveland, OH,[8]Facility of Epidemiology and Biostatistics, Fondazione Policlinico Universitario A. Gemelli IRCCS,, Roma, Italy,[9]Department of Medical Oncology, Fondazione Policlinico Universitario A. Gemelli IRCCS,Universita' Cattolica del Sacro Cuore, Roma, Italy

Background: The use of circulating tumor (ct) DNA testing allows to detect resistant and actionable somatic alterations and it could be associated with the incidental identification of germline mutations. An univocal variant allele frequency (VAF) threshold to distinguish germinal form somatic mutations has not been assessed yet. We aimed to correlate BRCA1/2 ctdNA detected mutations with germline mutational status to determine potential VAF cutoff.
Materials and methods:We retrospectively analyzed the incidence of both somatic (*s*) and germinal *(g) BRCA1/2* alterations in a multiinstitutional retrospective breast cancer (BC) cohort to assess the VAF threshold for the likelihood of germline mutations' detection by ctDNA next-generation sequencing (Guardant 360) testing. Clinical variables were analyzed using descriptive analyses and receiving operating characteristic (ROC) curves were generated to determine the VAF cutoff.
Results: Two hundred and fourteen patients (pts) with *sBRCA1/2* mutations (including variant of uncertain significant and synonymous) detected by ctDNA testing, referred to the enrolling centers between January 2015 to May 2023 were included in the analysis. The median age at diagnosis was 50 years old (Interquartile range (IQR)43,5-61.5), 43% had a family history of cancer. Hormone receptor positive/HER2 negative was the most represented subtype (68%) followed by the HER2 positive (16%) and triple negative (16%) ones. At ctDNA baseline, 95.8% of pts had a metastatic disease; the main sites of metastases were bone (67.4%) and visceral (59.3%). Ninetyfour (43.9%) and 137 (64%) pts had a *sBRCA1* and *sBRCA2* alterations respectively, while 17 (7.9%) had a co-mutation in *BRCA1* and *BRCA2*. The mean VAF value for *sBRCA1* alterations was 10.1% (standard deviation (SD) 19.5%, range [0.04%-84.3%]) while for *sBRCA2* alterations was 10.8% (SD 18.9%, range [0.21%-80.3%]). The germinal testing, performed per standard of care, was available for 100 pts (46.7%). Among these, 42 (42%) had at least a pathogenic variant detected. A *gBRCA1* mutation was present in 11 (11%) pts while 25 (25%) had a *gBRCA2* mutation. Comparing the somatic and germinal testing, 9/100 pts had a concordance for *BRCA1* detection, the 2 discordant cases had both a low allele frequency *sBRCA2* alterations; the concordance for *BRCA2* detection was instead 100%. An optimal cutoff of 38.4% (AUC 0.98) for *BRCA1* and 19.5% (AUC 0.96) for *BRCA2* was assessed by ROC analysis as the likelihood of a germline meaning of a somatic mutation detected by ctDNA analysis.
Conclusion: The identification of *BRCA1/2* alterations in ctDNA could guide the use of germline testing. The VAF cutoff identified for the likelihood of a germinal mutation is lower than expected, suggesting that a wider population should be screened for germinal mutation with relevant impact on the therapeutic choices and family screening.

#0978 Functional characterization and a real-world clinical laboratory pilot of the Foundation for the National Institutes of Health's (FNIH) circulating tumor DNA (ctDNA) quality control materials (QCMs).

C. P. Paweletz[1], T. D. Forbes[2], G. A. Heavey[1], L. M. Yee[3], H.-J. He[4], Z. He[4], D. E. Connors[5], D. Stetson[6], S. Keating[7], K. D. Cole[4], G. J. Kelloff[3], R. T. McCormack[8], M. P. Williams[2], C. Karlovich[2];

[1]Dana-Farber Cancer Institute, Boston, MA, [2]Frederick National Laboratory for Cancer Research, Frederick, MD, [3]National Cancer Institute, Bethesda, MD, [4]National Institute of Standards and Technology, Gaithersburg, MD, [5]Foundation for the NIH, Bethesda, MD, [6]AstraZeneca, Waltham, MA, [7]CCS Associates, Inc., McLean, VA, [8]Independent, Chester, NJ

Background: Analysis of ctDNA now permits assessment of targetable mutations (e.g. *EGFR* L858R/Ex19del) using noninvasive blood tests. There are several FDA-approved tests using digital PCR (ddPCR) or next-generation sequencing (NGS) and many more laboratory developed tests in use. The FNIH Biomarkers Consortium identified the absence of validated standards to qualify the performance of ctDNA assays as a critical need and set out to aid in the characterization of QCMs. Here we report on a commutability study comparing the performance of three commercial QCMs to clinical samples at or above LoD (limit of detection) and update on a real-world assessment of these QCMs by 11 clinical laboratories spanning 4 continents and 3 assay modalities.

Methods: QCMs were provided by Horizon Discovery (H), Thermo Fisher (T) and SeraCare (S). Clinical samples with known *EGFR* L858R and Ex19del mutations were prepared by diluting specimens at known concentrations into cell-free DNA (cfDNA) from healthy donors. The functional characterization compared detection of the mutations in QCM to clinical samples and consisted of 2 parts: (1) Evaluation of *EGFR* L858R/Ex19del (range 0.1% to 5% allele frequency [AF]) by ddPCR, amplicon and hybrid-capture NGS; (2) Evaluation near the LoD of the amplicon NGS assay at the assay LoD95 of 0.3% AF. For the clinical pilot, participants were sent QCM pools formulated at 0.5% and 1% AF by ddPCR. Some participants also tested clinical specimens with *EGFR* L858R and Ex19del at 0.5% and 1% AF by ddPCR. All participants were blinded to AF and identity of the manufacturer.

Results: For Part 1, QCM results from hybrid-capture NGS of *EGFR* L858R were similar to ddPCR; for Ex19del, QCM AF trended lower compared to ddPCR. In contrast, L858R clinical samples showed a strong positive bias compared to ddPCR. For amplicon NGS, QCMs performed similarly to clinical samples, with amplicon NGS AF closest to ddPCR AF for T QCM. For Part 2, the observed hit rates mostly approximated expected values. For H QCM, observed LoD95 (10% for EGFR L858R; 50% for Ex19del) and subsequent dilution hit rates were lower than expected. For the clinical pilot, median Ex19del AF of amplicon NGS were higher than for hybrid-capture NGS for both the 1% QCM formulations and 0.5% QCM formulations. Median QCM L858R AF were similar for amplicon and hybrid-capture NGS, with greatest contributor to variance being inter-lab differences.

Conclusions: This project, unprecedented in the number of participants and analytical rigor, revealed unexpected differences in performance of both assays and QCMs. These findings merit consideration by laboratories that rely on QCMs to develop and perform assays for ctDNA testing as diagnostics.

#0979 Cell-free DNA fragmentomics and second malignant neoplasm risk in patients with *PTEN* hamartoma tumor syndrome.

D. Liu[1], L. Yehia[2], A. Dhawan[3], Y. Ni[3], C. Eng[2];

[1]Cleveland Clinic Lerner College of Medicine, Cleveland, OH, [2]Cleveland Clinic Lerner Research Institute, Cleveland, OH, [3]Cleveland Clinic, Cleveland, OH

Individuals with *PTEN* hamartoma tumor syndrome (PHTS) harbor germline *PTEN* variants that confer a significantly increased lifetime risk of various organ-specific cancers, and a 7-fold increased risk of second primary malignant neoplasms (SMNs). Currently, there is no reliable biomarker that can accurately predict which individuals with PHTS will develop malignancies, let alone SMN. Currently, there is no reliable biomarker that can accurately predict which individuals with PHTS will develop malignancies, let alone SMN. Despite the highly promising value of cell-free DNA (cfDNA) as a biomarker for underlying sporadic cancers, the utility of cfDNA in individuals with hereditary forms of cancer remains poorly understood. Thus, we performed a retrospective study in prospectively accrued patients with PHTS investigating whether plasma cfDNA profiles can be leveraged as a predictive marker of cancer risk. We performed ultra-low pass whole genome sequencing of cfDNA of archived plasma samples from patients with PHTS without cancer (N = 50), and those with cancer (N = 49). Those with cancer included patients with only a single primary malignant neoplasm (PMN, N = 23) and patients with second malignant neoplasms (SMN, N = 26). To investigate cfDNA profiles in patients with PHTS and subclinical cancer, we included nine patients with plasma archived before their cancer diagnosis. We observed that patients with PHTS and SMNs have significantly decreased proportion of di- and tri-nucleosome-associated cfDNA fragments compared to patients with PMNs and those without cancer. Furthermore, SMN status was associated with increased genome-wide fragmentation (ratio of short to long fragments) of mono- (OR 2.37, 95% CI [1.09, 7.27]; P = 0.025) and di-nucleosome-associated (OR 3.03, 95% CI [1.07, 15.7]; P = 0.029) cfDNA fragments, even after controlling for age at plasma draw and phenotypic burden. Fragment end profiling was performed by calculating the frequencies of the first 4-nucleotide sequence (4-mer end motif) at each 5' end of cfDNA fragments. We identified 35 differentially abundant 4-mer end motifs when comparing patients with SMN to those without cancer. Patients with PHTS and SMNs were characterized by a decrease in A-end motifs with concurrent increases in G- and T-end motifs. Increased frequency of C-motifs—namely CC- and CA-end motifs—appeared to be unique to patients who had plasma drawn before their SMN diagnosis, a potential marker for active cancer. Our findings provide evidence that cfDNA fragmentomic features can be leveraged as a potential marker of individual SMN risk in PHTS. These results may facilitate earlier cancer detection and intervention as well as prevent unnecessary high-risk cancer surveillance and prophylactic surgeries in this vulnerable population.

#0980 Plasma tumor fraction is an independent prognostic marker of response to front line chemotherapy in high-grade serous epithelial ovarian cancer: The MITO-16a/MANGO-OV2a/ clinical trial experience.

S. Marchini[1], L. Paracchini[1], L. Arenare[2], G. Scambia[3], C. Pisano[4], R. Zadro[1], L. Mannarino[1], A. Ferrero[5], P. Chiodini[6], D. Califano[7], S. Pignata[8], M. D'Incalci[9]; [1]Humanitas Research Hospital, Milano, Italy, [2]Clinical Trial Unit, Istituto Nazionale Tumori, IRCCS, Fondazione G. Pascale, Naples, Italy, Naples, Italy, [3]IRCCS Policlinico Gemelli,, Rome, Italy, [4]Istituto Nazionale Tumori, IRCCS, Fondazione G. Pascale, Naples,, Naples, Italy, [5]University of Torino, Mauriziano Hospital, Tourin, Italy, [6]Universita degli Studi della Campania, Naples, Italy, [7]Istituto Nazionale Tumori IRCCS e Fondazione G. Pascale, Naples, Italy, [8]Istituto Nazionale Tumori, IRCCS, Fondazione G. Pascale, Naples, Italy, [9]Humanitas University, Milano, Italy

Background. Although 80% of high grade serous ovarian cancer (HGSOC) patients are initially responsive to platinum (Pt)-based chemotherapy, the majority of them experience relapse with a progressive Pt-resistant disease. One of the most challenging issue that hampers the possibility to effectively treat relapsed disease is the lack of biological information about tumor recurrence. To date, the Pt-free interval (PFI), an empirical measure of the time lagging between the end of front-line chemotherapy and relapse, is the only and widely accepted parameter to predict patient outcome and sensitivity to Pt second-line chemotherapy. We have previously demonstrated that analysis of circulating tumor DNA (ctDNA) by low pass whole genome sequencing (sWGS) is a suitable tool to predict patient outcome and to intercept early signs of relapsed disease (Paracchini et al . PMID:33323403). In the present study, we quantified the percentage of tumor fraction (TF) in plasma of patients enrolled within the frame of a phase III clinical trial (MITO-16A/MaNGO-OV2A-EUDRACT number: NCT01706120) to demonstrate, at baseline, the prognostic value of untargeted ctDNA analysis.

Methods. 172 eligible patients enrolled with the frame of the MITO-16A/MaNGO-OV2A clinical trial, for whom plasma sample was collected at chemotherapy before chemotherapy, were selected for the study. For each plasma sample, circulating-free DNA (cfDNA) was purified and whole genome libraries (HyperPlus, Roche) sequenced (mean coverage 0.5X). ichorCN algorithm was used to infer the percentage of TF, as previously published (Paracchini et al . PMID:33323403).

Results. In 168 out of 172 plasma samples analyzed, the TF was detectable and it ranged from 2.4% to 47%. Cox-model univariate analysis with patients' overall survival (OS) and Progression-Free Survival (PFS), indicates association of TF levels with both OS and PFS ($p<0.001$). The prognostic relevance of TF was also confirmed in multivariate analysis, where, considering CA-125, residual tumor, stage of disease, histology and age as co-variables, TF maintained its statistical significance in PFS (HR = 2.1, CI 95%, p-value < 0.003).

Conclusion. Retrospective analysis of baseline plasma samples collected within the frame of the MITO-16A/MaNGO-OV2A clinical trial, demonstrated that the percentage of TF is an independent prognostic marker of relapse. This finding confirms the importance of liquid biopsy analysis based on untargeted sWGS tool as an innovative approach to predict response to front line therapy and patient's outcome

#0981 Robustness of fragmentation-based cell-free DNA approaches to clonal hematopoiesis.

S. Cristiano[1], B. Alipanahi[1], J. E. Medina[1], L. Rinaldi[1], N. Dracopoli[1], R. B. Scharpf[2], A. Leal[3], V. E. Velculescu[2], J. Tom[1];
[1]Delfi Diagnostics, Baltimore, MD, MD, [2]Johns Hopkins University, Baltimore, MD, MD, [3]New York University Grossman School of Medicine, New York, NY, NY

INTRODUCTION: Clonal hematopoiesis (CH) is the result of the clonal expansion of hematopoietic stem cells which acquire and pass on somatically gained mutations, including SNVs as well as arm level losses and gains, defined here as mosaic deletions and amplifications (mDAs). The proportion of blood cells in circulation containing CH alterations increases with age and environmental exposures such as smoking, leading to a higher prevalence in many high-risk cancer screening populations. CH remains a major confounder for mutation-based liquid biopsy tests evaluating circulating cell-free DNA (cfDNA), since these assays are unable to discriminate between mutations originating from the tumor as opposed to CH. While the impact of CH mutations on fragmentation-based methods of detecting ctDNA appears to be limited, the effect of mDAs has not yet been explored.

METHODS: To assess the impact of mDAs on screening efforts using whole genome sequencing (WGS) of cfDNA, we performed copy number analyses on cfDNA from plasma collected from 895 individuals consisting of high-risk individuals meeting the USPSTF guidelines for annual lung cancer screening using low-dose computed tomography. From a subset of 203 available donors (157 without cancer and 46 with lung cancer), matched genomic DNA from white blood cells (WBCs) were extracted from the isolated buffy coat and WGS was performed to evaluate whether ploidy in cfDNA plasma is derived from WBCs. Genome-wide fragmentation features (short to long ratios and fragment size densities), coverage-based statistics, and copy number (CN) statistics adjusting for mDAs were calculated (CN_{adj}). Machine learning models to calculate the probability of cancer based on these features were then derived.

RESULTS: 3.8% (95% CI 0.9%-6.8%) of individuals without cancer had an mDA in their WBCs that were also observed in the plasma ($p < 0.01$, permutation test). Fragmentation features were not different in regions with mDAs in individuals without cancer ($p = 0.619$; permutation test) but were altered in regions of tumor-derived chromosomal changes in patients with cancer ($p < 0.01$; permutation test). Coverage-based statistics were impacted by mDAs ($p < 0.01$; Wilcoxon test). Machine learning models fit with CN_{adj} showed improved performance over CN. However, machine learning models fit with fragmentation features compensated for this difference overall showing robustness to mDAs ($p = 0.45$; bootstrap) demonstrating the robustness of cfDNA fragmentomes for detecting lung cancer.

CONCLUSIONS: While coverage-based statistics of WGS analyses of cfDNA may be affected by mDAs, fragmentation-based approaches relying on cfDNA fragment length are robust to effects of CH. CN_{adj} is an improved statistic for detecting tumor-derived chromosomal copy number changes in cfDNA, providing increased specificity by conditioning on fragment size distributions.

#0982 Variation of cell-free DNA concentrations in liquid biopsies.

S. Short[1], A. V. Annapragada[1], J. E. Medina[1], Z. H. Foda[1], D. Mathios[2], C. Hruban[1], E. J. Chiao[1], K. Boyapati[1], A. Bartolomucci[1], K. Boyapati[1], V. Adleff[1], R. B. Scharpf[1], V. E. Velculescu[1], J. Phallen[1];

[1]Johns Hopkins Sidney Kimmel Comprehensive Cancer Center, Baltimore, MD, [2]Washington University School of Medicine Siteman Comprehensive Cancer Center, St. Louis, MO

Introduction: Liquid biopsies are promising noninvasive tools for cancer detection. Variation in cell-free DNA concentrations (cfDNA-conc) has been observed between individuals with and without cancer. We assessed cfDNA-conc in 2287 treatment-naive individuals including those without cancer, with benign or high-risk conditions, or with one of eight cancer types.

Methods: Plasma (0.3 to 9.8 mL) was separated from whole blood collected in Streck or EDTA tubes from individuals with bile duct, breast, colorectal, gastric, ovarian, liver, lung, pancreatic, or metastatic cancer (n=23, 54, 28, 26, 264, 75, 180, 31, 22, respectively) as well as benign or high-risk conditions (n=550, 133, respectively) such as cirrhosis or hepatitis B or C virus infection (HBV/HCV), and without cancer (n=901). cfDNA was extracted using the Qiagen QIAamp Circulating Nucleic Acid Kit. Quality and quantity were assessed using the High Sensitivity DNA assay on the Agilent Bioanalyzer. Total amount (ng) of cfDNA from all nucleosomal peaks was evaluated per volume (mL) of plasma to assess significance across cohorts using unpaired two-sample Wilcoxon tests.

Results: We observed that in individuals without cancer, cfDNA-conc increased with age (Pearson R^2=0.59; 18-40yrs vs 41-55yrs, vs 56-65yrs, vs 66-85yrs; p=2.31E-09, 1.50E-12, 8.31E-17, respectively). No difference was observed between cfDNA-conc from EDTA and Streck plasma from the same individual (n=9, p=0.359, Wilcoxon signed-rank test two-tailed). Individuals with benign adnexal masses or cirrhosis had similar cfDNA-conc compared to those without cancer while individuals with benign lung lesions or HBV/HCV had significantly different cfDNA-conc (p=0.70, 0.35, 6.96E-04, 1.88E-09, respectively). These observations were not affected by age. Individuals with cancer had significantly higher cfDNA-conc compared to those without cancer (bile duct p=2.08E-14, breast p=4.44E-16, colorectal p=6.04E-10, gastric p=5.93E-04, ovarian p=9.99E-16, liver p=1.22E-15, lung p=0, pancreatic p=8.57E-03, metastatic p=1.18E-06). Ovarian cancer exhibited higher cfDNA-conc than benign adnexal masses which was more pronounced in later stage disease (I/II p=3.83E-06, III/IV p=8.18E-08). Compared to cirrhosis or HBV/HCV we observed a stepwise increase in cfDNA-conc in liver cancer with progressing stage (0/A p= 6.50E-04, B p= 5.69E-10, C p= 1.47E-08). Higher cfDNA-conc were also observed with higher stage of lung cancer compared to benign lung lesions (I/II p=4.99E-03, III/IV p=3.89E-06). Using cfDNA-conc (ng/mL) as a single feature, we distinguished individuals with and without cancer with an AUC of 0.72 (95% CI=0.70-0.75).

Conclusions: In a cohort of 2287 individuals, we observed cfDNA-conc increases with age and cancer stage that varied across cancer types. As a classifier, cfDNA-conc can be predictive of cancer status, yet further work is needed to understand the contribution of other comorbidities.

#0983 Epigenomic analysis of plasma cell-free DNA identifies stemness features associated with worse prognosis in AR-altered lethal metastatic castration resistant prostate cancer.

P. S. Chauhan[1], I. Alahi[1], S. Sinha[1], R. Mueller[1], A. L. Shiang[1], J. Webster[1], H. X. Dang[1], D. Saha[1], L. Greiner[1], B. Yang[1], E. M. Ledet[2], R. K. Babbra[3], W. Feng[1], P. K. Harris[1], F. Qaium[1], E. B. Jaeger[2], P. J. Miller[2], S. A. Caputo[2], O. A. Sartor[4], R. K. Pachynski[1], C. A. Maher[1], A. A. Chaudhuri[1];
[1]Washington University in St. Louis, St. Louis, MO, [2]Tulane University School of Medicine, New Orleans, LA, [3]Wilmot Institute Cancer Center, University of Rochester Medical Center, Rochester, NY, [4]Mayo Clinic, Rochester, MN

Background: Metastatic castration-resistant prostate cancer (mCRPC) resistant to androgen receptor (AR)-targeted agents is often lethal. Unfortunately, biomarkers for this deadly disease remain under investigation, and underpinning mechanisms are ill-understood. Here, we applied epigenomic approaches to identify cell-free (cf) DNA features associated with these lethal AR-resistant mCRPC patients.
Methods: Plasma from 99 mCRPC patients was collected from two independent institutions, either prior to first-line AR-targeted therapy (n = 63) or during treatment (n = 36). We applied EnhanceAR-Seq to detect alterations in the *AR* locus including the upstream enhancer. We then applied genome-wide cfDNA epigenomics to 43 pre-treatment plasma samples and performed both fragmentomics and methylation sequencing to delineate the biology of *AR*/enhancer-altered lethal mCRPC. Finally, we identified stemness genes by applying CytoTRACE to external single-cell RNA-seq data from mCRPC, and applied these to cfDNA via promoter-level methylation analysis. We then assessed these stem-associated genes in tumor bulk RNA-seq data from an independent mCRPC cohort.
Results: *AR*/enhancer alterations were detected in 44% of pre-treatment cfDNA samples and correlated with significantly worse progression-free survival (PFS) (HR = 2.12, P = 0.01) and overall survival (OS) (HR = 2.48; P = 0.02). *AR*/enhancer alterations were detected in 19% of on-treatment cfDNA samples and were also associated with profoundly worse PFS (HR = 15.38, P = 0.0003) and OS (HR = 15.53, P = 0.002). Further, genome-wide cfDNA fragmentomic analysis revealed that binding sites for developmentally relevant transcription factors such as *FOXA1*, *NKX-3* and *HOXB13* were significantly more accessible in *AR*/enhancer-altered lethal mCRPC patients. Gene set enrichment analysis of the 20 most accessible transcription factors revealed several pathways associated with stem cell development. Interestingly, the 10 most stem-associated genes obtained using CytoTRACE applied to an external cohort of single-cell RNA-seq data from mCRPC (He et al. 2021) were promoter-hypomethylated in the plasma cfDNA of *AR*/enhancer-altered lethal mCRPC patients (P = 0.005). Further, metagene analysis of these stem-associated genes revealed worse PFS by Kaplan-Meier analysis (P = 0.04), which was confirmed by multivariate cox proportional hazards modeling. Our stemness metagene further stratified overall survival (P = 0.03) when applied to an external cohort of 80 mCRPC patients from Abida et al. 2019.
Conclusions: Alterations in *AR* including the upstream enhancer are remarkably prognostic in mCRPC with pre-treatment predictive potential. The mechanism can be inferred via cfDNA epigenomic analysis and appears to involve increased tumor cell stemness in *AR*-altered lethal mCRPC.

#0984 Optimizing first-line systemic therapy selection in advanced hepatocellular carcinoma (HCC): A biomarker approach using circulating cell-free DNA (cfDNA) (atezolizumab plus bevacizumab vs. lenvatinib vs. sorafenib).

S. Park[1], B. Kim[2], Y.-e. Lee[3], J. Shim[1], D. Lee[1], J. Choi[1], E.-H. Cho[3];
[1]Asan Medical Center, University of Ulsan, Seoul, Korea, Republic of, [2]National Cancer Center, Goyang, Korea, Republic of, [3]GC Genome, Yongin, Korea, Republic of

Background: With the emergence of new immune checkpoint inhibitors and tyrosine kinase inhibitors for advanced HCC, determining the optimal first-line therapy is challenging due to the lack of precise biomarkers. This underscores the urgent need for biomarker-based strategies for treatment decisions.
Methods: This prospective biomarker study analyzed plasma cfDNA from 267 advanced HCC patients treated with first-line sorafenib (S) (n=212), lenvatinib (L) (n=32), or atezolizumab plus bevacizumab (AteBev) (n=23). Low-depth whole-genome sequencing was performed on cfDNA to identify genome-wide copy number alterations (CNAs). The 'I-score' was established to quantify genomic instability, calculated as the sum of absolute Z-scores of sequenced reads for each chromosome. The treatment outcomes of the three different therapies were compared based on the I-score. The I-score cutoff to differentiate high from low genomic instability was set the level separating progressive disease (PD) from non-PD at the first response evaluation
.Results: Patient demographics and disease characteristics were predominantly male (90.6%) with a median age of 59 years. The majority had an ECOG performance status of 1 (55.4%), HBV etiology (81.3%), and were classified as Child-Pugh class A (88.8%), with most presenting at BCLC stage C (95.1%). The high I-score group (n=164) exhibited a higher prevalence of macrovascular invasion (56.8% vs. 24.6%; p<0.001), lymph node metastasis (39.6% vs. 27.2%; p=0.038), and bone metastasis (14.6% vs. 4.9%; p=0.012) but lower peritoneal metastasis (5.5% vs. 12.6%; p=0.039) compared to the low I-score group (n=103). The high I-score group showed a worse disease control rate (50.6% vs. 74.8%; p<0.001), shorter time to progression (TTP) (median, 2.1 vs. 4.3 months; p<0.001), and poorer overall survival (OS) (6.0 vs. 18.5 months; p<0.001) compared to the low I-score group. Treatment efficacy varied within the high I-score group, with AteBev showing the most favorable outcomes: the median TTP was 6.0 months for AteBev vs. 4.1 months for L vs. 1.8 months for S (p=0.005), and the median OS was not reached for AteBev vs. 7.6 months for L vs. 5.4 months for S (p=0.036). However, in the low I-score group, there were no significant differences in TTP and OS among the treatment types: the median TTP was 9.4 months for AteBev vs. 3.9 months for L vs. 4.2 months for S (p=0.665), and the median OS was not reached for AteBev vs. 9.9 months for L vs. 18.8 months for S (p=0.412).
Conclusions: The I-score, reflecting genome-wide CNA in cfDNA, has potential as a prognostic biomarker for outcomes in advanced HCC patients receiving first-line treatments. It may be instrumental in guiding the selection of the most appropriate therapy.

#0985 An effective cfDNA methylation-based assay in discriminating primary liver cancer from cirrhosis or chronic hepatitis virus infection: marker discovery, phase I pilot, and phase II clinical validation.

Yang Tian[1], Yanan Wang[2], Mingxin Pan[3], Lei Zhang[4], Qiancheng You[4], Bingsi Li[4], Shangli Cai[4], Feng Shen[1], Guoyue Lv[5]

[1]Department of Hepatobiliary Surgery, Eastern Hepatobiliary Surgery Hospital, Navy Medical University, Shanghai, China,[2]Phase I Clinical Trials Unit, First Hospital of Jilin University, Changchun, China,[3]Department of Hepatobiliary Surgery II, General Surgery Center, Zhujiang Hospital, Southern Medical University, Guangzhou, China,[4]Burning Rock Biotech, Guangzhou, China,[5]Department of Hepatobiliary and Pancreatic Surgery, General Surgery Center, First Hospital of Jilin University, Changchun, China

Background: Early detection of primary liver cancer (PLC) in individuals with liver cirrhosis (LC) or chronic hepatitis virus infection (CHVI) improves survival. Timely, effective, and affordable tools with high sensitivity are urgently needed in clinical practice.
Methods: Tissue and/or plasma samples from 159 healthy individuals and 89 PLC, LC, or CHVI patients were sequenced by a targeted methylation panel (~70,000 CpGs) to screen candidate methylated DNA markers (MDMs). In phase I, the performance of each selected MDM was validated in 175 plasma samples (PLC, n=101; LC/CHVI, n=74) by a CO-methylation aMplification rEal-Time PCR (COMET) assay. Logistic models were then trained and validated in phase II with 310 plasma samples (hepatocellular carcinoma [HCC], n=212; combined hepatocellular-cholangiocarcinoma [cHCC-CC], n=12; LC/CHVI, n=106; training vs. validation, 2:1).
Results: The methylation levels of eleven selected MDMs with top performance showed a significant increase in PLC compared with LC/CHVI in both tissue and plasma samples ($P<0.05$). In phase I, eight of the above eleven MDMs with an area under the curve (AUC) over 0.80 to differentiate PLC and LC/CHVI were chosen for further investigation. In phase II, the MDM-based logistic model achieved sensitivity of 87.2% (95% confidence interval [CI], 80.8%-92.4%) and 88.0% (78.4%-94.4%), at respective specificity of 97.1% (90.1%-99.7%) and 100% (90.3%-100%) in the training and validation sets. In the validation set, sensitivity in patients with BCLC stage 0, diameter<3 cm, AFP-negative, and PIVKA-II-negative was 90.0% (55.5%-99.7%), 88.9% (65.3%-98.6%), 80.6% (64.0%-91.8%), and 81.3% (54.4%-96.0%), respectively. The classifier achieved similar sensitivity in patients with or without HBV/HCV infection (88.2% vs 90.0%). Additionally, our model detected 19 of 24 (79.3%, 57.8%-92.9%) intrahepatic cholangiocarcinoma. Combining AFP and PIVKA-II, the model achieved higher sensitivity of 93.3% (85.1%-97.8%) and specificity of 100.0% (90.3%-100%).
Conclusion: In conclusion, the present study demonstrated the feasibility of using an easy-to-implement cfDNA methylation assay (COMET) to discriminate early-stage liver cancer from other liver diseases, with superior accuracy over AFP and PIVKA-II. Notably, the combination of the COMET, AFP, and PIVKA-II increased the overall sensitivity, indicating the potential benefit of integrating these approaches in clinical practices. Moving forward, further investigation is needed to validate these findings in larger prospective clinical studies.
Keywords: primary liver cancer, early detection, liver cirrhosis, chronic hepatitis virus infection, methylated plasma DNA marker.

#0986 Mathematical modeling of ctDNA dynamics to predict utility of ultrasensitive MRD assays in early stage non-small cell lung cancer (NSCLC).

J. S. Goldstein[1], C. Abbosh[2], A. A. Alizadeh[1], M. Diehn[1], D. M. Kurtz[1];
[1]Stanford University, Stanford, CA, [2]AstraZeneca, Cambridge, United Kingdom

***Background*:** ctDNA assay use for minimal residual disease (MRD) detection in early stage NSCLC has been limited by suboptimal sensitivity of first generation assays. It is unclear how improving assay limit of detection (LOD) would translate to improvements in clinical sensitivity. Here, we performed mathematical modeling of ctDNA dynamics after curative-intent treatment in early stage NSCLC to predict the clinical impact of MRD assays with improved analytical sensitivity.
***Methods*:** We analyzed a recently reported dataset of post-surgical ctDNA MRD surveillance in early stage NSCLC (Abbosh et al., Nature 2023) to investigate ctDNA growth dynamics. Of 70 relapsed patients in this cohort, 23 had 3 consecutive ctDNA-positive samples with no intervening therapy. We used these to generate patient-specific mathematical models for ctDNA variant allele fractions (VAF) over time, initially assuming exponential growth. We assessed this assumption by creating log-linear models for ctDNA increase in these cases. Using slopes of the log-linear models, we calculated patient-specific doubling times and assessed their relation to stage, histology, and outcome. We used the log-linear models to simulate a VAF distribution each day after surgery, enabling projection of clinical sensitivities and estimation of lead times for recurrence detection at varying LODs.
***Results*:** For the 23 cases with 3+ consecutive ctDNA positive samples, we developed log-linear models for ctDNA VAF growth, which were strongly correlated ($r > 0.5$) in 18/23 (78%) patients (median $r = 0.89$), supporting that ctDNA can be modeled as exponential growth. We calculated ctDNA doubling times for the 18 patients with exponential ctDNA kinetics and 10 patients with 2 consecutive ctDNA positive samples. Doubling times were remarkably consistent with median 51 days (IQR 40-79). Doubling times were longer for stage I tumors compared to stage II/III ($p = 0.04$) but were not different between NSCLC subtypes. Doubling time correlated with time to clinical relapse, with patients having more rapid ctDNA growth relapsing earlier ($r = 0.52$, $p=0.03$).
Finally, we used patient-specific log-linear models to project ctDNA VAFs at a landmark 30 days after surgery. By improving the LOD for ctDNA detection from 10^{-4} to 10^{-6}, the projected clinical sensitivity doubled (from 43% to 86%). Simulations predicted that this improvement in sensitivity would increase median lead time from 183 days for LOD=10^{-4} to 349 days for LOD=10^{-6} ($p<0.0001$).
***Conclusion*:** For most relapsed NSCLC patients, the natural history of ctDNA MRD growth can be reliably modeled with exponential growth kinetics. ctDNA doubling time is associated with stage and clinical outcome. Ultrasensitive MRD assays with LOD of 10^{-6} are predicted to meaningfully improve clinical sensitivity at the post-surgical landmark and to increase the lead time for MRD detection before relapse.

#0987 Novel ALK mutations in EML4::ALK+ NSCLC resistant to TKIs identified by liquid biopsy.

Federica Malighetti[1], Matteo Villa[1], Elisa Sala[2], Geeta Sharma[1], Giulia Arosio[1], Maria Gemelli[2], Chiara Manfroni[1], Diletta Fontana[1], Nicoletta Cordani[1], Raffaella Meneveri[1], Alfonso Zambon[3], Rocco Piazza[1], Fabio Pagni[1], Diego Cortinovis[1], Luca Mologni[1]

[1]University of Milano-Bicocca, Monza, Italy,[2]Fondazione IRCCS San Gerardo dei Tintori, Monza, Italy,[3]University of Modena and Reggio Emilia, Modena, Italy

The identification of Anaplastic Lymphoma Kinase (ALK) chromosomal translocations led to the development of effective targeted therapies in a subset of Non-Small Cell Lung Cancer (NSCLC) patients. Several drugs are currently in clinical practice for advanced ALK+ NSCLC. However, resistance remains a challenge in these patients. The possibility to analyze circulating tumor DNA (ctDNA) with non-invasive methods can greatly improve prognostic capabilities, by allowing early detection of relapse and of drug-resistant mutations from peripheral blood. We report a series of 15 consecutive relapsed NSCLC patients (12 ALK+, 3 ROS1+) treated at the Fondazione IRCCS-San Gerardo dei Tintori (Monza, Italy) that were investigated by liquid biopsy at tyrosine kinase inhibitor (TKI) failure, through amplicon deep sequencing of the *ALK/ROS1* kinase domains. Median DNA yield was 4.8 ng per ml of plasma and mean fragment size was 176 bp. Mutational hotspot coding regions of ALK and ROS1 genes were amplified by high-fidelity PCR and sequenced. Mean coverage of called variants was 24,687x. The threshold for mutation calling was set at 0.6%, after correcting for mapping quality, minimum coverage, and strand bias. Analysis of background signal on healthy control DNA identified 0.0024 mismatches per mapped base. Overall, plasma ctDNA analysis detected an ALK mutation in 7/18 relapse samples from 7/15 patients. No ROS1 mutations were found in ROS1 fusion-positive patients. Among 12 patients carrying an EML4::ALK fusion, 10 variants potentially driving resistance were found. Along with mutations that were previously identified (L1196M/G1202R, E1154K, F1174L), novel ALK variants were detected such as L1198R, T1211I, C1235R, C1237Y, L1196P. Mutations were characterized for sensitivity to ALK inhibitors in a BaF3-EML4::ALK cell model, using cell proliferation assays and western blotting to evaluate the effects on ALK phosphorylation. C1237Y and L1196P mutants appeared to resist all TKIs; hence, we further tested their sensitivity to novel investigational drugs, zotizalkib and repotrectinib. Both mutants demonstrated resistance, suggesting that these two mutations confer broad resistance to TKIs. Molecular modelling of C1237Y and L1196P mutants was run to elucidate the mechanisms of resistance. The ADP-C1237Y complex showed a much smaller root-mean-square deviation than ADP-WT, indicating a higher affinity/activity of the mutant. L1196 interacts hydrophobically with a methyl group of lorlatinib, P1196 is predicted to lose such interaction, while ATP binding is not affected. The presence of C1237Y and L1196P variants, is a relevant finding due to their resistance, even after the exposure to the fourth-generation inhibitor zotizalkib. The clonal selection of these mutations, made by second/third generation ALK TKIs may lead to a complete refractory status, which would then render TKIs useless in a sequential therapeutic strategy.

#0988 Genome-wide repeat landscapes in cancer and cell-free DNA.

A. Annapragada, N. Niknafs, J. R. White, D. C. Bruhm, C. Cherry, J. E. Medina, V. Adleff, C. Hruban, D. Mathios, Z. H. Foda, J. Phallen, R. B. Scharpf, V. E. Velculescu;
Johns Hopkins University School of Medicine, Baltimore, MD

Introduction: Repeat sequences comprise >50% of the human genome and structural and epigenetic changes in these regions are implicated in cancer. However, no systematic analysis of the compendium of repeat sequences has ever been performed in human cancer or cell-free DNA (cfDNA), largely due to the inability to identify and quantify repeat sequences genome-wide. We describe here the first comprehensive analysis of genome-wide repeat landscapes in cancer and demonstrate their utility in cfDNA liquid biopsies.
Methods: We developed ARTEMIS (Analysis of RepeaT EleMents in dISease) an alignment-free, genome-wide approach for analyzing repeat landscapes in short read sequencing. This approach uses a *de novo* search of short sequences (kmers) in the telomere to telomere (chm13) reference genome to identify 1.2 billion 24-mers uniquely defining 1280 individual repeat types occurring genome-wide across 57 subfamilies and 6 families. We analyzed ARTEMIS kmers in whole genome sequences of 525 matched tumor/normal pairs from breast, colorectal, liver, lung, ovarian, cervical, prostate, thyroid, head and neck, gastric, and bladder cancers in the Pan Cancer Analysis of Whole Genomes (PCAWG), and in low coverage (1-2x) whole genome sequences of 1450 cfDNA samples from individuals with and without 8 types of cancer.
Results: Analysis of ARTEMIS kmer repeat landscapes in 525 PCAWG tumors identified changes in all 1280 repeat element types, including 820 novel elements not previously known to be altered in cancer. A median of 807 repeat elements (range 246-1280) were altered in each tumor compared to its matched normal. The majority of changes were in repeat elements not previously described as altered in tumorigenesis and were most frequently found within Satellites, LINEs and SINEs, though changes were also observed in LTRs, Transposable Elements, and RNA Elements. A cross-validated cfDNA model using repeat landscapes (ARTEMIS) and fragmentation features (DELFI) detected individuals in a diagnostic cohort (n=287) across all stages of lung cancer with high performance (AUC 0.91, 95% CI 0.88-0.95) and was externally validated in a separate population (n=513). The locked model generated scores that correlated with circulating tumor mutant allele fractions for patients (n=19) undergoing targeted lung cancer therapy ($r=0.80$, $p<2.2e-16$), and stratified progression-free survival ($p<0.001$). ARTEMIS repeat landscape analyses of cfDNA also detected liver cancer in a high-risk cohort (n=208) of individuals with cirrhosis or viral hepatitis (AUC 0.91, 95% CI 0.87-0.95), and identified tissue of origin among seven tumor types (n=423).
Conclusions: ARTEMIS reveals genome-wide repeat landscapes in human cancer, including in 820 novel elements not previously known to be altered in tumorigenesis. These repeat landscapes that can now be described are evaluable in the circulation and provide an avenue for noninvasive detection and characterization of cancer.

CLINICAL RESEARCH: Clinical Research in Special Populations
Poster Session

#0991 Unraveling the role of nicotinamide adenine dinucleotide precursors in pancreatic cancer biology.

F. Nakazzi[1], M. Zarei[1], H. J. Graor[1], A. W. Loftus[2], O. Hajihassanni[1], J. M. Winter[2];
[1]Case Western Reserve University, Cleveland, OH, [2]University Hospitals, Cleveland, OH

Introduction: Pancreatic cancer has the lowest 5-year survival rates among all cancers because of the challenges with early detection, its aggressive nature, and resistance to chemotherapy; this makes prevention a promising approach for reducing related mortalities. The disease is predominantly diagnosed in individuals over 60, suggesting that age-related physiological decline impacts its onset; therefore, delaying aging hallmarks may delay its onset. Nicotinamide dinucleotide (NAD+) precursors may hold a unique advantage over other geroprotectors because they target multiple aging hallmarks. Heron, we investigated how NAD+ supplementation impacts normal human pancreatic ductal epithelial cells (HPDE) under stress as a surrogate for cancer prevention in vitro. We also examined the paradoxical impact of NAD+ precursor supplementation on pancreatic cancer growth during chemotherapy.
Methods: In vitro, we mimicked age-related NAD+ decline in the media. We stressed HPDE cells under these conditions and evaluated the effect of supplementation with the NAD+ precursor, Nicotinamide mononucleotide (NMN). We assessed cell viability using the PicoGreen assay, mitochondrial function, and reactive oxygen species (ROS) using the Seahorse XF Analyzer and the mitoSox kit, respectively, DNA repair and DNA damage using a western blot for Poly ADP ribose (PAR) and gamma H2AX, respectively, and SIRT3 expression was determined using a western blot. To evaluate the impact of NAD+ supplementation on pancreatic cancer cells, we treated pancreatic cancer cells with NMN and oxaliplatin. We then assessed the mitochondrial function, ROS levels, DNA damage, and repair. We implanted MiaPaCa-2 xenografts into athymic nude mice and treated them daily with 300mg/Kg of NMN and biweekly 5mg/kg of Oxaliplatin.
Results: Experiments revealed that NMN is not toxic to HPDE cells, even at high concentrations. There was increased cell survival of HPDE cells under stress (nutrient deprivation and alkylating agents) following NMN supplementation. We also noted reduced ROS levels, increased SIRT3 expression, and PARylation. Pancreatic cancer cells were less sensitive to Oxaliplatin following NMN supplementation and showed an increased oxygen consumption rate, increased PARylation, and reduced ROS levels. There was reduced sensitivity to oxaliplatin treatment in the mice with MiaPaCa-2 xenografts treated with NMN.
Conclusion: These findings demonstrate a cytoprotective role of NAD+ precursor supplementation in normal pancreatic ductal epithelial cells, with implications for possible cancer prevention. NAD+ supplementation also rescued cancer cells under cytotoxic stress, meaning that geroprotectors like NMN, in conjunction with chemotherapy, may unintentionally promote cancer progression. Future studies will directly test NAD+ precursor supplementation in genetically engineered pancreatic cancer models.

#0992 The impact of tamoxifen on autophagic and epigenetic regulation in endometrial cancer.

S. Thota, R. Begum, N. Chintala, A. Pandit, B. Sapkota, J. Francis;
Louisiana State University, Baton Rouge, LA

Background: Endometrial cancer, predominantly endometrioid adenocarcinoma, ranks as the fourth most common cancer in women globally, with an increasing incidence over the last two decades. Tamoxifen, well-known for its antiestrogenic characteristics in the treatment of breast cancer, paradoxically increases the risk of endometrial cancer. Understanding this dual role of tamoxifen is crucial for optimizing breast cancer therapy while mitigating endometrial cancer risk. This study aims to elucidate the molecular alterations induced by tamoxifen in endometrial thickening and its potential to induce cancer, particularly focusing on autophagy, epithelial-mesenchymal transition (EMT), and cancer stem-like cells (CSCs).
Methods: In this study, female BALB/c mice were administered tamoxifen (20 mg/ml) orally for five consecutive days. We monitored changes in EMT markers, autophagy-related genes, and stem cell markers over 1 to 5 months. Furthermore, we investigated the epigenetic modulation of key genes involved in these processes.
Results: Tamoxifen treatment led to altered expression of both epithelial and mesenchymal EMT markers, autophagy-related genes (p62, LC3B, Beclin-1, mTOR, ATG12, ATG16), and stem cell markers (Nanog, SOX2, ALDH1). Notably, we observed significant epigenetic changes, including increased methylation of E-cadherin and decreased methylation of Twist. Furthermore, we observed hypermethylation (a process often linked to the silencing of tumor-suppressing genes) in MGMT (Methylguanine methyltransferase), a DNA repair enzyme involved in chemoresistance, and DAPK (Death-associated protein kinase), a kinase associated with apoptosis, autophagy, and inflammation. We also observed hypermethylation in the CpG promoter regions of autophagy-related genes (Beclin-1 and LC3B) highlighting a potential mechanism for tamoxifen-induced tumorigenic changes.
Conclusion: Our findings demonstrate tamoxifen's influence on cellular and molecular pathways, highlighting the complex interplay between drug treatment and cancer progression. The observed epigenetic changes provide insight into the mechanisms by which tamoxifen may contribute to endometrial cancer risk, suggesting potential targets for therapeutic intervention.

#0993 Comprehensive immunophenotypic strategies to enable equity in remote settings for improved cancer prognosis.

N. J. Smith[1], M. Cohen[2], J. Alipaz[2], C. Loh[2], D. King[2], B. Fazekas de St Groth[1], **H. M. McGuire**[1];
[1]The University of Sydney, Sydney, Australia, [2]Standard Biotools, South San Francisco, CA

Improved cancer prognosis begins with insights obtained from high quality data during clinical trials. Execution of longitudinal clinical trials in flow cytometry is complex, primarily due to logistical challenges in high quality sample collection. For instance, highly remote indigenous population centers are both disadvantaged in access to healthcare and often underrepresented in clinical trials. This paradox is highlighted in the case of Australian First Nations communities, for which lung cancer prevalence peaks in males at twice the magnitude of the general population. Our group has developed a novel blood “immune signature” that robustly predicts failure to make a clinical response to checkpoint therapies targeting the PD-1/PD-L1 pathway. Encouraged by these groundbreaking findings, which were achieved through applying a comprehensive 38-plex immunophenotyping CyTOF panel to biobanked cancer samples, recent advances in CyTOF technology now give us the opportunity to expand our clinical implementation to remote settings, with a further expanded panel to 50+ markers. CyTOF is the only technology that allows easily implemented remote asynchronous sample collection and the largest immunophenotyping panel that yields reproducible results. Asynchronous collection is uniquely enabled using a stable lyophilized large-scale staining panel and achieving comprehensive marker coverage in one panel minimizes blood sample required. Furthermore, the new technology enables a highly simplified workflow including blood collection and processing in remote locations to enable the simplest clinical trial infrastructure complexity and cost, easily implemented in current hospital lab environments. As such, this study is designed to ultimately demonstrate both clinical impact of the large panel and utility of CyTOF technology for highly simplified and robust workflow for multi-site clinical trials. This project has 3 phases; i) implementation and evaluation of the collection, analysis technique and data management of this new approach across multiple sites, ii) collection of samples for analysis both pre- and post- initiation of therapy to establish efficacy and optimize as necessary, and iii) blinded clinical trial. We will report on the first phase of this project which is implementing new workflow across clinical collection site, data integration and analysis. This workflow would enable highly simplified collection to access indigenous and under-served populations spread across remote sites in Australia.

#0995 Preservation of patient whole blood preserves cancer immune cell biology at single cell resolution.

K. Martin, C. Kunihiro, J. Abousoud, T. Drennon, Y. Li, S. Marrache, N. Raman, V. Rodriguez, P. Lund, J. Durruthy Durruthy, S. Taylor, A. Kohlway, P. Smibert, D. Walter, J. Herschleb;
10X Genomics, Pleasanton, CA

Blood is an easily accessible clinical sample type that helps inform treatments, investigate disease mechanisms, and monitor outcomes. Logistical challenges in the transportation and processing of blood samples impact data output from single cell RNA sequencing (scRNA-seq). Recent scRNA-seq studies have shown that significant changes in gene expression and immune cell populations occur in as little as a few hours post collection. Thus, there is a need for rapid preservation of blood upon collection before biological changes can occur. Existing preservation approaches compromise the cell membrane, making samples incompatible with single cell transcriptomic analyses. Here, we describe a novel workflow for fixation and long-term storage of whole blood, and isolation of peripheral blood mononuclear cells (PBMCs) from the fixed blood using a readily available, low-cost, high-throughput procedure. We then profile the gene expression of these cells using the fixation-compatible Single Cell Gene Expression Flex workflow. Importantly, this novel blood collection and preparation workflow eases blood transportation logistical constraints, allowing distributed sample collection and batched shipping of blood samples for scRNA-seq and potentially enabling large-scale translational research studies. We compared whole blood fixed immediately after collection using our workflow with clinical blood samples stored at ambient temperature. This revealed that immune cell populations and biological pathways shift significantly as early as five hours following sample collection, if not immediately stabilized. Across a time course of ambient temperature storage of whole blood without immediate stabilization, we observe significant upregulation of stress-related genes (FOS, JUN, CIRBP) in samples using Single Cell Gene Expression Flex profiling. Additionally, expression of a proto-oncogene TNFAIP3 was upregulated in whole blood stored at 20°C compared to samples stored at 4°C for the same lengths of time, unless samples were stabilized using the novel workflow shown here. This novel whole blood fixation method, coupled with automatable cell isolation methods and Single Cell Gene Expression Flex-enabled multiplexed single cell sequencing, will usher in a new age of economical, large-scale translational research studies that result in valuable clinical insights.

#0996 Predicting early mortality in a large ethnically diverse phase I clinical trial program.

H. Erfani[1], S. Woll[1], A. Luong[1], G. Guerra[1], A. Kharrat[2], R. Umayam[1], A. Martynova[1], L. Brunette[1], L. Roman[1], N. Izadian[1], T. Bustos[1], D. Hanna[1], A. El-Khoueiry[1], J. Thomas[1];

[1]USC - University of Southern California, Los Angeles, CA, [2]Brown University, Providence, RI

Background: Various scoring systems are developed to optimize patient selection for phase I clinical trials. We evaluated the Royal Marsden Hospital (RMH), Princess Margaret Hospital Index (PMHI), and MD-Anderson Cancer Center (MDACC) prognostic scores and compared their power to predict 90-day mortality (90DM) in an ethnically diverse population enrolled in the USC Norris Comprehensive Cancer Center (NCCC) Phase I Program.

Methods: We queried our database of patients enrolled in phase I clinical trials at the NCCC from 2015-2022 which includes demographics, treatment details and outcomes. The enrollment occurred at all NCCC sites including the Los Angeles General Medical Center, a safety net hospital. Prognostic scores were calculated: RMH (albumin < 35 g/L, LDH > ULN, > 2 metastatic sites), PMHI (albumin < 35 g/L, ECOG > 0, > 2 metastatic sites), MDACC (albumin < 35 g/L, LDH > ULN, ECOG > 0, > 2 metastatic sites, GI tumor type). Kaplan-Meier analysis was used to calculate median survival in each group. ROC analysis was performed to assess the 90DM prediction.

Results: 611 patients (15 breast, 344 GI, 20 GU, 29 GYN, 110 Lung/H&N, 88 other) were accrued to 88 phase I trials. Patients had a median age of 61 (25-87) and a median of 3 prior lines of therapy (0-10). 31.9% of pts were Hispanic, 44.1% non-Hispanic white, 3.7% black, and 20.4% Asian. The 90DM rate was 24.9%. The objective response rate was 8.3%, and 41.5% had stable disease. For all systems, higher scores had shorter survival (p<0.001). The MDACC system had the largest AUC to predict 90DM (AUC: 0.678, p < 0.001). Score of 4-5 (high risk) per MDACC system corresponds to a specificity of 94.5% (91.1-97.2) and positive likelihood ratio of 3.6 (1.8-7.2).

Conclusion: In our highly diverse phase I population, higher scores on the RMH, PMHI, and MDACC scoring systems were associated with worse prognosis and 90DM. Careful consideration should be given to potential patients with higher scores prior to enrollment in phase I trials.

Characteristics and outcomes of the study participants (N = 611).

Variable		**Median (IQR)/ N (%)**	**Scoring system**		**N (%)**	**Median survival days (95% CI)**	**p-Value**
Age (yr)		61 [54-68]	**RMH score**				**< 0.001**
Female gender		288 (47.1%)		**0**	151 (36.7%)	505 (378-631)	
Safety net participant		120 (19.6%)		**1**	184 (44.8%)	509 (324-693)	
Non-English speaking		177 (29%)		**2**	64 (15.6%)	176 (107-244)	
Performance status	**ECOG 0**	153 (33.3%)		**3**	12 (2.9%)	44 (12-76)	
	ECOG 1	302 (65.7%)		**Area under ROC curve**	**(95% CI)**	0.650 (0.579-0.721)	**< 0.001**
	ECOG 2	5 (1.1%)					
Number of prior lines	**0-2**	298 (48.8%)	**PMHI score**				**< 0.001**
	>= 3	313 (51.2%)		**0**	118 (25.7%)	603 (405-800)	
Tumor type	**Breast**	15 (2.5%)		**1**	214 (46.5%)	462 (378-545)	
	GI	344 (56.8%)		**2**	115 (25.0%)	254 (117-390)	
	GU	20 (3.3%)		**3**	13 (2.8%)	87 (52-122)	
	Gyn	29 (4.8%)		**Area under ROC curve**	**(95% CI)**	0.629 (0.560-0.697)	**< 0.001**
	Lung/H&N	110 (18.2%)					
	Others	88 (14.5%)	**MDACC score**				**< 0.001**
Type of trial	**Chemotherapy**	112 (18.3%)		**0** (low risk)	26 (7.9%)	Not estimated	
	Immunotherapy	227 (37.2%)		**1** (low-intermediate risk)	84 (25.5%)	597 (429-768)	
	Targeted therapy	272 (44.5%)		**2** (intermediate risk)	116 (35.2%)	471 (115-827)	
>2 metastatic sites		146 (23.9%)		**3** (high-intermediate risk)	75 (22.7%)	297 (142-452)	
90-day mortality		152 (24.9%)		**4** (high risk)	25 (7.6%)	119 (108-130)	
Best response by RECIST	**Stable disease**	225 (41.5%)		**5** (high risk)	4 (1.2%)	Not estimated	
	Partial response	39 (7.2%)		**Area under ROC curve**	**(95% CI)**	0.678 (0.611-0.745)	**< 0.001**
	Complete response	6 (1.1%)					
	Progressive disease	272 (50.2%)					

#0997 Bringing the first prehabilitation program to American Indian cancer patients.

J. Erdrich[1], A. Hernandez[2], J. W. Bea[2], C. A. Thomson[2];
[1]University of Arizona, College of Medicine, Tucson, AZ, [2]University of Arizona, Mel and Enid Zuckerman College of Public Health, Tucson, AZ

Purpose. American Indian/Alaska Native (AI/AN) people have the worst cancer survival rates of any US racial group, are underrepresented in clinical trials and research, and have never been recruited for participation in any published prehabilitation (prehab) intervention conducted prior to cancer surgery.
Description of Procedure. We are collaborating with tribal partners to design the first prehab translational clinical trial for AI patients diagnosed with obesity-related cancer, to be implemented prior to surgical resection of the tumor. Program components have been developed with community input through semi-structured interviews and guidance from the sponsoring tribal health facility, the San Carlos Apache Healthcare Corporation. Patients preparing for cancer surgery will engage in a 3-week multimodal intervention that entails home-based exercise, supervised fitness sessions, promotion of anti-inflammatory foods, and health education materials adapted for and by community members. Serum and tissue biomarkers, as well as lifestyle behavioral measures, will be compared pre and post intervention to assess responsiveness. In respect of tribal sovereignty, the experimental procedure includes protocol refinement and approval by the tribal health facility's IRB and tribal council.
Summary of Data. Our qualitative data reveal AI cancer survivors from the partnering tribal community have high interest in prehab and attest they would have participated if offered (100%). Their consensus feedback fashioned the specifics of the prehab translational clinical trial: 30 minutes daily walking, 60 minutes supervised resistance training twice weekly, 2 ounces walnut consumption daily, nutrition counseling, transportation assistance, and education/encouragement from staff and peers. Biospecimen sampling can be a sensitive topic for AI audiences, which we addressed early and found 75% of the interviewed survivors agreed to biospecimen collection without stipulation; this increased to 100% support once the rationale for biospecimens was explained.
Conclusions: Published prehab studies in other populations administered for 3-5 weeks between diagnosis and surgery have shown improvements in functional capacity, attenuation of surgery-induced losses, alterations of inflammatory biomarkers, and patient safety. Our community-informed prehab translational clinical trial for AI patients is the first of its kind, and anticipated to demonstrate feasibility, patient acceptability, behavioral changes in lifestyle, and the potential to modulate inflammatory biomarkers.

#0998 Pursuing leadership in literacy to ameliorate head and neck cancer disparities.

Joni D. Nelson[1], Irene M. Lubker[2]

[1]Biomedical and Community Health Sciences, The Medical University of South Carolina, Charleston, SC,[2]Academic Affairs, MUSC Libraries , The Medical University of South Carolina, Charleston, SC

Overview of Proposed Research. Head and neck cancers are a deadly cancer that ranks among the six most common cancers worldwide. (American Cancer Society, 2021). Studies have shown greater disease burden among minority populations for head and neck cancer, higher mortality rates and lower oral cancer knowledge, but limited evidence has defined the underlying causes of late stage diagnoses and access to the healthcare system (Suzuki et al, 2019). More specifically, in comparison to the national rates, South Carolina is among the top ten for head and neck cancers (Community Outreach, Hollings Cancer Center, MUSC, 2019). Dental and primary care play a critical role delivering quality patient education, prevention, risk reduction and treatment regimes. However, there is a paucity of information published on the value of designing and implementing a health literacy program to prioritize head and neck cancer screening and prevention. Rural communities face unique challenges to achieving optimal oral health, impacted mainly by geographic location and socioeconomic status (IOM&NRC, 2011). More specifically, rural southern states such as SC continues to have a tremendous shortage of primary care providers. SC currently has 44 of 46 counties designated as geographic Primary Care and Dental Health Professional Shortage Areas and approximately 25% of SC citizenry are living in rural areas (HRSA, 2018). Because the vast majority of the state has challenges with availability of primary care and dental providers, this potentially exacerbates access to care inequities for rural and underserved minority populations. To enhance the quality and equity of oral cancer prevention in rural SC, it is critical that we prioritize strategies to elevate the significance of head and neck cancer risks. Therefore, the need to design and deliver innovative strategies to increase opportunities that intersect the healthcare system and community is inevitable. In this regard, we propose PULL A-HEAD, Pursuing Leadership in Literacy to Ameliorate HEAd and neck cancer Disparities. PULL A-HEAD is aimed to develop and implement a community-centered approach design for increasing the health literacy and efficacy of navigating the healthcare system for early detection of head and neck cancers. In this presentation we will share outcome and impact results of a community-centered, health literacy program in collaboration with our Regional Medical Library - Region 2 (RML2), National Library of Medicine partners at the Medical University of South Carolina. The program (i.e. PULL A-HEAD) will emphasize the delivery of health literacy education and health systems navigation tools to improve the early detection of head and neck cancers.

#0999 Clinical trial matchmaking: Connecting sites to sponsors.

L. Griffin[1], L. Shivakumar[1], L. Boehmer[1], S. Dodson[1], E. Plotkin[1], S. Pal[2], A. B. Benson III[3];
[1]Association of Community Cancer Centers, Rockville, MD, [2]City of Hope Comprehensive Cancer Center, Duarte, CA, [3]Robert H. Lurie Comprehensive Cancer Center of Northwestern University, Chicago, IL

Background: Oncology programs may encounter many challenges engaging in clinical trials. The Association of Community Cancer Center's (ACCC) Community Oncology Research Institute (ACORI) conducted a survey to gather insights on barriers to clinical trial provision and implementation, patient recruitment, and identifying resources to support cancer programs.
Methods: A survey of 29 questions was administered via Qualtrics. The survey focused on research-naïve sites (i.e., sites with little to no clinical research experience). Survey recipients were identified from ACCC's membership database, and the survey was open from May 5 to October 10, 2023. One survey response was captured per program.
Results: Of the 350 respondents, most were physicians, investigators, or oncology fellows (20%), directors/administrators (16%), patient navigators (12%), and APPs (12%). Responding programs were categorized as a comprehensive community cancer program (28%), community practice (26%), or academic medical center (21%). Eighty percent of respondents indicated their program currently conducts clinical research. The most common challenges included: patient recruitment (40%), limited staffing (36%), limited clinician time (32%), and lack of training in research administration and conduct (25%). The top 3 resources desired were communication about clinical research opportunities (65%), connections to clinical trial sponsors (49%), and clinical research coordinator training (41%).
Conclusions: Survey results showed a clear need for improved communication regarding clinical research opportunities, connections to clinical trial sponsors, and education around clinical trial implementation. Data from this survey will be used to match sites with trial sponsors, especially sites that serve patients with cancer from under resourced geographic, socioeconomic, racial, and ethnic groups. Future efforts will seek to engage clinical trial sponsors in improving trial engagement and feasibility, workforce support, training, and clinical mentorship.

#1000 Clinician and clinical trial staff perspectives on factors that impact enrollment of Black women in breast cancer trials.

Christen Sandoval[1], Eliza Brumer Cohn[2], Leslie R. Carnahan[3], Vida Henderson[2], Tigist Mersha[1], Neha Hippalgaonkar[4], Joe Horowitz[5], Sarah Khan[6], Kauthar Salum[2], Ana Williams[3], Lolita Coleman[7], Beluah Brent[7], Anne Marie Murphy[1], Paris Thomas[8], Paramjeet Khosla[6], Kent Hoskins[3], Ryan Nguyen[3]

[1]School of Public Health, University of Illinois Chicago, Chicago, IL, [2]Fred Hutch Cancer Center, Seattle, WA, [3]University of Illinois Cancer Center, Chicago, IL, [4]Division of Hematology/Oncology, University of Illinois Chicago, Chicago, IL, [5]College of Medicine, University of Illinois Chicago, Chicago, IL, [6]Sinai Chicago, Chicago, IL, [7]Sisters Working It Out, Chicago, IL, [8]Equal Hope, Chicago, IL

Background: Black women (BW) are more likely to present with advanced-stage disease and to die following a breast cancer (BC) diagnosis compared with women from other racial and ethnic groups, yet BW are underrepresented in BC clinical trials (CT). Clinicians and CT staff play a key role in patient participation in CT, however, there is limited data on their perspectives on facilitators and barriers for BW in BC trials.
Objective: The goal of the FOR ME (Fostering Opportunities in Research through Messaging and Education) study is to develop, optimize, and test a decision-aid intervention (web-based video) for clinical care teams to use with BW who have been recently diagnosed with BC to promote shared decision-making and CT participation. We provide insight into the facilitators and barriers from clinicians and CT staff to effectively discuss and enroll BW in BC trials. The identified themes will be used to inform video content and dissemination strategies.
Methods: Key informant interviews (KIIs) (n=20) were conducted by phone and video conferencing. Each KII was recorded and professionally transcribed. Thematic analysis and inductive coding approaches were used to analyze the data. First, a subset of transcripts was annotated, and then annotations were compiled into a preliminary codebook. Inter-coder reliability was established to improve quality and to establish the final codebook. Dedoose was used to analyze quotations and code co-occurrences, application frequencies, and relationships.
Results: In total, 16 clinicians and 4 clinical trial staff across academic and community practices were interviewed. Participants expressed multiple opportunities and barriers to CT participation. Facilitators included formal training on communication around clinical trials among clinical trial staff, previous exposure to discussing and enrolling patients in CT during fellowships and other training, institutional support for CT databases, reviewing CTs during tumor boards, and the presence of dedicated research support staff. Barriers included a lack of formal training in communicating CT to patients among clinicians, lack of institutional investment in CT infrastructure, time constraints of clinical visits, and the clinician's perception of the patient's willingness and ability to complete a CT.
Conclusions: Clinicians and clinical trial staff have a unique and important role to play in CT participation for BW who have BC, however, there are barriers, including training, time, awareness of available trials, and institutional support. Clinical trial staff report formal training in communicating clinical trial information to patients, while there is a lack of this type of training for clinicians. Future research in the FOR ME study will integrate patient, clinician, care team, and advocate perspectives into a web-based decision aid.

#1001 Association between oral cancer screening and knowledge of head and neck cancer symptoms and risk factors among Arab Americans.

N. Al-Antary, R. Siddiqui, M. Gilbert, L. Fakhoury, M. Nair, F. Siddiqui, E. Adjei Boakye;
Henry Ford Health System, Detroit, MI

Background: Head and neck cancer (HNC) has been increasingly affecting individuals of different ages, significantly contributing to the annual cancer burden in the US. While most HNC cases present at late-stages and are more likely to require aggressive surgical interventions with higher mortality, those who present with premalignant clinical signs or early-stages have a 5-year survival of 70%-90%. Moreover, current HNC public awareness is poor with lack of data on cultural and ethnic minorities. This study evaluated the association between oral cancer screening (OCS) recommendation and receipt and HNC symptoms and risk factors knowledge among Arab Americans in Michigan.

Methods: This was a cross-sectional study of adult Arab Americans conducted between March and July 2023. Surveys were available in English and Arabic per participants preference. Outcome variables were knowledge of three main HNC risk factors—alcohol, cigarette smoking, and HPV— and four of the most common HNC symptoms—nonhealing oral ulcers, dysphagia/odynophagia, voice changes and neck/throat masses—defined as yes/no. OCS was captured as receiving provider-given recommendation for screening and undergoing a screening test (yes/no). Multivariable logistic regression models estimated the associations between OCS and HNC symptoms and risk factor knowledge adjusting for socioeconomic factors.

Results: A total of 295 respondents were included in the study, 9% had received recommendation for OCS and 11% had undergone a screening test. In adjusted models, respondents who *did not* correctly identify nonhealing oral ulcers (aOR=0.20; 95% CI 0.06-0.67) as HNC symptoms or HPV (aOR=0.15; 95% CI 0.04-0.55) as risk factor of HNC were less likely to have received provider-given recommendation for OCS compared to those who identified the symptom and risk factor. Similarly, respondents who *did not* correctly identify nonhealing oral ulcers (aOR=0.13; 95% CI 0.04-0.42), dysphagia or odynophagia (aOR=0.22; 95% CI 0.07-0.70), voice changes (aOR=0.27; 95% CI 0.09-0.81), and neck/throat masses (aOR=0.24; 95% CI 0.06-0.91) as HNC symptoms or HPV (aOR=0.07; 95% CI 0.02-0.29) and alcohol (aOR=0.17; 95% CI 0.05-0.58) as HNC risk factors were less likely to have undergone OCS compared to those who identified the symptoms and risk factors.

Conclusion: Respondents who reported limited knowledge of HNC symptoms and risk factors were less likely to be exposed to screening recommendations or testing. Combining screening with education on premalignant and early-stage clinical signs and risk factors might facilitate reduction of HNC incidence and late diagnosis. Further interventions are needed to increase Arab Americans education and identification of high-risk groups by their providers. As HNC screening efficacy remains controversial, future efforts should be directed towards deepening our understanding in this area.

#1002 The historically black colleges and universities cancer trial consortium: A way forward to diversifying cancer clinical trials.

S. L. HOLDER[1], R. A. Winn[2], W. S. El-Deiry[1];
[1]Legorreta Cancer Center, Providence, RI, [2]Massey Comprehensive Cancer Center, Richmond, VA

The National Comprehensive Cancer Center Network cancer guidelines state that the best management for a cancer patient is on a clinical trial. However, the demographics of 74 registration trials for oral cancer therapies from 2009 - 2019 show only 2.5% of participating patients were Black. Similarly, of the 3,593 patients enrolled in all registration trials for new cancer drugs approved by the FDA in 2019, only 4% were Black patients. A third analysis showed that between 2008 and 2018, only 3.1% of cancer trial patients were Black.

The underrepresentation of Black patients in cancer clinical trials is a complex issue that requires a multifaceted solution. Complicated, interdependent causes include, but are not limited to system, provider, and patient bias. Increasing globalization of clinical trials also contributes to a widening gap in Black patient enrollment. Achieving diversity among clinical trial participants requires intention in study design regarding accrual sites and outreach, and involvement of a diverse trial workforce.

The ideal clinical trial system would minimize system, provider, and patient biases. Such a system already exists in the Historically Black Colleges and Universities (HBCU) system. HBCUs represent 3% of institutions of higher education in the USA, yet they enroll 16% of Black students and confer 24% of all baccalaureate degrees earned by Black students. 40% of Black engineers, 50% of Black lawyers, 70% of Black physicians, and a staggering 80% of Black judges attended an HBCU. HBCUs are exceptional at impacting communities of Color and have been doing so for centuries.

The HBCU Cancer Trials Consortium (HBCU CTC) is a network of HBCUs and Ally institutions that aims to bring innovative cancer clinical trials to historically underserved communities and honor the legacy of HBCUs, which have consistently and successfully served underserved communities for over a century. The HBCU CTC will oversee and conduct cancer clinical trials at member institutions. We envision founding flagship members to include HBCUs that provide graduate medical education and training, such as Howard, Meharry, Charles Drew, and Morehouse. Non-HBCUs committed to the mission are invited to join the consortium as Ally institutions (eg. MSIs). Membership is not exclusive of membership in other cancer consortia. The HBCU CTC will provide shared resource services for member institutions that lack expertise or funding to conduct services locally (eg. data management, DSMB, biostatistics, a cancer focused IRB, central radiology, and central pathology). The Consortium will also work to develop local infrastructure support for the conduct of cancer clinical trials at member institutions.

#1003 Contact registry for health-related cancer research: Promoting inclusion in research.

F. Webb[1], I. Guzman[2], B. Hensel[2], E. Ibarra[3], C. Aristizabal[3], J. Luque[4], R. Barahona[3], D. Wilkie[5], M. C. Stern[3], L. Baezconde-Garbanati[3], S. Suther[4]; [1]University of Florida, Jacksonville, FL, [2]University of Florida, Orlando, FL, [3]University of Southern California, Los Angeles, CA, [4]Florida A&M University, Tallahassee, FL, [5]University of Florida, Gainesville, FL

Contact Registries can serve as key tools in connecting community members to cancer health research opportunities. Members of underrepresented groups who enroll in a contact registry can choose to participate in studies they find interesting, provided they are an ideal candidate for participation. However, limited information exists regarding the types of studies underrepresented groups would want to participate in. The Florida-California Cancer Research, Education, and Engagement (CaRE^2) Health Equity Center Community Outreach Core (COC) created a contact registry of community members self-identifying as Black/African American (B/AA) and/or Hispanic/Latinx (H/L) persons who are interested in learning about future research studies conducted at CaRE^2 institutions. The CaRE^2 Contact Registry was implemented in August 2022 by the CaRE^2 COC, one of the six (6) key cores within the CaRE^2 Center. COC's primary objective is to increase the number of persons participating in cancer research, which ultimately produces findings more applicable to the broader, diverse population of B/AA and H/L communities in both Florida and California. Our study team promotes the registry at local community events and through our center's social media accounts and website (https://care2healthequitycenter.org/the-care2-contact-registry/). Recruitment consists of both in-person and online methods provided in both Spanish and English with data stored on REDCap, an online data repository system. For in-person enrollment, a consent/authorization form and OPT-IN survey are completed; meanwhile, our online recruitment requires additional screening to ensure eligibility. Eligibility requires that the person resides in 1) either California or Florida, 2) be 18+ years old, and 3) identify as B/AA or H/L. In addition to collecting contact and demographic information, participants can choose their research study interests. For example, they can choose to participate in surveys, community forums, focus groups, a cancer advocacy training program, and/or to provide a hair, saliva, or blood sample. A $10.00 gift card, either in a physical or electronic format, was provided to each confirmed enrollee. As of November 13, 2023, 1,269 persons have enrolled, representing 63% of the 2,000 enrollment goal. While 92% of registry enrollees are willing to participate in health research involving surveys, only 20% are willing to participate in health research studies requiring saliva (23%), hair (22%), or blood (20%) donations. In conclusion, registry enrollees, regardless of race or ethnicity, have a high interest in participating in studies involving completing surveys or attending focus groups. However, efforts must continue to increase participation willingness for research involving biospecimen donation. Future efforts will also include connecting enrollees to cancer health-related research studies of their interest.

#1004 Establishing lung adenocarcinoma cell lines to mitigate lung cancer health disparities.

S. Lugo[1], C. Leon[1], M. Gladstone[1], C. Yan[1], N. S. Lamango[2], I. A. Offringa[1], K. Ofosu-Asante[2], Y. Huang[3], J. K. Mensah-Mamfo[2];
[1]University of Southern California, Los Angeles, CA, [2]Florida A&M University, Tallahassee, FL, [3]University of Florida, Gainesville, FL

Lung cancer remains the leading cause of cancer death worldwide and is a pronounced source of cancer health disparities. Black/African American (B/AA) individuals demonstrate the highest lung cancer death rates when compared to other ethnic/racial groups. B/AA males exhibit a 15% higher lung cancer death rate and a 12% higher lung cancer incidence when compared to White males. Lung adenocarcinoma (LUAD) is the most common histological subtype in all races including B/AA. To study lung cancer and its related disparities, essential tools such as lung cancer cell lines are important; they can be used for molecular studies of lung cancer development, progression, development of new therapies and pre-clinical drug testing. We reviewed the literature (Leon *et al.* 2023, Frontiers in Oncology, Vol. 13, p. 1187585, 2023) and identified only 30 unique B/AA cell lines out of ~800 cell lines available, with the majority of cell lines being from White and Asian patients. Moreover, only 6 B/AA cell lines were derived from patients with LUAD. We are in the process of developing additional LUAD cell lines from patients as well as alveolar epithelial cell lines that can be used to model LUAD development. In addition, we are generating multiple independent isogenic cell line variants from existing lung cancer cell line NCI-H23, derived from a B/AA male patient harboring a $KRAS^{G12C}$ heterozygous mutation. We are using CRISPR/Cas-9-based genome editing to replace the $KRAS^{G12C}$ mutation with other *KRAS* mutations found in B/AA patients, including $KRAS^{G12V}$, $KRAS^{G12D}$, $KRAS^{G12A}$, and $KRAS^{G13C}$. We will perform whole genome sequencing to exclude off target effects of the CRISPR engineering. We will use isogenic cell lines to test the efficacy of polyisoprenylated cysteinyl amide inhibitors (PCAIs) and other drugs on cell lines bearing the different *KRAS* mutations. PCAIs were developed to target cells carrying mutant *KRAS*. Our efforts will provide tools to limit cancer health disparities and serve as a foundation for future research.

Supported by grants U54CA233396, U54CA233444, and U54CA233465 from the National Institutes of Health (NIH)/National Cancer Institute (NCI) and the Norris Comprehensive Cancer Center core grant, award number P30CA014089 from the NIH/NCI.

#1005 A three-decade-long community-based participatory research among India and Bhutan's ethnic minorities led to the discovery of 32 unique medicinal plants having anti-cancer properties.

S. Sandhya[1], R. Das[2], P. Dutta[2], A. Chowdhury[2], P. Das[3], S. Das[4], T. Baishya[5], L. Pathak[1], D. Dutta[1], N. Das[1], P. Sarma[2], I. Pulu[6], U. Mahanta[7], D. Bora[8], H. Bhai[9], **B. Das**[10];

[1]KaviKrishna Laboratory, IIT Guwahati Research Park, Guwahati, India, [2]KaviKrishna Center of Indian Knowledge System, Sualkuchi, Assam, India, [3]KaviKrishna Center of Indian Knowledge System, Sualkuchi, India, [4]Thoreau Laboratory for Global Health, Lowell, MA, [5]KaviKrishna Telemedicine Care, Sualkuchi, Assam, India, [6]Research Institute of World Ancient Traditions Cultures and Heritage, Roing, Arunachal Pradesh, India, [7]Sri Sri Ishwar Hatisatra, Sualkuchi, Assam, India, [8]Ek Saran Bhagawati Samaj, Nagaon, Assam, India, [9]Shanti Sadhana Ashram, Guwahati, India, [10]KaviKrishna Laboratory, Research Park, Indian Institute of Technology, Guwahati, India

The country of Bhutan, and India's Northeast is an economically deprived region inhabited by diverse groups of indigenous and underserved communities. They live in mostly rural areas, where cancer disparity is very high. On the other hand, they have rich traditional knowledge systems including tantra philosophies (remnant of the Vedic age philosophy), herbal medicinal practice, and spiritual practices that can be traced back to India's Vedic age. To harness this traditional knowledge to reduce cancer disparity, we have taken an indigenous knowledge system (IKS) based approach (1) and initiated a community-based participatory research (CBPR) program in 1998 to conduct public health research in tuberculosis and cancer (2,3). Using this CBPR program, we have unraveled a Vedic age philosophy of Vedic Jiva Upkara Cikitsha Tantra (Vedic altruism-based medicinal system) (2,3). Specially, using the CBPR program we seek to identify novel herbal medicinal agents having anti-cancer activities.

Methodologies: We used the CBPR methodologies of focused group discussion (FGD), debate, and community social work with various indigenous communities living in the Sualkuchi-Hajo cultural complex of Assam, Roing of Arunachal Pradesh, and Mongar of Bhutan. Since 1994, BD has conducted CBPR through the KaviKrishna Telemedicine Care. We have retrospectively analyzed the data of FGD, and suppositional reasoning (tarka) with the community healers, various Hindu, and Buddhist ethnic spiritual organizations of the region. Thematic analysis and the grounded theory method were applied to organize the data. The resulting database of herbal medicinal plants was searched in the scientific database to find the scientific names. Out of the 36 medicinal plants, we have prepared herbal extracts of 10 medicinal plants and then tested for their anti-cancer efficacy at the KaviKrishna Laboratory.

Results: We have found the names of 32 plants used by the indigenous healers practicing the Vedic Jiva Upakara Cikitsha Tantra. We also found that these healers used curd-made whey protein concentrate, special soil, and fecal extracts to treat cancer (3). Our CBPR process also led to the research capacity building in the Sualkuchi-Hajo community.

Conclusion: The study unraveled a unique cancer-care-related philosophy of Vedic Altruism. Our work indicates that IKS-based CBPR can equitably involve researchers and community members to develop a partnership for the process of knowledge emergence. We found that CBPR-based research takes new meaning because of the unique perspectives that inform the ways that research studies take shape for knowledge emergence.

References: 1. Pathak L et al AACR abstract 3342, 2019. 2. Baishya T et al. https://zenodo.org/records/8062404. 3. Pathak et al AACR abstract 2772, 2023

#1006 Revitalizing the accrual of women and minorities: Unique drivers of therapeutic clinical trial enrollment for underrepresented patients with diffuse glioma.

M. Mehari[1], G. Warrier[1], S. Reihl[2], A. Dada[1], A. Kabir[1], M. Negussie[1], C. Nava Gonzales[1], U. Chukwueke[3], A. Porter[4], S. Hervey-Jumper[1];
[1]University of California, San Francisco, Department of Neurosurgery, San Francisco, CA, [2]University of California, Los Angeles, Department of Neurosurgery, Los Angeles, CA, [3]Center for Neuro-Oncology, Dana-Farber Cancer Institute, Department of Neurology, Harvard Medical School, Boston, MA, [4]Mayo Clinic, Division of Neuro-Oncology, Department of Neurology, Phoenix, AZ

Introduction: Despite the enactment of the 1993 NIH Revitalization Act to improve accrual of women and minorities in clinical trials, these groups remain underrepresented. This study aims to uncover drivers of therapeutic clinical trial enrollment that are unique to women and minority patients with low- and high-grade glioma.
Methods: Adult glioma patients who received care from the UCSF Brain Tumor Center between 1997-2017 were identified in a prospective registry. Dividing the cohort into subgroups by gender and NIH-designated minority status, factors associated with therapeutic clinical trial enrollment on univariate logistic regression ($p<0.2$) were selected for multivariate logistic regression.
Results: There were 351 trial participants (41% women, 12% minority) and 627 non-trial participants (44% women, 17% minority). Among women only, seizure at presentation (OR 2.10, p=0.008) was associated with increased odds of trial enrollment. In contrast, among men only, higher median household income (OR 1.09 per $10,000 increase, p=0.006), higher WHO tumor grade (OR 1.89, p=0.045), and occupational status according to the International Standard Classification of Occupations [professionals (e.g., physicians) vs managers (e.g., supervisory positions), OR 2.87, p=0.043] were associated with increased odds of trial enrollment. Among both women and men, lack of insurance (women: OR 0.49, p=0.02; men: OR 0.55, p=0.031) and no treatment with chemotherapy (women: OR 0.18, p=0.001; men: OR 0.34, p=0.002) were associated with decreased odds of clinical trial enrollment, whereas higher KPS (women: 90 vs <80, OR 3.16, p=0.003; men: 90 vs <80, OR 3.15, p=0.002) was associated with increased odds of trial enrollment. Among NIH-designated minority patients, older age (OR 0.66 per 10-year increase, p=0.033) and non-English preferred language (OR: 0.30, p=0.035) were associated with decreased odds of trial enrollment on univariate analysis, but not on multivariate analysis. Among non-minority patients, lack of insurance (OR 0.58, p=0.008) and no chemotherapy treatment (OR 0.25, p<0.001) were associated with decreased odds of trial enrollment, whereas seizure at presentation (OR 1.80, p=0.001), higher neighborhood household income (OR 1.07 per $10,000 increase, p=0.004), higher WHO grade (4 vs 2-3, OR 1.86, p=0.015), higher KPS (90 vs <80, OR 3.21, p<0.0001), and lower extent of tumor resection (80-89% vs 100%, OR 2.16, p=0.047) were associated with increased odds of trial enrollment.
Conclusion: Drivers of trial enrollment differed for women and minority patients with glioma. Non-English-speaking minority patients may face additional barriers to trial enrollment requiring targeted interventions. Our findings can revitalize and tailor efforts to recruit women and minority patients to therapeutic clinical trials in neuro-oncology.

#1007 Breast cancer related lymphedema patient characteristics and treatment patterns in a Hispanic majority population.

S. A. Shaker, L. P. Rahman, M. Mazo Canola;
University of Texas Health Science Center San Antonio, San Antonio, TX

Background: Studies have shown an increased risk of Breast Cancer Related Lymphedema (BCRL) in Hispanic populations, however there are limited studies examining factors specific to BCRL in this minority population. This retrospective study aims to characterize and analyze treatment and demographic related factors associated with BCRL in the Hispanic majority population of San Antonio.

Methods: This is a retrospective, single institution study of patients with BCRL between 2017-2020 at Mays Cancer Center in San Antonio, Texas, a city with a majority minority Hispanic population.**Results:** 110 subjects with BCRL were identified with a median age of 62 years old. 52.7% were Hispanic while 47.3% were non-Hispanic. The median BMI was 31 with over 75% of subjects with BCRL categorized with BMIs of overweight or obese. 89.1% received some form of chemotherapy, whether neoadjuvant or adjuvant, and 80.9% were exposed to some form of taxane. The majority underwent more invasive procedures and surgeries: 69.1% had axillary lymph node dissection and 71.2% underwent mastectomy. The median number of lymph nodes removed were 12. 62.7% of BCRL patients were exposed to nodal radiation. Regarding BCRL severity, 29.4% were classified as grade 1 while 11% classified as grade 3. Of note, there was a statistically significant correlation between more severe lymphedema (grade 2 and 3) and use of chemotherapy (P-value = 0.04.)**Conclusion:** The demographic composition of patients with BCRL closely mirrors the ethnically diverse population of San Antonio, with a large Hispanic predominance. Within this cohort of patients of BCRL, a large portion demonstrated factors of elevated BMI, more invasive surgical interventions, and exposure to chemotherapy, specifically taxane. The examination of these factors in a Hispanic-centric urban setting such as San Antonio offers crucial insight into a patient population at heightened risk for developing BCRL.

#1008 Pilot evaluation of an online course for primary care providers on preparing patients for cancer discussions with their oncologists.

A. Crowe[1], E. S. Weiss[2], M. Michaels[3], D. Durante[4], M. Sae-Hau[2], A. Cassells[5], C. L. Fisher[1], J. Arnold[4], T. Vasquez[6], A. Natale-Pereira[7], R. Mailhot[1], Z. Zhang[8], C. L. Bylund[1];

[1]University of Florida College of Medicine, Gainesville, FL, [2]The Leukemia & Lymphoma Society, Rye Brook, NY, [3]Health Access & Action Consulting, Boston, MA, [4]University of Florida College of Education, Gainesville, FL, [5]Clinical Directors Network, New York, NY, [6]University of Florida College of Journalism and Communications, Gainesville, FL, [7]Rutgers New Jersey Medical School, Newark, NJ, [8]University of Florida Health Cancer Center, Gainesville, FL

Introduction: Cancer clinical trial (CCT) accrual is only 5-8%, and barriers to participate can be more acute for underserved groups. Enrollment of racial/ethnic minorities, older adults, adolescents, and young adults is not adequate to understand treatment outcomes unique to these populations. Education before seeing an oncologist can increase patients' willingness to ask and consider receiving treatment through a CCT. Because primary care providers (PCPs) interact with patients during diagnosis, provide ongoing care, and are a trusted source of information, they can educate and normalize inquiries about therapeutic CCTs. The aim of this study was to pilot test an innovative, tailored online CCT course for PCPs.

Methods: To participate, PCPs (MD, DO, NP, or PA) had to provide care in an outpatient setting, refer patients to a cancer treatment specialist in the past year, and be an English speaker residing in the U.S. or its territories. PCPs were recruited from Clinical Directors Network, University of Pennsylvania, and University of Florida. The 1-hour online course includes four modules hosted by a PCP and radiation oncologist with video segments of a CCT expert who summarized CCT recruitment research. Participants interact with patient scenarios and learn about the patient's cancer diagnosis and medical/personal background. Videos of actors playing the roles of patient and doctor demonstrate communication skills taught in the course. PCPs completed short surveys prior to and immediately after completing the course.

Results: 28 PCPs participated. PCPs were mainly MDs (88.9%), residents (17, 60.7%), White (46.4%), non-Hispanic/Latino (92.9%), and 50% women. Mean *knowledge of CCTs scores* (0-100%) increased significantly from pre (M=56.7, SD=17.5) to post (M=82.1, SD=12; p<.001) indicating that PCPs answered more true/false statements about CCTs correctly after training. Using a 1-5 scale with 5=strongly agree, PCPs' *attitudes and beliefs scores* also increased significantly from pre (M=4.2, SD=.6) to post (4.7, SD=.4, p<.001) indicating that PCPs were more likely to agree they have a role in their patients' cancer treatment, including CCTs, after training. Using the same scale, PCPs' *willingness to communicate about CCTs* increased significantly from pre (M=4.4, SD= .5) to post (M=4.7, SD=.5, p=.007), indicating that PCPs were more willing to engage with patients diagnosed with cancer before referring them to a cancer specialist after training.

Conclusions: Significant pilot findings in knowledge, attitudes and beliefs, and communication scores demonstrate that the online course was effective at educating PCPs about CCTs, and improving PCPs' attitudes about the CCT referral process, and their willingness to engage in their patients' cancer care. Future research will include a larger sample and explore the course's impact on PCP's referral behavior.

#1009 Direct partnering with employers and unions diversifies cancer center access.

Michele Waters, Greg Crewse, Cole Manship, Abigail Baldwin-Medsker, Chris Fong, Nikolaus Schultz, Sergio Giralt, Benjamin Roman, Michelle Johnson, Francesca Gany, Carol Brown, Bob T. Li, Justin Jee

Memorial Sloan Kettering Cancer Center, New York, NY

Treatment at academic cancer centers can further research and improve patient outcomes. Interventions improving access to treatment across racial, ethnic, and socioeconomic boundaries might increase the generalizability of studies conducted at such centers and reduce healthcare inequities. Memorial Sloan Kettering (MSK) is an academic cancer center based in New York and New Jersey (NY/NJ). Like many other NCI-designated cancer centers, it has historically served a population within its geographic catchment, with limited diversity. MSK Direct is a national cancer benefits program that partners with employers and unions to provide a direct referral service for their employees or members and their families, including in-person care and remote second opinions outside NY/NJ. Whether such programs diversify access to academic cancer care is understudied.

To evaluate whether the service diversifies access to academic cancer care, we examined the self-identified race and ethnicity, geographic composition, and imputed socioeconomic status (Yost Index) of MSK Direct and non-MSK Direct (Control) patients with at least one assessment note at MSK since program inception in 2016 until September 21, 2023. We further stratified MSK Direct patients based on referral by employers vs. unions. Groups were compared using Chi-square or Student T tests.

The MSK Direct patient population (N=8,604) was more racially diverse than the Control population (N=283,434), with 9.0% Black/African American patients compared to 6.9% Control ($p<0.001$) patients and 9.3% Asian-Far East/Indian Subcontinental patients compared to 7.5% Control patients ($p<0.001$). Of MSK Direct patients, 10.5% identified as Hispanic or Latino vs. 7.5% of Control patients ($p<0.001$). Among MSK Direct patients, 14.2% of union-member patients self-identified as Black vs. 6.1% of non-union members, while Asian patients comprised 12.1% of company-referral patients vs. 5.8% of union patients. Hispanic patients represented 17.4% of union-referral patients vs. 6.5% of company referrals. The median Yost Index of union MSK Direct patients was 25 vs. 12 (non-union) and 17 (Control, $p<0.001$), signifying a less privileged socioeconomic status for union-referred patients. A total of N=336 MSK Direct patients received guidance through remote second opinions across 41 states, with the most common home states being Georgia, Arizona, and Florida.

Addressing healthcare disparities in diverse populations is a complex and systemic challenge. Direct partnerships with employers and unions are a new paradigm that may expand access to academic cancer care outside a center's usual geographic and sociodemographic catchment. Different partnering strategies may enhance the representation of specific patient populations.

#1010 Feasibility of serial microbiome collection in a multi-site neoadjuvant pancreatic cancer clinical trial allowing for a diverse patient population.

S. Rogers[1], R. Thomas[1], I. Nassour[1], I. Sahin[1], B. Ramnaraign[1], K. Russell[2], S. Hughes[1], K. Hitchcock[1], O. Kayaleh[3], A. Turk[4], M. Ratcliff[1], T. George[1];
[1]University of Florida College of Medicine, Gainesville, FL, [2]Tallahassee Memorial Hospital, Tallahassee, FL, [3]Orlando Health, Orlando, FL, [4]Indiana University, Indianapolis, IN

Background: Pancreatic cancer portends a very poor prognosis. It is the third leading cause of cancer deaths in the United States. African Americans have a 50-90% increased incidence of pancreatic cancer in comparison to other racial groups. 20% of patients present with operable disease and will have a median overall survival of 2.5 years if able to undergo surgical resection. There is a desperate need to discover novel ways of treating pancreatic cancer. Understanding of the microbiome may be informative to overcoming chemotherapy resistance, toxicity and improving outcomes and disparities. The aim of this study is to (1) identify changes in the microbiota during neoadjuvant treatment of pancreatic ductal adenocarcinoma that correlate with treatment response and (2) identify changes in the microbiota during neoadjuvant treatment of pancreatic ductal adenocarcinoma that correlate with treatment toxicity in a diverse patient population.
Methods: Patients with resectable or borderline resectable pancreatic cancer who are enrolled in a multi-site clinical trial (NCT03483038) receiving neoadjuvant NEO-Nali-IRI (oxaliplatin, liposomal irinotecan and 5- FU) followed by surgical resection were asked to provide serial microbiome collections of saliva, urine (collected in clinic), and stool with a dietary log during the following four (or five) time points: at baseline, mid-therapy (after C4), at completion of chemotherapy (after C8), after radiation if applicable, and at 4-6 weeks post-operative. Participants were given stool collection kits during clinic visits for home sample acquisition. All stool samples were mailed to the University of Florida Health Cancer Center Microbiome Biorepository. Demographics, stage, medical history and concurrent medications including antimicrobics and probiotics, chemotherapy dose-reductions, delays, discontinuations, adverse events, safety adverse events, attribution of causality, and hospitalizations were obtained. Outcomes include imaging response using RECIST criteria, CA 19-9 trend, development of metastatic disease, and the ability to proceed to definitive surgical resection. DNA will be extracted from stool and analyzed using 16S rRNA sequencing methods to determine signatures and alpha/beta biodiversity. Descriptive statistics and correlative analysis will be reported. Continuous and categorical variables will be compared with Student's t-test and Chi-squared test. Multiple groups will be compared by ANOVA. Kaplan-Meier logistic regression will be performed to compare outcomes between the different microbiota groupings.
Conclusion: Serial microbiome collection from a multi-site clinical trial is feasible during neoadjuvant chemotherapy for pancreatic cancer and can increase the diversity of the sample population.

#1011 A comprehensive comparative analysis of African Americans' early onset and late onset colorectal cancer: A 60 year study in underserved population serving hospital.

S. Challa[1], M. Deverapalli[1], N. Farjana[1], L. Gayathri Chirumamilla[1], R. Oskrouchi[2], S. Mynedi[3], M. Rashid[1], k. senthilvelan[3], B. Shokrani[3], R. Zafar[3], A. Kibreab[3], F. Aduli[3], A. Laiyemo[3], z. Sharif[3], H. Brim[1], **H. Ashktorab**[1];
[1]Howard University, Bethesda, MD, [2]Kuwait, Kuwait, Kuwait, [3]Howard University, Washington, DC

Background: The incident of early onset of colorectal cancer (EOCRC) is increasing in adults including in African Americans (AA).
Aim: To investigate differences between EOCRC compared to late onset colorectal cancer (LOCRC) in AA patients.
Methods: We reviewed demography, pathology and colonoscopy records of patients seen at Howard University Hospital from 1959 to 2023. This retrospective cohort consists of 175 EOCRC cases (<45 years) and 2025 LOCRC cases (>45 years). The age-adjusted rates for EOCRC and LOCRC were calculated for the age categories <45 and above 45.
Results: The cohort comprised predominantly AA individuals (>85%). Gender distribution showed slightly more females (1074, 53%) than males, with no significant difference observed between EOCRC and LOCRC groups (p=0.94). Initial symptoms at presentation were prevalent in both EOCRC (93.8%) and LOCRC (92.6%). Notably, EOCRC exhibited a higher incidence of abdominal pain (23.3% vs. 17.2%, p=0.05) and changes in bowel habits (24.4% vs. 14%, p=0.05) compared to LOCRC. However, other symptoms such as melena, hematochezia, weight loss, and anemia were less prevalent in EOCRC than in LOCRC. Additionally, comorbidities like hypertension (HTN), diabetes mellitus (DM), and inflammatory bowel disease (IBD) were less frequent in EOCRC compared to LOCRC. Family history of colon cancer in first-degree relatives was notably higher in EOCRC (15.5%) compared to LOCRC (3.2%, p=0.01). Pathology reports indicated a higher occurrence of neuroendocrine tumors in EOCRC (2.8%) than in LOCRC (1.4%). Complications such as gastrointestinal bleeding and abdominal CT abnormalities were more frequent in EOCRC. Location-wise, EOCRC was primarily observed in the left sigmoid and rectosigmoid regions (p=0.01). Metastasis to other organs was more prevalent in EOCRC than in LOCRC (p=0.04) suggesting more aggressive and advanced lesions. Surgical interventions were slightly more common in EOCRC (80.4%) than in LOCRC (79.1%). Type of polyps and stage distribution showed some variations between the two groups. Interestingly, the incidence of colorectal cancer showed fluctuations over the years, peaking between 1980 and 1989 before declining in recent years, probably as a result of colonoscopy popularization.
Conclusion: CRC incidence is increasing among young AA who display highly advanced and more metastatic tumors in comparison with LOCRC. While current screening programs seems to have decreased CRC prevalence in individuals older than 45, special attention needs to be addressed to young AA adults as well, to counter the observed trend, as they have the highest incidence of CRC among young population groups by race/ethnicity. Detailed analysis of the molecular landscape of EOCRC AA tumors is needed to understand the differential pathways and mechanisms defining these early onset cancers.

#1012 Colorectal cancer in the American Indian and Alaska Native community: A holistic review.

A. R. Monetathchi, W. Carson, A. Little, F. M. Cordova-Marks, J. Erdrich;
University of Arizona, Tucson, AZ

Colorectal cancer (CRC) is ranked third in the United States for both cancer incidence and mortality. Despite a decline in both categories, CRC continues to be a great concern in American Indian/Alaska Native (AI/AN) communities. AI/AN populations have also experienced the largest increase in early-onset colorectal cancer, have the second highest CRC incidence rates, and the AN community has the highest rates of CRC worldwide. AI/AN populations face numerous barriers and are susceptible to risk factors that may contribute to these findings. Currently, a significant amount of research is on screening efforts. Through conducting a literature review of 63 articles, as well as an additional 11 supplemental sources, this manuscript aims to look at several aspects of CRC including demographics, diet, screening, and the impact of geography. This review presents and organizes available research on CRC in the AI/AN population and explores research beyond screening because a more comprehensive and population-specific fund of knowledge on the totality of the subject is critical to directing more effective prevention, earlier detection, and management. Evaluating different components of CRC honors the holistic approach to health practiced by AI/AN communities.

#1013 Strengths, weaknesses, opportunities, and threats of conducting clinical trials in Nigeria: The IRONMAN study.

O. O. Bolajoko[1], P. Fathi[1], O. Toye[2], D. D. Fulwood[1], A. Popoola[3], C. Ogo[4], H. Dogo[5], O. Fatiregun[6], A. Sowumi[7], P. Jibrin[3], M. A. Jimoh[8], F. Mohammed[9], F. Odedina[1], Prostate Cancer Transatlantic Consortium;

[1]Mayo Clinic, Jacksonville, FL, [2]Prostate Cancer Transatlantic Consortium, Ilorin, Nigeria, [3]University of Ilorin Teaching Hospital, Ilorin, Nigeria, [4]Federal Medical Center, Abeokuta, Nigeria, [5]University of Maiduguri Teaching Hospital, Maiduguri, Nigeria, [6]Lagos State Teaching Hospital, Lagos, Nigeria, [7]Lagos University Teaching Hospital, Lagos, Nigeria, [8]Lagos State University Teaching Hospital, Lagos, Nigeria, [9]Amadu Bello University, Zaria, Nigeria

Background: The need to increase understanding of prostate cancer (CaP) is ever increasing. Unfortunately, there is limited understanding of how CaP affects men of African ancestry (MAA) despite significant disparities in CaP prevention, diagnosis, and treatment due to genetic and sociobehavioral factors. Conducting CaP clinical trials (CTs) in Africa presents multiple opportunities to improve upon collective knowledge of CaP in MAA experiences, expand patient access to CTs, and provide opportunities for African scientists and urologists to contribute to research on the global stage. The International Registry of Men with Advanced Prostate Cancer (IRONMAN) seeks to reduce CaP disparities by sponsoring sites throughout Africa. Four Prostate Cancer Transatlantic Consortium (CaPTC) institutions in Nigeria currently participate in IRONMAN: University of Ilorin Teaching Hospital, Federal Medical Center, University of Maiduguri, and Lagos State University Teaching Hospital. Because CTs of this scale are infrequently conducted in Africa, there are special considerations when conducting CTs in low-middle-income countries (LMICs) like Nigeria.

Methods: Hourlong interviews dedicated to site staff were conducted via Zoom in Spring 2023 (four total). Interviews utilized a Strengths, Weaknesses, Opportunities, and Threats (SWOT) analysis approach. Each interview was recorded, transcribed, and validated by study staff for accuracy. Themes from each were inductively coded and then collated across all four sites.

Results: The urologists, oncologists, phlebotomists, pathologists, nurses, research coordinators that make up the study teams identified the holistics of conducting the IRONMAN study at their sites. Strengths included a large patient population to recruit from and appropriate resources to conduct the study (ex., lab space, clinical knowledge, staffing levels). Weaknesses included the social determinants of health that negatively impact patient participation, limited biorepository space to store samples, and the need for patient-physician trust. The greatest opportunity presented was Nigerian institutions joining more CTs in the future, particularly multi-site global trials. Described threats included staff turnover, national stability, and increased economic disparities.

Discussion: While increasing the overall number of CTs in Africa is a noble cause, sponsors and institutions should note the unique circumstances in implementing CTs in Africa when designing CTs and recruiting sites. Listening to the experiences of study teams is pivotal in ensuring CTs are Africa-minded - they will be complimentary to established research infrastructure, appropriately funded, and culturally responsive all in the name of equitable research. By doing so, ethical compliance and quality data collection will ensue and reduce disparities at the micro, mezzo, and macro levels.

#1014 Disparities of triple negative breast cancer in Mississippi.

N. Kaur[1], J. A. Khan[1], J. Mao[2], D. Melvin[3], M. M. Hassan[1], X. Zho[1];
[1]University of Mississippi Medical Center, Jackson, MS, [2]Tougaloo College,, Tougaloo, MS, [3]Tougaloo College, Tougaloo, MS

Background: Triple-negative breast cancer (TNBC) accounts for about 10-15% of all breast cancers nationwide with disparities of incidence and outcomes among races, geographic locations, and other factors. This study is aimed to analyze the differences in the rate of TNBC, patient conditions at time of diagnosis, and death from TNBC among women in Mississippi.
Methods: A retrospective study was conducted to serially review breast cancer cases diagnosed in the University of Mississippi Medical Center during May 2016 to May 2023. The entire breast cancer population was then stratified by race. The rate of TNBC, age and BMI at time of diagnosis, the rate of expiration were compared between African American (AA) and Caucasian American (CA) women with breast cancer. Two-tailed Student's T-test was used to calculate the difference in mean values, and Chi-Square Test was used to compare the difference in rates or percentages. The significant p value was set at $p<0.05$.
Results: In total 291 women with breast cancer, AA patients were 195 (67.01%), CA patients were 88 (30.24%), and other were 8 (2.75%). The mean age of all patients was 58.3 years-old (ranged 24-97). The mean BMI was 31.19. The patients with TNBC were 109 (37.46%) in entire studied population. A total of 32 (1.6%) patients, including 14 TNBC and 18 non-TNBC were expired with an average age of 61.84 and an average survival time of 20 months from diagnosis to expiration. As compared to CA patient population, AA breast cancer patients had onset at younger age (58.08±0.88 vs. 59.18±1.36), had a higher BMI (31.79±0.62 vs. 28.25±1.05, p=0.017), higher percentage of TNBC (41.54% vs. 30.68%, p=0.082 and OR=1.605), and higher rate of expiration (11.28% vs. 9.1%). Also, as compared to CA expired patients with breast cancer, AA expired patients had higher BMI (29.57 vs. 28.61), shorter survival time (17.5 months vs. 19.4 months), and died at younger age (61.84-year old vs. 66.38-year old) with a higher proportion of TNBC subtype (54.6% vs 12.5%, p=0.045, OR=9.6).
Conclusions: Breast cancer is greatly disparate racially between AA and CA and geographically between Mississippi and US national average. The disparities are manifested in the proportion of TNBC subtype, age at onset of breast cancer, BMI at time of diagnosis, and death rate.

#1015 Potential of kava in reducing lung cancer risk and associated disparities: Mechanism-based biomarker discovery and analysis.

C. Xing[1], B. Freeman[1], J. Mamallapalli[1], A. Lynch[1], N. Fujioka[2], R. G. Salloum[1], J. Malaty[1], F. Orlando[1], Z. Huo[1];
[1]University of Florida, Gainesville, FL, [2]University of Minnesota, Minneapolis, MN

Background: Lung cancer is the leading cause of cancer-related deaths. Tobacco smoke is well-recognized as the dominant risk factor. Stress, lung inflammation, air pollution and other factors also contribute to the risk of developing lung cancer Racial/ethnic disparities in lung cancer risks exit as well. The quantitative contributions of different these risk factors to lung cancer and associated disparities, however, have not been systematically characterized. One major barrier is the lack of tools to non-invasively and objectively quantify these risk factors, which precludes the identification of high-risk individuals and the development of effective prevention. Data from our group, particularly results from a pilot clinical trial, suggest that kava, traditionally consumed in the South Pacific Islands as a beverage to reduce stress and promote relaxation, may holistically reduce lung cancer risk by impacting multiple factors that contribute to lung cancer risk.

Aim: This study aims to discover mechanism-based non-invasive biomarkers reflective of different lung cancer risk factors and explore their potential roles in lung cancer risk disparities. Such biomarkers are also employed to characterize the holistic effects of kava in reducing lung cancer risk and its potential in mitigating associated disparities.

Results and Analysis: One-week of kava significantly reduced the level of nicotine exposure among smokers, quantified by the Total Nicotine Equivalents (TNE) in the 24-h urine sample. Excitingly the reduction in TNE appeared to be higher among African American smokers in comparison to participants of other race/ethnicity. Biomarkers for stress (plasma cortisol and urinary total cortisol equivalents (TCE)) were significantly reduced upon one-week kava use, which may mechanistically contribute to the reductions in tobacco use. The reduction in plasma cortisol and TCE were higher among African American smokers as well. One-week kava exposure also increased urinary excretion of total NNAL and reduced urinary 3-methyladenine (3-mA) in participants, suggestive of its ability to reduce the carcinogenicity of nicotine-derived nitrosamine ketone (NNK). Kava effects on NNAL and 3mA were again more pronounced among African American smokers.

Conclusion and future directions: These results demonstrate the potential of mechanism-based biomarkers in investigating lung cancer risks and associated disparities. Such biomarkers may also facilitate the translational development of effective and targeted interventions, such as kava, which may not only reduce lung cancer risk but also mitigate the associated disparities. Additional mechanism-based biomarkers on other tobacco carcinogens and inflammation are currently under development. Two clinical trials are ongoing that the current clinical samples will help validate these discoveries.

#1016 Food insecurity among patients with cancer in the US.

A. R. Marrero-Gonzalez[1], A. Crawford[1], F. Draper[2], A. Incudine[2], S. T. Lindau[3], E. M. Graboyes[1];
[1]The Medical University of South Carolina (MUSC), Charleston, SC, [2]Family Reach, Boston, MA, [3]The University of Chicago, Chicago, IL

Introduction: Food insecurity (FI) is common among cancer patients and can lead to decreased treatment adherence, worse quality of life, and increased recurrence and mortality. Although some studies suggest that patients with cancer are particularly susceptible to FI, these studies have been limited by their small sample size, narrow sampling of cancer types and stages, and limited geographic scope. To address this gap, this study leverages data from a supportive care organization to characterize FI prevalence and associated risk factors in a nationwide sample of patients with diverse types of cancer.
Methods: This cross-sectional study included adults with cancer undergoing treatment referred to Family Reach, a national organization that provides financial support to cancer patients and their families, from 2020-2023. The primary outcome was FI, defined as a self-reported concern that the family would run out of food before getting enough money to buy more. Estimates of FI were provided for the cohort stratified by cancer type; multivariable logistic regression was used to evaluate the association of cancer type (primary independent variable) with FI, adjusted for oncologic and demographic covariates.
Results: Of 6,615 patients with cancer, 62.9% reported FI. Across cancer types, FI prevalence ranged from 56% (brain) to 68% (gynecologic). FI did not vary significantly by cancer type on multivariable logistic regression adjusted for oncologic, geographic, and demographic factors (**Table 1**). A variety of demographic factors were associated with FI (**Table 1**).
Conclusion: Nearly two-thirds of patients with cancer served by a large national cancer support organization reported FI. FI was common across all types of cancer and was associated primarily with demographic characteristics. These FI prevalence and risk factor data can be used by researchers, clinicians, and community-based organizations to understand and address FI among patients with cancer.

Table 1. Characteristics of Patients with Cancer With Food Insecurity Referred to Family Reach and Factors Associated with Food Insecurity Using Multivariable Logistic Regression Analysis.

Outcome	N (%)	aOR	(95% CI)	Outcome	N (%)	aOR	(95% CI)	Outcome	N (%)	aOR	(95% CI)
Cancer Type				Age, y				Region of US			
• Breast	1,348 (32.4)	Ref	-	• 18-64	3,887 (93.3)	Ref	-	• Pacific	465 (11.2)	Ref	-
• Brain	118 (2.8)	0.84	(0.61 - 1.16)	• ≥65	279 (6.7)	0.38	(0.3 - 0.48)	• Mountain	246 (5.9)	0.94	(0.71 - 1.23)
• Gastrointestinal	500 (12)	1.13	(0.92 - 1.38)	Gender				• West South Central	489 (11.7)	1.09	(0.87 - 1.38)
• Genitourinary	115 (2.8)	1.1	(0.78 - 1.55)	• Male	1,298 (31.2)	Ref	-	• West North Central	213 (5.1)	1.09	(0.82 - 1.44)
• Gynecologic	274 (6.6)	1.21	(0.95 - 1.54)	• Female	2,859 (68.6)	1.04	(0.91 - 1.19)	• East South Central	302 (7.2)	1.6	(1.21 - 2.13)
• Head and Neck	82 (2)	1.08	(0.72 - 1.62)	• Other	9 (0.2)	1.07	(0.25 - 4.6)	• East North Central	466 (11.2)	1.02	(0.81 - 1.29)
• Hematologic	958 (30)	0.95	(0.79 - 1.15)	Race and Ethnicity				• South Atlantic	941 (22.6)	1.14	(0.93 - 1.4)
• Lung	247 (5.9)	0.99	(0.77 - 1.26)	• Non-Hispanic White	1,725 (41.4)	Ref	-	• Middle Atlantic	851 (20.4)	0.76	(0.62 - 0.94)
• Melanoma/Sarcoma	200 (4.8)	0.97	(0.74 - 1.28)	• Non-Hispanic Black	1,249 (30)	1.6	(1.4 - 1.83)	• New England	193 (4.6)	1	(0.74 - 1.36)
• Other	324 (7.8)	1	(0.79 - 1.25)	• Hispanic White	832 (20)	1.63	(1.36 - 1.96)	Preferred Language			
Stage				• Asian or Pacific Islander	130 (3.1)	1.1	(0.82 - 1.49)	• English	3,686 (88.5)	Ref	-
• I	415 (10)	Ref	-	Health Insurance				• Spanish	328 (7.9)	1.69	(1.26 - 2.28)
• II	652 (15.7)	1.01	(0.81 - 1.25)	• Private/commercial	718 (17.2)	Ref	-	• Other	61 (1.5)	1.26	(0.81 - 1.98)
• III	814 (19.5)	1.11	(0.9 - 1.37)	• Self-pay	240 (5.8)	2.35	(1.74 - 3.16)				
• IV	1,254 (30.1)	1.07	(0.87 - 1.32)	• Medicaid	1,588 (38.1)	1.87	(1.62 - 2.16)				
• Not applicable	1,031 (24.7)	0.87	(0.69 - 1.08)	• Medicare	536 (12.9)	2.23	(1.81 - 2.76)				
Relapsed				• Medicare + Medicaid	122 (2.9)	2.98	(2.06 - 4.3)				
• Yes	631 (15.1)	Ref	-	• Other	782 (18.8)	1.45	(1.23 - 1.7)				
• No	3,535 (84.9)	1.11	(0.95 - 1.29)	Employment							
				• Dual employment	1,343 (32.2)	Ref	-				
				• Single employment	2,428 (58.3)	1.24	(1.1 - 1.38)				
				• Dual unemployment	261 (6.3)	1.7	(1.31 - 2.21)				

#1017 Characterizing immune cell infiltration in colorectal cancer tumor microenvironment among Native Hawaiians.

Y. Fu, G. Quintal, M. Nasu, M. Jijiwa, S. K. Rai, I. Mohd-Ibrahim, Y. Chen, H. Yang, Z. Wang, C. Wai, O. Chan, B. Y. Hernandez, Y. Deng;
University of Hawaii at Manoa, Honolulu, HI

Background Colorectal cancer (CRC) is recognized as a heterogeneous disease, ranking third in new cancer diagnoses and second in cancer-related deaths globally and nationally. CRC incidence is higher in the state of Hawaii compared to the U.S. overall. This study focuses on profiling immune cell infiltration in Native Hawaiian(NH)-specific CRC tumor microenvironments. Identifying the race-specific tumor infiltrating microenvironment may uncover potential mechanisms for CRC development in the NH population.

Methods Deidentified, archival formalin-fixed paraffin-embedded tumor samples from Native Hawaiian patients diagnosed with primary CRC between 1990 and 2006 were obtained from the Hawaii Tumor Registry. RNA was extracted from tumor and adjacent normal tissues. RNA-seq data from Caucasian American (CA) CRC samples were obtained from The Cancer Genome Atlas (TCGA) and the Gene Expression Omnibus (GEO). Differentially expressed genes for each cohort were identified via DESeq2 with Benjamini-Hochberg multiple testing q-value<0.05 and a cutoff of 2-fold change. From the gene expression profiles, we applied the ESTIMATE algorithm to calculate the overall immune cell infiltration score for each sample. Based on a deconvolution algorithm, known as CIBERSORT to estimate the abundance of 22 immune cell types, we profiled the tumor-infiltrating immune cells present in each cohort's paired samples, respectively. To improve the accuracy, p-value and root mean squared error were counted for each sample. Data with $p<0.05$ were filtered and selected for the next analysis. The fraction of immune cell subpopulations was evaluated and compared between paired tumor and adjacent normal tissues in NH and CA cohorts.

Results In the NH cohort, we found the overall immune cell infiltration score was significantly lower in cancer tissues than the adjacent normal tissues ($p<0.05$), and there were significantly higher fractions of activated dendritic cells, resting natural killer (NK), and follicular helper T cells in tumor tissues compared to adjacent non-tumor tissues ($p<0.05$). Furthermore, the fractions of activated NK cells and plasma cells were significantly lower in tumor tissues than in adjacent non-tumor tissues in NH ($p<0.05$). Resting NK cells are upregulated in both the NH and the CA cohorts, while plasma cells are the only immune cell type downregulated in either cohort. In the NH cohort, activated dendritic cells and follicular helper T cells are exclusively upregulated, while activated NK cells are downregulated relative to the CA cohort.

Conclusion This study demonstrates that the NH cohort displays distinctive immunological variances between tumor and adjacent non-tumor tissues which distinguishes them from the CA cohort. This emphasizes the significance of acknowledging population-specific genetic variations which may help understand race specific difference in CRC.

#1018 Characteristics and outcomes of patients with cystic fibrosis and pancreatic cancer: A population-based comparative analysis.

S. Manchkanti[1], S. J. Gaddam[2], **U. S. Grewal**[3];

[1]Carver College of Medicine, University of Iowa, Iowa City, IA, [2]Louisiana State University Health Sciences Center, Shreveport, LA, [3]University of Iowa Hospitals and Clinics, Iowa City, IA

Introduction: Advancements in diagnosis and treatment of cystic fibrosis (CF) has allowed improvement in overall survival which also in part explains the increasing incidence of malignancies among these patients, particularly, gastrointestinal cancers. Existing data related to the characteristics and outcomes of patients with CF and pancreatic cancer (PC) are limited to small case series. We sought to investigate the same using a large population-based database.
Methods: We used TriNetX, a national database comprising approximately 74 million patients across 54 healthcare organizations in the United States. We retrospectively identified patients with CF who also had a diagnosis of PC (using ICD-10 codes). We then performed an age, sex and race-matched analysis to compare patients with CF+PC to patients with CF alone. To study the impact of CF diagnosis on PC-related outcomes, we performed a propensity matched analysis between cohorts of patients with CF+PC and patients with PC alone. Kaplan Meier estimates were used for survival analysis. A p-value of <0.05 was considered statistically significant.
Results: We identified a total of 41,655 patients with CF, out of which 198 patients had a diagnosis of PC (0.48 %). A total of 180 patients were included in the propensity matched comparative analysis. Patients with CF and PC had a significantly higher prevalence of type 2 diabetes mellitus (42.8% vs 5.6%, p<0.001), hypertension (58.3% vs 5.6%, p<0.001) and hyperlipidemia (40% vs 5.6%, p<0.001) than patients with CF with no PC. No differences in the prevalence of liver cirrhosis were noted (8.9% vs 5.6%, p=0.22). Patients with PC and CF had a significantly lower prevalence of bronchiectasis (15.8% vs 28.7%, p=0.004). In a propensity matched analysis between patients with CF and PC and PC alone, CF did not impact survival among patients with resectable [HR=1.042 (0.35-3.11), p=0.79] or unresectable/advanced PC [HR=1.17 (0.62-2.22), p=0.09].
Conclusion: To our knowledge, this is the largest analysis investigating the characteristics and outcomes of patients with CF and PC. The prevalence of PC in patients with CF is higher than reported prevalence among general population. We found a significantly higher prevalence of diabetes, hypertension and hyperlipidemia and a significantly lower prevalence of bronchiectasis among patients with CF and PC. CF does not appear to impact overall survival among patients with resectable or unresectable or advanced PC. Our findings may inform risk prediction models for PC among patients with CF.

#7454 Cognitive function in older breast cancer survivors after chemotherapy.

R. Kim, K.-P. Liao, S. Peterson, D. Zorzi, L. Li, M. Chavez MacGregor, S. Giordano;
UT MD Anderson Cancer Center, Houston, TX

Background: In the United States, over 60% of breast cancer survivors are 65 years and older; however, little is known about patient-reported symptoms and the effect that cancer treatments could have on survivors years after their primary treatment and diagnosis. This study evaluated perceived cognitive function in older breast cancer survivors and whether prior chemotherapy was associated with cognitive outcomes.
Methods: Breast cancer patients aged 65 years and older, diagnosed 2012-2013, with local and regional stage disease, were identified through the linked Texas Cancer Registry-Medicare dataset (TCR). Survivors were mailed a survey to assess their cognitive function through the Functional Assessment of Cancer Therapy-Cognitive Function (FACT-Cog V3) instrument (section G of the survey). The survey also collected demographic and clinical data and was collected between April 2018 and October 2019. Utilizing the data from the self-administered questionnaires, TCR, and Medicare claims, the cognitive function and quality of life among elderly patients were evaluated to assess whether prior chemotherapy and/or endocrine therapy impacts long-term health. A linear regression model was used to examine the significance of receiving chemotherapy to FACT-Cog V3 primary score while controlling for respondent sociodemographic and clinical variables.
Results: Of 4,448 eligible patients, 1,954 (43.9% response rate) responded to section G. Of these, 1,065 respondents completed all 4 sections, 37 questions. Eighty of those 1065 respondents self-reported disease recurrence which excluded them from the analyses in order to avoid biases, leaving a total of 985 cases for this study. Median time from diagnosis to survey completion was 68 months (IQR 62-73). Receipt of chemotherapy was associated with a slightly lower FACT-Cog score. In total, those with chemotherapy scored, on average, 105.6 (SD 21.2) while those without scored 107.1 (SD 22.3). The largest difference in mean scores is attributed to the Perceived Cognitive Impairment subsection (scored from 0-72) where those with chemotherapy scored, on average, 57.2 (SD 13.8) and those without scored 58.7 (SD 14.0).
Responsible Conduct Of Research: We need to ensure that the privacy of our patients will be protected when using their information from the surveys.
Conclusion: Adjuvant chemotherapy was associated with more self-reported cognitive impairment in older breast cancer survivors, even 5-6 years after diagnosis. However, the difference between patients who received chemotherapy versus those who did not was modest, suggesting limited clinical significance. Further research is needed to determine the long-term impact of cancer treatments, particularly in older cancer survivors.

CLINICAL RESEARCH: Diagnostic Biomarkers 1
Poster Session

#1021 Defining total protease activity profiles in pancreatic cancer using a FRET substrate array.
M. Stewart, A. Quentel, J. Montoya Mira, E. Manalo-Hall, S. Ranganathan, B. Branchaud, F. Civitci, E. Tu, J. Fischer, Y.-J. Chiu, A. Yildirim;
Knight Cancer Institute, Oregon Health & Science University, Portland, OR

Proteases are an important component of many biological processes in the human body, and as such makes them a well-known subject to explore when investigating a variety of disease states from cancer to cardiovascular disease. In all stages of cancer, including early development, proteases play critical roles in almost every aspect for processes such as invasion, promotion of tumor growth, and metastasis. This makes screening of circulating proteases a potentially powerful tool for early detection and prognosis for a variety of cancers. The human proteome, however, is very complex, with around 600 proteases in total, and at least 234 of them found in circulation. Additionally, proteases often act on more than one substrate, cross reactively cleaving several substrates at different rates, further adding to the complexity of cleavage patterns of the human proteome. Previous liquid biopsies for cancer detection based on protease cleavage patterns focused mainly on detecting the activities of specific proteases, using single substrates to examine the effects of well-studied cancer-related proteases such as MMPs and cathepsins. In this study, we developed a method for screening cleavage patterns of proteases active in plasma samples that deviated from this norm. Due to the complexity of the human proteome, rather than developing a specific substrate for a specific protease, we utilized a large array of substrates to screen for cleavage patterns in plasma samples of cancer patients aimed at not one specific protease, but a wide range that may be present. In this proof of concept study, we used a commercially available internally quenched set of 360 substrates composed of 8 amino acids and a FRET pair. Initially, we optimized this assay to measure protease activity in the complex plasma environment. Next, we screened several plasma samples collected from patients with pancreatic ductal adenocarcinoma (PDAC) or pancreatitis, and screen negative samples using the 360 substrate set assay and identified 5 top substrates that were proficient in identifying PDAC from other conditions. Finally, we performed a validation study with a larger cohort (45 screen negative, 26 PDAC, 19 pancreatitis) using the selected substrates to determine the diagnostic performance of the assay. All five of the selected substrates showed 1.3-1.8-fold increase in fluorescence signal in PDAC compared to screen negative and pancreatitis. Amongst the cancer samples, the substrates showed no significant difference between stage, supporting possible applications for early detection. Additionally, area under the curve analysis of the five substrates gave a score of 0.8. In summary, in this study, we reported a novel approach for the detection of cancer exploiting the protease cleavage patterns in plasma samples. We believe that this approach holds great potential for detecting substrates and proteases for early detection of PDAC and other cancers.

#1022 Integration of cerebrospinal fluid methylome and proteome can obviate the need for biopsy in central nervous system lymphoma.

A. P. Landry[1], J. A. Zuccato[1], V. Patil[2], M. Voisin[1], J. Z. Wang[1], Y. Ellenbogen[1], C. Gui[1], A. Ajisebutu[1], F. Nassiri[1], G. Zadeh[1];
[1]University of Toronto, Toronto, ON, Canada, [2]University Health Network, Toronto, ON, Canada

Background: The diagnosis of intra-axial brain tumors requires histopathological examination of tissue obtained by neurosurgery in current clinical practice, which comes with inherent risks. Some patients, particularly those with primary CNS lymphoma (PCNSL), only undergo surgery to obtain a diagnosis and do not derive any therapeutic benefit from surgical resection or debulking. Less-invasive techniques for diagnosis, such as liquid biopsy, therefore provides an opportunity to mitigate surgical risk in these patients.
Methods: Patients with histopathology confirmed glioblastoma (GBM, IDH wild type), brain metastases (BM), and PCNSL with accompanying cerebrospinal fluid (CSF) samples were included in our study. Cell-free DNA methylation profiling and shotgun proteomics were obtained for all patients and used to train classifiers to distinguish each tumour entity from others. Specifically, binomial elastic net regression models were built by combining both data modalities using established early and late integration paradigms and performance was compared to classifiers built from individual data types alone. Each model was repeated 100 fold and performance assessed on an untouched testing subset.
Results: Our cohort includes 20 patients with GBM, 17 with BM, and 14 with PCNSL, each with matching CSF cell-free DNA methylation and shotgun proteomic profiling. We show that these data can be integrated to fully discriminate PCNSL from its major diagnostic counterparts with a perfect median AUC of 1.00 (95% CI 1-1) and 100% specificity. Integrated "lymphoma vs other" models significantly outperform models trained on methylation or protein data alone, though the same dramatic improvement was not demonstrated in GBM or BM, suggesting synergistic biological information is specific to lymphoma.
Conclusions: There is a critical need to diagnose patients with intra-axial tumours, particularly PCNSL, without relying on invasive and costly surgery. We present the most specific and accurate CNS lymphoma classifier to date by integrating the methylome and proteome of CSF. This has the potential for immediate clinical utility, eliminating the need for biopsy in an important subset of these patients.

#1023 Whole-genome methylation analysis using liquid biopsy for pancreatic cancer diagnosis.

T. Ito[1], T. Iwasawa[2], S. Takeda[2], C. Okamoto[2], T. Motohashi[2], S. Ueda[1], H. Kato[1], R. Yamamoto[1], A. Koizumi[1], Y. Murai[1], K. Nihei[1], M. Itakura[1], R. Akima[1], M. Sakurada[1], K. Tanaka[1], T. Kushida[1], K. Sato[1];

[1]Juntendo Shizuoka Hospital, Juntendo Univ. School of Medicine, Izunokuni-shi, Japan, [2]Shizuoka Medical Research Center for Disaster, Juntendo Univ. School of Medicine, Izunokuni-shi, Japan

Objective: Pancreatic cancer is one of the highly malignant tumors. Its diagnosis requires invasive ultrasound endoscopic biopsy or endoscopic retrograde cholangiopancreatography (ERCP). However, these methods are limited by false-positive results and complications. Liquid biopsy, which uses blood to detect *KRAS* mutations in cancer, can be used to overcome these hurdles. However, only about 30% of cases can be detected as a diagnostic marker by *KRAS* mutations using plasma from patients with stage I-II pancreatic cancer, and its clinical application remains a challenge. Therefore, in this study, we focused on diagnosing pancreatic cancer using methylated DNA in plasma cell-free DNA (cfDNA) obtained from pancreatic cancer and non-cancer patients.
Subjects: Plasma was collected before the start of the treatment from six patients diagnosed with pancreatic cancer from 2019 to 2023 at our hospital, and six non-cancer patients simultaneously.
Methods: Whole-genome bisulfite sequencing (WGBS) using next-generation sequencing (NGS) was performed using the cfDNA obtained from the plasma of pancreatic cancer and non-cancer patients.
Results: The cfDNA fragments obtained by WGBS revealed that promoter regions were mostly deleted, and no difference was observed between cancer and non-cancer patients. The methylation rate of cfDNA fragments by WGBS differed between cancer and non-cancer patients, with multiple methylation sites (>100 sites) in intergenic regions.
Discussion: Although attempts have been made to diagnose cancer using genetic mutations and liquid biopsy, only a few studies are available on using methylation markers in the plasma cfDNA of pancreatic cancer patients, and the effectiveness of this method remains unclear. In the present study, we found that promoter regions were deleted by WGBS, and several distinct hypermethylated regions were present in the intergenic region between pancreatic cancer and non-cancer samples, suggesting the presence of certain markers that can distinguish between pancreatic cancer and non-cancer patients.
Conclusion: This small number of cases suggests that hypermethylation of the intergenic regions could be helpful in the diagnosis of pancreatic cancer. We will need more cases in the future to verify the usefulness of hypermethylation of intergenic regions in the diagnosis of pancreatic cancer.

#1024 Differential gene expression of colorectal cancer biomarkers in Hispanic individuals.

E. V. Caraballo-Rivera[1], **H. Centeno-Girona**[1], G. De Jesus-Astacio[2], C. Zenon-Melendez[1], B. Torres-Velasquez[1], M. Martir-Ocasio[1], M. R. Cruz-Correa[3]; [1]University of Puerto Rico Comprehensive Cancer Center, San Juan, PR, [2]Ponce Health Sciences University, San Juan, PR, [3]University of Puerto Rico, San Juan, PR

Colorectal cancer (CRC) is a leading cause of cancer death among men and women in Puerto Rico and the United States. About 60-70% of CRC cases are found at advanced stages (III/IV), suggesting limited adherence to available screening methods. Several molecular biomarkers have been identified as discriminatory for CRC (e.g., KRAS, NRAS, MSI), improving CRC management and patient outcomes. This study evaluates the differential expression patterns of DKK3, PKM2, IGFBP2, and SEPT9 genes between matched CRC tumors and adjacent mucosa samples. The secondary outcome was to examine the association between the presence of the selected biomarkers in tissue compared to blood samples. Using a retrospective study design, we examined 112 tissue samples of Hispanic individuals with a pathology-confirmed CRC diagnosis recruited throughout the Puerto Rico Familial Colorectal Cancer Registry (PURIFICAR). We quantified expression levels of target genes by RT-qPCR normalized with endogenous control GAPDH, using TaqMan Gene Expression Assay in the QuantStudio 3 (Applied Biosystems). Wilcoxon signed-rank test was used to calculate differences between gene expression from tumor and adjacent mucosal tissue samples. Additionally, 39 paired blood and tissue samples were analyzed to explore the association between biomarkers in these two types of samples. Protein biomarkers were measured using a commercially available ELISA kit according to manufacturer protocols (Thermo Scientific Federick, MD and Biosource San Diego, CA). mSEPT9 was measured using the Epi proColon® 2.0 CE test. The association between biomarker presence in tissue and blood samples was assessed using the Chi-square test of independence, with biomarker concentrations dichotomized at the median value. Statistical analyses were performed using Stata 17 and R version 4.3.1. DKK3 and IGFBP2 expression levels were higher among CRC tumor samples. However, expression levels of PKM2 and SEPT9 genes were slightly lower. DKK3 was the only target gene significantly different ($p<0.05$) when comparing overall gene expression between the matched samples. Upon comparison between early and advanced CRC stages, DKK3 expression levels were higher in advanced-stage tumor samples when compared to adjacent mucosal tissue samples ($p<0.05$). Moreover, a significant association between IGFBG2 presence in tissue compared to blood was detected at a 90% confidence level (p-value<0.10). This association was evident in early-stage CRC cases; there is a relationship between IGFBG2 biomarker presence in tissue and IGFBG2 biomarker presence in blood ($p<0.05$). Our findings indicate DKK3 and IGFBP2 as potential biomarkers for CRC progression and early detection. The study's insights into the differential expression patterns of these biomarkers can inform targeted screening strategies. Further research is needed to assess their potential to enhance early tumor detection in Hispanics.

#1025 An AI based CT scan classifier for predicting extranodal extension and nodal metastasis of HPV-associated oropharyngeal carcinoma.

B. Song[1], k. yang[2], S. Pan[1], L. Li[1], Q. Liu[3], J. Lee[2], S. Stock[2], N. F. Saba[1], M. Bilen[4], M. R. Patel[4], A. Madabhushi[1];
[1]Emory University, Atlanta, GA, [2]Cleveland Clinic, Cleveland, OH, [3]California State University, Los Angeles, CA, [4]Winship Cancer Institute, Atlanta, GA

Background: Pathologic extranodal extension (ENE) and nodal metastasis (NM) are of prognostic significance in human papillomavirus (HPV)-associated oropharyngeal squamous cell carcinoma (OPSCC). The pretreatment identifications of these two factors through computed tomography (CT) imaging are of clinical importance since they could guide treatment de-escalation protocols and select candidates suitable for surgery. In an effort to enhance pretreatment decision making, we developed and validated an AI model (specifically a multi-layer perceptron (MLP)-based deep learning model) to predict radiologic NM and pathologic ENE in HPV-associated OPSCC patients.

Methods: Radiographic CT scans for 290 OPSCC patients treated with definitive chemoradiation were acquired from The Cancer Imaging Archive (TCIA) and divided into training (D_1) and validation (D_2) cohorts for NM prediction. Radiologic NM for D_1 and D_2 were reviewed by two radiologists. Only nodes with concordant NM judgments from both radiologists were included for analysis. An additional 46 OPSCC patients treated with surgery at Emory Winship Cancer Institute were collected to form the test cohorts (D_3) for ENE prediction. The largest metastatic or normal nodes were annotated for D_1 and D_2 while all visible nodes with pathology confirmation of ENE from D_3 were annotated. We present a novel deep-learning model utilizing U-shaped multi-layer perceptron mixer (MLP-Mixer) to capture both global and local feature representations by spatially aggregating image patch information through a procedure called token-mixing. The model was trained for 20 epochs with learning rate of0.0001 and batch size of 64. The diagnostic performance of the AI model was evaluated on D_2 and D_3 using accuracy and area under the ROC curve (AUROC).

Results: There were 121 NM negative and 130 NM positive nodes in D_1, 14 NM negative and 25 NM positive nodes in D_2 and 46 ENE negative and 20 ENE positive nodes in D_3. On D_2 for NM prediction, the AI model achieved overall accuracy of 0.77 and AUROC of 0.78. On D_3 for ENE prediction, the AI model achieved overall accuracy of 0.71, AUROC of 0.69, positive predictive value of 0.52 and negative predictive value of 0.86.

Conclusions: The new AI--based deep learning model was able to identify HPV-associated OPSCC NM and ENE with satisfactory diagnostic performance and shows promise to assist clinicians in treatment decision-making. Additional, multi-site prospective validation of the approach is warranted.

#1026 Post-surgery sequelae unrelated to disease progression and chemotherapy revealed in follow-up of stage III colon cancer patients.

A. Kudriavtsev[1], A. Mirandola[1], C. I. Cofre Munoz[2], R. Comas Navarro[3], M. Macagno[4], B. Pastor[1], E. Pisareva[1], M. Sanchis Marin[3], J. Gonzalo Ruiz[3], A. Sapino[4], A. Bartolini[4], M. Di Maio[5], C. Sanchez[1], Y. Gricourt[6], X. Capdevila[7], G. Lossaint[8], E. Crapez[8], M. Ychou[8], R. Salazar Soler[2], E. Fenocchio[4], P. X. Fernandez Calotti[2], P. Cuvillon[6], T. Mazard[8], C. Santos Vivas[2], E. M. E. Elez[3], F. Di Nicolantonio[4], **A. R. Thierry**[1];

[1]INSERM U896 - IRCM (Montpellier), Montpellier, France, [2]Institut Catala d'Oncologia (ICO) - IDIBELL,, Barcelona, Spain, [3]VHIO Vall d'Hebron Institute of Oncology,, Barcelona, Spain, [4]Istituto di Candiolo - Fondazione del Piemonte per l'Oncologia - IRCCS,, Candiolo, Torino, Italy, [5]University of Torino, Torino, Italy, [6]Centre Hospitalo-Universitaire (CHU), Nimes, France, [7]Montpellier University Hospital, Montpellier, France, [8]Institut du Cancer de Montpellier, ICM, Montpellier, France

A gap currently exists in our understanding of causes of elevated total circulating DNA (cirDNA) levels in cancer patients following tumor resection, and the influence of anesthesia or surgery on cirDNA release. Indeed, the post-surgery dynamics of cirDNA have been largely overlooked to date, despite their importance in determining the optimal timing for assessment of minimal residual disease (MRD). Since cirDNA levels were recently found to be associated with neutrophil extracellular traps (NETs) formation in various cancers, we investigated NETs and cirDNA post-surgery.We conducted two clinical studies to explore the dynamics of cirDNA quantity and of neutrophil extracellular traps (NETs) markers: (1) a peri-surgery study over a duration of up to 72 hours, which involved stage I-III colon (n=10), prostate (n=10), and breast (n=9) cancer patients; and (2) a post-surgery study that extended up to two years post-surgery, and which involved 74 stage III colon cancer patients. We assessed plasma levels of cirDNA using qPCR, and assessed two protein markers of NETs using ELISA, in both cancer patients and control group of healthy individuals (HI) (N=114). This second study is the first prospective, multicenter, blinded study of the dynamics of the total cirDNA post-surgery, for a period of up to two years.We observed that (i), NETs formation contributes to post-surgery conditions; (ii), peri- and post-surgery cirDNA levels were highly associated with NETs formation in colon cancer; (iii), each tumor type showed a specific pattern of the peri-surgery dynamics of cirDNA and NETs markers; peri-operative levels of these markers are significantly lower in breast cancer patients as compared to prostate and colorectal cancer patients; (iv), a significant proportion of patients showed pre- (58.1%) and post-surgery (80.4%) median marker values higher than in HI, even after 2 years following tumor resection, (v) these markers were either equal to or greater (23.2%) than their pre-surgery counterparts; and (vi), elevated values of these markers did not derive from chemotherapy toxicity.We provide evidence that, for cancer patients in the post-surgery period, cirDNA originates mainly from NETs. This finding calls into question the current method of assessing MRD according to the fraction of mutant cirDNA, given that the level of NETs formation appears to be patient dependant. The peri-surgery dynamics of NETs formation and cirDNA release vary according to the surgical procedure and cancer type. In a significant part of patients with colon cancer, NETs continue to persist for more than a year after surgery, irrespective of disease progression or chemotherapy use. Nevertheless, cirDNA and NETs marker levels vary in cases with post-surgery inflammatory/thrombotic adverse events. Our work highlights the existence of long-lasting “sequelae” effects of cancer, previously unreported.

#1027 Immunohistochemistry (IHC) to assess tumor cell-associated OX40 expression in lymphoma PDXs.

J. Lin[1], X. Tu[1], L. Zhang[1], H. Yu[1], C. Jiang[1], T. Yang[2], **H. Q. Li**[2];
[1]Crown Bioscience, Suzhou, China, [2]Hanx Bio, Hangzhou, China

Background. Tumor necrosis factor receptor superfamily member 4, or OX40, is an immunostimulatory receptor usually expressed in activated T-cells. The OX40-OX40L (ligand of OX40) interaction plays a crucial role in the enhancement of T-cell proliferation, survival, and cytokine production, including those in tumor microenvironment (TME) leading to increased anti-tumor immunity[1]. OX40 agonist antibodies have been widely tested for immunotherapy for solid tumors[2,3]. Interestingly, in the treatment of lymphoma, the situation may become more complicate, where OX40 could also be found to be expressed on lymphoma cells, in addition to TME. This phenomenon might or might not impact OX40 agonist therapy. This report aims at developing an immunohistochemistry (IHC) assay to assess tumor-associated OX40 by utilizing morphology approach to understand OX40 expression in lymphoma cells, as opposed on tumor-infiltrate T-lymphocytes (TILs) present in TME. FFPE samples from patient-derived xenografts (PDXs), recapitulating the main pathological features of the original tumors, but exclusive of human TILs, were used as the first stage of the assay development, avoiding TIL interference prior to human sample testing.

Methods. Ninety leukemia and lymphoma PDXs are comprehensively annotated, including RNAseq and histopathology (HuBase™; *https://hubase.crownbio.com*). IHC staining of PDX FFPE slides or TMA (tissue microarray) of various cancers was performed using a commercial OX40 antibody (CST, #61637) and Bond RX Automated IHC/ISH Staining System (Leica Biosystems), followed by whole slide imaging by NanoZoomer NDP2.0-HT Digital Slide System (Hamamatsu) and quantitative analysis by HALO™ image analysis software (Indica labs). OX40 IHC scores were also compared to the RNA expression determined by RNAseq.

Results. A total of 90 leukemia and lymphoma PDXs were comprehensively evaluated. RNASeq data (human mRNA) indeed revealed OX40 gene expression (cutoff as Log2 (FPKM)>3) in 8.9% of models (8/90 models); on the other hand, IHC data also confirmed these OX40 protein expression; and the IHC scores largely correlated with the RNA data. Together, our data firmly confirmed the expression of OX40 in certain hematological cancers, beyond just in TME. The ongoing studies is investigating the characteristics of the OX40 positive lymphoma/leukemia, and the preliminary data will be presented in the annual conference. Furthermore, we are also using the same assay to explore other cancer types beyond hematological cancers.

Conclusion. A tumor associated OX40 expression IHC workflow was preliminarily established and validated to facility the OX40 immunotherapy development.

#1028 Assessment of the diagnostic accuracy of Oncuria-Detect® for detection of upper tract urothelial carcinoma.

T. Sakatani[1], **S. Tanaka**[1], K. Fujita[2], J. Linehan[3], K. Murakami[1], R. Lee[4], I. Pagano[4], C. J. Rosser[1], H. Furuya[1];
[1]Cedars-Sinai Medical Center, Los Angeles, CA, [2]Kindai University, Osaka, Japan, [3]Saint John's Cancer Institute, Santa Monica, CA, [4]University of Hawaii Cancer Center, Honolulu, HI

Introduction and Objective: Due to insufficient accuracy, urine-based assays currently have a limited role in the management of patients with upper tract urothelial carcinoma (UTUC). The application of a robust urine-based multiplex assay, Oncuria-Detect®, to aid in the detection of UTUC has the potential to address this deficiency and to assist with accurate, non-invasive diagnosis.

Methods: To evaluate the performance of Oncuria-Detect®, a multiplex immunoassay capable of querying a voided urine sample for 10 protein biomarkers associated with urothelial carcinoma (A1AT, APOE, ANG, CA9, IL8, MMP9, MMP10, PAI1, SDC1 and VEGFA). Its application to UTUC was evaluated in a multi-institutional cohort of 35 prospectively collected subjects presenting for evaluation of upper tract mass along with 46 prospective collected matched controls (i.e., non-tumor bearing). The ability of the test to identify patients harboring UTUC was assessed. UTCU status was confirmed by endoscopy and tissue biopsy or definitive surgery. Diagnostic performance was assessed using ROC curves.

Results: Oncuria-Detect® provided an AUC of 0.886 (95% CI: 0.807-0.964) with an overall sensitivity of 91.4%, specificity of 73.9%, NPV 91.9% and PPV 72.7%. Sensitivity values of the diagnostic panel for low-grade UTUC, high-grade UTUC, non-invasive UTUC and invasive UTUC were 86.7%, 90.9%, 88.9% and 94.1%, respectively. Urinary cytology or selective ureteral washing/cytology was associated with an overall sensitivity of 54.2%, specificity of 100%, NPV 63.3% and PPV 100%. Sensitivity values of cytology for low-grade UTUC, high-grade UTUC, non-invasive UTUC and invasive UTUC were 100%, 100%, 100%, and 77.8%, respectively.

Conclusions: Urinary levels of a biomarker panel enabled the accurate discrimination of UTUC and controls non-tumor bearing individuals. The multiplex Oncuria-Detect® test can achieve the efficient and accurate detection of UTUC in a non-invasive patient setting.

#1029 Role of *PCDHGA12*/*PRRX1* methylation for the diagnosis of lung cancer using bronchial washing fluid.

J. Son[1], T. Oh[2], M. Lee[1], C. Park[3], S. An[2];

[1]Konyang Univ. College of Medicine, Daejeon, Korea, Republic of, [2]Genomictree, Inc., Daejeon, Korea, Republic of, [3]Ulsan University Hospital, University of Ulsan College of Medicine, Ulsan, Korea, Republic of

Bronchoscopy is a frequently used initial diagnostic procedure for patients with suspected lung cancer (LC). Cytological examinations of bronchial washing (BW) samples, obtained during bronchoscopy, often yield inconclusive results in the diagnosis of LC. Aberrant DNA methylation has previously been shown to be a useful biomarker for LC. DNA methylation analysis in BW specimens could serve as a valuable clinical adjunct to cytology. In this study, to identify potential methylation biomarkers for LC, methylation microarray analyses were performed on primary tumors and compared with adjacent non-tumor tissues of 13 patients with LC at various stages (I - IV). A stepwise validation process using bisulfite-pyrosequencing of cell lines and tissues identified six methylated genes (*ADAMTS20*, *FOXC2*, *NKX2-5*, *OLIG3*, *PCDHGA12*, and *PRRX1*) associated with LC. To assess methylation in BW samples, a highly sensitive and accurate 3-plex Linear Target Enrichment (LTE)-quantitative methylation-specific PCR (qMSP) in a single closed tube was developed. Clinical validation was performed using BW samples from patients with LC (*n* = 68) and non-LC (benign) (*n* = 33) and identified *PCDHGA12* and *PRRX1* methylation as the best performing marker combination for detecting LC. The 2-marker combination exhibited a sensitivity of 82.4% and a specificity of 87.9%, with an area under the curve of 0.891. Notably, its sensitivity was 100% for small cell LC. The 2-marker combination had a positive predictive value of 93.3% and a negative predictive value of 70.7%. Its sensitivity outperformed cytology. The methylation status of the 2-marker showed no correlation with gender, age or stage, but was associated with tumor location and histology. In conclusion, we identified *PCDHGA12* and *PRRX1* methylation as high potential biomarkers for LC diagnosis. This study shows that these biomarkers could be used as a diagnostic adjunct to cytology in the clinical practice for diagnosing LC in BW specimens.

#1030 Concordance between the DESTINY-Breast04 clinical trial assay (4B5[CDx]) and other HER2 IHC assays for HER2-low breast cancer in real-world practice: First phase of a large-scale, multicenter global ring study.

H.-U. Schildhaus[1], S. Badve[2], C. D'Arrigo[3], G. Farshid[4], A. Lebeau[5], V. Peg[6], F. Penault-Llorca[7], J. Rueschoff[1], W. Yang[8], N. Atkey[9], J. Baumann[10], E. Beyerlein[11], **A. Hanlon Newell**[12], A. Penner[1], A. Moh[12], G. Viale[13];

[1]Discovery Life Sciences Tissue Biomarker Services GmbH, Kassel, Germany, [2]Emory University School of Medicine, Atlanta, GA, [3]Poundbury Cancer Institute, Dorchester, Dorset, United Kingdom, [4]Royal Adelaide Hospital, Adelaide, Australia, [5]University Medical Centre Hamburg-Eppendorf, Hamburg-Eppendorf, Germany, [6]University Hospital Vall d'Hebron, Barcelona, Spain, [7]Centre Jean Perrin, Universite Clermont Auvergne, INSERM, Clermont-Ferrand, France, [8]Fudan University, Shanghai, China, [9]Diaceutics PLC, Belfast, United Kingdom, [10]AstraZeneca, Gaithersburg, MD, [11]Daiichi Sankyo Europe GmbH, Munich, Germany, [12]Daiichi Sankyo Inc., Basking Ridge, NJ, [13]IEO European Institute of Oncology IRCCS, Milan, Italy

Background: DESTINY-Breast04 (DB-04) showed that trastuzumab deruxtecan improves survival vs chemotherapy in patients with human epidermal growth factor receptor 2 (HER2)-low (immunohistochemistry [IHC] 1+ or IHC 2+ with in situ hybridization negative) metastatic breast cancer (BC). The VENTANA 4B5(CDx) IHC assay, now approved in the United States (US) as a companion diagnostic, was used as the clinical trial assay (CTA) in DB-04. Real-world differentiation of HER2-low vs HER2 IHC 0 BC with non-CTAs is difficult. This is the first phase of a study assessing agreement between CTA and non-CTA scores.

Methods: 50 clinical BC samples with HER2 IHC scores of 0, 1+, 2+, and 3+ were sent to laboratories in Europe, Canada, and the US for HER2 IHC testing per ASCO/CAP 2018 guidelines. After routine protocol scoring, pathologists were trained and rescored the samples 2 weeks later. Post training scores were compared with reference CTA scores determined by a central laboratory and a panel of experts. The primary endpoint was positive percentage agreement (PPA) and negative percentage agreement (NPA) between CTA and non-CTA scores, assessed after training, considering HER2-low as positive and HER2 IHC 0 as negative.

Results: A total of 3449 post training non-CTA scores were available for analysis. PPA for HER2-low vs HER2 IHC 0 was 87.5% and NPA was 61.9%, with Cohen κ of 0.51 (Table). HER2-low vs HER2 IHC 0 agreement between CTA and non-CTA varied across subgroups. PPA >95% was shown with 4B5 Laboratory Developed Tests (LDTs) and HercepTest (Omnis), NPA of 80% with Leica, and overall agreement >80% with HercepTest (Link48), 4B5 LDTs, and German, French, and Italian laboratories.

Conclusions: The degree of concordance between the CTA and non-CTAs varied among assay types and laboratory locations. A low NPA for some non-CTAs suggests the need for further assay optimization for HER2 IHC 0 evaluation.

Post training non-CTA results		**HER2-low vs HER2 IHC 0 BC Post training scores**			
		PPA (95% CI), %	**NPA (95% CI), %**	**Overall percentage agreement (95% CI), %**	**Cohen κ (95% CI)**
Overall non-CTA test results (N = 3449)		87.5 (86.0-89.0)	61.9 (58.9-64.9)	78.7 (77.1-80.1)	0.51 (0.48-0.54)
Non-CTA subgroups	**HercepTest (Omnis) (n = 467)**	95.5 (92.3-97.7)	36.9 (28.9-45.4)	75.2 (70.8-79.4)	0.37 (0.28-0.46)
	HercepTest (Link48) (n = 790)	88.5 (85.2-91.2)	64.3 (57.8-70.4)	80.3 (77.2-83.2)	0.55 (0.48-0.61)
	Leica (n = 96)	59.3 (45.0-72.4)	80.0 (61.4-92.3)	66.7 (55.5-76.6)	0.35 (0.17-0.53)
	Non-4B5 LDTs (n = 1609)	83.8 (81.2-86.1)	67.8 (63.5-72.0)	78.2 (75.9-80.3)	0.52 (0.47-0.57)
	4B5 LDTs (n = 487)	96.0 (93.0-98.0)	58.8 (50.4-66.8)	83.0 (79.1-86.4)	0.59 (0.51-0.68)
Country subgroups	**Germany (n = 340)**	93.1 (88.5-96.3)	64.4 (54.2-73.6)	83.1 (78.3-87.2)	0.61 (0.51-0.70)
	France (n = 342)	95.4 (91.5-97.9)	64.4 (54.4-73.6)	84.7 (80.1-88.6)	0.64 (0.55-0.73)
	Italy (n = 395)	89.9 (85.2-93.5)	72.5 (63.6-80.3)	83.9 (79.6-87.6)	0.64 (0.55-0.72)
	Spain (n = 567)	83.0 (78.4-86.9)	64.2 (56.6-71.3)	76.3 (72.3-80.0)	0.48 (0.40-0.56)
	US/Canada (n = 1029)	86.6 (83.6-89.2)	61.8 (56.1-67.3)	78.2 (75.4-80.8)	0.50 (0.44-0.56)
	Europe, other (n = 776)	85.0 (81.3-88.2)	52.8 (46.2-59.3)	73.8 (70.3-77.1)	0.40 (0.32-0.47)

#1031 Targeting genomic biomarker in voided urine for prostate cancer detection.

M. L. Thakur, V. S. Tomar, E. Dale, L. G. Gomella, H. T. Navarro, O. Kolesnikov, J. Leong, O. Dahlgren, E. J. Trabulsi;
Thomas Jefferson University, Philadelphia, PA

Introduction: Prostatic cancer (PCa) is the second most prevalent disease in men globally. In 2020 it lead to >14 million new cases and >375,000 deaths worldwide. Despite numerous detection methods, detecting PCa reliably and non-invasively continues to be challenging. PCa malignant cells (MC) express VPAC (combined for Vasoactive Intestinal Peptide and Pituitary Adenylate Cyclase Activating Peptide) in high density. A VPAC specific PACAP analogues ($Kd=3.1x10^{-8}M$) developed in our laboratory was conjugated with a fluorophore and named TP4303. The goal was to assess if TP4303 will image PCa-MC shed in voided urine and present severity of PCa as grade group (GG).

Method: Consenting PCa patients (N=110) scheduled for radical prostatectomy provided voided urine. Urine was cyto-centrifuged. Cells on glass slide were fixed, incubated with TP4303, washed, treated with DAPI (4,6-diamidodino-2-phenylindole), cover slip placed and analyzed with Zeiss Axio Observer microscope, coupled with ZENN Microscopy software. The software determined percentage of PCa MC shed by each patient. The results were corroborated as per GG, determined by post-surgical histopathology and analyzed statistically.

Results:TP4303 imaged PCa in all subjects. The percent MC shed in urine increased from 13.1±14.4% for GG1 to 25.3±21.07% for GG3 ($p=0.05$) to 50.5±26.7% for GG5 ($p=0.002$). Similarly, the fluorescence intensity increased from 43.8±2.2 for GG1 to 48.8±7.0 for GG3 ($p=0.01$) to 51.5±14.4 for GG5 ($p=0.15$).

Conclusions: The data strongly suggests that TP4303 may not only detect PCa reliably and noninvasively, but may also predict the severity of PCa.

Supported by NIH: NC5R01CA249921

#1032 Development of a novel companion diagnostic immunohistochemistry antibody for claudin 18.2-targeted therapies.

J. Chen[1], S. Bai[1], Y. Bai[1], Z. Hu[1], P. Chen[2], J. Mei[3], B. Shan[3], **B. Hou**[3];
[1]Antengene Biologics Co., Ltd., Hangzhou, China, [2]Antengene Corporation Co., Ltd., Shanghai, China, [3]Antengene Corporation Co., Ltd., Shaoxing, China

Background: CLDN18.2, the isoform 2 of CLDN18, is physiologically confined to gastric mucosa tight junctions, the epitopes of which would be exposed on the cancer cell surface upon malignant transformation and is highly expressed in a significant proportion of cancers, e.g., gastric and pancreatic adenocarcinomas, which makes it a promising drug target for cancer therapy. Currently, multiple drug modalities, such as monoclonal antibodies, ADCs, and CARTs targeting CLDN18.2 are being evaluated in clinical trials. A substantial correlation exists between the expression of CLDN18.2 and the efficacy of the these therapies. However, to date, no companion diagnostic (CDx) antibodies that are specific to CLDN18.2 have been approved. Therefore, it is important to promptly develop an anti-CLDN18.2 CDx antibody with a high specificity, sensitivity, and suitability for immunohistochemistry (IHC). In this study, we present the discovery and validation of a novel, highly sensitive IHC antibody that selectively identifies CLDN18.2.
Methods: 3 CLDN18.2 specific peptide fragments from extracellular domain of human CLDN18.2 were conjugated with KLH. Antibodies were discovered by immunizing BALB/c and SJL mice with these peptides-KLH conjugates. Screening and selection process was relied on positive ELISA results against the immunogen, as well as FACS and Acumen Explorer Microplate staining of CLDN18.2-experssing cells. Hit antibodies were evaluated for IHC on formalin-fixed paraffin-embedded CHOK1 cells expressing full-length CLDN18.2 or CLDN18.1. The antibodies were further validated on human gastric cancer tissue samples to establish the analytical sensitivity and specificity of the IHC assay.
Results: The mAb clone 43F11 exhibited binding to a fusion polypeptide comprising the first extracellular loop of human CLDN18.2 (aa32-53) at a half maximal effective concentration (EC50) of 0.212 nM. 43F11 showed positive cell surface IHC staining on CLDN18.2-experssing cells after fixation but demonstrated no staining on CLDN18.1-experssing cells. The IHC test method was established by utilizing clinical tumor tissues and PDX samples that had predetermined expression levels of CLDN18.2. The 43F11 antibody accurately identified the expression level of CLDN18.2 in the IHC assay, with a minimum concentration of 0.25 µg/mL. When compared to the commercial CLDN18.2 IHC antibody EPR19202, 43F11 demonstrated greater sensitivity, allowing for positive staining on cancer tissues that have significantly lower levels of CLDN18.2 expression.
Conclusion: 43F11 exhibits specific recognition of human CLDN18.2 in IHC assays, while showing no reactivity towards CLDN18.1. It demonstrated superior sensitivity compared to the benchmark antibody. These data suggest that 43F11 has the capacity to serve as an effective diagnostic tool for identifying patients who positively express CLDN18.2.

#1033 Evaluation of autoantibodies to proteins encoded by cancer driver genes as biomarkers for prostate cancer.

C. Qiu[1], X. Wang[1], C. A. Casiano[2], J.-Y. Zhang[1];
[1]The University of Texas at El Paso, El Paso, TX, [2], Loma Linda University School of Medicine, Loma Linda, CA

Prostate cancer (PCa) is a complex disease driven by genomic alterations, and understanding the immune response to these alterations can provide valuable insights into its pathogenesis. This study aimed at exploring the immunogenicity of proteins encoded by PCa driver genes and identifying corresponding autoantibodies as potential PCa biomarkers. Bioinformatics analysis, enzyme-linked immunosorbent assay (ELISA), and immunohistochemistry (IHC) were conducted in this study. A comprehensive screening process involving bioinformatics analysis and published studies identified a set of PCa driver genes for further investigation. Three strategies were employed to identify candidate driver genes: (1) utilizing the IntOGen database (Martínez-Jiménez et.al, Nature Reviews Cancer 2020), nine cohorts comprising 1503 primary PCa patient samples were analyzed, resulting in the identification of 63 PCa driver genes, with the top 20 genes exhibiting high mutation rates and frequencies in these cohorts; (2) employing the Kyoto Encyclopedia of Genes and Genomes (KEGG) database, 16 driver genes that were enriched in prostate cancer pathways were identified from the initial 63 genes; (3) referring to a published article (Dietlein et.al, Nature Genetics 2020), the top 17 driver genes that highly related to prostate cancer across 28 tumor types were selected. A final set of 15 PCa driver genes, which appeared in at least two of the screening strategies, were included in subsequent analyses. ELISA was then performed to assess the presence of autoantibodies targeting proteins encoded by these 15 PCa driver genes. Autoantibodies were evaluated using serum samples from 203 PCa patients and 93 normal controls. The results revealed that seven out of the 15 autoantibodies showed significantly elevated levels in the sera of PCa patients compared to normal controls. Notably, the autoantibody targeting SPOP (speckled-type POZ protein) exhibited the highest frequency of 42.4%, followed by the autoantibody to PTEN (phosphatase and tensin homolog) at 37.4% in the PCa group. Finally, the SPOP protein was analyzed by IHC on the prostate tissue microarray containing PCa tissues, prostate simple hyperplasia tissues, cancer adjacent prostate tissues, and normal prostate tissues further to explore the consistency of SPOP expression in antigen-antibody reactions. High expression of SPOP protein was found in the PCa tissues. These findings suggest that proteins encoded by PCa driver genes may possess immunogenic properties due to neoepitopes possibly generated by mutations, leading to the production of corresponding autoantibodies. Identifying specific autoantibodies associated with PCa driver genes could offer novel opportunities for discovering autoantibody-based biomarkers in PCa. Further validation of these autoantibodies is warranted to evaluate their diagnostic potential in PCa.

#1034 SIGMAR1 as a novel potential prognostic biomarker that regulates PD-L1 expression in oral cancer.

P. Shimaoka Chagas, Sr.[1], G. da Silva[1], G. Ribeiro de Sousa[1], C. Bernadelli Garcia[1], L. Oliveira Sousa[1], R. Cabral Marcelino[2], R. Luiz Lobo da Silva Souza[1], L. Luongo de Matos[3], L. Paulo Kowalski[3], E. da Silva Lopes Salles[4], L. P. Wang[4], B. Baban[4], A. Machado Leopoldino[1];

[1]University of Sao Paulo, Ribeirao Preto, Brazil, [2]Federal University of Alfenas, Alfenas, Brazil, [3]University of Sao Paulo, Sao Paulo, Brazil, [4]Augusta University, Augusta, GA

Background: The SIGMAR1 receptor is a regulator of immunity and inflammation. Together, these key processes can support or restrain cancer progression and response to therapy. Nevertheless, the effect of SIGMAR1 on the modulation of oral cancer (OC) immunity is largely unknown. Here, we investigated not only the prognostic value of SIGMAR1 in OC but also, its impact on antitumor immunity response.

Methods: Were included in this study data from TCGA (Pan-Cancer analysis), multiple large datasets of OC (GSE30784; GSE42743; GSE37991, GSE31056, our cohort-based study of human OC samples and OC cell lines. Taken together, were used to performed the bioinformatics analysis and the experimental verification by several in vitro assays. The CIBERSORT analysis and Luminex assay were used to evaluate the infiltration degrees of different immune cells and also to validate the presence of chemokines and immune-stimulators, respectively, in human OC samples. To assess the role of SIGMAR1 in the modulation of the -PD-L1 expression, SIGMAR1-shRNA OC cell lines were used.

Results: We found that overexpression of SIGMAR1 was associated with poor survival rates in OC. Further, we observed that SIGMAR1 deficiency inhibited Ca2+ influx and clonogenic growth and decreased chemoresistance to cisplatin in human OC cells. Next, the SIGMAR1 expression levels were associated with infiltration degrees of M1 macrophages, Natural Killer cells and T cells (memory and helper CD4+ activated, and CD8+ cytotoxic T cells). Regarding comparison of the analytes between patients with SIGMAR1 high/low expression group, we found significant differences in the CX3CL1 (chemokine), and in immune-stimulators as CD27, CD40, and PD-L1 expression level. Importantly, this research also showed that SIGMAR1 inhibition in human OC cell lines decreases the abundance of PD-L1, both at the total protein and surface expression levels.

Conclusions: Our findings suggests SIGMAR1 not only as an emerging biomarker with promising therapeutic values to OC patients, but also gave a new insight into a potential immunotherapy strategy.

Keywords: Oral cancer; SIGMAR1; PD-L1, Immune checkpoint inhibitors.

#1035 Identification of fibroblast growth factor receptors (FGFRs) alterations (alts) at DNA and RNA-level by one-step next-generation sequencing (NGS) panel.

M. Qing[1], X. Chen[2], W. Su[2], X. Zhuo[3], T. Shen[1], C. Xiong[1], X. Lyu[1], R. Tate[4], Q. Wu[1], L. Zhou[1], S. Thomas[4], W. Ning[2], J. Wang[2], H. Yan[2], Z. Yin[2], Z. Huang[2], Y. Xue[2], **C. Zhu**[2];

[1]Janssen Research & Development, Shanghai, China, [2]Amoy Diagnostics, Xiamen, China, [3]Janssen Research & Development, Beijing, China, [4]Janssen Research & Development, Spring House, PA

Background: FGFR inhibitors are currently in clinical development or approved for urothelial cancer and cholangiocarcinoma with *FGFR* fusion (FUS) or/and mutation (MUT). AmoyDx FGFR 1-4 NGS Panel (FGFR-P) was developed for FGFR alts detection based on both DNA and RNA. The goal of this study is to validate and assess the performance of FGFR-P in pan-cancer *FGFR* alts detection by comparing with an AmoyDx comprehensive genomic profiling test (CGP) and a health authority approved DNA-based NGS panel (DNA-P).

Methods: Both FGFR-P and CGP are DNA (MUT) and RNA (FUS) based for detecting *FGFR* alts with optimized bioinformatics pipeline to eliminate baseline noise caused by deamination events, which is commonly found in aged FFPE samples. Cell lines, cell line/patient derived xenografts (CDXs/PDXs) and 397 samples of 26 cancer types (90 samples >10 years) were used for validation of FGFR-P. Total 382 and 50 pan-cancer samples were respectively tested to compare FGFR-P with CGP and DNA-P.

Results: To validate accuracy, 36 FFPE samples from cell lines and CDXs/PDXs with known FGFR status (25 FUSs, 5 MUTs, 6 wild-types) were tested by FGFR-P with concordance rate 100%. In clinical sample testing, FGFR-P also showed high agreement with CGP (99.5%) and DNA-P (98.0%). Conflicting result confirmed by FISH revealed 1 FUS missed by DNA-P but detected by FGFR-P, which demonstrated advantage of *FGFR* alts detection by DNA+RNA. In addition, an optimized bioinformatics pipeline by mimic samples with deamination events effectively filtered out C:G>T:A false positive signals. FGFR-P achieved high success rate in testing pan-tumor samples (89.9%) including samples >10 years (75.6%).

Conclusions: FGFR-P provides a novel opportunity to identify *FGFR* alt pan-cancer patients using a robust DNA+RNA NGS platform, which shows high success rate even in aged samples and will be a potent tool for sensitive and reliable detection of *FGFR* alts for clinical diagnostics.

	CGP			
FGFR-P	**MUT**	Positive	Negative	Total
	Positive	29	0	29
	Negative	1	194	195
	Total	30	194	224
	FUS	Positive	Negative	Total
	Positive	20	1	21
	Negative	0	137	137
	Total	20	138	158
The overall percent agreement		99.5%		

#1036 Development of a comprehensive RNA-based NGS panel for detecting tyrosine kinase fusion genes associated with primary hypereosinophilia.

B. Lee[1], A. Chern[1], A. Zhang[1], C. M. Lu[2], M. Y. Sha[1];
[1]DiaCarta, Inc., Pleasanton, CA, [2]University of California and VA Health Care System, San Francisco, CA

Hypereosinophilia (HE) is a medical condition diagnosed when the count of eosinophils in the blood is greater than $1.5X10^9$ per liter. Primary HE is a clonal stem cell disorder manifesting as myeloid and/or lymphoid malignancies and is typically driven by aberrant fusion genes involving a tyrosine kinase (TK) gene (e.g., PDGFRA, PDGFRB, FGFR1, JAK2, FLT3, ABL1). The precise identification of the underlying molecular genetic abnormalities is crucial for timely diagnosing and managing primary HE. There has been no HE-specific assay that can concomitantly detect all known or novel TK fusion genes. We've developed an RNA-based panel for detecting TK fusion genes in HE. This panel, developed using 5' RACE technology, allows for the identification of fusion transcripts in total RNA extracted from whole blood sample. It covers 48 known TK fusion genes and also has the capability of detecting novel gene fusions. We balanced and optimized the panel using an in-house fusion RNA mix containing 11 fusion transcripts. We additionally validated the panel using samples from five patients with hematopoietic neoplasms and two fusion-positive cell lines to ensure its accuracy. The Limit of Detection (LoD) was established by analyzing the in-house RNA mix and normal whole blood RNA. It was found that the minimum RNA input required to detect all 11 fusion transcripts was 3540 copies in the presence of a background of 10 ng normal whole blood RNA. The panel successfully identified two fusion transcripts using 10 ng of total RNA obtained from cancer cell lines. The panel was then used to test five patient RNA samples extracted from whole blood. We successfully confirmed the presence of BCR-ABL1 fusion in 3 patient samples and ETV6-PDGFRB fusion in 1 patient sample, respectively. In summary, we developed HE-specific NGS panel for detecting all known and novel TK fusion genes and demonstrated its analytical accuracy and clinical effectiveness. The next phase of our study is to further validate the tests on a large patient cohort.

#1037 Clinical application of next-generation digital PCR capable of real-time analysis to HER2 measurement as a novel diagnostic in breast cancer: A multicenter retrospective study.

H. Kim[1], S. Park[1], S. Yang[1], M. Song[1], D. Kim[1], J. Chang[2], Y. Kim[2], H.-J. Choi[2], N. Heo[3], H.-Y. Won[4], J.-H. Park[4], M. Song[4], S.-S. Shin[4], D. Lee[4], S.-H. Jang[3], J.-Y. Lee[2], H. Ryu[1];

[1]Seoul National University, Seoul, Korea, Republic of, [2]Hanyang University, Seoul, Korea, Republic of, [3]Soonchunhyang University Cheonan Hospital, Cheonan-si, Korea, Republic of, [4]OPTOLANE Technologies Inc., Seongnam-si, Korea, Republic of

HER2 testing is still challenging due to the subjective natures of immunohistochemistry (IHC) and in situ hybridization (ISH), standard methods for determining HER2 status. Here, we developed a clinically reliable HER2 testing method enabling ultra-fast detection of HER2 gene amplification with high accuracy by using the digital real-time PCR (drPCR) system. To test the clinical validity and standardize procedures of drPCR-based HER2 status evaluation, three independent breast cancer cohorts from different institutions were enrolled, which assigned as a training (SCHU hospital, n = 103) and two validation sets (SNU hospital, n = 170; CNUH hospital, n = 45), and the drPCR assay was compared with current standard HER2 testing methods. In the training cohort, the HER2/CEP17 ratio values from FISH and drPCR tests were highly correlated (r^2 = 0.81; *P* < 0.001), and the drPCR results displayed 98.1% concordance to HER2 status defined by IHC and/or FISH with 92.6% sensitivity and 100% specificity. Eight samples further verified by targeted NGS showed 100% concordance of dPCR to NGS. Consistently, two validation cohorts also showed high concordance of drPCR to IHC and/or ISH results (accuracy = 97.1% and 97.8% in SNU and CNUH cohorts, respectively). The optimal cutoff for HER2 positivity in the drPCR assay was set as a HER2/CEP17 ratio ≥ 1.9 with AUC of 0.963 based on the results from training cohort, and the same cut-off for drPCR was applicable to two independent validation cohorts, supporting the clinical validity of our drPCR-based HER2 assessment. In some discordant cases, low tumor purity (≤ 25%) was observed and microdissection partly improved the drPCR results. The discordance between drPCR and ISH results was also found in marginal HER2+ cases with HER2/CEP17 ratio 2-3, but these cases showed inter-observer variability when re-evaluating the ISH/IHC data due to intratumoral HER2 heterogeneity. Of note, in HER2 IHC3+ cases with negative drPCR results, re-evaluation of IHC using an artificial intelligence (AI)-based HER2 scoring system revised the HER2 IHC 3+ score to 2+, and ISH assessment also confirmed that these cases are indeed HER2-negative, proving the high accuracy of HER2 CN drPCR assay. In conclusion, given the advantages of drPCR-based HER2 assessment with high accuracy, sensitivity, and simplicity, the drPCR assay could be a complementary or alternative method to IHC and ISH to greatly improve current HER2 testing.

#1038 Identification of diagnostic biomarkers for colon adenocarcinoma by analyzing proteins in human-derived extracellular vesicles and particles.

Y. Seo[1], Y. Han[2], L. Bojmar[3], K.-A. Kim[1], Y. Seo[1], D. Lyden[4], H. Kim[1];

[1]Graduate School of Medical Science, Brain Korea 21 FOUR Project, Yonsei University College of Medicine, Seoul, Korea, Republic of, [2]Yonsei University College of Medicine, Seoul, Korea, Republic of, [3]Linkoping University, Linkoping, Sweden, [4]Drukier Institute for Children's Health, Meyer Cancer Center, Weill Cornell Medicine, New York, NY

There is an unmet medical need for circulating biomarkers to improve early cancer detection in colon adenocarcinoma (COAD). We investigated the proteomic profile of extracellular vesicles and particles (EVPs) from the colon tissue explants and plasmas in COAD. The research aims to overcome the limitations of traditional serum Carcinoembryonic Antigen (CEA) testing and invasive procedures like colonoscopy. We analyzed EVPs sourced from tumor and adjacent non-tumor tissues and preoperative and postoperative plasma in COAD patients to identify potential EVP-based tumor diagnostic markers. In the Discovery phase with 50 COAD patients, we conducted a proteomic analysis using liquid chromatography-tandem mass spectrometry (LC-MS/MS), identifying approximately 50 markers each from tissue explants and plasma. These markers were validated in an independent cohort of 104 participants, including 84 COAD patients and 20 healthy controls. We utilized ELISA to quantify 11 selected EVP proteins. Notably, seven of these proteins exhibited significant differential expression in preoperative and postoperative plasma, highlighting their diagnostic relevance. These seven proteins also showed marked elevation in preoperative plasma compared to healthy controls, reinforcing their potential as diagnostic markers. The study extended to evaluate the diagnostic accuracy of these seven proteins, referred to as "EV-7 levels", across various stages of COAD. Their performance was compared with serum CEA levels and plasma cfDNA mutation rates, as detected by an FDA-approved liquid biopsy assay. The EV-7 levels demonstrated superior detection rates in the early stages of COAD, particularly in Stages I and II, in contrast to the serum CEA method. Among the 84 patients, 73 (86.9%) exhibited EV-7 levels exceeding the established cut-off. In the validation cohort, EV-7 levels were more accurate across different COAD stages than serum CEA levels and cfDNA mutation rates. CEA levels above 5 ng/ml were 27%, 45%, 42%, and 64% for Stages I through IV. cfDNA somatic mutation rates were 60%, 80%, 75%, and 75%. EV-7 levels exceeding the cut-off were 73%, 100%, 88%, and 84%, respectively, with Stages I and II having the highest detection rate among the three methods. ROC curve analysis for EV-7 levels in Stages I to IV showed statistically significant, with AUC values of 0.913, 1.000, 0.985, and 0.984, respectively. Our findings indicate that the seven EVP proteins are significantly present in the plasma of early-stage COAD patients. Integrating these markers with current diagnostic approaches could improve early cancer detection, showing promise for practical application in clinical settings.

#1040 Development of a novel RNA-based microsatellite stable predictive response signature (MSS-PRS) to identify MSS colorectal cancer (CRC) patients with a microsatellite instability-high (MSI-H) molecular phenotype.

K. Pappan, G. Mayhew, J. Shepherd, Y. Guo, K. Beebe, **J. Eisner**, M. Milburn;
GeneCentric Therapeutics, Inc., Durham, NC

Introduction: MSI-H and mismatch repair deficient (dMMR) tumors are associated with favorable immune checkpoint inhibitor (ICI) responses (PMID: 3326454). However, up to 95% of CRC tumors are MSS/proficient MMR (pMMR) leading to poorer prognosis and treatment outcomes than MSI-H/dMMR patients (PMID: 12867608, 26028255). In MSS/pMMR metastatic CRC, multiple combination therapies are being investigated despite a lack of biomarkers to guide therapy. Therefore, we developed an RNA-based MSS-PRS with a primary objective to identify MSS tumors that have MSI-H/dMMR molecular features indicative of ICI response.

Experimental Procedures: The MSS-PRS was developed using the TCGA CRC cohort (COAD; n=268). Training labels were assigned using the MSI Mantis score and mutation status from 8 genes with reported MSI association. Samples called “activated” had both a gene mutation and an MSI Mantis score > 0.4 (i.e., MSI-H), and samples called “non-activated” were wild type for all genes and had MSI Mantis score < 0.4. All other samples were designated “ambiguous” and excluded from training. Two thirds of the non-ambiguous samples were assigned to the classifier training set and all remaining samples were assigned to the test set. Using ClaNC software (PMID: 16269418) and cross-validation in the training set, a nearest centroid classifier was developed from a set of high mean, high variance candidate genes to select an optimal gene set to separate activated and non-activated groups. The classifier performance was evaluated in the test set.

Results: The MSS-PRS contained 112-genes enriched for mismatched DNA binding, DNA damage repair, PD-L1, innate and adaptive immune response, cellular immunity, and cytokines. In the test set, the classifier called 44 of 46 MSI-H samples activated; of the remaining 77 samples that were MSS tumors, 38 were called activated and 39 were called not activated. Visual inspection of heat maps of tumor by MSI/MSS-PRS status and their association with TMB and CRC-related mutations suggest greater differences between MSS tumors called activated and MSI-H tumors than between MSS tumors called activated and MSS tumors called not activated. In contrast, immune marker expression profiles in MSS tumors called activated were markedly more similar to MSI-H tumors compared to MSS tumors called non-activated.

Summary and Conclusions: Herein we described the development of a novel MSS-PRS that captures an MSI-H/dMMR-like molecular phenotype in a subset of patients with MSS tumors despite their lack of high TMB or overt MSI defects. Based upon these initial findings, further development of the MSS-PRS and its clinical validation as a tool to select patients with MSS tumors who may benefit from ICI-containing treatment regimens is warranted.

#1041 Spatial concordance between genome and proteome in oncology: A systematic review.

Laura K. M. Sysivirta, Franziska Niemeyer, Veera Kurki, Inkalilja Pirinen, Laura Savolainen, Ceren Seref-Vujaklilja, Andrew Erickson

University of Helsinki, Helsinki, Finland

We recently reported that spatial transcriptome data can be used to spatially detect copy number alterations (Erickson et al., Nature, 2022). Given that copy-number alterations may also be reflected by altered protein expression in human cancers, we sought to determine what the empirical concordance of the spatial proteome and genome in human cancer samples. We performed a systematic review of Immunohistochemistry (IHC) & Fluorescence/Chromogenic In-Situ Hybridization (FISH/CISH) across human cancers. We performed a PUBMED query for records up to April 1st, 2023, yielding 9,294 records. Our inclusion criteria included human sample studies that performed both IHC and FISH/CISH against the same target, with a minimum of two samples. We excluded case reports, RNA ISH- and non-human studies, studies without IHC/ISH performed on the same target, and articles not in English or inaccessible. We screened 9,294 PUBMED article abstracts using the AS Review active learning model (van de Schoot et al., 2021), and used a pre-defined threshold of 5 % consecutive irrelevant abstracts to stop screening. A total of 1,309 abstracts were manually excluded using the AS Review, directing the active learning model to automatically exclude 3,413 abstracts out of the original 9,294. Of the 4,572 articles assessed for full-article screening, 1,167 were excluded for being out of scope, 303 for access issues, 227 for language incompatibility, and 236 for imprecise information, primarily due to non-representative samples or incorrect gene/protein target identification. Ultimately, out of 2,413 articles assessed for eligibility, 2,294 did not meet inclusion criteria, leaving 119 studies for our analysis. From these articles, we manually extracted kappa values for analysis and visualization in R. We identified articles from 19 different cancers with the majority studying Breast Cancer, Non-Small Cell Lung Cancer, Gastric Cancer, and Mesothelioma. We observed high Cohen's Kappa values in Breast Cancer (median = 0.76), Non-Small Cell Lung Cancer (median = 0.91) and Mucinous Ovarian Carcinoma (median = 0.93). We identified studies from 14 different genes with majority being HER2, ALK and MYC. We observed high Cohen's Kappa values in HER2 (median = 0.80), ALK (median = 0.80), ROS1 (median = 0.95) and MDM2 (median = 0.72). Our preliminary analysis indicates significant heterogeneity between tumor types for protein expression and copy-number alterations. To our knowledge, there are no previously reported systematic reviews that have empirically assessed the spatial concordance of proteome and genome, in human cancer samples. The authors often reported IHC/FISH results at patient, or section level, potentially introducing selection bias by not accounting for intra-tumoral heterogeneity at single-cell resolution. Future efforts are needed to spatially resolve gene-copy number and protein expression at single-cell resolution.

#1042 Multi-exposure high dynamic range microscopy obviates the requirement for matching camera exposure to reagent concentration in high-plex spatial biology applications.

J. S. Schwarz, M. H. Ingalls, X. Meshik, A. Northcutt, O. Braubach;
Canopy Biosciences-A Bruker Company, St. Louis, MO

High-plex immunofluorescence imaging allows researchers to perform deep cellular phenotyping with spatial context. However, high-plex immunofluorescence imaging requires the end user to painstakingly optimize antibody concentrations and image acquisition settings before producing reproducible imaging data with sufficient and quantifiable dynamic range. Mismatches of reagent concentration and camera exposures will result in under and over-saturated images, and both outcomes are detrimental for signal quantification and downstream interpretation. As the number of markers deployed in spatial biology increases, it becomes necessary to develop strategies that streamline or automate parameter setting that is needed to capture data with optimal dynamic range.
The CellScape™ platform for Precise Spatial Multiplexing, featuring ChipCytometry™ technology, utilizes multi-exposure high dynamic range (HDR) microscopy as a tool to produce data with consistent and reliable detection of biomarker signals. CellScape replaces the standard single exposure with an exposure series calibrated to the physical limitations of the detector system. Each exposure series captures linear data, ranging from the dimmest to the brightest signals that the system can detect, as well as everything in between. HDR capture is thus akin to capturing an image at every possible exposure length, and it thus includes data from the ‘optimal’ matched exposure. By these means, HDR obviates the need for exposure selection by covering the entire exposure gamut.
Here, we use CellScape to collect a high-plex immunofluorescence spatial biology dataset. Analysis of the dataset highlights the extended linear dynamic range of the integrated luminance HDR data, including a calculation of the expected ‘best-matched’ exposure. Further, we extend this analysis to show how HDR can handle biological variation and allow normalization that is not possible with single exposure imaging. Finally, we examine a reagent concentration series to demonstrate how HDR can be used to maximize the sensitivity of the assay by allowing increasing detection reagent concentration without compromising overall dynamic range for the signal. Our data demonstrates that HDR microscopy supports the deployment of spatial biology as a tool to interrogate the tumor microenvironment, unravel responsiveness to drug treatments and cell therapies, and ultimately stratify patients for targeted treatment and clinical trial enrollment.

#1043 Identification of the novel immune synapse-localized proteome for immuno-oncology using Microscoop-induced targeted photo-biotinylation.

W.-M. Chong, C. Li, C.-K. Huang, C. Cheung, H.-J. Chang, C.-W. Chung, J.-C. Liao;
Syncell Inc., Taipei, Taiwan

Although tens of immune synapse (IS) protein species are known, there remain many unknown IS-localized protein species. Understanding the proteome of the IS between a target cell and a lymphocyte is crucial for advancing immuno-oncology. The low abundance of ISs and the lack of a definitive enrichment marker have limited efficient proteomic profiling. Here, we used Microscoop™, an innovative system that integrates microscopy, machine learning, and targeted photo-biotinylation to enable precise and spatially specific enrichment of IS proteins, thereby facilitating proteomic discovery of the IS. We utilized Raji B cells as antigen-presenting cells (APCs) and induced IS formation with Jurkat T cells. The system first employed immunofluorescence imaging of CD3, a common IS marker in Jurkat T cells, and used a convolutional neural network-based deep learning algorithm to train the recognition of ISs from CMTPX-stained Raji B cells. Our automated system then successfully achieved spatially-targeted biotin-tagging of proteins at ISs through thousands of fields of view of imaging, deep learning-driven pattern generation, and photochemical labeling. Subsequent streptavidin pull-down and mass spectrometry analysis enabled the identification of IS-specific proteins. Remarkably, our spatial proteomic approach led to the isolation and identification of hundreds of different species at the IS interface, including proteins associated with key components of T-cell receptor (TCR) signaling pathways such as the TCR/CD3 complex, Src and Tec family tyrosine kinases, and pivotal NF-kB signaling proteins. Beyond these, we also identified a significant enrichment of proteins not previously associated with the IS. Our study not only illuminates previously unknown aspects of immune regulation at the IS interface, but also shedded light on proteins potentially important for immuno-oncology. These insights have significant implications for cancer research, particularly in understanding and manipulating immune responses for therapeutic purposes.

#1044 Low-cost, high-sensitivity InSituPlex® mIF assays on the Parhelia Omni-Stainer™.

K. Hwang[1], L. Duro[1], A. Veith[1], N. Wedin[2], N. Samusik[2], J. H. Lee[1];
[1]Ultivue, Inc., Cambridge, MA, [2]Parhelia Biosciences, Austin, TX

Background: Multiplex immunofluorescence (mIF) is an important tool for extracting complex phenotypic information from normal or diseased tissues, and provides accurate and predictive insights on the tissue microenvironment faster. For patient samples in translational and clinical research, high sensitivity, specificity, and reproducibility are critical; however, throughput and cost considerations are also important in designing clinical studies. Enabling an easy-to-use high-performance assay such as InSituPlex® on robust and affordable auto-stainers like the Parhelia Omni-Stainer™ can allow researchers to gain a deeper understanding of the tissue micro-environment through high-quality multiplexed biomarker detection in a fraction of the time and cost.
Methods: We performed Ultivue InSituPlex® assays with OmniVUE™ panels using the Parhelia Omni-Stainer™, a low-cost, high-throughput tissue auto-stainer with reduced requirements for reagents with a minimal dead volume. We compared the whole-slide staining performance across replicates using human tonsil and tumor tissue arrays across multiple independent runs over multiple days. The stained slides were scanned using the Zeiss AxioScan.Z1 high-throughput imaging system, and image batches were processed using Ultivue's UltiStacker.AI and UltiAnalyzer.AI software.
Results: Tighter temperature control of the slide in the Omni-Stainer supports optimal InSituPlex® signal amplification. Intra-run and inter-day analysis on serial sections of human tonsil and tumor tissue arrays demonstrated a high degree of consistency in InSituPlex® assay performance, specifically with marker-specific signal intensities and cell densities. The Omni-Stainer facilitates the use of low reagent volumes at each step of the assay due to its efficient reagent use, thus lowering the cost of reagents per slide.
Conclusions: This study demonstrated a fast, simple and robust workflow to perform high-performance InSituPlex® mIF assays on the low-cost, high-throughput Parhelia Omni-Stainer™. Ultivue's configurable OmniVUE™ mIF panels can be run on the Omni-Stainer with reduced associated reagent costs per slide. This workflow can support larger clinical and translational studies in a more cost-effective fashion, leading to in-depth analysis of tissue microenvironment through highly precise multiplexed biomarker detection.

#1045 A freely expandable 20-plex immuno-oncology antibody core panel for spatial biology experiments on human FFPE cancer sections: REAplex IO Core for MICS technology.

J. Femel[1], E. C. DiBasio[2], K. Schonborn[1], M. Buttner[1], T. Duking[1], **M. Habich**[1], T. Wantenaar[1], S. Eulitz[1], A. Bosio[1];
[1]Miltenyi Biotec B.V. & Co. KG, Bergisch Gladbach, Germany, [2]Miltenyi Biotec North America, Inc., Waltham, MA

Spatial biology is integral to understanding the dynamics of immune cells, tumor microenvironment (TME), and therapeutic responses in cancer research. Ultra-high-plex immunofluorescence has transformed deep phenotyping and cell neighborhood analysis, providing unprecedented insight into complex and heterogeneous samples such as the TME. Many spatial biology platforms reduce operator hands-on time by automating image acquisition. However, determining the most appropriate markers to distinguish key cell types, finding application-compatible antibody clones and optimizing their dilution remains a tedious manual process. To streamline the panel-building process, we have developed a series of pre-defined, commercially available antibody panels for the MACSima™ Imaging Cyclic Staining (MICS) technology. So far, these have covered the spectrum from ultra-high-plex screening panels with up to 205 antibodies (REAscreen™ MAX) to the more focused REAscreen Immuno Oncology antibody panel with 61 cancer and immune-related antibodies for the comprehensive analysis of various different human FFPE samples. Here, we introduce a new, 20-plex, pre-defined antibody panel. Organized along essential marker groups, it can function as a stand-alone panel that allows the identification of the major tumor-infiltrating leukocyte populations with a focus on T-cells, and providing insight into TME architecture, tumor neovascularization, and cellular activity. Because it can be combined and expanded with any number of antibodies or even entire panel modules, it can be used as a standardized basis for highly multiplexed custom panels optimized for the research question at hand. We demonstrate its performance and broad applicability across several cancer types analyzed with the MICS technology. Finally, preset template examples for panel-specific data processing with MACS iQ View analysis software demonstrate the simplicity yet power of an integrated end-to-end workflow.

#1046 Prevalence of MTAP deficiencyin human cancer: A tissue microarray study on 17,078 cancers from 149 different tumor types.

N. Gorbokon[1], **M. Lennartz**[1], D. Hoeflmayer[1], S. Dwertmann Rico[1], S. Kind[1], V. Reiswich[1], F. Viehweger[1], F. Lutz[1], C. Fraune[1], A. M. Luebke[1], C. Hube-Magg[1], F. Buscheck[1], A. Menz[1], R. Schlichter[1], T. Krech[1], A. Hinsch[1], E. Burandt[1], G. Sauter[1], R. Simon[1], S. Steurer[1], A. H. Marx[2], P. Lebok[1], D. Dum[1], S. Minner[1], F. Jacobsen[1], T. S. Clauditz[1], C. Bernreuther[1], M. Kluth[1];

[1]University Medical Center Hamburg-Eppendorf, Hamburg, Germany, [2]Academic Hospital Fuerth, Fuerth, Germany

The S-methyl-5′-thioadenosine phosphorylase (MTAP) gene is located at 9p21 and is often co-deleted with CDKN2A. Because homozygous MTAP deletions result in a complete expression loss, MTAP immunohistochemistry (IHC) can be used for detection of homozygous deleted cells. MTAP IHC is of diagnostic utility for the distinction of mesotheliomas (often 9p21 deleted) from benign mesothelial proliferations. Moreover, evidence is emerging that MTAP deficiency results in a critical vulnerability of cancer cells towards drugs targeting several different pathways that depend on a functional MTAP gene and also causes resistance to immune checkpoint inhibitors.

To determine the prevalence of complete MTAP expression loss and to assess the diagnostic utility of MTAP IHC, a tissue microarray containing 17,078 samples from 149 different tumor entities and 608 samples of 76 different normal tissue types was analyzed by IHC. All cases with complete MTAP loss were validated by fluorescence in situ hybridization (FISH).

In normal tissues, MTAP was ubiquitously expressed resulting in a cytoplasmic and nuclear MTAP staining. At least one case with a complete MTAP expression loss was observed in 87 of 149 (58%) tumor categories. MTAP staining was most commonly lost in neuroendocrine neoplasms of various sites (up to 80%), Hodgkin's lymphoma (38%), mesothelioma (24-30%), bilio-pancreatic adenocarcinomas (9-36%), urothelial neoplasms (19-29%), malignant melanoma (14-21%), mucinous carcinoma of the ovary (27%), squamous cell carcinomas of various organs of origin (up to 24%), various types of sarcomas (up to 20%), adenocarcinoma of the lung (11%), gastro-esophageal adenocarcinomas (2.6-11%), and in various types of non-Hodgkin's lymphomas (up to 14%). FISH validation identified homozygous 9p21 deletions in 90-98% of cases with MTAP expression loss in most tumor categories including urothelial neoplasms, mesotheliomas, and pancreatic cancers, and others. There were, however, also tumor types such as neuroendocrine tumors and Hodgkin's lymphomas that always lacked 9p21 deletions.

In summary, our data provide a comprehensive overview on MTAP expression in cancer and show a strong link between MTAP expression loss and homozygous 9p21 deletions in most tumor entities. These cancers might most benefit from cancer drugs targeting MTAP deficiency. The absence of 9p21 deletions in other entities with frequent MTAP expression loss demonstrates that other mechanisms can cause significant MTAP downregulation. Whether these tumors benefit from targeting MTAT deficiency remains to be determined.

#1047 Expression of TYMS in cancer: A tissue microarray study involving 6,613 cancers from 127 tumor entities.

F. Lutz[1], N. Leege[1], K. Moller[1], F. Viehweger[1], R. Schlichter[1], A. M. Luebke[1], M. Kluth[1], C. Hube-Magg[1], A. Hinsch[1], C. Bernreuther[1], G. Sauter[1], D. Dum[1], A. H. Marx[2], R. Simon[1], T. Krech[1], T. S. Clauditz[1], F. Jacobsen[1], E. Burandt[1], S. Steurer[1], P. Lebok[1], C. Fraune[1], S. Minner[1], N. Gorbokon[1], **M. Lennartz**[1];
[1]University Medical Center Hamburg-Eppendorf, Hamburg, Germany, [2]Academic Hospital Fuerth, Fuerth, Germany

Thymidylate synthase (TS, TYMS) is an enzyme that catalyzes the conversion of deoxyuridine monophosphate (dUMP) to deoxythymidine monophosphate (dTMP) which is one of the nucleotides forming the DNA. TYMS is thus essential for DNA synthesis and represents an important target for several chemotherapeutic drugs including 5-fluorouracil (5-FU) and methotrexate. It has been suggested that tumors with low-levels of TYMS may show a better response to 5-FU than those with high-level expression. Literature data on TYMS expression in different cancer types is controversial, however. To better comprehend the role of TYMS expression in cancer, TYMS was analyzed by immunohistochemistry (IHC) on tissue microarrays (TMAs) containing 9,015 samples from 127 different tumor types as well as 8 samples each of 6 different normal tissue types. TYMS immunostaining was always cytoplasmic and/or nuclear. It was only detectable in a minority of normal cell types and was strongest in a subset of lymphoid cells, especially in germinal centers and in the thymus as well as in hematopoetic cells of the bone marrow. Detectable TYMS staining occurred in 3,749 (46.7%) of the 8,030 analyzable tumors, including 2,958 (36.8%) with weak, 609 (7.6%) with moderate, and 182 (2.3%) with strong positivity. A total of 114 of 127 tumor categories showed TYMS expression in at least one case, 64 tumor categories showed TYMS staining ≥50% of cases, and 47 tumor categories included at least one case with strong TYMS positivity. The frequency of TYMS positivity was highest in various subtypes of B- and T-cell lymphoma (80-100%), sarcomas, carcinosarcomas and sarcomatoid carcinomas (33.3-100%), primary and metastatic malignant melanoma (70.5-90.7%), adenocarcinoma of the uterine cervix (78.3%), squamous cell carcinomas of various sites of origin (57.1-77.9%), and testicular germ cell tumors (19.4-67.4%). In all four tumor entities for which clinico-pathological data could be assessed, high TYMS expression was associated with features of aggressive disease. High TYMS expression was linked to high histologic grade ($p<0.0001$) in endometrioid endometrium carcinoma, advanced pT stage ($p=0.0061$) in high-grade serous ovarian carcinoma, poor histologic grade ($p<0.0001$) in squamous cell carcinomas of 11 different organs of origin, and to advanced stage ($p<0.0001$), tumor invasion in blood and lymph vessels ($p\leq0.0064$) as well as microsatellite instability ($p<0.0001$) in colon cancers. TYMS is often overexpressed as compared to normal tissues in a broad range of different cancer entities. Our data suggest that high-level of TYMS expression is a feature of cancer aggressiveness in many different cancer types.

#1048 Loss of MTAP expression is strongly linked to homozygous 9p21 deletion, unfavorable tumor phenotype and non-inflamed microenvironment in urothelial bladder cancer.

N. Gorbokon[1], N. Wo?ner[1], V. Ahlburg[1], S. Schallenberg[2], H. Plage[2], S. Hofbauer[2], K. Furlano[2], S. Weinberger[2], P. G. Bruch[2], F. Ro?ner[2], S. Elezkurtaj[2], **M. Lennartz**[1], N. C. Blessin[1], A. H. Marx[3], H. Samtleben[3], M. Fisch[1], M. Rink[4], M. Slojewski[5], K. Kaczmarek[5], T. Ecke[6], S. Hallmann[6], S. Koch[6], N. Adamini[7], S. Minner[1], R. Simon[1], G. Sauter[1], H. Zecha[7], D. Horst[2], T. Klatte[2], T. Schlomm[2], M. Kluth[1];

[1]University Medical Center Hamburg-Eppendorf, Hamburg, Germany, [2]Charite - Universitatsmedizin Berlin, Corporate Member of Freie Universitat Berlin, Humboldt-Universitat zu Berlin and Berlin Institute of Health, Berlin, Germany, [3]Academic Hospital Fuerth, Fuerth, Germany, [4]Marienhospital Hamburg, Hamburg, Germany, [5]Pomeranian Medical University, Szczecin, Poland, [6]Helios Hospital Bad Saarow, Bad Saarow, Germany, [7]Albertinen Hospital, Hamburg, Germany

9p21 deletions are common in urothelial carcinoma and mostly include S-methyl-5′-thioadenosine phosphorylase (MTAP) a critical enzyme for DNA and RNA synthesis. Homozygous MTAP deletions result in a complete loss of expression which can be visualized by immunohistochemistry (IHC). Evidence is emerging that MTAP deficiency results in a critical vulnerability of cancer cells towards drugs targeting multiple different pathways that depend on a functional MTAP gene and causes resistance to immune checkpoint inhibitors. To determine the prevalence and clinical significance of MTAP deficiency and its relationship with the tumor microenvironment in urothelial bladder carcinomas, more than 2,500 tumors were analyzed by fluorescence in-situ hybridization (FISH) and IHC in a tissue microarray format, and the data were compared with existing data on intratumoral lymphocyte subsets and PD-L1 expression. The cohort included 1,826 patients that underwent radical cystectomy for muscle-invasive disease (pT2-4). 9p21 deletion was homozygous in 364 (21.3%) and heterozygous in 334 (19.5%) of 1,711 analyzable tumors. The rate of 9p21 deleted tumors increased from pTa G2 low (9.2% homozygous, 25.8% heterozygous) to pTa G2 high (32.6%, 20.9%; p<0.0001) but was slightly lower in pTa G3 (16.7% each). In pT2-pT4 carcinomas, 9p21 deletions were homozygous in 23.3% and heterozygous in 17.9%. Within muscle-invasive cancers, 9p21 deletions were tied to high pT (p=0.0014) and poor overall survival (p=0.0461). MTAP expression loss was strongly linked to homozygous 9p21 deletions. Complete absence of MTAP staining was seen in 96.1% of homozygous deleted cancers while only 4 of 249 MTAP negative cancers had retained at least one 9p21 copy (p<0.0001). Accordingly, absence of MTAP staining was also linked to advanced pT status and poor overall survival (p<0.05 each). Tumors with heterozygous 9p21 deletion did often show preserved but low-level expression of MTAP. 9p21 deletions were associated with low numbers of PD-L1 positive tumor cells (p<0.0001), CD8 (p=0.01) and CD4 positive lymphocytes (p=0.009), M2-macrophages (p<0.0001), and dendritic cells (p=0.0007). A similar tendency was observed for MTAP expression loss, but the level of significance was only reached for PD-L1 positive tumor cells (p<0.0001), M2 macrophages (p=0.001) and dendritic cells (p=0.012). Complete MTAP expression loss is common in urinary bladder cancer and strongly tied to homozygous 9p21 loss, aggressive disease, and non-inflamed microenvironment. Drugs targeting MTAP-deficiency may be highly useful in bladder cancer. MTAP IHC is an excellent surrogate for the detection of MTAP deficiency in this tumor entity.

#1049 Prevalence of KDM6A expression loss in human cancer: A tissue microarray study on 6,560 cancers from 114 different tumor types.

F. Viehweger[1], N. Gorbokon[1], **M. Lennartz**[1], V. Reiswich[1], F. Lutz[1], T. Krech[1], A. M. Luebke[1], C. Hube-Magg[1], G. Sauter[1], R. Simon[1], S. Steurer[1], A. H. Marx[2], C. Bernreuther[1], M. Kluth[1], S. Minner[1];

[1]University Medical Center Hamburg-Eppendorf, Hamburg, Germany, [2]Academic Hospital Fuerth, Fuerth, Germany

KDM6A, also known as UTX (ubiquitously transcribed X chromosome tetratricopeptide repeat protein) is an epigenetic regulator constituting a critical part of the COMPASS-like complex. KDM6A mutations occur commonly in cancer. These are of interest because KDM6A loss results in a dependency on EZH2, a potential therapeutic target. Most data on KDM6A have been obtained by next generation sequencing (NGS). However, since most KDM6A mutations are truncating and KDM6A is located on the X chromosome, many mutations result in a complete expression loss which can be detected by immunohistochemistry (IHC). To learn more on the prevalence of KDM6A expression loss and its role in cancer, a tissue microarray containing 6,560 samples from 114 different tumor entities and 608 samples of 76 different normal tissue types was analyzed. In normal tissues, KDM6A staining was rather ubiquitously seen in nuclei. In cancer, KDM6A staining was considered weak (1+) in 581 (11.2%), moderate in 1,927 (37%), and strong in 2,362 (45.4%) of 5,206 interpretable tumors. A complete loss of KDM6A staining occurred in 336 (6.5%) of tumors. At least one case with a complete KDM6A expression loss was observed in 51 of 114 tumor categories. KDM6A staining was most commonly lost in different categories of urothelial carcinomas (19.5-39.2%), squamous cell carcinomas of the esophagus (27.1%), hepatocellular carcinoma (18.4%), gastric carcinoma (3.2-12.5%), papillary renal cell carcinoma (9.5%), adenocarcinoma of the prostate (5.9-9.4%), chromophobe renal cell carcinoma (8.9%), Ewing sarcoma (8.3%), pheochromocytoma (8.3%), and metastatic malignant melanoma (8%). A KDM6A expression loss in less than 8% of cases was observed in 32 further tumor entities. KDM6A expression loss was more than twice as frequent in tumors from male (8.4% of 2,526) than in tumors from female patients (3.9% of 2,024; $p<0.0001$). It is concluded that KDM6A IHC is a suitable method for the detection of truncating KDM6A mutations, especially in males. These make up for about 2/3 of all KDM6A mutations and may exert specific biological effects than differ from the various KDM6A missense mutations known to also occur.

CLINICAL RESEARCH: Early Detection Biomarkers 1
Poster Session

#1053 The Influence of PD1 and TIM3 Expression on CD4+CD103+ and CD8+CD103+ Cells in Glioblastoma Progression.

L. Gabriele[1], G. Romagnoli[1], Q. G. D'Alessandris[2], I. Capone[1], A. Tavilla[1], I. Canini[1], C. Lapenta[1], M. Buccarelli[1], M. Giordano[2], V. Tirelli[1], M. Sanchez[1], A. Fragale[1], S. Giannetti[3], R. Di Bonaventura[2], L. Lauretti[2], M. Biffoni[1], L. Ricci-Vitiani[1], R. Pallini[2];
[1]Istituto Superiore di Sanita, Rome, Italy, [2]Fondazione Policlinico Universitario A. Gemelli IRCCS, Rome, Italy, [3]Universita Cattolica del Sacro Cuore, Rome, Italy

Glioblastoma (GB), IDH-wildtype, is the most common and aggressive high-grade primary malignant brain tumor with extremely poor outcome. Although the use of immune checkpoint inhibitors (ICIs) in GB has shown disappointing results, the identification of a small subgroup of responders underpins the role of the intratumoral immune contexture, in particular tumour-infiltrating lymphocytes (TILs), in determining disease outcome. This study aims to define the features of TIL subpopulations correlating with GB prognosis, and to establish in parallel the predictive roles of peripheral T cell subsets. A single cohort observational study, including patients undergoing GB resection and standard therapeutic and follow-up approaches in Neuro-Oncology, was conducted. Of the 45 patients, histologically confirmed WHO grade 4, 26 had MGMT promoter methylation (60.0%), 24 were male (53.3%) and the median age of young patients (≤63 years) vs elderly patients (>63 years) was 57 vs 71, respectively. Predictors of OS were KPS (≥70 vs <70: 14.7 vs 7.5 months, p=0.0007) and GTR (GTR vs non-GRT: 15 vs 9 months, p=0.004) whereas patients with methylated MGMT promoter had non-significant longer median OS compared to those with unmethylated promoter (14.5 vs 10.5 months). Patients were characterized for the expression of lineage, differentiation, memory, activation, and inhibition markers on intratumoral and peripheral CD4+ and CD8+ T cell subpopulations, and the correlation of an array of CD4+ and CD8+ T cell subsets with OS or PFS was evaluated by multiparametric flow cytometry and uni/multivariate analyses. Intratumoral immune infiltrate was positively associated with CD8+CD103+ tissue-resident memory T cells (Trm), and in particular with CD8+CD103+ Trm expressing PD1 and TIM3 rather than CD4+ Trm. Low CD8+CD103+PD1+ Trm resulted significantly associated with better OS and PFS (p=0.02 and 0.0031, respectively) and even higher significant was the correlation with better OS and PFS of low CD8+CD103+TIM3+ Trm (p=0.0002 and 0.0033, respectively) and CD8+CD103+PD1+TIM3+ Trm (p<0.0001, both). On multivariate analysis, low CD8+CD103+PD1+TIM3+ Trm and KPS ≥70 were confirmed to be the most predictive independent factors associated with longer OS (hazard ratios - HR [95%CI]: 0.14 [0.04 - 0.52] p<0.001, 0.39 [0.16 - 0.96] p=0.04, respectively). Moreover, CD8+CD103+ Trm subpopulations resulted age-related predictors for GB survival. Consistent with this finding, in vitro PD1 and TIM3 blockade released the capability of intratumoral T cells to produce the effector cytokines IFN-γ and TNF-α, and the cytotoxic factor GrzB. Conversely, T cells expressing PD1 and TIM3 of peripheral blood did not show any prognostic significance. In conclusion, low frequency of Trm expressing PD1 or TIM3 or both markers defined TIL subsets as independent positive prognostic factors for patient survival.

#1054 Reciprocal circRNA-miRNA expression axes indicative of early tumor initiation in breast.

N. A. H. Maatouk, S. H. H. Marei, A. B. A. Kurdi, N. S. K. Hamade, R. R. Nasr, R. S. Talhouk;
American University of Beirut, Beirut, Lebanon

Cancer prevention and early detection are the most effective tools for cancer control. In this study, we adopt a novel approach of identifying a network of proteins/mRNA-circRNA-miRNA axes. We hypothesize that mutation of oncogenes or tumor suppressor genes during pre-oncogenic stage result in aligned change in levels of circular RNAs-derived genes, as well as, reciprocally, in corresponding sponged miRNAs. These epigenetic risk predictive proteins/mRNA-circRNA-miRNA axes serve as potential tool for early detection of changes leading to breast cancer (BC) and can be further used as non-invasive screening biomarkers of patients' blood in populations susceptible to cancer. BC patients in GDC Data Portal, TCGA-BRCA project are selected based on several criteria such as their age at diagnosis (20-50 years old), early clinical stage of cancer (stage I) and disease type (ductal and lobular neoplasms). Differentially expressed genes are acquired from mRNA sequencing data by comparing Stage I Breast cancer versus normal primary tissues using R Studio. Then, mRNAs whose expression is aligned with the differentially expressed circRNAs and their host genes acquired from Gene Expression Omnibus (GEO) (GSE182471, Triple Negative Breast cancer tissues versus normal tissues) are selected. Differentially expressed miRNAs, in reciprocal expression with circRNAs, are defined using miRNA sequencing data of the same previously chosen TCGA BRCA patients. Selected miRNAs are hypothesized to be sponged with high confidence by selected circRNAs based on a context percentile binding score in CircInteractome. Using KM Plotter, the survival analysis of corresponding miRNAs in grade I BC patients is examined. The predicted miRNA expression was correlated with lower survival rates among stage I BC patients in KM Plotter. MiRNA-enrichment analysis is used to further validate the involvement of selected miRNAs in early tumorigenic events through exploring in which molecular pathways their downstream genes are enriched. We have constructed more than 20 potential proteins/mRNA-circRNA-miRNA axes for non-invasive screening of patients' body fluid (i.e. Blood) in populations susceptible to BC using RNA and miRNA sequencing data available in online databases and further validate the proposed axes using in-silico tools. The described axes, once validated in clinical samples could provide a potential tool for early-stage BC prediction and prevention.

#1055 ORF1p expression from LINE-1 occurs in clear cell ovarian carcinoma precursors and is detectable in patients' plasma samples.

P. R. de Santiago[1], S. Sato[1], Y. Zhuravlev[1], H. S. Rendulich[1], M. S. Taylor[2], C. Wu[3], M. C. Dougher[4], L. Schwartz[4], D. R. Walt[2], K. H. Burns[5], R. Drapkin[1]; [1]University of Pennsylvania, Philadelphia, PA, [2]Mass General Brigham, Boston, MA, [3]Life Sciences Institute, University of Michigan, Ann Arbor, MI, [4]Hospital of the University of Pennsylvania, Philadelphia, PA, [5]Dana-Farber Cancer Institute, Boston, MA

Long interspersed element 1 (LINE-1) retrotransposons are repetitive genomic sequences able to move across the genome by an autonomous "copy and paste" mechanism. Given the mutagenic potential of LINE-1, benign cells restrict its expression, although the molecular mechanisms involved are usually impaired in cancer. Clear cell ovarian carcinoma (CCOC) accounts for ~5-10% of ovarian cancers and is believed to arise from endometriosis. Women have a poor prognosis when it presents at an advanced stage, which emphasizes the need for a better understanding of the disease. In the present study, we found that ~85% of CCOC tumors express ORF1p, one of two proteins encoded by LINE-1. We show that CCOC cell lines retain ORF1p expression and release it into the extracellular media. By using single molecule array (Simoa) assays, we detected ORF1p in patient plasma, proposing ORF1p as a non-invasive biomarker for this disease. Finally, we found that LINE-1 retrotransposon de-repression is an early event in CCOC, as ORF1p is enhanced during the transition from typical to atypical endometriosis and that is retained in the invasive cancer.

#1056 Development of a B-cell epitope classifier for early detection of renal cell carcinoma.

Thomas W. Campbell[1], Christian R. Hoerner[2], Elizabeth Alli[3], John T. Leppert[4], John C. Shon[1], Alice C. Fan[2]

[1]Serimmune Inc., Goleta, CA,[2]Division of Oncology, Department of Medicine, Stanford School of Medicine, Stanford, CA,[3]Department of Cancer Biology, Wake Forest University School of Medicine, Winston-Salem, NC,[4]Department of Urology, Stanford University, Goleta, CA

A blood biomarker for early detection of renal cell carcinoma (RCC) would help decrease the burden of 15,000 deaths annually in the U.S. (1). Antibodies against tumor (neo)antigens are thought to arise early in cancer development and might serve as a more sensitive biomarker for RCC than tumor-derived biomolecules. Serum Epitope Repertoire Analysis (SERA) of human serum/plasma uses a random bacterial peptide display library and next generation sequencing to allow for unbiased highly multiplexed profiling of B cell epitopes. In combination with bioinformatic methods and machine learning, a classifier was trained to predict the presence of RCC using a cohort of 163 treatment-naïve patients (median age 62, stage: I 35%, II 5%, III 20%, IV 40%) with clear cell RCC (ccRCC) and 438 age-matched healthy controls (median age 61). Classifier performance was evaluated by sensitivity, specificity, and receiver operator curve (ROC) area under the curve (AUC) analysis in an independent validation cohort of 43 treatment-naïve patients with ccRCC (age 22-86, median 63, stage: I 33%, II 2%, III 26%, IV 39%) and 1,759 healthy controls (age 18-89, median 40). A total of 1,465 individual B cell epitope features were discovered and enriched in ccRCC vs. controls and included in a random forest model. In the validation cohort, the ROC-AUC was 0.65, and sensitivities of 9%, 16%, 30%, and 36% were achieved at specificities of 99%, 98%, 95%, and 90%, respectively. Performance was better in both early stage ccRCC and low tumor grade (grade 1 or 2). For stage I, the ROC-AUC was 0.88, and sensitivities of 7%, 14%, 36%, and 57% were achieved at specificities of 99%, 98%, 95%, and 90%, respectively. For low tumor grade, the ROC-AUC was 0.86, and sensitivities of 10%, 20%, 50%, and 60% of were achieved at specificities of 99%, 98%, 95%, and 90%, respectively. The classifier did not miscategorize benign renal lesions as ccRCC (Mann-Whitney p-value 0.52, ROC-AUC 0.54) in a separate cohort of 23 patients with benign renal tumors vs. the 1,759 healthy controls. This preliminary performance for a B cell epitope-based classifier is promising: the better performance in early stage ccRCC suggests that B cell epitope biomarkers may complement the lower sensitivity of cell-free DNA for detecting early-stage cancer (2). Future work will further validate these results in larger multi-institutional cohorts to improve classification performance and explore if B cell epitope biomarkers can be combined with existing assays to develop an early detection composite biomarker for RCC and tumor grade.

(1)Siegel RL, Miller KD, Wagle NS, Jemal A. Cancer statistics, 2023. CA Cancer J Clin. 2023 Jan;73(1):17-48.(2)Francini, E.; Fanelli, G.N.; Pederzoli, F.; Spisak, S.; Minonne, E.; Raffo, M.; Pakula, H.; Tisza, V.; Scatena, C.; Naccarato, A.G.; et al. Circulating Cell-Free DNA in Renal Cell Carcinoma: The New Era of Precision Medicine. *Cancers* 2022, *14*, 4359.

#1057 A blood-based multi-omics test for multicancer early detection: Combined retrospective and prospective studies.

M. Mao[1], S. Li[1], Q. Ren[2], Y. Luan[3], W. Liang[4], S. Geng[5], D.-L. Huang[1], D. Zhu[5], Y. Chang[5], W. Wu[1], Y. Zhang[4], L. Zhang[4], Y. Wang[4], Y. Feng[1], B. Wei[6], J. Ma[6], C. Duan[3], G. Long[2];

[1]Research & Development, SeekIn Inc, Shenzhen, China, [2]Peking University Shenzhen Hospital, Shenzhen, China, [3]Sun Yat-sen Memorial Hospital, Sun Yat-Sen University, Guangzhou, China, [4]The First Affiliated Hospital of Zhengzhou University, Zhengzhou, China, [5]Clinical Laboratories, Shenyou Bio, Zhengzhou, China, [6]Henan Cancer Hospital, The Affiliated Cancer Hospital of Zhengzhou University, Zhengzhou, China

Background: Recent studies have demonstrated that blood-based multi-cancer early detection (MCED) approaches may hold promise for identifying asymptomatic cancer patients from general population. However, most studies only exploit a single aspect of cancer hallmarks, which is challenging for the biological reasons as cancer is a heterogenous disease with a wide spectrum of pathological and clinical behaviors. Here we report a multi-omics MCED assay named SeekInCare, a CE-IVD Mark blood test, which incorporates genomic hallmarks: copy number aberrations, fragment size, end motifs and oncogenic viruses via shallow whole genome sequencing from cfDNA, and seven plasma protein tumor markers in 8 ml blood.

Methods: SeekInCare was developed using several retrospective cohorts and the method has been described in a publication (DOI: 10.1016/j.jmoldx.2021.06.003) IF: 4.1 Q2 .

Results: We present the validation in a retrospective cohort consisting of 584 non-cancer individuals and 617 cancer patients covering 27 cancer types. SeekInCare achieved 65.5% sensitivity at 97.9% specificity, resulting in an AUC of 0.936. The sensitivities were 46.9%, 60.0%, 68.9%, 81.8% in stage I, II, III, IV patients. The sensitivities of 10 common cancer types are as the following: breast (46.2%), stomach (46.4%), colorectum (56.5%), gallbladder (60.0%), lung (62.8%), pancreas (64.7%), lymphoma (68.5%), esophagus (70.0%), liver (77.5%), and leukemia (86.7%). These cancer types account for 73.5% of cancer incidence and 81.8% of cancer-related mortality in China. We prospectively evaluated SeekInCare in a real-world cohort consisting of 1203 individuals who received the test as a laboratory developed test (median follow-up time: 753 days) in which it achieved 60.0% sensitivity, 96.1% specificity, 11.5% PPV and 99.7% NPV.

Conclusion: The performances of SeekInCare in both retrospective and prospective studies demonstrate that SeekInCare is an effective blood-based MCED test with similar performance as Grail’s Galleri test, which paves the way for clinical utility as a cancer screening test in average-risk populations.

#1058 Immune biomarkers for recurrence in stage II and III melanoma to guide patient stratification.

Gerardo A. Espinoza[1], Chenxin Zhang[2], Jee-Young Moon[2], Divya B. Kenchappa[1], Matteo Abbruzzese[3], Lydia Bioh[1], Yadriel M. Bracero[1], Sharmin Sultana[1], Ajay Singh[1], Thazin Aung[4], John J. Krolewski[5], Robyn D. Gartrell[6], Larisa J. Geskin[7], Lawrence W. Leung[1], Tammie Ferringer[8], Rui Chang[9], Basil Horst[10], Kent Nastiuk[11], **Yvonne M. Saenger**[1]

[1]Cancer Center, Albert Einstein College of Medicine, Bronx, NY,[2]Epidemiology and Population Health, Albert Einstein College of Medicine, Bronx, NY,[3]Medicine, Albert Einstein College of Medicine, Bronx, NY,[4]Pathology, Yale School of Medicine, New Haven, CT,[5]Biology and Interdisciplinary Unit for Data Science & Analytics, Buffalo State University, Buffalo, NY,[6]Pediatrics, Columbia University Irving Medical Center, New York, NY,[7]Dermatology, Columbia University Irving Medical Center, New York, NY,[8]Dermatopathology, Geisinger Medical Laboratories, Danville, PA,[9]Nuerology, University of Arizona College of Medicine, Tuscon, AZ,[10]Pathology and Laboratory Medicine, The University of British Columbia, Vancouver, BC,[11]Cancer Genetics and Genomics, Roswell Park Comprehensive Cancer Center, Buffalo, NY

Stage II-III melanoma patients lack needed biomarkers to avoid over-treatment and determine need for combination immunotherapy. A “hot” tumor immune micro-environment (TIME) is predictive of survival and immunotherapy benefit in multiple tumor types. We have previously identified the ratio of CD8+/CD68+ cells as well as a 53-gene melanoma immune panel (MIP) as indicative of a favorable “hot” TIME. CD8/CD68 ratio and MIP were evaluated in specimens from 213 previously untreated patients including 164 from Roswell Park Comprehensive Cancer Center (RPCCC) and 49 from Geisinger Health Systems (GHS, n=36). Tumors were stained with Sox10, CD8, CD68, MPO, PDL1 and HLA-DR using the MOTiF workflow (Akoya Biosciences, AB). Image analysis was completed using inForm software (AB). RNA was extracted and NanoString analysis performed using published methods. Receiving Operator Curves (ROC) were generated and KM curves using cutoffs selected using maximally selected log-rank statistics to quantify survival benefit. We tested whether the CD8/CD68 ratio correlated with disease specific survival (DSS) and distant metastatic recurrence (DMR). In the RPCCC cohort (n=164), 138 specimens were evaluated by a pathologist and stained of which 15 were excluded based on tissue quality, and inForm analysis was completed on 80. Of these 80, 16 had DMR of whom 8 had died. ROC showed CD8/CD68 ratio to correlate with DMR (p=0.0397). KM analysis showed high CD8/CD68 ratio correlated with DMR free survival (p=0.00079). Within the GHS samples, 36 of 49 patients had sufficient quality tissue, of whom 13 had died. DMR data was not available. A high CD8/CD68 ratio correlated with DSS by ROC curve (p=0.027) and KM analysis (p=0.0009). MIP was run on 166 patients of whom 147 passed quality control for analysis. MIP correlated with DSS in the RPCCC cohort by ROC analysis (p=0.025) and cutoff defined based on prior cohort showed correlation with DSS (p=0.01) and trend towards correlation with DMRFS (p=0.065). To include diverse samples in the training set, MIP was retrained with the addition of 81 patients from Columbia University (CUMC). KM analysis performed using the retrained signature showed a favorable signature correlated with DSS (p=0.032) and DMRFS (p=0.00077). Immune based biomarkers including CD8/CD68 ratio and immune gene signature have potential to assist clinicians in selecting early-stage melanoma patients for more intensive immunotherapy regimens. Full analysis of the data from the RPCCC and GHS cohorts will be presented at the conference.

#1059 Biomarkers analysis on samples from patients in EVT801 clinical trial: Patient characterization and immunomonitoring.

L. Davenne[1], M. Fitzgerald[2], P.-B. Ancey[1], O. Delpuech[1], C. Poussereau-Pomie[1], M. Esquerre[1], M. R. Paillasse[1], M. Mandron[1], P. Rochaix[3], M. Ayyoub[3], C. Scarlata[3], C. Caux[4], C. Caux[4], P. Cassier[4], C. Gomez-Roca[3], J.-P. Delord[3], J. Friend[2], **P. Fons**[1];
[1]Evotec International GmbH, Toulouse, France, [2]Kazia Therapeutics, Sydney, Australia, [3]Institut Universitaire du Cancer Toulouse-Oncopole, Toulouse, France, [4]Centre Leon Berard, Lyon, France

Introduction: EVT801 is a highly selective small molecule inhibitor of VEGFR3 that acts by inducing tumor (lymph)-angiogenesis normalization in and around the tumor. EVT801 has shown compelling activity in a wide range of cancer models showing a decrease of tumor hypoxia and an increase of $CD8^{pos}$ T-cells infiltration into the tumor micro-environment. EVT801 was well-tolerated in preclinical toxicology studies. A phase I study is underway focusing primarily on understanding the safety, tolerability, and pharmacokinetics of EVT801 across a range of doses (NCT05114668).
Methods: The first stage of the phase I trial aims to determine the maximum tolerated dose (MTD) and recommended Phase II dose (RP2D) for EVT801. Clinical samples from enrolled patients have been collected to explore preliminary signals of the biological activity of the drug and characterize tumor phenotypes. Patient characterization includes histology and mRNA signature in archival biopsies. Target engagement and pharmacodynamics effects are investigated by immunomonitoring as well as assessment of a defined set of proteins as markers of inflammation and angiogenesis as identified in preclinical *in vivo* models.
Conclusion: Our first biomarkers analyses on a subpopulation of patients with High Grade Serous Ovarian Cancer (HGS-OC) enrolled in the first stage of the study showed that levels of VEGFR3 expression had a negative correlation with CD8 positive T-cells infiltration in the tumor microenvironment and a tendency to positive correlation with a PD1 mAb resistance signature. VEGFR3 expression also tends to be correlated with higher levels of hypoxia (CAIX labelling). Our working hypothesis is that patients with hypoxic HGS-OC tumors with high VEGFR3 expression may benefit from EVT801 treatment; this will need to be reinforced by inclusion of additional patients in dedicated PD biomarkers cohorts during stage 2 of the clinical trial.

#1060 Circulating early myeloid derived suppressor cells as biomarkers for early detection of lung cancer.

O. Fortunato[1], B. Bassani[2], M. Lecchi[1], P. Verderio[1], U. Pastorino[1], G. Sozzi[1], M. Colombo[1], **S. Sangaletti[1]**;
[1]Istituto Nazionale dei Tumori, Milano, Italy, [2]Multimedica, Milano, Italy

Background. Lung cancer (LC) patients, despite innovative cancer treatments such as target and immune-therapies, still have the poorest five-year survival rate. In this context the possibility of an early detection can anticipate therapeutic intervention, avoiding aggressive therapies thus prolonging disease-free and overall survival. Therefore, the identification of new circulating early biomarkers still represents a relevant clinical need.
Methods. Lung cancer (LC) patients (n=63) and heavy smokers (HS) cancer free-subjects (n=52) were evaluated for the enrichment of specific subtypes of myeloid cells. Circulating early myeloid derived suppressor cells (eMDSCs) and low-density neutrophils (LDNs) were assessed by flow cytometry on peripheral blood mononuclear cells (PMBCs). Early MDSCs were defined as CD11b+CD33+CD15-CD14- cells among Lineage negative (Lin-) HLA-DR- PBMCs, whereas LDNs were defined as CD66b+CD15+ cells within the gate of CD11b+ PBMCs. Mature and immature subtypes were discriminated according to the expression of CD10.
Results. Performing a sex- and smoking -matched case-control analysis in 39 LC and 39 HS subjects we were able to compare the capacity of specific myeloid population to discriminate lung cancer patients from heavy smokers. The analysis showed significantly higher values of eMDSC (OR=1.12; 95% Confidence Interval (CI) 1.03-1.21), total LDN (CD66b+CD15+; OR=1.23; 95%CI 1.04-1.45) and of mature CD10+ LDN (OR=1.30; 95%CI 1.05-1.61). Moreover, within the overall cohort of 63 LC patients, we analyzed the distributions of the different myeloid populations according to stage (I-II vs III-IV). In this comparison, total LDN (CD66b+CD15+; Kruskal-Wallis (KW) Test p-value=0.014), and mature CD10+ LDN (KW test p-value=0.006) showed significant different distributions according to tumor stage, observing higher values in patients with advanced stage. On the contrary, no difference among stages was observed for the eMDSC population.
Conclusions. These findings point to eMDSCs as an early marker for lung cancer detection whereas LDN could be as well associated with disease progression.

#1061 Diagnostic application of a novel blood CDH17 immunoassay in the detection of colorectal adenoma.

N. Lui[1], F. Hon[2], S. Sun[2], P. Leung[2], D. Ho[2], J. M. Luk[3], **D. C. Foo[1]**;
[1]The University of Hong Kong, Hong Kong, Hong Kong, [2]Tiberias Technology (HK) Limited, Hong Kong, Hong Kong, [3]Arbele Corp, Seattle, WA

Background: Colorectal cancer (CRC) is the most prevalent gastrointestinal (GI) cancer and contribute significantly to global cancer deaths. The mechanism of CRC development is a complex multistage process from hyperplastic lesions to the formation of adenomas, followed by the progression into malignancy. Hence, early detection during hyperplastic and adenomatous stages warrants new screening tests for effective interception of malignancy progression. Cadherin-17 (CDH17) is a biomarker characterized by its overexpression in several GI cancers, but restricted expression in intestinal mucosal epithelium of normal tissues. We have developed a blood immunoassay using a panel of RUO grade antibodies that unveiled CDH17 as a potential marker with high detection sensitivity and specificity for detecting adenomas. Our immunoassay is useful in identifying high-risk individuals with adenomas that may develop into CRC, which can significantly improve the diagnostic efficiency of colonoscopy that is currently lacking.
Methods: The study recruited 66 patients (54 adenoma and 12 hyperplasia) and 39 normal samples (no abnormality by colonoscopy). CDH17 level in plasma samples were measured using the CDH17 immunoassay.
Results: The novel CDH17 diagnostic assay showed an operating dynamic range from 90ng to 123pg. We observed a progressive and significant increase in the circulating CDH17 level from normal samples to the hyperplasia group, followed by the adenoma group (mean: 1.66ng/mL, 3.20ng/mL, 4.93ng/mL, respectively P<0.0001). The assay performance by ROC curve demonstrated an AUC of >0.9, with a sensitivity of 85% and specificity of 86%. NPV and PPV were 84% and 87%, respectively. The assay outperforms two market available FIT-DNA tests at predicting adenomas (Table. 1).
Conclusion: The novel CDH17 immunoassay is potentially a powerful tool for the detection of aberrant plasma CDH17 expression, improving the surveillance and the detection of high-risk individuals for CRC.

CDH17 immunoassay outperforms market availalble FIT-DNA tests at detecting hyperplasia and adenoma

		FIT-DNA test 1	FIT-DNA test 2	CDH17 blood immunoassay
		Age 40-74	Age 50-84	Age 45-93
Sensitivity (%)	Advanced adenoma	63.5	42.4	85.0
	Non-advanced adenoma (i.e Hyperplasia)	Unavailable	17.2	58.3
Specificity (%)	Normal control (no abnormality by colonoscopy)	87.1	89.8	86.1
NPV (%)	Advanced adenoma	Unavailable	Unavailable	83.8
	Non-advanced adenoma (i.e Hyperplasia)	Unavailable	Unavailable	86.1
PPV (%)	Advanced adenoma	Unavailable	Unavailable	87.2
	Non-advanced adenoma (i.e Hyperplasia)	Unavailable	Unavailable	58.3

#1062 Clinical validation: A blood-based biomarker for early lung cancer detection based on circulating DNA fragmentomics.

P. Mazzone[1], P. B. Bach[2], **L. B. Cotton**[2], C. A. Schonewolf[2];
[1]Cleveland Clinic, Cleveland, OH, [2]DELFI Diagnostics, Inc., Baltimore, MD

PURPOSE: Screening for lung cancer using a biomarker blood test has the potential to overcome the currently low adherence rates in the US, offering patients a convenient and accessible option. Integrating routine blood draws into lung cancer screening could boost participation, mirroring the success of non-invasive tests in colorectal screening. Numerous proof-of-concept studies indicate that analyzing genome-wide cfDNA fragmentation patterns can effectively distinguish between individuals with and without lung cancer. We conducted a multi-institutional case-control study to train and validate a fragmentome based cfDNA classifier for lung cancer early detection.
METHODS: The DELFI-L101 study (NCT04825834) is a prospective, multi-site, observational case-control study designed to develop and validate an early detection test for lung cancer. The DELFI (DNA Evaluation of Fragments for Early Interception) method utilizes low-pass whole genome sequencing, a cost-effective approach that examines cell-free DNA (cfDNA) fragmentation patterns associated with lung cancer. Enrolled participants were aged ≥50 y, smoking history of ≥20 pack-years, and had undergone or had planned chest CT imaging. Medical histories were documented, and blood samples were collected for DELFI analysis. A classifier, developed through supervised machine learning, was created to distinguish between samples from individuals with lung cancer and those without. Performance was assessed through repeated 10-fold cross-validation in the training set and then subsequently assessed in an independent split-study clinical validation set. The classifier was optimized for the sensitivity detection of lung cancer in the screening-eligible population. Performance was evaluated across patient and tumor characteristics, adjusting the stage distribution to match that of LDCT screening populations.
RESULTS: In an analysis of 958 participants from both the lung cancer and non-cancer control groups, the sensitivity of the test remained consistent across various participant demographics, comorbidities, and tumor characteristics, increasing with higher group, T, and N stages. The stage weighted sensitivity for the screening population was 80% (95% CI: 75%-86%), with a specificity of 53% (95% CI: 43%-64%). At a prevalence of 0.7%, the negative predictive value was 99.7%.
CONCLUSIONS: Clinical validation of the DELFI-based blood test demonstrates its potential to detect lung cancer within the screening eligible population. A negative result is associated with a high negative predictive value. Given the limited adoption of low-dose computed tomography (LDCT) screening, especially among socio-economically disadvantaged individuals, this clinically validated, blood-based cfDNA test could significantly increase LDCT screening participation.

#1063 IsomiR relative proportion (IRP) within miRNA family as an efficient biomarker for noninvasive colorectal cancer detection.

Y. Hu[1], W. Lu[1], C. Liu[1], X. Dai[2], J. Xu[1], X. Kong[1], Y. Zhu[3], Y. Ye[1], L. Chen[1], X. An[2], F. Wu[2], S. Ma[2], N. Wang[2], Q. Xiao[1], J. Liu[2], **K. Ding**[4];
[1]Ministry of Education, The Second Affiliated Hospital, Zhejiang University School of Medicine, Zhejiang University Cancer Center, Hangzhou, China, [2]New Horizon Health Research Center, Hangzhou, China, [3]Haining Hospital of Traditional Chinese Medicine, Haining Cancer Prevention and Treatment Research Institute, Haining, China, [4]The Second Affiliated Hospital, Zhejiang University School of Medicine,Center for Medical Research and Innovation in Digestive System Tumors, Ministry of Education, Cancer Center of Zhejiang University, Hangzhou, China

Background: Cell free miRNA has been widely used for disease diagnosis, particularly in cancers. The latest research has also demonstrated that isomiRs (isoform miRNAs) can serve as superior markers, displaying enhanced diagnostic performance in cancer diagnosis. However, the low detection sensitivities of miRNA/isomiRs in previous methods in plasma have limited their broad implementations for screening purpose. In this study, we propose a new isomiRs feature of isomiR relative proportion (IRP), which was validated with high performance in Colorectal Cancer (CRC) early diagnosis.
Methods: A total of 1036 participants were enrolled from the National Colorectal Cancer Cohort (NCRCC), and 836 participants were eligible for plasma collection, including 238 controls, 373 CRC patients, 41 inflammatory bowel disease (IBD), 5 intramucosal carcinoma (Tis) and 179 advanced precancerous lesions (APL). Total circulating small RNA was extracted, followed by library preparation using UMI-based approach. Subsequently, small RNA sequencing was conducted using DNB-seq, and bioinformatic analysis was performed thereafter. The samples were randomly assigned into training (49%), test (30%) and validation (21%) sets. Models based on isomiR relative proportion (IRP), isomiR relative expression (IRE) or both features were constructed by beam search and random forest algorithms in training and test sets, and results were verified in validation set.
Results: Differential IRP or IRE features were identified between cancer and controls. IRP identified 132 specific differential expressed isomiRs. Models constructed using either IRP or IRE features showed high performance (both AUC > 0.9). However, there was improvement in IRP feature model in the validation set (sensitivity of IRP: 0.923, sensitivity of IRE: 0.859) compared with IRE model. We then found that there may be complementarities between IRP and IRE features, and the combination model (34 IRP+IRE features) improved cancer detection performance (AUC: 0.953). Finally, the risk scores predicted by this combination model increased gradually across CRC progression (R=0.921), and the sensitivity of APL was 0.626.
Conclusion: We improved the small-RNA sequencing method and developed an IRP method, and present that IRP as a new feature not only demonstrate the ability of CRC early detection, but also revealed the CRC progressing process. Besides, the combination of IRP and IRE improved the performance of diagnosis. These results highlight the potential value of the IRP feature in early cancer detection.

#1065 Two-step method for early detection of ovarian cancer with high specificity via platelet RNA.

E. Ahn[1], S. Kim[2], S. Park[1], S. Kim[1], Y. Kim[3], E. Huang[3], S. Lee[3], D. Hwang[2], H. Kim[4], H. Jo[4], U. Cho[4], J. Lee[5], T. Ahn[3], Y.-S. Song[6];
[1]ForetellMyHealth, Inc., Seoul, Korea, Republic of, [2]Seoul National University College of Medicine, Seoul, Korea, Republic of, [3]Handong Global University, Pohang, Korea, Republic of, [4]Cancer Research Institute, Seoul National University College of Medicine, Seoul, Korea, Republic of, [5]Cancer Research Institute, Seoul National University College of Medicine,, Seoul, Korea, Republic of, [6]Myongji Hospital, Goyang, Korea, Republic of

Owing to lack of disease-specific symptoms and screening methods, most of patients with ovarian cancer are diagnosed at an advanced stage. Recent technology based on platelet RNA aids in detection of tumors at the early stages. Also, for population screening of low-prevalence diseases like cancer, accurate detection with high specificity is essential to improve diagnostic methods. Thus, we proposed platelet RNA-based early ovarian cancer detection with great specificity. It is a two-step method for detecting ovarian tumors with more than 99% specificity using exon-exon junction features and sampling invariant normalization and finding their malignancy with more than 99% negative predictive value using exon-exon junction and hematology parameters. First, we downloaded public platelet transcriptome data of gynecological cancer including ovarian cancer (n=151), benign tumor (n=30), and healthy counterparts (n=218) from GEO (GSE158508, 89843, and 183635). Second, we prospectively enrolled patients with gynecological cancer (n=31), benign tumors (n=20), and healthy women (n=18) at Seoul National University Hospital (SNUH) and Boaz Medical Center and obtained platelet transcriptome data (FMH data). Feature selection and model development were conducted using public training set (n=243), public validation set (n=156), and FMH training/validation set (n=47). The batch-invariant normalization was performed, and 198 splice junctions were selected as features from training/validation set for the bootstrap aggregation of the SVM model diagnosing the existence of an ovarian tumor. The model performance was assessed from a separate test set only composed of FMH data (n=22). Our model that demonstrated 96.8% sensitivity, 100.0% specificity, with a predetermined cut-off value. Next, FMH training/validation set was used for model development of following malignancy test. 10 splice junctions and 19 hematology parameters were selected and SVM models were separately developed for splice junctions and hematology parameters using 5-fold cross validation. The predictions were combined using a logical OR operation to obtain the final prediction result. The result showed its diagnostic performance with 100% sensitivity or NPV, and 50.0% specificity in the test data set with a predetermined cut-off value. We proposed a two-step method to operationally improve the existing protocol for ovarian cancer screening. Our model initially excludes most healthy individuals who do not have ovarian tumors and excludes patients with benign ovarian tumors who do not necessitate medical testing. To conclude, our model allows physicians to identify a subset of ovarian tumor patients with a higher risk of malignancy even at early stages; it exhibits potential in enhancing early diagnosis of ovarian cancer, leading to increase of treatment effectiveness and ultimately augmenting the survival of patients with ovarian cancer.

#1066 Colocalization of ovarian cancer-associated biomarkers in tumors, cancer cells and extracellular vesicles.

A. D. Couvillon[1], E. S. Winn-Deen[1], S. Thornton[2], S. Liu[2], M. DeRan[3], M. Pacula[4], S. Banerjee[1], D. Gusenleitner[1], L. T. Bortolin[1], J. Grosha[1], T. Santos-Heiman[1], G. Sangiuliano[1], K. M. Biette[1], C. R. Sedlak[1], B. Hamzeh[1], D. M. Byrne[1], P. A. Duff[1], J. Ho[2], D. Gao[2], A. Jamieson[2], L. T. Cuoco[1], M. S. King[1], D. R. Mattoon[1], T. Guettouche[1], J. N. McAlpine[2], D. Huntsman[2];

[1]Mercy Bioanalytics, Waltham, MA, [2]University of British Columbia, Vancouver, BC, Canada, [3]Diamond Age Data Science, Somerville, MA, [4]Flagstaff Solutions, Acton, MA

Introduction: We have previously shown that ovarian cancer can be detected with high specificity and sensitivity by interrogating colocalized membrane-associated cell-surface biomarkers on single tumor-associated extracellular vesicles (EVs). Our blood based Ovarian Cancer Test (OC Test) is composed of 5 cancer-associated biomarkers (BST-2, FOLR1, MUC-1, MUC-16, and sialylated Thomsen-nouveau antigen (sTn)) known to be overexpressed in ovarian cancer relative to healthy tissues. The test employs these 5 biomarkers in 3 combinations to capture and detect EVs from human plasma to distinguish high-grade serous ovarian carcinoma (HGSC) from both benign ovarian tumors and normal samples. Using super-resolution microscopy on ovarian cancer cell lines and EVs and multiplex immunohistochemistry of ovarian benign and tumor tissue, our study aimed to show that the 5 ovarian cancer biomarkers show 1) colocalization on ovarian cancer cells, 2) colocalization on the surface of EVs, and 3) colocalization on cancer cells within ovarian tumor biopsies.

Methods: Super-resolution microscopy was employed to visualize stained biomarkers on the cell surface of a collection of ovarian cancer cell lines as well as on the surface of extracellular vesicles released by these cell lines. 58 HGSC (17 Stage I, 30 Stage II, and 10 Stage III) and 17 benign ovarian tumor K_2EDTA plasma samples and paired FFPE tissue were sourced from the Ovarian Cancer Research Program (OVCARE, Vancouver BC, Canada). A tumor microarray from identical tissue samples was stained with an Opal multiplex-IHC (mIHC) assay comprised of antibodies to BST2, MUC1, sTn, and pan-cytokeratin and a DAPI counterstain. Machine learning based image analysis was utilized to determine colocalization of the biomarkers at the cellular level within benign and tumor tissue. RNA sequencing was carried out to assess expression levels of the biomarkers in each FFPE tissue sample. OC Tests were run on each plasma sample.

Results: Super-resolution microscopy showed colocalization of OC Test combination biomarkers on ovarian cancer cells and EVs derived therefrom. Machine learning-based image analysis of tumor and benign tissue microarrays stained for BST2/MUC1/sTn using mIHC, showed strong evidence for colocalization of these biomarkers on single cells within ovarian tumor tissue, particularly in early-stage tumors, but not on benign tissue. RNA sequencing analysis showed good correlation of biomarker RNA expression levels and with the OC Test results.

Conclusions: The results presented here demonstrate that the OC Test biomarkers are colocalized on tumor tissue, ovarian cancer cells, and EVs from ovarian cancer cell lines. RNA and protein expression levels show good correlation with OC Test results. These results provide further evidence that colocalized biomarkers on EVs can be utilized for early detection of cancer.

#1067 Label free Raman spectroscopy of extracellular vesicles for early stage liquid biopsy cancer detection.

R. P. Carney[1], M. Navas-Moreno[2], A. Birkeland[1];
[1]UC Davis, Davis, CA, [2]illumifyDx, Broomfield, CO

Aim: To improve patient outcomes, there remains a critical need to develop faster, less invasive platforms capable of identifying biomarkers. Multi-omics approaches, while promising, are high in cost and complexity, low throughput, slow, and require large sample volumes, thus are impractical for many stages of clinical care. Raman spectroscopy (RS) addresses many of these needs: it requires little to no sample preparation, is non-destructive, does not need exogenous dyes or labelling agents, and can be performed directly in aqueous solutions. Surface enhanced Raman spectroscopy (SERS) offers further improvements in terms of sensitivity but increases complexity. In this study we carried out comprehensive RS and SERS measurements on a >100-person cohort of blood and saliva from head and neck cancer (HNC) patients and benign controls. Analyses were carried out on whole biofluids, in addition to extracellular vesicles (EVs) isolated from the biofluids to investigate the added value. EVs are emerging biomarkers of interest found in high numbers in circulating biofluids with great promise to increase the specificity of diagnostic platforms.
Results: We analyzed a robust clinical dataset of HNC patient saliva and plasma to build a diagnostic model. We found distinct Raman and SERS signatures of metabolites in all cancer samples uniquely present compared to non-cancer controls. Raman spectral measurements fused together for EVs and whole biofluids across saliva and plasma delivered accuracies of >95% using a novel machine learning module based on convolutional neural networks. Our platform features an automated method to isolate EVs amenable to rapid clinical use.
Conclusions: The results of this study indicate an exciting step in validating Raman as a robust diagnostic tool revealing that complementary chemical information spread out across biofluids and biomarkers of interest can strongly improve simple, quick Raman based diagnostics of whole biofluids and EVs.

#1068 Plasma metabolite biomarkers for EGFR-mutated non-small cell lung cancer (NSCLC).

L. Thamlikitkul[1], S. Manocheewa[1], S. Limjiasahapong[1], K. Wanichthanarak[1], A. Panya[2], N. Poungvarin[1], Y. Pomyen[3], S. Khoomrung[1];
[1]Faculty of Medicine Siriraj Hospital, Mahidol University, Bangkok, Thailand, [2]National Center for Genetic Engineering and Biotechnology (BIOTEC), Pathumthani, Thailand, [3]Chulabhorn Research Institute, Bangkok, Thailand

Background: Lung cancer is the leading cause of cancer death. More than half of the patients are diagnosed in the advanced stage for which the 5-year survival is below 10%. Lung cancer screening using low-dose CT scan reduced lung cancer mortality among heavy smokers. However, no standard screening method exists for non-smokers. Up to 35% and 90% of male and female lung cancer patients in Southeast Asia, respectively, do not smoke. Half of NSCLC patients in this region harbor EGFR mutations, which is common in women and non-smokers. Thus, we sought to explore novel biomarkers that help to identify lung cancer patients and those who have EGFR mutation. Metabolic reprogramming is one of the hallmarks of cancer. It leads to changes in metabolite levels in the blood. Hence, we conducted plasma metabolomic analysis to identify potential metabolite biomarkers in lung cancer patients.
Methods: Plasma samples were collected from 69 lung cancer patients at Siriraj hospital and 10 healthy individuals during 2018-2022. Plasma metabolites from 29 treatment-naïve EGFR-mutated NSCLC patients, 30 treatment-naïve EGFR-wild-type NSCLC patients, 10 treatment-resistant EGFR T790M-mutated NSCLC patients, and 10 healthy individuals were profiled using GC-MS and untargeted LC-MS with Metlin database matching. EGFR mutation was detected from plasma ctDNA using real-time PCR. Negative plasma EGFR mutation results were confirmed with corresponding tumor tissues. Metabolomics data were processed by the metabox R package.
Results: Among 114 candidate metabolites that passed the variable importance in projection (VIP) cutoff of 1.5, the top ten metabolites that differentiate NSCLC patients with EGFR mutation from those without were shown in Table 1. Many of them can also separate between NSCLC patients and healthy individuals.
Conclusions: Plasma L-Histidinol, tryptophan, PC(20:0/24:0), and formic acid are potential metabolite biomarkers for NSCLC patients harboring EGFR mutation.

Table 1. ROC curve analysis

Discriminant metabolites (Mutated EGFR vs Wild-type EGFR NSCLC)	**AUC**	**Accuracy**	**Sensitivity**	**Specificity**
PG(a-13:0/i-12:0)	0.8000	0.7833	0.8333	0.7333
Nervonic ceramide	0.7736	0.6772	0.7259	0.6333
Valine	0.7678	0.7298	0.7259	0.7333
L-Histidinol	0.7644	0.7281	0.7222	0.7333
Leucine	0.7563	0.7632	0.7259	0.8000
Tryptophan	0.7425	0.6289	0.5593	0.7000
8-methylcaffeine	0.6793	0.6096	0.6222	0.6000
Formic acid	0.6759	0.6447	0.5889	0.7000
PC(20:0/24:0)	0.6506	0.6614	0.8259	0.5000
Sucrose	0.6471	0.6596	0.7593	0.5667
Discriminant metabolites (NSCLC patients vs Healthy individuals)	**AUC**	**Accuracy**	**Sensitivity**	**Specificity**
Tryptophan	0.9986	0.9867	1.0000	0.9848
PC(20:0/24:0)	0.8609	0.9505	0.6111	1.0000
L-Histidinol	0.8572	0.9625	0.7778	0.9861
Formic acid	0.6696	0.9262	0.6667	0.9704

#1069 Interrogating the role of the cGAS/STING pathway fallopian tube transformation.

D. H. Al-Rawi, D. Norkunaite, S. Bakhoum, S. Shah;
Memorial Sloan Kettering Cancer Center, Manhattan, NY

Ovarian Cancer is the deadliest gynecologic malignancy. Despite recent advances in cancer diagnostics, it is a cancer that is often detected late and the vast majority of patients are diagnosed at Stage III and Stage IV. After treatment with debulking surgery and chemotherapy, 80% of patients have tumor relapse with increasing resistance. Early detection efforts have been largely unsuccessful and the only effective prevention strategy in high risk patients is surgical removal of the fallopian tube and ovaries. Careful pathologic studies of prophylactic risk reducing bilateral salpingo-oophorectomy (RRSO) has demonstrated that HGSC originates in the fallopian tube. Within the fallopian tube, secretory cells within the fimbriae are believed to be the origin of HGSC based on numerous lines of correlative evidence including the identification of histologically and molecularly abnormal regions in the fallopian tube called serous tubal intraepithelial cancer (STIC) in 3-5% of patients undergoing RRSO, and the presence of STIC in approximately half of patients undergoing debulking surgeries for HGSC. Finally, p53 mutations have been found to be identical in STIC and in the concurrent invasive disease indicating that HGSC and the STIC likely arise from the same clone. TCGA analysis has demonstrated that HCSC is a disease characterized by genomic and chromosomal instability harboring copy number alteration, including amplifications, deletions and more complex chromosomal rearrangements which impact multiple genes and pathways. Aberrantly segregating chromosomes that lag behind the spindle apparatus fail to become part of the primary nucleus (PN) and are instead enclosed by a self-assembled nuclear membrane, creating a structure called the micronucleus (MN). Spontaneous breakdown of the MN causes cytoplasmic DNA sensing and activation of the cGAS-STING pathway, an important innate cellular defense mechanism to foreign cytoplasmic DNA. To better understand the early genomic and signaling events in the development of HGSC, we are interrogating tissue from our archives from MSKCC patients who have undergone RRSO, hormone ablation surgeries or surgical debulking and were found to have benign fallopian tube, STIC lesions or invasive HGSC with STIC. We have performed a pilot experiment of 20 patient samples of different germline genetic backgrounds. Intriguingly, cGAS signaling was observed only rarely in the STICs indicating low rates of CIN in STICs we have evaluated, however we note that even in early invasive disease, we observe cGAS positivity. Taken together, these data are consistent with a model where CIN and subsequent cGAS/STING pathway activation drives the transition from pre-invasive to invasive disease.

#1070 Overcoming deficiencies in the early detection of high grade serous ovarian cancer: Evaluating exosomal proteins as novel biomarkers of disease.

M. Lightfoot[1], **K. Dorayappan**[2], L. Yu[2], C. Hisey[2], T. Sakaue[3], M. Anbalagan[4], C. M. Cosgrove[2], L. G. Maxwell[5], P. Thaker[6], B. Y. Karlan[7], D. O'Malley[2], R. E. Pollock[2], D. E. Cohn[2], R. Gogna[8], S. Karuppaiyah[2];

[1]NYU Grossman School of Medicine, New York, NY 10016, NY, [2]The Ohio State University, Columbus, OH, [3]Kurume University School of Medicine, Kurume, Japan, [4]Tulane University School of Medicine, New Orleans, LA, [5]Inova Fairfax Hospital, Virginia, VA, [6]Washington University School of Medicine, St. Louis, MO, [7]University of California, Los Angeles, CA, [8]Virginia Commonwealth University, Richmond, VA

Introduction: High-grade serous ovarian cancer (HGSOC) accounts for over 75% of all epithelial ovarian cancer and has a high mortality rate due to a lack of early detection methods. Many biomarkers have been proposed; however, none have been shown to improve detection at an early stage in this patient population. The purpose of this study is to assess whether there are unique extracellular vesicle (EV) protein signatures of early-stage HGSOC that could serve as early detection biomarkers.

Methods: 250 serum samples were obtained from a multi-institutional retrospective cohort of patients with all stages of HGSOC and healthy controls. LC-MS/MS and PEA of serum samples from patients with early-stage HGSOC identified differentially expressed EVs proteins in HGSOC versus controls. Tob candidate proteins are validated by ELISA.

Results: We have identified the top 10 EVs candidate proteins based on their fold change and statistical significance. When comparing early-stage HGSOC and controls using ELISA, CFH, PCP, and CCNE1 exhibited the highest Area Under the Curve (AUC) values of 0.94, 0.91, and 0.83, respectively. In contrast, MUC16 (also known as CA-125) exhibited an AUC of only 0.42 in whole serum. Furthermore, MUC16 distinguished between controls and both early and advanced-stage HGSOC in EVs, while in whole serum, it was only differentially expressed between controls and advanced-stage disease. Our results demonstrate that the predictive performance of the combined biomarkers surpasses that of any individual biomarker. Further, we integrated the ten aforementioned biomarkers, deriving the optimal combination biomarker by maximizing the corresponding Sum of Harmonic Means (SHUM) function by utilizing data from all 70 patients, results showed the optimal coefficients of the biomarkers, which maximize the diagnostic accuracy for early-stage HGSOC. The overall true positive rate (TPR) of 0.943, false positive rate (FPR) of 0.000, and Mathew's correlation coefficient (MCC) were presented for both the combined biomarker approach and individual biomarkers. The results demonstrated that the predictive performance of the combined biomarkers surpassed that of any individual biomarker.

Conclusion: Expression of EV-based protein biomarkers is significantly different in early-stage HGSOC compared to both control and late-stage HGSOC. This work can be readily translated to clinical use and potentially improve the early detection of HGSOC substantially.

#1071 Circulation of rare events in the liquid biopsy for early detection of lung mass lesions.

A. Shah, K. Resnick, J. Mason, P. Kuhn, J. Nieva, S. Shishido;
USC - University of Southern California, Los Angeles, CA

Lung cancer screening with low-dose CT scans (LDCT) has reduced mortality for patients with high-risk smoking histories. However, this method of screening remains imperfect. High rates of false positive scans expose patients to additional morbidity as they pursue subsequent diagnostic evaluation. Real-world application of screening LDCT remains low. Finally, current screening guidelines exclude those without smoking histories, a population which comprises up to a quarter of lung cancer patients. We sought to explore the utility of liquid biopsy (LBx) in lung cancer patients and its use in early cancer screening and diagnosis. Using the third generation High-Definition Single Cell Assay (HDSCA3.0) workflow, we analyzed 99 peripheral blood samples divided into three cohorts: Normal Donors (ND, n=50) who were healthy volunteers with no known pathology, Screening CT patients (CT, n=25) who underwent standard LDCT screening with resultant Lung-RADS 1-2, Biopsy patients (BX, n=24) who had abnormal CT scans requiring tissue biopsy. The ND group was used to characterize baseline epithelial, mesenchymal, endothelial, and immune cells, alongside acellular events (oncosomes). For the CT and BX patients, demographic information including age, gender, and average BMI was roughly equivalent, however average pack-years smoked differed owing to 10 (42%) patients in the BX group who had no prior smoking history. A total of 14 (58%) BX patients were diagnosed with primary lung cancer (BX+), of which 11(75%) were adenocarcinoma, 2 (19%) were squamous cell carcinoma and 1 (6%) was small cell. Across the cohorts we observed intra- and interpatient heterogeneity of rare events including multiple phenotypic rare cell populations and oncosomes. The comparison of the rare event enumerations between the ND, CT, BX+, and BX- cohorts revealed a greater incidence of total events, total rare cells and oncosomes, as well as specific cellular phenotypes in the CT and BX cohorts compared to the ND cohort. LBx analytes were detected at a significant elevation in the BX samples compared to the CT samples, but there was no significant difference between BX+ and BX- samples. The data supports the utility of the LBx in distinguishing patients with an alveolar mass lesion from those without, providing a mechanism for screening prior to LDCT to better inform clinical workup and avoid unnecessary radiation exposure and biopsy.

#1072 The *EsomiR* project: A case control study to assess the role of exosomal miRNAs in breast cancer cancerogenesis.

B. Cardinali[1], P. Piccioli[1], F. Boccardo[2], A. Rubagotti[2], L. Zinoli[1], A. Sciutto[1], S. Coco[1], G. Chiorino[3], P. Ostano[3], E. Sehovic[3], Z. Cavalieri[1], C. Bruzzo[1], S. Marconi[1], R. Tasso[2], R. Quarto[1], D. Ceresa[1], P. Malatesta[2], L. Del Mastro[1];

[1]IRCCS Ospedale Policlinico San Martino, Genova, Italy, [2]University of Genova, Genova, Italy, [3]Fondazione Edo ed Elvo Tempia, Biella, Italy

Introduction: One of the unmet needs in Breast Cancer (BC) prevention is how to identify women at higher risk of developing this disease, who might benefit from periodic surveillance and/or from chemoprevention. The goal of this retrospective study is to assess the role miRNAs isolated from extracellular vesicles (EV-miRNAs) as possible early biomarkers for identifying patients with higher risk of developing BC, in order to personalize their screening programme. To this goal, EV-miRNAs from cyst fluid derived from women with Gross Cyst Disease of the Breast (GCDB - a benign disease of the mammary gland associated with a 2-4-fold increase in the risk of developing BC) have been analysed.

Methodology: Cyst fluids have been selected among samples from a cohort of 600 patients diagnosed with GCDB between 1985 and 1993, some of whom developed BC during follow-up. EV-miRNAs have been extracted from cyst fluid using the exoRNeasy midi kit (Qiagen), qualitatively evaluated by Bioanalyzer (Agilent) and quantified by Qubit™ using the microRNA Assay Kit (Thermo Fisher Scientific). The MiRNome profiles have been assessed by microarray using an optimised protocol on Agilent platform (labelling and hybridization on SurePrint Human miR Microarrays 8×60 K and images acquisition by G2565CA scanner).

Results: A total of 117 samples (58 cases and 59 controls, paired on the bases of clinical and pathological variables) have been analysed. Single variable logistic regression analysis on the most expressed EV-miRNAs (logFC >= 6 (n=329)), selected six EV-miRNAs (miR-6076, miR-202-3p, miR-6872-3p, miR-769-3p, miR-5195-3p, miR-4443) and one (miR-4713-3p) negatively and positively associated with BC development, respectively (raw p-value <0.05). A risk score combining the seven EV-miRNAs was derived by multivariable logistic regression modelling and reported an AUC=0.73 (95% [CI] 0.6427-0.8231). The model was refined including clinical variables and applying step-wise logistic regression analysis. The combination of 3 EV-miRNAs (miR-6076, miR-6872-3p, miR-5195-3p) with menopausal status, familiarity and type of cyst yielded an AUC of 0.8 (95% [CI] 0.7015-0.8847). Logistic regression was also performed on Type I cysts (n=78), that are correlated with a higher risk of developing BC, pointing in evidence 3 EV-miRNAs with a negative (miR-6076, miR-6872-3p) or positive (miR-4515) correlation with BC development risk (AUC = 0.74, 95% [CI] 0.6278-0.8475). In the model comprehensive of clinical variables, two of those EV-miRNAs (miR-6872-3p, miR-4515) together with familiarity and menopausal status were selected, giving an AUC of 0.8 (95% [CI] 0.6961-0.8991).

Conclusion: This study allowed the identification of a EV-miRNA-based BC risk signature obtained by liquid biopsy on cyst fluid. The final purpose of this project is to transfer this signature in the clinic by testing it prospectively on plasma samples.

#1073 AI-assisted high-dimensional cytological single cell analysis distinguishes normal and malignant urine samples using cell morphology images with high accuracy at the single cell level.

T. P. P. van den Bosch[1], G. J. van Leenders[1], S. Sinnadurai[1], Z. Lian[2], R. Carelli[2], M. Nakaki[2], V. Lu[2], M. Ray[2], J. Cruz[2], K. R. Miller[2], M. Salek[2], M. Masaeli[2], **P. J. van der Spek[1]**;

[1]Erasmus Medical Center, Rotterdam, Netherlands, [2]Deepcell, Inc, Menlo Park, CA

Background: Urothelial cancer (UCC) is the 4th most common malignancy in men. The current clinical problem in UCC management is the high interobserver variability of tissue UCC grading and the low sensitivity of urine cytology for early detection of recurrences and progression. We hypothesize that assessing urine samples and UCC tissues with detailed quantitative image analysis based on artificial intelligence has strong potential in both urine-based early detection of tumor recurrence and progression as well as tissue-based pathological grading.

Methods: Here, we utilized the Deepcell® Human Foundation Model (HFM), a self-supervised deep learning model, to assess a cohort of urine samples from 54 normal healthy cases, 19 atypical cases, and 4 UCC cases. High resolution images of label-free single cells were captured and analyzed using the HFM to identify distinct morphological characteristics of cells from different urine origins. The urine samples were loaded onto a single-use microfluidic cartridge as part of the Deepcell® REM-I platform and brightfield images of single cells were captured in real-time. For data analysis, images of all cells run through the REM-I instrument are automatically sent to the Deepcell® Axon Suite, which provides an analysis platform to visualize cell images from specific runs, generate UMAPs of the embedding space, and run additional deep neural network models on samples in silico.

Results: High-dimensional analysis of 115 deep learning and morphometric features reveals 12 morphotypes among the pooled urine samples, as represented by morphology UMAP plots. Morphology analysis reveals distinct morphotypes in normal compared to pathological urine samples. Confusion matrix showed deep learning model performance in classifying atypical versus UCC with 89.1% (Atypical (n = 8642), UCC (n = 12637)). This indicates high model performance accuracy for AI prediction of atypical versus UCC samples at the single cell level.

Conclusions: The Deepcell® REM-I platform performs well with urine samples and identified numerous cell clusters among normal and pathological urines. AI-assisted high-dimensional morphology analysis distinguishes atypical urine samples from UCC cases with 89.1% accuracy at the single cell level. Future applications of this study include early detection or monitoring of UCC cases using non-invasive patient samples such as urine.

#1074 Plasma EV profiling facilitates low abundance biomarker discovery in pancreatic cancer.

S. Bansal[1], S. Wang[1], Y. Li[1], S. Bansal[1], J. Smith[1], J. B. Tyburski[2], k. Unger[1], **A. Cheema**[1];
[1]Georgetown University Medical Center, Washington, DC, [2]Nelson Scientific Labs, Gaithersburg, MD

The lack of reliable biomarkers for early detection of pancreatic ductal adenocarcinoma (PDAC) results in poor prognosis due to advanced disease at diagnosis. Biopsies for pancreatic cancer are known to be particularly difficult to perform because of the location of the pancreas and low volume of primary tumors that metastasize aggressively. Currently, there is no blood test or other screening modality in use, for stratification of individuals with higher-than-average risk (5-8-fold) of developing PDAC in their lifetime. Given this existing void in the US and worldwide, an FDA-compliant, minimally invasive, quantitative biomarker test for the early detection of PDAC would be critical for screening subpopulations with, a) inherent genetic or familial predisposition; history of chronic pancreatitis; c) precursor lesions of pancreas; and d) older patients (>50 years) with new onset diabetes or sudden weight loss. Extracellular vesicles (EVs) are shed by normal and cancer cells and carry a rich molecular cargo that can be leveraged for biomarker discovery. Whereas molecular profiling of bio-fluids poses intrinsic limitations for detection of low abundant, disease-specific biomarkers due to matrix effects; EVs, on the other hand, offer promise as a robust and minimally invasive biomarker resource. Mass spectrometry data were developed in our laboratory, based on multi-omics (proteomics, lipidomics and metabolomics) analyses of plasma EVs derived from patients diagnosed with early-stage PC (N=60), pancreatitis (N=39), precursor lesions of pancreas (N=45) as well as normal controls (N=50). These clinically annotated samples were made available by the Georgetown University Medical Center (GUMC) repository. Feature selection using a training-validation design allowed the development of a multiplexed biomarker panel comprising of 12-analytes (5-lipids, 2-metabolites and 5-proteins) that can robustly stratify early-stage PC from normal controls with high accuracy (AUC>95%). Availability of a FDA compliant, multi-analyte-based classification algorithm that can stratify patients with precursor lesions of the pancreas that are at potential risk of progression to PC with > 90% specificity and sensitivity is a critical clinical need. Refinement of panel to improve positive predictive value as well as identification of markers predictive of progression of precursor lesions to malignant transformation is ongoing.

#1075 Buccal mucosal remodeling predicts esophageal cancer risk.

A. Yokoyama[1], T. Hirano[1], K. Watanabe[1], M. Tamaoki[1], K. Hirohashi[1], Y. Ishida[1], Y. Inoue[1], Y. Takeuch[1], Y. Kishimoto[1], S. Kim[2], C. Katada[1], Y. Nanya[3], H. Seno[1], S. Ogawa[1], M. Muto[1], N. Kakiuchi[1];

[1]Kyoto University, Kyoto, Japan, [2]Kobe Asahi Hospital, Kobe, Japan, [3]The University of Tokyo, Tokyo, Japan

Lifestyle habits, including alcohol consumption, tobacco smoking, and germline variants of *ALDH2* and *ADH1B*, increase the risk of developing esophageal squamous cell carcinoma (ESCC). However, current prediction methods that rely on self-reported lifestyle information lack accuracy. We previously demonstrated that driver-mutated clones remodel the esophageal epithelium with age and that this remodeling is accelerated in heavy drinkers and smokers. Nonetheless, predicting cancer from clonal expansion in normal tissues remains challenging, due to limited sample availability beyond the blood. The squamous epithelium continuously covers the esophagus, throat, and oral cavity. Therefore, we evaluated buccal mucosal remodeling by mutant clones and its potential as a predictive biomarker of ESCC. A total of 387 buccal mucosa samples were collected from 110 subjects, including 62 with ESCC and 48 without, using swabs of three different sizes, followed by error-corrected sequencing targeting 26 driver genes that showed positive selection in samples from ESCC and physiologically normal esophageal tissues, as well as *ALDH2* and *ADH1B*. Somatic mutations were detected in all samples (median, 27 (1-134)). In total, 13,235 mutations, including 12,085 nonsynonymous and 1,150 synonymous mutations, with VAFs ranging from 0.0016-0.12 (median, 0.0025), were detected. Ten of the 26 genes, *TP53*, *CHEK2*, *NOTCH1*, *CDKN2A*, *NOTCH2*, *FAT1*, *AJUBA*, *PPM1D*, *ARID1A*, and *ZNF750* showed positive selection (dN/dS >1, q<0.1). Correlation analysis demonstrated that driver mutations in *TP53*, *FAT1*, and *PPM1D* were positively correlated with not only germline risk variants of ALDH2 but also alcohol consumption. The impact of alcohol consumption on the number and sum of VAFs of mutations in each of the three genes was analyzed and stratified by the presence or absence of the germline risk variant of *ALDH2*, and positive correlations were observed only among subjects with risk variants. Compared to subjects without ESCC, patients with early-stage or advanced ESCC displayed significantly higher numbers and sums of VAFs of driver mutations (p<0.05). These results indicated that buccal mucosal remodeling driven by positively selected mutations is associated with lifestyle and germline risk factors for ESCC, thus motivating the establishment of a predictive model for ESCC using genetic swab data. The prediction model for ESCC using sequencing data outperformed a model using self-reported lifestyle and alcohol flushing reaction and a model using lifestyle and germline risk variants (AUC of 0.94, 0.72, and 0.88, respectively). In conclusion, this is the first study to use clonal expansion in normal tissues to predict the presence of solid organ cancer, and our study successfully established a prediction model for ESCC based on buccal mucosal remodeling and germline variants.

#1076 Single nucleus RNA-sequencing using normal human salivary glands revealed a potential etiologic relationship between each salivary gland cell and salivary gland malignancies.

T. Nakagawa[1], C. Nasamran[2], J. Hu[2], P. Sen[2], T. Guo[2], K. Fisch[2], J. Califano[2];
[1]Chiba Univ., Chiba, Japan, [2]UC San Diego, La Jolla, CA

Salivary glands are composed of several types of cells, and each cell type is predicted to be involved in the carcinogenesis of different types of cancers including Adenoid cystic carcinoma (ACC), Acinic cell carcinoma (AciCC), salivary duct carcinoma (SDC), myoepithelial carcinoma (MECA) and other histology. In this study, we performed single nucleus RNA-seq on three human salivary gland samples to clarify the gene expression profile of each complex cellular component of the salivary glands and related these expression patterns to expression found in salivary gland cancers (SGC) to infer cell of origin. By single nucleus RNA-seq, total 13,643 salivary gland cells were stratified into four clusters: acinar cells, ductal cells 1, ductal cells 2, and myoepithelial cells/stromal cells, with differentially expressed genes of each group. The localization of each cell group was anatomically validated by IHC of each cluster marker gene, and one group of ductal cells was found to represent intercalated ductal cells labeled with HES1. Gene ontology analysis for this group included “epithelial cell differentiation” confirming the intercalated duct. Furthermore, to elucidate the potential etiologic relationship between normal salivary glands cell type and salivary gland carcinoma histology, we compared the expression of each cluster marker to SGC public RNA-seq data. In comparison between AciCC and ACC, we used normalized RNA-seq data of 54 ACC and 21 AciCC. ACC had significantly less expression of acinar cells markers (STATH, CST2, and LPO) compared to other markers expression(***$P = 4x10^{-51}$), unlike AciCC ($P = 0.54$), suggesting a possible contribution of acinar cells to the carcinogenesis of AciCC. In another cohort, we compared 16 SDC, and 38 MECA with publicly available RNA-seq data. Remarkably, HES1 and ELF3, each of two different ductal cell markers, were significantly upregulated in SDC consistent with origin of SDC from ductal cells (P=0.001, P=0.0007, respectively). Consistent with bulk RNA-seq results, expression of HES1 in IHC using clinical human SDC and MECA samples was higher in SDC than MECA, suggesting that the expression of the derived cells is involved in salivary gland carcinogenesis. Cell type expressions in specific SGC histology are similar to those found in normal salivary gland populations, indicating a potential etiologic relationship. On the other hand, there was no significant difference in myoepithelial marker ACTA2 expression between SDC and MECA, suggesting that the markers of origin are not always highly expressed, depending on cancer subtypes. Although publicly available SGC RNA-seq data used in this study are limited, the results remarkably reflect the diverse modes of carcinogenesis of SGC. These findings might provide a better understanding of the molecular basis of SGC and treatment strategies for SGC.

CLINICAL RESEARCH: Pediatric Sarcomas and Other Solid Tumors: Translational
Poster Session

#1080 Using genome-wide CRISPR screening to develop novel combination therapies for high-risk Ewing's sarcoma.

D. Ravindrarajah[1], S. Krishan[1], K. Simpson[2], T. Gulati[2], B. B. Cheung[1], G. M. Marshall[1];
[1]Children's Cancer Institute Australia, Sydney, Australia, [2]Peter MacCallum Cancer Centre, Melbourne, Australia

Ewing's sarcoma (EWS) is an aggressive bone and soft-tissue cancer, characterized by a hallmark fusion oncoprotein comprising the amino terminus of a FET gene and the carboxy terminus of an ETS gene, most commonly (85%), the EWSR1-FLI1 t (11,22) fusion.TK-216 is a first-in-class EWSR1-FLI1 inhibitor currently in phase II clinical trials for EWS. Although TK-216 was designed to target the fusion protein interaction directly, it has demonstrated limited efficacy as a monotherapy. Thus, more effective TK-216 combination therapies are needed. We have used genome wide Clustered Regularly Interspaced Short Palindromic Repeats (CRISPR) Knockout screening in EWS cells treated with TK-216 to identify novel synthetic lethality. We have identified 97 genes whose deletion potentially enhances the action of TK-216 in EWS cells. We have also identified several druggable targets, such as USP9X and the oxidative phosphorylation (OXPHOS) pathway as synthetic lethal interactions for TK-216. USP9X is known to deubiquitinate and stabilize the EWS-FLI1 fusion protein. USP9X and EWS-FLI1 protein expression levels were found to be positively correlated in EWS clinical specimens. USP9X siRNA-mediated gene silencing reduced EWS cell viability. Most importantly, USP9X siRNA-mediated gene silencing sensitized EWS cells to TK-216 treatment. In addition, inhibition of USP9X with a small-molecule inhibitor WP1130, led to significant cell death in EWS alone and in combination with TK-216 with wide therapeutic indices. The molecular mechanism of synergy and *in vivo* efficacy of the novel TK-216 combination will be determined in our study for future clinical translation.

#1081 A role for the oncogenic driver fusion protein EWS-FLI1 in the targeting of DR5 by INBRX-109 in Ewing sarcoma.

C. C. Parker[1], L. M. Gaetano[1], E. A. Boguslawski[1], S. Kinn-Gurzo[1], R. Kaufman[1], M. C. Stout[1], C. Deveraux[2], P. J. Grohar[1];
[1]Children's Hospital of Philadelphia, Philadelphia, PA, [2]Inhibrx, Inc., La Jolla, CA

Background: Tumor necrosis factor receptor superfamily member 10b (TNFRSF10b, also known as DR5) agonists are attractive targeted agents for cancer cells because these agents activate cellular apoptosis. Ewing sarcoma (ES) is a bone and soft-tissue sarcoma occurring in adolescence defined by a t(11;22)(q24;q12) balanced chromosomal translocation that results in chimeric transcription factor and oncogenic driver protein, EWS-FLI1. Independent studies and unbiased cell line screens have reported ES to be sensitive to DR5 targeting. INBRX-109 is a tetravalent, DR5-targeted antibody. Here, we analyzed the sensitivity of ES models to DR5 targeting by INBRX-109 and explored how the EWS-FLI1 transcriptional program impacts the continuum of sensitivity-resistance to this targeting.
Methods: In a panel of 11 ES lines, in vitro sensitivity was assessed to both single agent and INBRX-109 combinations. A screen of 1,363 FDA approved compounds identified cooperative combinations that were prioritized mechanistically. Differential sensitivity for single agent and in combination with irinotecan was confirmed in vivo in xenograft models. Resistant clones were isolated from in vivo experiments and evaluated for DR5 expression and sensitivity. Cellular factors associated with sensitivity and resistance were determined by siRNA knockdown and Cleavage Under Targets and Tagmentation assay (CUT and Tag).
Results: ES models showed variable sensitivity to INBRX-109, with a GI90 as low as 10 picomolar in some models. All models showed robust expression of DR5, but absolute expression of DR5 did not correlate with sensitivity. In vitro sensitivity was replicated in vivo, with all 7 mice bearing RD-ES xenografts demonstrating initial complete tumor regression and 3 of 7 mice demonstrating no recurrence beyond 90 days. Importantly, cells isolated from recurrent tumors showed a novel mechanism of resistance: direct repression of DR5 by EWS-FLI1. INBRX-109 was ineffective as a single agent at 10 nM in resistant ES models. However, there was striking synergy in vitro with SN38, the active metabolite of irinotecan, and this effect translated into tumor regressions of a resistant TC32 xenograft in vivo. The FDA compound screen captured novel synergy with a panel of agents.
Conclusion: INBRX-109 is an exciting candidate for ES as a single agent in subsets of tumors or in combination with irinotecan, which is currently being evaluated in the clinic. Investigation of the exact relationship between EWS-FLI1 and sensitivity to DR5 targeting is ongoing. Initial findings suggest EWS-FLI1, combined with other disease modifying mutations, is a key mediator of this sensitivity. Further, EWS-FLI1 plays a direct role repressing DR5 in the setting of therapeutic challenge in one model in vivo. These findings highlight the potential for INBRX-109 in combination with irinotecan or novel candidates as therapies for ES patients.

#1082 Exploiting lurbinectedin-driven nucleolar relocalization of EWS-FLI1 to develop novel combination therapies for Ewing sarcoma.

S. M. Veluvolu[1], **R. D. Lopez**[1], J. M. Gedminas[2], E. A. Boguslawski[1], E. R. Wilson[1], B. P. Caiello[3], M. E. Murphy[4], P. J. Grohar[1];
[1]Children's Hospital of Philadelphia, Philadelphia, PA, [2]University of Iowa Stead Family Children's Hospital, Iowa City, IA, [3]University of Pennsylvania, Perelman School of Medicine, Philadelphia, PA, [4]The Wistar Institute, Philadelphia, PA

Background: Ewing sarcoma (ES) is a malignant bone tumor characterized by the oncogenic fusion protein EWS-FLI1. EWS-FLI1 acts as an aberrant transcription factor, inducing and silencing genes involved with increasing cell proliferation and survival. We have previously shown that lurbinectedin, a trabectedin analog, effectively inactivates the transcriptional activity of EWS-FLI1 by redistributing it within the nucleus to the nucleolus. Interestingly, this process activates a gene signature like that of the DNA damage response (DDR) to UV light, which was also shown to induce nucleolar translocation of WT Ewing sarcoma breakpoint 1 (EWSR1). However, the mechanism governing the nucleolar translocation of EWS-FLI1 induced by these drugs has yet to be elucidated. In addition, novel approaches to exploit this relocalization mechanism as a means to broaden the therapeutic window have yet to be established.
Methods: We used immunoblotting, RT-qPCR, viability assays, cell fractionation, confocal microscopy, proximity ligation assays (PLA), mass spectrometry, genomics, and immunoprecipitation to investigate the mechanism of action of trabectedin/lurbinectedin-induced nucleolar relocalization of EWS-FLI1.
Results: Through interrogation of the pathways triggered by trabectedin/lurbinectedin, we found that this mechanism is in part mediated by HSP70. Viability assays also revealed profound synergy between HSP70 inhibitors (HSP70is) and lurbinectedin. Immunoprecipitated EWS-FLI1 subjected to mass spectrometry revealed an association of EWS-FLI1 and several HSP70 isoforms after trabectedin treatment which was confirmed with PLA. Trabectedin/lurbinectedin treatment also revealed an upregulation of EWS-FLI1-suppressed targets and suppression of induced targets. Confocal microscopy showed that EWS-FLI1 “trapping” in the nucleolus was potentiated by combination treatment with HSP70is.
Conclusion: Our results underscore the synergistic effect of combining HSP70is with trabectedin or lurbinectedin treatment to attenuate several aspects of ES tumorigenesis *in vitro*. *In vivo* experiments with patient-derived xenografts are underway to corroborate the synergy of HSP70is and trabectedin/lurbinectedin. Together, our data highlights the potential for a novel “EWS-FLI1 nucleolar trap” as a means to inhibit and sustain EWS-FLI1 repression with this class of compounds.

#1083 Cell membrane-anchored and tumor-targeted IL12 T-cell therapy destroys cancer-associated fibroblasts and disrupts extracellular matrix in heterogenous osteosarcoma xenograft models.

J. Hu, A. Lazar, W.-L. Wang, W. Zhang, Z. Jia, D. Ragoonanan, J. Wang, X. Xia, K. Mahadeo, R. Gorlick, S. Li;
UT MD Anderson Cancer Center, Houston, TX

Background: The extracellular matrix (ECM) and cancer-associated fibroblasts (CAFs) play major roles in tumor progression, metastasis, and the poor response of many solid tumors to immunotherapy. CAF-targeted CAR-T cell therapy cannot infiltrate ECM-rich tumors such as osteosarcoma.
Method: In this study, we used RNA sequencing to assess whether the recently invented membrane-anchored and tumor-targeted IL12-armed (attIL12) T cells, which bind cell-surface vimentin (CSV) on tumor cells, could destroy CAFs to disrupt the ECM. We established an *in vitro* model of the interaction between osteosarcoma CAFs and attIL12-T cells to uncover the underlying mechanism by which attIL12-T cells penetrate stroma-enriched osteosarcoma tumors.
Results: RNA sequencing demonstrated that attIL12-T cell treatment altered ECM-related gene expression. Immunohistochemistry staining revealed disruption or elimination of high-density CAFs and ECM in osteosarcoma xenograft tumors following attIL12-T cell treatment, and CAF/ECM density was inversely correlated with T-cell infiltration. Other IL12-armed T cells, such as wild-type IL12- or tumor-targeted IL12-T cells, did not disrupt the ECM because this effect depended on the engagement between CSV on the tumor cell and its ligand on the attIL12-T cells. Mechanistic studies found that attIL12-T cell treatment elevated IFNγ production upon interacting with $CSV^{\pm}$ tumor cells, suppressing TGFβ secretion and in turn upregulating FAS-mediated CAF apoptosis. CAF destruction reshaped the tumor stroma to favor T-cell infiltration and tumor inhibition.
Conclusions: This study unveiled a novel therapy—attIL12-T cells—for targeting CAFs/ECM. These findings are highly relevant to humans because CAFs are abundant in human osteosarcoma. **What is already known on this topic:** As the major source of ECM factors in tumors, the $FAP^{\pm}\alpha SMA^{\pm}$ subtype of CAFs within tumors induce production of ECM factors, preventing antitumor T cells from accessing the core regions of tumors. **What this study adds:** Our group demonstrated that attIL12-T cell transfer (US Patent: 11421010) induced T-cell infiltration into and eliminated large osteosarcoma PDX tumors. Comparison of gene expression in sensitive or resistant PDX models to attIL12-T cell therapy elucidated the ECM-targeting mechanism of attIL12-T cells. Our *in vitro* system further determined that the CSV-attIL12 interaction mediated IFNγ upregulation, which triggered FAS induction in CAFs to induce CAF apoptosis. In sum, attIL12-T cell treatment shifts tumor stroma from a TGFβ-dependent CAF-promoting phenotype to an IFNγ-induced immune-inflamed phenotype. **How this study might affect research, practice or policy:** attIL12-T cell transfer is a novel anti-ECM strategy that renders ECM-rich tumors more susceptible to T cell-mediated tumor killing.

#1084 Preclinical testing of a cell adhesion molecule 1 (CADM1) targeting antibody-drug conjugate in osteosarcoma and other pediatric solid tumor models.

Z. Zhang[1], Y. Wang[2], W. Zhang[1], X. Tian[1], Q. Wang[1], R. Lazcano Segura[1], M. Roth[1], J. Gill[1], D. Harrison[1], Z. Xu[1], Y. Yi[1], S. Jusu[1], G. Longo[1], X. Zhou[1], J. Wang[1], R. Gorlick[1];

[1]UT MD Anderson Cancer Center, Houston, TX, [2]Boston University Boston Medical Center, Boston, MA

Introduction: Survival outcomes of osteosarcoma have remained stagnant for decades, emphasizing the urgent need to identify new cell surface targets and develop novel therapies. Antibody-drug conjugates (ADCs), known for their targeted delivery of cytotoxic agents to specific targets, present an attractive therapeutic class for potential use in osteosarcoma.

Methods: We previously identified Cell Adhesion Molecule 1 (CADM1) is highly expressed on the cell surface in osteosarcoma using an integrated proteomic and transcriptomic surfaceome profiling approach. As a proof of concept, a humanized CADM1 antibody (clone PTA021-A1) was conjugated with Tesirine (SG3249), a pyrrolobenzodiazepine (PBD) dimer payload. The antitumor activity of this CADM1 ADC was validated in vivo in 8 osteosarcoma patient-derived xenografts (PDXs). CADM1 is also highly expressed in other pediatric solid malignancies such as neuroblastoma and Wilms tumor. The CADM1 ADC was tested in vitro in neuroblastoma and Wilms tumor models. Negative controls included a CD19 targeting ADC with the same payloads and CADM1 negative Ewing sarcoma models.

Results: The expression of the CADM1 was validated by flow cytometry in osteosarcoma, neuroblastoma, and Wilms tumor cell lines, and by immunohistochemistry (IHC) in osteosarcoma patient samples and PDX models. In vivo testing of CADM1 ADC in 8 osteosarcoma PDX models showed that the ADC was well-tolerated and significantly prolonged progressive-free survival in all osteosarcoma models. Complete response (CR) and maintained CR was observed in 3 models. In vitro testing for neuroblastoma and Wilms tumor is ongoing, and preliminary data suggest promising antitumor activities.

Conclusions: CADM1 is highly expressed in osteosarcoma and other pediatric solid tumors. CADM1 ADC demonstrated promising antitumor *in vitro* and *in vivo* activity in osteosarcoma, and initial *in vitro* studies in neuroblastoma and Wilms tumor show similarly promising responses. These data support the need for further studies assessing the potential of a CADM1 ADC as a novel agent for the treatment of pediatric solid cancers.

#1085 Exploiting bioenergetic vulnerabilities in chemotherapy resistant osteosarcoma.

Valerie U. Nguyen[1], Laurie Graves[2], Veronica Colmenares[3], Abol Macabangon[4], Casey Syal[4], Kelsey Fisher-Wellman[5], William C. Eward[6], So Young Kim[7], Jason A. Somarelli[1]

[1]Department of Medicine, Duke Cancer Institute, Durham, NC,[2]Department of Pediatrics, Division of Hematology/Oncology, Duke University Medical Center, Durham, NC,[3]Duke Cancer Institute, Durham, NC,[4]Department of Medicine, Duke University, Durham, NC,[5]Department of Physiology, East Carolina University, Greenville, NC,[6]Department of Orthopedic Surgery, Duke University Medical Center, Durham, NC,[7]Department of Molecular Genetics and Microbiology, Duke University, Durham, NC

BACKGROUND: Osteosarcoma (OS) is the most common bone cancer in children and young adults. Standard treatment involves chemotherapy and surgical resection, yet nearly 4 in 10 patients experience disease relapse, and almost all of these patients are resistant to additional chemotherapy. Therefore, there is an urgent need to understand the biology of chemo-resistant OS and identify new therapeutic strategies to treat this therapy-resistant disease state.
METHODS: Using a CRISPR-Cas9 based lineage tracing system, RNA sequencing, and Seahorse XF assays in chemo-naïve, -resistant, and -released human 143b and patient-derived 173x OS cell lines, we modeled the evolution of chemoresistance and release from the selective pressure of chemotherapy in osteosarcoma. The phenotype of each cell state was assessed through *in vitro* and *ex vivo* cell proliferation assays, a comparison of cell viability upon re-challenge to standard-of-care chemotherapy, and comparison of cell viability in response to novel therapies targeting alterations in cell respiration.
RESULTS: Chemo-resistant OS cells demonstrate a decrease in expression of proliferation-associated gene pathways and shift their resources toward expression and maintenance of multi-drug resistance ABC transporters. Chemo-released cells maintain elevated expression of ABC transporters while re-activating proliferation. Across the spectrum of chemotherapy exposure, OS cells demonstrate changes in respiratory capacity, with unique bioenergetic phenotypes observed in chemo-naïve, -resistant, and -released cells.
CONCLUSIONS: Chemo-resistant and chemo-released OS cells demonstrate unique bioenergetic patterns that correlate with gene expression signatures and growth phenotypes. Evolution imposed by the selective pressure of chemotherapy may render OS cells vulnerable to therapies that disrupt cellular energetics and exploit multi-drug resistant ABC transporters.

#1086 ZFP36L2 is expected to be a potential prognostic marker in IL-1β+ osteosarcoma patients.

P. Hao[1], P. Luo[1], Z. Ren[1], S. Xu[2], J. Han[1], X. Nan[1];

[1]Anhui Medical University, Hefei, China, [2]Department of Orthopedics, The First Affiliated Hospital of Anhui Medical University, Hefei, China

Background: Osteosarcoma (OS) is the most common bone malignancy affect children and young adults. For decades, the long-term survival for patients with recurrences and metastases remains ~30%. There's an urgent need for new prognostic marker and therapeutic options. ZFP36L2, a member of the tristetraprolin (TTP) family of CCCH zinc finger proteins, stands out for its pivotal role in post transcriptional modifications and modify tumor microenvironment (TME). Notably, ZFP36L2 contributes to the recruitment of macrophages, specifically the M1 subtype, which are known for their ability to secrete IL1β and exhibit anti-tumor functions. Our study reveals that, ZFP36L2 can be used as a predictor of prognosis in OS patients with enriched IL1B expression. This study aims to elucidate the interaction between ZFP36L2 and IL1B in modification of TME and shed light on its potential of prognosis prediction and therapeutic in IL1β positive OS patients.

Methods: Firstly, we conducted a comprehensive exploration of ZFP36L2 expression across TCGA cohorts. Then, we performed IHC staining to confirm the evaluated expression of ZFP36L2 in cancerous tissues. Immune infiltration analysis, including QUANTISEQ, TIMER, and CIBERSORT, was conducted. KM plot was employed to analyze the prognosis of OS patients. Finally, qPCR and western blot were used to validate transcriptional and translational changes of key molecules across OS cell lines.

Results: Our findings demonstrate that ZFP36L2 exhibits specific expression across various cancer types, with a notable elevation in sarcoma tissues, as confirmed by IHC. Importantly, this high expression of ZFP36L2 in sarcoma tissues is correlated with metastasis. We found ZFP36L2 significantly correlates with tumor metastasis but failed in patient overall survival. Immunoinfiltration analysis indicates a significant correlation between ZFP36L2 and macrophages, as well as T cells, suggesting a role in the TME. Prognostic analysis reveals that ZFP36L2 can serve as a predictive marker for IL1β positive patients. The wetlab experiments demonstrated that ZFP36L2 leads to IRGM mRNA degradation, ultimately affecting $IL1\beta^{\pm}$ macrophages.

Conclusion: This study delineates the tumor-specific elevated expression of ZFP36L2 and its potential as a prognostic marker in $IL1\beta^{\pm}$ OS patients. We hypothesize that ZFP36L2 affects $IL1\beta^{\pm}$ macrophages through IRGM degradation. Besides, IRGM also has an impact on cytotoxic T cells. Therefore, the ZFP36L2-IRGM axis plays an important role in remodeling OS TME. These results indicated ZFP36L2, not only serves as a marker, but also can be a therapeutic target in IL1β enriched patients.

#1087 Synergistic mechanisms against pediatric bone sarcoma models: Trabectedin enhances oncolytic virotherapy intratumoral spread and antitumor immune activation.

E. Ringwalt[1], M. Currier[2], A. Glaspell[2], M. V. Cannon[2], C.-Y. Chen[2], A. C. Gross[2], M. Cam[2], P.-Y. Wang[2], R. D. Roberts[1], T. P. Cripe[1];
[1]Nationwide Children's Hospital & Ohio State University, Columbus, OH, [2]Nationwide Children's Hospital, Columbus, OH

Osteosarcoma and Ewing sarcoma are the most common pediatric bone malignancies and, despite decades of research, efforts to treat patients with advanced disease remain dismal. To address this inadequacy, we leverage oncolytic herpes simplex virotherapy as a double-edged attack against tumors through 1) tumor cell-specific lysis and 2) antitumor immune stimulation. However, previous trials of oncolytic herpes simplex virotherapy in pediatric sarcomas displayed limited responses, likely due to the observed presence of immunosuppressive monocytes and macrophages. To improve efficacy, we combined oncolytic herpes simplex virotherapy with trabectedin, an FDA-approved DNA-binding agent known to disrupt gene expression and deplete monocytes and macrophages. Surprisingly, we found that the efficacy of this combination far surpassed our predictions, inducing complete and partial regressions in multiple models of Ewing sarcoma and osteosarcoma. To explore potential mechanisms driving this high degree of synergy, we performed single cell RNA sequencing on tumors of mice treated with monotherapy or combination therapy. Interestingly, trabectedin synergized with the oncolytic virotherapy through two unexpected mechanisms. Our analysis revealed that trabectedin increased intratumoral oncolytic virus spread by disrupting expression of the intrinsic antiviral response in human Ewing sarcoma cells. Additionally, trabectedin not only reduced immunosuppressive macrophages but also stimulated cytotoxic granzyme expression in infiltrating T and NK cells in immunocompetent osteosarcoma models. These effector NK and T cells were necessary for the regressions of osteosarcoma allografts treated with trabectedin and oncolytic virotherapy. Thus, trabectedin enhanced both the oncolytic effect of herpes simplex virotherapy and the effector function of cytotoxic lymphocytes that become activated in response to the virus. The combination of trabectedin and oncolytic herpes simplex virotherapy offers the potential to unite these mechanisms against bone tumors to achieve better outcomes for children.

#1088 An evaluation of patritumab deruxtecan (HER3-DXd, U3-1402) against pediatric PDX models for hepatoblastoma and rhabdomyosarcoma - A report from the NCI PIVOT Program.

R. Kurmasheva[1], P. Houghton[1], V. Del Pozo[1], S. Ghilu[1], R. Nakamura[2], P.-D. Fan[3], E. Jocoy[4], T. Stearns[4], S. Neuhauser[4], J. Chuang[4], C. J. Bult[4], B. A. Teicher[5], M. A. Smith[5],

[1]UT Health San Antonio, San Antonio, TX, [2]Daiichi-Sankyo Co., Ltd., Tokyo, Japan, [3]Daiichi-Sankyo Co., Ltd., Hillsdale, NJ, [4]The Jackson Laboratory, Bar Harbor, ME, [5]National Cancer Institute, Bethesda, MD

Introduction: HER3-DXd is an ADC consisting of a fully human monoclonal antibody to HER3 attached to a topoisomerase I inhibitor payload (DXd, an exatecan derivative) that has demonstrated clinically meaningful efficacy with durable responses in adults with non-small cell lung cancer. Two childhood cancers with HER3 expression are rhabdomyosarcoma (RMS) and hepatoblastoma (HB), and the goal of this work was to evaluate the activity of HER3-DXd against PDX models for these cancer types.

Methods: IHC testing was conducted on FFPE tissue (slides or TMA) using HER3/ErbB3 (D22C5) XP rabbit mAB and membrane expression was determined. HB models were evaluated using HER3-DXd and control IgG ADC (C-ADC) with a DXd payload, both at 10 mg/kg weekly x 3. RMS models were evaluated using HER3-DXd and C-ADC at 3 mg/kg and 10 mg/kg administered weekly x 3. Activity was assessed by the PIVOT objective response measure (ORM) targeting partial, complete, or maintained complete responses (PR, CR, and MCR) as compared to stable disease (SD) or progressive disease, with or without growth delay (PD2 and PD1, respectively).

Results: For 11 HB models, HER3 expression was 0 (n=2), 1+ (n=5), 2+ (n=1), and 3+ (n=3). For 8 RMS models, median IHC scores were 0 (n=1), 1+ (n=5), and 2+ (n=2). HER3-DXd activity by ORM is shown in the table. Three of 4 HB models treated with HER3-DXd showed MCR, while one had PD. The 3 HB models with MCR responses to HER3-DXd showed lesser responses to C-ADC. HER3-DXd was highly active against RMS models at 3 and 10 mg/kg with most models having MCR. C-ADC was also highly active against RMS models at both dose levels. At 10 mg/kg HER3-DXd, 2 of 4 HB models and 3 of 6 evaluable RMS models had time to event > 100 days.

Conclusions: Many HB and RMS models show HER3 expression by IHC. HER3-DXd is highly active against both HB and RMS models. The high activity of C-ADC for RMS models suggests exquisite sensitivity of RMS models to the DXd payload

Treatment response categories to treatment of pediatric PDX models with HER3-Dxd

	PD1	PD2	SD	PR	CR	MCR
HB (HER3-Dxd, 10 mg/kg)	1	-	-	-	-	3
HB (C-ADC, 10 mg/kg)	2	1	-	1	-	-
RMS (HER3-Dxd, 3 mg/kg)	-	1	-	-	-	5
RMS (C-ADC, 3 mg/kg)	-	-	-	1	2	2
RMS (HER-Dxd, 10 mg/kg)	-	-	-	-	-	6
RMS (C-ADC, 10 mg/kg)	-	-	-	-	2	4

#1089 Endogenous HiBiT-tagging of PAX3-FOXO1 reveals downregulation of the fusion oncogene by CDK inhibitors and has synergy with vincristine.

Y. Kim[1], k. Jia[1], M. Churiwal[1], T. Hawley[2], S. Pomella[1], C. Evans[3], R. Chari[3], D. Milewski[1], R. Sinniah[1], Y. Song[1], H.-C. Chou[1], X. Wen[1], C. Thomas[4], M. Ceribelli[4], J. Wei[1], R. Hawley[5], J. Khan[1];

[1]National Cancer Institute, Bethesda, MD, [2]National Institute of Allergy and Infectious Diseases, Bethesda, MD, [3]Frederick National Laboratory for Cancer Research, Frederick, MD, [4]National Center for Advancing Translational Sciences, Bethesda, MD, [5]George Washington, Washington, DC

Background: Oncogenic fusion genes are attractive therapeutic targets due to their tumor-specific expression and driver roles in cancers. PAX3-FOXO1 (P3F) is the dominant oncogenic driver of fusion-positive rhabdomyosarcoma (FP-RMS) with no current targeted therapy. We developed methods to directly measure endogenous P3F protein levels amenable to high-throughput drug screens.

Method: HiBiT tag, an 11 amino acid peptide of NanoLuc luciferase, was inserted into the endogenous P3F using CRISPR in FP-RMS cell lines RH4 and SCMC. Western blot was used for HiBiT tag validation. RNA-seq and ChIP-seq were used to assess transcriptomics and DNA binding of HiBiT-tagged P3F (P3F-HiBiT). High-throughput drug screen using Nano-Glo luciferase assay was performed using the Mechanism Interrogation PlatE (MIPE 5.0) drug library, a 2,480 drug library with known mechanisms of action. CellTiter-Glo was used to monitor cell viability. Mouse xenograft models of FP-RMS were used to investigate in vivo efficacy.

Results: We validated HiBiT tagging of P3F by Western. Both P3F-HiBiT and unmodified P3F activated the same gene sets in fibroblasts by RNA-seq Gene Set Enrichment Analysis (GSEA). ChIP-seq using HiBiT antibody for P3F-HiBiT matched the genomic locations from ChIP-seq with P3F antibody in RH4 and SCMC. Using a cutoff value of > 90 (Area Under the Curve (AUC) of CellTiter-Glo minus AUC of Nano-Glo), in both RH4 and SCMC, we identified 182 compounds which downregulate P3F before cell death. Filtering for drugs with ≥ 3 hits for the same target identified 14 drug classes that suppressed P3F including HDAC inhibitors (3), BRD4 inhibitors (3), and CDK inhibitors (8). FP-RMS was sensitive to CDK1/2, CDK4/6, CDK9, and multi-CDK inhibitors. A multi-CDK inhibitor TG02, currently in human trials, downregulated P3F and RNA-seq GSEA showed marked suppression of P3F targets. TG02 also significantly delayed tumor progression in mouse xenograft model of FP-RMS without weight loss. Interestingly, the commonly used chemotherapeutic Vincristine (VCR) also downregulated P3F in vitro. TG02 with VCR showed synergy by Loewe analysis. In vivo, testing showed significant delay in tumor progression by the combination compared to TG02 or VCR alone. Of note, tumor RNA-seq GSEA following treatment with TG02, or VCR alone, and in combination significantly downregulated P3F targets.

Conclusion And Future Directions: By HiBiT tagging the fusion oncogene P3F, we identified 182 drugs that suppress P3F levels of which TG02 was a top hit. TG02 showed in vivo efficacy indicating that FP-RMS is susceptible to CDK inhibition. We also found synergy between TG02 and VCR, resulting in a significant delay in FP-RMS tumor progression compared to single agents. Interestingly, we found that VCR alone can downregulate P3F and its targets. Combination therapy of TG02 with VCR shows promise for clinical translation in FP-RMS.

#1090 GPC2 directed CAR T cells are efficacious against fusion-positive and fusion-negative rhabdomyosarcomas.

R. Shraim[1], P. M. Schuerch[1], A. Giudice[1], K. L. Conkrite[1], A. K. Weiner[1], A. B. Radaoui[1], B. Mooney[2], R. T. Kurmasheva[3], P. J. Houghton[3], G. B. Morin[2], Y. B. Mosse[1], P. H. Sorensen[2], B. A. Garcia[4], A. Sacan[5], J. M. Maris[1], K. R. Bosse[1], S. J. Diskin[1];

[1]Children's Hospital of Philadelphia, Philadelphia, PA, [2]BC Cancer Research Institute, Vancouver, BC, Canada, [3]The University of Texas Health Science Center at San Antonio, San Antonio, TX, [4]Washington University School of Medicine, St. Louis, MO, [5]Drexel University, Philadelphia, PA

Background: Rhabdomyosarcoma (RMS) is an aggressive pediatric solid tumor with poor survival and new targeted therapies are needed.
Aims: Using an integrative proteogenomic quantitative approach, we sought to identify candidate immunotherapeutic targets then validate top targets in RMS preclinical models.
Methods: We first performed plasma membrane enrichment followed by mass spectrometry (MS) to define the surfaceome of 7 fusion-positive (FP) and 14 fusion-negative (FN) RMS patient-derived xenograft models. Surface proteins were scored by IMMUNOTAR, our custom pipeline which extracts and integrates quantitative features from diverse proteogenomic and annotation datasets to provide a score for each protein, using mean-average-precision for score optimization. Cell surface expression of IMMUNOTAR-prioritized proteins was validated using flow cytometry, focusing on targets with immunotherapies in development. CAR T cells targeting the lead protein were engineered and studied in RMS preclinical models.
Results: A total of 847 and 882 high confidence cell surface proteins were detected in FP and FN RMS surfaceome, respectively, with 94% of proteins overlapping the phenotypes. IMMUNOTAR ranked anaplastic lymphoma kinase (ALK), a putative immunotherapeutic target in FP RMS, as the top FP target. Glypican 2 (GPC2), a differentially expressed cell surface proteoglycan identified in neuroblastoma and other neural-derived tumors, targetable with CAR T cells and antibody-drug conjugates [Bosse et al. Cancer Cell 2017], ranked as the top protein in FN and 5th protein in FP RMS. Overall, GPC2 was abundantly expressed in 16 of 21 RMS models profiled. Flow cytometry revealed expression of GPC2 comparable to neuroblastoma in 5 of 8 RMS cells lines. Additionally, both FP and FN GPC2+ RMS cell lines (FN: RH36, SMS-CTR; FP: RH41, RH30) activated GPC2 CAR T cells with either a CD28 or a 4-1BB costimulatory domain, inducing release of IFN-gamma and IL-2 upon co-incubation across different E:T ratios as quantified by ELISA. Further, GPC2 CAR T cells induced potent RMS cell cytotoxicity compared to control CD19 CAR T cells with near 100% specific cytotoxicity at 1:1 E:T ratio. In a pilot study, GPC2 CAR T cells with 4-1BB costimulatory domains induced significant tumor regression ($p=0.03$) and prolonged progression-free survival ($p=0.01$) compared to CD19 CAR T cells in an established murine RH41 flank xenograft model.
Conclusion: In summary, we probed the RMS surfaceome using MS and identified candidate proteins amenable for immunotherapeutic targeting using our IMMUNOTAR algorithm. We validated GPC2 as a candidate target in FP and FN RMS and are corroborating our findings in additional pre-clinical RMS models. Demonstration of GPC2 CAR efficacy in these models could lead to inclusion of RMS in our ongoing phase 1 clinical trial (NCT05650749) in a planned expansion phase.

#1091 Distinct mechanisms of orthotopic tumor control by alpha$_V$beta$_3$and HER2 CAR Ts support development of a bispecific CAR T cell therapy for pediatric rhabdomyosarcoma.

A. M. Lulu, N. Park, J. J. Caruso, D. A. Cobb, D. W. Lee;
University of Virginia, Charlottesville, VA

Goal: Evaluate αvβ3 and HER2 as antigens for a bispecific chimeric antigen receptor T (CAR T) cell therapy in pediatric rhabdomyosarcoma.
Background: Current treatments are ineffective against relapsed/refractory or metastatic rhabdomyosarcoma (RMS). Antigen loss or modulation on tumor cells commonly leads to tumor escape across diverse cancer types after CAR T therapy targeting different antigens. We hypothesize that simultaneously targeting two RMS antigens with a bispecific CAR T will reduce the likelihood of tumor escape. The integrin alpha$_V$beta$_3$ (αvβ3) plays a role in cancer progression, metastasis and neovascularization in several malignancies. HER2 also contributes to cancer progression and metastasis.
Methods: Control of intramuscular RMS tumors by αvβ3 or HER2 CAR Ts was assessed in NSG mice, with non-specific CD19 CAR Ts as controls. Tumor burden was assessed weekly by bioluminescence imaging. Persistence and phenotype of CAR Ts were evaluated by flow cytometry. CAR T cell infiltration, tumor antigen expression and residual disease were determined by immunohistochemistry.
Results: Six of six pediatric patient-derived RMS cell lines express αvβ3 and/or HER2. αvβ3 and HER2 CAR Ts kill RMS cells *in vitro* at low effector-to-target ratios. αvβ3 and HER2 CAR Ts independently control—and nearly eliminate—orthotopic RMS tumors. Fewer HER2 CAR Ts ($5x10^6$) are needed to control tumors than αvβ3 CAR Ts ($10x10^6$), but this is not due to lack of persistence or exhaustion of αvβ3 CAR Ts. Tumor control by αvβ3 CAR Ts is delayed (>21 days) compared to that by HER2 CAR Ts (7 days), and is robust, despite initial tumor progression following treatment. Importantly, despite strong tumor control by both CAR Ts, at 7 weeks post-treatment residual tumor nests are evident by histology. At this time, CAR Ts are still abundant, are not exhausted and express memory markers, suggesting that the remaining tumor cells are no longer susceptible to CAR T killing. We are currently evaluating the hypothesis that the remaining tumor cells have down-regulated antigen expression. Delayed tumor control by αvβ3 CAR Ts was ameliorated by engineering αvβ3 overexpression in RMS tumors.
Conclusions: αvβ3 and HER2 CAR Ts control orthotopic RMS tumors by distinct mechanisms with changes in αvβ3 antigen expression, likely due to tumor progression, one prevalent factor. This is consistent with our prior reports of αvβ3 CAR Ts preventing breast cancer metastases, which naturally upregulate αvβ3 compared to the primary tumor. Despite near elimination of tumors, residual nests of tumor cells are likely to rebound as CAR T resistant tumors, similar to what is seen in patients treated with monospecific CAR Ts. These data support the incorporation of αvβ3 and HER2 CAR Ts into a bispecific CAR T approach to mitigate antigen escape. Our data also support investigation into the role of αvβ3 in RMS.

#1092 RUNX2 inhibition alters PAX3::FOXO1 driven fusion-positive rhabdomyosarcoma cell state and growth.

Elizabeth A. Mendes[1], Audrey L. Chambers[1], Samantha J. Weitzel[1], Michael Deel[2], Aanandi Munshi[2], Christopher M. Counter[1], Seth Zimmerman[1], John Bushweller[3], Corinne M. Linardic[2]

[1]Pharmacology and Cancer Biology, Duke University School of Medicine, Durham, NC, [2]Pediatric Hematology/Oncology, Duke University School of Medicine, Durham, NC, [3]Molecular Physiology and Biophysics, University of Virginia Medical School, Durham, VA

Investigation: Fusion-positive rhabdomyosarcoma (FP-RMS) is an aggressive pediatric cancer of skeletal muscle lineage. While the incidence of RMS is ~4.5 patients per million individuals aged <20 years, 5-year survival for high-risk children is <30%, and <8% when metastatic. The *PAX3::FOXO1 (P3F)* fusion gene, resulting from *t*(2:13), is the most prominent fusion oncogene that drives FP-RMS. P3F is a fusion transcription factor and supports FP-RMS by keeping it in a persistent myoblastic state. We found P3F functions in part by suppressing MST kinase activity in the Hippo tumor suppressor pathway, a developmental pathway involved in cell fate and organ size. To investigate how this may rewire gene expression to support FP-RMS, we performed ATAC-seq analysis of a myoblast-based model of FP-RMS in which MST was further inhibited and found the *RUNX2* gene locus was more accessible. Since RUNX2 is a pioneer transcription factor known to interact with the "WW" domains of Hippo pathway members to support mesenchymal cell fate, we hypothesize that RUNX2 maintains these relationships to support FP-RMS cell state and survival.

Methods & Results: Inquiry of in silico databases and previously published literature unveiled that sarcomas including RMS have a high dependency on RUNX2 and that P3F directly binds a RUNX2 enhancer. Interrogation of a proximity labeling proteomics study from our collaborators in the Counter lab found that RUNX2 was part of the protein interactome of 7/7 FP-RMS fusions including P3F. Additionally, Co-IP experiments confirmed that there is a direct protein-protein relationship between RUNX2, P3F, and TAZ. Next, we performed *in vitro* genetic loss of function (LOF) of RUNX2 using RNAi, which showed that suppression of RUNX2 caused cell death, growth inhibition, increased TAZ expression, and induction of both myogenic and osteogenic markers. We also performed complementary pharmacologic LOF using two available small molecules, AI-14-91 (Bushweller lab) *in vitro,* and CADD522 (commercially available) *in vitro* and *in vivo*. We found that these partially phenocopied the genetic LOF and that CADD522 reduces tumor volume and growth.

Conclusions: RUNX2 is a vulnerability in RMS based on *in silico*, *in vitro,* and *in vivo* investigation, and may act to prevent osteogenic and myogenic differentiation via protein-protein relationships in the Hippo pathway. The next step will be assessing mechanistic relationships between the Hippo pathway and RUNX2, as well as the genome wide changes upon RUNX2 LOF by performing ChIP-seq, RNA-seq, and scRNA-seq experiments.

#1093 Small molecule inhibitors of the PAX3::FOXO1 fusion protein in rhabdomyosarcoma.

T. Shaw, K. Nakazawa, P. Tiwari, E. Nelson, J. Formen, C. Wolf, J. Toretsky, A. Uren;
Georgetown Lombardi Comprehensive Cancer Center, Washington, DC

Rhabdomyosarcoma (RMS) is the most common pediatric soft tissue sarcoma. It is commonly divided into subtypes based on histopathological appearance. The oncogenic fusion proteins PAX3::FOXO1 or PAX7::FOXO1 are present in the alveolar subtype of RMS (ARMS). These chimeric proteins are formed by reciprocal chromosomal translocations and consist of an N-terminal portion of the PAX3 or PAX7 transcription factor fused to a C-terminal portion of the FOXO1 transcription factor. These fusion proteins have been shown to drive malignant transformation in ARMS, and patients with fusion-positive ARMS have a worse prognosis than patients with fusion-negative ARMS and embryonal RMS. We recently reported that piperacetazine, a phenothiazine derivative and first-generation antipsychotic, is capable of binding to and inhibiting the transcriptional activity of PAX3::FOXO1, reducing the expression of PAX3::FOXO1 target genes, and inhibiting the ability of fusion-positive RMS cells to grow in soft agar. We hypothesize that other phenothiazine derivatives may have stronger binding affinity for PAX3::FOXO1 and greater ability to reduce tumor growth in vivo. We employed a structure-activity relationship campaign to develop new phenothiazine derivatives that may be more potent inhibitors of PAX3::FOXO1 than piperacetazine. We synthesized and tested 10 new compounds, in addition to 9 existing FDA-approved phenothiazine derivatives, for their ability to bind to PAX3::FOXO1 and inhibit its transcriptional activity and target gene expression as well as inhibiting the growth of fusion-positive RMS cells in 3D culture. Seven derivatives inhibited PAX3::FOXO1 reporter activity better than piperacetazine, nine of them performed worse, and three of them showed comparable activity to piperacetazine. We demonstrated that piperacetazine does not alter PAX3::FOXO1 levels, subcellular localization, binding to a PAX3::FOXO1 target DNA sequence, or phosphorylation at Ser256 in the FOXO1 portion of the fusion protein. We therefore hypothesize that piperacetazine may be disrupting interactions between PAX3::FOXO1 and its partner proteins. We are employing a proximity-based biotinylation method to identify proteins that are competed away from PAX3::FOXO1 by piperacetazine. Our data suggest that it is possible to target PAX3::FOXO1 protein using small molecules that can directly bind to it and inhibit its activity in fusion-positive RMS cells.

#1094 Utilizing CRISPR-Cas13 as a novel functional genomics tool to characterize PAX3-FOXO1 in alveolar rhabdomyosarcoma.

A. Zhao[1], L. M. Brown[1], M. Fareh[2], P. G. Ekert[1];
[1]CCIA, Sydney, Australia, [2]Peter MacCallum, Melbourne, Australia

Background: CRISPR-Cas13 (Cas13) is an RNA editing system that can knockdown gene transcripts with higher efficiency and specificity than RNA interference technologies. We are exploring the utility of Cas13 as a robust novel functional genomics tool to understand the biology of the PAX3-FOXO1(P3F1) gene fusion in alveolar rhabdomyosarcoma (ARMS). Our goal is to identify gene dependencies and novel druggable targets. [LB1]
Aim: This study aims to functionally characterize P3F1 in paediatric cancer cell lines using Cas13. [LB2]
Methods & Results: Transient transfection and viral transduction of Cas13 vector systems were used to demonstrate that Cas13 knockdown of target gene expression can be achieved in ARMS cell lines. We developed guides to specifically target P3F1 expression and tested their efficiency in HEK293T cells. Cas13 function was validated with a mCherry knockdown proof-of-concept expression in the ARMS cell lines Rh5 and Rh30. 90-95% knockdown efficiency was seen over three independent experiments. Ten P3F1 breakpoint targeting guides were designed and screened first in a HEK293T P3F1 overexpression model to select optimal high efficiency targeting guides. The highest efficiency targeting guide showed a GFP reduction of 70% in three independent experiments. High-efficiency Cas13 guides were taken forward into Rh5 cells to knockdown endogenous P3F1 expression which were validated by western blotting and RT-PCR. Western blots of Cas13 sorted Rh5 cells showed that guide 1150 was able to knockdown P3F1 protein expression by ~70%.
Discussion/Conclusion: These findings demonstrate the high efficiency and specificity of the Cas13 system to silence P3F1, and other oncogenic fusion drivers. Further studies will utilize Cas13 to characterize the molecular and cellular consequences of P3F1 gene-silencing in patient-derived ARMS cell lines.

#1095 Prox1 transcription factor and its downstream signaling - A new therapeutic target for rhabdomyosarcoma.

N. Y. Gizaw, T. Bohling, M. Sampo, K. Alitalo, R. M. Kivela;
University of Helsinki, Helsinki, Finland

Rhabdomyosarcoma (RMS) stands as the predominant soft tissue sarcoma in children, characterized by a high-grade neoplasm composed of cells resembling skeletal myoblasts. Despite being prevalent, patients with metastatic or recurrent rhabdomyosarcoma still experience poor outcomes, underscoring the necessity for novel treatments. We have recently shown that PROX1 is a critical factor in RMS tumor growth and myogenic characteristics (Gizaw NY, et al. PNAS 2022). As PROX1 has previously been associated with tumor metabolism in colorectal cancer, we investigated further its role in RMS metabolism. Our findings demonstrate that PROX1 plays a crucial role in regulating RMS cell metabolism. Specifically, silencing of PROX1 resulted in decreased lipid and oxidative metabolism, which was accompanied by an increase in glycolysis and triglyceride accumulation. RNA sequencing and Gene Set Enrichment Analysis revealed downregulation of all genes involved in the cholesterol synthesis pathway in PROX1-silenced RMS cells. Our studies further reveal that inhibiting cholesterol synthesis, akin to PROX1 silencing, can effectively inhibit RMS cell growth. Our results provide novel insights into the role of PROX1 in RMS metabolism and highlight the potential of PROX1-regulated metabolic pathways as promising targets for the development of novel RMS therapies.

#1096 Enhancing effector function in T cell adoptive cell therapy in murine models of pediatric sarcomas.

J. P. Sanchez[1], E. Davila[2], B. H. Ladle[1];

[1]Johns Hopkins University, School of Medicine, Baltimore, MD, [2]University of Colorado, Anschutz Medical Campus, Aurora, CO

New treatment approaches for high-risk pediatric sarcomas are desperately needed. Immunotherapy advances with adoptive cell therapy in hematologic malignancies have not yet translated to pediatric solid tumors including sarcomas. Hallmarks of the immune microenvironment in pediatric sarcomas include the presence of immunosuppressive cytokines and immune cells and a lack of potent T cell activation. We are seeking ways to overcome these barriers to effective adoptive cell therapy in pediatric sarcoma. We are exploring introduction of a novel synthetic co-receptor, CD8a:MyD88, that can augment tumor-specific T cell effector function and potentially improve outcomes in murine models of sarcoma. Tumor-antigen specific T cells or tumor-infiltrating T cell populations are transduced ex vivo to express the CD8a:MyD88 synthetic co-receptor resulting in MyD88 signaling when T cells encounter their cognate MHC I/epitope complex. We have studied the effects of CD8a:MyD88 expression on cytokine production and lytic activity against murine sarcoma cell lines in vitro. Initial experiments utilized the OT1 T cell model (specific to the model antigen chicken ovalbumin) which we introduced into our murine sarcoma cell lines (KPSarc pleomorphic sarcoma and M3-9M rhabdomyosarcoma). Using GFP as a marker of T cell transduction, the production of effector cytokine interferon gamma was measured following T cell activation compared with GFP-negative non-transduced T cells. CD8a:MyD88 expressing T cells expressed higher levels of interferon gamma at basal levels and following antigen-specific activation when co-cultured with Ova-expressing sarcoma cells. Improved tumor-specific lytic function in CD8a:MyD88 expressing T cells was also observed in co-culture experiments compared to untransduced or control vector- transduced T cells. We further hypothesized that skewing T cell differentiation toward an effector phenotype with the addition of interleukin-12 during T cell expansion would increase the anti-tumor effect of the CD8a:MyD88 expressing T cells. Co-culture with our murine sarcoma cell lines showed increased tumor-lytic function in T cells primed with IL-12. We have ongoing experiments studying the in vivo effects of the CD8a:MyD88 expressing T cells in model antigen-expressing murine sarcoma models. In addition, the ability of the CD8a:MyD88 co-receptor to augment the effector function of polyclonal sarcoma infiltrating T cells is being explored. These results will further define the obstacles and potential solutions to successful adoptive T cell therapy for pediatric sarcomas.

#1097 CD73 contributes to the pathogenesis of fusion-negative rhabdomyosarcoma through the purinergic signaling pathway.

K. G. Cano Hernandez, A. Shah, V. Lopez, V. Tagliabracci, K. Chen, L. Xu, R. Bassel-Duby, E. Olson, N. Liu;
University of Texas Southwestern Medical Center, Dallas, TX

Rhabdomyosarcoma (RMS) is the most common type of soft tissue sarcoma in children and adolescents. Fusion-Negative RMS (FN-RMS) accounts for more than 80% of all RMS cases. The long-term event-free survival rate for patients with high grade FN-RMS is below 30%, highlighting the need for improved therapeutic strategies. CD73 is a 5' ectonucleotidase that hydrolyzes AMP to adenosine and regulates the purinergic signaling pathway. We found that CD73 is elevated in FN-RMS tumors that express high levels of TWIST2. While high expression of CD73 contributes to the pathogenesis of multiple cancers, its role in FN-RMS has not been investigated. We found that CD73 knockdown decreased FN-RMS cell growth while upregulating the myogenic differentiation program. Moreover, mutation of the catalytic residues of CD73 rendered the protein enzymatically inactive and abolished its ability to stimulate FN-RMS growth. Overexpression of wildtype CD73, but not the catalytically inactive mutant, in CD73 knockdown FN-RMS cells, restored their growth capacity. Likewise, treatment with an adenosine receptor A_{2A-B} agonist partially rescued FN-RMS cell proliferation and bypassed the CD73 knockdown defective growth phenotype. These results demonstrate that the catalytic activity of CD73 contributes to the pathogenic growth of FN-RMS through the activation of the purinergic signaling pathway. Therefore, targeting CD73 and the purinergic signaling pathway represents a potential therapeutic approach for FN-RMS patients.

#1098 Identification of SUMO2 as a novel therapeutic target for synovial sarcoma.

R. Iyer, P. Akula Bala, R. Murad, A. J. Deshpande;
Sanford Burnham Prebys Medical Discovery Institute, San Diego, CA

Synovial Sarcoma (SySa) is a rare soft tissue sarcoma that accounts for 5 - 10% of all soft tissue sarcomas. It disproportionately affects children, adolescents and young adults with tumors emerging in muscles, tendons, nerve tissue and joints. Current treatment involves radiation and radical surgery including limb amputation with overall survival around 50% highlighting the urgent need to develop targeted therapies for these patients. In this study, we hypothesized that the fusion SS18-SSX protein found in SySa transcriptionally rewires the tumor cells creating a dependence on specific genes that if uncovered can be exploited therapeutically. To study genes that are selectively essential to SySa, we analyzed the dependency maps (DepMap) whole genome RNAi and CRISPR screening datasets consisting of ~1750 human cancer cell lines including 9 SySa cell lines. We identified 368 target genes that specifically impact the proliferation of SySa when compared to other tumor cell lines. To interrogate these genes systematically, we designed pooled CRISPR libraries and conducted *in vitro* as well as *in vivo* screens in SySa cell line HS-SY-II. Our screens revealed that Small Ubiquitin like-modifier 2 (SUMO2) was one of the most significant dependencies in both the *in vitro* as well as *in vivo* screens. We tested the SUMO2 inhibitor, TAK-981, a clinical stage small molecule inhibitor specific for E1 SUMO-activating enzyme (SAE), against a panel of SySa cell lines with HS-SY-II and SYO1 showing an EC_{50} in the low nanomolar range. Furthermore, TAK-981 treatment potently induced apoptosis and reduced the proportion of cycling cells in both HS-SY-II as well as SYO1 cell lines. Strikingly, transcriptomic studies on HS-SY-II and SYO1 cell lines showed that TAK-981 treatment substantially altered the oncogenic signatures of SySa. This was evident both in the HS-SY-II cell line expressing the SS18-SSX1 fusion as well as the SYO1 cell line expressing the SS18-SSX2 fusion protein. These data strongly indicate that SUMO2 is critical for the transcriptional activity of the different SS18-SSX chimeric oncoproteins. In addition, TAK-981 treatment showed a highly significant downregulation of genes associated with cell cycle progression as well as a modulation of genes of the BAF and PRC1/PRC2 complexes that have been implicated in SySa pathogenesis. Taken together, we developed an integrated computational and experimental screening approach to prioritize and validate selective dependencies in synovial sarcoma. Our studies identify SUMO2 as a novel, selective vulnerability in this cancer and since SUMO2 inhibitors are currently in Phase 1/2 clinical trials for other malignancies, our findings present a novel potential avenue for targeted treatment of synovial sarcoma.

#1099 Combined MEK and RET inhibition overcomes resistance to single agent RET inhibition in medullary thyroid cancer.

Arwa Fallatah[1], Abdelrahman Rahmy[1], Sophia Khan[2], Hsien-chao Chou[3], Kerstin Heselmeyer-Haddad[3], Darawalee Wangsa[3], David Milewski[3], Yong Kim[1], Robert Hawley[3], Young Song[3], Xiaohu Zhang[4], Craig Thomas[4], Jun S. Wei[3], Jong-In Park[5], John Glod[2], Javed Khan[3]

[1]Genetics Branch, Pediatric Oncology Branch, NIH-NCI, Bethesda, MD,[2]Pediatric Oncology Branch, NIH-NCI, Bethesda, MD,[3]Genetics Branch, NIH-NCI, Bethesda, MD,[4]National Center for Advancing Translational Sciences, NIH, Bethesda, MD,[5]Medical College of Wisconsin, Milwaukee, WI

Medullary thyroid carcinoma (MTC) is a rare neuroendocrine cancer, caused by activating mutations in the *RET* proto-oncogene, contributing to 13% of all thyroid cancer mortalities. Patients with metastatic MTC treated with RET inhibitors (RETi) can develop resistance through mechanisms currently being investigated. We aim to understand the molecular mechanisms of acquired resistance to RETi and develop novel combination therapies to circumvent resistance to these drugs. We used TT, an MTC cell line, to develop vandetanib-resistant (VanR) lines, at two independent sites, the Medical College of Wisconsin (MCW) and the Pediatric Oncology Branch (POB) at the NCI. We applied a multiomic approach to investigate the mechanisms of resistance, including Spectral karyotyping (SKY) and multiplex interphase Fluorescence in situ Hybridization (miFISH) to study the karyotype, ploidy, and heterogeneity at a single-cell level. Whole exome and RNA-sequencing was done to identify genetic alterations such as acquired mutations, copy number variations, and gene expression changes. In parallel, we performed genome-wide CRISPR gene knockout (KO) in TT cells treated with selpercatinib or vehicle to develop potential synergistic targeted combination therapy with RETi. Additionally, we performed a cytotoxicity screening using the Mechanism Interrogation Plate (MIPE6.0) library containing 2803 investigational drugs, novel agents, and FDA-approved drugs with known mechanisms of action. SKY and miFISH results showed that, for the parental TT_POB cell line, there were 4 copies of chromosome 10 (location of the *RET* gene), whereas there were 3 copies in TT_POB VanR. This was associated with an increase in the *RET* variant allele frequency, indicating a loss of heterozygosity of the wildtype allele as a mechanism of resistance, which was confirmed by whole exome sequencing. For TT_MCW VanR, we identified a new *RET* solvent front (G810S), as well as an increased copy number of *RET* with an increase in expression. CRISPR KO demonstrated that the knockout of NF1 led to resistance and survival to selpercatinib treatment. The MIPE6.0 screening confirmed resistance to RETi in TT_MCW VanR and sensitivity to multiple MEK inhibitors. *In vivo* testing in a xenograft mouse model confirmed the synergistic/additive activity of combined selpercatinib with trametinib, a MEK inhibitor. In conclusion, using a multiomic approach, we show that resistance to RETi occurs by an adaptive increase in RET signaling through secondary mutations in *RET*, and an increase in expression or dose of the mutant *RET* allele. These genetic events are associated with an activation of RAS signaling, in VanR cell lines, through the ERK/MAPK pathway. Furthermore, we demonstrate that the combination of RET and ERK/MAPK inhibition is synergistic against *RET*-mutant MTC. Future plans include translating our findings through clinical trials at the NCI.

#1100 Fascin-1 inhibitor decreases hepatoblastoma cells tumorigenicity via YAP 1.

L. DIF, A. Martin, S. Basbous, G. Manaud, V. Moreau;
Bordeaux Institut of Oncology, Bordeaux, France

Introduction: Hepatoblastoma (HB) is a liver tumor that arises in children. It's a sporadic malignancy that is often overly aggressive. The current treatment consists of chemotherapy. However, chemotherapy in young patients has disastrous and long-term side effects such as ototoxicity, cardiomyopathy, and infertility. Thus, alternative strategies are needed. One hint is to target the most common mutations in HB. It has been demonstrated that 90% of HB tumors are mutated for the Wnt pathway effector ß-catenin. This mutation leads to an aberrant constitutive activation of Wnt/ß-catenin signaling. Here, we investigate one of ß-catenin transcriptional targets, Fascin-1 that is found up-regulated in many tumors. Fascin1 affects actin organization into bundles, and this leads to cell migration and invasion. Whereas Fascin-1 is absent from normal hepatocytes, we found its expression associated to the poor prognosis C2 subtype of HB. In both human and murine HB samples, Fascin-1 is associated to undifferentiated tumor cells. We further demonstrated that Fascin-1 expression modulates tumor hepatocyte differentiation status through gene expression. In this study, we investigate how Fascin-1 can regulate tumor cell plasticity and whether Fascin-1 is a druggable target in HB tumors.
Methods: We use two classical HB model cells Huh6 and HepG2 and 3 Patient-Derived-Xenograft cell lines. We explore the effect of Fascin-1 actin-bundling activity impairment by using inhibitors, on invasion and migration using Trans-well and wound-healing assays. We follow proliferation and cell death by Flow cytometry and investigate gene expression by PCR and reporter assay. We investigate Fascin modulation of the kinome with PamGene technology.
Results: We show that the inhibition of Fascin actin-binding activity decreases cell invasion and migration as well as proliferation. We show an increase of cell death in Huh6/HepG2 cells but not in the PDX models. A cell cycle arrest is induced, and the cells become senescent. Differentiation genes are overexpressed and EMT genes are repressed. Yap expression is downregulated; Yap promoter activity is downregulated, and Yap is found translocated into the cytoplasm upon Fascin-1 inhibition. These data suggest that Fascin inhibition decreases tumors cell invasion, induces cell senescence, and favors a switch towards a differentiated and these effects on the cells are mediated via the Hippo pathway. The kinome is also modulated.
Conclusion: Fascin-1 is an interesting target in hepatoblastoma, commercialized phase-2 drugs are available, and this study will confirm the potential use of those drugs in HB treatment and elucidate by which mechanism Fascin-1 inhibition impacts tumors.

#1101 A patient-derived xenograft in vitro platform identifies panobinostat as the most efficient drug to treat high-risk hepatoblastoma patients.

S. Demir[1], E. Indersie[2], S. Branchereau[3], E. Hiyama[4], S. Cairo[5], **R. Kappler**[1];
[1]Ludwig Maximilians University, Munich, Germany, [2]XenTech, Evry, France, [3]Bicetre Hospital, Paris, France, [4]University Hospital, Hiroshima, Japan, [5]Champions Oncology, Rockville, MD

Hepatoblastoma is the most common pediatric liver tumor, and the treatment of patients with preoperative chemotherapy and surgical resection of the tumor has led to survival rates of up to 83%. However, resistance of the primary tumor towards chemotherapy and the persistence of metastases still represents major challenges to achieve complete remission in high-risk patients, which is associated with poor prognosis. In order to identify new treatment options, we have used a newly developed in vitro drug-testing platform comprised of conventional cell lines and cultures from dissociated patient-derived xenografts of pediatric liver cancers to test standard-of-care medications used in the current PHITT trial as well as compounds targeting a wide range of different cellular pathways. We identified histone deacetylase (HDAC) inhibitors as a promising drug family to reduce tumor cell growth in a dose-dependent manner, with panobinostat being the most effective drug tested. Subsequent in vitro assays showed that panobinostat reduced short- and long-term proliferation, retarded three-dimensional spheroid growth and ultimately induced apoptosis of hepatoblastoma cells. RNA sequencing indicated that panobinostat results in downregulation of MYC target genes and upregulation of the dual specificity phosphatase 1. Of clinical relevance, the combination of panobinostat with doxorubicin revealed a strong synergistic effect, even stronger than the one of cisplatin and doxorubicin, which is currently given to high-risk hepatoblastoma patients. Moreover, increased expression of *HDAC4* and *HDAC11* in primary tumor tissues was significantly associated with metastatic disease. Our results strongly suggest panobinostat to be used in future therapeutic trials for high-risk hepatoblastoma patients, especially when combined with doxorubicin.

#1102 Amentoflavone enhances regorafenib-induced apoptosis and -inhibited invasion via inactivating STAT3/NF-KB signaling pathway in Hepatocellular carcinoma.

Y. TSAI[1], Y.-T. Chen[2], F.-T. Hsu[1], J.-J. Tsai[3], Y.-C. Liu[4];
[1]China Medical University, Taichung City, Taiwan, [2]National Yang Ming Chiao Tung University, Taipei City, Taiwan, [3]Taipei Veterans General Hospital, Yuan-Shan/Su-Ao Branch, Taipei City, Taiwan, [4]Chang Bing Show Chwan Memorial Hospital, Changhua City, Taiwan

Hepatocellular carcinoma (HCC) is an aggressive tumor and ranks as the third leading cause of cancer-related deaths worldwide. Amentoflavone, a biflavonoid compound, possesses antiviral, angiogenesis-inhibitory, and anticancer properties. Prior studies have illustrated that amentoflavone effectively restrains tumor growth and promotes apoptosis in various cancers, including brain cancer and osteosarcoma. Regorafenib, a small molecule inhibitor of multi-kinases, can inhibit angiogenesis, tumor growth, and anti-tumor metastasis. While regorafenib is a targeted drug approved for the treatment of metastatic colorectal cancer and has also been approved for use in HCC, its effectiveness in HCC is limited. Consequently, our goal is to investigate whether amentoflavone may enhance the sensitivity of regorafenib in treating HCC and explore the underlying mechanisms. In our study, through the combined treatment and combination index analysis, we proved that the combination of regorafenib and amentoflavone may induce cytotoxicity more effectively compared to monotherapy, as assessed by the MTT assay in Huh7 and HepG2 cells. The invasion and migration assays also demonstrated a superior inhibitory effect in the combination group. Additionally, apoptosis markers such as "cleaved caspase-3, -8, -9, Fas and FasL" assayed by flow cytometry, confirm that the combination treatment may induce the extrinsic/intrinsic apoptosis pathway in HCC. In our Western blotting analysis, we observed that the phosphorylation of STAT3 and NF-κB proteins was effectively suppressed by the combination of regorafenib and amentoflavone in Huh7 and HepG2 cells, respectively. Furthermore, our in vivo study confirmed a superior tumor inhibition rate and control rate with the combination of regorafenib and amentoflavone. Importantly, no signs of general toxicity were observed in any of the treatment groups, as evidenced by body weight monitoring and Hematoxylin and Eosin stain (H&E) pathology evaluation. We believe that the combined treatment of these two drugs effectively triggers cell death and suppresses metastatic patterns through the inactivation of the STAT3/NF-κB signaling pathway. These results suggest that amentoflavone has the potential to serve as an adjuvant that sensitizes regorafenib for the treatment of HCC without causing any side effects.

#1103 Molecular signature for treatment-responsive and recurrent Wilms tumors.

J. Jiang, D. B. Allison, R. Burikhanov, S. Ganguly, R. A. Goettl, J. Liu, C. Wang, A. F. Saltzman, T. Tucker, P. H. Spielmann, E. B. Durbin, J. A. D'Orazio, V. M. Rangnekar;
University of Kentucky, Lexington, KY

Wilms tumor is the most common solid renal malignancy in children. To better understand the biology of Wilms tumors and develop drugs especially against tumors that relapse, we sought to identify mutations in the exome, differential gene expression patterns, and tumor suppressor expression status of Wilms tumors in Kentucky. The Kentucky Cancer Registry (KCR) Virtual Tissue Repository identified 29 cases of Wilms tumor diagnosed between 2015 and 2021 at hospitals across the Commonwealth of Kentucky. The Markey Cancer Center Biospecimen Procurement and Translational Pathology Facility prepared tumor microarrays (TMAs) using Wilms tumor and matching normal tissue cores for immunohistochemistry (IHC) analysis. RNA-Seq analysis performed at the Markey Cancer Center Oncogenomics Facility identified a gene signature that was further validated by IHC and reverse-transcription quantitative-PCR (RT-qPCR). Outcome data provided by KCR indicated that increased expression of an anti-apoptotic protein in the tumor counter-intuitively provided better prognosis and outcome to treatment, indicating that the treatments either directly or indirectly targeted this protein. Loss of function of the tumor suppressor proteins in Par-4/PAWR, WT1 and p53 did not explain the higher expression of the cell survival protein. Our multidisciplinary team approach involves basic science/translational researchers, population scientists, biomedical informaticists, and clinicians and has resulted in well-characterized, Wilms tumor tissue microarrays. The next phase of the study is generating patient derived xenografts (PDXs) for a better understanding of Wilms tumor biology in children.

CLINICAL RESEARCH: Radiation Oncology
Poster Session

#1107 Prospective observational study to evaluate the efficacy of oxygen saturation endoscopic imaging for radiotherapeutic response in head and neck squamous cell carcinoma.

K. Tomizawa[1], A. Motegi[1], H. Hirata[1], H. Yamashita[1], H. Sunakawa[1], W. Okano[1], T. Enokida[1], T. Fujisawa[1], S. Zenda[1], M. Nakamura[1], H. Hojo[1], S. Abe[2], M. Sakuramachi[2], H. Igaki[2], Y. Saito[2], K. Matsuura[1], M. Tahara[1], T. Yano[1], T. Akimoto[1];
[1]National Cancer Center Hospital East, Kashiwa, Japan, [2]National Cancer Center Hospital, Tokyo, Japan

Background: Radiotherapy (RT) has a pivotal role in the management of head and neck squamous cell carcinoma (HNSCC), providing effective tumor control and functional preservation. Hypoxia is a cause of radioresistance in HNSCC. We have developed an oxygen saturation endoscopic imaging (OXEI) method to assess real-time tissue oxygenation levels. However, the clinical significance of OXEI in patients with HNSCC receiving RT remains unclear. We evaluated the association between pretreatment tumor oxygen saturation (StO_2) quantified by OXEI and clinical outcomes of patients with HNSCC receiving RT.
Methods: We prospectively recruited patients with HNSCC scheduled to receive RT at 2 institutions. The primary endpoint was the association between pretreatment tumor StO_2 and complete response (CR) rate 8 weeks after completion of RT. Secondary endpoints evaluated the impact of StO_2 on 1-year overall survival (OS) and progression-free survival (PFS) rates after RT initiation. We also evaluated the cumulative incidence of local failure (LF). To explore the relationship between tumor hypoxia assessed by OXEI and gene expression profile, we performed RNA sequencing of 4 tumor samples collected from 2 patients (2 samples/patient) before RT. The hypoxia score for each sample was calculated by gene set variation analysis based on HNSCC mRNA-based hypoxia signatures. We performed gene set enrichment analysis (GSEA) to evaluate whether the biological pathways (Hallmark, Reactome, and KEGG gene sets) showed significant associations with tumor hypoxia.
Results: Of the 50 patients enrolled from March 2019 to February 2022, we analyzed 37 who underwent RT and OXEI. Thirty-six (97%) patients received current platinum-based chemotherapy. The median (range) pretreatment tumor StO_2 of 60 (45-84)% was lower than that of normal mucosa, 66 (56-84)% ($P < 0.01$). Patients with tumor $StO_2 < 60\%$ were classified as the hypoxia group (n =19), and those with tumor $StO_2 \geq 60\%$ as the non-hypoxia group (n =18). The CR rate 8 weeks after RT was not significantly different between the hypoxia and non-hypoxia groups (84% vs. 100%, respectively; $P = 0.23$). After a median (range) follow-up of 33 (9-45) months, the hypoxia group had worse 1-year PFS (74% vs. 94%, $P = 0.017$) and OS (89% vs. 100%, $P = 0.015$) and higher LF rates (21% vs. 6%, $P = 0.036$) compared with the non-hypoxia group. RNA sequencing confirmed that tumor StO_2 reflected expression-based hypoxia scores. GSEA showed upregulation of reactive oxygen species (ROS) and KEAP1-NFE2L2 pathways in hypoxic samples (StO_2 of 59%) compared with non-hypoxic samples (StO_2 of 70%; adjusted $P < 0.01$), consistent with the fact that hypoxic stress increases ROS production.
Conclusion: Our findings suggest that pretreatment tumor StO_2 quantified by OXEI correlates with 1-year PFS, OS, and LF rates of patients with HNSCC receiving RT.

#1108 The impact of adjuvant radiotherapy (ART) and survival prediction by machine learning in intracranial hemangiopericytoma (HPC).

S. Alshwayyat[1], A. A. Al-Khalili[1], A. Erjan[2], H. Kamal[1], T. Abdulsalam[1], M. Alshwayyat[1];
[1]Jordan University of Science & Technology, Irbid, Jordan, [2]King Hussein Cancer Foundation, Amman, Jordan

Background: Intracranial HPC is a rare brain tumor that accounts for less than 1% of all primary central nervous system malignancies. Surgery is the primary treatment, and while radiation may reduce the risk of local recurrence, its overall effectiveness remains uncertain. Therefore, it is crucial to develop reliable predictions for personalized care and improved management. In this study, we used machine learning (ML) techniques to predict the survival of patients with intracranial HPC.

Methods: Data were obtained from the Surveillance, Epidemiology, and End Results (SEER) database (2000-2019). Patients with other malignancies or lack of pathological diagnosis were excluded. T-tests and chi-square tests compared variables, while Kaplan-Meier, log-rank tests, and Cox regression identified prognostic factors for overall survival (OS) and cancer-specific survival (CSS). Patient records were randomly divided into training (80 %) and validation (20 %) sets. Univariate Cox regression and least absolute shrinkage and selection operator were used to identify the significant factors linked to survival, which were used to establish a nomogram for predicting the 3- and 5-year OS and CSS.

Results: Of the 367 included patients, 121 underwent surgery and 246 underwent surgery + ART. The median survival time was 54 months. Patients who underwent surgery had 5-year OS rates of 61% and 86% for CSS, while those treated with surgery + ART had 81% and 96% survival rates, respectively. The two treatment groups showed significant differences in the OS and CSS ($p<0.022$ and $p<0.017$, respectively). Age ≥ 50 years was a poor prognostic factor for OS, whereas ART, localized stage and regional stage were good prognostic factors. No significant factors were associated with CSS. To construct the OS Nomogram, three predictors, age, stage, and treatment method, were chosen. In the training and validation sets, the C-indices are 0.799 and 0.736, respectively. The receiver operating characteristic curves (AUCs) for the 3- and 5-year OS in the training set were 0.594 and 0.617, respectively, whereas those in the validation set were 0.56 and 0.59. For the CSS nomogram, two factors, age and stage, were utilized. The C-indices for the training and validation sets are 0.814 and 0.774, respectively. In the training set, the AUCs for 3- and 5-year CSS were 0.585 and 0.605, respectively, and 0.563 in the validation set. The most important risk factor was the distant stage, while the most important protective factor was age less than 50 years.

Conclusion: This study shows that ART has a significant impact on the treatment of Intracranial HPC and provides better survival outcomes. ML has been used to create prediction models to support personalized patient care. These findings provide valuable insights into the management of this rare brain tumor and the potential of data-driven approaches to improve treatment and outcomes.

#1109 LINC01770 stabilizes TEAD1 expression to mediates nasopharyngeal cancer radiation resistance rendering tumor cells vulnerable to ferroptosis.

Q. Xu, C. Sun, S. Zhang, X. Li, L. Chen, M. Chen;
Sun Yat-sen University Cancer Center, Guangzhou, China

Background: Long noncoding RNAs (lncRNAs) regulate various essential biological processes, including cell proliferation, differentiation, apoptosis, migration, and invasion. However, in nasopharyngeal carcinoma (NPC), the clinical significance and mechanisms of lncRNAs in malignant progression are unknown.
Methods: LINC01770 expression was determined using quantitative real-time reverse transcription PCR, and its prognostic value was evaluated using Kaplan-Meier survival analysis. RNA sequencing and bioinformatic analysis were used to determine the potential function of LINC01770, and its biological effects were investigated using *in vitro* and *in vivo* experiments. Mass spectrometry-coupled RNA pull-down assays and western blotting identified LINC01770 interacting proteins, followed by confirmation using RNA immunoprecipitation (RIP) assays. Ferroptosis and lipid peroxidation were detected using flow cytometry.
Results: LINC01770 was overexpressed in NPC tissues according to microarray screening. Patients with NPC showing high LINC01770 expression experienced shorter survival and worse prognosis. *In vitro* and *in vivo* experiments suggested that knockdown of LINC01770 expression significantly inhibited the proliferation, migration, and invasion of NPC cells. Sequencing and functional complementation experiments showed that LINC01770 regulates the proliferation and metastasis of NPC through TEA domain transcription factor 1 (TEAD1). Meanwhile, RIP and PCR experiments suggested that LINC01770 and TEAD1 were common targets of microRNAs miR-615-5p and miR-1293. Overexpression of LINC01770 promoted ferroptosis *in vitro* and *in vivo* through the TEAD1/Acyl-CoA synthetase long chain family member 4 (ACSL4)/transferrin receptor (TFRC) pathway.
Conclusions: LINC01770 is a prognostic biomarker for NPC and participates in the regulation of TEAD1 signaling pathway through competitive binding to miRNA-615-5p and miRNA-1293, resulting in NPC metastasis and progression. Radiation resistant cells are in a delicate balance between lipid peroxidation and increased vulnerability to ferroptosis, suggesting that ferroptosis could be used to kill NPC cells and reverse their radiotherapy resistance during the malignant progression of NPC caused by high expression of LINC01770. Thus, inducing ferroptosis could be used to treat recurrent and refractory NPC.

#1110 Estrogen receptor β signaling induced radio-resistance in bladder cancer.

H. Ide[1], T. Murakami[1], E. Kashiwagi[2], S. Kitaoka[3], A. Komatsuda[3], C. Nishimura[3], S. Funakoshi[3], M. Oya[1], H. Miyamoto[4];
[1]Keio University, Tokyo, Japan, [2]Kyushu University, Fukuoka, Japan, [3]Saiseikai Central Hospital, Tokyo, Japan, [4]University of Rochester Medical Center School of Medicine and Dentistry, Rochester, NY

Introduction and Objective: Although radiotherapy (RT) combined with chemotherapy shows comparable outcomes to surgery, women tend to have higher mortality from bladder cancer (BC) compared to men. Emerging evidence indicated the involvement of estrogen receptorβ (ERβ) signaling in BC progression and the association of ER signaling with DNA repair pathways which are involved in radio-resistance. Therefore, we evaluated the association between ERβ signaling and the sensitivity to BC cells.
Methods: We compared the inhibitory effect of RT on BC cell viability between ERβ positive [5637 and T24 expressing control short-heparin RNA (shRNA)] and ERβ negative (5637 and T24 expressing ERβ-shRNA) cells. Moreover, we compared DNA double-strand breaks (DSB) via γ-H2AX foci formation, as well as the expression levels of DNA repair genes, in these cells after RT. Finally, in a mouse xenograft model, we evaluated it on the growth of ERβ positive tumor treated with radiation combined with mock or tamoxifen treatment.
Results: *In vitro* experiment showed that ionizing radiation reduced the numbers of viable cells in ERβ negative cells more significantly than those in ERβ positive cells. Moreover, tamoxifen treatment reduced the numbers of viable cells more than mock treatment in ERβ positive cells, while tamoxifen didn't show significant effects in ERβ negative cells. The down-regulation of ERβ resulted in a delay in DSB repair 4-24 hours after RT. We then established radio-resistant cells and confirmed considerable elevation of the expression of ERβ as well as DNA repair genes including RAD51 and RAD54. Estradiol treatment induced the expression of these genes and tamoxifen abolished these effects. Finally, in vivo experiment showed that tamoxifen enhanced the cytotoxic effects of RT in xenograft bearing mice.
Conclusions: These results indicated that ERβ signaling inversely correlated with sensitivity to RT in BC. Thus, ERβ inhibition have a potential of enhancing the cytotoxic effects of radiation, especially in ERβ positive BC cells.

#1111 Poor radiation sensitivity and potential radiosensitizers for betel-nuts related head and neck squamous cell carcinoma in Taiwan.

J.-P. Chen, J.-Y. Chang, R.-L. Hong;
National Taiwan University Hospital, Taipei, Taiwan

Background: Betel nut chewing might contribute to strong invasion & treatment refractoriness in HNSCC from Taiwan. Betel-nuts exposed HNSCC cell line, TW2.6, had high PDL1, defective p53 mutation, p16 loss, & BCL2 overexpression. In our studies, PI3K/AKT/mTOR inhibitors, anti-angiogenesis therapies, CDK4/6 inhibitors, DDR interventions, epigenetic modifications, and immunotherapy-containing regimens will be future combination options. The genomic signature of TW2.6 has been figured out in our study(AACR2020 & 2023), too, mainly with PIK3CA H1047R mutation, high TMB(8.42 muts /Mb)/MSS, VEGF-A amplification, p53/MYC/HRAS/DDR2/ PDGFRbeta/EPHB1/ATM mutations, FAT1 loss, amplification of TERT/ FGF10/CCND3/SOX9/IL-7R/SDHA/RICTOR/FLCN, CDK12/PTPRD loss of function, CDK8 mutation, & deletions of STK11/ARID1B/MITF/TNFAIP3 and molecularly-guided novel interventions will be designed. Purpose & Methods: Polo-like kinase 1 inhibitor(volasertib), gluconate(blocking citrate transport & glucose metabolism), IAP inhibitor(Debio1143), glutaminase 1 inhibitor(CB839) were tested on TW2.6 to evaluate synergistic effects with radiation. Results: TW2.6 was resistant to volasertib, gluconate, or radiation alone; but sensitive to Debio1143 and CB839. Volasertib significantly enhanced radiation. The flow cytometry revealed volasertib and radiation resulted in a significant G2/M arrest. Western blotting showed volasertib and radiation increased p-histone3, p-CDK1, & cyclin B levels and induced apoptosis. Gluconate, CB839, or Debio1143 each had significant synergistic effects with radiation. The radiosensitization efficacy would be volasertib>gluconate>CB839>Debio1143. Conclusions: In Taiwan, patients with R/M HNSCC progressing within 3 months after CCRT could be rescued by early ICIs. Recently, sequential CCRT followed by ICI or Debio-1143 with CCRT showed potential survival benefits. In our studies, novel agents such as PLK inhibitor, gluconate, and CB839 had even better radiosensitization compared with Debio1143. Sequential CCRT with novel agents followed by ICI will be the future trend, esp. in biology-aggressive betel-nuts related locally advanced HNSCC in Taiwan.

#1112 Modulated dNTP pools and their influence on DNA repair mechanisms and apoptosis in therapy resistant cancers.

D. Monroe, M. Kehinde-Ige, E. Usoro, A. Williams, E. Steinbeck, S. Aycox, H. Shi, W. Daddacha;
Augusta University, Augusta, GA

Glioblastoma (GBM) is a deadly primary tumor of the brain, accounting for almost half of all diagnosed malignant gliomas. Ionizing radiation (IR) and some chemotherapeutics strategically target cancer cells by causing DNA double-strand breaks (DSBs). However, cancers like GBM often develop resistance to DSB-inducing therapeutics due to dysregulated DNA repair. Homologous Recombination (HR) is an error-free DSB-repair process consisting of proteins that are often dysregulated in GBM, causing overactive DNA-repair, therapy resistance, and poor patient outcomes. Proteins involved in the HR-repair process have been extensively investigated; however, therapeutic resistance remains common. Here, we provide an alternative approach to target DSB-resistant GBM by modulating the dNTP pool instead of solely targeting DNA-repair proteins. Our goal is to understand the interplay between dNTP pools and DSB- repair. dNTPs are a necessary constituent to repair DSBs; however, the role of the dNTP pool in DNA damage repair is not fully understood. Previous research shows that the dNTP pool remains unchanged after inducing DSBs, highlighting the importance of a tightly regulated dNTP pool. Using a neutral comet assay, we quantified accumulated double-stranded breaks in different treatment groups. We then analyzed these groups using immunofluorescent microscopy to examine distinct proteins involved in HR-mediated repair. We carried out RNA sequencing analysis to determine differential gene expression. We quantified cell viability and apoptotic cell populations via flow cytometry and Alamar blue assays. We determined protein interactions using immunoblotting and immunoprecipitation assays. We found that increasing the dNTP pool prior to IR treatment led to impaired DNA DSB repair in GBM cells as determined by a neutral comet assay. When analyzing key proteins involved in HR via immunofluorescence, we observed a significant decrease in RPA70 localization to the DNA damage site, indicating a disruption in end resection, a necessary phase of HR. Our RNA sequencing results show that increasing the dNTP pool in LN229 GBM cells prior to IR treatment caused significant changes in gene expression when compared to IR treatment alone. The most impacted pathways most were apoptosis, p53 cell cycle arrest, and DNA repair. The pathway analysis has identified genes of interest in the synergistic dNTP + IR treatment model. Significant increases in apoptosis and decreases in viability were observed 48 hours after inducing DSBs in LN229 cells with elevated dNTP pools. Not only do these data suggest that HR efficiency is reduced due to end resection impairment, but they also show that as a result, cell viability is destabilized due to prolonged DNA damage, resulting in apoptosis. The identification of this impairment may be essential in finding novel therapeutic approaches to sensitize therapy resistant GBM.

#1114 Evaluating strategies to harness metabolic vulnerabilities in cervical.

Julie K. Schwarz[1], Nishanth Gabriel[1], **Aunannya Banik**[2]

[1]Washington University School of Medicine, St Louis, MO,[2]Sweet Briar College, Sweet Briar, VA

Tumor cells frequently alter their metabolism to generate biomolecular intermediates for tumor maintenance and proliferation. Previous reports from Dr. Julie Schwarz's laboratory have shown that cervical cancer cells with altered AKT/mTOR pathways show increased reliance on glucose and exogenous glutamine. The laboratory has introduced PIK3CA E545K mutation and PTEN null mutation in cervical cancer cell line SiHa. Further, to evaluate the role of glutamine metabolism in these genotypes, these cells were cultured in sequentially lower levels of glutamine until these cells were able to proliferate without exogenous glutamine supplementation. These isogenic long-term glutamine-deprived (QD) cells allow us to tease out the role of these specific mutations in cellular metabolism. In our study, long-term glutamine deprivation inhibits the proliferation of rapidly proliferating PI3K-AKT-altered cell lines. Even though glutamine is required for GSH synthesis, which quenches reactive oxygen species, QD cells were refractory to cisplatin and irradiation. Since PI3K-AKT altered were dependent on exogenous glutamine, it was expected that QD cells would have lower GLS levels to inhibit glutaminolysis. However, GLS levels in WT and QD were similar. Altogether, these data indicate that in PI3K-AKT altered cervical tumor glutamine antagonists can reduce tumor proliferation. Further glutamine reduction does not alter GLS levels and hence GLS can be targeted as well to further improve treatment outcomes. To evaluate the alternate metabolic dependencies in cervical cancer tumors, both cellular as well as secreted metabolites were evaluated. To identify alternative pathways that are activated in these glutamine-deprived cell lines, we cultured these cells in uniformly labeled 13C glucose. Mass spectrometric studies also evaluated the protein levels of various metabolic intermediates in glutamine-deprived cell lines compared to control cells. To confirm our observations, we used kit-based assays to evaluate metabolites in the cells. To further confirm the change in the metabolite pathway we evaluated changes in transcriptional changes of regulating proteins/enzymes. This pre-clinical study reinforced efforts that are anticipated to reveal new metabolic vulnerabilities of cancer cells that can be targeted by therapeutic interventions. This study also helped us evaluate druggable metabolic targets that can be targeted for effective tumor eradication along with conventional treatment. This understanding will help advance the pre-clinical trials persistent to the cure of cervical cancer.

#1115 Enhancing lung cancer sensitivity to chemotherapy, radiation, and chemo-radiation through inhibition of a mitotic checkpoint kinase BUB1.

S. Thoidingjam, S. Sriramulu, S. L. Brown, F. Siddiqui, B. Movsas, S. Gadgeel, S. Nyati;
Henry Ford Health, Detroit, MI

Non-small cell lung cancer (NSCLC) and small cell lung cancer (SCLC) represent two major subtypes of lung cancer, marked by challenging treatment resistance. Our study explores the inhibition of BUB1, a critical mitotic checkpoint kinase, in conjunction with radiotherapy and chemotherapy. This approach has the potential to overcome resistance, thus enhancing the efficacy of treatment and improving treatment outcomes for lung cancer patients. We analyzed BUB1 expression in lung cancer using TCGA datasets and patient tissue microarrays (TMAs). In vitro experiments used four NSCLC and two SCLC cell lines with BUB1 inhibitor (BAY1816032), Paclitaxel, Cisplatin and Olaparib. Cells were irradiated (2, 4, or 6 Gy), and assays measured proliferation, long-term effects, DNA damage, and repair. Bioinformatic analysis in NSCLC subtype, lung adenocarcinoma (LUAD) demonstrated marked overexpression of BUB1, correlated with cancer stage, tumor grade and survival. Lung cancer TMAs revealed elevated expression of BUB1 protein in SCLC that correlated with poorer survival. BUB1 inhibition (BUB1i) induced cytotoxicity in LUAD cell lines at micromolar concentrations, while nanomolar concentrations enhanced cell death significantly when combined with radiation. Furthermore, BUB1i sensitized LUAD cells to different classes of chemotherapy (Paclitaxel, Cisplatin), and PARP inhibitor (Olaparib) alone (chemo-sensitization) or with radiation therapy (chemo-radiosensitization). H2030 and H1975 demonstrated higher chemo-radiosensitization efficacy compared to A549, likely due to genetic differences, potentially including a p53 mutation that improves sensitivity by affecting DNA repair and cell cycle regulation. Preliminary investigations revealed DNA double-strand breaks, indicated by prolonged γH2AX foci, and the inhibition of the NHEJ DNA damage repair pathway after BUB1 ablation. Among SCLC cell lines, NCI-H1876 demonstrated higher radiosensitivity upon BUB1 ablation compared to NCI-H2198, potentially due to genetic differences/mutations affecting radiation response. The study highlights the potential of BUB1i in enhancing the sensitivity of NSCLC and SCLC cells to radiotherapy and chemotherapy and provide rationale to explore BUB1i as a novel approach to enhance lung cancer therapy in clinical trials.

#1117 To investigate the effect of fluoxetine combined with radiation therapy on hepatocellular carcinoma.

B.-X. Chen[1], T. Liao[2], R.-E. Lu[1], F.-T. Hsu[1], Y. Chang[3],

[1]China Medical University, Taichung, Taiwan, [2]National Yang Ming Chiao Tung University, Taipei, Taiwan, [3]Taipei Medical University-Shuang Ho Hospital Ministry of Health and Welfare, New Taipei City, Taiwan

Hepatocellular carcinoma (HCC) is a highly prevalent and lethal primary liver tumor. It commonly occurs in individuals with chronic liver diseases, such as hepatitis B or C related cirrhosis. Despite conventional treatments, such as surgery and chemotherapy, the prognosis for HCC remains poor. The optimal treatment for patients with HCC is contingent on various factors, including the size and location of the tumor, the functional capacity of their liver, and their overall health status. Radiation therapy (RT) is a prevalent cancer treatment modality that targets rapidly dividing tumor cells by utilizing high-energy radiation. It is frequently administered alongside other treatments, such as surgery and chemotherapy, to improve the likelihood of successful cancer management. The timing of RT may vary, as it can be delivered before, during, or after other therapies depending on the patient's specific clinical situation. It's important to note that there are limits to the amount of radiation a patient's body can safely receive over their lifetime. For this reason, RT is often combined with other cancer treatments to enhance its effectiveness in sensitizing HCC cells. Fluoxetine is an anti-depressant drug that has also been shown to inhibit the growth of HCC. However, the potential role of fluoxetine in combination with RT for the treatment of HCC remains uncertain. In this study, we aim to identify whether fluoxetine may sensitize HCC to RT and evaluate its underlying mechanism. In this study, we employed the MTT assay and colon information to assess the cytotoxic effects of fluoxetine and radiotherapy (RT) at varying doses on HCC. Our findings, obtained through flow cytometry, revealed that the combination treatment can elicit extrinsic/intrinsic apoptosis in HCC cells. Specifically, this combination led to the loss of mitochondrial membrane potential, activation of cleaved-caspase-3, -8, -9, Fas, and FasL. Additionally, flow cytometry analysis showed an increase in the activation of PARP-1 and TUNEL, signifying DNA damage induction. Furthermore, we observed that fluoxetine not only enhances this DNA damage but also inhibits DNA repair, as shown through flow cytometry by the suppression of p-ATM and p-CHK2. Our western blotting assay confirmed that fluoxetine effectively inhibits HCC progression by activating LC3B, indicating the induction of autophagy in HCC cells. Moreover, the combined treatment, as demonstrated by transwell and wound healing assays, significantly reduced the migration and invasion capabilities of HCC cells. To conclude, the induction of apoptosis, DNA damage, and autophagy emerges as a crucial mechanism contributing to the heightened sensitivity of HCC cells to RT when combined with Fluoxetine. These results suggest that the combination of Fluoxetine with RT presents a promising novel approach for the treatment of HCC.

#1118 Mitigating radiation-induced lymphopenia using interleukin-15: Preclinical rationale for clinical translation.

Priti Gupta, Min Wang, Steven Lin

Radiation Oncology, UT MD Anderson Cancer Center, Houston, TX

Background: Radiation therapy is a common treatment for cancer patients, with nearly 50% of them undergoing this procedure. While radiation is effective at targeting tumor cells, it also has the unintended consequence of killing lymphocytes, which are among the most sensitive cells to radiation within the erythroid, myeloid, and lymphoid lineages. This phenomenon is known as radiation-induced lymphopenia (RIL) and is considered a negative prognostic factor in various malignant solid tumors. It occurs severely in over 40% of solid tumor patients who receive radiotherapy. Some previous studies have shown promising results with IL15 therapy in increasing circulating lymphocytes in cancer patients. However, until now, no studies have investigated the impact of IL15 in the context of radiation-induced lymphopenia. Our study aims to investigate whether IL15 can boost lymphocyte numbers and decrease tumor burden following radiation treatment in a mouse model.

Methods: To conduct our study, we subcutaneously injected TSA tumor cells into the flank region of mice. Once the tumors reached a palpable size, approximately 50mm^3, we divided the mice into four groups: Control (Con), Irradiation (IR), Control with IL15 (Con+IL15), and Irradiation with IL15 (IR+IL15). The irradiated mouse groups received a radiation dose of 2 Gray in the thorax and 1 Gray in the spleen for five consecutive days, simulating the severe radiation-induced lymphopenia observed in cancer patients. After the radiation treatment, the IL15-treated groups received IL15 in combination with recombinant IL15 in a 1:6 ratio weekly. Throughout the experiment, we monitored the circulating lymphocytes and tumor growth. After two weeks following the last radiation dose, we euthanized the mice, collected blood, spleen, and tumor samples, and identified immune cells using flow cytometry.

Results: The radiation treatment significantly increased tumor growth while decreasing the number of lymphocytes, including B cells, T cells, and NK cells, in the blood. IL15 administration led to an increase in the number of lymphocytes both in the blood and within the tumor compared to the irradiated group. We observed a trend toward reduced tumor growth in the group that received both IL15 and radiation (IR+IL15) compared to the group that received radiation alone (IR).

Conclusion: IL15 effectively boosted the number of lymphocytes in both the bloodstream and tumors, resulting in slower tumor growth in the IL15-treated group compared to the irradiated group. This study is of significant importance as it demonstrates the potential of IL15 to counteract radiation-induced lymphopenia in mice with TSA tumors. Further testing of these findings is currently underway in MC38 tumor-bearing mice, a cell line known to be more radiation-sensitive.

#1119 Novel fibroblast activation protein targeting radioligand for imaging and radiotherapy of solid tumors.

R. Mukkamala, L. D. Spencer, C. J. Daniel, P. Tudi, M. N. Kaine, A. Horner, S. Madduri, P. S. Low;
Purdue University, West Lafayette, IN

Fibroblast activation protein has emerged as an attractive biomarker for the imaging and therapyof ~90% of human epithelial cancers due to its expression on cancer associated fibroblasts (CAFs), but not on fibroblasts in healthy tissues. Not surprisingly, several small molecules and peptide-based radioligands that target FAP have been introduced into human clinical trials, but preclinical and clinical data suggest that these radioligand therapies suffer from inadequate tumor uptake, short tumor residence times, or unwanted uptake in the healthy tissues. Hence, there remains an unmet need for development of new FAP-targeted radioligands with improved therapeutic properties. For this purpose, we have designed and synthesized a higher affinity and specificity FAP-targetingligand (FAP8) and linked this ligand via a PEG spacer to both a well-known metal chelator (DOTA)and a 4(-iodo)-phenyl butyric acid pharmacokinetic extender to yield the trifunctional conjugate, FAP8-IP-DOTA. Binding affinity and FAP specificity studies reveal that FAP8-IP-DOTA exhibits high affinity and selectivity for FAP (IC_{50} = 1.6 nM) relative to its ubiquitous homologs' prolyloligopeptidase (IC_{50} = 16.5 nM) and dipeptidyl peptidase-IV (IC_{50} = 865.0 nM). Moreover, ^{177}Luand ^{111}In radiolabeled forms of the conjugate were found to bind a FAP-transduced cell line (HEK-FAP) with a K_d = 3.0 ± 2 nM, and this binding was completely suppressed upon co-incubation with unlabeled conjugate, i.e., further confirming FAP's specificity. SPECT/CT imaging studies following intravenous injection of ^{111}In labelled FAP8-IP-DOTA into mice expressing HT29, MDA-MB-231, KB or 4T1 tumors then demonstrated high tumor uptake and remarkably prolonged tumor retention of >8 days. Biodistribution studies of the ^{177}Lu labelledFAP8-IP-DOTA conjugate in mice implanted with either FAP-negative 4T1 tumor cells or FAP-transduced HEK tumor cells at different time points further revealed declining tumor radioactivity from 12.0 to 2.0 % ID/g and 21.0 to 12.0 %ID/g between 1h and 168h post injection, respectively. Importantly, uptake of the same conjugate in the healthy tissues was minimal over this time course, with most radioactivity clearing rapidly. Comparative dosimetry analyses showed tumor: healthy tissues ratios of >5-fold for all major organs. Finally, analysis of tumor inhibiting activity demonstrated that ^{177}Lu-FAP8-IP-DOTA suppressed tumor growth between 60% and 100% in all xenograft models tested (HT29, MDA-MB-231, KB and 4T1), with remarkably improved overall survival rates compared to untreated groups. Based on these promising results, we suggest that FAP8-IP-DOTA warrants further evaluation for possible translation into human clinical trials.

#1120 CD8 ImmunoPET imaging identifies an immunogenically active tumor microenvironment following radiotherapy in primary TNBC.

P. N. Song[1], S. E. Lynch[1], C. T. DeMellier[1], A. Mascioni[2], J. Fang[2], A. G. Sorace[1];
[1]University of Alabama at Birmingham, Birmingham, AL, [2]Imaginab, Inglewood, CA

Background: Tumor immune composition has been shown to drive therapy response in triple negative breast cancer (TNBC). Radiation is a component of standard-of-care treatments for TNBC, however immune populations have not been studied in the context of radiation resistance in breast cancer. Positron emission tomography (PET) allows for quantifying molecular signatures of the tumor microenvironment, which can precede anatomical changes in tumor volume. Recently, development of immune-targeted imaging approaches has allowed for noninvasive quantification of immune cells, allowing for quantification and long-term therapy response. Preclinical studies have demonstrated that combining therapies, such as radiotherapy and immunotherapy, could be beneficial in treating cancer. The goal of this study is to quantify changes in immune infiltration with [^{89}Zr]-CD8 ImmunoPET following radiation therapy to determine variations in immune activation that can affect therapeutic response in radiation sensitive or radiation resistant tumors.

Methods: Syngeneic radiation sensitive 4T1 or a radiation-resistant 4T1 tumors were treated with fractionated radiation (2 Gy/day) from day 0-5, injected with [^{89}Zr]-CD8 minibody on day 6, and imaged with [^{89}Zr]-CD8 PET on day 7. Following imaging, tumors were excised for biological assays (N = 20) or monitored for longitudinal changes in tumor volume (N = 15). Biological assays included CD8 immunofluorescence or assessment of immune population differences with flow cytometry against T-cells (CD3, CD4, CD8, IFN-gamma), macrophages (CD45, F4/80, CD86 and CD206), and natural killer cells (CD56 and CD16). A non-parametric T-test was used to assess for statistical differences.

Results: In radiation sensitive tumors, [^{89}Zr]-CD8 PET indicated that radiation significantly increases CD8 immune infiltration ($p = 0.02$) compared to controls, which was correlated with immunofluorescence ($p < 0.01$). Immune infiltration was increased in radiation sensitive tumors when treated with radiation therapy (4.6-fold increase in CD86+ M1-like macrophages, 4.7-fold increase in CD206+ M2-like macrophages, 5.3-fold increase in CD8 T-cells and 4.3-fold increase in CD4 T-cells) compared to control tumors. Radiation was observed to increase cytotoxic CD8 immune infiltration in radiation sensitive tumors. In radiation resistant tumors, no significant difference was observed in either CD8 immune infiltration or tumor volume in treated tumors compared to controls ($p = 0.63$).

Conclusions: [^{89}Zr]-CD8 ImmunoPET reveals significant increases in CD8 immune infiltration in a radiation sensitive model of TNBC and identifies an immune altered tumor immune microenvironment. Fractionated radiotherapy was also observed to significantly increase the infiltration of innate and adaptive immune cells.

#1121 Targeting the DNA damage response in high-risk medulloblastoma.

A. DeCarlo, C. Fernandes da Silva, L. Shen, V. Ramaswamy, U. Tabori;
SickKids, Toronto, ON, Canada

Medulloblastoma (MB) is the most common malignant pediatric brain tumour and is currently treated with surgery, external beam radiation and chemotherapy however, current treatments are woefully inadequate, with survival of only 50% but morbidity approaching 100%. A very-high risk group of SHH-activated MB harboring TP53 mutations (TP53mut-SHH) account for a substantial proportion of treatment failures after radiotherapy with a uniformly fatal outcome. Through optimizing radiation as a selection pressure and employing a functional genetic approach through whole-genome CrisprCas-9 dropout screening, the present study aims to identify drivers of radiation resistance and uncover unique vulnerabilities to sensitize these tumours to therapy. The dropout screen was conducted across a panel of established in vitro models of sporadic murine TP53mut-SHH, which resemble the human disease with profound radio-resistance. Initial results reveal that targeting the DNA damage response confer radiation sensitization. However, consistent hits across all models demonstrate non-homologous end-joining (NHEJ) as being synthetically lethal with radiation specifically in TP53mut-SHH. Genetic knockout experiments confirm genes encoding main proteins involved in NHEJ are synthetically lethal in combination with radiation. A small molecule drug screen targeting NHEJ revealed such vulnerabilities may be therapeutically exploited in TP53mut-SHH and are able sensitize these tumours to radiation. Using our unique approach of leveraging newly established models of TP53mut-SHH with a combination of functional genetic screening and small-molecule drug screening, this study highlights the genetic mechanisms of treatment resistance and reveals novel approaches for radiation sensitization. Here, we develop a novel approach to identify targets that are synthetically lethal with radiotherapy and identify multiple synthetically lethal targets at the genetic level which can be therapeutically targeted, allowing the development of new treatments to overcome current barriers.

#1122 Inhibition of HDAC6 enhanced radiation therapy induced antitumor response in melanoma.

X. Li[1], M. Suresh[1], H. Coulibaly[1], D. Quiceno-Torres[1], N. Gajendran[1], K. Tan[1], S. Noonepalle[1], S. Grindrod[2], A. Dritschilo[2], A. Villagra[1];
[1]Georgetown University, Washington, DC, [2]Shuttle Pharmaceutical Inc, Gaithersburg, MD

Patients with advanced melanoma are often treated with radiation therapy (RT) in combination with immunotherapies. Immunogenic tumor cell death induced by radiation is known to activate innate and adaptive immunity. Macrophage activity in the irradiated tumor microenvironment (TME) has been implicated to play a critical role in post-RT innate immune responses. However, tumor-associated macrophages (TAMs) due to their phenotypic plasticity convert from initial antitumor M1 phenotype to protumor M2 macrophages resulting in relapse and metastasis of any surviving tumor cells. Therefore, strategies regulating tumor macrophages post-radiation can enhance the therapeutic effectiveness of radiation therapy. Here, we report targeting HDAC6 function with a novel selective inhibitor (SP-2-225) as a potential therapeutic candidate for combination with RT. When administered intraperitoneally at a dose of 25mg/kg, SP-2-225 resulted in significant tumor suppression in the immunocompetent SM1 murine melanoma model. Phenotyping of tumor immune infiltrate indicated a profound decrease in M2 macrophages resulting in an M1/M2 macrophage ratio and an increase in CD8 effector memory T-cells. Further, in-vitro co-culture studies using trans-well assays indicated that irradiated tumor cells attract M2 macrophages, and treatment with SP-2-225 abrogated the M2 macrophage migration but did not alter M1 macrophage migration. In addition, 24 hours post-RT, intratumor administration of SP-2-225 treated M1 macrophages as adoptive cell therapy resulted in diminished tumor growth. The combination of conditioned M1 macrophages with an irradiated tumor microenvironment resulted in an increased M1/M2 ratio and infiltration of effector memory and central memory CD8 T-cells underscoring the influence of transplanted macrophages on the local antitumor immunity. Therefore, our findings demonstrate the ability of HDAC6 inhibitors to regulate macrophage function and phenotype as a cell therapy for use in combination with radiation therapy.

#1123 Genomic characterization of radiotherapy-associated bladder cancer.

N. Wijetunga[1], K. H. Gessner[1], K. Kanchi[1], S. E. Wobker[1], D. Corcoran[1], M. D. Galsky[2], M. I. Milowsky[1], W. Y. Kim[1], T. L. Rose[1], **J. S. Damrauer[1]**;
[1]University of North Carolina, Chapel Hill, NC, [2]Icahn School of Medicine at Mount Sinai, New York, NY

Background: Bladder cancer (BCa) is the 4th most common cancer diagnosed in men, with 82,290 new cases predicted in 2023. As BCa frequently occurs at an advanced patient age, its diagnosis may follow radiotherapy (RT) for the treatment of prostate cancer. Currently, data is limited regarding the influence of RT on the clinical course and genomic landscape of subsequent BCa, mainly due to a paucity of samples. From prior studies, pelvic radiation confers an increased risk of BCa, with resulting tumors that are largely genomically similar to non-RT tumors with the exception of an increase rate of genomic insertions. Our current study looks to expand on these findings by characterizing the genomes of the largest cohort of RT-associated bladder cancers to date.
Methods: We identified BCa cases from patients with a prior history of pelvic radiation for prostate cancer, and tumor only targeted sequencing was performed using Foundation Medicine (FMI) on FFPE tissue (n=41). For control cases (CTRL), patients with no prior record of pelvic radiation and who had previously underwent standard of care FMI sequencing were included (n=41). Sequencing data were re-aligned to hg38 and mutation calling was performed on the newly aligned sequences.
Results: CTRL and RT cohorts had similar distributions of patients based on race and smoking status. While cT stage was similar between the two cohorts, the CTRL cohort was biased toward higher cN and cM stages with no difference in overall survival (median OS: CTRL = 20m, RT = 23m), though the advanced stage of the CTRL cohort could mask a worse prognosis in the RT cohort. Latency specific analysis revealed short latency tumors (<10 years from RT) had a significantly shorter overall survival than long latency tumors ($p<0.01$, HR=5.59, CI=1.81-17.3), and a numerically, but not significantly, shorter survival than CTRL patients ($p=0.17$, HR=1.55, CI=0.82-2.94). Long latency tumor patients had a significantly longer overall survival than CTRL patients ($p<0.01$, HR = 0.22, CI=0.07-0.63). In line with prior studies, RT samples had increased numbers of insertions ($p<0.01$). In addition, we also detected an increase in SNVs in the RT samples ($p<0.01$). Of note, *KDM6A* alterations were enriched within the RT cohort (CTRL = 10/41, RT = 30/41, $p<0.001$), with series of splice site mutations exclusive to RT samples ($p<0.001$).
Conclusion: Patients diagnosed with BCa within a short interval following pelvic radiation have a worse prognosis. Genomic analysis showed RT-associated tumors having an increased number of insertions, SNVs, and *KDM6A* splice site mutations compared to non-RT tumors. Overall, the spectrum of recurrent alterations within the cohorts were consistent with previous studies, with the exception of the KDM6A mutations. To our knowledge, this is the first report of a RT-associated alteration in a specific gene in bladder cancer and additional studies will be needed to validate and understand the consequences of this finding.

#1124 Prevention of radiation-induced malignancies in Li-Fraumeni syndrome.

P. Psarianos[1], N. Fischer[2], D. Malkin[2];
[1]University of Toronto, Toronto, ON, Canada, [2]The Hospital for Sick Children, Toronto, ON, Canada

PURPOSE: Li-Fraumeni Syndrome (LFS) is a genetic disorder associated with a significant risk of early-onset cancer. This condition is driven by germline mutations in the *TP53* gene which plays a primary role in the regulation of the radiation response. Aberrant TP53 function contributes to radiation vulnerability and a greater risk of secondary, radiation-induced malignancies (RIMs). As a result, therapeutic options for LFS patients are often limited to exclude radiotherapy (RT), which may otherwise be beneficial for the treatment of certain primary tumors. Data from our lab demonstrate an aberrant transcriptomic response to irradiation (IR) in mutant p53 patient skin fibroblasts compared to wildtype; however, it is unknown whether reprogramming this radiation response can decrease the risk of RIM in LFS. Metformin, a commonly prescribed anti-diabetic drug, is associated with lower cancer incidence and may decrease cancer-related mortality in murine LFS models. In addition to its potential anti-tumorigenicity, studies have shed light on the ability of metformin to prevent IR-induced damage in normal tissue; hence, we hypothesize that metformin can reprogram the radiation response to protect against radiation injury and delay the onset of RIM in LFS.
METHODS: To establish a murine model of RIM in LFS, and to investigate whether metformin can delay tumor onset in this model, whole-body or localized IR were administered to mice harboring a hotspot *Trp53*$^{R172H/+}$ mutation in the presence and absence of metformin. Serial MRI was conducted to monitor for tumor development. To understand the effect of metformin on the mutant p53 radiation response *in vivo*, a similar murine workflow was established and irradiated skin was collected longitudinally from untreated and metformin-treated cohorts for whole transcriptome sequencing. Sequencing data were functionally validated in a separate cohort of mice using flow cytometry. In parallel, we performed RNA sequencing on LFS patient fibroblasts to characterize the effect of metformin on the human radiation response.

RESULTS: We demonstrate that IR decreases tumor latency in TP53$^{R172H/+}$ mice, and that metformin significantly delays tumor onset within the radiation field. Moreover, transcriptomic data revealed that metformin upregulates apoptosis following IR in TP53$^{R172H/+}$ mice. Flow cytometry analysis of the radiation response validated these findings, demonstrating that metformin promotes the apoptosis-driven clearance of damaged, potentially tumorigenic cells following IR. Transcriptomic data from patient cell lines will be presented.
CONCLUSIONS: Overall, we show that metformin may delay RIM in LFS mice, and have begun to characterize the biology underpinning this reprogrammed response to IR. This study is the first to highlight metformin as a radioprotective agent in the context of germline mutant p53, with the potential to broaden RT treatment options for LFS patients.

#1125 TNIK induced chemoradiation resistance in small cell lung cancer.

D. Dutta Chowdhury[1], E. Imada[2], N. Connis[3], T. Nguyen[1], J. Chang[1], D. Council[1], A. Lafargue[1], M. Rezaee[4], P. T. Tran[1], L. Marchionni[2], C. L. Hann[3]; [1]University of Maryland School of Medicine, Baltimore, MD, [2]Weill Cornell Medicine, New York, NY, [3]Johns Hopkins University School of Medicine, Baltimore, MD, [4]Johns Hopkins University, Baltimore, MD

Chemoradiation (CRT) is the standard first-line therapy for limited stage small cell lung cancer (LS-SCLC), which is characterized by early metastasis, intrinsic-acquired CRT resistance and tumor recurrence. CRT confers a 20-25% 5-year overall survival in patients with LS-SCLC. In this study, we utilized patient-derived xenograft (PDX) models to demonstrate CRT resistance of SCLC and identified CRT resistance candidate genes from various SCLC PDX that represent the majority of molecular subtypes (n=4 that include SCLC-A and SCLC-N subtypes). RNA-seq data identified *TNIK* (Traf2- and Nck-interacting kinase) as one such gene that is consistently upregulated in SCLC PDXs exposed to CRT compared to single modality treatments. Copy number gains of *TNIK* were also present in human SCLC samples. Overcoming this CRT resistance is crucial in improving treatment outcomes and patient survival. Genetic depletion or pharmacological inhibition of TNIK reduced the *in vitro* clonogenic survival of $TNIK^{high}$ SCLC cells, NCI-H446 and makes them increasingly sensitive to CRT. *In vivo,* pharmacological inhibition of TNIK with the inhibitor NCB-0846, enhances the CRT sensitivity of NCI-H446 cell line-derived xenografts (CDX) in NOD SCID immunodeficient mice. Furthermore, pharmacological inhibition of TNIK *in vivo* demonstrated sensitivity to CRT in LX33 PDX. In conclusion, our results indicate that *TNIK* plays a role in conferring resistance to CRT *in vitro* in SCLC cell lines and *in vivo* in SCLC CDX and PDX models and therefore, can be a potential therapeutic target in limited stage SCLC.

#1126 Extracellular vesicle mediated radioresistance in H3K27M-diffuse midline glioma.

V. Oza, S. Sampathi, Y. Chernyavskaya, K. Flores, J. Blackburn;
University of Kentucky, Lexington, KY

H3K27M-Diffuse Midline Gliomas (DMGs) are a subset of uncurable malignant pediatric gliomas and the deadliest form of brain tumors in children worldwide. Radiation therapy, the current standard of care, is initially effective but all tumors become resistant within 4-6 months. H3K27M-DMGs are heterogenous, comprised of an average of 6 genetically distinct subclones. Some subclones harbor mutations in genes previously linked to radiation resistance, such as *TP53*. We have found subclones are also functionally distinct, with some clones harboring intrinsic radiation resistance. Extracellular signaling between clones is linked with therapy resistance and tumor progression in other tumors, and we hypothesized that radioresistant H3K27M-DMG release small extracellular vesicles (sEVs) that impact the radiosensitivity of neighboring tumor cells. We found that all patient-derived H3K27M-DMG samples examined (n=6) produced sEVs (< 220nm), indicating this is a common feature in this tumor type. We isolated sEVs from a radioresistant (RR) patient-derived H3K27M-DMG cell line and used them to treat radiosensitive (RS) DMG cells. Using flow cytometry to profile sEV uptake dynamics, we found that RR-sEVs are internalized by RS cells within 2 hours of exposure and are retained at 18 hours ($p<0.001$, compared to control). This uptake can be significantly abrogated by proteinase K treatment of the sEVs, ($p<0.001$), indicating that uptake involves sEV surface proteins. We then applied a biosensor approach to assess single-cell phenotypic changes in RS DMG after RR-sEV treatment on radiation-induced cell death, DNA damage, and cell senescence, three dynamic processes. Using a genetically encoded death indicator (GEDI), we found that RR-sEVs significantly enhanced the survival of RS cells after acute radiation exposure ($p<0.001$). This was due to enhanced DNA damage repair as measured by 53BP1 foci ($p<0.01$). Small RNA sequencing of sEV cargo demonstrated that RR-sEVs express multiple miRNAs that are involved in oncogenic signaling such as the miR-7 family, miR-1246, and miR-1290 at several log fold higher than RS-sEVs. Overall, this data reveals the first functional role for sEVs in the context of radiation induced tumor transformation in DMG. We plan to further investigate the primary route of sEV uptake and define the mechanism through which sEV cargo alters radiosensitivity. This study provides new insight into the impact of heterogeneity and sEVs in mediating radioresistance in H3K27M-DMG and may lead to the development of novel radiosensitizers, which are critically needed for all patients.

#1127 Single cell network-based analyses reveal dose-dependent increase in myeloid suppressive cell sub-populations in response to radiation therapy.

A. Krishnan, S. Bansal, S. Sarti, M. D. Kissner, C. Karan, A. Califano, A. Z. Obradovic, C. S. Spina;
Columbia University Irving Medical Center, New York, NY

Background: More than half of all cancer patients undergo radiation therapy (RT) with curative or palliative intent. With the widespread use of immunotherapy to treat cancer, immune effects of radiation are an important consideration in design of sequential and combination therapies. While radiation has been found to deplete lymphocytes, less is known about its effects on the myeloid compartment, which includes both immune activating and suppressive populations. We hypothesized that a network-based analysis of single cell proteogenomic data generated from tumor-infiltrating immune cells can identify druggable proteins in pathways driving unwanted immunosuppressive changes with radiation, particularly among myeloid cells.
Methods: Proteogenomic (CITE-Seq) analysis was conducted on CD45+ immune cells from unirradiated and irradiated orthotopic 4T1 murine mammary tumors three- and ten-days after tumor irradiation (8 Gy x 1 or 8 Gy x 3). Based on expression of select surface proteins, analysis of the CITE-Seq data resulted in eight distinct immune clusters, including three myeloid clusters — monocytes, macrophages, and granulocytes. Using VIPER (virtual inference of protein activity by enriched regulon), an algorithm that infers protein activities from weighted expression on each protein's downstream targets, we identified distinct functional subpopulations within these eight clusters. Further profiling subclusters enriched by RT using the OncoTarget algorithm, we identified druggable proteins with significant inferred activity as potential targets of therapeutic interest.
Results: As expected, lymphocytes were persistently depleted after RT on both radiotherapy schedules. However, three distinct subclusters of myeloid cells with immune-suppressive phenotype became enriched following tumor irradiation, with greater enrichment at the lower radiation dose of 8 Gy x 1: TAM2, PMN1, and PMN4. Surface protein expression enabled us to define the immunophenotype and isolate these three cell clusters from murine 4T1 tumors as well as human renal cell carcinoma tumors for further functional analyses. OncoTarget identified a number of druggable targets, including PARP1 for the PMN1 subcluster.
Conclusion: Suppressive myeloid subpopulations induced by radiation were identified among the immune cells. Combining radiation therapy with inhibitors of these cell populations may provide therapeutic benefit over radiation therapy alone or in combination with checkpoint inhibitor immunotherapies. Future work will experimentally determine if inhibition of druggable protein targets in these myeloid subpopulations improves the overall efficacy of RT.

#1128 Association between gut microbial change and acute gastrointestinal toxicity in patients with prostate cancer undergoing definitive radiation therapy.

B.-S. Jang[1], **D. Lee**[2];
[1]Seoul National University Hospital, Seoul, Korea, Republic of, [2]College of Medicine, The Catholic University of Korea, Seoul, Korea, Republic of

Purpose: This prospective cohort study investigated the association between gut microbial changes and acute gastrointestinal toxicities in prostate cancer patients undergoing definitive radiation therapy (RT).
Methods: Seventy-nine fecal samples were analyzed. Stool samples were collected at the following timepoints: pre-RT (prRT), 2 weeks after the start of RT (RT-2w), 5 weeks after the start of RT (RT-5w), 1 month after completion of RT (poRT-1m), and 3 months after completion of RT (poRT-3m). We computed the microbial community polarization index (MCPI) as an indicator of RT-induced dysbiosis.
Results: Patients experiencing toxicity had lower alpha diversity, especially at RT-2w (P=0.037) and RT-5w (P=0.003). Compared to patients without toxicity, the MCPI in those experiencing toxicities was significantly elevated (P=0.019). In terms of predicted metabolic pathways, we found linearly decreasing pathways including carbon fixation pathways in prokaryotes (P=0.035) and the bacterial secretion system (P=0.005), in patients who experienced toxicities.
Conclusions: We showed RT-induced dysbiosis among patients who experienced toxicities. Reduced diversity and elevated RT-related MCPI could be helpfully used for developing individualized RT approaches.

#1129 A multifaceted study of X-Ray radiation therapy across diverse mouse tumor models.

J. Huang, W. Li, X. He, W. Cheng, L. Zhang, G. Li, Q. Li, Y. Wang, X. Ren, Z. Wei, L. Shi, Y. Wei, J. Jin, L. Li, W. Yun;
Pharmaron, Inc., Beijing, China

In this study, we showcase the application of X-ray radiation therapy of tumor-bearing mice across 13 syngeneic tumors, one intracranial tumor, and in combination with radiosensitizing drugs, aiming to develop potent cancer treatment strategies. 1.We examined the effects of different radiation levels on multiple tumor models using a therapeutic device delivering targeted radiation to the tumor site. 2.We investigated the combined benefits of radiation with the radiosensitizer Gemcitabine on the H22 liver tumor model. 3.We assessed the impact of radiation sensitization on the HCC1975-luc intracranial tumor model in combination with AZD0156, a drug that cannot cross the blood-brain barrier. The integrity of the blood-brain barrier and the presence of the pharmacodynamic marker pRAD50 of AZD0156 were evaluated. The results show that X-ray radiation has anti-tumor effects across diverse models, with combination drug treatment with both Gemcitabine and AZD0156 showing enhanced therapeutic effects. Furthermore, pRAD50 showed decreasing trend in the single dose PD study in HCC1975-luc intracranial model. We conclude that our platform provides robust methods for evaluating the therapeutic effects of X-Ray radiation, offering invaluable insights for the creation of new cancer therapies.

CLINICAL RESEARCH: Spatial Proteomics and Transcriptomics
Poster Session

#1134 Dissecting pancreatic cancer tumor-immune microenvironment crosstalk using spatial transcriptomics.

A. Pankaj[1], M. J. Raabe[1], B. K. Patel[1], E. R. Lang[1], J. R. Kocher[1], K. H. Xu[1], L. T. Nieman[1], W. L. Hwang[2], A. C. Kimmelman[3], D. P. Ryan[2], T. S. Hong[2], M. J. Aryee[4], **D. T. Ting**[1];

[1]Massachusetts General Hospital, Charlestown, MA, [2]Massachusetts General Hospital, Boston, MA, [3]NYU Langone Health, New York, NY, [4]Dana-Farber Cancer Institute, Boston, MA

Background: Pancreatic ductal adenocarcinoma (PDAC) often fails to respond to immune therapies due to various factors, including the role of Epithelial to Mesenchymal Transition (EMT) plasticity in conferring broad resistance to diverse therapies. However, the relationship between cancer cell heterogeneity and the tumor immune microenvironment remains unclear. To address this, we utilized single cell RNA-seq and spatial transcriptomics to uncover the landscape of these cell-cell interactions in human PDAC. Here, we applied to specimens from a clinical trial testing Losartan, an indirect TGF-beta inhibitor with FOLFIRINOX chemotherapy and nivolumab (anti-PD1) in a randomized multi-institutional clinical trial for PDAC (NCT03563248).
Methods: Using the NanoString GeoMx Digital Spatial Profiler, we selected multiple regions of interest in formalin-fixed paraffin-embedded (FFPE) human PDAC specimens. Immunofluorescent antibody-guided isolation of RNA and protein from cancer cells (pan-cytokeratin), cancer-associated fibroblasts (alpha-SMA), and immune cells (CD45) were performed. Utilizing the whole transcriptome assay (WTA; 18,000+ protein-coding genes) and a new IO Proteome Atlas (IPA; 500+ plex proteins), we ventured to understand the relationship between tumor cells and the surrounding microenvironment.
Results: PDAC cells, CAFs, and immune cells were successfully characterized using NanoString GeoMx in clinical trial specimens. Analysis revealed associations between cancer cell plasticity, TGF-beta signaling mesenchymal subtypes in PDAC cells. These TGF-beta enriched mesenchymal PDAC cells were enriched in Arm 1 (FOLFIRINOX) compared to Arm 2 (FOLFIRINOX+losartan). Immune deconvolution analysis identified variations in immune infiltrates, showing an anti-correlation between macrophages and T-cells. The IPA analysis revealed lower MHC I protein levels in short compared to long term survivors in Arm 3.
Conclusions: Spatial transcriptomics and proteomics reveal insights into the spatial relationship between PDAC tumor cell EMT plasticity, CAFs, and immune infiltrates. This enables the discovery of novel immune response biomarkers and potential therapeutic avenues to target tumor and microenvironment interactions.
Trial Registration: DF/HCC protocol 18-179: Losartan and Nivolumab in Combination With FOLFIRINOX and SBRT in Localized Pancreatic Cancer. NCT03563248
Ethics Approval: All studies presented were approved by the Dana-Farber/Harvard Cancer Center IRB protocols 18-179.

#1136 Tumor genomic and transcriptomic profiling of patients (pts) with metastatic castration sensitive prostate cancer (mCSPC) who do versus do not achieve an optimal PSA response to androgen deprivation therapy intensification (ADTi).

V. Mathew Thomas[1], B. Chigarira[1], G. Gebrael[1], C. Chehade[1], A. Narang[1], N. Sayegh[1], N. Tripathi[1], Y. Jo[1], C. Tandar[1], A. Srivastava[1], R. Ji[1], E. Dal[1], G. Fortuna[1], H. Li[2], B. L. Maughan[1], U. Swami[1], N. Agarwal[1];

[1]University of Utah Huntsman Cancer Institute, Salt Lake City, UT, [2]University of Kansas Cancer Center, Salt Lake City, UT

Background: Pts with mCSPC receiving ADTi and achieving PSA nadir ≤0.2 ng/mL (PSA-L) have better overall survival (OS) compared to those with a PSA nadir > 0.2 ng/mL (PSA-H). We investigate differences in genomic and transcriptomic profiling between PSA-L and PSA-H.

Methods: In this IRB-approved retrospective study, eligibility criteria included confirmed mCSPC receiving ADTi and having comprehensive genomic profiling (CGP) performed by a CLIA-certified lab (Foundation Medicine and Tempus). Transcriptomic profile was evaluated from Tempus cohort. Pts were divided into 2 groups: PSA-L and PSA-H based on achieving a PSA nadir ≤0.2 ng/mL at any time during treatment course. The DEseq2 pipeline was used to analyze differentially expressed genes between the groups. The data included the Log2 fold change, Wald-Test p-values, and Benjamini-Hochberg adjusted p values (q values) for each differentially expressed gene. These results were subjected to Gene Set Enrichment Analysis (GSEA) to identify pathways enriched in each cohort. All bioinformatic analysis was undertaken using R studio v4.2.

Results: 248 pts were eligible for genomic analysis (PSA-L=166, PSA-H=82). The top 5 most commonly altered genes were *TMPRSS2, TP53, PTEN, APC,* and *SPOP.* Genomic analysis did not reveal significant differences between PSA-L and PSA-H. 78 pts were eligible for transcriptomic analysis (PSA-L=55, PSA-H=23). Table shows differences in the expression of pathways between PSA-L and PSA-H.

Conclusion: While there were no significant differences in genomic aberrations between PSA-L and PSA-H, gene expression profiling showed significant variations in crucial pathways, particularly the AR pathway, which might explain the better outcomes in PSA-L. After external validation, these findings may help personalize medicine prior to initiation of therapy.

Differential gene set expression scores in PSA-L vs. PSA-H

Pathway	**Normalized Enrichment Score (NES)***	**p-value**	q-value
TNF-α signaling via NFKB	2.5	<0.01	<0.01
Androgen Response	1.7	<0.01	<0.01
Estrogen Response	1.7	<0.01	<0.01
Interferon-α	1.5	<0.01	<0.01
Bile Acid Metabolism	-1.5	<0.01	<0.01
Coagulation	-1.7	<0.01	<0.01
Epithelial Mesenchymal Transition	-1.9	<0.01	<0.01

#1137 Spatial expression profile of mucinous cystic neoplasm indicates a divergent malignant marker patterns in ductal and stromal regions.

A. Ghodrati, C. S. Gopinath, A. Parvizi, M. Gnanamony, L. Demirkhanyan, C. S. Gondi;
University of Illinois College of Medicine (Peoria), Peoria, IL

Mucinous cystic pancreatic neoplasms (MCPN), initially characterized as benign, present a unique challenge, with the five-year survival rate dropping from 100% to 57% if malignancy occurs. In this study, we using spatial genomic expression analysis of MCPN, and focus on the correlations between marker expression patterns in stroma and ductal region. Tissues obtained from surgical samples of a 69-year-old patient with a pancreatic head cystic mass and a history of pancreatitis (staged as T3N1Mx) were embedded in paraffin. These tissues were then sectioned, collected onto subbed slides, and subjected to probe hybridization, ligation, and extraction onto Visum slides following the manufacturer's instructions (10X Genomics). Genomic expression was extracted using established protocols, processed through SpaceRanger, and further visualized in Loupe Browser (10X Genomics). A comparison was conducted between the ductal and stromal regions, both with and without cystic involvement. Our study reveals a significant 5.1 $\log_2$ fold increase in MUC5AC expression in the ductal region, regardless of cystic involvement, suggesting implications for apoptosis regression and cadherin-dependent cell adhesion in MCPN progression. Further analysis indicates a significantly higher expression of TMSB4X exclusively in the ductal region, extending into the surrounding stroma, potentially stimulating MCPN progression by fostering pro-inflammatory cytokine environments. The novel marker IGKC, indicating favorable prognosis and PDAC treatment efficacy, shows high expression in the stroma (1.8 $\log_2$ fold higher). However, around the duct with cystic involvement, its expression is notably reduced (-1.7 $\log_2$ fold lower), suggesting pathways that may contribute to MCPN's progression towards a more invasive PDAC phenotype. Additionally, our study reveals a 1.9 $\log_2$ fold elevated expression of FN1, a biomarker associated with poor outcomes in PDAC patients, in the stroma around the cyst, hinting at a possible pathogenic role of FN1 in cell adhesion, migration, and progression of MCPN to PDAC. Co-expression of FN1 with COMP and TIMP3 within MCPN suggests a concerted effort in the microenvironment, influencing tissue development, maintenance, and extracellular matrix remodeling. Co-localization of FN1 with COMP and TIMP3, particularly within degenerating acinar cells, hints at a potential mechanism in the intricate progression of MCPN to PDAC. These findings contribute to a deeper understanding of the molecular landscape of MCPN, offering potential avenues for targeted interventions to thwart its progression to PDAC, guiding novel diagnostic and therapeutic strategies for pancreatic neoplasms. Further expression data will be presented.

#1138 A single-cell spatially resolved atlas of immune-mediated control of lung adenocarcinoma using 1,000-plex single-cell spatial molecular imaging in a transgenic mouse model.

T. Panciera[1], F. Zanconato[1], M. Cordenonsi[1], M. Forcato[1], G. Vanni[1], S. Bicciato[1], J. Preciado[2], S. Ilcisin[2], K. V. Raay[2], M. Hoang[2], M. Patrick[2], **S. He**[2], J. Beechem[2], S. Piccolo[1];

[1]University of Padua School of Medicine, Padua, Italy, [2]Nanostring Technologies, Seattle, WA

Background: Lung adenocarcinoma is one of the leading causes of cancer-related mortality. One of the most frequently occurring mutations in lung cancer is KRAS mutations. Recent development of chemical inhibitors that specifically target oncogenic variants of Ras, particularly the commonly mutated KRAS-G12D isoform, represents a significant breakthrough in targeted therapeutics. The tissue-level mechanisms underlying the cell-autonomous and non-cell-autonomous effects of KRas-G12D inhibitors are poorly understood. Additionally, the effectiveness of KRas-G12D inhibitors in lung cancer models remains unknown. To address these gaps in knowledge, we analyzed the spatial interactions between cancer cells and the surrounding tissue microenvironment during the process of tumor eradication mediated through KRas-G12D inhibitors.

Methods: We utilized a genetic mouse model of non-small cell lung cancer (NSCLC), driven by the activation of KRas-G12D in combination with the loss of p53. We investigated the immune-mediated tumor recognition following the targeting of KRas-G12D in an immunocompetent setting. Lung samples were collected from control mice and treated. Spatial transcriptomic analysis (CosMx™ SMI 1,000-plex Mouse Universal Cell Characterization Panel) were employed to obtain a high-plex, single-cell, temporal and spatially resolved molecular atlas of lung tumor regression.

Results: Prior to Kras inhibitor treatment, mice displayed both LuAD and lung adenomas. Lesion size and histological grade progressively decrease during pharmacological treatment with Kras inhibitor. 906 unique genes were detected above background on intact FFPE tissue slides, along with 4 protein markers for optimal single-cell segmentation results. Concordance between CosMx SMI and scRNAseq was assessed and demonstrated high assay sensitivity and specificity of the CosMx assay. LUAD cell subtypes were identified and showed distinct spatial features. Molecular states, and receptor-ligand interactions, within niche-specific signaling networks were investigated to underline molecular mechanism of immune attack and eventual eradication of tumors.

Conclusion: This study provides novel insights into the temporal and spatial dynamics of KRas-G12D inhibitor-mediated tumor regression in lung cancer, shedding light on the previously unknown cell-cell interactions occurring during this process. By investigating these spatiotemporal aspects, we aim to enhance our understanding of lung cancer biology and potentially identify new immunotherapeutic biomarkers. Moreover, the research tools used in this study have implications for the design of future preclinical studies exploring the potential of immuno-oncology combination therapies. FOR RESEARCH USE ONLY. Not for use in diagnostic procedures.

#1139 Unravelling tumor heterogeneity in patients with HER2-low hormone receptor-positive breast cancer using spatial transcriptomics.

D. Fimereli[1], M. Serra[1], M. Rediti[1], F. Lifrange[2], N. Occelli[1], L. Collet[1], D. Vincent[1], G. Rouas[1], L. Craciun[1], D. Larsimont[1], D. Venet[1], M. Vikkula[3], F. P. Duhoux[4], F. Rothe[1], C. Sotiriou[1];

[1]Institut Jules Bordet, Brussels, Belgium, [2]University Hospital Center of Liege, Liege, Belgium, [3]de Duve Institute, Brussels, Belgium, [4]Institut Roi Albert II, Cliniques universitaires Saint-Luc, Brussels, Belgium

Background: The current binary distinction between HER2-positive and HER2-negative breast cancer (BC) has recently been challenged by the emergence of the HER2-low entity. Antibody-drug conjugates targeting HER2 have shown efficacy in both HER2-positive and HER2-low BC, while some preliminary evidence showed efficacy also in patients with HER2-zero BC. Here, by combining spatial transcriptomics (ST) and morphological annotation, we aimed to investigate the inter- and intra-tumor heterogeneity of ERBB2 expression in relation to breast cancer IHC subtypes.

Methods: We performed ST (Visium 10X Genomics) on frozen tumor samples from patients with hormone receptor positive (HR+) ductal BC with HER2 IHC staining and FISH. Hematoxylin/eosin slides were morphologically annotated integrating manual and machine learning-based approaches reaching single-cell resolution (QuPath software). The relative histomorphological categories composition of each spot across the ST slide was computed as percentage of pixels. Spots were defined as tumoral if the percentile of pixels in that spot surpassed the 80th percentile of all the tumor spots in the cohort.

Results: Our cohort consisted of 56 HER2-zero (IHC 0), 30 HER2-low (IHC 1+) and 20 HER2-positive (IHC 2+/FISH positive or IHC 3+) samples. HER2-zero samples contained a significantly higher percentage of acellular stroma spots compared to HER2-low (pvalue=0.04), while no other morphological annotation showed a difference, including tumor spots. Only tumor spots were retained for downstream analysis. A difference in the ERBB2 gene expression was found at the spot level, with a higher expression in HER2-low samples compared to HER2-zero samples (median expression 0.4, 0.7 and 3.1 in HER2-zero, HER2-low and HER2-positive, respectively). Inter-sample heterogeneity was observed, with 27% of the HER2-zero samples having equal or higher mean ERBB2 expression that the mean ERBB2 expression of the HER2-low cohort. Variability within individual samples was observed, revealing two peaks in ERBB2 expression, one characterized by low levels and the other by medium-high levels. This pattern was frequently observed in samples classified as HER2-zero and HER2-low, indicating the existence of tumor spots with diverse ERBB2 expression.

Conclusions: Our results revealed inter- and intra-tumor heterogeneity of ERBB2 expression in HER2-zero and HER2-low BC. The use of spatial transcriptomics can provide more details of the spatial distribution of ERBB2. Further validation is warranted.

#1140 A spatially mapped gene expression signature for intestinal stem-like cells identifies high-risk precursors of gastric cancer.

I. A. Wichmann[1], R. J. Huang[1], A. Su[2], A. Sathe[1], M. V. Shum[1], S. M. Grimes[1], R. Meka[1], A. Almeda[1], X. Bai[1], J. Shen[1], Q. Nguyen[2], M. Amieva[1], J. Hwang[1], H. P. Ji[1];

[1]Stanford University School of Medicine, Stanford, CA, [2]The University of Queensland, Brisbane, Australia

Gastric intestinal metaplasia (GIM) is a precursor lesion for the intestinal subtype of gastric cancer (GC). A risk stratification tool is the Operative Link on GIM (OLGIM), a system that relies on histopathologic annotation of gastric biopsies. Advanced OLGIM (stages III and IV) have the highest risk of progression to GC. Molecular biomarkers for advanced OLGIM are lacking. We explored transcriptomics biomarkers for advanced OLGIM to aid risk assessment efforts among GC precursors.We used clinical and genomic data from four cohorts: 1) GAPS, a cohort of OLGIM-staged patients (N=303); 2) a subset of confirmed intestinal-type GC from The Cancer Genome Atlas (TCGA, N=198); 3) a compilation of scRNA-seq data (N=40), and 4) a spatial transcriptomics cohort (N=5) with annotated H&E-stained histopathology slides from GC or OLGIM-staged patients.We separated the GAPS bulk RNAseq gene expression dataset into independent discovery (N=88) and validation (N=215) sets. Through a combination of differential expression analysis and co-expression analysis, we identified a discrete set of 100 significantly upregulated genes characterizing advanced OLGIM that were confirmed in the validation set. Importantly, these genes were overexpressed both in the corpus and antrum of the stomach. We leveraged spatial transcriptomics assays to refine this signature to genes overexpressed specifically in GIM foci. We interrogated the TCGA dataset and confirmed these genes to be also expressed in gastric tumors. The final high-risk signature included 26 genes. Single-cell RNAseq analysis revealed these genes to be expressed by aberrant intestinal-like lineages. Further, reference-mapping identified cells resembling mature enterocytes and goblet cells that expressed 16 of these genes, whereas 10 genes from the high-risk signature pinpoint immature intestinal stem-like cells at varying stages of differentiation (duodenum stem cells, duodenum differentiating stem cells, and duodenum transit amplifying cells). Finally, we confirmed expression of 12 of these genes by single-molecule fluorescence *in situ* hybridization (smFISH), that distinguish differentiated from stem-like lineages in metaplasia and are absent in normal gastric glands in intact tissue sections from GC precursors.Our study identified as signature of 26 genes that are: i) characteristically over-expressed in advanced OLGIM stages, ii) localize specifically to metaplasia, iii) are expressed in gastric tumors, and iv) distinguish differentiated from stem-like cells in GIM. These results provide transcriptomics biomarkers that indicate the establishment and expansion of intestinal stem-like cells in advanced OLGIM, with profound translational implications, as these cells may harbor and expand mutations that predispose advanced OLGIM patients to GC.

#1141 Spatial-specific gene signatures to predict immunotherapy outcomes in lung cancer.

T. N. Aung[1], M. Moutafi[2], I. Trontzas[1], A. Kulasinghe[3], J. Monkman[3], N. Gavrielatou[2], I. Vathiotis[4], J. H. Warrell[5], D. L. Rimm[1];

[1]Department of Pathology, Yale University School of Medicine, New Haven, CT, [2]School of Medicine, National and Kapodistrian University of Athens, Anthens, Greece, [3]Frazer Institute, Faculty of Medicine, The University of Queensland, Brisbane, Australia, [4]Oncology Unit, 3rd Department of Internal Medicine, Sotiria Hospital, National and Kapodistrian University of Athens, Anthens, Greece, [5]Department of Molecular Biophysics and Biochemistry, Program in Computational Biology and Bioinformatics, Yale University, New Haven, CT

The widespread use of immunotherapy in lung cancer, and its more recent approval for early stages, underscores the need for biomarkers that can identify the most responsive patients. Spatial transcriptomics, which maps gene expression in its spatial tissue context, offers a unique approach over bulk transcriptomics. By incorporating spatial information, the predictive power of the signature can be enhanced. Here, we aim to develop spatially informed gene signatures that could be translated into clinical RNA in situ assays, distinguishing patients unlikely to benefit from immunotherapy and thereby sparing them unnecessary side effects. We utilized the NanoString GeoMX Whole Transcriptome Atlas for spatially resolved transcriptomic profiling of retrospectively collected lung cancer tissue samples from patients treated with immunotherapy in an advanced-stage setting (N=60). By targeting 18,190 genes within distinct areas of interest (AOIs)—including stromal (macrophages/CD68+ and leukocytes/CD45+) and tumor (cytokeratin, CK+) cells—we developed AOI-specific gene signatures to predict objective responses. These were derived from a robust computational framework employing LASSO logistic regression on a split-sample approach, yielding predictive models for treatment outcome.We achieved high predictive accuracy on the training set, with the area under the curve (AUC) exceeding 0.86 for all AOI-specific spatial signatures, indicating strong potential for clinical application. Validation against an independent cohort (N=42) corroborated the efficacy of these signatures. Our 6-gene tumor signature was validated with an AUC of 0.73 (95% CI: 0.67-0.89, p = 0.009**), while the CD45 5-gene signature showed an AUC of 0.75 (95% CI: 0.53-0.97, p = 0.022*). Our 18-gene CD68 signature trended towards validation but lacked statistical significance. A combined CD68 and CD45 signature predicted outcomes with greater accuracy, achieving an AUC of 0.79 (95% CI: 0.62-0.98, p = 0.0088*). Following gene set enrichment analysis on our differentially expressed and signature genes, we identified genes with positive coefficients in both tumor and stroma signatures that were associated with glucocorticoid response and glycolytic processes linked to T-cell homeostasis, while genes with negative coefficients were associated with epithelial cell differentiation and cytokine production. These associations are concordant with the observation that genes with positive coefficients are predictors of treatment response, while those with negative coefficients indicate resistance.Our findings indicate that AOI-specific signatures predict the immunotherapy outcome in lung cancer with high accuracy, suggesting that spatial assessment can provide substantial predictive information. The high performance of these signatures indicates their potential for prospective clinical applications.

#1142 Spatial decomposition of lung adenocarcinoma expression subtypes reveals tumor microenvironment characteristics.

S. He[1], C. Alba[2], S. Kounelis-Wuillaume[3], T. J. Franks[4], M. L. Doughty[3], R. F. Browning[5], C. D. Shriver[5], C. L. Dalgard[6], APOLLO Research Network, M. D. Wilkerson[6];

[1]John P. Murtha Cancer Center Research Program, Uniformed Services University; Henry M. Jackson Foundation for Military Medicine, Bethesda, MD, [2]Center for Military Precision Health, The American Genome Center, Uniformed Services University; Henry M. Jackson Foundation for Military Medicine, Bethesda, MD, [3]Department of Anatomy Physiology and Genetics, Uniformed Services University, Bethesda, MD, [4]Pulmonary & Mediastinal Pathology Department of Defense, The Joint Pathology Center, Silver Spring, MD, [5]John P. Murtha Cancer Center Research Program, Uniformed Services University, Bethesda, MD, [6]Center for Military Precision Health, The American Genome Center, Uniformed Services University; Department of Anatomy Physiology and Genetics, Uniformed Services University, Bethesda, MD

The expression subtypes of lung adenocarcinoma (LUAD) capture tumors with distinct pathway activity, mutations and histopathology and also differentiate clinical outcomes. The microenvironments of these subtypes, proximal-inflammatory (PI), proximal-proliferative (PP), and terminal respiratory unit (TRU), have been described generally as immune hot, immune moderate and immune cold, respectively, but otherwise have not been analyzed at high resolution. Here, we aimed to characterize and compare tumor microenvironments between LUAD subtypes. Using spatially barcoded arrays and cDNA libraries (10x Genomics), we sequenced the spatial transcriptomes of a 6.5mm^2 plane of 14 LUAD tumors from the Applied Proteogenomics and Organizational Learning Outcomes (APOLLO) program. Spatial transcriptomes had a median of 3,560 spots and a median of 4,026 genes detected per spot. First, collapsing the spatial array to a bulk measurement per sample, we applied our published expression subtype predictor classifying 4 PI, 5 PP, and 5 TRU cases. We then decomposed each tumor's spatial expression profile by unsupervised clustering, followed by signature scoring and collapsing into tumor, immune, and stroma tumor microenvironment (TME) components. Twelve of the fourteen tumors harbored multiple components while two tumors had one component. The region areas of TME components showed trends among the subtypes, with PI having the greatest immune area and PP having the greatest tumor area. Within each tumor, we calculated differentially-expressed genes between each TME component. Comparing TME genes to the subtype predictor genes, we found significant overlap (chi-square $p << 0.001$). This indicates that genes that are variable among bulk tumors also have variability within tumors. We then predicted expression subtype for decomposed compartments. Five tumors had the same expression subtype across their TME components, which we refer to as single subtype tumors. However, six tumors had more than one expression subtype prediction among the tumor's TME components, which we call 'multi-subtype tumors'. Multi-subtype tumors had lower bulk subtype prediction scores than single-subtype tumors ($p < 0.01$), indicating that the TME diversity among tumors affects the bulk expression subtype. Interestingly, the six multi-subtype tumors were in the PP and PI subtypes, suggesting greater TME component diversity than TRU. Calculating the spatial compactness of the tumors through continuity indices, we found that PI subtype trended with greater intermixing of TME components. In summary, the bulk LUAD expression subtypes capture differences between tumors and within tumors related to the tumor microenvironment. The views expressed in this abstract are solely of the authors and do not reflect the official policy of the Departments of Army/Navy/Air Force, Department of Defense, USUHS, HJF, or U.S. Government.

#1143 Dissection of melanoma and cutaneous lymphoma spatial molecular architecture by multimodal single-cell and spatial transcriptomics with generative AI.

Z. Liu[1], X. Song[2], J. He[3], J. He[3], J. Balasi[4], J. H. Chuang[1], P.-L. Chen[4];
[1]The Jackson Laboratory for Genomic Medicine, Farmington, CT, [2]H. Lee Moffitt Cancer Center & Research Institute, Tampa, FL, [3]Vizgen, Cambridge, MA, [4]Moffitt Cancer Center, Tampa, FL

Advances in single-cell multiomic technologies have revolutionized our understanding of how heterogeneous cell types and cell states shape the tumor microenvironment (TME). However, dissociated single cell profiling lacks spatial context. To resolve the organization, cell-cell communication, and granular structures in the TME, new single-cell spatial transcriptomic (ST) characterizations are needed. Here, we dissected the spatial molecular architecture of the melanoma (30 tumors, 30 patients) and transformed cutaneous T-cell lymphoma (tCTCL, 12 tumors, 6 patients) TMEs by Multiplexed Error-Robust FISH (305 gene MERFISH), with benchmarking scRNAseq data from matched tissues (6 melanoma scFFPEseq, 6 tCTCL scVDJ/RNAseq) for cross-platform validation. We profiled 565,122 cells in melanoma and 92584 cells in tCTCL by MERFISH. We interrogated both datasets using a novel computational framework that includes cell typing by Leiden clustering and marker genes, spatial neighborhood and receptor-ligand (R-L) analyses, and spatial/scRNA imputation via deep learning. In the melanoma dataset, we identified tumor cells, major TME cell types, and rare immune cell types (TCF7+ stem-like T-cells and CD3+TCRα+PAX5+CD79a+ B/T dual-expressor lymphocytes enriched in tertiary lymphoid structures). All cell types were validated in scFFPEseq. As immune R-L interactions are critical therapeutic targets, we developed a novel computation method to quantify spatial R-L interactions by accounting for cell-cell distance, identifying spatially informed R-L pairs that differ from dissociation-based inferences. CNV inference from melanoma scFFPEseq revealed intratumoral heterogeneity (ITH). We therefore adapted the conditional variational autoencoder ENVI to simultaneously incorporate scRNA and MERFISH spatial data into a unified latent embedding. ENVI-ITH successfully learned ITH subgroup information, enabling imputation of phylogenetic lineages on spatial MERFISH. CTCL MERFISH data revealed major TME cell types, yet separation of malignant vs benign T-cells by clustering and marker approaches is hindered by their overlapping gene expression. To overcome this barrier, we deployed ENVI to impute patient-specific malignant and benign TCR clonotypes by training on the matched scVDJ/RNA data, yielding an ENVI-TCR pipeline that can delineate malignant vs benign T-cells *in situ*. We validated the spatial pattern of malignant T-cells by patient-specific *in situ* TCR probes. In sum, we have interrogated the melanoma and CTCL TME by MERFISH and presented a novel computational framework for robustly co-embedding scRNA data with imaging-based ST to spatially resolve melanoma ITH and malignant/benign T-cell populations. We believe this approach will be highly impactful for melanoma and CTCL and can be broadly applied to other solid tumors and lymphomas.

#1144 Glioblastoma cells increase expression of neurodevelopmental programs and synaptic connectivity in the tumor periphery.

D. Harwood[1], V. Pedersen[1], N. S. Bager[1], A. Y. Schmidt[2], T. O. Stannius[2], A. Areskeviciute[2], K. Josefsen[2], D. S. Noroxe[1], D. Scheie[1], H. E. Rostalski[1], U. Lassen[1], F. O. Bagger[2], J. Weischenfeldt[1], D. H. Heiland[3], K. Vitting-Seerup[4], S. R. Michaelsen[1], B. W. Kristensen[1];

[1]University of Copenhagen, Copenhagen, Denmark, [2]Rigshospitalet, Copenhagen, Denmark, [3]University of Freiburg, Freiburg, Germany, [4]Technical University of Denmark, Copenhagen, Denmark

Glioblastoma remains one of the deadliest brain malignancies. First-line therapy consists of maximal surgical tumor resection, accompanied by concomitant and adjuvant temozolomide chemotherapy and radiotherapy. Malignant cells escape surgical resection by migrating into the brain parenchyma, where they give rise to the recurrent tumor. Based on gene expression, the tumor core can be subtyped into mesenchymal, proneural and classical areas, each being associated with differences in genetic alterations and cellular composition. In contrast, the tumor periphery where migrating tumor cells infiltrate brain parenchyma is less characterized in patients. Using spatial transcriptomics (n = 11), we show that specific malignant states colocalize in tumor core areas with necrosis and microvascular proliferation. Malignant cells within proneural or mesenchymal subtyped cores displayed, as expected, many differences in genetic expression, although such differences disappeared in the tumor periphery. Malignant cells residing in the tumor periphery had increased expression of genes related to neurodevelopmental pathways and synaptic connectivity. Our findings show similarities in cellular states across tumor subtypes with implications for post-operative treatment and provide an updated view of the spatial landscape of glioblastomas.

#1145 Comparative spatial transcriptomic analysis of tumor microenvironment responses to conventional chemotherapy and immunotherapy in triple-negative breast cancer.

D.-E. Gu[1], J. Hyeon[2], E. Seo[2], H. Jung[2], J. Yu[2], S. Kim[2], Y.-H. Im[2], J.-Y. Kim[2], W.-Y. Park[2];
[1]Sungkyunkwan University, Seoul, Korea, Republic of, [2]Samsung Medical Center, Seoul, Korea, Republic of

Background: In triple negative breast cancer (TNBC), pembrolizumab in combination with cytotoxic chemotherapy has proven its efficacy and improved survival outcome. Previous studies demonstrated that PD-L1 expression, tumor mutational burden as well as certain neo-antigens were associated with response to pembrolizumab but there were no biomarkers predicting the response of pembrolizumab of TNBC in neoadjuvant setting. Therefore, tumor microenvironment (TME) evaluation would be warranted to understand the mechanism of action of pembrolizumab in TNBC.
Methods: We employed the Xenium In Situ platform, a cutting-edge spatial transcriptomics tool, capable of mapping hundreds of transcripts within individual cells. Using a 380-plex gene panel, we analyzed formalin-fixed, paraffin-embedded TNBC sections treated with weekly paclitaxel with carboplatin followed by doxorubicin with cyclophosphamide (CTx) with/without pembrolizumab in neoadjuvant setting. We analyzed detailed cellular compositions of tumors, encompassing immune and stromal cells, across over one million cells and we attempted to identify various cell types and states, previously characterized through single-cell RNA sequencing, and assess their spatial heterogeneity within the TME with regard to treatment strategy and the response to treatment.
Results: We collected 19 serial samples from 13 patients including 12 pre-treatment and seven post-treatment samples. Among seven post-treatment samples, one was collected after three weeks of the first treatment and one was after disease relapse. Of 13 patients, seven patients had received pembrolizumab with cytotoxic chemotherapy and four out of seven have achieved pathologic complete response (pCR). In six patients treated with only cytotoxic chemotherapy, only two achieved pCR. Our analysis revealed significant alterations in the spatial organization of cells in both the pembrolizumab with CTx and CTx-only groups. Notably, an increase in CD8 T cells and plasma cells following treatments was pronounced in post-treatment samples from patients in the pembrolizumab with CTx group. We also observed treatment-specific variations in ligand-receptor interactions between immune cells and cancer cells.
Conclusion: This study provides an in-depth analysis of the TME in TNBCs in response to pembrolizumab with CTx. Utilizing the Xenium In Situ platform, we uncovered significant disparities in the immune cell population according to the application of pembrolizumab. Our findings underscore the complexity of TME responses and highlight the potential of spatial transcriptomics in informing tailored treatment strategies for TNBC.

#1146 Pan-cancer characterization of cancer cell state and plasticity using spatially resolved transcriptomics.

G. Pei[1], K. S. Cho[1], Y. Liu[1], S. Alejandra[1], R. Lazcano[1], E. Dai[1], G. Han[1], F. Peng[1], D. Zhang[2], Y. Chu[1], A. F. Sinjab[1], J. Jiang[1], M. Li[2], C. Yee[1], A. Futreal[1], A. Lazar[1], H. Kadara[1], J. Gao[1], L. M. Soto[1], A. Maitra[1], J. Ajani[1], L. Wang[1];

[1]UT MD Anderson Cancer Center, Houston, TX, [2]University of Pennsylvania, Philadelphia, PA

Cancer cell state heterogeneity constitutes a foundational characteristic of cancer, posing a formidable barrier to the discovery of biomarkers and the efficacy of therapeutic interventions. However, current understanding of cancer cell heterogeneity and plasticity remains limited, especially in the spatial context. Previous studies underscored that cancer cell states are not strictly governed by genetics, but rather display a remarkable degree of plasticity. Recent pan-cancer single-cell studies have unveiled dozens of recurrent cancer cell states. Nevertheless, the relationship between these cancer cell states and tumor microenvironment (TME) remains poorly understood, especially when considering the diversity across different tumor types. Recent advancements in spatial transcriptomics (ST) have paved the way for a novel approach to spatially profile cell location, organization, and interaction within the tumor microenvironment. In this study, we curated ST data (Visium, 10x Genomics) from public repositories and in-house datasets, encompassing a total of >200 tissue sections across 11 cancer types. By incorporating histological annotations and inferred copy number variations, we systematically investigated the spatial heterogeneity of cancer cell states and inferred clonal architectures of cancer cell-enriched spots. Non-negative matrix factorization was applied to identify highly recurrent cancer states and transcriptional hallmarks associated with intra-tumor heterogeneity. By employing this approach, we uncover a diverse curated gene set of meta-programs. Notably, we observe a high level of reproducibility of these meta-programs when compared to the findings from single-cell level. Furthermore, we observe significant variations of cell states across different cancer types, even among two cancer subtypes within a specific tissue. We noted a unique distribution of 'hypoxia' and 'epithelial-mesenchymal transition' in the basal lineage tumor. Following this, we perform single-cell and ST co-embedding using available tools, including CellTrek and CytoSPACE. We noticed the cell type composition of tumor's neighbor spots play a significant role in influencing tumor states, especially for myofibroblastic CAFs and the tumor state in epithelial-mesenchymal transition. These findings contribute valuable insights into the relationship between cancer cell state plasticity and interactions with the TME, offering potential targets for further exploration and therapeutic intervention.

#1147 Sub-cellular spatial resolution of immune and stromal interactions underlying prostate cancer progression.

C.-K. Mo, R. G. Jayasinghe, A. Abedin do, X. Li, C. Weimholt, E. H. Kim, R. Pachynski, F. Chen, L. Ding;
Washington University in St. Louis, St. Louis, MO

Prostate cancer boasts a complex morphological structure and diverse cellular composition, yet current technology falls short in resolving the detailed spatial interactions among cells within the environment. In this study, we employed the Xenium platform, coupled with the 3D reconstruction tool Mushroom, to examine high-resolution spatial cellular interactions within the prostate cancer microenvironment. Our investigation focused on the transition of molecular characteristics from normal to high-grade prostatic intraepithelial neoplasia (HGPIN, pre-cancer), spanning the spectrum of Gleason Grades 3 to 4 and advancing to metastatic prostate cancer. We identified genes with unique spatial and grade-dependent expression profiles, including MYC, CP, and UHCL1. Evaluating sub-cellular imaging facilitated a comprehensive characterization and quantification of immune and stromal interactions, unveiling distinct spatial niches across transition stages. These findings underscore the nuanced immune interactions within the tumor microenvironment and offer crucial insights into the development of immunotherapeutic approaches tailored to the specific spatial and immune dynamics observed in advanced prostate cancer. This research contributes to the evolving understanding of prostate cancer progression, providing a foundation for the development of targeted therapies that disrupt specific cellular interactions.

#1148 Multimodal spatial transcriptomics and proteomics analysis of the resectable NSCLC ecosystem following neoadjuvant chemoimmunotherapy.

Z. Rahal[1], T. Zhou[1], S. Yang[1], A. Serrano[1], J. Feng[1], A. Sinjab[1], J. T. Le[1], X. Sun[1], M. Wang[1], W. Hu[1], J. Zang[1], T. Bruno[2], H. T. Tran[1], S. G. Swisher[1], C. H. Leung[1], H. Y. Lin[1], J. J. Lee[1], J. Wang[1], J. V. Heymach[1], D. L. Gibbons[1], I. I. Wistuba[1], A. Weissferdt[1], J. K. Burks[1], L. M. Solis Soto[1], H. Kadara[1], T. Cascone[1];

[1]The University of Texas MD Anderson Cancer Center, Houston, TX, [2]University of Pittsburgh, Pittsburgh, PA

Neoadjuvant and perioperative immunotherapy with checkpoint inhibitors (ICIs), combined with chemotherapy (CT), have improved outcomes for patients with resectable non-small cell lung cancer (NSCLC). Pathologic tumor response has been utilized in clinical trials as a surrogate of clinical efficacy. Yet, over half of treated patients experience non-response, highlighting the need for novel markers to identify those who are most likely to derive therapeutic benefit.

To dissect the spatial complexity of the tumor-associated immune landscape following neoadjuvant chemoimmunotherapy (CT+ICI), we selected patients (n =3) with a range of residual viable tumor (%RVT) - pathological complete response (pCR; 0% RVT), partial response (20% RVT), and no-response (100% RVT). We performed multimodal spatial transcriptomics (ST) and proteomics (using a 35-plex protein panel) on the same tissue sections using the Visium CytAssist from 10X Genomics. We also examined spatial patterns of 20-plex panel of immune and stromal markers at single-cell resolution in the same samples using the COMET Lunaphore platform. In the pCR patient, we studied two tumor areas to assess the impact of tumor response heterogeneity on the immune landscape.

Our analysis identified distinct immune profiles across three patients with varying %RVT, reflecting the heterogeneity of the immune response. We found robust gene-protein correlation, such as *MS4A1* gene expression and CD20 protein levels, in our multimodal spatial-omics analysis. Intriguingly, the arrangement of B cells and their interaction with surrounding plasma cells (PCs) varied notably across patients. Unlike in the patients with partial or no response, pronounced tertiary lymphoid structure (TLS) formation and signatures were observed in the pCR patient, with the CXCL13-CXCR5 axis overlapping with the TLS profile, suggesting a functional interplay that may be crucial in mediating response to therapy. Intriguingly, in the pCR patient, PCs uniquely arrayed around dense B cell aggregates, marked by *MS4A1*, *CR2*, *FCER1*, and *CXCL13*. PCs were not only less abundant in non-PCR patients but they also did not array around lymphoid aggregates.

Our high-resolution and multimodal analysis identified spatially-resolved expression and patterns for B lineage cells that may be associated, and thus, underlie response of resectable NSCLC to neoadjuvant CT+ICI. Ongoing efforts on this expanding cohort will shed further light on transcriptional states and immunogenomic roles of B lineage cells in neoadjuvant CT+ICI-treated NSCLC.

#1149 Spatial transcriptomic analysis of tumor microenvironment in patients with triple negative breast cancer with residual disease after neoadjuvant chemotherapy with immune checkpoint inhibitor.

J.-Y. Kim[1], K. Park[2], Y. Choi[1], J. Lee[1], B. Chae[1], J. Yu[1], S. Kim[1], S. Nam[1], J. Ahn[1], W.-Y. Park[2], Y. Park[1];
[1]Samsung Medical Center, Seoul, Korea, Republic of, [2]Samsung Genome Institute, Seoul, Korea, Republic of

Recent advance of treatment strategy for triple negative breast cancer (TNBC) including immune checkpoint inhibitor improved survival outcome. Especially, adding pembrolizumab on neoadjuvant chemotherapy (NAC) increased pathologic complete response (pCR) rate at the time of curative surgery. Previous studies suggested that PD-L1 expression in both tumor and immune cells was associated with the response of pembrolizumab in TNBC, but PD-L1 expression state were not associated with pembrolizumab response in NAC setting. In addition, neoadjuvant pembrolizumab increased event-free survival (DFS) rate after NAC even though they had not achieved pCR. However, there were no biomarker for EFS increasement of using pembrolizumab. We designed prospective translational research for evaluating tumor microenvironment (TME) of residual TNBC which had treated with NAC followed by curative surgery. We collected formalin fixed paraffin embedded (FFPE) surgical specimens after NAC with or without pembrolizumab. TNBC samples were used for spatial transcriptomics (ST) analysis, with H&E staining and inspection by an experienced pathologist. Libraries were prepared using Visium Spatial Gene Expression Reagent Kit protocol for FFPE (10x Genomics). Sequencing was conducted on the NovaSeq 6000 System (Illumina). From February 2023 to October 2023, 23 TNBC specimens from 22 patients were collected. Twenty specimens were breast tissues and three were lymph nodes, 18 TNBCs had been treated with NAC with pembrolizumab and four with only NAC, and five had residual cancer burden(RCB) class I, 11 of RCB class II and one of RCB class III. We collected BC and LN samples from BC with class III. Of 23 samples, we performed spatial transcriptomic analysis in 12 samples. In intrinsic subtyping, eight specimens were categorized into normal like, two of basal like and two of luminal A BC subtypes. In TNBC subtyping, mesenchymal stem cell like (MSL) were in six specimens, three of stem cell like (SL), two of luminal androgen receptor (LAR) and one of immunomodulatory (IM). We also performed cell type annotation with unsupervised method and categorized into 11 cell types; three cancer cell types, two macrophages, B and T cells, adipocytes, normal epithelium and perivascular-like and cancer associated fibroblasts. Among these 11 cell types, increasement of immune cells including B cells, T cells and macrophage proportions was associated with pembrolizumab treatment in NAC setting. In our study, we evaluated TME state of TNBC after NAC with or without pembrolizumab. We suggested that MSL or SL TNBC subtypes were associated with residual disease after NAC regardless of pembrolizumab use and pembrolizumab may recruit more immune cells in TME of TNBC. For concreating our suggestion, further analyses would be warranted.

#1150 Unveiling the spatial landscape of tumor and stroma heterogeneity in colorectal cancer with spatial transcriptomics.

J. Zhou[1], T. B. Sheridan[2], S. Domanskyi[1], S. L. Cowles[2], S. Park[1], I. Putra[2], O. Anczukow[1], J. H. Chuang[1], J. C. Rubinstein[3];
[1]The Jackson Laboratory for Genomic Medicine, Farmington, CT, [2]Hartford Hospital, Hartford, CT, [3]Hartford HealthCare Cancer Institute at St. Vincent's Medical Center, Bridgeport, CT

Heterogeneity in colorectal cancer (CRC) manifests in the diversity and interactions among tumor cells, support stroma, and immune components, critically impacting patient prognosis and therapeutic efficacy. In this study, spatial transcriptomics (ST, 10x Genomics Visium Spatial Gene Expression) was performed on 40 retrospectively collected CRC samples, along with detailed clinicopathological parameters and long-term clinical outcomes, with the goal of unraveling the molecular topography of the tumor and surrounding stromal compartments, and associating their spatial interactions to clinical outcomes. Five primary RNA groups were identified through unsupervised clustering on ST data, correlating with tissue classes detected in H&E-stained images via a pre-trained deep learning model. Markers and pathways specific to these tissues were identified. Furthermore, immune cell infiltration in these regions was deconvoluted using reference single-cell RNA sequencing (scRNA-seq) data. Sub-clustering within the tumor groups revealed five major tumor subtypes, each characterized by a distinct set of differentially expressed marker genes. Enrichment analysis across these subtypes highlighted distinct activation and suppression in pathways including KRAS, p53, MAPK, and Integrin. Tumors exhibited intra- and inter-tumoral heterogeneity. Location-specific tumor subtypes were observed, with those in right-sided CRC displaying increased immune cell infiltration, linked to enriched pathways such as Type II Interferon Signaling and Cytokine Signaling. Conversely, left-sided CRC subtypes had reduced immune cell presence, and were characterized by enhanced pathways related to vascular development, Hypoxia, and p53 Signaling. Inferred clonal lineages from copy number variation (CNV) using ST suggested a spatially structured phylogenetic organization corresponding to transcriptional clusters. Additionally, the ST data unveiled distinct spatial distribution patterns across various cancer-associated fibroblast (CAF) phenotypes, such as matrix, inflammatory, vessel-associated, tumor-promoting, and antigen-presenting CAFs. Transcriptional patterns uncovered through scRNA-seq, including epithelial-mesenchymal transition (EMT) signatures and consensus molecular subtypes (CMS), displayed unique spatial layouts within the tumor microenvironment. To our knowledge, this is the most comprehensive study to date on spatial transcriptomic heterogeneity within CRC patients, revealing distinct tumor, stroma and immune compositions and spatial structures. This spatially detailed map provides novel insights into CRC heterogeneity, critical for advancing personalized treatment.

#1151 Reconstruction of the spatial ecosystem of glioblastoma reveals relationships between tumor cell states and microenvironment.

B. Adabbo[1], S. Migliozzi[1], L. Garofano[1], F. D'Angelo[1], P. Davila[1], S. H. Gultekin[1], D. Bilbao Cortes[1], B. Currall[1], S. L. Williams[1], M. Sanson[2], F. Bielle[2], A. Di Stefano[3], M. Ceccarelli[1], A. Lasorella[1], A. Iavarone[1];

[1]University of Miami Sylvester Centr.-I, Miami, FL, [2]Sorbonne University, Paris, France, [3]Ospedali Riuniti di Livorno, Livorno, Italy

Glioblastoma multiforme (GBM) is the most aggressive form of primary brain tumor, with no curative treatment options. Multiple studies have characterized at single cell resolution the GBM as being composed of transcriptional cell states interconnected with components in the tumor immune microenvironment (TME). Our group proposed and validated the first single cell guided functional classification of GBM in four tumor-intrinsic cell states which informed clinical outcome and delivered therapeutic options. However, single cell technologies are unable to unravel the spatial relationships among the cell states of GBM and between GBM cell states and TME. Spatially resolved transcriptomic technologies are emerging as powerful tools to reconstruct the spatial architecture of a tissue. We performed spatial transcriptomics of multicellular regions of interest (ROI) in 6 primary IDH wild-type GBM and 2 recurrent GBM with both CosMx Spatial Molecular Imager, which analyzes 1,000 RNA probes and 64 proteins at single cell resolution, and GeoMx Digital Spatial Profiler which profiles the whole transcriptome (~18,000 genes) at ROI resolution. The development of computational tools aimed to integrate spatial proximity and CosMx derived single-cell transcriptomics revealed spatial segregation of the tumor cell clones and cellular states and highlighted recurrent patterns of cell states, distinct TME cell types associated with coherent histopathological features across multiple samples. The development of a spatial informed intercellular communication algorithm and the reconstruction of ligand-receptor-target networks will allow the discovery of tumor cell states-TME cross-talks and the biological signaling regulated by these interactions that are driving the heterogeneity of GBM and therefore potentially therapeutically targetable. Analysis of matched regions of interest profiled by GeoMx and spatial proteomics with CosMx further cross-validated the spatial ecosystem of glioblastoma as reconstructed at single-cell resolution. Our studies established a scalable approach to resolve the transcriptional heterogeneity of GBM and reconstruct the architecture of GBM cell states and tumor microenvironment.

#1152 Pan-cancer single-cell and subcellular characterization of lymphoid aggregates and tertiary lymphoid structures using high-plex spatial molecular imaging.

Y. Liu[1], Y. Zhang[1], G. Han[1], G. Pei[1], K. Cho[1], E. Dai[1], Y. Chu[1], J. Jiang[1], A. Sinjab[1], L. M. S. Soto[1], A. Serrano[1], J. Gao[1], H. Kadara[1], C. Fridman[2], W. H. Fridman[2], L. Wang[1];

[1]UT MD Anderson Cancer Center, Houston, TX, [2]Universite de Paris, Paris, France

Tertiary lymphoid structures (TLSs), clusters of immune cells that form in non-lymphoid tissues, are frequently identified in a wide range of solid tumors. They function as immunological “hubs”, driving anti-tumor responses. Previous studies have demonstrated that the presence of TLSs is often associated with improved responses to immunotherapy and superior clinical outcomes. Despite these insights, our understanding of their phenotypic diversity, spatial organization, intercellular communication, and interactions with cancer cells and the tumor microenvironment remains incomplete. Existing methods lack the resolution, depth, and scale required for a thorough understanding of these complex structures. We have obtained in-house and public spatial multi-omics data generated on various tissues across 9 different cancer types using the cutting-edge single-cell spatial transcriptomics and high-plex spatial molecular imaging platforms. We have developed innovative computational approaches for the detailed characterization of TLSs at single-cell and subcellular resolution and carried out an extensive analysis of lymphoid aggregates (LAs) and TLSs in tissue sections across these different solid cancer types. We defined the phenotypic state of each individual cell within TLSs including B/ plasma cells, follicular helper/regulatory/stressed/exhausted T cells, follicular dendritic cells, fibroblasts and high endothelial venules. Then, we performed unbiased phenotyping and classification of TLSs based on their cellular states, compositions and organization patterns across various types of tissues. Additionally, we performed spatial neighborhood analysis, characterized the neighboring cells of each TLS and analyzed their cell-cell communication networks. Our approach allowed an unprecedented examination of the spatial phenotypes of TLSs in large, complex tissues at super resolution, in ways that were not previously described. We comprehensively characterized TLSs across different solid tumor types. Our analysis revealed a high degree of spatial and phenotypic heterogeneity in LAs and TLSs. We created a comprehensive spatial atlas of LAs and TLSs across solid tumor types, profiled TLSs at various maturation states with distinct cellular composition and organization patterns, and discovered new TLS states. Notably, we observed distinct communication networks associated with TLS phenotypic states. Our innovative methods and analytical approaches offer a more comprehensive way to study LAs and TLSs, enhancing detection capabilities and providing deeper insights into their spatial interaction and functional phenotypes. This research holds the potential to significantly advance our understanding of TLSs and their roles in immunobiology and immunotherapy responses across a broad range of cancers and diseases.

#1153 Using spatial transcriptomics to dissect cell to cell cooperation in lung adenocarcinoma.

R. Jamshidi, L. Griffiths, R. Johnston, V. Parihar, F. Schneider, A. Marcus;
Winship Cancer Institute, Emory University School of Medicine, Atlanta, GA

Lung cancer is the second most common cancer in the United States and the leading cause of cancer related deaths in this country. Unfortunately, efficacious treatments for lung cancer remain suboptimal. Lung cancer is characterized by several distinct subtypes of which lung adenocarcinoma is the most common, comprising about 40% of this malignancy. The hallmark gene mutations of lung adenocarcinoma include *TP53*, *RAS*, and *STK11*. LKB1 is a serine-threonine kinase (coded by the gene *STK11*) that largely functions as a tumor suppressor, and is mutated in 20-30% of non-small cell lung cancers (NSCLCs). The diversity between and within lung cancer subtypes, as well as within a patient (i.e. metastases vs primary tumor), makes treating this cancer very challenging. Lung adenocarcinoma, in particular, has collective invasion packs of cells adjacent to the primary tumor that correlate with metastatic disease in mouse models. We hypothesize that the transcriptomic profile of the collective invasion packs in lung adenocarcinoma patients varies significantly from the adjacent primary tumor and represents a targetable metastatic sub-population. This work will help to identify specific cell signaling pathways that have the translational potential to develop novel therapeutics for metastatic disease, ultimately improving patient outcomes through precision medicine. Utilizing patient lung adenocarcinoma samples with KRAS and KRAS+LKB1 mutations, we identified regions of interest including bulk tumor and surrounding invasion packs. Then, using GeoMx digital spatial profiling technology (by Nanostring) and next-gen sequencing, we generated transcriptomic profiles from bulk tumor and invasion packs. Preliminary results indicate region specific transcriptomic differences, highlighting the heterogeneity of these cell populations. More specifically, collective invasion packs exhibit upregulation of gene networks involving immune cell differentiation, function, oxidative phosphorylation, tumor invasiveness, and mitochondrial structure. To discern the metastatic potential, transcriptomic profiles and biological functions will be compared between invasion packs, tumor bulk vs invasion packs, and finally, inter-patient differences. Successful completion of this project will characterize transcriptomes of metastatic lung cancer and has the potential to ultimately identify biomarkers of aggressive disease. Lastly, this foundational study will pave the way for future studies on the transcriptomic landscape of metastatic pediatric cancers and cancer predisposition syndromes.

#1154 Spatial profiling of the tumor microenvironment in head and neck squamous cell carcinoma revealed immune cell type infiltration into the TME as a predictor of immunotherapy response.

H. Sadeghirad[1], C. Tan[2], N. Liu[2], J. Monkman[1], C. Cooper[3], K. O'Byrne[3], M. Davis[2], B. Hughes[4], A. Kulasinghe[1];
[1]The University of Queensland, Brisbane, Australia, [2]The Walter and Eliza Hall Institute (WEHI), Melbourne, Australia, [3]The Princess Alexandra Hospital, Brisbane, Australia, [4]The Royal Brisbane and Women's Hospital, Brisbane, Australia

Background: Immunotherapy has shown promising results in advanced head and neck cancer patients, however, only a subset of patients are responsive to immune checkpoint blockade therapy. The molecular and cellular characterization of the tumor microenvironment (TME) may reveal clues as to why some head and neck tumors are responsive or resistant to the therapy.
Methods: Formalin-fixed paraffin-embedded (FFPE) tissue samples were collected from 34 patients at two major Queensland Hospitals with advanced head and neck squamous cell carcinoma (HNSCC), prior to immunotherapy. To investigate the cellular and molecular characteristics of the HNSCC TME, we used the Nanostring GeoMx Digital Spatial Profiler (DSP) spanning modules in an immune-oncology panel, which included immune cell typing and profiling, cell death, PI3K/AKT signaling, drug target, immune activation, and pan tumor protein biomarkers. A deeper structural analysis was performed using the Nanostring whole transcriptome atlas (WTA) panel of tertiary lymphoid structures (TLSs) and germinal centers (GCs).
Results: Out of 34 patients, 3 had a complete response (CR), 7 had a partial response (PR), 5 had stable disease (SD), and 19 had progressive disease (PD), based on the Response Evaluation Criteria in Solid Tumors (RECIST). When we compared patient responders (patients with CR, PR, and SD) to patient non-responders (patients with PD), we found that the former had a higher infiltration of immune cell type markers representatives of $CD8^{+}$ T cells, dendritic cells, and macrophages, into their tumor microenvironment than the latter. Then, to investigate differentially expressed genes between patients with complete response and patients with partial response to immunotherapy, we performed DE analyses and we found that patients with PR had higher Ki-67 expression than those with CR. Spatial transcriptomic mapping of TLS's (peripheral, intra-tumoral) and normal germinal centers revealed interferon pathway enrichment in the TLS's. In a subset, these appear to be linked with HPV viral infection.
Conclusion: In this study, we found that immune cell type infiltration into the tumor microenvironment of head and neck cancers could be predictive of response to immunotherapy. Furthermore, it was revealed that patients with a high expression of Ki-67 might be less likely to respond completely to immunotherapy. Spatially resolved whole transcriptome analysis of HNSCC tissues revealed the presence of tertiary lymphoid structures with a higher enrichment of interferon pathway genes.

#1155 Spatial colocalization and molecular crosstalk of myofibroblastic CAFs and tumor cells shape lymph node metastasis in oral squamous cell carcinoma.

K. Furudate[1], S. Kasai[1], T. Yoshizawa[1], Y. Sasaki[2], K. Fujikura[3], S. Goto[1], R. Ito[1], T. Tanaka[2], H. Kijima[1], K. Kubota[1], K. Itoh[1], W. Kobayashi[1], K. Takahashi[2]; [1]Hirosaki University Graduate School of Medicine, Hirosaki, Japan, [2]The University of Texas MD Anderson Cancer Center, Houston, TX, [3]Kobe University Graduate School of Medicine, Kobe, Japan

Lymph node metastasis (LNM) is a critical prognostic factor for patients with oral squamous cell carcinoma (OSCC). While previous research has implicated partial epithelial-to-mesenchymal transition (p-EMT) of tumor cells and cancer-associated fibroblasts (CAFs), specifically myofibroblastic CAFs (myCAFs), in LNM, the underlying molecular mechanisms remain poorly understood. Furthermore, the lack of diagnostic and prognostic biomarkers related to LNM has impeded the improvement in clinical outcomes for patients with OSCC. Here, we conducted a comprehensive molecular analysis integrating original and publicly available OSCC data of the bulk genome and transcriptome analyses, single-cell transcriptome profiling, and spatial transcriptome analyses. We found that myCAFs were both quantitatively and functionally activated in LNM-positive samples and spatially colocalized with OSCC cells within the invasive tumor front (ITF), providing a niche that may facilitate LNM. We validated spatial colocalization of myCAFs and OSCC cells using 50 additional Immunohistochemistry (IHC) samples. Mechanistically, myCAFs provided increased extracellular matrix (ECM) signals, such as *COLLAGEN*, *Fibronectin1(FN1)*, and *LAMININ* to OSCC cells. Consequently, OSCC cells upregulate ECM receptors such as *αβ integrins (ITGA-B)*, *syndecans (SDC)*, and *CD44*, leading to upregulating stemness-related genes in OSCC cells. Further analysis using CRISPRGeneEffect data from DepMap found that *ITGB1*, *ITGA3*, and *CD44* are among the most essential genes for the survival and growth of OSCC cells. By analyzing the spatial transcriptomic data of matched primary tumor sites (HUH001-P1 and HUH001-P2) and metastatic site (HUH001-met) from the same patient, we identified the origins of metastatic cells in the primary tumor site. We further extracted a 23-gene signature from the metastatic origin in ITF, where OSCC and myCAFs colocalize. This spatially-resolved 23-gene signature predicted LNM status and poor overall survival (OS) in clinical OSCC patients. The prognostic significance of the 23-gene signature we extracted from the spatial analysis was also validated in separate clinical cohorts from TCGA study and two other microarray datasets. Our findings provide novel insight into the molecular crosstalk between myCAFs and OSCC cells that facilitates LNM and identifies clinically valuable biomarkers for better prognostication in patients with OSCC.

#1156 A systematic comparison of common multiplex immunohistochemistry (mIHC) methodologies to the novel SignalStar™ assay in the characterization of the tumor microenvironment (TME).

J. Ziello, D. Papalegis, L. Vu, K. Goldman, J. Loebelenz, S. Sponaugle, S. Tkachev, S. Klein;
Cell Signaling Technology, Inc., Danvers, MA

The emergence of an increasing number of immunotherapy biomarkers and their importance within the spatial context of the TME has resulted in a concomitant need for reliable and accurate mIHC assays. Many of the currently available mIHC technologies do not offer amplification, resulting in the loss of detection of low expressing cells, while others require deposition and cycling of antibodies, which can lead to epitope masking and degradation, respectively. The SignalStar mIHC assay from Cell Signaling Technology is a novel methodology used to label, amplify and visualize up to 8 targets within the same formalin fixed, paraffin-embedded carcinoma (FFPE) tissue section without the need for fluorophore deposition or antibody cycling.

In this study, the SignalStar mIHC assay was used to simultaneously label 8 targets including TIM-3, PD-1, PD-L1, LAG3, CD3, CD68, CD8 and Pan-Keratin in FFPE carcinoma tissue. A network of complementary, fluorescently-labeled oligonucleotides was used to amplify the signal of the first 4 antibody-oligo conjugates followed by tissue imaging. The fluorescent signal was then removed, and the process repeated.The resulting two 4-plex images were then computationally aligned with QuPath. This methodology was compared to the Tyramide Signal Amplification (TSA) deposition assay, as well as to indirect and direct immunofluorescent detection with respect to mean fluorescence intensity (MFI) per cell and percent positivity of cells in matched regions of interest in serial sections. All mIHC strategies were in turn compared to the canonical chromogenic IHC assay. Furthermore, the fluorescent signal from the 8-plex SignalStar assay was removed and the same tissue was stained with fluorescent direct conjugates to achieve even higher plex.

Our data demonstrates that the SignalStar assay detected similar percentages of cells when compared to chromogenic and TSA staining. Alternatively, the SignalStar assay often outperformed indirect and direct immunofluorescent detection. SignalStar was also successfully combined with a panel of direct Alexa Fluor® dye conjugates, showing the complementarity of these assays in such a way that both plex and flexibility can be increased. Ultimately, we demonstrate that SignalStar mIHC is a useful tool in the characterization and analysis of the complex TME. SignalStar mIHC outshines existing technologies as it does not require deposition in order to amplify the signal of multiple colocalizing targets, including low abundance proteins, while also maintaining dynamic range.

#1157 Molecular signatures associated with the progression from DCIS to IDC.

S. Chen, A. Karpova, P. Lal, E. Storrs, R. Jayasinghe, M. Iglesia, A. Houston, Y. Zhao, A. Shinkle, C.-K. Mo, J. Herndon, F. Chen, W. Gillanders, L. Ding; Washington University School of Medicine in St. Louis, St. Louis, MO

Patients with ductal carcinoma in situ (DCIS) are frequently overtreated. Identifying markers that accurately predict which cases of ductal carcinoma in situ (DCIS) would progress to invasive ductal carcinoma (IDC) is crucial to personalized medicine but remains a challenge. Deciphering the process of DCIS progression at cellular, molecular and genetic levels helps identify biomarkers, allowing for better informed clinical decision-making. To study molecular signatures associated with the progression from DCIS to IDC, we collected samples from breast cancer patients with co-occurring DCIS and IDC, and performed Visium spatial transcriptomics (ST), single-nucleus RNA sequencing and multiplex imaging on these samples. We identified *MGP*, *SLC39A6*, *PLAT*, *MLPH*, *AZGP1*, *TFF1* and *TFF3* as showing significant differential expression levels in DCIS compared to IDC from ST analysis, which was confirmed with snRNA analysis. Notably, in multiplex imaging, MGP and PLAT showed consistently higher expression in DCIS compared to IDC at the protein level. Moreover, we evaluated these molecular signatures using MMTV-PyMT genetic mouse models at various breast cancer progression stages (3, 6, 12, 15, and 20 weeks) with snRNA-seq and multiplex imaging platforms. Collectively, our findings highlight the importance of identifying biomarkers at the molecular level, and provide potential predictive biomarkers for DCIS progression.

#1158 Spatially resolved cell profiling unveils tumor metabolic states associated with immunotherapy response in NSCLC.

James Monkman[1], Rotem Czertok[2], Shai Bookstein[3], Becky Arbiv[4], Yuval Shachaf[5], Ron Elran[5], Kenneth Bloom[5], Oscar Puig[5], Ken O'Byrne[6], Ettai Markovits[5], **Arutha Kulasinghe**[1]

[1]University of Queensland, Brisbane, Australia,[2]NucleAI, Tel Aviv, Israel,[3]NucleAI, Tel-Aviv, Israel,[4]Nucleai, Tel-Aviv, Israel,[5]Nucleai, Tel Aviv, Israel,[6]Princess Alexandra Hospital, Brisbane, Australia

Background. Only a subset of non-small cell lung cancer (NSCLC) patients benefit from immune checkpoint inhibitors (ICIs). Thus, there is a clinical need to develop predictive biomarkers for ICIs. Deeper insights from the tumor microenvironment (TME) can lead to identification of spatial features associated with clinical responses to immune checkpoint inhibitors (ICI). In this study, we investigated functional profiles within cell subtypes as a surrogate for ICI clinical endpoints.

Methods. We profiled a retrospective cohort of 39 NSCLC tissue cores from 27 patients treated with ICI, using highly multiplexed immunofluorescence (mIF) stained by the Phenocycler Fusion platform (Akoya Biosciences) capturing 45 proteins. Utilizing a deep learning based multiplex imaging analysis pipeline, cells were classified to 15 cell types by known marker expression and were further subclassified by unsupervised clustering. Cells were assigned to the tumor area or TME and more than 1000 spatial features were calculated based on cell type, marker positivity, and area assignments, and were compared between responders and non-responders to ICI therapy using Fisher's exact and logrank tests.

Results. Unsupervised cell subtyping of the 15 cell types identified 43 cell subsets, which were mostly segregated by their metabolism and activation status. Interestingly, all lymphocytes showed a similar pattern of clustering resulting in two clusters of metabolically active and inactive cells. The most significantly differentially expressed proteins between these cell types were oxidative phosphorylation proteins such as CS, SDHA and ATPA5, and other metabolic enzymes such as HK1, GLUT1 and LDHA. We found a direct connection between metabolic state, effector functions and tissue localization as the metabolically active lymphocytes exhibited higher levels of PD-1, MHC class I and II and CD44 positivity, and were more abundant within tumor infiltrating lymphocytes (TILs) and tertiary lymphoid structures (TLS). Unsupervised clustering of tumor cells demonstrated segregation to three main metabolic states - OXPHOS+, OXPHOS- and a third cluster (PPP+) which was characterized by upregulation of ASCT2, a glutamine transporter, as well as pNRF2 and G6PD, regulators of the pentose phosphate pathway. These cells also exhibited higher proliferation rate and CD44, a tumor stemness marker, positivity. All tumors with high content of PPP+ tumor cells (>40%) were resistant to PD-1 blockade (0/8 vs. 10/18 response rate in other tumors, p=0.009) and showed reduced overall survival (OS) rates (median OS of 27.6 vs 90.3 months, p=0.02).

Conclusions. Taken together, this study reveals connections between metabolic states, effector functions, and immunotherapy outcome and contributes to the evolving landscape of predictive biomarkers for ICI therapies.

#1159 Machine learning integrating spatial omics uncovers humoral immunity patterns in intratumoral tertiary lymphoid structures in pancreatic cancer pathologic responders.

D. N. Sidiropoulos, S. M. Shin, A. Girgis, D. H. Shu, J. Montagne, A. Deshpande, J. A. I. Johnson, L. Dequiedt, V. Jacobs, A. Ogurtsova, G. Mo, X. Yuan, G. Stein-O'Brien, M. Yarchoan, Q. Zhu, A. Kiemen, E. M. Jaffee, L. Zheng, W. Ho, R. Anders, E. J. Fertig, L. T. Kagohara;
Johns Hopkins University, Baltimore, MD

Background: In pancreatic ductal adenocarcinoma (PDAC), rare long-term survivors correlate with high intratumoral tertiary lymphoid structure (TLS) density. This finding prompted our investigation of clinically viable strategies to induce TLS in patients with immune-excluded tumors. We previously reported the induction of intratumoral TLS following administration of a neoadjuvant GM-CSF-secreting allogeneic vaccine (GVAX) to PDAC patients (NCT00727441). However, no clinical benefit was observed, likely owing to immune tolerance mechanisms governing the PDAC tumor microenvironment (TME). We previously observed upregulation of both the PD-1 and 4-1BB pathways with GVAX, and thus in a subsequent neoadjuvant trial combined GVAX with PD-1 blockade and 4-1BB agonism (NCT02451982) which was associated with pathologic responses. We hypothesized this combination strategy induced TLS of higher maturity and anti-tumor activity compared to GVAX alone.

Methods: To explore how this therapeutic strategy affected TLS morphology and intercellular crosstalk, we leveraged the Visium spatial transcriptomics platform and a 35-marker customized TLS panel for imaging mass cytometry. We generated cellular and molecular maps of the TME after neoadjuvant treatment in 26 PDAC patients (GVAX n=19, GVAX+aPD1 n=2, GVAX+aPD1+a41BB n=5). To compare TLS maturation in parallel with secondary lymphoid organ-mediated tumor immunity, we also profiled tumor-adjacent lymph nodes. We applied unsupervised learning with non-negative matrix factorization (NMF) and trained AI-enabled image classification models to characterize cellular states within tissue structures of interest.

Results: We identified spatial gene expression NMF patterns in PDAC TLS spanning across distinct morphologies and neoadjuvant treatment arms. Intratumoral TLS after GVAX were found to propagate activated B cells expressing immunoglobulins that infiltrated into malignant cellular niches. TLS NMF patterns were also associated with autoimmune disease signatures, such as diabetes, in a subset of patients. We scored TLS using tumor-draining lymph nodes as a reference and found increased maturation of TLS after PD-1 blockade, while addition of 4-1BB agonism significantly boosted the cytotoxic NK/T cell compartment compared to GVAX alone.

Conclusions: We present machine learning approaches for spatial multi-omics analysis to characterize the TLS-enriched TME. We mined genome-wide spatial TLS gene expression patterns elucidating the spatial dynamics of humoral immunity of rare immunotherapy pathologic responders in PDAC. Altogether our findings shed light on the plasticity of TLS in neoadjuvant immunotherapy and suggest future immunotherapy approaches should target both humoral and cytotoxic NK/T cell compartments to augment responses in solid tumors.

#1160 Investigating spatial gene expression profiling in colorectal cancer: Tumor and stroma comparison between primary lesions and matched liver metastases.

J. Lee[1], Y. Kim[1], H. Ryu[1], J. Sim[1], C. Kim[1], J. Park[1], A.-R. Lim[1], J. Kim[1], H. Sung[1], X. Guo[2], J. Choi[1], **J. Choi**[1];
[1]Korea University Medical Center, Seoul, Korea, Republic of, [2]Vanderbilt University Medical Center, Nashville, TN

The nanoString GeoMx® Digital Spatial Profiling (DSP) enables the investigation of spatial assessment of tumors through high-plex profiling at the RNA and protein levels. Recent genomic analyses have revealed the intertumor heterogeneity between primary and metastatic lesions in colorectal cancer (CRC) patients. In CRC with liver metastases, current treatment strategies are mainly based on the parameters of primary tumors, and metastatic heterogeneity is a challenge since molecular heterogeneity contributes to therapeutic resistance. Furthermore, spatial intratumor heterogeneity exists within a single tumor between cancer cells (tumor) and their microenvironment (stroma) in human cancers. However, whether there are distinct spatial gene expression patterns of tumor and stroma between primary lesions and liver metastases remains unclear in CRCs.

We examined 24 formalin-fixed paraffin-embedded tissue samples, including primary lesions and matched liver metastases from 12 patients (6 with synchronous and 6 with metachronous metastases) using NanoString GeoMx® DSP. The best regions of interest (ROI) with the invasive front boundary of the tumor were selected by pathologists. The ROI was segmented into PanCK-positive (tumor) and PanCK-negative (stroma), followed by a collection of indexed oligonucleotides and sequencing on Illumina instrument. Differential expression and pathways enrichment analyses were performed using R BioConductor package standR, limma, and GSEABase. Statistical significances were based on $|\text{Log}_2$ fold change$| > 1$ and Benjamini-Hochberg-corrected $P < 0.05$. Immune cell abundance was estimated using the SpatialDecon package.

In 12 metastatic patients (mean age, 61 years ± 7 [standard deviation]), liver metastatic stroma was associated with 68 upregulated and 93 downregulated genes compared to the primary stroma, with enrichment of 'Immune response' terms in gene set enrichment analysis (GSEA). A higher proportion of CD4 T memory cells and increased expression of cytotoxic genes (*IL7R* [2.02-fold], *CD3E* [1.75-fold], *KLRB1* [1.68-fold], and *GZMK* [1.54-fold]) were observed in liver stroma compared to primary stroma. Conversely, liver metastatic tumors were associated only with 23 upregulated and 6 downregulated genes compared to primary tumors, with 'humoral response' terms enriched in GSEA. Similar patterns were observed in stratified analyses with synchronous and metachronous metastases, although a more prominent ‘immune response’ was observed in synchronous metastatic stroma compared to the primary stroma.

We revealed that higher immune cell proportion and cytotoxic activity were observed in liver metastatic stroma compared to CRC stroma, providing novel insights into a unique etiology and may yield clinical implications for developing targeted treatment modalities for liver metastatic CRC patients.

#1161 Deep spatial proteomics: A new approach for obtaining insight into the glioblastoma microenvironment.

K. Saxena[1], R. Daucke[2], V. Pedersen[1], P. H. klausen[3], E. Schoof[2], B. W. Kristensen[1];
[1]University of Copenhagen, Kobehavn N., Denmark, [2]Technical University of Denmark, Lyngby, Denmark, [3]Copenhagen University Hospital, Rigshospitalet, Kobehavn N., Denmark

Glioblastoma is the most frequent and malignant brain tumor, with a median survival of approximately 14 months. The tumor microenvironment is composed of different cell types and is known to support the glioblastoma cells and contribute to poor patient prognosis. Since accumulating studies report discordance between mRNA and protein abundances both on population and single-cell levels, and since proteins are the effector molecules of the cells and the actual target molecules of most drugs, our aim is to dissect the tumor microenvironment by spatial LC-MS based proteomics. Glioblastoma formalin-fixed paraffin-embedded (FFPE) tissue was sectioned and placed on membrane glass slides suitable for laser capture microdissection (LCM), followed by precise isolation of single cells from the heterogeneous tumor microenvironment. We used the Zeiss Palm MicroBeam laser microdissection instrument, combined with an Orbitrap Eclipse Tribrid Mass Spectrometer running our in-house sensitivity tailored Data Independent Acquisition method (WISH-DIA) to analyze and quantify the proteomes. We obtained up to 3000 proteins out of only 100 cells and were able to demonstrate the feasibility of collecting and analyzing various cell types at the single-cell level. The proteins identified belonged to many different classes/families of proteins and were able to distinguish the different cell types. In conclusion, this on-going study demonstrates our ability to isolate single cells from the highly heterogeneous tumor microenvironment of glioblastoma with ultra-high sensitivity, thereby allowing the characterization of the proteome of the glioblastoma microenvironment followed by identification of potential therapeutic and/or diagnostic targets.

#1162 Tumor-immune microenvironment associated with obesity in triple-negative breast cancer in the Mayo Clinic cohort.

S. Pang[1], Y. Liu[1], Y. Ma[1], Z. Li[1], R. A. Leon-Ferre[2], D. Zahrieh[2], D. W. Hillman[2], J. C. Boughey[2], J. N. Ingle[2], K. R. Kalari[2], F. J. Couch[2], M. P. Goetz[2], K. L. Knutson[1], S. Chumsri[1], E. Thompson[1];

[1]Mayo Clinic, Jacksonville, FL, [2]Mayo Clinic, Rochester, MN

Background: Previous studies demonstrated that obesity is associated with poor outcomes and significantly worse pathological complete response (pCR) in triple-negative breast cancer (TNBC) treated with conventional chemotherapy. Emerging studies described a phenomenon termed the obesity paradox, which referred to improved outcomes observed in obese patients treated with immune checkpoint inhibitors (ICIs). Our study aimed to determine distinct immune features in TNBC across body mass index (BMI).

Methods: Characteristics and outcomes of TNBC patients treated with neoadjuvant pembrolizumab-based chemotherapy at Mayo Clinic were collected. Normal BMI was defined as 18-25 kg/m^2, overweight 25-30, and obese BMI ≥ 30. NanoString CosMx, a spatial multi-omics single-cell imaging (SMI), was performed in 75 samples from the Mayo Clinic TNBC cohort (Leon-Ferre BCRT 2018). Differential expression as log 2-fold change (FC) was estimated from the linear mixed model with significance defined as two-sided p< 0.05.

Results: Between 2021-2023, there were 108 TNBC patients treated with neoadjuvant pembrolizumab. 25.9% were obese, 32.4% were overweight, and 41.7% had normal BMI. In contrast to previous studies with conventional chemotherapy, obese patients numerically had a higher pCR rate of 71.4% with pembrolizumab-based chemotherapy compared to 55.6% in normal and 62.9% in overweight patients. However, this difference did not reach statistical significance (obese vs. normal weight, OR 2.26, 95%CI 0.89-6.06, p 0.094). We further evaluated spatially-resolved immune features associated with obesity using CosMx SMI in 75 samples from the MC TNBC cohort. Obese patients had significantly higher intratumoral B cells (log2FC 1.88, p 0.017), stromal B cells (log2FC 2.79, p 0.001), stromal plasmablasts (log2FC 1.94, p 0.047), and stromal macrophages (log2FC 1.80, p 0.017) compared to patients with normal BMI. Obese patients also had significantly lower intratumoral myeloid dendritic cells (mDC) (log2FC -1.27, p 0.037). Similar trends were observed after standardizing cell counts per 100 tumor or stromal cells, including higher intratumoral B cells (log2FC 3.00, p 0.001), intratumoral plasmablasts (log2FC 2.00, p 0.006), intratumoral natural killer (NK) cells (log2FC 1.66, p 0.044), and stromal B cells (log2FC 1.50, p 0.008). Differential gene analyses for intratumoral B cells revealed that genes (CD74, HLA-C, HLA-DRB1, HLA-DRA, HLA-DRB) associated with the positive regulation of type 2 immune or chemokine response were upregulated.

Conclusions: Using in-depth analysis with spatially defined context, our study showed that obese TNBC patients had significantly higher B cell infiltration, which is associated with improved outcomes with ICIs. Future research on how obesity alters the immune microenvironment is needed to identify potential pathways to improve outcomes with ICIs in TNBC.

#1163 Increased spatial coupling of integrin and collagen IV in the immunoresistant clear cell renal cell carcinoma tumor microenvironment.

A. C. Soupir[1], M. T. Hayes[1], T. C. Peak[1], O. E. Ospina[1], N. H. Chakiryan[2], A. E. Berglund[1], P. A. Stewart[1], J. Nguyen[1], C. M. Moran-Segura[1], N. L. Francis[1], P. M. Ramos-Echevarria[1], J. Chahoud[1], R. Li[1], K. Y. Tsai[1], J. A. Balasi[1], Y. Caraballo-Perez[1], J. Dhillon[1], L. A. Martinez[1], W. E. Gloria[1], N. Schurman[3], S. Kim[3], M. Gregory[3], J. J. Mule[1], B. L. Fridley[1], B. J. Manley[1];

[1]H. Lee Moffitt Cancer Center, Tampa, FL, [2]Knight Cancer Center, Portland, OR, [3]Nanostring, Seatle, WA

Immunotherapy (IO) has improved the survival of patients with clear cell renal cell carcinoma (ccRCC); however, most patients will not have a durable complete response and will die from their disease. Our understanding of the development of IO resistance for ccRCC is very limited. We employed spatial transcriptomics (ST) with single cell resolution on patients with IO naïve tumors and IO exposed tumors to characterize spatial properties and differences between these two populations. Fourteen matched tumor and adjacent stromal fields of view (FOV) from surgically resected primary kidney specimens were analyzed using CosMx Spatial Molecular Imager (SMI). Non-tumor cell phenotyping was performed using the Kidney Cell Atlas. A generalized linear model was developed to identify malignant tumor cells in kidney tissues and validated by a pathologist. Differential cell abundance, clustering, and gene expression for each cell phenotype were compared between the two groups. Spatial gene set enrichment (GSEA) of modified hallmark gene sets were also compared. CD8+ T cells were more abundant in IO exposed vs IO naïve tumor FOVs. *YES1* expression in the malignant tumor cells was significantly higher in IO exposed samples compared to IO naïve samples (false discovery rate [FDR] = 0.084). Spatial GSEA showed significant clustering of many gene sets (cells of high enrichment closer together than expected by chance), most notably epithelial-mesenchymal transition (EMT) pathway. Next, a post-hoc analysis of genes belonging to known ligand-receptor pairs in the EMT pathway was completed using bivariate Moran's I to estimate spatial autocorrelation. We found significantly higher spatial autocorrelation of *ITGAV-COL4A1* in the stroma of IO exposed FOVs than IO naïve FOVs (FDR = 0.008). Cell types with the highest expression of *ITGAV* and *COL4A1* were found to be fibroblasts, endothelial, and tumor cells. Protein validation with multiplex immunofluorescence (mIF) confirmed cells positively stained for anti-integrin alpha-V were more abundance on stromal FOVs ($p < 0.001$) in IO exposed samples. Fibroblast (SMA+) cells in stromal FOVs were more likely to be positively stained for anti-integrin alpha-V ($p < 0.001$) in IO exposed than IO naïve FOVs. ITGAV protein is involved in migration from primary to metastatic disease in several cancers, and its inhibition increases T cell killing indicating ccRCC endothelial and tumor cells may be using this signaling for immune evasion and disease progression. Further, collagen and cancer associated fibroblasts (CAFs) play a role in tumor growth. To our knowledge, this is the first study to leverage single-cell resolution ST to identify potential ways by which ccRCC tumors become resistant to IO therapy.

CLINICAL RESEARCH: Tumor Immune Response 1
Poster Session

#1167 Prospective analysis of pretreatment circulating CD4 memory T cell features associated with severe immunotherapy toxicity.

A. Usmani[1], N. Earland[1], W. Zhang[2], P. K. Harris[1], A. Bacchiocchi[3], C. M. Sachs[1], A. Nene[3], D. Y. Chen[1], M. Sznol[3], R. Halaban[3], A. M. Newman[2], A. A. Chaudhuri[1];

[1]Washington University in St. Louis, St. Louis, MO, [2]Institute for Stem Cell Biology and Regenerative Medicine, Stanford University, Stanford, CA, [3]Yale University School of Medicine, New Haven, CT

Introduction: Immune checkpoint inhibitors (ICIs) have revolutionized melanoma treatment, significantly improving outcomes. Nevertheless, too many melanoma patients undergoing ICI treatment experience severe and often debilitating immune-related adverse events (irAEs). In a retrospective melanoma cohort treated with ICIs, we previously found that elevated baseline levels of circulating CD4 effector memory T (TEM) cells were associated with the development of severe irAEs, irrespective of the affected organ system (Lozano et al., Nature Medicine, 2022). Here, we present data from an extended prospective validation cohort from 47 patients across two academic medical centers.
Methods: Of 47 patients, 26 received combination anti-PD1/anti-CTLA4 ICIs, 3 combination anti-PD1/anti-LAG3 ICIs, 17 anti-PD1 ICI, and 1 anti-CTLA4 ICI. Peripheral blood mononuclear cells (PBMCs) were prepared from pretreatment (Cycle 1 Day 1) blood samples obtained from all patients. We performed mass cytometry (CyTOF) on PBMCs using a 38-marker panel to deeply profile immune subsets. We further leveraged bulk RNA-seq from 24 patients to (i) deconvolve CD4 memory T cell abundance using CIBERSORTx and (ii) determine T cell receptor (TCR) diversity using Shannon entropy following MiXCR clonotype assembly. irAEs were graded on a 5-point scale using the Common Terminology Criteria for Adverse Events v5.
Results: After treatment initiation, 14 patients experienced severe irAEs (grade 3+) at a median of 12.1 weeks (range 4-54), including 4 with life-threatening (grade 4) irAEs. CyTOF revealed elevated circulating CD4 TEM cells in patients that developed severe irAEs ($P<0.0001$; AUC=0.87), including those treated with combination ICIs ($P=0.0001$; AUC=0.89). We further observed a continuous relationship between increasing CD4 TEM levels and irAE grade ($P=3e-6$, Jonckheere-Terpstra test). We then combined CD4 memory T cell abundance and TCR diversity derived from bulk RNA-seq on 24 of these patients using logistic regression (trained on data from Lozano et al.) to yield a composite model score. The pretreatment composite model score was strongly associated with severe irAE development ($P=0.0009$, AUC=0.88), and in a median split, identified patients with shorter time to severe irAE development (3 months vs. not reached; $P=0.006$; HR=10.5). Notably, composite model features and the overall score had no significant association with immunotherapy benefit.
Conclusion: In this prospective study, both circulating CD4 TEM levels determined by CyTOF and a composite model score measured by RNA-seq were strongly associated with severe irAE development, independent of response status. These findings hold promise for future pretreatment risk stratification of ICI therapy.

#1168 Anti-CSF1R antibody monotherapy inhibits minimal residual disease in a novel immunocompetent murine colorectal cancer metastasis model.

A. M. T. Mohamed, K. Cho, M. Soeung, A. Anderson, J. Alshenaifi, G. Manyam, O. Villareal, J. Davis, W. Norton, S. Gao, C. Bristow, F. Carbone, S. Napolitano, O. Coker, I. Khanduri, J. Huang, D. M. Maru, M. Di Pilato, R. Sun, L. Wang, D. G. Menter, G. Genovese, G. Draetta, N. Fowlkes, S. Kopetz;
The University of Texas MD Anderson Cancer Center, Houston, TX

Background: The high mortality rate of colorectal cancer (CRC) is primarily due to metastatic disease. Microscopic minimal residual disease (MRD) detected in patients by circulating tumor DNA (ctDNA) may remain radiographically undetectable and persist following therapeutic intervention, resulting in recurrence. Preclinical models are urgently needed to elucidate the mechanisms whereby MRD escapes anti-tumor immune surveillance. We have developed and characterized a preclinical liver MRD model that recapitulates immune response, with the goal to discover novel strategies to improve outcomes for patients with ctDNA+ MRD.

Methods: We generated genetically engineered mouse colonic organoids CDX2 CRE; Rosa26 LSL-CAS9-GFP with APC and TP53 mutation and performed intrasplenic injection in syngeneic C57BL/6 mice to recapitulate microsatellite stable CRC metastasis to the liver. Mice were monitored for radiographically detectable disease using MRI. Tumors were resected at various timepoints, with comparison between metastases at various sizes of development (dichotomized as micro- and macro-metastases). We performed multiplex immunofluorescence staining, single cell RNA seq, and spatial transcriptomic analysis to delineate the immune compartments of micro- and macro-metastasis in untreated mice. After identifying colony stimulating factor -1 receptor (CSF1R) as a target, we performed a vehicle controlled anti-CSF1R monotherapy study for 4 weeks. Treatment began at either 7 days before metastasis is radiographically detectable to mimic treatment of MRD, or 21 days post tumor engraftment.

Results: Immune exclusion was confirmed through intratumoral CD45+ leukocyte densities, with transition to an immune excluded phenotype occurring above 0.5mm in size (defined as macro-metastases). In our preclinical model, immunosuppressive populations of macrophages (IBA1+CD163+) dominated in the micro-metastases. This observation was confirmed in 13 patients with paired micro- and macro-metastases to the liver ($p=0.0065$). Strikingly, anti-CSF1R treatment in the murine model eradicated IBA1+CD163+ macrophages ($p<0.0001$) and induced complete remission of liver micro-metastasis (0/7 mice with residual disease), in contrast to limited efficacy for macro-metastases (5/5 mice with progressed radiographically disease). Additionally, a long-term study confirmed 100% survival (5/5 mice) and no evidence of disease via MRI at 6 months upon anti-CSF1R treatment compared to vehicle (0/5 mice).

Conclusions: We established a reproducible preclinical model of MRD with similar immunopathological features of MRD in patients. Our data further identified infiltration of immunosuppressive macrophage populations as an early determinant of MRD progression and indicated CSF1R as a potential new clinical therapeutic target for ctDNA+-defined MRD patients.

#1169 Increased immunotherapy sensitivity associated with damaging IFN-gamma pathway mutations in NSCLC.

Alexander Azizi[1], Arvind Ravi[1], Natalie Vokes[2], Stephen-John Sammut[3], Justin Gainor[4], Gad Getz[1]

[1]The Broad Institute of Harvard and MIT, Cambridge, MA, [2]Department of Thoracic/Head and Neck Medical Oncology, MD Anderson Cancer Center, Houston, TX, [3]Breast Cancer Now Toby Robins Research Centre, The Institute of Cancer Research, London, United Kingdom, [4]Henri and Belinda Termeer Center for Targeted Therapies, Massachusetts General Hospital, Cambridge, MA

Introduction: In vivo CRISPR screens across multiple murine models of malignancy revealed that loss of interferon gamma (IFN-γ)-mediated sensing predisposes to immune elimination. We assessed the association between damaging mutations in the IFN-γ pathway and clinical outcomes after immune checkpoint inhibition in the Stand Up to Cancer-Mark Foundation non-small cell lung cancer (NSCLC) cohort.

Methods: The sensitizing IFN-γ pathway genes were defined as *IFNGR1*, *IFNGR2*, *JAK1*, *JAK2*, *STAT1*, *IRF1* & *IRF9*. Damaging mutations (including missense mutations) in any of these genes was considered as loss of pathway activity. We used the best observed response (measured by RECIST v1.1 criteria across time points) to define outcome. Complete and partial response were categorized as responses (R), while stable and progressive disease were categorized as non-responses (NR). The percentage change in target lesions (CTL) was also assessed. Response data was analyzed using additive logistic (LogR) and linear regression (LinR). Overall survival (OS) and progression-free survival (PFS) were analyzed using Cox proportional-hazards models. Three predictor variable groups were established; the final models comprised IFN-γ pathway loss, tumor mutational burden (TMB), programmed death-ligand 1 (PD-L1) tumor proportion score (TPS), prior platinum chemotherapy, age, sex, histological subtype, initial tumor stage, and smoking pack years.

Results: 309 patients had evaluable whole-exome sequencing data, treatment with PD-(L)1 inhibitor regimens, and matched radiological responses (121 R [39%], 188 NR [61%]); 306 had matched OS data; 297 had matched PFS data; and 227 had matched CTL data. 27 (7%) patients had damaging mutations in the IFN-γ pathway [*IFNGR1* (3); *IFNGR2* (1); *JAK1* (6); *JAK2* (8); *STAT1* (3); *IRF1* (1); *IRF9* (3); and *JAK2* & *IRF9* (1)]. Significant relationships were observed in univariable models between IFN-γ pathway loss and both response (LogR: OR 0.17, $p=2x10^{-4}$*; LinR: OR 0.70, $p=4.8x10^{-4}$*) and survival (PFS: HR 0.45, p=0.0067*; OS: HR 0.51, p=0.037*). IFN-γ pathway loss is significantly associated with TMB ($p=9.7x10^{-8}$*, Wilcoxon signed rank test). Multivariable models incorporating TMB and PD-L1 TPS confirmed the significance of IFN-γ pathway loss in both response (LogR: OR 0.29, p=0.050*; LinR: OR 0.71, p=0.0052*) and survival (PFS: HR 0.37, p=0.036*; OS: HR 0.27, p=0.030*). These relationships persisted in the final multivariable models (LogR: OR 0.32, p=0.11; LinR: OR 0.69, p=0.012*; PFS: HR 0.39, p=0.068; OS: HR 0.15, p=0.0038*). Random gene sets, of similar total protein coding sequence length, significantly associated with TMB but not with multivariable models of response or survival.

Conclusion: In this NSCLC cohort, damaging IFN-γ pathway mutations associate with increased immunotherapy sensitivity, independently of TMB and other co-variates, as evidenced by multiple clinical outcomes.

#1170 An off-the-shelf vaccine activates mutant KRAS-specific T cells in patients with resected pancreatic cancer.

A. L. Huff, A. Girgis, S. D. Haldar, E. Davis-Marcisak, T. Heumann, G. Longway, L. Andaloori, A. Hernandez, M. F. Konig, B. Mog, L. Danilova, L. T. Kagohara, J. M. Nauroth, A. M. Thomas, E. J. Fertig, W. Ho, E. M. Jaffee, N. Azad, N. Zaidi;
Johns Hopkins University, Baltimore, MD

Background: Oncogenic mutations in KRAS (mKRAS) are expressed in up to 90% of pancreatic ductal adenocarcinomas (PDAC) therefore representing a promising immunotherapeutic target. We developed a pooled mKRAS peptide vaccine targeting the 6 most common mutations in PDAC: G12V, G12A, G12C, G12R, G12D, or G13D (NCT04117087). In a phase I study, we evaluated mKRAS-specific T cell responses raised by the vaccine when given in combination with immune checkpoint inhibitors to PDAC patients following resection and adjuvant chemotherapy.

Materials and Methods: Patients received the pooled mKRAS peptide vaccine (0.3mg/peptide and 0.5mg poly-ICLC weekly for 4 doses in combination with ipilimumab and nivolumab followed by boosters every 8 weeks with nivolumab. To detect vaccine-induced mKRAS-specific T cells, pre- and post-vaccine peripheral blood mononuclear cells (PBMCs) were restimulated with control or individual mKRAS peptides and IFNγ release was measured by ELISPOT. mKRAS-specific T cell activation, proliferation, memory, and exhaustion profiles were assessed by CyTOF and cytokine secretion was determined by ELISA. For a subset of patients, mKRAS-specific T cells were expanded *in vitro* and T cell receptor (TCR) β chain sequencing and scRNA/TCRseq were used to identify the KRAS mutation-specific TCR repertoires and define their phenotypes in circulation.

Results: mKRAS-specific T cells were detected by IFNγ ELISPOT post-vaccination for all patients, although magnitude and mutation-specific responses varied between patients. CyTOF analysis identified mKRAS-specific Th1 CD4+ central memory (cm, CCR7+IFNγ+) and effector memory (em, CCR7-IFNγ +IL2+ TNFα+) responses as well as CD8+ effector (eff, CD137+GZMBhiKi67hi) and effector memory (CCR7-CD137+GZMB+) responses. mKRAS-specific T cells were also detectable in the extended booster phase of treatment (>1 year post initial vaccination). *In vitro* expanded mKRAS-specific T cells mapped to CD4+ Tcm/em and CD8+ Tem populations within single cell datasets of unstimulated PBMCs collected post-vaccine. 5-25% of the mKRAS-specific T cells significantly expanded to more than one mKRAS antigen suggesting potential cross-reactive T cell clonotypes. In addition, shared public mKRAS-specific T cell clonotypes were identified across patients.

Conclusions: This study demonstrates mKRAS vaccine induction of *de novo*, high quality mKRAS-specific polyfunctional CD4+ and CD8+ T cells. mKRAS-specific TCR analysis identified shared public TCRs across vaccinated patients that have important implications for future “off the shelf” adoptive therapy approaches. Ongoing studies are aimed to validate antigen specificity and map HLA-restriction of mKRAS-specific T cells. Overall, this study demonstrates a positive immunogenic signal of this pooled mutant KRAS vaccine that may be amenable for interception vaccination strategies against PDAC.

#1171 Estimating sensitivity of exploratory cellular biomarkers in oncology clinical trials.

C. Xue, C. D. Swenson, T. W. Mc Closkey;
ICON Clinical Research, Inc., Farmingdale, NY

Background: In the prolonged and complex process of assessing immunotherapeutic oncology drug candidates, flow cytometry plays an essential role. In oncology studies, biomarker measurement requires robust and reliable flow cytometric assays. A crucial element of these assays is to understand the lower limits of measurable surface biomarkers.
Methods: We incorporated into the development and validation of flow cytometry assays the measurement of the lower limit of quantitation (LLOQ). The LLOQ is the lowest number of a reportable parameter in a blood or bone marrow study sample that can be quantitatively determined with acceptable precision and accuracy. Two steps are necessary to determine the LLOQ. First in these assessments a measurable range of lower limits of a particular cell type or receptor is estimated. That is, in validating an assay LLOQ, there are three options to select cells expressing target surface biomarkers of interest: using cultured or bioengineered cells, using samples of known high expression of a biomarker, or using pre-titered positive samples. Then decreasing concentrations of the target cell or receptor may be used to precisely determine the LLOQ of a specific assay reportable parameter.
Results: By acquiring at least ten negative control sample results, the limit of the blank (LOB) and limit of detection (LOD) of a biomarker is determined. LOB is calculated as mean +1.645 SD, and LOD as mean +3 SD. The negative control samples either lack the fluorescent monoclonal antibodies against the markers of interest or lack the target cell population. Different reportable parameters, detected by one or more biomarkers have varying LLOQ. The LLOQ for a reportable parameter is a precise measurement of a parameter above or equal to the LOD. We found that typical LLOQ values are from 4 to 145 positive cells, with a frequency of 0.01 to 0.1% among a parent population. For example, in the case of tetramer assays, flow cytometry can reliably detect as few as 25 CD8+ antigen-specific cells among three million lymphocytes.
Conclusions: LLOQ determinations for exploratory flow cytometry biomarkers are required for clinical research in cancer immunotherapy and cancer vaccine development. This valuable information allows for interpretation of data at the low end of a measurable range.

#1172 Association between CD8+ PD-1+ T cell infiltration levels and improved response to total neoadjuvant therapy in mismatch-repair proficient locally advanced rectal cancer.

C. Lee, C.-T. Chen, N. Urganci, F. Wu, C. Firat, H. Williams, E. Seffar, P. Malekzadeh, W. K. Chatila, J. Shia, J. Garcia-Aguilar, F. Sanchez-Vega;
Memorial Sloan Kettering Cancer Center, New York, NY

Background: The tumor microenvironment plays a major role in colorectal cancer progression, dissemination, and response to therapy. As a mechanism of tumor immunity, CD8+ tumor infiltrating lymphocytes have been shown to express PD-1 in response to clonal neoantigens of tumors. We hypothesized that high levels of CD8+ PD-1+ T cell infiltration prior to treatment initiation may correlate with improved response to total neoadjuvant therapy (TNT) in patients with locally advanced rectal cancer (LARC).
Methods: We analyzed untreated endoscopic biopsies from 159 patients diagnosed with stage II (n=25) or III (n=134), mismatch-repair proficient rectal adenocarcinoma. All patients were treated with TNT, consisting of either induction chemotherapy followed by chemoradiation (n=108) or chemoradiation followed by consolidative chemotherapy (n=51). FFPE blocks from each biopsy were sectioned into slides for H&E and immunohistochemistry staining with antibodies for CD8 and PD-1 in a CLIA certified lab. CD8+ and PD-1+ cells were quantified using established protocols from the College of American Pathologists. We evaluated associations between response to TNT and tertiles of intratumoral CD8 and PD-1 expression (low/mid/high). Disease free survival (DFS) from the start of TNT and rate of sustained complete response (CR, either clinical or pathologic) were used as primary endpoints.
Results: Median follow-up was 40.3 months. The overall CR rate was 42% and the 5-year DFS rate was 77%. Intratumoral CD8 levels were significantly correlated with improved response rates (56% in the top tertile vs. 27% in the bottom tertile, p=0.003, Fisher's test) and improved 5-year DFS (92% vs. 67% for the top vs. bottom tertiles, respectively; p=0.006, log-rank test). Patients in the highest tertile of intratumoral PD-1 expression also had improved response (56% vs. 25%, p=0.002) and DFS (88% vs. 67%, p=0.034). CD8 and PD-1 levels were strongly correlated with each other (R=0.72, p<0.001, Spearman correlation). Finally, the 41 patients who met criteria for top tertiles of CD8 and PD-1 expression had higher CR rates (66% vs. 32%, p<0.001) and better 5-year DFS (97% vs. 70%, p=0.002) than the other patients.
Conclusions: Higher levels of CD8+ and PD-1+ tumor infiltrating lymphocytes on pre-treatment biopsies are associated with improved response to TNT and disease free survival in LARC patients.

#1173 T cell receptor diversity in buffy coat samples from subsets of breast and ovarian cancer patients.

Corinna Keup[1], Cornelia Kolberg-Liedtke[1], Song Tian[2], Samuel J. Rulli[2], Siegfried Hauch[3], Paul Buderath[1], Oliver Hoffmann[1], Rainer Kimmig[1], Sabine Kasimir-Bauer[1]

[1]Essen University Hospital, Essen, Germany,[2]QIAGEN GmbH, Frederick, MD,[3]QIAGEN GmbH, Hilden, Germany

Background: Immunotherapy, mainly by the use of immune checkpoint inhibitors (ICI), has been established as a standard option for both, solid tumors and hematological malignancies. Unfortunately, this success has only been replicated in a subset of patients (pts) with gynecological cancers. In ovarian cancer (OC), response rates to ICI monotherapy were low and in breast cancer (BC), only the subgroup of triple-negative BC (TNBC) pts showed an improved outcome by the addition of ICI. One reason for limited success of immunotherapy might be an impaired immune system. In this regard, monitoring the T cell receptor (TCR) repertoire could provide key insights into adaptive immune responses to ultimately understand disease initiation, progression and treatment response. Here we elucidated TCR alpha, beta, gamma and delta in buffy coats of pts with non-metastatic OC as well as non-metastatic and metastatic TNBC and compared the results with healthy donors (HDs).

Methods: RNA was isolated from buffy coat samples of 20 HDs, 10 treatment-naïve primary OC pts, 14 treatment-naïve, non-metastatic TNBC pts (participating in the phase II neomono trial) and 19 pts with metastatic TNBC by a modified QIAamp RNA Blood Mini protocol. A survey of the TCR diversity and mapping of common and unique TCRs was done using the QIAseq Targeted RNA Panel Human TCR panel for all known T-cell receptors (alpha, beta, gamma, delta).

Results: Regardless of the cancer entity, a significant reduction in TCR diversity was observed compared to HDs with the greatest differences observed in the delta receptors. When OC samples were compared with HDs, the difference in diversity was highly significant for all TCR subtypes (TCRalpha: p=0.013; TCRbeta: p=0.008; TCRgamma: 0.008; TCRdelta: 0.006). Similar results were obtained for non-metastatic TNBC (TCRalpha: p=0.0002; TCRbeta: p=0.0001; TCRgamma: p=0.002; TCRdelta: p=0.002) as well as metastatic TNBC patients (TCRalpha: p=0.001; TCRbeta: p=0.001; TCRgamma: p=0.005; TCRdelta: p=0.003) when their TCR diversity was compared to HDs. Interestingly, no significant differences in diversity were obtained when treatment-naïve non-metastatic TNBC pts were compared with heavily pretreated metastatic TNBC pts. The lowest diversity was found in BC pts compared to the OC pts.

Conclusion: We have initiated a survey of the TCR diversity in TNBC and OC patients. Further evaluations will include the correlation of these findings with clinical characteristics and outcome. Whether the reduced TCR diversity represents T cell exhaustion or T cell specialization cannot yet be deduced from the results. Nevertheless, the addition of a TCR diversity score could provide an additional metric which may help provide patient guidance when integrated into a multi-modal molecular test.

#1174 Incorporation of multisector analysis into the design of personalized DNA vaccines for patients with newly diagnosed glioblastoma.

E. A. R. Garfinkle[1], K. E. Miller[1], A. J. Livingstone[2], R. Perales-Linares[3], N. Cooch[3], A. Perales-Puchalt[3], S. Rochestie[3], J. Peters[3], N. Y. Sardesai[3], W. E. Gillanders[2], E. R. Mardis[1], G. P. Dunn[4], T. M. Johanns[2];

[1]Nationwide Children's Hospital, Columbus, OH, [2]Washington University School of Medicine, St. Louis, MO, [3]Geneos Therapeutics, Plymouth Meeting, PA, [4]Massachusetts General Hospital, Boston, MA

Glioblastoma (GBM) is the most common malignant central nervous system (CNS) tumor in adults. Despite multimodality treatment including surgery, radiation, and chemotherapy, patients with GBM have a median survival of less than 2 years. Recent clinical trials have reported promising results using cancer vaccines to stimulate a tumor-directed immune response in several histologies. The majority of trials targeted tumor neoantigens derived from a single tumor sample, which limits the antigen pool in spatially heterogeneous cancers like GBM. Our group previously implemented multisector sequencing into the design of personalized peptide vaccines to increase the candidate pool of targetable neoantigens (NCT03422094). Although the peptide vaccine treatment was successful in stimulating an effector T cell response, it was limited by a long turnaround time from vaccine design to administration and a low peptide production rate. Therefore, we incorporated multisector sampling into the design of a personalized DNA-based GBM vaccine (NCT04015700). An average of 33% of the candidate targetable neoantigens were spatially restricted to a single sampled region, which would have been missed without multisector sequencing. DNA-based vaccines are potentially advantageous over peptide-based vaccines because they enable a higher neoantigen payload and faster manufacturing time with potent immunogenicity. Here, we report the results from 9 subjects enrolled onto the study. Spatially distinct tumor regions were subjected to whole exome sequencing (WES) and RNA-sequencing (RNA-seq), data from which were used to identify neoantigens through the pVACseq algorithm (http://pvactools.org). An average of 32 neoantigens were included in each DNA vaccine, compared to an average of only 9 for the peptide vaccine, and the turnaround time from date of surgery to administration of the DNA vaccine was about half the time. Three subjects had radiographic evidence of tumor progression prior to vaccination, highlighting the aggressive nature of GBM and the need for short manufacturing timeframes. PBMCs pre- and post-DNA vaccination were collected from 7/9 subjects. All subjects presented detectable responses and 6/7 tested revealed a sustained increment in T cell reactivity against tumor neoantigens post-treatment by IFN-γ ELISpot. Intracellular staining showed a neoantigen-specific antitumor CD8/CD4 T cell cytolytic (CD69+, CD107a+) and proliferative (Ki67+) profile. Post-vaccination tumor resections were performed for 2 subjects who also were treated with PD1 blockade upon progression, providing an opportunity to explore vaccine-induced changes in the tumor microenvironment. Herein, we demonstrate the advantages of incorporating multisector sequencing into the development of DNA-based GBM vaccines and provide insights into the resulting immune responses.

#1175 Differential patterns of immune infiltration in the tumor immune microenvironment associate with therapeutic response in primary prostate cancer following chemohormonal therapy.

E. Heninger, J. M. Sperger, K. Weinstein, B. P. Johnson, P. G. Geiger, S. Wells, S. Y. Cho, W. Huang, P. Tsourkas, S. McIlwain, I. M. Ong, S. C. Kerr, D. F. Jarrard, D. J. Beebe, J. M. Lang;
University of Wisconsin, Madison, WI

There is a critical need to develop novel therapeutic strategies and diagnostic tools to precisely deliver treatments to improve survival for men with prostate cancer. To support this development, improved strategies are needed to better understand heterogenous tumor microenvironments and tumor biology that associate with variable treatment responses. We hypothesized that the tumor immune microenvironment (TIME) plays a critical role in treatment resistance. In this study we aimed to evaluate TIME signatures of treatment response and resistance utilizing a novel, integrated technological tool to identify response patterns and enable precision sampling for comparative cellular and molecular analysis.

30 patients with newly diagnosed, locally advanced, high-risk, primary prostate cancer underwent ^{18}F-DCFPyL PSMA PET/MRI with multiparametric MRI scans followed by 3 cycles of chemohormonal therapy (NCT03358563). Repeat PSMA PET/MRI was performed prior to prostatectomy and scans were used to categorize lesions as complete response (CR), partial response (PR), no response (NR) or normal tissue. MRI scans were used to print a 3D mold of the prostate to allow microdissection of regions of interest from the resected prostate. Cellular infiltrates were analyzed by flow cytometry in 3 to 5 tissue specimens per patient. Statistical analysis was performed with One-way ANOVA with Tukey-correction.

The frequency of CD8$^{\pm}$ T cells in the total CD45$^{\pm}$ infiltrate was highest in normal and CR areas and was significantly reduced in PR vs CR ($p<0.01$). CXCR3$^{\pm}$CD8$^{\pm}$ and CD103$^{\pm}$CD8$^{\pm}$ T cell frequencies were also reduced in PR vs CR foci ($p<0.01$, $p<0.05$, respectively). Meanwhile, the frequency of CXCR3$^{\pm}$CD8$^{\pm}$ T cells was highest and significantly elevated in CR vs normal tissue. A tendency of reduced CCR6$^{\pm}$, CXCR5$^{\pm}$, and CCR4$^{\pm}$CD8$^{\pm}$ T cells was observed in PR vs CR foci, while those frequencies remained higher in normal and CR areas. An increase in total CD8$^{\pm}$ and CD103$^{\pm}$CD8$^{\pm}$ T cells associated with longer progression-free survival. Additionally, the analysis of EpCAM$^{\pm}$ cells showed a significant increase in B7H3 expression in PR vs CR lesions ($p<0.05$) and a tendency of reduced HLA I expression in foci that associated with treatment resistance. We are currently integrating analysis of myeloid cells and transcriptomic analysis of sorted CD4$^{\pm}$, CD8$^{\pm}$ and CD11b/CD14$^{\pm}$ cells to further dissect patterns of therapeutic response in our study cohort.

In conclusion, PSMA/PET MRI based precision sampling of tumor tissue associated with differential therapeutic response patterns captured differences in the TIME infiltrates and these observations may provide hypothesis to test biological mechanisms to expedite discovery of targetable mechanisms to improve tumor stratification and targeting in high-risk prostate cancer.

#1176 Identification of circulating and spatial dynamics of immune cells response to to immune checkpoint inhibitors in triple-negative breast cancer at single-cell resolution.

E. Seo, H. Jung, K. Kim, K. Park, E. Ko, B. Chae, J. Lee, E. Cho, J.-Y. Kim, W.-Y. Park;
Samsung Medical Center, Seoul, Korea, Republic of

Background: Triple-negative breast cancer (TNBC) have had significantly worse survival outcome compared to other BC subtypes even though treatment strategies of TNBC have been advanced. The advent of immune checkpoint inhibitors (ICIs), especially pembrolizumab, a PD-1 inhibitor, has started to revolutionize TNBC treatment, showing encouraging effects in improving survival outcomes regardless of treatment settings. In neoadjuvant setting, pembrolizumab with cytotoxic chemotherapy achieved 13.6 % of pathologic complete response rate improvement and 36% of three-year event reduction. Therefore, pembrolizumab has highlighted new dimensions of TNBC's immunogenic characteristics. However, no immunogenic characteristics to predict the response of pembrolizumab have not been revealed.

Methods: This study was designed as prospective, translational research for stage II or III TNBC patients scheduled for neoadjuvant chemotherapy with or without pembrolizumab followed by curative surgery. Tissue and blood samples were collected at baseline, 1 or 3 weeks after the first treatment initiation and curative surgery. We employed various single-cell and bulk RNA techniques for our multiomic analysis, including peripheral blood mononuclear cell (PBMC) single-cell RNA sequencing, T cell receptor sequencing (scTCR), high-resolution single-cell spatial transcriptomics (Xenium) targeting 380 genes, and bulk PBMC and tissue TCR analysis

Results: From March 2023 to October 2023, 37 patients were enrolled in this study. Of 37 patients, we collected 36 blood and BC tissue samples at baseline, as well as 35 blood and 14 BC tissues at follow-up. These samples were analyzed and also compared with sex and age-matched healthy controls (n = 65). Of 37 patients, two patients were treated with only cytotoxic chemotherapy without pembrolizumab. We observed substantial increases in both systemic and localized immune responses, primarily marked by an upsurge in activated T cells and a decrease in regulatory T cells. A notable rise in TCR diversity post one week of treatment was followed by clonal expansion of activated T cells after three weeks in both blood and tissue. In addition, we observed a significant enrichment of pathways related to inflammatory response in classical monocytes following treatment.

Conclusion: The findings from this study significantly enhance our understanding of the dynamics of circulating and local immune cells in TNBC, analyzed at a single-cell level with spatial information. These insights reveal how pembrolizumab alters the immune landscape and correlates these changes with treatment responses. Importantly, the data provide valuable indicators for predicting which TNBC patients are more likely to respond to neoadjuvant pembrolizumab therapy.

#1177 The chronology of immune-related adverse events (irAEs)-mechanistic implications.

F. Mazahreh, H. Safar, L. Mazahreh, A. Safar;
University of Arkansas for Medical Sciences, Little Rock, AR

Immune Oncology (IO) is a novel component of the oncology armamentarium given its distinct mechanism of action, and by extension, unique mechanisms of toxicity (Tx). To recognize these unusual Txs, the term irAEs was popularized in clinical trials. Most organs have been involved by irAEs and autoimmunity has been implicated commonly by practicing oncologists. The onset of irAEs has not been studied well, however. We reasoned that autoimmune phenomena would be expected early after IO, since this is the timeframe within which T-cells expand to exert their effects on tumor and other 'self' tissues. It follows that if autoimmunity is the sole mechanism of irAEs, such toxicities should be reported early. Mechanism(s) of irARs may prove important for IO duration discussions. In some cases, tumor antigenic epitopes may mimic self-tissues, and in such cases irAEs develop early after initiation of IO. We *hypothesized* that irAEs have distinct chronology: earlier events representing autoimmunity (unavoidable); later events reflecting an intercurrent exposure to an antigen (e.g., virus) and therefore are avoidable by limiting duration of IO. Methods: We reviewed published IO monotherapy trials if individual patient data (swimmers' plot) were reported. We derived the timing and frequency of Tx. We used therapy discontinuation without progressive disease as a surrogate for Tx if reported before the planned 24 months IO therapy.Results: Table depicts the data on included clinical trialsConclusion: The emergence of irAEs after IO extends over a protracted periods with 86% of events occurring beyond 4 months of IO. Though responses occasionally develop late after IO, for Tx consideration, T-cell expansion starts within days of IO initiation, and if autoimmunity is the mediator of Tx, irAEs would emerge only early. Our results suggest dual mechanisms and provide one more impetus to consider shortening IO duration.

Tumor	Author	Discontinued IO (n)	Months of IO Discontinuation										
			0-2	3-4	5-6	7-8	9-10	11-12	13-14	15-16	17-18	19-20	21-22
NSCLC	Topalian	12	1		1	4		1	1			3	1
	Dart	11	3	4		3					1		
	Warburton	56	2	2	7	8	7	22	1	3	1	2	1
Melanoma	Topalian	13				4	1	2	1	2	2	1	
	Weber	2				1		1					
	Demetriou	66	8	4	6	5	6	10	6	10	6	5	
RCC	Topalian	3			1			2					
Total		163	14	10	15	25	14	38	9	15	10	11	2
			8%	6%	9%	15%	8%	23%	5%	9%	6%	7%	1%

#1178 Tissue nanomechanics as a novel, clinically translatable predictive early biomarker of response in combination immunotherapy.

G. Srivastava[1], S. Nizzero[2], M. Wasley[2], M. Kim[3], K. Graham[2], P. D. Ndiaye[1], M. Gachechiladze[1], N. Puebla-Osorio[4], P. Oertle[1], T. Appenzeller[1], V. Cristini[5], M. Loparic[1], M. Plodinec[1], J. W. Welsh[4];

[1]Artidis AG, Basel, Switzerland, [2]Artidis Inc, Houston, TX, [3]MD Anderson, Houston, TX, [4]MD Anderson Cancer Center, Houston, TX, [5]Houston Methodist Research Institute, Houston, TX

Background: Recently, the successful integration of immunotherapy with other treatment modalities has demonstrated its efficacy in enhancing immune activation and suppressing tumors in solid cancers. The most promising of such efforts include the use of low dose radiation (LD-XRT) to prime the tumor microenvironment and enhance the T cell infiltration and activation [Barsoumian HB, et al., 2020; Patel RR, et al., 2021; He K, et al., 2023]. With these advancements, there is an urgent need to develop clinical biomarkers to predict response and optimize treatment decisions. Recent evidence underscores the importance of nanomechanical alterations within the tumor microenvironment as mechanistic indicators of aggressiveness [Plodinec M, et al., 2012]. This study aims to demonstrate the value of ARTIDIS nanomechanical signature as early predictor of elucidate of response to combination LD-XRT/immune checkpoint inhibitors (ICI). Our measurement protocol in mice follows the same settings for biopsies acquired in routine biopsy collection protocol, thus supporting prompt clinical translation and integration.

Methods: We established a mouse model of 344SQ lung adenocarcinoma tumors that exhibited resistance to anti-PD1 treatment in 129Sv/Ev mice. These mice underwent treatment protocols involving a combination of anti-PD1 and anti-CTLA4 antibodies, both with and without LD-XRT pre-treatment. Throughout the study, we closely monitored survival rates and tumor growth across diverse experimental groups. Employing the ARTIDIS platform, a cutting-edge technology that integrates atomic force microscopy with proprietary artificial intelligence algorithms, we extracted a multiparametric nanomechanical signature and we evaluated its outcome prediction value. This signature was then complemented by histopathology, multiplex immunofluorescence, and Nanostring assays to elucidate mechanisms of stroma remodulation and immune infiltration.

Results: This study identifies the unique nanomechanical signature predictive of response to immunotherapy alone or in combination with radiation. Using the tissue nanomechanical signature as a predictive biomarker, we achieved precise differentiation between responders and non-responders, boasting a 90% sensitivity, 99.1% specificity, and a 96% AUC. To our knowledge, this study is the first to demonstrate the response-predicting power of a tissue derived nanomechanical signature for immune checkpoint inhibitors administered in combination with LD-XRT. These findings support clinical translation of the ARTIDIS nanomechanical signature as a pivotal tool for clinically predicting and evaluating responses to integrated radiation and immunotherapy approaches.

#1179 A single-cell atlas of human gastric malignancy reveals CD8+ T cell rejuvenation as a mediator of immunotherapeutic response.

H. Liang[1], J. Chen[2], Y. Luo[3], M. Kang[2], W. Liu[1], L. Wang[2];
[1]UT MD Anderson Cancer Center, Houston, TX, [2]Zhejiang University, Hangzhou, China, [3]Baylor College of Medicine, Houston, TX

Immune checkpoint inhibition (ICI) has emerged as a mainstream treatment for patients with advanced stage gastric cancer (GC). Cellular heterogeneity in the tumor microenvironment (TME) has a profound impact on the therapeutic responses to ICI. Here we characterize the kinetics of tumor-infiltrating immune populations in GC patients treated with anti-PD-1 using single-cell RNA and TCR sequencing (scRNA/TCR-seq), including primary tumors and metastases. Integrated with public GC scRNA-seq datasets, we construct the largest multi-omic atlas of GC cell states to date that captures the full trajectory of GC malignancy and comprises >320,000 cells derived from 73 samples. We demonstrate the rejuvenation of exhausted CD8$^{\pm}$ T cells into a proliferative state marked by the loss of *LAYN* expression as a major mediator of ICI response in the TME. In parallel, we observe enhanced immunogenicity of cancer cells in post-ICI tumors, thus highlighting the coordination between tumor-intrinsic and microenvironmental factors elicited by ICI. Our study provides a valuable resource of investigating the tumor response to anti-PD-1 treatment and suggests novel strategies for combination therapy and patient stratification.

#1180 Asparagine deprivations enhance CD8+ T cell antitumor activity and ICB immunotherapy via ROS-mediated NFAT nuclear localization.

Hsuan Chia Chang, Kwang-Huei Lin, Huang Yu Yang

Chang Gung University, Taoyuan City, Taiwan

Metabolic reprogramming plays a crucial role in the differentiation and activation of T cells. Both oxidative phosphorylation (OXPHOS) and glycolysis are upregulated to meet the high energy demands. However, the impact of amino acid metabolism on T cell activation remains unclear. Our study demonstrates that asparagine deprivation enhances the antitumor activity of CD8+ cytotoxic T lymphocytes (CTLs) and increases the flux of glycolysis and the tricarboxylic acid (TCA) cycle. Mechanistically, asparagine deprivation induces the production of reactive oxygen species (ROS) through mitochondrial complex I deficiency and leads to nuclear localization of NFAT, subsequently affecting cytokine production and T cell activation. In the animal model, we found that the clinical drug leunase exhibits antitumor activity that relies on the immune response of T cells. Leunase treatment promotes the activation of tumor-infiltrating lymphocytes (TILs) in vivo. Furthermore, the combination therapy of leunase and anti-PD1 demonstrates a synergistic effect. In patients with nasopharyngeal carcinoma (NPC), leunase therapy enhances the cytokines production and activation of CD8+ T cell. In summary, our findings offer valuable insights into how T cells adapt to changes in their nutritional environment.

#1181 Therapeutic efficacy by *Streptococcus salivarius* as a probiotic in a preclinical model of oropharyngeal carcinoma.

J. Diaz[1], M. R. Rivera[1], K. A. A. Del Valle[1], E. E. A. Pinero[1], F. G. Vitorino[1], J. R. G. Ortiz[2], S. M. D. Estremera[1];
[1]University of Puerto Rico - Medical Sciences Campus, San Juan, PR, [2]University of Puerto Rico - Comprehensive Cancer Center, San Juan, PR

Streptococcus salivarius is a gram-positive, non-pathogenic bacteria found in the oral cavity and upper respiratory tract. This bacterium has been shown to possess antimicrobial properties with the potential to cause activation of natural killer (NK) cells and induction of anti-tumorigenic cytokines such as interferon-gamma and interleukin-12 (IL-12). There is a high abundance of this bacteria in the saliva in oral squamous cell carcinoma patients. Moreover, *Streptococcus-reactive* cytotoxic T cells were associated with recurrence-free survival. Nevertheless, there is a considerable lack of information regarding the impact of *S. salivarius* on intratumoral immune responses and its potential as a cancer therapeutic. This study aimed to characterize the immune responses in the tumor microenvironment by *S. salivarius* in combination with programmed cell death protein 1 (anti-PD-1) therapy and its therapeutic efficacy. We expect that *S. salivarius* will cooperate with immune checkpoint inhibitors, activating antitumor immune responses. For this project, we used a preclinical murine model where an HPV+ oropharyngeal cancer cell line named mEER was implanted subcutaneously or in the tongue of the mice. We treated with or without *S. salivarius* and/or anti-PD-1. First, *S. salivarius* was administered intratumorally on subcutaneous tumors and treated or not with anti-PD-1 therapy administered intraperitoneally. We measured tumor volume and quantified different immune cells by flow cytometry. While anti-PD-1 treated mice showed a continuous increase in tumor volume, the ones treated with anti-PD-1 and *S. salivarius* reduced the growth rate starting at day 20. Mice treated with anti-PD1 and *S. salivarius* showed increased CD4+ T cells and myeloid-derived suppressor cells (MDSCs) compared to anti-PD-1 treatment alone. Secondly, we implanted the mice with tongue tumors and applied *S. salivarius* topically in the oral cavity with or without anti-PD-1. The use of *S. salivarius* contributed to an increase in CD4+T cells and activation of CD8+T cells and NK cells. The combination of anti-PD-1 with *S. salivarius* did not further enhance the activation of these cells. Nevertheless, 80% of mice receiving anti-PD-1 with *S. salivarius* responded to the therapy, whereas 63% responded while receiving only anti-PD-1. In conclusion, *Streptococcus salivarius* as a probiotic, affected tumor development and immune cell infiltration in oropharyngeal cancer. Future analyses will allow us to explore the effect of the probiotic on the tumor microenvironment and improve colonization in the oral cavity.

#1182 PDC*lung01: An innovative therapeutic cancer vaccine induces specific immune responses in combination with anti- PD-1 treatment in patients with non-small cell lung cancer.

J. Plumas[1], A. Sibille[2], I. Demedts[3], E. Pons-Tostivint[4], C. Van de Kerkhove[5], S. Derijcke[6], W. Theelen[7], B. Biesma[8], F. Borm[9], E. Wauters[10], M. Collodoro[1], K. Al Badawy[1], C. Duchayne[1], C. Debruyne[1], B. Devos[1], B. Colinet[11], D. Moro-Sibilot[12], M. Perol[13], E.-L. Buchmeier[14], M. Skrzypski[15], K. Cuppens[16], J. Vansteenkiste[17];

[1]PDC*line Pharma, Liege, Belgium, [2]University Hospital of Liege, Liege, Belgium, [3]AZ Delta, Roesalare, Belgium, [4]Nantes University, Nantes, France, [5]Vitaz Sint-Niklaas, Sint-Niklaas, Belgium, [6]AZ Groeninge Kortrijk, Kortrijk, Belgium, [7]Nederlands Kanker Instituut, Amsterdam, Netherlands, [8]Jeroen Bosch Hospital, GZ's-Hertogenbosch, Netherlands, [9]Leiden University Medical Center, Leiden, Netherlands, [10]University Hospital KU Leuven, Leuven, Belgium, [11]Grand Hopital de Charleroi, Charleroi, Belgium, [12]Grenoble-Alpes University Hospital, Grenoble, France, [13]Leon Berard Cancer, Lyon, France, [14]Lungenklinik Koeln-Merheim, Koeln- Merheim, Germany, [15]Medical University of Gdańsk, Gdańsk, Poland, [16]Jessa Hospital, Hasselt, Belgium, [17]University Hospitals KU Leuven, Leuven, Belgium

We have developed an innovative cancer vaccine for the treatment of advanced NSCLC patients in combination with checkpoint inhibitors. This PDC*lung01 product based on an irradiated plasmacytoid dendritic cell line loaded with HLA-A*02:01 restricted peptides (NY-ESO-1, MAGE-A3, MAGE-A4, Multi-MAGE-A, MUC1, Survivin and Melan-A) is able to prime and expand peptide-specific CD8+ T cells *in vitro* and *in vivo*, and is synergistic with anti-Programmed Death (PD)-1 (Plumas et al, 2022; Hannani et al, 2023, NCT03970746). In study PDC-LUNG-101 with EudraCT number 2018-002382-19, PDC*lung01 is injected intravenously and subcutaneously for 6 times at two dose levels, 14 million, or 140 million cells in stage II/IIIA (cohort A1 & A2, monotherapy) or stage IV with TPS≥50% (cohort B1 & B2; in combination with pembrolizumab) patients. We report here the analysis of immune response of 3 cohorts (A1, A2, B1) of patients and the first 19 patients out of 42 (cohort B2) treated with high dose of PDC*lung01 in combination with Pembrolizumab at baseline and 3 timepoints post injection. Several circulating immune parameters have been evaluated at different times before and after vaccination using different assays we have developed: leukocyte count and determination of circulation peptide specific CD8+ T cells by flow cytometry using multimer tools without prior *in vitro* culture. The assay made on purified CD8+ T-cells allowed us to define a limit of quantification (LOQ) to accurately assess the fold changes of the cell expansion. In addition, tumor microenvironment (TME) was analyzed by multiplex fluorescence immunochemistry. The data of 42 patients for who an immune response has been evaluated (cohorts A and B) will be presented. No major changes in circulating main lymphocyte frequencies (B cells, NK cells, CD4+, CD8+, or Treg T cells) were observed during treatment. In addition, no major cell activation (CD25+, CD54, or DR+) was noted. In contrast, in a significant number of patients, PDC*lung01 induced circulating peptide-specific CD8+ T cell expansion in all 4 cohorts at different levels and time points against at least one out of seven peptides used. The percentages of patients for who an expansion of antigen-specific T-cell were observed were 50%, 64%, 66.7% and 68.4% in A1, A2, B1 and B2 cohorts respectively. The intensity of the immune response was proportional to the dose of PDC*lung01 and to the combination with pembrolizumab. When possible, total and peptide-specific CD8+ T cells were sorted for analysis of TCR repertoire, illustrating the modelling and dynamics of the immune response. The TME features will also be illustrated. To conclude, treatment with PDC*lung01 induces an anti-tumor immune response in a significant number of patients which appears to be enhanced by the combination with pembrolizumab.

#1183 A first-in-class and SHP1 allosteric inhibitor, SB8091, shows a good efficacy and safety profile in preclinical models.

J. Kim, K. Ryu, J. Cho, D. Kim, D. Seong, K. Kim, I.-S. Jang, J. Shin, S. Jeong, M. Jang, H. Han, J. Hwang, D. Lee, C. Ryu, S. Lee, H. Kim, H. Lee, H. Lee, T.-D. Han, S. Yang, H. Doh;
Dong-A ST, Yongin-si, Korea, Republic of

Introduction: Src homology 2 domain-containing phosphatase 1 (SHP1) is a cytoplasmic protein tyrosine phosphatase (PTP) that is primarily expressed in hematopoietic cells and is commonly recognized as a negative regulator of multiple signaling pathways[1]. Previously, we showed that inhibition of the phosphatase activity of SHP1 by a novel SHP1 allosteric inhibitor, SB6299, results in the activation of innate and adaptive immune cells and enhanced anti-tumor immune responses[2]. Here, we report SB8091, an advanced SHP1 allosteric inhibitor with a promising initial safety profile and improved pharmacokinetic properties.

Methods: SHP1 inhibitors were developed through a structure-based drug design approach, and optimized for cellular activity on target, in vitro ADME, and in vivo pharmacokinetic properties. Pharmacokinetic (PK) and preliminary toxicity studies were performed with mice. The lead series was assessed in in-vitro studies with mouse or human primary immune cells. *In-vivo* efficacy and pharmacodynamic data were generated using mouse syngeneic tumor models.

Results: Structurally, SB8091 seemed to stabilize the autoinhibitory form of SHP1 as an allosteric inhibitor, in a nanomolar range and which can explain the outstanding selectivity compared to other PTP enzymes, including SHP2. In several human primary immune cell types, SB8091 significantly increased cytokine responses and demonstrated significantly enhanced activity in NK cells and macrophages against various cancer target cells. As a single agent, this compound exhibited inhibitory effects on tumor growth when administered orally, and the efficacy was further enhanced when co-administered with anti-PD1 antibodies in various syngeneic tumor models. Notably, this effect was associated with a pharmacodynamic response marked by increased levels of phosphorylated substrates regulated by SHP1. SB8091 exhibited favorable pharmacokinetic properties for oral administration, and SafetyScreen data showed a very low potential for off-target activity and drug-drug interactions. Additionally, during a 2-week repeat pilot toxicity study in mice, SB8091 demonstrated excellent tolerability even at high doses, indicating a high therapeutic index (TI > 100).

Conclusion: Our advanced compound, SB8091, is a potent, highly selective, and orally bioavailable allosteric inhibitor of SHP1. It has demonstrated excellent efficacy as a monotherapy or in combination with immune checkpoint blockers, with favorable drug properties and safety profiles. Research to advance to the clinical stage is being conducted.

References: 1. Watson HA, SHP-1: the next checkpoint target for cancer immunotherapy? Biochem Soc Trans. 2016. 2. AACR-NCI-EORTC 2023; A first-in-class and highly selective SHP1 allosteric inhibitor exhibits robust anti-tumor immunity and synergizes with PD-1 blockade; poster#34172

#1184 Combination pembrolizumab and radiotherapy induces anti-tumor immune responses in immunologically-cold non-small cell lung cancer.

J. Huang[1], W. S. M. Theelen[2], Z. Belcaid[1], M. Najjar[1], C. Cherry[1], A. Balan[1], J. R. White[1], N. Niknafs[1], J. Wehr[1], M. van den Heuvel[3], R. Karchin[1], P. Baas[2], V. E. Velculescu[1], V. Anagnostou[1];

[1]Johns Hopkins University School of Medicine, Baltimore, MD, [2]Netherlands Cancer Institute, Amsterdam, Netherlands, [3]Radboudumc, Nijmegen, Netherlands

Introduction: Primary resistance to immune checkpoint inhibition (ICI) is in part driven by a “cold” tumor microenvironment in the context of low PD-L1 expression, low tumor mutation burden or oncogenic mutations that drive tumor immune exclusion. Radiation has the potential to sensitize tumors to ICI through extra-tumoral T cell activation in response to tumor antigens released from irradiated cancer cells (abscopal effect). Here, we investigate tumor microenvironment and T cell repertoire reshaping leveraging serial biospecimens from a phase 2 randomized clinical trial of stereotactic body radiation therapy followed by pembrolizumab (SBRT arm) vs. pembrolizumab alone (control arm) in non-small cell lung cancer (NSCLC; NCT02492568).

Methods: We employed whole exome sequencing, RNA sequencing and T cell receptor (TCR) sequencing to analyze 293 serial tumor and peripheral blood samples collected at baseline and after 8 weeks of treatment from 72 patients in the control (n=35) and SBRT (n=37) arms. Immunologically-cold tumors were defined as low TMB (<300 mutations per exome, n=43), PD-L1 null (0% expression on immunohistochemistry, n=41), or WNT-activated (presence of mutations affecting genes in the WNT pathway, n=10). TCR clonotypic differential abundance analyses and RNA sequencing deconvolution and gene set enrichment analyses were performed on baseline and on-therapy blood and tumor samples from the control and SBRT arms.

Results: Patients with immunologically-cold tumors in the SBRT arm had significantly longer progression free survival compared to the pembrolizumab monotherapy arm (log rank p=0.029 for TMB-low, p=0.022 for PD-L1-null, p=0.037 for the WNT-activated subsets). Induction of interferon-gamma, interferon-alpha, antigen processing and presentation, and inflammatory response gene sets was significantly enriched on-therapy in the SBRT arm (FDR adjusted p<0.01 for TMB-low, PD-L1-null, and WNT-activated tumors). We observed greater enrichment in newly expanded TCR clones on-therapy intratumorally and in peripheral blood in the SBRT arm compared to the control arm (mean 16.17 vs 7.54 clonotypes, p=0.022 in tumor; mean 4.56 vs 1.00, p=0.039 in blood; Mann-Whitney U test). Similarly, we noted greater expansion of pre-existing TCR clones in the SBRT arm than within the control arm (mean 34.83 vs 18.69, p=0.021 in tumor; mean 21.61 vs 8.15, p=0.009 in blood; Mann-Whitney U test). Within the SBRT arm, there was no significant difference in T cell expansion between TMB-stratified (<300 mutations vs >=300 mutations) or PD-L1-stratified (0% vs >= 1% expression) groups.

Conclusions: SBRT followed by pembrolizumab was associated with priming and augmenting anti-tumor immune responses in immunologically-cold NSCLC, which opens a therapeutic window of opportunity for radiotherapy to overcome primary resistance to immune checkpoint inhibition.

#1185 Novel association of an autoimmune-related axis and anti-CTLA-4-based toxicities in adjuvant immunotherapy-treated melanoma patients.

K. R. Monson[1], R. Ferguson[1], J. Handzlik[1], J. Xiong[1], S. Dagayev[1], L. Morales[1], V. Chat[1], A. Bunis[1], C. Sreenivasaiah[1], S. Dolfi[2], D. Tenney[2], I. Osman[1], J. Weber[1], T. Kirchhoff[1],

[1]NYU Langone Health, New York, NY, [2]Bristol Myers Squibb, Princeton, NJ

Intro: Immune checkpoint inhibition (ICI) for metastatic unresectable melanoma has markedly improved survival, and has shown benefit as adjuvant (AT) and neoadjuvant (NAT) therapy. Although ICI treatments confer survival benefit, they frequently induce immune-related adverse events (irAEs), which are a substantial clinical problem, particularly in AT/NAT, where ICI is used in less advanced disease to prevent recurrence. As such, the biomarkers predicting irAE risk, in particular in AT/NAT, are urgently needed to improve patient outcomes.

Methods: We assessed RNA from pre-treatment peripheral CD4+ and CD8+ T cells from adjuvant clinical trial patients (CheckMate-915; n=212 patients) treated with Nivolumab (n=130) or Ipilimumab/Nivolumab (Combo) (n=82). We performed RNA-seq differential expression analysis to identify baseline differences in the immune profiles of patients with no/mild toxicity (grade 0-2) versus severe toxicity (grade 3-5).

Results: Gene ontology analysis of the differentially expressed genes (DEGs) among those with severe toxicity reveals significant enrichment of immune-related pathways (IL-2, IFN-gamma, T-cell receptors, Toll-like receptors). These are shared among cell types (CD4+/CD8+) and between treatments (Nivo/Combo). From predicted DEG protein-protein interactions, we identified a treatment- and cell-type-specific expression signature associated with irAE development in CD4+ cells from Combo-treated patients. This signature, involving genes in the spleen tyrosine kinase (SYK) pathway, correctly predicts severe irAE patients with 73% accuracy (chi-squared p-value=0.001). The signature also identifies patients with mild to moderate irAEs in organ systems previously found in autoimmune traits to be associated with SYK upregulation (including skin, GI, liver, and pancreas), with 96% of all predicted patients experiencing at least one of these SYK-related toxicities, and 79% experiencing two or more. Importantly, the signature is not associated with disease recurrence (p=0.79).

Conclusions: We have identified baseline expression differences in key immune pathways in peripheral T cells from ICI-treated patients with severe irAEs, and defined an SYK-related gene signature correctly identifying over half of severe irAE patients in the Combo-treated cohort. This finding aligns with our previous work linking anti-CTLA-4 irAEs with a germline variant associated with high SYK expression. This gene signature may not only serve as a baseline biomarker of severe irAEs, but it may also help guide treatment decisions, reducing toxicity while retaining efficacy, which will be particularly important in the adjuvant setting.

#1186 Moving beyond conventional autoimmune thyroiditis autoantibodies to predict immune checkpoint inhibitor induced hypothyroidism.

K. Blenman[1], O. Blaha[1], C. Gibson[1], S. Qiu[1], H. Rushmeier[1], M. Ibrahim[2], S. Qiu[2], M. Krosgsgaard[2], I. Osman[2];
[1]Yale University, New Haven, CT, [2]NYU Langone Health, New York, NY

INTRODUCTION
Treatment emergent adverse events (TEAEs) thyroiditis/thyrotoxicosis and hypothyroidism occur in up to 40% of patients treated with immune checkpoint inhibitors (ICIs). Conventional autoimmune thyroiditis autoantibodies (AutoAbs) (thyroglobulin (TG); thyroid peroxidase (TPO)) do not predict these TEAEs. We previously reported that pretreatment serum AutoAb profiles were associated with all severe TEAEs for melanoma patients treated with ICIs. Herein, we test if pre-existing AutoAbs could predict ICI induced hypothyroidism (TEAE ThyDis).
METHODS
NYU Melanoma Program patients with stage IV metastatic melanoma treated with ICIs (Ipilumumab, Pembrolizumab, Nivolumab, or Combination) who had TEAE ThyDis (N = 14) or No TEAE (N = 11) were included. The HuProt™ human proteome microarray was used to profile proteins on cell surfaces or preferentially in extracellular spaces (N = 1061) in pretreatment and posttreatment (within ~4 months of ICI start) serum. Wilcoxon Rank Sum test was used to determine statistical significance ($p < 0.05$).
RESULTS
17 pretreatment pre-existing AutoAbs were detected (**Table**). All were higher in patients with TEAE ThyDis versus those with No TEAE. The pre-existing AutoAbs impacted immune cells (41%), extracellular matrix (ECM) (65%), or both (24%). P3H4 ($p = 0.01$) and ABCA2 ($p = 0.01$) were the only pre-existing AutoAbs that were statistically different posttreatment and were >10x higher in patients with TEAE ThyDis. They are both associated with intracellular vesicles but can be found in plasma membranes and extracellular spaces. No pre-existing AutoAbs were higher in patients with No TEAE ThyDis compared to those with TEAE ThyDis. However, posttreatment there was an increase in CSF1 AutoAbs that were not pre-existing ($p = 0.05$).
CONCLUSIONS
Our data suggest that serum AutoAbs beyond TG and TPO can predict ICI TEAE ThyDis. Larger studies in other cancers (e.g., Breast) are required to validate these results.

Pretreatment VS Posttreatment

Pretreatment				
Pre-Existing Autoantibody Gene Name	Impact	TEAE ThyDis Present_median (N=14)	TEAE ThyDis Absent_median (N=11)	p-value
COL14A1	ECM	17.35	7.99	0.01
DKK3	Cancer cells/ECM	14.74	3.75	0.01
LRFN1	Neurons	9.87	3.54	0.01
ABI3BP	ECM	2.80	1.69	0.02
SELPLG	Immune Cells	6.26	3.39	0.02
SMPDL3B	Immune Cells/ECM	3.52	1.82	0.02
P3H4	Fibroplasts/ECM	13.41	6.29	0.02
C1QTNF2	Adipocytes/ECM	10.81	5.01	0.03
EMP1	Apoptosis	6.61	3.58	0.03
TMEF1	Neurons	6.44	3.03	0.03
CAPNS1	Cytoskeleton/ECM	3.27	2.13	0.04
FGFR2	Cancer Cells/ECM	2.96	1.62	0.04
GZMH	Immune Cells	2.46	1.45	0.04
FSTL1	Immune Cells (autoantigen)/ECM	5.76	3.17	0.04
ABCA2	Immune Cells	11.81	7.00	0.05
ENPP1	Immune Cells/ECM	2.00	1.33	0.05
FGL2	Immune Cells/ECM	4.17	2.21	0.05
Posttreatment				
P3H4	Fibroplasts/ECM	61.82	6.09	0.01
ABCA2	Immune Cells	106.97	6.69	0.01
CSF1	Immune Cells	4.89	10.31	0.05

#1187 Sensitization to chemo-immunotherapy by targeting TGF-β in preclinical triple negative breast cancer models.

Laura Kalfeist[1], Fanny Ledys[1], Stacy Petit[1], Samia Kada-Mohammed[1], Mickael Rialland[2], Francois Ghiringhelli[1], Emeric Limagne[1], Sylvain Ladoire[1]

[1]Centre Georges-Francois Leclerc, Dijon, France, [2]U1231 INSERM University of Burgundy, Dijon, France

Metastatic triple-negative breast cancer (mTNBC) is refractory to anti-PD-(L)1 immunotherapy. In order to sensitize it, preclinical data show the value of adding chemotherapy treatment for its ability to induce immunogenic cancer cell death (Kroemer et al, 2013). This would enable the recruitment of cytotoxic T-CD8^{+} lymphocytes (CTL) and thus initiate an antitumor immune response to sensitize tumors to immunotherapy. Nevertheless, the results of clinical trials using chemo-immunotherapy combinations are divergent (IMpassion 130 and 131). The IMpassion 130 trial demonstrated the efficacy of nab-paclitaxel and atezolizumab (anti-PD-L1) in PD-L1^{+} patients, but unfortunately, IMpassion 131 with paclitaxel did not replicate these results. The choice of chemotherapy to combine with immunotherapy appears to be crucial for inducing an antitumor immune response. Optimizing chemo-immunotherapy combinations is a major challenge in the management of TNBC.

The initial aim of this project was to evaluate the immune effects of an experimental chemotherapy doublet, based on two drugs used in mTNBC: cisplatin (CDDP) and eribulin. The idea was to find an alternative to the use of taxanes in combination with anti-PD-(L)1.The effect of the two molecules, alone or in combination, was evaluated on immunogenic death stigmata, modulation of effector or immunosuppressive immune populations and stromal populations, and sensitization to anti-PD-L1 immunotherapy in the immunologically "cold" model: 4T1. The *in vivo* studies has been realized by generation of orthotopic 4T1 tumors, the analysis of the immune infiltration was performed by RT-qPCR, IHC and flow cytometry.

In vitro, our results indicate that CDDP, and more intensely in combination with eribulin, significantly induces the various immunogenic death stigmas. *In vivo,* the therapeutic effect of chemotherapies is limited, with a superior effect of CDDP and the combination. Nevertheless, CTL recruitment and functionality induced by CDDP are significantly enhanced by eribulin. Despite these data pointing to a potential therapeutic synergy with anti PD-L1 immunotherapy, chemo-immunotherapy treatment fails to induce a superior treatment effect. The significant increase in a TGF-β signature induced by the combination in parallel with CTL recruitment explains this resistance. The results show that inhibition of TGF-β, combined with chemo-immunotherapy in the 4T1 model, leads to a reduction in tumor immunosuppression and intratumoral fibrosis, as well as an increase in CTL infiltration and cytotoxicity, enabling tumor sensitization.

Overall, this project highlights the benefits of using an experimental doublet of CDDP and eribulin-based chemotherapies. This project demonstrates that management of chemo-induced immunosuppression mechanisms is necessary to overcome tumor resistance to immunotherapy.

#1188 Identification of CXCL10-inducing chemotherapy/targeted therapy combinations for PD-1 blockade sensitization in “cold” triple negative breast cancer.

L. Kalfeist[1], S. Petit[1], L. Galland[1], C. Poirrier[1], R. Aucagne[2], F. Ghiringhelli[1], S. Ladoire[1], E. Limagne[1];
[1]Centre Georges-Francois Leclerc, Dijon, France, [2]University Hospital Francois Mitterand, Dijon, France

Metastatic triple-negative breast cancer (mTNBC) currently has the poorest prognosis among subtypes, with limited treatment options due to molecular characteristics that render conventional targeted therapies ineffective. Immunotherapy, specifically anti-PD-(L)1 (ICIs), has revolutionized certain cancer treatments, but its efficacy in mTNBC has been disappointing. To enhance tumor responses to ICIs, combining them with immunogenic chemotherapy has been explored. Studies like IMpassion130 and KEYNOTE 522 indicate benefits of chemo-immunotherapy based on taxanes, especially in PD-L1^{+} tumors. PD-L1 expression often correlates with TILs infiltration, particularly cytotoxic T lymphocytes (CTLs), indicating an activated immune response in the tumor. However, tumors with poor CTL infiltration, known as "Cold" phenotype, are often associated with a lack of induction of CXCR3-associated chemokines (CXCL9, 10, and 11), crucial for CTLs recruitment in the tumor microenvironment. The limited efficacy of chemo-immunotherapy in PD-L1-negative tumors may stem from chemotherapy's inability to induce immunogenic cancer cell death, CXCR3-associated chemokines, and CTL recruitment. Internal data from a 4T1 TNBC murine model demonstrated that the taxane paclitaxel failed to induce CXCL10, CTL recruitment, and sensitization to PD-L1 blockade. The preclinical research project aimed to identify a combination therapy, inspired by current clinical practices, capable of inducing CXCL10 expression and restoring CTL recruitment in the 4T1 "cold" mTNBC model. We initially screened standard TNBC chemotherapies and selected carboplatin for its *in vitro* potential to induce CXCL10 production and its clinical use in association with ICIs in the TNBC. Combining carboplatin with a library of over 400 targeted therapies, we identified histone deacetylase (HDAC) inhibitors as significantly enhancing CXCL10 secretion. *In vivo*, this combination demonstrated therapeutic additivity, increasing immune recruitment, particularly CD8+ T lymphocytes, with the therapeutic effect reduced by CXCR3 blockade. Mechanistic exploration in vitro revealed that the combination activated the type I interferon pathway, inducing CXCL10 secretion. *In vivo* confirmation validated the role of the type I interferon pathway and CXCL10 in the combination's efficacy. This data outlines a chemotherapy and HDAC inhibitor combination capable of inducing CTL recruitment via increased CXCL10 production. Future project phases will focus on understanding HDACi's mechanism of action on CXCL10 production and the combination's potential to sensitize tumors to ICIs. Overall, this project underscores the role of epigenetic modifications in amplifying carboplatin-induced CXCL10 secretion, potentially converting "cold" ICI-resistant tumors into a "hot" phenotype.

#1189 Modulation of the MSS and MSI colorectal cancer immune microenvironment with FOLFOX and FOLFIRI -/+ anti-PD-1 immunotherapy.

L. Carlsen, **M. Pinho-Schwermann**, L. Zhang, A. Elliott, K. E. Huntington, W. J. MacDonald, B. Verschleiser, L. Jinxuan Wu, W. S. El-Deiry;
Brown University, Providence, RI

Metastatic colorectal cancer (mCRC) is a deadly disease with a five-year survival rate of 14%. Most patients receive 5-FU (F) and folinic acid (FOL) combined with oxaliplatin (OX), irinotecan (IRI), or both (OXIRI). Immune checkpoint inhibitors (ICIs) are effective against microsatellite instable (MSI) tumors, but 95% of mCRC tumors are microsatellite stable (MSS) and ICI-resistant. Though the primary targets of 5-FU, irinotecan, and oxaliplatin are well-understood, their effects on the tumor microenvironment (TME) remain incompletely characterized. Chemotherapy-mediated immune stimulation in MSS CRC has been observed in preclinical models and clinical trials. We hypothesize that combination chemotherapy treatment modulates the immune microenvironment of CRC -/+ ICI, with differences across subtype and treatment regimen. Chemotherapy-dependent changes in cancer cell gene expression, PD-L1 levels, cytokine secretion, and T cell activation were measured using *in vitro* models of MSS and MSI CRC. A preliminary evaluation of spleen and tumor T cells and dendritic cells (DCs) in murine models of MSS and MSI CRC after immunotherapy -/+ chemotherapy was conducted. CD8+ T cells, DCs, PD-L1, CD69, and GM-CSF expression were measured in clinical specimens of chemotherapy-treated MSS mCRC patients. In MSS CRC, FOX increased GM-CSF and activated CD8+ T cells *in vitro* and activated splenic CD8+ and CD4+ T cells *in vivo*. FOX and FIRI suppressed an anti-PD-1-mediated enhancement of type 1 cDCs in the tumor *in vivo*. FOLFOX was associated with increased tumor CD8+ T cells and decreased GM-CSF in MSS mCRC biopsies. FIRI treatment increased PD-L1 *in vitro*. FOLFIRI was not associated with increased tumor CD8+ T cells in MSS mCRC biopsies. In MSI CRC, FOX increased tumor CD8+ T cells *in vivo*. Here, we elucidate novel effects of clinically relevant chemotherapy combinations on the TME in MSS and MSI CRC. These data point to a FOX-specific mechanism by which CD8+ T cell infiltration into MSS mCRC tumors is enhanced, but their activation is halted potentially by GM-CSF suppression and/or type 1 cDC depletion in the TME. These findings contribute to our understanding of the mechanisms of chemotherapy-dependent immune modulation and bring the field closer to harnessing these effects for therapeutic gain.

#1190 NK cell subsets as potential correlates of antitumor immunity in HPV+ cancers.

M. O'Hara, J. Sastry;
The University of Texas MD Anderson Cancer Center, Houston, TX

High-risk type human papillomaviruses (HPV) are associated with genital and oral cancers, and the incidence of head and neck squamous cell cancers is fast increasing in the USA and worldwide. Survival rates for patients with locally advanced disease are poor and variable after standard of care (SOC) chemoradiation treatment (CRT). Identifying the antitumor host immune mediators important for treatment response and designing strategies to promote them are essential for improving clinical outcome. Antitumor immunity comprises of adaptive and innate immune effectors. The immediate innate immune response by natural killer (NK) cells is a critical component for antitumor efficacy. The effector function of NK cells is modulated by various receptors via a wide array of activation or inhibitory signals. Among these receptors is HLA-DR, a recognized activation marker on CD8 T and NK cells. Literature studies refer to HLA-DR+ NK cells as pre-mNK. Preclinical data demonstrated therapeutic vaccine mediated induction of pre-mNK equivalent to contribute to tumor-free long-term survival. In our studies with clinical samples from HPV+ cancer patients, we've observed a dysfunctional phenotype of circulating pre-mNK when compared to healthy donors, demonstrated by flow cytometry methods. The correlates for dysfunction include increased PD-1 expression, a known inhibitory receptor, and reduced CD16, an NK receptor for Antibody Dependent Cellular Cytotoxicity (ADCC). Further, we observed circulating pre-mNK cells in HPV+ head and neck patients gain functionality post-treatment, as shown by significant increases in granzyme B and CD16, both known contributors for NK cytotoxicity. In cervical cancer patients, we had the opportunity to analyze the tumor microenvironment (TME). Interestingly, we found a significant increased frequency of cytotoxic pre-mNK cells, shown by granzyme B, in the TME that was not present in circulation. Overall, pre-mNK represent a uniquely activated immune subset for antiviral and antitumor immunity.

#1191 Personalized neoantigen DNA vaccine GNOS-PV02 and pembrolizumab as second-line treatment for advanced hepatocellular carcinoma.

M. Yarchoan[1], E. J. Gane[2], T. U. Marron[3], R. Perales-Linares[4], J. Yan[4], N. Cooch[4], D. Shu[1], E. J. Fertig[1], L. T. Kagohara[1], G. Bartha[5], J. Northcott[5], J. Lyle[5], S. Rochestie[4], J. Peters[4], J. Connor[6], E. Jaffee[1], A. Perales-Puchalt[4], D. B. Weiner[7], I. Csiki[4], N. Y. Sardesai[4];

[1]Sidney Kimmel Comprehensive Cancer Center, Johns Hopkins University School of Medicine, Baltimore, MD, [2]University of Auckland, Auckland, New Zealand, [3]Icahn School of Medicine at Mount Sinai, New York, NY, USA, New York, NY, [4]Geneos Therapeutics, Philadelphia, PA, [5]Personalis, Inc., Fremont, CA, [6]Confluence Stat, LLC, Cooper City, FL, [7]The Wistar Institute, Philadelphia, PA

Background: PD-1 inhibitors have modest efficacy as monotherapy in hepatocellular carcinoma (HCC). A personalized therapeutic cancer vaccine (PTCV) tailored against neoantigens identified in an individual's tumor may enhance responses to PD-1 inhibitors through the induction of tumor-specific immunity. Here, we present results from a single-arm Phase Ib/2a trial evaluating a DNA plasmid (GNOS-PV02) encoding up to 40 neoantigens co-administered with plasmid-encoded IL-12 (pIL12) in combination with pembrolizumab (PEMBRO) in patients (pts) with advanced HCC.**Methods**: Pts were eligible for study therapy upon progression or intolerance with a 1L tyrosine kinase inhibitor (TKI). The PTCV [GNOS-PV02 (1mg) and pIL12 (0.34mg)] was administered intradermally via in vivo electroporation Q3w x 4 doses, and Q9w thereafter. PEMBRO was administered at 200mg IV Q3w. The primary endpoints were safety and immunogenicity. To evaluate the secondary endpoint of ORR per RECIST 1.1 by investigator review with a null hypothesis of an ORR of 16.9% (KN-240, *Finn et al ASCO 2019*), 36 pts were included to provide 80% power to reject the null hypothesis at the one-sided 0.10 level, assuming the true ORR rate of 33.1%. The data cut date was August 18, 2023.**Results**: Among the 36 enrolled pts who received at least one dose of treatment, there were no DLTs or treatment-related grade ≥3 events. The most common treatment-related adverse events were injection site reactions, observed in 41.6% of pts. ORR (mITT) per RECIST 1.1 was 30.6% (11/36; 9 confirmed and 2 unconfirmed) with 8.3% (3/36) of pts achieving a CR. This achieved statistical significance with a one-sided p-value = 0.031 (1-sided 90% CI 20.4%-100%) The mOS was 19.9 months. ctDNA changes correlated with radiographic responses and preceded them. A complete molecular response (100% ctDNA clearance) was detected in 7 pts including the 3 radiographic CRs, and 4 additional pts who continue to show durable tumor control (3PR, 1 SD). Immunological analyses confirmed the induction of neoantigen-specific T cell responses by IFNγ-ELISpot in 19/22 (86.4%) evaluable pts, and pts with a larger ELISpot response showed a trend towards longer OS. Multi-parametric cellular profiling and single-cell analysis revealed active, proliferative, and cytolytic vaccine-specific CD4+ and CD8+ effector T cells in the blood of immunized pts. In 14/14 (100%) of pts with paired pre- and on-treatment blood and tumor biopsies, we identified by TCRβ bulk sequencing expanded T cell clones in the peripheral blood that also trafficked into the tumor. **Conclusions**: Our results show that a PTCV plus PEMBRO is well tolerated and has clinical activity in pts with advanced HCC, and support the PTCV mechanism of action based on the induction of anti-tumor T cells in peripheral blood and tumor. A confirmatory phase 3 clinical study assessing OS is planned.

#1192 Diversity of TCR repertoire on peripheral CD8$^{\pm}$PD-1$^{\pm}$ T-cell predicting the PFS of chemoradiotherapy followed by durvalumab maintenance in unresectable locally advanced NSCLC patients..

M. Shirasawa[1], T. Yoshida[1], Y. Takeyasu[2], T. Matsutani[3], S. Yagishita[4], S. Kitano[5], H. Kuroda[6], T. Hida[6], T. Kurata[2], Y. Ohe[1];

[1]National Cancer Center Hospital, Tokyo, Japan, [2]Kansai Medical University Hospital, Hirakata, Japan, [3]Repertoire Genesis, Inc., Osaka, Japan, [4]National Cancer Center Research Institute, Tokyo, Japan, [5]The Cancer Institute Hospital of JFCR, Tokyo, Japan, [6]Aichi Cancer Center Hospital, Nagoya, Japan

Background: Chemoradiotherapy (CRT) followed by Durvalumab consolidation has been the standard treatment for unresectable locally advanced non-small cell lung cancer (LA-NSCLC) patients. This study aimed to evaluate how CRT changes TCR repertoire on peripheral CD8$^{\pm}$PD-1$^{\pm}$ T-cells, and the change affects the clinical outcomes of CRT followed by durvalumab treatment.

Methods: This was a prospective cohort study conducted from November 2019 to May 2021 in three institutes (National Cancer Center Hospital, Kansai Medical University Hospital, and Aichi Cancer Center Hospital) in Japan. We revealed the diversity of TCR repertoire (diversity evenness 50 [DE50]) on PD-1$^{\pm}$CD8$^{\pm}$ T cells, and CD8$^{\pm}$ T cell phenotype in PBMCs before and after CRT treatment.

Results: A total of 40 patients treated with CRT were included. Of these patients, 32 patients received durvalumab consolidation treatment after CRT (Durva cohort). The diversity and usage of T cell Receptor Beta Variable (TRBV) and T-cell receptor beta joining gene (TRBJ) usage were significantly positively correlated before and after CRT (TRBV usage: r=0.62, p<0.001, TRBJ usage: r=0.55, p<0.001). Regarding the association of TCR repertoire diversity with CD8$^{\pm}$ T cell phenotype, DE50 and frequencies of CD8 naive were significantly positively correlated before CRT (p=0.049), while there was no correlation between PD-L1 expression and TCR repertoire before CRT (r=0.03, p=0.89) In Durva cohort, DE50 in patients with non-recurrence was higher than those with recurrence both before and after CRT (Before CRT: 0.0032 vs. 0.0019, p=0.13, After CRT: 0.0026 vs. 0.0014, p=0.06). The progression-free survival (PFS) of patients with $DE50_{High}$ before CRT was significantly greater than those with $DE50_{Low}$ (NR vs. 14.3 months; p=0.01). Moreover, when the patients were exploratory classified based on the PD-L1 expression status and the diversity of TCR repertoire, the PFS of the CRT followed by durvalumab apparently differed ($DE50_{High}$, PD-L1 TPS≥1%, NR, and $DE50_{Low}$, PD-L1 TPS<1%, 5.9 (4.6-7.3) months, p=0.001).

Conclusions: TCR diversity of peripheral CD8$^{\pm}$PD-1$^{\pm}$ T-cell predicted the recurrence in unresectable locally advanced NSCLC patients treated with chemoradiotherapy followed by durvalumab maintenance. Additionally, the TCR diversity combined with PD-L1 expression status could more accurately predict the efficacy of the CRT followed by durvalumab.

#1193 Peripheral immune analyses from phase I trial of HPV vaccine PRGN-2009 in combination with bintrafusp alfa in patients with HPV-associated cancers.

M. Goswami[1], C. S. Floudas[1], J. Strauss[1], D. E. Brough[2], A. R. Lankford[2], C. Jochems[1], J. L. Gulley[1], J. Schlom[1], R. N. Donahue[1];
[1]National Cancer Institute (NCI), Bethesda, MD, [2]Precigen Inc., Germantown, MD

Background: PRGN-2009 is a novel gorilla adenovirus vaccine targeting HPV16/18, and bintrafusp alfa (BA) is a bifunctional anti-PD-L1/TGFβ fusion protein. Patients with pretreated advanced HPV-associated malignancies received PRGN-2009 vaccine ($5x10^{11}$ particle units, subcutaneous administration) q2 weeks for 3 administrations and biweekly 1200mg BA followed by q4 weeks vaccine and biweekly BA (NCT04432597), with an overall response rate of 30%. We report here correlative analyses from this first-in-human Phase I study using peripheral blood from 10 patients with HPV16+ (n=8), HPV18+ (n=1), or HPV45+ (n=1) disease to identify immune correlates associated with clinical response.

Methods: Peripheral HPV-specific T cell responses, HPV circulating tumor DNA (ctDNA) from plasma, serum cytokines and soluble factors, and peripheral immune cell subsets were assessed to evaluate changes induced with treatment and peripheral correlates associated with clinical activity. Patients with complete response (CR, n=1), partial response (PR, n=2; 1 confirmed) or stable disease (SD, n=1) (n=4 total) were compared to patients with progressive disease (PD, n=6).

Results: Eighty percent (8/10) of patients developed either HPV16 or HPV18-specific T-cell responses after repeat administration of PRGN-2009 with BA. Eight of 10 patients had detectable HPV16 or 18 ctDNA at baseline and changes in ctDNA load with treatment generally correlated with outcomes. Early transient increases in IL-8, TNFα, and IFNγ occurred, with greater increases in IL-8 at 2 weeks and TNFα at 4 weeks in patients with PD compared to CR/PR/SD. The patient who achieved a durable CR had HPV45+ disease, and had a) a 50% increase in CD8+ T cell frequency at 2 weeks, b) increases in frequencies of CD8+ naïve T cells expressing Ki67+ and central and effector memory T cells expressing 4-1BB, PD-1, or TIM-3, and c) considerable increases in HPV18-specific T cell responses through 484 days after treatment start, indicating durable antigen-specific T cell activity.

Conclusions: The majority of patients developed HPV16/18 specific T-cell responses after repeat administration of PRGN-2009 in combination with BA. Transient increases in IL-8 and TNFα 2-4 weeks after start of treatment were associated with worse outcomes, suggesting that early changes in cytokines may reflect disease course. Furthermore, the early expansion of CD8+ T cell subsets in the patient developing a CR with HPV45+ disease after receiving a vaccine targeting HPV16 and HPV18 epitopes suggest a broadening and boosting of T cell responses that enabled potent anti-tumor activity. A high degree of homology between HPV18 and HPV45 may have contributed to the expansion of HPV18 specific T cells in the patient with CR. These data highlight the importance of assessing peripheral blood in immunotherapy trials to reveal important immunological phenomena.

#1194 Understanding radiation and immunotherapy induced cell state shifts in the pancreatic tumor microenvironment.

M. Parikh[1], R. Park[1], A. R. Parikh[2], J. L. Koenig[2], L. Pappas[2], M. Sade-Feldman[1], L. Bi[3], N. Carzo[2], T. M. Grillo[2], I. Baiev[2], O. Asupoto[4], I. Gushterova[2], T. LaSalle[2], A. Gonye[2], E. Blaum[2], D. P. Ryan[2], D. T. Ting[2], T. S. Hong[2], D. Pe'er[5], N. Hacohen[2], A. Mehta[1];

[1]Broad Institute of MIT and Harvard, Cambridge, MA, [2]Massachusetts General Hospital, Boston, MA, [3]Harvard Medical School, Boston, MA, [4]Boston Medical Center, Boston, MA, [5]Sloan Kettering Institute, New York, NY

Pancreatic ductal adenocarcinoma (PDAC) is a lethal disease with few effective treatment options. It is characterized by a highly desmoplastic tumor microenvironment and a paucity of dendritic cells, leading to low immune cell infiltration and poor outcomes with immunotherapy treatments that are highly effective in other cancers. In a recent pilot study, metastatic PDAC patients who had progressed on chemotherapy were treated with a combination of dual immune checkpoint blockade (ICB) therapy and radiation which resulted in an 18% overall response rate (ORR) and 29% disease control rate (DCR). This led to a phase 2 study in order to further test this combination with the goal of deep correlative analysis to understand the determinants of immunotherapy response and resistance. In this follow up there was a 3.6% ORR, 10.7% DCR, progression free survival (PFS) of 2.3 months, and a single patient with complete response. We collected 36 samples from 23 patients including primary pancreas tumor tissue and liver metastases, and 13 pairs of pre and on treatment biopsies. We performed single-nucleus and paired single-cell RNA and TCR sequencing on these samples to provide comprehensive insight into the cell types and biology present in this unique tumor microenvironment. Using supervised non-negative matrix factorization we have identified both previously established and novel gene programs that co-vary between cell types. Within the various tissue sites we have identified differing proportions of basal to classical tumor cell types and a distinct shift towards the classical state post-radiation. Of particular interest is a group of interferon related gene programs present within epithelial cell subtypes, C1QC+ and MHCII+ macrophages, and CD14+/CD16+ monocytes that indicate cell type specific responses to treatment. Focusing on the T cells, we found a distinct shift towards exhausted or proliferating states on treatment and using TCR sequencing data we have identified novel and expanding clones on treatment, largely consisting of those same cell subtypes. We also collected spatial transcriptomics data on a subset of patient samples, and analysis is ongoing to further confirm the cell type relationships identified in single-cell resolution data, along with spatial localization of basal to classical tumor states. This vast multimodal dataset allows us novel insight into the radiation and dual ICB induced cellular state shifts in the tumor microenvironment.

#1195 Prospective study for the identification of nivolumab biomarkers via analyses of pre-treatment plasma exosome mRNAs from head and neck cancer patients (BIONEXT).

M. Masuda[1], S. Toh[1], M. Matsuo[2], M. Sugasawa[3], K. Yamazaki[4], U. Yushi[5], T. Nakashima[6], H. Uryu[6], T. Ono[7], T. Ueda[8], H. Umeno[7], S. Kano[9], K. Tsukahara[10];

[1]National Kyushu Cancer Center, Fukuoka, Japan, [2]Graduate School of Medical Science, Kyushu University, Fukuoka, Japan, [3]International Medical Center, Saitama Medical University, Hidaka, Japan, [4]NiNigata University Graduate School of Medical and Dental Sciences, Niigata, Japan, [5]Niigata University Graduate School of Medical and Dental Sciences, Niigata, Japan, [6]National Hospital Organization Kyushu Medical Center, Fukuoka, Japan, [7]Kurume University School of Medicine, Kurume, Japan, [8]Graduate School of Biomedical and Health Sciences Hiroshima University, Hiroshima, Japan, [9]Faculty of Medicine and Graduate School of Medicine, Hokkaido University, Fukuoka, Japan, [10]Tokyo Medical University, Tokyo, Japan

Nivolumab paved a new way in the treatment of recurrent or metastatic (RM) head and neck squamous cell carcinoma of (HNSCC). However, the limited rates of long-term survivors (< 20%) demand a robust prognostic biomarker. This nationwide multi-centric prospective study aimed to identify a plasma exosome (PEX) mRNA signature, which serves as a companion diagnostic of nivolumab and as well provides a biological clue to develop effective therapies for a majority of non-survivors. Pre-treatment plasmas (*N* = 104) were subjected to comprehensive PEX mRNA analyses for prognostic marker discovery and validation. In parallel, paired treatment naïve tumor and plasma samples (*N* = 20) were assayed to elucidate biological implications of the PEX mRNA signature. A combination of 6 candidate PEX mRNAs plus neutrophil-to-lymphocyte ratio precisely (*P* = 0.000124) distinguished non-survivors from >2-yr survivor (0% vs 57.7%) with a high hazard ratio (2.878; 95% confidence interval 1.639-5.055; *P* = 0.0002348). In paired samples, high PEX *HLA-E* mRNA (a non-survivor-predicting marker) reflected the increased HLA-E protein expression (*P* = 0.0191) and the dense population of tumor-infiltrating NK cells (*P* = 0.024) in the corresponding tumor. It is estimated that the effects of PD-1blockade is canceled by the HLA-E-NKG2A immune checkpoint in patients with high PEX *HLA-E* mRNA. The combination of NKG2A antibody (i.e., monalizumab) and nivolumab may be a promising strategy for non-survivors predicted by a RT-qPCR-based pre-treatment measurement of PEX mRNAs. A candidate companion diagnostic of nivolumab that indicates a possible treatment option is identified.

#1196 Peripheral immune analyses correlate with clinical outcome: A phase II trial of nivolumab, capecitabine, or the combination in patients with triple negative breast cancer.

N. J. Toney[1], F. Lynce[2], C. Mainor[3], C. Isaacs[4], J. Schlom[1], R. N. Donahue[1];
[1]National Cancer Institute, Bethesda, MD, [2]Dana-Farber Institute, Boston, MA, [3]MedStar Georgetown University Hospital, Boston, MA, [4]Georgetown University, Bethesda, MD

Introduction: Patients with triple negative breast cancer (TNBC) with residual disease after neoadjuvant chemotherapy have a higher risk of recurrence and worse outcomes than patients achieving pathologic complete response. Here, we report on immune correlates from the OXEL study (NCT03487666), an open label randomized phase II trial in TNBC patients with residual disease following neoadjuvant chemotherapy, who were treated with post-neoadjuvant nivolumab (360 mg intravenously every 3 weeks, Arm A), capecitabine (1,250 mg/m^2 orally twice daily on days 1-14 of each 3-week cycle, Arm B), or the combination of nivolumab and capecitabine (Arm C). The primary endpoint was to assess the immunologic effects of nivolumab, capecitabine, or the combination.
Methods: Peripheral blood mononuclear cells were evaluated at baseline and after 6 and 12 weeks of therapy in patients from Arm A (n=15), B (n=14), and C (n=13) by flow cytometry to identify 158 immune cell subsets. Peripheral immunoscores reflective of enhanced immune cell function were calculated to evaluate changes in the immune profile induced by each therapy, and the association between the immune profile at baseline and disease recurrence.
Results: At 6 weeks versus baseline, an increase in immune cell function was seen in patients on Arms A+C compared to Arm B. Additional distinct immune subsets showed statistical changes after 6 and 12 weeks of therapy that were specific to each arm. At baseline, a higher peripheral immunoscore was associated with a lack of eventual disease recurrence in patients on Arm A or Arms A+C, but not for patients on Arm B. Patients on Arm A (p=0.0003) or Arms A+C (p=0.0085) with a peripheral immunoscore above the median also had a longer interval of disease-free survival than patients at or below the median; this association was not seen in Arm B. Distinct immune subsets at baseline also associated with development of recurrence in each arm; higher levels of naïve CD8$^+$ T cells and HLA-DR$^+$ Tregs and lower levels of NKp30$^+$ NK and PD1$^+$ NKT cells associated with recurrence in Arm A, while in Arm B, greater levels of intermediate and nonclassical monocytes associated with recurrence. In Arm C, higher frequencies of multiple Treg subsets were associated with recurrence.
Conclusions: Patients receiving nivolumab, with or without capecitabine, showed enhanced immune cell function. A peripheral immunoscore based on the immune profile at baseline was associated with disease recurrence only in patients receiving immunotherapy. These data highlight the importance of assessing peripheral blood to reveal important immunologic phenomenon and potential associations with clinical outcome.

BIOINFORMATICS / COMPUTATIONAL BIOLOGY / SYSTEMS BIOLOGY / CONVERGENT SCIENCE: Algorithms, Platforms, and Emerging Concepts Minisymposium

#1200 A novel algorithm for deconvolving cancer allele-specific clone copy number and copy number evolution.

P. Pawlik[1], K. K. Grigoriadis[2], A. Bunkum[1], S. Zaccaria[1], N. McGranahan[1], C. Swanton[2];
[1]University College London (UCL) Cancer Institute, London, United Kingdom, [2]The Francis Crick Institute, London, United Kingdom

Both single nucleotide variants (SNVs) and somatic copy number alterations (SCNAs) accumulate in cancer cells during tumor development, fuelling clonal evolution. However, accurate inference of their coevolution from bulk DNA sequencing is challenging. We present ALPACA (ALlele-specific Phylogenetic Analysis of clone Copy number Alterations), a novel algorithm to allow the practical inference of SNV and SCNA coevolution. ALPACA is framed as an optimisation problem, that takes as input bulk tumor sample copy number mixtures and the tumor phylogenetic tree constructed from SNVs, and deconvolves the optimal, allele-specific integer copy number profiles for every distinct clone present in the tumor. To circumvent the challenge of joint SNV/SCNA inference, we postulate that in high mutation burden tumors all relevant SCNA clones are identifiable by their unique SNVs, hence ALPACA leverages phylogenetic trees constructed from bulk tumor sequencing data using SNVs. Secondly, to restrict the clone-specific copy number search space, ALPACA leverages constraints imposed by multisample sequencing, specifically in cases where clones are present across multiple samples or clones from different samples are phylogenetically related. Finally, ALPACA relies on parsimony and biologically informed constraints to further guide the deconvolution process.
We demonstrate that ALPACA infers the copy number evolution of complex simulated tumors with higher accuracy than current state-of-the-art methods. We apply ALPACA to the large, multisample non-small cell lung cancer (NSCLC) cohort from the recent longitudinal, prospective TRACERx421 study, and show that ALPACA uncovers loss of heterozygosity and amplification events in minor subclones that were previously missed using standard approaches. ALPACA's assignment of SCNA driver events to branches of the phylogenetic tree reveals the evolutionary ordering of SNVs and SCNAs during NSCLC tumor evolution, such as late focal amplifications affecting the TERT gene locus occurring in subclones which expand and dominate a tumor sample. ALPACA enables an in-depth analysis of the coevolution of mutations and SCNAs in the tumor's evolutionary history, revealing distinct patterns of copy number evolution. Notably, ALPACA identifies common patterns of copy number changes across the genome characterizing metastatic seeding clones, revealing that they harbor an increased number of SCNAs compared to clones that do not metastasize. Additionally, ALPACA uncovers subclonal enrichment for CCND1 amplification in primary tumor subclones that seed metastasis, and an overall increase of SCNA events occurring in both tumors with polyclonal seeding and extrathoracic metastases.
Clone-level results obtained with ALPACA can offer new clinical insights and enable new types of analysis, e.g. copy number signature analysis including temporal order of SCNA acquisition.

#1201 Pervasive HLA disruption fuels cancer evolution.

C. Puttick[1], T. P. Jones[2], M. Leung[2], O. Pich[1], F. Galvez Cancino[2], J. Liu[2], M. Varas-Godoy[2], A. Rowan[1], C. Martinez-Ruiz[2], R. Bentham[2], K. K. Dijkstra[3], R. Rosenthal[4], N. Kanu[2], K. Litchfield[2], R. Salgado[5], D. A. Moore[1], P. Van Loo[6], M. Jamal-Hanjani[2], S. A. Quezada[2], N. McGranahan[2], C. Swanton[1];
[1]The Francis Crick Institute, London, United Kingdom, [2]University College London, London, United Kingdom, [3]Netherlands Cancer Institute, London, Netherlands, [4]Achilles Therapeutics, London, United Kingdom, [5]Peter MacCallum Cancer Centre, Melbourne, Australia, [6]MD Anderson Cancer Center, London, TX

Disruption of the human leukocyte antigen (HLA) molecules has important implications for immune evasion and tumor evolution. However, although genomic loss of HLA is frequent in non-small cell lung cancer (NSCLC) and in some types of breast cancer, the extent and importance of transcriptomic disruption to HLA presentation, including transcript repression and alternative splicing (AS), remains unclear. To address this, we developed MHC Hammer, a tool to call HLA allele-specific mutations, loss of heterozygosity (LOH), transcriptional repression, and alternative splicing.

We first assessed HLA allelic expression and the prevalence of AS in normal tissue. Applying MHC Hammer to 510 normal lung samples and 407 normal breast samples from the Genotype-Tissue Expression cohort, we identified extensive heterogeneity in HLA allelic expression depending on both the allele and tissue type. In addition, HLA allelic AS, occurring in at least 20% of the allele transcripts, was observed in 19% of normal lung and 13% of normal breast samples.

Next, we applied MHC Hammer to 413 TRACERx NSCLCs and 743 TCGA breast tumours. While mutations were uncommon, HLA LOH was a frequent event, occurring in 32% of lung adenocarcinomas (LUAD) and 57% of lung squamous cell carcinomas (LUSC). We observed a similar rate of HLA LOH in estrogen receptor positive (ER+) and negative (ER-) tumors (ER+: 14%, ER-: 15%), while in triple negative breast tumours we observed a higher rate of LOH (31%). Due to the heterogeneity in HLA expression observed in the normal samples, to measure tumor specific HLA repression and alternative splicing, we restricted our analysis to tumours with WES, tumor and tumor-adjacent normal RNAseq data. This resulted in a cohort of 88 NSCLCs from the TRACERx study as well as 44 ER+ breast tumours from the TCGA cohort. 61% of LUAD, 75% of LUSC and 35% of ER+ tumours harbored class I HLA transcriptional repression that could not be explained by underlying genomic loss. 27% of LUAD, 7% of LUSC and 55% of ER+ breast tumor patients exhibited no HLA disruption. Tumor specific AS affecting HLA exons 2, 3 or 4, potentially disrupting HLA antigen presentation, was identified in 8% of LUADs, 11% of LUSC and 7% of ER+ breast tumours. Tumor specific AS of exon 5, yielding soluble HLA molecules without a transmembrane domain was identified in 20% of LUAD, 14% of LUSCs and 18% of ER+ breast tumours.

LUAD and LUSC tumor regions without HLA LOH or repression were enriched for somatic HLA AS events and alleles with somatic HLA AS had a higher neoantigen burden than those without. We found no relationship between survival and HLA expression or AS in the normal tissue. However, consistent with the importance of HLA dysfunction in tumor evolution, LUADs with low HLA expression in at least one tumor region were associated with shorter disease-free survival, HLA LOH was more common in LUAD's that metastasized and HLA repression was enriched in LUSC primary regions seeding metastases.

#1202 Signatures of selection for biallelic inactivation in tumor suppressor genes across cancer types.

Mark R. Zucker[1], Maria A. Perry[2], Arielle Elkrief[2], Anton Safonov[2], Rohit Thummalapalli[2], Samuel I. Gould[3], Debyani Chakravarty[2], Rose Brannon[2], Marc Ladanyi[2], Pedram Razavi[2], Mark T. A. Donoghue[2], Yonina R. Murciano-Goroff[2], Francisco J. Sanchez-Rivera[3], Yuan Chen[2], Ronglai Shen[2], Sarat Chandarlapaty[2], David B. Solit[1], Nikolaus Schultz[2], Michael F. Berger[1], Adam J. Schoenfeld[2], Jason Chang[2], Ed Reznik[2], Chaitanya Bandlamudi[2]

[1]Epidemiology and Biostatistics, Memorial Sloan Kettering Cancer Center, New York City, NY, [2]Memorial Sloan Kettering Cancer Center, New York City, NY, [3]Massachusetts Institute of Technology, Cambridge, MA

Background: The canonical model of tumor suppressor gene (TSG)-mediated oncogenesis, Knudson's "two hit hypothesis," posits that loss of both alleles is necessary for TSG inactivation. Many key TSGs accordingly exhibit near universal biallelic loss in associated cancers (e.g., APC in colorectal cancer and RB1 in retinoblastoma). However, because the majority of large-scale cancer genomics studies have utilized non-allele-specific copy number analysis methods, neither the extent of biallelic inactivation across TSGs, nor patterns of selective pressure for biallelic inactivation of TSGs, nor the functional and translational consequences of biallelic inactivation, are well-understood.

Methods: Here, through allele-specific analysis of sequencing data from 48,179 cancer patients, we define the prevalence, selective pressure for, and functional consequences of biallelic inactivation across TSGs. We classify TSGs according to their patterns of selection for or against biallelic inactivation across cancer types. Finally, we investigate in detail the association of biallelic status with gene expression and clinical outcome for two TSGs, KEAP1 (in lung adenocarcinoma) and APC (in lung and prostate adenocarcinoma).

Results: TSGs largely assort into distinct classes associated with either pan-cancer (Class I) or lineage-specific (Class II) patterns of biallelic loss, while some TSGs, mostly transcription factors, were predominantly monoallelic (Class III/IV). We discover that gene expression and co-mutation patterns indicate selection for biallelic losses in noncanonical contexts, including *APC* in lung and prostate adenocarcinomas. Selection for biallelic inactivation is also significantly elevated among variants of unknown significance (VUS) of several TSGs, including in *KEAP1* in lung adenocarcinoma, nominating these VUS as worthy of in depth functional characterization. Patients with KEAP1 VUS also show similarly poor survival and response to chemoimmunotherapy to patients with known KEAP1 driver mutations, indicating that *KEAP1* VUSs phenocopy established *KEAP1* oncogenic alleles, and that zygosity, rather than variant classification, is prognostic of therapeutic response.

Conclusion: TSGs vary significantly in their patterns of biallelic inactivation, and can be classified according to whether and how consistently, across cancer types, they are selected for loss of both copies. Additionally, taking into account the zygosity of TSG alteration events is often necessary to understand their phenotypic and clinical consequences, and can be useful in identifying novel driver events.

#1203 Mushroom: a tool for identification of 3D cellular neighborhoods in multi-modal spatial datasets.

E. Storrs, S. Chen, C.-K. Mo, A. Houston, A. Shinkle, A. Southard-Smith, F. Simin, A. Targino, X. Li, A. Abedin, R. Jayasinghe, A. Karpova, J. Liu, J. Herndon, D. Fenyo, F. Chen, R. Fields, T. Ju, B. Raphael, L. Ding;
Washington University School of Medicine in St. Louis, Saint Louis, MO

A comprehensive understanding of the spatial localization of cellular processes is necessary to fully describe tissue biology. Numerous techniques exist to identify cellular neighborhoods in spatial datasets, however, these techniques are limited in that they either only capture two-dimensional phenomena - and can't describe the full, 3-dimensional tumor volume, or they are restricted to one spatial technology (i.e. IF, 10X Visium, Xenium, MERFISH, etc.). To address this, we developed Mushroom, a tool for identification of three-dimensional cellular neighborhoods in serial-sectioned multi-modal datasets. Mushroom's methodology consists of two main steps: 1) registration of multi-modal technologies taken in serial sections (such as multiplex imaging, H&E, or spatial transcriptomics), and 2) identification of 3-dimensional cellular neighborhoods comprising the tissue volume that has been serially sectioned. Keypoint registration is performed with BigWarp, after which the resulting dense displacement field (DDF) is used to register neighboring serial sections - including those from different data modalities. We then implement a neural network to identify three dimensional cellular neighborhoods. The network is a variational autoencoder (VAE) with a vision transformer (VIT) backbone that has been adapted to work with multiple spatial data modalities. Features extracted from the VIT backbone are then clustered to identify cellular neighborhoods unique to each input data type. With 3D neighborhoods in hand, biological questions not answerable in traditional 2D approaches can be investigated, such as z-dimensional changes in morphology and cellular interactions. Further, seamless characterization of cellular neighborhoods by simultaneous technologies at multiple levels of spatial and genomic resolution becomes possible.

#1204 Neoantigen MHC presentability ratios influence the tumor microenvironment and response to immunotherapy.

T. J. Sears[1], K.-H. Lee[1], M. Pagadala[1], A. Castro[2], M. Zanetti[1], H. Carter[1];
[1]University of California San Diego - UCSD, San Diego, CA, [2]University College London, London, United Kingdom

Introduction: Recent literature suggests that neoantigens presented via MHC-II induce a CD4+ T Cell mediated immune response, and MHC-I presented neoantigens expand CD8+ cytotoxic T Cells populations. We developed an algorithm to stratify patients into MHC-I Reliant and MHC-II Reliant immune checkpoint blockade (ICB) responders.
Experimental Procedures: Our algorithm generates patient mean harmonic best rank scores (PHBR) of each neoantigen in a tumor to estimate the proportion of neoantigens that are likely well presented by each MHC complex, given a patient's specific HLA alleles. From there, the ratio of neoantigens presented by each MHC (class-I and class-II) can be used to stratify patients into MHC-I or MHC-II Reliant groupings. The primary goals of our study were to investigate tumor immune microenvironment and survival differences between these groups. First, we used CIBERSORTx infiltration estimates of the ratio of these CD4/CD8 T cell populations across our MHC Reliance categories and by response vs nonresponse in two separate cohorts: Discovery (110) and Validation (77).
Results: We first observed that the CD4/CD8 ratio is higher in MHC-II responders than in MHC-I responders (Fig 6. A, P=~0.0057 Discovery; P=0.025 Validation), but no such a difference was found in nonresponders. Using an alternate digital cytometry tool (xCell) we obtained similar results (MHC-II vs MHC-I responders discovery P=0.44; validation P=0.0015) (Fig. S7). We applied an identical methodology to immune-hot ICB-naive cancer samples from TCGA and found that there was a powerful protective effect of the CD4/CD8 ratio in TCGA MHC-II Reliant patients (Fig S6. HR=-0.76, P=0.0092), there was a significantly harmful effect of that same ratio in TCGA MHC-I Reliant patients (Fig S6 HR=0.59, P=0.0352). These data demonstrate a benefit to having some level of concordance between CD4/CD8+ T cell infiltration and MHC-II/MHC-I neoantigen presentability ratios. Since CD4 memory based immune responses have a longer duration of action over more transient CD8 cytotoxic immune responses (cite), we compared the survival of responders in MHC-II vs MHC-I Reliance groups. MHC-II Reliant responders had a significantly longer overall survival in both discovery and validation cohorts (Fig 6. B-C, discovery P=0.0073; validation P=0.0398).
Conclusions: While neoantigens are already used in ICB stratification in the context of tumor mutational burden, we demonstrate that the balance of which MHC is presenting a set of neoantigens is relevant to immune infiltration and treatment outcome.

#1205 Inferring allele-specific copy number aberrations and tumor phylogeography from spatially resolved transcriptomics.

C. Ma[1], M. Balaban[1], J. Liu[2], S. Chen[2], L. Ding[2], **B. J. Raphael**[1];
[1]Princeton University, Princeton, NJ, [2]Washington University, St Louis, MO

Tumors evolve through the acquisition of somatic mutations over time and across space. While the temporal aspects of tumor evolution can be inferred by applying phylogenetic techniques to bulk or single-cell DNA sequencing data, the spatial aspects of tumor evolution remain understudied. Spatially resolved transcriptomics (SRT) measures gene expression at thousands of spatial locations in a tumor, but does not directly measure genetic aberrations. Thus, SRT data has not yet been fully utilized for tumor evolution studies. We introduce CalicoST, an algorithm that simultaneously infers allele-specific copy number aberrations (CNAs) and derives a phylogeographic model of tumor evolution from SRT data. By modeling CNA-induced perturbations in both gene expression and allele frequencies, CalicoST identifies important types of CNAs - including copy-neutral loss of heterozygosity (CNLOH) and mirrored subclonal CNAs - that are invisible to total copy number analysis. On SRT data from nine patients from the Human Tumor Atlas Network (HTAN), CalicoST achieves an average accuracy of 86%, approximately 21% higher than existing methods. On two of these patients with multiple adjacent slices, CalicoST reconstructs a tumor phylogeography that describes the spread of cancerous clones in three-dimensional space. CalicoST analysis of multiple SRT slices from a cancerous prostate organ reveals five spatially coherent clones, with mirrored subclonal CNAs distinguishing clones on the two sides of the prostate, and a bifurcating phylogeography in both genetic and physical space that suggests a polyclonal cancer.

#1206 Three-dimensional immune atlas of pancreatic cancer precursor lesions reveals large inter- and intra-lesion heterogeneity.

A. L. Kiemen[1], C. Almagro-Perez[2], V. Matos-Romero[2], A. M. Braxton[1], J. Mahesh-Babu[1], E. D. Thompson[1], T. C. Cornish[3], P. Wu[2], L. D. Wood[1], A. Munoz-Barrutia[4], R. H. Hruban[1], D. Wirtz[2];

[1]Johns Hopkins School of Medicine, Baltimore, MD, [2]Johns Hopkins University, Baltimore, MD, [3]University of Colorado, Denver, CO, [4]University of Carlos III, Madrid, Spain

Immunotherapies are generally ineffective in pancreatic ductal adenocarcinoma (PDAC). Paradoxically, inflammation is believed to play a key role in PDAC development and invasion: patients suffering from chronic pancreatitis have a 13-fold increase in risk of developing PDAC. PDAC cells are surrounded by a dense network of fibrotic tissue containing immunosuppressive cells such as regulatory T cells, tumor-associated macrophages, and cancer-associated fibroblasts. Better understanding of the role of inflammation in PDAC could lead to the design of effective immunotherapies. Pancreatic intraepithelial neoplasia (PanIN) is a precursor to PDAC. While most of us will develop PanINs, few of these lesions will progress to invasive cancer. Efforts to determine which PanINs are likely to progress have shown that the size, incidence, and genetic variation of these lesions is high. Here, we add to these efforts through in-depth quantitative analysis of the pancreatic immune microenvironment. CODA is a novel 3D imaging technique used extensively to study the structure, transcriptomic signatures, and genetic heterogeneity of PanINs. In serial histological samples, CODA integrates image registration, cell detection, and segmentation of nine pancreatic structures: PanIN, normal ducts, islets, acini, nerves, vasculature, fat, stroma, and immune aggregates. Through integration with CD45, CD3, and FoxP3 labelled images, we explored immune infiltration in 48 large (cm^3) samples of human pancreas tissues containing >1,000 PanIN lesions to describe spatial correlations between local immune hotspots, 3D tumor morphology, and the surrounding pancreas structures. We quantified inter- and intra-sample heterogeneity in immune response to pancreatic cancer precursor lesions. We determined that this cohort varied greatly in both the number of PanIN (range 3 - 92 per cm^3) and overall immune cell density (range 3,000 - 40,000 immune cells / mm^3). We determined that, while PanIN size is not related to local immune cell density, overall PanIN burden is highly correlated to global immune cell density. This suggests that PanIN content does not have a short-range relationship to inflammation, but does have a long-range relationship with pancreatic structures and immune infiltration. As chronic inflammation in the pancreas shows correlation with development of pancreatic cancer, increased knowledge of the heterogeneous, local immune cell environment in precancerous samples will help us determine the role of inflammation in reacting to and controlling malignant progression.

CLINICAL RESEARCH: Biomarkers Predictive of Therapeutic Benefit
Minisymposium

#1207 Immune subtyping identifies a subset of HR+HER2- early-stage breast cancer patients with a very high likelihood of response to neoadjuvant immunotherapy (IO): Results from 5 IO arms of the I-SPY2 TRIAL.

D. M. Wolf[1], C. Yau[1], L. Pusztai[2], R. Nanda[3], J. Chien[1], E. Stringer-Reasor[4], R. Shatsky[5], C. Isaacs[6], M. Liu[7], H. Han[8], H. Soliman[9], M. Campbell[1], A. Glas[10], A. Barcaru[10], L. Mittempergher[10], M. Kuilman[10], L. Brown Swigart[1], G. Hirst[1], H. Yu[11], P. Beineke[11], A. Basu[1], I-SPY2 Investigators, D. Yee[12], W. Symmans[13], A. DeMichele[14], J. Perlmutter[15], A. Delson[16], L. Huppert[1], H. Rugo[1], A. Clark[14], N. Hylton[1], P. Pohlmann[13], L. Esserman[1], L. van 't Veer[1];
[1]UCSF - University of California San Francisco, San Francisco, CA, [2]Yale University, New Haven, CT, [3]University of Chicago, Chicago, IL, [4]University of Alabama, Birmingham, AL, [5]University of California San Diego, San Diego, CA, [6]Georgetown University, Washington DC, DC, [7]Mayo Clinic, Rochester, MN, [8]Moffit Cancer Center, Tampa, FL, [9]Moffitt Cancer Center, Tampa, FL, [10]Agendia, Inc, Amsterdam, Netherlands, [11]Quantum Leap Healthcare Collaborative, San Francisco, CA, [12]University of Minnesota, Minneapolis, MN, [13]University of Texas MD Anderson Cancer Center, Houston, TX, [14]University of Pennsylvania, Philadelphia, PA, [15]Gemini Group, Ann Arbor, MI, [16]Research Advocate, San Francisco, CA

Background: Neoadjuvant immunotherapy (IO) has become standard of care for early-stage triple negative breast cancer (TNBC). I-SPY2 was the first randomized trial to examine the efficacy of IO therapy in high-risk HR+HER2- breast cancer, where most IO arms showed improved efficacy relative to control. We also previously showed immune-gene expression signatures associate with pathologic complete response (pCR) in HR+HER2- treated with IO; and developed a clinically applicable Immune classifier (ImPrint) predicting response to IO that is now being used in I-SPY2.2 as part of the Response Predictive Subtypes. Here we report the performance of ImPrint in HR+HER2- patients from 5 IO arms.
Methods: 204 HR+HER2- (MammaPrint high risk) patients from 5 IO arms (anti-PD1, anti-PDL1/PARPi, anti-PD1/TLR9 dual-IO, and anti-PD1 +/- LAG3 dual-IO) and 191 patients from the control arm were included in this analysis. Patients were classified ImPrint+ (likely sensitive) vs. ImPrint- (likely resistant), by Agendia, Inc, using pre-treatment mRNA. Performance of ImPrint for predicting pCR to IO was characterized and compared to that of MammaPrint (ultra) High2 risk (MP2) and tumor grade (III). Based on the DRFS of pCR vs. non-pCR HR+HER2-/ImPrint+ patients (median follow up ~4.5yr), we predicted the DRFS in the IO vs. control arms using an exponential model as a function of the pCR rates.
Results: Overall, the pCR rate over the 5 IO arms was 33%. 28% of HR+HER2- patients were ImPrint+; and pCR rates with IO were 76% in ImPrint+ vs. 16% in ImPrint-, with the highest pCR rate >90% in a dual-IO arm. In the control arm, pCR rates were 33% in ImPrint+ and 8% in ImPrint-.
Based on the pCR rates in the IO vs. control (76% vs. 33%), the predicted DRFS of HR+HER2-/ImPrint+ patients are 91% vs 80% at 5 years, respectively. This translates to a risk reduction of 52% for the IO arm relative to standard chemotherapy in HR+HER2-/ImPrint+ patients.
We also compared MP2 and tumor grade (III) to ImPrint+ as pCR predictors, as these markers have been used or proposed as selection markers for neoadjuvant IO trials in HR+HER2-. The pCR rates for MP2, Grade III, at 56%, 45%, respectively, are much smaller than that for ImPrint+ at 75% pCR; thus ImPrint appears to be a more precise predictive biomarker for neoadjuvant IO therapy in the HR+HER2- breast cancers.
Conclusion: These results suggest that a subset of high risk HR+HER2- breast cancers is highly sensitive to immunotherapy, and by using a specific and sensitive selection strategy patients could achieve pCR rates similar to what is seen with best neoadjuvant therapies in TNBC and HER2+ (i.e., pCR rate > 65-70%). ImPrint, an FDA IDE-enabled assay currently being further evaluated in I-SPY2, may represent the way to identify patients for IO that best balances likely benefit vs risk of serious immune-related adverse events.

#1208 Plasma proteomics-based models for predicting therapeutic benefit and immune-related adverse events in non-small cell lung cancer patients treated with immunotherapy.

M. Harel[1], P. Christopoulos[2], I. Puzanov[3], J. Bar[4], I. Kamer[4], N. Reinmuth[5], I. Koch[5], M. Moskovitz[6], A. Levy-Barda[7], A. Zer[8], M. Lotem[9], D. Farrugia[10], R. Katzenelson[11], G. Price[12], A. Agbarya[13], H. Cheley[14], A. Hassani[15], M. Abu-Amna[16], T. Geldart[17], A. Chatterjee[18], A. Polychronis[19], M. Gottfried[20], Y. Lou[21], T. Harkovsky[22], A. Brewster[23], I. Wolf[24], E. Tepper[25], B. Yellin[1], I. Sela[1], C. Lahav[1], Y. Elon[1], R. Leibowitz[26], A. P. Dicker[27], Y. K. Chae[28], R. J. Sullivan[29], D. Carbone[30], D. Gandara[31], **J. Naidoo**[32];

[1]OncoHost, Binyamina, Israel, [2]Thoraxklinik Heidelberg gGmbH, Heidelberg, Germany, [3]Roswell Park Comprehensive Cancer Center, Buffalo, NY, [4]Sheba Medical Center, Ramat Gan, Israel, [5]Asklepios Kliniken GmbH, Gauting, Germany, [6]Rabin Medical Center, Petah Tikva, Israel, [7]Biobank Rabin Medical Center, Petah Tikva, Israel, [8]Rambam Medical Center, Haifa, Israel, [9]Hadassah Medical Center, Jerusalem, Israel, [10]Cheltenham General Hospital, Cheltenham, United Kingdom, [11]Kaplan Medical Center, Rehovot, Israel, [12]Aberdeen Royal Infirmary Grampian NHS, Aberdeen, United Kingdom, [13]Bnai-Zion Medical Center, Haifa, Israel, [14]Swansea Bay UHB, Swansea Bay, United Kingdom, [15]South Tyneside and Sunderland NHS Foundation Trust, South Tyneside District, United Kingdom, [16]Haemek Medical Center, Afula, Israel, [17]Royal Bournemouth Hospital, Bournemouth, United Kingdom, [18]The Shrewsbury and Telford Hospital, Shrewsbury, United Kingdom, [19]Mount Vernon Cancer Centre and Lister Hospital, Northwood and Stevenage, United Kingdom, [20]Meir Medical Center, Kfar-Saba, Israel, [21]Mayo Clinic, Jacksonville, FL, [22]Barzilai Medical Center, Ashkelon, Israel, [23]Withybush Hospital Hawel Dda UHB, Haverfordwest, United Kingdom, [24]Sourasky Medical Center, Tel-Aviv, Israel, [25]Assuta Medical Center, Tel-Aviv, Israel, [26]Shamir Medical Center, Zerifin, Israel, [27]Thomas Jefferson University, Philadelphia, PA, [28]Northwestern University, Evanston, IL, [29]Massachusetts General Hospital, Boston, MA, [30]The Ohio State University, Columbus, OH, [31]University of California Davis Comprehensive Cancer Center, Sacramento, CA, [32]Beaumont RCSI Cancer Centre, Dublin, Ireland

Background: Immune checkpoint inhibitors (ICIs) have significantly improved outcomes for patients with metastatic non-small cell lung cancer (NSCLC). However, clinical management is challenging. The PD-L1 biomarker does not optimally guide the choice between ICI monotherapy and combination ICI-chemotherapy, and there are currently no biomarkers to predict immune-related adverse events (irAEs). Here, we describe a versatile platform based on plasma proteomics and machine learning for generating predictive tools to support treatment decisions.

Methods: Pre-treatment plasma samples were collected from 616 NSCLC patients receiving ICI-based therapy (NCT04056247). Clinical benefit (CB) data and irAEs were recorded. Proteomic profiling of plasma samples was performed using the SomaScan® assay, covering ~7000 proteins per sample. Proteins associated with Clinical Benefit (progression-free survival at 12 months) were classified as resistance-associated proteins (RAPs). Proteins associated with grade ≥3 irAEs occurring within the first 100 days of treatment were classified as toxicity-associated proteins (TAPs). RAPs and TAPs were integrated into two separate machine learning-based models, yielding CB and irAE probabilities, respectively. The CB model used a CB probability threshold to assign patients a PROphet-positive or PROphet-negative result. Bioinformatic analysis was performed on RAPs and TAPs.

Results: CB and irAE models displayed strong predictive performance with a high correlation between predicted probability and observed CB or irAE rate (CB model: R2=0.98; p-value<0.0001; irAE model: R2= 0.92; p-value <0.0001). In the CB model, patients classified as PROphet-positive achieved significantly longer overall survival (OS) than PROphet-negative patients, with a median OS of 25.9 vs. 10.8 months (hazard ratio, HR = 0.51; p-value<0.001). Furthermore, patients with PD-L1 ≥50% tumors and a PROphet-negative result had significantly longer OS with ICI-chemotherapy in comparison to ICI monotherapy (HR=0.23, p-value = 0.0003), suggesting that combination therapy is preferable for such patients despite high PD-L1 levels. Bioinformatic analysis showed that RAPs related to immune regulation, angiogenesis, chemo-resistance, and other potential resistance mechanisms displayed higher expression levels in patients who did not benefit from treatment. Neutrophil- and inflammation-related proteins were significantly enriched in patients who experienced irAEs.

Conclusions: We describe two machine-learning based predictive tools that may be used separately or in combination to inform treatment decisions based on the patient's likelihood to benefit from ICI therapy and to develop serious irAEs. Our findings also provide biological insights related to treatment resistance and immune-related toxicity.

#1209 Tumor informed circulating tumor DNA monitoring for early treatment response and survival outcomes on trastuzumab + pertuzumab.

R. Kurzrock[1], M. Childress[2], W. Li[3], A. Muse[3], J. Malato[4], Y. Wang[4], M. Liu[5], A. Aleshin[5], R. S. P. Wang[3], J. Thierauf[3], C. J. Sweeney[6], J. Hainsworth[7], T. Szado[4], A. Young[3], K. Schulze[4], D. Spigel[7], F. Meric-Bernstam[8], C. Swanton[9], H. A. Burris III[7];

[1]Medical College of Wisconsin, Wauwatosa, WI, [2]Foundation Medicine, Inc., Nashville, TN, [3]Foundation Medicine, Inc., Boston, MA, [4]Genentech, San Francisco, CA, [5]Natera, San Carlos, CA, [6]South Australian Immunogenomics Cancer Institute, Adelaide, Australia, [7]Sarah Cannon Research Institute, Nashville, TN, [8]MD Anderson Cancer Center, Houston, TX, [9]Francis Crick Institute, London, United Kingdom

Background: Advances in cancer treatment have led to the rise of targeted therapies as practice-changing modalities, demonstrating significant efficacy in molecularly selected patients. However, depth of response and survival benefit is variable. Limitations in radiographic imaging create challenges in determining a clinical response. Circulating tumor DNA (ctDNA) is a promising minimally-invasive, predictive biomarker. Here we explore the utility of tumor-informed, on-treatment ctDNA dynamics for early response monitoring and prognostication in patients with HER2-positive tumors of various histologies receiving trastuzumab + pertuzumab on the phase II basket trial, MyPathway (NCT02091141).

Methods: In this retrospective study, 58 patients were included based on availability of tissue comprehensive genomic profiling (CGP) results and baseline/on-treatment plasma. FoundationOne® Tracker was utilized to detect and quantify ctDNA, selecting 2-16 tumor-derived variants from tissue CGP and monitoring the corresponding patient's plasma with multiplex PCR. ctDNA was assessed at baseline and Cycle 3 Day 1 (C3D1) of therapy. Correlations between ctDNA changes and objective response, progression-free survival (PFS) and overall survival (OS) were made using Kaplan Meier analyses and landmarked at C3D1. Patients ctDNA- at baseline and C3D1 were excluded.

Results: Of the 58 patients, personalized ctDNA assays were successfully designed for 52 (89.7%) representing 14 unique tumor histologies. Of 52, 48 (92.3%) had ctDNA results available for baseline analysis with a median of 100.7 mean tumor molecules per mL (MTM/mL); 89.6% were ctDNA+ with a median of 119.5 MTM/mL. A total of 39 patients had both baseline and C3D1 results for ctDNA response analyses. On-treatment ctDNA decline >90% (N=10) was associated with longer survival compared to <90% decline (N=16) or any increase (N=13) in ctDNA (OS: NR, 9.4 months (mo); P= 0.007). CtDNA dynamics remained predictive in a disease specific analysis of colorectal cancer (N=18; OS: NR, 10.2 mo; P= 0.04). Similar results were seen when stratifying patients by baseline ctDNA level (above/below median MTM/mL) or HER2 *(ERBB2)* mutation vs amplification. ctDNA increase at C3D1 preceded radiographic progression by a median of 1.3 mo. In patients with stable disease, >90% decline in ctDNA was associated with longer OS compared to <90% decline or any increase (NR, 9.4 mo; P= 0.01).

Conclusion: Tumor-informed ctDNA monitoring provides insight into early treatment response and survival outcomes in patients with diverse HER2 amplified or mutated tumors receiving HER2 targeted therapy. On-treatment ctDNA dynamics refine and can potentially detect response/progression ahead of standard of care response assessments, suggesting early ctDNA monitoring as a valuable complementary tool for real-time treatment response monitoring.

#1210 High-throughput time-resolved single-cell analysis of T-cell activation.

S. J. J. Kwok[1], S. Forward[1], E. Assita[1], T. Brown[1], M. Fahlberg[1], P. Chattopadhyay[2];
[1]LASE Innovation, Woburn, MA, [2]Talon Biomarkers, Whippany, NJ

How immune cells respond to stimuli is fundamental in developing adoptive cell therapies, vaccines, and other immunotherapies. T cells dynamically undergo activation, exhaustion, expansion, phenotype switching, and cell killing. Flow cytometry is the gold standard method for characterizing these at high throughput, typically by comparing T cell populations before and at different timepoints after treatment. This approach is limited to population-level analyses and overlooks any heterogeneity of individual T cell responses over time, which may contribute to variability in response. Here, we describe the development of a novel flow cytometry-based method (Time-lapse flow™) to characterize immune cell responses over time at the single cell level.

To measure the same cells repeatedly on a flow cytometer, we employed a new optical barcoding technology called laser particles (LPs) that provide individual cells with a unique spectral signature that can be tracked over the course of multiple measurements. Using a custom flow cytometer with fluorescence and LP detection, we performed a multi-day assay to capture how T cell marker expression changes over time after CD3/CD28 activation. Specifically, we used releasable antibodies to quantify PD1, CD69 and CD25 at each time-point and correlated these expression kinetics with cell function at the end of the assay by measuring cytokine secretion (IFNg, IL2, TNFa) after PMA/ionomycin stimulation.

We found significant cellular heterogeneity in kinetic profiles of PD1, CD69 and CD25 expression, with different dominant ‘kinetic modes’ present for each marker. For example, while a large proportion of PD1 expression was transient (positive on day 1, but not on days 2 and 3), nearly all cells that express CD69 on day 1 retained their expression on day 2. We also found that T cells with late expression of PD1 had significantly more cytokine secretion compared to cells that were initially positive for PD1. These results were replicated with at least 3 replicate samples for multiple donors. Differences in kinetic phenotypes were not explained by conventional phenotyping with CD4, CD8, CD45RA and CCR7.

To date, immune cell phenotyping with flow cytometry involves classifying cell types through their marker expression profiles at a single time-point. Here, we introduce a novel approach for acquiring time-resolved single-cell data with a flow cytometer and applied it to study T cell activation. We found novel kinetic phenotypes of T cells defined by their marker expression over time, which also correlated to their functional potential (cytokine secretion). These kinetic phenotypes could not be identified with conventional flow cytometry. Our approach could have significant implications for immunotherapy development, particularly in identifying the most suitable cell populations to use, understanding mechanisms of exhaustion and persistence, and elucidating the basis of donor variability.

#1211 Biomarker analysis of pembrolizumab and ramucirumab neoadjuvant therapy for PD-L1-positive stage IB-IIIA lung cancer: EAST ENERGY trial.

K. Nomura[1], S. Kumagai[1], S. Koyama[1], K. Aokage[2], Y. Shimada[3], K. Yoh[2], M. Wakabayashi[2], M. Fukutani[2], H. Furuya[2], T. Miyoshi[2], K. Tane[2], J. Samejima[2], T. Taki[2], T. Hayashi[4], J. Matsubayashi[3], G. Ishii[2], N. Ikeda[3], H. Nishikawa[1], M. Tsuboi[2];

[1]National Cancer Center, Kashiwa, Japan, [2]National Cancer Center Hospital East, Kashiwa, Japan, [3]Tokyo Medical University, Tokyo, Japan, [4]Juntendo University School of Medicine, Tokyo, Japan

Background: Neoadjuvant treatments with novel combination immunotherapies for resectable non-small cell lung cancer (NSCLC) are being developed. Combination therapy with antiangiogenic agents and anti-PD-1/PD-L1 antibody has shown enhanced antitumor effects. EAST ENERGY is a single-arm multicenter phase 2 trial of neoadjuvant pembrolizumab and ramucirumab in patients with PD-L1-positive stage IB-IIIA NSCLC (NCT04040361). In this study, we aimed to identify biomarkers that predicts the efficacy of the neoadjuvant therapy. Furthermore, we aimed to elucidate the effect of the neoadjuvant therapy on the tumor microenvironment (TME).

Methods: Patients enrolled in the EAST ENERGY trial (n=24) for whom pre- and post-treatment specimens were available (n=20) were included in this study. RNA-sequencing and multiplex immunohistochemistry (mIHC) were used to examine the association between the immunological phenotype of the TME and major pathological response (MPR), and changes in the TME before and after treatment.

Results: MPR was achieved in 50.0% (12/24) of patients. Biomarker analyses with RNA-sequencing revealed that high expression of cancer-associated genes, and upregulation of interferon-gamma and interferon-alpha response in pre-treatment tumor were associated with MPR (q value<0.001). mIHC in pre-treatment samples revealed that abundance of $CD8^{\pm}$ T cells in the pre-treatment TME was associated with MPR (p=0.039). On the other hand, infiltration of immunosuppressive cells such as Treg or M2-macrophages were not associated with resistance for the treatment (p=0.836, 0.639, respectively). Next, to clarify the effect of the neoadjuvant therapy on the TME, comparative analyses of pre- and post-treatment samples was performed. In gene set enrichment analysis, the neoadjuvant therapy enhanced gene set associated with interferon-gamma response (q value=0.051). Furthermore, angiogenesis-related gene set were downregulated after the treatment (q value=0.090). mIHC analyses revealed that the number of $CD8^{\pm}$ T cells in the TME was significantly increased after the neoadjuvant therapy (p<0.001). Notably, Tregs / $CD8^{\pm}$ T cells ratio and the number of M2-macrophage in the TME were significantly decreased after the neoadjuvant therapy (p=0.032, 0.003, respectively).

Conclusion: In the neoadjuvant therapy with pembrolizumab and ramucirumab, immune-activated status before treatment serves as a potential biomarker for predicting treatment response. Moreover, combining ramucirumab with pembrolizumab reduced immunosuppressive cells in the TME and inhibited tumor angiogenesis. These results suggest that this combination therapy modifies the TME and augments antitumor immunity. Larger clinical trial is warranted to assess the efficacy of neoadjuvant therapy with ramucirumab and pembrolizumab in patients with PD-L1-positive NSCLC.

#1212 Impact of KEAP1/STK11 co-mutations and NRF2 signaling on resistance to adagrasib in advanced NSCLC.

M. V. Negrao[1], D. Molkentine[1], A. G. Paula[1], L. Hover[2], M. Nilsson[1], N. Vokes[1], L. Engstrom[3], A. Calinisan[3], L. Waters[3], D. M. Briere[3], J. Hallin[3], G. R. Blumenschein[1], F. Skoulidis[1], S. E. Kopetz[1], D. S. Hong[1], D. L. Gibbons[1], P. Olson[3], J. Christensen[3], J. V. Heymach[1];
[1]UT MD Anderson Cancer Center, Houston, TX, [2]Monoceros Biosystems, San Diego, CA, [3]Mirati Therapeutics, San Diego, CA

Background: KRAS G12C inhibitors (G12Ci) are revolutionizing the therapeutic landscape of advanced NSCLC, but mechanisms of limited clinical efficacy observed in some patients (pts) merit continued exploration. In the largest cohort of advanced KRAS G12C-mutant (K^{G12C}) NSCLC pts treated with G12Ci, we demonstrated *KEAP1* and *STK11* co-mutations are enriched in early progression to G12Ci. Yet the independent predictive role of *KEAP1* and *STK11* co-mutations and the impact of enhanced NRF2 signaling in clinical outcomes to G12Ci remains incompletely characterized.
Methods: Clinico-genomic data were collected from 129 pts with advanced K^{G12C} NSCLC treated with adagrasib (ada) (KRYSTAL-1 - NCT03785249). NRF2 signaling was estimated by NRF2 score (*HTG transcriptome panel*). Kaplan-Meier estimates of PFS and OS were assessed with log-rank test. Hazard ratios (HR) were estimated using Cox regression model. K^{G12C} NSCLC cell lines and CDX/PDX models were used for pre-clinical experiments.
Results *KEAP1* and *STK11* co-mutations were each associated with significantly shorter survival upon ada treatment (*KEAP1*: PFS 4.1 vs 9.9 mo, HR 2.7, p<0.01; OS 5.4 vs 19.0 mo, HR 3.6, p<0.01; *STK11:* PFS 4.2 vs 11.0 mo, HR 2.2, p<0.01; OS 9.8 mo vs not reached [NR], HR 2.6, p<0.01). $KEAP1^{WT}/STK11^{WT}$ status identified a group of pts with significantly longer PFS (16.85 mo) and OS (NR) upon treatment with ada. In cell viability and colony formation assays, KEAP1 re-expression sensitized all $KEAP1^{MUT}/STK11^{MUT}$ K^{G12C} NSCLC cell lines to ada treatment. Similar results were observed with *STK11*/LKB1 re-expression. $KEAP1^{MUT}$ was linked to limited response to ada across a broad panel of NSCLC PDX/CDX. *In vivo* drug anchored CRISPR screens in the ada-sensitive LU99 cell line identified *KEAP1* as the most significant gene promoting resistance to ada. *KEAP1* KO in the LU99 model determined early onset of ada resistance. *In vitro* drug screens showed high synergy scores and higher anti-tumor activity for mTOR inhibitor (mTORi) and ada combinations in K^{G12C} $KEAP1^{MUT}/STK11^{MUT}$ NSCLC. High NRF2 score was associated with significantly shorter survival with ada (PFS: 4.2 vs 8.4 mo, HR 2.0, p=0.02; OS: 6.5 vs 19.0 mo, HR 2.8, p<0.01) even in $KEAP1^{WT}$ NSCLC pts. Integration of $KEAP1^{WT}$, $STK11^{WT}$ and low NRF2 score status identified pts - 32% - with significant and meaningfully longer survival when treated with ada (PFS 12.0 vs 4.2 mo, HR 0.2, P<0.01; OS NR vs 8.0 mo, HR 0.1, p<0.01).
Conclusions: Co-mutations in *KEAP1* and *STK11* and NRF2 signaling define a subgroup of K^{G12C} NSCLC pts with markedly distinct outcomes upon treatment with ada. The mTORi and ada combination shows high efficacy for targeting K^{G12C} NSCLC harboring *KEAP1* and *STK11* co-mutations. The clinical safety and efficacy of mTORi nab-sirolimus and ada will be determined in the ongoing KRYSTAL-19 trial (NCT05840510).

#1213 Tissue-specific thresholds and microenvironment correlates of tumor mutation burden associated with immunotherapy benefit and prognosis in microsatellite stable cancers.

M. Muquith[1], M. Espinoza[1], A. Elliott[2], J. Xiu[2], A. Seeber[3], W. El-Deiry[4], E. S. Antonarakis[5], S. Graff[4], M. J. Hall[6], H. Borghaei[6], D. S. Hoon[7], S. V. Liu[8], P. C. Ma[9], R. R. McKay[10], T. Wise-Draper[11], J. Marshall[8], G. W. Sledge[2], D. Spetzler[2], H. Zhu[1], D. Hsieh[1];

[1]UT Southwestern, Dallas, TX, [2]Caris Life Sciences, Dallas, TX, [3]Medical University of Innsbruck, Innsbruck, Austria, [4]Brown University, Providence, RI, [5]Masonic Cancer Center, Minneapolis, MN, [6]Fox Chase Cancer Center, Philadelphia, PA, [7]Saint John's Cancer Institute, Santa Monica, CA, [8]Georgetown University, Washington, DC, [9]Penn State Cancer Institute, Hershey, PA, [10]Moores Cancer Center, San Diego, CA, [11]University of Cincinnati, Cincinnati, OH

Background: Immune checkpoint inhibitors (ICIs) targeting anti-PD-1/L1 have expanded the treatment landscape against cancers, but are only effective in a subset of patients across all cancer types. Tumor mutation burden (TMB) is postulated to be a generic determinant of ICI dependent-tumor rejection. Here, we clarify the association between TMB and survival outcomes among microsatellite-stable cancers in a real-world clinicogenomic cohort including 70,698 patients distributed across 27 histologies.

Methods: Patients were segregated into mutually exclusive anti-PD-1/L1 (N=14,736, immune checkpoint inhibitor, ICI) and non-ICI cohorts (N=55,962) if they had received pembrolizumab, nivolumab, atezolizumab, durvalumab, avelumab, or cemiplimab, and non-ICI therapies, respectively, during the course of treatment for individual cancer types. Patients treated with chemo-immunotherapy combination regimens were included in the ICI cohorts, but anti-CTLA-4 agents were excluded from both cohorts. For both ICI and non-ICI cohorts, patients were reiteratively categorized as TMB-high or -low using increasing TMB thresholds up to the 90th percentile TMB for individual cancer types. Outcomes were then assessed using Cox regression analyses of overall survival (OS).

Results: Across 27 histologies, 12 cancer types had at least one TMB cutoff associated with survival benefit upon ICIs (melanoma, NSCLC, SCLC, bladder, cervical, colorectal, gastric, ovarian, head and neck, vulvar cancers, as well as carcinoma of unknown primary, and sarcoma), and these associations were generally conserved across sex and age groups, although not necessarily significant in all cases. In two cancer types (cholangiocarcinoma and neuroendocrine tumors), TMB cutoffs were associated with worse OS with ICIs. The lowest TMB cutoff in which a survival benefit could be detected with ICIs ranged from 2 mut/Mb in melanoma to 9 mut/Mb in colorectal cancer. TMB thresholds with the greatest predictive value (defined as the lowest survival hazard ratio) were frequently near the highest TMB examined for individual cancer types, suggesting that TMB may scale with ICI benefit.

Conclusion: TMB was associated with survival benefit or detriment depending on tissue and treatment context. Detectable survival benefits were noted over a broad range of TMB cutoffs across cancer types, and a dose-dependent relationship between TMB and outcomes was observed in a subset of cancers. These results may have implications for cancer-agnostic and universal TMB cutoffs to guide the use of anti-PD-1/L1 therapies, and underline the importance of tissue context in the clinical development of ICI biomarkers.

EXPERIMENTAL AND MOLECULAR THERAPEUTICS: Biological Therapeutic Agents
Minisymposium

#1214 Investigating therapeutic strategies to promote immune rejection of KRAS^{G12C} inhibitor-resistant subpopulations in lung cancer.

M. Tomaschko, C. Moore, C. E. Pillsbury, K. Ng, S. de Carne, S. Rana, A. de Castro, P. Anastasiou, **M. Molina-Arcas**, J. Downward;
The Francis Crick Institute, London, United Kingdom

Oncogenic KRAS signaling not only promotes progression and survival of cancer cells, but it can also play a major role in suppressing anti-tumor immunity through several mechanisms, including secretion of cytokines, reduction of antigen presentation and suppression of tumor-intrinsic interferon responses. Consequently, treatment with KRAS^{G12C} inhibitors alleviates oncogenic KRAS driven immune suppression, resulting in a profound remodeling of the tumor microenvironment (TME). In immunogenic mouse models, these changes can lead to the generation of some complete responses which are dependent on the engagement of the immune system. In this project we aim to investigate whether the induction of immune responses triggered by KRAS^{G12C} inhibition can effectively target inhibitor-resistant subclones. To achieve this, we mimic the development of drug resistance by combining reporter-traced isogenic KRAS^{G12C} and KRAS^{G12D} mutant lung cancer cells, where the KRAS^{G12D} mutant cells are inherently resistant to KRAS^{G12C} inhibitors. Growth of resistant cells was monitored via in vivo luciferase imaging and end point flow cytometry. KRAS^{G12C} inhibition as monotherapy, either with the active-state KRAS^{G12C} inhibitor RMC-4998 or the inactive-state inhibitor adagrasib, led to a proliferative advantage of the drug-resistant subpopulation, suggesting that any immune response to KRAS^{G12C} inhibition in the bulk tumor population was insufficient to target the resistant cell subclones. To investigate if immune mediated elimination of resistant cells could be achieved using combinations, we assessed two strategies commonly evaluated in clinical trials with KRAS^{G12C} inhibitors: anti-PD1 blockade and SHP2 inhibition. Of note, KRAS^{G12D} mutant cells do not respond to these therapies when grown subcutaneously. Treatment of RMC-4998 in combination with either anti-PD1 or the SHP2 inhibitor RMC-4550 was able to induce complete eradication of both KRAS^{G12C} and KRAS^{G12D} mutant lung cancer cells, despite the resistant cells being insensitive to these therapies when treated in the absence of sensitive cells. Furthermore, both combinations induced immune memory towards the resistant cells. These long-term effects were dependent on the immune system as they were not observed in immune deficient mice. Immune profiling of treated tumors revealed that both combinations can result in a more profound remodeling of the TME and potentiate the immune responses. Overall, our preclinical results demonstrate that the anti-tumor responses generated by the combination of KRAS^{G12C} inhibitors with SHP2 inhibition and/or immune checkpoint blockade can result in the bystander immune mediated killing of subclones of KRAS^{G12C} inhibitor resistant cells, providing a paradigm for the development of therapeutic combinations that may be more able to counter the development of inhibitor resistance.

#1215 DIRAS3 inhibits oncogenic RAS signaling and RAS-dependent cell growth driven by prevalent KRAS hot spot mutations.

G. Bildik[1], J. Liu[2], W. Mao[1], H. Yang[1], J. F. Hancock[2], R. C. Bast, Jr.[1], Z. Lu[1];
[1]The University of Texas MD Anderson Cancer Center, Houston, TX, [2]The University of Texas Medical School at Houston, Houston, TX

RAS mutations are found in 30% of human cancers and are characterized by hotspot mutations at codons G12, G13, and Q61. This results in constitutively activated RAS proteins. Despite recent advances in drug design and the emergence of covalent inhibitors, effectively targeting mutant RAS remains challenging. Our group previously identified the tumor suppressor protein DIRAS3, which directly binds Ras and inhibits its function by disrupting KRAS dimers/nanoclusters and blocking effector activation. DIRAS3 expression reduced cancer cell growth in pancreatic and ovarian cancers. To determine whether DIRAS3 plays a definitive role in inhibiting mutant KRAS, we comprehensively characterized DIRAS3's RAS-inhibitory effects using RASless mouse embryo fibroblast (MEF) cells as a model system lacking endogenous RAS isoforms. We ectopically expressed various KRAS mutations in these cells and then examined DIRAS3's effect on each KRAS mutant clone. We analyzed downstream RAS signaling, colony formation, cell viability, and toxicity. Our results showed that DIRAS3 significantly inhibited RAS-dependent colony formation in KRAS mutant (G12C, G12D, G12V, G13D, G12R, Q61R, Q61L) but not wild-type KRAS clones. However, when we added epidermal growth factor (EGF) to the medium, DIRAS3 expression inhibited wild-type KRAS activity, decreasing colony formation. This suggests that DIRAS3 selectively affects the active, GTP-bound form of KRAS and downstream signaling. Additionally, DIRAS3 expression decreased Erk1/2 phosphorylation in MEF cells with mutant KRAS, but not in the cells with a BRAFV600E mutation. This indicates that DIRAS3 specifically inhibits the KRAS-mediated MEK/ERK signaling, cell proliferation, and cytotoxicity. Moreover, to determine the critical region for DIRAS3's RAS-inhibitory function, we compared wild-type DIRAS3 and deletions (ΔNTE, ΔCTE, ΔNCTE). Our results showed both termini are required to effectively suppress clonogenic growth, emphasizing the requirement for DIRAS3 to anchor to the plasma membrane and interact with the RAS dimer interface to inhibit RAS-dependent tumor growth. In conclusion, our findings underscore the potent and specific inhibitory effects of DIRAS3 on RAS-driven oncogenesis, positioning it as a promising pan-RAS inhibitor for RAS-mutant cancers.

#1216 Pan-RAS inhibition by a tumor-targeted biotherapeutic.

G. L. Beilhartz[1], H. Liang[1], M. Udaskin[2], C. Ng[1], N. Radulovich[2], R. A. Melnyk[1];
[1]The Hospital for Sick Children, Toronto, ON, Canada, [2]University Health Network, Toronto, ON, Canada

Oncogenic RAS signaling drives tumor growth in about 30% of human malignancies. In recent years the first mutant-specific inhibitors of KRAS G12C (sotorasib and adagrasib) entered the clinic. While some durable responses were noted in KRAS-mutant non-small cell lung cancer, the clinical experience of KRAS G12C inhibitors is marked by rapid drug resistance, either intrinsic or acquired, causing re-activation of the MAPK pathway. Common resistance mechanisms include compensatory signaling through the related RAS isoforms NRAS and HRAS, as well as the selection of non-G12C KRAS mutations, among others. The bacterial peptidase RRSP potently cleaves all RAS mutants and isoforms in the conserved Switch I region. We have shown that receptor-mediated intracellular delivery of RRSP using an engineered protein delivery system (RASx) can inactivate all RAS signaling in a cell, causing apoptosis in RAS-addicted tumor cells *in vitro* and *in vivo*. Since systemic pan-RAS inhibition is not likely to be tolerated therapeutically, precise tumor targeting is a necessary feature of a true pan-RAS inhibitor. Here, we describe the unique ability of the RASx system to specify the cell surface receptor used by RRSP to enter cells, allowing exquisite targeting and killing of KRAS, NRAS and HRAS-driven tumor cells while sparing healthy tissues. We screened a panel of patient-derived tumor organoids (PDOs), to demonstrate broad tumor cell killing across pancreatic and colorectal cancer-derived PDOs. 97% of KRAS mutant organoids were sensitive to RASx, independent of the specific mutation. Intriguingly, 46% of wildtype RAS PDOs were sensitive to RASx, including organoids with activating mutations in EGFR. In contrast, PDOs with mutations downstream of RAS such as BRAF V600E were resistant to RASx. Indeed, RASx is effective not only against RAS-addicted tumors, but also wildtype RAS tumors driven by upstream receptor tyrosine kinases, potentially expanding the clinical utility of this platform. RASx is a first-in-class, tumor-targeted pan-RAS inhibitor that represents a unique entry into the growing armamentarium against oncogenic RAS.

#1217 Defining the anti-tumor activity and immune effects of the RAS^{MULTI}(ON) inhibitor RMC-7977 in preclinical models of NRAS-mutant melanoma.

L. A. D. Carvalho, M. S. Phadke, K. S. Smalley;
Moffitt Cancer Center, Tampa, FL

Introduction: Mutations in the small GTPase NRAS are the second most common oncogenic driver in cutaneous melanoma, being found in ~25% of cases. Targeted therapy strategies are currently lacking for NRAS-mutant melanoma. Here, we characterized the anti-tumor activity and immune effects of RMC-7977, a RAS^{MULTI}(ON) preclinical tool compound, representative of the investigational agent RMC-6236, in preclinical mouse and human models of NRAS-mutant melanoma.

Methods: The *in vitro* potency of RMC-7977 was determined using mouse and human NRAS-mutant melanoma cell lines. Recovery of signaling was quantified by Western Blot and receptor tyrosine kinase (RTK) arrays. *In vivo* anti-tumor activity of RMC-7977 was determined in two syngeneic mouse melanoma models (SW1 NRAS^{G13D} and NRAS#5 NRAS^{Q61R}), and tumor immune infiltrate quantified using multiplexed IHC and flow cytometry. Mechanisms of resistance were defined using RNA-seq.

Results: RMC-7977 had good activity *in vitro* against human cancer cell lines and in mouse models of NRAS-mutant melanoma. Time-course studies demonstrated RMC-7977 rapidly inhibited phospho-ERK signaling, which then began to recover after 8 hr of treatment. There was also evidence of adaptive receptor tyrosine kinase signaling by 48 hr. In syngeneic mouse models of NRAS-mutant melanoma, RMC-7977 led to a rapid inhibition of tumor growth, increased expression of tumor MHC class I and PD-L1 and an increase in CD4+ and CD8+ T cell infiltrate into tumors. Therapeutic escape was associated with decreased CD4+ and CD8+ T cell infiltration and increased numbers of immunosuppressive MDSCs. Cells collected from tumors resistant to RMC-7977 *in vivo* did not show any shift in sensitivity to the inhibitor when re-challenged *in vitro*, suggesting that the resistance observed *in vivo* resulted from mechanisms specific to the tumor microenvironment, for example adaptive RTK signaling or immune escape. RNA-seq and IHC analysis suggested that resistance was associated with decreased MHC expression and antigen presentation, as well as reduced co-stimulation of T cells. Combination studies of RMC-7977 with anti-PD-1 are ongoing to identify potential synergistic interactions in these preclinical models.

Conclusion: RMC-7977 has anti-tumor activity in syngeneic mouse models of NRAS-mutant melanoma, associated with a robust immune response.

#1218 CDK9 inhibitors modulate the transcriptional landscape of colorectal cancer to suppress MAPK signaling and synergizes with BRAF inhibitors to treat BRAF-mutant colorectal cancer.

C. Kuang[1], N. Wei[1], M. Mohammadi[1], M. A. Bhat[1], T. Li[1], P. Patil[2], O. Wiltz[1], R. Huang[1], K. Ooka[1], M. Quintal[1], E. Chu[1];
[1]Montefiore Einstein Comprehensive Cancer Center, Bronx, NY, [2]Montefiore Medical Center, Bronx, NY

Background: Colorectal cancer (CRC) is the second leading cause of cancer deaths in the US, and it remains a significant public health burden. Metastatic CRC (mCRC) is usually treated with combination chemotherapy and targeted therapy regimens, but eventually becomes chemotherapy refractory. Thus, novel and more effective treatments for mCRC are urgently needed. Cyclin-dependent kinase 9 (CDK9) is a key activator of RNA Pol II transcription and promotes the expression of many cancer driver genes, making CDK9 a promising target for cancer therapy.
Methods: Human CRC cell lines, patient-derived organoids (PDOs), cell line xenografts, and patient-derived xenografts were used to investigate the efficacy and mechanisms of action of the CDK9 inhibitors AZD4573, enitociclib, and NVP-2, as well as the BRAF inhibitors encorafenib and dabrafenib. *In vitro* viability was measured by chemical cell proliferation assays and *in vivo* tumor sizes were measured by calipers. *In vitro* mechanisms of action were assessed by RNA sequencing, real time polymerase chain reaction, and Western blotting. *In vivo* mechanisms of action were assessed by immunohistochemistry.
Results: CDK9 inhibitors potently inhibited CRC cells and PDOs. In contrast to hematologic malignancies, we did not observe consistent suppression of the oncogenes c-MYC and MCL-1 by CDK9 inhibitor treatment. Instead, CDK9 inhibitors suppressed several other key cancer pathways in CRC, such as MAPK, mTOR, and PI3K signaling pathways. Importantly, multiple targets within the MAPK pathway were strongly suppressed, including EGFR, KRAS, and BRAF. We hypothesized that combination treatment with CKD9 inhibitors and MAPK pathway inhibitors can synergistically treat CRC. As proof-of-concept, we investigated the combination of CDK9 and BRAF inhibitors in models of BRAF-mutant CRC, a particularly aggressive type of CRC. We found this combination to synergistically suppress CRC growth *in vitro* and *in vivo*. Compared to single agents, combination treatment led to significantly stronger induction of apoptosis and suppression of MAPK pathway signaling. Our results suggest that concurrent treatment with CDK9 inhibitors plus established MAPK pathway inhibitors, such as BRAF inhibitors, can significantly improve upon single agent treatment. Conclusions: We have found CDK9 inhibitors to potently suppress CRC growth and survival through a unique mechanism of action, by vertical suppression of the MAPK signaling pathway. We demonstrate that CDK9 inhibitors can synergize with BRAF inhibitors in the treatment of BRAF-mutant CRC models. Thus, CDK9 inhibitors are a promising class of drugs warranting further investigation, including early-phase clinical trials, in mCRC.

#1219 In vivo delivery of CRISPR-Cas9 using lipid nanoparticles enables ATAD3A gene depletion to enhance RAS-targeted therapy.

F. Chen[1], L. Lang[2], Y. Li[3], W. Zheng[1], **Y. Teng**[1];

[1]Emory University, Atlanta, GA, [2]Augusta University, Augusta, GA, [3]Upstate Medical University, Syracuse, NY

Targeting mitochondrial oncoproteins presents a new concept in developing effective cancer therapeutics. ATAD3A is a nuclear-encoded mitochondrial enzyme that contributes to mitochondrial dynamics, cholesterol metabolism, and signal transduction. Our previous study has demonstrated elevated expression of ATAD3A in head and neck squamous cell carcinoma (HNSCC) primary tissues and cultured cell lines. Loss of function suppresses HNSCC cell growth and elicits tumor regression in orthotopic tumor-bearing mice. Mechanistically, ATAD3A interacts with ERK1/2 in the mitochondria of HNSCC cells in the presence of VDAC1, and the ATAD3A-ERK1/2 signaling axis drives HNSCC development in a RAS-independent fashion. CRISPR-Cas9 has revolutionized genome engineering and has been intensively used to modify cancer-associated genes. However, challenges remain as CRISPR editing components must be transported into cells to exert their function. There is a need to explore effective in vivo delivery systems to accelerate the clinical use of CRISPR-Cas9. As no drug is available to target ATAD3A directly, we developed CRISPR-based ATAD3A-targeting nanodrugs by loading Cas9 mRNA and anti-ATAD3A sgRNAs into lipid nanoparticles (LNPs) that have become clinically acceptable delivery system due to low toxicity and high delivery efficacy and biocompatibility. As expected, treatment tongue tumors established in NSG mice with LNP-sgATAD3A remarkably repressed tumor growth. Most interestingly, the addition of LNP-sgATAD3A to the RAS inhibitor salirasib potentiated anticancer activity for HNSCC compared with the efficacy resulting from single-arm treatment. These novel and significant findings demonstrate a novel approach to inhibiting ATAD3A in tumor cells and provide a possible therapeutic strategy to enhance the success of multimodality therapy in cancer patients.

#1220 Deep mutational scanning of EGFR reveals potential domain-specific TKI sensitivities in lung cancer and glioblastoma.

T. Hayes[1], E. Aquilanti[2], E. Kim[2], N. Persky[3], L. Brenan[3], A. Goodale[3], T. Sharpe[3], D. Alan[3], R. Shue[2], L. Golomb[4], B. Silverman[2], Y. Li[2], L. Westlake[3], F. Piccioni[5], A. Cherniack[3], X. Yang[3], D. Root[3], J. Hicks[6], A. Chi[7], J. Dietrich[8], D. Cahill[8], C. Johannessen[9], T. Batchelor[10], M. Meyerson[2];
[1]UCLA - University of California Los Angeles, Los Angeles, CA, [2]Dana-Farber Cancer Institute, Boston, MA, [3]Broad Institute, Cambridge, MA, [4]Dana-Farber Cancer Institute, Los Angeles, MA, [5]Merck, Boston, MA, [6]Moffitt Cancer Center, Tampa, FL, [7]Bright Peak Therapeutics, San Diego, CA, [8]Massachusetts General Hospital, Boston, MA, [9]Novartis, Cambridge, MA, [10]Brigham and Womens Hospital, Boston, MA

The epidermal growth factor receptor, EGFR, is frequently activated in lung cancer and glioblastoma by genomic alterations including missense mutations. The different mutation spectra in these diseases are reflected in divergent responses to EGFR inhibition: significant patient benefit in lung cancer, but limited in glioblastoma. Here, we report a comprehensive mutational analysis of EGFR function. We performed saturation mutagenesis of EGFR and assessed function of ~22,500 variants in a human EGFR-dependent lung cancer cell line. This approach revealed enrichment of erlotinib-insensitive variants of known and unknown significance in the dimerization, transmembrane, and kinase domains. Multiple EGFR extracellular domain variants, lacking approved targeted therapies, were sensitive to dacomitinib. Strikingly, at least two glioblastoma patients with G598V dimerization domain mutations showed responses to dacomitinib treatment together with subsequent off-target resistance in one case. In summary, this comprehensive screen reveals novel functional EGFR variants and suggests broader clinical investigation of EGFR inhibition for cancers harboring extracellular domain mutations.

EXPERIMENTAL AND MOLECULAR THERAPEUTICS: Conquering Drug Resistance by Innovative Research Minisymposium

#1221 Selective translational activation of PBK (PDZ- binding kinase) reveals a molecular vulnerability of drug-tolerant persister cells to targeted therapies in *EGFR*-mutant lung adenocarcinoma.

C. Leonce[1], A.-L. Desage[2], N.-H. Mourksi[1], G. De Souza[1], B. Vanbervliet[1], C. Charrondiere[1], C. Nicq[1], J. Neri[1], A. Swalduz[3], L. Tonon[1], E. Cumunel[1], N. Gadot[1], G. Ichim[1], J.-J. Diaz[1], C. Lovly[4], J. Mazieres[5], M. Tabutin[6], M. Perol[6], S. Lantuejoul[6], O. Calvayrac[7], F. Forest[8], V. Marcel[1], P. Saintigny[3], **S. Ortiz-Cuaran**[1];

[1]Univ Lyon, Claude Bernard Lyon 1 University, INSERM 1052, CNRS 5286, Centre Leon Berard, Cancer Research Center of Lyon, Lyon, France, [2]Univ Lyon, Claude Bernard Lyon 1 University, INSERM 1052, CNRS 5286, Centre Leon Berard, Cancer Research Center of Lyon, Department of Pulmonology and Thoracic Oncology, North Hospital, University Hospital of Saint-Etienne, Saint-Etienne, Lyon, France, [3]Univ Lyon, Claude Bernard Lyon 1 University, INSERM 1052, CNRS 5286, Centre Leon Berard, Cancer Research Center of Lyon, Department of Medical Oncology, Centre Leon Berard, Lyon, France, [4]Vanderbilt-Ingram Cancer Center, Vanderbilt University Medical Center, Nashville, TN, [5]Department of Pulmonology, Toulouse University Hospital, Cancer Research Centre of Toulouse, INSERM UMR1037, CNRS UMR5071, University Toulouse III-Paul Sabatier, Toulouse, France, [6]Department of Medical Oncology, Centre Leon Berard, Lyon, France, [7]Cancer Research Centre of Toulouse, INSERM UMR1037, CNRS UMR5071, University Toulouse III-Paul Sabatier, Toulouse, France, [8]Department of Pulmonology, Toulouse University Hospital,, Saint-Etienne, France

In lung adenocarcinoma (LUAD), EGFR-targeted therapies often result in incomplete tumor responses followed by disease progression caused by acquired resistance. As *EGFR* mutations are truncal (*i.e.*, present in every cell of a tumor), it remains unclear why a fraction of tumor cells can survive in the presence of drug treatment. It is increasingly recognized that drug-tolerant persister cells (DTPCs) can escape selective drug pressure and are important drivers of therapy failure and tumor relapse. The mechanisms underlying tumor cell adaptation and survival of DTPCs during therapy are not fully understood.Using *EGFR*-mutant LUAD cell lines treated with osimertinib, we unexpectedly observed that DTPCs display uncoupled mRNA and protein variations of PBK (PDZ Binding Kinase), a spindle assembly serine/threonine protein kinase. Mechanistically we discovered that although global protein synthesis is decreased upon osimertinib treatment, *PBK* translation is selectively maintained in DTPCs.The establishment and survival of DTPCs following EGFR inhibition is critically dependent on PBK, as genetic depletion of *PBK* reduces persistence to osimertinib treatment *in vitro*. PBK knockout leads to suppression of ERK1/2 reactivation following EGFR inhibition, and results in decreased expression of ZEB1 and Vimentin, key effectors of epithelial-to-mesenchymal transition (EMT), a hallmark of the DTPC phenotype. Consistently, combined treatment with osimertinib and OTS514 (PBK inhibitor) *in vitro*, reduces the DTPC fraction and decreases the enrichment of EMT-related transcriptional signatures. Similar results were obtained in LUAD patient-derived organoids, used to recapitulate the phenotype of residual disease in patients. In PDX treated with osimertinib, PBK is activated at both residual disease and acquired resistance. Concordantly, combined EGFR/PBK pharmacological inhibition was also effective in reverting osimertinib acquired resistance *in vitro*. Finally, in matched diagnosis and relapse samples from 7 *EGFR*-mutant LUAD patients treated with EGFR inhibitors, we observed increased PBK activation at the time of acquired resistance in 5 cases, including 3 $EGFR^{T790M}$-positive cases, suggesting that PBK activation may co-occur with genetic resistant alterations.Our findings unveil a novel mechanism by which *EGFR*-mutant lung cancer DTPCs selectively translate *PBK* mRNA as an adaptive survival mechanism to persist during osimertinib treatment; and provide a therapeutic target of non-genetic drug resistance otherwise unlooked-for in routine transcriptomic analyses. A deeper understanding on the mRNA translational reprogramming in DTPCs is currently performed to uncover therapeutic vulnerabilities to reduce residual disease and delay or revert the emergence of acquired resistance.

#1222 Mechanisms of succinate-mediated drug resistance in ER+ breast cancer.

J. HOGSTROM[1], B. Petrova[2], C. Perea[1], M. Ward[1], G. Wulf[1], L. Collins[1], N. Kanarek[2], T. Muranen[1];
[1]Beth Israel Deaconess Medical Center, Boston, MA, [2]Boston Children's Hospital, Boston, MA

Breast cancer is the most prevalent cancer among women worldwide with estrogen receptor-positive (ER+) cancer constituting 70% of all breast cancers. Although ER+ breast cancers initially respond well to ER-targeted therapies and CDK4/6 inhibitors, approximately 30% patients acquire resistance to targeted therapies. In addition to intrinsic resistance that tumors develop, cancer-associated fibroblasts (CAFs) residing in the tumor microenvironment, also contribute to treatment-resistance and poor survival. The role of secreted metabolites by CAFs has been poorly studied in the context of targeted drug resistance. Therefore, to investigate the mechanism of stroma-mediated resistance to CDK4/6-inhibitors, we propagated patient-derived organoids (PDOs) and CAFs from treatment-naïve and treatment-resistant ER+ breast tumors. Our data show that the CAF conditioned media containing the polar metabolite fraction stimulates resistance to CDK4/6 inhibitors. Therefore, to identify metabolites that drive resistance, we performed an untargeted metabolomics on CAF conditioned media. We observed that the CAF conditioned media was enriched for TCA cycle intermediates, including succinate. Succinate is an oncometabolite that has an essential function in energy metabolism. Aside from causing metabolic reprogramming, succinate can be transported out of the mitochondria to perform other biological processes, such as epigenetic modifications and pseudohypoxia. Furthermore, succinate in the extracellular space binds to the succinate receptor SUCNR1 and induces G-protein coupled receptor-mediated signaling in cells expressing SUCNR1. To assess mechanism of resistance that these metabolites might induce, we treated breast cancer cells with the most enriched metabolites we had identified in our metabolomics assay. These experiments identified succinate as driver of CDK4/6 inhibitor resistance in ER+ breast cancer cells. Furthermore, treating tumor cells with SUCNR1 antagonist increased their sensitivity to CDK4/6-inhibitors, showing that succinate mediated resistance is conveyed via SUCNR1. This suggests that CAF secreted succinate plays a role in supporting a pro-tumor environment by promoting drug resistance towards CDK4/6 inhibitors. Defining this mechanism of resistance will elucidate potential therapeutic targets to augment patient response to therapy.

#1223 KDM6A orchestrates NK cell response *via* CD38/48 regulation in multiple myeloma.

J. Liu[1], L. Xing[2], J. Li[3], k. Wen[1], N. Liu[4], Y. Liu[1], A. Gulla[1], N. Munshi[1], T. Hideshima[1], K. C. Anderson[1];
[1]Dana-Farber Cancer Institute, Boston, MA, [2]Shandong Cancer Hospital and Institute, Shandong First Medical University and Shandong Academy of Medical Sciences, Jinan, China, [3]The Seventh Affiliated Hospital of Sun Yat-Sen University, Shenzhen, China, [4]Shanghai Ocean University, Shanghai, China

Daratumumab (Dara), a first-in-class humanized monoclonal antibody targeting CD38, demonstrates notable efficacy in both newly diagnosed and relapsed/refractory multiple myeloma (MM) when administrated alone or in combination with other agents. However, the development of Dara resistance and subsequent relapse is common.To identify the tumor-intrinsic genes involved in resistance to NK-mediated cytotoxicity in the presence of Dara in MM cells, we conducted an *in vitro* genome-wide CRISPR-Cas9 knockout (KO) screen and found 433 genes exhibiting a positive correlation with MM cytotoxicity elicited by Dara and primary NK cells. Remarkably, 16 of these genes demonstrated a consistent correlation with cytolytic activity across the majority of the 36 cancer types in the TCGA database.The efficacy of Dara is closely linked to the expression of CD38, with nonresponders exhibiting low CD38 expression. Therefore, we conducted another CRISPR screen to identify the genes whose KO resulted in diminished CD38 expression. The genes that overlapped in these two screens are implicated in regulating both Dara-mediated ADCC and CD38 expression. Our focus turned to KDM6A among the overlapping genes. We validated that *KDM6A* KO significantly decreased CD38 expression and that reintroducing *KDM6A* into *KDM6A* KO cells restored the expression of CD38 and Dara-induced cytotoxicity.KDM6A demethylates lysine 27 of histone H3 (H3K27) to promote gene expression. Our ChIP-seq data unveiled that *KDM6A*-KO cells exhibited an increased H3K27me3 level at the CD38 promoter area than control cells. Remarkably, this pattern was consistent with Dara-resistant cell lines, which displayed reduced CD38 expression alongside elevated levels of H3K27me3 at the CD38 promoter. Interestingly, we found that CD38 overexpression only partially restored the sensitivity of *KDM6A* KO cells to Dara treatment, implying the existence of an additional mechanism. We performed RNA-seq in *KDM6A* KO cells and found CD48, an NK-activating ligand, was significantly repressed. Overexpression of CD48 in *KDM6A* KO cells resulted in a substantial increase in the secretion of Granzyme B and Perforin by NK cells and restored the activity of NK cells and re-sensitized *KDM6A* KO cells to Dara treatment. These data suggest that KDM6A mediates Dara-mediated ADCC sensitivity through the dual regulation of CD38 and CD48. KDM6A acts to oppose the EZH2/PRC2 complex by demethylating H3K27me3, and we found that Tazemetostat (Taze), an FDA-approved EZH2 inhibitor, increased the expression of CD38 and CD48, especially in *KDM6A*-KO cells. Importantly, Taze also restored the sensitivity of *KDM6A* KO cells to Dara-mediated NK cell cytotoxicity. In summary, our findings illuminate the dual role of KDM6A in enhancing the efficacy of Dara in MM. Imitating KDM6A function using an FDA-approved inhibitor holds promise in overcoming Dara resistance and improving patient outcomes in MM.

#1224 3D models of chemotherapy- and PARPi-resistant ovarian cancer indicate essential roles for JAK/STAT signaling in mediating drug resistance.

E. Rodman, X. Wang, H. Smith, X. Hou, S. Kaufmann, J. Weroha, J. Hawse;
Mayo Clinic, Rochester, MN

Ovarian cancer is the deadliest gynecological cancer with a low 5-year overall survival rate that affects over 300,000 women globally each year. Given lack of routine screening procedures, ovarian cancer patients are frequently diagnosed with late-stage disease that rapidly progress despite initial responses to front line therapy. PARPi and VEGFi targeted therapies have improved progression free survival in small subsets of patients but have largely failed to improve overall survival. Since the robust uptake of PARPis in the front line setting, resistance to this class of drugs is a growing problem. The literature is filled with many novel treatment approaches, but the vast majority fail to gain traction in pre-clinical models and early phase trials. A contributing factor to these disappointments relates to the prevalent use of 2D monoculture model systems that do not recapitulate the tumor microenvironment. To address this issue, we utilized the Rastrum 3D cell printer to grow ovarian cancer cells and PDX models in bio-functional matrices which provide optimal stiffness and extracellular matrix components specific to the ovarian tumor microenvironment. We found that ovarian cancer cells grown under these conditions exhibit dramatic up-regulation of the JAK/STAT signaling pathway, including autocrine/paracrine signaling factors, which correlated with increased sensitivity to JAK/STAT inhibitors. This affect was lost when STAT1 and STAT3 knockout cell lines were grown in this 3D environment. Ovarian tumors are known to be rich in cancer-associated fibroblasts (CAFs) and tumor-associated macrophages (TAMs). We incorporated primary CAFs into this 3D culture system and found they could promote ovarian cancer cell growth only in cancer cells with intact JAK/STAT signaling further indicating the essential role of this pathway in mediating tumor progression. Co-culture with M2 macrophages was also found to induce ovarian cancer cell growth, particularly in resistant models. Conversely, co-culture with M1 macrophages inhibited treatment naïve ovarian cancer cell growth but not resistant cell line growth. Single-cell RNAseq of the complex 3D cultures elucidated profound differences in the cross-talk between these cell types that is dependent on cancer cell sensitivity to standard-of-care agents. Finally, the addition of JAK/STAT inhibitors was found to substantially alter this cross-talk between cell types and inhibit cancer cell viability. These data further implicate the importance of JAK/STAT signaling, specifically in clinically relevant 3D models, in supporting ovarian cancer progression and response to chemotherapy and PARPi treatment. Ongoing studies are aimed at confirming these findings in pre-clinical mouse models and to elucidate the most effective JAK/STAT inhibitors *in vivo* with the goal of informing the design of future clinical trials.

#1225 Novel cellular barcoding to dissect melanoma heterogeneity and drug resistance.

H. Li, Y. Chen, J. Kaster, N. Promi, M. Herlyn;
The Wistar Institute, Phialdelphia, PA

Melanoma is the most common cause of death in skin cancer. While the development of targeted therapies (MAPK pathway inhibitors) led to a substantial improvement in overall survival of patients with melanoma harboring the BRAFV600E mutation, approximately 40% of treated patients acquire resistance and experience tumor recurrence after one year. Melanoma drug resistance is mediated by drug-tolerant persister (DTP) cell subpopulations present in tumors. DTP cells are either intrinsically rare sub-populations pre-existing prior to therapies, or adaptive sub-populations that acquire genetic and epigenetic alterations during treatments. Our lab has established six PDX models that responded to the treatment of BRAF/MEK inhibitor combination then relapsed in six to 40 weeks. We combined cell lineage barcoding and single-cell transcriptomics to trace the emergence of DTP cells in melanoma recurrence. The recent development of cellular barcoding facilitates the labelling of tens to millions of cancer clones and enables the identification of the complex mechanisms associated with clonal fate in response to therapy and in different microenvironments. We have constructed a library of approximately 15 million barcodes into a lentiviral vector. Melanoma cells were infected with the barcode library to ensure each cell carried a unique barcode. Labelled melanoma cells were injected into NSG mice, which were then treated with BRAF/MEK inhibitors, and they developed drug resistance with prolonged treatments. Treated tumors were harvested at different timepoints until relapse. The barcodes are localized close to the polyA tail of the expressed mRNA, the 3' end sequence of which could be retrieved simultaneously through single-cell RNA sequencing (scRNAseq). Thus, we can trace the clonal information from the relapsed tumor back to earlier timepoints such as the treatment naive tumor and minimal residual disease (MRD) stage. Our data showed that the diversity of barcodes in MRD stage had no significance compared to treatment naive tumor, while the diversity of barcodes in the relapsed tumor decreased around 10-fold from the MRD stage. The most dominant sub-populations in MRD arose from minor sub-populations in the treatment naive tumor, while most of the dominant sub-populations in the relapsed tumor were daughter cells from minor sub-populations in MRD stage. The top three sub-populations dominated 25% of the relapsed tumor. The three dominant drug-resistant sub-populations shared a similar phenotype shown by scRNAseq clusters. The data indicate that the heterogeneity of melanoma is maintained in the early treatment stage but is lost in acquired resistance. And the lineages of DTP cells change continuously under prolonged BRAF/MEKi drug pressure.

#1226 Genomically encoded lineage plasticity drives resistance to EGFR targeted therapy in lung adenocarcinoma.

M. Zatzman, A. Quintanal-Villalonga, S. Salehi, C. Falcon, N. Ceglia, S. P. Shah, C. M. Rudin, H. A. Yu;
Memorial Sloan Kettering Cancer Center, New York, NY

EGFR-mutant lung adenocarcinoma (LUAD) represents 20% of all non-small cell lung carcinomas, with most patients presenting with incurable metastatic disease. Treatment with mutant-selective EGFR tyrosine kinase inhibitor (TKI) therapies such as osimertinib, the current standard of care for metastatic EGFR-mutant LUAD, results in greater overall and progression-free survival. However, all patients eventually relapse. Uncovering the mechanisms driving primary and acquired resistance to osimertinib is therefore critical to improving disease management. Here, we use clinical genomic sequencing (n=47) and single-nucleus RNA (snRNA) sequencing (n=62) to profile a cohort of unmatched treatment-naïve (n=26), on-treatment (n=6), and post-treatment relapsed (n=30) EGFR-mutant LUADs treated with osimertinib. Relapsed tumors are marked by increased tumor mutation burden, along with elevated rates of genome doubling and loss-of-heterozygosity. We derived expression-based signatures of LUAD, lung squamous cell carcinoma (LUSC), and small cell lung carcinoma (SCLC) and applied them to tumor cells across our cohort. Relapsed tumors had a marked decrease in LUAD gene signature expression compared to untreated tumors and accompanying increases in epithelial-mesenchymal transition (EMT) and stemness markers, consistent with dedifferentiation. Notably, tumors harboring secondary mutations to EGFR, MET, or other MAPK pathway genes and showing sustained MAPK signaling retained a more differentiated state. Patients lacking these secondary on-target or bypass mutations were more likely to experience relapse with histological transdifferentiation, marked by complete loss of LUAD signatures, and accompanying increases in LUSC or SCLC signatures. Phenotype matching of tumor cells to normal cells from the developing fetal lung revealed enrichment of airway progenitor populations in non-histologically transformed treatment-resistant patients, in contrast to a proportion of late bud-tip and club-like epithelial cells which predominated in treatment-naïve samples. In rare cases, we observed subpopulations of basal stem-like progenitors in otherwise well-differentiated pre-treatment tumors. In summary, single-cell mapping of histological and developmental phenotypes has revealed divergent evolutionary trajectories during the acquisition of resistance to osimertinib, defined by MAPK signaling reactivation or by loss of LUAD identity and histological transformation respectively.

#1227 Novel combination therapies to overcome non-genetic/adaptive menin inhibitor resistance in AML with MLL1r or mtNPM1.

W. C. Fiskus[1], C. P. Mill[1], J. Piel[2], M. Hentemann[2], C. E. Birdwell[1], K. Das[1], J. A. Davis[1], H. Hou[1], T. M. Kadia[1], N. Daver[1], S. Loghavi[1], B. Cuglievan[1], C. D. DiNArdo[1], K. N. Bhalla[1];

[1]UT MD Anderson Cancer Center, Houston, TX, [2]Foghorn Therapeutics, Cambridge, MA

In AML with MLL1 rearrangement or MLL1 fusion proteins (FP), the N-terminus of MLL1 becomes fused to over 80 partner proteins resulting in an aberrant leukemic transcriptional program including dysregulated expression of HOXA9, MEIS1, PBX3, FLT3, MEF2C and CDK6. On the other hand, in mutant NPM1 AML cells, wild type MLL1 is the main regulator of HOXA9, MEIS1 and FLT3, promoting self-renewal of myeloid progenitor cells. Menin inhibitors have been developed that disrupt the binding of Menin to MLL1 leading to reduced activity of HOXA9 and MEIS1 and repression of MLL1 or MLL1-FP target genes. Clinical trials have demonstrated that Menin inhibitors (MI) are well-tolerated and clinical remissions have been observed in patients with relapsed/refractory AML harboring MLLr. Unfortunately, most patients either fail to respond or eventually relapse. MI-resistance in AML with MLL1r or mtNPM1 is either due to recently described mutations in the MI-binding domain of Menin or is non-genetic/adaptive, due to dysregulated epigenome/transcriptome/proteome. In the present studies, through repeated shocks with LD_{90} dosing of MI, followed by drug washout and recovery, we have generated MLL1r (MV4-11-MITR) and mtNPM1 (OCI-AML3-MITR) AML cell lines that are tolerant/resistant (TR) to MI with LD_{50} values greater than 1 μM. Whole exome sequencing confirmed that these cells were lacking in new driver mutations. We determined that resistance in the MITR cells was not due to presence of hotspot mutations in Menin. ChIP-Seq analysis of H3K27Ac showed that the activities of super enhancers and core transcriptional regulatory circuitry was altered in both MITR cell types. Non-genetic/adaptive resistance to MI also concordantly reduced genome wide ATAC-Seq and RNA-Seq peaks in the OCI-AML3-MITR cells with significant depletion of MEIS1, IGF2BP2, BCL2, and PBX3, with concomitant induction of leukemia stem cell associated CLEC12A and CD244 expressions. A domain-specific CRISPR screen in MV4-11-MITR cells identified several druggable co-dependencies (e.g. EP300 and MOZ) and co-enrichments (SMARCA4, CREBBP and BRD4) with MI, suggesting them as potential mechanisms of non-genetic/adaptive MI resistance. Consistent with these findings, co-treatment with SMARCA2/SMARCA4 (chromatin remodeler ATPases) inhibitor FHD-286 and the BETi OTX015 or the MI SNDX-50469 exerted synergistic lethality in MV4-11-MITR and OCI-AML3-MITR cells as well as in PD MITR AML cells with MLL1r or mtNPM1. Co-treatment with CBP/p300 inhibitor GNE049 or GNE781 was also synergistic with MI in these cells. In vivo treatment with FHD-286 and OTX015 or SNDX-5613 significantly reduced the AML burden in mice bearing OCI-AML3-MITR xenografts. These findings underscore preclinical activity of epigenetically-targeted agent-based combinations and highlight their promise in overcoming MI resistance in AML with MLL1r or mtNPM1.

EXPERIMENTAL AND MOLECULAR THERAPEUTICS: Novel Antitumor Agents 1
Minisymposium

#1228 Selective FGFR4 inhibitor Irpagratinib (ABSK011) exhibits broad synergistic and combinatory anti-tumor effects with other therapeutic agents in preclinical HCC models.

N. Zhang, B. Shen, Z. He, C. Dai, J. Wang, J. Zhang, M. Liu, Y. Zhang, Z. Chen;
Abbisko Therapeutics Co., Ltd., Shanghai, China

Background: Hepatocellular carcinoma (HCC) is the most common primary liver cancer, ranking as the sixth most prevalent cancer and the third leading cause of death worldwide. Approved therapeutic drugs, including chemotherapy, anti-angiogenesis agents and immunotherapy-based combination regimen (atezolizumab plus bevacizumab), have shown suboptimal clinical benefits for patients with HCC. There are critical unmet medical needs for additional therapeutic options to address this challenge. Deregulation of FGF19-FGFR4 signaling accounts for roughly 30% of HCC and plays a pivotal role in driving HCC tumorigenesis. To date, several FGFR4 inhibitors have advanced to the clinical stage for the treatment of HCC patients. Among them, a recently discovered novel and highly selective inhibitor, Irpagratinib (ABSK011), has demonstrated the potential to become a first-in-class or best-in-class FGFR4 inhibitor. It showed promising anti-tumor activity in an ongoing phase Ib clinical study, with an ORR of 40.7% observed in FGF19 overexpressed late line HCC patients in cohorts treated with BID regimens. To further expand the therapeutic potential of irpagratinib, we carried out an array of combination treatments and revealed its broad synergistic effects with various immune and targeted agents in treating HCC.
Methods: We evaluated the combination effects of Irpagratinib with a variety of therapeutic agents, covering both targeted and immune-oncology agents, in preclinical HCC *in vivo* models. The tested agents, including lenvatinib, atezolizumab plus bevacizumab, anti-PD-(L)1, SHP2 inhibitors and EGFR antagonists, were assessed across a range of preclinical models, such as cell-derived or patient-derived xenografts, engineered syngeneic models and humanized models.
Results: Synergistic anti-tumor effects of irpagratinib were observed in combination with the indicated agents, demonstrating more profound effects than either single agent alone in the selected preclinical *in vivo* models. This resulted in significant effects on inducing tumor regression or inhibiting tumor progression.
Conclusions: In summary, these findings collectively illustrate very broad synergistic anti-tumor effects of irpagratinib when combined with various other therapeutic agents. These results may pave the road for potential novel combinatory therapeutic strategies that could expand the utility of irpagratinib and provide innovative and more effective therapies to HCC patients.

#1229 BDTX-1535: A MasterKey EGFR inhibitor targeting classical and non-classical oncogenic driver mutations and the C797S acquired resistance mutation to address the evolving molecular landscape of EGFR mutant NSCLC.

E. Dardenne[1], M. O'Connor[1], M. Nilsson[2], J. He[2], X. Yu[2], J. V. Heymach[2], X. Le[2], E. Buck[1];
[1]Black Diamond Therapeutics, Cambridge, MA, [2]MD Anderson Cancer Center, Houston, TX

The molecular landscape of EGFR mutated NSCLC has evolved over time in response to changing treatment practices with EGFR inhibitors and through the expanding use of NGS. With the replacement of first-generation reversible EGFR tyrosine kinase inhibitors (TKIs) by the third generation covalent TKI osimertinib as front-line therapy for patients with NSCLC expressing classical EGFR mutations, acquired resistance mutations have shifted with the near disappearance of EGFR-T790M and the emergence and growing incidence of EGFR-C797S. Our understanding of the EGFR mutation landscape has also continued to mature with comprehensive sequencing across all EGFR exons and with the vast majority of patients now undergoing sequencing. We now see how classical oncogenic drivers represent only a subset of oncogenic EGFR driver mutations and where other non-classical driver mutations are numerous and represent a major unmet medical need. Furthermore, there is a growing appreciation of the differences between the classical EGFR-L858R and EGFR-Ex19 deletion (Ex19del) mutations. For patients expressing L858R, many co-express non-classical drivers and this may explain the weaker relative activity for osimertinib in patients expressing L858R versus Ex19del. For patients expressing Ex19del, the co-expression of non-classical mutations is less common. In contrast, patients with Ex19del more often gain C797S as an acquired resistance mutation. Using the Foundation Medicine's FoundationInsights™ web-based platform, we present real world evidence (RWE) to define the molecular landscape of classical, non-classical, and acquired resistance mutations from a survey of >80,000 sequenced cases of NSCLC, including >12000 EGFR altered cases. We further present the profile for BDTX-1535 as a MasterKey EGFR inhibitor designed to address this evolved EGFR mutational landscape and tested against over >50 EGFR mutations. We also show how BDTX-1535 can address classical EGFR mutations in addition to on target mechanisms of resistance post osimertinib with potency against C797S as well as non-classical mutations affecting both the intracellular and extracellular domains, including L718X, E709X, S784F, V834L and A289V.

#1230 MTX-531, a first-in-class pan-PI3K inhibitor spares hyperinsulinemia yielding durable tumor regressions and resilience to adaptive resistance.

C. E. Whitehead[1], E. K. Ziemke[2], C. L. Frankowski-McGregor[2], R. A. Mumby[2], J. Chung[2], J. Li[3], N. Osher[3], O. Coker[4], M. Norris[5], S. Kopetz[4], V. Baladandayuthapani[3], M. Hollingshead[5], S. Verma[5], **J. S. Sebolt-Leopold**[2];

[1]Mekanistic Therapeutics, Inc., Ann Arbor, MI, [2]University of Michigan Medical School, Ann Arbor, MI, [3]University of Michigan School of Public Health, Ann Arbor, MI, [4]MD Anderson Cancer Center, Houston, TX, [5]NCI, Rockville, MD

Adaptive resistance mechanisms compromise the long-term effectiveness of kinase-targeted agents dictating the need for strategic combination approaches. MTX-531 was computationally designed to selectively target both PI3K and wild type EGFR. MTX-531 exhibits low nanomolar potency against the PI3K isoform family and EGFR with a high degree of specificity predicted by co-crystal structural analyses. Full kinome screening confirmed that MTX-531 is exquisitely selective for its intended targets. We evaluated the pharmacological profile of MTX-531, whereupon single agent treatment with this lead molecule elicited a high incidence of durable tumor regressions in a broad panel of PIK3CA mutant CDX and PDX squamous head and neck (HNSCC) models. The combination of MTX-531 with RAS pathway inhibitors, including agents directed against KRAS G12C, led to durable regressions of KRAS mutant colorectal and pancreatic xenografts, resulting in striking increases in median survival. MTX-531 is exceptionally well tolerated in mice and uniquely does not lead to hyperglycemia and hyperinsulinemia commonly seen with predecessor pan PI3K inhibitors. MTX-531 acts as an agonist of PPARγ, a structural feature of the molecule that is thought to mitigate hyperglycemia induced by PI3K inhibition. This unique attribute of MTX-531 confers a favorable therapeutic index not typically seen with PI3K inhibitors. To the best of our knowledge, MTX-531 is the first reported pan-PI3K inhibitor that does not lead to hyperglycemia. The pharmaceutical profile of MTX-531 includes favorable cross-species oral bioavailability, microsomal stability, and a facile 3 step chemical synthesis. MTX-531, which has the unique capability of concurrently and selectively inhibiting PI3K and EGFR, illustrates the power of rational computational drug design to target multiple adaptive resistance mechanisms in a single molecule. The versatility of MTX-531 in both the single agent and combination settings offers a breadth of development strategies that continue to evolve as new combination candidates become available. MTX-531 is currently undergoing advanced preclinical development for anticipated first in human clinical trials in late 2024.

#1231 First-in-class AR-V7/AR-fl small molecule molecular glue degrader for prostate cancer treatment.

C. C. Au[1], C. Estrella[1], P. Vatsa[1], M. Naidoo[1], M. Miller[2], P. T. Meinke[2], D. M. Nanus[3], P. Giannakakou[3];
[1]Weill Cornell Medicine, New York, NY, [2]Tri-Institutional Therapeutics Discovery Institute, New York, NY, [3]Meyer Cancer Center, Weill Cornell Medicine, New York, NY

Metastatic castration resistance prostate cancer (mCRPC) is a lethal disease due to the development of treatment to androgen receptor (AR) signaling inhibitors (ARSi) and taxane chemotherapy. Treatment resistance occurs partly due to the expression of AR splice variants that lack the ligand binding domain (LBD) and are constitutively active in the nucleus. AR-V7 is the most prevalent variant conferring clinical resistance to both ARSi and taxanes. Currently, there is no selective AR-V7 inhibitor leaving patients with limited therapeutic options. Thus, the development of selective AR-V7 inhibitors is a high priority, clinically unmet need. To identify AR-V7 pharmacologic inhibitors, we performed a high throughput small molecule phenotypic screen using enzymatic complementation and nuclear AR-V7 as the assay endpoint. Our primary screen of ~170K compounds (z score = 0.8), followed by a cell-toxicity counter screen and a secondary GFP screen identified hit **compound 7907**, **as a dual AR-V7/AR-fl protein degrader**, with unique chemotype compared to all known AR modulators. Hit to lead optimization by medicinal chemistry/SAR studies identified **lead compound 15,** with increased potency compared to 7907. Mechanistically, we showed that compound **15** shortened AR-V7 protein half-life by activating the ubiquitin-proteasome pathway and inducing proteasomal degradation of both AR-V7/AR-fl, without affecting their transcription. Importantly, compound **15** induced degradation occurred within 3hr of treatment and was blocked by the clinically approved proteasome inhibitor, bortezomib. TurboID proximity ligation assay identified distinct E3 ligases, uniquely interacting with AR-V7 or AR-fl. Using AR-V7/AR-fl deletion mutants we further showed that compound **15** activity is mediated by the N-terminal domain of AR, present in both proteins. Remarkably, compound **15** sensitized LNCaP95 cells (endogenous AR-V7/AR-fl expression) to enzalutamide suggesting potential therapeutic synergism and ability to reverse enzalutamide resistance. Ongoing studies aim to narrow down the binding site of compound **15** as well as identify the E3 ligases mediating its activity. Together, these data support a molecular glue degrader mechanism of action, consistent with published studies showing that molecular glue degraders are ideal for targeting classically “undruggable” proteins lacking an LBD or containing intrinsically disordered domains, as is the case for AR-V7. Currently, all AR-directed therapies target the LBD of AR-fl, inhibiting AR signaling. AR-V7 expression is a direct outcome of this inhibition, leading to AR-fl and AR-V7 co-expression in patient tumors. We posit that our drug candidate, by offering **dual AR-V7/AR-fl inhibition in a single treatment**, has the potential to not only benefit patients with mCRPC but also patients with hormone-sensitive disease, and delay AR-V7 expression.

#1233 Novel inhibitor targeting triple integrated stress response kinase HRI, PERK, and GCN2 provides new insights into overcoming resistance to proteasome inhibitors in multiple myeloma.

Y. Inoue[1], K. Hikami[2], S. Ebara[2], M. Sugiyama[2], R. Oda[2], A. Mizutani[2], M. Yoshida[2], H. Yamakawa[2], S. Yagishita[3], A. Hamada[3], H. Hayashi[1], M. Ri[4], S. Iida[4], **D. Morishita[2]**;

[1]Nagoya City University, Nagoya, Japan, [2]Chordia Therapeutics Inc., Fujisawa, Japan, [3]National Cancer Center Research Institute, Tokyo, Japan, [4]Nagoya City University Graduate School of Medical Sciences, Nagoya, Japan

The introduction of novel treatments for Multiple myeloma (MM), particularly proteasome inhibitors (PI) such as bortezomib (BTZ), has greatly improved outcomes. However, many patients eventually experience relapse. Therefore, new approaches for managing patients with resistance to PI should be explored. The integrated stress response (ISR) is an evolutionarily conserved intracellular signaling network that is activated in response to both intrinsic and extrinsic stresses. Stresses are sensed by four specialized kinases: HRI, PERK, PKR, and GCN2, which converge on the phosphorylation of eIF2α. This phosphorylation triggers the translation of ATF4, thus promoting cell survival and homeostasis. Recent studies investigating the contribution of the four ISR kinases in overcoming resistance to PI treatment, have revealed the potential of a selective GCN2 inhibitor to overcome this resistance. Here, we observed that PI simultaneously induced mitochondrial stress, ER stress, and amino acid starvation, leading to the activation of HRI, PERK, and GCN2, respectively. However, the contribution of crosstalk among ISR kinases has not been considered thus far. To gain a comprehensive understanding of ISR kinases in BTZ resistance, we generated single or combination patterns of double and triple KO of the four ISR kinases and reevaluated their contribution to BTZ treatment. Sensitivity screening using the HAP1 single, double, and triple KO cell library showed that HRI primarily, and to a lesser extent, PERK and GCN2, contribute to BTZ resistance. Consistent with the HAP1 KO screening, MM cell line-derived KO cells revealed a similar dependency on these three kinases. Building upon our observation of the significance of the HRI/PERK/GCN2 triple kinase, we developed a novel and orally available small molecule, CRD-1367799, which inhibits these triple kinases in cells. CRD-1367799 effectively dampened the activity of these ISR kinases, leading to a complete inhibition of eIF2α phosphorylation and ATF4 activation. Additionally, we observed a distinct anti-growth effect when combined with BTZ in vitro and in vivo, which was not replicated by the GCN2 or PERK-selective inhibitor. Furthermore, we uncovered the mechanism of cell death induction in combination with proteasome inhibitors. Notably, the apoptosis inducers NOXA and CHOP were upregulated, but the mechanism did not seem to rely on previously known processes such as ATF4-mediated transcriptional induction. In summary, our novel findings on the contribution of the triple ISR kinase provides us with new insights for overcoming resistance to proteasome inhibitors with HRI/PERK/GCN2 inhibitor. To the best of our knowledge, the use of a triple kinase inhibitor in this context has not been reported thus far, making CRD-1367799 a new therapeutic strategy for MM with PI.

IMMUNOLOGY: Tumor-Targeted Immune Cell Engagers
Minisymposium

#1235 Impact of anti-CD3 and tumor-target binder affinities on *in-vitro* potency, *in-vivo* efficacy, and cytokine release.

O. Abdelmotaleb[1], A. Schneider[1], T. Hofer[1], J. Sam[1], M. Lechmann[2], I. Waldhauer[1], A. Bransi[1], M. Eigenmann[3], A. Freimoser-Grundschober[1], C. Gassner[2], A. Odermatt[4], P. Brunker[1], S. Colombetti[1], C. Klein[1];
[1]Roche Innovation Center Zurich, Schlieren, Switzerland, [2]Roche Innovation Center Munich, Penzberg, Germany, [3]Roche Innovation Center Basel, Basel, Switzerland, [4]University of Basel, Basel, Switzerland

Background: First generation T cell bispecifics (TCBs) were developed by utilizing high CD3 and tumor target binder affinities to induce a potent response. Instrumentalizing this, TCBs have clinically proven to elicit efficacious target cell killing and anti-tumor efficacy, but they encountered hurdles related to cytokine release. Recent studies suggested that reducing CD3 binder affinity could lead to an efficient tumor killing with lower cytokine levels. However, the answer to whether cytokine release is mainly dependent on CD3 binder affinity or a multifactorial phenomenon remains ambiguous. Here, we aim to characterize the efficacy-safety relationship of different TCBs through investigating the interplay between CD3 binder affinity and the affinity of the tumor target-specific binder. For that purpose, a series of TCBs with varying CD3 affinities, and two target binders of high and low affinities were generated in the 2:1 TCB format, resulting in a bivalent binding to the tumor antigen and a monovalent one to CD3, which offers a unique opportunity to enhance the activity of TCBs.
Methods: Firstly, 2:1 TCBs comprising either the high or low affinity target binder and varying CD3 binder affinities were co-cultured *in-vitro* with human peripheral blood mononuclear cells (PBMCs), and human tumor cell lines, in order to assess T cell mediated cytotoxicity and cytokine release at different time points. Additionally, the impact on *in-vivo* efficacy, cytokine release, and pharmacokinetics was assessed in humanized mice implanted with a patient-derived xenograft model.
Results: Based on the dose-response in the cytotoxicity assay, the CD3 binders were classified into high, intermediate, and low levels of affinity. As expected, we observed that the *in-vitro* T cell cytotoxicity, *in-vivo* tumor growth inhibition (TGI), and cytokine release levels were maximal with the highest affine CD3 binder. Simultaneously, we have observed a decrease in cytotoxicity response with decreasing CD3 affinity compared to the high affinity binder. However, this was accompanied by an atypical decrease in cytokine release. Particularly, the TCB comprising the intermediate CD3 affinity binder illustrated a comparable *in-vitro* cytotoxicity and *in-vivo* TGI to the high affinity binder with a marked decrease in cytokine release [4x reduction *in-vitro* and 6x reduction *in-vivo*]. Upon testing the TCBs comprising the low affinity target binder with the same CD3 binders, we observed an additional decrease in cytokine release with the decreasing CD3 affinity.
In conclusion, we designed and generated TCBs with varying affinities in both the CD3 and target binding arms. Reducing cytokine release while maintaining adequate efficacy is feasible through CD3 binder affinity attenuation; however, the target binder affinity should be taken into consideration when interpreting our findings and designing new molecules.

#1236 Characterization of CBX-250, a first-in-class TCR-mimetic-based T-cell engager targeting a cathepsin G peptide-HLA complex for the treatment of myeloid leukemia.

G. Paulus[1], B. Lee[1], P. Sankaran[1], T. Rahman[1], J. Jimenez[1], D. O'Connor[1], S. Yue[1], Y. Huang[1], M. Bikowitz[1], S. Jaffe[1], S. O'Malley[1], B. Ban[1], G. Gabriely[1], T. Wang[1], A. Mak[1], M. Princiotta[1], C. Shi[2], H. He[2], N. Feng[2], J. Yan[2], T. Heffernan[2], G. Alatrash[2], J. Molldrem[2], D. Wiederschain[1];
[1]Crossbow Therapeutics, Inc., Cambridge, MA, [2]The University of Texas MD Anderson Cancer Center, Houston, TX

While T-cell engaging therapies have demonstrated clear clinical benefit in the treatment of B-cell malignancies, their application to myeloid malignancies remains a challenge due to the limited repertoire of suitable tumor specific surface antigens. Targeting HLA-restricted peptides (pHLA) derived from intracellular cancer antigens provides an opportunity to explore the entire cancer proteome. CG1 (FLLPTGAEA) has been validated as an HLA-A*02:01 restricted leader peptide from Cathepsin G (CTSG) and is abundantly presented by leukemic versus normal myeloid cells. TCR-mimetic (TCRm) antibodies are ideally suited to target pHLA with high potency and specificity and can be engineered and manufactured using standard antibody technologies. Here we report the preclinical characterization of CBX-250, a novel CG1/HLA-A2 TCRm-CD3 bispecific T-Cell Engager (TCE).

CBX-250 induced potent T-cell activation and T-cell mediated killing of leukemia cell lines with varying levels of target antigen density with sub-nM EC50 *in vitro*. *In vivo*, a closely related precursor of CBX-250 demonstrated potent tumor control in various AML and CML CDX models at doses as low as 0.01mpk.

Although CTSG is a serine protease stored in neutrophil azurophilic granules, the CG1 peptide is preferentially presented by leukemia cells, as validated by mass spectrometry. Moreover, when co-culturing PBMCs with HLA-A2 neutrophils, we did not observe any CBX-250-mediated T-cell activation or IFNγ production.

In silico predictions identified HLA-A2-restricted human peptides that share sequence or structural similarity to CG1. We determined the cross-reactivity risk of CBX-250 to be low, based on T-cell activation and T-cell mediated cytotoxicity assays against cells pulsed with supra-physiological concentrations of these peptides. Moreover, we observed no activity against target-negative cancer cells, including a CTSG-KO cell line. To further assess the specificity of CBX-250, we screened a panel of normal cells and found no meaningful T-cell activation or IFNγ production at CBX-250 concentrations exceeding its EC90. Finally, the CBX-250 precursor molecule demonstrated favorable safety in a double transgenic mouse model expressing human HLA-A2 and CG1.

Following sequence optimization, CBX-250 demonstrated robust serum and pH stress stability and a favorable melting temperature, while retaining excellent potency and specificity. A full suite of analytical and biophysical assessments supports CBX-250's favorable developability profile.

In summary, these data provide strong preclinical evidence of the potency, specificity, safety, and developability of CBX-250, a novel, first-in-class, off-the-shelf, TCRm-based TCE for the treatment of myeloid malignancies.

#1237 IGM-2644, a CD38xCD3 bispecific IgM T cell engager, shows enhanced anti-tumor activity compared to daratumumab in preclinical models of multiple myeloma.

K. C. Hart, D. Santos, K. Li, R. Yun, M. Chai, A. Kabai, G. Li, P. Yakkundi, R. P. Funke, Y. Guan, T. Manley, L. Liu, A. M. Sinclair, A. F. Candia, B. Keyt, M. F. Kotturi;
IGM Biosciences, Inc., Mountain View, CA

Multiple myeloma (MM) is a hematologic malignancy characterized by the accumulation of monoclonal plasma cells in the bone marrow. CD38 is an attractive therapeutic target for MM due to its high expression on plasma cells, but it is also expressed on multiple subsets of normal immune cells. Approved therapies including anti-CD38 monoclonal antibodies such as daratumumab are available, however resistance inevitably develops, and toxicities such as reduced immune cell counts put patients at increased risk for infections. To address this and other issues associated with current therapies, we are developing IGM-2644, an engineered high affinity, high avidity bispecific anti-CD38xCD3 IgM T cell engager (TCE) antibody for the treatment of plasma cell disorders. IGM-2644 kills CD38-expressing tumor cells through complement-dependent cytotoxicity (CDC) and T cell-dependent cellular cytotoxicity (TDCC). Live cell imaging of tumor cells in the presence of normal human serum as a source of complement has shown that IGM-2644, compared to daratumumab, has exhibited superior CDC with faster kinetics and higher maximal killing, as well as increased activity on tumor cell lines that express low levels of CD38. IGM-2644 also has displayed enhanced cellular dependent cytotoxicity over daratumumab across tumor cell lines with a range of CD38 expression levels in vitro. In ex vivo assays with MM patient bone marrow mononuclear cells (BMMC), IGM-2644 has shown superior tumor cell depletion compared to daratumumab even with low T cell to tumor cell ratios. Furthermore, IGM-2644 can deplete tumor cells in BMMC from daratumumab-refractory MM patients. Similarly, using in vivo humanized xenograft tumor mouse models with various levels of CD38 expression, greater anti-tumor activity with IGM-2644 over daratumumab was observed. When compared to daratumumab, IGM-2644 demonstrated lower immune cell fratricide in an in vivo xenograft tumor mouse model, suggesting a potentially differentiated safety profile. In summary, IGM-2644 is a bispecific anti-CD38xCD3 IgM TCE antibody that demonstrates superior tumor cell killing when compared to daratumumab in vitro and especially in xenograft tumor models in vivo with low CD38 expression while having low immune cell depletion, potentially reducing the risk of infections. The safety and efficacy of IGM-2644 has been initially studied in a phase 1 clinical trial for relapsed/refractory (r/r) MM. Applicability of IGM-2644 for the treatment of other plasma cell disorders is currently being explored, including autoimmune diseases.

#1238 ISB 2001, a BCMA and CD38 dual targeting T cell engager, demonstrates superior cytotoxicity relative to teclistamab in the samples of patient relapsing from CD38 and BCMA targeted immunotherapies.

L. Carretero-Iglesia[1], M. Pihlgren[1], J. Berret[1], A. Drake[1], D. Pais[1], C. Dreyfus[1], V. Menon[2], T. Matthes[3], C. Edwards[4], J. Edwards[4], C. Pellat-Deceunynck[5], P. Moreau[6], C. Touzeau[6], T. Matsuura[7], P. van der Graaf[7], L. Pacaud[2], C. Konto[2], E. Zhukovsky[1], **M. Perro**[1];

[1]Ichnos Sciences Biotherapeutics SA, Epalinges, Switzerland, [2]Ichnos Sciences Biotherapeutics SA, New York, NY, [3]University Hospital Geneva, Geneve, Switzerland, [4]University of Oxford, Oxford, United Kingdom, [5]Nantes Universite, Nantes, France, [6]Service d'Hematologie Clinique, Unite d'Investigation Clinique, Nantes, France, [7]Certara UK Limited, Canterbury, United Kingdom

Immune therapies targeting single tumor associated antigens (TAA) demonstrated efficacy against multiple myeloma (MM). However, durable responses are still limited[1] potentially due to expansion of clones with low target expression[2] We have previously demonstrated that simultaneous targeting of BCMA and CD38 on MM tumor cells with heterogenous expression of these antigens using dual targeting ISB 2001, enables superior killing relative to mono-targeting T cell engagers (TCE) [3]. Here we present a further characterization of a dual targeting TCE utilizing bone marrow aspirates from multiple myeloma patients. In relapsed/refractory (r/r) patients, which received CD38 targeted therapy, daratumumab cytotoxicity was substantially reduced due to low CD38 expression. Teclistamab is considered the next line of treatment in such patients. However, ISB 2001 consistently demonstrated increased cytotoxicity compared to teclistamab in both newly diagnosed patient and r/r patient samples. Remarkably, ISB 2001 also induced stronger cytotoxic response in one patient relapsing after BCMA targeted therapy, suggesting that the dual targeting ISB 2001 TCE can overcome the escape mechanisms. ISB 2001 was also compared to the combination of teclistamab and daratumumab in cytotoxic assay using healthy donors. ISB 2001 shows superiority to both teclistamab and daratumumab as single agents, as well as when they were used in combination. Additionally, ISB 2001 was compared against a combination of daratumumab and teclistamab in a humanized mouse model of multiple myeloma with a low expression of both CD38 and BCMA, mimicking potential tumor escaping clones. ISB 2001 induced complete eradication of the tumors in almost all animals, whereas the combination only showed partial tumor protection, underscoring that dual targeting by a TCE is superior to two therapeutic agents individually targeting the same antigens. Based on the promising preclinical in vitro, ex vivo and in vivo data, we have advanced ISB 2001 into clinical studies. For calculating the first-in-human (FIH) dose, we have developed a quantitative systems pharmacology (QSP) model. The calculated FIH dose was 50-100 fold higher than that generated by a traditional minimum anticipated biological effect level calculation. Therefore, using this approach will substantially reduce patient exposure to sub-efficacious doses of ISB 2001. This plan was accepted by the HREC in Australia and the FDA in the US to initiate a Phase 1 FIH study of ISB 2001 for the treatment of relapsed/refractory multiple myeloma (NCT05862012)[4].

1. Munshi, N. C. *et al.* **384**, 705-716 (2021).
2. Nijhof, I. S. *et al. Blood* **128**, 12 (2016).
3. (https://doi.org/10.1182/blood-2022-159353)
4. Abstract# 3396 , ASH 2023, Hanlon Sia at al.

#1239 SAIL66, a next generation T cell engager targeting CLDN6, potentiates efficacy by binding to CD3/CD137.

M. Yoshimoto[1], **N. Kimura**[1], T. Kamikawa[1], S. Ishii[1], M. Muraoka[1], K. Taniguchi[1], R. Uchikawa[1], M. Okuda-Miura[2], S. Akai[1], T. Kodama[3], H. Sakumoto[1], S. Kawai[3], M. Shimada[1], M. Kamata-Sakurai[1], H. Aburatani[4], T. Kitazawa[1], T. Igawa[3],

[1]Chugai Pharmaceutical Co., Ltd., Yokohama, Kanagawa, Japan, [2]Chugai Pharmaceutical Co., Ltd., Kita-ku, Tokyo, Japan, [3]Chugai Pharmaceutical Co., Ltd., Chuo-ku, Tokyo, Japan, [4]The University of Tokyo, Meguro-ku, Tokyo, Japan

Background: Claudin-6 (CLDN6), one of over 20 known human CLDN family members, is upregulated in many solid tumors but shows minimal or no expression in healthy adult tissues. This makes it an ideal target for cancer therapy. Although several therapeutic modalities targeting CLDN6 are currently under investigation—including T cell engagers (TCE), CAR-T, and antibody drug conjugates—a more potent therapeutic option is still desirable. TCEs are a promising avenue within cancer immunotherapy, but their current efficacy and safety must be improved, particularly against solid tumors.

Methods and Results: To enhance immune activation and achieve successful clinical outcomes against solid tumors expressing CLDN6, we generated SAIL66, a CLDN6-targeting next generation TCE, using a new technological format called Dual-Ig®. SAIL66 is a tri-specific monoclonal antibody designed to bind to CLDN6 on cancer cells with one Fab arm and to both CD3 and CD137 with the other Fab arm. The preclinical characterization of SAIL66 was performed in a series of in vitro and in vivo studies which included comparisons to a conventional TCE targeting CLDN6 and CD3. SAIL66 demonstrated high specificity for CLDN6 despite its similarity to CLDN3, CLDN4, and CLDN9, suggesting a lack of off-target toxicity in patients. Using a Jurkat cell system harboring NFAT or NF-κB reporter genes, we confirmed that SAIL66 exerts CD3 and CD137 signal induction activity depending on CLDN6 expression. SAIL66 induced activation of T cells, release of cytokines, and lysis of CLDN6-positive cancer cells. In vivo studies with a humanized mouse (huNOG) model showed that SAIL66 had better anti-tumor efficacy in eliminating CLDN6-positive cancer cells than a conventional TCE. Flow cytometry analysis in the huNOG model revealed that SAIL66 also more significantly increased CD3+ T cell infiltration of tumor tissue and resulted in a smaller percentage of exhausted T cells in tumor. Moreover, transcriptome analysis in the huNOG model showed that both SAIL66 and the conventional TCE increase expression of genes associated with immune activation, with a durable increase observed especially with SAIL66. Further, we clarified that T cells repeatedly stimulated with SAIL66 had a greater ability to inhibit the growth of CLDN6-positive cancer cells than T cells stimulated with the conventional TCE in vitro.

Conclusion and Discussion: Our study shows that SAIL66 has better anti-tumor efficacy against CLDN6-positive cancer cells than a conventional TCE. This is due to effective immune activation by SAIL66 which triggers CD3 signaling (signal 1) combined with CD137 co-stimulatory signaling (signal 2) in T cells. Thus, SAIL66 represents a promising therapeutic option for solid tumors expressing CLDN6. A clinical trial for CLDN6-positive cancer patient is now ongoing (NCT05735366).

#1240 Enhancing NK cell function in the 'cold' tumor microenvironment of prostate cancer with a novel tri-specific killer engager.

S. Phung, Y. Soignier, N. Zorko, R. L. Waller, J. Walker, T. Nelson, C. Selleck, L. Bendzick, P. Kennedy, J. S. Miller, M. Felices;
University of Minnesota, Minneapolis, MN

Introduction: Natural killer (NK) cells are associated with good prognosis in patients with metastatic castration-resistant prostate cancer (mCRPC). However, NK cell function is hindered in the immunosuppressive and hypoxic tumor microenvironment (TME) of mCRPC. To improve NK cell-mediated responses against mCRPC, we designed a novel Tri-specific Killer Engager (TriKE®) that engages with NK cell activating receptor CD16, binds to prostate-specific membrane antigen (PSMA) that is highly and specifically expressed on mCRPC, and has an interleukin (IL)-15 moiety that is essential for NK cell survival, proliferation, and priming.

Methods: PSMA TriKE was produced using the mammalian expression system and tested using healthy donor and prostate cancer patient-derived NK cells. Flow cytometry-based functional and dye dilution proliferation assays were used to compare activation and proliferation of NK cells treated with PSMA TriKE or IL-15. NK cell cytolytic capacity against C4-2 cells, a PSMA-expressing prostate cancer line, was measured using IncuCyte live cell imaging. In various assays, hypoxic (1% oxygen) culture condition and cytokine-induced myeloid-derived suppressor cells (MDSC) were incorporated to better examine PSMA TriKE function in the physiological setting of mCRPC. In vivo testing of the PSMA TriKE was performed using C4-2 xenograft model and expanded NK cells in NSG mice.

Results: PSMA TriKE significantly enhanced expansion of peripheral blood NK cells derived from healthy donors up to 8-fold. Additionally, PSMA TriKE induced significantly higher NK cell degranulation and intracellular IFNγ and TNFα buildup, when compared to IL-15 treatment, after incubation with C4-2 cells. Responses of NK cells derived from prostate cancer patients were equivalent to healthy controls. Although NK cell activation was not observed against PSMA knockout (KO) C4-2, indicating specificity of PSMA TriKE treatment, bystander killing of PSMA-KO C4-2 was achieved with PSMA TriKE treatment when wildtype C4-2 cells were cocultured. This suggests potential PSMA TriKE benefit in controlling tumor antigen escape, through natural cytotoxicity once primed. In settings that mimic the TME of mCRPC, NK cells treated with PSMA TriKE in prolonged exposure to hypoxia showed retention of cytotoxicity against C4-2 while IL-15 treated NK cells showed greatly impaired cytotoxicity. Similarly, MDSC suppressed NK cell cytotoxicity in the presence of IL-15, but PSMA TriKE treatment abrogated MDSC-induced suppression. Finally, PSMA TriKE enhanced tumor control and improved survival of mice as compared to IL-15 and no treatment groups in vivo.

Conclusion: PSMA TriKE demonstrates potential in overcoming suppression of NK cells in the TME of mCRPC and is a promising candidate for advanced prostate cancer therapy.

#1241 Enhancing NK cell therapy for head and neck cancer within the solid tumor microenvironment using a B7H3-targeting tri-specific killer engager (TriKE).

M. Khaw[1], N. A. Zorko[1], C. Selleck[1], L. Bendzick[1], Z. Davis[1], P. Hinderlie[1], M. Shackelford[1], A. Lu[2], J. Lim[2], N. Fujioka[1], M. MacMillan[1], J. Wagner[1], M. Felices[1], J. S. Miller[1];

[1]University of Minnesota, Minneapolis, MN, [2]Xcell Biosciences, San Francisco, CA

With an annual incidence rate exceeding 660,000 cases, and a death toll surpassing 325,000 per year, head and neck cancer (HNC) ranks as the seventh most common cancer in the world. Surgery, radiation and chemotherapy are used to treat HNC patients with modest and variable clinical success. However, these treatments prove less effective for human papillomavirus negative (HPV-) HNC patients, a subset of HNC patients with markedly worse prognosis. While significant advancements have been made in cancer immunotherapy over the past decade, its success also remains elusive for HNC due to factors such as the hypoxic solid tumor microenvironment (TME). To address the critical need for an improved therapeutic intervention, we leveraged the ability of natural killer (NK) cells in killing cancer cells without prior sensitization by developing a novel tri-specific killer engager (TriKE) that can direct NK cell killing of tumor within the hypoxic solid TME. The TriKE is composed of three domains: a humanized nanobody arm binding the activating receptor CD16 on NK cells, an interleukin (IL)-15 moiety that can drive expansion of NK cells, and a nanobody arm binding B7H3, a protein which high expression can be negatively correlated with overall survival of HPV- HNC patients. B7H3 is a prime target candidate because it is highly expressed on HPV- HNC cells, but minimally expressed on healthy tissues. *In vitro* testing using HPV- HNC patient blood samples revealed that B7H3 TriKE enhances activation (measured by NK cell degranulation and interferon-gamma production) and expansion of NK cells from these patients at levels equivalent to those observed in healthy controls. Furthermore, B7H3 TriKE is efficacious in its ability to drive high NK cell cytotoxicity in both acute (<48-hours) and prolonged (7-days) hypoxic (1% oxygen) models of HNC. Under acute hypoxia, B7H3 TriKE induces significantly more killing of targets by NK cells compared to IL-15 treatment, where NK cell cytotoxicity is impaired. In addition, B7H3 TriKE can boost the killing efficacy of NK cells exposed to prolonged hypoxia, surpassing limitations seen with IL-15 treatment. These findings strongly suggest that the B7H3 TriKE can bypass hypoxic suppression of NK effector functions in the solid TME. *In vivo* studies using immunocompromised mice engrafted with HPV- HNC cells revealed that B7H3 TriKE treatment significantly extends the survival of mice, compared to IL-15 treatment. Moreover, NK cells persisted in the blood of B7H3 TriKE-treated mice 28 days post-NK cell injection, highlighting the promising clinical translation of this immunotherapy. More in-depth characterization of NK cells from HPV- HNC patients are underway but altogether, these robust pre-clinical data present a novel avenue for the management of HNC for these patients. We plan to translate results from these studies to clinical trials in fall 2024.

MOLECULAR/CELLULAR BIOLOGY AND GENETICS: Cancer Epigenetics
Minisymposium

#1242 Foxa1/2-dependent epigenomic reprogramming drives lineage switching in lung adenocarcinoma.
K. Gillis, W. Orellana, E. Wilson, G. Fort, H. Essel Dadzie, T. Parnell, X. Zhang, E. Snyder;
University of Utah Huntsman Cancer Institute, Salt Lake City, UT

The ability of cancer cells to alter their identity is essential for tumor survival and progression. Loss of the pulmonary lineage specifier NKX2-1 within KRAS-driven lung adenocarcinoma (LUAD) enhances tumor progression and results in a pulmonary-to-gastric lineage switch that is dependent upon the activity of pioneer factors FoxA1 and FoxA2; however, the underlying mechanism remains largely unknown. Here, we perform transcriptional and epigenetic assays to show that FoxA1/2 reprogram the chromatin landscape of NKX2-1-negative LUAD to facilitate a gastric differentiation program. Using sequential recombination models, we find that FoxA1/2 are required for demethylation of gastric-defining genes after *Nkx2-1* deletion. FoxA1 colocalizes with TET3, an enzyme that mediates DNA demethylation, in NKX2-1-negative tumors. Deletion of *Foxa1/2* results in loss of TET3 occupancy at key gastric marker genes, indicating that FoxA1/2 recruit TET3 to lineage-specific sites. H3K27ac ChIP-seq and HiChIP show that FoxA1/2 also control the activity of enhancers and promoters as well as their 3D interactions at gastric target genes following NKX2-1 loss. Furthermore, oncogenic KRAS is required for the FoxA1/2-dependent epigenetic reprogramming in NKX2-1-negative LUAD. This work demonstrates the role of FoxA1/2 in rewiring the methylation and histone landscape and cis-regulatory dynamics of NKX2-1-negative LUAD to drive cancer cell lineage switching.

#1243 Shifted mSWI/SNF complex assembly and function underlie therapeutically targetable dependencies in endometrial carcinoma.

Jessica Diane St. Laurent[1], Grace Xu[2], Alexander Ying[2], Bengul Gokbayrak[3], Ajinkya Patil[2], Akshay Sankar[2], Chae Young Shin[4], Daniel Same Guerra[2], David Kolin[5], David Huntsman[6], Yemin Wang[4], Cigall Kadoch[2]

[1]Brigham and Women's Hospital/ Dana Farber Cancer Institute/Harvard Medical School, Boston, MA,[2]Dana Farber Cancer Institute/Harvard Medical School, Boston, MA,[3]University of British Columbia, Vancouver, BC, Canada, BC, Canada,[4]University of British Columbia, Vancouver, BC, Canada,[5]Brigham and Women's Hospital/Harvard Medical School, Boston, MA,[6]University of British Columbia, Vancouver, BC

The mammalian SWI/SNF (mSWI/SNF) family of chromatin remodelers govern cell type-specific chromatin accessibility and gene expression and assemble as three distinct complexes: canonical BAF (cBAF), Polybromo-associated BAF (PBAF), and non-canonical BAF (ncBAF). ARID1A and ARID1B are paralog subunits that specifically nucleate the assembly of cBAF complexes and are the most frequently mutated mSWI/SNF components in human cancer, including in endometrial cancer. However, the biochemical and functional impacts of ARID1A/B loss, and hence cBAF complex disruption, on remaining PBAF and ncBAF complex activities, chromatin architecture, and gene expression remain poorly understood. Here, we define the molecular consequences of complete cBAF loss in models of aggressive de-differentiated endometrial carcinoma (DEC) harboring dual ARID1A/ARID1B mutations. Notably, re-expression of ARID1A in DEC cellular model systems biochemically restores cBAF complex assembly while reducing that of PBAF and ncBAF complexes, implicating functional contributions of differential mSWI/SNF family stoichiometry. We observe genome-wide increases in DNA accessibility at distal enhancer regions following ARID1A rescue, coupled with transcriptional changes at nearest genes including those associated with epithelial lineage differentiation, estrogen receptor signaling, and PI3K/AKT pathway signaling. Importantly, differential gene regulatory changes aligned with simultaneous cBAF restoration and reduction in ncBAF, and PBAF complex function mirror signatures derived from well-differentiated (WEC) and dedifferentiated (DEC) compartments of a collection of n= 15 primary human DEC cases profiled. Reduced ncBAF- and PBAF-mediated chromatin regulation resulting from either ARID1A rescue or ncBAF/PBAF genetic disruption attenuated oncogenic gene signature features such as MYC target genes, cell cycle checkpoint and DNA repair pathways and significantly reduced proliferative capacity. Finally, treatment of ARID1A/1B-mutant and ARID1A-mutant endometrial cell lines in culture and PDX models in vivo with a clinical-grade SMARCA4/2 ATPase inhibitor, FHD-286, markedly attenuated both cell proliferation and tumor growth. Further, FHD-286 synergized with carboplatin, leading to significant reduction in tumor burden in ARID1A- and ARID1A/B-mutant PDX models. Taken together, these findings reveal the oncogenic contributions of shifted of mSWI/SNF family complex abundance and chromatin-level gene regulatory function and suggest therapeutic utility of mSWI/SNF complex small molecule inhibitors in endometrial carcinoma and other cBAF-disrupted cancer types.

#1244 Exploiting the pathogenesis of endogenous retrovirus to tackle squamous cancers.

Y. Lyu, **Y. Ge**;
UT MD Anderson Cancer Center, Houston, TX

Retrotransposons are the evolution relic of ancestrally invaded retroviruses interspersed through our genome. Mostly domesticated as host regulome, retrotransposons shape lineage gene expressions or donate coding functions. A few rare evolutionarily young species remain virally active, leading to germline mutations and modulating immune functions. Aberrant retrotransposon activities have been widely observed in adult diseases, although the extent to which they ensue active viral form and function under those contexts is unclear. Their molecular trigger in adult pathophysiology is poorly defined. To address these questions, we use murine skin as our model, given its well-characterized, abundant and highly accessible adult stem cells, not only mediating postnatal remodeling and homeostatic regeneration, but also responding to stress by driving tissue repair and adaptations. By analyzing a genetic model lacking a known retrotransposon suppressor, histone methyltransferase Setdb1, which we found to be essential in the adult skin, we saw hair loss and hair follicle stem cell exhaustion phenotype, accompanied by a robust and selective surge of endogenous retroviruses (ERVs). When combined with squamous cell carcinoma drivers, Setdb1 loss significantly blocked tumor progression in vivo. Interestingly, compared to relatively mild or no induction of commonly observed evolutionarily young ERVs, the most induced species in our model is a class I ERV, murine leukemia virus (MuLV). We detected abundant retroviral peptides originated from its full-length copies through mass spectrometry and viral-like particles through transmission electron microscopy that are immunoreactive to a monoclonal MuLV *env* antibody. Similar viral-like particles were broadly evident across several epithelial tissues beyond skin, implicating its conserved function across squamous cancers. Epithelial originated ERVs elicit tissue wide inflammatory response, and can be ameliorated by pharmacological or genetic inhibition of retroviral activity. Physiologically, viral-coding ERVs arise as the epigenetic machinery declines in response to age-associated stress, and plummet when host safeguard prevails in UV induced skin hyperplasia. As an evolutionary conundrum, viral-coding ERVs pose a threat to host fitness and yet, they've resisted extinction persisting in the mammalian genome. Our findings suggest viral-coding ERVs wrestle with the host surveillance programs to regulate adult tissue physiology and pathology, thus providing a key target in eliciting innate immunity and tackling squamous cancers.

#1245 The histone methyltransferase KMT2D mediates subtype-specific transcriptional regulation and therapeutic response in prostate cancer.

S. Kittane[1], E. Ladewig[2], T. Li[3], J. Love[4], A. Arruabarrena-Aristorena[5], X. Guo[6], M. Sallaku[7], L. Garcia-Martinez[8], R. Blawski[3], J. Carmona Sanz[9], C. Simpkins[3], W. Chen[3], B. Vokshi[3], P. Zhao[10], N. Kelkar[1], L. Baldino[11], I. Kalemi[3], P. Castel[12], E. Cocco[8], L. Morey[8], C. Sawyers[2], H. Ji[1], M. Scaltriti[13], A. Battle[3], C. Leslie[2], W. Karthaus[4], E. Toska[3];

[1]Johns Hopkins Bloomberg School of Public Health, Baltimore, MD, [2]Memorial Sloan Kettering Cancer Center, New York, NY, [3]Johns Hopkins School of Medicine, Baltimore, MD, [4]Ecole Polytechnique Federale de Lausanne, Lausanne, Switzerland, [5]IKERBASQUE. Basque Foundation for Science, Bilbao, Spain, [6]University of Southern California, Los Angeles, CA, [7]Loxo Oncology at Lilly, New York, NY, [8]University of Miami-Miller School of Medicine, Miami, FL, [9]Vall d? Hebron Institute of Oncology, Barcelona, Spain, [10]KU Leuven, Belgium, Belgium, [11]SUNY Optometry, New York, NY, [12]NYU Grossman School of Medicine, New York, NY, [13]AstraZeneca, Gaithersburg, MD

Primary prostate cancer is characterized by its dependence on androgen receptor (AR) and often has hyperactive PI3K signaling, most frequently through loss of PTEN. PI3K/AKT pathway inhibitors are in late-stage clinical development in combination with anti-AR therapy. Androgen deprivation therapy is a cornerstone of treatment for advanced prostate cancer, but the development of castration-resistant prostate cancer (CRPC) eventually occurs. CRPC remains largely dependent on AR for growth with a subset of CRPC that lose AR dependence. There is an urgent need to study the molecular pathways leading to AR activation and the loss of AR reliance in order to identify therapeutic targets. KMT2D is a histone methyltransferase and an important regulator of gene expression. Here we found that KMT2D establishes the chromatin competence necessary for the recruitment of AR and FOXA1 transcription factors (TFs) to activate AR-dependent transcription in AR-high prostate models. In AR-low models such as the stem cell-like (SCL) subtype, KMT2D controls residual AR-FOXA1 gene expression programs and AP-1 TFs such as FOSL1, a driver of the SCL subtype. In SCL, single cell RNA-seq and single cell chromatin assays confirm a key role for KMT2D in the maintenance of a mixed lineage cell state through the regulation of AP-1 and FOXA1 TFs. Combined suppression of PI3K/AKT and KMT2D reduces cell proliferation in prostate cancer cells and patient derived organoids, providing a rationale for epigenetically informed combination therapies with PI3K/AKT inhibitors in PTEN-deficient prostate cancer. Together, these data establish KMT2D as a major mediator of subtype-specific chromatin accessibility and transcriptomic landscape in CRPC, required for prostate cancer growth and therapeutic response.

#1246 Erg-driven prostate cancer emerges from a basal subset of cells with luminal transcriptomic features.

E. Ladewig, W. Feng, C. Leslie, C. Sawyers;
Memorial Sloan Kettering Cancer Center, New York, NY

Translocations of the ETS family transcription factor *ERG* are found in nearly 150,000 newly diagnosed prostate cancers (PCas) each year in the United States underscoring the importance of defining the mechanism by which *ERG* promotes prostate epithelial transformation. A consequence of nearly all *ERG* translocations is the aberrant expression of ERG in prostate luminal cells under transcriptional control of *TMPRSS2*. Multiple lines of evidence implicate *ERG* translocations as an initiating event in prostate cancer. *ERG* expression is seen in prostatic intraepithelial neoplasia (PIN) and proliferative inflammatory atrophy; expression in cancers is typically uniform; and, in the context of PI3K pathway activation, *ERG* is sufficient to induce cancers in mice. Yet, despite extensive research the mechanism by which *ERG* initiates prostate cancer is unclear. To gain insight into how ERG translocations cause prostate cancer, we performed both transcriptional profiling (scRNA-seq) and chromatin accessibility via Assay for Transposase-Accessible Chromatin using sequencing (snATAC-seq) in single cells of an autochthonous mouse model at an early stage of disease initiation. Surprisingly, we observed in prostate epithelial cells broadly expressing *ERG* enhanced proliferation primarily in a hybrid subpopulation of cells having basal identity but with luminal morphology and cytokeratin expression. Through a series of lineage tracing and primary prostate epithelial transplantation experiments, we confirmed tumor initiating activity resided within a subpopulation of basal cells expressing luminal genes (e.g., *Tmprss2* and *Nkx3-1*). A trajectory analysis from single-cell Chromatin accessibility indicated Erg+ cells began to lose basal (*Trp63*) accessibility and gained in *STAT/NFAT* TFs while retaining the ability to rapidly differentiate into luminal cells that reflect the lineage of *ERG*-positive cancers. These findings help resolve a preexisting debate about the cell of origin of *ERG*-driven prostate cancer and narrow the focus for future mechanistic studies to a basal-luminal subpopulation of tumor initiating cells.

#1247 PPARsing epigenetic memory in intestinal stem cells: High-fat diet and oncogenic susceptibility.

D. R. Saiz, T. Hartley-McDerrmott, Y. Barrera-Millan, K. F. Castro-Ochoa, A. Shukla, M. Torel, M. D. Mana;
Arizona State University, Tempe, AZ

Diet has a profound impact on health and susceptibility to cancer. Adaptation to a Western diet is strongly associated with increased colorectal cancer (CRC) and obesity prevalence. This study demonstrates the epigenetic changes in intestinal stem cells (ISCs) induced by a pro-obesity high-fat Western diet (HFD) and the heightened risk of oncogenic transformation. A HFD induces a phenotype characterized by increased ISC frequency, proliferation, regenerative capacity, and ability to initiate adenomas. We hypothesized that a HFD generates lasting epigenetic alterations in ISCs thereby enhancing oncogenic susceptibility. We evaluated the chromatin landscape of intestinal stem cells (ISCs) and the reversibility of the epigenetic changes. Mice carrying a fluorescent reporter of the ISC marker Lgr5, were subjected to a control diet, HFD, or HFD with a return to control. We isolated ISCs by flow cytometry and used an assay for transposase-accessible chromatin sequencing (ATAC-seq) to identify differentially accessible genomic regions correlated with the ISC phenotype. We found that a HFD induces distinct changes in the chromatin landscape that persist after removal from the HFD. These accessible regions are associated with genes involved in lipid metabolism and are enriched with PPAR (Peroxisome Proliferator-Activated Receptor) binding motifs. We demonstrate that these lipid metabolism regulators, PPAR-delta and PPAR-alpha, are necessary for the majority of significant accessible regions. We further show that HFD-induced accessibility significantly correlates with early chromatin alterations seen by loss of tumor suppressor APC. Our data supports a mechanistic pathway for diet-induced epigenetic reprogramming due to PPAR activity and suggests that the HFD imposes a preneoplastic stem cell chromatin state that stokes the risk of oncogenic change.

#1248 The BRD8/p53 epigenetic switch re-establishes tumor suppression in glioblastoma.

Xueqin Sherine Sun, **Alea A. Mills**

Cold Spring Harbor Laboratory, Cold Spring Harbor, NY

Glioblastoma (GBM) is the most common and deadly adult primary brain malignancy. Median survival is just 12-14 months, with only about 5% of GBM patients surviving 5 years after diagnosis. This picture has not substantially improved over decades and there is an urgent need to discover more specific and effective treatments for this deadly malignancy. We discovered the bromodomain-containing chromatin regulator BRD8 as essential to GBM lacking p53 mutations *(TP53*^{WT}*)*, which make up ~71% of cases (1). BRD8 maintains malignancy by crippling p53-mediated tumor suppression in a way distinct from previously described mechanisms: it reprograms the p53 network through the EP400 histone acetyltransferase complex and by bromodomain-directed occupancy of the histone variant H2AZ at p53-induced targets, enforcing a repressive chromatin state that prevents p53-mediated transactivation. Importantly, targeting BRD8 in *TP53*^{WT} GBM remodels chromatin by evicting H2AZ and enhancing chromatin accessibility, enabling p53 to bind and transactivate its targets. This chromatin remodeling cascade (referred to as the “BRD8/p53 epigenetic switch”) re-establishes p53 activity in *TP53*^{WT} GBM, normalizing gene expression, evoking cell cycle arrest, inhibiting gliomagenesis, and prolonging survival in xenograft models of *TP53*^{WT} GBM. Our recent work: (i) reveals that BRD8 opposes p53 function in non-malignant brain cells; (ii) shows that the bromodomain of BRD8 is unique amongst the bromodomain-containing protein family, as it is the only one that selectively reprograms the p53 network; and (iii) demonstrates that targeting BRD8 works synergistically with MDM2 inhibition. Our findings present a previously unappreciated mechanism by which cancer cells side-step p53, indicate that targeting BRD8 re-establishes p53-mediated tumor suppression in *TP53*^{WT} GBM, highlight unique features of the bromodomain of BRD8, and propose therapies using co-inhibition of BRD8 and MDM2 as a dual-level tactic for boosting up p53. Thus, our work sheds light on new principles of chromatin biology and offers new promise for treating patients with this devastating malignancy.

(1)Sun *et al.*, 2023 *Nature* 613 (7942):195-202.

AACR PROJECT GENIE: Advancing Cancer Research Through an International Cancer Registry: AACR Project GENIE Use Cases Minisymposium

#1249 cBioPortal for Cancer Genomics.

T. Mazor[1], **I. de Bruijn**[2], R. AlHamad[2], C. Chennault[2], C. Dubin[3], J. Easton-Marks[1], Z. Fu[1], B. Gross[2], C. Haynes[4], D. M. Higgins[4], J. Hwee[2], P. K. Jagannathan[5], M. Kalafati[6], K. Kalletla[3], J. Ko[2], T. Kuijpers[6], S. Kumar[6], P. Kumari[3], R. Kundra[2], B. Lai[2], X. Li[2], J. Lindsay[1], A. Lisman[2], Q.-X. Lu[3], R. Madupuri[2], A. Ochoa[2], Y. Z. Ozgul[7], O. Plantalech[6], M. N. Pon[6], B. A. Satravada[2], J. Singh[6], S. Sumer[2], P. van Nierop[6], F. Vleugels[6], A. Wang[2], M. Wilson[2], H. Zhang[2], G. Zhao[2], U. Dogrusoz[7], A. Heath[4], A. Resnick[4], T. J. Pugh[5], C. Sander[8], E. Cerami[1], J. Gao[3], N. Schultz[2];
[1]Dana-Farber Cancer Institute, Boston, MA, [2]Memorial Sloan Kettering Cancer Center, New York, NY, [3]Caris Life Sciences, Irving, TX, [4]Children's Hospital of Philadelphia, Philadelphia, PA, [5]Princess Margaret Cancer Centre, Toronto, ON, [6]The Hyve, Utrecht, Netherlands, [7]Bilkent University, Ankara, Turkey, [8]Harvard Medical School, Boston, MA

cBioPortal for Cancer Genomics is an open-source platform for interactive, exploratory analysis of large-scale clinico-genomic data. cBioPortal provides a suite of user-friendly visualizations and analyses, including OncoPrints, mutation lollipop plots, variant interpretation, group comparison, survival analysis, expression correlation analysis, alteration enrichment analysis, cohort and patient-level visualization.

The public site (https://www.cbioportal.org) is accessed by >35,000 unique visitors each month and hosts data from >390 studies spanning individual labs and large consortia. All data is available in the cBioPortal Datahub: https://github.com/cBioPortal/datahub; in 2023 we added 35 studies (~16,000 samples). In addition, >86 instances of cBioPortal are installed at academic institutions and companies worldwide.

We also host a dedicated instance for AACR Project GENIE, enabling access to the GENIE cohort of >197,000 clinically sequenced samples from 19 institutions (https://genie.cbioportal.org). The GENIE Biopharma Collaborative (BPC) enables the collection of comprehensive clinical annotations including response, outcome, and treatment history, which can all be visualized in cBioPortal. BPC cohorts for non-small cell lung cancer (~2,000 samples) and colorectal cancer (~1,500 samples) are available, with more cancer types to come.

This past year, we significantly enhanced existing features. Group comparison now includes a Mutations tab showing a mirrored lollipop plot and outcomes analysis now supports hazard ratios and landmark analysis. Arm-level copy number can now be compared across groups, as can any data in the generic assay format.

We also enhanced the study view. Users can now add charts to summarize the copy number of a specific gene across the cohort. The option to add custom data charts now supports numerical data as well as categorical data. Filters in study view can now be manually submitted, which provides a performance improvement when applying multiple filters in a large cohort. Larger-scale performance improvements are currently underway.

We continue to improve support for multimodal datasets incorporating derived data elements, including cell type counts and fractions per sample from imaging or single cell data. The MSK-SPECTRUM ovarian cancer study has samples profiled with bulk sequencing, scRNASeq, H&E and mpIF imaging. Through integrations with CELLxGENE (single cell data) and Minerva (imaging), users can explore these data modalities in detail in isolation and query them jointly in cBioPortal.

cBioPortal is open source (https://github.com/cBioPortal/). Development is a collaborative effort among groups at Memorial Sloan Kettering Cancer Center, Dana-Farber Cancer Institute, Childrens Hospital of Philadelphia, Princess Margaret Cancer Centre, Caris Life Sciences, Bilkent University and The Hyve. We welcome open source contributions from others in the cancer research community.

#1250 Activating *PIK3CA* mutations and hedgehog signaling may confer resistance to KRAS inhibition in colorectal cancer.

S. Chowdhury[1], J. Ahmed[2], V. Haridas[1], D. S. Hong[1], S. Kopetz[1], J. Shen[1];

[1]UT MD Anderson Cancer Center, Houston, TX, [2]National Cancer Institute (NCI), National Institute of Health (NIH), Bethesda, MD

Background: Treatment with $KRAS^{G12C}$ inhibitors results in an objective response in only small fraction of patients with $KRAS^{G12C}$ mutant colorectal cancer (CRC) (7.1% and 22% objective response rates (ORR) in two prospective trials), in contrast to lung cancer where the ORR exceeds 35%. We hypothesize that co-mutation of other oncogenes and/or transcriptomic factors may contribute to the resistance of $KRAS^{G12C}$ CRC to KRAS inhibitors.

Methods: Mutation profiles of CRC patients were obtained from the AACR Project-GENIE v14 CRC cohort (N = 9441). The impact of *KRAS* knockout in 59 CRC cell lines was queried from the DepMap database. $KRAS^{G12C}$-mutant CRC cell lines SW837 and SW1463 were treated with Sotorasib ($KRAS^{G12C}$ inhibitor), Vismodegib and Taladegib (Hedgehog inhibitors), and cell viability was measured up to 96 hours after treatment.

Results: In the AACR Project-GENIE CRC (N = 9441) cohort, $KRAS^{G12C}$ tumors (2.6%, 245/9441) were significantly co-mutated with $PIK3CA^{mut}$ (19.2%, 47/245; Odds ratio = 1.7 (95% CI: 1.2 - 2.4), Chi-Square test, p-value = 0.002). Dependence on *KRAS* in CRISPR knockout viability assays was higher in $KRAS^{mut}$ vs. wildtype CRC cell lines (median CERES score -1.3 vs -0.5, p-value < 0.001). Interestingly, $KRAS^{mut}$ cell lines with *PIK3CA*-co-mutation (n=10) were more resistant to *KRAS* knockout than $PIK3CA^{wt}$ cells (n=22) (median -1.0 vs -1.4, p-value = 0.03). The SW837 and SW1463 cell lines initially displayed high sensitivity to Sotorasib (IC50: 0.92 µM and 0.90 µM). However, overexpression of $PIK3CA^{E545K}$ mutant induced resistance to the same treatment (IC50: 5.18 µM and 6.45 µM). Furthermore, gene set enrichment analysis (GSEA) showed that Hedgehog signaling was significantly enriched in *KRAS* knockout resistant $KRAS^{mut}$ CRC cell lines. SW837 cell line treated with Sotorasib (S) and a fixed dosage of 25 µM of Vismodegib (V) or Taladegib (T) showed higher sensitivities in combination treatment assays (IC50 decreased: ~11 folds in S+V vs S; and ~15 folds in S+T vs S) as compared to Sotorasib (S) treatment alone. Similar results were seen for the SW1463 cell line (IC50 decreased: ~18 folds in S+V vs S; and ~15 folds in S+T vs S).

Conclusion: Resistance in CRC to $KRAS^{G12C}$ inhibitors may be attributed to activated *PIK3CA* mutations and the Hedgehog signaling pathway. The future study will focus on detailed investigations involving comprehensive transcriptome and exome profiles in tumors and PDX models treated with anti-KRAS drugs in monotherapy and combination therapy.

#1251 Tobacco smoke alters the adaptive landscape of lung adenocarcinoma and influences the strength of epistatic interactions.

Krishna Dasari, Jorge Alfaro-Murillo, Jeffrey Townsend

Biostatistics, Yale University, New Haven, CT

Tobacco smoke produces both mutagenic and physiological effects, altering the mutation rate of cells and the selection acting on them in the damaged lung environment, and facilitating its role in driving cancer progression. In addition to these gene-by-environment interactions, gene-by-gene epistatic interactions also shape the adaptive landscape, influencing the evolutionary trajectories of cancer. Understanding the influence of tobacco smoke on the epistatic trajectories of lung cancer progression would help guide the development of targeted therapies that are more effective for smoker or never-smoker populations. To address this need, we constructed a continuous-time Markov chain model for the evolutionary trajectories of lung adenocarcinoma (LUAD), the most common subtype of lung cancer and the most frequent subtype among never-smokers. Using thousands of tumor sample sequences aggregated across studies, we profiled the trajectories of LUAD in smokers and never-smokers and estimated the rates at which mutations are gained from each possible set of pre-existing mutations, or genetic states. We then accounted for differences in baseline mutation rates to quantify the selective benefit of mutations. We find that epistasis is prevalent in LUAD, with several strong synergistic interactions—such as between RB1 and EGFR mutations- and antagonistic interactions-such as between EGFR and KEAP1 or KRAS mutations. Additionally, we identify non-additive epistatic effects: STK11 mutations are synergistic with KEAP1 and KRAS mutations but do not experience additional selection when both are mutated. In contrast, GNAS mutations are not synergistic with KEAP1 or RBM10 mutations alone but are synergistic with their co-mutation. Smoking has a large influence on the adaptive landscape, with several common mutations being preferentially selected in never-smoker cancers, including EGFR, SMAD4, GNAS, and PIK3CA mutations. KEAP1, STK11, and KRAS mutations are preferentially selected in smoker cancers. Smoking's physiological influence also affects the strength of certain epistatic interactions, such as between STK11 and KEAP1 mutations. Overall, we find that smoking not only increases the mutation rate of lung cells but also substantially alters the adaptive landscape of lung adenocarcinoma, leading to clinically relevant differences in selection on mutations between smoker and never-smoker cancers. We additionally detect frequent pairwise and higher-order epistatic effects in LUAD that may inform the personalized application of targeted therapies.

#1252 AI-derived predictions improve identification of real-world cancer driver mutations.

T. N. Tran, C. Fong, K. Pichotta, A. Luthra, R. Shen, Y. Chen, M. Waters, S. Kim, G. Riely, D. Chakravarty, N. Schultz, J. Jee;
Memorial Sloan Kettering Cancer Center, New York, NY

AI-based variant effect predictors (VEPs), such as AlphaMissense, which is based on the protein structure prediction method AlphaFold, have gained significant attention for their potential to predict pathogenic effects of mutations. However, the utility of these methods for identifying pathogenic mutations in cancer remains unknown.

We sought to quantify the prevalence of variants of unknown significance (VUSs) across the pan-cancer, multi-institution AACR GENIE cohort (N=160,965 samples) and test the utility of VEPs (SIFT, PolyPhen, MutationAssessor, REVEL, CADD, and AlphaMissense), using publicly available mutation annotations from each method, for 1) Annotating known pathogenic somatic cancer variants across the GENIE cohort, using known benign single nucleotide polymorphisms as negative controls 2) Identifying VUSs associated with overall survival (OS) in two cohorts of patients with non-small cell cancer (NSCLC), the MSK-IMPACT NCSLC (N=8,690) and non-MSK AACR GENIE Biopharma Collaborative NSCLC (N=977) cohorts, and 3) Identifying VUSs associated with known genomic patterns of mutual exclusivity in the MSK-IMPACT NSCLC cohort.

In the GENIE cohort, 79% of mutations identified were VUSs according to an FDA-recognized molecular knowledge database, with a wide range of VUS frequencies across genes. Among VEPs trained without prior human-annotated knowledge, CADD and AlphaMissense had the highest AUROCs (0.940, 95%CI 0.937-0.943 and 0.917, 95%CI 0.913-0.922 respectively) for predicting known cancer drivers, demonstrating the power of protein structure modeling or functional genomic data for enhancing cancer drivers prediction. All VEPs identified known driver mutations in tumor suppressor genes more accurately than oncogenes, highlighting the challenge in identifying gain-of-function mutations.

We tested whether VUSs reclassified as pathogenic by VEPs are associated with prognosis using inverse probability of treatment-weighted Cox's propensity hazard models controlling for tumor mutational burden, treatment history, and other factors. VUSs reclassified as pathogenic by AlphaMissense and other VEPs in KEAP1 and SMARCA4 correlated with worse OS, comparable to that of known oncogenic mutations in those genes. Patients with tumors containing VUSs annotated as benign had similar OS to patients without analogous driver mutations. Finally, VUSs reclassified as oncogenic by AlphaMissense in genes within the RTK/RAS and NRF2 pathways followed expected patterns of mutual exclusivity, further suggesting biological validity.

Despite not being trained to predict somatic effects in cancer, AI-derived mutation annotations can broaden the subset of annotated pathogenic variants in cancer and contribute to a more complete understanding of cancer genetics. Real-world outcomes and alteration patterns are additional benchmarks to consider when assessing the utility of VEPs in cancer.

#1253 Pan-cancer comparative and integrative analyses of driver alterations using Japanese and international genomic databases.

Sara Horie[1], Yuki Saito[2], Yasunori Kogure[2], Kota Mizuno[3], Yuta Ito[2], Mariko Tabata[4], Koichi Murakami[3], Junji Koya[2], Keisuke Kataoka[3]

[1]Department of Gastroenterology, Keio University School of Medicine, Tokyo, Japan,[2]Division of Molecular Oncology, National Cancer Center Research Institute, Tokyo, Japan,[3]Division of Hematology, Department of Medicine, Keio University School of Medicine, Tokyo, Japan,[4]Department of Urology, Graduate School of Medicine, The University of Tokyo, Tokyo, Japan

Recent large-scale pan-cancer genome projects have broadened our understanding of the cancer genome. However, these projects mainly consisted of White patients, with a limited focus on Asian populations. In addition, while pairwise relationships between driver alterations can provide valuable functional insights, the majority of these analyses are limited to those using The Cancer Genome Atlas (TCGA) dataset.

Here we present a pan-cancer landscape of driver alterations in Japanese patients with advanced solid tumors using targeted sequencing data of 48,627 samples from the Center for Cancer Genomics and Advanced Therapeutics (C-CAT) in Japan. This data set had a greater number of samples from Asian-prevalent cancer types, such as intrahepatic cholangiocarcinoma and stomach adenocarcinoma, compared to the Genomics Evidence Neoplasia Information Exchange (GENIE) cohort. In the C-CAT cohort, the most frequently mutated gene was *TP53* (56%), followed by *KRAS* (25%), *APC* (17%), and *PIK3CA* (12%). Gene fusions were detected in 1,166 samples (2%), including *ERG* fusions in prostate adenocarcinoma (*n* = 129), and *RET* and *ALK* fusions in lung adenocarcinoma (*n* = 30 and 32). At least one clinically actionable genetic lesion was found in 16% of patients, with well-differentiated thyroid cancer having the highest proportion.

A comparative analysis of somatic mutation frequencies was conducted between the C-CAT cohort and the White population in the GENIE cohort. Among 352 driver gene-cancer type combinations, 14 and 4 were significantly higher and lower in the C-CAT cohort (> 10% difference with *q*-value < 0.01). Notably, *TP53* mutation frequencies were elevated in the C-CAT cohort across 10 cancer types, suggesting racial differences in *TP53* mutation frequencies.

We then integrated C-CAT, GENIE, and TCGA data consisting of more than 150,000 patients to conduct a meta-analysis of co-occurring and mutually exclusive relationships between 1,790 cancer-driver combinations. This analysis not only validated 215 previously reported relationships but identified 484 novel ones. Interestingly, we found significantly co-occurring mutations within the epigenetic pathway, with 13 epigenetic regulators co-occurring in ten cancer types. Gene set enrichment analysis using RNA-sequencing data in TCGA revealed that accumulation of mutations in epigenetic regulators causes increased proliferation-related transcriptomic signatures. In addition, loss-of-function mutations in epigenetic drivers suppresses proliferation in wild-type cell lines, but this effect is reduced in cells with mutations in both the same and other epigenetic drivers.

Our multi-cohort analyses uncover differences in the driver landscape between Asian and White populations, provides valuable resources for precision cancer medicine, and offers insights into epigenetic regulator-associated oncogenesis.

#1254 Integration of human omics analysis and new syngeneic tumor organoid models reveals that aberrant RAS/PI3K crosstalk triggers refractoriness in high-grade serous carcinoma.

T. Tamura[1], K. Masuda[1], S. Nagai[1], K. Imaeda[1], J. Yamasaki[2], E. Sugihara[2], H. Nobusue[2], Y. Otsuki[2], R. Yamaguchi[3], K. Sakurada[1], W. Yamagami[1], H. Saya[2], O. Nagano[2];

[1]Keio University School of Medicine, Shinjuku, Japan, [2]Fujita Health University, Toyoake, Japan, [3]Aichi Cancer Center Research Institute, Nagoya, Japan

Refractory high-grade serous carcinoma (HGSC) is one of the most severe clinical problems in gynecology, but we have barely grasped the underlying mechanism of aggressiveness and chemo-resistance. Previous study has shown that homologous recombination genes, *BRCA1/2*-unmutated HGSC patients possess the potential to be in refractory condition, and their primary response to chemotherapy was heterogenous; thus, there can be subtype-specific determinant factors hatching refractoriness in *BRCA1/2*-unmutated HGSC patients. To explore the determinant factors, we performed gene set variation analysis and comprehensive log-rank tests on TCGA advanced serous ovarian cancer datasets. As a result, regulation of small GTPase signaling prominently correlated with poor prognosis uniquely in *BRCA1/2*-unmutated HGSC patients (p-value < 0.001), and eventually, pathway clustering analysis by variational Bayesian Gaussian mixture model discovered aberrant RAS/PI3K crosstalk as peculiar poor prognostic signature of *BRCA1/2*-unmutated HGSC patients. To elucidate the mechanism of poor progression triggered by RAS/PI3K, we utilized our syngeneic HGSC organoid models newly established from murine fallopian tube epithelium by making *Myc* overexpressing, and knocking out *Trp53* and *Rb1*; as a supplement, the propriety of these genetic alterations to develop HGSC models was backed up by genetic profiles of high-grade serous ovarian cancer patients in AACR Project GENIE. After that, we knocked out *Nf1* and *Pten* whose deletions were detected relatively with high frequency in HGSC to induce aberrant RAS/PI3K crosstalk in the primitive HGSC model. *In-vivo* evaluation and growth comparison indicated that aberrant RAS/PI3K crosstalk transformed *Brca1/2*-unmutated HGSC modeling cells into aggressive phenotypes such as poor survival (p-value < 0.01) and high growth rate (p-value < 0.001). Chemo-sensitivity assay also showed that the genetic manipulation made *Brca1/2*-unmutated HGSC modeling cells more tolerant to anti-tumor agents like carboplatin (p-value < 0.001), paclitaxel (p-value < 0.01), and olaparib (p-value < 0.01). To investigate biological processes that induce the aggressive and chemo-resistant phenotype, we performed gene set enrichment analysis among our HGSC models. The result showed that aberrant RAS/PI3K crosstalk induces cell cycle acceleration and downregulation of apoptosis in the HGSC cells, which backed up aggressive phenotype and chemo-resistance in our HGSC models. In conclusion, aberrant RAS/PI3K crosstalk transforms *Brca1/2*-unmutated HGSC modeling cells more aggressive and chemo-resistant, which was well recapitulated by our HGSC modeling organoids. The integration of our computational approach and experimental models will lead us to detect peculiar therapeutic targets against refractory HGSC.

MULTIDISCIPLINARY: Genetic and Cellular Mediators of Tumor Progression
Minisymposium

#1256 RPL22 is a tumor suppressor in MSI-high cancers and a key splicing regulator of MDM4.

H. N. W. Weinstein[1], K. Hu[1], L. Fish[1], Y.-A. Chen[1], P. Allegakoen[1], K. S. F. Hui[1], J. H. Pham[1], M. B. Baco[2], H. Song[1], A. O. Giacomelli[3], F. Vazquez[2], M. Ghandi3[2], H. Goodarzi[1], F. W. Huang[1];

[1]University of California - San Francisco, San Francisco, CA, [2]Broad Institute of MIT and Harvard, Boston, MA, [3]Princess Margaret Cancer Center, Toronto, ON, Canada

Microsatellite instability high (MSI-H) tumors are marked by 30% or more mutations in microsatellite regions and are generated by somatic or germline alterations in DNA mismatch repair machinery. Despite a high tumor mutational burden, MSI-H tumors do not frequently harbor mutations in TP53. Notably, a frameshift mutation (*p.K15fs*) in the gene *RPL22* is among the most recurrent mutations in MSI-H tumors. RPL22 and its paralog, RPL22L1, form part of the large subunit of the 60S ribosome and are known to affect protein synthesis as well as splicing of genes and transcription factors that affect development and tumorigenesis. Here we explore the result of *RPL22* loss on the regulation of MDM4, an upstream target of p53. MDM4 protein expression is mediated through alternative mRNA splicing of its sixth exon, which leads to two isoforms, the exon 6-inclusive MDM4-FL and the exon 6-exclusive MDM4-S, which is prone to degradation. To date, no mutational events have been associated with this alternative splicing event. We show the prevalence of *RPL22fs* mutations is more than 70% in certain MSI-H cell lines (e.g. colon, endometrial) and tumors (e.g. stomach adenocarcinoma) in the CCLE and TCGA. *RPL22* copy number loss and *RPL22* frameshift mutations are strongly correlated with MDM4 exon 6 inclusion in TCGA samples, and *RPL22* knockout increases *MDM4* exon 6 inclusion and MDM4 protein in multiple cell lines. *RPL22* loss increases cell proliferation and augments resistance to the MDM inhibitor Nutlin-3a. Downstream targets of p53 (p21, BBC3) are downregulated due to *RPL22* loss and Nutlin-3a inhibition, suggesting mutation of *RPL22* and subsequent overexpression of MDM4 promotes resistance to Nutlin-3a. CLIP-seq revealed that RPL22 binds the *MDM4* 3'-UTR. We find that *RPL22* loss is associated with an alternative 3'-splicing event in *RPL22L1* adjacent to exon 3 and results in the expression of the full-length transcript of *RPL22L1*. In summary, we identify RPL22 as a key modulator of *MDM4* splicing through an alternative splicing switch in exon 6. Furthermore, RPL22 represses the expression of its paralog, RPL22L1, by mediating the splicing of a cryptic exon corresponding to a truncated functional transcript. Therefore, we propose that damaging mutations in *RPL22* drive oncogenic MDM4 induction and reveal a common splicing circuit in MSI-H tumors that may inform therapeutic targeting of the MDM4-p53 axis and oncogenic RPL22L1 induction. Our results also suggest that the presence of RPL22 may act as a rheostat to maintain *MDM4* exon 6 skipping under normal cellular contexts.

#1257 CHD5 suppresses glioblastoma by inhibiting MYC.

X. Sun, A. Mills;
Cold Spring Harbor Laboratory, Cold Spring Harbor, NY

Fundamentally, cancer is a disease caused by genetic and epigenetic alterations that converge to reprogram gene expression networks, leading to unrestrained proliferation. Glioblastoma (GBM) is the most prevalent and aggressive primary brain cancer, median survival being approximately one year and the 5-year survival rate being only 5%. Despite decades of effort, this devastating picture has not appreciably improved and effective therapies have been elusive for GBM patients. A better understanding of GBM biology is essential for developing more effective therapies. Although several genetic alterations have been implicated in gliomagenesis, driving genetic factors responsible for GBM are still obscure, and the interplay between genetic alterations and epigenetic dysregulation is largely undocumented during the gliomagenic process. Here, we show that *CHD5* — a gene mapping to the 1p36 chromosomal region that is notoriously deleted in many cancers, is recurrently deleted in over 20% of GBM cases and is further downregulated through epigenetic means. To delineate how CHD5 loss promotes gliomagenesis, we established a glioma-prone mouse model harboring conditional alleles of *Pten*, *Trp53*, and *Chd5*. We developed an engineered mouse neural stem cell (NSCs)-based strategy to elicit glioma formation, as NSCs are the major cell-of-origin for GBM. We show that Chd5 loss significantly impairs NSCs differentiation while promoting proliferation, transformation, and gliomagenesis *in vivo*. Mechanistically, Chd5 forms a Chd3-containing but Chd4-independent NuRD complex that directly binds the *Myc* promoter and super enhancers to govern *Myc* expression in normal NSCs, with the Snf2 domain of Chd5 playing the most critical chromatin regulating role in the context of GBM. Chd5 loss triggers the remodeling of chromatin, enhances accessibility, and augments *Myc* expression, leading to the formation of highly aggressive glioma. Furthermore, reactivating CHD5 in human GBM xenograft models significantly extends survival. This work demonstrates the tumor suppressive role of CHD5 in gliomagenesis, providing therapeutic insights for cancers with 1p36 deletions. In parallel, this work presents a powerful strategy for rapidly interrogating gene function during gliomagenesis using engineering NSCs, and the generation of novel mouse models with classic clinical features of GBM, offering new approaches for elucidating GBM biology that can inform on therapeutic opportunities for treating patients with GBM.

#1258 A cholesterol metabolite can modulate neutrophil-derived extracellular vesicles to promote breast cancer cell epithelial to mesenchymal transition (EMT) and stemness.

N. J. Krawczynska[1], Y. Wang[1], A. Das Gupta[1], J. Drnevich[1], J. Ostrander[2], E. R. Nelson[1];
[1]University of Illinois at Urbana-Champaign, Urbana-Champaign, IL, [2]University of Minnesota Medical School, Minneapolis, MN

Breast cancer is the second leading cause of cancer-related death in women, with mortality most often due to metastatic recurrence. Elevated cholesterol is associated with poor prognosis, with several potential mechanisms proposed. Work in murine models found that many of the pro-metastatic actions of cholesterol required the enzymatic conversion of cholesterol to 27-hydroxycholesterol (27HC), which functions as a ligand for both the estrogen receptors (ERs) and liver X receptors (LXRs). Importantly, we have found that 27HC promotes metastasis, in part through its actions on neutrophils. When examining mechanisms, we have made the observation that 27HC resulted in increased secretion of small extracellular vesicles (sEVs) from neutrophils. These 27HC-neutrophil-sEVs independently promote metastatic colonization. Since we have found that breast cancer cell lines can take up neutrophil-derived sEVs, we hypothesized that 27HC results in altered cargo within sEVs which leads to functional changes within cancer cells, the ultimate consequence of which being their increased metastatic potential. Using a non-biased small RNA-seq approach we have found that sEVs from 27HC-treated neutrophils had an altered miRNA signature. Bioinformatic analysis revealed several downregulated miRNAs from the let-7 subgroup. Let-7 miRs are known to target several genes associated with the WNT/β-catenin pathway, a pathway strongly implicated in epithelial to mesenchymal transition (EMT) and cancer cell stemness. Strikingly, breast cancer cells treated with sEVs from neutrophils treated with 27HC lost their adherent properties and adopted a mesenchymal and stem-like phenotype. In order to elucidate the mechanism by which these sEVs promote EMT and stemness, we performed comprehensive transcriptomics through time. Weighted gene co-expression network analysis (WGCNA) confirmed these phenotypic shifts, and implicated the WNT/β-catenin pathway, providing support to our hypothesis that the loss of let-7 miRs is the upstream mediator. Collectively, our data suggests that 27HC increases metastasis in part through its effects on neutrophils, by shifting sEVs cargo towards a loss of protective microRNA, resulting in increased EMT and stemness, and thus the ability of cancer cells to migrate, invade and metastasize. Funding: National Cancer Institute (ERN: R01CA234025) Department of Defense (ERN: BCRP Era of Hope Award), and Beckman Institute for Advanced Science and Technology (NK)

#1259 HMGA1: An epigenetic gatekeeper of Wnt signals during colon tumorigenesis and regeneration.

B. West[1], L. M. Resar[1], L. Z. Luo[1], L. Xian[1], I. Herrera[1], S. Wu[1], J.-H. Kim[1], Y. Feng[2], J. Calderon-Espinosa[1], E. R. Fearon[2], C. Sears[1];
[1]Johns Hopkins University School of Medicine, Baltimore, MD, [2]University of Michigan Medical School, Ann Arbor, MI

Cancer cells undergo epigenetic reprogramming to co-opt stem cell networks and drive tumor progression, although how this occurs remains unclear. The *High Mobility Group A1* (*HMGA1*) gene encodes an architectural transcription factor that binds to DNA at AT-rich sequences where it recruits chromatin complexes to modulate gene expression. *HMGA1* is highly expressed during embryogenesis and in adult stem cells, but silenced in differentiated cells. *HMGA1* becomes re-expressed in aggressive cancers where high levels portend adverse outcomes. In colorectal cancer (CRC), *HMGA1* is among the genes most highly overexpressed compared to normal colon epithelium. We previously discovered that *HMGA1* is required for oncogenic phenotypes in CRC cell lines by inducing genes involved in an epithelial-mesenchymal transition. *Hmga1* transgenic mice also develop aberrant proliferation and polyposis of small intestinal epithelium where Hmga1 amplifies Wnt signals to enhance self-renewal. To determine how HMGA1 functions in colon epithelial homeostasis and tumorigenesis, we examined mouse models with overexpression or deficiency of *Hmga1*. Here, we uncover a previously unknown role for HMGA1 as an epigenetic gatekeeper of Wnt signals in colon epithelial cells, both during tumorigenesis driven by mutant *APC* or stress-induced tissue repair. Strikingly, loss of just a single *Hmga1* allele within the colon epithelium disrupts tumorigenesis while prolonging survival in two models of colon tumorigenesis driven by *APC* mutation, including *CDX2P-CreER*^{TC}*Apc*$^{fl/fl}$ and *APC*^{Min} mice inoculated with pro-carcinogenic, enterotoxigenic *Bacteroides fragilis*. Single cell RNA sequencing in *Apc* mutant crypt epithelial cells reveals that intact Hmga1 is required for expansion in the *Lgr5*$^{+}$ stem cell pool, deep secretory cells, and tuft cells during tumorigenesis. *Hmga1* deficiency impacts the stem cell pool the greatest, decreasing Lgr5+ stem cells with skewing to more proliferative, transit amplifying-like cells. Single cell transcriptomic analyses together with assays of single cell chromatin accessibility demonstrate that Hmga1 maintains accessible chromatin to activate gene loci involved in Wnt signals, including *Ascl2*, a stem cell master regulator, Wnt agonist receptors, and Wnt downstream effectors. Surprisingly, either depletion or overexpression of *Hmga1* has no impact on colon epithelial regeneration under homeostatic conditions, although *Hmga1* overexpression enhances tissue repair and survival following injury induced by inflammation or irradiation. Together, our results establish HMGA1 as an epigenetic gatekeeper of Wnt signals in colon stem cells during APC-driven tumorigenesis or injury, but not steady state homeostasis, highlighting its role as a promising therapeutic target for both cancer and regenerative medicine.

#1260 Collapse of cancer cell micronuclei from oxidative damage.

M. Di Bona[1], Y. Chen[1], A. Agustinus[1], M. Deyell[2], M. A. Duran[1], C. Hong[1], J. Hickling[1], D. Bronder[1], S. Martin[3], N. Riaz[1], B. Diplas[1], M. Jalan[1], N. Lee[1], A. Ordureau[1], B. Izar[4], A. Laughney[2], S. Powell[1], S. Santaguida[3], J. Maciejowski[1], T. Jeitner[2], S. Bakhoum[1];
[1]Memorial Sloan Kettering Cancer Center, New York, NY, [2]Weill Cornell Medicine, New York, NY, [3]European Institute of Oncology, Milan, Italy, [4]Columbia University, New York, NY

Chromosomal instability, a hallmark of aggressive cancers, disrupts genome integrity through multiple hits by ongoing missegregation of chromosomes. These chromosomes, inherited only by one daughter cell, are subsequently encapsulated in micronuclei (MNi). Micronucleation is detrimental for replication fidelity not only because it sustains chromosomal missegregation, but also because MNi frequently undergo irreversible collapse during interphase exposing their enclosed chromatin to the cytosol. This exposure catalyzes chromosomal rearrangements and heritable epigenetic abnormalities that have been shown to further bolster cancer evolution and therapeutic resistance. Moreover, MNi collapse is known to promote distant metastasis and poor prognosis through eliciting a non-canonical response of otherwise inflammatory signaling pathways. Despite the fundamental role played by MNi catastrophe in compromising genome integrity and sustaining cancer progression, and the subsequent therapeutic potential of targeting this process, the mechanisms underlying MNi collapse are poorly understood. Here, we identify mitochondria-derived reactive oxygen species (ROS) as the main cause of MNi rupture. Notably, we observe that MNi that locate closer to mitochondria are more prone to rupture. Accordingly, increasing ROS chemically and by H_2O_2 addition increment rupture in a panel of 5 different tumor cell lines, while decreasing ROS using pan-cellular or mitochondrial specific scavengers reduce the frequency of ruptured MNi. By using a combination of advanced super-resolution microscopy, proteomics, transcriptomics, *in vitro* biochemistry assays, and extensive mutagenesis, we reveal the exact pathway leading to MNi collapse. We demonstrate that ROS promote a noncanonical function of the membrane repair ESCRT-III complex scaffolding protein, CHMP7. ROS reduce CHMP7 interaction with ESCRT-III promoting CHMP7 oligomerization and its binding to the inner nuclear membrane protein, LEMD2. CHMP7, while aggregating, physically pulls the micronuclear envelope together with the LEMD2-associated lamina, thereby disrupting MNi integrity. Finally, we show that hypoxic conditions promote ROS-dependent CHMP7-LEMD2 interaction, inducing MNi rupture and inflammatory signaling. Thus, we observe that human tumors characterized by hypoxia have a significantly increased predominance of ruptured MNi, providing a mechanistic link between tumor hypoxia and downstream processes that drive cancer progression.

#1261 *In vitro* medulloblastoma leptomeningeal metastasis models reveal adhesion signaling as a therapeutic vulnerability.

L. Jimenez Garcia, A. C. Gross, R. D. Roberts, J. B. Reinecke;
Nationwide Children's Hospital, Columbus, OH

Introduction: How tumor cells colonize an inherently distinct environment and survive the pressures of therapeutic treatment during metastasis is incompletely understood. In patients with medulloblastoma, the most common malignant pediatric brain tumor, mortality is almost exclusively dictated by metastasis to the leptomeninges, the inner covering of the brain and spinal cord. We aim to mechanistically understand the molecular drivers of leptomeningeal colonization, including how leptomeningeal adhesion mediates therapy resistance.

Experimental approach: Progress in leptomeningeal metastasis research has been hindered by the scarcity of matched primary and metastatic tissue from patients given the lack of clinical benefit to obtaining metastatic tissue. Furthermore, end points from pre-clinical human xenograft mouse models are often driven by primary cerebellar tumors, not leptomeningeal dissemination. These barriers underscore the necessity for novel *in vitro* leptomeningeal metastasis models that allow for rigorous experimental analysis. These models must simultaneously recapitulate tumor cell-host and tumor cell-environment interactions driving colonization to produce translatable findings. Accordingly, our lab has developed two novel *in vitro* leptomeningeal metastasis models that allow for cell-based experimental analysis: a primary meningeal cell-medulloblastoma organotypic co-culture and an acellular leptomeningeal matrix mimetic monoculture.

Results: Proteomic analysis identified that leptomeningeal cells promote medulloblastoma chemotactic honing to the leptomeninges through CXCL12-CXCR4 signaling. Additionally, loss of CXCL12/CXCR4 signaling impaired medulloblastoma adhesion to the leptomeninges. CXCL12/CXCR4 are known to mediate adhesion of stem cells in stromal niches via activation of integrin receptor ITGA4/ITGB1 (VLA4) binding to stromal VCAM1. Indeed, the VLA4-VCAM1 axis is required for medulloblastoma leptomeningeal adhesion and requires activation by CXCL12/CXCR4 signaling. From a translational perspective, we found that leptomeningeal adhesion promotes therapy resistance and that inhibition of adhesion signaling sensitized adherent medulloblastoma cells to therapy.

Conclusions: These findings provide proof-of-concept that appropriate *in vitro* models of metastasis can be developed and utilized to define the biology driving adhesion and chemotherapy resistance in medulloblastoma metastasis. Furthermore, we show that medulloblastoma leptomeningeal adhesion is mediated by a CXCL12/CXCR4-VLA4/VCAM1 axis. Finally, we demonstrate the therapeutic potential of targeting this axis in sensitizing medulloblastoma metastases to current therapies.

#1262 Comparative analysis of *TP53* alleles in pancreatic ductal adenocarcinoma.

A. Tang[1], S. Agabiti[2], H. Chung[2], M. D. Muzumdar[2];
[1]Yale University, New Haven, CT, [2]Yale University School of Medicine, New Haven, CT

The transcription factor p53 is a tumor suppressor capable of inducing cell cycle arrest, senescence, and apoptosis. Both truncating loss-of-function mutations and point mutations of the *TP53* gene (mouse gene *Trp53*), which encodes for the p53 protein, are frequently observed across human cancers. While point mutations in p53 result in loss of canonical tumor suppressor function, recent studies suggest that these mutated proteins acquire pro-tumorigenic gain-of-function properties. For example, $Trp53^{R172H}$ mutations (the murine homolog of $TP53^{R175H}$, the most common human *TP53* variant) enhance metastatic spread relative to deletion mutations in mouse models of advanced pancreatic ductal adenocarcinoma (PDAC). To further explore the differential functions of p53 point and deletion mutants in cancer progression, we performed a rigorous comparative analysis of *Trp53* alleles *in vivo* using **M**osaic **A**nalysis with **D**ouble **M**arkers (MADM) in mice. MADM uses stochastic mitotic recombination to induce two genotypically distinct daughter cells - created at 1-to-1 ratios - expressing different *Trp53* variants dependent on the genotype of the mouse (+/+ vs. -/-, *R172H/R172H* vs. +/+, *R172H/R172H* vs. -/-) and simultaneously label them with unique genetically encoded fluorescent markers (TdTomato vs. GFP). We integrated MADM into a faithful *Kras*-driven model of pancreatic tumorigenesis and used fluorescence microscopy to trace subclonal populations with various p53 alleles within the same mouse. By analyzing the ratio of TdTomato+ to GFP+ cells, we studied the functional differences between alleles in driving pancreatic cancer at various stages of progression. We found that $Trp53^{-/-}$ cells exhibited greater tumor initiation of preinvasive pancreatic intraepithelial neoplasia (PanINs) and early PanIN cell expansion compared to $Trp53^{+/+}$ cells. Surprisingly, $Trp53^{R172H/R172H}$ cells were comparable in number to $Trp53^{+/+}$ cells in early PanINs but were outcompeted by $Trp53^{-/-}$ cells.In contrast, both $Trp53^{R172H/R172H}$ and $Trp53^{-/-}$ cells were capable of facilitating the transition to advanced PDAC with comparable survival times. These phenotypic differences imply that $p53^{R172H}$ retains tumor suppressive properties in early pancreatic tumorigenesis, but similar to the loss of p53, it is incapable of constraining progression to advanced disease, arguing that $p53^{R172H}$ is a separation of function mutation *in vivo*. Ongoing studies examining the molecular differences between *Trp53* alleles by fluorescence-activated cell sorting and RNA-sequencing will shed further light onto the underlying mechanisms that explain these phenotypic differences.

PREVENTION / EARLY DETECTION / INTERCEPTION: Multi-Cancer Early Detection Testing: Where Are We?
Minisymposium

#1263 Interim results from a large-scale, prospective cohort study (JINLING) for multi-cancer early detection test in average-risk asymptomatic patients.

S. Yang, H. Bao, X. Chen, M. Wu, S. Tang, R. Yang, D. Zhu, X. Wu, W. Tang, S. Chang, P. He, X. Xu, Y. Jiang, S. Wu, S. Liu, X. Zhang, X. Wu, Y. Shao; Nanjing Geneseeq Technology Inc., Nanjing, China

Background: Previously, we reported that a multi-cancer early detection (MCED) test CanScan, which utilizes plasma cfDNA genome-wide fragmentomics-related features that can detect cancer signals and tissue of origin (TOO) signals across thirteen cancer types at 99% specificity in individuals with cancer. Here, we report the interim results of a first large-scale prospective clinical study in an asymptomatic population with average risk of cancer, the JINLING Cohort (NCT06011694).
Methods: This ongoing prospective clinical study is enrolling participants aged between 45 and 75 years old without cancer-related symptoms, initiated in June 2022. Each participant will undergo peripheral blood collection for CanScan test and annual routine physical exams once a year for three consecutive years, with an additional two years of follow-up. The primary objective of the study was to evaluate the diagnostic performance of the CanScan test in the early detection of multiple cancers. Secondary objectives include the evaluation of TOO accuracy, its efficiency and clinical utility, lead-time relative to clinical diagnosis, and participants' attitudes and adherence to this test compared to standard care screening methods.
Results: By June 2023, a total of 3724 participants with analyzable samples were included in the analysis. At the data cut off time of Sept 2023, 29 participants were clinically diagnosed with cancer, including 8 that were not in the 13 targeted cancer types. The majority of the cancers were found in the early stages (Stage I or II; 89.6%, 26/29). The CanScan test detected a cancer signal at a sensitivity of 55.2% (16/29; stage I: 10/21, 47.6%; stage II: 4/5, 80.0%; stage III: 2/3, 66.7%). For detected cancers, the prediction accuracy of the top predicted origin was 61.5% (95% CI [38.5%,84.6%]; stage I: 62.5% [5/8]; stage II: 1/3, 33.3%; stage III: 2/2, 100%). The accuracy was 84.6% (95% CI [61.5%,100.0%]; I: 87.5% [7/8]; II: 66.7% [2/3]; III: 100.0% [2/2]) when taking into account the top two predicted origins. Specificity was 97.9% (3619/3695) in non-cancer participants.
Conclusions: In this one-year interim analysis of the large-scale, prospective, clinical cohort study, we investigated the efficacy of the MCED test within an asymptomatic population with an average-risk of cancer. the CanScan test demonstrates capability in detecting a wide range of cancer types and predicting TOO at early stages, highlighting an exceptional level of sensitivity and accuracy while maintaining a high level of specificity. Therefore, the MCED test holds significant potential for early cancer screening in asymptomatic populations, potentially transforming preventative healthcare and improving patient outcomes.

#1264 A targeted methylation-based multi-cancer early detection blood test preferentially detects high-grade prostate cancer and minimizes overdiagnosis.

B. Mahal[1], M. Margolis[2], E. Hubbell[2], C. Chen[2], J. M. Venstrom[2], J. Abran[2], J. J. Karlitz[2], A. W. Wyatt[3], **E. A. Klein**[2];
[1]University of Miami Miller School of Medicine, Miama, FL, [2]GRAIL, LLC, Menlo Park, CA, [3]University of British Columbia, Vancouver, BC, Canada

Background: Indolent prostate cancer (PCa) is prevalent in men in the intended use population (adults aged 50-79 years) for blood-based multi-cancer early detection (MCED) tests. It is thus important to understand detectability of PCa by MCED tests across the spectrum of disease aggressiveness, including detection of indolent disease.
Methods: PCa detectability by a targeted methylation-based MCED test that interrogates circulating cfDNA was assessed in 2 studies: 1) the Circulating Cell-free Genome Atlas (CCGA, NCT02889978), a case-control study (Substudy 3) that demonstrated detection of a shared cancer signal across > 50 cancer types and accurate prediction of cancer signal origin (CSO) with an observed false positive rate of 0.5%; and 2) PATHFINDER (PF, NCT04241796), a return of results cohort study in the intended use population without clinical suspicion of cancer. MCED test performance was assessed by Gleason grade group (GG) and clinical stage, and the association between tumor methylated fraction (TMeF) and cancer detectability was investigated.
Results: The CCGA3 study included 420 recently diagnosed PCa cases with a median age of 65 years (IQR, 59-70). Test sensitivity for PCa was 11.2% (47/420), and CSO accuracy was 91.5% (43/47). Median PSA was higher in detected cases (14 ng/dL, IQR 7-38 vs 6 ng/dL, IQR 5-9, $p < 0.05$). The MCED test detected no low grade (GG1, 0/58), 1.9% (3/157) of favorable intermediate grade (GG2), 5.1% (4/78) of unfavorable intermediate grade (GG3), and 31.9% (36/113) of high grade (GG4 & GG5) cancers. Clinical staging showed detection of 3.2% (3/95) of Stage I, 4.7% (11/235) of Stage II, 14.9% (7/47) of Stage III, and 81.5% (22/27) of Stage IV cases. Non-detected cases had better overall survival (HR 0.263, CI 0.104 - 0.533, $p<0.05$), and detected cases had similar survival (HR 0.672, CI 0.323 - 1.21, $p=0.2$) compared to SEER estimates matched for age, stage and GG. Median TMeF was higher for detected cases (0.002106, IQR 0.000350 - 0.024376 vs 0.000024, IQR 0.00001 - 0.000038, $p < 0.05$). Performance was similar in PF (median age 66 years, IQR 58 -70) with overall sensitivity for PCa of 5.9% (1/17), including no (0/12) detected GG1-2 cases and one of five GG3-5 cases. No Stage I or II (0/15) and 1/2 (50%) Stage III & IV cases were detected.
Conclusion: In two independent prospective studies, this MCED test preferentially detected high grade, clinically significant PCa. A cancer signal detected test result with a prostate CSO prediction generally indicates the presence of aggressive PCa and should lead to a prompt diagnostic work-up. Use of this test in population-based screening programs is unlikely to exacerbate overdiagnosis of indolent PCa.

#1265 Comparison of mortality- vs. stage-based endpoints in randomized trials of cancer screening: A systematic review with implications for multi-cancer screening trials.

X. Feng[1], H. Zahed[1], J. Onwuka[1], M. Johansson[1], R. Etzioni[2], M. E. J. Callister[3], **H. A. Robbins**[1];
[1]International Agency for Research on Cancer, Lyon, France, [2]Fred Hutchinson Cancer Center, Seattle, WA, [3]Leeds Teaching Hospitals, Leeds, United Kingdom

Background: Randomized controlled trials (RCTs) assessing the endpoint of late-stage cancer incidence, rather than the gold-standard of cancer-specific mortality, are proposed for evaluation of multi-cancer early detection tests.
Methods: We conducted a systematic review to assess whether stage-based endpoints can provide a valid alternative for mortality-based endpoints (registration: PROSPERO CRD42023411132). We searched PubMed to identify RCTs of cancer screening interventions published in English before January 20, 2023. Inclusion required that RCTs report, by study arm, numbers of cancer-specific deaths and cancer cases distinguishable between stages I-II vs. III-IV. Data extraction was done by 2 separate reviewers and included the numbers of cancer cases, deaths, and participants by study arm. For each trial, we calculated the percentage reduction in the cumulative (a) late-stage cancer incidence and (b) cancer-specific mortality between the intervention and control arms. We compared these two endpoints based on Pearson correlation coefficients, fixed-effects meta-analysis, and binary statistical significance.
Results: We analyzed 41 trials ranging in size from 2,500 to 409,000 participants. Correlation between the reduction in cancer-specific mortality vs. stage III-IV cancer was strong for lung (Pearson's ρ=0.92, n=12), breast (ρ=0.70, n=6), and 'other' cancers (ρ=0.69, n=8) but weak for colorectal (ρ=0.39, n=11) and prostate cancers (ρ<0, n=4). The overall correlation by fixed-effects meta-analysis across cancer types was 0.71 (95%CI=0.47-0.86) (I^2=0.55). In larger trials, there was a smaller deviation between the observed reduction in cancer-specific mortality and that predicted, by cancer type, based on the trial's reduction in stage III-IV cancer (p=0.02). Of 12 trials demonstrating a statistically significant reduction in stage III-IV cancer incidence (p<0.05), 5 also showed reduced cancer-specific mortality (42%).
Conclusions: In screening RCTs, reductions in late-stage cancer vs. cancer-specific mortality are correlated, but with important differences by cancer type. Screening interventions that reduce late-stage cancer incidence do not necessarily reduce cancer-specific mortality.

#1266 Development and performance of a multi-cancer early detection test utilizing plasma cfDNA fragmentomics: A large-scale, prospective, multicenter study.

H. Bao, X. Chen, M. Wu, S. Tang, X. Wu, W. Tang, D. Zhu, S. Yang, S. Chang, P. He, X. Xu, J. Zhang, Y. Shen, S. Wu, Y. Jiang, S. Liu, X. Zhang, X. Wu, Y. Shao;
Nanjing Geneseeq Technology Inc., Nanjing, China

Background: The implementation of the multi-cancer early detection (MCED) test offers a valuable adjunct to existing screening methods, enabling more efficient detection of cancer and potentially leading to improved treatment outcomes and prognoses for patients. Here, we report on the performance of an MCED test, which utilizes plasma cfDNA and leverages genome-wide fragmentomics-based characteristics to identify cancer signals and predict the signal origin across a diverse range of cancer types.
Methods: Plasma cfDNA from evaluable blood samples was analyzed using an MCED blood test called MERCURY, a robust machine learning classifier leveraging the low-coverage whole-genome sequencing and a comprehensive set of genome-wide features derived from cfDNA fragmentomics. A carefully selected cohort of 3076 cancer patients representing 13 cancer types, in addition to 3477 healthy controls, were pre-specified into the training and internal validation sets to train and internally validate the models to assess cancer and tissue of origin (TOO). The classifier was trained to a target specificity of 99% and locked before analysis of the independent validation set. The independent validation was enrolled prospectively and consists of 1465 participants (cancer: n= 732; non-cancer: n= 733).
Results: The performance metrics in the internal validation set demonstrated that the sensitivity and specificity for cancer detection were 0.865 (95% CI [0.840, 0.887]) and 0.989 (95% CI [0.980, 0.994]), respectively. These impressive results were further substantiated in the independent validation set, where the overall sensitivity and specificity were found to be 0.874 (95% CI [0.848, 0.897]) and 0.978 (95% CI [0.965, 0.987]) respectively. Notably, the sensitivity showed an incremental increase with the stage of cancer (Stage I: 0.769, 95% CI [0.708, 0.821]; Stage II: 0.840, 95% CI [0.784, 0.886]; Stage III: 0.923, 95% CI [0.874, 0.954]; Stage IV: 0.971, 95% CI [0.901, 0.995]. Regarding the TOO model, a total of 10 cancer types with more than 100 patients in the model construction cohort were considered. The TOO model achieved a prediction accuracy of 83.5% (95% CI [80.7%, 86.6%]) and 91.8% (95% CI [89.6%, 94.1%]) for the top predicted origin and the top two predicted origins, respectively, amongst the true positive cases in the independent validation set.
Conclusions: In this pre-specified, large-scale study, the MCED test, utilizing cfDNA fragmentomics, demonstrates its remarkable ability to assess cancer signal with an elevated level of sensitivity and specificity across 13 distinct types of cancer. Moreover, it displays noteworthy accuracy in predicting the tissue of origin. The performances are to be further validated in a prospective cohort study (NCT06011694).

#1267 Projected impact of liquid biopsy screening strategies with high sensitivity in focused populations and high specificity in broad populations.

P. B. Bach, N. U. Trivedi, L. Cotton;
Delfi Diagnostics, Baltimore, MD

Purpose: Two 'liquid biopsy' cancer screening approaches exist: Focused and Broad. The Focused approach targets specific cancers and populations lacking adequate screening, emphasizing high sensitivity. The Broad approach aims to detect various cancers in the population, prioritizing high specificity to minimize false-positives but potentially compromising sensitivity. The public health impact and testing burden of these approaches remain unexplored.
Methods: Projected cancer mortality reduction and annual test volumes are based on published data for liquid biopsy tests. Focused screening is modeled for patients not undergoing guideline-recommended screening for lung, liver, and colorectal cancers. Broad screening is modeled for individuals aged 50-80, assuming the detection of all cancer types. Averted deaths are calculated by combining published mortality reduction estimates or assumed at 20% if not available. Reductions are adjusted for reported test sensitivities. Liquid biopsy cannot prevent deaths from cancers recommended for screening if the person has already undergone the recommended test.
Results: Focused and broad screening strategies annually prevented around 20,000 cancer deaths. Focused screening necessitated testing only one-fifth of the people compared to broad screening (30MM vs. 150MM). The projected reduction in mortality for focused testing relied entirely on randomized studies, while the equivalent statistic for the broad strategy was 53%.
Conclusions: Equivalent reductions in cancer deaths can be achieved with focused screening at high sensitivity and broad screening at high specificity, with only one-fifth of the testing burden. The influence of false positives in focused testing and false reassurance in broad testing may impact these findings, which could also be influenced by testing and follow-up costs.

Table 1

Annual cancer deaths averted (thousands)	Focused cancer testing	Broad cancer testing
Lung	10-12	4-8
Liver	4-5	1
Colorectal	3-4	1
Other screened cancers*	Not modeled	1-2
Unscreened cancers	Not modeled	6-10
Total	17-20	14-22
Annual test volume (millions)	30	150
*Other screened cancers includes prostate, breast, cervical. Range reflects the application of reported Stage I or overall sensitivity, respectively.		

#1268 Immune activation characterization via amino acid concentration signatures for multi-cancer early detection and CDKi treatment response prediction.

C. Tang[1], P. Corredeira[1], S. Casimiro[1], W. Sukdao[2], L. Costa[1], E. Yates[2], G. Bernardes[3];
[1]Instituto de Medicina Molecular Joao Lobo Antunes, Lisbon, Portugal, [2]Proteotype Diagnostics Ltd, London, United Kingdom, [3]Yusuf Hamied Department of Chemistry, University of Cambridge, Cambridge, United Kingdom

Early detection of cancer can increase survival rates by 5-10 times. In the US, a significant portion of cancers are still detected at a late stage, for example, 32.1% of breast cancer, 45.5% of lung cancer, 22.8% of colon cancer patients were diagnosed at advanced stage. Early detection is challenging because many cancers are asymptomatic in early stages, although cancer screening can detect cancer before symptoms emerge. Current standard-of-care screening programs are limited and directed to single types of cancer. Non-invasive multi-cancer early detection (MCED) is urgently needed because it can screen for several cancer types with a single blood test, increasing cancer screening coverage while avoiding cumulative false positive rates.
Developmental MCED approaches usually rely on detection of circulating tumor DNA (ctDNA) released from tumors. However, ctDNA signals scale with tumor burden limiting sensitivity and specificity, particularly for early-stage cancers, while also limiting applicability to precision oncology.
Here we report a MCED approach with superior sensitivity and specificity, which can also be used to predict treatment response. We introduce a novel strategy for detecting cancers from blood plasma, profiling the immune response to disease development rather than relying on detection of emerging diseased tissue. The platform is designed to detect alterations in the ratio of immunoglobulins and albumin, as well as class-switching among immunoglobulins, by measuring the overall concentration of amino acid residues incorporated into proteins in patient plasma. By using our biorthogonal chemistry labeling tool, we were able to measure and characterize amino acid concentration signatures (AACS) within the neat blood samples, including cysteine, free cysteine, lysine, tryptophan and tyrosine, which allowed us to observe distinct signatures for varying cancers including breast, prostate, colorectal and pancreatic cancers. We could identify 84% of cancers with <0.5% false positive rate (N=93). In this study, cancer AACS signatures were distinct from signatures measured with non-cancerous immune activation, including autoimmune diseases and infection.
Moreover, AACS was also correlated to clinical features, such as cancer metastatic statuses and therapy response. With Cyclin-dependent Kinase 4/6 Inhibitors-treated advanced breast cancer patients as an example, we achieved 100% correct prediction of responding patients and 91.7% accurate predictions of non-responding patients by using AACS in treatment-naïve samples.
Altogether, the novel AACS approach is a powerful combination of bioorthogonal chemistry and machine learning analysis in clinical practice, and it can be potentially used for cancer screening and support clinical decisions for treatment selection and patient stratification in new indications.

#1269 Large-scale validaton studies of a blood-based effective and affordable test for multicancer early detection.

M. Mao[1], B. Wei[2], Q. Xu[2], Y. Shen[2], R. Brandao[3], S. Li[1], W. Wu[1], P. Xing[4], Y. Chang[4], D. Zhu[4];

[1]Research & Development, SeekIn Inc, Shenzhen, China, [2]The Affiliated Cancer Hospital of Zhengzhou University and Henan Cancer Hospital, Zhengzhou, China, [3]First Clinic, Sao Paulo, Brazil, [4]Clinical Laboratories, Shenyou Bio, Zhengzhou, China

Cancer early detection aims at reducing cancer deaths. Unfortunately, many established cancer screening methods are not suitable for use in low- and middle-income countries (LMICs) due to cost, complexity, and dependency on extensive medical infrastructure. Nearly 10,000 participants (2003 cancer cases and 7888 non-cancer cases) were divided into one training and five independent validation cohorts across different races, sample types and platforms. One tube of peripheral blood was collected from each participant and quantified using a panel of seven protein tumor markers (PTMs) consisting of AFP, CA125, CA15-3, CA19-9, CA72-4, CEA and CYFRA 21-1 by common clinical immunoassay analyzers. An algorithm named OncoSeek was established using artificial intelligence (AI) to distinguish cancer cases from non-cancer cases by calculating the probability of cancer (POC) index based on the quantification of the seven PTMs and clinical information including sex and age, and to predict the possible affected tissue of origin (TOO). The conventional clinical method that relied only on a single threshold for each PTM would make a big problem when combining the results of those markers as the false positive rate would accumulate as the number of markers increased. Nevertheless, OncoSeek was empowered by AI to significantly reduce the false positive rate, increasing the specificity from 54.0% to 93.0%. The overall sensitivity of OncoSeek was 51.7%, resulting in 84.6% accuracy. The performance was consistent in the training and the five validation cohorts from three countries (Brazil, China and United States) including two sample types (plasma and serum) and three different platforms (Roche, Luminex and ELISA). The sensitivities ranged from 39.0% to 77.6% for the detection of the nine common cancer types (breast, colorectum, liver, lung, lymphoma, oesophagus, ovary, pancreas and stomach), which account for 59.2% of global cancer deaths annually. Furthermore, it has shown excellent sensitivity in several high-mortality cancer types for which there are lacking routine screening tests in the clinic, such as the sensitivity of pancreatic cancer was 77.6%. The overall accuracy of TOO prediction in the true positives was 65.4%, which could assist the clinical diagnostic workup. OncoSeek significantly outperforms the conventional clinical method, representing a novel blood-based test for multicancer early detection (MCED) that is non-invasive, easy, efficient and robust. Moreover, the accuracy of TOO facilitates the follow-up diagnostic workup. OncoSeek is affordable (~$20) and accessible requiring nothing more than a blood draw at the screening sites, which makes it adoptable in LMICs.

TUMOR BIOLOGY: Metastasis
Minisymposium

#1270 p53-R172H mutation confers gain-of-function properties and promotes metastasis in squamous cell carcinoma.

G. Efe[1], K. Cunningham[1], R. Navaridas Fernandez de Bobadilla[1], K. J. Dunbar[1], K. Sugiura[1], N. Nishiwaki[1], S. Carcamo[2], L. Resnick-Silverman[2], D. Hasson[2], A. J. Klein-Szanto[3], A. M. Taylor[1], J. J. Manfredi[2], C. Prives[4], A. K. Rustgi[1];
[1]Columbia University Irving Medical Center, New York, NY, [2]Icahn School of Medicine at Mount Sinai, New York, NY, [3]Fox Chase Cancer Center, New York, NY, [4]Columbia University, New York, NY

INTRODUCTION: Metastasis is associated with more than 90% of cancer-related mortality, and thus, there is a compelling need for innovative therapeutic breakthroughs. *TP53* mutations are present in 60-70% of human cancers, especially in squamous cell cancers. For example, *TP53* mutations are detected in up to 80% of esophageal squamous cell carcinomas (ESCCs). Accumulating evidence suggests that certain missense mutant forms of p53 such as R175 (R172 in mouse), R273 and R282 can acquire neomorphic pro-oncogenic activities that are referred to as gain-of-function (GOF). To elucidate novel mutant p53-dependent mechanisms in promoting metastasis, we conducted RNA-Seq, p53 ChIP-Seq and H3K27ac CUT&RUN-Seq on primary and metastatic tumor cells harvested from our mouse model of ESCC harboring *Trp53*$^{R172H/-}$, *Trp53*$^{-/-}$ and *Trp53*$^{+/+}$. Herein, we have identified p53-R172H gene targets in metastatic ESCC. One of the dominant effectors of p53-R172H-mediated metastasis was Colony stimulating factor-1 (Csf-1) signaling through its cognate receptor (Csf-1r), which we recently published in Cancer Discovery (PMID: 37676642). Overall, this study aims to investigate the GOF properties and mediators of mutant p53 in promoting ESCC metastasis.

RESULTS/DISCUSSION: Using *ex vivo* cultures and *in vivo* tail-vein injections, we demonstrated increased colonization and metastatic capabilities of ESCC cells harboring p53-R172H in comparison to the tumor cells with null and wild-type p53. p53-R172H occupies more genes in the metastatic ESCCs than in the primary tumors that is independent of p53 expression levels. We identified 72 unique targets of p53-R172H with altered gene occupancy and expression that occurs during the transition from primary tumor to metastasis. Such targets in metastatic ESCC are exemplified by *Csf-1* and *Birc5* (encoding anti-apoptosis protein Survivin) that are also enriched with H3K27ac in their promoters. They are upregulated during metastasis compared to the primary tumors dependent upon p53 mutation status, which is reinforced by TCGA data and ESCC patient-derived tissue microarrays (TMAs). Interestingly, other frequently detected “hotspot” p53 mutations including R282W and R273C, which we introduced into the ESCC cells using base editing promote differential pro-tumorigenic activities. Indeed, the analysis of SCC datasets in TCGA reveals that specific p53 mutations are associated with altered overall survival, as well as differences in the enriched pathways.

CONCLUSION: We have demonstrated GOF properties and mediators of p53-R172H in promoting ESCC metastasis that may be applicable to other SCCs. We are further expanding our analyses to additional “hotspot” p53 mutations to dissect the mechanisms of distinct p53 mutations in fostering ESCC metastasis, which can open up new avenues for therapeutic applications.

#1271 PMEPA1 acts as a switch to modulate cooperative cellular invasion and drive NSCLC tumor progression.

T. O. Khatib[1], B. A. Pedro[2], C. M. Knippler[1], V. Y. Matsuk[1], S. F. Webster[1], S. Bombin[1], B. Dwivedi[1], J. Kowalski[3], H. R. Johnston[1], J. K. Mouw[1], A. I. Marcus[1]; [1]Emory University, Atlanta, GA, [2]Johns Hopkins School of Medicine, Baltimore, MD, [3]University of Texas at Austin, Austin, TX

Metastatic disease drives cancer patient mortality. One primary mode of metastasis is collective invasion, whereby cohesive groups of cells invade into the adjacent stroma while maintaining cell-cell contacts. Importantly, these cellular packs harbor genetically and phenotypically heterogeneous subpopulations that cooperate to drive invasion. To deconstruct how phenotypic cellular heterogeneity facilitates distinct molecular profiles within a single tumor, we established the technique Spatiotemporal Cellular and Genomic Analysis (SaGA). SaGA is an image-guided approach that optically highlights phenotypically defined cell(s) for live fluorescence-activated cell sorting and analysis. To elucidate the transcriptional heterogeneity across invasive packs within a 3D physiologically-relevant microenvironment, we combined SaGA with single cell RNA sequencing for isolation and analysis of actively invading cells. This novel single cell transcriptomics approach reveals that - during cellular invasion into the microenvironment - the follower subpopulation supplies TGFβ to heterogeneously stimulate both autocrine canonical and paracrine noncanonical signaling pathways. This cooperative exchange facilitates a symbiotic relationship between tumor subpopulations in non-small cell lung carcinoma both *in vitro* and *in vivo*. *In vitro*, we determine that PMEPA1 protein levels mitigate TGFβ downstream effector signaling within heterogeneous tumor cells to modulate JAG1 expression and activity. *In vivo*, we show that a reduction in JAG1 levels decreases primary tumor cell invasion and progression. We mechanistically define a TGFβ-PMEPA1-JAG1 signaling axis across leader and follower subpopulations critical for tumor cell invasion and cancer progression. Together, these data highlight the importance of cellular heterogeneity and subpopulation communication required for tumor progression.

#1272 Spatial profiling of human colorectal cancer brain metastasis identifies chromosomal instability with adaptive niche cellular reorganization and reprograming.

A. Sathe[1], A. Khan[1], J. Kang[1], R. Meka[1], S. M. Grimes[1], A. S. Luksik[2], M. Lim[1], C. Petrisch[1], C. M. Jackson[2], H. Vogel[1], M. Gephart[1], S. Han[1], H. P. Ji[1]; [1]Stanford University School of Medicine, Palo Alto, CA, [2]Johns Hopkins University School of Medicine, Baltimore, MD

Brain metastasis in colorectal cancer (mCRC) poses a significant clinical challenge with poor outcomes. Our study, the largest spatial analysis reported to date, aimed to uncover unique cellular and genomic features facilitating metastatic lesion development. Employing spatial transcriptomics on 60 patients' surgical resections, we validated our findings with single-cell RNA sequencing (scRNA-seq), whole-genome sequencing (WGS), and *ex vivo* functional studies in tumor slice cultures. We obtained spatially distinct gene expression profiles of metastatic tumor cells, tumor microenvironment (TME) and brain parenchymal lineages. Our analysis identified spatially heterogenous upregulation of PI3K, MAPK, EGFR, p53, and TGFβ signaling in metastatic tumor cells. Tumor cells had high levels of chromosomal instability (CIN) marked by recurrent amplifications in chromosomes 6, 7, 17, and 20. WGS from three independent cohorts revealed significantly higher CIN in mCRC brain compared to primary CRC or mCRC from other organs. Spatial neighborhood analysis identified an immune desert phenotype with lack of proximity between lymphocytes and metastatic tumor cells. However, mCRC brain contained abundant plasma cells identifying a unique TME niche feature. Significant proximity between tumor cells and endothelial cells underscored their potential role in tumor seeding and growth. Spatially aware differential expression analysis demonstrated adaptive responses in the brain parenchyma. This included increased Golgi-ER processing and Rho GTPase signaling in neurons and astrocytes adjacent to metastatic tumor cells, respectively. Macrophages were characterized by high expression of pro-fibrogenic genes. Increased *SPP1* ligand expression from these macrophages interacted with corresponding receptors on spatially proximal fibroblasts, identifying a key niche reorganization feature that can promote metastatic lesion growth. To evaluate the translational potential of our findings, we examined the effects of perturbating the metastatic niche using scRNA-seq. We established a tumor slice culture from a mCRC brain surgical resection, which maintained all original cell states. Despite elevated signaling pathway activity, metastatic tumor cells were resistant to regorafenib, a multi-receptor tyrosine kinase inhibitor. In contrast, pirfenidone, an anti-fibrotic and anti-inflammatory small molecule, successfully reduced extracellular matrix-associated gene expression programs in fibroblasts in the TME. Our analysis identified distinct properties of mCRC brain that can serve as therapeutic targets, including high levels of chromosomal instability, remodeling of brain parenchyma, lymphocyte evasion, plasma cell abundance and macrophage-fibroblast interactions.

#1273 Tumor progression and tumor microenvironment of pancreas cancer ascites revealed by scRNA-seq and spatial transcriptomics.

S. Umeda, E.-R. Karnoub, F. Balogun, A. Jimenez-Sanchez, C. A. Iacobuzio-Donahue;
Memorial Sloan Kettering Cancer Center, New York, NY

Peritoneal metastasis of pancreas cancer is one of the ultimate modes of spread in the cancer. Little is known about how cancer cells spread into abdominal cavity and what is different from hematogenous metastasis. It is also not well characterized how tumor microenvironment prevent cancer cells from spreading in abdominal cavity. We performed single-cell RNA-seq analysis and special transcriptomic analysis to clarify the progression and environment of the cancer. We collected and processed ascites samples of 20 PDAC samples from 19 patients. Sixteen ascites samples were obtained from abdominal paracentesis and two cases in the postmortem period. For one patient ascites was collected both pre and postmortem. All but one patient received chemotherapy prior to ascites collection. Routine clinical cytology evaluation of ascites samples from 17 patients indicated it was malignant in 11 patients and nonmalignant in six patients. All ascites samples were purified by gradient centrifuge using Ficoll-Paque Plus to remove erythrocytes and necrotic debris. For the platform, we adopted the 10x Genomics Chromium Single Cell Gene Expression platform for single-cell RNA-seq library preparation. Spatial transcriptomics was performed for eight FFPE samples from the two autopsy patients with paired cancer ascites using 10x Visium. The CytAssist was used to transfer transcripts of pre-sectioned and pre-stained tissues with 11 x 11 mm Visium Capture Area slides. The sample locations were metastatic tumors to bowel wall, rib bone, mesentery, iliac nerve, diaphragm, peritoneum, pelvis, and primary pancreas tumor. A total of 248,263 cells were analyzed in single-cell RNA-seq. Cell population in pancreas cancer ascites consisted of macrophages, lymphocytes, dendritic cells, plasma cells, plasmacytoid dendritic cells, mesothelial cells, and cancer cells. Cancer cells were detected in twelve samples whereas no cancer cells were detected in eight samples. Gene ontology and gene set enrichment analyses showed macrophages in ascites with cancer cells involved neutrophil activation while those in ascites without cancer cells retained antigen presentation capacity and inducing interferon gamma pathway. Mesothelial cells in ascites with cancer cells showed more apoptosis and lymphocyte proliferation while those in ascites without cancers cells triggered fibrosis and mitosis. These data suggest that macrophage and mesothelial cells could be categorized into anti-tumor cells and tumor associated cells. Ongoing investigations are exploring ligand-receptor relationships. We are going to compare the expression profile of tumor cells in ascites fluid and in tissue from various organs by integrating single cell RNA-seq data and special transcriptomics data.

#1274 Investigating PLOD2 as a therapeutic target to overcome metastasis in radiorecurrent prostate cancer.

Gavin Frame[1], Hon Leong[2], Roni Haas[3], Xiaoyong Huang[2], Jessica Wright[1], Paul C. Boutros[3], Thomas Kislinger[4], Stanley K. Liu[2]

[1]Medical Biophysics, University of Toronto, Toronto, ON, Canada,[2]Sunnybrook Research Institute, Toronto, ON, Canada,[3]University of California, Los Angeles, Los Angeles, CA,[4]University Health Network, Toronto, ON, Canada

Prostate cancer (PCa) is the second most common cancer in males, with 1 in 8 men developing the disease in their lifetime. For PCa, a common treatment strategy is external beam radiation therapy to the prostate. However, when cancer recurs (radiorecurrent PCa), it often behaves aggressively by invading into surrounding organs or spreading distantly. Radiorecurrent PCa metastasis is therefore a significant cause of morbidity and mortality that must be overcome to improve survival of advanced PCa patients. Proteomic analysis revealed the procollagen enzyme Lysyl Hydroxylase 2 (PLOD2) to be upregulated in our radiorecurrent, and highly aggressive, conventionally fractionated DU145 (DU145-CF) PCa cell line. Given its established function as a mediator of invasion in various other cancers, we sought to characterize the role of PLOD2 in the aggressive phenotype of our radiorecurrent PCa cells. Bioinformatic analysis of clinical data revealed PLOD2 genomic amplification to be significantly associated with biochemical recurrence in PCa patients. Upon further examination in vitro, it was revealed that PLOD2 knockdown significantly reduces matrigel invasion and migration in our radiorecurrent DU145-CF cell line, in addition to numerous other PCa cell lines, including primary cells we derived directly from PCa patients. Using the in vivo chick Chorioallantoic Membrane (CAM) model, we confirmed that PLOD2 knockdown significantly reduces the ability of DU145-CF cells to extravasate from the CAM vasculature into the surrounding stroma, a critical step of the metastatic cascade. To explore mechanisms of metastatic cellular reprogramming downstream of PLOD2, RNA sequencing of DU145-CF cells was conducted; a total of 681 genes were discovered to be dysregulated by PLOD2 knockdown, with their functional analysis suggesting changes in cellular metabolism and respiration. Finally, since PLOD2 is known to be regulated by hypoxia-induced protein HIF1α, we explored whether PLOD2 expression could be inhibited by the HIF1α inhibitor, PX-478. Treatment with PX-478 reduced both HIF1α and PLOD2 protein expression, and significantly reduced invasion, migration, and in vivo extravasation in DU145-CF cells, thereby indicating its potential as a pharmacological inhibitor of HIF1α-associated PLOD2 in radiorecurrent PCa. Together, our results demonstrate for the first time the role of PLOD2 in radiorecurrent PCa invasiveness, and point towards its potential as a therapeutic target to reduce metastasis and improve survival outcomes in PCa patients.

#1275 *In vivo* functional CRISPR screens identifies metabolic dependencies mediating triple negative breast cancer lung metastasis.

Xiaoyong Wang, Shu-ting Chou, Verra Ngwa, Yoonha Hwang, Breelyn Karno, Deanna Edwards, Jin Chen

Medicine, Vanderbilt University Medical Center, Nashville, TN

Metastasis is responsible for about 90% of cancer-related mortality. Throughout the metastatic cascade, cancer cells requires substantial metabolic rewiring to adapt the nutrient micro-environmental changes enabling dissemination and seeding in distant organs. Recent insights into importance of the tumor-intrinsic metabolic reprograming has been implicated in immune escape, yet altered immune responses imposed by tumor metabolism during metastasis are poorly understood. Here, we generated genetic perturbations in triple-negative breast cancer cells using metabolism-focused CRISPR knockout library and performed in vivo screens in both immunocompetent and immunodeficient mice. By comparing enriched sgRNAs in lung metastases or primary tumors, we identify loss of one gene related to long chain fatty acid (LCFA) β-oxidation (FAO) potentiates metastatic dissemination in immunocompetent mice but no in immunodeficient mice, suggesting that impaired FAO in tumor cells promotes breast cancer lung metastasis through an lymphocytes-dependent manner. We confirmed individual sgRNAs targeting this FAO gene from the primary screen dramatically accelerate metastasis in different breast cancer orthotopic models. Specifically, we find that low expression of this gene in primary tumors of advanced breast cancer patients with high grade tumors and positive lymph nodes (LN+) is associated with reduced overall survival. In addition, deletion of this gene generates an immunosuppressive microenvironment in the lung metastatic tumors with increased neutrophils, monocytes and decreased $TNF\alpha^{+}$-$IFN\gamma^{+}$ $CD8^{+}$ T cells. Mechanistically, impaired FAO in tumor cells causes mitochondria imbalance under lipid metabolism stress, consequently triggers inflammatory response on establishing a neutrophil-rich metastatic niche via mitochondrial nucleic acid-driven innate immunity. Altogether, our data provides a new insight on how tumor cell lipid metabolism impacting immune interplay during metastatic progression, nominating potential anti-tumor immunotherapies.

#1276 Kindlin-2: a novel target of Parkin regulating cancer metastasis.

M. Yeon, I. Bertolini, D. C. Altieri;
The Wistar Institute, Philadelphia, PA

Although targeted therapies in prostate cancer have clinically shown successful outcomes, resistance to these therapies and acquisition of lineage plasticity pose challenges for fully treating prostate cancer. Among several microscopic perspectives to solve these obstacles, much evidence has emerged indicating that mitochondria dynamics are closely associated with tumor metastasis and tumor progression in various types of cancer.

The E3 ubiquitin ligase Parkin is associated with PINK1-mediated mitophagy, allowing cells to control mitochondria damages and generate the needed energy to survive in harsh physiological conditions.

Interestingly, we found that Parkin potentially ubiquitinates proteins independently of PINK1-associated mitophagy. By SALIC analysis, we found that K681 and K582 of Kindlin-2 is one of the potential ubiquitination sites by Parkin in prostate cancer cells.

Kindlin-2 is a cytoskeletal membrane protein and is a component of the focal adhesion complex. Computational modeling suggested that N-terminal region of Kindlin-2 binds to Parkin, with K581 and K582 of Kindlin-2 exposed outside for ubiquitination. Our studies showed that Kindlin-2 is ubiquitinated and degraded by wild-type Parkin but not by the catalytic site, C431S, mutant Parkin. Furthermore, K581A and K582A mutant Kindlin-2 did not exhibit poly-ubiquitination under conditions of Parkin overexpression. Surprisingly, in our immunofluorescence study, Kindlin-2 was recruited to the mitochondria and co-localized with Parkin. From a mitochondrial functional perspective, wild-type Kindlin-2 reduced mitochondria dynamics, whereas mutant Kindlin-2 didn't in the presence of Parkin. This suggests that the cytoskeletal protein Kindlin-2 might play a role in mitochondrial dynamics that mediates tumor metastasis.

Wild-type Kindlin-2 reduced both focal adhesion generation and decay, unlike mutant Kindlin-2 under Parkin-induced condition. Additionally, this pattern was observed in the single cell lamellipodia dynamics through live cell imaging. 2D and 3D cell invasive assays supported the evidence that Parkin decreases tumor metastatic potential by ubiquitinating Kindlin-2 and regulating mitochondria and focal adhesion dynamics.

Our findings indicate that Parkin reduces tumor metastatic potential by ubiquitinating Kindlin-2 and demonstrate the possibility as a therapeutic agent for advanced and immune suppressive tumors. Furthermore, Parkin could be a promising agent for Parkin suppressed tumor patients in line with personalized cancer therapy development.

TUMOR BIOLOGY: Microbes and Tumors: Time for Mechanisms
Minisymposium

#1277 Unveiling the impact of intratumoral microbiota in the treatment efficacy of soft tissue sarcoma.

L. Tiraboschi[1], D. Braga[2], A. Melacarne[1], V. Ferrari[3], G. Vella[1], A. Mozzarelli[4], A. Lo Cascio[1], G. Fornasa[1], M. Lizier[1], S. Carloni[5], G. Martano[1], S. Timo[1], A. Bernardinello[1], S. L. Renne[5], F. Cananzi[5], A. Bertuzzi[1], G. Penna[1], M. Rescigno[5];

[1]IRCCS Humanitas Clinical and Research Center, Rozzano, Milan, Italy, [2]Institute of Oncology Research, Bellinzona, Switzerland, [3]Institute for Research in Biomedicine, Bellinzona, Switzerland, [4]New York University, Langone Health, New York, NY, [5]Humanitas University, Rozzano, Milan, Italy

Tumor resident microbiota is an emerging component of the tumor microenvironment with unclear biological function. Among all microorganisms harbored within tumor tissue, bacteria are currently the most studied due to their ability to interact with the host. To date, the tumor microbiome is reported as composed of tumor type-specific bacteria, commonly found within host cells, which can affect tumor biology as well as play a role in cancer formation, progression, and response to therapy. So far, the contribution of intratumoral microbiota in the context of soft tissue sarcoma (STS) has been underestimated; therefore, this project aims to characterize the STS microbiota and understand if it can impair the sensitivity to chemotherapeutic regimens. STS are heterogeneous cancers with more than 100 histological subtypes, different in molecular alterations, which make its personalized therapy very complex. Thus, doxorubicin is the gold standard of chemotherapy for advanced STS but it is effective for less than 50% of patients. Doxorubicin is a natural anthracycline produced by different strains of *Streptomycetaceae* which exploit the toxic properties of this molecule for inter-specific competition. Hence, the hypothesis that certain bacteria developed drug-inactivating mechanisms seems evolutionarily plausible. Targeting the bacterial 16S rRNA gene through a Fluorescence in situ hybridization, we were able to detect bacteria within different histotypes of sarcoma. In addition, we analyzed the microbiome composition of sarcoma tissues and adjacent healthy tissues showing that sarcomas harbor a distinct microbiome composition. Besides, comparison of different sarcoma histotypes revealed that microbiome composition seems to be shaped according to histological features. Moreover, we isolate live bacteria harbored within sarcoma tissues. To date, isolated bacteria were mainly strictly or facultative anaerobes; thus, well adapted to live in the hypoxic environment of tumors. These bacteria gave us the opportunity to investigate their ability to interfere with chemotherapy. We exposed several sarcoma-isolated bacteria strains to doxorubicin, we found that certain bacteria strains were responsible for drug degradation. This result was confirmed with functional experiments evaluating drug toxicity after bacterial exposure. In addition, we showed *in vivo* that the intratumoral presence of doxorubicin-degrading bacteria is sufficient to provoke the occurrence of chemoresistance in a doxorubicin-sensitive mouse model of fibrosarcoma. This study offers new insights about the relationship between the intratumoral microbiota and the occurrence of chemoresistance in cancer therapies, suggesting that microbial communities hosted within the tumor should be deeply investigated, and then manipulated, to improve the outcome of therapies.

#1278 Differential urinary microbiome and its metabolic footprint in bladder cancer patients following BCG treatment.

Kyungchan Min[1], Xuan-Mei Piao[2], Young Joon Byun[2], Chuang-Ming Zheng[2], Seon-Kyu Kim[3], Seong-Hwan Park[3], Sungmin Moon[4], Kyeong Kim[4], Ho Won Kang[4], Won Tae Kim[4], Seok Joong Yun[4], Hansoo Park[1]

[1]Gwangju Institute of Science and Technology, Gwangju, Korea, Republic of,[2]Department of Urology, Chungbuk National University College of Medicine, Cheongju, Korea, Republic of,[3]University of Science and Technology, Department of Bioscience, Daejeon, Korea, Republic of,[4]Department of Urology, Chungbuk National University Hospital, Cheongju, Korea, Republic of

Introduction & Objectives: Recent insights reveal a urinary microbiome, challenging prior beliefs about urine's sterility. Using 16S rRNA gene sequencing, a pivotal tool in mapping this microbiome, our study delves into the interplay between bladder cancer (BCa), BCG therapy, and the urinary microbiome. We analyzed bacterial profiles in benign and malignant samples, considering various clinical parameters.

Materials & Methods: A total of 88 patients participated in the study, comprising 30 individuals with benign diseases and 58 BCa patients. Urine samples were collected from patients with benign conditions and from BCa patients before and after BCG treatment. Malignant samples obtained before the completion of the intravesical BCG induction cycle were labeled 'Pre-BCG', while those collected after this cycle were termed 'Post-BCG'. Following collection, DNA was extracted and underwent 16S rRNA gene sequencing. The sequencing data was then utilized for bioinformatic analyses, which included metagenomic profiling and metabolic pathway inference.

Results: Significant differences in bacterial compositions were observed between benign and malignant samples, with a metabolic signature suggesting toluene degradation pathway may mitigate bladder cancer development. In the post-BCG samples, we inferred elevations of 2-oxoglutarate, a BCG derivative, and L-methionine, which is associated with therapeutic benefits, compared to their pre-BCG counterparts. Furthermore, post-BCG samples showed microbial differences in responders and increased quinolone synthesis compared to non-responders. This is of significance due to quinolone's role in modulating DNA topoisomerase and mitochondrial functions, both pivotal in bladder cancer progression.

Conclusions: Utilizing 16S rRNA gene sequencing, we drew comparisons between the urinary microbiomes of benign and malignant samples and suggested a potential pathway for bladder cancer occurrence. Following intravesical BCG treatment, certain microbial metabolic pathways seemed to offer therapeutic benefits to responders. Our study provides insights into the microbial influences on bladder cancer development and the varying responses to BCG treatment.

#1280 Role of the tumor microbiome in the lung adenocarcinoma immune microenvironment through multi meta-omics analysis.

I. Valdes[1], A. Martin[2], E. Martinez[3], d. Carvajal Hausdorf[4], E. Riquelme[1];
[1]Pontificia Universidad Catolica de Chile, Santiago, Chile, [2]Universidad San Sebastian, Santiago, Chile, [3]Corporacion CGNA, Temuco, Chile, [4]Clinica Alemana Santiago, Santiago, Chile

Lung cancer is the leading cause of death by cancer worldwide. The tumor microbiome has shed light on its role, influence, and modulation in cancer immunosurveillance, where the tumor-bacterial component emerges as a potential mediator for the antitumoral-immune response. Nevertheless, the complexities and functional mechanisms underlying this interaction remain elusive. Here, we outline how the tumor microbiota can impact the host´s immune response to lung adenocarcinoma (LUAD). We explored the microbiome within LUAD tumors and non-tumoral adjacent tissues (NAT) from Chilean patients. We used 10 paired (LUAD and NAT) fresh-frozen samples, 20 exclusively tumor fresh-frozen samples, and 40 exclusively tumor formalin-fixed paraffin-embedded samples. Using 16S rRNA gene sequencing, we assessed revealed variations in alpha diversity, with an intra-tumoral microbiome enriched in *Gammaproteobacteria* and *Actinobacteria*, particularly genera *Pseudomonas* and *Corynebacterium* in undifferentiated LUAD samples. Notably, a consistent depletion of *Verrucomicrobiota* with genus *Akkermansia* was evident in samples where cell differentiation was lost. Metaproteomics analysis revealed bacteria-associated peptides from *Pseudomonas* and *Streptomyces* enriched in the tumor, linked to Major facilitator superfamily (MFS) transporters and Glutathione S-transferase N-terminal domain-containing protein, both associated with transport activity and negatively correlated with cancer. The bacterial metabolic analysis uncovered 10 enriched microbial-associated metabolites in the tumor, highlighting adenosine and inosine, two known inducers of immunosuppression on T-cells in the tumor microenvironment. Host proteomics gene-ontology analysis highlighted an enrichment of proteins in the Interferon pathways. Concurrently, a downregulation of proteins like T-cell surface-glycoprotein CD8 and HLA-class I histocompatibility antigen was observed, linked to MHC protein complex binding function, and associated with immune evasion through diminished antigen presentation. Furthermore, upregulated proteins such as macrophage migration inhibition factor (MIF) and eIF-2-alpha kinase GCN2, known to stimulate cell proliferation, were identified. In summary, our multi-omics and bioinformatic analyses unveil a distinct intra-tumoral microbiome and microbe-derived metabolites could induce immune suppression, altering the metabolic profile in the LUAD tumor microenvironment and collectively contribute to tumor progression.
Funding information: This work was supported by FONDECYT1231629 and ANID-Subdirección de capital humano/Doctorado Nacional/2023/21231386.

#1281 Antibiotics aerosolization shrinks intratumoral Tregs and impairs lung tumor growth by perturbing the taxonomic structure of tumor-associated microbiota.

Giancarla Bernardo[1], Valentino Le Noci[2], Elena Montanari[2], Emerenziana Ottaviano[3], Giorgio Gargari[4], Elisa Borghi[3], Simone Guglielmetti[4], Federico Ambrogi[5], Tiziana Triulzi[2], Elda Tagliabue[2], Serenella M. Pupa[2], Michele Sommariva[1], Lucia Sfondrini[1]

[1]Department of Biomedical Sciences for Health, University of Milan, Milano, Italy,[2]Department of Experimental Oncology, Fondazione IRCCS Istituto Nazionale dei Tumori, Milano, Italy,[3]Department of Science of Health, University of Milan, Milano, Italy,[4]Department of Food, Environmental and Nutritional Sciences (DeFENS), University of Milan, Milano, Italy,[5]Department of Clinical Sciences and Community Health,, University of Milan, Milano, Italy

The lung has been traditionally regarded as a sterile environment. Emerging evidence has overturned this belief unveiling the existence of a specific lung microbiota that plays a pivotal role in modulating lung immune tolerance. Recent research also sheds light on how the tissue microbiota is significantly altered by the presence of a growing tumor. Here, we investigated the compositional changes in lung-colonizing bacterial populations associated with the growth of LLC1 lung carcinoma cells in C57BL/6 mice, by analyzing the lung 16S rRNA profiling. While overall microbial diversity and structure were similar in tumor-bearing and healthy lungs, abundance analysis of amplicon sequence variants (ASVs) revealed that 48 ASVs were differentially modulated at significant level (FDR ≤ 0.05). Notably, local treatment with aerosolized vancomycin/neomycin antibiotics starting 4 days after tumor injection caused a different representation of 47 ASVs (FDR ≤ 0.05), mostly reducing those ASVs specifically emerging in the lung by the tumor growth, belonging to Bacterioidales, Clostridiales, Lactobacillales and Enterobacteriales. A different microbial composition was also suggested by the results of Partial Least Squares Discriminant Analysis (PLS-DA) that clustered lung tumor samples as saline or antibiotic-aerosolized. Based on the reported ability of some bacteria belonging to these orders to induce immunosuppressive cells in the gut, we examined the impact of antibiotic aerosol on tumor-associated Tregs in the lung. The presence of the tumor promoted the appearance of Tregs expressing CD69 and PD-1 activation markers, but vancomycin/neomycin aerosol treatment strongly dropped Treg frequency in tumor-bearing lungs, compared to saline. In a therapeutic setting, aerosolization of antibiotics starting 4 days after LLC1 tumor intravenous injection significantly reduced the number of lung metastases (p=0.0116). This effect was associated with an increased cytotoxic activity of immune infiltrating effector cells suggesting that the modulation of the lung microbiota impairs tumor growth and enhances antitumor immune response. Some cultivable bacterial strains, that were in agreement with metataxonomic profile results, were isolated from tumor-bearing lungs, but not from healthy lungs. Ongoing experiments suggest an effect of their in vivo transfer in the lung by aerosol on tumor growth and the ability to induce Treg expansion in vitro. Overall, this study unveils that the growth of the murine LLC1 tumor shapes the lung microbial composition by favoring the expansion of microbes with potential immunosuppressive activity eventually affecting the tumor progression. Moreover, our findings unravel the therapeutic potential of localized antibiotics to revert the immunosuppressive microenvironment by targeting tumor-associated bacteria.

#1282 Gavage with *Candida albicans* leads to fungal colonization of colorectal tumors and decreased response to radiotherapy.

D. J. Grencewicz III[1], A. Loncar[1], R. Hoyd[1], A. Pallerla[1], N. Williams[1], M. Benej[1], M. Kreamer[1], Y. Mehra[1], S. Jahanbakhshi[1], M. Anderson[2], N. Denko[1], D. Spakowicz[1];

[1]The Ohio State University College of Medicine, Columbus, OH, [2]University of Wisconsin-Madison, Madison, WI

The host microbiome in the gut and tumors have been shown to affect tumor growth and therapeutic response in cancer. Furthermore, the presence of specific fungal taxa are associated with tumor hypoxia, tumor progression, therapeutic response, and clinical outcomes in colorectal cancer (CRC). Preliminary data from our group found that the presence of *Candida* species increased tumor hypoxia and decreased overall survival in CRC. However, whether intratumoral *Candida* drive, support, or simply inhabit tumors with poor prognoses remains unclear. Here, we investigate a casual role for *Candida albicans* in tumor progression and therapy response using a syngeneic mouse model of microsatellite-instability high (MSI-H) colorectal cancer.

We subcutaneously implanted MC38 colorectal cancer cells into C57BL/6 mice and then orally gavaged these mice with *C. albicans*, *Saccharomyces cerevisiae*, or PBS. The site of tumor formation was locally irradiated once (7.5 Gy), and growth of the tumor was measured over time. Differences in tumor volume were assessed by longitudinal mixed-effect models. Tumor sections were stained for fungi using calcofluor white (CFW) and underwent bulk RNA sequencing to detect differential gene expression, which were interpreted using gene set enrichment analysis (GSEA).

Mice gavaged with *C. albicans* showed decreased response to radiation compared to mice gavaged with either *S. cerevisiae* ($p<0.05$) or PBS ($p<0.001$). Additionally, hyphae were observed in murine tumors gavaged with *C. albicans*, suggesting translocation of gavaged *C. albicans* from the gut to tumors. Further, tumors from mice gavaged with *C. albicans* displayed unique gene expression profiles, including decreased interferon alpha and IL-6 and STAT3 signaling, decreased oxidative phosphorylation, and decreased apoptosis-related gene expression.

Here, we show that *C. albicans* may confer resistance to radiation therapy and affects immune and cancer cell activity in the MC38 (MSI-H) syngeneic *in vivo* model of colorectal cancer. Further, we show that hyphal fungi can be visualized in heterotopic murine tumors from our *C. albicans* gavage condition. These data establish that fungi can translocate from the gut to distal tumor sites, and that upon translocation, changes in gene expression and therapy response are observed. Future directions will explore the mechanism by which these effects occur and whether these findings can be leveraged to improve radiotherapy outcomes.

#1283 Digital spatial profiling of metastatic brain tumors reveals association of the tumor microbiome with immune alterations in the tumor microenvironment.

G. Morad, A. V. Damania, B. Melendez, M. C. Wong, P. V. Sahasrabhojane, S. B. Johnson, M. Chelvanambi, F. Dimitriou, J. S. Losh, N. J. Ajami, S. D. Ferguson, J. A. Wargo;
UT MD Anderson Cancer Center, Houston, TX

Introduction: Metastatic brain tumors are associated with significant morbidity and mortality. The microbiome has emerged as a novel hallmark of cancer, with a prominent role in tumor immunity and response to treatment. However, the role of the microbiome in brain tumors, and in particular brain metastasis, is largely unknown. We hypothesized that distinct microbial communities are associated with alterations in the tumor microenvironment in metastatic brain tumors.
Methods: To evaluate the role of different microbial communities in brain metastasis, matched stool, saliva, and tumor samples were collected prospectively from patients with metastatic brain tumors who underwent surgical tumor resection at the University of Texas MD Anderson Cancer Center. Stool and saliva samples were sequenced via metagenomic shotgun sequencing and tumor samples were analyzed through 16S rRNA gene sequencing. The tumor microbiome was further characterized through confocal and electron microscopy and culture techniques. Lastly, we conducted digital spatial profiling using the NanoString GeoMx® platform to determine the spatial association of the tumor microbiome with tumor and immune transcriptome. Spatial single-cell transcriptome analysis of bacteria-positive and bacteria-negative cells within the tumor microenvironment is currently in progress using the CosMx® platform (NanoString Inc.).
Results: Our computational and experimental analyses demonstrated that bacterial signals could be detected in metastatic brain tumors and exhibit an intracellular localization. Interestingly, we found that the tumor bacterial signatures in brain metastases were composed of commensal oral bacterial taxa but had limited overlap with the gut microbiome. Spatial transcriptome analysis demonstrated that tumor areas with high bacterial signal were associated with innate-immune mediated anti-bacterial responses, suggesting an active host response to intra-tumoral bacteria in metastatic brain tumors.
Conclusion: Overall, this work demonstrates the presence of intracellular bacterial signal coupled with an anti-bacterial response within the tumor microenvironment of brain metastases. These findings offer a new perspective on the dynamic interaction between cancer, microbiome, and the brain microenvironment and can inform future mechanistic and translational studies to improve the outcome of brain tumor patients.

Monday, April 8, 2024

SCIENCE AND HEALTH POLICY: Science and Health Policy
Poster Session

#1287 The ACCESS consortium: Advancing childhood cancer experience, science and survivorship in Canada.

C. J. Williams[1], S. A. Grover[2], A. Co-Dyre[3], D. Malkin[2], J. A. Whitlock[2], on behalf of the ACCESS consortium;
[1]Ontario Institute for Cancer Research, Toronto, ON, Canada, [2]The Hospital for Sick Children, Toronto, ON, Canada, [3]King's University College at Western University, London, ON, Canada

In Canada, >4,300 children, adolescents and young adults are diagnosed with cancer each year. 1/3 have refractory/metastatic disease or will relapse with an expected 5-year survival rate of <15%. The prognosis for most pediatric cancers has stagnated in the past 30 years and Canada trails the US and Europe in providing accessible clinical trials and improved outcomes. Advocacy for change by patients and families led to a federal government investment of $30M in pediatric cancer research. $23M was allocated to establishing a national pediatric cancer consortium. “ACCESS: advancing childhood cancer experience, science and survivorship” is the new multi-stakeholder network created with a vision that every Canadian child with cancer has access to the latest scientific advances, diagnostic tools, therapies and supportive care leading to better outcomes and quality of life.
ACCESS will connect the Canadian pediatric cancer community, build partnerships, leverage research and clinical expertise across cancer types and ages, implement transformative change and create a unified national strategy. To date, >350 clinicians, researchers, policymakers, advocates, people with lived experience (PWLE; patients, families and survivors) and other stakeholders have been engaged, with a goal of representing Canada's ethno-cultural, socioeconomic and geographic diversity. ACCESS is building partnerships between children, families, professionals, and existing programs to collaborate in coordinated research and knowledge mobilization. The goal is to implement transformative change in the delivery of fair, fast, effective and safe cancer care for all Canadian children.
ACCESS has developed a statement of its values that includes patient/survivor and family centred; collaborative; anti-oppressive; innovation and excellence; accountable. Uniquely, ACCESS is an interdisciplinary and inclusive organization that directly engages and collaborates with PWLE at all levels of research and governance.
ACCESS is organized into 7 themes that will address gaps, advance research and educate through all phases of the pediatric cancer journey: cancer biology; clinical trials; access to innovative therapies and optimal care; regulation, policy and economics; education and training; ethical, legal, societal implications and implementation science; and psychosocial and survivorship. In addition, there are two cross cutting groups focusing on Knowledge mobilization and Social justice, Indigenization and Inclusion.
Collaborations with local, provincial, national and international initiatives are being established through the development of a partnership strategy. Cross-consortium priorities are being implemented, and a data management strategy is in development. The publication of a strategic and sustainability plan for ACCESS is anticipated in 2024.

#1288 Evaluating gender and country of origin diversity on editorial boards in thoracic, gastrointestinal, and breast oncology journals.

Z. L. Arter[1], R. Hsu[2], D. Benjamin[3];

[1]University of California Irvine medical center/Chao Family Comprehensive Cancer Center, Orange, CA, [2]University of Southern California/Norris Comprehensive Cancer Center, Los Angeles, CA, [3]Hoag Family Cancer Institute, Newport Beach, CA

Background: The composition and diversity of editorial board members in oncology journals are critical indicators of the field's inclusivity and global perspective. Despite a historical trend of female underrepresentation on editorial boards of peer-reviewed medical journals, the extent of diversity within oncology's various subspecialties remains less understood. This study aims to elucidate the landscape of gender and economic diversity among editorial boards in three major oncology subspecialties: thoracic, gastrointestinal (GI), and breast oncology.

Methods: 5 top oncology journals in thoracic, GI, and breast oncology were selected based on 2022 Journal Citation Reports impact factors (Clarivate). Editorial board members, identified from each journal's website, were assessed for economic diversity using the World Bank's 2024 high-income country classification and gender based on academic profile data. Chi-square tests evaluated the gender and economic diversity differences.

Results: A total of 762 editor positions from 15 journals were analyzed across the 3 subspecialties. In thoracic oncology, 64.6% were men, 33.5% women, with 7.3% from non-high-income countries. In GI oncology, 84.5% were men, 10.5% women, with 11.1% from non-high-income countries. In breast oncology, 59.3% were men, 39.7% women, with 2.8% from non-high-income countries. Significant disparities in gender and geographical origin were noted ($\chi^2 < 0.01$). A majority of GI oncology journal editors are based in Asia (66.1%), while in thoracic and breast oncology, most editors are located in North America and Europe. Among 17 editors-in-chief, 88.2% were men, all from high-income countries.

Conclusion: The study highlights a significant gender imbalance and a predominance of editors from high-income countries in oncology journals. This imbalance underscores the need for greater inclusivity and diversity in the editorial boards of prominent oncology journals.

Gender and country of origin representation among thoracic, GI, and breast oncology Journals

Editors in Subspecialties	Male	Female	Unknown Gender	Originating from High-Income Country	Originating from Middle- or Low-Income Country	Continent
Thoracic Oncology (N=206)	133 (64.6%)	69 (33.5%)	4 (1.9%)	191 (92.7%)	15 (7.3%)	Asia: 37 (18.0%) Africa: 1 (0.5%) Australia: 7 (3.4%) Europe: 73 (35.4%) North America: 86 (41.7%) South America: 2 (1.0%)
GI oncology (N=342)	289 (84.5%)	36(10.5%)	17 (5%)	304 (88.9%)	38 (11.1%)	Asia: 226 (66.1%) Africa: 1 (0.3%) Australia: 2 (0.6%) Europe: 71 (20.8%) North America: 40 (11.7%) South America: 2 (0.6%)
Breast Oncology (N=214)	127 (59.3%)	85 (39.7%)	2 (0.9%)	208 (97.2%)	6 (2.8%)	Asia: 10 (4.7%) Australia: 10 (4.7%) Europe: 63 (29.4%) North America: 130 (60.7%) South America: 1 (0.5%)

#1289 Disparities in healthcare utilization and access among female cancer survivors in Maryland.

A. E. Connor[1], M. Jin[2], K. Visvanathan[1];

[1]Johns Hopkins Bloomberg Sch. of Public Health & Sidney Kimmel Comprehensive Cancer Center, Baltimore, MD, [2]University of North Carolina, Chapel Hill, Chapel Hill, NC

Background: Healthcare utilization can be defined as how often healthcare is used, through what venue, and if access is available. There are medically vulnerable groups of cancer survivors, such as racial/ethnic minorities and economically disadvantaged populations, that may underutilize healthcare throughout cancer survivorship compared to non-vulnerable groups. Factors associated with survivorship care access/utilization should be evaluated to identify at-risk groups and reduce risk of poor health outcomes. Among female cancer survivors in Maryland, we examined the associations between race/ethnicity, obesity, measures of economic stability, and healthcare utilization-related outcomes (including access to care providers, type of doctor provides majority of care, and unmet health care needs because of cost).

Methods: Survey data were analyzed for 1,353 non-Hispanic white (NHW) and 280 non-Hispanic Black (NHB) women with a self-reported history of cancer living in Maryland who completed the Maryland Behavioral Risk Factor Surveillance Survey between 2011-2020. Multivariable logistic regression models were used to estimate odds ratios (ORs) and 95% confidence intervals (CI) for the associations between independent factors and healthcare utilization outcomes.

Results: On average, survivors were 66.8 (standard deviation (SD)=12.8) years of age at time of survey and 53.5 (SD=15.6) years of age at time of cancer diagnosis. Breast cancer was the most common cancer reported (58.9%). While most women reported being retired (50.6%), 30.6% reported being employed and 10% were unemployed. Most women were homeowners (81.5%) and 40.1% had household incomes >$50,000/year. Overall, race/ethnicity was not associated with any of the outcomes. Unemployed survivors (compared to employed) were 3.90 times more likely (95% CI 1.38-11.04, p=0.01) to report not being able to see a doctor because of cost. Survivors who were not homeowners (compared to homeowners) were 0.39 times less likely (95% CI 0.22-0.67, p <0.001) to report having a general/family practitioner for majority of cancer survivorship care. Survivors with household incomes ≤$50,000/year (compared to >$50,000/year) were 2.36 times more likely (95% CI 1.20-4.65, p=0.01) to not have seen a doctor in the past year. Lastly, obese survivors, compared to non-obese, were 0.25 times less likely (95% CI 0.07-0.84, p=0.02) to not have at least one healthcare provider.

Conclusions: While race/ethnicity was not associated with healthcare access/utilization, our results do demonstrate various disparities in access to care and healthcare utilization during cancer survivorship by employment status, home ownership, and income. Our findings can inform interventions in collaboration with healthcare providers caring for female cancer survivors to address challenges associated with access to survivorship care among medically underserved survivors in Maryland.

#1290 Racial and ethnic representation and disparities on clinical guideline panels in oncology.

J. M. Loree[1], A. Dasari[2], M. Shaheed[3], H. Gothwal[4], K. Singh[5], H. Shaheed[6], R. Mangal[4], S. Gothwal[7], J. Willis[2], M. J. Overman[2], S. Kopetz[2], **K. P. Raghav**[2]; [1]BC Cancer, Vancouver, BC, Canada, [2]The University of Texas MD Anderson Cancer Center, Houston, TX, [3]McMaster University, Hamilton, ON, Canada, [4]Adesh Institute of Medical Science and Research, Bathinda, India, [5]Government Medical College, Patiala, India, [6]The University at Buffalo, Buffalo, NY, [7]Texas A&M University, College Station, TX

Purpose: Culturally competent diverse workforce is critical to equitable and progressive cancer care. Yet, racial bias, permeates practice and research in oncology. The National Comprehensive Cancer Network (NCCN) panels recommend guidelines that determine standards for patient care in the United States (US). We investigated the extent of racial/ethnic representation/disparity amid this higher echelon of cancer leadership.

Methods: We collected data from publicly available NCCN (https://www.nccn.org) guidelines (version: 1.2023-5.2023) published between 11/2022-11/2023. Six research team members extracted data. Race/ethnicity (NIH categories: White, Black, Hispanic/Latinx, Asian) was identified by advanced AI detection software tools (Namsor and Kairos, utilizing names and facial recognition to infer US race). Gender was determined using name/pronoun (if available). All information was confirmed using online databases (institutional profiles, biographical paragraphs, social media) and group consensus (in case of discrepancies). Data regarding active US physicians was obtained using Association of American Medical Colleges (AAMC) 2022 physician specialty data report. The primary objective was to determine the racial/ethnic composition of panels and association between race/ethnicity and chairs/co-chairs/vice-chairs (lead positions or leads) within panels. Descriptive statistics were used. Proportions were compared using Fisher-exact or Chi-squared test (odds-ratio [OR] and 95% confidence intervals [95%CI] were reported).

Results: We reviewed 63 panels corresponding to 63 distinct disease sites. A total of 1223 unique individuals [475 (38.8%) females and 748 (61.2%) males] accounted for 2162 panel members with a median of 34 members (range: 25-42) per panel. Racial/ethnic representation was 1455 (67.3%) Whites, 570 (26.4%) Asians, 93 (4.3%) Hispanics/Latinx, and 44 (2.0%) Blacks, which was comparable to racial/ethnic makeup of active US physicians (64%, 21%, 7% and 6%, respectively). Among these 2162 member positions, 129 (6.0%) were lead positions. In these leads, racial/ethnic representation was 105 (81.4%) Whites, 5 (11.4%) Blacks, 17 (3.0%) Asians, and 2 (2.2%) Hispanics/Latinx. Notably, no significant difference was seen between proportion of female (5.2%) and male (6.4%) leads (OR: 0.80; 95%CI:0.55-1.16; P=0.26). However, the proportion of Whites in lead positions was significantly higher than Non-whites (7.2% vs. 3.4%; OR: 2.2; 95%CI: 1.4-3.5; P < 0.001).

Conclusions: Although, overall membership of NCCN panels shows favorable racial/ethnic diversity, underrepresentation and bias appear to subsist for non-White race/ethnicity, when it comes to leadership positions within this key decision-making body that influences cancer care. Further efforts to improve this disparity within oncology is an essential step to shaping equity within the field.

#1291 ASPIRE: Advocates and Scientists Partner in Research Education.

Laurie Betts[1], Jennifer Potter[2], Veronica Carlisle[2], Patricia A. Spears[3]

[1]Patient Advocates for Research Council, UNC Lineberger Comprehensive Cancer Center, Mebane, NC,[2]UNC Lineberger Comprehensive Cancer Center, Chapel Hill, NC,[3]Patient Advocates for Research Council, UNC Lineberger Comprehensive Cancer Center, Chapel Hill, NC

UNC Lineberger Comprehensive Cancer Center (LCCC) has a robust and growing cancer patient advocacy community. UNC Lineberger is the flagship publicly funded comprehensive cancer center in North Carolina. We are constantly looking for ways to educate patient and community advocates on recent advances in cancer biology research and clinical trials. Our advocates are also valuable partners for our basic and clinical researchers that may be early in their career. We developed and implemented an inaugural research education program for new advocates. We model this program partly on the highly successful and popular AACR Scientist Survivor Program that recently celebrated it's 25th anniversary. Some of the UNC LCCC advocates participate in the SSP and were motivated to develop our own local program.

We will showcase our pilot 2024 ASPIRE education program that brings together cancer patient and community advocates and cancer researchers to learn from each other. The basic itinerary of the ASPIRE program is:

1.Three separate one-hour online presentations by UNC Lineberger researchers with a patient advocate moderator. The topics covered are:

Cancer 101 : cancer biology, diagnosis, staging, treatment.

Clinical Trials 101: clinical trials, phases, patient protection, progress with for example accrual of representative populations.

Research 101: bench research, bioinformatic, AI, how research works and how it may lead to new treatments. To showcase a tissue donation program being developed by UNC Patient Advocates that will benefit researchers.

2.The lecture series is followed by a breakfast roundtable discussion for all the participants to discuss their experiences. There will be short presentations and discussions in small groups of researchers and cancer patient advocates.

We will summarize our ASPIRE pilot experience, how our participation in the SSP program motivated this local program, and how we plan to incorporate feedback from participants to inform future programs. We hope this will lead to more informed patient advocates that can then be even more powerful in research advocacy.

#1292 ProTALKS: A community outreach project founded by a graduate of the CaRE^2 Community Scientist Research Advocacy training program, Mrs. Lynn Jones-Turpin.

Lynn Jones-Turpin[1], Ileana Guzman[2], Brooke Hensel[2], Fern Webb[1]

[1]University of Florida, Jacksonville, FL,[2]University of Florida, Orlando, FL

ProTALKS was created and led by a community member committed to reducing prostate cancer health disparities. ProTALKS stands for Prostate Cancer Outreach, Opinions, and Opportunities and is designed to increase awareness of prostate cancer prevention, research, and treatment as well as highlight the health disparities observed in Black communities. According to the Florida Department of Health, prostate cancer incidence and mortality rates among Black men living in Duval County are higher compared to men of other races and ethnicities. Therefore, there is a need for programs like ProTALKS that focus on early detection strategies and promoting community resources. In collaboration with the Prostate Health Education Network (PHEN), The American Legion Post 197, and Florida Blue, ProTALKS has increased access to services such as prostate cancer screening and evidence-based information. Community events implemented by ProTALKS bring together oncologists, researchers, key community leaders, health educators, and providers to educate and promote positive health behavior changes among high-risk communities. In addition to hosting health fairs, ProTalks has hosted grilling competitions and community awareness walks to further educate the community about prostate cancer prevention, screening, and research. ProTALKS also shares information through the local newspaper, *The Jacksonville Free Press*, The Lynn & Friends radio show, and social media platforms. Since its start in 2021, with support from the Florida-California Cancer Research, Education, and Engagement (CaRE^2) Health Equity Center, ProTALKS has implemented more than 10 community events with over 1,000 community members from Jacksonville, Florida. ProTALKS, in collaboration with CaRE^2, continues to disseminate information about cancer screening, the importance of clinical trial participation, and donating biospecimens for cancer research. Although ProTALKS has been successful in its mission, there have been challenges throughout its implementation. For example, one challenge has been increasing the number of community members attending events and using appropriate marketing techniques to promote ProTALKS' activities. Future implications to avoid challenges include recruiting more volunteers, and partnering with other community organizations in Duval County.

#1293 Uncovered: The breast cancer journey of a Black woman from advocacy to awareness to action.

M. Audoin;
Michelle Audoin (Individual Patient Advocate), Toronto, ON, Canada

Background: There have been 3 significant life events guiding my journey from being a young, Black mother with stage 4 breast cancer and thyroid cancer to an engaged patient partner. The first was having a benign breast tumor removed at age 14. The second was my 2017 mBC diagnosis, including my bilateral mastectomy and the lack of images and information available for Black women concerning reconstruction and scar management. The third is exclusion from and the lack of diversity in clinical trials.
Objective: In order to address the disparities in cancer and my unmet needs, I use my story and experiences as a catalyst for change primarily in three forms, which have evolved over time: advocacy, awareness, and action.
Methods: Advocacy: To unburden myself from the shame about my breast health and the scar from my surgery at age 14, I vocalized my concerns and needs as an adult navigating my breast reconstruction options after my 2017 cancer diagnosis. Ongoing frustration that my needs were not being addressed led me to create Uncovered: A Breast Recognition Project, in collaboration with Rethink Breast Cancer. Uncovered, a digital and print resource, shines a light on the disparities and challenges that Black, Indigenous and people of color face in breast cancer care.
Awareness: The 2020 edition started with my story and those of 7 Black women. After Uncovered launched, other racialized women reached out with similar experiences. The resource was expanded in 2021 to include stories and images of an Inuk woman, Black women, and women of color. This confirmed a systemic need to raise awareness and address racialized communities and inequities in breast cancer care.
Action: As a result of the slow progress towards systemic change, I, along with the women of Uncovered, co-created the Wish List in 2021. The Uncovered Wish List is 6 accessible and actionable items that should be a priority for ending disparities in breast cancer care. Due to the complexity of my diagnosis, which limits my clinical trial options, and the historical underrepresentation of racialized communities in clinical trials, I now partner with cancer institutions and organizations that focus on research to address ongoing unmet needs with the goal to improve equity, diversity and inclusion.
Results: Uncovered is a first-of-its-kind resource in Canada. To date, it has had a global reach of over 70 million through conferences, panels, podcasts, resource links, presentations, and various media. The recognition of my story, Uncovered, and the Wish List allows me to form collaborative connections, and become an engaged patient partner committed to systemic change.
Conclusion: Despite systemic barriers, it is possible for Black women with breast cancer to advocate, raise awareness and take action towards change in meaningful ways.

#1294 Cancer related fatigue and the additive effect of treatment in the context of lymphoma and CLL: An analysis of Lymphoma Coalition's 2022 Global Patient Survey.

S. E. Kalloger, A. Watson, S. Sajkowski, L. Warwick;
Lymphoma Coalition, Kingston, ON, Canada

Introduction: Cancer related fatigue (CRF) continues to be a challenging phenomenon that is often underreported and poorly understood. With etiologies in both disease and treatment manifesting as a symptom and a side-effect respectively, CRF is highly incident and presents a significant clinical problem that impacts survivorship. We sought to explore CRF in a large multinational cohort of patients with lymphoma and Chronic lymphocytic leukemia (CLL).
Methods: Lymphoma Coalition deployed the Global Patient Survey in 2022 targeting patients with lymphoma and CLL and their caregivers. Responses were collected from 8637 respondents over 79 countries. Respondents indicated if they experienced fatigue as a symptom, side-effect or both. Data were enumerated and segregated into the following categories: No Fatigue / Treated (A), No Symptom / No Treatment (B), Symptom / No Treatment (C), Symptom Only / Treated (D), Side-effect Only (E), Symptom and Side-Effect (F). Data were stratified across lymphoma subtypes and categorical percentages were computed. An approximation of the contribution of treatment to CRF was calculated using the following equation: (F) + (E) - (D).
Results: Valid responses were obtained for 6758 respondents. The majority of respondents for most subtypes reported CRF as both a symptom and a side-effect of treatment. Across the 13 subtypes examined, the attributable incidence of CRF related to treatment was found to be highest in: DLBCL (58%), Hodgkin (54%), Peripheral T- Cell (53%) and Mantle Cell (50%). The subtypes with the lowest attributable incidence of CRF included: Chronic Lymphocytic Leukemia (3%), Hairy Cell (12%), Cutaneous (25%) and Marginal Zone (26%).
Conclusions: The majority of patients in this study cited CRF as a significant issue. The calculated fraction of fatigue attributable to treatment suggests that certain treatments may have a larger effect on fatigue than others. A limitation of this study is that we are relying upon patient reported outcomes and we acknowledge that patients may be unable to reliably differentiate fatigue from being a symptom or a side-effect. Our future work in this area will seek to map the intensity of fatigue from diagnosis through treatment in order to get a better understanding of the dynamic nature of this phenomenon. However, we are of the opinion that the compounding effect of CRF related to both disease and treatment yields opportunities to individualize treatment to patients based upon their symptomatic CRF.

#1295 CancerCare coping circle workshop for patients with cancer and covid-19.

Christine Verini[1], **Sarah Paul**[1], Rebecca Ashkenazy[2], Brittany Wolf Gianares[2]

[1]CancerCare, New York, NY, [2]Pfizer, New York, NY

Background: Despite an end to the US COVID-19 public health emergency, COVID-19 remains an ongoing public health priority (1). Patients with cancer can be at increased risk of progression to severe COVID-19 due to their cancer type or to receipt of immunosuppressives or treatment (2). Their mental and emotional well-being have also been impacted negatively (3). There is a need for awareness and education on managing and navigating risk of COVID-19 infection in patients with cancer.

Method: Coping Circle Workshop series webinar 'Navigating the Ongoing Impact of COVID-19 on Cancer Patients' was designed for patient/caregivers to reduce feelings of isolation caused by ongoing challenges associated with COVID-19; provide attendees with the tools to communicate effectively with medical teams; offer tips on utilizing and enhancing their support systems; and help develop adaptive coping mechanisms and provide resources for support. Pre- and post-webinar polls were analyzed to assess webinar impact. Training was provided by a social worker and a mindfulness practice was incorporated.

Results: Webinar had 11 attendees; 91% had skipped a cancer medical appointment due to COVID-19. Post-webinar, all participants responded that the webinar provided new topic information or insights at a level of ≥3 (scale 0-5; Table 1). Attendees' confidence in understanding and managing their potential risks associated with COVID-19 infection increased from 5.8±1.3 (mean± standard deviation) pre-survey to 8.2±1.8 post-survey (scale 0-10).

Conclusions: Delivery of COVID-19 education by an aligned provider supports enhanced scientific discourse and disease management resource utilization and awareness. It may also serve to reduce time and resource burden on oncology providers when engaging in educating patients and improve patients COVID-19 care and management. Conclusions are limited by small participation size.

References: 1.End of PHE. Accessed Nov 2023;2.CDC. Accessed Nov 2023;3.Madan et al, Can Med. 2020;9:9205-18

Table 1: Webinar "COVID-19 and Cancer" - Pre and post webinar questions and responses

Pre-poll, N=11	**Scale**	**Number of patients responded**	**% of patients responded**	**Post-poll, N=11**	**Scale**	**Number of patients responded**	**% of patients responded**
In the past three years, how many times have you skipped a medical appointment due to concerns or fear related to COVID-19?	1-3 times	2	18.18	The webinar provided me with new information or new insights about this topic. Scale of 0-5; 0-strongly disagree, 5-strongly agree	0	0	0
	3-5 times	2	18.18		1-2	0	0
	5-7 times	3	27.27		3	2	18.18
	7-10 times	3	27.27		4	5	45.45
	Unknown	0	0		5	4	36.36
	Never	1	9.09		-	-	-
How would you rate your knowledge about the impact of COVID-19 on people diagnosed with cancer? Scale of 0-10; 0-no knowledge, 10- High knowledge	0	0	0	I am now more aware of the precautions and measures to take to manage the risk of COVID-19. Scale of 0-5; 0-strongly disagree, 5-strongly agree	0	0	0
	1-3	0	0		1-2	0	0
	4	3	27.27		3	1	9.09
	5	3	27.27		4	2	18.18
	6	1	9.09		5	6	54.54
	7	1	9.09		-	-	-
	8	2	18.18		-	-	-
	9	0	0		-	-	-
	10	0	0		-	-	-
How confident do you feel in managing the potential risks associated with COVID-19 as a patient or caregiver? Scale of 0-10; 0-not confident, 10- High confident	0	0	0	How confident do you feel in managing the potential risks associated with COVID-19 as a patient or caregiver? Scale of 0-10; 0-not confident, 10- High confident	0	0	0
	1-3	0	0		1-3	0	0
	4	2	18.18		4	1	9.09
	5	3	27.27		5	0	0
	6	2	18.18		6	1	9.09
	7	3	27.27		7	0	0
	8	1	9.09		8	3	27.27
	9	0	0		9	4	36.36
	10	0	0		10	2	18.18

#1296 Evaluating the accuracy and reproducibility of ChatGPT models in answering lung cancer patient queries.

A. Allibhai[1], **A. Allibhai**[1], A. Brade[2], Z. Allibhai[1];
[1]Southlake Hospital, Newmarket, ON, Canada, [2]University of Toronto, West Mississauga, ON, Canada

Large language models (LLMs) such as ChatGPT can imitate human conversation and produce rapid, coherent responses, which may mask their potential for inaccuracies. With patients increasingly turning to the internet for medical information, the use of LLM chatbots for cancer-related queries risks spreading misinformation. Our study assessed ChatGPT's accuracy and reproducibility in offering valid information and treatment advice for lung cancer in line with established guidelines.

In the evolving landscape of AI-driven healthcare support, the ability of language models to provide accurate and reliable information is crucial. Our study delves into the effectiveness of OpenAI's ChatGPT models (versions 3.5 and 4.0) in responding to patient inquiries about lung cancer across various domains including general information, clinical presentation, risk factors, screening, diagnosis, staging, treatment options, prognosis, post-treatment follow-up, lifestyle recommendations, and psychosocial/educational aspects.

We conducted a structured assessment, posing identical sets of questions to both ChatGPT 3.5 and 4.0. A total of 47 questions were posed with each query being repeated twice per model to evaluate both the accuracy and reproducibility of the responses. The scoring system focused on the accuracy and comprehensiveness of each response.

Our findings revealed a notable disparity in the performance of the two models. GPT 4.0 demonstrated higher consistency and accuracy, with 41 out of 47 (87.2%) responses deemed accurate and comprehensive, compared to 36 out of 47 (76.6%) for GPT 3.5. In terms of reproducibility, both models exhibited strong performance: 42 out of 47 (89.3%) for GPT 3.5 and 45 out of 47 for GPT 4.0 (95.7%). When comparing responses between the models, we observed good reproducibility in 38 out of 47 questions (80.8%).

A key observation was that GPT 4.0 significantly outperformed its predecessor GPT 3.5 in terms of both accuracy as well as reproducibility within its own responses, indicating a more reliable and consistent performance. The area most lacking in accuracy for both models was lung cancer staging, indicating a need for further refinement in this domain. Another key observation was the models' tendency to incorporate empathetic language, often beginning responses with expressions of sympathy and consistently advising confirmation with a medical professional.

Our study underscores the potential and limitations of current AI models in patient education and support, highlighting areas for improvement and the importance of empathetic communication in AI interactions with patients. As the model continues to be trained on a larger and more comprehensive set of data, it is reasonable to anticipate further improvements in its ability to provide precise, detailed, and contextually appropriate responses.

#1297 Patient engagement: Improving the at home care for cancer patients in treatment.

R. Blomquist;
CareBOX Program, Austin, TX

CareBOX Program is an Austin-based non-profit founded in 2014 to address a serious gap in cancer care for patients in the Central Texas area. It provides essential nutritional supplements and supplies to help prevent malnutrition, infections, and injuries from falls as patients continue at-home recovery during treatment and following surgery. About 80 percent of the supplies CareBOX Program provides are not covered by insurance. Many patients could not afford to purchase these items on their own. Volunteers deliver the CareBOXes to the clients' homes. CareBOX Program has always been an inclusive organization. We operate on the basis that all cancer patients in Central Texas in need of our services will receive them as long as we have the funding to do so. Our youngest patient has been 3 months old and our oldest patient has been 93 years old. Currently we are serving more women (61%) than men (39%). Approximately 67% of patient households report annual income of less than $35,000. To date, CareBOX program volunteers have delivered more than 3,800 CareBOXes

#1298 Assessing the impact of Medicaid expansion on colorectal cancer preventative services utilization.

P. Omeaku;
VCU Massey Comprehensive Cancer Center, Richmond, VA

Introduction: Colorectal cancer (CRC) is the second leading cause of cancer mortality. CRC screening rates have steadily risen and incidence rates around the nation have declined. To date, forty-one states have expanded Medicaid across the United States, with 9 states remaining that have not expanded. Although, access through insurance has increased, colorectal disparities in screening and mortality persist. Other studies have shown that screening guideline concordance can be inconsistent based on insurance type. Data suggests Medicaid enrollees are more likely to present advanced-stage cancers than those privately enrolled. The screening differences throughout the United States emphasize how complex colorectal cancer disparities are and how insurance may play a role.
Aims: Our study aims to investigate the impact of Medicaid expansion on timely CRC screenings, specifically examining whether these effects differ by African Americans, Hispanics, and White Americans.
Methods: Data was utilized from the Behavioral Risk Factor Surveillance System (BRFSS) to analyze timely CRC screening data of adults below 138% of the federal poverty level (FPL) of states with different Medicaid expansion statuses. Most recently available data was used in our analysis spanning the years 2014-2022 in all 50 states. States were stratified by dummy variables for Medicaid expansion and non-expansion status. Timely CRC screenings were determined by eligible respondent responses. Difference-in-difference analyses were used to study the effect of Medicaid expansion on timely CRC screenings in states with different Medicaid expansion statuses.
Results: Our sample included 60.52% White Americans, 12.22% African Americans, and 16.41% Hispanics in both Medicaid expanded and non-expanded states. Sex and race had significant associations to Medicaid expansion status and timely CRC screenings, particularly when analyzing race for Hispanics and White Americans. Between 2014 and 2022, timely CRC screening for low-income adults in Medicaid expansion states was at 33.15% compared to 23.17% from non-expansion status states. Notably, adults aged 45-64 demonstrated the highest differences in timely CRC screenings for Medicaid-expanded states (12.26% and 18.98%) compared to non-expanded states (9.27% and 13.96%, respectively).

#1299 Cost-effectiveness analysis of circulating tumor DNA-based molecular profiling platforms for the detection of *EGFR* mutations in lung cancer.
P. Rozendal, P. van der Leest, E. M. J. van der Logt, N. Rifaela, I. Platteel, F. J. G. Scherpen, H. J. M. Groen, L. C. L. van Kempen, E. M. D. Schuuring; University Medical Center Groningen, Groningen, Netherlands

Background The detection of mutations in circulating tumor DNA (ctDNA) in blood plasma of lung cancer patients can be used to monitor the tumor-response to therapy and for the early detection of resistance mechanisms. In 2017, the Roche Cobas® EGFR Mutation Test v2 for the detection of the *EGFR* c.2369C>T p.(T790M) mutation in plasma-derived ctDNA was FDA-approved to identify patients eligible for osimertinib treatment. Today, different platforms are available for *EGFR* mutation testing in plasma-derived cell-free DNA (cfDNA). In this study we compared the clinical utility of five platforms for the detection of *EGFR* mutations in cfDNA offering insights into their operational costs, target coverage, hands-on-time and turn-around-time.
Methods Four PCR-based platforms and one NGS-based approach for the detection of *EGFR* mutations were compared. Operational, maintenance, material and personnel costs were calculated for each platform and used as input variables for our recently developed ctDNA micro-costing framework (doi.org/10.1016/j.jmoldx.2022.10.004). This was compared to target coverage and turn-around-time of each platform in the context of therapy resistance.
Results Per sample costs decreased for all platforms at maximal weekly throughput. The BioCartis Idylla™ demonstrated the shortest turn-around-time while the Roche Cobas® was the least expensive. Despite being the most expensive and time-consuming, the AVENIO ctDNA Expanded kit covered the most known resistance mechanisms to *EGFR* inhibitors, many of which are targetable with other TKIs.
Conclusion *EGFR* ctDNA mutation analysis is only cost-effective when the throughput is high. This implies that centralization of cfDNA-testing is necessary to optimize cost-efficiency. With the advent of ctDNA analysis beyond *EGFR* in the context of targeted therapies for lung cancer, multigene detection assays will become more cost-effective with high throughput.

Overview of results

Platform	Turn-around time at maximal weekly throughput	Per sample cost at maximal weekly throughput	Coverage of resistance mutations in *EGFR* [1]Additional testing necessary	Coverage of genome-wide resistance mutations to *EGFR*-TKI [1]Additional testing necessary
BioCartis Idylla™ ct*EGFR* Mutation Assay	2,5 hours	€571	33%	12%[1]
Roche Cobas® *EGFR* Mutation Test v2	4 hours	€497	33%	6%
Bio-Rad QX200 droplet digital PCR (ddPCR)	7,5 hours	€766	100%[1]	24%[1]
Agena MassARRAY® UltraSEEK® Lung Panel	2 days	€613	53%	12%
Roche AVENIO ctDNA Expanded kit	1 week	€1551	100%	65%

#1300 A collaborative approach to enhance tissue donation for cancer research; the UNC Patients and Researchers Together (PART) Program.

P. A. Spears, M. Van Lokeren, V. Branch, J. A. Potter, R. Robinson, Patient And Researchers Together (PART) Team;
University of North Carolina at Chapel Hill, Chapel Hill, NC

Introduction: Tumor tissue-based cancer research is essential to translate scientific discoveries to improve treatments for cancer. Tissue donation programs require a partnership: patients donating tissue and researchers using tissue for translational research. Lineberger Comprehensive Cancer Center (LCCC) has established a program called Patients and Researchers Together (PART) to value and increase the number of patients who agree to donate tissue for research. The PART Program is a patient-centered partnership between patients, community members, oncologists, surgeons, researchers, as well as staff and faculty from the clinical trials office, tissue procurement facility and UNC health communications to increase tissue donations for cancer research by valuing the patient's contribution.

Methods: The PART program began in 2021 by convening a group of diverse partners with a common goal of valuing patients as partners in biospecimen research. Creating an environment of bidirectional communication and exchange of ideas to 1) inform patients about the benefits of donating tissue for research, 2) inform the public about the importance of tissue to help researchers learn more about cancer, and 3) ensure researchers at UNC have access to tissue for their research. In the initial phase, the PART team evaluated the tissue research needs at LCCC by conducting surveys, interviews and focus groups with key partners. This set the foundation for the focus of current activities. One of the key focus areas is to communicate to patients and the public about the value of using tissue in research. The PART program established a working group to develop patient materials. The working group developed a template for educational materials, study summaries and a rigorous review process. The development of materials and iterative review process includes content experts, health literacy experts, patients and community members, and communications experts.

Results: The PART working group developed a series of educational materials about tissue donation for research. Understanding the importance of donating tissue for research is the first step in engaging with patients. The team developed a template and a multi-step process to review documents. PART used this information to develop a website to promote tissue donation for research to the public. The team has been developing summaries of studies focused on tissue donation. We developed or consulted on 2 general education flyers and 8 study summaries in a variety of cancer types. There is a continuous queue of studies in progress and plans to develop more general education materials.

PART patients and community members are leading the effort to educate patients and the public about tissue use in research. LCCC values patients who donate their tissue to research to improve the lives of all cancer patients.

#1301 Comparing VA and safety-net hospital patient-reported care metrics and provider recommendations to address social determinants of health and demographics.

N. Hippalgaonkar[1], M. Weinfeld[1], C. Weldon[2], J. Trosman[2], C. Chan[3], S. Khan[4], S. Paduri[4], V. Reddy[4], A. Sakhuja[4], P. Khosla[4], M. Pasquinelli[1], L. Feldman[1]; [1]University of Illinois at Chicago, Chicago, IL, [2]Center for Business Models in Healthcare, Glencoe, IL, [3]Jesse Brown VA Medical Center, Chicago, IL, [4]Sinai Chicago, Chicago, IL

Background: The Jesse Brown Department of Veterans Affairs Medical Center (JBVA) and Sinai Chicago, a safety-net hospital nearby, serve veterans and patients with significant social needs on Chicago's South and West sides. Both institutions are adopting the 4R Oncology Model (Right Info/Care/Patient/Time) for patient-facing care planning and self-management, proven to enhance supportive and health maintenance care delivery (Trosman JCOOP 2021). This abstract depicts a baseline survey of JBVA veterans' and Sinai Chicago patients' experiences in planning and delivering guideline-directed supportive and health maintenance care for new cancer diagnoses, informing 4R implementations.
Methods: Patients at JBVA and Sinai Chicago were surveyed from February to September 2023 with participants receiving a $25 gift card. An analysis was conducted using Fisher's two-tailed exact test.
Results: The two institutions yielded a 67% survey response rate. Key patient demographics and oncologic and supportive care metrics are outlined in the table below. At JBVA, fewer than 50% of veterans knew their cancer stage at diagnosis, and 63% were aware of their care goals. Furthermore, only 17% of veterans received recommendations for support services offered by JBVA. "Emotional distress or worry" support recommendations were received by < 50% of patients at both institutions.
Conclusions: The baseline survey uncovered gaps in care planning, supportive services, and health maintenance care in both institutions, catering to patients with challenging social determinants of health. The implementation of the 4R Oncology Model is designed to address these gaps, providing a personalized care sequence that establishes a clear roadmap through the patient's care trajectory, ultimately enhancing patient-centered care. Further results will be shared when available.

Metric	Combined% of pts(n=60)	JBVA% of pts (n=30)	SINAI% of pts(n=30)	PVALUE
Patient knew stage of their cancer	67	43	86	**0.0005**
Patient knew goal of their care	77	63	86	**0.0442**
Cancer care provider recommended to:				
Get Nutrition consult about how to eat during cancer treatment	35	27	42	0.2997
Talk to your primary care provider about staying as healthy as possible during care treatment	62	57	67	0.4523
Get support for transportation, food, housing, insurance, or other practical needs	44	17	67	**0.0001**
Get help to stop smoking or vaping*	29	28	31	1.0
Get help for emotional distress or worry*	37	24	46	0.1078
Demographics				
Age	59	66	53	**0.0001**
Male	69	93	39	**0.0004**
Black	59	83	39	**0.0001**
Hispanic	32	0	58	0.1103
High School education or less	68	57	78	0.1854
Household income less than $30,000 **	70	59	81	0.1305
Live Alone	37	47	29	**0.0001**

*of those who reported needing help, **of those who shared income level

#1302 Development and implementation of a systematic approach to measure patient-reported outcomes in early-phase cancer trials.

A. L. King, J. E. Levine, E. Vera, Y. Gandhi, E. Novakovich, T. Yu, S. Berhanu, C. Locke, K. Julmeus, T. Mendoza, T. S. Armstrong;
National Cancer Inst. - Bethesda Campus, Bethesda, MD

Background: There has been a shift in the clinical trial landscape toward early-phase studies where data from well-designed and pivotal phase I/II trials is leading to accelerated drug approval. Our goal was to develop a standardized approach to the measurement and reporting of patient-reported outcomes (PROs) in early-phase trials to improve assessment of tolerability, address noted barriers to inclusion, and enhance patient-provider communication to inform treatment decisions and ultimately improve outcomes.

Methods: The Office of Patient Centered Outcomes Research (OPCORe) was established in 2022 within the Center for Cancer Research at the National Cancer Institute (NCI) with the mission to advance understanding of the clinical benefit and tolerability of cancer therapies by integrating patient-centered approaches into CCR clinical trials by fostering education and collaboration with stakeholders. Implementation of regulatory/consortia guidelines related to use of core constructs, assessment frequency, and hypothesis-driven objectives and analysis plans through protocol template, development of data capture, email-based alerts and data visualization for clinical providers was developed and standardized templates for protocol language, research staff education, tools for workflow, and tracking implemented.

Results: The OPCORe protocol template includes measurement of 3 constructs, including tolerability, clinical benefit and disease-specific impact, as well as anchors of meaningful change. Core symptomatic toxicities are measured to inform understanding across trials with agent/class-specific symptomatic toxicities added to assure relevance. Baseline and standardized weekly electronic capture of tolerability during early cycles with alerts to clinical research staff if moderate-severe toxicities reported helps facilitate patient check-ins. Repeat PROs assessments in later cycles are expanded to include disease-specific assessments and align with disease evaluation to further inform clinical impact. To date, we have collaborated with 7 research groups and developed approaches for first-in-human, phase I, and phase II studies with trial start-up and data collection in process.

Conclusion: The value of including PROs in cancer trials is increasingly recognized by regulators, clinicians, patients, and advocates to advance understanding of the clinical benefit & tolerability of emerging therapies. Standardization and incorporation of PROs in earlier phase trials may enable PROs to be optimized, improve later phase trial design, and help inform health policy, support drug approval, and promote shared decision making between providers and patients to inform treatment decisions.

#1303 Harness the power of data to improve cancer care - Understanding the complex landscape of health policies and regulations.

Y. Huang, H. Basehore, E. S. Boja, J. M. Guidry Auvil;
National Cancer Institute, Rockville, MD

In the era of big data and artificial intelligence, biomedical research and healthcare have been presented with unprecedented opportunities for improving the understanding of cancer biology. In addition, the Open Science Initiative aims to shift the current paradigm of research practice towards broad sharing and public access to research findings as the norm. Big data in oncology usually includes a combination of genomic sequencing, proteomics, medical imaging, electronic health records, payor records, and other data sources from pharmaceutical research, wearables, and medical devices. While combining, linking, and analyzing data from different sources across research and healthcare enterprises is key to realizing the promise of big data and a health learning system, it poses tremendous challenges for researchers and implementers to understand the nuances of relevant policies, laws, and regulations while striving for broad, equitable, timely and responsible data sharing, as well as tackling issues in data quality, harmonization, interoperability, and security. Herein, we aim to shine a light on the ever-evolving landscape of data privacy regulations, laws, and policies that govern different touch points of a patient's journey where data are collected for research and healthcare purposes throughout the lifecycle that would impact data-sharing outcomes. We hope the illumination of a complex landscape of data governance framework to consider for many data sources will facilitate broad community engagement including data scientists and technologists, patients and advocacy groups, and policymakers to maximize open data and science while protecting patient privacy and confidentiality.

#1304 Employing widening funds to address inequity in cancer research - example of the STEPUPIORS collaborative rectal cancer project.

M. Cavic[1], A. Djuric[1], M. Marinkovic[2], A. Stanojevic[1], M. Tanic[1], S. Bjelogrlic[1], J. Spasic[1], A. Damjanovic[1], M. Djordjic Crnogorac[1], A. Vuletic[1], K. Mirjacic Martinovic[1], M. Radulovic[1], S. Stojanovic-Rundic[2], A. Krivokuca[1], R. Jankovic[1], S. Castellvi-Bel[3], J. Zoidakis[4], R. J. A. Fijneman[5];
[1]Institute for Oncology and Radiology of Serbia, Belgrade, Serbia, [2]Institute for Oncology and Radiology of Serbia; Faculty of Medicine, University of Belgrade, Belgrade, Serbia, [3]Fundacio Clinic per la Recerca Biomedica-Institut d'Investigacions Biomediques August Pi i Sunyer (FRCB-IDIBAPS), Centro de Investigacion Biomedica en Red de Enfermedades Hepaticas y Digestivas (CIBERehd), Hospital Clinic, University of Barcelona, Barcelona, Spain, [4]Biomedical Research Foundation, Academy of Athens; National and Kapodistrian University of Athens, Greece, Athens, Greece, [5]The Netherlands Cancer Institute-Antoni van Leeuwenhoekziekenhuis, Amsterdam, Netherlands

Introduction: Treatment of locally advanced rectal cancer (LARC) using neoadjuvant chemoradiotherapy (nCRT) improves local control and survival, but response varies. Patients treated at the Institute for Oncology and Radiology of Serbia (IORS) who undergo surgery upon complete response might be exposed to risks and poor quality of life. A consortium dedicated to redefining prognostic and predictive biomarkers in rectal cancer was formed within the framework of the STEPUPIORS Horizon Europe project. The current study evaluated whether employing collaborative widening funds might lead to sustainable strategies for cancer treatment, lowering inequity and steering societal impact, especially in countries with limited resources, using a pilot rectal cancer project.
Patients and Methods: The analysis was performed in the period Oct 01, 2022, to Oct 01, 2023, with a Serbian coordinating institution and partners from Spain, Greece, and the Netherlands as expert twinning centers. RT was administered to 75 patients with LARC using volumetric modulated arc therapy-simultaneous integrated boost approach/concomitant chemotherapy (5FU/Leucovorin, week 1&5) for the first time in Serbia. A comprehensive approach towards building human capacities on biobanking, multiomics analyses and project management was developed through intensive training and expert visits. Consensus consortium decisions were reached on regular partner meetings.
Results: Patients with clinical complete response (16.0%) and initially distant-located tumors were enrolled in the watch and wait approach and are under follow up. Developed pipelines for multiomics analyses led to 4 high-quality papers on new predictive biomarkers to nCRT in LARC and the deposition of omics data in open-science repositories following FAIR data principles. A first Serbian cancer biobank was successfully installed. Fifteen IORS researchers (87% female), were certified in biobanking. A grant management office was established to provide and support the sustainability of future research projects. This led to 5 new grant applications and enrollment of 1 female project member in a Masters program for Management in the Health Care System.
Conclusion: This study showed that even within the first 12 months, implementation of a 3-year collaborative grant dedicated to a specific research problem, might significantly change educational and treatment strategies enabling better patient care (OCEBM level of evidence 3). The results highlight that disparities in cancer outcomes and health equity might only be addressed by progressing beyond descriptions of said outcomes and taking specific action. Systematic, long-term strategic initiatives and collaborations among relevant stakeholders and ethical, legal and societal structures are needed in more countries.
Acknowledgements: Horizon Europe Project STEPUPIORS (101079217).

#1305 Comparison of HPV-DNA testing to PET-CT imaging as prognostic test following definitive treatment for cervical cancer: A retrospective proof-of-concept study.

C. Huddleston, A. Fakhreddine, S. Stroever, R. Young, N. Sah, K. Palle, M. Reedy;
Texas Tech University Health Sciences Center, Lubbock, TX

Cervical cancer is a significant global health issue, with oncogenic HPV-High Risk (HPV) responsible for over 99% of cases. Despite the prevalence of HPV-related malignancies, current guidelines by the National Comprehensive Cancer Center (NCCN) do not recommend post-treatment HPV-DNA testing. Instead, PET-CT imaging is recommended as a prognostic test. This retrospective proof-of-concept study aims to evaluate current NCCN guidelines and examines whether post-treatment HPV-HR DNA testing is a cost-effective, reliable alternative to PET-CT imaging in cervical cancer prognosis.

Methods: The study included female patients diagnosed with cervical or vaginal carcinomas (2011-2021), ensuring comprehensive records of both pre-treatment and post-treatment high-risk HPV (HPV-HR) testing, alongside PET-CT imaging results. Utilizing the FDA-approved HPV-HR DNA test, capable of detecting 14 oncogenic HPV strains, the study conducted rigorous statistical analyses via STATA software to determine significance of the study results.

Results: Our analysis of 53 patients who met the inclusion criteria demonstrated that post-treatment assessments using both HPV status and PET-CT imaging exhibited high levels of sensitivity and specificity, as well as impressive negative and positive predictive values (NPV and PPV, respectively). There was a statistically significant correlation between the likelihood of cancer recurrence and the results obtained from HPV status and PET-CT imaging post-treatment (p-value < 0.001). A critical observation was the superior sensitivity and improved NPV of post-treatment HPV status compared to PET-CT scans. Specifically, the sensitivity for HPV status post-treatment was quantified at 92.31, surpassing the 76.92 sensitivity rating of PET-CT scans. Furthermore, the NPV for post-treatment HPV status was measured at 97.44, which is better than the 92.31 NPV for PET-CT scans. Notably, no patients with negative post-treatment HPV-HR tests had a recurrence.

Discussion: The results of this study underscore the clinical significance of assessing HPV-HR DNA status post-treatment, particularly when HPV-HR DNA is negative. If future prospective studies confirm these findings, it may eliminate the need for post-treatment PET-CT scans, providing significant survivorship benefits for patients by reducing follow-up visits and eliminating unnecessary imaging. This would also result in substantial financial savings, estimated to be over $75,000,000 per year in the US alone, based on 2023 data. The limitations of the study include small sample size, single-institution data, and biases associated with retrospective studies. Future multi-institutional prospective studies are necessary to improve current guidelines further and validate the findings of this study.

#1306 Preferences for survivorship care among AYA cancer survivors and challenges of cancer specialist-led follow up.

Y. Kojima, Y. Ando, Y. Nogami, S. Iwata, T. Suzuki, E. Satomi;
National Cancer Center Hospital, Tokyo, Japan

Background: The number of cancer survivors is increasing substantially. Survivorship care, including long-term health care, for adolescent and young adult (15-39 years) (AYA) cancer survivors is not standardized. AYA cancer survivors have unique challenges that differ from those of other generations. The purpose of this study was to highlight challenges regarding survivorship care for AYA cancer survivors.
Methods: This study assessed survivorship care challenges for AYA cancer survivors based on questionnaire data in two configurations. We surveyed AYA cancer survivors diagnosed with various cancer types at our hospital regarding the actual status and challenges of survivorship care. Questionnaires assessed schooling and employment status, place of residence, length of hospital visits, cost of transportation to hospital, department and reason for visits, and issues related to survivorship care. We then surveyed cancer specialists who provide survivorship care about the actual status and challenges of survivorship care, including issues identified in the AYA cancer survivor survey.
Results: Ninety-eight AYA cancer survivors responded; 42 survivors (42.9%) were aged 20-29 and 45 (45.9%) were aged 30-39. The median time since completion of cancer treatment was 3.7 years. Most survivors (85.7%) hoped for long-term follow-up for surveillance of cancer recurrence. There were 27 survivors (27.6%) who received survivorship care in more than one department, and 26 (26.5%) received survivorship care in cooperation with other departments in the other hospital. Due to schoolwork and jobs, 52.0% of survivors felt that time for outpatient visits was scarce, and 51.0% of survivors indicated that they would prefer online survivorship care. On the other hand, the survey for cancer specialists was completed by 45 respondents (70.3%). More than 60% of cancer specialists providing follow-up care for AYA cancer patients felt that knowledge and experience in reproductive medicine and life events was necessary. Furthermore, regarding the challenges of long-term follow-up care for AYA cancer patients, more than 80% of physicians felt that mental, endocrine-related, and sexual function-related care and management were difficult in their own practices.
Conclusion: AYA cancer survivors with schoolwork and jobs felt that they had challenges in visiting outpatient clinics for survivorship care. Meanwhile, cancer specialists found it difficult to provide mental, endocrine, and reproductive care for AYA cancer survivorship care on their own. These require standardization of medical treatment content and systems for survivorship care for AYA.

#1307 Community-driven support platform BlueHQ: An innovative solution to address the needs of patients with colorectal cancer.

K. L. Newcomer;
Colorectal Cancer Alliance, Washington, DC

Background: Colorectal cancer (CRC) is the third-most commonly diagnosed cancer and the second-leading cause of cancer death in men and women combined in the United States. To manage the disease, patients and caregivers turn to various tools and resources for financial assistance, information dissemination, emotional and peer support, and treatment planning, among other critical issues and needs they face. The Colorectal Cancer Alliance (the Alliance) created BlueHQ to provide patients and caregivers with a resource solution encompassing all potential areas of need.
Methods: A survey aimed at understanding needs, barriers, and quality improvement opportunities was disseminated via the Alliance's Blue Hope Nation community for two weeks and by email. One hundred sixty-seven colorectal cancer patients and forty caregivers of colorectal cancer patients completed the survey.
Results: Patients and caregiver respondents report reliance on external tools and resources to manage disease and support information. Of the support methods, patient respondents reported using social media (46.11%); notebooks, journals, and planners (45.41%); online articles (44.91%); the Blue Hope Nation Facebook group (41.32%); cancer discussion boards (35.33%); and spiritual or religious advice (29.94%). Patients sought financial assistance, local peer support and groups, and mental health help to minimize diagnosis-related stressors. To provide more efficient care and limit stress, the community suggested financial help, communication and support from other patients and caregivers, and informational resources.
Conclusions: These survey results are consistent with other published learnings about patient and caregiver reliance on support tools and highlight the myriad resources that patients and caregivers currently use for managing CRC. BlueHQ is a support solution that provides patients and caregivers with access to information and resources tailored to users' specified profiles, including molecular characteristics of the tumor. Users can also store documents and information from healthcare encounters, creating a longitudinal record and tracking disease progression. In the age of precision oncology, BlueHQ ensures patients and users are presented with personalized educational materials and multimedia resources to help manage their disease and bridge the gaps in patient support. BlueHQ was explicitly designed to connect the CRC community to the latest therapeutic and clinical research resources to improve outcomes and quality of life for all CRC patients.

#1308 Policy guiding secondary findings from genome sequencing pertinent to cancer: Results from a systematic review.

S. Majeed[1], C. Johnston[1], S. Saeedi[2], C. Mighton[1], V. Rokoszak[2], I. Abbasi[2], S. Grewal[2], V. Aguda[2], D. Malkin[3], Y. Bombard[1];
[1]University of Toronto, Toronto, ON, Canada, [2]Unity Health, Toronto, ON, Canada, [3]The Hospital for Sick Children, Toronto, ON, Canada

Background: While genomic sequencing has personalized patient care across disciplines like oncology, secondary findings (SFs) unrelated to the primary indication are a common complicating factor. SFs relevant for oncology are categorized as cancer-related potentially leading to a cancer diagnosis (CA-SFs) or non-cancer findings revealing important medical conditions, predispositions, or carrier status in cancer patients (NC-SFs). These SFs can inform disease prevention, early detection, or management decisions, but may cause distress, overdiagnosis, and overuse of resources if actionability is limited. There is a lack of consensus for identifying, analyzing, and interpreting the clinical relevance of SFs. This significantly impacts cancer care, where paired tumor-normal sequencing is standard practice. Widespread practice variation can lead to detrimental impacts on patient outcomes and overall health. We synthesized policy guiding the clinical investigation of SFs for cancer to help providers navigate decisions regarding SFs.
Methods: We carried out a systematic review of international guidance directing the identification, analysis, and management of SFs from genomic sequencing, and analyzed the subset of policies specifically relating to oncology. We searched the grey literature (IFHGS members) and academic databases including MEDLINE, Embase and Cochrane. Two reviewers independently assessed policy documents for screening, data extraction and quality assessment (using AGREE-II).
Results: We identified 7 policies guiding the investigation of SFs relating to cancer across the general population (n=4), adults (n=1), pediatrics (n=1) and research (n=2) contexts. Most policies included guidelines for SF variant selection (identification; n=5) and management (n=4), with a minority detailing analysis processes (n=2). Recommended CA-SFs included medically actionable cancer predisposition variants, while suggested NC-SFs were variants important for drug therapies *(identification)*. Laboratories were advised to ensure adequate coverage and read depth during SF analysis *(analysis)*, while policies recommended that a medical genetics healthcare provider return results, specifically discussing their clinical utility *(management)*.
Conclusions: To our knowledge, our review is the most comprehensive synthesis of policy guiding SFs for cancer. Policies outline the types of SFs to investigate from genome sequencing in cancer and non-cancer patients, and related strategies for disclosure. However, best practices for SF analyses and patient follow-up including SF surveillance, treatment, etc. remain poorly described. This synthesis will help cancer care providers navigate critical decision points based on current evidence and direct policymakers on gaps to fill in the future.

#1309 Assessment of geographic and socioeconomic factors in primary brain tumor patient accrual to a natural history study.

Y. Kim[1], M. L. Stockdill[2], E. Vera[2], H. Miller[2], J. B. Vo[2], M. R. Gilbert[2], T. S. Armstrong[2], O. Celiku[2];

[1]Wayne State University School of Medicine, Detroit, MI, [2]National Cancer Institute, National Institutes of Health, Bethesda, MD

Purpose: To better understand neuro-oncology trial access barriers in the United States (US), we assessed the role of geography, population density, and socioeconomic factors in the accrual of adult primary brain tumor patients in the Natural History Study (NHS, NCT02851706) at the National Institutes of Health (NIH).

Methods: Participant addresses were linked to zip code geography and population data from the US Census and the Neighborhood Atlas Area Deprivation Index (ADI; 1 to 100 from least to most disadvantaged). Locations with population density greater than 1000 inhabitants per square mile were considered urban. Locations were categorized based on their distance from NIH as local (<50 mi), short-distance (50-200mi) and long-distance (>200 mi). T-tests, chi-square tests, and multivariate logistic regression compared socioeconomic and urbanity factors.

Results: 667 NHS participants arrived from 43 states and territories, with the majority (61%) from Maryland and neighboring states, and other states contributing no more than 5% of the participants each. The home locations of the participants were disproportionately urban (60% versus 19% of all US locations, p <0.001) and socioeconomically advantaged (mean ADI 26.94 versus 57.30 across all US locations, p<0.001). Local participants (49%) had greater racial and ethnic diversity (73% White, 11% Black, 9% Asian, 2% other; 11% Hispanic/Latino) compared to short-distance participants (11% total; 96% White, 3% Black, 0% other; 0% Hispanic/Latino) and long-distance participants (39% total; 89% White, 3% Black, 3% Asian, 2% Other; 6% Hispanic/Latino). Local participants lived in the most socioeconomically advantaged locations (mean ADI 16.39) compared to short-distance (mean ADI 40.88, p<0.001) and long-distance (mean ADI 39.69, p<0.001) participants. Short-distance participants were from disproportionally non-urban areas (69%) compared to local (28%, p<0.001) and long-distance (46%, p<0.001) participants. Multivariate analysis also confirmed that local participants were more likely to live in more advantaged areas than short-distance (OR=0.90, p<0.001) and long-distance (OR=0.93, p<0.001) participants, and short-distance participants were less likely to live in urban areas compared to local (OR=0.19, p<0.001) and long-distance (OR=0.44, p=0.008) participants.

Conclusion: The trial enrolled patients across the US, albeit with most participants arriving from neighboring states and socioeconomically advantaged, urban areas. Greater rural patient participation from nearby areas reflects the positive impact of NIH subsidies in reducing the financial challenges linked to participating in clinical trials. Current trends indicate that continued and targeted efforts to enable participation from local disadvantaged communities can ameliorate access to neuro-oncology clinical care and research.

#1310 Social determinants of migrant health factors impacting prostate cancer care and survivorship among sub-Saharan African immigrant men diagnosed with prostate cancer.

E. Kaninjing[1], G. Asiedu[2], K. Van Voorhis[1], M. Young[3], E. Erefah[4], E. Agboola[4], F. Odedina[3], R. Dronca[3], K. Ashing[5], S. Rotimi[6], C. Ngufor[2], A. Merriweather[7], J. McCall[5], A. Hill[3];

[1]Georgia College & State University, Milledgeville, GA, [2]Mayo Clinic, Rochester, MN, [3]Mayo Clinic, Jacksonville, FL, [4]Florida A&M University, Tallahassee, FL, [5]City of Hope, Duarte, CA, [6]Covenant University, Otta, Nigeria, [7]American Legion, Jacksonville, FL

Background: Sub-Saharan African Immigrants (SSAI) represent one of the fastest-growing segments of the immigrant population in the United States (US). Between 2010 and 2018, the SSAI population in the US increased by 53%, significantly outpacing the 12% growth rate for the overall foreign-born population in the US during that time frame. Despite these growing numbers, little is published about the extent to which SSAIs adapt to health behaviors more common in the US or remain immersed in the values, beliefs and practices reflective of their country of origin. Importantly, no study has comprehensively examined the Social Determinants of Health (SDOH) among this population relative to their migration experiences and their influence on health-seeking behaviors and decision-making regarding prostate cancer care and treatment options.

Methods: This qualitative study employed grounded theory and the social determinants of migrant heath framework to better understand the needs of SSAI prostate cancer survivors in the United States and how to effectively support these survivors. In-depth interviews were conducted with 8 survivors who live in the states of Florida and Minnesota.

Findings: Some participants reported limited access to care and financial challenges paying for drugs. In terms of coping with diagnosis and treatment, most of the participants relied on their faith, a positive outlook about survivorship and support of family members. Some participants relied on the coaching and support of a loved one who experienced prostate cancer in the past. Erectile dysfunction severely impacted the sexual life of most participants as they experienced difficulty getting an erection.

Conclusion: Participants expressed the benefit of belonging to support groups with other survivors for social and emotional support. As the number of immigrants from sub-Saharan continue to rise, so too will the demand for culturally tailored care to address and reduce disparities in survivorship among this sub-population.

#1311 Planning for health equity in oncology trials: Expectations and feasibility.

H. G. Skinner, C. Marra, A. I. Alexandrow, H. L. Subramaniam, N. C. Nussbaum, J. B. Franklin, E. P. Simard, A. P. Abernethy;
Verily Life Sciences LLC, South San Francisco, CA

Achieving diverse representation in oncology studies is an ongoing challenge., Responding to calls to advance health equity in clinical trials, Congress amended the Food Drug and Cosmetic Act to require trial sponsors to submit a “diversity action plan” to the FDA with a study’s protocol. This requirement to plan for diverse trial recruitment drives a need to innovate approaches for site selection and trial recruitment that go beyond mirroring race-ethnicity distributions from the US Census or disease prevalence. We present a novel framework that nests clinical trials in a longitudinal patient registry to achieve diverse representation across multiple domains, evaluate site-selection and recruitment strategies, and examine health equity across the cancer patient journey.

Implementing a registry to support longitudinal data collection (i.e., a cohort study), we establish a continuous view of participant characteristics including demographic and social determinants of health, treatment received, and relevant outcomes. Nesting clinical trials within the structure of the cohort, we can select sites and recruit for diverse representation to achieve equity goals. This framework involves a multi-layer analysis of external population statistics and internal reference registry to gauge the pool of eligible participants and calibrate the sampling strategy and recruitment expectations to the realities of clinical representation. Moreover, where clinical representation differs from population statistics, the registry offers an opportunity to report benchmarks for diversity and compare to site-level and study-level realized enrollment and feasibility.

In conclusion, the path to health equity in oncology trials depends on a capacity to ask and answer the right questions in planning. What specific aspects of diversity are we aiming to capture? How do these aspects impact outcomes? We advocate for a dynamic planning process that continuously reevaluates goals and strategies in the face of enrollment data and evolving population demographics. By utilizing a registry with longitudinal follow-up, we can set forth clear expectations, transparently report on the progress of inclusion efforts, and candidly address feasibility challenges. We present a structured framework for trial sponsors to not only comply with the forthcoming requirement for diversity action plans, but ultimately to advance the goal of equitable cancer care through research that truly reflects the complex intersectional diversity of those impacted by the disease.

#1312 A study of the clinical utility of NTRKs only vs. comprehensive gene fusion panel testing from a single assay platform.

C. Duong, S. Lau-Rivera, R. Jackson, P. Kanagasunderam, R. Hariri, N. Montgomery, D. Lyle, F. Lopez Diaz;
NeoGenomics, Fort Myers, FL

Background: Gene fusions have important implications for therapeutic selection and patient quality of care, and though they have a low prevalence individually, many fusions are targeted effectively, agnostic of any tumor type. Unfortunately, patients in the community oncology setting are most often only tested for NTRK fusions, which have a prevalence of around 1%. Here, we compared side by side the actual clinical actionability differences using real-world testing data between broad vs. NTRK fusion only panels offered by our clinical laboratory, both with identical assay performance characteristics, reimbursement, and cost levels.

Methods: Clinical samples(n=8307) from 33 tumor types were tested for known and novel RNA fusions using our hybridization capture RNA-seq based Solid Tumor Fusion Panels in our clinical laboratory, which targets RNA breakpoints at 1104 genes. Deidentified results were analyzed before or after filtering for fusions based on either a Targeted Solid Tumor NGS fusion Panel (16 drug targetable genes) or only NTRKs fusions. Deidentified patient data presented was analyzed according to an IRB-approved protocol.

Results: The prevalence of fusions in the cohort was 30.5% involving any of the 1104 targeted genes by the assay (27% in frame, 20% out of frame, and 41% others). Druggable fusions were present in 5.1% (422) of patients, where 53% were female with a median age of 68 years old, and 47% were male with a median age of 70. However, when filtering only for NTRK fusions, only 104 patients had an NTRK fusion (38 NTRK1, 10 NTRK2, 56 NTRK3), while an additional 318 patients had detected fusions from the Targeted Panel. These druggable fusions had the following prevalences; ALK 0.6 %, BRAF 0.3%, FGFR1 0.2%, FGFR2 0.3%, FGFR3 0.4%, FGFR4 0.0% n=4, MET 0.4%, NOTCH1 0.0% n=1, NOTCH2 0.2%, NRG1 0.2%, PDGFB 0.0% n=3, PDGFRA 0.1%, PDGFRB 0% n=0, RAF1 0.2%, RET 0.5%, ROS1 0.2%, excluding NTRK positive cases. The incidence of NTRK 1/2/3 fusions was 1.25%, while 3.8% of patients have other fusions included on the Targeted Panel in the absence of an NTRK fusion. Two (2, 0.02%) patients had both an NTRK fusion and an additional fusion covered on one of the other 16 genes in the Targeted NGS fusion panel.

Conclusion: Actionable fusions showed a combined prevalence in the clinical setting of 5.1%. This study demonstrates that when fusion testing is performed, four times more patients can benefit from a therapeutic option than when testing for these 16 genes compared to the widespread panel of the current clinicians' favorite choice of only NTRK fusions. More data and education are needed to change the testing paradigm of treating physicians to test broader sets of fusions when assay performance and financial considerations are equal to increase cancer care access.

#1313 Racial disparities in colorectal cancer incidence across US ethnic groups: A comprehensive analysis.

A. Chaudhuri, R. Gray;
Stillman College, Tuscaloosa, AL

Colorectal cancer (CRC) ranks as the third most prevalent global cancer and the fourth leading cause of cancer-related deaths. Racial disparities in CRC within the United States pose a significant public health concern, affecting incidence, mortality rates, and screening rates. This study investigates the impact of racial disparities on CRC incidence across various US states, utilizing CRC data from the National Cancer Institute (NCI) at the Centers for Disease Control and Prevention (CDC). Analysis with GraphPad Prism 5 software and Student's t-test reveals a consistent trend of higher CRC incidence in males compared to females, irrespective of ethnicity. Notably, the Black and American Indian ethnic groups demonstrate the highest CRC incidences among all races, especially in individuals aged 65 and above. Certain states, including Iowa and Mississippi for Black populations, and Alaska, Minnesota, Montana, Oklahoma, and South Dakota for American Indian populations, exhibit significantly elevated CRC incidences compared to the national average. County-specific analysis in Alabama reveals varying CRC incidence rates across ethnic groups, with higher rates in specific counties, such as Clarke County for Black males. Limited reports for American Indian, Asian Pacific, and Hispanic ethnic groups indicate potential disparities in access to testing, awareness, and funding for CRC detection and prevention. This study concludes that Black and American Indian males and females experience a higher incidence of colorectal cancer, possibly influenced by genetic factors or other variables contributing to CRC development. The observed disparities are multifaceted, arising from a combination of social, economic, and healthcare system factors. Addressing these complexities is crucial for mitigating CRC disparities and promoting equitable healthcare access and outcomes. Additional research, including molecular screening studies, is essential to substantiate disparities in cancer-related health and enhance public health and cancer awareness within the community.

Key Words: Cancer, Colorectal Cancer, Health Care, Racial Disparities

#1314 SCHEQ Foundation (STEMM & Cancer Health Equity): Increasing STEMM diversity and outcomes for patients navigating cancer.

E. Manley, Jr.;
SCHEQ Foundation, New York, NY

Health inequities are estimated to cost $320B annually, while racial and ethnic disparities are estimated to cost $42B in productivity. There are systemic issues at play that contribute to these disparities. These include lack of diversity in Science, Technology, Engineering, Mathematics, and Medicine (STEMM) fields; bias in healthcare delivery and access; underinsurance in patients from low-income backgrounds; and lack of training that advances those from historically underrepresented groups. The SCHEQ Foundation (STEMM & Cancer Health Equity) is a black-founded nonprofit organization that seeks to increase STEMM workforce diversity and improve outcomes for underrepresented, underserved, marginalized, and invisible populations across the cancer care continuum. Herein we describe the formation of SCHEQ Foundation and our core domains that we seek to make change. We seek to increase STEMM access and exposure, increase STEMM workforce diversity, and improve outcomes for underserved populations navigating the cancer care continuum. This will be accomplished in part by 1) engaging professional in STEMM from their lived background and experiences, 2) developing training, mentoring, and professional developing programs across the academic continuum to increase success of minoritized scholars; and 3) providing information and resources in culturally responsive manners to help underserved patient navigate cancer and advocate for the standard of care they deserve. We will change how we convey content, information, and resources to underserved populations by utilizing a combination of multimedia, infographics, webinars, info sheets, and community engagement. The goal is to increase survival for groups that historically have the greatest cancer disparities.

#1319 In vivo programming of natural killer cells and T cells using mRNA delivered cytotoxic chimeric antigen receptors.

N. Diwanji, D. Getts, Y. Wang;
Myeloid Therapeutics, Cambridge, MA

Introduction: Current generation of adoptive cell therapy relies on ex vivo engineering of immune cells with tumor-targeting chimeric antigen receptors. In addition to manufacturing challenges, ex vivo engineered cells such as CAR-NK and CAR-T show limited tumor infiltration and persistency within tumor microenvironment. A method leveraging mRNA-based delivery for in-vivo engineering of these cells could address these issues but has not been established. Conventional mRNA/LNP when infused systemically result in significant accumulation in liver tissue and the CAR has no immune cell specificity in their expression or function.

Method: Many immune receptors are heterodimeric complexes composed of a ligand binding subunit (e.g. CD16 and TCR) and a signaling adaptor containing Immunoreceptor Tyrosine-based Activation Motif (ITAM) (e.g. FcRγ and CD3ζ). Notably, the cell surface expression of the ligand binding subunit often depends on the expression of the ITAM adaptor. Based on this we fused HER2-targeting scFv to multiple activating receptors whose expression is restricted to NK cells and T cells, and evaluated their expression and anti-tumor function.

Results: We developed a series of Natural Cytotoxic Receptor (NCR)-based in vivo CAR constructs by fusing HER2-targeting scFv to the native extracellular and transmembrane sequences of the receptor NKp30, NKp44 and NKp46, These CARs engage signaling adaptor FcRγ or DAP12 expressed in NK cells, and exhibit potent tumoricidal activity against HER2+ ovarian cancer cells as well as mediate tumor-induced cytokine and chemokine response. Using Huh7 liver cell as a model for off-target expression in hepatocytes, we found that NKp44 and NKp46-based CAR requires their cognate signaling adaptors for stable cell surface expression. We also showed that similar strategy can be used to design receptors for selective expression on the surface of T cells utilizing CD3ε chain fused with tumor targeting scFv.

Conclusion: These results demonstrated the feasibility of engineering primary NK cells with CARs based on the NCR family of receptors NKp44 and NKp46, whose expression requires the immune-restricted signaling adaptors. These CAR-NK receptors do not contain intracellular signaling motifs but can engage and activate their signaling natural adaptors to initiate tumor killing and cytokine response. An mRNA/LNP based delivery of NKp44-based CAR for cancer treatment is currently under clinical development.

#1320 Engineered expression of HLA-E and HLA-G protects iPSC-derived cells from killing by primary NK cells.

A. Lebid, D. Kim, G. Greco, H. Jessup, A. Suarez, S. Brown, N. Alexander, M. Desai, B. Gurung, B. Morse, D. J. Perry, M. F. Naso, H. Levitsky; Century Therapeutics, Philadelphia, PA

Background: A major challenge to off-the-shelf allogeneic cell therapies is the HLA-targeted elimination of genetically dissimilar cells. To combat this, HLA Class I can be deleted through transgene insertion at the beta-2 microglobulin (B2M) locus, while HLA Class II can be deleted by disruption of the gene encoding MHC Class II Transactivator (CIITA). Lack of HLA Class I expression, however, marks cells for elimination by natural killer (NK) cells, which normally receive inhibitory signals from this protein family. HLA-E and HLA-G are non-classical HLA Class I molecules that are far less polymorphic than HLA-A/B/C. They can inhibit natural killer cell-mediated activation by engaging NKG2A, KIR2DL4, ILT2, and ILT4. The objective of this study was to assess allo-evasion from NK cells by iPSC-derived cells engineered to overexpress HLA-E and -G.

Methods: Allo-evasion by HLA-E, -G or both was first assessed in the chronic myelogenous leukemia K562 cell line, which expresses very low HLA Class I and is highly susceptible to NK-mediated killing. K562 cells were engineered using CRISPR/CAS9 to express chimeric molecules encoding either HLA-E or HLA-G heavy chains tethered to a defined nominal self-peptide and B2M, or HLA-E/peptide/B2M-P2A-HLA-G/peptide/B2M. Along with parental K562, these were used as targets in co-cultures with allogeneic PBMCs (n=22 donors) at different E:T ratios. Target killing was observed using flow cytometry and normalized to parental K562. Phenotyping of effector PBMCs for NK frequency and expression of HLA-E and -G receptors (NKG2A, KIR2DL4, ILT2, and ILT4) was performed to study correlations with killing efficiency and allo-evasion. IPSCs with endogenous B2M knocked out were also engineered to overexpress HLA-E and -G with the constructs described above. These were then differentiated into NK cells and gamma delta T cells using proprietary processes. Allo-evasion of these cells from killing by the same PBMC cohort was evaluated by flow cytometry.

Results: While NK cells across donors expressed heterogeneous combinations of HLA-E and -G receptors, the strongest correlation with PBMC allo-responsiveness was NK frequency. K562 and iPSC-derived cells lacking HLA were susceptible to killing by PBMCs. Overexpression of HLA-E and -G offered protection to K562 and iPSC-derived cells against all tested donors. HLA-E offered more protection than HLA-G, and the combination of both HLA-E and -G was most potent.

Conclusion: When genetically dissimilar HLA Class I protein family must be deleted to prevent graft rejection, expression of the more-conserved HLA-E and -G can effectively protect allogeneic drug products from elimination. These Allo-evasion^{TM} edits may increase the in vivo persistence and enable multi-dosing of our iPSC-derived allogeneic cell therapies.

#1321 *In vivo* immune cell programming using mRNA-LNP chimeric antigen receptors.

S. Argueta, F. K. Melber, M. Gorgievski, N. Divangi, E. Cochran, T. Chu, Y. Wang, J. Ding, D. Getts;
Myeloid Therapeutics, Cambridge, MA

Introduction: The tumor microenvironment (TME) is a dynamic and multifaceted system that comprises largely myeloid lineage immune cells including monocytes, neutrophils, macrophages, and dendritic cells. Reprogramming the myeloid compartment within the context of cancer therapy presents an attractive strategy to overcome current limitations in solid tumor treatment. We have developed a novel approach that harnesses the natural ability of Myeloid cells to take up mRNA loaded lipid nanoparticles, to reprogram these cells with chimeric antigen receptors (CAR's) that arm these cells to recognize and kill tumor cells.
Methods: Current LNPs technology is sufficient to deliver significant mRNA cargo to numerous cell types, including B cells, T cells and myeloid cells. Leveraging this phenomenon we have developed a new class of chimeric antigen receptors (CARs), using protein biology that imparts targeted immune cell expression and functionality, specifically in Myeloid cells. These CARs harness Immunoreceptor Tyrosine-based Activation Motif (ITAM) signaling adaptors expressed exclusively in immune cells, achieving immune cell-type specific CAR-directed tumor lysis and cytokine responses. With a FcaR I (CD89) based CAR design, we have developed a CAR that is dependent on the common Fc receptor gamma chain, primarily restricted to myeloid cells, for stable expression and function.
Results: We have demonstrated specific expression of CD89-based CAR in myeloid cells in mouse and monkey following systemic mRNA/LNP delivery, and in human myeloid cells following *in vitro* treatment with mRNA/LNPs. Systemic mRNA/LNP delivery of CD89-based CAR has demonstrated robust anti-tumor efficacy against multiple tumor antigens in various xenograft mouse models of human breast cancer, hepatocellular carcinoma, and ovarian cancer. Furthermore, in syngeneic mouse tumor models, robust anti-tumor immune responses, characterized by tumoral infiltration of activated CD8+ T cells, diminished tumor-associated Tregs, systemic enhancement of dendritic cells and anti-tumor IgG production, were observed for treated animals.
Conclusions: Taken together, we present CAR designs that achieve expression and function in targeted immune cell populations, capable of eliciting anti-tumor efficacy against multiple target antigens by leveraging innate and adaptive immune responses, and demonstrating a class of novel CAR designs to overcome limitations faced by current *in vivo* mRNA/LNP delivery strategy. A phase I clinical trial is currently on-going to assess the safety and preliminary efficacy of CD89-based CAR against TROP2+ epithelial malignancies.

#1322 A cryopreserved allogeneic anti-BCMA CAR-NK cellular therapy exhibits both innate and CAR-mediated MM cell killing *in vitro* and *in vivo*.

L. Talarico[1], C. Wong[1], C. Pang[1], T. Hickman[1], C. Hu[1], A. Shaw[1], E. Wisniewski[1], S.-C. Lai[1], P. Sharma[1], S. Moore[1], L. Nguyen[1], K. Rhuda[1], S. Patel[1], P. Lin[2], R. Basar[2], S. Cogan[1], K. Sofjan[1], A. Ramamurthy[1], A. Handler[1], K. Fraser[1], Y. Wang[1], K. Rezvani[2], M. D. Curley[1];

[1]Takeda Pharmaceutical Company Ltd. (U.S.), Cambridge, MA, [2]The University of Texas MD Anderson Cancer Center, Houston, TX

Introduction Multiple myeloma (MM) is the second most prevalent hematopoietic malignancy with an overall 5-year survival rate of 58%. B cell maturation antigen (BCMA) is selectively expressed on normal and malignant plasma cells, making it an attractive MM target. Anti-BCMA chimeric antigen receptor (CAR) T cell therapy and T cell engagers have shown promise as treatment options for certain MM patients; however, potential toxicities associated with these anti-BCMA therapies, such as cytokine release syndrome (CRS), have limited broader utilization. Much like T cells, natural killer (NK) cells are cytolytic and have demonstrated an innate capacity to reduce tumor burden while exhibiting a more favorable safety profile in clinical testing. To that end, we developed a cryopreserved allogeneic cell therapy comprised of genetically modified human umbilical cord blood-derived (CB) NK cells transduced with a gammaretroviral vector, which incorporates genes for an anti-BCMA CAR and soluble human interleukin-15 (sIL-15). Referred to hereafter as anti-BCMA CAR-NK, it exhibits both innate NK- and CAR-mediated killing *in vitro* and robust *in vivo* activity against established MM tumors.

Methods CBNK cells were isolated from donor cord blood units, propagated using feeder cells, transduced with a gammaretroviral vector to express an anti-BCMA CAR and soluble human IL-15, and propagated further before harvest and cryopreservation. Donor-equivalent untransduced (UTD) NK cells were generated via the same process but without the transduction step. Cryopreserved anti-BCMA CAR-NK and UTD NK cells were used for in vitro studies, including short-term killing, as well as for evaluation of activity against established MM tumors *in vivo* using the MM.1S-Luc4 model.

Results The anti-BCMA CAR was successfully expressed across all batches of anti-BCMA CAR-NK generated. Results from an *in vitro* cytotoxicity assay indicated that anti-BCMA CAR-NK kills BCMA expressing MM.1S-Luc4 tumor cells and secretes IFNγ, TNFα, and granzyme B at greater amounts compared to donor-equivalent UTD NK. Anti-BCMA CAR-NK and UTD NK cells also demonstrated equivalent cytotoxicity towards BCMA non-expressing cell lines, JJN3-Luc BCMA KO and NCI-H520, in an effector:target cancer cell dependent manner, highlighting the potential for treatment with anti-BCMA CAR-NK post-prior BCMA therapy. In *in vivo* studies, anti-BCMA CAR-NK exhibited robust anti-tumor activity in an MM.1S-Luc4 NSG mouse xenograft model, with no signs of anti-BCMA CAR-NK related body weight loss.

Conclusion A cryopreserved allogeneic anti-BCMA CAR-NK cellular therapy exhibits both innate and CAR-mediated killing in vitro and robust in vivo activity in MM tumor models. Preclinical data supports future clinical evaluation in relapsed/refractory MM patients who have received prior BCMA therapy and IND enabling studies are ongoing.

#1323 Anti-B7-H3 chimeric antigen receptor NK cells suppress the growth of atypical teratoid/rhabdoid tumor orthotopic xenografts.

J. Choe, S. Chakravarti, N. Holl, R. Rahnama, M. Zinsky, D. G. Jones, S. Vorri, A. Modi, E. H. Raabe, C. L. Bonifant;
Johns Hopkins University School of Medicine, Baltimore, MD

Background: Atypical teratoid/rhabdoid tumors (AT/RTs) are the most common malignant CNS tumor in infants. AT/RT patients have a 5-year overall survival rate of ~35% and high rates of relapse, emphasizing a dire need for new safe and effective therapies. These therapy-resistant tumors frequently overexpress the immune checkpoint cell surface molecule B7-H3 (CD276). CAR-T cell studies have an established safety profile in pediatric patients. We developed B7-H3 targeted chimeric antigen receptor (CAR) natural killer (NK) cells as a tumor-specific cell therapy for aggressive pediatric brain tumors. CAR-NK cells have several advantages over CAR-T cells. NK cells can be obtained from healthy donors and produced as an “off-the-shelf” product. NK cells also have a lower risk of inflammatory toxicity and graft-versus-host disease compared to T-cells when transferred across the HLA barrier from healthy donors to patients.
Methods: We have designed a library of variable affinity B7-H3-targeted CARs, produced replication incompetent γ-retroviral vector, and used this for generation of B7-H3 CAR-NK cells. We verified B7-H3 expression in a panel of AT/RT cell lines, and further engineered firefly luciferase expressing AT/RT (CHLA06.ffLuc, BT12.ffLuc, BT37.ffLuc) as well as a CHLA06-derived B7-H3 knockout. We developed an orthotopic CHLA06.ffLuc xenograft model. We tested CAR-NK cell functionality using *in vitro* co-culture and cytotoxicity assays. *In vivo* study was performed in our xenograft with intratumoral delivery of CAR-NK cells.
Results: B7-H3 targeted CAR-NK cells demonstrate target-specific cytotoxicity when compared to untransduced NK cells (36.8±12.5% vs. 72.4±24.2% at effector:target ratio of 1:1, n=3). CRISPR/Cas9 mediated knockout of B7-H3 in target cells abolished the difference in CAR vs. no-CAR NK-mediated target killing. When delivered intracranially to CHLA-06 orthotopic xenograft bearing mice, B7-H3 CAR NK cells eliminate tumor cells and prolong survival, whereas unmodified NK cells did not (log-ranked median survival = 20 vs. 84 days, $p<0.0001$). We are currently testing intracranial delivery of our B7-H3 CAR NK against other AT/RT orthotopic xenografts.
Conclusions: Targeting pediatric brain tumors with an anti-B7-H3 CAR-NK cell therapy may provide a safe and effective treatment for patients who have extremely limited therapeutic options. Direct intracranial injections of cell therapies into pediatric patients is currently being explored in clinical trials. As B7-H3 is a tumor associated antigen found to be overexpressed in a large variety of tumor types, this strategy may also be useful for treatment of other B7-H3 expressing cancers.

#1324 Superior anti-tumor activity of GL205, an allogeneic anti-CD5 CAR-NK for treating T-cell malignancies.

Miyoung Jung, Seung Min Kim, Eunsol Lee, Hyunseung Sun, Jaeyoung Yoo, Hwi Wan Choi, Subin An, Sunglim Cho, Bokyung Min

GC Cell, Yongin-si, Gyeonggi-do, Korea, Republic of

T cell malignancies are rare and intractable diseases with fewer treatment options and higher unmet needs compared to B-cell lymphomas. Chemotherapy such as CHOP has been used as the standard therapy for treatment of T cell malignancies, but clinical outcome is not a promising and alternative treatments are needed. Currently, Brentuximab Vedotin, an antibody-drug conjugate that targets CD30 is widely used for Hodgkin lymphoma, ALCL and CTCL. However, the application is limited to specific subtypes because CD30 expression is restricted to some subsets of T-cell lymphoma. CD5 is an attractive target for cancer immunotherapy because it is commonly expressed in most of T cell malignancies. Although CD5 CAR-T cell products have demonstrated the anti-cancer efficacy, there are several disadvantages including 1) challenges due to difficulties in manufacturing process caused by fratricide, 2) product contamination by CAR-introduced patient's malignant T cells, 3) severe side effects such as CRS and neurotoxicity. Therefore, CD5 CAR-NK as allogeneic anti-tumor therapy can be an alternative for treatment of T cell malignancies. GL205, cord blood-derived CD5 CAR-NK, is genetically modified to express CD5-directed CAR and simultaneously produce IL-15 which supports the NK survival and proliferation. GL205 is ex-vivo expanded, cryopreserved cell therapy product comprising of pure NK cells (> 99%) with high CD5 CAR expression (> 90%). GL205 showed significantly higher *in vitro* direct-killing efficacy against $CD5^{\pm}$ tumor cells compared to donor matched CBNK. IFN-γ and IL-15 release from GL205 was significantly increased after co-incubation with $CD5^{+}$ tumor cells. In xenograft mouse model, GL205 administration exhibited a greater survival rate and low tumor burden compared to vehicle group. In addition, GL205 was detected in blood for 3 months, demonstrating *in vivo* long-term persistence. In conclusion, GL205 could be a valuable and off-the-shelf allogeneic therapeutic option for treating T cell malignancies.

#1325 CD19 CAR-expressing iPSC-derived NK cells effectively enhance migration and cytotoxicity into glioblastoma by targeting to the pericytes in tumor microenvironment.

D. Kong[1], D. Kwon[2], B. Moon[2], D.-H. Kim[3], K.-S. Kang[1];
[1]Seoul National University, Seoul, Korea, Republic of, [2]Research Institute in Maru Therapeutics, Seoul, Korea, Republic of, [3]Sungshin Women's University, Seoul, Korea, Republic of

In cancer immunotherapy, targeting specific antigens with chimeric antigen receptors (CARs) has emerged as a potent tool for cell-based therapy. After being accessed by CARs, the selective anticancer lysis by CAR-natural killer (NK) cells through ‘missing-self’ and ‘induced-self’ mechanisms can mitigate off-tumor toxicity, a contrast to CAR-T cells. This specificity can be advantageous in the heterogeneous milieu of solid tumors. In the tumor microenvironment of glioblastoma (GBM), pericytes not only support tumor growth but also contribute to immune evasion, underscoring their potential as therapeutic targets in GBM treatment. Indeed, we examined and observed the presence of CD19-positive pericytes derived from GBM in patient samples, particularly within the perivascular niche, highlighting CD19 as a possible therapeutic target. Given this context, our study aimed to target the GBM tumor microenvironment, with a special focus on pericytes expressing CD19, to evaluate the potential effectiveness of CD19 CAR-iNK cells against GBM. In this study, we generated induced pluripotent stem cell-derived NK (iNK) cells with CD19 CAR. To determine whether CD19 CAR targets the tumor microenvironment pericytes in GBM, we developed GBM-blood vessel assembloids (GBVA) by fusing GBM spheroids with blood vessel organoids. When co-cultured with GBVA, CD19 CAR-iNK cells migrated towards the pericytes surrounding the GBM, inducing tumor lysis through NKp44 upregulation. Using a microfluidic chip, we observed that post-infused CD19 CAR-iNK cells targeted pericytes in a perfusion-like setting, facilitating an examination of CD19 CAR-driven migration and their tumor-specific cytotoxicity on the GBM. Therefore, we conclude that CD19 CAR-iNK cells may effectively target the pericytes in the GBM tumor microenvironment, suggesting their potential therapeutic value for GBM treatment.

#1326 Pre-clinical development of ARB011: A CDH17 targeting allogeneic nonviral RNA-based *"Flash"* CAR-NK therapy for gastrointestinal cancer.

J. Roy[1], N. Lin[1], K. Chow[1], C. Y. Yang[2], J. C. Lin[2], J. M. Luk[3], K. F. Wong[1];

[1]Arbele Limited, Hong Kong SAR, Hong Kong, [2]Medigen Biotechnology Corp., Taipei City, Taiwan, [3]Arbele Corporation, Seattle, WA

Background: Treatment for advanced gastrointestinal (GI) cancers has remained challenging, therefore, novel immunotherapies using chimeric antigen receptor (CAR)-T cells are being developed as a new hope for the patients. However, despite the clinical successes in hematologic malignancies, the overall safety and efficacy against solid tumors of CAR-T cells have yet to be established, and the manufacturing of autologous CAR-T cells requires lengthy cell expansion and viral transduction processes. In view of these technical challenges, we have developed ARB011, an RNA-based allogeneic CAR-NK therapy targeting GI cancers expressing cadherin-17 (CDH17), a promising therapeutic target with its overexpression associated with poor prognosis in patients with GI cancers. The use of allogeneic NK cells would mitigate the risk of graft-versus-host disease. Moreover, engineering NK cells with nonviral CAR-encoding mRNA would provide a rapid large-scale manufacturing platform with minimal risk of abnormal genetic alteration mediated by viral integration.

Methods: To generate the ARB011 CAR-NK cells, ex vivo expanded human peripheral blood NK (Magicell-NK, Medigen, Taiwan) cells were electroporated with mRNA encoding a humanized anti-CDH17 scFv fused with transactivation domains. Flow cytometry, in vitro cytotoxicity assay, and cytokine release assay were performed to evaluate the expression and functionality of ARB011. To examine the developability of ARB011 as an off-the-shelf cell product, cryopreservation and large-scale electroporation were also studied.

Results: Flow cytometry analysis revealed efficient electroporation with a high level of CDH17 CAR expression (>80%) and optimal CAR-NK cell viability (60%-80%). Following electroporation, cytotoxicity of ARB011 was tested against gastric (AGS and NCI-N87), colorectal (DLD-1 and T84), and liver (MHCC-97H) cancer cells by co-culturing at 1:1 and 2:1 effector/target ratio for 12-24h. ARB011 showed significant cytotoxicity against CDH17+ but not CDH17- cancer cells. The CDH17-sepcific cytotoxicity was accompanied with elevated levels of CD107a or LAMP-1 expression on CAR-NK cells and IFN-γ and TNF-α releases. Interestingly, cryopreserved ARB011 maintained optimal cell viability, CAR expression, and potent CDH17 target-specific cytolytic activity. Lastly, large-scale electroporation showed the establishment of up-scaling process of ARB011 production for clinical application.

Conclusions: Overall, the findings suggest that ARB011 could be a novel off-the-shelf, CAR-NK therapy that warrants further studies in animal models and in clinical trials.

#1327 Affinity tuning anti-CD123 chimeric antigen receptor natural killer cell therapy to treat acute myeloid leukemia.

M. Kizerwetter[1], H. Yang[2], R. Rahnama[1], C. Bonifant[1], J. Spangler[1];
[1]Johns Hopkins University School of Medicine, Baltimore, MD, [2]Johns Hopkins University, Baltimore, MD

Acute myeloid leukemia (AML) is a highly prevalent blood and bone marrow cancer characterized by the uncontrolled growth of abnormal myeloblasts. Current treatments for AML often result in systemic toxicities for patients, many of whom will still experience relapse. There is thus an unmet need to develop safer and more effective therapies targeting AML. Chimeric antigen receptor (CAR) T cells, which are engineered to express a cancer-targeting extracellular antibody single-chain variable fragment (scFv) linked to an intracellular T cell-activating domain, have shown promise in treating B cell leukemias, but their success has been limited in myeloid leukemias. This is due in part to the lack of AML-specific target antigens. Moreover, impaired T cell function, a hallmark of AML, is also problematic when relying on autologous T cell activation upon reinfusion. We overcame the limitations of CAR T therapy in AML by developing CAR-expressing natural killer (NK) cells targeting CD123. While present on both healthy and AML cells, CD123 is expressed at >10-fold higher levels on malignant cells. Furthermore, use of NK allows use of fully functional allogeneic cells from healthy donors, since NK cells do not induce graft-versus-host-disease. To optimize the tumor cell selectivity of CAR NK cells, we employed the yeast display directed evolution platform to isolate anti-CD123 scFvs with varying affinities and are identifying and characterizing clones that maximize the interaction with $CD123^{high}$ AML cells over healthy $CD123^{low}$ cells, as determined by binding, cytotoxicity, cytokine secretion, and intracellular signaling studies. Collectively, our efforts introduce a new paradigm for engineered cell therapeutics with significant promise for AML treatment.

#1328 AccuBase™ (ceBE), a second-generation high-fidelity base editor, can proficiently modify genes in a human primary NK cells with minimizing off-target effect.

H. Ying[1], C. Yao[2], C. Fang[2], G. Li[3], L. Wang[2], Y. Zhou[2], C. Gong[2], J. Li[3], Y. Wang[3], W. Fan[3], F. Lv[3], X. Shao[3], H. Zhao[3], L. Wang[3], J. Yan[3], T. Xu[3], S. Zhu[2]; [1]Base Therapeutics (US) Co., Ltd., San Mateo, CA, [2]Shanghai University of Traditional Chinese Medicine, Shanghai, China, [3]Base Therapeutics (Shanghai) Co., Ltd., Shanghai, China

Natural Killer (NK) cells hold great promise for cancer therapy owing to their innate ability to detect cells expressing signs of stress or infection. However, NK cell-based therapeutics face significant challenges: limited expansion and genetic modification resistance. In response to these challenges, we present our pioneering work in the development of Base Editing-Directed NK (BED-NK) cell products, referred to as NK510, which is an off-the-shelf allogeneic cell therapy product containing peripheral blood mononuclear cell (PBMC)-derived TIGIT knock-out NK cells. Through a meticulously planned optimization process, we have achieved over 80% editing efficiency in NK510s using our high-fidelity Base Editor, AccuBase™. By knocking out TIGIT (an inhibitory receptor in NK cells), we have prompted tumor cell-derived CD155 (an inhibitory ligands in tumor cells) to engage with CD226 (an activating receptor in NK cells), triggering activating signals in NK510s. Our results showed that CD155 positive tumor cells were more susceptible to NK510s than CD155 negative tumor cells. And target killing percentage is positively related to CD155 expression level in tumor cells. This transformation effectively converted an inhibitory ligand into an activating one, resulting in tumor regression in multiple mouse models, including non-small cell lung cancer (NSCLC) and sarcoma. We developed a GMP-compliant NKBoost+ expansion system to generate a millionfold expansion of NK510 within a 21-day expansion protocol. To investigate the safety of NK510 product, we conducted repeated dosing toxicity, tumorigenicity, and oncogenicity study in a GLP facility, and the results validated the safety of NK510. Additionally, we developed an analytical protocol based on Droplet Digital PCR (ddPCR) technology to investigate the pharmacokinetics (PK) and biodistribution of NK510s in NSCLC tumor-bearing mice. We observed an enrichment of NK510-derived genomic DNA (gDNA) in lung tissues of tumor-bearing mice at day 1. The concentration of NK510-derived gDNA was up to 2000 copies/ug DNA. The concentration of NK510-derived gDNA sharply decreased from day 2 to day 6, and then decreased to below the lower limit of quantification (LLOQ). Distinct from the PK data of NK510s, the concentration of NK510-derived gDNA started low at day 1 and reached peak concentration at day 2 (in blood samples) and at day 4 (in liver tissues), respectively. These results demonstrated the efficacy and safety of BED-NK product and underscore the feasibility of combining base editing with ex vivo expansion of NK cells, significantly enhancing their therapeutic potential in clinical settings.

#1329 Development of the first optimised “off the shelf” MAGE-A4 targeting TCR-NK cells for advancement into the clinic for the treatment of solid tumors.

S. Vollmers, A. Cieslar-Pobuda, J. Kmiecik, G. Malachin, M. L. Satersmoen, F. Hosoien Haugen, M. Boieri, M. Sandve, D. Clement, I. Cardoso, P. Wanichawan, M. E. Haugstoyl, A. Oldenburg, L. Christ, P. Oberoi, L. Mora-Velandia, A. Holm, N. J. Hassan, E. Gauthy, J. Ino, S. Pollmann, L. U. Weigand; Zelluna Immunotherapy AS, Oslo, Norway

T cell receptor (TCR)-T based therapies, such as MAGE-A4 TCR-T cells, have shown compelling data demonstrating effective infiltration into and targeting of solid tumors with clinical responses across various solid cancers. However, heterogeneity and down-regulation of target antigen and HLA expression limit the durability and curative potential of these types of treatments. On the other hand, owing to their clinical potency, favorable safety profile and applicability as “off the shelf” therapy, natural killer (NK) cells have emerged as promising modalities in recent years. Unguided NK cells have shown limited potential against solid cancers, due to lacking infiltration into tumors. With our proprietary TCR-NK platform, we combine the solid tumor targeting capabilities of TCRs with the pan-cancer sensing and cytotoxic potential of highly potent killer cells, redirecting and arming NK cells with a fully functional TCR-CD3 complex. Here we present our lead product, an optimized TCR-NK cell product, ZI-MA4-1a, expressing an affinity enhanced TCR (KVL-a) directed to the HLA class I-restricted clinically validated cancer-testis antigen MAGE-A4, that is broadly expressed across solid tumors. The KVL-a TCR was successfully engineered from a naturally occurring wild-type TCR, increasing the affinity to MAGE-A4-peptide-HLA complex and resulting in enhanced recognition of tumor cells expressing the target antigen. ZI-MA4-1a is produced by transducing healthy peripheral blood derived NK cells with the full CD3 complex, the KVL-a TCR and a CD8 coreceptor. The process has been optimized to enrich TCR-NK cells, increasing process robustness, diminishing the impact of donor variability, and producing a higher performing TCR-NK cell product. We show the dual functionality of ZI-MA4-1a: TCR driven cytotoxicity as well as innate NK sensing of antigen knockout or HLA negative cancers. We demonstrate killing of heterogenous tumor cell models in vitro, as well as the multifunctionality of ZI-MA4-1a with killing, degranulation and multicytokine secretion. Interestingly, we observe enhanced proliferation of ZI-MA4-1a cells after activation by MAGE-A4 expressing tumor cells, indicating that TCR-NK cells acquire further proliferative capacity when the TCR is triggered. Finally, we demonstrate higher activity of ZI-MA4-1a compared to KVL-a and benchmark TCR transduced T cells against antigen positive targets, and activity against antigen negative tumor cells escaping TCR-T cell recognition.

#1330 Universal and potent chimeric antigen receptor-natural killer (upCAR-NK) cells for B-cell malignancy treatment.

D. Kwon[1], B. Moon[1], M. Han[1], T.-W. Lee[1], J.-H. Lee[1], K.-S. Kang[2];

[1]Maru Therapeutics Co., Ltd., Seoul, Korea, Republic of, [2]Seoul National University, Seoul, Korea, Republic of

Patient-specific CAR-T cells treatment is an innovative new drug that has shown excellent therapeutic effects against B cell blood cancer. However, side effects such as cytokine release syndrome and immune effector cell-associated neurotoxicity syndrome and ultra-high treatment costs must be overcome, and off-the-shelf CAR-NK cells can be a good alternative. The purpose of this study was to combine cellular reprogramming, gene editing, and differentiation technologies to produce full-off-the-shelf NK cells derived from iPSCs and verify their efficacy and safety. To this end, somatic cell-derived iPSCs were produced, seven genes were edited using CRISPR/Cas9 technology (5 kinds of knockout and 2 kinds of overexpression), and differentiated into NK cells. upCAR (universal and potent chimeric antigen receptor)-iPSCs with seven genes edited showed bialleic INDEL in the coding sequence of five genes and no off-target effect. In addition, normal transcriptome and genetic stability were maintained. High-efficiency differentiated upCAR-NK cells showed a very high differentiation yield, *in vitro* proliferation, and freezing / thawing were possible. In addition, upCAR-NK cells secrete interferon-γ when they meet cancer cells, showing cytotoxic effects *in vitro* and *in vivo*. upCAR-NK cells themselves showed no obvious toxicity *in vivo*. In conclusion, this study developed upCAR-iPSCs and upCAR-NK cells platform technologies that are less likely to have side effects and can be economically developed for B cell blood cancer than CAR-T. In the future, this technology can be useful in developing full-off-the-shelf CAR-NK cells anti-cancer immune cell therapy with low side effects, high efficacy, and low price.

#1331 MiNK-215, an IL-15 armored FAP-targeting CAR iNKT cell therapy, effectively treats human organoid models of treatment-refractory MSS colorectal cancer (CRC) liver metastases.

S. Krishnan[1], B. Joshi[1], J. Keith[1], R. Frazier[1], B. Kalinowska[1], J. Choi[2], S. Sanders[2], S. Boi[3], O. Le Tonqueze[3], N. Kushner[3], K. Soh[1], R. Stein[1], T. J. Curiel[4], M. A. van Dijk[3], E. Kim[2], E. Chantzoura[3], N.-P. Rudqvist[1], D. Chand[1];

[1]Agenus Inc, Lexington, MA, [2]Biorg, Winston-Salem, NC, [3]MiNK Therapeutics, New York City, NY, [4]Agenus Inc and Dartmouth-Hitchcock Medical Center, Lexington, MA

The presence of liver metastases in patients with microsatellite-stable (MSS) or mismatch repair proficient (pMMR) colorectal cancer (CRC) is associated with poor response to current pharmacological treatments, including immune checkpoint blockade (ICB). The tumor microenvironment (TME) of CRC liver metastases is characterized by a highly immunosuppressive phenotype that includes poor immunogenicity, a paucity of dendritic cells, elimination of tumor-specific effector T cells, and an abundance of immunosuppressive intrahepatic Kupffer cells and myeloid-derived suppressor cells. This underscores the urgent need for innovative therapeutic approaches targeted specifically to patients with CRC liver metastases. Here we describe MiNK-215, an IL-15 armored FAP-targeting CAR iNKT cell therapy, derived from the AgenT-797 allogeneic iNKT platform, as a potential novel therapeutic approach for patients with CRC liver metastases.

To better model ICB refractory human MSS CRC liver metastases, we developed an ex vivo human organoid model that recapitulates the histological and immunological features of human disease. Organoids were comprised of MSS CRC cells engineered to express nuclear GFP and HLA-A2-NY-ESO-1, hepatocytes, Kupffer cell-enriched non-parenchymal cells, and HLA-matched peripheral blood mononuclear cells (PBMCs) supplemented with NY-ESO-1-reactive T cells. Organoid models of CRC lung metastases, which are traditionally more responsive to ICB therapy were also developed to compare the models to clinical experience and further validate their usefulness. Models were treated with Fc-enhanced anti-CTLA-4 (botensilimab) and anti-PD-1 (balstilimab) antibodies, or MiNK-215 to assess tumor killing and immune activation.

Botensilimab and balstilimab enhanced T cell activation and cytotoxicity of CRC tumor cells in the absence of “normal” liver cells and in lung organoids. However, they were less effective in organoid models of CRC with liver metastases consistent with clinical observations. In contrast, MiNK-215 potently enhanced tumor killing by T cells in models of CRC with liver metastases. Tumor killing in CRC liver organoid models by MiNK-215 was associated with depletion of immune suppressive FAP-expressing stellate cells and increased $CD8^{\pm}$ T cell infiltration.

Our findings demonstrate that in treatment-refractory CRC-liver metastatic organoid models, MiNK-215 overcomes the limitations of ICB therapy to home to sites of disease, reprogram the TME, recruit tumor-reactive T cells and enhance tumor killing. *Ex-vivo* human CRC liver and lung metastatic organoid models are a novel platform that can be leveraged to rapidly identify new therapeutic approaches for potential clinical evaluation.

#1332 Allogeneic CD19-directed CAR-iNKT cells and their phenotypic subsets for the treatment of CD19+ hematological malignancies.

K. Ponnusamy[1], S. Poon[2], N. van der Weerden[2], R. Dossa[2], M. J. Baker[2], M. Bharathan[2], A. Karadimitris[1];
[1]Imperial College, London, United Kingdom, [2]Arovella Therapeutics, Victoria, Australia

Invariant Natural Killer T (iNKT) cells are a unique subset of innate lymphocytes, constituting <1% of human T cells. iNKT cells express a semi-invariant TCR (iTCR) recognizing glycolipids presented by the monomorphic, MHC-like molecule CD1d. Previous studies indicate that due to distinctive TCR constitution and antigen recognition properties, iNKT cells do not induce acute graft-versus-host disease. Based on the CD4 and CD8 expression, mature human iNKT cells can be classified into CD4+CD8-, CD4-CD8- & CD4-CD8+ subsets with overlapping and distinct functions. The functional profiling of CAR19-iNKT cell subsets serves the dual purpose of ensuring their safety and efficacy as a therapeutic intervention. Here we characterized the phenotypic and functional profile of CD4+ and CD4- CAR19-iNKT cells. iNKT cells were isolated with >99% purity from healthy donors' peripheral blood and were transduced with a CD19 CAR-encoding 3rd generation lentivirus. After expansion, the CAR19-iNKT cells were cryopreserved and later analyzed post-thawing. Differential expression of CD27 and PD1 was noted in CAR+CD4+ and CAR+CD4- iNKT cells compared to other markers. For functional profiling, CAR+CD4+ iNKT cells were positively selected, and 24h cytotoxicity assays were performed using several tumor cell lines including SEM, Ramos and C1R-CD1d (+/- α-GalCer). The CAR+CD4- iNKT cells exhibited superior cytotoxicity to multiple tumor cell lines compared to that of CAR+CD4+ iNKT cells from two donors. However, both subsets lysed α-GalCer pulsed C1R-CD1d cells in a comparable manner indicating the potential of these subsets to recognize antigen through the iTCR. Subsequently, we assessed the proliferation ability of the CAR+CD4+ and CAR+CD4- subsets by exposing the cells to three rounds of stimulation, 24h apart, using SEM (CD19+CD1d-) or K562 (CD19-CD1d-) tumor cells with or without IL-15. Proliferation was assessed seven days following the first stimulation. The CAR+CD4+ subset of CAR19-iNKT cells demonstrated faster proliferation than CAR+CD4- cells in the presence of IL-15 after repeated exposure to tumor cells. Ongoing RNA seq analysis of CAR+CD4+/CAR+CD4- cells will further elucidate differences between these subsets. The outcomes of these studies have shown encouraging results, indicating the potential benefit of having diverse subsets among CAR19-iNKT cells for treating CD19+ cancers. The therapeutic potential of CAR+CD4+ iNKT cell subset could be enhanced to match that of CAR+CD4- subset with the use of α-GalCer. In summary, inclusion of both CD4+ and CD4- iNKT cells is critical for the functionality of allogeneic CAR-iNKT cell therapy. Extensive characterization is crucial for clinical translation, but additional research, including preclinical and clinical trials, is essential to determine the safety and effectiveness of CAR19-iNKT cell therapy in real-world applications.

#1333 Preclinical data supporting the Phase 1 trial design of SENTI-202, a next generation allogeneic logic-gated selective CAR NK cell therapy, engineered to overcome key limitations of first generation cell therapies in AML.

D. Kaveri, P. Chinta, E. Leitner, L. Naitmazi, G. Yucel, M. Tian, N. Almudhfar, H. Deng, Y. Li, A. Lam, C.-T. Lee, E. Hong, R. Emery, B. Garrison, **A. N. Nguyen**, K. Rajangam;
Senti Biosciences, South San Francisco, CA

First generation natural killer (NK) and chimeric antigen receptor (CAR) NK cell products are well-tolerated and have clinical activity (~20-60% CR) in patients with AML. CRs generally increase with the inclusion of CARs or cytokines, increased cell doses, and when Flu/Ara-C lymphodepletion (LD) is used for conditioning. Key clinical limitations have been low PK of the infused NK cells, short durability of the observed responses potentially due to immune evasion of leukemic stem cells (LSCs), and manufacturing challenges precluding higher or multiple doses.

SENTI-202 is a next generation allogeneic logic-gated selective CAR NK cell therapy specifically designed to address these limitations and to augment endogenous NK anti-AML activity. SENTI-202 expresses a bivalent activating CAR (aCAR) that targets CD33 and FLT3 on bulk AML blasts and LSCs. As FLT3 is also expressed on healthy hematopoietic stem cells (HSCs), SENTI-202 is further engineered to express an inhibitory CAR that recognizes endomucin expressed on HSCs, thereby conferring protection from aCAR-mediated cytotoxicity even in the presence of FLT3/CD33. SENTI-202 expresses a calibrated-release IL15 that provides both auto- and paracrine cytokine support, mediating expansion, activation, and persistence of SENTI-202 and host immune cells. SENTI-202 demonstrated robust and specific killing of primary AML blasts, LSCs, and AML cell lines in vitro. SENTI-202 protected HSCs from CAR-mediated cytotoxicity while preserving their function. In vivo, SENTI-202 revealed robust efficacy that increased with higher E:T ratio and with 3 weekly vs 1 dose. Preclinically, 3 doses of SENTI-202 that were > 60-fold the planned starting clinical trial dose were well tolerated in acute and chronic toxicology studies with no CAR NK-related body weight, laboratory, or histopathology findings. SENTI-202 non-clinical PK revealed greater than dose proportional exposure, which was ~2-fold greater compared to non-engineered NK cells. Pretreatment of CD33/FLT3 negative AML cell lines with Ara-C resulted in upregulation of CD33 and FLT3 expression, sensitizing cells to robust SENTI-202-mediated killing, providing additional rationale for the use of Ara-C-based LD. In the presence of exogenous IL2, persistence, cytotoxicity, and serial killing activity of SENTI-202 were increased, supporting the use of low dose IL2 to further augment SENTI-202 clinical activity.

Taken together, these results support the Phase 1 trial design of SENTI-202-101 in patients with R/R CD33 and/or FLT3 positive malignancies including AML, which uses Flu/Ara-C as LD followed by 3 weekly doses of SENTI-202 and includes the option of enrolling patients into cohorts that additionally receive low dose IL2 following SENTI-202 administration.

#1334 Evaluation of NK cell combination therapies in mouse models of cancer.

K. Franciszkiewicz[1], P. Rettman[1], B. Gauthier[2], L. Noblet[1], C. Nicolazzi[1], A. Kunert[3], R. Igarashi[3], L. Calvet[1], V. Fantin[4], **S. Sidhu**[1];
[1]Sanofi R&D, Vitry-sur-Seine, France, [2]Sanofi R&D, Montpellier, France, [3]Sanofi R&D, Amsterdam, Netherlands, [4]Sanofi R&D, Cambridge, MA

Adoptive immunotherapy with natural killer (NK) cells has emerged as a promising innovative approach against hematological malignancies and solid tumors. To enhance the functional aspects of NK cells and to achieve stronger, sustained anti-tumor responses, combination strategies are under development. They are focused on optimization of NK cell potency, persistence and tumor targeting using monoclonal antibodies, multi-specific NK cell engagers and immune modulators like cytokines. SAR445419 is a universal off-the-shelf allogeneic human NK cell (hNK) product made using Sanofi's proprietary platform with potential broad application across hematologic and solid tumor indications. We evaluated the therapeutic potential of these NK cells in combination with internal assets and standard of care treatments in preclinical mouse models. The studies were performed in immunodeficient NOG mouse strains transgenic for hIL-15, supporting long-term engraftment of functional hNK cells. We demonstrated the therapeutic advantage of NK cell combination with an anti-CD20 monoclonal antibody (mAb) in a disseminated lymphoma model. We also reported prolonged lifespan of leukemia-bearing animals treated with NK cells and pegenzileukin, a PEGylated non-alpha rhIL-2 variant engineered to preferentially bind to the IL-2 βγ receptors and promote NK cell function. The anti-tumor response correlated with pegenzileukin-induced increase in NK cell numbers in the blood. A combination of CD38KO NK cells with an anti-CD38 mAb was also investigated in a model of multiple myeloma (MM). FcγR-KO immunodeficient mice were used in these studies to limit the confounding contribution of residual murine immune cells engaging with the Fc-competent therapeutic antibody and to specifically detect hNK-cell mediated activity. The comparison of CD38KO versus WT NK cell numbers in the blood of animals treated with an anti-CD38 mAb showed a significant decrease in CD38-expressing NK cell count that was mitigated by the genetic deletion of CD38. Obtained results suggest that CD38KO NK cells are resistant to anti-CD38 mAb-mediated fratricide and provide a rationale for the combination of CD38KO NK cells with anti-an CD38 mAb against MM. Overall, these preclinical in vivo studies have a pivotal role in the evaluation of NK cell combination therapies against cancer and reveal their therapeutic potential.

#1335 Generating functional CAR-NK cells for cancer immunotherapy.

Karina Di Gregoli[1], Henry Leonard[1], Dan Rocca[1], William Morley[2], Sabrina de Munnik[3], Gemma Moiset[3], Raluca Dumitru[4], Wassim Basheer[4], Brianna Schoen[4], Robert Nunan[1], Lauren Schewitz-Bowers[1], **Louise Brackenbury**[1]

[1]Charles River Laboratories, Bristol, United Kingdom,[2]Charles River Laboratories, Portishead, United Kingdom,[3]Charles River Laboratories, Leiden, Netherlands,[4]Charles River Laboratories - Cell Solutions, Northridge, CA

Chimeric Antigen Receptor-Natural Killer (CAR-NK) cells are rapidly emerging as a promising cellular therapeutic overcoming the potential life-threatening adverse events that may result from CAR-T therapy, including cytokine release syndrome (CRS), neurotoxicity and graft-versus-host disease (GVHD). Due to their intrinsic characteristics, NK cells can kill tumor cells without the requirement for recognition of antigen in the context of MHC. This removes the constraint of HLA matching and supports antigen independent cytotoxicity through NK cell intrinsic mechanisms. As such CAR-NK cells kill via both CAR-dependent and -independent mechanisms. For these reasons, they offer the advantage of being an “off-the-shelf” product; satisfying the requirement for large-scale production of cancer immunotherapies, with the potential to reach more patients at a reduced cost. The frequency of NK cells in the blood is low (~ 2-5%), therefore improving their *in vitro* expansion is key to generating sufficient material to offer a viable CAR-NK cell therapy. Here we outline an *in-vitro* method to generate, expand, and test primary human CAR-NK cells using engineered feeder cells, and go on to demonstrate the efficacy of the CAR-NK against target cancer cells. Primary human NK cells were cultured and expanded in the presence of irradiated K562 cells (iK562) modified to express 4-1BBL and membrane bound IL-21. Following initial expansion, NK cells were transduced with a clinically tested CD19-targeting CAR lentiviral vector (LV) or GFP expressing LV; as an empty vector transduced control. Following transduction, CD19 CAR-NK and GFP-NK were enriched by FACS sorting to reach >80% purity and further expanded in the presence of 4-1BBL/mbIL21 iK562 feeder cells. Following sufficient expansion, cytotoxicity of fresh or cryopreserved CD19 CAR-NK cells was tested *in vitro* in a Tumor Killing Assay (TKA) against CD19+ or CD19- target cells. As expected, CD19 CAR-NK cells showed increased on-target cytotoxicity, increased degranulation and IFNγ secretion compared to controls. This effect was not observed with CD19 negative cancer cells, strongly suggesting CD19 CAR engagement of the target antigen to mediate killing. Taken together these data show the generation, expansion, and enrichment of CD19 CAR-NK cells with enhanced cytotoxic activity towards CD19+ target cells. This approach provides a platform for *in vitro* characterization of novel CAR-constructs, allied with *in-vitro* safety assessment and *in vivo* pharmacology testing. Together, this offers the potential to further develop new and more widely available cellular therapeutics to treat cancer.

#1336 Verification of the effect of human allogeneic iPS cell-derived gene-engineered NK cells (eNK cells HLCN061) on mesothelioma.

S. Matsumoto[1], Y. Fujita[1], K. Goto[2], Y. Sato[2], F. Nishigaki[2], Y. Higashi[2], H. Kimura[2], K. Tamura[2];
[1]Hyogo Medical University, Nishinomiya, Japan, [2]HEALIOS K.K., Kobe, Japan

Malignant pleural mesothelioma is a malignant tumor that is caused by exposure to asbestos. Because it is a rare cancer, there are few drugs that can be used to treat it. Healios is developing iPSC-derived NK cells (eNK cells) (HLCN061) engineered with NKG2D, DAP10, IL-15, CD16, CCL19, and CCR2B genes for the treatment of refractory solid tumors. This study evaluated the antitumor effect of eNK cells against human malignant pleural mesothelioma cell lines.(Method) The antitumor effect of eNK cells on human malignant pleural mesothelioma cell lines in vitro was evaluated using the Viability/Cytotoxicity Multiplex Assay Kit (WST-8/LDH).In vivo, immunodeficient mice were subcutaneously inoculated with human malignant pleural mesothelioma cell lines. After subcutaneous tumor formation, eNK cells were inoculated into or near the tumor, the size of the subcutaneous tumor was measured, and the tumor volume was compared with that of an untreated group. After the study was completed, the tumors were removed and the tumors in the untreated group and the eNK cell-administered group were analyzed using RNA-seq.(Results) The antitumor effect of eNK cells against human malignant pleural mesothelioma cell lines was confirmed in vitro. In a mouse subcutaneous tumor model, the eNK cell treatment group suppressed tumor growth compared to the untreated group ($p \leqq 0.05$). RNA-seq showed increased expression of granulysin, IL2RB, cathepsin W, etc. in subcutaneous tumors treated with eNK cells.

#1337 Characterization of anti-AXL CAR-NK cell therapy for the treatment of melanoma.

W. Hibler, G. Merlino, Y. Yu;
NIH-NCI, Bethesda, MD

AXL is a receptor tyrosine kinase (RTK) that is commonly expressed in metastatic melanoma and several other forms of cancer. Activation of AXL signaling is linked to tumor cell growth, invasion, metastatic transformation, drug resistance, and immune response regulation. However, treatment of metastatic melanoma continues to present clinical challenges due to its capacity to rapidly develop drug resistance, which manifests under the influence of AXL signaling. As such, AXL may be a viable antigen target for immunotherapies. Despite their successes in hematological malignancies, chimeric antigen receptor (CAR)-T cell therapies remain limited by their susceptibility to causing off-target toxicity. In contrast, natural killer (NK) cells are not associated with such risks, which makes them clinically appealing as an alternative to T cells. However, studies on the application of CAR-NK cells to treat solid tumors remain acutely scarce. To explore the clinical viability of CAR-NK cells for the treatment of metastatic melanoma, AXL-specific CAR-NK cells were generated by transfecting NK cells obtained from NK cell lines. Preliminary data from a cytotoxicity assay indicated that the cytotoxicity of CAR-NK92-MI cells against AXL-positive melanoma cell lines was significantly stronger (up to a 10-fold difference) than the corresponding parental cells. Further in vitro characterization of this CAR-NK cell line and other CAR-NK cell lines, as well as in vivo evaluation of their efficacy in a mouse xenograft model of melanoma metastasis, is underway.

#1338 Novel activation domains coupled to chimeric ILT receptors (CIR) enhance NK cell targeting of HLA-G$^{\pm}$leukemic and solid tumor cells.

M. Duong, J. Park, R. Ognar, S. Wain-Hobson, **H. Bayle**;
NKILT Therapeutics, Houston, TX

Human leukocyte antigen-G (HLA-G) suppresses lymphoid and myeloid immune systems by binding ILT2 and ILT4 respectively and activating ITIM signaling. HLA-G is abundantly expressed in placental cytotrophoblasts to block fetal rejection. HLA-G is not expressed in most normal cells but is derepressed in in about 50% of malignancies. We engineered ILT2 and ILT4 to produce activating signals as Chimeric ILT Receptors or CIR. Preliminary results indicated robust killing of Acute Myeloid Leukemia (AML) cells by Natural Killer (NK) cells expressing either ILT2 or ILT4 CIRs. Here, we evaluated the effect of alteration of activating domains in the CIR constructs to produce signals that mimic the effect of IL-18 signaling in CIR-NK cells to enhance cytotoxicity, NK cell growth and persistence. Further, HLA-G expression and CIR-NK cell targeting of primary human cell types were rigorously screened.

Activated NK cells derived from peripheral blood (2 to 5 donors) were transduced with γ-retroviruses directing expression of CIR proteins (CIR.X.Y or CIR.Y.X) where X stimulates cytotoxicity through CD3ζ, DAP10 or DAP12, and Y directs coactivation through 4-1BB, fusion of the MyD88 death domain or recruitment of endogenous MyD88 with receptor-derived TIR domains and soluble IL-15. CIR-NK cells were cocultured with GFP*ffluc*-expressing AML and solid tumor target cell lines or normal primary human cells. NK cell proliferation and cytotoxicity of CIR-NK cells was monitored by Incucyte microscopy and supernatants were analyzed for cytokine release by ELISA.

At low E:T (1:20 - 1:40) in 7-day cocultures, mock-transduced NK cells displayed innate killing activity against HLA-G$^{\pm}$ Molm13 and Kasumi1 AML cells that was augmented by CIR constructs containing direct fusions of MyD88 and DAP10 or DAP12 (mock = 2.06E7 ± 4.53E6 vs. CIR-ILT4.MyD88.DAP10 = 1.03E7 ± 5.46E6) with 7-fold elevation of IFN-γ production. CIR constructs that recruited endogenous MyD88 signaling through the TLR2 TIR domain (4-1BB.DAP10.TLR2) also exhibited enhanced anti-HLA-G activity (9.13E6 ± 5.33E6). Against HLA-G$^{\pm}$ HT-1376 bladder cancer cells (E:T = 1:10-1:20), CIR-NK cells also displayed enhanced tumor cell killing with enhanced NK cell growth. Conversely, CIR-enhanced killing was not observed against HLA-G^{-} HCT-116 colorectal cancer cells. The persistence of CIR-NK cell potency after 4 weeks of expansion varied markedly with different activation domains employed. When screened against primary human cells (cardiomyocytes, hepatocytes, hepatic endothelial cells, corneal, colon and lung epithelial cells), no CIR-specific targeting was observed at high E:T ratios (1:1 and 1:5).

In conclusion, CIR-NK cells exhibit potent and specific anti-tumor activity against HLA-G$^{\pm}$ solid and leukemia cells. Alteration of CIR-NK cell intracellular signaling can optimize the potency and persistence of NK cell anti-tumor activity.

#1339 Pre-clinical development of IAMA-004, a tri-specific antibody targeting innate immune receptors and tumor targets.

L. Liu, Z. Han, Y. Fan, Q. Pan;
Nanjing JSIAMA Biopharmaceuticals, Ltd., Nanjing, China

Immune check-point inhibitor (ICI) such as anti-PD1 or anti-PDL1 antibody, which enhances the adaptive immunity via re-energizing exhausted T cells, has become the foundational therapy for many cancers. However, due to variety of other immunosuppressive tumor microenvironments, it is efficacious only in 15-30% of the patients. It is well known both the innate immunity and the adaptive immunity are required for full control of cancer growth. Thus, therapeutics harnessing the innate immunity will be complementary to ICI and improve the cancer response rate when used in combination. Currently therapeutics harnessing the innate immunity mainly involve bispecific antibodies with one arm targeting tumor antigen and one arm connecting to innate effector cells such as NK cells or macrophages, represented by CD30-CD16a bispecific and Her2-CD47 bispecific respectively. Considering that cancer patient's immune status are heterogenous, varying from T cell exhaustion, macrophage disfunction (M2 bias), Treg cell presence to NK cell deficiencies, it would be advantageous to combine several innate immunity enhancers into one therapeutic molecule. Here we describe a long-acting tri-specific antibody termed IAMA-004 that targets Her2 as the primary target and CD47 and CD16a as effector cell engagers. CD47 is also a co-target on some tumor cells (CD47-Her2 double positive tumors). We have characterized this molecule both *in vitro* and *in vivo*. The *in vitro* experiments tested the molecule's ability to kill Her2 high, Her2 low and Her2 negative tumor cell lines including BT-474, SK-OV-3, NCI-N87, OE19, HCC1954, MDA-MB-231, MDA-MB-468, in human PBMC ADCC assays with DS-8201 and Trastuzmab as the comparator molecules. In all of these ADCC experiments, IAMA-004 showed superior tumor cell killing activities to those mediated by DS-8201 or Trastuzmab. When combined with IAMA-005 (a Fc-IL2-IFN-α fusion cytokine), the tumor cell killing activities were dramatically increased. In addition, IAMA-004 was also tested in patient-derived *Ex-Vivo* fluids (one malignant pleural effusion and one malignant asities) and demonstrated tumor cell killing efficacies; and the killing activity could be attributed to the specific arms of the molecule. These results suggest that it is feasible to combine more than one innate engager in one molecule to carry out specific functions in the heterogeneous immune status for the treatment of advanced cancer patients.

#1340 Modulation of the natural killer cell immune response to tumor with a synthetic tumor -immune cell agonist, NK-TICA™.

F. Dufort, T. Ezell, A. Rezvaya, K. Ho, C. Leitheiser, P. Brandish, K. McDonnell, N. Keen;
Bicycle Therapeutics, Cambridge, MA

Natural Killer (NK) cells are highly responsive cytotoxic immune cells of the innate immune system with well characterized anti-tumor properties. Their ability to directly kill malignant cells and elicit an adaptive immune response makes them a promising candidate for a precision guided immunotherapy in oncology. Bicycle® peptides are small (ca.1.5kDa), chemically synthetic, structurally constrained peptides discovered via phage display and optimized using structure-driven design and medicinal chemistry approaches. We have applied the Bicycle® platform technology to discover and evaluate a new class of fully synthetic molecules termed NK tumor immune cell agonists (NK-TICA™). The NK-TICA™ consists of chemically coupled Bicycle® peptides that bind specifically to the key activating receptor, NKp46, and to tumor antigens, that results in highly potent, antigen-dependent receptor activation and NK cell function. We demonstrate potent, selective binding of our Bicycle® peptides to receptor-expressing cells and the capability of the bifunctional molecule to induce NK cell function in vitro. With Bicycle's novel NK-TICA™ compound, we demonstrate the engagement of NK cells, the specific activation and function of NK cells, and enhanced tumor cytotoxicity in a tumor target- and dose-dependent manner. In conclusion, NK-TICAs drive NK cell-mediated tumor cell killing and cytokine production in vitro and as such have the potential to catalyze the development of durable anti-tumor immunity in tumor types not well served by current therapies. We hypothesize that utilization of Bicycle® NK-TICA™ as a multifunctional immune cell engager will promote the modulation and anti-tumor activity of peripheral and intra-tumoral NK cells to solid tumors.

#1341 SM2235: A bispecific EGFR x CD16A innate immune cell engager for enhanced treatment of EGFR-expressing solid tumors, regardless of RAS mutation status.

H. Geng, W. Song, X. Liu, S. Lu, H. Zhou, S. Yang, S. Xie, Y. Wei, X. Zhang, S. Zhou, **Y. Liang**;
Beijing StarMab BioMed Technology, Ltd., Beijing, China

Background: Monoclonal antibodies (mAbs) targeting the epidermal growth factor receptor (EGFR) are frontline therapies for numerous EGFR-dependent epithelial tumors. However, their efficacy faces challenges due to on-target skin toxicity and intrinsic or acquired resistance. Within the tumor microenvironment, innate immune cells, including macrophages and natural killer (NK) cells, play a significant role but are hindered by the lack of specific cancer cell targeting and a suppressive microenvironment. To enhance innate immune cell cytotoxicity, we have developed SM2235, a humanized tetravalent bispecific VHH antibody. SM2235 partially blocks EGFR and EGF interaction while conditionally activating innate immune cells through CD16A upon engagement with cancer cells.
Methods: SM2235 was engineered by combining a partially blocking EGFR single-domain antibody with a high-affinity CD16A-activating single-domain antibody on an inactivated human IgG1 Fc backbone. The binding affinity and specificity were confirmed using bio-layer interferometry and ELISA with recombinant proteins, followed by flow cytometry with EGFR+ human cancer cell lines and CD16A+ primary NK cells. SM2235's efficacy in blocking EGFR-EGF interaction and downstream signaling was assessed through competitive ELISA and proliferation assays in both EGFR-dependent and independent cancer cell lines. Its ability to induce target-dependent NK cell and macrophage activation was evaluated through activation markers as well as cytotoxicity and phagocytosis assays. In vivo efficacy of SM2235 against EGFR+ human tumors was measured using xenograft assays in NSG mice, covering cetuximab-sensitive and resistant cancer cell lines. Preliminary pharmacokinetics and safety studies were conducted in cynomolgus monkeys.
Results: SM2235 exhibits sub-nanomolar affinity for EGFR+ human cancer cell lines and CD16A+ primary human NK cells. It partially inhibits EGFR-dependent cancer cell proliferation. Compared to cetuximab, SM2235 significantly enhances target-dependent CD16A-mediated NK cell and macrophage activation and cytotoxicity against EGFR+ cancer cells in ADCC and ADCP assays in vitro. SM2235 effectively inhibits EGFR+ xenograft tumors in vivo, irrespective of KRAS mutation status. In cynomolgus monkeys, SM2235 demonstrates excellent tolerance with a 20-hour serum half-life of approximately 20 hours and no dose-dependent skin toxicity.
Conclusions: Preclinical characterization of SM2235 shows promising in vivo efficacy against EGFR+ human cancers, regardless of KRAS mutation, with a favorable safety profile marked by minimal skin toxicity.

#1343 BSI-111, a highly selective anti-CD16a monoclonal antibody with potent agonist activity for building a NK cell engager platform.

J. Liu[1], W. Dai[1], H. Li[1], **X. F. Liu**[2], J. Li[1], S. Xia[1], Q. Lyu[1], H. M. Davis[2], M. Chen[1], Z. Peng[1];
[1]Biosion, Inc., Nanjing, China, [2]Biosion USA, Inc., Newark, DE

Background: Natural killer cells (NK) are innate lymphocytes endowed with the ability to recognize and kill cancer cells. CD16a, a well-characterized activating receptor predominantly expressed on NK cells, is a low-affinity receptor for the IgG Fc domain and is crucial for stimulating NK cell-mediated tumor cell killing. Unlike CD16a, CD16b is mainly expressed on granulocytes as a GPI-anchored receptor and is not involved in the lysis of tumor cells although CD16a and CD16b share 97% sequence identity in their extracellular domains. Due to the high homology of extracellular domains of CD16a and CD16b, it is extremely challenging to develop CD16a-specific agonistic antibodies without binding $CD16b^{\pm}$ granulocytes, the most abundant subset in leukocytes. Here we report the development of an anti-CD16a-specific monoclonal antibody with potent NK cell activation.

Experimental procedures: Humanized mice were immunized with recombinant CD16a-ECD-Fc. The Biosion proprietary H^3 (High-throughput, High-content and High-efficiency) antibody screening platform was used to identify an anti-CD16a monoclonal antibody lead candidate - BSI-111. The target binding specificity, binding activity, and affinity of BSI-111 were evaluated by protein-based ELISA, cell-based FACS and Biacore-based SPR. A cell-based agonist reporter assay and a primary NK cell activation assay were used to evaluate the bioactivity of BSI-111.

Summary: BSI-111 is a fully human monoclonal antibody with the following critical properties: (1) specifically binds to CD16a without recognizing CD16b; (2) binds the two allelic variants of CD16A - 158F and 158V with similar high affinities; (3) shows cross-reactivity to cynomolgus CD16a; (4) can significantly activate NFAT signaling in a cell-based reporter assay; (5) exhibits strong activity on activating primary NK cells; and (6) has potentially longer half-life and silenced Fc-effector function through Fc-engineering.

Conclusion: BSI-111 demonstrates great biophysical properties and functional characteristics, supporting the development of anti-CD16a-based NK cell engagers for potential benefit of cancer patients.

#1344 Improvement of the anti-tumor activity of NK cells and the efficacy of anti-CD20 monoclonal antibodies in the therapy of B cell-derived malignancies..

A. Zerrouqi[1], A. Zdanowicz[1], A. Torun[1], A. Ciechanowicz[1], B. Pradhan[1], G. Rymkiewicz[2], D. Efremov[3], **B. Pyrzynska[1]**;
[1]Medical University of Warsaw, Warsaw, Poland, [2]Maria Sklodowska-Curie National Research Institute of Oncology, Warsaw, Poland, [3]International Centre for Genetic Engineering and Biotechnology, Trieste, Italy

Resistance of tumor cells to immunotherapy with monoclonal antibodies (mAbs) often relies on the reduced level of the antigen targeted by the particular mAb. We have therefore screened for the compounds able to upregulate selected antigens on the surface of lymphoma/leukemia cells, to minimize the possibility of resistance acquired by the tumor cells. We have found that members of a specific class of antibiotics, known as cation carriers, namely salinomycin (SAL), monensin (MON), narasin, and nigericin exhibit great CD20 antigen-upregulating abilities. A variety of Burkitt's lymphoma and diffuse large B-cell lymphoma (DLBCL) cell lines as well as patients-derived primary malignant cells, such as DLBCL and chronic lymphocytic leukemia (CLL) cells exhibited upregulation of surface CD20 upon the treatment with SAL and MON at concentrations as low as 250nM and 50 nM, respectively. As a consequence, these compounds appeared to be beneficial for the therapy of lymphoma/leukemia with anti-CD20 mAbs, both *in vitro* and in animal models.Moreover, the proteomics analysis revealed that besides CD20, cation carriers upregulated a number of different proteins on the surface of tumor cells, including proteins implicated in the interaction with immune cells. These included ICAM1, HLA-A/B/C, CD155, CD80, CD86 and ULBP2/5/6. Particularly important appears to be the upregulation of antigens interacting with the activating receptors on NK cells, helping them to overcome the inhibitory signals and stimulate the lysis of tumor cells. Thus, the results of proteomics analysis explained why SAL- or MON-pretreated tumor cells were efficiently eliminated by NK cells, even in the absence of therapeutic mAb. In light of our discoveries, it seems reasonable to consider the cation carriers as promising drug candidates for the improvement of NK cell anti-tumor activity and potential treatment of B-cell non-Hodgkin lymphoma patients, in combination with anti-CD20 mAbs.Funding: National Science Centre (NCN, Poland), grants 2019/35/B/NZ5/01445 and 2020/39/B/NZ6/03513.

#1345 NAV-201, an orally bioavailable small molecule NK cell activator enhancing antibody-mediated cancer therapies.

N. C. Nicolaides, L. Grasso, J. Kline;
Navrogen, Glen Mills, PA

Tumors employ a number of mechanisms to suppress a patient's immune anti-tumor responses. Recently, we uncovered an immunosuppression mechanism that tumors employ to avoid humoral immune responses that involves tumor-produced proteins, called Humoral Immuno-Oncology (HIO) factors. These HIO factors are able to suppress antibody-mediated tumor cell killing via direct binding to antibodies that alter their Fc domain interactions with the C1q protein to suppress complement dependent cytotoxicity (CDC) and reduce antibody engagement with CD16a Fc receptors on immune-effector cells, including NK cells, to suppress antibody dependent cellular cytotoxicity (ADCC). HIO factor immunosuppression of ADCC appears to involve the reduced binding affinity of antibody to CD16a Fc receptors. In an attempt to identify agents that may enhance antibody-CD16a binding affinity to overcome HIO factor immunosuppression, we sought to identify agents that can restore this interaction by screening natural small compound libraries via an IgG1-CD16a based ELISA assay. One lead compound was identified that was subsequently optimized by structural activity relationship analysis. This compound, named NAV-201, specifically binds CD16a and enhances the affinity of antibody binding to both the low affinity CD16a-158F and high affinity CD16a-158V allotypes. Moreover, we found that NAV-201 can also bind to the mouse CD16a ortholog and enhance its antibody binding affinity, making NAV-201 suitable for efficacy testing in mouse models. *In vivo*, NAV-201 was found to be well tolerated up to at least 120 mg/kg when administered orally and daily to mice, have a serum half-life of 18 hours, enhance systemic levels of the NK cell produced INF-γ and TNF-α cytokines, and enhance the therapeutic efficacy of antibodies in mouse xenografts. Together, these data support the further development of NAV-201 for human testing to improve and/or enhance the efficacy of antibody-based therapies in HIO factor positive cancers.

#1346 Combined role of interleukin-15 stimulated natural killer cell-derived extracellular vesicles and carboplatin in Osimertinib resistant H1975 lung cancer with EGFR mutations.

A. Nathani[1], L. Sun[2], I. Khan[1], M. Aare[1], A. Bagde[1], Y. Li[3], M. Sachdeva[1];

[1]Florida A&M University College of Pharmacy & Pharmaceutical Sciences, Tallahassee, FL, [2]Florida State University, Tallahassee, FL, [3]FAMU-FSU College of Engineering, Tallahassee, FL

Extracellular vesicles (EVs) derived from immune cells (e.g., NK cells, dendritic cells) may be able to treat malignancies that are resistant to other treatments (e.g., chemotherapy) relying on the hypothesis that EVs carry almost the same cargo of the parent cells. In this study, we evaluated IL-15 stimulated natural killer cell-derived EVs (NK-EVs) as therapeutic agents in vitro and in vivo in Osimertinib resistant lung cancer (H1975R) with EGFR mutations(L858R). NK-EVs were isolated by ultracentrifugation and nanoparticle tracking analysis revealed a size distribution of 89.5 ± 3.4 nm, zeta potential of -31.38 ± 0.25 mV. Atomic force microscopy imaging revealed vesicles with a spherical form and comparable sizes, meeting the criteria of exosomal EVs. Further, western blot studies demonstrated the presence of regular EV markers along with specific NK markers (perforin and granzyme). EVs were also characterized by using proteomic analysis which demonstrated that EVs had proteins for natural killer cell mediated cytotoxicity (Granzyme B) and T cell activation (Perforin and Plastin-2). Gene oncology (GO) analysis also showed that these are differentially expressed proteins (DEPs) that are involved in programmed cell death and positive regulation of cell death. Further, isolated NK-EVs ($1*10^{11}$ particles/mL) were cytotoxic to H1975R cells in vitro with 55% and 68% cell viability in 2D and 3D cell cultures respectively against control. Carboplatin's IC_{50} was reduced by approximately 1.9 and 1.7-fold (p less than 0.001) in 2D and 3D cell culture respectively when combined with NK-EVs. The EVs were then combined with carboplatin (25 mg/kg) and administered by i.p. route to H1975R tumor xenografts and significant reduction in tumor volume in vivo (≈1000 mm^3 compared to ≈2000 mm^3 of control group, p less than 0.001) was observed after 10 days. Our findings show for the first time that NK-EVs target the PD-L1/PD-1 immunological checkpoint and induce apoptosis and anti-inflammatory response by downregulation of SOD2, PARP, BCL2, SET, NF-κB and TGF-ß. MicroRNAs regulating cytotoxic proteins like perforin, granzyme and plastin were also identified using sequencing and the miRNAs: hsa-miR-5193/149-5P/3133/193-5p are picked for further studies. These miRNAs have been encapsulated in NK-EVs by electroporation and will be evaluated against Lung PDX xenografts along with carboplatin loaded NK-EVs. These miRNAs are directly involved in T cell or NK cell mediated cytotoxicity and are being currently investigated. The ability to isolate functional NK-EVs on a large scale and using them with platinum-based drugs may lead to new clinical applications. The results of the present study suggest the possibility of the combination of NK-cell-derived EVs and carboplatin as a viable immunochemotherapeutic strategy for resistant cancers.

IMMUNOLOGY: Immune Checkpoints and Inhibitory Molecules 1
Poster Session

#1350 KD6001: A promising new anti-CTLA-4 human monoclonal antibody for cancer therapy.

Y. Chen[1], P. Li[2], G. Fang[2], H. Wu[2], C. Zhang[2], Z. Cai[1];
[1]Shanghai Kanda Biotechnology Co. Ltd., Shanghai, China, [2]Shanghai Celgen Bio-Pharmaceutical Co. Ltd., Shanghai, China

Cytotoxic T lymphocyte antigen-4 (CTLA-4) is a crucial immune checkpoint that negatively regulates T cell activation. Inhibiting this negative regulation through CTLA-4 blockade has emerged as a promising therapeutic strategy against cancer. Herein, we present the preclinical pharmacology study of KD6001, a novel anti-CTLA-4 IgG1 kappa human monoclonal antibody with superior properties compared to ipilimumab, a currently approved anti-CTLA-4 mAb. Surface plasmon resonance (SPR) analysis revealed that KD6001 exhibits a higher affinity for CTLA-4 compared to ipilimumab (KD = 0.57 nM vs 1.20 nM). Competition ELISA experiments demonstrated that KD6001 is significantly more potent than ipilimumab in disrupting CTLA-4 interactions with CD80 (IC50 = 16 ng/mL vs 93 ng/mL) and CD86. Further, amino acid point mutation analysis indicated that two specific residues following the CD80/CD86 binding site (99MYPPPY104) are critical for ipilimumab binding, whereas mutation of the two residues had minimal impact on KD6001's CTLA-4 binding activity. These findings suggest that KD6001 and ipilimumab bind distinct epitopes on CTLA-4. In vitro experiments demonstrated that KD6001 enhances the production of IL-2 and IFNγ in PHA-activated human lymphocytes and exhibits synergistic anti-tumor effects when combined with anti-PD-1/L1 antibodies. Moreover, in vivo studies utilizing syngeneic murine tumor models established in human CTLA-4 gene knock-in mice revealed that KD6001 effectively inhibits or delays tumor growth in colon cancer MC38, melanoma B16, and hepatocellular carcinoma Hepa1-6 models. Additionally, KD6001 demonstrated synergistic anti-tumor effects when combined with a mouse anti-PD-1 antibody or ibuprofen. Toxicity evaluation in cynomolgus monkeys revealed that KD6001 was generally well-tolerated at doses ranging from 1 mg/kg to 10 mg/kg administered intravenously once weekly for four weeks. The primary pathological changes observed were lymphocyte/monocyte infiltration or increased lymphocyte/monocyte infiltration in several organs, consistent with KD6001's mechanism of action. Notably, the similar affinity of KD6001 for human and cynomolgus monkey CTLA-4 suggests that the toxicity profile observed in monkeys accurately reflects the dose-toxicity relationship in human. The promising preclinical data presented herein support the further clinical development of KD6001 as a potential therapeutic agent for cancer treatment. Currently, clinical trials evaluating KD6001 in patients with advanced melanoma are ongoing.

#1351 Preclinical characterization of BMS-986288, a novel non-fucosylated (NF) anti-cytotoxic T lymphocyte antigen-4 (anti-CTLA-4) Probody® therapeutic.

A. Jhatakia[1], M. Nasser[1], A. Mukhopadhyay[1], K. Kang[1], C. Newsome[2], N. Gupta[1], R. Z. Mandawe[1], F. Findeisen[1], J. A. Lohre[1], L. Leung[1], Y. Wei[1], J. Dobroff[1], K. Price[2], J. Engelhardt[1], M. Selby[1], A. J. Korman[1], N. Wilson[1];

[1]Bristol Myers Squibb, Redwood City, CA, [2]Bristol Myers Squibb, New Brunswick, NJ

Introduction: Blockade of the CTLA-4 pathway with ipilimumab (IPI), alone and in combination with nivolumab (anti-programmed death-1 antibody), has shown clinical benefit in multiple tumor types. However, not all tumors respond to IPI ± nivolumab, and peripheral effects can lead to immune-related adverse events. To enhance the therapeutic index of CTLA-4-directed therapy, a proprietary Probody® therapeutics technology platform was used to develop a modified version of IPI. BMS-986288 is an anti-CTLA-4 antibody that combines a Probody® therapeutic masking peptide and protease-cleavable linker, designed to localize anti-CTLA-4 activity to the tumor microenvironment, with an NF Fc region hypothesized to enhance antigen-presenting cell (APC)-mediated T-cell priming and regulatory T cell (Treg) modulation via increased binding to the FcγRIIIA (CD16) receptor. Here, we present the characterization of the mechanism of action and pharmacodynamic (PD) response of BMS-986288 in preclinical models.

Methods: APC-mediated T-cell priming and antigen-specific responses were evaluated in a superantigen model using peripheral blood mononuclear cells (PBMCs) and human CTLA-4 knock-in (KI) mice. Antitumor activity and immune cell population changes were assessed in an MC38 tumor model implanted in human CTLA-4 KI mice. Intratumoral Treg depletion was further investigated using patient-derived dissociated tumor samples as a physiologically relevant model. Peripheral PD effects and tolerability of BMS-986288 were evaluated in a non-human primate (NHP) Ad5 vaccine model.

Results: Protease-cleaved BMS-986288 demonstrated enhanced APC-mediated T-cell priming compared with IPI in superantigen-stimulated PBMCs. Similarly, administration of superantigen staphylococcal enterotoxin B (SEB) peptide elicited an increased antigen-specific T-cell receptor (Vβ8+) T-cell response after treatment with cleaved BMS-986288 vs IPI in human CTLA-4 KI mice. In the MC38 tumor-bearing mouse model, BMS-986288 showed enhanced antitumor activity as compared to IPI, with tumor clearance in all mice. Although BMS-986288 enhanced intratumoral CTLA-4+ Treg depletion in the MC38 model, limited Treg depletion was observed in the patient-derived dissociated tumor model with an NF anti-CTLA-4 antibody without the masking peptide, potentially reflecting differences in CTLA-4 expression on human vs mouse Tregs. BMS-986288 reduced PD effects in the peripheral blood compartment and increased tolerability in NHP relative to IPI.

Conclusion: BMS-986288 leverages unique characteristics to differentiate it from IPI, enhancing APC-mediated T-cell priming and anti-tumor activity while also reducing peripheral activity in preclinical models. These data support an ongoing phase 1/2 clinical trial of BMS-986288 (NCT03994601) in patients with advanced solid tumors.

#1352 Computational design of a cyclic peptide that inhibits the CTLA4 in T cells and the growth of lung carcinoma in mice.

R. Thakkar[1], D. Upreti[2], S. Ishiguro[2], G. Magnin[2], K. Sudasinghe[2], A. Hall[2], **S. DeVader**[2], M. Tamura[2], J. Comer[2];
[1]University of California, Berkeley, CA, [2]Kansas State University, Manhattan, KS

Proteins involved in immune checkpoint pathways, such as CTLA4, PD-1, and PD-L1, have become important targets for cancer immunotherapy; however, the development of small molecule drugs targeting these pathways has proven difficult due to the nature of their protein-protein interfaces. Here, using a hierarchy of computational techniques, we designed a cyclic peptide that binds CTLA4 and follow this with experimental verification of binding and biological activity, using bio-layer interferometry, cell culture, and a lung cancer mouse model in immunocompetent mice. Beginning from a template excised from the x-ray structure of the CTLA4:B7-2 complex, we generate several peptide sequences using Rosetta, a protein modelling program. These peptides are cyclized head-to-tail to improve structural and proteolytic stability and screened using molecular dynamics simulation and MM-GBSA calculation. The standard binding free energies for shortlisted peptides are then calculated in explicit-solvent simulation using a rigorous multistep Binding Free Energy Estimator (BFEE). The most promising peptide, cyc-EIDTVLTPTGWVAKRYS (hereafter CTLA4-ip), yields the standard free energy -6.6 ± 3.5 kcal/mol, which corresponds to a dissociation constant of 15 μmol/L. The binding affinity of this peptide for CTLA4 is measured experimentally (31 ± 4 μmol/L) using bio-layer interferometry. Pharmacokinetics of CTLA4-ip in a cell culture with Lewis lung carcinoma (LLC) cells and in mice revealed that this peptide is significantly more stable in both cell culture and in mice as compared to a control non-cyclic scrambled-sequence. Treatment with CTLA4-ip inhibited cancer cell growth in a co-culture of LLC cells and LLC cell-antigen primed murine T cells. Intraperitoneal administration of the CTLA4-ip (10mg/kg/day, every other day totaling 4 doses) markedly inhibited lung tumor growth in mice with an orthotropic LLC allograft model. Efficacy of the tumor growth inhibition by the CTLA4-ip was similar to that by an anti-PD-L1 antibody (10mg/kg/day, every two days totaling 3 doses). These results strongly suggest that this novel CTLA4-ip works as an immune checkpoint inhibitor to CTLA4 and is usable for lung cancer treatment. This research was supported by Kansas State University Johnson Cancer Research center (MT), Midwest Biomedical Accelerator Consortium (MT, JC), National Cancer Institute MT, JC) and the National Science Foundation (JC).

#1353 Potentiating salvage radiotherapy in radiorecurrent prostate cancer through anti-CTLA4 therapy: Implications from a syngeneic model.

H. Wang[1], L. Gong[1], X. Huang[2], S. D. White[1], H. T. Chung[3], D. Vesprini[3], T. N. Petchiny[1], E. Fokas[4], H. He[1], R. S. Kerbel[5], S. K. Liu[6];
[1]University of Toronto, Toronto, ON, Canada, [2]Sunnyrook Research Institute, Toronto, ON, Canada, [3]Sunnybrook Health Science Centre, Toronto, ON, Canada, [4]Goethe University Frankfurt, Frankfurt, Germany, [5]Sunnybrook Research Insitute, Toronto, ON, Canada, [6]Sunnybrook Research Institute, Toronto, ON, Canada

Background: Advanced prostate cancer (PCa) is a leading cause in cancer death and can elicit significant morbidity and mortality. A common treatment modality for advanced PCa is radiation therapy (RT). Currently, salvage of local disease recurrence after RT is a major clinical problem. Emerging evidence indicates the importance of the immune system in governing RT response. In support of this, immune checkpoint inhibitors (ICIs), which enhance immune activation, have demonstrated clinical therapeutic promise in combination with RT in certain advanced cancers. Irradiation (IR) combined with ICIs may prime the immune system to recognize and target recurrent cancer.
Purpose: Investigate the therapeutic efficacy of ICIs in combination with RT for radiorecurrent PCa in a syngeneic pre-clinical model.
Methods: TRAMP-C2 cells were treated with 10 Gy of radiation over 5 fractions (similar to clinical hypofractionated (HF) schedule) to generate TRAMP-C2 HF cells. Immune-competent mice were transplanted subcutaneously with TRAMP-C2 HF cells. Once tumors reached palpable size, mice were administered either ICIs (anti-PDL1 or anti-CTLA4) alone or in combination with RT. Tumor volume was monitored to determine the treatment effect. Correlative studies on excised tumors and secondary lymphoid organs included flow cytometry and NanoString gene expression panel to evaluate immunological mechanisms that contribute to anti-tumor effects.
Results: TRAMP-C2 HF cells were validated for radiation resistance and exhibited a more aggressive phenotype (reduction in senescence, increase in clonogenicity) similar to clinically recurrent PCa. Radiation resistance of TRAMP-C2 HF tumors was validated in vivo. Administration of anti-PDL1 and anti-CTLA4 as monotherapy or in combination did not achieve significant tumor growth delay compared to control. IR alone produced an observable tumor growth delay compared to ICIs alone. The combination of anti-PDL1 and IR did not yield additional growth delay compared to IR alone. Strikingly, significant tumor growth delay was seen with the combination of IR and anti-CTLA4 compared to IR alone, while also resulting in complete cure in a third of the mice. mice. Lymph nodes and tumors from mice treated with IR and anti-CTLA4 vs. IR and isotype control demonstrated differential expression of genes in T cell functions and enrichment in both CD4+ and CD8+ T cell populations.
Conclusion: We generated the first syngeneic radiorecurrent PCa model and demonstrated that combining anti-CTLA4 and IR results in synergistic tumor response. Combined therapy resulted in augmented immune response, most notably enhancement of CD8 T cell activity.
Significance: These findings contribute to our understanding of immunological events associated with RT and ICIs in the context of radiorecurrent PCa and support new avenues for salvage therapy in clinical trials.

#1354 Anti-CTLA-4 generates memory T-cells with greater expansion and functionality than anti-PD-1.

S. Mok, H. Liu, N.-A. A. Anang, J. J. Mancuso, D. A. Cobanoğlu, J. P. Allison;
UT MD Anderson Cancer Center, Houston, TX

Distinct effects on T-cell differentiation arise from immune checkpoint inhibition targeting cytotoxic T-lymphocyte-associated antigen 4 (CTLA-4) and programmed death 1 (PD-1). However, the effect of these immunotherapies on the immunological memory response remains unclear. Our investigation into the effects of anti-CTLA-4 and anti-PD-1 on memory T-cell formation in mice revealed that anti-CTLA-4 generates a more effective memory antitumor response than anti-PD-1. Memory T-cells arising after anti-CTLA-4 treatment exhibit greater expansion, cytokine production, and antitumor activity than those from anti-PD-1. Notably, anti-CTLA-4 preserves more TCF-1+ T-cells during priming, while anti-PD-1 leads to more TOX+ T-cells. Experiments using conditional TCF-1- or TOX-knockout mice highlight TCF-1 is essential for memory response generated by anti-CTLA-4, whereas TOX deletion alone in T cells has no effect on response to anti-PD-1. Deepening our understanding of how checkpoint inhibition affects memory response is crucial for advancing our understanding of the enduring impacts of these immunotherapies on the immune system.

#1356 The VISTA blocking antibody HMBD-002 promotes type-I interferon signaling and drives anti-tumor responses through macrophage reprograming and cytotoxic CD8+ T cell activation.

B. Dharmadhikari, O. Zharkova, D. Thakkar, R. Tirado-Magallanes, K. Paszkiewicz, P. J. Ingram, J. D. Boyd-Kirkup;
Hummingbird Bioscience Pte Ltd, Singapore, Singapore

VISTA, a predominantly myeloid immune checkpoint, promotes an immunosuppressive tumor microenvironment and has been associated with resistance to approved checkpoint therapies. While blockade of VISTA with antibodies has shown anti-tumor efficacy in preclinical models, the biological mechanisms that underlie this effect remain poorly understood. To investigate the mechanistic basis of anti-tumor responses, we performed single-cell RNA sequencing of tumor infiltrating leukocytes from the cell-derived murine colon carcinoma xenograft model, CT26, which is known to be sensitive to VISTA blockade. We used HMBD-002, a uniquely blocking but non-depleting clinical-stage IgG4 anti-VISTA antibody, to identify the key immune cells and pathways impacted by VISTA blockade in the absence of Fc-mediated cell depletion. The translatability of these findings was validated in a human PBMC mixed leukocyte reaction assay. Subsequently, targeted depletion or inhibition of the identified immune populations and pathways was performed to confirm their contribution to the anti-tumor efficacy of HMBD-002.The blockade of VISTA by HMBD-002 significantly increased CD8+ T cells in the CT26 tumors, promoting an activated cytotoxic Tc1 program without inducing exhaustion. Concurrently, a substantial increase in proinflammatory M1 tumor-associated macrophages (TAMs) was noted within treated tumors, while other immune cell populations remained unaffected. Among the signaling pathways, the type-I interferon (IFN) response exhibited a significant upregulation, particularly in TAMs, indicating a type-I IFN-driven M1 reprogramming by HMBD-002. Validation experiments further demonstrated that the depletion of TAMs or CD8+ T cells, but not CD4+ T cells, abrogated the efficacy of HMBD-002. Moreover, blocking the type-I IFN signaling effectively impeded HMBD-002-induced TAM reprogramming and subsequent anti-tumor efficacy, thus confirming the pivotal roles of CD8+ T cells, TAMs, and type-I IFN signaling in driving the anti-tumor response to VISTA blockade. In conclusion, VISTA blockade with HMBD-002 promotes an anti-tumor response by type-I IFN mediated reprogramming of TAMs and activation of cytotoxic CD8+ T cells.

#1358 Elucidating the contribution of T cell-intrinsic VISTA to the suppression of antitumor T cell immunity.

Sachin Patnaik[1], Elizabeth Delaney[1], Cassandra Gilmour[1], Keman Zhang[1], Amin Zakeri[1], Hieu M. Ta[1], Prerana B. Parthasarathy[2], Tyler Alban[2], Timothy Chan[2], Li Lily Wang[1]

[1]Department of Translational Hematology and Oncology Research, Cleveland Clinic Foundation, Cleveland, OH,[2]Center for Immunotherapy and Precision Immuno-Oncology, Cleveland Clinic Foundation, Cleveland, OH

Immune checkpoint receptors (ICRs) negatively regulate antitumor immune responses. While significant advances have been made in understanding the mechanisms of well-established ICRs such as PD-1 and CTLA-4, other checkpoint proteins remain incompletely characterized and may be targeted to synergistically boost antitumor immunity. One such protein is V-domain immunoglobulin suppressor of T-cell activation (VISTA), an ICR whose expression curtails the function of several lymphoid and myeloid lineages, including tumor-reactive cytotoxic T cells. Globally blocking VISTA elicits potent T cell-mediated antitumor immunity and systemic myeloid cell-mediated inflammatory responses. Mechanistically, VISTA has been shown to inhibit T cell activation by acting as an inhibitory ligand on antigen-presenting cells. However, the impact of T cell-intrinsic VISTA on modulating tumor-reactive T cell responses has not been thoroughly investigated, and it remains unclear whether blocking T cell-specific VISTA is adequate for revitalizing T cell-mediated tumor control. In this study, we utilized VISTA conditional knockout mice models to examine the relative contribution of T cell-intrinsic VISTA versus myeloid-derived VISTA in the regulation of antitumor immunity. We present evidence that blocking VISTA on T cells alone is insufficient to induce strong antitumor immune responses, whereas blocking VISTA on myeloid cells counteracts its dominant role in orchestrating T cell suppression.

#1359 Rewiring CD8$^{\pm}$T cell responses to PD-1 immune checkpoint blockade in PDAC by preventing terminal exhaustion via the inhibitory receptor PSGL-1.

J. L. Hope[1], Y. Zhang[2], H. A. F. Hetrick[2], G. Romano[1], S. Roy[2], M. Lin[2], A. B. Palete[2], S. Maganti[2], D. C. Otero[2], C. Commisso[2], L. M. Bradley[2]; [1]Drexel University College of Medicine, Philadelphia, PA, [2]Sanford Burnham Prebys Medical Discovery Institute, La Jolla, CA

Pancreatic ductal adenocarcinoma (PDAC) is an aggressive, poorly immunogenic cancer with increasing incidence and a poor 5-year survival rate of 12%. PDAC tumors are refractory to all currently available treatments, including immune checkpoint blockade (ICB) therapies, and demonstrate limited infiltration of cytotoxic CD8$^{\pm}$ T cells that kill tumor cells. There is therefore an urgent, unmet need for novel therapeutic options. Analysis of single-cell RNA-sequencing data of patient PDAC revealed high expression of the novel immune checkpoint, PSGL-1, on infiltrating CD8$^{\pm}$ T cells. We hypothesize that PSGL-1-mediated immune suppression is a critical barrier to effective anti-tumor immunity in PDAC. To test this, we utilized a preclinical model of PDAC where orthotopic injection of the KPC.4662 tumor cell line into pancreata recapitulates patient tumor responses with limited T cell infiltrates and uncontrolled tumor growth in C57BL/6 (wildtype) control mice and compared to PSGL-1^{KO} (C57BL/6 background) mice. At endpoint, tumor burden in PSGL-1^{KO} mice was reduced by >50% compared to controls, with 45% of PSGL-1^{KO} animals exhibiting >70% reduction. Total immune infiltration (CD45$^{\pm}$) was 2-fold greater in tumors from PSGL-1^{KO} mice, with a significant increase in infiltrating CD3$^{\pm}$ T cells. Detailed analyses revealed that infiltrating CD8$^{\pm}$ T cells from PSGL-1^{KO} mice were not only more abundant, but also less differentiated towards terminal exhaustion with sustained TCT-1 expression compared to controls. Moreover, PSGL-1^{KO} mice showed protection against metastatic disease. Since our data support a critical role for T cell driven anti-tumor immunity to PDAC, we transiently depleted CD4$^{\pm}$ T cells, CD8$^{\pm}$ T cells, or both just prior to tumor cell implantation. While depletion of CD8$^{\pm}$ T cells did not impede tumor control by PSGL-1^{KO} mice, depletion of all T cells or only CD4$^{\pm}$ T cells resulted in the loss of PDAC tumor growth inhibition, demonstrating a key role of CD4$^{\pm}$ cells in the response. Given our previous studies demonstrating an intrinsic role for PSGL-1 in development of terminal T cell exhaustion in melanoma, including loss of TCF-1$^{\pm}$ CD8$^{\pm}$ T cells, we hypothesized that PSGL-1-deficiency would promote responsiveness to PD-1 ICB, which is ineffective as a monotherapy in PDAC patients and mouse models. To test this prediction, PD-1 ICB was therapeutically administered to control and PSGL-1^{KO} mice. While treatment with anti-PD-1 had no effect on the tumor growth in the control animals, PD-1 ICB resulted in complete tumor ablation in 85% of PSGL-1^{KO} animals, demonstrating a profound synergistic effect of PD-1 inhibition in the absence of PSGL-1. From these studies, we conclude that PSGL-1 is a critical inhibitor of T cell anti-tumor responses in PDAC. PSGL-1 therefore represents a novel ICB target with high translational potential for promoting immune responses to PDAC tumors.

#1360 TIGIT blockade combined with local radiotherapy and PD-1 blockade in a murine triple-negative breast cancer model.

S. Kim[1], S. Jeon[2], I. Kim[2],

[1]Integrated Major in Innovative Medical Science, Seoul, Korea, Republic of, [2]Seoul National University Bundang Hospital, Seongnam, Korea, Republic of

Background: Immune checkpoint blockades (ICB) improve outcomes of patients with some solid tumors such has melanoma and lung cancer, however the efficacy of ICB alone showed limited efficacy in many other tumors such as breast cancer. Radiation therapy is a promising combination partner of ICB as a strong immune stimulator so called *in situ* tumor vaccine, however it also can increase immune suppressive repertoires. TIGIT (T cell Immunoglobulin and ITIM domain) is an inhibitory receptor expressed on activated T cells and NK cells. We evaluated the effects of TIGIT blockade in addition to local RT and PD-1 blockade as a strategy to overcome therapeutic resistance of ICI in a murine breast cancer model. Materials and Methods: 4T1-Luc tumors were treated with various strategies including control, RT, anti-PD-1, anti-TIGIT, RT+anti-PD-1, RT+anti-TIGIT, anti-PD-1+anti-TIGIT, and RT+anti-PD-1+anti-TIGIT. A total of 24 Gy in 3 fractions at 1 week was delivered to the tumor at hindlimb (primary tumor) while the tumor at flank (secondary tumor) was left unirradiated. 10 mg/kg of anti-PD-1 blocking antibodies and 10 mg/kg of anti-TIGIT blocking antibodies were intraperitoneally injected for 6 times for 2 weeks. Flow cytometry, IHC staining, and ELISA were performed to assess the immunologic status after treatments.

Results: The triple combination therapy (TCT) group showed the most superior growth delay of primary and secondary tumor growth among treatments. The number of metastatic lung nodule was significantly reduced by TCT as well. Plasma levels of interferon-β and interferon-γ were the highest after TCT. Moreover, TCT significantly increased the proportion of splenic $CD8^+$ dendritic cells among myeloid cells, and effector-memory ($CD44^+CD62L^-$) cells among splenic $Foxp3^-$ non-regulatory $CD4^+$ and $CD8^+$ T cells. Furthermore, expression of CD226, which is an activating counter-receptor of TIGIT, on splenic $CD8^+$ T cells was elevated by TIGIT blockade, possibly suggesting the activation of systemic immune response by addition of TIGIT blockade to local RT and PD-1 blockade. Meanwhile, TCT decreased splenic $Foxp3^+$ regulatory T cells, as well as the expression of CD39 on splenic $Foxp3^+$ regulatory T cells. The increase of $CD8^+$ T cell infiltration in primary and secondary tumors was most prominent in TCT group.

Conclusion: TIGIT blockade elicits systemic immune responses in a murine triple-negative breast cancer model. when combined with local RT and PD-1 blockade, which were correlated with significant delay in the growth of both irradiated and unirradiated tumors. These results suggest that TIGIT blockade could be a viable approach to increase the efficacy of RT and immune checkpoint inhibitors in breast cancer which is a relatively immunologically cold tumor. (Work supported by a grant from National Research Foundation of Korea #2023R1A2C3003782 to In Ah Kim).

#1362 IOMX-0675, a LILRB1 and LILRB2 cross-specific antibody, effectively repolarizes immunosuppressive myeloid cells and activates T cells leading to potent tumor cell killing.

C. Hartl, J. Zantow, I.-P. Maser, M. Stebegg-Wagner, S. Friedrich, J. Schilz, S. Kaden, R. Milde, E. Korotkova, M. Maraslis, B. Langer, M. Swiat, C. Ginzel, C. Ammerhauser, L. Albert, L. Majunke, A. Huth, K. Sudan, M. Yule, C. Rothe, H. Loferer, M. Aigner, A. Marziale, **S. Bissinger**;
iOmx Therapeutics AG, Martinsried / Planegg, Germany

Recently, myeloid checkpoints in the tumor microenvironment have gained increased attention in the context of tumor immune evasion. LILRB1 (ILT2) and LILRB2 (ILT4) are immunosuppressive receptors of the leukocyte immunoglobulin-like receptor (LILR) family that recognize both classical and non-classical MHC-I molecules (e.g., HLA-G). While tumor-infiltrating myeloid cells express both LILRB1 and LILRB2, lymphoid cells are restricted to LILRB1 expression. LILRB1 and LILRB2 are frequently co-expressed with immune-activating LILR family members LILRA1 and LILRA3 in several tumor indications and upregulated in patients non-responsive to T cell checkpoint blockade. Furthermore, the non-classical MHC-I molecule HLA-G, a major ligand of LILRB1 and LILRB2 in the tumor environment, is overexpressed and associated with poor prognosis in multiple solid cancer types.
IOMX-0675, a fully human, Fc-silenced, monoclonal immunoglobulin G1 (IgG1) antibody with a highly differentiated binding profile, that binds selectively with high affinity to the inhibitory receptors LILRB1 and LILRB2, while binding only weakly to the closely related immune-activating LILR family members LILRA1 and LILRA3, was identified from iOmx' proprietary phage display library. A high-resolution Fab-based Octet assay was established to monitor the IOMX-0675-mediated blocking of LILRB1 or LILRB2 binding to HLA-G. The LILRB1/2 cross-specific antibody promotes phagocytic and pro-inflammatory activity of various macrophage subtypes, which was monitored by flow cytometry and cytokine profiling. In co-cultures of monocyte-derived macrophages with autologous T cells, IOMX-0675 shows high potential to reprogram dose-dependently immunosuppressive macrophage, to further activate pro-inflammatory macrophage subtypes and thereby rescues the activity of the lymphoid immune compartment. Even in environments dominated by LILRA1/A3, IOMX-0675 shows a strong binding capacity to the immunosuppressive LILRB1/B2 receptors and significantly repolarizes the immune environment.
In summary, we discovered IOMX-0675, a cross-specific antibody antagonizing both LILRB1 and LILRB2 with high selectivity, that exhibits potent reprogramming of the immunosuppressive myeloid compartment and restores cytotoxic T cell activity in the tumor microenvironment. Negligible binding to immune-activating LILR family members by IOMX-0675 could unleash full anti-tumor activity. The differential binding profile of IOMX-0675 provides best-in-class potential and may maximize anti-tumor efficacy for the benefit of patients with high-unmet medical need, who are resistant to T cell checkpoint blockade.

#1363 Blocking inhibitory receptor ILT3 by an antibody with enhanced Fc function promoted adaptive immunity against hematopoietic malignancy independent of ADCC.

S. Ye[1], D. Zhang[1], M.-Z. Wu[1], H. Raghu[1], D. Cohen[1], M. Romero[1], S.-S. Tan[1], D. Choi[1], J. Hickson[2], J. Engelhardt[1], A. Shoemaker[2];
[1]AbbVie Bay Area, South San Francisco, CA, [2]AbbVie Inc., North Chicago, IL

Immunoglobulin-like transcript 3 (ILT3) is an inhibitory receptor that is expressed by mature monocytes, dendritic cells (DC), plasma blasts, and the malignant cells arising thereof including acute myeloid leukemia (AML), B cell lymphoma and multiple myeloma (MM). We developed an anti-ILT3 blocking monoclonal antibody (mAb) 17G8 to test the hypothesis that blockade of ILT3 on hematopoietic malignant cells might drive anti-cancer responses through several mechanisms such as cell migration, ADCC, and T cell driven immune responses. Blockade of ILT3 using 17G8 without Fc effector function impaired AML cell line THP1 dissemination into distant sites *in vivo* and using 17G8 with enhanced Fc function through afucosylation further reduced the tumor burden. This effect of afucosylated 17G8 appears to be mediated by a mechanism other than ADCC, since afucosylated 17G8 showed modest tumor inhibition in ICR mice carrying ILT3 positive AML and MM xenografts. In immune competent mice carrying murine syngeneic AML cell C1498 expressing human ILT3, 17G8 also showed modest anti-tumor effects as a single agent, however, when combined with anti-PD1, afucosylated 17G8 increased $CD8^{+}$ effector memory T cells, reduced proportion of cells with an exhausted phenotype and significantly improved survival when compared to different controls. Since T cells don't express ILT3, the effects of 17G8 on T cells are hypothesized to be mediated by blocking ILT3 expressed on myeloid cells. The expression of ILT3 on immature human monocyte-derived DC (moDC) is higher than on mature moDC. Blocking ILT3 with afucosylated 17G8 on immature moDC potentiated maturation of moDC when compared to the controls *in vitro*. Surprisingly, afucosylated 17G8 stimulated IFNγ production from moDC during maturation. The enhanced DC function induced by afucosylated 17G8 was subsequently found to be translated into enhanced T cell function in an allogeneic mixed lymphocyte reaction (allo-MLR) assay, in which afucosylated 17G8 significantly increased IFNγ production when combined with anti-PD1. The activation of effector T cells was also monitored through a cytotoxicity assay by mixing THP-1 cells with human PBMC in culture. Afucosylated 17G8 induced strong cytotoxicity on THP-1 cells with minimal effects on normal ILT3 positive cells such as monocytes or moDC, suggesting that blockade of ILT3 with afucosylated 17G8 induced more potent T cell mediated allogeneic cytotoxicity than innate cell mediated ADCC killing. In summary, ILT3 is a highly selective M4/M5 AML target. Developing a blocking antibody with enhanced Fc function could add an additional therapeutic strategy of inducing host anti-tumor immunity to current AML treatments which induce direct tumor killing, such as chemotherapy, targeted therapy, and antibody drug conjugate.

#1364 Characterization of CHS-1000, an Fc-modified anti-ILT4 monoclonal antibody for reprogramming suppressive myeloid cells in solid tumors.
N. Rajasekaran, X. Wang, S. Klakamp, S. Ravindranathan, S. Tatarewicz, J. Du, B. Nguyen, K. Widmann, N. Hawkins, D. J. Chin, T. LaVallee, V. Kapoor; Coherus Biosciences Inc., Redwood City, CA

Tumor resident immunosuppressive myeloid cells play a significant role in inducing resistance to cancer immunotherapy and are associated with poor prognosis in several solid tumors. The leukocyte immunoglobulin-like receptor B2 (LILRB2), also known as ILT4, is primarily expressed on myeloid cells and is a negative regulator of myeloid cell activation. ILT4 and its primary ligands (HLA-G, HLA-A) are widely expressed in various solid tumors and are associated with disease progression, tumor metastasis and poor clinical outcome. Abrogating inhibitory signals mediated through ILT4 and its ligands is a promising strategy to reprogram suppressive myeloid cells and enhance efficacy of immune checkpoint therapies. Here we report IND-enabling preclinical characterization of CHS-1000, a novel recombinant humanized Fc-modified IgG1 antibody with attenuated Fc-gamma receptor (FcγR) binding, that specifically targets immunoglobulin-like transcript 4 (ILT4). CHS-1000 selectively binds to human ILT4 with high affinity and potently blocks ILT4 interactions with its primary ligands (HLA-A, HLA-G). Functionally, CHS-1000 promotes re-polarization of suppressive myeloid cells to a pro-inflammatory phenotype and enhances activation of dendritic cells and T cells. Combinations of CHS-1000 with PD-1 inhibitors or other immunotherapy agents hold particular promise for enhanced anti-tumor activity. These preclinical characterization data support clinical development of CHS-1000 in combination with toripalimab (a commercial stage anti-PD-1 antibody) as an immunotherapy treatment for patients with solid tumors.

#1365 INB03: a new immune checkpoint inhibitor that reprograms macrophage polarization, boosts ADCP and reverts T-cell exhaustion markers.

S. Bruni, M. F. Mercogliano, R. Schillaci;
Instituto de Biologia y Medicina Experimental, Buenos Aires, Argentina

Trastuzumab resistance is an important clinical issue in HER2+ breast cancer (BC), and few actionable targets are available. We demonstrated that soluble TNF (sTNF) upregulates mucin 4 (MUC4) expression, which shields trastuzumab epitope on HER2 hindering its therapeutic effect, and that sTNF blockade with INB03 decreases MUC4 expression which, together with trastuzumab, triggers an effective antitumor immune response based on antitumoral macrophage-NK cell collaboration. Because immune checkpoint molecules (ICP) and T cell exhaustion foster tumor immune escape, we addressed whether INB03 could modulate macrophage polarization, T cell exhaustion, and ICP expression in both populations to boost an antitumor immune response. For *in vitro* assays, human monocytes and T cells were isolated from buffy coats and enriched with specific RosetteSep. Macrophages (Mϕ) were differentiated for 6 days with M-CSF (10 ng/ml) to M0, and polarized for 48h to the M1-like subtype with LPS (50 ng/ml)+IFNγ (20 ng/ml), or to the M2-like subtype with IL-4 (20 ng/ml)+IL-10 (20 ng/ml). Then, INB03 was added (10 µg/ml) for 96h with corresponding cytokines to already-polarized Mϕ to test its ability to revert polarization. Also, Mϕ antibody-dependent cellular phagocytosis (ADCP) against human HER2+ breast cancer cell line JIMT-1 was assessed. T cells were activated with CD3/CD28 beads and cultured for 7 or 14 days. INB03 was added at those times for 48h to test its ability to modulate ICP and exhaustion markers. For *in vivo* assays, tumor-free mice or bearing the HER2+ C4HD tumor were treated with vehicle or INB03 (10 mg/kg, i.p.) for 21 days. Polarization, exhaustion and ICP markers were studied in Mϕ and T cells from spleen and tumor. Adding INB03 to already-polarized human Mϕ enhanced polarization towards M1-like ($CD86^{\pm}CD206^{-}$). Polarized Mϕ exposed to INB03 showed decreased PD1 and PDL-1 expression. Also, the expression of ADCP-inhibitory markers B7H4 and SIRPα was diminished when INB03 was present. These Mϕ exhibited increased ADCP against JIMT-1 cells treated with INB03, which showed downregulation of the inhibitory signal CD47. Murine Mϕ from tumor-bearing mice treated with INB03 showed increased polarization to the M1-like phenotype. Human $CD8^{\pm}$ T cells showed decreased expression of PD1, PD-L1, LAG3, TIM3 and TIGIT. However, only TIM3 and PD1 were downregulated in murine $CD8^{\pm}$ T cells of tumor-bearing mice treated with INB03. In all, sTNF blockade skews Mϕ to the M1-like phenotype and reprograms already-polarized pro-tumoral M2-like Mϕ to antitumoral ones. INB03 can tailor the tumor microenvironment by promoting Mϕ ADCP against tumor cells and by acting as an ICP inhibitor for $CD8^{\pm}$ T cells, possibly relieving their exhaustion. $HER2^{\pm}MUC4^{\pm}$ BC patients could benefit from the administration of INB03 to boost targeted therapy efficacy and overcome tumor-induced macrophage and T-cell immune escape.

#1366 Dual immune checkpoint inhibition enhances the anti-tumor activity of trastuzumab deruxtecan in preclinical models.

Liam Jenkins[1], Laura Kazlauskas[1], Matt Wilson[2], Scott A. Hammond[3], Theresa Proia[1], Jerome Mettetal[1]

[1]AstraZeneca, Waltham, MA,[2]AstraZeneca, Cambridge, United Kingdom,[3]AstraZeneca, Gaithersburg, MD

Background

Trastuzumab deruxtecan (T-DXd) is an antibody-drug conjugate (ADC) composed of an anti-human epidermal growth factor receptor 2 (HER2) antibody, a cleavable tetrapeptide-based linker, and a topoisomerase I inhibitor payload. Recent clinical trials such as BEGONIA have highlighted the potential therapeutic benefit in combining T-DXd with immuno-oncology (IO) agents such as the PD-L1 inhibitor durvalumab. Here, we report preclinical findings demonstrating enhanced anti-tumor activity when T-DXd is combined with dual immune checkpoint inhibition.

Methods

HER2-expressing human cancer cell lines were treated in vitro with T-DXd and assessed for induction of immunogenic cell death (ICD) markers and expression of NK cell-activating ligands. Human macrophages and T cells were incubated with supernatants from treated cancer cells, and their activation status evaluated via flow cytometry. In vivo, the effects of T-DXd in combination with inhibitors of PD-L1, CTLA-4, and a monovalent bispecific anti-PD-1/TIGIT antibody - a murine surrogate of rilvegostomig - on tumor growth were evaluated in BALB/c mice bearing human HER2-low EMT6 murine mammary tumors. The anti-tumor activity of T-DXd in combination with volrustomig, a monovalent bispecific antibody targeting PD-1 and CTLA-4, was also assessed in hu-CD34+ NSG mice bearing HER2-low Caki-1 renal cell carcinoma tumors.

Results

In vitro, T-DXd induced ICD via DXd-mediated extracellular release of inflammatory mediators ATP and HMGB1, and cell surface exposure of calreticulin. This was associated with a greater than 2-fold increase in expression of NK cell-activating ligands, and activation of both macrophages and T cells. In immunocompetent mice bearing human HER2 expressing EMT6 tumors, T-DXd treatment drove tumor growth inhibition (53%, P <0.001) that was associated with an increase in tumoral T cells (2.6-fold, P <0.05) and increased CD8+ T cell expression of the immune checkpoints PD-1, TIGIT, and TIM-3. Tumor growth inhibition relative to vehicle-treated mice was enhanced when T-DXd was combined with inhibitors of PD-L1 (108%, P <0.001), PD-L1 plus CTLA-4 (172%, P <0.001), or a bispecific PD-1/TIGIT inhibitor (181%, P <0.001). Pharmacodynamic analysis revealed how the combination of T-DXd and PD-1/TIGIT inhibition increased tumoral NK cells (3.2-fold, P <0.001) and CD8+ T cells (3.8-fold, P <0.001) relative to vehicle. Consistent with findings in syngeneic models, the combination of T-DXd with a bispecific PD-1/CTLA-4 inhibitor also enhanced tumor growth inhibition in a humanised Caki-1 model (121%) compared to T-DXd alone (72%) (P <0.001).

Conclusions

These data provide insight into the clinical activity observed with T-DXd and provide scientific rationale for combination strategies with novel, bispecific IO agents targeting CTLA-4 or TIGIT in addition to the PD-1/PD-L1 axis.

#1367 PD1 signaling uncovers a pathogenic subset of cytotoxic T cells.

S. Bukhari[1], S. Lerrer[1], J. Straube[2], R. Winchester[1], B. Henick[1], M. Dragovich[1], **A. Mor**[1];
[1]Columbia University Irving Medical Center, New York, NY, [2]Martin Luther University Halle-Wittenberg, Halle, Germany

PD-1 drives its fame for serving as a pivotal immune checkpoint receptor on T cells. Within the realm of cancer immunotherapy, blocking this receptor triggers the T cell activation, leading to the immune response against tumors. Conversely, in autoimmunity, PD-1 agonist is a prime candidate for effectively suppressing the T-cell-driven auto-reactivity and self-tissue damage. Despite a decade of exploration and unlike cancer immunotherapy, the efficacy of PD-1 agonists in treating autoimmunity remains a challenge. To overcome this hurdle, innovative methods must be devised to look beyond the PD-1 receptor engagement and uncover the downstream effectors involved in PD-1 signal transduction. A comprehensive genome-wide CRISPR/Cas9 screen was also conducted to pinpoint genes linked to PD-1 signaling. An in-depth exploration of genes associated with PD-1 signaling was undertaken, utilizing publicly accessible bulk and single-cell RNA sequencing datasets of patients with melanoma treated with PD-1 blockade and in patients with inflammatory arthritis. We employed flow cytometry of T cells derived from peripheral blood and synovial fluid to validate the results.Our screening process validated established regulators in the proximal PD-1 signaling pathway and unveiled an additional 1,112 unique genes associated with PD-1's capacity to hinder T-cell functions. These genes demonstrated a robust correlation with the response of cancer patients to PD-1 blockades and exhibited high scores for tumor immune dysfunction and exclusion, affirming their downstream involvement in PD-1 signaling. Functional annotation underscored the significance of these genes in established immune regulation processes. Intriguingly, T cells isolated from patients with inflammatory arthritis exhibited a significant downregulation of the same genes, emphasizing their overarching inhibitory role. Examining single-cell RNA sequencing data revealed that five specific genes, KLRG1, CRTAM, SLAMF7, PTPN2, and KLRD1, were notably downregulated in activated and effector T cells from synovial fluids. Back-gating these genes to canonical cytotoxic T cell signatures identified PD-1^{+} HLA-DR^{HIGH} KLRG^{LOW} T cells as a novel inflammatory T cell subset that should be targeted with immunotherapies. Our findings suggest that PD-1 $^{+}$ HLA-DR^{HIGH} KLRG^{LOW} T cells are promising targets for prospective PD-1 antagonists and agonists in treating inflammatory diseases. This study not only reveals novel genes linked to PD-1 downstream functions but also serves as a valuable resource, offering insights for further investigations essential to delineate the role of PD-1 within immune responses.

#1368 Novel mRNA encoding anti-PD-L1 monoclonal antibodies for cancer immunotherapy.

E. Chung, Y. Bong, R. Chen, M. Zhang, S. Long, **D. Shen**;
RNAimmune, Inc., Baltimore, MD

The difficulties with antibody-based therapies stem from their steep costs, complex procedures, and contamination risks. We investigate the use of in vitro transcription (IVT) for mRNA production, presenting a novel approach to traditional antibody treatments by promoting internal protein or antibody synthesis. We aim to create innovative mRNA-based anti-PD-L1 antibodies with strong immunotherapeutic effectiveness. The study begins with mouse immunization and hybridoma generation. Immunizing mice with the glycosylated extracellular domain of PD-L1 produces mouse antibodies against human PD-L1. Hybridomas, derived from post-immunization splenocytes, yield monoclonal antibodies screened for PD-L1 binding affinity via flow cytometry. A neutralizing assay identifies 22 antibodies with similar IC50 values and shared binding epitopes. M1, chosen for glycospecificity, affinity, and neutralizing activity, undergoes additional evaluation for the expression and anti-tumor efficacy of mRNA-encoded antibodies. The expression of M1 and atezolizumab antibodies is facilitated through an mRNA-lipid nanoparticles (LNPs) delivery system. Following intravenous administration in mice, sustained serum levels of M1 (ranging from 100 to 700 μg/mL at 24 hours post-injection) are observed. Serum concentrations of M1 and atezolizumab antibody peak at the first timepoint (24 or 48 h) after mRNA-LNP injection, respectively, and then significantly decrease within the next 4 days, with a gradual decline over the next 2 weeks. Conversely, the serum concentrations of M1 or atezolizumab protein decline significantly 24 hours post-injection and consistently stay at a baseline level (t1/2 of 94 and 4 h for M1 mRNA-LNP and protein, respectively). This indicates that the injection of encoded mRNA in mice can stably and continuously express antibodies.Administering Atezolizumab mRNA-LNP through two intravenous injections leads to a significant decrease in MC38 tumor growth, exhibiting a dose-dependent effect (TGI% = 8.1, 43.1, and 62.8 for doses of 0.2, 0.6, and 1 mg/kg, respectively). A complete tumor regression was observed up to day 19 following injection with a 2 mg/kg dose of mRNA-LNP (TGI% = 90.8%). Remarkably, a 3 mg/kg dose of atezolizumab antibody demonstrates a similar reduction in tumor growth as 0.6 mg/kg of the mRNA-LNP formulation in this model. In conclusion, this research underscores the potential of LNP-formulated mRNA as a transformative approach, converting the human body into a site for the continuous, stable expression of antibodies, offering a promising alternative to traditional protein-based therapies for combating cancer. This innovative approach shows promise in overcoming the limitations associated with traditional antibody production and clinical utilization.

#1369 PD-1 directly suppresses macrophage metabolism to restrict anti-tumor immunity in an obesity-cancer connection.

J. Bader, J. Rathmell;
Vanderbilt University Medical Center, Nashville, TN

Obesity has been established as a leading risk factor for many cancers and can drive tumor progression and metastasis. Paradoxically, obesity has in some cases been associated with better survival and improved response to immune checkpoint blockade therapies. The role of the immune system in the obesity-cancer connection and how obesity affects immunotherapy responses, however, have been unclear. Here we show that obesity enhanced PD-1 expression on macrophages to reduce phagocytosis and antigen presentation to T cells that correlated with reduced T cell expansion and function. This obesity associated immune dysfunction, however, primed for enhanced anti-tumor response to PD-1 blockade. Single cell RNAseq showed obesity remodels myeloid and T cell populations but does not impact non-immune cell populations such as fibroblasts and epithelial cells. Specifically, obesity increased the overall number of tumor-associated macrophages (TAM) while effector T cells were decreased in abundance. Interestingly, the frequency of macrophages expressing PD-1 increased, while the remaining T cells maintained similar or reduced PD-1 expression and appeared less activated. Further, T cell depletion from the tumor microenvironment, enhanced macrophage PD-1 expression and worsened PD1-associated TAM dysfunction in an obesity enhanced manor. Obesity associated cytokines and adipokines including IFN-ã, leptin and insulin induced PD-1 expression on macrophages. This expression is associated with mTOR and c-myc activation signaling pathways; as such inhibiting these signaling pathways blocked PD1 expression. Bulk RNA sequencing analysis revealed PD-1^{+} TAMs had an altered gene profile compared to PD-1^{-} TAMs. PD1 expressing macrophages exhibited increased mitochondrial respiration and expression of oxidative phosphorylation, increased lipid uptake and increased cell cycling related genes. Conversely PD1- TAMs exhibited increased phagocytosis and antigen presentation. PD-1/PDL1 interaction directly regulated TAMs, as recombinant PDL-1 reduced glycolysis and phagocytosis in purified macrophages, and these effects could be reversed with blocking PD-1 antibody. Conversely, PD-1$^{-/-}$ TAMs had reduced lipid uptake but high rates of glycolysis, phagocytosis, and expression of MHC-II. Myeloid-specific PD-1 deficiency correlated with slower tumor growth and decreased LAG3 and increased CD69 on CD8 T cells. In addition, myeloid specific PD1 deficiency enhanced TAM antigen presentation through OVA specific CD8 T cell activation. These findings identify PD-1 as a metabolic regulator in TAM dysfunction and reveal a unique PD-1 mediated and macrophage-specific mechanism for immune tumor surveillance and checkpoint blockade. This may contribute to improved immunotherapy response in TAM-enriched tumors and obesity.

#1371 SLAMF9 promotes tumor progression and immunotherapy resistance by reshaping the tumor microenvironment.

T. Fan, C. Xiao, Z. Deng, W. Cai, H. Tian, L. Wang, C. Li, J. He;
National Cancer Center/National Clinical Research Center for Cancer/Cancer Hospital, Chinese Academy of Medical Sciences and Peking Union Medical College, Bei jing, China

Tumor prognosis and immunotherapy efficacy coincides with the infiltration ratio and functional status of immune cells in the tumor microenvironment (TME). Signaling lymphocytes activating molecule factors (SLAMFs) has been reported to play a key role in regulating tumor immunity. Herein, using multi cohorts, in vitro and in vivo experiments, we showed that SLAMF9 worsens tumor and suppresses immune therapy responses by remodeling TME. A pan-cancer analysis showed that SLAMF9 had relatively high transcriptional levels within tumor tissues compared with normal tissues across most cancer types. High SLAMF9 expression is associated with poor prognosis and anti-PD-L1 therapy resistance in advanced clear cell renal cell carcinoma cohorts and metastatic urothelial cancer cohorts. SLAMF9 expression was markedly upregulated in anti-CTLA-4-resistant murine B16 melanoma compared with parental tumors. In particular, SLAMF9 expression was generally negatively correlated with CD8+T cell infiltration score in 12159 patients of 40 cancer types even using different immune cell infiltrating algorithms. Although in vitro experiments have shown that SLAMF9 knockdown has almost no effect on the malignant phenotype of tumor cells, subcutaneous melanoma and lung adenocarcinoma with SLAMF9 deficiency grew slowly, which featured with increased infiltration of CD8+T and PD-1+cells. More importantly, SLAMF9-knockdown significantly increases the sensitivity of subcutaneous melanoma to anti-CTLA-4 inhibitor or anti-PD-L1 antibodies and improved the survival benefits of tumor-bearing mice. This work highlights SLAMF9 as a new target in reshaping the tumor immune microenvironment by controlling the functional status of CD+8 T cells and to improve the efficacy of immunotherapy.

#1372 BTN1A1 regulates T cell-mediated cancer immunotherapy by interacting with Galectin-9, PD-1, and TIM3.

S. Lee, Y.-S. Kim, C. Wu, A. Park, S. S. Yoo;
STCube Pharmaceuticals Inc., Gaithersburg, MD

Butyrophilin 1A1 (BTN1A1) is a novel immune checkpoint protein belonging to the butyrophilin family and is expressed on immune cells such as macrophages, B cells, or activated CD8 T cells and in human tumors. Our results indicate that BTN1A1 and PD-L1 expression are mutually exclusive in various human solid tumors. Furthermore, it was observed that BTN1A1 had a significantly higher detection level than PD-L1 in cancer patient samples. We have reported that BTN1A1 plays an immunomodulatory role in T cell activation and proliferation. BTN1A1 inhibited the proliferation of T cells that are activated by anti-CD3 and anti-CD28 antibodies *in vitro*. Overexpression of BTN1A1 in PC3 cells also inhibits T cell-mediated killing of cancer cells. BTN1A1 is a bona fide immune checkpoint inhibitor and has anti-tumor activity in a human immune setting. BTN1A1 represents a novel cancer immunotherapy target that goes beyond the low expression levels of PD-1/PD-L1 in tumors. BNT1A1 is an immune checkpoint and cell membrane protein that, together with its binding partners, serves as a starting point for signaling pathways. The BNT1A1 complex, which has various abilities by combining with a specific partner, plays a vital role as an immune checkpoint. In this study, we identified binding partners of BTN1A that regulate immune activity in a mutually interaction relationship with BTN1A1 in various ways. We identified binding partners for the extracellular domain of human BTN1A1 using cell microarrays from Retrogenix (Whaley Bridge, UK). Through this screening approach, we found that BTN1A1 binds to galectin-1 (Gal1), galectin-9 (Gal9), and neuropilin 2 (NRP2). These three putative binding partners could specifically bind to wild-type BTN1A1 but not to this protein's unglycosylated (2NQ) form. Of these three targets, immunoprecipitation and Biacore binding assays revealed that Gal9 exhibited the greatest affinity for human BTN1A1. Since Gal9 is a known PD-1 and TIM3 binding protein, we predicted the potential formation of a BTN1A1/Gal9/PD-1 or BTN1A1/Gal9/TIM3 complex. Indeed, it reveals that immunoprecipitation and confocal microscopy assays performed using cells expressing Myc-tagged versions of these four proteins demonstrated the formation of BTN1A1/Gal9, PD-1/Gal9, TIM3/Gal9, BTN1A1/Gal9/TIM3, and BTN1A1/Gal9/PD-1 complexes. In T cell activation assay using these complexes, when present BTN1A1 alongside the complex inhibits activated T cells. As high Gal9 expression levels are correlated with poor prognosis in multiple cancers, our results highlight this BTN1A1-Gal9-PD-1 or BTN1A1-Gal9-TIM3 axis as a novel therapeutic target for immunotherapeutic drug development.

#1373 Gene expression correlation of immune checkpoint molecules Siglec-15 and PD-L1 varies widely by cancer indication.

K. Watkins, L. Diao, M. Crochiere, J. Pinkas;
Pyxis Oncology, Boston, MA

Siglec-15 is a novel target for immunotherapy in cancer and exhibits low mRNA expression in normal tissues but broad expression across cancer indications, specifically on tumor-associated macrophages and tumor cells [1]. Expression of Siglec-15 and the immune checkpoint molecule PD-L1 have previously been reported to be mutually exclusive [1][2]. However, a large-scale meta-analysis of this claim has not been undertaken across cancer indications. Here, RNA-Seq analyses were performed across single cells, cell lines, and bulk tumor samples for Siglec-15 and PD-L1 mRNA expression. Data and meta-data from TCGA, CCLE, and primary tumor samples from 62 studies were obtained through OmicSoft OncoLand and single cell analysis was performed on the BioTuring Talk2Data platform. Analyses were limited to non-small cell lung cancer (NSCLC), cholangiocarcinoma, breast, thyroid, head and neck, colon, rectal, bladder, kidney, and endometrial cancers. Expression values were binned separately into percentiles across all indications and samples in increments of 10%. These analyses revealed individual gene expression levels of Siglec-15 and PD-L1 in bulk tumor samples varied substantially by indication, while co-expression of Siglec-15 and PD-L1 varied across indications. Analysis of gene expression of Siglec-15 and PD-L1 from the TCGA database showed a positive correlation in several indications including NSCLC, head and neck, kidney, and thyroid cancers. Analyses from additional studies in primary tumor samples confirmed co-expression of Siglec-15 and PD-L1 in NSCLC and head and neck cancer. Cell lines showed a similar trend of positive correlation with varying levels of Siglec-15 and PD-L1 expression. However, when examining expression at the single cell level (not bulk tumor), in 30 single cell studies spanning >1.3M cells, only 731 cells in 20 studies were found to co-express Siglec-15 and PD-L1 on the same cell while each gene was expressed individually on other cells. The majority of the cells co-expressing the genes were macrophages (n=~350), followed by CD4 (n=~115) and CD8 T cells (n=~50). This study demonstrates that at the bulk tumor level, Siglec-15 and PD-L1 mRNA expression are not broadly mutually exclusive across cancer indications and instead expression of each gene varies broadly within a given indication. Additionally, their expression is frequently positively correlated, including in NSCLC, head and neck, kidney, and thyroid cancers. These results also demonstrate that Siglec-15 and PD-L1 are rarely found co-expressed on same cell. These associations enable a better understanding of the landscape of target expression in patients across a wide variety of cancer indications and can inform combination strategies with anti-Siglec-15 therapies. [1] Sun J, et al. *Clin Cancer Res*, 2021;27(3):680-688. [2] Wang J, et al. *Nat Med,* 2019;25(4):656-666.

#1374 Targeting CD47/SIRPα axis in urologic cancer triggers enhanced phagocytosis of tumor cell and induces tumor growth inhibition.

F. Shen, M. Praharaj, A. J. Lee, T. R. Nirschl, X. Wang;
Johns Hopkins University School of Medicine, Baltimore, MD

Signal regulatory protein-α (SIRPα; CD172a or SHPS-1) is a transmembrane molecule that highly expressed on myeloid population. Binding of CD47 (integrin-associated protein, IAP) to SIRPα inhibits phagocytosis in macrophages, which acts as a mechanism of maintaining homeostasis. Tumor cells however, often time upregulate CD47 to evade immune response. Using publicly available dataset, we found that human prostate cancer cells upregulate expression of both CD47 and calreticulin, a “eat me” signal when engaged with Low density lipoprotein receptor-related protein 1 (LRP1). In addition, macrophages, monocytes and dendritic cells in human prostate cancer do have relatively high level of SIRPα and LRP1 expression. This finding provides the rationale of targeting CD47/SIRPα axis in prostate cancer to shift the balance between pro-phagocytosis and anti-phagocytosis signaling. We then moved to RM1 and B6Cap, two syngeneic prostate cancer models in immunocompetent mice. Significant tumor growth inhibition was seen in both models with anti SIRPα blocking antibody. Furthermore, we observed in vitro that CD47 or SIRPα blockage led to enhanced PC3 cell line phagocytosis by human monocyte derived macrophages (HMDMs). Same finding was found using mouse bone marrow derived macrophages (BMDMs). We then utilized ovalbumin expressing MB49 bladder cancer cell line and cocultured those with BMDMs. CD8+ T cell from OT1 mice exhibited higher expression of activation makers when cocultured BMDMs treated by either anti CD47 or SIRPα antibody, indicating that enhanced phagocytosis subsequently increases antigen cross presentation in macrophages. In summary, we identified that CD47 is overexpressed in human prostate cancer; blocking CD47/SIRPα did inhibit tumor growth through enhanced phagocytosis and antigen presentation.

#1375 Abundance of *KLRB1*+ (CD161) T cells in anti-PD1 non responders coupled with enhanced tumor cytotoxicity of anti-CD161 (IMT-009) with anti-PD1 makes it a rational target for combination with anti-PD-(L)1 immunotherapy.

A. Kar[1], T. Nieuwenhuis[2], M. Duan[3], S. Tabrizi[1], M. Huggins[1], E. Scanlon[1], C. Hession[1], M. Bernstein[1], M. Ross[1], M. Tang[1], S. Malu[1];
[1]Immunitas Therapeutics, Inc., Waltham, MA, [2]AstraZeneca, Waltham, MA, [3]Novartis Institute of Biomedical Research, Cambridge, MA

Background: Intra-tumoral CD4+ and CD8+ T cells expressing inhibitory receptor CD161 have an effector memory phenotype with high cytotoxic potential. CD161 inhibits T and NK cell function in the presence of its ligand, CLEC2D. This suppression can be recovered by treatment with IMT-009, a first in class anti-CD161 antibody. Single cell transcriptomic analysis of anti-PD1 refractory microsatellite stable colorectal tumors identified presence of CD161+ CD4+ cytotoxic T cells and CD161+ PD1+ exhausted CD8 T cells suggesting that anti-CD161 treatment may provide benefit in these tumors both as a monotherapy and in combination with anti-PD1. It was also observed that CD161+ CD4/CD8T cells are more abundant in anti-PD1/L1 non responders compared with responders in hepatocellular carcinoma, cutaneous squamous cell carcinoma, clear cell renal carcinoma and breast cancer, providing a rationale for targeting CD161. Using engineered ex-vivo tumor models and dissociated human tumors, we have demonstrated that IMT-009 reverses CLEC2D mediated inhibition and restores primary T cell function. Additionally, co-treatment of IMT-009 with anti-PD1 further enhanced T cell mediated cytotoxicity, providing rationale for studies combining IMT-009 and anti PD1 in the clinic.

Methods: Using the Snakemake pipeline developed in house, we processed publicly available scRNAseq data. Cells were clustered by Louvian method followed by cell type annotation by Seurat, and gene expression and gene signature levels per cluster were plotted. For ex-vivo assays, antigen specific CD8 T cells expanded from HLA-A2:01 donors were co-cultured with HLA-A2:01 expressing MDA-MB 231 triple negative breast cancer cell line or Raji Burkitt Lymphoma model with HLA-A2:01 allelic overexpression. Target tumor cells were engineered to express the ligands CLEC2D or PDL1. These cell lines were made to overexpress luciferase for monitoring target cell death using a luminescence readout. Additionally, dissociated tumor cells (DTCs) were cultured in presence of the treatment molecules. Intracellular staining of cytotoxic T cells along with detection of IFNγ, IL-2, TNFα and Granzyme B levels in culture supernatants by MSD/ELISA were used to assess activation profile of tumor infiltrated T cells.

Results: Combining anti-PD1 and IMT-009 significantly enhanced cytotoxic benefit compared to individual monotherapy in both Raji and MDA-MB-231 target cell line models. IFNγ levels in supernatants of DTCs treated with this combination were elevated as compared to individual monotherapy. Together with scRNAseq data of increased abundance of *KLRB1* (CD161) expressing T cells in anti PD1 non-responder patients, our data provide rationale for testing combination of IMT-009 with anti-PD1 in patients that may not respond to anti PD1 alone.

#1376 Engineered exosomes for the delivery of PD-L1 siRNA for lung cancer immunotherapy.

R. Kandimalla[1], D. N. Moholkar[2], M. Wallen[3], C. Ding[1], R. C. Gupta[1], F. Aqil[1];

[1]Brown Cancer Center, University of Louisville, Louisville, KY, [2]University of Louisville, Louisville, KY, [3]3P Biotechnologies, Louisville, KY

Cancer immunosurveillance involves a dynamic interplay between the host's innate and adaptive immunity. The regulation of programmed death ligand-1 (PD-L1) expression on cancer cells has emerged as an attractive approach for cancer treatment. However, challenges such as the immunosuppressive tumor microenvironment, ineffective trafficking, and tumor antigen heterogeneity limit the applications of cancer immunotherapy for solid tumors. Small interfering RNA (siRNA) against PD-L1 presents a compelling alternative to antibody treatment to reduce *PD-L1* presentation on cancer cells, thereby enhancing T-cell detection and preventing tumor progression. Bovine milk/colostrum serve as a biocompatible source for exosomes for delivery biologics such as siRNA. Here, we demonstrate exosomes mediated delivery of si*PD-L1* for lung cancer immunotherapy. Exosomes were isolated from bovine colostrum powder using ultracentrifugation. The average particle size of exosomes was 66 ± 2.5 nm, with polydispersity index (pdi) 0.27 ± 0.01 and a zeta potential -9.2 ± 0.70 mV, as analyzed by Zetasizer and validated by atomic force microscopy (AFM) and transmission electron microscopy (TEM). Formulations of exosomes with polyethyleneimine (EPM) and siRNA (1 - 20 µg), when mixed with 5'-^{32}P-labeled siRNA as a tracer resulted in over 90% entrapment of siRNA. Biodistribution studies of exosomes and EPM, with or without the tumor-targeting ligand folic acid (FA), revealed predominantly similar distribution patterns. Notably, FA-EPM exhibited enhanced tumor accumulation compared to EPM, attributed to the overexpression of folate receptors on tumor cells.To assess the functionality of EPM-siRNA, we screened 4 different siPD-L1 sequences in LLC-1 and A549 lung cancer cells. Following 48 h of EPM-siPD-L1 treatment, cells were harvested. Analysis of protein lysates by western blot showed a significant downregulation of the PD-L1 expression, ranging from 55% - 80% in LLC-1 cells and over 80% in A549 cells. *In vivo* mouse study with orthotopic Lewis lung carcinoma (LL/2-Luc2) tumors is underway to validate the effective silencing of PD-L1 and its effect on tumor inhibition and immune markers. In summary, our targeted EPM technology represents a novel nanoplatform for siRNA therapeutics delivery. As milk/colostrum are the most abundant sources of exosomes, clinical translatability of this novel approach is eminent.

Funding: This research work was supported from the Kentucky Lung Cancer Research Program (GB170558) and Immunotherapy CCII CoBRE pilot project (P20GM135004).

Keywords: Exosomes, siPD-L1, siRNA delivery, Lung cancer, Immunotherapy

#1377 The role of TIM3 and PD1 blockades in head and neck cancer.

M. Shaikh, A. Karimi, P. Zeng, H. Pan, J. Barrett, A. Nichols;
University of Western Ontario, London, ON, Canada

Background: Our group has recently developed and validated a novel prognostic score for human papillomavirus (HPV+) oropharyngeal cancer called UWO3, which stratifies patients into low risk (immune rich), intermediate risk (immune mixed), and high risk (immune desert) groups. The high-risk immune desert group had a paucity of immune cells, however, that population of lymphocytes expressed high levels of the checkpoint molecule TIM3. To follow up on this, we assessed the therapeutic effect of anti-TIM3 mAb alone and in combination with anti-PD-1 in a syngenic murine HPV+ head and neck cancer model using the mERR. T-cell immunoglobulin mucin 3 (TIM3) and Programmed death 1 (PD-1) are negative immune checkpoint receptors that are expressed on tumor-infiltrating lymphocytes (TIL), play a crucial role in tumor-induced immune suppression. Given the critical role that the tumour microenvironment (TME) has on the prognosis of head and neck squamous cell carcinoma (HNSCC), immune checkpoint inhibitor immunotherapy approaches, specifically anti-PD1 and/or anti-TIM3 antibody therapy, may be very effective treatment strategies and may offer improved survival outcomes.

Methods:Immunocompetent C57BL/6 mice were injected in one flank with the syngeneic mouse HPV+ cell line, mEERL (10^6 cells), for tumour generation. Mice were then treated with either IgG2a isotype control, anti-PD1 (200µg), anti-TIM3 (200 µg) antibodies or a combination of anti-PD-1 and anti-TIM3 were administered via intraperitoneal injection 3 times per week following tumour establishement for 6 weeks (n = 7 mice per arm, total of 28 mice). Tumour volumes were measured every 2 days. Three representative tumors from each treatment group were collected for bulk RNA sequencing, scRNA-seq, and flow cytometry to characterise immune cell populations and transcriptional changes and monitor their impact on the TME of HNSCC.

Results:Anti-PD1 and anti-TIM3 both restricted tumour growth by size and weight relative to the IgG2a control ($p<0.01$, linear mixed model [lmm]). The combination of anti-PD1 and anti-TIM3 was more effective than either monotherapy alone ($p<0.05$, lmm). RNA sequencing analysis revealed differential abundance in CCL6, CCL9, CFD, and MAP3K5 transcripts relative to control for anti-PD1, anti-TIM3, and combination checkpoint inhibition.

Conclusion:Targeting both PD-1 and TIM3 enhanced the anti-tumor immune response in HPV+ head and neck tumours, providing further support for dual targeting of these molecules for more effective cancer immunotherapy. Our results suggest that immune checkpoint inhibitor therapy (PD1 and TIM3 blockades) could be a promising treatment strategy for HPV+ HNSCC, and the expression of these immune checkpoint molecules could serve as a predictive biomarker of patient outcome in HPV+ HNSCC.

IMMUNOLOGY: Inflammation and Cancer in Metastasis
Poster Session

#1381 Characterization of the 12-lipoxygenase expression in the megakaryoblastic cell line, Dami.

L. H. Boudreau[1], V. L. Gauvin[1], J. Richard[1], M.-F. N. Soucy[1], M. P. Hebert[1], E. P. Allain[2];
[1]Universite de Moncton, Moncton, NB, Canada, [2]Vitalite Health Network, Moncton, NB, Canada

Megakaryocytes are myeloid cells produced primarily in the bone marrow and are best known for releasing platelets in the blood stream. In the platelet production process, megakaryocytes transfer their bioactive content, including the 12-lipoxygenase (12-LO) enzyme, into newly formed platelets. The 12-LO has been shown to be implicated in platelet activation and is overexpressed in several chronic inflammatory conditions, including several types of cancers. The 12-LO is responsible for the conversion of the arachidonic acid into the 12(S)-hydroxyeicosatetraenoic acid (12(S)-HETE), a key lipid mediator implicated in several steps of the metastatic cascade. While 12-LO is expressed in mature human megakaryocytes, we recently identified two megakaryoblast cell lines isolated from leukemia patients lacking 12-LO expression. However, only one of the two cell lines expresses functional 12-LO protein upon megakaryocyte maturation. The goal of this study is to characterize the 12-LO expression during the megakaryocyte maturation process. We hypothesize that 12-LO expression is increased during cell maturation and that inhibition of the 12-LO expression will result in dysfunctional platelets. Both the Dami cell and MEG-01 cells were induced with the co-incubation of both phorbol myristate acetate and eltrombopag, a thrombopoietin receptor agonist. The maturation and viability of the cells were confirmed by flow cytometry. Expression of the 12-LO was assessed by RT-qPCR and immunoblot. Quantification of the 12(S)-HETE was performed by reversed-phase high performance liquid chromatography. Platelet release was quantified by flow cytometry using CD41 fluorescent labelled antibodies. We observed a 3-fold increase in 12-LO protein expression following cell maturation in the Dami cell line. Interestingly, mRNA expression between the undifferentiated Dami cells and mature Dami cells remained unchanged. Furthermore, we did not detect any 12-LO protein expression in the MEG-01 after the cell's maturation. Finally, we identified a specific 12-LO antisens non-coding RNA that is implicated in the regulation of the protein expression in megakaryocytes. Our study reports the first mechanistic regulation of 12-LO expression implicated in the megakaryocyte maturation process. Since both platelets and platelet-specific 12-LO play an important role in cancer biology, it is important to better understand how megakaryocytes package the enzyme inside these small cells. It remains elusive whether 12-LO enrichment in platelet correlates with the disease severity.

#1382 Activation of the cGAS-STING pathway by large oncosomes induces type I IFN inflammation in mesenchymal stem cells that triggers an immunosuppressive phenotype in neutrophils.

Taylon F. Silva[1], Diana Kitka[1], Blandine Victor[1], Chen Qian[1], Minhyung Kim[1], Tatyana Vagner[1], Giorgia Guerra[1], Catherine Grasso[1], Sungyong You[1], Fayyazz Sutterwala[1], Caroline Jefferies[1], Paola de Candia[2], Michael Freeman[1], Helen Goodridge[1], Karen Cavassani[1], Jlenia Guarnerio[1], Dolores Di Vizio[1]

[1]Cedars-Sinai Medical Center, Los Angeles, CA,[2]University of Naples Federico II, Naples, Italy

Extracellular vesicles (EVs) have been recognized as key players in cancer progression and metastasis, particularly large oncosomes (LO), secreted by invasive cancer cells, represent a distinct class of EVs with unique features. Previous research by the Di Vizio lab revealed LO's ability to alter recipient cell behavior, induce vascular morphogenesis, and carry cancer-specific biomolecules. Our preliminary studies point to a new mechanism of intercellular communication that involves the release of LO-containing DNA from PC cells. Notably, LO from prostate cancer exhibits enhanced potency in reprogramming bone marrow-derived mesenchymal stem cells (BM-MSCs) compared to exosomes (Exo) as observed by RNAseq. When evaluating the response to LO and Exo of BM-MSC, which are emerging as important drivers of bone metastasis, LO induces a robust inflammatory response, including metastasis-relevant chemokines and transcription factors involved in type I IFN response such as IRF7 and RASD2. Further, REACTOME pathway analysis of the differentially expressed genes revealed enrichment of the cGAS-STING pathway in BM-MSCs treated with LO, indicating a potential link between DNA/RNA sensors and the inflammatory response. BM cells isolated from WT and mutant Sting1gt/J mice demonstrated that up-regulation of IRF3 and IFNA1 genes induced by LO is inhibited when STING is absent. Suggesting that nucleic acid sensors engage in the LO-induced immune response in BM cells. Gene ontology analysis (GO) also identified several chemokines involved in neutrophil chemotaxis. In line with the observation from GO, neutrophil chemotaxis was significantly promoted by PC-derived LO-treated BM-MSC. Interestingly, human blood-derived neutrophils exposed to a conditioned medium from EVs-treated BM-MSC significantly increased the percentage of a population of LOX-1^{high} and CD62L$^{low/-}$ after 6h of culture. This was observed in concert with increased expression of Arginase1 and IL-10, suggesting their differentiation into polymorphonuclear-myeloid-derived suppressor cells (PMN-MDSC). An experimental orthotopic model using the breast cancer bone metastatic 4T1.2 cell line, with increased capacity to shed LO, demonstrated an increase in the presence of PMN-MDSC in the bone marrow of tumor-bearing mice in addition to a complete lack of lymphocyte populations, indicating their immunosuppressive activity that could lead to a pre-metastatic niche formation. This comprehensive study unveils the molecular pathways underlying the immune response to LO in the bone marrow, shedding light on mechanisms that could influence metastatic progression in prostate cancer. The findings underscore the unique role of LO in modulating the BM microenvironment, providing potential targets for therapeutic intervention and biomarkers for early disease detection.

#1383 Investigation of biological role and cytokine axis of cancer-associated fibroblast (CAF) in lung cancer brain metastasis.

N. Kim, S. Salam, E. Jahan, E.-J. Ahn, T.-Y. Jung, J.-H. Lee, J. Rhee, S. Kim, **K.-H. Lee**, K.-S. Moon;
Chonnam National University Medical School, Jeollanam-do, Korea, Republic of

Background: Brain metastases (BM) are among the most lethal forms of cancer globally. Lung cancer BM are frequently encountered and are associated with poor prognosis, decreased survival rates, and therapeutic resistances. Cancer-associated fibroblasts (CAFs) have emerged as important players of the brain metastases tumor microenvironment (TME). Mechanistic roles of brain metastases CAFs (hBM-CAFs) in tumorigenesis and therapeutic resistances remain unclear.

Material and Methods: In the present study, the patient's BM surgical sample was subjected to primary culture to isolate CAF. The hBM-CAF induced EMT and stemness phenotype was investigated by western blot. Biological role of hBM-CAF in tumorigenesis was evaluated using indirect co-culture method in vitro. FACS analysis was performed to investigate the changes in cisplatin cytotoxicity and radiation susceptibility of lung cancer cell lines when co-cultured with hBM-CAF. CX3CL1 and IL26 expression was confirmed by ELISA along with transcriptomic analysis of hBM-CAF. Molecular events were validated by using neutralizing CX3CL1 and IL26. The tumorigenicity and response to chemotoxicity of lung cancer cells were examined by co-injecting them with hBM-CAF in a mouse xenograft model.

Results: Our experiments demonstrated that hBM-CAFs significantly enhanced EMT and stemness phenotype by upregulating transcription factor SNAIL1, TWIST1, Slug and CD133, CD44 respectively in lung cancer cells. We also observed that hBM-CAFs decreased cisplatin cytotoxicity and enhanced radiation resistance, as measured by FACS analysis of apoptotic cells. *In vivo* experiments using xenograft mouse models revealed that co-injection of lung cancer cells with hBM-CAFs led to faster tumor growth and increased cisplatin resistance. Transcriptomic analysis of hBM-CAFs revealed a distinct genomic signature compared to normal fibroblast (hNFs), with significant overexpression of IL26 and CX3CL1 genes in the hBM-CAFs secretome, as validated by ELISA. Moreover, we found that lung cancer cells expressed high levels of the IL26 receptor IL10Rβ and ILR20α, and CX3CL1 receptor CX3CR1. Our hBM-CAF significantly upregulated JAK-STAT3 and Akt-mTOR pathway. Eventually, we have confirmed that neutralizing IL26 and CX3CL1 inhibit phosphorylation of JAK-STAT3 and Akt-mTOR respectively and revoked the IL26-CX3CL1 induced EMT and stemness phenotype of lung cancer cells.

Conclusion: Patient derived hBM-CAF promote aggressive phenotype of lung cancer cells by upregulating EMT and stemness transcriptome factors. Overexpression of IL26 and CX3CL1 cytokine led to the therapeutic resistance through JAK-STAT3 and Akt-mTOR signaling pathway respectively. Targeting IL26-CX3CL1 might be a novel therapeutic efficacy for lung cancer brain metastasis patients.

#1384 Highly metastatic PDAC adopts mesenchymal morphology and spatially coordinates endothelial cells with macrophages.

N. E. Gross, S. Charmsaz, J. W. Lee, C.-C. Huang, A. G. Hernandez, S. M. Shin, E. M. Coyne, C. Cannon, X. Yuan, L. D. Wood, E. M. Jaffee, W. Ho; Johns Hopkins University School of Medicine, Baltimore, MD

Background: Patients with pancreatic ductal adenocarcinoma (PDAC) often have metastatic disease at diagnosis and are highly resistant to cytotoxic and immunotherapies. Increased presence of myeloid cells, specifically high myeloid-to-T cell ratios, correlates with worse prognoses. However, mechanisms by which myeloid cells regulate cancer invasion and metastasis remain poorly understood. To study the role of immunosuppressive myeloid cells in driving metastasis, we employed murine PDAC models in conjunction with organoid systems and imaging mass cytometry (IMC).

Methods: We used two murine cell lines driven by *Kras*^{G12D} and *Trp53*^{R172H} under *Pdx1*-Cre, KPCY 2838c3 and KPCY 6419c5, which exhibit low-metastatic and high-metastatic propensities, respectively. To characterize differences in the metastatic cascade between these cell lines, flow cytometry, histological analysis, and 3D organoid modeling were used. IMC was also used to interrogate the tumor microenvironment and identify spatial relationships.

Results: These cell lines were orthotopically injected into syngeneic C57BL/6J mice to generate tumors that naturally metastasize to the liver. Flow cytometry analysis of livers from mice bearing 2838c3 or 6419c5 pancreatic tumors validated the higher propensity for metastasis with the 6419c5 cells ($p=0.0484$). Furthermore, the steps along the metastatic cascade contrasted significantly between 6419c5 and 2838c3. Highly metastatic PDAC adopted mesenchymal rather than collective invasion, increased intravasation, and more robust metastatic outgrowth. Notably, IMC revealed that highly metastatic PDAC had increased endothelial cell abundance (***$p \leq 0.001$), lower cytotoxic CD8+ T cell to CD4+ regulatory T cell ratios (***$p \leq 0.001$), and lower M1-like to M2-like tumor associated macrophage (TAM) ratios (*$p \leq 0.05$). Furthermore, spatial analysis demonstrated that highly metastatic PDAC excluded lymphocytes from the tumor and situated Arginase-1+ TAMs near Ki67+ tumor cells and CD31+ endothelial cells. In contrast, low-metastatic PDAC had closer lymphocyte proximities to tumor and greater distances between Arginase-1+ TAMs, tumor, and endothelial cells.

Conclusions: The highly metastatic PDAC tumor line utilizes mesenchymal invasion, has increased intravasation, and robust metastatic outgrowth compared to the low-metastatic PDAC cells. The TME of the highly metastatic model had disproportionate abundances of T regulatory cells and M2-like macrophages, poor lymphocyte infiltration, and enhanced vascularization. These overabundant M2-like macrophages (Arginase-1+) were also spatially coordinated with proliferating tumor cells and vasculature, suggesting a potential role for macrophages in tumor cell invasion and/or angiogenesis.

#1385 Crosstalk between hepatocyte and myeloid-specific IL17 signaling in colorectal cancer metastasis.

Katarzyna Chojnacka[1], Dan Kamen[1], Katrina M. Reyes[2], Hana Tomizawa[2], Sergei I. Grivennikov[1]

[1]Department of Medicine and Department of Biomedical Sciences, Cedars-Sinai Medical Center, Los Angeles, CA, [2]University of California Los Angeles, Los Angeles, CA

Advanced colorectal cancer (CRC) is resistant to current immunotherapies and prone to metastasis. Chronic inflammation mediated by cytokines such as interleukin (IL)17 activates the oncogenic pathways in cancer cells, promoting sporadic and inflammation-associated CRC. Increased levels of IL17A in early stages of CRC portends poor prognosis indicating its potential involvement into metastasis. We and others previously showed that IL17A signaling is required for early CRC tumorigenicity in a variety of models and that in early CRC, its ability to signal to epithelial cells is essential. What remains unknown is whether IL17 signaling to other cell types within the tumor microenvironment (TME) is essential to control tumor progression and metastasis. Using a model of colitis-associated cancer (CAC) we found that “late” IL17A neutralization decreases tumor burden, possibly acting through regulation of myeloid cells and chemokine network essential for the control of immunosuppressive TME. Next, using models of colorectal cancer liver metastasis (CRLM) including intraportal cell injection and cecum transplantation of organoids with distinct set of oncogenic mutation we found that IL17 neutralization reduces metastasis. FACS analysis revealed that IL17A promotes the recruitment of tumor-associated macrophages and other key myeloid subsets into the metastatic liver environment. Interestingly, ablation of IL17RC (receptor) in myeloid cells only (using *Il17rc*$^{f/f}$-LysMCre mice) led to reduction in metastasis and reshaping of metastatic myeloid cell compartments. Meanwhile, IL17 signaling in hepatocytes was required for early metastasis and pre-metastatic niche formation, as the ablation of IL17RC in hepatocytes (using *Il17rc*$^{f/f}$-AlbCre mice) led to a reduction of metastatic numbers but not growth. This coincided with reduced neutrophil recruitment and enhanced activation of cytotoxic innate lymphoid cells and CD8 T lymphocytes, indicating the role of hepatocyte specific IL17 signaling in blunting anti-tumor immunity. Our findings illuminate the role of inflammatory cytokine IL17 into CRC progression and metastasis and imply its distinct cell type specific role within the metastatic liver TME.

#1386 CD1d-restricted iNKT cells promote liver metastasis from colon cancer.

Marc Nater[1], Giulia Lucchiari[1], Michael Brugger[2], Tomas Valenta[2], Virginia Cecconi[1], Geo Forni[1], Stephan Benke[3], Maries van den Broek[1]

[1]Institute of Experimental Immunology, Universitat Zurich, Zurich, Switzerland,[2]Department of Molecular Life Sciences, Universitat Zurich, Zurich, Switzerland,[3]Flow Cytometry Facility, Universitat Zurich, Zurich, Switzerland

The liver is a prominent site for metastasis, yet little is known about the role of liver immunity in antimetastatic defense. Compared to other organs, the liver harbors a unique immune environment characterized by the abundance of innate cell lineages, including CD1d-restricted invariant natural killer T (iNKT) cells. To investigate the influence of iNKT cells on metastasis, we established an orthotopic model of colorectal cancer (CRC) with spontaneous dissemination to the liver. We induce the primary tumor by implanting CRC organoids into the colon mucosa of syngeneic C57BL/6 mice, resulting in hepatic macrometastases within 5 weeks. We observed that liver metastasis hardly occurred in mouse strains lacking iNKT cells (*Cd1d*$^{-/-}$ and *Traj18*$^{-/-}$ mice), while the growth of the primary tumor was comparable to that in wild-type mice. These results indicate a tumor-promoting function for hepatic iNKT cells. We uncovered that hepatic iNKT cells respond to disseminating cancer by producing IL-4 and IL-13, two cytokines known to activate hepatic stellate cells (HSCs) into fibrogenic myofibroblasts. Indeed, we saw rapid activation of HSCs and deposition of extracellular matrix upon arrival of cancer cells in the liver of wild-type but not iNKT cell-deficient mice. We propose that hepatic iNKT cells contribute to the formation of a supportive niche for disseminated tumor cells by activating HSCs early in the development of hepatic metastasis. Taken together, our findings highlight an essential tumor-promoting role for iNKT cells during the development of liver metastasis and contribute to our understanding of immune regulation of metastasis.

#1387 SETD2 loss promotes macrophage infiltration and metastasis in RCC.

E. N. Arner[1], M. M. Wolf[2], L. Vlach[2], J. C. Rathmell[1], W. Rathmell[1];
[1]Vanderbilt University Medical Center, Nashville, TN, [2]Vanderbilt University, Nashville, TN

Across human cancer, tumors that are high grade, poorly differentiated, and have undergone epithelial-to-mesenchymal transition (EMT) carry a worse prognosis with a high likelihood of metastasizing to distant organs. Despite significant research efforts, metastatic cancers and relapse remain the primary cause of cancer related deaths. In renal cell carcinoma (RCC), metastasis is present in one-third of patients at the time of diagnosis, and one-third of patients who initially present with locally advanced disease eventually develop local or distant recurrence following resection of the primary tumor, highlighting the need for new RCC therapies and further insight into the metastatic process. Using RCC patient biopsies, we found that patients with more epithelial tumors have a significantly lower risk of recurrence. Additionally, tumors that had a mesenchymal protein signature had significantly increased macrophage infiltration, which was significantly associated with a higher stage at diagnosis and worse overall survival, suggesting that macrophages may play an important role in EMT and metastasis in ccRCC. Whole exome sequencing of these patient samples revealed that mutational loss of SETD2, a histone methyltransferase that is lost in about 20% of RCC patients, correlated strongly with increased macrophage infiltration within the primary tumor and was necessary for the correlation between macrophages and EMT. SETD2 loss in syngeneic kidney cancer mouse models confirmed that SETD2 loss within tumor cells resulted in increased EMT, macrophages within the primary tumor microenvironment (TME), and spontaneous metastasis, further supporting the role of macrophages in promoting metastasis in the absence of SETD2. Further characterization of the gene signatures and immune cell infiltrate in RCC will lead to a better understanding of metastasis in an oncogene- and tissue-specific manner and thus lead to more efficacious therapies for metastatic patients.

#1388 Spatial transcriptome analysis of EMT trait and corresponding immune composition study in HNSCC.

C.-H. Chung, M.-H. Yang;
National Yang Ming Chiao Tung University, Hsinchu, Taiwan

Head and neck squamous cell carcinoma (HNSCC) is a prevalent malignant cancer worldwide. Conventional treatments for this type of cancer involve surgical resection, radiation therapy, and chemotherapy. However, in cases where the tumor recurs or metastasizes distantly, rendering surgical resection or radiation therapy impractical, the only viable option is the utilization of targeted drugs in conjunction with chemotherapy. Despite such interventions, the prognosis remains grim. Hence, the identification of genetic characteristics or biomarkers associated with easy metastasis or recurrence in the early stages of the tumor has become imperative for effective head and neck cancer treatment. The objective of this study is to analyze tumor specimens from the primary site and lymph node metastasis post-surgical resection in HNSCC patients. We employed the GeoMx Digital Spatial Profiler (DSP) for imaging-based digitized gene expression analysis. The DSP provides gene expression information at specific locations we selected, such as the primary tumor center core, primary tumor invasion borders, and lymph node metastasis specimens. The GeoMx DSP spatial analysis tool illustrates the cancer transcriptome atlas (CTA), encompassing the expression of 1825 genes related to cancer and immunity from the primary site to the metastatic site. We identified tissue-specific EMT gene expression patterns in paired tumor regions of interest (ROIs). ITGB1 emerged as the most significant co-expression marker in the primary outer tumor and metastatic tumor. Distinct EMT signature genes expressed in the HNSCC primary site and lymph node metastatic site were also discovered. Additionally, we conducted CTA profiling in correlated stroma ROIs. Through myeloid activity analysis in HNSCC paired samples, we identified distinct myeloid activation signatures in primary and metastatic site stroma cells. These results will provide crucial insights into head and neck cancer treatment strategies based on different tumor site characteristics.

#1389 Understanding the differential role of an IL-6 family cytokine in varying subtypes of breast cancer patients for novel therapeutic intervention.

C. L. Wolf, K. Tawara, C. L. Jorcyk;
Boise State University, Boise, ID

In the United States, it is estimated that over 295,000 women will be diagnosed with breast cancer, and over 43,000 breast cancer deaths in 2023. Mortality in breast cancer is due in large part due to distant metastasis to organs such as the bone, lung, liver, and brain. Our laboratory has identified that the IL-6-family cytokine oncostatin M (OSM) plays a crucial role in initiating metastasis by secreting pro-metastatic molecules such as VEGF, LOXL2 and IL-6, and increasing circulating tumor cell numbers and metastases to bone and lung *in vivo*. More recent work within our lab has identified unique roles for OSM in varying subtypes of breast cancer patients, particularly between estrogen receptor positive (ER+) and ER- patients. It is well known that patients with ER- breast cancer, specifically triple negative breast cancer (TNBC; ER- PR- HER2-), have limited therapeutic options. However, the divergent role OSM plays in ER+ and ER- breast cancer and the mechanism by which this occurs has yet to be fully understood. Thus, we aimed to fully elucidate the difference between OSM in ER+ versus ER- breast cancer. RNA sequencing analysis on OSM-treated human ER+ cells and ER- TNBC cells discovered significant differences in gene expression between both cell lines upon treatment with OSM, including alteration in DNA-replication and cell cycle pathway genes. Afterwards to evaluate the correlation between OSM and DNA synthesis and this role on metastasis, we evaluated the role of a novel anti-OSM therapeutic and its correlation with decreased metastasis. This research aims to elucidate the unique role OSM plays in ER+ and ER- breast cancer and will provide a molecular understanding of how this occurs and will provide detailed information on which patients will benefit most from anti-OSM therapeutics.

#1390 Pulmonary viral infection promotes the awakening of dormant metastatic breast cancer cells in lungs.

S. Chia[1], B. Johnson[1], M. Boorgula[1], V. Sreekanth[1], A. Goodspeed[1], B. J. Davenport[1], J. Hu[1], D. Gao[1], M. Papanicolaou[2], T. E. Morrison[1], J. A. Aguirre-Ghiso[2], M. Rincon[1], J. V. DeGregori[1],

[1]University of Colorado Anschutz Medical Campus, Aurora, CO, [2]Albert Einstein College of Medicine, New York, NY

Background: Breast cancer is the most common form of cancer and the second cancer-causing death in females. Although remission rates are high if detected early, survival rates drop substantially when breast cancer becomes metastatic. The most common sites of metastatic breast cancer are bone, liver, and lung. Respiratory viral infections inflict illnesses on countless people, as evidenced by annual flu seasons and the latest pandemic caused by SARS-CoV-2. Respiratory viral infections result in increased inflammation with immune cell influx to facilitate viral clearance. Prior studies have shown that inflammation can contribute to dormant cancer cells awakening and outgrowth. However, how respiratory viral infections contribute to breast cancer lung metastasis remains to be unraveled.

Methods: MMTV/NEU mouse model of dormant breast cancer was used, with influenza virus as the model respiratory virus. Lungs and bronchoalveolar lavage fluid were harvested for immunohistochemistry, flow cytometry, cytokines, and single-cell RNA-seq analysis. Flatiron Health Database was mined for epidemiological data to assess the risk of breast cancer metastasis to lung with COVID infection.

Results: We have shown a dramatic increase in disseminated cancer cell (DCC) awakening in the lungs following influenza and SARS-CoV-2 infections. Influenza infection results in loss of a pro-dormancy mesenchymal phenotype and increased proliferation of DCC in the lungs within days post-infection, with a more than 1000-fold expansion of carcinoma cells over a couple of weeks. Strikingly, by 15 days post-infection, the lesions that expanded from solitary HER2$^{\pm}$ DCCs almost homogeneously return to a quiescent state. Our preliminary data indicate that post-infection increases in IL-6 are required for DCC expansion post-influenza. Acute influenza infection also contributed to an accumulation of CD4$^{\pm}$ T cells around expanding tumor cells for as long as 28 days after the initial infection. Depletion of CD4$^{\pm}$ T cells but not CD8$^{\pm}$ cells during infection with influenza virus prevents the expansion of the DCCs in the lung. Co-depletion of CD8 cells with CD4 cells partially restored the DCC burden in the lungs, indicating a role for CD8 cells in eliminating DCCs when released from CD4-mediated suppression. Single-cell RNA-seq analyses of CD8$^{\pm}$ T cells with CD4 depletion showed an increased IL2/STAT5, MTORC1, and Ox/Phos activation by 15 dpi. The analyses also showed an immunosuppressive effect by the tumor cells. Finally, analysis of female breast cancer patients who tested positive with SARS-CoV-2 after their initial diagnosis exhibited a hazard ratio of 1.44 (p=0.043) for subsequent diagnosis of metastatic breast cancer in lungs.

Conclusions: These studies reveal the potential risks to cancer survivors who experience respiratory viral infections, with mechanistic insight that could lead to novel prevention or intervention strategies.

#1391 Therapeutic salmonella induces long-term protective trained immunity in NK cells against metastasis.

L. Rong, J. Huang;
The University of Hong Kong, Hong Kong, Hong Kong

Immune memory is a trait commonly associated with adaptive immunity. Nevertheless, it has been observed that activation of the innate immune system can also result in enhanced responsiveness to subsequent triggers, a form of innate immune memory known as trained immunity. This *phenomenon* has been primarily explored in the context of host defense against infectious disease, where myeloid cells, including monocytes, macrophages, and their precursor cells, are conditioned by specific stimuli such as β-glucan, LPS, or the bacillus Calmette-Guérin (BCG) to boost protection against microbial pathogens. However, the induction of trained immunity in innate lymphocytes, particularly through these known or yet-to-be-discovered stimuli and its explicit contribution to tumor immunity, remain insufficiently characterized. Metastasis accounts for 90% of cancer-related deaths, and no effective clinical therapies are currently available to halt the metastatic cascade. Based on multiple cancer metastasis mouse models and immunological analysis, we found that a single dose of therapeutic Salmonella YB1, an engineered oxygen-sensitive strain, provides extensive and persistent protection against metastasis by inducing protective trained immunity in NK cells, consistently observed irrespective of the mouse genetic background or cancer cell lines. Following inflammatory resolution, salmonella YB1-trained NK cells exhibit an enhanced capacity to release IFN-γ upon secondary stimulation and increased cytotoxicity towards cancer cells, which is associated with epigenetic changes. Further investigation using single-cell transcriptomic profiling indicates that the formation of long-term anti-metastatic trained immunity in NK cells by Salmonella YB1 is dependent on IL12 and IL18. Additionally, Salmonella YB1-trained NK cells outperform common immune checkpoint therapies like PD1 blockade and TIGIT blockade in suppressing metastasis. In summary, our results revealed a novel anti-metastatic function of trained NK cells induced by therapeutic Salmonella, suggesting the induction of trained immunity in NK cells as a potential anti-tumor strategy.

#1392 Neutrophil extracellular trap (NET)-induced pancreatic tumor metastasis requires integrin-linked kinase (ILK) signaling.

P. C. McDonald[1], S. J. Awrey[1], H. Tavakoli[1], R. Carroll[1], Z. J. Gerbec[1], J. M. Karasinska[2], D. F. Schaeffer[2], D. J. Renouf[2], S. Dedhar[1];
[1]BC Cancer Research Institute, Vancouver, BC, Canada, [2]Pancreas Centre BC, Vancouver, BC, Canada

Neutrophil extracellular traps (NETs) are an important contributor to the immunosuppressive tumor microenvironment and facilitate metastasis of solid cancers. NETs have been shown to stimulate breast and colon cancer cell metastasis through a mechanism potentially involving an interaction between integrin-linked kinase (ILK) and the cell surface receptor coiled-coil domain containing protein 25 (CCDC25). Here, we have interrogated whether ILK is required for NET-induced metastasis in pancreatic ductal adenocarcinoma (PDAC), an inflammation-driven tumor that is difficult to treat. Evaluation of the circulating neutrophil to lymphocyte ratio (NLR) in the blood samples of patients presenting with metastatic PDAC showed that a higher baseline NLR is associated with significantly shorter overall patient survival. Western blot and immunofluorescence analyses demonstrated that human PDAC cell lines, patient-derived xenograft cells, cells derived from the KPCY genetic model of PDAC and patient-derived organoids co-express CCDC25 and ILK. Co-immunoprecipitation analyses showed that CCDC25 and ILK associate in both mouse and human PDAC cells, and that exposure of the cells to NETs results in an increased amount of ILK associated with CCDC25. Exposure of human and KPCY mouse PDAC cells to NETs increases phosphorylation of GSK3-β and ERK, increases activation of Rac1 and Cdc42 and upregulates markers of epithelial-to-mesenchymal transition (EMT), including ZEB1 and Snail, in a time and concentration-dependent manner. Furthermore, time-lapse imaging using Incucyte-based wounding assays showed that exposure to NETs induces pseudopodia-like protrusions, migration and invasion by these cells. RNAi-mediated suppression of ILK expression or inhibition of ILK activity using a highly selective inhibitor of ILK, QLT-0267, significantly inhibits the NET-induced increase in GSK3-β phosphorylation, Rac1/Cdc42 activation, migration and invasion of PDAC cells. *In vivo*, co-localization of CCDC25 and ILK is observed in tumors and metastases from KPCY mouse and MIA PaCa-2 human PDAC xenograft models stained by multispectral immunofluorescence and analyzed by confocal microscopy. Tumors and metastases show the presence of infiltrating neutrophils and NETs as indicated by staining for myeloperoxidase and citrullinated histone H3. Importantly, doxycycline-inducible shRNA-mediated suppression of ILK expression by luciferase-positive PDAC cells following injection of these cells through the tail vein of mice administered LPS intranasally results in a significant reduction in metastasis as measured by bioluminescence-based imaging, compared to control animals. Collectively, these data identify NET-induced ILK signaling as an important contributor to PDAC progression and suggest the potential for targeting this axis to prevent PDAC progression and metastasis.

#1393 Tumor-infiltrating monocyte-like cells create metastasis-promoting immunosuppressive microenvironment via THBS1 production in aggressive colorectal cancer.

M. Omatsu[1], Y. Nakanishi[1], K. Iwane[1], N. Aoyama[1], T. Maruno[1], H. Kasashima[2], M. Yashiro[2], A. Fukuda[1], H. Seno[1];
[1]Kyoto Univ. Graduate School of Medicine, Kyoto City, Japan, [2]Osaka Metropolitan Univ., Osaka City, Japan

Mesenchymal subtype of colorectal cancer (CRC) is characterized by high metastatic potential, poor prognosis and an immunosuppressive tumor microenvironment (TME). Although tumor-infiltrating myeloid cells constitute the primary population of immune components in the TME, targeting myeloid cells remains highly challenging owing to the developmental and functional heterogeneity of their subsets. Thus, a deeper understanding of how tumor-infiltrating myeloid cells contribute to the creation of a tumor-promoting TME is needed to identify rational strategies against CRCs with aggressive phenotypes. Recent studies have revealed that multiple inflammatory signatures are elevated in mesenchymal CRCs, suggesting a strong association between inflammation and stromal activation. In this study, we focus on thrombospondin-1 (THBS1), which is a matricellular protein, typically expressed in inflammatory processes. Immunostaining and RNA in situ hybridization on human CRC samples revealed a clear localization of THBS1 expression in tumor stroma. Analyses of the cancer genome atlas (TCGA) and tissue microarray of human CRCs show a positive correlation between increased expression of THBS1 and the mesenchymal phenotype, immunosuppression, and poor prognosis in human CRCs. Utilizing immunocompetent orthotopic implantation systems with aggressive mouse tumor organoids (MTO) on wild-type and *Thbs1* knockout (*Thbs1*$^{-/-}$) mice, we demonstrated that loss of THBS1 in the TME suppressed metastatic formation accompanied by an increased infiltration of tumor-infiltrating CD8^{+} T cells. Depletion of CD8^{+} T cells by neutralizing antibody restored metastases in MTO-bearing *Thbs1*$^{-/-}$ mice, indicating that THBS1 promotes metastatic formation by suppressing CD8^{+} T cell-mediated anti-tumor immunity. Analyses of single cell RNA sequencing data of human CRCs and orthotopic MTO tumors revealed that bone marrow (BM)-derived monocyte-like cells are the primary source of THBS1. This notion was further supported by analyzing the orthotopic MTO tumors in chimeric mice generated by bone marrow transplantation. Finally, we identified stroma-derived CXCL12 as a key chemokine for the recruitment of THBS1-producing monocyte-like cells by analyzing orthotopic MTO tumors treated with CXCL12 inhibitor. Our study contributes to a better understanding of the processes underlying THBS1 production by monocyte-like cells that mediates immune evasion that confer aggressive features to CRCs. These findings provide insights for the treatment of this poor-prognosis malignancy.

#1394 The CXCL10-CXCR3 axis as Jekyll and Hyde: A regulator of metastasis and immune response in osteosarcoma.

B. B. Gyau[1], X. Chen[1], J. Wang[1], M. A. Clement[1], A. M. Major[2], J. Xu[1], M. Hicks[1], T.-K. Man[1];
[1]Baylor College of Medicine, Houston, TX, [2]Texas Children's Hospital, Houston, TX

The CXCL10-CXCR3 axis is known to promote tumor growth and metastasis via autocrine signaling, while it can also elicit anti-tumor responses by paracrine signaling. However, its roles are still elusive in osteosarcoma (OS), the most common malignant bone tumor in children. In this study, we utilized in vitro assays, mouse models, and gene expression analysis to characterize the roles of the CXCL10-CXCR3 axis in OS. To understand the autocrine signaling, we performed in vitro phenotypic assays on three OS cell lines with and without CXCL10. The results showed that the chemokine increased AKT phosphorylation and tumor cell migration. Using a CRISPR-based CXCR3 deletion mutant, we demonstrated that the lack of the receptor inhibited OS tumor growth and pulmonary metastasis in an orthotopic xenograft mouse model. The results indicate that the CXCL10-CXCR3 axis is sufficient and necessary to promote aggressive phenotypes in OS via autocrine signaling. Next, using gene expression datasets from two cohorts of OS patients, we showed that high expression of CXCL10 or its cognate receptor CXCR3 was associated with a better prognosis. Since CXCL10 is known to recruit CXCR3+ immune cells to fight against cancer, we further found that the expression of the T cell marker CD3D was associated with a better prognosis. These results suggest that the chemokine may also play a protective role in osteosarcoma by recruiting anti-tumor immune cells via paracrine signaling. Lastly, we have previously reported that a high circulating level of CXCL10 correlates with a poor prognosis in osteosarcoma patients. In this study, we demonstrated that increasing the circulating CXCL10 level in immunodeficient orthotopic xenograft mouse models of OS did not significantly promote the development of pulmonary metastases, suggesting circulating CXCL10 may exert its chemotactic effect mainly on immune cells, not on tumor cells. Taken together, we propose a model that tumor expression of CXCL10 promotes osteosarcoma growth and metastasis development via autocrine signaling. The increase of the local level of CXCL10 attracts CXCR3+ immune cells to the tumor site and promotes anti-tumor function via paracrine signaling. Metastatic cells colonize the lungs and cause tissue damage and inflammation, which increases the production of CXCL10 in the circulation. The higher circulating CXCL10 recruits T cells away from the primary tumor site and indicates the occurrence of metastasis and, hence, correlates with a worse outcome in patients. Our research highlights the importance of understanding the opposite effects of CXCL10 on tumor and immune cells as well as in the tumor microenvironment and circulation. Identification of the mechanistic differences in the CXCL10-CXCR3 signaling between tumor and immune cells will provide a novel therapeutic approach against tumor cells while promoting anti-tumor immune response in OS.

#1395 Unraveling the interplay between tumor heterogeneity and microenvironment in pancreatic ductal adenocarcinoma evolution and its clinical implications.

H. Kim[1], H.-o. Jeong[2], S.-H. Lee[1], K. Lee[1], K. Lee[1], J. Lee[1], M. Lee[1], S. Lee[2], J. Park[1];
[1]Samsung Medical Center, Sungkyunkwan University School of Medicine, Seoul, Korea, Republic of, [2]Ulsan National Institute of Science and Technology, Ulsan, Korea, Republic of

Intratumoral heterogeneity (ITH) and tumor microenvironment (TME) of pancreatic ductal adenocarcinoma (PDAC) play important roles in tumor evolution and patient outcomes. However, the precise characterization of diverse cell populations and their crosstalk associated with PDAC progression and metastasis is still challenging. We performed single-cell RNA sequencing of primary PDAC samples with and without paired liver metastasis samples to understand the interplay between ITH and TME in the PDAC evolution and its clinical associations. We discovered that even a small proportion (~30%) of basal-like ductal cells in primary PDAC was associated with poor chemotherapy response and patient survival and that epithelial-mesenchymal transition programs were largely subtype specific. The clonal homogeneity significantly increased with more prevalent and pronounced copy number gains of oncogenes, such as KRAS and ETV1, and losses of tumor suppressor genes, such as SMAD2 and MAP2K4, along PDAC progression. Diverse immune cell populations, including naive SELL^{hi} regulatory T cells (Tregs) and activated TIGIT^{hi} Tregs, contributed to shaping immunosuppressive TMEs of PDAC through cellular interactions with malignant ductal cells. The proportion of basal-like ductal cells negatively correlated with that of immunoreactive cell populations, such as cytotoxic T cells, but positively correlated with that of immunosuppressive cell populations, such as Tregs. Overall, our study provides a valuable resource for better understanding the roles of ITH and TME in PDAC evolution and their clinical relevance in the treatment of PDAC.

#1396 Targeting immune suppressive myeloid cells in prostate cancer recurrence and metastasis.

S. Mei, H. Zhang, T. Hirz, N. E. Jeffries, S. Wu, C. Wu, D. M. Dahl, P. J. Saylor, D. B. Sykes;
Massachusetts General Hospital, Boston, MA

Metastatic prostate cancer is a leading cause of cancer-related deaths worldwide and therefore an urgent inadequately addressed clinical problem. We have approached this problem primarily by studying immune cells within the tumor microenvironment rather than the tumor cells themselves. One critical cell subset that seems to be contributing to the aggressive behavior of clinically significant prostate cancers is the immune suppressive myeloid cells (MDSC) within the tumor microenvironment. MDSC have been shown to promote tumor metastases by participating in the formation of pre-metastatic niche, promoting angiogenesis, tumor cell invasion, and mediating immune suppression. Understanding the heterogeneity and function of these myeloid cells is an essential step toward developing effective therapeutic strategies to target them and enhance anti-tumor immune responses that have thus far been so elusive. We utilized previously generated scRNAseq data and combined it with publicly available prostate cancer scRNAseq datasets. The analysis included a total of 96 samples at different disease stages, including healthy prostate tissue, adjacent-normal tissue, low-grade tumors, high-grade tumors, as well as local and bone metastatic tumors. In addition, GeoMx spatial profiling was performed on 24 high-grade prostate cancer patients to assess immune cell spatial infiltration. This meta-analysis provided comprehensive insights into the molecular characteristics of prostate cancer. We characterized multiple MDSC subpopulations and revealed the dynamics of tumor associated macrophages (TAMs) during tumor progression and metastasis. We found that a specific type of TAM, known as APOE+ SPP1+TAM, is significantly enriched in metastatic tumors. They are transcriptionally similar to the TAMs found in the bone metastasis niche of prostate cancer. Moreover, we found APOE+ SPP1+TAMs within primary/localized tumors tumors alone could predict prostate cancer recurrence despite curative-intent local therapy. We validated the accumulation of APOE+ SPP1+TAMs in a prostate cancer mice model. We are currently studying the role of the specific subset of TAMs in tumor metastases by focused analysis of the communication between these TAMs, T cells, and tumors. Additionally, we are exploring the therapeutic potential of blocking APOE+ SPP1+TAMs in a mice model of prostate cancer. Our analyses provide a comprehensive picture of myeloid cell linage across different prostate cancer stages, highlighting the potential for therapeutic targets that disrupt the metastatic process via their effects on tumor associated macrophages.

#1397 Metabolic CRISPR-Cas9 screening identifies loss of mitochondria*Gene M*in triple-negative breast cancer to promote lung metastasis via immune modulation.

S.-T. Chou, X. Wang, D. N. Edwards, J. Chen;
Vanderbilt University Medical Center, Nashville, TN

Triple-negative breast cancer (TNBC) is a heterogenous breast cancer characterized by an aggressive phenotype and high risk of metastatic occurrence. Metastasis is a multifaceted process that involves metabolic reprogramming, selection, and adaptation. Although studies have shown that alterations of metabolic processes can influence TNBC phenotype and sensitivity to treatments, less is known about how changes in metabolic enzymes in the tumor cells affect crosstalk between tumor and immune cells during metastasis. Here, we performed a high-throughput CRISPR-Cas9 screening of metabolic genes in an orthotopic basal-like mammary carcinoma 4T1 mouse model to identify key metabolic enzymes in the tumor cells that are associated with TNBC lung metastasis by affecting the tumor microenvironment (TME). The CRISPR-Cas9 screening showed an enrichment of sgRNA for mitochondria *Gene M* in the metastasized lungs of wild-type mice but not *Rag1*$^{-/-}$ mice, indicating that loss of *Gene M* could modulate adaptive immune cells in the TME or distant organs to promote 4T1 lung metastasis. Further pilot experiments revealed that loss of *Gene M* in 4T1 cells increased murine basal-like carcinoma lung metastasis *in vivo* and decreased population of B cells, CD4+ T cells, M2 macrophages, monocytes, and CXCR2+ neutrophils in the metastasized lungs without affecting the growth rate of the primary tumors. Overall, our preliminary results demonstrated that *Gene M* deficiency in 4T1 cells affects immune cell profile and drives lung metastasis of murine basal-like carcinoma cells, but the molecular and cellular mechanisms by which loss of *Gene M* grant tumor cells with metastatic advantage requires further investigation.

#1398 The role of ST8SIA2 & ST8SIA4 in melanoma progression and metastasis.

Amirali Amirfallah, Kayla Gallant, Maria Cavallo, Zongguan Huang, Edward Hartsough

Drexel University College of Medicine, Philadelphia, PA

Melanoma is the deadliest form of skin cancer; while early detection affords patients a 5-year survival rate greater than 90 percent, survival for metastatic patients is poor. Metastatic dissemination is reliant on melanoma's ability to escape immune surveillance and migrate to distant organs. These processes are heavily influenced by cell surface proteins, which themselves can be regulated by post-translational modifications (PTM) like protein glycosylation. An understudied glycosylation that may affect immune evasion and cancer progression is polysialylation (polySia). Here, a long-chained polymer of sialic acid moieties is formed by the polysialyltransferases ST8SIA2 and ST8SIA4. In silico analysis suggests that compared to normal skin, primary cutaneous melanoma has elevated expression of both ST8SIA2 and ST8SIA4. Interestingly, although ST8SIA4 is upregulated in metastatic samples, its expression is associated with increased survival. Further analysis revealed a positive correlation between CD8+ T cell infiltrates and ST8SIA4 expression. Furthermore, analysis of ST8SIA2 expression shows an inverse correlation with survival and T Cell CD8+ cells infiltration, suggesting ST8SIA2 and -4 differentially regulate the tumor immune microenvironment. One potential polySia modified cell surface protein, mediating these effects is Cell Adhesion Molecule 1 (CADM1). CADM1 is a target of ST8SIA2 and may also be modified by ST8SIA4. Loss of CADM1 increases the invasive properties of melanoma cells and our recent point mutational analysis reveals that the adhesive function of CADM1 might be regulated by polySia at Asp 113. In addition to its role in cancer migration and invasiveness, CADM1 expression may also affect the tumor immune environment. Further investigations are needed to untangle the complex relationship between PolySia modification and melanoma immune evasion and metastasis.

#1399 The role of CCN5 in regulation of tumor-infiltrating lymphocytes (TILS) in triple-negative breast cancer (TNBC) cells.

U. Biswas, A. Kambhampati, N. Haideri, A. De, S. Upadhyay, S. Banerjee, S. Banerjee;
Kansas City VA Medical Center, Kansas City, MO

TNBC accounts for about 15-20 percent of all breast cancer cases, with a high incidence in young and African-American women. TNBC lacks the expression of estrogen receptor, progesterone receptor, and normal human epidermal growth factor receptor type 2 (HER2) copy number with expression. Thus, TNBC is not sensitive to endocrine and targeted molecular therapies. Therefore, surgery and systemic chemotherapy are the primary treatment methods for TNBC. The adjuvant therapy regimen includes anthracycline, paclitaxel, or both in (Neo-) early TNBC. However, this treatment is often ineffective after recurrence or metastasis. Therefore, continuously searching for new targeted therapies and immunotherapies becomes a focus in TNBC treatment in patients with diverse communities. The studies showed that TNBC is more immunogenic than other subtypes of breast cancers with tumor-infiltrating lymphocytes (TILs) in its microenvironment. More importantly, Cytotoxic CD8+ TILs of the adaptive immune system are the most potent effectors in the anticancer immune response and constitute the backbone of cancer immunotherapy. Therefore, a high number of CD8+TILs in TNBC patients' tumors are considered a better prognosis following neoadjuvant chemotherapy. Hence, increasing and activating CD8+ TILs could be an exciting and appropriate approach to treating TNBC. Blocking immune checkpoints can inverse the microenvironment immunosuppressive state and enhance the function of tumor cell clearance. One of the major immune checkpoint therapies has involved a monoclonal antibody against programmed cell death-1 (PD-1)/programmed cell death-ligand 1 (PD-L1), expressed in various tumor cells, including TNBC and immune cells. The studies found that PD-1/PD-L1 negatively regulates CD8+ TILs in cancers, and blockade of PD-1 can induce CD8+ TILs responses in advanced melanoma. Interestingly, PD-1/PD-L1 immunotherapy has also progressed in suppressing TNBC growth and progression. However, the currently available immune checkpoint therapies have therapeutic limitations with the toxicity of the drugs. Thus, new therapeutic options are urgently needed. Our studies found that the expression of CCN5, an anti-invasive gene, correlates with the number of cytotoxic CD8+ TILs in ER+ and HER-2 positive breast cancer samples. Furthermore, we also observed that PD-L1 (programmed death-ligand 1), which was found to have high and low expression in MDA-MB-231 and 4T1, respectively, was suppressed in MDA-MB-231 and 4T1 TNBC cell lines by CCN5 recombinant protein treatment for 48 h. These findings might provide a novel immune checkpoint mechanistic explanation of CCN5 that mediates TNBC growth and progression suppression.

IMMUNOLOGY: Inflammation, Host Factors, and Epigenetic Influences on Cancer Development and Treatment
Poster Session

#1403 The role of Dclk1-expression cells in normal pancreas and in pancreatic tumor progression.
G. Valenti, P. Laise, **F. Wu**, H. Kobayashi, Q. T. Waterbury, R. Takahashi, T. Ruan, Z. Jiang, Y. Ochiai, L. B. Zamechek, T. C. Wang;
Columbia University Irving Medical Center, New York, NY

Background: Tuft cells, marked by Doublecortin-like kinase-1 (Dclk1), are rare in the healthy pancreas but increase markedly during pancreatic tumorigenesis. While Group 2 innate lymphoid cells (ILC2s) are known to modulate inflammation and immunity, their specific roles in cancer-related immunity and immunotherapy interactions with pancreatic tuft cells remain unknown.
Methods: To investigate tuft cells during early pancreatic neoplasia, we used a Dclk1 reporter mouse model and single-cell RNA-seq to study Dclk1-expressing cells in normal pancreas and neoplasia using Mist1/Kras mouse. We treated mice with IL-13 peptides and anti-IL-13 antibodies to explore the IL-13-ILC2 axis in tuft cell regulation.
Results: Within the normal pancreas, Dclk1 expression marked several specialized epithelial cell types, including tuft-like cells, neuroendocrine cells, and a small number of acinar progenitor cells. A notable increase in Dclk1-expressing cells was observed at the onset of early PanIN lesions, with a subsequent decline in advanced PanIN stages and PDAC. Using flow cytometric analysis, we observed an increase in ILC2 cells in the Mist1/Kras pancreas in response to IL33 produced by pancreatic cancer-associated fibroblasts (CAFs). Blocking ILC2 activation with anti-IL33 antibodies reduced Dclk1 cell hyperplasia during PanIN progression. Given the known association between tuft cells, ILC2 cells, and the IL13/IL4 signaling pathways in the intestine, we discovered that Dclk1-expressing cells highly expressed the IL4 receptor (IL4ra). IL-13 levels increased during PanIN progression, and we found that ILC2s comprised the primary source of IL-13 within pancreatic tumors. In vitro, studies showed that the presence of IL-13 maintained the expansion of Dclk1-expressing tuft-like cells in pancreatic organoids derived from Dclk1-DTR-ZsGreen mice. Correspondingly, the in vivo administration of anti-IL-13 resulted in reduced Dclk1 expression.
Conclusion: Previous studies have shown that pancreatic tuft cells inhibit pancreatic cancer progression. Our study reveals a novel regulatory mechanism wherein IL-13 secreted by ILC2s modulates Dclk1 tuft cell expression during pancreatic tumorigenesis. The IL13-ILC2 axis appears to be a potential therapeutic target to regulate Dclk1 cell activity, which could influence the course of pancreatic tumorigenesis. Future investigations will further explore the interaction between the IL13/ILC2 axis and Dclk1 in pancreatic cancer development.

#1404 Blood-based transcriptomics provides novel insights into Sjögren's syndrome-associated lymphomagenesis.

A. Gjyrezi[1], C. Skarlis[2], P. Zumbo[3], D. Betel[3], I. E. Stergiou[2], M. Voulgarelis[2], C. P. Mavragani[2], P. Giannakakou[4];
[1]Weill Cornell Medicine, New York, NY & National Kapodistrian University of Athens, Athens, Greece, [2]National and Kapodistrian University of Athens, Athens, Greece, [3]Weill Cornell Medicine, New York, NY, [4]Meyer Cancer Center, Weill Cornell Medicine, New York, NY

Sjögren's syndrome (SS) is a debilitating autoimmune disorder that carries the highest risk of progressing to lymphoma among all autoimmune diseases, with up to 10% of patients developing SS-associated lymphoma. However, the underlying mechanisms are unknown, and there are currently no actionable targets for prevention and therapeutic intervention.To elucidate the mechanisms associated with SS-lymphoma, we performed RNA-Seq in peripheral blood from SS patients without (n=11) or with lymphoma (n=8). Differential gene expression and pathway analysis identified TNF-α signaling via NF-κB, inflammatory response and interferon gamma (IFN-γ) response as the top pathways enriched in SS-lymphoma patients. Interestingly, the enriched IFN-γ response pathway is consistent with our published work identifying elevated IFN-γ transcript levels in salivary gland tissues from SS patients with lymphoma. Central to SS pathogenesis is the elevation of TNF-α signaling, triggering NF-κB pathway activation and subsequent inflammation, along with inflammasome activation, in line with prior observations. Our data reveal significant upregulation of these pathways in SS-lymphoma patients, which together with the inflammatory response and IFN-γ pathway enrichment, support the idea that persistent autoimmune-related chronic inflammation fosters a microenvironment conducive to lymphomagenesis.Next, we sought to assess the impact of SS immune landscape in SS-lymphoma by performing an immune modular analysis using an established framework of 97 whole blood transcriptomics modules (Pascual), derived from transcripts co-expressed in blood across various autoimmune conditions. This analysis revealed a significant downregulation of T-cell and enrichment of B-cell modules in SS-lymphoma compared to SS patients. These findings are consistent with our biopsy results, showing lower T cell counts in high-grade *vs*. low-grade SS patients. As patients with high-grade SS are more likely to develop SS-lymphoma, these data possibly suggest that suppressed T-cell responses are involved in lymphomagenesis. In addition, the significant enrichment in B-cell transcriptional modules mirrors the observed clinical increase in B cell counts during the transition to SS-lymphoma. Germline mutations in B-cells are thought to drive the clonal expansion of malignant B cells, which may contribute to the observed increase of B cell transcriptomes in SS patients developing lymphoma. We are currently investigating the gene mutation landscape in these datasets to better understand their contribution to SS-lymphomagenesis.This study provides preliminary evidence that chronic inflammation along with dysregulation of T and B compartments in SS significantly contributes to lymphoma progression, emphasizing the need for further research to uncover the molecular basis and develop early diagnostic/intervention tools.

#1405 Development of a humanized anti-IL-22 antibody for cancer and inflammation therapy.

J. Chen, C. Chang, G. Frey, H. Liu, J. Wang, W. J. Boyle, J. M. Short;
BioAtla, San Diego, CA

Interleukin-22 (IL-22) is an inflammatory cytokine involved in the pathology of autoimmune diseases such as psoriasis, atopic dermatitis, and ulcerative colitis. IL-22 has also been shown to promote epithelial cell proliferation, stemness and tumorigenesis in cancer, and is associated with a more aggressive phenotype in a variety of cancers including inflammatory colon cancer models. IL-22 plays a central role in this pathogenic process by driving activation of STAT3 and other signaling cascades. Recent studies demonstrated that neutralization of IL-22 reduced dysplasia and tumor development in preclinical models. However, there has not been a clear application for anti-IL-22 therapy for cancer and autoimmune diseases, likely due to identifying the right disease indication and their low potency and efficacy. Thus, there remains an opportunity to explore the potential of more potent anti-IL-22 therapeutics.

We have developed humanized anti-IL-22 antibodies with high affinities to human, cynomolgus and mouse IL-22 using BioAtla's proprietary antibody discovery and engineering platforms. *In vitro* data demonstrated that our anti-IL-22 antibodies inhibited IL-22-induced p-STAT3 activities. In addition, our antibodies showed a 10-fold increased binding activity to human IL-22 compared to Fezakinumab, which was previously developed by Pfizer for the treatment of autoimmune diseases. To test the functions of our antibodies *in vivo*, we established an inflammation-driven sporadic colitis-associated colorectal (CAC) cancer mouse model. Our humanized anti-IL-22 antibody, a potent, species cross-reactive anti-IL-22 blocking antibody, significantly reduced tumor progression in CAC model. These data suggest that targeting IL-22 reduces tumor occurrence by reducing inflammation-induced tumorigenesis. In addition, we evaluated our anti-IL22 antibodies in an imiquimod-induced psoriasiform skin inflammation mouse model. The mice treated with anti-IL22 antibodies had significantly reduced skin lesions compared to isotype antibody-treated mice. Q-PCR analysis of the mouse skin demonstrated that treatment with our anti-IL-22 antibody led to significantly decreased RNA levels of the imiquimod-induced inflammatory marker CXCL3. In conclusion, the development of a potent, species cross-reactive anti-IL-22 antibody using BioAtla's antibody discovery and engineering platforms addresses the past challenges of anti-IL-22 therapeutics and allows for translational studies in relevant animal efficacy and safety models.

#1406 Plk1 attenuates colon inflammation and tumorigenesis.

Xinyi Wang, Daheng He, Fengyi Mao, Yifan Kong, Chaohao Li, Sai Wu, Jia Peng, Chi Wang, Zhiguo Li, Xiaoqi Liu

University of Kentucky, Lexington, KY

Inflammation-associated colon cancer, linked with long-standing colon inflammation, is often seen in patients with inflammatory bowel diseases (IBD), such as Crohn's disease and ulcerative colitis. Typically, these patients are diagnosed at a younger age compared to those with sporadic colon cancer. Despite some advancements, the detailed molecular mechanisms driving cancer development in IBD remain unclear. Polo-like kinase 1 (Plk1), a serine/threonine kinase and cell cycle regulator, is recognized as an oncogene in various cancers. Intriguingly, higher Plk1 expression correlates with better survival rates in colon cancer patients. Besides, Plk1 also elevates in IBD cases, suggesting its significant role in both colitis and colon cancer. Our study explores Plk1's role in IBD-associated colon cancer using the azoxymethane (AOM)/dextran sulfate sodium (DSS) mouse model, revealing Plk1's suppressive impact on both colitis and related colon cancer.

#1407 Investigating the effect of an aged liver microenvironment on immune surveillance and predisposition to cancer.

A. Aabish Gandhi[1], F. A. Hoffmann[2], M. LaPorte II[3], A. Havas[1], A. Rajesh[1], A. Davis[1], M. G. Teneche[1], J. Proulx[1], S. Kaech[3], P. D. Adams[1];
[1]Sanford Burnham Prebys Medical Discovery Institute, La Jolla, CA, [2]Stanford University, Stanford, CA, [3]Salk Institute of Biological Studies, La Jolla, CA

The incidence of liver cancer is increasing and there is an urgent need for new therapies and preventative strategies. Age is a major risk factor for liver cancer, the reasons for which are not well defined. One of the hallmarks of aging is immune dysfunction which affects liver homeostasis potentially making it prone to cancer. To understand the role of immune dysfunction in aging liver, we analyzed immune cells from young and old livers. As is reported before, in aged livers we observed an increase in $CD101^{\pm}PD1^{\pm}CD8^{\pm}$ T cell population as well as an increase in an $IFN\gamma^{\pm}TNF\alpha^{\pm}$ population suggesting an increase in T cell response in an aging liver. We next sought to understand the cause of T cell exhaustion in aged livers. Cell cluster analysis of the young (4-month-old) and old (22 month old) livers by scRNA seq revealed a cell population unique to the aged livers, showing increased expression of immune checkpoint ligands as well as tumor-initiating cell markers. We validated this data by flow cytometry. We next functionally probed the immune environment of aged liver, by testing the effect of cognate antigen expression in young and old hepatocytes on adoptively transferred activated P14 $CD8^{\pm}$ T cells isolated from a young P14 mouse. Analysis of the *ex vivo* activated P14 $CD8^{\pm}$ T cells from young and old antigen-expressing livers by flow cytometry and scRNA sequencing revealed increased exhaustion and cytokine-deficiency in old mice as compared to the young mice. This study explores the age-associated alterations in the immune cells in the liver, aiming to alter liver-resident immune cells and their metabolic states in a way that promotes anti-tumor immunity in an aging liver.

#1408 Intrahepatic IgA complex induces polarization of cancer-associated fibroblasts to matrix phenotypes in the tumor microenvironment of HCC.

P. Sung;
Catholic University of Korea, Seoul, Korea, Republic of

Background and Aims: Cancer-associated fibroblasts (CAFs) are activated fibroblasts that play key roles in the tumor microenvironment (TME). Immunoglobulin A (IgA) contributes to inflammation and anti-tumor immunity dismantling in the human liver. We investigated the effects of the IgA complex on CAFs in the TME of hepatocellular carcinoma (HCC).
Approach and Results: CAF dynamics in HCC TME were analyzed via single-cell RNA sequencing of HCC samples. CAFs were isolated from 40 HCC samples. The isolated CAFs were treated with mock or serum-derived IgA dimers. Following treatment with the mock or serum IgA dimers in vitro, co-culture experiments were performed using CAF and $CD8^{\pm}$ T cells. Single-cell analysis showed that sub-cluster proportions in the CAF-fibroblast activation protein-α (FAP) matrix were significantly increased in patients with high serum IgA levels. We were performed flow cytometry on fresh surgical tissues and observed a significant increase in the mean fluorescence intensity (MFI) of FAP in the $CD68^{\pm}$ cells from patients with high serum IgA levels compared to those with low serum IgA levels ($p<0.001$). We validated that the transferrin receptor (CD71) is expressed in CAFs ($p<0.01$). IgA-treated CAFs exhibited higher programmed death-ligand 1 (PD-L1) expression levels than mock-treated CAFs ($p<0.05$). Co-culture with CAFs induced the attenuation of the cytotoxic function of activated $CD8^{\pm}$ T cell, and these cells co-cultured with IgA-treated CAFs exhibited increased expression levels of programmed death-1 (PD-1) compared to those co-cultured with mock-treated CAFs ($p<0.05$).
Conclusions: Intrahepatic IgA induces polarization of HCC CAFs into more malignant matrix phenotype and attenuates cytotoxic T cell function. Our study uncovers five dynamic CAF subpopulations within HCC tissues and highlights their potential roles in tumor progression and immune suppression.

#1409 The role of liver receptor homolog 1<LRH-1>in regulating breast cancer progression by modulating the immune response.

Y. Wang[1], B. Duong[1], N. Krawczynska[1], S. V. Bendre[1], C. P. Schane[1], E. Weisser[1], L. Kockaya[1], Y. Fei[1], A. Das Gupta[1], H. E. Vidana Gamage[1], A. T. Nelczyk[2], E. R. Nelson[1];

[1]University of Illinois at Urbana-Champaign, Urbana, IL, [2]Helixon US Inc, Champaign, IL

Breast cancer remains the second leading cause of cancer-related death among American women, with the majority of morality being associated with metastatic disease. At this stage, immunotherapy is only approved for a small subset of patients whose tumors are of the triple negative subtype <TNBC> that stain positive for PD-L1. However, the majority of these tumors prove refractory. Thus, it is imperative to develop novel therapeutic targets to improve the immune response in breast cancer. Since cholesterol metabolism is important for myeloid immune cell function, we launched studies to identify proteins involved in cholesterol homeostasis that are amenable to small molecule intervention. Liver Receptor Homolog 1 <LRH-1/NR5A2> is highly expressed in myeloid cells, particularly neutrophils. We have found that elevated LRH-1 expression in breast cancer patients is associated with increased overall and recurrence-free survival rate. Thus, we hypothesized that LRH-1 acts as an immune modulator in myeloid cells, with subsequent effects on breast cancer progression. We initiated a series of experiments to characterize the role of LRH-1 in important aspects of neutrophil function: migration, NETosis, phagocytosis and influence on T cells. Neutrophils and neutrophil NETosis has previously been implicated in breast cancer progression including reemergence from dormancy and metastatic recurrence. Interestingly, we found that LRH-1 inhibits neutrophil migration towards cancer cells, a finding that may have important implications regarding infiltration of immune-suppressive myeloid cells. Furthermore, neutrophils treated with an LRH-1 agonist demonstrated decreased NETosis, while an antagonist resulted in increased NETosis. On the other hand, LRH-1 agonist treatment strongly decreased the neutrophil phagocytotic ability, while treatment with an antagonist did not significantly impact this process. Finally, T cells had increased expansion when cocultured with neutrophils that had been previously treated with an LRH-1 agonist, and reduced proliferation in the presence of neutrophils pretreated with an LRH-1 antagonist or inverse agonist. This was especially apparent in CD4+ helper T cells and later divisions. Ongoing work is aimed at determining the pathological relevance of these findings.

Collectively, our data indicate that LRH-1 plays important roles in regulating different neutrophils functions, including migration, NETosis, phagocytosis, and T cell expansion. Overall, these findings suggest that LRH-1 in neutrophils regulates the immune response, and therefore can be a potential therapeutic target for cancer patients.

Funding: National Cancer Institute (ERN: R01CA234025) Department of Defense (ERN: BCRP Era of Hope Award)

#1410 An effect of Phenylalanine hydroxylase (PAH) deficiency on cancer development in kidney.

S. Kim[1], J. Park[1], J. Park[1], C. Kang[1], K. Moon[2], S. Han[3], Y. Koh[3], S.-S. Yoon[3];

[1]Seoul National University College of Medicine, Seoul, Korea, Republic of, [2]Seoul National University Hospita, Seoul, Korea, Republic of, [3]Seoul National University Hospital, Seoul, Korea, Republic of

Several studies have noted the importance of amino acid metabolism in cancer progression. Preliminary research using public cancer multi-omics data has revealed associations between heterozygous germline mutations in genes associated with amino acid metabolism and cancer development. In particular, the heterozygous status of the PAH gene enhances the risk of developing kidney cancer by more than three times. Phenylalanine hydroxylase (PAH) is an enzyme that converts phenylalanine to tyrosine. It is highly expressed in the liver and kidneys. Analysis of the blood metabolome in prospectively collected PAH heterozygous carriers indicates that heterozygous status causes metabolome fluctuations in the body. By the way, renal cell carcinoma (RCC) is an immunogenic tumor mainly infiltrated by T cells. Accordingly, we suggest that defects in the PAH gene change the metabolites in the body, leading to a reduction in immune function and an increased risk of developing kidney cancer. First, the expression of the PAH protein was confirmed through immunohistochemistry in a tissue microarray from RCC patients, and the results were then compared with clinical information. Next, we simulated the environment of PAH deficiency in vitro by treating the cells with phenylalanine (Phe) and its metabolite, phenylpyruvate (PRA), which accumulates during PAH dysfunction. The cytotoxicity of Phe and PPA was investigated using the WST assay. The Jurkat T cell line was cultured long-term in a medium containing Phe or PPA and then stimulated with PHA/PMA. Cytokine secretion was confirmed in these supernatants. In addition, purified primary human pan T cells were stimulated with Anti-CD3/CD28 in the medium containing either Phe or PPA. Proliferation was evaluated using CFSE staining. The IHC was performed on 467 tissues from RCC patients aged 29 to 101 years. We classified the cases into three scale scores based on the percentage of PAH intensity. Approximately 73% of cases were PAH-negative, and only 27% were positive (score 1+ or 2+). A comparison of IHC results with clinical information showed that lower PAH expression was associated with a lower relapse-free survival rate. Next, Phe and PPA exhibited minimal cytotoxicity. The secretion of representative proinflammatory cytokines IL-2 and TNF- α were dose-dependent and significantly decreased with Phe and PPA treatment. Additionally, cell proliferation, a critical step in acquiring effector functions of T cells, was inhibited by treatment with Phe and PPA, particularly in the CD8+ T cell population compared to CD4+ T cells. These results suggest that metabolite changes within the tissue microenvironment of the kidney, caused by Pah defects, may suppress anti-tumor immunity by impairing the function of immune cells. This novel discovery may contribute to the importance of the PAH gene as a new biomarker for diagnosing kidney cancer and to the development of kidney cancer therapy.

#1411 Cell-type-specific transcriptomic immune aging clocks reveal clinically relevant associations with chronic illnesses including cancer.

Y. Gurevich-Schmidt[1], **K. Wang**[1], D. Wu[1], S. Madan[1], V. Gopalan[1], S. Sinha[2], B. Wang[1], S. Dhruba[1], A. A. Schaffer[1], E. Ruppin[1];
[1]NIH-NCI, Bethesda, MD, [2]NCI-Designated Cancer Center Sanford Burnham Prebys Medical Discovery Institute, San Diego, CA

The aging of the immune system has profound implications for individual immune responses, yet precise quantification of immune age remains a challenge. Analyzing single-cell peripheral blood mononuclear cells (PBMC) transcriptomics data from 981 healthy individuals, we developed IMMClock (IMMune Clock), a human immune age clock derived from single cell transcriptomics. IMMClock is the first to accurately assess the age of three major immune cell types, CD8+ T cells, CD4+ T cells and NK cells, at the individual level. Testing the ability of these clocks to capture the dynamic aging process, we show that they reliably predict individuals' chronological ages across seven publicly available single-cell transcriptomics datasets and the large Framingham bulk transcriptomics cohort. IMMClock identifies cell type specific age-related pathways including apoptosis, interferon gamma response, and cytokine response. The application of IMMClock reveals several associations between immune aging of different cell-types and key clinical phenotypes during aging: it recapitulates the established observation of higher immune age in males compared to females and uncovers higher immune age in CD8+ T cells of smokers and individuals with chronic illnesses including cancer. Analyzing cancer patients' data, IMMClock readings strongly correlate with CD8+ T cell exhaustion levels, and, quite strikingly, highlights an elevated immune age in the tumor microenvironment compared to blood.

#1412 Immune and metabolic control of Th17 cells by TMEM176B: Potential implication in cancer immunotherapy.

S. Russo, M. Malcuori, M. Segovia, M. Hill;
University of the Republic, Faculty of Medicine, Montevideo, Uruguay

Helper $CD4^{+}$ T cells are key players in the adaptive immune response that differentiate into different subpopulations. One of these subpopulations are T helper 17 (Th17) cells. In cancer, the role of Th17 cells is still controversial. The dual effect that Th17 cells seem to have in cancer can be explained by the great heterogeneity and/or plasticity of these cells. Two different subpopulations of Th17 cells have been reported: regulatory or “non-pathogenic” Th17 cells and effector or “pathogenic” Th17 cells. We currently know that this dual behavior depends on the cytokine microenvironment in which Th17 cells differentiate. However, the molecular basis of how, when, and why Th17 cells differentiate into effector or regulatory populations, as well as its *in vivo* relevance, are still poorly understood. Here we show that intrinsic expression of TMEM176B can determine the fate of Th17 cells. TMEM176b is a druggable immunoregulatory ion channel which function was first described by our team. We have found that in *in vitro* differentiated Th17 cells, *Tmem176b* is over-expressed in regulatory Th17 cells compared to effector Th17 cells, in agreement with its immunoregulatory properties. Furthermore, we found that *Tmem176b* influence Th17 polarity, since Th17 *in vitro* differentiation with IL-6+TGF-β from naïve *Tmem176b*$^{-/-}$ $CD4^{+}$ T cells results in an enhanced IFN-γ production. Same results were obtained by pharmacological inhibition of TMEM176B in WT $CD4^{+}$ T cells. Functional evaluation of these cells showed a decreased regulatory capacity compared to WT Th17 cells. Thus, WT Th17 cells inhibited $CD8^{+}$ T cell proliferation whereas *Tmem176b*$^{-/-}$ Th17 cells showed poor inhibitory capacity. Supporting this effector-like phenotype, *Tmem176b*$^{-/-}$ Th17 cells have higher basal pAKT/AKT ratio compared to WT Th17 cells. Furthermore, *Tmem176b*$^{-/-}$ Th17 cells have a better metabolic fitness than WT Th17 cells, with higher glycolysis and oxidative phosphorylation. It was reported that the effector role of Th17 cells is dependent on the IL-1β production through ASC-NLRP3-caspase 8 activation. Here we show that *Tmem176b*$^{-/-}$ Th17 cells stimulated with ATP have a higher Caspase-8 activation compared to WT Th17 cells. All these results suggest that *Tmem176b* deficiency leads to an effector-like Th17 cell phenotype when cells are differentiated in a regulatory cytokine microenvironment. Moreover, co-culture of *Tmem176b*$^{-/-}$ Th17 cells with *in vitro* generated exhausted $CD8^{+}$ T cells results in a reduction of the frequency of terminal exhausted $CD8^{+}$ T cells and of mitochondrial reactive oxygen species production compared to co-culture with WT Th17 cells. Therefore, *Tmem176b*$^{-/-}$ Th17 may have enhanced anti-tumor properties compared to WT Th17 cells. In conclusion, we have identified a new intrinsic regulator of Th17 cells, TMEM176B, which may constitute a molecular target to pharmacologically modulate these cells.

#1413 BRCA1 loss is synthetic lethal with double stranded RNA: A genome wide CRISPR screen to identify mechanisms of RNASEL independent death.

D. Trastulli, G. Vozza, V. Pinamonti, **L. Mazzarella**;
IEO - European Institute of Oncology, Milan, Italy

Double-stranded RNAs (dsRNAs) are potent immunostimulatory nucleic acids of viral origin but also physiologically produced by mammalian cells. Recent studies demonstrated that elevating dsRNA levels, either exogenously through dsRNA mimetics like Polyinosinic-polycytidylic acid (pI:C) or endogenously through epigenetic modulation of retroviral elements, can elicit anticancer effects. In response to dsRNA, cells elicit a dual response consisting in Interferon (IFN) production and translational shutdown associated, in some cells, with cell death. These two responses are linked in a feed-forward loop in which induced cytokines themselves enhance dsRNA sensing by the death-inducing pathway, complicating our understanding of the cell-intrinsic mechanisms at play. The 2,5-oligoadenylate synthetase (OAS)-RNASEL system is widely thought to be the main responsible for dsRNA-induced cell death, but it remains unclear how its activity leads to cell death.To elucidate these mechanisms, we decided to minimize the impact of interferon modulation by studying dsRNA-induced death in interferon-saturated conditions. RNASEL-KO A549 cells were, as expected, refractory to IFN+pI:C induced cell death; however, inhibiting protein synthesis or RNA transcription with Cycloheximide (CHX) or Actinomycin D (ActD) abolished the need for RNASEL causing RNASEL-KO cells to undergo apoptosis, although CHX/ActD alone had no effect. In addition, HT-29 cells revealed no clear dependence on RNASEL for dsRNA-induced cell death. Transient ablation through siRNA showed that this novel death-inducing pathway is independent of other canonical dsRNA sensors such as RIG-I, MDA5 and PKR. We then performed a genome-wide CRISPR screen for factors involved in dsRNA-induced death in our interferon-saturated conditions in HT29 cells. Pathway enrichment analysis of screen hits revealed that RNA surveillance, RNA Polymerase II Transcription Initiation, Mitochondrial translation and respiratory chain and DNA Repair genes have a protective role against dsRNA increase. In particular, we validated the synthetic lethality of IFN+pI:C with BRCA1 by CRISPR. Ongoing research is aimed at validating this interaction in vivo models.Our work shed light on potential new mechanisms involved in dsRNA dependent cell death, revealing a connection with DNA damage and BRCA1. If confirmed, these findings may pave the way for the use of dsRNA mimetics, possibly in conjunction with immune checkpoint inhibitors, in the treatment of BRCA1-mutated tumors.

#1414 HBM9014, a first-in-class fully human anti-LIFR antibody with excellent preclinical efficacy and safety profile.

Jue Zeng[1], Dongxu Zhang[2], Louis Liu[1], **Lingbing Zhang**[2]

[1]Harbour BioMed, Natick, MA,[2]Yinuoke, Ltd., Nanchang, China

Background: Leukemia inhibitory factor (LIF) and cardiotrophin like cytokine factor 1 (CLCF1) are multi-functional cytokines from IL-6 family. They are reported to be highly expressed in a variety of human cancers such as pancreatic carcinoma, cholangiocarcinoma, NSCLC, GBM, head and neck cancer etc. Their expression is associated with poor prognosis and survival. LIFR is the key component of LIF/CLCF1 receptors. Antibody targeting LIFR has the advantage to block both LIF and CLCF1 pathways thus inhibiting tumor growth more effectively than products to block single cytokines.
Methods: Fully human Anti-LIFR antibodies were generated from H2L2 Harbour Mice® transgenic platform. *In vitro* function of the antibodies was tested for their abilities to block LIF/CLCF1 induced downstream signaling pathway and tumor spheroid proliferation. *In vivo* efficacy was tested in multiple tumor models as monotherapy and in combination with cisplatin. DRF toxicokinetics was evaluated on NHP with a 4-week repeat-dose toxicity study.
Results: HBM9014, a fully human anti-LIFR antibody generated by H2L2 Harbour Mice®, specifically binds LIFR thus blocks the interaction between LIF/CLCF1 and their respective receptors, inhibits downstream STAT3 phosphorylation, and reduces exogenous and endogenous LIF induced tumor spheroid proliferation in vitro. Furthermore, HBM9014 shows potent anti-tumor activity in multiple tumor models in vivo. In a GLP NHP 4-week repeat-dose toxicity study, HBM9014 is well tolerated up to 150 mg/kg with no discernable drug-related toxicity.
Conclusions: HBM9014 specifically binds to the key component of LIF and CLCF1 receptor, LIFR, thus blocks both LIF and CLCF1 signaling pathways. HBM9014 shows significant cell proliferation inhibition alone or in combo with small molecule inhibitors in 3D culture of multiple cancer cell lines. It also shows significant in vivo antitumor efficacy as monotherapy, and enhanced efficacy in combination with Cisplatin in multiple mouse models. Importantly, despite the benefits of double blocking, HMB9014 has an excellent safety profile. Taken together, HMB9014 is a promising drug candidate for advanced cancer with favorable efficacy and safety profiles that warrant clinical validation.

#1415 Reduction in photoimmunotherapy-induced edema with COX-2 inhibition: Combatting clinically relevant adverse events without compromising efficacy.

G. Ma, M. Gordon, J. Lapetoda, A. Lozano, C. M. Amantea, T. Osada, A. H. Thorne;
Rakuten Medical, San Diego, CA

ASP-1929 photoimmunotherapy (PIT), an investigational drug-device combination, consists of an epithelial growth factor receptor (EGFR)-targeting drug, cetuximab, conjugated to a light-activatable dye, IRDye® 700DX, and a laser light. Localized illumination results in rapid and selective tumor necrosis in the preclinical setting, and early clinical studies demonstrate a manageable safety profile in patients with head and neck squamous cell carcinoma. In the ongoing clinical trials, however, edema is a commonly reported adverse event and laryngeal edema, requiring prophylactic tracheostomy, has been noted in some patients. Thus, a critical need exists to provide clinicians with tools to manage ASP-1929 PIT-associated edema to ensure optimal patient outcome. To evaluate edema following cancer-targeted PIT, we developed a mouse tumor model and used it to characterize the mechanism of edema development and evaluate various methods for edema reduction. Briefly, cohorts of mice bearing syngeneic LL/2 tumors engineered to express Ephrin A2 (EphA2) were administered an anti-EphA2 antibody conjugated to IR700 (conjugate) or saline control. Light was applied 24h following administration and edema was measured by caliper. In control mice, light alone did not generate edema; however, mice treated with conjugate plus light showed a light-dose dependent increase in edema volume which peaked at 6h post light delivery. We next evaluated a series of inflammatory cytokines and immune cell populations in the blood and tumor region at the onset (2h), peak (6h), and resolution (24h) of PIT-induced edema. We found a striking increase in neutrophils (500-fold greater than control mice, n=10, $p<0.0001$) in the blood at the peak of edema formation coinciding with a significant increase in IL-6 (n=5, $p<0.001$) and IL-10 (n=5, $p<0.05$), indicating the onset of a heightened inflammatory response. To combat the edema formation, we next evaluated the effect of various anti-inflammatory drugs commonly used in the clinical setting. Cohorts of mice were administered conjugate plus light in the presence or absence of steroids or the selective COX-2 inhibitor meloxicam. Results show there is no reduction in edema by steroids regardless of timing of administration. Conversely, the addition of meloxicam resulted in a significant reduction in edema at all time points and light doses evaluated: 40-50% reduction at both 2h and 6h post-PIT when administered prophylactically and 25% reduction at 6h post-PIT when administered post-light (all settings, n=10, $p<0.0001$). Importantly, we found the reduction in edema with meloxicam was not associated with a loss of therapeutic benefit based on measurement of tumor growth. In conclusion, the use of COX-2 inhibitors may be directly translated to the clinic for the benefit of patients receiving ASP-1929 PIT and should undergo further evaluation.

#1416 Resolvins enhance immunotherapy to induce Fanconi anemia tumor regression via inflammation resolution.

K. Quinlivan[1], H. Yang[2], D. R. Bielenberg[3], S. I. Wells[4], C. N. Serhan[5], D. Panigrahy[1];

[1]Beth Israel Deaconess Medical Center, Harvard Medical School, Boston, MA, [2]College of Food Science and Nutritional Engineering, China Agricultural University, Beijing, China, [3]Boston Children's Hospital, Harvard Medical School, Boston, MA, [4]Cancer and Blood Diseases Institute, Cincinnati Children's Hospital Medical Center, Cincinnati, OH, [5]Brigham and Women's Hospital, Harvard Medical School, Boston, MA

Fanconi anemia (FA) is a disorder characterized by early-onset solid tumors unresponsive to chemotherapy and radiation. Unresolved inflammation is a hallmark of FA, the mechanisms underlying the initiation and resolution of inflammation in FA are poorly characterized. We hypothesized that FA tumor progression is controlled by dysregulated resolution metabolomes and a systemic pro-inflammatory eicosanoid storm of inflammation-initiating mediators. Using a novel transplantable murine FA tumor model, we show that Fancc-/- HNSCC (head and neck squamous cell carcinoma) progression disrupts the resolution of inflammation via an imbalance between specialized pro-resolving lipid mediators (SPMs) and eicosanoids. Fancc-/- tumor-bearing mice exhibited an increase in eicosanoids, including leukotriene B_4 (LTB_4) and thromboxane B_2 (TXB_2) in the spleen and a 113% increase in prostaglandin E metabolite (PGEM), a marker of PGE_2 production, in the plasma compared to non-tumor-bearing (NT) mice. Fancc-/- tumor-bearing mice exhibited a loss in the SPM/LTB_4 ratio including RvD1/LTB_4, RvD2/LTB_4, and MaR1/LTB_4, compared to NT mice. Given the activity of immune checkpoint blockade in mismatch repair deficient tumors including head and neck cancers, immunotherapy may be relevant to FA-induced cancers. Importantly, the number of absolute T cells and CD4+ T cell function is preserved in individuals with FA. We combined stimulation of the resolution of inflammation (i.e., treatment with RvDs) with immunotherapy in a new transplantable murine FA tumor model. While treatment with RvD4, RvD5, or anti-PD1 immunotherapy alone delayed tumor growth compared to control at treatment day 20, the tumors did escape monotherapy by treatment day 30. Remarkably, RvD4 or RvD5 combined with anti-PD1 immunotherapy induced sustained Fancc-/- tumor regression. Moreover, RvD4 and/or anti-PD1 immunotherapy inhibited orthotopic Fancc-/- tumor growth compared to control. Resolvins and immune checkpoint blockade synergistically induced *Fancc-/-* tumor regression via macrophage phagocytosis of apoptotic debris, counter-regulation of pro-angiogenic cytokines, and inhibition of angiogenesis. Triggering Receptor Expressed on Myeloid cells-2 (TREM2)-antagonism combined with resolvins and immunotherapy restored SPM/eicosanoid ratios in *Fancc*$^{-/-}$ tumor-bearing mice to pre-cancer levels. SPMs and eicosanoids provide potential early biomarkers and biological targets in FA-induced cancer progression. Stimulating the resolution of inflammation via pro-resolution lipid mediators to enhance immunotherapy is a novel host-centric therapeutic approach to prevent FA-induced cancer progression via debris clearance and cytokine suppression. These results provide evidence for targeting the resolution of inflammation via resolvins to enhance immunotherapy to prevent and/or reverse FA-induced cancer progression.

#1417 IRF8 driven reprogramming of the immune microenvironment enhances anti-tumor adaptive immunity and reduces immunosuppression in murine glioblastoma.

Megan Montoya, Sara A. Collins, Pavlina Chuntova, Noriyuki Kasahara, Hideho Okada

Neurological Surgery, UCSF - University of California San Francisco, San Francisco, CA

Glioblastoma (GBM) has an extremely immunosuppressive microenvironment, primarily mediated by the recruitment of immature myeloid cells (IMCs) to the tumor. IMCs suppress T cell function and dampen the anti-tumor response. In this study, we sought to “reprogram” IMCs into antigen-presenting cells (APCs) to enhance anti-tumor T cell responses. To induce IMC differentiation into APCs, we utilized a retroviral replicating vector (RRV) expressing IRF8, a master regulator of type 1 conventional dendritic cell (cDC1) development. We evaluated the impact of IRF8 RRV on *in vivo* tumor growth kinetics, survival, immunosuppression, and immune microenvironment. Because RRV transduction requires the proliferation of target cells, we assessed the proliferative capacity of myeloid cells in murine and human GBM samples. We utilized the SB28 cell line, a poorly immunogenic murine GBM model. We pre-transduced SB28 cells with IRF8 RRV and implanted them intracranially into syngeneic C57BL/6 mice; controls expressed an empty vector. Intratumoral myeloid cells were proliferative in both murine and human samples. In vivo, tumor and myeloid cells are infected proportionately to their respective levels of proliferation. Mice with IRF8 RRV pre-transduced intracranial tumors had significantly longer survival (median 28 days) compared to controls (median 19 days) ($p < 0.0001$). Additionally, tumor growth was delayed in IRF8 RRV mice. IRF8 RRV mice had significant enrichment of dendritic cells ($p = 0.0145$), cDC1s ($p < 0.0001$), T cells ($p = 0.0025$) and CD8+ T cells ($p < 0.0001$). Both monocytic and granulocytic IMCs had decreased expression of the immunosuppressive markers Arginase 1 and IDO1. Further, *ex vivo* co-culture of intra-tumoral myeloid cells with naïve T cells showed a functional decrease in immunosuppression in IRF8 RRV tumors compared to controls ($p < 0.0001$).

To study the mechanism of action, we assessed whether IRF8 transduction of tumor cells alone or both tumor and immune cells, was necessary for the observed survival benefit. To inhibit RRV spread from infected cells to other cells, we treated mice with azidothymidine, a reverse transcription inhibitor. A robust survival benefit and tumor growth inhibition were seen only in mice where the RRV could spread freely ($p = 0.0005$). This finding shows that both tumor and immune cells must be infected to cause the phenotype and suggests that reprogramming immune cells is required for therapeutic efficacy.

Our novel approach used RRV to deliver a myeloid transcriptional regulator in intracerebral GBM. This therapy achieved significant survival benefits and increased intratumoral cytotoxic T cells and APCs, while decreasing myeloid immunosuppression. Further studies will expand upon the mechanism of action and test combination therapies.

#1418 Priming of the glioblastoma tumour microenvironment via copper chelation to enhance the efficacy of immunotherapies.

Tyler Shai-Hee[1], Toni Rose Jue[2], Riccardo Cazzoli[2], Jourdin R. C. Rouaen[2], Filip Michniewicz[3], Jessica Bell[2], Tessa Gargett[4], Michael P. Brown[4], Orazio Vittorio[1]

[1]School of Clinical Medicine, Faculty of Medicine & Health, UNSW Sydney, Kensington, Australia,[2]Children's Cancer Institute, Lowy Cancer Research Centre, UNSW, Kensington, Australia,[3]School of Biomedical Sciences, Faculty of Medicine & Health, UNSW Sydney, Kensington, Australia,[4]Translational Oncology Laboratory, Centre for Cancer Biology, SA Pathology and University of South Australia, Adelaide, Australia

Glioblastoma, a highly aggressive brain tumor with a dismal prognosis necessitates novel therapeutic approaches as current standard treatments yield limited success. Despite the transformative impact of immune checkpoint blockade in various malignancies, its efficacy in glioblastoma remains elusive. Similarly, chimeric antigen receptor T (CAR-T) cell therapy, while successful in hematological malignancies, faces challenges in solid tumors. This study addresses the immunosuppressive barriers hindering the effectiveness of immunotherapies in glioblastoma. Highlighting copper's pivotal role in glioblastoma, our research group demonstrated its elevation and influence on PD-L1 expression. Given the success of copper chelators in treating Wilson's Disease, in which neurological manifestations are alleviated following treatment, we hypothesized that copper chelation therapy could be a promising strategy for glioblastoma, especially when combined with immunotherapies. Flow cytometry analysis revealed a significant increase in the tumor-associated antigen GD2 following treatment with the copper chelator trientine (TETA), suggesting its potential synergy with GD2-targeted immunotherapies. In an immunocompetent murine glioblastoma model, combination therapy with GD2-targeted CAR-T cells and TETA effectively slowed tumor growth, demonstrating enhanced efficacy. Additionally, TETA as a monotherapy significantly improved survival compared to the control. The combination of TETA with anti-PD1 antibody therapy also exhibited promising results in inhibiting tumor growth and subsequently prolonging survival, with some mice demonstrating complete tumor regression. Importantly, TETA decreased copper levels in the brains of the mice, indicating the drug can act on the brain, a crucial therapeutic hurdle that is hampering the efficacy of novel therapies in glioblastoma. Further exploration of immune cell populations using OPAL Multiplex immunohistochemistry following TETA, anti-PD1, and GD2-targeted CAR-T cell treatments will underscore the potential of copper chelation in reshaping the tumor microenvironment. Our findings suggest that copper chelation, with agents like TETA, can be repurposed as a viable anticancer therapy when combined with immunotherapies. This study provides a compelling rationale for further pre-clinical validation, offering a potential breakthrough in the quest for effective glioblastoma treatments.

#1419 Locoregional delivery with engineered stem cells modulates immunosuppressive tumor microenvironment in brain leptomeningeal metastasis.

N. Kanaya[1], W. Seddiq[2], K.-S. Chen[2], Y. Kajiwara[2], L. Moreno Lama[2], S. Kuroda[1], T. Fujiwara[1], H. Wakimoto[3], K. Shah[2];
[1]Okayama University Graduate School of Medicine, Dentistry, and Pharmaceutical Sciences, Okayama, Japan, [2]Harvard Medical School/Brigham and Women's Hospital, Boston, MA, [3]Harvard Medical School/Massachusetts General Hospital, Boston, MA

Leptomeningeal metastasis (LM) is one of the severe disease conditions in brain metastasis (BM) and results in poor prognosis and reduction of quality of life. Immunotherapies such as anti-Programmed cell Death (PD)-1 antibodies have shown improved overall survival against non-small cell lung cancer (NSCLC).. However, the clinical benefit of patients with NSCLC derived LM is still limited due to poor penetration of therapeutic agents into the brain and cerebrospinal fluid (CSF) and lack of understanding of the tumor microenvironment in LM. In this study, we first developed immune-competent mouse models of LM which show significantly decreased immune cells and increased PD-1+ T cells in the tumor microenvironment as compared to primary NSCLC tumors, thus mimicking primary and LM NSCL in patients. Next, we explored the use of oncolytic herpes simplex virus (oHSV) that selectively replicate in tumor cells and illicit an antitumor effect via oncolysis and production of neoantigens for targeting LM NSCLC. Given that virus neutralization, and inefficient extravasation are the major barriers to the effective systemic delivery of oHSV to target metastatic tumor lesions in the brain, we utilized mesenchymal stem cells (SC) and created two population of mesenchymal SC types: one for loading oncolytic herpes simplex virus (oHSV) and another one, engineered with knockout of Nectin-1 receptor by CRISPR/Cas9 technique to be resistant to oHSV, for secreting single-chain variable fragment (scFv) anti-PD-1. We show that locoregional treatment improved therapeutic outcomes by inducing oHSV-mediated immunogenic cell death, and activation of anti-tumor T cell signaling in mouse NSCLC LM tumors. Our novel SCs based immunotherapeutic strategy provides a roadmap towards treatment of lung to brain leptomeningeal metastatic patients.

#1420 Mechanism of NPRL2 gene therapy induced antitumor immunity in KRAS/STK11^{mt} aPD1 resistant metastatic NSCLC.

I. M. Meraz, M. Majidi, R. Song, F. Meng, L. Gao, Q. Wang, J. Wang, E. Shpall, J. A. Roth;
UT MD Anderson Cancer Center, Houston, TX

NPRL2/TUSC4 is a tumor suppressor gene whose expression is reduced in many cancers including NSCLC. Restoration of NPRL2 induces cell cycle arrest and apoptosis. We investigated the antitumor immune responses to NPRL2 gene therapy in aPD1 resistant KRAS/STK11^{mt} NSCLC in a humanized mouse model. Humanized mice were generated by transplanting human cord blood-derived CD34 stem cells into NSG mice. Mice harboring > 25% human CD45 cells were considered humanized. Lung metastases were developed in humanized mice by injecting KRAS/STK11^{mt}/aPD1^{R} A549 cells, which were treated with i.v. injection of NPRL2 nanoparticles (DOTAP-NPRL2) with or without pembrolizumab (aPD1). NPRL2 treatment reduced lung metastases, whereas pembrolizumab was ineffective. The antitumor effect was greater in humanized than non-humanized mice suggesting the role of immune cells. The antitumor effect was associated with increased infiltration of human cytotoxic immune cells and decreased numbers of Treg in tumors. NPRL2+ pembrolizumab was not synergistic in this resistant model but was synergistic in KRAS^{wt}/aPD1^{S} H1299 tumors. Cytotoxic immune cells in tumors were associated with the antitumor effect. Consistent with A549, NPRL2 showed a significantly strong antitumor effect on other KRAS^{mt}/aPD1^{R} syngeneic LLC2 tumors whereas aPD1 was not effective. The antitumor effect of NPRL2 was correlated with HLA-DR$^{\pm}$ DC, CD11c DC, TILs and NK cells in TME. The antitumor effect of NPRL2 was abolished upon in-vivo depletion of CD4, CD8 T, and MΦ in the LLC2 tumor model. However, no effect was found on in-vivo depletion of NK cells. Nanostring analysis on lung metastasis resulted in a distinct pattern of human gene expression by NPRL2. T cell functional genes, including IFNγ, CD8b, CD7, TNFSF18, ITGA1, GATA3 and TBX21 were significantly increased. Conversely, the negative regulatory genes, including FOXP3, TGFB1, TGFB2, and IL-10RA were inhibited. NPRL2 also downregulated T cell co-inhibitory molecules, including CTLA4, ICOS, LAG3, PDCD1, CD274, IDO1, PDCD1LG2, CD47, and KLRB1. Stably expressing NPRL2 clones were established, and tumors in humanized mice with these clones exhibited significantly slower growth compared to controls. TME analysis showed an upregulation of human CD45, CD3, CD8 T, HLA-DR+ DC and a downregulation of Tregs, CD3$^{\pm}$PD1$^{\pm}$T, MDSC, and CD163$^{\pm}$ TAM in tumors expressing NPRL2. The stable cells showed a substantial increase in both colony formation inhibition and apoptosis. Stable clones showed heightened sensitivity to carboplatin in colony formation, apoptosis, and PARP cleavage assays. Stable expression of NPRL2 resulted in the downregulation of both AKT-mTOR and MAPK pathways by inhibition of pAKT, pmTOR, pPRAS40, p4E-BP1, pS6, and pERK1/2. Taken together, NPRL2 gene therapy induces antitumor activity on KRAS/STK11^{mt}/aPD1^{R} tumors through DC-mediated antigen presentation and cytotoxic immune cell activation

#1421 The HDAC6-specific inhibitor AVS100 (SS208) blocks M2 polarization of tumor associated macrophages and potentiates immunotherapy in preclinical tumor models.

D. Kovalovsky[1], S. Noonepalle[2], M. Suresh[2], D. Kumar[1], M. Berrigan[3], A. Horvath[3], A. Kim[3], D. Quiceno-Torres[2], K. Musunuri[1], A. Villagra[2];
[1]Avstera Therapeutics Corp., Malvern, PA, [2]Georgetown University, Washington, DC, [3]The George Washington University, Washington, DC

Inhibition of HDAC6 was associated with an increased proinflammatory tumor microenvironment and an antitumoral response. Here, we show that a highly specific HDAC6 inhibitor AVS100 (SS208), blocks M2 polarization in murine and human macrophages while partially affecting M1 polarization. AVS100 effects were observed as blocked upregulation of M2-related gene signature under M2 polarizing conditions and blocked generation of $CD206^{\pm}$ and $Arg1^{\pm}$ macrophages. Oral administration of AVS100 had an antitumoral effect in SM1 melanoma and CT26 colon cancer models and increased the efficacy of anti-PD1 treatment, leading to complete remission in melanoma and increased response in colon cancer. Flow cytometry and scRNAseq analysis of tumor-infiltrating immune cells revealed an increase of proinflammatory/anti-inflammatory ratio in tumor-associated macrophages as well as an increase of intratumoral CD8 effector T-cells after AVS100 treatment. Interestingly, cured mice didn't relapse and became resistant to a subsequent tumor challenge, suggesting acquired antitumoral T-cell immunity. T-cell repertoire analysis of effector/memory T-cells in cured mice revealed a higher number of immunodominant T-cell clones after AVS100 treatment, indicating increased T-cell expansion. Finally, AVS100 has demonstrated no mutagenicity and a strong safety profile in rats and dogs, leading to its recent U.S. FDA clearance of an Investigational New Drug (IND) application and planned initiation of Phase Ia/b clinical trials targeting locally advanced or metastatic solid tumors in the first half of 2024. Altogether, we have performed the preclinical characterization of a novel small molecule inhibitor targeting HDAC6 for solid cancers. AVS100 had an antitumoral effect as single agent and improved the efficacy of immune checkpoint inhibition by blocking the immunoregulatory tumor microenvironment and increasing T-cell immunity.

#1422 A novel gut microbiota therapeutic approach for enhancing immune checkpoint inhibitor therapy.

P. Del Valle, G. Nguyen, Y. Choi, P. Sabaeifard, W. Li, J. Lichterman, L. Coughlin, N. Poulides, A. Sanjuan, A. Y. Koh;
UT Southwestern Medical Center, Dallas, TX

Immune checkpoint inhibitor therapy (ICT) has revolutionized cancer care, but up to 50% of patients do not respond to ICT. A host factor implicated in variable ICT response is the gut microbiome: a) germfree/antibiotic-treated mice do not respond to ICT; b) human ICT responders have distinct gut microbiome signatures compared to non-responders; and c) fecal microbiota transplants are safe and potentially effective in cancer patients previously unresponsive to ICT. We have previously established that ICT induces translocation of gut microbiota into secondary lymphoid tissues (particularly the mesenteric lymph nodes) and tumor which is required to enhance extraintestinal anti-tumor immunity (PMID: 36867675). Here, we have developed a novel gut microbiota therapy (GMT) which circumvents the challenges and limitations of conventional microbiome therapies that use live microbes. GMT utilizes specific components derived from commensal gut microbiota identified in our published clinical study (PMID:28923537) that can be administered parenterally (subcutaneous/intravenous) to safely and reproducibly enhance ICT efficacy in multiple preclinical cancer models (B16-F10 with anti-PD-1 and/or CTLA-4, MC38 with or without anti-PD-1, humanized mouse with human melanoma and human anti-PD-1). GMT acts by agonizing the pattern recognition receptors hTLR1/2/6, hNOD2 and hSTING. GMT induces anti-tumor cytokines (IL-12) but does not significantly increase sepsis associated cytokines (IL-6, TNFa) in both human immune cells and in non-human primates. Mechanistically, GMT acts via dendritic cells, and potentially through increased expression of delta-like ligand protein 4 (DLL4), a Notch signaling ligand that activates Notch 1/4 in T cells and promotes Th1 and Th17 differentiation. Current efforts to identify the active components of GMT are underway in which we have used serial liquid-liquid extractions (ethyl acetate followed by water:methanol:chloroform) and subsequent reverse phase chromatography to identify the most active fractions and identification of the bacterial components/constituents within these fractions. Together, these results demonstrate that GMT has the potential to serve as an innate immune adjuvant (akin to vaccine adjuvants) that enhances the effect of immunotherapy for possibly many cancer types.

#1423 Harnessing the gut microbiome to modulate immune checkpoint blockade response in triple-negative breast cancer.

Kenysha YJ. Clear[1], Adam S. Wilson[1], Elizabeth R. Stirling[1], Yu-Ting Tsai[2], Valerie Payne[1], David R. Soto-Pantoja[2], Katherine L. Cook[2]

[1]Department of Surgery, Wake Forest University School of Medicine, Winston-Salem, NC,[2]Department of Cancer Biology, Wake Forest University School of Medicine, Winston-Salem, NC

Triple-negative breast cancer (TNBC) is one of the most aggressive subtypes of breast cancer. The discovery that this subtype has the highest levels of tumor-infiltrating immune cells and programmed death ligand 1 (PD-L1) expression in the tumor microenvironment (TME) has propelled the use of anti-PD-1 immune checkpoint blockade (ICB) therapy, in combination with chemotherapy, as a treatment for TNBC patients. This has advantageously impacted TNBC patient outcomes such as survival, yet there remains a need to improve patient response to ICB therapies. The gut microbiome, in particular, increased abundance of *Akkermansia muciniphila* was associated with ICB therapy response in other cancer types. *A. muciniphila* can degrade mucins and produce short-chain fatty acid (SCFA) metabolites. Therefore, we investigated the interplay between *A. muciniphila*, SCFAs, and ICB therapy efficacy in TNBC models. As diet is the main modifier of the gut microbiome, we first investigated diet-gut microbiome interactions on ICB efficacy. Using the EO771 syngeneic murine model of TNBC, female C57BL/6 tumor-bearing mice consuming a low-fat control, or high-fat Western, or Mediterranean diet, were treated with 3 doses of 200µg of IgG or anti-PD-L1 antibodies and tumor progression was monitored. To assess changes in tumoral immune cell populations, end-of-study tumor tissue was used for immunohistochemistry (IHC). To evaluate modulation on the gut microbiome, metagenomic sequencing was performed on DNA isolated from fecal samples collected at the end-of-study, and targeted SCFA metabolomic analysis was performed on plasma collected at the study endpoint. Results show mice consuming a Mediterranean diet treated with anti-PD-L1 had significant increases in the abundance of gut *A. muciniphila* and plasma SCFAs, as well as significantly reduced primary tumor volume and increased immune cell activity within the TME. To then investigate if direct supplementation of *A. muciniphila* or SCFAs could enhance ICB efficacy, EO771 tumor-bearing mice were treated with 3 doses of 200µg of IgG, anti-PD-L1 or anti-PD-1 antibodies with a subset of mice stratified to also receive *A. muciniphila* or exogenoussupplementation of SCFAs. Tumor progression was measured and changes in tumoral immune cell populations were assessed with end-of-study tumor tissue prepared for flow cytometry and IHC. Results show mice supplemented with *A. muciniphila* and treated with anti-PD-L1 therapy demonstrated response to treatment, with a significant reduction in tumor volume as well as increased levels of immune cell populations in the TME. Mice supplemented with SCFAs and treated with a combination of anti-PD-1 and chemotherapy demonstrated enhanced response to treatment, with a significant reduction in tumor volume. In conclusion, data from our lab suggest that increased levels of gut *A. muciniphila* and SCFAs drive ICB efficacy in TNBC.

#1424 Epigenetic activation of tumoral IFNγresponse and pyroptosis overcomes immunotherapy resistance in hepatocellular carcinoma.

Y. Tu[1], H. Wu[1], C. Zhong[2], Z. Xiong[1], J. Wang[1], P. P. Wong[1], W. Yang[1], J. Lu[1], Z. Liang[1], S. Chen[1], L. Zhang[1], S. Chen[1], J. Zhou[1], K.-F. To[1], J. J. Sung[3], S. L. Chan[1], D. Kerr[4], N. L. Thangue[4], A. S. Cheng[1];

[1]The Chinese University of Hong Kong, Hong Kong, Hong Kong, [2]Renji Hospital Affiliated to Shanghai Jiao Tong University, Shanghai, China, [3]Nanyang Technological University, Singapore, Singapore, [4]The University of Oxford, Oxford, United Kingdom

Background: Immune checkpoint blockade (ICB) therapies by antibodies have revolutionized the treatment paradigm for a variety of cancers. Although subsets of people exhibit durable responses, resistance and relapse are common in hepatocellular carcinoma (HCC). We therefore aim to delineate the mechanism underlying the failure of ICB therapy in HCC, and more importantly to identify ICB-sensitizing therapeutic approaches.

Methods: ICB-resistant orthotopic-grafted murine models were established via a serial selection of HCC cells in ICB-treated mice. Integrated multi-omics analysis (single-cell RNA-seq, single-cell ATAC-seq and ChIP-seq) were applied to decode the mechanisms underlying the ICB resistance and an epigenetic-mediated ICB response.

Results: We successfully established the ICB-resistant murine models of HCC, in which tumor intrinsic interferon-gamma (IFNγ) response was most significantly suppressed and characterized by a “cold” tumor microenvironment with decreased lymphocyte activation and intratumoral infiltration. On the other hand, single cell RNA-seq analysis of human HCC biopsies revealed that patients with HDAC1/2/3-high HCC exhibit poor survival upon ICB therapy. Notably, we found that a novel specific HDAC1/2/3 inhibitor CXD101 synergized with PD-(L)1 antibody to induce immunogenic cell death, eradicate tumor and prolong survival in our ICB-resistant mouse models, which was accompanied by enhanced intratumoral infiltration, activation and anti-tumor memory formation of cytotoxic lymphocytes. Mechanistically, CXD101 combined with PD-(L)1 inhibition synergistically reactivated tumor IFNγ pathway via enhancing chromatin accessibility of downstream genes associated with antigen presentation and lymphocytes recruitment. Moreover, the activated immune system induced tumor cell pyroptosis, further igniting antitumor immunity and ICB response.

Conclusions: Our findings suggest that corruption of tumor intrinsic IFNγ signaling may confer ICB resistance upon ICB therapy, which can be rectified by class I HDAC inhibitor mediated IFNγ response and tumor cell pyroptosis. Based on these findings, we have commenced a Phase II clinical study of a new epigenetic immunotherapy (CXD101 plus anti-PD-1) for HCC patients resisting anti-PD-(L)1 alone. This project is supported by the CRF (C4045-18W), GRF (14115820), TRS (T11-706/18-N), Li Ka Shing Foundation, CUHK Strategic Seed Funding for Collaborative Research Scheme. We also acknowledge support (funding and study medications) by Celleron Therapeutics.

#1425 Epigenetic modulation synergizes with a novel TCR β chain directed antibody-fusion molecule to suppress checkpoint-refractory tumors irrespective of MHC I status.

K. E. Lothstein[1], A. S. Khelifa[1], M. Miyamoto[1], C. M. Minnar[1], L. Poppe[1], N. Roller[1], A. Bayliffe[2], K. Liu[2], J. Moisan[2], M. Katragadda[2], Z. Su[2], J. Schlom[1], S. R. Gameiro[1];

[1]National Cancer Institute, Bethesda, MD, [2]Marengo Therapeutics, Cambridge, MA

Background: Epigenetic silencing of MHC-I, and poor T cell infiltration and function in the tumor microenvironment (TME) are prevalent in solid malignancies and associate with lack of response to immune checkpoint blockade (ICB). Novel combination therapies may overcome these barriers, thereby providing clinical benefit across solid tumors. STAR0602 is a first-in-class bifunctional therapeutic molecule, that simultaneously engages a nonclonal mode of T cell receptor (TCR) activation with costimulation to promote activation and expansion of αβ T cell subsets expressing distinct variable β (Vβ) TCR chains. Here, we examined the tumor-suppressive ability and mode of action of a murine surrogate of STAR0602 (mSTAR1302) in combination with the class I HDAC inhibitor Entinostat, an epigenetic modulator that enhances tumor immune cell recognition, in multiple tumor models, including ICB-refractory.

Methods: mSTAR1302 and/or Entinostat were administered to mice bearing ICB-responsive breast EMT6 wild-type (wt) and ICB-refractory EMT6 β2-microglobulin (B2m)-deleted and CT26 (Kras $G12D^{mut}$ colon) tumors. Anti-tumor efficacy, survival, and protective memory were monitored. Immune cell depletion studies were conducted. Comprehensive proteomic and immune profiling of tumor, tumor-draining lymph node (tdLN), and spleen cell populations was conducted. Antigen-specific IFNg T cell responses were evaluated by ELISpot.

Results: Combination therapy demonstrated significant enhancement in tumor suppression and prolonged survival in CT26 ($MHC\text{-}I^{\pm}$), EMT6 wt ($MHC\text{-}I^{\pm}$) and EMT6 β2m-deleted ($MHC\text{-}I^{null}$) tumors relative to single agent therapy, as well as enhanced tumor-specific protective memory responses. Tumor suppression was independent of $CD4^{\pm}$ T cell immunity and associated with sustained activation and expansion of Vβ13 $CD8^{\pm}$ T cells.

Conclusions: Ongoing mechanistic studies indicate combination therapy to elicit complimentary mechanisms of tumor suppression beyond $CD8^{\pm}$ T cells. Ongoing proteomic and single-cell transcriptomic investigation of MHC-I competent and null tumors will provide a deeper insight into the mode of action of this combination therapy. Collectively, these data support the use of STAR0602 in combination with Entinostat for the treatment of solid malignancies, including for patients harboring ICB-refractory tumors devoid of MHC class I.

#1426 Lipid-mediated epigenetic activation of PPAR-gamma signaling promotes immune-checkpoint resistance in hepatocellular carcinoma.

Z. Xiong[1], S. L. Chan[1], J. Zhou[1], X. Zeng[1], W. Yang[1], H. Wu[1], J. Cao[1], J.-T. Low[2], M. W. Chan[2], K. Y. Yip[3], J. J. Sung[4], A. S. Cheng[1];
[1]The Chinese University of Hong Kong, Hong Kong, China, [2]National Chung Cheng University, Min-Hsiung, Taiwan, [3]Sanford Burnham Prebys Medical Discovery Institute, La Jolla, CA, [4]Nanyang Technological University, Singapore, Singapore

Background: Although use of immune-checkpoint inhibitors (ICI) has yielded impressive results in cancer patients, resistance to ICI therapies has increasingly been observed, especially in hepatocellular carcinoma (HCC).
Materials and Methods: We generated a novel anti-programmed death-ligand 1 (PD-L1) treatment resistant mouse hepatoma cell Hepa1-6 (PD-L1R) by 7-generation of *in vivo* selection. To dissect tumor cell-intrinsic resistant mechanism, we performed single-cell RNA-sequencing (scRNA-seq) from anti-PD-L1-treated tumors generated from parental or PD-L1R cells. Expression level of target genes was detected by QPCR, western blot and immunohistochemical analyses. Lipid content and fatty acid uptake was examined by Oil Red O and BIODIPY staining. *Peroxisome proliferator-activated receptor gamma* (*PPARγ*) promoter methylation level was analyzed by bisulfite pyrosequencing. To investigate the tumor cell-extrinsic factors, we profiled the myeloid and lymphoid lineages by flow cytometry.
Results: ScRNA-seq revealed significant gene enrichments in lipid metabolism and PPARγ signaling pathway in PD-L1R tumors, which could be verified in both mRNA and protein levels. Moreover, we observed evident lipid accumulation in the PD-L1R tumors when compared to the parental tumors by Oil Red O staining. Consistently, PD-L1R tumor cells exhibited higher lipid content and enhanced fatty acid uptake *in vitro*, as demonstrated by $BODIPY^{493/503}$ and BODIPY-C16 analyses. Of note, palmitic acid could dose-dependently increase *Pparg* mRNA expression in parental cells to a similar level with the PD-L1R cells, supporting an important role of lipids in inducing PPARγ expression. Pyrosequencing analysis indicated that PD-L1R cells exhibited lower PPARγ methylation level compared with parental cells. Notably, 5-Azacytidine treatment in parental cells significantly reduced the promoter DNA methylation and increased *Pparg* mRNA expression to similar extent with the PD-L1R tumor cells, thus indicating DNA hypomethylation-driven PPARγ up-regulation. Flow cytometry analysis showed that ICI resistance was associated with lower cytotoxic $CD8^{+}$ T cells but higher intermediate Th17 cells, myeloid-derived suppressor cells and T regulatory cells in the tumor microenvironment (TME).
Conclusions: Our study suggested that lipid exposure may epigenetically up-regulate PPARγ transcription in the development of anti-PD-L1 resistance. Detailed investigation on the crosstalk between aberrant lipid metabolism and immunosuppressive TME is ongoing.
Acknowledgment: This study is supported by RGC General Research Fund (14120621 and 14119023), Li Ka Shing Foundation and CUHK Strategic Seed Funding for Collaborative Research Scheme.

TUMOR BIOLOGY: Animal Models of Cancer
Poster Session

#1430 Development of transparent transgenic zebrafish model to study anti-cancer drug induced *in vivo* cardiotoxicity.
S. K. Rajpurohit, T. Gossman, S. Nasanally, K. Bhatt, A. Van Derhei, S. Hotwani, D.-A. Manhiani, R. Pasi, J. Mi, V. Arora, B. Lokeshwar; Augusta University, Augusta, GA

Cardiotoxicity is the second leading cause of death among cancer survivors and can manifest as arrhythmia, acute coronary syndrome, acute heart failure, or pericarditis/myocarditis. Chronic myocyte damage and apoptosis can transition from an asymptomatic phase to adaptive myocardial hypertrophy, followed by decreased left ventricular ejection fraction, and eventual heart failure. Cardio-oncology is an emerging field that studies cancer therapy-associated cardiotoxicities. The development of reliable and effective preclinical models for cardiotoxicity prediction and prevention is essential to improving the long-term cardiac health of cancer patients. Zebrafish are a promising animal model for the field of cardio-oncology and have emerged as an invaluable tool for investigating genetic and molecular aspects of cardiovascular research. Zebrafish heart cells are like human heart cells at the molecular level, making them an ideal system for studying the genetic underpinning of cardiac function. Zebrafish myl7 gene, a myosin light chain-7 gene, is a regulatory gene of heart orthologs to human MYL7. In-vivo imaging is limited due to the opacification of skin and subdermal structures. To conduct in-vivo whole organism imaging studies, skin transparency is a primary requirement, necessitating the blocking of pigmentation. The Zebrafish Casper mutant maintains skin transparency throughout its life, offering the ideal combination of sensitivity and resolution for in-vivo analyses and imaging. In this study, we have developed a novel transparent transgenic zebrafish model and established time-lapse in-vivo confocal microscopy to study cellular phenotype/pathologies of cardiomyocytes. The newly developed homozygous transparent transgenic Casper/ myl7:RFP; annexin-5:YFP/NF-kB: GFP/mpeg1:mcherryFP, allows us to study cell death process (Annexin5) and inflammatory activity (NF-kB) in microglia and cardiomyocytes. We have successfully established in vivo fluorescence and confocal microscopy in this newly developed strain, enabling the study of cellular morphology and function changes under various conditions. This will allow us to elucidate cell death patterns, and cardio-inflammatory and cardiotoxicity pathways.

#1431 Generation of transparent transgenic zebrafish strain to study cardiovascular functionin translational cardio-oncology research.

S. K. Rajpurohit[1], T. Gossman[1], **R. Pasi**[1], S. Nasanally[1], K. Bhatt[1], A. Van Derhei[1], S. Hotwani[1], D.-A. Manhiani[1], K. Kimmerling[2], V. Arora[3], B. L. Lokeshwar[1]; [1]Augusta University, Augusta, GA, [2]FiteBac Technology, Marietta, GA, [3]Medical College of Georgia, Augusta University, AUGUSTA, GA

Transgenic zebrafish lines have been extensive use in biomedical research and their primary applications. The zebrafish has proven to be an ideal tool for direct In-vivo observations of developmental processes. In vertebrates, including zebrafish and humans, the ability to obtain high-resolution, in-vivo imaging is limited due to the natural opacification of skin and subdermal structures. To conduct in-vivo whole organism imaging studies, skin transparency is a primary requirement, necessitating blocking of pigmentation. Zebrafish casper mutant maintains skin transparency throughout its life, offering the ideal combination of sensitivity and resolution for in-vivo analyses and imaging. Our Laboratory is developing a novel transparent transgenic zebrafish model to address basic and translational cardio-oncology and experimental therapeutics. The fli1 promoter in zebrafish having an enhanced expression reporter gene of green fluorescent protein, GFP. This model allows for the in-vivo examination of the vascular system by using fluorescent and confocal microscopy. In this study, we developed transparent transgenic strain of Caspe/fli1:EGFP and integrating with recently developed *casper*/myl7/annexin-*5:YFP and* casper/*fli1:EGFP* strain through crossbreeding of casper and transgenic zebrafish. We have generated F1 generation of newly developed strains of Caspe/fli1:EGFP and *casper*/myl7/annexin-*5:YFP and* casper/*fli1:EGFP.* The presence of fluorescence expressions RFP, YFP and GFP, in crossbred progeny identified through the screening of larvae at 72 HPF stage. Expression of these fluorescent proteins determines the presence of the reporter genes. *Positive transgenic larvae validated by confocal microscopy. The progenies of the F1 generation are heterozygous in nature and allow them to grow into adults to breed transparent transgenic strain to get F2 generation. This process will be continued to F2, F3, F4 and F5 generation until obtain homozygous progeny of newly developed strain.* The development of *casper*/myl7/annexin-*5:YFP x* casper/*fli1:EGFP* will aid new dimensions in Cardio-oncology research for cardiac injury and Vasotoxicity induced by anticancer drug treatment in cancer patients.

#1432 Development of transparent transgenic zebrafish model to study CNS microglia and NF-kB activity in glioblastoma.

S. K. Rajpurohit[1], S. Nasanally[1], **S. Hotwani**[1], T. Gossman[1], K. Bhatt[1], A. Van Derhei[1], R. Pasi[1], D.-A. Manhiani[1], K. Kimmerling[2], B. L. Lokeshwar[1]; [1]Augusta University, Augusta, GA, [2]FiteBac Technology, Marietta, GA

Microglia are resident macrophages of the central nervous system (CNS) and have crucial roles in normal brain homeostasis, function, and immune response. Microglia play key roles in the healthy brain, ranging from phagocytosis of dying neurons and CNS debris to modulating adaptability. The role of microglia has been well documented but their specific contributions to the development and progression of cancers, such as glioblastoma, have recently garnered wide attention. The zebrafish have proven novel tool for modeling innate immune responses. A macrophage-specific marker mpeg1 and its promoter are used in mpeg1-driven transgenes. mpeg1-driven transgenes mpeg1:mCherryFP are expressed in macrophage-lineage cells that do not express neutrophil-marking transgenes. These zebrafish transgenes contribute to the fields of inflammation, infection, and leukocyte biology. We have recently developed a novel transparent transgenic homozygous strain Tg(6xNF-kB:EGFP); Casper(roy−/−, nacre−/−) of zebrafish to the in-vivo study of NF-kB activity under normal and inflammation stage at the cellular, organ-specific and whole organism level. To perform an in-vivo study of microglial function, we are developing Casper;*mpeg1:mCherryFP* microglia specific strain and integrating with newly developed Tg(6xNF-kB:EGFP); Casper(roy−/−, nacre−/−) strain through crossbreeding of Casper and transgenic zebrafish. We have generated F1 generation of newly developed strains of Casper;*mpeg1:mCherryFP and Tg(6xNF-kB:EGFP);Casper*. The presence of fluorescence mCherry and GFP, in crossbred progeny was identified through the screening of larvae at 72 HPF stage. The expression of these fluorescent proteins determines the presence of the reporter genes. *F1 generation confirmed heterozygous and allowed them to grow into adults to breed transparent transgenic strain to get F2 generation. This process will be continued to F2, F3, F4, and F5 generation until achieving homozygous progeny.* This model allows for in-vivo examination of microglia functional morphology by using fluorescent and confocal microscopy. This novel transgenic model will be applied to identify novel anti-inflammatory drug inhibitors in NF-kB pathophysiology for glioblastoma and cardio-oncology experimental therapeutics.

#1433 FOXA1 alterations distinctively drive prostate tumorigenesis or therapy resistance in mice.

S. Eyunni, A. Parolia, E. Young, J. M. George, R. Mannan, S. E. Carson, Y. Zhang, J. Tien, M. Jaber, J. Luo, M. Pang, R. Mehra, X. Cao, F. Su, R. Wang, M. Cieslik, D. K. Lee, J. Xu, A. M. Chinnaiyan;
University of Michigan, ann arbor, MI

Androgen receptor (AR) signaling is critical for survival of prostate cancer (PCa) cells, thus making androgen deprivation therapy (ADT; e.g., castration) as the mainstay for treatment. Notably, oncogenic functions of AR rely on chromatin-binding regulatory proteins, which includes a pioneer transcription factor called FOXA1. FOXA1 de-compacts chromatin to enable AR's binding to the DNA and expression of it's target genes. Recently, our lab found FOXA1 alterations to recur within three distinct structural classes in over 35% of metastatic castration resistant PCa (mCRPC) in Caucasian men. Subsequent studies found FOXA1 mutations to be prevalent in over 40% of primary PCa in Chinese men, positioning FOXA1 as a principal oncogene in this disease. Yet, hitherto, no studies have defined the pathobiology of FOXA1 alterations in mouse models. Here, we have developed the first-in-field transgenic mice with conditional overexpression of FOXA1 mutants in the prostate luminal epithelia. We found truncal FOXA1 Class1-mutants to initiate luminal hyperplasia in a monogenic model, or hyperproliferative prostate adenocarcinoma in a compound Trp53-deficient genetic background. Mechanistically, Class1 mutants concurrently upregulate the AR and mTORC1/2 pathways to drive transformation, with this being the first report of FOXA1-driven PCa formation in mice. In contrast, FOXA1 Class2 mutants—which are acquired in mCRPC—do not drive prostate luminal transformation. Instead, single-cell multi-omics (RNA+ATAC) profiling of Class2-mutant mouse prostate tissue uncovered extensive transcriptional remodeling of epithelial cells into a luminal stem-like cell fate, leading to a dramatic 15-20-fold expansion of the progenitor population vs control tissue. These luminal stem cells are similar to the Club/Hillock cells detected in the human prostate that have been implicated in driving resistance to ADT. Consistently, we found Class2-mutant prostates to show minimal atrophy upon castration, with immunohistological assessment uncovering a higher density of Ki67+ luminal epithelial cells relative to wild type and Class1 tissues. Class2-mutant organoids also showed higher subcutaneous grafting ability in mice in limiting dilution assays. Mechanistically, we found the cistromically-dominant Class2 mutants to pioneer over 40,000 *neo*-enhancer elements harboring motifs of stemness-associated transcription factors, which in turn instruct the ADT-resistant luminal progenitor gene program. Altogether, findings from our mouse models uncover FOXA1's versatility as a driver oncogene that, depending on the mutation type, either activates enhancer-wired luminal tumorigenesis (Class1-initiating event) or therapy resistance-associated stemness (Class2-promoting alteration) gene programs in the mouse prostate tissue.

#1434 Modeling the 3q26 OncCassette using genetically engineered mice.

K. M. Meneses, Y. Liu, C. R. Weems, L. Jamieson, D. T. Nguyen, V. Justilien, N. R. Murray, A. P. Fields;
Mayo Clinic, Jacksonville, FL

Lung squamous cell carcinoma (LUSC) is a devastating disease, accounting for ~30% of all lung cancer diagnoses and ~40,000 deaths annually in the United States alone. LUSC patients suffer from high prevalence of relapse and a dismal 5-year survival of only ~24%. The lack of animal models that reflect the salient features of human disease to assess the safety and efficacy of drugs, and to explore the underlying molecular mechanisms of LUSC tumor biology, is a major impediment for LUSC patients. We have identified concomitant 3q26 copy number gain (CNG) and *TP53* loss as a defining genetic alteration present in ~90% of LUSC tumors. Furthermore, we have identified and characterized three 3q26 oncogenes (*PRKCI, ECT2 and SOX2)* that genetically and biochemically collaborate to drive LUSC tumor formation. Using syngeneic mouse modeling, we have demonstrated that coordinate overexpression of *Prkci, Ect2* and *Sox2*, and loss of *Trp53* in *ex vivo* cultures of lung basal stem cells (LBSCs; a cell of origin for LUSC) drives transformation of these cells into tumors of exclusively LUSC histopathology. These findings lead to the hypothesis that *PRKCI, ECT2* and *SOX2* represent a multigenic driver of 3q26 CNG-driven LUSC, which we term the 3q26 OncCassette. Based in these findings, we have developed and begun characterizing the first autochthonous genetically engineered mouse model (GEMM) to study 3q26 OncCassette-driven tumorigenesis. Our novel immune competent GEMM will provide critical insight into tumor initiation and progression of preneoplastic lesions to malignant LUSC and allow characterization of the immune landscape in these tumors.

#1435 Utilization of CLDN18.2 syngeneic mouse models to study chimeric antigen receptor T cells in immunocompetent mice.

S. Breen, R. Carrasco, K. McGlinchey, B. Janocha, P. Zanvit, L. Ortiz, B. Clark, A. Toloczko, M. Cobbold, G. Moody, E. Bosco, A. Barrett; AstraZeneca US, Gaithersburg, MD

CLDN18.2 expression has been observed in pancreatic, gastric and esophageal cancers, whereas normal tissue expression of CLDN18.2 is mostly restricted to differentiated gastric mucosal epithelial cells. This expression profile renders CLDN18.2 an ideal tumor associated antigen (TAA) for CAR-T targeting and an armored targeted CAR-T, AZD6422, is in clinical development. While CAR-T are beginning to show clinical promise in solid tumors, a consistent challenge is to overcome the immunosuppressive tumor microenvironment (TME) where immune and stromal cells secrete high levels of TGFb. Since the majority of pre-clinical CAR-T efficacy data is generated utilizing immunocompromised mouse models, which lack a proper TME, the team utilized syngeneic xenograft models to circumvent this challenge. In vitro studies showed that CLDN18.2 targeted murine CAR-T cells generated by retroviral transduction induced efficient cytolysis of target positive mouse tumor cells accompanied by cytokine release. To model the clinical scenario, tumor-bearing mice were lymphodepleted with total body irradiation (TBI) to enhance CAR-T engraftment. The dosage of TBI used in these studies was predetermined to have caused leukopenia and minimal impact on tumor growth. We observed substantial tumor control and extended tumor efficacy in mice treated with mCAR-T cells compared to those infused with untransduced T cells or in non-target bearing control tumors in the absence of gross toxicities. This syngeneic mouse model platform will additionally allow us to investigate how mCAR-T cells perform within a fully competent TME in combination with other therapeutic agents targeting cancer cells via altered mechanism of action.

#1436 Cancer associated fibroblast dependency in a model of bladder cancer.

H. Valentine, U. Satyal, L. Bukavina, H. Uddin, Y. Beyamin, R. Arya, P. Abbosh;
Fox Chase Cancer Center, Philadelphia, PA

Introduction: The relationship between genotype and phenotype in targeted therapy has proven to be crucial for most kinase inhibitors. In bladder cancer, the PI3K/AKT/mTOR pathway is widely activated by mutation but untargeted. Our study focuses on developing an immunocompetent, CRISPR-edited bladder cancer mouse model that mirrors common PI3K/AKT/mTOR mutations. We aim to establish genotype-effective kinase inhibitor pairings using *in vitro* CRISPR-edited organoids and Cancer Associated Fibroblasts (CAFs) to create a pro-tumorigenic environment *in vivo*.

Methods and Results: Urothelial cells were isolated from the bladder of Rosa26 Lox-Stop-Lox-Cas9/GFP transgenic mice to develop organoids. These organoids were co-edited for *Trp53* and *Rb1* KO, and further editing of the *Pten* gene resulted in a nine-fold increase in sensitivity to the kinase inhibitor ipatasertib. Despite successful engraftment into mouse bladder, these edited cells regressed before tumor formation, and intradermal injection did not yield subcutaneous tumors. An alternate model featuring a *9p21* deletion with *Trp53* KO also displayed similar regression post-engraftment into bladder or skin. However, co-injection with skin-cancer-derived CAFs subcutaneously yielded palpable subcutaneous tumors that grew for 12 weeks. Enhancing orthotopic model fidelity, we established a BBN bladder-tumor-derived CAF line, leading to the formation of tumors with squamous differentiation upon intramural co-injection with edited organoids. These models displayed immune-excluded architecture and a predominance of M2 over M1 macrophages. Following our accomplishments in establishing bladder tumors, we aimed to enhance our model's adaptability by introducing common PI3K/AKT/mTOR mutations, specifically *TSC1*/*TSC2* KO and *Pik3ca* hotspots, into our *9p21*/*Trp53* KO model. While *TSC1*/*TSC2* KO lines exhibited elevated P-S6K signaling, they displayed resistance to Torin 1, Voxtalisib, and Everolimus—kinase inhibitors targeting mTORC1/2. In parallel, we employed CRISPR-mediated HDR to successfully introduce a *Pik3ca* H1047R hotspot into our *9p21*/*Trp53* KO model, as evidenced by increased Phosphorylation of AKT compared to wild-type *9p21*/*Trp53* KO cell lines.

Conclusions: Our research establishes the crucial role of CAFs in bladder tumor formation. Our now established customizable model of bladder cancer is suitable for direct targeting by kinase inhibitors while providing a platform for understanding the genotype-phenotype relationship in bladder cancer.

#1437 Generating primary mouse models of diffuse midline glioma through a combination of the RCAS/tv-a retrovirus system and CRISPR/Cas9 gene editing.

S. R. Wu[1], H. Q. Liu[2], J. Tolliver[2], S. M. Maingi[2], V. Valentine[2], N. T. Williams[2], Z. J. Reitman[2];
[1]Duke University, Durham, NC, [2]Duke University Medical Center, Durham, NC

Diffuse midline gliomas (DMGs) are deadly brain tumors that arise in the brainstem of children and young adults, resulting in a median survival of less than two years. Genetically engineered mouse models (GEMMs) are critical to studying tumorigenesis and tumor-immune interactions in DMG, which may inform the design of new urgently-needed treatment approaches. One approach to generate DMG GEMMs uses RCAS/tv-a, an avian retrovirus gene delivery system to express transgenes in specific brain cell lineages in the mouse brain. However, this approach often requires resource-intensive breeding to generate mice with the desired genetic alterations in their germline. As a result, we aimed to establish a new approach that combines this system with CRISPR/Cas9 gene editing technology. This methodology has been described for model adult supratentorial gliomas in mice but has not been described for pediatric or brainstem gliomas. To express Cas9 and the avian retrovirus receptor TVA in mouse neural stem cells, we bred mice of genotype Nestin-TVA; Nestin-Cre; LoxP-STOP-LoxP-Cas9-EGFP. RCAS retrovirus plasmids were generated containing various guide RNAs (gRNAs) targeting DMG-relevant genes for disruption by Cas9, including *Trp53*, *Cdkn2a*, *Atm*, *Ppm1d*, *Pten*, and a non-targeting control (Cntl). For each gRNA, two plasmids were generated, one with a platelet-derived growth factor beta ligand (PDGFB) oncogene driver and one with a blue fluorescent protein (BFP) marker. In a pilot experiment, avian fibroblast cells transduced with RCAS-Trp53_gRNA_BFP and RCAS-Cntl_gRNA-PDGFB were injected into postnatal day 4 mouse brainstems of the aforementioned genotype and observed for tumor formation. High grade tumor formation was observed. We also observed high grade tumors in mice of genotype Nestin-TVA; LoxP-STOP-LoxP-Cas9-EGFP when injected with an additional RCAS-Cre construct, indicating that Cre can be expressed from the mouse germline or delivered via a retrovirus payload to drive tumorigenesis. Immunohistochemistry confirmed tumor features that model human DMG, expression of Cas9 and PDGFB, and loss of p53. Thus, RCAS/tv-a and CRISPR/Cas9 can be combined to model pediatric glioma tumorigenesis in the mouse brainstem. This approach to mouse modeling will streamline future GEMM DMG research by allowing new genes of interest to be rapidly perturbed by simply generating RCAS retrovirus constructs. The workflow may also enable sophisticated experiments such as pooled *in vivo* genetic experiments that screen gRNAs targeting various tumor suppressor genes or therapeutic targets.

#1438 Investigating the roles of EMT in small cell lung cancer tumorigenesis and chemoradiation response.

T. Nguyen[1], J. Chang[2], K. Gabrielson[3], A. Shetty[4], Y. Song[4], A. Lafargue[2], S. Jagtap[3], D. Council[2], A. Chan[2], D. Dutta Chowdhury[2], M. Khan[2], N. Connis[3], F. Carrieri[3], E. Imada[5], D. Sforza[3], E. Gardner[5], C. McFarland[6], L. Marchionni[5], M. Rezaee[3], C. Hann[3], P. Tran[2];

[1]Johns Hopkins Bloomberg School of Public Health, Baltimore, MD, [2]University of Maryland School of Medicine, Baltimore, MD, [3]Johns Hopkins School of Medicine, Baltimore, MD, [4]University of Maryland Institute for Genome Sciences, Baltimore, MD, [5]Weill-Cornell Medicine, New York, NY, [6]Case Westerns Reserve University, Cleveland, OH

In this study, we investigated the contributions of the epithelial-mesenchymal transition (EMT) program to small cell lung cancer (SCLC) tumorigenesis and chemoradiation (CRT) response. SCLC is a highly aggressive and deadly neuroendocrine malignancy. Two major factors that contribute to the high mortality of SCLC are (1) early metastasis and (2) rapid development of therapy resistance. Recent research suggests upregulation of EMT and the EMT transcription factor Twist1 correlated with accelerated tumor progression and CRT resistance in SCLC. Due to the lack of suitable animal models, the causal relationship between the EMT program and SCLC tumorigenesis and therapy response has not been rigorously investigated. To this end, we have generated a novel genetically engineered mouse model (GEMM) termed RPGT (*Rb1*^{Flox}*; Trp53*^{Flox}*; ROSA26*$^{LSL\text{-}rtTA\text{-}IRES\text{-}EGFP}$*; Twist1-TetO*$_7$*-Luc*). The RPGT GEMM enables the generation of autochthonous SCLC tumors after induction with Cre recombinase adenovirus. By withdrawing or providing doxycycline to mice, we can control Twist1 expression to activate or inactivate EMT in tumors. Upon characterizing mouse tumor samples with histological and molecular analyses, we observed that both control (no Twist1 overexpression) and Twist1-overexpressing RPGT mice developed neuroendocrine SCLC tumors. While SCLC-A was the predominant subtype in both cohorts, RPGT tumors exhibited more heterogeneity. Importantly, although no difference in tumorigenesis was observed, Twist1 overexpression dramatically increased the metastatic incidence in RPGT (87-100%) compared to control (25-50%) animals, indicating an important role of EMT in SCLC dissemination. Furthermore, transcriptomic profiling of primary tumors and matching metastases in RPGT mice revealed downregulation of Twist1 and EMT in metastases, suggesting that EMT suppression was necessary for metastatic outgrowth. To evaluate the impact of EMT activation on SCLC sensitivity to CRT, we performed *in vitro* viability assays on primary tumor cell lines established from RPGT tumors. We found that repressing Twist1 expression enhanced SCLC susceptibility to CRT. To validate these results *in vivo*, we treated RPGT mice with vs. without Twist1 overexpression with CRT. Consistent with our *in vitro* results, our *in vivo* data indicated that Twist1 overexpression promoted CRT resistance in SCLC tumors. Overall, our data suggest that the EMT program plays an important role in SCLC differentiation, metastasis, and resistance against chemo-radiotherapy.

#1439 Elucidation of the pathogenesis of prostate cancer harboring mutations of epigenetic factor UTX using genetically engineered mice.

N. MURAMOTO[1], M. Iwasaki[2], Y. Sera[2], H. Ide[1], S. Mukai[3], T. Fukushima[4], S. Horie[1], H. Honda[2];
[1]Juntendo University Graduate School of Medicine, Tokyo, Japan, [2]Tokyo Women's Medical University, Tokyo, Japan, [3]University of Miyazaki, Miyazaki, Japan, [4]University of Miyazaki, Tokyo, Japan

Introduction and Objective: Histone modifications are important for tissue homeostasis, and their mutations are involved in carcinogenesis. Mutations in a histone modifier, UTX (KDM6A) are common in prostate cancer (PCa), which is frequently associated with loss of its counterpart UTY (KDM6C). However, mechanisms underlying the development of UTX-deficient PCa are not clear. We aimed to address this issue by generating and analyzing genetically-engineered mice.
Methods: We generated mice with deletion of both *Utx* and *Uty* in the prostate tissue (*Utx*Δ, *Uty*Δ) and crossed with mice with a heterozygous deletion of *p53* (*p53*+/−) to create *Utx*Δ, *Uty*Δ and *p53*+/− compound mice. High-fat diet (HFD) that is known to promote cancer growth was administered to mice. We found that *Utx*Δ, *Uty*Δ, *p53*+/− mice treated with HFD developed PCa with Gleason score (GS) = 3+3. Isolated prostate tissues were subjected to pathologic, molecular, and cellular analyses. In addition, RM-2 mouse PCa cells which do not express UTY were knocked down for *Utx* (si*Utx*) and *control* (si*NC*) by siRNAs to assess changes in the abilities of proliferation and migration.
Results: RM-2 si*Utx* cells showed increased proliferation and migration compared with RM-2 si*NC* cells. By performing high-throughput RNA sequencing (RNA seq) and gene set enrichment analysis (GSEA) using mouse prostate tissues, we found that loss of UTX in the prostate activated inflammatory pathways, whereas inactivated DNA damage repair pathways. Immunostaining prostate tissues with an antibody to a macrophage marker, F4/80, exhibited significant accumulation of macrophages in *Utx*Δ, *Uty*Δ, *p53*+/+ mice compared to *Utx*+, *Uty*Δ, *p53*+/+ mice. In addition, immunofluorescent staining of irradiated prostate tissues with an antibody against a DNA repair marker, γH2AX, revealed that the time required for DNA damage repair was markedly prolonged in *Utx*Δ, *Uty*Δ, *p53*+/+ mice compared with *Utx*+, *Uty*Δ, *p53*+/+ mice.
Conclusions: These results suggest that loss of UTX contributes to prostate cancer development through promoting inflammation and impairing DNA damage repair, which may serve as novel therapeutic targets in PCa patients with UTX mutations.

#1440 Retinoblastoma binding protein 9 regulates intestinal inflammation and inflammation-associated carcinogenesis.

Y. Nakanishi[1], K. Hamada[1], M. Omatsu[1], K. Iwane[1], H. Kitamoto[1], M. Okabe[1], Y. Muta[1], S. Yamamoto[1], A. Fukuda[1], H. Kasashima[2], H. Seno[1];
[1]Kyoto Univ. Graduate School of Medicine, Kyoto, Japan, [2]Osaka Metropolitan University, Osaka, Japan

The intestinal epithelium constitutes the mucosal barrier, and its dysfunction promotes microbial invasion from the gut lumen, which further induces the intestinal inflammation. Chronic intestinal inflammation, as observed in poorly controlled inflammatory bowel diseases (IBD), leads to the development of inflammation-associated cancer. Thus, a deeper understanding of the regulatory system that controls intestinal homeostasis is essential. Retinoblastoma-binding protein 9 (RBBP9) is expressed in a range of human cancer cells. RBBP9 was initially reported to have the ability to regulate the cell cycle pathway. More recent studies have identified RBBP9 as a serine hydrolase (SH) that promotes cancer progression by subverting the anti-proliferative function of TGFβ in a pancreatic cancer model. However, little is known about the roles RBBP9 plays in the development of intestinal cancer. In this study, we investigated the role of RBBP9 in inflammation and inflammation-associated cancer in the intestine. Analyses of surgically resected human samples and publicly available datasets demonstrated that RBBP9 expression was reduced in patient samples of ulcerative colitis (UC) and colitis-associated cancer (CAC). Genetically knockout mice for Rbbp9 (*Rbbp9*$^{-/-}$) were susceptible to experimental colitis induced by dextran sulfate sodium (DSS). Furthermore, *Rbbp9*$^{-/-}$ mice exhibited enhanced azoxymethane/DSS-induced tumorigenesis, a model for human CAC. Mechanistically, RNA sequencing of these tumors showed increased enrichment of inflammation-associated signatures, including interferon signaling pathways. Ex vivo organoid experiments revealed the suppressive function of RBBP9 in interferon signaling-mediated apoptosis of the intestinal epithelium. Simultaneous inhibition of RBBP9 and STAT1, a downstream transcription factor of interferon signaling, reverted the apoptotic phenotype of *Rbbp9*$^{-/-}$ organoids. Collectively, our data provide insight into the understanding of the crucial role of RBBP9 in protecting against intestinal inflammation and inflammation-related tumorigenesis via regulating the interferon signaling-mediated apoptotic pathway.

#1441 Establishing a novel clinically relevant disease model of glioblastoma.

K. Connor[1], K. White[1], J. Clerkin[2], K. Sweeney[2], L. Shiels[1], T. van Brussel[3], I. Arijs[3], D. Lambrechts[3], G. Shankar[3], F. de Smet[3], S. G. Maher[4], L. Marignol[4], P. Dicker[1], J. Prehn[1], D. O'Brien[2], A. T. Byrne[1];

[1]Royal College of Surgeons in Ireland, Dublin, Ireland, [2]Beaumont Hospital Dublin, Dublin, Ireland, [3]KU Leuven, Leuven, Belgium, [4]Trinity College Dublin, Dublin, Ireland

Introduction: GBM is the most common primary malignancy of the CNS. Historically pre-clinical models have failed to predict response in humans, despite promising preclinical data. Moreover, current models seldom incorporate surgical resection and/or standard of care chemotherapy treatment. These models also commonly employ young animals exclusively, whose immune contexture differs from older patients. We therefore sought to establish an improved, orthotopic, preclinical GBM model, which better recapitulates patient response to standard-of-care and targeted treatments.

Methods: NFpp10a-Luc2 GBM cells were orthotopically implanted into C57BL/6-mice (aged[>18months] and young[6-8weeks]) and weekly bioluminescence imaging performed to monitor tumor growth. Overall survival (OS) and tumor growth were assessed in response to (1) Surgical Resection, (2) Temozolomide (TMZ) (3) anti-PD1 (4) neoadjuvant anti-PD1 and (5) Regorafenib (REGO) therapy. Tissue collected post-mortem underwent bulk RNA sequencing followed by analysis via microenvironment cell population counter (MCP) and gene set enrichment (GSEA) to determine changes in the GBM-TME following treatment.

Results: We demonstrated OS advantage in aged mice undergoing surgical resection (Resection:33.5 days vs Non-Resection: 18 days; p=0.0166) and observed age to be a significant prognostic factor (Young:62 days vs Aged: 22 days; p=0.0002). Subsequently, we observed that TMZ and anti-PD1 monotherapies had no impact on NFpp10-Luc2 growth (p=0.9001, p=0.7933) or survival (p=0.3035, p=0.6328). Neoadjuvant anti-PD1 treated mice demonstrated no significant survival advantage compared to IgG control (33 days vs 35 days; p=0.9429). Lastly, REGO treatment demonstrated a trend towards improved OS vs Vehicle (p=0.096). MCP analysis revealed both neoadjuvant anti-PD1 and REGO treatment induced influx of CD8+ T cells, B cells and monocytes into the TME, with neoadjuvant anti-PD1 associated with an upregulation of CXCR3 (p=0.0045).

Conclusions: We have, for the first time, established and characterized response of the NFpp10a-C57BL/6 model to surgical resection, TMZ, anti-PD1 and REGO therapy in both young and aged mice. We have shown the model is markedly insensitive to intervention with chemotherapy and immune checkpoint therapy, mirroring what is seen clinically in patients. The model may therefore be employed in future pre-clinical studies to guide clinical trials in the setting of mesenchymal GBM.

#1442 Establishing a papillary renal cell carcinoma mouse model with activating Met mutation.

Preet Lal[1], Li Ding[2], Feng Chen[1]

[1]Department of Medicine-Nephrology, Washington University In St. Louis, Saint Louis, MO,[2]Department of Medicine-Oncology, Washington University In St. Louis, Saint Louis, MO

Renal cell carcinoma (RCC) is a heterogeneous group of cancers of the nephron. Papillary renal cell carcinoma (PRCC) is the second most common type of RCC. c-Met activating mutations have been associated with Type 1 PRCC which are made up of small cells containing basophilic cytoplasm covering papillae and tubular structures. In patients with PRCC, c-MetH1112Y missense mutations are associated with both somatic and germline mutations. Previous functional studies indicate codon H1112 plays an important structural role in maintaining c-Met in the inactive conformation and alterations at this codon, including H1112Y, likely disrupt this interaction facilitating constitutive activation with increased c-MET activity. A c-MetH1112Y (c-MetHY) transgene with tetO promoter sequence was micro-injected into the mouse oocyte. Transgenic mice carrying this transgene have the ability to express this activated Met protein in cells expressing rtTA (reverse tetracycline-controlled transactivator) and when doxycycline is present. Mutant mice harboring this transgene along with additional trp53 mutations showed glomeruloid like Type 1 PRCC. Our in vivo studies confirmed the expression of c-MetHY gene within the kidney and Lrp2 and Ki67 staining indicated that PRCC arises from PT (proximal tubule). PRCC canonical markers CK7, AMACR and MET expression confirmed the Type1 PRCC in our mouse model. Additionally Pan-CK, E-Cad positive expression in mutant mice further confirmed PRCC arises from epithelial cells. We have generated and described type 1 PRCC mouse model with activating-MetHY mutation. This mouse model will help illustrate the oncogenic mechanism of Met activation and identify the critical events during progression of PRCC.

#1443 The PI3K-AKT-mTOR axis persists as a therapeutic dependency in KRAS^{G12D}-driven non-small cell lung cancer.

W. J. McDaid[1], L. Wilson[1], H. Adderley[2], M. Baker[1], J. Searle[1], T. Budden[1], A. Viros[1], M. Aldea[3], A. Marinello[3], J. Aredo[4], B. Besse[3], H. A. Wakelee[4], C. R. Lindsay[5], A. Malliri[1];

[1]Cancer Research UK Manchester Institute, Manchester, United Kingdom, [2]Department of Medical Oncology, The Christie NHS Foundation Trust, Manchester, United Kingdom, [3]Gustave Roussy, Paris, France, [4]Stanford University, Stanford, CA, [5]The Christie NHS Foundation Trust, Manchester, United Kingdom

Direct inhibitors of KRAS^{G12C} and more recently KRAS^{G12D} are currently under clinical evaluation and may represent the beginning of a major translational breakthrough for non-small cell lung cancer (NSCLC) and RAS addicted cancers in general, targeting the most commonly mutated oncogene in this disease. However early reports of resistance with inactive state-selective KRAS^{G12C} inhibitors have highlighted the pressing need for rational combination partners. While preclinical combination strategies to enhance KRAS^{G12D} inhibition and combat innate resistance have already been reported for pancreatic and colorectal cancer, the application of KRAS^{G12D} inhibitors alongside combination partners in KRAS^{G12D}-driven NSCLC has not been investigated. Here we compared KRAS^{G12C}- and KRAS^{G12D}-initiated lung tumorigenesis using isogenic genetically engineered mouse models and human and mouse cell models of KRAS^{G12C} and KRAS^{G12D}-driven NSCLC initiation to compare oncopotency and signaling of each subtype. We then examined whether signaling differences observed at initiation persist in established tumors. We identified that KRAS^{G12D} is more potent than KRAS^{G12C} in inducing tumor formation. This higher potency was accompanied by co-operative activation of the PI3K-AKT-mTOR signaling axis. Disruption of this pathway using either an AKT inhibitor or mTORC1-specific inhibitor (RMC-6272, a preclinical tool compound representative of the clinical candidate RMC-5552) led to a greater reduction in transformation and proliferation in a KRAS^{G12D}-driven lung initiation model compared to the KRAS^{G12C} counterpart. Although differences between these oncogenic phenotypes become less distinguishable once tumors are established, signaling dependencies and vulnerabilities are still preserved. For instance, KRAS^{G12C}-lung tumor cells are relatively more susceptible to ERK and MEK inhibition, while KRAS^{G12D}-lung tumor cells are more susceptible to AKT and mTORC1 inhibition. Inhibiting the PI3K-AKT-mTOR axis alongside KRAS^{G12D} inhibition (MRTX1133) induced a robust, synergistic apoptotic response in KRAS^{G12D} tumor cell lines of varying sensitivity to KRAS^{G12D} inhibition alone, highlighting a potential combinatorial approach to override intrinsic resistance to KRAS^{G12D} inhibitors. Our preclinical data identify treatment vulnerabilities and suggest patient selection strategies for combination approaches that should be i) contextualized to individual RAS mutants, and ii) tailored to their downstream signaling programs.

#1444 Modeling *Twist1* overexpression in a pancreatic ductal adenocarcinoma mouse model.

M. A. Khan[1], J. Chang[1], T. Nguyen[2], D. N. Council[1], D. Dutta Chowdhury[1], A. Shetty[1], Y. Song[1], A. Chan[1], C. Lam[2], P. Patel[1], L. Tran[1], J. Chen[2], K. Nugent[2], M. Ballew[2], G. Lemtiri-Chlieh[2], F. A. Carrieri[2], R. Malek[2], H. Wang[2], N. R. J. Thielman[3], K. Li[4], L. Zheng[2], K. Gabrielson[2], P. T. Tran[1], A. Lafargue[1]; [1]University of Maryland, Baltimore, MD, [2]Johns Hopkins University, Baltimore, MD, [3]Lake Erie College of Osteopathic Medicine, Erie, PA,, PA, [4]Sichuan university, Chengdu, China

Pancreatic ductal adenocarcinoma (PDAC) is an extremely lethal cancer characterized by very poor survival outcomes. Genomic sequencing of human PDAC tissues and cell lines have identified four molecular subtypes: quasimesenchymal (QM), pancreatic progenitor, immunogenic, and aberrantly differentiated endocrine exocrine (ADEX). QM-PDAC has the worse prognosis, but no *in vivo* models exist for this molecular subtype. Our preliminary analysis using publicly available data demonstrated that the epithelial-to-mesenchymal transition (EMT) transcription factor *TWIST1* is upregulated in QM-PDAC. We hypothesized that the *TWIST1*-dependent plasticity program was a key regulator of QM-PDAC subtype development. We created a tetracycline-inducible tissue specific *Twist1* PDAC genetically engineered mouse model (GEMM). Tumor development in the mouse pancreatic ductal epithelium was directed using the *Pdx1 promoter-Cre* (P) allele leading to stable native expression of the *LSL-Kras*^{G12D} oncogene (R) and *LSL-rtTA-IRES-GFP* (G) alleles. The non-*Twist1* GEMM (PGR) was crossed with the *Twist1-tetO-Luc* (T) mouse to create the PGRT model which allows inducible expression of *Twist1* and *luciferase* in pancreatic epithelium under doxycycline treatment (Tet-ON system). Tumor progression, lineage tracing and metastatic invasion are followed by fluorescence (GFP) and bioluminescence (BLI) imaging. The characterization of this novel PGRT mouse model showed decreased overall survival compared to control non-*Twist1* containing mice (~35 weeks PGRT (n=17) vs ~60 weeks PGR (n=10)). Histological and immunohistochemistry analyses showed the PGRT pancreatic tumors resemble the QM-PDAC subtype and vimentin overexpression correlates with *Twist1*-dependent induction of EMT. We attempted to confirm the QM-PDAC profile via cellular markers: GATA6-, HNF1A-, KRT81+, KRT17+, KRT20+, P63+ and ΔP63+. The PGR and standard KPC (*Kras*$^{+/LSL\text{-}G12D}$*; Trp53*$^{+LSL\text{-}R172H}$*; Pdx1-Cre*) PDAC model were also profiled. We observed that 75% of the PGRT tumors displayed a QM-PDAC profile, contrasting with the absence of such profile in both PGR and KPC tumors. Examining the tumors from PGR and KPC, 100% of the PGR and 72.27% KPC tumors exhibited a non-squamous PDAC profile while an intermediate squamous profile was observed in 25% PGRT tumors and 27.27% KPC tumors. Furthermore, *Twist1* induction resulted in intra-abdominal and lung metastases. We observed that 87.5% of the PGRT mice were positive for metastases while we observed no positivity for PGR mice and 63.64% positivity in KPC mice. In conclusion, these data suggest that *Twist1* overexpression cooperates with *Kras*^{G12D} for PDAC tumor development mimicking the human QM-PDAC subtype to promote progression towards metastasis and early lethality. Potential uses of this novel model include testing treatment strategies to ultimately improve patient outcomes with QM-PDAC.

#1445 Emergence of frameshift mutations during tumorigenesis in VCMsh2 mouse model of Lynch syndrome.

Y. Song[1], L. Wei[2], S. S. Baxter[1], B. Somerville[1], H. Loomans-Kropp[3], C. Sanders[1], R. N. Baugher[1], S. D. Mellott[1], T. B. Young[1], H. E. Lawhorn[1], T. M. Plona[1], Q. Hu[2], S. Liu[2], A. Hutson[2], S. Difilippantonio[1], L. Pinto[1], S. M. Lipkin[4], M. Kloor[5], S. Sei[3], R. H. Shoemaker[3];
[1]Frederick National Laboratory for Cancer Research, Frederick, MD, [2]Roswell Park Comprehensive Cancer Center, Buffalo, NY, [3]National Cancer Institute, Bethesda, MD, [4]Weill Cornell Medical College, New York, NY, [5]University of Heidelberg, Heidelberg, Germany

Monoallelic germline mutations in MMR genes (e.g., *MLH1*, *MSH2*, *MSH6*, and *PMS2*) predispose individuals to Lynch syndrome (LS) with microsatellite instability (MSI) throughout the genome. Mutations at coding mononucleotide repeats (MNR) usually result in frameshift mutations (FSMs). Recurrent FSMs are thought to play a central role in the increased risk of different types of cancer. Neoantigens produced by FSMs have been shown to elicit immune responses, which is the basis for frameshift neoantigen-based vaccines. To develop a prophylactic vaccine and prevention strategy for this high-risk population, we assessed FSMs during tumorigenesis from histologically normal mucosa and fecal DNA of a LS mouse model using targeted sequencing and a panel of FSMs in MNR regions. *Msh2*$^{LoxP/LoxP}$;*Villin-Cre* mice (VCMsh2) started developing detectable tumors at 7-8 months and median survival was 11.5 months with 100% penetrance. Interestingly, FSMs were detectable not only in tumors and mucosa at 7-8 months, but also in young mice (1 month), embryos and pups although FSMs detected and variant allele frequency (VAF) were very low, indicating that FSMs accumulated over time, and FSMs alone may be not sufficient for tumorigenesis since tumors emerge at older age. To determine whether Msh2 was absent in embryos and pups, immunohistochemical (IHC) analysis was performed. Msh2 was lost in almost all intestine epithelial cells in 2-month-old mice but still present in young pups and embryos with very few cells absent of Msh2, indicating that emerging FSMs in these young pups may be due to decreased Msh2 expression because of delayed Cre function. To determine whether low Msh2 expression could lead to the emergence of FSMs, intestine mucosa from 8-, 10-, and 12-month-old *Msh2*$^{LoxP/+}$;*Villin-Cre* heterozygous mice was sequenced. FSMs were detectable with low VAF, although they didn't develop tumors. IHC staining revealed that Msh2 was absent in only a few intestine epithelial cells in these heterozygous mice, suggesting that loss of heterozygosity was a late event and rare at 12 months. To determine whether MSI emerged in young VCMsh2 pups and heterozygous mice due to haploinsufficiency of *Msh2*, MSI was assessed using seven markers and fragment size analysis. One marker (mBat67) showed instability in the intestinal mucosa of heterozygous mice and three showed instability in fecal DNA of one month old VCMsh2 mice. Interestingly, mucosal and fecal samples from a time course study in VCMsh2 mice showed progressive increase in MSI with a good correlation between MSI and FSMs during the tumorigenesis process. In summary, FSMs emerged at an early stage of tumorigenesis in VCMsh2 mice, which correlated with MSI status. Our data indicates that FSMs and MSI status can be used to monitor the tumor development of LS colorectal cancer.
Funded by the National Cancer Institute, National Institutes of Health, under Contract No. HHSN261201500003I

#1446 Gastric cancer with microsatellite instability: Ex vivo generation of syngeneic mouse models.

Daniela Conticelli[1], Gabriele Picco[2], Cristina Migliore[1], Claudia Orru[1], Fabrizio Maina[3], Emanuela Boccuni[1], Simona Corso[1], Silvia Giordano[1]

[1]Department of Oncology, University of Turin, Candiolo Cancer Institute, FPO-IRCCS, Candiolo, Italy,[2]Wellcome Sanger Institute, Hinxton, United Kingdom,[3]Candiolo Cancer Institute, FPO-IRCCS, Candiolo, Italy

The DNA mismatch repair (MMR) system is a highly conserved pathway crucial for maintaining the genomic integrity. MMR impairment in sporadic tumors is due to *MLH1* epigenetic silencing or mutations in other MMR genes (such as *MSH2, MSH6, PMS2*) and leads to microsatellite instability (MSI). Two independent molecular classifications reported the existence of a MSI subgroup in gastric cancer (GC), including 22-23% of all cases. GC MSI inter and intra-tumoral heterogeneity represents a significant challenge for precise patient stratification and treatment. Even if MSI status in GC is usually associated with a good prognosis, some reports described a subpopulation of MSI GC patients displaying a worse outcome. Moreover, while clinical trials testing immune checkpoint inhibitors in MSI tumors showed effectiveness across all treatment lines, the outcomes in GC patients were not as remarkable as in other cancer types. From the analysis of MSI GC patients enrolled in phase III clinical trials testing anti-PD1 monotherapy, it emerged that nearly half of the tumors are intrinsically resistant and complete and long-lasting responses are achieved in very few cases. Tumor mouse immunocompetent models allow to mimic the complex interactions between a fully functional immune system and a developing tumor. MSI GC syngeneic mouse models could thus represent a valuable tool to better understand the molecular complexity and predict the clinical behavior of this subgroup. To obtain MSI GC mouse models, we generated non-transformed organoids from normal gastric mucosa of BALB/c mice as a starting point for the induction of a neoplastic transformation *ex vivo*. To induce MMR deficiency, we inactivated either *Mlh1* or *Msh2* genes using CRISPR/Cas9 genome editing. Importantly, we did not introduce any other alteration in known oncogenes and tumor suppressor genes, thus allowing the natural emergence of driver mutations in the context of the genetic instability. Over time, MMR deficient models, but not the WT controls, exhibited MSI and increased their mutational burden. Furthermore, when cultured in stringent culture conditions (two-dimensional culture, growth factor deprivation), only MMR deficient cells generated tumor masses upon subcutaneous injection in immunodeficient NOD SCID mice. Importantly, cells retrieved from the tumor masses (n = 8) exhibited mutations in a relevant fraction of genes associated with the MSI subgroup by TCGA (21 out of 35) – including *Kras, Arid1a, Erbb3* and *Tpr53* – thus offering a good representation of the human MSI GC mutational landscape. Given the immunogenicity of the Cas9 protein, we finalized our models optimizing the genome editing protocol to avoid a persistent Cas9 expression. Cas9-free MMR deficient models were able to generate tumors in immunocompetent BALB/c mice, thus representing a valuable resource to investigate tumor development, progression and responses to immunotherapy *in vivo*.

#1447 Development of advanced preclinical modeling for a comprehensive characterization of cardiac angiosarcoma biology.

Rosalba Minelli, Luigi Perelli, Benjamin J. Bivona, Sanjana Srinivasan, Desiree Catania, Bianca E. Amador, Frederick S. Robinson, Johnathon L. Rose, Christopher T. Terranova, Alejandro Hernandez Martinez, Charles E. Deckard, Courtney N. Le, Kuo-Shun Hsu, Michael Peoples, Aparna Subramaniam, Hannah C. Beird, Ningping Feng, Joseph R. Daniele, Christopher Vellano, Joseph Marszalek, Vinod Ravi, Alexander J. Lazar, Andrew Futreal, Timothy P. Heffernan, Giannicola Genovese, Virginia Giuliani

UT MD Anderson Cancer Ctr., Houston, TX

Cardiac angiosarcoma (CAS) is an extremely rare malignant cardiac tumor known for its propensity for early metastasis and poor prognosis. CAS frequency is around 1-2% of all angiosarcoma cases and mostly arise in the right atrium. At present, there are no effective treatments and the survival rate is less than 10% at 5 years. Furthermore, the dearth of preclinical models has limited the advancement of biological insights into CAS. To address this challenge, we developed a somatic mosaic genetically engineered mouse model (smGEMM) with the aim of accurately mirroring the biological features of CAS. This model will be a crucial instrument for acquiring in-depth insights into the disease and steering the development of impactful therapeutic strategies. To develop a CAS smGEMM, we leveraged an endothelial-specific CRE recombinase to activate a fluorescent reporter in a tissue-dependent manner and CRISPR/Cas9 technology to engineer somatic drivers of CAS tumorigenesis. Using this strategy, all endothelial cells express tdTomato fluorescent reporter and spCas9. We then administered adeno-associated viral (AAV) particles carrying selected tandem sgRNAs with two different approaches: a direct approach where AAV particles were administered by ultrasound-guided injection in the cardiac wall of the smGEMM; and an *ex-vivo* approach where primary endotheliocytes derived from cardiac tissue of our smGEMM were first transduced with AAV particles *in vitro*, and then transplanted orthotopically by ultrasound-guided injection. With the latter strategy, we successfully generated the first cardiac angiosarcoma model that faithfully recapitulates angiosarcoma features, including lung dissemination. Cell lines from primary and metastatic tumors were also established, characterized and utilized for genome-wide CRISPR Cas9 screening. Current efforts are focused on prioritizing hits for validation, aiming to glean insights that can inform potential therapeutic strategies.

#1448 Investigating the effects of estrogen on the initiation of prostate cancer.

Nash S. Denic, Ashlyn Swift-Gallant, Kenneth R. Kao

Medicine, Memorial University of Newfoundland, St. John's, NL, Canada

Background: Prostate cancer (PCa) is responsible for ~10% of cancer-related deaths in men. *Nkx3.1* is an androgen-regulated gene expressed primarily in the prostate, which encodes a tumor suppressor protein important for male reproductive development. Loss of nkx3.1 is thought to lead to prostatic intraepithelial neoplasia (PIN), the pre-invasive form of prostatic adenocarcinoma. Previous evidence suggests that estrogenic dysregulation and testosterone imbalance play a significant role in PCa initiation and progression.

Objectives/Aims: We aimed to investigate how estrogen impacts the progression of PIN in the anterior prostate of mice lacking nkx3.1.

Methods: To investigate the effect of long-term exposure to 17β-estradiol (E2), nkx3.1$^{+/+}$ and nkx3.1$^{-/-}$ 12-week-old mice were given 2 mg/day of E2 over 90 days by subdermal implantation of 90-day extended-release tablets. After 90 days, the anterior prostate lobes of the mice were harvested and analyzed post-treatment for signs of pre-cancerous tissue. The immediate, early effect of E2 exposure was also investigated by the subcutaneous injection of 8- and 20-week-old mice with 0.300 mg/kg of E2. Within two hours, the anterior prostate lobes were harvested, and ~500 ng/µL of RNA was isolated from the tissues. cDNA was reverse-transcribed, in triplicate, from the RNA and the expression of c-myc, p53, estrogen receptor ERα (ESR1), and ERβ (ESR2) were assessed via qRT-PCR. Three technical replicates from three biological replicates were performed for each treatment.

Results: Nkx3.1$^{-/-}$ mice chronically exposed to elevated E2 developed PIN following E2 treatment, while the placebo group had tissue hyperplasia. Nkx3.1$^{+/+}$ mice had normal prostate tissue regardless of E2 treatment. In response to immediate exposure to E2, the prostates of 8-week-old nkx3.1$^{+/+}$ mice showed reduced c-myc expression. 8-week-old nkx3.1$^{-/-}$ mice showed no changes in expression of any of the four genes assayed, in response to E2 as compared to the placebo treatment. In contrast, regardless of exposure to E2, c-myc, p53, and ESR2 were significantly elevated in these mice compared to the nkx3.1$^{+/+}$ groups. Furthermore, c-myc and p53 expression was suppressed in 20-week-old nkx3.1$^{-/-}$ mice in response to E2, while ESR1 and ESR2 remained unchanged.

Conclusion: Our evidence suggested that prolonged exposure of wild-type mice to E2 had no pathohistological impact on the anterior prostate tissue. In nkx3.1-deficient mice, however, E2 exposure promoted the onset of PIN, and caused immediate differential expression of estrogen-responsive genes, suggesting a role of nkx3.1 in protecting the prostate in the presence of a hormonal imbalance.

#1449 Targeting squalene epoxidase for breast cancer brain metastasis: The evaluation of a new therapeutic target for brain extravasation and colonization using animal models.

P. Y. Lee[1], K.-Y. Lin[1], C.-D. Chang[1], S.-Y. Cheng[1], Y.-W. Hung[1], C.-C. Yang[1], Y.-H. Chang[1], C.-C. Shen[1], J.-Y. Yeh[2], Y.-L. Yu[2], S.-P. Wang[3];
[1]Pharmacology Discovery Services Taiwan, Ltd., New Taipei City, Taiwan, [2]China Medical University, Taichung, Taiwan, [3]Academia Sinica, Taipei, Taiwan

Breast cancer brain metastasis is one of the most common forms of breast cancer metastasis and a major cause of morbidity and mortality. Patients who develop brain metastases tend to be associated with progressive neurologic deficits and short overall survival, which represents an unmet medical need. Extensive research has been conducted to elucidate the mechanism of cancer metastasis with limited information gained as to how cancer cells extravasate and colonize to the brain. Recently, we identified a novel mechanism by which squalene epoxidase (SQLE), the second rate-limiting enzyme in cholesterol biosynthesis, plays a critical role in the process of breast cancer metastasis to the brain. Thus, toward a better understanding of the underlying molecular mechanisms and applications of molecular target(s) for brain metastasis therapy, murine models were employed for investigation of brain extravasation and colonization with intracardiac or direct intracranial injections of GFP/FLuc-labeled human MDA-MB-231 metastatic breast carcinoma cells. The MDA-MB-231 cells were found to metastasize to the brain and other organs following intracardiac implantation into nude mice and were further isolated from each tissue. Interestingly, the isolated brain-metastasized tumor cells (MDA-MB-231-BrM) exhibited a significant upregulation of SQLE expression when compared with those that metastasized to other distal sites. The essential role of SQLE in the specific steps of the breast cancer-to-brain metastatic process was evaluated by *ex vivo* immunofluorescence analysis and immunohistochemistry staining of brain slices from the study subjects. Our data demonstrate that high SQLE expression is essential for MDA-MB-231-BrM to extravasate into the parenchyma, as well as the formation of micro- and macro-metastases in the brain. Interestingly, we found that blood vessel co-option and the surrounding neuronal cells play key roles in supporting MDA-MB-231-BrM to develop brain macro-metastases. *In vitro* blood-brain barrier (BBB) models further demonstrated the critical role of SQLE in promoting tumor cell invasion and penetration through the BBB. To verify SQLE as an oncogenic factor that can be selected as a potential therapeutic target in suppressing breast cancer brain metastasis, we evaluated the inhibitory effects of terbinafine (a SQLE inhibitor) in both the MDA-MB-231-BrM orthotopic and intracardiac mouse models. Pharmacologic inhibition of SQLE by terbinafine suppressed MDA-MB-231-BrM tumor growth at the mammary fat pad and distal metastases to the brain, suggesting that targeting SQLE represents a therapeutic opportunity for breast cancer brain metastasis.

#1450 Novel whole slide imaging modes for imaging mass cytometry reveal cellular and structural composition of mouse glioblastoma.

Q. Raza, N. Zabinyakov, **T. D. Pfister**, N. Parsotam, D. Howell, L. Lim, C. Loh;
Standard BioTools, Markham, ON, Canada

Mouse tumors have become widely used models in translational research of brain malignancies, helping to address the difficulties related to studying the human brain. Mouse brain can be regarded as a miniaturized model of the human brain, permitting visualization of the whole tissue to provide spatial cellular context. Imaging Mass Cytometry™ (IMC™) is a highly relevant tool capable of quantitative evaluation of the multiparametric protein composition in brain tumor microenvironment (TME) without the complications of autofluorescence, tissue degradation, and spectral overlap. The Hyperion XTi™ Imaging System (Standard BioTools™) utilizes IMC technology to simultaneously assess more than 40 individual structural and functional markers in tissue, providing insight into the organization and function of the TME.

We demonstrate the whole slide imaging (WSI) application using a 40-marker panel composed of the Maxpar OnDemand™ Mouse Immuno-Oncology IMC Panel Kit and the Maxpar® Neuro Phenotyping IMC Panel Kit on mouse normal and glioblastoma (GBM) brain tissue. The panel was composed of mouse-specific antibodies, which highlight tumor and immune components of the mouse TME. We performed imaging using two new features of Hyperion™ XTi. Ultrafast preview mode (PM) was applied to rapidly screen entire brain sections for marker expression signatures associated with various immuno-oncology processes. This enabled biomarker-guided selection of areas in tumor tissue that were imaged using region of interest-based IMC and analyzed using single-cell analysis (SCA). In parallel, a high-throughput tissue mode (TM) was applied to perform a detailed whole-slide scan of normal and GBM mouse brain tissues that were quantified using pixel-based analysis (PBA) to unravel the composition of the TME.

Using TM, we were able to successfully visualize the entire coronal and sagittal sections of normal mouse brain as well as mouse GBM tissue. PBA on TM data provided quantitative spatial expression patterns of structural and immune markers across the whole tissue. In normal tissue, we visualized the highly organized structure of the normal brain and detected neurons, oligodendrocytes, vascular-adjacent astrocytes, and axonal tracks. In GBM tissue, necrotic cores, areas with high immune infiltration, extracellular matrix deposits, and activated tumor cells were detected. SCA of GBM tissue demonstrated expansive vascularization, replicating $Olig2^{+}$ cells, activation of Ras signaling, and high abundance of infiltrating immune cells.

Overall, we demonstrate the successful application of two novel WSI modes and highlight the power of IMC technology to simultaneously explore dozens of relevant biological outputs to better understand the TME of GBM and other tumors.

For research use only. Not for use in diagnostic procedures.

#1451 Replication repair deficient mouse models provide insights into gliomagenesis and response to immunotherapy.

Z. Aamir[1], M. Galati[1], E. Gattoni[1], O. Crump[1], N. M. Nunes[1], A. Das[1], N. Fernandez[1], N. Fernandez[1], A. K. Q. Wong[2], J. Fortin[3], L. Stengs[1], V. Bianchi[1], M. Edwards[1], L. Negm[1], C. Hawkins[1], D. Malkin[1], S. Egan[1], U. Tabori[1];

[1]The Hospital for Sick Children, Toronto, ON, Canada, [2]Queen's University, Kingston, ON, Canada, [3]Princess Margaret Cancer Centre, Toronto, ON, Canada

Background: Replication Repair Deficiency (RRD), caused by germline monoallelic (Lynch Syndrome) or biallelic (Constitutional Mismatch Repair Deficiency, CMMRD) mutations in MMR genes, is present in 5-10% of glioblastomas in children, adolescents, and young adults. RRD glioblastomas are chemoradiation-resistant, but respond favorably to immune checkpoint inhibition (ICI). Representative immunocompetent animal models are urgently needed for 3 recently identified subgroups based on specific somatically-acquired mutations, survival, and immunotherapy response (RRD1: MMRD with *POLE* mutations, RRD2: MMRD associated with *TP53* mutations, and RRD3: MMRD harboring *IDH1* mutations).

Methods: Using germline mutations and brain-specific *Cre*-drivers, we genetically engineered mouse models that recapitulate each human RRD-subgroup.

Results: All mouse models robustly developed brain tumors displaying phenotypic variation.

RRD1 (*Nestin-* and *Olig2-Cre*$^{+}$*/ Msh2*$^{LoxP/LoxP}$*/Pole*$^{S459F/+}$ and *LSL-Pole*$^{P286R/+}$): CMMRD-like *Nestin-Cre*-driven mice develop posterior-fossa glioma-like or embryonal (EB)-like tumors at ~2.7 months. *Olig2-Cre*-driven mice display hemispheric gliomas at ~10 months, suggesting distinct cell-of-origin.

RRD2 (*Nestin-Cre*$^{+}$*/Trp53*$^{LoxP/LoxP}$ and *Msh2*$^{LoxP/LoxP}$ or *Mlh1*$^{-/-}$): tumors develop primarily in the hindbrain in germline *Mlh1* mice, and majority arise in the forebrain of *Nestin-Cre/Msh2* mice, highlighting the timeline of mutagenesis. Strikingly, germline *Mlh1* tumors occur earlier than *Nestin-Cre*-driven RRD2 tumors, indicating early developmental mutation accumulation in CMMRD-patients. Lynch-like RRD1/2 mice succumb exclusively to gliomas >13 months ($p<0.0001$).

RRD3 (*Olig2-Cre*$^{+}$*/Msh2*$^{LoxP/LoxP}$*/Trp53*$^{LoxP/LoxP}$*/LSL-Idh1*$^{R132H/+}$): mice succumb to brain tumors at >11 months and are hemispheric.

Significance: These observations recapitulate human data, where CMMRD-patients develop glioblastoma/EB earlier than Lynch-patients (8.6 vs. 14-years; $p<0.0001$), and posterior-fossa glioblastoma/EB presents earlier than hemispheric gliomas ($p=0.04$). Additionally, tumor onset and location vary by subgroup (RRD1: 7.6-years, RRD2: 8.3-years, both hemispheric/posterior-fossa; RRD3: 12-years, hemispheric; $p=0.005$). In both mice and humans, RRD1 exhibits ultra-hypermutation, high immune infiltration, and response to ICI, whereas RRD2 harbors lower mutational burden, are immune-cold, and ICI-monotherapy resistant. Temporal dynamics of RRD tumor development is currently being tracked by serial MRI to define previously undetermined biologically relevant time points of tumor progression.

Conclusion: Our models accurately mimic the human condition and provide unique insights into RRD tumorigenesis, allowing optimization of subgroup-tailored therapeutic approaches.

#1452 A *PIK3CA*-driven mouse model of metaplastic breast carcinoma to assess potential therapeutic strategies.

P. Roa[1], V. Foglizzo[1], M. R. de Marchena[1], S. Chandthakuri[1], E. Cocco[1], P. Castel[2];
[1]University of Miami Miller School of Medicine, Miami, FL, [2]NYU Grossman School of Medicine, New York, NY

Metaplastic Breast Carcinomas (MBC) are rare and aggressive breast cancers with mesenchymal or squamous components. While histologically heterogeneous, MBC are typically triple negative: they lack expression of ER, PR and HER2. Importantly, approximately 40% of MBC harbor oncogenic gain-of-function mutations in *PIK3CA*, the gene encoding for the catalytic subunit of PI3K. These alterations are targetable by an array of inhibitors of the PI3K-AKT-mTORC1 pathway. However, few animal models of MBC are available, and it is currently difficult to study MBC biology and response to therapy. Here, we describe the generation of a new mouse model of MBC driven by the *PIK3CA* H1047R mutation. We histologically and biologically characterize this model and assess potential therapeutic strategies. We used genetically-engineered mouse models to express the human *PIK3CA* H1047R mutation under the control of the MMTV promoter, which is mostly expressed in the mammary epithelium. Tumors developed in mice in about 1 year. We histologically characterized these tumors and generated cell lines, organoids, and tumor grafts in immunocompromised mice. The resulting model, termed MMTV-102, was evaluated for the response to PI3K-AKT-mTOR pathway inhibitors, both *in vitro* and *in vivo*. The MMTV-PIK3CA^{H1047R} tumor was a high grade poorly differentiated MBC negative for ER, PR, and HER2. It presented squamous components, keratin depositions, mitotic figures, and vascular invasion and stained positive for the basal marker CK14. In addition, due to the presence of the *PIK3CA* H1047R mutation, it stained positive for phosphorylated AKT, PRAS40, and S6RP, indicating constitutive activation of the PI3K-AKT-mTORC1 pathway. MBC derived cell lines and organoids were confirmed to be triple negative and could form tumors in mice. In addition, these cellular models were sensitive to PI3Kα, pan-PI3K, and mTORC1 inhibitors *in vitro* and *in vivo*, but the mTORC1 inhibitor everolimus exhibited the strongest effect. When resistance to everolimus eventually developed *in vivo*, we established cell lines from these resistant tumors. In addition, we generated an everolimus resistant cell line following chronic drug exposure *in vitro* (MMTV-102 Par res). Both cellular models were tested for their sensitivity to the next-generation mTORC1 inhibitor RMC-5552 by proliferation and clonogenic assays. We show that our mouse model can originate MBC with an active PI3K pathway. These tumors are amenable to transplantation into immunocompromised mice and to generate cell lines and organoids, allowing us to develop a simple, versatile, and rapid model of MBC. Tumors derived from our model are sensitive to PI3Kα and mTORC1 inhibitors, but eventually develop resistance to these agents. The use of next-generation mTORC1 inhibitors can overcome resistance in some cases, providing a rationale for their implementation in the treatment of patients with MBC.

#1453 Development and evaluation of subcutaneous and orthotopic PC3M metastatic prostate cancer xenograft model in SRG rats for therapeutic assessment.

K. Draheim, E. Rainbolt, B. John, C. Clouse, K. Shinn, J. Avery, K. Aw Yong, C. Hall, P. Fadden, **A. Avrutskaya**;
Charles River Laboratories, Inc., Wilmington, MA

Introduction: Prostate cancer is the most prevalent cause of cancer deaths in American males after lung cancer. The establishment of clinically relevant prostate cancer models is crucial for advancing our understanding of the disease and evaluating potential therapeutics. Oncology studies in rats provide a secondary species to mice with the advantage of extensive longitudinal blood sampling and tumor biopsies in pharmacodynamics analysis. This *in vivo* study evaluates the behavior of subcutaneous and orthotopic luciferase (luc) tagged metastatic PC3M-luc cells in immunodeficient SRG rats (Hera Biolabs) for tumor growth kinetics, metastasis, and response to paclitaxel and carboplatin alone and in combination.
Methods: PC3M-luc cells were implanted subcutaneously into the right flank or orthotopically into the prostate of SRG rats. Subcutaneous tumor progression and treatment responses were monitored using calipers and bioluminescent imaging (BLI), with the capacity to detect developing metastases prior to necropsy. Orthotopic implants were monitored exclusively using BLI. Tolerability was evaluated based on biweekly changes in body weight, daily observations for signs of tumor- or treatment-related clinical signs, necropsy results, and complete blood count (CBC) and clinical chemistry marker comparisons with immunocompetent CD rats.
Results: PC3M-luc prostate carcinoma was successfully established orthotopically and subcutaneously in SRG rats, with similar growth rates and the development of spontaneous metastases to distant organs, modeling metastases observed in prostate cancer patients. Paclitaxel treatment was less tolerated in SRG rats in comparison to nude rats, enhanced toxicity was observed when combined with carboplatin. Comparison of CBC and clinical chemistry blood markers in naïve immunocompetent CD and immunodeficient SRG rats differed mainly in White Blood Cell (WBC) counts that were significantly lower in SRG rats, as expected due to the lack of mature B, T, and NK cells in these animals.
Conclusion: The development of orthotopic and subcutaneous PC3M-luc prostate cancer models in rats provides a valuable alternative platform for assessing the effectiveness of established and novel therapies. This rat-based models offers a secondary species for comparison of prostate cancer behavior in mice, successfully mimics the clinical development of metastases, and provides additional insights into disease progression and therapeutic strategies. Future studies will focus on the assessment of tolerability and combination therapy strategies for improved treatment outcomes.

#1454 Expanding the therapeutic application of PARP inhibitor: AI evaluation of real-word clinico-genomic data from spontaneous canine tumors.

L. Rodrigues[1], K. Wu[2], G. Harvey[1], G. Post[1], A. Hull[1], A. Miller[1], L. Lambert[1], C. Lopes[1], J. Zou[2];
[1]FidoCure - One Health Company, Palo Alto, CA, [2]Department of Biomedical Data Science, Stanford University, Stanford, CA

The widespread application of Poly-ADP ribose polymerase (PARP) inhibitors in anti-cancer therapy is constantly increasing their role as a treatment strategy across various neoplasms, the majority of which are linked with BRCA deficiency. While the most significant advantages are observed in cancers with BRCA1/2 mutations, it is evident that the benefits extend beyond this specific group. Preclinical evidence encourages the exploration of PARP inhibitors in neoplasms demonstrating BRCAness or homologous recombination deficiency (HRD), both as monotherapy and in combination with chemotherapy. This study employs spontaneous canine tumors as a complementary model for cancer research, aiming to seamlessly bridge the transition from preclinical investigations to clinical application. Leveraging the FidoCure® Precision Medicine Platform, we identified biomarkers associated with prognosis and treatment prediction, specifically with the PARP inhibitor olaparib, facilitating a smoother translation from laboratory findings to practical clinical use. Analyzing real-world clinico-genomic data from 1278 dogs with cancer revealed intriguing insights of specific targeted treatments developed for humans showing a positive prognosis when applied to canine tumors with specific genomic alterations. Notably, olaparib exhibited efficacy in TP53 and BRCA1-mutated cases (OS HR 0.34, $P < 0.001$; HR 0.39, $P = 0.004$), while rapamycin (mTOR inhibitor) demonstrated promising outcomes in TP53 and RB1-mutated canine tumors (OS HR 0.73, $P = 0.028$; HR 0.32, $P = 0.024$). Further stratification by tumor types unveiled noteworthy correlations. TP53 mutant osteosarcomas exhibited improved prognosis with olaparib treatment (OS HR 0.11, $P < 0.001$), and soft tissue sarcomas with TP53 mutations demonstrated favorable responses to rapamycin and olaparib therapy (OS HR 0.11, $P = 0.012$; HR 0.07, $P = 0.011$). These findings underscore the potential of leveraging canine tumor models and clinico-genomic analyses to inform targeted treatment strategies, offering valuable insights for advancing precision medicine in both veterinary and human oncology. Further investigation into the association between TP53 mutation and olaparib response is warranted. The intriguing aspect lies in the role TP53 mutation has been linked in previous studies to heightened chromosomal instability and elevated HRD scores. Utilizing real-world evidence and data tools within the FidoCure dataset, we have effectively pinpointed correlations between gene mutations and survival, particularly in relation to responses to targeted therapy treatment. Canine models, mirroring human diseases with intact immune systems and comparable tumor genomic profiles, as verified by the FidoCure database, expedite clinical studies of novel treatments that face significant scalability challenges.

#1455 *In vitro* blood brain barrier model for evaluation of brain metastasis.

S. Noda-Narita, A. Aiba;
The University of Tokyo, Tokyo, Japan

Introduction: Brain metastasis significantly reduces the patient's quality of life and survival, but there are only a few choices of treatment for brain metastasis. The research for brain metastasis is difficult because of its complex and unique microenvironment, including blood-brain barrier (BBB). The BBB maintains strong cell adhesion of the vascular endothelial cells (ECs) to protect the brain parenchyma. The BBB is composed of three cell types: vascular endothelial cells, pericytes, and astrocytes. As the role of pericytes in maintaining the BBB function has become more evident, the reconstituted models of the BBB in which ECs, pericytes, and astrocytes are seeded on the front and back of the insert membrane have gotten our attention. In the field of cancer, the role of not only ECs but also wall cells, corresponding to pericytes in the brain, has been focused on. In this study, we aimed to create the *in vitro* BBB models and elucidate the interaction of the BBB and the metastasizing cancer cells.
Methods: We applied a reconstituted model of the BBB consisting of ECs, pericytes, and astrocytes of human immortalized cells (Ito R, et al. *Mol Pharm* 2019) and created the co-culture system for evaluating brain metastasis. We constructed four co-culture systems and compared the migration ability of MDA231 in those models: EPA model (ECs, pericytes, and astrocytes), E0A model (ECs and astrocytes), EP0 model (ECs and pericytes), and E00 model (ECs only). We also analyzed the migration ability of the pairs of parental and brain metastatic (BrM) cell lines.
Results: The BBB reconstituted model (EPA model), in which ECs were co-cultured with pericytes and astrocytes, showed higher trans-epithelial electrical resistance and lower permeability than the other co-culture models. When cancer cells were seeded, the EPA model strongly inhibited metastatic invasion of cancer cells compared to the other models. It suggests that both pericytes and astrocytes are essential for regulating cancer cell invasion. In addition, when the BrM cells of MDA231 and Ex3LL were seeded, the BrM cells invaded the EPA model more easily than the parental cells. It indicates that this model can reproduce *in vivo* brain vascular functions.
Conclusion: We created the BBB reconstituted model which mimics the brain vascular microenvironment. This model reproduced the *in vivo* BBB function to protect brain from cancer cells and evaluated the brain metastatic ability of the cancer cells. Using this model, we showed that pericytes and astrocytes were essential for the BBB barrier function against the cancer cells. We need further investigation to elucidate the mechanism of brain metastasis using this BBB model.

#1456 First successful engraftment of human liver cancer cell line in highly robust immunocompromised porcine model to test the tumor ablation efficacy by histotripsy.

T. Paul[1], K. Imran[1], J. Gannon[1], B. Trusiano[1], K. Eden[1], H. Ivester[1], M. Mott[1], M. Powar[1], M. Edwards[1], C. Byron[1], S. Clark-Deener[1], K. Lee[2], E. Vlaisavljevich[1], I. Allen[1];

[1]Virginia Tech, Blacksburg, VA, [2]University of Missouri, Columbia, MO

Liver tumor, commonly called Hepatocellular carcinoma(HCC), is the most common type of primary liver malignancy. It is the fourth leading cause of cancer-related deaths. Late diagnosis, location of the tumor, tumor burden, and metastases makes liver tumor very challenging to treat by liver transplantation, surgical procedures, and other ablation techniques like cryoablation and thermal ablation. Also, the absence of a preclinical animal model makes it challenging to develop and explore the feasibility of treatment modalities. Histotripsy is a non-invasive, non-ionizing, non-thermal, image-guided focused ultrasound ablation treatment method that uses high-pressure pulses to create acoustic cavitation, a “bubble cloud,” at the target. The bubble cloud expands and collapses, which ablates the tissue into an acellular homogenate. Pigs are ideal animal models as they closely resemble human anatomy and are significant in improving the translation to human patients. This study aimed to establish the feasibility of successfully ablating liver tumors by histotripsy using an immunocompromised porcine model to generate HepG2 human liver cancer cell line tumors in the liver of the immunocompromised pigs. The orthotopic porcine model was established using RAG2/IL2RG double knockout immunocompromised pigs. HepG2 cells were injected orthotopically into the liver of immunocompromised pigs. Three weeks after the injections, CT images and necropsy indicated successful engraftment and growth of liver tumors in the pigs. The ultrasound images and post-histotripsy treatment histology images showed confirmed ablation zones in the liver. Therefore, in conclusion, our preliminary results in the study could demonstrate, for the first time, a highly robust model of human liver cancer in a large animal model. Soon, we plan to conduct more such studies and explore all the possible utilities of these immunocompromised porcine models to develop therapeutic strategies to increase the efficacy of liver tumor ablation by histotripsy.

#1458 Anti tumoral role of PDX1 on pancreatic ductal adenocarcinoma aggressiveness.

J. Mosna, F. Garde, M. Stinson, C. Pastore, P. Sanchis, A. Carcagno;
CONICET - IQUIBICEN, Buenos Aires, Argentina

Pancreatic ductal adenocarcinoma (PDAC) represents a very aggressive type of pancreatic cancer (9% survival rate at 5 years). PDX1 is an important transcription factor for embryonic development of the pancreas, endocrine lineage differentiation and the maintenance of mature beta cells. Notably, in PDAC patients, the expression of PDX1 is downregulated in tumor cells compared to adjacent non-tumoral tissue. Interestingly, increasing tumor PDX1 expression has been shown to enhance the overall survival rate in PDAC patients. Therefore, our aim was to analyze the role of PDX1 on tumor aggressiveness of PDAC cells. To induce PDX1 expression, PANC1 cells were treated with BRD7552 (a PDX1 inducer) for 9 days. Overexpression of PDX1 was confirmed by Western Blot analysis and no cytotoxic effects were observed by MTT or Trypan Blue exclusion assays on treated cells compared to control. Wound healing and transwell migration assays showed a significant reduction in the migration rate compared to the control group. A higher proportion of cells in G1 phase was observed in treated cells compared to control by propidium iodide staining followed by flow cytometry assay. Furthermore, the cell confluence assay showed a significant reduction in proliferation rate in treated cells compared to control, but no differences were observed on the proportion of $KI67^{+}$ and $PH3^{+}$ cells by immunostaining. To assess the *in ovo* effects of BRD7552, treated PANC1 cells were implanted onto the chorioallantoic membrane of chick embryos and tumor growth was measured at different stages observing a significant reduction in tumor growth in PANC1 cells compared to control between days 3 and 8 post implantation. No significant differences in morphology or color were observed between treated and control implanted cells. Hematoxylin-eosin staining showed reduced invasion of treated cells into the chorioallantoic membrane compared to control. In conclusion, the overexpression of PDX1 affects cell cycle, reduces proliferation rate and inhibits migratory potential *in vitro*. Moreover, in an *in ovo* model this overexpression diminished tumor growth and invasion in PANC1 cells. In conclusion, the overexpression of PDX1 induced by BRD7552 drives pancreatic ductal adenocarcinoma to a less aggressive tumoral phenotype.

#1459 The immuno-AVI-PDX, am innovative patient-derived xenograft model for preclinical immuno-oncology studies.

M. Lacourrege, Jr., C. Costechareyre, Jr., L. Jarrosson, Sr., **R. Teinturier, Sr.**, F. Berget, Sr., C. Delloye-Bourgeois, Sr., V. Castellani, Sr.;
ONCOFACTORY, Lyon, France

Over the last decade, the success of immunotherapy in treating numerous solid and hematological tumors is unprecedent. However, the poor preclinical predictive power of current model systems explains in part the failures during late-stages clinical drug development for the numerous potential immunotherapies. Thus, there is a crucial need for innovative technologies offering fast and reliable evaluation of immunotherapies on patient-derived models. Using its proprietary process of micro-implantation of patient tumor cells within selected organs of series of avian embryos, Oncofactory developed two humanized avian xenograft models, namely IMMUNO-AVI-patient derived xenograft (iAVI-PDX™) and IMMUNO-AVI-cell line derived xenograft (iAVI-cellDX™). These models, consisting in the co-implantation of human peripheral-blood mononuclear cells (PBMC) and human cancer cells were validated through a sequence of experimental steps. First, we found that transplantation of PBMCs into avian tissues exhibited good survival and low allogenicity against the avian embryonic organism. Second, in embryos engrafted with tumoral cells, we established that intravenously injected PBMCs successfully populated the tumor. Third, to reduce the dilution of immune cells in the embryonic tissues and to better standardize the number of implanted cells in between embryos, we optimized the process by direct co-implantation of both PBMCs and cancer cells. We analyzed the immune cell contingent sorted from dissected tumors and found that all major immune cells populations, including T and B lymphocytes, monocytes as well as NK cells were preserved post-grafting, when compared to pre-grafted PBMCs. The AVI-cellDX™ and AVI-PDX™ models initially developed by Oncofactory allows fast and reproducible tumor growth with statistical evaluation of molecule efficacy already at 24 hours post-injection. To assess whether our humanized models retain these advantages, we analyzed the outcome of anti-PD1 antibody (Pembrolizumab) intravenous injection in series of avian embryos co-engrafted with human PBMCs and PDL1-expressing breast and colorectal cancer cell lines. Twenty-four hours post vehicle or Pembrolizumab exposure, we analyzed the tumor volumes in grafted embryos using light sheet microscopy. In all three cancer models, we found a statistically significant reduction of the volume upon pembrolizumab, compared with vehicle. Using a panel of molecular markers in flow cytometry, we found that the Pembrolizumab efficiently targeted T lymphocytes in the tumors. Finally, we validated the efficiency of Pembrolizumab treatment in models of co-implantation of human PBMCs with melanoma and colorectal patient samples. Thus, humanized iAVI-cellDX™ or -PDX™ technology bring powerful and fast alternative to mouse models, to strongly accelerate preclinical developments in immuno-oncology.

TUMOR BIOLOGY: Chemical, Environmental, and Virus-Induced Carcinogenesis
Poster Session

#1463 Characterizing inflammation-induced epigenetic and transcriptomic alterations driving NSCLC using lung organoid models.
N. Wang, K. Lombardo, R. Padaki, R.-W. Chiu Yen, M. V. Brock, L. Cope, H. Easwaran, S. B. Baylin, M. Vaz;
Johns Hopkins University School of Medicine, Baltimore, MD

Chronic inflammation is a major driver of lung cancer and contributes to its pathogenesis by inducing genetic and epigenetic alterations. These, in turn, modulate the microenvironment to facilitate emergence of tumor promoting immune evasive mechanisms. The evolution of epigenetic events and their role, both alone, and in association with lung cancer specific genetic drivers in initiation of lung cancer is not well delineated. Specific pathological subtypes of non-small cell lung cancer (NSCLC) have distinct cells of origin, suggestive of cell type-specific changes in driving their development. We employed lung organoid models with chronic exposure to cigarette smoke condensate (CSC) to elucidate sequential, cell type-specific epigenetic and transcriptomic alterations and their role in co-operating with genetic events to drive development of NSCLC. We examined epigenomic and transcriptomic alterations over a 6-month exposure period by DNA methylation arrays, ATAC-seq, and RNA-seq. We observe that CSC exposure causes distinct morphological changes in organoid structure and composition, accompanied by an increase in proliferative potential. Using flow cytometry and immunofluorescent staining approaches, we demonstrate a chronic inflammation-driven shift in stem cell populations accompanied by reduction in differentiated cell types. Bulk and single-cell RNA sequencing approaches identified distinct temporal changes in transcriptional signatures in CSC exposed organoids suggestive of evolution of an immune evasive and pro-tumorigenic phenotype. Gene set enrichment analysis revealed a downregulation of interferon signaling and upregulation of Myc targets and oxidative phosphorylation pathways in CSC treated organoids. Notably, co-culturing organoids with key immune cell populations, demonstrate the ability of the CSC exposed organoids to modulate shifts in immune cells from a pro- to anti- inflammatory state. In accordance with this shift in immune cell phenotype, CSC treated organoids secreted decreased levels of pro-inflammatory cytokines as measured by multiplex ELISA assays. Genome wide DNA methylation analysis reveal that CSC methylated genes were associated with differentiation and cell fate commitment as well as transcription factor activity. Finally, we demonstrate that introduction of key NSCLC-specific driver events at the 6-month time point sensitize only CSC treated organoids to tumor formation in vivo, leading to the development of distinct genetic driver-specific subtypes of NSCLC. Altogether, our results demonstrate the ability of chronic inflammation to drive key cell type-specific transcriptomic and epigenetic changes leading to the development of distinct subtypes of NSCLC. Our findings will help identify molecular correlates for early detection and aid development of novel therapeutic strategies for disease interception.

#1464 Smoking carcinogen-induced inflammation promotes lung carcinogenesis via IRAK4 activation.

R. K. Aggarwal[1], S. Sidoli[1], S. Sahu[1], S. Aluri[1], C. Vegivinti[1], D. Verma[1], S. Gordon-Mitchell[1], B. Agarwal[2], T. Verma[1], D. T. Starczynowski[3], U. G. Steidl[1], B. Halmos[1], L. M. LaFave[1], H. Cheng[1], A. Verma[1], Y. Zou[1];

[1]Albert Einstein College of Medicine, Bronx, NY, [2]Genome RX, Philadelphia, PA, [3]Albert Einstein College of Medicine, Cincinnati, OH

Lung cancer is globally the most common cancer, and most cases are associated with smoking. Smoking exposes respiratory epithelial tissues to various carcinogens. Evaluating the effects of these carcinogens administered intratracheally in mouse models would allow us to study lung carcinogenesis in a relevant manner and determine therapeutically targetable pathways.

Cigarette smoking exposure was mimicked in vivo using a smoke machine and the condensate was subjected to chemical analysis. In addition to nicotine, cigarette smoking condensate included significant levels of the carcinogens, Nicotine-derived nitrosamine ketone (NNK) and Benzo(α)pyrene (BP). Next, a mouse model of cigarette smoking-induced carcinogenesis was developed by exposing ICR mice to intratracheal exposure to NNK and BP three times a week for 18 months.

Mice chronically exposed to NNK and BP developed epithelial dysplasia at 4 months of exposure and lung cancers at 8-12 mo. of exposure at significantly increased rates relative to controls. Histology revealed myeloid inflammation in murine lung tissues. Exposure of lung epithelial cells to cigarette smoking condensate led to increased production of pro-inflammatory IL-1β. Downstream mediator of IL-1β signaling, Interleukin 1 receptor associated kinase-4 (IRAK4), was overexpressed in murine lung tissues exposed to carcinogens in vivo. Two-thirds of human tissue sections obtained from archived lung cancers also exhibited overactivated IRAK4 expression.

In lung cancer cell lines, IRAK4 immunofluorescence revealed a microtubule like pattern of expression in lung cancer cells. Immunoblotting confirmed IRAK4 colocalization within purified microtubules. Using mass spectrometry on isolated microtubules, we observed that phosphorylation decreased in various tubular proteins after IRAK4 inhibition. Inhibition of IRAK4 using small molecule specific inhibitors resulted in decreased invasion in lung cancer cell lines.

These data show that chronic intratracheal exposure of smoking associated carcinogens leads to dysplasia and malignancies in mouse models. This exposure also leads to myeloid inflammation and activation of IRAK4 in lung tissues. Therapeutic targeting of IRAK4 can have potentially beneficial effects in lung cancer models.

#1465 Studying basal cell adaptation in the airways in response to chronic tobacco exposure.

D. Osuna de la Pena[1], Z. Stoichkova[1], M. Przybilla[2], C. Percival[1], S. E. Clarke[1], K. H. Gowers[1], P. J. Campbell[2], S. M. Janes[1];
[1]University College London (UCL), London, United Kingdom, [2]Wellcome Sanger Institute, Hinxton, United Kingdom

Premalignant lesions in the airways are preceded by the accumulation of cells with a high mutational load, many of which carry driver mutations. Our previous work suggests this is a dynamic process: tobacco smoking increases the size of mutated clones, which contain shorter telomeres and higher Ki67, while smoking cessation appears to be associated with the expansion of clones with near-normal mutational burden and an overall reduction in Ki-67 expression. To understand how these long-term changes take place, we have performed ex vivo functional assays to quantify the competitive advantage imparted by smoke. We have then explored the transcriptomic landscape of these cultures to determine how differential smoke exposure modulates epithelial cell dynamics before and after smoking cessation.

Primary basal cells from bronchial explants were co-cultured following different regimes of exposure to cigarette smoke extract (CSE). We find that, upon acute exposure, pre-exposed cells have a ~20% higher chance of proliferating per week than smoke-naïve cells. To test this in a more physiological model, long-term epithelioid cultures were established with chronic exposure to low-dose CSE for months. As before, we observe that over time, pre-exposed cells outcompete the smoke-naïve, suggesting that smoke imparts a beneficial adaptation on re-exposed cells even at low doses. To elucidate this mechanism, we performed RNA sequencing of 48 different combinations of acute and chronic exposure to CSE. Genes were classified into distinct modules according to their regulation following exposure, re-exposure and cessation. Differential expression analysis and gene set enrichment analysis showed that metabolic pathways, including both nutrient and detoxification pathways, are predominantly enriched in these modules. In particular, following cessation, cells with the highest cumulative exposure to CSE displayed senescent-like features which are suppressed with chronic re-exposure. Further analysis and in vivo validation of these results will help elucidate how these changes affect the likelihood of premalignancy and may provide valuable targets for cancer prevention.

#1466 Tobacco carcinogen impacts redox pathway to facilitate pancreatic ductal adenocarcinoma (PDAC) initiation and progression.

X. Lin[1], M. Stamp[2], A. Fowler[2], C. Bottomley[2], S. Okhovat[2], K. Peck[2], D. Engle[2];

[1]University of California San Diego - UCSD, San Diego, CA, [2]Salk Institute for Biological Studies, San Diego, CA

The 5-year survival rate for pancreatic ductal adenocarcinoma (PDAC) is only 10%. PDAC is projected to soon become the second leading cause of cancer death. Tobacco is one of the main risk factors for PDAC. Incidence of PDAC increases 2-fold among tobacco users, and 20-35% of PDAC cases are attributed to smoking. However, the specific pathways activated by tobacco carcinogens remain elusive.This research project addresses the impact of carcinogens in pancreatic cancer etiology. We hypothesize that carcinogens in tobacco increase reactive oxygen species (ROS), which elevates the Nrf2 redox pathway to facilitate PDAC initiation and progression. Specifically, we focus on two major subclasses of carcinogens: the heavy metal cadmium (Cd) and the polycyclic aromatic hydrocarbon (PAH) benzo(a)pyrene (BaP). Using mouse pancreatic ductal organoid cultures, we found that acute carcinogen exposure increases Nrf2 activity, which is sustained after "intermediate" exposure (5 passages). Intriguingly, chronic exposure (10 passages) downregulates Nrf2 activity, which has been shown to be associated with acquired metastatic potential. Furthermore, we found an upregulation in NFkB and EGFR signaling after intermediate exposure, which are involved in microenvironment remodeling and increased proliferative potential. Overall, we demonstrate that acute carcinogen exposure elevates ROS levels and activates the Nrf2 pathway, whereas prolonged exposure upregulates NFkB and EGFR pathways. Furthermore, we have established a novel carcinogenesis model using 3D organoid culture to recapitulate each step in pancreatic tumorigenesis. Collectively, this project contributes to our understanding of tobacco-related PDAC pathogenesis.

#1467 Contribution of estrogen metabolites to never-smoking lung cancer.

Mitchell Cheung, Lisa A. Vanderveer, Daniel Krzizike, J. Nicholas Bodor, Joseph Treat, Joseph R. Testa, Margie L. Clapper

Fox Chase Cancer Center, Philadelphia, PA

There has been a consistent rise in the incidence of non-small cell lung cancer (NSCLC) among individuals who have never smoked. Remarkably, over 50% of diagnosed female cases and 15-20% of male cases are never-smokers. Notably, NSCLC in never-smokers exhibits distinctive clinical and pathological features, notably a higher incidence of tumors with EGFR mutations, setting it apart from its counterpart in smokers. Despite the improved disease-free survival observed with EGFR-tyrosine kinase inhibitors, eventual relapse and limited responsiveness to immunotherapy are common, underscoring the urgency to comprehend the molecular mechanisms driving the escalating prevalence of NSCLC in never-smokers and develop targeted preventive and interceptive therapeutic strategies. The preponderance of females among NSCLC patients who never smoked has prompted an exploration into the potential contribution of estrogen to lung tumorigenesis. In contrast to prevailing research focused on estrogen receptor-mediated signaling, our investigations have yielded compelling evidence supporting the involvement of estrogen metabolism in lung carcinogenesis among never-smokers. This group is the first to report that estrogen is metabolized extensively in both mouse and human lungs, resulting in the generation of various derivatives, including the potential carcinogen 4-hydroxyestrogen (4-OHE). Notably, recent findings from our laboratory indicate that prolonged exposure of nonneoplastic human bronchial epithelial cells to 17β estradiol or 4-OHE, at concentrations approximating physiological levels, induces the accumulation of double-strand DNA breaks and cellular transformation. A comprehensive analysis was performed to further elucidate the mechanisms underlying the transformation process. Isolated transformed clones obtained after 9, 18, and 22 wks of exposure to 4-OHE were subjected to karyotyping, F.I.S.H., and RNA and exome sequencing. A longitudinal progression of aberrant chromosomal rearrangements and copy number alterations was observed, that increased with time of 4-OHE exposure. In addition, RNA-Seq analyses revealed the epithelial-mesenchymal transition pathway was highly enriched at the early timepoint (9 wks), while replicative stress-related signaling pathways were induced at all timepoints. To determine if the differentially expressed genes were also dysregulated in clinical lung cancer cases, TCGA lung adenocarcinoma (LUAD) data were examined. Interestingly, many of the genes upregulated after estrogen exposure were similarly overexpressed in the LUAD samples and often associated with a worse prognosis. In conclusion, our data support the role of estrogen metabolites in promoting lung cancer among never-smokers. (Supported by CA217161 and generous contributions from the Hellendall Family Foundation, Gregory G. Lawton and the Timothy and Aurora Hughes Cancer Research Fund.)

#1468 Low exposures to amphibole or serpentine asbestos in germline *Bap1*-mutant mice induce mesotheliomacharacterized by an immunosuppressive tumor microenvironment.

Y. Kadariya, E. Sementino, M. Ruan, M. Cheung, A. J. Klein-Szanto, K. Cai, J. R. Testa;
Fox Chase Cancer Center, Philadelphia, PA

The purpose of this study was to determine if minimal exposures to amphibole (crocidolite) and serpentine (chrysotile) asbestos fibers significantly increase the incidence and rate of malignant mesothelioma (MM) onset in mice with a germline heterozygous *Bap1* mutation, and to assess the effect of the resulting gene × environment interactions on the tumor immune microenvironment (TIME). The studies were carried out by chronically injecting intraperitoneally *Bap1*+/- and *Bap1*+/+ (wild-type, WT) mice with minimal doses of asbestos (in some experiments, as low as 0.0125 mg x 8 injections; total, 0.1 mg/mouse) and then monitoring the mice for tumor formation for up to 90 weeks. Pro-inflammatory and pro-tumorigenic factors in the TIME were evaluated by immunohistochemistry (IHC) and immunofluorescence (IF) for immune cell markers. With either type of asbestos and at each dose tested, MMs occurred at a significantly higher rate and earlier onset time in *Bap1*-mutant mice than in WT littermates. MMs from mice injected with chrysotile, but less so with crocidolite, had widespread adhesions in the peritoneal cavity owing to an overwhelming immune response, particularly at the higher dose used. IHC staining demonstrated an increased number of immune cells in granulomas and MMs. In particular, pro-inflammatory M1 macrophages were found mainly in granulomas, whereas pro-tumorigenic M2 macrophages were predominant in MMs. IF staining revealed that the relative number of M2 macrophages was strikingly greater in chrysotile-induced than crocidolite-induced MMs, suggesting that chrysotile induces a more profound immune response. MMs from *Bap1*-mutant mice showed upregulation of both CD39/CD73-adenosine and Ccl2/Ccr2 pathways, which collectively are known to mechanistically create favorable conditions for neoplastic transformation, invasion, and the development of an immunosuppressive TIME, in part by attracting M2 macrophages. This implies that chemoprevention and immunotherapy strategies targeting these pro-tumorigenic immune pathways could be beneficial in *BAP1* mutation carriers. In conclusion, we provide evidence that low-level exposures to either chrysotile or crocidolite in germline *Bap1* heterozygous mice result in a markedly increased risk of MM characterized by an immunosuppressive tumor microenvironment. Drawing parallels to humans, these experimental findings suggest that exposure of *BAP1* mutation carriers to even minimal doses of different forms of asbestos may be associated with significantly enhanced susceptibility to MM.

#1470 Advancing cancer research: A novel PanCancer digital PCR tool for simultaneous detection of multiple hallmark mutations in BRAF and EGFR.

C. Kappmeier, S. Edward, C. Hochstein, E. I. Bruske, F. Di Pasquale, **R. Kellner**;
QIAGEN GmbH, Hilden, Germany

The paradigm shift towards precision medicine in oncology emphasizes the importance of identifying specific genetic mutations driving cancer. Some hallmark mutations in cancer-associated genes, such as BRAF and EGFR, are important in analyzing many cancer types. With the emergence of digital PCR (dPCR) technology, high-sensitivity and quantitative mutation analysis can be performed, lending valuable support to cancer research. In this work, we introduce a new and innovative dPCR method, the dPCR PanCancer assays (RUO), designed for concurrently detecting multiple hallmark mutations in BRAF and EGFR.
This work includes two novel PanCancer assays for BRAF and EGFR, each tailored to target a spectrum of mutations associated with these genes, facilitating a comprehensive mutation analysis. The dPCR assay for BRAF targets multiple V600 hallmark mutations, and the dPCR assay for EGFR targets various important deletions on exon 19. This also includes a reference gene as a control for PCR efficiency in the duplex reaction. Here, we present our initial data from various sample types, including blood, plasma and FFPE samples. Through a meticulously optimized dPCR setup, we achieved exceptional sensitivity and specificity, enabling the detection of multiple mutations in a single channel at allelic frequencies below 1%.
Both dPCR PanCancer Kits (RUO) have potential use in research for pre-screening samples (e.g., prior to next-generation sequencing) or monitoring cancer cells. They simultaneously assess the mutations, reducing time and costs and saving sample material. Additionally, our technology is adaptable to other cancer-associated genes, where similar assays can potentially be developed. Overall, we have demonstrated that our dPCR PanCancer Kits (RUO) provide a robust, fast and efficient technology to identify critical mutations, ultimately enhancing our understanding of BRAF and EGFR-driven cancers.
The dPCR PanCancer Kit is for research use only. Not for the diagnosis, prevention, or treatment of a disease.

#1471 A novel mouse model of upper tract urothelial carcinoma influenced by gut microbiota.

A. Yamamoto[1], A. Kawashima[1], K. Jingushi[2], S. Nesrine[1], Y. Horibe[1], A. Yoshimura[1], M. Tani[1], L. Yutong[1], t. Oka[1], Y. Okuda[1], t. Uemura[1], G. Yamamichi[1], Y. Ishizuya[1], Y. Yamamoto[1], T. Kato[1], K. Hatano[1], N. Nonomura[1];

[1]Graduate School of Medicine Osaka University, Osaka, Japan, [2]Graduate School of Pharmaceutical Science Osaka University, Osaka, Japan

Introduction & Objective: Recently, it has been revealed that bladder cancer (BC) and upper tract urothelial carcinoma (UTUC) are biologically distinct diseases. Mouse models of BC carcinogenesis have been established using N-butyl-N-(4-hydro-oxybutyl) nitorosamine (BBN) for a long time, but there are few reports of UTUC carcinogenesis with high incidence. Therefore, the UTUC carcinogenesis mouse model is expected. The aim of this study is to establish a novel mouse model of UTUC carcinogenesis and to identify the characteristics of this model.

Methods: We used two strains (C57BL/6 and BALB/c) of male and female mice and fed 0.05% BBN from 6 weeks old to the harvest day. Both sides of upper urinary tract from mice drinking BBN or tap water were subjected to whole exome sequencing and whole transcriptome sequencing (WTS) to assess its genetic similarity to human UTUC. Microbiome in gut were assessed by 16S ribosomal RNA gene sequencing (16S rRNA-seq). Metabolic differences in feces, serum and liver between UTUC mice and healthy mice were evaluated by comprehensive metabolomic analysis. Inflammatory mediators were assessed by quantitative polymerase chain reaction (qPCR).

Results: Only BALB/c female showed higher incidence of UTUC than BC, while the other strains rarely had UTUC. This model showed SBS5-like mutational pattern. The frequent mutated gene list showed similarity to human UTUC. In terms of gene expression, this model belonged basal subtype. We detected 593 differentially expressed genes between cancerous side and non-cancerous side of upper urinary tract in this model, which could also classify human UTUC and adjacent normal samples. The cancerous side of upper urinary tract enriched several inflammation related pathways such as Nfkb and Tnf pathway. We validated the upregulation of inflammatory gene expression in upper urinary tract (*Il6*, *Il1b*, *Tnfa*, *Relb*) by qPCR (all: $p < 0.05$). 16S rRNA-seq revealed that *Firmicutes* was enriched in feces. Metabolomic analysis revealed that some amino acids in feces and FAD in serum were upregulated. Feeding with amino acid mediated diet changed gut environment. *Firmicutes* in feces and FAD in both feces and serum were downregulated consistently. This diet suppressed inflammatory gene expression in upper urinary tract (*Il6*, *Il1b*, *Tnfa*, *Relb*, *Cd38*, *Tnfrsf1b* and *Kdm1a;* all: $p < 0.05$). Finally, UTUC was disappeared but not BC in this model treated by BBN with amino acid mediated diet.

Conclusion: We have established a novel mouse model developing UTUC with high incidence that genetically mimics human UTUC. In addition, amino acid mediated diet can change both microbiome and metabolome in gut of this model, downregulate host's inflammatory reaction to BBN in upper urinary trat and suppress the UTUC carcinogenesis.

#1472 APOBEC-induced non-coding hotspot mutations near *LEPROTL1* contribute to the tumorigenicity of bladder cancer via deregulation of *LEPROTL1*, *DCTN6* and *SARAF*.

B. Lone, K. Butler, A. Dobbins, D. Yesudhas, A. Chakraborty, E. Hickman, S. Boudjadi, A. Apolo, R. Banday;
National Cancer Inst. - Bethesda Campus, Bethesda, MD

In bladder cancer, APOBEC3 deaminases are major drivers of genomic mutagenesis, with most of these mutations occurring in synonymous or non-coding regions of the genome. The impact of these mutations on tumorigenesis has not been explored. This study aimed to investigate two non-coding hotspot mutations, likely induced by APOBEC3A near *LEPROTL1*—chr8: 29,952,919 G>A and chr8: 29,952,921 C>T—in bladder cancer. Using dual-luciferase reporter assays, we found that these mutations enhance both promoter and enhancer activities. Employing multi-omics approaches, including RNA-seq, ChiP-seq, and Hi-C, identified *LEPROTL1, DCTN6,* and *SARAF* as target genes co-regulated by a common enhancer where these hotspot non-coding mutations manifest. Isogenic cell lines, generated through CRISPR-mediated base editing to introduce these mutations, exhibited upregulation of target genes, and displayed oncogenic characteristics, such as increased cell growth, proliferation, invasiveness, and resistance to cisplatin. Moreover, these mutations exert their effect on cell proliferation by promoting cell cycle progression. These results suggest that recurrent non-coding somatic mutations upstream of *LEPROTL1* disrupt the coregulation pattern of the three genes, thereby promoting bladder tumorigenesis.

#1473 Exposure of arsenic promotes malignant stemness and induces bladder malignancy in preclinical models.

Bhawna Tyagi, Mohit Vashishta, Neha Tyagi, Balaji Chandrasekaran, Vaibhav Shukla, Ashish Tyagi, Chendil Damodaran

Texas A&M University, College Station, TX

Numerous epidemiological and scientific studies have consistently demonstrated that populations exposed to arsenic (As) concentrations ranging from >10 ppb to 2500 ppb in their drinking water face an elevated risk of urogenital cancers, with a particular emphasis on bladder cancer (BCa). Hence, the goal of the study is to investigate the underlying mechanisms that trigger malignant transformation in the bladder using physiologically relevant arsenic concentrations observed in BCa patients. In our results, we observed significantly elevated levels of arsenic in the urine of BCa patients, ranging from 20 to 50 mg/L, in stark contrast to the levels observed in healthy controls (>10 mg/L) and the recommended guidelines set by the Environmental Protection Agency (EPA) and Centers for Disease Control and Prevention (CDC). We used a median physiological concentration of arsenic (30 PPM) in drinking water-induced bladder hyperplasia in male and female mice over six months. Likewise, chronic exposure of healthy bladder epithelial cells (TRT-HU1) to similar arsenic concentrations (250nM:30 PPM) for 12 months resulted in malignant transformation, and arsenic-transformed cells (AsT) were capable of inducing tumors in xenografted and orthotopic models. Nonetheless, the molecular mechanism responsible for this malignancy remains to be elucidated. Our molecular analysis has pointed towards the activation of stem cells, notably ALDH1A1 (with a 50,000-fold increase), as a pivotal factor driving this transformation. Furthermore, our research has demonstrated that the activation of ALDH1A1 is contingent on the induction of Metal Response Element-Binding Transcription Factor-1 (MTF1). Consequently, silencing MTF1 inhibited the expression of ALDH1A1 and its associated malignant properties in As-transformed cells, strongly suggesting that MTF1 functions as the master regulator in As-induced bladder carcinogenesis. We have also observed similar molecular signatures (MTF1 and ALDH1A1 expression) in arsenic-exposed versus non-exposed mice and bladder cancer patients. In conclusion, our studies suggest that activation of stem cells is a critical step in arsenic-induced bladder carcinogenesis.

#1474 Interleukin-8 and NF-κB mediated signaling axis: A potential driver for cadmium-induced prostate carcinogenesis..

K. Gupta[1], R. K. Singh[2], J. R. Seremak[1], V. B. Lokeshwar[1], B. L. Lokeshwar[1];
[1]Augusta University, Augusta, GA, [2]Integra Biosciences, Princeton, NJ

Cadmium (Cd) is a toxic heavy metal, ubiquitous in nature, and an industrial pollutant. Cadmium exposure can cause irreversible damage to lungs, liver and kidney including cancers. Alarmingly, abnormally high levels of cadmium are found in human prostate tissues. Studies on rodents have shown cadmium exposure causes liver, lung, and prostate cancers. The mechanism of carcinogenesis caused by Cd is multifactorial and specific organ carcinogenesis remains unclear. We and others have reported that the CXC-chemokine IL-8 drives cancer progression in prostate cancer (PCa). We tested a hypothesis that chronic cadmium-exposure induces upregulation of proinflammatory cytokines, such as IL-1β, IL-6, and IL-8, which individually or combined promote carcinogenesis and progression. The study used two non-transformed prostate epithelial cell lines (RWPE-1 and NHPrE1) to test whether continuous exposure to Cadmium chloride ($CdCl_2$) perturbs cytokine expression pattern and selective silencing of elevated cytokines delays carcinogenesis and invasive potential. The $CdCl_2$ exposed cells and culture conditioned media were analyzed regularly for changes in inflammatory milieu and for hallmarks of carcinogenesis. These studies measured changes in cell proliferation, production of cytokines (IL-8, IL-1β, IL-6, IFN-γ, TGF-β, and others), activation of Nuclear Factor-kB (NF-κB), and pro-tumorigenic factors, e.g., vascular endothelial growth factors (VEGF-A and B), cellular motility, and invasive potential, etc. Cells exposed to $CdCl_2$ showed increased cell proliferation and clonogenic potential and specifically, increased expression of IL-8, it's receptors (CXCR1 and CXCR2), IL-1β, and other cytokines & related genes. While un-exposed RWPE-1 cells did not express IL-8, it was the first cytokine to increase when exposed to $CdCl_2$, followed by activation of NF-κB (p65-rel), VEGF-A, & B, CXCR1 and other markers. Gene silencing of IL-8 suppressed motility, invasion, and survival activity. These data supported that immediate-early IL-8 expression probably upregulates NF-κB mediated inflammatory signaling axis which is critical for Cd-induced carcinogenesis and may expose targets for countermeasures to prevent metal-induced toxicity & carcinogenesis.

#1475 Investigating the carcinogenic effects and the mechanism of cadmium exposure on WPMY-1 prostate myofibroblast cell line.

Sakshi V. Bansod, Gnanasekar Munirathinam

Biomedical Sciences, University of Illinois College of Med. at Rockford, ROCKFORD, IL

Prostate cancer (PCa) is the second most common cancer among males with an incidence rate of PCa is 288,300 new cases annually. Risk factors include age, genetics, and lifestyle, but the underlying stimuli remain largely uncertain. One potential emerging cause of PCa is exposure to metal carcinogens as cadmium (Cd) which is now classified as a group I human carcinogen. Chronic exposure to Cd on epithelial cells has been extensively shown to induce carcinogenesis, making it a likely contributor to PCa development. In this study, we expand this information by examining how chronic Cd exposure affects prostate-derived myofibroblast (WPMY-1) cells transforming into a cancer-associated fibroblast like phenotype. To study the transformation, WPMY-1 cells were treated with 500nM of Cd for a period of 11 months establishing the WPMY-1 Cd model. Fibroblasts are a crucial tumor microenvironment (TME) component and potentially contribute to PCa progression when transformed and activated into cancer-associated fibroblasts (CAFs). To begin, we used an MTT assay to measure the effect of Cd toxicity on normal prostate myofibroblasts versus WPMY-1 Cd. The data showed that 10µM Cd solution was toxic to WPMY-1 cells, but WPMY-Cd cells depicted high cell viability at 50 µM dose, conferring to chronic Cd exposure improved resiliency to Cd toxicity. We analyzed the expression of CAF-specific markers in WPMY-Cd cells, such as vimentin, FAP, α-SMA, and PDGFR-β. WPMY-Cd cells showed a distinct upregulation for these markers when compared to untreated WPMY-1 cells, suggesting that chronic exposure to Cd promotes CAF-like phenotypic transformation in WPMY-Cd. To further ascertain the cancer-promoting properties of WPMY-Cd, an *in vitro* 3-D spheroid assay was performed by growing the cells on a Matrigel scaffold. The WPMY-Cd cells formed many more tumor-like spheroid structures than WPMY-1 and exhibited sprouting. The sprouting spheroids displayed lamellipodium and filopodium-like structures, demonstrating the initiation of migratory phenotype in WPMY-Cd. Additionally, previous research suggests that CAFs may play a role in PCa progression by promoting tumor growth via the secretion of cytokines and growth factors. We tested this theory by exposing Cd-treated epithelial (BPH-Cd) cells to conditioned media containing secretions from CAFs and WPMY-Cd. WPMY-1 Cd conditioned media in conferring cell migration on epithelial BPH-Cd cells was confirmed by a wound healing assay wherein BPH-Cd cells treated with WPMY-1 Cd conditioned media led to complete wound closure in 24 hours as compared to WPMY-1 and CAF conditioned media. Overall, there is considerable evidence that Cd exposure in fibroblasts may play a crucial role in PCa disease progression and is a promising area for researching PCa treatment strategies against a crucial component of the tumor microenvironment.

#1476 OSBPL3 facilitates endoplasmic reticulum stress and stemness in triple negative breast cancer.

S. Pu, H. Zhang, Y. Ren, J. He, N. Hao;
First Affiliated Hospital of Xi'an Jiaotong University, Xian, China

Background: Triple negative breast cancer (TNBC) is a type of aggressive breast cancer with a poor survival. Endoplasmic reticulum (ER) stress, induced by exposed to intrinsic (e.g. oncogenes) and external factors (e.g. chemotherapies), is an important factor in both tumor progression and responses to chemotherapies. Recent studies have demonstrated that the progression of ER stress may result in the emergence of cancer stem cells (CSC), which also arise as a consequence of metastasis. However, the mechanism of targeting ER stress signaling in cancer stem cells remains to be investigated.
Aim: (i) To investigate the mechanistic role of Oxysterol binding protein-like 3 (OSBPL3) in TNBC and its links with breast cancer mortality, particularly caused by chemotherapeutic resistance and metastasis; and (ii) to test a hypothesis that OSBPL3 facilitates the abnormal activation of ER stress and cancer stemness, result in the resistance to chemotherapy and metastasis in TNBC.
Methods: The expression level of OSBPL3 in TNBC was determined by immunohistochemical staining and the mRNA expression profiles from the TCGA database. Roles of OSBPL3 in cancer cell growth, metastasis, stemness and activation of ER stress were determined by molecular and cell biology methods. Immunoprecipitation was used to examine the binding of proteins and chromatin immunoprecipitation (ChIP), promoter luciferase reporter assay was included for detecting the transcription of OSBPL3 in TNBC. TNBC xenograft nude mice were used to study the inhibition of tumor development.
Results: OSBPL3 is a novel TNBC target, which is overexpressed in TNBC tissues and significantly associated with clinical pathology of advanced TNM stage and poor prognosis of tumor patients. Mechanistically, Increased OSBPL3 induced ER stress and ER stress agonist (tunicamycin) treatment results in the translocation of XBP1, an ER stress sensor, into the nucleus to induce OSBPL3 expression through direct binding to the OSBPL3 promoter. In addition, OSBPL3 facilitates the stemness induced by ER stress via phosphorylating GSK3β and transporting accumulated β-catenin to the nucleus to promote the expression of stemness-related transcriptional factors, ultimately resulting in tumor metastasis and resistance to chemotherapy. Furthermore, OSBPL3-specific siRNAs encapsulated by jetPEI nanocarriers prominently inhibit tumor growth and epirubicin-induced resistance in vivo.
Conclusion: We identified an important role of OSBPL3-ER stress-XBP1 feedback loop in the stemness and resistance to chemotherapy, representing a future biomarker and therapeutic target of TNBC.

#1477 Acrylamide exposure in obesity enhances mammary epithelial DNA damage via the activity of its metabolite, glycidamide, and increased oxidative stress.

B. Walton, L. Arendt;
University of Wisconsin-Madison, Madison, WI

Obesity is a world-wide epidemic, with 39% of adults considered overweight and 13% obese, and rates are rising. Obese women are at greater risk for developing breast cancer than lean women, however the mechanisms of how obesity increases breast cancer risk are not well understood. There is also limited knowledge on how environmental toxins may interact with obesity to promote breast cancer. Acrylamide, a probable carcinogen, is a biproduct in starchy foods cooked at high temperatures, which are prevalent in the obesity-inducing Western diet. Acrylamide is metabolized by the CYP2E1 enzyme into the epoxide, glycidamide, which is known to induce DNA damage. CYP2E1 activity is elevated in obesity, which could enhance DNA damage in obese individuals. Acrylamide exposure is associated with an increased risk of breast cancer in epidemiologic studies, but the evidence has been contradictory. To investigate how acrylamide impacts DNA damage in the obese mammary gland, three-week-old FVB female mice were randomized to receive a low-fat (LFD; 16% kcal from fat) or high-fat diet (HFD; 60% kcal from fat) and either 0.7 mM acrylamide water or control water. HFD-fed mice gained significantly more weight than LFD-fed mice, and exposure to acrylamide did not impact weight gain compared to respective controls. Mammary epithelial cells from acrylamide-treated mice had increased DNA damage compared to controls measured by COMET assays, with the highest DNA damage present in epithelial cells from obese acrylamide-treated mice. Mammary epithelial cells from acrylamide-treated mice also had enhanced oxidative DNA damage, measured by 8-OHdG adducts, and an additive effect was observed between acrylamide exposure and obesity. To investigate the impact of acrylamide *in vitro*, COMMA-D mammary epithelial cells were treated with vehicle, 9.8 µM acrylamide, or 0.5 mM glycidamide for 24 hours, then COMET assays and immunohistochemistry for markers of DNA damage were performed. COMMA-D cells treated with acrylamide-metabolite glycidamide showed significantly increased double strand DNA breaks compared to vehicle-treated cells, however acrylamide-treated cells did not. Interestingly, acrylamide-treated cells demonstrated significantly higher levels of intracellular reactive oxygen species compared to both glycidamide and vehicle-treated cells. These studies suggest acrylamide exposure enhances DNA damage in mammary epithelial cells via conversion to the genotoxic metabolite glycidamide and through generation of oxidative stress, which is exacerbated by obese conditions. These studies suggest that long-term acrylamide exposure through foods common in the Western diet may enhance DNA damage in mammary epithelial cells, potentially enhancing obesity-induced breast cancer risk.

#1478 Chronic perfluorooctanesulfonic acid exposure promotes proliferation of colorectal cancer cells.

J. Durham, J. Weber Tessmann, B. Hennig, Y. Zaytseva;
University of Kentucky, Lexington, KY

Background: Chronic exposure to long-term exposures to per- and polyfluoroalkyl substances (PFAS), widely known as “forever chemicals”, has been associated with multiple negative health outcomes including increased risk of cancer. Perfluorooctanesulfonic acid (PFOS), a “long-chain” subtype of PFAS, has high bioaccumulation potential with a long elimination half-life. PFOS is frequently detected in drinking water leading to its high absorption through the gastrointestinal tract. Recent studies demonstrate that PFAS exposures promote intestinal inflammation and gut barrier dysfunction. However, how a long-term PFOS exposure affects colorectal cancer (CRC) progression is not known. Therefore, the purpose of this study is to delineate the effect of PFOS exposure on CRC cell proliferation and test the potential mitigation strategy for the harmful effects of PFOS.
Methods: SW480 and HCT116 cells have been treated with 1 ug/mL PFOS and proliferation was measured at 1, 2, and 3 months using the Presto Blue Cell Viability Reagent fluorescence assay. Proliferation markers were assessed by qPCR and Western blot. Control and PFOS exposed cells were treated with sulforaphane, a nuclear factor erythroid 2-related factor 2 (Nrf-2) inducer, at concentration 5, 10 and 20 uM for 72 hours.
Results: We show that chronic, low-dose PFOS exposure promotes proliferation of SW480 and HCT116 cell lines starting at 3 months since the first exposure. The increase in proliferation is associated with upregulation of Cyclin D, pAkt and FASN. We also show that sulforaphane significantly decreases proliferation of HCT116 and SW480 cells, and its efficacy is significantly higher in PFOS exposed CRC cells. The current studies show no effect on sulforaphane on normal colon epithelium cells.
Conclusion: Our studies suggest that chronic PFOS exposure promotes proliferation of CRC cells by increasing pro-carcinogenic gene expression and signaling. Furthermore, our findings suggest that supplementation of diet sulforaphane can potentially mitigate the harmful effects from PFOS exposure. Our studies warrant further investigation of the mechanisms behind the effect of PFOS exposure on cancer progression that would guide development of effective intervention strategies to mitigate the harmful effects of the exposure to “forever chemicals”.

#1479 ABCC3 (MRP3)-mediated export of deoxycholic acid regulates MAPK signaling in colorectal adenoma and adenocarcinoma.

Y. Sato[1], **M. Kobayashi**[1], M. Ohira[2], R. Funayama[1], M. Maekawa[3], H. Karasawa[1], S. Ohnuma[1], M. Unno[1], K. Nakayama[1];
[1]Tohoku University Graduate School of Medicine, Sendai, Japan, [2]Tohoku University School of Medicine, Sendai, Japan, [3]Tohoku University Hospital, Sendai, Japan

ABCC3 (also known as MRP3) is an ATP binding cassette transporter and it works as a bile acids transporter. We previously elucidated that ABCC3 expression is downregulated in colorectal cancer through the Wnt/β-catenin signaling pathway. However, it remained unclear how downregulation of ABCC3 expression contributes to colorectal carcinogenesis. We here explored the role of ABCC3 in the progression of colorectal cancer-in particular, focusing on the regulation of bile acid export. First, we performed experiments with clinical samples of familial adenomatous polyposis (FAP) patients to confirm whether ABCC3 expression is already downregulated in colorectal adenomas. Next, we investigated the effect of ABCC3 expression on intracellular bile acid concentrations using ABCC3 knockdown and overexpression colorectal cancer cell lines (HT-29, SW620). The intracellular concentration of deoxycholic acid, which is known to have carcinogenic effects, was verified with fluorescently labeled deoxycholic acid. Then, we tested whether activation of oncogenic signaling by deoxycholic acid is affected by ABCC3 expression changes. Finally, we examined the effect of nonsteroidal anti-inflammatory drugs (NSAIDs), which have been suggested to inhibit the carcinogenesis of FAP, on the expression of ABCC3 in experiments with colorectal cancer cell lines. Gene and protein expression analysis of colorectal adenomas isolated from FAP patients revealed that ABCC3 were downregulated as early as at the stage of adenoma formation, and many other genes related to bile acid efflux were also downregulated. Knockdown or overexpression of ABCC3 increased or decreased intracellular concentration of deoxycholic acid in colorectal cancer cells, respectively. Forced expression of ABCC3 suppressed deoxycholic acid-induced activation of MAPK signaling. Finally, we found that several NSAIDs increased ABCC3 expression in colorectal cancer cells, suggesting that ABCC3 could be one of the targets for therapeutic intervention of FAP. Our data thus suggest that downregulation of ABCC3 expression contributes to colorectal carcinogenesis through the regulation of intracellular accumulation of bile acids and activity of MAPK signaling.

#1480 Perfluorooctanesulfonic acid exposure promotes pathological changes in normal intestinal tissues which may lead to an increased risk of colorectal cancer development.

J. Weber Tessmann, J. Durham, R. Goettl, D. He, C. Wang, P. Deng, B. Hennig, Y. Zaytseva;
University of Kentucky, Lexignton, KY

Introduction: Long-term exposures to per- and polyfluoroalkyl substances (PFAS) have been increasingly linked to negative health outcomes including metabolic disorders, reduced immune responses, and increased risk of cancer. PFOS, one the most frequently detected PFAS in drinking water, is readily absorbed in the GI tract and distributes predominantly to the plasma and liver. Even though recent studies demonstrate that PFOS can cause an imbalance of cecal gut microbiota, alter microbiota diversity, and promote inflammation and gut barrier dysfunction, there is still not much known about the effects of PFOS exposure on normal and pre-malignant intestinal tissues and its contribution to carcinogenesis. Therefore, the goal of this study is to investigate the effects of PFOS on normal (I) and malignant intestinal cells (II).
Methods: The effect of PFOS on gene expression profile was assessed by RNAseq analysis in intestinal tissue of C57BL/6 mice. Tumor organoids were established from Apc/VillinCre mice (adenoma models). Organoid cultures, colorectal cancer (CRC) and primary normal intestinal cell lines have been treated with 1µg/ml of PFOS. To access the mechanisms involved in PFOS-induced intestinal alterations, qRT-PCR, western blot, immunofluorescence, cytokine array and metabolomics analysis have been performed.
Results: The RNAseq analysis showed that PFOS exposure is associated with transcriptome alterations with exacerbated changes in pathways involved in lipid metabolism, immune system regulation and pro-carcinogenesis signaling. PFOS exposure leads to a significant decrease in expression of 3-hydroxy-3-methylglutaryl-Coa synthase 2 (HMGCS2), a rate limiting ketogenic enzyme, in intestinal tissues. We also showed that PFOS exposure upregulates fatty acid synthase, a key enzyme of *de novo* lipogenesis, programmed death-ligand, an immune checkpoint inhibitor, and altered the levels of pro-inflammatory cytokines and metabolites. Using HMGCS2 knockout cells, we identified the possible contribution of HMGCS2 in cytokine regulation and activation of oncogenic pathways.
Conclusion: In summary, our data suggests that PFOS may induce gastrointestinal pathological changes that can increase the risk of CRC development. Further studies are warranted to determine the functional significance of PFOS-mediated downregulation of HMGCS2 and upregulation of lipid metabolism in intestinal cells. Delineating the effects of PFOS on intestinal epithelium may contribute to development of interventional strategies to eliminate harmful effects of these environmental pollutants.

#1481 Disparity landscapes of HBV integration in hepatocellular carcinoma: Mechanistic characterization and functional implications.

X. Lyu, K. M. Sze, J. M. Lee, A. Husain, I. O. Ng, D. W. Ho;
University of Hong Kong, Li Ka Shing Faculty of Medicine, Hong Kong, China

Hepatocellular carcinoma (HCC) is the most common type of primary liver cancer and is a common malignancy worldwide. About half of all new liver cancers worldwide each year occur in China due to a high prevalence of hepatitis B virus (HBV) infection. HBV DNA integrates into the human genome, disrupting the endogenous tumor suppressors/regulatory genes or enhancing the activity of proto-oncogenes. It would be useful to examine the different NGS-based databases to provide a more unbiased and comprehensive survey of HBV integration. We aimed to take advantage of publicly available datasets of different regional cohorts to determine the disparity landscapes of integration events among sample cohorts, tissue types, chromosomal positions, individual host and viral genes, and genic locations. By comparing HCC tumor with non-tumorous liver, landscape of HBV integration was delineated at gene-independent and gene-dependent manners. Moreover, we performed mechanistic investigations on how HBV-*TERT* integration led to *TERT* activation and derived a score to predict patients' prognostication according to their clonal disparity landscape of HBV integration. We revealed a global geographical disparity of HBV integration that the landscape of HBV integration between HCC and non-tumorous liver varied in regional cohorts, suggesting the different degrees of clonal enrichment. In the Mainland China, Hong Kong and Mongolia cohorts, HCC tumors had higher numbers of events than the non-tumorous livers, whereas in the French and US cohorts, the reverse was true. Moreover, most HBV integrations were positionally enriched at the telomeres and centromeres, and this highlighted the novel co-involvement of HBV integration at these regions, which likely introduces greater genomic instability. Furthermore, we constructed a large meta-cohort of multiple ethnicities to refine the landscape of HBV integration. This enabled the identification of events at key HCC-related genes (e.g., *TERT*, *KMT2B,* and *CCNA2*) and gene families (e.g., cyclin, cadherin, and contactin). As *TERT* is the most frequently integrated gene by HBV, we further investigated the mechanistic modulation of *TERT* transcription activation by combining and analyzing our in-house sample cohort with a previous report and luciferase reporter assays. This revealed the positive concurrent influence by both the orientation and relative distance of HBV integration (closer to transcription start site) from the *TERT* gene. Additionally, we observed clonal disparity of HBV integration among patients and the higher level of the clonal disparity score correlated with poor prognostication of HCC patients. Our study uncovered the different levels of clonal enrichment of HBV integration and identified mechanistic insights and prognostic biomarker. This strengthens our understanding of HBV-associated hepatocarcinogenesis.

#1482 FKBP52 drives diverse HCC phenotypes through context-dependent targeting of p53.

X. Wang, J. Wu, C. Tang, X. Li, L. Zhu, Y. Liu;
Fujian Medical University, Fuzhou, Fujian province, China

p53 is notably the most frequently mutated protein in hepatocellular carcinoma (HCC), one of the major causes of cancer-related fatalities globally. These mutations often result in some of the most adverse outcomes in HCC, making p53 a prime target for therapeutic intervention. The concept of “hyperstability”of p53 is essential in understanding its gain-of-function and dominant-negative effects in tumorigenesis. However, the mechanisms driving this hyperstability are not completely understood. In this study, we have identified FKBP52, a member of the FK506-binding protein family, as a crucial factor in stabilizing and accumulating p53, irrespective of the type of mutation. Furthermore, our study suggests that FKBP52 could be a valuable biomarker for predicting HCC outcomes. We observed a notable link between FKBP52 levels and the histological differentiation in HCC samples. To corroborate these observations, we performed a series of in vitro and in vivo experiments using liver cancer models. These experiments highlighted the dual nature of FKBP52’s impact on hepatocytes, which varies according to cell type. Given its connection to HCC severity, FKBP52 seems to contribute negatively to the disease’s progression. The insights gained from this study on how FKBP52 influences p53 stabilization are critical. We suggest that targeting the processes upstream of FKBP52 could lead to more effective HCC treatments. These findings emphasize the importance of further investigating this pathway, potentially paving the way for new strategies in liver cancer therapy.

#1483 Sugar analogs inhibit KSHV replication by blocking N-glycosylation and inducing the unfolded protein response.

M. Schlesinger[1], **C. McDonald**[1], A. Ahuja[1], C. Alvez-Canete[1], Z. Nunez Del Prado[1], J. Naipauer[2], T. Lampidis[3], E. Mesri[3], N. Shembade[3];
[1]University of Miami Miller School of Medicine, Miami, FL, [2]Universidad de Buenos Aires, Buenos Aires, Argentina, [3]University of Miami, Miami, FL

Background: Kaposi´s Sarcoma (KS) herpesvirus (KSHV) is one of the seven known human oncogenic viruses. KSHV infection precedes the development of KS, an AIDS-associated malignancy. While the incidence of AIDS-KS globally has seen a decline, this endothelial cancer is refractory to treatment. The standard of care for AIDS-KS has gone virtually unchanged for over 20 years and effective treatments against the oncovirus KSHV have yet to be developed. 2-DG (2-deoxy-D-glucose), 2-FDG (2-fluoro-deoxy-D-glucose), and2-DFM (2-deoxy-2-fluoro-D-mannose) are sugar analogs. 2-DG and 2-FDG are D-glucose analogs and strong glycolysis inhibitors. 2-DG is also a D-mannose analog so that can inhibit N-glycosylation. In this work we aimed to further characterize and compare the inhibition of the three drug analogs on KSHV replication and pathogenesis.
Design/Methods: We determined the ability of each drug to inhibit KSHV reactivation and infection by flow cytometry using the KSHV producer cell line iSLK.219 Virus titers were measured by de novo infection of naïve AdHEK293 cells and quantifying the number of AdHEK293 infected cells. We further characterized sugar analog inhibition assessing viral glycoprotein expression by western blot and quantifying virion production by qPCR. To show that N-glycosylation impairment is the main contributor of virus replication inhibition, we carried out D-mannose rescue experiments and analyzed activation of the unfolded protein response (UPR). When UPR cannot be resolved, it leads to either apoptosis or autophagy. For this reason, we analyzed the cellular fate of reactivated sugar analog-treated cells by western blot using apoptotic and autophagic markers. Additionally, we calculated the cell death index using the IncuCyte® machine.
Results: All three sugar analogs negatively affected KSHV replication and virion infectivity, but 2-DFM displayed the strongest inhibition. Viral glycoproteins K8.1 and gB were down-regulated and virion production was diminished especially with 2-FDG and 2-DFM sugar analogs. D-mannose could rescue viral glycoprotein expression and virion infectivity, but could not reverse the number of reactivated cells, indicating that N-glycosylation is the main target of the drugs. In line with this, all analogs triggered UPR and even overcame KSHV-induced suppression of the PERK pathway. Finally, 2-DG, 2-FDG, and 2-DFM played a protective role in reactivated cells, displaying the autophagic marker instead of the apoptotic signature observed in the untreated cells.
Conclusion: Collectively, this work identifies the non-toxic inhibition of N-glycosylation by sugar analogs as an important viral target and reinforces the potential of 2-DG as an antiviral for KSHV and other enveloped viruses. We also found that 2-DFM is a more potent and target-oriented compound and a promising therapeutic antiviral agent against an oncogenic virus.

#1484 5-Aza-4'-thio-2'-deoxycytidine induces C to G transversions in a specific trinucleotide context and leads to acute lymphoid leukemia.

R. M. Bertoli, Y. Chung, M. Difilippantonio, A. Wokasch, M. R. B. Marasco, H. Klimaszewski, S. Garber, Y. Zhu, R. L. Walker, D. Cao, J. Doroshow, P. Meltzer, P. D. Aplan;
NIH-NCI, Bethesda, MD

Myelodysplastic syndromes (MDS) are a diverse group of blood cancers characterized by peripheral blood cytopenias and dysplastic blood cell morphology. Up to 40% of patients with high risk MDS will transform to acute myeloid leukemia (AML), an aggressive blood cancer with significant morbidity and an overall 5-year survival of less than 35%. Both MDS and AML have been linked to hypermethylation of cytosine residues. Hypermethylation in the 5' regulatory region can result in epigenetic downregulation of gene expression, and it has been speculated that hypermethylation of tumor suppressor genes can contribute to malignant transformation. DNA methyltransferase inhibitors (DNMTi), most commonly cytidine analogs, are compounds that are used clinically to decrease 5'-cytosine methylation, with the aim of inducing the re-expression of tumor suppressor genes resulting in a halt of tumor progression. 5-Aza-4'-thio-2'-deoxycytidine (Aza-TdCyd or ATC) is a cytidine analog that incorporates an aza modification (nitrogen in place of carbon) of the cytosine base and a thioether modification of the deoxyribose sugar. ATC is a promising new DNMT1i that has demonstrated efficacy in preclinical studies of solid tumors. Based on these prior studies, we sought to characterize the potential therapeutic effect of ATC in MDS.Mice that express a NUP98::HOXD13 (NHD13) transgene develop an MDS that closely recapitulates all of the key features of human MDS, including pancytopenia, dysplastic morphology, and transformation to AML. We transplanted NHD13 and wild-type (WT) hematopoietic stem and progenitor cells into WT recipients, and used this model of MDS to investigate the therapeutic potential of ATC. We found that ATC treatment led to both T and B lineage lymphoid leukemia (ALL) originating from the NHD13 cells. Surprisingly, ATC treatment also led to T and B lineage ALL in the WT cells, and further experiments demonstrated that non-transplanted, healthy WT mice developed T and B cell ALL after treatment with ATC. In sum, all mice that received at least 8 cycles of ATC therapy at the 1.0 mg/kg dose developed leukemia. Whole exome sequencing of tumors revealed thousands of acquired mutations, almost all of which were C>G transversions in a previously unrecognized, specific 5'-NCG-3' context. These mutations involved a number of genes well-known to be involved in human lymphoid leukemia, such as Notch1, Pten, Pax5, Trp53, and Nf1. Treatment of the human U937 and CEM cell lines in vitro showed thousands of acquired C>G transversions in a similar context. Taken together, these findings demonstrate that ATC can be a potent mutagen in human and mouse cells, both in vitro and in vivo.

#1485 Hallmarks of APOBEC3 mutagenesis in normal, pre-leukemic, and myeloproliferative neoplasm cell populations.

J. M. Isquith, T. Whisenant, J. Pham, L. Alexandrov, C. Jamieson;
UC San Diego School of Medicine, San Diego, CA

Changes in gene expression and subsequent editing patterns of APOBEC3 (apolipoprotein B mRNA editing enzyme catalytic polypeptide-like) cytosine deaminases have been shown to be present in solid tumor cancer evolution, however, the context specificity and mechanisms by which APOBEC3 enzymes promote cancer initiation and progression require further elucidation, especially in the hematopoietic niche. Building on advanced sequencing data of healthy, pre-leukemic, and myeloproliferative neoplasm patient samples, we seek to uncover normal and malignant patterns of APOBEC3C overexpression in hematopoietic cells. Overexpression of lentiviral APOBEC3C and an editase-mutated APOBEC3C in normal cord blood, healthy bone marrow, and MPN patient hematopoietic stem/progenitor cells (HSPCs) allows us to study the effects of deaminase dysregulation in hematopoietic cells. In addition to APOBEC3, we are exploring the upregulation of adenosine deaminase acting on RNA1 (ADAR1), as we have previously shown that these two innate immune deaminases are synchronously upregulated in the high-risk myelofibrosis (MF) stem cell population compared to normal aged bone marrow. These overexpression studies show novel differential gene expression changes, RNA hyper-editing sites, and DNA mutation signatures induced by APOBEC3 mutagenesis, which can be cross-referenced to gene expression and mutation signatures seen in hematopoietic malignancies and solid tumor cancers. In addition to mutation patterns, the regulation of LINE-1 elements has been shown to be another important function of APOBEC3 enzymes. In these studies, we examine the effects of APOBEC3 overexpression on repetitive element expression in hematopoietic cell populations and have found that there are strong cell type and context patterns across the APOBEC3 family and between cell types within the hematopoietic system. We will use this comprehensive study of APOBEC3 deregulation to uncover predictive biomarkers of malignant transformation.

TUMOR BIOLOGY: Contributors to Metastatic Organotropism
Poster Session

#1488 Spatial characterization of the tumor microenvironment of metastatic triple-negative breast cancer.

M. Bhargava[1], J. Kaur[2], G. Saini[1], J. Zheng[3], Y. Xu[3], S.-H. Chen[3], P.-Y. Pan[3], E. Rewcastle[4], U. Kiraz[4], E. A. M. Janssen[4], R. Aneja[1];
[1]University of Alabama at Birmingham, Birmingham, AL, [2]Georgia State University, Atlanta, GA, [3]Houston Methodist Research Institute, Houston, TX, [4]Stavanger University Hospital, Health Stavanger HF, Stavanger, Norway

Triple-negative breast cancer (TNBC) is an aggressive subtype of breast cancer associated with high rates of recurrence and metastasis, which contribute to poor overall survival. The challenges in treating TNBC stem from its high intratumor heterogeneity and lack of expression of the estrogen receptor, progesterone receptor, and human epidermal growth factor receptor 2 druggable targets. The tumor microenvironment (TME) plays a crucial role in disease progression. Within the TME, complex spatial interactions among tumor cells, immune cells, stroma, angiogenesis- and hypoxia-inducing factors collectively contribute to the advancement and spread of TNBC. In-depth understanding of the TME and interactions of the various components within can elucidate newer therapeutic targets, enhancing the prognosis of TNBC patients. Imaging mass cytometry (IMC) enables detailed analysis of cell-cell and cell-matrix interactions within the TME at the single-cell level. In this study, we aim to characterize the spatial relationships among various cell types within the TNBC TME using IMC, while also investigating differences in the TME of TNBC patients who developed distant metastasis (DM) compared to those who remained non-metastatic (NM). IMC was performed on formalin-fixed paraffin-embedded TNBC primary resection tissues (n= 16; DM= 7, NM= 9) from Stavanger University Hospital, Norway, using a panel of 25 metal-conjugated antibodies. Regions of interest were marked by the pathologist and the slides were laser ablated using Hyperion Imaging System. DeepCell was used to segment single cells based on surface markers. Mean intensity values of all markers for each cell were extracted and consolidated in R scripts for unsupervised clustering. Cell clusters were annotated based on phenotypic markers. Normalized expression of markers was compared for each cell type across DM and NM patients, including markers for cell proliferation, angiogenesis, hypoxia, and cell migration. Neighborhood analysis examined spatial associations between different cell types, highlighting differences in DM and NM patients. The IMC panel successfully provided spatial insights into the TME, including the characterization of tumor cells, immune cells (B cells, T cells, macrophages), endothelial cells, and proliferating cells. We identified 18 unique phenotypic cell clusters that were present at different frequencies in DM and NM patients. These clusters demonstrated different expression profiles of functional markers. t-SNE plots revealed distinct patterns of cell type distribution and unique protein expression profiles, highlighting significant differences between the two groups. Our data suggest a distinct spatial organization of the TME in TNBC patients who develop metastasis. This warrants further investigations to determine the role and interplay of TME features in predicting the risk of distant metastasis in TNBC.

#1489 The role of EPAS1 and TEAD1 in gastric cancer liver metastasis.

D. Lee[1], H. Park[2], J.-H. Cheong[1], H. Gee[1];

[1]Yonsei University College of Medicine, Seoul, Korea, Republic of, [2]Yonsei University, Seoul, Korea, Republic of

Gastric cancer ranks fifth in incidence and fourth for cancer-related mortality worldwide. While the liver is widely recognized as the leading site of metastasis in gastric cancer, the intricate mechanisms underpinning its tropism toward the liver and the hematogenous metastasis process remain poorly understood and demand further investigation.

Hematogenous metastasis encompasses the generation of circulating tumor cells from the primary tumor site and their subsequent attachment to the metastatic niche. This process involves the transition between adherent and suspension states. In our investigation of anchorage dependency, we identified 20 transcription factors upregulated in suspension cells compared to adherent cells and 18 transcription factors upregulated in adherent cells relative to suspension cells, respectively.

To investigate factors involved in gastric cancer metastasis, RNA sequencing of paired primary and metastatic tissue samples obtained from 15 patients diagnosed with advanced gastric cancer was conducted, which disclosed the selective upregulation of EPAS1 and TEAD1 in metastatic liver tissue compared to the matched primary tumor tissue and the metastatic tissue originating from other sites.

Through in vitro analysis, we observed a portion of adherent cells transitioning into suspension cells when subjected to a hyperdense environment. We also observed cell reattachment upon harvesting and replating these suspension-state transited cells. Comparing EPAS1 and TEAD1 expression in these states unveiled increased expression of EPAS1 and TEAD1 in reattached cells relative to suspension-state cells.

We established a gastric cancer metastasis mouse model introducing gastric cancer cells into the mouse circulatory system via intracardiac injection to validate our findings. In vivo imaging was utilized to confirm systemic metastasis. After fluorescence-based cell sorting, EPAS1 and TEAD1 expression in cancer cells collected from the blood, liver, and ovary were assessed. We detected higher expression of EPAS1 and TEAD1 in liver metastasis compared to the circulating tumor cells. Furthermore, EPAS1 and TEAD1 were upregulated in liver metastatic cancer cells compared to ovarian metastatic cancer cells.

Our findings underscore EPAS1 and TEAD1 as pivotal factors governing gastric cancer liver tropism and metastasis, offering insights that may contribute to targeted interventions in the clinical landscape.

#1490 Elucidating the effect of glutamine metabolism in breast to bone metastasis.

B. A. Karno[1], Y. Hwang[2], R. Johnson[2], J. Chen[2], D. Edwards[2];
[1]Vanderbilt University, Nashville, TN, [2]Vanderbilt University Medical Center, Nashville, TN

Bone-metastatic lesions will develop in approximately 65-75% of patients with metastatic breast cancer and are associated with high morbidity and mortality. Despite our limited understanding of how breast-to-bone metastases form, the recent emergence of metabolic adaptation as a critical factor in metastasis is a promising development. Breast cancer cells are particularly reliant on glutamine, a key amino acid that is metabolized by the enzyme glutaminase (GLS) to facilitate many downstream metabolic processes. Bone-tropic breast cancer cell lines significantly enhance their glutamine uptake, suggesting that glutamine metabolism may be a significant factor in bone metastasis. In addition to tumor cells, glutamine metabolism is critical for osteoblasts, important bone-resident cells that contribute to the “vicious cycle” of bone destruction during metastatic outgrowth in the bone niche. In this study, we sought to evaluate the role of glutamine metabolism in breast cancer bone metastasis by examining the effect of GLS function in metastasizing tumor cells and bone-native osteoblasts. Using an intracardiac inoculation model of bone metastasis, we found that breast cancer cells lacking GLS (GLS KO) failed to effectively form bone metastatic tumors. We also observed that GLS KO bone tumors show a reduction in osteolysis using a direct intratibial injection model. Mechanistically, we have found that GLS KO breast cancer cells develop a “senescence-like” phenotype that may limit metastatic outgrowth within the bone. To investigate the importance of glutamine metabolism in the bone niche, we developed a conditional genetic mouse model to delete GLS in osterix-expressing in osteoblast progenitors and mature osteoblasts (GLS^{OBKO}). Remarkably, we observed reduced bone destruction in GLS^{OBKO} mice after intratibial injection of syngeneic breast cancer cells. We also report a reduction in the number of osteoclasts at the bone/tumor interface in these mice, suggesting that loss of osteoblast GLS could temporarily halt the “vicious cycle” of bone metastasis. Together, this work suggests that glutamine metabolism may promote breast-to-bone metastasis via both intrinsic and extrinsic mechanisms. These findings raise the possibility of using pre-existing cancer therapies targeting glutamine metabolism to ameliorate bone metastatic burden in breast cancer.

#1491 The enhanced formation of neutrophil extracellular traps (NETs) may contribute to the exacerbation of peritoneal metastasis in a diabetic host.

R. Takahashi, H. Ohzawa, Y. Kaneko, M. Matsumiya, Y. Futoh, K. Tamura, K. Takahashi, Y. Kimura, A. Saito, H. Miyato, N. Sata, J. Kitayama;
Jichi Medical University, Tochigi, Japan

Background: Diabetes is associated with increased risk of cancer development and progression. Recent studies have shown that neutrophils in diabetic patients are prone to forming neutrophil extracellular traps (NETs) which have been reported to capture circulating cancer cells, leading to the promotion of liver and lung metastasis. This study aims to clarify the causative relationship between NETs and the peritoneal metastasis (PM) in diabetic condition.
Methods: Outcome of the diabetic patients who received curative gastrectomy for gastric cancer from 2010 to 2021 in our institute was comparatively investigated with those without diabetes. Neutrophils were isolated from the bone marrow from C57BL/JHamSlc-ob/ob mouse (type 2 diabetes model) and wild type mouse using Ly6G-based positive immunomagnetic selection. The neutrophils were stimulated with 100nM of PMA for 4 hours and NETs formation was evaluated by the addition of Sytox Green under fluorescent microscope. A mouse gastric cancer cell, YTN16P (5×10^5 cells) was intraperitoneally (IP) injected, the number of metastatic nodules on mesentery was comparatively evaluated two weeks later.
Results: Disease-free survival (p=0.004, HR=1.65) and overall survival (p=0.035, HR=1.46) of 203 diabetic patients were significantly worse those of 975 non-diabetic patients. Neutrophils isolated from ob/ob mice produced markedly increased NETs than that from wild-type mice. NETs produced by neutrophils obtained from the peritoneal cavity of ob/ob mice after IP injection of a 9% casein solution effectively captured many YTN16P in vitro. The concentration of double strand DNA (dsDNA) in plasma in ob/ob mice compared with their counterparts (676ng/mL vs 590ng/mL, p=0.036, n=3). The number of PM in ob/ob mice was significantly more than that in wild-type controls (39.1 vs 15.5, p=0.027, n=10).
Conclusion: Enhanced NETs formation in diabetic conditions may be associated with an increased risk of PM in gastric cancer.

#1492 Unveiling the re-programming of choroid plexus and leptomeningeal metastasis.

A. Nobre, H. Wang, R. Estrera, I. Osei-Gyening, A. Boire;
Memorial Sloan Kettering Cancer Center, New York, NY

Leptomeningeal metastasis (LM) is an increasingly common, fatal complication of breast and lung cancer. Despite aggressive treatment, neurologic deficits accumulate rapidly, and patients generally succumb to LM within months. We must expand our limited mechanistic knowledge of this disease.
Under homeostatic conditions, choroid plexus (ChP), highly vascularized structures within the brain ventricles, restrict the entry of macromolecules and cells into the leptomeninges; however, select cancer cells can cross this barrier and grow within the leptomeningeal space. We hypothesize that interactions between cancer and ChP niche cells alter both the niche and the cancer cells, ultimately supporting LM.During neurogenesis, the ChP display substantial extracellular matrix (ECM) remodeling, which is elegantly modulated by dynamic spatiotemporal regulation of MMPs, Wnt signaling, among other effector proteins. Similarly, 2-photon imaging of ChP collected from mice harboring LM revealed a profound ECM remodeling of the ChP when compared with naïve mice. This remodeling was accompanied by increased levels of MMP2 and MMP9 in LM mice. Upon pharmacological inhibition of MMP2 and MMP9 *in vivo*, we observed a decrease in LM burden and increase in overall survival, which correlates with a decrease in ChP permeability. Interestingly, human CSF from patients with leptomeningeal metastases is also enriched in collagen 1 fragments, MMP2, MMP9 and TIMP1. TIMP1, a MMP9 natural inhibitor, is not present in complex with MMP9, suggesting a role of TIMP1 as a cytokine in LM progression. TIMP1 neutralization and knockout from the cancer cells leads to a decrease in LM burden and increase in overall survival. Together, these data suggest a provocative link between proteolysis and inflammation in LM progression.
The use of clinically-annotated human samples and mouse models of LM, and the integration of transcriptomics and proteomics enabled us to identify key signaling pathways, and capture the re-programming of ChP niche and cancer cells that unlock the leptomeningeal space to cancer cells. The timeframe for this evolution will be further revealed by analysis of mouse and human samples at different stages of cancer progression.

#1493 Secretory function of neuroendocrine-like prostate cancer cell enhances therapy resistance and metastatic potential of adjacent adenocarcinoma.

J. Mishra, S. Bodas, S. Bhattacharya, D. Das, S. UnNazir, S. Dutta, K. Datta;
University of Nebraska Medical Center, Omaha, NE

Background: Castration-resistant prostate cancer (CRPC) is advanced non curable disease associated with poor prognosis and survival n patients. Androgen receptor pathway inhibitors (ARSIs) are used to treat advanced prostate cancer, but in majority of patients it progresses by developing resistance to AR-directed therapies and is referred to as CRPC. Adenocarcinoma cells in CRPC tumor often undergoes lineage switch and become neuroendocrine-like cancer cells (NEPC) with small-cell histology, characterized by the loss of Tp53 and Rb1 genes. NEPC cells are frequently present as scattered foci along with prostatic adenocarcinomas and are secretory in nature.
Objective: The primary objective is to determine how these NEPC cells influence surrounding adenocarcinoma and aids in disease progression.
Methods: We performed Mass spec and cytokine array experiments from NEPC conditioned media to determine its secretory phenotype. We orthotopically implanted NEPC and adeno cells in the nude mice and performed colony formation assay on flow sorted adeno cells from the tumor. We also checked the effect of NEPC on the adeno cells and TME components.
Results: Our analysis of the RNA-seq data from SU2C-PCF cohort and NE-like cells revealed that functions related to secretion were significantly enriched in NE-like PCa. NE-like cells gain the ability to secrete neuropeptides, growth factors, and cytokines to establish cell-cell communication. This secretory function is tightly regulated by the Neuropilin2 (NRP2) axis. We studied for the effect of NE-like cells on the adenocarcinoma cells in the mice tumor model and found that the presence of NE-like cells facilitated the adenocarcinoma cells to acquire aggressive characteristics. This could be due to both direct and/or through the modulation of the tumor microenvironment (TME). The direct effect could be by enhancing the therapy resistant ability of the surrounding adenocarcinoma, and the indirect effect is through the tumor microenvironment especially through neurons and macrophages that promote metastatic potential.
Conclusions: Overall, our results prove that NE-like cancer cells influence the adjacent adenocarcinoma cells directly by making them resistant to treatment and indirectly make them more metastatic by utilizing macrophage-neuron axis.

#1494 Clonal dominance defines metastatic dissemination in pancreatic cancer.

I.-L. Ho[1], C.-Y. Li[1], F. Wang[1], L. Zhao[1], J. Liu[1], E.-Y. Yen[1], C. Dyke[1], R. Shah[1], Z. Liu[1], A. Cetin[2], F. Citron[1], S. Attanasio[1], V. Giuliani[1], T. Heffernan[1], K.-A. Do[1], G. Gargiulo[2], G. Draetta[1], A. Carugo[1], R. Lin[1], A. Viale[1];

[1]UT MD Anderson Cancer Center, Houston, TX, [2]Max-Delbruck-Centrum fur Molekulare Medizin, Berlin, Germany

Tumors represent ecosystems where subclones compete during tumor growth. While extensively investigated, a comprehensive picture of the interplay of clonal lineages during dissemination is still lacking. Using patient-derived pancreatic cancer cells, we created orthotopically-implanted clonal replica tumors to trace clonal dynamics of unperturbed tumor expansion and dissemination. This model revealed the multifaceted nature of tumor growth, with rapid changes in clonal fitness leading to continuous reshuffling of tumor architecture and alternating clonal dominance as a distinct feature of cancer growth. Regarding dissemination, a large fraction of tumor lineages could be found at secondary sites each having distinctive organ growth patterns as well as numerous undescribed behaviors such as abortive colonization. Paired analysis of primary and secondary sites revealed fitness as major contributor to dissemination. From the analysis of pro- and non-metastatic isogenic subclones, we identified a transcriptomic signature able to identify metastatic cells in human tumors and predict patients' survival.

#1495 Lipocalin-2 promotes breast cancer metastasis via tumor cell intrinsic and extrinsic mechanisms.

J. Gamez[1], F. Sanchez[1], G. Ortiz-Soto[2], J. Cox[1], A. Gerami[3], **J. A. Kelber**[2];
[1]California State University, Northridge, Northridge, CA, [2]Baylor University, Waco, TX, [3]Western University of Health Sciences, Pomona, CA

While metastasis is the primary factor predicting poor outcomes in solid tumors, survival is lowest in patients initially diagnosed with a localized malignancy that then progresses to metastatic disease. Notably, nearly 25% of early-stage breast cancers (BCs) metastasize during treatment or following an initial positive response to therapeutic intervention. To define the molecular and cellular factors that contribute to metastatic progression of BC, we previously developed the Py230-C57Bl/6 syngeneic experimental metastasis model for interrogating mechanisms by which soluble factors condition premetastatic lung tissue to potentiate BC cell seeding/expansion. Using this model and the TCGA, we identified lipocalin-2 (Lcn2) as a molecular candidate that is upregulated in lung-tropic Py230 cells and other human triple-negative breast cancer (TNBC) cells, and that predicts poor outcomes in human BCs. While Lcn2 has been previously reported to mediate BC progression in genetically engineered mouse models, its mechanism(s) of action remain undefined. Here, we demonstrate that Py230 cell-secreted Lcn2 is necessary for optimal reprogramming of the premetastatic lung during metastatic progression. In agreement with these data, we defined a cell intrinsic role for Lcn2 in BC cell organoid assembly/invasion and expression of proinflammatory factors. To define BC cell extrinsic roles for Lcn2 in remodeling the premetastatic lung, we collected global transcriptome and single-cell spatial proteome data for lung tissue from C57Bl/6 mice systemically educated with mock media or media conditioned with Py8119 ($Lcn2^{low}$) or Py230 ($Lcn2^{hi}$) BC cells. Mice receiving Py230 conditioned media treatments were further divided between two groups – one receiving an isotype control IgG and the other receiving an Lcn2 immunoneutralizing antibody. Global transcriptome data was used to determine novel gene set enrichment signatures and clinically relevant interactomes – notable candidates predicted to cooperate with Lcn2 in decreasing patient survival were affiliated with cilia biogenesis and function. Single-cell spatial proteome data were analyzed for 28 different cell populations within the premetastatic lung. Interestingly, Py230 cell-derived Lcn2 did not affect the percentage of ciliated epithelial cells indicating that the global transcriptome data referenced above represent a real increase in expression of cilia-related genes and not an increase in cilia-positive cell types. Notably, we identified that Lcn2 increased the percentage of $CD45^{neg}/Des^{pos}$ mechanomodulatory cells and proliferating $CD45^{pos}/CD3^{pos}/CD4^{neg}/CD8^{pos}$ cytotoxic T cells in the premetastatic lung. Taken together, these data define new targets around which new therapeutic strategies can be developed to improve BC patient outcomes.

#1496 The role of endothelial ACKR1 in breast cancer metastasis.

S. T. Roach, R. Patel, S. Thomas, C. Ewenighi-Amankwah, J. Dufraine, L. A. Naiche, J. Kitajewski;
University of Illinois at Chicago, Chicago, IL

Background: Tumor cells can co-opt mechanisms of leukocyte extravasation. Atypical Chemokine Receptor 1 (ACKR1) expression in endothelial cells has an established role in promoting leukocyte extravasation; however, the potential for endothelial ACKR1 to facilitate the metastatic process through the extravasation of tumor cells has not been studied.
Methods: To understand ACKR1 function, we investigated endothelial ACKR1 expression at the distant metastatic site of the lung, a common site of breast cancer metastasis. We analyzed lung endothelial ACKR1 expression using immunofluorescent staining of lung vasculature during tumor progression in immunocompetent mice bearing orthotopically implanted E0771.LMB breast tumor cells. We assessed the timing of metastatic tumor cell arrival in the lung and evaluated the spatial relationship between disseminated tumor cells and ACKR1-positive vessels. To investigate secreted tumor factors that may mediate ACKR1 regulation in the lung, we performed intratracheal injections of TNF-alpha. We developed an endothelial cell specific ACKR1 conditional knockout mouse model (ACKR1 ECKO) to understand the impact of endothelial ACKR1 on primary tumor growth and subsequent lung metastasis in breast cancer.
Results: Our results reveal a significant upregulation of ACKR1 in the lung endothelium of mice implanted with breast cancer cells in the mammary fat pad. Tumor-dependent ACKR1 expression was specifically localized to pulmonary venule endothelium, a common site of leukocyte and tumor cell extravasation. Lung endothelial ACKR1 expression became evident by day 13 after implantation, persisting through endpoint at day 28. Notably, ACKR1 upregulation occurred prior to tumor cell arrival in lungs of tumor bearing mice. We observed spatial clustering of disseminated tumor cells in proximity to ACKR1-positive vessels, implying a preferential site of tumor cell extravasation. In the absence of primary tumors, intratracheal delivery of TNF-alpha induced ACKR1 expression within lungs. When tumors were orthotopically implanted into our ACKR1 ECKO mouse model, we observed a marked decrease in lung metastases compared to control mice.
Conclusion/Future Directions: We have determined that pulmonary ACKR1 expression is induced by breast tumors, and vessels expressing ACKR1 appear to act as entry points for lung metastasis. Loss of endothelial ACKR1 reduced metastasis, suggesting that endothelial ACKR1 regulates tumor cell extravasation at distant metastatic sites. We will upregulate lung endothelial ACKR1 expression and directly test its requirement for extravasation using an intravenous tumor cell injection metastasis model.

#1497 Humanized mouse model unveils niche conditioning in gastric cancer peritoneal metastasis.

J. J. Zhao[1], D. K. Chia[2], Z. Her[3], H. Ma[4], X. Ong[4], S. Tay[4], J. B. So[2], Q. Chen[3], P. Tan[4], R. Sundar[1];

[1]National University Cancer Institute, Singapore, Singapore, [2]University Surgical Cluster, National University Health System, Singapore, Singapore, [3]Agency for Science, Technology and Research (A*STAR), Singapore, Singapore, [4]Duke-NUS Medical School, Singapore, Singapore

Background: Peritoneal metastases (PM) in gastric cancer (GC) portend a poor prognosis. Yet, biological mechanisms underpinning peritoneal colonization and transcoelomic metastases remain unclear. Utilizing a novel humanized mouse model of GCPM, we seek to understand the evolution of the peritoneum to allow for peritoneal dissemination. The humanized mouse model, defined as mice engrafted with functional human cells or tissues, was selected as the host immune system appears to play a significant role in the mechanisms of transcoelomic metastases.

Methodology: Humanized (humice) and NOD-scid Il2rynull (NSG) mice models were injected with GSU (diffuse type) GC cell lines in the flank (subcutaneous), stomach (orthotopic) and directly into the peritoneum (intra-peritoneal). After 1 month, the mouse models were sacrificed and samples from the primary tumor (PT), PM and adjacent peritoneum were retrieved. The tumors were then harvested, along with normal/adjacent peritoneum and bulk RNA-seq was performed and analyzed.

Results: Fifty-six samples including PT, PM were harvested from 10 humice and 11 NSG models and were analysed with whole transcriptome sequencing. All models with orthotopic inoculation were found to create PM while no gross PM were appreciated in models with flank inoculation. Principal component analysis mapping of samples demonstrated transcriptomic distinction between normal peritoneum from the flank humice model and adjacent normal samples in the orthotopic and intra-peritoneal humice model. Compared to adjacent peritoneum of the intra-peritoneal humanized mouse model, the orthotopic model appeared to be more tumorigenic with enriched epithelial mesenchymal transition (EMT), stromal and immune infiltration, inflammatory response (IL2-STAT5, IL6-JAK-STAT3, TGF-β signaling), IFN-γ response signatures. Enrichment scores of these pathways were likewise more pronounced in adjacent normal peritoneal samples in the orthotopic humanized mouse model when contrasted against other sample types. Higher expression of M2 macrophages, B cells and T regs, dendritic cells (activating and resting) was found in adjacent peritoneum in the orthotopic model. Collectively, these describe a phenomenon in which the adjacent uninvolved peritoneum has evolved into a tumorigenic environment to facilitate transcoelomic metastasis. These unique niche changes of the peritoneum were conversely not appreciated in the NSG model.

Conclusion: We unveil novel insights that delve into the mechanistic role of the host immune system in orchestrating tumorigenic microenvironmental alterations to support peritoneal organotropism. These provide functional proof alluding to the phenomenon of peritoneal niche conditioning in GC PM.

#1498 TGFβ signaling in cancer-associated fibroblasts drives a hepatic gp130-dependent pro-metastatic inflammatory program in CMS4 colorectal cancer.

S. Abudukelimu, T. J. Harryvan, S. G. T. Janson, I. Stouten, E. M. E. Verdegaal, L. J. Hawinkels;
Leiden University Medical Center (LUMC), Leiden, Netherlands

Background: Colorectal cancer (CRC) is characterized by a metastatic pattern that shows tropism towards the liver which is the major cause of CRC-related deaths. The current CRC classification, Consensus Molecular Subtypes (CMS), suggests an association between transforming growth factor (TGF)-β signaling, cancer-associated fibroblasts (CAFs), and the risk of liver metastasis. However, the key downstream effectors of TGFβ signaling in CAFs and their role in hepatic metastases remain poorly understood.
Methods: The aim of this study was to investigate the TGF-β/CAF dependent cross talk with the hepatocytes in pre-metastatic niche formation. CAFs from 18 primary CRC tissues and 7 liver-metastasized CRC were stimulated with TGFβ1 and qPCR arrays/ELISAs were performed to identify differentially expressed genes. Results were cross-referenced with RNAseq expression data of CMS-classified CRC and in fresh samples from CRC patients. To investigate CAF-liver crosstalk hepatocytes were stimulated with the TGFβ primed CAF-derived cytokines and the effect on pro-inflammatory gene expression and neutrophil migration was determined. Subsequently, blockade of these pathways via chemical inhibition and CRISPR/Cas9 genetic ablation was performed to study the molecular mechanism involved in the induction of this hepatic pro-inflammatory program.
Results: TGFβ signaling in primary CRC-derived CAFs leads to increased expression of different IL-6 cytokine family members, which was also reflected in human CRC samples. CAF-derived IL6 family members induce upregulation of myeloid chemoattractants, including SAA1, in hepatocytes and increased neutrophil-to-hepatocyte migration in vitro. Chemical blockade and genetic ablation of the IL-6 family cytokine signaling pathway showed the critical role of the gp130 co-receptor in the regulation of this inflammatory response in hepatocytes and the potential formation of a premetastatic niche.
Conclusion: TGFβ signaling in CAFs actively contributes to the formation of a neutrophil-dependent, pre-metastatic hepatic niche, and this mechanism might play a role in CMS4 subtype CRC.

#1499 Senescent stromal cells drive lung metastases of breast cancer.

A. Melam, J. Ye, S. A. Stewart;
Washington University in St. Louis, Saint Louis, MO

In 2022 in the United States, there were nearly 300,000 women diagnosed with breast cancer (BC) with the risk increasing significantly after age 50. The overall 5-year survival rate dramatically decreases, from 99% for patients with stage I, to a devastating 25% for those with stage IV (metastatic) BC, making distal metastasis the leading cause of BC mortality. This mortality rate has not changed in decades with lungs being one of the most common sites for distal metastasis of BC. The BC microenvironment is a complex mix, consisting of tumor cells and numerous nontumor cells including distinct subpopulations of cancer-associated fibroblasts (CAFs): vascular (vCAFs), inflammatory (iCAFs), and myofibroblastic CAFs (myCAFs), which can play pro- or anti-tumor roles. Senescent fibroblasts, which accumulate with age typically express $p16^{INK4A}$ and can modulate the cells around them via the secretion of a cadre of pro-tumorigenic factors including cytokines, chemokines, and extracellular matrix (ECM) modulating enzymes, collectively called the senescence-associated secretory phenotype (SASP). To investigate how p16+ senescent cells impact tumorigenesis, we mated the well-characterized MMTV-PyMT mouse, to the INK-ATTAC (INK) mouse, wherein treatment with AP20187 (AP) selectively eliminates p16+ senescent cells. Preliminary data showed that elimination of p16+ aSMA+ senescent fibroblasts (senCAF) resulted in a significant decrease in primary tumors, lung tumor foci and lung metastatic burden. Further, we found that senescent CAFs (senCAFs) were the only stromal cells eliminated in the PyMT-INK mouse treated with AP, suggesting that this CAF subtype is a key contributor to tumor progression. To determine if senCAFs directly impacted lung metastasis, EO771-LG Luc mammary tumor cells were injected in the tail vein of INKATTAC mice that were treated with AP to eliminate p16+ senCAFs. We found that metastatic tumor burdens were significantly reduced in INK+ versus control mice and immunohistochemical analysis revealed that tumor burden and foci was significantly reduced, suggesting that senCAFs in the lung promoted tumor cell seeding and outgrowth.

#1500 Breast cancer-derived extracellular vesicles modulate the endocytic metabolism and morphodynamics of the endothelial cells of the blood-brain barrier.

S. Busatto, G. Morad, M. Moses;
Boston Children's Hospital, Boston, MA

Breast cancer, particularly the triple-negative subtype, is the primary cause of brain metastasis in women, affecting 10-20% of breast cancer patients. Breast cancer patients who develop brain metastasis have few treatment options and a dismal prognosis with a median survival time of 6-16 months. We demonstrated, for the first time, that EVs derived from brain-seeking breast cancer cells (BrEVs) breach the intact blood-brain barrier (BBB) via transcytosis and cause a significantly increased incidence of breast-to-brain metastasis. Within this context, we are now studying the interactions between BrEVs and the endothelial cells (ECs) of the BBB. BrEVs were isolated by ultracentrifugation, characterized following the latest guidelines published by the International Society of Extracellular Vesicles (MISEV 2018) and tested *in vitro* using primary human brain ECs and *in vivo* using our mouse model of breast-to-brain metastasis. ECs were treated with BrEVs and analyzed using antibody-based assays, impedance measurements, genetic engineering and fixed and live cell imaging. The imaging results were analyzed using novel machine learning approaches to detect and describe, for the first time, EV-mediated morphodynamic changes at the brain EC barrier level. *In vivo*, we administered BrEVs intravenously to our models of breast-to-brain metastasis, followed by the analysis of mouse brains and their cerebral microvessels to examine microscopic structure and protein expression. Our studies show that (1) BrEVs target BBB ECs both *in vitro* and *in vivo*, causing significant variations of multiple proteins involved in the intracytoplasmic vesicles' long-recycling loop, (2) BrEVs are responsible for specific EC barrier function and morphodynamic changes and (3) BrEVs mediate, at least in part, their effect(s) through the delivery of specific micro RNAs. Taken together, our studies demonstrate that BrEVs have a significant impact on brain EC endocytic metabolism and morphodynamics, promoting transcytosis and sustaining breast-to-brain metastasis. Our findings increase our understanding of the early events that facilitate brain metastasis and have the potential to identify key regulators of brain metastasis formation. These results also inform and contribute to the development of EV-based therapeutic and diagnostic strategies for brain metastasis. (This work was supported by NIH R21 CA253051-01, the Breast Cancer Research Foundation, NIH T32 5T32HL007917-22 and the Nile Albright Research Foundation.)

#1501 Engineering tissue models to elucidate prostate cancer bone metastasis dynamics.

B. Han, Z. Yang, S. Zhao, G. Liang, B. X. Hoang, J. Fang;
Keck School of Medicine of USC, Los Angeles, CA

Prostate cancer (PCa) ranks as the second most frequently diagnosed cancer in men and the fifth leading cause of male cancer-related deaths globally Advanced PCa exhibits a propensity for bone metastasis which significantly contributes to morbidity. It is challenging to understand its mechanisms and develop effective treatments due to complicated tumor microenvironments. The current study addresses this gap by focusing on the construction of in vitro and in vivo models to mimic tissue-specific microenvironments resembling primary prostate tumor sites and metastatic bone tissue, shedding light on the complex processes of cancer cell dissemination, osteomimicry, and bone metastasis. To recapitulate the complex interplay between primary tumor sites and bone microenvironments, the study employs a combination of tunable extracellular matrix mechanics, bone-derived growth factors, and bone marrow-derived stromal cells. These engineered niches emulate the contexts of both primary tumor and bone tissue. LNCAP-C4-2B prostate cancer cells are introduced into these niches to analyze various aspects, including cell proliferation, osteoblastic differentiation, dissemination, and in vivo tumor formation. The study introduces a 3D organoid culture that mimics the pre-metastatic niche, providing a platform for studying PCa cell proliferation and dissemination. A negative relationship is observed between 3D matrix stiffness and cell proliferation, while a positive link is identified with cell dissemination. Bone matrix-derived soluble factors (BMSF) are identified as key modulators of LNCAP-C4-2B cell behavior, suppressing LNCAP-C4-2B proliferation but enhancing osteomimicry in vitro, Notably, bone marrow-derived stromal cells, primed with bone matrix-derived growth factors, amplify tumor cell proliferation and chemotaxis in vitro, contributing to increased tumor formation in vivo. In vivo experiments demonstrate BMSFs eliciting local inflammatory responses and inhibiting in vivo tumor formation. Moreover, osteogenic bone marrow stromal cells are shown to play a promotive role in LNCAP-C4-2B proliferation and migration, emphasizing the influence of the bone microenvironment on the prostate-to-bone progression of PCa cells. In conclusion, this study highlights the potential of the engineered tissue models for dissecting tumor progression and screening therapeutic interventions. By leveraging tissue-engineered soft and hard tissues, our approach offers a versatile toolbox for comprehensively investigating PCa progression and bone metastasis. These insights extend to potential therapeutic screening applications, providing a valuable resource for advancing our understanding of cancer pathogenesis and treatment strategies.

#1502 Deciphering the spatial and temporal dynamics of premetastatic niche in lung mediated by Treg and myeloid cell interactions.

Y. Tian[1], J.-R. Li[2], B. Zhu[1], J. Fradette[1], H. Chen[1], C. Li[1], L. Rodriguez[1], D. Kraushaar[2], L. Solis[1], A. Reuben[1], I. Wistuba[1], D. L. Gibbons[1], C. Cheng[2], J. Zhang[1];

[1]UT MD Anderson Cancer Center, Houston, TX, [2]Baylor College of Medicine, Houston, TX

Introduction: The lung is a frequent site for metastases, where pre-metastatic niches (PMN) form in anticipation of tumor cell arrival. A deeper understanding of the molecular and immune features underlying the PMN formation may facilitate developing innovative strategies to prevent and treat metastasis more effectively in its early stages.

Methods: In this study, we developed mouse models by subcutaneously implanting the 344SQ cell line, derived from the metastasis of a genetically engineered mouse model (GEMM) harboring *Kras*$^{G12D/+}$; *p53*$^{R172H/+}$ mutations, which reliably metastasizes to the lungs. We collected paired samples of the subcutaneous tumors, peripheral blood mononuclear cells (PBMCs), and lung tissue at pre-metastatic, early-metastatic, and late-metastatic phases. These samples were subjected to single-cell RNA sequencing (scRNA-seq), single-cell TCR/BCR sequencing (scTCR/BCR-seq), and spatial gene expression profiling with 10X Genomics Visium technology.

Results: ScRNA analysis revealed large-scale comprehensive longitudinal changes in cell components throughout the invasion and metastasis cascade, which were validated by spatial gene expression. Furthermore, analysis of Visium data deduces the spatial information of these dynamic changes.We identified a subset of tumor-associated Tregs (TA_Tregs, enriched in the subcutaneous tumor tissues) that existed in small amounts in the lung tissue in the pre-metastatic phase when there are no tumor cells detectable in the lung. These cells were characterized by high expression of Treg-associated suppressive genes (Tnfrsf9, Tnfrsf4, Tnfrsf18, Traf1, Nfkbia), inhibitory molecules (Ikzf2, Il2ra, Tight, Pdcd1), cytokines and chemokines (Ccr5, Ccr8, Ccl5, Cxcr6) and other Treg effector molecules (Id2, Hif1a, Rora, Il1r2, Itgav, Stat1, Icos, Areg). The scTCR-seq results and trajectory analysis revealed the TA_Tregs might derive from minor clones of lung resident Tregs (LR_Tregs) and play an active role in remodeling an immunosuppressive microenvironment by closely interacting with other cell components in the TME. We also observed a significant alteration in the ratio of macrophage subpopulations between Macro_Spic and Macro_Vcan. This ratio exhibited a continuous decrease in lung tissues, which could be an early indication of the initiation of pre-metastatic niche (PMN) conditioning.

Conclusion: By simultaneously characterizing cellular gene expression, immune repertoires, and their corresponding spatial information, we revealed the dynamic changes of the lung tissue microenvironment (LTME) during from a normal state to pro-metastasis state at single-cell resolution. The LTME of metastatic organs may be primed before the establishment of metastasis.

#1503 Melanoma-derived lymphatic extracellular vesicles suppress dendritic cell differentiation and maturation in the sentinel lymph node.

S. Suman[1], W. K. Nevala[1], J. W. Jakub[2], R. Guo[2], A. A. Leontovich[1], R. M. Moore[1], C. L. Atherton[1], L. Geng[1], J. E. Johnson[1], S. A. McLaughlin[2], S. N. Markovic[1],

[1]Mayo Clinic, Rochester, MN, [2]Mayo Clinic, Jacksonville, FL

Spread to regional lymph nodes is the most common site of metastasis from melanoma and almost all solid tumors. Lymphatic metastases begin in the first lymph nodes draining from the primary tumor, i.e., the sentinel lymph nodes (SLN), preceded by the development of the premetastatic niche (PMN) initiated by primary cutaneous melanoma. Melanoma mediators are known to play a critical role in developing the PMN through the immune subversion in SLN. The DCs are a vital component of LN immunity that directly relates to eliciting T-cell functions. Our multiplex immunofluorescence (MxIF) analysis of SLNs indicates significantly decreased levels of DCs and cytotoxic-T cells in both core and interface areas of tumors in recurred patients treated with immunotherapy compared to non-recurred melanoma patients. The goal of this study is to determine whether the lymphatic extracellular vesicles (L-EVs) of melanoma patients regulate DC tolerization in SLN in order to stimulate the development of PMN. To identify whether L-EVs stimulate DC suppression, we extracted L-EVs from the lymphatic fluid of patients with melanoma downstream of primary cutaneous melanomas, compared it with controls (non-malignant post-operative fluid collected from the lymph node dissection field, and evaluated their effect on DC maturation by challenging these L-EVs in monocytic (CD14+) and hematopoietic stem cells (CD34+) cells. We found that L-EVs derived from melanoma patients suppress differentiation of CD11c+HLA-DR+ DCs and their maturation (defined by CD83 and CD86) compared to control L-EVs in CD14+ based DC maturation assay. We also found a reduction of conventional type 1 DC (cDC1) in CD34+-based DC maturation assay those challenged with patients' L-EVs compared to control. To understand the mechanism of DC suppression in patients' L-EVs, we also conducted a total RNA sequencing analysis of subsets of DCs from maturation experiments to evaluate differently regulated transcriptomic profiles. The gene ontology analysis indicates that patient-derived L-EVs interfere with tRNA processing, oncostatin M & IL-10 signaling, and other immunoregulatory pathways to alter the hematopoietic cell lineage pathways in the DC maturation. Furthermore, the proteomic analysis of L-EVs also indicated several differentially regulated cargo-identified proteins in patient L-EVs, which are associated with immunomodulation, including regulation of DC function compared to control L-EVs. In conclusion, our study revealed that the patient's L-EVs carry differential proteomic cargoes secreted by cutaneous melanoma, which may be involved in regulating DC differentiation and maturation to diminish their functions and support the developing PMN in SLN.

#1504 Tumor microenvironment-mediated regulation of early dissemination and colonization in breast cancer via BAZ2A-containing remodeling complexes.

Miriam Kokal-Ribaudo[1], Nora Jahnen[2], Saba Sameri[1], Fulvia Ferrazzi[3], Renato Liguori[3], Christoph A. Klein[1], Gernot Langst[2], Hedayatollah Hosseini[1]

[1]Experimental Medicine and Therapy Research, University of Regensburg, Regensburg, Germany,[2]Biochemistry Center Regensburg, University of Regensburg, Regensburg, Germany,[3]Bioinformatics and Computational Pathology, University of Erlangen, Erlangen, Germany

The molecular mechanisms governing invasion, dissemination, extravasation, and early metastatic colonization remain incompletely understood. In the BALB-neuT mouse model, we found that most metastases originate from disseminated cancer cells (DCCs) that left the primary site early in tumorigenesis, i.e. when lesions are still small. Consequently, we investigated whether cellular density and the tumor microenvironment synergize to generate the plasticity needed during metastasis.

RNA-sequencing analyses of murine breast cancer cells in low cellular density (LD) and high cellular density (HD) conditions revealed distinct profiles of differentially expressed genes. Notably, we identified the enrichment of ribosomal RNA (rRNA) and chromatin remodeling pathways in LD conditions. Interestingly, once these cells were treated with Wnt4 and Rankl, factors secreted by the tumor microenvironment, the expression profile of genes involved in proliferation, migration and stemness as well as epigenetic-related factors changed drastically. Specifically, cells in LD conditions treated with Wnt4 and Rankl displayed induced migration and stemness phenotypes, whereas under HD conditions, these signals induced proliferation. Among the chromatin-remodeling pathways, we found that BAZ2A along with the rRNA regulating network were primarily upregulated in migratory cancer cells. Immunostaining of primary and metastatic lesions in murine and human breast cancer samples showed an upregulation of BAZ2A in early/microlesions compared to more advanced and proliferative macroscopic lesions.

Taken together, these results indicate that cell density, tumor microenvironmental factors and BAZ2A-containing chromatin regulating complexes play pivotal roles in regulating cancer cell plasticity in breast cancer. Additional sequencing and functional analyses will be performed to dissect the specific components of this mechanism and evaluate their impact on the *in vivo* colonization of breast cancer models.

#1505 Unraveling diepafitaxis: Investigating ECM stiffness and microarchitecture in tumor spheroid migration.

H.-P. Chen, Y.-C. Tsai, T.-Y. Tu;
National Cheng Kung University, Tainan City, Taiwan

Background: Metastasis, accounting for up to 90% of cancer-related deaths, remains one of the least understood aspects of cancer progression. Recent research has shifted focus from solely biological hallmarks to the physical characteristics of cancer, such as the stiffness and microarchitecture of the extracellular matrix (ECM), which play pivotal roles in metastatic advancement. We previously introduced the concept of 'diepafitaxis' to describe a unique mechanism driving the interface-mediated tropism of tumor spheroids at matrix-surface boundaries. This phenomenon suggests that cancer cells preferentially migrate along a 2D 'interfacial' track formed by heterogeneous 3D ECM structures, facilitating invasion and dispersion. However, the exact mechanisms by which interfacial components, stiffness, and structural attributes influence cell movement remain debated. To investigate this, we have developed a microfluidic chip with a precisely controlled stiffness of the hydrogel matrix-matrix interface (MMI), aiming to shed light on specific diepafitatic behaviors.
Method: We developed a polydimethylsiloxane (PDMS)-based microfluidic chip using a traditional photolithographic process. This chip features three channels, with the center channel designed to precisely control various MMI stiffness combinations: stiff vs soft (t-o), stiff vs stiff (t-t) and soft vs soft (o-o). MDA-MB-231 breast cancer spheroids (BCS), representing an in vitro tumor model, were embedded in the top gel. We observed the dynamic behavior of these cancer spheroids over a 24-h period using differential interference contrast (DIC) microscopy.
Result: The study revealed that BCS exhibited more pronounced dispersion in a soft homogeneous ECM compared to a stiff ECM in 3D environments. Interestingly, when BCS were near an MMI, a stiffer MMI (t-t) significantly enhanced BCS invasiveness and single-cell migration, more so than t-o, and notably more than o-o. We previously described this phenomenon as '2.5D migration,' where cells migrate in a ventral 2D manner within a sandwiched 3D gel structure. This diepafitatic behavior was further analyzed for its response to gravitational effects and the influence of chemotaxis, induced by introducing VEGF on one side of the microfluidic channel.
Conclusion: Conclusively, our study demonstrates that the stiffness and structure of the ECM, particularly at MMI, significantly influence the invasive behavior and migration patterns of BCS, underscoring the critical role of mechanical microenvironments in cancer metastasis.

#1506 Diminished migration potential of MDA-MB-231Br (brain-seeking) breast cancer cell line with integration of keratin 18 gene.

A. Johnson[1], T. Liu[2], P. Lockman[3], G. Szalai[1];

[1]Burrell College of Osteopathic Medicine, LLC, Las Cruces, NM, [2]West Virginia School of Osteopathic Medicine, Lewisburg, WV, [3]West Virginia University School of Medicine, Morgantown, WV

Triple-negative breast cancer is considered to have one of the poorest prognostic outcomes of the breast cancer subtypes, with brain metastasis resulting in a survival rate of less than a year. Determining and eventually targeting the cause of the triple-negative breast cancer cells that seek the brain would improve life expectancy and quality of life by preventing the ramifications of brain pathology. Through a novel mouse model, previous research has demonstrated that one sub-line of the MDA-MB-231 (triple-negative breast cancer cell line) cells, MDA-MB-231Br, preferentially metastasizes to the brain. Additionally, lower levels of expression of the keratin 18 gene were observed in the MDA-MB-231Br cells, which prompted the analysis of the transcriptional control of the keratin 18 gene. In our previous study, we analyzed the pattern of chromatin occupation of transcription factors FLI1 and ETS1 to understand the transcriptional control of keratin 18 within the parental MDA-MB-231 cell line and MDA-MB-231Br brain-seeking counterpart. Notably, the ETS1 transcription factor was enriched in the MDA-MB-231Br cells, and the FLI1 transcription factor was enriched in the MDA-MB-231 cells. In this study, using transient and stable transfection, we incorporated keratin 18 cDNA into the MDA-MB-231Br cells and examined the effect on their migration capabilities. We hypothesized that with the introduction of keratin 18 cDNA into the MDA-MB-231Br cells, their migration capabilities would match that of their parental counterpart.

The MDA-MB-231Br cells were cultured in the Burrell research laboratory, and transfections were performed using Lipofectamine™ 3000 Transfection Reagent by Thermo Scientific with GFP as a control. Migration assays were performed using a transwell migration assay (Millipore) and with a wound healing assay. Ultimately, our results from both migration and wound healing assays demonstrated a diminished migration capability after keratin 18 was re-introduced into the MDA-MB-231Br cells through transfection. In the wound healing assay, the MDA-MB-231Br cells transfected with keratin 18 closely resembled the pattern of migration demonstrated by the parental MDA-MB-231 cells, while the MDA-MB-231Br cells transfected with GFP followed the pattern of the untouched MDA-MB-231Br cells. Additionally, the migration assay showed significantly less migratory capability of the MDA-MB-231Br cells expressing keratin 18 compared to the MDA-MB-231Br cells expressing GFP as a control ($p < 0.05$). The invasion capabilities of these cells with and without the presence of keratin 18 will be evaluated next to further elucidate the effects of re-expressing keratin 18.

#1507 Involvement of GABAergic signaling in enhanced tumor cell invasion in a mechanically dynamic tumor microenvironment.

C. Strelez[1], R. Perez[1], J. S. Chlystek[1], C. Cherry[2], B. Haliday[3], A. Yoon[1], C. Shah[3], R. X. Sun[1], R. Lau[1], A. Schatz[1], J. Neman[4], H. Josef-Lenz[3], J. Katz[1], **S. M. Mumenthaler**[3],

[1]Ellison Institute of Technology, Los Angeles, CA, [2]C M Cherry Consulting, Baltimore, MD, [3]USC - University of Southern California, Los Angeles, CA, [4]University of Southern California, Los Angeles, CA

Metastasis is a major contributor to cancer morbidity and mortality. However, studying this complex, multi-step, multi-organ process is challenging. There is a pressing need to dissect the contributions of the tumor microenvironment (TME) on this process in a controlled and precise manner. Fortunately, the utilization of microfluidic “organs-on-chips” (OOC) in cancer research is facilitating such investigations. Moreover, by combining organoids and organs-on-chips we can enhance the progress of these studies in a patient specific manner. In this study, we have developed a cancer-on-chip model aimed at investigating early metastatic spread within the colon milieu. To achieve this, we employ colorectal cancer (CRC) cell lines as well as patient-derived CRC organoids chosen from our biorepository to encompass diverse representations across race/ethnicity, sex, and mutational profiles. The tumor cells are introduced into the upper chamber of the OOC model, while human microvascular endothelial cells (HIMECs) are introduced into the lower chamber to establish a tube-like structure resembling a blood vessel. These two chambers are separated by a porous membrane, and the chip is flanked by vacuum chambers to introduce stretch-like motions, simulating peristalsis in the gastrointestinal track.

Creating a mechanically dynamic microenvironment facilitates the exploration of neurotransmitters and their impact on tumor cell behavior. Recent studies have suggested that tumor cells may exploit physiological processes, such as neurotransmitter signaling, to their benefit. By utilizing mass spectrometry-based metabolomics we detected dynamic and patient organoid-specific changes in neurotransmitter levels (i.e., serotonin, aspartate, glutamate, γ-aminobutyric acid (GABA)) in the effluent of our CRC-on-chip model. Coupled with live-cell imaging, we discovered tumor cell-derived GABA, a major inhibitory neurotransmitter, serves as an energy source for supporting tumor cell intravasation. This finding was most pronounced in KRAS-mutant tumor cells and further supported by analysis of CRC patient samples from The Cancer Genome Atlas (TCGA) database. We were able to reverse the GABA-mediated invasion effect by inhibiting 4-aminobutyrate aminotransferase (ABAT), the enzyme responsible for GABA catabolism. In summary, our cancer-on-chip model holds promise for exploring various aspects of the metastatic process and uncovering potential therapeutic targets, such as neurotransmitters.

#1508 Membrane heparan sulfate proteoglycans work with cadherins to establish the directional orientation of migrating cancer cells.

Lorenzo Depau, Jlenia Brunetti, Chiara Falciani, Marta Garfi, Maria Francesca Paolocci, Alessandro Pini, **Luisa Bracci**

Department of Medical Biotechnologies, University of Siena, Siena, Italy

A role of heparan sulfate proteoglycans (HSPGs) in cancer cell differentiation, proliferation and migration has been recognized and related to their ability to specifically interact with growth factors, morphogens, and extracellular matrix proteins, mainly through sulfated groups on their glycosaminoglycan (GAG) chains. Due to the considerable diversity of HSPGs and of their GAG chains, and to the lack of specific ligands, a precise molecular characterization of the biological role of HSPGs in cancer cells is still lacking. HSPGs, besides working as coreceptors for growth factors and morphogens, may have a determinant and autonomous role in cancer signaling events, regulating cell adhesion, migration, and invasiveness. Being overexpressed and over sulfated in cancer cells, HSPGs may become attractive tumor targets for cancer diagnosis and therapy. We had used the tetra-branched peptide NT4, which binds sulphated GAG chains of HSPGs, to validate HSPGs as potential tumor associated antigens in different human solid tumors. The same NT4 peptide had been tested as a tumor targeting agent for either cancer cell imaging or therapy, in vitro and in vivo [1]. Once identified the sulfated GAG specificity of NT4, the peptide has also been used as a specific tool for studying the role of HSPGs in cancer cell migration and invasiveness, with the aim of proposing HSPG as potential drug targets for interfering with cancer invasiveness and metastatic potential [2,3]. We found that NT4 inhibits adhesion, oriented migration, and colony formation in different human cancer cell lines. We investigated the role of HSPGs in migration of different human cancer cell lines, displaying either single-cell mesenchymal migration (PANC-1 pancreas adenocarcinoma, and MDA-MB-231 breast adenocarcinoma) or collective migration (MCF-7 breast adenocarcinoma). After assessing the expression of HSPG and of E- and N- cadherin in each cell line, their specific cellular distribution was detected by confocal microscopy in migrating cells, in wound healing experiments. We found that distribution of either E- or N- cadherins on the membrane of migrating cells is complementary to that of HSPG. This is particularly clear in collective migration, where HSPGs are exclusively located on the migration front of leader cells, whereas cadherins are only expressed by follower cells. Our results suggest that HSPG may have a crucial role in defining the front of migrating cells, while cadherin-mediated cell-cell contacts on the opposite site, may contribute to inducing protrusion formation at the front of migrating cells, as already suggested [4]. [1]- Brunetti J et al. Sci. Rep. 2015, 5, 17736; [2]- Brunetti J et al. Sci. Rep. 2016, 6, 27174; [3]- Depau L et al. J Med Chem 2020, 63, 15997; [4]- Grimaldi C et al Nat Commun 2020, 11, 5397

#1509 Microglial dominance in glioma dissemination: Unraveling TAMs' impact and therapeutic implications through modulating cathepsin activity.

S.-Y. Wu, C.-S. Chiang;
National Tsing-Hua University, Hsinchu, Taiwan

Introduction: It is well known that tumor-associated macrophages/microglia (TAMs) play a vital role in brain tumor progression. Our previous studies suggested that the activated microglia could reduce the cytotoxic effect of chemotherapeutic drugs on glioma cells in a 2D/3D model. This study delves into TAMs within diverse brain TME regions, emphasizing the distinction of resident microglia from infiltrating macrophages in invasion areas and their role in glioma migration and invasion.

Material and Method: We employed the murine orthotopic astrocytoma model (ALTS1C1), dissecting brain tumor tissues into normal, invasion, edge, and core regions. Immunofluorescence staining, utilizing TMEM119 and CD68 markers to identify resident microglia and infiltrating macrophages, respectively. The IHC results were analyzed with QuPath software and validated via flow cytometry. Microglia (BV2) and macrophage (RAW264.7) cell lines were directly co-cultured with ALTS1C1 in 2D and 3D migration/invasion models. Bulk RNA sequencing analysis unraveled the differences between BV2 and RAW264.7. Bone marrow-derived macrophages (BMDM) were used for the TAMs activation test, and the cathepsin inhibitor, E64, was applied to elucidate cathepsin's role in microglia within co-culture models.

Results: The IHC results reveal more TMEM119^{+} microglia than CD68^{+} infiltrating macrophages in the tumor invasion area. On the other hand, there are more CD68+ infiltrating macrophages than TMEM119^{+} microglia in the tumor core regions, signifying a specific role of microglia in tumor invasion. Flow cytometry further supported that more CD11b^{+}CD45^{low} microglia prevalence in tumor surrounding tissues than in tumor core. ALTS1C1 astrocytoma cells, in the presence of microglia, exhibited more increased invasion and migration ability than the presence of macrophages in 2D/3D models. RNA sequencing highlighted M2 activation and cathepsin gene upregulation in microglia over macrophages. M2-polarized TAMs enhanced 2D migration, while cathepsin inhibition significantly decreased glioma's 3D invasion potential.

Conclusion: This study identifies microglia as primary TAMs in brain tumor invasion areas and their roles in glioma cell survival and dissemination. Notable differences in activation states and the critical impact of cathepsin in microglia for their roles on brain tumor invasion and survival offer promising therapeutic avenues. Targeting cathepsin in microglia emerges as a novel glioma prevention and treatment strategy. These findings contribute valuable insights to enhance clinical interventions for glioma patients.

#1510 Cell-cell contacts regulate HER2 cellular localization and the transitions between migration and proliferation in breast cancer cells.

H. Hosseini[1], S. Sameri[1], S. Shahrivari[1], C. Fisch[1], M. Kokal[1], M. Schletter[1], P. S. Hahn[1], L. Seider[1], M. Schubel[1], D. Das[2], M. Hoffmann[2], C. Werno[2], K. Weidele[2], V. Milosevic[3], A. Ostman[3], S. Sarhadi[4], J. Wegener[5], S. Michaelis[5], F. Weber[1], A. Bruckmann[1], E. R. Tamm[1], Y. Li[6], C. A. Klein[1];

[1]University of Regensburg, Regensburg, Germany, [2]Fraunhofer Institute for Toxicology and Experimental Medicine ITEM, Regensburg, Germany, [3]University of Bergen, Bergen, Norway, [4]Technical University of Munich, Munich, Germany, [5]Fraunhofer Institute for Electronic Microsystems and Solid State Technologies EMFT, Regensburg, Germany, [6]Shenyang Pharmaceutical University, Shen Yang, China

Introduction: Epithelial-to-mesenchymal transition (EMT) is widely recognized as the primary mechanism regulating invasion and metastatic dissemination in carcinomas. In contrast, the mechanisms triggering single disseminated cancer cells (DCC) to reacquire their epithelial identity at ectopic sites, initiating metastasis formation, remain unclear. Since we had previously noted that HER2 expression levels and cellular density impact on migration and proliferation, we sought to determine whether they are involved in molecular mechanisms regulating transitions between proliferation and migration.

Methods: To control HER2 expression levels we generated inducible cell models. Cell density was assessed by the number of cell-cell contacts or by the number of cells per area. Pathway analyses were performed by gene expression analysis, protein interactions by western blotting and mass spectrometry. Migration and proliferation were analyzed by functional assays including in vitro live cell imaging.

Results: Migrating epithelial cells undergo reduced protein trafficking, resulting in a perinuclear deposition of HER2. This was accompanied by increased calcium ion regulation via phospholipase-C in the endoplasmic reticulum (ER). Upon the establishment of cell-cell contacts, particularly between cells expressing desmosome cadherin proteins, HER2 is redirected to the cell surface through direct physical binding with desmoplakin, facilitating proliferation signals. Then, PIP2 to PIP3 is converted through the activation of the PI3K pathway, concomitant with the upregulation of PDPK1. The PH domain of PDPK1 exhibits a high binding affinity to PIP2 molecules. Consequently, membrane localization of HER2 significantly diminishes PIP2 availability for the PLC pathway, redirecting cells towards proliferation. Patient sample analysis confirmed the loss of membrane-bound HER2 in solitary circulating tumor cells (CTCs), which was paralleled by increased plakoglobin, elevated ZEB1, and reduced KI67 protein levels.

Conclusion: Cell-cell contacts determine the cellular localization and function of growth factor receptors like HER2. Single disseminating cancer cells therefore need to establish such contacts at metastatic sites to activate proliferation programs. Our data are in line with findings that circulating tumor cell clusters are associated with higher metastatic rates, the impact of specific metastatic niches for outgrowth and have implementation for the targeting of single DCC.

TUMOR BIOLOGY: Immune Cells in the Tumor Microenvironment 1
Poster Session

#1514 A novel workflow to assess the T-cell and patient-derived organoid interaction.
Z. Tong, A. Lim, O. Sirenko;
Molecular Devices, LLC (Moldev), San Jose, CA

Immunotherapy is increasingly popular as a type of cancer treatment. These therapies include the use of Chimeric Antigen Receptor-engineered T-cells (CAR T-cells), tumor-infiltrating lymphocytes (TIL), and other genetically modified T-cells to specifically target the cancer cells. Although much success has been achieved with immunotherapy for treatment of blood cancers, its efficacy remains limited in solid tumors. One of the reasons for the low success rate is attributed to the solid tumor microenvironment (TME) where suppressive cytokines limit the tumor killing ability of T-cells. Thus, understanding the role the TME plays in T-cell responses is essential for the development of effective cancer therapies. The benefits of using 3-dimensional (3D) PDOs lie in the physical and chemical cues present within the TME that cannot be mimicked in traditional 2D monolayer cultures. Studies show that PDOs show similar responses to drugs as original tumors, suggesting the value of using PDOs to improve therapeutic outcomes. Thus, PDOs can provide more relevant physiological and pathological cancer models that recapitulate the basic features of primary tumors and is more suited for assessing the effectiveness of T-cell killing than 2D cell models. Despite the benefits associated with the use of PDOs, there are significant barriers to widespread adoption of PDOs in drug discovery. Organoid production is a costly and highly labor-intensive process. Moreover, organoid culture is a skilled manual process, and thus there can be significant variability between operators. To address the challenges associated with the use of PDOs in large scale applications, a semi-automated bioprocess has been developed for the large-scale expansion of assay ready organoids. Here, we developed a method to assess the effectiveness of T-cell invasion in solid tumors using patient derive organoids (PDOs). Using bioreactor expanded patient-derived colorectal cancer organoids (CRCs), activated PBMCs (human peripheral blood mononuclear cells) stained with CellTracker were added to CRCs (stained with MitoTracker) in a 96well microtiter plate and monitored on every 4 hours for 3 days using high content imager. To quantify T-cell invasion, we developed an image analysis method to measure the distance of each T-cell to the nearest organoid (interaction distance). We find that stimulated T-cell resulted in smaller interaction distance than non-stimulated T-cells. The results demonstrate the utility of the bioreactor-expanded organoids in large scale T-cell based screens.

#1515 Tertiary lymphoid structures restrain cancer evolution by supporting stem-like CD8+ T cells for sustained anti-tumor immunity.

P. Wang[1], C. Zhou[2], Z. Wei[2], Y. Wang[1], Y. Gao[2], F. Meng[2], J. Zhou[1], J. Fan[1], Q. Liu[2], Y. Sun[1];
[1]Zhongshan Hospital Fudan University, Shanghai, China, [2]School of Life Sciences and Technology, Tongji University, Shanghai, China

Currently, our understanding of the mechanism underlying the immune response on extending the survival of patients with aggressive tumors remains limited. In this study, we generated multi-regional genomic and transcriptional data coupled with digital pathology from 28 long-term survivors (LTSs) and 34 stage-matched short-term survivors, with intrahepatic cholangiocarcinoma (iCCA). Our investigation unveiled that mature tertiary lymphoid structures (TLSs) within the tumors of LTSs exerted significant immune pressure on the tumor, leading to the restriction in generating clonal mutations and increased subclonal diversity. Employing single-cell profiling, we identified significant enrichment of IgM^{+} naïve B cells and TCF7^{+} stem-like CD8^{+} T cells in TLS-positive tumors. Spatial profiling further highlighted that TCF7^{+} stem-like CD8^{+} T cells preferentially localized in TLS, facilitating reduced vulnerability to unfavorable environmental factors. Functionally, TCF7^{+} stem-like CD8^{+} T cells displayed strong capacity to differentiate into effector subsets while maintaining a diverse T-cell receptor repertoire. Mechanistically, we identified that naïve B cells promote activation and differentiation of stem-like CD8^{+} T cells within the TLS niche through IgM-FcμR axis, which primed these T cells for enhanced anti-tumor immunity. In summary, our findings underscore that TLS plays a pivotal role in orchestrating enduring and effective anti-tumor immunity, which yield strong immune stress on cancer evolution and ultimately contributing to better prognosis of patients.

#1516 Large scale, transcriptome-based analysis of TCR clonality reveals functional immunity in non-small cell lung cancer.

H. Yu[1], A. Magoulopoulou[2], M. Hori[3], A. Lindberg[1], M. Backman[1], H. Brunstrom[4], M. Marincevic Zuniga[1], J. Mattsson[1], A. Saito[5], K. Leandersson[4], M. Nilsson[2], R.-M. Amini[1], P. Micke[1], C. Strell[1];

[1]Uppsala University, Uppsala, Sweden, [2]Stockholm University, Stockholm, Sweden, [3]Kanazawa University, Kanazawa, Japan, [4]Lund University, Lund, Sweden, [5]The University of Tokyo, Tokyo, Japan

Tumor-related T-cell activation and subsequent clonal expansion are essential for an effective anti-cancer immune response. Thus, quantifying the clonal distribution of T-cells in cancer tissue from patients might provide prognostic and predictive information, particularly in high immunogenic tumors like non-small cell lung cancer (NSCLC). We evaluated TCR clonality in the tumor microenvironment of NSCLC, its relation to the *in situ* immune phenotype, and its clinical impact in a cohort of 182 resected NSCLC patients. The α and β TCR clones were determined based on RNA sequencing data, and the Gini index was used to weight individual clonal distribution. We used matched FFPE cancer tissue for multiplex immunofluorescence cell analysis and *in-situ* sequencing of T-cell clones. The analysis revealed a broad spectrum of TCR clonality patterns, including tissue with high TCR diversity and high evenness (low Gini coefficient) and tissue with clonal dominance with low evenness (high Gini coefficient). Highly expended clones were detected in 15/182 patients, whereas 43/182 revealed no clonal enrichment. A low TCR clone evenness (high Gini coefficient) was significantly more frequent in normal lung areas than in the corresponding tumor areas (n=20, p=0.02). In the cancer tissue, a high Gini index further correlated with high tumor mutational burden, indicating neoantigen-induced T cell clone expansions. Correspondingly, high TCR clonality was associated with an inflamed tumor phenotype associated with PD-1+ immune cells, CD3+, CD8A+, CD163+, and CD138+ cells, as well as higher expression of genes connected to immune activation (PRF1, GZMB, GZMH) and T cell exhaustion (PD-L1, LAG3, TIGIT). Cancer tissue with dominant T-cell clones also showed higher numbers of mature tertiary lymphoid structures with germinal centers. *In situ* sequencing suggested a close spatial relation between specific T cell clones and tumor cells. Finally, NSCLC patients with dominant T-cell clones showed strong responses and longer survival when treated with immune checkpoint inhibitors. This suggests that TCR clonality analysis is a strong candidate for precision diagnostics. Plausibly, the dominant clones found in NSCLC are responsible for a specific but malfunctioning anti-tumor response that can be unleashed by immune checkpoint inhibition.

#1517 Tc1 cytotoxic T-cells and Th1 helper T-cell rich tumor microenvironment is a hallmark of MSI colorectal cancers.

T. Mandelkow, Z. Huang, E. Bady, J. H. Muller, G. Sauter, J. Ebner, M. Lennartz, N. Gorbokon, R. Simon, M. Kluth, C. Hube-Magg, S. Minner, N. C. Blessin; University Medical Center Hamburg-Eppendorf, Hamburg, Germany

Background: Microsatellite instability (MSI-h) is a strong biomarker to predict response to immune checkpoint therapy and patient's outcome in colorectal cancer. Although enrichment of distinct T-cell subpopulations, such as type 1 cytotoxic T-cells (Tc1) or type 1 helper T-cells (Th1), have been identified to impact patient's outcome and response to immune checkpoint therapy, only little is known about the underlying changes in the composition of the immune tumor microenvironment.

Material and Methods: To assess the density, composition, degree of functional marker expression, and spatial interplay of T-cell subpopulations in 93 MSI and 1153 microsatellite stable (MSS) colorectal cancers, a tissue microarray as well as large sections were stained with antibodies directed against CD3, CD4, CD8, FOXP3, T-bet, GATA3, RORγT, BCL6, CD27, CD56, TIM3, PD-1, CTLA-4 Granzym B, and Ki67 using our BLEACH&STAIN multiplex fluorescence immunohistochemistry approach. A deep learning-based framework comprising two different convolutional neuronal networks (U-Net and DeepLabv3+) was used for image analysis.

Results: The composition of Type 1 (T-bet$^{\pm}$), Type 2 (GATA3$^{\pm}$), Type 17 (RORγT$^{\pm}$), NKT-like (CD56$^{\pm}$), regulatory (FOXP3$^{\pm}$), and follicular (BCL6$^{\pm}$) cytotoxic (CD3^{+}CD8$^{\pm}$) or helper (CD3^{+}CD4$^{\pm}$) T-cells showed marked differences between MSI and MSS patients. For instance, the density and proportion of Tc1 as well as Th1 was significantly higher ($p<0.001$ each) in MSI compared to MSS patients. In contrast, the density and composition of Tregs, Th2, Th17 T-cells was significantly lower in MSI compared to MSS patients in the intraepithelial tumor compartment. In addition, among the MSI colorectal cancers, NKT-cells showed the highest level of Granzyme B that was significantly higher than in MSS patients ($p<0.05$). The degree of immune checkpoint expression (i.e., TIM3, PD-1, CTLA-4) was significantly higher in MSI compared to MSS patients for most T-cell subpopulations ($p<0.05$ each). The additional analysis of 10 large sections confirmed the observations from the TMA analysis and revealed that the alterations in the T-cell composition seen in the center of the tumor largely reflect the T-cell composition at the invasive margin in both MSI and MSS patients.

Conclusion: This study identified a higher proportion of Tc1 cytotoxic T-cells and Th1 helper T-cells accompanied by a paucity of regulatory T-cell subpopulations, Th17 and Th2 T- helper cells in MSI colorectal cancers compared to MSS patients.

#1518 Understanding the role of VISTA in regulating T cells function and the therapeutic potential of blocking VISTA in triple negative breast cancer.

M. Abudula, Y. Astuti, M. Raymant, T. Luckett, P. Freeman, M. Schmid, A. Mielgo Iza;
University of Liverpool, Liverpool, United Kingdom

Immune checkpoint inhibitors (ICIs) targeting immune modulatory molecules have been widely used and have shown therapeutic efficacy in treating multiple malignancies in the last decade. However, in triple-negative breast cancer (TNBC), only around 5 % of patients showed a durable response to ICIs. While the response rates were increased up to 10% by combining ICIs with conventional chemotherapy, the majority of the patients did not respond to the treatment. Thus, there is a need to improve our understanding of the mechanism underlying unequal response to ICIs in TNBC and develop/discover new treatments to improve patient outcomes. The lack of response to ICIs has been attributed to the increased infiltration of immunosuppressive cells (including MDSCs, neutrophils and TAMs), as well as the presence of additional immune checkpoint receptors/ligands that may further suppress cytotoxic T cells (CD8+ T cells) in the tumor microenvironment (TME). V-domain Ig suppressor of T-cell activation (VISTA) is one of the immune checkpoint molecules attracting increasing attention in the context of anti-tumor immunity due to its broad expression across various cancer types and increased expression upon development of immune checkpoint resistance. However, the role of VISTA in the anti-tumor immune response and its therapeutic potential in TNBC remains unclear. In our study, we observed that VISTA is expressed in TNBC patients, with higher expression in neutrophils and macrophages. In the Py230 murine breast cancer model, VISTA expression increased upon paclitaxel (PTX), anti-PD-L1 and paclitaxel combined with anti-PD-L1 treatment compared to the control group, suggesting its potential role as a resistance mechanism in further inhibiting T cells. In the Py230 model, VISTA blockade increased the infiltration and activation of CD8+ T cells, as evidenced by the higher number of CD8+ T cells, increased CD69+CD8+ T cells, and Granzyme B production, indicating that VISTA blockade improved CD8+ T cells mediated anti-tumor immunity. To functionally test the role of VISTA, we stimulated CD8+ T cells and co-cultured them with naïve macrophages or tumor educated macrophages in the presence or absence of VISTA blocking antibody. Tumor-educated macrophages showed increased immunosuppressive activity which is abrogated with VISTA blockade. Moreover, we found that the immunosuppressive effect of macrophages on T cell activation needs direct cell interaction between VISTA on macrophages and T cells. In conclusion, this study shows the mechanism of action of VISTA in the regulation of T cells mediated anti-tumor immune response, and provides the rationale for blocking VISTA in TNBC.

#1519 Effect of obesity on CD4$^+$ T cells in the tumor immune microenvironment of colorectal cancer.

M. Ando, K. Yamada, M. Saito, K. Yamashita, T. Tsuneki, Y. Adachi, T. Abe, T. Mukoyama, R. Sawada, Y. Koterazawa, H. Harada, N. Urakawa, H. Goto, H. Hasegawa, S. Kanaji, T. Matsuda, Y. Kakeji;
Kobe University Graduate School of Medicine, Kobe, Japan

Background: The number of new cases and deaths from colorectal cancer (CRC) is increasing rapidly, and obesity is considered one of the risk factors. Obesity-associated cancers are related to the overproduction of hormones, induction of reactive oxygen species (ROS) production by free fatty acids, and changes in the gut microbiome. Obesity also promotes immune cell dysfunction in the tumor immune microenvironment (TIME). The increase of fatty acid levels due to obesity causes metabolic reprogramming and decreases the cytotoxic activity of natural killer (NK) cells and CD8$^+$ T cells, which accelerate tumor progression. However, the impact of obesity on CD4$^+$ T cells in the TIME remains unclear. Therefore, this study aimed to clarify how obesity affected the number and the anti-tumor activity of CD4$^+$ T cells in CRC using mouse models.

Methods: Seven-week-old male C57BL/6J mice were randomly divided into two groups and fed the control diet (CD) or high-fat diet (HFD) for nine weeks. Blood samples were collected from the buccal vein of the mice every four weeks after feeding for analysis. MC38 CRC cells of 4×10^6 were subcutaneously inoculated in the middle of the backs of mice to analyze tumor progression. Three weeks after tumor cell inoculation, the mice were sacrificed, and the immune cells of the tumor, blood, and various organs were analyzed.

Results: After nine weeks of feeding, the HFD-fed mice had a significantly increased body weight compared to CD-fed mice. Flow cytometry results revealed that the number and frequency of CD4$^+$ T cells in the blood were significantly reduced in HFD-fed mice compared to those in CD-fed mice, and the expression of programmed death-1 (PD-1) in CD4$^+$ T cells in HFD-fed mice was significantly higher than that in CD-fed mice at eight weeks. Three weeks after tumor inoculation, HFD feeding accelerated tumor growth and decreased the survival rate. The number of CD4$^+$ T cells in the tumors was significantly reduced in HFD-fed mice compared to that in CD-fed mice (55.9 vs 18.2 cells/mg; 95% CI 14.9-60.3 cells/mg; $P = 0.006$). The number of CD8$^+$ T cells in the tumors was also reduced, which was more pronounced for CD4$^+$ T cells than for CD8$^+$ T cells. In addition, the production of cytokines such as IFN-γ and TNF-α was significantly reduced in CD4$^+$ T cells and CD8$^+$ T cells of HFD-fed mice. In a depletion analysis of CD4$^+$ T cells, the feeding-dependent acceleration of tumor growth was not observed in each group. This result indicated that CD4$^+$ T cells were involved in accelerating tumor growth due to HFD-induced obesity.

Conclusion: We showed that the reduced number and dysfunction of CD4$^+$ T cells due to obesity led to a decreased anti-tumor response of both CD4$^+$ and CD8$^+$ T cells, ultimately accelerating the progression of colorectal cancer. Our findings may elucidate the pathogenesis for poor outcomes of colorectal cancer associated with obesity.

#1520 A novel cluster of cytolytic alpha/beta TCR$^{\pm}$CD4^{-}CD8^{-}T cells originating from CD8$^{\pm}$T cells with potent innate-like T cell killing ability: implicating adoptive T cell transfer therapy for hepatocellular carcinoma.

Cheng-Heng Wu[1], Te-Wei Tseng[2], Chen-Yang Huang[3], Ping-Hsun Ou[4], Yi-Chen Lin[4], Pin-Jung Chen[4], Po-Ting Lin[4], Chan-Keng Yang[3], Wei Teng[4], Tsung-Han Wu[5], Yung-Chang Lin[3], Chun-Yen Lin[6]

[1]School of Medicine, Chang Gung University, Taoyuan, Taiwan, [2]Internal Medicine, Chang Gung Memorial Hospital, Taoyuan, Taiwan, [3]Division of Medical Oncology/Hematology, Chang Gung Memorial Hospital, Taoyuan, Taiwan, [4]Division of Gastroenterology, Chang Gung Memorial Hospital, Taoyuan, Taiwan, [5]General Surgery, Chang Gung Memorial Hospital, Taoyuan, Taiwan, [6]College of Medicine, Chang Gung University, Taoyuan, Taiwan

Tumor immunotherapies represent promising strategies for treating various cancers, including hepatocellular carcinoma. In this context, immune cells, including the adoptive T cell transfer treatment, become the focus of interests. Notably, alpha/beta TCR$^{\pm}$CD4^{-}CD8^{-}T (DNT) cells is a subgroup of T cells that is ignored for a long time but was re-focused recently. These DNT cells are a group of cells with opposite functions in different condition, including pro-inflammatory or suppressive functions and possibly originated from over-stimulation of peripheral CD4$^{\pm}$T cells/CD8$^{\pm}$T cells or a special group of T cells formed in thymus. In our research results, we have found these DNT cells increased in murine hepatoma model, especially in the tumor microenvironment. In addition, these DNT cells from tumor microenvironment of murine hepatoma possessed potent tumor-killing ability. Furthermore, we analyzed the transcriptome profile of T cells in tumor microenvironment by single cell RNAseq approach (CITE-seq). We found DNT cells could be categorized into two main clusters, one is cytolytic DNT cells, resemble the potent CD8$^{\pm}$T cells, and another is the CD4$^{\pm}$T cell-like DNT cells. These cytolytic DNT cells are not exhausted but with high expression of cytolytic molecule and low hypoxia-inducible factor-1alpha (HIF-1a) expression. By trajectory analysis, cytolytic DNT cells come from the conventional CD8$^{\pm}$T cells but following a unique developmental pathway that is different from the exhausted CD8$^{\pm}$T cells. Interesting, these cytolytic DNT cells also expressed high level of Fcer1g molecule, a marker of innate CD8+T cells. In addition, these DNT cells could be generated and expanded in-vitro by IL-15 without TCR activation. In conclusion, we identified a cluster of cytolytic DNT cells, originated from CD8$^{\pm}$T cells, exhibits innate T cells behavior and potent killing ability. In addition, these cytolytic DNT cells could be generated and expanded in-vitro for the adoptive T cell transfer treatment of hepatoma.

#1521 Chromatin remodeler ACTL6A in CD8$^{\pm}$ T cells promotes antitumor immunity.

B. Wu[1], W. Thant[1], E. Bitman[1], T. Liu[1], L. W. Ellisen[2];
[1]Harvard Medical School/Massachusetts General Hospital, Boston, MA, [2]Harvard Medical School/Massachusetts General Hospital, Ludwig Center at Harvard, Boston, MA

Chromatin remodeling plays a pivotal role in dictating epigenetic and transcriptomic regulation governing cytotoxic T lymphocyte differentiation and effector function. However, the regulatory mechanisms underlying chromatin remodeler assembly and actions remains unclear. Actin-like gene family members have been implicated in the organization of chromatin landscapes, however their role in T cell functional regulation remains unknown. We identified Actin-like protein 6A/Actl6a as the most upregulated gene within actin-like family members upon CD8$^{\pm}$ T cell activation across multiple species. Additionally, *ACTL6A* is highly expressed in human tumor-infiltrating CD8$^{\pm}$ mitotic tissue-resident memory T cells, suggesting a functional importance of *ACTL6A* in this subset. Deletion of mouse *Actl6a* in mature T lymphocytes impairs immune responses to transplanted syngeneic mouse tumors. T cell-specific *Actl6a* deletion mice exhibit a reduced effector memory population and attenuated cytotoxicity in their tumor infiltrating CD8$^{\pm}$ T cells. Heterozygous deletion of *Actl6a* displays an intermediate reduction of effector memory population and cytotoxicity between that of wildtype and homozygous knockout, indicating that ACTL6A acts in a dose-dependent manner to promote CD8$^{\pm}$ effector cell fate. T cell adoptive transfer further corroborates a CD8$^{\pm}$ T cell-intrinsic role of *Actl6a* on antitumor adaptive immunity. Currently, we are investigating the chromatin landscape and transcriptomic changes upon loss of *Actl6a* using ATAC-seq and RNA-seq. Furthermore, the dose dependency of Aclt6a on CD8$^{\pm}$ T cell effector function suggests that pharmacological or genetic approaches to increase Actl6a expression in CD8$^{\pm}$ T cells may have the potential to boost immune based anticancer therapies including CAR-T therapies.

#1522 Tumor-associated fibrosis leads to an increase in T-cell exhaustion and impairs tumor control in non-small cell lung cancer.

U. Y. Panni, V. Shenoy, B. Knolhoff, F. Ahmed, B. Herzog, W. G. Hawkins, J. A. Olson, D. G. DeNardo;
Washington University in St. Louis, St.Louis, MO

Lung cancer is the leading cause of cancer-related mortality with non-small cell lung cancer (NSCLC) being the most predominant type. Recent studies have shown the efficacy of anti-PD1 inhibitors which improved overall survival. However, this efficacy is limited to a subset of patients due to the intrinsic tumor resistance to immune checkpoint inhibitors. Our group recently demonstrated that tumor-associated fibrosis negatively correlates with T cell-mediated immune response in lung cancer. This is largely dependent on Col13a1-expressing cancer-associated fibroblasts (CAFs), which result in recruiting the immunosuppressive macrophages and regulatory T cells while limiting dendritic cells and CD8 T cell infiltration. Here, we characterize the effect of fibrosis on the TME including TILs and macrophages using an orthotopic KRAS and P53-driven murine NSCLC model (KPL86-mCher model) with FITC-induced fibrosis.Fibrosis significantly increased the number of cancer-associated fibroblasts and collagen density in KPL86-mCher lung tumors. Following carboplatin + pemetrexed and Anti-PD1 treatment, we observed no increase in tumor-infiltrating $CD4^+$ and $CD8^+$ T cells or decrease in tumor burden when compared with the non-fibrotic tumors. Rather, we observed a significant increase in exhausted T cells marked by high Tim3, PD1, and TOX in fibrotic KPL86-mCher tumors. Corresponding to these impaired T-cell responses, we found an increase in tumor-infiltrating alveolar macrophages with immunosuppressive phenotype under fibrotic tumor conditions. Our data suggests that tumor-associated fibrosis leads to an increase in CD8+ T cell exhaustion as well as immunosuppressive macrophage infiltration in our spontaneously derived murine model on NSCLC. Overall, this indicates that targeting tumor fibrosis may significantly improve the efficacy of immunotherapy which would have translational implications for patients with immunotherapy-resistant NSCLC.

#1523 The predictive potential of gamma-delta T cells and germinal B cells in cancer therapy for enhanced clinical outcomes.

A. Segura[1], **M. Dicome**[1], L. Song[2], X. S. Liu[3], A. Sahu[1];
[1]University of New Mexico Health Sciences Ctr., Albuquerque, NM, [2]Geisel School of Medicine at Dartmouth, Hanover, NH, [3]Dana-Farber Cancer Institute, Boston, MA

Introduction: Immune Checkpoint Blockade (ICB) therapy elicits clinical responses in a subset of patients in multiple cancer types, yet predicting response remains an open problem. While CD8-T cells remains to be focus, emerging evidence suggests role of other immune cell subtypes in favorable outcome of patients. This study presents the abundance of gamma-delta T (gdt) cell subpopulations in responders and non-responders. The analysis further contrasts differential abundances under immunotherapy and non-immunotherapy regimens across diverse cancers.
Methods: We performed joint analysis of data from 250 non-immunotherapy cohorts and 17 ICB cohorts. To infer differential abundance in each cohort, we first identified genes robustly upregulated in tumors of patients with favorable outcome, and then unbiasedly evaluated upregulated genes for enrichment for immune cell populations. The topmost differential abundant subpopulations were validated by de novo assembly and single cell analyses.
Results: Our analysis revealed similarities in the immune microenvironment across responders, irrespective of immunotherapy or non-immunotherapy modalities, strongly suggesting shared factors influencing response. Notably, gdt cells emerged as consistent predictors of better prognosis, being associated with favorable responses to ICB therapy and improved long-term survival in non-immunotherapy-treated cancer patients. Two independent validation approaches reinforce these findings. First, taking advantage of the fact that gamma and delta receptors are unique to gdt cells, we obtained precise estimates of gdt cells in tumors from their RNA-seq using de novo assembly. The assessment recapitulated our finding that favorable prognosis of tumors with of gdt cell levels. Second, analysis of several single-cell RNA-sequencing cohorts showed that patients with favorable prognoses consistently exhibit high gdt cell levels within tumors.
Conclusion: The study underscores a strikingly consistent responder immune microenvironment, whether under immunotherapy or non-immunotherapy setting, suggesting a shared response and resistance mechanisms. The likelihood of cross-resistance has implications when clinicians decide whether immunotherapy should be administered before or after the traditional therapies for patients. Our study also elucidates the role of gdt cells as potent biomarkers for ICB therapy and their broader significance in enhancing patient survival across various cancer types. Ultimately, these insights may refine patient selection and inform tailored treatment strategies, could elevating clinical outcomes in the realm of precision oncology.

#1525 Integration of high-plex tumor-Immune phenotyping and checkpoint interactions for deeper spatial characterization of human cancer tissues.

S. Bodbin[1], A. Viratham[2], R. Stad[2], **N. Ma**[2], A. Pratapa[2], N. Nikulina[2], J. Monkman[3], N. Jhaveri[2], H. Elofsson[1], S. Basu[1], A. Zieba-Wicher[1], A. Kulasinghe[3];
[1]Navinci Diagnostics, Uppsala, Sweden, [2]Akoya Biosciences, Marlborough, MA, [3]University of Queensland, Brisbane, Australia

Background: Immune evasion is a key cancer hallmark, and one of the primary mechanisms is the PD-1/PD-L1 checkpoint axis. While immunotherapies that target these interactions have reshaped cancer treatment, the variable efficacy in patients is not fully understood. Due to the weak correlation between PD-1/PD-L1 expression measured by single-plex assays and observed clinical outcomes, there is a need to understand protein interactions at the cellular and subcellular level. Proximity Ligation Assays, detecting spatial interactions between ligand-receptor targets, provide insights into the activation of signaling pathways. Coupled with high-plex spatial phenotyping with tumor and immune profiling biomarkers, the integration of cellular and functional information will be beneficial for a deeper characterization of the tumor microenvironment (TME), understanding immune responses, and identifying spatial signatures for patient stratification and targeted treatment strategies.
Methods: In this study, we phenotyped biopsies from head and neck cancer patients enrolled in immune checkpoint inhibitor therapies. We integrated Naveni® PD-1/PD-L1 proximity ligation assays and a customizable high-plex PhenoCode™ Signature Panel (CD3ε/CD8/CD20/CD68/PanCK) for high-throughput profiling of the TME utilizing the PhenoImager® HT 2.0 platform. Comprehensive bioinformatic analyses were conducted for whole-slide segmentation, identifying cellular phenotypes, spatial neighborhoods, functional interactions, and distinct spatial signatures via the open-source image analysis software QuPath.
Results: Our analyses revealed key differences in the localization of the PD-1/PD-L1 interactions within the TME of head and neck cancers. Areas of PD-1/PD-L1 interactions are associated with immune cell types on the periphery of the tumor and some within the tumor-infiltrating lymphocytes. The PhenoCode Signature panels helped resolve the localization of PD-1/PD-L1 interactions to immune cell types within the TME and provided a dual workflow for spatial co-localization of interacting receptor/ligand interactions and cell phenotypes within the TME.
Conclusions: By combining spatial immune profiling with Akoya's PhenoCode Signature panels and protein-protein interaction data from Navinci's Naveni® PD-1/PD-L1 assay, deep correlative insights of the TME can be applied to improve predictions of clinical outcomes. This innovative approach enriches our comprehension of underlying mechanisms and stands as a promising tool for refining patient selection and optimizing treatment outcomes in immunotherapy.

#1526 The distinct tumor microenvironment of advanced hepatocellular carcinoma with high PVR or high PD-L1 expression.

L.-C. Lu, Y.-H. Lee, T.-h. Liu, Y.-Y. Shao, A.-L. Cheng, C.-H. Hsu;
National Taiwan University Hospital, Taipei, Taiwan

Background: The combination of anti-PD-L1 and anti-VEGF has been the standard-of-care for advanced hepatocellular carcinoma (HCC), while additionally targeting TIGIT is under active investigation. We aimed to explore the expression and clinical significance of PVR (CD155), the ligand of TIGIT, within the tumor microenvironment (TME) of advanced HCC.

Methods: All HCC tumor specimens were obtained at the advanced stage of HCC. Immunohistochemistry (IHC) was employed to evaluate membranous staining of PVR and PD-L1 of tumor specimens, and semiquantitative scores with IHC 0, 1, 2, or 3 were given if < 1%, ≥1% but < 5%, ≥5% but < 10%, or ≥10% of tumor cells (TCs) and tumor-infiltrating immune cells (ICs) were PVR or PD-L1 positive. Selected tumor specimens underwent immune gene expression profiling using the nCounter Analysis System (NanoString Technologies, Inc.) with the PanCancer Immune Profiling Panel.

Results: The study enrolled 67 advanced HCC patients, with median age of 59.2 years (male:female = 57:10). Forty-eight (71.6%) of the patients were hepatitis B virus (HBV) surface antigen positive, and 23 (34.3%) had received sorafenib before the study. Thirteen (19.4%) and 18 (26.9%) tumor tissues showed positive PVR expressions (IHC scores ≥1) in TCs and ICs, respectively; Seventeen (25.4%) and 36 (53.7%) tumor tissues showed positive PD-L1 expressions in TCs and ICs, respectively. The expressions of PVR in TCs or ICs showed no association with clinical factors, such as sex, age, HBV infection, sorafenib treatment, or overall survival. Interestingly, in both TCs and ICs, the intensities of PVR and PD-L1 expression were inversely correlated for those with at least IHC scores ≥1 in either PVR or PD-L1 (TCs, $n = 26$, $r = -0.6966$, $p < 0.0001$; ICs, $n = 46$, $r = -0.4548$, $p = 0.0015$). Immune profiling of the selected tumor specimens showed that those with high PVR but low PD-L1 expressions had significantly lower CD8 T cells scores, lower cytotoxic cells scores, and lower CD8/Treg ratio than those with high PD-L1 but low PVR expressions.

Conclusions: There was an inverse correlation observed between expressions of PVR and PD-L1 in the advanced HCC tissues. The TME of those with high PVR expression was distinct from those with high PD-L1 expression. These findings may have important clinical implications for developing combination immunotherapy in advanced HCC. (This work is supported by grants from the Ministry of Science and Technology, Taiwan, MOST 110-2314-B-002-204-MY3).

#1527 Exploring the role of tertiary lymphoid structure in the tumor microenvironment of cholangiocarcinoma.

S.-Y. Chung[1], M.-H. Chen[1], Y.-C. Yeh[1], Y.-C. Chang[2], Y.-C. Wang[2];
[1]Taipei Veterans General Hospital, Taipei, Taiwan, [2]National Yang Ming Chiao Tung University, Taipei, Taiwan

Cholangiocarcinoma is the second most common hepatobiliary malignant tumor besides liver cancer, grows from bile duct epithelial cells. However, surgery is the only hope for most patients with cholangiocarcinoma, but the effectiveness of treatment is not outstanding. Even though other methods of treatment, such as chemotherapy and radiation therapy, have limited effects. The immunotherapy and precision treatment have become the latest expectations of patients. Here, we analyzed the TCGA and GEO database to classify the cold and hot tumor using hierarchical clustering. The MCP counter results demonstrated that two genes, MS4A1 and CD79A, could identify the hot and cold tumor subgroups after TCGA data training and similar results show in GEO database. We also performed the tissue array for 105 cholangiocarcinoma tissue samples and found patients with high expression levels of MS4A1 or CD79A have better disease free survival (DFS) and progression free survival (PFS) (p value =0.0131 and 0.0017). In addition, we tested the tertiary lymphoid structures (TLS) signatures in tissue array sections, which is associated with the present of MS4A1 and CD79A. The results shows that patients who received the immunotherapy with TLS signatures have longer overall survival (OS) and PFS (p value =0.017 and 0.006). Collectively, B cell lineages or TLS could be an ideal biomarker to lead the clinical treatment and wish can broader applications in other diseases.

#1528 Flowcytometric based approach to investigate prostate tumor microenvironment.

karishma sajnani, Sini Eerola, Konsta Kukkonen, Hanna Rauhala, Tapio Visakorpi, **Alfonso Urbanucci**

Faculty of Medicine and Health Technology, Tampere University, Faculty of Medicine and Health Technology, Tampere, Finland

Prostate cancer (PC) and its tumor microenvironment (TME) are heterogenous and evolving along with the treatment patients are exposed to. Modelling of the TME represents an attractive approach to understand how PC evolves and spreads. Flow cytometry is a technique for quantitative measurement of single cell profiling based on the cell surface as well as intracellular markers. We designed a flowcytometric based approach to investigate the interplay between the PC cells and immune cells in a direct coculture. Cells are fluorescently tagged with a cell tracer and the analysis is performed separately on the adherent and non-adherent cells. To optimize the readout method, we investigate the interplay between Jurkat cells and PC cells (LNCaP) as well as immortalized prostate epithelial cell models modified to mimic early events in prostate carcinogenesis (RWPE-1 cells overexpressing androgen receptor, RWPE-1-AR, and having PTEN deletion, RWPE-1-AR-PTENdel).Jurkat (suspension culture) cocultured with LNCaP (adherent culture) exhibited 40% decrease in viability but only 30% of LNCaP dying cell in the floating population compared to LNcaP only which is 60%. When Jurkat were activated using Phorbol 12-myristate 13-acetate (PMA), we observed an increase in LNCaP cell death. Jurkat viability was not impacted in presence of RWPE-1 neither when exposed to RWPE1-AR-PTENdel. In summary our Flowcytometric-based approach will help to understand the interplay between immune cells and prostate cancer cells.

#1529 Development of lymphoid aggregates in metastatic uveal melanoma tumors treated with tebentafusp.

T. Sato[1], C. Britton-Rivet[2], S. Khakoo[2], A. Easton[3], A. Kazachenka[2], L. Collins[2], E. Leach[2], A. Benlarech[2], S. Stanhope[2], M. O. Butler[4]; [1]Thomas Jefferson University, Philadelphia, PA, [2]Immunocore Ltd., Abingdon, United Kingdom, [3]University of Oxford, Oxford, United Kingdom, [4]Princess Margaret Cancer Centre, Toronto, ON, Canada

Tebentafusp (tebe), targeting gp100, is the first TCR-CD3 bispecific to demonstrate overall survival (OS) benefit and is approved for the treatment of metastatic uveal melanoma (mUM). We have previously shown B cell recruitment into the tumor associates with OS on tebe [1]. We explored further the formation of lymphoid aggregates (LA) within the tumor microenvironment in response to tebe. HLA-A*02:01+ 2L+ adult patients (pts) with mUM were treated with tebe (NCT02570308). Paired tumor biopsies were collected at baseline (n=70), after 3 doses of tebe (n=48), and at radiographical progression (n=17). Presence of B cells, T cells and macrophages was assessed by immunohistochemistry, using antibodies against CD20, CD3 and CD163 respectively, and digitally quantified. Using digital density analysis, aggregates of ≥10 CD20+ B cells within CD3+ T cell area in a 100µm radius were defined as LA. At progression pts were categorized by OS ≥12 or <12 months. Mean fold change (FC) was used. At baseline, B cells were detected in 90% of pts (median 5 B cells/mm^2) with those pts having no more than 2 LA/mm^2 (17% pts with 1 LA/mm^2 and 3% pts with 2 LA/mm^2). The median number of B cells in the biggest LA per sample was 24.B cells were recruited into the tumor after 3 doses of tebe (median 32 B cells/mm^2, FC 3, p=6.5e-05). The LA density increased up to 6 LA/mm2 (23% pts with 1 LA/mm^2, 8% pts with 2 LA/mm^2, 6% pts with 3 LA/mm^2 and 2% pts with 6 LA/mm^2) with a trend for an increase in LA size (median B cell number in biggest LA = 30, p = 0.67). Tumors with a low baseline CD163+ macrophage to CD3+ T cell ratio, which was previously associated with longer OS on tebe, tended to have more LA/mm^2 at baseline and on-treatment than those with a high ratio. At progression, pts with long OS had more B cells in the tumor compared to short OS (median 20 vs 2 B cells/mm^2; FC 5, p=0.05). Additionally, more pts with long OS had LA than pts with short OS (6/12 pts vs 1/5 pts respectively) with a density not exceeding 1 LA/mm^2. LA size was larger in pts with long OS compared to short OS (median B cell number in biggest LA 30 vs 10 respectively). LA in the short OS patient was found in the normal adjacent tissue compared to the LA in long OS patients which were located in the tumor and invasive margin. Tebe enhanced the formation of LA in the tumor microenvironment, notably in the low immunosuppressed tumors, which is consistent with the hypothesis that it results in epitope spread. These observations provide deeper insight into the mechanism of action of tebe and helps to explain prolonged survival of mUM pts beyond radiographical progression. [1] Greenshields-Watson A. et al., 619, SITC 2022

#1530 Tumor cell line-derived xenograft subtype shapes tumor microenvironment composition in BRGSF-HIS mice.

P. Martin-Jeantet, S. Hedir, F. Sonego, G. Martin, Y. Cherifi, **K. Thiam**;
genOway, Lyon, France

The relevance of preclinical models has vastly improved with mice bearing a human immune system, especially in the context of immunotherapy. BRGSF (Balb/C Rag2$^{-/-}$, IL2Rγ$^{-/-}$, SIRPαNOD and Flt3$^{-/-}$) is a highly immunodeficient mouse featuring reduced murine myeloid cells. BRGSF mice reconstituted with human cord blood CD34^{+} cells (BRGSF-HIS) develop functional lymphoid and myeloid compartments. This engraftment is stable for over a year (Labarthe *et al.*, 2019) and mice do not develop GvHD. Myeloid compartment can be transiently boosted with exogenous human Flt3L injections. In contrary to other models overexpressing human cytokines to develop human myeloid cells, Flt3L-treated BRGSF-HIS mice do not show side effects. BRGSF-HIS mice are permissive to mouse and human cancer cell lines engraftment and represent a valuable preclinical model to study cancer development and test novel therapeutics. Effect of Flt3L-induced boost on myeloid compartment is seen in a non-small cell lung cancer (A549) tumor model. A single boost prior to tumor cell inoculation associates with increased tumor-infiltrating T-cells (mainly CD8^{+} T-cells) and myeloid cells, and reduced tumor-infiltrating NK cells in the tumor microenvironment (TME). Human triple negative cancer cell (TNBC) MDA-MB-231 and human pancreatic adenocarcinoma HPAFII cell lines are widely used in cancer research and drug development. We show that upon implantation in BRGSF-HIS mice, *in vivo* growth of human cell line-derived xenograft (CDX) is CD34^{+} donor independent and the TME composition varies according to cell line used. As seen in TNBC patients (Zheng *et al.*, 2021); TME of MDA-MB-231 bearing BRGSF-HIS mice is enriched in myeloid cells, mostly CD206^{+}/CD163^{+} M2 macrophages. CD163-expressing M2 macrophages represent the main tumor-associated macrophages, and are known to promote breast cancer initiation, angiogenesis, invasion, and metastasis by generating an immunosuppressive TME. Interestingly, TME composition evolves over time, with increased T cells frequency in later stage (tumor volume over 1000 mm^3 compared to 500 mm^3) depicting cancer cell plasticity. Conversely, TME of HPAFII bearing mice is mainly composed of T cells enabling T cells-based therapy. Treatment of BRGSF-HIS mice bearing HPAFII tumor cells with combotherapy based on CD3xTAA + CD28xTAA efficiently reduces tumor growth *in vivo* compared to vehicle-treated mice or mice injected with CD3xTAA alone. Induced systemic immunomodulation is observed in the TME where increased numbers of both CD4 and CD8 T cells are observed upon combotherapy. Remarkably, while no CD34^{+} donor effect is observed in CDX growth kinetic, response to treatment appears to be donor dependent with apparition of “weak” and “good” responders. This heterogeneity of response mimics what is observed in clinic and enables further investigations of treatment mode of action and immune escape mechanisms.

#1531 TIL analysis demonstrates different mechanisms underlying PD-1 resistance in animal models.

S. Qiao, Y. Liu, W. Liu, W. Pan, X. Zhou, L. Wang, M. Chai, Y. Liu, H. Yang, **Z. Yu**;
Biocytogen Pharmaceuticals (Beijing) Co., Ltd., Beijing, China

Despite the tremendous success of PD-1 immunotherapy in treating cancer, resistance to the therapy is an inevitable risk. One of the major mechanisms underlying this resistance is alterations in the tumor microenvironment, including tumor-infiltrating lymphocyte (TIL) profiling changes after anti-PD1 treatment. To better understand the mechanism of PD-1 resistance, characterization of TILs in the tumor microenvironment was explored. First, immune cell profiling was performed in syngeneic tumor models established by 19 cancer cell lines without anti-PD-1 treatment. Depending on the tumor model, absolute numbers of $CD45^+$ cells and immune cell subsets varied. Moreover, stratifying the analysis based on tumor size (100 mm^3 to 3000 mm^3) revealed alterations in the proportion of immune cell percentages in MC38 tumors, which implies alterations in TIL frequency during cancer progression. Next, we investigated the TIL profile in two PD-1 resistant models: a hPD-1 antibody-induced resistant model and a syngeneic model in aged mice. The hPD-1 antibody resistant model was induced by multiple rounds of hPD-1 antibody retreatment on MC38 tumor-bearing humanized B-hPD-1/hPD-L1 mice. Efficacy results from this model further validated their resistance to hPD-1 treatment (0% tumor growth inhibition (TGI)), while the control group, which was not serially treated, showed substantial tumor inhibition (82.2% TGI). Next, mPD-1 antibody resistance was evaluated in aged wild-type mice. While mPD-1 efficacy on MC38-bearing young mice was approximately 85.5% TGI, the efficacy of this treatment in aged mice yielded only 6% TGI. TIL analysis in these models was subsequently performed: in the hPD-1-treated control mice that were responsive to anti-PD1 treatment, the numbers of total T cells, cytotoxic T cells ($CD8^+$) and MHC II positive cells were increased, while the anti-tumor effector cells in the serially treated resistant mice were either unchanged (total T cells and MHC II positive cells) or decreased ($CD8^+$ cells); strikingly, an increase in inhibitory myeloid-derived suppressor cell (MDSC) populations was also observed in the resistant model post-treatment. In the anti-PD1 treated aged mice, the frequency of TILs was unchanged upon mPD-1 treatment, suggesting that resistance in aged mice may be due to non-responsiveness of the immune cells. In sum, our results demonstrate different mechanisms underlying anti-PD-1 resistance, and suggest that a more thorough analysis of the TILs present in the tumor microenvironment could predict the responsiveness to PD-1 therapy and inform treatment strategies.

#1532 Improved reproducibility in multiplex immunofluorescence analysis of the tumor microenvironment using a novel quenching solution.

M. Levin, J. Heath, A. Schrank-Hacker, S. Dunn, M.-C. Vu, I. Hamza, D. Schwartz;
Leica Biosystems, Vista, CA

Formalin-fixed, paraffin-embedded (FFPE) tissues are commonly used in histopathology because the fixed tissues are stable and easy to store. In the context of immunofluorescence detection, however, endogenous autofluorescence of FFPE tissues can significantly reduce or mask immunofluorescent signals. The autofluorescence of FFPE tissues is caused by a variety of factors, including the presence of endogenous fluorophores, tissue fixation, and processing. While there are several methods that can be used to quench autofluorescence in FFPE tissues, chemical quenchers, which absorb or scatter light, are most frequently used for multiplex IF. Examples of chemical quenchers commonly used in manual multiplex staining include Sudan Black B and TrueBlack; however, these are not chemically compatible for use on automated platforms such as the Leica Biosystems BOND RX. Due to the need for increased throughput and decreased hands-on time, automation has risen in popularity versus manual staining, leading to a need for a versatile quenching solution compatible with automation. Here we demonstrate that NovaPlex Quenching Solution (NPQS), a novel proprietary quenching agent, reduces the background caused by autofluorescence and enhances the signal of the Cell IDx UltraPlex multiplex immunofluorescent (mxIF) assay across tissue types. Qualitative studies showed a decrease in autofluorescent signal in FFPE mouse spleen stained with antibodies against B220/Foxp3/CD3e, suggesting the utility of NPQS in mouse models of cancer and immunity. Similarly, nonspecific background was decreased across FFPE human tissue types, including lung adenocarcinoma stained for CD8/Foxp3/CD3e/CD4 and tonsil stained for CD8/Foxp3/PD-1/CD4. Further statistical studies in FFPE human tonsil tissue stained with CD8/Foxp3/PD-1/CD4 showed there was no significant decrease in dye intensity across all four markers and channels, resulting in a significant increase in signal-to-noise ratio for both CD8 at 490nm and PD-1 at 650nm ($p<0.05$). These experiments using Cell IDx/LBS UltraPlex mxIF technology demonstrate an effective method to improve the signal-to-noise ratios of fluorophores without reducing signal intensity from any of the target proteins in these parallel multiplex immunofluorescent assays.

#1533 Characterizing tumor-immune surveillance in Li-Fraumeni syndrome.

Camilla Giovino, Nicholas Fischer, Noel Ong, Ashby Kissoondoyal, Ran Kafri, David Malkin

Hospital for Sick Children, Toronto, ON, Canada

Li-Fraumeni Syndrome (LFS) is a cancer predisposition syndrome associated with germline *TP53* mutations and increased lifetime risk of developing multiple cancers. p53, the protein encoded by *TP53*, plays a role in regulating various aspects of immune cell biology. Accordingly, inactivation of p53 in tumor cells shapes interactions with the immune system and influences the anti-tumor immune response. Mutation or deletion of p53 in immune cells also favors tumor development and progression. However, to date, a comprehensive study of immune cell populations and the anti-tumor immune response has not been undertaken in the context of LFS. We hypothesized that germline *TP53* mutation carriers possess dysfunctional immune cells and/or immune responses, supporting LFS-associated tumor progression. Our preliminary data indicate a profound defect in tumor-immune surveillance in an LFS murine model. We observed that MC38 cancer cells develop significantly faster into tumors when injected into LFS mice (harboring a gain-of-function mutation $Trp53^{R172H/WT}$) compared to wildtype (WT) control-mice. Importantly, we identified significant alterations in immune cell compositions and phenotypes within the tumor microenvironment as well as immune organs using flow cytometry. We are currently using *ex vivo* proliferation assays and cytotoxicity assays to investigate the impact of mutant p53 on the tumor-killing ability of immune effector cells. Altogether, an improved understanding of anti-tumor immune dysfunction in the context of germline *TP53* mutation may reveal the potential for innovative therapies to target different facets of the immune system to intercept cancer progression in LFS patients.

#1534 The tumor immune microenvironment at different stages of non-small cell lung cancer.

M. Hansen[1], Q. Zhou[2], Y. S. DeRose[2], M. Kovacsovics[2], B. Brintz[2], B. L. Witt[2], K. L. O'Neill[1], S. Hu-Lieskovan[2];
[1]Brigham Young University, Provo, UT, [2]University of Utah, Salt Lake City, UT

Introduction: To better understand the immune microenvironment in non-small cell lung cancer (NSCLC), we evaluated immune cell populations within the tumor parenchyma and their interaction at the periphery of the tumors at different stages of disease.
Methods: 27 whole tumor slides were collected from NSCLC patients of all stages after surgical resection. Tissue slides were stained with multiplex Opal immunofluorescence for CD8, CD68, CK, PD-1, PD-L1, FoxP3, and DAPI using a Leica Bond automated stainer. Slides were scanned at 20x magnification by Akoya Polaris whole slide scanner and spectrally unmixed. Spatial analyses were performed on the HALO software.
Results: Density of CD8 T cells, T regulatory (Treg) cells, and macrophages were significantly higher ($p=0.001$) in the interface region compared to the tumor and stroma. There is abundant CD8 T cell infiltration in the tumor at early stage I and this decreased significantly ($p=0.05$) at higher stages. PD-1− CD8 T cells significantly dropped with higher stage, while PD-1+ CD8 T cells did not. On the other hand, macrophage infiltration increased as stage increased, with most of the increase driven by PD-L1− macrophages. No statistically significant trends were observed in Treg cells across stages, but they appeared to be higher in stage II. No differences in immune infiltration were observed between the NSCLC subtypes adenocarcinoma and squamous cell carcinoma. No correlation was found between proximity of immune cell subsets to tumor cells and stage.
Conclusion: The tumor microenvironment in NSCLC is rich in CD8+ cells at early stage and their density decreases as the stage of the disease increases, while macrophage infiltration increases as the disease stage progresses.

#1535 Differential immune microenvironments in triple-negative breast cancer and hormone receptor-positive HER2-negative breast cancer: A spatial analysis via multiplex immunofluorescence.

Y. Cha, I. Park, S.-J. Shin;
Yonsei University College of Medicine, Seoul, Korea, Republic of

Objective: To elucidate differences in immune cell (IC) composition and their spatial distribution between triple-negative breast cancer (TNBC) and hormone receptor-positive HER2-negative breast cancer (HR+HER2-BC), and to evaluate the effect of PD-L1 status on these parameters.
Methods: We selected 32 patients with ≥60% tumor-infiltrating lymphocytes (TIL) (TNBC, n=18; HR+HER2- BC, n=14). Multiplex immunofluorescence was employed on resected tumor tissues. Using markers such as CK, CD20, CD8, CD4, and FOXP3, IC types and tumor cells (TC) were identified in both stromal and tumor areas. We analyzed and compared cellular density and proportional distribution of IC, and spatial interactions (both IC-TC and IC-IC) based on tumor subtype and PD-L1 status.
Results: TNBC exhibited a unique IC composition with a higher proportion of CD8+IC (stroma: 27% vs 17%, p<0.001; tumor: 54% vs 31%, p<0.001) and CD4+FOXP3+IC (stroma: 3.9% vs 3.0%, p=0.036) than HR+HER2-BC. Among PD-L1 positive cases, TNBC had a denser stromal population of CD4+FOXP3+IC (146.4±67.1/mm2 vs 114.3±146.9/mm2, p=0.036). Both tumor subtypes displayed varied IC compositions based on PD-L1 status. Density plots revealed a pronounced clustering of IC near TC in TNBC, especially in PD-L1 positive cases. Analysis of cell-cell interactions showed diverse adjacency patterns between TC and various IC combinations with frequencies differing by tumor subtype and PD-L1 status.
Conclusion: The immune landscape, typified by IC composition and spatial distribution, varies between TNBC and HR+HER2- BC, with PD-L1 status further modulating these patterns.

#1536 Deciphering the crosstalk within the tumor microenvironment of NSCLC by a virtual microdissection approach.

S. Parab[1], F. Napoli[1], D. Cora[2], G. Doronzo[1], V. Communanza[1], L. Righi[1], L. Primo[1], V. Monica[1], L. Manganaro[3], B. Selene[3], P. Bironzo[1], G. Scagliotti[1], F. Bussolino[1];

[1]University of Turin, Turin, Italy, [2]Piemonte Orientale University, Novara, Italy, [3]Aizoon Technology Consulting, Turin, Italy

Introduction: Non-small cell lung cancer (NSCLC) is a highly heterogenous disease with the largest number of cancer-related mortality worldwide, one of the reasons for this is the complex and diverse tumor microenvironment (TME) comprising of numerous cell types. Several studies have already highlighted the importance of TME in dictating progression steps and response to therapies; however, a transcriptome-based molecular subtyping of patients in lung adenocarcinomas (LUADs) and lung squamous cell carcinomas (LUSCs) can further determine the distinct tumor immune microenvironment (TiME), which can eventually provide a systematic overview to improve the diagnosis and prognosis of patients.

Material and method: To elucidate such nature of interactions between tumor cells and cells comprising the TME, we exploited the transcriptome of 300 early stages (Ib-IIIa) NSCLC recruited in the prospective observational clinical trial PROMOLE. With the help of a clustering approach, initially we performed a molecular-based virtual stratification/dissection on the NSCLC patients. Next, to elucidate the relative cell-type abundance, a deconvolution approach was applied to identify the possibility of tumor infiltrating immune cells within these subgroups. Immunohistochemistry (IHC) was then used to substantiate these predictions on tumor cells.

Results and discussion: The resulting subgroups of LUADs and LUSCs are biologically well-characterized by mutational and gene expression profiles. Cell-type abundance approach identified samples which are enriched with tumor infiltrating immune cells like Neutrophils, Tcells, macrophages, etc. These findings were positively confirmed by IHC with multiple cell markers such as MPO, CD4, CD8, CD68, etc. Integrating these two results highlighted the proportion of TiME in the two different sub-populations along with shedding some light on the crosstalk happening between different cancer-/immune- cell lines.

Conclusion: The in-silico predictions on bulk RNA data by virtual micro-dissection, distinguished the two distinct NSCLC subtypes, each associated with clinical and molecular features. Furthermore, the immune cells infiltration suggests a possible role of infiltrating tumor immune cells with the prognosis of patients. Our analysis successfully performed an intra-sample and inter-sample comparison, which can unveil new prognostic markers that can provide relevant information for cancer immunotherapy.

#1537 CD63 acts as a key modulator of tumor progression and innate immune evasion in non-small cell lung cancer.

T. Lerbs[1], L. Cui[2], C. De Souza[2], R. Buettner[1], G. Wernig[2];
[1]University Hospital of Cologne, Bonn, Germany, [2]Stanford University, Stanford, CA

Introduction: Lung cancer is a major reason for cancer-related mortality worldwide, causing more than two million cancer deaths per year. Over the last decade, new therapies have allowed long-term survival for patients even in advanced stages. However, only a minority of patients benefits from these therapies and patients often grow resistant over time. An important mechanism that contributes to cancer growth and the development of therapy resistances is the cross-talk between cancer cells and their tissue microenvironment, in particular fibroblasts and macrophages. In this context, we explored whether the tetraspanin CD63 - which is commonly found on intra- and extracellular membranes - stimulates cancer growth and mediates pro-tumorigenic functions of the tissue microenvironment in NSCLC.
Methods: We analyzed patient tissue via immunohistochemistry and in-situ-hybridization. We deleted CD63 in cancer cell lines (A549, H810, LC19) and primary fibroblasts via CRISPR-Cas9. To assess phagocytosis, we used in vitro EdU assays and adaptive transfer models in vivo, and identified changes in cell signaling via mass spectrometry. We used an in vitro phagocytosis assay to determine the effect of CD63 on cancer cell phagocytosis through macrophages and analyzed the expression of M1 and M2-associated surface markers through flow cytometry upon co-culturing PBMC with cancer cells over one week.
Results: In patient sections, cancer tissue did not only express more CD63 on the gene expression and protein level but a stronger CD63 expression also correlated with a denser macrophage infiltrate. Looking for pro-tumorigenic functions, deleting CD63 in three cancer cell lines reduced cancer cell growth both in vitro and in an adaptive transfer model in vivo. Additionally, deleting CD63 impaired the pro-tumorigenic focal adhesion signaling in primary fibroblasts. Concerning the interaction between cancer cells and macrophages, deleting CD63 reduced the macrophage-mediated phagocytosis of cancer cells and co-culturing primary monocytes with CD63-deficient lung cancer cells induced the expression of M1-associated surface markers on the PBMC.
Conclusion: In conclusion, these results demonstrate that the tetraspanin CD63 drives NSCLC growth by stimulating cancer cell proliferation - in part by interfering with focal adhesion signaling - and facilitating immune evasion by preventing cancer cell phagocytosis through macrophages and inducing an immunosuppressive phenotype in macrophages.

#1538 Impact of C-reactive protein on the efficacy of immune checkpoint inhibitors in non-small cell lung cancer.

W. Li[1], H. Guo[2];

[1]The First Affiliated Hospital of Xi'an Jiaotong University, Xi'an, China, [2]The Second Affiliated Hospital of Xi'an Jiaotong University, Xi'an, China

Background: Immune checkpoint inhibitors (ICIs) therapy has achieved remarkable success in the treatment of non-small cell lung cancer (NSCLC). Clinical studies have suggested a correlation between C-reactive protein (CRP) levels and treatment efficacy, but it remains unclear whether CRP can directly impact the efficacy. Therefore, we investigated the imapct of CRP on the efficacy of ICIs in NSCLC.

Methods: The tumor growth model was established in CRP knockout and wildtype mice by injecting LLC cells to evaluate the effect of CRP on tumor proliferation. The frequencies and phenotypes of macrophages and T cells in mouse tumors were detected by flow cytometry. The impact of CRP on macrophage polarization was evaluated using flow cytometry and IF, while its impact on T cell chemokines CCL5, CXCL9, and CXCL10 was analyzed by ELISA and qRT-PCR. mCRP and α-PD-1 were implemented in C57/BL6 mice injected with LLC cells to evaluate the effect of mCRP on tumor immunotherapy. The frequencies of T cells in mouse tumors were detected by flow cytometry. Expression of mCRP and infiltration of immune cells in human NSCLC tissues were analyzed using IHC.

Results: We found that tumor progression was enhanced and the proportion of tumor-infiltrated M1 macrophages was decreased in CRP knockout mice. Using human PBMC-derived macrophage and RAW264.7 cell lines, we demonstrated that the monomeric form of CRP, known as mCRP, induced M1 polarization of macrophages, leading to increased secretion of CCL5, CXCL9, and CXCL10. In tumor bearing mice, mCRP treatment enhanced anti-tumor immunity and suppressed tumor progression by increasing $CD4^+$ and $CD8^+$ T cell recruitment. Surprisingly, the combined treatment of mCRP and α-PD-1 induced more significant tumor regression than α-PD-1 treatment alone. Additionally, high level of mCRP in NSCLC tissues is correlated with a more inflamed tumor microenvironment phenotype.

Conclusion: mCRP can enhance the efficacy of immune checkpoint inhibitors in NSCLC by activating anti-tumor immunity.

#1539 A comprehensive analytical validation framework for antibodies used in the CellScape multiplex immunofluorescence assay.

C. E. Jackson[1], A. Christians[2], J. Boog[2], M. H. Ingalls[1], X. Meshik[1], A. Northcutt[1], K. E. Cashion[1], J. S. Schwarz[1], O. Braubach[1];
[1]Canopy Biosciences-A Bruker Company, St. Louis, MO, [2]Canopy Biosciences-A Bruker Company, Hannover, Germany

Background: Multiplex immunofluorescence (mIF) is a powerful tool that enables deep phenotyping of cells within the tumor microenvironment (TME). Careful optimization of multiplex antibody panels for specificity, sensitivity and reproducibility is crucial to achieving robust data and is a precondition for assay repeatability and standardization. We describe our validation procedure for VistaPlex™ multiplex assay panels.
Methods: Experiments were performed using the CellScape™ platform for precise spatial multiplexing. The platform enables automated cyclic mIF for readily available fluorophore-conjugated antibodies compatible with fresh frozen or FFPE tissues. The use of high dynamic range imaging further facilitates quantitative phenotyping, while excellent imaging resolution provides single-cell discrimination with high accuracy. To design a ready-to-use panel for immune cell phenotyping, individual antibodies were first screened for specificity and then optimized for labeling sensitivity. Signal-to-noise, inter-assay reproducibility, and intra-assay precision were evaluated across serial sections in a multi-stage testing matrix to validate each antibody in isolation and assembled into a panel. Resulting from this effort, we introduce a 15-plex ready-to-use VistaPlex immune profiling panel for human FFPE tissues.
Results: Image analysis of signal-to-noise ratios demonstrated robust performance of multiplexed antibodies across multiple tissue sections and tissue types. Measurements of both signal and quantitative immune phenotyping across technical replicates showed a high degree of intra-assay precision and inter-assay reproducibility. The 15-plex panel was validated on human tonsil, lung, breast, and colon tissues.
Conclusions: The CellScape platform enables simultaneous detection of multiple protein biomarkers on a single tissue section for deep immune cell profiling in the TME. Rigorously validated VistaPlex panels further streamline this spatial biology workflow and will aid in the generation of consistent and reliable results for end users.

#1540 The dendritic cell receptor DNGR-1 shapes immunity to cancer.

K. H. J. Lim[1], E. Giampazolias[2], B. Frederico[1], N. C. Rogers[1], P. Chakravarty[1], G. Kelly[1], A. Cardoso[1], E. Nye[1], A. Suarez-Bonnet[3], S. Priestnall[3], R. Goldstone[1], C. Science Technology Platform[1], S. Lee[1], O. Schulz[1], J. Strid[4], L. Zapata[5], C. Reis e Sousa[1];

[1]The Francis Crick Institute, London, United Kingdom, [2]Cancer Research UK Manchester Institute, Manchester, United Kingdom, [3]The Royal Veterinary College, Hatfield, United Kingdom, [4]Imperial College London, London, United Kingdom, [5]The Institute of Cancer Research, London, United Kingdom

Background: Central to the success of $CD8^{+}$ T cell-mediated anti-cancer response are type 1 conventional dendritic cells (cDC1s), acting as professional antigen presenting cells. In both mouse and human, DNGR-1 (a.k.a. CLEC9A) is a dedicated cDC1 receptor that, upon binding to its physiological ligand filamentous-actin (F-actin) exposed upon cell death, prime cytotoxic $CD8^{+}$ T cells specifically against dead cell-associated antigens. Here, we interrogate the role of DNGR-1 in shaping the tumor microenvironment during carcinogenesis.

Methods: We utilized two models of chemical carcinogenesis: 3-methylcholanthrene (MCA)-induced sarcoma, and azoxymethane (AOM) and dextran sodium sulfate colitis (DSS)-associated carcinoma. *Rag1*$^{-/-}$ (no B and T cells), *Clec9a*$^{gfp/gfp}$, *Clec9a*$^{cre/cre}$ and WT (wildtype) mice on C57BL/6 background were used. Primary MCA-sarcoma cell lines were generated and subsequently tested in a series of transplantation experiments in naïve syngeneic WT mice. Whole exome and RNA sequencing were performed to elucidate the mutational landscape and decipher the immunopeptidome of these primary cell lines.

Results: Upon challenge with MCA, there is shorter latency for tumorigenesis in DNGR-1-deficient mice (n=46), like in *Rag1*$^{-/-}$ mice (n=43), in contrast to immunocompetent WT hosts (n=59) (median: 95 vs 113 days, hazard ratio: 1.72, 95% CI 1.11-2.68, p=0.008). DNGR-1-deficient mice also display increased susceptibility to AOM-DSS carcinogenesis compared to co-housed WT mice. Majority (n=16/24, 68%) of MCA-induced primary sarcoma cell lines derived from DNGR-1-deficient hosts are highly immunogenic and were controlled/rejected at a similar rate, upon challenge in secondary naïve WT recipients, like those derived from *Rag1*$^{-/-}$ mice (n=13/19, 68%). Whole-exome sequencing of cell lines derived from DNGR-1-deficient hosts revealed that they harbor high mutational burden, including mutations in F-actin-binding proteins that have been previously associated with better survival outcomes in patients with cancer (Giampazolias *et al. Cell*, 2021). Collectively, these data argue that DNGR-1 protects against carcinogenesis and selects for less immunogenic tumor cells. To evaluate the degree of immunoediting which occurred in the respective primary host mice, we applied the evolutionary metric based on the ratio of nonsynonymous to synonymous mutations (dN/dS), and found that they are less immunoedited compared to cell lines derived from WT hosts.

Conclusion: Our findings highlight DNGR-1 as a novel immune checkpoint that couples cell death sensing and (neo-)antigen cross-presentation to functional tumor-specific $CD8^{+}$ T cell responses during cancer immunoediting. Understanding the mechanism by which DNGR-1 sculpts the mutational landscape of tumors may further inform the dynamics of cancer evolution and may have translational therapeutic implications in directing effective immunotherapy strategies.

#1541 Heterogeneity of the hormone receptor-positive breast tumor immune microenvironment according to patient's body mass index.

H.-L. Nguyen[1], T. Geukens[2], M. De Schepper[2], K. Van Baelen[1], M. Maetens[1], G. Zels[1], A. Mahdami[1], E. Isnaldi[1], S. Hatse[1], J. Verbeke[1], C. Matthys[1], B. Thienpont[1], E. Vanderheyden[3], T. Van Brussel[3], R. Schepers[3], G. Philips[3], B. Boeckx[3], D. Lambrechts[3], G. Floris[2], F. Richard[1], C. Desmedt[1];
[1]KU Leuven, Leuven, Belgium, [2]University Hospitals Leuven, Leuven, Belgium, [3]VIB-KU Leuven, Leuven, Belgium

Background: Obesity is a risk factor for postmenopausal hormone receptor-positive (HR+) breast cancer (BC) and is associated with poorer outcomes. "Obesity-paradox", a phenomenon where obesity (BMI ≥ 30) is associated with better outcomes in patients treated with immune checkpoint inhibitors (ICI), has been observed in several cancer types. It is however under-explored in BC, especially HR+ BC. Emerging data from recent trials (KEYNOTE-756 and CheckMate 7FL) have shown the potential benefits of ICI for treating early HR+ BC. This prompted the need for better insights into the biological link between obesity and HR+ BC, particularly its tumor immune microenvironment (TIME).

Patients & Methods: A monocentric cohort of 33 patients (11 lean, 11 overweight, 11 obese) with early HR+ BC was selected for the study, whose tumor tissues were collected and subjected to snRNA-seq. Unsupervised clustering and cluster annotation were performed on the processed data leading to identification of cell types and subtypes. We then performed differential gene expression (DGEA) and gene set enrichment analyses (GSEA) according to BMI category for each of the immune cell types.

Results: We identified a total of 76,773 immune cells belonging to six major cell types, namely B/plasma cell, dendritic cell (DC), mast cell, monocyte/macrophage (mono/macro), T cell, and natural killer (NK) cell. Their proportions varied between patients, however immune cellular composition was not associated with BMI. DGEA and GSEA revealed highly cell type-specific obesity-associated differences in the expression profile of immune cells. Notably, an enrichment of B cell-mediated immune activities, substantiated by the upregulation of Ig genes, was observed in B cells and plasma cells. This was however coupled with an overexpression of the checkpoint *BTLA* in B cells. CD8+ and CD4+ T cells showed a lower level of activation (higher *LEF1, TCF7*, lower *ANXA1, IL4R*), and NK cells a decreased cytokine production (*CD96, CD226*) and conflicting differential expression of cytotoxic molecules (lower *NKG7*, higher granzymes). Checkpoint genes such as *PDCD1, CTLA4, TIGIT, LAG3, HAVCR2* did not show significant changes in their expression in T/NK cells. Mast cells displayed a downregulation of antigen presenting genes (*CD74, HLA-A/B/E*). DC and mono/macro populations also exhibited both up- and down-regulation of genes involved in different immune pathways.

Conclusion: Our current data suggested that obesity was associated with multi-directional changes in the immune activities, possibly implying an unresolved inflammation in the HR+ BC tissue. Further investigation incorporating other cell types and their interaction with immune cells in both tumor and matched normal mammary tissues is warranted and on-going, which could provide more understanding of HR+ breast TIME and lead to speculation on therapeutic implications.

#1542 Epithelial cell adhesion molecule induces canonical Wnt pathway to promote stemness in colorectal cancer.

H.-C. Wu[1], S. Panda[1], K.-C. Chen[1], C.-C. Lee[1], H. Hsieh[2], Y.-J. Su[1];
[1]Academia Sinica - Institute of Cellular & Organismic Biology, Taipei, Taiwan, [2]National Health Research Institutes - Institute of Biotechnology and Pharmaceutical Research, Miaoli, Taiwan

Epithelial cell adhesion molecule (EpCAM) is a pleiotropic type-1 transmembrane glycoprotein and known cancer stem cell marker, yet its tumorigenic mechanisms remain elusive. Cancer stem cells (CSC) have been implicated in cancer progression and recurrence, but targeting them with therapeutics is a major challenge. It is known that EpCAM is highly expressed in CSCs of different cancer types. Here, we studied the role of EpCAM in colorectal cancer (CRC) stemness. First, we show that the extracellular domain of EpCAM (EpEX) functions as a ligand for Wnt receptors, frizzled6/7 and LRP5/6, while the intracellular domain (EpICD) upregulates transcription of these receptors. Further, EpEX-induced Wnt signaling activates TACE and γ-secretase enzymes to augment shedding of EpEX and EpICD, establishing a positive feedback loop. Importantly, we show that the EpCAM-neutralizing antibody, EpAb2-6, targets the Wnt pathway to attenuate stemness characteristics in colorectal cancer (CRC). Our EpCAM-neutralizing antibody (EpAb2-6) and a porcupine inhibitor (LGK974) each partially attenuated cancer stemness, while their combination abolished stemness-related endpoints, induced apoptosis *in vitro* and markedly diminished tumor progression in animal models of human CRC. From these findings, we conclude that EpCAM stimulates Wnt signaling to promote cancer stemness, and the combination of EpAb2-6 and porcupine inhibitors may represent an effective CRC treatment, including for KRAS-mutant cancers. Our findings reveal an opportunity to combat drug resistance in tumor stem cells. Thus, the mechanistic insights gained from our study may be useful to improve existing treatments or to develop novel anticancer therapeutics.

#1543 40-color spectral flow cytometry for comprehensive immunophenotyping of murine cancers.

A. J. Kare, L. Nichols, R. Zermeno, M. N. Raie, S. K. Tumbale, K. W. Ferrara;
Stanford University, Stanford, CA

Introduction: High-dimensional immunoprofiling is essential for studying host response to cancer immunotherapy. Synergistic agents often induce systemic changes in leukocyte abundance/function due to targeting, dosage, or delivery, necessitating multi-tissue analyses to decipher immune response mechanisms. We set out to dissect leukocyte composition in lymphoid tissues and tumors by using spectral cytometry, a multiplexed, high-throughput technology.
Methods: We engineered a 40-color spectral flow cytometry panel to immunophenotype all major leukocytes and their functional subsets. Naïve and tumor-burdened C57BL/6 mice treated with combinations of agonist CD40 (aCD40) and checkpoint inhibitors were sacrificed, and tissues were processed. Stained cells were acquired on a 5-laser CyTEK Aurora. Unmixing accuracy and resolution was validated via 780 NxN plots, and high-dimensional analysis was performed.
Results: Spectral cytometry affords resolution of 43+ parameters compared to 26 or less in conventional systems. We first designed a 25-marker backbone panel to identify all immune lineages. Additional channels were assigned to functional markers, allowing for profiling of migration, maturation, and activation in tumor-infiltrating leukocytes (TILs). In naïve secondary lymphoid tissues (SLTs), 35 distinct $CD45^{+}$ populations were resolved. Germinal center B cells (17% vs. ~0.3% of $CD45^{+}$ in other SLTs) and T follicular cells (31% vs. ~1-5% of CD4+ T cells in other SLTs) were mostly found in the Peyer's patches, representing a hypothesized model tissue for studying tertiary immune structures in tumors. Peripheral blood contained the highest frequency of NK cells (4%), monocytes (6%), basophils (0.3%), eosinophils (4%), and neutrophils (7%) as a percentage of $CD45^{+}$ cells. The spleen held the largest reservoir of CD4/8 central/effector memory cells (5% of $CD45^{+}$) while ~80% of all T cells in the lymph nodes were naïve. In primary lymphoid tissues (PLTs), 12 distinct thymocyte and 7 B cell populations were resolved. Wanderlust trajectory analysis revealed CD24 and CD127 as key developmental regulators in lymphocyte differentiation. Autofluorescence extraction was essential for myeloid phenotyping. With this approach, we found monocytes comprised ~60% of TILs following aCD40 treatment (~8% in non-treatment and checkpoint only controls) and had altered macrophage differentiation fates. aCD40-treated tumors also contained higher frequencies of activated $CD40/80/86^{+}$ DCs (~80/86/60% vs. ~60/51/50% of DCs in NTCs).
Conclusion: This work describes a novel tool that efficiently resolves leukocytes on the axes of time, tissue, and treatment. Applications range from serial monitoring of circulating blood, endpoint analysis, validation of multiplexed-IHC, and cell sorting. PLT and SLT data has been made publicly available to serve as a training tool and reference proteomic atlas in future work.

#6869 Paired single-cell B-cell transcriptomics and receptor sequencing reveal activation states and clonal signatures that characterize B cell immunity in acute myeloid leukemia.

S. Guo[1], **G. S. Mohan**[2], B. Wang[2], T. Li[1], N. Daver[2], Y. Zhao[1], P. K. Reville[2], D. Hao[1], H. A. Abbas[2];
[1]Harbin Medical University, Harbin, China, [2]UT MD Anderson Cancer Center, Houston, TX

Acute myeloid leukemia (AML) is the second most common adult leukemia with a five-year survival rate around 30%. For decades, AML treatment has centered around intensive chemotherapy frequently followed by allogeneic stem cell transplant (Allo-SCT). The power of Allo-SCT to induce lasting remission has been attributed to a potent graft-versus-leukemia effect and has inspired efforts to stimulate host immunity against AML via immune checkpoint blockade (ICB). Thus far, these studies have yielded mixed results. While tumor-infiltrating T-cells have long been the focus of immunotherapy investigations, a growing body of data points to a central role of B-cells in mediating anti-tumor immunity, and a comprehensive assessment of B lymphocytes within the AML immune microenvironment has never been carried out with single cell clonal resolution. We performed paired single-cell transcriptomic and B cell receptor (BCR) analysis on 52 bone marrow aspirate samples. These samples included 6 from healthy bone marrow donors (normal), 24 from newly diagnosed AML patients (NewlyDx), and 22 from 8 relapsed or refractory AML patients (RelRef), who underwent assessment both before and after ICB with azacitidine/nivolumab. We first used transcriptomic data to delineate canonical B-cell subpopulations and observed a reduction in nascent B cells and an expansion of differentiated B cells in AML patients (RelRef>NewlyDx). Overlaying BCR sequencing and clonotypic analysis revealed clonal expansion, low clonotypic diversity, and extensive somatic hypermutation in the RelRef samples, suggesting antigen-driven affinity maturation within the tumor microenvironment. Furthermore, we identified robust AP-1 expression (a marker of activation) in B-cells from NewlyDx patients and a marked loss of AP-1 in RelRef patients, suggesting that B-cell exhaustion may be a key immunologic feature of AML relapse. Importantly, we observed that AP-1 activity is restored and that specific B-cell clones expand after ICB, but only among patients who clinically respond to ICB. In line with these observations, we also noted the clonal expansion of AML-associated plasma cells and loss of clonotypic diversity among ICB clinical responders, pointing to an antitumor role for these clones. Finally, we characterized atypical memory B cells which demonstrate high antigen presentation activity, close interaction with AML cells and are associated with unfavorable clinical outcomes, suggesting that they play a direct role in aiding AML survival and immune escape. Collectively, our findings establish the dynamic landscape of AML-associated B-cells while identifying specific B-cell subpopulations and B-cell-AML interactions that may be targeted by the next generation of AML-directed immunotherapies.

TUMOR BIOLOGY: Metastasis Promoting and Suppressing Genes
Poster Session

#1547 Melanotransferrin (*MELTF*, CD228) as a determinant of melanomagenesis: *MELTF* expression attenuates melanoma progression in the A375-luc2 murine metastasis model and human patients.

J. Jandova, **G. T. Wondrak**;
R Ken Coit College of Pharmacy and UA Cancer Center, The University of Arizona, Tucson, AZ

The cell-surface glycoprotein melanotransferrin (MELTF, CD228) is a member of the iron-binding transferrin superfamily expressed in human melanocytes and other cell types. Dysregulated *MELTF* expression in malignant melanoma has been reported before but its specific role in tumorigenesis has remained elusive. Following our interest in the role of the transferrin receptor (TFRC) in melanomagenesis, our initial TCGA-analysis suggested that high *MELTF* expression is associated with increased melanoma patient survival. In order to explore the mechanistic role of *MELTF* in melanoma we performed CRISPR/Cas9-based *MELTF* deletion in A375-luc2 human malignant melanoma cells. ICP/MS-analysis indicated no difference in iron-content between *MELTF*_WT and *MELTF*_KO cells. NanoString nCounter™ ('PanCancer-Progression-Panel'; 770 genes) comparative transcriptomic profiling (*MELTF*_KO versus *MELTF*_WT) demonstrated an upregulation of EMT-related expression networks in *MELTF*_KO cells, an observation consistent with phenotypic detection of enhanced matrigel invasiveness; likewise, inclusion of recombinant glycosylated MELTF (Gly20-Gly711 His-tag; 92 kDa; 10-100 nM) attenuated invasiveness of *MELTF*_KO cells. In SCID mice, subcutaneous growth of *MELTF*_KO exceeded that of *MELTF*_WT xenografts, and intracardial injection followed by non-invasive bioluminescent monitoring revealed an increase in lung metastatic burden associated with decreased survival of the *MELTF*_KO group. These data support a heretofore unrecognized tumor-suppressive function of *MELTF* expression in melanoma progression, a mechanistic role consistent with a potential survival benefit associated with high *MELTF* expression observed in human melanoma patients.

#1548 Olfactomedin 4 deficiency promote de novo progression of prostate cancer in TRAMP mouse model.

H. Li, W. Liu, J. Zhu, K. Chin, G. P. Rodgers;
NIH National Heart, Lung & Blood Institute, Bethesda, MD

Prostate cancer is the most diagnosed solid tumor and the second leading cause of cancer-related death in American men. Olfactomedin (*OLFM4*) plays tumor suppressor roles and is associated with the initiation, growth, and clinical outcome of human prostate cancer. *Olfm4*-null mouse sporadically developed prostate epithelial neoplasia through up-regulated hedgehog signaling pathways. In this study, we have generated *Olfm4*$^{+/+}$*/GFP/TRAMP* and *Olfm4*$^{-/-}$*/TRAMP* mouse models to investigate *Olfm4* gene biological functions underlying prostate cancer de novo progression. We have observed that *Olfm4*$^{-/-}$*/TRAMP* mice developed more advanced prostate cancer at 47.6% (20/42) compared to *Olfm4*$^{+/+}$*/TRAMP* at 11.9 % (5/42) and had poor survival compared to *Olfm4*$^{+/+}$*/TRAMP* mice ($P<0.01$). Histopathological and immunofluorescent staining revealed that tumor tissues containing more heterogeneous cells such as Ar+/Ck8+ epithelial or Syn+ neuroendocrinal cells or Vim+/Ck8+ epithelium mesenchymal transition cells in the primary tumors obtained from *Olfm4*$^{-/-}$*/TRAMP* mouse. We found more tumor angiogenesis and metastases into lymph nodes, liver, lung, kidney, and soft tissues in *Olfm4*$^{-/-}$*/TRAMP* mice. The accumulations of the dendritic cell population in primary tumor and lung metastasis tumors were detected. The primary tumor was sensitive to androgen deprivation therapy by using castration with both *Olfm4*$^{+/+}$*/GFP/TRAMP* and *Olfm4*$^{-/-}$*/TRAMP* mice. However, castration-resisted EMT tumor cells or expressing neuroendocrine marker cells regrew after castration 7-8 months in both *Olfm4*$^{+/+}$*/GFP/TRAMP* and *Olfm4*$^{-/-}$*/TRAMP* mice. Furthermore, we tested JQ1, a BET bromodomain inhibitor, as an epigenetic targeted therapy reagent and found that JQ1 significantly inhibited tumor cell growth of *Olfm4*$^{-/-}$*/TRAMP* mouse tumor in the organoids culture. Taken together, we have provided novel evidence that *Olfm4* plays a tumor-suppressing role during prostate cancer de novo progression.

#1549 Molecular mechanism of CD146 nanobody in tumor metastasis inhibition mediating by IL-6/JAK/STAT3 signaling in triple-negative breast cancer.

K. Huang[1], H. Sun[1], C. Wu[1], D. Lin[2], J. Chen[1], Y. Chen[1], X. Fang[1], S. Chen[1], Y. Liang[1], H. Lin[1];
[1]First Affiliated Hospital of Shantou University Medical College, Shantou, China, [2]Cancer Hospital of Shantou University Medical College, Shantou, China

Background: CD146, an adhesion molecule involved in inflammatory regulation, is linked to increased aggressiveness in Triple Negative Breast Cancer (TNBC). Yet, the molecular mechanisms of CD1146-driven TNBC metastasis in an inflammatory context remain elusive. We synthesized CD146 nanobody (anti-CD146 #112-2), which degraded CD146 protein specifically, inhibiting IL-6-mediated JAK/STAT3 activation and suppressing TNBC metastasis. This study aims to elucidate the mechanisms of CD146 degradation by 112-2 and the role of CD146 in mediating inflammatory responses leading to TNBC metastasis.
Methods: CD146 knockout and overxpression cell models were created using CRISPR/Cas9 or lentiviral techniques. Lung metastasis was evaluated by injecting luciferase-labeled cells into the tail veins of Balb/c-nu mice, monitored with the IVIS Kinetic system. The impact of CD146 on TNBC metastasis in an inflammatory environment was explored through cell-adhesion assays and trans-endothelial migration assays using CD146 knockout models and HUVEC cells. Transwell assays assessed the influence of IL-6 and 112-2 on TNBC. CD146 mutant vectors with specific truncations were generated to confirm the binding sites between CD146 and 112-2. ELISA and immunofluorescence assays examined CD146 protein internalization. CD146 degradation by 112-2 was confirmed using proteasome inhibitor MG132 and lysosome inhibitor Bafilomycin A1, along with western blotting and immunofluorescence experiments. **Results:** Stimulation of TNBC cells with IL-6 increased CD146 expression and tumor metastasis. Knocking down CD146 significantly reduced IL-6 secretion by TNBC cells, leading to reduced tumor-endothelial cell adhesion and trans-endothelial migration. CD146 knockout or 112-2 treatment inhibited IL-6-mediated JAK/STAT3 activation and tumor metastasis. Experiments with CD146 mutants and molecular docking identified the specific 112-2 binding site at leucine positions 331-332 of CD146 protein. 112-2 treatment led to CD146 protein internalization and cleavage, resulting in an 80 kDa fragment recognized by both 112-2 and C-terminus-specific CD146 antibodies, ultimately inhibiting the activation of IL-6/JAK/STAT3 signaling. Notably, the inhibition of proteasome or lysosome activity failed to reverse the 112-2-induced reduction in CD146 protein levels. However, inhibiting lysosomal acidification resulted in significant co-localization of CD146 with lysosomes, suggesting a potential role of lysosomes in 112-2-mediated cleavage of CD146. **Conclusion:** CD146 promotes TNBC metastasis by modulating IL-6/JAK/STAT3 activation. The nanobody anti-CD146 #112-2 specifically binds to CD146 extracellular domain induces the proteolysis of CD146 protein, thereby inhibiting the tumor-promoting effect of IL-6.

#1550 Identification of a novel squalene epoxidase function in breast cancer brain metastasis.

S.-P. Wang[1], J.-Y. Yeh[2], Y.-L. Lee[3], K.-Y. Lin[3], C.-D. Chang[3], C.-C. Yang[3], S.-Y. Cheng[3], Y.-W. Hung[3], Y.-H. Chang[3], Y.-F. Li[4], Y.-L. Yu[2];
[1]Academia Sinica, Taipei, Taiwan, [2]China Medical University, Taichung, Taiwan, [3]Pharmacology Discovery Services Taiwan, Ltd., New Taipei City, Taiwan, [4]National Defense Medical Center, Taipei, Taiwan

Brain metastases are serious complications of breast cancer, especially in triple-negative breast cancer (TNBC) patients. There is currently no effective treatment due to the unique brain microenvironment and limitation for drugs to cross the blood-brain barrier (BBB). BBB limits access of nutrients from the circulation and thereby makes the brain hypoxic and depleted of metabolites, growth factors and proteins. However, it remains poorly understood how breast cancer cells manipulate for adaption and colonization in the brain. To probe the molecular mechanism of breast cancer brain metastasis (BCBM), we compared gene signatures in primary breast tumors and BCBM tumors, and identified that *SQLE* (encodes squalene epoxidase, the second rate-limiting enzyme in the cholesterol biosynthesis) could be a leading-edge gene in breast cancer brain metastasis. To explore the role of SQLE in BCBM, we established the brain metastatic TNBC MDA-MB-231 (MDA231-BrM) cell line from brain metastatic subpopulation that originated from its parental MDA-MB-231 (MDA231) cell line. We found that SQLE expression was greatly upregulated in MDA231-BrM cells compared with the parental MDA231 cells. Using MDA231-BrM and MDA231 cell lines expressing *SQLE* shRNAs, we evaluated the effects of SQLE loss on cancer cell migration, invasion, and stemness by wound-healing, transwell invasion/migration, and tumorsphere formation assays. While loss of SQLE greatly attenuated cell invasiveness and stemness in both MDA231 and MDA231-BrM cells, loss of SQLE could only affect the cell migration activity on MDA231 cells but not MDA231-BrM cells. Our RNA-seq data further identified a subset of SQLE-affected genes that is uniquely enriched in MDA231-BrM cells and favors brain extravasation and colonization. To explore the potential function of SQLE in brain extravasation and colonization, we established *in vitro* BBB models and *ex vivo* mouse brain slice organotypic cultures. We showed that loss of SQLE inhibited the ability of MDA231-BrM cells to across the BBB-mimic astrocyte-endothelial structures as well as impaired the co-option with blood capillaries in the mouse brain slices. Although SQLE-deficient MDA231-BrM cells could still spread on the surface of the blood vessels, they seemed to undergo apoptosis. Since the ability to invade, migrate, and penetrate is critical for invasion of cancer cells, our results strongly imply the novel function of SQLE in breast cancer cell invasion, penetration, and even colonization in the brain through blood vessel co-option. In summary, our data reveal a novel role for SQLE in two critical requisites for breast-to-brain extravasation and colonization - the ability to penetrate through BBB and to co-opt brain vessels for metastatic expansion. Our findings indicate that targeting SQLE may represent a therapeutic opportunity for breast cancer brain metastases.

#1551 Succinyl-CoA synthetase Beta-A: A novel metastasis promoting factor in lung cancer.

J. Kang, J. Hwang, A. C. Boese, S. Shuff, J. Kim, K. Eun, **S. Kang**;
Emory University, Atlanta, GA

Changes in metabolism occur when cancer cells disseminate from primary sites and metastasize. Mitochondrial metabolism plays an essential role in various biological processes of cancer cells, but the underlying mechanism through which mitochondrial factors contribute to cancer metastasis remains largely elusive. Anoikis is a form of apoptosis induced by loss of cell adhesion, and metastatic tumor cells must be anoikis resistant to survive during circulation before forming metastatic foci in distant organs. We performed an unbiased RNAi screen using a customized mitochondrion shRNA library and identified succinyl-CoA synthetase beta-A (A-SCS, also called SUCLA2), which is known to catalyze the reversible conversion of succinyl-CoA and ADP to succinate and ATP in the TCA cycle as an essential factor that promotes the survival of disseminated cancer cells during metastasis. We demonstrate that A-SCS manages redox balance during tumor metastasis, and this metabolic contribution is independent of its role in the TCA cycle. Mechanistically, A-SCS relocates from the mitochondria to the cytosol and binds to stress granules, promoting stress granules to express the redox-scavenging enzyme catalase upon cell detachment. This mitigates oxidative stress and makes cancer cells survive through anoikis, eventually promoting metastasis. A clinical correlation study comparing primary and metastasized tumors collected from lung cancer patients demonstrated that A-SCS levels align with catalase expression as well as the metastatic progression of lung cancer. Our finding provides an academic basis for developing new treatment targets against metastasis, which strikes elevated mitochondrial metabolism during cancer cell dissemination.

#1552 Tumorigenesis of basal muscle invasive bladder cancer was mediated by PTEN protein degradation resulting from *SNHG1* upregulation.

C. Huang, T. Li, H. Jin;
Oujiang Laboratory and Wenzhou Medical University, Wenzhou, China

hosphatase and tensin homolog deleted on chromosome ten (PTEN) serves as a powerful tumor suppressor, and has been found to be downregulated in human bladder cancer (BC) tissues. Despite this observation, the mechanisms contributing to PTEN's downregulation have remained elusive. In this study, we discovered that mice exposed to N-butyl-N-(4-hydroxybu-tyl)nitrosamine (BBN), a specific bladder chemical carcinogen, exhibited primary basal muscle invasive BC (BMIBC) accompanied by a pronounced reduction in PTEN protein expression *in vivo*. Utilizing a lncRNA deep sequencing high-throughput platform, along with gain- and loss-of-function analyses, we identified small nucleolar RNA host gene 1 (*SNHG1*) as a critical lncRNA that might drive the formation of primary BMIBCs in BBN-treated mice. Cell culture results further demonstrated that BBN exposure significantly induced *SNHG1* in normal human bladder urothelial cell UROtsa. Notably, the ectopic expression of *SNHG1* alone was sufficient to induce malignant transformation in human urothelial cells, while *SNHG1* knockdown effectively inhibited anchorage-independent growth of human BMIBCs. Our detailed investigation revealed that *SNHG1* overexpression led to PTEN protein degradation through its direct interaction with HUR. This interaction reduced HUR binding to ubiquitin-specific peptidase 8 (USP8) mRNA, causing degradation of USP8 mRNA and a subsequent decrease in USP8 protein expression. The downregulation of USP8, in turn, increased PTEN poly-ubiquitination and degradation, culminating in cell malignant transformation and BMIBC anchorage-independent growth. *In vivo* studies confirmed the downregulation of PTEN and USP8, as well as their positive correlations in both BBN-treated mouse bladder urothelium and tumor tissues of bladder cancer in nude mice.Our findings, for the first time, demonstrate that overexpressed *SNHG1* competes with USP8 for binding to HUR. This competition attenuates USP8 mRNA stability and protein expression, leading to PTEN protein degradation, consequently, this process drives urothelial cell malignant transformation and fosters BMIBC growth and primary BMIBC formation.

#1553 S1PR1 directs tumorsphere proliferation in ovarian cancer.

N. Gendrau-Sanclemente[1], A. Figueras[1], K. Gracova[1], E. Alsina-Sanchis[1], J. Marin-Jimenez[1], J. Casas[2], A. Vidal[3], X. Matias-Guiu[3], S. Fernandez-Gonzalez[3], M. Barahona[3], L. Marti[3], J. Ponce[3], F. Vinals[1];

[1]Catalan Institute of Oncology; Institut d'Investigacio Biomedica de Bellvitge (IDIBELL), Barcelona, Spain, [2]Institute for Advanced Chemistry of Catalonia (IQAC-CSIC), Barcelona, Spain, [3]University Hospital of Bellvitge, Barcelona, Spain

Despite the clinical efforts to improve detection and treatment of high-grade serous ovarian cancer (HGSOC), half of diagnosed women will die every year because of this disease. Notably, nearly all of them present with ascites at diagnosis, which is directly associated with poor prognosis. Malignant ascites production occurs when ovarian cancer cells shed from the primary tumor, creating a selective pressure environment that threatens their survival. Therefore, cancer cells cluster into tumorspheres, the main metastatic units in HGSOC. In recent years, valuable insights into the mutational and immunological landscapes of HGSOC have been gained. However, there is scarce evidence on the precise molecular mechanisms that enable tumorspheres to surpass the ascites bottleneck and metastasize. In this work, our group addresses this knowledge gap by deciphering the role of S1PR1 in ovarian tumorsphere biology. In this study, ascites samples and Formalin-Fixed Paraffin-Embedded (FFPE) tumors and peritoneal metastases from a cohort of 32 treatment-naïve HGSOC patients have been used. Furthermore, 3D spheroid models from four different ovarian cancer cell lines have also been developed for *in vitro* and *in vivo* assays. Our results indicate that up to 60% of cells within HGSOC tumorspheres are proliferating due to an increased expression of pro-proliferative receptors. Thus, cancer cells within tumorspheres that overexpress these receptors might benefit from autocrine and paracrine signaling through release of their ligands. In this work, we have identified S1P-S1PR1 as one of these ligand-receptor axes, which promotes an autocrine positive loop that increases the intermediates of sphingolipid metabolism in ovarian cancer spheroids. Here, we demonstrate that S1PR1 is highly expressed in ascites tumorspheres and, in consequence, overexpressed in metastases in comparison with primary tumors. Furthermore, we also report that proliferation levels of ovarian cancer spheroids positively correlate with S1PR1 endogenous expression. Consistently, these levels are significantly reduced when S1PR1 is knocked out or pharmacologically inhibited. In addition, our results indicate that MEK1/2-ERK is the key downstream pro-mitogenic pathway of S1PR1 in HGSOC tumorspheres, and that its pharmacological inhibition is effective in reducing growth and number of disseminations *in vivo*. Conclusively, our group is the first one in reporting that the axis S1P-S1PR1-MEK1/2 is the main proliferative mechanism in HGSOC tumorspheres, providing them with a selective advantage and, consequently, a greater metastatic potential. The preclinical findings presented here may represent an opportunity to further explore targeted therapeutic strategies to hamper disease progression in ovarian cancer patients with the poorest outcome.

#1554 *LIM Domain 7* (*LMO7*) splice variant influences prostate cancer biology.

M. Al Abo[1], D. J. George[2], Z. Wang[3], S. R. Patierno[2], J. A. Freedman[2], A. Jiang[4];
[1]Duke Cancer Institute, Durham, NC, [2]Duke University, Durham, NC, [3]Shanghai Institute for Nutrition and Health, Shanghai, China, [4]Washington University, St. Louis, MO

LIM Domain 7 (LMO7) has been shown to participate in cell-cell junction formation through interaction with afadin and α-actinin. It has also been reported to collaborate with Rho kinase to regulate actin filament formation and to activate the Rho-myocardin-related transcription factor serum response factor pathway. Additionally, LMO7 itself may function as a transcription factor, regulating the expression of genes involved in Epithelial Mesenchymal Transition (EMT). Alternative splicing of *LMO7* has the potential to modulate its function. Previously, we reported *LMO7* as a target that is alternatively spliced in prostate cancer (PCa) between self-reported Black and White patients. In addition, by analyzing expression of *LMO7* splice variants in The Cancer Genome Atlas (TCGA) data, we previously reported increased expression of a *LMO7* splice variant skipping exon 12 in breast, lung and liver cancer compared with paired normal tissues. In the present study, we found that *LMO7* is downregulated in metastatic PCa specimens within the Stand Up To Cancer cohort. To investigate the functional impact of expression of the *LMO7* splice variant skipping exon 12 in PCa, we utilized CRISPR-Cas9 methodology to delete *LMO7* exon 12 in PCa cells and assessed resulting alterations in PCa cell biology. The *LMO7* exon 12 deleted PC3 PCa cells exhibited enhanced migratory potential compared with parental PCa cells. An Immunofluorescence (IF) assay showed weak staining of cell-cell junctions in *LMO7* exon 12 deleted PCa cells compared with parental PCa cells. Moreover, IF staining showed retardation in f-actin in *LMO7* exon 12 deleted PCa cells compared with parental PCa cells. As E-Cadherin is often inhibited during EMT, we assessed the level of E-Cadherin by western blot and real-time polymerase chain reaction (PCR). These analyses revealed that E-Cadherin protein as well as messenger RNA is suppressed in *LMO7* exon 12 deleted PCa cells compared with parental PCa cells. These findings suggest a role for skipping of *LMO7* exon 12 in disrupting PCa cell-cell junctions, down-regulating E-Cadherin in PCa and enhancing PCa cell migratory potential, consistent with EMT.

#1555 Nuclear accumulation of cell surface programmed cell death ligand 1 promotes metastatic outgrowth in triple-negative breast cancer cells.

Y. Gohara, N. Tomonobu, R. Kinoshita, K. Yamamoto, H. Murata, M. Sakaguchi;
Okayama Univ. Graduate School of Med., Dentistry & Pharm. Sci., Okayama, Japan

PD-L1 presented on the cancer cell surface is well known for its role in immune checkpoint regulation by interacting with PD-1 on immune cells. On the other hand, it has been reported that PD-L1 is localized in the cancer cells' nuclei, where the nuclear PD-L1 (nPD-L1) is conducive to cancer outgrowth and motility. However, there has yet to be reported about the mechanistic insight into the event. In this study, we, therefore, aimed to clarify still unidentified points in the nPD-L1-mediated event. Our efforts revealed that the upregulation is induced by a functional suppression of nuclear protein X (tentative name), which we identified as a novel binding protein with nPD-L1 at its cytoplasmic tail. Their nuclear interaction also abolished an aggressive cancer proclivity, epithelial-mesenchymal transition (EMT). The mechanism is helpful to the complex nature of PD-L1 in plural cancer cell behaviors.

#1556 AMIGO2 is associated with the peritoneal dissemination in serous ovarian cancer by enhancing its adhesion to peritoneal mesothelial cells.

Y. Iida, S. Sato, K. Yamamoto, K. Hikino, M. Okawa, M. Hosokawa, M. Sawada, H. Komatsu, A. Kudoh, H. K. Seong, R. Izutsu, M. Osaki, F. Okada, F. Taniguchi;
Tottori University, Yonago, Japan

Amphoterin-induced gene and open reading frame 2 (AMIGO2) has been associated with the prognosis of colorectal, gastric, and cervical cancer. However, its relationship with ovarian cancer remains unclear. This study aimed to clarify the role of AMIGO2 in ovarian cancer. The research involved evaluating AMIGO2 expression in patients with ovarian serous carcinoma using immunohistochemistry. The AMIGO2-high group exhibited significantly shorter progression-free survival (PFS) compared to the AMIGO2-low group. The predictive index of the AMIGO2-high group was considerably higher than that of the AMIGO2-low group. The rate of complete cytoreductive surgery was lower in the AMIGO2-high group than in the AMIGO2-low group. Furthermore, in vitro studies showed that four serous ovarian cancer cell lines expressed AMIGO2 expression and adhesion to mesothelial cells. Adhesion to mesothelial cells was attenuated by AMIGO2 knockdown in SKOV3 cells. Moreover, in a murine model, AMIGO2 downregulation in SKOV3 cells significantly suppressed peritoneal dissemination. These findings suggest that high AMIGO2 expression in serous ovarian carcinoma cells contributes to a poor prognosis by promoting peritoneal metastasis through enhanced cell adhesion to mesothelial cells.

#1557 Loss of lncRNA XIST promote brain metastasis by reshaping tumor lipid metabolism via upregulation of ACSL4.

Y. Liu, M. R. Smith, Y. Wang, R. D'Agostino, Jr., J. Ruiz, G. L. Kucera, L. D. Miller, W. Li, M. D. Chan, M. Farris, D. Zhao, F. Xing;
Wake Forest University School of Medicine, Winston-Salem, NC

Metastatic disease is the main cause of cancer death, and the brain is one of the major sites of breast tumor metastasis. The median survival of breast cancer patients who developed brain metastases (BrM) is less than a year even with the advanced treatment such as stereotactic radiosurgery (SRS). Regardless of high clinical significance, the pathological mechanism of brain metastasis is still poorly understood. Previously, we found that loss of lncRNA XIST robustly promote metastasis and specially brain metastasis in breast cancer. However, the underlying molecular mechanism was not fully understood. In following study, we found that loss of XIST has significantly altered lipid metabolism of breast cancer cells specifically increasing lipid droplet amount and PUFA incorporation. Instead of *de novo* syntheses, XIST^{low} cancer cells acquire fatty acid by uptake from exogenous. We found that one X-linked gene, Acyl-CoA Synthetase Long Chain Family Member 4 (ACSL4) which are highly upregulated after loss of XIST is responsible for the altered lipid metabolism. ACSL4 activated the free polyunsaturated fatty acids (PUFAs) and lead to increased incorporation of PUFAs into phospholipids. On one hand, elevated ACLS4 expression leads to relative low PPAR pathway activation by decreasing the cellular free PUFA level which directly binds and activate PPAR. PPAR pathway is known to inhibit the expression of inflammatory cytokines which are important for cancer cells to establish brain metastasis. On the other hand, elevated ACSL4 expression enable cancer cells to metabolize the abundant PUFAs in the brain environment, thereby gaining survival advantage. However, increased PUFA incorporation into lipids especially phospholipids produce excess lipid ROS and sensitize cells to ferroptosis inducer such as RSL3. Our study has find out that brain microenvironment not only supports the outgrowth of *XIST* ^{low} cells by providing PUFAs for maintaining their metastatic properties but also sensitizes those cells to ferroptosis inducers, a potential therapy for treating this devastating disease.

#1558 Deciphering the role of ribosomal paralogs RPL39/RPL39L in metaplastic breast cancer.

M. F. Chervo, **M. Li**, C. Mancino, K. A. Ortega Martinez, V. V. Shah, W. Qian, J. Zhou, L. Guzman-Rojas, P. Matre, F. Taraballi, K. W. Brannan, J. C. Chang; Houston Methodist Research Institute, Houston, TX

Metaplastic breast cancer (MpBC) is a rare, highly aggressive, and metastatic malignancy that accounts for <5% of all breast cancer diagnoses. Most MpBCs display a triple-negative breast cancer (TNBC) phenotype (ER-/PR-/HER2-). MpBCs exhibit the most dismal prognosis of all breast cancer subtypes. The standard of care for metastatic MpBC remains systemic chemotherapy, despite known resistance to most cytotoxic drugs. MpBCs are enriched with epithelial-to-mesenchymal transition (EMT) and cancer stem cell (CSC) markers. We previously described a unique molecular signature for breast cancer stem cells (BCSCs) derived from patient biopsies and identified ribosomal protein L39 (RPL39) as a critical driver of treatment resistance, BCSCs self-renewal, and lung metastases in TNBC/MpBC. Growing evidence has also demonstrated aberrant expression of the testis-specific ribosomal protein paralog 39L (RPL39L) in several cancer types. Here, we hypothesize that RPL39 and its paralog RPL39L alter ribosome composition and function to initiate a specific translational landscape that promotes tumor growth and enhanced metastatic potential in MpBC. We first examined the relative expression of RPL39 and RPL39L in TNBC/MpBC cell lines and patient-derived xenografts (PDXs) using real-time qPCR. We detected co-expression of RPL39/RPL39L transcripts, however, RPL39L mRNA levels were significantly lower than RPL39. These results suggest that both RPL39 and RPL39L contribute to ribosome heterogeneity in TNBC/MpBC. To investigate the function of RPL39/RPL39L transcripts, we designed a small interfering RNA (siRNA)-strategy targeting their differential 5' untranslated region (5’ UTR). Selective downregulation of RPL39 and RPL39L mRNA inhibited in vitro cell proliferation in TNBC/MpBC models. Notably, combined targeted silencing of both RPL39 and RPL39L further decreased cell proliferation in comparison to individual siRNAs. We next evaluated the efficacy of RPL39/RPL39L dual blockade in vivo using MpBC PDXs. MpBC PDX4664 was implanted into the mammary fat pad of NSG mice. Once tumors were established (100-150 mm^3), mice received phosphate buffered saline (PBS controls) or 0.5 mg/kg RPL39/RPL39L siRNAs encapsulated into liposome-like nanoparticles (NPs) via tail vain (i.v.) injection. Animals were treated thrice a week for 21 days and sacrificed 48 h after the last injection. We found that siRNAs-NP formulation silenced RPL39/RPL39L expression in vivo and significantly reduced tumor growth. Overall, our findings support the notion that RPL39/RPL39L ribosome heterogeneity may confer preferential translation of oncogenic and BCSC-related genes, facilitating tumor progression and metastasis in MpBC. Ongoing studies are directed to validate ribosome heterogeneity by proteomic analysis and evaluate the role of RPL39/RPL39L on global translation by ribosome profiling.

#1559 IKZF1 plays a crucial role in the spread of melanoma.

J. Oh[1], D. Lee[1], S. Lee[1], H. Park[2], H. Gee[1];

[1]Yonsei University College of Medicine, Seoul, Korea, Republic of, [2]College of Life Science and Biotechnology Yonsei University, Seoul, Korea, Republic of

Melanoma is one of the most fatal type of skin cancer. If melanoma has spread to distant sites, it is refractory to existing therapies with the 5-year survival rate declining to 17%. Metastasis remains as the main barrier to successful therapy, persisting as the main cause of cancer-related death. Thus, understanding metastasis mechanism is vital.

First, we confirmed that IKZF1 gene was more increased in circulating tumor cells than primary tumor cells. Using GFP+ B16F10, we generated an orthotopic melanoma mouse model and isolated GFP+ tumor cells of primary footpad, blood, and lung. In single cell RNA sequencing, IKZF1, IRF8, NFE2 genes were more upregulated in circulating tumor cells than primary tumor cells. We also found these correlations in human melanoma cell line orthotopic mouse model and Braf/Pten mouse model.

Next, we conduct intervention study to find causality in IKZF1 and metastasis. IKZF1 KO led to fewer CTCs and IKZF1 inhibitor, lenalidomide, reduced metastasis in mice.

Collectively, we demonstrate that IKZF1 could contribute the formation of CTC and IKZF1 could be a target for metastasis treatment.

#1560 *In vivo* CRISPR/Cas9 transcriptional activation screen leads to discovery of INAFM2, a novel driver of metastasis.

A. Molotkova, E. Deniz, M. Swift, E. Glasgow, J. Toretsky, A. Uren;
Georgetown University Medical Center, Washington, DC

Metastasis is the main cause of mortality in cancer patients and accounts for about 90% of cancer deaths, which has not changed in the past 50 years. This indicates a significant need for further study of metastasis pathways to find novel druggable targets. Ewing sarcoma (ES) is an aggressive childhood cancer that occurs in the bones or soft tissue. The five-year survival rate for Ewing sarcoma patients diagnosed with metastatic disease is still only 25%, making ES a good model for studying metastasis. We performed a genome-wide CRISPR/Cas9 transcriptional activation screen in a zebrafish xenograft model to discover genes whose activation leads to increased metastasis. The screen identified a number of genes that may accelerate ES metastasis; we chose *INAFM2* for further study because multiple unique INAFM2-targeting gRNAs were enriched in the screen and we discovered a potential link to metastasis and patient survival in publicly available clinical data. Overexpression of INAFM2 in six different cancer cell lines (four ES, one hepatocellular carcinoma, and one stomach adenocarcinoma) caused increased cell migration and chemotaxis *in vitro*, and increased intravasation in zebrafish xenografts. INAFM2 knockdown in four cancer cell lines (two ES, one clear cell renal cell carcinoma, and one stomach adenocarcinoma) decreased chemotaxis and rescue of INAFM2 expression restored the cells' ability to migrate. Analysis of patient tumor RNA sequencing data from many different types of cancers revealed correlations between INAFM2 expression and both an increased metastatic phenotype and poor patient survival. Further *in vivo* studies by tail vein injection of ES cells in immunodeficient mice demonstrated significantly increased gross metastases with INAFM2 overexpression and decreased gross metastases with INAFM2 knockdown compared to the respective control groups. This provides strong evidence for a substantial role of INAFM2 in cancer metastasis. Human *INAFM2* is an unstudied gene and our preliminary work has revealed that the INAFM2 protein localizes to the cell membrane, is glycosylated, and may be involved in Wnt and/or MAPK pathway signaling. Inafm2 silencing by morpholino in zebrafish embryos lead to significant mortality, necrosis, and developmental delays/defects including severe cardiac edema. Current studies are focused on further discerning the molecular pathways that mediate the role of INAFM2 in promoting metastasis using *in vitro* and *in vivo* models as well as characterizing the functional significance of the direct protein binding partners and post-translational modifications for INAFM2.

#1561 Identification of tumor-associated macrophages promoting early-stage metastasis during peritoneal dissemination in gastric cancer.

W. Kawase[1], Y. Hiroshima[1], I. Hashimoto[2], S. Onuma[2], M. Furuta[2], N. Machida[2], T. Oshima[2], Y. Miyagi[1];
[1]Kanagawa Cancer Centre Research Institute, Yokohama, Japan, [2]Kanagawa Cancer Centre, Yokohama, Japan

Peritoneal dissemination (PD) is the most frequent metastasis pattern in gastric cancer (GC) and is a significant predictor of poor prognosis. However, the mechanisms underlying PD formation remain unclear, and a PD-specific signature has not been identified. PD development is thought to be influenced by various changes occurring in GC tumor cells and immune cells present in the peritoneal cavity. We previously performed RNA-seq analysis of cell components in cytology-positive (CY1) gastric cancer ascites. The results suggested that tumor-associated macrophages (TAMs) infiltrate the abdominal cavity together with GC tumor cells and might be involved in PD development. In this study, we aimed to identify the specific TAMs responsible for promoting metastasis during the early stage of PD in GC. We demonstrated the abundant presence of TAMs in CY1 GC ascites using flow cytometry analysis and identified several genes that were significantly expressed in CY1 TAMs using single-cell RNA-seq analysis. Furthermore, we evaluated the potential of these genes to serve as therapeutic targets for the treatment of PD in GC.

#1562 HMGA2 regulates GPX4 expression and oxidative stress.

P. E. Dike[1], T. Campbell[2], M. Awolowo[1], V. Odero-Marah[1];
[1]Morgan State University, Baltimore, MD, [2]Clark Atlanta University, Atlanta, GA

Prostate cancer (PCa) is a leading cause of mortality, primarily due to its ability to metastasize to the bone. The High Mobility Group AT-Hook 2 (HMGA2) plays a crucial role in regulating gene expression and has been implicated in tumorigenesis and the metastatic process. Our recent study revealed that overexpression of the wild-type/full-length HMGA2 isoform in PCa cells promotes cancer progression by triggering epithelial mesenchymal transition (EMT), whereas truncated HMGA2 isoform promotes progression through oxidative stress signaling. We hypothesize that HMGA2 regulates GPX4 expression and oxidative stress in PCa. We studied the expression of HMGA2 and GPX4 in various PCa cell lines including enzalutamide resistant cell line (C4-2B MDVR), LNCaP cells overexpressing HMGA2 isoforms (wild type and truncated HMGA2). Our analysis of HMGA2 and GPX4 expression in diverse PCa cell lines, shows an inverse relationship between HMGA2 and GPX4 levels. Elevated HMGA2 expression coincides with reduced GPX4 expression, leading to heightened oxidative stress and susceptibility to ferroptosis. Moreover, treatment of enzalutamide resistant cell line C4-2B MDVR with ferroptosis inducer RSL3, further suppresses GPX4 expression, resulting in decreased cell proliferation. Our results unveils the intricate relationship between HMGA2, GPX4 regulation and oxidative stress in the context of prostate cancer progression. Exploiting this oxidative stress pathway offers a promising therapeutic approach for cancer treatment, especially for enzalutamide-resistant cancer cells.

Acknowledgements: These studies were supported by NIH/NIGMS/RISE SR25GM060414 and NIH/NIMHD 2U54MD007590; 5U54MD013376.

#1563 Anoikis associated metabolic modulation by UCA1 in CRC.

S. Leslie, K. Doxtater, S. Lopez, B. Hafeez, T. Oraby, T. Loy, M. K. Tripathi;
University of Texas Rio Grande Valley, McAllen, TX

Colorectal Cancer (CRC) is the second most lethal cancer in estimated deaths for 2023 according to the American Cancer Society. This is partially due to the low survival rate once CRC is diagnosed at a distant location. This warrants early diagnostic markers and an understanding of the mechanisms underlying the metastatic process, anoikis resistance being one of them. Our laboratory analysis of the TCGA database comprising 519 human CRC tissues shows lncRNA UCA1 overexpressed in tumors compared to normal, and higher expression of lncRNA UCA1 is responsible for the progression, metastasis, and poor survival of CRC patients. In our anchorage-independent growth model (anoikis resistant), using isogenic (oncogenic and metastatic) cell lines, we observed a very high expression of lncRNA UCA1 along with GluT1 with increased cell survival. Cancer cells, however, appear to rapidly increase their glucose uptake and directly ferment it into lactate, even in the presence of oxygen and functional mitochondria. UCA1 has been found to play an essential role in the development of metastasis and dysregulation of glycolysis in various cancers. To verify if lncRNA UCA1 modulates anoikis resistance and glucose metabolism, we generated SW480+UCA1 overexpression (OE) and SW620+shUCA1 knockdown (KD) stable cell lines using lentiviral transduction. The OE GFP-expressing cell lines were further sorted, and grown in puromycin. The KD cell lines were selected with puromycin for the generation of stable cell lines. The stable cell lines were characterized through different phenotypic assays. UCA1 OE cell lines have a higher glucose uptake and the UCA1 KD cell lines have a lower glucose uptake. The lactate production is high in the KD and low in OE cell lines. The OE and KD cell lines along with the control cell lines were subjected to an anoikis model, and glucose and lactate analysis were performed accordingly. RT-PCR and western blot analysis were performed for the target genes responsible for cell survival, stemness, and glucose metabolism. We are analyzing the Extracellular Acidification Rate (ECAR), Oxidative Consumption Rate (OCR), ATP production rate the rate and potential max rate of glycolysis, and the mitochondrial stress of the recombinant cell lines using the “Agilent Seahorse XF”. The role of lncRNA UCA1 in anoikis resistance leading to metastasis and modulating glucose metabolism will provide new insights into the pathophysiology of CRC metastasis. This information will be beneficial for developing more unique strategies for the treatment of this metastatic disease.

#1564 NEU4-mediated desialylation ignites the oncogenic receptors for the dissemination of ovarian carcinoma.

J. Shi[1], R. Zhou[1], S. Wang[1], Y. Liu[1], B. Tian[1], Y. Liu[1], Y. Chen[1], T. Hu[1], Y. Mu[1], S. Wang[1], X. Shao[1], J. Yan[1], P. Qu[2], W. Ding[2], S. Yang[1], Y. Shi[1], J. Li[1], L. Wang[1];

[1]The School of Medicine, Nankai University, TianJin, China, [2]Department of Gynecological Oncology, Tianjin Central Hospital of Obstetrics and Gynecology, TianJin, China

Background: Glycosylation profoundly influences the interactions between cancer cells and microenvironmental stromal cells during the peritoneal disseminated metastasis of ovarian carcinoma (OC), which is the major cause of cancer-related death. Although the characteristic cancer glycoconjugates are widely used as biomarkers for cancer diagnosis, our knowledge about cancer glycome remains quite fragmented due to the technique limitations in analyzing glycan chains with tremendous structural and functional heterogeneity.

Method: Given the dysregulated cancer glycome is defined by the altered glycosylation machinery, here we performed a systematic loss-of-function screen on 498 genes involved in glycosylation for key regulators of OC dissemination. We identified neuraminidase 4 (NEU4), an enzyme capable of hydrolyzing terminal sialic acid from glycoconjugates, as a vital peritoneal dissemination-promoting modifier of OC glycome. What's more, we also identified membrane proteins whose sialylation was able to be modified by NEU4 in OC cells by pull down and mass spectrum to investigate the functional significance of NEU4-mediated desialylation.

Results: In human patients with high-grade serous OC (HGSOC), increased NEU4 was detected in the disseminated OC cells when compared with that in the primary tumor cells, which significantly correlated with the worse survival. Among three alternative splice-generated isoforms of human NEU4, we revealed that only the plasma membrane-localized NEU4 isoform 2 (NEU4-iso2) and intracellular isoform 3 promoted the peritoneal dissemination of OC by enhancing the cell motility and epithelial-mesenchymal transition. We also identified NEU4-iso2-regulated cell surface glycoproteome and found that NEU4-iso2 desialylated the epithelial growth factor receptor (EGFR), in particular at N196 residue, for the hyperactivation of EGFR and its downstream tumor-promoting signaling cascades.

Conclusion: Our results provide new insights into how the OC glycome is dysregulated by NEU4 during OC progression and reveals a functionally important glycosite on EGFR for its abnormal activation in cancer.

#1565 USP13 influences metastatic features in fallopian tube-originated high-grade serous carcinoma.

B. Mok[1], J. Kwon[1], J. Zhang[1], S. Allsup[1], H. Choi[2], C. Han[1];
[1]Georgetown University School of Medicine, Washington, DC, [2]Konkuk University, Seoul, Korea, Republic of

High-grade serous ovarian carcinoma (HGSOC), originating from the fallopian tube, stands as a formidable challenging gynecologic malignancy with the highest mortality rate worldwide. Ubiquitin-specific peptidase 13 (USP13) has garnered attention due to the highly frequent *USP13* gene copy amplification in human ovarian cancer. However, its precise pathological role in ovarian cancer remained elusive. To uncover the underlying role of USP13 in HGSOC, we developed a novel genetically engineered mouse model (GEMM) of HGSOC. *Ovgp1-iCreER*^{T2};*Trp53*$^{flox/flox}$;*Pten*$^{flox/flox}$ mouse (OPT) was crossed with Rosa26$^{-LSL-Usp13}$ knockin mouse model (U), generating *Ovgp1-iCreER*^{T2};*Trp53*$^{flox/flox}$;*Pten*$^{flox/flox}$; Rosa26$^{-LSL-Usp13}$ mouse model (OPTU). Usp13 overexpression with loss of p53 and Pten was induced specifically in fallopian tube secretory epithelial cells in OPTU mice. OPTU mice demonstrated the development of STIC and early HGSOC in the fallopian tube as well as invasive metastatic HGSOC. While OPT tumors largely retained mucinous and HGSOC subtypes, displaying limited metastatic behavior, OPTU tumors exhibited more complex ovarian tumor subtypes, including mucinous, HGSOC, and Mixed Mesodermal Mullerian Tumor (MMMT) histology. Furthermore, OPTU tumors showed invasive and metastatic phenotypes, characterized by an increased incidence of ovary invasion, metastasis to distant organs, and ascites development. Importantly, OPTU-driven HGSOC tumors closely resemble human HGSOC histology features, making the OPTU model a valuable tool for exploring fallopian tube-originated ovarian cancer. Primary ovarian cancer cells established from ascites of the OPTU mouse reproduced metastatic HGSOC tumorigenesis in the syngeneic mouse study. Stable USP13 knockdown in OPTU cells exhibited reduced cell proliferation and metastatic abilities in 2D and 3D cultures. In summary, this study underscores the pivotal role of USP13 in facilitating metastasis in fallopian tube-originated HGOSC. Our findings may provide a promising avenue for future therapeutic strategies aimed at mitigating the aggressive nature of USP13-amplified fallopian tube-originated HGOSC.

#1566 Cancer metastasis and stemness: The metastasis-inducer MACC1 regulates LGR5 to promote cancer stem cell-like properties in colorectal cancer.

M. Erdem[1], K. Lee[1], M. Hardt[1], J. Regan[2], D. Kobelt[1], W. Walther[1], C. Regenbrecht[3], **U. S. Stein[1]**;
[1]Max Delbruck Center for Molecular Medicine, Berlin, Germany, [2]Charite Berlin, Berlin, Germany, [3]CELLphenomics GmbH, Berlin, Germany

Colorectal cancer (CRC) is one of the leading causes of cancer-related deaths worldwide. The high mortality is directly associated with metastatic disease which is thought to be initiated by colon cancer stem cells according to cancer stem cell (CSC) model. Consequently, early identification of those patients who are at high risk for metastasis is crucial for improved treatment and patient outcome. Metastasis-associated in colon cancer 1 (MACC1) is a novel prognostic biomarker for tumor progression and metastasis formation independent of tumor stage. We previously showed an involvement of MACC1 in cancer stemness in the mouse intestine of our transgenic mouse models. However, the expression of MACC1 in human CSCs and possible implications remain elusive. Here, we explored the molecular mechanisms by which MACC1 regulates stemness and CSC-associated invasive phenotype based on patient-derived 3D cell culture models (PD3D), patient-derived xenografts (PDX) and human CRC cell lines. We showed that CD44-enriched CSCs from PD3D models express significantly higher levels of MACC1 and display higher tumorigenicity in immunocompromised mice. Similarly, RNA sequencing performed on PD3D and PDX models demonstrated significantly increased MACC1 expression in ALDH1(+) CSCs, highlighting its involvement in cancer stemness. We further showed the correlation of MACC1 with CSC markers CD44, NANOG and LGR5 in PD3D models as well as established cell lines. Additionally, MACC1 increased stem cell gene expression, clonogenicity and sphere formation. Strikingly, we showed that MACC1 binds as a transcription factor to the LGR5 gene promoter uncovering the long-known CSC marker LGR5 as novel essential signaling mediator used by MACC1 to induce CSC-like properties in human CRC patients. Our *in vitro* findings were further substantiated by significant positive correlation of MACC1 and LGR5 in CRC cell lines as well as CRC patient tumors. Taken together, this study indicates that the metastasis-inducer MACC1 act as a cancer stem cell-associated marker. Interventional approaches targeting MACC1 would potentially improve further targeted therapies for colorectal cancer patients to eradicate CSCs, prevent cancer recurrence and distant metastasis formation.

#1567 Honing in on the metastasis machinery.

J. Chen, T. C. Fugere, F. Mazahreh, B. Fugere, E. Delgiacco, A. M. Safar;
University of Arkansas for Medical Sciences, Little Rock, AR

A prevailing 'principal' in oncology posits that metastases is the last step in a strict sequence of tumorigenic events. However, despite decades of widespread breast & colon cancer (CA) screening and interceptive surgeries, there hasn't been any decrease in metastatic (M) stages, a discrepancy that undermines the validity of this principle. Others suggested unlinking tumorigenesis from metastasis, supporting an evolutionarily convergent model. We reasoned that cells' ability to circulate (physiologic in white blood cells) is mediated by putative gene(s)-encoded metastatic apparatus (MA), hence subject to alteration during the genomic turmoil of tumorigenesis. It follows that essential components of MA cannot be chromosomally deleted in M CAs; stage I CA may indicate deactivated MA. The overarching goal here is to identify genes encoding the putative MA. Chromosomal deletions are relevant since they are definitive, testable and inform mutational and epigenetic events. Of note, the retained gene list (RGL) in any CA includes cell-viability genes (CVG).
Methods: The Cancer Genome Atlas (TCGA) is a well-curated, clinically annotated public database. We examined copy number variation to determine the RGL1 in stage 1 cancers (CVG); and RGL2 in metastatic CAs. To account for possible heterogeneity or redundancy in MA in different CA types, we performed the RGL2 analysis within organ systems. By TCGA's criteria, deletion was defined as a microarray expression of <-0.3. Regions of interest, therefore, were RGL2 excluding RGL1.
Results: Table lists RGL2 excluding RGL1 per CA site

RGL2 (excluding RGL-1 2,405 regions): unique genes that are never deleted in any of the listed metastatic cases in TCGA per site (n) and the number of overlapping genes for further testing consideration											
Gastrointestinal Exocrine		Gastrointestinal Mucosa		Lung		Genitourinary		Breast		Head & Neck		Thyroid	
Pancreas	392 (100)	Esophagus (49)	1982	Adenocarcinoma (169)	2800	Bladder (216)	434	BC (191)	341	H&N (337)	275	Thyroid (224)	8292
		Gastric (52)	7773	Squamous (90)	2101	Kidney (111)	10189						
Number of Overlapping unique genes	392	825		368		87		341		275		8292	
Pan-CA Overlap	ZERO												

Conclusion: We present a plausible mechanistic approach to identify RGL encoding the putative MA for interrogation by gene-editing experiments. Our data suggest plurality of the MA given zero overlap for the entire set. Performing the analysis in additional cases within embryonal ontogeny or by driver oncogene might be useful in this pursuit. This work has implications for screening, diagnostic, prognostic surgical/adjuvant CA therapy, and novel antineoplastics.

#1568 Her2 promotes early dissemination of breast cancer by suppressing the p38 pathway through upregulation of Wip1.

Nan Wang

Wake Forest Baptist Medical Center, Winston-Salem, NC

(a)Metastasis is the leading cause of cancer-related deaths. Increasing evidence shows that cancer cells can disseminate from early primary lesions that are impalpable, but the pathways are poorly understood. Her2 promotes breast cancer early dissemination by suppressing p38, but how Her2 downregulates p38 is unclear. In this study, we investigated the mechanism underlying suppression of p38 by Her2 in breast cancer early dissemination using cell models and xenograft models of early lesions of breast cancer.
(b)We studied the role of Wip1, a p38 phosphatase, in disseminating phenotypes in cell line models of breast cancer early lesions, including cell motility measured in transwell assays, cell invasion measured by percentage of organoids with outward invading cells, and epithelial-to-mesenchymal transition (EMT) measured by levels of EMT markers in Western blotting analysis and immunofluorescence (IF) staining assays.
(c)We demonstrate that high levels of Wip1 correlated with Her2+ status, and reduced phosphorylation of p38 and its downstream effectors MK2 and Hsp27 in tissue samples from early lesions of human breast cancer. In addition, ectopic expression of Wip1 reduced phosphorylation of p38, MK2 and Hsp27 in cell models of breast cancer early lesions.We found that Wip1 promoted migration, invasion and EMT, while Wip1 knockdown abrogated the ability of Her2 to induce these disseminating phenotypes, in cell line models of early lesion breast cancer. Thus, Wip1 induction is both sufficient, and necessary for Her2, to promote migration, invasion and EMT in early lesion breast cancer cells. In an attempt to identify the Wip1 downstream effectors involved in disseminating phenotypes, we found that ectopic expression of the constitutively active mutants of p38 reversed the ability of Wip1 to suppress MK2 and Hsp27 phosphorylation and to induce migration, invasion and EMT in early lesion breast cancer cells. These results suggest that Wip1 promotes breast cancer early dissemination by suppressing p38. We investigate the mechanism by which Her2 induces Wip1 expression. Ectopic expression of Her2 did not alter the level of Wip1 mRNA or the Wip1 protein stability, suggesting that Her2 promote Wip1 expression by regulating its translation. We are currently investigating the mechanism by which Her2 induces Wip1 translation.Moreover, inhibitors of Her2, Wip1 and Skp2 can each reduce the disseminating phenotypes in cells models of breast cancer early lesions ectopically expressing Her2, Wip1 or Skp2.
(d)Our findings identify the Her2-Wip1-p38-Mk2-Hsp27 cascade as a novel mechanism mediating breast cancer early dissemination and provide a basis for new therapies targeting early metastatic dissemination in Her2+ breast cancer using inhibitors for Her2, Wip1 or Skp2.

#1569 Keratin X promotes cell metastasis and sorafenib resistance via the AMPKα/Snail axis in hepatocellular carcinoma.

Y.-H. Lin, C.-T. Yeh;
Chang Gung Memorial Hospital - Linkou branch, Taoyuan City, Taiwan

A great majority of liver cancers are developed from cirrhotic livers. The key molecules involved in cirrhosis-mediated hepatocarcinogenesis have not been clearly defined. Understanding the oncogenic pathways and their associations with cancer growth, metastasis and drug resistance may help scientists devise new effective therapeutic agents. In the present study, we identified the intermediate filament-forming protein keratin X (KRTX) as a key factor in cirrhosis-mediated hepatocarcinogenesis. KRTX was highly expressed in HCC tissues and correlated with poor survival outcomes. Experimental verification revealed that overexpression of KRTX enhanced cell growth, tumor cell metastasis, glycolysis and sorafenib resistance. Conversely, knockdown of KRTX led to opposite effects. Mechanistically, KRTX inhibited AMPKα phosphorylation, thereby enhancing Snail protein stability. Additionally, TGFβ1 positively regulated *KRTX* expression, resulting in a KRTX/AMPKα (Thr172)/Snail axis-mediated increase in cell motility. Treating with 2-deoxyglucose reversed the KRTX-induced metastasis and sorafenib resistance. In clinic, KRTX expression is positively correlated with Snail overexpression and high KRTX/Snail expression had poor prognosis in HCC patients. Our data revealed a signaling pathway from TGFβ1, KRTX, through p-AMPKα (Thr172) to Snail. Targeting KRTX and its pathway may be effective for treating patients with metastatic HCC.

#1570 Lipid metabolism alterations promote TNBC metastasis and immunotherapy resistance via PD-L1 internalization and signaling.

W. O. Wofford, J. Kim, D. Kim, A. H. Janneh, H. G. Lee, F. C. Atilgan, N. Oleinik, E. Hill, O. Saatci, S. Gencer, P. Chakraborty, S. Mehrotra, O. Sahin, B. Ogretmen;
The Medical University of South Carolina, Charleston, SC

Programmed death-ligand 1, PD-L1 (CD274), is an immune checkpoint protein upregulated by cancer cells to facilitate immune evasion. PD-L1 also performs oncogenic functions within cancer cells, but the underlying mechanisms of PD-L1 internalization and signaling remain largely unknown. Here, we report a new mechanism whereby altered ceramide metabolism via ceramide synthase 4 (CerS4) drives PD-L1 internalization to potentiate a TGFβ/Shh/β-catenin signaling axis to drive triple-negative breast cancer (TNBC) migration and metastasis. In response to altered ceramide metabolism, we observed that PD-L1 is internalized via clathrin-mediated endocytosis and depends on S278/S279 in its cytoplasmic domain. Once internalized, PD-L1 directly interacts with Caprin-1, an RNA-binding protein previously unassociated with PD-L1 signaling. Through our analysis of clinical specimens, we established a positive association between PD-L1/Caprin-1 interaction and metastatic progression in human TNBC. In terms of mechanism, we determined that the PD-L1/Caprin-1 complex plays a pivotal role in mediating CerS4-dependent cell migration. This complex selectively binds and stabilizes mRNA, resulting in heightened TGFβ/Shh/β-catenin signaling. Conversely, CerS4 restoration in metastatic TNBC cells impaired cellular migration and the interaction between PD-L1 and Caprin-1. Genetic depletion of CerS4 enhanced lung metastasis derived from 4T1 orthotopic allografts and transgenic MMTV-PyMT breast tumors concomitant with PD-L1/Caprin-1 interaction and TGFβ/Shh/β-catenin signaling. Bioinformatics analysis of clinical datasets was used to validate the impact of the CerS4/PD-L1/Caprin-1 axis on metastatic progression in human TNBC. In alignment with enhanced tumor progression, CerS4 depletion in tumors promoted regulatory T-cell infiltration, suggesting an immunosuppressive tumor microenvironment (TME). Treatment with sonidegib, an FDA-approved Hedgehog (Hh) inhibitor, effectively prevented PD-L1 internalization and its interaction with Caprin-1. We hypothesized that sonidegib could synergize with immune checkpoint blockade to sensitize TNBC to immunotherapy, which typically has low response rates. Sonidegib, in combination with αPD-L1 therapy, was significantly more effective in controlling TNBC primary and metastatic tumor growth, especially when Cers4 was downregulated, compared to αPD-L1 monotherapy. Our data also suggested that this potent anti-tumor effect was due to immunotherapy sensitization after combined flow cytometry, multiplexed immunofluorescence, and bulk RNA-sequencing analyses. Altogether, these findings demonstrate a mechanism to define intracellular PD-L1 signaling in response to altered ceramide metabolism, providing a new therapeutic strategy to target TNBC metastasis and improve response to immunotherapy.

#1571 Upregulation of phosphoglyceric acid mutase (PGAM)-1 is related to lymph node metastasis in gastric cancer.

H. Wang[1], Z. Liu[1], L. Wang[1], Z. Wang[2], C. Jamieson[3], **N. A. Cacalano**[2];
[1]The First Hospital of Jilin University, Jilin, China, [2]UCLA David Geffen School of Medicine, Los Angeles, CA, [3]University of California San Diego, Los Angeles, CA

Gastric cancer (GC) is the most common malignancy of the digestive system, causing over 750,000 deaths worldwide. Gastric cancer mortality is largely due to its high level of invasiveness and metastasis to distal organs. Thus, it is an urgent priority to identify mechanisms underlying GC metastasis to improve cancer diagnosis develop of effective biological targeting agents. In this study, we demonstrate that phosphoglyceric acid mutase-1 (PGAM1) was preferentially over-expressed in lymph node metastasis (LNM) tissues of GC patients and correlated with poor prognosis. PGAM1 knock down in two human GC cell lines resulted in impaired cell proliferation and increased cell cycle arrest. Further, PGAM knockdown inhibited migration of both GC cell lines, which correlated with decreased expression of MMP2, MMP9 and ICAM-1. In a murine xenograft model, GC cells with a PGAM1 knockdown displayed decreased growth capacity *in vivo.* Western blot analysis showed that PGAM1 knockdown in SGC7901 and BGC823 decreased the phosphorylation of Src, FAK and Paxillin relative to the parental cell lines. These results indicate that PGAM1 may play an important role in promoting GC lymph node metastasis by driving cell proliferation and activating cytoskeletal reorganization and cell migration through the regulating Src/FAK/Paxillin pathway.

#1572 *POU5F1B* is a human-restricted ROCK inhibitor-sensitive oncoprotein that restructures membrane nanodomains to increase cell adhesion.

L. Simo-Riudalbas[1], S. Offner[1], L. Abrami[1], E. M. Unterauer[2], J. Duc[1], E. Planet[1], R. Jungmann[2], G. van der Goot[1], D. Trono[1];
[1]Ecole Polytechnique Federale de Lausanne, Lausanne, Switzerland, [2]Ludwig Maximilian University, Munich, Germany

Evolution confers new species with distinctive biological features, which can translate in purely mechanistic speciation or in novel phenotypic traits. *POU5F1B* arose by retrotransposition of *POU5F1 (OCT4)* in the last common ancestor of modern Hominoidae. Its human product is endowed with oncogenic properties, notably promoting gastrointestinal cancer growth and metastasis. Here, we reveal that the oncogenic action of POU5F1B requires ubiquitination of lysine residues found only in the human protein. This post-translational modification is essential for POU5F1B to localize to the cytoplasm and become acylated by the DHHC17 palmitoyltransferase. This leads to POU5F1B association with detergent-resistant membrane subdomains, where it triggers the accumulation of integrins and signaling molecules, and to a stimulation of cell focal adhesion. Finally, we determined that POU5F1B stability is critically dependent on ROCK, a crucial regulator of cytoskeletal dynamics and cell motility.

TUMOR BIOLOGY: Pancreatic Cancer Microenvironment
Poster Session

#1576 The heterogeneity between pancreatic ductal adenocarcinoma with & without lymphovascular invasion.
Y. Zou, Y. Xie, S. Gao, T. Zhou, J. Yu, J. Hao;
Tianjin Medical Univ. Cancer Inst. & Hospital, Tianjin, China

Background Pancreatic ductal adenocarcinoma (PDAC) is one of the deadliest malignant solid tumors, with a five-year survival rate less than 10%. Lymphovascular invasion (LVI) is a poor prognostic indicator for PDAC, yet the difference between tumors with or without LVI is unclear.
Methods We used scRNA-seq analysis on the PDAC tissue of 24 patients obtained from the National Genomics Data Center (Project number: PRJCA001063) to compare T-cell, macrophage, & cancer-associated fibroblast (CAF) heterogeneity between LVI-positive & LVI-negative PDAC. To validate the scRNA-seq results, complementary techniques, including multiple immunofluorescence assays & flow cytometry, were used. Additionally, we analyzed the characteristics of LVI-positive PDAC tumor cells.
Results LVI-positive PDAC thrives in an immunosuppressive microenvironment. We discovered that CD8+ T cells were more deficient in LVI-positive PDAC than in LVI-negative PDAC. Furthermore, the effective & cytotoxic markers (such as GZMB & IFN-γ) of CD8+ T cells also decreased in LVI-positive PDAC. M2 macrophage polarization was found to be higher in LVI-positive PDAC compared to LVI-negative PDAC. In addition, we discovered a more fibrotic TME signature in LVI-positive PDAC. LVI-positive tumor cells, in particular, had a mesenchymal transition phenotype & a hypoxic microenvironment.
Conclusions This study adds to our understanding of the intricate heterogeneity seen in LVI-positive PDAC. It sheds light on the distinct characteristics of LVI-positive PDAC & advances our understanding of its underlying biology.

#1577 Cancer associated fibroblast - tumor cell crosstalk enhances epithelial to mesenchymal transition and promotes a classical to basal switch in human pancreatic ductal adenocarcinoma.

S. Guinn, B. Perez, J. Patel, J. Lee, D. Zabransky, W. J. Ho, E. J. Fertig, E. Kartalia, J. Tandurella, R. Burkhart, J. W. Zimmerman, E. Jaffee;
Johns Hopkins Medicine, Baltimore, MD

Introduction: Cancer associated fibroblasts (CAF) drive a complex tumor microenvironment (TME) in pancreatic ductal adenocarcinoma (PDAC) through incompletely understood interactions. Two major CAF subtypes, myofibroblastic (myCAF) and inflammatory (iCAF), dominate the tumor landscape and have been defined by gene expression profiles. There is significant plasticity between subtypes and alterations in CAF behavior likely drive changes in tumorigenicity and immune evasion. Additionally, PDAC tumor cells usually present with a predominant classical or basal phenotype that is associated with clinical outcomes. We hypothesized that CAF phenotype impacts tumor cell gene expression and alters the clinically-relevant tumor subtyping.

Methods: We interrogated cellular crosstalk in the PDAC TME using a novel three-dimensional, patient-matched coculture system of patient-derived organoids (PDO) and CAFs, established from 12 patients undergoing surgical resection. Molecular characterization included bulk RNA sequencing, proteome profiling (107 factor), flow cytometry, multiplex RNA Scope, imaging mass cytometry (IMC), and RT-qPCR.

Results: PDO gene expression analysis from bulk RNAseq demonstrated CAF coculture induced phenotypic shifts in the Moffitt subtype from a classical to a basal phenotype. Further, CAF coculture enhanced epithelial to mesenchymal transition (EMT) across all patients, even those with a baseline basal phenotype. We hypothesized this could be due to both cell-cell crosstalk and secreted factors. We therefore treated PDO with CAF-conditioned media (CM) and demonstrated that CM is sufficient to drive the observed classical-to-basal shift by RT-qPCR. Secretome analysis of CM derived from 3 CAF lines identified HGF, FGF19, and IL-8 as factors contributing to this transcriptional change. Next, we used spatial - omics (transcriptomics and proteomics) to examine the validity of these findings in source patient tissue. Using RNA Scope, we discovered distinct tumor neighborhoods expressing basal mRNAs KRT17 and KRT6a surrounded by CAFs compared to those expressing classical genes TFF1 and GATA6. We then used IMC to further explore CAF subtypes in patient tumors and found FAP+ myCAF regions corresponded to basal tumor regions, while CXCL12+ iCAFs were found in classical regions.

Conclusions: PDAC tumor biology is likely driven by interactions between cancer cells and CAFs. Potential mediators of these interactions include both cell-cell contact and secreted factors. We introduce a novel approach combining *in vitro* coculture with tissue-based assays, demonstrating that modern culture techniques preserve cell type heterogeneity and plasticity. Together, these data demonstrate that a CAF-rich TME drives tumor cell plasticity not only towards EMT but also a more basal disease phenotype.

#1578 RAS-GTP inhibition modulates Hedgehog signaling, suppressing myCAFs and promoting iCAFs in pancreatic ductal adenocarcinoma.

M. Hasselluhn, L. Tomassoni, U. Wasko, A. Curiel-Garcia, T. Dalton, S. A. Sastra, C. Palermo, A. Califano, **K. P. Olive**;
Columbia University Irving Medical Center, New York, NY

More than 90% of human pancreatic ductal adenocarcinoma (PDAC) cases are driven by activating mutations in KRAS. RMC-7977 is a potent inhibitor of GTP-bound RAS proteins (RAS(ON), including both wild type and mutant variants of KRAS, NRAS, and HRAS. The related investigational agent, RMC-6236, is a first-in-class, potent, orally bioavailable, RAS^{MULTI}(ON) inhibitor currently in Phase 1/1b clinical trials (NCT05379985). We performed preclinical studies in a range of models of PDAC, including the highly chemoresistant K-$ras^{LSL.G12D/+}$, $p53^{LSL.R172H/+}$, $Pdx1Cre^{tg/+}$ (KPC) genetically engineered mouse. RMC-7977 exhibited broad anti-tumor activity at tolerable doses, provoking radiographic responses in KPC pancreatic tumors and extending overall survival by 3-fold, the largest response observed yet in this model. RMC-7977 dosing produced a metronomic effect on RAS signaling in tumor and normal tissues. This yielded tumor-selective effects on apoptosis and proliferation, consistent with RAS oncogene addition in PDAC.

PDAC tumors are characterized by an expansive stroma that harbors multiple subtypes of cancer associated fibroblasts (CAFs) that manufacture a fibrotic, inflammatory extracellular matrix. CAF proliferation is driven by signals emanating from the malignant epithelial cells, such as Sonic Hedgehog (SHH), a secreted ligand that drives downstream Hedgehog pathway signaling in myofibroblastic CAFs (myCAFs). To understand the impact of RAS-GTP inhibition on paracrine signaling to CAFs in PDAC, To understand the dynamic responses of malignant epithelial cells following GTP-RAS inhibition, we performed single cell RNA sequencing (scRNAseq) on KPC pancreatic tumors treated with RMC-7977 or vehicle at multiple timepoints. Using the ARACNe and VIPER algorithms, we performed single cell regulatory network analysis on the expression profiles of >210,000 cells to calculate the activities of thousands of transcriptional regulatory protein in each cell.

We found that the RAS-GTP inhibition blocked SHH expression in malignant epithelial cells, resulting in loss of downstream Hh pathway activity in CAFs within 24 hours of treatment. By one week of treatment, myCAFs were significantly depleted whereas inflammatory CAFs (iCAFs) were significantly accumulated. Strikingly, CAF heterogeneity was restored in KPC pancreatic tumors that acquired resistance to RMC-7977, despite continued suppression of Hedgehog pathway signaling. Consistent with prior studies of Smoothened inhibitors, the depletion of myCAFs from RAS-GTP inhibition was associated with the rapid opening and hypersprouting of intra-tumoral blood vessels. Ongoing studies using the mutant-selective $KRAS^{G12D}$ inhibitor RM-044 should discriminate between direct effects of wild type RAS inhibition in CAFs versus the paracrine consequences of mutant RAS inhibition in malignant epithelial cells.

#1579 Macrophage infiltration and polarization in pancreatic ductal adenocarcinoma following stereotactic body radiation therapy.

E. D. Gonzalez Marrero[1], L. Wang[2], B. R. Schrank[2], A. C. Koong[2];

[1]University of Puerto Rico School of Medicine, San Juan, PR, [2]The University of Texas MD Anderson Cancer Center, Houston, TX

Introduction: Stereotactic body radiation therapy (SBRT) has emerged as a promising treatment modality for pancreatic ductal adenocarcinoma (PDAC) due to its precise delivery and potential to improve local control. Beyond its direct impact on tumor cells, accumulating evidence suggests that SBRT may also modulate the tumor microenvironment (TME), influencing immune responses. Macrophages play a crucial role in the TME with their polarization into pro-inflammatory (M1) or pro-tumoral (M2) phenotypes significantly impacting cancer progression. Studying the TME and developing immune therapies may be helpful for metastatic PDAC, which currently only has non-curative treatment. The TME, in particular the polarization of macrophages, has not been well studied following radiation treatment. Therefore, our work aims to study how SBRT affects the infiltration and polarization of macrophages in the PDAC TME in a time-dependent manner.
Methods: To establish and study PDAC C57BL/6J mice were orthotopically injected with a luciferase-labeled KPC tumor cell line. SBRT was administered to tumor-bearing mice following a schedule of 10Gy radiation per fraction in total of 5 fractions on days 10-14 post tumor implantation. Mice were euthanized on day 1, 3 and 7 after irradiation. Tumor tissues were collected for immunohistochemistry (IHC) staining and flow cytometry with antibodies targeting CD68, CD11b, CD86 (M1 marker), and CD206 (M2 marker). Images were analyzed and quantified using ImageJ and GraphPad Prism.
Results: Via the use of IHC staining, we found no significant difference in the number of cells stained with the CD68 antibody (macrophage marker) when compared throughout groups. Additionally, we found no significant difference in the number of macrophages stained with the M2 marker. However, we did observe a significant increase in the number of macrophages stained with the M1 marker in the group receiving SBRT. Through flow cytometry of the tumor tissues we observed an increasing trend, as time passed, in the number of macrophages expressing the M1 marker. The same trend was observed in macrophages expressing both the M1 and M2 markers. However, a change in the total number of macrophages or those expressing only the M2 marker was not observed.
Conclusions: SBRT does not affect the total number of infiltrated macrophages in the TME or the amount of M2 macrophages. However, we did observe that the percentage of M1 macrophage increases significantly as time passes after SBRT. We theorize that the increase in M1 macrophages may be due to an M2 to M1 transition in the M2 population. Our study provides preliminary rationale to use macrophage-targeted immune therapy to potentiate the efficacy of SBRT for PDAC treatment, though we understand that further follow-up studies with a larger sample size and longer time course are required to obtain significant and meaningful results.

#1580 Investigating the tumor microenvironment of pancreatic ductal adenocarcinoma with BRCA2 mutation.

F. Al-Musawi, C.-i. Hwang;
UC Davis, Davis, CA

Pancreatic ductal adenocarcinoma (PDAC) is one of the most aggressive and deadliest cancers with a survival rate of less than 12% at 5 years. It is estimated that around 14% of human PDAC contain mutations in genes involved in DNA Damage Repair (DDR), including BRCA1/2, ATM, and others. Additionally, PDAC has an extensive network of extracellular matrix components surrounding the tumor in the stroma, such as cancer-associated fibroblasts, which promote cancer cell growth. The interactions of the tumor with its tumor microenvironment and stroma can bring vulnerabilities that could be targeted if identified. New therapeutic strategies to those targets can be developed for specifically PDAC with DDR mutations.

Using publicly available RNA-seq dataset of PDAC patients from The Cancer Genome Atlas (TCGA), I computationally estimated the infiltration of immune and stromal cell types into the tumor. From the analyses, I found that there was a significant difference in the migration of Common Lymphoid Progenitor (CLP) cells into PDAC with mutations to DDR genes. CLP cells usually divide into T-cells, B-cells, and NK cells, suggesting that DDR mutations could cause a more immunogenic environment. There was also a decrease in the infiltration of stromal elements, mainly fibroblasts, into PDAC with mutations to DDR genes.

In the experiment I am currently working on, I hypothesize there are also in vivo differences in the infiltration rates of certain immune cell types and fibroblasts into BRCA2-mutated PDAC, since BRCA2 is the most commonly mutated DDR gene in PDAC.

For my current experimental design, the mice in the experimental group will be orthotopically implanted with PDAC with Brca2 knockout. The control group will have mice orthotopically implanted with PDAC without Brca2 knockout. After letting the tumors grow for 3 weeks, the mice will be sacrificed and the pancreatic tumors will be collected and stained through trichrome staining. Trichrome staining probes for the stromal cancer-associated fibroblasts. Furthermore, immunohistochemistry (IHC) staining will be done to look for specific populations of cells, such as specific types of fibroblasts, effective and immunosuppressive immune cells including T-cells, B-cells, and NK cells. The aim is to see whether the computational findings in regards to the tumor microenvironment are also reflected in vivo. I will have the data from this experiment by the time of the conference in April 2024.

Overall, my project is about investigating the tumor microenvironment and fibroblast abundance in PDAC with BRCA2 knockout mice, using computational data, IHC staining and trichrome staining.

#1581 Colony-stimulating factor-1 receptor as a potential therapeutic target in pancreatic ductal adenocarcinoma.

S. Chaudhuri, D. A. Deming, C. A. Pasch, K. A. Johnson, C. K. Sievers, P. B. Emmerich;
Univ. of Wisconsin Madison Sch. of Med. & Public Health, Madison, WI

Background:
Pancreatic ductal adenocarcinoma (PDAC) is associated with poor prognosis, rising incidence and suffers from limited existing treatment options. Currently, salient features of PDAC are being investigated that can potentially predict immunotherapy outcomes, to identify small patient populations that can benefit from such strategies. Preliminary studies show that colony-stimulating factor-1 receptor (CSF1R), a surface receptor tyrosine kinase that drives survival, function, proliferation and differentiation of several myeloid lineage cell types can be a potentially interesting target for combination immunotherapy.

Methods:
PDAC patients from the TCGA PanCancer Atlas were stratified into $CSF1R^{hi}$ and $CSF1R^{lo}$ cohorts and clinically relevant characteristics were compared between the two. The mRNA expression of CSF1R and immunological markers of interest were evaluated and Gene Set Enrichment Analysis (GSEA) was run on the two groups to analyze differential expression of gene sets.

Results:
mRNA expression z-scores were used to classify 129 patient samples in the TCGA PanCancer Atlas dataset into $CSF1R^{hi}$ (z-score>1, n=20) and $CSF1R^{lo}$ (z-score<0, n=109) cohorts. Both have similar disease staging, MSI MANTIS scores, tumor mutation burden, median diagnosis age, sex and race distribution. However, the $CSF1R^{hi}$ cohort has a distinct, non-conventional PDAC driver gene mutation profile (genomic alteration frequencies in $CSF1R^{hi}$ vs $CSF1R^{lo}$ cohorts respectively: a) *KRAS: 30% vs* 73% b) *CDKN2A*: 15% vs 57% and c) *SMAD4*: 5% vs 42%) (p-value<0.01 for each). CSF1R correlates with markers of CD8+ T-cell function (R^2 values: *CD8A:* 0.683, *GZMB:* 0.508, *PRF1:* 0.673), CD8+ T-cell infiltration (*CXCL9:* 0.596, *CXCL10:* 0.483, *CCL5:* 0.666) and expression of immune checkpoint genes (*PDCD1:* 0.602, *CD274:* 0.544, *CTLA4:* 0.613). *CD8A, GZMB, PRF1, CXCL9, CXCL10, CCL5, PDCD1, CD274, CTLA4* are significantly upregulated in the $CSF1R^{hi}$ group (log2Fold changes respectively: 2.07, 1.57, 1.48, 2.51, 1.71, 1.75, 1.63, 1.34, 1.80). GSEA against the hallmark gene set database shows that *KRAS* signaling, Inflammatory response, IL6 JAK STAT3 and Interferon-gamma signaling are significantly upregulated in the CSF1R high patient group (FDR q-value <0.01 for each).

Conclusion:
Preliminary *in silico* analysis suggests that PDAC patients with higher levels of CSF1R may be more immune infiltrated. Future studies will evaluate the potential of CSF1R as a biomarker to identify an immune infiltrated subset of PDAC patients *ex vivo* and the mechanism of immune infiltration in $CSF1R^{hi}$ PDACs *in vivo*.

#1583 Neutrophil pro-tumorigenic role in progression and therapy resistance in pancreatic ductal adenocarcinoma.

Reegan Sturgeon[1], Esther Johnson[1], Caitlin Molczyk[1], Paran Goel[2], Parker Tinsley[3], Lauren Abrahams[4], Michael Maher[5], Rakesh K. Singh[1]

[1]University of Nebraska Medical Center, Omaha, NE,[2]University of Alabama at Birmingham, Birmingham, AL,[3]Wayne State University, Wayne, NE,[4]Tufts University, Medford, MA,[5]Creighton University, Omaha, NE

Pancreatic cancer (PC) continues to be a challenge for today's therapeutics, with a meager 5-year survival rate of 12%. Due to the pancreas' location, patients often receive diagnosis late, leaving them with limited treatment options. Often, they fail to respond to chemotherapy regimens or develop resistance to those therapies. Tumor-promoting inflammation is a hallmark of cancer, contributing to tumor cells' survival and proliferation. Infiltrating leukocytes and pro-inflammatory cytokines released into the tumor microenvironment (TME) often cause this inflammation. My lab has previously linked increases in pancreatic ductal adenocarcinoma (PDAC) progression and chemotherapy resistance to inflammation and the CXCR2 pathway. In the present study, we examined the role of neutrophil recruitment in PDAC progression using patient samples and KRAS-dependent KC and KPC murine models. Our data suggest a positive association between tumor-associated neutrophils (TANs) and PDAC progression. *In vitro*, we observed neutrophil-PDAC interaction enhancing the survival of both neutrophils and PDAC cell lines. Moreover, this survival was mediated by cellular aggressiveness and therapy resistance. Concerning survival, we saw increased expression of anti-apoptotic genes in the neutrophils upon PDAC cancer cell conditioned media treatment. We also observed modulated expression of immunoregulatory molecules. Our data suggest that increased recruitment of TANs supports PDAC progression and survival, and PDAC cell-neutrophil interaction modulates neutrophil survival and immunoregulatory phenotype.

#1584 The interplay between natural killer cells and pancreatic stellate cells in pancreatic ductal adenocarcinoma.

R. E. A. Fincham[1], P. Periasamy[2], C. R. Joseph[2], J. Meng[2], J. Lim[2], F. Wee[2], K. Stasinos[1], M. R. Goulart[1], J. Ye[2], L. Chong[2], D. Goh[2], J. P. S. Yeong[2], H. M. Kocher[1];

[1]Barts Cancer Institute, London, United Kingdom, [2]Agency for Science, Technology and Research (A*STAR), Singapore, Singapore

Natural Killer (NK) cells have been shown to possess potent anti-tumor activity against multiple cancer types and consequently have been harnessed as a cellular cancer immunotherapy. Furthermore, targeting of pancreatic stellate cells has received increasing interest in the treatment of pancreatic ductal adenocarcinoma (PDAC), with several clinical trials testing the hypothesis that rendering activated pancreatic stellate cells/cancer associated fibroblasts (aPSC/CAF) into a quiescent state (qPSC) can enhance anticancer treatment. Despite this interest, our understanding of the interplay between these two cell types remains limited. We hypothesized that PSC/CAF may exhibit a dynamic interaction with NK cells that may be harnessed for therapeutic strategies and patient stratification. Employing a series of *in vitro* assays, we demonstrate a significant bi-directional interaction between natural killer cells and pancreatic stellate cells in the context of PDAC. NK cells were found to effectively target and eliminate both aPSC and qPSC, with PSC activation conferring some protection from NK-lysis. Furthermore, we highlight a significant myofibroblastic shift in PSCs regardless of previous activation status when cultured with NK cells; an interaction that was direct contact dependent. NK cells were also found to demonstrate cellular modulation of NKG2A and TIM3 in response to PSC co-culture. Drawing on Luminex ELISA analysis, we suggest that engagement of the IFN-γ signaling pathway may be driving phenotypic modulation. Global proteomic analyses demonstrated differential protein changes induced by NK cells in aPSC compared to qPSC, as well as alterations in the NK cell proteome upon such co-culture. Utilizing multiplex immunohistochemical analysis of PDAC patient samples, we highlight differential spatial distribution of phenotypically distinct NK cells and PSC/CAF subtypes in patient samples between long- (n=16) and short- (n=48) survivors. Moreover, NK-PSC proximity, and not total immune infiltrate, was found to play a prognostic role in PDAC. Our work provides a global overview of the cross-talk between NK and PSC in PDAC, demonstrating a significant bi-directional relationship which offers novel insights into potential therapeutic avenues. Furthermore, we demonstrate, for the first time to our knowledge, the prognostic role of NK-PSC proximity in patient survival and suggest its potential for patient stratification.

#1585 Tenascin C in pancreatic cancer-associated fibroblasts enhances epithelial mesenchymal transition and is associated with resistance to immune checkpoint inhibitor.

S. Furuhashi, Y. Morita, A. Matsumoto, S. Ida, R. Muraki, R. Kitajima, M. Takeda, H. Kikuchi, Y. Hiramatsu, H. Takeuchi;
Hamamatsu University School of Medicine, Hamamatsu, Japan

Backgrounds: Tenascin C (TNC) is an extracellular matrix glycoprotein that is abundantly expressed in cancer stroma and its overexpression correlates with tumor progression in various types of cancer including pancreatic adenocarcinoma (PAAD). However, the role of TNC in regards to response to immune checkpoint inhibitor (ICI) still remains to be identified. In this study, we aimed to investigate the potential involvement of TNC in the response to ICI among PAAD patients.
Materials and Methods: Transcriptomic profiles were downloaded by TCGA and GTEx database and TNC mRNA levels were compared between tumors and normal tissues. These transcriptomic data were deconvoluted using CIBERSORTx to identify specific enriched pathways in cancer cells and cancer-associated fibroblasts (CAFs) in PAAD patients. Bioinformatic programs were used to predict paracrine communications between cancer cells and cancer-associated fibroblasts (CAFs), and the Tumor Immune Dysfunction and Exclusion (TIDE) score was calculated to predict response to ICI treatment in PAAD patients. An independent immunotherapeutic cohort was applied to validate prediction values for immunotherapy.
Results: TNC mRNA levels were significantly upregulated in tumors compared to normal tissues in eight cancer types including PAAD. TNC-high (TNC-H) PAAD patients (n = 138) had significant shorter overall survival than TNC-low (TNC-L) patients (n = 40) (p = 0.0125, Log-rank test). Using CIBERSORTx, TNC was estimated to be predominantly expressed in CAFs in PAAD. In pathway analysis, both cancer cells and CAFs had significant enrichments of the epithelial mesenchymal transition pathway in TNC-H patients. Ligand-receptor interaction analysis showed that TNC produced in CAFs had the highest interaction potentials to bind to integrin families such as ITGαV and ITGβ3 in cancer cells. In an independent immunotherapy data cohort, patients with TNC-H and ITGαV-high or ITGβ3-high expression were associated with poor response to ICI treatment and had shorter overall survival than those with both low expressions.
Conclusions: In conclusion, these findings suggest that TNC-high CAFs can play a crucial role in tumor progression and resistance to ICI therapy in PAAD patients, and targeting TNC and its interactions with cancer cells may provide a potential strategy for improving the efficacy of ICI therapy in PAAD.

#1586 Unraveling the importance of pancreatic cancer extracellular signaling to endothelial cells within the tumor microenvironment.

J. M. Finan[1], Y. Guo[1], A. Q. Bartlett[1], K. MacPherson[1], V. Calvert[2], M. D. Hedberg[1], E. Petricoin[2], R. Sears[1], J. R. Brody[1];
[1]Oregon Health & Science University, Portland, OR, [2]George Mason University, Fairfax, VA

In many solid tumors, including pancreatic ductal adenocarcinoma (PDAC), the secretion of extracellular vesicles (EVs) has been shown to support tumor progression, chemotherapeutic resistance, and metastasis. Importantly, PDAC tumors are composed of up to 80% non-tumor cells and an extracellular matrix, yet no studies have been performed to determine which cells within PDAC tumors internalized PDAC EVs. Further, the RNA-binding protein HuR plays an important role in PDAC cells, supporting the stability and translation of transcripts that aid tumor cell stress responses. Our lab has recently found that EVs harbor distinct mRNA and phosphorylated protein cargoes from donor cells. Further, HuR knockout (KO) cells produce EVs with significantly different mRNAs and phosphorylated proteins that EVs isolated from HuR wildtype (WT) cells. Specifically, proteins relating to endothelial function and angiogenesis were significantly differentially phosphorylated. Considering the functional impact of EV cargoes on recipient cells, our study aims to identify the specific cell types in the tumor microenvironment that import PDAC EVs and investigate the role of PDAC cell HuR in this signaling process. We have generated human PDAC and mouse $Kras^{G12D}$ $Trp53^{R172H}$ driven (KPC) PDAC cell lines to express an EV reporter, PalmGRET. Utilizing these cells lines in an immunocompetent mouse model of PDAC, we found that endothelial cells are major importers of PDAC EVs. We next performed bulk RNA-sequencing on endothelial cells sorted from these tumors that have (GFP+) versus have not (GFP-) imported PDAC EVs to assess the functional impact of PDAC EVs. Subsequent studies will focus on delineating the importance of this signaling axis by ablating EV secretion in addition to assessing endothelial cell function when treated with EVs from HuR WT vs. KO cells. Collectively, our study sheds light on the preferential uptake of PDAC EVs by endothelial cells and highlights the potential role of tumor cell-intrinsic HuR in this signaling process. These findings expand our understanding of the interactions between PDAC and the tumor microenvironment, potentially paving the way for targeted therapeutic interventions in this devastating disease.

#1587 Multimodal spatial transcriptomics uncover distinct tumor microenvironment states and cell-cell communication networks in molecular pancreatic cancer subtypes.

S. Baerthel[1], C. Falcomata[2], V. Goelling[3], D. Lucarelli[4], R. Gindra[5], C. Schmitt[1], J. Swietlik[6], F. Meissner[7], M. Schmidt-Supprian[8], D. Saur[1];
[1]DKFZ German Cancer Research Center, Munich, Germany, [2]Icahn School of Medicine at Mount Sinai, New York, NY, [3]Institute of Experimental Hematology, School of Medicine, Technical University of Munich, Munich, Germany, [4]Chair of Translational Cancer Research and Institute of Experimental Cancer Therapy, Klinikum rechts der Isar, School of Medicine, Munich, Germany, [5]Chair of Translational Cancer Research and Institute of Experimental Cancer Therapy, Klinikum rechts der Isar, School of Medicine, Munich, Germany, Munich, Germany, [6]Experimental Systems Immunology Laboratory, Max Planck Institute of Biochemistry, Martinsried, Germany, [7]Institute of Innate Immunity, Department of Systems Immunology and Proteomics, Medical Faculty, University of Bonnr, Bonn, Germany, [8]Institute of Experimental Hematology, School of Medicine, Technical University of Munich, Munich, Germany, Munich, Germany

The tumor microenvironment (TME) presents a complex ecosystem comprising a diversity of immune and stromal cell populations that influence tumor progression, drug delivery and therapy outcome. High levels of inter- and intra-tumor heterogeneity in TME state are driven by molecular tumor phenotypes. Pancreatic ductal adenocarcinoma (PDAC), one of the most lethal cancer types, displays a high genetic heterogeneity along with an immunosuppressive TME. However, it remains largely elusive how distinct TME states are mechanistically influenced, and which molecular processes dictate the emergence of different modes of immunosuppression within the TME of molecular PDAC subtypes.Here, we performed a systematic analysis of functional associations between the major molecular PDAC subtypes, the classical and mesenchymal subtype, and their TME states. We describe the TME composition and complex cell-cell communication networks within PDAC subtypes using a multimodal integration of spatial transcriptomics (ST) with complementary approaches, such as scRNA-seq, MS-based Secretomics and multiplexed histocytometry. We generated ST data sets (Visium) of a tumor cohort derived from a *Kras*-driven PDAC mouse model. To analyze TME composition as well as spatial niches and cell type communities, we computationally enhanced the spot-resolution of ST datasets, followed by cell type deconvolution and cell-cell communication analysis to identify subtype-specific TME communities and communication networks.To this end, we generated a large resource of PDAC mouse models which represent molecular subtypes of the disease and mimic the heterogeneity of TME states found in human PDAC cohorts. This analysis revealed that a set of subtype-specific secreted factors shape the immunosuppressive PDAC TME via direct and indirect communication networks with immunosuppressive myeloid and T cells in molecular PDAC subtypes. Multimodal ST analysis delineated spatial subtype-specific TME communities as well as spatial communication patterns. We functionally investigate the tumor cell intrinsic regulation of the identified subtype-specific secreted factors, providing potential therapeutic vulnerabilities for more effective combinatorial subtype-specific therapies including immunotherapeutic approaches.

#1588 Identification of new signaling pathways between fibroblasts & tumor cells in pancreatic cancer.

A. Al Shoukari[1], M. Batardiere[1], N. Movahed[2], C. beaussier[1], J. Baig[1], M. gonzalez[1], P. Moraille[1], E. Bonneil[1], L. Rousseau[3], S. turcotte[3], K. Delgiorno[4], M. Tan[5], A. Means[5], E. Dianati Ajibisheh[1], Q.-h. Trinh[1];

[1]University of Montreal, Montreal, QC, Canada, [2]Concordia University, Montreal, QC, Canada, [3]CHUM, Montreal, QC, Canada, [4]Vanderbilt University, Tennessee, TN, [5]Vanderbilt University Medical Center, Tennessee, TN

We explore the unstudied role of nanoparticles (NPs), recently discovered secreted non-vesicular nanoparticles, in signaling between pre-cancer associated fibroblasts (preCAF), CAFs, and tumor cells. We generated two novel primary lines preCAF PFUM1 from a patient with high-grade intraductal papillary mucinous neoplasms and CAF FUM2 from a patient with pancreatic ductal adenocarcinoma, all tests performed between passages 2 and 3, fibroblast purity validated by RT-PCR and ACTA2 immunofluorescence. Small extracellular vesicles (sEVs), exomeres, and supermeres (the two main forms of NPs) were isolated by the ultracentrifugation method from PF-UM1 and F-UM2 with n=2-3 experiments. To validate the isolation, we used nanoparticle tracking, electron, and fluid-phase atomic force microscopy. Proteins were quantified by BCA assay. Liquid chromatography-mass spectrometry characterized the cargo from each fraction. Human cancer lines MIAPACA2 and SU8686 were treated with 10 µg of each fraction and cell proliferation was tested by phase-contrast images (Cytation 5), analyzed by Ilastik-based 1.4.0 machine-learning. We performed fluorescent Ki-67 and vimentin staining and quantified in QuPath 0.4.3. Non-parametric statistics were performed in Prism GraphPad.

NPs constitute the major fraction of small particles released by fibroblasts, containing 80.5% (PFUM1) and 77.5% (FUM2) of the protein load by quantification. Mass spectrometry reveals enrichment of growth factors, epithelial-to-mesenchymal (EMT) transition, and metabolism-associated proteins in the NPs compared to sEVs. At 72 hours, cell proliferation for Su8686 reveals a proliferative effect for all fractions from both PFUM1 and FUM2 (19-63% increase compared to controls, p=0.049 to <0.0001). For MIAPACA2, only supermeres from PFUM1 and FUM2 consistently increased proliferation (9.5-35% increase, p=0.0051 to <0.0001). Ki-67 expression in MIAPACA2, increased by 9.6-23.0% following treatment by NPs (all p<0.0001) and by 2.9-9.2% with sEVs (p=0.011 to <0.0001). EMT was estimated by vimentin in MIAPACA2, as all preCAF fractions from PFUM1 reduced vimentin expression (p<0.001), while CAF FUM2 NPs increased vimentin expression (p<0.0001) while sEVs had no effect (p=0.075).

In conclusion, the majority of pancreatic tumor-associated fibroblast small secretome is composed of NPs, exhibiting significant functional pro-tumoral effects.

#1589 Integrated multiomics analysis revealed the significance of Transgelin in driving pancreatic cancer-associated fibroblast-mediated cancer progression.

K. Shinjo[1], X. Wang[1], K. Kumegawa[2], R. Maruyama[2], S. Mii[1], Y. Murofushi[1], M. Suzuki[1], A. Enomoto[1], Y. Kondo[1];
[1]Nagoya Univ. Graduate School of Medicine, Nagoya, Japan, [2]Japanese Foundation for Cancer Research, Tokyo, Japan

Pancreatic ductal adenocarcinoma (PDAC) is primarily characterized by a desmoplastic reaction, mainly consisting of cancer-associated fibroblasts (CAFs). In order to investigate the heterogeneity of CAFs, we initially conducted single-cell Assay for Transposase-Accessible Chromatin with high-throughput sequencing (scATAC-seq) using pancreas tissue from 12-week-old KPC (K-rasLSL.G12D/+; Trp53R172H/+; Pdx-1-Cre) PDAC mouse models. We identified three clusters enriched with myofibroblast CAF (myCAF) gene markers and one cluster enriched with inflammatory CAF (iCAF) gene markers. Next, we performed single-cell RNA sequencing (scRNA-seq) on pancreas tissues from KPC mice. scRNA-seq revealed four distinct fibroblast clusters, each exhibiting characteristic gene expression profiles of normal fibroblasts, iCAF, myCAF and antigen-presenting CAF (apCAF). These findings suggest that CAFs in the myCAF cluster identified in scATAC-seq may have potential to differentiate into either myCAFs or other CAF subtypes based on certain cues. Next, we focus on the expression of myCAF marker genes, particularly two commonly used markers, *Tagln* and *Acta2*. Among myCAFs, two subtypes were identified: *Tagln*-positive and *Acta2*-positive CAFs, and *Tagln*-negative and *Acta2*-positive CAFs. To confirm our findings, we conducted Immunohistochemical analysis (IHC) on KPC pancreas samples. We observed CAFs that were positive for both Talng and αSMA exclusively in close proximity to tumor cells. Fibroblast expressing only αSMA mostly located in normal area. Tagln is known as an actin-binding protein and plays an important role in activated fibroblasts. Orthotopic PDAC mouse models using Tagln homozygous knockout mice showed a significant reduction in tumor weight compared to the wild-type mice (P = 0.0076). Indeed, we found that high *TAGLN* expression in PDAC samples was associated with poor survival, as demonstrated by the analysis of the TCGA dataset. These data suggest that myCAFs expressing TAGLN contribute to the promotion of PDAC growth. Targeting stromal TAGLN might be a potential therapeutic strategy to counteract PDAC progression.

#1590 The role of mucosal associated invariant T (MAIT) cells in pancreatic cancer liver metastasis.

Jugmohit Toor[1], Peter Dimitrion[1], Rachel Krevh[2], Kalpana Subedi[2], Bobby Zuniga[2], Jie Wang[2], Li Zhou[2], Qing-Sheng Mi[2]

[1]Cancer Biology, Henry Ford Health System / Wayne State University, Detroit, MI, [2]Henry Ford Health System, Detroit, MI

Pancreatic cancer liver metastasis (PCLM) is present in 50% of patients diagnosed with pancreatic ductal adenocarcinoma (PDAC) and leads to a median survival of <6 months. Here, we sought to identify urgently needed therapeutic options for treating PCLM by targeting mucosal associated invariant T (MAIT) cells, an invariant T cell restricted to MHCI related protein (MR1). MAIT cells are a unique subset of T cells that are classified as “protumor” MAIT17 and “antitumor” MAIT1 cells. We hypothesize that the PCLM tumor microenvironment (TME) induces direct MAIT cell activation via MR1 which primes MAIT cells towards a “protumor” phenotype. Using publicly available TCGA data, we found that PDAC tumors were enriched for MR1 gene expression compared to healthy tissue and patients with lower tumor MR1 expression had better overall survival. Next, immunostaining of MR1 on tumor samples from primary PDAC and PCLM revealed that that MR1 protein expression is highly enriched in the TME and localized to the surface of tumor cells. This suggests that MAIT cells in the PCLM TME are being activated directly via an MR1 dependent pathway. Next, we performed hemi-spleen injection of mouse pancreatic cancer cells into WT and MR1 KO (lacks MAIT cells) mice to model PCLM. Interestingly, MAIT cells in the WT PCLM mice were shifted towards the “pro-tumor” MAIT17 phenotype. Furthermore, the lack of MAIT cells in MR1 KO mice significantly reduced tumor burden compared to WT mice. Lastly, we found that MR1 KO mice had a reduction in exhausted NK and NKT cells which likely promoted anti-tumor immunity. Overall, we find that the PCLM TME promotes “pro-tumor” MAIT17 cells via MR1 mediated activation and these MAIT17 cells inhibit anti-tumor cells such as NK and NKT cells. This work identifies targeting MAIT cells as a novel immunotherapy approach for PCLM.

#1591 Hepatocytes compensate for the loss of PHGDH in pancreatic cancer cells during liver metastasis.

K. Ganguly[1], K. Yamamoto[2], J. Encarnacion Rosado[1], A. Sohn[1], D. Biancur[1], E. Lin[1], E. White[1], A. C. Kimmelman[1];
[1]NYU Langone Health Perlmutter Cancer Ctr., New York, NY, [2]The University of Tokyo, Bunkyo City, Tokyo, Japan

Background: Pancreatic cancer (PC), one of the deadliest malignancies, exhibits a high rate of distant metastasis that directly correlates with the mortality rate. Liver serves as one of the most predominant sites of metastasis in PC patients. The nutrient availabilities at the metastatic organ and the metabolic dependencies of the invading tumor cells play pivotal role in shaping the metastatic tumor microenvironment (TME) and establishing metastatic colonies. We observed an elevated expression of PHGDH, the first rate-limiting enzyme of the serine (Ser) biosynthesis pathway, in the hepatocytes (most abundant liver-resident cells) isolated from murine pancreatic liver-metastasis (LM), as compared to normal livers. Hence, we hypothesized that hepatocytes may promote the growth of PC cells by sufficing for their Ser-requirement during LM.
Methods: Murine PC line (HY19636 derived from LSL-KrasG12D; p53 L/+, Ptf1a-Cre+ tumors), were used to generate LMs in B6 mice via hemi-splenic route. PHGDH was knocked-out by lentiviral and AAV-mediated delivery of CRISPR-Cas9 gRNAs *in vitro* and *in vivo*, respectively. RNA-seq, immunoblot, immunohistochemistry, confocal microscopy, ELISA, flow cytometry, chromatin immunoprecipitation and promoter-reporter analyses were performed to identify the molecular axis, followed by functional validations using genetic and pharmacologic inhibitions in murine and human lines. Frozen homogenates with matched formalin-fixed sections of LMs from PC patients provided a unique correlative platform for the study.
Results: A significant portion of the LM tissues (68% in our cohort of 32 PC patients) demonstrated no to very low expression of PHGDH in the cancer cells, rendering them as exogeneous Ser (exSer)-dependent. Notably, loss of PHGDH in the tumor cells induced an elevated PI3K/AKT signaling, downstream of a CXCL5/CXCR2 axis, in the neighboring hepatocytes. This led to FOXO3A's cytoplasmic sequestration and decline in its occupancy on PHGDH promoter, causing a transcriptional upregulation of PHGDH in these hepatocytes, which enabled them to supply Ser and support the growth of exSer-dependent cancer cells in the liver. Abrogation of each node in the CXCR2-PI3K-FOXO3A axis and hepatocyte-specific deletion of PHGDH, led to a significant decline in the metastatic burden of exSer-dependent cells in the liver with a significant increase in overall mice survival, particularly under Ser-deprived dietary conditions.
Conclusion: Our findings demonstrate a novel cancer cell-hepatocytes crosstalk necessary for the growth of PC cells in Ser-depleted conditions. Here, we have identified several actionable signaling nodes in the liver that serve as compensatory metabolic allies for PC cells during liver metastasis, and can be considered as potential therapeutic targets in adjuvant setting.

#1592 Single-cell transcriptomics reveals unique stromal and metabolic heterogeneity in liver metastatic pancreatic cancer.

R. Singh, C. Halbrook;
University of California, Irvine, Irvine, CA

Pancreatic ductal adenocarcinoma (PDA) is the 3rd leading cause of cancer related death in the US. This mortality is strongly linked to the complex PDA tumor microenvironment that drives resistance to chemotherapy and immune suppression. Most patients succumb to metastatic disease, with liver being the most frequently colonized organ. Despite this, most pre-clinical studies have focused on primary PDA models to study the disease. Accordingly, the extent that the liver metastatic niche promotes immune evasion and resistance to treatment remains unclear.To directly compare primary vs. metastatic tumors in PDA tumors, we have optimized a syngeneic experimental model to contrast primary vs. metastatic lesions. To define the similarities and differences between cell types present in these tumors, we employed a single-cell transcriptomics approach. Our analysis has identified shared populations of malignant epithelial, stromal, and immune cells between lesions, allowing for a direct comparison of programming. Here, we have observed that the dominant populations of PDA cells in pancreas vs. liver tumors engage in distinct metabolic programs that suggest different actionable vulnerabilities.Beyond these, we also observed fibroblasts and myeloid sub-populations that are exclusive to liver tumors. These data further support our hypothesis that alternative mechanisms of metabolic, immune, and stromal interactions take place in the metastatic tumor microenvironment. To define these crosstalk networks, we employed the interactome tool CellChat, which has uncovered unique signaling interactions between the CAF and cancer cell populations in pancreatic or liver tumors. Overall, these data have the potential to lead to new avenues to directly target cancer cells or engage an effective immune response that can be designed to treat metastatic pancreatic cancer- an urgent clinical need.

#1593 Intercellular network in immune suppressive microenvironment of pancreatic cancer.

K. Aoki, H. Fukuda, Y. Mizoguchi, K. Arai;
National Cancer Center Research Institute, Tokyo, Japan

Despite constant efforts to improve treatment, the prognosis remains poor, with an overall survival rate of 6% (ranges from 2% to 9%) due to lack of efficient chemotherapy, radiotherapy, and targeted therapy. Immune checkpoint inhibitors (ICIs) has been reported to be effective in various solid cancers, such as melanoma, lung cancer, and renal cell carcinoma. However, pancreatic ductal adenocarcinoma (PDAC) is resistant against ICIs. The responsiveness of immune therapy is mainly determined by immune tumor microenvironment (TME) composed of tumor-infiltrating lymphocytes (TIL) and stromal cells. PDAC possesses unique TME, which is abundant of fibrosis, termed of desmoplasia, and the role of fibrosis in constructing immune suppressive TME remains unclear. First, in this study, to examine the immunological characteristics of TME, we constructed an integrated data base of TIL profiling, RNA-seq and whole exome seq using 31 fresh resected tissues of PDAC. An unsupervised clustering of based on numbers and percentages of 12 TIL types analyzed by flow cytometry showed that PDAC was divided into 2 types of cluster (myeloid cell-, T cell-dominant type), and the prognosis of myeloid type was significantly poorer than T cell-type. Myeloid type contained the high frequency of myeloid cell lineage including monocytes, macrophages and myeloid-derived suppressor cells (MDSC). Only MDSCs were significantly associated with poor prognosis among various immune cell types. Furthermore, gene enrichment analysis identified activated and suppressed pathways in each immune type, and in myeloid cell-dominant type, the immune-related pathways were significantly down-regulated. Then, to understand the characteristics of MDSCs infiltrated into pancreatic cancer tissues, single cell RNA-seq with surgical specimens was performed, and the analysis showed that a specific subtype of MDSCs infiltrated into cancer tissues. In addition, activation status of cancer-associated fibroblasts (CAFs) was related with MDSC recruitment and activation, indicating that the interaction between MDSCs and CAFs is crucial to create MDSC-rich TME. Inhibition of interaction between MDSCs and CAFs is expected to overcome immunosuppressive TME can be a therapy in PDAC.

#1594 Pancreatic cancer and T-cell crosstalk-induced MUC4 expression attenuates T-cell-mediated response.

X. Li, I. Khan, R. Kehrberg, Z. W. Alsafwani, R. Bhatia, S. Kumar, S. K. Batra;
University of Nebraska Medical Center, Omaha, NE

Background: While T-cell-based immunotherapy emerged as a promising tool for cancer management, clinical trials and translational studies revealed that cancer cells develop resistance by modulating tumor microenvironment and cell-intrinsic mechanisms. Pancreatic cancer (PC), consisting of dense stroma, immunosuppressive environment, and aberrant mucin expression, has a dismal survival rate and responds poorly to immunotherapies. MUC4, a member of the mucin family, has been reported to block lymphokine-activated killer cells and induce apoptosis of cytotoxic T-cells, suggesting its possible role in immune modulation. However, how the T-cell secretome influences MUC4 expression in PC and its role in modulating the T-cell response is poorly investigated.
Method: The scRNA-seq data analysis and primary T-cell conditioned media (CM) were utilized to investigate the MUC4 and T-cell crosstalk. T-cell CM-treated murine PC cell line (KCT-3266) was analyzed by RNA-seq analysis followed by MUC4 silencing studies to investigate its role in evading T-cell response. The subcutaneous murine model was utilized to investigate the influence of MUC4 KO on immune cells and cytotoxic cell infiltration. The RNA isolated from tumor tissues from $Kras^{G12D/+}$, $Trp53^{R127H/+}$, Pdx-1-Cre (KPC), and Muc4 knockout (KPMC) murine models were used for PanCancer immune profiling.
Results: The scRNA-seq analysis suggests that intratumoral T-cells positively correlate with MUC4 expression in PC patients. The activated T-cell CM consisting of predominantly IL-2, IFN-γ, and TNF-α cytokines, significantly induce the expression of MUC4 transcriptionally and translationally in both human (SW1990 and COLO357) and murine (KCT-3248 and KCT3266) PC cell lines. RNA-seq analysis from T-cell CM-treated cancer cells revealed that T-cell secretome induced the pathways related to cancer cell death. The CRISPR knockout of MUC4 in PC cells showed increased expression of cleaved caspase-3 after T-cell CM treatment, indicating that MUC4 plays a protective role against the T-cell CM-mediated killing. Subcutaneous implantation of MUC4 proficient and deficient PC cells on the flanks of C57BL/6 immunocompetent mice demonstrated a significantly higher infiltration of CD3 positive and cytotoxic T-cell infiltration in the MUC4 deficient tumors, resulting in significantly lower tumor weight. The PanCancer immune profiling also showed that depletion of Muc4 increases the T-cells and cytotoxic T-cell signaling scores in the KPMC tumor tissues compared to KPC.
Conclusion: T-cell secretome induces MUC4 expression in pancreatic cancer cells, and the increased MUC4 expression reduces T-cell infiltration and protects PC cells against T-cell-mediated killing.

#1595 Persistence of fetal gene signatures along the mesenchymal lineage trajectory defines heterogeneity and function of pancreatic cancer associated fibroblasts.

L. Han[1], T. Walter[1], J. Beaudet[1], C. Everett[1], K. Fang[2], M. Zimmermann[2], A. Mathison[2], R. Urrutia[2], V. Jin[2], G. Leone[2], M. Ostrowski[1];
[1]The Medical University of South Carolina (MUSC), Charleston, SC, [2]Medical College of Wisconsin, Milwaukee, WI

In pancreatic ductal adenocarcinoma (PDAC), cancer associated fibroblasts (CAFs) play critical and complex roles in the tumor microenvironment. CAFs are also a major cell type in the desmoplastic stroma in PDAC and may account for half of the entire tumor tissue. Here we aimed to investigate the origin, diversification, and function of CAFs. We constructed a dual-DNA-recombinase mouse genetic model carrying *Kras*$^{G12D/+}$; *Trp53*$^{frt/+}$; *Pdx1*$^{Flpo/+}$; *Isl1*$^{creER/+}$; *R26*$^{Tomato/+}$ alleles, referred to as *KPFIT*. The DNA recombinase FlpO directs expression of an oncogene Kras (G12D mutation) and loss of a tumor suppressor p53 in pancreatic epithelial cells, while creER recombines the Tomato reporter in the splanchnic mesenchyme and its descendants. The splanchnic mesenchyme is a layer of fetal tissue surrounding the endoderm where the pancreatic epithelium arises. This approach capitalized on the independent functions of FlpO/Frt and CreER/LoxP systems, allowing us to lineage trace Tomato labeled splanchnic progenies (via *IT*) in a spontaneous pancreatic cancer model (via *KPF*) within the same mouse. Our study identified the splanchnic mesenchyme as the fetal origin of pancreatic fibroblasts during homeostasis and tumorigenesis. Notably, the other two postulated origins, bone marrow and epithelial cells, have minimal contributions to fibroblasts. Importantly, single cell transcriptomic analysis indicated persistent and dynamic gene expressions along the pancreatic mesenchymal trajectory during development, homeostasis, precancer lesion and cancer. Intriguingly, certain splanchnic factors are expressed in only subtypes of adult pancreatic fibroblasts in temporally and spatially distinct patterns. Furthermore, we constructed mouse genetic models to delete one of the splanchnic factors, *Gata6,* specifically in CAFs, which resulted in increased tumor burden in the pancreas. This suggests a non-cell autonomous function of GATA6 in CAFs to restrain pancreatic cancer progression. In summary, this study delineated a continuous cell trajectory of the mesenchymal lineage in the pancreas across different life stages. Moreover, persistent gene expressions along the mesenchymal trajectory contributes to pancreatic CAF heterogeneity. Importantly, such persistence may constitute an inherent mechanism to suppress pancreatic cancer. The enhancement of this mechanism could be explored further for therapeutic benefits.

#1596 Disrupting local immunosuppression by combined myCAF/myeloid targeting in pancreatic cancer.

M. C. Hasselluhn[1], D. Thomas[2], L. Vlahos[1], A. Curiel-Garcia[1], A. R. Decker-Farrell[1], T. C. Dalton[1], S. A. Sastra[1], C. F. Palermo[1], A. Califano[1], K. P. Olive[1]; [1]Columbia University Irving Medical Center, New York, NY, [2]QuantX Biosciences, Princeton, NJ

Immunotherapy has revolutionized clinical care for many patients, but some cancers, such as pancreatic ductal adenocarcinoma (PDAC) remain stubbornly resistant. Local immunosuppression (LIS) is one of the striking hallmarks of PDAC due to the combined effects of multiple different immunosuppressive cell types in the tumor microenvironment (TME). There is great need for an increased understanding of the cellular crosstalk within tumors to understand how stromal cells coordinate in their suppression of immune responses. Oncogenic KRAS activation in tumor cells promotes the invasion and proliferation of tumor-supporting stromal cells, while excluding cancer-targeted cytotoxic T cells. Prior attempts to reverse LIS in PDAC by targeting individual stromal cell populations have been unsuccessful, alluding to the contributions of multiple distinct cell types. Here we examine the interactions of cancer-associated fibroblasts (CAFs) and myeloid-derived suppressor cells (MDSCs) and how they coordinate to suppress immune responses in the PDAC TME. We interrogate PDAC stromal cell biology by using targeted therapies to perturb various cell populations both *in vivo* using genetically engineered mouse models, and *ex vivo* using PDAC tumor explants. Explants are short-term slice cultures that enable experimental study of intact tumor sections with a full complement of cell types. Importantly, PDAC explants maintain their histopathological architecture and cellular diversity over time. This medium-throughput platform allows for testing of multiple drugs and mechanistic hypotheses in the native PDAC TME. We show in preliminary data that Smoothened inhibition (SMOi) decreases the proliferation and activity of myCAFs, but provokes the expansion of CD11b-positive myeloid cells *in vivo*. Thus, we hypothesize that LIS in PDAC is maintained by a balance between myCAFs and myeloid cells, preventing effective T cell invasion. Single cell RNA-seq data comparing ctrl vs. SMOi-treated murine PDAC elucidates stromal subpopulations involved in the LIS phenotype and guides the identification of myeloid subtypes emerging after SMOi. Strikingly, we demonstrated that simultaneous SMOi and targeting myeloid cells via anti-Gr1 or CCR1 inhibition significantly elevates cytotoxic T cell numbers within the TME. We are currently investigating whether the activity of these T cells may be further potentiated through combination with immunomodulatory agents. By testing various treatment combination in the same TME, we will identify the best synergistic effects for future immunotherapy approaches in human PDAC. In summary, we are elucidating the complex mechanism behind LIS in PDAC by employing our novel explant culture system alongside *in vivo* studies. We aim to develop a translatable regimen to neutralize LIS, reactivating the cytotoxic T cells in the tumor periphery to invade, proliferate, and attack cancer cells.

#1597 CD144$^{\pm}$cancer-associated fibroblasts drive the malignancy of pancreatic cancer via stimulating inflammatory paracrine.

X. Sun, J. Yu, T. Zhao, J. Hao;
Tianjin Medical University Cancer Institute and Hospital, Tianjin, China

Purpose: Cancer-associated fibroblasts (CAFs) are highly heterogeneous in pancreatic ductal adenocarcinoma (PDAC). We previously reported that CAFs can acquire an endothelial phenotype under stress. Thus, we hypothesized that there are CAFs highly expressing endothelial markers and substantiated a novel subtype of CAFs promoting tumor progression.

Experimental design: We performed single-cell RNA sequencing to identify the existence of CD144$^{\pm}$CAFs. The prospective and retrospective analysis were combined to figure out the correlation between CD144$^{\pm}$CAFs proportion and clinical outcome. The proliferation and invasion assay of cell lines, organoids and pancreatic cancer xenograft model were used to detect the effect of CD144$^{\pm}$CAFs on tumor progression. Cytokine array assay, RNA-sequencing, IP-mass spectrum, Ch-IP and luciferase analysis were conducted to elucidate the underlying mechanism. siRNA delivery nanosystem was designed and administrated to precisely target CD144$^{\pm}$CAFs *in vivo*.

Results: CD144$^{\pm}$CAFs were present in tumor microenvironment of PDAC and breast cancer and patients with a higher CD144$^{\pm}$CAFs proportion have worse prognosis in PDAC. CD144$^{\pm}$CAFs can promote the metastasis of PDAC through enhancing epithelial-mesenchymal transition. CD144-β-catenin-STAT3 signaling axis was activated and downstream inflammatory secreted cytokines were transcriptionally upregulated to maintain the functions and phenotype of CD144$^{\pm}$CAFs. A novel CAF-targeting siRNA delivery nanosystem, loading FAPα and siCDH5, was designed and administrated to precisely target CD144$^{\pm}$CAFs, which substantially inhibited the protumoral roles *in vivo*.

Conclusion: CD144$^{\pm}$CAFs can promote the growth and metastasis of PDAC by activating CD144-β-catenin-STAT3 signaling axis and stimulating inflammatory secretion. CAF-targeting siRNA delivery nanosystem can inhibit tumor progression by precisely targeting CD144+CAFs.

#1598 Individualized longitudinal assessment reveals therapy-induced tumor and microenvironment dynamics in preclinical pancreatic cancer models.

J. T. Siveke, R. Fang, P.-Y. Cheung, J. Yang, J. Peng, K. Althoff, K. Savvatakis;
German Cancer Research Center, Essen, Germany

Background & Aim: Progression and therapeutic resistance in pancreatic cancer depends on the ability of cancer cells to adopt specific cell states. These phenotypes largely depend on environmental tissue niches. Here, we investigated therapy-induced tumor dynamics in vivo at single-cell spatial and temporal resolution in different subtypes of PDAC using several genetically engineered mouse models, which reflect distinct human PDAC ecosystems.
Methods & Results: We established orthotopic tumor models of pancreatic cancer with distinct tumor microenvironment (TME) formation (reactive vs deserted stroma), which were monitored for tumor growth to define tumor response patterns under MAPK inhibition. Serial ultrasound-guided biopsy sampling was performed to collect tissues from the same tumors at pre-treatment, responsive and recurrence periods.Transcriptomic analysis of biopsies using the Mfuzz algorithm delineated highly dynamic gene and pathway activities during treatment. Reactive, but not deserted, TME showed an upregulation of immune-related pathways (antigen presentation, T cell receptor, NK cytotoxicity) immediately after MAPK inhibition in regressed tumors that dropped dramatically during recurrence of tumors, in which upregulation of TGF-b signaling was observed. In the deserted stroma model, on the other hand, an enrichment in drug metabolic pathways during recurrence was observed.CAF cluster deconvolution analysis revealed an increase in a LRRC15+ CAF cluster, which was TGF-b-driven and immunosuppressive, during recurrence period only in the reactive model. The dynamic changes of immune cells and CAFs were validated at protein level by multiplex immunofluorescent imaging. Cmputational spatial analysis revealed a tumor-encapsulating and CD8+ cytotoxic T cell-repelling pattern exhibited by LRRC15+FAP+ CAFs, implying a potential role of this CAF subset in T cell suppression during recurrence in reactive subtype. Using spectral cell sorting with CellView image technology, specific CAF subsets, tumor cells as well as immune cell subsets based on 30+ markers and cell morphology were isolated, characterized and assessed by *ex vivo* functional assays to confirm the immunosuppressive and tumor protective mechanism mediated by CAFs.
Conclusion: Longitudinal in vivo assessment of distinct PDAC subtypes provides deep mechanistic insights to accurately unlock specific response patterns of tumors with heterogeneous TME dynamics upon therapeutic perturbation, leveraging identification of key nodes for intervention.

#1599 Metabolism as a key regulator of macrophage phenotype in pancreatic cancer.

C. Anaraki, C. Halbrook;
University of California, Irvine, Irvine, CA

Pancreatic Ductal Adenocarcinoma (PDAC) is the 3rd leading cause of cancer-related deaths in the US, with a five-year survival rate of 12%. Barriers to treatment include the highly fibrotic tumor microenvironment (TME), the high interstitial pressure which acts to collapse the blood vessels, and the influx of immunosuppressive immune cells. Within this immune milieu, we find that the most abundant are tumor-associated macrophages (TAMs). These TAMs display a phenotype similar to anti-inflammatory (M2-like) macrophages. Despite TAMs exerting an immunosuppressive function within the TME, there is not a complete overlap with the characteristics associated with M2 macrophages. Interestingly, TAMs still display many markers associated with the pro-inflammatory (M1-like) macrophages. This dichotomy suggests there may be a level of plasticity within the macrophage compartment that can be exploited to lead to better tumor control. Previous studies have shown a connection between arginine metabolism and macrophage effector function along the M1/M2 axis. In macrophages, arginine can be broken down in two ways: via iNOS into nitric oxide, which aids in effector function, or via Arginase 1 (Arg1) into ornithine and later proline, which is an essential component of the extracellular matrix (ECM). This study seeks to elucidate how metabolic perturbations influence macrophage function and phenotype. Here we observed that changes in oxygen availability and glucose abundance shifted macrophage expression of iNOS and Arg1. In vivo we found that conditionally knocking out Arg1 in the myeloid compartment leads to lower fibrosis when inducing inflammation in the pancreas. Furthermore, macrophages polarized with PDAC cancer-conditioned media display a sharp increase in Arg1 expression as compared to unpolarized macrophages, as well as increased resistance to both glycolytic inhibitors and mitochondrial inhibitors. This preliminary data demonstrates an important link between macrophage metabolism and function in the context of pancreatic disease.

#1600 Interception of pro-tumorigenic glycan signaling in pancreatic cancer.

Jasper Hsu, Hyemin Song, Kristina Peck, Chelsea Bottomley, McKenna Stamp, Shira Okhovat, Dannielle D. Engle

Salk Institute, La Jolla, CA

Pancreatic cancer is a deadly malignancy. We have setup a pipeline to interrogate cancer cell intrinsic and extrinsic mechanisms contributing to treatment response. Using a combination of mouse and human organoids models together with *in vivo* investigation, we have systematically dissected key signaling hubs driving pro-tumorigenic cancer cell intrinsic features as well as remodeling of the tumor microenvironment (TME). We found that the glycan epitope, CA19-9, drives pancreatic inflammation, cancer, and metastasis. CA19-9 drives pro-tumorigenic intrinsic features in part through CA19-9 modification of the secreted glycoprotein Fibulin 3. We have also discovered direct and indirect mechanisms through which CA19-9 causes remodeling of the TME. Specifically, CA19-9 elevation causes expansion of all cancer associated fibroblast (CAF) subtypes, including an increase in antigen presenting CAFs and resulting increase in regulatory T cells. Further, there are dramatic increases in tumor associated macrophages (TAMs) derived from both inflammatory monocytes as well as tissue resident macrophages. To delineate the mechanisms by which these TME changes are mediated, we use novel co-culture model incorporating macrophages, organoids, and fibroblasts (MOrF). Blocking CA19-9 signaling *in vitro* and *in vivo* reverses these TME alterations. These changes to the TME are mediated through indirect effectors as well as previously unknown CA19-9 modified proteins. Overall, we elucidate previously unexplored mechanisms driving pancreatic tumorigenesis while also uncovered vulnerabilities for therapeutic exploitation.

#1601 The role of complement in pancreatic cancer cachexia.

A. C. D'Lugos, C. Callaway, S. M. Judge, **A. R. Judge**;
University of Florida, Gainesville, FL

Cancer cachexia is a multifactorial condition characterized by skeletal muscle atrophy and dysfunction that impairs longevity and quality of life for the vast majority of cancer patients. Recently, we discovered through unbiased proteomic analyses that the complement system is activated in the skeletal muscle of cachectic pancreatic cancer patients. Therefore, the purpose of this study was to investigate the role of complement in pancreatic cancer cachexia. To accomplish this, we obtained genetically modified, C57Bl6/J congenic mice lacking the central regulator of complement, C3 ($C3^{-/-}$ mice). Wild-type (C57Bl6/J, WT, n=12) and $C3^{-/-}$ mice (n=11) (male, 12 weeks old) received orthotopic injections of mouse pancreatic cancer cells (KPC) into the pancreas, and as non-cancer controls, WT (n=8) and $C3^{-/-}$ (n=4) mice received injections of PBS into the pancreas. Mice were monitored daily and euthanized at IACUC-mandated tumor endpoint (body condition score ≤ 2; range: 14-15 days). *In-vivo* diaphragm function was assessed immediately prior to euthanasia via M-mode ultrasound. Skeletal muscles (soleus, SOL; *tibialis anterior*, TA; diaphragm, DIA) were harvested and *ex-vivo* contractile function was assessed on strips of costal diaphragm. Diaphragmatic excursion and respiratory rate were reduced with KPC tumor burden in WT mice, but preserved in $C3^{-/-}$ mice. Deletion of C3 did not influence the KPC-induced reduction of body mass or KPC tumor growth. Atrophy of limb muscle mass (SOL, TA) and fiber size (TA) during KPC tumor burden was attenuated in $C3^{-/-}$ mice. Maximal specific force of DIA was greater in $C3^{-/-}$ versus WT KPC-bearing mice. KPC tumor burden increased collagen content in the DIA of WT mice, but not $C3^{-/-}$ mice. Diaphragm fiber size was reduced in WT KPC-bearing mice, but preserved in $C3^{-/-}$ mice. KPC tumor burden induced significant increases in immune cell (CD45+) infiltration and fibroadipogenic progenitor cell (PDGFRa+) abundance in the DIA of WT tumor-bearing mice, but to a lesser extent in $C3^{-/-}$ mice. These findings suggest complement activation is causative in pancreatic cancer-induced skeletal muscle wasting and dysfunction. Inhibition of complement during cancer cachexia may possess therapeutic potential for the preservation of skeletal muscle mass and function.

#1602 Leukemia inhibitory factor (LIF)-factor XIIIA mediated macrophage-stromal crosstalk in pancreatic cancer.

N. Jaferi[1], S. Mehra[2], V. Krishnamoorthy[2], S. Jinka[2], A. Bianchi[2], V. T. Garrido[2], L. A. Nivelo[2], B. Yuguang[2], N. S. Nagathihalli[2];
[1]Yale College, New Haven, CT, [2]University of Miami, Miller School of Medicine, Sylvester Comprehensive Cancer Center, Miami, FL

Background: Pancreatic ductal adenocarcinoma (PDAC) is a lethal malignancy marked by a highly immunosuppressive tumor microenvironment (TME). Macrophages are known to promote immunosuppression and exhibit a profibrotic transcriptional profile with potential involvement in extracellular matrix (ECM) remodeling. Previously, we identified hyperactivation of cancer cell intrinsic cyclic AMP response element binding protein 1 (CREB) regulates leukemia inhibitory factor (LIF) to mediate macrophage infiltration and polarization within the TME of PDAC. Subsequently, we observed that disrupting LIF-LIF receptor (LIFR) signaling therapeutically not only diminishes the infiltration of tumor-associated macrophages (TAMs) but also results in a decrease in ECM deposition. This study delves into the potential regulatory pathway through which LIF induces remodeling of the ECM within the PDAC TME.

Methods: We targeted LIF-induced macrophage-stromal crosstalk using the LIFR antagonist (EC359) in an orthotopically tumor implanted LSL-$Kras^{G12D/+}$; $Trp53^{R172H/+}$; $Pdx1^{Cre/+}$ (KPC) mice model of PDAC. Sirius red staining in tumor sections was performed to assess ECM (collagen) deposition. Moreover, we performed RNA transcriptomics-based analysis of recombinant (rLIF) induced bone marrow derived macrophages harvested from syngeneic C57BL/6 mice. The Cancer Genome Atlas (TCGA) pancreatic cancer (PAAD) data set along with single-cell RNA sequencing (scRNA seq) were employed to assess the expression of major downstream targets of LIF. To validate the RNA-seq results, we conducted immunohistochemical analysis (IHC) on mouse PDAC tissue sections and quantitative polymerase (qPCR) analysis on RAW 264 macrophage cell line treated with rLIF or KPC $CREB^{WT}$ PDAC tumor cells conditioned media.

Results: We observed a drastic decrease in both TAM infiltration and, of note, ECM deposition in orthotopically implanted KPC pancreas tumor mice tissue treated with EC359 as compared to vehicle. Mechanistically, our RNA-seq analysis unveiled a significant upregulation of *Factor XIIIA* (FXIIIa), a major downstream target of LIF. Notably, TCGA data revealed that *FXIIIa* mRNA expression is upregulated across PDAC tumors marked by poor survival outcomes. Moreover, scRNA seq and IHC established that TAMs highly express FXIIIa in the PDAC TME. In exploring the effect of LIF-LIFR signaling in the ECM, mouse RAW 264.7 macrophage lines incubated in high LIF conditions confirmed transcriptional upregulation of ECM-associated proteins such as *FXIIIa* as well as fibronectin.

Conclusion: Our investigation provides valuable insights into the possible mechanism by which LIF triggers ECM remodeling, thereby contributing to the desmoplastic stroma. Significantly, our findings propose that LIF-regulated FXIIIa signaling in macrophages serves as a plausible mediator of the LIF-induced ECM remodeling in PDAC.

#1603 Intra-pancreatic fat promotes the progression of PDAC by activating thermogenesis.

X. Yin, Y. Chen, R. Xu, C. Hu, **C. Wang**, Y. Zhao;
Peking Union Medical College Hospital (PUMCH), Beijing, China

Background: The presence of minimal intra-pancreatic fat deposition (IPFD) in the healthy human pancreas has been demonstrated in numerous studies. But excess IPFD, or fatty pancreas disease, leads to a wide array of diseases, including but not limited to diabetes, pancreatitis, and pancreatic ductal adenocarcinoma (PDAC). Remarkably, PDAC patients with excessive intra-pancreatic fat accumulation are commonly associated with a poor prognosis compared to those with minimal deposition. However, the interaction between tumor and intra-pancreatic adipose tissue remains elusive. Here, we evaluated the pancreatic fat infiltration in normal people and patients with PDAC respectively, and explored the mechanism of how intra-pancreatic fat affects the progression of PDAC.

Methods: Magnetic resonance imaging (MRI) and clinical biopsy specimens were used to assess the degree of pancreatic fat infiltration in PDAC patients and healthy control individuals. The C57BL/6J mice injected orthotopically with KPC cells and adipocytes, high-fat diet (HFD)-induced obesity *KC (Pdx1-Cre; $Kras^{LSL\text{-}G12D/WT}$)* mice, and *KC; ob/ob* mice were established to dynamically observe how adipocytes affect tumor progression in vivo. The snRNA-seq of tumor samples and proteomics of conditional medium of PDAC cell lines were performed to identify the mechanism of interaction between cancer cells and adipocytes.

Results: We found that patients with PDAC presented excess intra-pancreatic fat deposition more frequently than healthy individuals, and the degree of fat infiltration was positively correlated with the tumor burden of PDAC patients. HFD-induced obesity *KC* mice and *KC; ob/ob* mice showed a higher degree of IPFD, which contributed to tumor growth and low survival rates of mice. Additionally, the expression of uncoupling protein 1 was upregulated in PDAC patients and *KPC (Pdx1-Cre; $Kras^{LSL\text{-}G12D/WT}$; $p53^{LSL\text{-}R172H/WT}$)* mice compared to normal controls. Constantly, the snRNA-seq of PDAC samples demonstrated the increase in thermogenic signature. In vitro, C3H10T1/2 cells treated with conditional medium from pancreatic cancer cell lines or co-cultured with pancreatic cancer cell lines showed increased expression of browning markers and elevated oxygen consumption rate. Specifically, combined analysis of the proteomic of T3M4 and CFPAC-1 conditional medium and the snRNA-seq revealed that pancreatic cancer cells secreted integrin β4 (ITGB4) to improve the thermogenesis of intra-pancreatic adipocytes (IPA), which in turn promoted cancer cell progression.

Conclusion: Parts of PDAC patients present excess intra-pancreatic fat accumulation, a process associated with tumor growth and poor prognosis. Mechanistically, pancreatic cancer cells activate the thermogenesis of IPA by secreting ITGB4, and then the thermogenetic adipocytes fuel the progression of the tumor in response.

#1604 Cancer-associated fibroblasts modulate T cell killing activity & phenotype in PDAC.

F. Zayou[1], H. Pearce[1], S. Nicol[1], S. Margielewska-Davies[1], S. Powell-Brett[2], R. Brown[2], J. Zuo[1], K. Roberts[2], H. M. McGettrick[1], P. Moss[1];
[1]College of Medical and Dental Sciences, University of Birmingham, Birmingham, United Kingdom, [2]Queen Elizabeth Hospital Birmingham, University Hospital Birmingham NHS Foundation Trust, Birmingham, United Kingdom

Background: Pancreatic ductal adenocarcinoma (PDAC) is highly aggressive malignancy characterised by its abundant extracellular matrix and diverse stromal cell components such as cancer associated fibroblasts (CAFs). CAFs play a pivotal role in shaping the tumour microenvironment and influencing the behaviour of immune cells, particularly T cells, through various mechanisms. The impact of CAFs on T cells is multifaceted as they can exert both pro- and anti-tumoral effects, influencing the delicate balance between immunosurveillance and immune evasion. In this study, we examined the phenotype and function of T cells when co-cultured with CAFs and Adjacent-normal fibroblasts (ANF) isolated from primary PDAC tissue following surgical resection.
Methods: Tumour and juxta-tumoral tissue from patients underwent digestion into a single cell suspension. Subsequently, the isolated fibroblasts were cultured and stained with a 22-plex antibody panel designed for flow cytometry. Additional functional assays involved co-culture of CAFs and ANFs with unstimulated or anti-CD3/CD28 stimulated allogeneic T cells. Cell proliferation rates were quantified through the CFSE assay, while the T cells were simultaneously stained to distinguish CD4+ and CD8+ T cells subpopulations. Additionally, the expression of key co-stimulatory molecules: CD69, NKG2D and DNAM-1 and the co-inhibitory molecule: PD-1 were assessed, providing a thorough examination of the immune dynamics within the tumour microenvironment.
Results: Flow Cytometry analysis revealed a distinct expression profile in CAFs compared to ANFs, with CAFs expressing higher levels of FAP and CD29. The CFSE assay further revealed that CAFs induced T cell proliferation of resting T cells with no significant increase in stimulated T cells. Notably, this co-culture led to a highly differentiated phenotype in both unstimulated and stimulated CD4+ and CD8+ T cells, characterised by elevated expression of activating markers (CD69 and NKG2D) and the inhibitory molecule PD-1. These findings suggest a dynamic interplay between fibroblasts and T cells in the tumour microenvironment, influencing both the proliferation and phenotypic aspects of T cell behaviour.

#1605 Oncolytic hsv-1(vc2) gm-csf regulates the proinflammatory profile suggestive of an immunomodulatory effect in PDAC cells.

N. Chintala Ramulu, S. Thota, B. Stanfield, K. Kousoulas, J. Francis;
Louisiana State University, Baton Rouge, LA

Pancreatic ductal adenocarcinoma (PDAC) is a highly aggressive disease that is projected to be the second leading cause of cancer-associated deaths by 2030. Owing to its intrinsic immune evasive tumor microenvironment (TME), PDAC is regarded as an immunologically “cold” tumor with a significant therapeutic challenge. Although 5-fluorouracil or gemcitabine-based chemotherapy is considered as standard of care, harnessing immunological pathways may potentially convert PDAC to a “hot” tumor, thereby providing survival advantage to patients. Lately, the use of oncolytic virus has proven to be an alternative strategy to activate the innate immune response within the TME coupled with its cytotoxic effect against the cancer cells. The FDA approval of T-VEC for the treatment of stage IIIB/IV melanoma validates the preceding argument. In this study, we have investigated the effect of herpes simplex virus type-1 (HSV-1) (VC2) overexpressing granulocyte-macrophage colony-stimulating factor (GMCSF), HSV-1VC2GM-CSF in the murine KRAS, p53, and Cre (KPC), and human MIA PaCa-2 pancreatic carcinoma cells. Following a 24h infection of the KPC and MIA PaCa-2 cells with the HSV-1VC2GM-CSF, the observed cytopathic effects (CPE) included cell rounding, detachment, and aggregation as compared to the wild-type HSV-1VC2 treated or the uninfected control cells. The CPE effect of HSV-1VC2GM-CSF was proven to be a more direct and dynamic response against these cells. In the next steps, the viral titers were determined to be 9.6E7 pfu/ml, 1.26E7 pfu/ml for HSV-1VC2 and VC2GM-CSF respectively. The infection of VC2GM-CSF 0.1, 1.0 and 10 MOI in KPC cells resulted in a significant increase in the expression of proinflammatory markers including interleukin 10 (IL-10), cyclooxygenase -2 (COX-2) and iNOS at the gene level in contrast to the uninfected controls. This was coupled with an increase in the expression of Fas ligand (FasL) in the treated cells. Intriguingly, the treated cells showed a significant upregulation of programmed death ligand (PD-L1). Interestingly, in a 3D-coculture of KPC and RAW264.7 cells the expression of PD-L1 was significantly upregulated. Based on the evidence presented here, it is speculated that VC2GM-CSF-induced proinflammatory profile in KPC and Mia PaCa-2 cells converts to an immunomodulatory one characterized by the regulation of FasL and PD-L1. The effect of VC2GM-CSF in a PDAC organoid model to understand the interplay between the tumor and the stromal cells in response to the virus is currently underway.

TUMOR BIOLOGY: Tumor Evolution in Space and Time
Poster Session

#1609 Inferring the T cell repertoire dynamics in non-small cell lung cancer metastases.

C. Richard[1], S. Hessey[1], C. Naceur-Lombardelli[1], S. Veeriah[1], G. Nageswaran[2], C. Hiley[1], S. Quezada[1], B. Chain[2], TRACERx and PEACE Consortia, C. Swanton[3], M. Jamal-Hanjani[1];
[1]University College London (UCL) Cancer Institute, London, United Kingdom, [2]University College London (UCL) Division of Infection and Immunity, London, United Kingdom, [3]The Francis Crick Institute, London, United Kingdom

Non-small cell lung cancer (NSCLC) is a highly complex disease, characterized by extensive genomic heterogeneity and dynamic evolution under therapeutic pressure. This evolution can lead to alterations in the antigens expressed by cancer cells, thereby influencing the T cell repertoire (TCR) as T cells expand in response to foreign antigens. Despite the central role of TCR in cancer progression and treatment response, only few studies have investigated the temporal and spatial changes in the TCR repertoire. In this study, we delve into the role of the TCR repertoire in metastatic progression in NSCLC. We conducted TCR sequencing of multiregion primary tumors, normal-adjacent tissues, and post-mortem metastases sampled from a cohort of 22 patients enrolled in the TRACERx and PEACE studies. Our findings reveal that primary tumor regions and normal-adjacent tissues exhibit similar fractions of expanded clonotypes. However, a higher proportion of expanded intratumoral TCRs were privately expanded in the tumor samples, suggesting a unique TCR landscape within the tumor microenvironment. The TCR repertoire across multiregion primary tumor samples was largely homogenous, with most expanded clonotypes shared across at least two regions. However, only a small fraction of these clonotypes were tracked in metastases, indicating a significant shift in the TCR repertoire during metastatic progression. Notably, the expanded clonotypes that persisted over time from early to late stage disease were significantly enriched for clonotypes ubiquitously expanded in the primary tumor across all regions. This was not shown to be associated with an increased likelihood of generation via VDJ recombination, suggesting a tumor-specific immune response. The expanded TCR repertoire in the postmortem metastases clustered mainly by anatomical site, suggesting an immune response driven by tissue-resident T cells. Moreover, we found a significant positive correlation between repertoire dissimilarity and genomic distance, suggesting that T cell clones track with tumor clones across spatial sites within patients. Our study demonstrates the significant spatiotemporal dynamics of the TCR repertoire during the metastatic progression of NSCLC, orchestrated by both tissue-resident T cells and the genomic evolutionary trajectory of tumors. Such an exploration could provide valuable insights to inform future strategies for immunotherapy treatments and enhance clinical monitoring of patients.

#1610 Elucidating tumor evolution and heterogeneity in metastatic bladder cancer from rapid autopsies.

P. Itagi[1], S. Arora[1], T. Persse[1], M. Yang[1], P. Galipeau[1], Y. Lin[2], F. Vakar-Lopez[3], J. K. Lee[4], P. Grivas[3], R. B. Montgomery[3], J. L. Wright[3], H.-M. Lam[3], A. Hsieh[1], G. Ha[1];

[1]Fred Hutchinson Cancer Center, Seattle, WA, [2]Aarhus University, Aarhus, Denmark, [3]University of Washington, Seattle, WA, [4]David Geffen School of Medicine at UCLA, Los Angeles, CA

Background: Bladder Cancer is a highly prevalent cancer with staggering mortality of about 20%. Metastatic BLCA (mBLCA) with variant histologies are aggressive and have a poor prognosis. The extent and impact of tumor heterogeneity in these variant subtypes are not fully understood. This work explores the intricate characterization of intra-patient and inter-patient tumor heterogeneity through genomic and transcriptomic analyses, drawing insights from a unique rapid autopsy cohort comprising 20 patients. The resulting revelations provide critical perspectives on heterogeneity and clonal evolution in mBLCA, underscoring the essential role of understanding these dynamics for the development of personalized treatment strategies.

Approach: Our research focuses on the genetic and molecular characteristics of these tumors, including the vast landscape of tumor heterogeneity, clonal evolution, genomic alterations, mutational signatures, and structural variants. Within the tumor microenvironment, we identified diverse cell populations with distinct genetic profiles. A detailed examination of mutational signatures sheds light on the specific processes underlying genetic alterations, while the investigation of structural variants elucidates their consequential role in cancer development and progression. Advanced bioinformatics tools are deployed to process and interpret the vast genomic and transcriptomic datasets, facilitating the identification of clonal populations, their genetic features, and the trajectory of clonal evolution. Furthermore, statistical models are employed to discern correlations between mutational signatures, treatment responses, and clinical outcomes.

Summary: The study unveils substantial inter-patient heterogeneity and discernible differences in mutational signatures, revealing intriguing correlations with treatment responses. These variations are intricately connected to underlying genomic alterations, copy number alterations, and gene expression patterns, offer a detailed perspective on the molecular landscape of mBLCA.

Conclusion: This multi-omics exploration stands as the most extensive study of its kind, leveraging rapid autopsy samples of metastatic variant histology BLCA. The research provides unprecedented resolution of genomic alterations and intra- and inter-patient tumor heterogeneity. The exploration of clonal evolution enhances our appreciation of the temporal dynamics of tumor progression, establishing a robust foundation for future therapeutic interventions precisely targeting evolving tumor clones. As we advance into an era of personalized medicine, these findings pave the way for tailored therapeutic strategies in the challenging landscape of metastatic variant histology Bladder Cancer.

#1611 DNA methylation co-operates with genomic alterations during non-small cell lung cancer evolution.

F. Gimeno-Valiente[1], C. Castignani[2], E. L. Cadieux[2], N. E. Mensah[2], O. Chervova[3], M. Jamal-Hanjani[1], N. McGranahan[1], S. Beck[3], J. Demeulemeester[4], M. Tanic[1], C. Swanton[3], P. Van Loo[2], **N. Kanu**[1];

[1]University College London (UCL), London, United Kingdom, [2]The Francis Crick Institute, London, United Kingdom, [3]University College London, London, United Kingdom, [4]VIB - KU Leuven Center for Cancer Biology,, Leuven, Belgium

Aberrant DNA methylation patterns have been described in nearly all human cancers, yet their interplay with genomic alterations during tumor evolution is poorly understood. To explore this crosstalk, we performed reduced representation bisulfite sequencing on 217 tumor regions from 59 patients from the TRACERx study, all with matched adjacent normal tissue, to deconvolve tumor methylation rates. We combined two new metrics for integrative evolutionary analysis with DNA and RNA sequencing data. I-TMD (intra-tumoral methylation distance) quantifies intra-tumor DNA methylation heterogeneity. MR/MN classifies genes based on the rate of hypermethylation at regulatory (MR) versus non-regulatory (MN) CpGs, to identify driver genes exhibiting recurrent functional hypermethylation. We observed early DNA methylation of VIPR2 and ZNF714 co-occurring with driver mutations in CDKN2A and STK11, respectively. Finally, we found DNA methylation-linked dosage compensation of essential genes co-amplified with neighboring oncogenes. Our identification of hypermethylated driver genes under positive selection may open new avenues for therapeutic stratification of patients with non-small cell lung cancer.

#1612 Timing ecDNA acquisition across cancer.

A. R. Lynch, P. Van Loo;
UT MD Anderson Cancer Center, Houston, TX

Extrachromosomal DNA (ecDNA) are acentric, circular DNA fragments which form after DNA double strand breaks. They segregate randomly during mitosis, promoting high-level amplifications of positively selected oncogenes such as *EGFR* and *MYC*. The prevalence of ecDNA across several cancer types, such as glioblastoma and sarcoma, has made promising therapeutic targets. However, while DNA damage is a hallmark of nearly all cancers, the formation of ecDNA is not, and the determinants for ecDNA acquisition are unclear. Furthermore, whether the timing of tumors' acquisition of ecDNA (i.e., early or late clonal or sub-clonal) affects patient survival and drug resistance is unclear. Here, we leverage orthoganol information from ecDNA amplicons, such as mutation allele frequency and sequence synteny, to develop computational methods for elucidating the evolutionary history of ecDNA. Applying these to several cancer subtypes in TCGA, we find that most ecDNAs arise early in tumor evolution. We expect these results will help identify determinants of ecDNA acquisition and its temporal influence on patient survival.

#1613 Evolution of mutations in the antigen presentation machinery across cancers.

W. Chen[1], T. Baker[2], Z. Zhang[1], P. Van Loo[1], **S. S. Gu**[1];
[1]UT MD Anderson Cancer Center, Houston, TX, [2]The Francis Crick Institute, London, United Kingdom

Immune escape is a critical hallmark of cancer progression. Under immunosurveillance, a subset of cancer-associated antigens or neoantigens are presented to the cancer cell surface via the antigen presentation machinery (APM) for recognition by antigen-specific T cells. During clonal evolution, cancer cells can evade such immunosurveillance by suppressing or ablating the APM. The defects in APM can further cause resistance to cancer immunotherapies and is associated with worse prognosis. Understanding how the defects in APM emerge and further shape the evolution of cancers is critical for devising strategies to overcome such immune escape mechanisms. However, it is not known when mutations in the APM occur along the history of cancer clonal evolution. We utilized a molecular archeology of cancer approach to reconstruct the evolution history of mutations in APM across 38 cancer types using whole-genome sequencing data from PCAWG. Genetic alterations in the APM occur in nearly 30% of patients, with varying frequencies and associations with immune infiltration across cancer types. Employing a League model to compare the timing of genetic events, we found that APM mutations can be early clonal, late clonal, or subclonal along cancer development. Further examination of individual tumors identified driver mutations that can happen before or after APM mutations along cancer development. Our study reveals the evolution of APM mutations in different cancers in a genetic context-aware manner. This information can contribute to optimizing personalized immunotherapy.

#1614 Macroscopic clonal expansion with driver mutations in normal human endometrium.

K. Watanabe[1], N. Kakiuchi[1], K. Ieiri[1], H. Maeda[1], T. Hirano[1], S. Kitamura[1], M. Taki[1], K. Yamanoi[1], R. Murakami[1], K. Yamaguchi[1], J. Hamanishi[1], H. Tanaka[2], S. Miyano[2], M. Mandai[1], S. Ogawa[1];

[1]Kyoto University, Kyoto, Japan, [2]Tokyo Medical and Dental University, Tokyo, Japan

Introduction: The epithelial cells of the endometrium undergo rapid proliferation and shedding each month under the influence of estrogen and progesterone. Recent studies have demonstrated pervasive driver mutations in the endometrium with ageing. However, previous observations have been limited to the microscopic scale, and it is still unclear how clonal expansion occurs over the entire endometrium and what driver mutations are responsible therein. To address these issues, we performed multisampling of the endometrium with extensive spatial mapping.

Methods: We collected multiple endometrial glands from normal endometrium in a 5mm lattice in 19 patients aged 30 to 85 years who underwent hysterectomy (3-31 samples per case), followed by DNA extraction, detected somatic mutations by whole exome sequencing, to identify large clones that spread across samples based on shared mutations.

Results: In total, 213 bulk endometrial glands were analyzed. The number of detected somatic mutations per sample ranged from 4 to 81 (mean±SD: 32.5±14.1), with at least one known driver gene mutation detected in 204 of 213 samples (mean±SD: 3.03±1.78). The mutational signature analysis revealed the predominance of the age-related SBS1 and SBS5 signatures. dN/dS analysis identified 20 genes that were positively selected in normal endometrium, including *PIK3CA, PIK3R1, KRAS, PPP2R1A, ARHGAP35,* and *FBXW7*, most of which are also known as driver genes for endometrial cancer. The number of mutations and their frequency for each driver gene did not differ by background diseases: endometriosis, endometriosis-associated ovarian cancer and other non-endometrial related diseases. In contrast to the high frequency of driver gene mutations, copy-number alterations were found in only 3 samples, such as +1q, +7, +10 and +12. We found clones showing a large expansion involving multiple samples in 8 cases, most of which harbored one or more driver mutations, such as *PIK3CA* and *KRAS*. The size of the largest clone carrying a *KRAS* mutation, which was found in a 32-year-old woman with cervical cancer, spanned as long as 10 mm in diameter. This suggests that clonal expansion in the endometrium could be very rapid even in healthy women, which contrasts to the observations that clonal expansion in other organs is usually seen in aged individuals.

Conclusion: We confirmed the high frequency of driver mutations in the normal endometrium, most of which overlapped to those found in endometrial cancers, suggesting that these driver genes
are involved in the early phase of the development in the endometrial cancer. Some of the driver-mutated clones expanded in macroscopic size. Our findings provide an interesting insight into the clonal structure and underlying genetic variation in the normal endometrium.

#1615 Balanced molecular feature selection unveils universally tumor-lineage informative methylation sites in colorectal cancer.

X. C. Li[1], Y. Liu[1], A. A. Schaffer[1], S. M. Mount[2], S. C. Sahinalp[1];
[1]National Cancer Institute, Bethesda, MD, [2]University of Maryland, College Park, MD

In the era of precision medicine, performing comparative analysis over diverse patient populations is a fundamental step toward tailoring healthcare interventions. However, the critical aspect of equitably selecting molecular features across multiple patients is often overlooked. To address this challenge, we introduce FALAFL (FAir muLti-sAmple Feature seLection), a novel algorithmic approach based on integer linear programming. FALAFL is designed to bridge the gap between molecular feature selection and algorithmic fairness, ensuring a balanced selection of molecular features across different patient samples.
We have applied FALAFL to the problem of selecting lineage-informative CpG sites within a cohort of 9 colorectal cancer patients subjected to low-coverage single-cell methylation sequencing. Our results demonstrate that FALAFL excels at rapidly determining the optimal set of CpG sites, which are well covered by cells across the vast majority of the patients, while ensuring that each patient contributes a similar number of sites to the final selection. An analysis of the FALAFL-selected CpG sites reveals that their lineage informativeness exhibits a strong association across diverse patient profiles, suggesting the non-stochasticity and universality of methylation changes in tumor evolution. Furthermore, these universally lineage-informative sites exhibit subclonal level alterations in the colorectal cancer primary tumors and are strongly associated with lineage-specific gene expression patterns.
By integrating equity considerations into the molecular feature selection process, FALAFL is poised to propel equitable healthcare data science practices and advance our understanding of cancer and other complex diseases.

#1617 Tumor evolution during therapy in ovarian cancer.

S. K. Hautaniemi[1], J. Oikkonen[1], A. Lahtinen[1], M. Nguyen[1], G. Marchi[1], K. Lavikka[1], A. Rajavuori[2], S. Hietanen[2], A. Virtanen[3], J. Hynninen[2];
[1]University of Helsinki, Helsinki, Finland, [2]University of Turku and Turku University Hospital, Turku, Finland, [3]University of Helsinki and HUS Diagnostic Center, Helsinki, Finland

The evolution of tumors from diagnosis to relapse in ovarian high-grade serous carcinoma (HGSC) patients is poorly understood. Consequently, it is unknown whether diagnostic samples are representative enough to guide treatment directions at relapse, or whether acquired changes during therapy provide targets in patients with relapses. To answer these questions and characterize tumor evolution during treatment, we used data from >700 tissue and plasma samples from 200 HGSC patients belonging to the observational, longitudinal DECIDER trial (NCT04846933).
Mutations from whole-genome sequencing data from tissue samples (2-12 per patient) were used to construct phylogenetic trees. The trees were corrected by the copy-number alterations and curated to integrate circulating tumor DNA (ctDNA) exome- and targeted-sequencing data from plasma samples. Evolutionary states presenting within and between sample heterogeneity were evaluated through clonal complexity and divergence. Additionally, genetic differences between persistent and non-persistent subclones were studied to identify features affecting treatment resistance.
Our results indicate that the majority of subclones survive chemotherapy treatment and major subclonal replacement takes place in only a few patients. Within-sample heterogeneity was higher in plasma samples than in ascites, highlighting the importance of ctDNA samples to estimate persistent subclones.
Additionally, our recently reported evolutionary states (Lahtinen et al. Cancer Cell 2023) were often altered by the treatment induced selection pressure. At late relapses, subclone compositions typical of maintaining evolutionary state tumors were less common, and a higher number of acquired subclones were detected, suggesting further evolution of the persisting clones.
In summary, chemotherapy does not suppress heterogeneity in HGSC tumors. Interestingly, patients with the worst prognosis have a stable composition of multiple clones in their tumors, and tumors with low heterogeneity responded better to primary treatment. Relapse samples show lower within-sample heterogeneity and further evolution. Furthermore, we detected several evolutionary trajectories from stable, persistent cancer subclone populations to highly dynamic subclone structures. This renders diagnostic samples suitable to guide relapse treatment decisions in a subset of patients with HGSC but not for all.
Our characterization of the dynamics of tumor clonal heterogeneity during treatment allows to define better therapeutic interventions for HGSC patients with relapsed disease.

#1618 Highly populated phylogenetic reconstruction in patients with hormone receptor positive - HER2 non-amplified metastatic breast cancer.

F. Richard[1], T. Geukens[1], M. De Schepper[1], A. Mahdami[1], K. Van Baelen[1], M. Maetens[1], G. Zels[1], H.-L. Nguyen[1], A. Pabba[1], S. Leduc[1], E. Isnaldi[1], J. Van Cauwenberge[1], K. Borremans[1], H. Izci[1], I. Bachir[2], S. Hatse[1], P. Vermeulen[3], E. Vanderheyden[1], B. Boeckx[1], D. Lambrechts[1], A. Smeets[4], I. Nevelsteen[4], K. Punie[3], P. Neven[4], H. Wildiers[4], W. Van Den Bogaert[4], J. Demeulemeester[1], E. Biganzoli[5], G. Floris[4], C. Desmedt[1];

[1]KU Leuven, Leuven, Belgium, [2]Bordet Institute, Brussels, Belgium, [3]GZA Hospitals, Antwerp, Belgium, [4]UZ Leuven, Leuven, Belgium, [5]University of Milan, Milan, Italy

Background: Tumor progression still needs to be further elucidated in hormone receptor positive (HR+) breast cancer, the most common subtype of breast cancer. Here, leveraging the extensive sampling approach of our postmortem rapid tissue donation program UPTIDER (NCT04531696), we used phylogenic reconstruction to analyze disease progression.

Patients and Methods: Thirteen patients with HR+/HER2 non-amplified primary breast cancer, recruited in UPTIDER between 12/2020 and 05/2022, were considered. Shallow whole-genome sequencing was performed on 495 solid samples including a matched germline DNA and archived primary tumor sample for each patient. Log2 coverage ratios were computed with CNVkit and profiles with median absolute pairwise deviation < 0.35 were co-segmented per patient using the copynumber R package. Purity and ploidy were assessed by ABSOLUTE and manually reviewed. Samples with purity > 30% were kept for downstream analysis. Phylogenetic reconstruction was performed using MEDICC2 for each patient. Metrics derived from the trees were: (i) tree length, (ii) trunk length, (iii) trunk ratio as trunk length/tree length*100. Overall survival (OS) was defined as time between primary diagnosis and death. Comparison was done using Wilcoxon test, time to event analysis using cox regression. Endocrine resistance was defined as per the ESMO guidelines (PMID:34678411).

Results: 81% (399/495) of the samples passed QC. Phylogenies included a median of 28 samples per patient (range: 9-59) and 10/13 phylogenies included primary samples at diagnosis. Multi-seeding from the primary tumor was observed in 7 patients, suspected in 1, and a single seeding was observed in 2 patients. Median OS was 8.0 years. Higher trunk ratios tended to associate with poorer OS (Hazard ratio: 1.08 per 1% increase, 95% confidence interval: 0.99-1.16, p=0.06). In organs where multiple metastatic lesions were sampled (n= 73 organs, median of 3 samples/organ, range: 2-18 and median of 5 organs per patient, range: 1-10) seeding from at least 2 organs was detected in 48% (35/73) of the organs. Phylogenies from patients with secondary endocrine resistance (7 patients) tended to have a shorter trunk compared to patients with primary endocrine resistance (5 patients, median of 18 and 48 alterations respectively, p=0.15).

Conclusion: Branching evolution from the primary tumor was more frequently observed than linear evolution. Phylogenies revealed extensive tumor heterogeneity, questioning treatment decisions based on a single biopsy. Additionally, evaluation of multiple metastatic samples per organ showed seeding from multiple organs in 48% of organs evaluated, indicating greater disease heterogeneity than previously thought. Phylogenetic differences were also noted according to the type of endocrine resistance (primary versus secondary).

#1620 Multiregion spatial sequencing of early-stage head and neck squamous cell carcinoma revealed theranostic intratumor heterogeneity.

G. Marret[1], S. Vacher[1], **C. Lamy**[1], L. Ahmanache[1], L. Courtois[1], C. Kamoun[2], M. Halladjian[1], Z. El Beaino[1], J. Klijanienko[1], C. Martinat[1], E. Jeannot[1], J. Martin[1], G. Rougier[1], N. Badois[1], M. Lesnik[1], A. Dubray-Vautrin[1], O. Choussy[1], W. Ghanem[3], R. Taouachi[3], J. Masliah Planchon[1], N. Servant[2], M. Kamal[1], I. Bieche[1], C. Le Tourneau[1];

[1]Institut Curie, Paris, France, [2]INSERM U900, Paris, France, [3]Institut Curie, Saint-Cloud, France

Introduction: Head and neck squamous cell carcinoma (HNSCC) is characterized by substantial intratumor heterogeneity (ITH) at the molecular level that may foster tumor evolution, adaptation, and therapeutic failure. Personalized-medicine strategies mostly rely on single tumor-biopsy samples which might not capture the mutational burden of heterogeneous tumors. We investigated genetic ITH portrayed from multiregion spatial sequencing in early-stage HNSCC patients.
Patients and Method: Seventy-eight early-stage HNSCC patients treated with upfront curative-intent surgery in the prospective biobanking SCANDARE study (NCT03017573) were included. We developed a pathological measure of ITH, based on the relative contribution of multiple poorly and well-differentiated intratumor regions (n = 199) in resected tumor samples. To characterize genetic ITH, we performed targeted next-generation sequencing on multiple spatially separated intratumor regions by using a custom panel of 571 genes (named DRAGON), in combination with 3'-Tag RNA sequencing and pathway enrichment analysis.
Results: Fifty-nine patients displaying a minimum of two sequenced intratumor regions (total, n = 180) were analyzed. We observed genetic ITH in 22/59 patients (37%), of whom 6/22 (27%) based on theranostic molecular alterations. Three of the six patients exhibited molecular alterations in *PIK3CA* (n = 2) and *TSC2* (n = 1) that have supporting clinical evidence of actionability in some cancer types (OncoKB level 1) and three patients exhibited actionable molecular alterations in *PTEN* (n = 2) and *CDKN2A/B* (n = 1) supported by substantial research evidence (OncoKB level 4). Two patients exhibited molecular alterations in *SMARCA4* that is likely oncogenic, albeit not yet annotated by OncoKB. The pathological measure of ITH accounted for a significant source of variation in gene expression. Notably, we identified 346 differentially expressed genes imposing p-values ≤ 0.05 and |log fold-change| ≥ 1 involved in several Reactome's signaling pathways, including the cell junction organization (R-HSA-446728) and the tight junction interaction (R-HSA-420029) pathways.
Conclusions: We reported clinically relevant genetic ITH in early-stage HNSCC, which can lead to underestimation of the mutational landscape portrayed from single tumor biopsy and may present major challenges to precision medicine. Our findings uncovered the biology behind ITH and may have translational implications for biomarkers discovery in HNSCC.

#1621 Integrated analysis of genetic, transcriptional and TME evolution of ccRCC: TRACERx Renal.

A. Fernandez Sanroman[1], L. Au[1], B. Jek Yang Tan[1], **C. Spencer**[1], A.-L. Catin[1], I. Lobon[1], H. Pallikonda[1], K. Litchfield[2], F. Byrne[1], J. Larkin[3], A. Fendler[1], S. Turajlic[1];

[1]The Francis Crick Institute, London, United Kingdom, [2]UCL Cancer Institute, London, United Kingdom, [3]The Royal Marsden Institute, London, United Kingdom

Background: Genetic evolution of clear cell renal cell carcinoma (ccRCC) follows distinct trajectories, with varying levels of intratumor heterogeneity (ITH) and chromosomal complexity (WGII). While these patterns associate with clinical outcomes, it remains unknown whether they fully reconcile tumor behavior and how genetic and transcriptional features co-evolve in relation to the tumor microenvironment (TME).

Methods: To analyze the patterns of transcriptional and TME heterogeneity, we performed bulk whole-transcriptome sequencing on 244 samples, including 22 metastatic and 12 tumor-adjacent normal samples, from 79 ccRCC patients recruited to the TRACERx Renal study. We integrated transcriptional data with previously published genetic, phylogenetic, spatial and clinical information.

Results: Transcriptional distances between paired samples from the same primary tumor mirrored but were not fully determined by genetic distance (p-value < 0.001); and increased from primary-primary to primary-metastasis and primary-normal pairs. Within primary-metastasis pairs, metastasis-seeding primary tumor regions were transcriptionally closest to their matched metastasis (p-value < 0.001), suggesting that an important fraction of metastatic transcriptional traits were acquired in the primary tumor. Regarding the tumor clonal structure, transcriptional evolution followed a conserved path through increasing cell proliferation and oxidative phosphorylation and downregulating DNA repair from earlier to later clones. Further, within tumors with increasing WGII we observed upregulation and downregulation of repressors and downstream effectors, respectively, of the canonical cGAS-STING pathway. Combining the presence of this transcriptional pattern with WGII predicted shorter PFS in TRACERx Renal (p-value < 0.001) and in TCGA-KIRC (p-value < 0.001).

Clonal evolution was also linked to changes in TME, with each of the previously defined genetic evolutionary trajectories associated to a specific TME (p-value < 0.001). For example, ccRCCs on a PBRM1-SETD2 trajectory demonstrated increased infiltration of cytotoxic immune cells. TME ITH was pervasive and associated with shorter PFS (p-value = 0.03). A recurrent trend from earlier to later clones was progressive T cell depletion (p-value < 0.001). The evolution of the TCR repertoire mirrored the tumor clonal structure (p-value = 0.002), suggesting the thus far elusive antigenic source in ccRCC is heritable. Accordingly, the TCR repertoire in metastasis-seeding primary tumor regions resembled the closest the TCR repertoire of matched metastasis (p-value = 0.06).

Conclusion: Integrated analysis of genetic and transcriptional data in TRACERx Renal showed i) transcriptional and TME ITH not fully recapitulated by genetic ITH, ii) conserved paths of transcriptional and TME evolution and iii) a heritable nature of part of the ccRCC antigen source.

#1622 Characterization of the phylogenetic relationships in bilateral breast angiosarcoma.

M. Kim[1], J. Youk[2], S. Kim[1], M. Kim[2], B. Keam[2], T. Kim[2], D.-W. Kim[2], M. Song[3], J. Koh[4], J. Bae[4], H.-G. Moon[2], S.-A. Im[2];

[1]Cancer Research Institute, Integrated Major in Innovative Medical Science, Seoul National University College of Medicine, Seoul, Korea, Republic of, [2]Cancer Research Institute, Seoul National University Hospital, Seoul National University College of Medicine, Seoul, Korea, Republic of, [3]Biomedical Research Institute, Seoul National University Hospital, Seoul, Korea, Republic of, [4]Department of Pathology, Seoul National University Hospital, Seoul, Korea, Republic of

Background: Breast angiosarcoma represents around 20% of all angiosarcomas, and often spread to lung, liver, and bones. Driver mutations of angiosarcoma, specifically *PTPRB*, and *PLCG1*, are well-known as reported previously. Notably, contralateral breast is another metastatic site of the breast angiosarcoma, where an unusual location for other soft tissue sarcomas. However, it remains uncertain whether the contralateral disease originates from the primary tumor or emerges independently. Here, we present a 75-year-old woman with bilateral breast angiosarcomas to investigate the genetic relationship between the tumors.
Methods: Irregular and heterogeneous masses were synchronously detected through breast sonography. Whole genome sequencing (WGS) was conducted at 60X coverage using bilateral total mastectomies, along with a matched normal blood sample (n=1). Single nucleotide variants (SNVs) and small indels were identified using Strelka2 and Varscan2. Subsequent filtering was performed using custom Python scripts to establish high-confidence variants. A phylogenetic tree was then reconstructed based on SNVs to trace clonal evolution and distinguish between de novo primary and metastasis. Following this, COSMIC mutational signatures were analyzed to characterize the genomic profile.
Results: For the left breast angiosarcoma, we found 1,086 SNVs and 101 indels, while the right breast angiosarcoma had 921 SNVs and 92 indels. Despite their small size (<1.0 cm) and low FNCLCC grade (G1), these two cancers shared 600 SNVs and 135 indels as “truncal events”, indicating that one side metastasized from the other. According to the phylogenetic tree and the molecular clock of the two angiosarcomas, we estimated that the metastasis occurred during the middle stages of cancer evolution. Additionally, we identified 7 nonsynonymous SNVs (*ADAMTS7, RPS15, CYP2A6, OR1S2, ARHGAP23, GNAQ, UGT2B7*), five of which were shared. Remarkably, the GNAQ driver mutation exhibited a mutation at codon 209, a hotspot mutation not previously reported in breast angiosarcoma. The dominant Cosmic mutational signatures were SBS1/5 and ID1/2, all of which were associated with aging.
Conclusion: Our findings demonstrate that bilateral breast angiosarcomas metastasized from one side to the other, as evidenced by the WGS data. This study underscores that the capability of WGS to distinguish between oligometastatic disease and multiple primary cancers, which has implications for predicting patients’ prognosis.

#1626 Clonal expansion in bile duct associated with chronic inflammation.

H. Maeda[1], N. Kakiuchi[1], T. Ito[1], E. Ogawa[1], M. Shiokawa[1], N. Uza[1], H. Tanaka[2], Y. Nannya[3], H. Makishima[1], Y. Kodama[4], E. Hatano[1], S. Miyano[2], S. Ogawa[1];

[1]Kyoto University, Kyoto, Japan, [2]Tokyo Medical and Dental University, Tokyo, Japan, [3]The University of Tokyo, Tokyo, Japan, [4]Kobe University, Kobe, Japan

Introduction: Chronic inflammation has been implicated in cancer development in many tissues and has recently been associated with promoted clonal expansion in non-cancer tissues. Primary sclerosing cholangitis (PSC) is a chronic progressive disease of unknown etiology affecting the bile ducts and has been associated with a substantially increased risk of cholangiocarcinoma. Clonal dynamics in the normal bile duct and PSC epithelium remains poorly understood because of the limited accessibility to normal/inflamed bile ducts. In this study, we established a method to detect somatic mutations accumulated in the bile duct epithelium and investigated a mutation rate in normal bile duct cells and clonal expansion in PSC epithelium.

Methods: We established single cell-derived organoids from bile, which were subjected to whole genome sequencing to measure the age-related mutation rate in normal epithelial cell in the bile ducts. We next established organoids from multiple sites in perihilar bile ducts and collected epithelial samples from intrahepatic bile ducts obtained by laser-capture microdissection (LCM) from patients with PSC who underwent total hepatectomy for liver transplantation, for which we performed whole exome sequencing to investigate clonal expansion in PSC-involved bile ducts.

Results: In total, 14 single cell-derived organoid lines were established from 2 patients with PSC and 3 control individuals. Based on the whole genome sequencing of those organoids, the number of mutations found in non-PSC bile duct epithelium increases with age at an annual mutation rate of 34.3 mutations per genome per year, which did not substantially differ from the rate in the PSC epithelium, suggesting that the inflammatory process in PSC hardly affected the mutations in PSC epithelium. To further investigate clonal expansion in the PSC epithelium, a total of 120 bulk organoid samples from perihilar bile ducts in 3 PSC patients and 111 LCM samples from intrahepatic bile ducts in 4 PSC patients were analyzed. In perihilar bile duct-derived organoids, we detected a median of 13 [1-30] somatic mutations per exome in samples derived from perihilar bile ducts and 20 [5-41] mutations per exome in those from intrahepatic LCM samples. Most mutations were detected in a single sample but some mutation clusters were shared by adjacent samples, which expanded in an area as large as 13 mm in length. Expanded clones harbored mutations in known cancer-driver genes, such as *ARID1A* and *KRAS*, which were enriched in segmental bile ducts, suggesting their role in the clonal expansion.

Conclusions: Here, we established the method to detect somatic mutations accumulated in the normal/inflamed bile duct epithelium using an organoid-based analysis of clonal somatic mutations. Our results revealed clonal expansion existing in PSC epithelium and open up a way to the better understanding of carcinogenesis in the bile duct.

#1627 Persistence and dynamics of mutation, selection, and epistasis during the somatic evolution of low-risk, high-risk, and metastatic prostate cancer.

M. Rajaei[1], A. Yang[1], C. N. Cross[1], J. N. Fisk[2], E. B. Perry[1], J. D. Mandell[1], S. G. Gaffney[1], T. N. Yamaguchi[3], J. Livingstone[3], V. L. Cannataro[4], P. Humphrey[1], J. Costa[1], P. C. Boutros[3], J. P. Townsend[1],

[1]Yale University, New Haven, CT, [2]University of Rhode Island, Kingston, RI, [3]University of California Los Angeles, Los Angeles, CA, [4]Emmanuel College, Boston, MA

Driver genes and mutations responsible for prostate cancer tumorigenesis have been identified, but research has not previously quantified the effects of prostate cancer driver mutations, or how the magnitude of those effects vary with cancer stage and epistatic interactions among genes. Using 2699 prostate cancer tumor exomes, genomes, and panel sequences (1648 primary tumors and 1051 metastatic samples), we calculated the cancer effect size (CES)—the each mutation confers to lower-risk (Grade Group 1/2) and higher-risk (Grade Group 3/4/5) tumorigenesis and metastasis. The lower-risk, higher-risk, and metastatic tumors exhibited similar neutral rates at which mutations were introduced into DNA, with these underlying gene mutation rates generally increasing from lower-risk to higher risk to metastatic tumors. However, lower risk, higher risk, and metastatic tumors noticeably differed in the genes and specific somatic variants that were most highly selected for within each group. Therefore, to assess whether differences in natural selection that we observed among low-risk, high-risk, and metastatic tumor types were at least partly due to epistatic interactions, we applied a model of pairwise epistasis that quantified the effect of the presence or absence of a mutation in one gene on the selection for mutations in another gene. We found significant evidence of epistatic effects among driver genes. Our results indicate a very early role for SPOP in the development of prostate cancer: strength of selection for SPOP mutations is tightly associated with the degree to which the mutation ablates contact with the BRD3, and these disruptive mutations in turn increase the selection for mutations in several other tumor suppressors and oncogenes such as RHOA. Previously identified gene-gene interactions such as that between SPOP and PIK3CA were supported by this analysis, and we also identified novel gene-gene interactions such as those between AR and MUC16 occurring during metastasis. In conclusion, we have demonstrated that rates of mutation and strengths of selection on these driver mutations vary dynamically along the trajectories to lower-risk, higher-risk, and metastatic prostate cancer, and that powerful selective epistasis among driver genes provides an explanation for these differences. Because precision therapeutic targeting of somatic variant genes is fundamentally targeting the selective benefit obtained from that variant at the time of treatment, understanding these changes in stage-specific and somatic genotype-specific selective strengths will enable better therapeutic targeting in translational and clinical science.

MOLECULAR/CELLULAR BIOLOGY AND GENETICS: Cell Cycle, DNA Repair, and Telomere Biology
Poster Session

#1631 A homogeneous assay system for discernment of proliferative, antiproliferative, and cytotoxic effects in culture.
D. F. Lazar, K. R. Kupcho, A. L. Niles, J. J. Cali;
Promega, Madison, WI

We describe a novel homogeneous cell-based assay developed for the quantitative detection of Ki-67 protein, a recognized marker of cell proliferation, utilizing Lumit™ immunoassay technology. This luminescent assay has been effectively multiplexed with a fluorescent measure of cell death, employing a cell-impermeant fluorogenic DNA dye. This multiplex allows for the clear distinction between antiproliferative activity and overt cytotoxicity in cell culture models. Through varying lytic conditions, we demonstrated effective cell lysis and detection of nuclear Ki-67 protein. Specifically, Lumit™ Lysis Buffer II provided efficient recovery of Ki-67 protein without compromising assay performance, including the requisite binding of labeled antibodies to the target protein. This assay exhibited excellent signal-to-background (up to 40-fold) and signal linearity ($R^2 = 0.99$) in wildtype HeLa cells (~1000 to 80,000/well), while the signal in Ki-67 knockout HeLa cells was comparable to the no-cell background, indicating excellent specificity for Ki-67 protein. Due to the unavailability of recombinant full-length Ki-67 protein, two different recombinant Ki-67 protein fragments were used to corroborate assay sensitivity of <1 pM Ki-67 protein. The assay's suitability for human Ki-67 protein detection, not mouse, was observed through further cell-based testing. The proliferation/cytotoxicity assay multiplex was validated in both suspension and adherent cell lines, as well as primary cell culture, detecting antiproliferative and proliferative responses. CDK4/6 inhibitors are a class of antiproliferative agents of significant interest for their potential in treating cancer. In Jurkat cells, treatment with the CDK4/6 inhibitor palbociclib led to a dose-dependent reduction in Ki-67 protein expression with an EC_{50} of 88 nM, and total Ki-67 elimination at 2 µM compound concentration. Notably, there was no cytotoxicity detected at the tested doses and treatment duration (up to 48 h), but a significant reduction in viable cell number at maximal palbociclib concentrations, aligning with an antiproliferative mechanism. This work establishes a rapid, simple, luminescent assay for determining Ki-67 levels that can be paired with a fluorogenic readout of cell death, facilitating efficient and quantitative discernment of altered proliferation in mammalian cell culture using standard microplate readers.

#1632 Dissecting AMBRA1-cyclin D axis deregulation in embryonal tumors of the central nervous system.

G. Milletti[1], G. Cadeddu[2], A. Adelantado Rubio[1], C. Ferraina[3], A. Maya-Mendoza[1], F. Cecconi[1];

[1]Danish Cancer Society Research Center, Copenhagen, Denmark, [2]Universita degli studi di Tor Vergata, Roma, Denmark, [3]Ospedale Pediatrico Bambino Gesu, Roma, Italy

Dissecting AMBRA1-cyclin D axis deregulation in embryonal tumors of the centralnervous systemEmbryonal tumors of the central nervous system (CNS) are malignant growths originating from embryonic neural stem cells, primarily affecting pediatric patients. These tumors pose a significant threat to children's health, leading to high morbidity and mortality rates. To improve survival rates and reduce morbidity, there is a critical need for advanced molecular diagnostics and innovative therapies. Among these tumors are medulloblastomas (MB) and other embryonal tumors, previously classified as primitive neuroectodermal tumors (CNS-PNET). These malignancies are characterized by uncontrolled cell proliferation, primarily driven by abnormalities in cell cycle proteins. Consequently, targeting cell cycle regulators has emerged as a promising approach for their treatment. Two key signaling pathways, namely the MYC and the cyclin D-CDK-RB pathway, govern the decision-making process related to genome replication. Mutations in both MYC and the CDK4/6/cyclin D pathway, leading to the functional inactivation of RB, have been identified as relevant factors in the development of CNS-PNET and medulloblastomas. Our seminal research has highlighted the crucial role of AMBRA1, an upstream master regulator orchestrating the transition from G1 to S phase (Maiani & Milletti et al., 2021). Specifically, AMBRA1 modulates the abundance of D-type cyclins and MYC by facilitating their proteasomal degradation, thereby ensuring genomic stability during DNA replication.Based on these discoveries, we propose that AMBRA1 functions as a multifaceted tumor suppressor across various cancer types. An unbiased Sleeping Beauty analysis identified AMBRA1 as a genetic driver of CNS-PNET, providing a strong foundation for investigating its role further (Beckmann et al., 2019). We hypothesize that the simultaneous deletion of AMBRA1 and p53 in an inducible knockout mouse model can lead to the spontaneous development of CNS-PNET or medulloblastoma, contingent on the specific targeted cell lineage. Additionally, our research demonstrates that AMBRA1 deficiency confers resistance to CDK4/6 inhibitors while creating a synthetic lethality with CHK1 inhibitors. Consequently, we propose that a comparative analysis of AMBRA1, D-type cyclins, and Myc family expression levels could serve as a diagnostic marker. This marker could facilitate patient-based stratification for CHK1 inhibitor treatment efficacy, enabling the differentiation of non- responsive cases to CDK4/6 chemotherapy.

#1633 A phenotype risk score to define patients with a 'long-telomeropathy' and at risk for a novel cancer-like syndrome.

s. hebbring, P. Alaire;
Marshfield Clinic, Marshfield, WI

Introduction: In human populations, telomere length (TL) displays a large inter-individual variability. At the population level, the most predictive variable for TL is age. Rare loss-of-function mutations in telomere maintenance genes are known to cause telomeropathies, a group of deadly diseases triggered by critically short telomeres. Over the last few decades, GWASs have uncovered many common variants associated with TL. More recently, a small number of PheWASs have suggested short-TL is associated with risk for a wide spectrum of phenotypes whereas long-TL is primarily associated with increased risk for several different neoplasms. We hypothesized that genetic variation contributing to long-TL may cause a unique and heritable telomeropathy, distinguishable from classical telomeropathies, that we refer to as a long-telomeropathy resulting in a cancer-like syndrome. To test this hypothesis, we studied telomere genetics in two large independent cohorts linking genomics with electronic health records data.
Methods: Discovery cohort consisted of approximately 70,398 individuals from the All of Us (AoU) Research Program. Marshfield Clinic's PMRP Biobank of 19,443 individuals served as a replication set. Previously published GWAS results (161 common variant) were utilized to produce a weighted polygenic risk score for TL (TL-PRS). A PheWAS of TL-PRS in AoU identified 19 significant phenotypes that passed a Bonferroni-adjusted p-value threshold (P<2.71E-5). Notably, risk for all 19 phenotypes were associated with long-TL and were categorized as neoplasm or neoplasm-like phenotypes. PheWAS results were used to generate a phenotype risk score for long-telomeropathy (longTL-PheRS), and this model was replicated in PMRP.
Results: The validated longTL-PheRS was used to screen rare variants that may contribute to increased risk for a telomere dependent cancer-like syndrome. When focusing on 293 telomere related genes in AoU, SKAT identified *ATM* (P=8.8E-7) and *DCLRE1B* (P<1E-10) as statistically significant risk genes. Whereas *ATM* has been previously implicated in multiple cancer types, *DCLRE1B* has not. SKAT results were influenced largely by a single missense variant in each gene [P=2.43E-15 (*ATM,* p.Leu2307Phe) and =1.78E-12 (*DCLRE1B,* p.Asn510Tyr)]. Neither variant was previously reported as pathogenic.
Conclusion: Many decades of research in telomere biology has demonstrated the health consequences associated with telomere shortening. This study builds on a growing body of evidence that long telomeres also have significant negative health implications. Individuals who have a genetic predisposition to long telomeres influenced by both common and rare variants may be at risk for a spectrum of tumors. These findings may lead to new diagnostic or preventative measures for individuals at risk for a long-telomeropathy and a cancer-like syndrome.

#1634 Cyclin D1 induces Akt1 activity in RB deficient prostate cancer.

X. Jiao[1], A. W. Ashton[2], Z. Li[1], R. Harish[1], D. Li[1], G. Robertson[3], D. Shen[4], X. Ju[5], K. Chen[5], W. Zhang[6], S. Archilefu[7], K. A. Iczkowski[8], H. Rui[5], B. Knudsen[6], P. Timpson[9], M. Nobis[9], **R. G. Pestell**[1];

[1]Baruch S. Blumberg Institute, Wynnewood, PA, [2]Lankenau Institute for Medical Research, Wynnewood, PA, [3]BC Cancer Agency, Vancouver, BC, Canada, [4]Washington University, St. Louis, MO, [5]Thomas Jefferson University, Philadelphia, PA, [6]University of Utah, Salt Lake City, UT, [7]University of Texas Southwestern Medical Center, Dallas, TX, [8]UC Davis Health, Sacramento, CA, [9]Garvan Institute of Medical Research & The Kinghorn Cancer Centre, Sidney, Australia

Background: Prostate cancer (PCa), the second leading cause of death in American men, is a genetically heterogeneous disease. The aberrant activation of AKT is one of the most frequent alterations in human cancers, and an elevated level of phosphorylated AKT at Ser473 site (pSer473) is associated with metastatic cancers (1). In prostate cancer (PCa), PI3K/AKT activation induces tumorigenesis (2), androgen receptor (AR)-mediated signaling, enzalutamide resistance and stemness, synergizing with other pathways including the notch intracellular domain (NICD). The *cyclin D1* gene (*CCND1*), which is overexpressed in PCa, conveys canonical function by encoding the regulatory subunit of a holoenzyme that phosphorylates the retinoblastoma gene (RB) product, and non-canonical functions through phosphorylating other substrates and transcriptional activities. Cyclin D1 expression augments growth of some castrate-resistant PCa (CRPC) and clinical trials are targeting the cyclin D1 related CDK kinase activity in pRB^{+} PCa. Several Rb-independent mechanisms of action have been described (3). In recent studies the effect of CDK inhibitors was similar in patients with Rb^{+} vs. Rb^{-} PCa (4). Whether Rb expression is required for the antiproliferative effects of CKD4/6 inhibition in PCa remains to be established.

Methods: The kinetics of Akt1 induction by mitogens was assessed using the phosphorylation of the dichromic fluorescent (DCF) dye substrate LS456. We used cyclin D1 shRNA to show endogenous cyclin D1 augmented AKT1 signaling in response to mitogens.

Results: Cyclin D1 reintroduction into cyclin $D1^{-/-}$ cells augmented Akt1 phosphorylation, requiring the cyclin D1 K112 residue. CDK inhibitors reduced Akt activity in RB^{+} and RB^{-} human prostate cancer cell lines. Prostate-specific epithelial cell deletion of cyclin D1 (probasin-CRE-cyclin-$D1^{fl/fl}$) reduced prostate epithelial cell Akt1 activity assessed by immunohistochemical (IHC) staining. $pAkt^{Ser473}$ was reduced in cell nuclei and the cytoplasm of both epithelial cells and stromal fibroblasts without a significant change in the abundance of Akt1. The downstream targets of Akt signaling ($pTSC2^{Ser939}$, and $pFKHR^{Ser319}$) and $AR^{Ser213P}$ were reduced in both epithelial cells and stromal fibroblasts. Genetic deletion of both epithelial cell and stromal cyclin D1 further reduced Akt1 activity, prostate epithelial cell proliferation, and markers of cancer stem cells. Proteomic analysis of cyclin D1-expressing stroma identified heterotypic chemokine signals that augment PCa AKT activity.

Conclusions: Cyclin D1 induces Akt1 activity in both RB^{+} and RB^{-} PCa cells which may contribute to tumor progression and therapy resistance.

Reference: (1) Chen YL, Law PY, Loh HH. Curr Med Chem Anticancer Agents 2005;5:575-892. (2) Stoyanova T, *et al.* Proc Natl Acad Sci U S A 2013;110:20111-63. (3) Chen K, *et al.* Cell Rep 2020;32:1081514. (4) de Kouchkovsky I, *et al.* Clin Cancer Res 2022;28:1531-9

#1635 Inhibition of FANCA Suppresses Breast Cancer Development by Regulating Cell Cycle Progression.

L. Luo, W. Liu, F. Yuan, F. Li, A. Palovcak, D. Calkins, K. Briegel, Y. Li, C. Mason, Z.-J. Liu, S. Daunert, Y. Zhang;
University of Miami Miller School of Medicine, Miami, FL

FANCA is one of the 22 known Fanconi anemia (FA) pathway genes that are involved in interstrand crosslink (ICL) repair. We have also shown that and FANCA plays a role in double strand break repair by promoting strand annealing and exchange. In this report, we describe that FANCA expression in breast cancer is significantly elevated within TCGA databases and in patient tumors-derived sections on both transcription and translation levels and this elevation is associated with poor outcomes of the breast cancer patients. Importantly, we have found that overexpressing FANCA in breast cancer cell line MDA-MB-231 promotes tumor growth both *in vitro* and *in vivo*. We have also demonstrated that FANCA inactivation by knocking out or knocking down inhibits growth of MDA-MB-231 *in vitro* and *in vivo* by causing cell cycle arrest at G1 phase resulting from hypophosphorylation of Rb protein. Our RNA-seq data has indicated that E2F targets are also downregulated in FANCA knockout (KO) cells compared to the wildtype (WT) MDA-MB-231 cells, which is consistent with the G1/S cell cycle arrest and Rb hypophosphorylation. Intriguingly, heterozygous FANCA KO in a breast cancer mouse model MMTV-PyMT model has shown reduction of breast tumor formation and volume. Our goal is to elucidate the role of FANCA in breast cancer development and to evaluate the potential of FANCA as a target for breast cancer treatment.

#1637 EPHB4 is a key regulator of G1/S transition in hepatocellular carcinoma.

A. Husain, E. Y. T. Chiu, H.-T. Ma, D. W. H. Ho, K. M. F. Sze, L.-K. Chan, I. O. L. Ng;
University of Hong Kong, The - Li Ka Shing Faculty of Medicine, Pok Fu Lam, Hong Kong

Effective therapeutic regimens against advanced hepatocellular carcinoma (HCCs) have recently improved but it remains very limited. Targeting receptor tyrosine kinases (RTKs) has proven to one of the main ways of achieving better survival outcome in HCC patients, yet the precise mechanism for this success remains to be elusive. We have systematically investigated the expression profiles of RTKs transcriptomic datasets i.e. The Cancer Genome Atlas - Liver hepatocellular carcinoma (TCGA-LIHC) (n=371) and our in-house cohort of paired i.e. HKU-QMH (n=41), and identified EPHB4 as one of the most abundantly expressed and frequently mutated RTKs in human HCCs. EPHB4 expression was found to be significantly correlated with Alpha Fetoprotein (AFP) expression, a factor commonly used in the diagnosis of HCCs. Furthermore, EphB4 has been demonstrated to play a regulatory role in VEGF/VEGFR-mediated angiogenesis, critical targets for current successful drugs. We confirmed abundant membrane EphB4 expression in HCC clinical specimens and human HCC cell line models using immunohistochemistry. Clinicopathological correlation analysis of EPHB4 mRNA expression revealed that its overexpression is associated with aggressive tumor features including presence of tumor microsatellite, liver invasion, venous invasion, and absence of tumor encapsulation. Functionally, stably knocking down EPHB4 (shEPHB4) resulted in a strong reduction of proliferation and self-renewal rates of multiple HCC cell lines *in vitro*. It significantly reduced tumor growth rates in subcutaneous and liver orthotopic models *in vivo*. Furthermore, limiting dilution assay showed EPHB4 plays a role in tumor initiation property of HCC cells. Mechanistically, we performed Gene Set Enrichment Analysis (GSEA) of transcriptome profiles for shEPHB4 with respective controls and found that knocking down EPHB4 causes HCC cells undergo drastic changes in several cell cycle checkpoints including G1/S transition. Using thymidine blockade, we further confirmed that knockdown of significantly hinders the transition of HCC cells from G1 to S phase of cell cycle. Our data suggests a strong link between EphB4 and cell cycle. Conclusion: We found EphB4 plays a functional role in regulating G1/S transition in human HCCs and understanding regulatory role of EphB4 on cell cycle progression may provide mechanistic insights into the how to effectively target HCC in the clinic.

#1638 Regulation of spindle pole integrity by the MASTL-ENSA-aurora a pathway during mitosis.

S. Kim, K. Jun, Y.-H. Kim, **J. Kim**;
Korea Institute of Radiological & Medical Sciences (KIRAMS), Seoul, Korea, Republic of

The preservation of spindle pole integrity is crucial for proper spindle assembly and chromosome segregation in mitosis, yet the precise mechanisms governing spindle pole integrity remain elusive. During mitosis, phosphorylated Ensa (p-ENSA) localizes to spindle poles, and the inhibition of ENSA leads to a range of mitotic defects, including misaligned chromosomes, multipolar spindles, asymmetric bipolar spindles, and centrosome aberrations, resulting in a delayed mitotic progression. Remarkably, the mitotic delay induced by ENSA inhibition is alleviated upon depletion of PP2A-B55α, but spindle pole defects persist. Significantly, we have observed an interaction between ENSA and Aurora A during mitosis, and the inhibition of ENSA diminishes Aurora A expression at the mitotic spindle poles. Intriguingly, the injection of MKI-2-sensitized tumors is associated with heightened chromosomal instability and downregulation of the MASTL-ENSA-Aurora A pathway in an orthotopic breast cancer mouse model. These findings offer new insights into the regulation of spindle pole integrity through the MASTL-ENSA-Aurora A pathway during mitosis, emphasizing the pivotal role of ENSA in recruiting Aurora A to the spindle pole, independently of PP2A-B55α.

#1639 Telomere dynamics in aging and cancer by nanopore long-read sequencing.

T. T. Schmidt[1], C. Tyer[2], P. Rughani[2], C. Haggblom[1], J. Jones[1], X. Dai[2], K. A. Frazer[3], F. H. Gage[1], S. Juul[2], S. Hickey[2], J. Karlseder[1];
[1]Salk Institute For Biological Studies, La Jolla, CA, [2]Oxford Nanopore Technologies, Inc., New York, NY, [3]University of California San Diego, La Jolla, CA

Telomeres are the protective, nucleoprotein structure at the ends of linear eukaryotic chromosomes. The accurate measurement of both telomeric length and composition of individual telomeres in mammalian cells has been challenged by the length and repetitive nature of telomeres. With the advent of third generation sequencing technologies, it is now technically possible to sequence entire telomeres and map them to individual chromosome arms. Here, we report a reliable method to enrich, sequence and analyze human telomeres using Oxford Nanopore Technologies long-read sequencing. To enrich for telomeric sequences we combine the ligation of adapters complementary to the telomeric G-overhang with restriction enzyme digest to sequence the telomeric C-strand and part of the adjacent subtelomere. The subtelomeric information is harvested to map individual telomeric reads to specific chromosome arms and even alleles. We have measured bulk, chromosome-arm-specific telomere length dynamics during cellular aging of cultured primary cells and in a patient-derived aging cohort. To address the impact of the telomere maintenance mechanism on telomere length and composition, we have sequenced matched pairs of fibroblasts and induced pluripotent stem cells, as well as five well-established telomerase- and ALT-positive cancer cell lines. Our results suggest that based on nanopore telomere long-read sequencing ALT-positive cells can be easily discriminated from normal and telomerase-positive cancer cells. Further, telomere sequencing allows to evaluate the methylation status of the subtelomeric CpG islands adjacent to telomeres.
In summary, nanopore telomere long-read sequencing allows to measure the length and composition of individual telomeres and their mapping to specific chromosome arms. Telomere long read sequencing methods will be valuable tools to study telomere biology during aging and cancer.

#1640 The role of CDC20 in the progression of colorectal cancer.

Nouran Abualsaud, Nada Gazzaz, Amal Alhamid, Deemah Alenizy, Bahauddeen M. Alrfaei, Mana Alshehri

Blood and Cancer Research, King Abdullah International Medical Research Center, Riyadh, Saudi Arabia

Colorectal cancer (CRC) is the one of most common cancers and a major leading cause of cancer-related death worldwide. CDC20 is a key cell cycle regulator required during mitosis. Pathologically, CDC20 has been found to be overexpressed in cancer cells of various malignancies including breast, lung, brain and hepatic cancers and high level of CDC20 expression is associated with poor prognosis and disease progression in these cancers. Although it has been reported that CDC20 is associated with CRC progression and metastasis, it is still largely unknown how CDC20 regulates CRC cancer progression. Thus, the goal of this study is to identify the role of CDC20 in the progression of colorectal cancer. Our gene expression analysis revealed that CDC20 is highly expressed in colon cancer tissues compared to their adjacent normal colon in a cohort of CRC patients, suggesting the involvement of CDC20 in the CRC progression. To further understand the role of CDC20 in CRC progression, we experimentally targeted CDC20 genetically and pharmacologically. To perform CDC20 Loss of function studies, we screened various CRC cell lines for CDC20 protein levels and CDC20 highly expressing cell lines were utilized to establish CDC20-knockdown cells using shRNA targeting CDC20 and scrambled shRNA as controls. CDC20 Down-regulation levels were confirmed using both western blot and RT-PCR analysis. The effect of CDC20 knockdown/CRC cells on CRC cell proliferation was investigated using xCELLigence real-time cell analysis instrument and colony formation assay. Our results revealed that CDC20 knockdown CRC cells have lower proliferation capacity compared to the control, suggesting involvement of CDC20 in regulating tumorigenic phenotypes of CRC cells. Pharmacologically, we targeted CDC20 using a specific molecular inhibitor, Apcin and we assessed the Apcin treatment effect on cell viability and migration of CRC cells. Our results showed that Apcin significantly reduced CRC cell viability and migration in a dose-dependent manner. Taken together, our results suggest that CDC20 is a key regulator in the tumorigenic behavior of CRC and is considered a potential therapeutic target for treating patients with CRC.

#1641 Clobetasol differentially effects the vulvar cancer cell line, UMSCV-4, causing both increases in apoptosis while maintaining a subpopulation in quiescence.

J. E. Lewis, M. Ogden, G. Minnuto, K. Haering, L. North;
SUNY Geneseo, Geneseo, NY

Vulvar cancer is a rare but aggressive form of cancer that remains understudied. Our results show that treatment of the vulvar cancer cell line, UMSCV-4, with the glucocorticoid, clobetasol, increases apoptosis. Clobetasol is often used to treat a common inflammatory disease of the vulva known as vulvar lichen sclerosus (VLS) and up to 65% of vulvar carcinomas arise in the background of VLS. This would indicate clobetasol may also decrease the progression of vulvar cancer, if our observations reflect what is happening in vivo. However, our studies also show that apoptosis is not universal for the clobetasol treated UMSCV-4 cells. A subpopulation appears to enter a state of quiescence as evidenced by the return of some of the cells to normal cell proliferation upon removal of clobetasol. We previously showed that $p27^{Kip1}$ is upregulated in the clobetasol treated cells. Cells that were incubated in clobetasol for three months and then removed from clobetasol (UMSCV-4 LT), allowing them to reenter the cell cycle, no longer expressed high levels of $p27^{Kip1}$ upon re-exposure to clobetasol. We are now examining the differential phosphorylation states of $p27^{Kip1}$ in the untreated and treated cells as well as identifying other genes important to clobetasol induced quiescence using RNAseq.

#1642 NuMA exclusive post-translational modification in epithelial cancer cells is a novel target for cell eradication.

M. Cohen-Armon;
Tel Aviv University, Tel Aviv, Israel

The post-translational modification of proteins implicated in mitosis in healthy and in cancer epithelial cells was measured by 2-D gels analysis. The post-translational modifications of NuMA in a variety of human epithelial cancer cells was prevented by treatment with a small phenanthridine, PJ34, while not impaired in similarly treated healthy epithelial cells. NuMA in the cancer cells was phosphorylated by pim1 kinase, and was polyADP-ribosylated by Tankyrase1. These post-translational modifications are inhibited by PJ34. Tankyrase1 is not expressed in healthy epithelial cells, and pim1 kinase was hardly expressed in these cells. Preventing the post-translational modification of NuMA in the epithelial cancer cells also suppressed the protein binding capacity of NuMA. NuMA clustering in the mitotic spindle poles, which stabilizes the mitotic spindle, and is required for the alignment of chromosomes in the spindle mid-zone was impaired. In epithelial cancer cells treated with PJ34, the mitotic spindle poles were distorted, extra-centrosomes were not clustered in multi-centrosomal cancer cells, and chromosomes were dispersed. Chromosomes dispersion violated mitosis termination. Mitosis arrested in the anaphase led to mitotic catastrophe cell death. PJ34 treated epithelial cancer cells were eradicated during 72-96 hours, regardless of their mutations, while treated healthy epithelial cells were not affected, and continued to proliferate.

#1643 Relative telomere length analysis in breast cancer patients with *TP53* p.R337H and *XAF1* p.E134* germline variants.

Larissa M. Okano[1], Stefanne M. J. Bortoletto[1], Mariana Paraizo[1], Aline S. Fonseca[1], Bonald C. Figueiredo[1], Enilze M F. S. Ribeiro[2], Ariana Centa[1], Luciane R. Cavalli[1]

[1]Faculdades Pequeno Principe, Research Institute Pele Pequeno Principe, Curitiba, Brazil,[2]Genetics Department, Universidade Federal do Parana, Curitiba, Brazil

Background: Telomere deregulation is one of the forms of genomic instability, an enabling characteristic of the cancer hallmarks. The *TP53* gene plays a fundamental role in genome integrity maintenance by controlling cell cycle, apoptosis, senescence, and DNA repair. The germline variant *TP53* p.R337H, a low penetrance variant, has been described in several types of cancer, including sporadic and familial breast cancer. The *XAF1* p.E134*, a germline variant of the tumor-suppressor gene X-linked inhibitor of apoptosis (XIAP)-associated factor 1 (*XAF1*), is a genetic modifier of p53 function and was found to co-segregate with *TP53* p.R337H variant on the 17p13 region. The main objective of this study was to determine the impact of the *TP53* p.R337H and *XAF1* p.E134* germline variants on the relative telomere length (RTL) in breast cancer patients.

Materials and methods: Peripheral blood samples from three distinct groups of patients were collected: patients with breast cancer (BC; n=56) (test group), patients with other types of cancer (non-BC; n=59), and individuals without cancer and cancer family history (non-CA; n=100) (control groups). The samples were genotyped for the *TP53* p.R337H and *XAF1* p.E134* variants. The RTL analysis was performed by RT-qPCR, using primers for the TEL gene (T) and *36B4* gene (S) (reference) and calculated based on the T/S ratio.

Results: BC cases with *TP53* p.R337H variant exhibited higher RTL compared to cases without the variant. No RTL differences were observed for the *XAF1*p.E134* variant or for the concomitant presence of these variants. However, in the non-BC cases higher RTL were observed in all the cases positive for the variants compared to the negative cases. The same was observed for the BC and non-BC cancer cases combined (CA cases). In the non-CA cases no difference in the RTL was observed in relation to the variants. The stratification of the cases by age (≤ or >45 years old), showed that the *TP53* p.R337H variant was significantly associated to longer telomeres in the BC and CA patients across all ages. *XAF1* p.E134* showed age-dependent effects, with longer telomeres in BC and CA patients ≤ 45 years. Non-BC cases had similar results.

Conclusion: This study indicates that *TP53* p.R337H significantly impacts telomere length in BC cases, while *XAF1* p.E134* shows age-dependent effects. Despite the observed variability, these findings highlight an association between these germline variants and telomere length regulation. Further research is needed to elucidate the functional impact and underlying mechanisms of these variants, particularly in the context of breast cancer.

#1644 Exploring the role of a *TERT* intronic tandem repeat in regulating cell proliferative responses to environmental factors and cancer risk.

M. Ho[1], O. Florez-Vargas[1], M. Hogshead[1], B. Papenberg[1], C. Lee[1], C. Zhang[1], K. Forsythe[1], W. Yan[1], R. Chari[2], L. Prokunina-Olsson[1];
[1]National Cancer Institute, Rockville, MD, [2]Frederick National Laboratory for Cancer Research, Frederick, MD

The chr 5p15.33 genomic locus encoding telomerase reverse transcriptase (*TERT*) is structurally complex, with several highly polymorphic intronic variable number tandem repeats (VNTRs). A germline VNTR located in *TERT* intron 6 (VNTR6-1, 38 bp repeat unit) has previously been associated with *TERT* alternative splicing but its potential role in regulating cellular functions and disease risk is unclear. To functionally characterize VNTR6-1, we deleted this region (1-2 kb) using CRISPR/Cas9 in UMUC3 (bladder cancer cell line). Cell count growth tracking of parental and VNTR6-1 knockout (VNTR6-1 KO) cells via automated live-cell monitoring revealed different relative growth rates under serum starvation vs. normal conditions, suggesting that VNTR6-1 might be sensitive to growth factors present in culture media. Evaluation of growth in media with full vs. charcoal-stripped (CS) serum, showed significant differences, with higher cell counts in parental vs. VNTR6-1 KO in CS-serum (P=4.1e-3), parental vs. parental in full (P=1.57e-4) or CS-serum (P=4.76e-2), but not in parental vs. VNTR6-1 KO in full serum (P=0.378). After 5-6 days of growth, cells in CS-serum also rapidly began outgrowing cells in full serum. We observed that VNTR6-1 KO dampened the outgrowth response in cells lacking growth factors in CS-serum. Proliferation-specific growth assays tracking the dilution of an incorporated dye in cells by flow cytometry further showed that VNTR6-1 KO leads to more pronounced proliferation differences due to the presence or absence of serum-supplied factors. Overall, cell growth patterns appear to be sensitive to serum in interaction with VNTR6-1, suggesting a potential VNTR6-1-dependent response to extracellular signaling. In human populations, we have identified two VNTR6-1 groups: Short (24-27 copies) and Long (40.5-66.5 copies). In the PLCO dataset (n=100,445 cancer cases and controls), logistic regression showed that VNTR6-1-Long group was associated with a decreased risk in male-prevalent cancers such as bladder and prostate, but an increased risk in female-prevalent cancers such as breast, endometrial and ovarian. These results support a link between the *TERT* region, and potentially VNTR6-1, with hormone signaling and cancer risk. Motif analysis within VNTR6-1 predicted binding sites for several transcription factors, including those associated with development and cell growth. Together, these results suggest that VNTR6-1 may be involved in regulating cell growth, potentially by facilitating responses to extracellular signaling pathways. Additionally, given the location of VNTR6-1 within a multi-cancer GWAS region, our findings provide functional context for the role of this polymorphic repeat in differential risk and outcomes in certain cancers.

#1645 Telomere-related genes associated with clinical-pathological in pancreatic ductal adenocarcinoma.

E. Curiel Gomez, Sr.[1], V. Maldonado Lagunas[2], J. Melendez Zajgla[2];

[1]Universidad Nacional Autonoma de Mexico (UNAM), Mexico City, Mexico, [2]Instituto Nacional de Medicina Genomica, Mexico City, Mexico

Pancreatic ductal adenocarcinoma (PDAC) stands as one of the leading causes of cancer deaths worldwide. Studies have suggested that telomeres shortening is linked to genetic instability, higher risk of developing pancreatic cancer and pancreatic tumorigenesis. However, previous research has predominantly focused on either telomere length or specific telomere-related genes in pancreatic cancer. Therefore, it is essential to elucidate the association between telomere-related genes and pancreatic cancer to identify novel therapeutic strategies and establish prognostic biomarkers. Telomere-relevant genes were downloaded from the TelNet database. Expression data from primary tumour of The Cancer Genome Atlas-PAAD (TCGA-PAAD) cohort, the Genome Sequence Archive CRA001160 dataset and the GTEx database were obtained for screen for differentially expressed genes (DEGs). Gene set enrichment analisis was performed using the Enrichr software. The gene essentiality queried from the gene dependency database of the Achilles-DepMap project was also assessed. Finally, data of The Cancer Genome Atlas-PanCancer CaPa cohort and healthy pancreas from the GTEx database, obtained from the UCSC Xena project, were used to correlate gene expression with stemness signatures and clinical-pathological variables. We identified 300 telomere-associated DEGs, Of these, 73 genes were common to studies and they were to be enriched in biological processes related to the cell cycle and telomere homeostasis. The differentially expresed of ASS1, S100P, IGF2BP2, MET, ABCC3 and RAC1 genes were significantly associated with overall survival and recurrence-free survival, conferring them prognostic value. Furthermore, the expression profiles of these genes are significantly associated with the histological grade of the disease, as well as with tumour T-N classification, the presence of residual tumour, the degree of response to treatment and stemness signatures. Among these, three genes of particular interest (KLF3, RAC1 and ABI1) were identified and shown to be highly essential in pancreatic cancer cell lines. In summary, we have identified a telomere gene-related signature for pancreatic cancer, highlighting the prognostic value of KLF3, RAC1, and ABI1 genes. This signature is significantly associated with clinical-pathological variables of the disease, potentially offering new insights for individualized therapy.

#1646 IL-23R is a regulator of the mitotic spindle and is critical for cell viability in AML.

N. Duong[1], D. H. Khan[1], G. E. Thomas[1], R. Hurren[1], J. Lee[2], J. St-Germain[1], L. Drimmer[1], Y. Yan[1], N. Maclean[1], M. Gronda[1], V. Rondeau[1], B. D. Brown[3], C. L. Jones[1], H. Chang[2], A. Arruda[1], M. D. Minden[1], L. Zhang[2], S. M. Kornblau[3], B. Raught[1], V. Spadavecchio[4], A. D. Schimmer[1];

[1]UHN Princess Margaret Cancer Centre, Toronto, ON, Canada, [2]UHN Toronto General Hospital, Toronto, ON, Canada, [3]MD Anderson Cancer Center, Houston, TX, [4]Interlinked Therapeutics LLC, Portland, OR

To identify novel biological vulnerabilities in AML, we searched for gene ontologies that were upregulated in AML compared to normal hematopoietic cells. Of the upregulated processes, the mitotic spindle ontology was a top hit. Unexpectedly, expression of the IL-23 receptor (IL-23R) showed a strong positive correlation with the mitotic spindle ontology. IL-23R is a cell surface cytokine receptor that is canonically expressed on T cells, but not known to have a role in AML. In 7 of 7 tested AML cell lines and 15 of 20 primary AML patient samples, IL-23R protein was expressed >2 fold higher compared to mean IL-23R in normal mononuclear hematopoietic cells (n=5) and CD34+ cells (n=3). IL-23R is classically a T cell surface receptor and we confirmed localization to the cell surface in T cells. However, only small amounts of IL-23R were present on the cell surface of AML cell lines and primary AML samples. Rather, in AML cells, primary AML samples, and AML stem cells, IL-23R was located intracellularly as determined by 4 different modalities and 4 different antibodies directed against 4 different epitopes of the receptor. Of note, only the full-length IL-23R protein was detected by immunoblotting. We also detected IL-23R's heterodimeric partner, IL12Rβ1, in AML cells. To understand the function of intracellular IL-23R, we used BioID mass spectrometry to identify proteins that interacted with IL-23R. Pathway analysis of interacting proteins identified mitotic spindle formation as the top pathway. Using Proximity Ligation Assays, we validated interactions with mitotic spindle proteins, and BioID hits, NUMA, TMEM201, TACC1, and BAG6 in AML cells. By confocal microscopy, we demonstrated that IL-23R colocalized with the mitotic spindle and centrosomes in AML cells and primary AML samples. IL-23R interacted with the mitotic spindle via its (S/T)x(I/L)P motif (amino acids 588-591). IL-12Rβ1 was also found in complex with IL-23R at the mitotic spindle in AML cells. Additionally, it was discovered that the cytokine, IL-23, promoted translocation of IL-23R to the mitotic spindle through clathrin-mediated endocytosis. Knockdown and knockout of IL-23R in AML cells led to dysregulation of the mitotic spindle with multipolarity, lagging chromosomes, and other spindle defects. Knockdown of IL-23R also reduced proliferation, clonogenic growth, and marrow engraftment of AML cells and primary AML samples. In contrast, knockdown of IL-23R in normal CD34+ cells did not impair engraftment. Likewise, constitutive homozygote IL-23R knockout mice had no difference in complete blood counts and stem cell number/function compared to wild type. In summary, IL-23R interacts with the mitotic spindle and centrosome where it regulates mitotic spindle formation and is critical for AML cell viability. Thus, we discover a novel function for IL-23R and a potential therapeutic target for this disease.

#1647 Plk4 phosphorylates the distal tip complex to promote centriole growth.

A. Amoiroglou, J. M. Ryniawec, D. W. Buster, G. C. Rogers;
University of Arizona, Tucson, AZ

The centrosome is the major microtubule-organizing center of the cell with a key role in forming the mitotic spindle. The centrosome consists of two core duplicating elements, the centrioles, surrounded by pericentriolar material, a cloud of proteins that nucleates microtubules. Centrioles are barrel-like structures composed of microtubule bundles and are essential to maintain centrosome number. Therefore, centriole duplication and growth are tightly regulated to ensure proper centrosome number throughout the cell cycle. Alterations in centrosome number lead to an abnormally shaped mitotic spindle that often mis-segregate chromosomes, thereby causing chromosomal instability, a hallmark of cancer. Defects in centriole growth, such as over-elongation, can increase centrosome numbers (known as 'centriole amplification', an overproduction of centrioles frequently observed in cancer cells). For example, over-elongation of the centriolar barrel can cause multiple ectopic daughter centrioles to assemble or simply fragment, producing multiple smaller (but functional) centrioles. Thus, understanding how centrioles grow and define length is a major question in the field. Centrioles elongate at their distal ends and, in *Drosophila*, elongation is regulated by a group of proteins, Cep97, CP110 and Klp10A. Elongation is negatively regulated by Cep97 and CP110 which cap centrioles at their distal end to maintain centriole length, by counteracting the microtubule depolymerizing kinesin, Klp10A. Recently, we identified a new centriole regulator, Cep104, that also localizes to the centriole distal tip. We discovered that Cep104 promotes centriole elongation through its microtubule-binding TOG domain. Additionally, Cep104 localization to the centriole distal ends is dependent on Cep97. Furthermore, Cep97, CP110, Cep104 and Klp10A form a complex and we have mapped their sites of interaction. Collectively, we refer to this as the Distal Tip Complex (DTC). Although the DTC is first recruited to new daughter centrioles during G1/S-phase, the majority of centriole elongation occurs during mitosis. Here, we explore the mechanisms that regulate the DTC to promote centriole growth during mitosis. We hypothesize that Polo-like kinase 4 (Plk4), the master regulator of centriole duplication, phosphorylates and inhibits the DTC to promote elongation of nascent centrioles. Notably, we found that centrioles are longer in cells overexpressing Plk4. Using tandem mass spectrometry, we identified multiple sites that Plk4 phosphorylates on each DTC protein. Analysis of DTC phosphomutants revealed that the phosphorylation state of Klp10A, Cep97 and CP110 affect centriole number. We are currently investigating how Plk4 phosphorylation regulates the activities of these conserved centriole length factors.

#1648 RB represses cohesin-dependent loop formation and activates E2F-independent transcription.

H. Lee[1], I.-M. Gkotinakou[1], B. Krishnan[2], N. J. Dyson[1], M. S. Lawrence[1], I. Sanidas[1];
[1]Massachusetts General Hospital, Charlestown, MA, [2]Whitehead Institute for Biomedical Research, Cambridge, MA

The retinoblastoma protein (RB) suppresses the activity of the E2F transcription factor family, controlling cellular proliferation. Recent studies, however, indicate that RB's role in chromatin organization, which is not yet fully understood, might be distinct from this E2F-dependent regulation. Employing chromosome conformation capture at a single nucleosome resolution, we identified RB as a cell cycle-regulated repressor of cohesin-dependent loop formation at topologically associating domain (TAD) boundaries. RB depletion increased the number and size of cohesin-dependent loops and strengthened topologically associating domains (TADs). This phenomenon was specific to the G1 phase and was not observed in the S phase, indicating that this novel RB function is regulated by the cell cycle. Mechanistically, RB showed extensive colocalization with cohesin in the human genome, and it impacted cohesin's distribution on the chromatin. Active RB reduced cohesin from RB-bound TAD boundaries and decreased cohesin activity therein, as assessed by the increased K105/106 acetylation of the cohesin subunit SMC3. This led to reduced insulation in chromosome conformation capture assays. Importantly, by weakening the insulation activity of the adjacent insulators, RB non-canonically enhanced the expression of non-E2F target genes salient for cell adhesion and extracellular matrix organization. When RB was lost, cells showed a more rapid cellular detachment rate and an elevated migration rate, indicating that this novel RB function controls specific transcriptional programs rather than arbitrary genes to regulate the process of cell adhesion and migration. Overall, we conclude that RB has a central role in the interplay between cell cycle and chromatin organization, by repressing the cohesin-dependent loop formation at TAD boundaries. This RB function safeguards E2F-independent transcriptional programs driven by active enhancers and helps maintain cellular adhesion to the extracellular matrix.

#1649 Large scale multi-omics concordance study of cyclin E1 identifies high expressing tumors lacking CCNE1 gene alterations across multiple tumor indications.

Sophie E. Willis[1], Gemma N. Jones[2], Shaan Gill[2], Emma V. Jones[2], Amelia Raymond[3], Barrett Nuttall[3], Sophie Kirschner[2], Sakshi Gulati[2], Paola Marco-Casanova[2], Benedetta Lombardi[2], David Jenkins[3], Felicia S. L. Ng[2], James Hadfield[2], Paul Waring[2], Helen K. Angell[2], Heike Laman[1]

[1]University of Cambridge, Cambridge, United Kingdom,[2]AstraZeneca, Cambridge, United Kingdom,[3]AstraZeneca, Waltham, MA

Cyclin E1 is a key regulator of the G1/S transition and is thought to cause excessive entry into the cell cycle. *CCNE1* is amplified in a range of tumor indications, and its amplification is associated with poorer prognosis and resistance to chemotherapy. Cyclin E1 is also being investigated as a potential biomarker for inhibitors targeting the replication stress response. Understanding the best way to quantify cyclin E1 overexpression is fundamental to support patient selection approaches for these inhibitors. In many cases, gene amplification correlates with increased cyclin E1 protein expression; however, there are a proportion of high-grade serous ovarian cancer and basal-like breast cancer cases where cyclin E1 protein overexpression does not correlate with gene amplification. In this study, we investigate if this phenomenon is observed in other cancers and some of the potential mechanisms causing cyclin E1 overexpression. We used a multi-omics approach to assess cyclin E1 expression in 1417 formalin-fixed paraffin-embedded (FFPE) patient tumor resections across 6 indications (SCCHN, Bladder, NSCLC, TNBC, Ovarian & SCLC). We used copy number variation (CNV) determined by next generation sequencing (NGS), NanoString nCounter RNA analysis and protein expression by immunohistochemistry (IHC). 830 were evaluable for all 3 methods and demonstrated *CCNE1* gene amplification by NGS (CNV normalized log2 ratio ≥1.5) in 3.3% cases. Using a threshold of mRNA z-score >2, 17% cases had high *CCNE1* mRNA and 29% had high cyclin E1 protein (H-score ≥100). 15.7% (130/830) cases had high protein expression without gene amplification or gain, crucially this was found across all 6 indications (n=20/102 SCCHN, n=29/166 Bladder, n=34/232 NSCLC, n=15/76 SCLC, n=15/143 TNBC & n=17/118 Ovarian). Impaired protein degradation has been proposed as a mechanism that may result in high Cyclin E1 expression. From a panel of 1600 genes, we assessed the relationship between cyclin E1 and mRNA expression of 57 genes involved in the ubiquitin-proteasome pathway in 1239 samples across the 6 indications. We assessed mutations which could impair ubiquitination in 915 samples across the 6 indications. We also assessed the methylation status of 893 genes associated with ubiquitin ligases or deubiquitinases in a cohort of 170 TNBC samples. Further investigation into other mechanisms causing cyclin E1 overexpression is required. IHC provides an ideal platform to build our understanding of cyclin E1 expression spatially. Our results indicate that assessing Cyclin E1 protein overexpression instead of *CCNE1* gene amplification could greatly broaden the population of patients who could benefit from replication stress response kinase inhibitors, as cyclin E1 overexpression correlates with genomic instability and replication stress.

#1650 Characterization of nucleolar biological functions via Auxin inducible degron-mediated acute depletion in triple negative breast cancer cells.
N. Samadi Rad, J. Mills, A. Tessari, D. Sunil Kumar, V. Anastas, S. Lamba, A. Reers, I. Cosentini, Z. Zhu, T. Magliery, E. Cocucci, L. Rizzotto, D. Palmieri; The Ohio State University, Columbus, OH

Nucleoli are large nuclear sub-compartments where vital cellular processes, such as rRNA production and ribosome assembly, take place. Aggressive tumor types, such as Triple Negative Breast Cancer (TNBC), require increased ribosome biogenesis to support their enhanced proliferation. Therefore, it has been suggested that the nucleolus could be a valid anti-neoplastic target. However, we still have a limited understanding of the cancer-specific functions of the nucleolar components, preventing the effective development of therapeutic agents. The characterization of nucleolar proteins is technically challenging. Several nucleolar proteins are essential, and their complete abrogation cannot be achieved through conventional RNAi or CRISPR-KO approaches. Additionally, many nucleolar proteins display peculiar biophysical properties, and their functions are connected to their abundance. Therefore, artificial overexpression systems might not fully recapitulate their endogenous biological functions. To overcome these challenges, we implemented an Auxin Inducible Degron (AID) system to acutely abrogate endogenous nucleolin, one of the most abundant nucleolar proteins, and asses its impact on the proliferation of TNBC cell lines. We used CRISPR/Cas9 editing in TNBC cell lines to modify the endogenous NCL gene, fusing it with an AID tag. Then, we stably transduced the cells with a modified Oryza Sativa TIR1 (OsTIR1-F74G) E3 ubiquitin ligase. In response to the synthetic phytohormone phenyl-auxin, OsTIR1 leads to the proteasomal degradation of AID-containing endogenous nucleolin in less than 6h, sparing any other human protein. RNA sequencing analysis showed that nucleolin degradation significantly alters the expression of genes involved in cell cycle progression. Accordingly, nucleolin degradation reduces cancer cell proliferation in vitro, associated with increased propidium iodide staining, suggestive of a G2/M cell cycle arrest. However, immunofluorescence analyses revealed that nucleolin abrogation leads to the accumulation of bi-nucleated cells with actin patches. These findings are indicative of potential cytokinesis defects due to altered spindle tension during mitosis. Notably, nucleolin abrogation increased the efficacy of chemical inhibitors of the Anaphase Promoting Complex on suppression of cell proliferation. To the best of our knowledge, this study is the first reporting the acute abrogation of an endogenous, highly abundant nucleolar protein, using the AID system. This approach allowed the characterization of nucleolin biological functions with unprecedented temporal resolution, shedding light on new biological functions in the regulation of cell division. Finally, our results suggest that nucleolin inhibition could enhance the therapeutic activities of drugs affecting cell cycle progression in TNBC.

#1651 Targeting intermediates of the PRMT5/BRG1 axis as a combination therapy.

A. Shaykevich, I. Silverman, A. Siegman, R. Maitra;
Yeshiva University, New York, NY

Over 40% of colorectal cancer (CRC) patients harbor a mutation in the *KRAS* gene, leading to a worse prognosis. PRMT5 and BRG1 are proteins considered potential therapeutic targets for cancer. Our lab has previously reported that both PRMT5 and BRG1 are overexpressed in *KRAS* mutant CRC when compared to *KRAS* wild-type CRC. It is therefore proposed that the PRMT5-BRG1 axis may be a strong therapeutic target for CRC. In this study, several key proteins that potentially mediate crosstalk between the PRMT5-BRG1 axis and *KRAS* were investigated.A literature review was first conducted to determine how the PRMT5-BRG1 axis acts in cancers. Additionally, pathways that may be involved in mediating the potential crosstalk between BRG1 and *KRAS* were discussed. Initial findings indicated that the PRMT5-BRG1 axis facilitates cancer oncogenesis. At the same time, the axis suppresses Myc/Max/Mad expression, leading to a dual role of the PRMT5-BRG1 axis depending on the tumor status. BRG1 was also found to work alongside mutant *KRAS* to affect tumor levels, with the effect differing by tumor type. The STRING database to determine the connection between the PRMT5-BRG1 axis and *KRAS*. It was determined that PRMT5, BRG1, and *KRAS* all interact with *PBRM1*, *SMARCB1*, *ARID1A*, and *ARID2*, with a combined interaction score >0.5. The UCSC Xena software was then used to analyze the mRNA data of CRC patients from The Cancer Genome Atlas (TCGA) database. Xena was utilized to determine which proteins are over expressed in CRC patient tumor samples compared to non-cancerous colon and rectum patient samples. Levels of *PBRM1* and *ARID1A* were observed to significantly decrease in CRC patients as compared to non-cancerous samples by approximately 15% (adjp < 0.0001 and 0.05, respectively). However, *SMARCB1* expression increased by 12% (adjp < 0.05). The Gene Expression Profiling Interactive Analysis (GEPIA) software was then used to analyze the correlation between the intermediary genes and PRMT5, BRG1, and *KRAS* in CRC patient tumor samples. *PBRM1*, *SMARCB1*, *ARID1A*, and *ARID2* all demonstrated positive correlation with PRMT5, SMARCA4, and *KRAS* (R greater than 0.75 for nearly all correlations and p =0) in CRC patient tumor samples. Our study thus showcases the possible disrepair of the PRMT5/BRG1 axis in relation to *KRAS*. Key downstream proteins are decreased in CRC and may lower the potential crosstalk between PRMT5, BRG1, and *KRAS*. These findings are significant, and these key intermediate proteins may be strong therapeutic targets via inducing expression. Further research is currently in progress to outline the molecular processes behind the therapeutic role of revitalizing the SMARCA4/BRG1 axis when the downstream proteins are induced.

MOLECULAR/CELLULAR BIOLOGY AND GENETICS: Cell Signaling Components as Therapeutic Targets
Poster Session

#1654 Anti-tumor activity of orally-available cyclic peptide LUNA18 through direct RAS inhibition in RAS-altered tumors.

H. Sase[1], S. Michisaka[2], Y. Tachibana[2], M. Hasegawa[2], T. Fujii[2], K. Takei[2], T. Kanei[2], N. Murao[2], S. Kuramoto[2], N. Shibahara[2], A. Ohta[2], M. Tanada[2], T. Shiraishi[2], H. Iikura[2], T. Kitazawa[2], H. Tanaka[2];

[1]Chugai Pharmaceutical Co., Ltd., Chuo-ku, Tokyo, Japan, [2]Chugai Pharmaceutical Co., Ltd., Yokohama, Kanagawa, Japan

RAS is the one of the most frequently altered genes in human cancer and contributes to the growth of tumors. Recently, KRAS G12C inhibitors were approved as the first molecular targeting agents for RAS, but there are still huge unmet medical needs in RAS-mutated cancers because drugs targeting non-KRAS G12C tumors have not yet been approved and efficacy by even approved KRAS G12C inhibitors is not satisfactory. LUNA18 is the cyclic peptide that binds to RAS mutants and wildtype, including KRAS, NRAS and HRAS, thereby inhibiting protein-protein interaction (PPI) between the inactive form of RAS and GEFs (guanine nucleotide exchange factors). LUNA18 decreased the active form of KRAS and phosphorylated ERK and AKT, and cell proliferation in RAS-mutated cancer cells with nM order of cellular IC50s irrespective of tumor types and amino acid substitutions except for Q61 mutants. On the other hand, LUNA18 did not inhibit proliferation of cells with active mutations downstream of RAS (BRAF and MEK), suggesting LUNA18 selectively inhibited growth of RAS-dependent cells. Consistent with in vitro cellular activity, oral administration of LUNA18 showed durable RAS signal inhibition up to 24-48 hours and tumor regression in RAS-mutated xenograft models. In addition to KRAS-mutated cells, LUNA18 also showed in vitro and in vivo robust efficacy in KRAS-amplified cells. These data indicated LUNA18 is the versatile compound that selectively suppressed cellular signaling from RAS G12/G13 mutants as well as RAS wildtype amplification through inhibition of PPI between the inactive form of RAS and GEFs, and it can be applicable to a wide range of RAS-altered tumors. Rebound of the MAPK pathway is reported to be the one of the cause for attenuating efficacy of KRAS G12C inhibitors. We also observed the rebound of ERK activation 24-72 hours after the treatment with a KRAS G12C inhibitor in cells with the KRAS G12C mutation though suppression of KRAS activity was maintained. On the other hand, LUNA18 persistently suppressed ERK activity as well as KRAS activity up to 72 hours. The combination of the KRAS G12C inhibitor with siRNA for RAS wildtype showed durable inhibition of ERK activity, suggesting that RAS wildtype plays a key role for the rebound of ERK activity and inhibitory activity to RAS wildtype by LUNA18 contribute to the persistent inhibition of RAS signaling by LUNA18. We orally administered LUNA18 and a KRAS G12C inhibitor to a xenograft model, which showed temporal response and then acquired resistance to a KRAS G12C inhibitor, and found that LUNA18 significantly suppressed emergence of resistance to a KRAS G12C inhibitor. These results supported that the combination of the KRAS G12C inhibitor with LUNA18 could be a promising option to patients with KRAS G12C mutation by suppressing resistance to a KRAS G12C inhibitor through the suppression of rebound of the MAPK pathway.

#1655 Targeting lipid metabolism disrupts KRAS oncogenesis in pancreatic cancer.

Neha Arora[1], Hong Liang[1], Alex Reed[2], Jeffrey T. Chang[1], Benjamin F. Cravatt[2], Yong Zhou[1]

[1]Integrative Biology and Pharmacology, McGovern Medical School at UTHealth Houston, Houston, TX,[2]Department of Chemistry, The Scripps Research Institute, La Jolla, San Diego, CA

Background: KRAS mutations are chief genetic event in pancreatic cancer. Recently approved inhibitors, sotorasib and adagrasib specifically target $KRAS^{G12C}$, a minor mutation in pancreatic cancer. Further, patients developed acquired resistance by generating secondary KRAS mutations, posing an added obstacle for allele specific inhibitors, warranting alternative strategies to tackle KRAS-dependent cancers. KRAS forms proteolipid signaling platforms on plasma membrane (PM) termed nanoclusters. We have shown mutant KRAS nanoclusters selectively enrich phosphatidylserine (PS) lipid, being particularly receptive to unsaturated PS, suggesting lipid acyl chain metabolism is crucial for KRAS function. In cells, lysophosphatidylcholine acyltransferases 3 (LPCAT3) preferentially catalyzes synthesis of unsaturated PS. We tested the hypothesis that inhibition of LPCAT3 depletes unsaturated PS in the PM, perturbs the PS-dependent PM interactions and oncogenic functions of KRAS.

Methods: LPCAT3 knockdown (KD) mediated by siRNA in doxycycline (Dox) inducible $KRAS^{G12D}$ murine cells (iKRAS) and CRISPR-Cas9 in human pancreatic tumor line (MiaPaCa-2). LPCAT3 inhibition achieved using small molecule inhibitors (SMIs): HTS3 and HTS4. Shotgun lipidomics characterized re-modeling of PS lipidomes. PM distribution and nanoclustering of KRAS was evaluated by super-resolution electron microscopy (EM). Anti-tumor effect of LPCAT3 inhibition was examined *in vitro* by proliferation, colony formation and soft agar assays and cellular signaling by western blot.

Results: LPCAT3KD decreased polyunsaturated PS levels in MiaPaCa-2 and mislocalized mutant $KRAS^{G12V}$ on the PM with a 4-fold reduction in KRAS PM distribution ($p<0.0013$) and disrupted KRAS nanoclustering, without affecting that of $HRAS^{G12V}$ in transformed MiaPaCa-2. LPCAT3KD reduced colony formation ability in MiaPaCa-2. LPCAT3 siRNA reduced KRAS-dependent MAPK signaling, and significantly reduced colony formation only upon Dox-induced expression of $KRAS^{G12D}$, while having no effect in uninduced iKRAS. An integrated knowledgebase tool canSAR.ai generated a druggability score of 77% suggesting LPCAT3 is highly druggable by chemistry-based assessment. Indeed, recently discovered LPCAT3 inhibitors, significantly reduced MAPK signaling, proliferation and colony formation in mutant KRAS-dependent tumor cells while having no significant effect in WT KRAS cells corroborating mutant KRAS specificity of LPCAT3.

Conclusion: We demonstrate targeting unsaturated PS lipid metabolism by inhibiting LPCAT3 disrupts KRAS signaling platform and perturbs its oncogenic functions in pancreatic cancer cells. Since various KRAS mutants require unsaturated PS to propagate signaling, our approach targets diverse KRAS mutants, uniquely addressing drug resistance issue. Further, we will optimize the LPCAT3 inhibitors and study their efficacy in xenograft mouse models.

#1656 ISM6331, a novel and potent pan-TEAD inhibitor, exhibits strong anti-tumor activity in preclinical models of Hippo pathway-dysregulated cancers.

Q. Li[1], J. Wan[1], J. Liu[1], J. Shang[1], J. Yu[1], W. Zhu[1], C.-J. Chen[1], J. Qiao[1], L. Wang[1], M. Zhang[1], X. Ding[1], S. Bavadekar[2], **S. Rao**[2], F. Ren[1], A. Zhavoronkov[2]; [1]Insilico Medicine, Shanghai, China, [2]Insilico Medicine, New York, NY

The Hippo-YAP/TAZ-TEAD signaling pathway plays critical roles in tumorigenesis and tumor progression. Genetic alterations of Hippo pathway regulators, such as NF2 or LATS1/2, have been shown to induce YAP/TAZ-TEAD transcriptional activity, promoting initiation and progression of many solid tumors. In addition, many studies have shown that YAP/TAZ-TEAD activation mediates resistance to multiple targeted therapies, particularly EGFR-KRas-MAPK pathway inhibitors. The TEAD family of transcription factors (TEAD1/2/3/4) share structural similarity and have overlapping functions in tumor development and TEAD auto-palmitoylation is critical for its interaction with YAP/TAZ and its transcriptional function. Therefore, blocking TEAD palmitoylation and allosterically disrupting YAP/TAZ-TEAD-mediated transcriptional regulation, is emerging as a promising approach for the treatment of tumors with Hippo pathway dysregulation.
In this work, ISM6331, a novel and potent TEAD inhibitor with excellent inhibition against TEAD1/2/3/4 was identified leveraging an AI generative model. ISM6331 reversibly binds to the TEAD palmitoylation site and significantly suppresses TEAD transcriptional activity. ISM6331 potently and selectively inhibited the growth of many Hippo pathway-dysregulated tumor cells and dose-dependently suppressed the expression of TEAD target genes *in vitro*. In NF2-deficient or LATS1/2-mutant *in vivo* mesothelioma models, ISM6331 exhibited promising anti-tumor efficacy as monotherapy in a dose-dependent manner from 3 to 30mg/kg. ISM6331 also showed synergism with EGFR or KRasG12C inhibitors in inhibiting tumor cell growth and overcame drug resistance in *in vitro* and *in vivo* models. In addition, ISM6331 showed excellent pharmacokinetic properties in multiple preclinical species and was well-tolerated in GLP-toxicity studies. In summary, ISM6331 has promising potential to treat Hippo pathway-dysregulated tumors as monotherapy as well as in combination with targeted therapies.

#1657 Microfluidics-based screening platform identifies a novel therapeutic approach to targeting EML4-ALK driven cancers.

R. C. Centore[1], M. Watson[2], J. Doh[1], J. Cattin[2], C. Sgambato[2], A. Alex[2], J. Sawant[1], P. Radhakrishnan[1], J. Cornish[2], A. Howarth[2], N. Bharatham[2], W. E. Arter[2], S. Qamar[2], K. L. Saar[2], D. Williamson[2], A. Seeber[1], N. Groenewegen[2], M. Czekalska[2], T. Kartanas[2], N. Ermann[2], A. Taher[2], T. Knowles[2], S. Arora[1]; [1]Transition Bio, Inc., Watertown, MA, [2]Transition Bio, Inc., Cambridge, United Kingdom

To achieve proliferative dysregulation, a hallmark of cancer, tumor cells utilize a variety of mechanisms to maintain constitutive oncogenic signaling in the absence of extracellular cues. One such mechanism occurs in cells expressing the EML4-ALK fusion protein. This fusion, found in about 4% of non-small cell lung cancer (NSCLC), is a result of an inversion within chromosome 2, placing the 3' end of the *ALK* (anaplastic lymphoma kinase) gene downstream of the 5' end of the *EML4* (echinoderm microtubule associated protein-like 4) gene. The resulting fusion protein contains the oligomerization domain and additional disordered sequence elements of EML4 upstream of a functional ALK kinase domain. EML4-ALK is a critical driver for these tumors, promoting aberrant ALK-dependent oncogenic signaling. While tumors harboring the EML4-ALK fusion initially respond to ALK tyrosine kinase inhibitors (TKIs), resistance remains a significant clinical challenge requiring new therapeutic approaches. Recently, it has come to be understood that rather than responding through extracellular proliferative cues, the EML4-ALK fusion protein elicits constitutive ALK signaling through the formation of cytoplasmic biomolecular condensates. These condensates are the result of phase separation and have been shown to be causal for disease phenotypes in cell and animal models driven by EML4-ALK, establishing condensate modulation as a novel means by which to treat TKI-resistant tumors. Here, we have developed a novel proprietary microfluidics-based high throughput screening platform (termed PhaseScan™) to identify small-molecule modulators of EML4-ALK condensates. Using this technology, we identified compounds that disrupt EML4-ALK condensates *in vitro* and in cells through a novel mechanism, distinct from that of known ALK TKIs, providing utility in both TKI-resistant as well as TKI-naïve tumors. Further profiling of the mechanism of action (MoA) revealed specific modification within the disordered region of EML4, disruption of EML4 oligomerization, and defective ALK signaling in cancer cells. Thus, our PhaseScan™ methodology enabled the identification of novel, functionally active chemical matter that would have otherwise been challenging to identify utilizing any conventional hit identification methodology.

#1658 CFT1946, a potent, selective BRAF V600X mutant-specific degrader demonstrates superior activity as a single agent to clinically approved BRAF inhibitors and standard of care combinations in preclinical models of BRAF V600X melanoma, CRC, NSCLC, and brain metastasis.

B. Kreger, J. R. Stephenson, M. E. Sowa, S. A. Perino, L. L. Poling, E. Hurh, M. J. Thomenius, Y. Liang, S. L. Fisher, R. M. Pollock;
C4 Therapeutics, Watertown, MA

Activating mutations in BRAF at residue V600 (typically V600E) lead to dysregulation of the MAPK pathway and occur in approximately 8% of all human cancers including 60% of melanoma, up to 12% of colorectal cancer (CRC), and 4% of NSCLC. Currently approved BRAF inhibitors (BRAFi) are selective for BRAF V600X mutant proteins and are typically used in combination with MEK inhibitors (MEKi) in melanoma and NSCLC, or anti-EGFR antibodies such as cetuximab in CRC. However, their activity is limited by primary or acquired resistance often mediated by RAF dimer-inducing mechanisms. Furthermore, progression of BRAF V600X melanoma after BRAFi/MEKi treatment frequently involves brain metastasis, and currently approved BRAFi have relatively poor brain penetration. CFT1946 is a potent, orally bioavailable, cereblon-based BiDAC^{TM} degrader that selectively degrades BRAF V600X mutant protein and is currently under investigation in a Phase I clinical trial. CFT1946 has the potential to overcome limitations of clinically approved BRAFi, as degradation of BRAF V600X should abrogate RAF dimer-driven resistance and paradoxical activation. Indeed, we have previously demonstrated that CFT1946 is efficacious in an A375 BRAF V600E/NRAS Q61K xenograft model of BRAFi resistant melanoma. Here we substantially expand our preclinical characterization of CFT1946 across multiple models of BRAF V600X-driven cancers including BRAF V600X-driven CRC and NSCLC, additional BRAFi-resistant melanoma models, and a brain metastatic melanoma model. Single agent CFT1946 outperformed the SOC encorafenib + cetuximab combination in a panel of BRAF-V600X CRC xenograft models. Pathway analysis in BRAF V600X CRC models revealed that CFT1946 suppresses EGFR-mediated MAPK pathway reactivation, a mechanism known to diminish the impact of approved BRAF inhibitors in this indication. CFT1946 also demonstrated regression in a BRAF-V600X NSCLC PDX model where the SOC dabrafenib + trametinib showed only modest tumor growth inhibition. Consistent with our previous results in the A375 melanoma model, single agent CFT1946 showed superior activity versus the SOC dabrafenib + trametinib combination in all additional melanoma models tested, with complete regression achieved using a CFT1946 + trametinib combination in a PDX model bearing a BRAF-V600E kinase duplication that showed minimal response to dabrafenib + trametinib. Finally, using an A375 intracranial model, treatment with CFT1946 gave robust, dose dependent efficacy and survival advantage over encorafenib. The promising activity of CFT1946 in a broad range of BRAF V600X preclinical models supports its ongoing clinical investigation in BRAF V600 mutant solid tumors (NCT05668585).

#1659 Phosphorylation of cell cycle and apoptosis regulatory protein (CARP)-1 by stress-activated protein kinase P38γ is a novel mechanism of apoptosis signaling by genotoxic chemotherapy.

J. Venkatesh[1], M. Muthu[1], V. T. Cheriyan[1], S. C. Sekhar[1], N. C. P. Acharige[2], E. Levi[3], H. Assad[1], M. K. H. Pflum[2], **A. K. Rishi[1]**;
[1]Barbara Ann Karmanos Cancer Institute, Detroit, MI, [2]Wayne state University, Detroit, MI, [3]Department of Veterans Affairs Medical Center, Detroit, MI

CARP-1, a perinuclear phospho-protein, regulates cell survival and apoptosis signaling induced by genotoxic drugs. However, kinase(s) phosphorylating CARP-1 and down-stream signal transduction events remain unclear. Here we find that CARP-1 Serine (S)^{626} and Threonine (T)^{627} substitution to Alanines (AA) inhibits genotoxic drug-induced apoptosis. CARP-1 T^{627} is followed by a Proline (P), and this TP motif is conserved in vertebrates. To further elucidate chemotherapy-activated, CARP-1-dependent signaling mechanisms, we UV cross-linked protein extracts from Adriamycin-treated HeLa cervical cancer cells with a CARP-1 (614-638) peptide, and conducted liquid chromatography-tandem mass spectrometry (LC-MS/MS) analyses of the peptide-bound protein complexes. This experiment revealed SAPK p38γ interaction with CARP-1 (614-638) peptide. Our studies further revealed that SAPK p38γ phosphorylates CARP-1 T^{627} in cancer cells treated with genotoxic drugs. CARP-1 T^{627} phosphorylation was also noted in breast tumors from patients treated with radiation or endocrine therapies. Loss of p38γ abrogates CARP-1 T^{627} phosphorylation, and results in enhanced survival of breast cancer cells by genotoxic drugs. We conclude that genotoxic drugs activate p38γ-dependent CARP-1 T^{627} phosphorylation and cell growth inhibition.

#1660 Tumor pharmacokinetics and pharmacodynamics assessment of TEAD inhibitor VT03989 in patient-derived xenograft models of glioblastoma.

T. Margaryan, Y.-W. Chang, J. Molloy, B. Hopkins, M. Elliott, E. Luna Melendez, C. White, N. Sanai, A.-C. Tien, A. Tovmasyan, S. Mehta;
Barrow Neurological Institute, Phoenix, AZ

Background: The Hippo-YAP/TAZ pathway regulates cell proliferation, cell growth and migration. The major effectors of the Hippo pathway are the TEAD transcription factors, which are deregulated in several cancers, including glioblastoma (GBM). In this study, we evaluated the pharmacokinetics and pharmacodynamics of VT03989, a highly potent TEAD inhibitor, in orthotopic patient-derived xenograft (PDX) models of GBM.
Methods: Mice with intracranial PDX GBM tumors were randomized into two cohorts to receive 10 mg/kg (oral) VT03989 or placebo for 4 days. VT03989 levels in plasma, tumor, and contralateral brain tissue were measured by liquid chromatography tandem mass spectrometry (LC-MS/MS) at 2, 6, and 12 hours after the last treatment of VT03989. Unbound fractions were determined by equilibrium dialysis. Quantitative RT-PCR was performed to assess levels of TEAD target genes, CTGF and CYR61. Immunohistochemistry of Ki67 and cleaved caspase 3 (CC3) was performed.
Results: The median unbound concentrations of VT3989 were 27 nM in plasma and 26 nmol/kg in the tumor. The median brain-to-plasma and tumor-to-plasma partition coefficients of unbound VT03989 were 0.65 and 0.99, respectively - indicating favorable brain and tumor penetration ability of VT03989. A decrease in CTGF and CYR61 indicated TEAD inhibition and was accompanied by an increase in CC3 (+) cells.
Conclusion: VT03989 is well tolerated, achieves pharmacologically relevant unbound concentrations in GBM PDX models, and is associated with significant target modulation. Ongoing studies are evaluating *in vivo* survival benefits from combining VT03989 inhibition with radiation therapy

#1661 Preclinical characterization of HMPL-295, a potent and selective ERK 1/2 inhibitor.

J. Hu, J. Ni, Y. Lv, W. Li, H. Zhang, X. Li, Y. Yu, Z. Zhong, J. Wang, Y. Sai, W. Qing, Y. Ren, M. Shi, W. Su;
HUTCHMED, Shanghai, China

Background: Although therapeutic agents targeting alterations in the MAPK pathway have achieved great clinical success, the overall benefit is still suboptimal. Several studies have shown that reactivation of MAPK signaling is the main basis to compromise the efficacy. Thus, co-inhibition of ERK, the terminal master kinase of MAPK pathway, and the upstream targets may effectively shut down the MAPK signaling cascade and induce deeper and more durable anti-tumor activities. Herein, we present the preclinical characterization of HMPL-295, a potent and selective ERK 1/2 inhibitor, discovered and being currently developed in phase I clinical trial (NCT04908046) by HUTCHMED.

Methods: The inhibition on ERK 1/2 kinase was determined using Z-LYTE™ kinase assay. The selectivity of HMPL-295 was evaluated against 394 kinases (KinaseProfiler^{TM}) and 86 safety-related proteins (SafetyScreen87^{TM}) by Eurofins. Cellular target inhibition on phosphorylation of RSK (p-RSK) was detected by ELISA. *In vitro* anti-proliferation activity of HMPL-295 as a single agent was measured by CCK-8 or CellTiter-Glo luminescent assay. Colony formation assay was used to evaluate the combination effect of HMPL-295 with targeted therapy. Multiple tumor models with RAS/RAF/MAPK pathway activation were applied in immune-deficient mice to investigate the anti-tumor activity of HMPL-295 as a single agent or in combination with either chemotherapy or targeted therapy.

Results: HMPL-295 strongly inhibited ERK1 and ERK2 kinase activities with equal IC_{50} at 4 nM. In human colon cancer cell line COLO 205 harboring *BRAF*^{V600E} mutation, HMPL-295 inhibited p-RSK, a direct substrate of ERK1/2, with an average IC_{50} of 180 nM from 3 independent experiments. With the inhibition of ERK and its downstream substrates, HMPL-295 treatment induced tumor cells arresting at G0/G1 phase via down-regulation of cyclin D1/p-RB signaling and consequently attenuated cell growth in a panel of MAPK pathway dysregulated tumor cell lines, but barely affected the growth of normal cells. Furthermore, HMPL-295 demonstrated favorable selectivity in the kinase and safety pharmacology profiling, indicating a low off-target risk. For *in vivo* studies, oral administration of HMPL-295 induced time- and dose-dependent inhibition of p-RSK and resulted in dose-dependent anti-tumor activity in several tumor models harboring *KRAS* or *BRAF* mutations. Moreover, HMPL-295 significantly improved the anti-tumor activity of standard-of-care chemotherapy as well as targeted agents in *KRAS*- or *BRAF*-mutant tumor models both *in vitro* and *in vivo*.

Conclusion: HMPL-295 is a potent and selective ERK1/2 inhibitor which demonstrates strong anti-tumor activity in preclinical models, supporting further clinical evaluation.

#1662 Evaluation of TEAD inhibitor, VT03989 treatment on growth of aggressive meningioma preclinical models.

S. Desai, A. Thaghalli Shivanna, M. Stavnichuk, E. Hayes, S. Patel, J. McNamara, A. DeSantis, N. Sanai, A.-C. Tien, S. Mehta;
Barrow Neurological Institute, Phoenix, AZ

Background: Aggressive meningiomas (WHO grade II/III) are incurable brain tumors and despite surgery and radiation therapy, tumors recur frequently without approved systemic treatment options. Hence, there is an unmet need for targeted inhibition therapy and biomarkers that predict vulnerability to targeted therapies in aggressive meningioma patients. Hippo signaling pathway has been shown to be dysregulated in meningioma, resulting in activation of its target TEAD as a transcriptional factor. We hypothesize that targeted inhibition of TEAD in recurrent high-grade meningioma with *NF2* loss will lead to increased inhibition of tumor growth. Here, we investigated the effect of VT3989, a potent TEAD inhibitor, in meningioma cell lines with *NF2* wild-type or *NF2* loss genotype.

Methods: Two meningioma cell-lines: IOMM-Lee (*NF2* wild-type) and MG309, a grade III meningioma patient-derived cell line with *NF2* loss were treated with various doses of VT3989 and cell viability was assessed. Relative expression of direct targets of TEAD including CTGF and CYR61 was determined with quantitative PCR (qPCR) to ensure target engagement. Global transcriptomic changes were examined via RNAseq analysis on RNA isolated from MG309 cells treated with VT03989 compared to vehicle treated cells.

Results: VT3989 treatment significantly decreased viability of both IOMM-Lee and MG309 cells. Canonical downstream targets of TEAD such as CTGF, CYR61, BIRC5, BCL-2 were downregulated in VT3989 treated cells compared to control. Furthermore, VT03989 treatment resulted in downregulation in cell cycle regulation and DNA damage response (DDR) pathway genes. Ongoing work is focused on combining VT3989 with agents targeting cell cycle and DDR pathways.

Conclusion: VT3989 treatment led to downregulation of TEAD direct targets CTGF and CYR61 and inhibited cell viability of both IOMM-Lee cell and MG309 meningioma lines. RNA-seq analysis identified cell cycle and DDR pathway genes to be downregulated upon TEAD inhibition.

#1663 Single-cell signaling analysis reveals that major vault protein facilitates RasG12C inhibitor resistance.

J. Z. Zhang, S.-E. Ong, D. Baker, D. J. Maly;
University of Washington, School of Medicine, Seattle, WA

Covalent inhibitors of RasG12C are the first clinically-approved drugs for targeting mutant Ras-driven cancers. However, the rapid development of clinical resistance to current Ras G12C inhibitors is common. It has been demonstrated that a subpopulation of cancer cells facilitate drug resistance but the mechanistic basis of this heterogenous response is not well understood. Here, we utilized recently developed Ras sensors to profile the environment of active Ras and to measure the activity of endogenous Ras to pair structure (Ras signalosome) to function (Ras activity), respectively, at a single-cell level. With this approach, we found that a subpopulation of KRasG12C cells treated with RasG12C-GDP inhibitors underwent oncogenic signaling and metabolic changes driven by WT Ras at the golgi and mutant Ras at mitochondria, respectively. Our Ras sensors identified Major Vault Protein (MVP) as a mediator of Ras activation at both subcellular locations by scaffolding Ras signaling pathway components and metabolite channels. We found that recently developed RasG12C-GTP inhibitors also led to MVP-mediated WT Ras signaling at the golgi, demonstrating that this a general mechanism of RasG12C inhibitor resistance. Overall, single-cell analyses enabled the discovery of a RasG12C inhibitor-resistant subpopulation driven by MVP, providing insight into the complex and heterogenous rewiring that confers drug resistance in cancer.

#1664 Combination of LUNA18, a novel RAS inhibitor, with KRAS G12C inhibitors augments anti-tumor activity via inhibition of MAPK pathway reactivation.

S. Michisaka, H. Sase, Y. Tachibana, M. Hasegawa, T. Fujii, S. Kuramoto, N. Shibahara, A. Ohta, M. Tanada, T. Shiraishi, H. Iikura, T. Kitazawa, H. Tanaka; Chugai Pharmaceutical Co., Ltd., Kanagawa, Japan

RAS gene alterations, found in approximately 15% of all cancers and known oncogenes, are recognized as promising therapeutic targets. KRAS G12C inhibitors were the first FDA-approved RAS targeting agent, but their efficacy of monotherapy is limited. Reactivation of the MAPK pathway is reported to be the one of the causes for attenuating efficacy of KRAS G12C inhibitors. LUNA18 is the cyclic peptide that binds to RAS mutants and wildtype, including KRAS, NRAS and HRAS, thereby inhibiting protein-protein interaction (PPI) between the inactive form of RAS and GEFs (guanine nucleotide exchange factors).We observed the rebound of ERK activation 24-72 hours after the treatment with a KRAS G12C inhibitor in cells with the KRAS G12C mutation though suppression of KRAS activity was maintained. This rebound was not suppressed by the KRAS G12C inhibitor retreatment. On the other hand, LUNA18 persistently suppressed ERK activity as well as KRAS activity up to 72 hours. LUNA18 also suppressed ERK reactivation caused by long-term treatment with the KRAS G12C inhibitor. The combination of the KRAS G12C inhibitor with siRNA for RAS wildtype showed durable inhibition of ERK activity, suggesting that RAS wildtype plays a key role for the rebound of ERK activity and inhibitory activity to RAS wildtype by LUNA18 contribute to the persistent inhibition of RAS signaling by LUNA18. In the experiment model that with strong RAS wildtype activation by stimulation with GFs (growth factors), the KRAS G12C inhibitor also did not suppress ERK activation. Conversely, LUNA18 suppressed it. Cell proliferation induced by GF stimulation was more strongly inhibited by LUNA18 than by the KRAS G12C inhibitors. Our data indicates that MAPK pathway reactivation via WT-RAS activation leads to resistance to KRAS G12C inhibitors and that the combination of LUNA18 and KRAS G12C inhibitors has the potential to overcome this resistance mechanism. In the in vitro cell growth assay, combination of LUNA18 and the KRAS G12C inhibitor showed more potent cell growth inhibition than single agents. We orally administered LUNA18 and the KRAS G12C inhibitor to a xenograft model, which showed temporal response and then acquired resistance to the KRAS G12C inhibitor, and found that LUNA18 significantly suppressed emergence of resistance to the KRAS G12C inhibitor. These results suggest that LUNA18 could be a promising candidate for combination therapy with KRAS G12C inhibitors.

#1665 Investigating Daple-FLT3 gene fusion in leukemia cells and its response to kinase inhibitors.

E. Nguyen, J. Ear;
California State Polytechnic University of Pomona, Pomona, CA

Gene fusions are frequently found in leukemia and other cancers. The signaling scaffold protein, Daple (CCDC88C), has been found to undergo gene fusion to the receptor tyrosine kinase, FLT3. Specifically, a fragment of the coiled-coil domain from Daple and tyrosine kinase domain (TKD) of FLT3 are found fused together. How the gene product from this gene fusion functions in rewiring the signaling network in cells and whether this gene product can be targeted though pharmacological inhibitions remain unclear. Cell surface receptors, such as receptor tyrosine kinases (RTKs), activate cell signaling and genetic mutations that lead to constitutive receptor activation can promote unregulated cell proliferation, survival, and migration. Leukemia patients with hyperactive RTKs are treated with tyrosine kinase inhibitors (TKIs), such as Imatinib and Sorafenib. Here we demonstrate how TKIs can directly block the activation of Daple-FLT3 and prevent hyperactivation of its downstream pathways. Our studies unveil a strategy to identify other compounds which may serve as an additive, or alternative, approach to treating patients with Daple gene fusion.

#1666 A novel sox-based continuous and homogeneous assay for the discovery of inhibitors of inactive and active AKT.

S. Cornell-Kennon, D. Urul, M. Hakar, H. McMahon, K. Huynh, E. May, E. Schaefer;
Assayquant Technologies, Inc., Marlborough, MA

Introduction: The activity of protein kinases plays a critical role in the aberrant activation of oncogenic signaling pathways which can drive tumorigenesis and malignant transformation in cancer. AKT has been shown to be both upregulated and mutated in cancer cells allowing it to serve as a driver of cancer cell growth and progression. Inhibition of AKT activation and activity are both attractive targets for effective cancer drug discovery.
Experimental Procedures: We developed continuous, homogeneous assays for unactive AKTs. A peptide substrate, modified with a sulfonamido-oxine fluorophore (Sox), utilizes chelation-enhanced fluorescence to enable a real-time readout of AKT-driven phosphorylation. First, a subset of 30,000 Sox-containing sequences were evaluated for AKT substrate candidates, selecting for assay robustness and specificity. A physiologically relevant peptide substrate was identified and used to develop a kinetic assay to monitor AKT1 activation and activity. Unactive AKT1 was incubated with DOPS/DOPC and PIP3, which mimics the plasma membrane, allowing the PH domain of AKT to bind, leading to a conformational change that enables full activation of AKT by PDK1 and MK2. Upon assay initiation, active AKT phosphorylates the sensor peptide, and the resulting signal is read in kinetic mode using a fluorescence intensity readout. First derivative plots for each progress curve were generated; the slope of the linear regions of each plot, representing acceleration towards a steady-state, were used to determine relative rates of activation for each AKT.
Results: We developed a novel assay for AKT activation and substrate phosphorylation utilizing AQT0076, DOPS/DOPC, PIP3, PDK1, and MK2. With a mix of classical AKT inhibitors and allosteric inhibitors that rely on an inactive “PH-in” conformation, we demonstrated inhibition and quantified inhibitor potency of both active “PH-out” AKT activity and inactive “PH-in” AKT activation via dose-response measurements of steady-state rate and rate acceleration, respectively.
Conclusions: A robust, homogeneous assay was developed to simultaneously monitor AKT activation and substrate phosphorylation kinetically over time. Through a continuous assay, we captured both steady-state rates and rate acceleration as a function of inhibitor concentration, allowing for accurate quantitation of both classes of AKT inhibitors in a single experimental format. With some inhibitors, we observed potencies that matched reported literature values, while with others we observed marked differences that may reflect a more physiological context that could translate through to higher efficacy in the clinic. This novel assay format provides a new tool that can be used in drug discovery to generate more effective next generation inhibitors of both AKT activation and subsequent substrate phosphorylation to prevent cancer cell growth and progression.

#1667 The role of CCN1 in mutant K-RAS addiction in pancreatic cancer.

A. Kambhampati, A. De, I. Haque, S. Banerjee, S. K. Banerjee;
Kansas City VA Medical Center, Kansas City, MO

Mutant K-RAS addiction of pancreatic ductal adenocarcinoma cells (PDAC) coordinates their transformation, proliferation, and survival. Therefore, initially, it had an impression that targeting mutant K-RAS could be an ideal strategy to treat PDAC. However, after decades of studies, no effective RAS inhibitors reached the clinic, indicating that RAS-oncoprotein is an undruggable target in PDAC. Thus, identifying a new target linked with K-RAS signaling was most needed. Using genetically engineered cell lines and K-RAS-driven genetically engineered mouse models (KC or KPC) with or without pancreas-specific CCN1 conditional knockout background, we identified a positive feedback circuit between CCN1 and mutant K-RAS expression. Moreover, blocking this feedback via conditional knockout of CCN1 in the pancreas significantly reduced invasive phenotypes, PDAC growth, and metastasis in the lung in KC and KPC mice. Mechanistically, we found that the K-RAS-CCN1 feedback circuit is regulated by microRNA miR-145 via a feedforward mechanism. Collectively, these studies highlight the clinical potential of targeting CCN1 in PDAC. (VA Merit Grant supports this work)

#1668 Association of stem cell-like phenotype with isoform specific functions of AKTs in hepatocytes.

I. Slarve, Y. Wang, M. Alba, L. He, B. Stiles;
USC - University of Southern California, Los Angeles, CA

Introduction: Liver cancer is the sixth most common cancer and the third leading cause of cancer-related deaths worldwide. It is associated with abnormal activation of the phosphatidylinositol 3-kinase (PI3K)/AKT pathway, which is implicated in regulation of cancer stem cells (CSCs). The present study investigated the effects of AKT loss on stem cell-like phenotype in immortalized mouse hepatocytes.

Methods: Immortalized hepatocytes were established from mice with *Akt1* (*Akt1*$^{-/-}$; *Akt1*-null) or *Akt2* (*Akt2*$^{-/-}$; *Akt2*-null) whole-body deletion. Cell morphology was assessed via microscopy. Cell proliferation was evaluated with hemacytometer count and MTT assay. Cell migration towards a chemoattractant was assessed via transwell assay. Cell viability was evaluated in response to chemotherapy treatment. The ability of cells to

Results: When compared to WT cells, which exhibited cuboidal epithelial-like features, *Akt1*-null and *Akt2*-null cells demonstrated elongated mesenchymal-like morphology. Loss of either isoform was associated with a significantly decreased cell growth ($p<0.05$). *Akt1*-null cells migrated faster towards a chemoattractant in the transwell assay, were significantly more resistant to sorafenib, and formed a significantly higher number of spheres in the sphere formation assay ($p<0.01$). Proteomic analysis revealed that both *Akt1*-null and *Akt2*-null cells exhibited increased expression of CSC marker CD44, along with other proteins associated with liver cancer, including PDGFRA, CDH2, MMP14, and COX2 ($p<0.05$). Additionally, *Akt1*-null cells exhibited elevated levels of ANXA1 and ANXA3 ($p<0.01$).

Conclusions: Loss of both AKT isoforms resulted in decreased cell proliferation and elevated expression of proteins with a previously reported role in liver cancer invasion, migration, and epithelial-mesenchymal transition. AKT1 loss correlated with an enhanced stem cell-like phenotype, including increased migration towards a chemoattractant, higher resistance to chemotherapy, and enhanced ability to form spheres. These results contribute to the understanding of the role of AKT isoforms in regulating stemness in liver cancer and may serve as a basis for investigation into isoform specific inhibitors. Further investigation into cellular mechanisms governing these phenotypes is required.

#1669 KRAS G12X mutants display differential preferences in downstream effector binding.

L. J. Ash[1], O. Bourdain[2], D. Lam[2], S. S. Pallas[2], A. L. Wolfe[2];

[1]The Graduate Center of the City University of New York, New York, NY, [2]Hunter College of the City University of New YorK, New York, NY

KRAS is among the most frequently mutated oncogenic driver proteins in human cancers including lung, colorectal, and pancreatic cancers. Activating KRAS mutants cause increased cell proliferation through direct binding and overactivation of effector proteins. Effector activation preference is driver mutation specific, as KRAS G12D and G12C purportedly bind both RAF and PI3K, whereas G12R has been reported to bind RAF but not PI3K. The mechanisms of effector binding of G12S action are under-investigated. Furthermore, most KRAS mutations remain clinically untreatable, as clinically approved KRAS inhibitors (KRASi) are currently limited to specifically targeting G12C. While experimental non-G12C inhibitors are being developed, resistance mechanisms to non-G12C mutations—including G12D/R/S/V—remain relatively understudied.

We set out to characterize the binding efficiency of KRAS to RAF1 and the PI3K subunit p110α, and to understand how isoforms differ in inhibitor resistance strategies. Our findings suggest that significant variances in KRAS mutation-specific effector binding preference exist and are cell line dependent. We performed proximity ligation based immunofluorescence assays (PLA) on an isogenic panel of human colorectal SW48 KRAS cells with G12C/D/R/S/V or wildtype. SW48 cells with G12S significantly prefer the KRAS-RAF1 mode of binding over otherwise isogenic WT cells, and G12V homologs prefer PI3K. Our findings suggest that in this model, G12R cells have no specific preference of one binding mode over the other. We hypothesize that G12 chemistry drives effector binding preference and that G12X inhibitor resistant cell cultures will demonstrate variant mechanisms of resistance in line with their preferred binding partner. Ongoing studies will further characterize understudied RAS isoform biology and evaluate the links between isoform chemistry and mechanisms of inhibitor resistance. These studies will expand our mechanistic knowledge of the interplay between G12X chemistry and adaptive resistance in human cancer.

#1670 Mechanistic insight into mTOR signaling identifies RNA splicing machinery as a potential therapeutic target for cancer.

G. Rondeau, M. Opichka, K. White, J. M. Yeakley, D. J. Eastburn, **B. Seligmann**;
BioSpyder, Carlsbad, CA

Aberrant signal transduction regulating cell growth and proliferation is a hallmark of many cancers. Activation of mTOR signaling is common and is an attractive therapeutic target with mechanistically different mTOR inhibitors in clinical use. One consequence of exposure to the mTOR inhibitor rapamycin is an alteration of gene expression through a global increase in alternative exon inclusion (Cheng et al. 2022, doi.org/10.3390/ijms232012416). To examine the mechanisms underlying this effect, we utilized the TempO-Seq targeted sequencing platform to profile both the whole transcriptome and a selection of alternatively spliced RNA targets in the rapamycin sensitive and resistant breast cancer cell lines MCF-7 and MDA MB 231 following exposure to 13 mTOR inhibitors, some closely related and some from distinct chemical classes. Recent publications have demonstrated that high quality dose response data can be obtained using this sequencing platform (Harrill et al. 2021, doi: 10.1093/toxsci/kfab009; Ramaiahgari et al. 2019, doi: 10.1093/toxsci/kfz065) and TempO-Seq has been widely adopted in toxicology for deriving compound-specific expression signatures to identify mechanisms of action and long-term toxicity. Treated cells were also profiled using TempO-LINC, a novel high-throughput single-cell assay based on the same platform. We observed that certain mTOR inhibitors induced both common and cell-specific differential expression as well as widespread alternative exon inclusion, as expected. Intriguingly, transcripts with the most significant changes in splicing upon treatment were those encoding members of the SR family of splicing factors, often overexpressed or amplified in breast cancers (Park, et al. 2019, doi: 10.1016/j.celrep.2019.10.110). This is significant because SR protein expression is autoregulated by alternative inclusion of an exon containing a premature stop codon in a feedback loop leading to nonsense-mediated decay (NMD) and lowered protein levels. Indeed, NMD is known to be inhibited by rapamycin (Martinez-Nunez, et al. 2017, doi: 10.1093/nar/gkw1109), which would lead to the observed accumulation of these transcripts. Thus, monitoring a targeted selection of alternative splicing events and regulators revealed mTOR regulation of mRNA isoform abundance consistent with regulation of the NMD RNA turnover process and with overexpression of SR proteins in breast cancers. Importantly, targeted bulk and single-cell TempO-Seq assays enable efficient sequencing and simplified data analysis without the expense and bioinformatic burden of RNAseq, making them particularly well-suited for drug discovery. These results support the use of this approach for further characterization of cell-specific effects of mTOR inhibitors and their mechanisms of action.

#1671 Exploring the mechanism of PP2A regulated cell death via macropinocytosis in pancreatic cancer.

I. Doraivel, G. Baral, C. M. Pfeffer, B. L. Allen-Petersen;
Purdue University, West Lafayette, IN

Pancreatic Ductal Adenocarcinoma (PDAC) is the 4th leading cause of cancer-related death in the United States. KRAS is an oncogene mutated in 90% of PDAC patients. Oncogenic KRAS leads to aberrant cell proliferation and survival. KRAS is considered hard to target because resistance mechanisms to KRAS inhibitors are common highlighting the need to understand alternative strategies. PDAC tumor microenvironment evolves with cancer cell progression leading to vascular remodeling and blood vessel collapse. This makes the tumors nutrient deplete. To circumvent this, cells employ KRAS-dependent macropinocytosis- a nutrient scavenging pathway. Macropinocytosis is the process by which cells take up extracellular material by membrane ruffling to form vesicles which then fuse with lysosomes to release nutrients. Targeting KRAS-driven macropinocytosis can be crucial to limiting nutrients to the cell to prevent tumor growth. Protein Phosphatase 2A (PP2A), a heterotrimeric Serine/Threonine phosphatase, is a downstream regulator of KRAS. Its activity is repressed by mutated KRAS. We have seen that the activation of PP2A with small molecular activator, DT061, prevents macropinosomes from fusing with lysosomes which leads to cell death. But how DT061 regulated PP2A activity affects the macropinocytosis pathway is still unknown. The purpose of this study is to understand the mechanism of cell death brough upon by the activation of PP2A with DT061. Membrane ruffling is critical for the initiation of macropinocytosis. Rac is a GTPase usually involved with membrane ruffling. To show that Rac is needed for DT061 mediated macropinocytosis, we used EHT 1864, a Rac family inhibitor. Cells were treated with EHT 1864 before being treated with DT061 and stained with crystal violet. The inhibition of Rac prevented DT061 driven cell death, indicating that Rac is crucial to DT061 driven cell death. High molecular weight TMR-Dextran can only be taken up by the cells through macropinocytosis. Cells were treated with TMR-Dextran and EHT 1864. Cells with Rac inhibition showed lower uptake of TMR-Dextran than cells that were treated with DT061. Together these findings indicate to us that Rac plays a crucial role in the initiation of macropinocytosis and the regulation of cell death caused by the activation of PP2A. Understanding the pathway of DT061 mediated cell death can be vital to developing this concept as a therapeutic method of treatment for PDAC patients who currently have the lowest 5-year survival rate (12%) of all cancers.

#1672 PKC-ι and 14-3-3 are crucial regulators of c-Raf and the Erk pathway in human medulloblastoma.

L. Lajmi, W. S. Ratnayake, J. Palathinkal, S. Breedy, A. Todman, M. Acevedo-Duncan;
University of South Florida, Tampa, FL

Medulloblastoma is the second most common childhood cancer, behind leukemia, and the most common pediatric brain tumor, comprising 20% of all childhood brain cancers. Current treatment options are limited to radiation therapy, surgical resection, and chemotherapy, which are extremely invasive. This underscores the need for more targeted and effective therapeutic treatments to improve patient outcomes. The following study will focus on exploring the PKC-ι specific inhibitor 5-amino-1-((1R,2S,3S,4R)-2,3-dihydroxy-4-methylcyclopentyl)-1H-imidazole-4-carboxamide (ICA-1S) and its effects on medulloblastoma cell lines Daoy and ONS-76. Our *in-vitro* treatments showed that PKC-ι functions an oncogenic protein that is necessary for Daoy and ONS-76 cell proliferation and that ICA-1S was found to be cytostatic to both Daoy and ONS-76 cells. The inhibition of PKC-ι in both cell lines resulted in a decreased phosphorylation of PKC-ι as well as downregulation of 14-3-3 and crucial components of the c-Raf/Erk pathway including total and phosphorylated levels of c-Raf, Mek1/2, and Erk1/2. This comes as a result of ICA-1S blocking the association of PKC-ι with 14-3-3 while PKC-ι and c-Raf were not found to directly associate with each other, indicating indirect modulation of c-Raf by PKC-ι. Additionally, PKC-ι inhibition decreased its association with Stat3. Expression levels of Stat1, Stat3, c-Fos, and c-Myc transcription factors were significantly downregulated, which is likely the result of reduced transcriptional activation due to upstream inhibition of PKC-ι and Erk signaling. Treatment with ICA-1S was also shown to substantially decrease cellular invasion of Daoy and ONS-76 cells and induce apoptosis. Taken together, these data suggest that PKC-ι likely plays a critical role in the regulation of the c-Raf/Erk pathway, which controls the proliferation and invasion of human medulloblastoma.

#1673 KRAS dependency, a gene editing approach.

C. Marcireau[1], F. Lacroix[1], D. Hoffmann[2], M. Cindhuchao[2], L. Calvet[1], Y. Ruffin[1], L. Debussche[1];
[1]Sanofi, Vitry-Sur-Seine, France, [2]Sanofi, Cambridge, MA

The RAS family genes encode small GTP-binding cytoplasmic proteins that are important signaling molecules. They regulate cell growth, survival and differentiation by coupling receptor activation to downstream effector pathways. Activating mutations of oncogenic RAS pathway genes are frequently detected in human cancers. The role of KRAS in tumor formation is not questionable. It's implication in tumor maintenance is less well validated. The KRAS dependency is a key question to answer before to develop KRAS inhibitor. Targeted genome editing using CRISPR/Cas9 is a relatively new, revolutionary technology allowing for efficient and directed alterations of the genome. CRISPR is a genome-editing platform that makes use of the bacterially-derived endonuclease Cas9 to introduce DNA double-strand breaks at precise locations in the genome using complementary guide RNAs. These double strand breaks can be repaired by homologous recombination DNA repair mechanisms thank to a donor DNA template. By this way mutations can be introduced at desired loci, DNA fragment can be deleted or introduce at the desired location. We aimed at investigating the KRAS dependence and we applied the CRISPR-Cas9 technology to engineer isogenic cancer cells harboring a "conditional KRAS gene knockout" by exchanging the KRAS endogenous promoter. This promoter replacement approach can be used also to validate new targets.

#1674 Inhibition of oncogenic nras signaling in acute myeloid leukemia cell lines through directed transcriptome alterations.

Michael Roberts, Sophia Kovatsis, Amelia Harper, Megan Cravinho, Kishan Mangru, Sher Bahadur, Keagan Hesse, Katy Meta, Cuong Nguyen

Dickinson College, Carlisle, PA

Oncogenic mutations in genes involved in proliferative signaling are hallmarks of malignant transformation. The Ras family of signal transducing proteins are involved in the activation of several proliferative pathways and therefore are found to be oncogenically mutated in a variety of cancer types. The NRAS-directed pathways resulting in Erk1/2 activation are dysregulated in a significant percentage of acute myeloid leukemia (AML), metastatic melanoma, Hodgkin lymphoma, and thyroid cancers. The consequence of oncogenic NRAS signaling is the establishment of a transcriptome commanding constitutive proliferation and survival. It has long been known that phorbol ester treatment of AML cell lines, resulting in activation of protein kinase C (PKC), causes phenotypic changes that include cell cycle arrest, myeloid differentiation, and apoptosis. The paradox is that numerous studies identify PKC as an activator of RAS/ERK signaling. Here we show that phorbol ester treatment of NRAS-driven AML cell lines results in the transcriptional upregulation of genes encoding negative regulators of RAS signaling including *DUSP1,2,4,5,6, SPRY2, SPRED1, RASA1, PEA15, RPS6KA1,* and *RASSF5.* Additionally, phorbol ester treatment eventually results to ERK1/2 inactivation through dephosphorylation. Several of these negative regulators, when overexpressed in AML cell lines, dampen proliferation, and induce senescence. We propose that the induction of RAS negative regulators alters the AML transcriptome to a non-proliferative state in part through the transcriptional regulation of genes such as *CDKN1A, CDKN2B, ZFP36L1,* and *MYC.* As gene therapy strategies develop, designed to provide negative regulators of proliferative signaling pathways that are repressed in the malignant cell, we imagine the RAS/ERK pathway as a target for transcriptome reprogramming.

#1675 Investigating the role of SRC-family kinases in MPNST tumorigenesis.

E. Zereg[1], L. Voisin[1], K. Grenier[2], M. Courcelles[1], S. Jung[2], P. Thibault[1], S. Meloche[1];
[1]Institute for Research in Immunology and Cancer (IRIC), Montreal, QC, Canada, [2]Department of Pathology, McGill University Health Centre, Montreal, QC, Canada

Purpose: Malignant peripheral nerve sheath tumor (MPNST), an aggressive soft-tissue sarcoma, is the leading cause of mortality in patients with neurofibromatosis type 1. Over the past two decades, significant advancement has been made in understanding the pathogenesis of MPNST. Still, this progress has not improved overall survival of patients. Therefore, ongoing efforts to identify alterations contributing to the transformation, progression, and metastasis of MPNST are essential for pinpointing targetable oncogenic signaling pathways for this cancer. Previous studies have revealed an increase in YAP/TAZ activity through both LATS1/2-dependent and LATS1/2-independent mechanisms, suggesting that YAP/TAZ hyperactivity may act as a convergence point for MPNST pathogenesis. YES and SRC, two members of the SRC-family kinases (SFKs), were shown to phosphorylate LATS1/2 and YAP/TAZ, and stimulate the transcriptional activity of YAP/TAZ by promoting their nuclear accumulation in hepatocellular carcinoma and colorectal cancer cells. Thus, we have investigated whether YES and SRC are involved in the pathogenesis of MPNSTs.
Experimental Design: To assess whether the SFK-YAP/TAZ signaling axis is implicated in the development of MPNST, we have used genetic and pharmacological approaches to investigate the roles of YES and SRC in the proliferation of a subset of human MPNST cell lines, and in the growth of xenografted MPNST tumors in ectopic and orthotopic mouse models. We also performed a phosphoproteome and a transcriptome analysis of YES and SRC-depleted MPNST cells to assess their oncogenic signaling network. Lastly, we evaluated the clinical significance of phospho-SFK and YAP in human MPNST TMAs.
Results: Our findings reveal that YES and SRC activity play an essential and redundant role in sustaining the proliferation of human MPNST cell lines. Further, the simultaneous depletion of both kinases impedes tumor growth in xenograft MPNST mouse models. Transcriptomic analyses identified YAP and TAZ as potential effectors of SFKs, as well as other family of transcription factors. Finally, TMA data suggested a correlation between the expressions of YAP, YAP/TAZ, and phospho-SFK and the progression of MPNST.

#1676 A continuous kinetic assay to quantitate specific protein kinase activity in unfractionated cell lysates.

V. Nemmara, S. Cornell-Kennon, Z. Lu, G. Pikul, Z. Belisle, M. Hakar, J. Chin, E. Schaefer, E. May;
Assayquant Technologies, Inc., Marlborough, MA

Protein kinases form a network of signaling pathways and are modified by multiple post-translational modifications, including phosphorylation, which regulate the kinase enzymatic activity, protein complexes formation, and its cellular location. Given this rich target complexity, >30% of all drug development is focused on kinases. However, these target only 15% of the human kinome and are primarily just one type (ATP-competitive) that can readily result in off-target inhibition and the development of resistance during cancer treatment. Most kinase inhibitor development is carried out *in vitro* assays with an epitope-tagged recombinant kinase. As a result, efficacy in patients can be limited due to poor inhibitor performance under physiological conditions (e.g., mM ATP and kinases being complexed with other proteins). In contrast, *in vitro* assays using unfractionated cell lysates provide a close approximation of the native kinase environment, including the complexity of interactions with other cellular components. Being able to selectively quantify the enzymatic activity of all protein kinases in crude cell or tissue homogenates would enable an improved understanding of kinase signaling biology, drug development, and personalized medicine. However, despite the large amount of literature on kinase assays, only a fraction is compatible with unfractionated lysates since most peptide substrates are not selective for a given kinase. To that end, we utilized a continuous assay format coupled with high-throughput Sox-sensor-peptide library synthesis using physiological sequences to identify selective sensor peptide substrates for multiple high-profile kinases implicated in cancer. As an example, we identified a highly selective sensor peptide for ERK1 and 2 mitogen-activated protein kinases (MAPKs) involved in pro-growth/oncogenic signaling. We demonstrated selectivity initially with the recombinant enzymes for ERK1/2 and a panel of other related MAPKs or CMGC kinases. Next, we extended the selectivity screen to 392 kinases using a large panel kinome profiling service. The screen also demonstrated high selectivity for ERK1/2 isoforms. We then tested our best sensor peptide substrate for ERK1/2 using unfractionated lysates from the HEK293T cell line with ERK2 overexpression and demonstrated high activity that could be increased 50-fold by the addition of recombinant MEK1 or 2, the upstream kinase that activates ERK1 and 2, and completely blocked with the addition of an ERK2-selective inhibitor. These results demonstrate a method to systematically generate a selective sensor peptide for ERK1/2 to continuously monitor this kinase activity in crude cell or tissue lysates. This poster will fully describe the methods and results pertaining to ERK-selective sensor peptide development and validation, and the ability to extend to other kinases of interest.

#1677 The emerging role of the Plasminogen-Apple-Nematode (PAN) domain in cancer therapy.

K. De, D. Pal, W. Muchero;
Oak Ridge National Laboratory, Oak Ridge, TN

The Plasminogen-Apple-Nematode (PAN) domain, with a core of four to six cysteine residues, is found in more than 28,000 proteins across 959 genera. However, its role in protein function still needs to be elucidated. Numerous proteins initially characterized the PAN domain, including a well-known master regulator for cancer cell proliferation, HGF (Hepatocyte growth factor). Abnormal regulation of HGF-mediated signaling results in multiple deadly cancers. The binding of HGF to its cell surface receptor, c-MET, triggers signaling pathways, which leads to cancer. Here, we show that mutating four core cysteine residues in the HGF PAN domain reduces c-MET interaction, subsequent c-MET autophosphorylation, and phosphorylation of its downstream targets, perinuclear localization, cellular internalization of HGF and its receptor, c-MET, and c-MET ubiquitination. Furthermore, transcriptional activation of HGF/c-MET signaling-related genes involved in cancer progression, invasion, metastasis, and cell survival was impaired. Thus, targeting the PAN domain of HGF may represent a mechanism for selectively regulating the binding and activation of the c-MET pathway. Additionally, we found this domain in the tumor suppressor gene, MST1 (macrophage stimulating 1), and mutating the domain altered the protein function through protein stability and ubiquitination. In another study, we show that cysteine residues in the vestigial plasminogen-apple-nematode (PAN) domain of NRP1 are necessary for SARS-CoV-2 spike protein internalization. Mutating novel cysteine residues in the PAN altered NRP1 stability and downstream activation of the extracellular signal-regulated kinase (ERK) signaling pathway, impairing its interaction with the spike protein. These results show the diverse critical role of the PAN domain beyond cancer therapy.

#1678 Docetaxel induces Rac1 and Cdc42 Rho GTPase activation in prostate cancer cells.

A. P. Lopez Gonzalez[1], J. Colon Gonzalez[1], M. C. Santa Maria Fuentes[1], S. Dharmawardhane[1], C. J. Diaz Osterman[2];
[1]University of Puerto Rico School of Medicine, San Juan, PR, [2]University of Puerto Rico Comprehensive Cancer Center, San Juan, PR

Prostate cancer (PCa) is a major health burden that affects the quality of life of men worldwide. In the United States, PCa is the second leading cause of mortality among cancers that affect men. Treatment of advanced PCa aims to suppress androgen signaling and proliferation in cancer cells using anti-androgens and chemotherapy. However, the development of drug resistance is a major limitation to curing advanced prostate cancer and strategies to block mechanisms of therapy resistance would enhance treatment efficacy and potentially improve patient prognosis. Cdc42 and Rac1, members of the family of Rho GTPases, have been associated with the progression of different types of hormone-associated cancer, such as breast, ovary, and prostate, among others. The current study was designed to evaluate the role of Cdc42 and Rac1 in chemoresistant prostate cancer cells, including under castration-resistant and androgen-independent conditions. We did not observe significant differences in active (Rac-GTP) or total Rac1 levels in chemoresistant compared to parental PC3 or DU145 cells; similar findings were observed for Ccd42. Treatment of drug-naïve cells with a sublethal dose of docetaxel (10uM) induced gradual increases in Rac1-GTP up to 30 minutes in 22rv1, 60 minutes in LNCaP and DU145, and 24 hours in PC3 cells. Cdc42-GTP levels also increased with subacute docetaxel treatment up to 24 hours in 22rv1 and DU145. Chemoresistant 22rv1, PC3, and DU145 exhibited similar sensitivity to Rac1 and Ccd42 inhibitors including MB1-167, MBQ-168, EHop-097, with an IC50 of about 1uM for each compound and line. Ongoing studies are evaluating the role of these Rho-GTPases in 3-dimensional growth and survival.

#1679 Understanding the mechanism of Daple-PDGFRB gene fusion in leukemia.

A. C. Ibarra, V. Ly, J. Ear;
California State Polytechnic University of Pomona, Pomona, CA

Gene fusion between the scaffolding protein Daple and cell-surface receptor PDGFRB have been identified in several patients with leukemia. Patients with Daple-PDGFRB gene fusion are responsive to tyrosine kinase inhibitors, suggesting that the kinase domain on the receptor is active. How the Daple-PDGFRB gene fusion is activated and affects leukemia cells is poorly understood. It is hypothesized that the PDGFRB kinase domains found in gene fusion remain constitutively active, leading to hyperactivation of cell-signaling downstream of receptor tyrosine kinases (RTKs). To test this, identified Daple-PDGFRB mutants found in patients were ectopically expressed in cells and kinase activation were determined using a phospho-specific antibody. We demonstrated that indeed, the kinase domain on the gene fusion were active, and partake in rampant cell signaling. Because drug resistance is common in cancers such as leukemia, the implications from this work may uncover additional methods of therapeutic interventions for patients harboring these types of mutations.

#1680 Roles of EphA2 receptor signaling in prostate cancer development and progression.

R. Lingerak[1], A. Petty[2], H. Guo[1], H. Lin[1], X. Shi[1], S. Kim[1], B. Wang[1];
[1]Case Western Reserve University, Cleveland, OH, [2]The Cleveland Clinic, Cleveland, OH

Aggressive forms of prostate cancer (PCa), while initially responsive to androgen deprivation therapy (ADT), inevitably become resistant to therapy and are considered castration resistant PCa (CRPC). A major goal of PCa research has been to broadly identify molecular and cellular mechanisms that aid this progression to identify potential therapeutic targets. Using a combination of human data and unique animal models, we found that the receptor tyrosine kinase (RTK) EphA2 is overexpressed specifically in castration resistant and advancing prostate cancers. Furthermore we show that in metastatic PCa the receptor undergoes ligand-independent oncogenic signaling mediated by phosphorylation of EphA2 at S897. Together our data indicate a potential mechanism in PCa progression in which EphA2 becomes overexpressed and aids acquisition of castration resistance via acting as a driver of cell migration, invasion, and proliferation.

#1681 Characterizing signaling and localization of Daple-FLT3 gene fusion in leukemia cells.

M. Acquazzino, J. Ear;
California State Polytechnic University of Pomona, Pomona, CA

Receptor tyrosine kinases (RTKs) are cell surface receptors that regulate cell survival, cell proliferation, and cell migration upon ligand binding. Genetic mutations leading to hyperactivation of RTKs are often seen in cancer and allow signaling pathways to be constitutively active. In some hematological malignanices, the coiled-coil domain (CCD) of Daple, a cell signaling scaffold protein, has been found in gene fusions with the RTKs FLT3 and PDGFRB, and to the intracellular kinase JAK2. It is hypothesized that this gene fusion product causes the tyrosine kinase domain of FLT3 to become activated and mislocalizes in the cell, leading to rampant cell signaling of either the MAPK, AKT, and STAT5 signal transduction cascades. Using fluorescently tagged Daple-FLT3, it was shown that the gene fusion product is subcellularly localizes to the peri-centrosome space across all leukemia cell lines tested. Ectopic expression demonstrated activation of the kinase domain and subsequent increases in phosphorylation of STAT5α and AKT, but no significant increase in the phosphorylation of MAPK was observed. Further investigation is needed to identify direct substrates of the Daple-FLT3 gene fusion and transcriptional changes. Identifying the direct kinase substrates and insights gained through understanding the gene fusion localization, affects on cell signaling, and changes in gene expression, may unveil novel therapeutic strategies into targeting this protein in cancer.

MOLECULAR/CELLULAR BIOLOGY AND GENETICS: Chromatin Organization and Regulators of Chromatin Biology
Poster Session

#1685 Investigating PAX8 interactions in ovarian cancer.
K. Sereti, A. Russo, R. Raisner, K. Gascoigne;
Genentech, Inc., South San Francisco, CA

Ovarian cancer is the most lethal gynecological cancer and there is a critical unmet need to develop novel therapies. The transcription factor, PAX8, is upregulated in ~80% of renal, ovarian, endometrial and thyroid tumors and its overexpression correlates with higher risk of death and recurrence. PAX8 represents a promising target because of its high specificity and low expected toxicity, but how it promotes tumorigenesis remains elusive. Using proximity labeling followed by mass spectrometry, we identified a list of PAX8 binding partners and have further confirmed these interactions at the genomic level through ChIP-seq and ATAC-seq. Our findings reveal novel PAX8 interactions and a potential therapeutic approach for ovarian cancer treatment.

#1686 Dissecting the 3D enhancer-promoter hubs in prostate tumorigenesis.

H. Cao, Z. Wu, L. Gonzalez-Smith, S. Yang, S. K. Rhie;
Norris Comprehensive Cancer Center, Keck School of Medicine of University of Southern California, Los Angeles, CA

The transcription process is controlled by regulatory elements that are often located in non-coding regions. Among regulatory elements, activities of enhancers that are bound by cell-type specific transcription factors (TFs) are tightly linked to cell identity. Enhancers loop to interact with the promoters of target genes at a distance to drive different cell fates. Evidently, transcriptional dysregulation linked to enhancers that are differentially activated in cancer is an underlying factor in tumorigenesis. To identify enhancers linked to prostate tumorigenesis, we analyzed hundreds of in-house and public H3K27ac ChIP-seq data generated from normal prostate and prostate cancer cell lines and tissues. We identified thousands of prostate cancer-specific enhancers (PSEs) that were activated exclusively in cancer conditions. To further identify the target genes of PSEs, we performed 3C-derived assays, such as Hi-C and Micro-C, and mapped genome-wide interactions. However, they were limited by the resolution to detect enhancer-promoter interactions. The recent development of Region Capture Micro-C (RCMC), a hybridization-based capture Micro-C method, allowed us to deeply map the highly nested interactions between regulatory elements. By utilizing RCMC, we generated high-resolution, focal contact maps that revealed comprehensive enhancer-promoter interactions near PSEs in prostate cancer cells. Interestingly, we found that PSEs loop to other PSEs clustered in the proximal genomic region, in addition to promoters of significantly upregulated genes in cancer compared to normal cells. We termed these regions as multi-connected "3D enhancer-promoter hubs". To mechanistically dissect these hubs, we deleted 5+ PSEs one by one using the CRISPR/Cas9 system and performed multi-omics analyses, including RNA-seq and ChIP-seq. We found that single deletions of a subset of PSEs led to the downregulation of multiple genes looped to the deleted PSE as well as to other PSEs. Moreover, we found that deletion reduced the activity of other connected PSEs. When we further evaluated the chromatin contacts of regulatory elements in the PSE-deleted cells, we observed that many chromatin contacts remained unaffected. Finally, we identified TFs that bind to PSEs, and we are currently in the process of investigating enhancer-promoter hub connectivity by performing knockdown experiments on these TFs. Furthermore, we are using molecular assays to identify PSEs that could exert a phenotypic shift in cancer cell identity to drive prostate tumorigenesis. Overall, our study not only provides mechanistic insights into the spatial regulation of 3D enhancer-promoter hubs but also identifies new non-coding drivers in prostate tumorigenesis.

#1687 Targeted degradation of MECOM in high-risk acute myeloid leukemia reveals a novel repressive function that is amenable to therapeutic small-molecule rewiring.

T. J. Fleming[1], M. Gundry[1], R. Voit[1], M. Antoszewski[1], W. J. Gibson[2], A. Sadagopan[2], V. G. Sankaran[1];
[1]Harvard Medical School, Boston, MA, [2]The Broad Institute, Cambridge, MA

Hematopoiesis relies on an intricate balance between stem-cell self-renewal and terminal maturation of blood cells. Disrupting this balance can lead to the development of deadly blood cancers, like acute myeloid leukemia (AML). Increasing evidence suggests that acquiring hematopoietic stem cell (HSC) gene expression programs in AML confers a particularly poor prognosis and increases risk of relapse with conventional therapy. Acquisition of these features in AML is commonly driven by dysregulation of MECOM, a transcription factor and master regulator of HSC self-renewal. To define the role of MECOM in AMLs, we engineered cell-line models of high-risk AML by endogenously tagging MECOM with an FKBP12^{F36V} degron. These models enable targeted degradation of MECOM which we employed in concert with multi-omic readouts to assess changes in nascent transcription and chromatin accessibility to identify direct transcriptional targets of MECOM. We demonstrate that MECOM degradation results in a rapid increase in chromatin accessibility at MECOM-bound sites and increased expression of cognate genes to establish a pro-differentiation gene program. These findings suggest a previously unappreciated mechanism for MECOM in repressing differentiation-promoting cis-regulatory elements (cisREs) and their cognate target genes in AML. We then employed a pooled CRISPR inhibition (CRISPRi) screen to functionally characterize the role that each cisRE plays in promoting high-risk features in AML. Utilizing CRISPRi to repress MECOM-bound cisREs in concert with dTAG-mediated MECOM degradation, we examined if repression of over 500 individual MECOM-bound cisREs is sufficient to maintain AML progenitors in the absence of MECOM. This functional dissection revealed that the individual repression of three cisREs that regulate *CEBPA, GFI1B, and RUNX1* is sufficient to maintain AML progenitor cells in the absence of MECOM. This result implicates MECOM as a direct repressor of known regulators of myeloid differentiation. Given these findings, we hypothesized that small molecule-based recruitment of a transcriptional coactivator to MECOM could rewire its repressive function to activate myeloid differentiation and subsequent leukemia cell death. To test this approach, we treated a MECOM-FKBP12^{F36V} AML degron model with the bifunctional small molecule NICE-01 (AP1867-PEG2-JQ1) to recruit an epigenetic activator (BRD4) to MECOM to functionally rewire this transcriptional network. NICE-01 treatment induced significant differentiation of AML progenitor cells relative to JQ1 treatment alone. Our work highlights the utility of targeted protein degradation to mechanistically interrogate the function of a key driver of high-risk AMLs and suggests the potential for small molecule-rewiring of stem cell gene regulatory networks to confer therapeutic benefit.

#1688 Nuclear receptor coactivator SRC-1 promotes colorectal cancer immune escape by enhancing PD-L1 transcription and protein stability.

Y. Hong[1], Q. Chen[2], Z. Wang[1], Y. Zhang[1], B. Li[1], X. Kong[1], P. Mo[1], N. Xiao[1], J. Xu[3], Y. Ye[4], C. Yu[1];

[1]Xiamen University, Xiamen, China, [2]Ningbo University, Ningbo, China, [3]Baylor College of Medicine, Houston, TX, [4]Fujian Cancer Hospital, Fuzhou, China

Programmed death-ligand 1 (PD-L1), one of the immunosuppressive molecules, overexpresses in multiple cancers and is critical for their immune escape. We previously showed that the nuclear coactivator SRC-1 promoted colorectal cancer (CRC) progression by enhancing CRC cell viability; however, the role of SRC-1 in CRC immune escape is unclear. Here, we demonstrated that SRC-1 was positively correlated with PD-L1 in human CRC specimens. SRC-1 deficiency significantly inhibited PD-L1 expression in both human and murine CRC cells and retarded murine CRC growth in subcutaneous grafts by enhancing CRC immune escape via increasing tumor infiltration and antitumor activity of effector $CD8^+$ T cells. Genetic ablation of SRC-1 in mice also decreased PD-L1 expression in AOM/DSS-induced murine CRC. These results suggest that tumor-derived SRC-1 promotes CRC immune escape by enhancing PD-L1 expression. Mechanistically, SRC-1 activated JAK-STAT signaling by inhibiting SOCS1 expression and coactivated STAT3 and IRF1 to enhance PD-L1 transcription as well as stabilized PD-L1 protein by inhibiting proteasome-dependent degradation mediated by speckle type POZ protein (SPOP). Pharmacological inhibition of SRC-1 improved the antitumor effect of PD-L1 antibody in both subcutaneous graft and AOM/DSS-induced murine CRC models. Taken together, our findings highlight a crucial role of SRC-1 in facilitating CRC immune escape and targeting SRC-1 in combination with PD-L1 antibody immunotherapy may be an attractive strategy for CRC treatment.

#1689 CRISPR functional genetic screening for immune enhancers of inhibitor receptors in human primary CD8 T cells.

P. Wang, J. R. Giles, H. Huang, J. Shi, E. Wherry;
University of Pennsylvania, Philadelphia, PA

The restrained efficacy of T cell therapies in cancer treatment is associated with T cell exhaustion (T_{EX}), an impaired effector function state that is marked by distinct epigenetic landscape. These unique epigenetic features promoted the progression of T_{EX}, hindered reinvigoration of T_{EX} state and controlled the abnormal expression of inhibitor receptors (IRs), which could serve as target sites in cancer treatment. Thus, deciphering the regulatory elements in primary human T cells will deeply reveal the mechanism controlling T_{EX} and provide novel therapeutic strategies to promote clinical response. However, how enhancers can be effectively applied in anti-cancer treatment is still poorly understood because high throughput identifying the functional enhancers of inhibitor receptors at scale is technically limited in human T cells. Here, we first developed a pooled screening platform that employs a compact CRISPRi system and enabled efficient one-step delivery of pooled screening libraries to primary human T cells. Leveraging this platform, we screened large genomic regions (~300kb) at saturation around key T_{EX} genes, two IRs—*PDCD1*, *HAVCR2* and one transcription factor (TF)—*TBX21* to interrogate functional enhancers in human primary CD8 T cells. We identified two enhancers for *PDCD1*, three enhancers for *HAVCR2* and three enhancers for *TBX21*, all of which are located over 12kb away from each gene's transcription start sites. Then, to parse the essential sequences that fulfill enhancer function, we employed Cas9-based in-situ saturation mutagenesis screening to the identified enhancers of *PDCD1* and *HAVCR2*. We found disrupt essential sequences impaired the entire enhancer function, quantitatively phenocopied the effect of targeting the entire enhancer with CRISPRi. Transcription factor motifs analyses of these sequences revealed potential regulation of ZFX for controlling *PDCD1* expression and STAT for *HAVCR2* expression. Finally, we explored the functional consequences of applying enhancers to anti-cancer treatment. Indeed, targeting the identified enhancers of *PDCD1* and *HAVCR2* in CAR T cells lead to enhanced cancer cell killing efficiency in vitro. Together, our study provides a platform and paradigm to interrogate functional enhancers in human T cells, illuminated the great potential of manipulating enhancers in T cell therapies.

#1690 LSD1 and CoREST2 demethylate STAT3 to promote enteroendocrine cell differentiation in mucinous colorectal cancer.

C. A. Ladaika, A. H. Ghobashi, W. C. Boulton, H. M. O'Hagan;
Indiana Univerisy, Bloomington, IN

Across different cancer types, tumor heterogeneity has been shown to drive tumor progression, metastasis, and therapeutic resistance. Adenocarcinoma to neuroendocrine lineage transition is an emergent mechanism of targeted therapy resistance in several cancer types, including lung and prostate cancer. Therefore, understanding the dynamics and mechanisms driving neuroendocrine cell fates in cancer is critical. Mucinous colorectal cancer accounts for upwards of 20% of colorectal cancer cases and is characterized by tumors with mucous accounting for at least 50% of the tumor volume. The normal colon epithelium consists of several specialized cell types, including hormone secreting enteroendocrine cells (EECs), which are the neuroendocrine cell of the intestine. We have previously shown that EEC progenitors are enriched in mucinous colorectal cancer and promote cancer cell survival via secreted factors. Additionally, we have shown that lysine specific demethylase 1 (LSD1) promotes EEC differentiation in these tumors; however, the mechanism by which LSD1 promotes EEC differentiation has remained unknown. Typically to carry out its enzymatic function, LSD1 must be a part of a transcriptional regulatory complex. One such complex is the CoREST complex, which contains LSD1, HDAC1, and one of three CoREST protein family members. Here we report that LSD1 and CoREST2 promote EEC differentiation by demethylating the transcription factor signal transducer and activator of transcription 3 (STAT3) to promote STAT3 chromatin binding. Additionally, we demonstrate that knocking down CoREST2 decreases tumor growth and lung metastases of mucinous colorectal cancer cells injected orthotopically into the colons of immunocompromised mice. Furthermore, we utilized single cell multi-omics that combines single cell RNA sequencing with single cell ATAC sequencing to show that during EEC differentiation there is an increase in chromatin accessibility at regulatory regions of known EEC-promoting transcription factors. Finally, through our single cell multi-omics analysis we identify a new rare cell type with neuron-like but not secretory characteristics. Mucinous colorectal cancer is an aggressive and chemotherapeutically intractable form of CRC that is enriched for EEC progenitors. Our data demonstrates that LSD1 and STAT3 promote EEC differentiation, suggesting that inhibiting LSD1 and or STAT3 may have benefits for patients with mucinous colorectal cancer.

#1691 p300 catalytic inhibition selectively targets IRF4 oncogenic activity in multiple myeloma.

M. R. McKeown[1], G. Giorgetti[2], W. F. Lenoir[1], M. J. Kobylarz[1], T. D. Hopkins[1], W. L. Glore[1], M. G. Shum[1], Y. Calderon[1], K. R. Mori[1], H. Gao[1], L. A. Carvajal[1], N. D. Obholzer[1], B. W. Trotter[1], C. D. Dinsmore[1], N. C. Munshi[2], P. B. Rahl[1], M. Fulciniti[2], **C. Y. Lin**[1];
[1]Kronos Bio, Inc., Cambridge, MA, [2]Dana-Farber Cancer Institute, Boston, MA

Multiple myeloma (MM), an incurable plasma cell malignancy, is addicted to oncogenic transcription factor (TF) IRF4 signaling. Lineage TFs like IRF4 are difficult to drug but represent high value oncology targets owing to the depth and context selectivity of their genetic dependency. Using a transcription regulatory network (TRN) based approach to integrate a high dimensional multi-platform dataset, we defined the key regulatory activity of IRF4 and its druggable co-factors. This unbiased analysis identified p300 lysine acetyl transferase (KAT) function as the nearest selective neighbor for therapeutic intervention, with more potent and selective effects than historically observed with p300/CBP bromodomain inhibitors.

To further probe this biology, we developed a highly selective inhibitor of the KAT domain of p300 and its close homolog CBP. p300 KAT inhibition led to selective downregulation of IRF4 at the mRNA and protein level as well as reduction in acetylation at highly specific sites co-localized with IRF4, in contrast to more general agents like BET inhibitors. Gene expression reduction was most pronounced at IRF4/p300 co-bound genes, in particular IRF4 itself and MYC. IRF4 and p300 also directly bind to each other and other key MM nodes regulating them at the chromatin, mRNA, and protein levels.

p300 KAT inhibition exhibits strong antiproliferative activity across *in vitro* MM models regardless of cytogenetics or resistance to other therapies. Moreover, this relationship is mediated by the KAT domain and not its acetyl-lysine recognizing bromodomain. Comparative pharmacology studies found that a p300 KAT inhibitor downregulated the IRF4 TRN and induced apoptosis in MM cells more effectively than existing standard of care agents, including IMiDs and glucocorticoid receptor agonists, or p300/CBP bromodomain inhibitors. Combinations of a p300 KAT inhibitor with clinically active molecules such as IMiDs and glucocorticoid agonists showed synergistic impacts on reducing key MM TFs and cell line viability.

Ex vivo treatment of primary patient samples demonstrated broad anti-proliferative activity with loss of IRF4 and induction of apoptosis in relapsed-refractory MM patient samples, independent of prior lines of therapy. Importantly, the induction of MM cell apoptosis occurs in the milieu of CD138 negative bone marrow stromal cells while also sparing them from toxicity, supporting a potential therapeutic index.

Finally, p300 KAT inhibition demonstrated activity in *in vivo* MM models with robust tumor growth inhibition at tolerated doses and exposures correlated to reduced p300-dependent substrate acetylation. IRF4 dependency is a hallmark of MM that has been challenging to target with existing therapies, motivating further development of p300 KAT targeting therapeutics.

#1692 MAPK and NF-kappaB signaling converge on the epigenome to transcriptionally activate genes involved in pancreatic cancer metastasis.

J. E. Aggrey-Fynn[1], M. Manjunath[2], S. A. Johnsen[2];

[1]Mayo Clinic Graduate School of Biomedical Sciences, Robert Bosch Center for Tumor Diseases (RBCT), Rochester, MN, [2]Robert Bosch Center for Tumor Diseases (RBCT), Stuttgart, Germany

Pancreatic ductal adenocarcinoma (PDAC) is a highly aggressive and lethal type of pancreatic neoplasm. Unfortunately, most patients are diagnosed with unresectable or metastatic disease, making current treatments insufficient. As a result, the 5-year survival rate for PDAC is below 10%.Pancreatic neoplasms are primarily initiated by the KRAS mutation, accounting for 95% of cases. However, the progression of PDAC to a highly aggressive and therapy-resistant cancer is accelerated by chronic inflammation. The role of mutant KRAS signaling and NF-κB inflammatory signaling in promoting PDAC progression has been extensively studied. Yet, the transcriptional mechanism of their cooperation remains unclear. Additionally, the interaction between PDAC tumor cells and signals in the tumor microenvironment (TME) is not yet fully understood. Our study demonstrates that the simultaneous activation of KRAS/MAPK and NF-κB by epidermal growth factor (EGF) and TNFα, respectively, increases cell migration as shown through live-cell imaging analysis. An integrated analysis of epigenetic and transcriptomic data (ChIP-seq and RNA-seq) was performed after dual stimulation of both pathways. This revealed a high occupancy of the active mark, H3K27ac at transcription start sites of a subset of genes involved in cell migration and subtype switch. Through gain and loss-of-function studies, FOSL1 and RELA were identified as the key transcription factors. The epigenome mapping of FOSL1 and RELA after the stimulation of both pathways revealed their occupancy at RELA-dominant and FOSL1/RELA co-occupied regions. Inhibitor treatments and loss-of-function studies revealed that RELA binding controls RNA polymerase recruitment for transcription initiation and enhances cell migration. Further analysis of RNA-seq data on PDAC cell lines and cells from patient-derived xenografts highlighted that active inflammatory signaling contributes to a subtype switch from the classical to the more migratory basal subtype. Our study, combined with single-cell RNA-seq analysis of published data, shows that macrophages in the tumor microenvironment supply TNFα that activates NF-κB signaling, leading to changes in cell migration. Our study has provided a comprehensive understanding of the mechanism by which mutant KRAS and inflammatory signaling contribute to the progression of PDAC. These findings could offer a new perspective in the development of mechanism-based therapeutic approaches that can improve the efficacy of chemotherapeutic agents and make tumors more amenable to surgical resection.

#1693 Mitochondrial-associated DNAJA3 variant and its role in NASH-driven hepatocellular carcinoma.

Y. Shiode, C.-W. Chang, X. W. Wang;
National Cancer Institute, Bethesda, MD

Nonalcoholic fatty liver disease (NAFLD) is increasingly recognized as a major risk factor for hepatocellular carcinoma (HCC). Despite the known progression from NAFLD to nonalcoholic steatohepatitis (NASH) and eventually HCC, the genetic underpinnings driving this transition remain underexplored. A comprehensive genomics assessment was conducted, encompassing a genome-wide study of variants linked to body fat distribution in 344,369 individuals. Correlating these, significant variants associated with NASH and HCC were discerned in a cohort of 1,009 participants from the NCI-UMD study. Candidate variants underwent further eQTL analysis. Our investigation unveiled the rs3747579-TT variant emerged as significantly associated with NASH-related HCC, serving as an eQTL for mitochondrial DNAJA3. HCC patients harboring this variant presented with diminished DNAJA3 expression, correlating with an unfavorable prognosis. Exploration into the 3D genome architecture has identified potential chromatin topology sites that may influence the regulation of DNAJA3 by rs3747579. Specifically, enhancer loops exhibit allele-specific interactions with rs3747579 in the regulation of DNAJA3. Notably, the rs3747579-CC variant was found to interact with RBFOX2. Beyond its known RNA splicing functions, RBFOX2 might have implications in the chromatin landscape, influencing chromatin dynamics and gene transcription. RBFOX2 knockdown experiments showcased significantly reduced DNAJA3 expression, and luciferase assays highlighted increased activity for the rs3747579-CC allele versus its TT counterpart. In summary, our findings spotlight the rs3747579-TT variant as a potential oncogenic factor in DNAJA3, elucidating its role in the genesis of NASH and progression to HCC. This understanding could pave the way for novel therapeutic interventions in HCC stemming from NAFLD/NASH.

#1694 Using high-throughput screening to identify DNA response elements that sense cancer dysregulated pathways.

E. Stroebele, Y. Zhang, I. Podar, C. Xia, A. Rojc, D. Wodziak, M. Louie, D. Suhy;
Earli Inc., Redwood City, CA

Earli is developing a highly sensitive, orthogonal approach that is designed to be delivered via IV injection and uses a genetic construct to usurp dysregulated pathways, and actively forces cancer cells to drive the expression of a detectable 'synthetic' biomarker. The key element of our cancer-activated construct that drives specificity and sensitivity of expression is a promoter sequence, synthetically engineered to leverage transcription factors (TFs) activated in cancer pathways. Acting as a molecular sensor for dysregulated TF levels, the DNA construct expresses a measurable biomarker in cancer cells, while remaining transcriptionally silent in normal adjacent tissues and benign lesions. Previously, we described a multiomics factor analysis (MOFA) to interrogate 200 non-small cell lung cancer (NSCLC) and matched normal adjacent tissue samples comprised of RNA-seq based transcriptional profiling, and MS-based proteomics and phospho-proteomics from the Clinical Proteomic Tumor Analysis Consortium (CPTAC) dataset, and generated a list of top TFs dysregulated in NSCLC. In this study, we show the capability to design, engineer, and test cancer specific activity of combinations of response elements using a Massively Parallel Reporter Assay (MPRA) high-throughput pooled screening (HTS) method. More than 2,000 unique sequences of homotypic or heterotypic TF binding sites corresponding to the top 100 TFs were arrayed with diverse spacing and individually barcoded for the high-throughput screens in NSCLC cell lines. To validate our top hits, we individually tested 10 sequences from the top 25% and 8 sequences from the bottom 25%. Nine of the top sequences produced signals 5-10X higher than the background, whereas only one of the eight bottom sequences produced signal higher than the background. We have individually validated 30 different response elements and found that 28 of 30 drove the expected expression, with the majority of response elements (n=20) showing expression 5-10X higher than background. Remarkably, two of the engineered response elements were able to drive expression 20-30X higher in a specific cell line activated by WNT-signaling, suggesting that these response elements can sense specific cancer dysregulated pathways. Our lead response elements are being tested across a broad range of *in vitro* primary tumor lines with diverse genetic backgrounds and transcriptional profiles prior to *in vivo* testing using our imaging platform to distinguish malignant lung nodules. In summary, we have established a robust screening platform to identify response elements that can be activated by cancer dysregulated pathways. We are currently expanding this platform to other cancer models and indications, and leveraging this to explore more complex response elements that use combinations of TFs and natural spacing.

#1695 Genomic clustering tendency of transcription factors reflects phase-separated transcriptional condensates at cancer super-enhancers.

Z. Wang, S. Wang, **C. Zang**;
University of Virginia, Charlottesville, VA

Many transcription factors (TFs) have been shown to bind to super-enhancers, forming transcriptional condensates to activate transcription in various cellular systems including cancer. However, the genomic and epigenomic determinants of phase-separated transcriptional condensate formation remain poorly understood. Questions regarding which TFs tend to associate with transcriptional condensates and what factors influence their association are largely unanswered. Here we systematically analyzed 528 DNA sequence motifs across the human genome and 6,650 TF binding profiles across different cell types to identify the molecular features contributing to the formation of transcriptional condensates. We found that the genomic distributions of sequence motifs for different TFs exhibit distinct clustering tendencies. Notably, TF motifs with a high genomic clustering tendency are significantly associated with super-enhancers. TF binding profiles showing a high genomic clustering tendency are further enriched at cell-type-specific super-enhancers. TFs with a high binding clustering tendency also possess high liquid-liquid phase separation abilities. Compared to non-clustered TF binding, densely clustered TF binding sites are more enriched at cell-type-specific super-enhancers with higher chromatin accessibility, elevated chromatin interaction, and stronger association with cancer outcomes. Our results indicate that the clustered genomic binding patterns and the phase separation properties of TFs collectively contribute to the formation of transcriptional condensates at cancer super-enhancers.

#1696 ACTL6A deficiency drives cell death through KLF4-involved chromatin accessibility changes in colorectal cancer.

H.-J. Yang[1], E.-J. Kim[1], S.-H. Song[1], T.-Y. Kim[2];

[1]Seoul National University, Seoul, Korea, Republic of, [2]Seoul National University Hospital, Seoul, Korea, Republic of

ACTL6A is a subunit of the SWI/SNF and INO80 chromatin remodeling complexes and plays roles in neural development and cancer cell proliferation. Additionally, it is known to be upregulated in various types of cancer and is associated with a decrease in patient survival rates. However, the mechanism of how chromatin remodelers including ACTL6A cause cell death has yet to be defined. Therefore, we would like to investigate how the depletion of ACTL6A promotes cell growth reduction by mediating changes in the epigenetic landscape in colorectal cancer cells. We engineered ACTL6A knockout by CRISPR-Cas9. We performed Assay for transposase-accessible chromatin using sequencing (ATAC-seq), RNA sequencing (RNA-seq), and Chromatin Immunoprecipitation sequencing (ChIP-seq) for SMARCB1 and INO80, as representative members of their respective families, and KLF4. Moreover, HCT116 cells stably transduced with doxycycline-inducible shGFP or shACTL6A were implanted into the flank of nude mice. One week after tumor implantation, mice were randomly allocated to 4 groups (n=13-15 per group) and doxycycline treated group was administered with doxycycline (1mg/ml) and 5% sucrose in the drinking water. Tumor volume was measured with calipers. Upon depletion of ACTL6A, the regions of increased chromatin accessibility were correlated with the upregulated genes. After the loss of ACTL6A, there was a significant increase in KLF4 expression and genomic binding largely increased, coinciding with an increase in newly accessible regions containing KLF4 motifs. Interestingly, there is a strong positive correlation between changes in chromatin accessibility and overall changes in the binding of KLF4, SWI/SNF, and INO80 complexes. We find that changes in chromatin accessibility are co-regulated by KLF4, the SWI/SNF and the INO80 complex, while SWI/SNF and INO80 complex have a low correlation in binding between the SWI/SNF and INO80 complexes at newly accessible regions, indicating no physical interactions between these two chromatin complexes. Overall, we demonstrated that the redistribution of ACTL6A-deficient two chromatin remodeling complexes and KLF4 is associated with changes in chromatin accessibility, which are also linked to upregulated genes that promote the p53 pathway. These findings revealed the role of KLF4 along with the SWI/SNF and INO80 complexes, in regulating the chromatin landscape and gene expression in ACTL6A-depleted colorectal cancer cells.

#1697 Phase separation of BHLHE40 up-regulates SREBF1 and inhibits ferroptosis in pancreatic cancer cells.

Y. Cao, X. Wang, Y. Liu, P. Liu, J. Qin, Y. Zhu, S. Zhai, M. Shi, W. Wang, X. Deng, C. Peng, H. Chen, R. Ren, L. Jiang, B. Shen;
Ruijin Hospital Affiliated to Shanghai Jiao Tong University School of Medicine, Shanghai, China

Pancreatic cancer (PCa) is one of the most lethal malignancies in human cancers. The enhanced infiltration of stromal tissue of PCa tumor microenvironment limits the identification of key tumor-specific transcription factors and epigenomic abnormalities in malignant epithelial cells. Integrated transcriptome and epigenetic multi-omics analysis of paired PCa organoids indicated that the basic helix-loop-helix transcription factor 40 (BHLHE40) was significantly upregulated in tumor samples. Increased chromatin accessibility at promoter region and enhanced mTOR pathway activity contribute to the elevated expression of BHLHE40. Integrated analysis of chromatin immunoprecipitation (ChIP)-seq, RNA-seq and high-through chromosome conformation capture (Hi-C) data together with chromosome conformation capture (3C) assay indicate that BHLHE40 not only regulates the sterol regulatory element-binding factor 1 (SREBF1) transcription as a classic transcription factor, but also links the enhancer and promoter regions of SREBF1 via forming liquid-liquid phase-separated droplets. Then, we find the BHLHE40-SREBF1-stearoyl-CoA desaturase (SCD1) axis protects PCa cells from ferroptosis, leading to the reduced accumulation of lipid peroxidation in cells. Moreover, SREBF1 inhibitor, Fatostatin, significantly suppresses the cell growth of PCa tumors with higher expression of BHLHE40. This study highlights the important roles of BHLHE40 mediated lipid peroxidation in inducing ferroptosis of PCa cells and provides a novel mechanism underlying the SREBF1 overexpression in PCa.

#1699 Defining the impact of aberrant transcription on the chromatin structure.

N. Thomas[1], T. E. Reznicek[2], E. Aiden[3], M. Rowley[2], E. Wagner[4], G. Nir[1];
[1]University of Texas Medical Branch (UTMB), Galveston, TX, [2]University of Nebraska Medical Center, Omaha, NE, [3]Baylor College of Medicine, Houston, TX, [4]University of Rochester Medical Center, Rochester, NY

Genome organization in humans is governed by two major mechanisms: loop extrusion by cohesin and CTCF and the spatial compartmentalization of the chromosomes. These folding mechanisms have been shown to regulate several genomic functions, including gene expression. However, how transcription might regulate the chromatin structure remains a subject of many ongoing investigations. In this study, we use the Integrator protein complex as a tool to understand the impact of aberrant transcription on the 3D structure of the genome. During transcription initiation, RNA Polymerase-II (Pol-II) often pauses proximally to the promoter before further elongating transcripts. The Integrator protein complex regulates this checkpoint by its endonuclease and phosphatase activity. This protein complex is essential in premature transcription termination in hundreds of protein-coding genes. It also facilitates the synthesis of non-coding (ncRNA), such as enhancer RNAs (eRNAs) and long non-coding RNAs (lncRNAs), which have been shown to support loop extrusion domains, and their absence may disrupt these domains. Using HiC sequencing, we found that depleting Integrator proteins can interfere with forming and maintaining loop domains. This study aims to be the first to decipher the relationship between chromosome structure and Integrator protein activity and address our very little knowledge of how misregulation of transcription termination may influence the folding of chromosomes.

#1700 Interplay of pioneer and chromatin remodeling factors: New insights into breast cancer mechanisms.

M. Takaku, M. Cooper, M. Saotome;
University of North Dakota, Grand Forks, ND

Eukaryotic cells utilize chromatin to package their genomic DNA, which can hinder transcription factor binding and gene activation. Pioneer factors, which can activate silent chromatin by binding to nucleosomes in closed (inactive) chromatin regions, thereby increasing chromatin accessibility, are essential in multiple developmental pathways. Their misregulation has been linked to various human diseases, including cancer. Yet, the involvement of pioneer factor mutations in tumorigenesis and tumor progression remains largely unexplored. GATA3 is one of the most frequently mutated genes in breast cancer. We and other groups found that a subset of GATA3 mutations promote tumor growth by redirecting luminal transcriptional network governed by Estrogen Receptor alpha (ER-alpha), FOXA1, and GATA3. Our genomics data also suggested that GATA3 requires multiple co-factors to maintain and establish active enhancers. Through IP-mass spectrometry, we identified several chromatin remodeling factors as potential GATA3 binding partners, with CHD4 being particularly notable. Our genomic data, including ChIP-seq, ATAC-seq, and RNA-seq, suggest that during GATA3-induced mesenchymal-to-epithelial transition (MET), CHD4 plays a critical role in maintaining closed chromatin structure, particularly at enhancer regions. Depletion of CHD4 results in the activation of chromatin and genes that are not essential for successful MET. Furthermore, we observed functional interactions between GATA3 and PARP1 in both luminal and basal breast cancer cells, with notable changes in GATA3 mutant cells. Through these studies, we aim to uncover epigenetic vulnerabilities in GATA3-altered breast cancer cells, ultimately contributing to the development of new breast cancer treatments.

#1701 ABI1 regulates prostate tumor plasticity through chromatin remodeling and transcriptional regulation.

L. Kotula;
SUNY Upstate Medical University, Syracuse, NY

Background: Prostate cancer remains a challenging issue affecting men worldwide. In contrast to localized disease, metastatic prostate cancer tumor is incurable. Progression to metastatic disease is characterized by tumor heterogeneity and plasticity regulated by epigenetic changes of tumor cells. While tumor heterogeneity is often associated with gene mutations, tumor plasticity is ascribed to transcriptional regulation and chromatin activity. The latter is modulated by treatment of prostate cancer leading to treatment resistance. Here, we identified a novel mechanism of epigenetic regulation in prostate cancer by an actin regulatory and signaling protein, Abelson Interactor 1 (ABI1).
Methods: To demonstrate the ABI1-DNA binding, we employed in vitro binding assays, NMR spectroscopy, and ChIP-seq. from cells expressing alternatively spliced isoforms of ABI1 that contain or lack the DNA binding HHR domain. To determine the ABI1 interactions with several transcriptional factors, we used immunoprecipitation and/or proximity ligation assay (PLA). We used ATAC sequencing to determine the chromatin accessibility in the presence or absence of ABI1 gene. RNA-seq established the activity of transcriptional factors and signaling pathways regulated by ABI1.
Results: Using NMR spectroscopy, we established that ABI1 demonstrated DNA binding dependent on the presence of alternatively spliced Exon 4. Exon 4 is located within the homeobox homology region (HHR). The DNA binding activity was confirmed using in vitro binding assays; the assay results confirmed the role of ABI1 HHR. Moreover, cells lacking ABI1 or expressing ABI1 lacking Exon 4 show low accessibility and activity of chromatin. In contrast, cells expressing ABI1 containing Exon 4 show active chromatin. RNA-seq analysis demonstrated that ABI1 regulated transcription in an Exon 4-dependent manner.
Conclusions: We uncovered a role of ABI1 in chromatin stability, that is dependent on the presence of the DNA binding region. Notably, ABI1's contribution to transcriptional activity occurs via a transient yet precisely defined interaction between its intrinsically disordered region and DNA. This regulatory control plays a pivotal role in managing tumor plasticity by establishing connections between the actin cytoskeleton, cellular signaling, and transcriptional regulation. Based on these findings, we propose that ABI1 functions as an epigenetic regulator, maintaining transcriptional homeostasis in prostate cancer.

#1702 Loss of KEAP1 promotes R-loop formation independent of NRF2.

P. Mukhopadhyay, N. Bassani, A. J. R. Bishop;
UT Health San Antonio Greehey Children's Cancer Res. Inst., San Antonio, TX

This study investigates the mechanism of R-loop formation as a consequence of KEAP1 depletion. R-loops, described as three-stranded nucleic acid structures consisting of a DNA:RNA hybrid and a non-template single-stranded DNA, are assemblies often attributed with pathological consequences like genomic instability and replication stress. However, they have significant physiological roles, inter alia, regulation of transcription initiation, splicing and termination. Loss in R-loop resolution factors (like RNaseH nucleases, senataxin) can result in “unscheduled” or “pathological” R-loops, which can compromise genome stability. R-loops are commonly associated with an active transcription bubble, with nascent RNA trailing the RNA polymerase re-annealing to the template DNA strand. Increased transcriptional stress can lead to accumulation of R-loops. In a 2016 eLife study by Stork et al., estrogen induction resulted in concomitantly increased transcription and R-loop formation in the same subset of genes. Similar to estrogen induction, activation of the NRF2/KEAP1 pathway upon oxidative stress causes NRF2 to be released from KEAP1 and enter the nucleus to turn on transcription of its target genes. Kelch-like ECH associated protein 1, encoded by the *KEAP1* gene, is a canonical binding partner of NRF2. Under basal conditions, KEAP1 binds NRF2 and targets it for degradation. Mutations in *KEAP1* and epigenetic modifications have been reported in lung and breast cancer phenotypes. In lieu of chemical manipulation, NRF2 can be activated by knocking down KEAP1 via RNAi. We therefore asked whether transcription activation downstream of the NRF2/KEAP1 pathway can lead to accumulation of R-loops.We have observed the consequences of depleting KEAP1 (for NRF2 activation) with RNAi on global transcription using ethynyl uridine (EU) incorporation with click-iT chemistry and flow cytometry, on R-loop levels using S9.6 antibody immunocytochemistry and on transcriptional profile changes with RNA-seq. We observe that loss of KEAP1 leads to an increased accumulation of R-loops. Surprisingly, this is not accompanied by an expected increase in transcription as measured quantitatively with EU flow cytometry. This phenomenon was found to consistently occur in various cell lines across cancer types (breast, lung). Interestingly, depleting NRF2 cannot mitigate the effects of KEAP1 loss, suggesting that KEAP1 loss-associated R-loop formation is independent of NRF2 activation. Analysis of RNA-seq data shows that TOP2 is downregulated in KEAP1 deficient cells. As TOP2 has been previously known to regulate R-loop formation, we predict that KEAP1 loss can sensitize cells to topoisomerase inhibitors.In conclusion, interaction of KEAP1 with other players in its interactome outside of NRF2 may regulate R-loop formation and therefore R-loop-induced genome instability.

#1703 SMARCA2/4 degraders relieve the differentiation block in AML via changes in chromatin looping and accessibility.

S. Aminov[1], K. Pradhan[1], S. Sahu[1], S. Gordon-Mitchell[1], E. Rabinovich[1], A. Fromowitz[1], J. Chakraborty[1], S. Aluri[1], R. Zhao[1], N. Haque[1], M. Carbajal[1], A. Shastri[1], U. Steidl[1], S. Samajdarr[2], A. Kumar[2], M. Ramachandra[2], R. A. Coleman[1], K. Stengel[1], A. K. Verma[1];

[1]Albert Einstein College of Medicine, Bronx, NY, [2]Aurigene Oncology Limited, Bangalore, India

Acute Myeloid Leukemia (AML) is characterized by the unfettered proliferation and poor differentiation of myeloid cells causing reduced survival. The mammalian BAF complexes (also known as SWI/SNF) are important regulators of *MYC* and the cell cycle. There are three BAF complexes (cBAF, ncBAF and pBAF) that share several subunits. SMARCA2 and 4 are mutually exclusive ATPase subunits within the BAF complexes that use ATP hydrolysis and helicase activity to remodel chromatin via nucleosome sliding and removal. PBRM1 is a SMARCA4 associated factor present in pBAF. The association of SMARCA4 with regulatory elements of transcription factors makes it an intriguing target for AML. To evaluate the role of SMARC2/4 in AML, we analyzed RNA transcripts from highly purified primary AML initiating populations and control samples. Sorted leukemia stem cells (Lin-ve, CD34+, CD38-) overexpressed SMARCA2/4 when compared to healthy cells. A novel and highly selective SMARCA2/4 and PBRM1 PROTAC degrading agent AU-15330 was used to investigate the therapeutic effectiveness of targeting BAF complexes as well as the role of SMARCA2/4 in leukemic pathogenesis. Our data demonstrate that AU-15330 effectively degrades SMARCA2/4 and PBRM1 in human leukemia cell lines with varying mutational profiles; MV4-11 was the most sensitive cell line. When evaluating healthy CD34+ HSPCs as well as patient derived AML cells in colony assays, AU-15330 treatment increased differentiation in patient AML samples with minimal effects on healthy CD34+ cells. A xenograft of patient derived AML cells in irradiated mice was performed to determine the requirement of SMARCA2/4 in leukemia stem cell maintenance. Mice treated with AU-15330 had greater myeloid differentiation, fewer human cells in their bone marrows and reduced leukemia stem cell activity, seen in secondary transplants. To understand the underlying mechanism of how SMARCA2/4 and PBRM1 promote leukemic pathogenesis, we used a multi-omic analysis of transcription and chromatin dynamics in MV4-11 cells: ATAC-seq and RNA-seq identified downregulated genes with decreased accessibility, PRO-seq determined early transcriptional changes and HiChIP showed changes in enhancer promoter loops with SMARC2/4 degradation. Several leukemia related transcription factors as well as inflammatory genes were identified from these analyses as possible targets of the BAF complexes in the context of AML. Finally, to determine the effect of SMARCA2/4 degradation on pBAF association with chromatin, single cell imaging was performed of U2OS cells with HALO-tagged PBRM1 treated with the degrader or DMSO. pBAF in the degrader treated cells improved engagement with target chromatin however, a decrease in the stability of the complex binding to the nucleosome when compared to DMSO treated cells was shown. Taken together, these studies will determine the role of SMARCA2/4 in leukemia disease.

#1704 Interplay of MITF and NCOA3 in orchestrating oncogenic transcriptional network in uveal melanoma.

A. Rusin[1], M. E. R. Echartea[1], S. P. R. Manikonda[1], D. G. Skapura[1], C. M. Davis[2], E. A. Ehli[2], S. L. Grimm[1], C. Coarfa[1], S. Kaochar[1];
[1]Baylor College of Medicine, Houston, TX, [2]Avera Genetics, Sioux Falls, SD

Uveal melanoma (UM) originates from melanocytes residing in the uveal tract of an eye. Despite effective local control, 50% of patients develop metastatic disease responding poorly to chemotherapy, targeted therapy, and immunotherapy. The molecular basis of events leading to initiation of UM is related to mutations in G alpha proteins GNAQ or GNA11, rendering them constitutively active and activating downstream PKC, ERK and AKT pathways sustaining cell proliferation.

In our previous work, we showed that NCOA3 regulates proliferation of UM cells in vitro and the growth of UM xenografts in vivo downstream of GNAQ or GNA11. The critical role of NCOA3 in UM is manifested by transcriptional regulation of proliferation-related genes that are massively suppressed by NCOA3 knockout or knockdown. Here, we interrogated transcription factors that NCOA3 interacts with in UM to execute oncogenic programs and identified Melanocyte inducing transcription factor (MITF) as its critical partner.

Chromatin immunoprecipitation (ChIP) using an NCOA3 recognizing antibody followed by sequencing was performed to determine NCOA3 binding sites in the human genome. The known transcription binding motifs within NCOA3 peaks were discovered using HOMER algorithm. Co-immunoprecipitation was performed to examine direct NCOA3 and MITF interaction. ChIP sequencing for MITF was performed to determine co-localization of NCOA3 and MITF at chromatin. Proliferation of UM cells after inhibition of MITF by either siRNA mediated knockdown or MITF inhibitor ML329 was evaluated using MTT assay. Functional enrichment analysis of transcriptome was used to identify classes of genes regulated by MITF, with specific attention to the subset regulated by MITF partnered with NCOA3.

NCOA3 chromatin peaks are highly enriched in MITF binding motifs, and 77% of the NCOA3 peaks co-localizes with the MITF peaks. NCOA3 co-immunoprecipitates with MITF. Among transcriptional programs regulated by MITF in UM are those related to melanocyte biology, differentiation, and melanin production, but also those related to melanoma growth, especially cell division, DNA replication, myc response, purine and pyrimidine metabolism, and mTOR signaling. Strong suppression of these transcriptional signatures by inhibition of MITF using siRNA-mediated knockdown or pharmacological inhibition correlates with dramatic loss of cell viability. Clinical data indicate that higher expression of MITF-positively regulated genes correlates with lower survival rates of UM patients. Importantly, the transcriptional programs regulated by MITF cooperating with NCOA3 were related to TGF beta signaling, cell adhesion, ECM interaction and actin cytoskeleton.

Importance of MITF as an oncogene is manifested in uveal melanoma cell lines and clinical data. Oncogenic function of MITF is partially dependent on its interaction with a transcription co-activator NCOA3.

#1705 3D growth modulates the competition between STAT3 and STAT5 in breast cancer.

A. E. Temple, S. R. Walker;
University of New Hampshire, Durham, NH

Approximately 13% of women are diagnosed with invasive breast cancer. Signal Transducer and Activator of Transcription 3 (STAT3) is a transcription factor that is often inappropriately activated in breast cancer and is frequently associated with Triple Negative Breast Cancer (TNBC). STAT5 can also be activated and inappropriate activation of STAT5 alone or with STAT3 is generally correlated with a more favorable prognosis, a lower grade tumor, and a better response to therapies compared to inappropriate activation of STAT3 alone. Therefore, knowing the activation status of STAT5 and understanding how STAT5 activation can attenuate STAT3-driven breast cancers could help guide therapeutic choices and patient treatment. STAT3 and STAT5 can regulate a set of overlapping target genes. For example, STAT3 and STAT5 can regulate BCL6 expression, where STAT5 represses expression and STAT3 enhances it. Importantly, STAT5 outcompetes and preferentially binds in the presence of activated STAT3. This suggests that the overlapping target genes could play an important role in understanding how activation of STAT5 can lead to a more favorable breast cancer compared to activation of STAT3 alone. This previous work was conducted in a 2D cell culture model; however, 3D models can better mimic clinical settings and the use of 3D models can help bridge the gap. Therefore, understanding the relationship between STAT3 and STAT5 in 3D is important. SK-BR-3 cells (HER2+ cells with low basal STAT3 activity) and MDA-MB-231 cells (TNBC cells with constitutive STAT3 activity) are being compared between 2D cell culture and 3D media suspension. We have shown using chromatin immunoprecipitation that STAT3 DNA-binding is enhanced in 3D at certain binding sites, whereas STAT5 is not. STAT5 has reduced dominance and preferential binding over STAT3 for BCL6 in 3D compared to 2D. In other cases, STAT3 binding is decreased upon STAT5 activation in 3D but not 2D. To begin to understand these differences, we analyzed phosphorylation of these STATs in 2D and 3D. Phospho-STAT3 levels were similar between 2D and 3D in SK-BR-3 cells when activated with LIF stimulation but were higher in 3D in the MDA-MB-231 cells which contain constitutive STAT3 activity. STAT5 activation by prolactin stimulation did not directly affect STAT3 phosphorylation in 2D or 3D but does affect STAT3 binding in 3D growing cells. However, prolactin induced phospho-STAT5 seems to be reduced in 3D in both cell lines. We are currently analyzing additional binding sites to better define the differences between STAT3 and STAT5 mediated gene regulation in 2D and 3D since STAT phosphorylation does not fully address it. Overall, our data suggests that differences between 2D and 3D breast cancer models will be important for translation to patient tumors and understanding the relationship between STAT3 and STAT5 will help elucidate how STAT5 activation status can be used when treating patients with breast cancer.

#1706 Investigating the interaction between ETS family members and mutant p53.

S. Metcalf, P. Hollenhorst;
Indiana University School of Medicine, Bloomington, IN

Cancer cases are on the rise globally requiring a deeper understanding of the disease and identification of novel therapeutic targets. Mutations in genes often result in tumor formation. TP53 encodes p53, a tumor suppressive transcription factor, and is mutated in nearly 50% of all cancer cases. Once mutated, p53 loses its tumor suppressive function while simultaneously gaining oncogenic function. p53 mutations disrupt direct p53 binding to DNA and promotes p53 binding to regulatory regions of oncogenes via protein-protein interactions with other transcription factors. One of these interacting partners is ETS2, a member of the ETS transcription factor family. ETS binding sites are present in 50% of all mutant p53 occupied regulatory elements. Other ETS family members have also been linked to mutant p53 but these interactions have either been deemed weak (ETS1) or have yet to be identified as direct (ERG). It is my aim to determine the scope of interaction between the ETS family and mutant p53 and to elucidate whether this interaction is required for the observed oncogenic phenotypes of ETS proteins and mutant p53.To determine which ETS proteins interact with mutant p53 purified ETS proteins were used for affinity pull-down of purified mutant p53. The entire ETS family interacted with mutant p53 to some degree, and several ETS proteins had stronger interactions than ETS2. Truncation studies were used to determine interaction domains. One interacting region was the conserved DNA binding domain, which may explain interaction across the entire family. ERG and ETS2, both strong mutant p53 interactors, had two interaction interfaces. I hypothesize that the second interaction interface defines strong interactors. To determine if interacting ETS are responsible for targeting mutant p53 to the genome, chromatin immunoprecipitation sequencing measured mutant p53 binding in the presence or absence of different ETS factors. These data indicate that each of the conditions resulted in different p53 binding patterns and that there is a requirement for ETS in mutant p53 binding. Lastly, I wanted to determine if there was a correlation between p53 mutation and expression of strong mutant p53 interactors in certain cancer types. Analysis of TCGA samples showed that in ovarian cancers with p53 mutations, ETS factors that are strong mutant p53 interactors were upregulated in a mutually exclusive pattern, while weak interactors tended to be downregulated, or unchanged. Similar trends were observed among some other cancer types. My studies have shown that several ETS proteins interact with mutant p53 in vitro, recruit p53 to the genome, and that this interaction pattern correlates with expression in mutant p53 driven cancers. Additionally, studies are ongoing to determine phenotypes related to this interaction. Ultimately, if ETS/mutant p53 interactions are deemed important for oncogenesis, these will be attractive targets for drug development.

#1707 YAP-driven epigenetic reprogramming in head and neck cancer.

A. Officer[1], F. Faraji[1], S. Ramirez[2], A. Goren[3], P. Tamayo[1], J. Gutkind[1];
[1]UCSD Moores Cancer Center, La Jolla, CA, [2]La Jolla Institute for Immunology, La Jolla, CA, [3]University of California San Diego, La Jolla, CA

The ability to measure tumor evolution is difficult due to a lack of model systems able to capture tumor initiation, development, and invasion. We have developed a Dox-inducible spatiotemporally controlled HPV- and YAP-driven model of head and neck squamous cell carcinoma (HNSCC) with a well-defined cancer stem cell population. In order to better understand the epigenetic reprogramming associated with tumorigenesis we have systematically characterized the chromatin accessibility, histone landscape and YAP binding sites in this model.

Cell lines were generated from tongue epithelia of normal and Dox-induced tumor-containing mice. Gene expression was measured using RNA-seq and chromatin accessibility was measured using ATAC-seq. CUT&Tag for H3K27me3, H3K27ac, and YAP was used to measure epigenetic reprogramming and YAP-DNA interactions.

Differential gene expression shows that genes involved in hormone signaling, glutathione-related metabolism, fatty acid metabolism and p53 signaling were highly enriched in the normal tongue suggesting a change in metabolism upon tumorigenesis.Differential ATAC-seq peaks with higher binding levels in the normal tongue showed enrichment for p53 motifs as well as homebox motifs including Otx2, GSC and CRX suggesting p53 signaling is lost upon carcinogenesis and lineage determination is altered. Motifs for TEAD, AP-1, and KLF5 were enriched in the tumor-specific ATAC-seq peaks showing that YAP is involved in chromatin accessibility changes. CUT&Tag for YAP shows clear YAP binding near canonical YAP target genes including Axl, Ccn1, Ccn2 and Birc3. YAP peaks with higher binding in the normal tongue cell line were enriched for RUNX2 and p63 motifs and peaks higher in the tumor contained KLF5 motifs showing YAP is directly involved in the reprogramming of lineage determination. Multi-omics integration shows YAP-driven chromatin remodeling is associated with differential expression of genes involved in keratin production, EGFR and ER signaling.

Direct epigenetic characterization of YAP involvement in tumor initiation is key to understanding the mechanisms of tumorigenesis in head and neck cancer. This work shows that YAP directly binds and affects the expression of genes involved in lineage determination and growth factor signaling to induce cancer progression and generate a cancer stem cell population.

#1708 Transposable element derived enhancers in ovarian cancer.

L. L. Nguyen[1], A. Ivancevic[1], B. G. Bitler[2], E. B. Chuong[1];
[1]University of Colorado, Boulder, Boulder, CO, [2]University of Colorado, Anschutz, Denver, CO

There is global epigenetic dysregulation during transformation from normal to cancerous cells. One of the many consequences of this global epigenetic dysregulation is the reactivation of transposable elements (TEs). TEs compose roughly half of the human genome and are normally repressed through epigenetic mechanisms such as DNA methylation and histone modifications. Endogenous retroviruses (ERVs) are a class of TEs that contain long terminal repeats (LTRs) with putative gene regulatory motifs. LTRs can be co-opted to be pro-tumorigenic by becoming non-canonical promotors for oncogenic genes. While several examples of TE-derived promotors have been reported in cancer, the potential significance of TE-derived enhancers remains largely unexplored. Here, we utilized publicly available multi-omics datasets (bulk and single-cell ATAC-seq, bulk and single-cell RNA-seq, and chromatin profiling) in the context of ovarian cancer to determine if there are tumor specific, TE-derived-enhancers that have gene regulatory function. We used CRISPRi technology to functionally validate a putative TE-derived enhancer and gene regulatory axis. We discovered that on the bulk tissue level, several TE families are enriched at open chromatin sites and sites marked by H3K27Ac (enhancer mark) of ovarian tumors, suggesting the presence of tumor specific, TE-derived enhancers. On the single-cell level, we discovered that ovarian cells have the highest expression of these TE transcripts compared to stromal and immune cells in the tumor microenvironment, suggesting that the increased TE-derived enhancer activity observed on the bulk level are specific to ovarian cells. Lastly, when we silenced a specific LTR18 locus upstream of a gene, *TIPARP*, TIPARP gene expression was also repressed, suggesting that these putative TE-derived enhancers have gene regulatory function. Determining the regulatory role of these TE-derived enhancers will provide novel insights into cancer-related transcriptomes.

#1710 DPF3 over-expression oncogenic effect in renal cancer is through SWI/SNF BAF complex.

L. A. Costa[1], A. G. Souza[1], V. C. Silvestrini[1], T. Myers[2], V. M. Faca[1], S. Chanock[2], L. M. Colli[1];
[1]University of Sao Paulo - FMRP, Ribeirao Preto, Brazil, [2]National Cancer Institute - NIH, Bethesda, MD

Renal Cancer (RCC) is the seventh most common type of cancer in the United States, and most part of these tumors do not respond to radiation and chemotherapy treatments. A Genome Wide Association Study (GWAS) identified 13 regions that are related to the risk of developing RCC, and one of this regions is the 14q24 region, a region that has already been shown to have a Single Nucleotide Polymorphism (SNP) involved in the development of RCC, by which the presence of the risk allele is capable of increase the expression of *DPF3* and this increase is capable of regulated the RCC cell line proliferation. It is very published the oncogenic effect of *DPF3* in RCC, however, the mechanism by which *DPF3* is acting is not very knew. Our objective is to understand the mechanisms by which *DPF3* regulate renal cancer development. For this, we did a co-immunoprecipitation of DPF3 with nuclear extract of RCC cell line that overexpress DPF3 and analyze the interactions between DPF3 and other proteins of SWI/SNF Complex. We did a proteomic analyzes in Targeted Mass Spectrometry (MRM) for see the proteins levels. We could see an increase in expression of other SWI/SNF BAF Complex proteins in RCC cell line that overexpress DPF3, such like SMARCA2, SMARCE1 and ARID1A, suggesting a relation between DPF3 and SWI/SNF BAF Complex and evidencing that DPF3 is acting through BAF Complex. To extend the evaluation of DPF3 we inhibit the expression of the SNP associated with the 14q24 region, rs4903064, in renal cancer cell lines (UOK121, SN12C and 786-O) using the CRISPRi technic and analyze the role of this SNP in *DPF3*, *CEMIP* and *IL23R* expression. Our initial results demonstrate that in the UOK121 and SN12C lineage, the inhibition of the SNP was able to decrease the expression of *DPF3*, and in the SN12C cell line we also see a decrease in *CEMIP* expression. When we analyze the 786-O cell line, we see that the blockade of SNP does not change the expression of *DPF3*, nor of the other genes, indicating that the action of the SNP on *DPF3* occurs only in the presence of the risk allele for RCC. We also use a murine (Renca) RCC cell line that overexpress *DPF3* under regulation of TetOn promoter and we did an *in vivo* experiment in mouse (Balb/c and Balb/c Nude), for analyze the function of *DPF3* in tumor growth, migration and proliferation. When we inject (s.c) in Balb/c Nude we could see an increase in tumor growth, in tumor volume and weight in the group treated with doxycycline diet when compare with de control group, suggesting that *DPF3* is capable of increase RCC growth. We also analyze the *DPF3* function in RCC invasion and migration, and when we inject (intrarenal) in Balb/c we could see a metastatic signal in the lung. The lung of the animals treated with doxycycline diet presents an increase in volume and weight when compare with the control group. In this way, the study of genetic and proteomic behind DPF3 function and RCC development is essential for a biomarker discovery and help in the patient prognosithes and treatment.

#1711 Rearranged active enhancers and promoter-enhancer contacts promote lipid metabolic reprogramming during secondary trastuzumab adaptation of HER2 positive breast cancer.

N. Duan[1], Y. Hua[2], Y. Yin[1];

[1]Jiangsu Province Hospital, Nanjing, China, [2]Nanjing Medical University, Nanjing, China

Background: The development of secondary trastuzumab resistance signifies an evolutionary adaptation within HER2-positive breast cancer during anti-HER2 treatment. Our research reveals a comprehensive metabolic reprogramming, with a particular emphasis on the synthesis of unsaturated fatty acids and the degradation of arachidonic acid, accompanying this adaptation. Non-mutational epigenetic variations, particularly alterations in active enhancers, coupled with the rearrangement of enhancer-promoter contacts, demonstrate robust correlations with lipid metabolic reprogramming. These findings suggest that non-mutational epigenetic variations play a crucial role in driving the adaptation to trastuzumab.

Materials and Methods: In a prior investigation, we successfully generated secondary trastuzumab-resistant SKBR3_HR cells. In our current study, total RNA was extracted from both trastuzumab-resistant SKBR3_HR and trastuzumab-sensitive SKBR3 cells for transcriptome analysis. Additionally, mass spectrometry was employed to analyze cellular metabolism in both resistant and sensitive cell populations. Simultaneously, we utilized the CUT&Tag kit with an anti-H3K27ac antibody to create a sequencing library for active enhancer measurement. Furthermore, the Micro-C kit was applied to generate a sequencing library for genome contact measurement.

Results: In our study, secondary trastuzumab-adaptive SKBR3_HR cells demonstrated a reduction in cellular unsaturated fatty acids, with more than 110 UFAs or UFA-containing lipids showing decreases, while only 36 exhibited increases. This phenomenon may be attributed to the downregulation of SCD, FADS2, and HACD2. Simultaneously, the upregulation of PTGS1 and PTGES may contribute to a higher conversion of arachidonic acid to prostaglandin E2 (PGE2), resulting in immune inhibition. In SKBR3 and SKBR3_HR cells, 10,955 and 10,889 non-promoter H3K27me3 peaks, respectively, were identified as active enhancer regions. Among them, 379 enhancers became silent, and 313 transitioned into an active state during the formation of trastuzumab adaptation. Trastuzumab adaptation led to an increase in intra-chromosomal interactions, particularly short-distance contacts (< 1MB). By employing the activity-by-contact (ABC) algorithm, we observed significant variant contacts between PTGES and SCD promoters and enhancers within 1MB genomic regions in SKBR3_HR cells compared to SKBR3 cells.

Conclusion: The formation of secondary trastuzumab adaptation involves the rearrangement of active enhancers and promoter-enhancer contacts, serving as an effective force to drive lipid
metabolic reprogramming, especially the synthesis of unsaturated fatty acids and PGE2 production, reshaping the cellular fatty acid composition and anti-tumor immunity.

#1712 Identifying a novel alternative promoter usage in HDAC9: Implications for LUAD prognosis and therapy.

A. Bolatkan[1], K. Asada[1], S. Kaneko[2], M. Komatsu[1], R. Hamamoto[1];
[1]RIKEN, Chuo City, Japan, [2]NCC, Chuo City, Japan

Promoters are key elements in gene regulation. It has been estimated that more than half of protein-coding genes in the human genome possess multiple promoters. Aberrant expression and dysregulated activity of alternative promoters have been correlated with numerous diseases, especially cancer. In this study, we utilized RNA-seq data from 608 lung adenocarcinoma (LUAD) patients and systematically analyzed promoter activities using the proActiv algorithm. Of the expressed genes in LUAD, approximately 57% have at least two distinct promoters. In addition, we identified 1852 tumor-specific alternative promoters that showed a significant shift (2-fold changes) in promoter activity without any notable changes in the expression of corresponding 1603 genes between tumor and adjacent non-tumor tissues. Functional enrichment analysis showed that these genes were associated with key cellular functions such as signaling pathways, cell cycle, and cell junctions. Unsupervised clustering of patients based on altered promoters revealed a significant prognostic value. Among them, we observed a major promoter switch in *HDAC9*, which mainly utilizes three promoters: prmt3280, prmt3283, and prmt3287 in our LUAD dataset. Notably, prmt3287 was exclusively active in tumor samples and functioned as the dominant promoter, while prmt3283 served as the main promoter in adjacent non-tumor samples. Intriguingly, even though the overall expression of HDAC9 mRNA lacked prognostic relevance both in our dataset and in the TCGA dataset, higher expression of the alternative promoter prmt3287 (using ≥50% activity level as a cutoff) was associated with adverse outcomes in LUAD patients. We further compared the DNA methylation level around the *HDAC9* domain between paired tumor and non-tumor samples and found that positions with the most significant differences ($p<0.001$) overlapped with the prmt3287 region. Moreover, DNA methylation levels around prmt3287 significantly decreased in prmt3287 high-activity patient groups. Next, we investigated the ChIP-seq levels over the *HDAC9* region, and ChIPseeker successfully annotated the alternative promoters of *HDAC9*. In addition, the alternative promoter prmt3287 exhibited the highest active enhancer signals. Furthermore, we performed PCR to determine the expression of six distinct transcript isoforms from alternative promoters in four different LUAD cell lines, and we observed high expression of isoform 10, which is possibly generated by prmt3287 in all cell lines. The impact of prmt3287 on cell proliferation, cell cycle, and cell migration will be further addressed. Our results indicate that alternative promoter usage can capture insights that might be missed at the overall gene expression level, and alternative promoter usage in *HDAC9* could be a novel biomarker and a promising therapy target.

MOLECULAR/CELLULAR BIOLOGY AND GENETICS: Epigenetic Targets in Oncology
Poster Session

#1716 A proteome-wide association study identifies putative causal proteins for breast cancer.

T. Zhao[1], S. Xu[1], J. Ping[1], G. Jia[1], Y. Dou[2], B. Zhang[2], X. Guo[1], Q. Cai[1], X.-O. Shu[1], W. Zheng[1], J. Long[1];
[1]Vanderbilt University Medical Center, Nashville, TN, [2]Baylor College of Medicine, Houston, TX

Background: Genome-wide association studies (GWAS) have identified over 200 breast cancer risk associated genetic loci, yet the causal genes and biological mechanisms for most loci remain elusive. Proteins, as final gene products, are pivotal in cellular function. In this study, we conducted a proteome-wide association study (PWAS) to identify proteins in breast tissue in relation to breast cancer risk.
Methods: We profiled the proteome in breast tissue samples from 120 cancer-free European-ancestry women from the Susan G. Komen Tissue Bank. Protein expression levels were log2 transferred and then normalized via quantile and inverse-rank transformations. The *elastic net* method was used to build statistical models to predict protein expression levels via genetic variants. The prediction models were then applied to the GWAS summary statistics data of 133,384 breast cancer cases and 113,789 controls to assess the associations of genetically predicted protein expression levels with breast cancer risk overall and its sub-types using the S-PrediXcan method.
Results: A total of 6,388 proteins were detected in the normal breast tissue samples from 120 women with a high detection false discovery rate (FDR). Among the 5,823 proteins detected in more than 80% of participants, prediction models were successfully built for 2,041 proteins with R>0.1 and P<0.05. Among these 2,041 proteins, six proteins were significantly associated with overall breast cancer risk at an FDR P< 0.05. Among these six proteins, the corresponding genes for proteins DCTN3 and DDX6 were located at least 500kb away from the GWAS-identified breast cancer risk variants. Both DCTN3 and DDX6 were associated with a decreased risk of breast cancer with P values of 8.46×10^{-4} and 2.27×10^{-4}, respectively. The corresponding genes for the remaining four proteins, LMNA, LSP1, RPS6KA5, and DNAJA3, were located in previously GWAS-identified breast cancer risk loci. After adjusting for GWAS-identified risk variants, the associations for LMNA and RPS6KA5 were still significant ($P=2.54 \times 10^{-7}$ and 2.79×10^{-5}, respectively), however, the associations for LSP1 and DNAJA3 became weaker with P values of 0.65 and 2.10×10^{-4} respectively.Stratification analyses by breast cancer subtypes identified three proteins, LMNA, LSP1, and NCKAP1L, associated with luminal A, luminal B, and ER-positive subtypes. NCKAP1L was located at least 500kb away from risk loci. After adjusting for GWAS-risk variants, the associations for LMNA were still significant ($P=2.58 \times 10^{-5}$ and 4.08×10^{-6} for luminal A and ER-positive respectively).
Conclusion: We conducted the first breast-tissue-based PWAS and identified seven proteins associated with breast cancer, including six proteins that were not previously implicated. These findings help improve our understanding of the underlying genetic mechanism of breast cancer development.

#1717 RAS and PP2A co-regulated phosphosite on KDM1A dictates its substrate specificity & transcriptional outcome.

M. Sharma[1], A. Aakula[1], J. Kamila[1], R. Natkin[2], T. Bonaldi[3], S. Minucci[3], M. Nykter[2], J. Westermarck[1];
[1]University of Turku, Turku, Finland, [2]Tampere University, Tampere, Finland, [3]Istituto Europeo di Oncologia, IEO, Milan, Italy

RAS-mediated human cell transformation requires simultaneous inhibition of tumor suppressor phosphatase PP2A; however, the target phosphosites co-regulated by RAS and PP2A are poorly characterized. In this study, we describe the phosphoregulation of an epigenetic regulator, KDM1A, by RAS and PP2A. KDM1A is a lysine-specific demethylase that can act as a transcriptional activator or inhibitor, depending on its specific activity toward various histone marks. However, the post-translational modifications regulating the substrate specificity of KDM1A are poorly addressed. We found that KDM1A physically interacts with PP2A through a conserved binding motif, and that mutating the motif residues decreased its interaction with PP2A. Additionally, PP2A activation or RAS inhibition led to increased chromatin recruitment of KDM1A. This enhanced chromatin recruitment of KDM1A was recapitulated upon CRISPR/CAS9-mediated substitution of the PP2A/RAS-targeted serine to alanine. Using histone proteomics, we further identified that the RAS/PP2A-regulated phosphosite determines the substrate specificity of KDM1A. This is evidenced by an increased demethylation of histone H3K9me2/3, a marker of gene activation. The differential gene expression profile of the phosphorylation mutants of KDM1A predominantly showed increased gene expression, further validating our findings. The gene expression profiles of KDM1A phosphomutant RAS mutant cells demonstrate gene level specificity indicating that this newly discovered KDM1A phosphoswitch has an important role in specifying KDM1A function in cancer. Collectively, our results demonstrate that RAS and PP2A activities converge on phosphoregulation of epigenetic machinery in cancer cells. This RAS and PP2A co-regulated phosphosite on KDM1A dictates both its histone mark specificity and transcriptional outcome.

#1718 The lysine demethylase KDM2A regulates tumor cell clustering to potentiate metastasis.

C. Kravitz[1], K. D. Patel[1], W. L. Cai[2], A. Arnal-Estape[1], D. Zhao[1], E. Wingrove[1], L. Stevens[1], T. F. Westbrook[3], Q. Yan[1], D. X. Nguyen[1];
[1]Yale University, New Haven, CT, [2]University of Pittsburgh, Pittsburgh, PA, [3]Baylor College of Medicine, Houston, TX

Approximately 70% of patients diagnosed with non-small cell lung cancer (NSCLC) are not eligible for curative resection, often due to disseminated disease at diagnosis. Thus, the advent of novel therapeutics, especially those efficacious for metastatic disease, is of primary importance. Metastasis correlates with epigenetic alterations that drive tumor plasticity and adaptive heterogeneity in response to the multiple microenvironments metastatic cells see, yet the molecular mechanisms underlying these epigenetic alterations remain poorly understood.

We performed a functional genomic screen and identified the lysine 36 on histone H3 (H3K36) demethylase KDM2A as a mediator of *in vivo* and *in vitro* metastatic competence in multiple models of NSCLC. KDM2A depletion in highly metastatic NSCLC cell lines reduces their capacity to form multi-tumor cell clusters. *In vivo*, KDM2A depletion does not impact lung orthotopic tumor cell growth or the total number of circulating tumor cells (CTCs) but does reduce their ability to colonize distant metastatic sites. This is consistent with the fact that human CTCs found in clusters are more metastatic than CTCs which disseminate as single-cells.

Because the molecular and biological consequences of H3K36 regulation are context dependent, we performed for the first time an integrated transcriptomic-epigenomic analysis of target gene regulation, KDM2A genomic binding, H3K36 methylation, and H3K27 acetylation, in metastatic cell clusters. KDM2A enhances the expression of cell adhesion and anti-oxidant genes, while suppressing inflammatory gene responses, and this regulation preferentially occurs in tumor cell clusters. Transcriptomic analysis of CTCs from patients confirms that KDM2A regulated transcriptional responses correlate with metastatic relapse across multiple cancer types. Moreover, KDM2A may function both as a transcriptional activator and repressor in metastatic clusters. As KDM2A encodes for several domains which can independently regulate E3-ubiqutin ligation, H3K36me2 demethylation, and DNA methylation, we have also performed a structure function analysis of K2MDA in the context of metastatic phenotypes. Thus, the distinct biochemical functions of KDM2A in relation to its regulation of CTC gene transcription and histone modification will also be presented.

In conclusion, we have identified KDM2A as a novel regulator of NSCLC metastatic spread. The ability to inhibit KDM2A with small molecule inhibitors may be translated into effective therapeutic interventions for NSCLC patients with metastasis disease.

#1719 Targeting H3.3 serine 28 phosphorylation as a novel therapeutic strategy for diffuse midline glioma.

Y. Yan;
Mayo Clinic, Rochester, MN

Background: Diffuse midline glioma (DMG) is a highly aggressive pediatric brain cancer with a poor prognosis [1]. Mechanistically, DMG harbors a lysine-to-methionine substitution at position 27 of histone H3.3 (H3.3K27M), which leads to global hypomethylation and a dramatically altered epigenetic landscape [2, 3].
Aim: This study aims to explore the H3.3K27M mutation from a novel perspective by investigating its effects on H3.3 ubiquitination, with the goal of identifying effective, novel therapeutic targets.
Methods: Mass spectrometry was used to identify potential E3 ligases for H3.3, while immunoprecipitation to verify this interaction. Cell viability and survival were determined by MTS and clonogenic survival assays, respectively. Nucleosome fractionation was performed to detect the distribution of wild-type (WT) or K27M mutant H3.3 histones.
Results: Mass spectrometry identified UBR7, an E3 ligase, as exhibiting a stronger binding affinity with WT H3.3 than its K27M mutant counterpart. Further nucleosome fractionation assay revealed that K27M histones are more likely deposited in nucleosomes than WT H3.3. Further analysis demonstrated that a non-phosphorylation mimic mutation (serine to alanine) at amino acid 28 (S28A) restored the binding affinity of K27M mutant H3.3 with UBR7. Importantly, this mutation disrupted H3.3 phosphorylation and significantly diminished cell survival, whereas the constitutively activated phosphorylation mutation (S to glutamine (E)) on S28 (S28E) mimics K27M mutation in promoting cell proliferation and survival.
Conclusion: These findings suggest that S28ph impairs UBR7-mediated K27M ubiquitination and promotes DMG cell growth, suggesting that targeting S28ph is an effective therapeutic strategy. However, the underlying mechanisms by which K27M interplays with S28ph in promoting tumorigenesis require further investigation.

#1720 53BP1 regulates heterochromatin through liquid-liquid phase separation (LLPS).

X. Geng, Y. Zhang;
Case Western Reserve University, Cleveland, OH

As compacted DNA, heterochromatin represses abnormal gene expression by inhibiting DNA transcription and maintains genome integrity by protecting aberrant chromosome segregation. Therefore, abnormalities in heterochromatin function are commonly found in cancer. However, how exactly heterochromatin preserves the genome integrity remains poorly understood due largely to the complex structure of heterochromatin. Recently, increasing evidence suggests that heterochromatin factors, including HP1α, KAP1, and SUV39H1/2, could drive the soluble heterochromatin into phase-separated droplets/condensates to promote gene silencing, which is referred to as liquid-liquid phase separation (LLPS). TP53-binding protein 1 (53BP1) has traditionally been a critical factor in DNA double-strand break (DSB) repair. We recently reported an unexpected finding that under normal growth conditions, 53BP1 regulates heterochromatin function through LLPS, which is independent of its DSB repair function. Our studies reveal a new paradigm in studying 53BP1, heterochromatin, and genome stability. However, an important question remains unanswered: how 53BP1 is recruited to heterochromatin to undergo LLPS and the associated broad biological impact. To address this question, we performed a special crosslinking coupled mass spectrometry to uncover potential factors in the 53BP1 condensates assembled on heterochromatin. We identified many factors associated with DNA methylation and histone modification, which are the two main steps in restoring heterochromatin epigenetic modification. Their interactions with 53BP1 at heterochromatin were confirmed by different approaches. We further focused on one of the key factors, PCNA, and carried out a detailed analysis of the interaction between PCNA and 53BP1 and the role of such interaction in 53BP1 LLPS, DSB repair, and heterochromatin function. These findings reveal the previously uncharacterized function of 53BP1 at heterochromatin during normal DNA replication.

#1721 Epigenetic heterogeneity of osteosarcoma reveals distinct cellular states driven by enhancer regulation.

E. Lopez Fuentes, A. Clugston, A. Lee, L. Sayles, M. Pons, A. Sweet-Cordero;
UCSF - University of California San Francisco, San Francisco, CA

Osteosarcoma (OS) is characterized by structural rearrangements and copy number changes which drive considerable heterogeneity. What is less clear is how these genetic rearrangements alter are in turn regulated at the epigenetic level to drive gene expression. Defining the epigenetic circuitry of osteosarcoma could help to understand the role of chromatin accessibility in determining cell plasticity. Chromatin accessibility can prime gene expression and define a cellular state. As chromatin accessibility is a major determinant of epigenetic transcriptional regulation, understanding the variability of chromatin accessibility could identify clinically-relevant subtypes and biomarkers of therapy response in Osteosarcoma, a disease that has seen few advances in therapy for over 40 years. Using ATAC-seq, we identified two epigenetic subtypes (EC1 and EC2) of OS with distinct chromatin accessibility. These studies were done in a panel of 11 PDX-derived cell lines and 9 established OS cell lines. We also performed ATACseq on the matching PDX for the 11 PDX-derived lines as well as 8 primary tumor samples. Analysis of transcription factor (TF) motifs and footprints of ATAC-seq peaks identified transcription factors distinctly activated in these two subtypes. For example, EC1 is characterized by high level of activity of developmental transcription factors including RUNX2, MEF2C and homeobox TFs. In contrast, EC2 is characterized by high activity of AP1 transcription factors such as FOSL1 and FOSL2. In order to understand the underlying transcriptional circuitry of these cell states, we performed CUT&RUN assay for the complete panel of PDX-derived cell lines. We found that the subtypes are driven by enhancer regulation (H3K27ac). We defined the specific Core Regulatory Circuitry (CRC) per subtype by defining the superenhancers by ROSE. We overlapped ATAC-seq data in the acetylated regions to demarcate TF binding regions dramatically and reduce the search space for TF cis-regulatory sites. In parallel, we used our PDX-derived cell line panel to screen cluster-specific targeted therapies and found differential responses dependent on cellular states defined by chromatin accessibility. For example, cell lines in the EC2 cluster are marked by upregulation of AP1 transcription factors, have evidence of ERK activation and are highly responsive to ERK inhibitors. In contrast cell lines in the EC1 cluster are sensitive to AURKA and AURKB inhibitors. Single-cell RNAseq analysis indicates that these subtypes may coexist within a single tumor. In summary, we discovered two epigenetically distinct cell states that are controlled by a state-specific collection of transcription factors, creating a gene signature that may aid in distinguishing osteosarcoma subclasses and predicting treatment response.

#1722 Subtype classification of small cell lung cancer (SCLC) tissues using the EpiCheck methylation sensitive restriction-based PCR platform.

O. Savin[1], **D. Netanely**[1], S. Heeke[2], C. M. Gay[2], M. R. Estecio[2], S. Danan[1], S. Zaouch[1], A. Shuali[1], M. Ehrich[3], L. A. Byers[2], J. V. Heymach[2], A. Wasserstrom[1], D. Frumkin[1];

[1]Nucleix, Rehovot, Israel, [2]The University of Texas MD Anderson Cancer Center, Houston, TX, [3]Nucleix, San Diego, CA

Small cell lung cancer (SCLC) is an aggressive neuroendocrine malignancy with poor survival rates. Despite molecular and clinical heterogeneity, SCLC is currently treated as a single entity without guidance of predictive biomarkers leading to expectedly poor outcomes. A recent study suggested classifying SCLC into four subtypes (“A”, “N”, “P” and “I”), each with unique molecular features and therapeutic vulnerabilities. While initially this classification was based on gene expression (RNA-seq) data, subsequent data suggest it can be recapitulated using reduced-representation bisulfite sequencing (RRBS) methylation profile. While the classification system accurately predicts responses to therapies, including immunotherapies, in retrospective analysis, both tissue-based RNAseq and RRBS are cumbersome, time-consuming and impractical for prospective treatment assignment in an aggressive malignancy. In this pilot study, we developed a methylation-based PCR assay for classification of SCLC subtypes based on the EpiCheck platform, which combines methylation-sensitive restriction endonuclease (MSRE) digestion with qPCR amplification to detect differential methylation at the DNA level. We developed a 13-marker assay and successfully classified, in a blinded study, 96.55% of FFPE tissue samples originating from SCLC patient of A, N and P subtypes. First, a bioinformatic analysis identified 41 candidate biomarkers that are differentially methylated between pairs of SCLC subtypes (A-N, A-P, and N-P) using RRBS data from 56 RNA-seq classified SCLC tumor samples (34 “A”, 19 “N”, 3 “P”). Development of primers and probes for these markers was followed by a biochemical selection process, identifying 13 markers that displayed optimal performance. A PCR EpiCheck assay, employing these 13 markers, was applied to a blinded set of 29 DNA samples from SCLC FFPE tumor tissues (21 “A”, 6 “N”, 2 “P”). Each sample received two ranks based on methylation levels of 5 A-N and 9 P-AN markers and was classified using determined thresholds for each rank. Finally, when comparing PCR-based and RNA-seq-based classifications, the 13-marker PCR assay classified 28/29 (96.55%) of the samples concordantly, misclassifying one "P" sample as "A".

This pilot demonstrates the potential of a simple PCR EpiCheck-based assay to accurately differentiate between SCLC subtypes. For complete subtype classification, “I” markers need to be added to the panel, and the assay should be further validated using a larger cohort, particularly for the “P” subtype. Early detection and classification are critical for timely personalized therapy, and such an assay, performed on cfDNA samples, could potentially be used to shorten the time between a patient diagnosis and tailored treatment initiation or clinical study inclusion from a month in best case scenarios to a few days.

#1723 Targeting SMARCA1 in rhabdomyosarcoma: Potential therapeutic implications.

A. Aljabri[1], K. Hebron[1], Y. Kriga[2], J. Caravaca[2], A. Althobaiti[3], S. Stauffer[1], A. Kim[1], L. Stoak[1], M. Porter[1], J. Shetty[1], B. Tran[1], M. Geisler[3], J. Davie[3], M. Yohe[1];

[1]National Institutes of Health, Frederick, MD, [2]National Institutes of Health, HHS, Frederick, MD, [3]Southern Illinois University, Carbondale, IL

Background: Rhabdomyosarcoma (RMS) is the most common soft tissue in pediatric sarcoma, and studies demonstrate that RMS arises from skeletal muscle precursor cells. RMS, genetically divided into two subtypes: PAX-FOXO1 fusion positive RMS (FP-RMS), which is driven by chromosomal translocation involving PAX3 or PAX7 genes with FOXO1 and PAX-FOXO1 fusion negative RMS (FN-RMS), which is marked by mutations in RAS isoforms and some other genes. Chromatin was one of the earliest identified targets for cancer therapy. Several chromatin remodeling proteins are associated with cancer progression processes such as proliferation, differentiation, apoptosis, and tumorigenesis. Components of chromatin remodeling complexes have been classified as both oncogenes and tumor suppressors. The ISWI family protein, SMARCA1 has been implicated in tumorigenesis for several cancer types. ISWI complexes regulate cell differentiation and proliferation in other cell systems, but their impact on myogenesis is not well understood.
In this study, we will characterize the function of SMARCA1 in RMS cells and skeletal muscle.
We hypothesize that SMARCA1 acts to modulate chromatin accessibility and drive RMS tumorigenic growth.
Methods: We employed RNA-seq, ATAC-seq, and CUT&RUN to study the impact of SMARCA1 in RMS cells. Furthermore, phenotypic experiments were performed to determine the influence of SMARCA1 on differentiation and proliferation.
Results: SMARCA1 is expressed at a high level in RMS tissues but not in muscle tissues. Our findings show that SMARCA1 is modestly upregulated during differentiation in normal myogenesis. Upon treatment with trametinib, FP-RMS cell lines with SMARCA1 knockout exhibited a dramatic decrease in cell confluency and viability. Intriguingly, the control FP-RMS cell lines demonstrated increased SMARCA1 protein levels in response to trametinib, which could suggest a resistance mechanism to the treatment. Trametinib also affected SMARCA1 mRNA expression in FN-RMS cells. Additionally, it was discovered that the elimination of SMARCA1 not only resulted in a reduction in cell migration but also led to a failure of these cells to develop spheres, unlike the control cells, where the migration gap healed in the usual manner and the spheres were observed. These findings may align with our hypothesis that SMARCA1 regulates chromatin accessibility, potentially impacting adhesion properties and signaling pathways. Analysis of gene clusters in RMS transcriptomic data indicated that SMARCA1 co-expresses with a RAS effector, RALA. SMARCA1 is also clustered with HDAC2. In addition, SMARCA1 interacted with HDAC2 in RMS cells, as determined by co-immunoprecipitation experiments.
Conclusions: Our findings suggest that SMARCA1 may influence RMS tumor growth. This study might contribute to a deeper understanding of SMARCA1's role in RMS and support its credentialing as a novel therapeutic avenue.

#1725 Role of PRMT5 in neuroendocrine prostate cancer development.

H. S. Nam, X. Deng, C.-D. Hu;
Purdue University, West Lafayeette, IN

Background: Neuroendocrine prostate cancer (NEPC) is a lethal subtype of prostate cancer responsible for an estimated 20-30% of castration resistant prostate cancer (CRPC) deaths. While NEPC can arise de novo, the majority of these cases emerge as treatment-induced NEPC (tNEPC). Our data establish PRMT5:MEP50 as a key epigenetic regulator in NEPC and provide a potential predictive biomarker for tNEPC.
Methods: Here we generated an in vitro cell culture model and mouse model to mimic the clinical conditions in androgen signaling inhibitor (ASI) or androgen deprivation treatment (ADT) We developed an *in vitro* cell culture and *in vivo* model to mimic the clinical conditions in enzalutamide-resistant prostate cancer. Regulation and role of protein arginine methyltransferase 5 (PRMT5) and its cofactor methylosome protein 50 (MEP50) were determined by treating cells and mice tumors with doxycycline inducible-shRNAs and catalytic inhibitors followed by analysis of cell viability, neurite growth, and effects on neuroendocrine related gene transcription. Pro-NEPC development effects were analyzed by immunofluorescence, immunohistochemical analysis, and western blot. PRMT5:MEP50-dependent methyltransferase activity was further validated by observing histone deposition levels via western blot and ChIP-qPCR. For clinical correlation, PRMT5 and MEP50 expression levels were comprehensively analyzed in both CRPC and NEPC patient prostate tissue samples.
Results: Our clinical and computational analyses have identified increased expression of PRMT5:MEP50 in NEPC. Overexpression of PRMT5 and MEP50 in prostate cancer cells is sufficient to induce neuroendocrine differentiation (NED) in prostate cancer cells. Gene depletion of PRMT5 and MEP50 prevented the NE phenotype induced by androgen receptor inhibition and resensitized the prostate cancer cells to ASI/ADT. PRMT5 and MEP50 facilitate chromatin modulation through the dimethylation of H4R3, which is highly correlated with the NED phenotype. Moreover, overexpression of PRMT5 and MEP50 in mouse prostate induces NEPC development, and gene downregulation can prevent NED in a xenograft mouse model. Elevated PRMT5 and MEP50 correlated with increased recurrence in prostate cancer patients receiving ADT and their recurrence probability after the treatment.
Conclusion: Our data establish PRMT5:MEP50 as a key epigenetic regulator in NEPC and provide a potential predictive biomarker for tNEPC.

#1726 Targeted epigenomic control of MYC as a strategy to treat EGFR inhibitor-resistant NSCLC.

E. Lee, P. Flahardy, C. Vergato, S. Siecinski, J. Chen, C. O'Donnell, G. Hodgson, D. Yarar, T. McCauley;
Omega Therapeutics, Cambridge, MA

EGFR tyrosine kinase inhibitors (EGFRi) have improved outcomes for non-small cell lung cancer (NSCLC) patients harboring activating *EGFR* mutations. However, patients receiving EGFRi therapy frequently relapse with an EGFR T790M mutation. While osimertinib, a third generation EGFRi, blocks EGFR T790M activity, resistance eventually develops through various EGFR-dependent and EGFR-independent mechanisms, such as acquiring additional mutations in EGFR (e.g. C797S), activating bypass signaling pathways, or undergoing an epithelial to mesenchymal transition (EMT). MYC is a master transcription factor critical for mediating oncogenic signal transduction and has been implicated in EGFRi resistance, suggesting that MYC targeting may overcome multiple EGFRi resistance mechanisms. To evaluate this, we have developed a NSCLC-specific programmable epigenomic mRNA therapy, termed a MYC epigenomic controller (NSCLC MYC-EC), designed to selectively target regulatory elements in MYC's insulated genomic domain and downregulate MYC expression. We have previously shown that NSCLC MYC-EC effectively decreases MYC expression pre-transcriptionally and have demonstrated that MYC-EC combination with osimertinib synergistically reduces viability of EGFR mutant NSCLC cells. Here, we demonstrate NSCLC MYC-EC activity in models that have developed EGFRi resistance through EGFR-dependent and -independent mechanisms. To test the effect of NSCLC MYC-EC in NSCLC cells with T790M mutant EGFR, we treated H1975 (L858R, T790M) and PC9-T790M cells (del19, engineered T790M) with MYC-EC alone or in combination with osimertinib. MYC-EC combination with osimertinib enhanced MYC protein downregulation and synergistically reduced cell viability in both models. To evaluate the effect of MYC-EC in osimertinib-resistant cells, we engineered H1975 and PC9-T790M cells with an EGFR C797S mutation. While osimertinib treatment did not impact cell viability in these models, MYC-EC maintained activity, downregulating MYC levels and reducing cell viability. To investigate MYC-EC activity in cells with alternative resistance mechanisms, we generated osimertinib-resistant H1975 cells by stepwise dose escalation. Protein analysis showed highly reduced phospho-EGFR levels, suggesting an EGFR-independent mechanism of survival. RNA-sequencing analysis revealed that EMT pathway was highly activated in these resistant cells. Importantly, this model retained sensitivity to NSCLC MYC-EC treatment, demonstrating that selectively targeting MYC can treat osimertinib-resistant NSCLC cells with a mesenchymal phenotype. Together, these data demonstrate that pre-transcriptional downregulation of MYC through NSCLC MYC-EC treatment effectively inhibits viability of EGFRi-resistant NSCLC through both EGFR-dependent and -independent mechanisms and supports the development of NSCLC MYC-EC in EGFRi-resistant NSCLC.

#1727 Silencing of novel m6A reader PRRC2A as a therapeutic strategy for oral cancer.

B. Kannan, V. P. Jayaseelan, S. M, P. Arumugam;
Saveetha Dental College and Hospitals, Saveetha Institute of Medical and Technical Sciences (SIMATS), Saveetha University, Chennai, India

Background: Oral squamous cell carcinoma (OSCC) poses a substantial global health challenge characterized by limited treatment options and unfavorable prognoses. Recent research has illuminated the pivotal role of N6-methyladenosine (m6A) modification and its regulators in cancer biology. However, the precise involvement of a novel m6A regulator (m6A reader), PRRC2A in OSCC remains inadequately understood.
Objective: This study aims to unravel the role of PRRC2A in OSCC and ascertain its potential as both a diagnostic biomarker and a therapeutic target.
Methods: We collected 76 OSCC tumor samples and 38 adjacent non-tumor samples from OSCC patients. Comprehensive analyses, including RT-qPCR, western blotting, histopathological examination, and associations with clinicopathological features, were performed to assess PRRC2A expression in cancer tissues. Furthermore, we explored its links with key factors like metastasis and its implications for patient prognosis. *In vitro* experiments were conducted using OSCC cell lines and human normal oral keratinocytes (NOKs). PRRC2A knockdown in OSCC cell lines was assessed for its effects on cell proliferation, apoptosis, cell cycle, migration, invasion, and sphere-forming abilities. The study also delved into its impact on immune cell infiltration and involvement in biological pathways.
Results: Our investigation unveiled significant overexpression of PRRC2A in OSCC tissue samples and cell lines, relative to adjacent non-tumor tissues and NOKs ($P < 0.001$). These findings were further validated by the Cancer Genome Atlas - Head and Neck Squamous Cell Carcinoma (TCGA-HNSC) dataset. PRRC2A expression displayed significant correlations with nodal metastasis, higher tumor grades, and advanced cancer stages in OSCC samples, suggesting its crucial role in driving cancer progression and aggressiveness. Silencing PRRC2A *in vitro* led to reduced metastasis, diminished tumor colony formation, and increased apoptosis in oral cancer cell lines. Furthermore, the study uncovered PRRC2A intricate connections with immune regulatory genes, highlighting its potential to influence the tumor immune microenvironment.
Conclusion: PRRC2A emerges as a promising candidate for both diagnosis and therapeutic intervention in OSCC. Its pronounced overexpression in oral cancer tissues, coupled with its associations with metastasis and intricate interactions with immune regulatory networks, underscores its significance in the context of oral cancer malignancies. This research offers valuable insights into the multifaceted role of PRRC2A in OSCC and lays the groundwork for future investigations and potential clinical applications.

#1728 Senescent cancer-associated fibroblast drives colorectal cancer progression in a METTL1-dependent manner.

J. Weng, X. Wang, X. Liu, Y. Luo, **H. Yu**;
The Sixth Affiliated Hospital of Sun Yat-sen University, Guangzhou, China

Background: Colorectal cancer (CRC) is a leading cause of cancer-related mortality worldwide. More comprehensive studies of key molecular alterations were urgent. Cancer-associated fibroblasts (CAFs) exhibit the senescence-associated secretory phenotype (SASP) which contributes to the progression of cancer through the transcriptomic reprogramming at their senescent states. N7-methylguanosine (m7G), one of the most common RNA modifications, is catalyzed by Methyltransferase-like 1 (METTL1) in human RNA. We therefore investigated the role of METTL1-mediated transcriptomic reprogramming in the crosstalk between senescent CAFs (s-CAFs) and cancer cells.
Methods: The SA-β-gal staining and immunofluorescence assays were conducted to characterize the senescent cells. The transwell, wound scratch and organoids assays were preformed to test the abilities of viability, migration and invasion. The concentrations of cytokines and chemokines were determined by Luminex liquid suspension chip. The methylated RNA immunoprecipitation and dot blot assays were performed to characterize the RNA m7G levels in the transcriptome.
Results: Through the activation of mTOR signaling, the expression of P16 gene was significantly up-regulated in s-CAFs which was treated by H_2O_2, accompanied by an increased proportion of SA-β-gal+ cells and altered expression level of METTL1 protein. Luminex liquid suspension chip analysis revealed a significant increase in SASP cytokines such as TNF-α and PDGF-BB in the conditioned media of s-CAFs. Co-culturing CRC cell and organoids with s-CAFs resulted in down-regulation of METTL1 expression and significantly enhanced its invasion and migration abilities, while organoids exhibited increased activity and proliferated more rapidly. TNF-α and PDGF-BB down-regulated the METTL1 expression in CRC cell, while inhibitors targeting TNF-α and PDGF-BB rescued this trend. Interestingly, the regulatory effect on METTL1 of CRC cell by s-CAFs which treated by rapamycin was disappeared. These results indicated that METTL1 modulates RNA m7G modifications influenced by SASP cytokines for promoting CRC metastasis flow.
Conclusions: In summary, our findings illustrated that METTL1 plays a role in relaying tumor-promoting signals from s-CAFs in response to SASP cytokines. This ultimately contributes to the tumor-promoting signal flow from s-CAFs. This highlights the importance of understanding the molecular mechanisms underlying the communication between different cell types in the tumor microenvironment. In addition, it also provides a novel strategy for clinical treatment in advanced CRC.
Keywords: METTL1, Epigenetic regulation, Senescent CAFs, Tumor microenvironment

#1729 SUV420H1 depletion reveals therapeutic potential in HPV-negative head and neck squamous cell carcinoma.

Arfa Moshiri[1], Sohyoung Kim[2], Marie Luff[1], Vassiliki Saloura[1]

[1]Thoracic and GI Malignancies Branch, National Cancer Institute, Bethesda, MD,[2]Laboratory of Receptor Biology and Gene Expression, National Cancer Institute, Bethesda, MD

Human Papilloma Virus (HPV)-negative head and neck squamous cell carcinoma (HNSCC) poses a significant clinical challenge with limited treatment options. *SUV420H1*, which encodes for a protein lysine methyltransferase (PMT) that methylates H4K20 (H4K20me3), is recurrently amplified in ~5% of HPV-negative HNSCC tumors and is the second most frequently amplified PMT in this disease, suggesting an oncogenic function in this subset of HPV-negative HNSCC patients. Gene set enrichment analysis using the TCGA database of HPV-negative HNSCC tumors revealed that SUV420H1 overexpressing tumors showed enrichment in the mitotic spindle related pathways, and repression of immune-related pathways. To assess whether SUV420H1 depletion affects the proliferation of HPV-negative HSNCC cells, CCK8 and colony formation assays were pursued after siRNA-mediated knockdown of SUV420H1 in five SUV420H1-overexpressing HPV-negative HNSCC cell lines and revealed a significant reduction in cell proliferation and colony forming capacity. SUV420H1 CRISPR knockout (KO) HPV-negative HNSCC human and mouse cell lines were generated. Proliferation and colony formation assays with the SUV420H1 KO cell lines are ongoing to validate the aforementioned phenotypes. To identify oncogenic mechanism of SUV420H1, genome-wide mapping of H4K20me3 after siRNA-mediated depletion or enzymatic inhibition of SUV420H1 (A-196) was pursued using CUT&RUN assays combined with RNA-seq in a *SUV420H1* amplified cell line (SCC-151), and analysis is ongoing. Preliminary RNA-seq analysis revealed upregulation of a number of type I IFN response genes after siRNA-mediated knockdown of SUV420H1. In vivo mouse experiments using SUV420H1 KO mouse cell lines are planned in a syngeneic HPV-negative HNSCC flank mouse model (MOC1) with or without anti-PD-1 treatment with the goal to assess whether SUV420H1 depletion affects tumor growth and/or sensitizes cancer cells to anti-PD-1 therapy. These data provide preliminary support for the function of SUV420H1 as an oncogene in HPV-negative HNSCC.

#1730 Unraveling the oncogenic potential of KDM2A with gastric organoids.

Shilpa S. Dhar, Calena Brown, Constantin Zod, Jaffer A. Ajani, Min Gyu Lee

UT MD Anderson Cancer Center, Houston, TX

Background: Gastric adenocarcinoma (GAC), prevalent and often lethal, imposes a serious global health challenge. Therefore, it is critical to identify novel oncogenes (drivers) that can be therapeutically targeted. Of epigenetic modifications, histone lysine methylation is a hallmark of epigenetic and transcriptional regulation of gene expression. Therefore, investigating the involvement of histone methylation modifiers in GAC is paramount to gaining a comprehensive understanding of the disease but also to discover novel targets. Our analysis of the GAC genome indicates that these epigenetic modifiers are amplified in GAC.
Objective and Hypothesis: The overall objective is to define the oncogenic role of KDM2A in GAC pathogenesis and progression. The central hypothesis is that KDM2A promotes GAC by upregulating the expression of oncogenic proteins via the activation of epigenomic signatures/pathways.KDM2A (FBXL11) is a histone lysine demethylase that demethylates H3K36me2 and represses target genes involved in various biological processes, including cell proliferation, DNA damage repair, and stem cell maintenance. Previously, we reported that KDM2A was necessary for the tumorigenic and metastatic capabilities of non-small lung cancer cells through transcriptionally repressing the expression of DUSP3 and HDAC3, which led to activation of ERK signaling and upregulation of cell cycle-associated genes.
Results: Our analysis of the GAC genome indicates that KDM2A is one of the top demethylases frequently amplified and overexpressed (14%). In addition, *KDM2A* expression was significantly higher in GAC samples than in normal tissues, and high expression of KDM2A was associated with poor survival in GAC patients. To examine the effect of KDM2A knockdown on characteristics of GAC, we used gastric organoids generated from KDM2A$^{flox/flox}$ mouse stomach. We expressed wild-type (Flag-KDM2A) and catalytic mutant (Flag-KDM2A-mut) in these organoids. Ectopic expression of KDM2A wild-type, but not mutant, increased the proliferation of organoids. We showed that KDM2A knockdown decreased the proliferation and invasion of two GAC cells, GA0518 and AGS. In addition, we determine the effect of overexpression of KDM2A on cell proliferation by comparing the control organoids to KDM2A overexpressed using IHC staining of Ki-67 (a proliferation marker) and other activated oncogenic signaling PI3KCA/mTOR/AKT, EGFR. We showed that GA5018 cells were very sensitive to the KDM2A inhibitor (daminozide) alone and in combination with erlotinib (EGFRi inhibitor) and RAD001 (RAD1 mTOR inhibitor).
Significance and Innovation: In contrast to advances in cellular signaling pathways in GAC pathogenesis, how GAC development is epigenetically regulated remains largely unknown. Our results from using organoids indicate that KDM2A is an oncoprotein.

#1732 Linker histone h1 inhibits topoisomerase IIa *in vitro* and *in vivo*.

S. Lasater, H. Hamdan, P.-Y. Ho, T. Wu, K. Cao, R. Yang, Y. Zhang, **Y. Fan**;
Georgia Institute of Technology, Atlanta, GA

H1 linker histones play a crucial role in organizing chromatin into higher-order structures and regulating gene expression, contributing significantly to various cellular processes. Topoisomerase IIa (TopoIIa) is essential for multiple cellular functions via regulating DNA topology. Here, we report a direct interaction between H1 linker histones and TopoIIa through both N- and C-terminal domains of H1 variants. H1 suppresses the decatenation enzymatic activity of TopoIIa *in vitro* in a dose-dependent manner. Overexpressing specific H1 variants in HeLa cells results in a marked decrease in cell proliferation and a dramatic increase in the occurrence of cells displaying abnormal mitotic chromosomes. Additionally, we find that the inhibitory effect of the specific H1 variant on TopoIIa activity occurs prior to the formation of DNA-TopoIIa complexes. These results reveal a novel mechanistic link between histone H1 and Topo IIa in the regulation of chromatin function.

#1733 SET-NUP214 rearranges the DNA-methylation landscape to upregulate the HOX-gene cluster in acute myeloid leukemia.

S. Roy Choudhury, A. Kaushal;
University of Arkansas for Medical Sciences, Little Rock, AR

The SET-NUP214 (S/N) fusion gene, which results from either cryptic t(9:9) (q34;q34) or del(9) (q34.11q34.13), is found in a very narrow spectrum of patients diagnosed with Acute Myeloid Leukemia (AML) or T-cell acute lymphoblastic leukemia (T-ALL). AML patients with S/N fusion were reported to have relatively poor prognostic outcomes despite receiving myeloablative conditioning. While previously, the fusion has been described to overrepresent HOX cluster genes, the underlying mechanism of gene regulation that contributes to the pathology remains elusive due to the rare incidence of the disease. The current study used the MEGAL (ACC719, DSMZ) cell line, identified as the solo megakaryocytic AML line expressing the S/N-fusion, for determining genome-wide DNA methylation (DNAm) and gene expression using 935K Infinium MethylationEPIC v2.0 BeadChip array and RNA-sequencing, respectively. The differential DNAm and expression data were analyzed and compared to the hematopoietic stem progenitor cells (HSPC) or normal megakaryocytes (MK). The ChIP-sequencing data from the S/N positive T-ALL cell line LOUCY has been used to represent the coincidence of regulatory chromatin marks and differentially methylated CpG (mC) sites. We observed n=1934 genes upregulated and n=2396 downregulated in MEGAL, compared to both HSPC and MK. The direction of expression changes between MEGAL and HSPC and MEGAL and MK showed a high correlation (r=0.92, p< 0.01). Per the previous literature, we observed an overrepresentation of *HOX* genes (n=19) in MEGAL. Based on DNAm profiling, we noticed a propensity of hypermethylation in MEGAL across the promoters (93%±0.6), bodies (93%±0.8), and intergenic (85%±0.3) regions, compared to HSPC/MK. Next, we integrated the mC and expression at the promoters and identified that the majority (75%±3) of the genes belong to the hyper-down (n=2563 against HPSC; n=1907 against MK) or hyper-up (n=965 against HPSC; n=923 against MK) clusters. We further investigated the *HOXB* (*HOXB7, HOXB8, HOXB9*) and *HOXC* (*HOXC10, HOXC12, HOXC13, HOXC13-AS, HOXC4, HOXC5, HOC6, HOXC8, HOXC9, HOXC-AS1, HOXC-AS2*, and *HOXC-AS3*) cluster genes, where hypermethylated CpGs mainly were concentrated at the CpG islands and overlapped with active promoter (H3K4me3, H3K4me1) signatures or enhancer-like (CTCF bound) elements. We also observed frequent overlaps between mC and H3K36me3 across the observed genes. The differentially expressed genes in this AML subtype were enriched for the hippo-signaling pathway, calcium signaling, focal adhesion, and PI3-Akt pathways. Collectively, our data showed that S/N favors genome-wide hypermethylation, which, in conjunction with the cis-regulatory elements, induces overrepresentation of the HOX cluster genes. These novel epigenetic vulnerabilities are worth pursuing for investigating the cellular function and pathophysiology of the disease.

#1734 Dissecting the bifaceted function of SMYD3 as a transcriptional activator and repressor in HPV-negative HNSCC.

J. Akhtar, S. Kim, V. Saloura;
National Institute of Health, Bethesda, MD

Background: Approximately 75% of Human-papilloma-virus (HPV)-negative head and neck squamous cell carcinoma (HNSCC) tumors carry genetic and expression alterations in the family of protein methyltransferases and demethylases, underscoring the importance of these enzymes in the pathogenesis of HNSCC. SMYD3 a lysine methyltransferase that is overexpressed in HPV-negative HNSCC. We recently reported that nuclear SMYD3 plays dual role in immune-related gene regulation through H3K4me3 or H4K20me3, leading to gene activation or silencing, respectively in HPV-negative HNSCC. While SMYD3 has been reported to write and bind to H3K4me3 activating target gene expression, its function in gene silencing is understudied. This study aims to determine the mechanism(s) through which SMYD3 functions both as a transcriptional activator and a repressor within the same cell context, specifically in HPV-negative HNSCC. **Methods:** immunoprecipitation (IP) of SMYD3 was performed from nuclear extracts isolated from HN-6 cells to identify candidate interacting partners of SMYD3. The nuclear immunoprecipitates were sent for MS analysis to identify candidate nuclear interacting partners of SMYD3. CUT&RUN assays for selected candidate interacting proteins and SMYD3 will be performed in control HN-6 cells versus SMYD3 KO cells to assess genomic co-occupancy with SMYD3. Further, CUT&RUN assays for repressive marks H4K20me3, H3K27me3 and H3K9me3 have been performed in HN-6 and SMYD3 KO cells to assess co-occupancy with SMYD3 as well as its effect of SMYD3 on the genome-wide mapping of these marks. Finally, CUT&RUN assays for SMYD3 followed by re-CUT&RUN of repressive histone marks are ongoing to identify co-occupied loci. **Results:** Preliminary analysis of our nuclear SMYD3 IP results has identified a chromatin modifier with known repressive function. Co-immunoprecipitation experiments to validate this interaction are planned. CUT&RUN assays for repressive histone marks in HN-6 versus SMYD3 KO cells have revealed impact on H4K20me3 and H3K27me3. **Conclusions:** Our preliminary results suggest that SMYD3 may exert its silencing function by regulating the genome-wide deposition of H4K20me3.Our nuclear SMYD3 IP analysis has identified candidate interacting
partners that may assist SMYD3 in promoting the deposition of these repressive marks. CUT&RUN assays for SMYD3 followed by re-CUT&RUN for H4K20me3 and H3K27me3 bound chromatin may provide further insight about whether SMYD3 co-occupies specific genomic regions together with these repressive marks. This project is expected to provide mechanistic insights into the bifaceted functions of SMYD3 within the same cell context using HPV-negative HNSCC cell lines as an experimental model system..

#1735 DNA demethylating agents have cell type-specific effects on viability and *BRCA2* alternative splicing.

J. Werner[1], H. Siddiqui[1], S. Syed[1], O. Khan[1], S. Casillas Garabito[2], **J. D. Fackenthal**[1];
[1]Benedictine University, Chicago, IL, [2]College of DuPage, Glen Ellyn, IL

Introduction: *BRCA2* is one of two principal tumor suppressors responsible for hereditary breast/ovarian cancer syndrome (HBOC). Patients with strong family histories of breast/ovarian cancer may carry *BRCA2* DNA sequence variants of unknown clinical significance (VUSs). To evaluate which of these VUSs may contribute to cancer risk by altering splicing patterns, naturally occurring *BRCA2* mRNA alternate splicing events have been extensively characterized, but it is not yet known which if any of these alternate splicing events plays a role in *BRCA2* function. One variant lacking exon 3 (Δ3), which maintains the full length translational reading frame, lacks sequence encoding EMSY and PALB binding domains as well as transactivation function. Previous work has shown that, while some VUSs associated with increased levels of Δ3 in lymphoblastoid cell lines are not pathogenic, germline deletions that eliminate *BRCA2* exon 3 are associated with increased breast cancer risk. It is therefore of interest to characterize the factors that influence the frequency of naturally occurring *BRCA2* exon 3-skipping, including cell types and therapies. DNA demethylating agents are used as cancer therapy to promote expression of tumor suppressor genes that may be epigenetically silenced in tumors. However, DNA methylation has been shown to be more frequent in exonic than intronic regions of protein-coding genes, suggesting that methylation may play a role in recruiting spliceosomal components to nascent pre-mRNA. It is therefore of interest to determine whether genomic demethylation affects alternative splicing patterns. Here, we explore whether *BRCA2* exon 3 alternative splicing patterns are altered by demethylating agents.

Methods: To determine whether DNA demethylating agents can alter the levels of Δ3, MCF7 and/or the non-cancer breast cell line MCF 10A was treated with 5-aza 2'-deoxycytidine (5-AzadC) or 5-Azacytidine (5-AzaC), and isoform-specific RT-PCR was used to compare relative levels of splice junctions containing or skipping exon 3.

Results and Conclusions: 1) While the IC_{50} for both 5-AzadC and 5-AzaC in MCF 10A was similar (less than 1 μM), MCF7 showed considerably more resistance to 5-AzaC than 5-AzadC (IC_{50} of ≥ 5 μM vs ≤ 0.2 μM). 2) 5-AzaC treatment reduces the proportion of MCF 10A cultures in apoptosis but does not increase the proportion of viable cells, indicating it causes cell death by some other means. 3) While both 5-AzaC and 5-AzadC reduce relative levels of Δ3 in MCF7, 5-azadC does not reduce relative levels of Δ3 in MCF 10A, suggesting there may be a cell type-specific splicing response to genomic demethylation therapies.

#1736 Elucidating the oncogenic mechanisms in diffuse midline glioma: Comparative analysis of h3k27m mutation and k27 methylation loss on gene expression profiles via RNA sequencing.

S. Bhattarai[1], F. L. Hakkim[1], C. Day[1], F. Grigore[2], A. Langfald[1], E. Hinchcliffe[1], J. Robinson[1];
[1]The Hormel Institute, University of Minnesota, Austin, MN, [2]New York Presbyterian Hospital, New York City, NY

Background: Diffuse Midline Glioma (DMG), a severe pediatric brain tumor, is characterized by its aggressive nature and poor prognosis. Common in brain midline structures like the thalamus and brainstem, DMGs often harbor H3K27M mutations, leading to reduced histone trimethylation at lysine 27 and loss of serine 31 phosphorylation. Building on these findings, our laboratory has undertaken a novel approach by engineering a knockout of the Polycomb Repressive Complex 2 (PRC2) in selected cell lines. This was achieved using CRISPR-Cas technology to target the EZH1 and EZH2 methyltransferases (PRC2KO), alongside the introduction or reversal of histone H3.3 mutations. The goal of this study is to investigate the effects of K27 Methylation loss and H3.3 mutations on gene expression in DMG to better understand DMG pathogenesis and potential therapeutic avenues.
Methods: RNA and ATAC sequencing were performed on DMG cell lines including H3.3WT, H3.3 S31A, H3.3K27M, and PRC2KO. Utilizing 150 bp paired-end reads, 25 to 45 million unique reads were mapped to the human genome (hg38) using STAR. Differential gene expression was analyzed using DESeq2 in R, complemented by ATAC-sequencing to explore potential epigenetic changes.
Results: The analysis identified 2,564; 2,946; 4,618; and 5,490 differentially expressed genes (DEGs) in the K27M, S31A, K27M-PRC2KO, and WT-PRC2KO cell lines, respectively, when compared to WT. A four-way Venn diagram analysis identified unique and shared gene cohorts among the different mutations. H3K27M cells showed 414 downregulated and 385 upregulated genes, mainly affecting cell migration. In contrast, PRC2KO cells, characterized by a complete loss of histone methylation, showed extensive changes with 1,302 genes downregulated and 1,779 upregulated, primarily impacting cell cycle and developmental processes. The S31A cells displayed a unique profile with 548 genes uniquely downregulated and 547 genes upregulated. The lack of enrichment in specific pathways for these genes suggests their involvement in a broader range of affected pathways. A significant discovery was the identification of a set of genes common to both S31 and K27M cells, but absent in PRC2 knockouts. This cohort, consisting of 350 downregulated and 389 upregulated genes, may represent a molecular link between serine phosphorylation and the K27M mutation. Additionally, ATAC-sequencing analysis was conducted to determine if the expression changes were a direct result of epigenetic dysregulation or an indirect effect.
Conclusion: This study delineates the intricate gene regulation in DMG resulting from H3K27M mutations beyond loss of loss of K27 Methylation. It highlights unique and overlapping pathways influenced by, providing valuable insights into the molecular basis of DMG and guiding future therapeutic strategies.

#1737 METTL3-mediated m^{6}A modification promotes tumor progression in upper tract urothelial carcinoma.

L.-J. LIN[1], P.-H. PENG[2], K.-W. HSU[1];

[1]China Medical University, Taichung, Taiwan, [2]Chang Gung Memorial Hospital, Taoyuan, Taiwan

Upper tract urothelial carcinoma (UTUC), comprising 5% of urothelial neoplasms, is a rare malignancy arising from the transitional epithelium of the renal pelvis and ureter. Its rarity and diverse histology pose diagnostic and therapeutic challenges, often lead to delayed diagnoses. The absence of targeted therapies, coupled with a limited understanding of molecular pathogenesis, underscores the ongoing research in urological oncology for effective UTUC management. N6-methyladenosine (m^{6}A) is the predominant RNA methylation in mammalian cells, with its inscription primarily orchestrated by METTL3, a crucial methyltransferase. METTL3 has been implicated in various cancers, affecting critical processes like proliferation, migration, and tumor progression. However, the specific mechanisms and biological function of how METTL3/m^{6}A regulates the progression of UTUC remain unclear. In our study, we found that m^{6}A modification and METTL3 expression were elevated in aggressive UTUC, both are negatively correlated with unfavorable clinical outcomes and poor patient survival. By overexpressing METTL3 in less aggressive UTUC cell lines BFTC909 and KTCC28, the abilities of cell proliferation, migration, invasion, and colony formation increased. Notably, overexpression of METTL3 also increased tumor growth and metastasis in the in vivo orthotopic mouse model. In contrast, knockdown of METTL3 decreases tumor progression in a highly aggressive UTUC cell line KTCC28M. Furthermore, our comparative analysis of RNA-seq and m^{6}A MeRIP-seq datasets unveiled the regulation of 1660 genes by METTL3. This diverse set includes genes associated with tumor growth and metastasis (such as *MYC*, *JAK2*, and *STAT3*), as well as RNA processing-related genes which their critical roles in modulating mRNA stability and splicing (such as *GEMIN5* and *PABPC1L*). Together, we noticed METTL3/m^{6}A is a crucial protagonist in the oncogenic landscape of UTUC, which suggested that it can be used as a target for novel therapeutic strategy for UTUC treatment.

#1738 Precise detection of benign and malignant renal tumor via epigenetic characteristics of urinary cell-free DNA.

W. Kong[1], **H. Dong**[2], H. Tang[2], P. Du[2], S. Jia[2], J. Zhang[1];

[1]Shanghai Jiao Tong University School of Medicine, Shanghai, China, [2]Huidu (Shanghai) Medical Sciences, Ltd., Shanghai, China

Early detection of clear cell renal cell carcinoma (ccRCC) and accurate differentiation between malignant and benign lesions pose clinical challenges. Profiling the epigenetic pattern of patients through liquid biopsy offers a promising strategy for non-invasive cancer identification. This study utilizes the methylation characteristics of urinary cell-free DNA to enhance the precise diagnosis of ccRCC. In this study, 32 patients with malignant RCC, 20 patients with benign kidney lesions, and 28 age- and sex-matched healthy donors were enrolled. Urine samples were collected and applied by PredicineEPIC assay to analyze the whole genome methylation profiles. We assessed the methylation differences on cancer-specific altered regions and constructed a machine learning model for malignant and benign classification. Beta values were calculated for differentially methylated regions identified through literature mining and our current work. These features carry methylation signals that are recognized by gradient boosting machine and used for classification training. The leave-one-out cross-validation method compensated for the shotage of sample size. The sensitivity and specificity of the optimal model in the training set are both greater than 0.97, and it can achieve an accuracy of 0.95 on the validation set. This performance surpasses traditional diagnostic methods such as contrast-enhanced CT and MRI. This study demonstrated the technical feasibility of leveraging epigenetics profiles to discriminate malignant from benign lesions, suggesting a promising liquid biopsy-based approach for the precise detection of renal cell carcinoma.

#1739 Detection of regulatory T cells, a comparison of flow cytometry and epigenetic qPCR immunophenotyping using healthy donor and oncology patient whole blood.

U. Baron, L. Lozza, **A. Bisconte**, E. Raschke, D. Phippard, S. Olek;
Precision for Medicine, Frederick, MD

Human regulatory T cells (Tregs) are part of the adaptive immune response and play a pivotal role in suppressing both the immune and anti-tumor responses. Infiltration of Tregs into the tumor microenvironment has been associated with poor clinical prognosis. In addition, increased peripheral Treg frequency is associated with disease progression. Monitoring Tregs in both the blood and in the tumor of patients is being used to evaluate clinical prognosis and response to treatment in immuno-oncology studies. The key challenge is the ability to detect Tregs with high accuracy and precision. Here, we have used epigenetic qPCR (Epiontis ID®) as a method to detect and quantify Tregs in peripheral whole blood and compared it with flow cytometry. Flow cytometry is the current gold standard for immunophenotyping. For method comparison, we analyzed 113 whole blood samples from healthy donors. We have demonstrated equivalence and shown a strong correlation between epigenetic qPCR and flow cytometry-based data, indicating that Epiontis ID® is a robust and sensitive DNA-based method for Treg quantification. This epigenetic qPCR method does not require fresh samples or intact cells, since DNA can be extracted from frozen blood. We then evaluated Treg levels in blood samples from solid tumor cancer patients by epigenetic qPCR to demonstrate the clinical application and relevance for immune monitoring. Here, Treg frequencies were reported as relative (%) and absolute counts (cells/µL) values. Epigenetic qPCR for immune monitoring mitigates the operational and technical challenges of monitoring Tregs in the periphery for immuno-oncology studies which traditionally been performed by flow cytometry. This Epiontis ID® method provides the sensitivity and accuracy needed for determining patient response in progressive disease.

#1740 Histone proteomic profiling of EMT-transformed MCF10A breast cells demonstrates a loss in novel histone arginine methylation sites via dual p53 and PTEN deletion.

C. B. McGuinness[1], M. A. Wilson[1], M. V. Leonard[1], M. Ouzounova[2], H. Korkaya[3], A. Y. Shull[1];
[1]Presbyterian College, Clinton, SC, [2]Cancer Research Center of Lyon, Lyon, France, [3]Karmanos Cancer Institute, Wayne State University, Detroit, MI

Metastatic potential of basal-like breast cancers typically is initiated by genetic alterations that lead to a process known as epithelial-mesenchymal transition (EMT). However, much is currently not understood regarding the role of epigenetic modifications that lead to invasive characteristics and EMT phenotype of metastatic breast cancers. Based on the previous notion connecting epigenetic changes to breast cancer metastasis, we performed DIA-based mass spectrometry of isolated histones from an isogenic panel of MCF10A breast cell lines where the tumor suppressor genes TP53 and PTEN were silenced and induced EMT. With this approach, we determined which histone modifications were differentially enriched in the non-EMT and EMT-induced MCF10A cell lines. From approximately 72 histone modifications identified and annotated from our mass spectrometry results, we were able to identify 5 histone events that were differentially enriched in our MCF10A cell line panel. Two events of note were histone H3 lysine-14 acetylation (H3K14ac) significantly increasing and histone H4 arginine 55 dimethylation (H4R55me2) significantly decreasing in our EMT-transformed MCF10A p53-/PTEN- cell lines when compared to the parental, non-tumorigenic MCF10A cell line, showing these events are differentially affected during the EMT process in breast cancer cells. Furthermore, significant arginine demethylation of H4R55me2 & H3.1R83me in the EMT-transformed MCF10A p53-/PTEN- cell lines corresponded with JMJD6, an established histone arginine demethylase, being overexpressed in basal-like breast cancer cell lines as well as basal-like breast cancer patients from The Cancer Genome Atlas (TCGA) and METABRIC datasets. Based on histone proteomic profiling of our isogenic cell line model, the loss of specific histone arginine methylation events corresponding with JMJD6 overexpression could highlight the potential for a targetable epigenetic mechanism in breast cancer metastasis.

#1741 AlidaBio EpiPlex: A platform for multiplexed detection of RNA modifications in clinical samples.

A. Price[1], Z. Miles[1], J. Chevillet[1], B. Purse[1], R. I. Gregory[2], **G. Stengel**[1];
[1]Alida Biosciences Inc., San Diego, CA, [2]Harvard Medical School, Boston, MA

It is becoming increasingly appreciated that RNA modifications are widespread in development and homeostasis, regulating RNA stability and translation, and that alterations to these modifications are associated with cancer development and progression. Although 170 different RNA modifications have been identified using mass spectrometry, there is a paucity of convenient, validated tools immediately available to cancer researchers to explore these modifications using relevant clinical samples in sufficient numbers, and accurately determine their suitability for use as diagnostic or drug targets. In addition, most existing methods concentrate only on m6A, the most prevalent modification in mRNA. Alida Bio has developed an end-to-end assay platform with an integrated bioinformatics solution that detects multiple modifications in the same reaction. This platform exploits targeted, multiplexed barcoding to reveal the quantitative abundance of modified transcripts, co-localization of multiple RNA modifications to the same gene, and gene expression profiles. Alida Bio's mission is to equip translational researchers with tools that will significantly improve their understanding of gene regulation through seamless measurement of RNA modifications.

#1742 A universal spike-in normalization strategy for CUT&RUN, CUT&Tag and ATAC-seq.

S. Traynor, B. Townsley, J. Weber, M. Jelinek, B. Egan, **B. Delatte**;
Active Motif, Calrlsbad, CA

The development of simple and efficient genome-wide approaches has recently democratized the study of epigenetics. For instance, CUT&RUN and CUT&Tag were developed as fast and affordable alternatives to ChIP-seq, whereas ATAC-seq readily identifies regions of open chromatin. These methods are ideal to look for genome-wide alterations in chromatin structures but are only semi-quantitative and can miss global changes when performed without normalization spike-ins. In fact, many standard computational pipelines fail to detect a reportedly substantial global H3K27me3 decrease in the presence of *GSK126*, a therapeutic target for lymphoma and potent inhibitor of the EZH2 methyltransferase. To overcome this challenge, we developed a spike-in approach using *Drosophila melanogaster* nuclei for normalization of ATAC, CUT&RUN and CUT&Tag experiments using human cells. The addition of the spiked-in nuclei allowed for the detection of the expected global changes in open regions of chromatin (ATAC-seq), H3K27me3 (CUT&Tag), R-loops (CUT&Tag), EED and p53 binding (CUT&RUN) upon treatment of K562 cells with GSK126. By contrast, these same changes were all missed when omitting the spike-in nuclei. This streamlined spike-in normalization strategy can be easily applied to any number of cells and on a large variety of conditions.

#1743 Pan-cancer review of TP53 somatic alterations as a function of tumor type: Sometimes lost, sometimes gained, frequently altered.

Ubaid A. Tanveer[1], David N. Hayes[1], Julie George[2], Jeremiah R. Holt[1], Martin Peifer[2], Roman Thomas[2]

[1]Hematology and Oncology, University of Tennessee Health Science Center, Memphis, TN,[2]University of Cologne, Cologne, Germany

Background: TP53 is the gene most frequently disrupted by somatic alterations in cancer. Mutations include single nucleotide variants resulting in functional alterations, as well as premature stop codons, splice variants, and cryptic alterations. TP53 gene dosage is disrupted by heterozygous and homozygous deletions, copy-neutral loss of heterozygosity, and other structural changes such as intragenic deletions and fusions. TP53 is altered by epigenetic events and viral oncogenes, such as E6 expressed by the human papillomavirus. The readout of altered TP53 includes decreased gene expression of either variant or wild-type alleles. Epistatic alteration of TP53 pathway components have also been described, with the E3 ubiquitin ligase MDM2 being the canonical example. Depending on the type of TP53 alteration, there may be differential signaling consequences, ranging from loss of function and dominant negative to oncogenic signaling.
Hypothesis: Patterns of TP53 mutations will vary based on tumor type. Differential alterations of TP53 will suggest differential pathway dependence and downstream pathophysiology that may be relevant to signaling and therapeutic potential.
Methods: We analyzed extensive cancer genomics repositories, such as the Pan-Cancer Atlas (10,000+ tumors, >30 cancer types) from The Cancer Genome Atlas project and the International Cancer Genome Consortium. Assessing genes in the TP53 pathway, we examined somatic mutations, copy number alterations, structural changes, and gene expression. Epigenetic data was considered when available.
Results: A significant pattern amongst sarcomas, prostate cancers, and urothelial carcinomas emerged, revealing that certain tumors exhibited a predominant classic tumor suppressor gene genotype. This genotype featured frequent homozygous deletions, inactivating mutations, and relatively low TP53 gene expression, often accompanied by epistatic MDM2 amplification. By contrast, other tumors demonstrate an atypical pattern in which TP53 mutations were rarely if ever associated with loss of TP53 gene expression with low levels of homozygous TP53 gene deletion. Likewise, atypical TP53 mutant tumor types rarely demonstrated MDM2 amplifications, and in opposition to typical TP53 cases, MDM2 amplification was positively associated with TP53 mutation rather than anti-correlated. Head and neck squamous cell carcinoma, uterine carcinoma, and pancreatic adenocarcinoma followed this pattern. Investigation within selected tumor types such as lung squamous cell carcinoma suggested that both typical and atypical TP53 mutation patterns could be observed.
Conclusions: TP53 mutation patterns were strongly associated with tumor type and may suggest differential pathway activation according to the somatic alteration status.

MOLECULAR/CELLULAR BIOLOGY AND GENETICS: Genomic Characterization of Cancers and Cancer Subgroups
Poster Session

#1746 KRAS mutant lung adenocarcinoma is associated with distinct mutational signature profiles.

L. C. Woodhouse[1], A. Hawari[1], A. J. Gruber[2], C. R. Lindsay[1], D. C. Wedge[1];
[1]University of Manchester, Manchester, United Kingdom, [2]University of Konstanz, Konstanz, Germany

Background: Lung cancer is the 3rd most common cancer in the UK and leading cause of cancer mortality worldwide. Somatic *RAS* mutations are the most common oncogenes in human cancer, and *KRAS* mutations are the largest molecular subset of lung adenocarcinoma (LUAD). Each cancer genome accumulates a unique combination of somatic mutations, and these mutational signatures provide a genetic imprint of mutational processes that have occurred during tumorigenesis. Mutational signatures provide information on tumor aetiology/maintenance and could highlight potential therapeutic targets. This is the largest study to date to profile *KRAS* mutant LUAD mutational signatures using whole genome sequencing (WGS) data.
Methods: Paired tumor and germline WGS data were obtained through the 100 000 Genomes Project (Genomics England). *KRAS* mutations were profiled using Ensembl Variant Effect Predictor (VEP) v109.0. Single base substitution (SBS), doublet base substitution (DBS), small insertion and deletions (ID) and copy number (CN) mutational signature extraction was performed using SigProfiler (COSMIC version 3.3). Statistical analysis and plotting were performed in R; a two-tailed p-value <0.05 was considered statistically significant.
Results: 680 LUAD patients were included; 301 *KRAS* mutant (44%), 379 *KRAS* wild type (63%). Common *KRAS* variants were present, including *G12C (38.9%), G12V (15.9%) and G12D (14.0%)*. 17 SBS, 9 DBS, 10 ID and 9 CN signatures were extracted and present in both *KRAS* mutant and wild type cohorts. *KRAS* mutant samples were enriched in smoking related signatures (SBS4, DBS2, ID3; odds (OR) ratio 5.54, 3.80, 4.97 respectively, p <0.001) and diploid CN signature (CN1, OR 1.41, p = 0.03). Conversely, *KRAS* mutant samples were less likely to have clocklike (ID5, OR 0.61, p = 0.012; ID8, OR 0.44, p <0.001), APOBEC (SBS2, OR 0.49, p <0.001; SBS13; 0.50, p <0.001), chromosomal instability (CN9, OR 0.63, p = 0.019), loss of heterozygosity (CN14, OR 0.47, p = 0.015), or homologous recombination deficiency (CN17, OR 0.58, p <0.001) signatures.
Discussion: These results show distinct mutational signature profiles between *KRAS* mutant and wild type LUAD. As previously described, *KRAS* mutant LUAD is dominated by smoking related signatures; however, the majority of remaining signatures were more common in the *KRAS* wild type cohort where there was a statistically significant difference. This data suggests different mutational processes are observed in *KRAS* mutant compared to wild type LUAD. *KRAS* mutations are commonly clonal and thought to initiate tumorigenesis: timing signatures relative to *KRAS* mutations is necessary to further our understanding of *KRAS* cancer evolution and the subject of future work. Combined with clinical data integration, mutational signatures could provide prognostic information and inform predictive models.

#1747 The mutational landscape and its longitudinal dynamics in relapsed and refractory Hodgkin lymphoma.

H. Witte[1], A. Kunstner[2], T. Hahn[3], V. Bernard[4], S. Stoelting[4], K. Kusch[4], K. Nagarathinam[2], N. von Bubnoff[3], C. Khandanpour[5], A. Bauer[1], M. Grunert[1], A. Arndt[1], K. Steinestel[1], H. Merz[4], H. Busch[2], A. Feller[4], N. Gebauer[3];

[1]Bundeswehrkrankenhaus Ulm, Ulm, Germany, [2]University of Luebeck, Lubeck, Germany, [3]University Hospital Schleswig Holstein Campus Lubeck, Lubeck, Germany, [4]Hematopathology Lubeck, Lubeck, Germany, [5]University Hospital Schlesiwg Holstein Campus Lubeck, Lubeck, Germany

Introduction: In classical Hodgkin-lymphoma (cHL), only a few cases recur, and only a limited fraction of patients is primary-refractory to standard-polychemotherapy. Underlying genomic features of unfavorable clinical courses remain sparsely characterized. Here, we investigated the genomic characteristics of primary-refractory/relapsed cHL in contrast with long-term-responders (LTR).

Methods: Therefore, ultra-deep next-generation panel-sequencing was performed on a total of 59 samples (20 LTR, 26 relapsed (rHL: 11 initial-diagnosis, 15 relapse) and 13 primary-refractory (prHL: 8 initial-diagnosis, 5 progression) from 44 cHL-patients applying a hybrid-capture approach. We compared samples associated with distinct disease courses concerning their oncogenic drivers, mutational signatures, and perturbed pathways.

Results: Compared to LTRs, mutations in genes such as *PMS2, PDGFRB, KAT6A, EPHB1,* and *HGF* were detected more frequently in prHL/rHL. Additionally, we observed that in rHL or prHL, *BARD1*-mutations occur, whereas *ETV1, NF1,* and *MET*-mutations were eliminated through clonal selection. A significant enrichment of non-synonymous variants was detected in prHL compared to LTRs and a significant selection process in favor of NOTCH-pathway mutations driving rHL or prHL was observed.

Conclusion: This study delineates distinct mutational signatures between LTR and rHL/prHL, whilst illustrating longitudinal dynamics in mutational profiles using paired samples. Further, several exploitable therapeutic vulnerabilities for rHL and prHL were identified.

#1748 Dearth of smoking-induced mutations in oncogene-driven NSCLCs despite smoking exposure.

C.-Y. Huang[1], N. Jiang[2], M. Shen[3], G. Lai[3], A. Tan[3], A. Jain[3], S. Saw[3], M.-K. Ang[3], Q. Ng[3], D.-T. Lim[3], R. Kanesvaran[3], E.-H. Tan[3], W. Tan[3], B.-H. Ong[4], K. Chua[3], D. Anantham[5], A. Takano[5], T. Lim[5], W. Tam[6], N. Sim[7], A. J. Skanderup[7], D. Tan[3], S. G. Rozen[8];

[1]Chang Gung Memorial Hospital - Linkou Branch, Taoyuan City, Taiwan, [2]Duke-NUS Medical School, Singapore, Singapore, [3]National Cancer Centre Singapore, Singapore, Singapore, [4]National Heart Centre Singapore, Singapore, Singapore, [5]Singapore General Hospital, Singapore, Singapore, [6]National University of Singapore, Singapore, Singapore, [7]Genome Institute of Singapore, Singapore, Singapore, [8]Duke University School of Medicine, Durham, NC

Non-small cell lung cancers (NSCLCs) in non-smokers are mostly driven by mutations in the oncogenes *EGFR, ERBB2,* and *MET*, and fusions involving *ALK* and *RET*. We term these “non-smoking-related oncogenes” (NSROs). NSRO-driven tumors account for approximately half of NSCLCs in East Asia, and, alarmingly, their age-adjusted incidence is increasing for unknown reasons. In addition to occurring in non-smokers, NSRO-driven tumors also occur in smokers. However, the clonal architecture and genomic landscape of these tumors remain largely unexplored. Here, we investigated genomic and transcriptomic alterations in 173 tumor sectors from 48 patients with NSRO-driven or typical-smoking NSCLCs. Overall, NSRO-driven NSCLCs in smokers and non-smokers had similar genomic landscapes and clonal architectures that were distinct from those in typical-smoking NSCLCs. Surprisingly, even in patients with prominent smoking histories, the mutational signature caused by tobacco smoking was essentially absent in NSRO-driven NSCLCs. We confirmed this unexpected finding in two large NSCLC data sets from other geographic regions. However, we observed differences in the tumor transcriptomes of NSRO-driven NSCLCs in smokers and non-smokers, with tumors in smokers displaying higher transcriptomic activities related to regulation of the cell cycle. This suggested that smoking does have an impact on tumor phenotype in NSCRO-driven NSCLC, likely through non-genetic mechanisms. We concluded that NSRO-driven NSCLCs, whether in non-smokers or smokers, constitute an important disease entity that is very different from typical-smoking NSCLC.

#1749 Esophageal adenocarcinoma single-cell resolution ecotypes and subtypes mediate chemoradiation resistance.

R. Ye, Y. Qiao, S. Bai, E. Sei, M. Hu, J. He, N. Li, Y. Wang, P. Lopez, W. Zhang, F. Ye, B. Weston, E. Coronel, W. Ross, P. Ge, B. Manoop, N. Navin, S. Lin; UT MD Anderson Cancer Center, Houston, TX

Esophageal adenocarcinoma (EAC) is an aggressive and lethal disease with a 5-year survival rate less than 20%. The current standard of care for locally advanced EAC patients is neoadjuvant chemoradiation (CRT) followed by surgery and the pathological response rate is low in clinic. An unresolved question is how the cancer cells and their tumor microenvironment (TME) mediate CRT resistance in EAC. To address this question, we performed single-cell RNA sequencing on 84 longitudinal samples from a cohort of patients (N=47) containing 20 good responders (GR) and 27 non-responders (NR). In total, we obtained 302,918 single cells which enabled us to delineate the phenotypic heterogeneity landscape in EAC at baseline, and identify reprogramming in both the immune and tumor cells during treatment that lead to CRT resistance. We identified 4 major cell type compartments in the EAC TME: lymphoid cells (T cells, NK cells, B cells, and plasma cells), myeloid cells (macrophages, neutrophils, dendritic cells, and mast cells), stromal cells (fibroblasts and endothelial cells) and epithelial cells. Our data shows that the TME enriched in lymphoid cells, including resident and effector memory CD8 T cells, follicular helper CD4 T cells, and B cells was associated with better CRT responses. Moreover, a significant myeloid cell infiltration was observed across most patients during CRT and the infiltrated macrophages from GR harbored a more pro-inflammation phenotype. In addition, we identified 4 major ecotypes of the TME cells and 4 major expression subtypes of the cancer cells. Notably, the interactions between TME ecotypes and cancer subtypes are significantly associated with CRT responsiveness. In summary, this study has provided valuable insights into the biology of EAC CRT response, and identified novel predictive biomarkers and actionable targets to enhance CRT efficacy.

#1750 Decoding breast cancer: Unraveling subtype and model differences through multi-model single-cell RNA sequencing data integration.

J. E. Altman[1], C. J. Walker[1], E. K. Zboril[1], N. S. Hairr[1], R. K. Myrick[1], D. C. Boyd[1], J. E. Koblenski[1], M. Puchalapalli[1], B. Hu[1], M. G. Dozmorov[1], X. Chen[2], Y. Chen[3], C. M. Perou[4], B. D. Lehmann[2], J. E. Visvader[3], A. L. Olex[1], J. Harrell[1],

[1]Virginia Commonwealth University, Richmond, VA, [2]Vanderbilt University Medical Center, Nashville, TN, [3]Walter and Eliza Hall Institute of Medical Research, Melbourne, Australia, [4]University of North Carolina at Chapel Hill, Chapel Hill, NC

Breast cancer's complex transcriptional landscape requires a deep understanding of sample and cell diversity to identify effective treatments. In this study, we amalgamate single-cell RNA sequencing data from breast cancer patient-derived xenografts (PDX), organoids, cell lines, patient tumors and reduction mammoplasties resulting in a comprehensive dataset of 117 samples with 506,719 total cells. These samples encompass hormone receptor positive (HR+), human epidermal growth factor receptor 2 enriched (HER2E), and triple-negative breast cancer (TNBC) subtypes. We aimed to delineate similarities and distinctions across model systems and patient samples while also exploring stratification of therapeutic drug efficacy based on subtype proportions within tumors. Mammary tumor PDXs, organoids, and established cell lines exhibited higher proliferation and lower heterogeneity observed via UMAP dimensionality reduction compared to most patient tumors or normal breast epithelium. TNBCs had elevated proliferative and pro-metastatic signatures compared to HR+ and HER2E samples. Interestingly, compared to matched PDX tumors, organoids from these same models were found to exhibit stark differences in gene expression, including upregulation of metabolically active aldo-keto reductase family genes, highlighting differences in the model systems with implications for pre-clinical drug testing. Single-cell tumor subtyping analyses with scSubtype and TNBCtype methods found that therapeutically treated samples had shifts in the proportions of cell-wise subtype annotations when compared to matched untreated samples. Similarly, patient lymph node metastasis when compared with matched primary tumors were significantly linked to decreases in Basal-like and HER2-enriched cell-wise annotations in untreated ER+ samples. In vitro assessment of anti-cancer compounds on PDX cells showed significant correlation of subtype proportion with cell viability following treatment with targeted therapeutic agents. This subtyping methodology offers a powerful tool to monitor the evolving gene expression landscape within samples and predict responses to therapeutic agents. We present here a dynamic approach to cell-wise sample annotation and a substantial multi-model dataset for use facilitating informed decision-making in preclinical research and therapeutic development.

#1751 Deep multi-omics analysis of uterine leiomyosarcoma reveals defective HRD signature, a novel gene fusion and the amplification of the poor-prognosis CTHRC1 gene.

R. M. Falcao[1], J. E. de Souza[1], W. Mathieson[2], J. W. Carlson[3], T. B. Petta[3];

[1]Universidade Federal do Rio Grande do Norte, Natal, Brazil, [2]Integrated Biobank of Luxembourg, Dudelange, Luxembourg, [3]University of Southern California, Los Angeles, CA

Uterine leiomyosarcoma (uLMS) is a rare and aggressive cancer representing approximately 2-5% of all uterine malignancies. The molecular heterogeneity and pathogenesis of uLMS are notwell understood. To unravel the intricate molecular landscape of uLMS, we conducted a multi-omics workflow consisting of 4 high-throughput sequencing technologies; short- and long-readwhole genome sequencing (WGS), RNA-Seq, and Tandem mass tag (TMT) labeling enablingmassively parallel proteome proteomic analyses. Our study cohort consisted of 97 fresh frozentissue samples collected from 68 female patients, with 19 uLMS, 37 leiomyoma (LM), and 41normal myometrium (MM). A deep analysis of somatic variants with clinical impact revealed 46variants present in 90% of samples and two actionable therapeutic targets: IDH1_p.Arg132Cysand KRAS_p.Gly12Val. Also, 80% of the samples presented a chromothripsis signature and 60%presented the SBS3 COSMIC signature related to homologous recombination deficiency (HRD).Analysis of the proliferation score in RNA-Seq data revealed a notable difference among thetumor groups, signifying a higher proliferation index in the uLMS group, suggesting a moreaggressive growth pattern with implications for clinical behavior and disease progression. Afterapplying a customized workflow to identify balanced chromosomal abnormalities of genefusions with clinical impact, the proto-oncogene eukaryotic elongation factor 1 alpha (EEF1A1)emerged as a prominent fusion partner. Eight fusions in 7 samples were identified withtranscriptional overexpression in positive cases. At the proteomic level the enrichment analysisunveiled activated pathways associated with the innate immune system, while suppressedpathways pertained to extracellular matrix (ECM) organization and smooth muscle contraction.With an integrated bioinformatics pipeline, we identified copy number amplification of theCTHRC1 gene in 80% of the samples, accompanied by increased gene expression and proteinlevels. This gene is related to collagen remodeling and degradation and has been demonstratedto be upregulated in some solid tumors and is closely associated with malignancy. Survivalcurve analysis highlighted a significantly poorer prognosis in uLMS exhibiting CTHRC1 geneamplification with potential clinical relevance of CTHRC1 amplification as a prognostic indicatorin uLMS. Taken together these results show the overall suppression of ECM and collagenremodeling in uLMS associated with poor prognosis. Additionally, these data provide the firstevidence that the EEF1A1 gene has a strong selective pressure in uLMS underscoring theindispensable role of precision genomics in advancing precision medicine.

#1752 Comprehensive genomic profiling of advanced breast cancer subtypes: Insights from liquid biopsy analysis and implications for personalized therapies.

X. Liu[1], Y. Liu[1], C. Jia[2], Y. Zhang[2], F. Xie[2], H. Tang[2], S. Jia[2], H. Li[1];

[1]Key laboratory of Carcinogenesis and Translational Research (Ministry of Education/Beijing), department of breast oncology, Peking University Cancer Hospital & Institute, Beijing, China, [2]Huidu (Shanghai) Medical Sciences, Ltd., Shanghai, China

Background: Breast cancer stands as the most prevalent malignancy affecting women's health. The disease consists of three subtypes, including hormone receptor (HR) positive, HER2-positive, and triple-negative breast cancer (TNBC). In recent years, the advent of targeted therapies such as PI3K inhibitors has significantly improved the prognosis of breast cancer patients. However, the detection of relevant molecular markers, such as PIK3CA mutations, relies on tissue samples, which imposes limitations on the clinical application of these therapies. Consequently, this study presents a comprehensive analysis of genomic profiling that compares breast cancer patients across distinct pathological classifications, utilizing a liquid biopsy approach.

Methods: In this retrospective study, 214 patients with advanced breast cancer were recruited. Plasma samples collected prior to first line treatment were analyzed using PredicineCARE, a targeted next-generation sequencing (NGS) liquid biopsy assay, to detect somatic alterations in ctDNA of blood, including single nucleotide variations (SNVs), gene fusions, and copy number variations (CNVs).

Results: Based on the IHC classifications of tumor tissue, this cohort comprised 119 HR-positive, 61 HER2-positive, and 34 TNBC patients. The assay identified a total of 1456 mutations and 2357 gene copy number variants in plasma samples. Among these, the most frequently mutated genes and those with copy number variations (top 5) in HR-positive patients were TP53 (40%), PIK3CA (39%), ATM (22%), ERBB2 (19%), and FGFR1 (19%). In HER2-positive patients, they were TP53 (39%), PIK3CA (31%), ERBB2 (30%), NTRK1 (20%), and RAD50 (20%). For TNBC patients, the top genes were TP53 (59%), ERBB2 (44%), PIK3CA (35%), NTRK1 (35%), and BRCA2 (26%). Regarding the PIK3CA gene, the most prevalent mutation site was H1047, occurring in 12.61% of HR-positive patients, 14.75% of HER2-positive patients, and 11.76% of TNBC patients. Similarly, both E542 (4.20% in HR-positive, 3.28% in HER2-positive, and 2.94% in TNBC patients) and E545 (3.36% in HR-positive, 3.28% in HER2-positive, and 2.94% in TNBC patients) showed equivalent prevalence across the three classifications. These findings suggest the potential efficacy of PI3K inhibitors in various pathological types of breast cancer.

Conclusions: This study offers insights into the genomic landscape of advanced breast cancer subtypes through liquid biopsy. The observed prevalence of PIK3CA mutations supports the potential efficacy of PI3K inhibitors across these diverse types of breast cancer, laying the groundwork for personalized therapeutic strategies and biomarker identification for prognosis and targeted therapies.

#1753 *SHOC2* is a genetic dependency in *NRAS*-mutant melanoma.

A. Y. Gu[1], T.-W. Lee[1], A. Khan[1], F. W. Hunter[2], D. C. Singleton[1], **S. M. Jamieson**[1];
[1]University of Auckland, Auckland, New Zealand, [2]Janssen Research and Development, Spring House, PA

Melanoma is the most lethal form of skin cancer, with over 300,000 new cases worldwide every year. Specifically, melanoma with *NRAS* mutations are of particular clinical concern due to their association with a poor prognosis and lack of specific treatment options. Therefore, there is a pressing need for novel approaches to address the treatment of *NRAS*-mutant melanoma. A current approach to identify novel drug targets is based on the genetic concept of induced essentiality, where functional interactions that occur in response to oncogene addiction create a dependency on another gene. To identify genetic dependencies in *NRAS*-mutant melanoma, whole-genome CRISPR-Cas9 knockout screens were conducted in 6 *NRAS*-mutant and 7 *NRAS*-wild-type (wt) early-passage New Zealand melanoma (NZM) cell lines that were established and maintained at 5% oxygen to mimic physiological oxygen conditions. The NZM cell lines were stably transduced with the whole-genome Brunello lentiviral single guide (sg) RNA library and screened for up to 35 days. BAGEL (Bayesian Analysis of Gene Essentiality) analyses of the NZM whole-genome knockout screens, alongside CRISPR-Cas9 screening data using the Avana sgRNA library from an additional 28 melanoma cell lines, available on the Cancer Cell Line Encyclopaedia (CCLE) database, revealed prospective gene candidates that exhibit greater detrimental effects on the fitness of *NRAS*-mutant cell lines compared to the *NRAS*-wt lines. These genes are being further validated as essential genes for *NRAS*-mutant melanoma cells through custom sgRNA library knockout screens and *in vitro* individual gene knockout studies. In particular, we demonstrate that knockout of *SHOC2*, a gene that encodes a scaffold protein essential for activation of the MAPK signalling pathway, results in the prevention of ERK phosphorylation and a more substantial reduction in cell growth in *NRAS*-mutant NZM cell lines when compared to *NRAS*-wt lines. These results support previous studies that have identified SHOC2 as a potential therapeutic target for *RAS*-driven cancers and suggest that targeting of SHOC2 may have utility in *NRAS*-mutant melanoma, where greater treatment options are urgently needed.

#1754 Test-the-test: Clinical utility of comprehensive whole exome sequencing (WES) and RNA-seq for lymphoma patients.

D. Chihara,[1], K. Balakrishnan,[1], G. Masand[1], A. Novokreshchenova[2], A. Bagaev[2], N. Kotlov[2], E. Postovalova[2], E. Shugaev-Mendosa[2], Y. Gracheva[2], A. Love[2], K. Nomie[2], N. Fowler[2], C. R. Flowers[1], J. Westin[1];

[1]The University of Texas MD Anderson Cancer Center, Houston, TX, [2]BostonGene Corporation, Waltham, MA

Background: Due to the rapidly evolving landscape of targeted therapies, there is an unmet need for comprehensive molecular profiling to guide treatment decisions for patients with lymphoma. To meet this need, we designed a pilot study to assess the feasibility and turnaround time (TAT) of a comprehensive WES and whole transcriptome sequencing (RNA-seq) assay (BostonGene Tumor Portrait™ test) in large B-cell lymphoma (LBCL) patients for clinical decision-making (NCT05464823).

Design: Patients aged ≥18 years with histologically documented LBCL requiring therapy were eligible. Formalin-fixed paraffin-embedded tissues underwent WES, RNA-seq, and copy number analysis (CNA) with concomitant peripheral blood or saliva for germline DNA sequencing. Samples with <20% tumor purity and median coverage of <142x for tumor and/or <95x for normal samples were labeled as quantity not sufficient (QNS). Genomic and transcriptomic data were profiled to uncover clinically relevant biomarkers and match patients with clinical trials on ClinicalTrials.gov.

Results: To date, 63 patients received WES and RNA-seq, with 45 full Tumor Portrait™ test clinical reports delivered and 3 partial reports for QNS samples. Cell of origin (COO, n = 41), LymphGen (n = 41), and lymphoma microenvironment (LME, n = 42) classifications were applied. The median TAT was 8 days for advanced reports, and 76% of reports had a TAT ≤9 days.

WES identified frequent *TP53* (n = 13) and CDK2NA (n = 5) alterations. COOs were designated as activated (n = 16, 39%) or germinal center (n = 25, 61%) LBCL. The LymphGen classifier showed the EZB MYC- (n = 9, 22%), A53 (n = 6, 15%), and MCD (n = 6, 15%) subtypes as the most prevalent. LME classification revealed most LMEs as mesenchymal (n = 30, 71%). Immune-depleted (n = 7, 17%), immune-inflamed (n = 4, 10%), and germinal center-like (n = 1, 2%) LMEs were less prevalent, but the immune-depleted LME was more common in patients with relapse. Clinically significant findings, such as ABC COO (n = 16), *TP53* loss (n = 13), DHITsig+ (n = 6), and *CARD11* mutations associated with ibrutinib resistance (n = 3), were identified in 33 samples. On average, 8 clinical trials were identified per delivered report.

Conclusion: Our results show the clinical utility and acceptable TAT of using a comprehensive WES and RNA-seq assay on a cohort of lymphoma patients. The produced BostonGene Tumor Portrait™ test reports included findings on significant alterations, LymphGen and LME subtypes, COOs, and potential clinical trial matches. These robust findings, coupled with the rapid TAT, demonstrate the feasibility of using integrated WES and RNA-seq to guide clinical decision-making in lymphoma patients.

#1755 Integrative genomic and transcriptomic profiles from a prospective cervical cancer study (RAIDs).

M. Kamal[1], S. Barraud[1], L. Lecompte[2], M. Halladjian[1], E. Jeannot[3], E. Girard[2], S. Baulande[4], P. Legoix[4], F. Lecuru[5], L. Pauly[5], M. Saint-Ghislain[1], S. Cyrille[6], C. Dupain[1], C. Lamy[1], O. Chouchane-Mlik[7], A. Oniga[7], M. Mittelbronn[7], C. Le Tourneau[8], A. Latouche[6], N. Servant[2], S. Scholl[1], I. Bieche[9],

[1]Department of Drug Development and Innovation (D3i), Institut Curie, Paris, France, [2]Bioinformatics and Computational Systems Biology of Cancer, PSL Research University, Mines Paris Tech, INSERM U900, Paris, France, [3]Department of Genetics, Institut Curie, PSL Research University; Department of Pathology, Institut Curie, PSL Research University, Paris, France, [4]Institut Curie, Genomics of Excellence (ICGex) Platform, PSL Research University, Paris, France, [5]Department of Breast, Gynecological and Reconstructive Surgery, Institut Curie, Universite Paris Cite, Paris, France, [6]INSERM, U900, Institut Curie, PSL Research University; Conservatoire National des Arts et Metiers, Saint Cloud, France, [7]National Center of Pathology (NCP), Laboratoire National de Sante (LNS), Dudelange, Luxembourg, [8]Department of Drug Development and Innovation (D3i), Institut Curie; INSERM U900 Research Unit, Institut Curie, Paris, France, [9]Department of Genetics, Institut Curie, PSL Research University; INSERM U1016, Paris Descartes University, Faculty of Pharmaceutical and Biological Sciences, Paris, France

Background: Cervical cancer (CC) remains a leading cause of gynecological cancer related mortality worldwide and constitutes the third most common malignancy in women. We have previously reported a “metagene” of genomic markers in the PI3K pathway and epigenetic regulators associated with poor outcome. Immune therapy recently showed promising results yet new biomarkers for targeted therapeutic approaches in this type of cancer remain to be determined.

Patients & Methods: Patients included in this study were enrolled in BioRAIDs [NCT02428842]. Whole exome sequencing (WES), shallow whole genome sequencing (sWGS) and RNA sequencing were performed on quality-controlled primary frozen tumor samples in 297, 306 and 280 patients, respectively who subsequently had received primary radio chemotherapy. Multi-omics bioinformatics analyses were performed to identify alterations representing new valid drug targets in CC. Tumor-stromal characteristics such as transcriptome deconvolution, CD8+, CD45+, CD68+ staining cells, PD-L1 expression, tumor infiltrating lymphocytes (TILs) together with the degree of tumor necrosis were assessed.

Results: 273/306 were HPV positive (89%). Most frequently altered (≥10%) oncogenes were *PIK3CA* (30%) and *TERT* promoter (14%). Most frequently altered (≥10%) tumor suppressor genes were *FBXW7* (14%), *KMT2D* (11%), *KMT2C* (11%) and *FAT1* (11%).Microsatellite instability (MSI) was detected in 8/297 (3%) patients, homologous recombination deficiency (HRD)-high status in 8/297 (3%) patients and TMB-high (>10mut/Mb) in 32/297 (11%) patients. The most frequent mutational signatures were APOBEC, deaminase and MMR (DNA mismatch repair deficiency (74%, 28% and 11% respectively). Interestingly, *FGFR3 f*usions were detected in 8/297 patients (3%). Transcriptomic analyses showed 510 differentially expressed genes between HPV positive and HPV negative CC (adjusted p-value<0.01 and |log2FC|>1). No significantly differentially expressed genes were detected between FIGO 2018 stages (I/II *vs* III-IV). Both stages as well as tumor necrosis were highly significantly associated with progression-free survival (PFS), with tumor necrosis as an independent prognostic factor in a multivariable analysis (p<0.001).Presence or absence of CD8-positive lymphocytes, or CD68-positive cells of the myeloid cell compartment, histopathological subtype or number of TILs did not correlate with PFS.

Conclusion: Our results confirm the high level of altered genes involved in chromatin remodeling with or without PI3K pathway mutations suggesting the relevance of epidrugs in CC. *FGFR3* fusions and HRD tumors - although being rare (3%) - to be considered as new targeted approaches. Additionally, MSI and TMB high are of interest for immunotherapy beyond PD-L1 expression. Integrative analyses of omics and pathology data and correlation with PFS are ongoing and will be presented in the meeting.

#1756 Characterizing the mutational spectrum of metastatic mucinous adenocarcinoma of the appendix.

D. J. Gironda[1], M. Leung[2], G. Jin[1], L. Liu[1], K. I. Votanopoulos[1], E. A. Levine[1], L. D. Miller[1];

[1]Wake Forest University School of Medicine, Winston Salem, NC, [2]The Atrium Health Wake Forest Baptist Comprehensive Cancer Center, Winston Salem, NC

Background: Appendiceal cancer (AC) is an orphan malignancy with only 1-2 cases per 100,000 people in the US. The genomic composition of metastatic, mucinous AC is yet to be resolved at the whole exome level and few groups have assessed the clinical actionability of target genes. Here we performed whole-exome sequencing (WES) on AC specimens to 1) elucidate the mutational spectrum of AC, 2) identify recurrent mutations at frequencies unique to AC or in common with colorectal cancer (CRC), and 3) uncover recurrent AC mutations that are associated with patient survival outcomes.

Methodology: Twenty-four FFPE samples, one from each of 24 AC patients treated at our institution with cytoreductive surgery (CRS) followed by heated intraperitoneal chemotherapy (HIPEC), were collected from our tumor bank with IRB approval. DNA from tumor and corresponding normal tissue (PBMCs) was extracted, assessed for integrity and quantity, then analyzed by WES using the Illumina NextSeq 6000 platform. The resulting data were processed using both GATK and DRAGEN pipelines. The frequencies of recurrent mutations in AC were compared with those of CRC from cBioPortal and statistically compared by Fisher's Exact Test. Logrank test was performed to estimate survival associations based off mutation status. Mutational signatures derived from the Pan-Cancer Analysis of Whole Genomes (PCAWG) Consortium were cross-compared to our cohort to identify previously unknown mutational processes in AC.

Results: The most frequent mutations were found in MUC6 (63%), KRAS (58%), HLA-B (54%), PABPC1 (50%), and MUC5AC (50%). Distinct from a 534-patient CRC cohort, AC had lower rates of alteration in APC (4% vs 73% CRC, $p<0.001$) and TP53 (21% vs. 62%, $p<0.001$), with higher rates of alteration in HLA-B (54% vs 3%, $p<0.001$), GNAS (38% vs 5%, $p<0.001$), and ABCA1 (29% vs 7%, $p=0.001$). Notably, ABCA1 mutation frequency was higher in mucinous CRC (n=56) when compared to non-mucinous CRC (n=478, 20% vs 7%; $p<0.001$), suggesting that ABCA1 may be uniquely altered in bowel cancers of mucinous phenotype. Alterations in Rho-A were a statistically significant predictor of poor survival in both AC ($p<0.001$) and CRC ($p=0.05$). PCAWG analysis showed that the predominant mutational signature in AC most resembles SBS5, suggesting that the mutational etiology of AC may be linked to age and/or smoking status.

Discussion: Here we present the largest whole-exome sequencing analysis of AC analyzed to date and identify previously undescribed recurrently mutated genes unique to AC as compared to CRC. We demonstrate novel associations between altered genes and patient survival, which opens discussion regarding the clinical utility of molecular markers in AC for assisting treatment decision making.

#1757 Pan-cancer analysis identifies signatures of HRD-positivity in germline BRCA1/2 mutated non-BRCA associated cancers.

D. M. Muldoon, M. Mehine, S. Tischfield, A. Brannon, M. Ladanyi, Z. K. Stadler, D. B. Solit, A. Drilon, M. F. Berger, Y. Murciano-Goroff, C. Bandlamudi; Memorial Sloan Kettering Cancer Center, New York City, NY

Introduction: BRCA-associated cancers (breast, ovarian, pancreas, and prostate) with germline pathogenic mutations in *BRCA1/2* (*gBRCA1/2*) are associated with homologous recombination deficiency (HRD) and benefit from platinum/PARPi. However, the role of *gBRCA1/2* in non-BRCA assoc. cancers is poorly understood. HRD tumors present with 'genomic scars' that can be quantified in tumor profiling ("HRD-sum" score). We reasoned that the HRD-sum score together with germline mutation status (including loss of wild-type) is a strong correlate of HRD-positivity. Leveraging 42,448 prospectively sequenced patients across 63 cancer types, we sought to characterize the prevalence of the HRD-positivity in non-BRCA-assoc. cancers.

Methods: Allele-specific copy number data was inferred using FACETS. HRD-sum was calculated as a sum of the numbers of telomeric imbalances, large-scale transitions and genome-wide losses of heterozygosity. Calculating each score was iteratively optimized to improve detection of the scars using MSK-IMPACT targeted sequencing data using patient-matched WES data from 1841 tumors as reference. Germline mutations were identified by a clinically validated pipeline and annotated for pathogenicity using ClinVar. After excluding low quality tumors, 27,375 patients were retained for analysis. "HRD-positive" tumors are those with *gBRCA1/2* mutations, loss of wild type, and an HRD-sum score >=42.

Results: Expectedly, g*BRCA1/2* mutations were more frequent in BRCA-assoc. cancers (7.2%, 558 of 7,737 patients) compared to non-BRCA-assoc. cancers (2.6%, 500 of 19,638) (p=5e-60). Among non-BRCA-assoc. cancers, g*BRCA1/2* were most common in esophagogastric (3.9%), lung (3%), hepatobiliary (2.9%), and bladder (2.8%) cancers. Although biallelic loss in g*BRCA1/2* patients was sig. higher in BRCA-assoc. cancers (80% vs. 37% in non-BRCA-assoc.), several cancer types showed high rates of loss of wild-type including g*BRCA1* tumors in hepatobiliary (5/5) and endometrial (10/11) cancers. HRD-sum scores in all *gBRCA1/2* biallelic tumors were sig. higher (median 58) compared to monoallelic (26) or wild-type (25) tumors. Notably, the non-BRCA assoc. cancers with biallelic *gBRCA1/2* harbored higher HRD-sum scores compared to monoallelic (median 51 vs. 22, p<0.0001). These include cancer types such as endometrial (64 vs. 37, p= 0.0014) and esophagogastric (62 vs. 45, p=0.0017). In all, 68% of *gBRCA1/2* patients in BRCA-assoc. cancers showed HRD-positivity. Interestingly, 18% (91/500) of *gBRCA1/2* patients in non-BRCA-assoc. cancers also showed HRD-positivity. These included 52% of esophagogastric, 28% of lung, and 22% of bladder cancer patients with *gBRCA1/2*.

Conclusion: Using a robust measure to detect HRD scars from MSK-IMPACT panel data, we demonstrate evidence for BRCA-mediated tumorigenesis in an expanded spectrum of cancers with potential therapeutic relevance.

#1758 Chromosome 3 copy number loss alone drives tumor evolution to aggressive disease in uveal melanoma.

S. Srinivasan[1], J. Rose[1], R. Minelli[1], C. Terranova[1], P. Shah[1], J. R. Daniele[1], M. Peoples[1], M. He[1], C.-Y. Liu[1], J. Gay[1], M. Soeung[1], S. Soni[2], F. Wang[1], C. Bristow[1], K. Wani[1], L. Perelli[1], D. Loza[1], N. Feng[1], M. Tarabichi[3], P. Van Loo[1], A. Futreal[1], S. Woodman[1], A. Lazar[1], C. P. Vellano[1], J. Marszalek[1], G. F. Draetta[1], T. Heffernan[1], A. Carugo[4], G. Genovese[1], V. Giuliani[1],

[1]UT MD Anderson Cancer Center, Houston, TX, [2]Rice University, Houston, TX, [3]Universite Libre de Bruxelles, Bruxelles, Belgium, [4]IRBM, Rome, Israel

Uveal Melanoma (UM) is a rare tumor characterized by mutations in GNAQ or GNA11, followed by a mutation in BAP1, SF3B1 or EIF1AX. Notably, a large subset of BAP1 mutant patients present with a unique chromosome 3 copy-number (CN) loss and higher likelihood of metastases. The biology underlying the causes and consequences of Monosomy 3 (M3), and its role in metastases is largely unexplored. This can be partially attributed to the relatively few numbers of preclinical models of UM, and the inability to delineate M3 from BAP1 loss. To address this, we derived a preclinical isogenic model of chromosome 3 CN loss through CRISPR-based centromere targeting in a well characterized UM cell line lacking a BAP1 mutation. Clones with and without chromosome 3 loss were derived from these efforts. Recent studies have evaluated genomic events in primary UM and described five CN aberration-based subtypes expanding beyond M3, with the fifth subtype being called the “ultra-high-risk UM” based on poor survival and extremely high metastatic rate. Whole genome sequencing across our clones confirmed chromosome 3 CN loss, and in addition to this, recapitulated all of the core genomic features characteristic of the ultra-high-risk UM group. In comparison, our models without chromosome 3 CN loss maintained a genomic profile more characteristic of lower risk UM subtypes. The genomic landscape of our isogenic low risk (LR) and high risk (HR) clones suggest that chromosome 3 CN loss alone in the absence of BAP1 mutations can be the driver for acquisition of downstream genomic events seen in aggressive UM. Further, using single cell DNA sequencing on the parental model, LR and HR clones, we confirmed that chromosome 3 CN loss in our clones was engineered, and not a pre-existing subclone in the parental cell line. Bulk RNAseq on our LR and HR clones demonstrate concordance with genomic regions of losses and gains, while also highlighting upregulation of pathways such as cell cycle and DNA damage response in the HR clones. Next, we developed patient derived xenograft (PDX) models demonstrating differential behavior in paired *in vivo* settings, where HR clones had higher fitness advantage and metastatic potential, specifically to the mouse liver. This modeling has enabled us to employ spatial transcriptomics in a PDX setting, adapt existing methodology to infer chromosomal copy number events in our system and inform transcriptional and genomic phenotypes akin to the aggressive HR clones. Thus, using our engineered preclinical models, we demonstrate that chromosome 3 loss, in the absence of BAP1 mutations is capable of driving aggressive disease in UM, characterized by genomic evolution, transcriptional reprogramming and *in vivo* invasiveness.

#1759 Integrative longitudinal genomic analysis of therapy-resistant and metastatic pediatric cancers.

H. J. Martell[1], A. T. Shah[1], A. G. Lee[1], S. G. Leung[1], S.-J. Cho[1], M. Pons Ventura[1], A. Golla[1], A. E. Marinoff[1], E. P. Young[1], B. Tanasa[1], I. Behroozfard[1], H.-Y. Liu[1], A. Spillinger[1], M. L. Turski[1], N. Elzie-Tuttle[1], C. Espinosa-Mendez[1], A. Rangaswami[1], T. M. Cooney[1], C. Kline[1], A. Agrawal[1], J. Michlisch[1], E. Stieglitz[1], M. Loh[1], A. J. Sabnis[1], K. T. Vo[1], S. Spunt[2], N. Lacayo[2], H. C. Beal[3], F. K. Hazard[2], S. Salama[3], D. Haussler[3], O. M. Vaske[3], M. R. Breese[1], E. Sweet-Cordero[1]; [1]UCSF - University of California San Francisco, San Francisco, CA, [2]Stanford University, Stanford, CA, [3]UCSC - University of California Santa Cruz, Santa Cruz, CA

Pediatric cancer patients are commonly profiled with gene-panel sequencing tests that yield few actionable results, in part due to the complex genomic alterations that define these malignancies. We hypothesized that integration of whole-genome (WGS) and RNA sequencing (RNAseq), would lead to a more comprehensive understanding of these diseases. Our study is uniquely focused on metastatic and relapsed disease, whereas previous studies focused on primary cases. We also prioritized longitudinal profiling, including with deep sequencing, to capture tumor evolution across primary and metastatic sites and to quantify the utility of resampling.

We assembled a cohort of 219 high-risk pediatric oncology patients, including solid tumors, CNS tumors, leukemias/lymphomas, patients with relapsed/refractory disease (75), metastatic disease at diagnosis (7), rare diagnoses (17), prior cancer history, and estimated overall survival <50%. We characterized 286 samples with WGS (tumor ~60X; germline ~30X) and/or RNAseq (polyA selected, ≥20 million reads), including 95 samples taken from 44 patients at different time points (diagnosis, relapse, etc.). Variants, structural rearrangements, mutational signatures, and copy-number alterations were identified using WGS. RNAseq was used to profile gene expression outliers, gene fusions, and expression of variants. Integrated results were used to prioritize potentially actionable variants. For 20 patients (44 samples), we performed targeted deep sequencing of the DNA (~500X).

RNAseq identified potentially druggable outlier gene expression and fusions, including 102 novel fusions where the 3' gene is overexpressed. WGS identified aneuploidy, loss of heterozygosity and whole genome duplication across histotypes. Mutational burden and mutational signatures analyses identified profound effects from platinum drugs on tumor evolution, but treatment effects were not universal. Multiple sampling per patient uncovered drastic spatial and temporal differences in the genomes and transcriptomes of these tumors. Custom deep sequencing confirmed these findings, captured evolution missed by WGS, and furthered our understanding of the complex impacts of treatment on clonal evolution. Histotypes differed by whether actionability was higher for WGS or RNAseq alone, but in 66% of samples modality integration increased actionability. Integration also identified a subset of tumors that may be amenable to immunotherapy, but which lack canonical markers of response. Longitudinal analysis highlighted both the opportunities and risks of targeted therapy, with targetable variants gained and lost between timepoints. Our study shows that integrated multi-modality sequencing can elucidate novel insights into the biology of pediatric cancers and identify potential therapeutic targets not detected using gene-panel testing alone.

#1760 Mutational landscape of the canine acute myeloid leukemia exome.

R. Harris, E. Conaway, A. Avery;
Colorado State University, Fort Collins, CO

Over 21,000 newly diagnosed cases of human acute myeloid leukemia (hAML) and 10,000 hAML-related deaths are reported in the United States every year. hAML is considered a highly diverse aggressive hematopoietic malignancy, with over 16 recurrent gene rearrangements, 60 recurrent point mutations, and hundreds of rarely mutated genes. There are large ongoing multi-institutional studies devoted to advancing medical management for hAML by providing targeted therapeutics to patients based on their molecular characteristics. A preclinical spontaneous large animal model for testing novel therapies could accelerate the development of better treatments in people. Dogs spontaneously develop AML with similar clinical features and outcomes. As such, the dog may be a useful pre-clinical model, but little is known about the molecular landscape and/or drivers of canine AML (cAML). The goal of this work was to identify somatic mutation candidates in cAML and determine the overlapping features with hAML. We utilized whole exome sequencing at 300x coverage to identify candidate mutations in 51 cAML samples. Somatic variant calling was performed per the GATK best practice recommendations using Mutect2 and a reference panel of normals (n=77) and a variant call file of canine germline variants. We focused our analysis on novel variants predicted to have a moderate to high impact and that occurred in genes implicated in cancer. At least one variant was identified in genes involved in the RTK/RAS pathway (e.g. *NRAS, KRAS, PTPN11, FLT3, KIT*) in over 75% of cAML samples, a trend that is also found in people. Additionally, recurrent point mutations were predicted in *NRAS* and *KRAS*, and some of which, such as the codon changes G13R and Q61R/H in *NRAS*, were noted to be shared between hAML and cAML. Mutations in *DNMT3A* were uncommon (n=3/44) and *NPM1* mutations were not identified in our cohort, both of which are common hAML-associated genes. However, mutations in other epigenetic modifiers, such as *KDM5C* and *KDM6A*, occurred at a high frequency. This data provides insight into the candidate mutations potentially driving cAML pathogenesis and highlights the overlapping molecular features with hAML.

#1761 Comprehensive profiling of the FAT3-associated gene signature in deciphering immunophenotypes of gastrointestinal cancers: Analysis of institutional cohort and TCGA dataset.

P. Ahluwalia, T. Leeman, A. Mondal, A. Vashisht, H. Singh, R. Kolhe;
Augusta University, Augusta, GA

Gastrointestinal (GI) cancers are among the most prevalent cancers affecting the US population. Anatomically, GI cancer includes cancers of the organs in the digestive tract, from the esophagus to the rectum. Advances in molecular oncology have started to transform the therapeutic landscape and offer tremendous promise for patients across diverse lineages. However, the equitable benefit of this approach has been hampered due to tumor heterogeneity and the lack of accurate, tumor-agnostic biomarkers with prognosis and predictive utility. Thus, there is a need to identify novel biomarkers that affect gastrointestinal malignancies to improve the management of cancer patients. This study analyzed a single institution's whole genome sequencing dataset to explore the genomic variation in GI cancers. Between 2020 and 2022, 302 AU patients underwent molecular profiling, including whole-exome sequencing (WES) profiling at Caris Life Sciences. WES is an NGS assay that analyzes the DNA sequences of all protein-coding exons in the genome, representing approximately 1-2% of the human genome with coverage of over 22,000 genes. We analyzed the TCGA dataset for comparative analysis, which included cancer data from >1800 GI cancer patients. In addition, survival and network analyses were performed to identify a 6-gene *FAT3*-related signature for GI cancers. In our cohort, we identified *FAT3* (Fat atypical cadherin 3) as the most frequently mutated gene after *TP53*, *APC*, and *KRAS*. *FAT3* encodes a cadherin protein involved in cell-cell interactions and adhesion. In the institutional cohort, *FAT3* was found to be mutated in 16% of all GI cases. Further analysis of TCGA datasets comprising 1808 GI cancer patients revealed *FAT3* mutations in 12% of the cases. To identify additional prognostic biomarkers associated with *FAT3*, we performed network analysis and identified a 6-gene *FAT3*-related signature (*FAT3*, *RYK*, *FAT2*, *EGFLAM*, *NTRK3*, *IGSF9*, and *HMGA2*) that significantly stratified GI cancer patients based on overall survival, progression-free survival, and disease-specific survival. The perturbation profile of the 6-gene signature was associated with 509 patients or 28% of total GI patients. Further, immune deconvolution analysis of stratified patients revealed increased infiltration of immune cells with immunosuppressive phenotypic properties in GI cancer patients with higher expression of the *FAT3*-related gene signature. In summary, this analysis reveals the distribution of *FAT3* mutational profiles in GI patients and identifies a gene signature that stratifies patients based on survival outcomes. This analysis can provide new tools for patient stratification and therapy implementation, leading to better outcomes for cancer patients.

#1762 Characterization of somatic copy number deletion of chromosome 22q in papillary thyroid carcinoma.

Olivia W. Lee[1], Danielle Karyadi[1], Stephen Hartley[1], Weyin Zhou[1], Mitchell Machiela[1], Mykola Tronko[2], Tetiana Bogdanova[2], Liudmyla Zurnadzhy[2], Lindsay Morton[1], Stephen Chanock[1]

[1]National Cancer Institute, Rockville, MD,[2]V.P. Komisarenko Institute of Endocrinology and Metabolism of the National Academy of Medical Sciences of Ukraine, Kyiv, Ukraine

Deletion in the long arm of chromosome 22 (22qDEL) is the most prevalent somatic copy number alteration (SCNA) observed in papillary thyroid carcinoma (PTC). Despite its recurrence, the specific characteristics and role of 22qDEL in PTC have not been fully studied. We conducted a pooled analysis of 22qDEL by integrating patient and clinical information and molecular profiles from 1,094 primary PTC tumors across four major published PTC genomic studies: The Cancer Genome Atlas (TCGA) PTC profile study, the National Cancer Institute (NCI) post-Chornobyl PTC study, the Memorial Sloan Kettering Cancer Center Integrated Mutation Profiling of Actionable Cancer Targets (MSKCC-IMPACT) PTC cases, and the Seoul National University (SNU) thyroid cancer profile study. The majority of PTC with 22qDEL demonstrated arm-level loss of heterozygosity (86%). Even in PTC cases with partial 22qDEL, we observed a loss across 70% of chromosome 22, encompassing regions 22q12 and 22q13, which harbors known cancer genes (*NF2* and *CHEK2*). More than 90% of 22qDEL co-occurred with established oncogenic drivers of PTC, though a full assessment of PTC drivers was not available for all cases. 22qDEL occurred more frequently with *RAS* point mutations (50.4%) than other drivers (9.3%). A higher fraction of 22qDEL was clonal in *RAS*-driven PTCs (78.3%), suggesting 22qDEL occurs early in *RAS*-driven tumor development. We did not observe any association between 22qDEL and established PTC risk factors such as age, sex, and radiation, nor with clinical features including tumor size, multifocality, and metastasis (p-values>0.22). RNA sequencing gene expression analysis based on 22qDEL status revealed downregulation of most genes residing on chromosome 22q and significant differential expression activity of immune-related genes, further implicating a role of immune dysregulation in PTC. Our study suggests that 22qDEL may not act as a primary driver of PTC but plays an important role as a co-factor of *RAS* point mutations, which could further drive PTC development.

#1763 Long-read sequencing of pediatric leukemia identifies clinically relevant genomic rearrangements.

B. Yoo[1], A. Keskus[2], C. Bi[1], L. Lansdon[1], T. Ahmad[2], I. Pushel[1], A. Walter[1], M. Gibson[1], E. Guest[1], T. Pastinen[1], M. Kolmogorov[2], M. S. Farooqi[1];
[1]Children's Mercy Kansas City, Kansas City, MO, [2]National Cancer Institute, Bethesda, MD

Clinical detection of genomic rearrangements currently depends on a range of complementary and overlapping methods including fluorescence *in situ* hybridization (FISH), karyotyping, and DNA and/or RNA sequencing. This requirement for multiple tests results in higher total costs, extended analysis time, and increased usage of sometimes limited tumor material. In our laboratory, we apply long high-fidelity reads to human samples using PacBio circular consensus sequencing (HiFi-GS) of 12-18kb DNA fragments, which offers better structural variant detection relative to short-read sequencing. Here, we assess the ability of HiFi-GS to detect clinically relevant genomic rearrangements (CRGRs) in pediatric leukemia.

We selected 11 pediatric leukemia cases with corresponding normal (remission) samples, including 7 cases of B-cell acute lymphoblastic leukemia (B-ALL) and 4 cases of acute myeloid leukemia (AML); 5 of these 11 leukemia cases had known CRGRs as below. The remaining 6 leukemia cases had also undergone clinical genetic profiling via karyotyping, FISH, microarray, and sequencing yet a clinical grade genomic driver was not identified. DNA from each sample was sequenced on a Revio instrument (PacBio, Menlo Park, CA) to a target depth of 30x. The PacBio Human Whole Genome Sequencing (WGS) workflow was used to process HiFi reads for haplotagged alignment and phasing, followed by somatic structural variant calling using Severus. Subsequent analysis focused on the presence of break ends in known cancer-relevant genes.

We found that HiFi-GS detected the known CRGRs in all 5 cases with prior findings, providing precise break ends and clarifying sometimes unclear cytogenetic observations (such as exact partner genes), in these cases. These included detection of an *ETV6-RUNX1* fusion, *NUP98-NSD1* fusion, *KMT2A-AFF1* fusion, *KMT2A-AFDN* fusion, and *RUNX1-RUNX1T1* fusion. HiFi sequencing also detected CRGRs in 2 of the 6 “undiagnosed cases”; namely, one case of *ZNF384-TCF3* fusion and one case of *KMT2A-MLLT10* fusion. The former can be cytogenetically cryptic, while the latter can often be missed due to its potentially complex nature.

Our results demonstrate that HiFi-GS can reliably detect CRGRs, bringing us closer to the promise of a single comprehensive genetic test for cancer characterization. Additional work examining other somatic structural and copy number variants (i.e., inversions, deletions, and duplications) in these cases, as well as oncogenic sequence variants, is ongoing.

#1764 Long read sequencing allows comprehensive molecular profiling of complex karyotype acute myeloid leukemia (CKAML) with 5q deletions.

F. Schick[1], E. Slonova[2], E. Straeng[1], S. Huet[3], M. Raso[1], M. Tilgner[1], F. Damm[1], P. Sujobert[3], O. Blau[1], L. Bullinger[1], A. Dolnik[1];
[1]Charite - University Medicine Berlin, Berlin, Germany, [2]German Cancer Research Center (DKFZ) and German Cancer Consortium (DKTK), Berlin, Germany, [3]Hospices Civils de Lyon, Lyon, France

Background Acute myeloid leukemia with complex karyotype (CKAML) does frequently show del(5q), deletion of chromosome 5q. Previous work in MDS and AML showed that CKAML form clusters distinguishing del(5q) cases with commonly retained regions (CRRs) in the telomeric (≥5q34) and centromeric (≤5q14.2) ends from cases with loss of the telomeric and/or centromeric regions. Interestingly, del(5q) patients with CRRs were shown to have less genomic lesions and were associated with a better prognosis than other 5q-deleted CKAML cases.
Aim: Combining the advantages of two different long read sequencing technologies, Pacific Biosciences (PacBio) and Oxford Nanopore Technologies (ONT), we aimed to more comprehensively characterize the molecular landscape of CKAML with del(5q). Our integrative workflow enabled an in-depth characterization of copy number variations (CNV), genomic rearrangements, transcriptomic and epigenomic changes.
Methods: Low coverage whole genome sequencing (WGS) using ONT was performed on 209 patients with CKAML to identify del(5q) cases for further in-depth analysis. For 10 selected cases with known CRR status, genomic deep sequencing using PacBio Revio and ONT PromethION was performed, as well as PacBio Revio MAS-seq for fusion transcript detection.
Results: A mean sequencing depth of 3-fold (range 0.4-17.3-fold) was obtained by low coverage WGS of the 209 CKAML cases. With a resolution of 0.1 Mbp n=134 del(5q) cases were identified in our CKAML cohort (64%) and commonly deleted regions on 5q could be resolved at 5q21.2 to 5q23.3 and 5q33.3 to 5q35 (Fisher test, FDR Benjamini-Hochberg, $p<10^{-30}$). These regions separated del(5q) in n=52 cases showing CRR retention and n=82 showing partially no CRR, (either the centromeric or telomeric regions, n=74, or of both regions, n=8 involved). Subsequent co-occurrence analysis provided evidence of an association between the loss of telomeric 5q region with a 3p12-25 deletion. In-depth analysis (30-50 fold) of ten distinct del(5q) cases by PacBio and ONT revealed additional insights into the complex clonal composition of del(5q) cases. For example, one case showed two distinct subclones with 5q14.2-5q35.1 deletion and with translocation t(3;5)(p14;q14) respectively. Moreover, we could demonstrate that 5q-aberrations are far more complex than initially thought showing, e.g. inverted terminal duplications that resulted in fusion transcripts involving *PDE4D* and leading to its deregulated expression.
Conclusion: Using our long read deep sequencing approach we could further delineate the structural complexity of del(5q) CKAML. While gene expression profiling, methylation analysis and correlation of findings with clinical outcome are ongoing and will be presented at the meeting, our results help to further pinpoint the biology underlying del(5q) and to further refine this heterogeneous CKAML subgroup.

#1765 The genetic landscape of head and neck cancer using brush biopsy.

E. John[1], T. Lesluyes[2], T. Baker[2], M. Tarabichi[3], P. Van Loo[1], X. Zhao[1];
[1]UT MD Anderson Cancer Center, Houston, TX, [2]The Francis Crick Institute, London, United Kingdom, [3]Universite Libre de Bruxelles, Brussels, Belgium

Oral premalignant lesions (OPLs) with genomic alterations have a heightened risk of evolving into oral squamous cell carcinoma (OSCC). Currently, genomic data are obtained through invasive tissue biopsy. Brush biopsy has been utilized for diagnosing dysplasia but its effectiveness in reflecting the complete genomic landscape of OPLs remains uncertain. This study investigates the potential of brush biopsy samples in accurately reconstructing the genomic profile of OPLs. The evolution and heterogeneity were assessed by assessing SNVs, copy number analysis, and subclonal architecture reconstruction of paired tissue-brush biopsy samples of oral epithelium, dysplastic lesion, and OSCC lesion. We found that brush biopsy accurately reflects the genomic landscape of oral lesions, mirroring about 90% of SNVs and comparable CNA profiles found in tissue biopsies. Genomic profiling with brush biopsy was tissue-specific, as SNVs identified in OPL or OSCC lesions were not found in adjacent normal mucosa. Shared SNVs and CNAs were observed between OPL and OSCC samples. This suggested a common ancestor giving rise to these lesions. Subclonal architecture reconstruction confirmed that both lesion types shared a common ancestor clone and then diverged evolutionarily. These findings underscore the potential of brush biopsies in accurately reconstructing the genomic profile of OPL and OSCC, highlighting their usefulness in understanding the biological processes involved in tumor evolution.

#1766 *CREBBP*, *NOTCH2* and *GNAS*mutational profile in uterine sarcomas.

L. G. dos Anjos, G. N. Quevedo, E. C. Baracat, **K. C. Carvalho**;
University of Sao Paulo, Faculty of Medicine, Sao Paulo, Brazil

Background: Uterine sarcomas (US) present clinical challenges due to their dynamic behavior and limited treatment options. Representing 1-3% of uterine cancer cases, these tumors exhibit rapid growth, high recurrence rates, and resistance to the standard treatments. The present study aimed to validate several Loss-of-function mutations (LOF), obtained by NGS analysis in the *CREBBP*, *NOTCH2*, and *GNAS* sequences, in US through Sanger sequencing. **Methods:** Twenty-five samples of US were collected between 2000 and 2015 for genomic DNA extraction. An initial genetic screening of the samples by NGS method was followed by Sanger sequencing validation. Bioinformatics analysis through SnapGene confirmed the results. **Results:** A c.4063G>A mutation was confirmed in uterine leiomyosarcomas (ULMS), in the both strands. Notable variations in the forward strand, such as a C>G substitution at position 38 of the alignment and a degenerate base S at position 113, differentiated ULMS from uterine sarcomas (US). Two ULMSs exhibited the highest substitution rates: one with 18 and another with 6 substitutions. Despite the absence of the c.5527T>C *CREBBP* mutation, ULMS displayed increased insertions and deletions. Assessing the *NOTCH2* gene in US revealed a complex genetic landscape, with a unique SU-specific duplication in the forward strand. The reverse strand maintained high genetic stability. Mutation c.6094C>A was exclusive to one US sample. Notably, the c.7223T>A mutation in *NOTCH2* was not identified. Shared mutations between ULMS and US suggest genomic similarities in these regions. In the *GNAS* analysis, the c.2381A>C mutation was not found. However, in the forward sequence of one US sample, a deletion at the expected substitution site was detected, suggesting a specific genetic alteration. The c.706G>A mutation was consistently present in sample ULMS, indicating genetic stability in this sample. US exhibited a G>C substitution in the reverse sequence, hinting at a unique pattern of genetic variation. These findings underscore the complexity of genetic alterations in these critical gene regions. **Conclusion:** Our analysis identified specific alterations in ULMS and US. ULMS showed the c.4063G>A *CREBBP* mutation and unique variations, while US had a specific c.6094C>A *NOTCH2* mutation. The absence of the c.2381A>C *GNAS* mutation in both ULMS and US, along with distinct genetic patterns (c.706G>A in ULMS and G>C substitution in US), underscores significant mutational differences in these critical gene regions. These findings enhance our understanding of uterine sarcoma genetics, prompting further exploration for potential diagnosis, prognosis and therapeutic advancements.

#1767 Molecular subclassification of gastrointestinal stromal tumors by genomic backgrounds.

H. Yamamoto, E. Nakada, S. Kawano, F. Kato, C. Fukano, M. Futagawa, Y. Urakawa, R. Ohsumi, S. Ueno, H. Yanai, A. Hirasawa;
Okayama University Hospital, Okayama, Japan

Gastrointestinal stromal tumors (GISTs) are the most common gastrointestinal mesenchymal tumors. While about 10% of GISTs are known to be developed from the *KIT* or *PDGFRA* gain-of-function mutations, the rest, which is the majority of GISTs, is so-called as wild-type GISTs. There are attempts to make subclassification of wild-type GISTs in syndromic or non-syndromic group as promising for understanding of heterogeneity or treatment strategy. Genomic states of succinate dehydrogenase B (SDHB) and neurofibromatosis type 1 (NF1) have been raised as candidates for subclassification of wild-type GISTs. In this presentation, we will discuss our recent three cases of wild-type GISTs, carrying germline pathogenic variants in *SDHB* or *NF1*. Two cases with *SDHB* germline pathogenic variants showed stomach GISTs with good clinical course, the maintained performance status and long survival nevertheless of the recurrence. The other case with an *NF1* germline pathogenic variant showed multiple GISTs in small intestine which was controlled surgically and the late onset of other clinical symptoms of NF1. These cases might clinically suggest potential prognostic and predictive markers in genomic alterations of *SDHB* or *NF1* for the cases with wild-type GISTs.

#1768 Investigating oncogene amplifications in brain metastasis of esophageal adenocarcinoma samples.

Nora Lawson[1], Lingqun Ye[2], Bo Zhao[2], Andy Futreal[2], Kadir Akdemir[3]

[1]School of Health Professions, The University of Texas MD Anderson Cancer Center, Houston, TX,[2]Genomic Medicine, The University of Texas MD Anderson Cancer Center, Houston, TX,[3]Neurosurgery-Research, The University of Texas MD Anderson Cancer Center, Houston, TX

Esophageal Adenocarcinoma (EAC) exhibits a rising incidence and dismal survival rate in the US, primarily attributed to frequent distant metastases. Brain metastasis, though uncommon is an aggressive tumor type, remains poorly understood in EAC. To address this knowledge gap, we conducted a comprehensive analysis of 9 brain metastasis samples, profiling their whole-genome with matched normal and comparing them to the primary EAC tumors, other EAC metastasis types and other brain metastasis types, including the Hartwig Institute and PCAWG. Overall, our sample size comprised over 4,500 tumor whole-genome data and we utilized a uniform data analysis pipeline for robust comparisons between cohorts. Our analysis revealed that brain metastasis samples have significantly higher single-nucleotide variants, however, the structural variant burden in brain metastases closely resembled those observed in the primary tumor. Notably, the incidence of whole genome doubling is significantly higher in brain metastasis compared to other primary cancer types and metastases. This significant difference stems from the higher WGD incidence in primary EACs compared to other tumor types. Mutational signature analysis revealed no significant changes compared to the primary tumor, and we observed an enrichment of SBS 17a/b, previously associated with tumor progression in primary esophageal adenocarcinoma, along with a prevalent presence of the APOBEC mutagenesis signature in most samples. Notably, ERBB2 and TP53 emerged as prominent driver genes present in most brain metastasis samples. We also observed an upregulation of ERBB2 expression in brain metastasis samples. Interestingly, ERBB2 appeared to play a more significant role in brain metastasis progression compared to the primary tumor and other metastasis types, suggesting its potential as a therapeutic target. These findings advance our comprehension of brain metastasis in EAC, providing crucial insights into genomic alterations and mutational processes that could inform future therapeutic strategies and clinical management for this previously understudied metastatic type.

#1769 Pan-cancer genomic characterization of human papillomavirus associated tumors reveals patterns of somatic alteration that associate with virus status and anatomic site.

J. R. Holt[1], P. Little[1], H. Jo[1], X. Zhao[1], H. Choi[1], V. Walter[2], B. Wahle[3], J. P. Zevallos[4], A. Mazul[4], K. A. Hoadley[5], M. Hayward[6], D. N. Hayes[1];
[1]University of Tennessee Health Science Center, Memphis, TN, [2]Penn State College of Medicine, Hershey, PA, [3]Washington University School of Medicine, St. Louis, MO, [4]University of Pittsburgh, Pittsburgh, PA, [5]University of North Carolina School of Medicine, Chapel Hill, NC, [6]UNC Lineberger Comprehensive Cancer Center, Chapel Hill, NC

Human papilloma virus (HPV) infection causes over 600,000 human cancers yearly and accounts for nearly all cervical cancers, increasing rates of head and neck squamous cell carcinomas (HNSCC), and many anogenital cancers - all with varying clinical outcomes due to a lack of personalized care. While recent integrative genomic studies have described molecular features of individual cancer types, few studies have compared genomic changes between HPV(+) and HPV(-) cancers across anatomic sites. Here, we conducted the first pan-cancer genomic analysis of HPV-associated tumors across multiple anatomic tumor types using whole exome and transcriptome data from The Cancer Genome Atlas (TCGA) cohorts of cervical (n=254) and HNSCCs (n=514), and targeted exome sequencing of 800 cancer genes plus full length HPV16/18 genomes in a clinical cohort of squamous tumors from the head and neck (n=458), cervix (n=78), vulva (n=23), anal canal (n=5), and vagina (n=2). Somatic variant calling and filtering, followed by an integrative pathway analysis of commonly altered targets, defined the catalog of somatic mutations and copy number alterations (CNAs) that drive HPV(+) and HPV(-) tumorigenesis. Sequencing reads from viral RNA or DNA determined HPV status, and HPV type, genome structure, integration events, and viral load were characterized in a subset of samples via de novo assembly of viral aligned reads followed by copy number analysis, breakpoint identification, and the calling of structural variants. Overall HPV positivity was 50% (668 out of 1334 total), with HPV16 accounting for 96%, 89%, and 60% of all HPV(+) anogenital, head and neck, and cervical tumors respectively. Significant differences in somatic mutation frequency between HPV(+) and HPV(-) tumors were observed in the full cohort, as well as in analyses stratified by anatomic site. Interestingly, we noticed recurrently mutated “hotspots” attributable to increased APOBEC-mutagenesis in HPV(+) samples across anatomic sites (PIK3CA:E545K, FGFR3:S249C, EP300:D1399N), while hotspot mutations likely caused by tobacco smoking predominate HPV(-) HNSCC (PIK3CA:H1047R/L, CDKN2A:R80*, TP53:R282W). Focal and arm level CNAs were distinctive, including gains of 11q22 in HPV(+) cervical and HPV(-) HNSCC, and losses of 11q22 in HPV(+) HNSCC. Biological pathways commonly altered include epithelial differentiation, cell death, innate immunity, growth factor/kinase signaling, and cell cycle control. In summary, pan-cancer genomic analysis revealed distinct patterns of somatic alteration of conserved biological pathways that associate with HPV status and anatomic site. These findings improve our understanding of tumor biology unique to HPV-associated cancers and may lead to novel treatment and classification strategies to improve patient outcomes in the clinical setting.

#1770 Right oncogene, wrong tumor - CBL mutations in pediatric CNS and solid tumors.

L. M. Brown[1], C. Mayoh[1], P. Acera Mateos[1], A. De Weck[1], R. Salomon[1], T. Sadras[2], N. Manoharan[3], M. Wong[1], M. J. Cowley[1], P. G. Ekert[1];
[1]Children's Cancer Institute, Sydney, Australia, [2]Peter MacCallum Cancer Centre, Parkville, Australia, [3]Sydney Children's Hospital, Randwick, Australia

The molecular analysis of individual patient tumors by personalized medicine programs like the Zero Childhood Cancer Program (ZERO) enables the detection of potentially targetable lesions, unlocking new therapeutic opportunities for patients. Somatic mutations in the E3-ubiquitin ligase, CBL, are known to activate receptor tyrosine kinases (RTKs) in cancer and have been exclusively characterized in hematological malignancies. This includes acute myeloid leukemia, where CBL mutations lead to FLT3 activation. Using molecular data from ZERO we have identified known and novel *CBL* variants in novel tumor contexts. Our findings raise the possibility that CBL mutation may be a marker of RTK activation in a range of paediatric cancer types and may represent a group of patients who could benefit from tyrosine kinase inhibitor (TKI) therapy.

We analyzed whole genome and RNA sequencing data from the ZERO cohort and identified 26 somatic *CBL* variants in 22 individual patients, the majority of which were in CNS tumors (14 patients). In 8 patients with CNS tumors, we identified missense and splicing variants, which were either novel or not previously seen in this tumor type, that are predicted to have a functional impact on CBL E3 ligase activity due to their location in the linker region or RING finger domain of CBL. Interestingly, most of these patients did not fall into a pre-defined DNA methylation-based subtype classification of CNS tumors and had no significant upregulation of RTK genes.

In addition to the novel variants, we identified an established oncogenic CBL deletion variant, CBL exon 8/9 deletion (CBL ex8/9Δ), in novel tumor types - neuroblastoma and a germ cell tumor. Functionally, we show that overexpression of CBL ex8/9Δ enhances cell proliferation and maintains EGFR signaling by blocking CBL mediated degradation of phosphorylated EGFR in neuroblastoma cells.

In this study, we demonstrate that CBL is mutated in a range of pediatric cancer types beyond hematological malignancies and may represent a marker of RTK activation and a new target for high-risk patients with limited therapeutic options.

#1771 NYU Langone Genome PACT - Genome Profiling of Actionable Cancer Targets (LG-PACT) for clinical patient molecular diagnostics and treatment.

V. Vasudevaraja, Y. Yang, J. Serrano, K. Wrzeszczynski, M. Snuderl;
NYU Langone Health, New York, NY

Next-generation sequencing (NGS) for the detection of somatic variants has become the tool of choice in a variety of molecular oncology fields and in the clinic. Its use ranges from sequencing entire tumor genomes and transcriptomes to targeted clinical diagnostic gene panels. The NYU Langone Genome PACT assay is a qualitative in vitro diagnostic test that uses targeted next generation sequencing of formalin-fixed paraffin-embedded (FFPE) tumor tissue matched with normal specimens from patients to detect gene alterations in a 607-gene panel. Indications for testing are cancer (solid tumors or hematological malignancies) where a mutational profile from multiple genes would be informative for disease stratification, prognosis, or treatment options including targeted therapies and eligibility for clinical trials. The test is intended to provide information on somatic mutations including point mutations, copy number aberrations, and small insertions/deletions (indels) for diagnostic and treatment decisions. LG-PACT is a United States Food and Drug Administration (FDA) approved diagnostic test. The clinical interpretation of sequencing data of molecular tumor markers from NGS encompasses automated variant calling tools with human interpretation. The final mostly manual review of data is intensive, involving highly trained scientists, encompassing literature review, interpretation and tier classification by pathologists, who then provide a complete molecular diagnostic report to the treating oncologists. Since January 2022 to present (October 2023) we have provided clinical genomic reports for 1029 oncological cases from 124 different cancers and their subtypes, including Brain (489 cases incl. meningioma, glioma and glioblastoma), Gastrointestinal (123), Lung (114), among others. We first present the technical challenges of validating an NGS oncological diagnostic targeted assay for appropriate clinical grade accuracy and sensitivity acceptable for patient care. We show how copy number alterations provide a more comprehensive description of the tumors genomic profile. We then outline the actionability of targeted panel sequencing for our current patient cohort. Where analysis of variant detection has led to 47% (490) of our clinical tumor samples containing known tier 1 therapeutic variants. We conclude with presenting case studies that identify both the clinical utility and informatic challenges of variant calling specific to gene panel sequencing e.g., i) the capture of potential targetable rare and novel indels and multivariant mutations in exons 19 and 20 of EGFR, and ii) a unique KIT tandem duplication event in a gastrointestinal stromal tumor (GIST). We demonstrate the value in precision oncology for multiple cancer types and how the capture of unique variants can provide better targeted treatment options to cancer patients.

#1772 A naturally occurring canine model of peripheral T-cell lymphoma, not otherwise specified.

E. Owens, A. Harris, A. Avery;
Colorado State University, College of Veterinary Medicine & Biomedical Sciences, Fort Collins, CO

Despite being the most common subtype of human peripheral T-cell lymphoma (PTCL), PTCL-not otherwise specified (PTCL-NOS) remains a poorly understood diagnosis of exclusion with poor survival times and treatment responses. Canine PTCL clinically and immunophenotypically resembles human PTCL-NOS, and PTCL is more common in dogs than humans, leading to their interest as a naturally occurring preclinical model. Canine models of cancer offer several unique advantages: in contrast to traditional rodent models, these are spontaneous tumors in genetically diverse and immunocompetent animals living in a shared environment with humans, but relative to their human counterparts, they offer accelerated lifespans with shorter clinical courses of disease. Here, we analyzed the gene expression profile of 96 canine CD4+ PTCLs to determine similarities to human PTCL-NOS and investigate a possible cell of origin. Bulk RNA-seq was performed on lymph node aspirates of 96 cases of canine CD4+ PTCL diagnosed by flow cytometry and sorted CD4+ nodal lymphocytes and CD4+ thymocytes from healthy control dogs. Raw reads were aligned to the Ensembl canine reference genome (ROS_Cfam_1.0) and tabulated. Data normalization and differential expression analysis was conducted with DESeq2, and differentially expressed genes were compared to human PTCL-NOS and various stages of T-cell development via gene set enrichment analyses (GSEA). Global gene expression in canine CD4+ PTCL was analogous to that of human PTCL-NOS (NES = 2.3, $p < 0.001$). Additionally, canine CD4+ PTCL had increased expression of *GATA3* (log2fc = 1.9, padj = 6.5e-07) and was enriched for gene signatures associated with downregulation of PTEN (NES = 1.7, p = 0.0001) and upregulation of PI3K/AKT/mTOR signaling (NES = 1.5, padj = 0.0007), resembling the more aggressive human GATA3-PTCL subtype. Canine CD4+ PTCL was also enriched for human and murine gene signatures associated with early thymocyte progenitor cells and had increased expression of genes of immaturity, including *CD34* (log2fc = 7.8, padj = 2.6e-14), *KIT* (log2fc = 3.3, padj = 7.7e-05), and *CCR9* (log2fc = 4.8, padj = 3.9e-11), although surface CD34 expression is not detected by flow cytometry. These findings were confirmed when we compared the canine PTCL gene expression programs to a canine single cell transcriptomic atlas of hematopoietic precursors and T cells across canine bone marrow, thymic, and lymph node tissues. Canine CD4+ PTCL cells were significantly ($padj < 0.05$) enriched for gene signatures associated with early thymic and bone marrow precursors (NES 1.3-2.1), and negatively enriched for gene signatures associated with naïve nodal CD4+ T cells (NES = -3.2, padj = 0.006). In conclusion, the gene expression profile of canine CD4+ PTCL resembles human PTCL-NOS, supporting its potential as a naturally occurring preclinical model, and a subset of these neoplasms may arise from a thymic precursor cell of origin.

#1773 Deciphering the roles of germline predisposition variants and somatic mutations on breast cancer cells and the tumor microenvironment.

F. Martins Rodrigues, K. Gallant, R. Jayasinghe, M. Iglesia, A. Houston, S. Chen, P. Lal, R. Fields, W. Gillanders, F. Chen, L. Ding;
Washington University in St. Louis, Saint Louis, MO

While great progress has been made in the understanding and treatment of cancer, tumor heterogeneity remains a diagnostic and prognostic challenge. Single-cell sequencing techniques and high-resolution cellular imaging now afford researchers the ability to investigate the effects of germline variants (especially when compared to somatic mutations) on molecular characteristics of cancer cells and non-cancer cells in the tumor microenvironment (TME). Here, we investigated a breast cancer (BRCA) cohort of over 100 individuals, for which we have generated sc/sn RNA-seq, snATAC-seq, and CODEX imaging data as well as bulk whole exome sequencing and RNA-seq data. We identified 21 BRCA cases carrying pathogenic and likely pathogenic rare germline variants in known cancer predisposition genes, such as BRCA2, BRIP1, ATM, and TP53. These predisposition genes showed diverse expression patterns across stromal and immune cell types, indicating roles in cell types beyond breast epithelia. For cases carrying pathogenic germline variants in such genes, we use snRNA-seq/snATAC-seq to assess gene expression changes and pathway alterations (e.g.,HRD and apoptosis) across all cell types and investigate phenotypic changes associated with pathogenic germline variants in cancer cells compared to stroma and immune cells in the TME. By evaluating chromatin accessibility changes and allele-specific expression, we reveal the connection between epigenetic regulators and differential roles of germline variants across cell types. Finally, the integrated analysis of germline variants and somatic mutations from predisposition genes at single cell resolution broadened our understanding of the role of germline variants in TME during tumorigenesis.

#1774 Examination of variants of unknown significance (VUSs) and co-occurring mutations from comprehensive genomic profiling (CGP) results in a cross tumor model.

T. Simon, R. Oliver, R. Harrell, P. Conkling, E. Paul;
Ontada, Boston, MA

Data from Comprehensive Genomic Profiling (CGP) generates both actionable and non-actionable results for oncology patients. While the actionable results are included in reports, the non-actionable are less often investigated. This study explored the results of both actionable and non-actionable mutations as well as the co-occurrence of mutations in a pan-tumor model.In this study, we explored data generated from 41 oncology practices where patients (+ 18yo) were tracked within the iKnowMed EHR and had received CGP as part of their care. CGP is defined as a large-scale (300+ genes) NGS-based assay. As part of this study, results between 2017 - present were collected across tumor types and stages.Assessment of the data pool demonstrated that a majority of the 44,769 profiles were generated from Stage IV patients (n=24,545) and NSCLC, colorectal, and breast cancers were the highest representing disease populations in the cohort. The tested gene targets aligned with the diseases that were most represented, with EGFR, PIKC3A, ERBB2, and KRAS genes as the most common genes to have documented results . Exploration of the actionable biomarkers showed the expected pathogenic mutations in the relevant disease context. When exploring the remaining reported variants, it was found that CGP results yield a significant ($p \leq 0.05$) number of VUSs as well (n=23106). The complexity of mutations was also examined on an intra- and intergenic basis. Intragenic assessment for variants focused on complex mutations, qualified by 2+ mutations including multiple SNV, multiple indels, or SNVs and deletions in the same gene. Trends of co-occurring alterations were not obvious, with TP53 having the most reported occurrences of complex mutations (n=7491). Exploration moved to intergenic assessment and, while disease-bounded exploration did not reveal trends, a disease-agnostic approach revealed co-occurrences of mutations. The top 5 genes with co-existing mutations are TP53, KRAS, APC, PIK3CA, and ATM. Co-occurrence of alterations in any gene with tumor agnostic markers was also explored, notably TMB. The presence of mutation with TMB-high was similar to that of intergenic complex mutations and the same genes had high co-incidence levels. This study has demonstrated that CGP data provide insights beyond actionable biomarkers, and that a pan-tumor approach allows new trends to be observed. Real-world data bias for reported biomarkers skewed the results observed. Taking the results out of disease context allows us to visualize new possibilities for identifying variants implicated in disease processes. Future studies could allow the exploration of unreported data from raw files, overlaid with cellular pathways on complex patient profiles to identify exploitable targets. Inclusion of treatment and outcome data can demonstrate the influence of genetics on a patient journey.

#1775 The profiling of *MTAP* homozygous deletion (MTAPhd) in a Chinese pan-cancer cohort.

Shuirong Zhang, Wenjin Liu, Mingmin Wang, Caiping Chen, Xiaowei Dong, Aodi Wang, **Kai Wang**

OrigiMed, Shanghai, China

Background: Protein arginine methyltransferase 5 (PRMT5) is an enzyme that catalyzes the transfer of methyl groups from S-adenosylmethionine (SAM) to the arginine residues on histones and other proteins. The dysregulation of this methylation is critical in the development of certain cancers. MTAPhd can cause anti-tumor effect of PRMT5 inhibitor via a synthetic lethality mechanism.
Methods: 9,202 cases were collected and subjected to NGS for genomic alteration detection. The testing was carried out by a College of American Pathologists (CAP) accredited and Clinical Laboratory Improvement Amendments (CLIA) certified laboratory, Shanghai, China. The hybrid capture panel covered 450 genes, heterozygous snps were used for MTAPhd identification, the detection rate of MTAPhd was measured and fisher's exact test was used for analyzing the correlation with age, stage, subtype and gender.
Results: In total, 6.8% (626/9202) cases had MTAPhd. In 626 dataset, 220 was female and 406 was male. Age was from 3 to 91 with median 63. 25, 43, 74 and 119 was in clinical stage I, II, III, IV, respectively. Patients with age < 60 had lower odds (OR 0.60; 95% CI 0.51-0.71; p < 0.001) of occurring MTAPhd compared to age >= 60. Clinical stage I and II had lower odds (OR 0.59; 95% CI 0.44-0.79; p < 0.001) compared to stage III and IV. Adenocarcinoma had lower odds (OR 0.17; 95% CI 0.14-0.21; p < 0.001) compared to squamous carcinoma. Female had lower odds (OR 0.70; 95% CI 0.59-0.83; p < 0.001). MTAPhd occurred in multiple cancers, among which it was more likely to occur in esophageal carcinoma (72/298; 24.2%), brain tumor (14/66; 21.2%) and bladder urothelial carcinoma (67/348, 19.3%). The detection rates of the top three cancer types in the sample size were lung cancer (208/2743, 7.6%), pancreatic cancer (48/794, 6.0%) and colorectal carcinoma (7/756, 0.9%), respectively. Lung squamous cell carcinoma (LUSC) (13.5% vs 19.3%, p = 0.008) and bladder urothelial carcinoma (BLCA) (19.3% vs 25.5%, p = 0.045) of Chinese cohort had lower rate of MTAPhd compared to TCGA cohort. 53 out of 626 had no driver mutations associated with recommended drug use currently. One lung adenocarcinoma patient received crizotinib (*MET* amplification) in 2021, then changed to osimertinib (*EGFR* exon19del), underwent chemotherapy in 2023, developed hip metastases, and was currently undergoing radiotherapy.
Conclusion: This study, for the first time, revealed that MTAPhd were found in approximately 6.8% of Chinese patients across different tumors. Patients with age >= 60, stage III and IV, squamous carcinoma and male, were more likely to occur MTAPhd. Esophageal carcinoma and brain tumor had a higher detection rate. Chinese cohort had lower detection rate of MTAPhd for LUSC and BLCA compared to TCGA cohort. Our results indicated that PRMT5 inhibitors would be a potential therapeutic strategy to be considered for Chinese patients with MTAPhd in the near future.

MOLECULAR/CELLULAR BIOLOGY AND GENETICS: Metabolic Pathways 2
Poster Session

#1779 *De novo* purine pathway enzyme ATIC promotes tumor progression and modulates metabolic reprogramming in breast cancer.
D. Murthy, K. S. Attri, J. Park, B. A. Kaipparettu;
Baylor College of Medicine, Houston, TX

Breast cancer (BC), a complex and heterogeneous disease, poses a significant global health challenge with a pressing need for enhanced prognostic markers and therapeutic targets. This study focuses on 5-Aminoimidazole-4-carboxamide ribonucleotide formyltransferase/IMP cyclohydrolase (ATIC), an enzyme essential in *de novo* purine biosynthesis and previously implicated in myeloma and hepatocellular carcinoma progression. Leveraging publicly available datasets, including TCGA, METABRIC, and GENT2, we identified elevated ATIC expression in BC tissues compared to normal tissues. Notably, patients with elevated ATIC expression displayed significantly diminished overall survival rates, underscoring ATIC's potential as a prognostic marker. Functional assays involving ATIC downregulation in BC cell lines revealed suppressed cell growth, migration, and increased sensitivity to chemotherapeutic drug, Doxorubicin, implicating ATIC in BC progression. Further, RNA-sequencing analysis of ATIC knockdown (KD) BC cell lines revealed a positive correlation between ATIC expression and the activation of MYC and E2F-regulated pathways. The marked attenuation in cell growth and various tumor properties upon ATIC KD provides mechanistic insights into the role of ATIC in fueling BC progression, potentially through the modulation of MYC and E2F target gene expression. Gene Set Enrichment Analysis (GSEA) on differentially expressed genes identified between tumors with high ATIC expression and low ATIC expression in BC patients from the TCGA cohort revealed a notable enrichment of genes associated with MYC and E2F targets, providing additional support for the observed molecular associations in our experimental model. Intriguingly, ATIC KD in Triple Negative BC cell line unexpectedly led to an increase in fatty acid β-oxidation (FAO), uncovering a metabolic vulnerability in these cells. In conclusion, this study unravels the multifaceted role of ATIC in BC, demonstrating its influence on BC tumor progression and metabolism. The observed increase in FAO upon ATIC KD presents a novel metabolic vulnerability that could be explored for targeted therapeutic interventions in BC. This comprehensive analysis contributes valuable insights toward understanding ATIC as a potential therapeutic target and prognostic indicator in BC.

#1780 Utilizing bisbiguanide compounds to disrupt metabolic heterogeneity in non-small cell lung cancer.

V. Y. Matsuk, C. M. Knippler, J. L. Arnst, I. E. Robinson, T. O. Khatib, M. Shanmugam, T. Ganesh, J. K. Mouw, A. I. Marcus;
Emory Winship Cancer Institute, Atlanta, GA

Metastasis accounts for 90% of cancer-related deaths; however, the molecularmechanisms by which cancer cells invade and metastasize remain poorly understood.Around 80% of lung cancer patients present with metastatic disease and have only a 5%5-year relative survival. Metastases are often seeded by heterogeneous cells that invadecollectively in cellular packs. However, most studies and treatments focus on bulk cellularpopulations leaving subpopulations that drive metastasis masked. We previouslypublished on metabolic heterogeneity within collectively invading lung cancer cells andidentified the bisbiguanide compound alexidine as a disrupter of lung cancermitochondrial metabolism and invasion. To expand on these findings, we developed newbiguanides and identified promising candidates, AX-4 and AX-7. These analogs inducemitochondrial structural defects and cause metabolic rewiring. Treated lung cancer cellsexhibited reduced oxygen consumption and increased lactate production. Importantly,AX-4 and AX-7 reduced collective cell invasion, highlighting the potential of these newbiguanides to limit cancer metastasis. Taken together, we have developed new chemicaltools to disrupt mitochondrial metabolism. These tools will be useful to further parse theroles of metabolically heterogenous cancer cells on tumor growth and metastasis.

#1781 Elucidation of glutathione related dipeptide metabolism in cancer.

F. Alimohammadi[1], F. Hecht[1], M. Zocchi[1], E. Tuttle[1], G. Asantewaa[1], T. Scales[1], N. Ward[2], G. DeNicola[2], I. Harris[1];
[1]University of Rochester Medical Center, Rochester, NY, [2]Moffitt Cancer Center, Tampa, FL

There is a long-standing belief that supplementation with antioxidants could potentially treat diseases like cancer. Recent year studies showed, however, that they can behave like a double-edged sword and can also increase tumor proliferation and metastatic progression. The exact mechanism behind antioxidants' impact on tumors is poorly understood. Glutathione (GSH), the most abundant antioxidant in mammalian cells, is a tripeptide containing glutamate, cysteine, and glycine. GSH levels are reported to be significantly elevated within the extracellular space of the tumor. Our preliminary findings show that the breakdown of extracellular GSH can support tumor cell survival under cystine-free conditions. Extracellular GSH catabolism releases cysteinylglycine, which can enter the cell through a dipeptide transporter and be further broken down to supply cysteine and glycine to cells. Alternatively, cysteinylglycine can also be broken down extracellularly into cysteine and glycine, allowing for the uptake of these individual peptides. The molecular mechanisms surrounding the utilization of GSH-breakdown products by the tumor cell are largely unknown. We hypothesize that the proteins responsible for the supply of cysteinylglycine to the tumor cell are required for tumor growth and survival. To test this, we will use unbiased genetic and pharmacologic screening approaches to elucidate the proteins involved in cysteinylglycine processing. Preliminarily, we have found that inhibitors of dipeptidases prevent the ability of cysteinylglycine to support tumor cell survival under cystine starvation, suggesting that tumors require downstream utilization of GSH products. By identifying the mechanisms involved in cysteinylglycine breakdown and supply to tumor cells, we will potentially reveal novel therapeutic targets for cancer treatment, including those not relied upon by normal tissues. Further, our studies will potentially provide a better understanding of how antioxidants impact tumor growth and progression.

#1783 Understanding lipogenesis in bladder cancer.

J. Leak, D. Matye, E. Abbott, B. Woolbright, J. A. Taylor III;
University of Kansas Medical Center, Kansas City, MO

Cancer cells are known to have different metabolic needs for growth and survival and by understanding these demands of individual cancers, targeted novel therapies may be developed. Lipogenesis and ß-oxidation serve to balance lipid levels in the cell. Lipogenesis is rate limited by a series of reactions that include enzymes fatty acid synthase (FASN) and acetyl-CoA carboxylase (ACC1) that facilitate lipid formation; whereas ß-oxidation is rate limited by the transporter carnitine palmitoyltransferase 1 (CPT1) and the enzyme thiolase that catalyzes the final step of the ß-oxidation cycle. Many cancers are dependent on lipogenesis, but the role of these factors in BCa is poorly defined. The Cancer Genome Atlas was used to assess levels of relevant metabolic proteins in normal and cancerous BCa tissue, and showed FASN levels were elevated in BCa tissue and were associated with worse survival. The purpose of this project is to better understand the metabolic demands of bladder cancer (BCa) cell lines, and we hypothesized lipogenesis is a major metabolic pathway for BCa cell growth. T24, HTB-5, and HTB-9 BCa cell lines were used to evaluate the role of metabolism. CPT1 was inhibited with etomoxir, thiolase with trimetazidine, FASN with cerulenin, and ACC1 with 5-(Tetradecyloxy)-2-furoic acid (TOFA). Cell viability was assessed at 48 and 72 hours with an enzymatic activity assay measuring ß-hexosaminidase activity as a surrogate for cell proliferation. The IC50 (concentration of a drug to reduce cell proliferation by 50%) was calculated from this data. At 48 hours, cerulenin-treated cells had an IC50 of 11.80 µM, 13.28 µM, 18.31 µM for HTB-9, T24, and HTB-5 respectively. At 48 hours, TOFA-treated cells had an IC50 of 64.25 µM, 59.29 µM, 32.03 µM for HTB-9, T24, and HTB-5 respectively. Cellular proliferation was not inhibited by CPT1 or trimetazidine at enzymatic IC50 concentrations consistent with their known levels of efficacy. When adding the lipid palmitate (20µM) to TOFA-treated cells, it appeared to mediate a rescue of cell proliferation almost to control, although statistical significance was not achieved. Crystal violet assays were performed to assess long-term cell viability. There was visible reduction in colony formation in a dose-dependent manner at 5 µM and 10 µM cerulenin in T24 cells at 14 days of culture, and there were similar results in HTB-9 cells treated with 20 µM and 40 µM TOFA at 17 days. In both cerulenin and TOFA-treated cells, there was elevated cleaved caspase-3 protein expression, indicating initiation of apoptosis. In conclusion, inhibition of lipogenesis in BCa cell lines reduces cell viability by reducing proliferation and inducing apoptosis whereas inhibitors of ß-oxidation did not produce the same effect at relevant concentrations. These data indicate lipogenesis is a key metabolic pathway for BCa cell growth.

#1784 Glucose metabolism and *de novo* palmitate synthesis under normoxia and hypoxia in breast cancer cells that preferentially metastasize to lung and liver.

M. A. Layosa[1], M. Conrad[1], S. Hursting[2], D. Teegarden[1];
[1]Purdue University, West Lafayette, IN, [2]University of North Carolina at Chapel Hill, Chapel Hill, NC

Cancer cells are exposed to variable oxygen and nutrient availability during the metastatic process which can influence metabolic adaptations of cancer cells to metastasize to distant sites. Thus, we investigated the metabolic adaptations of breast cancer cells that preferentially metastasize to lung (metM-Wnt^{Lung} cells; MLg) and liver (metM-Wnt^{Liver} cells; MLr) in normoxia and hypoxia and at different glucose concentrations. In normoxia, ^{14}C-glucose uptake is similar, but mRNA abundance of hexokinase, the initial rate-limiting step in glycolysis, was 22% higher in MLg cells. This is consistent with higher $^{13}C_6$-glucose flux into glycolytic metabolites pyruvate (M+3) and lactate (M+3) in MLg compared to MLr. Also, *de novo* palmitate synthesis from $^{13}C_6$-glucose was 7.6% higher in MLg and was accompanied by higher mRNA expression of ATP-citrate lyase (ACLY), which converts citrate to acetyl-CoA for fatty acid synthesis. These suggest greater glucose metabolism in MLg compared to MLr in normoxia, consistent with reduced viability of MLr by 39% in high glucose (25 mM) concentrations. Further, mRNA abundance of CPT1A, a rate-limiting step in fatty acid oxidation, is 23% higher in MLg. Moreover, the fatty acid oxidation inhibition (etomoxir) reduced viability of MLg by 26.7% compared to MLr, suggesting that fatty acid synthesis and oxidation are critical for MLg. Protein expression of HIF1α, a transcription factor that induces glycolysis during hypoxia, is 1.5-fold higher in MLr than MLg in normoxia, consistent with higher MLr mRNA abundance of pyruvate dehydrogenase kinase (PDK1), a target of HIF1α that inhibits pyruvate dehydrogenase (PDH) activity. Surprisingly, mRNA abundance of pyruvate carboxylase (PC), the enzyme that converts pyruvate to oxaloacetate, is also higher in MLr (39%) than MLg, thus supporting a potential alternative mechanism for glucose metabolites to enter the TCA cycle in normoxia in MLr. In hypoxia, viability of MLr, relative to MLg, increased by 11% at high glucose concentration. This was accompanied by higher hexokinase (33%) and PDK1 (83%) mRNA abundance suggesting MLr's shift towards a glycolytic phenotype. However, *de novo* palmitate synthesis from $^{13}C_6$-glucose is higher in MLg, suggesting that palmitate synthesis is maintained in MLg even in hypoxia. Altogether, results demonstrate that glucose utilization shifts in breast cancer cells that preferentially metastasize to lung vs liver, but *de novo* fatty acid synthesis is higher in MLg in different oxygen conditions. Thus, targeting breast cancer cells' adaptation to glucose and *de novo* fatty acid synthesis may be a potential strategy to prevent breast cancer progression to distant organs.

#1785 The role of *BRCA1* on metabolic pathways in an *in vivo* system.

S. L. Hembruff, A. Dekonenko, J. Thyfault, M. Sardiu, M. Washburn, R. A. Jensen, L. M. Harlan-Williams;
University of Kansas Medical Center, Kansas City, KS

The role of *BRCA1* in cellular metabolism is not well characterized and what we do understand has been mostly demonstrated *in vitro*. Our studies aim to fully characterize the role of *BRCA1* in metabolic pathways in a whole-body system. *In vivo* studies using C57BL/6 wild-type and transgenic humanized *BRCA1* mice demonstrate the effect of human *BRCA1* on the whole-body metabolic phenotype and start to elucidate the mechanism by which this occurs. We used Promethion metabolic chambers and glucose tolerance tests to measure a number of metabolic outputs of male and female mice that had either normal mouse *Brca1* gene expression (wild-type/WT mice) or a knock-out mouse *Brca1*/knock-in human *BRCA1* (humanized/HU mice). Humanized *BRCA1* mice are more lean, hyperactive and demonstrate a sexual dimorphism in glucose tolerance when compared to wild-type mice on the same genetic background. To begin to elucidate the mechanisms behind the observed metabolic phenotype, we used a metabolic tissue, female mouse skeletal muscle, to perform mass spectrometry, SuperArray, and Western blot analysis. Proteomic samples were sent to the IDeA National Resource for Quantitative Proteomics at the University of Arkansas Medical Sciences for processing and analysis. Proteomic and genomic analysis showed changes in a number of metabolic pathways that may be implicated in the observed whole body metabolic phenotype. We can conclude that changing the expression levels of *BRCA1* in an *in vivo* model altered the overall metabolic profile of C57BL/6 mice. This is the first *in vivo* evidence demonstrating the effects of *BRCA1* expression in whole body metabolism.

#1786 Metabolic rewiring induced by protein or calorie restriction provides unique therapeutic vulnerabilities in translocation and select clear cell renal cell carcinomas.

S. A. Orsi[1], C. Rupert[1], S. Colligan[1], M. Chang[1], A. Jawadwala[1], I. Delle Fontane[1], F. de Nigris[2], R. Pili[1];
[1]University at Buffalo, Buffalo, NY, [2]University of Campania L. Vanvitelli, Naples, NY

While the approval of several combinations with immune checkpoint inhibitors have significantly improved the outcome of kidney cancer patients, advanced clear cell and non-clear cell renal cell carcinoma (RCC) remain a clinical challenge. There has been a longstanding interest in using dysregulated metabolism as a therapeutic target due to its association with the pathogenesis and progression of several cancer types. As one of these highly metabolic tumors, RCC has the potential to greatly benefit from strategies targeting tumor metabolism. Dietary interventions are an innovative adjunct therapy that has the potential to induce a wide range of anti-cancer effects by disrupting metabolism due to the role diet plays in providing tumors with macromolecules for energy metabolism. Unfortunately, tumor cell plasticity, intratumor heterogeneity, and a lack of understanding regarding metabolic vulnerabilities in tumors limit the efficacy of implementing these strategies and a fundamental gap in the field remains as to how basic metabolic requirements of the tumor can be targeted with specific dietary interventions. In this study, the inherent metabolic phenotypes of translocation RCC (tRCC) and clear cell RCC (ccRCC) were characterized by integrating *in vivo* metabolomics and transcriptomics data, assessing mitochondrial and glycolytic activity *in vitro* via Seahorse, and performing immunohistochemical analyses of patient samples. Interestingly, the respective mitochondrial and glycolytic dependencies in tRCC and ccRCC patient-derived xenograft (PDX) models appear to influence the response to nutrient deprivation as seen by *in vitro* assays conducted after amino acid or glucose restriction. Importantly, these results indicate that dietary interventions may be able to selectively target metabolic vulnerabilities in tRCC and ccRCC. Ongoing combination studies with either protein or calorie restriction and targeted therapies, such as standard of care receptor tyrosine-kinase inhibitors, suggest the benefit of using dietary interventions as an adjunct therapy in RCC. Overall, these studies reveal that selective dietary interventions alter the metabolic landscape of RCC and expose vulnerabilities that can be exploited with targeted therapy. As dietary interventions are a safe, affordable, and potentially well tolerated adjunct therapy, we anticipate that the results of these studies will provide the biologic and mechanistic support for translating this strategy to advanced RCC patients.

#1787 The β3-adrenergic receptor as novel target of metabolic phenotype in Ewing sarcoma.

Cristina Banella[1], **Francesco Carrozzo**[1], Laura Zocca[1], Amada Pasha[1], Gianluca Mattei[2], Marina Mola[1], Lara Ballerini[1], Nicla Lorito[3], Annalisa Tondo[1], Claudio Favre[1], Maura Calvani[1]

[1]Meyer Children's Hospital - IRCCS, Firenze, Italy,[2]University of Florence Department of Information Engineering, Firenze, Italy,[3]University of Florence, Department of Experimental and Clinical Biomedical Sciences, Firenze, Italy

Purpose of study: Metabolic targeted therapies may represent an innovative strategy in Ewing sarcoma (ES).
Introduction: Ewing sarcoma (ES) is highly aggressive round cell mesenchymal neoplasm, most often occurring in children and young adults. Metabolic peculiarities of ES cells are indeed involved in tumor growth, survival and resistance to therapy. We have further investigated apoptotic role of ***β***;;3-adrenergic receptor (***β***;;3-AR) SR59230A (SR) antagonist for its ability to reduce cells viability due increased oxidative stress, now we underline the metabolic role of SR.
Materials & Methods: The metabolic profile after SR administration in A673 ES cell model was studied using the Seahorse XF Analyzer. Viability was evaluated with MTS. Changes in gene expression was evaluated with RNA sequencing. Western blot analysis and Immunofluorescence was performed for redox signature and metabolic alteration. Ros production and cell death was assessed by flow cytometry.
Results: Metabolic analysis reveals glucose and fatty acid dependency in A673 cells using the Fuel Flex Test of Seahorse XFe Analyzer. Quantification of transcript abundance using Salmon in A673 after SR treatment showed decrease in response to reactive oxygen species, increase of Thioredoxin Interacting Protein (TXNIP) inhibits the antioxidative function of thioredoxin, moreover reduced glucose uptake, consequently, decrease NADPH/NADP resulting in the accumulation of ROS coincident with a decrease of GLUT1, SOD2, TrDX an increase of LC3IIA protein expression. SR enhances A673 pyruvate dependency, and decrease glyco and mito ATP production rate, more over observed under glucose deprivation. Furthermore, apoptotic effect was significantly amplified when cells were under nutrient starvation, revealing a 56% apoptotic rate after 24 hours of SR treatment.
Conclusion: SR antagonist of ***β***;;3-AR and combination of SR with BUF could be an innovative therapeutic option to raise awareness ES.

#1789 Machine learning-based method to analyze metabolic fluxes of patient tumors.

B. Meghdadi, A. Mittal, A. J. Scott, S. Palavalasa, D. R. Wahl, D. Nagrath;
University of Michigan, Ann Arbor, MI

Personalized oncology must overcome the complex challenge of distinct cancer phenotypes in each patient, formed in part in response to unique metabolic crosstalk among cells in the tumor microenvironment which can be a determining factor in therapeutic response. Although isotope tracing sheds light on differences of metabolite enrichments in tumor and normal tissues, quantifying the metabolic fluxes in patients remains elusive. The conventional metabolic flux analysis tools are unable to estimate patient metabolic fluxes because we are limited to a single time point enrichment datapoint from each patient's in-vivo measurement at isotopic non-steady state. We overcame this challenge by generating training data from the limited patient data and implementing a machine learning model to predict fluxes. To generate training data, we first simulated constrained random fluxes and enrichment patterns at different time points using patient circulating metabolites enrichment via an isotopic non-stationary metabolic flux analysis framework. Using this data, we trained a convolutional neural network to predict flux ratios. To validate our model, we compared predicted flux ratios to the experimental data from mouse models for two different treatments. Our recent findings from a glioblastoma (GBM) mouse model study using conventional metabolic flux analysis revealed higher de novo guanosine monophosphate (GMP) synthesis in GBM than normal cortex. These tumors can be sensitive to mycophenolate mofetil (MMF) which inhibits inosine monophosphate dehydrogenase, but only if the major source of GMP production is de novo synthesis and not salvage. Our machine learning model can discriminate between sources of GMP synthesis in patients, thus enabling prediction of potential responders. Furthermore, we previously showed that serine uptake is higher in GBM than normal cortex, and a serine- and glycine-restricted diet slows tumor growth in mice. While both circulating serine and microenvironment-derived serine could account for serine uptake in GBM, we hypothesized that the circulating serine dependence would better predict response to dietary serine depletion. Hence, we combined patient scRNA-seq and metabolomics data to feed our neural network framework to estimate microenvironmental and circulating serine uptake in six patients with brain cancer. Thus, we have shown that our model can identify patients who will benefit from MMF treatment or a serine- and glycine-restricted diet, enabling administration of highly effective personalized treatments for GBM patients.

#1790 Pyruvate carboxylase regulates tumor progression through central carbon metabolism and immunosuppression.

M. F. Coleman[1], E. Kulkoyluoglu Cotul[2], A. J. Pfeil[1], A. N. Ho[1], E. N. Devericks[1], M. H. Safdar[2], H. Chen[2], N. Attaar[1], V. A. Kiesel[1], D. Teegarden[2], S. D. Hursting[1], M. K. Wendt[3],

[1]UNC Chapel Hill, Chapel Hill, NC, [2]Purdue University, West Lafayette, IN, [3]University of Iowa, Iowa City, IA

The tumor microenvironment (TME) is characterized by metabolic reprogramming and immune evasion, essential features in tumor progression. Tumor metabolic dysregulation, particularly the high production of lactate, plays a pivotal role in suppressing antitumor immunity within the TME. Pyruvate carboxylase (PC), responsible for converting pyruvate to oxaloacetate, is a critical determinant for lung metastasis in triple-negative breast cancer (TNBC). Herein we test the hypothesis that PC-mediated regulation of central carbon metabolism controls TME immunosurrveilance. Wild-type C57BL6/J and NSG mice received orthotopic injections of E0771 or M-Wnt tumor cells with shRNA targeting PC or a scramble control. RNA from tumors underwent transcriptomic profiling using Affymetrix Clariom D microarray (n=3-6/group per experiment). Gene set enrichment analysis identified pathways enriched in each condition, including a PC-associated hypoxia signature. Immunohistochemistry with anti-CD3 antibody and full spectrum flow cytometry assessed T cell infiltration and TME immune cell composition. Untargeted metabolomics, extracellular flux analysis, and high-resolution respirometry determined how loss of PC altered cellular metabolism. We found that suppressing PC expression increased primary tumor growth (~2 fold), potently drove immunosuppression, and remodeled cellular metabolism towards lactate production. Injection of PC-suppressed cells increased regulatory T cell levels in wild type mice. Importantly, PC-suppressed cells injected into NSG mice, which lack T, B, and NK cells, demonstrated slower, rather than accelerated, tumor growth. PC-suppression reduced oxygen consumption rate (OCR), but supply of anaplerotic carbon through exogenous malate or oxaloacetate restored OCR. Conversely, both the rate of and reliance on lactate production was increased by PC suppression. Notably, loss of immunosurveillance following downregulation of PC was reversed by inhibiting lactate transport. Additionally, lower PC expression was associated with increased hypoxia in tumors, supporting in vitro evidence of PC-repression by hypoxia. In summary, hypoxia-induced PC suppression emerges as a crucial mechanism through which primary tumors hinder antitumor immunity, partly via increased lactate production. These findings underscore the significance of PC-directed tumor metabolism as an understudied nexus in the interplay between tumor progression and antitumor immunity.

#1791 Metabolic rewiring promotes metastatic potential upon glutamine deprivation in STK11 null KRAS-driven lung adenocarcinoma.

S. Prior, L. Sands, S. Lenahan, H. Sarausky, M. Scheiber, D. Seward, P. Deming;
University of Vermont, Swanton, VT

Lung adenocarcinoma (LUAD) with concurrent oncogenic KRAS and STK11 loss-of-function mutations define an aggressive subtype characterized, in part, by increased metastasis. Loss of STK11, a tumor suppressor and nutrient sensor, leads to dysregulation of many critical cellular processes, including metabolism. As such, STK11 null cancers are “glutamine addicted” to support proliferative properties and the tumor microenvironment therefore becomes glutamine depleted. We hypothesize that conditions of glutamine stress promote metastatic potential in STK11 null KRAS-driven LUAD due to metabolic rewiring. To test this hypothesis, we utilized a cell culture model of KRAS-driven LUAD cell lines and corresponding STK11 knockout cell lines (ΔSTK11). Parental and ΔSTK11 cells underwent the Seahorse mitochondrial stress test in full and glutamine-deficient media to obtain parameters of mitochondrial respiration at baseline and under conditions reflective of the tumor microenvironment, respectively. At baseline, ΔSTK11 cells had a hypermetabolic phenotype associated with enhanced glutamine utilization. Deprivation of glutamine resulted in decreased mitochondrial respiration along with a significant increase in live, detached ΔSTK11 cells compared to the parental line. Upon further examination, the detached ΔSTK11 cells maintained the ability to re-adhere and proliferate in full media while the detached parental cells did not. Additionally, expression of pro-survival, anti-apoptotic and EMT markers in ΔSTK11 cells were increased upon glutamine deprivation. To determine the mechanism(s) underlying this pro-metastatic phenotype, we employed heavy nitrogen labeling which revealed an upregulation of the hexosamine biosynthetic pathway (HBP). The HBP is an offshoot of glycolysis that serves as a central hub to regulate many cancer fitness pathways via O-GlcNAcylation; the addition of a GlcNAc moiety to serine/threonine residues of target proteins. Further assessment of O-GlcNAcylation levels via western and far western blot analysis revealed that parental cells had decreasing HBP flux concordant with decreasing glutamine concentration while ΔSTK11 cells, conversely, had enhanced HBP flux upon decreasing glutamine availability. These observations suggest ΔSTK11 cells utilize the HBP as a protective shunt under decreased glutamine availability. We are currently characterizing the invasive potential and anchorage-independence of parental and ΔSTK11 LUAD cells upon glutamine deprivation. Future studies aim to establish the impact of HBP perturbation, both genetically and pharmacologically, on the described measures of metastatic potential. Overall, this work reveals novel insight into the molecular mechanisms altered downstream of STK11 loss that link glutamine metabolism with metastatic properties in KRAS-driven LUAD.

#1792 Synthetic lethal vulnerabilities stemming from inhibition of one carbon metabolism in anaplastic thyroid cancer.

A. Forrest, A. Ahsan, **A. Di Cristofano**;
Albert Einstein College of Medicine, Bronx, NY

Reprogramming of metabolic processes by tumor cells is essential to cope with their increased proliferative activity, and with the challenges of the unique microenvironment they inhabit. These metabolic alterations are attractive targets to design novel therapeutic approaches.The most aggressive subtype of thyroid cancer, Anaplastic Thyroid Cancer (ATC), is often unresectable at presentation, highly resistant to therapy and usually lethal. We have recently discovered that ATCs overexpress several genes encoding enzymes involved in one-carbon metabolism (1C-Met), which utilizes serine and dietary folates to produce glycine and tetrahydrofolate-bound one-carbon units, required for nucleotide biosynthesis and for NADPH and glutathione (GSH) production. We have shown that i) the increased activity of the 1C-Met pathway supports the high purine demand of ATC; ii) inhibition of 1C-Met impairs tumor growth in vitro and in vivo, leading to growth arrest; iii) inhibition of 1C-Met renders thyroid cancer cells glycine-auxotroph.We now demonstrate that the profound addiction of ATC cells to 1C-Met creates a series of targetable vulnerabilities that can be harnessed to induce massive ATC cell death.Our new data demonstrate that:1- The purine depletion consequent impaired 1C-Met induces replicative stress and triggers the DNA Damage Response (DDR). Activation of DDR, coupled with the absence of functional TP53 in the vast majority of ATCs, leads to synthetic lethality between inhibition of 1C-Met and G2/M checkpoint kinases.2- Inhibition of 1C-Met in ATC cells generates an absolute dependence on extracellular glycine uptake. We have identified and validated the main glycine transporter(s) in ATC cells and show that inhibition of 1C-Met is synthetic lethal with inhibition of glycine uptake.3- Impaired 1C-Met leads to increased oxidative stress and decrease of NADPH and glutathione levels. These alterations create a synthetic lethality relationship with the glutathione-depleting activity of PRIMA-1 (APR246), a small molecule originally identified as a compound restoring mutant p53 conformation and function, but later shown to be converted within cells into the reactive electrophile methylene quinuclidinone, which acts in a p53-independent manner through a variety of mechanisms, including reduction of cellular GSH levels.Our data shed light on the molecular consequences of 1C-Met upregulation in ATC and support the efficacy of novel rationally designed therapeutic approaches with curative intent not only for ATC, but also for other aggressive, dedifferentiated solid tumors.

#1793 Transmembrane serine protease TMPRSS11B promotes tumorigenesis in lung squamous cell carcinoma through enhanced lactate export and modulation of the tumor microenvironment.

H. Sunil[1], B. L. Updegraff[2], J. Zhu[1], L. Thomas[1], B. M. Evers[1], J. R. Clemenceau[3], I. Barnfather[3], J. D. Minna[1], R. J. Deberardinis[1], T. G. Oliver[4], T. Hwang[3], K. A. O'Donnell[1];

[1]University of Texas Southwestern Medical Center, Dallas, TX, [2]Seagen, Bothell, WA, [3]Mayo Clinic, Jacksonville, FL, [4]Duke University, Durham, NC

Lung cancer is the leading cause of cancer-related deaths worldwide. Existing therapeutic options have limited efficacy, underscoring the critical need for the identification of new actionable therapeutic targets. We previously identified the Transmembrane Serine Protease *TMPRSS11B* as a novel gene that promotes the transformation of human bronchial epithelial cells *in vitro* and induces tumorigenesis *in vivo*. TMPRSS11B promotes extracellular release of Basigin, an obligate chaperone of the lactate monocarboxylate transporters MCT1/4, enhancing lactate export and glycolytic metabolism, and thereby promoting tumorigenesis. Importantly, *TMPRSS11B* is frequently overexpressed in human lung squamous cell cancers (LSCC) and high expression is associated with poor patient survival. Moreover, as a cell surface protein and enzyme, TMPRSS11B represents a tractable target for therapeutic intervention. To investigate whether TMPRSS11B activity impacts the host immune system and the tumor microenvironment (TME), we evaluated the effect of *Tmprss11b* depletion in a syngeneic LSCC mouse model, KLN205. *Tmprss11b* loss of function in KLN205 LSCC cells significantly reduced tumor burden in immunocompetent mice and triggered an accumulation of CD4+ T cells. We are currently extending these studies by investigating the effect of *Tmprss11b* loss of function using CRISPR/Cas9 editing in the *Rosa26*$^{\text{LSL-Sox2-IRES-GFP}}$; Nkx2-1$^{\text{fl/fl}}$; *Lkb1*$^{\text{fl/fl}}$ (SNL) mouse model of LSCC. Tumor burden analysis and pH-sensitive fluorescent imaging are ongoing to assess changes in lactate accumulation. Moreover, RNA FISH analysis and spatial transcriptomics revealed that *Tmprss11b* expression is highly enriched in lung squamous tumors compared to lung adenocarcinomas and normal lung in SNL mice. Spatial analysis of the transcriptome is currently ongoing to assess the effects of *Tmprss11b* expression on the TME. Collectively, these studies will elucidate the molecular mechanisms through which TMPRSS11B promotes tumor growth and alters the tumor microenvironment in LSCC.

#1794 PAF1 reprograms metabolism in pancreatic cancer by interacting with HIF1α.

A. O. Ogunleye, N. Gayen, S. Marimuthu, R. Nimmakayala, S. Rauth, Z. Alsafwani, J. L. Cox, S. K. Batra, M. P. Ponnusamy;
University of Nebraska Medical Center, Omaha, NE

Background: Reprogrammed cellular metabolism has been refocused on in the past decade, as many cancer cells rewire various metabolic pathways to facilitate their survival, unlimited cell growth, and division. RNA Polymerase II-Associated Factor 1 (PAF1)/Pancreatic Differentiation 2 (PD2) is a core subunit of the human PAF1 Complex (PAF1C) that regulates the RNA polymerase II function during transcriptional elongation in normal cells; however, its overexpression has been implicated in promoting pancreatic tumorigenesis and metastasis through epigenetic regulation, chemoresistance, radioresistance and maintenance of cancer stem cells. While most of these studies have provided evidence of the multifunctional nature of PAF1/PD2 in PDAC progression, no study has investigated the role of PAF1/PD2 during the metabolic rewiring of cancer.
Methods: In this study, we sought to examine the role of PAF1/PD2 in the metabolic rewiring of cancer cells in pancreatic ductal adenocarcinoma (PDAC) and decipher how PAF1/PD2 mediates this metabolic reprogramming in PDAC. Pancreatic cancer cell lines were transfected with shRNAs to knock down PAF1/PD2. Metabolic genes regulated by PAF1/PD2 were identified by qPCR and western blot upon PAF1/PD2 depletion. Metabolic assays were performed to investigate the role of PAF1/PD2. Immunoprecipitations identified proteins that interact with PAF1/PD2. Confocal microscopy confirmed the co-localization of PAF1/PD2 with its protein partners. We performed chromatin immunoprecipitation (ChIP) - Polymerase chain reaction to confirm the binding of the PAF1 sub-complex to its target gene.
Results: Our results showed that pancreatic cancer cells depleted PAF1/PD2 downregulate genes involved in aerobic glycolysis compared to control cells. Also, the lactate release assay indicated that more lactate was produced in control cells than in cells with PAF1/PD2 knockdown. Interestingly, we identified that HIF1α interacts with PAF1, specifically in pancreatic cancer cells. PAF1 and HIF1α co-localization was observed in pancreatic cancer cell lines. We also observed that the PAF1/PD2- HIF1α complex bound to the promoter region of LDHA to regulate the expression of LDHA in pancreatic cancer cells, reprogramming the metabolism to utilize the aerobic glycolysis pathway preferentially.
Conclusions: In conclusion, our study shows that PAF1/PD2 rewires the metabolism of PDAC by interacting with HIF1 α to regulate the expression of LDHA, which is the rate-limiting step of aerobic glycolysis.

#1795 Tumor-targeting *Salmonella* A1-R selectively delivers recombinant methioninase and inhibits syngeneic-cancer mouse models.

Y. Kubota[1], Y. Aoki[1], N. Masaki[1], K. Obara[1], S. Morinaga[1], K. Mizuta[1], M. Sato[1], M. Zhao[1], Q. Han[1], B. Michael[2], T. Tsunoda[3], R. M. Hoffman[1];
[1]AntiCancer Inc., San Diego, CA, [2]University of California San Diego, San Diego, CA, [3]Showa University School of Medicine, Tokyo, Japan

Background: Methionine addiction, termed the Hoffman effect, is a general hallmark of cancer. Methionine restriction (MR) using an MR diet or recombinant methioninase (rMETase) is effective for all types of cancer. However, methionine restriction also inhibits the activity of CD8-positive T-lymphocytes. Therefore, we hypothesized that methionine depletion in the tumor only may be more effective for cancer therapy. We previously developed *Salmonella* A1-R, which selectively targets and kills tumors. In the present study, we established rMETase-producing *Salmonella* A1-R, by transfer of the *Pseudomonas putida* methioninase gene, to target and inhibit syngeneic cancer mouse models.

Methods: A plasmid containing the *Pseudomonas putida* methioninase gene was extracted from rMETase-producing *E. coli* and inserted into *Salmonella* A1-R using electroporation. The rMETase-producing *Salmonella* A1-R (A1-R-rMETase) infected several cancer cell lines in vitro, including HT29, PC-3, MDA-MB-435, and Lewis Lung Carcinoma (LLC). LLC was chosen for in vivo studies as it supported extensive growth of A1-R-rMETase. We determined 10^8 A1-R-rMETase was a safe dosage in C57BL/6 mice. LLC cells (10^6) were injected in male C57BL/6 mice aged 4-6 weeks subcutaneously. After tumor growth, 18 mice were divided into three groups of 6. One group was injected with phosphate-buffered saline (PBS) via the tail vein, twice per week as a control. Another group was injected with 10^8 Salmonella A1-R via the tail vein, twice per week. Another group was injected with 10^8 A1-R-rMETase via the tail vein, twice per week for two weeks. Tumor size was measured with calipers three times per week for 3 weeks. On day 22, tumor methionine level was measured using HPLC in the PBS control and the mice injected with A1-R-rMETase.

Results: The mean LLC tumor size of each group on day 22 was as follows: The PBS control: 741.5 mm^3; mice injected with A1-R: 566.3 mm^3; and mice injected with A1-R-rMETase: 198.8 mm^3. Turkey's multiple comparisons test showed a significant difference between the PBS control and mice injected with A1-R-rMETase ($p<0.0001$) and between mice injected with A1-R and mice injected with A1-R-rMETase ($p=0.0036$). However, the PBS control and the mice injected with A1-R did not show a significant difference ($p=0.1794$). The mice injected with A1-R-rMETase showed a significantly lower mean methionine level than mice injected with PBS (5.9 nM/mg protein vs. 11.1 nM/mg protein, $p=0.0095$, Mann Whitney test).

Conclusion: Tumor-targeting *Salmonella* A1-R modified to express the *Pseudomonas putida* methioninase gene (A1-R-rMETase), inhibited LLC tumor growth in a syngeneic mouse model and reduced the methionine level in the tumor. A1-R-rMETase combines the tumor targeting and killing capability of A1-R itself and restriction methionine selectively in tumors.

#1796 Role of FASN in pancreatic neuroendocrine cancer cells survival.

B. M. Evers[1], Z. Chow[1], Y. Zaytseva[1], E. Y. Lee[1], C. M. Townsend, Jr.[2], T. Gao[1], B. Evers[1], P. G. Rychahou[1];
[1]University of Kentucky, Lexington, KY, [2]University of Texas Medical Branch, Galveston, TX

Introduction. Pancreatic neuroendocrine tumors (pNETs) are among the most frequently occurring neuroendocrine neoplasms. Up-regulation of fatty acid synthase (FASN) has been reported in many cancers, but the role of lipid metabolism in pNETs remains unclear. The purpose of this study was to determine whether FASN inhibition can be used as a target for pNET treatment.
Methods. Immunohistochemistry and western blot analysis were used to determine protein levels of FASN in pNET tissues and cell lines. Expression of FASN was evaluated in pancreatic neuroendocrine primary and metastatic tumors and scored by a pathologist. Neutral lipid droplet levels in pNET cell lines were determined with BODIPY 493/503 staining. Clonogenic and SRB assays were used to evaluate cytotoxic effects of FASN inhibition by TVB-3664 in QGP-1 and BON pancreatic NET cell lines. Western blot analysis was used to determine levels of cleaved PARP and cyclin D1 after FASN inhibition. FASN knockdown was used to determine the effects of FASN downregulation on proliferation and lipid synthesis.
Results. FASN expression was determined at the maximum scores of 6 and 5 in 98% of patient samples. BON, QGP-1 and NT-3 cell lines were stained with BODIPY 493/503; the highest levels of neutral lipid droplets were observed in the BON cell line. BON and QGP-1 cells were treated with TVB-3664 in either complete media with fatty acids (FA+) or complete media prepared with fatty acid depleted FBS (FA-). Treatment with TVB-3664 resulted in significant inhibition of BON and QGP-1 cell proliferation and cyclin D1 expression in both FA+ and FA- conditions. Depletion of extracellular FA enhanced the effect of TVB-3664 therapy on NET cells, especially in the BON cell line. FASN inhibition with TVB-3634 suppressed pNET cell proliferation and colony formation.
Conclusions. Our study identified high protein levels of FASN in pNET patient samples and cell lines. Moreover, we demonstrated variability in the response of pNET cells to FASN inhibition. QGP cell viability was significantly decreased with FASN inhibition even in the presence of extracellular lipids. FASN inhibition in BON cells had only a minimal effect on cell viability and required depletion of extracellular lipids to achieve a decrease in cell viability and cyclin D1 expression. These data demonstrate that de novo lipid synthesis is involved in the pathogenesis and progression of pNETs. Importantly, our findings show that some pNETs are highly sensitive to FASN inhibition, suggesting that FASN inhibition may be considered as a treatment option in selected pNETs.

#1797 Investigating the significance of OXPHOS activity in non-small cell lung cancer brain metastases.

N. G. Hammond, M. Alsamraae, M. Kaur, R. Zuckerman, B. Chang, R. Cameron, A. Dyas, B. Faubert;
University of Chicago, Chicago, IL

Background: Brain metastasis is a common and devastating occurrence for patients with non-small cell lung cancer (NSCLC). NSCLC patients with brain metastases have a poor median overall survival of 2-3 months, highlighting the urgency for novel treatment strategies. One approach to understanding and potentially targeting metastasis is via cancer metabolism. During the metastatic cascade, cancer cells must survive and adapt to the differential nutrient environments they encounter, including the brain. The blood brain barrier limits the availability of many metabolites, leading metastatic cells to alter their nutrient use to survive. RNA sequencing analyses of NSCLC brain metastases suggest that increased oxidative phosphorylation (OXPHOS) may be one such metabolic adaptation in the brain. The aim of this study was to determine the necessity of OXPHOS activity as a metabolic adaptation for NSCLC cells to proliferate in the unique metabolic environment of the brain.

Materials and Methods: NSCLC cells were cultured in media mimicking the metabolic environments of the brain and blood. Expression of mitochondrial markers were evaluated by immunoblot in cells cultured across media conditions. The effects of the OXPHOS inhibitor IACS-010759 were assessed by cell growth as well as stable isotope tracing with [U-^{13}C] glucose. Patient derived xenografts (PDXs) were derived from a cohort of patients with NSCLC who underwent stable isotope tracing with [U-^{13}C] glucose. Mice bearing subcutaneously implanted PDXs were treated daily with 5mg/kg IACS-010759 and metastatic burden was measured by flow cytometry and histology.

Results: Tracing studies in patients revealed that high enrichment in OXPHOS-related metabolites in the primary tumor correlated with worse patient outcomes. Compared with other media conditions, cells cultured in media replicating the metabolic environment of the brain have increased expression of mitochondrial proteins, increased ^{13}C glucose labeling in the TCA cycle, and a larger reduction in proliferation with IACS-010759 treatment. Using our PDX models, inhibition of OXPHOS with IACS-010759 had little effect on subcutaneous tumor growth but reduced metastasis in the lung and the brain.

Conclusions: OXPHOS activity may be enhanced in NSCLC brain metastases due to the unique metabolic environment of the brain. This elevated OXPHOS activity may be necessary for NSCLC brain metastasis growth, as OXPHOS inhibition reduced metastasis in the brain. NSCLC cells may undergo mitochondrial biogenesis to support survival in this unique metabolic environment, and this may represent an area of therapeutic vulnerability for brain metastases.

#1798 Glyoxalase 1 (*GLO1*) as an oncometabolic enabler of prostate cancer progression: CRISPR/Cas9-based *GLO1*-deletion from human DU145-Luc2 cells blocks EMT and bone metastasis in SCID mice.

J. Jandova[1], A. E. Cress[2], **G. T. Wondrak[1]**;
[1]R Ken Coit College of Pharmacy and UA Cancer Center, The University of Arizona, Tucson, AZ, [2]College of Medicine and UA Cancer Center, The University of Arizona, Tucson, AZ

Glyoxalase 1 (encoded by *GLO1*) is a glutathione-dependent enzyme detoxifying the glycolytic byproduct methylglyoxal (MG), an oncometabolite involved in metabolic reprogramming. Recently, we have demonstrated that *GLO1* is overexpressed in human prostate cancer cells and patient tumors. In order to inform the ongoing debate on the role of *GLO1* as an oncometabolic enabler of tumor glucose metabolism and malignant progression, we performed CRISPR/Cas9-based *GLO1*-deletion in human DU145-Luc2 malignant prostate cancer cells. NanoString nCounter™ ('PanCancer-Progression-Panel') comparative gene expression profiling (*GLO1*_KO versus *GLO1*_wt) revealed a significant downregulation of EMT-related pathways in *GLO1*_KO cells; concordantly, phenotypical screening indicated a pronounced attenuation of matrigel invasiveness observable in *GLO1*_KO cells. Likewise, inclusion of MG or a small molecule GLO1 inhibitor (TLSC-702) blocked invasiveness of DU145 *GLO1*_wt cells. Downregulation of EMT-related genes (including *MMP3, SPP1, CXCL8*) was accompanied by increased expression of *TXNIP* (thioredoxin-interacting protein), a master regulator of cellular energy metabolism and redox homeostasis. In a bioluminescent SCID mouse bone metastasis model (intracardial injection of DU145-Luc2 *GLO1*_wt and *GLO1*_KO cells), *GLO1* expression was necessary to cause mandibular bone metastases (as evidenced by the complete absence of bone metastases after *GLO1* deletion). Given the availability of drug-like small molecule inhibitors of GLO1 enzymatic activity these data suggest that GLO1 represents a novel molecular target for the pharmacological suppression of prostate cancer bone metastasis.

#1799 Regulation of epidermal stem cell proliferation and adhesion by ACSS2.

Nicholas K. Chamberlain, Xiaomin Bao

Molecular Biosciences, Northwestern University - Evanston, Evanston, IL

Acetyl-CoA Synthetase Short-Chain Family Member 2 (ACSS2) is an enzyme that converts acetate into acetyl-CoA, a crucial metabolite required for protein acetylation and lipogenesis. Acetyl-CoA is membrane-impermeable and must be synthesized in the compartment in which it will be used. Among ACSS enzymes, ACSS2 alone is found in the nucleocytoplasmic compartment rather than the mitochondria. This enzyme shows dynamic localization dependent on cell nutrient status, with nutrient stress promoting nuclear localization where ACSS2 activity promotes cell growth and survival. Emerging evidence suggests ACSS2 may also play roles in promoting metastasis, and has been proposed as a potential therapeutic target. However, the role of ACSS2 in controlling normal tissue homeostasis is understudied. Addressing this knowledge gap is critical to ensure safety and efficacy of cancer therapeutics. As 80% to 90% of human cancers originate from epithelial tissues, we have leveraged human epidermal stem cells to further interrogate the role of ACSS2. As progenitor keratinocytes differentiate, they detach from the basal lamina and migrate from the metabolically privileged basal layer to the more challenging environment at the surface of the epidermis. Using shRNA-mediated knockdown, we first found ACSS2 knockdown dramatically decreases progenitor keratinocyte clonogenicity, abolishing proliferative capacity. Analysis of RNA sequencing data following ACSS2 knockdown with five constructs showed significant increases in expression of genes related to cell adhesion, extracellular matrix organization, collagen catabolism, and cell migration, in addition to keratinocyte differentiation. Downregulated genes were associated with cell division, DNA repair, and DNA replication. Live cell imaging revealed knockdown cells show striking differences in cell adhesion compared to control. These results indicate a role for ACSS2 in regulating keratinocyte proliferation and adhesion during the maintenance of epidermal homeostasis.

#1800 Cytosolic NADK is conditionally essential for folate-dependent nucleotide synthesis in human cells.

K. M. Flickinger, K. S. Huggler, J. R. Cantor;
University of Wisconsin - Madison, Madison, WI

The genes that are required for the growth of mammalian cells can depend on an interplay of cell-intrinsic factors and environmental context. However, there is often little investigation into how nutrient availability impacts gene essentiality. Moreover, efforts such as DepMap have catalogued genes that contribute to cancer cell fitness using *in vitro* CRISPR screens in hundreds of cancer cell lines cultured in traditional media that poorly recapitulate the nutrient availability of human blood. Previously, we developed Human Plasma-Like Medium (HPLM), a physiologic medium designed to better model the nutrient availability of human blood. We recently tested the hypothesis that nutrient availability influences gene essentiality. By performing paired CRISPR-based screens in human blood cancer cells, we identified sets of genes that are differentially required to support cell growth in HPLM versus traditional media such as RPMI. Among the strongest scoring HPLM-essential genes was NAD kinase (*NADK*), which encodes an enzyme critical for the generation of cytosolic NADPH. NADK has been previously suggested as an anti-cancer therapeutic target, given the central importance of NADPH for enabling proliferative metabolism through macromolecule synthesis and ROS management. Interestingly, *NADK* has been annotated as an essential gene in only 1% of the cell lines included in DepMap, suggesting that the essentiality of *NADK* may have been largely masked by the nutrient conditions used to generate the DepMap. To investigate the conditional CRISPR phenotype for *NADK*, we engineered *NADK*-knockout cells and found that they showed a 50% stronger growth defect versus control cells in HPLM relative to RPMI. Next, we used localization and activity studies to confirm that cytosolic NAD^+ kinase activity is required for the conditionally essential role of *NADK*. We then employed systematic approaches in media engineering and metabolomics to identify the medium component(s) that contribute to the *NADK* gene-nutrient interaction and to gain insights into the conditionally essential role of *NADK*. Through these studies, we traced the cause of *NADK* essentiality to an inhibition of folate-dependent nucleotide synthesis linked to differential folic acid availability. Finally, we examined the pre-translational potential of NADK as an anti-cancer therapeutic target by demonstrating that the reported NADK inhibitor thionicotinamide largely phenocopies *NADK*-knockout in a folic-acid dependent manner in the K562 cell line. Collectively, our work improves understanding of how *NADK* contributes to human cell growth and reveals how the relative importance of cytosolic NAD^+ kinase activity can depend on nutrient availability.

#1801 Rewiring of cortical glucose metabolism fuels human brain cancer growth.

Andrew J. Scott[1], Anjali Mittal[1], Baharan Meghdadi[1], Sravya Palavalasa[1], Abhinav Achreja[1], Alexandra O'Brien[1], Ayesha Kothari[1], Weihua Zhou[1], Jie Xu[1], Angelica Lin[1], Kari Wilder-Romans[1], Donna M. Edwards[1], Vijay Tarnal[1], Nathan Qi[1], Theodore S. Lawrence[1], Sriram Venneti[1], Nathalie Y. R. Agar[2], Costas A. Lyssiotis[1], Wajd N. Al-Holou[1], Deepak Nagrath[1], Daniel R. Wahl[1]

[1]University of Michigan, Ann Arbor, MI,[2]Dana-Farber Cancer Institute, Boston, MA

The brain avidly consumes glucose to fuel neurophysiology. Cancers of the brain, such as glioblastoma (GBM), lose aspects of normal biology and gain the ability to proliferate and invade healthy tissue. How brain cancers rewire glucose utilization to fuel these processes is poorly understood. Here we perform infusions of ^{13}C-labeled glucose into patients and mice with brain cancer to define the metabolic fates of glucose-derived carbon in tumor and cortex. By combining these measurements with quantitative metabolic flux analysis, we find that human cortex funnels glucose-derived carbons towards physiologic processes including TCA cycle oxidation and neurotransmitter synthesis. In contrast, brain cancers downregulate these physiologic processes, scavenge alternative carbon sources from the environment, and instead use glucose-derived carbons to produce molecules needed for proliferation and invasion. Targeting this metabolic rewiring in mice through dietary modulation selectively alters GBM metabolism and slows tumor growth.

#1802 Melanoma addiction to GCDH.

N. Nadig, S. Verma, Z. A. Ronai;
Sanford Burnham Prebys Medical Discovery Institute, La Jolla, CA

Rewiring of metabolic pathways often underlies the malignant state, including melanoma. In our previous studies we have demonstrated melanoma addiction to Gutaryl Co-dehydrogenase (GCDH), an enzyme in the lysine catabolism pathway. Our studies revealed that blocking GCDH activity in melanoma, but not colon, lung or breast cancer cells, led to cell death which abolished growth both in culture and in vivo. Important cellular component which was found to mediate melanoma addiction to GCDH was the transcription factor NRF2, which exhibited tumor suppressor function upon GCDH inhibition. Notably, coinciding with NRF2 tumor suppressor role seen upon GCDH inhibition was its glutarylation, a post translational modification which acquired NRF2 stability and ability to induce transcription of ATF4, ATF3 and CHOP which led to extensive cell death program. Knockdown of NRF2, ATF3 or DTHDK-1 effectively blocked the cell death phenotype seen upon GCDH knockdown. Analyses of patient data confirmed that low GCDH expression coincided with prolonged survival of melanoma but not colon, breast or prostate cancer patients. These findings led us to perform an unbiased screen to identify cellular components, which underlie melanoma addiction to GCDH. The results of this analysis will be discussed.

#1803 ACOD1 is a key regulator of immunosuppressive MDSCs, prostate cancer progression, and resistance to immunotherapy.

C. S. Mak, X. Liang, J. Suh, D. Liang, M. Zhu, **G. Wang**;
UT MD Anderson Cancer Center, Houston, TX

Although Immune checkpoint therapy (ICT) is highly effective in a wide range of malignancies, patients with metastatic castration-resistant prostate cancer (mCRPC) are largely resistant to ICT. Yet, the cellular and molecular basis of the poor response to ICT in lethal prostate cancer remain poorly defined. Polymorphonuclear myeloid-derived suppressor cells (PMN-MDSCs) have emerged as a key driver of prostate cancer progression and resistance to immunotherapy. Yet the molecular mechanisms underlying the immunosuppressive activities of PMN-MDSCs remains poorly defined. By performing single-cell RNA-sequencing (scRNA-seq) of prostate tumors, we identified *Acod1*, a gene that encodes cis-aconitate decarboxylase (ACOD1) and catalyzes the synthesis of itaconate from cis-aconitate in the tricarboxylic acid (TCA) cycle, is among the top 5 metabolic-related genes that are overexpressed in PMN-MDSCs. Moreover, bulk RNA-seq and microarray datasets revealed that intratumoral and splenic PMN-MDSCs express a significantly higher level of *Acod1* compared to less immunosuppressive bone marrow PMN-MDSCs. Importantly, high ACOD1 expression is strongly associated with significantly shorter overall survival and higher Gleason scores in human mCRPC. Using an autochthonous whole-body *Acod1*-KO mouse model, we showed that Acod1 KO in TRAMP mice led to a reduction in tumor burden and an increase in overall survival. Furthermore, using syngeneic prostate cancer models, we showed that whole-body or PMN-specific *Acod1*-KO delayed tumor progression. As expected, Acod1 KO dramatically reduced the production of itaconate in bone marrow-derived MDSCs (BM-MDSC) as shown by targeted metabolic profiling. Importantly, we found that *Acod1* KO impaired immunosuppressive activities of BM-MDSC and an increase in CD3+ and CD8+ T cell infiltration in the tumors. Also, Acod1-KO in BM-MDSC led to a reduction of H2DCFDA staining intensity suggesting a reduction in the production of reactive oxygen species (ROS). Gene set enrichment analysis (GSEA) revealed that *Acod1*-KO MDSCs have hyperactive oxidative phosphorylation (OXPHOS) compared to *Acod1*-WT BM-MDSCs. KO of *Acod1* also leads to suppression of key MDSC functions signaling such as TNFα/NFκB, IL6/JAK/STAT3, and C/EBPβ pathways. In summary, our data suggests that the upregulation of ACOD1 in PMN-MDSCs has a vital role in prostate cancer progression and resistance to ICT by regulating their immunosuppressive activities through metabolic reprogramming. Also, our data suggest that targeting ACOD1 could be an effective therapeutic strategy for lethal prostate cancer as a monotherapy and in combination with immunotherapy.

CHEMISTRY: Lead Identification and Optimization
Poster Session

#1806 Induction of KRAS G13D dimers as a therapeutic strategy for colorectal cancer.
D. Angira, L. Li, Z. Zhou, S. Lee, J. Ready, K. Westover;
UT Southwestern Medical Center, Dallas, TX

Colorectal cancer (CRC) is the third leading cause of cancer deaths. Most CRCs arise from polyps in the colon/rectum that acquire gene mutations, including frequent activation of the oncogene Kirsten rat sarcoma virus (KRAS) observed in 40% of cases, particularly at codons 12, 13, and 61. KRAS oligomerization is critical for MAPK pathway signaling, which drives CRC pathogenesis. This study evaluated compounds that bind mutant KRAS G13D to induce non-physiological dimerization. Screening of a 4.1 billion compound DNA-encoded library led to the identification of pyridinylpiperazine/quinoline compounds. These compounds demonstrated the ability to induce RAS dimer formation, subsequently reducing MAPK signaling, exhibiting similarities to BI-2852, which is known to induce formation of non-physiologic RAS dimers. Structure-activity studies yielded indole, piperidine, and morpholine variants showing improved activity in thermal shift assays (DSF) and in cell-based assays evaluating RAS signaling (p-ERK inhibition).

#1807 New strategies to target the pseudokinase receptor PTK7 in the Wnt pathway.

J.-P. Borg[1], M. Pierre[1], L. Ganier[1], A. Daulat[1], A. Molliex[2], J. Duez[2], M. Sanchez[1], E. Lallemand[2], A. Goncalves[1], G. Bollot[1];
[1]Centre de Recherche en Cancerologie de Marseille (CRCM), Marseille, France, [2]Synsight Inc., Paris, France

Colorectal cancer (CRC) remains the second cause of death by cancer worldwide and its survival is currently estimated at 60%[1]. There is therefore a crucial need to identify biomarkers and new targets for therapy. In 90% of CRC, the Wnt/β-catenin pathway is constitutively activated due to mutations of *β-catenin*, *APC* (Adenomatous Polyposis Coli) or *axin-1*[2]. These alterations cause an accumulation of β-catenin and lead to an over-transcription of target genes involved in tumorigenesis[3-4]. Studies of our team pointed out an overexpression of the Protein Tyrosine Kinase 7 (PTK7) in CRC, an event associated with metastatic development, reduced metastases-free survival, and resistance to chemotherapy. In CRC cells, the pseudokinase PTK7 has pro-metastatic and pro-migratory functions, and thus appears to be a promising new therapeutic target[5-6]. The role of PTK7 in the Wnt/β-catenin pathway has been demonstrated in several studies[7-8]. Our group identified β-catenin as a partner of PTK7. We selected a first series of small molecules inhibitors targeting PTK7/β-catenin interaction[9]. This strategy could represent, in the future, a new therapeutic strategy to inhibit CRC cell growth dependent on the Wnt signaling pathway. However, the compounds identified had weak activity, with an IC_{50} of around 10-25 mM. We have set up a new method with SYNSIGHT to select more potent chemical inhibitors targeting PTK7/β-catenin in CRC in order to counteract the Wnt/β-catenin signaling pathway deregulation. References : [1]Colorectal cancer (Source : Globocan 2020) ; [2]Cancer Genome Atlas Network. *Nature*. 2012 ; [3]He, T. C. *et al. Science*. 1998 ; [4]Tetsu, O. & McCormick, F. *Nature*. 1999 ; [5]Lhoumeau, A.-C. *et al. PLOS ONE*. 2015 ; [6]Lhoumeau, A.-C. *et al. J. Immunol.* 2016 ; [7]Puppo, F. *et al. EMBO Rep.* 2011 ; [8]Peradziryi, H. *et al. EMBO J.* 2011 ; [9]Ganier, L. *et al. ACS Chem. Biol.* 2022 ; [10]Daulat, A. M. & Borg, J.-P. *Trends Cancer*. 2017 ; [11]Stamos, J. L. & Weis, W. I. *Cold Spring Harb. Perspect. Biol.* 2013.

#1808 Discovery of highly selective novel MTA-cooperative PRMT5 inhibitors for the treatment of cancers.

W.-L. Wu[1], T. Hu[1], Z. Deng[1], H. Li[2], Q. Shen[2], L. Zhang[2], X. Ma[2], P. Sun[2], C. Cheng[1], F. Liu[1], X. Chen[1], Y. Hua[1], B. Huang[1];
[1]BioNova Pharmaceuticals, Shanghai, China, [2]PharmaResources Co., Shanghai, China

Protein arginine methyltransferase 5 (PRMT5), a type II PRMT catalyzing the formation of symmetric dimethylation of arginine residues on histone and non-histone proteins, regulates many biological pathways in mammalian cells, including cell growth and differentiation. Methylthioadenosine phosphorylase (MTAP) is required for the methionine salvage pathway, deletion of MTAP leads to the accumulation of inhibitory PRMT5 cofactor methylthioadenosine (MTA). MTAP gene is adjacent to and frequently co-deleted with CDKN2A gene, the most commonly deleted tumor suppressor gene in human cancers. The increase in MTA significantly reduced PRMT5 activity in MTAP-deficient cancer cells, rendering them more vulnerable to PRMT5 inhibition than normal cells. Selective Inhibitors of PRMT5-MTA complex (MTA-cooperative) are supposed to exhibit an increased therapeutic index compared to first generation PRMT5 inhibitors for the treatment of MTAP-deleted (MTAP-del) cancer patients. Guided by computation-aided drug design (CADD), binding mode analysis of known PRMT5 inhibitors has led to the design and synthesis of a novel series of MTA-cooperative PRMT5 inhibitors. Many compounds within this series were found to inhibit PRMT5/MEP50 complex with single digit nM of IC_{50} in enzymatic assay. Cell based activity of these compounds was assessed by measuring the symmetric demethylarginine (SDMA) and 10-day cell proliferation assays. Several compounds exhibited low double-digit nM of cellular potency in HCT116 MTAP-del cells, the inhibition of SDMA and anti-proliferation activities in HCT116 MTAP-del cells over HCT116 MTAP-WT cells have excellent selectivity (80 - 400 fold). Further optimization of *in vitro* and *in vivo* pharmacokinetic properties has yielded candidate compounds suitable for evaluation of pharmacodynamic effect in the LU99 MTAP-del NSCLC xenograft model. Tumor growth inhibition (TGI) was observed in a dose-dependent manner, accompanied by a reduction of PRMT5-mediated SDMA levels in both the tumor and bone marrow. In summary, we have identified compounds with novel scaffolds that are potent and highly selective MTA-cooperative PRMT5 inhibitors. Further development of the second-generation PRMT5 inhibitors for treatment of cancers is also planned.

#1809 Discovery of novel AXL and MER inhibitors as potential anticancer and immunomodulatory drugs.

H.-P. Hsieh[1], M.-C. Li[1], W.-C. Yen[1], S.-Y. Wu[1], T.-K. Yeh[1], C.-C. Kuo[1], S.-H. Ueng[1], H.-C. Wu[2];
[1]National Health Research Institutes, Miaoli County, Taiwan, [2]Academia Sinica, Taipei, Taiwan

In cancer progression, abnormal AXL expression can promote tumor growth, metastasis, and chemotherapy resistance, while MER can identify apoptotic cancer cells and induce immune suppression in the tumor microenvironment. Combining AXL and MER inhibitors could generate a synergistic effect, enhancing antitumor responses, and further suppressing resistance formed by monotherapy with AXL selective or MER selective inhibitors. According to the explicit function of AXL and MER, the development of dual AXL and MER inhibitors may provide tremendous advantages to cancer patients. Drawing on our experience in the discovery of an anti-EGFR and anti-HER2 clinical candidate, we introduced several AXL-active and MER-active pharmacophores into DBPR112. Furthermore, we modified the scaffold and the solubilizing groups to improve the drug-like properties. Our comprehensive structure-activity relationship study led to the discovery of several potent dual AXL and MER inhibitors. Among approximately 200 synthesized compounds, BPR5K230 demonstrated strong inhibitory activities against AXL and MER, along with favorable oral bioavailability (F% = 55%) and promising *in vivo* antitumor effects in various mouse xenograft models, including MDA-MB-231, 4T1, and MC-38 tumor models. BPR5K230 effectively addressed sorafenib resistance in the Hepa 1-6 model and exhibited significant synergistic antitumor effects when combined with an anti-PD-L1 antibody in the EMT-6 model. As a result, BPR5K230 represents a promising dual AXL/MER kinase inhibitor, and further preclinical evaluation is underway for its development as a potential anticancer and immune-modulating drug.

#1810 Development of new phthalic hydrazide scaffold for potent TNKS inhibitors.

H. Ryu[1], H.-R. Seo[1], J. Lee[2], K. Lee[3], **J. Ahn**[1];

[1]Korea Institute of Radiological & Medical Sciences (KIRAMS), Seoul, Korea, Republic of, [2]Korea Research Institute of Chemical Technology, Daejeon, Korea, Republic of, [3]Korea Research Institute of Chemical Technology, Seoul, Korea, Republic of

Tankyrase 1 and 2 (TNKS1/2) catalyze post-translational modifications of target proteins through poly-ADP-ribosylation. Inhibition of TNKS stabilizes AXIN and induces β-catenin degradation in adenomatous polyposis coli (APC)-mutated colorectal cancer (CRC) cells. Therefore, TNKS emerges as a therapeutic target for APC mutant CRC, and there is a critical need for drug development against it. Tankyrase 1 and 2 (TNKS1/2) catalyze the post-translational modification of target proteins through poly-ADP-ribosylation. Their inhibition stabilizes AXIN and induces β-catenin degradation. Therefore, TNKS is a therapeutic target for APC mutant colorectal cancer (CRC), and there is a need for drug development against it. However, reported TNKS inhibitors have serious limitations in that they cause intestinal toxicity. To address these issues and enhance efficacy, we synthesized 60 compounds based on the tetrahydrophthalazine scaffold using protein structure modeling-AI technology. Using an in vitro TNKS1 and TNKS2 enzyme assay and derivatizing Hit compounds, we confirmed that TI-61987 significantly inhibits TNKS enzyme activity at low nanomolar levels. TI-61987 stabilized AXIN2, reduced active β-catenin, and downregulated β-catenin target genes in COLO320DM, APC-mutated CRC cells. Additionally, TI-61987 exhibited excellent anticancer effects not only in COLO320DM cells but also in in vivo xenograft mouse models. Our findings demonstrate that TI-61987 is a therapeutic candidate targeting TNKS for the treatment of APC-mutated CRCs, and this anticancer drug may represent an effective therapy regimen for APC-mutated CRCs.

#1811 Efficient identification of new small molecules targeting succinate dehydrogenase in non-small cell lung cancer.

L. Silva[1], N. Skiados[1], N. Murugavel[1], N. Luna[1], K. Cover[1], M. K. Gupta[1], S. C. Contreras[2], T. E. O'Brien[2], W. Zhang[1];
[1]University of Central Florida, Orlando, FL, [2]Atomwise Inc., San Francisco, CA

Efficient lung cancer treatment remains challenging due to the lack of therapeutic targets. The succinate dehydrogenase (SDH) enzyme plays a critical metabolic role as an intermediate between the citric acid cycle and the electron transport chain associated with the cancer disease state. Although several existing compounds have been applied to target metabolic diseases in vitro, modulating SDH for lung cancer treatment is still elusive. By integrating the AtomNet® technology for compound identification with mitochondria- and cell-based enzyme activity assays, we identified two new small molecules from 96 predicted candidates. Cellular thermal shift assay confirmed that these small molecules bind directly to SDH subunits in lung cancer cells. Mechanistically, treatment with these small molecules increased cellular and mitochondrial reactive oxygen species, accumulated succinate, and DNA damage-induced apoptosis in lung cancer cell lines. Functionally, these small molecules reduced the growth, migration, and formation of 3D organoids in vitro in lung cancer cell lines, both in the short and long term. Our study sheds light on the function of SDH in metabolic dysfunction related to cancer and highlights the potential of modulating SDH as a viable therapeutic strategy for targeting lung cancer and other cancer types. LS, NS, and WCZ contributed equally to this work.

#1812 Development of novel topoisomerase 1 inhibitor PBX-7 payload-based ADC including tandem cleavable linker system.

Y. Chun, A. Go, H. Cho, B. Lee, S. Shin, J. Lee, S. Kweon, H. Han, S. Park, D. Jung;
PINOTBIO, Inc., Suwon-si, Korea, Republic of

Antibody-Drug Conjugates (ADC) employing camptothecin-based payloads are gaining high interests as a new modality to treat various cancers, especially solid tumors. Among them, novel ADCs containing synthetic camptothecin-based payloads specially optimized for ADC applications (e.g., DXd) are of special interest due to their successful clinical results. Despite the remarkable success of ADCs exploiting these payloads, such as Enhertu (DS-8201a), there are still clear unmet needs, including the improvement of safety profile (minimization of ILD and neutropenia) and the development of novel ADCs with multiple MoA payloads to combat cancer heterogeneity.

To address these unmet needs, we have synthesized and evaluated a series of PBX-7 payloads, derived from novel camptothecin FL118, a potent, dual inhibitor of Top 1/anti-apoptotic pathway known for its favorable safety profile. These compounds showed strong *in vitro* cytotoxicity across various cancer cell lines and inhibition of Top 1 comparable to DXd or other related camptothecin compounds. They had excellent safety profile in the preliminary toxicity study in mice that can be attributed to their physicochemical properties.

PBX-7 series payloads based ADC exhibited superior cellular cytotoxicity and *in vivo* tumor regression compared to Enhertu in Her2-positive cell line and CDX mouse model. Notably, PBX-7 based ADC demonstrated remarkable efficacy in reducing tumor volume more than Enhertu in the T-DM1-resistant JIMT-1 xenograft mouse model. Furthermore, PBX-7 based ADC have bystander effects similar to Enhertu, leading to reduced viability of antigen-negative cells when co-cultured with antigen-positive cell lines. In NHP toxicity study in Cynomolgus monkeys, no sign of toxicity was observed when dosed with Trastuzumab-PBX-7016 up to 30mg/kg.

As another way of addressing unmet needs, we synthesized novel linker including tandem cleavage site to reduce payload mediated toxicity. Two distinct enzyme, beta-glucuronidase and cathepsin B cleave linker sequentially. This linker system has a higher stability during circulation in the body and higher specific payload release in the tumor tissue than single cleavable linker.

In conclusion, our research shows the promising potential of novel camptothecin PBX-7 based ADCs and tandem cleavable linker system as potent and safe ADC candidates for cancer therapy. These advancements hold great promise in addressing the current challenges in ADC development with their enhanced safety profiles and targeted efficacy.

#1813 Discovery, biomarker validation, and pre-clinical profiling of a novel PKMYT1 inhibitor.

A. Brennan, J. Lanz, D. S. Miller, O. Vipond, N. Harrison, J. Aaronson, A. Hercot;
Evariste Ltd, London, United Kingdom

Protein kinase membrane-associated tyrosine/threonine 1 (PKMYT1) is a negative regulator of CDK1 activity and has been identified as a putative synthetic lethal target in cancers which upregulate cyclin E (CCNE1). We used high-throughput virtual screening to identify inhibitors of PKMYT1 with high lipophilic ligand efficiency (LLE), which were rapidly optimized to potent leads with exceptional selectivity over a key off target, WEE1. Machine learning-driven optimization rapidly reduced mouse hepatocyte clearance to acceptable levels, delivering a compound with best-in-class potency, selectivity, and pharmacokinetic profiles in relevant animal models. Tool compounds from this series were used to validate a differentiated biomarker for sensitivity to PKMYT1 inhibition in cellular models, which could significantly expand the potential patient population. In vivo proof-of-concept studies are ongoing in a variety of cell line- and patient-derived xenograft models which represent the novel biomarker previously identified, to further validate our therapeutic strategy.

#1814 Development and evaluation of Hsp90β-selective inhibitors to overcome the safety challenges associated with pan-Hsp90 inhibitors.

S. Mishra[1], T. Reynolds[2], B. Blagg[2];
[1]Grannus Therapeutics Inc., South bend, IN, [2]University of Notre Dame, Notre Dame, IN

The 90 kD heat shock proteins (Hsp90) are molecular chaperones that are responsible for the folding of select proteins, many of which are directly associated with cancer progression. Consequently, inhibition of the Hsp90 protein folding machinery results in a combinatorial attack on numerous oncogenic pathways. More than 20 small-molecule inhibitors of Hsp90 have entered clinical trials for the treatment of cancer, all of which bind the Hsp90 N-terminus and exhibit pan-inhibitory activity against all four Hsp90 isoforms (Hsp90a, Hsp90β, Grp94 and TRAP-1). Most of these clinical trials have failed as pan-Inhibition of Hsp90 appears to be detrimental with toxicities reported alongside induction of the pro-survival heat shock response, which leads to additional dosing challenges/toxicities. The cytosolic Hsp90 isoforms Hsp90a and Hsp90β are the major contributors to cancer growth/survival. It has been established that inhibition of Hsp90a is associated with cardiac toxicity, retinal toxicity, and induction of the heat shock response. Therefore, the development of Hsp90β -selective inhibitors represents an alternative approach for the treatment of cancer with limited side effects. Towards this goal, Hsp90β-selective inhibitors that exhibit >150-fold selectivity over Hsp90a have been developed, which exhibit efficacy against select cancers while overcoming the safety challenges associated with previous Hsp90 inhibitors. The results from such studies will be presented.

#1815 Optimization of Lin28 inhibitors: A promising therapeutic approach for the suppression of cancer cell proliferation, stemness properties, and spheroid growth.

V. M. Matias-Barrios, M. Radaeva, G. Rosellinny, A. Cherkasov, X. Dong;
University of British Columbia, Vancouver, BC, Canada

Background: The pluripotency factor known as Lin28 plays a crucial role in the regulation of cancer cell stem-like characteristics, hence facilitating the formation of cancer and the evolution of therapy-resistant tumors. The protein exerts its function by utilizing its cold shock domain and zinc knuckle domain (ZKD) to engage with the Let-7 pre-microRNA and impede the process of Let-7 production. The implementation of chemical agents to hinder the interaction between Lin28 and Let-7 has been proven as a therapeutic approach for treating aggressive tumors.
Methods: Computer-aided drug design techniques were employed in the development of a novel series of small molecule inhibitors, which are derivatives of our previously identified lead compounds Ln115, Ln15, and Ln7. Fluorescent Polarization Assay (FP), and Electrophoretic Mobility Shift Assay (EMSA) were used to screen the chemicals as Lin28-Let7 interaction disruptors using Lin28A/B ZKD domain. To further screen the chemicals, the Incucyte cell proliferation assay was performed using two Lin28A and Lin28B positive cells, IGROV-1, and DuNE cells, respectively. The inhibition of Lin28 activity was subsequently evaluated by measuring Let-7 micro-RNA and Lin28 protein levels using RT-PCR and Western Blot. Then, the metabolism profile was explored using Microsomal Stability Assay. Incucyte proliferation assay and MTS assay determined the IC50 of lead compound in Lin28 positive cells. The anti-stemness properties of the lead compound were subsequently evaluated through assays for stem gene expression levels and colony formation. To evaluate the potential of the lead compound to further move into animal studies, we tested it on a newly developed 3D Neuroendocrine Prostate Cancer (NEPC) model.
Results: In this study, we provide a novel set of derivatives, within which, Ln268 was chosen as the lead compound. Ln268 shows higher metabolic stability with a half-life time of 462 min and clearance rate of 5 ul/min/mg, compared to its father compound at 347 min and 46 ul/min/mg, respectively. Ln268 treatment resulted in a time-dependent inhibition of cell growth with an IC50 of 2.5 uM at 72 hrs. Ln268 reduces mRNA levels of stemness and neurodifferentiation markers such as CHGA, CHG, SYP, SCGN, OCT3/4, NANOG, ID4, FOXC1, ALDH1A2, and FOXO3. In the 3D NEPC model, Ln268 suppresses spheroid growth in a dose- and time-dependent manner. Ln268 achieved 100% spheroid growth inhibition at the concentration of 100 uM, while the current commercially available C1632 only reached 50%.
Conclusion: We discovered a novel Ln15 derivative named Ln268, which has a better metabolism profile and increased inhibitory activity to distrust Lin28-Let7 interaction and cancer cell proliferation. Ln268 has the potential to be improved and used as an anti-cancer treatment for a variety of malignancies, such as prostate cancer.

#1816 In silico design of novel multitarget small molecule inhibitor LCI139 for the treatment of PTEN-mutant endometrial carcinoma.

V. Mujumdar, R. Delara, H. Dryden, D. Pal, K. Maddeboina, P. M. Arditti, B. Yada, R. W. Naumann, Y. Casablanca, E. Crane, J. Brown, D. Durden, C. McHale; Atrium Health Levine Cancer, Charlotte, NC

Background: Previously we described multitarget CDK4/6-CDK9 inhibitor, LCI133 for the treatment of endometrial carcinoma (EC). We have optimized LCI133's chemical properties to increase PI3K p110α potency to better target epithelial-derived cancers, resulting in nanomolar potent LCI139. We characterized LCI139's in vitro potency, target specificity, activity in in vitro EC models, safety against normal cell lines.
Methods: LCI139's chemical structure was determined using nuclear magnetic resonance and high-resolution mass spectrometry. Specific target inhibition was assessed by cell-free kinase hotspot/lipid kinase assay and selectivity profile. LCI139 (0.001-10μM) was screened against EC cell lines AN3CA, RL95-2, Ishikawa, KLE, HEC-1-A and -B for 48 hours; IC50 values determined by CellTiter-Glo Assay. EC cells were treated with LCI139 or single agent control for 24 hours and stained with Annexin V/7-AAD to assess apoptosis by cytometer. Representative PTEN wildtype (HEC-1) and mutant (AN3CA) EC cell lines were chosen for mechanistic studies and treated 6 to 24 hours with multitarget or single agent inhibitor. RNA was isolated to determine gene expression by qRT-PCR, cells were stained with Vybrant DyeCycle Violet to determine cell cycle arrest by cytometer, or cellular lysates were prepared for Western blot (WB).
Results: LCI139's has a molecular weight of 502.57Da and is a highly potent PI3Kα-CDK4/6-CDK9 inhibitor by cell-free kinase assays: 0.070μM (PI3Kα), 0.461μM (PI3Kγ), 0.214μM (PI3Kδ), 0.0015μM (CDK4), 0.0036μM (CDK6), 0.000039μM (CDK9). KINOMEscan revealed a favorable S(35) selectivity score of 0.221 screened against 403 non-mutant kinases. PTEN mutant AN3CA (IC50 243.6nM), RL95-2 (IC50 22.8nM), Ishikawa (IC50 9.8nM) had nanomolar LCI139 IC50 values, while PTEN-wild type cell lines were insensitive up to 10μM; confirmed by dose-dependent apoptosis and colony-forming assays. WB revealed LCI139 treatment ablated MCL-1 expression, decreased phosphorylation of AKT, Rb, Rpb1 (Ser2), induced significant amounts of cPARP. MCL-1 ablation correlated to decreased Mcl1 expression ($p<0.0010$) assessed 6 hours post treatment. LCI139 generated heterogenous cell line specific effects on cell cycle progression and arrest. LCI139 displayed a favorable toxicity profile against normal human kidney cells (HEK-293) compared to single agent controls.
Conclusions: Triple PI3K-CDK4/6-CDK9 inhibitor, LCI139, is nanomolar potent against PTEN mutant EC cell lines and displays decreased toxicity compared with CDK9 inhibitor reference compounds, AZD4573 and flavopiridol. Our results merit further mechanistic dissection of PTEN interaction with PI3K pathway signaling, cell cycle machinery, CDK9-mediated transcriptional control. These data support extensive in vivo potency, toxicity, PK/PD studies to assess LCI139's clinical utility in treating EC.

#1817 Association of nuclear morphometrical variables with drug cytotoxicity: A proof of principle using NCI-60 anti-cancer drug screening panel.

G. Klorin[1], L. Rodriguez[2], E. Sabo[3], G. Izmirlian[2], A. Amit[1], P. Meltzer[2], A. Roschke[2];
[1]Rambam Medical Center, Haifa, Israel, [2]National cancer Institute, Bethesda, MD, [3]Carmel Hospital, Haifa, Israel

The National Cancer Institute's panel of 60 cancer cell lines (NCI-60) have been extensively used to screen compounds for anti-cancer activity in a wide range of molecular and pharmacologic assays. We completed a detailed analysis of the nuclear morphometric variables of 57 cancer cell lines from this drug-discovery panel using recently developed computerized method that allows simultaneously assess 42 variables related to morphology/texture of the cell nuclei. The goal of this study was to determine whether unique nuclear patterns seen in cancer cells can effectively predict response to anti-cancer therapies. Stained sections prepared from paraffin cell blocks were used to measure each cell nucleus by size (e.g. area, perimeters); by shape (e.g. area box, fractal dimensions, roundness); and by optical density of the pixels and texture (e.g. margination, heterogeneity). The obtained values were then summarized at the cell line level, generating a dataset comprising 84 variables, represented by mean values and coefficients of variation. We filtered the complete set of chemical compounds, tested on the NCI-60 panel, based on sufficient GI50 variability, narrowing the list down to 4,839 compounds. These compounds were further refined using the Benjamini-Hochberg false discovery rate (FDR) method at 1% FDR, based on the p-values from "goodness of fit" tests. This process identified 1,314 compounds where the inclusion of morphometric variables significantly improved the fit of our models. To determine which variables were highly predictive for GI50 in each compound, we performed lasso regression per compound of logged GI50 versus dummied tissue of origin and morphometric variables. We tabulated the proportion of compound models selecting each variable as well as the median relative strength for each variable. This procedure identified 10 promising compound models, in which the top 5 values of relative strength from each of the tested variables emerged. Our primary objective in this analysis was to find associations between certain nuclear morphometric parameters of tumors cells and drug sensitivity. Better defining how to use these previously untapped clues may pave the way for future studies able to predict sensitivity to cancer drugs and to help in the selection of the best anticancer treatments. Additionally, our work may draw new attention to compounds not now used for anticancer treatments, but whose increased cytotoxicity can be linked to abnormal morphometric parameters that indicate possible anti-tumor activity.

#1818 Novel efficient isolation and water-soluble prodrug preparation of anti-cancer natural product narciclasine.

A. Kornienko, R. Rutledge;
Texas State University (San Marcos Campus), San Marcos, TX

Narciclasine is a promising anti-cancer agent produced by plants of the family *Amaryllidaceae*. Narciclasine has been shown to be a potent anti-cancer agent against a variety of cancers carrying dismal outcomes, including glioblastoma, non-small cell lung cancer, and non-Hodgkin's lymphoma. It is particularly effective in animal studies of brain cancer both primary, such as glioblastoma, metastatic tumors to the brain, such as melanoma and non-small cell lung cancer. Its isolation from plants has generally been accompanied with variable success as it depends on the plant species, their location and the time of plant collection. In this study, an optimized procedure for the extraction of narciclasine yielding 300 mg/kg of dried plant material. This represents a crucial step towards the development of optimized narciclasine derivatives, as the price of narciclasine from commercial sources ranges from $100-$500 per milligram. Additionally, clinical advancement of narciclasine and its derivatives has been severely thwarted, potentially owing to its sparing water-solubility. Insolubility in water makes administration at therapeutic dosages difficult and can lead to unfavorable pharmacokinetic and pharmacodynamic characteristics. To this effort, the synthesis of five prodrug esters of narciclasine is presented, with the target of a water-soluble narciclasine prodrug.

#1819 Esculetin modulates SLC31A1 and ATP7B to influence copper homeostasis and trigger cell death in colorectal cancer.

Fangyue Guo, Mengying Liu, Kaihe Zhu, Jiapeng Ru, Pei Li, **Shanfeng Zhang**

Basic Medical Experimental Center, School of Basic Medical Science, Zhengzhou University, Zhengzhou, Henan, China

Background: Esculetin is a naturally occurring dihydroxycoumarin with anti-inflammatory, antioxidant, and anti-tumor activities. Copper ion transport proteins, notably SLC31A1 and ATP7B, are essential in maintaining intracellular copper homeostasis, averting disruptions that might lead to copper-induced cell death under normal physiological conditions. However, prior research has not explored Esculetin's role in inducing copper-induced cell death. Hence, this study aims to investigate the biological process of Esculetin-induced cell death and the molecular mechanism underlying dysregulation of intracellular copper ion homeostasis.
Methods: Initially, the CCK-8 assay was used to determine the IC50 values of Esculetin on colorectal cancer cell lines (HCT116, HT29, SW480) and normal colonic epithelial cell lines (NCM460). In terms of biological behaviors, the effects of Esculetin on the proliferation of colorectal cancer cell lines were assessed using CCK-8, colony formation assay, and EdU staining. Flow cytometry was used to examine the impact of Esculetin on apoptosis and cell cycle distribution in colorectal cancer cells. A subcutaneous xenograft tumor model in nude mice was employed to evaluate the in vivo anti-tumor effects of Esculetin, while IHC staining was conducted to detect Ki-67 levels, and Western blotting was performed to assess EMT-related protein expression. To investigate copper ion homeostasis, qPCR was used to measure the expression levels of copper ion transporters SLC31A1 and ATP7B before and after Esculetin treatment.
Results: The CCK-8 results revealed that the IC50 of Esculetin for normal colonic epithelial cell lines was significantly higher than that for colorectal cancer cell lines. Meanwhile, a notable inhibitory effect of Esculetin on the proliferation of colorectal cancer cells was observed. Additionally, Esculetin treatment suppressed colony formation and reduced the proportion of EdU-positive cells in colorectal cancer cells. Flow cytometry demonstrated an increase in apoptosis and S-phase arrest following Esculetin treatment. The subcutaneous xenograft tumor model showed significant inhibition of tumor growth by Esculetin, as evidenced by reduced Ki-67-positive cells in the Esculetin-treated group. Western blot analysis revealed a significant decrease in the expression levels of Vimentin and N-Cadherin and an increase in E-Cadherin expression. Furthermore, qPCR analysis post-Esculetin treatment showed an elevation in the inward copper transporter SLC31A1 levels, while the outward transporter ATP7B expression decreased.
Conclusion: Esculetin induces dysregulation of intracellular copper ion homeostasis by upregulating SLC31A1 expression and downregulating ATP7B expression, leading to intracellular copper accumulation and subsequent disruption of copper homeostasis, thereby inducing copper-induced cell death.

#1820 Investigating the anticancer effects and pharmacological mechanisms of phenanthridine Amaryllidaceae alkaloid in bladder cancer.

Y.-C. Su, **M.-C. Chen**;
Taipei Medical University, Taipei, Taiwan

Bladder cancer (BC) ranks as the tenth most common malignancy worldwide. Despite the improved five-year survival rate of around 80% for bladder cancer patients, 25% of cases progress to muscle-invasive bladder cancer with associated metastases, leading to a notable five-year survival of 5%. This underscores the urgent clinical necessity for the development of novel therapeutic strategies in the management of bladder cancer. In this study, we demonstrate the anticancer potential of a *phenanthridine* Amaryllidaceae *alkaloid (PAA)*, and investigate its underlying mechanisms in bladder cancer. The data demonstrates the selective cytotoxicity of *PAA* towards bladder cancer cells, revealing IC_{50} values of 2.47 μM in RT112 cells and 8.99 μM in normal uroepithelial SV-HUC-1 cells. Protein array analysis further showed that *PAA* attenuated phosphorylation of several kinases, which functions as critical regulators of cell survival and proliferation. *PAA* induces S phase retardation and increases the phosphorylation of ATM, potentially enhancing DNA damage capability. Furthermore, *PAA* induced apoptosis, as evidenced by the accumulation of sub-G1 cells and caspase activation. In summary, our findings demonstrate that *PAA* exerts diverse effects on cell cycle regulation and apoptosis. These results suggest that *PAA* holds promise as a potential candidate for the treatment of bladder cancer.

#1821 Conessine inhibits cell proliferation, migration and invasion, and induces apoptosis in liver cancer cells.

Sheng-I Lee[1], Chia-Yang Li[1], Yu-Sheng Lin[2]

[1]Graduate Institute of Medicine, Kaohsiung Medical University, Kaohsiung City, Taiwan,[2]School of Medicine, Kaohsiung Medical University, Kaohsiung City, Taiwan

Cancer-related deaths from hepatocellular carcinoma (HCC) rank first worldwide. Although many attempts have been made to treat HCC, the survival rate remains unsatisfactory. Many plants from the family *Apocynaceae*, such as *Holarrhena floribunda*, contain conessine, a steroidal alkaloid. Several studies have indicated that conessine acts as an antihistamine with cancer therapy and antimicrobial resistance, but it hasn't been tested for its anti-cancer activity against liver cancer. Our study aimed to investigate the anticancer properties of conessine against liver cancer. We tested the effects of conessine on cell proliferation, migration, invasion, and epithelial-mesenchymal transition (EMT) markers using both Huh7 and Mahlavu cells. Our experimental results indicated that conessine inhibited cell proliferation, migration, motility, and invasion in Huh7 and Mahlavu cells. Results of Western blot analysis showed that conessine induced apoptosis and EMT in liver cancer cells. Taken together, our results demonstrated that conessine exhibits anticancer activity in liver cancer through suppressing cell proliferation, migration, and invasion, and inducing apoptosis, suggesting it may have benefits for liver cancer treatment.

#1822 *Artemisia annua L*polyphenols augment b-lapachone effects on oxaliplatin-resistant HCT 116 colorectal cancer cells by downregulating TERT, CD44, EGFR and oxaliplatin resistance-related proteins of OXP-R-Hct 116 cells.

W. Lee[1], E. Jung[1], H. Kim[2], S. Shin[2], G. Kim[2], J.-M. Jung[1], S. Hong[1], C. Kim[2];
[1]Gyeongsang National Univ. Hospital, Jinju, Korea, Republic of, [2]Gyeongsang National Univ., Jinju, Korea, Republic of

We previously demonstrated that β-lapachone (β-Lap) exerts stronger anticancer activity on oxaliplatin-resistant HCT116 colorectal cancer cells (Oxp-R-HCT 116 cells) than parental HCT116 cells (p-HCT 116 cells) by downregulating the oxaliplatin resistance-related upregulated proteins (Oxp-RR-Proteins) proteins in Oxp-R-HCT 116 cells, such as SOD1, MAPK, and nucelophosmin. We also demonstrated polyphenols extracted from Korean Artemisia annua L. (pKAL) exerts anticancer activity on radio-resistant MDA-MB-231 human breast cancer cells by suppressing stem cell phenotype, β-catenin, and MMP-9. In this study, we found that pKAL significantly enhanced the anticancer activity of β-lapachone (β-Lap) on oxaliplatin-resistant (Oxp-R) HCT116 colorectal cancer cells. The aim of this study is to elucidate how pKAL enhance the anticancer effects of β-Lap on Oxp-R-HCT 116 cells. CCK-8 assay, phase-contrast microscopy analysis, and morphological analysis with hematoxylin stain revealed that the anticancer effect of β-Lap is more enhanced by pKAL on Oxp-R-HCT 116 cells over 60 hr. This phenomenon was associated with suppression of oxaliplatin resistance-related upregulated proteins (Oxp-RR-Proteins) (p53, ERK, and β-catenin), and downregulation of cell survival- and stemness-related proteins (TERT, CD44 and EGFR) that were not up-regulated in Oxp-R-HCT 116 cells. Protein-protein interaction network analysis of the 21 proteins that showed large difference in expression between before and after the combined treatment of pKAL and β-Lap in HCT116-OxPt-R cells revealed that the enhanced anticancer effect of β-Lap by pKAL was related to the inhibition of negative regulation of apoptotic process and the induction of DNA damage through TERT, CD44, and EGFR-mediated multiple signaling networks. The detailed western blot analysis for anti-cancer effects of pKAL revealed that pKAL alone also suppressed the expression of TERT, CD44 and EGFR in p-HCT 116 cells as well as Oxp-R-HCT 116 cells while β-Lap alone did not influence the expression of them. In addition, for some of the Oxp-RR-Proteins of Oxp-R-HCT 116 cells (p53, ERK, and β-catenin) were suppressed by pKAL alone, but not others. However, some other Oxp-RR-Proteins of Oxp-R-HCT 116 cells that were not suppressed by pKAL alone were significantly suppressed by the combination treatment of pKAL and β-Lap. These findings suggest that pKAL enhanced the anti-cancer effects β-Lap by suppressing TERT, CD44, and EGFR-mediated multiple signaling networks as well as some of the Oxp-RR-Proteins of Oxp-R-HCT 116 cells. In conclusion, this study suggests that pKAL enhance the anticancer effects of β-Lap on OXP-R-Hct 116 cells by downregulating CD44, EGFR and some of the Oxp-RR-Proteins of Oxp-R-HCT 116 cells.

#1823 *In vitro* evaluation of novel pyrimidine nucleosides for the treatment of pancreatic cancer.

R. Bulusu[1], J. Okoro[1], E. Frimpong[1], B. Han[2], S. Rogers[3], X. Zhu[1], E. Agyare[1];
[1]Florida A&M University, College of Pharmacy and Pharmaceutical Sciences, Tallahassee, FL, [2]KECK School of Medicine, University of Southern California, California, FL, [3]University of Florida College of Medicine, Gainesville, FL

The **purpose** of the study is to synthesize and characterize novel 5-FU analogs (AGY_1 and AGY_2) and investigate their anticancer activity against pancreatic cancer cell lines.

Methods: 5-FU derivatives were synthesized and characterized using Nuclear magnetic resonance (NMR), high-performance liquid chromatography (HPLC), and elemental analysis to determine the presence of new bond formation and the purity of the derivatives or analogs. 2D cell viability, 3D models, cell migration, and cell cycle studies were performed on MiaPaCa-2 (MP-2) cells and PANC-1 cells. Apoptosis was performed on PANC-1 cells by staining with Acridine Orange and Ethidium Bromide. The metabolic stability of the analogs was determined by using human liver microsomes. PARP, p53, and BAX expressions in PANC-1 were determined by Western Blot.

Results: NMR data showed the conjugation of alkyl and tetrahydrofuran groups to the 5-FU ring confirming the formation of AGY_1 and AGY_2. The elemental analysis of AGY_1 and AGY_2 showed 99.6% and 99.5 % purity respectively. The IC_{50} value of the AGY_1 against 2D MP-2 was found to be 12.2 ± 1 µM, while the IC_{50} value of AGY_2 was determined to be 2.9 ± 0.2 µM. Both AGY_1 and AGY_2 anticancer activities were significantly higher than 5-FU (18.5 ± 1.1 µM). However, AGY_2 was more effective compared to AGY_1. A similar trend was observed for AGY_2 analog where the IC_{50} value for treated 2D PANC-1 was 3.1 ± 0.29 µM and demonstrated a higher anticancer activity compared to AGY_1 (6.4 ± 0.38 µM) or 5-FU (7.5 ± 1.1 µM). For cell migration studies, AGY_2 (43 ± 5.5) exposed MP-2 cells showed significant arrest towards the wound gap compared to AGY_1 (74 ± 18.5) and 5-FU (86 ± 15.6). A similar result of cell migration arrests AGY_2 was observed in PANC-1 treated-AGY_1, AGY_2, and 5-FU. Organoid and spheroid models demonstrated high and comparable anticancer activity of AGY_1 and AGY_2 compared to 5-FU treated organoid and spheroid models. The cell-cycle analysis showed that AGY_2-treated MP-2 cells at 1µM concentration showed a higher G_1 population arrest (64.25%) compared to AGY_1 (54.2%) and 5-FU (55.75%). Similarly, in PANC-1 cells, AGY_2 at 1µM concentration showed a higher S-phase arrest (53.86%) compared to AGY_1 (50.76%) and 5-FU (36.14%). Metabolic stability data showed higher stability of AGY_2 (95% intact) compared to AGY_1 (85% intact) compared to 5-FU (55% intact) after 2 hour of human liver microsomal incubation. The expressions of p53 and BAX proteins in PANC-1 cells were significantly upregulated and PARP was downregulated at higher concentration when treated with AGY_1 and AGY_2 compared to 5-FU.

Conclusion: We demonstrate that AGY_2 showed more promising anticancer activity compared to AGY_1 and 5-FU against pancreatic cancer cells. AGY_2 has the potential to improve 5-FU's metabolic stability and enhance its therapeutic efficacy.

#1824 Hexadecanoic acid mediated cell cycle arrest involving inhibition of cell migration.

S.-g. A. Wright, W. Aiken, H. Asemota, K. Foster, R. Delgoda;
University of the West Indies, Kingston, Jamaica

The Caribbean region accounts for the highest incidence and mortality rates of prostate cancer in the world. This warrants the need for targeted therapy as currently the most prevalent and effective option include chemotherapeutic drugs. Previous studies showed that an enriched sample extracted from the Jamaican Round Leaf yellow yam exhibited antiproliferative effects on DU145 prostate cancer cells. Based on the results obtained, this present study aims at exploring the underlying mechanism of action as well as the antimetastatic activities that the yam derived hexadecanoic acid may exhibit. Flow cytometry analysis was used to assess cell cycle arrest exhibited by hexadecanoic acid on the hormone insensitive DU145 prostate cancer cells. The western blot analysis was then utilized to determine the effects of the hexadecanoic acid enriched sample on cyclins in the cells. Transwell migration assays were then used to evaluate cell metastatic capabilities. Hexadecanoic acid enriched sample induced G1 S cell cycle arrest in the hormone insensitive prostate cancer cell line. Western blot assays also indicated that cell death was possibly induced through the cell cycle regulatory protein, cyclin D1 as its expression was downregulated in the treatment groups. Additionally, the observed metastatic inhibition of prostate cancer cells due to the action of the hexadecanoic acid in the wound healing assay may be attributed to a mechanism involving cyclin D1 as studies have indicated that abnormal Ccnd1 Cdk4 expression promotes tumor growth and metastasis. These results are substantial as it indicates a mechanistic pathway through which hexadecanoic acid is able to cause antiproliferative effects through a cell cycle arrest of hormone insensitive prostate cancer cell lines.

#1825 Synthesis and biological evaluation of novel 5-FU analogs against pancreatic cancer.

E. Frimpong[1], R. Bulusu[1], J. Okoro[1], A. Inkoom[1], N. Ndemazie[1], S. Rogers[2], X. Zhu[1], B. Han[3], E. Agyare[1];
[1]Florida A&M University College of Pharmacy & Pharmaceutical Sciences, Tallahassee, FL, [2]Department of Medicine, Division of Hematology and Oncology, University of Florida College of Medicine, Gainsville, FL, [3]Department of Surgery, Keck School of Medicine University of Southern California, Los Angeles, CA

Purpose: 5-Fluorouracil (5-FU) is one of the standard chemotherapy drugs used to treat pancreatic cancer. However, treatment only extends survival modestly, and disease recurrence is typical due to systemic instability, drug resistance, severe adverse effects, and limited benefits in patients with locally advanced tumors. These shortcomings have necessitated new strategies to develop safer and more effective anticancer agents. The study's objective was to synthesize, characterize, and evaluate the cytotoxic effects of novel 5-FU analogs in pancreatic cancer cells.

Methods: The analogs, XYZ-I-71 and XYZ-I-73, were synthesized by introducing a tetrahydrofuran ring on 5-fluorocytosine (a precursor of 5-FU) and conjugation with octanoyl chloride and lauroyl chloride, respectively. They were characterized by NMR, HPLC, micro-elemental analysis, and mass spectrometry. Cytotoxicity and cell migration studies were performed to determine the effectiveness of the analogs against MiaPaCa-2, PANC-1, and BxPC-3 pancreatic cancer cells. PARP apoptosis study was conducted in MiaPaca-2 cells using the analogs and 5-FU. The metabolic stability of analogs was determined by using human liver microsomes and quantified by HPLC.

Results: Analysis of the ^{1}H-NMR spectra displayed amide bonds at 7.80 ppm and 7.73 ppm, confirming the conjugation of octanoyl and lauroyl chloride to 5-fluorocutosine, respectively. The purity of both analogs was 99.6%. We found that the XYZ-I-73 (IC_{50} 3.6 ± 0.4μM) analog was most effective against MiaPaCa-2 cells compared to XYZ-I-71(IC_{50} 12.3±1.7μM), GemHCl (IC_{50} 24.2 ± 1.3 μM), Irinotecan (IC_{50} 10.1 ± 1.5 μM**)** and 5-FU (IC_{50} 13.2 ± 1.1 μM**)**. For PANC-1 cell growth inhibition, XYZ-I-73 (IC_{50} 3.9 ± 0.5) was again observed as the most effective agent compared to XYZ-I-71(IC_{50} 8.7±0.9 μM), GemHCl (IC_{50} 10.07±0.9), 5-FU (IC_{50} 20.43±1.2) and Irinotecan (IC_{50} 11.6 ±1.1). A similar pattern of XYZ-I-73 (IC_{50} 5.9±0.7) anticancer activity against BxPC-3 cells was found to be higher than XYZ-I-71(IC_{50} 7.7 ± 0.8), GemHCl (IC_{50} 10.95±0.9), 5-FU (IC_{50} 14±1.1) and Irinotecan (IC_{50} 9.5±1.0). For 24-hour MiaPaCa-2 cell migration studies, XYZ-I-73 (5μM) analog significantly reduced migration (# of migrated cells, 168±2.9) followed by XYZ-I-71(315±2.1), Gem-HCl (762±3.1) and 5-FU (710±3.2). PARP studies demonstrated significant inhibition of PARP expression of XYZ-I-73 treated cells compared to 5-FU and XYZ-I-71. Further, BAX and p53 expressions were significantly increased in cells treated with XYZ-I-73 compared to 5-FU and XYZ-I-71. Metabolic stability studies showed that 80 ± 5.9 % of XYZ-I-71 and XYZ-I-73 remained intact after 2-hour exposure in liver microsomal solution compared to 5-FU.

Conclusion: XYZ-I-73 demonstrated a remarkable cytotoxic effect and improved in vitro metabolic stability over the selected standard drugs and may have potential anticancer activity against pancreatic cancer.

#1826 New inhibitors of oncology targets discovered using the affinity-mediated selection of DNA-encoded chemical libraries followed by machine-learning.

A. D. Keefe, M. AbouZleikha, A. Baghaie, M. A. Clark, M.-A. Guie, J. P. Guilinger, R. Walsh, Y. Zhang;
X-Chem Inc., Waltham, MA

X-Chem's DNA-Encoded Chemical Library platform generates a large amount of binding data for each target it is screened against. Here, we report the application of machine learning to these large datasets with case studies that include the identification of novel inhibitors of two oncology targets. One, ERα, is an estrogen-activated receptor that controls transcription and stimulates breast cell proliferation including in breast cancer. The second, DCAF1, is the substrate-recognition component of an E3 ligase complex that is associated with the proliferation of colon cancer cells. Over 100 billion DNA-Encoded compounds were synthesized and screened for their affinity to each target. The selection output data was then featurized and used to train multiple machine-learned models. Models with demonstrated predictive power were then used to score virtual catalogue compounds which were subsequently acquired and tested. A range of successful data-science strategies will be described including those that lead to double-digit nM inhibitors of each of DCAF1 and ERα.

#1827 Exploring the feasibility and pharmacological mechanism of bufadienolides for the treatment of non-muscle invasive bladder cancer.

C.-C. Tu[1], M.-C. Chen[2], **C.-H. Chen**[1];

[1]College of Medicine, Taipei Medical University, Taipei, Taiwan, [2]College of Pharmacy, Taipei Medical University, Taipei, Taiwan

The majority of diagnosed bladder cancer (BC) patients is presenting with non-muscle-invasive bladder cancer (NMIBC). Although NMIBC generally exhibits a favorable prognosis, a considerable number of patients suffer from short-term recurrence, and high risks of progression to the more aggressive muscle-invasive bladder cancer (MIBC). Therefore, there is an urgent need for innovative treatments to improve outcomes for patients with NMIBC. For centuries, traditional Chinese medicine (TCM) has played a significant role in Asian society, with ongoing research to investigate the intricate relationship between TCM and treatment of cancers. Bufadienolides, the principal active components in Chansu, are derived from the aqueous extract of the parotoid glands and the dried secretion of the Asiatic toad. Bufadienolides have been reported to demonstrate significant antitumor and anti-inflammatory activities. This study aims to evaluate the feasibility and elucidate the pharmacological mechanisms that underlie the anticancer effects of bufadienolides in NMIBC. Our experiments show that bufadienolides significantly decrease cell viability, induce cell-cycle arrest at the sub-G1 phase, and activate apoptosis in NMIBC cells (RT112 and RT4). Protein analysis reveals the activation of apoptosis-related proteins (PARP, caspase-3, -8, -9) by bufadienolides in NMIBC cells. In conclusion, our findings suggest that bufadienolides present promising potential as therapeutic agents for NMIBC treatment.

#1828 Development and evaluation of novel gemcitabine analog for the treatment of pancreatic cancer.

J. Okoro[1], R. Bulusu[1], E. K. Frimpong[1], S. Rodgers[2], B. Han[3], X. Zhu[1], E. Agyare[1];
[1]Florida A&M University College of Pharmacy and Pharmaceutical Sciences, Tallahassee, FL, [2]Department of Medicine, Division of Hematology and Oncology, University of Florida College of Medicine, Gainesville, FL, [3]Department of Surgery, Keck School of Medicine University of Southern California, Los Angeles, CA

Purpose: Gemcitabine acts against pancreatic cancer and a wide range of solid tumors and it is known to be rapidly deaminated or metabolized in the blood to an inactive metabolite. To increase its therapeutic levels, gemcitabine is administered at high doses causing severe side effects. To improve its metabolic stability, increase cytotoxic activity, and limit the phenomena of resistance many alternatives have emerged, such as modifying gemcitabine. The purpose of this study was to develop and characterize a novel gemcitabine analog with improved stability and enhanced anticancer activity against pancreatic cancer.
Methods: A novel analog of gemcitabine (GemAGY) was designed and synthesized through chemical modification of gemcitabine hydrochloride (GemHCl) at position 4 with hydroxylamine. Gem AGY was characterized using nuclear magnetic resonance (NMR), micro-elemental analysis, and purity determined using High-Performance Liquid Chromatography (HPLC). Pancreatic cancer cell lines (MiaPaCa-2, BxPC3, and PANC-1) were treated with GemHCl and GemAGY. Cytotoxicity, cell migration, clonogenic assay, cell cycle, and apoptosis studies were performed to evaluate the effect of GemAGY against pancreatic cancer cell lines.
Results: The percent purity of GemAGY was over 99.6%. GemAGY demonstrated a higher cytotoxic effect against pancreatic cancer cells with a lower half-maximal inhibitory concentration (IC_{50}) value (2.5-fold high) compared with GemHCl. For MiaPaCa-2 cells, the IC_{50} value of GemAGY was found to be 1.63 ± 0.15 µm compared to GemHCl (4.0 ± 1.7 µm). GemAGY also exhibited higher cytotoxicity in PANC-1 (IC_{50}: 1.7 ± 0.2µm) compared to GemHCl (IC_{50}: 5.6 ±1.3 µm) and the IC_{50} value of GemAGY (3.2±1.1µm) in BxPC-3 cells was significantly better than GemHCl (5.5±1.0 µm). The cell cycle analysis indicated that GemAGY-treated MiaPaCa-2 cells at 1.50 µm concentration had a higher G_0/G_1 population (60.24%) compared to GemHCl-treated cells (55%). The cell migration studies showed that GemAGY-treated MiaPaCa-2 cells at 12.5 µm concentration significantly inhibited cell mobility towards the wound area with migrated cells found to be 65 ± 6 compared to Gem HCl (174.3 ± 4.0) (GemAGY vs GemHCl; $p<0.0001$). Similarly, GemAGY-treated PANC-1 cells at 12.5 µm concentration significantly inhibited cell mobility towards the wound area with (98 ± 5.1) compared to Gem HCl (254 ± 6.6). The quantitative analysis of apoptosis studies showed that GemAGY significantly induced higher apoptosis in a dose-dependent manner in MiaPaCa-2 cells compared to GemHCl as concentration increases (GemAGY vs GemHCl; $p <0.0001$).
Conclusion: This study demonstrates that GemAGY increases the anticancer activity of gemcitabine and may have the potential to improve the chemotherapeutic efficacy of gemcitabine in the treatment of pancreatic cancer.

#1829 Brusatol overcomes tyrosine kinase inhibitors resistance in myeloid leukemia cells by inhibiting translation of fast turnover protein cyclin D1 and Mcl-1.

H. Hua[1], Y. Yang[1], G. Lin[1], J. Zhang[1], S. Waxman[2], Y. Jing[1];

[1]Shenyang Pharmaceutical University, Shenyang, China, [2]Icahn School of Medicine at Mount Sinai, New York, NY

Myeloid leukemia is characterized with fast proliferation and apoptosis evasion, which are controlled by mutant or activated tyrosine kinase signalings. Tyrosine kinase inhibitors (TKI) targeting BCR-ABL in chronic myeloid leukemia (CML) and FLT3-ITD in acute myeloid leukemia (AML) significantly improved the therapy, but not cure, due to the general resistance. Overactivated mTOR protein translation pathway is believed to be one of the mechanisms causing resistance and that targeting protein translation should be one effective approach to overcome resistance. Brusatol is a quassinoid extracted from the fruit of *Brucea javanica* and an inhibitor of protein translation. We tested its antiproliferation and apoptosis induction in a variety of AML and CML cell lines as well as in TKI resistant cell lines. Brusatol effectively inhibits the growth of seven leukemia cell lines with GI_{50} values less than 20 nM. Brusatol induces apoptosis in AML cell lines and induces G0/G1 phase arrest in CML cell lines. Brusatol decreases the levels of fast turnover protein cyclin D1 and Mcl-1. In FLT3-ITD inhibitor sorafenib resistant MOLM-13/Sor cell line brusatol exhibits similar growth inhibition and apoptosis induction with the parental MOLM-13 cells, associated with inhibition of Mcl-1 and FLT3-ITD proteins. In BCR-ABL inhibitor imatinib resistant K562/STI cell line brusatol is effective as in parental K562 cells, associated with inhibition of cyclin D1 and BCR-ABL proteins. Brusatol at 2 mg/kg effectively inhibit tumor growth of K562 xenografts without causing toxicity to normal organs. These data indicate that brusatol inhibits oncogenic protein translation and has potential to be used to treat TKI resistant leukemia.

#1830 Bergenin inhibits growth of human cervical cancer cells by decreasing galectin-3 and MMP-9 expression.

M. Singh[1], R. Chauhan[1], L. Malhotra[2], A. Gupta[1], G. Dagar[1], D. Das[3], S. Uddin[4], E. A. Samath[1], M. A. Macha[5], A. Akil[6], A. A. Bhat[6];
[1]All India Institute of Medical Sciences, Delhi, India, [2]Sri Venkateswara College, Delhi, India, [3]NYU Langone Health, New York, NY, [4]Hamad Medical Corporation, Doha, Qatar, [5]Watson Crick Center for Molecular Medicine, Islamic University of Science and Technology, Pulwama, India, [6]Sidra Medicine, Doha, Qatar

Cervical cancer is still the leading of cancer mortality worldwide, even after introducing a vaccine against Human papillomavirus (HPV), due to low vaccine coverage, especially in the developing world. Cervical cancer is primarily treated by Chemo/Radiotherapy, depending on the disease stage, with Carboplatin/Cisplatin-based drug regime. These drugs being non-specific, target rapidly dividing cells, including normal cells, so safer options are needed for more targeted therapy and lower off-target toxicity. Natural products offer an attractive option compared to synthetic drugs due to their well-established safety profile and capacity to target multiple oncogenic hallmarks of cancer like inflammation, angiogenesis, etc. In the current study, we investigated the effect of Bergenin (C-glycoside of 4-O-methylgallic acid), a natural polyphenol compound that is isolated from medicinal plants such as *Bergenia crassifolia*, *Caesalpinia digyna,* and *Flueggea leucopyrus*. Bergenin has been shown to have anti-inflammatory, anti-ulcerogenic, and wound healing properties. Still, its anticancer potential has been realized only recently. We performed a proteomic analysis of cervical carcinoma cells treated with bergenin and found it to influence multiple hallmarks of cancers, including apoptosis, angiogenesis, and tumor suppressor proteins. It was also involved in many different cellular processes unrelated to cancer, as shown by our proteomic analysis. Further analysis showed bergenin to be a potent -angiogenic agent by reducing key angiogenic proteins like Galectin 3 and MMP-9 (Matrix Metalloprotease 9) in cervical carcinoma cells at cellular level as shown by western blotting assay. Further understanding of this interaction was carried out using molecular docking analysis, which indicated MMP-9 has more affinity for Bergenin as compared to Galectin-3. Cumulatively, our data provide novel insight into the anti-angiogenic mechanism of Bergenin in cervical carcinoma cells by modulation of multiple angiogenic proteins like Galectin-3 and MMP-9 which warrant its further development as an anticancer agent in cervical cancer.

#1831 Reduction of PMN-MDSC level/activity following the consumption of white button mushroom in prostate cancer murine models and patients: A translational study to mitigate cancer progression.

X. Wang[1], S. Ma[1], P. Twardowski[2], C. Lau[1], Y. Chan[1], K. Wong[1], J. Wang[1], X. Wu[1], P. Frankel[1], T. G. Wilson[2], T. W. Synold[1], C. Presant[1], J. Yu[1], S. Chen[1]; [1]City of Hope National Medical Center, Duarte, CA, [2]Saint John's Cancer Institute, Santa Monica, CA

Frequent consumption of edible mushrooms, such as white button mushrooms (WBM), has been associated with a lower risk of prostate cancer [1]. Our laboratory at City of Hope has over 20 years of collective experience in defining the anticancer mechanisms of WBM [2, 3]. Previous studies have indicated that WBM consumption has anti-androgenic activities in prostate cancers in both preclinical models [4] and clinical trials [5]. In our first-in-human phase 1 trial on prostate cancer patients, we ensured the safety of consuming WBM in humans. In addition to observing a therapeutic-responsive decline in prostate-specific antigen (PSA), the levels of myeloid-derived suppressor cells (MDSCs) reduced in responders to WBM treatments [5]. These observations led us to hypothesize that WBM may mitigate the progression of prostate cancer in part by modulating the immune response. In the current study, we conducted translational research in syngeneic murine models and in prostate cancer patients from an ongoing phase 2 trial, aiming to define the immunomodulatory activity and mechanisms of WBM. We confirmed that WBM consumption in mouse models altered the number and function of immunosuppressive cells (MDSCs) and anti-tumor immune cells (T & NK cells), ultimately enhancing the intratumor and systemic immune responses. At a bulk-transcriptional level, we observed the elevated expression of programmed cell death protein 1 (PD-1) in xenograft tumors. In our single immune cell profiling of patients' blood specimens following 3 months of WBM consumption in freeze-dried tablets form, we investigated the transcriptional landscape of circulating immune cells in response to WBM interventions. The level of circulating neutrophil-associated PMN-MDSCs decreased, and the remaining cells showed transcriptional profiles associated with "neutrophil chemotaxis", "leukocyte aggregation", and "regulation of inflammatory response", as functions associated with enhanced anti-tumor activity. Lastly, we also showed in a mouse model that WBM consumption synergistically enhances the anticancer activity of anti-PD1 drugs, indicating that WBM may be used as adjuvant therapy with immune checkpoint inhibitors. In summary, our results from prostate cancer patients and murine models show the immunomodulatory effects of WBM consumption and provide a scientific foundation for the application of WBM in alleviating prostate cancer progression.

References 1. Zhang S., et al. *Int. J. Cancer.* 2019; 146:2712-2720. 2. Chen S., et al. *Cancer Res.* 2006; 66:12026-12034. 3. Adams L.S., et al. *Nutr. Cancer.* 2008; 60:744-756. 4. Wang X., et al. *J. Nutr. Biochem.* 2021; 89:108580.5. Twardowski P., et al. *Cancer.* 2015; 121:2942-2950.

#1833 Antioxidant and antiproliferative activities of *Ipomoea cairica* extracts on three breast cancer cell lines.

A. M. Adegoke[1], D. Kyagaba[1], N. Hadebe[1], N. Mabaso[1], R. Lefojane[2], H. Baijnath[3], O. Odunola[4], M. Sekhoacha[1];
[1]University of the Free State, Bloemfontein, South Africa, [2]Central University of Technology, Bloemfontein, South Africa, [3]University of KwaZulu-Natal, Durban, South Africa, [4]University of Ibadan, Ibadan, Nigeria

Introduction: Breast cancer was the top cause of cancer deaths in 2020 with a death toll of 685 000 worldwide. Breast cancer treatments are based on drug specificity for unique receptors on the surface of some breast cancer types, there is a search for alternative treatments that are inclusive of different breast cancer types. Evidence suggests that antioxidants offer a protective effect against certain cancers. Studies on *Ipomoea cairica* have reported potential anticancer activity, hence this study aimed to assess the antioxidant and antiproliferative potentials of the extracts of *Ipomoea cairica* on three breast cancer cell lines.

Materials and Methods: The study protocol was approved by the University of the Free State Health Sciences Research Ethics Committee (HSREC), with approval number: UFS-HSD2022/0353/2607-0001. *Ipomoea cairica* stem and leaves were harvested and identified by Prof. H. Baijnath, Department of Conservation Science, School of Life Sciences, University of KwaZulu-Natal, Durban, South Africa, with specimen number 29 30 DD housed at the Ward Herbarium. The dried plant was extracted sequentially using organic solvents ranging from non-polar to polar and water. The extracts were filtered and concentrated using a rotary evaporator and then evaporated to dryness/lyophilized. Cells were cultured according to standard established procedure. The extracts were subjected to phytochemical analyses. FRAP, DPPH, and ABTS assays were done to examine antioxidant activity and MTT assays were used to evaluate the antiproliferative/cytotoxicity of the extracts against normal (Vero) and breast cancer cell lines (MCF-7, MDA-MB-231, and 4T1).

Results and Discussion: Extracts of *Ipomoea cairic*a possess alkaloids, saponins, phenols, flavonoids, phytosterols, tannins, triterpenoids, and anthraquinones. The results from the DPPH and ABTS assays revealed that the methanol and ethyl acetate fractions had significantly the highest antioxidant potentials while the methanol stem extract exhibited the most significant antioxidant activity in the FRAP assay. The DCM stem extract showed the highest antiproliferative activity against all tested cell lines.

Conclusion: Extracts of *I. cairica* possess significant antioxidant properties and antiproliferative activities against a wide array of breast cancer types including the most challenging triple-negative breast cancer. The plant would make for a strong herbal candidate for adjuvant therapy with breast cancer medication.

#1834 Discovery of a novel and highly selective PARP7 inhibitor for cancer immunotherapy.

X. Liu, Y. Wang, D. Xia, W. Zhang, S. Tian, Y. He, X. Feng, X. Yang, Q. Zhang, S. Jiang, M. Wu, J. Deng, Y. Wang, Y. Su, M. Yao, W. Yuan, X. You; Beijing Pharscin InnoBio Co., Ltd., Chongqing, China

Poly-ADP-ribose polymerase 7 (PARP7) is a member of the wider PARP enzyme family that modulate protein function by using nicotinamide adenine dinucleotide (NAD^+) as a substrate to transfer an ADP-ribose monomer onto specific amino acid acceptor residues of target proteins. PARP7 acts as a key repressor of type I interferon (IFN) signaling. Its inhibition combats tumor regression by enhancing antitumor immunity that depends on STING pathway. Therefore, PARP7 is emerging as a promising drug target for new immunotherapy. Using structure-based drug design and optimization, we discovered a novel PARP7 inhibitor, HSN002066, with high inhibitory potency (Enzyme assay IC50 = 0.96 nM) and high selectivity for PARP7 over PARP1/2/12/5A/5B/10 (IC50 =163.4/4.7/345.2/1790/110.2/>10000 nM, respectively). In addition, HSN002066 has excellent ADMET profiles with CYPs inhibition, IC_{50} >10 μM, human LMS $T_{1/2}$ > 60 min, hERG inhibition, IC_{50} > 30 μM,mouse oral bioavailability (F) 98.1%. Notably, HSN002066 and RBN-2397, the only PARP7 inhibitor currently in Ph 1/2 clinical development, displayed differentiated antiproliferative activities in cell line NCI-H1373 (IC_{50} are 387.8 nM and 15.2 nM, respectively). However, HSN002066 revealed remarkable antitumor effects as monotherapy (TGI 77% at 100 mg/kg) or combination with PD-1 antibody in CT-26 allograft model. The structure of HSN002066 was not presented and will not be disclosed at the time of presentation at AACR meeting.

#1835 Discovery of HSN003839, a highly potent inhibitor of ubiquitin-specific protease USP21 for cancer therapy.

X. Liu, Y. Wang, D. Xia, W. Zhang, Y. He, S. Tian, X. Feng, X. Yang, Q. Zhang, F. Liu, S. Jiang, R. Hu, M. Tang, X. Tang, Y. Liu, W. Yuan, X. You; Beijing Pharscin InnoBio Co., Ltd., Chongqing, China

USP21 belongs to the ubiquitin-specific protease (USP) subfamily of deubiquitinating enzymes (DUBs), which catalyze the removal of ubiquitin chain from targeted proteins. Numerous efforts over the last decade have identified a wide range of USP21 substrates and revealed the momentous and multifaceted role of USP21 in physiological and pathological states, especially in tumorigenesis, indicating that USP21 is an appealing target for the therapy of many correlative diseases. Nevertheless, progress in the development of potent USP21 inhibitors remains limited. Herein, we present the discovery of HSN003839, a highly potent and selective USP21 inhibitor with excellent anticancer activity and drug-like properties. Following screening tool compounds to identify hits and subsequent optimization, we discovered a series of compounds with strong enzymatic inhibition for USP21 with IC_{50} < 100 nM. Among them, HSN003839 displayed low nanomolar cancer cells proliferation inhibitions and excellent ADMET properties. The mouse oral bioavailability (F) is 76.5% at 10 mg/kg. In a preliminary mouse CDX model, monotherapy of HSN003839 showed 105% tumor growth inhibition (TGI) at 30 mg/kg with no obvious body weight reduction. Further biological characterization, efficacy and toxicity studies are ongoing.
The structure of HSN003839 was not presented and will not be disclosed at the time of presentation at AACR meeting.

CHEMISTRY: Proteomics and Mass Spectrometry 1
Poster Session

#1838 Advancing cancer research with Next-Generation Protein Sequencing™ on Platinum™ by Quantum-Si .
K. D. Q. Nguyen;
Quantum-Si, San Diego, CA

Protein sequencing has the potential of playing a crucial role in advancing cancer research by providing insights into the specific proteins involved in cancer pathways. New discoveries from protein sequencing advance our understanding of cancer and potential targeted therapies. Here, we demonstrate the power of next-generation protein sequencing™ using the insight-generating Platinum™ platform. Individual peptides are digested from proteins and immobilized on a semiconductor chip and probed by dye-labeled N-terminal amino acid (NAA) recognizers, followed by subsequent aminopeptidase cleavage to expose each NAA in the peptide for recognition. By recording and analyzing fluorescent intensity, lifetime, and binding kinetics of each NAA binding event, we can decipher single amino acid substitutions and modifications.
To demonstrate the versatility of this methodology across proteins associated with cellular biology, we sequenced a series of interleukins: IL4, IL6, IL7, IL13, IL20, and IL34. Interleukins, a group of cytokines that play a vital role in cancer by modulating immune responses, promoting inflammation, and influencing tumor microenvironment, impacting tumor growth and the efficacy of treatments. We have successfully sequenced all the mentioned interleukins individually or within protein mixtures. Furthermore, we were able to sequence IL6 that was enriched through immunoprecipitation from human serum. Finally, we demonstrated the unique potential of Platinum in detecting post-translational modifications (PTMs) relevant to cancer, as exemplified by the successful identification of arginine citrullination in vimentin, an onco-protein that promotes cancer cell mobility and invasion into surround tissues.
These results demonstrate the transformative potential of next-generation protein sequencing using Platinum™ in enabling the identification of proteins in complex mixtures and biofluids, as well as the detection of critical PTMs implicated in human pathophysiology, offering valuable insights into cancer research.

#1839 Proteomic and glycoproteomic differences associated with prostate cancer in urine.

N. Shamsher[1], F. Garcia-Marques[1], A. Bermudez[1], M. R. Flory[2], S. J. Pitteri[1];

[1]Stanford University School of Medicine, Palo Alto, CA, [2]Knight Cancer Institute, Oregon Health & Science University, Portland, OR

Background and Aims: Prostate cancer is one of the most common cancers affecting men in the United States, with ~288,300 new cases and 34,700 deaths in 2023 alone. Prostate-specific antigen (PSA), the most widely used prostate cancer biomarker, lacks specificity and sensitivity, leading to unnecessary biopsies, overdiagnosis, and overtreatment. There is an urgent unmet clinical need to find new biomarkers that can distinguish patients with benign disease from those with prostate cancer. Urine is an attractive source for these biomarkers as prostate-derived proteins are more highly concentrated in urine than in blood. To better understand both global proteomic and glycoproteomic molecular signatures that could lead to improved diagnostics for prostate cancer, we analyzed urine samples from unaffected men, men with benign prostatic hyperplasia (BPH), and men with prostate cancer.

Methods: Urine samples (N = 58 total) were collected from unaffected men (N = 17), men with BPH (N = 24), and men with prostate cancer (N = 17). Samples were digested with trypsin and analyzed with high-resolution liquid chromatography-tandem mass spectrometry (LC-MS/MS) for shotgun proteomics analysis. Association with cancer was determined through supervised analysis using Pearson correlation. For glycoproteomics analysis, intact glycopeptides were enriched using strong anion exchange-electrostatic repulsion hydrophilic interaction chromatography, fractionated using high pH reversed-phase chromatography, and analyzed with LC-MS/MS. Association with the three conditions was determined through several rounds of supervised analysis using Pearson correlation.

Results: In total, 3542 human proteins were identified, and 78 proteins ($p < 0.01$) were significantly associated with prostate cancer. The glycolysis pathway and lysosome pathway were enriched in samples from men with prostate cancer. In the glycoproteomics analysis, 36 proteins ($p < 0.05$) had altered glycan diversity in one of the three conditions, and the complement and coagulation cascade pathway and the lysosome pathway were highly enriched. Six proteins ($p < 0.05$) had significantly increased glycan diversity in the cancerous samples than in the BPH and normal samples.

Conclusions: This study identifies a set of interesting proteomic and glycoproteomic differences in urine from men with prostate cancer compared to BPH and non-cancer samples, which warrant further investigation in additional sample cohorts as potential novel biomarkers.

#1840 MYBBP1A AMPylated by SELO to influence its function.

W. Li;
Tianjin Medical University, Tianjin, China

Introduction: MYBBP1A, named Myb-binding protein 1A, is a protein that mainly locates in nucleolar and shuttles between the nucleus and cytoplasm, nuclear import may be mediated by KPNA2, however export depend partially on XPO1/CRM1. It activates or represses transcription via interactions with sequence specific DNA-binding proteins. Repression may be mediated at least in part by histone deacetylase activity (HDAC activity). Acts as a corepressor and in concert with CRY1, represses the transcription of the core circadian clock component PER2. Preferentially binds to di-methylated histone H3 'Lys-9' (H3K9me2) on the PER2 promoter. MYBBP1A overexpressed in tumor than normal and have a significantly negative correlation with patient overall survival. We aim to explore the role of MYBBP1A in PDAC progression and underlying mechanism. In our research, we find and prove the novel AMPylating enzyme SELO-AMPylate MYBBP1A inhibits PDAC progression and modified site in S1353 and further influence downstream relative RNA, such as 18s rRNA, 28S rRNA.

Methods and Materials:

1. The function of MYBBP1A in tumorigenesis at the organismal and cellular levels.

MYBBP1A is widely expressed in different tissues. Firstly, we explored the correlation between MYBBP1A expression level and PDAC through TCGA database and Kaplan-Meier plotter. We then established MYBBP1A gene knockout mice mating with PDX/$P53^{K172H}$/$KRAS^{G12C}$ to induced a primary PDAC model to analyze the progression of pancreatic cancer. The effect of MYBBP1A on tumor cell growth and proliferation was explored through cell proliferation analysis and a nude mouse tumor xenograft model.

2. The MYBBP1A AMPylated by SELO influence MYBBP1A function in cell proliferation was investigated at the molecular and cellular levels.

AMPylation-specific antibodies were used to confirmed MYBBP1A AMPylated by SELO in both cell lysates and purified proteins through experiments such as CO-IP and WB. Stably expressed MYBBP1A WT/S1353A were constructed to verify the function in cell proliferation or migration by SELO. The signaling molecules were further explored through CO-IP and WB to identify the changed molecular by SELO-AMPylate-MYBBP1A, revealing the entire signaling pathways of AMPylation-mediated regulation of PDAC proliferation.

Conclusion: We have demonstrated the function of MYBBP1A in the formation of pancreatic cancer, and further revealed SELO-AMPylate-MYBBP1A importance in the process of reversing MYBBP1A's role, which has played a certain significance for the treatment of pancreatic cancer and the exploration of related therapeutic targets.

#1841 Investigating mechanisms of tumor eradication by blocking SIAH E3 ligase, a major tumor vulnerability, in EGFR/RAS-driven human cancer.

J. M. Baker[1], A. Howell[1], A. Hannah[1], J. Wulfkuhle[2], N. Stahr[1], R. Gallagher[2], E. Petricoin[2], A. Tang[1];
[1]Eastern Virginia Medical School, Norfolk, VA, [2]George Mason University, Manassas, VA

Introduction: Hyperactivation of the EGFR/RAS pathway is a major driver of tumorigenesis and metastasis. It has been difficult to design effective therapies contravening the compensatory EGFR/RAS downstream effector pathways to achieve curative antitumor efficacy. Seven in absentia homologues ($SIAH_1$ and $SIAH_2$) are RING-domain E3 ubiquitin ligases that function as the most downstream signaling gatekeeper of the EGFR/RAS pathway. Our prior studies demonstrated that SIAH inhibition led to tumor eradication of multiple malignant human cancers cell lines in xenograft models. We propose that SIAH is a major tumor vulnerability/actionable drug target for inhibiting persistent EGFR/RAS pathway activation; we aim to elucidate the molecular mechanisms underpinning antitumor efficacy of our SIAH inhibitor.

Methods: Reverse phase protein arrays (RPPAs) in conjunction with Principal Component Analysis (PCA) were used to quantify fold-changes of 300 proteins/phospho-proteins that were significantly up- or down-regulated in response to SIAH inhibition ($p < 0.001$). Independent RPPA assays were performed in triplicate on doxycycline (DOX)-inducible MiaPaCa, MDA-MB-231, MDA-MB-468, HeLa, and A459 cell lines in which our SIAH inhibitor, $SIAH_2^{PD}$, expression was induced by a Tet-ON/OFF system. Four experimental conditions were used: Tet-ON control cells without DOX (group A) and with DOX induction (group B), Tet-ON-$SIAH_2^{PD}$ cancer cells without DOX (no $SIAH_2^{PD}$ inhibitor expression in group C) and with DOX induction ($SIAH_2^{PD}$ inhibitor expression in group D). The ratios of D/C/B/A, D/C, D/B, C/A, and B/A were calculated in a pairwise comparison after normalization to GAPDH as an internal control. To validate identified targets of interest, immunoblotting of biological quadruplicate cell lysates for each respective cell line were performed for group C and D at 3-, 5-, and 7-days post DOX induction; target proteins' expression normalized to β-actin, α-Tubulin, or GAPDH respectively, and the pathway alterations induced by SIAH2 inhibition were standardized, quantified, and analyzed.

Results: RPPA analyses identified 6 proteins (NFκB, Caspase-7, PARP, Cofilin, PD-L1, and Collagens) exhibiting differential expression in response to SIAH2 blockade. Western blot analyses independently confirmed their altered expression patterns, further supporting their roles as the biological readout of $SIAH_2$ loss-of-function in human cancer cells.

Conclusion: The RPPA-based cancer pathway mapping provides valuable molecular insight into the antitumor efficacy and reveals a major tumor vulnerability in human cancer pathway/network rewiring when SIAH2 is blocked in late-stage malignant cells. The kinomic data support our innovative strategy to design anti-SIAH-based anti-EGFR/RAS target therapies to control and eradicate undruggable and incurable human cancers in the future.

#1842 Global proteomics reveals integrin signaling as a driver of infiltration in glioblastoma.

L. J. van Winden, R. S. Sajid, O. A. Borhani, E. R. Kamski-Hennekam, N. Gopal, A. Leon, P. Diamandis;
University of Toronto, Toronto, ON, Canada

Background: Glioblastoma (GBM), a notably aggressive brain cancer, presents significant treatment challenges due to its propensity for deep, diffuse infiltration into healthy brain tissue. This trait enables GBM to resist and survive following surgery and conventional adjuvant therapies. Emerging evidence suggests that signaling between GBM stem cells (GSCs) may be instrumental in this invasive behavior. Our study aimed to unravel the intricacies of these intercellular communication networks within glioblastoma by employing comprehensive proteomic profiling across a diverse array of patient-derived GSC lines.
Methods: We conducted our study using a sex-stratified cohort comprising 17 patient-derived GSC lines. Proteomic profiling encompassed analyses of both GSC lysates and conditioned media under various oxygen conditions (normoxia at 20% O_2, hypoxia at 1% and 0.2% O_2). Additionally, we incorporated the glioma cerebral organoid (GLICO) system, facilitating co-cultures of GSCs with human cerebral organoids. For in-depth proteomic analysis, we utilized advanced TMT-based liquid chromatography-tandem mass spectrometry (LC-MS/MS; Q-Exactive, Thermo Fisher).
Results: Our findings corroborate that GSCs adhere to the tripartite model of proliferation, invasion, and hypoxic response. A salient discovery was the consistent enrichment of integrin signaling pathways in GSCs under hypoxic conditions. Specifically, we observed a significant association between upregulation in integrin signaling (BIOCARTA_INTEGRIN_PATHWAY) and elevated KRAS activity (SWEET_KRAS_TARGETS_UP: $r=0.43$, $p<0.01$), as well as hypoxic responses (WINTER_HYPOXIA_UP: $r=0.76$, $p<0.0001$) in GSCs. Notably, in the GLICO model, both integrin signaling and KRAS pathways were markedly upregulated in the presence of GSCs compared to cerebral organoids alone ($p<0.05$).
Conclusions: This research highlights the pivotal role of integrin signaling in mediating the invasive attributes of glioblastoma. The data underscore the importance of further exploring key modulators within the integrin signaling pathway, presenting a promising avenue for the discovery of novel therapeutic targets in glioblastoma treatment.

#1843 Integrating machine learning with microfluidic technologies for proteomic profiling of extracellular vesicles in triple-negative breast cancer.

M. Kim[1], J. Kim[1], Y. Kim[1], S. Lee[1], S. Moon[1], J.-y. Hyon[2], K.-A. Hyun[3], Y. Yang[2], S. Ha[4], S. Park[4], H. Gawk[4], H. Lee[2], E. Han[2], J. Kim[2], H.-I. Jung[4], Y.-H. Chung[2], S. Kim[1];

[1]Yonsei University College of Medicine, Seoul, Korea, Republic of, [2]Korea Basic Science Institute, Cheongju, Korea, Republic of, [3]Korea Electronics Technology Institute (KETI), Seongnam, Korea, Republic of, [4]Yonsei University, Seoul, Korea, Republic of

Accurate diagnosis of breast cancer using circulating biomarkers present in plasma remains an important challenge. In particular, protein changes in tumor-derived extracellular vesicles (tdEVs) have emerged as potential biomarkers for breast cancer diagnosis because they accurately reflect dynamic changes in tumors. In this study, we compared the proteomes of extracellular vesicle (EV) isolated from the plasma of 100 breast cancer patients and 30 healthy individuals who visited Severance Hospital between Mar 2010 and Dec 2015. Microfluidic chip-based protocol that facilitates the removal of contaminants such as albumin and immunoglobulins was used for the extraction of enriched tdEVs with small amounts of plasma. Comparative analysis of the proteomes identified 26 significant biomarkers that could indicate differences between breast cancer patients and healthy individuals. Using the LsBoost-CNN-SVM hybrid machine learning algorithm, we especially identified key EV protein biomarkers for detecting triple-negative breast cancer (TNBC), a breast cancer subtype with a poor prognosis and a high recurrence rate, as well as lacking therapeutic and diagnostic targets. Remarkably, a signature consisting of three EV proteins, specifically extracellular matrix protein 1 (ECM1), mannose-binding lectin 2 (MBL2), and biotinidase (BTD), effectively distinguished TNBC patients from healthy individuals. In our proteomic analysis set (n=73), this signature exhibited impressive performance, achieving a sensitivity of 93.3% and specificity of 93% in the accurate discrimination of TNBC from the control group. The validation set (n=40) confirmed these findings, with 100% sensitivity and 80% specificity. This signature not only served as a diagnostic tool but also provided valuable insights into the risk of recurrence and patient prognosis. We found a novel diagnostic approach that holds the potential to revolutionize breast cancer diagnostics by enhancing the reliability of tumor-related information obtained from blood samples.

#1844 Proteomic characterization of decitabine resistance in acute myeloid leukemia reveals signaling pathway crosstalk dampens the effectiveness of combination therapy.

J. C. Pino[1], C. Posso[1], S. Sharzehi[2], S. Gosline[1], C. Hutchinson-Bunch[1], E. Traer[2], P. D. Piehowski[1], K. D. Rodland[1], J. W. Tyner[2], T. Liu[1], A. Agarwal[2]; [1]Pacific Northwest National Laboratory, Richland, WA, [2]OHSU, Portland, OR

Acute myeloid leukemia (AML) is a deadly form of blood cancer primarily characterized by genetic abnormalities that guide treatment strategies. In recent years, several new therapies have emerged to target these genetic abnormalities such as gilteritinib or quizartinib, which target an internal tandem duplication (ITD) of the FLT3 gene. Additional drugs have been developed to target core cellular processes, such as venetoclax and the decitabine. Despite initial positive responses to these treatments, patients eventually relapse as they develop resistance to the individual drugs. One common approach to drug resistance is to add an additional drug to the treatment protocol. However, patients then develop further resistance to not just a single drug but multiple. As such, understanding the origins of both single and multi-drug resistance is crucial for improving treatment efficacy and clinical outcomes. Here, we present a collection of cell lines that have developed resistance to single, double, and triple drug combinations of gilteritinib, venetoclax, and decitabine. Through comprehensive global and phospho proteomics analyses under multiple conditions together with computational pathway interrogation, we unravel the underlying molecular mechanisms responsible for resistance. Leveraging our previous model of early and late drug resistance, we investigate the emergence of resistance to drug combinations involving gilteritinib alone, gilteritinib with venetoclax, gilteritinib with decitabine, and gilteritinib with venetoclax and decitabine. Through the characterization of molecular signatures for each drug combination, we identify molecular signals that are specific to combination treatments. Specifically, we find that the emergences of decitabine resistance alters the cellular pathways to effectively downregulate targets of venetoclax and gilteritinib, ultimately dampening the response to these drugs, regardless of co-administration. These findings provide a potential explanation for the limited success of combination treatments involving hypomethylating agents, as observed in recent clinical trials. Our results underscore the importance of monitoring proteome-level changes in single and combination drug treatments and shed light on the simple and intuitive reasons behind the lack of synergy often observed in combination therapies. In conclusion, we establish cell line models of resistance to various combinations of venetoclax, gilteritinib, and decitabine. By integrating global and phospo proteomic measurements, we gain a comprehensive understanding of the intricate molecular mechanisms underlying resistance.

#1845 11,000-plex aptamer based proteomics of colorectal cancer stools for the discovery of novel disease biomarkers.

C. Mohan[1], K. Vanarsa[1], J. Castillo[1], R. Bresalier[2], N. Chia[3];
[1]University of Houston, Houston, TX, [2]MD Anderson Cancer Center, Houston, TX, [3]Mayo Clinic, Rochester, TX

Given the morbidity and mortality associated with colorectal cancer, novel biomarkers are clearly warranted, especially for early detection, particularly for advanced adenomas. An earlier 1317-plex aptamer-based proteomic screen of stool proteins revealed 92 proteins to be significantly elevated in CRC stool, with the most discriminatory proteins being MMP9, haptoglobin, myeloperoxidase, fibrinogen, and adiponectin (PMID: 34117903). Results from a recent 2000-plex proteomic screen of CRC stools are detailed below, while a 11,000-plex aptamer based proteomic screen is in progress. Comprehensive proteomic screening revealed 116 proteins to be differentially expressed in CRC stool compared to control stool, with 45 being elevated 2-fold or higher. 37 of these proteins were ELISA validated in 3 independent cohorts. Stool MMP-8, MMP-9, Hemoglobin, PGRP-S, Haptoglobin, Myeloperoxidase and Fibrinogen emerged as being most discriminatory for distinguishing CRC from healthy controls (AUC: 0.91-0.95), while Stool Fibrinogen, MMP-9, Hemoglobin, MMP-8, and PGRP-S best distinguished advanced adenoma from healthy control (HC) stool, with stool Fibrinogen topping the list with an ROC AUC value of 0.86, as detailed in Table 1. Functional pathway analysis revealed a significant over-representation of pathways related to anti-oxidant activity, integrin/receptor binding, cytokines, blood coagulation, and lipoprotein biosynthesis in patients with CRC compared to HC. Nuclear Factor IC (NFIC) and IKZF2 were identified as key regulators of the molecular cascades over-represented in CRC. Stool Fibrinogen, MMP-8, MMP-9, PGRP-S, Haptoglobin, and Myeloperoxidase emerge as promising biomarkers for distinguishing CRC/advanced adenomas/healthy stools, outperforming Hemoglobin. Thus, comprehensive proteomics and independent ELISA validation have uncovered novel stool biomarkers for identifying CRC and advanced adenomas, that warrant further head to head comparison against current diagnostic tests.

#1846 Integrative histopathologic, proteomic, phosphoproteomic, genomic, and transcriptomic characterization of renal cell carcinoma.

W. Kwon[1], C. Kim[1], H. Koo[2], W. Bae[3], E. Hwang[3], W. Ham[1], N. Cho[1], J. Sa[4], J. Park[2], S. Rha[1];
[1]Yonsei University College of Medicine, Seoul, Korea, Republic of, [2]National Cancer Center, Goyang, Korea, Republic of, [3]Chonnam National University Medical School, Hwasun, Korea, Republic of, [4]Korea University College of Medicine,, Seoul, Korea, Republic of

Although histologically defined subtypes exist, renal cell carcinoma (RCC) is a heterogenous disease, resulting in various treatment outcomes and prognosis. Here, we conduct comprehensive profiling of RCC with histopathologic, proteomic, phosphoproteomic, genomic, and transcriptomic analyses on tumor and paired adjacent normal tissues from 113 patients. RCC tumors are distinctly separated from corresponding normal tissues through multi-omics clustering, a distinction further supported by pathway analysis. In addition, various hallmarks of cancer were differentially observed at the individual patient level, highlighting the intertumoral heterogeneity of RCC. Proteomic subtyping classifies RCC tumors into four subtypes (C1-4) with distinct phosphoproteomic, genomic, and transcriptomic characteristics with prognostic and predictive implications. Among these subtypes, C1-3 were almost composed of clear cell RCC (ccRCC; 96.8%), whereas C4 was composed of non-clear cell RCC (nccRCC) or other types of cancer (100.0%). Among each subtype, C1 (N=37) exhibits the strongest adaptive immune response and angiogenesis with favorable prognosis after surgical resection. C2 (N=39) was characterized with enrichment in DNA repair pathways and alteration in *VHL* (100.0%) along with *BAP1* (24.0%) genes. C3 (N=19) was associated with enrichment in inflammatory response with dismal prognosis and therapeutic resistance to tyrosine kinase inhibitors targeting vascular endothelial growth factor receptors. C4 (N=18) was exclusively enriched with nccRCC with active mitochondrial and oxidation phosphorylation. Transglutaminase 2 (*TGM2*), a crosslinking enzyme, is identified as a potential marker with therapeutic implication for ccRCC. Collectively, this study reports a large-scale multi-omics-based approach of RCC, providing insights into biologic underpinning and evidence for rational treatment selection as well as linking the multi-omics-derived phenotypes to clinical outcomes of ccRCC.

#1847 Human protein atlas: A resource for target expression across 19 tissues.

S. Schaer, M. Tognetti, R. Bruderer, P. Shichkova, **Y. Feng**, L. Reiter;
Biognosys AG, Schlieren, Switzerland

Proteins are the primary targets and off-targets of therapeutics such as small molecule and biologics. Thus, a thorough understanding of their expression profiles across various human tissues in health and disease is essential through all stages of drug development. However, generating such a comprehensive proteome profile for each tissue poses a major analytical challenge due to the large dynamic range of protein abundance within a tissue and the enormous complexity introduced by distinct proteoforms. These proteoforms may arise from genetic variations (e.g. mutations), posttranscriptional events (e.g. isoforms from alternative splicing) or posttranslational modifications, resulting in more than a million protein species from 20,000 protein-coding genes. Thanks to advancements in sensitivity and speed in the recent years, mass spectrometry (MS)-based proteomics can now be routinely applied to quantify ten thousand of proteins in biological samples. Taking advantage of MS being an unbiased and matrix-agnostic method, we pivoted the generation of a high quality and uniform protein expression atlas of 19 healthy human tissues and 3 cancerous tissues. We constructed the atlas in two parts aiming to address the following two aspects respectively: 1) a deep library providing evidence for protein/proteoform presence in each of the 22 tissues; 2) quantitative profiles for cross-comparison in all tissues. For the first part, each tissue sample was subjected to an extensive fractionation process followed by MS analysis of each of the fractions. In total, we identified 20’025 protein groups mapped to 17’715 protein-coding genes, providing protein-level evidence for > 90% of all protein-coding genes annotated in the neXtProt repository. Among all identified proteins, 10’755 were detectable across all tissues. Notably, we identified 37 proteins mapping to putative genes. In part two of the atlas, quantitative expression profiles were generated for 15’772 protein groups using TrueDiscovery DIA-MS across the 22 tissues. These data allow us to investigate ubiquitous vs. tissue-restricted protein expression of various protein classes such as surface receptors or kinases. Moreover, we performed correlation analysis between protein expression and mRNA abundance across 19 tissues, demonstrating that for a significant portion of the proteome, mRNA level-information is not an adequate proxy for protein expression. Collectively, this MS-based resource alleviates dependency on antibody-based reagents. We envision that the tissue atlas can be expanded to cover various disease indications, providing valuable insights for target discovery and assessment of target/off-target tissue distribution.

#1848 The Cellular Thermal Shift assay and its applications in Target ID, MoA determination and biomarker discovery.

T. Friman, A. Chernobrovkin, T. Tolvanen, E. Gilson, S. Lundgren, V. Brehmer, **D. Martinez Molina**;
Pelago Bioscience, Stockholm, Sweden

With the Cellular Thermal Shift Assay (CETSA) celebrating its first decade since the PoC publication, the method has gained much interest in the basic science field as well as become an industry standard in applied drug discovery setting. In the last few years it has become apparent that in addition to providing information about drug-protein interaction, CETSA based thermal profiling of cells can help describe additional aspects of cell biology as it gives insight into the activating and rewiring of protein-protein interaction networks inside the cell upon stimuli. In the work presented here, we have used CETSA coupled to high resolution mass spectrometric readout to profile the response patterns of about 8000 proteins to several hundred molecular probes and marketed drugs. The goal has been to provide a map of wanted and unwanted effects following treatment and to correlate it to alternative readouts, by for example cellular imaging and cell death assays.

We have applied the CETSA protocol for close to five hundred compounds, many in several cell-lines (HepG2, U87MG and K562). The experimental setup includes the step of treating the cells with a certain compound at a fixed concentration. After incubation for an hour, we heated the cells to a range of temperatures, followed by a lysis protocol and pooling of the samples. After this, the samples have been centrifuged to separate the soluble from insoluble fraction. The soluble fraction has then been prepared for MS acquisition using TMT based multiplexing.

Typically, this allowed us to monitor changes in thermal stability among more than 8,000 proteins, as a consequence of compound treatment. This data reveals specific compound “fingerprints” that can be used to decipher mode of action and identify biomarkers. Despite the short incubation time, proteins with compound-induced thermal stability shifts are not only targets/off-targets (direct binders), but also downstream, and sometimes upstream, pathway members and general cellular responses. All data combined makes the basis of the Target Engagement Atlas. Here we can see clusters of compounds, sharing similar protein binding profiles. Among the most prominent ones are mTOR inhibitors, NSAIDs, as well as tubulin binders. Alternatively, one can use this resource to reveal clusters of “pharmacologically” associated protein networks. We show that pharmacological perturbation allows identification of clusters representing tight protein complexes (for example ribosomes), known metabolic pathways (folate biosynthesis), molecular functions (kinases), as well as networks of proteins linked only by ligand binding specificity.

CETSA MS allows for unbiased, cellular, and molecular profiling of compound effects. Together with data from clinical settings, as well as in vivo/in vitro end point assays it is possible to correlate the CETSA patterns to wanted but also unwanted responses.

#1849 High throughput interactome profiling of small bioactive peptides.

C. D. Warren, N. Yardeny, J. B. Geri;
Weill Cornell Grad. School of Medical Sci., New York City, NY

Interactions between individual biomolecules give rise to emergent signaling and regulatory networks that govern complex and varied biological processes. Disruption of these finely tuned interactions can result in imbalanced cellular states that drive diseases; for example, many metastatic cancers become desensitized to checkpoints encoded by molecular contacts. Still, numerous interaction networks remain unmapped within the cell, namely those between cryptic endogenous peptides and their protein targets. This is primarily due to the lack of investigation around translation events that occur from “noncoding” genetic material and limited knowledge of how translated polypeptides can mature into functional proteolytic fragments. Moreover, technologies to map protein-peptide interactions in an efficient and reliable manner are limited, leaving a gap in knowledge of how many bioactive peptides regulate cellular homeostasis. We aim to map the interactions of short (30 > amino acid), bioactive peptides that are (1) translated from noncanonical open reading frames or (2) generated through proteolytic cleavage of nascent proteins. To achieve these goals, we are leveraging the recently developed MicroMap technology and label-free mass spectrometry-based proteomics. A scalable and reliable platform to discover peptide binding targets will uncover the elusive functional roles of understudied endogenous peptides in cell signaling and their part in driving cancer cell survival.

#1850 From proteomic analysis to early investigations of combining inhibitors targeting PCNA and histone deacetylase.

C. M. Li[1], K. Garcia-Mansfield[2], R. G. Lingeman[1], L. Gu[1], R. J. Hickey[1], P. Pirrotte[2], L. H. Malkas[1];
[1]Beckman Research Institute of City of Hope, Duarte, CA, [2]Translational Genomics Research Institute, Phoenix, AZ

Proteomic changes were investigated in a neuroblastoma cell line, SK-N-AS, treated with a small molecule inhibitor, AOH1996, designed to specifically bind proliferating cell nuclear antigen (PCNA) in cancer. PCNA is crucial to DNA replication, DNA repair, transcription, cell cycle control, and chromatin organization through interactions with different proteins. Pathway analysis of differential protein expressions between treated and untreated cells revealed less G2/M DNA damage checkpoint regulation and decreased assembly of RNA polymerase complex. Phosphoproteomic analysis by PTM Signature Enrichment Analysis (PTM-SEA) identified signatures of kinase activities, signaling pathways, and perturbations. Specifically, the histone deacetylase inhibitors belinostat and vorinostat were identified as enriched perturbation signatures. Both inhibitors were tested in combination with AOH1996 in SK-N-AS as well as cell lines derived from breast, lung, ovarian, and pancreatic cancer, revealing drug synergies at specific dose combinations. Western blot analysis showed that belinostat decreased protein expression of PCNA, suggestive of mechanistic synergies with AOH1996+belinostat combination therapies. Our proteomic analysis reveals a therapeutic potential of combining AOH1996 and histone deacetylase inhibitors for treating cancer with possibly lower drug dose and toxicities compared to single drug treatment.

#1851 Comprehensive multi-level proteomics characterization of gastric cancer.

Y. Wang, Clinical Proteomic Tumor Analysis Consortium (CPTAC);
Johns Hopkins University School of Medicine, Baltimore, MD

Gastric cancer is the leading cause of cancer related deaths worldwide, accounts for over 700,000 deaths each year. There is an urgent need for advancing therapeutic strategies for patients with gastric cancer. Addressing this need, the Clinical Proteomics Tumor Analysis Consortium (CPTAC) has conducted a comprehensive characterization of gastric cancer, aiming to elucidate the complex molecular mechanisms driving this cancer type, and to discover underlying cancer biology that will form the basis for developing new approaches for precision medicine. This comprehensive study includes an integrated multi-level proteomics analysis of 165 surgically resected gastric cancer and 41 normal adjacent tissues. We employed a multi-faceted approach, analyzing the proteome, phosphoproteome and glycoproteome, along with other protein modifications including ubiquitination, acetylation, and tyrosine phosphorylation. Furthermore, we extended our research to include 74 pairs of early-onset gastric cancer and normal adjacent tissues, analyzed using a proteomic approach. We can totally identify more than 12,000 protein groups with median identification of 9750 protein groups per sample. This expansive dataset helps constructing a comprehensive multi-omics atlas of gastric cancer, offering a deep understanding into the disease's molecular landscape. The depth of this study was enhanced by incorporating multi-level proteomics data across 6 tiers, facilitating an unprecedented multi-level proteomics analysis. Our integrated approach allows us to illustrate the changes in protein expression, protein modifications, signaling pathways, and protein networks during tumorigeneis. This analysis uncovers potential therapeutic targets for personalized treatments. Overall, our study provides a multi-omics atlas for gastric cancer, a profound insight into gastric cancer biology, contributing significantly to the understanding of its pathogenesis. It could pave the way for precise treatments for gastric cancer, underscoring the potential of multi-level proteomics analyses in advancing personalized medicine.

#1852 NCI's Clinical Proteomic Tumor Analysis Consortium: A proteogenomic cancer analysis program.

M. Mesri, E. An, X. Zhang, J. Bavarva, A. I. Robles, T. Hiltke, H. Rodriguez;
National Cancer Institute, Rockville, MD

The National Cancer Institute's Clinical Proteomic Tumor Analysis Consortium (NCI's CPTAC) is a national effort to accelerate the understanding of cancer biology through the integration of large-scale proteome and genome analysis, or proteogenomics. The program which is composed of a Tumor Characterization Program and a Translational Research Program (proteomics.cancer.gov) aims to leverage the investments made in cancer research by understanding the molecular changes by proteogenomically characterizing cancers and accelerating the basic discovery toward clinical impact. All data and analytical tools are made broadly available to the research community through public databases to maximize utility and public benefit.CPTAC teams have characterized a plethora of treatment-naïve tumor types, including colorectal, ovarian, breast, clear cell renal cell carcinoma, uterine corpus endometrial carcinoma, lung adenocarcinoma, lung squamous cell carcinoma, brain (including adult, pediatric, and adolescent and young adult), head and neck squamous cell carcinoma, and pancreatic ductal adenocarcinoma (proteomics.cancer.gov/resources/milestones-and-publications). Ongoing projects include acute myeloid leukemia (AML), cutaneous melanoma, sarcoma, oligodendroglioma, gastric, prostate, liver, and thyroid cancers. In the PTRC Program, CPTAC is partnering with NCI-sponsored clinical trials to support clinically relevant research projects that would elucidate biological mechanisms of therapeutic response, resistance, and/or toxicity in cancers including AML, multiple myeloma, melanoma, and lung cancers.

All mass spectrometry-based proteomic, genomic, and imaging data (histopathology and radiology) are made publicly available at the CPTAC Proteomic Data Commons (pdc.cancer.gov), Genomic Data Commons (gdc.cancer.gov), and the Cancer Imaging Archive (cancerimagingarchive.net) / Imaging Data Commons (imaging.datacommons.cancer.gov) respectively. CPTAC is also supporting development of new proteogenomic data analysis tools (proteomics.cancer.gov/resources/computational-tools). In addition, the CPTAC Assay Portal (assays.cancer.gov) is a public resource populated with mass spectrometry-based targeted proteomic assays developed by the consortium for quantitatively measuring proteins of interest, including those discovered through comprehensive tumor characterization. Lastly, well-characterized monoclonal antibodies targeting cancer-specific proteins and peptides are also made available at CPTAC's Antibody Portal (antibodies.cancer.gov).

#1853 Prostate specific membrane antigen (PSMA) glycoforms and prostate cancer progression.

S. Mackay, I. O. Oduor, T. C. Burch, D. A. Troyer, O. J. Semmes IV, **J. O. Nyalwidhe**;
Eastern Virginia Medical School, Norfolk, VA

Introduction: Prostate cancer (PCa) is the most common non-skin malignancy and the second leading cause of cancer related death in men. Prostate cancer is a heterogeneous disease with diverse clinical outcomes ranging from indolent asymptomatic cases to very aggressive and potentially lethal metastatic forms of the disease. Early detection of PCa is predominantly through determination of serum PSA levels and digital rectal examinations (DRE). Subsequently, biopsy based Gleason Grade Scores and TNM staging, tumor size or mpMRI are used to assess disease severity and progression. However, due to the low specificity of PSA concentration in diagnosis and prognosis, biopsy complications, and high mpMRI costs, there is still a critical need to identify and develop novel noninvasive biomarkers that discriminate indolent from aggressive PCa upon diagnosis. Our long-term objective is to discover biomarkers for aggressive PCa, develop and to implement them into robust clinical testing minimally invasive assays for PCa risk stratification at diagnosis. The current focus is on Prostate-Specific Membrane Antigen (PSMA), a membrane bound glycoprotein, that is significantly over-expressed in aggressive and metastatic prostate carcinomas and with poor patient prognosis. The role of its glycosylation status and composition in disease progression and its glycoforms on biomarker development and therapeutics is unknown. Aberrant glycosylation of glycoproteins occurs in many cancers, and it influences disease progression. We rationalize that differential glycosylation of PSMA correlate with progression to aggressive PCa and that PSMA glycopeptides and glycoforms can be used as diagnostics and prognosticators for aggressive disease.

Methods/Results: PSMA was isolated from risk Grade Group stratified post-DRE urines, seminal plasma and prostate cancer cell lines with different metastatic phenotypes cell line lysates. Intact glycopeptides were isolated, purified and analyzed by qualitative and quantitative mass spectrometry to identify site specific glycoforms. Our data demonstrate differential expression of unique PSMA glycoforms that correlate with disease risk and severity. Conclusions: Differential glycosylation of PSMA correlates with PCa disease progression to aggressive phenotypes and may have utility in disease stratification. Ongoing studies focus on determining if these qualitative and quantitative changes have diagnostic/prognostic value and if these be integrated with other PCa biomarkers to improve their prognostic power in discriminating aggressive PCa.

Acknowledgements: This work was supported by the DOD, USAMRAA, through the Prostate Cancer Research Program under Award No. W81XWH18-1-0228. Opinions, interpretations, and conclusions are those of the author and are not necessarily endorsed by the USAMRAA.

#1854 Plasma proteomic biomarkers identify non-responders and reveal biological insights about the tumor microenvironment in melanoma patients after PD1 blockade.

Samuel J. Wright[1], Deepika Yeramosu[1], Milan Parikh[1], Marijana Rucevic[2], Ngan Nguyen[3], Russell W. Jenkins[4], Keith T. Flaherty[4], Nir Hacohen[4], Genevieve M. Boland[4], Arnav Mehta[1]

[1]Broad Institute of MIT and Harvard, Cambridge, MA,[2]Olink Proteomics, Watertown, MA,[3]Teiko.bio, Salt Lake City, UT,[4]Massachusetts General Hospital, Boston, MA

Most patients treated with immune checkpoint blockade (ICB) do not have durable treatment responses, stressing a critical need to identify early non-invasive biomarkers of response. Circulating biomarkers provide easy access for serial monitoring and can provide insight on the mechanisms of response to ICB. We performed plasma proteomics (~3000 proteins) on 250 metastatic melanoma patients before and on ICB treatment and performed analysis to identify response- and time point-associated peripheral protein biomarkers. We next generated patient-matched peripheral blood lymphocyte (PBL) surface proteomic data and tumor sample bulk transcriptomic data to build a multimodal dataset. We leveraged these data to train machine learning models for unsupervised analysis and to classify treatment responses and learned features predictive of survival and patient endotypes. Using univariate linear models to predict protein abundance based on time point, response and the interaction term for time point and response, we identified 343 time point-associated proteins, 141 response-associated proteins, and one interaction-associated protein. We further investigated response-related proteins by fitting multivariate logistic regression and cox proportional hazards regression models to further investigate the ability of these proteins to predict response, progression-free survival (PFS), and overall survival (OS) and identify those proteins that are most important in predicting response. We calculated covarying modules of proteins that were found to be either response-associated or time point-associated to discover underlying biological networks at different treatment time points and disease response states. Additionally, we leveraged these modules to endotype patients and identified trends in protein modules across patient subsets, including modules related to biological processes such as immune infiltration, apoptosis, metaplasia and cell adhesion. To understand the contribution of different compartments on plasma proteomic abundance, we studied correlations of plasma protein abundance with PBL surface protein abundance and tumor bulk mRNA-sequencing expression. Finally, we integrated our data modalities and fit various statistical models to evaluate the relative importance of plasma protein biomarkers in predicting response compared to PBL surface proteins and tumor bulk mRNA-sequencing expression. Together, these data represent one of the deepest peripheral biomarker studies using paired samples in melanoma patients treated with anti-PD1 therapy.

#1855 Proteomics driven biomarker discovery for high-grade serous ovarian carcinoma from archived tissue specimens.

A. Shenoy, **G. Arad**, D. Kovalerchik, A. Manor, N. Simchi, D. Daitchman, K. Pevzner, E. Seger;
Protai, Tel Aviv, Israel

High-Grade Serous Ovarian Carcinoma (HGSOC) is a highly aggressive and heterogeneous cancer with variable treatment responses. Current treatment strategies, including surgical resection and chemotherapy, are often ineffective due to a lack of molecular markers to predict drug sensitivity and patient prognosis. Mass spectrometry-based proteomics analysis is a powerful tool for biomarker discovery, but it is restricted by the availability and quality of archived clinical specimens.

In this study, we developed a proteomics-based biomarker discovery pipeline that optimizes the extraction and sample preparation from archived tissue specimens of HGSOC patients. Macrodissection of the tumor rich tissue areas of interest ensured sample purity and statistical power for comparative analysis. Using liquid chromatography-tandem mass spectrometry (LC-MS/MS), we conducted a comprehensive, global proteomics analysis of FF tissue specimens from 25 HGSOC patients to associate proteomic profiles with patient outcomes. Combining high-resolution mass spectrometry proteomics of clinical samples with advanced computational tools for clinical data mining, we were able to identify pathways associated with HGSOC that hold clinical significance.

Our unique biomarker discovery platform provides a novel strategy for detecting cancer vulnerabilities from archived tissue samples and identifying proteomic biomarkers linked with treatment response and patient prognosis beyond BRCA mutation status.

EXPERIMENTAL AND MOLECULAR THERAPEUTICS: Antibody-Based Technologies and New Inhibitors
Poster Session

#1857 Development of monoclonal antibodies against CD44v specifically expressed in cancers.

Yukinari Kato, Hiroyuki Suzuki, Mika K. Kaneko

Tohoku University Graduate School of Medicine, Sendai, Japan

CD44 is a transmembrane glycoprotein that binds to the extracellular matrix including hyaluronic acid. Human CD44 has 19 exons, 10 of which are commonly present in all isoforms. CD44 standard isoform (CD44s) is composed of the common exons, and is expressed in many cell types. CD44 variants (CD44v) are produced by alternative splicing, in which the remaining nine variant exons are inserted into the CD44 standard isoform in various combinations. The CD44 isoforms have overlapping and unique functions. Both CD44s and CD44v harbor hyaluronan-binding motifs that promote interaction with the tumor microenvironment, which activate various signaling pathways in tumor cells. CD44v is mainly expressed in epithelial cells and is involved in cell adhesion, proliferation, and survival. Overexpression of CD44v is observed in many solid tumors and plays an important role in invasion, metastasis, and acquisition of stemness. In this study, we employed the Cell-Based Immunization and Screening method (CBIS method), and established highly sensitive anti-CD44 monoclonal antibodies (mAbs) using CD44v3-10-overexpressed cell lines as immunogens. After that, we determined the epitopes by enzyme-linked immunosorbent assay and investigated their applications. As a result, we successfully established eight mAbs against each CD44v (v3 to v10), which can be used for flow cytometry, western blotting, and immunohistochemistry. Furthermore, some of them exhibited cancer specificity against pancreatic cancers, colorectal cancers, gastric cancers, or oral cancers, indicating that established anti-CD44v mAbs are useful for the antibody therapies.

#1858 Discovery of AT86474, a highly efficacious anti-ROR1 ADC utilizing a proprietary payload.

B. Tan, X. Zhang, Y. Wu, Y. Cheng, S. Liu, P. Du, C. Zhong, B. Zou;
Axcynsis Therapeutics, Singapore, Singapore

ROR1 is a pseudo kinase that is involved in the non-canonical Wnt signaling pathway and is highly expressed during early embryonic development. In adult tissues, ROR1 is expressed at very low levels but its increased expression is observed in hematological cancers and a broad range of solid tumors. AT86474 is a highly homogeneous antibody drug conjugate incorporating AxcynCYS^{TM} technology that allows reproducible site-specific conjugation with DAR4 composition greater than 97%. AT86474 utilizes a proprietary payload derived from an FDA approved drug that was optimized in-house for increased potency and with altered PK properties to limit systemic exposure. In vitro, the payload displays broad sub-nanomolar activity across multiple cancer cell lines, including those resistant to paclitaxel, DM1, MMAE and DXd. The payload is conjugated via an enzyme-cleavable linker optimized for solubility, stability, and high drug to antibody ratios. AT86474 uses a humanized and optimized monoclonal antibody that demonstrates selective binding to ROR1-positive cells and subsequent internalization, sub-nanomolar potency in vitro and strong bystander effects. AT86474 was evaluated in a preclinical CDX mouse model of ovarian cancer, where substantial tumor growth inhibition was observed with two weekly doses at as low as 1 mg/kg. As ROR1 over-expression is also observed in many solid tumors, such as pancreatic, gastric, breast and lung cancers, the use of AT86474 can be expanded to benefit a large patient population.

#1859 Diverse CD28-binding IgG and heavy chain-only antibodies for T-cell engager development.

K. Lam, S. Zhi, L. Kraft, E. Vigano, W. Wei, C. Faralla, E. Odekunle, K. Bullock, E. Marshall, M. Cid, G. Leung, **L. DeVorkin**, S. Duncan;
AbCellera, Vancouver, BC, Canada

Engagement of the CD28 co-receptor by T-cell engager (TCE) molecules can enhance activation, proliferation, and anti-tumor activities, particularly in immunosuppressive tumor microenvironments. In this study, we present data on a diverse panel of CD28-binding IgG and heavy chain-only (HCAb) antibodies for T-cell co-stimulation. Our diverse panel of CD28-binding antibodies add co-stimulatory building blocks to our TCE repertoire. Using single B cell-screening, we identified fully human IgG and HCAb binders to human and non-human primate CD28 with a high degree of sequence diversity. We selected a subset of antibodies for expression and assessed binding to both human and cynomolgus CD28-expressing cells. These antibodies displayed a wide range of binding avidities in the sub-nanomolar to micromolar range, and epitope binning analysis identified seven epitope communities. Co-stimulatory activity for a subset of molecules was assessed *in vitro*. Antibodies displayed a wide range of crosslinked T-cell activation with the majority showing no activation independent of crosslinking. Data presented here describe a diverse set of CD28-binding antibodies ready for engineering into co-stimulatory TCEs. Combining these molecules with our TCE platform or other T-cell activating strategies will enable development of novel TCE modalities with co-stimulatory function for diverse tumor targets.

#1860 The smallest antibody class: Cow ultralong CDR3 knobs as a new class of biomolecule for therapeutics and diagnostics.

V. Smider;
Applied Biomedical Science Institute, San Diego, CA

Engineered antibodies, including bispecifics and ADCs, are now a major drug class for oncology and other therapeutic areas. There are two fundamental antibody fragments: the Fv (heavy and light chain variable region fragments, derived from most species), and VHH (heavy chain 'only' V regions, derived from camelids and sharks). Cows produce antibodies with an unusually long VH CDR3 region, which can be up to seventy amino acids in length and is comprised of a β-ribbon "stalk" and disulfide-bonded "knob" minidomain which sits atop the stalk. The knob region is highly diverse and can bind cryptic epitopes with high affinity. We recently developed the technology to produce knob domains independently of the antibody, and at ~5 kDa are the smallest functional antibody fragment (https://doi.org/10.1073/pnas.2303455120). The high stability and small size could enable improved tissue penetration and development of novel therapeutics, including knob-drug conjugates or extremely small bispecific molecules.

#1862 ZW191 - a FRα-targeting antibody drug conjugate with strong preclinical activity across multiple FRα-expressing indications.

S. Lawn, A. Hernandez Rojas, R. Colombo, J. Wong, K. Wu, V. Fung, M. Lasalle, M. E. Petersen, L. Degefie, A. Sagoe-Wagner, D. Urosev, L. Yang, A. Wu, C. Kim, A. Chua, K. Stahl, G. C. Winters, J. C. H. Fann, J. Rich, S. Barnscher;
Zymeworks Inc., Vancouver, BC, Canada

Background: Folate Receptor alpha (FRα) is a validated cancer target that is prevalently expressed in multiple cancers with high unmet need, including ovarian cancer and other gynecological cancers, NSCLC, endometrial cancer and TNBC. Due to FRα's favorable expression profile, multiple antibody-drug conjugates (ADCs) are being explored in this setting. Here we present the preclinical characterization of a new anti-FRα ADC, ZW191. ZW191 is a bystander active antibody drug conjugate (ADC) comprised of a humanized IgG1 antibody conjugated to a novel camptothecin-based topoisomerase 1 inhibitor (TOPO1i) payload, ZD06519, via a maleimidocaproyl (MC) anchor and a glycyl glycyl phenylalanyl glycyl (GGFG)-aminomethyl (AM) cleavable linker at a drug-to-antibody ratio (DAR) of 8. ZW191 is projected to undergo IND submission in 2024.

Materials and Methods: The novel antibody and drug-linker components of ZW191 were generated, characterized, and optimally integrated. The apparent binding affinity and cellular internalization of the ZW191 antibody were determined in FRα-expressing cells. Tumor spheroid cancer cell cultures were utilized to determine ZW191's degree of tissue penetration and its cytotoxicity. The bystander activity of ZW191 was assessed using antigen positive and negative co-culture experiments. The anti-tumor activity of ZW191 was evaluated in a panel of ovarian cancer, NSCLC, endometrial cancer and TNBC patient-derived xenografts (PDX) spanning a range of FRα expression. ZW191 was evaluated in toxicology and pharmacokinetic (PK) studies performed in non-human primates (NHP).

Results: The antibody component of ZW191 features a favorable binding profile with strong binding to FRα, and drives superior tumor spheroid penetration, cellular internalization, and payload delivery compared to FRα targeted antibodies used in multiple other ADCs. ZW191 demonstrates potent activity in FRα expressing cell cultures and effective bystander activity. In a panel of PDX models representing a range of FRα expression, ZW191 demonstrates compelling anti-tumor activity across ovarian and endometrial cancers, NSCLC and TNBC. ZW191 demonstrates an encouraging tolerability profile in NHP, with favorable PK. The promising efficacy, tolerability, and PK support the potential of ZW191 as a novel therapeutic agent that may help address unmet need in patients with high and low FRα expressing cancers.

#1863 α-ABN501, a novel antibody targeting claudin-3, demonstrates the potential to be a new therapeutic option for small cell lung cancer.

J. Choi[1], S. Hong[1], H. Park[1], J. Kim[1], S. Lee[1], M.-R. Seo[2], S.-B. Bang[2], H.-J. Shin[2], K.-i. Jeong[1], H. Yang[3], S. Hong[4], J. Choi[1], N. Kim[1], Y. Shin[2], S. Lee[1]; [1]ABION Inc., Digital-ro, Guro-gu, Seoul, Korea, Republic of, [2]Department of Molecular Medicine and Biopharmaceutical Sciences, Graduate School of Convergence Science and Technology, Seoul National University, Seoul, Republic of Korea, 1 Gwanak-ro, Gwanak-gu, Seoul, Korea, Republic of, [3]College of Pharmacy, Kyungsung University, 309, Suyeong-ro, Nam-gu, Busan, 48434, Republic of Korea., 309, Suyeong-ro, Nam-gu, Busan, Korea, Republic of, [4]College of Pharmacy and Research Institute of Pharmaceutical Sciences, Seoul National University, Seoul 08826, Republic of Korea, 1 Gwanak-ro, Gwanak-gu, Seoul, Korea, Republic of

Small Cell Lung Cancer (SCLC) is the most aggressive and lethal type of lung cancer, characterized by a poor prognosis, with a 5-year survival rate of only 7% for overall SCLC patients. Limited treatment options such as chemotherapy and immune-checkpoint inhibitor therapy are available for SCLC patients, very often followed by rapid recurrence and metastasis. Thus, new effective treatment options for SCLC remain high unmet medical needs. Overexpression of claudin-3 (CLDN3), one of the tight junction proteins, is observed in various types of cancers. The abnormal conformation of tumor cell growth leads to the external exposure of CLDN3, in contrast, the normal cells that maintain high polarity do not expose CLDN3 externally. Therefore, CLDN3 could be a potential therapeutic target and biomarker. Based on the analysis of the expression pattern of CLDN3 using a single-cell RNA sequencing dataset derived from SCLC patients, we found that CLDN3 could be a superior and unique target of SCLC compared to others (e.g., DLL3 and B7H3). Hence, we developed a fully human monoclonal antibody, afucosylated ABN501 (α-ABN501), which has high specificity and strong affinity to CLDN3-expressing cells. The α-ABN501 antibody showed CLDN3-dependent killing effects against the SCLC cells, expressing different levels of CLDN3, as assessed via the antibody-dependent cellular cytotoxicity (ADCC) assay wherein using NK cells expressing CD16a (NK-92MI-CD16a), peripheral blood mononuclear cells (PBMC), and primary NK cells. Further, the efficacy study in the CLDN3-expressing SCLC cell derived xenograft mouse model revealed that α-ABN501 was highly efficacious in inhibition of tumor growth. Collectively, we elucidated that the ADCC activity of α-ABN501 was dependent on the expression level of CLDN3 and especially specific to the SCLC cells, which underlines significant suppression of tumor growth. Present study data sets suggest that the α-ABN501 can be a potential new therapeutic option for SCLC. In addition, the α-ABN501 antibody is currently under way of development into new drug platforms for further applications.

#1864 New generation of fully human anti-progranulin monoclonal antibodies inhibiting migration and tumor formation of non-small cell carcinoma cells.

G. Serrero[1], J. Dong[1], B. Yue[1], M. Oshimura[2], C. Dong[3], J. Hayashi[3],
[1]A&G Pharmaceutical, Inc., Columbia, MD, [2]TransChromosomics, Inc, Yonago, Japan, [3]Precision Antibody, Columbia, MD

Advanced carcinomas of the lung or the breast are characterized by invasiveness and poor survival. Identifying novel targeted therapies to potentiate standard of care (SOC) therapy, remains an unmet need. In the past 4 years, numerous targeted therapies in Oncology have been approved by the Food and Drug Administration (FDA). However, the identification of targeted therapies against direct tumor biological drivers remains important. Progranulin (PGRN/GP88) is a biological driver of tumorigenesis, survival, and drug resistance in multiple cancers including breast and lung cancers. PGRN/GP88 tissue expression is an independent prognostic factor of recurrence and mortality while elevated serum PGRN/GP88 level is associated with poor outcomes such as progression of disease and shortened survival. The importance of inhibiting PGRN/GP88 expression or action effect on the proliferation and tumor growth of several cancers has been established by several laboratories including ours. In the current study, in association with Precision Antibody, we developed anti-PGRN/GP88 fully human monoclonal antibodies by immunizing TC transgenic humanized mice with recombinant human progranulin. Within 60 days following the start of immunization, several fully human anti-progranulin monoclonal antibodies were developed, characterized by several functional assays including neutralization, inhibition of PGRN/GP88 cell surface binding, proliferation, migration *in vitro* and tumor formation *in vivo*. Results: The inhibition of PGRN/GP88 action by fully human monoclonal antibodies inhibited cell proliferation and migration in a dose-and time-dependent fashion. Octet analysis determined Kd in the range of 10^{-11} M to 10^{-10} M. Transwell assay showed that anti-PGRN treatment inhibited migration of non-small cell lung cancer cells such as H1299 and A549 cells. In vivo xenograft studies with H1299 cells injected in athymic nude mice showed that fully human anti-PGRN antibodies inhibited tumor growth when compared to antibody control treated mice. Conclusion: PGRN/GP88 represents a therapeutic target for non-small cell carcinoma with two companion diagnostics (tissue test and ELISA to measure GP88 circulating levels). The use of the TC transgenic mice allows for the rapid development of fully human high affinity monoclonal antibodies bypassing the need for chimerization or humanization and affinity maturation of monoclonal antibodies raised in mice or other humanized systems.
This work is supported by SBIR grants R44 CA 224718 and R44CA162729 from the National Cancer Institute to GS.

#1865 HDP-102 - a CD37-targeting Amanitin-based-ADC for the treatment of NHL - non-clinical data package.

S.-J. Neuberth[1], K. Decker[2], C. Orlik[1], I. Dranova[1], A. Palfi[1], T. Hechler[1], A. Pahl[2], M. Kulke[2];
[1]Heidelberg Pharma Research GmbH, Ladenburg, Germany, [2]Heidelberg Pharma AG, Ladenburg, Germany

Background: Antibody-drug conjugates (ADC) are gaining importance as anti-cancer therapy. Most ADCs are based on cytotoxic warheads targeting only proliferating cells. In contrast, HDP´s proprietary ATAC platform utilizes amatoxins as payload. Amatoxins are specific inhibitors of eukaryotic RNA polymerase II, suppressing a key function in the protein metabolism not limiting their cytotoxicity to proliferating cells. Furthermore, there are no known resistance mechanisms against amatoxins in mammalian cells (i.e. multi drug resistance transporters), making ATACs a promising new class of anti-cancer ADCs. Here we present pre-clinical data on the anti-CD37 ATAC HDP-102. CD37 is a transmembrane protein expressed exclusively on immune cells, mainly mature B-cells, and in many B-cell malignancies, including Non-Hodgkin's Lymphoma (NHL).
Material and Methods: HDP-102: anti-CD37 ADC based on cysteine-reactive, site-specific amatoxin-linker constructs produced by HDP
Cytotoxicity assays: CellTiter Glo 2.0 (Promega) assays on $CD37^{pos}$ cell lines MEC-2, Raji-luc, Ramos and $CD37^{neg}$ Nalm-6 cells
Efficacy studies: Disseminated MEC-2 and Raji-Luc mouse xenograft tumor models in single dose experiments
Tolerability study in Cynomolgus monkeys: i.v. HDP-102 treatment on days 1 and 22; blood sampling for PK analysis; necropsy and histopathology on days 28 and 64
Results: HDP-102 showed full-blown cytotoxicity with EC_{50} values in the low nanomolar range in all $CD37^{pos}$ cell lines *in vitro* but no cytotoxicity on $CD37^{neg}$ cells. *In vivo*, the anti-tumor efficacy of HDP-102 was evaluated in disseminated CDX models of NHL. A single dose of 0.5 mg/kg HDP-102 already led to complete tumor remission in all animals in a Raji-luc model and 60% survival on day 100 in a MEC-2 model, demonstrating the high potency of HDP-102 in NHL models. In a tolerability study in Cynomolgus monkeys, i.v. administration of HDP-102 was well tolerated up to 2.5 mg/kg without clinical signs of toxicity. Microscopically, decreased cellularity in lymphoid tissue was the main finding, caused by the targeted effect of HDP-102 on $CD37^{pos}$ cells. The HNSTD of 2.5 mg/kg together with the potent anti-tumor efficacy of HDP-102 leads to a therapeutic window of ~200 for HDP-102.
Conclusion: CD37 is an ideal target for ADCs due to its high prevalence in B-cell malignancies and limited expression on healthy cells. We have demonstrated that the anti-CD37 ATAC HDP-102 is a promising drug candidate for the treatment of NHL. HDP-102 showed excellent anti-tumor efficacy in CDX models even after single doses. Pharmacological activity of HDP-102 was also seen in Cynomolgus monkeys as evidenced by depletion of B-cells in lymphoid organs. Furthermore, HDP-102 was well tolerated in monkeys. Taken together, based on pre-clinical data, HDP-102 is a promising new treatment option for NHL patients combining a good safety profile with strong anti-tumor efficacy.

#1866 Discovery of mutation-independent EGFR degrading bispecific antibodies that suppress tumor growth in preclinical tumor models.

J. Sitrin, L. Marshall, H. Tran, K. Ng, K. Hoi, J. Gramespacher, Z. Huang, A. Goodrich, F. Housley, M. Dayao, M.-T. Wang, K. Pance, A. Chen, K. Carlin, L. Zhang, J. Lee, R. Hannoush, K. Flanagan, M. Vinogradova, I. Rondon, S. Gardai;
EpiBiologics, San Mateo, CA

Extracellular targeted protein degradation (eTPD) has emerged as a promising new drug modality focused on targeted elimination of extracellular and transmembrane proteins. In contrast to intracellular protein degraders, such as proteolysis targeting chimeras (PROTACs) and molecular glues which require ubiquitin-proteosome cellular degradation pathways, extracellular protein degraders can additionally harness endosomal-lysosomal protein degradation. Two recently published examples of extracellular protein degraders include AbTACs (antibody-based PROTAC) which co-engage a protein of interest (POI) and transmembrane E3 ligases, and KineTACs (cytokine receptor-targeting chimeras) which utilize endogenous cytokine receptors to degrade extracellular POIs. These bispecific antibody degrader platforms not only have advantageous pharmacological and drug-like manufacturing properties, but can also be engineered for tissue-specificity and to address multiple complementary targets, with the goal of increased efficacy and decreased toxicity. To that end, we have greatly expanded the extracellular degrader repertoire beyond AbTACs and KineTACs, with a novel bispecific antibody degrader platform called TrainTACs (tissue receptor antigen internalization targeting chimeras). To demonstrate the potential of this novel extracellular degrading platform, we developed degraders for the canonical receptor tyrosine kinase epidermal growth factor receptor (EGFR). EGFR is an oncogenic driver, that has been clinically validated in lung, colorectal and head and neck cancers, but patient benefit has been limited by treatment-related acquired resistance mutations and on-target/off-tumor dose-limiting toxicities. The potential of our TrainTACs, AbTACs and KineTACs to overcome the limitations of current therapeutic modalities was assessed. Gene expression profiles from tumor and normal tissues were evaluated to identify potential degraders co-expressed with EGFR in tumors. More than 70 unique bispecific antibody constructs spanning 20 receptors were generated and screened in tumor cell-based assays to evaluate EGFR antagonism, internalization, and degradation. TrainTACs, AbTACs and KineTACs degraded EGFR in multiple tumor cell lines covering a range of EGFR mutations. Degradation of EGFR led to deep inhibition of EGFR signaling, robust inhibitory effects on tumor spheroids, and in xenograft mouse tumor models. In conclusion, eTPD represents a promising new drug modality, and TrainTACs, AbTACs and KineTACs have expanded the toolbox of extracellular targeted protein degraders that can be utilized in a target-, tissue- and disease-specific manner.

#1867 LBL-049: A novel neutralizing antibody against GDF15 for the treatment of cachexia.

Baohui Wang, Xiao Huang, Mi Ding, Jing Huang, Yurong Qin, Fengxia Li, Jing Guan, Jianming Sun, Guojin Wu, Xiaoxiao Liu, Jordan Zhu, Shoupeng Lai, Xiaoqiang Kang, **Hong Ling**

Nanjing Leads Biolabs Co.,Ltd., Nan Jing, China

Background: Cachexia is a disorder characterized by loss of body weight with specific losses of skeletal muscle and adipose tissue and occurs in the progression of many diseases, especially in cancer. Growth differentiation factor 15 (GDF15) belongs to the transforming growth factor β (TGFβ) superfamily. GDF15 can bind to the glial cell-derived neurotrophic factor (GDNF) family receptor α-like (GFRAL) protein, which is primarily expressed in the hindbrain. This interaction activates the GFRAL-RET signaling pathway, which transmits anorectic neural signals, leading to weight loss, affecting fat and muscle degradation, and inducing cachexia. Anti-GDF-15/GFRAL antibodies have the potential to reverse this response, making them vital therapeutic targets for cachexia. Herein, a novel humanized GDF-15 neutralizing antibody (LBL-049) was developed with higher efficacy and better specificity than ponsegromab, the same target antibody from Pfizer, in pre-clinical studies.

Methods: LBL-049 was generated from mouse hybridoma, humanized by CDR grafting, the Fc region was further engineered to silence Fc effector. The binding affinity and specificity were detected by Fortebio and ELISA respectively. The function of blocking GDF15/GFRAL/RET signaling was examined in the reporter-gene cell assays. The in vivo efficacy of restoring cachexia was demonstrated in both tumor-induced and cisplatin-induced mouse cachexia models, in which preliminary pharmacokinetics (PK) and pharmacodynamics (PD) studies were also conducted. And a single-dose PK study was conducted in rats.

Results: LBL-049 had high binding affinities to both human and cynomolgus GDF-15 proteins with high specificity, did not bind with other TGF family members as compared with ponsegromab. In reporter-gene cell assays, LBL-049 blocked GDF15/GFRAL signaling more potently than ponsegromab. In HT1080 tumor-induced or cisplatin-induced mouse cachexia model, LBL-049 prevented weight loss by neutralizing circulating GDF-15 in a dose dependent manner, at low dose of 1 mpk in HT1080 cachexia model, LBL-049 was more efficacious than ponsegromab to restore the body weight loss. The PK profile was excellent after single dosing of LBL-049 in rats. LBL-049 also showed good developability, i.e., low viscosity and good stability.

Conclusion: LBL-049, a novel GDF15 neutralizing antibody with high affinity and specificity, showed great potency to inhibit GDF15/GFRAL/RET signaling in vitro and prevent weight loss in various mouse cachexia models, which are encouraging for future development for the treatment of cachexia.

#1868 Target-dependent considerations for the design of bispecific T-cell engagers.

Matt Mai, Raffi Tonikian, Peter Bergqvist, **Michael Kennedy**, Alaa Amash, Nathalie Blamey, Gabrielle Conaghan, Valentine de Puyraimond, Patrick Farber, Allison Goodman, Ahn Lee, Jessica Fernandes Scortecci, Cindy-Lee Crichlow, Akram Khodabandehloo, Tova Pinsky, Kate Caldwell, Jessica Patterson, Philippe Pouliot, Davide Tortora, Oscar Urtatiz, Ping Xiang, Irene Yu, Kirstin Brown, Kelly Bullock, Andrea Chee, Stephanie K. Masterman, Neil Aubuchon, Lindsay Devorkin, Bryan C. Barnhart, Tim Jacobs

AbCellera, Vancouver, BC, Canada

In this study, we present data from four T-cell engager (TCE) programs in which we leveraged our highly diverse CD3-binding antibodies to generate functional bispecifics for each tumor target. By aggregating tumor-cell killing and cytokine data across four tumor targets with different properties and target expression levels, we have gained novel insights into target-specific considerations for the development of CD3 TCEs. TCEs recapitulate a synapse between T cells and target cells. T cell function downstream of this synapse is determined by the complex interplay between multiple independent factors. These include properties of the CD3- and tumor-binding arms, such as binding kinetics and epitope, as well as target-dependent factors such as cell type and target density. We used our diverse CD3 antibodies to engineer bispecific TCEs against four solid tumor targets: PSMA, B7-H4, 5T4, and the peptide-MHC target MAGE-A4. For each target, we engineered and characterized hundreds of bispecific molecules using high-throughput assays, including T-cell dependent tumor-cell killing, cytokine release, developability assessments, and structural studies. Here, we compare data from across these programs to elucidate the impact of target-dependent parameters on TCE function. These data provide important insights for the selection of appropriate TCE targets and efficient design of bispecific antibodies with high therapeutic potential.

#1869 The AI-powered KisoSeek™ platform identifies functional anti-TROP2 heavy-chain antibodies with potent anti-cancer activity.

S. E. Cousineau[1], A. Subedi[2], R. Wargachuk[1], J. The[1], X. Wang[2], W. Hou[1], A. Nair[1], W. Qiu[1], A. Zhou[2], T. Cheng[2], M. Babaie[3], B. Gojogh[3], M. Montero[1], H. Zahreddine[1], E. Undzys[2], L. Lai[1], G. Ngan[1], L. Da Cruz[1], D. Young[1];

[1]KisoJi Biotechnology Inc., Montreal, QC, Canada, [2]KisoJi Biotechnology Inc., Toronto, ON, Canada, [3]KisoJi Biotechnology Inc., Waterloo, ON, Canada

Functional heavy-chain antibodies (HCAbs) are promising therapeutic agents for targeted cancer therapy. Since they do not have a light chain, HCAbs have a small antigen-binding domain that can unlock new functionalities by reaching epitopes that are inaccessible to classical antibodies. HCAbs can be obtained by immunizing camelids, but this approach is expensive, time-consuming, and results in a limited antibody repertoire. Previously, we engineered the KisoMouse™- a transgenic mouse with multi-camelid species VHH/VH genes and the complete alpaca D and J gene segments integrated into the mouse IgH locus, along with a functional loss of the heavy chain CH1 domain to eliminate light chain pairing. KisoMouse™ are healthy and generate a robust serum HCAb response against a diverse range of immunogens.

Trophoblast cell surface antigen-2 (TROP2) is a membrane protein overexpressed in numerous solid tumor types such as breast, colon, and lung cancers. TROP2 is associated with tumor aggressiveness and decreased survival and has emerged as an attractive therapeutic target. An anti-TROP2 antibody-drug conjugate has been approved for breast and bladder cancer, but challenges related to payload toxicity and resistance highlight the need for alternative therapeutics.

We had previously identified an anti-TROP2 HCAb with high potency in *in vivo* preclinical models of human breast and colorectal cancer. Conventional antibody discovery approaches are resource-intensive and can fail to identify rare antibodies. To overcome such limitations, we developed the KisoSeek™ platform, a proprietary AI-powered toolkit that categorizes antibodies in an immune response based on their structural and biophysical features. With KisoSeek™, we analyzed the entire antibody repertoire generated from KisoMouse™ immunized with TROP2 and rapidly identified HCAbs with similar features as the high potency reference antibody described above. We selected three additional antibodies based on their *in vitro* TROP2 affinity, competitiveness for the reference antibody's epitope, and yield in CHO cells. These candidates showed comparable potent efficacy in inducing regression in human breast and colorectal xenograft models, akin to the original reference antibody.

In summary, the KisoSeek™ platform identified novel anti-TROP2 HCAbs out of the KisoMouse™ antibody repertoire that were similar to our original reference antibody. This demonstrates how KisoMouse™ and KisoSeek™ are two powerful complementary platforms for novel clinical antibody discovery. By categorizing the entire antibody repertoire and identifying antibodies with similar characteristics as known functional antibodies, KisoSeek™ has the potential to leverage existing discovery efforts to uncover many more rare yet potent therapeutic antibodies - the proverbial needles in a haystack.

#1870 LCB36, a bi-specific antibody drug conjugate (BsADC) utilizing ConjuAll conjugation technology and proprietary prodrug payload selectively activated in cancer cells for treating B-cell blood cancers expressing CD20 and/or CD22.

Wihak Kim, Namjeong Choi, Cul-Woong Chung, Hwanhee Oh

LegoChem Biosciences, Inc, Daejeon, Korea, Republic of

Although frontline chemoimmunotherapy elicits responses in many B-Cell malignancy patients, treatment options remain limited, and clinical outcomes are suboptimal for those with relapsed or refractory diseases. Minimal residual disease (MRD) can lead to disease relapse despite achieving complete remission through targeted therapy, and tumor heterogeneity is responsible for MRD and compromises the efficacy of targeted therapy, especially in B-cell malignancies. Antibody-drug conjugates (ADCs) play a crucial role in oncology indications, and bispecific antibodies (BsAbs) represent one of the fastest-growing classes of next generation antibody therapeutics for cancer therapy. Several advantages of targeting dual tumor-associated antigens (TAAs) with BsAbs and bi-specific antibody drug conjugates (BsADCs) have been proposed, including improved efficacy, heightened tumor cell specificity, and reduced side effects in normal tissues. Notably, the ability of BsADCs to bind to cancer cells expressing even just one antigen has prompted further investigation into their efficacy in heterogeneous cancer models. LCB36 is a BsADC composed of a BsAb targeting both clinically validated CD20 and CD22, which are expressed in B-Cell malignancy, and a proprietary DNA cross-linking PBD prodrug that is site-specifically conjugated to the BsAb using ConjuAll technology. We assessed the expression levels of CD20 and CD22 in the cancer cell lines. While most cells expressed both antigens, some populations showed a low expression level of CD20 and a high expression level of CD22, while others exhibited the opposite pattern, suggesting heterogeneous expression of the two antigens within the same cell line. To confirm the heterogeneity of the two antigens in blood cancer patients, we analyzed single-cell sequencing data [GSE132509]. Each patient had CD20 and CD22 double-positive cells along with CD20 or CD22 single-positive cells, suggesting the possibility of relapse due to MRD following CD20 or CD22 single-targeted therapy. LCB36 demonstrated superior efficacy in CD20 and CD22 double-positive cell lines and cell-line derived xenografts (CDXs) models compared to ADCs targeting either CD20 or CD22, while showing comparable efficacy to single-target ADCs in CD20 or CD22 single-positive cancer cell lines and CDXs. Pharmacokinetic and toxicokinetic studies of LCB36 were analyzed in rats and Cynomolgus monkeys, respectively, using LC-MS/MS bioanalysis. Preliminary toxicity studies in rats and Cynomolgus monkeys demonstrated that LCB36 is well tolerated. In conclusion, LCB36, composed of a BsAb that binds to two clinically validated targets, showed efficacy at well-tolerated doses and has the potential to increase event-free survival periods by reducing MRD.

#1871 Discovery and characterization of NXV01c, an EGFR×cMET bispecific nanobody drug conjugate with potent anti-tumor activity.

R. Wu[1], P. Yuan[1], **Y. Xie**[2], J. Guo[1], F. Zhang[1], F. Liu[1], T. B. Guo[3];
[1]neoX Biotech, Beijing, China, [2]neoX Biotech, Boston, MA, [3]neoX Biotech, Shanghai, China

EGFR and cMET are proven cancer targets co-expressed in diverse tumor types. EGFR×cMET bispecific antibody has been approved for the treatment of NSCLC, supporting a simultaneous targeting strategy. In addition to this dual targeting benefit, bispecific antibody drug conjugates (ADCs) targeting EGFR and cMET have also been developed to further improve anti-tumor activity and tissue selectivity. Sufficient target affinity, good cellular internalization and high tumor infiltration are critical for an ADC to mediate therapeutic activity. To this end, we developed the first EGFR×cMET bispecific nanobody conjugated with monomethyl auristatin E (MMAE) as payload (NXV01c). Lead nanobodies against EGFR and cMET were respectively selected from immune libraries by phage display, followed by highly efficient humanization and optimization by neoX's computation platform. The bispecific nanobody with Fc (NXV01) was constructed by "knobs-into-holes" heterodimerization and then homogeneously conjugated with MMAE via a lysosomal cleavable valine-citrulline dipeptide linker. The resulting bispecific nanobody drug conjugate (NDC), NXV01c, was evaluated in multiple tumor cell lines and tumor xenograft models. NXV01, the pre-conjugate bispecific nanobody, bound EGFR and cMET with nanomolar potency (BLI) and inhibited the phosphorylation of cellular EGFR and cMET with nanomolar IC50 (ELISA). Moreover, it did not activate cellular cMET. Importantly, the NDC NXV01c is highly homogeneous: it has an average DAR of 3.87 and >95% of NXV01c has a DAR of 4. To examine stability of conjugation, NXV01C was incubated in human plasma (37℃) for 14 days, the maximum free drug release rate (by LC/MS/MS) is 0.68%, which is much lower than that of DS8201. In vitro, NXV01c was rapidly internalized into H1975 cells which co-expressed EGFR and cMET. It inhibited the growth of H1975 (lung) and SNU5 (gastric) cancer cells with picomolar activity but spared normal keratinocytes. NXV01c also inhibited the proliferation of additional cell lines derived from lung, gastric, esophageal, and liver cancer, and the level of inhibition positively associated with the expression density of both targets. In an H1975 cell line-derived xenograft model, NXV01C exhibited potent and dose-dependent anti-tumor activity. Treatments at 3 and 10 mg/kg once per week for 2 weeks led to shrinkage and complete regression of tumor, respectively. In patient-derived xenograft models of NSCLC and esophageal cancer, NXV01C led to tumor regression and elimination without noticeable toxic effects. EGFR×cMET bispecific nanobody drug conjugate NXV01c has favorable drug-like properties and demonstrated superior anti-tumor effect in vitro and in vivo. The results suggest NXV01C can be an effective solution for EGFR/cMET bearing tumors commonly found in diverse malignancies.

#1872 A next generation treatment for Nectin-4 positive cancers - Preclinical characterization of LY4052031, an anti-Nectin-4 antibody, conjugated to a novel camptothecin payload.

D. Sagar[1], M. Srinivasan[2], K. Lindquist[2], Q. Guo[1], W. Wong[1], M. B. Lebron[1], R. Sattler[1], J. Zhou[2], W. Helms[3], J. Boyles[4], P. Verdino[5], X. Zhao[2], Y. Mak[2], J. Park[2], R. Holmgaard[1], K. Driscoll[1], O. Duramad[2], K. Bedard[2];
[1]Loxo@Lilly, New York, NY, [2]Loxo@Lilly, South San Francisco, CA, [3]Loxo@Lilly, Silver Springs, MD, [4]Eli Lilly and Company, Indianapolis, IN, [5]Eli Lilly and Company, San Diego, CA

Nectin-4 is an immunoglobulin-like antigen overexpressed in a variety of cancers including bladder, breast, NSCLC, and gastric. Normal tissues including skin, salivary glands, bladder and esophagus express only low to medium levels of Nectin-4 making the protein an attractive target for cancer therapies. The approval of enfortumab vedotin-ejfv, an anti-Nectin-4 based antibody-drug conjugate (ADC) with a microtubule inhibitor payload, either as a single agent or in combination with pembrolizumab has been a significant advancement in the treatment of metastatic urothelial cancer. We have developed a novel anti-Nectin-4 ADC with a novel topoisomerase I (TOPO 1) inhibitor drug payload. Topoisomerase inhibitor payload-based ADCs offer potential advantages compared to microtubule payload-based ADCs including a different toxicity profile and the differentiated susceptibility to resistance mechanisms, such as P-gp mediated drug efflux. LY4052031 is a fully human monoclonal anti-Nectin-4 antibody conjugated to a novel TOPO 1 inhibitor by a cleavable peptide linker at a homogeneous drug antibody ratio (DAR) of 8:1. *In vitro*, both LY4052031 and its unconjugated parental antibody specifically bind to Nectin-4 expressing cell lines and are quickly and efficiently internalized. LY4052031 demonstrated potent cytotoxicity on tumor cells with high and low Nectin-4 expression. Additionally, bystander activity exerted by LY4052031 on antigen negative cells co-cultured with antigen positive cells was greater than that observed with the clinical benchmark enfortumab vedotin-ejfv. *In vivo* studies in xenografts expressing low to high levels of Nectin-4 showed significant tumor growth inhibition following treatment with LY4052031 as monotherapy. Overall, LY4052031 exhibits specificity, selectivity, potency, and effectiveness as a next generation therapy to treat Nectin-4 positive tumors. An IND submission is planned for 2024.

#1873 AST-05X: A novel GCN2 inhibitor as a promising anti-cancer approach for sarcoma.

Y. Choi[1], J. Lim[1], H.-H. Park[1], J. Kang[1], H. Kim[2], K. Yun[2], H. Jung[1];
[1]Aston Sci., Seoul, Korea, Republic of, [2]Yonsei Cancer Center, Seoul, Korea, Republic of

Background Integrated stress response (ISR) is an adaptive signaling pathway that responds to stress and plays an important role in cell fate determination. This pathway enables cellular adaptation and survival under stress conditions by activating specific genes that reduce protein synthesis. Tumors exist in a state characterized by heightened intrinsic and extrinsic stress, heavily relying on a balanced ISR to manage the metabolic demands for rapid growth. ISR (Integrated Stress Response) consists of four major kinases: GCN2, PERK, HRI, and PKR. GCN2 is activated by stress due to amino acid deprivation. Amino acids are crucial for cell survival, and cancer cells, require higher amounts than normal cells, particularly depending on conditionally essential amino acids like glutamine, asparagine, and arginine. GCN2 activation acts as a key mechanism for cancer cells to overcome amino acid deficiencies, making GCN2 a potential target, especially in conjunction with anticancer drugs like asparaginase. In this study, we aimed to identify a potential GCN2 inhibitor to explore a promising anti-cancer approach in sarcoma, a rare cancer with no new therapeutic alternatives.
Method The activity verification of ISR kinases was characterized using *in-vitro* enzyme assays. *In-vitro* panel assays were employed to determine the selectivity profiling for oncology kinases. The modulation of the ISR pathway was validated using a sarcoma cell line (HT-1080) and a cell line derived from sarcoma patients. Western blot or ELISA assays were employed to measure phospho-GCN2, ATF4, phospho-eIF2a, and CHOP under both basal conditions and amino acid starvation conditions. Gene expression profiling (GEP) of sarcoma patient tissue samples(n=17) was conducted through RNA sequencing (RNAseq) analysis.
Results AST-05X is a selective and potent GCN2 inhibitor. AST-05X inhibits the expression of GCN2 and ISR downstream factors (p-eIF2a, ATF, CHOP) in vitro cell-based experiments under amino acid deprivation. In addition, based on the results of ISR-related gene expression profiling GEP analysis, we identified potential CDx biomarkers for evaluating the diagnosis and treatment response of sarcoma.
Conclusion This study is currently investigating the efficacy of the drug in sarcoma patient-derived xenograft models. AST-05X is a GCN2 inhibitor that has the potential to validate the inhibition of GCN2 as a promising anti-cancer approach for sarcoma, a rare cancer with limited therapeutic alternatives.

#1874 Common vulnerabilities of stem cells along the Barrett's-dysplasia-adenocarcinoma sequence.

Wa Xian[1], Frank McKeon[1], Christopher Crum[2], Jaffer Ajani[3], Peter Davies[4], Matthew Vincent[5], William Bachovchin[6], Hung-Sen Lai[6], Shuang Pan[6], Amber Su[1], Ashley Hoffman[1], Raul Caballero Montes[1], Melina Khorrami[1], Melika Khorrami[1], Yusuke Yamamoto[7]

[1]University of Houston, Houston, TX,[2]Harvard University, Boston, MA,[3]MD Anderson Cancer Center, Houston, TX,[4]Texas A&M, Houston, TX,[5]Tract Pharmaceuticals, Inc., Houston, TX,[6]Tufts University, Boston, MA,[7]National Cancer Institute, Tokyo, Japan

Barrett's esophagus (BE) is an early precursor of esophageal adenocarcinoma and therefore a relevant target of preemptive therapeutics. Using robust stem cell cloning technologies, we have cloned stem cells from patient-matched biopsies of BE, low-grade dysplasia (LGD), high-grade dysplasia (HGD), and esophageal adenocarcinoma (EAC) from multiple patients. Whole exome sequencing of these stem cells reveals the mutational maturation along the sequence of BE, LGD, HGD, and EAC at unprecedented resolution of both copy number and single nucleotide variation. In vitro differentiation and xenografting of these clones recapitulates their original histology and shows that only the EAC stem cells yield robust tumors in immunodeficient mice. Leveraging the intrinsic immortality of these stem cells, we have performed high-throughput screens for small molecules that selectively kill BE stem cells without harming patient-matched normal esophageal stem cells. These screening efforts evolved into synthetic lethal strategies that identified drug combinations that selectively eliminate, in vitro, BE stem cells from 20 of 23 cases. Remarkably, this same synthetic lethal drug combination also eliminated in vitro stem cells of LGD, HGD, and EAC that were not components of the original screens. We have used synthetic chemistry to generate a series of novel molecules based on the identified drug combination that significantly improved the in vitro efficacy to sub-nanomolar levels. These novel molecules directed to the stem cell component of BE, LGD, HGD, and EAC also show potent effects against tumors generated from EAC stem cells in immunodeficient mice. We anticipate that these synthetically lethal drug combinations will have potential utility against precursor lesions to preempt EAC as well as against EAC itself.

#1875 Enhanced lung cancer treatment using AOH1996, a potent PCNA inhibitor.

R. G. Lingeman, R. J. Hickey, L. H. Malkas;
Beckman Research Institute of the City of Hope, Duarte, CA

AOH1996 targets a cancer-associated form of PCNA (caPCNA) by altering the protein-protein interface between caPCNA and its many binding partners. AOH1996 does this by inserting into the PCNA-interacting protein-box (PIP-box) pocket that is, in part, defined by the interdomain connecting loop (IDCL), the site of interaction between PCNA and most of its many binding partners. As a result, AOH1996 inhibits PCNA functions such as DNA replication, DNA repair, and transcription-replication conflict (TRC) resolution leading to cell cycle arrest and apoptosis. These effects are cancer specific and AOH1996 has little effect on non-cancerous cells even at 6-fold the effective dose in cancer cells. AOH1996 was developed in our lab and is currently in Phase I human clinical trials. Six patients have been enrolled in the trial and have not experienced AOH1996-related toxicities as the doses have been escalated to levels found to be efficacious in preclinical animal studies. Resistance to EGFR tyrosine kinase inhibitors (TKIs) poses a significant challenge in the treatment of non-small cell lung cancer (NSCLC) patients harboring EGFR activating mutations. Initially, EGFR TKIs like gefitinib, erlotinib, afatinib and osimertinib deliver remarkable responses, inducing tumor regression and improving overall survival. However, the emergence of resistance mechanisms, such as secondary EGFR mutations and bypass signaling pathway activation, hampers the efficacy of these drugs over time. The functional relationship between PCNA and EGFR has implications for the treatment of lung cancer patients with activating EGFR mutations. Membrane-localized EGFR modulates the PCNA-centric process of DNA replication through signaling pathways such as the Ras-Raf-Mek-Erk, PI3K/AKT, and PLCγ1/PKC signaling pathways. Nucleus-localized EGFR enhances PCNA stability by phosphorylating PCNA on tyrosine 211 (Y211), which prevents its degradation. In addition, phosphorylation at Y211 by EGFR results in decreased association of PCNA with MutS, which results in reduced mismatch repair (MMR). In this study, we combine AOH1996 and osimertinib as an innovative approach to treating NSCLC cancers with activating EGFR mutations and find that the drug combination: 1.) enhances the killing of NSCLC cell lines with activating EGFR mutations and acquired resistance to TKIs; 2.) enhances the destabilization of PCNA on chromatin; and 3.) causes changes in the localization and colocalization of PCNA and EGFR. We conclude that the combination of AOH1996 and osimertinib holds much potential as an improved treatment regimen for lung cancer patients with activating EGFR mutations.

#1876 Development of therapeutic antibodies targeting the GLUT-1 transporter to restrict cancer cell growth.

S. Tahk[1], K. Virumae[1], K. Anton[1], P. Hermet[1], R. Pau[1], M. Plaas[2], M. Abel[1], D. Belitskin[1], L. Galdieri[3], S. Garner[3], J. Krings[3], K. Collver[3], E. Schultz[3], K. Powers[3], A. King[3], F. Neethling[3], A. Planken[4], M. Ustav[1], J. Terya[1], A. Mannik[1], M. Ustav, Jr.[1];

[1]Icosagen Cell Factory OU, Tartu maakond, Estonia, [2]University of Tartu, Tartu, Estonia, [3]Eurofins Discovery, St. Charles, MO, [4]North-Estonian Medical Centre, Tallinn, Estonia

Background: Upregulated glucose metabolism is one of the strategies cancer cells use to fuel their abnormal cell growth and division. Targeting the cancer-specific glucose transporter GLUT-1 is a promising approach to restrict glucose uptake and challenge the metabolic needs of tumor cells. Antibodies, as opposed to small molecule inhibitors, are an attractive modality to therapeutically target complex muti-pass membrane transporters. Here we report the development of antibodies that very specifically block the function of only GLUT-1.

Methods: Monoclonal antibodies against GLUT-1 were generated using virus-like particles. For immunization, chickens were used as they are evolutionarily distant from mammals and can produce antibodies with prolonged CDR3-s in VH, which could facilitate their binding to the limited extracellular region of GLUT-1. Antibody discovery was performed with HybriFree B cell cloning technology followed by functional screens with 2-deoxyglucose uptake interference or cell proliferation measurements.

Results: The discovered antibodies specifically bind to GLUT-1 with low nanomolar EC50 values and do not target other glucose transporters. The lead candidate, ICO-33, inhibits glucose uptake and rewires the metabolism of GLUT-1-dependent cancer cells to rely on oxidative phosphorylation. This results in a significantly synergistic cancer proliferation inhibition with ICO-33 and OXPHOS inhibitor combinations in doses that do not inhibit proliferation as single agents. ICO-33 and OXPHOS inhibitor treatment is well-tolerated and demonstrates a drastic tumor growth inhibition in *in vivo* colorectal and pancreatic cancer models.

Conclusions: We describe the discovery of highly specific monoclonal antibodies targeting GLUT-1. We further demonstrate that the restriction of the much-needed glucose uptake by ICO-33 makes cancer cells highly susceptible to OXPHOS inhibitor co-therapy both *in vitro* and *in vivo*, validating the antibody as a promising candidate for clinical development.

#1878 CTPS1: An unexplored vulnerability in breast and ovarian cancer.

X. Wang[1], M. Emch[1], L. Voll[1], R. Russell[1], E. Rodman[1], N. Pearson[1], X. Hou[1], S. Kaufmann[1], S. Weroha[1], P. Beer[2], J. Hawse[1];
[1]Mayo Clinic, Rochester, MN, [2]Step Pharma, Saint-Genis-Pouilly, France

Breast and ovarian cancer represent the most common cancer types in women worldwide and are among the top fatal cancers. Despite the use of cytotoxic chemotherapy and targeted agents, recurrence is frequent and survival rates for patients with advanced metastatic disease are dismal. These realities highlight the need to identify novel biomarkers and therapeutic vulnerabilities in such tumors and to develop alternative treatment strategies. We took an unbiased approach to tackle this problem in which we leveraged publically available (DepMap) and in-house generated genome-wide CRISPR screens conducted in over 1000 cancer cell lines. We initially focused on the identification of essential genes that were unique to triple-negative breast cancer (TNBC) cells and whose expression levels were associated with worse patient outcomes. This interrogation revealed six genes (CTPS1, RHOA, PRKRA, RAD9A, HUS1, and RAD1) meeting these initial criteria. The essentiality of these genes was validated using gene-specific siRNAs in a panel of TNBC cells and knockdown of CTPS1 was shown to elicit the most inhibitory effect. CTPS1 depletion resulted in a rapid S-phase cell cycle arrest followed by apoptosis, not only in TNBC cells but also in highly aggressive ovarian cancer cells which share many molecular features with TNBC. CTPS1 converts uridine triphosphate to cytidine triphosphate, forming an essential nucleic acid required for multiple cellular processes. CTPS1 mRNA expression was substantially elevated in tumor vs. normal tissue, for both breast and ovarian cancer. Using over 40 breast and ovarian cancer cell lines, RT-PCR analyses confirmed increased expression of CTPS1 in TNBC and most ovarian cancer cell lines compared to other disease sub-types and “normal” cell line/tissue controls. Interestingly, chemoresistant and PARP inhibitor-resistant models exhibited the highest levels of CTPS1 among all cells analyzed. We subsequently identified and acquired STP938, a first-in-class highly selective CTPS1 inhibitor being developed by Step-Pharma. STP938 was found to elicit potent anti-cancer effects at nM concentrations across many cell line and patient-derived models, in both 2D and 3D culture systems. RNAseq analysis in aggressive cell line models following STP938 treatment or CTPS1 knockdown revealed significant regulation of genes related to DNA replication and the cell cycle pathways suggesting that combinatorial/sequential treatments of STP938 with replication stress/DNA damage response related drugs may be synergistic. STP938 is currently being developed for the treatment of lymphoma, and our findings support the repurposing of STP938 for breast and ovarian cancer, an avenue that we are currently developing.

#1879 A novel therapeutics accelerator for the brain cancer community: Early lessons learned.

Charlotte Kate Aitken[1], Katie Bushby[1], Petra Hamerlik[2], Nicky Huskens[1], Edward Kaye[3], Dione Kobayashi[4], **Juanita Lopez**[5], Ryan Mathew[6], John McCall[7], Javad Nazarian[8], Ruth Plummer[9], Steven Pollard[10], Ruman Rahman[11]

[1]Tessa Jowell Brain Cancer Mission C.I.C., London, United Kingdom,[2]University of Manchester, Manchester, United Kingdom,[3]Stoke Therapeutics, Bedford, MA,[4]Mass General Brigham, Boston, MA,[5]The Royal Marsden NHS Foundation Trust, London, United Kingdom,[6]University of Leeds Teaching Hospitals NHS Trust, Leeds, United Kingdom,[7]University of Wisconsin, Madison, WI,[8]University Children's Hospital,, Zurich, Switzerland,[9]Newcastle University, Newcastle upon Tyne, United Kingdom,[10]University of Edinburgh, Edinburgh, United Kingdom,[11]University of Nottingham, Nottingham, United Kingdom

Developing a comprehensive translational program for brain tumors is a complex task that involves numerous challenges. These challenges include significant obstacles surrounding the delivery of pre-clinical studies, safety, clinical trial design, and routes to commercialization. Recognizing that this journey is difficult, in 2023 the Tessa Jowell Brain Cancer Mission launched the Brain Tumor Research Novel Therapeutics Accelerator (BTR-NTA). The BTR-NTA is a new international accelerator program that provides independent and comprehensive expert guidance to de-risk therapeutic development through systematic, multidisciplinary evaluation and feedback for academic or industry researchers who are developing a therapeutic or technology for brain tumors. The BTR-NTA was modeled on the TREAT-NMD Advisory Committee for Therapeutics, which has yielded impressive results in the neuromuscular disease field. The ultimate goal of the BTR-NTA program is to enable researchers with a potential therapy or technology for brain tumors to navigate the development journey and successfully make it to the clinic in an efficient and timely way. The international, multidisciplinary BTR-NTA Expert Committee spans the entire therapeutic development pathway to avoid a siloed approach to research. Thanks to charitable funding, the BTR-NTA is free for academics and available at low cost for industry. Researchers at any stage of pre-clinical or clinical work can apply to the BTR-NTA, and, if accepted, their application will proceed as follows: 1. The applicant completes an application form covering work to date and future plans under a strict confidentiality agreement that protects the applicant; 2. Depending on the types of applicants, additional experts are recruited to ensure that each applicant gets a robust and tailored review 3. The applicant’s work is reviewed by an international, multidisciplinary committee 4. The applicant and BTR-NTA Expert Committee meet in-person to further discuss the applicant’s work; and 5. The applicant receives a comprehensive written report from the BTR-NTA Expert Committee, with feedback on strengths and weaknesses and guidance on next steps. The BTR-NTA Expert Committee dedicates half a day to review the applicant’s work in-person, and extensive time pre- and post-meeting. This is a low cost to applicant, high impact process designed to provide valuable feedback and support. The BTR-NTA aims to help overcome barriers for applicants by highlighting potential pitfalls or risks, providing multi-disciplinary feedback on work to date and constructive guidance on next steps, and by strengthening international collaboration in the brain tumor field. Following the launch of the BTR-NTA program in 2023 and review of the first group of therapeutics and technologies, we report on our early learnings, impact, and how we hope to grow the program to help accelerate new brain tumor therapies globally.

#1880 Ecubectedin and PM54 demonstrate antitumor activity in patient-derived xenograft models of soft tissue sarcoma.

D. Gorgels[1], A. Wozniak[1], C.-C. Wang[1], P. M. Aviles[2], M. J. Guillen[2], C. Cuevas[2], P. Schoffski[3];
[1]KU Leuven, Leuven Cancer Institute, Leuven, Belgium, [2]PharmaMar, Madrid, Spain, [3]University Hospitals Leuven, Leuven Cancer Institute, Leuven, Belgium

Objective: Soft tissue sarcoma (STS) is a heterogenous group of rare, malignant tumors arising from mesenchymal tissue. Doxorubicin (DOX)-based chemotherapy is the standard for advanced or metastatic STS, despite low response rates and poor disease control. We explored the antitumor activity of two novel compounds, ecubectedin (ECU; PM14) and PM54 (PharmaMar), in two patient-derived xenograft (PDX) models of STS, leiomyosarcoma (LMS) and *CIC*-rearranged sarcoma (CRS). Mode of action of ECU and PM54 is similar to lurbinectedin (LUR), inhibiting oncogenic transcription by eviction of oncogenic transcription factors from gene promotors' recognition sequences, while inducing the generation of double strand breaks through DNA adduct formation.
Methods: Female NMRI *nu/nu* mice (n=104) were transplanted bilaterally with STS PDX: UZLX-STS134 (CRS) and UZLX-STS22_2 (LMS). Xenografted mice were randomized to six treatment groups: 1) vehicle (VEH) (5% dextrose) 5 mL/kg once weekly (QW) intravenously (IV); 2) DOX 5 mg/kg QW IV; 3) trabectedin (TRA) 0.15 mg/kg QW IV; 4) LUR 0.18 mg/kg QW IV; 5) ECU 1.2 mg/kg QW IV; 6) PM54 1.2 mg/kg QW IV. Treatment lasted 16 days and antitumor activity was assessed by tumor volume (TV) analysis, histopathology and western blot. The Mann-Whitney U test was used to compare groups, the Wilcoxon test to compare to baseline.
Results: ECU and PM54 caused TV shrinkage in UZLX-STS134, while TV in other groups grew significantly on day 16 (Table 1). VEH treatment led to the largest TV increase on day 16, compared to any treatment. PM54 treatment showed TV stabilization in UZLX-STS22_2, and significantly smaller tumors than VEH and TRA treated tumors ($p<0.05$ and $p<0.01$, respectively). Histopathological evaluation corroborate the results from the relative TV analysis.

Table 1: TV change on day 16 versus baseline, and comparison of proliferative and apoptotic activity

	Tumor volume change		Proliferative activity (pHH3)		Apoptotic activity (cPARP)	
Subtypes	**UZLX-STS134**	**UZLX-STS22_2**	**UZLX-STS134**	**UZLX-STS22_2**	**UZLX-STS134**	**UZLX-STS22_2**
VEH(5 ML/kg)	387%***	349%**	n/a	n/a	n/a	n/a
DOX (5 mg/kg/QW IV)	177%***	243%**	↓***	↓	↑**	↑
TRA(0.15 mg/kg/QW IV)	230%**	254%***	↓**	↓**	↑**	↑***
LUR(0.18 mg/kg/QW IV)	202%**	232%**	↓***	↓***	↑***	↑**
ECU(1.2 mg/kg/QW IV)	41%***	181%**	↓***	↓***	↑***	↑***
PM54 (1.2 mg/kg/QW IV)	76%***	162%	↓***	↓***	↑***	↑

Conclusion: Novel drugs exhibit promising results in the PDX models tested, supporting ongoing exploration in additional PDX models of synovial sarcoma and dedifferentiated liposarcoma.

#1881 Screening of Rac1 and Cdc42 inhibitors as anti-metastatic compounds.

J. Colon Gonzalez[1], M. C. Santa Maria Fuentes[2], C. Vlaar[1], S. Dharmawardhane[1];
[1]University of Puerto Rico Medical Sciences Campus, San Juan, PR, [2]University of Puerto Rico Rio Piedras Campus, San Juan, PR

Metastasis is responsible for >90% of cancer-related deaths and is a key cause of failure of cancer therapy. The development of effective targeted therapy to prevent and treat metastasis has been challenging. Homologous Rho GTPases Rac and Cdc42 are viable metastasis targets because they have a crucial role in the signaling pathways that regulate cell survival, proliferation, and migration, so dysregulation of these proteins leads to cancer progression and metastasis of diverse cancer types. Therefore, targeting these regulatory proteins results in anticancer and antimetastatic activity, as observed with our dual Rac/Cdc42 inhibitor, MBQ-167, in triple-negative breast cancer. MBQ-167 has an IC_{50} of ~100nM for Rac and Cdc42 activation inhibition and a GI_{50} of 130nM. MBQ-167 inhibits the binding of guanine nucleotides to Rac and Cdc42 with similar efficacy. The purpose of this study was to identify MBQ-167 derivatives with similar or greater efficacy and specificity, with a range of inhibitory mechanisms, that may be specific to the different guanine nucleotide exchange factors expressed in distinct cancer cell types. Currently, over 30 different compounds with potential Rac1 and Cdc42 inhibitory activity are being evaluated. So far, some of the evaluated compounds have shown comparable GI_{50} values to MBQ-167 in metastatic breast cancer cell lines. From this screening, CPV-337 was selected as a compound with a GI_{50} of ~55nM and ~70% Rac activation inhibition at 50nM, therefore being 2X more effective than our leading compound MBQ-167. However, evaluation of CPV-337 in the viability of the MCF-10 non-tumorigenic epithelial cell line demonstrated a GI_{50} of ~63nM, which is similar to that of breast cancer cells. Therefore, CPV-337 may have cytotoxic effects on breast cancer. We are continuing to screen the library of MBQ-167 derivatives in breast, pancreatic, lung, and prostate cancer cell lines.

#1882 DXC024, a novel anti-TROP2/EGFR bispecific antibody and tubulysin conjugate, for targeted treatment of highly TROP2- or EGFR-expressing tumors.

Jingjing Zhu, Junxiang Jia, Huihui Guo, Xiangfei Kong, Yong Du, Zhicang Ye, Lingli Zhang, Yongxiang Chen, Lu Bai, Yunxia Zheng, Wei Zheng, Jun Zheng, Juan Wang, Wenjun Li, Yuanyuan Huang, Zhongliang Fan, Mengmeng Liu, Binbin Chen, Meng Dai, Fang Du, Miaomiao Chen, Zhixiang Guo, Qingliang Yang, **Robert Y. Zhao**

Hangzhou DAC Biotechnology Co., Ltd., Hangzhou City, China

Antibody drug conjugates (ADCs) which combine the precision of targeted therapy with the cytotoxic effects of chemotherapy have become a promising drug class in cancer therapy. Epidermal growth factor receptor (EGFR) is overexpressed in a wide diversity of epithelial tumors, promoting cell proliferation and survival pathways. Tumor-associated calcium signal transducer 2 (Trop2) is also expressed in a wide range of solid tumors and has been used as a transport gate for cytotoxic agents into cells in antibody-drug conjugate constructions for clinic applications. However, the approved Trop2 ADC, sacituzumab govitecan, only showed an objective response rate (ORR) of 17% and median OS of 9.5 months for lung cancers. In addition, both EGFR-ADC and Trop2-ADC had exhibited strong side effects in clinical trials due to their expression on some normal tissues, such as skin, mouth, eyes, etc. We generated bispecific Fab/scFv antibodies targeting both TROP2 and EGFR using the knob-into-hole technology, which presumably have wider efficacy, less on-target toxicity in comparison to the ADCs constructed based on the fully individual EGFR and Trop2 IgG antibodies having strong affinity to either EGFR or Trop2 antigens. Indeed, many of generated anti-TROP2/EGFR BsAbs showed strong binding activity in $TROP2^{high}EGFR^{high}$ cells and demonstrated over 60% internalization rate within 60 min in vitro. The selected BsAbs were subsequently conjugated with tubulysin B analogs with varieties of peptidyl linkers to generate bispecific ADC (DXC024) candidates, two of which exhibited strong killing activity in A431, MDA-MB-468, Calu3, MCF-7 cells with IC_{50} of single to ten digital pM. In vivo, they showed very good durable antitumor response at dose as low as 4.6 mg/Kg for one injection in Calu3 ($TROP2^{high}EGFR^{moderate}$) xenograft model, and demonstrated enhanced anti-tumor efficacy in comparison to those of the same payload conjugated to the monoclonal TROP2 or EGFR ADCs. These results indicated that DXC024 would be a promising ADC candidate for targeted treatment of highly either TROP2- or EGFR-expressing tumors.

#1883 A MUC1 antibody-conjugated with a tubulysin B analog, DXC005, demonstrates excellent synergistic effect in combination with gemcitabine for treatment of pancreatic tumors.

X. Cai, M. Cao, H. Guo, Q. Yang, Y. Chen, X. Kong, Y. Du, Z. Ye, Z. Guo, L. Zhang, L. Bai, J. Jia, Y. Zheng, W. Zheng, J. Zheng, W. Li, Y. Huang, Z. Fan, B. Chen, Y. Yang, M. Dai, **R. Y. Zhao**;
Hangzhou DAC Biotechnology Co., Ltd., Hangzhou City, China

Pancreatic cancer is a malignant tumor with high incidence and mortality. It is difficult to diagnose and detect in the early stage, with low surgical resection rate and high recurrence and metastasis rate after surgery. At present, the clinical therapeutic strategy is extremely limited. The first-line Standard of Care (SOC) for unresectable pancreatic cancer is chemotherapy. The preferred regimen includes gemcitabine combined with albumin paclitaxel or FOLFIRINOX (5-FU+Oxaliplatin+Irinotecan). Due to the limited long-term benefits and toxic side effects of chemotherapy, targeted therapy combined with chemotherapy has become a new therapeutic strategy. MUC1 is a highly glycosylated transmembrane mucin located on the lumen surface of epithelial cells. It can protect cells from extreme factors and plays an important role in tumor cell metabolism, apoptosis, epithelial-mesenchymal transition (EMT) and metastasis. Previous studies have confirmed that MUC1 is highly expressed in a variety of tumors, including pancreatic cancer, and is closely related to poor prognosis. DXC005 is a novel MUC1-targeting antibody-drug conjugate (ADC), generated by conjugating a Tubulysin B analogue to a recombinant humanized anti-Muc1 monoclonal antibody. DXC005 is the first MUC1-ADC IND in China, and is currently in phase I clinical trials. Preclinical studies have confirmed the efficacy of DXC005 monotherapy (2.5 mg/kg, 5 mg/kg, 10 mg/kg in one administration) in the HuPrime ® pancreatic cancer PDX model (PA1194). The tumor growth inhibition (TGI) was 42.53 %, 70.77 %, and 95.58 %, respectively. We want to further clarify whether DXC005 combined with chemotherapeutic drug Gemcitabine can ensure or even improve the efficacy while reducing the dosage of Gemcitabine. In PA1194 xenograft model, DXC005 (3 mg/kg or 6 mg/kg) in combination with Gemcitabine (10 mg/kg) showed significant anti-tumor efficacy with 58.77% and 93.17% TGIs, respectively. In contrast, the treatment with 10 mg/kg of Gemcitabine alone exhibited much less TGI. Furthermore, complete response (CR) was observed in some animals after treatment with DXC005 (6 mg/kg) plus Gemcitabine (10 mg/kg). All groups of treatment are tolerated well, no abnormal animal behavior and body weight loss were observed in the study. The above results concluded that DXC005 combined with Gemcitabine can achieve synergistic effect even with reduced dose of Gemcitabine, which will serve as a support for synergistic application in clinical studies.

#1884 DXC006, Anti-CD56-CPT113 ADC displays favorable anti-tumor efficacy, pharmacokinetic and safety profiles in preclinical studies.

X. Kong, H. Guo, Y. Du, Z. Ye, Y. Chen, Z. Guo, L. Zhang, L. Bai, J. Jia, Y. Zheng, W. Zheng, J. Zheng, W. Li, Y. Huang, Z. Fan, M. Liu, B. Chen, M. Dai, J. Wang, F. Du, M. Chen, Q. Yang, **R. Y. Zhao**;
Hangzhou DAC Biotechnology Co., Ltd., Hangzhou City, China

CD56, also known as neural cell adhesion molecule 1 (NCAM1), is a type I plasma membrane glycoprotein involved in cell-cell and cell-matrix adhesion. It is overexpressed in almost all neuroblastomas, 95% of small cell lung cancers and 78% of multiple myeloma patients[1], whereas CD56 is less frequently or less abundantly expressed in normal tissues, making it a potential target for tumor therapy. So far, no CD56-targeting ADCs have entered late-stage clinical trials.DXC006 is an antibody-drug conjugate of a humanized anti-CD56 antibody (DXA006) linked to the topoisomerase I inhibitor CPT113 through a cleavable peptidyl linker and CROSSCONJU™ technology. The pharmacologic activity and mechanism of action of DXC006 were investigated in several human cancer cell lines and xenograft mouse models. Pharmacokinetic and safety profiles were also assessed in rats and cynomolgus monkeys.DXC006 binds specifically to CD56 and internalizes into tumor cells, after intracellular trafficking to lysosome and CPT113 releasing, induces DNA damage. In vitro cell based assays showed that DXC006 remarkably inhibited the cell growth of CD56-positive cell lines of IMR-32 (neuroblastoma), NCI-H526 (small cell lung cancer), and NCI-H929 (multiple myeloma), with IC_{50} of 0.0046~0.061 nmol/L. Although DXC006 also binds to CD56 expressed NK cells, we found that the inhibition of DXC006 to human NK cells was much less effective, with IC_{50} higher than 675 nmol/L, which is ten thousand-folds less potent than that of targeted abnormal cells. In vivo, DXC006 demonstrated good durable antitumor activities in three CD56-positive xenograft models of IMR-32, NCI-H526 and NCI-H929 cell lines, with a single dose of 2 mg/Kg, 3 mg/Kg, and 5 mg/Kg, respectively. No animal death or moribund outcome was observed in two months during preclinical safety studies in 150 mg/Kg Q2W dosed rats. For cynomolgus monkeys, the highest non-severely toxic dose (HNSTD) of DXC006 was 20 mg/Kg, in Q2W, four times of administration. PK profiles of both DXC006 the naked antibody DXA006 were comparable in both rats and monkeys. In summary, DXC006 demonstrated strong antitumor activity in various types of cancer cells both in vitro and in vivo, and good pharmacokinetic and safety profiles in rat and monkeys, a potential to be explored in clinical applications.

[1] Yang Feng, Yanping Wang, Zhongyu Zhu, et al. Differential killing of CD56-expressing cells by drug-conjugated human antibodies targeting membrane-distal and membrane-proximal nonoverlapping epitopes. mAbs 2016; 799-810.

#1885 Developing a biparatopic anti-ROR1 antibody drug conjugate BR111 for hematological and solid tumor treatment.

X. Zhao[1], J. Zhu[1], z. Wu[2], Y. Li[1], J. Li[1], Y. Zhou[2], L. Nie[2], H. Wang[2], G. Chen[1];
[1]BioRay Pharmaceutical Corp., San Diego, CA, [2]BioRay Pharmaceutical Ltd., San Diego, CA

ROR1 is a type I transmembrane protein that belongs to the ROR family. It is a receptor for Wnt family signaling molecules Wnt5a, and plays a critical role in various cellular processes, such as cell proliferation, survival, and migration. Being an oncofetal protein, ROR1 exhibits limited expression in most normal tissues. However, it is abnormally expressed in various hematological and solid cancers, contributing to the development and progression of many types of cancer. Due to its overexpression in cancer, ROR1 presents as a highly attractive target for antibody-drug conjugate (ADC) therapy. The current clinical results of ROR1 ADCs have been promising in treating patients with relapsed and/or refractory (R/R) hematologic malignancies.
BR111 is anti-ROR1 ADC that consists of a biparatopic antibody, stably conjugated to an antimitotic agent. The biparatopic antibodies demonstrate superior binding affinity to ROR1-expressing cancer cells compared to single epitope antibodies. Notably, our unique and innovative conjugation platform CysX™, not only prevents payload detachment during circulation and reducing the off-target toxicity, but also enables a uniformed drug-to-antibody ratio (DAR) of 4.
Both *in vitro* and *In vivo* studies have highlighted the remarkable antitumor activity of BR111. Preclinical data have shown great safety profile in cynomolgus monkeys. BR111 demonstrated a wider therapeutic window for cancer treatment, outperforming the lead anti-ROR1 ADC currently in phase II/III trial. The promising outcome holds great potential as a therapeutic treatment for hematological and solid cancers, offering a better safety profile. BR111 has great potential in further clinical evaluations.

#1886 BRY812, an anti-LIV-1 antibody drug conjugate with novel conjugation method for cancer therapeutics.

X. Zhao[1], J. Zhu[1], Y. Zhou[2], J. Li[1], L. Nie[2], H. Wang[2], G. Chen[1];

[1]BioRay Pharmaceutical Corp., San Diego, CA, [2]BioRay Pharmaceutical Ltd., Hangzhou, China

LIV-1, also known as SLC39A6 or ZIP6, belongs to the zinc transporter family and was initially identified as an estrogen-inducible gene in breast cancer. Immunohistochemical (IHC) analysis have revealed escalated LIV-1 expression in estrogen receptor-positive (ER+), hormone-treated tumors (both primary and metastatic sites) as well as ER-/PR-/Her2- (triple-negative) breast cancers. Notably, healthy human tissues exhibit limited LIV-1 expression, primarily in hormone regulated organs (prostate, uterus, and breast). The escalated expression of LIV-1 in breast and prostate cancer, as well as melanoma and other tumors, positions LIV-1 as an excellent target for ADC therapeutics.

BRY812 is a monomethyl auristatin E (MMAE)-conjugated humanized IgG1 ADC against LIV-1. With Bioray's irreversible conjugation method CysLink™, BRY812 enables superior *in vivo* stability and eliminates off-target payload migration. The PK studies in rat and monkey demonstrated that the free MMAE released from ADC is 1 to 2 logs lower compared with approved ADCs prepared by the standard conjugation method. BRY812 is well tolerated in cynomolgus monkeys with repeated doses. With best-in-class anti-tumor efficacy in various models, BRY812 demonstrated a wider therapeutic window for cancer treatment. BRY812 is currently in Phase Ia dose escalation stage clinical trial to explore the maximum tolerate dosage (MTD) from 0.25 to 3.6 mg/kg Q3W in patients with advanced malignancies.

EXPERIMENTAL AND MOLECULAR THERAPEUTICS: Antibody-Drug Conjugates and Bispectific Antibodies
Poster Session

#1890 HMA800067, a novel CD38-targeting antibody-drug conjugate (ADC), demonstrated superior anti-tumor activity to daratumumab in preclinical B-cell malignancies models.

Y. Xu, J. Liang, S. Jiang, H. Yang, H. Zhang, F. Mao, J. Zhu, J. He, N. Yang, J. Wang, W. Zhang, Y. Ren, W. Su;
HUTCHMED, Shanghai, China

Introduction: Daratumumab (Dara), an anti-CD38 monoclonal antibody, has been widely used in the treatment of multiple myeloma (MM). However, some of MM patients exhibit primary or acquired resistance to Dara therapy. A CD38 targeting antibody-drug conjugate (ADC) HMA800067 is developed, in which Dara was conjugated with cytotoxic payload via a novel linker, aiming to have superior anti-tumor efficacy to Dara, even in the subjects with resistance to Dara treatment.
Methods: HMA800067 was characterized by ELISA-based binding assay, cell internalization assay, antibody-dependent cell-mediated cytotoxicity (ADCC) and antibody-dependent cellular phagocytosis (ADCP) assays. The *in vitro* anti-tumor potency was assessed against a panel of 24 MM and B cell lymphoma cell lines with various CD38 expressions. Bystander effect of HMA800067 was evaluated in co-culture of $CD38^-$ SU-DHL-2 cells with $CD38^\pm$ Ramos cells. *In vivo* anti-tumor efficacy was investigated in the multiple MM and Diffuse Large B-cell Lymphoma (DLBCL) subcutaneous xenograft models, including some non-responsive to Dara.
Results: HMA800067 displayed comparable binding affinity and internalization capability to Dara in $CD38^\pm$ Ramos cells. And HMA800067 maintained the ability of Dara to induce the death of $CD38^\pm$ Daudi cells by ADCC and ADCP, which indicated that conjugation did not change the property of Dara in the ADC upon antigen binding. HMA800067 exhibited a CD38-dependent cytotoxic activity with median IC_{50} of 0.46 nM against a panel of tumor cell lines, with a trend that the higher CD38 expression, the stronger potency could be seen. Bystander killing effect of HMA800067 was observed in $CD38^-$ cells when co-cultured with $CD38^\pm$ cells *in vitro*. Furthermore, with the low release of payload in plasma and sustainable high exposure of payload in the tumor, HMA800067 demonstrated dose-dependent and superior anti-tumor efficacy to Dara in all tested models, and 10 mg/kg induced complete tumor regression in MM RPMI-8226, DLBCL SU-DHL-6 and SU-DHL-10 models. For example, in SU-DHL-6 xenograft model, the treatment of intravenous injection of HMA800067 at 10 mg/kg single dose induced complete tumor regression in all the animals within 10 days of administration, which was maintained until the end of study (day 49), while 10 mg/kg Dara twice a week for 2 weeks inhibited tumor growth within 20%-40% without any tumor regression during a four-week observation post initial dosing.
Conclusion: HMA800067 demonstrated potent anti-tumor activities *in vitro* and *in vivo* in multiple B-cell malignant tumor lines, including those with poor response to Dara. These results supported further development of HMA800067, as a superior therapeutic option for treatment of patients with $CD38^\pm$ B cell malignancies.

#1891 Preclinical characterization of ADRX-0706: A next-generation anti-Nectin-4 antibody-drug conjugate with improved therapeutic window.

A. M. Hau[1], M. Shahmoradgoli[1], D. Lee[1], W. Sisson[1], A. Wang[1], P. P. Challita[1], E. Nye[1], M. M. -. Kuo[1], A. Mahloch[1], M. Leung[1], O. Betancourt[1], A. Chu-Kung[1], M. Guo[2], H. Li[1], S. Rottmann[1], P. M. Challita-Eid[1];

[1]Adcentrx Therapeutics, Inc., San Diego, CA, [2]Adcentrx Therapeutics, Inc., Shanghai, China

Nectin-4 is a well validated tumor target, which is highly expressed in several solid cancers such as urothelial, head-and-neck, breast, lung, pancreatic, ovarian, and cervical cancer, while expression in normal tissues is limited. A first-generation antibody-drug conjugate targeting Nectin-4, called enfortumab vedotin-ejfv (EV), was granted accelerated FDA approval in 2019 for urothelial cancers, and is currently approved for frontline therapy in cisplatin-ineligible patients with locally advanced or metastatic urothelial carcinoma, providing groundbreaking improvement in patient survival. However, clinical use of EV has also revealed safety-driven limitations, which result in reduced and/or interrupted drug exposures impacting efficacy. To overcome these limitations in therapeutic window and to maximize on the potential of Nectin-4 as a tumor target beyond urothelial cancers, Adcentrx has developed ADRX-0706, a Nectin-4-targeting next-generation ADC with a drug-antibody ratio of 8. ADRX-0706 is comprised of a novel fully human IgG1k monoclonal antibody linked to an optimized tubulin inhibitor payload AP052 through a proprietary cleavable linker. ADRX-0706 has strong binding affinity and selectively induces cytotoxicity in Nectin-4-expressing tumor cells. Importantly, ADRX-0706 is designed to have improved bystander effect, which allows tumor regression even in cases of heterogeneous Nectin-4 expression. This translates to superior in vivo efficacy of ADRX-0706 over EV in multiple mouse xenograft models of other indications beyond bladder cancer. In a mouse clinical trial of patient-derived cervical cancers with a range of Nectin-4 expression levels, ADRX-0706 reaches a 73% ORR. Since peripheral neuropathy is a main platform toxicity for this payload class, ADRX-0706 is assessed in an in vitro co-culture model to evaluate its neurotoxic potential. While EV displays a 75% decrease in neurite outgrowth, ADRX-0706 strikingly has no impact at concentrations up to 1mg/ml, suggesting a lower risk of peripheral neuropathy in humans for ADRX-0706. In preclinical repeat dose toxicology study, ADRX-0706 reaches an HNSTD of 18mg/kg in NHPs well above therapeutic exposures in mouse pharmacology studies, indicating a tremendous increase in the therapeutic index compared to EV. In summary, the highly selective and potent anti-tumor activity in multiple tumor types and wide preclinical therapeutic index of ADRX-0706 support clinical evaluation of this next generation anti-Nectin-4 ADC. ADRX-0706 is currently in a phase 1a/b study (NCT06036121).

#1892 KK2260: A fully human tetravalent bispecific antibody targeting TfR1 and EGFR for the treatment of EGFR-expressing tumors.

K. Mitamura[1], H. Otsuki[2], K. Nakahashi[2], A. Kitagawa[2], M. Kamigaki[1], Y. Kurio[1], M. Inoue[1], Y. Uemura[1];
[1]Kyowa Kirin Co., Ltd., Machida-Shi, Tokyo, Japan, [2]Kyowa Kirin Co., Ltd., Sunto-gun, Shizuoka, Japan

Background: TfR1 is a transmembrane glycoprotein involved in iron uptake and regulation of cell growth. High TfR1 expression has been reported in different types of cancers, therefore recognized as a target molecule for cancer therapy. Despite the promise of potent efficacy of TfR1-targeted agents, there is a risk of side effects (*i.e.*, severe anemia), since TfR1 is also highly expressed in certain normal cells (*e.g.*, reticulocytes). KK2260 is a fully human tetravalent bispecific antibody (bsAb) based on REGULGENT™ technology targeting TfR1 and EGFR. This bsAb was designed for EGFR-expressing cell selective anti-cancer drug which could not be achieved by conventional monospecific Ab. In this study, we evaluated the mechanism of action (MOA), anti-cancer effect, and toxicity of KK2260.

Methods: Binding activity of KK2260 to TfR1 and EGFR was evaluated by surface plasmon resonance method. Ligand blocking activity was evaluated by binding competition on esophageal squamous cell carcinoma (ESCC) OE21 cells. Growth inhibitory activity of KK2260 on cancer cells or hematopoietic progenitor cells was evaluated by proliferation inhibition assay. In some studies, excessive iron or anti-EGFR parent Ab was added. Effect on the cell surface target expression levels was evaluated by flow cytometry. The intracellular iron level was evaluated by cell imaging. Effect on EGF induced EGFR phosphorylation was evaluated by Western blotting. The *in vivo* efficacy of KK2260 was evaluated in cell line-derived and patient-derived xenograft (PDX) models of ESCC selected for high EGFR expression level. The toxicity of KK2260 was evaluated in cynomolgus monkeys.

Results: KK2260 bound to TfR1 and EGFR with no ligand binding inhibition. KK2260 inhibited cell growth of moderate to high EGFR-expressing cancer cells, but not against EGFR-negative cancer cells or hematopoietic progenitor cells. KK2260 downregulated TfR1 expression on OE21 cells and the intracellular iron level decreased, but no effect was observed on EGFR phosphorylation. The growth inhibitory activity of KK2260 was abolished by adding excessive amounts of iron or reduced by inhibiting the binding to EGFR. Potent anti-tumor activity was observed in the ESCC PDX models with tumor regression. In the intermittent-dose toxicity study of cynomolgus monkeys, KK2260 was well-tolerated.

Conclusions: KK2260 demonstrated potent anti-cancer effect both *in vitro* and *in vivo*. Intriguingly, KK2260 did not inhibit EGFR phosphorylation while EGFR-binding dependent TfR1 downregulation resulted in intracellular iron deficiency, which was considered as the MOA of KK2260. KK2260 was well tolerated in non-human primates. These preclinical data suggest the unique property of KK2260 is expected to provide significant benefit to patients with advanced ESCC and other EGFR-expressing tumors and Phase 1 study is currently on going in Japan (jRCT2031230372).

#1893 OBI-992, a novel TROP2 targeting antibody-drug conjugate, displayed excellent antitumor efficacy in various animal models.

W.-F. Li, M.-F. Chiang, H.-C. Weng, J.-J. Yang, H.-S. Wu, C.-J. Lin, P.-T. Chiu, M.-T. Lai;
OBI Pharma, Inc., Taipei, Taiwan

Background: TROP2 is a validated therapeutic target for cancer treatment. OBI-992 is an antibody-drug conjugate (ADC) derived from a novel TROP2 antibody linked with a topoisomerase 1 inhibitor payload, exatecan, through conjugation with an enzyme-cleavable linker. Upon binding to TROP2 on the surface of cancer cells, OBI-992 is internalized into the cell and trafficked to lysosomes where the linker is cleaved by cathepsin B, releasing the payload exatecan to kill the cancer cells. This study aims to evaluate the antitumor efficacy of OBI-992 *in vitro* and *in vivo*, including cell-based cytotoxicity, cell line-derived xenografts (CDX), and patient-derived xenografts (PDX) models.

Methods: The cytotoxicity of OBI-992 was evaluated in cell lines with different levels of TROP2 expression. *In vivo* efficacy was evaluated using CDX and PDX models of various cancer types. Bystander killing effect of OBI-992 was examined in a xenograft model containing a premixture of TROP2 positive and TROP2 negative cancer cells. Moreover, the impact of overexpression of P-glycoprotein (Pgp) or breast cancer resistance protein (BCRP) on the antitumor efficacy of TROP-2 ADCs was evaluated. OBI-992 in combination with PARP inhibitors such as olaparib and talazoparib was examined for potential synergistic effects in a homologous recombination deficiency (HRD) xenograft model.

Results: The cytotoxicity of OBI-992 was positively associated with the TROP2 RNA levels in different cell lines. In various CDX and PDX models, a single dose of OBI-992 at 3 or 10 mg/kg exhibited remarkable tumor growth inhibition. Notably, the antitumor efficacy of OBI-992 surpassed that of datopotamab deruxtecan (Dato-DXd) across different CDX and PDX models. OBI-992 demonstrated a bystander killing effect as OBI-992 was able to kill TROP2-negative xenografts in the presence of nearby TROP2-positive cells. OBI-992 showed superior efficacy to Dato-DXd in the CDX model overexpressing Pgp or BCRP. These findings suggest that OBI-992 was not affected by the Pgp- and BCRP-mediated multidrug resistance. In the HRD CDX model at suboptimal doses, combination of OBI-992 with olaparib or talazoparib displayed remarkable synergistic effects.

Conclusions: OBI-992 exhibited excellent antitumor efficacy and outperformed the benchmark Dato-DXd in CDX and PDX models of various cancer types. A strong bystander killing effect indicated that OBI-992 will be effective for tumors with heterogenous expression of target antigen. OBI-992 retained its antitumor effect upon overexpression of Pgp and BCRP, suggesting that OBI-992 may overcome the multidrug resistance. Outstanding synergistic effect with the combination of OBI-992 with PARP inhibitors was observed. These results warrant further studies of OBI-992 in the clinical setting.

#1894 Preclinical development of YL205, a novel NaPi2b-targeting antibody-drug conjugate (ADC) with novel topoisomerase I inhibitor-based linker-payload for treatment of solid tumors.

L. Xiao[1], W. Lian[1], Q. Liu[1], Q. Zong[1], S. Song[1], S. Stann[2], J. Cai[1], T. Xue[1];
[1]MediLink Therapeutics (Suzhou) Co., Ltd., Suzhou, China, [2]MediLink Therapeutics USA, INC., Boston, MA

MediLink's TMALIN (Tumor Microenvironment Activable LINker-payload) platform incorporates the proprietary protease-cleavable tripeptide linker and novel DNA topoisomerase I inhibitor, enables the release payload both in the tumor cell intracellularly and in the tumor microenvironment extracellularly. YL205 is built on the TMALIN platform, which is comprised of an anti-NaPi2b humanized monoclonal antibody and conjugated in a site-specific manner to yield a uniform DAR 8 product. NaPi2b, encoded by the SLC34A2 gene, is a cell surface sodium-dependent phosphate transporter that is highly expressed in certain cancers, including ovarian, lung, thyroid, and breast cancers, with limited expression in normal tissues. This study evaluated the drug properties, efficacy, safety and pharmacokinetic profiles of YL205 in nonclinical studies. YL205 achieved a high drug-to-antibody ratio through homogeneous conjugation with hydrophilic TMALIN linker-payload, which showed limited impact on the hydrophilicity of the antibody, prolonged the retention time *in vivo* and eventually enhanced the *in vivo* potency of ADC. Additionally, YL205 exhibited strong potency, high internalization, potent cytotoxicity and bystander-mediated cell killing toward tumor cells. Significant dose-dependent antitumor activities, including complete tumor regressions with no observable toxicity, were noted in NaPi2b low to high expression ovarian and NSCLC tumor xenograft mouse models. YL205 showed a favorable PK profile evidenced by the overlapping ADC and TAb curves in SD rat and cynomolgus monkey studies. Despite high levels of expression in normal lungs of non-human primates, YL205 exhibited a good safety profile with toxic findings unrelated to normal tissue target expression. Toxicity studies using cynomolgus monkeys showed that YL205 is well tolerated with calculated therapeutic index (TI, HNSTD versus MED) of >80 for repeat dosing. No drug-related adverse findings were found in the lungs, liver or kidneys when tested in all doses. The highly stable nature of TMALIN linker, together with the high potency of the payload, likely mitigates the potential liability of this normal tissue expression. Based on these results, it demonstrates that YL205's advanced ADC design results in an increased therapeutic margin, and YL205 may help address unmet medical need in patients with NaPi2b-expressing tumors.

#1896 Therapeutic potential of TORL-4-500, an antibody-drug conjugate directed against delta like non-canonical notch ligand 1 (DLK1).

M. S. J. McDermott, N. A. O'Brien, M. Lu, J. Zhang, K. Gong, B. Hoffstrom, T. Luo, M. Liang, W. Jia, K. Chau, L. Presta, J. Glaspy, D. J. Slamon;
UCLA David Geffen School of Medicine, Los Angeles, CA

Delta like non-canonical Notch ligand 1 (DLK1) is a transmembrane protein that belongs to the NOTCH non-canonical ligand family. It has been implicated in adipogenesis, the regulation of stem cell pools, tissue differentiation during development, cancer differentiation, and cancer stem-like cell maintenance. DLK1 is highly expressed in adrenocortical, uterine, and testicular cancers as well as in a large portion of pancreatic, sarcoma, liver and squamous lung cancer patient samples. In contrast there is limited normal tissue expression beyond the normal adrenal gland, pituitary, and ovarian tissue samples. This expression profile makes DLK1 an attractive target for development of a therapeutic antibody-drug conjugate (ADC). This study describes the generation and preclinical characterization of TORL-4-500, an ADC consisting of a humanized anti-DLK1 monoclonal antibody coupled to monomethyl auristatin E (MMAE) via a cleavable linker.

TORL-4-500 showed strong binding to DLK1 by flow cytometry in DLK1 native and artificial overexpressing cell lines. In contrast no binding was observed in DLK1 non-expressing cell lines. TORL-4-500 exhibits nanomolar binding affinity for both human and cynomolgus monkey DLK1 and is rapidly internalized in DLK1 expressing cells. TORL-4-500 exhibited selective efficacy in cell line xenograft models of DLK1 positive human cancers. Treatment with TORL-4-500 induced significant regressions in four DLK1 expressing human cancer cell line xenograft studies encompassing liver, small cell lung cancer (SCLC) and sarcoma cancer. Furthermore, anti-tumor responses were sustained in each of the DLK1 expressing models for several weeks post-final dose. In the case of the two SCLC cell lines, complete regressions of xenograft tumors were measured out past 100 days in the TORL-4-500 treated animals. No significant impact on xenograft tumor growth was observed in either a DLK1 non-expressing colon cell line xenograft or in a DLK1 non-expressing melanoma xenograft study. Each of the doses tested in this study was well tolerated in mice with no dose-limiting toxicity observed. The nonclinical pharmacokinetics and toxicokinetics of TORL-4-500 were characterized in mice and monkeys and results support dosing in humans.

In summary, TORL-4-500 is a novel therapeutic for DLK1 positive cancers and on the basis of these promising preclinical efficacy results, a first in human trial to evaluate safety, tolerability, pharmacokinetics, and antitumor activity of TORL-4-500 has been launched in patients with advanced cancer and is currently ongoing (NCT06005740).

#1897 Preclinical development of MGC028, an ADAM9-targeted, glycan-linked, exatecan-based antibody-drug conjugate for the treatment of solid cancers.

J. A. Scribner[1], J. G. Brown[2], T. Son[2], L. Jin[2], C. McKenzie[2], V. Nam[2], C. Bush[2], D. Quinonez[2], D. Ford[2], V. Gonzalez[2], J. Tamura[2], S. Gorlatov[2], H. Li[2], S. Butler[2], E. Bonvini[2], D. Loo[1];

[1]MacroGenics, Inc., San Mateo, CA, [2]MacroGenics, Inc., Rockville, MD

Introduction: Antibody-drug conjugates (ADCs) seek to increase the therapeutic window of potent cytotoxic agents by linking them with monoclonal antibodies (mAbs) to selectively deliver cytotoxic payloads to tumor cells. The effectiveness and safety of ADCs rely on both the mAb specificity, and the linker-payload employed. Several approved ADCs using microtubule inhibitor payloads are impacted by ocular adverse events that have been observed both preclinically and in patients. A class of linker-payloads incorporating topoisomerase 1 inhibitors (TOP1i) has emerged recently as an effective alternative to tubulin inhibitor-based ADCs. To date, TOP1i ADCs have not been associated with dose-limiting ocular toxicity seen with microtubule inhibitor payloads. Here we report the preclinical development of an ADAM9 (a disintegrin and metalloprotease domain 9)-targeted ADC that incorporates a novel glycan-linked TOP1i. ADAM9, a member of the ADAM family of multifunctional type 1 transmembrane proteins, plays a role in tumorigenesis and cancer progression and is overexpressed in multiple cancers, making it an attractive target for cancer treatment.

Methods: MGC028 incorporates the cleavable linker-payload, bicyclononyne carbamoyl sulfamide Val-Ala-PABC exatecan (SYNtecan E™), site-specifically conjugated at asparagine 297 of the heavy chain through enzymatic glycan remodeling and metal-free click chemistry using Synaffix's GlycoConnect™ technology. *In vivo* efficacy studies were performed in immunodeficient mice with ADAM9-expressing human tumor cell-line (CDX) or patient-derived (PDX) xenografts. A non-human primate toxicology study was conducted in which MGC028 was administered by 15-minute IV infusion every two weeks at dose levels of 22.5 and 55 mg/kg for a total of two doses.

Results: MGC028 exhibited specific, dose-dependent *in vivo* antitumor activity toward ADAM9-positive CDX models representing gastric, lung, pancreatic and colorectal cancer, and head and neck squamous cell carcinoma. Furthermore, MGC028 demonstrated antitumor activity toward ADAM9-positive PDX models of lung and pancreatic cancer, and cholangiocarcinoma. MGC028 was well tolerated in a repeat-dose non-human primate toxicology study, up to 55 mg/kg, the highest dose level tested. Observations were limited to mild, reversible increases in liver enzymes, without microscopic correlates, and decreased lymphoid cellularity in the thymus. In particular, ocular toxicities were not observed.

Conclusions: MGC028 exhibited potent antitumor activity in *in vivo* models representing various solid cancer indications and was well tolerated in non-human primates at exposure levels exceeding those required for antitumor activity. Our findings support continued investigation of MGC028 as an ADC therapeutic for the treatment of ADAM9-expressing solid cancers.

#1898 LNCB74 is a potent and safe next-generation antibody-drug-conjugate utilizing a cancer selective linker for the treatment of B7-H4 expressing cancers.

Daniel P. Fitzgerald[1], Duc N. Doan[1], Riley B. Peacock[1], Shannon M. Kahan[1], Suvendu Lomash[1], Stephen Slocum[2], Kwang Hwa Jung[3], Hwanhee Oh[3], Ingrid Meza[1], Yanira Manzanarez[1], Shanmugam Selvam[1], Dallas B. Flies[1], Chul-Woong Chung[3], **Sol Langermann**[1]

[1]NextCure, Inc., Beltsville, MD,[2]AntibodyChem Biosciences, Boston, MA,[3]LegoChem Biosciences, Daejeon, Korea, Republic of

The B7 family protein B7-H4 is highly expressed on a range of solid tumors including breast, ovarian, and endometrial cancers, where it may play a role in immune evasion. In non-cancerous tissues, B7-H4 expression is limited, suggesting it may be a potential target for an antibody drug conjugate (ADC). LNCB74 is a human IgG1 antibody conjugated to the potent microtubule disrupting payload monomethyl auristatin E (MMAE) with a drug-to-antibody ratio of 4 (DAR4). The ADC employs a highly selective B7-H4 antibody based upon NextCure's expertise in B7-H4 tumor biology coupled with a glucuronidase-cleavable, site-specific linkage to an engineered cysteine in the antibody light chain via LegoChem Biosciences' ConjuAll™ technology. This improves the safety profile and therapeutic index of the agent by a) increasing stability in circulation, b) selectively releasing payload in tumor cells, and c) reducing payload release in off-target cells. LNCB74 was further engineered with a "LALA"-mutant Fc region to minimize uptake and toxicity to immune cells. In a nonhuman primate (NHP) toxicity study, LNCB74 was well tolerated for repeat dosing and provides evidence for a superior safety profile without noticeable side effects. LNCB74 is rapidly internalized by B7-H4-expressing tumor cells, and demonstrates potent, target-specific cytotoxicity on multiple cancer cell lines. *In vivo* studies demonstrate a strong bystander effect following a single dose administration of LNCB74. A rapid and durable anti-tumor response has been demonstrated in multiple cell-line derived (CDX) and patient-derived xenograft (PDX) tumor models. In summary, LNCB74 is a promising ADC enabling specific targeting of B7-H4 positive cancers across a spectrum of indications.

#1899 Novel combinations of aplitabart, a DR5 agonist IgM antibody, with ADCs or chemotherapeutic agents lead to robust anti-tumor responses in solid tumor models.

M. Desbois[1], S. E. Calhoun[1], K. C. Hart[1], C. R. Denson[1], P. Yakkundi[1], T. J. Matthew[1], M. K. Leabman[1], S. Bilic[2], G. Hernandez[1], E. W. Humke[1], A. F. Candia[1], B. Keyt[1], A. M. Sinclair[1], M. F. Kotturi[1], **B. T. Wang**[1];
[1]IGM Biosciences, Inc., Mountain View, CA, [2]Vanadro, West Des Moines, IA

Agonism of death receptor 5 (DR5), a tumor necrosis factor receptor superfamily member, induces the killing of tumor cells via the extrinsic apoptotic pathway upon receptor multimerization. We have engineered a multivalent IgM DR5 agonist antibody, aplitabart (IGM-8444), that induces robust anti-tumor activity in both in vitro and in vivo preclinical models. We also demonstrated potent synergistic in vitro activity of aplitabart with different classes of chemotherapeutic agents including microtubule inhibitors, nucleoside analogs and topoisomerase inhibitors in a range of solid cancer cell lines. Preliminary results from an ongoing phase 1a/ab clinical study show that aplitabart has an encouraging safety profile and promising activity in combination with FOLFIRI ± bevacizumab in heavily pretreated metastatic colorectal cancer patients. To further explore the combination therapies for aplitabart in lung and breast cancers, we evaluated standard of care chemotherapies, such as paclitaxel, carboplatin, and antibody drug conjugates (ADCs) *in vitro* on a range of human lung and breast cancer cell lines. We observed dose-dependent synergistic cytotoxic effects of aplitabart on tumor cells when combined with these agents. Additionally, these agents increased the expression of DR5 on tumor cells and could explain their synergistic combinatorial activity with aplitabart. Representative cancer cell lines were selected to evaluate these combinations *in vivo* using xenograft mouse models where robust anti-tumor responses were demonstrated in the xenograft lung and breast cancer models, resulting in enhanced tumor growth inhibition and extended survival. Our findings demonstrate potent in vitro synergistic cytotoxicity and enhanced anti-tumor response in preclinical models *in vivo* by combining aplitabart with ADCs, or carboplatin and paclitaxel. These results support the combination of DR5 agonist IgM antibodies with agents known to upregulate DR5 expression on solid tumors. Aplitabart is currently under evaluation in a randomized clinical study in combination with FOLFIRI + bevacizumab in comparison with FOLFIRI + bevacizumab in patients with colorectal cancer (NCT04553692).

#1900 TORL-3-600, a novel antibody drug conjugate directed against cadherin 17 (CDH17), has preclinical efficacy in colorectal, gastric, and pancreatic cancer.

N. A. O'Brien, M. S. McDermott, J. Zhang, M. Lu, K. Gong, B. Hoffstrom, W. Jia, T. Luo, A. M. Madrid, M. Liang, J. A. Glaspy, D. J. Slamon;
UCLA - University of California Los Angeles, Los Angeles, CA

Cadherin 17 (CDH17) is a cell-to-cell adhesion protein that is a member of the cadherin superfamily. In normal tissues, expression of this single pass transmembrane protein is restricted to the lateral surfaces of intestinal and pancreatic ductal epithelial cells. However, in cancer, CDH17 is frequently overexpressed in tumors of the colon, stomach, and pancreas. The selective expression of this cell surface protein in these hard-to-treat cancer makes it an attractive target for the development of antibody-based therapeutics. Here, we describe the preclinical development of TORL-3-600, a novel CDH17-targeting antibody drug conjugate (ADC). CDH17 specific monoclonal antibodies were generated using traditional hybridoma technology and splenocytes isolated from mice immunized with cocktails of NIH3T3 cells overexpressing full length hCHD17 plus purified mammalian expressed hCDH17 extracellular domain protein (aa 23-787). Selective mAb binding was confirmed by flow cytometry and mAb internalization rate was assessed by immunofluorescence (IF). TORL-3-600 was generated from a fully humanized CDH17 mAb by MMAE conjugation with a cleavable linker. Cell membrane staining of CDH17 in patient tumor microarrays (TMAs), cell line (CDX) and patient derived xenografts (PDX) was evaluated by IHC assay. Selective binding of the TORL-3-600 to CDH17 was confirmed in human cancer cell lines and cells engineered to overexpress CDH17. Binding of TORL-3-600 to cell surface CDH17 induced Internalization and translocation to the lysosome of the protein-ADC complex for release of the MMAE payload. Treatment with TORL-3-600 induced significant regressions and tumor growth inhibition (TGI) in four CDH17-positive (CDH17+) human colorectal cancer (CRC) CDXs (103.6 - 140.4% TGI) and three CDH17+ CRC PDXs (63.3 - 102.2% TGI). Responses in these models were sustained for up to nine-weeks following cessation of treatment. Sustained inhibition of xenograft tumor progression was also observed in a cell line model of CDH17+ pancreatic cancer (85.8% TGI). In contrast, greatly reduced responses (37.3 - 58.2% TGI) to TORL-3-600 were observed in the CDH17- human colon cancer CDX and PDX models. Each of the doses tested in this study were well tolerated in mice with no dose-limiting toxicities observed. Analyses of large human patient TMAs by CDH17 IHC assay demonstrated detectable expression of CDH17 in 90.1% (173/193) of CRC, 51.8% (86/166) of gastric and 20.4% (69/331) of pancreatic cancers. These numbers suggest that an ADC directed against CDH17 could provide benefit to a significant number of patients diagnosed with these cancers. These data support the clinical development of TORL-3-600 for the treatment of CDH17+ cancers. TORL-3-600 has completed IND enabling toxicity studies with acceptable PK and toxicity profiles and is now in phase 1 clinical testing (NCT05948826).

#1901 Disitamab vedotin, a clinical stage HER2-directed antibody-drug conjugate, shows potent antitumor activity as a monotherapy in preclinical urothelial cancer models.

Renee Hein, Kelsi Willis, Gina LoMastro, Suhas Vasaikar, Vinita Gupta, Katie Snead, Sharsti Sandall, Anita Kulukian

Seagen, Bothell, WA

Disitamab vedotin (DV, RC48-ADC) is an antibody-drug conjugate (ADC) that selectively delivers cytotoxic drug to HER2-expressing cancer cells. DV is composed of disitamab, a HER2-directed monoclonal antibody, and a vedotin linker-payload system, which enables conjugation of the microtubule-disrupting agent monomethyl auristatin E (MMAE) to the antibody via a protease-cleavable linker. The proposed mechanism of action (MOA) of DV occurs through direct cytotoxicity of HER2-expressing tumor cells following internalization of DV and intracellular release of MMAE. DV may also induce antitumor activity through bystander-mediated cytotoxicity of neighboring cells and via the inhibition of HER2 signaling pathways. Moreover, cellular response to MMAE includes the induction of immunogenic cell death and recruitment of immune cells to the tumor site. DV is currently being evaluated globally in subjects with HER2-expressing locally advanced or metastatic urothelial carcinoma (la/mUC) and has gained conditional approval in China following an overall response rate of 50.5% (pooled analysis from studies NCT03507166 and NCT03809013). RNA sequencing data from a large cohort of urothelial cancer patient tumors revealed expression of HER2 in many urothelial tumors; however, the relationship between HER2 expression and efficacy of DV is not well understood. Here, we sought to evaluate the antitumor activity of DV monotherapy in preclinical urothelial cancer models with varying levels of HER2 expression. Multiple patient-derived xenografts (PDX) and patient-derived 3D *in vitro* urothelial cancer models showed potent antitumor response to DV monotherapy in tumors with varying HER2 expression levels including HER2-low tumors. Overall, these findings support ongoing clinical trials in subjects with HER2-expressing la/mUC and provide scientific rationale to further explore DV monotherapy in HER2-positive and HER2-low urothelial cancer clinical settings.

#1902 ADRX-0706 Nectin-4 antibody-drug conjugate PK/PD characterization elucidates its widened therapeutic window.

M. Shahmoradgoli, A. Hau, D. Lee, A. Wang, P. P. Challita, O. Betancourt, W. Sisson, M. M. -. Kuo, K. Zhang, A. Goldson, S. Janssen, P. Datta, F. Acosta, A. Chu-Kung, H. Li, P. M. Challita-Eid, S. Rottmann;
Adcentrx Therapeutics, Inc., San Diego, CA

Nectin-4 is a well validated tumor target, which is highly expressed in several solid cancers, while expression in normal tissues is limited. A first-generation antibody-drug conjugate targeting Nectin-4, called enfortumab vedotin-ejfv (EV), was granted accelerated FDA approval in 2019 for urothelial cancers, and is currently approved for frontline therapy in cisplatin-ineligible patients with locally advanced or metastatic urothelial carcinoma, providing groundbreaking improvement in patient survival. However, clinical use of EV has also revealed safety-driven limitations, which result in reduced and/or interrupted drug exposures impacting efficacy. To overcome these limitations in therapeutic window, Adcentrx has developed ADRX-0706, a Nectin-4-targeting next-generation ADC with a drug-antibody ratio (DAR) of 8. ADRX-0706 utilizes a novel tubulin inhibitor payload AP052 with a proprietary cleavable linker utilizing Adcentrx' proprietary i-ConjugationTM technology, which results in excellent biophysical features. Most noteworthy, ADRX-0706 displays a very stable PK profile with overlapping curves for total antibody and ADC as well as full DAR retention in circulation as determined by mass spectrometry. This translates to superior efficacy of ADRX-0706 over EV in multiple in vivo cancer cell line- and patient-derived xenograft mouse models across indications. Detailed PK/PD characterization of ADRX-0706 validates the mechanism of action as an anti-mitotic agent inducing cell cycle arrest and apoptosis. In addition, ADRX-0706 treatment leads to increased PD-L1 expression in mouse pharmacology models, which is a consequence of immunogenic cell death as described for this payload class. These findings are in line with emerging data on EV and provide rationale for combination regimens with checkpoint inhibitors. Besides the improvement in efficacy, ADRX-0706 was also designed for superior safety. A payload distribution study in tumor-bearing mice reveals a preferential and increased delivery of payload to tumors and lower payload delivery to normal tissues as well as lower free payload levels in plasma for ADRX-0706 compared to EV. Taken together, these data provide association of the improved drug-linker stability of ADRX-0706 to an improved Nectin-4 directed delivery of AP052 payload to the tumor and lower exposure in normal tissues, which may translate to an improved therapeutic window. In summary, the preclinical efficacy and safety properties of ADRX-0706 support clinical evaluation of this next generation anti-Nectin-4 ADC. ADRX-0706 is currently in a phase 1a/b study (NCT06036121).

#1903 Zenocutuzumab, a HER2xHER3 bispecific antibody, is effective in cancer models with high NRG1 expression.

M. N. O'Connor[1], R. C. J. Schackmann[2], I. Odintsov[3], S. Fatrai[1], A. B. Brinkman[1], S. Walker[1], J. J. Lammerts van Bueren[1], C. A. W. Geuijen[1];
[1]Merus N.V., Utrecht, Netherlands, [2]Genmab B.V., Utrecht, Netherlands, [3]Memorial Sloan Kettering Cancer Center, New York, NY

Neuregulin 1 (NRG1) is a ligand that binds to HER3, promotes HER2/HER3 dimerization and PI3K/AKT/mTOR signaling, and causes malignant transformation. Zenocutuzumab (Zeno, MCLA-128) is a humanized IgG1 bispecific antibody that docks on HER2, preventing heterodimerization with HER3, while also blocking NRG1 interaction with HER3, and potently inhibiting NRG1-induced HER2:HER3 proliferation and survival signaling of cancer cells. High NRG1 expression arising from autocrine signaling or gene amplification is associated with poor prognosis in certain cancers, and resistance to standard therapies. The clinical efficacy and safety of Zeno in patients with NRG1 fusion-driven cancer who were enrolled in the ongoing global multicenter eNRGy study and Early Access Program were recently presented. Treatment with Zeno led to durable responses across multiple different previously treated NRG1 fusion tumor types. Zeno utilizes the Merus Dock & Block® mechanism to inhibit HER2/HER3 dimerization and the NRG1/HER3 tumor-signaling pathway and is effective at high NRG1 concentrations. Here, we examined the efficacy of Zeno in preclinical models representing different tumor types expressing high NRG1 levels. Zeno treatment of the lung cancer cell line HCC95, which harbors an NRG1 gene amplification, effectively inhibited signaling pathways involved in the regulation of proliferation and survival, including the PI3K/AKT/mTOR pathway and inhibited cell proliferation. The anti-tumor efficacy of Zeno in vivo against a panel of 28 patient-derived xenograft (PDX) models representing different tumor types was examined. Zeno significantly inhibited tumor growth in seven high-NRG1-expressing PDX models. These results show that Zeno is effective in tumor cell killing in vitro and in vivo in high NRG1-expressing cancer models representing multiple different tumor types.

#1904 Preclinical development of MGC026, a glycan-linked, exatecan-based antibody-drug conjugate (ADC) targeting B7-H3 for solid cancer.

J. A. Scribner[1], J. G. Brown[2], T. Son[2], L. Jin[2], C. McKenzie[2], V. Nam[2], C. Bush[2], D. Quinonez[2], J. Tamura[2], S. Gorlatov[2], H. Li[2], S. Butler[2], E. Bonvini[2], **D. Loo**[1];

[1]MacroGenics, Inc., San Mateo, CA, [2]MacroGenics, Inc., Rockville, MD

Introduction: Antibody-drug conjugates (ADCs) have emerged as an important class of therapeutic agents for the treatment of cancer. A duocarmycin-based B7-H3-targeted DNA-alkylating ADC, vobramitamab duocarmazine (vobra duo), has shown encouraging clinical activity in the treatment of metastatic castration-resistant prostate cancer. Given the broad spectrum of tumor indications addressable by targeting B7-H3, we developed MGC026, an ADC incorporating a B7-H3-targeting antibody and a novel glycan-linked topoisomerase 1 inhibitor (TOP1i). With distinct mechanisms of action, vobra duo and MGC026 can address different cancers, tumor stages, or be used in combination with alternate agents to enhance their clinical utility.

Methods: MGC026 is comprised of the cleavable linker-payload, bicyclononyne carbamoyl sulfamide Val-Ala-PABC exatecan (SYNtecan E™) site-specifically conjugated at asparagine 297 of the heavy chain through enzymatic glycan remodeling and metal-free click chemistry, using Synaffix's GlycoConnect™ technology. In vivo efficacy studies were conducted in immunodeficient mice with human tumor cell-line or patient-derived xenografts to identify the spectrum of MGC026-sensitive tumors and the relationship between exposure and antitumor activity. A toxicology study was conducted in cynomolgus monkeys in which MGC026 was administered by 15-minute IV infusion once every three weeks. Pharmacokinetic (PK) analysis and detailed toxicology evaluation was performed.

Results: MGC026 demonstrated specific, dose-dependent in vivo antitumor activity toward B7-H3-positive tumor xenografts representing lung, pancreatic, and prostate cancers, head and neck squamous cell carcinoma, and melanoma. Additionally, MGC026 demonstrated antitumor activity toward B7-H3-positive patient-derived xenograft models of lung and prostate cancer, with additional indications under investigation. MGC026, administered to cynomolgus monkeys at dose levels of 10, 30, and 50 mg/kg every 3 weeks for a total of 3 doses, exhibited approximate dose-proportional PK and high stability in circulation. MGC026 was well tolerated, with no lung toxicity observed, and the highest dose level tested (50 mg/kg) was declared as the highest non-severely toxic dose.

Conclusions: MGC026 exhibited a favorable preclinical profile, with potent in vivo activity toward B7-H3-expressing tumor xenografts representing a range of cancer indications. MGC026 was tolerated in cynomolgus monkeys, a relevant toxicology model, at exposure levels exceeding those required for antitumor activity. These data support clinical development of MGC026 for the treatment of B7-H3-expressing solid cancers.

#1905 The ROR1 antibody-drug conjugate, MK-2140, enhances the efficacy of established drugs in preclinical models of pediatric acute lymphoblastic leukemia.

R. B. Lock[1], K. Evans[1], B. Watts[1], E. P. Bowman[2], S. Neuhauser[3], T. Stearns[3], J. H. Chuang[3], V. M. Phillip[3], K. A. Jessen[4], E. L. Jocoy[5], C. J. Bult[3], B. A. Teicher[6], M. A. Smith[6],

[1]UNSW Medicine & Health, UNSW Centre for Childhood Cancer Research, UNSW Sydney, Sydney, Australia, [2]Merck & Co., Rahway, NJ, [3]The Jackson Laboratory, Bar Harbor, ME, [4]Formerly VelosBio, Inc., San Diego, CA, [5]The Jackson Laboratory, Sacramento, CA, [6]National Cancer Institute, Bethesda, MD

Introduction: Children diagnosed with acute lymphoblastic leukemia (ALL) experience ~90% likelihood of cure. However, the outcome for high-risk ALL and children who relapse remains poor. Receptor tyrosine kinase like orphan 1 receptor (ROR1) is a cell surface antigen primarily expressed in embryonic tissue, but also overexpressed in hematological malignancies. UC961 is a humanized IgG monoclonal antibody with high affinity for ROR1. MK-2140 (Zilovertamab vedotin/VLS-101) and VLS-211 are antibody-drug conjugates (ADCs) of UC961 with monomethyl auristatin-E or PNU payloads, respectively. This study evaluated the in vivo efficacy of MK-2140 and VLS211 against pediatric ALL patient derived xenografts (PDXs).

Methods: PDXs were selected based on ROR1 mRNA (RNA-seq) and cell surface (flow cytometry) expression and grown as orthotopic disease in immune-deficient NSG mice. Engraftment and drug responses were assessed by flow cytometric enumeration of the proportion of human versus mouse $CD45^{\pm}$ cells in peripheral blood (%$huCD45^{\pm}$). Events were defined a priori as the %$huCD45^{\pm}$ exceeding 25% or leukemia-related morbidity. MK-2140 (2.5 and 5.0 mg/kg) and VLS-211 (0.25 and 0.5 mg/kg) were administered intravenously, weekly x 3 weeks. Vincristine (0.15 mg/kg once weekly), dexamethasone (5 mg/kg daily x 5) and Lasparaginase (1,250 U/kg daily x 5) (VXL) were administered intraperitoneally for 3 weeks, followed by MK-2140 (5 mg/kg weekly x 3 weeks). Drug efficacy was assessed by event-free survival of treated (T) and control (C) groups and by stringent objective response criteria. In receptor occupancy/pharmacokinetic studies, a single dose of MK-2140 was administered and samples collected for analysis at discrete timepoints thereafter.

Results: ROR1 mRNA and cell surface expression showed a significant correlation (R=0.83, P=0.021). MK-2140 significantly delayed disease progression in 4/7 PDXs compared to vehicle control (T-C, -2.6 to 20.0 days). At the highest dose, MK-2140 elicited objective responses (remissions) in two PDXs. VLS-211 significantly delayed disease progression in 5/7 PDXs (TC, -1.8 to 70.5 days), including 3 objective responses. Prior treatment with VXL followed by MK-2140 significantly delayed disease progression compared to VXL alone (T-C, 56.8 versus 35.2 days). MK-2140 bound to $ROR1^{\pm}$ cells with near 100% occupancy within two hours of treatment, which was sustained for up to 96 h. Consistent with the receptor occupancy data, plasma levels of MK-2140 were maintained at ≥100 nM for at least 96 h after a single dose (5 mg/kg).

Conclusions: MK-2140 and VLS-211 exerted significant single-agent *in vivo* activity against a panel of pediatric ALL PDXs. MK-2140 significantly enhanced the efficacy of an induction-type regimen and should be considered for further evaluation in a minimal residual disease setting.

#1906 UNO-A001 (A001), a clinical candidate CD38 x CD3 bispecific with a novel structure, potently kills multiple myeloma cells *in vitro* and is highly effective *in vivo*.

M. Anderson[1], Y. Ling[1], M. L. Chiu[2], P. Cheung[1];
[1]Unogen Biotech Limited, Harrisburg, PA, [2]Tavotek Biotherapeutics, Spring House, PA

CD38 is a validated target for the treatment of multiple myeloma (MM) as evidenced by the important clinical activity of CD38 targeting monoclonal antibodies. Bispecific T Cell Engagers (TCEs) kill cancer cells by distinct mechanisms as compared to standard format antibody therapeutics and several TCEs have demonstrated impressive clinical activity, and have been approved for clinical use, in hematologic malignancies. Here we describe a novel bispecific leveraging the potent killing mechanism of TCEs to target CD38 bearing cancer cells. UNO-A001 is a TCE binding the cell surface receptor CD38 on target human cancer cells and CD3 on T cells. The molecule has a differentiated format, binding CD38 with a high affinity humanized camelid VHH moiety and CD3 on T cells through a unique antibody Fab arm. The affinities of each arm were optimized so that the CD38 arm bound with high affinity and the CD3 arm with much lower relative binding affinity. This configuration was designed to engage CD38 bearing target cells with multiple TCE molecules at lower doses and concentrations while minimizing T cell binding in the periphery, and in the absence of cell surface CD38. A001 potently and specifically killed human CD38 bearing multiple myeloma cell lines in T cell killing assays in vitro with EC50s in the 2.7-6.6 pM range. This potency, despite the designed lower affinity to CD3, may be due to the unique structure of A001 enabling a productive immunologic synapse between T cells and the target cancer cells, and an optimal TAA/CD3 binding affinity ratio. A001 was also highly effective in inhibiting tumor growth in H929 xenograft models. In a flank model of H929 tumor growth A001 dose dependently inhibited tumor growth with complete growth inhibition of established tumors at the highest dose level tested. In a systemic disease model with NCI-H929-luc cells A001 was also highly effective and improved survival relative to control treated animals. In preparation for clinical studies a robust and high yield production cell line was created and characterized. It achieved high expression levels of quality monodisperse UNO-A001 product that was stable in all relevant storage conditions. A001 has similar affinities for human and cynomolgus macaque CD38 and CD3. Dose ranging studies in cynomolgus macaques demonstrated tolerability consistent with clinically approved TCEs, and the expected dose dependent pharmacodynamic effects on CD38 expressing myeloid and lymphoid cell populations. These data support planned clinical testing of A001 in multiple myeloma and other CD38 bearing hematologic malignancies, including mantle cell lymphoma, T cell lymphoma, and acute myelogenous leukemia.

#1907 MYTX-011: A pH-dependent anti-cMET ADC with increased payload delivery in vivo and potent activity against cMET-expressing tumors of various epithelial origins.

D. Kanojia, W. Comb, W. Israelsen, F. Colombo, L. Nie, N. Gera, T. Chittenden, B. Fiske;
Mythic Therapeutics, Waltham, MA

cMET is an oncogenic receptor tyrosine kinase overexpressed in multiple types of solid tumors, including non-small cell lung cancer (NSCLC), gastric, head and neck, liver cancer and others. Several cMET-directed therapies including antibody-drug conjugates (ADCs) have been developed that may benefit a subset of patients with tumors that have high cMET expression, *MET* amplification, or dependency on cMET signaling. MYTX-011 is an investigational, pH-sensitive, vcMMAE-based ADC that is designed to potentially benefit not only patients whose tumors express high levels of cMET, but also a broader set of patients whose tumors express low to moderate levels of cMET. MYTX-011 is engineered to rapidly dissociate from cMET only at the acidic pH of endolysosomes. We have previously demonstrated that MYTX-011 drives increased internalization and cytotoxicity in tumor cells expressing moderate cMET levels compared to a matched parent non-pH sensitive ADC. MYTX-011 also demonstrated markedly superior efficacy in NSCLC xenografts with moderate cMET expression as compared to either the parent ADC or benchmark ADCs representing clinical-stage anti-cMET ADCs with vcMMAE and maytansinoid payloads. MYTX-011 was efficacious in NSCLC PDX models with moderate cMET expression of adenocarcinoma/squamous histology and in heterogeneous cMET-expressing EGFR mutant models. In these studies, we demonstrate that MYTX-011 exerts enhanced efficacy by delivering increased levels of payload to cMET+ tumors compared to the parent ADC. MYTX-011 treatment induced significantly increased levels of phospho-histone H3 (pHH3), a pharmacodynamic marker of MMAE cytotoxicity, in moderate cMET expressing NCI-H1975 NSCLC xenograft tumors compared to the parent ADC. Further, increased levels of free MMAE were detected in tumors from mice treated with MYTX-011 compared to a matched dose of the parent ADC, indicating that the pH dependent binding engineered into MYTX-011 translated to increased payload delivery to tumors in vivo. To explore the potential efficacy of MYTX-011 in other cMET-expressing tumor types, we tested the activity of MYTX-011 in a panel of cell lines derived from gastric and head and neck cancers. MYTX-011 demonstrated increased cMET-dependent cytotoxicity compared to the parent ADC. MYTX-011 was also highly active in cMET+ xenograft models derived from gastric (non-*MET* amplified), esophageal, and head and neck cancers. Together, these findings highlight the potential of MYTX-011 as a therapeutic candidate for treating a broader range of cMET-expressing malignancies.

#1909 Advancing a novel tubulin-inhibitor ADC technology: The Adcentrx auristatin platform offers enhanced efficacy and safety profiles compared to vedotin technology.

D. Lee[1], S. Rottmann[1], A. Wang[1], P. P. Challita[1], A. M. Hau[1], W. Sisson[1], M. M. -. Kuo[1], K. Zhang[1], M. Leung[1], A. Mahloch[1], E. Nye[1], P. Datta[1], S. Janssen[1], F. Acosta[1], O. Betancourt[1], M. Shahmoradgoli[1], A. Chu-Kung[1], M. Guo[2], P. M. Challita-Eid[1], H. Li[1];
[1]Adcentrx Therapeutics, Inc., San Diego, CA, [2]Adcentrx Therapeutics, Inc., Shanghai, China

Auristatins represent an important class of anti-mitotic antibody-drug conjugate (ADC) payloads with potent cytotoxic effects on rapidly dividing cancer cells. Most notably, monomethyl auristatin E (MMAE) stands as the most extensively validated compound, laying the foundation for the vcMMAE (vedotin) linker-payload technology that has contributed to the approval of several ADCs, including brentuximab vedotin, polatuzumab vedotin-piiq, tisotumab vedotin-tftv, and enfortumab vedotin-ejfv. However, while these first-generation ADCs have paved the way for a paradigm shift in cancer treatment away from traditional chemotherapy, there remains a discernible opportunity for improvement in both efficacy and safety. In this context, we introduce the Adcentrx auristatin platform, which substantially expands the therapeutic window of auristatin-ADCs beyond the vedotin technology. Through systematic exploration, we have synthesized >100 proprietary auristatin analogues with a range of distinctive properties. We identified optimized linker-payloads by strategically pairing lead payload candidates with our proprietary i-ConjugationTM, an irreversible, stable cysteine conjugation technology, and fine-tuned linkers. The resulting ADCs with a drug-to-antibody ratio (DAR) of 8 were extremely hydrophilic with excellent in vivo pharmacokinetics, and sustained DAR retention for a period of 21-days. Comparative assessments against vedotin-ADCs revealed that Adcentrx-ADCs demonstrated superior efficacy across multiple targets and indications in various mouse xenograft models. In Sprague-Dawley rats, Adcentrx-ADCs exhibited remarkable tolerability, albeit their high drug loading of 8. In summary, our preclinical studies underscore the significant enhancement in the therapeutic index achieved by the Adcentrx auristatin platform. Furthermore, this technology presents a promising alternative mode of action to camptothecins, exhibiting tolerance to targets expressed in non-proliferative normal tissues but without the burden of severe dose-limiting toxicities such as interstitial lung disease.

#1910 Advancing therapeutic interventions for NUT carcinoma: Orchestrating the precision of CRISPR/Cas9-mediated NUTM1 suppression and synergistic ADC strategies.

J. Choi[1], H. Yi[1], H. Park[2], M. Lee[3], D. Kim[1], S. Hong[2], Y. Shin[2], Y.-I. Choi[3];
[1]Sungkyunkwan University, Seoul, Korea, Republic of, [2]Seoul National University, Seoul, Korea, Republic of, [3]Samsung Medical Center, Seoul, Korea, Republic of

Purpose: NUT carcinoma (NC) is aggressive carcinoma defined by translocations involving the *NUTM1* and frequent squamous differentiation. *NUTM1* gene encodes a testicular nuclear protein (NUT), exclusively expressed in the testis. The fusion of *NUTM1* leads to abnormal cell growth, resulting in the development of NC. This study aims to discover advanced approaches for inducing the death of cancer cells, specifically targeting those expressing NUT proteins.
Methods: Spatial Transcriptome analysis and RNA sequencing were applied to formalin-fixed paraffin-embedded *NUTM1* fusion-positive cancer tissues. Virus-like particles were used to introduce CRISPR/Cas9 into cells expressing the *NUTM1* fusion oncoprotein. The inhibitory effect was confirmed through multiple in vitro assays. The effectiveness of Anti-Trophoblastic cell-surface antigen (TROP-2) Antibody-Drug Conjugate (ADC) was demonstrated in vivo and in vitro in cells with increased TROP2 expression subsequent to NUT suppression.
Results: NCs revealed a relatively uniform pattern of gene expression, forming six unique groups. Notably, the NUT protein predominantly located in the inner regions of the tumor tissues. We employed CRISPR/Cas9 technology to specifically target cells harboring the NUTM1 fusion gene. The precise genetic editing was remarkably effective, achieving up to 90% success in the targeted area. This led to a notable decrease in both RNA and protein levels of NUT expression, effectively disrupting associated downstream pathways. The cell growth rate was reduced in several NC cell lines, and differentiation, accompanied by morphological changes, was observed in most edited cells. RNA sequencing analysis of these edited cells uncovered a substantial increase in expression of cytosolic molecules, with a marked increase in TACSTD2 expression. Interestingly, when we combined this genetic editing approach with a targeted therapy - the TROP2-ADC loaded with interferon-beta - the results were even more striking. Cells treated with this combination showed almost double the rate of growth inhibition compared to those receiving only a single form of treatment.
Conclusion: This study provides valuable insights into identifying novel therapeutic targets and elucidating potential mechanisms by analyzing NUT cancer tissues using various assays. Our results support that CRISPR/Cas9-mediated targeting of *NUTM1* could be a useful approach for NUT oncoprotein ablation, especially when used in combination with other therapies such as ADCs. Further studies are needed to investigate the efficacy of NUT inhibition in preclinical and clinical settings. the elimination of tumor cells facilitated by CRISPR/Cas9, along with additional tumor markers targeted by ADCs, holds potential for developing treatment strategies against incurable cancers driven by genetic alterations.

#1911 Dato-DXd mediates anti-tumor activity in preclinical TROP2-expressing intracranial tumor model.

K. Jones, M. Suksomboon, S. rosenthal, J. Gordon, C. Reimer, M. Sung, **C. Rane**;
AstraZeneca, Waltham, MA

Datopotamab deruxtecan (Dato-DXd) is an antibody-drug conjugate (ADC) consisting of a humanized anti-TROP2 monoclonal antibody linked to a potent DNA topoisomerase I (TOP1) inhibitor payload via a plasma-stable, tumor-selective, tetrapeptide-based cleavable linker. Dato-DXd is currently under clinical investigation for the treatment of patients with solid tumors including non-small cell lung cancer (NSCLC), hormone receptor positive (HR+ BC) and triple negative breast cancer (TNBC). Pharmacotherapy of brain tumors can be limiting due to restricted drug delivery across blood brain and blood tumor barrier. Enhertu®, that uses the same DXd ADC technology, has reported clinical activity in patients with brain metastases from HER2+ breast cancer, but very little information is available on what drives ADC biodistribution and activity in CNS-involved cancers. Here, we investigated whether systemically administered ADCs can penetrate the brain microenvironment and mediate anti-tumor activity in a preclinical model. Luciferase-tagged H1373 (TROP2-expressing NSCLC) tumor cells were intracranially implanted into NSG mice. Tumor-bearing mice were dosed with Dato-DXd or matched isotype Control IgG-ADC (DAR4) at 10mpk 7 days or 14 days post intracranial tumor implant. Dato-DXd inhibited intracranial tumor growth better than Control ADC (Day 7: 105% TGI vs 38% TGI; Day 14: 65% TGI vs <10% TGI, respectively, compared to Vehicle). Immunohistochemistry analysis of brain tissue validated localization of Dato-DXd in the tumor, suggesting Dato-DXd can distribute into the local tumor microenvironment in this preclinical tumor model. Additionally, treatment with Dato-DXd provided a significant survival benefit over Control ADC (Median survival of 63 days vs 43 days, P=0.0002). This preclinical study supports the inclusion of Dato-DXd in treatment of patients with CNS-involved tumors. Understanding the pharmacological determinants of Dato-DXd activity in the CNS will help outline strategies to implement Dato-DXd-based treatment of patients with CNS-involved tumors.

#1912 Targeting Trop-2 with sacituzumab govitecan (IMMU-132) suppresses the tumor growth in diffuse large B cell lymphoma.

J. Ting, M.-F. Wei, H.-W. Lee, K.-H. Lan, A.-L. Cheng, S.-H. Kuo;
National Taiwan University College of Medicine, Taipei City, Taiwan

Introduction: Sacituzumab govitecan (SG), also termed IMMU-132, is an antibody-drug conjugate, linking an anti-Trop-2 antibody and the topoisomerase I inhibitor, SN-38. Clinically, SG has shown promising therapeutic effects in patients with human epidermal growth factor receptor 2 (HER2)-negative metastatic breast cancer. However, the efficacy of SG in diffuse large B-cell lymphoma (DLBCL) remains unexplored. In this study, we sought to determine whether SG can efficiently inhibit cell proliferation and tumor growth of DLBCL by using both *in vitro* and *in vivo* models.

Methods: We examined the cytotoxicity of SG in the activated B-cell like (ABC)-subtype-DLBCL cell lines, Riva (Ri-1), HBL-1, and SU-DHL-2, and the germinal center B-cell (GCB)-subtype-DLBCL cell lines, SU-DHL-4, SU-DHL-5, and SU-DHL-6 by MTT assay. We assessed the distributions of cell cycle phase and apoptosis in the aforementioned DLBCL cell lines treated with SG for 24 h or 48 h using flow cytometry and Annexin V staining. We confirmed apoptosis (cleavage of poly ADP-ribose polymerase [PARP] and caspase-3) and detected DNA damage (γH2AX and 53BP1)-related protein expression in SU-DHL-2 and SU-DHL-6 cell lines treated with SG at various concentrations for 48 h using western blotting, compared to untreated cells. To examine the anti-tumor effect of SG *in vivo*, NOD-SCID nude mice of Riva-xenograft mouse models were randomized into a control group and an SG-treated group.

Results: Flow cytometry and western blotting revealed overexpression of Trop-2 on the surface of untreated ABC-DLBCL and GCB-DLBCL cell lines. In this study, we showed that SG treatment reduced cell viability in all six DLBCL cell lines with nanomolar IC_{50} values. Exposing SG to DLBCL cells significantly increased cell cycle arrest at the G2/M and sub-G1 phases of all six DLBCL cell lines. Annexin V staining revealed that SG induced apoptosis in all six DLBCL cell lines. Western blotting confirmed apoptosis induction by showing a dose-dependent upregulation of cleaved PARP and cleaved caspases-3 by SG treatment, along with decreased expression of survivin in both SU-DHL-2 and SU-DHL-6 cells. SG also upregulated the expression of γH2AX and 53BP1 in both SU-DHL-2 and SU-DHL-6 cells. Furthermore, we found that tumor growth of Riva cells *in vivo* was significantly reduced by treatment with SG when compared with untreated control.

Conclusion: SG suppresses tumor growth of ABC-DLBCL and GCB-DLBCL cells in both *in vitro* and *in vivo* models by inducing cell cycle arrest, apoptosis, and DNA damage. These findings provide a rationale for transitioning SG to clinical trials for treating patients with relapsed or refractory DLBCL.

#1913 KD5005: HER-2 dependent strong potent anti-tumor activity of an anti-HER-2 mAb-TNFaimmunocytokine.

Y. CHEN[1], P. LI[2], G. FANG[2], H. WU[2], C. ZHANG[2], Z. CAI[2];

[1]Shanghai Kanda Biotechnology Co. Ltd., Shanghai, China, [2]Shanghai Celgen Bio-Pharmaceutical Co. Ltd., Shanghai, China

Tumor necrosis factor alpha (TNFα) is a pleiotropic cytokine with diverse biological functions, including apoptosis, cell survival, inflammation, and immunity. While recombinant human TNFα has demonstrated therapeutic efficacy in isolated limb perfusion for soft tissue sarcoma and melanoma, its systemic administration is limited by severe toxicities, including hypotension. Tumor-specific targeting and enhancement of TNFα's tumor cell killing activity hold promise for improving its therapeutic index. To address these challenges, we developed KD5005, a novel HER-2-targeted immunocytokine fusion protein comprising an anti-HER-2 IgG1 monoclonal antibody (trastuzumab) and human TNFα. Tissue distribution studies revealed that KD5005 specifically accumulated in HER-2-expressing tumors, demonstrating its tumor-targeting capability. In vitro, KD5005 exhibited reduced TNFα-mediated apoptosis in L929 cells compared to recombinant TNFα, indicating its lower non-specific toxicity. Notably, KD5005 induced apoptosis of HER-2-positive human gastric cancer NCI-N87 cells at significantly lower concentrations than trastuzumab, TNFα, or their combination, demonstrating its enhanced tumor cell killing activity. The potent apoptotic activity of KD5005 was HER-2-dependent, as it did not show increased apoptotic activity in WT mouse forestomach carcinoma (MFC) cells and had similar apoptotic activity compared to the combination of trastuzumab and TNFα. This HER-2 dependency further supports the tumor-specific targeting of KD5005.In vivo, KD5005 demonstrated superior anti-tumor efficacy compared to the combination of trastuzumab and TNFα in syngeneic tumor models using CT26 tumor cells transfected with the human HER-2 gene. KD5005 induced robust tumor regression and durable cure in 7 of 8 mice, while the combination of trastuzumab and TNFα elicited weaker therapeutic responses, resulting in tumor rejection in only 3 of 8 mice. Pharmacokinetic and toxicity studies of KD5005 were conducted in cynomolgus monkeys. KD5005 exhibited a significantly prolonged in vivo half-life compared to TNFα, indicating its improved pharmacokinetic profile. KD5005 was administered intravenously every two weeks to the same animal in a dose-escalation study at 0.3 mg/kg, 1.0 mg/kg, 3 mg/kg, 10 mg/kg, and 30 mg/kg. The toxicity study results showed that the maximum tolerated dose for KD5005 in cynomolgus monkeys is 10 mg/kg, indicating its favorable toxicity profile. In summary, we have developed KD5005, a HER-2-targeted immunocytokine fusion protein with enhanced tumor-killing activity, improved pharmacokinetic properties, and a favorable toxicity profile. These preclinical findings support the further clinical development of KD5005 as a promising therapeutic agent for HER-2-positive cancers.

#1914 Amivantamab efficacy in wildtype EGFR NSCLC tumors correlates with levels of ligand expression.

R. Rivera-Soto[1], B. Henley[1], M. Pulgar[1], S. Lehman-Tenuto[1], H. Gupta[1], M. Weindorfer[1], S. Vijayaraghavan[1], T.-W. Yao[2], S. Laquerre[1], S. Moores[1];
[1]Johnson & Johnson Innovative Medicine, Spring House, PA, [2]Johnson & Johnson Innovative Medicine, La Jolla, CA

Amivantamab (RYBREVANT™) is an FDA-approved, low-fucose IgG1 bispecific antibody targeting EGF and Met receptor tyrosine kinases, with proven clinical activity against EGFR mutant non-small cell lung cancer (NSCLC). Preclinical studies demonstrated that three context-dependent mechanisms of action (MOA) contribute to amivantamab efficacy: immune cell-mediated killing by antibody-dependent cellular cytotoxicity and trogocytosis, receptor internalization and degradation, and inhibition of ligand binding to both EGF and Met receptors. In tumors lacking known cancer-driver genetic aberrations, ligand binding to wildtype EGFR ($EGFR^{WT}$) and/or Met^{WT} may activate downstream signaling pathways, inducing pro-tumorigenic processes. Among the EGFR ligands, we demonstrated that amphiregulin (AREG) is highly expressed in $EGFR^{WT}$ NSCLC primary tumors, with significantly higher circulating protein levels in NSCLC patients than in healthy volunteers, and induces EGFR phosphorylation, promoting downstream signaling and increasing cell proliferation. Importantly, treatment of AREG-stimulated $EGFR^{WT}$ cells/tumors with amivantamab, or an AREG-targeting antibody, inhibits ligand-induced signaling and cell/tumor proliferation/growth. Across 10 $EGFR^{WT}$ NSCLC patient-derived xenograft mouse models, amivantamab efficacy correlated with *AREG* RNA levels, suggesting AREG as a potential predictive marker for amivantamab activity in this population. Interestingly, in these xenograft models, amivantamab anti-tumor activity was independent of amivantamab's Fc engagement with immune cells, suggesting that, in this context, the amivantamab's ligand-blocking function is sufficient for its efficacy. Juxtaposedly, we previously demonstrated that low fucose amivantamab, active Fc domain, was necessary for maximal anti-tumor activity against tumors with EGFR or Met activating mutations. Altogether, these results demonstrated amivantamab context-dependent MOA for efficacy. In conclusion, these data 1) highlight EGFR ligand AREG as a driver of tumor growth in some $EGFR^{WT}$ NSCLC models, 2) illustrate the preclinical efficacy of amivantamab in ligand-driven $EGFR^{WT}$ NSCLC, and 3) identify AREG as a potential predictive biomarker for amivantamab against anti-$EGFR^{WT}$ therapies.

#1915 A scalable pancancer antigen target discovery platform for precision oncology.

E. Fox, G. Appe, A. Behdenna, L. Meunier, A. Nordor, S. Weill, **C. Marijon**;
Epigene Labs, Paris, France

With the emergence of precision oncology as a new paradigm in cancer care, there is an urgent need to develop tools capable of mining the massive amounts of rich omic data generated every year. To support target discovery programs at scale, we developed a pan-cancer bioinformatics platform combining patient data with extensive biological and pharmaceutical knowledge for the identification and prioritization of novel antigen targets. Our pipeline was first validated with the discovery of new antigen targets amenable to CAR-T therapy for relapsed/refractory multiple myeloma. Here, we are exploring AML, a type of leukemia with several unmet needs.

First, we identified and integrated 36 relevant microarray datasets from the GEO database using a proprietary data identification and integration pipeline. The clinical data was curated using our proprietary oncology ontology, machine learning models, and domain expert quality control processes. The molecular data was normalized and the datasets aggregated into a virtual patient cohort of unprecedented size and quality, comprising 2,995 AML patients and 220 healthy controls. To both find a clinically relevant patient sub-population and reduce the cohort heterogeneity, AML patients were stratified based on their transcriptomic profile using a consensus clustering analysis, which we interpreted thanks to the curated clinical data. Among multiple others, we identified a highly stable cluster enriched in AML-M3 patients, a very distinct and aggressive subtype of AML caused by a t(15;17) translocation. A differential gene expression analysis was performed comparing this cluster with the control group and 574 genes were found to be overexpressed. We then applied proteomic filters to exclusively focus on cell surface-bound protein targets demonstrating an acceptable level of anticipated cytotoxicity. Finally, the 23 short-listed antigen targets were prioritized with additional multi-omic patient and cell line data to optimize their safety and efficacy profiles as well as expression robustness. Interestingly, well-known targets, such as CD96 and ABCC1, were found in the top targets.

Developing scalable pipelines will be instrumental in the advent of precision oncology. Combining unbiased data-driven tools with cancer biology-driven approaches, our state-of-the-art pipeline can be used for any cancer type and antigen-targeting modality, including CAR-T and antibody-based therapies. The present study illustrates the potential of our platform when applied to AML, one of the most heterogeneous groups of neoplastic disorders. Leveraging our large and unique AML patient cohort, we were not only able to detect a relevant subgroup of patients, but also identified novel antigen target candidates for this specific population, which were then prioritized based on domain expertise. A broader study addressing other cancer indications, including solid tumors, is underway.

#1916 Discovery of a novel Nectin4 IPSC-derived cell therapy for the treatment of solid tumors.

J. M. Carton, **C. Dower**, M. Miller, J. Wheeler, S. Heron, H. J. Millar, D. Walker, D. J. Perry, A. Lebid, L. Cocka, D. Kim, B. Morse, B. Gurung, M. Harris, A. Jethon, M. Naso, H. Levitsky;
Century Therapeutics LLC, Philadelphia, PA

Century Therapeutics is developing a Nectin4-targeting IPSC-derived cell therapy for the treatment of Nectin4 expressing solid tumors. The Nectin proteins (Nectin1, Nectin2, Nectin3 and Nectin4) are members of the calcium independent immunoglobulin superfamily of cell adhesion molecules (CAMs) involved in adhesive processes that help in the growth and development of tissues. Nectin 1, 2 and 3 are normally found in adult tissue whereas Nectin4 is mainly found in normal placental and embryonic tissue. Nectin4 is also expressed in different types of cancer including urothelial, ovarian, lung and head/neck cancers. Nectin4 is established as a biomarker for worse prognosis in cancers and is linked with carcinogenesis and disease severity. These features establish Nectin4 as a promising target for anti-tumor drug development. Enfortumab vedotin, an antibody drug conjugate targeting Nectin4 positive tumors, has demonstrated benefit in clinical trials and is FDA approved for treatment of advanced bladder cancer. We have identified novel single-domain antibodies (VHH) that bind to multiple epitopes on Nectin4 extracellular domain. The VHH antibodies were engineered into chimeric antigen receptor (CAR) formats and characterized for expression, cell activation through antigen engagement, and cytotoxicity activity in primary T-cells. Selected binders demonstrated efficacy in multiple CAR formats in primary T-cells in a mouse xenograft model using OVCar-3 tumor cells. The lead CARs engineered into primary T-cells demonstrated tumor inhibition similar to a reference CAR using the ASG-5ME antibody (Enfortumab) as the Nectin4 binder. The CARs were engineered into our IPSC-derived iNK and iT cells and demonstrated cytotoxicity activity against a panel of cell lines with a range of cell surface expression of Nectin4. Based on these studies, Century Therapeutics is advancing the lead Nectin4 binder for development of an IPSC-derived cell therapy to treat Nectin4 positive solid tumors.

#1917 HER2-FGFR1 interaction induced by bispecific molecules: A novel strategy for treating breast cancer.

M. A. Krzyscik, K. Hristova;
Johns Hopkins University, Baltimore, MD

Breast cancer poses a significant global health challenge, demanding effective therapies targeting specific receptors. In our prior study, we engineered molecules capable of binding to both HER2 and FGFR1, pivotal receptors in breast cancer progression. By combining the high-affinity Affibody $Z_{HER2:2891}$ for HER2 with a modified, stable form of FGF2 binding to FGFR1, we created the bispecific protein (Af_{HER2}-lFGF2). This innovative molecule could simultaneously recognize HER2 and FGFR1, exhibiting enhanced cell penetration. When coupled with the potent cytotoxic agent monomethyl auristatin E (MMAE), it demonstrated exceptional efficacy in eliminating cancer cells expressing HER2, FGFR, or both receptors. Our current investigation focused on quantifying the interaction between HER2 and FGFR1 receptors on the cell surface upon treatment with these bispecific molecules. Leveraging fully quantified spectral imaging FRET (FSI-FRET), a technique utilizing spectrally resolved two-photon microscopy. We directly monitor the association of HER2 and FGFR1 in the plasma membrane. Our findings revealed that the bispecific Af_{HER2}-lFGF2 molecule forces interaction between HER2 and FGFR1 on the cell surface. Furthermore, we analyzed the activation of the HER2-FGFR1 complex and subsequent downstream signaling pathways using western blotting. In summary, our research uncovers the ability of the Af_{HER2}-lFGF2 bispecific protein to foster direct interaction between HER2 and FGFR receptors on the cell membrane. By employing state-of-the-art techniques like FSI-FRET, we elucidated the mechanisms governing this interaction and, by western blotting, downstream signaling pathways. These insights emphasize the potential of A_{fHER2}-lFGF2 as a promising therapeutic agent for targeting HER2, FGFRs, and HER2/FGFRs-positive cancers. This approach paves the way for targeted therapies in addressing the prevalent global health challenge of breast cancer.

#1918 LX-101, a novel, clinical stage, payload-bearing targeted therapy directed to the insulin-like growth factor receptor (IGF-1R), demonstrates potent preclinical anti-tumor activity against multiple cancer types with well-established ties to the IGF-1/IGF-1R pathway.

M. Hoberman[1], A. Z. Dudek[2];

[1]Lirum Therapeutics, New York, NY, [2]Mayo Clinic, Rochester, MN

Objective: LX-101 is a next-generation, targeted therapy directed to the insulin-like growth factor 1 receptor (IGF-1R). LX-101 consists of a proprietary IGF-1 variant coupled to a cytotoxic methotrexate payload. LX-101 was previously evaluated in Phase 1 trials of adult patients with advanced, pretreated cancers, where it was well-tolerated and demonstrated single agent activity. Neither a dose limiting toxicity, nor a maximum tolerated dose was reached, leaving potential room for additional dose escalation and schedule optimization. Multiple aggressive cancers of unmet need have genetic alterations affecting the IGF-1R pathway and/or high IGF-1R expression that correlates with poor outcomes, including certain cancers of the breast, head and neck, Ewing's sarcoma, osteosarcoma, and others. Prior attempts at inhibiting IGF-1R with non-payload bearing naked monoclonal antibodies or small molecules produced a range of clinical outcomes including some partial and complete responses. None of these agents, however, were ultimately approved, potentially due to suboptimal potency that allowed for escape mechanisms, including redundant signaling pathways, and the lack of enrichment for select tumor types with strong ties to the IGF-1/IGF-1R pathway. Herein, we investigated the anti-tumor activity of the payload-bearing agent LX-101 against IGF-1R-involved cancer cell lines.

Methods: Cell lines were incubated with LX-101 (~1.6 - 2500nM). Cell viability was assessed by CellTiter-Glo after 4 days. IC_{50}s were calculated using GraphPad PRISM software.

Results: LX-101 displayed potency against head and neck cancer (FaDu, IC_{50} = 9 nM), triple negative breast cancer (BT-20, IC_{50} = 17 nM), Ewing's sarcoma, including EWSR1-FLI1 gene fusion-positive cell lines RD-ES (IC_{50} = 10 nM), A-673 (IC_{50} = 14 nM), and SK-ES-1 (IC_{50} = 29 nM) and EWSR1-ERG gene fusion-positive cell line CADO-ES1 (IC_{50} = 14 nM). LX-101 was also potent against PAX3-FOXO1 gene fusion positive alveolar rhabdomyosarcoma (SJCRH30, IC_{50} = 23 nM), osteosarcoma (143B, IC_{50} = 6 nM; HOS, IC_{50} = 7 nM; U2OS, IC_{50} = 32 nM), and neuroblastoma (SK-N-AS, IC_{50} = 16 nM; IMR-32, IC_{50} = 20 nM; SH-SY5Y, IC_{50} = 30 nM).

Conclusion: These results demonstrate that LX-101 has potent preclinical anti-tumor activity against multiple cancer cell lines with well-established ties to the IGF-1/IGF-1R pathway, including with different genetic and epigenetic alterations. These data support further clinical development of LX-101 in IGF-1R-involved cancers. New clinical trials are planned.

#1919 Activity and affinity tuning next-generation immunotoxins for targeted therapy.

H. Liang[1], G. L. Beilhartz[2], S. Cao[1], R. A. Melnyk[2];
[1]University of Toronto, Toronto, ON, Canada, [2]Hospital for Sick Children, Toronto, ON, Canada

Classic cancer-associated receptors, such as EGFR and Her2, are often overexpressed on malignant cells relative to healthy cells. Numerous molecules have been developed to leverage this differential expression with the goal of developing specific and safe targeted therapies, including antibody-drug-conjugates and immunotoxins. The general schematic of these molecules is to fuse toxic payloads -either small molecules or proteins - with a targeting moiety that binds to the cancer-specific receptor. Despite the general success of this approach, even low levels of these receptors on healthy tissues result in on-target/off-tumor toxicity thus limiting the dose of therapeutic molecules available to tumors. Targeted therapies with greater on-tumor efficacy and reduced toxicity are urgently needed in order to further advance therapeutic outcomes. To achieve this, we set out to exploit the unique features of bacterial toxins as highly modular protein delivery systems to design next-generation targeted therapies. We demonstrate the capacity of the immunotoxin platform to deliver various therapeutic proteins, with distinct activities from inhibiting protein synthesis to degrading oncogenic signaling pathways, such as the RAS/MAPK pathway. Further, we show how modifying the affinity, valency, and specificity of the receptor-binding moieties, as well as tuning the enzymatic activity of the toxic enzyme payloads interact to affect the on-target efficacy and off-target toxicity of the targeted molecules. Altogether, these data demonstrate the potential of immunotoxins as highly flexible and tunable platforms for the development of a new class of anti-cancer therapeutics.

EXPERIMENTAL AND MOLECULAR THERAPEUTICS: Drug Resistance 2: Ras GTPase
Poster Session

#1923 Cytoplasmic localization of KRAS in Her2-amplified colorectal cancer induces an altered dependency of the oncogenic signaling pathway from RAS/MAPK to PI3K/AKT.

K. Maruyama, S. Nagayama, R. Katayama;
Japanese Foundation for Cancer Research, Tokyo, Japan

Nowadays, KRAS-G12C specific inhibitor has been used for the treatment of patients with KRAS mutated non-small cell lung cancer, but not for colorectal cancer (CRC) patients. Recent clinical trials have shown that the efficacy of a single KRAS inhibitor treatment was limited for CRC due to multiple primary/adaptive resistance mechanisms. In the CRC, clinical trial with dual inhibition of KRAS-G12C and EGFR has demonstrated that combination therapy had improved partial response rate, suggesting that primary resistance to KRAS inhibitor is mainly caused by EGFR-mediated adaptation. Meanwhile, more than half of the primary resistance mechanisms are still unknown. To understand the intrinsic resistance mechanisms to KRAS inhibitors in CRC, KRAS G12C- or G12D-positive CRC patient-derived cells (PDCs) were established from surgically resected tumor specimens. Analysis of cell proliferation under KRAS inhibitor treatment or KRAS knockdown revealed these PDCs were not solely dependent on KRAS mediated growth signaling. To clarify the compensatory activated pathways in KRAS inhibitor, inhibitor library screening and sequencing analysis were performed among 8 KRAS-mutated PDCs. As a result, PDCs were categorized into EGFR inhibitor with KRAS inhibitor sensitive group and PI3K pathway activating group harboring PIK3CA mutation or/and ERBB2 amplification with KRAS mutation. To explore the novel intrinsic resistance mechanisms, we deeply analyzed one of the PDC named JC261, harboring PIK3CA, ERBB2, and KRAS alterations. We observed that PI3K pathway was highly activated in JC261 cells, and cell proliferation was mainly dependent on PI3K/AKT/mTOR pathway regardless the existence of KRAS-G12C mutation. To examine whether Her2 amplification contributes to the PI3K pathway dependency, we established Her2 knockout JC261 cells. Notably, *Her2* knockout suppressed Her2-Her3-PI3K signaling and restored KRAS-MAPK dependency. To analyze the mechanism of how KRAS-MAPK pathway was activated in Her2 knockout cells, we focused on KRAS localization, since the MAPK activation is known to initiate from plasma membrane localization of KRAS after appropriate modifications. Remarkably, immunofluorescence staining of KRAS revealed that KRAS was aberrantly localized in the cytoplasm in JC261, while KRAS localization was changed to the plasm membrane in Her2 knockout JC261 cells. In addition, the cytoplasmic KRAS localization was also observed in Her2-amplified, KRAS-WT PDC (JC69). These results suggest that Her2 amplification may induce aberrant KRAS localization, resulting in low dependence on the KRAS-MAPK pathway. Thus, KRAS localization may regulate the balance between MAPK and PI3K signaling intensity.

#1924 RTK signaling and WT RAS activity as vulnerabilities in tumors with acquired resistance to GDP-state selective KRAS^{G12C} inhibitors in preclinical models.

H. S. Solanki[1], H. Shah[2], D. Imbody[1], B. Desai[1], P. A. Stewart[1], B. Fang[1], Y. Stern[1], L. N. Darville[1], J. M. Koomen[1], A. Marusyk[1], E. Ahler[2], I. Aronchik[2], M. Singh[2], E. B. Haura[1];

[1]Moffitt Cancer Center, Tampa, FL, [2]Revolution Medicines, Inc. (RVMD), Redwood City, CA

Background: KRAS^{G12C}-GDP Inhibitors such as sotorasib and adagrasib have demonstrated clinical benefit in lung cancer patients harboring an oncogenic *KRAS^{G12C}* mutation. However, the durability of monotherapy benefit is limited by the development of resistance. Hence, identification of novel treatment approaches to overcome resistance and extend duration of benefit becomes necessary to address this unmet clinical need.

Experimental Design: We generated two NSCLC models of KRAS^{G12C}-GDP inhibitor acquired resistance, named sotorasib-R LU65 (cell-line derived, *in vitro*) and adagrasib-R LUN156 (PDX-derived, *in vivo*) following extended treatment with sotorasib and adagrasib, respectively. We then performed transcriptomic and mass spectrometry-based phosphoproteomics analyses on baseline and KRAS^{G12C}-GDP inhibitor-resistant samples to determine resistance and escape mechanisms.

Results: In the sotorasib-R LU65 cells, we discovered upregulation of various RTKs including HER2, HER3, and AXL using a mass spectrometry-based proteomics approach and Immunoblot analysis. Simultaneously, from a transcriptome analysis, we observed activation of RAS and PI3K/AKT signaling in these cells. In the adagrasib-R LUN156 model, increased phosphorylation of MET was observed via phospho-RTK array and by immunoblotting. Transcriptomic analysis revealed an enrichment for RAS pathway dependency in the adagrasib-R tumor models. RAS GTP-binding assessed by RAF-RBD pulldown and multiple reactions monitoring mass-spectrometry suggest increased GTP-bound RAS isoforms in sotorasib-R LU65 cells and active RAS signaling in adagrasib-R LUN156. Given the convergence of our findings on re-activation/maintenance of wild-type RAS signaling as a means of resistance to KRAS^{G12C}-GDP-state inhibitors, we hypothesized that RMC-7977, a tri-complex RAS^{MULTI}-GTP inhibitor, which inhibits signaling via mutant and wild-type RAS, had the potential to counteract these mechanisms. We tested RMC-7977 monotherapy, which drove complete tumor regressions in the adagrasib-R LUN156 model. Additionally, RMC-7977 attenuated tumor growth in sotorasib-R cell derived LU65 xenograft model wherein we observed co-activation of PI3K/AKT signaling. Thus, we tested a combination with the pan-PI3K inhibitor pictilisib and observed combinatorial activity consistent with our findings.

Conclusions: These data suggest that in KRAS^{G12C}-GDP inhibitor-resistant models RTK activation maintains MAPK dependency and in the case of one model, PI3K signaling. Consistent with these mechanisms, RMC-7977 as a single agent or in combination with pictilisib drove significant tumor regressions in these models. These preclinical results indicate RAS^{MULTI}-GTP inhibition alone or combination with PI3K inhibition has the potential to address KRAS^{G12C}-GDP inhibitor resistance.

#1925 Wild-type RAS signaling is an essential therapeutic target in *RAS*-mutated cancers.

Nancy E. Sealover, Bridget Finniff, Jacob Hughes, Hyun Lee, Robert L. Kortum

Uniformed Services University, Bethesda, MD

Single-agent targeting of RAS-mutated cancers using RAF/MEK/ERK or PI3K/AKT pathway inhibitors is ineffective; blocking one pathway relieves negative feedback control of RTK signaling and hyperactivates parallel effector pathways. While combined MEK and PI3K inhibition is effective in preclinical models, toxicity of this combination prevents its clinical use. Alternative strategies for treating RAS-mutated cancers are essential. Therapeutics directly targeting mutated RAS proteins have the potential to spare normal cellular function thereby lessening overall toxicity. Unfortunately, direct RAS inhibition as a monotherapy does not fully block RAS effector signaling. RAS proteins show differential activation of RAF and PI3K pathways: KRAS potently activates RAF but poorly activates PI3K, whereas HRAS effectively activates PI3K but poorly activates RAF. Further, mutant RAS inhibition relieves negative feedback controls leading to rapid hyperactivation of RTK−WT RAS signaling. A more comprehensive understanding of the interplay between mutant RAS and RTK−WT RAS signaling is essential to developing rational therapeutic approaches to treat RAS-mutated cancers. We found that WT RAS enhanced mutant RAS-driven transformation by activating RAS effectors poorly engaged by mutated RAS. Further, inhibition of RAS effectors activated poorly by mutant RAS synergized with and limited resistance to mutant HRAS and KRAS inhibitors. The mutant HRAS inhibitor tipifarnib blocked PI3K signaling and synergized with MEK inhibitors in HRAS-mutated cancer cell lines; covalent KRASG12C inhibitors blocked MEK signaling and synergized with PI3K inhibitors in KRASG12C- mutated cell lines. Synergy between inhibitors of mutant RAS and RAS effectors was dependent on intact RTK/WT RAS signaling and was lost in both RASless or SOSless MEFs. Dual knock-out of WT RAS isoforms in *KRAS*- and *HRAS*-mutated cancer cell lines reduced PI3K signaling in *KRAS*-mutant cell lines and MAPK signaling in *HRAS*-mutant cell lines and reduced proliferation, confirming our findings in MEF cells. Overall, our data highlight the critical role of WT RAS isoforms in supporting mutant RAS signaling and should be considered when designing combination therapies in *RAS*-mutated cancers.

#1926 MRAS the forgotten member of the GTPase superfamily plays a role in KRASG12Ci resistance.

V. Thatikonda, K. Kostyrko, S. Jurado, S. Lieb, M. Hinkel, D. Alpar, O. Bergner, A. Jeschko, M. Pearson, **M. H. Hofmann**;
Boehringer Ingelheim RCV GmbH & Co. KG, Vienna, Austria

$KRAS^{G12C}$ inhibitors have achieved impressive results in the clinic. However, intrinsic or acquired resistance to therapy invariably develops leading to disease progression in most treated patients. Emerging pre-clinical and clinical evidence points to multiple mechanisms being responsible for resistance to $KRAS^{G12C}$ inhibitors, including receptor tyrosine kinase (RTK) activation, $KRAS^{G12C}$ amplification, activation of alternative signaling pathways including PI3K, mTOR, YAP/TAZ, acquisition of KRAS mutations that would preclude compound binding (e.g. R68S, Y96C/D, H95D/Q/R), conversion of the G12C codon mutation, and additional activating KRAS mutations (G13D, Q61H). In the clinic, many of the described mutations were detected at low frequency, some patients displayed multiple mutations and in 40% of patients no potential driving mutations were identified. It is therefore likely that other non-genetic alterations are also involved in resistance to $KRAS^{G12C}$i monotherapy.

Here, we used preclinical models of $KRAS^{G12C}$ non-small cell lung cancer (NSCLC) and colorectal cancer (CRC) to study intrinsic and acquired resistance to $KRAS^{G12C}$ inhibitors. Increased expression of the RAS superfamily gene MRAS was observed in most $KRAS^{G12C}$-naïve tumor cells upon treatment with a $KRAS^{G12C}$ inhibitors. In line with this, we observed an increase of MRAS-GTP levels in cells treated with $KRAS^{G12C}$i *in vitro*. Interestingly, the increase in active MRAS did not lead to concomitant upregulation of MAPK signaling.

Long term treatment with adagrasib was used for generating in vitro and in vivo $KRAS^{G12C}$ models with acquired resistance to $KRAS^{G12C}$i . A strong increase in MRAS expression was observed under these conditions, that surpassed the levels seen with short term treatment in naïve models. This data suggests that activation of MRAS-SHOC2-PP1C complex may play a role in compensating for the $KRAS^{G12C}$-driven signaling in both the intrinsic and acquired resistance setting. Knockdown of SHOC2 to baseline levels resulted in re-sensitization to $KRAS^{G12C}$i monotherapy and to the effects of combinations in adagrasib-resistant NCI-H358 NSCLC cells. Pathway suppression was deepened by combining adagrasib with either a SOS1i (e.g. BI-3406) or SHP2i (e.g. TNO155) resulting in enhanced anti-tumor effects observed in the $KRAS^{G12C}$i-resistant models. Our findings underscore the role of MRAS in acquired resistance in KRASG12Ci and the potential to overcome this with vertical pathway combinations, such as SOS1i or SHP2i.

#1927 Resistance to RAS-GTP inhibition in models of pancreatic ductal adenocarcinoma arises downstream of RAS effectors.

U. N. Wasko[1], J. Jiang[2], Y. Wang[2], L. Tomassoni[1], L. Jiang[2], M. Menard[2], A. Curiel-Garcia[1], T. C. Dalton[1], M. Orlen[3], C. Edwards[4], C. Stalnecker[4], J. Dilly[5], S. Chang[2], S. A. Sastra[1], C. F. Palermo[1], T. Baslan[6], S. Tian[6], M. Holderfield[2], E. Quintana[2], Z. Wang[2], J. A. M. Smith[2], A. Califano[1], D. Wildes[2], A. J. Aguirre[5], R. H. Vonderheide[3], B. Z. Stanger[3], S. W. Lowe[6], C. J. Der[4], M. Singh[2], K. P. Olive[1],

[1]Vagelos College of Physicians and Surgeons, Herbert Irving Comprehensive Cancer Center, Columbia University Irving Medical Center, New York, NY, [2]Revolution Medicines, Redwood City, CA, [3]University of Pennsylvania Perelman School of Medicine, Philadelphia, PA, [4]Lineberger Comprehensive Cancer Center, University of North Carolina at Chapel Hill, Chapel Hill, NC, [5]Dana-Farber Cancer Institute, Boston, MA, [6]Sloan Kettering Institute, Memorial Sloan Kettering Cancer Center, New York, NY

More than 90% of pancreatic ductal adenocarcinoma (PDAC) cases are driven by activating mutations in KRAS that drive it into an active, GTP-bound state (KRAS(ON)), producing excessive signaling via MAPK and other effector pathways. RMC-7977 is a potent inhibitor of GTP-bound RAS proteins (RAS(ON)), including both wild type and mutant variants of KRAS, NRAS, and HRAS. The related investigational agent, RMC-6236, is a first-in-class, potent, orally bioavailable, RAS^{MULTI}(ON) inhibitor currently in Phase 1/1b clinical trials (NCT05379985). Exposure to RMC-7977 suppressed the MAPK biomarker p-ERK, reduced cell growth, and induced apoptosis in multiple human RAS-addicted cancer cell lines. Assessment of RMC-7977 in a series of PDAC preclinical model systems revealed broad anti-tumor activity and treatment was well tolerated at translatable doses. The K-$ras^{LSL.G12D/+}$, $p53^{LSL.R172H/+}$, $Pdx1Cre^{tg/+}$ (KPC) autochthonous mouse model was utilized to study the effects of Ras-GTP inhibition in both tumor and normal tissues. At doses that drove anti-tumor activity, RMC-7977 dosing produced a metronomic effect on RAS signaling in tumor and normal tissue, with full pathway inhibition at 4 h post treatment that was restored by 24 h. This pattern yielded tumor-selective effects on apoptosis and proliferation, consistent with RAS oncogene addition in PDAC. RMC-7977 treatment drove regressions and an unprecedented ~3-fold extension of overall survival in KPC mice. After an initial response, all tumors eventually developed resistance on treatment, affording the opportunity to study acquired resistance mechanisms to RAS-GTP inhibition. Strikingly, in all resistant tumors, acute inhibition of MAPK and PI3K signaling was still apparent following treatment. These results indicate that RAS signaling re-activation mechanisms that have been reported as clinical mechanisms of resistance to mutant-selective $KRAS^{G12C}$ inhibitors (e.g. second-site mutations or upregulation of upstream RTK) may be insufficient to confer resistance to a compound that inhibits all RAS isoforms. Rather, in this model we observed activation of alternative oncogenic mechanisms downstream of RAS effector signaling, including frequent focal amplification of Myc, focal amplification of Jun, and/or activation of Yap/Taz/Tead signaling in most resistant KPC tumors. Together these results demonstrate preclinical activity of RMC-7977 at tolerable doses, producing unprecedented responses even in highly chemoresistant PDAC models such as the KPC mouse. The observed range of potential resistance mechanisms suggests that RAS-GTP inhibition imposes a narrow evolutionary path to the development of acquired resistance in this context. These preclinical findings may help inform the ongoing development of investigational RAS inhibitors and the design of potential combinatorial treatment strategies to forestall resistance.

#1928 Targeting FAK to improve the therapy of KRAS G12C mutant cancers.

S. Liu, J. Shi, C. Lu, M. Zhang, Y. Xin, Y. Zhu, J. Li, **H. Luo**, Y. Sun;
Shouyao Holding (Beijing) Co., Ltd., beijing, China

Despite the pivotal role of KRAS G12C in tumor initiation and progression, currently available KRAS G12C inhibitors have relatively modest activity compared to other approved therapies targeting other classic oncogenic drivers. Fortunately, efforts to improve the anti-tumor response to KRAS G12C targeted therapy have benefited from the use of combination approaches. Here, we found that treatment with KRAS G12C inhibitors induces sustained activation of focal adhesion kinase (FAK) in KRAS G12C mutant cell lines from various cancer types, including non-small cell lung cancer, colorectal cancer, and pancreatic cancer. These results suggest a potential role for FAK in adaptive resistance to KRAS G12C inhibition and encourage us to explore the anticancer effects of combining the KRAS G12C inhibitor SY-5933 with a FAK inhibitor, CT-707. The cell viability and clonogenic assays using various KRAS G12C mutant cancer cell lines showed that the combination of SY-5933 and CT-707 synergistically inhibited cell growth. Mechanistically, this enhanced anti-proliferative effect is associated with a significant decrease in FAK activity and a more pronounced induction of cell cycle arrest and apoptosis. In vivo efficacy studies in multiple cell line derived xenograft (CDX) models, the combination of SY-5933 plus CT-707 consistently induced a more potent anti-tumor response than either monotherapy alone. In conclusion, our results demonstrate that CT-707 has the potential to enhance the efficacy of SY-5933 by suppressing adaptive FAK activation under KRAS G12C inhibition. This provides a rationale for an innovative combination therapy to improve outcomes in patients with KRAS G12C mutated cancers.

#1929 Acquired resistance to sotorasib in KRAS^{G12C} mutant NSCLC is vulnerable to PI3K-mTOR pathway inhibition and regulated by 4E-BP1.

I. M. Meraz[1], S. Wu[1], M. Majidi[1], C. Ren[1], Y. Xu[1], F. Meng[1], L. Gao[1], R. Song[1], R. Zhang[1], B. Fang[1], Q. Wang[1], Y. Xi[1], J. Wang[1], S. Jung[2], J. A. Roth[1]; [1]UT MD Anderson Cancer Center, Houston, TX, [2]Baylor College of Medicine, Houston, TX

Up to 40% of NSCLC patients with KRAS^{G12C} mutation respond to sotorasib. However, acquired resistance (AR) develops rapidly in all patients. The majority of AR is associated with unknown mechanisms. Twelve KRAS^{G12C} mutant NSCLC PDXs were developed from patient samples and characterized with WES, RNAseq, and RPPA analyses. Three PDXs treated with sotorasib showed complete tumor regression, and one showed growth inhibition. PDXs, PDX derived organoids (PDXO), and cell line derived xenografts (CDX) were with AR to sotorasib were generated. TC303AR and TC314AR PDXs were generated by prolonged continuous in-vivo treatment with sotorasib. Two isogeneic AR PDXOs from TC303 and TC314 PDXs were generated through continuous incremental dosing of sotorasib in organoid cultures. Both TC303AR and TC314AR PDXOs showed >100-fold resistance than sensitive counterparts. Over 100-fold resistance were also measured in two sotorasib resistant isogenic H23AR and H358AR cell lines. Both resistant PDXOs and cell lines showed resistance to adagrasib, another selective, KRAS^{G12C} inhibitor. H358AR CDXs were generated through continuous in-vivo treatment with sotorasib and multiple passages of CDX tissues. WES was performed for AR PDXs, CDX, PDXOs and cell lines and all retained the KRAS^{G12C} mutation, and no additional KRAS mutations were found. We performed RNAseq, RPPA, and mass spectrometry (MS) on TC303AR and TC314AR PDXs. Heatmaps showed significant sets of differentially regulated RNA and protein in AR vs. parental. Enrichment analysis found a significant upregulation of MTORC1 signaling in AR PDXs. Proteins involved in PI3K-AKT-mTOR pathway were significantly upregulated in AR. PI3K and AKT expression were also increased in H23AR and H358AR. Inhibition of PI3K, AKT and mTOR by copanlisib, MK2206 and everolimus respectively was synergistic with sotorasib in AR cells and PDXOs, with copanlisib being the most effective. Copanlisib significantly inhibited colony formation in AR cells. Downstream molecules in PI3K-AKT-mTOR pathway showed marked downregulation of pAKT, pmTOR, p70S6, pS6, pGSK3b, and pPRAS40 by copanlisib. The downstream 4E-BP1 and p4E-BP1 were remarkably high in AR cells, which was downregulated by copanlisib. To verify the role of PI3K, PI3Kα CRISPR-Cas9 knock-out clones were generated in both H23AR and H358AR cells. Absence of p4E-BP1 was associated with restoration of sotorasib sensitivity while high levels of p4E-BP1 phosphorylated by an mTOR independent pathway restored sotorasib resistance in the knock-out clones. When copanlisib was combined with sotorasib in treating the resistant TC303AR, TC314AR PDXs, H358AR CDX and H23AR xenograft tumors, antitumor effects were observed in every model. Inhibition of the PI3K pathway at different nodes is a vulnerability in KRAS^{G12C} mutant NSCLC with sotorasib AR and p4E-BP1 is a mediator of sotorasib resistance

#1930 Combination of KRASG12C and FGFR1 inhibitors as a resistance-overcoming therapeutic strategy for maximizing therapeutic impact of KRASG12C inhibitors.

A. Santos, P. Plaza, M. Jimenez, D. Gomez-Sanchez, L. Paz-Ares, I. Ferrer;
Fundacion Investigacion Biomedica Hospital 12 de Octubre, Madrid, Spain

INTRODUCTION: Lung cancer is the leading cause of cancer-related deaths worldwide. KRAS is the most frequent mutated driver gen in lung adenocarcinoma (LUAD). KRASG12C inhibitors (G12Ci) have revealed promising results in the clinic, having being approved two G12Ci for the treatment of LUAD patients, which marks the first approved targeted therapy for KRAS-mutant tumors. Nevertheless, these therapies face the same limitation as other targeted therapies, the therapeutic potential of these inhibitors can be impaired by resistance mechanisms. Deciphering resistance mechanisms to G12Ci is of prime relevance to predict which patients may benefit from these therapies and to propose resistance-overcoming therapeutic strategies for maximizing therapeutic impact of these inhibitors.

MATERIAL AND METHODS: We generated 10 acquired resistant LUAD cell lines to G12Ci (Sotorasib and Adagrasib), exposing sensitive cells to increasing concentrations of drugs. All the acquired resistant models were characterized at the proteomic (phospho-Array and Western Blot) and transcriptomic (WTS) levels to find signatures that define the resistance.The efficacy of G12Ci was tested *in vitro* in a panel of 8 cell lines and 7 PDX-derived organoids (PDXDO) models and *in vivo* in 7 patient-derived xenografts (PDX) models to classify them as resistant, sensitive or partially sensitive. The efficacy of the combination of FGFR1 and G12Ci was tested *in vitro* in the panel of 10 acquired resistant cell lines but also in the parental cell lines and PDXDOs (sensitive and intrinsic resistant) and *in vivo* in the intrinsic resistant PDXs.

RESULTS AND DISCUSSION: The characterization of 10 acquired resistant cell lines at the proteomic and transcriptomic levels showed differences in the expression and/or activation of Fibroblast Growth Factor Receptors (FGFRs) in more than 50% of them. The combination of KRASG12C and FGFR1 inhibitors in all acquired resistant cell lines showed efficacy, regardless of whether acquired resistance was mediated or not by FGFR1 overexpression/overactivation.In addition, the combination of KRASG12C and FGFR1 inhibitors showed more efficacy than the monotherapies in most intrinsically resistant cell lines, PDXDOs and PDXs models. Finally, we tested the combination with FGFR1i in sensitive or partially responsive models, observing an improvement in efficacy compared to monotherapy with G12Ci.

CONCLUSIONS: The activation or overexpression of FGFR1 acts as a mechanism of acquired resistance to KRASG12C inhibitors.-The combination of FGFR and KRASG12C inhibitors is effective as an acquired/intrinsic resistance-overcoming therapeutic strategy in cell lines, PDXDOs and PDXs models.-The combination of FGFR and KRASG12C inhibitors is also synergistic for sensitive models, which could maximize therapeutic impact of KRASG12C inhibitors.

#1931 Targeting YAP1/TEAD signaling re-sensitizes MAPK/ERK pathway inhibitors in KRAS- driven cancer cells.

X. Yang, G. Li, P. Ren, X. Shi, Y. Yu, B. Hao, P. Wang, M. Cheng, G. Dai;
HUTCHMED, Shanghai, China

Many TEAD small-molecule inhibitors (SMIs) have recently reported initial clinical evaluations on Hippo-mutated cancer types. Several studies have demonstrated that activation of the YAP1/TEAD transcriptional complex via a Hippo-independent manner can drive resistance to MAPK/ERK pathway inhibitors. Here, we elucidated the potential mechanism of TEAD inhibition overcoming MAPK/ERK pathway resistance with a TEAD SMI (hereafter abbreviated as TEADi). Firstly, the MoA of TEADi was validated in Hippo-mutated cells. TEADi inhibited cell growth of Hippo-mutated cancer cell lines NCI-H226 and NCI-H2052 but not that of MKN45, a YAP1-deletion cell line. Co-IP and qRT-PCR results demonstrated that TEADi disrupted the interaction between YAP1 and TEAD, and thus markedly repressed the expression of *CTGF* and *CYR61*, two downstream targets of YAP1/TEAD, in NCI-H226 cells. Secondly, we hypothesized that hyper-activation of TEAD confers resistance to KRAS mutant cancer types. To test this hypothesis, we generated two resistant cell lines. One is KARS G12C inhibitor Sotorasib-resistant NCI-H358 (NCI-H358-R). The other is MEK inhibitor Trametinib-resistant HCT116 (HCT116-R). Immunofluoresence assay showed that YAP1 nucleus translocation was enhanced in both resistant cells (NCI-H358-R and HCT116-R), but not in their parental counterparts (NCI-H358-P and HCT116-P). The enhanced YAP1 nucleus translocation resulted in increased transcription activities of TEAD in both resistant cells, as illustrated by luciferase reporter assay. Accordingly, *CTGF* and *CYR61* were observed upregulated in both resistant cells. The above data indicate that YAP1/TEAD mediated-transactivation plays a role in MAPK pathway resistance. Indeed, TEADi treatment alone displayed substantial difference in cell growth inhibition between parental and resistant cell lines in both NCI-H358 and HCT116, further confirming that the resistant cells are more dependent on YAP1/TEAD signaling. Finally, we evaluated the combinational efficacies of TEADi and MAPK/ERK pathway inhibitors in the resistant cells. It was observed that addition of TEADi could significantly restore the response of NCI-H358-R and HCT116-R to Sotorasib and Trametinib, respectively. Mechanistically, TEADi efficiently suppressed TEAD transcriptional activities and subsequently the expression of *CTGF* and *CYR61* in both resistant cells. Moreover, TEADi had almost no impact on ERK phosphorylation in either of the resistant cells, suggesting that re-sensitization of MAPK/ERK pathway inhibitors by TEADi is independent of primary onco-genetic signaling pathway. Taken together, our study demonstrates that inhibition of YAP1/TEAD signaling would be an efficient approach to overcome resistance to MAPK/ERK pathway inhibitors in the patients carrying KRAS mutations, and provides the scientific basis for development of combination therapy strategies.

#1932 Overcoming acquired resistance to KRAS(G12D) inhibition using a KRAS-HSP90 hetero-bifunctional small molecule therapeutic agent.

I. Pulido Endrino[1], L. gunder[1], Q. Luan[1], C. Ying[2], Z. Yang[2], J. Li[2], Y. Wang[2], Y. Sun[2], C. Liu[2], Y. Dai[2], H. Zhou[2], M. Massad[1], I. Papautsky[1], T. L. Prince[3], G. Wang[2], K. P. Foley[3], W. Ying[2];

[1]University of Illinois Chicago, Chicago, IL, [2]RANOK Therapeutics, Hangzhou, China, [3]RANOK Therapeutics, Waltham, MA

KRAS mutations are highly prevalent across many different cancer types. Recent advancements in KRAS-targeted drugs, such as the FDA-approved KRAS(G12C) inhibitors sotorasib and adagrasib for NSCLC patients, have shown great promise in the clinic. Nonetheless, these new agents fail to address other mutations, such as KRAS(G12D), which overall is the most common KRAS mutation in cancers, being found in 37% of pancreatic ductal adenocarcinomas, 12.5% of colorectal cancers and 4.9% of lung adenocarcinomas. Recently, MRTX1133 has been described as a selective, non-covalent inhibitor of KRAS(G12D) that shows promising preclinical efficacy and is undergoing clinical testing. However, based on prior clinical experience with sotorasib and adagrasib, acquired resistance to MRTX1133 may reasonably be anticipated. In fact, we find that KRAS(G12D)-mutated cell lines and a patient-derived organoid model exhibit varying degrees of inherent resistance to MRTX1133. To examine the consequences of blocking KRAS signaling, we employed a KRAS(G12D)-specific PROTAC, which simulated the effects of *KRAS* deletion. This demonstrated that receptor tyrosine kinase (RTK) activation could compensate for loss of KRAS signaling and was a key de novo resistance mechanism. This suggests that combination therapies may need to be individually tailored to treat patients resistant to KRAS(G12D)-targeted therapies. Additionally, we developed MRTX1133 resistant cells by culturing sensitive AsPC-1 pancreatic cancer cells in gradually increasing concentrations of the inhibitor. The resulting resistant cells displayed a complex RTK activation profile compared to parental cells. To counteract this, we employed KRAS(G12D)-CHAMP RNK08179, a hetero-bifunctional small molecule agent that simultaneously targets both KRAS(G12D) and HSP90, an RTK-regulating chaperone protein. RNK08179 effectively suppressed both KRAS signaling and RTK activation in MRTX1133-resistant cancer models, overcoming the compensatory resistance mechanisms observed with MRTX1133 alone. These findings highlight the potential of KRAS-CHAMPs as a novel, effective treatment strategy for KRAS-driven cancers, particularly those resistant to KRAS(G12D) inhibitors.

#1933 Dissecting acquired resistance to KRAS^{G12D} inhibition in a mouse model of pancreatic ductal adenocarcinoma.

J. Dilly[1], L. Abbassi[2], C. J. Hennessey[3], G. A. Uribe[3], B. Parent[3], A. Yang[3], K. S. Kapner[3], Z. Li[2], K. E. Evans[1], S. Dasgupta[3], M. T. Hoffman[2], L. Qiang[2], F. P. Hambitzer[2], S. Chugh[2], A. K. Shalek[4], S. K. Dougan[2], B. M. Wolpin[5], J. A. Nowak[6], S. Raghavan[7], P. S. Winter[8], A. J. Aguirre[9];
[1]Dana-Farber Cancer Institute, The Broad Institute of Harvard and MIT, Harvard Medical School, Boston, MA, [2]Dana-Farber Cancer Institute, Boston, MA, [3]Dana-Farber Cancer Institute, The Broad Institute of Harvard and MIT, Boston, MA, [4]Massachusetts Institute of Technology, The Broad Institute of Harvard and MIT, Koch Institute for Integrative Cancer Research, Cambridge, MA, [5]Dana-Farber Cancer Institute, Harvard Medical School, Brigham and Women's Hospital, Boston, MA, [6]Brigham and Women's Hospital, Harvard Medical School, Boston, MA, [7]Dana-Farber Cancer Institute, Harvard Medical School, Brigham and Women's Hospital, The Broad Institute of Harvard and MIT, Boston, Boston, MA, [8]The Broad Institute of Harvard and MIT, Cambridge, MA, [9]Dana-Farber Cancer Institute, Harvard Medical School, Brigham and Women's Hospital, The Broad Institute of Harvard and MIT, Boston, MA

KRAS is a major oncogenic driver in pancreatic ductal adenocarcinoma (PDAC) and is mutationally activated in approximately 90% of cases, with the glycine-to-aspartic acid substitution at position 12 (p.G12D) being the most prevalent alteration. Mutations in this oncogene have been associated with more aggressive disease and poorer outcomes and have remained “undruggable” for more than three decades. However, the recent development of mutant-specific small molecule inhibitors of KRAS has given hope for the treatment of this highly lethal and treatment-refractory malignancy. Here we evaluated the genomic and transcriptional mechanisms of resistance to MRTX1133, a first-in-class inhibitor of KRAS^{G12D}, in an autochthonous mouse model of PDAC. We leveraged single-nucleus RNA sequencing and whole-exome sequencing on 17 tumors from KPC mouse specimens (LSL-Kras$^{G12D/+}$; LSL-Trp53$^{R172H/+}$; p48-Cre) that were treated with either MRTX1133 or the vehicle, including 6 samples from mice that developed acquired resistance to KRAS^{G12D} inhibition. Our analysis has uncovered that resistance is multifaceted and characterized by both emergent genomic and transcriptional features. Genetically, resistant tumors harbored clonal and subclonal amplifications in the HIPPO pathway, cell cycle regulators, and ABC transporters. Transcriptionally, we employed non-negative matrix factorization and identified recurrent gene expression programs in resistant and vehicle samples. Using this approach, we uncovered the existence of an intermediate phenotype between classical and mesenchymal cell states that is enriched in tumors with evolved resistance to MRTX1133. In summary, our study provides a high-resolution genomic and transcriptional landscape of resistance to KRAS targeting in a preclinical *in vivo* model of PDAC, highlighting the complexity of treatment resistance and identifying various pathways and effectors that may serve as potential new targets for combination therapy.

#1934 The PLK1 inhibitor, onvansertib, is active as monotherapy and in combination with cetuximab in RAS wild-type colorectal cancer patient-derived xenografts.

M. Ridinger[1], P. Kanikarla Marie[2], F. Gao[2], Z. Liu[2], G. Maddalena[2], D. Menter[2], A. Sorokin[2], T. Smeal[1], S. Kopetz[2];
[1]Cardiff Oncology, San Diego, CA, [2]UT MD Anderson Cancer Center, Houston, TX

Background: Cetuximab and panitumumab are monoclonal antibodies targeting the epidermal growth factor receptor (EGFR), that provide clinical benefit to metastatic colorectal cancer (mCRC) patients with RAS wild-type (RAS^{WT}) tumors. Unfortunately, intrinsic or acquired resistance to these therapies limits their clinical effectiveness, necessitating the development of more efficient therapeutic strategies. Onvansertib is an oral, small molecule, selective inhibitor of the PLK1 kinase, currently in clinical development for KRAS-mutant mCRC. The aim of this study was to assess the anti-tumor activity of onvansertib monotherapy and in combination with cetuximab in RAS^{WT} CRC patient-derived xenograft (PDX) models.

Methods: Twenty RAS^{WT} CRC PDXs were selected and engrafted in nude mice. Once tumors reached 200-350-mm^3, mice were treated with vehicle, onvansertib (60mg/kg, QD), cetuximab (20mg/kg, BIW) or the combination for 18 days. PDX models were chosen based on their sensitivity to cetuximab, resulting in a selection of 7 cetuximab-sensitive (CetuxS) and 13 cetuximab-resistant (CetuxR) PDXs, including 7 with intrinsic resistance and 6 with acquired-resistance. Tumor volume change from baseline (TVC) was calculated as 100%x(Vt-Vo)/Vo and tumor growth inhibition (TGI) as 100%x(TVCcontrol-TVCtreated)/TVCcontrol. Tumor regression was defined as $TVC_{D18}<0$ and tumor stasis $0\leq TVC_{D18}<100$.

Results: Cetuximab sensitivity was confirmed in the selected models, cetuximab induced tumor regression in all the CetuxS PDXs, while no or limited activity was observed in the resistant models (median TGI=29%, IQR 16-61). Onvansertib exhibited potent anti-tumor activity in 17 (85%) PDXs, resulting in tumor regression (n=11) or tumor stasis (n=6). Onvansertib TGI at Day 18 was not significantly different in CetuxS PDXs (median TGI 102, IQR 76-103) compared to CetuxR PDXs (median TGI 108, IQR 74-124), supporting that onvansertib anti-tumor activity is independent of the sensitivity/resistance to cetuximab. The combination of onvansertib and cetuximab induced tumor regression in 18 (90%) PDXs. The combination showed significantly improved efficacy compared to individual therapies in some of the models.

Conclusions: Onvansertib monotherapy displayed potent anti-tumor activity in RAS^{WT} CRC PDX models, independently of their sensitivity to cetuximab. Additionally, onvansertib combined with cetuximab exhibited either comparable or superior anti-tumor activity than the monotherapies. Collectively, this data supports the clinical development of the PLK1 inhibitor onvansertib for RAS^{WT} mCRC.

#1935 The FAK/SRC axis mediates resistance to KRAS G12C inhibitors and its blockade can overcome KRAS inhibitor resistance.

Y. Shibata, H. Udagawa, M. B. Nilsson, J. Robichaux, A. Galan-Cobo, M. Negrao, D. P. Molkentine, J. He, A. Poteete, Y. Qian, Q. Huang, F. Skoulidis, J. V. Heymach;
UT MD Anderson Cancer Center, Houston, TX

Activating mutations in KRAS are found in approximately 30% of non-small cell lung cancer (NSCLC), and among all KRAS mutations, KRAS G12C is the most frequent variant in NSCLC, with a prevalence of approximately 14%. KRAS G12C inhibitors, sotorasib and adagrasib are FDA approved for locally advanced or metastatic KRAS G12C-positive NSCLC. However, clinical evidence suggests that there are various factors limiting the efficacy of KRAS G12C inhibitors in patients with KRAS G12C-positive NSCLC, highlighting the urgent need for novel treatment strategies or combinations to improve efficacy. Therefore, we sought to identify effective combinations to enhance the efficacy of KRAS G12C inhibitors using in vitro and in vivo models of KRAS G12C-positive NSCLC. Employing a high throughput in vitro drug screening effort using KRAS mutant NSCLC cell lines, we observed that Focal Adhesion Kinase (FAK) and Steroid Receptor Coactivator (SRC) inhibitors produced a synergistic effect when combined with KRAS G12C inhibitors adagrasib or sotorasib. As determined by reverse phase array and Western blotting, in H358, H23, HCC44, and H2122 cells, KRAS inhibitor treatment alone resulted in an initial suppression of RAS/MAPK and AKT pathway activation which was followed by upregulation of multiple receptor tyrosine kinases and integrins which contributed to the re-activation of the RAS/MAPK and AKT pathways after 24-48 hours. We identified FAK as a key downstream mediator of these bypass pathways. FAK/SRC inhibitors enhanced the efficacy of KRAS G12C inhibitors by preventing this feedback activation. Moreover, we observed increased FAK activation in H358 NSCLC cell lines with acquired resistance to adagrasib or sotorasib as compared to parental cells, and FAK/SRC inhibitors re-sensitized resistant cells to KRAS G12C inhibitors. Using a xenograft model of human KRAS mutant NSCLC, we determined that the combination of repotrectinib, a FAK/SRC inhibitor, and a KRAS G12C inhibitor significantly suppressed tumor growth as compared to KRAS G12C inhibitors alone, and this combination was well tolerated. Overall, our findings indicate that activation of FAK is a key mechanism of adaptive feedback and acquired resistance to KRAS G12C inhibitors in KRAS G12C-positive NSCLC and highlight the therapeutic potential of FAK/SRC inhibitors in combination with KRAS G12C inhibitors. These data support the clinical testing of the combination of FAK/SRC inhibitors and KRAS G12C inhibitors in patients with KRAS G12C-positive NSCLC.

#1936 KEAP1-NRF2 mediated resistance against KRAS^{G12D} inhibitor in pancreatic ductal adenocarcinoma.

W.-H. Chang[1], A. G. Stamey[1], A. M. Waters[2], K. L. Bryant[1], A. D. Cox[1], C. J. Der[1];
[1]University of North Carolina at Chapel Hill, Chapel Hill, NC, [2]University of Cincinnati, Cincinnati, OH

Pancreatic ductal adenocarcinoma (PDAC) is the third leading cause of cancer deaths in the US. Mutational activation of the KRAS oncogene is associated with 95% of PDAC and is essential for maintaining PDAC tumorigenic growth. Although inhibitors (sotorasib and adagrasib) targeting one KRAS mutation (G12C) have been approved for the treatment of KRAS^{G12C}-mutant lung cancer, the G12C mutation comprises less than 2% of KRAS mutations in PDAC. Recently, the clinical candidate KRAS^{G12D}-selective inhibitor MRTX1133 (G12Di) has been shown to potently suppress both activation of the RAF-MEK-ERK signaling pathway downstream of KRAS and tumorigenic growth of KRAS^{G12D}-mutant PDAC in vitro and in vivo. Since KRAS^{G12D} represents 40% of KRAS-mutant PDAC, G12D-selective inhibitors hold promise as an effective therapy for a significant fraction of PDAC patients. However, the efficacy of these inhibitors is hindered by persistent challenges related to both primary (innate) and acquired treatment-associated resistance, which curtails the long-term effectiveness of likely all KRAS inhibitors. Here, our studies focus on unraveling the mechanism of primary and acquired resistance to G12Di treatment in PDAC. We applied a loss-of-function CRISPR screen targeting the druggable genome on KRAS^{G12D}-mutant PDAC cells treated with a sublethal concentration of G12Di to identify genes that modulate G12Di sensitivity. We identified loss of genes (e.g., *CBL*, *RB1*, and *PTEN*) found previously in patients who relapsed on G12Ci treatment, providing validation of the screen. One gene also identified was *KEAP1*. KEAP1 is known as a substrate-specific adapter of an E3 ubiquitin ligase complex that promotes the degradation of NRF2, and the loss of KEAP1 is commonly associated with increased stability of NRF2, a transcription factor that promotes the transcription of many anti-oxidative stress and pro-cell survival genes. We found that knockout of *KEAP1* significantly compromised the ability of G12Di to inhibit PDAC cell proliferation in vitro. KEAP1 loss was associated with upregulated expression of NRF2, and concurrent CRISPR knockout of *NRF2* restored sensitivity of G12Di in PDAC. Interestingly, we determined that G12Di-resistant KEAP1-deficient PDAC cells exhibited high dependence on glutaminase (GLS), which converts glutamine to glutamate. We further discovered that combination treatment with a glutaminase inhibitor (CB-839) synergistically enhanced G12Di growth suppression not only of KEAP1-knockout but also of parental PDAC cells. In summary, our study establishes a role for KEAP1 loss as a mechanism that drives PDAC resistance to KRAS inhibitors and identifies GLS inhibition as a possible approach to overcome NRF2-driven resistance.

#1937 YAP-TAZ-TEAD transcriptional program is a prominent driver of acquired resistance to KRAS^{G12C}-based therapies in patients with metastatic colorectal cancer.

O. Coker[1], A. Sorokin[1], N. Akhave[1], K. Pan[1], F. Gao[1], Z. Liu[1], P. Kanikarla[1], H. Lee[1], O. Villarreal[1], J. Alshenaifi[1], G. Maddalena[1], A. Mohamed[1], D. Prescod[1], D. Menter[1], S. Chowdury[1], R. Corcoran[2], K. Rai[1], D. Hong[1], S. Kopetz[1];

[1]UT MD Anderson Cancer Center, Houston, TX, [2]Harvard Medical School, Houston, TX

Background: KRAS mutations are present in 50% of patients with metastatic colorectal cancer (mCRC) and play a critical role in mCRC tumor biology. KRAS^{G12C} mutations are present in 6% of patients with mCRC. While KRAS^{G12C} inhibitors (G12Ci) have entered the clinic, clinical responses to G12Ci are transient even when combined with EGFRi, highlighting the need to optimize therapeutic interventions. We have characterized our KRAS^{G12C} mCRC patient-derived xenograft (PDX) models and paired biopsies from progressing patients that have acquired resistance to G12Ci/G12Ci+EGFRi through an integrative multi-omics approach and have validated them through wet-lab experiments.

Experimental Procedures: qPCR analysis was performed on 13 PDX models that were established from paired tumor biopsies from patients pre and at progression of treatment. We also treated 5 KRAS^{G12C} mCRC PDX models with G12Ci +/- EGFRi until acquired resistance was achieved. Tumors were harvested post-treatment and whole-exome, RNAseq, and RPPA were performed on them. In parallel, 3 paired parental and G12Ci/EGFRi-resistant 2D/3D *in vitro* models were established and treated with G12Ci +/- EGFRi +/- pan-TEADi. Expression and response profiles were assessed through cell viability assays, western blot, qPCR, and IncuCyte analyses. We simultaneously re-established *in vivo* acquired resistance to G12Ci + EGFRi in 2 PDX models and treated them with pan-TEADi triple combo. Finally, we performed spatial transcriptomics (Xenium) from 6 paired pre-/post-treatment patient samples to characterize transcriptomic profiles at the single-cell resolution.

Results: In our PDX models, the acquisition of a new NRAS mutation and KRAS amplification in response to therapy were found, which are commonly known genomic resistance mechanisms to MAPK targeted therapies. 3 of the 5 PDX models ($p < 0.05$, $p < 0.001$) and 2 of 4 patients ($p < 0.01$, $p < 0.001$) from the PDX models established from paired tumor biopsies from patients pre and at progression of treatment exhibited YAP1-TEAD signaling as an acquired response to G12Ci-based therapies. In our *in vitro* work, pan-TEADi triple combo provided efficacy over G12Ci/therapy in 3D *in vitro* models while both 2D/3D *in vitro* resistant models were sensitized to pan-TEADi monotherapy, suggesting the combination drives a state change to be YAP dependent where YAP-TEAD signaling may now be driving MAPK signaling. Detailed spatial transcriptomic data will be presented.

Conclusion: Clinical responses to G12Ci are transient and require optimizing therapeutic modalities. In patients, where genomic mechanisms are not found, YAP-TAZ-TEAD signaling was found to be a common feature of resistance to inhibitors targeting the KRAS pathway. This work suggests that pan-TEADi may provide patients with improved therapeutic options.

#1938 WEE1 inhibition prevents and overcomes resistance to KRAS inhibitors in lung cancer by enhancing MCL1-mediated apoptosis.

G. Yamamoto, K. Tanaka, R. Kamata, T. Nakao, S. Mori, J. Liu, S. S. Kobayashi, A. Ohashi;
National Cancer Center Japan, Kashiwa, Chiba, Japan

Background: While novel covalent inhibitors of KRAS G12C have been approved in non-small-cell lung cancer (NSCLC), their efficacies are known to be limited. To enhance the therapeutic potential of KRAS inhibitors, combination strategies need to be developed. In this study, we conducted a large-scale screening to identify novel combination partners that induced synergistic efficacy with KRAS inhibitors. Additionally, mechanistic analyses were conducted to clarify the synergistic effects in combination and their role in conferring resistance to KRAS inhibitors.
Methods: To identify novel combination partners of KRAS inhibitors, we conducted high-throughput screening (HTS) using a chemical library composed of 1,400 kinase inhibitors. Sotorasib was used as a KRAS inhibitor. Anti-proliferative and apoptotic effects in vitro were assessed by ATP-based cell viability assay, and caspase 3/7 assay and/or Annexin V assay, respectively. Protein expression levels were assessed by immunoblotting. In vivo studies were performed using a H358 xenograft nude mouse model and a patient-derived xenograft model (PDX). PDX samples were provided by the National Cancer Center J-PDX library, Japan.
Results: HTS identified the WEE1 inhibitor AZD1775, a G2/M checkpoint abrogator in clinical-stage development, as a promising combination partner of KRAS inhibitors in KRAS G12C mutant NSCLC. Synergistic effects of KRAS and WEE1 inhibitors were confirmed across multiple KRAS G12C mutant NSCLC cell lines, independently of their co-occurring oncogenic mutation profiles. The combination treatment enhanced apoptotic cell death, being upregulated pro-apoptotic protein BIM, while downregulated anti-apoptotic protein MCL1. In vivo efficacy studies in combination with sotorasib and AZD1775 also demonstrated remarkable tumor regression and durable response in both CDX and PDX models. We also generated sotorasib-resistant H23 (H23-SR) cells, confirming upregulation of both WEE1 and MCL1 in the resistant cells. Ectopic overexpression of WEE1 in H23, on the contrary, conferred resistance to sotorasib. Furthermore, WEE1 inhibition re-sensitized H23-SR cells to KRAS inhibitors.
Conclusion: Our results suggest that the WEE1-MCL1 axis plays an important role in both the initial therapeutic efficacy and the acquired resistance to KRAS inhibitors. These findings could pave the way for a novel therapeutic strategy for KRAS G12C mutant NSCLC.

#1939 NT219, a dual inhibitor of IRS1/2 and STAT3, suppresses cancer stem cell mediated resistance to $KRAS^{G12C}$ and $KRAS^{G12D}$ inhibitors in solid tumors.

H. Reuveni[1], M. N. Al-Hallak[2], S. Motorwala[3], E. Beal[2], S. Kim[2], R. Beydoun[2], G. Dyson[2], B. El-Rayes[4], H. Chen[4], P. Philip[5], A. Shields[2], B. Pasche[2], K. Sigalov[1], H. Ben-David[1], D. Miron[1], A. Azmi[2],

[1]Purple Biotech Ltd., Rehovot, Israel, [2]Karmanos Cancer Institute Wayne State University, Detroit, MI, [3]Michigan State University, Detroit, MI, [4]University of Alabama, Birmingham, AL, [5]Henry Ford Health, Detroit, MI

Background NT219 is a novel small molecule, a dual inhibitor which uniquely triggers the degradation of Insulin Receptor Substrates 1/2 (IRS) and the dephosphorylation and suppression of STAT3, two major oncogenic targets that play a key role in drug resistance. Mutated KRAS (mKRAS) has long been referred to as undruggable until recently when $KRAS^{G12C}$ inhibitors were approved. While $KRAS^{G12C}$ is the most common oncogenic driver in NCSLC, $KRAS^{G12D}$ is found in 42% of pancreatic tumors. We present NT219 suppressive effect on mKRASi resistant and sensitive cells of both PDAC and NSCLC, as well as on cancer stem cells (CSC) known to contribute to disease recurrence.

Method The inhibitory effects of NT219 as a monotherapy or in combination with either $KRAS^{G12C}$ inhibitors (sotorasib/adagrasib) or $KRAS^{G12D}$ inhibitor (MTRX1133) were tested in 2D cell growth and colony formation assays using mKRAS inhibitor sensitive and resistant cancer cell lines. The effect of NT219 and mKRASi on cancer stem cells was assessed using 3D spheroid assay evaluating spheroid size (microscopic measurements), cell viability (CellTiterGlo) and stemness marker expression (FACS analysis).

Results NT219 in combination with either sotorasib or MTRX1133 suppressed established spheroids of NSCLC($KRAS^{G12C}$) and PDAC($KRAS^{G12D}$) respectively, in terms of size, disintegration and viability. In NSCLC H358, spheroid satellites appeared following treatment with sotorasib, while the combination with NT219 suppressed it. CSC marker ALDH increased 7-fold in NSCLC spheroids as compared to 2D grown cells, while NT219 and sotorasib suppressed it. The expression of SOX2 stemness marker was reduced by NT219 alone (5 fold), unexpectedly induced by sotorasib (4 fold) and suppressed by NT219+sotorasib (15 fold vs sotorasib alone). In addition, significant induction of STAT3, was observed following sotorasib treatment and completely reversed by the addition of NT219. We also demonstrate that NT219 induces growth inhibition in both $KRASi^{G12C}$ resistant PDAC and NSCLC, and $KRASi^{G12D}$ resistant PDAC cells. NT219 exhibited synergistic effects with adagrasib and MTRX1133, in suppressing the proliferation of $KRAS^{G12C}$ PDAC and NSCLC cells and $KRAS^{G12D}$ PDAC cells, respectively. This combination showed a synergistic effect in xenograft model.

Conclusion We first showed the effect of NT219 in suppressing cancer stem cells, known to promote resistance and tumor recurrence. Synergistic effect of NT219 and mKRAS inhibitors, G12Cand G12D, in NSCLC and PDAC respectively, was demonstrated. Initial results suggest involvement of NT219 target proteins in resistance to $mKRAS^{G12C/D}$ inhibitors. Treatment with sotorasib induced enhancement in stemness potential of $mKRAS^{G12C}$ NSCLC, which NT219 efficiently suppressed, suggesting a novel therapy for this unmet need and a novel mechanism to combat resistance to mKRAS inhibitors

#1940 Identifying resistant mechanisms to direct KRAS inhibitors in NSCLC.

S. T. Kundu, D. H. Peng, B. L. Rodriguez, E. L. McCarthy, D. L. Gibbons;
UT MD Anderson Cancer Center, Houston, TX

Mutations in the KRAS oncogenic driver gene are frequently found in malignancies such as pancreatic, colorectal, and lung cancers. The replacement of the amino acid glycine at position 12 (e.g., G12C, G12D, G12V) is a frequent mutation that traps the protein in an active state and promotes uncontrolled cell proliferation. KRAS was regarded as "undruggable" for many years due to insufficient drug-binding pockets on the protein's surface. Recent breakthroughs, however, have resulted in the development of covalent inhibitors capable of selectively targeting the KRAS G12C mutation, like Sotorasib (AMG510) and Adagrasib (MRTX849) which are approved by the FDA due to their encouraging effects in clinical trials. The identification of selective inhibitors of other oncogenic KRAS alleles, such as the noncovalent KRAS-G12D inhibitor, MRTX1133, and a pan-KRAS-inhibitor drug (BI2865) is also a promising next step in the treatment of KRAS-dependent malignancies. While these inhibitors have shown initial success, their use frequently leads to resistance, the mechanisms of which largely remain unknown. To fill this essential research gap, we are employing our pre-clinical syngeneic mouse models and KRAS mutant allele-specific cell lines to investigate the underlying molecular processes of acquired resistance to direct KRAS allele-specific inhibitors. Using these murine syngeneic cell lines and human NSCLC cell lines, we have generated a panel of cell lines with acquired resistance to these direct KRAS inhibitors. To elucidate the molecular underpinnings of acquired resistance to direct KRAS inhibitors, we performed proteomic profiling of the sensitive and resistant cells by RPPA analysis. Among the several proteins whose expressions were altered in the KRAS-inhibitor-resistant cells, we identified the YAP/TEAD1 pathway that was commonly upregulated in the cells resistant to MRTX849 (G12Ci) or MRTX1133 (G12Di). We also observed significant re-sensitization of the resistant cells to the specific KRAS inhibitors upon genetic or pharmacological inhibition of TEAD using siRNA or a TEAD-inhibitor, *in vitro.* Tumors from syngeneic mice that were implanted with KRAS inhibitor-resistant cells or their sensitive versions and treated with the specific KRAS inhibitors for 3-4 weeks, also exhibited increased nuclear YAP1 localization in the resistant tumors. We are currently performing *in vitro* and *in vivo* studies to understand the therapeutic efficacy of a TEAD inhibitor in combination with KRASi (MRTX849 or MRTX1133) to either reverse or prevent resistance to these direct KRAS inhibitors. We are also trying to identify alterations in the tumor immune microenvironment upon combination therapy targeting KRAS and TEAD. Successful completion of this research will help address the urgent need to understand ways to overcome resistance to KRAS inhibitors and increase their clinical efficacy.

#1941 AXL activation promotes adaptive resistance to KRAS-G12C inhibitors in KRAS-G12C-mutated non-small cell lung cancer.

K. Morimoto[1], T. Yamada[1], S. Hirai[1], Y. Katayama[1], K. Kunimasa[2], T. Sasaki[3], M. Nishida[4], S. Watanabe[5], S. Shiotsu[6], H. Uehara[7], K. Takayama[1]; [1]Kyoto Prefectural University of Medicine, Kyoto, Japan, [2]Osaka International Cancer Institute, Osaka, Japan, [3]Asahikawa Medical University Hospital, Hokkaido, Japan, [4]St. Marianna University School of Medicine, Kanagawa, Japan, [5]Niigata University Graduate School of Medical and Dental Sciences, Niigata, Japan, [6]Japanese Red Cross Kyoto Daiichi Hospital, Kyoto, Japan, [7]Institute of Biomedical Sciences, Tokushima University Graduate School, Tokushima, Japan

Background: KRAS is the most frequent targetable oncogene in non-small cell lung cancer (NSCLC). Recently, novel KRAS inhibitor have been clinically developed for treatment of KRAS G12C-mutated NSCLC patients. However, it is difficult to achieve complete remission of tumor. Therefore, the optimal combined therapeutic intervention with KRAS G12C inhibitors has a potentially crucial role in the clinical outcomes of patients. In this study, we focused on the mechanisms underlying adaptive resistance to KRAS G12C inhibitors and therapeutic strategies required to overcome them.
Methods: We used KRAS G12C-mutated NSCLC cell lines to evaluate the adaptive response to KRAS G12C inhibitors in vitro and in vivo. We also investigated the correlation between AXL expression in pre-treated tumors and clinical outcomes with sotorasib for KRAS G12C-mutated NSCLC patients.
Results: We revealed that AXL signaling leads to the adaptive resistance to KRAS G12C inhibitors in KRAS-G12C mutated NSCLC, activation of which is induced by GAS6 production via transcriptional coactivator YAP. AXL inhibition reduced the viability of AXL-overexpressing KRAS G12C-mutated lung cancer cells by enhancing KRAS G12C inhibition-induced apoptosis. In xenograft models of AXL-overexpressing KRAS G12C-mutated lung cancer treated with KRAS G12C inhibitors, initial combination therapy with AXL inhibitor markedly delayed tumor regrowth compared with KRAS G12C inhibitor alone or the combination after acquired resistance to KRAS G12C inhibitor. AXL was highly expressed in clinical specimens of KRAS G12C-mutated lung cancers and its high expression was associated with a low treatment response to sotorasib.
Conclusions: These results indicated pivotal roles for AXL activation and its inhibition in the intrinsic resistance to KRAS G12C inhibitor.

#1942 Characterization of a panel of CRISPR/Cas9 engineered KRAS G12C inhibitor-resistant tumor models.

J. Zhou[1], L. Hua[1], J. Feng[1], N. Bao[1], D. Zhang[1], J. Wang[1], M. Putker[2], L. Bourre[1];
[1]Crown Bioscience, Inc., San Diego, CA, [2]Crown Bioscience, Inc., Leiden, Netherlands

Introduction: KRAS is one of the most frequent mutated oncogenes and has been recognized as undruggable for many years. AMG510, the first therapy to directly target KRAS, was approved by the FDA to treat non-small cell lung cancer (NSCLC) bearing KRAS G12C mutation. However, the emergence of resistance in patients remains a challenge and limits its clinical benefits, which calls for next-generation targeted therapy or combination strategies to overcome the resistance to KRAS G12C inhibitors. A variety of secondary mutations in KRAS attributing to the resistance have been identified, which requires robust *in vitro* and *in vivo* preclinical models to validate potential therapeutics targeting these mutations. Therefore, we generated a panel of KRAS G12C inhibitor-resistant tumor models to facilitate the development of possible strategies to overcome such resistance.

Methods: First, a secondary KRAS mutation, including H95D, H95Q, H95R, Q61H and R68S, was introduced by using CRISPR/Cas9 technology in MIA PaCa cell line, which harbors a homozygous KRAS G12C mutation in addition to Y96D, Y96C and Y96S previously published by us. Point mutation knock-in was validated by sanger sequencing, and cell identity was confirmed by SNP assay. *In vitro*, the parental and mutated cells were treated with either AMG510 and MRTX849 and cell viability was measured by CellTiter-Glo. *In vivo* efficacy of KRAS G12C inhibitors, AMG510 and MRTX849, SOS1 inhibitor, BI-3406 and MEK inhibitor, Trametinib were evaluated in the Y96D mutated MIA PaCa subcutaneous xenograft.

Results: Homozygous secondary point mutation knock-in in MIA PaCa cells was confirmed by sanger sequencing. Similar growth rate and morphology was observed in selected clones compared to the parental line. Similar to Y96D mutation previously published, R68S mutation was highly resistant to both KRAS G12C inhibitors, with IC_{50} increased more than 100 fold for both MRTX849 and AMG510, whereas H95D, H95Q and H95R mutation was more resistant to MRTX849, while Q61H had a minimal effect on either one of the inhibitors. In addition, cells expressing KRAS G12C/Y96D were also resistant to AMG510 and MRTX849 in *in vivo* study, whereas combination of BI-3406 (single treatment: TGI of 27%) and Trametinib (single treatment: TGI of 76%) suppressed tumor growth significantly with TGI of 93% on day 17 after randomization compared to control group ($p<0.001$). Also, the combination showed significant improvement compared to BI-3406 single treatment ($p<0.001$) whereas no significant improvement was observed compared to Trametinib single treatment ($p>0.05$).

Conclusion: CRISPR/Cas9 engineered second site KRAS mutations in cells harboring KRAS G12C mutation displayed a differentially resistant profile to KRAS G12C inhibitors. Thus, H95D/Q/R, R68S and Y96D can be used as preclinical inhibitor-resistant models to evaluate clinical strategies to overcome resistance to KRAS-targeted therapies.

#1943 Discovery and characterization of potential drivers of resistance to the KRAS G12D inhibitor, MRTX1133, in cancer cell line models.

X. M. Helu[1], E. Griffiths[1], A. Calinisan[1], A. Hebbert[1], L. Yan[1], N. Hoffman[1], D. Trinh[1], L. Hover[2], J. Fernandez-Banet[2], D. M. Briere[1], E. Lifset[1], P. Olson[1], J. G. Christensen[1], **J. Hallin**[1];

[1]Mirati Therapeutics, San Diego, CA, [2]Monoceros Biosystems LLC, San Diego, CA

Introduction: *KRAS*^{G12D} is the most common *KRAS* mutation and is present in approximately 34% of pancreatic cancer, 10-12% of colorectal cancer, 4% of lung adenocarcinoma and in a number of other cancer types. We previously identified MRTX1133, a potent, selective, and non-covalent KRAS^{G12D} inhibitor. The advancement of MRTX1133 to clinical trials warrants continued study of the role of the *KRAS*^{G12D} mutation in cancer pathogenesis and progression.

Methods: Previous pharmacodynamic and pharmacogenomic profiling in sensitive and partially resistant models identified mechanisms implicated in limiting the anti-tumor response including signaling pathways that induce feedback reactivation and/or bypass KRAS dependence. Thus, cell lines (GP2D and SNU-1033, colorectal cancer; HPAC and AsPC-1, pancreatic cancer) were utilized to study acquired resistance to MRTX1133 following continuous treatment at increasing concentrations over time. These cell lines were confirmed to be stably resistant as determined by evaluation of response to MRTX1133 in vitro and in vivo. These cell lines were extensively profiled to determine underlying mechanisms of resistance utilizing molecular profiling strategies as well as drug combination screens to interrogate pathways that could circumvent resistance.

Results: In one of the four generated cell lines with acquired resistance, evidence of secondary *KRAS* mutations Y96N and H95Q were confirmed by RNAseq and are likely drivers of resistance in this cell line and are consistent with known mechanisms of KRAS^{G12C} inhibitor resistance. The three other MRTX1133 resistant cell lines did not show evidence of secondary *KRAS* mutations and were further evaluated for mechanisms that bypass KRAS dependence. Combinations of MRTX1133 with therapies that target pathways including upstream RTK signaling, mTOR, or AKT broadly enhanced the anti-tumor activity of MRTX1133 in both in vitro cell viability and in vivo efficacy studies in the resistant cell lines. Conclusion: Collectively, these data provide early insight onto potential mechanisms of resistance to selective KRAS^{G12D} inhibitors and demonstrate the importance of developing rational combination strategies designed to address drug resistance. In addition, these studies provide a catalogue of potentially druggable vulnerabilities that complement KRAS blockade.

#1944 Using patient-derived cancer organoids to determine the effects of the anti-EGFR therapy panitumumab in the presence or absence of *KRAS* mutation.

J. N. Stoecker, S. Udgata, A. A. Gillette, C. A. Pasch, M. C. Skala, D. A. Deming;
UW Madison, Madison, WI

Introduction: Tumor heterogeneity is a major cause of resistance to therapies in colorectal cancer (CRC). The anti-EGFR (epidermal growth factor receptor) therapies panitumumab (pani) and cetuximab, are now being investigated for the retreatment of patients when resistant subclones could be more abundant in a previously wild-type cancer. Here we utilize patient-derived cancer organoids (PDCOs) to investigate the potential implications of the abundance of resistant subclones on treatment and duration of response.

Methods: Two CRC PDCO lines, one pani sensitive (PS) and one pani resistant (PR), were cultured separately and then mixed to determine how different combinations of mutations altered the time for the overall culture to be resistant to pani. NGS was performed on these cells to determine the mutation profile. The two PDCO lines were cultured together with the following concentrations (v/v) of 100% PS; 20% PR+80% PS; 10% PR+90% PS, 5% PR+95% PS, 1% PR+99% PS, and 100% PR using Matrigel and fed with previously published CRC organoid media. Widefield imaging was performed for diameter change analysis at day 0 and day 4 using ImageJ. Upon a median growth of >20% at baseline/untreated, all mixed populations were treated at increments of 20% physiologic Cmax of pani each week. Once select mixed populations reached 100% Cmax and maintained a median growth of >20% for two consecutive weeks, they were determined to have reached complete resistance to the treatment.

Results: DNA sequencing of PDCOs showed PR has mutations associated with pani resistance (KRASG12V, PIK3CAH1047R) and the PS line did not. All the conditions except for 100% PS escalated to ≥40% Cmax within 7 weeks and reached complete resistance to pani by week 22. 100% PS remained at 20% Cmax through week 22. The 100% PR population reached complete resistance to pani the quickest at 100% Cmax at week 8. The conditions with the lowest percentages of PR (5% PR+95% PS and 1% PR+99% PS already started to show resistance above the PS line by 8 weeks and reached complete resistance to pani at week 12.

Conclusion: PDCO lines containing low concentrations of resistant clones can quickly lead to resistance to pani treatment, even below the typical level for clinical NGS detection. All KRAS mutant conditions (PR) reached resistance quicker than 100% PS condition. Further studies will evaluate even low concentrations of resistance clones across further CRC PDCO models and will evaluate the mechanism by which these clones are leading to resistance.

#1945 Mechanisms of acquired resistance to EGFR tyrosine kinase inhibitor osimertinib and KRAS-G12C inhibitor sotorasib in lung cancer..

Y. Yagami[1], T. Sato[1], H. Yamamoto, Sr.[1], M. Shirasawa[1], Y. Nakahara[1], W. Hideo[2], N. Katsuhiko[1];
[1]Kitasato Univ. School of Medicine, kanagawa, Japan, [2]Mount Sainai, New York, NY

A series of molecular targeted drugs have been developed for the treatment of non-small cell lung cancer (NSCLC) harboring driver gene alterations. Although the use of these drugs has substantially improved the clinical outcomes of patients with the genetically altered NSCLC, these patients ultimately develop resistance to the drugs. Various molecular mechanisms of resistance to the molecular target therapies have been reported, it is still a crucial challenge to overcome the drug resistance. Osimertinib, the most used third-generation EGFR tyrosine kinase inhibitor to target both common *EGFR* mutations and secondary T790M mutation, and sotorasib, a recently developed KRAS inhibitor to target *KRAS* G12C mutation, are no exception. In this study, we aimed to investigate the mechanisms of acquired resistance to osimertinib and sotorasib in NSCLC by profiling drug-resistant lung cancer cell lines, which were established from *EGFR*-mutant HCC827(del E756_A750) and *KRAS* G12C-mutant H23 through exposure to each of the molecular targeted drugs. Phospho-RTK array and western blot analyses revealed MET overexpression and phosphorylation in the osimertinib-resistant HCC827 (HCC827OR) as previous studies reported. Notably in our study, HCC827OR cells were incompletely sensitive to a selective MET inhibitor savolitinib without osimertinib, suggesting that HCC827OR partially lost its dependency on mutant EGFR and got addiction to MET signaling. When sotolasib was administered to the sotolasib-resistant H23 (H23SR) cells, KRAS-GTP, and the downstream ERK and AKT phosphorylation were suppressed. To identify novel mechanisms of the resistance, we performed epigenomic profiling of active enhancer in those cells and found a candidate transcription factor, at whose gene locus H3K27 acetylation signal was increased in H23SR cells compared to parent H23 cells. Immunoblotting showed that protein expression of the gene was indeed higher in H23SR cells than the parent cells. To confirm the involvement of this gene to the resistance, further investigation is warranted.

#1946 Elucidating the mechanisms of acquired resistance to AMG510 in cancer models harboring KRAS G12C mutations.

T. Ni, T. Huo, Y. Zhang, J. Wang, G. Liu, W. Shi, Q. Gu;
WuXi AppTec, Suzhou, China

GTPase KRas (KRAS), a critical oncogene, is known for its frequent mutations across a wide array of human cancers, most notably in pancreatic, lung, and colorectal cancers. Recent advancements in the field have led to the successful development of numerous inhibitors targeting the mutant KRAS. Clinical application of KRAS G12C inhibitors, such as AMG510 and MTRX849, represents major breakthroughs in addressing previously 'undruggable' cancer targets. Nevertheless, a subset of patients initially responsive to these inhibitors eventually exhibit treatment resistance. Uncovering the underlying mechanism would help to develop novel therapies that overcome the acquired drug resistance.

To elucidate the underlying mechanisms, we generated AMG510-resistant tumor models, namely AMG510-R-MIA PaCa-2 and AMG510-R CT26 KRAS G12C, by continuous administration of AMG510 to tumor-bearing mice. Upon comparison of sensitive parental tumors and resistant tumors, we found that highly expressed KRAS and constant activation of RAS-MAPK signaling pathway are critical for resistant tumor progression following AMG510 treatment. In addition, resistant tumor cells are responsible for the elevated secretion of CXCL2/3/5, which dramatically reconditions the tumor immune microenvironment and recruits immunosuppressive cells.

In summary, the exploration of the resistance mechanism in AMG510-induced resistant models provides insight into the development of new-generation KRAS-G12C inhibitors and novel combinatorial therapies.

#1947 Studies on pMEK inhibitors for the treatment of RAS-mutant cancers as a single agent or combinations.

X. Lv, M. Xu, Y. Hu, L. Zhao, X. Chen, Y. Chen, C. Yang, J. Li, C. Chen;
ABM Therapeutics, San Diego, CA

RAS mutations are the most common oncogene in human cancers and KRAS has the highest frequency in non-small cell lung cancer (NSCLC) and pancreatic cancer (PDAC). KRAS G12C inhibitors have been approved to treat NSCLC patients. However, drug-resistance is eventually developed for these treatments. Preclinical studies suggested MAPK pathway reactivation is one possible mechanism. Among many MEK inhibitors in clinical development, CH5126766 binds to MEK1 inactive conformation and blocks its phosphorylation and activation. We believe this compound should prevent MAPK “paradoxical activation” commonly observed in most RAF and MEK inhibitors such as vemurafenib and cobimetinib. We studied this compound in various in vitro assays and found its potential in combating the paradoxical activation, which might be the cause of drug-resistance for MAPK signal pathway inhibitors, including RAS-, RAF- MEK- and ERK-inhibitors, as a single agent or in combination with above-mentioned inhibitors. In addition, we are developing a series of compounds based on CH5126766, by improving the inhibition of MEK1/2 kinase activity in addition to its activation. In summary, studies on the pMEK inhibitor demonstrated that this class of compounds might mitigate the MAPK pathway reactivation and prolong drug efficacies in clinical. Detailed research results will be discussed.

#1948 Resistance to RAS inhibition promotes remodeling of the immunosuppressive microenvironment of pancreatic cancer.

H. Tiriac;
UC San Diego, San Diego, CA

Background: Pancreatic ductal adenocarcinoma (PDAC) remains one of the most lethal malignancies, largely due to acquired chemotherapy resistance. MRTX-1133, a promising KRAS-G12D inhibitor, has demonstrated initial efficacy; however, resistance analogous to that seen with KRAS-G12C inhibitors is an emerging challenge. The tumor microenvironment (TME) is increasingly recognized as a contributor to resistance, often fostering tumor survival and immune evasion.
Methods: To elucidate the resistance mechanisms to KRAS-G12D inhibition, we established resistant mouse and human PDAC cell lines derived from mouse and human models. These models were analyzed using flow cytometry and single cell RNA sequencing to define TME dynamics as resistant is acquired and after is has been established. We also analyzed cytokines released by resistant tumor cells using protein arrays and RNA sequencing.
Results: Our investigation revealed significant TME alterations associated with acquired resistance. Notably, there was a marked increase in the population CD4+ Tregs and neutrophil while activated CD8+ T cells are decreased in the resistant tumors. Concurrently, an increased secretion of chemokines such as CXCL1 and CXCL2 was observed in resistant tumor cells relative to their parental counterparts.
Conclusions: The adaptation of PDAC to circumvent KRAS inhibition involves a distinct reprogramming of the TME, attenuating immune surveillance and potentially facilitating tumor progression. Current efforts are directed towards delineating the key pathways implicated in these TME modifications to pioneer new therapeutic approaches for managing KRAS inhibitor resistant PDAC.

EXPERIMENTAL AND MOLECULAR THERAPEUTICS: Kinase and Phosphatase Inhibitors 2
Poster Session

#1952 Co-alterations in *PIK3CA* and ARID1A lead to enhanced sensitivity to PI3K inhibition.
S. Udgata, J. N. Stoecker, A. L. Lippert, C. A. Pasch, D. A. Deming;
University of Wisconsin-Madison, Madison, WI

Background: There is increasing interest in developing precision medicine strategies for cancers with *PIK3CA* mutations. Co-alterations in *PIK3CA* and ARID1A (AD) occur in ~1% of all cancers. Previously, patients with co-alterations in *PIK3CA* and AD have shown both an improved objective response rate and improved progression free survival following copanlisib (cop) treatment compared to cancers with *PIK3CA* mutations and wild-type AD. Here we evaluate potential mechanisms for this enhanced clinical benefit.
Methods: AD was knocked out in SW48 and SW48$^{PIK3CA\text{-}H1047R}$ (SW48PK) human 2D colorectal cancer cell lines using CRISPR (SW48AD; SW48PKAD). Knockouts were confirmed using PCR genotyping, amplicon sequencing, and western blot (WB). A cell proliferation assay (WST-1) was performed at increasing doses of cop for 48hrs to determine cell viability. WBs were performed at 6hrs and 24hrs after cop treatment to determine levels of phosphorylation of AKT, S6, and 4EBP1 and levels of apoptosis-related proteins (MCL-1, BCL-xL, BCL-2, PARP). Athymic nude mice were flank injected with SW48PK and SW48PKAD and treated with cop (10mg/kg in PEG400/acidified water (0.1N HCl, pH 3.5; 20/80, v/v) or vehicle for 25 days or until moribund.
Results: WST-1 assay showed highest sensitivity to cop in SW48PKAD cells compared to SW48, SW48PK and SW48AD. At 10nM ($p=0.01$), there was a significant difference in cell viability between SW48PK and SW48PKAD. No significant difference was seen in the phosphorylation (p) of AKT, S6, or 4EBP1 between SW48PK and SW48PKAD. Expression of MCL-1 protein decreased in SW48PKAD compared to SW48PK. No difference was seen in levels of BCL-xL and BCL-2. On treatment with cop, there was a greater reduction in pS6 in SW48PKAD at 24 hours compared to SW48PK, but no significant difference in pAKT and p4EBP1. There was a gradual increase in MCL-1, BCL-xL, and cleaved PARP in SW48PKAD overtime following cop treatment compared to SW48PK. *In vivo,* untreated SW48PKAD tumors grew more quickly than the SW48PK tumors (8-fold increase in tumor size in SW48PKAD compared to 5-fold increase in SW48PK by day 25, $p=0.06$). SW48PKAD mice had significant tumor reduction ($p=0.002$) on cop treatment by day 25; however, SW48PK mice did not.
Conclusions: ARID1A loss along with *PIK3CA* mutation leads to greater PI3K inhibition response most likely due to enhanced induction of apoptosis. Further confirmation of this enhanced sensitivity is required with better *in vitro* models such as patient-derived cancer organoids.

#1953 Posttranslational modification in glucocorticoid receptor in treatment resistant prostate cancers.

S. Gulla[1], E. Gardner[1], S. Sundar[1], P. Jaiswal[2], N. Gao[2], L. Bennet[2], S. Conzen[2], R. Adelaiye-Ogala[1];
[1]SUNY at Buffalo, Buffalo, NY, [2]University of Texas Southwestern Medical Center, Dallas, TX

Prostate Cancer (PCa) remains the most common cancer in men in the United States and the second leading cause of cancer-related death in men. An evolving concept that contributes to our understanding of resistance to androgen deprivation therapy (ADT) and AR antagonists in advanced PCa is the ability of cells to turn on compensatory hormone receptor signaling for survival. Preclinical and clinical studies demonstrate that induction of glucocorticoid receptor (GR) expression confers resistance to AR-targeted therapy. Previous studies from our lab demonstrated that the inhibition of AKT signaling blocks pro-oncogenic GR activity and overcomes resistance to AR-targeted therapy. AKT1 is predicted to phosphorylate GR at s134, however, the implications of pGR(s134) in advanced PCa remains unclear. Although ligands (e.g., Dex) activates GR, we have found GR activation modulated by post-translational modification (PTM) and persistent in treatment resistant PCa. Therefore, we hypothesize pro-oncogenic GR activation through AKT1-induced PTM. The rationale is that by inhibiting AKT signaling, we block residual GR signaling that can potentially drive lethal prostate cancers and consequently be re-sensitized to the standard of care. We validated our findings by Western blot analysis, we used an AKT1-specific inhibitor (AKT1i) and observed decreased AKT1 activity and decreased pGR(s134) without affecting total GR protein expression. Functional studies using shRNA against AKT1 showed reduced pGR(s134) expression without affecting the total GR expression Our preliminary data suggests that pro-oncogenic GR activity is modulated through the phosphorylation of GR on s134 by AKT1.

#1954 Development of highly potent, covalent, and selective inhibitors to target PI3Kα in cancer.

L. Raguz, T. A. Constantin, L. Bissegger, E. Keleş, C. Orbegozo, T. Schafer, R. Sriramaratnam, C. Borsari, M. P. Wymann;
University of Basel, Basel, Switzerland

Aberrant PI3K signaling is linked to various forms of cancer and proliferative disease. Approved clinical therapies targeting overactive PI3K are scarce and often accompanied by severe adverse effects due to lack of PI3K isoform selectivity. We recently reported a proprietary covalent proximity scanning (CoPS) approach to selectively target distant cysteines outside of the ATP-binding pocket in kinases. Using CoPS, we developed isoform specific, irreversible covalent PI3Kα inhibitors (cPI3Kαi) with outstanding target engagement profiles. Here, we report structure-guided scaffold and linker-optimizations resulting in cPI3Kαi with long-term and rapid inhibition of PI3Kα. Cellular activity was improved exploiting additional protein-inhibitor interactions inspired by X-ray crystallographic data, and introduction of structural elements to increase cell permeability. The cPI3Kαi series showed enhanced cellular potency and excellent on-target engagement. Kinetic parameters and covalent bond formation were determined using TR-FRET, nanoBRET tracer displacement assays, and LCMS/MS based proteomics. With our new cPI3Kαi, IC_{50}s of PKB/Akt phosphorylation, pPKB/Akt recovery after drug washout, and growth inhibition experiments were performed in cancer cell lines harboring activating PIK3CA or inactivating PTEN mutations. Efficient and long-lasting inhibition of PKB/Akt phosphorylation was observed in PIK3CA mutant cell lines, while loss of PTEN was associated with partial responses, consistent with contributions of other class I PI3K isoforms to signal reactivation. A dynamic FOXO cytosolic/nuclear translocation assay was used to monitor distal PI3K signaling: cPI3Kαi blunted PI3K signaling rapidly with rates identical to the reversible BYL719/alpelisib. After drug washout, inhibition by BYL719/alpelisib was relieved within minutes, while a complete and prolonged shutdown of downstream signaling events was observed in PIK3CA mutant cell lines but not in cell lines where PTEN function was lost. This relapse in downstream signaling explains the lack of efficacy of PI3Kα selective inhibitors in models with PTEN loss and demonstrates that persistent inhibition across the PI3K pathway is required for efficacy. In summary, the new cPI3Kαi display outstanding specificity and cellular activity in PIK3CA-mutated cancer cells, and support the further development of cPI3Kαi as future clinical candidates and an alternative to established reversible inhibitors.

#1955 Novel long-acting covalent PI3Kα inhibitors boost potential action in cancer.

T. A. Constantin[1], L. Bissegger[1], E. Keleş[1], L. Raguz[1], C. Orbegozo[1], T. Schaefer[1], I. Barlow-Busch[2], J. E. Burke[3], C. Borsari[1], M. P. Wymann[1];
[1]University of Basel, Basel, Switzerland, [2]University of Victoria, Victoria, BC, Canada, [3]University of Victoria, Vancouver, BC, Canada

Phosphoinositide 3-kinase (PI3K) is a key regulator of cell proliferation, survival, and metabolism. Hotspot mutations in the *PIK3CA* gene constitutively activate the catalytic subunit of the PI3Kα isoform and are found in 10-30% of solid tumors. The development of PI3K pathway inhibitors has been hampered by poor drug tolerance and release of negative feedback loops, leading to rapid reactivation of signaling in response to reversible inhibitors. To remedy these challenges, we developed highly selective covalent PI3Kα inhibitors that irreversibly bind to a non-conserved cysteine (C862) located 11 Å outside the ATP-binding site. Here we present the properties of an optimized drug-like covalent lead, dubbed compound 9, and describe the generation of a biotinylated probe developed to be used in conjunction with compound 9 to monitor PI3Kα target occupancy in relation to downstream PI3K signaling outputs. Biochemical investigations of compound 9 using TR-FRET assays showed high affinity binding (K_i), high reaction rates (k_{inact}) for covalent bond formation with PI3Kα, and negligible off-target reactivity. Cellular NanoBRET assays revealed that compound 9 diffuses three times more rapidly into cells as compared to BYL719 (alpelisib), and leads to rapid and potent on-target engagement. Covalent bond formation to residue C862 of PI3Kα was further confirmed by X-ray crystallography. In *PIK3CA* mutant cancer cell lines, covalent binding of PI3Kα occurred at low nanomolar concentrations and led to persistent inhibition of Akt/PKB phosphorylation for more than 72 hours after drug removal. Notably, investigation of PI3Kα re-synthesis after labeling with compound 9 showed a negligible reappearance in cancer cell lines, which indicates that persistent suppression of PI3Kα signaling by compound 9 results in a much longer half-life for PI3Kα than previously reported. The irreversible inactivation of PI3Kα by compound 9 provides a marked gain in growth inhibition potency (10-600-fold) in *PIK3CA* mutant cancer cell lines in comparison to clinical reversible PI3Kα inhibitors and allows for intermittent dosing without compromising efficacy. These data collectively demonstrate that compound 9 enables precise and selective targeting of PI3Kα with high potency and long-lasting efficacy in cancer models. The new class of irreversible PI3Kα inhibitors have a unique pharmacology among PI3K inhibitors characterized by strong decoupling of drug exposure from efficacy which may provide opportunities to lower treatment burden in patients.

#1956 Discovery of a novel and potent mutant-selective inhibitor of PI3Kα.

M. Gao, C. Qi, Z. Li, Q. Fan, L. Wang, F. Zhou, L. You, H. Zheng, Y. Li, L. Wu, W. Yao, P. C. C. Liu;
Synnovation Therapeutics, Inc., Wilmington, DE

Gain-of-function mutations in hotspots of PI3Kα including H1047R, E545K, and E542K are well-recognized oncogenic drivers in human cancers. Prevalence of these mutations is enriched in many human malignancies, particularly in hormone receptor-positive/human epidermal growth factor receptor 2-negative (HR+/HER2−) breast cancer. PI3Kα inhibition showed clear clinical benefit in treating HR+/HER2− breast cancer and has been approved in combination with fulvestrant. First generation PI3Kα inhibitors such as alpelisib and inavolisib, however, have limited selectivity against wild-type (WT) PI3Kα; therefore, are associated with a variety of on-target adverse effects including grade 3 hyperglycemia, skin rash, and gastrointestinal toxicities. Discovery of a highly-selective inhibitor of mutant PI3Kα could enable deeper target coverage while reducing undesired effects of inhibiting WT PI3Kα. SNV-002 is a novel, proprietary, and mutant-selective inhibitor of PI3Kα. In cellular assays, SNV-002 inhibited Ser473 phosphorylation of AKT (pAKT) with single digit nanomolar potency in PI3Kα H1047R-mutant T47D cells and displayed greater than 50-fold selectivity over SKBR3 WT control. Similar inhibition of pAKT was also observed in other cell lines carrying PI3Kα hotspot mutations, such as CAL33, NCI-H1048, EFM19, and HCC1954. SNV-002 maintained selectivity in helical domain E545K-mutant cell lines including MCF7 and MDA-MB-361. This selectivity was further confirmed using MCF10A isogenic cell lines carrying either WT or mutant PI3Kα (H1047R and E545K). In cellular assays to assess inhibition of other isoforms of PI3K (PI3Kβ, PI3Kγ, and PI3Kδ), the IC50 of SNV-002 was over 10,000 nM. Similarly, a broad kinome screen showed no inhibition of activity of 371 kinases. Compared with alpelisib, SNV-002 showed improved potency and prolonged residence time in T47D breast cancer cells. Importantly, assays using H1047R-mutant cells in the presence of human whole blood showed SNV-002 potency to be less than 100 nM, which was over 10-fold more potent than that of alpelisib. Treatment of breast cancer cells with SNV-002 suppressed PI3K-AKT-mTOR pathway, as evidenced by reduced levels of phospho-S6 ribosomal protein and associated with loss of cell viability in mutant lines. The pharmacokinetic profile of SNV-002 was excellent across multiple species. Oral administration of HCC1954 tumor-bearing mice with SNV-002 resulted in dose-proportional exposure and >90% pharmacodynamic inhibition of pAKT in the tumor with doses of 10 mg/kg, and no sign of glucose dysregulation in contrast to alpelisib. Together, these data show that SNV-002 is a highly-selective and potent inhibitor of mutant PI3Kα with good drug-like properties that support further development of SNV-002 for treatment of cancers driven by oncogenic PI3Kα mutations.

#1957 OPM-116, a highly potent and specific PI3Kγ inhibitor to enhance antitumor immunity.

K. Shoji, P. Blom, M. E. Riveiro, J. Hoflack;
Oncodesign Precision Medicine, Dijon, France

Tumor-associated macrophages are an integral part of the tumor microenvironment. They play a crucial role in cancer initiation and progression by orchestrating tumor proliferation, angiogenesis, extracellular matrix remodeling, metastasis, immunosuppression, and resistance to checkpoint blockade immunotherapy and chemotherapy (Gao J, 2022). On the other hand, when properly stimulated, macrophages can effectively interact with the innate and adaptive immune systems arms, promoting cancer cell phagocytosis and tumor destruction by T cell-mediated cytotoxicity (Mantovani A, 2022). PI3Kγ has a unique pattern of expression and biological function, and it has been investigated for a long time as a therapeutic target for different disorders, including cancer. Inhibition of PI3Kγ reprograms M2 macrophages into M1 cells in the tumor microenvironment which translates into the expansion of activated T cells by relieving macrophage suppression. Recent clinical data indicates the compelling role of PI3Kγ in combination with PDL1 in anti-tumor activity, irrespective of PDL1 status (Hamilton E, 2021). PI3Kγ selectivity has been difficult to achieve due to the high sequence homology across the class 1 PI3K isoforms (Drew SL, 2020). Macrocyclization of small molecules with a linear structure strongly reduces their conformational flexibility and alters a variety of their physicochemical and biological characteristics. The unexpected selectivity these compounds can exhibit, even amongst closely similar target molecules, is explained by the conformationally limited structure (Ma J, 2022). Here, we describe the discovery of a potent and selective, ATP-competitive inhibitor of PI3Kγ. OPM-116, macrocyclic compound display >300-fold selectivity for PI3Kγ over the other class I isoforms. Its selectivity in biochemical and cellular assays as well as in human PBMC assays is presented. In vitro, OPM-116 can inhibit the IL-4-induced polarization of M2 macrophages. Pharmacodynamic analysis performed in animals that received oral compound administration confirmed the absolute selectivity and good PK profiles of the drug. OPM-116 is a highly selective, PI3Kγ inhibitor that displays high potency and specificity and represents a promising step toward the identification of a clinical candidate.

Drew S.L., et al. Discovery of potent and selective PI3Kγ inhibitors. J. Med. Chem. 2020. Ma J., et al. Development of small macrocyclic kinase inhibitors. Futur. Med. Chem. 2022. Gao J., et al. Shaping polarization of tumor-associated macrophages in cancer immunotherapy. Front. Immunol. 2022. Mantovani A, et al. Macrophages as tools and targets in cancer therapy. Nat Rev Drug Discovery. 2022. Hamilton E, et al. Mario-3 phase II study safety run-in evaluating a novel triplet combination of eganelisib, atezolizumab, and nab-paclitaxel as first-line therapy for locally advanced or metastatic TNBC. AACR, Cancer Res 2021.

#1958 EGFR and mTOR signaling facilitate RET-independent resistance to selective RET-TKIs.

T. Takehara[1], M. B. Nilsson[1], X. Liu[1], H. Udagawa[2], N. Morikawa[3], A. Poteete[1], J. He[1], X. Yu[1], T. Arumugam[1], K. Goto[2], J. V. Heymach[1];
[1]The University of Texas MD Anderson Cancer Center, Houston, TX, [2]National Cancer Center Hospital East, Kashiwa, Japan, [3]Tohoku Rosai Hospital, Sendai, Japan

RET fusions are an oncogenic driver mutation occurring in 1-2% non-small cell lung cancer (NSCLC). Currently, RET-selective tyrosine kinase inhibitors (TKIs) selpercatinib and pralsetinib are approved for this patient population, demonstrating favorable antitumor activity and safety profiles in advanced RET fusion-positive NSCLC. However, tumors eventually become refractory to selective RET inhibitor monotherapy. We sought to identify signaling pathways which mediate RET-independent acquired resistance to RET inhibitors and effective therapeutic combinations to overcome resistance. Using LC-2/ad (CCDC6-RET) NSCLC cells, we assessed the expression and activation of critical signaling pathways at a proteomic level following RET knockdown using reverse-phase protein array. RET knockdown resulted in rapidly increased adaptive upregulation of EGFR, HER2, MET, mTOR and MEK pathway signaling; observations were confirmed by Western Blotting. To determine whether EGFR or MET signaling facilitate RET inhibitor resistance, LC-2/ad and NCCE-TH1101 (KIF5B-RET) NSCLC cells were treated with increasing concentrations of selpercatinib or pralsetinib with or without ligands for these receptors, EGF or HGF respectively, and after five days cell viability was measured by CellTiter Glo. EGFR and MET signaling promoted RET TKI resistance in both cell lines. Next, to evaluate whether blockade of EGFR or MET signaling could enhance the activity of RET inhibitors, we treated LC-2/ad and NCCE-TH1101 cells with RET TKIs alone or in combination with the EGFR TKI erlotinib or poziotinib, or the MET inhibitor SU11274. We observed an additive effect with EGFR but not MET inhibitors when combined with RET TKIs. Western blot analysis revealed that EGFR signaling could reactivate mTOR and MAPK signaling after RET TKI treatment. Therefore, we next tested whether inhibition of these downstream pathways might enhance RET TKI sensitivity. We observed that treatment of LC-2/ad and NCCE-TH1101 cells with an mTOR inhibitor (everolimus) or a MEK inhibitor (trametinib) in combination with RET TKIs increased the anti-tumor activity or RET inhibitors. Finally, we established cells with acquired resistance to selpercatinib and pralsetinib. RET TKI resistant cells did not harbor secondary RET fusion mutations but underwent epithelial to mesenchymal transition and exhibited pan-RET inhibitor resistance. Moreover, RET TKI resistant cells showed increased cell surface expression of EGFR and MET by flow cytometry. RET TKI resistant cells were sensitive to mTOR or MEK inhibitors in combination with RET TKIs. Collectively, our findings indicate that in RET-fusion positive NSCLC tumor cells, activation of bypass pathways including the EGFR, MAPK, mTOR pathways may facilitate RET inhibitor resistance and that blockade of bypass pathways may enhance the efficacy of selective RET inhibitors and overcome acquired RET TKI resistance.

#1959 BLU-222, a potent and highly selective CDK2 inhibitor, demonstrates antitumor activity as monotherapy and as combination treatment in *CCNE1*-aberrant endometrial cancer models.

N. House, V. Brown, L. Yuan, M. Chen, S. Lee, R. Wu, L. Muthuswamy, S. Ribich, P. Ramsden, K. Faia;
Blueprint Medicines Corporation, Cambridge, MA

Background: Many cyclin-dependent kinases (CDK) bind regulatory cyclins to control cell cycle progression. Aberrant CDK2 activation occurs in selected cancers (*e.g.*, ovarian cancer, endometrial cancer) through *CCNE1* amplification, leading to Rb phosphorylation, inactivation, and cell cycle checkpoint dysregulation. *CCNE1* amplification and subsequent cyclin E overexpression are associated with chemotherapy resistance and shorter progression-free and overall survival. Therefore, novel therapies are needed to inhibit aberrant CDK2 activation and elicit positive clinical benefit in these patients. BLU-222 is a potent, highly selective, orally bioavailable, investigational CDK2 inhibitor with demonstrated activity in preclinical *CCNE1*-amplified ovarian cancer models. Here, we explored additional, specific biomarkers to predict BLU-222 sensitivity in ovarian and endometrial cancer as monotherapy or in novel combination treatment strategies.

Methods: *In vitro* antiproliferative effect of BLU-222 was assessed by CyQuant in a panel of *CCNE1*-aberrant or *CCNE1*-normal ovarian and endometrial cell lines. Combination of BLU-222 and paclitaxel was evaluated by dosing matrix; synergy was calculated using SynergyFinder. *In vivo* antitumor activity of BLU-222 as a single agent or combined with paclitaxel was measured in *CCNE1*-aberrant endometrial cancer patient-derived xenograft (PDX) models (XenoSTART).

Results: In ovarian and endometrial cell lines, *CCNE1* amplification (copy number ≥ 6) predicted strong antiproliferative response to BLU-222. Using multivariate biomarker analysis, high p16 protein expression and wild-type Rb protein were identified as additional predictive markers for response to BLU-222 in *CCNE1*-aberrant cell lines. BLU-222 with paclitaxel was broadly active in endometrial cancer cell lines, with the strongest combination effect in cells with high *CCNE1* expression, wild-type Rb protein, and low p16 protein expression. *In vivo*, BLU-222 elicited strong monotherapy antitumor response in *CCNE1* copy number-aberrant endometrial cancer PDX models, and this effect was strengthened with the combination of paclitaxel.

Conclusions: In preclinical models of *CCNE1*-aberrant endometrial cancer, BLU-222 demonstrated enhanced activity in combination with paclitaxel. Furthermore, Rb and p16 protein expression can be used in conjunction with *CCNE1* copy number to predict response to both BLU-222 monotherapy and combination treatment. These data provide a rationale for using BLU-222 in combination with paclitaxel and demonstrate the potential benefit of using specific biomarkers to predict response.

#1960 CFON-026 is a potent non-covalent BTK inhibitor suitable for combination therapy with covalent BTK inhibitors for early eradication of resistance mutations.

J. de Man, M. Muller, J. Uitdehaag, F. van Cauter, S. van Gemert, M. Hoffmann, Y. van Mil, W. Mulder, M. Prinsen, J. Sterrenburg, D. Vu, J. de Wit, E. Ensing, R. Buijsman;
Crossfire Oncology B.V., Oss, Netherlands

Bruton's Tyrosine Kinase (BTK) inhibitor drugs are a mainstay in the treatment of CLL, WM and MCL. They are not curative because of the emergence of BTK inhibitor resistance mutations in as much as 67% of relapsed patients (in CLL) [1]. Frequently observed mutations include BTK^{C481S}, which abrogates covalent binding of irreversible drugs such as acalabrutinib, ibrutinib and zanubrutinib, and BTK^{T474I} and BTK^{V416L} which both abrogate binding of the non-covalent inhibitor drug pirtobrutinib [1, 2]. To combat resistance, third generation BTK inhibitors are needed, which must 1. bind to unique regions in the tumor driving kinases that are not marred by resistance mutations, 2. have sufficient potency for sustained inhibition of BTK signaling, and 3. be sufficiently selective to afford efficacious doses and suitable for a combination regimen. We have developed a platform called Energetically Privileged Ligands (EPriLs), based on a macrocycle scaffold that binds non-covalently in the kinase ATP pocket. Their unique binding mode involves connecting the N-terminal and C-terminal lobes of the general kinase fold in a continuous β-sheet, in this way avoiding hotspots for kinase inhibitor resistance mutations. The potent binding of the macrocycle ensures a very long residence time. Using the EPriL platform, we have developed CFON-026, a next generation non-covalent BTK inhibitor with a covalent-like residence time as demonstrated by surface plasmon resonance (SPR) and cellular washout experiments. The biochemical binding K_D to BTK^{WT}, determined by SPR, is 0.14 nM. CFON-026 binds mutants with K_Ds of 0.4 nM (BTK^{C481S}) and and 1.8 nM (BTK^{T474I}). X-ray crystal structures of CFON-026 bound to BTK^{WT} and BTK^{T474I} confirm the unique binding mode and water network around the active site. CFON-026 inhibits the growth of the BTK dependent cell lines TMD8 and Rec-1 with IC_{50}s of 0.45 nM and 1.7 nM, respectively. CFON-026 is very active on TMD8 variants containing endogenous BTK inhibitor resistance mutations (BTK^{C481S}, BTK^{V416L}, BTK^{T474I} and BTK^{L528W}, IC_{50} range 1-100 nM). CFON-026 has favorable metabolic stability, pharmacokinetic properties, and safety characteristics, and induces complete tumor regression in a TMD8 xenograft model. Since BTK resistance mutations can be detected diagnostically 12-18 months before clinical relapse, CFON-026 could be applied as combination partner to prolong progression free survival on first line BTK inhibitor therapy. Experiments with mixed populations of BTK mutant cell lines, to model a heterogenous tumor, show that CFON-026 can deepen the efficacy of ibrutinib, acalabrutinib and zanubrutinib. In conclusion, CFON-026 is a novel EPriL-based non-covalent BTK inhibitor that could enhance and prolong responses of existing covalent BTK inhibitor therapy. [1] Woyach *et al.*, J Clin Oncol (2017). [2] Wang *et al.*, N. Eng J Med (2022).

#1961 Discovery of a highly potent and brain penetrant fourth generation EGFR tyrosine kinase inhibitor.

s. kumar, j. wang, w. li, w. pan, z. wen, K.-L. yu, G. Zhao, t. yin;
Acerand Therapeutics US, Carmel, IN

Third generation EGFR tyrosine kinase inhibitors (TKIs) such as Osimertinib have emerged as first-line standard of care therapy to treat non-small cell lung cancer (NSCLC) patients with activating EGFR mutations (del19, L858R or T790M). However, within 12 to 18 months following treatment, 15-20% of the patients develop C797S mutation, which drives resistance to these drugs; with the progression of disease brain metastasis is observed in 40-70% of the EGFRm+ NSCLC patients. Here, we report a highly potent and brain penetrant fourth generation EGFR-TKI ACE-34237307, designed to overcome C797S mutation (del19/C797S and L858R/C797S), and common single point mutations (del19 and L858R). ACE-34237307 is also designed to potently inhibit the more prevalent non-canonical EGFR mutations such as G719S and L861Q. ACE-34237307 showed robust anti-proliferative activity against EGFR double mutations in Ba/F3 (EGFR-del19/C797S and EGFR-L858R/C797S) cell lines with IC_{50} values of 0.1 and 0.23 nM, respectively. In phospho-EGFR assay, ACE-34237307 demonstrates over 79-fold selectivity against A431 (EGFR-WT) cell line when compared to PC-9 (EGFR-del 19) cell line. ACE-34237307 is highly brain penetrant with B/P ratio of 2.3 in rat and 1.2 in mouse. It has an excellent pharmacokinetic profile in rat, mouse and dog with good bioavailability, a flat PK curve and reduced C_{max}, which will translate to a better safety profile. The *in vivo* anti-tumor efficacy was evaluated in Osimertinib resistant double mutant Ba/F3-EGFR-del19/C797S and L858R/C797S as well as del19 and L858R single mutant xenograft models. It has been shown that ACE-34237307 at doses of ≥ 0.6 mg/kg induces complete tumor regression or eradication in all tumor models tested. In brain tumor models with Ba/F3 (EGFR-del19/C797S) and PC-9 (EGFR-del19), ACE-34237307 showed complete inhibition or eradication of brain tumors and drastically extended animal survival at ≥ 0.6 mg/kg. In summary, ACE-34237307 is a potent fourth generation EGFR-TKI with high WT selectivity, excellent brain penetration, highly favorable DMPK profile, outstanding *in vivo* efficacy in subcutaneous and brain tumor models and low projected human dose amenable to QD dosing.

#1962 PH009-1, a highly potent, selective and brain-penetrable fourth-generation EGFR-TKI that overcome classic and resistant EGFR mutations in NSCLC.

F. Gao[1], J. Wang[1], B. Liu[1], Y. Wu[2], L. Jing[2], P. Zhang[1], Y. Gao[1], Z. Li[3], Y. Guo[1];
[1]Puhe Biopharma, Beijing, China, [2]Gongkang Bio, Suzhou, China, [3]Shiyu Children Foundation, Beijing, China

Background: Epidermal growth factor receptor (EGFR) inhibitors, especially 3rd Gen inhibitor such as osimertinib (Osi), have become the first line therapy for non-small cell lung cancer (NSCLC) patients with EGFR activating mutations. However, treatments with 3rd Gen EGFR inhibitors lead to occurrence of acquired C797S mutation in 10-24% of patients. Though studies showed that double mutations 19Del/C797S (DC) and L858R/C797S (LC) could be inhibited by 1st Gen EGFR TKIs, appearance of triple mutations 19Del/T790M/C797S (DTC) and L858R/T790M/C797S (LTC) always leads to treatment failure. In recent years, 4th Gen EGFR inhibitors have been developed such as BLU-945 and PH009-1. PH009-1 had been reported on AACR annual meeting 2023.
Methods: Cell activity and selectivity were determined in engineered Ba/F3 cell lines carrying EGFR wild type (WT, stimulated with EGF), 19Del (D), L858R (L), 19Del/T790M (DT), L858R/T790M (LT), DC, LC, DTC and LTC. The *in vivo* anti-tumor efficacy and PK-PD studies were performed in cell or patient derived xenograft (CDX or PDX) cancer models (HCC827, D; Ba/F3, LC; PDX, DTC). Brain penetration capability was tested in mice orally treated with PH009-1 for 7 days. Systemic safety of PH009-1 was evaluated in 28-day repeated dosing toxicity studies in rats and dogs following GLP guidelines.
Results: PH009-1 displayed potent anti-proliferation activity against Ba/F3 cells harboring EGFR mutations (L, D, LC, DC, LT, DT, LTC, DTC) with IC_{50} of 2.4, 1.3, 5.2, 1.2, 1.1, 1.5, 2.8, 1.9 nM, respectively, but had very weak effect on EGFR WT Ba/F3 cells (IC_{50}, 1135 nM), suggesting excellent potency and selectivity. In contrast, though BLU-945 potently inhibited DT, LT, DTC, LTC with IC_{50} less than 5 nM, but its activities on L, D, LC, DC were not strong with IC_{50} of 31.6, 81.2, 46.2, and 52.0 nM. In *in vivo* efficacy studies, PH009-1 at a dose of 20 mg/kg BID led to potent inhibition on tumor growth and EGFR phosphorylation, and tumor regression was observed at higher doses in all tested models. In HCC827 model with 19Del (first line therapy setting), mice were treated for more than 200 days, and one tumor relapsed in BLU-945 group but not in PH009-1 or Osi group. Also, deaths were observed in Osi group, but not with PH009-1. After treated mice with PH009-1 at efficacious dose for 7 days, concentrations in cerebrospinal fluids (CSF) at 0-8 h post final dose were more than enough (≥1.5 fold) to cover IC80 on all tested mutations. In GLP toxicity studies, no unexpected toxicity was observed. In dogs. the highest tested dose was determined as highest non-severely toxic dose (HNSTD) and based on high plasma exposure, wide safety margin was confirmed with PH009-1.
Conclusion: Our data suggested that PH009-1 overcome T790M/C797S resistant mutations, and also have potential to become a potent and safe approach for first line therapy of NSCLC with EGFR mutations.

#1963 BB102, a highly selective and potent reversible-covalent FGFR4 inhibitor effective in multiple xenograft tumor models.

Q. Wang, G. Duan, W. Hua, X. Wei, M. Li, J. Wang, X. Zhang;
BroadenBio Co., Ltd., Beijing, China

Introduction: Fibroblast growth factor receptor 4 (FGFR4) belongs to the FGFR family which interact with fibroblast growth factors (FGFs) to regulate cell proliferation, differentiation and apoptosis. Due to unique structural domain, FGFR4 is specifically bound by FGF19 with high affinity in the presence of co-receptor β-Klotho. Hyperactivated FGF19/FGFR4 signaling, induced by FGF19/FGFR4 overexpression and FGFR4 mutation, was reported to be associated with the growth, metastasis and invasion of various cancer. Thus, FGFR4 is considered as a novel target to treat cancer with hyperactivated FGF19/FGFR4 signaling. Here we report BB102 as a highly selective and potent reversible-covalent FGFR4 inhibitor.

Methods: BB102 was developed through structure-based drug design, and optimized by SAR analysis and medicinal chemistry iteration. Biochemical and cell assays were applied in evaluation of BB102 inhibitory activity. Preclinical studies including pharmacokinetic (PK) and toxicity were performed in rats and dogs. Xenograft tumor models in mice were conducted to demonstrate the *in vivo* efficacy of BB102.

Results: As a reversible-covalent FGFR4 inhibitor, about half compound of BB102 dissociated from FGFR4 kinase within 24 h, which was conducive to overcome the fast re-synthesis rate of FGFR4 (< 2 h) in hepatocellular carcinoma cells. BB102 only inhibited kinase activity of $FGFR4^{WT}$, $FGFR4^{N535K}$ and $FGFR4^{V550L}$ at nanomolar levels in 207 kinase panel screening. BB102 completely blocked the phosphorylation of the downstream protein ERK at 16.7 nM. BB102 exhibited strong inhibitory effects on the cell proliferation *in vitro* and tumor growth in mouse models inoculated with the high expression of both FGF19 and FGFR4, or FGFR4 mutated tumor cells. PK profile of BB102 showed good oral bioavailability (F>70%) with a nearly linear dose-dependent exposure. The compound had no effects on the respiratory and central nervous systems in rats, cardiovascular system in Beagle dogs or hERG liability *in vitro*. In comprehensive safety evaluation, the Severely Toxic Dose in 10% (STD_{10}) in rats was 300 mg/kg/day and the Highest Non-Severely Toxic Dose (HNSTD) in dogs were 100 mg/kg/day.

Conclusion: BB102 is a highly selective and potent reversible-covalent FGFR4 inhibitor with promising efficacy in high expression of both FGF19 and FGFR4, and/or FGFR4 mutated tumor models and good safety in preclinical studies. The phase I study of BB102 is in progress.

#1964 Furmonertinib is a brain-penetrant EGFR TKI highly active in uncommon EGFR mutations, including PACC and exon 20 insertions.

Monique B. Nilsson[1], Zineb Mounir[2], Luna Musib[2], Junqin He[1], Xiaoxing Yu[1], Qing Li[3], Huibing Luo[3], John V. Heymach[1], Jerry Y. Hsu[2], Stuart Lutzker[2], **Xiuning Le**[1], Marcin Kowanetz[2]

[1]The University of Texas MD Anderson Cancer Center, Houston, TX,[2]ArriVent Biopharma, Inc., Burlingame, CA,[3]Allist Pharmaceuticals Co., Ltd., Shanghai, China

Background: Furmonertinib (AST2818, furmo) is an oral, highly brain-penetrant, and broadly active mutation-selective EGFR inhibitor against both classical and uncommon EGFR mutations (mts). Furmo has demonstrated promising interim efficacy and safety in non-small cell lung cancer (NSCLC) patients (pts) with EGFR exon 20 insertion (ex20ins) mts (Han et al., 2023). Furmo is currently being studied in a global Phase 3 trial for 1st line pts with ex20ins in NSCLC (FURVENT; NCT05607550) and has received FDA Breakthrough Designation in this pt population. P-loop and αC-helix Compressing (PACC) mts represent another subset of uncommon EGFR mts (Robichaux et al., 2021) that are similar to ex20ins in narrowing the drug binding pocket; include e.g. G719X, S768I, E709X, L747X, V774M; and are found as single or compound EGFR mts. Treatment options for pts with PACC mts remain limited. In this study, we further characterized PACC mts as cancer drivers in NSCLC and evaluated the pre-clinical activity and binding mechanisms of furmo in PACC and ex20ins mts.
Methods: AACR Project GENIE and TEMPUS databases were used for mutation analysis. In vitro potency was determined in Ba/F3 cell lines for 33 PACC and 16 ex20ins mts. In vivo efficacy was conducted in pt-derived xenografts (PDXs). Molecular modeling was performed using MOE software.
Results: PACC prevalence was 2.4% vs. 1.6% for ex20ins and 14% for classical EGFR mts in all NSCLC, corresponding to 10.4% PACC and 7% ex20ins of all EGFR mts. Co-mutation analysis revealed that other oncogenes, such as p53, co-occurred alongside PACC to a similar rate as with ex20ins and classical EGFR mts which further supports the role of PACC mts as a similar cancer driver as other EGFR mts in NSCLC. Ba/F3 cell lines harboring PACC mts were highly sensitive to furmo which showed overall superior potency vs. osimertinib and similar activity to afatinib. When comparing the mutant/wild-type IC50 ratio, furmo showed promising and high activity against single (e.g. G719X) and compound (e.g. ex19del+L718V) PACC mts. IC50 values were similar for PACC as compared to ex20ins mts. Therefore, furmo is predicted to be broadly active across both PACC and ex20ins mutant pt populations at clinically achievable drug levels. Molecular modelling revealed that furmo's interaction with ex20ins and PACC mts is stabilized through hydrogen bonds with specific sites and its proximity to hydrophobic residues including L792 and P794 in the drug binding pocket. To further characterize furmo sensitivity in vivo against PACC mts, studies in PDXs are ongoing to evaluate efficacy, pharmacokinetics and pharmacodynamics and will be presented.
Conclusions: PACC mts are important and prevalent cancer drivers in NSCLC and furmo is similarly active preclinically against both PACC and ex20ins mts. The activity of furmo in EGFR PACC mutant NSCLC is currently being evaluated in a global study FURTHER (NCT05364073).

#1965 3HP-2827-high selective inhibitor of FGFR2, a best-in-class therapy for FGFR2-driven solid tumors.

S. S. Liu-Chen, J. Lin, J. Hu, Y. Liu, W. Zhang, Z. Zhang, Y. Ding, J. Liu, K. Chen, S. Hu;
3H Pharmaceuticals Co., Limited, Shanghai, China

FDA-approved pan-FGFR inhibitors bring encouraging results in solid tumors. However, resistance mechanisms and side effect profiles may limit their clinical utility. We designed 3HP-2827, a highly selective and potent small molecule inhibitor of FGFR2, to treat solid tumors harboring FGFR2 alterations, including amplifications, mutations, and fusions to overcome these limitations. 3HP-2827 inhibits FGFR2 enzyme activity with more than 1623-fold selectivity over FGFR1 and FGFR3. 3HP-2827 inhibits cell proliferation with IC50 <10 nM and 30 nM in FGFR2 amplified and FGFR2-mutant cancer cell lines, respectively. 3HP-2827 demonstrates high kinome selectivity for FGFR2 against a panel of 485 human kinases, resulting in 90.1% inhibition of FGFR2, and no other kinases showed greater than 75% inhibition. 3HP-2827 leads only modest activity at 10 μM against PDE4D2 and LCK in 44 distinct common adverse drug reaction targets, supporting its high degree of safety. 3HP-2827 also demonstrates a dose-dependent inhibition of phosphorylation of FGFR2 and FGFR2 signaling pathway nodes, including ERK and AKT, in the FGFR2-dependent cancer cell line. In vivo, 3HP-2827 demonstrates potent antitumor activity in cell- and patient-derived xenograft mouse models, including FGFR2-amplified gastric cancer, FGFR2-mutant (N549K) endometrial cancer, FGFR2 fusion ICC and gastric cancers. Strikingly, 3HP-2827 demonstrates superior activity in patient-derived ICC and gastric cancer, cell-derived endometrial cancer (CDX) in tumor and pFGFR2 inhibitions. In the ICC PDX model, 3HP-2827 also induces the regression of pemigatinib-resistant tumors. 3HP-2827 is well tolerated in the toxicology studies, and no hyperphosphatemia or tissue mineralization is observed at 150 mg/kg/kg/day in rats and 120 mg/kg/day in dogs. The data support that 3HP-2827, a potential to be a best-in-class selective FGFR2 inhibitor, will be studying clinically at the beginning of 2024.

#1966 The FLT3 tyrosine kinase receptor ITD mutation controls its expression and drug resistance in acute myeloid leukemia.

T. Alqahtani[1], D. MacEwan[2];

[1]King Khalid University, Abha, Saudi Arabia, [2]University of Liverpool, Liverpool, United Kingdom

In approximately 23% of AML patients, Fms-like tyrosine kinase 3 (FLT3) contains a gain-of-function, internal tandem duplication (ITD) mutation that is associated with an unfavourable prognosis. FLT3 is therefore seen as a promising therapeutic avenue for AML and as a result, a more complete understanding of its function and signalling may lead to additional targets and resistance mechanisms being identified. To date, several FLT3 inhibitors including Quizartinib (AC220), a second-generation ITD-selective tyrosine kinase inhibitor, have been developed, but single-agent clinical trials have not been overwhelmingly successful. In most preclinical studies, the inhibitory effects of FLT3 inhibitors are mainly evaluated using mutant-expressing models, however, most AML patients harbour both a wild-type and mutant FLT3 allele as well as presenting with high plasma levels of FLT3 ligand (FLT3L). We hypothesized that FLT3L could act through WT-FLT3 to influence the efficacy of FLT3 inhibitors in cells with heterozygous mutations. In this study, we have examined the role of FLT3 inhibition and FLT3L activation on the cellular localisation and downstream signalling in several AML cell lines, some of which express ITD mutations. We also looked at mechanisms by which FLT3L could impair the efficacy of FLT3 inhibitors. Our results revealed that the majority of FLT3 in the MV4-11 and MOLM-13 cells was intracellular. Inhibition of ITD-FLT3 with quizartinib led to a dramatic relocalisation of FLT3 to the cell surface. This effect was more pronounced in MV4-11 (FLT3ITD/ITD) than the heterozygous MOLM-13 (FLT3ITD/WT) cells that also express WT. This was accompanied by inhibition of ERK, AKT and STAT5 signalling pathways and resulted in cell death. Quizartinib induced cell death only in AML lines expressing FLT3-ITD mutations (MOLM-13 and MV4-11), and this could be antagonised by FLT3 ligand (FLT3L). The largest inhibitory effects were seen in heterozygous cells expressing a mutated and wild-type allele. FLT3 inhibition was associated with downregulation of the anti-apoptotic protein Mcl1 and upregulation of the pro-apoptotic BH3-only protein, Bim. Our experiments indicated that both of these proteins were regulated by both WT and ITD-FLT3 through the MAPK pathway. These results suggest that activation of FLT3 signalling by FLT3L confers resistance to quizartinib through upregulation of Mcl-1 and suppression of Bim expression. Taken together, our data suggest that FLT3 cell surface localisation and expression are controlled by ITD mutations and are key components of drug resistance. The data also suggests a novel therapeutic approach in patients with high plasma FLT3L levels, especially when using type II inhibitors such as quizartinib, is to co-target the MAPK/ERK pathway to abrogate the FLT3Lmediated resistance in FLT3-ITD AML.

#1967 IN-119873, the next-generation allosteric EGFR TKI, a potent and highly selective EGFR L858R for the treatment of osimertinib-resistant NSCLC.

J. Choi, D. Yoon, S. Kim, D. Kim, S. Kang, S.-I. Choi, S. Park, H. Lee, D. Kim, J. Lee, H.-J. Kim, B. Kim;
HK inno.N, Icheon-si, Korea, Republic of

EGFR mutations occur in approximately 50% of Asian patients and 20% of Caucasian patients with non-small cell lung cancer (NSCLC). The EGFR L858R mutation constitutes approximately half of the EGFR-mutated patients, and despite receiving first-line or second-line treatment with the 3rd generation EGFR TKI osimertinib, they continue to exhibit a poor prognosis. According to real-world analysis, the leading resistance mechanism to osimertinib is identified as EGFR C797S mutation. Furthermore, osimertinib is still associated with gastrointestinal and skin toxicity, despite its improved selectivity for EGFR WT compared to 1st-generation EGFR TKIs. Here, we show that IN-119873 can overcome C797S-mediated acquired resistance based on the results obtained by various in vitro and in vivo NSCLC models. IN-119873 binds to an EGFR allosteric site separate from the ATP-binding site with a remarkable preference for highly mutant-selective inhibition. It effectively targets EGFR L858R activating mutations while sparing the inhibition of EGFR WT, which sets it apart from ATP competitive inhibitors. Moreover, oral administration of IN-119873 showed excellent anti-tumor efficacy in a dose-dependent manner in a diverse of osimertinib-resistant CDX and PDX models. IN-119873 also demonstrated favorable blood-brain-barrier penetration with promising intracranial efficacy in the H1975-luc brain metastasis model both mono or in combination with osimertinib. As a selective, orally available, and CNS-penetrable next-generation allosteric EGFR-TKI, IN-119873 is currently undergoing IND-enabling studies and has the potential to demonstrate activity in both first-line and resistance settings, either as a monotherapy or in combination with 3rd generation EGFR TKI.

#1968 Discovery of a highly potent and selective FGFR2 inhibitor for FGFR2-driven cancers.

W. Li, B. Liu, J. Wang, T. Yin, K.-L. Yu, S. Kumar, Z. Wen, G. Zhao, W. Pan;
Acerand Therapeutics US, Carmel, IN

Fibroblast growth factor receptor 2 (FGFR2) is a clinically validated target and frequently altered in many solid tumors. The resulting oncogenic driver alterations often drive multiple solid tumors. Therefore, targeting FGFR2 has broad therapeutic potential. Currently, only pan-FGFR inhibitors are approved for FGFR2-driven intrahepatic cholangiocarcinoma, but not for other FGFR2-driven cancers. Due to the severe on-target toxicity associated with inhibition of FGFR1 and FGFR4, the use of the pan-FGFR inhibitors has been very limited. Thus, developing a selective FGFR2 inhibitor addresses the unmet medical need as the treatment options for FGFR2-altered cancers remain limited. Here we report the discovery and characterization of a highly selective FGFR2 inhibitor, ACE-16229210. This molecule potently inhibits FGFR2 (IC_{50} = 6.2 nM) and exhibits excellent selectivity (>133-fold) over other FGFR1 and FGFR4 in biochemical assays. It also potently (IC_{50} <1 nM) and selectively (≥500-fold) inhibits FGFR2-induced ERK phosphorylation in multiple cancer cell lines harboring FGFR2 fusions, amplification, and mutations, but not those harboring FGFR1, FGFR3, or FGFR4 genetic alterations (IC_{50} > 460 nM). Furthermore, this molecule, when evaluated in a panel of 24 cell lines, demonstrates potent anti-proliferative activity against the cell lines harboring FGFR2, but not FGFR3, and especially FGFR1, or FGFR4 genetic alterations. Thus, ACE-16229210 is a potent and selective FGFR2 inhibitor. Interestingly, it exhibits the most potent activity against gatekeeper and molecular brake mutations followed by fusions, amplification, and activation loop mutations. This molecule shows a robust broad spectrum of antitumor activity with significant tumor regression at low doses (1-10 mg/kg) in several tumor xenograft and PDX models representing the major FGFR2 relevant tumor histologies including gastric, breast, ovarian, and endometrial cancers harboring clinically important FGFR2 driver alterations with a well-defined pharmacokinetic/pharmacodynamic relationship. This molecule also demonstrates strong synergistic effects when combined with irinotecan and fulvestrant in a gastric tumor model and a breast cancer PDX model harboring FGFR2 amplification, respectively. Finally, ACE-16229210 did not significantly affect serum phosphorus levels in animals at the exposure levels that are >100-fold higher than the efficacious AUC, further confirming its excellent selectivity over FGFR1. Taken together, these *in vitro* and *in vivo* studies show that ACE-16229210 is a potent and selective FGFR2 inhibitor with the potential to be developed into a more effective treatment option for multiple cancers harboring FGFR2 oncogenic driver alterations.

#1969 Off-target autophagy inhibition by SHP2 allosteric inhibitors and therapeutic implications for aberrant RAS-driven cancers.

Yiming Miao[1], Yunpeng Bai[1], Jinmin Miao[1], Allison A. Murray[1], Jianping Lin[1], Jiajun Dong[1], Zihan Qu[1], Ruo-Yu Zhang[1], Quyen Nguyen[1], Shaomeng Wang[2], Zhong-Yin Zhang[1]

[1]Purdue University, West Lafayette, IN,[2]The University of Michigan, Ann Arbor, MI

Aberrant activation of RAS-MAPK signaling is common in cancer, and efforts to inhibit pathway components have yielded drugs with promising clinical activities. Unfortunately, treatment-provoked adaptive resistance mechanisms inevitably develop, limiting their therapeutic potential. As a central node essential for receptor tyrosine kinase mediated RAS activation, SHP2 has emerged as an attractive cancer target. Consequently, many SHP2 allosteric inhibitors are now in clinical testing. Here we discovered a previously unrecognized off-target effect associated with SHP2 allosteric inhibitors. We found that these inhibitors accumulate in the lysosome and block autophagic flux in a SHP2-independent manner. We showed that off-target autophagy inhibition by SHP2 allosteric inhibitors contributes to their anti-tumor activity. We also demonstrated that SHP2 allosteric inhibitors harboring this off-target activity not only suppress oncogenic RAS signaling but also overcome drug resistance such as MAPK rebound and protective autophagy in response to RAS-MAPK pathway blockage. Finally, we exemplified a new therapeutic framework that harnesses both the on- and off-target activities of SHP2 allosteric inhibitors for improved treatment of mutant RAS driven and drug resistant malignancies such as pancreatic and colorectal cancers.

#1970 Discovery and characterization of potent and selective HER2 exon20 insertion mutant inhibitors.

H. Nam, S. Jang, J. Jeon, H. Yoo, J. Byun, G. Lee, Y. Lee, Y.-Y. Kim, S. Jeon, Y. Ahn;
Hanmi Pharmaceutical Co., Ltd., Hwaseong-si, Korea, Republic of

Non-small cell lung cancer (NSCLC) is the most common type of lung cancer, accounting for over 85% of all cases. Among NSCLC, approximately 2-4% of patients have mutations in the HER2, a member of the ErbB family of receptor tyrosine kinases and key proliferation driver, with exon 20 insertions making up about 90% of these mutations. HER2 exon mutations can have various alterations, and among them, the most common HER2 mutation is in-frame insertions in exon 20, especially the A775_G776insYVMA insertion/duplication. These mutations can affect the structure and function of the HER2 protein and may contribute to tumor development and growth. HER2 mutations have often shown resistance to EGFR tyrosine kinase inhibitors (TKIs), further highlighting the need for HER2-specific treatments. Also, inhibitors targeting HER2 mutations are selective, meaning they specifically target HER2 alterations without causing toxicities or affecting $EGFR^{WT}$. Therefore, there is a need for the development of selective HER2 exon20 insertion mutant inhibitors. Herein, Hanmi has identified selective HER2 exon20 insertion mutant small molecule inhibitors, designed based on affinity and binding mode starting from a known crystal structure using GLIDE (Schrödinger), and the screening for the viability of cell lines including $HER2^{A775\_G776insYVMA}$, $HER2^{G776delinsVC}$, $HER2^{WT}$ and $EGFR^{WT}$ was investigated. Hanmi's HER2 exon20 insertion mutant inhibitors selectively target mutant HER2 receptor tyrosine domains through shared binding, sparing $EGFR^{WT}$ and minimizing EGFR-related toxicities. With highly selectivity against $EGFR^{WT}$ and desirable pharmacokinetic properties, the Hanmi compounds inhibit HER2 mutant cells and HER2 mutant enzymes. Additionally, the compounds have an oral administration-compatible DMPK profile and demonstrated anti-tumor activity in HER2 mutant and $HER2^{WT}$ tumor xenograft mice. In conclusion, based on our study, Hanmi compounds, a novel HER2 exon20 insertion mutant inhibitors could be suggested as an appropriate therapeutic agent for inhibitory activity against HER2 exon20 insertion mutant NSCLC.

#1971 Olverembatinib, a novel multikinase inhibitor, demonstrates superior antitumor activity in succinate dehydrogenase (SDH)-deficient neoplasms.

Yan Xiong[1], Eric Liang[2], Ping Min[1], Huidan Yu[1], Bingxing Wu[1], Jing Yang[3], Guoqin Zhai[1], Dajun Yang[1], Yifan Zhai[1]

[1]Ascentage Pharma (Suzhou) Co., Ltd., Suzhou, China,[2]Ascentage Pharma Group Inc., Rockville, MD,[3]Department of Experimental Research, Sun Yat-sen University Cancer Center, State Key Laboratory of Oncology in South China Collaborative Innovation Center for Cancer Medicine, Guangzhou, China

SDH deficiency, characterized by loss of SDHB, occurs in many tumors including paraganglioma, pheochromocytoma, renal, and gastrointestinal stromal tumor (GIST). Olverembatinib, a novel multikinase inhibitor, targets a broad spectrum of kinases and has promising efficacy in SDH-deficient GIST (Qiu H et al. *J Clin Oncol*. 2023). Here, we assessed antitumor effects of olverembatinib in preclinical models of SDH-deficient cancers and explored potential mechanisms of action (MOA). Antiproliferation assays were conducted using CellTiter-Glo®. MOA analyses were performed using western blotting. *In vivo* activity was evaluated using an SDHB knock-out [KO]-derived mouse xenograft model. Olverembatinib had superior antiproliferative activity (vs other approved TKIs) in SDH-deficient cell lines (IC_{50}, 0.129-5.132 μM), including Jurkat clone E6-1 (*SDHB* mutation [mut]), OS-RC-2 (*SDHA* and *SDHB* mut), RKO (*SDHA* mut), and rat pheochromocytoma PC12 cells with SDHB KO (PC12$^{\#}$5F7) (Table 1). In PC12$^{\#}$5F7 cells, olverembatinib decreased HIF-1α, HIF-2α, VEGFA, and FGFR1 protein levels and inhibited phosphorylation of FGFR1, IGF-1R, SRC, AKT, and ERK1/2. Increased cleavage of caspase-3 and PARP-1 was observed, suggesting induction of apoptosis. In PC12$^{\#}$5F7 (SDHB KO)-derived xenograft models, olverembatinib demonstrated dose-dependent antitumor activity at 10 and 20 mg/kg (QOD), with tumor growth inhibition rates of 27.4% and 52.2%, respectively. At 20 mg/kg, olverembatinib showed superior efficacy vs ponatinib (10 mg/kg) and rogaratinib (50 mg/kg). Results from western blot analyses were similar in both tumor tissues and cell lines. Olverembatinib exerts promising antitumor effects in SDH-deficient neoplasms and can modulate multiple signal pathways involved in angiogenesis, apoptosis, proliferation, and survival. The results provide a preclinical rationale for future development of olverembatinib in SDH-deficient cancers.

Table 1. Antiproliferation activity of TKIs in SDH-deficient cell lines

	IC_{50} μM, mean ± SD				
Cell lines	**Acute lymphoblastic leukemia**	**Renal cell carcinoma**	**Colon cancer**	**Rat pheochromocytoma carcinoma**	
	Jurkat, clone E6-1	OS-RC-2	RKO	PC12	PC12$^{\#}$5F7
SDH status*	SDHB: missense_variant, p.A15T	SDHA: missense_variant, p.G184R; SDHB: stop gained, p.W218Ter	SDHA: missense_variant, p.P279S	SDHB competent	SDHB exon 2+3 KO (heterozygote) by CRISPR-Cas9
Compound					
Olverembatinib (KIT, PDGFR, SRC, VEGFR, FGFR, FLT-3, RET)	0.149 ± 0.04	0.135 ± 0.083	0.129 ± 0.136	9.600 ± 1.407(n = 4)	5.132 ± 1.950
Imatinib (KIT, PDGFR)	> 10	> 10	> 10	> 10	> 10
Ripretinib (KIT, PDGFR)	1.559 ± 0.294	8.781 ± 1.725	1.247 ± 0.933	> 10	> 10
Avapritinib (PDGFRA exon 18 mut)	> 8.071 ± 2.728	> 10 ± 0	> 10 ± 0	> 10	> 10
Ponatinib (KIT, PDGFR, VEGFR, FGFR)	2.136 ± 2.107	0.809 ± 0.443	0.274 ± 0.241	> 10	8.537 ± 3.553
Dasatinib (KIT, SRC, PDGFR, FGFR)	2.025 ± 0.644	0.029 ± 0.003	0.382 ± 0.320	> 10	> 10
Sunitinib (VEGFR)	4.289 ± 0.280	> 5.099 ± 0.207	3.789 ± 0.385	> 10	> 10
Regorafenib (VEGFR)	> 10	5.110 ± 0.588	2.145 ± 0.812	> 10	> 10
Sorafenib (VEGFR)	> 10	3.581 ± 0.255	3.875 ± 0.170	> 10	> 10
Pazopanib (VEGFR, FGFR)	> 10	> 10	> 10	> 10	> 10
Rogaratinib (FGFR)	> 10	> 10	> 10	> 10	> 10
Infigratinib (FGFR)	4.581 ± 0.342	3.166 ± 0.791	2.374 ± 2.311	> 10	> 10
Pemigatinib (FGFR)	4.642 ± 1.842	> 10	> 10	> 10	> 10

*From CrownBio database.

#1972 Preclinical activity of the type II RAF inhibitor tovorafenib in tumor models harboring either a *BRAF* fusion or a *NF1*-LOF mutation.

S. Rastogi, S. Perino, M. Lal-Nag, Y. Wang, S. C. Blackman, E. Venetsanakos;
Day One Biopharmaceuticals, Brisbane, CA

Genomic alterations and dysregulation of the MAPK pathway have been described in many different types of cancers. BRAF V600 point mutations and *BRAF* fusions, which are found in both pediatric and adult cancers, are oncogenic drivers that drive constitutive activation of the RAF pathway (Jones 2009, Yaeger 2019). Neurofibromatosis 1 (*NF1*) loss-of-function (LOF) mutations, which occur in many cancer types, result in decreased neurofibromin GAP function, thus activating RAS (Basu 1992). Tovorafenib is an investigational, selective, CNS-penetrant, small molecule type II RAF inhibitor which inhibits both RAF monomers and dimers and has been shown preclinically to impact the *KIAA1549*::*BRAF* fusion (Sun 2017). In this study, the impact of tovorafenib alone or in combination with MEK inhibitor, pimasertib, was explored in adult or pediatric tumor models harboring *BRAF* fusions or *NF1*-LOF mutations. At clinically relevant doses, tovorafenib treatment resulted in tumor regression in an *AGK*::*BRAF* fusion melanoma patient-derived xenograft (PDX) model *in vivo*. In contrast, little anti-tumor activity was observed in response to tovorafenib *in vivo* in two tumor models harboring *NF1*-LOF mutations. Ongoing PK-PD studies in both the *AGK*::*BRAF* fusion model and the *NF1*-LOF models will assess the extent and duration of target inhibition. *In vitro*, anti-proliferative activity of tovorafenib was also evaluated in *NF1*-LOF mutant tumor cell lines or PDX models of different tumor types, including melanoma, lung and malignant peripheral nerve sheath tumor (MPNST). While tovorafenib was potent in the BRAF V600E tumor cell line, little activity was observed in the *NF1*-LOF tumor cell lines. Modulation of phosphorylated-ERK (pERK) was also assessed. At very low concentrations, modest induction of pERK was observed in the *NF1*-LOF tumor cell lines, with inhibition at higher concentrations. *In vitro* combination studies were conducted using pimasertib and tovorafenib, or a tool compound. Synergy was observed in a *NF1*-LOF embryonal rhabdomyosarcoma PDX model *ex vivo* and a *NF1*-LOF MPNST cell line *in vitro*, suggesting that vertical pathway inhibition is impactful in the *NF1*-LOF mutant setting. Tovorafenib is currently being evaluated as a monotherapy in relapsed or progressive pediatric low-grade glioma (pLGG) harboring *RAF* alterations (NCT04775485) and in combination with pimasertib in patients ≥12 years of age with recurrent, progressive, or refractory solid tumors harboring MAPK pathway alterations (NCT04985604). Ongoing preclinical translational work will continue to explore potential biomarker-defined tumor indications for these agents.

#1973 Discovery of the first-in-class SHP1 covalent inhibitor for cancer immunotherapy.

Z. Qu, F. Nguele Meke, Z. Zhang, Y. Bai, A. D. Krabill, C. S. Muli, B. A. Jassim, J. Dong, J. Li, N. Yuyen, A. W. Tao, D. T. Trader, Z.-Y. Zhang;
Purdue University, West Lafayette, IN

Cancer immunotherapy refers to the approach leveraging patients' immune system against tumor, which has gained tremendous progress hallmarked by immune checkpoint blockade and adoptive cell therapies. However, contemporary strategies suffer from limited responses, adverse side effects, and low tissue penetration due to utilization of macromolecules, calling for more efficacious and safer alternative strategies. SHP1 is a protein tyrosine phosphatase (PTP) primarily expressed in hematopoietic cells and has been shown to negatively regulate immune responses in T cells and natural killer (NK) cells, and SHP1 deletion in these cells has shown to promote their anti-tumor functions. Recent studies also demonstrated that inducible SHP1 knockout inhibited tumor growth *in vivo* through immune activation. Although presented as an attractive target, no high-quality small molecule inhibitors have been reported for SHP1 due to its undruggable nature. Through high-throughput screening and extensive medicinal chemistry, we have acquired the first-in-class SHP1 covalent inhibitor M029, which shows >25-fold selectivity against SHP2, its closest analogues and >60-fold selectivity against other PTPs and cysteine-based proteins. Further proteomics studies reveal that M029 is superiorly selective for SHP1 *in cellulo*. Additionally, M029 is stable in 100-fold excessive glutathione with a half-life of ≥35 hours and non-toxic up to 100 μM to healthy cells, such high stability was also reflected by its oral bioavailability with a F% of 10%. M029 treatment significantly activated T cell receptor signaling in T cells and NK cells killing effects *in vitro*. Furthermore, oral dosage of M029 significantly delayed tumor progression in mice bearing MC38 tumors through enhanced T cell and NK cell infiltration and activation and prolonging of T cell exhaustion. To validate that the compound acted through immune activation, we dosed the mice with anti-$CD8^{\pm}$ or anti-NK1.1 during M029 treatment, both of which abolished the compound efficacy, corroborating with its mechanism of action. Meanwhile, to assess the compound safety, we dosed the mice up to 100 mg/kg for 8 days, where no significant body weight change or cytokine storm were observed. Collectively, we have developed the first SHP1 covalent inhibitor with high selectivity and strong anti-tumor efficacy. This study is the first characterization of pharmacological SHP1 inhibition as cancer immunotherapy and solidified its potential as an immunotherapeutic target. The development of M029 will also enlighten drug discovery strategies against SHP1 or other undruggable PTPs.

#1974 Discovery of TRX-211-399, a potent, CNS-penetrant, highly selective inhibitor of EGFR exon 20 insertion mutations.

K. Chun, S. Lim, J. Lee, S. Choi, S. Kim, Y. Choi, A. Park, B. Kim, Y. Park, E. Choi, S. Lee, K. Lee;
Therapex, Seoul, Korea, Republic of

Lung cancer is the leading cause of cancer-related deaths worldwide, accounting for approximately 2 million new cases and 1.8 million deaths annually. Various types of EGFR-activating mutations are one of the most important oncogenic drivers in non-small cell lung cancer (NSCLC). Among NSCLC patients with EGFR mutations, 5-10% of patients have EGFR exon 20 insertion (ex20ins) mutations that are insensitive to clinically available EGFR tyrosine kinase inhibitors (TKIs). Recently, as mobocertinib (EXKIVITY®) failed to improve progression-free survival in Phase 3 clinical trial, there remains a high unmet medical need to develop new drugs with wider therapeutic window to treat NSCLC harboring EGFR ex20ins mutations. Herein, we report a novel EGFR-TKI, TRX-211-399, specifically designed to target ex20ins mutations. TRX-211-399 potently inhibited the proliferation of not only Ba/F3 cells overexpressing near-loop (A767dupASV, S768dupSVD) and far-loop (H773insNPH, H773dupH) mutations but also patient-derived NSCLC cell line. In particular, TRX-211-399 demonstrated high selectivity against wild-type EGFR. With favorable DMPK profiles, once-daily oral administration of TRX-211-399 showed significant tumor regression in multiple Ba/F3 xenograft models carrying different EGFR exon20ins mutations. Furthermore, in a PC-9-luc cell intracranial xenograft model, TRX-211-399 induced substantial anti-tumor effects and prolonged survival without body weight loss. TRX-211-399 is currently undergoing further preclinical evaluation as a potential candidate for clinical development for patients with EGFR exon20ins mutations.

#1975 Discovery of I-1000233, a potent, selective and brain permeable SHP2 allosteric inhibitor.

Francesca Puca, Danilo Fabbrini, Alina Ciammaichella, Antonino Missineo, Monica Bisbocci, Martina Nibbio, Annalise Di Marco, Claudia Apicella, Fabrizio Colaceci, Romina Sasso, Daniela Natale, Francesco Scalabri, Cristina Alli, Vincenzo Pucci, Christian Montalbetti, Alessia Petrocchi, Alessandro Carugo, Carlo Toniatti

IRBM Spa, Pomezia (RM), Italy

Background: SHP2 (Src homology region 2-containing protein tyrosine phosphatase 2) is a target of interest for cancer therapy due to its key role in the regulation of RAS/MAPK signal transduction downstream of Receptor Tyrosine Kinases (RTKs). We report here the identification of I-1000233, a novel, highly potent, orally available and brain permeable SHP2 allosteric inhibitor, with potential for the treatment of tumors with dysregulated RTK/RAS/ERK signaling pathways.

Material and Methods: High-throughput biological, biochemical and pharmacodynamic (PD) assays were used to inform Structure Activity Relationship studies which led to the identification of a chemical series of potent SHP2 inhibitors. Iterative optimization of physicochemical and pharmacological properties resulted in the identification of I-1000233, an orally available SHP2 inhibitor that showed excellent drug-like properties in preclinical studies.

Results: I-1000233 is a potent inhibitor of the SHP2 enzyme in vitro (IC_{50} = 2 nM) with an exceptionally long residence time on the target. When tested in cell lines, it exhibits significant anti-proliferation activity against brain tumor cells and multiple RAS or EGFR mutant models. It strongly inhibits pERK, a downstream marker of MAPK pathway activity, in a dose dependent manner. Further, in vivo preclinical data confirmed that I-1000233 penetrates the BBB and shows anti-tumor activity, supporting its potential in the treatment of CNS and brain-metastasized tumors.

Conclusions: I-1000233 is a potent, selective and orally available SHP2 inhibitor with potential for once-a-day dosing and its brain permeability in humans makes it a promising therapeutic agent against SHP2i responsive brain tumors and metastases.

#1976 Targeting metabolism in non-small cell lung cancer (NSCLC) with the novel multitarget small molecule PI3K-CDK4/6-CDK9 inhibitor LCI139.

Cody C. McHale[1], Anna V. Ivanina Foureau[2], Hailey L. Dryden[1], Krishnaiah Maddeboina[1], Dhananjaya Pal[1], Bharath Yada[1], Page Mangum Arditti[1], Fei Guo[2], Kathryn F. Mileham[3], David M. Foureau[2], Donald L. Durden[1]

[1]Molecular Targeted Therapeutics Laboratory, Atrium Health Levine Cancer, Charlotte, NC, [2]Translational Research, Atrium Health Levine Cancer, Charlotte, NC, [3]Section of Thoracic Medical Oncology, Atrium Health Levine Cancer, Charlotte, NC

Introduction: NSCLC is a heterogenous disease estimated to cause the majority of all 2023 United States cancer-related deaths. There is no broadly applicable targeted therapy to treat lung cancer and those FDA-approved drugs target patient-specific biomarker mutations such as *EGFR*, *ALK*, *ROS1*, etc. Targeting multiple oncogenic pathways to induce synthetic lethality is an attractive strategy for anticancer therapeutic development. Here, we describe the effects of novel multitarget small molecule PI3K-CDK4/6-CDK9 inhibitor LCI139 on a panel of human NSCLC cells of mixed histologic and mutational backgrounds.

Methods: LCI139 specific target inhibition was assessed by cell-free kinase hotspot/lipid kinase assay and KINOMEscan. LCI139 (0.001-10μM) was screened against NCI-H1975, NCI-H1703, NCI-H1373, NCI-H1781 and NCI-H226 human cell lines; IC_{50} values determined by CellTiter-Glo/WST-8 Assay and apoptotic rate by flow cytometry (Annexin V/7-AAD). Metabolomic profile of representative LCI139 sensitive ($LCI139^S$) and resistant ($LCI139^R$) NSCLC cells was evaluated by western blot.

Results: LCI139 is a highly potent inhibitor of PI3K-CDK4/6-CDK9: 0.070μM (PI3Kα), 0.461μM (PI3Kγ), 0.214μM (PI3Kδ), 0.0015μM (CDK4), 0.0036μM (CDK6), 0.000039μM (CDK9). NCI-H1703, NCI-H226, NCI-H1373 and NCI-H1975 were highly sensitive to LCI139 (0.68, 3.2, 35.27 and 342.4nM IC_{50}), while NCI-H1781 remained insensitive up to 10μM. Confirming those findings, LCI139 promoted robust apoptotic cell death in NCI-H1703, NCI-H226, NCI-H1373 and NCI-H1975 but not NCI-H1781. $LCI139^S$ H1703 cells displayed increased bioenergetic reliance on oxidative phosphorylation (OXPHOS), compared with the $LCI139^R$ H1781 cells. In the $LCI139^S$ H1703 cells, LCI139 treatment decreased expression of all mitochondrial complexes (I-IV) and glycolytic enzymes (HK2, GAPDH, LDHA). Conversely, LCI139 treatment of $LCI139^R$ H1781 cells only inhibited expression of mitochondrial complexes II and III, but increased glucose uptake (Glut1) and retained expression of other glycolytic enzymes.

Conclusions: Triple PI3K-CDK4/6-CDK9 inhibitor LCI139 is nanomolar potent against several NSCLC cells lines of mixed histologic and mutational backgrounds. NSCLC cells that are most reliant on OXPHOS to generate ATP, a classic metabolic adaptation to chemotherapy, appear to be most sensitive to LCI139. Taken together, these data support further drug characterization and mechanistic dissection to assess LCI139's potential clinical utility in treating advanced stage and recurrent NSCLC.

#1977 ACR-2316: A potentially first-in-class, potent, selective WEE1/PKMYT1 inhibitor rationally designed for superior single agent activity through synergistic disruption of cell cycle checkpoints.

C. Wigerup[1], H. Nilsson[1], L. Shi[2], J. Jung[2], J. Baddour-Sousounis[2], R. Cornelius[1], N. Lipjankic[1], U. Muralitharan[1], V. Siino[1], I. Arribas Diez[1], Z. Best[2], M. Pasetto[1], W. Dahlberg[2], S. Rafiei[2], P. Lombardo[2], M. E. Jakobsson[1], R. Improgo[2], C. Scherer[2], J. van Duzer[2], D. A. Proia[2], K. Masson[2], P. Blume-Jensen[2]; [1]Acrivon Therapeutics, Lund, Sweden, [2]Acrivon Therapeutics, Watertown, MA

WEE1 and PKMYT1 kinases play essential roles in cell cycle checkpoints and DNA damage response. Genetic interaction has been documented between WEE1 and PKMYT1, and clinical trials have reported clinical activity with inhibitors of WEE1 (adavosertib, azenosertib) and PKMYT1 (lunresertib). Here, we report the discovery and characterization of ACR-2316, a dual inhibitor of WEE1 and PKMYT1 specifically designed for optimal selectivity through co-crystallography and superior single agent activity uniquely enabled by Acrivon Predictive Precision Proteomics (AP3). Mass spectrometry-based AP3 profiling was conducted across several novel WEE1 and PKMYT1 inhibitor leads generated through co-crystallography-based rational drug design. Selective leads originating from one series were further optimized using AP3 for biological structure-activity relationship analysis. AP3 profiling revealed WEE1 inhibitor-upregulated phosphorylation sites across a subset of phosphoproteins that were oppositely regulated (quenched) by PKMYT1 inhibitors. Consensus sites for these included CDK1 T14, a direct PKMYT1 phosphorylation site, as well as CHK1 S296. A particular lead compound, ACR-2316, demonstrated a desirable potent, balanced ratio of cellular WEE1 (IC50 = 2 nM, IC90 = 10 nM) and PKMYT1 (IC20 = 44 nM) inhibition resulting in superior activation of the mitotic kinases CDK1, CDK2, and PLK1 compared to adavosertib and lunresertib, based on annotated kinase substrate relationships. ACR-2316 is more selective than adavosertib, azenosertib, and lunresertib based on >200 kinases profiled by AP3 and 468 kinases assessed by KINOMEscan. Cell cycle analyses demonstrated a drastic ACR-2316-induced S-G2/M accumulation qualitatively distinct from adavosertib or lunresertib. In a 19-cancer cell line proliferation assay (CellTiter-Glo), ACR-2316 demonstrated greater potency in all cell lines tested compared to adavosertib and lunresertib (mean IC50 = 70, 252 and 364 nM, respectively). Superior anti-cancer activity of ACR-2316 was observed in 12 ovarian cancer patient-derived xenograft models tested ex vivo (CellTiter-Glo 3D) compared to azenosertib and lunresertib (mean IC50 = 9, 248 and 1620 nM, respectively). Across human tumor xenograft mouse models, oral administration of ACR-2316 demonstrated superior, durable, dose-dependent efficacy compared to azenosertib and lunresertib and was well tolerated at all doses. Complete responses observed with ACR-2316 were associated with strong WEE1 and intermediate PKMYT1 inhibition in tumors. In conclusion, ACR-2316 is a potent, selective dual WEE1/PKMYT1 inhibitor with superior single-agent activity compared to clinical WEE1 or PKMYT1 inhibitors. ACR-2316 is progressing through IND-enabling studies in preparation for clinical monotherapy development.

#1978 The combination of neratinib with sotorasib is synergistic in models of HER2-amplified and KRAS^{G12C}-mutated cancer.

M. E. Castel[1], N. T. Conlon[1], N. Walsh[1], G. F. Bischof[2], J. P. Crown[3], D. M. Collins[1];
[1]Dublin City University, Dublin, Ireland, [2]Puma Biotechnology, Inc., Los Angeles, CA, [3]St Vincent's University Hospital, Dublin, Ireland

Introduction: Constitutive activation of KRAS through gain-of-function mutations, such as KRAS^{G12C}, is thought to reduce sensitivity to HER-targeted TKIs like neratinib (N), lapatinib (L) and tucatinib (T). Sotorasib (S) is a KRAS^{G12C} specific inhibitor clinically approved for the treatment of advanced KRAS^{G12C}-mutated non-small cell lung cancer. One identified resistance mechanism to sotorasib is the increase of multiple phosphorylated receptor tyrosine kinases, including EGFR and HER2. The objective of this study was to assess the *in vitro* efficacy of the single agents N, L, T and S, and the combination of N and S in HER2-amplified, KRAS^{G12C}-mutated cancer cell lines.

Methods: The antiproliferative effects of N, L, T and S were assessed in the HER2-amplified and KRAS^{G12C}-mutated KYSE-410 (esophageal) and NCI-H2030 (lung) cancer cell lines, and KRAS^{G12C}-mutated MiaPaca-2 (pancreatic) cell line by 5-day acid phosphatase assay. IC_{50} values were calculated using CalcuSyn software. To assess the synergy between N and S, matrix assays were performed and analyzed using Combenefit software. To further determine the efficacy of the drugs, changes in signaling pathways were assessed by Western blotting.

Results: N displayed nanomolar IC_{50} values (< 100 nM) in all three cell lines, while nanomolar IC_{50} values with L and T were only achieved in KYSE-410 (IC_{50} = 426.84 nM and IC_{50} = 363.38 nM respectively). S was most potent in MiaPaca-2 (IC_{50} = 6.04 nM), followed by NCI-H2030 (IC_{50} = 270.60 nM) and KYSE-410 (IC_{50} = 5.46 µM). Matrix assays showed that NS was broadly additive in MiaPaca-2 cells, and synergistic in both NCI-H2030 and KYSE-410 cell lines. N and NS numerically decreased HER2 levels compared to control in NCI-H2030 after 24h of treatment (6.4-fold, $p = 0.58$ and 2.5-fold, $p = 0.79$ respectively) but not in KYSE-410. KRAS levels were significantly increased (1.89-fold, $p \leq 0.05$) after treatment with NS in NCI-H2030. No significant effects were observed on the activation of HER2 and EGFR in either cell line at 24h. In NCI-H2030, NS had a significantly stronger inhibitory effect on pERK compared to N ($p \leq 0.0001$) and S ($p = 0.012$) alone. In KYSE-410, pERK levels were also slightly decreased with NS, but not significantly different from N ($p = 0.12$). However, pAkt levels in KYSE-410 were significantly reduced by N (1.3-fold, $p = 0.009$) and NS (1.7-fold, $p \leq 0.0001$) compared to control, with NS showing a significantly greater decrease than N ($p = 0.026$). It thus appears that the synergy between N and S occurs through a stronger inhibition of ERK activity in NCI-H2030, while it occurs through a stronger inhibition of Akt activity in KYSE-410.

Conclusion: NS is additive or synergistic in the three KRAS^{G12C}-mutated cancer cell lines examined. Further work is planned to investigate the basis of the synergy observed.

#1979 Preclinical characterization of NVL-330, a selective and brain penetrant HER2 tyrosine kinase inhibitor with broad activity on HER2 oncogenic alterations.

Y. Sun[1], K. L. Andrews[1], A. Tangpeerachaikul[1], T. M. Nguyen[1], B. Gerard[1], N. E. Kohl[2], J. C. Horan[1], H. E. Pelish[1];
[1]Nuvalent, Cambridge, MA, [2]Kohl consulting, Wellesley, MA

Background: Oncogenic mutations and gene amplifications in the HER2 receptor tyrosine kinase are detected in approximately 2 - 4% and 1 - 5%, respectively, of non-small cell lung cancers (NSCLC) in the US. Exon 20 insertion mutations (exon20ins) are the predominant HER2 mutations in NSCLC, and ~50% of HER2-mutant metastatic NSCLC patients develop brain metastases. The antibody drug conjugate trastuzumab deruxtecan (T-DXd) has received FDA accelerated approval for HER2-mutant NSCLC, but currently there are no approved tyrosine kinase inhibitors (TKIs) for this indication. NVL-330 is a novel, brain-penetrant, HER2-selective TKI, designed to address the combined medical need of treating HER2-mutant tumors, avoiding treatment related adverse events due to off-target inhibition of wild-type EGFR, and treating brain metastases. Here we characterized the preclinical pharmacological profile of NVL-330 in comparison to other investigational HER2-targeting TKIs and T-DXd.
Methods: TKIs were profiled in cellular phospho-HER2, phospho-EGFR, and viability assays. *In vivo* antitumor studies were performed in nude mice with HER2-altered subcutaneous or intracranial tumors. T-DXd concentration was measured in an ELISA assay. The unbound brain-to-plasma partitioning ratio (Kp,uu) was determined at one hour after oral 10 mg/kg dosing in Wistar Han rats.
Results: NVL-330 broadly inhibited HER2 oncogenic alterations, including amplified wild-type HER2, HER2 exon20ins and non-exon20ins mutants, with potency and selectivity over wild-type EGFR comparable to investigational HER2-selective TKI zongertinib. By contrast, NVL-330 had a higher Kp,uu than zongertinib in rats. In a patient-derived xenograft model harboring HER2 exon20ins, treatment with NVL-330 suppressed phospho-HER2 and downstream signaling, increased total HER2 and caused dose-dependent tumor regression at well tolerated doses. In the $HER2^{amp}$ NCI-N87 subcutaneous xenograft model, oral administration of 30 mg/kg NVL-330 twice per day induced tumor regression, similar to that achieved by intravenous administration of 10 mg/kg T-DXd once every three weeks, a human-relevant dose in mice. By comparison, in the intracranial setting with the same tumor model and dosing regimens, NVL-330 induced tumor regression, whereas T-DXd provided tumor stasis. Pharmacokinetic analysis in these intracranial tumor bearing mice indicated that NVL-330 had significantly higher brain penetrance than T-DXd.
Conclusions: NVL-330 was broadly and selectively active against HER2 oncogenic alterations *in vitro* and *in vivo*, and demonstrated brain penetrance in rodents exceeding that of HER2 investigational TKI zongertinib and T-DXd. This preclinical profile supports the potential for NVL-330 to address a medical need for patients with HER2-driven cancers, including those with brain metastases.

#1980 Validation of a novel Type II HER2 inhibitor through preclinical studies across various cancer models.

L. Kulyk, K. Chen, I. Botrous, C. Zhao, C. Zhao, M. Maestre, S. Wright, J. Dennis, J. Park, A. Adams, W. Derricotte, S. Yost, M. L. Anderson, F. Manby, T. Miller, C. Zhang, L. Gomez, Z. Huang;
Iambic Therapeutics, Inc., San Diego, CA

HER2 activation through amplification, overexpression or mutation drives many types of human cancers, and has been the target of several therapeutic approaches. The demonstration of clinical benefit of available pan-ERBB and HER2 inhibitors has been hampered by the dose-limiting side effects from their collateral or residual EGFR inhibition. Here we present IAM1363 (also known as ENT-H1), a highly potent and selective irreversible inhibitor of both HER2 wild-type and HER2 oncogenic mutants. IAM1363 binds to HER2 in a type II DFG-out conformation, the only example reported to date for this target. This binding mechanism underlies its strong interactions with HER2, including N-terminally truncated HER2 (p95HER2) and HER2 kinase domain mutants, with cellular IC50s in the low nanomolar range, while sparing WT EGFR. Oral administration of IAM1363 in mice led to tumor regression (TR) in a diverse set of HER2-driven tumor models at levels well below the maximum tolerated dose (MTD). Importantly, strong in vivo efficacy was observed in tumor models that exhibited resistance to the existing HER2-targeting agents. For example, in a p95HER2 xenograft model, IAM1363 caused significant TR, including complete responses, at 100 mg/kg dose, whereas tucatinib achieved at best tumor stasis at MTD and T-DXd showed marginal effect. Besides HER2 truncation, co-occurring EGFR and other receptor tyrosine kinase (RTK) amplification or overexpression can also lead to resistance to HER2-directed treatments. IAM1363 was tested in xenograft models using HER2-amplified/EGFR-high cell lines HCC1954 and SKOV3, and demonstrated robust TRs. Even more strikingly, IAM1363 led to TR in the HCC827 human lung cancer xenograft model with mid-level HER2, and high levels of EGFR and MET expression. The resistance combatting effect of IAM1363 goes beyond co-occurring RTK-mediated mechanism as IAM1363 also showed dose-dependent TR in KYSE410, a human esophageal squamous cancer xenograft model that harbors the KRAS G12C mutation and HER2 amplification. Taken together, IAM1363 represents a promising clinical candidate for the treatment of HER2-driven tumors. Its unique binding mechanism and potent pan-HER2 activity overcome multiple resistance mechanisms, and its strong EGFR avoidance widens the safety margin. Additionally, IAM1363 was found to be consistently enriched in xenograft tumors that had moderate to high HER2 expression levels, and those with HER2 activating mutations. This distinctive pharmacokinetic property facilitates optimal target engagement in tumors, including those occurring in the brain, while minimizing potential systemic side effects.

#1981 Profiling of protein interactome with cysteine-reactive libraries led to the discovery of EML4ALK dimerizers.

Diane Yang, Stefan Harry, Elizabeth Codd, Stefan T. Kaluziak, Alexander D. Carlin, Edwin Zhang, Zavontae Oppong-Holmes, Wenxin Yang, Abigail Smith, Dawn Mitchell, Mariko Hara, Siwen Zhang, Maristela Onozato, Liron Bar-Peled, Anthony J. Iafrate

Massachusetts General Hospital, Boston, MA

Cysteine covalent binders enable direct interactions with previously deemed undruggable protein targets, revolutionizing cancer therapeutics development. The primary focus has been on tailoring single-warhead compounds to target specific cysteine residues within the functional domains of target proteins. However, the biochemical properties including dimerization, induced conformational changes, and interactome disruption have been underexplored, presenting an ongoing limitation in current drug discovery approaches. In this study, we generated a library of 32 cysteine-reactive warhead compounds using various combinations of scaffolds and warheads to represent diverse reactivities. A combinatory assay approach, including cysteine druggability mapping (CDM) to discover reactive residues and SDS-PAGE fractionation assays to identify disrupted protein interaction events, was employed. Characterization of the library revealed distinct reactive cysteines and dimerization profiles among the 32 unique compounds. Compound 1C9, identified as a lead compound, demonstrated significant dimerization of EML4, a common fusion gene partner in lung cancer. Using the EML4ALK fusion gene as a proof of concept, we explored potential mechanisms underlying the compound-induced dimerization of EML4. Subsequent structure-activity relationship (SAR) studies and screening of 70 additional compounds were conducted to optimize ALK dimerization and minimize off-target effects. The enhanced compound disrupted the ALK cellular signaling pathways AKT and ERK upon dimerization of the EML4ALK fusion gene. Additionally, we discovered that covalent dimerization induced EML4ALK degradation without requiring a ubiquitin ligase like a PROTAC. In conclusion, our work has uncovered a novel class of cysteine covalent binders, which we believe are valuable tools to modulate protein-protein interactions in previously undruggable proteins in cancer. This discovery holds significant therapeutic potential for future drug development.

EXPERIMENTAL AND MOLECULAR THERAPEUTICS: Mechanisms of Drug Resistance 1
Poster Session

#1985 Ablation of adenylosuccinate lyase retarded the cell proliferation and induces mitochondrial dysfunction in endocrine therapy resistant breast cancer cells.

A. Yadav, L. Jin, R. Clarke, S. Sengupta;
The Hormel Institute, University of Minnesota, Austin, MN

Approximately 75% of breast tumors express estrogen receptors (ER+); recurrent ER+ breast cancer is generally incurable. Endocrine therapy (ET) is the mainstay of treatment for ER+ breast cancer and works by targeting either ER activity (Tamoxifen or Fulvestrant) or availability of its ligand estrogen (Letrozole, Exemestane). Unfortunately, endocrine therapies are limited by the emergence of resistance; resistance to endocrine therapies (ET) remains a significant clinical challenge. We have explored the role of adenylosuccinate lyase (ADSL), an enzyme of the *de-novo* purine biosynthesis pathway, in ET-resistant breast cancer cells. Protein expression of ADSL was significantly higher in two different ET-resistant cells (LCC9 and T47D-4HT) when compared with their respective parental ET-sensitive cells (MCF-7 and T47D). siRNA mediated ablation of ADSL in LCC9 and T47D-4HT cells blocked cell proliferation and both colony and spheroid formation. Depletion of ADSL in LCC9 cells obstructed cell cycle progression from G1 to S phase and elevated the protein expression of cyclin D1/D3, CDK2/4, and cyclin E. In T47D-4HT cells, ADSL depletion led to an accumulation of cells in S-phase with reduced protein expression of cyclin D1. Notably, ADSL ablation in LCC9 cells lead to DNA replication stress, resulting in activation (phosphorylation) of ataxia-telangiectasia-mutated-and-Rad3-related kinase (ATR) and its key downstream effector checkpoint kinase 1 (Chk1), which further limited the phosphatase activity of cdc25A leading to deactivation (phosphorylation) of Cyclin-Dependent Kinase 2 (CDK2). ADSL knockdown reduced the mitochondrial membrane potential and impaired the oxygen consumption (OCR) and extracellular acidification (ECAR) rates in both LCC9 and T47D-4HT cells. Of
note, addition of AICAR to ADSL-depleted LCC9 cells significantly increased cell proliferation, colony formation, and restored mitochondrial membrane potential. RNA sequencing data revealed the effect of ADSL depletion on enrichment of different pathways in LCC9 and TH47D-4HT cells. Importantly, p53 signaling was significantly enriched in LCC9 cells but not in T47D-4HT cells after ADSL knockdown (T47D cells have a mutated p53 gene). ER+ breast cancer patients treated with ET showed high ADSL expression that is associated with poor recurrence-free survival. In summary, our findings indicate that ADSL-mediated *de novo* purine synthesis is crucial for cell proliferation. Therefore, targeting ADSL may be a novel therapeutic approach for ER, ET-resistant breast cancer.

#1986 Acquisition of carboplatin resistance corresponds with reduced sacituzumab govitecan efficacy in triple negative breast cancer patient derived xenografts.

C. J. Walker, J. E. Altman, E. K. Zboril, R. K. Myrick, N. S. Hairr, D. C. Boyd, B. Hu, M. G. Dozmorov, J. Harrell;
Virginia Commonwealth University, Richmond, VA

Sacituzumab Govitecan (SG) is an antibody drug conjugate that targets the epithelial glycoprotein Trop-2. SG has been approved for the treatment of patients with triple negative breast cancer (TNBC) or estrogen receptor positive (ER+) breast cancer after they have received at least two previous systemic treatments. The objectives of this study were to identify biomarkers of SG response using breast cancer patient-derived xenografts (PDXs) and determine if SG efficacy changes when cells become carboplatin resistant (CR). Analysis of transcriptomic and proteomic levels of Trop2 using bulk RNAseq, scRNA-seq, and tandem mass tag spectrometry found that overall ER+ PDXs had significantly lower RNA (p-value less than 0.001) and protein (p-value less than 0.001) expression of Trop-2 than TNBC PDXs. Immunohistochemical assessment of 42 TNBC and 27 ER+ patient tumor samples identified variation in Trop-2 expression; within each cohort, expression varied from highly positive to completely negative. To test the association of Trop-2 with drug responsiveness, cells from 19 different PDXs were cultured in vitro and administered increasing doses of SG. TNBC cells were more responsive to SG treatments compared to ER+ cells (p-value equaling 0.005). Correlation analysis identified a positive relationship of drug response with protein abundance which was stronger in TNBC samples. In vivo studies with 7 TNBC PDXs found that over 70% were highly susceptible to SG treatments, with some tumors being completely eradicated or exhibiting a total inhibition of tumor growth which resulted in a long-term durable response after 10 weeks of treatment. In vivo across all the PDXs, Trop-2 expression alone did not strongly correlate with SG treatment success. Interestingly, CR sublines derived from 2 carboplatin sensitive PDXs were significantly less responsive to SG than their parental PDXs (p-value less than 0.001). These two CR sublines were also significantly less sensitive to the majority of 555 other drugs identified by the NCI compared to their parental PDXs. Ongoing studies are defining mechanisms of reduced SG efficacy in CR models. Overall, these studies find that SG is highly effective in many TNBC PDX models and should be utilized earlier in treatment protocols, especially in metastatic patients.

#1987 PARP inhibitor (PARPi) rechallenge shows differential sensitivity in PARPi olaparib-resistant *BRCA1*-mutated (BRCA1m) high-grade serous ovarian cancer (HGSC).

Chi-Ting Shih, Tzu-Ting Huang, Jayakumar R. Nair, Jung-Min Lee

National Institutes of Health (NIH), Bethesda, MD

Background: PARPis have changed the treatment paradigm in HGSC, particularly for women with *BRCA* mutations. PARPi, olaparib (O), is a standard of care maintenance therapy following platinum-based chemotherapy in newly diagnosed *BRCA*-mutated (BRCAm) HGSC. But patients ultimately develop resistance to O. We investigated whether rechallenge with different PARPi monotherapy could cause cytotoxicity in BRCAm HGSC after becoming O-resistant. We also aimed to identify possible mechanisms of actions of PARPi's differential sensitivity.
Methods: We developed a PARPi-resistant line (UWB-OlaJR) from BRCA1m PARPi-sensitive cells (UWB1.289) by gradient exposure of O with initial lower doses to a final concentration of 20 μM over 10 months. Four PARPis including O, niraparib (N), talazoparib (T), and veliparib (V) were tested. Cell growth was assessed using 5-day XTT and 10-day clonogenic assays. DNA damage and homologous recombination (HR) repair activity were evaluated using immunofluorescence (IF) staining of γH2AX and RAD51 foci, respectively. Replication fork (RF) dynamics was measured by DNA fiber assay. All data were repeated in triplicate and analyzed using t-test or one-way ANOVA. Data were shown as mean ± SD and $P < 0.05$ was considered statistically significant.
Results: 5-day XTT assay shows a 53.7-fold increase in resistance to O in UWB-OlaJR relative to UWB1.289 (IC_{50} 2.2 μM vs. 118.1 μM). Cross-resistance was observed with other 3 PARPis, showing increased IC_{50} values compared to its parental line (V: 23.4-fold, N: 160.5-fold, T: 229.6-fold). However, 10-day clonogenic assay showed no resistance against N (1.09-fold) and T (0.51-fold) in UWB-OlaJR, indicating differential sensitivity to different PARPis by a long-term cytotoxicity measure. Surprisingly, γH2AX foci did not increase in response to PARPis in UWB-OlaJR compared to UWB1.289 (O: 2.58-fold, V: 2.33-fold; N: 2.89-fold, T: 2.58-fold; all $P < 0.05$), suggesting possible restored DNA repair function. All four PARPis induced replication stress in both O-sensitive and -resistant cell lines as evidenced by decreased RF speed compared to untreated group (O: 0.57- and 0.7-fold, V: 0.68- and 0.74-fold, N: 0.47- and 0.47-fold, T: 0.47- and 0.52-fold; all $P < 0.001$). Notably, N and T treatments reduced fork speed to a greater extent than O and V in UWB-OlaJR. However, RF protection was not affected when UWB-OlaJR treated with different PARPis compared to UWB1.289 (O: 0.89-fold, V: 0.87-fold, N: 0.71-fold, T: 0.83-fold; all $P < 0.05$), suggesting that differential sensitivity to different PARPis was unlikely due to modulation of RF stabilization.
Conclusions: Our findings demonstrate different PARPis may induce varied levels of cytotoxicity and replication stress in O-resistant BRCA1m HGSC, possibly via modulating alternative RF dynamics besides RF protection.

#1988 Mass spectrometry profiling identifies ENO2 as a driver of lenvatinib resistance in hepatocellular carcinoma.

Sukbum Kim[1], Jia-Jian Loh[1], Huajian Yu[1], Ki-Fong Man[1], Kai-Yu Ng[1], Terence Kin-Wah Lee[2], Clive Yik-Sham Chung[1], Stephanie Ma[1]

[1]School of Biomedical Sciences, The University of Hong Kong, Hong Kong, Hong Kong, [2]Department of Applied Biology and Chemical Technology, The Hong Kong Polytechnic University, Hong Kong, Hong Kong

Hepatocellular carcinoma (HCC) is the predominant type of primary liver cancer, and lenvatinib is a multi-kinase inhibitor approved by the FDA as a first-line drug for advanced HCC since 2018. Lenvatinib demonstrated antitumor activity with a higher objective response rate, longer progression-free survival, and time to progression in a non-inferiority trial compared with sorafenib. However, the clinical benefits of lenvatinib remain limited as acquired resistance to lenvatinib during HCC treatment is inevitable. This highlights the need to understand the molecular mechanisms of lenvatinib resistance and to explore new therapeutic approaches to overcome this resistance. Tumor lineage plasticity, a recognized hallmark of cancer, is a phenomenon in which tumor cells dedifferentiate into a more stemness state to attain cellular plasticity, enabling them to evade targeted therapeutic interventions. However, the mechanism by which cellular plasticity contributes to lenvatinib resistance remains elusive. In this study, we employed proteomic mass spectrometry to investigate altered proteins in two pairs of parental lenvatinib-sensitive and their corresponding trained lenvatinib-resistant HCC cell lines. This analysis revealed that upregulation of enolase 2 (ENO2), a glycolytic enzyme that catalyzes the dehydration and conversion of 2-phosphoglycerate to phosphoenolpyruvate, is a critical contributor. ENO2 upregulation is frequently observed in HCC and is strongly correlated with aggressive clinical features, including poor survival, advanced tumor stage, and poor differentiation status. We further showed that ENO2 upregulation in HCC is positively correlated with stemness and hepatic progenitor marker signatures, as well as hypoxia, and subsequently demonstrated that ENO2 is regulated by hypoxia/HIF-1α, with hypoxia response element sequences located in the ENO2 promoter region. Research is underway to investigate the functional role and underlying molecular mechanisms associated with ENO2-driven lenvatinib resistance and cellular plasticity in HCC.

#1989 Intratumor heterogeneity in EGFR-mutant lung tumors mediates targeted therapy resistance and formation of drug tolerant microenvironment.

H. M. Haikala[1], B. Alsaed[1], J. Son[2], L. Lin[1], P. Gokhale[2], P. Janne[2];
[1]University of Helsinki, Helsinki, Finland, [2]Dana-Farber Cancer Institute & Harvard Medical School, Boston, MA

Introduction: Non-small cell lung cancers (NSCLC) harboring *EGFR* mutations are commonly treated with EGFR tyrosine kinase inhibitors (TKIs), but the emergence of drug resistance often leads to treatment failure. While various acquired resistance mechanisms have been identified, they are not always actionable. Furthermore, since drug resistance is typically studied after cancer relapse, little is known about the cellular or microenvironmental taking place during the formation of resistance at the stage of minimal residual disease (MRD). Therefore, it is necessary to understand the mechanisms leading to resistance during MRD and develop new ways to prevent drug resistance in *EGFR*-mutant cancers.
Methods: In this study, we discovered pre-existing intratumor heterogeneity in EGFR expression within *EGFR*-mutant NSCLCs and found that patient tumors contain clones with low mutant EGFR expression. To study the effect of this intratumor heterogeneity on drug response, we isolated low and high expressing cells and conducted longitudinal drug challenge assays in *ex vivo* and *in vivo* models. To dissect how the observed heterogeneity affects drug resistance and the tumor microenvironment during MRD, we employed patient-derived tumor cells and used novel tumor-on-a-chip co-culture approaches.
Results: Our findings reveal that EGFR-low cells are more tolerant to drug treatment and can survive the initial TKI insult, making them more likely to contribute to drug resistance in *EGFR*-mutant NSCLCs. Additionally, the surviving EGFR-low cells were able to modify the tumor microenvironment leading to fibroblast accumulation and immune suppression, contributing to the drug-tolerant tumor microenvironment. Importantly, we found that pharmacological induction of EGFR using epigenetic inhibitors was able to sensitize the drug tolerant cells to EGFR inhibition, suggesting a potential strategy to overcome TKI resistance in NSCLC patients.
Conclusions: In conclusion, our study sheds light on the critical role of intratumoral heterogeneity in treatment resistance and offers valuable insights into potential strategies to overcome this challenge. Our findings suggest that combination therapies that can alter the cellular phenotype during MRD have the potential to prevent intrinsic drug resistance. This underscores the importance of gaining a better understanding of the mechanisms underlying drug-tolerant microenvironment and developing more effective treatment strategies for patients with *EGFR*-mutant NSCLCs.

#1990 TIP60-mediated acetylation of ΔNp63α is associated with cisplatin resistance.

A. Hira, J. Zhang, M. Kemp, M. P. Kadakia;
Wright State University, Dayton, OH

The chemotherapeutic drug Cisplatin is often used to treat squamous cell carcinoma (SCC) patients, but low response rates and disease recurrence are common. About 5.4 million basal and squamous cell skin cancers are diagnosed each year in the US. ΔNp63α, a member of the p53 family of transcription factors, is overexpressed and considered oncogenic in non-melanoma skin cancer where it regulates cell survival, promotes proliferation, and inhibits cell apoptosis. ΔNp63α has also been shown to promote resistance to cisplatin by orchestrating the transcriptional regulation of several DNA damage response (DDR) genes. Our previous study showed that the histone acetyltransferase (HAT) TIP60 promotes SCC proliferation by positively regulating ΔNp63α protein levels in a manner reliant on the catalytic activity of TIP60. This observation suggested that TIP60 may contribute to the failure of platinum-based drugs in SCC and led us to hypothesize that TIP60-mediated acetylation of ΔNp63α regulates its stability and transcriptional activity to promote chemoresistance. We found that TIP60 levels positively correlated with ΔNp63α stability, protein levels, and cisplatin resistance. Further, silencing endogenous TIP60 led to a decrease in ΔNp63α transcript and protein levels in multiple cisplatin resistant SCC cell lines. Further, stable expression of TIP60 or ΔNp63α individually promoted resistance to cisplatin and reduced cell death, whereas loss of ΔNp63α or TIP60 induced G2/M arrest, increased cell death, and sensitized cells to cisplatin. Additionally, pharmacological inhibition of TIP60 reduced acetylation of ΔNp63α, decreased colony formation, and sensitized resistant cells to cisplatin. Finally, we demonstrated that ΔNp63α and TIP60 levels positively correlated with DNA repair capacity and negatively correlated with cisplatin-DNA adduct formation. Silencing of either TIP60 or ΔNp63α intensified cisplatin-DNA adduct formation and significantly reduced the expression of drug efflux transporters. Taken together, our data indicate that TIP60-mediated stabilization of ΔNp63α increases cisplatin resistance and provides critical insights into the mechanisms by which ΔNp63α confers cisplatin resistance in SCC. Our findings suggest that the inhibition of TIP60 may be therapeutically advantageous in overcoming cisplatin resistance in SCC and other epithelial cancers.

#1991 Leiomyosarcoma poly-aneuploid cancer cells form in response to chemotherapy, contribute to chemoresistance, and lead to higher rates of metastatic recurrence.

R. Kennington[1], G. Mitchell[1], E. Payne[1], N. Bhachech[1], J. A. Fletcher[2], T. Liu[3], M. van de Rijn[4], S. Amend[5], K. J. Pienta[5], J. D. Schiffman[1], L. M. Abegglen[1]; [1]University of Utah Huntsman Cancer Institute, Salt Lake City, UT, [2]Harvard University, Boston, MA, [3]University of Utah, Salt Lake City, UT, [4]Stanford University, Stanford, CA, [5]John Hopkins University, Baltimore, MD

Poly-aneuploid cancer cells (PACCs) or as also known as “giant cells”, are a treatment resistant stem cell-like cancer phenotype. PACCs have been identified in numerous cancer types, and their presence appears to play a significant role in chemoresistance and poor patient outcomes. PACCs employ a multitude of polyploidization programs to enter this transient state in response to stress. After removal of stress, PACCs give rise to non-PACC progeny through potential mechanisms of neosis or depolyploidization that maintain chemotherapeutic resistance. Leiomyosarcoma (LMS) is a difficult to treat sarcoma that grows in smooth muscle that often develops chemoresistance. Here we report the first description of PACCs in LMS cell culture, LMS xenografts, and LMS patient tumor microarrays. LMS cells treated (doxorubicin, docetaxel, and gemcitabine) in vitro and in vivo lead to the development of mononucleated and multinucleated polypoid cells as the predominant phenotype via polyploidization. Polyploidization mechanisms identified included endocycling, endomitosis, and cell-cell fusion. In vitro, LMS PACCs had a significant increase in size and DNA content as well as an increase in resistance to chemotherapy as compared to parents. LMS PACCs also repopulated the culture with non-PACC LMS progeny cells. The PACC progeny cells maintained a significantly decreased ($p<0.0001$) response to chemotherapy compared to parent cells. PACCs were also identified in clinical samples from patients with LMS. Twenty-nine percent of samples (N=289) contained abnormally large tumor cells and fifty-eight percent contained abnormal nuclei. A positive correlation was observed in patient tumor samples between PACCs in metastatic tumors and recurrence ($p=0.0277$) and survival ($p=0.0009$) than those patient tumors without PACCs. The high rate of functional loss of TP53 in LMS (>90%) may contribute to the ability of PACCs to form abnormal, multiple nuclei. We therefore transfected LMS PACCs to express TP53 and observed an increased apoptotic response. Additionally, combining functional TP53 expression with low doses of doxorubicin increases the apoptotic response of LMS cells, potentially by targeting PACCs. LMS PACCs may contribute to the lack of response in patients with LMS. Identifying therapeutic approaches that prevent or target LMS PACCs, including TP53 replacement, may improve response to chemotherapy and improve outcomes for patients.

#1992 A novel RB1 E3 ligase TRIM37 contributes to palbociclib resistance in breast cancer.

C. You, H. Tsoi, P. Man, L. Chow, W. Dai, U. Khoo;
The University of Hong Kong, Hong Kong, Hong Kong

The tripartite motif-containing 37 (TRIM37) is a RING finger E3 ubiquitin ligase and is a poor prognostic factor in breast cancer patients. The gene is located in chromosome 17q23, a region amplified in up to 40% of breast cancers. We observed that activation of androgen receptor (AR) could induce resistance to the CDK4/6 inhibitor Palbociclib, the mechanism yet to be clarified. ChIP-sequencing data suggested that AR binds to the TRIM37 promoter, with AR activation resulting in TRIM37 expression. We hypothesized that TRIM37 might be involved in Palbociclib resistance. Using an ER+ve cell line MCF7 and a TNBC cell line MDA-MB 453, we found that overexpression of TRIM37 could induce Palbociclib resistance. TRIM37 overexpression resulted in RB1 protein downregulation, which is the primary downstream target of CDK4/6, while TRIM37 knockdown enhanced RB1 protein expression. Ubiquitination assay demonstrated TRIM37 overexpression increased the level of RB1 protein ubiquitination. The co-immunoprecipitation (Co-IP) assay confirmed that TRIM37 protein could interact with the RB1 protein. These results suggest that TRIM37 could be the E3 ligase that regulates RB1 degradation. Various deletion mutants of TRIM37 were cloned for Co-IP experiments between these mutants and RB1. Results show that the MATH and c-terminal domains of TRIM37 was the essential region for the interaction. Overexpression of the mutant with the TRIM37 MATH and c-terminal domains (TRIM37-MATH/C) could enhance RB1 protein level. This might be due to competition of TRIM37-MATH/C with wild-type TRIM37 for RB1 binding. Our findings suggest TRIM37 is a novel RB1 E3 ligase, and it binds to the RB1 protein via the MATH and C-terminal domains to regulate protein degradation. Our study also suggests that high expression of TRIM37 mediated by AR activation could deplete RB1, which is the target of Palbociclib, eventually leading to resistance. These findings are supportive of the contribution of AR activation to Palbociclib resistance.

#1993 Cytosolic BAX dimerization as a mechanism of resistance to apoptosis and a novel target to potentiate BAX activation and apoptosis.

N. Gitego[1], B. Agianian[1], O. Mak[1], V. Kumar MV[1], E. Cheng[2], **E. Gavathiotis**[1];

[1]Albert Einstein College of Medicine, Bronx, NY, [2]Memorial Sloan-Ketetring Cancer Center, New York City, NY

BCL-2 family proteins are master regulators of cellular life and death and have become drug targets for the development of therapeutic agents to overcome the apoptotic blockade of cancer. BAX is a pro-apoptotic BCL-2 member that is a crucial mediator of apoptosis induced by diverse stimuli including various chemotherapeutic and targeted agents. BAX predominantly resides in the cytosol in a quiescent state and upon stress, it undergoes conformational activation and mitochondrial translocation leading to mitochondrial outer membrane permeabilization, a critical event in apoptosis execution. While cytosolic BAX is typically considered an inactive monomer, we previously reported structural and cell-based evidence of a cytosolic BAX dimer. However, it remains unclear how this regulates BAX. Moreover, we found that specific BAX mutants such as P168G and G67R formed inactive BAX dimers and mutations of P168A and G67R have been identified in AML patients and found to have impaired apoptotic activity and notably the BAX P168A mutant appeared in AML patients acquiring resistance to the BCL-2 inhibitor Venetoclax. Here, we investigated the role of the inactive BAX dimer in regulating apoptosis and pro-apoptotic drug treatments in various hematologic and solid tumor cancer cells. Surprisingly, cancer cell lines express cytosolic inactive BAX dimers and/or monomers. Expression of inactive dimers, results in reduced BAX activation, translocation and apoptosis upon pro-apoptotic drug treatments such as BH3 mimetics and chemotherapy drugs. Our findings support the notion that formation of the inactive BAX dimer is a mechanism adopted by cancer cells to further suppress BAX activation and gain survival advantage. Using the inactive BAX dimer crystal structure, we designed a pharmacophore-based drug screen, and identified a small-molecule modulator, BDM19 that binds and activates cytosolic BAX dimers and prompts cells to apoptosis alone or in combination with BCL-2/BCL-XL inhibitors. Moreover, we validated interactions of BDM19 and BAX, using structural, biochemical and cellular methods, critical for BAX activation. Our findings provide mechanistic insights into the regulation of BAX and resistance to apoptosis in cancer through inactive BAX dimerization. Further, we demonstrate a rational strategy to target BAX dimer for therapeutic modulation of BAX and overcoming resistance to apoptosis by pro-apoptotic agents.

#1994 Drug-induced cancer cell secretome promotes resistance in colon cancer.

S. R. Satapathy, S. Ghatak, A. Sjolander;
Lund University, Malmo, Sweden

Colorectal cancer (CRC) is the third most common cancer in the world, with a projection of increased lethality in the upcoming years. Adjuvant chemotherapy with biological agents is the most practiced standard of care today. However, patients with metastatic CRC (mCRC) do not benefit from the wide range of therapies available for CRC, which either owe to unresectability or co-morbidity or more importantly resistance to therapy. 5-fluorouracil (5-FU) combined with leucovorin, oxaliplatin, or irinotecan (FOLFOX or FOLFIRI) has been routinely employed as the first-line therapy in colon cancer, but patients often develop resistance to 5-FU. Additionally, tumor cell dormancy plays a major role in tumor relapse which leads to poor prognosis in the patients. Despite many advances, the understanding of therapy-induced resistance is still in its infancy. Here, we show that 5-FU-induced tumor cell secretome helps in the outgrowth and metastasis of 5-FU-resistant clones in colon cancer. We used parental and 5-FU-resistant colon cancer cell lines, and transgenic zebrafish embryos to test the hypothesis and perform the colon cancer cell-based functional assays. We observed that 5-FU resistant (5-FU-R) colon cancer cells showed an increase in proliferation and survival when cultured with the secretome of 5-FU exposed colon cancer cells compared to the DMSO-induced secretome. Interestingly, we also noted elevated migration and invasion in the 5-FU-R colon cancer cells exposed to 5-FU-induced secretome compared to the DMSO counterpart. Additionally, in zebrafish xenograft, we found that 5-FU-R colon cancer cells cultured with 5-FU-induced secretome showed higher tail-vein metastatic burden compared to the 5-FU-R cells cultured with DMSO-induced secretome. This provides a background to further study in detail the therapy-induced resistance as well as dormancy in colorectal cancer which will help to develop approaches to prevent or reverse chemoresistance in patients who receive systemic therapy for mCRC.

#1995 DUSP4 loss enhances resistance to encorafenib plus cetuximab in *BRAF* mutant colorectal cancer.

K. Needham, F. Chionh, S. Kaczmarczyk, C. Kearney, L. Jenkins, I. Luk, J. M. Mariadason;
Olivia Newton-John Cancer Research Institute, Melbourne, Australia

The 5-year survival rate for metastatic colorectal cancer (CRC) is less than 14%. Hyperactivation of the ERK/MAPK pathway occurs at a high frequency in CRC, due to mutations (RAS, BRAF) or overexpression/amplification (EGFR) of its signalling components. Aberrant activation of this pathway drives tumour growth and survival and several inhibitors of this pathway are now clinically utilized. The *BRAF* V600E activating mutation occurs in ~10% of CRC patients and is correlated with an extremely poor prognosis. Use of the small molecule BRAF inhibitor encorafenib in combination with the EGFR inhibitor cetuximab is now approved for *BRAF* V600E mutant patients, however, the objective response rate is only ~20% and the treatment is rarely curative. Therefore, there is an urgent need to identify predictive biomarkers of response to encorafenib+cetuximab treatment. Dual-specificity phosphatase 4 (DUSP4) is rapidly induced upon activation of ERK/MAPK signaling upon which it acts as a critical negative regulator of signaling output by directly de-phosphorylating ERK. We have observed that DUSP4 is highly expressed in *BRAF*-mutant CRC cell lines and primary tumours, although there is a range of expression. Whether DUSP4 expression status impacts on response to encorafenib+cetuximab therapy is unknown. The aim of this study therefore was to determine the role of DUSP4 on sensitivity of *BRAF*-mutant CRC cells to encorafenib+cetuximab treatment *in vitro*. To examine this, we determined the impact of DUSP4 knock-down, knock-out and re-expression on sensitivity of *BRAF*-mutant CRC cancer cell lines to encorafenib+cetuximab treatment. Screening a panel of BRAF mutant CRC cell lines for sensitivity to encorafenib+cetuximab revealed a subset of resistant cell lines had either low or undetectable DUSP4 protein expression, while all sensitive cell lines had high DUSP4 expression. siRNA-mediated knockdown of DUSP4 in DUSP4 expressing *BRAF*-mutant CRC cell lines increased pERK and pFRA1, suggesting activation of ERK/MAPK signalling. DUSP4 knockdown also reduced sensitivity of BRAF mutant CRC cell lines to encorafenib+cetuximab compared to control. These findings were further validated using DUSP4 knock-out with CRISPR-Cas9. Conversely, DUSP4 re-expression in *BRAF*-mutant CRC cell lines lacking DUSP4 expression, decreased pERK and increased sensitivity to encorafenib+cetuximab treatment. These results demonstrate that DUSP4 regulates ERK/MAPK signalling in BRAF mutant CRC cell lines and that loss of DUSP4 promotes resistance to encorafenib plus cetuximab treatment. These findings warrant investigation of DUSP4 expression status as a predictive biomarker of encorafenib+cetuximab response in patient samples.

#1996 Novel mechanism of temozolomide resistance in glioblastoma.

Y. Hung, M. Kiang, K. Leung;
The University of Hong Kong, Hong Kong, China

Intrinsic expression of PD-1 has been discovered in different types of tumurs, exhibiting either oncogenic or tumor-suppressing function. In glioblastoma (GBM), intrinsic PD-1 has been found to play a role in promoting the proliferation and self-renewal of brain tumor-initiating cells through nuclear factor κB without involving PD-L1 ligation, with unknown factors activating this signalling pathway. Meanwhile, TMZ resistance significantly contributes to treatment failure and an extremely poor prognosis for GBM. This study investigated whether intrinsic PD-1 is also expressed in differentiated human GBM cell lines and its role in GBM proliferation and temozolomide (TMZ) resistance. In vitro studies demonstrated the presence of PD-1 in both U87 and U251 TMZ-sensitive and -resistant cell lines, with a higher expression on TMZ-resistant cell lines. *PDCD1* knockdown led to decreased GBM progression, including cell proliferation, colony formation and cell migration, in TMZ-resistant U87 and U251 cell lines using cell viability assays. It also resensitizes these cell lines to TMZ. Overexpression of *PDCD1* in the *PDCD1*-knockdown cell lines increases their proliferation and restores their resistance to TMZ. Treatment of U87 and U251 TMZ-resistant cell lines with TMZ upregulated PD-1 expression. An orthotopic xenograft mouse model is further deployed by injecting previously cultured U87 and U251 cell lines into the mouse brains. A smaller tumour size is observed in the model with *PDCD1* knockdown model than the one without *PDCD1* knockdown when treated with TMZ. This study reveals that intrinsic PD-1 expression contributes to TMZ resistance in GBM and TMZ may be a factor activating the PD-L1-independent PD-1 signalling. PD-1 and its downstream signalling pathway, such as SHP-2 and IKK, may be potential therapeutic targets for GBM patients with TMZ resistance. Co-administration of TMZ and agents inhibiting the intrinsic PD-1 signalling pathway can potentially produce synergistic therapeutic effects. The higher expression of PD-1 on TMZ-resistant GBM than on TMZ-sensitive GBM also suggests that the intrinsic PD-1 level can be a predictor of TMZ outcome.

#1997 The small GTPase ARF6 augments BRAF and PI3K expression to promote melanoma survival.

J. Wang, C. Rich, A. Rogers, S. Holmen, R. Wolff, A. Grossmann;
University of Utah Huntsman Cancer Institute, Salt Lake City, UT

RAF and MEK inhibitors greatly benefit BRAF-mutant melanoma patients, but eventually, nearly 80% of patients relapse. Reactivation of MAPK signaling and activation of PI3K/AKT signaling play a major role in the development of targeted therapy resistance. Therefore, understanding how tumor cells regulate these signaling pathways may yield new insights into drug resistance. The small GTPase ARF6, a member of the RAS superfamily, influences oncogenic signaling by controlling cytoskeletal rearrangements and through endomembrane trafficking. We previously reported that ARF6 is aberrantly activated in metastatic melanoma and that activation of ARF6 is sufficient to promote invasion and accelerate spontaneous metastasis *in vivo* through WNT5A/beta-catenin and PI3K/AKT signaling. In contrast to ARF6 activation, herein we show that tumor-specific deletion of *Arf6* significantly limits development and progression of $BRAF^{V600E}$ melanoma *in vivo*. Mechanistically, we discovered these ARF6-dependent phenotypes may be attributed to a previously unknown role for ARF6 in augmenting $BRAF^{V600E}$ and PI3K protein levels. Specifically, pharmacologic or genetic activation ARF6 (ARF6-GTP) is sufficient to increase $BRAF^{V600E}$ and PI3K protein levels in both murine and human melanoma. As a result, ARF6-GTP is also sufficient to enhance activation of MEK, ERK and AKT. Importantly, murine tumors expressing constitutively active ARF6 ($ARF6^{Q67L}$) show increased expression of anti-apoptotic proteins compared to $ARF6^{WT}$ tumors. Together these data suggest that ARF6 promotes tumor survival through augmentation of the BRAF/MAPK and PI3K/AKT pathways. To test this, we pharmacologically activated ARF6 during serum withdrawal or vemurafenib treatment. In both conditions, ARF6 activation is sufficient to prevent apoptosis. Surprisingly, we found that vemurafenib treatment leads to ARF6 activation, suggesting that ARF6 may be an important component of the cellular machinery that reactivates MAPK signaling after RAF inhibition. Indeed, pharmacologic activation of ARF6 maintains MAPK signaling (pERK levels) in the presence of vemurafenib and enhances pERK and pAKT-mediated suppression of apoptotic signaling. In summary, our data suggest that in addition to well-established roles in tumor cell invasion, ARF6 is a crucial mediator of survival during tumor progression and in the context of BRAF targeted therapy. More work is needed to understand how ARF6 activation increases BRAF and PI3K expression and if ARF6 activation contributes to the development of persister cells in melanoma.

#1998 ABCB1 promotes uveal melanoma cell resistance to FR900359 and identifies a tumor cell subpopulation with a distinct gene expression signature.

S. D. Murray[1], J. D. Riordan[1], E. R. Anderson[1], M. D. Onken[2], K. J. Blumer[2], A. J. Dupuy[1], C. S. Stipp[1];
[1]University of Iowa Holden Comprehensive Cancer Center, Iowa City, IA, [2]Washington University School of Medicine, St. Louis, MO

Uveal melanoma (UM) is the leading form of intraocular cancer in adults and the second most common form of melanoma. Although rare, UM has a median survival rate of ~1 year after metastasis occurs. Metastatic UM is largely refractory to treatment and there are no effective pharmacological therapies, resulting in poor overall survival. In >90% UM cases, the oncogenic initiator proteins are constitutively active mutant GNAQ or GNA11 proteins (GNAQ/11). FR900359 (FR) is a natural compound that inhibits GNAQ/11 and has anti-proliferative effects on UM cells. To identify key oncogenic mechanisms downstream of mutant GNAQ/11, we performed a *Sleeping Beauty* (SB) transposon forward genetic screen to identify drivers of FR resistance. The SB screen identified ATP-binding cassette sub-family B member 1 (ABCB1) as one of the top genes upregulated by SB in FR-resistant UM cell populations. We determined that although ABCB1 does not provide immediate resistance to FR, the overexpression of ABCB1 leads to emergence of resistant colonies at a much higher rate than spontaneous resistance, validating ABCB1 as contributors to FR resistance. Unexpectedly, immunofluorescence revealed that a relatively small fraction of UM cells strongly expresses the transgenes after stable transfection. Immunoblotting confirmed that ABCB1 expression was initially modest in ABCB1-transfected populations but increased in the cells that developed resistance to FR. To examine the kinetics of FR resistance, population doubling versus time (PDVT) assays were performed in UM cells expressing ABCB1 or empty vector control treated with FR or vehicle. FR potently suppressed the proliferation of vector control cells. Drug-naïve ABCB1-transfected cells developed resistance to FR over time but accomplished fewer population doublings than vehicle-treated cells in the same time interval. Once transgenic populations emerged as resistant populations in FR, they grew similarly in drug or vehicle. Ongoing RNA-sequencing analysis from PDVT samples has identified distinct gene expression signatures associated with FR treatment and ABCB1 expression. These findings are expected to illuminate tumor cell heterogeneity amongst UM cell populations that may be related to drug resistance and metastasis.

#2000 Role of O-GlcNAc conjugation and TS translational repression in 5-FU/LV resistance in CRC and CF10 response.

C. C. Okechukwu, X. Ma, W. H. Gmeiner;
Wake Forest University School of Medicine, Winston-Salem, NC

Rationale: Fluoropyrimidine drugs (FPs; e.g., 5-FU) are widely used to treat colorectal cancer (CRC), the 3rd leading cause of cancer-related mortality. However, acquired resistance to 5-FU is a principal cause of treatment failure in the metastatic setting. Further, previous studies selected for cells resistant to single agent 5-FU however 5-FU is invariably used clinically in combination with the reduced folate leucovorin (LV). Our studies focus on resistance mechanisms upon treatment with 5-FU+LV in folate-restricted media and test if CF10, a novel polymeric FP being developed in our laboratory displays activity in CRC cells resistant to 5-FU+LV.

Experimental: We selected CRC cells (HCT-116, LS174T, HCT15, MC38) resistant to 5-FU+LV by selecting for survival upon culture in folate-restricted media with stepwise increased concentrations of 5-FU+LV over 5 months. Since elevated thymidylate synthase (TS) levels were observed in multiple studies selecting CRC cells for 5-FU resistance, we performed Western blot on cell lysates from parental and (5-FU+LV)-R cells. Since Myc and p53 expression are regulated in part via translational inhibition by TS binding to these mRNAs we also compared Myc and p53 levels in parental and (5-FU+LV)-R cells by Western blot. Further, since TS, Myc, and p53 protein stability are all regulated in part via O-GlcNAc conjugation we tested if OGT levels were changed in (5-FU+LV)-R cells. Resistance factors for CF10 were also determined in (5-FU+LV)-R cells.

Results: A surprising result was that basal TS levels were reduced in (5-FU+LV)-R cells relative to the parental cells. We also observed that TS levels were increased in both parental and (5-FU+LV)-R cells by 5-FU+LV treatment however the effect was much greater in (5-FU+LV)-R cells. We observed strongly decreased p53 and Myc levels in the (5-FU+LV)-R cells. CF10 treatment further decreased p53 and Myc levels in parental cells, but increased p53 and further decreased Myc in (5-FU+LV)-R cells. In contrast, 5-FU alone treatment in (5-FU+LV)-R cells increased Myc and decreased p53 levels and further decreased in combination with LV. CF10 retained strong activity in (5-FU+LV)-R cells.

Conclusions: Overall, we have validated that cancer cells can be cultured under conditions with human-like folate levels and selected for resistance to 5-FU+LV under folate-restricted conditions. The causes of 5-FU+LV resistance are multi-factorial and include TS overexpression induced by 5-FU+LV treatment that may be mediated by O-GlcNAc conjugation. We demonstrated that CF10 is more potent than 5-FU, and importantly its potency advantage is enhanced in cells selected for 5-FU+LV resistance. Our studies support CF10 translation for treatment of metastatic CRC in patients with progressive disease following treatment with combination therapy that includes 5-FU+LV.

#2001 Autocrine HGF maturation as a targetable regulatory step in cetuximab resistance in colorectal cancer.

V. Truong Jones[1], R. Graves-Deal[2], Z. Cao[2], G. Bogatcheva[2], M. A. Ramirez[2], S. J. Harmych[1], J. N. Higginbotham[2], C. C. Wahoski[1], N. Joshi[2], J. T. Roland[2], G. D. Ayers[2], Q. Liu[2], R. J. Coffey[2], J. W. Janetka[3], **B. Singh**[2];

[1]Vanderbilt University, Nashville, TN, [2]Vanderbilt University Medical Center, Nashville, TN, [3]Washington University School of Medicine, Saint Louis, MO

Although amplifications and mutations in receptor tyrosine kinases (RTKs) act as bona fide oncogenes, in most cancers, RTKs maintain moderate expression and remain wild-type. Consequently, cognate ligands control many facets of tumorigenesis, including resistance to anti-RTK therapies. Herein, we show that the ligands for the RTKs MET and RON, HGF and HGFL, respectively, are synthesized as inactive precursors that are activated by cellular proteases. Our newly generated HGF/HGFL protease inhibitors could overcome both *de novo* and acquired cetuximab resistance in colorectal cancer (CRC). Conversely, HGF overexpression was necessary and sufficient to induce cetuximab resistance and loss of polarity. Moreover, HGF-induced cetuximab resistance could be overcome by the downstream MET inhibitor, crizotinib, and upstream protease inhibitors. Additionally, HAI-1, an endogenous inhibitor of HGF proteases, (i) was downregulated in CRC, (ii) exhibited increased genomic methylation that correlated with poor prognosis, (iii) HAI-1 expression correlated with cetuximab response in a panel of cancer cell lines, and (iv) exogenous addition of recombinant HAI-1 overcame cetuximab resistance in CC-HGF cells. Thus, we describe a targetable, autocrine HAI-1/Protease/HGF/MET axis in cetuximab resistance in CRC.

#2003 Chromatin based targeting of a master regulatory complex in estrogen receptor epithelial ovarian cancer.

S. K. Jaiswal[1], K. Fedkenheuer[1], R. Khamar[1], H. Tan[1], V. Gotea[1], A. Elkahloun[1], C. Annunziata[2], L. Elnitski[1];
[1]National Human Genome Research Institute, Bethesda, MD, [2]National Cancer Institute, Bethesda, MD

Ovarian cancer remains a significant contributor to cancer-related mortality in the United States, with low survival rates over the past decades. Hormonal therapies targeting estrogen receptors have shown limited efficacy. To explore mechanism of the inefficacy, our approach involved investigating ESR1 degradation within the higher order chromatin structure formed by Megacomplex. We identified a 1.3MDa Megacomplex containing ESR1, FOXA1 and PITX1, with colocalization at 2,440 genomic positions within the PEO4 cell line. Unlike cytoplasmic ESR1, the nuclear form was degraded minimally by ICI182780 (ICI), moreover, ESR1 incorporated into the Megacomplex macromolecule was least degraded. We hypothesized that this resistance might be due to sequestration within the Megacomplex, thereby preventing ICI from effectively targeting ESR1. Addition of a small molecule inhibitor of active chromatin, JQ1, in combination with ICI effectively enhanced the degradation of ESR1 within Megacomplex. The combination stopped nuclear occupancy of ESR1 and also degraded the cytoplasmic protein, thus breaking the ESR1 signaling circuit responsible for tumor cell proliferation. Pathway enrichment results consistently identified similar gene sets obtained independently for RNA-seq analysis after ESR1 modulation, and ChIP-seq analysis of Megacomplex bound genes. Likewise, proteins enriched within the Megacomplex macromolecule, as revealed from mass-spec analysis, returned similar pathway enrichments, directly implicating Megacomplex in ESR1 ovarian cancer gene regulation. We conclude, ESR1 in Megacomplex is resistant to ICI and sensitized by combining ICI with JQ1. This combined treatment strategy showed inhibition of cell proliferation and viability by uncovering ESR1 within the Megacomplex, thus elucidating a novel drug resistance mechanism.

#2004 CDC7 inhibition prevents neuroendocrine transformation in the lung and prostate through MYC degradation.

A. Quintanal-Villalonga[1], F. Uddin[1], K. Kawasaki[1], E. Redin[1], V. Durani[1], A. Sabet[1], W. Karthaus[1], Y. A. Zhan[1], S. Zaidi[1], M. Shaffer[1], H. Sridhar[1], J. Qiu[1], P. Manoj[1], E. De Stanchina[1], M. C. Haffner[2], C. L. Sawyers[1], C. M. Rudin[1];

[1]Memorial Sloan Kettering Cancer Center, New York, NY, [2]Fred Hutchinson Cancer Research Center, Seattle, WA

Neuroendocrine (NE) transformation occurs as a mechanism of resistance to targeted therapy in up to 14% and 30% of *EGFR*-mutant lung and AR-dependent prostate adenocarcinomas, respectively, leading to poor prognosis. Even if we know the tumor population at high risk of transformation (*TP53/RB1*-mutated), no therapies to prevent NE relapse are currently available. To identify therapeutic vulnerabilities for tumors undergoing NE transformation, we performed an *in vitro* CRISPR screen in a NE-transformed lung tumor model. This screen identified CDC7, involved in DNA replication and DNA damage response, as a potential therapeutic target in this setting. Proteogenomic analyses revealed CDC7 upregulation in lung and prostate clinical samples undergoing NE transformation, detected already in pre-transformation adenocarcinomas. These results indicated that CDC7 expression is induced already at early steps of transformation. Consistently, TP53/RB1-mutated lung and prostate adenocarcinomas exhibited higher CDC7 expression than their double wild-type counterparts. Combined ChIP-seq and promoter reporter assays indicated that CDC7 expression was directly regulated by TP53 and RB1 inactivation. Importantly, TP53/RB1-inactivation induced sensitivity to the CDC7 inhibitor simurosertib, unraveling a therapeutic vulnerability in tumors at high risk of NE transformation. Thus, we tested the combination of simurosertib with targeted therapy *in vivo* in different lung and prostate patient-derived models of NE transformation, namely TP53/RB1-knock out adenocarcinomas known to undergo NE transformation on targeted therapy. In these, simurosertib was able to suppress NE transformation and dramatically delay tumor relapse. Trajectory analysis on single-cell transcriptomic data for such models revealed a NE transformation transcriptional program occurring already in the untreated tumors before transformation. Remarkably, simurosertib treatment reverted this transcriptomic state and induced a reversion to the original adenocarcinoma transcriptomic profile. CDC7 inhibition led to increased proteasomal activity and degradation of MYC, a stemness transcription factor involved in NE transformation. Ectopic overexpression of MYC^{T58A}, a proteasome degradation-resistant MYC isoform, rescued the NE phenotype in these transformation models, suggesting that CDC7 inhibition-induced MYC degradation is the mechanism by which NE transformation is prevented. In sum, CDC7 inhibition may suppress, or at least dramatically delay NE transformation in patients with lung and prostate adenocarcinomas at high risk of transformation, by inducing MYC proteasomal degradation. The clinical availability of CDC7 inhibitors, currently in phase II clinical trials after demonstrating tolerability and preliminary efficacy, will allow rapid translation of these results into the clinics.

#2006 Deciphering the interplay of β-catenin/YAP signaling and alveolar lineage plasticity during targeted therapy in non-small cell lung cancer.

Yu-Ting Chou[1], Wei Wu[2], Daniel Kerr[2], Macey Slota[3], Trever Bivona[1]

[1]Medicine/Cellular and Molecular Pharmacology/Helen Diller Family Comprehensive Cancer Center, University of California San Francisco; Chan-Zuckerberg Biohub, San Francisco, CA,[2]Medicine, University of California San Francisco, San Francisco, CA,[3]Urology, University of California San Francisco, San Francisco, CA

Molecularly targeted therapies have significantly enhanced clinical outcomes by directly addressing oncogenic driver mutations in genes such as EGFR. However, despite the success of treatments targeting these mutations, long-term patient survival remains limited. This study investigates the molecular mechanisms underlying drug-tolerance in response to targeted therapies in non-small cell lung cancer (NSCLC). Using single-cell RNA sequencing of oncogene-driven human NSCLCs at the residual disease (RD) state during active targeted therapy, our investigation reveals an increase of an alveolar type I/II (AT1/2) mixed lineage program in surviving cancer cells, resembling an alveolar cell-like state. We observed increased WNT3A/4 ligands, FZD2 receptors, β-catenin signaling, and AT1/2 signatures at the RD stage. Consistent with clinical results, AT1/2 signatures and target genes of β-catenin and YAP are increased in drug-tolerant persister (DTP) cells in preclinical models. Additionally, we discovered that β-catenin and YAP form a stable nuclear protein complex in DTP cells. Disrupting β-catenin/YAP protein expression and stability in DTP cells by knocking down FZD2 or interrupting the destruction complex of β-catenin/YAP leads to re-sensitization to the EGFR inhibitor Osimertinib, suggesting a potential therapeutic approach. Furthermore, this therapeutic strategy decreased AT1/2 gene signatures. Our results highlight an interdependence between β-catenin and YAP, with both proteins playing crucial roles in sustaining DTP cells and promoting the alveolar cell like lineage plasticity. These findings shed light on the complex interplay between β-catenin/YAP signaling and alveolar signatures in the residual cancer state, offering mechanistic insights and potential therapeutic strategies to address drug tolerance and improve clinical outcomes.

#2007 Neurolysin: A novel architect of the prostate cancer microenvironment and therapeutic resistance.

C. Wang, P. Mu;
UT Southwestern Medical Center, Dallas, TX

Introduction: Prostate cancer is the second leading cause of cancer-related death in American men, primarily driven by its ability to evade therapeutic interventions. This study uncovers a novel paradigm where neurolysin, a peptidase previously ascribed to neuronal function, orchestrates the tumor microenvironment (TME) by interfacing with cellular motor proteins. This interaction precipitates a series of events that not only fortify the cancer cells' survival but also underpin the resistance to antiandrogen therapies.

Experimental Procedures: We deployed advanced prostate cancer models to delve into the extra-neuronal influence of neurolysin, probing its role in the orchestration of the TME. An exhaustive suite of transcriptomic and proteomic analyses, complemented by comprehensive patient cohort studies, laid the foundation for unraveling the complex interplay between neurolysin, motor proteins, and the TME dynamics.

Results: Our data elucidates that neurolysin's depletion correlates with an altered TME, conducive to cancer proliferation and resilience against targeted therapies. This shift is mediated through neurolysin's interaction with cellular motor proteins, a liaison that appears to be a cornerstone in TME modulation. A significant subset of prostate cancer cases exhibits a neurolysin deficiency, paralleling more aggressive disease and therapeutic defiance, highlighting its role as a critical biomarker and a novel target for intervention.

Conclusions: Neurolysin steps into the limelight as a pivotal modulator of the TME, operating through mechanisms distinct from its known neuronal functions. Its interplay with motor proteins opens a novel avenue in prostate cancer biology, providing a unique perspective on the regulation of the TME and subsequent therapeutic resistance. Targeting this newly discovered regulatory axis presents a promising therapeutic strategy that could potentially redefine the clinical approach to managing prostate cancer and may have implications for other malignancies driven by similar TME alterations.

#2008 The N6-methyladenine-long noncoding RNA axis promotes drug resistance through PI3k signaling in leukemia.

Y. Tan[1], C. Zhou[1], S. Bian[1], W. Walter[2], J. Pang[1], T. Cheng[1], G. Huang[3], G. Hoermann[2], W. Tse[1], S. Liu[1];

[1]Case Western Reserve University, Cleveland, OH, [2]MLL Munich Leukemia Laboratory, Munich, Germany, [3]The University of Texas Health Science Center at San Antonio, San Antonio, TX

Disease recurrence characterized by drug resistance remains a major hurdle to the successful cancer treatment. Long noncoding RNAs (lncRNAs) and RNA N^6-methyladenosine (m6A) have been linked to cancer recurrence. However, if and how lncRNAs and m6A coordinately determine drug resistance in tyrosine kinase (TK)-driven cancers are still unclear. We hypothesize that upon exposure to TK inhibitors (TKI), the dynamic m6A methylation epitransciptomically allows a set of proliferation/anti-apoptosis-relevant lncRNAs bearing m6A motifs to be rapidly upregulated, thus facilitating a subpopulation of cancer cells to evade TKI killing. By performing transcriptomic and epitransciptomic profiling in long-term TKI (nilotinib)-deprived leukemia resistant cells, we show that many differentially expressed lncRNAs enrich m6A, and more lncRNAs tend to have higher m6A content in resistant cells. We further demonstrate a broad clinical relevance of our findings, showing that upregulation of specific top-ranked lncRNAs (e.g., SENCR, PROX1-AS1, LN892) in TKI-resistant cell lines also occurs in leukemia patients at the diagnostic stage, blast crisis phase or in those not-responding to TKI treatment compared to chronic phase or TKI responders, respectively. Some of the upregulated lncRNAs in leukemia patients pre- and post-TKI treatment predict unfavorable outcomes and are associated with shorter survival duration. Through proliferative and clonogenic assays, we demonstrate that knockdown of SENCR, PROX1-AS1 or LN892 impairs resistant cell growth and renders resistant cells sensitive to nilotinib-induced cell death. We further found that this lncRNA upregulation is attributed to FTO-dependent m6A hypomethylation that stabilizes lncRNA transcripts. Using ectopic expression or genetic/pharmacological inhibition, we demonstrate that lncRNA upregulation empowers resistant cell growth through an activated PI3K signaling as supported by overexpression of PI3K signaling mediators (e.g., ITGA2, F2R, COL6A1). Treatment with PI3K inhibitor alpelisib sensitizes TKI-resistant cells to TKI-induced cell death and reduces leukemia burden in mice via downregulation of F2R, ITGA2, and COL6A1. In conclusion, our findings add a new layer to the complexity of mechanisms regulating leukemia cell fate under TKI selection and raise the possibility that the m6A-regulated lncRNAs represents a new non-genetic factor to affect the development and maintenance of TKI resistance; our discoveries identify a promising therapeutic target, the m6A-lncRNAs axis, for specifically the most challenging patient subpopulations who are TKI non-responders/relapsed but do not carry the acquired mutations on top of BCR/ABL; our results also uncover a strong predictor, m6A-regulated lncRNA-PI3K axis, for poorer prognosis and failure in drug response which might be a pan-cancer mechanism.

#2009 Novel clinically relevant CLIP-170 variants display an extended conformation microtubule-lattice bound conformation associated with taxane resistance.

U. del Castillo, K. Sahu, W. G. Stone IV, M. A. Shah, P. Giannakakou;
Weill Cornell Medicine, New York, NY

Taxanes are microtubule (MT)-stabilizing drugs widely used for the treatment of solid tumors, including the highly prevalent cancers of the breast, the prostate and gastric cancer. However, despite their initial activity, taxane resistance invariably occurs, leaving patients with limited therapeutic options. Currently, the molecular determinants of clinical taxane resistance remain poorly understood. We recently identified CLIP-170S, a novel truncated variant of the MT plus-end binding protein CLIP-170, that confers taxane resistance *in vitro* and is associated with clinical taxane resistance in patients with gastric cancer. We further showed that CLIP-170S is aberrantly localized along the MT lattice, thus impairing taxane access to its binding site in the MT lumen. However, the mechanism underlying the resistance-inducing extensive lattice localization of CLIP-170S is unknown. The activity and MT binding properties of canonical CLIP-170 are regulated by conformational changes mediated by the interaction of its N- and C-terminal domains. In its inactive, “closed” conformation, CLIP-170 is soluble as the N- and C-terminal domains interact with each other. In the active “open” conformation, CLIP-170’s N- and C-terminal domains are apart, thus exposing its MT-binding domain and allowing MT plus-end binding. As CLIP-170S is missing part of its N-terminal domain, we hypothesized that CLIP-170S is constitutively displayed in an open conformation that promotes its extensive and aberrant localization to the MT lattice. To prove this hypothesis, we used the FKBP-rapalog-FRB system to “force” CLIP-170S to assume a “closed” conformation. We generated a fusion CLIP-170S protein tagged with FKBP and FRB domains in its N- and C-terminal, respectively. The addition of rapalog induced FKBP (N-ter) and FRB (C-ter) domains to interact, promoting CLIP-170S to adopt a “closed” conformation. CLIP-170S in this “closed” conformation resulted in its release from the MT-lattice and restored taxane binding to MTs. We next extended our search to other CLIP-170 clinically prevalent variants with sequence alteration predicted to bind to the MT-lattice and potentially interfere with taxane sensitivity. This search identified CLIP-170IR (an intron retention variant) and several other truncation mutants prevalent in gastric, breast and lung cancer cell lines. Experimentally, we showed that these variants not only phenocopy CLIP-170S binding to the MT- lattice but also confer taxane-resistance. Together, these data demonstrate a novel mechanism of taxane resistance mediated by CLIP-170 mutations that induce CLIP-170 to adopt a constitutively “open” MT-lattice binding conformation, which renders them susceptible to causing taxane resistance.

#2010 TRIM27 Interacts with KLF12 to regulate L1CAM expression, influencing cisplatin resistance and cancer metastasis in esophageal squamous cell carcinoma.

H. Zhang, **C. Li**, J. He;
Department of Thoracic Surgery, National Cancer Center/National Clinical Research Center for Cancer/Cancer Hospital, Chinese Academy of Medical Sciences and Peking Union Medical College, Beijing, China

Esophageal squamous cell carcinoma (ESCC) accounts for 85% of cases of esophageal cancer worldwide and is the predominant form of esophageal cancer in Asia. A significant number of patients with ESCC are diagnosed at an advanced stage, resulting in poor prognosis. Cisplatin resistance and cancer metastasis are the main clinical challenges in the treatment of advanced ESCC. KLF12 has been extensively characterized as a transcriptional repressor, and previous studies have unveiled its roles in angiogenesis, neural tube defect, and NK cell proliferation. However, the precise contribution of KLF12 to cancer treatment remains undefined. Here, we show that KLF12 is downregulated in various cancer types, and KLF12 downregulation promotes cisplatin resistance, cancer metastasis and recruitment of regulatory T cells (Tregs) in ESCC cell lines. Mechanistically, KLF12 binds to the promoters of L1CAM and represses its expression. Depletion of L1CAM abrogates cisplatin resistance, cancer metastasis, and Treg recruitment caused by KLF12 loss. Moreover, the E3 ubiquitin ligase TRIM27 binds to the N-terminal region of KLF12 and ubiquitinates KLF12 at K326 via K33-linked polyubiquitination. Notably, TRIM27 depletion enhances the transcriptional activity of KLF12 and consequently inhibits L1CAM expression. Overall, our study has firstly elucidated a novel regulatory mechanism involving TRIM27, KLF12 and L1CAM, which plays a substantial role in cisplatin resistance and cancer metastasis in ESCC, and targeting KLF12/L1CAM axis may be a promising approach for ESCC treatment.

#2011 MAOA Drives Anti Androgen Therapy Resistance in Advanced Prostate Cancer by Conferring Neuroendocrine Plasticity via a Twist1 BRN2 Signaling Pathway.

J. Wei, J. Wang, C.-h. Chen, W. Guan, B. Wu;
Washington State University, SPOKANE, WA

Background: Therapy resistance in cancer is often linked to cancer cell state or lineage changes. In prostate cancer (PCa), a subset of castration-resistant prostate cancer (CRPC) loses reliance on the androgen receptor (AR) signaling and gains neuroendocrine (NE) traits through a lineage switch along disease progression. However, the molecular mechanisms driving such cellular lineage plasticity remain unclear. This study investigated the functional and mechanistic role of monoamine oxidase A (MAOA) in driving adenocarcinoma (adeno)-to-NE lineage conversion in CRPC cells upon enzalutamide (ENZ), a FDA-approved newer-generation antiandrogen drug, and evaluated the efficacy of MAOA inhibitors for treating CRPC and overcoming ENZ resistance.**Methods:** ENZ-resistant C4-2B and CWR-R1 cells (C4-2B^{ENZR} and CWR-R1^{ENZR}) CRPC cells were transfected with a PSA promoter-driven GFP expression construct for isolating a PSA$^{lo/-}$ cell population distinct from PSA^{hi} cells, which was used for manipulation of MAOA expression levels and subsequent functional assays in vitro and in vivo. The MAOA expression levels were determined and correlated with NE parameters in PCa clinical samples by immunohistochemistry and data mining of multiple publicly available clinical datasets. **Results:** MAOA protein expression was significantly upregulated in the PSA$^{lo/-}$ ENZ-resistant cell population, accompanied by concomitant activation of NE markers and downregulation of luminal markers including AR and AR targets, compared to the PSA^{hi} counterpart. Elevated MAOA expression was also found in PCa patient samples associated with NE features from multiple independent cohorts. Silencing MAOA suppressed the proliferation, migration, invasion, stem-like properties and NE plasticity of both PSA$^{lo/-}$ C4-2B^{ENZR} and CWR-R1^{ENZR} cells. Moreover, co-culturing adeno LNCaP or C4-2B cells with MAOA-silenced PSA$^{lo/-}$ cells exhibiting a repressed secretory phenotype attenuated acquired induction of NE markers and proliferation of adeno cells as compared to controls. Mechanistically, MAOA induces Twist1, which directly activates the transcription and expression of BRN2, a master neural transcription factor known to confer NE differentiation and anti-AR therapy resistance in CRPC. Further, pharmacological inhibition of MAOA greatly enhanced the growth-inhibitory efficacy of ENZ with ENZ sensitivity restored in ENZ-resistant LuCaP PC PDX-derived organoids as well as a PSA$^{lo/-}$ CWR-R1^{ENZR} xenograft mouse model.**Conclusion:** Our results suggest MAOA as a potential therapeutic target for reversing ENZ resistance in CRPC treatment by blockade of NE transdifferentiation.**Funding Acknowledgements:** This work was supported by the NIH/NCI grants R37CA233658 and R01CA258634 (to B. Wu) and the DOD Department of Defense EIRA award W81XWH-21-1-0218 (to J. Wei)

#2012 Extrachromosomal DNA promotes drug resistance in pancreatic ductal adenocarcinoma cells.

T. Vorberg[1], M. Reitberger[1], B. Rodriguez-Martin[2], M. Starostecka[2], O. Kossi[1], V. Vogel[1], J. Korbel[2], A. Trumpp[1], M. Sprick[1];
[1]German Cancer Research Center, Heidelberg, Germany, [2]European Molecular Biology Laboratory, Heidelberg, Germany

Pancreatic ductal adenocarcinoma (PDAC) is the fourth leading cause of cancer-related deaths in Western Countries and has been predicted to become the second leading cause of cancer-related deaths by 2030. Difficulties in early detection as well as strong chemoresistance of the disease prevent the successful treatment of PDAC patients. Although we have previously identified CYP3A5 as a mediator of paclitaxel resistance, further targets remain elusive. Thus, we set out to identify these CYP3A5-independent mechanisms which could lead to the identification of novel biomarkers and drug targets to improve PDAC treatment. For this project, pancreatic cancer cell lines were derived from treatment-naive PDAC samples and exposed to increasing paclitaxel concentrations to induce resistance. The cells were characterized on a genomic and transcriptomic level using short-read sequencing as well as optical mapping to characterize potential candidate genes *in vitro*. In our results, multi-drug resistance protein 1 (ABCB1) was highly upregulated in our differential gene expression analysis and confirmed as a CYP3A5-independent mediator of acquired paclitaxel resistance. Its overexpression was mediated by extrachromosomal DNA (ecDNA) amplifications upon drug treatment. These circular DNAs were characterized by short-read sequencing as well as long-read optical mapping, which revealed the structures of the most abundant molecules. Furthermore, we investigated the biogenesis of the ecDNA. Current models propose different events such as chromothripsis or breakage-fusion-bridge cycles to initiate ecDNA formation, however, knowledge about the underlying mechanisms remains limited. To study the ecDNA dynamics, we generated ecDNA-negative cell clones from a paclitaxel resistant PDAC cell line. Interestingly, our clonal cell population appears to show the capacity for ecDNA *de novo* generation and quickly adapts to changing selective pressure such as therapy. This finding might unveil new insights into the triggers of ecDNA formation and its dynamic regulation. In conclusion, our results suggest the clinical relevance of ABCB1 as a mediator of paclitaxel resistance in PDAC and we currently validate our findings in patient samples. However, ABCB1 inhibition is associated with severe side effects. Instead, the regulatory pathways associated with enhanced ABCB1 expression and the formation of ecDNAs might provide therapeutic potential. Additionally, the characterization of ecDNA *de novo* generation might unveil new insights into how cancer cells adapt to changing selective pressures.

#2013 Extracellular vesicles transfer miR-181a to confer PARP inhibitor resistance and induce *STING* degradation in *BRCA*-mutated triple-negative breast and ovarian cancers cells.

M. A. Bustos[1], T. Yokoe[1], Y. Shoji[1], Y. Kobayashi[1], S. Mizuno[1], T. Murakami[1], S. C. Sekhar[2], M. Knarr[3], S. A. Vasilev[1], A. DiFeo[2], R. Drapkin[3], D. S. B. Hoon[1];

[1]Providence Saint John's Health Center, Santa Monica, CA, [2]University Michigan, Ann Arbor, MI, [3]University of Pennsylvania, Pensylvania, PA

Background: Patients with *BRCA*-mutated breast cancer (BC), including triple-negative BC (TNBC), and ovarian cancer (OvCa) are treated with poly (ADP-ribose) polymerase inhibitors (PARPi). BC and OvCa tumors develop similar mechanisms of resistance to platinum-based agents and PARPi. This study aimed to identify microRNAs (miRs) inducing PARPi resistance in cancer cells that can be transferred by extracellular vesicles (EV).

Methods: Olaparib-resistant (OlaR) cell lines were analyzed for 2,083 miRs using HTG miRNA Whole Transcriptomic Analysis (WTA) and NGS. Functional assays were performed in *BRCA1*-mutated TNBC and OvCa cell lines. *In-silico* analysis were performed using TCGA, GTEx, CCLE, GDSC, and GEO databases.

Results: The miR-181 family (including miR-181a, p=0.001) was significantly upregulated in OlaR TNBC cell lines. High miR-181a levels occurred in tumor tissues of TNBC patients (p=0.001). miR-181a binds to the stimulator of interferon genes (STING) mRNA to promote STING mRNA degradation in OvCa. We *hypothesized* that miR-181a downregulates STING and downstream proinflammatory cytokines, to mediate PARPi resistance. miR-181a-overexpression induced olaparib resistance and STING downregulation in *BRCA1*-mutated TNBC cell lines. EV isolated from OlaR TNBC cell lines horizontally transferred miR-181a to non-resistant parental cell lines, which conferred PARPi-resistance and decreased STING. In clinical settings, *STING* levels were positively correlated with interferon gamma (IFNG) response scores (p=0.01). Low-IFNG response scores in HER2-negative BC patients showed a worse response to neoadjuvant treatment (p=0.001). Consistently, OlaR TNBC cell lines showed resistance to platinum-based drugs. OvCa cell lines resistant to cisplatin showed resistance to olaparib; but miR-181a knockout significantly improved olaparib sensitivity (p=0.001).

Conclusions: High levels of miR-181a decrease STING pathway, correlate with IFNG scores, drive PARPi and platinum-based drug resistance. Horizontal miR-181a EVs transfer can facilitate drug resistance in cells. The miR-181a-STING axis can be used for predicting PARPi responses in TNBC and OvCa tumors.

#2014 Tumor glycosylation impacts the efficacy of HER2 targeting therapies.

Ana Ruiz-Saenz[1], Roos Vincken[1], Denise Wolf[2], Veronica Steri[2], Laura van't Veer[2], John Martens[3], Danny Huylebroeck[3], Mark M. Moasser[2]

[1]CIC bioGUNE, Bilbao, Spain,[2]UCSF, San Francisco, CA,[3]Erasmus University Medical Center, Rotterdam, Netherlands

Cancer progression remains a major obstacle to the successful treatment of cancer. In HER2+ breast cancer, targeting therapies against HER2 have revolutionized the treatment landscape. However, predictive factors for response are largely unknown and a significant number of patients develop resistance. An extensive body of work has revealed a plethora of mechanisms of resistance. However, a key aspect of cancer cells has been largely overlooked: their aberrant glycosylation profile. Aberrant glycosylation of proteins is a hallmark in cancer and has been linked to multiple processes such as invasion, angiogenesis and modulation of the immune response. Yet the influence of altered glycosylation on the efficacy of HER2-targeted therapies remains unknown. Therefore, here, we address this question using clinical data, 3D co-culture systems and advanced live microscopy. Bioinformatics analysis of SPY-2 clinical trial data reveals an association of specific glycogenes with response to HER2-targeting therapies in breast cancer patients. We validated these findings in resistance cell models generated in-vitro and in-vivo using gain and loss of function assays. Furthermore, to provide a more relevant cell model system, we implement the use of 3D co-cultures of cancer spheroids and immune cells. Thus, our research addresses a largely unexplored area in cancer biology combining clinical data from tumor biopsies, trastuzumab-resistant cancer cell models and, live imaging of 3D heterotypic cultures. This work holds the potential to identify new markers of response to therapies and highlights the importance of the interplay of cancer cells and their microenvironment on the efficacy of current treatments.

EXPERIMENTAL AND MOLECULAR THERAPEUTICS: Microenvironment, Immunity, and DNA Repair in Therapeutic Response
Poster Session

#2018 Tumor treating fields (TTFields) disrupt cancer cell invasion by impacting cell-ECM traction forces.
S. M. Short, H. J. Bowers, J. A. Weis;
Wake Forest University School of Medicine, Winston-Salem, NC

Introduction: Tumor Treating Fields (TTFields) are an anti-cancer treatment that use low intensity, alternating electric fields. Anti-mitotic treatment effects of TTFields have been, to date, considered the primary anti-cancer effect. Recent studies have shown additional impacts on cancer cell invasion and migration, among other effects, resulting in a complex anti-tumor response derived from a combination of factors. By deploying computational imaging tools to assess experimental conditions that apply TTFields treatment to 3D cancer multicellular spheroid cultures, the goal of our study is to elucidate important mechanisms and effect sizes on anti-tumor effects relating to the modulation of cancer cell-extracellular matrix (ECM) biophysical interactions.
Methods: 3D multicellular tumor spheroids (MTS) are cultured using GFP-tagged U-87 MG glioma cells. A single 3D MTS is placed in a cell culture insert and embedded in collagen I ECM at 2.25 mg/mL. Fluorescent polystyrene microspheres are dispersed in the ECM to facilitate subsequent tracking of displacement fields induced by the MTS-ECM construct. Fluorescence microscopy imaging is acquired for all spheroids prior to treatment initiation. Then, with 3 replicates in each treatment condition, TTFields are applied for a duration of 48 hours at 200 kHz frequency with a no treatment condition as a control. At 48 hours, we acquire fluorescence microscopy images to track spheroid growth and bead-field displacement. To determine deformation fields induced by the cancer spheroid, we compare each image at 48 hours to their respective baseline image. Deformation fields are analyzed using a custom-developed analysis code that performs an initial alignment of the baseline and specific time point images using a global rigid registration. Next, we perform a B-spline based nonrigid image registration to generate an estimate of the deformation field vector at each pixel location within the image. Deformation intensity is measured within a circular region of interest ($r = 900$ μm) centered at the spheroid core.
Results: The average magnitude of displacement for treatment and control groups is 0.52±0.2 μm and 1.07±0.1 μm, respectively. Analysis of deformation fields reveals a significant difference ($p < 0.1$) in the magnitude of deformation present between treatment and control groups.
Conclusions: Implementation of our computational imaging analysis methods using rigid and nonrigid registration, we observe a 69.6% decrease in the magnitude of deformation in TTFields treated spheroids compared to control spheroids. Due to the decrease in deformation induced by cancer spheroids treated with TTFields, we conclude that TTFields impact cancer cell traction forces applied to the ECM to disrupt cancer cell invasion.

#2019 Primary cancer associated fibroblasts increase the chemoresistance of triple negative breast cancer cells by mitochondria metabolic upregulation.

I. Hofer[1], A. Mencattini[2], Y. Kieffer[1], E. Martinelli[2], M. Parrini[1], F. Mechta-Grigoriou[1];
[1]Institut Curie, Paris, France, [2]University of Rome Tor Vergata, Rome, Italy

Breast cancers (BCs) are the most prevalent cancers occurring in women. Tumor reoccurrence attributed to chemotherapy resistance remains a main challenge in fighting disease relapse. Cancer associated fibroblasts (CAFs) are the most prominent component of the tumor microenvironment (TME) and have already been implicated in therapy resistances. Although the exact molecular mechanisms behind this resistance remain unclear. In this regard, we recently identified 4 CAF populations (S1-S4) in ovarian and BCs, and showed that only CAF-S1 promote immunotherapy resistance as well as metastasis. Based on these observations, we are now investigating the impact of CAF-S1 on the chemotherapy response of BCs. To study the interactions between CAF-S1 and BC cells, we developed a tumor on chip (ToC) device, mimicking the TME in 3D. Using ToC live imaging, we show that primary CAF-S1 mediate a chemoprotective effect over luminal and triple negative BC (TNBC) cells by significantly decreasing their apoptosis rate as early as 10h after Doxorubicin and 40h after Paclitaxel treatment. Interestingly, CAF-S1 display a highly heterogenous response to Doxorubicin, allowing the classification into chemo-sensitive and -resistant CAF-S1. Regardless of premature CAF-S1 cell death, the chemoprotective effect over BC cells is maintained for at least 3 days. This indicates a crucial CAF-S1 - cancer cell cross talk at early timepoints. Additionally, by applying machine learning algorithms on live imaging videos, we demonstrate that physical proximity of CAF-S1 to BC cells immediately after treatment initiation correlates with BC cell survival, even after several days of treatment. This again implies cancer cell priming by CAF-S1 as a possible mechanism of chemotherapy resistance. To investigate this molecular interplay further, we performed scRNA-seq of ToC extracted and treatment naïve CAF-S1 and TNBC cells as well as bulk RNA-seq of patient derived TNBC tumors before/after chemotherapy treatment. We identify mitochondrial metabolic pathways to be upregulated in TNBC cells after CAF-S1 co-culture inside ToC devices and in TNBC cells of chemo-resistant patients enriched in CAF-S1 at baseline. We are now validating the impact of target gene knock downs on the survival of TNBC cells in CAF-S1 co-cultures after chemotherapy treatment on chip. Overall, these results provide insights into molecular mechanisms by which CAF-S1 promote chemotherapy resistance of breast cancers.

#2020 Determination of parameters to understand the metabolism in the tumor microenvironment by *in vivo* microdialysis.

Mariette Suzan Heins, Gunnar Flik

Charles River Laboratories, Inc., Groningen, Netherlands

The tumor microenvironment presents a unique surrounding with more favorable conditions for the cancer cells to growth thrive and interact than for the host cells. To obtain a better understanding of cancer biology and pathophysiology, information about the physiological state of the tumor microenvironment is crucial. By using the *in situ* microdialysis technique we can quantitate relevant modulators in the interstitial space of the tumor.

The current set of experiments demonstrates the benefits of the use of microdialysis in freely-moving awake tumor-bearing animals. Following inoculation, growth was monitored continuously and upon an average tumor volume of 400 mm^3, the animals underwent surgical implantation of microdialysis probes. The next day, the sample collection was initiated by perfusion of the implanted probes with dialysate fluid. Samples were continuously collected over several hours and stored at -80C. Levels of analytes indicative of metabolic and physiological conditions of the tumor microdialysis were quantified by EIA and/or LC-MS/MS analysis.

The microdialysis technology combined with sensitive analytical methods allows us to quantify several analytes from the tumor microenvironment simultaneously and monitor changes over time. Metabolic activity is an important indicator of tumor growth speed. Depletion of energy can lead to increases in lactate levels and acidification of the tumor microenvironment. Resulting in a reduction of host immunological efficacy. Elucidation of the status of the tumor environment during tumor growth and treatment allows for better translational models.

#2021 The RXR agonist MSU-42011 and the MEK inhibitor selumetinib reduce pERK levels in NF1-deficient cells and inhibit cytokine production in macrophages.

P.-Y. Hung[1], J. A. Moerland[1], K. T. Liby[2];

[1]Michigan State University, East Lansing, MI, [2]IU School of Medicine, Indianapolis, IN

Neurofibromatosis type 1 (NF1) is a common genetic disease that predisposes approximately 50% of affected individuals to develop plexiform neurofibromas (PNFs), which can progress to highly aggressive malignant peripheral nerve sheath tumors (MPNSTs) in approximately 10% of patients. NF1 is caused by mutations in the tumor suppressor gene *NF1*, which encodes for neurofibromin, a negative regulator of RAS activity. Selumetinib, a specific inhibitor of MEK1/2, is the only FDA-approved drug for NF1-associated PNFs. However, the anti-tumor effects of selumetinib are limited in MPNSTs and have dose-limiting side effects. Deficiency of the *NF1* gene not only promotes tumorigenesis but also has broad effects on the immune cells and cytokine signaling driven by hyperactive RAS signaling. Because macrophages account for almost half of cells in NF1 lesions and their infiltration correlates with disease progression, we hypothesized that targeting tumor-promoting immune cells could be an alternative approach for treating NF1. The novel retinoid X receptor (RXR) agonist MSU-42011 reduces tumor growth in experimental Kras-driven cancers by decreasing pERK expression, reducing tumor-promoting immune cells like CD206+ macrophages and regulatory T cells, and increasing activated cytotoxic T cells. Here, we treated NF1-deficient cells and macrophages with MSU-42011 and selumetinib, either alone or in combination, using monoculture and conditioned media (CM) conditions. In human PNF cells and mouse MPNSTs, treatment with 200 nM MSU-40211 or 50 nM selumetinib for 3 hours reduced pERK protein levels compared with untreated controls, and the combination treatment enhanced this reduction in pERK protein levels. Additionally, there was a trend toward reduction in cell viability with increasing drug concentrations after 72 hours of the combination treatment. Moreover, CM from human and mouse PNF cells increased the mRNA expression of monocyte chemoattractant *CCL2* (C-C motif chemokine ligand 2) and the secretion of IL-6 and TNFα in human THP1 monocytes/macrophages and bone marrow derived macrophages (BMDM). Notably, MSU-42011 and selumetinib alone inhibited *CCL2* mRNA expression in THP1 macrophages and BMDM stimulated with CM from human and mouse PNF cells, respectively, and the inhibition of *CCL2* mRNA expression was greatest with combination treatment. The combination of MSU42011 and selumetinib also significantly reduced tumor burden in a LL2 model of lung cancer driven by an activating *Kras* mutation. Based on the similarities in RAS activation and immune cell infiltration in NF1 and lung cancer, our next step is to confirm the immunomodulatory and anti-tumor effects of MSU-42011 and selumetinib in a syngeneic model of PNF and MPNST.

#2022 E7386, a Wnt/β-catenin signaling modulator, suppresses the differentiation of regulatory T cells in combination with lenvatinib plus anti-PD-1 antibody.

J. Shen, R. Ishida, M. Kume, T. Kimura, Y. Adachi, Y. Kato;
Eisai Co., Ltd., Tsukuba, Japan

Background: E7386, a selective inhibitor of the interaction between β-catenin and CREB binding protein (CBP), showed antitumor activity in preclinical tumor models with aberrant activation of the Wnt/β-catenin signaling pathway. Previously, we reported the enhanced antitumor activity of a triple combination (E7386 in combination with Lenvatinib [LEN, a multiple receptor tyrosine kinase inhibitor mainly targeting VEGFRs and FGFRs] plus anti-PD-1 antibody) versus a 2-drug combination (LEN plus anti-PD-1 antibody). In this study, we further investigated the immunomodulatory functions of E7386 as a triple combination by single-cell RNA-sequencing (scRNA-Seq) analysis and subsequent functional assays.

Methods: Mice bearing subcutaneous RAG (mouse renal cell carcinoma) tumors were randomized into 4 groups (n=6 in each group), including ⑴ Nontreatment, ⑵ E7386 at 25 mg/kg (PO, QD), ⑶ LEN at 10 mg/kg (PO, QD) plus anti-PD-1 antibody at 10 mg/kg (IP, BIW), and ⑷ triple combination. Tumor tissues were collected after a 2-week treatment period. $CD45^{\pm}$ immune cells were isolated from the tumors by magnetic cell separation (MACS) and subjected to scRNA-Seq using 10x Genomics pipelines. Bioinformatics data analysis was conducted with Clarivate Analytics. To evaluate the effects of E7386 on Treg differentiation, an in vitro-induced regulatory T cells (Tregs) differentiation assay was conducted. Naïve $CD4^{\pm}$ T cells were isolated by MACS and plated under iTreg differentiation conditions (stimulation of TGF-β and IL-2) with or without treatment of E7386. Induced Tregs and conditional culture medium were collected for evaluation of Treg differentiation, including gene expression and protein analysis.

Results: $CD45^{\pm}$ immune cells were clustered into 14 cell-type groups. Increased proportion of monocytes, NK cells, Tregs, $CD4^{\pm}$ T cells, $CD8^{\pm}$ T cells, eosinophils, and neutrophils were observed after LEN plus anti-PD-1 treatment. Among these subpopulations, Treg were most significantly suppressed by E7386 plus LEN plus anti-PD-1. Gene expression analysis revealed that the triple combination suppressed the activated gene expression of the Stat5/Foxp3 axis in $CD4^{\pm}$ T cells, particularly Tregs, induced by LEN plus anti-PD-1 treatment. Consistently, the iTreg differentiation assay confirmed the suppressive function of E7386 on the Treg differentiation rate. Multiple subsequent in vitro assays also demonstrated the inhibitory effects of E7386 on TGF-β secretion and the expression levels of TGF-β downstream target genes.

Conclusion: In summary, these data suggest a suppressive role of E7386 on Treg differentiation, which leads to antitumor activity of E7386 in combination with lenvatinib and anti-PD-1 antibody in a preclinical tumor model.

#2023 Multiplex immunofluorescence profiling of the tumor microenvironment and CD73: Activity of neoadjuvant oleclumab in patients with non-small-cell lung cancer in NeoCOAST.

I. Bisha[1], T. Tan[1], M. Weitkunat[1], A. Andoni[1], I. Dino[1], P. Martin[2], M. Saraiya[1], K. DaCosta[1], P. Sontakke[1], M. Schick[1], M. Surace[2], J. Blando[2], I. Grenga[3], R. Kumar[2], L. McGrath[3];

[1]AstraZeneca, Munich, Germany, [2]AstraZeneca, Gaithersburg, MD, [3]AstraZeneca, Waltham, MA

Background: The NeoCOAST study (NCT03794544) investigated the efficacy of neoadjuvant immuno-oncology combinations in patients with resectable non-small-cell lung cancer (NSCLC), using major pathological response (MPR) as the primary endpoint (Cascone T, et al. *Cancer Discov* 2023;13:2394-411). Patients received a single cycle of the following treatments: durvalumab monotherapy (durva; anti-PD-L1), durva + oleclumab (ole; anti-CD73), or durva + monalizumab (mona; anti-NKG2A). Here we analyze the tumor microenvironment to investigate the mechanism of action of ole.

Methods: A cohort of 47 patients (17 durva, 13 durva + mona, 17 durva + ole) with tumor tissue samples from pre-treatment (baseline, n=31) and surgery (post-treatment, n=24; n=8 paired pre- and post-treatment samples) were evaluated. Tumor sections were stained with (1) multiplex immunofluorescence (Panel 1: CD8-PD-L1-PD1-CD68-Ki67-panCK, Panel 2: NKp46-CD20), (2) CD73 immunohistochemistry (IHC), and (3) NKG2A IHC. Stains were analyzed using deep learning algorithms, manual pathology, and digital pathology scoring, respectively.

Results: All arms showed similar infiltration of tumors by T cells (CD8), B cells (CD20), NK cells (NKp46), and macrophages (CD68) at the pre-treatment time point (Kruskal-Wallis, p=0.5-0.9 *n.s.*). Percent CD73+ tumor cells (TCs) at baseline was correlated with increased B cell, T cell, NK cell, and macrophage abundance (Spearman's Rho=0.4-0.6, p<0.05). Percent CD73+ TC and B cell abundance was higher in patients with MPR vs those without MPR in the durva + ole arm, but not in the durva monotherapy or durva + mona arms. Increased CD8 T cell and NK cell abundance was not associated with MPR in any arm. Moreover, comparison of baseline to post-treatment tumor samples revealed a greater increase in CD8 T cells in the durva + ole arm (FC=2.1, p=0.02), particularly in proliferating activated T cells (CD8+Ki67+PD-1+; FC=8.0, p=0.003), compared to durva alone (FC=1.8, p=0.4 and FC=2.9, p=0.04, respectively).

Conclusion: Increased abundance of CD73+ TCs is correlated with high B cells in the tumor microenvironment and associated with patients who experienced MPR in the durva + ole arm. Treatment with neoadjuvant durva + ole results in a greater increase in proliferating CD8 T cells than durva alone.

#2024 Deep and durable responses to ALK-targeted therapy require CD8+ T cells.

Greg Reis, Stevie Phelabaum, Andre Navarro, Emily Kleczko, Lynn Heasley, Raphael Nemenoff, **Erin L. Schenk**

University of Colorado Anschutz Medical Campus, Aurora, CO

Despite major advances in therapies for lung cancer, it remains the leading cause of cancer related deaths in the United States. Tyrosine kinase inhibitors (TKI) designed to inhibit oncogenic anaplastic lymphoma kinase (ALK) fusions have transformed the treatment of patients with ALK+ NSCLC and many survive for several years on TKIs. While most patients experience a decrease in tumor burden on initial alectinib therapy, for many, tumor shrinkage is incomplete and persistent, residual disease remains. Critically, the degree of tumor shrinkage and amount of residual disease that persists despite TKI associates with overall survival. Multiple cancer-cell intrinsic mechanisms of persistence despite TKI therapy have been reported, but they do not fully account for the heterogeneity of this initial tumor response, suggesting other determinants are present beyond inhibiting the primary oncogene. However, extrinsic mediators of persistent disease, such as immune cells within the tumor microenvironment (TME), have not been rigorously studied in ALK+ NSCLC as they are considered immunologically “cold” tumors. Using EA-1 and EA-2, two distinct murine ALK+ adenocarcinoma cells lines derived from immunocompetent C57BL/6J mice, we have demonstrated that ALK+ NSCLC response to alectinib requires the adaptive immune system. C57BL/6J mice bearing orthotopic EA-1 tumors experience tumor shrinkage but have persistent, residual disease on CT imaging; those bearing EA-2 tumors have no residual disease. In this model system, when alectinib treatment stops, no EA-2 tumors recur but all animals bearing EA-1 tumors experience tumor outgrowth. TME interrogations by multispectral tissue imaging demonstrated more CD8+ T cells in the EA-2 TME compared to EA-1 and no difference in CD4+ T cells. Flow cytometry revealed a significant increase in activated CD8+ T cells and CD86+ CD103+ dendritic cells within the TME of EA-2 tumors compared to EA-1. When implanted into nude mice, EA-1 and EA-2 both experience initial disease shrinkage on alectinib, but EA-2 tumors now exhibit residual disease on imaging. Notably for both cell lines, tumor outgrowth occurs in the nude mice despite continued TKI therapy. Using knock out animal models, we established that CD8+ T cells, but not CD4+ T cells, were required for response to alectinib. In animals lacking CD8+ T cells, EA-2 tumors shrink with alectinib therapy but are not eliminated as in the wild type controls. Notably, despite continued alectinib therapy, tumors grew out in the CD8+ knock out animals. In the EA-2 model, CD4+ T cells we not required for response to alectinib, and CD4+ knock out animals did not experience tumor outgrowth when alectinib was held. Taken together, these data suggest that the adaptive immune system, specifically CD8+ T cells, are required for a deep and durable response to molecularly targeted therapy for ALK+ NSCLC.

#2025 Zeb1 downregulation sensitizes pancreatic cancer-associated fibroblasts to killing by oncolytic reovirus through upregulation of the reovirus receptor junction adhesion molecule A.

N. Dam[1], T. J. Harryvan[1], B. Schmierer[2], L. J. Hawinkels[1], V. Kemp[1];
[1]LUMC, Leiden, Netherlands, [2]Karolinska Institutet, Stockholm, Sweden

Pancreatic tumors display an abundance of cancer-associated fibroblasts (CAFs), which negatively affect prognosis and therapy response. Oncolytic virotherapy exploits viruses that preferentially lyse epithelial cancer cells as opposed to normal cells. Interestingly, we have observed that oncolytic reoviruses are able to infect and lyse CAFs, in addition to epithelial cancer cells. Targeting CAFs, in addition to cancer cells, could be advantageous to increase therapy effectiveness. It could serve as a conduit for viral spread and simultaneously disrupt the desmoplastic barrier around tumors, thereby also accelerating the influx of other therapeutics and immune cells. We previously found that the proneness of CAFs to lysis by oncolytic reovirus correlates with the cell surface expression levels of the reovirus entry receptor junction adhesion molecule A (JAM-A). However, most pancreatic CAFs do not express JAM-A. Therefore, a genome-wide CRISPR/Cas9 screen was employed to identify the genes regulating JAM-A expression on fibroblasts, which can subsequently be targeted to sensitize CAFs to reovirus. Pancreatic stellate cells with a moderate JAM-A expression level were transduced with a gRNA library making a knockout of one gene per cell. The highest and lowest JAM-A expressing cells were sorted and sequenced to identify the gRNAs that regulate JAM-A expression. Clonal CRISPR/Cas9-generated knockouts of a top negative regulator were generated and infected with reovirus, followed by cell viability assays to quantify their susceptibilities to reovirus-induced cell death. F11R, the gene encoding JAM-A, was identified as the top positive regulator of JAM-A expression in the CRISPR/Cas9 screen, verifying the validity of the screen. The top negative regulators identified were Fibroblast Growth Factor Receptor 1 (FGFR1) and Zinc finger E-box Binding homeobox 1 (Zeb1), thereby serving as potential therapeutic targets to sensitize CAFs to reovirus treatment. Using clonal Zeb1 knock-outs, Zeb1 was confirmed as a strong regulator of JAM-A expression. Zeb1 knockout in JAM-A negative pancreatic fibroblasts caused a robust upregulation of JAM-A and sensitized these inherently resistant fibroblasts to reovirus-directed cytolysis. Additionally, the clinically approved drug Mocetinostat, previously described to inhibit Zeb1, upregulated JAM-A expression on CAFs and increased cell lysis by reovirus. Altogether, our data show that Zeb1 is a strong negative regulator of JAM-A expression on fibroblasts and that Zeb1 inhibition can sensitize CAFs to reovirus-induced cell death. This research provides a rationale for combining Zeb1 inhibitory drugs with oncolytic reovirus treatment to improve killing of CAFs, which in turn could boost overall tumor eradication.

#2026 Single-cell RNA-sequencing analysis of tumor endothelial cells reveals suppression of specific endothelial subtypes by the combination treatment of Wnt/β-catenin signaling modulator E7386 plus lenvatinib.

M. Kume, R. Ishida, Y. Ozawa, J. Shen, H. Konishi, M. Kuronishi, T. Kimura, Y. Adachi, Y. Kato;
Eisai Co., Ltd., Tsukuba, Japan

Background: Aberrant activation of Wnt/β-catenin signaling plays an important role in both carcinogenesis and modulation of the tumor microenvironment. E7386, a novel orally active antitumor agent, inhibits the interaction between β-catenin and CREB-binding protein (CBP) and thereby modulates Wnt/β-catenin signaling. We previously reported that E7386 in combination with lenvatinib (LEN), a multiple receptor tyrosine kinase inhibitor mainly targeting VEGFRs and FGFRs, showed a greater antitumor activity and reduction of tumor microvessels than each treatment alone in preclinical tumor models. Multiple clinical studies are in progress including the combination of E7386 plus LEN (NCT04008797). Here, we further tried to elucidate the mechanism underlying the antitumor and antiangiogenic effect of the combination of E7386 plus LEN by using single-cell RNA sequencing (scRNA-seq) of tumor endothelial cells (ECs).
Methods: Mice bearing subcutaneous RAG (mouse renal cell carcinoma cell line) tumors were treated with E7386 at 25 mg/kg and/or with LEN at 10 mg/kg by daily oral gavage for 8 days. Tumor ECs ($CD31^{+}/CD45^{-}$) were isolated by magnetic cell separation and flow cytometry and were subjected to scRNA-seq using 10x Genomics pipeline. Bioinformatics data analysis was conducted by Clarivate Analytics. After quality control and filtering, ECs were gated by their expression of pan-EC markers and were further classified into 9 subtypes (tip, capillary, arterial, venous, proliferating, immature, interferon, activated artery, and lymphatic) according to previously reported markers for each subtype.
Results: Among classified subtypes, proliferating and immature subtypes showed clear reduction in the percentage of total ECs with combination of E7386 plus LEN versus LEN monotherapy. In both proliferating and immature subtypes, a subset of Wnt/β-catenin downstream genes showed increased expression with LEN monotreatment. Conversely, these Wnt/β-catenin downstream genes were downregulated with the combination of E7386 plus LEN, suggesting that Wnt/β-catenin signaling may be associated with a drug resistance mechanism against LEN in these subtypes. Pathway analysis indicated that genes involved in cell proliferation and survival were downregulated by the E7386 plus LEN combination versus LEN monotreatment in both proliferating and immature subtypes.
Conclusion: Taken together, these results suggest a role for E7386 in suppressing the activation of Wnt/β-catenin signaling induced by LEN monotreatment in specific EC subtypes; this activity leads to enhanced antiangiogenic and antitumor activity with E7386 plus LEN combination therapy in a preclinical tumor model.

#2027 Serological assessment of cancer associated myo-fibroblast (myCAF) activity by collagen pro-peptide biomarkers provides high prognostic power.

N. Willumsen, N. I. Nissen, M. A. Karsdal;
Nordic Bioscience, Herlev, Denmark

Background: Myofibroblast Cancer Associated Fibroblasts (myCAFs) are the main tumor fibrosis drivers and hence different from inflammatory CAFs (iCAFs). MyCAFs are emerging as an important tool for understanding tumor biology. CAFs produce type III, V, VI and XI collagen that are the essential components of tumor fibrosis. Pro-peptides of these collagens can be quantified both in serum with the PRO-C3, PRO-C5, PRO-C6 and PRO-C11 biomarkers where they are prognostic for poor overall survival in patients with various solid tumor types and may be applied in vitro. Here we investigated the association and difference between myCAFs and iCAFs and their collagen expression profile and related that to data available data on serological assessments of PRO-C3, PRO-C5, PRO-C6 and PRO-C11, and cultured CAFs.
Methods: The collagen expression in CAF subtypes were established from publicly available single-cell RNA-Seq dataset from pancreas cancer (PMID: 31273297) and non-small cell lung cancer (PMID: 36973297). In addition, we generated a biomarker profile using PRO-C3, PRO-C5, PRO-C6 and PRO-C11 ELISA to measure in serum of 220 patients with various solid tumor types and 33 healthy controls. We cultured CAFs in vitro and measured the same biomarkers in conditioned medium. We compared the result to historical PRO-C3, PRO-C6 and PRO-C11 prognostic data for pancreas cancer patient data.
Results: Based on the single-cell RNA-Seq dataset, while type III and type VI collagen were found expressed in fibroblasts both from normal tissues and tumor tissues whereas type V collagen and XI collagen were found almost exclusively expressed in CAFs (tumor tissue). When further examining the CAF subtypes, type III collagen and VI collagen were found expressed in both myCAFs and iCAFs whereas type V collagen and XI collagen were found almost exclusively expressed in myCAFs and not iCAFs. Moreover, in the 220 patients, PRO-C3 and PRO-C6 was elevated in elevated in a few cancer types ($p<0.05$-0.01) with an inter-patient variation ~2-fold whereas PRO-C5 and PRO-C11 were elevated in all cancer types ($p<0.0001$) with a ~5-fold inter-patient variation. These four biomarkers identified different pancreas cancer patients endotypes all with poor overall survival, $P<0.001$. In direct alignment, collagen pro-peptides we highly upregulated in cultures of CAFs.
Conclusions: Profiling collagen expression in fibroblast from PDAC and NSCLC reveals that type V collagen and type XI collagen are exclusively found in myCAF not iCAF. Biomarkers of these collagens can be measured in serum from cancer patients and are prognostic for poor overall survival. Thus, these data suggest that cancer associated myo-fibroblast (myCAF) activity can be assessed non-invasively by specific collagen pro-peptide biomarkers.

#2028 The triterpenoid CDDO-Methyl ester requires Nrf2 to decrease lung tumor burden and to protect against the toxicity of chemotherapy in experimental lung cancer.

J. A. Moerland[1], K. T. Liby[2];

[1]Michigan State University, Lansing, MI, [2]Indiana University School of Medicine, Indianapolis, IN

The NRF2 cytoprotective pathway, a drug target for many inflammation-related diseases, regulates immune cell function. While the anti-inflammatory nature of NRF2 activation protects healthy cells from malignant transformation, cancer cells can utilize the pathway to promote resistance to anti-cancer drugs. Up to 30% of human lung adenocarcinomas acquire mutations in either *NFE2L2* or its negative regulator *KEAP1* which result in constitutive activation of the NRF2 pathway. However, despite our knowledge of the important immunomodulatory effects of NRF2, these effects are not well characterized in the context of cancer. With NRF2 activators now approved for clinical use, it is critical to understand the impact of these drugs in cancer. Triterpenoids including CDDO-methyl ester (CDDO-Me, also known as bardoxolone methyl) are potent pharmacological NRF2 activators with demonstrated anti-cancer activity in preclinical models. In an early-stage preclinical model of lung cancer, CDDO-Me significantly decreased tumor burden in a dose- and Nrf2-dependent manner and improved immune signatures within the tumor microenvironment. However, most human lung cancers are not diagnosed until more advanced stages. To test CDDO-Me in an established tumor intervention model, lung tumors were initiated with vinyl carbamate in A/J WT and Nrf2 knockout (KO) mice. Tumors were allowed to develop for 8 weeks post initiation, after which mice were fed either a vehicle control diet or CDDO-Me (50-100 mg/kg of diet) for an additional 8-12 weeks, alone or in combination with carboplatin and paclitaxel (C/P) at 50 mg/kg and 15 mg/kg, respectively, by IP injection every other week. CDDO-Me significantly ($p < 0.05$) decreased surface lung tumor counts 35-71% in a Nrf2-dependent manner, and C/P significantly ($p < 0.001$) reduced tumor burden 53-59% regardless of Nrf2 status. The combination of CDDO-Me + C/P reduced tumor burden in WT lungs by 84% ($p < 0.05$), more than either agent alone. Nrf2 KO mice had an approximately two-fold increase ($p < 0.001$) of surface tumors compared to WT mice in both studies, regardless of treatment. C/P reduced tumor burden similarly in Nrf2 WT and Nrf2 KO mice. Interestingly, the combination of CDDO-Me + C/P increased T cell infiltration into the lungs of WT mice, but this change was not observed in groups treated with either agent alone. Importantly, CDDO-Me did not decrease the efficacy of C/P but protected WT mice from mortality and weight loss and lowered white and red blood cell counts. These studies suggest that NRF2 activation in advanced lung cancers can still decrease tumor burden by favorably modulating the immune microenvironment and, importantly, complements the anti-tumor efficacy of conventional chemotherapy while decreasing drug toxicity.

#2029 Investigation of anti-tumor activity of porcine myeloperoxidase for urothelial carcinoma of the bladder.

J. Liu[1], R. C. Allen[2], J. T. Stephens, Jr.[3], P. Shah[1], H. Huang[1];
[1]Mayo Clinic, Rochester, MN, [2]Creighton University, Omaha, NE, [3]Exoxemis, Inc, Little Rock, AR

Introduction: Porcine myeloperoxidase (pMPO) is a cationic enzyme secreted by granulocytic leukocytes capable of selectively binding cancer cells due to their negative surface charge. In the presence of hydrogen peroxide (H_2O_2) and sodium chloride (NaCl), MPO catalyzes the production of electronically excited singlet molecular oxygen, which exerts focused cytotoxic activity against cancer cells.
Methods: Human bladder non-cancer (SV-HUC1) and cancer cells (T24 and 5637) were used to assess differential cytotoxic activity of pMPO. pMPO was combined with associated reagents, including H_2O_2, NaCl, and L-proline and glycine for 45 minutes to support the generation of singlet oxygen. MTS assay was used to assessed cell viability at day 3 post-treatment. Non-cancer and cancer cells were labeled with GFP and mCherry, respectively, via infection with lentivirus and cultured in tandem to allow for simultaneous treatment of both cell types. After the treatment, flow cytometry and microscopy were used to monitor the growth of the cells.
Results: No cytotoxicity was noted when SV-HUC1 cells were cultured with individual reagents pMPO, NaCl, L-Proline, or Glycine, and limited cytotoxicity was observed with H_2O_2. Notably, cell viability was nearly maximally preserved for SV-HUC1 cells. The combination of pMPO with associated reagents resulted in killing of 5637 and T24 cells, with tumoricidal activity maintained across increasing tumor cell density, with cell viability preserved for SV-HUC1 cells. Within the cell co-culture system, simultaneous treatment of both cell types with the pMPO treatment resulted in selective killing of tumor cells and preservation of SV-HUC1 cells. Mechanistic studies confirm specificity of pMPO binding to tumor cells, and further, high levels of expression of gammaH2AX and phospho-ATM in 5637 and T24 cells following treatment.
Conclusion: pMPO demonstrates selective and efficient killing of bladder cancer cells with minimal cytotoxicity against non-cancer urothelial cells. Given its reliance on direct surface contact with tumor cells for activity, pMPO may be developed as an intravesical therapy for treatment of non-muscle invasive bladder cancers.
Acknowledgements: This work was partially supported by Mayo funds provided to Dr. Haojie Huang.

#2030 N-cadherin-mediated activation of PI3K/Akt pathway following application of tumor treating fields (TTFields).

A. Klein-Goldberg, **T. Voloshin**, E. Zemer-Tov, R. Paz, L. Koren, K. Wainer-Katsir, A. Volodin, B. Koltun, B. Brant, Y. Barsheshet, T. Kan, C. David, T. Haj Khalil, A. Haber, M. Giladi, U. Weinberg, Y. Palti;
Novocure Ltd, Haifa, Israel

Introduction: Tumor Treating Fields (TTFields) therapy is FDA-approved for the treatment of glioblastoma and unresectable pleural mesothelioma, and has recently demonstrated benefit (together with an immune checkpoint inhibitor) for the treatment of metastatic non-small cell lung carcinoma (NSCLC) progressing on or after platinum-based therapy. The current study aimed to uncover cellular response mechanisms to TTFields.
Methods: A2780 ovarian cancer cells and H1299 NSCLC cells were treated with TTFields for 72 h (200 and 150 kHz, respectively; 1.7 V/cm RMS). Changes in signaling pathways were analyzed using the Luminex multiplex assay and validated by protein expression. Fluorescence microscopy, calcium switch assay, antibody neutralization assay, and immunoprecipitation were employed to investigate the mechanism of action. The efficacy of concomitant treatment with TTFields and a potential inhibitor was tested in cell lines (cytotoxic and clonogenic effects) and two orthotopic mouse models: MOSE-L-FFL ovarian cancer and LL/2 lung cancer. Immunohistochemistry was performed on tumor sections from both models.
Results: Increased AKT phosphorylation was observed in the cancer cells treated with TTFields. N-cadherin, known to be involved in the activation of the PI3K/AKT pathway, was elevated in the membranes of cells treated with TTFields. Elimination of calcium ions required for N-cadherin homophilic ligation abrogated TTFields-induced AKT phosphorylation, whereas calcium supplementation restored AKT phosphorylation. Inhibition of N-cadherin-mediated cell-cell contacts by neutralizing antibody resulted in a significant reduction in TTFields-induced AKT phosphorylation. Pull-down assays with an anti-N-cadherin antibody demonstrated increased recruitment of the p85 regulatory subunit of PI3K to N-cadherin complexes following TTFields application. TTFields-induced activation of AKT could be mitigated in cell cultures as well as in animal models by application of the PI3K inhibitor alpelisib. Co-treatment with alpelisib also enhanced the effectiveness of TTFields *in vitro* and *in vivo*.
Conclusions: The PI3K/AKT signaling pathway, activated via cell-cell N-cadherin interactions, plays a role in the cancer cell response to TTFields treatment. Inhibiting the PI3K/AKT pathway may potentially sensitize tumors to TTFields.

#2031 A phase 1b/2 clinical study of onvansertib in combination with FOLFIRI/bevacizumab revealed a new role of PLK1 in regulating the hypoxia pathway in KRAS-mutant colorectal cancer.

M. Ridinger[1], A. Karki[1], R. A. Subramanian[1], E. Samuelsz[1], D. Yemane[1], R. Kim[1], C.-C. Wu[1], F. F. Kabbinavar[1], T. Smeal[1], H.-J. Lenz[2];
[1]Cardiff Oncology, Inc., San Diego, CA, [2]University of Southern California, Los Angeles, CA

Background: Onvansertib (Onv) is an oral, small molecule, selective PLK1 kinase inhibitor that demonstrated clinical activity at tolerated drug exposures in combination with FOLFIRI/Bevacizumab (Bev) in the 2nd-line treatment of mutated KRAS (mKRAS) metastatic colorectal cancer (mCRC) (Lenz, JCO, 2022). Here we explored biomarkers of response to the combination therapy and their associated biology.
Methods: In a Phase 1b/2 study, mKRAS mCRC patients with prior exposure to oxaliplatin (with or without Bev) were treated with Onv (Days 1-5 and 15-19) in combination with FOLFIRI/Bev (Days 1 and 15) of each 28-day cycle (NCT03829410). Efficacy endpoints included objective response rate (ORR, RECIST v1.1), progression-free survival (PFS) and duration of response (DoR). Preclinically, the combination of Onv and Bev was tested in 3 mKRAS CRC xenograft models. The role of PLK1 in hypoxia was assessed through protein and RNA analyses of mKRAS CRC cell lines exposed to low oxygen levels and treated with Onv.
Results: As of 25-AUG-2023, 66 patients were evaluable for efficacy in the Phase 1b/2 and ORR of Onv + FOLFIRI/Bev was 28.8%. Patients had a median PFS of 9.8 months [95%CI: 7.6, 12.6] and median DoR of 11.7 months [95%CI: 9.0, NR]. An analysis of baseline characteristics revealed that patients not exposed to Bev in the 1st-line setting (Bev-naïve patients, n=15) achieved superior clinical benefit compared to Bev-exposed patients (n=51). Bev-naïve patients had significantly higher ORR (73.3% versus 15.7%, p<0.0001) and longer median PFS (14.9 months [95%CI: 10.5, NR] versus 7.8 months [95%CI: 5.6, 9.8], p=0.0013) than Bev-exposed patients. This data prompted us to assess the effect of Onv+Bev in mKRAS CRC xenograft models. Onv+Bev significantly reduced tumor growth in the 3 xenograft models tested. The combination resulted in a greater decrease in tumor vascularization and tumor cell proliferation, and a corresponding increase in apoptosis, compared to either monotherapy. Further, the effect of Onv on the hypoxia pathway was assessed in mKRAS CRC cell lines. Our findings indicated that under low oxygen levels, Onv inhibited the hypoxia pathway by reducing the expression of the hypoxia-inducible factor 1-alpha (HIF1α) protein, and the mRNA expression of its downstream targets.
Conclusions: Onv + FOLFIRI/Bev resulted in greater clinical benefit in Bev- naïve than Bev-exposed mKRAS CRC patients. Preclinical studies revealed synergistic effect of Onv and Bev in mKRAS CRC xenografts, and a new function of PLK1 in modulating the hypoxia pathway through the regulation of HIF1α. Collectively, this data supports a crosstalk between PLK1 and angiogenesis, and further exploration of Onv + FOLFIRI/Bev therapy in Bev-naïve mCRC patients with KRAS mutation.

#2032 Osteoblasts alter their protein expression profile in the presence of prostate cancer cells to facilitate their invasion.

A. J. Todman, W. S. Ratnayake, L. Lajmi, S. Breedy, A. H. Shourav, K. Bisht, M. Acevedo-Duncan;
University of South Florida, Tampa, FL

Bone metastasis is the leading cause of death in prostate cancer patients, for which there is currently no effective treatment. Since the bone microenvironment plays an important role in this process, attention has been directed to the interactions between cancer cells and the bone microenvironment, including osteoblasts. Here, we investigated the mechanism of interactions between prostate cancer cells (DU-145 and PC-3) and osteoblast cell line hFOB.1.19. We are investigating the broader effects of four different nucleoside reverse transcriptase inhibitor (NRTI) analogs 5-fluoro-1-((1R,4R)-4-hydroxycyclopent-2-en-1-yl)pyrimidine-2,4(1H,3H)-dione (KBMD-E), 3-benzoyl-5-fluoro-1-((1S,4S)-4-((tetrahydro-2H-pyran-2-yl)oxy)cyclopent-2-en-1-yl)pyrimidine-2,4(1H,3H)-dione (KBMD-G), 1-((1R,4R)-4-hydroxycyclopent-2-en-1-yl)-5-methylpyrimidine-2,4(1H,3H)-dione (KBMD-H) and 1-(5-hydroxymethyl)-2,5-dihydrofuran-2-yl)-5-methylpyrimidine-2,4(*1H,3H*)-dione (KBMD-S) along with aPKC specific inhibitors ICA-1S and ζ-Stat to develop as potential anti-cancer drugs. Our previous publications suggested that aPKC-ι and ζ are involved in prostate cancer progression and metastasis. Current data suggested that aPKC specific inhibitors along with KBMD compounds induced apoptosis and pyroptosis of DU-145 and PC-3 while having lesser effects on hFOB.1.19 cell line. Our data demonstrate that osteoblasts assist prostate cells to establish in the bone microenvironment by producing metastatic stimulating chemokines while upregulating responsible transcription factors such as c-Jun. In addition, our preliminary data suggested that PKC-ι and ζ are crucial for driving critical steps of the metastatic cascades of prostate cancer cells. Preliminary data suggested that all 6 compounds upregulated interleukin (IL)-18 and IL-1β while downregulating IL-8, IL-6 and CXCL-1. Upregulation of Caspase 8 with cleaved gasdermin D in prostate cells indicates an increase in pyroptosis. Our preliminary results suggest that all 6 compounds can be used to disrupt the main steps of prostate cancer bone metastasis which can be targeted to develop customized, tailored therapies for bone metastatic prostate cancer which merit further research.

#2033 Rigosertib promotes anti-tumor activity of cancer cells via CETSA revealed novel targets and activates NLRP3-dependent inflammatory responses.

P. Kechagioglou[1], C. Dupont[1], H. Yurugi[1], A. Chernobrovkin[2], R. Romero[1], R. Tweedell[3], T.-D. Kanneganti[3], S. Cosenza[4], S. M. Fruchtman[4], K. Rajalingam[1]; [1]University Medical Center of the Johannes Gutenberg University Mainz, Mainz, Germany, [2]Pelagobio Bioscience, Solna, Sweden, [3]St. Jude Children's Research Hospital, Memphis, TN, [4]Onconova Therapeutics Inc, Newtown, PA

Background: Rigosertib (ON 01910.Na) is considered a promising anticancer agent due to its ability to inhibit multiple disease signaling pathways, including RAS-MAPK signaling. Rigosertib is in a Phase 2 program in advanced squamous cell carcinoma complicating recessive dystrophic epidermolysis bullosa (RDEB-associated SCC) (NCT03786237, NCT04177498), and a Phase 2 trial in combination with pembrolizumab in patients with metastatic melanoma (NCT05764395). The aim of our study was to further elucidate the mechanism of action and to identify potential novel targets engaged by rigosertib.
Methods: A variety of biochemical, molecular and cell biological assays were performed to characterize the binding of rigosertib to previously proposed targets and its effect on RAS-MAPK signaling and tumor cell survival. A mass spectrometry-based Cellular Thermal Shift Assay (CETSA-MS) was conducted to identify potential new protein targets of rigosertib. Time-lapse microscopy was used for detection of ROS levels and tubulin polymerization in rigosertib treated lung cancer cells. Bone Marrow Derived Macrophages (BMDM) collected from C57/BL6 mice and human lung cancer organoids were treated with rigosertib and the cell death was determined by flow cytometry.
Results: Comparative CETSA profiling of rigosertib and colchicine, a classical tubulin depolymerizing agent, reveals unique targets of rigosertib in multiple tumor cell types. We identify two ROS-related proteins, ERO1A and NQO2 that potentially contribute to the induction of ROS-dependent JNK activation. Fluorescence live-cell imaging confirms the effect of ERO1A and NQO2 on rigosertib induced ROS generation. NEK7, a relevant protein for microtubule organization, is another potential target for rigosertib. NEK7 knock-down reveals reduced microtubule depolymerization in rigosertib treated lung cancer cells. While we confirm that rigosertib might affect microtubules at higher concentrations, the main cellular target(s) responsible for the induction of stress and JNK-mediated inhibition of RAS-RAF-MEK signaling needs to be further characterized. Rigosertib affects the tumor immune environment by activating NLRP3-dependent inflammatory responses and Caspase-1 to trigger IL-1β and IL-18 secretion in THP1 cells, as well as in human cancer organoids, and in wild-type, Casp1/11$^{-/-}$, Asc$^{-/-}$ and Nlrp3$^{-/-}$ BMDMs.
Conclusion: These findings indicate that rigosertib may represent an effective compound for inhibition of RAS-MAPK signaling through ROS-mediated JNK activation. The rigosertib-dependent mechanism for NLRP3 activation suggests a reprogramming of the tumor immune environment which may contribute to the synergistic effect seen with immune checkpoint inhibitors pre-clinically and clinically. Clinical trials in several difficult-to-treat cancers continue.

#2034 The NAE1 inhibitor MLN4924 sensitizes both BRCA1 wild type and mutant triple negative breast cancers to cisplatin by reducing the nucleotide excision repair protein XPC level..

S. Misra[1], M. Opyrchal[2], **A. Ray**[2];

[1]Ohio State University Medical Center, Columbus, OH, [2]Indiana University Melvin and Bren Simon Cancer Center, Indianapolis, IN

Background: Triple-negative breast cancer (TNBC) shows poor survival and prognosis, high recurrence, and poor response to conventional therapeutics. To develop novel therapeutics for TNBC, we explored the efficacy of the neddylation inhibitor, MLN4924. We showed that MLN4924 displayed increased sensitivity against TNBC compared to non-TNBC subtypes. Mechanistically, MLN4924 induced extensive re-replication and DNA damage leading to cell death. Furthermore, MLN4924 improved cisplatin efficacy by elevating the DNA damage levels. To demonstrate the mechanisms of MLN4924+cisplatin-mediated enhanced cell death, we examined the XPC level, a key factor in the nucleotide excision repair (NER) pathway, playing a central role in cisplatin damage repair. Neddylation of CUL4A promotes XPC ubiquitination which influences XPC binding to the DNA damage sites for NER.

Methods: We examined the XPC protein level by Western blot assay and RNA level by Real Time PCR using both BRCA1-wild type (MDA-MB-231) and BRCA1-mutated (MDA-MB-436) cell lines and mouse xenograft tumor samples. We evaluated if the proteosome inhibitor MG132 stabilizes XPC ubiquitination and protein levels by treating these cells with MG132 for various times. We also overexpressed XPC in these cell lines and examined the effect on survival upon MLN4924 and MLN4924+cisplatin treatments.

Results: Our results demonstrate that MLN4924 reduces XPC ubiquitination upon shorter drug treatment but reduces the protein level upon longer drug treatment in both BRCA1-wild type and BRCA1-mutated cell lines. MG132 treatment did not stabilize the XPC ubiquitination level upon shorter drug treatment but stabilized the protein level upon longer drug treatment. We also observed a reduction in the XPC protein level in tumor samples which correlated with the increase in the DNA damage level. Surprisingly, XPC overexpression improved the cell survival in both MLN4924- and MLN4924+cisplatin-treated BRCA1-wild type and mutated TNBC cells.

Conclusion: We hypothesize that a reduction in the XPC ubiquitination and protein levels plays a role in cisplatin-induced DNA damage repair reducing NER efficiency and consequently increasing the DNA damage upon MLN4924+cisplatin treatment. Since overexpression of XPC results in improved survival of both MLN4924-and MLN4924+cisplatin-treated cells, we anticipate that XPC not only regulates cisplatin damage repair through NER but may have a broader role in MLN4924 sensitization beyond the NER pathway. Importantly, MLN4924 treatment does not affect the XPC mRNA level emphasizing that neddylation influences the XPC protein level. In summary, our research uncovers novel insights into the role of XPC in both MLN4924 and MLN4924+cisplatin sensitization, shedding light on potential avenues for innovative therapeutic strategies for TNBC patients.

#2035 A Benzenesulfornamide with potential to improve chemoresponse of ovarian cancer through activation of AMPK and immunogenic cell death.

J. Kim, N. Montero, S. Sharma, M. Mansolf, K. Yang, T. Hartwich, Y. Yang-Hartwich;
Yale School of Medicine, New Haven, CT

Introduction: Ovarian cancer is a leading cause of death among women globally often characterized by poor prognosis and aggressive tumor growth. The therapeutic outcomes of ovarian cancer patients are limited by the development of acquired chemoresistance and the lack of targeted therapies. This study aimed to understand the mechanism in which a benzenesulfornamide named Y3 enhances the efficacy of chemotherapeutic agents. Y3 was previously identified by our team as an activator of AMPK with the activity to induce immunogenic cell death of ovarian cancer cells.
Material and Methods: Patient-derived ovarian cancer cell lines were pretreated with Y3 for 3 h before treatment of carboplatin or paclitaxel. Celltiter Glo assay was performed to determine the impact of Y3 pretreatment on the IC50 values of carboplatin or paclitaxel after 48 h. Apoptosis was evaluated using Annexin VI/PI staining and Caspase 3 activity assays. The role of AMPK pathway was assessed using AMPK siRNAs and western blot. The potential of Y3 to enhance immunogenic cell death induced by carboplatin or paclitaxel was evaluated in a syngeneic mouse model of ovarian cancer using a vaccination assay. The control group mice were vaccinated by subcutaneously injecting mouse ovarian cancer cells treated by carboplatin in vitro for 24 h into the left flank. The test group mice were vaccinated by injecting Y3-carboplatin co-treated cells. One week after vaccination, untreated live cancer cells were injected into the right flank of both groups. Tumor growth was monitored.
Results: Ovarian cancer cell lines pretreated with Y3 showed decreased IC50 values for carboplatin and paclitaxel treatments. The apoptotic cell populations stained by Annexin VI were increased in the Y3 pretreated in comparisons with the single treatment groups. Caspase-3 activity validated the results of Annexin VI/PI staining assay. AMPK knockdown by siRNAs effectively reduced the levels of phospho-AMPK that was induced by Y3, which also dampened the Y3-promoted chemotherapeutic effects on ovarian cancer cells. In the in vivo vaccination assay, tumor growth in the right flank was suppressed in the mice vaccinated with Y3-carboplatin co-treated cells to an extend that is more significant than the control group.
Conclusion: Y3 pretreatment increased the sensitivity of ovarian cancer cell lines to carboplatin and paclitaxel. The effects of Y3 on ovarian cancer cells depend on the activation of AMPK. Y3 enhances the immunogenicity of carboplatin-treated ovarian cancer cells.

#2036 Characterizing PARP inhibitor and next-generation anti-androgen therapy responses in advanced prostate cancer.

L. A. Moore, B. Correa Gonzalez, A. C. Gao, **A. P. Lombard**;
University of California, Davis Health, Sacramento, CA

PARP inhibitors (PARPi) have been shown to be effective in prostate cancer patients with certain DNA repair defects, thus ushering in the era of precision medicine for this disease. Despite this advance, barriers remain which impede further progress including an incomplete understanding of therapeutic response. Our previous and on-going work shows that PARP inhibition leads to both cell death and a more cytostatic, senescence-like arrest. We hypothesize that persistent cells may later promote progression and treatment resistance. Recent clinical trials such as PROpel and TALAPRO-2 have demonstrated success in combining PARPi's with next-generation anti-androgen therapies (NGAT) including abiraterone and enzalutamide. Whether NGAT's are synthetic lethal and cell death promoting with PARP inhibition is poorly understood. Additionally, given the evolving clinical landscape for prostate cancer, it is important to test whether prior NGAT exposure may preclude response to combination therapy. In this study, we sought to characterize these combinations to better understand tumor cell response to treatment and the placement of treatment within the overall therapeutic paradigm. We've previously used the C4-2B metastatic castration-resistant prostate cancer cell line as a model which responds well to PARP inhibition. Here, we additionally utilize the C4-2B-derived enzalutamide and abiraterone resistant lines MDVR and AbiR, respectively. The combination of olaparib with abiraterone (recently approved from results of PROpel) was significantly more efficacious than either monotherapy in all three models. Additionally, combination of talazoparib and enzalutamide (approved from results of TALAPRO-2) was also more effective than monotherapy. These data suggest that prior development of NGAT resistance does not prevent benefit from NGAT and PARPi combinations. Although both combinations were found to cause significantly less cell growth, cells appeared more cytostatic rather than apoptotic, suggesting NGAT's do not induce significant synthetic lethality with PARPi's. Our work suggests that combining a PARPi with an NGAT promotes a persistent cytostasis which may give rise to eventual tumor progression and the development of resistance. Future studies are directed at further characterizing combinations with PARPi's and the development of novel strategies to enhance their efficacy.

#2037 Enhanced chemosensitivity to DNA-damaging agents in human high-grade glioma through 2-DG treatment.

T. Miller[1], E. Jane[2], M. Halbert[2], T. Gatesman[2], S. Wendell[2], D. Mohanakrishnan[2], S. Agnihotri[2], D. Premkumar[2], I. Pollack[2];
[1]University of Pittsburgh School of Medicine, Pittsburgh, PA, [2]University of Pittsburgh Medical Center, Pittsburgh, PA

Background: Human high-grade gliomas are aggressive brain cancers known for their resistance to treatment. Targeted therapies with single agents have shown limited success, and the presence of tumor heterogeneity complicates treatment. Combining multiple chemotherapeutic agents has emerged as a potential strategy to overcome these challenges. 2-deoxy-D-glucose (2-DG) is a glucose analog known for its ability to disrupt glycolysis, protein folding, and the pentose phosphate pathway. This disruption renders cancer cells more susceptible to further damage from reactive oxygen species and DNA damage. Previous studies have demonstrated synergistic effects when combining 2-DG with chemotherapeutic drugs in various cancers. Our study examines combining 2-DG with DNA-damaging agents for high-grade gliomas to uncover potential synergies, theorizing that this combination enhances cell death and metabolic stress, offering insights for better treatments against these tumors.
Methods: The cell proliferation, clonogenic growth, and cell migration assays assessed viability, clonogenic formation, and migration. Additionally, the cell cycle and reactive oxygen species analysis were employed to evaluate cell division, oxidative stress, and antioxidant capacity. The Illumina NovaSeq 6000 platform measured transcript levels, and Liquid Chromatography-High-Resolution Mass Spectrometry analyzed metabolite changes in high-grade glioma cell lines following 2-DG treatment. The Agilent Seahorse Mito Stress Test evaluated alterations in cellular bioenergetics. SYNERGYFINDER 3 quantified synergistic effects of 2-DG with DNA-damaging agents, while the Annexin V-FITC Conjugates and a ROS multiplex assay assessed cell death and metabolic stress.
Results: Our findings demonstrate that when used as a single agent, 2-DG induces cell senescence and limits cell migration but is insufficient to trigger cell death. Moreover, 2-DG treatment shifts glioma cells towards oxidative phosphorylation for energy production, elevates ROS levels, and hampers DNA synthesis and repair mechanisms. Our synergy study reveals promising synergistic effects when combining 2-DG with DNA-damaging agents, including 5-FU, Methotrexate, Gemcitabine, and Lomustine. This combined therapy leads to significant ROS generation and increased cell death compared to single-agent treatments. Furthermore, prolonged exposure to 2-DG leads to increased levels of both glucogenic and ketogenic amino acids within glioma cells, potentially serving as an alternative energy source. This finding hints at a prospective therapeutic approach for targeting drug-resistant cells.
Conclusions: Our results suggest that the anticancer therapeutic effect of 2-DG is enhanced when used in combination with DNA-damaging agents, indicating this strategy as a potential approach for treating human high-grade glioma.

#2038 Combination therapy leads to decreased viability in cardiomyblasts cells.

A. N. Greenlee, E. J. Schwendeman, S. A. Smith;
The Ohio State University, Columbus, OH

Anti-cancer therapies (ACT) have been extremely effective in improving survival in cancer patients; however, they have also been known to cause cardiovascular diseases (CVD) in the same patients. Published research shows that ACTs are toxic to cardiomyocytes through decreased viability. However, they have mainly focused on drugs that are phasing out of clinical practice while newly generated tyrosine kinase inhibitors (TKIs) and immune checkpoint inhibitors (ICIs) have rarely been studied, despite their increase in popularity for treating multiple cancers as monotherapies and combination therapies. Additionally, most of the concentrations tested tend to be higher than the concentration that directly interacts with cardiomyocytes, therefore overestimating its effects. The goal of this project is to elucidate whether newly generated TKIs and ICIs, both by itself and in combination, lead to decreased viability in cells. We tested three TKIs (Axitinib, Cabozantinib, and Lenvatinib) and two ICIs (Nivolumab and Pembrolizumab), both solely and together, on rat ventricular myoblasts (H9c2) cells using clinically relevant concentrations by calculating the unbound serum drug concentrations found in cancer patients. After 24 hours, we tested cell viability using the cell counting kit-8 (CCK-8) assay. After 24 hours, neither TKIs nor ICIs by themselves caused decreased viability compared to the control group. However, there were significant decreases in viability when treated with combination of the two, with more than 50% depletion in the Lenvatinib/Pembrolizumab group. Our study indicates although TKIs and ICIs by themselves do not effect viability, they have significant effects after 24 hours when the drugs are combined, even at clinically relevant concentrations. We plan to further characterize whether these drug combinations lead to cardiomyocyte death and through which pathway. Additionally, our lab has successfully differentiated and validated human-induced pluripotent ventricular myocytes (hiPSC-CMs) and testing whether these monotherapies and combination therapies effect viability and functionality on human-induced pluripotent ventricular myocytes (hiPSC-CMs) is currently in progress.

#2039 Cellular characterization of small molecule PD-L1 inhibitors reveal their novel mechanisms of action.

W. Pan, Y. Zhang, F. Qi, W. Xin, Z. Feng, Z. Chen, **H. Ying**;
Abbisko Therapeutics, Shanghai, China

Introductions: Immune checkpoint inhibitors, including PD-1/L1, are key regulators of immune response and promising targets in cancer immunotherapy. Like anti-PD-1/L1 antibodies, small molecule PD-L1 inhibitors that have been discovered by us and others could also efficiently block PD-1 and PD-L1 interaction and exhibit anti-tumor efficacy in preclinical and clinically settings. In this study, we explore the cellular mechanism of small molecule PD-L1 inhibitors, unveiling their novel mechanisms of action in the regulation of PD-L1 and its functions.

Materials and Methods: The cellular effects of the small molecule PD-L1 inhibitor on PD-L1 protein and RNA levels were assessed through Western blot and real-time qPCR experiments. HTRF assay and cellular luciferase reporter assay were used to evaluate the blockade of PD-1 and PD-L1 interaction *in vitro* and in cells. Flow cytometry and confocal microscopy were used to investigate the internalization of PD-L1 upon treatment with inhibitors. MSD assay was used to evaluate the alteration of soluble PD-L1 proteins.

Results: Small molecule PD-L1 inhibitors discovered by Abbisko Therapeutics potently blocked PD-1/PD-L1 interaction *in vitro* and in cellular system. It could also rapidly and strongly induce PD-L1 internalization in cells. Further profiling suggested that small molecule PD-L1 inhibitors specifically disrupt PD-L1 N-glycosylation, resulting in aberrant PD-L1 glycosylation. This, in turn, may hinder the proper translocation of newly synthesized PD-L1 to the cell surface, thereby abolishing its interaction with PD-1 and functions in immune regulation.

Conclusion: Taken together, these results for the first time revealed the distinctive mechanisms of our small molecule PD-L1 inhibitors. With their multi-layer inhibitory effects stemming from various mechanisms, small molecule PD-L1 inhibitors may offer potentially improved activities and an alternative therapeutic treatment for the cancer patients.

#2040 Targeting MUS81 endonuclease to enhance chemo-immunotherapy response in head and neck squamous cell carcinoma.

A. A. Suwaidan[1], A. Pasto[1], C. McCarthy[1], T. Pan[1], J. Deng[1], L. Dolcetti[1], G. Alfano[1], R. Mustapha[1], J. Monypenny[1], M. Forster[2], T. Ng[1];
[1]King's College London, London, United Kingdom, [2]University College London, London, United Kingdom

Background: In advanced head and neck squamous cell carcinoma (HNSCC), immune checkpoint inhibitors are only effective in 15-20% of cases. Defects in replication stress response represent a promising avenue for enhancing the therapeutic efficacy of immunotherapy through DNA damage and the release of immunostimulatory DNA. MUS81, a DNA structure-specific endonuclease involved in resolving replication stress, is upregulated in many cancer types including HNSCC, and MUS81-associated cytosolic DNA is implicated in triggering cGAS-STING mediated innate immunity. The objectives of this study were to assess the impact of targeting MUS81 on HNSCC cell sensitivity to cisplatin, and investigate its role in enhancing immunotherapy response in HNSCC, through the cell viability and cell cycle analysis, differential gene expression, and DNA release within small extracellular vesicles (exosomes).
Methods and Results: We used HNSCC cell lines and patient-derived organoids (PDOs) to investigate the consequences of CRISPR/Cas9-mediated MUS81 knockout (KO). We demonstrated that MUS81 KO increased HNSCC cell sensitivity to cisplatin, inducing a G2/M cell cycle arrest. Transcriptomic analysis of differentially expressed genes (DEG) in MUS81 KO vs control cells highlighted upregulation of *ANXA6* (tumor suppressor gene encoding for Annexin A6), *MACROH2A2* (involved in the quiescent phenotype acquisition of malignant HNSCC cells) and *CDA* (encoding for cytidine deaminase, implicated in replication stress). MUS81 KO was also associated with downregulation of LCP1 (encoding for lymphocyte cytosolic protein 1, upregulated in oral cancer and controlling cellular proliferation, invasiveness, and migratory activities). Gene Set Enrichment Analysis (GSEA) of RNA-seq data, revealed positive enrichment in MUS81 KO cells treated with cisplatin in genes involved in the hallmark interferon alpha (Normalized Enrichment Score (NES) 3.03, p-value < 0.001) and interferon gamma (NES 2.83, p- value < 0.001) pathways, indicative of innate and adaptive immune responses. Additionally, the pathway of hallmark inflammatory response was positively enriched (NES 2.22, p < 0.001). In addition, cisplatin treatment in MUS81 KO was associated with notable alterations in the concentration and length of exosomal DNA, with implications for immune response modulation within the tumor microenvironment.
Conclusions: Our study underscores the potential significance of MUS81 as a novel therapeutic target in HNSCC. In addition to sensitizing HNSCC cells to chemotherapeutic agents, targeting MUS81 may influence the dynamics of the tumor microenvironment, thereby enhancing the prospects of immunotherapy in this context. Further in-depth investigations are imperative to validate these observations and facilitate the development of innovative therapeutic strategies tailored to targeting MUS81 in HNSCC.

EXPERIMENTAL AND MOLECULAR THERAPEUTICS: New Technologies
Poster Session

#2044 A live cell PRMT5 NanoBRET Target Engagement Assay querying competitive and uncompetitive modes of inhibition.

A. Michaud[1], E. Rothweiler[2], **C. Corona**[3], M. Beck[1], J. Wilkinson[1], J. Vasta[1], K. Huber[2], M. Robers[1];
[1]Promega Corporation, Madison, WI, [2]University of Oxford, Oxford, United Kingdom, [3]Promega Corporation, San Luis Obispo, CA

PRMT5 is an essential arginine methyltransferase that regulates a wide spectrum of cellular processes through the methylation of histone and non-histone substrates. In PRMT5 catalysis, SAM serves as the cofactor and methyl group donor, generating a methylated guanidinium moiety on the target substrate. In normal cells, the SAM pools are maintained through the methionine salvage pathway. In 15% of cancers, a key enzyme in this pathway (MTAP) is deleted, leading to an accumulation of the intermediate MTA, which inhibits PRMT5 activity. This genetic loss of function has therefore been pursued as a collateral vulnerability in MTAP deleted cancers. To exploit this synthetic lethality, a number of novel inhibitors have been developed that bind cooperatively at the PRMT5/MTA complex, offering a compelling pathway to precision medicine. Here we describe a novel, live cell NanoBRET Target Engagement assay that enables mechanistic studies on a variety of PRMT5 inhibitors. Using a cell-permeable NanoBRET probe directed to the substrate pocket of PRMT5, both substrate- and cofactor-competitive engagement can be quantified in cells. Moreover, this method can be used to quantify MTA-uncompetitive target engagement in cells, providing a platform to measure the potency of PRMT5-MTA-drug ternary complex formation. This method serves as a first-in-class method to quantify uncompetitive target engagement in live cells, which can be applied to other model systems.

#2045 Novel TFRC humanized mouse model for drug delivery to the brain.

F. Sonego[1], A. Pappalardo[1], G. Martin[1], B. Ozgur[2], P. Ravn[2], Y. Cherifi[1], F. Sotty[2], P. Isnard-Petit[1], **K. Thiam**[1];
[1]genOway, Lyon, France, [2]Lundbeck, Copenhagen, Denmark

Gliomas are the most common neoplasm in the central nervous system (CNS). Although immunotherapy has shown efficacy in several tumor types, no immunotherapies are approved by the US Food and Drug Administration for treatment of gliomas. One of the biggest challenges in using immunotherapies in the CNS is the existence of the blood-brain barrier (BBB), which limits drug delivery and the subsequent therapeutic drug efficacy. In addition to biodistribution, assessment of PK in preclinical models do not reflect the clinical findings. Conjugation of therapeutic agents with molecules binding to TRFC expressed along the BBB are being used as one of the alternative approaches to deliver drugs into the CNS. Herein, we describe a novel TFRC humanized mouse model (hTFRC), developed to enable assessment of compounds targeting human TFRC and aiming to deliver drug through the BBB. hTFRC model was developed by knock-in at the mouse endogenous locus to enable a physiological expression of TFRC. Splenocytes from hTFRC mice stimulated with labelled pHrodo Red human transferrin show internalization of human transferrin, suggesting that humanization of the transferrin receptor does not change the endocytosis process. *In vivo*, treatment of hTFRC mice with anti-BACE1/anti-TFRC antibodies enables the transfer of anti-BACE1 to the brain, while anti-BACE1 antibody is not. As a consequence of the drug delivery, mice treated with anti-BACE1/anti-TFRC show a marked reduction in Amyloid-β 1-40 levels in the brain. Altogether, the data suggest that hTFRC is expressed in the BBB and enables the efficient shuttling of therapeutic antibodies to the brain. While assessment of TFRC-targeting antibodies in a glioma model remains to be performed, the hTFRC model is a promising tool to assess delivery and efficacy of immunotherapies in gliomas. Moreover, the hTFRC model is also being intercrossed with the well-established hSA/FcRn humanized mouse model (Viuff *et al*., 2016), to enable a more translatable PK and biodistribution of compounds targeting TFRC.

#2046 Targeting cellular models of glioblastoma versus non-target and off-target cell populations using U87-MG membrane lipid-modified nanoliposomes.

K. Janton, D. Baamir, A. Patel, S. Boco, R. Campbell;
Massachusetts Col. of Pharmacy & Health Sci., Worcester, MA

Background: Glioblastoma Multiform (GBM) is an aggressive and malignant form of brain cancer known for its invasiveness and significant heterogenicity. The majority of GBM cases are linked to genetic mutations (ie. TP53, EGFR, and PTEN), which disrupt the normal regulation of cell growth and division, resulting in uncontrolled cell proliferation. The utilization of nanoparticles presents a promising approach for addressing the complexities associated with selective drug delivery to GMB and treatment. The purpose of this study was to investigate the effect of including U87-MG membrane lipid extracts in nanoliposomes using target, non-target, and normal healthy cellular populations in vitro.
Methods: The nanoliposomes employed for the experiments included various ratios of U87-MG lipid extracts (lipids derived from U87-MG cells), DOPC, Cholesterol, and DPPE-Rhodamine for fluorescence studies. The particle size and zeta potential values were measured and monitored throughout for consistency. Fluorescence intensity values (arbitrary units) were used to assess extent of cell binding, and uptake at the various time points. In vitro studies were employed to evaluate the cellular uptake activity of U87-MG-modified nanoliposome preparations using mixed ratios and compositions of lipid materials. Cell lines employed were, LN-18 (human glioma), T98G (human glioma), U87-MG (human glioma), 4TI (murine breast), and HBEC-5i (normal healthy) cells.
Results: The average size for the nanoliposomes (with and without lipid extract) fell within the range of 110 to 220 nm, while the zeta potential for the CLENs was negatively-charged. In vitro studies revealed that the inclusion of U87MG lipid extract in nanoliposomes increased cellular uptake in glioma cells when compared to control. Current investigations focus on different microenvironments, including non-target and off target cell populations. The findings from the cellular uptake analyses to date suggest that the *in vitro* cellular uptake of the CLENs varied in accordance with the total lipid extract content for all cell lines.

#2047 Scale up and scale down approaches for screening of 3D patient-derived cell models.

C. Paul[1], A. Chatman[1], A. Bullock[1], X. Yang[2], G. Wong[2], B. Balhouse[1], C. Yankaskas[1], E. Willems[2], M. Dallas[1], D. Kuninger[1];
[1]Thermo Fisher Scientific, Frederick, MD, [2]Thermo Fisher Scientific, Carlsbad, CA

3D cell culture is becoming more prevalent as scientists work to better model human physiology using in vitro systems. However, differences in handling 3D cell cultures compared to traditional 2D cell lines have limited adoption of 3D techniques in compound and cell therapy screening experiments. To facilitate use of patient-derived 3D tumoroid models, we developed protocols for both scale up and scale down of these models in Gibco™ OncoPro™ Tumoroid Culture Medium. OncoPro Tumoroid Culture Medium is a serum-free, conditioned medium-free culture medium designed to promote the growth of patient-derived 3D cancer models (tumoroids, cancer organoids). OncoPro medium is compatible with a suspension culture approach for easier handling compared to traditional embedded culture formats. We studied the growth of tumoroids in different flask sizes during suspension culture to optimize scale up for downstream assays. Tumoroid growth rates and morphologies were consistent across non-tissue culture treated flask sizes, and viable cell yield increased with surface area during scale up. In some cases, as many as $100x10^6$ dissociated tumoroid cells can be recovered from a single Nunc™ TripleFlask™ after a week of growth. After scaling up, tumoroids were dissociated and seeded in multiwell plates to test multiple screening conditions (compound identity, compound concentration) in parallel. Dissociated cells were seeded in 96-well plates using both manual and automated liquid handling (Tecan Fluent 780). Due to the tendency of 3D cell models to aggregate and fall out of solution, initial seeding in a 96-well flat bottom plate resulted in high well-to-well variability. Optimization of cell seeding protocols led to standard deviations in tumoroid metabolic activity, number, and size that were comparable to manual seeding, with a coefficient of variation of less than 3% between wells for multiple tumoroid lines when automation was implemented. Generally, variability in cell seeding was lower when using the optimized, automated cell seeding protocol compared to manual methods. After seeding, cells were grown for three days to form tumoroids prior to the addition of compounds. At this time point, there was low well-to-well variability in tumoroid metabolic activity (CV<2%). Compounds and reagents to analyze cell health could also be added using automated liquid handling prior to analysis on plate readers or high-content imaging platforms.

#2048 Integrated tumor models for immune oncology: Using live cell imaging for prediction of treatment efficacy *in vitro* and *in vivo*.

D. Kobelt, M. Stecklum, S. Rhein, W. Walther, J. Hoffmann;
Experimental Pharmacology and Oncology Berlin-Buch GmbH, Berlin-Buch, Germany, Germany

Background: The preclinical evaluation of novel cancer treatments demands comprehensive model systems in vitro that provide meaningful data before entering in vivo studies. Here we evaluate the capabilities of live cell imaging systems to evaluate novel immune therapies. Using integrated immune and tumor cell models in vitro we demonstrate, that these model systems can generate reliable data of pharmacodynamic activity of biologicals, small molecules or combinatorial approaches for further preclinical in vivo characterization.

Methods: Target tumor cell killing was assessed in vitro with immune cells (T- and NK-cells) and engagers. Tumor cells were transduced with a fluorescent marker to discriminate tumor cells from immune cells. The technology was used to determine inhibition of cell motility (re-invasion) after scratching of tumor cell monolayers. Cells were monitored using the IncuCyte. Dose-response-curves of single treatments and all combinations were generated in parallel. Active therapies were selected for further in vivo validation of immune cell killing. Humanized mice were generated by injection of CD34+ HSC or human immune cell subsets. Immune cell engraftment was monitored by FACS. To analyze the effect biologicals or small molecules, tumor cells were transplanted into these humanized mice. Tumor development and therapeutic effects were monitored by BLI measurements.

Results and conclusion: Tumor cell killing by immune cells and monolayer scratch assay in 96 well format were successfully monitored in the IncuCyte. Here, data can be generated over time without the need of new samples at every time point compared with conventional end point measurements. Using antibodies directing immune cells to attack target cells extensive cell killing was observed over time. These data predicted in vivo treatment outcome in mice co-engrafted with human immune cells. After successful humanization of mice, immune cells can be directed to kill target tumor cells. Small molecule combinations were tested in vitro utilizing the metastasis/2D scratch assay. After setup of dose-response curves for two molecules combinatorial treatments were tested. Here we found a synergistic increase in efficacy. These combinations were tested in vivo to evaluate their abilities to inhibit cell motility and distant metastasis. Here we show that the in vitro assays predicted correctly the highest efficacy of combined treatments compared to mono treatments.The IncuCyte System provides data that translate our integrated model systems into in vivo studies. We have shown that activated immune cells can kill target tumor cells in vitro. These data have been validated in vivo using immune cell humanized mice. Further, immune cells, biologicals and small molecule based treatments can be tested either alone or in combination, allowing the preselection of active combinations for further development.

#2049 Novel preclinical models for PROTAC evaluation: And beyond.

y. xu, J. Zhang, Y. Tian, Z. Chen, A. Wang, T. Ma, Q. Chen, Y. Yin;
Shanghai ChemPartner Co., Ltd., Shanghai, China

Proteolysis-targeting chimeras (PROTACs) are a novel class of small molecules that induce the degradation of target proteins. Unlike conventional inhibitors that disable target proteins by direct binding, PROTACs are event-driven, meaning that a single PROTAC molecule can induce the degradation of multiple target protein molecules. This catalytic mechanism allows PROTACs to achieve complete inhibition of target proteins at lower concentrations compared to conventional inhibitors, making them a promising therapeutic approach for previously considered "undruggable" targets.Despite their promise, the development of PROTACs faces several challenges. The large molecular weight of PROTACs can lead to poor cell permeability and bioavailability. Additionally, the lack of high-throughput, quantitative assays for evaluating PROTAC efficacy hinders structure-activity relationship (SAR) studies. The formation of the Protein-PROTAC-E3 ternary complex is crucial for PROTAC function, and reliable methods for assessing this interaction are essential for PROTAC development.In this poster, ChemPartner showcases a comprehensive suite of preclinical models for PROTAC evaluation, encompassing both in vitro and in vivo approaches. Using low-cost, high-throughput biochemical assays, we can provide valuable insights into PROTAC efficacy, facilitating SAR studies and elucidating the relationship between molecular structure and activity. Followed by in cell and in vivo function assays, we can test PROTAC PK/PD, toxicity, and efficacy. This suite of assays provides a powerful tool to speed up PROTAC development and reduce the fail rate.

#2050 Preclinical characterization of PRO1106, a novel and promising SLITRK6-directed sesutecan ADC.

W. Shen[1], H. Lu[1], Y. Xiao[1], X. Qiu[1], H. Liu[1], L. Wang[1], **Z. Chen**[2];
[1]ProfoundBio (Suzhou) Co., Ltd., Suzhou, China, [2]ProfoundBio US Co., Seattle, WA

SLITRK6 is a type I transmembrane member of the SLITRK family of proteins and is highly expressed in certain epithelial tumors including urothelial, lung, breast cancer and glioblastoma, with minimal-to-low expression in normal tissues. Recent studies with a vedotin-based SLITRK6-directed ADC, AGS15E, have offered clinical proof-of-concept of harnessing this target with the ADC modality for addressing high unmet need at least in bladder cancer. PRO1106 is comprised of a proprietary humanized SLITRK6-targeting IgG1 (dubbed as “mAb”) and the proprietary topoisomerase 1 inhibitor-based linker-drug, sesutecan. Sesutecan previously demonstrated promising characteristics in preclinical studies with multiple targets and conferred an encouraging benefit:risk profile in the clinic with a FRα-directed ADC (rinatabart sesutecan). PRO1106 and the parent mAb exhibited strong binding (with low nanomolar affinity) to recombinant human or cynomolgus monkey SLITRK6 on bio-layer interferometry. No binding was observed with human SLITRK1 or SLITRK4 or in additional negative-binding assays. Potent cellular binding (with sub-nanomolar EC_{50}) was also observed for the parent mAb and ADC with bladder, head and neck, and brain cancer cell lines as well as SLITRK6-overexpressing 293F cells. Target-binding was superior to sirtratumab (the parent antibody in AGS15E) and the binding epitope appeared to be distinct from that of sirtratumab in cross-block studies. PRO1106 displayed rapid internalization and elicited robust cytotoxicity (IC_{50} in the sub-nanomolar to low nanomolar range) in SLITRK6-expressing tumor cells but not target-negative cells. PRO1106 produced strong tumor growth inhibition in multiple cell-derived xenograft (CDX) models in mice representing bladder cancer and esophageal squamous cell carcinoma. PRO1106 showed a stable PK with much higher exposure compared to an in-house synthesized analog of AGS15E in rats. In an exploratory PK study in cynomolgus monkeys, PRO1106 at 5 mg/kg exhibited extended PK with minimal release of exatecan in circulation and with no apparent toxicity observed. In summary, PRO1106 is an ADC built on a clinically validated linker-drug directed at a clinically validated target, with promising data in preclinical pharmacology studies. As SLITRK6 expression in skin is negligible, PRO1106 may offer an exciting new option for patients with bladder cancer where the current standard-of-care ADC therapy (enfortumab vedotin) confers significant skin-related toxicity burden as well as for patients with additional cancer types.

#2051 Innovations in ADC technology platform with legumain-cleavable KSP-inhibitor payloads adaptable to various aspects of cancer biology.

H.-G. Lerchen[1], A.-S. Rebstock[1], M. Wiedmann[1], B. Stelte-Ludwig[1], A. J. Johnson[2], R. Izumi[2], A. Hamdy[2];
[1]Vincerx Pharma, Monheim, Germany, [2]Vincerx Pharma, Palo Alto, CA

Despite recent advances in the antibody-drug conjugate (ADC) field it remains challenging to achieve a sufficient therapeutic window. To address key issues of current ADCs such as aggregate formation and payload-related toxicities, we have developed a platform technology with tailored solutions for ADCs and small molecule-drug conjugates (SMDCs). Key features of the ADC technology comprise of kinesin spindle protein inhibitors (KSPi) as a novel payload class, a unique linker selectively cleaved by the tumor-associated protease legumain, and a CellTrapper® modification of the KSPi payload to reduce membrane permeability and provide accumulation in tumor cells beneficial for efficacy and safety[1,2]. Our advanced ADC VIP943 is targeting CD123 for the treatment of AML and MDS and is currently in Phase 1 clinical trial (NCT06034275). Here we show the extension and applicability of the platform in combination with various antibodies. Two case studies demonstrate how the payload-linker optimization increases the selectivity for tumor over healthy cells and potentially overcomes transporter-mediated drug resistance. Tuning the cleavable linker of cetuximab-ADCs for a higher challenge of legumain-mediated payload release resulted in a 52-fold improved selectivity of cytotoxicity against tumor cells versus HaCaT skin cells. A trastuzumab-ADC using a KSPi payload modified with the CellTrapper, shows low nanomolar potency against JIMT-1 cells resistant to trastuzumab-deruxtecan and thus may overcome resistance. An increased potency was not observed with an ADC releasing a permeable KSPi without CellTrapper. To address heterogenous target expression in solid tumors, novel antibody-2-drug conjugates (A2DCs) were synthesized to combine the advantages of intracellular accumulation of non-permeable payloads with the release of a second, membrane permeable KSPi payload. In vitro studies comparing the A2DCs with their respective mono-drug ADCs on 4 different targets shows the highest cytotoxicity achieved with A2DCs independent of the efficacy driver in mono ADCs. Lastly, synthesis of homogenous KSPi ADCs with a drug to antibody ratio of ~8 is compatible with different antibodies without significant aggregate formation. Furthermore, an easy and efficient process for ring-opening of the thiosuccinimide ring after conjugation was developed and shown to successfully avoid ADC de-conjugation via retro-Michael reaction. Selected examples of each of these subclasses were coupled to trastuzumab; all conjugates were highly efficacious and resulted in tumor regressions in the SKOV-3 model similar to trastuzumab-deruxtecan.

Conclusion: Our technology platform offers options for efficient and safe cancer treatments and allows for versatile adaptations to the various aspects of cancer biology. 1. Kirchhoff et al, *Cancers* (2020). 2. Lerchen et al, *Bioconj Chem*. (2020).

#2052 Screening novel format antibodies to design bispecific ADCs that address target heterogeneity.

S. D. Barnscher, D. Urosev, K. Yin, A. Hernandez Rojas, S. Lawn, V. Fung, J. Wong, A. Sagoe-Wagner, L. Degefie, A. Livernois, C. Kim, P. A. Moore, J. R. Rich;

Zymeworks Inc., Vancouver, BC, Canada

Addressing inter-patient and intra-tumoral target heterogeneity is a challenge for antibody drug conjugates (ADCs). The most common approach to mitigate intra-tumoral ADC target heterogeneity is to employ a bystander active payload. Once the ADC is internalized and metabolized, the payload can diffuse into tumor cells, independent of target expression. This strategy has proven effective, as evidenced by all but one of the eleven FDA-approved ADCs incorporating a bystander active payload. Nevertheless, it is important to note that in most cases there is clear evidence of an expression-response relationship, and the bystander approach does not specifically address inter-patient heterogeneity in target expression. Bispecific ADCs that can target two different tumor associated antigens (TAAs) are a promising approach to overcoming challenges associated with spatial and temporal target heterogeneity. A traditional bispecific ADC design employs a bivalent IgG where one paratope interacts with target A, and the other paratope interacts with target B. This design ensures that the molecule is maximally active when both targets A and B are present. However, this enhanced specificity approach has limitations, as it requires cellular co-expression of both targets to be effective. In contrast, a novel-format bispecific ADC targeting two different TAAs independently could increase the addressable patient population relative to a monospecific ADC. For example, a bispecific ADC with the potential for both independent and dual targeting of folate receptor alpha (FRα) and NaPi2b, established targets in ovarian cancers, could significantly expand the number of patients who could benefit relative to an ADC against either target alone. Here we describe a novel approach to the design and screening of a FRα x NaPi2b bispecific ADC library with the aim of targeting tumors that express either FRα, NaPi2b, or both targets. A library of 48 bispecific molecules was designed, employing multiple paratopes and variable antibody formats. The library comprised three valency bins, 1+1, 2+1, and 2+2, corresponding to the number of binding arms to each target. Bispecific antibodies were generated from 31 half antibodies containing Azymetric™ Het_Fc mutations. Complementary half-antibodies were combined and oxidized to generate interchain disulfide bonds, with bispecific antibody purity in the range of 90%. Antibodies and their corresponding ADCs, prepared through direct conjugation to a cytotoxic payload, were evaluated on a panel of FRα-expressing and Napi2b-expressing cancer cell lines. Key ADC parameters, including binding, internalization, and in vitro cytotoxicity, highlighted paratope combinations, valencies, and geometric formats that offer the unique potential to overcome target heterogeneity in ovarian cancer.

#2053 Spatiotemporal tumor immune modulation by localized delivery of cancer therapeutics using an implantable microdevice.

X. Li[1], J. Tessier[1], J. Lee[1], S. Garren[1], V. Cortez-Retamozo[1], M. Sharma[1], A. Jankowski[2], E. Zarazinski[2], A. Fiore[2], O. Jonas[3], C. Brenan[3], D. Shaffer[1], **A. Hadjipanayis**[1];

[1]Sanofi Oncology, Cambridge, MA, [2]Charles River Labs, Worcester, MA, [3]KiburMed, Inc., Cambridge, MA

Mechanism of action studies are imperative to translating oncology therapeutics into the clinic informing testable hypotheses and potential combination partners. This often involves large and time-consuming mouse studies to test a small number of compounds in an attempt to show statistically significant benefit. Likewise, testing multiple compounds and combination partners in these systems is limited by time, cost, and a desire to reduce the number of animals used in biological research. To overcome these limitations, we utilized an implantable microdevice (IMD) developed by KiburMed to measure intra-tumoral drug responses and to differentiate the mechanism of action of multiple cytokine agents in parallel in the MC38 mouse model. After sizable tumor growth in mice and implantation of the IMD device with 9 different therapeutic candidates, MC38 mice were taken down at different time points (24 hour, 4 days,7 days) to assess response. Local tumor response in the study was measured by cyclical immunofluorescence for deep cellular response phenotyping with a panel of 32 markers for comprehensive immune cell phenotyping. Among the candidate murine surrogate compounds in the device, SAR445877 (anti-PD-1-IL-15 mutein) was tested as a monotherapy, as a combination partner with anti-PDL1 and compared against anti-PD1 monotherapy. With further validation of this novel platform, results from this work are aligned with previous studies (1) showing a murine surrogate for SAR445877 in combination with anti-PDL1 increases immune cell populations more than either single agent alone. These analyses show CD3, CD4, and CD8 were significantly increased in SAR'877 murine surrogate + anti-PDL1 compared to SAR'877 alone or anti-PD1 alone. In addition, T cells could infiltrate at a distance away from treatment release region, well into tumor core. Other significant changes in immune cell markers include increases in CD45+, CD11b, CD11c, CD20 and CD27. In conclusion, we have shown that multiple oncology therapeutics can be screened simultaneously in a small number of mice using an implantable microdevice and data obtained with this technology is consistent with that obtained from traditional mouse tumor experiments.

(1) Preclinical characterization of SAR445877, an anti-PD-1 antibody-IL-15 mutein fusion protein with robust anti-tumor efficacy as monotherapy and in combination with PD-L1 blockade. Marie Bernardo; Yu-an Zhang; Dan Lu; Stella Martomo; Fatima Menas; Chen Zhu; Raymond Perez; Jeegar Patel; Donald Shaffer; Xiangming Li, *Cancer Res* (2023) 83 (7_Supplement): 2972.

*This work was supported and funded by Sanofi.

#2054 A sensitive and specific human primary stem cell-based *in vitro* assay for predicting the gastrointestinal toxicity risk of therapeutic agents.

J. Levi, R. Lorichon, L. Boone, M. Bunger, E. Boazak, **W. R. Thelin**;
Altis Biosystems, Durham, NC

Gastrointestinal (GI) toxicities are the most common drug-induced adverse events in human clinical trials. Drugs that cause GI toxicities often affect the proliferative stem and progenitor cell populations responsible for maintaining the cellular composition, self-renewing capacity, and barrier function of the intestinal epithelium. This disruption leads to impaired GI barrier integrity, culminating in a broad range of clinical symptoms, including diarrhea, inflammation, and increased risk of infection. The impact of GI toxicity is substantial and can cause dose-limiting clinical side-effects that may affect patient compliance and dosing adherence. Common nonclinical animal models, including rats, mice and dogs are often poor predictors of human GI toxicity and safety outcomes. Furthermore, in vivo animal testing poses limited screening throughput, which is particularly important in fields such as oncology, where matrices of double or triple drug combinations represent the standard of care. Additionally, existing cell-based model systems, such as Caco-2 cells, are of limited predictive value as they are tumor-derived and do not reprise native epithelium. Thus, there is a need for the development of assay systems that more accurately recapitulate human biology, have higher throughput testing capabilities, and ultimately improve clinical predictability. To this end, we have developed an assay to assess GI toxicity potential using the RepliGut Planar platform, which consists of a primary human stem cell-derived epithelium in a 96-well Transwell format. Quantitative dose-response curves were generated on proliferative and/or differentiated GI cultures for various test articles utilizing endpoints that assess GI proliferative capacity, cell viability, and epithelial barrier formation and maintenance. An initial set of marketed drugs (including diverse anti-proliferative, cytotoxic, or anti-inflammatory mechanisms) with known clinical incidence of diarrhea were over a 5-log dose range to enable modeling of the Toxic Concentration 50% (TC50). When benchmarked against the known human plasma concentrations (Cmax), this model was able to accurately predict clinical outcomes for diarrheagenic-drugs, as well as non-toxic negative controls, within 30-fold of the clinical Cmax. Overall, this model system provides straightforward and informative screening for GI toxicity that integrates sensitive and robust endpoints, enables screening to support early nonclinical development, and uniquely allows for mechanistic insights.

#2055 Delivery of oligonucleotide therapeutic drugs: Universal detection reagents specific for nucleic acid modifications.

T. Giardiello, **A. Anderson**, R. Salvo, C. Ascoli;
Rockland Immunochemicals Inc, Limerick, PA

Nucleic acid therapies, including oligonucleotide therapeutics (ONTs) and vaccines, have increased in development, respectively, since their inception as an emerging drug modality and after the first mRNA COVID-19 vaccine was granted EUA approval in 2020. RNA-based therapies, such as antisense oligonucleotides (ASO), RNAi, aptamers, and mRNA, are designed to modulate protein synthesis in patients and have applications in oncology, gene therapy, and infectious disease prevention. Strategies for ONT drug delivery have advanced over recent years with the goal of overcoming limitations when targeting extrahepatic tissues. Improving the “drug-likeness” of ONTs is facilitated by chemical modifications to the sugar-phosphate backbone and/or nitrogenous bases. Modifications are designed to increase ONT drug stability, uptake, and efficacy, but may increase the likelihood of toxicity. First generation chemical modifications include phosphorothioate (PS) modification of the phosphate portion of the backbone, whereas second generation modifications include adding substituent groups to the 2’ position of the ribose portion of the backbone, specifically 2’-O-methyl (OME), 2’-O-methoxy-ethyl (MOE), and 2’-fluoro modifications of RNA. Third generation modifications include peptide nucleic acids (PNA), locked nucleic acids (LNA), morpholino phosphoroamidate (PMO) modifications, and others. We have developed, optimized, and validated a library of monoclonal antibody reagents that detect these chemical modifications independent of nucleic acid composition, structure, strandedness, configuration, or platform. These “universal detection reagents” can be used in (1) immunohistochemistry (IHC) to determine biodistribution, (2) immunofluorescence (IF) to determine intracellular localization, (3) ELISA to determine anti-drug antibody binding, immunogenicity, and drug ranking, (4) immunoprecipitation to determine protein binding in serum and/or tissue lysates, (5) *in vivo* cell culture studies to determine potency, and (6) other immunoassays. While *in situ* hybridization (ISH) is an established method for the detection and localization of ONTs in cells and tissues, this method has limitations that include lack of utility (as unique probes must be designed individually for each ONT), high costs in time and materials to produce probes, the inability of ISH to bind and detect short ONT drug sequences, and difficulties encountered when repeated sequences are present within the ONT sequence. Here we report differential sensitivity and specificity of panels of antibodies specific for PS and MOE modifications. We demonstrate the performance of these antibodies by various *in vitro* assays that show the utility of these specialty reagents to facilitate the collection of analytical data to support ADMET studies useful to ensure ONT approval by regulatory agencies.

#2056 Click chemistry enabled selective activation of highly cytotoxic MMAE payload at tumors using TROP2 targeting agent.

G. Coricor, J. M. McFarland, S. Srinivasan, S. Wagner, T.-H. Nguyen, J. M. Mejia Oneto;
Shasqi Inc., San Francisco, CA

Shasqi is advancing the Click Activated Protodrugs Against Cancer (CAPAC®) platform based on click chemistry, a Nobel Prize winning technology. The platform is modular and comprises 1) an activator that target specific antigens, and 2) inert cancer drugs, protodrugs, which are selectively activated at tumors via click chemistry. The CAPAC technology separates the tumor targeting function from the payload and reunite them at the tumor creating the flexibility to optimize activity while limiting toxicity during preclinical and clinical development. The modularity of the platform enables the rapid development of new therapies as well as unlocking unique treatment benefits such as tunable combinations and payload cycling. We envision that CAPAC will expand the scope of potential targets, widen the therapeutic index of antibody drug conjugates (ADCs). Here we present a TROP2-targeting activator with a monomethyl auristatin E (MMAE) payload.

TROP2 expression has been observed in many cancers that express low-HER2. The clinical efficacy of anti-TROP2 ADCs is hindered by undesirable side effects, limiting their potential therapeutic window. We have developed the targeting activator SQT02, a TROP2 Fab binder conjugated with ~2.2 tetrazines per protein, and SQP22, an attenuated protodrug of MMAE coupled with *trans*-cyclooctene (TCO). The reaction between tetrazine and TCO moieties releases MMAE at the tumor site. Previously we have demonstrated that SQP22 is attenuated compared to free MMAE and in combination with a HER2 targeting activator led to significant tumor inhibition with no observable toxicity. The CAPAC platform's modular nature allows seamless exchange of targeting agents or payloads, thus enabling different therapeutic combinations to be generated quickly and efficiently, like SQT02 in combination with SQP22. Dosing of SQT02 occurs prior to dosing with SQP22 to reduce non-specific activation while enabling higher payload activation at the tumor site to induce tumor cell death. *In vitro*, SQT02 bound NCI-N87 human gastric cancer cells with similar EC_{50} (~0.07 µg/mL) to an antibody that binds to TROP2. *In vivo*, treatment of SQT02 followed by SQP22 led to 60% tumor growth inhibition compared to Sacituzumab govitecan's 35% inhibition in the NCI-N87 xenograft model. No body weight loss was observed in the animals treated with SQT02 in combination with SQP22.

We have demonstrated the use of click chemistry to deliver a highly potent cytotoxic agent to tumors, causing significant growth inhibition. The flexibility and adaptability of the CAPAC platform allowed us to quickly develop therapeutic combinations that can be deployed to accelerate the path to the clinic. Our findings provide evidence for developing SQT02 in combination with SQP22 for the treatment of TROP2 expressing cancers.

#2057 Monitoring cGAMP Biochemically and in cell using homogenous HTS formatted bioluminescent assay.

S. A. Goueli, k. Hsiao, N. Murray, d. Mikheil, M. Larsen, H. Wang;
Promega, Madison, WI

The STimulator of INterferon Genes (STING) is a transmembrane protein located at the endoplasmic reticulum, which serves as a molecular hub in response to cytoplasmic cyclic dinucleotide (CDN) second messengers such as cyclic GMP-AMP (cGAMP). Upon its generation via cyclic GMP-AMP synthase (cGAS) by a wide array of pathogens that provide extracellular microbial DNA and by intracellular (nuclear and mitochondrial) DNA, it binds directly to the STING protein resulting in the activation of the STING pathway. This activation by cytosolic DNA initiates a cascade of events, cGAS-STING-TBK1-IRF3 signaling, that induces type 1 IFN response, and eventually the signaling is terminated by degradation of pathway components and clearance of stimulatory DNA. Given its significant role as an adaptor for DNA sensors to pathogens and its involvement in immune sensing, tumor growth control, and control of autoinflammatory and autoimmune disorders, the STING pathway has become a very important drug target. Credible evidence suggests that the cGAS–cGAMP–STING pathway makes fundamental contributions to at least three major cancer therapies: radiation therapy, chemotherapy, and immunotherapy, and it thus represents a promising drug target. Therefore, there is a need to identify lead compounds that effectively modulate human STING for further drug development. Towards this goal, we have developed a bioluminescent assay to monitor the concentration of cGAMP in intracellular as well as extracellular compartments. The assay relies on the new concept of Protein Complementation Assay (PCA) using nanoluciferase (nanoluc) complementation technology where a small peptide (SmBiT) derived from nanoluc linked to cGAMP through a linker (cGAMP tracer) can be recognized by an anti cGAMP antibody that is linked to a nanoluc complementary fragment (LgBiT) resulting in bioluminescence upon the addition of nanoluc substrate. The presence of free cGAMP that is generated in the reaction competes with cGAMP tracer and decreases bioluminescence. We have optimized the assay for higher sensitivity down to less than 10 nM cGAMP and less than one ng of cGAS and thus, and it is suitable for testing compounds that modulate cGAS activity. We also improved cell lysis condition to increase recovery of cGAMP that is generated intracellularly using several cGAS activators and correlating its concentration with cytokine release. We envision using this assay to monitor cGAMP presence in sera and spinal fluids of patients who have ALS and Alzheimer diseases. The assay is homogenous, with minimal or no false hits using LOPAC screening and HTS formatted and can be completed in less than one hour. Thus, this assay provides valuable contribution for investigating modulators of the STING pathway and facilitates the search for novel therapeutics.

#2058 Compound library screening to identify modulators of alternative splicing in non-small cell lung cancer (NSCLC).

R. Cooley[1], M. V. Powers[1], A. G. Bond[1], P. Jensen[2], G. Newton[1], A. Scarpino[1], J. Braun[2], C. Esdar[2], P. A. Clarke[1];
[1]The Institute of Cancer Research, London, United Kingdom, [2]The Healthcare Business of Merck KGaA, Darmstadt, Germany

Alternative splicing is a molecular mechanism that allows a single gene to encode multiple proteins. It is a complex and highly controlled process used to regulate normal gene expression but is often dysregulated in cancer. Compounds that can modulate alternative splicing are currently being explored as a potential new class of therapeutic agent in cancer. This highlights the need for a deeper understanding of the splicing process, its regulation, and its impact. The discovery of novel and specific tool compounds that modulate splicing would therefore not only be beneficial in investigating the regulation and dysregulation of splicing in cancer but could also be exploited therapeutically.

To identify novel regulators of splicing, we generated a cell-based split luciferase screening assay based on alternative splicing of MCL-1 (myeloid cell leukemia-1 protein) pre-mRNA. The *MCL1* gene usually produces an mRNA encoding a 'long' variant (MCL1L) that is an anti-apoptotic protein often highly expressed in cancers. However, in some circumstances, for example following genetic knockdown of splicing factors, a pro-apoptotic 'short' variant (MCL1S) is expressed as a result of exon-skipping.

Here we engineered the human NSCLC cell line NCI-H1299 to express a luminescent-tagged version of the MCL1S splice variant to monitor its induction upon spliceosome modulation. Using this engineered cell line, we screened an unannotated library of 12,000 compounds selected to have low molecular weights and favorable properties for cellular uptake. The screen had an average Z' value of 0.89 over 45 microplates, indicating high assay robustness. Hits were identified as any compound with a luminescence of greater than the average + two standard deviations of the screening dataset. The compounds were validated by repetition in the screening assay, giving 34 candidate hits that were then triaged by qPCR assay to confirm splicing modulation of *MCL1*. One interesting hit was found to increase mRNA and cellular protein levels of MCL1S and induced altered splicing across the transcriptome that was distinct from the splicing profiles of a diverse panel of splicing modulators, including compounds targeting SF3B1, CLK, and RBM39. In addition, treatment with this hit compound resulted in accumulation of the splicing factor SC35 in cytoplasmic granules, an unusual phenotype not seen with known splicing modulators, that could explain the distinct splicing modulation we have observed.

Deconvolution and further characterization of screening hits and potentially unique new mechanisms of action could improve current understanding of alternative splicing and its regulation in NSCLC. The discovery of novel compounds to expand our current toolset of splicing modulators will be key in building the foundation for future splicing targeted drug discovery.

#2059 An image-based real time method to measure antibody-dependent cellular phagocytosis.

J. Wang, Y. Shi, Y. Sun, J. T. Koerber, A. Seki, S. Rutz;
Genentech, Inc., South San Francisco, CA

Antibody-dependent cellular phagocytosis (ADCP) is an important mechanism of action of therapeutic antibodies. *In vitro* quantification of macrophage phagocytosis has been technically challenging. Flow cytometry assays were traditionally used for ADCP activity measurements, these methods were static measurements at certain time point, thus provide no information about engulfment kinetics. Moreover, the flow cytometry assays require lifting the macrophage cells from the labware which may affect macrophage activities. We have developed a real time ADCP assay using a live cell analysis system. The target cells labeled with a pH sensitive dye only fluoresce when they are engulfed in acidic phagosomes in the presence of specific antibodies. Our assay is a plate-based with a simple mix and read protocol without disturbing the macrophages. The new method is quantitative and robust, can be readily used for high-throughput screening for functional antibodies. By studying the ADCP activities of different subtypes of macrophages, we found M2 microphages showed the strongest ADCP activity compare to M0 and M1 macrophages, due to their different expression levels of FcgRs. The assay is highly sensitive to differentiate the antibody variants with enhanced Fc function. It can also be used to study the kinetics and mechanisms of ADCP.

#2060 Automation of 3D cancer spheroid assay for compound screening.

O. Sirenko, A. Lim, A. Michlmayr, Z. Tong, E. Keidel, F. Spira;
Molecular Devices, LLC (Moldev), San Jose, CA

Finding efficient drug combinations to treat cancer patients is critical for therapy success. Accordingly, there is a critical need to develop methods for efficient testing drug efficacy to discover new therapeutic targets. 3D cancer models are highly valuable tools for cancer research and drug development. However, the complexity of performing 3D assays remains a hurdle for adopting these methods for compound screening. To alleviate the bottlenecks that come with labor-intensive manual protocols we developed cell culture automation methods using CellXpress.ai instrument. The instrument enables automation of 2D or 3D culture for prolonged complex workflows. The CellXpress.ai provides automated plating, passaging, media exchanges, monitoring organoids, alone with compound treatment and the end point assays with high content image analysis. In the present study we describe full automation of imaging, analysis, and cell culture process which enables scaling up complex 3D cell-based assays and compound screening. As an example of 3D protocol, we automated culture and imaging of colorectal cancer 3D spheroids formed from HCT116 cell line in U-shape low attachment plates. HCT116 cells were expanded in 2D, then spheroids were formed after automated dispensing of cell suspension into U-shape 96 or 384 plates. After 48h spheroids were treated with 12 anti-cancer compounds, at multiple concentrations for 3-5 days, then stained and imaged. Cell plating, compound additions, media exchange, and staining were performed automatically by CellXpressAI instrument. During the culture spheroids were monitored using transmitted light, with immediate analysis of phenotypic changes, including inhibition of growth or spheroid disintegration. For endpoint assay spheroids were stained with combination of Hoechst nuclear stain and viability dyes Calcein AM and EtHD, then imaged, and analyzed for multiple read-outs including spheroid size, marker intensities, and live-dead cell scoring. We observed concentration-dependent inhibition of spheroid growth and cell death in response to anti-cancer compounds and evaluated effective compound concentrations for cytotoxic or cytostatic effects. Cell culture process automation for 3D assays, powered by imaging and image analysis has a potential to bring 3D biology into another level, allowing to increase throughput and reproducibility, and enabling variety of high throughput drug discovery and precision medicine applications.

#2061 A proven activity-based workflow for the identification and characterization of time-dependent kinase inhibitors using a continuous assay format.

E. May[1], D. Urul[1], K. Huynh[1], S. Cornell-Kennon[1], V. Nemmara[1], Z. Lu[1], S. Hoare[2], M. Lyles[3], E. Schaefer[1];
[1]Assayquant Technologies, Inc., Marlborough, MA, [2]Pharmechanics LLC, Owego, NY, [3]Assayquant Technologies, Inc., Marlboro, MA

Time-dependent inhibitors (TDIs) of enzyme targets offer distinct advantages for the development of potent and selective compounds with favorable pharmacokinetic and pharmacodynamic properties. Such inhibitors are characterized by non-linear progress curves: after an initial inhibited velocity, a rate constant governs the transition to a final steady-state reaction rate of the inhibited enzyme. A final rate of zero indicates irreversible inhibition, whereas a non-zero final rate indicates slow-binding inhibition. Characterizing these inhibitory modes of action is enabled with a continuous assay format that avoids the common pitfalls and misleading results seen with end-point assays. A continuous assay format enables efficient and robust determination of the kinetic parameters required to drive structure-activity relationship optimization to streamline the development of more effective drugs. It is important to note that simple IC_{50}s for TDIs will not suffice, and can, indeed, also be misleading. We have developed a robust three-step workflow based on kinetic catalytic activity measurements to quickly identify and characterize TDIs. First, dose-response experiments are conducted with and without an enzyme-inhibitor preincubation step. The curvature of the reaction progress curve in the non-preincubated experiment and a shift in IC_{50} from the preincubated experiment are indicative of TDI. In the absence of TDI, simple IC_{50}s are reported with, if possible, K_i values. If TDI is present, a second experiment is conducted to assess compound reversibility using either a jump-dilution protocol or a novel free-compound clearance method that uses gel filtration spin columns or spin plates. In either protocol, forward progress curve analysis is used to monitor the recovery of enzymatic activity after dilution of inhibitor in solution. Lastly, the potency of the inhibitor is evaluated using kinetic experiments tailored to the nature of the inhibition – either reversible or irreversible. If reversible, then the rate constant from the reversibility experiment is used to determine the residence time of the molecule. If irreversible, then a 24-point dose-response experiment with serial 1.5-fold dilutions is performed, and all the progress curves are globally fit to determine k_{inact}/K_I, and, if possible, k_{inact} and K_I separately. The method will be fully described through the characterization of known EGFR inhibitors of three inhibition types: fast-off (Gefitinib), slow binding (Lapatinib), and irreversible (Osimertinib).

#2062 Identification of functional MAIT-specific TCRs using MR1 dCODE Dextramer® reagents and evaluating antigen presentation.

K. Lenogue, B. Hansen, K. Jacobsen, L. Brix, T. Holberg Blicher;
Immudex, Virum, Denmark

Objectives:

To support TCR discovery and enable evaluation of TCR target expression on the surface of cells, we have established a streamlined workflow allowing TCR Discovery, validation and evaluation of MHC-antigen expression on target cells. As proof of concept, MR1 dCODE Dextramer® reagents were used to identify antigen-specific MAIT cells using single-cell sequencing, TCR sequences were extracted from the resulting data and then cloned and expressed as TCR monomers. The specificity of the TCRs was subsequently validated as TCR Dextramer® reagents and used to evaluate target MHC-peptide presentation on cell surface.

Methods:

Mixed PBMC samples from three healthy donors were stained with antibodies targeting relevant phenotypic markers as well as MR1 dCODE Dextramer® reagents carrying the MAIT cell-specific ligand 5-OP-RU. Following staining, sorting, and partitioning on a BD Rhapsody™ Single-Cell Analysis System, the cells underwent sequencing for a characterization of gene and surface marker expression as well as paired alpha-beta TCR sequences. Single alpha and beta chains were individually expressed, refolded together and purified. Refolded TCR monomer functionality was validated using an artificial cell assay. The functional TCRs can be multimerized on a Dextramer® backbone and used to evaluate expression of target on cell surface.

Results:

The majority of the identified CD161+ MAIT cells (~70%) expressed typical TCRs consisting of TRAV1-2 and TRAJ33 as well as TRBV6/20, TRBD1/2, and TRBJ2 gene segments. Three alpha-beta TCR sequences were selected: Two TCRs having common TRAV+TRAJ, TRBV+TRBJ combinations and one having a rare TRAV+TRAJ one. TCR alpha and beta chains were successfully expressed for all selected TCRs but only 2 TCRs showed a correctly refolded TCR as demonstrated by proper recognition of MR1/5-OP-RU. Based on these two functional TCRs, TCR Dextramer® reagents were generated and used to evaluate expression of target antigen on cell surface.

Conclusion:

We demonstrate a workflow allowing: (i) Identification of MAIT cells and their corresponding TCR sequences. (ii) Generation of soluble TCR molecules based on the identified sequences and validation of their specificity. (iii) Generation of TCR Dextramer® reagents allowing identification of target expression on surface of cells.

This workflow is also useful for identification of other antigen-specific T cells and creates a new tool for evaluation of antigen-expression by MHC on surface of cells. By combining the high sensitivity of dCODE Dextramer® technology with TCR sequencing and creation of TCR Dextramer® reagents, both low-affinity interactions and rare cell types can be detected and studied in unique detail.

#2063 Using the edge wells in 96-well plates without increasing variability in cytotoxicity assays through thermal controls.

A. D. Henn, S. Darou, R. Yerden;
BioSpherix, Ltd., Parish, NY

There are very few things as fundamental to cancer research as the 96-well-plate, yet edge effect has continued to cause problems since its introduction. The most common remedy for edge effect is to avoid using edge wells altogether, which eliminates 37% of the plate from the assay. If all of those wells could be used, an estimated USD $119M could be saved in research costs annually across the globe. We have shown previously that maintaining constant thermal control of plating conditions reduces variability in stem cell toxicity assays. Here, we ask the question: can we use the edge wells in cancer screening assays if we control thermal changes that happen in the traditional lab as cells are plated at room temperature and incubated at 37 degrees C? We had the null hypothesis that including the edge wells would add variability to an A549 cytotoxicity assay, even if the cell handling and incubation temperatures were matched and held constant. We plated A549 cells at either room temperature (like a BSC) or at 37 degrees C using the Xvivo System, which maintains constant temperature, oxygen, CO2, and relative humidity levels around cell handling operations. The cells were treated with serial dilutions of peracetic acid/hydrogen peroxide solution. After incubation for 3 days, the plates were stained with Crystal Violet and assessed for cell density (n=3 separate experiments). The null hypothesis was disproven. We found that if the plates were maintained at 37 degrees C during cell handling as well as incubation, that cell distribution was random and even across all wells, even edge wells. We found that there was no statistical difference between edge well and center well results in cytotoxicity assays. Edge wells were usable without increasing variability in the assays. This is consistent with earlier findings showing that when temperature changes between cell plating and incubation were averted, stem cell distribution across the plate was random and the edge effect was eliminated.

#2064 Unveiling the correlation between gemtuzumab-ozogamicin efficacy and CD33+ expression in AML primary samples using the novel AML vitroscreen.

Mara Gilardi, Garima Kaushik, Brandon Walling, Paolo Schiavini, **Stefano Cairo**, Marianna Zipeto

Champions Oncology, Inc. (Hackensack, NJ), Hackensack, NJ

Acute myeloid leukemia (AML) poses a significant therapeutic challenge, with a rising incidence in recent times. This clonal hematopoietic disorder of progenitor and stem cells exhibits aggressive behavior, and despite initial remission, recurrence is common[1]. The conventional shift from chemotherapy to monoclonal antibodies and antibody-drug conjugates (ADCs) has been hindered by the absence of AML-specific antigens. Notably, CD33, expressed strongly in 80-90% of AML cells, has become a target for gemtuzumab-ozogamicin (Mylotarg), the sole FDA approved ADC for AML treatment[2]. While advancements in understanding AML molecular mechanisms have influenced clinical approaches, the lack of clinically representative models hinders therapeutic progress. Existing models, both in vivo and ex vivo, struggle to capture the heterogeneity and complexity of AML[3]. Addressing this, we present our proprietary assay, Champions AML VitroScreen®[4], designed for testing therapeutic candidates in primary AML samples. Our diverse bank of deeply characterized AML samples encompasses multiple subtypes, allowing evaluation of therapeutic responses through cell viability, proliferation, and clonal composition analyses. To validate our novel assay, we employed the VitroScreen platform to test Mylotarg across various AML subtypes, considering CD33 expression levels. By assessing more than 20 AML models, we determined the IC50 for Mylotarg and observed dose-dependent responses, where sensitivity to the drugh correlated with CD33 expression. Through multiple endpoints, including viability, proliferation, apoptosis, and phenotyping, we categorized primary AML models as responders, low responders, or resistant, establishing a strong positive correlation between Mylotarg sensitivity and CD33 expression. Our innovative approach, utilizing deeply characterized AML patient samples in the AML VitroScreen® platform, facilitates high-throughput drug testing. This system, serving as an ideal clinical translational setting in preclinical research, holds promise for developing tailored therapeutic strategies. Ultimately, this approach could significantly impact patient outcomes by offering improved strategies for both primary and recurrent AML cases.

#2065 Development of a genetically validated, cell-based reporter assay for ADAR1 editing activity.

V. Sapp, J. Bilakovics, A. Burr, F. Martins, P. Shashkin, V. Baron, H. Zhu, J. Park;
BPS Bioscience, San Diego, CA

Adenosine Deaminase Acting on RNA (ADAR) enzymes perform adenosine to inosine base editing in RNA, particularly targeting adenosines located within a specific double-stranded stem-loop motif. The ADAR1 gene encodes both a universally expressed isoform (p110) and an interferon-inducible isoform (p150), which plays a role in innate immunity by mediating interferon signaling. In the context of healthy, uninfected cells, ADAR1 performs A-to-I editing on endogenous double-stranded RNA to prevent it from activating downstream dsRNA sensors RIG-I and MDA5, which in-turn activate a pro-inflammatory response. Loss of function mutations in ADAR1 result in aberrant activation of the dsRNA sensors and are involved in autoimmune disorders. ADAR1 dysfunction also impacts cancer cell growth, proliferation, and response to immunotherapy. ADAR1 expression is increased in several types of cancer and ADAR1 knock-out has been demonstrated to improve the response to certain immunotherapies such PD-1/PD-L1 blockade and to circumvent tumor immunotherapy resistance mechanisms, making ADAR1 an attractive target for therapeutic development. We have developed and validated a high-throughput, cell-based assay for measuring ADAR1 editing activity. Several ADAR editing reporter constructs were designed and evaluated for their relative response to ADAR1 over-expression. They all feature an ADAR1 hairpin target with a stop codon (UAG) which is susceptible to ADAR1-mediated editing to a tryptophan (UUG), located upstream of a firefly luciferase gene. We show that increasing transient expression of ADAR1 led to proportional increased activity of the downstream firefly luciferase, indicating dose-dependent transcript editing by ADAR1. Selected reporters were used in conjunction with ADAR2 overexpression to identify an ADAR1-biased reporter. Thus, a reporter with low luciferase activity in response to ADAR2 expression was chosen to establish stable HEK293 cell lines (which express low levels of ADAR1) with and without constitutively expressed ADAR1 protein. ADAR1-overexpressing HEK293 cells displayed high luciferase activity, in accordance with high ADAR1-mediated editing of the reporter transcript, which was decreased in response to siRNA-mediated knockdown of ADAR1 expression or pharmacological inhibition of ADAR1 activity. Sequencing of the reporter RNA confirmed that changes in reporter activity were correlated with editing of the RNA transcript. Finally, these validated ADAR1 editing reporter cell lines were further engineered to constitutively express Renilla luciferase under the control of a CMV promoter, serving as an internal control for the toxicity of ADAR1 inhibitors. In conclusion, our robust cell-based assay provides a well-validated resource to identify modulators of ADAR1 editing activity in a cellular context.

#2066 Measuring the activity of SMUG1 DNA glycosylase with a novel sSTRIDE-SMUG1 assay.

K. Stepien, F. Sierpowski, Z. Prucsi, S. Koman, M. Jarosz, A. Waligorska, M. Kordon-Kiszala, K. Solarczyk;
intoDNA, Krakow, Poland

On average, spontaneous deamination of cytosine to aberrant base uracil happens 70-200 times per human genome per day. These mutagenic U/G mispairs are, however, corrected by error-free base repair (BER) initiated by uracil-DNA glycosylases. SMUG1 (single-strand selective monofunctional uracil DNA glycosylase), as one of the major glycosylases, removes uracil and oxidized pyrimidines from DNA. In spite of the name, SMUG1 removes uracil also from double-stranded DNA. Unrepaired by SMUG1 U/G mispairs are mutagenic, and alterations in SMUG1 expression levels have been linked to cancer development. Low SMUG1 transcripts are associated with poor prognosis in breast cancer and SMUG1 loss has been shown to cause PARPi resistance in HR-deficient background. Hence, tools describing SMUG1 activities in DNA damage response may provide new approaches for cancer cell treatment. We report here the development, optimization and validation of an assay measuring the activity of SMUG1. The new assay is based on the STRIDE platform technology, which enables direct and sensitive detection of single- or double-strand DNA breaks in situ, in fixed cells. sSTRIDE-SMUG1 assay detects DNA nicks localized in close proximity to the SMUG1 protein and can thus be utilized as a direct reporter of its activity. The experiments were performed in HAP1 cells. First, in untreated cells we have shown that the sSTRIDE-SMUG1 signals constitute ca. 1-2% of total single-strand DNA breaks foci detected by the classic sSTRIDE assay variant, while the negative controls have shown that the number of false-positive foci does not exceed 15% of the total number of signals. As expected, treatment of cells with a cytotoxic nucleotide hydroxymethyl-deoxyuridine (hmdU) resulted in an increase in the number of detected sSTRIDE-SMUG1 signals. To verify the specificity of the assay, SMUG1 was knocked-down in HAP1 wild-type cells using siRNA and then the level of sSTRIDE-SMUG1 signals was measured in both untreated and hmdU-treated cells. In all tested conditions, SMUG1 expression silencing has resulted in a decrease in sSTRIDE-SMUG1 foci. We believe that the sSTRIDE-SMUG1 assay can prove to be a very useful solution to study DNA repair mechanisms involving aberrant base excision. Additionally, sSTRIDE-SMUG1 measurements may be of the utmost importance in characterization of agents inducing synthetic lethality or trapping BER intermediates.

#2067 QUANTROseq, a transcriptomic based drug discovery platform using time-resolved gene expression profiling: Identification of inhibitors and degraders of transcription factors and cell signaling regulators.

Arianna Sabo[1], Nina Fasching Griesmayr[1], Tobias Neumann[1], Raphael Manzenreither[1], Maja Ivankovic[1], Rodrigo Pacheco Valamatos Costa[1], Sarah Rieser[1], Sara Scinicariello[1], Petr Triska[1], Anna Stingeder[1], Astrid Gruss[1], Ryan Cubero[1], Olga Frank[1], Ivica Sowemimo[1], Paul Kirchgatterer[2], Adriana Cantoran[3], Stefan Ameres[4], Johannes Zuber[2], Michael Bauer[1]

[1]QUANTRO Therapeutics GmbH, Vienna, Austria,[2]Research Institue of Molecular Biology, Vienna, Austria,[3]St. Anna Children's Cancer Research Institute, Vienna, Austria,[4]Max Perutz Labs, Vienna, Austria

Integrative analyses of CRISPR/Cas9 screening datasets from different sources revealed - besides known oncogenes - a series of transcriptional master regulators as most prominent context-specific dependencies in cancer that remained largely inaccessible to conventional drug discovery approaches. New chemical entities (NCEs) that specifically interfere with a transcription factor (TF) at any level should induce and be detectable based on selective effects on their primary biochemical activity - i.e., the transcriptional activation of specific target genes. However, the definition of direct targets of a TF and, more generally, the unbiased detection of direct transcriptional effects has remained challenging due to the limited time resolution of conventional techniques for gene perturbation and transcriptional profiling. To overcome this limitation, QUANTRO Therapeutics relies on SLAMseq technology that, by metabolic labeling de novo-synthesized RNA immediately after intervention and conserving the information for later readout, provides unprecedent time-resolution in transcriptomic analysis.

Aiming to target previously undruggable targets, we set out to first build definitive knowledge around their direct effect on transcription, inducing their quick protein degradation through the auxin-inducible degron (AID) technology followed by immediate transcriptional readout though SLAMseq -before any secondary, confounding effect could appear in the cell.

The targets´ mRNA fingerprints produced are then used as a reference and cross-compared with existing and new chemical entities to:

(i) benchmark the real mode of action of existing drugs; (ii) identify new drug candidates that specifically interfere with disease-causing transcriptional programs in cancer; (iii) interrogate the efficiency, selectivity, and potency of drug candidates during Hit-validation and Hit-to-Lead activities.

Proof of concept data demonstrated that time-resolved transcriptional profiling can reveal drugs´ mode of action with unprecedent precision and sensitivity, when drugs act on Targets that have a direct effect on transcriptional regulation - such as TFs and signaling pathways. Building on this knowledge, QUANTRO Therapeutics unleashed the unique potential of mRNA fingerprinting technology for HTS-compatible drug discovery by (1) establishing scalable and automated workflows for metabolic RNA labeling, treatment of cells, and RNA extraction; (2) developing algorithms for combinatorial mRNA fingerprint-readout that allow for the simultaneous assessment of TF signatures by multiplexed targeted RNA sequencing (QUANTROseq), thus transforming the precision and scope of cell-based compound screens.

#2068 Multi-pass flow cytometry for high-marker panels with minimal spillover spread.

T. Brown, S. Forward, E. Assita, G. Abbott, M. Fahlberg, S. J. J. Kwok;
LASE Innovation, Woburn, MA

Multiparametric flow cytometry on immune cells is essential in cancer research, disease diagnosis, and treatment monitoring. Collecting data on >10 markers at a time is ideal due to deeper cell characterization and assay sensitivity, however, high-marker panels are subject to significant spillover spread from spectrally overlapping fluorophores that compromise data quality, standardization, and interpretation. Clinical flow cytometry still relies on the use of multi-tube low-marker (<10) panels that minimize spillover spread and ease analysis and interpretation of results. To improve and expand the clinical utility of flow cytometry, there is a need for higher marker measurements without use of highly overlapping fluorophores, which would also serve to streamline the use of samples and reagents. Here, we present the development of a novel barcoding method using micron-sized laser particles (LPs) that confer an optical signature to individual cells at high-throughput, enabling tracking of cells through multiple passes in a flow cytometer. This process is possible using a custom cytometer equipped to detect LPs and capture samples. Sequential staining of samples with releasing or photobleaching antibodies/fluors between cycles enables merging of multiple smaller panels that each have minimal spillover, resulting in a high-marker dataset with drastic reduction in spillover compared to conventional single-acquisition flow cytometry.

We demonstrate the utility of this technology through three different assays. Human PBMCs were barcoded with LPs and stained with 1) a panel of releasable antibodies (Miltenyi Biotec, 10 markers, 2 passes), 2) a laboratory-designed panel that utilized photobleaching (32 markers, 3 passes), and 3) a panel of dried and validated DuraClone antibodies that utilized photobleaching (Beckman Coulter, 18 markers, 2 passes). For each assay, cells were stained, acquired, photobleached/released, captured, re-stained, re-acquired and steps were repeated either once (for 2 passes) or twice (for 3 passes). In all cases, we found drastically reduced spillover, better data quality, and identified the same cell subtypes detected by conventional flow cytometry. Reproducibility was high across multiple (3+) replicates with CVs <30% among all populations with >1% frequency of total. New cell populations were identified that would not be possible with separate acquisitions of each pass.

Recent advances in flow cytometry now allow more markers to be analyzed together, but at the cost of increasing spectral overlap and spillover spread. Multi-pass flow cytometry confines spillover to individual panels, reducing overall interference and simplifying analysis. This enhances data quality and usability while streamlining resources, facilitating the clinical uptake of complex flow cytometry in cancer research, diagnosis, and treatment.

#2069 High content imaging without sacrificing coverage, resolution or speed: Functional validation through multiple assays.

M. Boisvert, J. Kieler, D. DiSepio, D. Weldon;
Araceli Biosciences Inc., Portland, OR

Traditionally, high content screening (HCS) required compromise: sacrificing resolution, sample coverage or speed. This has limited high content screening's utility as a high throughput tool, as speed is essential to cancer research at scale. Using a new approach, Araceli Endeavor® offers a solution to this compromise. This system images 96, 384 or 1536 -well high content microplates in under 10 minutes with full well coverage and sub-micron resolution, enabling high content screening at high throughput speeds without compromising resolution or coverage. Paired with the Clairvoyance™ analysis software, plates are analyzed at similar speeds, going from images to object-level data in 5-25 minutes. As with any new technology, validation is needed. Here we validate Endeavor and Clairvoyance at the level of the bioassay, using a range of common high content assays across different modalities. Assays are chosen to quantifiably demonstrate sensitivity, breadth, and broad applicability. Performance was benchmarked by using well-characterized compounds, matching published EC50/IC50 values when possible. We examined submicron-level nuclear spot counting, measuring histone γH2Ax and micronuclei formation after genotoxic insult. Intensity-based assays include cellular positivity, here live/dead, and subcellular translocation with transcription factor NFKB after induction with cytokines Il1b and TNFα. Looking at cytosolic vesicle aggregation, we measured autophagic flux with two distinct modalities, comparative imaging and analysis of live cell dye and immunohistochemistry-based detection yielded consistent EC50 values between methods. Overall, these assays yield consistent, robust results corresponding to literature values, showing the importance of full well coverage and resolution. We demonstrate how assays that formerly took hours can be effectively imaged and analyzed without sacrificing quality in 10-30 minutes.

#2070 Engineered Inhalation nanoparticle formulation for lung cancer.

R. Tiwari, E. N. H. Ghali, N. Chauhan, V. Kashyap, S. C. Chauhan, **M. M. Yallapu**;
University of Texas Rio Grande Valley, McAllen, TX

Background: Lung cancer is a predominant cause of cancer-related morbidity and mortality across the world including in the United States. Treatment modalities for lung cancer include surgery, chemotherapy, radiotherapy, and/or targeted therapies depending on the cancer stage. Despite the survival benefits of chemotherapy, its value is offset by severe systemic side effects such as renal and/or hepatic toxicity or insufficient amounts of drug reaching to the target site. Such pitfalls can be handled by inhalable therapy which avoids first-pass metabolism and increases patients' compliance. In this study, we have investigated the inhalable therapy of cross-linked tannic acid-based nanoparticles (CTA NPs) into cancer cells and determined the synergistic effect of gambogic acid (GA) and gemcitabine (Gem).

Methods: The CTA NPs formulations were characterized for particle size, chemical composition, and drug loading efficiency using various physicochemical methods (FT-IR, DSC, SEM, and TGA). Cellular uptake of CTA NPs was evaluated in lung cancer cell lines (A549 and NCI-H1299) using fluorescence microscopy and flow cytometry analysis. Further, the therapeutic efficacy of GA-Gem encapsulated CTA NPs (G-G CTA NPs) formulation was determined by various *in vitro* assays (CCK-8, mucoadhesion Boyden chamber, and apoptosis assays). The molecular effects of G-G CTA NPs formulation were also observed in lung cancer cell lines.

Results: Our novel CTA NPs formulation provided an average size of 110 nm in dynamic light scattering with a sustained release of the drug(s). CTA NPs formulation showed a remarkable mucoadhesion and mucopenetration penetration potential in-vitro model(s). Cellular uptake studies show that CTA NPs formulation allows for effective endosomal release into the cytosol. Additionally, the G-G CTA NPs formulation showed superior *in vitro* anti-cancer activity in lung cancer cells (A549 and NCI-H1299) compared to free drugs.

Conclusions: Taken together, our results demonstrate that G-G CTA NPs formulation exhibits superior anti-cancer potential than free drug against lung cancer and could be a novel therapeutic modality for the management of lung cancer.

#2071 Pre-clinical evidence for new camptothecin-peptide conjugates in the treatment of sortilin-positive colorectal cancers.

S. Das[1], J.-C. Currie[1], M. Demeule[1], C. Charfi[1], A. Zgheib[2], A. Nayyar[1], A. Nguyen[1], B. Danalache[2], R. Beliveau[2], C. Marsolais[1], B. Annabi[2]; [1]Theratechnologies, Montreal, QC, Canada, [2]Universite du Quebec a Montreal, Montreal, QC, Canada

Limitations in current colorectal cancer (CRC) camptothecin (CPT)-based chemotherapy have mostly been attributed to low specificity and high systemic cytotoxic side effects. More effective therapies are therefore required to improve the clinical outcomes of patients with CRC. Here, we developed a selective and better anticancer drug delivery of CPT through conjugation to a peptide (TH19P01) that targets Sortilin (SORT1), a scavenging receptor expressed in various tumor tissues including CRC. In the current study, significant SORT1 expression was detected in various CRC cell lines as well as that of irinotecan analogs efflux pump (ABCG2) in LoVo and HT-29 cells. Considering this result, we used our proprietary peptide conjugation SORT1 technology to increase cell targeting selectivity and cell delivery efficacy of CPT analogs. Different peptide drug conjugates (PDCs) were generated linking the TH19P01 peptide to SN-38 (an irinotecan metabolite) or exatecan, which are two main CPT derivatives used in recent antibody drug conjugates (ADC) as payloads. *In vitro*, immunonofluorescent microscopy revealed that TH19P01 was rapidly internalized (<15 min) in a SORT1-positive human HT-29 CRC cell model. These PDCs also inhibited CRC cell proliferation at low nM concentrations (3-90 nM). *In vivo*, weekly administration of TH2101 (SN-38) and of TH2303 (exatecan) conjugates were well tolerated as they had little impact on mouse body weight but caused a more potent growth inhibition of the HT-29 CRC tumor xenograft model than did either unconjugated irinotecan or exatecan molecules. In fact, at their maximum tolerable dose, irinotecan and exatecan caused a tumor growth inhibition of only 48% and 45% whereas TH2101 and TH2303 inhibited the growth of HT-29 tumors by 83% and 91%, respectively. These results provide strong pre-clinical evidence for the future development of novel CPT PDCs therapeutics with targeting of SORT1-positive CRC cells.

#2072 Human liver patient derived organoids: Development and characterization of a new tissue mimetic model.

R. Bhowmick[1], M. Rahman[1], S. Wani[1], S. Malla[1], A. Chatterjee[2];
[1]MilliporeSigma, Temecula, CA, [2]MilliporeSigma, Burlington, MA

Liver is the largest solid organ and performs hundreds of vital functions including drug metabolism. Liver diseases, including viral infections, cancer and metabolic disorders account for about 2 million deaths annually, worldwide (1). Current models for studying liver biology and drug metabolism include 2D cultured primary cells/ cell lines, which do not represent the metabolic and structural complexity of human tissue. *In vivo* models for liver diseases are time consuming, cost prohibitive and often ineffective. Therefore, better tissue mimetic liver models are needed. Organoids are self-assembled 3D cultured cellular units that may mimic the corresponding human tissue structurally and functionally (2). Patient derived organoids (PDO) are developed from tissue of specific patients and may resemble the source tissue in molecular features, including recapitulation of patient specific responses to therapies. Here, we report development and characterization of novel liver PDO lines from vendor-sourced cryopreserved tissue. We have developed biobanks of undifferentiated as well as differentiated liver PDO models.Human cadaver-sourced liver tissue were obtained with explicit donor consent. Liver PDO were generated following modification of a previously established protocol (3). Briefly, samples were minced, digested to single cells, and filtered. Specific number of cells were mixed with diluted Matrigel (Corning) and added as small drops on cell culture plates and grown in liver PDO specific growth media. Whenever appropriate, PDO were differentiated by culturing in differentiation-specific media in multi-well plates. In all cases, PDO were monitored using brightfield microscopy (Olympus CK40) and live cell imaging (Muvicyte, Perkin Elmer); and passaged every 6-8 days. Undifferentiated PDO were cryopreserved/ thawed following in-house SOP to confirm viability. Liver-specific biomarker expression in the PDO lines were confirmed by confocal microscopy (ImageExpress, Molecular Devices). PDO lines were also assayed for ALT activity, albumin production and urea. PDO were cleared for microbial/ viral contamination and confirmed as unique lines using single tandem repeat analyses. Transcriptome profiles were analyzed using vendor services. So far, we have successfully generated 3 liver PDO lines, both undifferentiated as well as differentiated. Our liver PDO lines would be highly useful in understanding liver biology and disease models; and will have significant usage in drug testing, including DMPK and ADME/Tox studies. Future efforts would include scaling up, development of liver specific assays and developing PDO from specific liver diseases, including hepatocellular carcinoma, MASLD and NASH. References:1.Asrani, et al., 2019. J. Hepatol. 2.Zhao et al., 2022. STAR Protocols3.Broutier et al., 2016. Nature Protocols

#2073 Human breast patient derived organoids: Development and characterization of a new tissue mimetic model.

R. Bhowmick[1], S. Malla[1], S. Wani[1], A. Chatterjee[2];
[1]MilliporeSigma, Temecula, CA, [2]MilliporeSigma, Burlington, MA

Worldwide, breast cancer (BC), is the most frequently diagnosed cancer among women. In the US, 1 out of 8 women may expect to be diagnosed with BC In their lifetime. Current models for studying BC tumor biology and BC drug discovery include 2D cultured cell lines and patient derived xenografts (PDX). As 2D cultured cells do not represent the 3D complexity of human tissue, and PDX models are time consuming and cost prohibitive, better tissue mimetic models are needed. Organoids are self-assembled 3D cultured cellular units that may mimic the corresponding human tissue structurally and functionally (1). Patient derived organoids (PDO) are developed from tissue of specific patients and may resemble the source tissue in molecular features, including recapitulation of patient specific responses to therapies (2). Here, we report development and characterization of novel breast PDO lines from fresh (≤24h post-surgery) and cryopreserved (≤7 days post-surgery) tissue. Breast tumor and normal, tumor adjacent (NTA) tissue were sourced from consented patients. Breast PDO were generated following modifications to a published protocol (3). Briefly, tissue samples were minced, digested with collagenase, and filtered. The filtrate was resuspended in Matrigel (Corning) and small drops were added on cell culture plates. Both tumor and NTA PDO were cultured using the same media and organoids were monitored using brightfield microscopy (Olympus CK40) and live cell imaging (Muvicyte, Perkin Elmer). PDO lines were analyzed for expression and distribution of important breast-specific biomarkers using confocal microscopy (ImagExpress, Molecular Devices). PDO lines displayed hormone receptors (ER, PR), cell surface (EpCAM, CD49f), cytoskeletal (cytokeratin 14, 19, E-cadherin, vimentin) and cell proliferation (Ki67) markers. Transcriptome profiles were analyzed using vendor services (Azenta). PDO were also tested for their susceptibility to breast cancer drugs, e.g., Tamoxifen, chlorambucil and Docetaxel. We have successfully generated one NTA ER^{+}/ PR^{+}/ $HER2^{-}$ PDO line and one tumor ER^{+}/ PR^{+}/ $HER2^{-}$ PDO line from different donors. Our breast PDO lines would be highly useful in understanding tumor biology, BC progression, signal transduction, and drug discovery/ testing. Future efforts would include process scaling up and development of BC specific assays. References:1.Zhao et al., 2022. STAR Protocols 2.Bleijs, M. et al., 2019. EMBO J3.Dekkers et al., 2021. Nature Protocols

EXPERIMENTAL AND MOLECULAR THERAPEUTICS: Novel Targets and Pathways
Poster Session

#2077 Exploring the multifaceted efficacy of de novo lipogenesis inhibitor in cancer therapy.
D. Lowder, J. Shin, M. E. Ruiz-Echartea, J. Deng, A. Rusin, D. Skapura, M. Ittmann, S. Kaochar;
Baylor College of Medicine, Houston, TX

Cancer cells frequently exhibit altered lipid metabolism to sustain their rapid growth and proliferation.Sterol Regulatory Element-Binding Proteins (SREBPs) are key transcription factors that orchestratelipid biosynthesis and uptake in cells. Dysregulation of SREBPs is a common feature of many cancertypes, making them attractive targets for therapeutic intervention. In this study, we present acomprehensive exploration of the potential and rationale for targeting lipid metabolism in cancerthrough the use of a small molecule inhibitor that targets activation of SREBP. We illustrate that oursmall molecule inhibitor (SMI) exhibits potent anticancer activity and effectively targets SREBPsignaling in a variety of prostate cancer models as well as in non-prostate cancer models that arelipogenesis driven. Our novel SMI induces apoptosis and reduces PCa cell proliferation, suppressescell invasion and migration. Furthermore, we illustrate that in addition to suppressing the transcriptionfactor activity of SREBPs, these novel SMIs are highly effective in suppressing both the full length andvariant androgen receptor and their signaling in prostate cancer cells. Notably, in cell and organoidmodels, these novel inhibitors exhibit synergistic anticancer activity in combination with the ARsignaling inhibitor, Enzalutamide. The anticancer activity of these inhibitors extend beyond ARdependent prostate cancer and are also effective in organoid models of neuroendocrine PCa, aparticularly drug-resistant and aggressive PC subtype. Lastly, we illustrate excellent pharmacokineticsand potent anti-tumor effects of these novel SREBP activation inhibitors using *in vivo* castration-resistant prostate cancer CDX tumors. Given the urgent need for novel targets in PCa, our first-in-class inhibitor represents a promising therapeutic strategy with the potential to effectively targetdysregulated lipogenesis in cancer patients.

#2078 The imipridone ONC212 cooperates with MEK and immune checkpoint inhibition to elicit *in vivo* regression of KPC mouse pancreatic tumors.

J. Chan[1], A. J. Lannigan[1], G. Sun[1], V. V. Prabhu[2], R. Edwards IV[1], L. Zhang[1], L. Zhou[1], W. S. El-Deiry[1], A. G. Raufi[1];
[1]Brown University, Providence, RI, [2]Chimerix, Durham, NC

Background: Pancreatic ductal adenocarcinoma (PDAC) is an aggressive disease with limited therapeutic options. ONC212 is a second-generation imipridone with antitumor effects in human PDAC cell lines. ONC212 has been shown to bind to mitochondrial protease ClpP, suppress ClpX, and impair oxidative phosphorylation by decreasing ATP production. While ONC212 has been evaluated in immunocompromised mice xenografted with human pancreatic tumors, ONC212 has not been evaluated, either alone or in combination with MEK and/or immune checkpoint inhibition (ICI), in immunocompetent mice bearing notoriously aggressive *Kras*$^{LSL.G12D/+}$; *Tp53*$^{LSL.R172H/+}$; *Pdx1Cre*$^{tg/+}$ (KPC) murine PDAC tumors. We hypothesized that, like human PDAC cells, KPC cells would demonstrate sensitivity to ONC212 both *in vitro* and *in vivo*. Our group has previously shown that ONC212 synergizes with trametinib to induce tumor cell death in human PDAC cells. We therefore hypothesized that this combination, together with ICI, would enhance KPC tumor cell death *in vivo*.
Methods: We determined *in vitro* sensitivity of the KPC cells to ONC212 alone and in combination with trametinib using CellTiter-Glo® luminescent cell viability assays. Results were analyzed after 72 hours of incubation using Compusyn and Combenefit. *In vivo* experiments involved C57BL/6 mice that were injected subcutaneously with $3x10^5$ KPCy cells in 100 mL of PBS/matrigel. To determine the ideal ONC212 dose, we tested five different doses/dosing frequencies (50 mg/kg; 25 mg/kg; 12.5 mg/kg given by oral gavage weekly or twice weekly) in tumor-bearing (50-75 mm^3) mice. Mouse weight and tumor size was measured every four days. Treatment was stopped once tumor volumes reached 3,000 mm^3 or if ulceration occurred. Once the ideal dose of ONC212 was determined, a study treating KPC tumor-bearing C57BL/6 mice with ONC212, trametinib, and ICI (anti-PD-1 mAb) alone and all possible doublet/triplet combinations was performed using the same methods.
Results: We found that the combination of ONC212 and trametinib exhibited synergy in the KPC cell line *in vitro*. Our *in vivo* experiments revealed that ONC212 controlled KPC tumor growth in a dose-dependent manner, however, toxicity was also noted at higher, more frequent doses. While both 25 mg/kg and 50 mg/kg twice weekly were equally effective, 25 mg/kg was better tolerated and determined to be the ideal dose. In the combination therapy study, all treatments resulted in tumor reduction, as compared to the vehicle control; however, the triple therapy group had the lowest average tumor size at day twenty. Toxicity was noted in mice receiving at least two treatments, reflected by reduced weights and mobility. Further analysis of the tumor immune microenvironment using multiplex cytokine and immunofluorescence are ongoing.

#2079 Tumor-derived fibrinogen promotes pancreatic ductal adenocarcinoma progression.

D. Liu[1], L. Brubaker[1], Y. Niu[1], E. LaPlante[1], G. Van Buren[1], A. Milosavljevic[1], C. Chen[1], C. Zong[1], M. Cruz[2], Q. Yao[1];
[1]Baylor College of Medicine, Houston, TX, [2]Michael E. DeBakey VA Medical Center, Houston, TX

Background: Hypercoagulability is a common clinical manifestation in patients with cancers, especially in pancreatic ductal adenocarcinoma (PDAC). Over 20% of PDAC patients with advanced-stage and worse prognosis undergo a venous thromboembolism (VTE) incidence. Fibrinogen (FG) may contribute to VTE due to its high expression in advanced PDAC tumors. Here, we set to determine the biological roles of tumor-derived FG in PDAC. In addition, our previous study showed that Von Willebrand Factor (VWF) A2 domain can effectively bind to FG and reduce platelet clot formation. Therefore, the functional roles of A2 on FG in PDAC were also studied.

Methods: The correlation between survival rate and FG expression in PDAC was analyzed using RNAseq profiles of 149 PDAC patient samples from the TCGA database. PDAC subtyping of Baylor College of Medicine (BCM) PDAC patient-derived xenograft (PDX) cohort was performed using RNAseq data according to Moffitt's criteria. The FG (three chains FGA, FGB, FGG) overexpression (OE) and knock-out (KO) PDAC cell lines were established. The gene expression and biological functions of FG were performed in PDX and cell lines using IHC and immunoblot assays. The FG effect on PDAC progression *in vivo* was studied in mouse models.

Results: TCGA analysis showed that elevated tumor-derived FG gene expression is significantly correlated with worse overall survival and disease-free survival rates in PDAC patients. PDX lines RNAseq analysis clearly separated BCM PDAC PDXs into two subtypes: basal-like and classical PDACs. Basal-like PDXs showed significantly stronger FG staining than that in classical ones. Compared to the classical subtype, the basal-like subtype showed significantly upregulated genes that are associated with the epithelial-mesenchymal transition (EMT), IL6/JAK/STAT3, and TNFα signaling pathways. Accordingly, basal-like subtype PDAC exposed to IL6 or TNFα significantly increased FG and FG receptor expression with activated STAT3 and AKT pathways and elevated EMT markers, whereas classical subtype cells have minimal changes. In addition, we found that the FG-OE cells exhibit enhanced cell proliferation and migration properties whereas FG-KO cells reduced the effects. Consistent with *in vitro* data, FG-OE PDAC showed significantly higher tumor burdens than that of control PDAC in both orthotopic and subcutaneous PDAC mouse models. Furthermore, A2 protein treatment can effectively block the FG function and dramatically inactivate the FG-induced EMT process and AKT signaling pathway.

Conclusions: Tumor-derived fibrinogen is upregulated in a basal-like subtype of PDAC cells and may contribute to tumor growth and metastasis by activating aberrant signaling pathways and promoting EMT. Our findings imply that elevated fibrinogen in PDAC could contribute to tumor progression and the A2 protein which target to fibrinogen may be a promising therapy for basal-like subtype PDAC.

#2080 SOS1 inhibition is an effective therapeutic strategy in SOS1-mutant cancer.

M. J. Sale[1], N. Mukherjee[1], M. Koch[1], R. Ruzicka[2], R. Jacob[2], C. Albrecht[2], T. Zanin[2], T. Madensky[2], R. L. Schenk[2], A. Baum[2], K. Kostyrko[2], D. Gerlach[2], M. H. Hofmann[2], F. McCormick[1];

[1]UCSF - University of California San Francisco, San Francisco, CA, [2]Boehringer Ingelheim, Vienna, Austria

SOS1 is a principal guanine nucleotide exchange factor for canonical RAS GTPases and activates RAS signaling. Mutations in SOS1 are found in several prominent cancer types, including 2-4% of NSCLC, CRC, and melanoma. The recent development of novel SOS1 inhibitors (SOS1i), including BI-3406, that block interaction between SOS1 and RAS, presents a potential therapy for SOS1-driven cancers. Here we show that the majority of SOS1 mutations observed in patients enhance RAS guanine nucleotide exchange in cells and activate RAS-MAPK signaling. We treated 11 SOS1 mutant cancer cell lines without RAS co-mutation with a SOS1i and found that 10 were sensitive to SOS1 inhibition in 2D and/or 3D cell culture. In contrast, cell lines with SOS1 and RAS co-mutations were resistant to SOS1 inhibition. In vitro treatment of SOS1 mutant cells with a SHP2 inhibitor, which is presumed to inhibit the activity of both SOS1 and SOS2, revealed a subset of four cell lines that were more sensitive to SHP2 inhibition than SOS1 inhibition. This implied that, in certain contexts, SOS2 can compensate for the loss of SOS1 activity. Accordingly, these cells exhibited a SOS2-dependent rebound in RAS-MAPK signaling after treatment with SOS1i. SOS2 knock-down further sensitized these cells to SOS1 inhibition, resulting in responses equivalent to SHP2 inhibition. Thus, upon SOS1 inhibition relief of ERK1/2-dependent negative regulation likely contributes to receptor tyrosine kinase-driven SOS2 activation that may mediate SOS1 inhibitor resistance in some contexts. In vivo, SOS1i efficiently inhibited tumor growth in four SOS1-mutant NSCLC, CRC, and AML xenograft models. The tumor-suppressive effects of SOS1i in these models were comparable to or stronger than the effects of SHP2i or MEKi. Thus, our results suggest that SOS1 inhibition could be an effective therapeutic approach in RAS wild-type cancer patients with SOS1 mutations.

#2081 Biomarkers for CLK inhibitor CTX-712 treatment response in myeloid neoplasms: Paving the way toward clinical trials.

A. Yoda[1], D. Morishita[2], Y. Ochi[1], A. Mizutani[2], H. Tozaki[2], Y. Satoh[2], T. Mori[1], J. Takeda[1], H. Makishima[1], M. Nakagawa[1], Y. Nannya[1], S. Ogawa[1]; [1]Kyoto Univ. Graduate School of Medicine, Kyoto, Japan, [2]Chordia Therapeutics Inc., Fujisawa, Japan

Dysregulated RNA splicing is a molecular feature that characterizes almost all tumor types. Splicing is altered in cancer owing to both recurrent mutations and deregulated expression of trans-acting factors that catalyze and regulate splicing. Therefore, splicing can be targeted for the development of new drugs to treat cancers, particularly those with mutations in splicing factors. In myelodysplastic syndromes (MDS) and acute myeloid leukemia (AML), genes that encode splicing factors are among those with the highest mutation rates. These mutations are heterozygous and largely mutually exclusive, suggesting the possibility of synthetic lethality due to multiple splicing factor mutations. Such synthetic lethality can be applied as an innovative strategy to develop drugs for the treatment of MDS and AML. We have reported the development of a CLK kinase inhibitor, CTX-712, and evaluated its anti-leukemic activities both *in vitro* and *in vivo*. The mechanism of action of CTX-712 involves the suppression of the phosphorylation of multiple SR proteins, including SRSF2/3/4/6, alteration of nuclear speckle morphology, and switching of binding partners of SRSF2. RNA-seq analysis revealed that CTX-712 induced global alterations in splicing, typically resulting in exon exclusion (exon skipping) of cassette exons. Notably, the anti-leukemic effects of CTX-712 positively correlated with the degree of altered splicing, suggesting that CTX-712 inhibits RNA splicing. [Cancer Res (2022) 82 (12_Supplement): 5494., Blood (2022) 140 (Supplement 1): 489-490]. However, patient stratification markers for CTX-712 based on the above mechanism are still undefined. To identify biomarkers for CTX-712, we performed a comprehensive analysis by integrating both wet and dry DNA/RNA sequencing on more than 60 *ex vivo* primary samples from MDS/AML patients and 23 MDS/AML-derived xenografts (PDX). Unexpectedly, regardless of their splicing factor-mutation status, various types of primary AML cells and PDX models were highly sensitive to CTX-712. Both the primary cells and PDX models showed significant responses to CTX-712 and greater changes in splicing. Additionally, we performed biomarker analysis by comparing gene mutations and RNA splicing patterns between the sensitive and insensitive models and associating them with the anti-tumor effect. We identified several potential biomarkers that can indicate sensitivity to CTX-712. Mechanistic studies that aim to determine why these biomarkers could make cancer more sensitive to splicing perturbation by CTX-712 are ongoing. In conclusion, our results demonstrated a significant effect of CTX-712 on MDS/AML-derived models regardless of their splicing factor-mutation status. Additionally, we present novel biomarkers that could predict sensitivity to CTX-712.

#2082 Identification of nonsense-mediated decay inhibitors that alter the tumor immune landscape.

A. L. Cook, S. Sur, L. Dobbyn, E. Watson, J. D. Cohen, B. Ptak, B. S. Lee, S. Paul, E. Hsiue, M. Popoli, B. Vogelstein, N. Papadopoulos, C. Bettegowda, K. Gabrielson, S. Zhou, K. Kinzler, **N. Wyhs**;
Johns Hopkins University School of Medicine, Baltimore, MD

Despite exciting developments in cancer immunotherapy, its broad application is limited by the paucity of targetable antigens on the tumor cell surface. As an intrinsic cellular pathway, nonsense-mediated decay (NMD) conceals neoantigens through the destruction of the RNA products from genes harboring truncating mutations. We developed and conducted a high throughput screen, based on the ratiometric analysis of transcripts, to identify critical mediators of NMD. This screen revealed disruption of kinase SMG1's phosphorylation of UPF1 as a potent disruptor of NMD. This led us to design a novel SMG1 inhibitor, KVS0001, that elevates the expression of transcripts and proteins resulting from truncating mutations in vivo and in vitro. Most importantly, KVS0001 concomitantly increased the presentation of immune-targetable HLA class I-associated peptides from NMD-downregulated proteins on the surface of cancer cells. KVS0001 provides new opportunities for studying NMD and the diseases in which NMD plays a role, including cancer and inherited diseases.

#2083 Discovery of ETX-19477, a novel and selective PARG inhibitor with high potency against tumors with underlying replication stress.

J. P. Holleran, T. S. Rodems, S. Sharma, A. M. Santini, C. Wuerz, J. Liu, L. Tian, J. Dosch, J. Nader, R. Rivera, S. Herath, J. Marakovits, C. McBride, R. Stansfield, A. Salyards, J. M. Veal, J. A. Stafford, G. Bain;
858 Therapeutics, Inc., San Diego, CA

DNA damage response (DDR) is an important cellular process that is regulated by poly ADP ribosylation (PARylation). PARP1 binds to DNA break sites and then catalyzes PARylation, which leads to recruitment of repair factors and initiation of base-excision and single-strand break (SSB) repair. Removal of PAR chains is performed by PARG and is also critical for successful completion of DNA repair. Suppression of PAR chain hydrolysis via PARG depletion or inhibition leads to defective single-strand break repair, reduced kinetics of repair, and hypersensitivity to certain DNA damaging agents.

Cancer cells demonstrate high levels of replication stress, characterized as the slowing or stalling of replication forks during DNA replication. Replication stress generates DNA SSBs and exposes unligated Okazaki fragments which activate PARP1. PARP1 catalyzed PARylation slows replication fork progression as a protective mechanism, initiates damage repair, and promotes fork reversal. PAR chain removal, via PARG activity, enables completion of damage repair, replication fork restart, and recovery from replication stress. Under conditions of replication stress, PARP inhibition can result in unrestrained fork progression and the occurrence of DNA double strand breaks from fork runoff. In contrast, PARG inhibition causes prolonged slowing or stalling of replication fork progression, which can lead to replication catastrophe and cancer cell death. Because of these opposing roles, PARG inhibitors show distinct pharmacology as compared to PARP inhibitors in certain cancer cells including cancer cells that are *BRCA* wild type, homologous recombination proficient, and PARP inhibitor insensitive or resistant.

ETX-19477 is a novel inhibitor of PARG that demonstrates low nM, on-target activity in cells as measured by the accumulation of PAR chains. ETX-19477 induces death and/or inhibits the proliferation of multiple cancer cell types including ER+HER2- breast, serous and mucinous ovarian, lung, and gastric cancers and induces pan-nuclear γH2AX expression, a hallmark of replication catastrophe. Preclinical studies demonstrate that ETX-19477 is orally bioavailable with favorable pharmacokinetics. Oral treatment of mice with ETX-19477 is well tolerated and shows robust dose-dependent in vivo anti-tumor activity in breast and ovarian cell-line derived and patient-derived xenograft models. Efficacy is observed with either once or twice daily dosing and with a discontinuous dosing regimen. In mouse xenograft models, induction of γH2AX expression in tumor tissue correlates with tumor growth inhibition. Preclinical data show ETX-19477 demonstrates potent and specific anti-proliferative effects by exposing underlying existing replication stress vulnerabilities in cancer cells across multiple tumor types. ETX-19477 will be advanced into clinical trials in 2024.

#2084 Autocrine regulation of laryngeal cancer tumorigenesis by 24R,25(OH)$_2$D$_3$.

C. D. Dennis, D. Cohen, J. T. Dillon, B. D. Boyan, Z. Schwartz;
Virginia Commonwealth University, Richmond, VA

Vitamin D3 supplementation is becoming widely accepted as a therapeutic in many common estrogen responsive cancers. Previous studies in breast cancer showed that 24R,25-dihydroxyvitamin D$_3$ (24,25) regulates tumorigenesis via a caveolae membrane-associated signaling pathway involving phospholipase D [PLD] and palmitoylation of an unknown receptor. The goal of this study was to examine the effects of 24,25 in estrogen responsive laryngeal cancer tumorigenesis, investigate the mechanisms involved, and determine the ability of the tumor cells to produce 24,25 locally. Expression of CYP24A1 and CYP27B1 was measured in ERα66+ UM-SCC-12 (UM12) and ERα66- UM-SCC-11A (UM11A) laryngeal cancer cells. Cells were treated with 25(OH)D$_3$, and production of the vitamin D$_3$ metabolites 1,25(OH)$_2$D$_3$, 24,25(OH)$_2$D$_3$, and 1,24,25(OH)$_3$D$_3$ was measured using HPLC. The therapeutic potential of 24,25 was then assessed by treating the cells with 24,25 and measuring proliferation and apoptosis. In vivo, UM12 and UM11A cells were implanted into the cheek of NSG mice; the mice were treated with 24,25, and evaluated for survival and tumor volume. The signaling pathways involving PLD, palmitoylation, and caveolin-1 were investigated as driving mechanisms. CYP24A1 and CYP27B1 were present in ERα66+ UM12 and ERα66- UM11A cells, both of which are responsive to estrogen. When treated with 25(OH)D$_3$, UM11A cells produced more 24,25 than UM12s, comparable to the physiologically relevant levels in blood. Both cells produced similar levels of 1,25. 24,25 increased proliferation and inhibited apoptosis in ERα66+ UM12 cells in vitro, but had the opposite effect in ERα66- UM11A cells. 24,25 increased PLD activity in UM12 cells but decreased PLD activity in UM11A cells. Inhibition of PLD activity or palmitoylation, as well as silencing expression of caveolin-1, reduced the effects of 24,25 on P53 in both cell types, indicating they played a role. Mice with UM11A tumors given 24,25 exhibited reduced tumor burden and increased survival compared to vehicle-treated controls. In contrast, mice with UM12 tumors given 24,25 had an increased tumor burden and reduced survival compared to controls. The presence of CYP24A1 and CYP27B1, local production of 24,25, and demonstration that laryngeal cancer cells respond to 24,25, indicate that 24,25 acts in an autocrine/paracrine manner. 24,25 was pro-tumorigenic in ERα66+ laryngeal cancer cells while having the opposite effect in ERα66- cells, both in vitro and in vivo, demonstrating a dependence on ERα66 expression. 24,25 acts via a mechanism involving PLD, caveolae, and palmitoylation. These data show that 24,25 regulates laryngeal cancer tumorigenesis, which is mediated by membrane associated signaling pathways that may depend on ERα66 level, and suggest a major role of 24R,25-dihydroxyvitamin D$_3$ in laryngeal cancer.

#2085 Targeting the translation initiation complex component eIF4G1 in melanoma.

Y. Feng[1], M. Radaeva[2], H. Kim[1], A. Deshpande[1], A. Deshpande[1], P. Jovanovic[3], R. Murad[1], I. Topisirovic[3], S. Olson[4], A. Cherkasov[2], Z. Ronai[1];
[1]Sanford Burnham Prebys Med. Discovery Inst., La Jolla, CA, [2]Vancouver Prostate Centre and Department of Urologic Sciences, University of British Columbia, Vancouver, BC, Canada, [3]Lady Davis Institute, SMBD Jewish General Hospital, Gerald Bronfman Department of Oncology and Division of Experimental Medicine, McGill University, Montreal, QC, [4]Conrad Prebys Center for Chemical Genomics at Sanford Burnham Prebys Medical Discovery Institute, La Jolla, CA

The translation initiation factor 4F (eIF4F) complex assembly is a rate-limiting step in mRNA translation. eIF4F subunits including eIF4A, eIF4E, and eIF4G, are often upregulated in cancer and neurodegeneration diseases. Elevated eIF4F level/activity has been correlated with poor prognosis and drug resistance. Leveraging our findings with the small molecule SBI-756, which interacts with eIF4G1 and impairs eIF4F complex assembly, we set to map domains that are required for SBI-756 activity. A CRISPR screen using sgRNAs that target different sequences on eIF4G1 led to the identification of the MA3 domain, as a putative binding site for SBI-756. Deletion/mutation of the eIF4G1 MA3 domain attenuated melanoma cells and spheroids growth. Polysome profiling assays confirmed attenuated translation activity, which resembled those seen with SBI-756. In silico virtual screen identified 64 small molecules (out of >10 million) that interact with the MA3 domain. Of these, we have selected four that effectively attenuated melanoma growth in culture. Analogs developed for these four compounds were more potent in impairing the assembly of the eIF4F complex, inhibition of protein translation and the 2D and 3D growth of melanoma cells. RNA-sequencing analysis highlighted altered expression of genes implicated in apoptosis, UPR, cell cycle, and ROS pathways, leading us to test possible combination with pathways that may complement the above. Among those, autophagy inhibitors synergized with our lead compound, M19-6, resulting in efficient melanoma cell death, using notably lower concentrations of these inhibitors. Our findings identify the eIF4G1 MA3 domain as an important player in eIF4F assembly and a potential target for cancer therapy.

#2086 Effect of XPO1 inhibition on colorectal cancer tumorigenesis.

A. E. Evans, D. A. Dixon;
University of Kansas, Lawrence, KS

Colorectal Cancer (CRC) is the second leading cause of cancer-related death in the U.S. A subset of individuals faces a notably higher likelihood of developing CRC within their lifetime. Hence, there is a compelling need for innovative chemopreventive treatments aimed at minimizing CRC tumorigenesis. Exportin 1 (XPO1; also referred to as CRM1) plays a pivotal role in transporting proteins from the nucleus to the cytoplasm. The overexpression of XPO1 has been identified across several cancers, including CRC. XPO1 interacts with a diverse spectrum of more than 1000 proteins. The overexpression of XPO1 leads to the excessive removal of tumor suppressors from the nucleus, rendering these proteins functionally inert. To counteract the overexpression of XPO1 in tumors, a novel class of drugs known as Selective Inhibitors of Nuclear Export (SINE) has been developed. Among these, Eltanexor (KPT-8602) has emerged as a promising therapeutic agent, demonstrating fewer side effects compared to its precursors, and is currently under evaluation in Phase 1/2 clinical trials. The treatment effects of SINE compounds on CRC remain largely unknown. We have assessed Eltanexor's ability to limit CRC tumorigenesis using a genetic CRC model in *Apc*$^{min/+}$ mice. Our findings indicate that Eltanexor substantially reduces tumor burden by approximately 3-fold and induces a significant reduction of tumors exceeding 1mm in size. Furthermore, a xenograft experiment using the human CRC cell line, HCT116, reveals nearly a 3-fold reduction in tumor size upon Eltanexor treatment. In both CRC models, Eltanexor exhibits noteworthy tolerability. Additionally, XPO1 protein levels are consistently diminished in both models, aligning with our *in vitro* observations. To further ascertain Eltanexor's specificity for CRC tumors versus normal tissue, we conducted drug sensitivity assays using organoids derived from *Apc*$^{min/+}$ tumors and wild-type mice small intestine tissue. We found that *Apc*$^{min/+}$ tumoroids have heightened sensitivity to Eltanexor-treatments, when compared to wild-type organoids. In an endeavor to elucidate Eltanexor's potent *in vivo* tumorigenesis inhibitory effects, we conducted multiple assays which revealed a reduction in COX-2 RNA and protein expression levels in Eltanexor-treated cells and reduced COX-2 protein in the tumors of Eltanexor-treated *Apc*$^{min/+}$ mice. In CRC, COX-2 is implicated in CRC development and is currently the target of multiple CRC chemopreventive agents. Our observations reveal that Eltanexor-treated CRC cells exhibit reduced COX-2 gene expression through both inhibiting COX-2's promoter and its mRNA post-transcriptional stability. Collectively, our findings underscore XPO1 as a potent target for inhibiting CRC tumorigenesis. Future studies will aim to further assess how Eltanexor is impacting COX-2's promoter, while additionally testing Eltanexor's tumorigenesis-inhibiting potential in a colitis-induced CRC mouse model.

#2087 Targeting lipid metabolism in pancreatic cancer.

C. Cheng[1], J. P. Wisniewski[1], A. Korkaya[1], B. Jackson[1], R. Mannan[1], S. Mahapatra[1], N. Rossiter[1], R. Bhattacharyya[1], P. Morlacchi[2], S. Peters[1], Y. Qiao[1], C. A. Lyssiotis[1], A. M. Chinnaiyan[1];

[1]University of Michigan, Ann Arbor, MI, [2]Agilent Technologies, Inc., Lexington, MA

Background PIKfyve is a lipid kinase that serves as the sole source of cellular PI(3,5)P2 and PI5P, critical phosphatidylinositols for autophagy and lysosome function. Pancreatic ductal adenocarcinoma (PDAC) is known to upregulate and depend on lysosomal functions such as autophagy to exist in its harsh, nutrient-disrupted microenvironment. Thus, we aimed to establish PIKfyve as a therapeutic target in PDAC. Using a PIKfyve-knockout genetically engineered mouse model of pancreatic cancer (KC and KPC), we determined that PIKfyve was necessary for PDAC development. Given these results, we hypothesized that PIKfyve was critical for maintaining metabolic homeostasis in PDAC and that inhibiting PIKfyve would be an efficacious therapeutic strategy for PDAC.
Methods and results We first validated the known role of PIKfyve in regulating autophagy using CRISPRi mediated knockdown, PIKfyve inhibitors Apilimod and ESK981, and a PIKfyve degrader, which all demonstrated that PIKfyve perturbation disrupted autophagic flux and suppressed PDAC cell growth. Little is known about the metabolic impacts of PIKfyve inhibition in PDAC beyond disruption of autophagy. Thus, we paired RNA-seq and a metabolic CRISPR screen to discover that PIKfyve inhibition obligated PDAC cells to upregulate *de novo* lipid synthesis. Specifically, PDAC cells upregulated fatty acid synthesis genes *ACACA* and *FASN* upon PIKfyve inhibition. Additionally, these genes were synthetically critical in the context of PIKfyve inhibition. We further performed metabolomics and lipidomics which revealed accumulation of sphingolipids upon PIKfyve inhibition. Given this, we concluded that PIKfyve regulates lipid homeostasis in PDAC. To further establish PIKfyve as a target in PDAC, we investigated the role of PIKfyve upon inhibition of KRAS, which drives PDAC through MAPK pathway signaling. First, KRAS/MAPK inhibition diminished expression of *FASN* and *ACACA*, genes synthetically essential upon PIKfyve inhibition. Additionally, KRAS/MAPK inhibition upregulated autophagy which was attenuated upon concurrent PIKfyve inhibition. Given this metabolic conflict between KRAS/MAPK and PIKfyve, we assessed the effects of dual inhibiting KRAS/MAPK and PIKfyve in a syngeneic orthotopic model. Encouragingly, combination therapy of trametinib (MEK inhibitor) and ESK981 eliminated tumor burden in most of mice, while single treatments only had modest effects. Further, we established a patient-derived xenograft model and showed that while the treatment with individual compounds trametinib, MRTX-1133 ($KRAS^{G12D}$ inhibitor), and ESK981 all suppressed tumor growth, the combination of ESK981 and trametinib or ESK981 and MRTX-1133 caused substantial tumor regression in nearly all mice. Taken together, targeting lipid metabolism through inhibition of PIKfyve is a promising therapeutic strategy for PDAC, particularly in combination with the numerous KRAS/MAPK inhibitors in clinical development.

#2088 Targeting transcriptional factor IWS1 as a potential treatment of advanced dedifferentiated liposarcoma.

Marina Goryunova[1], Yiran He[2], Nipin Sp[1], Elizaveta K. Titerina[1], Sayumi Tahara[1], Carson Karakis[1], Alessandro La Ferlita[1], Michael Sorkin[1], Alex Kim[1], Hua Zhu[3], Christopher M. Hadad[2], Raphael E. Pollock[1], Joal D. Beane[1]

[1]Surgical Oncology, The Ohio State University Wexner Medical Center, Columbus, OH,[2]Department of Chemistry and Biochemistry, The Ohio State University, Columbus, OH,[3]Division of Cardiac Surgery, The Ohio State University, Columbus, OH

Introduction. Surgery remains the only curative treatment for patients with liposarcoma (LPS). The translation of novel therapies has been hampered, and there has been no significant improvement in prognosis for 30 years. Our recent findings demonstrate that IWS1, a transcription elongation and alternative splicing factor, is elevated in dedifferentiated LPS (ddLPS) patient tumor samples and is associated with worse survival and a shorter time to relapse in ddLPS. In this study, we present preliminary results on a novel treatment for advanced ddLPS: an IWS1 inhibitor, serving as a way to discover a spliceosome as a novel therapeutic target.

Methods. Utilizing computer-aided, structure-based virtual screening approaches, we identified a class of compounds that exhibited inhibitory potential. A subset of FDA-approved drugs was evaluated by molecular docking calculations, and compounds with the highest calculated theoretical potency were selected for further analysis. To assess the ability of specific compounds to disrupt IWS1/Spt6 binding, Co-immunoprecipitation (Co-IP) experiments on ddLPS cell line Lipo863 were conducted. Transwell invasion and migration assays were performed to evaluate the effect of the drug candidate on the metastatic potential of cells. Additionally, to evaluate the impact of IWS1 inhibition on spheroid formation, a matrigel extracellular matrix scaffold was employed.

Results. Through virtual screening, we identified a class of compounds characterized by a specific chemical pattern featuring a tricyclic fused-ring structure. This class of compounds includes the well-known FDA-approved drug Ketotifen, an antihistamine and mast cell stabilizer. Co-immunoprecipitation of IWS1/Spt6 complex after 48-hour treatment with Ketotifen showed a decrease of over 50% of the isolated complex. Migration and invasion of the ddLPS cell line, Lipo863, were reduced in a dose-dependent manner by 18-44% and 17-52%, respectively, when treated with Ketotifen, without affecting cell viability. In a 3D model, a 14-day treatment of Ketotifen significantly reduced spheroid formation, confirming its impact on tumor growth and cell proliferation.

Conclusion. Ketotifen effectively disrupted IWS1/Spt6 complex *in vitro*. Importantly, it did not affect cell viability while reducing the migratory and invasive potential of ddLPS. The dose-dependent effect of Ketotifen suggests that there may be an optimal *in vivo* concentration to prevent cells from invading nearby structures and/or metastasizing. We are currently testing the ability of these compounds in preclinical mouse models of ddLPS.

#2089 A pro-oncogenic RAS-GTP:RAN-GAP complex facilitates nuclear protein export and has clinical implications.

B. K. Tripathi[1], N. H. Hirsh[1], D. Hansen[1], X. Qian[1], M. E. Durkin[1], D. Wang[1], A. G. Papageorge[1], R. Lake[1], Y. A. Evrard[2], A. Marcus[3], S. S. Ramalingam[3], M. Dasso[4], K. Vousden[5], J. H. Doroshow[1], K. J. Walters[6], D. R. Lowy[1];

[1]National Cancer Institute, Bethesda, MD, [2]Frederick National Laboratory for Cancer Research, Frederick, MD, [3]Winship Cancer Institute, Emory University, Atlanta, GA, [4]National Institute for Child Health and Human Development, Bethesda, MD, [5]The Francis Crick Institute, London, United Kingdom, [6]National Cancer Institute, Frederick, MD

The majority of RAS oncogenic activity is thought to be mediated by its canonical signaling, mainly via RAS-GTP interactions with its effectors RAF and PI3K at the plasma membrane, which respectively activate MEK/ERK and AKT/mTOR pathways. However, in this study, we have identified a new, fundamental, pro-oncogenic, non-canonical activity of RAS-GTP that increases the Exportin 1 (XPO1)-dependent export of nuclear proteins into the cytoplasm and is independent of RAF/MEK and PI3K/AKT signaling. The nuclear protein export machinery is known to depend on a trimeric protein complex composed of RAN-GTP:XPO1:nuclear protein cargo. Unexpectedly, we have found that RAS-GTP forms a stable complex with RAN GTPase-Activating Protein 1 (RAN-GAP) at the nuclear envelope, which facilitates the release of nuclear protein cargo by increasing the hydrolysis of RAN-GTP to RAN-GDP. We have determined that RAS-GTP and RAN-GAP form this complex in primary human lung tumors, patient derived xenografts, and human lung cancer cell lines. Interestingly, the RAS-GTP:RAN-GAP complex is found at the nuclear envelope and in the cytoplasm, but not at the plasma membrane. The RAS-dependent step mediated by the RAS-GTP:RAN-GAP complex acts downstream of XPO1 by increasing RAN-GTP hydrolysis, which promotes protein cargo release. Our fundamental findings have important clinical implications. For example, in human lung cancer models that harbor a KRAS-G12C mutation, the combined inhibition of MEK and PI3K (MEKi + PI3Ki) does not inhibit tumor growth to the same degree as a KRAS-G12C inhibitor. Remarkably, adding an XPO1 inhibitor to MEKi + PI3Ki inhibits tumor growth to the same degree as the KRAS-G12C inhibitor. One critical pro-oncogenic target of the RAS-GTP:RAN-GAP complex is nuclear export of the EZH2 methyltransferase, whose increase in the cytoplasm leads to a direct methylation of the cytoplasmic DLC1 tumor suppressor protein, leading to ubiquitin-dependent proteasomal degradation of DLC1 protein. Analysis of a KRAS mutant cell line from which the DLC1 gene has been disrupted by CRISPR-Cas9 technology indicates that DLC1 makes an important contribution to the growth inhibition by inhibitors that reduce nuclear protein export. These findings establish nuclear protein export as a critical, pro-oncogenic, non-canonical RAS function that is mediated by the RAS-GTP:RAN-GAP complex and provide a mechanistic explanation for poor clinical responses to combined inhibition of MEK and PI3K, which do not regulate the nuclear protein activity identified in this study.

#2090 The GNAQ T96S mutation enhances the oncogenic properties of breast cancer.

M.-H. Wu, H.-C. Wang, W.-H. Wang, Y.-J. Lin, W.-R. Chen, S.-T. Chen, C.-W. Fu, E. Chuang;
Industrial Technology Research Institute, Hsinchu, Taiwan

Breast cancer (BC) is the most commonly diagnosed cancer in the world, and metastatic breast cancer (mBC) remains responsible for the majority of breast cancer deaths. In this study, we collected 615 cases of Taiwanese BC patient's tumor samples and used whole exome sequencing (WES) to clarify the genetic mutation landscape of this population. We have compared with various BC genomic databases such as TCGA, COSMIC, and MSKCC to identify 29 novel variants in 18 genes that were predicted to have a pathogenic effect. In these pathogenic variants, we found that the GNAQ T96S mutation (threonine 96 to serine alteration of the Gαq protein) was presented in 116 out of 615 BC patients (18.9%). To examine the effect of the GNAQ T96S mutation on BC, we transfected the MCF-7 and MDA-MB-231 cell lines with the wild-type or the mutant GNAQ T96S expression vector. Transfection with the GNAQ T96S expression vector enhanced cell proliferation, colony formation, migration, and activation of the MAPK pathways compared to wild-type GNAQ expression MCF-7 cells. We also found that the tumorigenicity, and tumor growth were significantly increased in the GNAQ T96S expressed MCF-7 xenograft model, and exhibited higher rates of lung metastasis in GNAQ T96S expressed MDA-MB-231 cells. Our data suggest that the GNAQ T96S mutation may play an oncogenic role in BC by potentiating the GNAQ signaling pathway. In this study, we also found several compounds that can inhibit in vitro cell proliferation and in vivo tumor growth of GNAQ T96S expressed MCF-7 cells. These compounds showed the potential to treat the mBC patients who have GNAQ T96S mutation.

#2091 Pharmacological inhibition of chaperone-mediated autophagy via NCoR1/RARα targeting is effective against non-small cell lung cancer.

M. McCabe, R. R. Khawaja, R. Bhattacharyya, A. Diaz, T. P. Garner, K. Lindenau, R. Sereda, O. Santiago-Fernandez, A. Cuervo, E. Gavathiotis;
Albert Einstein College of Medicine, Bronx, NY

Dysregulation of autophagy, the lysosomal degradation of intracellular components, has been universally described in cancer. While activity of macroautophagy changes in a context-dependent manner in cancers, the upregulation of chaperone-mediated autophagy (CMA) is well-described in all solid tumors studied to date. Upregulated CMA directly contributes to both tumor growth and protection against anti-oncogenic interventions in cancers. Selective degradation of anti-oncogenic and pro-apoptotic proteins, such as mutant p53 and PUMA, misfolded proteins, and glycolytic enzymes by CMA allows for increased survival, reduced cell death, increased stress resistance, and enhancement of the Warburg effect in cancer cells, respectively. As such, inhibition of CMA is an attractive target for anti-cancer therapeutics, but the field currently lacks protein targets specific to CMA and selective CMA inhibitors. We have previously demonstrated the regulatory effect of retinoic acid receptor alpha (RARα) and its coregulator, nuclear receptor corepressor 1 (NCoR1), on CMA through transcriptional upregulation of the CMA effector proteins (Bourdenx et al. Cell 2021, Gomez-Sintes et al, Nat. Commun. 2022). Here, we identified a high NCoR1/RARα expression ratio in human non-small cell lung cancer (NSCLC) tumors compared to healthy lung tissue. We further illustrated a dependency on NCoR1 expression and its interaction with RARα to maintain high CMA activity in NSCLC cell lines. Provided the reliance on NCoR1 repression of RARα for high CMA activity in NSCLC, we hypothesized that small molecule targeting of the druggable NCoR1/RARα interaction to disrupt the interaction may result in suppression of CMA effector proteins and CMA inhibition. Through a series of in-silico screens for predicted NCoR1/RARα targeting, and functional screens for CMA inhibition, we identified CIM7, a first-in-class potent and selective CMA inhibitor. We validated CIM7 function through binding to RARα and subsequent disruption of NCoR1 binding, resulting in alterations to CMA-related gene expression. CIM7 inhibits CMA *in vivo* with no observed toxicity in normal tissues. We additionally demonstrated the therapeutic potential of CIM7 through its ability to reduce tumor growth *in vivo* in mouse NSCLC xenografts. Our findings support the NCoR1/RARα interaction as a major regulator of CMA in NSCLC and demonstrate the potential of pharmacologic CMA inhibition as an anti-cancer therapeutic strategy.

#2092 Genomic and proteomic analysis of glioblastoma recurrences during TTFields exposure.

F. Cianci[1], G. Rey[1], D. Krex[2], D. Ceresa[3], P. Malatesta[3], **M. Mazzanti**[1];

[1]University of Milan, Milano, Italy, [2]Universitatsklinikum Carl Gustav Carus der Technischen Universitat, Dresden, Germany, [3]University of Genova, Genova, Italy

Glioblastoma (GB) is the most aggressive type of brain tumor, and current treatments are generally ineffective in preventing recurrence. Tumor Treating Fields (TTFields) are an innovative treatment that has been shown to improve patients' life expectancy in the last two decades. TTFields therapy has an antitumoral effect that involves different mechanisms and is an optional add-on to standard maintenance temozolomide. Although TTFields therapy initially slows tumor progression, it does not prevent tumor relapse in most patients. In the present investigation, we run a genomic and proteomic analysis of surgical material from 10 patients treated with TTFields. GB tissues were obtained from the primary tumor mass and from a second surgery after tumor relapse. All the patients, in addition to brain tumor standard therapies, were treated with TTFields for eighteen hours a day, the time span of treatment application was dependent on GB recurrence. Control samples were obtained from primary and secondary surgeries of 5 patients treated with standard therapy alone. The GB tissue extracts were analyzed with an RNAseq routine, and the results from the secondary surgery were compared with the data obtained from tumor specimens of the primary surgery. A common feature of transcripts among all the patients was the alterations of several pathways promoting the increase of intracellular oxidation and cell cycle regulation. In parallel with the analysis of patient specimens, we developed an *in vitro* GB cell relapse model. This was instrumental in investigating the beneficial contribution of TTFields action during tumor relapse, but also in uncovering the limitation of this therapeutic procedure. GB primary cultures obtained from patients' surgery were exposed for up to 12 days with 200 kHz TTFields stimulation using the inovitro™ system. After 12 days of continuous TTFields application, GB cells showed an average depolarization of the resting membrane potential, increasing oxidation, and acidification of the cytoplasm. Genomic analysis of treated cells compared with wild-type primary culture, denoted an increase of tumor stem cell markers, activation of several metabolic pathways, and upregulation of different ion channel protein transcripts. Our final goal is to identify specific molecular features enhanced by TTFields treatment to be used as a parallel therapy to fight GB recurrence.

#2093 Co-treatment with KRAS G12D inhibitor MRTX1133 plus TTFields against human pancreatic and Colorectal cancer cell lines results in synergistic up-regulation of cleaved PARP in KRAS G12D & unexpectedly in KRAS G12V as well.

V. Tajiknia, P. Srinivasan, M. PInho-Schwermann, W. MacDonald, C. Purcell, W. El-Deiry;
Legorreta Cancer Center at Brown University, Providence, RI

Background: Both colorectal and pancreatic cancers are major global health issues and among deadliest cancers with great disease burden. The most commonly mutated oncogenic alteration in human cancers is KRAS, which is prevalent in pancreatic malignancies. The KRAS G12D mutation subtype is present in more than 40% of pancreatic ductal adenocarcinoma (PDAC). To this date there is no available targeted therapy options for patients with KRAS subtype mutations. MRTX1133 has been identified as a non-covalent, potent, and selective inhibitor of KRASG12D. This small molecule inhibitor has been shown to suppress KRASG12D signaling in cells and in vivo. Tumor Treating Fields (TTFields) therapy is a novel approach to treating cancer, the electric fields alter the behavior of cancer cells and prevent them from growing and dividing. We hypothesize that the co-application of MRTX1133 with TTFields will enhance the effects of MRTX1133 in PDAC and colorectal cancer (CRC).
Martials and Methods: PDAC cell line CFPAC1 with KRAS G12 V mutation and LS513 CRC cell line with KRAS G12D Mutation were treated with same dose of MRTX1133 (500 nM) and were co-treated with 150kHz TTFields. After 48 hours western blot was used to probe for cleaved PARP, cleaved C3, phosphor-ERK and DUSP6.
Results: In both KRAS G12D & KRAS G12V cell lines, synergistic upregulation of cPARP was observed following 48-hour co-treatment. Synergistic inhibition of pERK happened in KRAS G12D cell line but no change in pERK level following TTFields or MRTX1133 treatment was seen. Upregulation of cC3 in KRAS G12D happened in only co-treatment conditions. DUSP6 levels increased following MRTX1133 treatment in KRAS G12V cell line.
Conclusions: The surprising synergistic upregulation of cPARP in both KRAS G12V and G12D cells following co-treatment of KRAS G12D inhibitor MRTX1133 and TTFields can bring hope for other KRAS mutation subtypes as well as G12D. the increase in cPARP in KRAS G12V with no effect on pERK is particularly interesting and demonstrates the need of more studies to investigate the mechanisms of this synergy.

#2095 Peptide-based pivoting of p53 to target metastatic breast cancer.

Diana Putavet[1], Marjolein P. Baar[1], Johannes H. Lehmann[1], Antoine Khalil[1], Tao Shi[1], Thijs Koorman[1], Tobias B. Dansen[1], Patrick WB Derksen[1], Michael Teifel[2], Tobias Madl[3], Nicholas Sarlis[2], Peterus L. J. de Keizer[1]

[1]UMC Utrecht, Utrecht, Netherlands,[2]Cleara Biotech B.V., Utrecht, Netherlands,[3]Medical University Graz, Graz, Austria

The inability to target distant metastases limits the treatment of late-stage cancers. At least in part, this is due to the lack of optimal targeted therapies and treatment resistance to the remaining standard of care consisting of chemo-/radio- therapy. Here, we show that cancer cells that are irreparably damaged can withstand cell death through a process we define as “scarring”. In scarred cells, p53 is phosphorylated at Ser46 and Ser392 and localizes into progressive multifocal leukemia (PML) nuclear bodies. We have identified scarring in over a quarter of metastatic breast, colon, stomach and ovarian cancer. Thus, pivoting scarred p53 towards cell death in scarred cancer could establish a novel broad-range therapeutic opportunity against metastatic cancer. Targeting p53 with small molecules has proven challenging. We developed cell-penetrating peptides that selectively bind scarred p53. One of our lead compounds, CL04177 dissociates p53 from its PML scaffold leading to its a nuclear exclusion and initiation of the transcription-independent mitochondrial apoptosis. To examine the role of scarring as a therapeutic target, we focused on triple-negative breast cancer (TNBC). TNBC cells are marked by the expression of p53 and PML compared to other breast cancer subtypes. In cytotoxicity experiments, CL04177 specifically targeted TNBC over other breast cancer subtypes. Further investigation into how this compound can target metastatic cells revealed that scarred features are upregulated in metastasis-initiating cells of organoids when induced to invade in contact with collagen and that CL04177 can induce apoptosis specifically in these invading strands. *In vivo*, CL04177 showed favorable pharmacokinetics and -dynamics and a clear safety profile. Importantly, when dosed at 10-fold below its Maximally Tolerated Dose, CL04177 strongly reduced primary tumor mass and metastatic dissemination to the liver of TNBC cell line-derived orthotopic xenografts. This data indicates a new concept of scarred p53 in cancer progression and metastasis. Moreover, peptides that release scarring markers from nuclear structures can eliminate aggressive cancers *in vitro* and, most importantly, *in vivo*, e.g., in p53-mutated, metastatic TNBC. This ability introduces a conceptually new therapeutic option, especially for types of cancer for which there is a high unmet medical need.

#2096 A novel, orally available ferroptosis inducer targeting Fe-S assembly with significant *in vivo* anti-tumor efficacy.

Y. Song Green[1], M. Ferreira dos Santos[2], S. Ciofi-Baffoni[3], X. Liu[2], **M. Koh[1]**;
[1]University of Utah, Salt Lake City, UT, [2]Kuda Therapeutics, Inc, Salt Lake City, UT, [3]University of Florence, Florence, Italy

Background: Ferroptosis is a novel form of cell death driven by iron-dependent lipid peroxidation, which disrupts cellular membranes resulting in immune-activating death. A variety of tumor types, particularly those associated with enhanced lipid and/or iron content, or which experience increased oxidative stress (including drug tolerant persister cells), are sensitive to ferroptosis, rendering ferroptosis a promising therapeutic strategy for cancer. However, currently available ferroptosis inducers show limited activity *in vivo*, suggesting a need for novel molecular targets to validate the clinical utility of ferroptosis induction. Clear cell renal cell carcinoma (ccRCC), the most common form of kidney cancer, is typically initiated by inactivation of VHL resulting in constitutive activation of HIF-1α and HIF-2α, which contribute to disease progression, including by promoting lipid accumulation that sensitizes ccRCC cells to ferroptosis.
Methods: We performed a high-throughput screen to identify small molecule inhibitors of HIF-2α followed by structure-activity-relationship studies for validation. The molecular target of these inhibitors was identified using the Drug Affinity Responsive Target Stability assay, and target validation was confirmed using siRNA and NMR. *In vitro* efficacy was determined in a panel of cancer cell lines and *in vivo* anti-tumor efficacy was verified using mouse models of cancer.
Results: We identified a novel molecule, KD061, which decreases HIF-1/2α and induces ferroptosis *in vivo* through oral administration by targeting Iron Sulfur Cluster Assembly 2 (ISCA2). ISCA2 is a component of the late mitochondrial Iron Sulfur Cluster (L-ISC) assembly complex and ISCA2 inhibition either pharmacologically or using siRNA triggers the iron starvation response, resulting in iron/metals overload and death via ferroptosis. ISCA2 inhibition also decreases HIF-2α protein levels by blocking iron-responsive element (IRE)-dependent translation, and at higher concentrations, also decreases HIF-1α translation. These studies reveal a novel function of ISCA2 in extra-mitochondrial Fe-S assembly that may be limiting in cancer due to the increased need for these proteins in DNA replication and maintenance. Outside of ccRCC, a 92-cell line screen reveals a variety of tumor types sensitive to ISCA2 inhibition including melanoma and clear cell ovarian cancer. Treatment of tumor-bearing mice with KD061 resulted in > 65% tumor growth inhibition, associated with significantly increased lipid peroxidation, thus confirming ferroptosis *in vivo*, and with decreased HIF-1/2α. The anti-tumor efficacy of KD061 exceeded that of α-PD1 and was well tolerated at the therapeutic dose.
Conclusions: We describe the first orally available inducer of ferroptosis with significant anti-tumor efficacy in ccRCC and other tumor types.

#2097 ABT co-dose accelerated target validation with a fit-for-purpose HPK1 inhibitor tool.

J. L. Methot, J. L. Chen, E. Yu, R. D. Otte, H. Xu, Z. Xu, B. Lacey, J. Laskey, R. Mcleod, D. Smith, A. Pasternak;
Merck & Co., Inc., Rahway, NJ

Target validation can be challenging when mouse efficacy studies require achieving a high therapeutic exposure of a tool compound, ideally with a low peak-to-trough (P/T) ratio to avoid Cmax-induced toxicity. Herein, we describe the daily co-administration of the CYP inhibitor aminobenzotriazole (ABT) as a well-tolerated PK enhancer for medium-term efficacy studies in mice, enabling faster decision-making in the early space with imperfect tools. Genetic studies in mice have suggested that HPK1 inhibition would lead to enhanced effector T-cell function, decreased tumor growth and enhanced αPD-L1 efficacy. However, it remains unknown whether immune activation by pharmacological inhibition of HPK1 will recapitulate the genetic deletions. We developed a fit for purpose tool compound with picomolar HPK1 potency, excellent kinome selectivity (98% >100x, ATP-Km corrected), dose-dependent inhibition of pSLP76, sustained IL2 elevation in PBMCs, and IL6/TNFa elevation in dendritic cells. The mouse PK for this tool was inadequate, having a low exposure (AUC 16 uM-hr at 100 mg/kg po) and a high P/T ratio of 13 that could lead to an erosion of kinome selectivity in vivo; complicating efficacy interpretation and limiting overall tolerability. However, when co-dosed with ABT (50 mg/kg po 2 h prior to the HPK1 inhibitor), improved exposure of our tool was achieved (AUC 63 uM-hr at 100 mg/kg po), 90% inhibition of pSLP76 was maintained at C(trough), and the P/T ratio was reduced to 3 to avoid Cmax-induced toxicity. The inhibitor was well-tolerated co-dosed with ABT for three weeks in mice, enabling studies sooner to probe HPK1 pharmacological inhibition in cancer immunotherapy as a monotherapy as well as in combination with a mouse anti-PD-1 antibody.

#2098 A novel GCN2 kinase activator demonstrates therapeutic efficacy in preclinical PDX models of human cholangiocarcinoma.

D. M. Carlson[1], H. Kuipers[1], A. Abdelrahman[1], E. Jessen[1], J. Roldan Kalil[2], J. Sample[1], J. Tomlinson[1], M. Truty[1], R. Smoot[1];
[1]Mayo Clinic Hospital-Rochester, Rochester, MN, [2]Puerto Rico School of Medicine, San Juan, Puerto Rico

Introduction Cholangiocarcinoma (CCA) is a highly lethal, heterogenous biliary malignancy. Despite the development of targeted therapies, treatment success has been hindered by primary or acquired resistance. New therapeutic strategies are necessary to improve outcomes in these patients. NXP800 is a GCN2 small-molecule activator that phosphorylates eIF2a inducing selective ATF4 transcription which stimulates stress-induced genes leading to apoptosis. NXP800 has been previously validated in ovarian cancers with *ARID1A* mutations, well-known players in cholangiocarcinoma. We sought to determine the treatment efficacy of novel NXP800 in CCA utilizing patient derived xenograft (PDX) preclinical models. Methods In our preliminary studies, four human and two murine CCA cell lines were tested for cell viability using CellTiter-Glo to determine the maximal inhibitory concentration (IC_{50}). Immunoblot analysis of HuCCT-1 cells incubated with 1 mM of NXP800 for 6 hours vs. vehicle was performed. We also evaluated response to GCN2 activation in multiple RNA sequenced PDX models. Xenografts were expanded into the flank of NOD/SCID mice and treatment begun when tumors averaged 120mm^3. Tumor bearing mice were treated with NXP800 (35 mg/kg) or vehicle via oral gavage five days on, two days off, for 28 days. Tumor volume and animal weight were collected twice weekly. Predicted sensitive signatures were determined using multi-omics. Results IC50 dose response curves showed nanomolar activity in all six cell lines, ranging from 5-170 nM. Immunoblotting demonstrated an upregulation of phosphorylated eIF2a and in turn upregulation of ATF4 with treatment of NXP800 compared to vehicle. Five PDX tumors from patients with intrahepatic or distal CCA was established and validated by histologic analysis. Molecular characterization of the tumor identified tumor mutation and a total tumor mutational burden. RNA sequencing was completed and identified 21-gene signatures related to *YAP* activity, which were cross-referenced against our existing PDX model tumor bank. Treatment with NXP800 was associated with a statistically significant decrease in tumor size in three of five PDX models tested, which included an *ARID1A, FGFR1*, and *ATM* mutants. Preliminary multi-omics on the PDX models revealed that sensitivity mechanisms were centered around EGFR signaling. Conclusion The novel GCN2 kinase activator, NXP800, has nanomolar efficacy in both human and murine CCA cell lines *in vitro*. Additionally, NXP800 demonstrated therapeutic activity in multiple cholangiocarcinoma PDX models *in vivo*. We are opening a Phase 1b clinical trial investigating the effects of NXP800 use in patients with advanced CCA. Future studies determining the cellular effect of GCN2 activation utilizing NXP800 are being conducted.

#2099 PELP1 inhibition enhances the therapeutic efficacy of topoisomerase inhibitors in triple-negative breast cancer.

K. Nassar, J. R. Sanchez, D. Panneerdoss, B. Ebrahimi, Y. Xue, U. P. Pratap, S. C. Alejo, G. R. Sareddy, S. Viswanadhapalli, R. K. Vadlamudi;
UT Health San Antonio, San Antonio, TX

BACKGROUND: Triple negative breast cancers (TNBCs) account for 15-24% of breast cancer deaths and are characterized by aggressive clinical course, a worse prognosis, and a higher propensity to metastasize. Proline, glutamic acid-, and leucine-rich protein 1 (PELP1) is an oncogene, its expression is deregulated in TNBC, and its status is a prognostic indicator of poor TNBC survival. Recently, a small molecule inhibitor of PELP1 (SMIP34) which binds to and degrades PELP1 was developed. The *Objective* of this proposal is to define the mechanism of action of PELP1 inhibitor SMIP34 in TNBC progression and to pave the path for a novel combination therapy.

METHODS: We tested the effectiveness of PELP1 inhibitor, SMIP-34, in combination with 140 FDA-approved medications on cell survival of multiple TNBC cell lines. The effect of SMIP34 combination therapy on cell survival was measured using MTT, colony formation, and Annexin V apoptosis assays. Mechanistic studies were done using RT-qPCR, immunoprecipitation, proximity ligation, mass spectrometry, gene reporter, immunofluorescence, and comet assays. Furthermore, the preclinical utility of combination therapy was evaluated using MDA-MB-231 xenografts, patient-derived organoids (PDOs) and explants (PDEs).

RESULTS: We performed an in vitro screening of 140 FDA-approved drugs in combination with SMIP34. Results revealed that SMIP34 sensitized TNBC cells to five FDA approved drugs. Of the five drugs, the three drugs Gemcitabine, Valrubicin, and Mitoxantrone, induced DNA damage by inhibiting topoisomerase, a protein that cleaves and reconnects DNA during replication. We validated the ability of SMIP34 to enhance the efficacy of TIs using two additional TNBC cell lines and confirmed their synergistic activity using several in vitro assays including cell viability, colony formation, and apoptosis. In agreement with the role of PELP1 in DNA damage response, Western blotting analyses showed higher levels of γ-H2AX in SMIP34+TI combination therapy when compared to monotherapy. Results from the comet assays further demonstrate increased DNA damage caused by the SMIP-34 + TIs combination therapy. Mechanistic studies using Proximity labelling followed by immunoprecipitation identified topoisomerase 2A and 2B (TOP2A and TOP2B) as potential interactors of PELP1. Furthermore, gene correlation analysis using TCGA datasets revealed that PELP1 expression is positively correlated with TOP2A, and TOP2B in TNBC. SMIP34 plus Mitoxantrone (TI) combination treatment significantly reduced the growth of TNBC PDEXs, and PDOs *in vitro,* and MDA-MB-231 xenograft tumor growth *in vivo,* compared to vehicle or monotherapy treatment.

CONCLUSION: Together, these results suggest a novel targeted therapy for the treatment of TNBC, involving the combination of topoisomerase inhibitors and the PELP1 inhibitor SMIP34.

#2100 Novel LIPA targeted therapy for treating inflammatory breast cancer.

Z. Fuentes[1], R. Gopalam[1], B. A. Romo[1], K. Nassar[1], X. Yang[1], B. Ebrahimi[1], P. Ramirez[1], C.-Y. Chen[2], S. Elmore[2], H. Nagandla[3], U. Pratap[1], C. Thomas[1], **S. Viswanadhapalli**[1], J.-M. Ahn[2], G. Raj[4], R. K. Vadlamudi[1];

[1]UT Health San Antonio, San Antonio, TX, [2]UT Dallas, Dallas, TX, [3]Houston Methodist, Houston, TX, [4]UT SouthWestern, Dallas, TX

Background: Inflammatory breast cancer (IBC) is a rare but incredibly aggressive subtype of breast cancer (BC). IBC accounts for 2-4% of all occurrences of breast cancer and results in 7-10% of breast cancer-related deaths. IBC is only partially treatable with current therapies such as chemotherapy, surgery, and radiotherapy. Identification of novel therapeutic targets is urgently required. The main organelle for the synthesis, folding, and modification of proteins is called the endoplasmic reticulum (ER). Since elevated basal ER stress (ERS) is usually found in many cancers including IBC, our hypothesis was that the high basal ERS in IBC constitutes a serious vulnerability that can be targeted. Recently, we developed a small molecule ERX41 that promotes ER stress by blocking Lysosomal acid lipase A (LIPA) function in ER of cancer cells. The goal of the project is to test the utility of ERX-41 in treating IBC.

Methods: To study the effect of ERX-41, we have used three well-established IBC model cells. We evaluated the efficacy of ERX-41 as a novel therapeutic for treating IBC using cell viability assays. The long-term effects of ERX-41 on IBC cell survival were evaluated using colony formation assays. Annexin V assays were used to measure apoptosis. Reporter assays, splicing assays, RT-qPCR, and Western blotting were used in mechanistic investigations. The effectiveness of ERX-41 was examined in vivo using KPL4 cell-based xenografts.

Results: ERX-41 significantly decreased the viability of all three IBC model cells (SUM149, SUM190PT, and KPL4), with an IC_{50} of about 125 nM in MTT assay. Additionally, ERX-41 treatment significantly decreased IBC cells capacity to form colonies and promoted apoptosis. Specificity of the ERX41 mediated actions were confirmed using LIPA KO cells. Using RTqPCR based splicing assays, we demonstrated increased splicing of XBP1 as early as 6 hours after ERX41 treatment. Western analyses showed robust induction of stress markers (CHOP, PERK, ATF4) in IBC cells upon treatment with ERX-41. In KPL4 xenograft studies, ERX-41 showed significant reduction in the tumor volume. IHC analyses confirmed decreased proliferation marker and increased ER stress markers.

Conclusions: Collectively, our results suggest that ERX-41 is a novel therapeutic agent that targets the LIPA with a unique mechanism of action and implicate ERX-41 binding to LIPA induces ER stress and promotes apoptosis of IBC cells.

#2101 Patient-derived cells (PDCs) and organoids (PDOs) as critical platforms for developing next therapeutic strategies for NSCLC.

S. Park[1], Y. Joo[2], J.-h. Lee[1], M. Yun[3], M. Yu[3], S. Oh[2], E. Lee[2], D. Kim[2], S. Lee[2], K. Lim[1], M. Hong[4], S. Lim[4], J. Lee[4], B. Cho[4];
[1]JEUK Institute for Cancer Research, Gumi-City, Korea, Republic of, [2]Brain Korea 21 PLUS Project for Medical Science, Seoul, Korea, Republic of, [3]Severance Biomedical Science Institute, Seoul, Korea, Republic of, [4]Division of Medical Oncology, Department of Internal Medicine and Yonsei Cancer Center, Seoul, Korea, Republic of

Purpose : Patient-derived cells (PDCs) and organoids (PDOs) are constructed from pleural effusions to mimic the biological features of patients. In cancer research, PDC/PDOs could be a critical tool because they can recapitulate tumor mutations. Since commercial cell lines have difficulty mimicking the heterogeneity of tumors, PDC/PDOs are widely used for predicting the preclinical drug efficacy. The aim of this study is to show that the PDC/PDOs can be used as effective tools for developing new therapeutic strategy on non-small cell lung cancer (NSCLC).
Experimental design : PDC/PDO models from malignant effusions were established as following. We succeeded the establishment with samples which are positive for malignancy in cytology tests and tumor colony formation. Mutations that cell harbors are confirmed by Sanger sequencing, Whole exome sequencing, or RNA-sequencing. Following the patient treatment history, we confirmed how does established patient derived model response to drugs that patient was treated.
Results : A total of 54 PDCs and 171 PDOs were established from NSCLC patients, including models harboring EGFR mutations, KRAS mutations, uncommon EGFR mutations. 8 models of PDC and 7 models of PDO harbor various mutations of resistance mechanisms to EGFR-TKIs (T790M, C797S/C797G, MET amplification). Also, 4 models of PDC and PDO harbor uncommon EGFR mutations (EGFR G719S, L861Q, G719C/S768I, G719S/S768I) and 12 models of PDO harbors KRAS mutation.
YUO-139 and YU-1092 are patient derived models that harbors uncommon EGFR mutation G719S and L861Q respectively. The models response to afatinib sensitively. IC_{50} of YUO-139 and YU-1092 to afatinib were 2.1 nM and 23.8 nM respectively. YUO-143 is a PDO model that harbors EGFR E19del/T790M/C797S which was derived from gefitinib and mavelertinib resistant patient revealed sensitivity to BLU-945 (IC_{50}, 43 nM), a novel fourth-generation EGFR-TKI.
Conclusions : Patient derived models could be a critical tool for developing therapeutic strategies for NSCLC.

#2102 Understanding the mechanism of action of rigosertib in recessive dystrophic epidermolysis bullosa-associated squamous cell carcinoma through single cellanalysis.

A. P. South, S. Han, P. Fortina;
Thomas Jefferson University, Philadelphia, PA

The allosteric inhibitor rigosertib (an experimental therapeutic) was previously identified as an effective inducer of G2M arrest and apoptosis in squamous cell carcinoma (SCC) keratinocytes isolated from patients with the rare genetic disease recessive dystrophic epidermolysis bullosa (RDEB), both in vitro and in vivo. Early clinical trial data treating RDEB-associated SCC with rigosertib has shown remarkable efficacy in a sub-set of patients and understanding the mechanism of action of rigosertib in this lethal cancer would provide rationale for patient stratification. Multiple mechanisms of action were previously attributed to rigosertib, including polo-like kinase-1 (PLK1), PI3-kinase, activated RAS and microtubule polymerization inhibition. Our published data comparing PLK1 siRNA with PI3-Kinase inhibitors, MAPK inhibitors and microtubule disruption favored PLK1 as a mechanism of action without definitive conclusion. We therefore sought to determine the mechanism of action using transcriptomic profiling. Flow cytometry experiments identified three main categories of time to increase G2M in nine separate RDEB SCC keratinocyte populations in culture ranging from 1 to 6 hours after exposure to 1uM rigosertib. Bulk-RNA sequencing of representative populations from time to G2M groupings failed to identify consistent transcriptional change after exposure to rigosertib. However, single cell sequencing was able to identify increases in sub-populations of cells associated with G2M as well as transient emergence of unique populations that were specific to individual patient populations after exposure to rigosertib in culture. Of note a transient population of RDEB SCC keratinocytes only present after 1 hour of exposure to rigosertib was characterized by increased expression of the potassium regulator *KCNRG* which has previously been associated with apoptosis in chronic lymphocytic leukemia. Ongoing work is determining the role this gene may play in the mechanism of apoptosis induction in RDEB SCC keratinocytes after exposure to rigosertib.

#2103 Small extracellular vesicles derived from macrophages show anti-tumor effects in MDA-MB-231 cells.

P. Desai[1], A. Kumari[2], S. A. Abdullah[2], K. Dellinger[2];
[1]University of North Carolina at Greensboro, Greensboro, NC, [2]North Carolina A&T State University, Greensboro, NC

Triple-negative breast cancer is the primary cause of death in women globally due to the absence of targeted receptors on the tumor, making it hard to treat. In addition, the rapid spread of triple-negative breast cancer makes it difficult to manage using current treatment options such as lumpectomies, mastectomies, radiation, and chemotherapy. The survival rate for patients with triple-negative breast cancer is only 8-16%. Therefore, there is a critical need to develop new and effective treatment options. The objective of this study was to investigate the potential of M1 macrophage-derived exosomes to induce cancer cell apoptosis. To test this, we isolated M1 macrophage-derived exosomes to see their effects on triple-negative breast cancer MDA-MB-231 cells. We induce polarization in RAW 264.7 macrophage cells via lipopolysaccharide (LPS). Macrophage polarization was characterized using an enzyme-linked immunosorbent assay (ELISA), real-time PCR, nitric oxide production, and bright field microscopy. We characterized exosomes using nanoparticle tracking analysis (NTA) and scanning electron microscopy (SEM). The apoptosis marker, caspase 3/7 activation, was assessed using confocal microscopy in MDA-MB-231 cells. M1 macrophage-derived exosomes were isolated, characterized, and incubated with breast cancer cells to see their anticancer effects. Data showed the induction of apoptosis in 48 hours in triple-negative breast cancer cells. We conclude that exosomes derived from M1 macrophages may have the capability to induce apoptosis in triple-negative breast cancer.

#2104 Targeting stem cell proteostasis pathways sensitizes acute myeloid leukemia to proteasome inhibitors.

K. Lam, Y. J. Kim, C. M. Ong, F. J. Zhou, A. Z. Liu, B. A. Chua, J.-H. Zhou, E. D. Ball, R. A. J. Signer;
UC San Diego, San Diego, CA

Proteasome inhibitors are highly effective for treating multiple myeloma, but exhibit little efficacy in other blood cancers. In this study, we set out to determine why acute myeloid leukemia (AML) is largely refractory to proteasome inhibition and if we could sensitize human AML to this class of drugs. Efficacy of proteasome inhibitors in myeloma partly depends on disruption of protein homeostasis (proteostasis). This is driven by an accumulation of misfolded proteins that activate the unfolded protein response (UPR) and integrated stress response (ISR). Due to their highly secretory nature, myeloma cells exhibit relatively elevated baseline endoplasmic reticulum stress, and are thus sensitive to proteasome inhibition as they readily activate a terminal UPR. However, we found that proteasome inhibition fails to significantly disrupt proteostasis in human AML cells. We recently discovered that hematopoietic stem cells utilize distinct pathways to regulate proteostasis, and we hypothesized that AML cells co-opt stem cell proteostasis pathways to cope with proteasome inhibition and preserve proteostasis. To test this, we first performed RNA-sequencing which revealed that AML cells respond to proteasome inhibition by activating two distinct proteostasis pathways normally utilized by hematopoietic stem cells: autophagy and the heat shock response. Concurrent proteasome and autophagy inhibition significantly increased unfolded protein content in multiple human AML cell lines. This proteostasis disruption was sufficient to induce a terminal ISR marked by activation of the eIF2α-ATF4-CHOP signaling axis that severely attenuated protein synthesis, reduced proliferation, and induced widespread apoptosis in human AML cell lines and primary AML patient samples. In contrast to AML cells, dual proteasome and autophagy inhibition was well tolerated by healthy human CD34+ hematopoietic stem and progenitor cells, suggesting a tractable therapeutic window for treating AML. Indeed, dual proteasome and autophagy inhibition was tolerated *in vivo*, and decreased leukemia burden in mice xenografted with human AML cell lines. Similar to autophagy inhibition, disabling the heat shock response by deleting Heat shock factor 1 (*HSF1*) sensitized human AML cell lines to proteasome inhibitors. Treatment of *HSF1*-deficient AML cells with a proteasome inhibitior induced a significant increase in unfolded protein, activated the ISR, reduced growth and protein synthesis, and led to severe apoptosis. Concurrent *HSF1* deletion and proteasome inhibition dramatically reduced AML disease burden *in vivo* and extended median survival from 40 to 140 days. Overall, this study revealed that AML cells hijack stem cell proteostasis pathways to promote growth, survival, and therapeutic resistance. Targeting the unique configuration of the proteostasis network is uncovering new therapeutic strategies to eliminate AML.

#2105 Targeting the “Achilles Heel” of androgen receptor activity in castration resistant prostate cancer.

Ashish Tyagi[1], Balaji Chandrasekaran[1], Arun K. Sharma[2], Chendil Damoadaran[1]

[1]Texas A&M Health Sci. Ctr. (Bryan-Col. Station), College Station, TX, [2]Penn State College of Medicine, Hershey, PA

Background: Each year, millions of men are diagnosed with prostate cancer (CaP). The unchecked activation of the Androgen Receptor (AR) spurs CaP development and progression. Mutations or the presence of AR splice variants can add complexity to tumor ecology, leading to chemoresistance. This study aims to develop novel inhibitors targeting the “Achilles Heel” of AR activity: the N-terminal domain (NTD). This would circumvent the limitations of LBD (Ligand Binding Domain) therapies and offer a superior treatment option for patients. Though the AR-NTD is an intrinsically disordered protein, which complicates structure-based drug design, we have developed a unique small molecule inhibitor, ASR600, which specifically targets AR-NTD and promotes AR and AR-variants degradation by ubiquitination at previously unknown sites.

Methods: Mass-spec analysis was performed to identify distinct ubiquitination sites in AR's NTD. To perform spatial transcriptome analysis, CytAssist Visium (10X genomics) was used. Furthermore, we used western blotting, immunofluorescence, immunoprecipitation, and PDX mice studies in CRPC mouse models to examine the impact of ASR600 on CRPC.

Results: Four AR ubiquitination sites: K845, K847, and K913 (LBD) and K311 (NTD) are already identified. Interestingly, ASR600 continued to inhibit AR expression even with mutated ubiquitination sites. Mass spectrometry analysis of ASR-mediated mono-ubiquitinated N-terminal AR identified K16 as a unique ubiquitin acceptor. Altering this ubiquitination site rescues AR expression from ASR600-mediated degradation, emphasizing AR N-terminus as an ASR600 target. To discern the role of the K16 ubiquitination site in AR protein turnover, we evaluated AR protein stability in LNCaP cells that stably expressed ARWT or AR-K16R constructs. Our data indicates the pivotal importance of K16 for AR transcriptional activity. Invivo, ASR600, when used as a sole agent, exhibited inhibitory responses in PDX of clinically aggressive, AR-expressing tumors. Spatial gene expression analysis revealed marked expression differences in AR signature genes between control and ASR600-treated PDX tissues. Crucially, AR signaling, and related markers mainly aligned with epithelial markers rather than stromal ones. In contrast, the ASR600-treated PDX tumor showcased reduced AR signaling within epithelial cells.

Conclusion: Targeting AR-NTD has received a lot of attention, but its innately disordered structure has hindered progress. ASR600 targets AR-NTD specifically by ubiquitinating the protein at a novel location, K16. Our in vivo, PDX studies, combined with the spatial analysis, lay a strong foundation for initiating IND-enabling TOX studies, followed by a phase-I clinical trial for ASR-600 in CRPC patients.

#2106 Creating a living public oncology drug resource using PRISM cell line viability screening.

M. G. Rees, M. Kocak, C. Mapa, D. Frederick, E. Nguyen, A. Kalathungal, A. Fazio, J. F. Davis, E. Reeves, A. Tucci, R. Barry, C. Harrington, J. Eskra, M. M. Ronan, W. R. Sellers, J. A. Roth;
Broad Institute, Cambridge, MA

Cancer treatment options are rapidly expanding, with many new targeted agents and therapeutic modalities under development. However, systematic characterization of the cellular effects of emerging drug candidates is limited. Screening such agents against the approximately 900 diverse cancer cell lines in the PRISM assay can provide insights into drug specificity and cancer subtype selectivity and, leveraging the rich genomic and functional characterization of PRISM cell lines, support for annotated mechanisms of action. Our goal was to generate a large, high-quality, oncology-focused dataset that can benefit the cancer research community by characterizing new test agents of high clinical relevance. In the past year, this effort has been utilized to screen a total of 180 test agents with plans to extend testing to an additional 140 over the next year. The collection includes biologics (e.g., cytokines, antibodies, antibody-drug conjugates), targeted protein degraders, and small molecules. Supporting the quality of the screening collection and the robustness of the PRISM assay, the majority of inhibitors (including mutant-selective KRAS inhibitors, and inhibitors targeting the WRN helicase, a preferential vulnerability in cancers with microsatellite instability) tested to date closely mimic the effects of genetic knockout and/or knockdown of their annotated target, as measured by CRISPR and shRNA data available through the Dependency Map Portal (depmap.org). Further, while we observe strong modality-independent co-clustering of test agents annotated to act on the same target(s) (e.g., tucatinib with the antibody-drug conjugates T-DM1 and T-DXd for HER2), intriguing differences in efficacy and selectivity emerge in individual cell line models. All PRISM reference screening data and analyses will be made publicly available through depmap.org to serve as a benchmark for new drug development candidates and to further the efforts of researchers worldwide to match emerging cancer therapies to the patients most likely to benefit.

EXPERIMENTAL AND MOLECULAR THERAPEUTICS: Pharmacodynamic Biomarkers of Drug Response
Poster Session

#2110 Characterization of the correlation between BTK degradation and tumor growth inhibition of the BTK target protein degraders using PK/PD modeling.

Y. Wu, **S. Li**, F. Wang, N. Hu, L. Yin, X. Song, J. Zhang, A. Xu, S. Yang;
BeiGene, Beijing, China

Introduction: Chimeric degradation activation compound (CDACs) are heterobifunctional molecules causing target protein degradation by simultaneously binding to the target protein as well as an E3-ubiquitin ligase. As an emerging new therapeutic modality, it is critical to understand the contribution of compound-specific parameters (e.g. drug exposure and binding potency to the target protein) and the system-specific parameters (e.g. target protein turnover) of CDACs to its in vivo effect. Method: To identify the key parameters for guiding compound optimization and to find the correlation between BTK degradation and the extent of tumor growth inhibition, a mechanistic PK/PD model was built (Phoenix WinNonlin 8.1) on a dataset generated from a BTK CDAC (Compound A). The PK/PD model was simplified mathematically compared to the full mechanistic models published previously1, since the binding affinity of Compound A to BTK was much higher than the binding affinity of CDAC to E3 ligase. This model can be linked to a tumor growth inhibition (TGI) mathematical model to find the correlation between target degradation and efficacy.Result: In mouse Rec-1 xenograft model, the BTK degradation and TGI was studied. The mice were dosed with Compound A orally at 0.3, 1, or 3 mg/kg, dose-dependent PK and BTK degradation in tumor was observed. After a single dose administration of Compound A, ~50% BTK degradation was observed in tumor at 24 h post dosing and the tumor BTK rebound to baseline at 72 hours post dosing at 3 mg/kg. The tumor BTK degradation was deeper after repeated dosing. A PK/PD model was built based on the data in this PK/PD study. The calculated BTK turnover half-life in Rec-1 model is about 16 h. In the efficacy study, Compound A was dosed orally once a day to the mice at 0.3, 1, or 3 mg/kg. The 3 mg/kg group achieved ~90% tumor growth inhibition in Rec-1 xenograft model. The PK/PD model was then linked with a mathematical model describing TGI2. A threshold level of BTK degradation in tumor to achieve tumor stasis was identified to be 96% for Rec-1 tumor model. At 90% tumor growth inhibition, average of 70% BTK was predicted to be degraded in tumor at steady state. The model was subsequently used to characterize the PK/PD relationship of BGB-16673. The efficacy of BGB-16673 was predicted using the model and it agreed with the observed value.Conclusions: The current model deepened our understanding of the PK/PD relationship of CDACs. The approach can be used to simulate different scenarios, e.g. different BTK turnover, potency or PK exposure. It can also be used in compound selection and optimization to predict repeated dose PD and efficacy from a single dose PK/PD data.1. J Pharmacokinet Pharmacodyn. 2021 Feb;48(1):149-163.2. Cancer Res. 2004 Feb 1;64(3):1094-101.

#2111 Impact of HER2 Expression on trastuzumab deruxtecan(T-DXd) efficacy.

W. Chen[1], J. Drago[2], A. Gupta[2], B. Liu[2], S. Chandarlapaty[2];

[1]Weill Cornell Graduate School of Medical Sciences/Memorial Sloan Kettering Cancer Center, New York, NY, [2]Memorial Sloan Kettering Cancer Center, New York, NY

Background: T-DXd is an FDA-approved anti-HER2 Antibody Drug Conjugate (ADC), which has shown clinical efficacy in breast cancers with either overexpression or low-level expression of HER2. The benefit of T-DXd across the spectrum of HER2 expression has called into question the relevance of HER2 expression level as relevant parameter for T-DXd sensitivity. We sought to experimentally address the relevance of HER2 expression level upon the degree of T-DXd response.

Methods: A series of isogenic models was generated that expressed different levels of surface HER2 using a doxycycline-inducible promoter. These were analyzed for impact of differential expression level upon T-DXd internalization and drug response. Human breast cancer samples were analyzed for HER2 expression levels and association with clinical response to T-DXd under an IRB approved protocol.

Results: Induction of different levels of HER2 at specified doxycycline concentrations was verified in multiple models using immunoblotting and FACS. These different levels appeared to correspond to clinical breast cancer immunohistochemistry (IHC) scoring levels to 0, 1+, 2+, and 3+. The models were analyzed for T-DXd response and showed increasing levels of HER2 led to increase lysosomal uptake of T-DXd ($p<0.0001$). Moreover, elevation of HER2 levels led to lower concentrations of T-DXd needed to suppress tumor growth. Analyses of the effects of increasing levels of HER2 upon xenograft response to T-DXd are ongoing. Finally, retrospective analyses of a cohort of 50 breast cancer patients treated with T-DXd revealed that higher levels of HER2 corresponded to longer time on treatment (time to progression).

Conclusion: We observe a consistent relationship between elevated expression of HER2 and breast cancer response to T-DXd. The findings highlight the relevance of HER2 expression level as a biomarker of T-DXd response and support the potential value of therapeutic strategies that can induce HER2 surface expression levels to enhance response.

#2112 Identification of biomarkers associated with sensitivity to a novel PCNA inhibitor (AOH1996) by CRISPRi screening.

L. Gu, M. Li, C.-W. Chen, R. J. Hickey, L. H. Malkas;
City of Hope National Medical Center, Duarte, CA

Proliferating cell nuclear antigen (PCNA) plays an essential role in regulating DNA synthesis and repair and is essential for cancer cell growth and survival. We discovered a cancer-associated isoform of PCNA (caPCNA), which is ubiquitously and highly expressed in a broad range of cancer cells and tumor tissues but is not significantly expressed in non-malignant cells. Further studies of this novel caPCNA isoform as an anti-cancer drug target led to the identification of a cancer distinct region of PCNA which is partly delineated by the L126-Y133 peptide sequence and the discovery of a small molecule (AOH1996), which binds to this cancer distinct region as shown by crystallization studies. By targeting caPCNA, AOH1996 selectively kills cancer cells by interfering with the resolution of transcription-replication conflicts (TRC). Importantly, it causes no discernable toxicity at 6 times of its effective dose in mice. AOH1996 is currently in a phase 1 clinical trial for adult solid tumors at City of Hope (IND 138273). To identify genes that may be used as biomarkers for patient selection or potential targets for combination therapies, we screened a CRISPR interference (CRISPRi) library, which targets genes that are involved in cell signaling and cell cycle regulation. After culturing transduced cells in the presence of DMSO or 250 nM AOH1996 (corresponding to IC20) in triplicates for 14 generations, we measured the relative abundance of each guide RNA (gRNA) construct. Significant changes in the abundance of the gRNA constructs in AOH1996-treated cells relative to that in DMSO-treated cells were determined by the MAGeCK method. The target genes of the depleted or enriched gRNAs are predominantly involved in DNA repair, cell cycle regulation, and transcription regulation, which is consistent with the action mechanism of AOH1996. We validated the effect of these genes on sensitivity to AOH1996 and identified a panel of target proteins whose up or down-regulation is associated with sensitivity to AOH1996. Some of these proteins are targets of known chemotherapeutic drugs, which may be used in combination with AOH1996 in the clinic.

#2113 HMPL-506, a novel, highly potent and differentiated menin-MLL inhibitor for the treatment of *MLL-rearranged* and *NPM1* mutant acute leukemia in preclinical models.

M. Cheng, L. Ge, Z. Gao, Z. Zhong, A. Jiang, W. Zhang, J. Hu, S. Jiang, N. Li, N. Yang, J. Wang, Y. Sai, W. Qing, Y. Ren, W. Su;
HUTCHMED, Shanghai, China

Background: Mixed-lineage leukemia (*MLL*, or *KMT2A*) gene rearrangements (*MLL-r*) occur in 5%-10% acute leukemias and are associated with poor prognosis. *Nucleophosmin 1* mutations (*NPM1m*) are the most common genetic alterations in acute myeloid leukemia (AML). Multiple studies have illuminated that those leukemogenesis are dependent on the interaction of menin-MLL, which controls downstream gene expressions associated with cell proliferation and differentiation, e.g. *HOXA9* and *CD11b*. Herein, we introduce HMPL-506, a novel and highly differentiated small molecule compound targeting menin-MLL interaction.

Methods and Results: Biochemical assay revealed that HMPL-506 potently blocked menin-MLL binding with IC_{50} of 1.0 nM. In cell lines carrying *MLL-r* or *NPM1m*, HMPL-506 substantially down-regulated menin-MLL target genes transcription of *MEIS1* and *HOXA9* and upregulated the differentiation marker of *CD11b* by RT-PCR assay, consequently, HMPL-506 attenuated tumor cell growth, with GI_{50} ranging from 3.0 to 12.1 nM in *MLL-r* cell lines (MV-4-11, MOML-13 and RS4;11) and 22.4 nM in *NPM1m* cell line (OCI-AML-3) in CellTiter-Glo cell viability assay. Notably, compared with the other 5 menin inhibitors in clinical stage, HMPL-506 showed the strongest inhibitory potency in *MLL-r* and *NPM1m* cell line models. *In vivo* studies demonstrated the dose- and exposure-dependent target regulation of *MEIS1* and anti-tumor efficacy following HMPL-506 treatment in multiple tumor xenograft models. For instance, in MV-4-11 subcutaneous model, once daily oral administration of HMPL-506 at 5, 10 and 25 mg/kg for 4 days in BALB/c nude mice induced dose-dependent inhibition of *MEIS1* gene expression, positively correlating with compound exposures in tumor tissues; continuous dosing of HMPL-506 at 5 mg/kg for 28 days reduced the tumor growth by 86%, which was comparable to the efficacy induced by SNDX-5613 at 50 mg/kg. Treatment of HMPL-506 at 10 mg/kg and 25 mg/kg resulted in tumor shrinkage in all treated animals, with tumor regression rates of 72% and 100%, respectively. Furthermore, HMPL-506 synergistically improved anti-tumor effect of azacytidine, venetoclax and gilteritinib against *MLL-r* leukemias both *in vitro* and *in vivo*. HMPL-506 displayed favorable PK profiles and high selectivity among multiple kinases, methyltransferases and safety related targets. More importantly, the IC_{50} of HMPL-506 on hERG patch clamp was over 60 μM, indicating low risk of QTc prolongation in human.

Conclusion: HMPL-506 is a novel and highly differentiated menin-MLL inhibitor with robust anti-tumor activities, favorable ADME properties and low risk of cardiac toxicity, warranting it further clinical development for treatment of *MLL-r* and *NPM1m* acute leukemias. HMPL-506 IND is expected to be cleared in H1 2024.

#2114 Enhancing therapeutic strategies for osimertinib-resistant EGFR-mutant NSCLC: A HER3 dual-payload ADC (dpADC) with topoisomerase I and EGFR tyrosine kinase inhibitor.

L. Wang, M. Xiong, X. Gao, C. Zhou, Y. Han, Y. Li, J. Wang, L. Shi, G. Qin, P. H. Song;
GeneQuantum Healthcare (Suzhou) Co., Ltd., Suzhou, China

Background: EGFR tyrosine kinase inhibitors (TKIs) have significantly improved the survival rate and the quality of life of the NSCLC patients with EGFR mutation in the first line setting. For example, Osimertinib, a potent third-generation EGFR TKI, has demonstrated exceptional efficacy in metastatic NSCLC with specific EGFR mutations. Despite its success, the emergence of drug resistance, often linked to elevated HER3 protein expression, remains a significant challenge. U3-1402 (HER3-Dxd), an HER3 ADC, demonstrates a promising result in managing Osimertinib-resistant NSCLC. It has been reported that combining U3-1402 with Osimertinib has shown enhanced efficacy in resistant cell lines and mouse models. Here, we explore a novel HER3 dual-payload ADC (HER3 dpADC), uniquely combining a Topoisomerase I inhibitor and an EGFR TKI within a single antibody structure using the enzymatic site-specific conjugation platform developed by GeneQuantum (GQ). This innovative approach demonstrates potent and synergistic anti-tumor effects in vitro and in vivo, presenting an alternative therapeutic strategy for EGFR-mutant NSCLC patients.

Results: GQ's dpADC platform technology employs two orthogonal enzymatic site-specific conjugations and stable linker technologies to efficiently generate the dual-payload ADC with high homogeneity and quality. For HER3 dpADC, HER3 Ab was conjugated with a novel Topoisomerase I inhibitor, TopoIx, and an EGFR tyrosine kinase inhibitor. In vitro DAR analysis revealed high linker stability, with minimal free payload release even after 96 hours of plasma incubation. Binding affinity assessments confirmed comparable affinity between HER3 dpADC and HER3 mAb in specific EGFR exon 19 deletion cell lines. Using various NSCLC cell lines in a 3D-spheroid culture system, HER3 dpADC demonstrated significant dose-dependent and synergistic anti-tumor activities. A robust bystander killing efficacy was observed in both HER3+/HER3- HEK293T cell coculture assays. Evaluation in CDX mouse models consistently demonstrated heightened in vivo efficacy by HER3 dpADC, aligning with the promising in vitro data. In NSCLC patient-derived xenograft (PDX) mouse models representing EGFR tyrosine kinase inhibitor-sensitive or resistant phenotypes, HER3 dpADC induced tumor regressions with no obvious toxicity, underscoring its potential as the next-generation HER3 targeting agent.

Conclusion: The innovative HER3 dpADC, leveraging an efficient dual enzymatic site-specific conjugation, exhibited robust anti-tumor efficacy in both in vitro and in vivo settings, surpassing single-agent treatments. Its synergistic mechanism of action presents a promising possibility for developing a more potent and the front-line therapeutic solutions in NSCLC patients who have progressed on standard therapies.

#2115 Assessing BCL2 protein complex level in peripheral blood mononuclear cells as a surrogate pharmacodynamic biomarker of BCL2 inhibitors in hematological cancers.

Hongwon Lee[1], **Byungsan Choi**[1], Saem Hong[1], Yunseo Lee[1], Tae-Young Yoon[1], Janghee Woo[2]

[1]Proteina Co., Seoul, Korea, Republic of,[2]Department of Hematology and Medical Oncology, Emory University School of Medicine, Atlanta, GA

In the last decade, cancer therapeutics have adhered to the practice of administering drugs at the maximum tolerated dose (MTD) selected from limited patient cohorts. The emergence of targeted therapies has disrupted this dose selection paradigm, as optimal efficacy may be achievable at lower dose than MTD. Recently, a regulatory agency initiated "OPTIMUS" to redefine the dose selection process, recommending quantitative assessments of drug efficacy in relation to the target protein throughout development and clinical trials.

ABT-199 is a protein interaction inhibitor that specifically disrupts the interaction of BCL2 protein. Consequently, the assessment of changes in the level of BCL2 protein complex is necessary to evaluate the ABT-199 efficacy for optimal dose selection. In this study, we adapted the Single-molecule Protein Interaction Detection platform for evaluating pharmacodynamics of BCL2 inhibitors in clinical samples.

We assessed the dissociation of two BCL2-related biomarkers, BCL2-BAX and BCL2-BIM, from a model system under various ABT-199 doses. Following one hour treatment with 300 nM of ABT-199, the BCL2-BAX complex dissociated almost by 40%, while 80% of the BCL2-BIM complex remained. The reduction of the BCL2-BIM complex was not changed when extending the treatment for 3 hours, indicating that the BCL2-BAX complex may serve as a more sensitive biomarker for assessing the target engagement of ABT-199. To determine the assay sensitivity, we evaluated the ABT-199 response across different cell numbers and found that 100,000 cells are sufficient for performing the BCL2-BAX assay. Subsequently, we validated the utility of our method in assessing clinical samples, specifically BMMCs and PBMCs. We collected 4 PBMCs and the corresponding BMMCs from hematological cancer patients and treated them with various doses of ABT-199 ex vivo. With 100,000 BMMCs and 1,000,000 PBMCs, we can generate dose-response curves for the BCL2-BAX complex at doses of ABT-199 ranging from 1 to 1,000 nM. To explore the feasibility of employing the BCL2-BAX complex in PBMCs as a surrogate biomarker for assessing ABT-199 engagement with BCL2 in BMMCs, we compared the averaged dose-response curves from 4 PBMCs with that of BMMCs. Remarkably, the two curves showed a coherent dissociation trend, indicating that the biochemical effect of ABT-199 on the BCL2-BAX complex may be conserved across different sample types.

Collectively, we have developed a target engagement assay for BCL2 inhibitors by measuring the BCL2-BAX complex. Notably, we observed a consistent dissociation pattern of the BCL2-BAX complex by ABT-199 treatment in both PBMCs and BMMCs. This molecular information offers an alternative way to assess the pharmacodynamics of BCL2 inhibitors, particularly in the case where collecting a series of BMMCs with sufficient amounts may not be feasible.

#2116 Telisotuzumab vedotin (Teliso-V)-mediated c-Met internalization, endolysosomal trafficking, and potent cytotoxic activity are unaffected by MET exon-14 skipping mutation.

I. Batth, R. Pandoy, S. Khaja, D. Maji, T. Uziel, A. Vasilopoulos, P. Ansell, P. Epling-Burnette;
AbbVie Inc., North Chicago, IL

Background: Telisotuzumab vedotin (Teliso-V) is an antibody-drug conjugate (ADC) composed of a c-Met (MET protein) antibody coupled to the microtubule inhibitor monomethyl auristatin E (MMAE). Teliso-V was granted FDA Breakthrough Therapy Designation for advanced/metastatic EGFR WT, NSQ NSCLC with high c-MET overexpression. For MMAE drug delivery, Teliso-V must first undergo receptor internalization and endolysosomal (EL) trafficking. Hepatocyte growth factor (HGF)-dependent MET EL trafficking and degradation depend on the E3 ubiquitin ligase Casitas B-lineage lymphoma (CBL). METex14 skipping and CBL-binding site mutations, which delete the binding site for CBL, occur in ~ 3% of NSCLC. The role of CBL in Teliso-V-MMAE delivery and activity was assessed in this work.

Methods: WT-human c-Met, c-Met-Y1003F/N (CBL binding site mutations in MET), and c-Met-ex14Δ (47 aa deletion to mimic ex14 skipping) or CBL-L620f, G807*, and W802* (CBL inactivating mutants) were expressed in NIH3T3, Ba/F3 cells, or A549 tumor cells using retroviral transduction. Genetically modified cells were then used to define the role of CBL in c-Met surface expression, intracellular signaling, EL trafficking (using pHrodo Red-labeled Teliso-V), and Teliso-V sensitivity in 2D/3D cell cultures.

Results: c-Met expression was required for Teliso-V cytotoxicity and intracellular payload delivery in all cell lines. While minimal changes in cell surface c-Met levels were observed, CBL binding mutants had increased phosphorylated c-Met in the absence of HGF, and ex14Δ-MET and CBL binding site mutants showed increased sensitivity to small molecule c-Met inhibitors. Compared to WT c-Met, ex14Δ and CBL-binding mutants showed similar EL trafficking and no change in sensitivity to Teliso-V. Co-treatment with a pan-CBL inhibitor also failed to alter Teliso-V EL trafficking and anti-tumor activity. Like most ADCs, EL trafficking was dependent on a dynamin-mediated process with reduced EL trafficking by co-treatment with Dyngo4a. To further understand the role of CBL in Teliso-V sensitivity, we expressed CBL inactivating mutations in A549 tumor cells. While the L602F and W802* mutants increased spheroid size, as well as activated p-MET, there was no change in sensitivity to Teliso-V.

Conclusions: Loss of CBL-binding sites on c-Met via ex14 deletion or Y1003F/N leads to increased MET-targeted TKI sensitivity and increased phospho-c-Met levels but does not impact Teliso-V sensitivity or EL trafficking. Our results indicate that Teliso-V traffics to the EL via a dynamin-mediated process. Therefore, Teliso-V delivers MMAE through a robust ADC-mediated EL-dependent mechanism that is independent of CBL, suggesting that high c-Met expression in Ex14skipping or CBL binding site mutant NSCLC patients should be further investigated for response to Teliso-V.

#2117 Elucidation of the fates of CDK2 inhibited aneuploid and residual lung cancers.

L. Tyutyunyk[1], Z. Chen[1], X. Liu[1], Y. Ng[2], A. Bhatawadekar[1], K. Narayan[1], R. Weigert[2], X. Liu[1], E. Dmitrovsky[1];
[1]Frederick National Laboratory for Cancer Research, Frederick, MD, [2]National Cancer Institute, Bethesda, MD

Genomic instability is a hallmark of cancer. Unlike normal diploid cells, cancer cells exhibit abnormal centrosome numbers and chromosomal instability. Mitosis with supernumerary centrosomes yields progeny with aberrant chromosome segregation and aneuploidy. While most progeny cells with abnormal chromosomes are eliminated through apoptosis, some have distinct fates with a growth advantage. These cancer cells can acquire resistance to antineoplastic agents. This confers an aggressive tumor biology and unfavorable clinical outcomes. Cyclin-dependent kinase 2 (CDK2) regulates cell cycle progression and the centrosome cycle. We previously reported that CDK2 inhibition prevents supernumerary centrosome clustering, causing multipolar mitosis and anaphase catastrophe in lung and other aneuploid cancers. This was associated with residual transplanted tumors in mice. To elucidate cell fates of progeny with multipolar mitosis after CDK2/9 inhibition with CYC065 (0.2 μM) treatment, a panel of murine and human lung cancer cells underwent time-lapse fluorescent microscopy. This elucidated multipolar mitotic events within the progeny. Intriguingly, distinct outcomes occurred after mitosis including formation of multipolar and multinucleated cells. Cell death of progeny is the predominant fate, but some progeny survive despite continuous CDK2 inhibition. Surprisingly, some of these cells fuse together. Those multinucleated cells can undergo multiple cell cycles without successful cytokinesis. To confirm these effects were through CDK2 inhibition, the selective CDK2 inhibitor Tagtociclib (PF-07104091, at the 2 μM dosage) was used. This treatment statistically-significantly increased multipolar lung cancer cells and increased apoptotic death during time-lapse fluorescent microscopy. Findings were independently validated by CDK2 shRNA knockdown. Focused ion beam scanning electron microscopy (FIB-SEM) and immunofluorescent staining revealed the ultrastructure of multinucleated cells. Insights into tumor biology came from intravital imaging of transplanted lung cancer cells in mice. Multipolar and multinuclear cells followed CDK2 antagonism. Incucyte® Live-Cell Analysis System and Artificial Intelligence-based imaging determined distinct growth responses in aneuploid as compared to non-aneuploid lung cancer cells after CDK2 inhibitor treatments. In summary, these findings are translationally relevant. CDK2 inhibition of aneuploid lung cancers yields distinct cell fates. This is linked to resistance to CDK2 antagonism and to formation of residual *in vivo* tumors.

#2118 SGN-CEACAM5C / SAR445953, a novel topoisomerase I inhibitor antibody-drug conjugate targeting CEACAM5, has potent anti-tumor activity in CRC, PDAC, GC and lung cancer tumor models.

Y. Baudat[1], C. Nicolazzi[1], J. Sigurjonsson[2], C. Amara[3], A. Clarke[2], R. Iyski[2], D. Meyer[2], V. Fantin[4], M. Chiron[1], S. Decary[1];
[1]Sanofi, Vitry-Sur-Seine, France, [2]Seagen, Bothell, WA, [3]Sanofi, Chilly-Mazarin, France, [4]Sanofi, Remote, NJ

Carcinoembryonic antigen cell adhesion molecule 5, CEACAM5, is a glycosylphosphatidylinositol-anchored glycoprotein expressed on the cell surface of most of the colorectal cancer (CRC) and pancreatic ductal adenocarcinoma (PDAC) and of more than 2/3 of gastric cancer (GC) and non-small cell lung cancer (NSCLC) while normal tissue expression is limited. The high prevalence of CEACAM5 expression prompted us to develop a novel CEACAM5 topoisomerase I inhibitor (Topo1i) antibody drug conjugate (ADC) with a DAR of 8, SGN-CEACAM5C / SAR445953. The anti-CEACAM5 antibody was chosen based on its high selectivity for CEACAM5 and its potential to direct cytotoxic payloads to tumor. The Topo1i payload was optimized for potency and enhanced bystander activity. SGN-CEACAM5C / SAR445953 is rapidly internalized and demonstrates *in vitro* cytotoxicity with EC50 values in the sub-nM range while it induces no toxicity on CEACAM5-negative cells. The potent anti-tumor activity is mediated by direct cytotoxicity on CEACAM5-expressing tumor cells and by a strong bystander effect due to the diffusion of the payload to the neighboring CEACAM5-negative tumor cells. Accordingly, the ADC incubated in a co-culture of CEACAM5-positive and -negative cells at a ratio of 1/1 induces a ~50% growth inhibition of CEACAM5-negative cells. Interestingly, with incubated ADC, only 1% of CEACAM5-positive cells in co-culture are sufficient to provide 11% growth inhibition of CEACAM5-negative cells. *In vivo*, SGN-CEACAM5C / SAR445953 is stable in circulation in SCID mice with a t1/2 close to 15 days. *In vivo* efficacy at 1, 3 and 10 mg/kg (single administration) was evaluated in panels of 4 CRC, 3 PDAC, 4 NSCLC and 3 GC patient-derived xenograft (PDX) models. At 10 mg/kg, the ADC elicits antitumor regression in 14/14 models. At 3 mg/kg, tumor regression occurs in 12/14 models. This potent, specific and dose dependent anti-tumor activity was further confirmed in Single Mouse Trials (SMT) of 20 CRC PDX models, 31 lung cancer PDX models and 19 gastric cancer PDX models. SMT consists in use of one animal per PDX model per treatment arm and for which the evaluation of efficacy is based on RECIST (Response Evaluation Criteria In Solid Tumors) criteria used in clinic. In CRC, gastric and lung cancer SMT, disease control rates are 95%, 84% and 87%, respectively with overall response rates of 55%, 68% and 71% including 15%, 10% and 26% of complete responses, respectively. The high anti-tumor activity across panels of PDX models of several CEACAM5 positive indications supports further evaluation of SGN-CEACAM5C / SAR445953 in patients with CRC, PDAC, GC and lung cancers (NCT06131840).

#2119 Translational research to facilitate development of novel therapeutic combinations of letrozole for the treatment of glioblastoma.

A. S. Karve, B. B. Gabani, S. N. Gadgil, S. P. Kulkarni, G. A. Gudelsky, P. B. Desai;
University of Cincinnati, Cincinnati, OH

Letrozole (LTZ), a third-generation aromatase inhibitor, appears to be a promising novel therapeutic for the treatment of glioblastoma (GBM). It synergistically enhances the efficacy of the DNA alkylating agent temozolomide, one of the few approved chemotherapeutics for GBM, against patient-derived GBM cells. RNA-seq analysis of tumor from recurrent GBM patients treated with LTZ prior to surgery in a “window of opportunity” phase 0/1 dose escalation clinical trial revealed that LTZ downregulates genes encoding for DNA-damage repair proteins (BRCA2) in a dose dependent manner. Our central hypothesis for this project is that combination of LTZ with targeted therapeutic agents that promote DNA damage results in synergistic effects against GBM. The objective of this study is to evaluate the effects of poly-ADP ribose polymerase (PARP) inhibitors in combination with LTZ against patient-derived GBM cells. Our secondary aim for this project is to delineate the blood-brain barrier (BBB) permeability of PARP inhibitors. Employing patient-derived G43, G75 and JHH-136 GBM lines we assessed the influence of PARP inhibitors (olaparib, pamiparib, veliparib and niraparib) in combination with LTZ on cell viability and neurosphere growth. We then utilized male CD-IGS rats (n=6; body wt., 250g) to assess plasma and brain extracellular fluid (ECF) pharmacokinetics (PK) of PARP inhibitors using cerebral microdialysis. The IC_{50} values for PARP inhibitors in these assays ranged from 0.06 to 11.31 µM. Treatment in combination with LTZ (0.05 µM), a non-cytotoxic concentration of LTZ in these lines, significantly decreased the IC_{50} values for PARP inhibitors (0.012 to 0.51 µM). Combination Index analysis indicated that this combination was strongly synergistic. Furthermore, the plasma and brain ECF PK analyses suggested that PARP inhibitors such as pamiparib and niraparib exhibit facile transport across the BBB barrier as reflected in $K_{p,uu,brain}$ (ratio of AUC_{ecf}/$AUC_{plasma,\ unbound}$) values of 0.98 and 0.45, respectively. Overall, these results provide a strong foundation for pursuing further development of combination therapy of GBM with LTZ and PARP inhibitors. A careful assessment of the clinical efficacy and safety profile of these agents will further guide shortlisting combination of LTZ for pre-clinical and clinical development.

#2120 Asparaginases-Treatment potential for the biomarker selected hepatocellular carcinoma (HCC) population.

E. Tyagi[1], M. Pohorecka[2], V. Duvivier[2], A. Studeny[2], D. Valour[2], N. Moulharat[2], H. Darville[2], N. Provost[2], P. Barbier Saint Hilaire[2], E. Hoeben[2], D. Simons[1]; [1]Servier BioInnovation, Boston, MA, [2]Servier, Gif Sur Yvette, France

Asparaginase is a key component of the therapeutic regimen used to treat patients with acute lymphoblastic leukemia (ALL). Calaspargase pegol (Asparlas) is composed of *E. coli* L-asparaginase and is PEGylated with approximately 5000 Da polyethylene glycol (PEG). Asparlas depletes asparagine (Asn) by deamination into aspartic acid. Asn synthetase (ASNS) is the key enzyme responsible for *de novo* Asn synthesis. In the absence of Asn in their direct environment, normal cells having adequate ASNS activity can survive with their own Asn supply while cancer cells lacking ASNS activity undergo apoptosis as they depend on extracellular sources of Asn. The *ASNS* gene has a typical CpG island in its promoter and its methylation status in tumor cells has been reported to be associated with asparaginase sensitivity clinically in T-ALL and in solid tumors preclinically. In this study we have investigated *ASNS* promoter hypermethylation as a biomarker for Asparlas activity in solid tumors and explored the feasibility of translating these results into the clinic. Analyses of the TCGA datasets indicated that a relatively high fraction of hepatocellular carcinoma (HCC) and gastric cancers are hypermethylated at the *ASNS* promoter. Testing Asparlas across a panel of HCC cell lines demonstrated that *ASNS* promoter-hypermethylated cell lines with lowest *ASNS* mRNA expression are the most responsive to Asparlas treatment in vitro. In vivo efficacy studies in mice bearing human *ASNS* promoter-hypermethylated xenograft models of HCC and gastric cancer showed that Asparlas treatment inhibited tumor growth in a dose-dependent manner and resulted in tumor rejections at the highest doses. Data from the HCC model was used to build a PK/PD efficacy model to project efficacious concentrations in patients. A panel of HCC PDX models with different levels of *ASNS* promoter methylation was evaluated to better understand the relationship between this biomarker and response to Asparlas. Treatment with Asparlas resulted in complete depletion of Asn in plasma and a partial depletion of Asn in the tumor for all models tested and strong anti-tumor activity against a model that had high methylation of the *ASNS* promoter. This activity was lost in models with lesser degrees of methylation indicating a strict threshold of promoter methylation for efficacy. These data confirm and extend previous findings that hypermethylation of the *ASNS* promoter has a synthetic lethal relationship with Asn-depleting therapies including Asparlas and highlight the need to carefully define the minimum threshold of hypermethylation to select HCC patients who could potentially benefit from Asparlas treatment.

#2122 Enhanced anticancer efficacy via ROS-dependent ferroptosis: Synergy between surufatinib and cisplatin in small cell lung cancer.

X. Li[1], Z. Zhang[1], Q. Tang[1], H. Xu[2];

[1]the First Affiliated Hospital of Nanjing Medical University, Nanjing, China, [2]Nanjing Medical University, Nanjing, China

Objective: Small cell lung cancer (SCLC), a highly malignant subset of neuroendocrine carcinoma, accounts for 13% of lung cancer cases and is characterized by its high aggressiveness and poor prognosis. The longstanding first-line treatment, a platinum-etoposide chemotherapy regimen, is increasingly compromised by resistance issues, highlighting the critical need for new therapeutic approaches. Surufatinib, an inhibitor selectively targeting vascular endothelial growth factor receptors (VEGFR) 1, 2, and 3, fibroblast growth factor receptor type 1 (FGFR1), and colony-stimulating factor-1 receptor (CSF-1R), has demonstrated efficacy in a spectrum of solid tumors, including neuroendocrine neoplasm, thyroid cancers and biliary cancers. Recently, ferroptosis, an iron-dependent cell death pathway, offers therapeutic promise, especially by inhibiting the xCT system, effective in pancreatic and lung adenocarcinomas. Yet, surufatinib's potential for inducing ferroptosis in SCLC remains to be investigated.

Methods: Cytotoxicity assays were performed on SCLC cell lines to assess the combinatorial effect of surufatinib and cisplatin, revealing a synergistic interaction. Ferroptosis inhibitors were applied to assess the reversal of cytotoxic effects. Mitochondrial morphology, reactive oxygen species (ROS) accumulation, membrane potential dissipation (JC-1 assay), lipid peroxidation (MDA levels), and intracellular iron accumulation (Fe2+ quantification) assays confirmed ferroptosis induction. Western blot analyses were conducted to explore the mechanistic pathways, supplemented by in vivo antitumor efficacy evaluations.

Results: In vitro assays revealed that surufatinib, when combined with cisplatin, exerts a pronounced synergistic effect on small cell lung cancer (SCLC) cell lines by inducing ferroptosis. The combination therapy strategically modulated ferroptosis-related pathways: cisplatin effectively decreased the expression of glutathione peroxidase 4 (GPX4), critical for cellular antioxidant defenses, while surufatinib increased the expression of acyl-CoA synthetase long-chain family member 4 (ACSL4), which is essential for the accumulation of lipid peroxides. This dual pathway engagement significantly amplified the ferroptotic response, culminating in heightened antitumor activity. Corroborative in vivo experiments substantiated these findings, validating the combined treatment's efficacy in a living model and underscoring its potential as a robust therapeutic strategy for SCLC.

Conclusion: Our findings reveal that surufatinib triggers ferroptosis in small cell lung cancer—a novel discovery. Additionally, it also unveils that surufatinib and cisplatin together enhance anti-cancer efficacy via the ROS-mediated ferroptosis pathway, marking a significant advance in SCLC therapy.

#2123 Validation of novel histone deacetylases (HDAC) specific nanoparticles using HDACs overexpressed human embryonic kidney cells.

S. Lohana, Y. Ramakrishnan, P. Balraj, M. Khan, M. Sanku, V. Sathish, M. Quadir;
North Dakota State Univ., Fargo, ND

Introduction: Histone deacetylase (HDAC) is a major enzyme system that is upregulated in numerous disease conditions including cancer. Harnessing the upregulation of HDAC can be a viable tool to design targeted therapy for these diseases. Nanoparticle technology has emerged as a powerful workhorse to suppress the survival of diseased cells selectively. As such, we aim to design a nanoscale, drug delivery platform that responds to HDAC enzymes to initiate drug release. In this poster, we show the pharmacological evidence that HDAC-sensitive nanoparticles are interacting with HDAC enzymes in vitro in time and concentration dependent pattern.

Methods: We synthesized HDAC-responsive nanoparticles via developing a block copolymer composed of a poly (ethylene glycol) block and a poly (L-acetylated lysine) block. Abbreviated as PEG-acPLK, these copolymers self-assemble as nanoparticles with negatively charged surface. Using in vitro culture of HEK 293 cells, we showed that the formed nanoparticles interact and interfere with HDAC enzymes. Cells were grown to 80-90% confluency in DMEM media w/ 10% FBS prior to experiments. HEK-293 cells were overexpressed with HDAC 7 & HDAC 8 using Lentiviral vectors. Western blot was done to prove the successful overexpression of the HEK cells. Cytotoxicity assay was done by MTT to analyze the efficacy of HDAC specific nanoparticle on control and overexpressed HEK-293 cells.

Results: Our work showed that, PEG-acPLK systems form nanoparticles with a hydrodynamic diameter (RH) of 120-150 nm. The particles were negatively charged on their surface, as such did not produce any non-specific toxicity to cells, such as damage of cell membranes. HEK-293 cells were infected with lentivirus vectors for HDAC 7 and HDAC 8. The medium was changed 8 h after infection. Forty-eight hours after infection, the positive cells were selected with 5 µg/mL puromycin. The lentivirus stable transformants of HEK-293 cells were collected and significant overexpression were confirmed by western blot. For the cytotoxicity study, control and overexpressed cells were treated with HDAC-nanoparticle and PEG-acPLKC (5 µg/mL to 70 µg/mL) for 24hrs. Both the HDAC-nanoparticle and PEG-acPLC (free form) showed more than 60% of toxicity at the concentration of 20 µg/mL. Whereas the HDAC 7 and 8 overexpressed HEK-293 cells did not showed any effects with nanoparticle and Ae-peg-PLKC, suggesting compensating effect due to highly available HDAC system in place and confirm the effectiveness of the HDAC nanoparticle.

Summary and Conclusion: Overall, these results showed that HDAC specific nanoparticle exhibited effects in HEK-293 HDACs overexpressed cells. Further molecular mechanistic studies will help to delineate how the HDAC-responsive particles can be used for drug delivery.

#2124 Validation of the intelligent glycotransferase-dependent conjugation (iGDC) platform: A groundbreaking approach for next-generation HER2-targeting ADC GQ1012 with enhanced druggability, potency, and safety.

M. Xiong, Z. Mu, M. Xu, C. Liu, B. Dai, J. Wang, X. Gao, L. Shi, P. H. Song, G. Qin;
GeneQuantum Healthcare (Suzhou) Co., Ltd., Suzhou, China

Background: Antibody glycan remodeling has emerged as a promising site-specific conjugation technology to develop ADCs, while most reported cases suffer from complicated CMC process and scalability challenges. We report herein an innovative, streamlined one-enzyme, one-step glycan remodeling technology, i.e. intelligent Glycotransferase-Dependent Conjugation (iGDC), that enables the site-specific conjugation of various biologic modalities including monoclonal antibody, bispecific antibody and Fc fusion proteins. Employing immobilized enzymes and a continuous-flow process, iGDC efficiently tethers payloads to the *N*-297 glycan site without requiring antibody engineering. In contrast to alternative conjugation techniques, iGDC offers superior versatility, product quality, process efficiency, scalability, and cost-effectiveness. Validation of the iGDC platform is exemplified by GQ1012, a HER2-targeting ADC featuring the potent Topoisomerase I inhibitor, TopoIx. Preclinical studies demonstrated GQ1012's outstanding anti-tumor efficacy in diverse in vitro and in vivo models, displaying robust synergistic effects with anti-PD-1 therapy and excellent tolerability in pre-tox studies involving monkeys with no signs of lung diseases, surpassing those of Enhertu. **Results:** GQ1012, developed through iGDC, utilized a highly hydrophilic, stable branch linker to conjugate TopoIx to an anti-HER2 antibody, achieving high conjugation efficiency confirmed by DAR analysis. The ADC maintained comparable antigen binding affinity and internalization compared to the parental antibody, exhibiting potent cytotoxicity against HER2-positive cancer cells. Despite glycan remodeling with iGDC leading to the removal of ADCC function, GQ1012 demonstrated no off-target cytotoxicity in HER2-negative cells and displayed a robust bystander killing ability in co-culture assays. In various in vivo models, GQ1012 demonstrated similar or superior antitumor efficacy compared to Enhertu, showcasing strong synergy with anti-PD-1 therapy. Stability studies confirmed GQ1012 maintains a highly stable linker, minimizing DAR reduction. Preliminary toxicity studies in monkeys following repeated intravenous infusions of GQ1012 showcased excellent safety and pharmacokinetics at specified doses and the potential for an extended therapeutic window compared to Enhertu. **Conclusion:** The validation of the iGDC platform through GQ1012 highlights its adaptability and efficiency in producing highly homogeneous next-generation ADCs without requiring antibody engineering. GQ1012 presents promising potential as a next generation HER2 ADC with an expanded therapeutic window compared to Enhertu, supported by extensive in vitro, in vivo assessments, and preliminary toxicity studies.

#2125 The use of intestinal organoids as a preclinical screen to assess gastrointestinal (GI) toxicity and barrier integrity.

V. Ubertini, S. Hall, F. Ponthan, J. Wilson;
Epistem Ltd., Manchester, United Kingdom

Gastrointestinal (GI) toxicity is a common and often severe limiting factor in the development of antineoplastic drugs. Symptoms include diarrhoea, dehydration and ulceration which increase susceptibility to infection, partly due to damage of crypt and/or villus structures in the small intestine, impairing the barrier function. As novel targeted therapies are emerging, assessment of their potential GI toxicity remains crucial. Small intestinal (SI) organoids are 3D *in vitro* models of the epithelium which recapitulate the structure and function of the small intestine. We have further developed and validated the organoid model as a screening tool to predict GI toxicity and subsequent mucosal regeneration in four species: mouse, rat, dog and human. The culture conditions have been designed to mimic the stem cell niche and allow cell differentiation and proliferation to occur. All intestinal lineages were present in the organoids derived from each species and the epithelial hierarchy closely resembled that observed *in vivo*. The toxic effects of antineoplastic drugs on the organoids were assessed by quantification of the total cell viability upon treatment, coupled to morphometric analysis of the organoids (size, area, perimeter, and branching efficiency). Immunofluorescence and RNAseq can be used to identify the targeted cells and the toxicity mechanisms of the drugs. To further assess the effect of drugs on barrier integrity, we have developed transwell-grown cell monolayers derived from normal human small intestinal organoids. This model allows direct access to both apical and basal surfaces, which is not possible when using organoids where their geometry prevents access to the apical surface. The monolayer formation was followed by live imaging and Trans-Epithelial Electrical Resistance (TEER) measurements and treatments with toxic drugs were applied after TEER reached a plateau. The direct effect on barrier integrity was evaluated by TEER reduction, increased FITC-Dextran permeability and analysis of TJ proteins by immunofluorescence. Furthermore, effects on cell death were assessed by measuring the levels of Lactate Dehydrogenase (LDH) released into the medium by dying cells. In conclusion, our models provide an innovative *in vitro* solution to further study the toxic effects of drugs on the normal small intestine and to analyse direct effects on barrier integrity. The monolayer assay may also be useful for developing models of transient TJ impairment to improve the bioavailability of orally administered antineoplastic drugs. The model can be considered more representative of the normal intestine than transformed cell lines such as CaCo2.

#2126 Efficacy and underlying mechanisms of surufatinib in non-small cell lung cancer treatment.

Y. Zheng, B. Shan, M. Wang, X. Wu, R. Cai, F. Niu, Y. Yuan, L. Liu, X. Zhu;
Affiliated Cancer Hospital & Institute of Guangzhou Medical University, Guangzhou, China

Background: The prevalence and fatality of lung cancer, especially non-small cell lung cancer (NSCLC), highlight the urgency for efficacious therapies. Surufatinib, an inhibitor of tyrosine kinases like VEGF receptors (VEGFR) 1, 2, and 3, Fibroblast growth factor receptor 1 (FGFR1), and CSF-1R, shows potential in augmenting chemotherapy efficacy and reducing adverse effects. Preliminary clinical studies (NCT04922658) have indicated survival benefits for NSCLC patients treated with surufatinib. This investigation seeks to delineate the therapeutic efficacy of surufatinib, correlating clinical benefits with mechanistic insights.
Methods: To elucidate mechanisms, proliferation assays (CCK8), migration (scratch assay), and apoptosis (flow cytometry) were conducted in A549 and H1299 cell lines. Angiogenesis and macrophage polarization were examined via vascular junction points and mRNA expression profiling. In nude mice, subcutaneous tumors were induced and treated with the study drugs, with tumor growth and angiogenic markers assessed.
Results: In vitro, surufatinib potently inhibited angiogenesis and exerted a dose-dependent suppression of proliferation and colony formation in lung cancer A549 and PC9 cell lines. It also enhanced apoptosis and cell migration. Additionally, surufatinib shifted macrophage polarization towards an M1 phenotype while diminishing M2 macrophages, thereby, contributing to a more robust anti-tumor immune milieu. In vivo studies corroborated these findings, with surufatinib and vinorelbine combination therapy significantly curtailing tumor growth and reducing CD31 expression in tumor tissues, highlighting its potential for substantial therapeutic gains in NSCLC management.
Conclusion: Surufatinib achieved notable antitumor effect consistent with clinical findings in NSCLC, effectively inhibiting cellular proliferation and migration, attenuating angiogenesis, and enhancing apoptosis. Significantly, it also modulated macrophage polarization to favor an M1/M2 balance, thus activating the immune response. Therapeutic strategies with surufatinib have underscored augmented antineoplastic efficacy, meriting additional clinical investigations.

#2127 Enhancing radiosensitivity in biliary tract cancer: The dual role of surufatinib in tumor suppression and macrophage reprogramming.

N. Wang, H. Ma, X. Mei, A. Huang, Y. Xiao, J. Yao;
Wuhan Union Hospital, Wuhan, China

Background: Biliary tract cancer (BTC) is notorious for its unfavorable clinical outcomes. Radiotherapy (RT) is a crucial component in BTC treatment. This study explores the radiosensitizing potential and mechanisms of Surufatinib (SF), an oral tyrosine kinase inhibitor, distinguished by its anti-angiogenic and immunomodulatory effects.
Methods: In a NOZ mouse xenograft model, tumor growth and expressions of Ki-67, CD31 were analyzed. NOZ and TFK1 BTC cells treated with SF and/or RT underwent assessments for viability, cycle, and apoptosis using CCK8, colony formation, and flow cytometry. Macrophage polarization in SF/RT-treated tumor cell-macrophage co-cultures was studied using Elisa, qRT-PCR, and flow cytometry.
Results: In vivo, SF impeded angiogenesis and bolsters the anti-tumor effect of radiotherapy. SF combined with RT significantly reduced subcutaneous tumor growth in nude mice, and diminished Ki-67 and CD31 expressions. In vitro, SF heightened cholangiocarcinoma cells' radio-sensitivity, causing DNA double-strand breaks and apoptosis. SF and radiotherapy combined notably increased γ-H2A expression and apoptosis levels ($P<0.05$). SF induced inflammatory response changes, favoring M2 to M1 macrophage polarization. In a tumor cell-macrophage co-culture, the SF-radiotherapy group showed increased IL-6 and decreased TGF-β ($P<0.05$), with upregulated M1 markers (IL-6, CXCL10) and downregulated M2 markers (TGF-β, CCL22, Arg-1) in macrophages ($P<0.05$). Both in vivo and in vitro, SF significantly reduced CD206+ M2-type macrophages ($P<0.05$).
Conclusion: Surufatinib alters the immune microenvironment in cholangiocarcinoma, reversing the immunosuppressive macrophage polarization induced by radiotherapy and reprogramming M2-type macrophages into M1-type, thereby enhancing the radiosensitivity of cholangiocarcinoma.

#2128 Surufatinib treatment in pancreatic cancer: unveiling the role of GPR34 in TAMs and enhancing immunotherapy efficacy.

X. Guo[1], Y. Liu[1], Y. Song[1], J. Huang[1], W. Zhu[1], P. Xu[2], J. Yu[1], S. Gao[1], J. Hao[1];

[1]Tianjin Medical University Cancer Institute and Hospital, Tianjin, China, [2]National Center for Nanoscience and Technology, Beijing, China

Background: Pancreatic cancer, often resistant due to its immunologically "cold" nature and tumor-associated macrophages (TAMs), presents challenges in chemotherapy and immunotherapy. This study uses single-cell transcriptomics to assess TAM subsets in response to surufatinib, an inhibitor targeting CSF-1R, FGFR1, and VEGFR1-3.

Methods: Surufatinib-treated patient samples were analyzed using single-cell RNA sequencing to identify altered macrophage subsets. Additional techniques, such as flow cytometry, tissue microarrays, co-culture assays, and macrophage-specific knockout mice, were used for further study. Western blot and immunofluorescence clarified the molecular functions of TAMs, and the impact of targeting these TAMs on PD-1 therapy was evaluated in a pancreatic cancer mouse model.

Results: Single-cell RNA sequencing revealed macrophage subsets with increased GPR34 expression following surufatinib treatment. The Gpr34fl/flLYZ2Cre mouse orthotopic-transplanted tumor model, treated with gemcitabine and albumin-bound paclitaxel, showed significantly reduced tumor growth compared to the control group, with notably lower percentages of exhausted T (Tex) cells and regulatory T (Treg) cells, and a significant increase in cytotoxic T cells in tumor tissue. LysoPS, produced by chronically injured pancreatic cancer cells, promotes the differentiation of bone marrow-derived monocytes (BMDM) into an immunosuppressive phenotype, an effect abolished after siGpr34 transfection. The LysoPS-GPR34 axis can significantly activate the NF-κB signaling pathway in BMDMs, potentially inducing the senescence-related secretory phenotype (SASP) and contributing to the macrophages' immunosuppressive phenotype. Combining a GPR34 antagonist with αPD-1 and PD-L1 inhibitors significantly curbed tumor growth and enhanced the immune environment in KPC mice.

Conclusions: Elevated GPR34 in TAMs enhances immunosuppression via the NF-κB pathway, affecting T cell distribution. GPR34's role could be key in optimizing surufatinib treatment for pancreatic cancer, indicating new therapeutic avenues.

#2129 Efficacy and underlying mechanisms of surufatinib combined with PD-1 monoclonal antibody and chemotherapy in pancreatic cancer.

N. Zhang, R. Jia, G. Dai;
Chinese PLA General Hospital (CPLAGH), beijing, China

Background: A phase 1b/2 study (NCT05218889) of surufatinib combined with camrelizumab, nab-paclitaxel, and S-1 (NASCA) as first-line therapy for metastatic pancreatic adenocarcinoma has shown promising results, potentially overcoming the limitations of current pancreatic immunotherapies. Animal studies are underway to further explore the synergistic effects and mechanisms of this combined therapeutic approach.
Methods: Genetically engineered KPC mouse cells were used to establish a subcutaneous transplantation tumor model in female mice, which were then divided into control group, AG group (nab-paclitaxel + gemcitabine), and NASCA group. Tumor metrics were recorded until euthanasia after 21 days. Blood and tumor samples were analyzed using Flow Cytometry.
Results: Compared with the control group, the NASCA and AG groups demonstrated tumor volume reductions of 14.7% (p=0.172) and -0.4% (p=0.972) on day 7, respectively. At day 14, the reductions were 48.8% and 29.9% (p<0.001*, p=0.002*). At day 21, the reductions were 37.4% and 21.5% (p=0.001*, p=0.144). The tumor growth inhibitions (TGIs) for NASCA and AG group were 56.7% (p<0.001*) and 21.2% (p=0.36), respectively. Compare to AG group, the tumor volume reduction in NASCA group were 15.1% (p=0.050*), 26.9% (p=0.001*) and 20.3% (p=0.116), respectively. And the TGIs for NASCA group compare AG group was 45.0% (p=0.020*). Distinguishingly, the NASCA group, when compared to the AG group, had a heightened proportion of M1 macrophages (28.5% vs. 15.5%, p=0.019*), mCD68+ Macrophages (99.7% vs. 99.1%, p=0,014*) and mPD-1+/mCD8+ T cells (24.8% vs. 9.8%, p=0.03*). Furthermore, T-regulatory cells (T-regs) in peripheral blood demonstrated uniformity across the groups, were no statistically. RNA-seq analysis revealed that the NASCA significantly suppressed multiple anti-angiogenic pathways while enhancing the cytokine pathway (p=0.005*), indicating potential immune system activation.
Conclusion: The NASCA group outperformed the AG group in controlling tumor growth and early tumor shrinkage, potentially due to macrophage polarization regulation. Further research is vital to understand the benefits of integrating targeted therapy, immunotherapy, and chemotherapy for pancreatic cancer.

#2130 Glioblastoma-derived extracellular vesicle cargo as a reporter of drug delivery and effect.

V. DeLuca[1], N. Tang[1], N. Hansen[1], A. Raju[1], C. Shaffer[1], Y. Hao[1], T. C. Burns[2], J. N. Sarkaria[2], I. Parney[2], P. Pirrotte[1], K. Van Keuren-Jensen[1], M. E. Berens[1];

[1]TGen (The Translational Genomics Research Institute), Phoenix, AZ, [2]Mayo Clinic, Rochester, MN

The selectivity of the blood-brain-barrier (BBB) can prevent therapeutics from reaching the brain, and this may contribute to the high failure rate of new drugs for tumors like glioblastoma (GBM) and brain metastasis. The capacity to detect BBB penetrance in real-time in a noninvasive manner would arguably aid the rate of therapeutic development. Extracellular vesicles, which are membrane bound particles secreted by all cell types in the body, have potential as a neuro pharmacodynamic reporter given that their protein and RNA cargo reflect the originating cell population. We hypothesized that the exposure of GBM cells to therapy results in altered EV cargo, and that the detection of this shift can be leveraged as a liquid biopsy from patients during early clinical trials to determine BBB penetrance and tumor engagement. To identify cargo shifts indicative of treatment, we exposed four short-term patient derived glioma cell lines to arsenic trioxide (an idiopathic toxin), MLN4924 (a neddylation inhibitor), and the alkylating agent temozolomide, then harvested EVs for unbiased mass spectrometry and RNA sequencing. Interestingly, we identified conserved upregulated and downregulated protein and RNA species across cell lines and across drug treatments, despite the diverse mechanisms of action. Candidate proteins were further validated by mesoscale immunoassays and exoview evaluation of tetraspanin-captured EVs. RNA species were validated by qRT-PCR. Overall, we demonstrate that GBM-derived EV cargo changes in response to therapy, supporting the development of EVs as a reporter of drug delivery in GBM. Ongoing and future work is focused on identifying enrichment handles in order to selectively evaluate GBM-derived EV cargo from patient biofluids. Thus far, B7H3, PTPRZ1, EGFRvII and IL13Ra2 have been screened as putative handles. Success in this pursuit could substantially enhance findings and accelerate drug testing in early-stage clinical trials in brain tumor patients by reporting drug accessibility to the tumor and engagement with drug targets.

PREVENTION / EARLY DETECTION / INTERCEPTION: Health Disparities Across the Cancer Continuum
Poster Session

#2134 Disaggregating breast cancer mortality trends in Asian American women from 2005-2020.

M. Marcotte[1], Y. Chauhan[1], **V. Penmetcha**[1], C. Thompson[2], C. Thompson[1], M. Srinivasan[1], G. Kim[1], X. Qi[1], R. Huang[1], A. Bacong[1];
[1]Stanford University School of Medicine, Stanford, CA, [2]University of North Caroline Chapel Hill, Chapel Hill, NC

Background: Breast cancer (BC) is the second leading cause of death among women and has disproportionately higher rates of mortality in certain racial groups, including Asian Americans (AA). While differences in BC mortality between AA and other racial groups have been identified, few studies have disaggregated nationwide AA mortality data.
Methods: Using National Vital Statistics System mortality data, BC-related deaths were analyzed among AA groups (Asian Indian, Chinese, Filipina, Japanese, Korean, Vietnamese), Native Hawiian and Pacific Islanders (NHPIs), and non-Hispanic Whites (NHWs) from 2005-2020. We calculated cancer proportional mortality ratios (PMRs), age-adjusted mortality rates (AAMRs), standard mortality ratios, and used JoinPoint regression for average annual percentage change (AAPC).
Results: Among 13677 AA, 522 NHPI, 501282 NHW descendants, 14.3% cancer deaths were due to BC. PMRs increased for all racial groups except Filipina. AAMRs significantly decreased in NHWs (AAPC -1.61; CI -1.70 to -1.48) while significantly increasing for aggregate AAs (AAPC 0.45; CI 0.08 to 0.94). Among AAs, Filipinas had the highest AAMR. AAMRs significantly increased for Asian Indians (AAPC 2.05; CI 1.20 to 3.46), Filipinas (AAPC 0.61; CI 0.15 to 1.46), Koreans (AAPC 2.72; CI 1.57 to 4.65) and Vietnamese women (AAPC 3.63; CI 2.26 to 6.20), but significantly decreased for Japanese (AAPC -1.41; CI -2.22 to -0.53).
Conclusions: We observed heterogenous and converging BC mortality trends across AA groups. These trends elucidate which populations within the broader AA group have disproportionately higher death rates and therefore should be targeted for BC prevention protocols (e.g., Asian Indian and Filipina). Identifying such trends can also help elucidate disparities in cancer care and the overall social determinants that affect women with BC. Understanding disaggregated trends can inform more inclusive screening practices and culturally tailored interventions and treatments to reduce BC deaths in vulnerable populations.

#2135 Racial disparities in symptom burden among women receiving early stage breast cancer chemotherapy.

E. Nasrollahi[1], H. Abujaradeh[2], S. Mazanec[3], J. O'Brien[2], I. M. Schlemmer[2], M. Rosenzweig[2];

[1]University of Pittsburg Medical Center, Pittsburgh, PA, [2]University of Pittsburgh School of Nursing, Pittsburgh, PA, [3]Case Western Reserve School of Nursing, Cleveland, OH

Purpose: The purpose of this study was to compare prevalent symptoms (pain, fatigue, and physical function) and changes over time between Black and White women undergoing chemotherapy for early-stage breast cancer (ESBC) employing a longitudinal, repeated measures design over the course of ESBC.

Methods: Data collected as per protocol of 1R01MD012245, comparing racial differences in chemotherapy tolerance and dose modifications during chemotherapy treatment at baseline, midpoint, and endpoint, tailored to each patient's individual chemotherapy schedule. Race was collected by patient self-report and chart review. Symptom burden (fatigue, pain, and physical functioning) was measured by the PROMIS-29 Profile v 2.0). Area deprivation was measured using the Area Deprivation Index (ADI). Linear mixed models were used to assess racial differences in symptom burden across timepoints, and changes in symptom burden over time, adjusting for ADI.

Results: A total of 147 patients participated in this study (36% Black and 64% white).

Pain: Black patients reported significantly higher pain scores than White patients at pretherapy (MD=3.7, p=.034), midpoint (MD=5.8, p: 0.002), and endpoint (MD=7.8, p<.001). Even after adjusting for area deprivation, this disparity persisted (F(1, 390)=29.43, p<.001), with Black patients having higher pain scores at midpoint (MD=4.7, p: 0.02) and endpoint (MD=7.8, p<.001). Pain scores worsened over time for Black patients, increasing significantly by the end of chemotherapy (MD_{T1-T3} =6.2, p=.010; MD_{T2-T3}=5.8, p=.024). No significant changes in pain scores were observed over time among White patients.

Fatigue: After adjusting for area deprivation, fatigue significantly increased at the endpoint (MD_{T1-T3}=8.9, p<.001) for Black patients. Among White patients, fatigue increased at midpoint (MD_{T1-T2}=5.7) and continued to worsen at the endpoint (MD_{T1-T3}=10.1, p<.001; MD_{T2-T3}=4.3, p=.017).

Physical Function: Black patients had significantly lower physical function than White patients at the midpoint (MD=4.0, p=.027). By the end of chemotherapy, physical function deteriorated significantly for Black patients (MD_{T1-T3}=7.8, p<.001), and White patients (MD_{T1-T3}=7.7, p<.001; MD_{T2-T3}=4.8, p=.002).

Correlations between the ADI and symptom severity and physical function revealed that living in more deprived areas was associated with greater pain severity (r=-.227, p=.002, 56.3 vs. 50.1) and worse physical function (r=-.190, p=-.035, 40.6 vs. 42.4) at the completion of chemotherapy.

Conclusions: The findings indicate that race and area deprivation are associated with symptom trajectories over the course of ESBC chemotherapy. Further research is warranted on how to best assess and relieve symptom burden among Black ESBC patients so that existing disparities in treatment and treatment outcomes are not perpetuated.

#2136 Genetic ancestry dependent variability in stromal cells: An unexplored player in breast cancer disparity.

P. Bhat-Nakshatri, H. Gao, C. Erdogan, Y. Liu, **H. Nakshatri**;
Indiana University School of Medicine, Indianapolis, IN

Genetic ancestry dependent variability in cancer incidence, mutation patterns, response to chemotherapy, and outcome has been documented. While an association between social determinants of health and breast cancer disparity has already been established, there is emerging evidence for genetic ancestry dependent variability in normal breast biology impacting breast cancer biology and potentially outcome. Tumor biology studies in the context of genetic ancestry and disparity have often focused on intrinsic properties of tumor cells or tumor infiltrating immune cells. However, other stromal cell types have received very little attention. Through immunohistochemistry of breast tissues from healthy women of African and European ancestry and primary cell culturing system, we had previously demonstrated enrichment of a stromal cell population called PZP cells (PROCR+/ZEB1+/PDGFRA+) with mesenchymal stem-like and fibroadipogenic properties in the normal breast tissues of women of African ancestry. In this study, we used single nuclei ATAC-seq and/or RNA-seq to further characterize stromal fibroblasts in the breast tissues of women of Ashkenazi Jewish-European, European, Indigenous American, Hispanic-European, African, and Asian ancestry. Among eight fibroblast cell clusters generated from women of African and European ancestry, only three cell clusters overlapped between two groups. While Complement Factor D (CFD, also called adipsin) expression was observed in unique fibroblast clusters of African ancestry, the expression of Insulin-like Growth Factor 1 (IGF1) was enriched in clusters unique to European ancestry. Interestingly, previous studies have demonstrated African ancestry-specific genomic variants for CFD linked to cardiometabolic disorders. Additional genes that showed genetic ancestry dependent variability in expression within fibroblasts include ABCA10, ABCA9, ABCA8, NEGR1 (enriched in African ancestry), MMP16, MAGI1, KIAA1217, PTPRK and SEMA5A (enriched in European ancestry). NEGR1 (Neuronal Growth Regulator 1) is a trans-neural growth promoting factor, whereas PTPRK (Protein Tyrosine Phosphatase Receptor Type K) is a negative regulator of EGFR signaling. These results suggest genetic ancestry dependent variability in stromal-epithelial cell communications under normal and cancerous conditions. These genetic ancestry dependent differences could impact intracellular signaling networks in epithelial cells with consequential effects on cancer incidence, mutation patterns, drug sensitivity, and outcome.

#2137 Racial disparities in triple-negative breast cancer (TNBC) mortality rates in Hampton Roads Virginia and the effects of SIAH expression on prognosis.

C. B. Piatak[1], T. N. Drake[1], A. Hannah[1], J. Baker[1], C. L. Dasom[2], E. L. Breeding[3], J. S. Winston[4], B. Samli[4], R. Jansen[5], M. Danso[6], R. A. Hoefer[7], A. H. Tang[1];

[1]Eastern Virginia Medical School, Norfolk, VA, [2]Stanford Medical, Stanford, CA, [3]Vanderbilt University Medical Center, Nashville, TN, [4]Sentara, Norfolk, VA, [5]University of Minnesota, Minneapolis, MN, [6]Virginia Oncology Associates, Norfolk, VA, [7]Sentara Cancer Network, Norfolk, VA

Background: While high-resolution imaging and advancements in therapies have significantly improved breast cancer survival rates, 43,170 breast cancer patients will die in the United States in 2023 alone. Triple-negative breast cancer (TNBC) is the most aggressive breast cancer subtype and disproportionately affects BRCA1 mutation carriers and young black women. Black/African American (AA) patients have the highest mortality and the shortest survival of any racial/ethnic group in the US. Persistent cancer racial disparities remain due to a variety of risk factors. The SEER/CDC data show an 8% lower breast cancer incidence rate and a 41% higher mortality rate in Black/AA patients compared to their white counterparts.

Methods: Chart review was conducted using Sentara MD Office/EPIC and VOA iKnowMedicine portals to update tumor relapse, metastasis, and survival in 577 TNBC patients. Supported by strong evidence in developmental, evolutionary, and cancer biology, we hypothesize that persistent EGFR/K-RAS/SIAH pathway activation is a major driving force of TNBC malignancy, racial disparity, early relapse, and high mortality. We propose to integrate SIAH expression to augment the existing clinicopathological parameters to improve patient risk stratification, therapy quantification, and relapse/survival prediction at the 1st-line neoadjuvant settings.

Results: We report that cancer disparity and high mortality rates are even more pronounced in our racially-diverse communities in Hampton Roads Virginia. We discovered that SIAH is a tumor-specific, therapy-responsive, and prognostic biomarker in TNBC. High SIAH expression in residual tumors reflects tumor-driving EGFR/K-RAS/SIAH pathway activation (ON) that will predict cancer disparity, treatment resistance, early relapse, and poor survival. Low SIAH expression in residual tumors reflect EGFR/K-RAS/SIAH pathway inactivation (OFF) that will predict tumor remission and prolonged survival.

Conclusion: We detect a major racial disparity of TNBC patients at Sentara-EVMS-VOA. Our local Black/AA TNBC patients have a 1.6-fold higher mortality rate than their White counterparts. Encouraged by our preliminary data, we aim to develop a SIAH-centered biomarker panel by measuring the EGFR/K-RAS/SIAH pathway activation (ON)/inactivation (OFF), and use SIAH as a new prognostic biomarker to risk stratify patients, detect cancer racial disparities, forecast tumor relapse, and predict patient survival at 1st-line neoadjuvant settings. By targeting SIAH, individualized treatments can be created to allow for increased survival rates in at risk individuals with more aggressive TNBCs.

#2138 Understanding the link between breastfeeding and the risk of breast cancer through comparative analysis of the murine-based model of mammary gland involution.

S. Mishra[1], N. Shinde[1], M. Cuitino[2], M. Bauer[1], D. Ahirwar[1], V. Bharti[1], K. Ormiston[1], R. Mawalkar[1], S. Alsammerai[1], G. Sarathy[1], X. Zhang[1], A. Vilgelm[1], R. Ganju[1], S. Majumder[1], B. Ramaswamy[1];

[1]The Ohio State University, Columbus, OH, [2]Medical University of South Carolina, Charleston, SC

Introduction: A meta-analysis of 47 global epidemiological studies highlights a higher breast cancer risk in women who did not breastfeed or breastfed for a short time. Further studies showed this is especially true for triple-negative breast cancer (TNBC) patients. Premenopausal AA women (AAW) have a lower prevalence of breastfeeding and a higher incidence of TNBC and mortality. Our previous study compares short-term breastfeeding, abrupt involution (AI) with prolonged breastfeeding called gradual involution (GI), revealing that AI alone induces ductal hyperplasia four months postpartum. Our current investigation delves into early events during AI *versus* GI, employing a comprehensive approach encompassing histology, gene expression, and myeloid cell involvement.
Methods: Utilizing FVB female mice, we conducted a comparative analysis of AI and GI. AI involved early pup removal, while GI was achieved through staggered weaning. The evaluation included analysis of histomorphology, gene/protein expression, and myeloid cell infiltration. Sequential mammary gland (MG) changes were monitored through H&E staining, TUNEL assay, and DNA damage analysis. 3D-organoid cultures of luminal progenitors (LPs) were employed to assess the impact of AI *versus* GI. qRT-PCR, IHC, Western blot, and flow cytometry/multiplex imaging were employed for the differential expression analysis of molecular and cellular factors associated with AI/GI.
Results: Our research showed that AI had early adipocyte repopulation, rapid cell death, DNA repair, and myeloid cell infiltration, resulting in a chronically inflamed microenvironment. In contrast, the GI triggers a controlled immune response and prolonged cell death, facilitating comprehensive remodeling of the MG. Our flow cytometric or multiplexing imaging analyses revealed that AI-affected glands exhibit an enrichment of CCL9-producing CD206+ M2-like macrophages and CD11b+Gr1+ myeloid-derived suppressor cells. Moreover, exogenous CCL9 treatment on LPs in 3D-organoid culture results in disorganized acinar-type organoids, mirroring morphological differences observed in LPs from AI mammary glands on day56 PPM. Further analysis of CCL9 treated organoids revealed the expansion of Esr1- LPs population in *ex-vivo* organoid culture which might indicate an increase in the putative cells of origin of TNBC.
Conclusion: Our studies comparing AI and GI demonstrate that AI is producing a pro-tumorigenic environment in the breast. It is important to note that prolonged breastfeeding protects the breast, although this cannot be a singular risk factor for TNBC. Therefore, understanding the mechanism will lead to prevention strategies to improve outcomes for all women but, has the potential to have a significant benefit in AAW.

#2139 Identifying molecular mechanisms in triple negative breast cancer disparities: Unveiling the role of Hedgehog signaling in non-Hispanic Black women.

J. V. Cabezas, S. Toure, M. Wilson, M. L. Stallings Mann, L. M. Pacheco-Spann, J. W. Ogony, M. E. Sherman, D. C. Radisky;
Mayo Clinic Florida, Jacksonville, FL

Triple negative breast cancer (TNBC) represents an aggressive and therapeutically challenging breast cancer subtype with higher incidence and mortality rates in non-Hispanic Black (NHB) women. This disparity persists even after adjusting for socioeconomic factors, tumor biology, and quality of care. The study aims to unravel specific molecular mechanisms underlying this disparity, with a focus on Hedgehog signaling pathways in premenopausal NHB women. Understanding these mechanisms is vital for developing targeted therapies and personalized medicine approaches to address these health disparities. Our research utilized a unique cohort of NHB and non-Hispanic White (NHW) women who underwent breast reduction surgery at the Mayo Clinic and donated breast tissue samples for our study. We isolated RNA from whole tissue sections from a cohort of 12 NHB and 40 NHW women who were parous and premenopausal at time of surgery. We performed gene expression profiling using NanoString BC360 and IO360 assays. This allowed us to identify a distinct gene expression signature characteristic of basal-like/TNBC and indicative of heightened activity in the Hedgehog signaling pathway. We also employed advanced cell culture techniques to generate tissue organoids and subculture human mammary epithelial cells (HMECs) that preserve the intrinsic characteristics of the original tissue samples. We found that significantly differential expression of IL20RA and SOX10, principal factors in the gene expression signature, were preserved in both the derived organoids and the HMECs. These results suggest a potential intrinsic difference in the activation of the Hedgehog pathway in the breast epithelial cells of NHB women. This activation may contribute to increased proliferation and transformation of basal stem cells within the breast, possibly fueling the development and progression of TNBC. The implication of activated Hedgehog signaling in NHB women opens new avenues for understanding TNBC disparities. IL20RA and SOX10 represent potential biomarkers for TNBC risk that may serve as a stratification tool for NHB women. The results of this study have the potential to improve assessment and management of TNBC risk among NHB women, thereby contributing significantly to reducing health disparities in breast cancer outcomes.

#2140 Untargeted lipidomics reveals racial differences in lipid species among women.

L. Li, G. Pourali, K. R. Getz, M. Jeon, J. Luo, C. Luo, **A. T. Toriola**;
Washington University School of Medicine in St. Louis, St. Louis, MO

Introduction: Lipids are important for many cellular processes and have been implicated in cancer development. Adopting a lipidomic approach has revealed sex-specific differences in lipid species but whether there are racial differences in lipid profiles remain unexplored. As a result, we investigated differences in lipid species between Non-Hispanic Black (NHB) vs Non-Hispanic White (NHW) women.

Methods: We performed lipidomic profiling on 705 premenopausal women who were recruited during their annual screening mammogram at Washington University School of Medicine, St. Louis, MO. A total of 982 lipid species were profiled at Metabolon (Durham, NC®). 125 lipid species missing in 300 or more women were excluded from the analysis. For the remaining missing values, we employed the nearest neighbor method for imputation. We investigated the race-differentiating lipid species concentrations using linear regression models, adjusting for age and body mass index (BMI). To satisfy the assumptions of normality and homoscedasticity, we log-transformed the lipid concentrations before performing regression analyses. The linear regression coefficients were then back-transformed as percentage differences. We accounted for multiple testings by applying the Bonferroni correction. Statistical significance was defined as a Bonferroni-adjusted p-value < 10^{-5}. Pathway enrichment analyses was conducted for differential lipid species for each sub pathway.

Results: Of the 705 women, 506 were NHW and 163 were NHB. In analysis adjusted for age and BMI, 278 lipid species were significantly lower in NHB, and one lipid specie (TAG58:10-FA20:4) was higher in NHB. These species belonged to triacylglycerols (TAG, n=213), phosphatidylcholines (PC, n=25), diacylglycerols (DAG, n=22), cholesteryl esters (CE, n=4), phosphatidylethanolamines (PE, n=4), lysophosphatidylcholines (LPC, n=3), lysophosphatidylethanolamines (LPE, n=3), sphingomyelins (SM, n=2), ceramides (CER, n=1), lactosylceramides (LCER, n=1) and phosphatidylinositols (PI, n=1) sub-pathways. The TAG sub-pathway was enriched with differential lipid species (213 significant out of 518 species, $p = 1.26\times10^{-11}$). Forty-three lipid species (42 TAGs and one DAG) exhibited an absolute percentage difference > 50% between NHB and NHW women. The top 3 TAG species with the largest absolute percentage differences were TAG44:0-FA14:0 (60.6% lower in NHB women, $p = 6.25\times10^{-8}$), TAG46:2-FA16:1 (59.8% lower in NHB women, $p = 1.11\times10^{-14}$) and TAG47:2-FA16:1 (59.4% lower in NHB women, $p = 8.66\times10^{-20}$). Conversely, TAG58:10-FA20:4 was 47.1% ($p = 5.79\times10^{-8}$) higher in NHB women.

Conclusions: Our study reveals novel substantial racial differences in lipid species among women, mostly in the TAG sub-pathway, highlighting the influence of race on the lipidome. Validation in a different study population is needed.

#2141 Prevalence of cervical high risk HPV serotypes not covered by the 9vt vaccine in a clinic-based sample of Hispanic women living in Puerto Rico.

Romaguera Josefina[1], Bianka Morales[1], Andrea Cortes[1], Ana Rosario[1], Andrea Padilla-Bou[1], Maria Frontera[1], Claudia Rosado[1], Daniela Cargas-Robles[1], Ana P. Ortiz[2], **Filipa Godoy-Vitorino**[1]

[1]University of Puerto Rico School of Medicine, San Juan, PR,[2]Comprehensive Cancer Center, University of Puerto Rico, San Juan, PR

Cervical cancer (CC) is the fourth most common female malignancy worldwide. Puerto Rico (PR) has the highest age-adjusted incidence of cervical cancer in the U.S. High-risk strains of human papillomavirus (hr-HPV) have been identified as common causative agents of CC. We aimed to characterize the prevalence of High-Risk HPV (HR-HPV) genotypes among a clinic-based sample of 368 HIV-negative women using a high-resolution approach. We used baseline data from IRB protocol 10510114. Cervical swabs underwent genomic DNA extractions followed by typification of HPV genotypes using a short-polymerase chain reaction-fragment assay (SPF10-LiPA) which detects 14 mucosal HR-HPV types (LiPA-25); 10 types (8 HR and 2LR) included in the 9-valent vaccine and 13 others not included on it. This process uses SPF10 primers to amplify a 65 bp fragment of the L1 open reading frame of HPV, followed by a reverse-hybridizationfor specific HPV genotypes by comparing the results to standardized kit controls. Cervical cytology was acquired for all participants. Data was collected from 186 women negative to intraepithelial lesions (NILM), 65 with low-grade lesions (LGSIL), 23 atypical squamous cells of undetermined significance (ASCUS) and 94 with high-grade lesions (HGSIL).Among study results, the prevalence of any HR-HPV infection was high overall (~71.5%) and higher in women who had either LGSIL or HGSIL. The top leading HR types detected were 51 (20.4%), 16 (18.5%), 52 (13.60%), 33 (13.00%) and 56 (11.00%, with other types including HPVs 35,39, 68 or 59.Nearly 34.00% of the identified cervical HR-HPV types, are not included in the 9-valent vaccine. The most common HPV types in HGSIL, included HR HPV types 16 (30.9%), 52 (18.10%), 51 (14.9%) and 33 (10.60%). In this group, only 35.20% were HPV16/18. The other 64.80% were other HR-HPV types and, based on the ASCCP guidelines, would not require a colposcopy, and could be observed in one year. Among these HGSIL (n=94) 48.9% of the HPV types were not included in the vaccine. HPV 51 was the most dominant in ASCUS (26.10%), LGSIL (20%), and women who were negative for intraepithelial lesions (NILM 22.6%). Additionally, the most prevalent HPV-HR serotypes across all cytology categories in the vaccinated cohort were 52 (11.14%), 16 (8.02%) and 31 (7.56%), whereas in the non-vaccinated cohort were HPV 16 (20.6%), 51 (17.55%), 33 (13.33%), 52 (12.29%), and 56 (11.94%).In conclusion, the high burden of other high-risk types not covered by the vaccine in women with high-grade lesions suggests that delaying immediate colposcopy might limit the identification of cervical lesions. Even though this is not a population-based study, the high prevalence of these other HR-HPV types calls for their inclusion in future generations of the vaccine.

Study sponsored by 2U54MD007600-36 (8538) Research Centers in Minority Institutions of the University of Puerto Rico (NIH/NIMHD).

#2142 Spatial distribution of high-risk human papillomavirus (HR-HPV) across 23 Chicago community areas and correlates.

G. Goba[1], J. Sun[1], Q. Class[1], J. Schwartz[1], S. Kim[1], K. Watson[1], L. Tussing-Hummphreys[1], Y. Molina[1], S. MacLaughlan[1], Z. Xu[1], B. Aldred[1], S. K. Kolar Rajanna[1], T. Alexander[1], A.-B. Moscicki[2];

[1]University of Illinois Cancer Center, Chicago, IL, [2]University of California, Los Angeles, Los Angles, CA

Background: Despite availability of effective vaccines and screening, cervical cancer claimed 4,280 lives in 2022. We explored the spatial distribution of high-risk human papillomavirus ("HR-HPV") infection across 23 Chicago Community Areas (CCAs) served by the University of Illinois Health Network (UI Health). Using a modified Warnecke et al Health Disparity Outcomes (HDO) model, we hypothesized that CCAs with higher rates of structural violence, the social, economic, and political systems exposing populations to risks and vulnerabilities, would correlate with increased HR-HPV.

Methods: Electronic medical records of patients receiving routine cervical cancer screening between January 1, 2015 and December 31, 2019 were reviewed. As per the 2014 ACS guidelines. HR-HPV test results were captured as HR-HPV positive, HR-HPV-16, HR-HPV-18 and non-16/18 HR-HPV, the latter consisting of 12 HR-HPV subtypes. Structural violence variables were used from Chicago Health Atlas (2015-2019) with percent poverty, hardship index score, easy access to fruit and vegetables, routine checkup, homicide, and primary care provider across CCAS. Univariate Poisson regression was used to compare the associations between selected structural violence factors and HR-HPV prevalence. Univariate multinomial logistic regression evaluated associations between structural violence indicators and HR-HPV subtypes Global p-values were obtained using ANOVA at 0.05 significance.

Results: 8,566 women met inclusion criteria out of 13,466 total women. 75% were Black or Hispanic. Overall prevalence of cervical HR-HPV infection was 20.3% (n=1,737), ranging from 8.7% to 27.2% across CCAs. Median age for women was 36. Percent with primary care provider was negatively associated with HPV infection (IRR = 0.99 with 95% CI (0.98, 1.00), adjusted p-value=0.023), indicating women living in CCAs with higher rates of primary care provider were less likely to have HR-HPV. Easy access to fruit and vegetables (adjusted p-value = 0.007) and percent with primary care provider (adjusted p-value = 0.009) were significantly associated with HR-HPV subtypes. Women living in CCAs with easy access to fruit and vegetables (OR = 0.99, with 95% CI (0.98,0.99)) as well as those with higher rates of primary care provider (OR = 0.98, with 95% CI (0.97,0.99)) were less likely to have non-16/18 HR-HPV.

Conclusion: HR-HPV is the most common sexually transmitted infection, and most women clear the infection naturally. As the origin of 99% of cervical cancer, understanding the reasons HR-HPV persists and progresses to cancer among certain individuals and groups is critical. Novel interventions like increasing access to fruit and vegetables could compliment widely available and effective vaccines.

#2143 Association between health insurance coverage and stage of diagnosis for cervical cancer among women in Indiana from 2011-2019.

M. Suresh Babu, M. L. Kasting, N. M. Rodriguez;
Purdue University, West Lafayette, IN

Introduction: Cervical cancer is one of the most common types of cancer among women and it is caused by infection from the human papillomavirus (HPV). The incidence rates of cervical cancer have increased in Indiana from 7.8 in 2008-2012 to 8.4 in 2013-2017. In 2020, the screening rate for cervical cancer among women in Indiana was 76% when compared to a national average of 78%. Women diagnosed at earlier stages for cervical cancer had higher relative survival of 0.98 than those diagnosed at later stages with a relative survival of 0.43. Health insurance status is an important determinant for health outcomes for patients with cancer. This study aims to assess the extent to which health insurance coverage is a contributing factor to the stage of cervical cancer diagnosis.
Methods: We examined reported cases of cervical cancer among women (N=2518) using cervical cancer registry data from the Indiana State Department of Health from 2011-2019. Using multinomial logistic regression model, we examined the associations of both race/ethnicity and insurance status with stage of diagnosis after adjusting for age at diagnosis.
Results: In this sample, the average age at diagnosis was 48.98 years (SD = 14.98). The largest proportion of the sample was between 45 to 64 years of age (41.7%), Non-Hispanic White (85.5%), had private insurance coverage (41.8%), had cervix uteri, NOS as the primary site of diagnosis (76.5%), lived in a metropolitan area (74.5%) and had squamous cell carcinoma (73.4%). The largest percentage of Non-Hispanic White patients had private insurance (50.9%), whereas the largest percentage of Black patients had Medicaid (39.3%). 20.2% of Hispanic patients were uninsured when compared to 7.7% Non-Hispanic White and 3.6% Black patients. The multivariate analysis shows that women who are uninsured (OR = 2.475) and those who have Medicaid (OR = 2.321) were significantly more likely to be diagnosed at the regional stage than the in-situ stage compared to women with private insurance. Additionally, women who are uninsured (OR = 4.432) and those who have Medicaid (OR = 3.007) were significantly more likely to be diagnosed at the distant stage than in-situ, compared to women with private insurance.
Conclusion: The findings show that insurance status is associated with the stage of diagnosis for cervical cancer and detection at regional or distant stages often leads to higher morbidity. Impact - Increased coverage for routine cervical cancer screening and preventive care services is recommended, especially for uninsured women and women with public insurance such as Medicaid or Medicare.

#2144 Disparities in gynecologic cancer survival outcome by treatment facility and region.

S. Bae[1], V. Pandya[1], C. Wang[2], H. Wang[2], R. C. Arend[1], C. A. Leath III[1], W. K. Huh[1];
[1]University of Alabama at Birmingham, Birmingham, AL, [2]Johns Hopkins University, Baltimore, MD

Objective: To explore five-year survival of patients with gynecologic cancers by region and treatment facility in the United States. Background: Research studies have examined the risk factors associated with gynecologic cancers, specifically cervical, ovarian, and endometrial, incidence and mortality. In addition to older age, Black/African American race, living in south, less income, less education, having comorbidity, stages of cancer, and lack of insurance have reported as risk factors for the incidence and mortality of gynecologic cancers. In addition, prior studies reported the possible effects from the distance to cancer care facilities on gynecologic cancer outcomes indicated varying results. In this study, we explore the impact of distance travelled by region and treatment facility on gynecologic cancer outcomes. Methods: This study aims to assess five-year cervical, ovarian, and endometrial cancer survival. Data were obtained from the National Cancer Database (NCDB) years 2004-2017, only from patients with a minimum 5-year follow-up. Women with races other than White or Black were excluded from the study. Demographics, region, treatment center type, distance to the treatment center, and cancer stage at diagnosis were analyzed by cancer type and 5-year survival status. Multivariate logistic regression model was used to assess the relationship between distance travelled to treatment facility by region and five-year survival. SAS version 9.4 was used for statistical analysis. Results: The distribution of the demographics across the three cancers were similar. Multivariate logistic models showed significant interactions between facility type and region on five-year survival among cervical, ovarian and endometrial cancer patients. Risk factors varied by region and treatment facility type. Age and cancer stage were significantly associated with survival among all cancers. Distance was significantly associated with survival in cervical and endometrial cancers. Conclusion: Cervical cancer patients in the South Atlantic who travel longer distances to Academic/Research Programs have poorer survival. Likewise, patients with endometrial cancer who live in New England region, and travel longer distances to Integrated Network Cancer Programs, as well as those who live in the West North Central region and travel longer distances to Community Cancer Programs have poorer survival. Further research is warranted to explore the specifics of region and treatment center types among different cancers to get a better understanding of the risk factors. Moreover, to improve the clinical outcomes, further study is needed to aim to identify which of these factors are actionable.

#2145 Genetic ancestry associations with pancreatic cancer mutational profiles from a diverse 9,274-patient real-world cohort.

B. Rhead[1], V. Vudatha[2], Y. Pouliot[1], E. Williamns[1], A. N. Riner[3], **F. M. De La Vega**[1], J. Trevino II[4];
[1]Tempus Labs, Chicago, IL, [2]Virginia Commonwealth University, Richmon, VA, [3]University of Florida College of Medicine, Gainesville, FL, [4]Virginia Commonwealth University, Richmond, VA

Pancreatic cancer is an aggressive malignancy associated with racial/ethnic disparities. Notably, Black patients have a higher incidence and mortality compared to their White counterparts. However, low representation of Black and Hispanic patients in cancer genomics studies hampers our understanding of genomic factors contributing to differential outcomes. Furthermore, comparisons between racial groups fail to capture differences in genomic ancestry. We studied the associations between genetic ancestry and race/ethnicity categories with mutational profiles, using a large, diverse real-world pancreatic cancer cohort. We analyzed 9,274 de-identified pancreatic cancer patients (8,483 with ductal adenocarcinoma, PDAC) who underwent tumor profiling with the Tempus xT 648-gene assay. We used 654 ancestry-informative markers to estimate continental ancestry for five regions: Africa (AFR), Americas (AMR), East Asia (EAS), Europe (EUR), and South Asia (SAS). We imputed Asian (ASN, n=431), Hispanic/Latino/Native American (HLN, n=593), Non-Hispanic Black (NHB, n=875) and Non-Hispanic White (NHW, n=7,309) categories from genetic ancestry using a previously published machine learning method. Associations between either race/ethnicity categories or ancestry proportions and somatic variants (copy number alterations or CNAs, small nonsynonymous, OncoKB L1/2 & R1, and predicted driver somatic mutations using boostDM) were assessed for 172 pancreatic cancer-related genes or gene sets using logistic regression models. Models with and without race/ethnicity or ancestry terms were compared with likelihood ratio (LR) tests, and p-values were adjusted to control the FDR at 5%. We tested for associations of race/ethnicity groups with TMB using a Kruskal-Wallis rank sum test. Tests of TMB and small variants used only patients with available matched normal tissue to avoid artifacts from misclassification of germline variants. Among pancreatic cancer patients, having either a CNA or small nonsynonymous mutation in a receptor tyrosine kinase (RTK) gene (*ERBB2, EGFR, MET, FGFR1*) was associated with genetic ancestry (LR adjusted p=0.027). Specifically, AMR ancestry was positively associated (OR=1.08 per doubling of ancestry proportion, p=0.004) and EUR negatively associated (OR=0.93, p=0.002). Associations in PDAC were similar but not significant. Race/ethnicity was associated with RTK changes in both groups, with ASN and HLN having more mutations than NHW, but the associations were not significant after correcting for multiple hypotheses. There was no association of race/ethnicity and TMB .Somatic changes in RTK genes were associated with AMR genetic ancestry; however, despite the relatively large cohort size, these results are modest, suggesting there is not a large somatic mutation component contributing to differences in pancreatic cancer outcomes by ancestry.

#2146 Race-related differential immunoreactivity of enolase autoantibodies in patients with prostate cancer.

K. Cheng[1], C. J. Diaz Osterman[2], K. Santiago[1], M. Reeves[3], D. Lozano[3], P. Ochoa[1], A. Duran[1], S. Mirshahidi[1], B. R. Hu[1], F. Almaguel[1], C. A. Casiano[1];
[1]Loma Linda University, Loma Linda, CA, [2]Ponce Health Sciences University, Ponce, Puerto Rico, [3]La Sierra University, Riverside, CA

INTRODUCTION AND OBJECTIVE: Enolase-1 (ENO1) and -2 (ENO2) are implicated in tumor metabolic and aggressive functions. Like prostate specific membrane antigen (PSMA), they localize to the tumor cell surface and are potential theranostics targets. ENO autoantibodies were reported by our group in prostate cancer (PCa) patients but their immunoreactivity to ENO1/2 isoforms was not defined. Differential ENO immunoreactivity in docetaxel-resistant (DR) PCa cells between African American (AA) and European American (EA) PCa patients was also reported. Our objective was to investigate the role of ENO isoforms in the race-related differential ENO immunoreactivity of PCa patients.

METHODS: PCa patient sera (41 AA, 68 EA) were obtained from Loma Linda University Biospecimen Laboratory. Western blotting (WB) analysis, using patient sera and monoclonal antibodies to ENO1 and ENO2, was done against lysates from docetaxel-sensitive (DS) and DR PCa cell lines and against recombinant (rec) ENO1 and ENO2 to assess ENO isoform expression and detect ENO autoantibodies. Scratch-wound assay was performed to evaluate AA and EA anti-ENO driven inhibition of DR PCa cell migration. Student's T-test and Chi-squared analyses were performed with $p<0.05$ deemed significant.

RESULTS: ENO1 expression was robust in all assessed DS and DR cell lines. ENO2 was detected in DS cells but was significantly reduced in DR cells. PSMA expression was lost in cells expressing ENO1 and neuroendocrine markers. Anti-ENO EA sera reacted in WB with the expected 50 kD band in both DS and DR PCa cells, but anti-ENO AA sera reacted preferentially with this band in DS cells. Strong immunoreactivity was noted against recENO1 in AA and EA sera (7% vs 28%, $p<0.01$) and against recENO2 in AA and EA sera (24% vs 35%, $p=0.23$). EA, but not AA, ENO autoantibodies significantly inhibited DR cell migration, and their pre-absorption with recENO1 diminished this inhibitory effect.

CONCLUSIONS: Autoantibodies to ENO1 and ENO2 were identified in EA and AA PCa patient sera. Weaker ENO1 immunoreactivity was seen in sera from AA PCa patients, corresponding with weaker inhibition of DR PCa cell migration compared to EA patient sera. Unlike PSMA and ENO2, ENO1 expression was robust in neuroendocrine-like DR PCa cell lines. Future studies will correlate the presence of ENO autoantibodies with clinicopathologic parameters in a larger patient cohort. Defining mechanisms underlying the race-related differential ENO immunoreactivity may identify novel biological determinants of PCa health disparities and uncover the theranostic potential of tumor surface ENO1.

#2147 Genetic ancestry associations with prostate adenocarcinoma mutational profiles: New Insights from a diverse 5,959-patient real-world cohort.

B. Rhead[1], Y. Pouliot[1], F. M. De La Vega[1], D. W. Craig[2], J. Carpten[2];
[1]Tempus Labs, Chicago, IL, [2]City of Hope, Duarte, CA

In prostate cancer, Black men face higher incidence rates, more advanced diagnoses and worse outcomes than White men. These disparities partially stem from environmental, socioeconomic, and healthcare access factors. Recent data highlight racial differences in prostate cancer molecular profiles, with tumors from Black men showing increased *SPOP* and decreased *PIK3CA* mutations and amplified androgen receptor signaling and inflammatory pathway activations. Thus, somatic mutation patterns may also contribute to these disparities. We sought to identify associations of mutational profiles in prostate adenocarcinoma (PRAD) with genetic ancestry instead of race and ethnicity categories, analyzing a de-identified cohort of 5,959 patients who underwent the Tempus xT 648-gene NGS tumor profiling test. We used 654 ancestry-informative markers to estimate genetic ancestry by calculating similarity to reference populations for five regions: Africa (AFR), Americas (AMR), East Asia (EAS), Europe (EUR), and South Asia (SAS). Associations between genetic ancestry proportions and somatic variants were assessed for 67 PRAD-related genes using logistic regression models. Analyses included copy number alterations (CNAs), oncogenic gene fusions, small splice and non-synonymous mutations (NS), OncoKB L1/2 & R1, and small missense driver somatic mutations predicted with boostDM. Likelihood ratio tests were employed to compare models with and without ancestry terms. The Benjamini-Hochberg method was utilized to adjust p-values and control the FDR at 5%. We confirmed reported associations in PRAD between AFR ancestry and *SPOP* NS mutations (OR=1.03 per doubling of AFR ancestry proportion, p=0.03) and decreased AFR with *PIK3CA* OncoKB and driver mutations (OR=0.94, p=0.02), *PTEN* CNAs (OR=0.95, p=0.0001), and *TMPRSS2-ERG* fusions (OR=0.95, p<0.0001). However, we also observed negative associations between AFR and *AR* CNAs (OR=0.95, p=0.004), EAS and *PTEN* CNAs (OR=0.96, p=0.01), and EAS and *TMPRSS2-ERG* fusions (OR=0.97, p=0.02). Additionally, a negative association was found between EAS and *TP53* driver NS mutations (OR=0.96, p=0.04), while positive associations with driver mutations in *FOXA1* (OR=1.06, p=0.03) and NS mutations in the PI3K/AKT/mTOR pathway genes (OR=1.04, p=0.01) were noted. Lastly, we identified novel positive associations between AMR and driver mutations in *PIK3C3A* (OR=1.12, p=0.0003) as well as small NS mutations or CNAs in the PI3K/AKT/mTOR pathway genes (OR=1.03, p=0.04). By analyzing a large, diverse real-world cohort and leveraging NGS-inferred genetic ancestry, our study confirms known associations between somatic alterations in PRAD cancer genes and race and ethnicity, while unveiling novel associations in understudied populations of potential significance for understanding disparities in disease outcomes.

#2148 Tumor-microenvironment from African-American prostate cancer exhibit methylation of multiple immune modulators.

S. Sankaran[1], J. Nguyen[1], T. Jennings[1], V. Kumar[1], M. B. Lilly[2], M. M. Ittmann[3], P. Castro[3], L. Song[1], T. Keane[2], W. Chu[1], X. Zi[1], O. Yazdanpanah[4], A. Rezazadeh Kalebasty[4], F. Rahmatpanah[1],

[1]University of California, Irvine, Irvine, CA, [2]Medical University of South Carolina, Charleston, SC, [3]Baylor College of Medicine, Houston, TX, [4]UC Irvine Medical Center, Orange, CA

Background: Non-Hispanic Black American patients (BA) with prostate cancer (PCa) tend to fare worse than their Non-Hispanic White American counterparts (WA), even with consideration of socioeconomic disparities. Clinically, BA face diagnosis at younger age with worse clinical outcomes. Stromal cells adjacent to the tumor, including carcinoma-associated fibroblasts (CAFs), play a critical role in tumorigenesis of PCa. Dysfunction in the tumor microenvironment play a crucial role in mediating prostate cancer tumorigenesis and is emerging as a key target for cancer therapy in solid tumors.

Methods: To investigate whether DNA methylation varies in tumor adjacent stroma (TAS) among PCa patients with different geographical ancestries, areas immediate adjacent to tumor (i.e., less than 1mm) removed for methylation analysis. A complete genome-wide DNA methylation of PCa stroma using 17 BA and 15 WA patients who had radical prostatectomy was carried out. Methyl-Captured (mCap) sequencing data was generated for TAS of prostate cancer FFPE tissues. Methylated sites were identified with the MACS2 callpeak function using a band width of 300 bp and a false discovery rate of $q < 0.05$. A consensus peak set was derived from the aligned reads of BA and WA prostate cancer stroma samples that were sequenced. Pathway analysis was performed using Ingenuity Pathway Analysis (IPA) tools. CAFs from primary tumors of BA and WA was prepared by tissue culture and treated with demethylating agent (i.e., 5-Azacytidine) for 24 hours followed by maintenance of the cells in drug-free medium for 7-10 days and subjected to mCap sequencing.

Results: We found racial disparities in genome-wide DNA methylation in TAS between the two populations in which BA PCa patients had significantly increased in global DNA methylation as compared to their WA counterpart (p value < 0.001). Hypomethylation occurred in CAFs from BA patients treated with 5-Azacytidine. We identified 1041 methylated sites corresponding to 409 unique genes that were differentially methylated in BA vs WA (p value < 0.05). Pathway analysis identified significant association between methylated genes in BA TAS and immune response pathways including IL-13, JACK/STAT, T cell receptors, NF-KB, and PD-1, PDL1 cancer immunotherapy. Evaluation of the methylome profile between patients based on the post-prostatectomy resection margins, negative (R0) vs positive (R1), showed that R0 resections had significantly greater (p value < 0.001) methylation than R1 resections. Further analysis identified 984 sites corresponding to 373 differentially methylated, unique genes (p value < 0.05).

Conclusion: Tumor-adjacent stroma of BA prostate cancer patients has a distinct methylome as compared to WA patients. Differences in immune response pathways suggests a distinct immune response in TAS in men of different races.

#2149 West African genetic ancestry and origin of the BRCA1 locus in Jamaican men with high grade prostate cancer.

S. M. Gaston, A. J. Griswold, O. N. Kryvenko, T. Gu, G.-N. Zhang, N. S. Prakash, Y. Avda, T. Ajami, C. R. Ritch;
University of Miami Miller School of Medicine, Miami, FL

Introduction: Men of West African (WA) ancestry are at higher risk for prostate cancer than men of European (EU) or Asian descent. Caribbean populations provide an opportunity to identify potential founder mutations that contribute to cancer risk. Jamaica has among the highest rates of prostate cancer incidence and mortality in the world and the majority of the population are of WA ancestry. However, there is a significant amount of genetic admixture of EU and Asian ancestry from historic migration patterns. Thus, the population provides a unique cohort for studying the complex interplay between genetic ancestry and prostate cancer. In this pilot study, we characterized the overall and gene locus-specific ancestry of Jamaican prostate cancer patients to explore potential associations with clinicopathologic disease features. We specifically focused this analysis on the BRCA1 locus based on its known association with inherited prostate cancer risk and also with breast cancer risk in patients from the Caribbean.
Methods: A retrospective cohort of 31 Jamaican men (non-US citizens/residents) who travelled to the University of Miami (2015-2020) specifically for robotic prostatectomy were included in the analysis. DNA was prepared from normal prostate tissue and analyzed using the Illumina Global Screening Array version 3 with Multi-Disease Drop-In that includes more than 650,000 genetic markers. Both overall genetic ancestry and allele specific ancestries were determined for each study subject. Clinical and pathological features (age, PSA, stage, grade group (GG)) were also recorded and analyzed using descriptive statistics.
Results: Median age was 67 years, median pre-op PSA was 6.7. The majority of patients were cT1c (91%) and GG 2 (29%) on biopsy. On final pathology most men were ≥pT3 (51%) and the proportion of GG 1, 2 and ≥ 3 was 3%, 52% and 45% respectively. The mean overall West African genetic ancestry was 51.2% (SD 28.4%). Overall % West African ancestry was not associated with pathological GG. In contrast, 50% of the men who were homozygous for African ancestry alleles at the BRCA1 locus had high-grade prostate cancer (GG 3, 4, 5) versus 37% of the men with non-African or heterozygous BRCA1 genotypes.
Conclusions: In a select cohort of Jamaican men, we found that half of patients with BRCA1 alleles derived from West African ancestry also have high grade prostate cancer. BRCA1 of African ancestral origin may contribute to the relatively high prevalence of aggressive prostate cancer in men from Jamaica. Work in progress focuses on an expanded study of associations between allele-specific genetic ancestry and prostate cancer in high-risk populations.

#2150 Spatial transcriptomic analysis of histologically matched regions adjacent to and within prostate cancer reveals RNA expression differences between African Americans and European Americans.

V. Kumar[1], D. Castaneda[1], J. A. Nguyen[1], G. A. Giannico[2], M. M. Ittmann[3], P. Castro[3], O. Yazdanpanah[2], A. Rezazadeh[2], T. S. K. Jennings[1], M. Mcclelland[1], F. Rahmatpanah[1],

[1]University of California, Irvine, Irvine, CA, [2]University of California, Irvine, Orange, CA, [3]Baylor College of Medicine, Houston, TX

Introduction. Prostate cancer (PCa) of American men of African ancestry (AA) is diagnosed at an earlier median age and more advanced stage with a poorer prognosis and significantly higher mortality than in Americans of primarily Northern European ancestry (EA). The mechanism of how ancestry contributes to aggressive PCa in AA patients is not well understood. Given the inherent heterogeneity and multifocality of prostate cancer, Spatial transcriptomics is of particular interest because it allows distinct cell populations within the tumor microenvironment to be characterized, and their possible effects on local tumors to be identified. Here we compare transcription between four AA and four EA patients in regions of peritumoral stroma, inflammation, Benign Prostatic Hyperplasia (BPH), and Gleason score patterns 3 (G3) and 4 (G4).

Methods: Formalin fixed, paraffin embedded (FFPE) prostatectomy tissue blocks were obtained from 8 patients (4 AA and 4 EA) prior to treatment of the patients and matched for clinical variables (i.e., biochemical relapse, age, Gleason score, and tumor stage). 10um tissue sections were mounted onto Visium Spatial Gene Expression Slides and processed following 10x Genomics protocol. Sample counts were processed through Space Ranger. 18000 unique genes, spatial barcodes, and clinician guided annotations were imported to the R program Seurat. Data was processed using SCTransform. Significance of each transcript differences between each tissue were calculated.

Results: Digital histologic slides of prostate cancer specimens from AA (n=4) and EA (n=4) patients were annotated by a urologic pathologist to identify regions of peritumoral stroma, inflammation, BPH, G3, and G4. Each spot was interrogated for the expression of 18000 transcripts, with an average of 17796 being detected per spot. Among the largest differences observed between AA and EA, G3 and G4 had distinct transcriptome profiles in the four AA as compared to G3 and G4 in four EA. Also, when differential expression (padj < 0.05) in peritumoral stroma was compared to G4 in AA, we identified 290 differentially expressed genes, whereas the same comparison in EA cohorts identified 600 differentially expressed genes.

Conclusion: Spatial transcriptomic analysis revealed differences in gene expression across multiple tissue types in prostate cancer patients of different ancestries.

#2151 Additional impact of genetic ancestry over self-reported race/ethnicity to prevalence of *KRAS* mutations and allele-specific subtypes in non-small cell lung cancer.

X. Wang[1], K. Hou[2], B. Ricciuti[3], J. V. Alessi[3], X. Li[1], F. Pecci[3], R. Dey[1], J. Luo[3], M. M. Awad[3], A. Gusev[3], X. Lin[1], B. E. Johnson[3], D. C. Christiani[1];
[1]Harvard T.H. Chan School of Public Health, Boston, MA, [2]University of California, Los Angeles, Los Angeles, CA, [3]Dana-Farber Cancer Institute, Boston, MA

Background: *KRAS* mutation is the most common oncogenic driver in patients with non-small cell lung cancer (NSCLC). However, the interplay between self-reported race and/or ethnicity (SIRE) and genetically inferred ancestry (GIA) on *KRAS* mutations and allele-specific subtypes is largely unknown.
Methods: A total of 3918 NSCLC patients from the Chinese OrigiMed (OM) cohort (n=2039) and Boston Lung Cancer Survival (BLCS) cohort (n=1879) were included, all of whom had baseline covariates including age, sex, clinical stage, SIRE, histology and smoking status. *KRAS* mutation and subtypes were determined by targeted NGS panels in each cohort, and *KRAS* mutation outcomes, including *KRAS* mutation, *KRAS* subtypes, and *KRAS* transversion and transition were analyzed. GIA was inferred from paired germline data for patients in the BLCS cohort. Multivariable and multinomial logistic regressions were employed to assess the associations between SIRE, GIA and *KRAS* outcomes.
Results: In the entire cohort, 804 (20.5%) patients harbored *KRAS* mutation, with a considerably higher prevalence of 31.5% observed in BLCS compared to 10.4% in OM cohort. Patients with self-identified Asian was associated with a significantly lower rate of *KRAS* mutation (OR = 0.44, 95% CI:0.22 - 0.81, P = 0.01), transversion substitutions (OR = 0.24, 95% CI:0.10 - 0.62, P = 0.003) and $KRAS^{G12C}$ (OR = 0.17, 95% CI:0.04 - 0.72, P = 0.02) compared to SIRE-White patients after adjusting for confounders including smoking status, sex and histology. The association of SIRE and *KRAS* driver mutation was further modified by sex, with Asian women demonstrating lower risk compared to Asian men, while the opposite trend was observed in SIRE-White patients. Increased European ancestry was associated with a higher risk of *KRAS* mutation (OR per 10% increase = 1.05, 95% CI:1.00 - 1.09, P = 0.03), particularly with more transition substitutions (OR per 10% increase = 1.10, 95% CI:1.01 - 1.21, P = 0.03) and $KRAS^{G12D}$ (OR per 10% increase = 1.18, 95% CI:1.04 - 1.34, P = 0.01). This association was even more pronounced in patients of increased Northern European ancestry. Furthermore, even among SIRE-White patients, a 10% increase in European ancestry was associated with an additional 6% increase in the likelihood of *KRAS* mutations (OR = 1.06, 95% CI: 1.01 - 1.12, P = 0.03), while a 10% increase in Admixed American ancestry was associated with a 6% decreased likelihood of *KRAS* mutations (OR = 0.94, 95% CI: 0.88 - 0.99, P = 0.04). Results were validated in an independent cohort of 1450 patients.
Conclusion: Self-reported race/ethnicity and genetic ancestry are both associated with *KRAS* driver mutations and allele-specific subtypes of NSCLC. This work highlights the significance of integrating both into population-based cancer research, aiming to refine clinical decision-making processes and mitigate health disparities.

#2152 Evaluating beliefs and perceived competence about tobacco cancer prevention practices in Texas local mental health authorities.

A. D. Siddiqi[1], M. Britton[2], T. A. Chen[3], I. Martinez Leal[2], A. Rogova[2], M. Z. Jafry[4], B. Kyburz[5], T. Williams[5], L. R. Reitzel[2];
[1]Rice University, Houston, TX, [2]MD Anderson Cancer Center, Houston, TX, [3]University of Houston, Houston, TX, [4]McGovern Medical School, Houston, TX, [5]Integral Care, Austin, TX

Tobacco use is causally associated with 18 cancers and is a leading cause of preventable death. Individuals experiencing mental illness use tobacco at an elevated rate and consequently suffer from greater cancer-related morbidity and mortality. Unfortunately, local mental health authorities (LMHAs), a common setting to receive mental health services, do not prioritize tobacco dependence treatment despite robust evidence that tobacco cessation can enhance mental health in addition to reducing cancer incidence. Beliefs (Health Belief Model) and competence (Self Determination Theory) both play an integral role in shaping behavior. Consequently, this study examined employee and provider tobacco-related beliefs and competence in LMHAs to contextualize their tobacco intervention practices. The frequency of beliefs and competence related to provision of evidence-based tobacco cessation care was collected by e-survey from organizational representatives of 30 of the 39 LMHAs in Texas in 2021. Queries included if respondents agreed that patients should concurrently quit drugs/alcohol and tobacco (N=30 employees) and if they believed patients want to quit cigarette and non-cigarette (i.e., other) tobacco products (n=16 direct service providers). Providers were also asked if they thought that they had the competence to help patients quit smoking and other tobacco use, if they could tailor cessation treatment to patient needs, and about their intervention practices. Only 40% of LMHA representatives endorsed that patients should quit tobacco at the same time as other drugs. Furthermore, only 50% of providers believed that patients want to quit smoking and other tobacco use, respectively. About 70% of providers believed that they have the skills to help patients quit smoking and other tobacco use, respectively, but only 56% reported that they can tailor treatment. Finally, only 56% and 38% of providers recommend that patients stop smoking or other tobacco use, respectively, with 25% recommending smokers switch to vapes or smokeless tobacco products. Contrary to LMHA employee and provider beliefs, research indicates that most patients want to quit tobacco use and that concurrent tobacco use treatment can enhance patient sobriety for non-nicotine substance use disorders. Results demonstrate high levels of misinformation on concurrent tobacco and substance use treatment in LMHAs, which can subvert the provision of evidence-based cessation care. Educational interventions are needed to shift these beliefs, increase competence, and increase tobacco use intervention provision. This will not only help to address cancer disparities among patients but also improve mental health- a critical goal of LMHAs. Future research should investigate how to target tobacco-related beliefs, competence, and intervention behavior in LMHAs to broaden the reach of cancer prevention strategies.

#2153 The impact of socioeconomic and racial segregation on cancer stage at diagnosis, treatment and mortality among patients with small cell lung cancer.

B. B. Bekele, M. Lian, Y. Liu;
Washington University in St Louis, St Louis, MO

Background: Although studies have revealed the adverse impact of residential segregation on early detection, treatment, and survival of non-small cell lung cancer—a predominant type of lung cancers, it remains unknown regarding the role of residential segregation in treatment and outcomes of small cell lung cancer (SCLC)—a rare type of lung cancer characterized by rapid growth and poor prognosis. Therefore, we examined the associations of racialized socioeconomic segregation with risks of extensive-stage diagnosis, non-adherence to guideline-recommended treatment, and mortality among non-Hispanic White (NHW) and non-Hispanic Black (NHB) patients with SCLC.
Methods: This population-based retrospective cohort study included patients who were diagnosed with SCLC as a first primary malignancy at age 20 and older between January 2007 and December 2015, followed through December 2016, and identified from the Surveillance, Epidemiology, and End Results. County-level racialized socioeconomic segregation was measured using the Index of Concentration at the Extremes (ICE). Multilevel logistic regression accounting for county-level clustering was used to estimate odds ratios (ORs) for extensive-stage diagnosis and non-adherence to guideline-recommended treatment. Hazard ratios (HRs) for lung cancer-specific mortality and all-cause mortality were computed using multilevel Cox regression.
Results: Among 38,393 patients, 90.1% were NHW and 9.9% were NHB. Patients dwelling in the counties with the highest concentration of low-income NHB households (highest ICE quartile) had higher risks of non-adherence to guideline-recommended treatment (OR=1.23, 95% CI: 1.08-1.40; P_{trend} <0.01), lung cancer-specific mortality (HR=1.08, 95% CI: 1.04-1.12; P_{trend} <0.01), and all-cause mortality (HR=1.13, 95% CI: 1.09-1.17; P_{trend} <0.0001) as compared with patients dwelling in the counties with the highest concentration of high-income NHW households (lowest ICE quartile). These associations were comparable between NHB and NHW patients. Racialized economic segregation was not significantly associated with extensive-stage diagnosis.
Conclusions: Residing in the segregated, low-income NHB counties had adverse impacts on stage-appropriate treatment for SCLC and survival outcomes. Future research on the pathway(s) linking residential segregation to SCLC treatment underutilization and poor outcomes is warranted.

#2154 *Actívatexto:*Feasibility and acceptability of a mobile intervention that promotes smoking cessation and physical activity among Latinos.

D. Lara[1], E. I. Alaniz-Cantu[1], A. Chavez-Iniguez[1], D. Fuller[2], S. McIntosh[1], D. J. Ossip[1], A. Cupertino[1], **F. Cartujano-Barrera**[1];
[1]University of Rochester Medical Center, Rochester, NY, [2]University of Saskatchewan, Saskatchewan, SK, Canada

The purpose of this study was to assess the feasibility and acceptability of a mobile intervention that promotes smoking cessation and physical activity among Latinos. Twenty Latino adults who smoked and did not meet recommended levels of physical activity were recruited using community-based recruitment strategies. Participants received *Actívatexto*, a theory-based, culturally accommodated, 12-week text messaging intervention (available in English and Spanish) that promotes both smoking cessation and physical activity. *Actívatexto* integrates four components: 1) a text messaging program that promotes both smoking cessation and physical activity, 2) a wearable device to monitor physical activity, 3) an online dashboard where the research team manages participants' incoming and outgoing data from both the text messaging program and wearable devices, and 4) smoking cessation pharmacotherapy (i.e., nicotine replacement therapies). We assessed self-reported 7-day point prevalence smoking abstinence (not smoking any cigarettes in the past seven days) at Month 3, weekly minutes of moderate to vigorous physical activity (MVPA), pharmacotherapy adherence, self-efficacy, and satisfaction. At baseline, participants' mean age was 47.3 years old (SD 16.0), 55% of participants were female, 80% had completed high school or lower educational level, and 60% indicated that Spanish was their language of preference. Most participants (75%) smoked 1-10 cigarettes daily, 35% smoked their first cigarette within five minutes after waking up, and 60% used menthol cigarettes. At Month 3, 14 participants (70%) self-reported 7-day point prevalence smoking abstinence (90% follow-up rate). Fitbit-assessed mean minutes of MVPA per week increased from 113 (SD 127; range 0-399) at Week 1 to 177 (SD 163; range 0-513) at Month 3, although the difference was not statistically significant ($p=0.15$). Sixteen participants (88.9%, 16/18) reported NRT use in the past 90 days. Mean scores of self-efficacy for smoking cessation increased from 31.2 (SD 10.6) at baseline to 47.8 (SD 13.0) at Month 3 ($p<0.01$). Mean scores of self-efficacy for physical activity increased from 12.3 (SD 3.9) at baseline to 14.6 (SD 4.4) at Month 3 ($p=0.2$). Most participants reported being satisfied or extremely satisfied with the intervention (88.9%, 16/18). In conclusion, *Actívatexto* resulted in a noteworthy cessation rate at Month 3 (70%), increased mean minutes of MVPA per week, produced high use of NRT, increased self-efficacy for smoking cessation and physical activity, and was well received by participants. Additional testing in a formal randomized clinical trial is warranted to assess the efficacy of the intervention.

#2155 The impact of urban residence on symptom duration, treatment initiation, and survival among primary brain tumor patients: A large cohort analysis.

M. L. Stockdill, J. B. Vo, O. Celiku, Z. Karim, Y. Kim, H. Miller, E. Vera, T. S. Armstrong;
National Cancer Institute, Bethesda, MD

Primary brain tumors (PBT) are rare, accounting for less than 2% of all cancers, present acutely, and often require specialized care to determine treatment approaches. Neuro-Oncology clinics are located in densely populated urban areas resulting in additional access barriers, such as longer travel time, for those in non-urban areas. To better understand how proximity to our facility affects patient outcomes among PBT patients enrolled in the National Institutes of Health (NIH) Natural History Study (NCT02851706, PI: Armstrong), we assessed the association of population density with symptom duration before diagnosis, time to first treatment, and overall survival among a cohort of 666 adult PBT patients. More urbanized areas were defined as areas with a core population density of more than 1,000 persons per square mile. T-tests and chi-squared tests were performed to assess differences in patient and tumor characteristics based on population density (more urbanized vs. less urbanized). We used ordinal logistic regression (odds ratio [OR], 95% confidence intervals [CI]) to assess the association between duration of presenting symptoms (<6 months, 6 months-1 year, ≥1 year) and linear regression (beta coefficient, 95% CI) for time to treatment and population density. We adjusted for age at cancer diagnosis and sex (male, female), and results were stratified according to residential distance to the NIH (short distance=<200 miles, long distance=200+ miles), to control for local referral patterns. Kaplan-Meier estimates were used to assess overall survival by population density levels, overall, and by residential distance. All models were then further stratified by tumor grade (low, high). Among 666 patients diagnosed with PBTs, 401 (60%) lived in more urbanized areas, 40% were long distance, and 24% had low-grade tumors. Patients living in more urbanized areas were more racially diverse ($p<0.001$), had higher educational attainment ($p<0.001$), and were more likely to be single ($p=0.008$). In the overall cohort and when stratified by distance to NIH or tumor grade, there were no associations between population density level and symptom duration prior to diagnosis. Time to treatment for radiation and chemotherapy was longer for PBT patients living in less urbanized areas and longer distances from the NIH ($\beta=0.63$; 95%CI=0.08,1.17) compared to those living in more urbanized areas. There were no differences in the 5-year survival rates between more or less urbanized groups. In conclusion, access to care for those in less urbanized areas was demonstrated, although survival was not impacted. Future consideration should be given to novel approaches to increase access to specialized care, particularly for PBT patients living further from urban areas.

#2156 Exploring barriers to colorectal cancer screening among adult male immigrants in Salt Lake City.

O. O. Onigbogi, K. Kah, K. Okuyemi;
University of Utah, Salt Lake City, UT

Background: The United States (U.S) foreign-born population aged 65+ increased substantially between 1990 and 2010 with migrants from Africa and the Middle East being a part of these new refugee admissions. According to 2010 data, socioeconomic disparities and reduced access to health care is common in this population with 16 percent of foreign-born elderly living below the poverty threshold in comparison with 8 percent of U.S.-born elderly. Colorectal Cancer (CRC) is the second leading cause of cancer related deaths in the U.S despite being easily preventable and treatable. Studies among male African Americans reveal a CRC incidence >20% higher than what obtains among whites. Since, genetic factors are believed to contribute as much as 35% to the overall risk of CRC, male adult immigrants aged 45 years and above from Africa and the Middle East may be at increased risk of developing the disease. Determining CRC screening uptake in this population will be critical in planning interventions which may ultimately reduce disparities in CRC-related morbidity and mortality in the future.

Methods: We conducted a mixed methods study comprising administration of questionnaires and organizing four Focus Group Discussion (FGD) sessions among adult males in Salt Lake City who identified as refugees from Africa or the Middle East. The sessions were audio-taped, transcribed and coded using the Dedoose software.

Results: We had thirty-one participants who were between 45 and 64 years of age. Twenty-five of them (83%) reported awareness of the existence of CRC screening tests. Ten participants (33%) had undergone a CRC test in the past. However, only nine participants (30%) indicated that they will be willing to participate (WTP) in CRC screening if offered for free. Increased WTP was associated with younger age (OR=1.45, 95% CI: 1.23-1.81), length of stay in the United States (OR=1.41, 95% CI: 1.13-1.78) and higher education (OR= 1.26, 95% CI 1.13-1.37). Three major themes identified in the FGDs include: (1) Mistrust - distrust of the US health system (2) Fear - fear of cancer and nature of test and (3) Fatalism - the belief that screening cannot lead to cancer cure.

Conclusion: The low level of WTP in CRC screening tests among the respondents may be associated with past experiences. There may be a need to consider the correlates of increased WTP and explore culture-specific CRC prevention measures in planning interventions designed to improve screening uptake in this population.

#2157 Evaluating cervical and lung cancer risk among Hispanic and Non-Hispanic Black women in three urban Texas counties.

M. L. Chu, I. E. Jayesh;
University of North Texas Health Science Ctr., Fort Worth, TX

This study examines if there is a statistically significant difference in the risk of being diagnosed with cervical and lung cancer between Hispanic and Non-Hispanic Black (NHB) women in Tarrant, Dallas, and Bexar county.
Pulling from the National Cancer Institute's Surveillance, Epidemiology, and End Results (SEER) Program, 2000-2020 trends in cancer diagnosis were measured by age-adjusted annual percent change (APC). Data was sorted by county and race/ethnicity and statistically insignificant measures were removed. APC measures were ranked relative to counties across Texas and the US. APC measures with 95% confidence intervals for Hispanic and NHB women in Tarrant, Dallas, and Bexar county were compared for a significant difference. Results from a previous study indicated that the slowest decreases in cervical cancer rates are found among Hispanic and African-American women in Tarrant and Dallas County. We built upon this study to assess if there was a statistically significant difference in the risk of developing cervical and lung cancer between these two groups. In Tarrant County (TC), the cervical cancer APC of Hispanic women was -1.8 [-3.4,0.1] and NHB women was -1.2 [-3.7, 1.3]. In Dallas County, the cervical cancer APC of Hispanic women was -2.1 [-3.4, -0.8] and NHB women was -1.8 [-3, -0.5]. This indicates that for both cities, Hispanic women saw a greater decrease in the APC in cervical cancer rates than NHB women. In Tarrant County (TC), the lung cancer APC of Hispanic women was -2.7 [-4.5, -0.9] and NHB women was -2.1[-3.1, -1.1]. In Dallas County, the lung cancer APC of Hispanic women was -2.3 [-4.2, -0.4] and NHB women was -1.8 [-2.5, -1]. This indicates that for both cities, while Hispanic women saw a greater decrease in the APC in lung cancer rates than NHB women, the decrease is not statistically significant due to the overlap of the confidence intervals. Even though the confidence interval (CI) overlaps indicates insignificance, the APC can still provide valuable information regarding diagnostic trends seen in urban cities. The results showed that there is no significant difference between these two groups, suggesting that other county-level factors may play a role in diagnostic disparities seen between these two racial groups.

#2158 Emerging epidemiological cancer trends among West African adults in Zaria, Nigeria (1972 to 2022).

F. Mohammed[1], D. J. Lee[2], K. Graef[3], A. H. Rafindadi[1], S. Ibrahim[1], S. M. Aminu[1], A. Adamu[1], A. Abdullahi[1], A. M. Suleiman[1], A. Mohammed[1], J. Idoko[4], A. L. Rafindadi[1], D. A. Ameh[1], B. A. Kumo[1], A. Bello[1], A. J. Randawa[1], O. O. Adekunle[1], U. M. Aminu[1], M. Manko[1], O. T. Tajudeen[1], L. M. D. Yusufu[1], M. D. Maigatari[1], L. Khalid[1], D. Ismail[1], A. A. Babadoko[1], A. T. Lawal[1], A. A. Mohammed[1], Y. Ukwenya[1], A. Mai[1], M. Y. Hussaini[1], A. Yahaya[1], C. Bishop[3], J. Dent[3], T. R. Rebbeck[5], Y. Iliyasu[4];

[1]Ahmadu Bello University, Zaria, Nigeria, [2]Massachusetts General Hospital, Boston, MA, [3]BIO Ventures for Global Health, Seattle, WA, [4]Ahmadu Bello University Teaching Hospital, Zaria, Nigeria, [5]Dana-Farber Cancer Institute, Boston, MA

Cancer incidence and mortality rates in Africa are increasing, with sub-Saharan Africa reporting 2.7-fold higher fatality than global averages. The incidence of cancer in Africa in 2020 was about 1.1 million new cases, with 711,000 deaths, indicating a mortality-to-incidence ratio (MIR) of 0.64. These cancer challenges in Africa necessitate a concerted approach towards effective cancer control and management. Here, we present an extensive report of emerging epidemiological cancer trends among West African adults seen between 1972-2022 in Zaria, Nigeria. We used the Zaria cancer registry of the Ahmadu Bello University Teaching Hospital (ABUTH) Zaria, Nigeria to obtain information on histologically diagnosed cancers from January 1st, 1972 to December 31, 2022. Records in the Zaria registry are indexed into a register paper-based and 2008 and transferred by CanReg4 software on the computer. We used WHO classification of tumors (WHO Blue Book) 5th edition to classify all the abstracted cancers for the purpose of this study. Time-trend analyses were performed by utilizing linear regression models. In the analysis of the Zaria cancer registry, 12,114 adults (42.2% male, 57.8% female) were diagnosed with histologically confirmed cancer between 1972 - 2022. The most common diagnosis among male cancer patients was prostate cancer, comprising a quarter of all cases. The median age of diagnosis for prostate cancer was 65 years, with an interquartile range (IQR) of 60 and 70. Among female cancer patients, the most common diagnoses were cervical cancer and breast cancer, together comprising 68.2% of all cases. Median age at diagnosis were 45 (IQR, 40-56) and 42 (IQR, 35-50), respectively. In time-trend analyses, the total number of new cancer cases diagnosed at ABUTH from 1972 to 2022 increased over time ($p<0.001$). In the analyses of individual cancers, those in which the number of new cases increased over time were neoplasms of the bones and joints, breast, cervix, prostate, colorectum and stomach, head and neck ($p<0.001$); esophagus ($p=0.006$); eye and orbit and soft tissue ($p=0.002$); and ovary ($p=0.005$). Cancers in which the number of new cases decreased over time were Hodgkin lymphoma, Non-Hodgkin lymphoma, melanoma of the skin, and non-melanoma cancer of the skin ($p<0.001$). The number of new adult cancer diagnoses recorded in the Zaria cancer registry have increased over time from 1972 to 2022. Prostate cancer accounted for a quarter of all cancer cases among males, whereas cervical cancer and breast cancer accounted for nearly 70% of all cases among females. Westernization with associated change in dietary habits, physical inactivity, obesity and reproductive behaviors and changes in the population size and life expectancy may be attributable factors to change in cancer in Zaria. Better understanding of these factors will inform cancer prevention and control strategies.

#2159 Testing of an educational tool kit for the Community Genetic Navigation Engagement Specialists, COGENES, Training Program.

Yaneth L. Rodriguez, Janet Rodriguez, Charite Ricker, Julie Culver, Daisy Hernandez, Natalia Guierrez, Yvonne Cardona, Rosa Barahona, Bianca Rosales, Mariana Stern, **Lourdes A. Baezconde-Garbanati**

Keck School of Medicine of USC, Los Angeles, CA

Introduction: There is a lack of culturally sensitive materials to educate the Hispanic/Latino/a/x (H/L) community on colorectal cancer (CRC), which is the second and third leading cause of cancer deaths among H/L men and women in the United States, respectively. For these reasons, an Educational Tool Kit was created for the Community Genetic Navigation Specialists (CoGENEs) program at the Center for Optimizing Engagement of Hispanic Colorectal Cancer Patients in Cancer Genomic Characterization Studies (COPECC) at the University of Southern California (USC). CoGENES is a train the trainer program geared towards the development of a local workforce of trained community engagement specialists, promotores de salud (community health workers) that will act as liaison agents to increase knowledge and create community awareness on genetic research, clinical genetic testing, counseling, biospecimen donation and participation in clinical trials for H/Ls CRC patients, and community at large.
Methods: The Tool Kit consisted of a newly developed educational handbook focused on CRC prevention, genetics, counseling, tumor testing, and patient navigation, as well as existing materials with resources for CRC and counseling. To test the handbook, five focus groups in Spanish/English were conducted with 44 participants, recruited via community agencies/clinics serving Los Angeles. Optimization probes focused on readability, knowledge, acceptability, barriers, and recommended changes. Content analysis was conducted with focus group transcripts to inform how to optimize the handbook. A Materials Review Optimization Scorecard was developed to evaluate materials on content, literacy, graphics, layout and typography, learning, stimulation and motivation, and cultural and language appropriateness. Fifteen pieces in the handbook were each rated by three community health workers. A final suitability score was calculated for each piece.
Results: Overall, the materials were well received, and participants understood the overall main message of the materials. Feedback included refining terminology, providing additional headings and subtitles, and clarifying images to optimize the illustration of mutations. Final suitability scores from community health educators ranged from 80 to 99% for all materials, translating into “superior materials.”
Conclusion: Overall materials were well received, and they were rated as “superior materials.” Participants’ feedback from CoGENES is shared with the Engagement Optimization Unit (EOU) and Patient Engagement Unit (PEU) to optimize ongoing education and research at COPECC. The MR-OS tool will be shared with other PEU’s at other center’s to encourage it use when developing educational materials.

#2160 Utilizing geospatial analytics to identify neighborhood cancer hot spots for recruitment of underserved populations in clinical prevention research.

M. S. Lee, R. Kaiser, R. Vyas, A. Vera, D. Flores Quetant, N. Elliott, V. Bethel, A. Rivera, S. Kumar, B. Mahal, E. Franzmann, E. Kobetz;
University of Miami Miller School of Medicine, Miami, FL

Background: The term “precision public health” has increasingly been used in literature to describe public health practices that utilize new technologies and big data to precisely target the most vulnerable populations for disease control. Following the principles of precision public health, we used geospatial technologies and population-based health data to identify the locations and socioeconomic status of neighborhoods with high cancer incidences for recruitment of participants in prevention research.
Methods: Using Florida cancer registry data, geospatial hot spot analyses were carried out to identify statistically significant clusters of census tracts with high incidences of prostate, gastric, and oral cancers within the catchment area of the Sylvester Comprehensive Cancer Center in South Florida. The locations, social determinants of health (US Census’ American Community Survey), and behavioral risk factor data (CDC’s Behavioral Risk Factor Surveillance System) of these hot spots were analyzed to identify the locations of underserved communities facing high risk for these three cancers.
Results: Hot spots with high incidences for each of these three cancers overlap in many neighborhoods with high proportions of Hispanic and Non-Hispanic Black populations and high levels of socioeconomic disparities, such as low income, low education level, rental housing, no vehicles, and no access to health insurance. These neighborhoods also have high rates for behavioral risk factors in smoking, lack of physical activity, obesity, and high incidence of cervical cancer (high risk areas for HPV-associated oral cancers). Mobile screening units called the Game Changer Vehicles have been deployed to the locations to recruit participants who were tested on-site for prostate specific antigen (prostate cancer), H. pylori (gastric cancer), or solCD44 (a soluble tumor marker for squamous cell carcinoma) and total protein levels in oral rinse specimens, which can distinguish individuals with molecular features at risk for oral cancers due to tobacco, alcohol use, and human HPV infection.
Conclusions: Geospatial analyses of population health data can be used to produce metrics that precisely target neighborhoods with high cancer risk and health disparities to recruit research participants. The same precision approach can also be applied for cancer screening purposes, such as offering cervical self-sample and fecal blood test kits in disadvantaged communities facing heightened risk for cervical and colorectal cancers.

#2161 Recruitment feasibility of Hispanic women in breast cancer survivorship research using state cancer registry procedures.

E. Lee, B. Sukhu, M. Griffin, R. Griffin, N. Mercado-Almodovar, N. Utrera, K. Bello, M. Lakshmanan;
University of Central Florida, Orlando, FL

Objectives: Hispanic populations are underrepresented in epidemiologic studies. Although the Florida State Cancer Registry's primary role is cancer surveillance and control, it can also aid in population-based epidemiologic studies of cancer survivors. This study aimed to evaluate the viability of using the Florida Cancer Data System's (FCDS) patient recruitment methods to enlist Hispanic women with breast cancer for a cross-sectional survey.
Methods: During August 2023 - November 2023**,** we recruited adult (age ≥ 20) women who were diagnosed with breast cancer at least six months ago before enrollment, self-identified themself as Hispanic, and currently living in Central Florida, using state-mandated recruitment procedure which includes two invitation letters sent via mail three weeks apart and calling to non-responders after three weeks, but up to 4 times. Potential interested participants were asked to complete a survey in English or Spanish via print or online packet, providing data on demographics, health, lifestyle, and quality of life. An Excel log was used to track the response and return dates.
Results: As of October 25, 2023, we sent the invitation letters to a total of 667 participants deemed eligible per FCDS. Most of them did not respond to the letters or follow-up telephone calls, with 364 being unreachable due to incorrect contact information, which led to 303 accessible participants. The accessible sample included 22 Cubans, 73 Puerto Ricans, 65 South/Central Americans, 20 Dominicans, 39 Mexicans, and 83 Other Hispanics, with 48.7% speaking Spanish. Among the accessible participants, 113 refused to participate, 34 were not eligible, 13 have not decided yet, 118 agreed to participate but have not completed the survey yet, and 25 agreed to participate and completed the survey as of November 15. Common reasons for not qualifying included "not being Hispanic," "dead," "not living in Central Florida," "not having cancer," or "inability to read English or Spanish." The most common reasons for refusal were "too sick," "too old," or "not interested." The average response time to the first and second invitations was 20.1 and 19.6 days, respectively, and most participants responded to the second or third call within 8.3 days of the first call.
Conclusions: The FCDS can be used to recruit Hispanics for epidemiology studies. However, the state-mandated patient recruitment procedure needs improvement. For example, the procedure should collect participants' email addresses in addition to their mail and telephone numbers, allow researchers to contact participants via email instead of written mail, and remove all dead individuals before sending the contact information to researchers.
(Supported by Florida Breast Cancer Foundation Scientific Research Grant 2023 and UCF SEED grant).

#2162 Framework and pilot testing for the recruitment of a U.S.-based prospective cohort study of 100,000 Black women.

A. V. Patel, L. R. Teras, E. Kirkland, J. McCrary, H. Vins, J. E. Bontemps-Jones, E. Larbi, M. L. Hall, P. J. Briggs, D. M. Dudas, C. Lichtman, L. E. McCullough; American Cancer Society, Atlanta, GA

Background: As of 2020, 46.9 million people in the United States (14.2% of the total population) identify as Black or African American. Collectively, Black Americans have the highest cancer death rate and shortest survival of any racial or ethnic group in the U.S. The drivers of cancer and other health conditions among Black women are likely multi-level, complex, and include contributions from environmental, behavioral, community, and system-level factors. Inadequate representation in research has limited the understanding of drivers of disparate outcomes, which, in turn, has hindered our ability to identify successful, culturally appropriate strategies for intervention.

Approach: The American Cancer Society is establishing a cohort of at least 100,000 Black women to better understand cancer risk and outcomes in this population. The cohort will include two recruitment arms: (1) an “at risk” group of 85,000 participants between the ages of 25-55 years old with no prior cancer history and (2) a “survivorship” group of 15,000 participants previously diagnosed with breast, colorectal, or endometrial cancers. Pilot enrollment of the “at risk” group launched in October 2023 and will focus on understanding the disproportionate burden of early-onset cancer among Black women. For the “survivorship” group, pilot enrollment will launch in late 2024. The cancers of focus account for 95% of the absolute cancer mortality rate difference for Black vs. White women and offer the greatest opportunity for learning how to reduce cancer mortality disparities. Enrollment will focus on Black women who reside in the District of Columbia or one of 20 U.S. states representing >90% of the U.S. Black population.

Results: Approximately 200 women were successfully consented into the cohort between October-November 2023. Study activities are conducted through an online portal optimized for mobile use. Through the portal, participants confirmed eligibility by completing an electronic survey, and reviewing and signing the informed consent. Upon consent, participants will complete a baseline survey and be sent follow-up surveys twice per year for at least 30 years. These surveys will track exposures, health outcomes, and participants’ lived experiences.

Conclusions: Pilot work in 2023 demonstrated feasibility to engage Black women into a prospective cohort study. Based on the early feasibility success, full launch of enrollment is planned for May 2024.

#2163 Socioeconomic status associates with epigenetic modulation of TET2: An emerging pathway in cardio-oncology.

Sonal Sharda[1], Yvonne Baumer[1], Alina P. S. Pang[2], Abhinav Saurabh[1], Billy S. Collins[1], Valerie M. Mitchell[1], Michael J. Corley[2], Tiffany M. Powell-Wiley[3]

[1]National Heart, Lung, and Blood Institute, National Institute of Health, Bethesda, MD,[2]Department of Medicine, Division of Infectious Diseases, Weill Cornell Medicine, New York City, NY,[3]National Heart, Lung, and Blood Institute & National Institute on Minority Health Disparities, National Institute of Health, Bethesda, MD

Introduction: Adverse social determinants of health (SDOH) are known to accelerate poor outcomes in cardiovascular disease (CVD) and cancer. Clonal Hematopoiesis (CH) is a mechanism implicated in these disease states, partially driven by epigenetic regulatory genes, including *TET2*. Yet, there is not much known about how epigenetic modulations of *TET2* itself may relate to the immune system and subsequent disease development.
Hypothesis: We hypothesize that socioeconomic status (SES), as a SDOH marker, relates to epigenetic modulation of *TET2*.
Methods: 60 African American adults (93.3% female, mean age 61) with CVD risk, living in the Washington, D.C. area self-reported their SES as household income. Immune system activity was assessed via splenic activity (SpleenA) by ^{18}FDG PET/CT. Serum cytokine levels were measured by ELISA and DNA methylation analysis evaluated the epigenetic modulations of *TET2*. Multivariable regression analysis adjusted for ASCVD 10-year risk score and BMI was used to examine associations.
Results: Out of 33 *TET2* methylation sites, we found 3 sites that were significantly related to SES. Notably, only *Tet2cg09666717* (SES β=0.310, p=0.038) was also associated with SpleenA (β=-0.453, p=0.036) and several cytokines: IL-17A, IL-1β and TNFα along with trending to significance with IFN-γ (Table).
Conclusion: Thus, we found that SES associates with hypomethylation of *Tet2cg09666717*, which further related to SpleenA and inflammatory markers. Our findings are hypothesis generating and suggest that lower SES may relate to inflammation and immune system dysregulation by the way of epigenetic modulation of TET2. These results should be examined in larger, functional studies with diverse population-based cohorts to determine the potential relationships of both SDOH and epigenetic markers in CH and cardio-oncology outcomes.

Associations between TET2 methylation sites, SpleenA, SES and Cytokines in DCCNHA cohort, 2014-17

	Tet2cg09666717	Tet2cg05094833	Tet2cg10594473
SES	0.310 **(0.038)**	-0.405 **(0.006)**	-0.283 **(0.060)**
Splenic Activity	**-0.453 (0.036)**	0.004 (0.985)	0.097 (0.654)
IL-6	-0.078 (0.558)	-0.211 (0.108)	-0.222 (0.084)
IL-8	-0.199 (0.153)	0.024 (0.865)	-0.004 (0.979)
IL-17A	**-0.373 (0.010)**	0.134 (0.370)	-0.434 **(0.017)**
IL-1β	**-0.382 (0.003)**	0.042 (0.757)	-0.143 (0.275)
TNFα	**-0.456 (0.000)**	-0.157 (0.244)	0.005 (0.969)
IFN-γ	-0.258 (0.062)	-0.037 (0.790)	0.022 (0.876)

Data are presented as standardized β coefficient (p-value). All data are adjusted for 10-year predicted ASCVD risk and BMI; **ASCVD** = atherosclerotic cardiovascular disease; **BMI** = body mass index; **IL-6** = interleukin 6; **IL-8** = interleukin 8; **IL-17A** = interleukin 17A; **IL-1β** = interleukin 1 beta; **TNF**α = tumor necrosis factor; **IFN-γ** = interferon gamma

PREVENTION / EARLY DETECTION / INTERCEPTION: Role of Diet, Nutrition, and the Microbiome Across the Cancer Continuum
Poster Session

#2167 Microbial bile acid, 3-oxo-LCA, inhibits colorectal cancer progression.
F. Sun, X. Dong, M. Qi, T. Fu;
University of Wisconsin-Madison, Madison, WI

Colorectal cancer (CRC) affects a significant number of individuals each year, ranking as a leading cause of cancer-related deaths in the U.S. Bile acids (BAs), natural compounds crucial for digesting dietary fats, not only influence the gut microbiota but are also involved in gut health through their interaction with the Farnesoid X Receptor (FXR). Recent findings have highlighted certain microbiota-generated BAs like 3-oxo-lithocholic acid (LCA) and IsoLCA, modulate host immunity, hinder the expansion of intestinal pathogens, and potentially anti-aging. Despite the advancements in identifying the gut microbes behind these BAs, their precise impact on intestinal cells (IECs) and their role in disease progression are largely unexplored. Our pilot investigation unveiled 3oxoLCA as an FXR agonist, restoring FXR signaling in both cancer cells and $APC^{min/+}$ mice (a classic CRC mice model). As a result, 3-oxo-LCA inhibits the growth of both human and mouse CRC cells, such as MC38, CT26 and HCT116. Additionally, 3-oxo-LCA also restrained the intestinal stem cells (ISCs)' proliferation in organoids from both wild-type and $APC^{min/+}$ mice, and patient-derived CRC organoids (PDCOs). Remarkably, treatment with 3-oxo-LCA decreased BAs levels, improved gut barrier function, reduced tumor load, and inhibited tumor progression in $APC^{min/+}$ mice. Furthermore, 3-oxo-LCA significantly suppressed tumor growth in cancer cell-derived xenograft model mice. Crucially, the 3-oxo-LCA-FXR interaction transcriptionally regulated key apoptotic genes, encouraging cancer cell death. These discoveries highlight the therapeutic promise of incorporating 3-oxo-LCA into strategies for treating CRC.

#2168 Intermittent fasting in combination with carboplatin in a pre-clinical model of obesity-driven endometrial cancer.

J. Haag, O. Lara, C. Zhou, S. D. Hursting, V. Bae-Jump;
University of North Carolina at Chapel Hill, Chapel Hill, NC

Objectives: Endometrial cancer (EC) incidence and mortality continue to rise, with obesity a well-known driver of this disease. Obesity is associated with excess estrogen, hyperinsulinemia, activation of the Akt/mTOR pathway, chronic inflammation, and a heightened capacity to harvest dietary energy, all of which contribute to the development and progression of EC. Intermittent energy restriction (IER) is thought to have anti-tumorigenic benefits and has been shown to have synergistic effects with chemotherapy and hormonal therapy in various cancer types. Thus, we evaluated the anti-tumorigenic effects of a switch from high fat diet (HFD) to either IER or low fat diet (LFD) with carboplatin treatment in a mouse model of obesity-driven endometrioid EC.

Methods: *Lkb1*$^{fl/fl}$*p53*$^{fl/fl}$ mice were fed either HFD or LFD starting at 4 weeks of age. At 12 weeks of age, the HFD-fed mice were randomized to three treatment groups: continuous HFD, HFD-LFD switch, and HFD-IER switch. The LFD-fed mice were continuously maintained on LFD. At 16 weeks of age, all mice were injected with AdCre into the left uterine horn to induce EC development. At 26 weeks of age, mice were treated with placebo or carboplatin (50 mg/kg intraperitoneally weekly) for 4 weeks (n=8-10 mice per group). EC incidence, tumor weight, and body weight were evaluated. EC gene expression was assessed by microarray analysis.

Results: EC incidence was lowest in the HFD-IER group (~60%) and highest in the HFD group (~80%); rates were similar in the other diet groups (~75%). The continuous HFD-fed mice demonstrated a 76% increase in tumor size relative to continuous LFD-fed mice ($p<0.001$). At sacrifice and after carboplatin treatment, mean body weights were significantly higher ($p<0.05$) in the HFD group (38g) than groups receiving continuous LFD (26g), HFD-LFD switch (28g), or HFD-IER switch (21g), although mean body weights were not significantly different within diet groups between placebo and carboplatin-treated mice. In placebo-treated groups, mean tumor weights were significantly lower in mice fed continuous LFD (0.62g), HFD-LFD switch (0.60g) and HFD-IER switch (0.26g) relative to continuous HFD-fed mice (1.10 g; $p<0.001$). When comparing gene expression between the HFD-LFD and the HFD-IER placebo groups, genes related to cholesterol metabolism, estrogen response, and inflammation were preferentially up-regulated in the HFD-IER group. Carboplatin treatment reduced EC tumor size 42-69% across all diet groups ($p<0.05$); tumor size was the smallest in the HFD-IER group (0.15g) relative to mice receiving continuous HFD (0.34g), HFD-LFD (0.29g) or continuous LFD (0.34g).

Conclusion: IER with carboplatin treatment may be an innovative combination treatment strategy in the management of EC, a highly obesity-driven cancer.

#2169 Dietary inflammatory potential and mortality among patients with MAFLD.

Z. Lyu, Y. Zhang, W. Li, G. Si, **K. Chen**;
Tianjin Medical Univ. Cancer Inst. & Hospital, Tianjin, China

Background: Inflammation is important in metabolic dysfunction-associated fatty liver disease (MAFLD) development and progression. However, evidence regarding the influence of dietary inflammatory potential and mortality among people with MAFLD is rare. This study aimed to elucidate the association of the energy-density dietary inflammatory index (E-DII) with all-cause and cause-specific mortality among MAFLD patients.
Methods: Data were obtained from the National Health and Nutrition Examination Survey (NHANES) (1988-1994, 1999-2010). MAFLD was defined as the evidence of hepatic steatosis with ≥1 of the following: type 2 diabetes (T2DM), overweight/obesity (OW, BMI ≥ 25 kg/m^2), or lean metabolic dysregulation (MD). Dietary intake was assessed through 24-hour dietary recalls. E-DII scores and component intakes were divided into tertiles, with T1 as the reference. Through linkage to National Death Index by December 31, 2019, mortality from all cause, cardiovascular disease (CVD), and cancer were identified. Multivariable Cox proportional hazards regression model and restricted cubic splines (RCS) were used to analyze the association between dietary inflammatory potential and mortality among MAFLD and its subtypes patients.
Results: A total of 6537 MAFLD patients were included in the present analysis. During the median follow-up of 16.8 years, 2281 total deaths (534 cancer-related, 750 CVD-related) were documented. Compared to high dietary inflammatory potential, low dietary inflammatory potential presented a inverse association with all-cause mortality risk in MAFLD patients ($HR_{T2\ vs.\ T1}$ = 0.83, 95% CI = 0.72-0.95, $HR_{T3\ vs.\ T1}$ = 0.88, 95% CI = 0.76-1.01, P_{trend} = 0.092) and OW subtype patients ($HR_{T2\ vs.\ T1}$ = 0.77, 95% CI = 0.63-0.93, $HR_{T3\ vs.\ T1}$ = 0.76, 95% CI = 0.63-0.92, P_{trend} = 0.009). No significant benefit was observed among T2DM and MD subtype patients. Further component analysis found that eicosapentaenoic acid (EPA) (HR = 0.74, 95% CI = 0.66-0.83), docosapentaenoic acid (DPA) (HR = 0.72, 95% CI = 0.65-0.80), docosahexaenoic acid (DHA) (HR = 0.85, 95% CI = 0.65-0.80), and linoleic acid (HR = 0.86, 95% CI = 0.79-0.94) were linked with reduced cancer mortality risk in MAFLD patients. Further RCS analyses found that the effect pattern of EPA, DPA, and DHA on both all-cause and cause-specific mortality was presented as “J shaped” ($P_{non\text{-}linear}$ < 0.05). Similar results were observed for all-cause and CVD mortality among both MAFLD and OW subtype patients. When excluding participants who died within five years, consistent results were presented.
Conclusions: The findings of this study suggest that keep low-inflammatory dietary pattern, especially appropriate level of PUFAs component (EPA, DPA, and DHA) intake were associated with a lower risk of cancer mortality in MAFLD patients. These findings may inform future public health guidelines regarding specific dietary consumption, and liver-related health promotion.

#2170 Effects of folic acid supplementation on early stages of colitis-associated carcinogenesis.

Ariane Rocha Bartolomeu, Wen-Chi Chang, Lisa Vanderveer, Kristen N. Harvey, Mitchell Cheung, Harry S. Cooper, Margie Lee Clapper

Cancer prevention and control, Fox Chase Cancer Center, Philadelphia, PA

Ulcerative colitis (UC) is a chronic inflammatory bowel disease (IBD) characterized by persistent mucosal inflammation extending throughout the colon. Due to compromised intestinal surface integrity and the prolonged use of medication, individuals with UC often develop a folate deficiency, requiring folic acid (FA) supplementation. Prior findings from this group indicate that FA supplementation, at clinically relevant levels, promotes UC-associated dysplasia. Supplementation with FA resulted in an increased multiplicity of dysplasia and a significant elevation in the expression of several inflammatory genes (e.g. IL-6, Cox-2, Iκκ-β) within the colonic mucosa of mice with UC. Genome-wide expression profiling of normal and dysplastic colonic epithelial cells from mice treated with different doses of FA revealed differentially expressed genes were enriched for members of the ERK and NF-κB pathways. Subsequent *in vitro* analyses, utilizing isogenic RKO colon adenocarcinoma cells exposed to various doses of FA, demonstrated the downregulation of ERK and p-ERK in wild type (WT) $p53^{+/+}$ cells, while an increase in expression was observed in $p53^{-/-}$ cells at the protein level. The goal of this study is to investigate the role of the MAPK/ERK pathway in the development of UC-associated neoplasms. An *in vitro* model that faithfully reproduces the inflamed microenvironment in the context of WT vs. mutant p53, the putative gatekeeper of UC-associated carcinogenesis, is needed to enhance our understanding of early changes in the colon that are induced by FA and drive tumor formation. Colon organoids are being generated by isolating crypts from WT $p53^{+/+}$ and mutant $p53^{+/515A}$ mice. These organoids are then co-cultured with mouse macrophages (RAW264.7 cells) in inserts to stimulate crosstalk between the macrophages and colonic epithelial cells, as in the inflamed colon. Analyses demonstrate that the macrophages express pivotal inflammatory cytokines characteristic of UC, including IL-1β, IL-10, TNF-α, and IL-6, irrespective of the presence or absence of LPS stimulation. Co-cultured organoids and macrophages will be exposed to different concentrations of FA for various lengths of time, and the impact of treatment on the levels of ERK, p-ERK, and p65 will be assessed. The ability of p-ERK to mediate the transcriptional activation of NF-κB and its downstream effector IL-6 will also be evaluated. Subsequent investigations employing this innovative experimental model will reveal the mechanisms by which FA supplementation promotes the progression of UC-associated dysplasia. Given the potential risks associated with FA supplementation in individuals with UC, there is an urgent need to translate these results to a clinical setting. (Supported by CA262551 and the Timothy and Aurora Hughes Cancer Research Fund).

#2171 Nutritional mediators of inflammation: A cause for increased surveillance.

J. Crook[1], E. Lee[1], R. Xie[1], O. Bolajoko[2], V. Loerzel[1];
[1]University of Central Florida, Orlando, FL, [2]Mayo Clinic, Jacksonville, FL

Background: Nutritional and inflammatory factors collected in routine cancer labs, neutrophil percentage to albumin ratio (NPAR), neutrophil lymphocyte ratio (NLR), monocyte lymphocyte ratio (MLR), and platelet lymphocyte ratio (PLR), have been shown feasible in identification of patients at risk of increased treatment complications, decreased cognition, anxiety and depression, and increased mortality. These have proven sensitive to multiple cancer types and stages, though little is known about causal pathways. The Vitamin/Mineral and Inflammatory Correlations To Understand Chronic Stress in the U.S. (The VICTUS Study) sought to elucidate a relationship between diet and food insecurity within these panels.
Methods: Using NHANES 2017/2018 surveys, adults > 18 years without renal or hepatic disorders, pregnancy, alcohol, or supplement use were included. NPAR, NLR, MLR, and PLR were categorized as quartiles and compared to demographic, food security, plasma micronutrient statuses [vitamins A, B9, C, D, E, calcium (Ca), ferritin (Fe), phosphorus (P), potassium (K), sodium (Na)], and smoking, activity level, and sun exposure, using chi-square and ANOVA. ANOVA models compared food security and poverty to NPAR, NLR, MLR, and PLR means.
Results: From 3,317 participants, 50.2% were male, 54.3% non-Hispanic White, 33.7%, food insecure, 51.1% food stamp recipients, 27.7% smokers, with a mean age of 42.5 (SD 0.44), poverty to income ratio 2.79 (SD 0.08), CRP 3.90 (SD 0.18), NPAR 14.1 (SD 0.14), NLR 2.07 (SD 0.04), MLR 0.28 (SD 0.003), and PLR 118.7 (SD 1.61). CRP was found to be statistically significantly associated with all biomarker ratios ($p < 0.018$). Significant micronutrient biomarker-inflammatory biomarker associations were identified in Fe [NPAR, MLR, PLR ($p < 0.001$)], P [NPAR, NLR, MLR, PLR ($p < 0.033$)], C [NPAR, NLR ($p < 0.008$)], E [MLR, PLR ($p < 0.016$)], K [NPAR, NLR, MLR, PLR ($p < 0.015$)], Ca [NPAR, PLR ($p < 0.04$)], A [NPAR ($p < 0.023$)] and D [NLR ($p < 0.035$)]. Significant micronutrient intake-inflammatory biomarker associations were detected in vitamin A [NPAR, PLR ($p < 0.013$)], lycopene [NLR, PLR ($p < 0.035$)], and B12 [NLR, PLR ($p < 0.031$)]. Age [NPAR, NLR, MLR, PLR ($p < 0.001$)], gender [NPAR, MLR, PLR ($p < 0.001$)], ethnicity [NPAR, NLR, MLR ($p < 0.006$)], and sedentariness [MLR, PLR ($p < 0.039$)] were also associated with inflammatory markers. Poverty was significantly associated with NPAR, NLR, MLR, and CRP ($p < 0.018$). Food insecurity was significantly associated with NPAR ($p < 0.001$) and CRP ($p < 0.001$).
Discussion: Food insecurity and poverty were significantly associated with NPAR, a ratio implicated in overall poorer cancer health outcomes. Multiple inadequate micronutrient intakes and plasma biomarkers were associated with inflammatory panels, though neither nutritional biomarker nor food insecurity statuses and their contributions to inflammatory processes are routinely surveilled within cancer disease and treatment.

#2172 Associations between plant- and animal-based dietary patterns and aggressive prostate cancer in the North Carolina-Louisiana prostate cancer project (PCaP).

J. Sainyo[1], S. E. Steck[1], L. Zhao[2], L. J. Su[3], L. Arab[4], D. Turner[5], E. N. Butler[6], J. T. Bensen[6], E. T. Fontham[7], J. L. Mohler[8];
[1]University of South Carolina, Columbia, SC, [2]Harvard Medical School, Boston, MA, [3]University of Texas Southwestern Medical Center, Dallas, TX, [4]University of California Los Angeles, Los Angeles, CA, [5]Virginia Commonwealth University, Richmond, VA, [6]Gillings School of Global Public Health, University of North Carolina at Chapel Hill, Chapel Hill, NC, [7]Louisiana State University Health Sciences Center, New Orleans, LA, [8]Roswell Park Comprehensive Cancer Center, Buffalo, NY

Objective: Results of studies examining the association between a plant-based diet or animal food intake and prostate cancer have been mixed. Few studies have focused on aggressive prostate cancer in a racially diverse population. We examined the association between healthy and unhealthy plant-based and animal-based diet scores and aggressive prostate cancer in the North Carolina-Louisiana Prostate Cancer Project, a case-only study of Black and White men in the United States.
Methods: Eighteen food groups were created and classified as healthy plant foods, unhealthy plant foods, or animal foods using dietary data collected from an interviewer-administered modified version of the National Cancer Institute Diet History Questionnaire among 909 Black and 991 White men with a histologically confirmed diagnosis of prostate cancer. High aggressive prostate cancer (n=332) was defined as Gleason sum ≥8; or PSA> 20ng/ml; or Gleason sum ≥7 and clinical stage T3-T4, and the comparison group was all other prostate cancer cases (n=1,568). Logistic regression was used to determine the odds ratio (OR) and 95% confidence intervals (95% CI) for high aggressive prostate cancer by tertiles of dietary pattern scores.
Results: A decreased odds of aggressive prostate cancer was observed among men in the upper compared to the bottom tertile for healthy plant-based diet score (OR: 0.82, 95% CI: 0.58, 1.15) and unhealthy plant-based diet score (OR: 0.89, 95%CI: 0.63, 1.25) while an increased odds was observed comparing extreme tertiles of the animal-based diet score (OR: 1.17, 95% CI: 0.84-1.65) after adjustment for multiple covariates, though confidence intervals were imprecise and not statistically significant. Associations tended to be stronger among White men than among Black men; e.g., for the animal-based diet score, ORs (95% CIs) were 1.41 (0.86, 2.37) and 1.02 (0.63, 1.66) for White and Black men, respectively.
Conclusions: Consuming a plant-based dietary pattern may be associated with lower odds of aggressive prostate cancer while an animal-based dietary pattern may be associated with higher odds, though associations were weak and not statistically significant.
Keywords: Healthy plant-based diet, unhealthy plant-based diet, animal-based diet, aggressive prostate cancer, racial disparities
Conflict of interest: None
Funding: PCaP is carried out as a collaborative study supported by the Department of Defense contract DAMD 17-03-2-0052. This research was made possible in part by Grant Numbers R01-CA259415 from NIH-NCI and T32-GM081740 from NIH-NIGMS. Its contents are solely the responsibility of the authors and do not necessarily represent the official views of the NIGMS or NIH.

#2173 Effect of colored fruits and vegetables intake on gastrointestinal cancer risk: A prospective cohort study.

Y. Cho, J. Lee, M. Gunathilake, J. Kim;
National Cancer Center - Korea, Goyang-si, Korea, Republic of

Background and Aim: Diverse antioxidant compounds found in colored fruits and vegetables have been linked to various health benefits. While anthocyanins, present in purple, red, and blue pigments, and chlorophyll, responsible for green pigments, are recognized for their antioxidant properties, limited evidence exists regarding their preventive effects on gastrointestinal (GI) cancers. In the year 2020, GI cancers constituted 29% of global cancer cases. To address this gap, this prospective cohort study investigates the association between the intake of colored fruits and vegetables and the risk of GI cancer in Korea.
Methods: The Cancer Screenee Cohort, comprising adults undergoing check-ups at the National Cancer Center Korea, was analyzed for GI cancer cases diagnosed between October 16, 2007, and December 31, 2020. Of the 10,741 eligible participants, 208 developed GI cancer and 10,533 did not. General and validated semi-quantitative food frequency questionnaires were used to collect demographic data and measure dietary intake. Fruit and vegetable intake (g/day) were categorized into four groups (white, green, orange/yellow, and red/purple) based on the color of the edible parts. Analyses were conducted on total fruits/vegetables, total fruits, total vegetables, and fruits/vegetables in each color category. The intake was divided into quintiles to compare the effects of low and high intake. Cox proportional hazard models were used to estimate hazard ratios (HRs) and 95% confidence intervals (CI). HRs were adjusted for variables, including age, gender, body mass index, smoking status, alcohol drinking, education, occupation, first-degree family history of any cancer, and marital status.
Results: High total fruit and vegetable intake was associated with reduced GI cancer risk (HR = 0.64, 95% CI: 0.42-0.98, *p* for trend = 0.022). No significant associations were found for total fruits, total vegetables, fruits and vegetables together and separately in green and orange/yellow colors in this study. However, a higher intake of white fruits and vegetables was found to be effective in preventing cancer with adjusted HRs (HR = 0.51, 95% CI: 0.31-0.85, *p* for trend = 0.019). Similarly, the inverse association was observed in red and purple vegetables with adjusted HRs (HR = 0.52, 95% CI: 0.32-0.84, *p* for trend = 0.022).
Conclusions: This cohort study suggests that the consumption of fruits and vegetables in white color, as well as vegetables in red and purple colors, may have a potential protective effect against GI cancer.
Key Words: Gastrointestinal (GI) cancer; fruits and vegetables; colors of fruits and vegetables; color food; cohort studies; Korea

#2174 Sample size estimations based on human microbiome temporal stability over six months: A shallow shotgun metagenome sequencing analysis.

S. Zouiouich[1], S. Karwa[1], Y. Wan[1], E. Vogtmann[1], C. Porras[2], C. C. Abnet[1], J. Shi[1], R. Sinha[1];
[1]National Cancer Institute, Rockville, MD, [2]Costa Rican Agency for Biomedical Research-INCIENSA Foundation, San Jose, Costa Rica

Introduction: Many biological factors can influence the human microbiome; thus, it is necessary to reasonably estimate sample size to have adequate power for future population-based studies.
Methods: We evaluated the temporal stability of fecal microbial diversity, species level composition, and genes and functional pathways based on shallow shotgun metagenome sequencing from a population-based study in Costa Rica with two fecal samples separated by an interval of six months. We quantified the biological variability over six months with intraclass correlation coefficients (ICC). We then estimated the numbers of cases, assuming 1:1 or 1:3 matched case-control study, required to detect an association at significance levels of 0.05 and 0.001 with 80% power, based on the number of fecal specimens collected per participant.
Results: For most alpha and beta diversity metrics, the temporal stability of fecal microbiome in samples collected at six months of interval was low to moderate, with ICCs of 0.6 or less. We observed heterogeneity in temporal stability for the proportions of species, genes and pathways, with ICCs varying between 0.0 and 0.9. For most microbiome measures from a single fecal collection, assuming an equal number of cases and controls at significance level of 0.05 (for alpha and beta diversity) or 0.001 (for species, genes and pathways), detecting an odds ratio of 1.5 per standard deviation of microbiome metric would require hundreds to thousands of cases. Specifically, detecting an association between alpha/beta diversity metrics and an outcome would require between 1,000-5,000 cases. In addition, for low prevalent species (5% - 10%, median ICC = 0.09), 15,102 cases would be required; in contrast, for species with high prevalence (>75%, median ICC = 0.41) 3,527 cases would be necessary; the same applies to genes and pathways. For an odds ratio of 1.5, assuming a 1:3 matched case-control study based on one fecal specimen per subject, 10,068 cases would be required for low prevalent species and 2,351 cases for species with high prevalence. Using the same study setting with multiple specimens per subject over time, the required sample size would be lower. Indeed, detecting an odds ratio of 1.5 for low prevalent species would require 15,102 cases with one specimen, 8,267 cases with two specimens, and 5,989 cases with three specimens.
Conclusion: Our calculations suggest that to detect modest disease associations we would need a substantial number of cases. Repeated prediagnostic samples could decrease the number of subjects required to detect these associations as well as matching cases to a great number of controls.

#2175 Multiple exposures to antibiotics and increased risk of colorectal cancer.

N. Jani, M. Richardson, K. Hogan, M. M. Pena;
University of South Carolina, Columbia, SC

Colorectal cancer (CRC) is the second leading cause of cancer related deaths in the United States and worldwide. In 2023, approximately 153,020 individuals will be diagnosed with CRC and 52,550 will die, including 19,550 cases and 3750 deaths in patients under 50 years of age. CRC in younger patients (less than 55 years) is known as early onset colorectal cancer (EOCRC). It is a growing global phenomenon whose incidence and mortality has incidence from 11% to 20% between 1995 to 2019 and is expected to increase by 140% by 2030. While it has been linked to known and established risks for CRC, the underlying causes and mechanisms are poorly understood. Based on our current knowledge of the disease, we propose that EOCRC results from exposure of children and young adults to exposome factors that have been increasing globally in the last four decades that may impact the microbiome causing dysbiosis and inflammation in the distal colon and rectum, the anatomical site of EOCRC. Among the likely factors is the use of antibiotics, particularly in infants and children. In this study we hypothesized that early life exposure to antibiotics causes dysbiosis and inflammation in the distal colon and rectum leading to increased mutations and epigenetic events that promote EOCRC development. Specifically, we examined the effect of the most commonly prescribed pediatric antibiotics on the gut microbiota and inflammatory environment in the colon, and their impact on tumor development upon exposure to a carcinogen. We treated A/J mice with multiples rounds of antibiotics and then exposed them to azoxymethane, a carcinogen to determine the effect on tumor development in the colon. The results showed that antibiotic exposure caused dysbiosis and inflammation in the colon of antibiotic treated mice as well as systemic inflammation in mice treated with antibiotics. Treatment with azoxymethane, a carcinogen in the presence of antibiotic-induced dysbiosis led to increased tumor burden in the distal colon. These results suggest a possible involvement of antibiotics on increased risk of EOCRC.

#2176 Differences in gut microbial composition alter pancreatic tumorigenesis.

R. M. Howell, J. Enriquez Ortiz, O. Le Roux, V. Chandra, L. Li, P. K. Bhattacharya, F. McAllister;
UT MD Anderson Cancer Center, Houston, TX

Pancreatic ductal adenocarcinoma (PDAC) is predicted to become the second leading cause of cancer-related deaths by 2030, and currently has a 5-year survival rate of roughly 10%. With long-term survival rates in patients being exceedingly low, understanding what factors delineate survival is imperative. When comparing spontaneous transgenic mouse models of pancreatic cancer housed in geographically distinct vivaria, regardless of a common lineage, we observed drastically different phenotype states in the respective locations. We hypothesize that the gut microbiome results in different gene expression profiles, leading to alterations in pancreatic tumorigenesis. Using various sequencing techniques, including 16s rRNA and RNA sequencing of the gut, we identified unique signatures at these respective institutions. Subsequent fecal microbiota transplantation and single bacterial species colonization experiments were performed to evaluate the ability of microbiomes/specific microbiota to alter the rate of tumorigenesis. In addition to probing the gut microbiome, circulating metabolites from individual mice were quantified, and correlated to phenotype state. Following identification of potentially tumorigenic bacterially derived metabolites, single bacteria colonization experiments were utilized to determine the downstream effects of identified metabolites as well as the ability of directly altering the metabolic landscape to drive tumorigenesis. Additionally, murine derived pancreatic cancer cells were exposed to both identified bacteria alone or bacterially produced metabolite and analyzed by metrics such as proliferation and relative expression of transcription factors associated with cancer development *in vitro*. Taken together, these data demonstrate the ability of distinct gut microbiomes to directly alter the metabolic landscape in mice, thus differentially altering the progression of pancreatic lesions. By better understanding the factors that stratify survivorship, we can begin to employ clinically actionable methodologies in the treatment or prevention of pancreatic cancer.

#2177 Postbiotic metabolites secreted by L. acidophilus reduce DNA damage in an experimental model of Barrett's tumorigenesis.

D. Joshi, C. Andl;
University of Central Florida, Orlando, FL

The origins of esophageal adenocarcinoma (EAC) are commonly attributed to the progression from gastroesophageal reflux disease (GERD) to Barrett's Esophagus (BE) and finally to esophageal adenocarcinoma. During GERD, various types of bile induce oxidative stress and generate reactive oxygen species (ROS), resulting in DNA damage and inflammation in cells. Although there has been much research documenting the shift in the esophageal microbiome from gram-positive to gram-negative bacteria during this progression, there has also been an observed increase in the presence of Lactobacillus, a gram-positive commensal bacterium with probiotic qualities, in the esophagus during the progression from GERD to BE and eventually to EAC. Our previous research has demonstrated the ability of Lactobacillus spp. to not only colonize the esophagus under *in vitro* conditions of GERD, but also their anti-inflammatory and anti-genotoxic properties on esophageal cells exposed to bile. To assess the extent of reflux-induced DNA damage and oxidative stress during the progression of BE, we exposed two BE cell lines, CP-B and BAR-T, and the EAC cell line FLO-1 to ox bile or deoxycholic acid. Both bile types demonstrated significant increases in phosphorylated H2AX, as a marker for pronounced DNA damage repair. Next, we supplemented both live *L. acidophilus* and its postbiotic metabolites to cells exposed to ox bile and deoxycholic acid. We show a significant reduction in DNA damage as measured by pH2AX with both the live treatment and the treatment with postbiotic metabolites when compared to untreated, bile-exposed cells at various stages of BE and EAC. Ongoing experiments include assessing anti-genotoxic effects of postbiotic metabolites through DNA repair protein RAD51, reductions in oxidative stress though ROS marker 8-oxo-guanine, and anti-inflammatory effects through NFkB-associated inflammation. BE and EAC cell viability and proliferation upon bile exposure and postbiotic metabolite administration will also be assessed. This study aims to determine the supplementation with Lactobacillus postbiotic metabolites in the prevention and intervention of esophageal adenocarcinoma development.

#2178 Metagenomic analysis unveils the microbial landscape of pancreatic tumors.

S. Khan[1], G. Banerjee[2], S. Setua[3], A. Dhasmana[1], P. Banerjee[2], M. M. Yallapu[1], S. W. Behrman[4], S. Chauhan[1], D. H. Jones[5], B. Chauhan[1];
[1]University of Texas Rio Grande Valley, Edinburg, TX, [2]University of Illinois at Urbana-Champaign, Chicago, IL, [3]University of Maryland, Baltimore, MD, [4]Baptist Memorial Hospital and Medical Education, Memphis, TN, [5]University of Tennessee-Knoxville, Knoxville, TN

The composition of resident microbes in the human body is linked to various diseases and their treatment outcomes. Although studies have identified pancreatic ductal adenocarcinoma (PDAC) associated bacterial communities in the oral and gut samples, herein we hypothesize the prevalence of microbiota in pancreatic tumor tissues is different as compared to their matched adjacent, histologically normal appearing tissues and these microbial molecular signatures can be highly useful for PDAC diagnosis/prognosis. In this study, we performed comparative profiling of bacterial populations in pancreatic tumors and their respective adjacent normal tissues using 16S rRNA-based metagenomics analysis. This study revealed a higher abundance of Proteobacteria and Actinomycetota in tumor tissues compared to adjacent normal tissues. Interestingly, the Linear Discriminant Analysis (LDA) scores unambiguously revealed an enrichment of *Delftia* in tumor tissues, whereas *Sphingomonas, Streptococcus*, and *Citrobacter* exhibited depletion in tumor tissues. Furthermore, we analyzed the microbial composition between different groups of patients with different tumor differentiation stages. The bacterial genera, *Delftia* and *Staphylococcus* were very high in G1 stages (well differentiated) compared to G2 (well to moderate/moderately differentiated) and G3/G4 (poorly differentiated). However, the abundance of *Actinobacter* and *Cloacibacterium* was found to be very high in G2 and G3, respectively. Additionally, we evaluated the correlation of PD-L1 expression with the abundance of bacterial genera in tumor lesions. Our results indicated that three genus such as *Streptomyces, Cutibacterium*, and *Delftia* have a positive correlation with PD-L1 expression. Collectively, these findings demonstrate that PDAC lesions harbor relatively different microbiota compared to their normal tumor-adjacent tissues, and this information might be helpful for the diagnosis and prognosis of PADC patients.

#2179 Microbiome-derived metabolites mediate carcinogenic alterations of breast tissue in the context of obesity.

M. Gaber[1], K. Neary[1], J. Holmes[1], A. S. Wilson[1], A. J. Katz[2], P.-A. Vidi[3], K. L. Cook[1];
[1]Wake Forest University School of Medicine, Winston-Salem, NC, [2]Wake Forest Baptist Health, Winston-Salem, NC, [3]Institut de Cancerologie de l'Ouest, Angers, France

Obesity increases the relative risk for breast cancer incidence. Multiple molecular mechanisms linked to obesity drive breast cancer progression. Obesity shifts the gut microbiome in ways that may increase breast cancer risk. Microbial-associated molecular pattern (MAMP)-proteins and metabolites could directly affect breast epithelial cell signaling. In this study, we focused on lipopolysaccharide (LPS), a structural component of the outer membranes of gram-negative bacteria and a toll-like receptor 4 (TLR4)-agonist. Systemic LPS levels are known to increase in obesity. We hypothesize that chronic low-grade inflammation caused by LPS contributes to breast cancer initiation. To test this hypothesis, we first quantified levels of LPS, along with a panel of adipokines/cytokines, in serum samples from women (n= 33; BMI range= 18.3-45.3 Kg/m^2; Age range= 18-51 years). Women with elevated serum LPS had significantly higher BMI, leptin, and leptin/adiponectin ratio, confirming a link between systemic LPS and metabolic markers of obesity. Other biomarkers of breast cancer risk include DNA damage. Analyses of non-cancerous breast tissue sections from matched donors revealed higher densities of DNA double-strand breaks (estimated based on 53BP1 foci counts) in women with high serum LPS. Experiments with HMT-3522 S1 breast acini showed that LPS increases DNA break frequencies and oxidative stress levels in 3D structures of mammary epithelium. Moreover, LPS increases oxidative lesions in the DNA (estimated based on 8-oxoguanine fluorescence in MCF-10A cells) that may lead to increased LPS-mediated DNA damage. Patient obesity status was associated with alterations in oxidative modifications in the breast proteome. We also found that LPS disrupts epithelial polarity, a hallmark of breast tissue homeostasis. In mammary epithelium, LPS activates the nuclear factor-kappa B (NFκB) pathway by binding to the TLR4 receptor, leading to an increased expression of inflammatory cytokines such as tumor necrosis factor-alpha (TNF-α). Interestingly, TLR4 blockade prevented the loss of apical polarity and DNA damage induced by LPS. Last, but not least, we show an association between LPS immunogenicity (anti-LPS IgA concentrations) and participant BMI in non-cancerous breast tissue samples. These novel findings show that LPS is a key systemic and local mediator of the obesity-modulated microbiome that increases breast cancer risk. The outcomes of our study underscore the importance of considering the microbiome in the prevention of breast cancer.

#2180 Modulation of immune infiltration patterns in inflammation-associated colorectal cancer through rice bran-based dietary strategies.

R. Kumar[1], L. Bugata[1], M. Kabir[1], R. Agarwal[2], E. P. Ryan[3], **K. Raina**[1];
[1]South Dakota State University, Brookings, SD, [2]University of Colorado Denver-Anschutz Medical Campus, Aurora, CO, [3]Colorado State University, Fort Collins, CO

The correlation between gut microbiota dysbiosis and inflammation-associated colorectal cancer (CRC) has generated considerable interest in dietary interventions targeting immune modulation. Our prior study demonstrated the colon cancer protective effects of rice bran (RB) and ex vivo Bifidobacterium longum fermented rice bran (FRB) diet intervention against azoxymethane/dextran sodium sulfate (AOM/DSS)-induced CRC in gut microbiota-intact specific pathogen-free mice (SPF). RB showed higher levels of protection compared to FRB against CRC, as evidenced by diminished neoplastic lesion size and restored colonic epithelial integrity. The major objective of the present study was to leverage cutting-edge multispectral imaging technique for simultaneous detection of multiple immune cells markers and for a comprehensive analysis of distinct immune landscapes. We also performed spatial correlations within the tumor microenvironment of AOM/DSS-SPF mice undergoing RB and FRB dietary interventions. The primary focus was on T cell subtypes including cytotoxic T cells, helper T cells, regulatory T (Treg) cells, natural killer (NK) cells, NKT cells, B cells and macrophages (MΦ) subtypes (M1 MΦ, and M2 MΦ) to uncover the intricacies of the immune landscape and the interplay for CRC prevention through dietary intervention. The results indicated that RB intervention for 15 weeks led to reductions in overall T cell subtypes in the colonic tissue, particularly Treg cells, which are associated with protecting tumors against immune surveillance in CRC. On the other hand, FRB intervention also resulted in reductions in overall T cell subtypes but exhibited higher infiltration of NK cells and proinflammatory M1 macrophages in the colonic tissue after 15 weeks. While an increased presence of NK cells might be beneficial in countering CRC, the infiltration of M1 macrophages could potentially lessen the impact of FRB compared to RB intervention in CRC protection. The outcomes suggest that the better protective efficacy of non-fermented RB diets is linked to the modulation of Treg cell infiltration, whereas the efficacy of the FRB diet is to some extent limited by the presence of M1 macrophages. Overall, this study provides valuable insights into the complex immune landscape influenced by RB and FRB interventions in a murine model of inflammation-induced CRC, and a novel mechanism for the immunomodulatory effects of dietary RB interactions with gut microbiota. In the future, observing immune modulation throughout diet intervention would enhance our understanding of the role played by these immune cells.

#2181 Endocrine-targeting therapies modify the breast microbiome to shift metabolism and reduce cancer risk.

A. Arnone[1], Y.-T. Tsai[1], J. M. Cline[1], A. S. Wilson[1], B. Westwood[1], M. E. Seger[1], A. Chiba[2], M. Howard-McNatt[1], E. A. Levine[1], A. Thomas[1], D. R. Soto-Pantoja[1], K. L. Cook[1];

[1]Wake Forest School of Medicine, Winston-Salem, NC, [2]Duke University School of Medicine, Durham, NC

Studies indicate that breast tissue has a distinct modifiable microbiome population. However, whether endocrine-targeting therapies modify the non-cancerous breast microbiome to impact tumorigenesis is unknown. To examine this question, we performed 16S bacterial sequencing on DNA isolated from female C57BL/6 mouse mammary glands (MG) administered tamoxifen citrate for 16 weeks and breast tissue from ovariectomized non-human primates administered tamoxifen citrate (TAM) for 2.5 years. In both models, we show that TAM significantly shifted β-diversity and increased Firmicutes proportional abundance. TAM elevated the proportional abundance of *Lactobacillus spp.*, *Streptococcus luticea*, and *Staphylococcus sciuri*. Female BALB/c mice received intra-nipple injections of *Lactobacillus* and MG were harvested at 1-, 3-, 7-, and 14-days post-injection to show bacteria colonization and modulation of metabolism-associated gene and protein expression. B6.MMTV-PyMT mice were injected with *Lactobacillus* bacteria into the MG. Elevating MG *Lactobacillus* reduced tumorigenesis with an associated decrease in tumor proliferation and shifts in non-cancerous MG tissue metabolism. To elucidate the effects of combining TAM and probiotic bacteria on breast cancer outcomes, 4T1.2ER+ tumor-bearing female BALB/c mice, fed either a control or Western diet were treated with TAM, *Lactobacillus* probiotic, or a combination of TAM + *Lactobacillus*. Results indicate that oral probiotic administration in combination with TAM reduced ER+ tumor growth. Plasma metabolomics revealed combination treatment elevated L-carnitine regardless of diet, suggesting drug-bug interactions modifying metabolite profiles. Cell viability assays on human MCF7 BC cells and non-cancerous mammary HMT-3522S1 cells treated with 1% probiotic-conditioned media (Pro-CM) revealed a significant decrease in cell viability in BC cells but not non-cancerous epithelial cells. Mitochondrial fuel oxidation Seahorse assay on murine 4T1.2ER+ cells treated with 1% Pro-CM, 1µm 4-hydroxytamoxifen (4-OHT) or combination revealed changes in metabolic substrate dependency, supporting role of microbial metabolites impacting metabolism. Tumor sections from patients with ER+ BC treated with aromatase inhibitors and/or Faslodex in the neoadjuvant setting were stained for Gram-positive bacteria, Gram-negative bacteria, and Ki67. Gram-positive bacteria negatively correlated with Ki67 immunoreactivity, suggesting endocrine-targeting therapies promote tumor Gram-positive bacteria associated with a decrease in proliferation. Taken together, our data indicates that endocrine-targeting treatments modify the breast microbiome associated with a shift in tissue metabolism to decrease proliferation and reduce ER+ BC risk.

#2182 15-lipoxygenase-1 modulation of colonic resolvin production to suppress colorectal carcinogenesis.

X. Zuo[1], Y. Kiyasu[2], Y. Liu[1], M. Moussalli[2], B. Wei[1], P. Yang[1], I. Shureiqi[2];
[1]UT MD Anderson Cancer Center, Houston, TX, [2]University of Michigan Rogel Cancer Center, Ann Arbor, MI

Docosahexaenoic acid (DHA) and eicosapentaenoic acid (EPA) are widely used dietary supplements and FDA-approved treatments. The reported impacts of fish oil, DHA, and EPA on colorectal carcinogenesis (CRC) have spurred debates, as certain studies suggest promotional effects while numerous others emphasize suppressive effects. Nevertheless, resolvins, oxidative metabolites of EPA and DHA, exhibit the ability to inhibit crucial pathways (such as TNF-α and IL-1β) that contribute to CRC. 15-lipoxygenase-1 (ALOX15) plays a crucial role in the oxidative metabolism of DHA and EPA, ultimately leading to the formation of resolvins. However, ALOX15 expression is commonly lost during human CRC. Whether loss of ALOX15 expression modulates the effects of DHA and EPA on CRC remains to be elucidated. We therefore conducted the experiments in preclinical CRC mouse models induced by Azoxymethane or *Apc* gene mutation to explore the hypothesis that ALOX15 expression in colonic epithelial cells regulates DHA and EPA metabolism to generate resolvins, subsequently influencing CRC outcomes. We found that 1) DHA and EPA exert differential effects on CRC, which can be further modified by factors such as their formulation (e.g., ethyl ester versus triglyceride); 2) targeted transgenic expression of ALOX15 in the intestines of mice (referred to as ALOX15-Gut mice) markedly augmented the production of resolvins and concurrently suppressed CRC; 3) the predominant products from the expressed ALOX15 enzymatic activity were identified as 17-HDHA and resolvin D5; and 4) the effects ALOX15 on increasing resolvin generation and suppressing CRC were consistent across various promoters used to drive ALOX15 transgenic expression in mice. These findings collectively underscore the profound importance of ALOX15 intestinal expression as a host-related factor in resolvin generation from EPA and DHA, which subsequently contributes to the suppression of CRC.

#2183 Immunomodulation by oxaliplatin is affected by the mycotoxin food contaminants alternariol and deoxynivalenol in opposite directions.

S. Hager[1], J. Gufler[1], W. Berger[2], P. Heffeter[2], D. Marko[1];
[1]University of Vienna, Vienna, Austria, [2]Medical University of Vienna, Vienna, Austria

Our diet does not only impact our risk for cancer, but might also affect the outcome of anti-cancer therapies. While interaction of natural food constituents or supplements with anticancer therapies are frequently investigated, studies on how food contaminants, such as mycotoxins, interfere with anticancer drugs is rare or lacking, despite the rise of mycotoxin occurrence in food worldwide. As the importance of the immune system during anticancer therapies is now well known, especially mycotoxins with immunomodulatory activity, such as alternariol (AOH) or deoxynivalenol (DON), which were reported as immunosuppressive and immunostimulatory, respectively, are of great concern. Thus, the aim of this study was to investigate possible disadvantageous or beneficial interactions of the mycotoxins AOH or DON with the clinically routinely-used oxaliplatin, a known stimulator of the anticancer immune response as well as immunogenic cell death inducer. Effects of the mycotoxin-oxaliplatin combinations on cell viability of different colon carcinoma cell models were analyzed via CellTiter Blue, showing a mostly additive increase of anticancer activity with both mycotoxins. As the immune system was reported to play an important role in the anticancer activity of oxaliplatin, the combined influence of mycotoxins and anticancer therapies on immune cell stimulation was analyzed. To that end, monocytic THP-1 Lucia NF-κB reporter cells were utilized and their activation, differentiation and polarization was monitored during combinatorial treatment, via luminescence, flow cytometry and qPCR, respectively. In line with its more immunostimulatory activities, oxaliplatin alone activated NF-κB signaling in monocytic THP-1 cells. However, this increase in signaling was significantly suppressed in combination with AOH, while DON further enhanced the activation significantly. In line, during polarization of THP-1 macrophages to pro- (M1) or anti-inflammatory (M2) mediators, oxaliplatin strongly induced M1 markers (IL-8, TNF-α and COX-2) on mRNA level, not altering the NF-κB activity but partly downregulating M2 marker IL-10. This M1 stimulation was potentiated in the combination with DON, whereas AOH stimulated M2 marker expression. In conclusion, AOH was able to suppress the immunostimulatory potential of oxaliplatin, whereas DON enhanced it. Consequently, mycotoxins might affect the outcome of especially immunologically-active therapies. This should not only be considered in future risk assessment of food contaminants, but might also be a chance to fine-tune the anticancer immune response.

#2184 A high-fat diet accelerates early-stage murine pancreatic carcinogenesis by influencing, in part, mesenteric adipose tissue metabolism.

A. Ead, J. Wirkus, G. G. Mackenzie;
UC Davis, Davis, CA

Increased adiposity represents a modifiable risk factor of pancreatic cancer. Multiple preclinical studies have shown that a high-fat and high-sugar diets on the acceleration of pancreatic carcinogenesis, in the context of obesity. However, the impact of diets resembling the omega-6 to omega-3 fatty acid (FA) ratio in a Western-style diet, remains unclear. Furthermore, the role of the mesenteric adipose tissue (MAT) in pancreatic carcinogenesis is poorly characterized. Thus, we aimed to determine the impact of a high-fat diet with a ratio of 9 parts omega-6 FA to each omega-3 FA, on early stages of pancreatic carcinogenesis in a genetically engineered LSL- KrasLSL-G12D; Ptf1aCre/+ (KC) model of pancreatic cancer, with an emphasis on evaluating the contribution of the MAT within the pancreatic microenvironment. For this purpose, cohorts of male and female KC mice (6-8 males and females per diet group) were randomly assigned to either a control diet (CD) group (9:1 of omega-6 FAs to omega-3 FAs) or a high-fat diet (HFD) group (9:1 of omega-6 FAs to omega-3 FAs) and fed their respective diets until three months of age. After eight weeks on their diets, HFD-fed mice had significantly increased body weight, fat mass, and elevated serum leptin levels. Furthermore, HFD-fed mice had increased acinar-to-ductal metaplasia, associated with increased PCNA expression, ERK and STAT3 phosphorylation and elevated pro-tumorigenic immune cell expression compared to CD-fed mice. Although no significant differences in MAT weight or adipocyte size were observed after 8 weeks between the groups, metabolomics analysis of the MAT revealed that HFD-fed mice had significant upregulation of many key metabolites linked to proliferative and inflammatory pathways. For instance, HFD-fed female KC mice had significant differences in α-linolenic acid metabolism and the biosynthesis of unsaturated fatty acids, while male mice had significant differences in arginine biosynthesis, amino acid metabolism, linoleic acid metabolism, and α-linolenic acid metabolism. HFD-fed female mice had a significant increase in α-linolenic acid and linoleic acid in MAT, concurrent with a reduction in inosine 5-monophosphate and α-tocopherol compared to female CD-fed mice. HFD-fed male mice displayed a more pronounced difference in metabolites, including an increase in α-linolenic acid, linoleic acid, malic acid, glutamine, isoleucine, and several other amino acids, with a concurrent reduction in lauric acid and palmitoleic acid compared to male CD-fed mice. In summary, a HFD accelerates pancreatic carcinogenesis through multifaceted mechanisms, including effects on the tumor and surrounding adipose depots. A HFD increases affects MAT metabolism in a sex-dependent manner, that might ultimately promote early-stage progression of pancreatic carcinogenesis.

#2185 Mechanism of antitumor effects of saffron in human prostate cancer cells.

M. Khan[1], **K. Hearn**[1], C. Parry,[1], M. Rashid[1], H. Brim[1], H. Ashktorab[2], B. Kwabi-Addo[1];
[1]Howard University, Washington, DC, [2]Howard University, Bethesda, MD

Prostate cancer is the most common malignancy in men in the USA and the second leading cause of cancer deaths. Several studies have suggested the antitumor properties of saffron in many types of cancers including prostate. The objective of this study was to carry out in vitro studies of saffron-treated prostate cancer cells to ascertain the effects of saffron on key intermediates in prostate carcinogenesis. Our studies demonstrate significant inhibition of cell proliferation of androgen-sensitive prostate cancer cell lines via apoptotic pathways. We also demonstrate statistically significant down-regulation of DNA methyltransferase; COMT, MGMT, EHMT2, and SIRT1 in saffron-treated prostate cancer cells. In addition, saffron-treated prostate cancer cells displayed statistically significant dysregulation of DNA repair intermediates; WRN, p53, RECQ5, MST1R, and WDR70 in a time-dependent manner. Furthermore, Western blot analysis demonstrated that saffron treatment induced changes in the expression of other key genes; DNMT1, DNMT3b, MBD2, CD44, HDAC3, c-Myc, NF-kB, TNFα, AR, N-RAS and PTEN in prostate cancer cells. Collectively, our findings demonstrate important mechanistic targets of saffron mediating anti-tumor properties in prostate cancer. These findings suggest that the use of saffron supplements alongside standard treatment protocols may yield beneficial effects for individuals with prostate cancer.

#2186 Bacterial lung cancer therapeutics from soil bacteria in New York City.

D. Deb, T. Danino;
Columbia University, New York, NY

The microbiome's diverse functions in human health have generated increasing interest in using live bacteria for cancer therapy. Due to their natural presence in colon, lung and breast tissue, bacterial therapies have been augmented using synthetic biology in order to treat infections, inflammation, and cancer. One major challenge is finding safe and effective host species and therapeutic payloads for a particular type of cancer. Here we explored the vast diversity of microbial isolates in the environment as a valuable source of novel therapeutic compounds that can be expressed by bacteria. Specifically, we isolated and identified soil bacteria from 25 local parks, and investigated their secreted compounds for anti-cancer activity using monolayer and 3D-spheroid cultures of lung cancer. Through metagenomic analysis, toxicology assays, varied growth conditions, and bacteria-cancer co-culture experiments, we found *Bacillus spp.* isolates from Manhattan parks' soil that secreted products with high, dose-dependent cytotoxicity against lung cancer models. We also demonstrate that *Bacillus subtilis*, a model organism for gram-positive bacteria, can colonize lung cancer tumor spheroids, pointing to its use as a viable strain for bacteria cancer therapy. The work presented here underscores the potential of harnessing environmental microbial diversity for the development of gram positive species and their compounds as cancer therapeutics.

#2187 Influences of high-fat diet on tumor biology in a mouse model of colorectal cancer.

A. Mahanty, **C. Wallingford**, R. Hammontree, M. Njoka, Z. Clark, M. Rekowski, M. Washburn, J. S. Davis;
University of Kansas Cancer Center, Kansas City, KS

Purpose: To test the influence of high-fat diet on tumor biology in the inducible *Kras*, *Apc* and *p53* (iKAP) model (Boutin, et al *Genes & Development* 2017, 31:370).

Methods: At weening, both male and female mice were fed either a high-fat (60%) or low-fat (10%) diet for 5-6 weeks prior to tumor induction. Mutant *Kras* expression was controlled using a tet-on system. Expression of mutant *Kras* was activated by the addition of doxycycline hyclate in the drinking water. Tumor growth was monitored by bi-weekly endoscopy and calculated as percent luminal occlusion. Tumor biology was assessed with proteomics and phospho-proteomics with comparisons by sex and diet.

Results: In the absence of mutant *Kras* expression (no doxycycline in drinking water), tumors were larger in females on high-fat diet compared to low-fat diet. Tumor sizes were not significantly different in males or in the presence of mutant *Kras* expression. Proteomics analyses of tumor tissue identified significantly different patterns by diet in female mice, including altered levels of KIF4, DAB2iP, JNK cascade and JUN kinase activity (Table).

Conclusion: Based on our preliminary data, high-fat diet may alter tumor kinase activities, even in a genetically engineered mouse model. Replication and validation studies are ongoing.

Table of significantly upregulated biologic processes in female mice on high-fat diet compared to lo

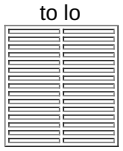

#2188 Tirzepatide treatment restores antitumor immunity in a model of obesity-driven cancer.

M. F. Coleman, E. M. Glenny, T. L. McFarlane, H. M. Malian, C. E. Gates, F. Chen, A. N. Ho, V. A. Kiesel, S. D. Hursting;
UNC Chapel Hill, Chapel Hill, NC

Obesity is a widely and increasingly prevalent disease and a risk factor for several cancers. Recent work has shown that weight loss following bariatric surgery is potently protective against obesity-associated cancers. However, little is known about the potential anticancer effects of weight loss achieved through incretin-based therapies. We therefore interrogated the effects of the dual glucagon-like peptide 1 and glucose-dependent insulinotropic polypeptide receptor agonist tirzepatide (TZP) on body weight and tumor progression in a mouse model of obesity and transplanted colon cancer cells. Moreover, we tested whether TZP-mediated weight loss can reverse obesity-associated suppression of CD8+ T cell immunity. Male C57BL/6J mice were fed either 60 kcal% fat diet (D12492) or a sucrose-matched 10 kcal% fat diet (D12450J) for ≥15 weeks to generate diet induced obese (DIO) or control mice, respectively. Once DIO mice reached a body weight of 47 g they were randomized to begin TZP treatment or receive a vehicle control every other day for 3 weeks (when stable body weights were reached for TZP mice). All mice then received subcutaneous injections with $2.5x10^5$ MC38 cells and continued to receive TZP or vehicle. To determine the role of CD8+ T cell mediated tumor control in driving the effects of TZP treatment, mice received either CD8-depleting antibodies or an isotype control at days -2, 0, 2 relative to tumor cell injection and subsequently every 4 days. Tumor mass was determined by digital scale. Fasting blood glucose, body weight loss, and body composition were monitored to determine the metabolic effects of TZP. Immune cell populations were measured by full spectrum flow cytometry. We found TZP reduced body weight, fasting blood glucose, and adiposity relative to DIO mice, as was expected. These metabolic improvements were accompanied by reduction of tumor mass in TZP mice relative to DIO mice. DIO mice had increased levels of exhausted T cells which were normalized by TZP treatment. Depletion of CD8+ cells did not alter the tumor mass of DIO mice, indicating negligible CD8+ T cell-mediated tumor control. In contrast, CD8+ cell depletion in control and TZP mice increased in tumor masses to the levels comparable to those of DIO mice. These results demonstrate that TZP can mitigate obesity-associated acceleration of tumor growth and restore markers of effective antitumor T cell immunity. Critically, we find that restoration of CD8+ T cell function is essential for TZP's ability to limit tumor growth in DIO mice. Taken together, these results demonstrate that the metabolic improvements achieved by TZP treatment are accompanied by mitigation of obesity-driven immunosuppression. These findings shed important light on the potential for TZP and other incretin-based therapies to limit obesity-associated cancer progression, and are especially timely given the growing population of patients utilizing incretin-based therapies.

#2189 Tirzepatide mitigates obesity-associated metabolic dysregulation and tumor progression in a mouse model of triple-negative breast cancer.

E. M. Glenny, A. N. Ho, V. A. Kiesel, F. Chen, C. E. Gates, E. M. Paules, R. Xu, C. Holt, M. F. Coleman, S. D. Hursting;
University of North Carolina at Chapel Hill, Chapel Hill, NC

Obesity is an established risk factor for breast cancer. Dietary and surgical weight loss interventions reduce breast cancer risk but have significant limitations to their widespread use as anticancer strategies. Incretin-based pharmaceuticals safely and effectively promote weight loss, but whether these drugs exert similar protective effects against cancer is unknown. Here we test whether weight loss induced by the glucagon-like peptide 1 (GLP-1)/glucose-dependent insulinotropic polypeptide (GIP) receptor agonist tirzepatide limits tumor growth in an orthotopic mouse model of triple-negative breast cancer. Ten-week-old female C57BL/6NCrl mice were randomized to either a 10 kcal% low-fat diet (control; n=14) or 60 kcal% high-fat diet to promote diet-induced obesity (DIO; n=43). After 18 weeks on diet, DIO mice were randomized by body weight to either i) remain on the high-fat diet (DIO; n=15); ii) lose weight with tirzepatide (TZP; n=13); or iii) lose weight with 30% daily calorie restriction relative to control mice (CR; n=15). All mice were subcutaneously injected with either TZP or vehicle every other day for 13 weeks with the following escalating dosing schedule: 3 nmol/kg TZP in week 1; 10 nmol/kg TZP in weeks 2-3; 20 nmol/kg TZP in weeks 4-7; 30 nmol/kg TZP in weeks 8-11; and 40 nmol/kg TZP in weeks 12-13. Fasting blood glucose and body composition was assessed after 9 weeks of weight loss, and 35,000 E0771 cells were orthotopically transplanted into the 4th mammary fat pad. Tumors growth was monitored for 4 weeks. TZP-treated mice lost on average >20% weight loss by week 4 and remained at or below 20% weight loss for the remainder of the study. Directly prior to E0771 tumor cell injections, TZP-treated mice had lost 23.6±8.9% body weight, versus 39.7±3.6% in CR mice. Relative to DIO mice, blood glucose control was restored in both weight loss groups (DIO: 149.5±18.5 mg/dl; TZP: 124.5±15.5 mg/dl; CR: 107.6±18.8 mg/dl) and >87.5% of the lost weight was attributed to fat mass, rather than lean mass, for TZP-treated and CR mice. Notably, tirzepatide suppressed tumor growth relative to DIO, but the CR group had a greater anticancer effect than TZP. Reduced tumor mass in both weight loss groups was accompanied by a significant reduction in circulating IGF-1, insulin, and leptin relative to DIO mice. These findings are timely and important because i) obesity is a highly prevalent metabolic disease that increases risk and progression of breast cancer and >13 other cancers; ii) incretin therapies, which show promise as highly effective weight loss drugs, are increasingly being prescribed; and iii) the tumor suppressive effects of tirzepatide described herein newly suggest incretin agonism as another propitious option for breaking the obesity-cancer link.

#2190 Transcriptomic signatures of obesity-driven colon cancer: A multi-species transdisciplinary approach.

E. M. Glenny[1], T. Lin[2], V. M. Bandera[2], B. Gigic[3], A. Tan[2], B. Mirminachi[4], S. S. Khumukcham[4], A. Carpanese[4], C. A. Warby[2], O. Aksonova[2], C. Himbert[5], J. Ose[2], C. Stubben[6], D. Nix[6], K. Boucher[2], P. Schirmacher[3], I. Strehli[2], J. Jedrzkiewicz[6], A. Brobeil[3], M. A. Schneider[3], C. Kahlert[3], E. M. Siegel[7], A. T. Toriola[8], D. Shibata[9], C. I. Li[10], J. C. Figueiredo[11], J. Roper[4], C. M. Ulrich[2], S. D. Hursting[1];

[1]University of North Carolina at Chapel Hill, Chapel Hill, NC, [2]University of Utah, Salt Lake City, UT, [3]Heidelberg University Hospital, Heidelberg, Germany, [4]Duke University, Durham, NC, [5]Harvard T.H. Chan School of Public Health, Boston, MA, [6]Huntsman Cancer Institute, Salt Lake City, UT, [7]H. Lee Moffitt Cancer Center and Research Institute, Tampa, FL, [8]Washington University, St. Louis, MO, [9]University of Tennessee, Memphis, TN, [10]Fred Hutchinson Cancer Research Center, Seattle, WA, [11]Cedars-Sinai Medical Center, Los Angeles, CA

Obesity is a highly prevalent metabolic disease and an established risk factor for colon cancer. However, critical biological pathways underpinning this relationship remain undetermined. Herein, we integrate human and murine colon tumor transcriptomic data to identify obesity-responsive pathways conserved between species. Human colon cancer samples (n=155) were collected as part of the clinical ColoCare Study, a prospective cohort study of patients newly diagnosed with colorectal cancer. Enrolled patients were diagnosed with stage I-III colon cancer and treatment naïve at time of tissue collection. Patients were classified as having a BMI <30 kg/m^2 (i.e., non-obese) or BMI ≥30 kg/m^2 (i.e., obese) at baseline. Age, sex, tumor stage, and collection site were adjusted for in all analyses. Patients were 63.3 ± 13.7 years, 51% male, and 34% had a BMI ≥30. C57BL/6J adult female mice were fed a low-fat control diet (Research Diets D12450J, n= 8) or a high-fat diet-induced obesity regimen (D12492, n=7) for ~23 weeks, at which time 700 *Apc-null;KrasG12D/+;Trp53-null;Smad4-null;tdTomato* (i.e., AKPS) organoids were orthotopically transplanted into the colonic submucosa via colonoscopy-guided injection. Obese mice weighed more than controls (controls 26.4 ± 3.7 g *vs.* DIO 45.9 ± 9.7 g) and had more mesenteric fat surrounding the colon (controls 201 ± 143 mg *vs.* 1176 ± 589 mg). Tumors were excised after 4 weeks of growth. RNA was extracted from bulk human tumor samples and from the epithelial-enriched EpCAM+ cell population in murine tumor samples for RNA sequencing. Genes differentially expressed between the reference and obese groups were identified using DESeq2. For gene set enrichment analysis, genes were preranked by log2 fold change for both human and mouse datasets. There were 76 and 132 differentially expressed genes (DEGs; FDRq<0.10) identified in the human and mouse datasets, respectively. None of these 208 DEGs were common to both datasets. Thirty-five Hallmark gene sets in the human dataset and 25 Hallmark gene sets in the mouse dataset were significantly enriched in the obese group; 18 of these gene sets were common to both mouse and human datasets. These overlapping pathways were largely related to inflammation (e.g., inflammatory response, IL6 JAK STAT3 signaling, TNFα signaling) and metabolism (e.g., cholesterol homeostasis, glycolysis, and fatty acid metabolism). Additional analysis revealed 204 genes common between the leading edges of both transcriptomic datasets. These transdisciplinary data suggest that obesity induces a set of metabolic and inflammatory processes and/or pathways in colon tumors which is conserved between mice and humans. Future studies will mechanistically evaluate the role of candidate genes and pathways in obesity-associated colorectal carcinogenesis in our AKPS orthotopic organoid transplant mouse model.

POPULATION SCIENCES: Diet, Alcohol, Tobacco Use, and Other Lifestyle Risk Factors
Poster Session

#2194 Association of metabolic syndrome conditions with risk of second primary cancer of any organ in breast cancer survivors.

A. Mukherjee[1], Z. Gu[1], L. Chen[1], A. Potosky[2], R. Haque[1];
[1]Kaiser Permanente - Southern California, Pasadena, CA, [2]Lombardi Comprehensive Cancer Center, Georgetown University Medical Center, Washington DC, DC

Purpose: Breast cancer survivors are at increased risk of developing second primary cancers; however, factors attributing to increased risk of second primary cancer in breast cancer survivors are under-studied. We evaluated the association of metabolic syndrome conditions with second primary cancer of any organ in breast cancer survivors.
Methods: In this retrospective cohort study, we included 37,222 patients diagnosed with breast cancer between 2008-2020 at Kaiser Permanente Southern California (KPSC), an integrated healthcare system. We extracted data on cancer-related variables, sociodemographic and clinical variables from KPSC's cancer registry and electronic health records. Among the metabolic conditions, we identified diabetes, hypertension, and dyslipidemia using ICD-10 diagnosis codes at or 1-year prior to breast cancer diagnosis; obesity was based on body mass index (BMI≥30kg/m^2). We included metabolic syndrome as a categorical variable: 0, 1-2, and 3+ metabolic conditions. We followed patients electronically from breast cancer diagnosis until patients developed second primary cancer of any organ, died, disenrolled from the health plan, or reached study's end (12/31/2021), whichever occurred first. Proportional hazards regression was used to report association [HR (95%CI)] between metabolic conditions and any second primary cancer.
Results: During a median (IQR) follow-up of 5.17 (2.75-8.58) years, 1701 (4.6%) patients developed any second primary cancer. More than half (53.1%) of the breast cancer survivors had 1-2 metabolic conditions at baseline; 19.4% had 3+ metabolic conditions, and the rest 27.5% did not have any metabolic condition. Hypertension was the most common metabolic condition (45.5%), followed by obesity (38.9%), dyslipidemia (36.5%), and diabetes (19.0%). Survivors with 0 and 1-2 metabolic conditions were 35% and 19% less likely to develop any second primary cancer than survivors with 3+ metabolic conditions, respectively [crude HR (95%CI): 0.65 (0.57-0.75) and 0.81 (0.72-0.91), respectively]. Reduced risk in survivors with 1-2 metabolic conditions persisted adjusting for age, race and ethnicity, breast cancer diagnosis year, breast tumor SEER summary stage, breast tumor estrogen-progesterone status, smoking status, and breast tumor treatment [adjusted HR (95%CI): 0.87 (0.77-0.99)].
Conclusion: Risk of second primary cancer of any organ was elevated in breast cancer survivors with three or more metabolic conditions.

#2195 Intrauterine device use and risk of invasive epithelial ovarian cancer: A population-based case-control study.

Minh Tung Phung[1], Yuting Wang[2], Alice W. Lee[3], Malcolm C. Pike[4], Anna H. Wu[5], Celeste Leigh Pearce[1]

[1]University of Michigan, Ann Arbor, MI,[2]Dartmouth College, Hanover, NH,[3]California State University, Fullerton, Fullerton, CA,[4]Memorial Sloan Kettering Cancer Center, New York, NY,[5]University of Southern California, Los Angeles, NY

Introduction: Ovarian, fallopian tube, and primary peritoneal cancers (hereafter referred to as ovarian cancer) are the most fatal gynecologic cancers. Thus, it is imperative to identify strategies that can reduce the risk of the disease. Several contraceptive methods have been shown to be associated with a reduced risk of ovarian cancer, including combined oral contraceptives, injectable progestins, and tubal ligation. However, the use of these contraceptive methods has been decreasing in the U.S., with a growing preference for intrauterine devices (IUDs) for pregnancy prevention. Previous case-control studies on the association between IUD use and ovarian cancer risk have found inconsistent results. Notably, previous studies had small sample sizes and did not restrict to invasive epithelial tumors. The current analysis assessed the association between IUD use and risk of invasive epithelial ovarian cancer in a large population-based case-control study.

Methods: This analysis used data from 1,713 people diagnosed with primary invasive epithelial ovarian cancer (cases) and 2,348 cancer-free people (controls) participating in a case-control study conducted in Los Angeles, CA from 1992-2010. The study consisted of four waves of recruitment with similar enrollment and data collection methods. Logistic regression models were fit to assess the association between IUD use and risk of invasive epithelial ovarian cancer. All models were adjusted for age, race/ethnicity, education, first-degree family history of ovarian cancer, endometriosis, body mass index, duration of combined oral contraceptive use, parity, duration of breastfeeding, tubal ligation, and study wave. Heterogeneity across the study waves and the ovarian cancer histotypes was evaluated using standard meta-analysis techniques.

Results: There was no statistically significant association between IUD use and risk of invasive epithelial ovarian cancer (odds ratio=1.09, 95% confidence interval 0.93-1.28). This result was consistent across the study waves and the ovarian cancer histotypes (p-values for heterogeneity>0.05).

Conclusion: IUD use was not associated with the risk of invasive epithelial ovarian cancer. Analysis by IUD type (i.e., hormone-releasing vs copper IUDs) was not possible in this study as these data were not collected. Future research should examine whether the type of IUD (i.e. copper versus hormone-releasing) may have different effects on risk of ovarian cancer.

#2196 Susceptibility to tobacco use among rural adolescents: Examining the role of tobacco marketing exposure and media use intensity.

S. J. Kim[1], K. Fugate-Laus[1], J. Barsell[1], E. K. Do[2], R. Hayes[1], D. Wheeler[1], B. Fuemmeler[1];
[1]Virginia Commonwealth University - VCU, Richmond, VA, [2]Truth Initiative Schroeder Institute, Washington, DC

Background: Rural youth have higher rates of electronic nicotine delivery systems (ENDS) and tobacco product use compared to their urban counterparts. Prior literature confirms that marketing exposure increases pro-tobacco attitudes and susceptibilities, yet the extent to which tobacco product marketing and advertising messages relate to tobacco use susceptibility among rural adolescents is understudied.
Objectives: To examine the association between tobacco marketing exposure and susceptibility to tobacco use and ever tobacco use among a population of rural youth.
Methods: Youth (aged 14-18 years), enrolled in grades 9-11, able to speak and write in English, and residing in rural counties in Virginia (n = 697) were recruited to participate in the Southern Virginia - Adolescents, Place, and Behavior study. At baseline, eligible participants were asked to answer survey questions, including demographics (e.g., age, race/ethnicity, and gender), tobacco product (e.g., e-cigarettes/vapes, cigarettes, and cigars), tobacco use susceptibility (e.g., “do you think you will try any type of tobacco product in the next year?”), digital media use (e.g., “how many hours do you spend visiting social networking sites on both a typical weekday and a typical weekend day?"), and interaction and exposure to tobacco advertisements.
Results: The majority of participants were female (51.9%), White (62.4%) and non-Hispanic (86.6%), with an average age of 15.1 years old (*SD* = .96). Less than a quarter (20.7%) of participants reported ever using any tobacco products. Heavy social media users and text users were more likely to be tobacco ever-users than those who were light social media users, $X^2(1) = 12.00$, $p < .001$. Multivariate logistic regression models report that exposure to online ads promoting tobacco products (OR: 2.03, 95% CI [1.37 - 3.03]) and higher grade level (OR: 1.77, 95% CI [1.29 - 2.43]) were significantly associated with the likelihood of ever using tobacco products, while controlling for mother’s education, gender, and ethnicity. Among adolescents who never used tobacco products, higher grade levels (OR: 1.40, 95% CI [1.05 - 1.86]) were associated with greater susceptibility to initiating tobacco product use while controlling for the covariates.
Conclusions: Greater social media use and exposure to ads promoting tobacco products were significantly associated with tobacco ever use. For never tobacco users, social media use or tobacco ad exposure was not associated with greater susceptibility to tobacco use. Higher grade levels were associated with both tobacco ever use and greater susceptibility to tobacco product use. Identification of these risk factors may help inform potential targets for future tobacco prevention campaigns.

#2197 Weight history and colorectal cancer risk in the Cancer Prevention Study-3 cohort.

C. Y. Um[1], C. C. Newton[1], A. Parikh[2], M. L. McCullough[1], A. V. Patel[1];
[1]American Cancer Society, Atlanta, GA, [2]Massachusetts General Hospital Cancer Center, Boston, MA

While the link between obesity and colorectal carcinogenesis is established, limited evidence suggests that early-life overweight/obesity may be an important consideration, particularly in the development of early-onset colorectal cancer (CRC). Using data from the American Cancer Society's Cancer Prevention Study-3 (CPS-3), we investigated the association of body weight across the life course and risk of CRC.

From 2006-13, over 300,000 participants (ages 30-65) enrolled in the CPS-3 cohort and provided a baseline waist circumference (WC) measure, self-reported baseline weight and height, weight at age 18, and weight at each decade of adulthood (20s to current age). Body shape phenotype (apple, pear, other) was self-reported in 2015. Excess body mass index (BMI)-years was calculated by subtracting a reference BMI of 25 from the reported BMI for each decade of life and aggregating excess BMI for the reported years of life. Through 2018, 424 incident cases of colorectal cancer were reported, of which 94 were younger than 50 years. Associations of BMI measures and WC with incident CRC were estimated using multivariable-adjusted Cox proportional hazards regression and stratified by sex and body shape.

After exclusions (n=248,804), 78% of participants were women, 85% were non-Hispanic white, 69% were never smokers, and 8% had a family history of CRC. The mean baseline age was 47.8 (women) and 48.5 (men) years. The mean baseline BMI, WC, and age 18 BMI were 27.6 kg/m^2, 91.9 cm, and 21.7 kg/m^2, respectively, among women and 28.3 kg/m^2, 103.8 cm, and 23.1 kg/m^2, respectively, among men. Baseline BMI was associated with 8% higher CRC risk (95% confidence interval (CI) 0.99-1.18) per 5 kg/m^2 increase. However, apple body shape was associated with higher CRC risk (hazard ratio (HR) per 5 kg/m^2 BMI = 1.18, 95% CI 1.02-1.38). WC was associated with higher CRC risk (HR 1.08, 95% CI 1.01-1.15) per 10 cm increase, and the association was higher for apple body shape (HR 1.14, 95% CI 1.01-1.28). BMI at age 18 was associated with 17% higher CRC risk (95% CI 1.03-1.32) per 5 kg/m^2 increase, and the association was higher for apple body shape (HR 1.36, 95% CI 1.12-1.65). Associations for non-apple body shapes were not statistically significant across all exposures. For early-onset CRC, associations with baseline BMI, WC, and age 18 BMI were suggestive of higher risk but not statistically significant. Participants in the highest category of excess BMI-years (women ≥35, men ≥81) relative to those in the lowest had 56% higher risk of overall CRC (95% CI 1.19-2.05), but the association with early-onset CRC was not statistically significant (HR 1.92, 95% CI 0.90-4.07).

These findings suggest that while obesity is associated with higher CRC risk, excess weight gain around the waist and at younger ages may be of importance. Studies are needed to confirm these findings and further investigate the potential role of early-life obesity in the development of early-onset CRC.

#2198 Poverty, food insecurity, and nutritional inflammatory mediators of allostatic load.

J. M. Crook[1], E. Lee[1], O. Bolajoko[2], R. Xie[1];

[1]University of Central Florida, Orlando, FL, [2]Mayo Clinic, Jacksonville, FL

Background: Though widely recognized in cancer pathogenesis, inflammatory pathways of allostatic load remain vaguely understood. A partial explanation may be found within the realm of food insecurity and micronutrient inadequacies, defined as nutrient intake less than the estimated average requirement. Many micronutrient deficiencies contribute to pro-inflammatory and immunocompromised milieus. Inadequacies, however, which may present without overt symptoms, are not currently well studied. The purpose of this study was to examine relationships between known inflammation-associated nutritional biomarkers of micronutrients and biomarker variables of allostatic load.

Methods: Using NHANES 2017/2018 surveys, adults > 18 years without renal or hepatic disorders, pregnancy, alcohol, or supplement use were included. Plasma levels of vitamins A, B9, C, D, E, calcium (Ca), ferritin (Fe), phosphorus (P), potassium (K) and sodium (Na) were grouped into deficiency, inadequate and adequate groups based on clinically recognized standards. Micronutrient prevalence was assessed and variables of allostatic load [blood pressure, glucose, albumin, creatinine, red cell distribution width (RDW), high density lipoprotein (HDL), low density lipoprotein (LDL), cholesterol and triglycerides] were analyzed for mean differences among micronutrient groups, food security and poverty.

Results: From 3,317 unique participants, inadequacy prevalence percentages were quantified as: vitamins A (0.4%), B9 (12.2%), C (58.3%), D (39.6%), E (21.0%), P (11.4%), K (3.4%), Na (24.2%), Ca (59.5%), and Fe (37.4%) [$p < 0.001$]. Statistically significant differences were identified in age [C, D, E, Ca, Fe, P, Na ($p < 0.004$)], race/ethnicity [B9, C, D ($p < 0.006$)], gender [C, E, Ca, Fe, P, K, Na ($p < 0.018$)], poverty [A, B9, C, D, E, Fe, K ($p < 0.025$)], and food security [B9, C, D, E, P ($p < 0.032$)]. Associations to allostatic load were discovered in: albumin [A, C, D, Ca, Fe, P, Na ($p < 0.025$)], glucose [C, E, Fe, P, Na ($p < 0.009$)], HDL [C, D, E, Fe, P, K ($p<0.045$)], LDL [E, Ca, Fe, Na ($p<0.028$)], creatinine [C, D, Ca, Fe ($p<0.001$)], triglycerides [B9, D, E, Fe ($p<0.033$)], cholesterol [C, D, E, Ca, Fe, Na ($p<0.006$)], B/P [C, E, Fe, P, Na ($p < 0.035$)], and RDW [C, D, Ca, Fe ($p < 0.001$)]. Poverty was significantly associated with all variables of allostatic load ($F = 2.85$, $p = 0.002$). Food security was significantly correlated with albumin ($p < 0.001$), glucose ($p = 0.005$) and HDL ($p < 0.001$).

Conclusion: Allostatic load, poverty, and food security were significantly associated with subclinical micronutrient statuses, which may not present with signs of deficiency and are not currently well assessed. Similarly, poverty was significantly associated with all variables of allostatic load, though food security was only identified to be associated with albumin, glucose, and HDL, suggesting that food security may not be currently adequately defined for surveillance.

#2199 Low-carbohydrate diet score and risk of bladder cancer: Findings from the Singapore Chinese Health Study.

Y. T. Pham[1], R. Wang[1], A. Jin[2], W.-P. Koh[2], J.-M. Yuan[1], H. N. Luu[1];

[1]University of Pittsburgh, Pittsburgh, PA, [2]National University of Singapore, Singapore, Singapore

Background. Bladder cancer is a leading tumor of urinary tract with annually 570,000+ new cases and 200,000+ deaths worldwide. In the United States, the current incidence rate of bladder cancer is 15.8 per 100,000 population with more than 82,000 new cases and more than 16,000 deaths each year. Although smoking is established as a major risk factor for bladder cancer development, accounting for 30-50% cases, the role of other modifiable risk factors, including dietary in bladder cancer remains unclear. Low-carbohydrate diet (LCD) is a dietary pattern to restrict carbohydrate and to favor protein and/or fat intakes that has recently been well-accepted for weight loss. While its short-term effect to support the weight loss has been popular, its long-term effect on chronic diseases, including cancer, needs to be elucidated. In the current analysis, we sought to determine the association between LCD scores and bladder cancer risk in the Singapore Chinese Health Study (SCHS), an ongoing prospective cohort study consisting of more than 63,000 Chinese Singaporeans, 45- 74 years of age at baseline enrollment period 1995-1998.

Methods. Total, animal-based and plant-based LCD scores were derived from the baseline dietary survey data, representing summed intake of carbohydrates, fats and proteins from all dietary, animal- and plant-food sources, respectively. Bladder cancer cases were ascertained using cancer registry. Cox proportional hazard regression model was used to calculate hazard ratios (HRs) and 95% confidence intervals (CIs) for different LCD score levels with risk of bladder cancer.

Results. By December 31, 2015, or after 17.6 years of follow-up, 250 bladder cancer cases were developed within the SCHS. Total LCD score was marginally associated with increased risk of bladder cancer ($HR_{Q4vs.Q1}$=1.43, 95% CI: 0.98-2.09, P_{trend} = 0.06). Animal-based LCD score was significantly associated with risk of bladder cancer. The HRs and respective 95% CIs of bladder cancer for quartiles 2, 3, and 4, compared with the lowest quartile, were 1.09 (0.76-1.56), 1.17 (0.81-1.70), and 1.53 (1.09-2.17) (P_{trend}=0.01). The positive association was only present in men, ever smokers, never drinkers and individuals without history of type 2 diabetes (All $P's_{heterogeneity}$>0.05).

Conclusions. In a prospective cohort study of more than 63,000 Chinese Singaporeans, we found that animal-based LCD score, representing a diet with lower carbohydrate and higher animal fat and protein, was significantly associated with increased risk of bladder cancer. Dietary modification is therefore suggested as an effective strategy for primary prevention of bladder cancer.

#2200 Plant-based diet and survival among patients with metastatic colorectal cancer: Findings from CALGB/SWOG 80405 (Alliance).

E. Cheng[1], F.-S. Ou[2], C. Ma[3], A. P. Venook[4], H.-J. Lenz[5], E. M. O'Reilly[6], P. T. Campbell[1], C. Kuang[1], B. J. Caan[7], K. Ng[3], J. A. Meyerhardt[3]; [1]Albert Einstein College of Medicine, Bronx, NY, [2]Mayo Clinic, Rochester, MN, [3]Dana-Farber Cancer Institute, Boston, MA, [4]University of California, San Francisco, San Francisco, CA, [5]University of Southern California, Los Angeles, CA, [6]Memorial Sloan Kettering Cancer Center, New York, NY, [7]Kaiser Permanente Northern California, Oakland, CA

Background: Plant-based diet is recommended by multiple cancer survivorship guidelines and was reported to be associated with better survival among patients with non-metastatic colorectal cancer. However, the association between plant-based diet and survival in metastatic colorectal cancer is unknown.
Methods: Using an NCI-sponsored systemic therapy trial conducted from 2005 to 2015 (CALGB/SWOG 80405), we included 1,279 patients who completed validated food frequency questionnaires at the initiation of treatment for metastatic colorectal cancer. To emphasize different impact of healthful plant foods, less healthful plant foods, and animal foods, we used 18 food groups to calculate three plant-based indexes (ranges: 18-90 points): overall plant-based diet index (PDI), healthful plant-based diet index (hPDI), and unhealthful plant-based diet index (uPDI). The primary outcome was overall survival, and the secondary outcome was progression-free survival. We estimated the associations of three indexes (quintiles) with survival using multivariable Cox proportional hazards regression.
Results: Of 1,279 patients (median follow-up: 6.1 years), mean (SD) age at diagnosis was 58.8 (11.7) years, 57.4% were men, 85.6% were White, and 1,096 deaths and 1,201 events of progression occurred. The mean (SD) points of three indexes were 51.2 (6.3) for PDI, 51.1 (6.7) for hPDI, and 51.2 (8.1) for uPDI. Compared to the lowest quintile (Q1), the highest quintile (Q5) of PDI was significantly associated with better overall survival (HR: 0.80 [0.65-0.99]) and progression-free survival (HR: 0.80 [0.65-0.98]). Similar findings were observed for hPDI, but uPDI was not significantly associated with worse survival.
Conclusions: Our findings suggest that plant-based diet is associated with better survival among patients with metastatic colorectal cancer, and plant-based dietary interventions should be considered for future trials in metastatic colorectal cancer.

Table. Adjusted Associations of Plant-Based Diet with Survival in Metastatic Colorectal Cancer

	Q1	Q2	Q3	Q4	Q5	P for trend
Overall Survival						
PDI	1.00	0.96 (0.80-1.16)	0.93 (0.77-1.14)	0.82 (0.67-0.99)	0.80 (0.65-0.99)	0.01
hPDI	1.00	0.95 (0.78-1.14)	0.94 (0.77-1.15)	0.86 (0.70-1.04)	0.84 (0.68-1.03)	0.07
uPDI	1.00	1.14 (0.95-1.39)	1.07 (0.87-1.31)	1.18 (0.97-1.45)	1.17 (0.95-1.45)	0.15
Progression-free Survival						
PDI	1.00	0.84 (0.70-1.01)	0.94 (0.78-1.14)	0.93 (0.77-1.12)	0.80 (0.65-0.98)	0.10
hPDI	1.00	0.86 (0.72-1.03)	0.83 (0.69-1.01)	0.80 (0.67-0.97)	0.80 (0.66-0.97)	0.03
uPDI	1.00	1.12 (0.94-1.34)	1.11 (0.91-1.34)	1.10 (0.91-1.34)	1.15 (0.94-1.41)	0.23

#2201 Population attributable fraction of alcohol consumption on cancer incidence in 2020 in the Republic of Korea.

Y. Min[1], Y. Park[1], **S. Byoun**[1], S. Park[2], K. Ko[3], S.-S. Sung[2], N. Kim[4], K. Jung[4], S. Jee[4], S.-I. Cho[5], M. Lim[6], S. Park[7], E. Park[8], H. Woo[9], K.-W. Jung[1], E. Yun[1], B. Kim[1], J.-K. Oh[1], Y. Choi[1], B. Park[1], H. Seo[1], Y.-J. Choi[1], J.-S. Im[1];

[1]National Cancer Control Institute, National Cancer Center, Goyang, Korea, Republic of, [2]Department of Preventive Medicine, Seoul National University College of Medicine, Seoul, Korea, Republic of, [3]Clinical Preventive Medicine Center, Seoul National University Bundang Hospital,, Seongnam, Korea, Republic of, [4]Department of Epidemiology and Health Promotion, Institute for Health Promotion, Graduate School of Public Health, Yonsei University, Seoul, Korea, Republic of, [5]Graduate School of Public Health and Institute of Health and Environment, Seoul National University, Seoul, Korea, Republic of, [6]Department of Social and Preventive Medicine, College of Medicine, Inha University, Incheon, Korea, Republic of, [7]Department of Biostatistics, Graduate School of Public Health, Yonsei University, Seoul, Korea, Republic of, [8]Preventive Medicine Department, Korea University College of Medicine, Seoul, Korea, Republic of, [9]Department of Precision Medicine, Korea National Institute of Health, Korea Disease Control and Prevention Agency, Cheongju, Korea, Republic of

Backgrounds: Alcohol consumption is the Group I carcinogen according to International Agency for Research on Cancer (IARC). In 2009, National Cancer Center Korea reported that 3.0% and 0.5% of total cancer incidence were attributable to alcohol consumption in men and women, respectively. Herein, we estimated population attributable fraction (PAF) of cancer incidence due to alcohol consumption as of 2020.

Methods: We organized the Consensus Committee to establish strategy and methodology of PAF estimation. Based on the consensus, cancer sites for PAF estimation were selected according to the IARC List of classification with sufficient evidence in human. PAF was calculated by using Levin's formula which incorporates exposure prevalence and relative risk (RR). Exposure prevalence was obtained from the Korea National Health and Nutrition Examination Survey (KNHANES) in 2005, assuming that latent period between exposure to alcohol consumption and diagnosis of cancer would be 15 years. Alcohol consumption was defined as non-drinking (<0.1g/day), light (0.1~30g/day), moderate (30~60g/day), and heavy (60~588g/day) drinking according to the definition by World Health Organization. We estimated RRs from the cohort data established by Korean Genome and Epidemiology Study, National Health Examination data provided by National Health Insurance Services, Korean Cancer Prevention Study-II, and KNHANES, while each cohort was linked with Korea Cancer Registry. RRs were estimated by using Cox proportional hazards model adjusted by age group and smoking status. RRs were then meta-analyzed to yield pooled RR by using random-effects model.

Results: A total of 4.1% and 1.2% of all cancer incidence were attributable to alcohol consumption in men and women. By cancer sites, 67.1% of esophageal cancer, 23.8% of oral cavity/pharyngeal cancer, 15.1% of laryngeal cancer, 12.0% of colorectal cancer, and 7.9% of liver cancer were attributable to alcohol consumption in men. In women, 54.1% of liver cancer, 10.3% of colorectal cancer, 7.8% of oral cavity/pharyngeal cancer, and 3.6% of breast cancer were due to alcohol consumption.

Conclusion: PAF of cancer incidence due to alcohol consumption has increased in 2020 compared to PAF in 2009. As alcohol consumption is an important cause of oral cavity/pharyngeal, esophageal, and laryngeal cancer in men, and liver and breast cancer in women, prevention measures are required to reduce alcohol consumption for cancer prevention in Korea. Funding Sources: This work was supported by the National Cancer Center Grant(NCC-2210840).

#2202 Association of multi-morbidity with incident cancer diagnoses.

M. C. Conroy, G. K. Reeves, N. E. Allen;
University of Oxford, Oxford, United Kingdom

Background: Multi-morbidity (MM), which is usually defined as a simple count of the number of different diseases an individual has, has previously been identified as a risk factor for some incident cancer diagnoses. This study aimed to use more sophisticated machine learning techniques to classify MM into disease clusters and to investigate their association with incident colorectal (CRC), breast (BC), lung (LC) and prostate (PrC) cancer diagnoses.
Methods: Participants in UK Biobank with a hospital (HES) record and no prevalent cancer were included in the study. Self-reported (SR), HES and primary-care (GP) recorded diseases were converted to phecodes. Sex-stratified latent class analyses (LCA) was used to identify disease clusters in the SR data. Associations between clusters and selected cancer diagnoses was undertaken using Cox proportional hazards modelling, adjusting for age, ethnicity, socio-economic status, year and region of recruitment, body mass index, smoking history, alcohol consumption and menopausal hormone therapy use (women only). The analyses were validated using HES and GP data.
Results: The analysis included 158,951 women and 127,406 men. Just over 30% (49,061) of women and 37% (48,110) of men had MM (≥2 diseases) at recruitment. LCA identified 10 disease clusters in women, the most common of which was related to respiratory disease, largely comprising asthma (9344; 19.1%). Nine disease clusters were identified in men, the most common of which was related to heart disease (9358; 19.5%), and largely comprising ischemic heart disease and hypertension. No association between disease cluster and incident CRC or BC was identified. In women, LC risk was associated with several disease clusters: respiratory (Hazard Ratio 1.57 (95% confidence interval 1.28 - 1.91) p<0.001), arthritis/gut (1.46 (1.15 - 1.85) p=0.002), hyperlipidemia (1.51 (1.19 - 1.92) p=0.001, cardiac (1.74 (1.40 - 2.17) p<0.001) and type 2 diabetes (T2DM) (1.56 (1.16 - 2.09) p=0.003). In men, LC was associated with disease clusters of hyperlipidemia/ hypertension (1.23 (1.02 - 1.48) p=0.03), cardiac (1.40 (1.18 - 1.66) p<0.001), T2DM (1.26 (1.02 - 1.56) p=0.03), respiratory (2.74 (2.21 - 3.39) p<0.001) and cardiometabolic/arthritis (1.81 (1.08 - 3.03) p=0.02). T2DM (0.80 (0.68 - 0.87) p<0.001) was associated with an inverse risk of PrC. Cluster distribution was similar in HES and GP data, with the association between the cardiac and the arthritis clusters replicated for LC in women, and the respiratory cluster for LC and T2DM cluster for PrC in men.
Conclusion: Clusters of MM were identified in a large cancer-free population, which were replicated using different sources of healthcare data. Several disease clusters were associated with incident LC and, to a lesser extent, PrC. Further work to understand the potential causal nature of these associations is needed.

#2203 Dietary patterns and prostate cancer risk in the Multiethnic Cohort Study.

W. Xiong[1], S.-Y. Park[2], A. Wang[3], P. Wan[1], L. R. Wilkens[2], L. L. Marchand[2], C. A. Haiman[1], F. Chen[1];
[1]USC - University of Southern California, Los Angeles, CA, [2]University of Hawaii Cancer Center, Honolulu, HI, [3]Harvard T.H. Chan School of Public Health, Boston, MA

Background: A growing body of research has shown the benefits of a healthy diet on a variety of cancer outcomes. Evidence is inconsistent for prostate cancer and research in diverse populations is limited.
Methods: In the Multiethnic Cohort Study (MEC), we conducted a prospective cohort analysis to investigate the association of four diet quality indices (DQIs; AHEI-2010, aMED, HEI-2015, DASH; a higher score indicates healthier diet), three plant-based diet indices (PDI, hPDI, uPDI), two inflammatory (DII, EDIP), and two insulinemic dietary indices (EDIH, EDIR) (a higher score indicates more pro-inflammatory or pro-insulinemic diet) with incidence of prostate cancer (PCa) in 79,930 men from five racial/ethnic groups (White, African American, Japanese American, Latino, and Native Hawaiian). All dietary scores were constructed from a baseline quantitative food frequency questionnaire. Outcomes examined included total PCa, high-grade PCa (Gleason score > 7), advanced PCa (regional or distant), aggressive PCa (high-grade or advanced), and lethal PCa (distant or death due to PCa). Hazard ratios (HR) and 95% confidence intervals (CI) per one standard deviation (SD) increase in the dietary score were estimated from Cox proportional hazards models, overall and by race/ethnicity. Associations were considered nominally significant at $P < 0.05$.
Results: During a mean follow-up of 18.9 years, a total of 9,759 incident PCa cases were identified, including 2,503 high-grade, 1,706 advanced, 3,430 aggressive, and 1,426 lethal PCa cases. None of the dietary scores was significantly associated with total PCa. We found a significant association between DII and advanced PCa (HR=1.08, 95% CI=1.01-1.15) overall and the association appeared to be the strongest in African Americans (HR=1.17, 95% CI=1.00-1.36) and Native Hawaiians (HR=1.29, 95% CI=0.98-1.68). We also observed weak associations of the four DQIs with advanced PCa (HR of 0.95-0.96, P of 0.07-0.10) in the overall population, among which a higher DASH score was significantly associated with a 15% (95% CI = 0.75-0.96) lower risk of advanced PCa in African Americans. In addition, we observed that several inflammatory (EDIP) and insulinemic (EDIH, EDIR) dietary scores were associated with lower incidence of advanced, aggressive, or lethal PCa (HR=0.89-0.95, P of 0.03-0.05), which requires further investigation.
Conclusions: Our findings suggest that diets with high proinflammatory potential may increase risk of advanced PCa while following a healthy dietary pattern may reduce the risk of advanced PCa. Further studies are needed to better understand the inconsistent results across studies on diet and PCa risk and whether our findings can be replicated in other populations.

#2204 Evaluating ovarian cancer risk factors in the Mexican Teachers' Cohort.

B. Trabert[1], L. Gomez Flores Ramos[2], M. Brochier[2], E. V. Bandera[3], J. A. Doherty[1], S. L. Gomez[4], L. H. Kushi[5], A. Mohar[6], **M. Lajous**[2];
[1]University of Utah Huntsman Cancer Institute, Salt Lake City, UT, [2]National Institute of Public Health, Cuernavaca, Mexico, [3]Rutgers Cancer Institute of New Jersey; Robert Wood Johnson Medical School, New Brunswick, NJ, [4]University of California, San Francisco, San Francisco, CA, [5]Kaiser Permanente Northern California, Oakland, CA, [6]National Cancer Institute (INCan), Mexico City, Mexico

Purpose: Ovarian cancer is the most lethal gynecologic cancer in North America, yet our understanding of ovarian cancer risk factors in Mexican women is limited. The aim of the present study was to prospectively evaluate associations between reproductive and lifestyle factors and incident ovarian cancer risk among Mexican women.
Methods: The Mexican Teachers' Cohort (ESMaestras) is a large, prospective, population-based cohort of women (n=115,306) living in a culturally, geographically, and economically diverse 12-state area in Mexico. Reproductive and lifestyle factors were collected on baseline questionnaires administered between 2006-2008, with additional questionnaires collected from the cohort in 2011, and 2014. During follow-up, 187 incident ovarian cancer cases were identified, including 101 via self-report on 2011 and 2014 questionnaires, as well as an additional 85 through linkage with mortality databases, and 3 via other administrative- and cancer registry-based linkages (2 of 3 were also identified via the mortality database linkage). Of the self-reported incident cases, 5 have been validated via mortality databases and 4 via linkage with an administrative database; validation of the remaining self-reported cases is ongoing. Primary analyses examined associations between established ovarian cancer risk factors and incident ovarian cancer. Age-adjusted hazard ratios (HRs) and 95% confidence intervals (CIs) were estimated using Cox proportional hazards regression.
Results: Women in the Mexican Teachers' Cohort that used hormonal contraceptives (HC), were parous, or had a tubal ligation experienced reduced ovarian cancer risks during follow-up (ever HC use vs. never HR 0.70 [95% CI 0.51-0.95], parous vs. nulliparous 0.48 [0.35-0.68], ever tubal ligation vs. never 0.87 [0.59-1.28]). Ovarian cancer risk was elevated among women with a positive family history of breast cancer (1.34 [0.76-2.36]). Women with a history of endometriosis were at increased ovarian cancer risk (3.43 [1.41-8.34]). Taller adult height (>159 cm vs <150 cm) was not associated with ovarian cancer risk among women in this cohort. Risk estimates were consistent and, in some instances, more pronounced (i.e., HC use and tubal ligation) when limited to incident ovarian cancer cases confirmed via linkage with mortality databases (n=90).
Conclusions: Ovarian cancer risk factors identified in the Mexican Teachers' Cohort were generally consistent with associations reported in predominantly non-Hispanic white populations. More research is needed to better understand ovarian cancer etiology among populations under-represented in cancer research.

#2205 Modifiable risk factors are associated with clonal hematopoiesis.

C. D. Young[1], A. K. Hubbard[1], P. Saint-Maurice[2], I. Chan[3], K. L. Bolton[3], S. J. Chanock[1], C. Matthews[1], S. C. Moore[1], E. Loftfield[1], Y. Cao[3], **M. J. Machiela**[1], D. Tran[3];

[1]NCI Division of Cancer Epidemiology & Genetics, Rockville, MD, [2]Champalimaud Foundation, Lisbon, Portugal, [3]Washington University School of Medicine, St. Louis, MO

Observational studies have implicated modifiable factors like smoking, alcohol intake, physical activity (PA), and sleep to cancer risk. Clonal hematopoiesis (CH), marked by clonal expansions of mutated hematopoietic progenitors with mosaic chromosomal alterations (mCAs) or clonal hematopoiesis of indeterminate potential (CHIP), has been associated with the risk of serval cancers and may shed light the interplay between these factors and early preneoplastic hematopoietic expansion.Leveraging genotyping array and whole-exome sequencing data of leukocyte-derived DNA from 485,028 participants without hematologic malignancies in the UK Biobank (UKBB), we performed genome-wide characterization of two common forms of CH—mCAs and CHIP. To assess associations between social deprivation, self-reported modifiable risk factors, and CH risk, we employed multivariable logistic regression models adjusted for potential confounders including age, sex, smoking history, and genetic ancestry.We identified 11,826 (2.4%) individuals with autosomal mosaic chromosomal alterations (auto mCAs), 15,499 (3.2%) with loss of the X chromosome (mLOX), 43,044 (8.8%) with loss of the Y chromosome (mLOY) and 22,508 (4.6%) with CHIP. Individuals with any CH subtype were on average older than CH-free individuals ($p < 9.11\times10^{-52}$). Multivariable models identified a significant negative association between mLOY and social deprivation in England (1 SD change in score: OR = 0.968 [0.956-0.980], $p = 4.88\times10^{-7}$), suggesting modifiable risk factors could influence risk of mLOY. We observed a positive association with ever smoking and CH, which decreased with increased years since smoking cessation. Current smokers were at higher risk for auto mCAs (Odds ratio (OR) = 1.23, 95% Confidence Interval (CI):[1.16-1.31], P-value (p) = 2.63×10^{-11}), mLOY (OR = 2.25, 95%CI: [2.17-2.33], $p < 9.11\times10^{-52}$), and CHIP (OR = 1.40, , 95%CI: [1.34-1.47] $p < 9.11\times10^{-52}$); and former smokers also exhibited significant associations for mLOY (OR = 1.16, 95%CI: [1.13-1.19], $p = 2.97\times10^{-32}$) and CHIP (OR = 1.11, 95%CI: [1.08-1.15], $p = 2.75\times10^{-13}$). Alcohol consumption was associated with a significant increase in the risk of mLOX in heavy drinkers (>2-3 drinks/day) compared to non-drinkers (OR = 1.16, 95%CI: [1.09-1.24], $p = 1.21\times10^{-5}$). Moderate and high PA levels (categorized as level 2 and 3 based on total activity), were positively associated with increased mLOY frequency (moderate: OR = 1.05, 95%CI: [1.02-1.08], $p = 8.6\times10^{-2}$, high: OR = 1.06, 95%CI: [1.03-1.08], $p = 1.6\times10^{-3}$). We observed no evidence for an association between sleep patterns and CH.Our investigation in a large cohort identified associations between CH and social deprivation, smoking, alcohol consumption and PA. As CH is an intermediate marker for hematologic cancer risk, our findings imply that modifiable exposures may contribute to hematologic cancer risk through clonal mechanisms.

#2206 Obesity and cancer outcomes among patients with lung cancer and cutaneous melanoma treated with immune checkpoint inhibitors and EGFR inhibitors.

S. O. Nduaguba, L. Hazlehurst;
Mary Babb Randolph Cancer Center and School of Pharmacy at West Virginia University, Morgantown, WV

Background: Obesity is a causal factor in cancer risk and progression. Immune checkpoint inhibitors (ICI) and EGFR inhibitors (EGFRi) are indicated for the treatment of several cancers, including non-small-cell lung cancer (NSCLC) and cutaneous melanoma (CM). Improved outcomes was observed with ICI in preclinical studies. We aimed to determine the association of obesity with progression-free survival (PFS) or overall survival (OS) among patients with NSCLC and CM treated with ICI or EGFRi.
Methods: This was a retrospective study utilizing 2011-2019 SEER-Medicare data of Medicare Parts A and B enrolled patients ≥66 years diagnosed with NSCLC or CM who received ICI or EGFRi (NSCLC only) within 1-year post-diagnosis. Patients were followed from treatment commencement until death, loss to follow-up, or end of study. Descriptive statistics and survival analysis were used to achieve study objectives.
Results: Among 2393 NSCLC patients receiving ICI, obese patients (N=281, 11.7%) were younger (73.4±5.2 yrs vs 74.4±5.9 yrs, p<0.01) with higher CCI scores (2 (IQR=1-4) vs 1 (IQR=0-2), p<0.0001) compared to non-obese patients (N=2,311, 89.2%). Time to progression(TTP) was 41% faster among obese patients (392 days (95% CI=330-468) vs 493 days (95% CI=464-525), p<0.01; HR=1.41 (1.13-1.76), p<0.01) with no significant difference in time to death (TTD) (443 days (404-488) vs 491 days (462-524), p=0.35). Among 880 CM patients, those with obesity (N=91, 10.3%)) were significantly younger (74.7±6.1 yrs vs 76.3±7.3 yrs, p=0.02) with higher CCI scores (2 (IQR=0-4) vs 0 (IQR=0-2), p<0.0001). TTP was 343 days (320-400). TTD was 1,409 days (1,107-2,136) with no association between obesity status and PFS or OS. Among 2,524 NSCLC patients receiving EGFRi, obese patients (126, 5.0%) were younger (73.7±6.1 yrs) vs 75.6±6.5 yrs, p<0.01), had higher CCI scores (2 (IQR=1-3) vs 0 (IQR=0-1), p<0.0001), and longer time to treatment (3 mths (IQR=1-7) vs 2 mths (IQR=1-6), p=0.02). A higher proportion were White (76.2% vs 61.3%, p<0.001). Risk of progression was 48% higher among obese patients (664 dys (496-778) vs 1,231 dys (1,127-1,379), p<0.0001; HR=1.48, 95% CI=1.11-1.97, p<0.01) with no significant difference in TTD (559 dys (440-763) vs 673 dys (639-707), p=0.35).
Conclusion: Obesity with associated with PFS but not OS among patients with NSCLC with no association observed among patients with CM. Given that the link between obesity and NSCLC risk remains controversial, the observed association with PFS may be linked to the absence of the paradoxical effect of improve outcomes that may be seen with cancers caused by obesity such as CM.

#2207 Fiber intake and risk of lethal prostate cancer among men at increased genetic risk.

Y. Zhang[1], K. H. Stopsack[2], L. A. Mucci[1], E. Giovannucci[1], A. Plym[3];

[1]Harvard School of Public Health, Boston, MA, [2]Massachusetts General Hospital and Harvard Medical School, Boston, MA, [3]Karolinska Institutet, Stockholm, Sweden

Introduction High fiber intake from grains may lower advanced prostate cancer risk by enhancing insulin sensitivity, lowering insulin-like growth factor 1 and systemic inflammation. Whether a high-fiber diet can lower risk of metastatic disease and prostate cancer death in men at high genetic risk is unclear.
Methods Using a new 400-SNP polygenic risk score (PRS) for prostate cancer, we quantified the genetic risk of 10,269 men with available genotype data in the Health Professionals Follow-up Study, followed between 1993 and 2019. Men in the top 50-100% PRS category were considered high-risk and included for analysis. Total fiber intake and different sources (cereal, fruits, vegetables) were assessed by validated food frequency questionnaires. Overall and lethal prostate cancer (metastatic disease/prostate cancer death) were analyzed using Cox proportional hazards models estimating hazard ratios (HRs) and 95% confidence intervals (CIs).
Results During 26 years of follow-up, we recorded 1,494 overall and 174 lethal prostate cancer events in the high genetic risk group. As expected, no associations were observed fiber intake with risk of overall prostate cancer. For lethal prostate cancer, the results varied according to the source of fiber. Higher cereal fiber intake was associated with a lower risk of lethal prostate cancer (per 3 g/d higher intake: 0.81 [0.68, 0.97], *P-trend*=0.02). We further observed a higher disease risk among men with higher fruit fiber intake (per 3g/d higher intake: 1.18 [1.02, 1.36], *P-trend*=0.03). The associations remained similar when mutually adjusted for each fiber type. No associations were observed for total or vegetable fiber intake.
Conclusion In this analysis of men at high prostate cancer genetic risk, we observed that higher cereal fiber intake was associated with lower lethal prostate cancer risk, whereas higher fruit fiber intake showed an opposite trend. Further studies in different populations and investigations into the underlying mechanisms are needed.

Fiber intake with risk of overall and lethal prostate cancer among men at high genetic risk.

Fiber type	Overall prostate cancer: No.event/PY	Overall prostate cancer: HR (95% CI)	Lethal prostate cancer: No.event/PY	Lethal prostate cancer: HR (95% CI)
All fiber, g/d				
T1, median=15.8	490/66047	ref.	42/73826	ref.
T2, median=21.8	484/62237	0.96 (0.83-1.11)	61/69849	1.16 (0.77-1.75)
T3, median=29.9	520/67374	1.02 (0.86-1.21)	71/75242	1.24 (0.75-2.05)
Per 3 g/d		0.98 (0.96-1.01)		1.00 (0.92-1.08)
P for trend		0.27		0.93
Cereal fiber, g/d				
T1, median=4.6	491/63911	ref.	49/72367	ref.
T2, median=6.7	512/66251	1.04 (0.91-1.20)	76/73384	1.30 (0.90-1.87)
T3, median=9.4	491/65496	0.92 (0.80-1.06)	49/73166	0.75 (0.50-1.12)
Per 3 g/d		0.96 (0.90-1.01)		0.81 (0.68-0.97)
P for trend		0.14		0.02
Fruit fiber, g/d				
T1, median=2.5	471/66306	ref.	33/74056	ref.
T2, median=4.5	514/63268	1.06 (0.92-1.22)	51/70430	1.21 (0.76-1.91)
T3, median=7.2	509/66085	1.00 (0.86-1.16)	90/74431	1.84 (1.18-2.87)
Per 3 g/d		0.97 (0.91-1.03)		1.18 (1.02-1.36)
P for trend		0.34		0.03
Vegetable fiber, g/d				
T1, median=4.8	481/64139	ref.	51/71594	ref.
T2, median=6.9	505/64938	1.04 (0.91-1.20)	66/72291	1.22 (0.84-1.78)
T3, median=9.6	508/66581	1.04 (0.90-1.20)	57/75031	0.98 (0.65-1.45)
Per 3 g/d		0.99 (0.93-1.05)		0.97 (0.82-1.15)
P for trend		0.72		0.74

#2209 Tattooing and risk of melanoma: A population-based case-control study in Utah.

R. D. McCarty[1], B. Trabert[1], M. M. Millar[2], D. Kriebel[3], L. Grieshober[1], M. E. Barnard[4], L. J. Collin[1], K. A. Lawson-Michod[1], J. A. Gilreath[1], D. Grossman[1], J. Hyngstrom[1], P. J. Shami[1], J. A. Doherty[1];

[1]University of Utah Huntsman Cancer Institute, Salt Lake City, UT, [2]University of Utah, Salt Lake City, UT, [3]University of Massachusetts Lowell, Lowell, MA, [4]Boston University, Boston, MA

Background: Carcinogens have been observed in many tattoo inks which can form new carcinogenic compounds when exposed to ultraviolet radiation and can accumulate in the lymph nodes and other organs. Tattooing can result in short- and long-term inflammatory and immune responses. At least 38 cases of melanoma have been reported in tattoos. The incidence of melanoma in Utah is the highest in the U.S., and potentially modifiable risk factors are of public health interest. In this study, we evaluated associations between tattooing and melanoma risk.

Methods: We utilized a population-based case-control study of 514 incident *in situ* (284 men and 230 women) and 534 invasive (285 men and 249 women) melanoma cases diagnosed in Utah between 2020-2021. Controls (n=5,240) were selected from respondents to the Utah Behavioral Risk Factor Surveillance System (BRFSS) survey and frequency matched to cases in a 5:1 ratio on sex, age, race, and ethnicity. We fit logistic regression models to compute odds ratios (ORs) and 95% confidence intervals (CIs) associating ever tattooing with *in situ* and invasive melanoma risk, adjusting for age, education level, race, and ethnicity, separately for women and men. We then fit logistic models stratified by education level (< four-year college degree/four-year college degree or more) and models stratified by age (< 50 years/50+ years), separately for women and men.

Results: Among men, the prevalence of tattooing was 7% for both *in situ* and invasive cases, and 11% for controls. Among women, tattooing prevalence was 20% for *in situ* cases, 15% for invasive cases, and 18% for controls. Ever tattooing was associated with decreased invasive melanoma risk among men (OR=0.62 [95% CI: 0.37-1.02]), particularly among those who had less than a four-year college degree (0.52 [0.28-0.99]), and among ages 50+ (0.36 [0.16-0.84]). Among men, the OR for ever tattooing and *in situ* melanoma was in the same direction as invasive melanoma, but the estimate was statistically imprecise (0.73 [0.45-1.19]). Among women, we did not observe an association between ever tattooing and invasive melanoma (0.83 [0.56-1.20]), while the association between ever tattooing and *in situ* melanoma was statistically imprecise (1.25 [0.87-1.80]). However, ever tattooing was associated with a nearly two-fold increased risk of *in situ* melanoma among women with a four-year college degree (1.98 [1.21-3.26]), but not for those without a college degree (0.89 [0.52-1.50]).

Conclusion: These findings do not suggest that there is an association between tattooing and melanoma. Associations between tattooing and health-seeking behaviors, which may vary by sex and other demographic factors, may influence associations with melanoma diagnosis, particularly for *in situ* melanoma. This study is the first step in investigating whether reported cases of melanoma arising in tattoos are coincidental or whether tattoos may be associated with an increased risk of melanoma.

#2210 Healthy dietary patterns and survival among men with prostate cancer.

B. Liu, J. B. Vaselkiv, C. Himbert, C. B. McGrath, L. Lucas, E. Giovannucci, M. J. Stampfer, K. H. Stopsack, Q. Sun, L. A. Mucci;
Harvard School of Public Health, Boston, MA

Background: While prostate cancer is the second leading cause of cancer death in U.S. males, most men with prostate cancer die from other causes. We prospectively examined the potential benefits of adhering to established healthy dietary patterns on overall and cause-specific mortality among men living with prostate cancer.
Methods: We studied men with incident prostate cancer in the Health Professionals Follow-up Study from 1986-2022. Five dietary indices-Alternative Healthy Eating Index (AHEI), the Mediterranean diet, Dietary Approaches to Stop Hypertension (DASH), anti-insulinemic, and anti-inflammatory diet scores-were derived from validated food frequency questionnaires administered every 4 years. Post-diagnosis scores were cumulatively averaged, and time-varying changes in scores from pre- to post-diagnosis were calculated. We used multivariable-adjusted Cox models to estimate hazard ratios (HRs, 95% CI) for associations between adherence to dietary patterns with overall and cause-specific survival adjusting for demographics, dietary and lifestyle factors.
Results: Among 6,086 prostate cancer patients with 71,783 person-years of follow-up, 3,406 deaths occurred: 578 from prostate cancer, 918 from cardiovascular disease (CVD), and 1910 from other causes. When comparing extreme quintiles of post-diagnosis diet scores, a healthy diet was associated with lower overall mortality for AHEI (0.76, 0.66-0.88) and the Mediterranean diet (0.84, 0.73-0.97). Moreover, comparing extreme quintiles of score change, patients who increased their adherence to these diets after diagnosis had better overall survival with HRs (95% CI) that ranged from 0.79 (0.70-0.89) for AHEI to 0.89 (0.79- <1.00) for the anti-inflammatory diet. No significant associations were observed for DASH. Regarding cause-specific survival, increased adherence to anti-insulinemic diet was associated with better CVD-specific survival (0.78, 0.61-0.99). No significant associations were found between these diet scores and prostate cancer survival. Stronger associations of post-diagnosis diet scores with overall survival were seen in men diagnosed before age 70, those classified as obese at diagnosis (BMI≥30 kg/m^2), consuming less alcohol (<7.8 g/d), and with lower grade (Gleason Score ≤7) or stage (T1/T2) tumors.
Conclusions: For men diagnosed with prostate cancer, adhering to a healthy dietary pattern after cancer diagnosis, such as the AHEI and Mediterranean Diet, was associated with better overall survival. Increasing adherence to these diets after cancer diagnosis was also associated with improved overall and CVD-specific survival.

#2211 ALDH2 deficiency and alcohol intake: Opportunity for precision cancer prevention.

D. Forman[1], M. Yang[2], R. Chien[2], H. Nguyen[2], C. Wong[2], J. H. J. Kim[2], A. Ziogas[2], H. L. Park[2];
[1]University of California, Los Angeles, Los Angeles, CA, [2]University of California, Irvine, Irvine, CA

Alcoholic beverages and the main metabolite of alcohol, acetaldehyde, are known carcinogens, according to the International Agency for Research on Cancer. Many studies have shown that alcohol consumption is a modifiable risk factor for breast, esophageal, colorectal, and other cancers, and that individuals deficient in metabolizing acetaldehyde are at higher risk for alcohol-associated cancers. A genetic variant in *aldehyde dehydrogenase 2* (*ALDH2*, G>A, rs671), the main enzyme responsible for breaking down acetaldehyde, results in decreased efficiency of ALDH2, or ALDH2 deficiency. This is the most common single genetic variation in humans worldwide, mostly found in some East Asian populations. While having one or both deficient alleles can lead to adverse physical effects when drinking, including facial flushing, nausea, and palpitations, studies done in Asian countries have shown that many affected individuals still consume alcohol, increasing their risk for some cancers. We sought to explore the scope and design of potential intervention in the U.S. by examining alcohol consumption behavior in individuals with and without ALDH2 deficiency within the All of Us Research Program, a current large, diverse, national U.S. cohort. Relationships between self-reported alcohol consumption and sociodemographic factors were examined among 380,845 participants. Genomic data was available for 296,254 of them. Overall, 72.7% of the cohort reported drinking alcohol in the past year, with the majority drinking moderately (≤1 drink/day for women and ≤2 drinks/day for men). Among those who drank, 42.7% reported at least one binge drinking episode (≥6 drinks on one occasion). Among our genomic cohort who identified as Asian individuals, 23.6% had at least one deficient *ALDH2* allele compared to <4% in all other groups. 63.7% of individuals with one deficient *ALDH2* allele and 25.4% with two deficient *ALDH2* alleles reported drinking in the past year. 29.9% of individuals with ALDH2 deficiency reported binge drinking in the past year. Multivariate analysis showed that male sex, younger age, higher education level, higher household income, and being born in the U.S. were associated with alcohol consumption among both individuals with and without ALDH2 deficiency. Our study shows that ALDH2 deficiency is fairly common among Asian Americans and that many affected individuals still drink alcohol. With the growing population of Asian Americans in the U.S. (currently >7% of the total U.S. population, projected to be ~38 million individuals by 2050), our findings suggest a significant opportunity for precision cancer prevention for a substantial portion of the population.

#2212 Global cancers attributable to modifiable risk factors: Dietary factors of animal origin.

Monireh Sadat Seyyedsalehi[1], Edward Giovannucci[2], Paolo Boffetta[3]

[1]University of Bologna, Bologna, Italy,[2]Harvard T.H. Chan School of Public Health, Boston, MA,[3]Stony Brook University, Stony Brook, NY

Cancer is the leading cause of death worldwide. Modifiable risk factors including diet have been linked to a wide range of malignancies. We estimated the global cancer population-attributable fraction (PAF) to established and suspected dietary cancer risk factors according to the Human Development Index (HDI).Diet-cancer associations were selected from WCRF, GBD and IARC report. Dietary factors of animal origin include red meat, processed meat, fish and dairy products; cancers include nasopharynx, esophageal, stomach, colorectal, pancreatic, lung, prostate, breast cancer. Gender-specific PAF were calculated based on 1) the total and gender-specific 2022 country-specific population from World Bank; 2) the country-specific average daily dietary factors intake (g/day) for 2000-2005 from the Global Dietary Database; 3) relative risks from the meta-analyses and WCRF reports; 4) country-specific 2020 cancer incidence from WHO. Estimates were also stratified by Human Development Index (HDI).Table 1 provides the results. The PAF for red meat and processed meat was higher in high HDI countries, while that for low dairy product intake was higher in low HDI countries. According to results, changes in selected dietary factors can prevent cancer-related incidence, particularly depending on where development status of countries and access to the source of their intake. Table1: Population attributable fractions for incidence of cancer in 2020 by gender.

Dietary factors and Related Cancers	Relative risk (g/day)	AF (N. global) – Both gender	AF (N. global)- Female	AF (N. global)- Male
Red meat				
Nasopharynx(L)	1.35(100)	0.103(13750.2)	0.102(3734.9)	0.104(10015.3)
Colorectal (S)	1.12(100)	0.040(78714.5)	0.040(33981.2)	0.041(44733.2)
Pancreatic (L)	1.11(100)	0.037(27420.3)	0.036(8479.8)	0.037(18940.4)
Lung (L)	1.22(100)	0.070(155986.9)	0.069(52442.6)	0.070(103544.4)
Prostate(L)	1.04(100)	0.014(20665.6)	-	0.014(20665.6)
Effect on total cancers *		0.016(296537.5)	0.011(98638.5)	0.021 (197898.9)
Processed meat				
Nasopharynx(L)	1.46(30)	0.164(22194.6)	0.154(5637.4)	0.173(16557.1)
Esophagus(L)	1.3(100)	0.036(22654.9)	0.034(6345.8)	0.038(16309.2)
Stomach(L)	1.21(50)	0.052(60325.8)	0.049(18161.7)	0.055(42164)
Colorectal (S)	1.18(100)	0.023(45460.9)	0.021(18522.8)	0.024(26938.1)
Pancreatic(L)	1.17(50)	0.043(21900.2)	0.040(9414.4)	0.046(12485.8)
Lung (L)	1.14(50)	0.036(82762.9)	0.034(26023.9)	0.038(56739)
Effect on total cancers *		0.014(255299.3)	0.010(84106)	0.018(171193.2)
Dairy products				
Colorectal(S)	0.87(400)	0.092(180063.4)	0.091(77598.8)	0.093(102464.6)
Breast (L)	0.95(200)	0.068(151960.9)	0.068(151960.9)	-
Prostate (L)	1.07(400)	0.016(24224.3)	-	0.016(24224.3)
Effect on total cancers *		0.019(356248.6)	0.026(229559.7)	0.013(126688.9)
Fish				
Colorectal (L)	0.89(100)	0.022(44882.9)	0.022(18705.9)	0.024(26177)
Effect on total cancers *		0.002(44882.9)	0.002(18705.9	0.003(26177)
Mean (g/day) of global intake Processed meat (B=14.2/M=15.1/F=13.3), red meat (B=36.5/M=36.9/F=36), fish(B=23/M=22.1/F=23.8), dairy products(B=77/M=74.9/F=79)S=strong evidenceL=limited evidence*All cancers excl. non-melanoma skin cancer (B= 18094716/ F=8751759/M=9342957)				

#2213 Vaping, smoking and lung cancer: A case-control study.

M. A. Bittoni, D. Carbone, R. Harris;
The Ohio State University, Columbus, OH

Introduction: Nicotine exposure through the use of electronic delivery systems (vaping) has been found to elevate the risk of certain conditions of the lungs, e.g., vaping associated lung injury. However, the potential impact of vaping on lung cancer risk remains largely unexplored. We, therefore, examined the association of vaping and cigarette smoking with lung cancer risk in a case-control study conducted at The Ohio State University in Columbus, Ohio.
Methods: Medical records examined from the James Cancer Hospital and Solove Research Institute revealed 4,975 cases with newly diagnosed, pathologically confirmed lung cancer during 2013-2021. These cases were compared to 27,294 controls without cancer that were group-matched on a 5:1 ratio to cases by age, gender, race and year of ascertainment. Descriptive statistics were calculated, and logistic regression analyses were performed to assess the associations between vaping, smoking and lung cancer.
Results: The lung cancer cases in this study were 55% male, 88% white, with mean age at diagnosis of 62 years. The adjusted odds ratio (OR) for individuals who reported vaping and smoking was OR=21.1 (95% CI=17.1, 26.1) versus OR=6.3 (95% CI=5.8, 6.8) for smoking only. Estimates for gender and histologic cell type of lung cancer, e.g., pulmonary adenocarcinoma, squamous cell carcinoma and small cell carcinoma, were consistently over threefold higher for vaping and smoking compared to smoking only ($p<0.001$), and the vaping effect persisted even after adjustment for comorbidities, COPD and cardiovascular disease.
Conclusion: Adjusted estimates of odds ratios (OR) revealed over threefold higher risk of lung cancer among individuals who had vaped and smoked compared to individuals who only smoked. Our results suggest that the addition of vaping to smoking greatly accelerates the risk of developing lung cancer. Future studies are needed to further confirm these results.

#2214 Impacts of habitual and recent alcohol intake on gut microbiome diversity and composition among Black Americans.

L. Liu, S. Nguyen, Q. Cai, M. Shrubsole, W. Zheng, D. Yu;
Vanderbilt University, Nashville, TN

Background: Alcohol intake can alter the gut microbiome, which may play a role in the development of cancer and other chronic diseases. However, there have been limited population-based studies investigating the associations of habitual and recent alcohol intake with the gut microbiome, particularly among Black Americans.

Methods: We investigated the association of alcohol intake with the gut microbiome among 538 Black American participants of the Southern Community Cohort Study (150 men and 388 women). Habitual and recent alcohol intake was assessed at cohort baseline (2002-2009) and stool collection (2018-2021), respectively. DNA was extracted from fecal samples for gut microbiome profiling using shotgun metagenomic sequencing. Generalized linear models were employed to evaluate the associations between alcohol intake and gut microbiome diversity and composition, with adjustments for sociodemographic characteristics, other lifestyle factors, and comorbidities. False discovery rate (FDR)<0.1 was considered statistically significant.

Results: The mean age at enrollment was 53.2 ± 7.7 years, with a mean interval of 13.8 years (range: 9.0-18.1 years) between baseline and stool collection. Neither habitual nor recent alcohol intake was associated with microbiome diversity indices, and recent alcohol intake was not associated with microbial taxa abundance either. However, habitual alcohol intake, both total amount and subtypes, showed significant associations with microbial taxa abundance primarily in men, including *Actinobacteria*, *Proteobacteria*, *Firmicutes*, and classes *Bacilli* and *Clostridia* within these phyla (all FDR<0.1). Specifically, total alcohol and red wine intakes were inversely associated with genus *MGYG-HGUT-02719* in class *Clostridia;* beer consumption was inversely associated with genus *Anaerostipes;* white wine intake showed negative associations with order *RF32* and genus *Eubacterium* and a positive association with genus *Paenibacillus*. Most of these associations remained significant after adjusting for BMI and history of cardiometabolic diseases or cancer.

Conclusion: We identified gut microbiome taxa associated with habitual alcohol intake among Black American men, including several with anti- or pro-gastrointestinal-cancer properties. However, the magnitudes of these associations were generally small. Further research is needed to determine if these bacteria play a mediating or modifying role in alcohol-disease relationships.

#2215 Effects of a high-fiber, high-fruit and -vegetable, low-fat dietary intervention on rectal tissue bacteria.

D. A. Byrd[1], M. Gomez[1], S. Hogue[1], A. Ortega-Villa[2], Y. Wan[2], A. Warner[3], B. Zhu[2], C. Dagnall[2], K. Jones[2], B. Hicks[2], P. Albert[2], G. Murphy[4], R. Sinha[2], E. Vogtmann[2];

[1]Moffitt Cancer Center, Tampa, FL, [2]NIH, Bethesda, MD, [3]NIH, Frederick, MD, [4]Imperial College of London, London, United Kingdom

Introduction. Emerging evidence suggests that the bacteria residing in colon and rectal tissue are plausibly associated with colorectal cancer (CRC). Prior studies investigated the effects of dietary interventions on the fecal microbiome but few assessed colorectal tissue microbiome endpoints. We investigated the effects of a high-fiber, high-fruit and -vegetable, low-fat dietary intervention on the rectal tissue microbiome in the Polyp Prevention Trial (PPT).

Methods. PPT is a 4-year randomized clinical trial, with specific goals including consuming: 1) ≥ 18g of fiber per 1,000 kcal/day; 2) ≥ 3.5 servings of fruits and vegetables per 1,000 kcal/day; and 3) <20% of kcal/day from fat. We extracted DNA from rectal biopsies using the AutoGen Animal Tissue DNA Extraction Kit and sequenced the V4 region of the 16S rRNA gene to characterize the bacteria in biopsies collected at baseline and the end of years 1 and 4 (N=233 in intervention arm and N=222 in control arm). We estimated effects of the intervention on rarefied alpha diversity and *a priori*-selected presence and relative abundance (presented as percentages summing to 100) of 10 bacteria most strongly historically associated with CRC presence using repeated-measures linear mixed-effects models. We also explored intervention effects on presence/abundance of all bacteria (with Bonferroni correction for multiple testing) and stratified the analysis among intervention arm participants who adhered to 75% of the dietary goals (super compliers) over the 4 years (N=48) and comparable participants in the control arm (N=64).

Results. The intervention did not statistically significantly modify rectal tissue alpha diversity. Compared to the control arm, relative abundance of *a priori*-selected *Porphyromonas* (absolute difference-in-difference (DiD) at T1 vs. T0 = -0.24 and T4 vs. T0 = -0.12; *P*=0.004) and *Prevotella* (absolute DiD at T1 vs. T0 = -0.40 and at T4 vs. T0 = -0.32; *P*=0.01) were more strongly decreased in the intervention arm. Other bacteria selected for exploratory analyses were not statistically significantly modified by the intervention after accounting for multiple testing. Among super compliers and comparable control arm participants, the findings were similarly weak.

Conclusion. Overall, our findings did not strongly support that a high-fiber, -fruit, and -vegetable, and low-fat diet intervention influences rectal tissue microbiome diversity nor the abundance of most bacteria, except for two oral-originating bacteria that were previously associated with CRC presence. It is possible that dietary exposures over longer periods of time (than 4 years) may more strongly influence the tissue microbiome. Future intervention studies, including tissue samples collected throughout the colon and rectum among larger, diverse study populations for longer periods of time are warranted to inform potential primary prevention strategies for CRC.

#2216 Population attributable fraction of tobacco smoking on cancer incidence in 2020 in the Republic of Korea.

S. Byoun[1], Y.-J. Choi[1], Y. Min[1], S.-K. Park[2], K. Ko[3], S. Sung[2], N. Kim[4], K. Jung[4], S. Jee[4], S.-I. Cho[5], M. Lim[6], S. Park[7], E. Park[8], H. Woo[9], K.-W. Jung[1], E. Yun[1], B. Kim[1], J.-K. Oh[1], Y. Choi[1], B. Park[1], H. Seo[1], J.-S. Im[1];

[1]National Cancer Control Institute, National Cancer Center, Goyang, Korea, Republic of, [2]Department of Preventive Medicine, Seoul National University College of Medicine, Seoul, Korea, Republic of, [3]Clinical Preventive Medicine Center, Seoul National University Bundang Hospital, Seongnam, Korea, Republic of, [4]Department of Epidemiology and Health Promotion, Institute for Health Promotion, Graduate School of Public Health, Yonsei University, Seoul, Korea, Republic of, [5]Graduate School of Public Health and Institute of Health and Environment, Seoul National University, Seoul, Korea, Republic of, [6]Department of Social and Preventive Medicine, College of Medicine, Inha University, Incheon, Korea, Republic of, [7]Department of Biostatistics, Graduate School of Public Health, Yonsei University, Seoul, Korea, Republic of, [8]Preventive Medicine Department, Korea University College of Medicine, Seoul, Korea, Republic of, [9]Department of Precision Medicine, Korea National Institute of Health, Korea Disease Control and Prevention Agency, Cheongju, Korea, Republic of

Backgrounds: Cancer is the most common cause of mortality in Korea. According to International Agency for Research on Cancer (IARC), tobacco smoking is the Group I carcinogen, and the National Cancer Center Korea reported in 2009 that 20.9% and 2.3% of total cancer incidence were attributable to tobacco smoking in men and women, respectively. As of 2020, we estimated population attributable fraction (PAF) of cancer incidence due to tobacco smoking.
Methods: We organized the Consensus Committee to develop strategy and methodology for PAF estimation. From the consensus, cancer sites for PAF estimation were selected based on the IARC list of classification with sufficient evidence in human. PAF was calculated by using Levin's formula which includes exposure prevalence and relative risk (RR). Exposure prevalence was collected from the Korea National Health and Nutrition Examination Survey (KNHANES) in 2005, assuming that latent period from risk exposure to cancer development was 15 years. Tobacco smoking was defined as a categorical variable including non-smokers, past smokers, and current smokers. Pooled RRs were estimated from meta-analysis of RRs obtained from Korean Genome and Epidemiology Study, National Health Examination data provided by National Health Insurance Services, Korean Cancer Prevention Study-II, and KNHANES, each of which was linked with Korea Cancer Registry. Cox proportional hazards model were used to estimate RRs, while adjusted by age groups and alcohol consumption.
Results: For men, 17.4% of all cancer cases were attributed to smoking, compared to 1.7% for women. Specifically, in men, 57.9% of lung cancer, 36.4% of bladder cancer, 31.9% of esophageal cancer, 39.1% of laryngeal cancer , 25.4% of oral cavity/pharyngeal cancer, 19.7% of liver cancer, and 19.5% of stomach cancer were attributed to tobacco smoking. In women, 51.7% of laryngeal cancer, 15.0% of esophageal cancer, 11.6% of lung cancer, 6.0% of bladder cancer, 5.1% of oral cavity/pharyngeal cancer, 5.0% of cervix cancer, and 4.6% of liver cancer were due to smoking.
Conclusion: Tobacco smoking is an important cause of esophageal, laryngeal, and lung cancer in men, and esophageal and laryngeal cancer in women, and comprises a substantial proportion of PAF in cancer incidence. Thus, intervention measures are needed to reduce smoking prevalence for cancer prevention in Korea. Funding Sources: This work was supported by the National Cancer Center Grant(NCC-2210840).

#2217 Associations between intrauterine device use and ovarian cancer risk among 11 population-based case-control studies.

Jennifer M. Mongiovi[1], Ana Babic[2], Naoko Sasamoto[3], Lauren Peres[4], Holly Harris[5], Mollie E. Barnard[6], Shelley S. Tworoger[7], Anita Koushik[8], Joellen M. Schildkraut[9], Jennifer A. Doherty[10], Kathryn L. Terry[3], the Ovarian Cancer Association Consortium & the African-American Cancer Epidemiology Study

[1]Harvard T.H. Chan School of Public Health, Boston, MA,[2]Dana Farber Cancer Institute, Boston, MA,[3]Brigham and Women's Hospital, Boston, MA,[4]Moffitt Cancer Center, Tampa, FL,[5]Fred Hutch, Seattle, WA,[6]Boston University School of Medicine, Boston, MA,[7]Oregon Health and Science University School of Medicine, Portland, OR,[8]McGill University, Montreal, QC, Canada,[9]Emory University Rollins School of Public Health, Atlanta, GA,[10]Huntsman Cancer Institute, Salt Lake City, UT

Background: Intrauterine device (IUD) use has increased while oral contraceptive (OC) use has decreased among premenopausal women. It is unknown whether IUDs offer protection against epithelial ovarian cancer (EOC), similar to OCs, or may increase risk. Therefore, we examined the association between IUD use and EOC risk.

Methods: Information on contraception use was obtained through questionnaires from 11 studies participating in the Ovarian Cancer Association Consortium and African-American Cancer Epidemiology Study. Study-specific odds ratios (OR) and 95% confidence intervals (CI) were calculated using unconditional multivariable logistic regression, and heterogeneity between studies was assessed using Cochran *Q* and I^2 statistics. There was no evidence of heterogeneity, thus data were pooled. We assessed potential effect modification by decade of birth, race, parity, and personal history of endometriosis by reporting stratum-specific estimates and tested for multiplicative interaction by comparing models with and without interaction terms via likelihood ratio test. Polytomous logistic regression was used to estimate histotype-specific associations.

Results: Results were pooled for 11,033 EOC cases and 13,358 controls. There were 2,656 (19.9%) IUD users (mostly non-hormonal) and 8,923 (66.8%) OC users among controls compared to 1,933 (17.5%) IUD users and 6,318 (57.3%) OC users among cases. IUD use was associated with lower risk of endometrioid (OR: 0.73, 95% CI: 0.62-0.86) and clear cell (OR: 0.63, 95% CI: 0.48-0.80), but not high-grade serous subtypes (OR: 1.05, 95% CI: 0.98-1.14), with significant heterogeneity by histotype (p=0.0006). Among studies that collected data on IUD type, we observed a non-significant inverse association between hormonal IUD use and EOC (OR: 0.72, 95% CI: 0.51-1.03); however, only 51 cases reported hormonal IUD use. Among those who used both IUD and OCs, there was no association with the order of contraception use and EOC. There were no major differences in the associations of age at first use, duration of use, or time since last use and EOC risk. Among parous women, IUD use before first pregnancy was associated with a non-significant reduced odds of EOC (OR: 0.82, 95% CI: 0.65-1.04). We also observed a statistically significant interaction between IUD use and endometriosis with reduced odds of EOC associated with IUD use among women with endometriosis (OR: 0.77, 95% CI: 0.60-0.98) but not those without endometriosis (OR: 0.96, 95% CI: 0.90-1.03, *p*-interaction=0.05).

Discussion: IUD use was associated with lower clear cell and endometrioid EOC risk and may be most protective among women with endometriosis. Future research should include cohorts of women with a higher prevalence of hormonal IUD use to determine the impact of changing contraceptive trends on ovarian cancer burden and identifying preventive strategies for women at high risk.

#2218 Dietary insulinemic potential and survival after breast cancer diagnosis.

A. Romanos-Nanclares[1], T. Wang[1], B. A. Rosner[2], M. D. Holmes[2], W. Y. Chen[3], W. C. Willett[2], R. M. Tamimi[4], A. Eliassen[1];
[1]Brigham and Women's Hospital and Harvard Medical School, Boston, MA, [2]Harvard T.H. Chan School of Public Health, Boston, MA, [3]Dana-Farber Cancer Institute, Boston, MA, [4]Weill Cornell Medicine, New York, NY

Background: Hyperinsulinemia may promote the growth and metastasis of breast cancers by activating the insulin/insulin-like growth factor 1 signaling pathways. Whether the insulinemic potential of the diet contributes to breast cancer prognosis has not been examined previously. Here, we focused on a food-based empirical dietary index for hyperinsulinemia (EDIH), an index previously designed as most predictive of fasting plasma C-peptide. We aimed to investigate whether EDIH (at different time settings) is associated with overall and breast cancer-specific mortality.
Methods: For 9,640 women with stage I-III breast cancer from the Nurses' Health Study (NHS) and Nurses' Health Study II (NHSII), we calculated the cumulative average EDIH, using repeated measures of post-diagnostic diet from food frequency questionnaires (FFQ). We also considered the pre-diagnostic EDIH score (using the last FFQ reported before diagnosis), the first postdiagnostic EDIH score, as well as a simple updated EDIH score. Information on diet and other factors was repeatedly measured in validated questionnaires every two to four years. Deaths were ascertained by report from family members or by searching the National Death Index. Multivariable-adjusted hazard ratios (HRs) and 95% confidence intervals (CI) were estimated using Cox proportional hazards models.
Results: Participants were followed up for a median of 12 years after breast cancer diagnosis. We documented 1,120 deaths due to breast cancer and 2,762 all-cause deaths. Women with higher post-diagnostic EDIH had a 40% higher risk of all-cause mortality (HR for quintile 5 vs. quintile 1 [$HR_{Q5vs.Q1}$], 1.40; 95% CI, 1.22, 1.61; P-trend<0.0001). EDIH was also associated with a 19% increased risk of breast cancer mortality, although the confidence interval included the null ($HR_{Q5vs.Q1}$, 1.19; 95% CI, 0.95, 1.48; P-trend=0.17). Findings for overall mortality were similar for EDIH measured at other timings/settings: last pre-diagnosis dietary assessment ($HR_{Q5vs.Q1}$,1.21; 95% CI, 1.06, 1.39; P-trend<0.0001) and first post-diagnosis dietary assessment ($HR_{Q5vs.Q1}$,1.23; 95% CI, 1.08, 1.40; P-trend<0.0001).
Conclusions: In this large prospective study of breast cancer survivors, higher hyperinsulinemic dietary scores (reflecting higher dietary insulinemic potential) were associated with worse survival outcomes following diagnosis. Thus, dietary recommendations emphasizing the importance of avoiding high insulinemic dietary patterns (i.e., processed meat and red meat) and prioritizing low insulinemic dietary patterns (i.e., coffee, whole fruit and green-leafy vegetables) as components of a healthy diet may improve overall survival.

#2220 Associations between post-diagnostic lifestyle and dietary patterns with prostate cancer survival in the Multiethnic Cohort.

A. Wang[1], E. L. Van Blarigan[2], I. Cheng[2], J. M. Chan[2], P. Wan[3], S.-Y. Park[4], F. Chen[3], L. Le Marchand[4], L. Wilkens[4], S. A. Kenfield[2], C. A. Haiman[3]; [1]Harvard T.H.Chan School of Public Health, Boston, MA, [2]University of California, San Francisco, San Francisco, CA, [3]University of Southern California, Los Angeles, CA, [4]University of Hawaii Cancer Center, University of Hawaii, Honolulu, HI

Background: Prostate cancer (PCa) remains a leading cause of cancer-related death among men despite high 5-year survival rates for localized and regional diseases. This study evaluated healthy lifestyle and dietary patterns in relation to PCa survival in a multiethnic population.
Methods: We prospectively followed 2,603 men with non-metastatic PCa in the Multiethnic Cohort (MEC) for a median duration of 10.9 years (497 African American, 754 Japanese American, 577 Latino, 129 Native Hawaiian, and 646 White men) starting in 1993. We documented 1,321 deaths, including 196 from PCa. Lifestyle pattern was assessed after diagnosis by a previously reported PCa Behavior Score, which includes BMI, physical activity, and smoking, and a modified version including diet (based on the sum of saturated fat, whole milk, alcohol, and processed meat intake). We also evaluated six indices of inflammatory and insulinemic potential of diet and lifestyle patterns (E-DII, EDIP, EDIH, ELIH, EDIR, and ELIR); and three indices of plant-based diets: an overall plant-based diet index (PDI), a healthful PDI (hPDI), and an unhealthful PDI (uPDI). We used Cox proportional hazards models to calculate hazard ratios (HR) and 95% confidence intervals (CI) for the relationship between each index with PCa-specific and all-cause mortality. We adjusted for education, race/ethnicity, smoking, BMI, physical activity (if not part of the score), family history of PCa, and first course of treatment.
Results: Across the five racial/ethnic groups, Japanese American men exhibited healthier lifestyle and dietary patterns post-diagnosis, while African American and Native Hawaiian men tended to have less healthy behaviors. The PCa Behavior Score was statistically significantly associated with a reduced risk of all-cause mortality (HR per point=0.71, 95% CI 0.63-0.80), and a similar trend persisted when incorporating diet into the score. The PDI was statistically significantly inversely associated with all-cause mortality (HR per SD=0.90, 95% CI 0.83-0.97), while the uPDI showed a positive association (HR=1.10, 95% CI 1.12-1.18). None of the lifestyle or dietary patterns were associated with PCa mortality (p-values>0.05). No clear trends were observed for inflammatory and insulinemic dietary patterns after PCa diagnosis with all-cause or PCa-specific mortality.
Conclusion: Adopting a healthy lifestyle and diet was associated with longer overall survival among men with PCa. We did not find these practices to be associated with a lower risk of PCa-specific mortality among men diagnosed with non-metastatic disease. However, 85% of the observed deaths during follow-up were due to other causes; this underscores the importance of counseling all men, including those with non-metastatic prostate cancer on health behaviors to manage comorbidities.

#2221 Reducing cancer disparity among indigenous people by locally prepared Whey protein isolates having selective cytoprotective ability against chemotherapy induced bone marrow stem cell toxicity.

N. Das[1], L. Pathak[1], B. Pal[2], R. Das[3], P. J. Saikia[1], S. Mitra[1], T. Baishya[3], R. Bhuyan[4], H. Li[4], B. Das[1];
[1]KaviKrishna Laboratory, Research Park, Indian Institute of Technology, Guwahati, India, [2]Thoreau Laboratory for Global Health, Lowell, MA, [3]KaviKrishna Telemedicine Care, Sualkuchi, India, [4]Forsyth Institute, Cambridge, MA

Background: Cancer disparity is a major problem for the indigenous people living in the rural area of Kamrup district of Assam, a remote north eastern state of India. Often, rural people are prescribed with expensive dietary supplements during chemotherapy by urban for profit medical centers, increasing disparity, as per a study conducted by KaviKrishna Telemedicine Care (KTC) (1). We seek to reduce cancer disparity by using locally available diet/nutrition of Sualkuchi-Hajo cultural complex, including the whey protein prepared by indigenous healers practicing Vedic Jiva Upakara Cikitsha Tantra (Vejiupacita) (2,3). However, the efficacy of the indigenous Vejiupacita Whey protein is not clearly known. Here we have performed pre-clinical and clinical studies to evaluate the therapeutic efficacy of Vejiupacita Chena Pani (VCP) whey protein in reducing cancer chemotherapy induced bone marrow stem cell niche toxicity.
Methods: Using a previously described pre-clinical model of cisplatin and busalphan induced BM stem cell niche toxicities (4), the cytoprotective activity of VCP Whey protein was evaluated. Commercially available whey proteins Ensure plus, and Immunocal were used for comparisons. Next, the indigenous cancer patients (n=55) of KaviKrishna Telemedicine Care taking the whey protein (20 gm twice daily for three months of chemo and or radiation) were monitored for hemoglobin, total blood count as well as Glasgow prognostic score (ratio of serum albumin and CRP) and ECOG performance score. Third, using a Vejiupacita based Sahasa-ojash scale of well being (3) patient's quality of life was evaluated.
Results: In the pre-clinical model of cisplatin-induced BM toxicity in black 6 mice (n=10 in each group), the VCP whey protein exerted cytoprotection of BM stem cells similar to Immunocal but 2-fold higher protection compared to Ensure plus. Serum glutathione and squalene level was significantly increased only in the VCP whey protein group. The hypoxic niche of CD271+ MSCs showed enhanced stem cell niche protection. Notably, VCP and Immunocal whey protein treatment increased the hypoxic BM stem cell niche defense against cisplatin-induced toxicity. Next, 34/55 patients taking the VCP whey protein (20 gm/twice daily for three months) showed increased hemoglobin level, increased total blood count, and increased weight gain. The Sahasa-ojash scale showed significant improvement in quality of life compared to the period when they did not take whey proteins in a manner similar to Glasgow prognostic score, and ECOG performance score.
Conclusion: The Vejiupcita based whey protein concentrate therapy exerts cytoprotection against chemotherapy induced toxicity.
References:1. Abstract 3342, AACR 2019. 2. Abstract 2772, 2023. 3. https://zenodo.org/records/8062404. 4. PMID: 18813359

#2222 Knowledge of risk factors and symptoms of head and neck cancers among Arab-Americans.

E. Adjei Boakye[1], R. F. Siddiqui[1], N. Al-Antary[1], M. Gilbert[1], L. Fakhoury[1], M. Vu[2], F. Siddiqui[1];
[1]Henry Ford Health System, Detroit, MI, [2]Northwestern University School of Medicine, Chicago, IL

Background: In 2023, approximately 66000 patients with head and neck cancers (HNC) will be diagnosed in the United States (U.S.). There are approximately 3.7 million Arab-Americans living in the U.S., with large concentration in Michigan (MI). For example, Dearborn, MI has the largest percentage of Arab-Americans (40% of people having Arab ancestry). Smoking, alcohol, and human papillomavirus (HPV) are the main causes of HNC. Common symptoms of HNC are lump in the neck/mouth, nonhealing ulcers, dysphagia or odynophagia, and change in voice. Currently, there is a scarcity of research on knowledge of HNC risk factors and symptoms among Arab-Americans. We examined knowledge of risk factors and symptoms of HNC among Arab-Americans residing in MI.
Methods: This was a cross-sectional study of adult Arab-Americans (≥18 years) conducted between March and July 2023. Survey questions were adapted from the National Cancer Institute and Centers for Disease Control and Prevention and offered in English and Arabic depending on respondent preference. Awareness of the symptoms of HNCs were assessed using 14 questions while risk factors were assessed using 10 questions. The questions were in the form of “Do you know that the following can be symptoms/risk factors of HNC?” Respondents selected “yes,” “no,” or “don’t know/not sure” for each answer choice.
Results: Of the 295 Arab-Americans survey respondents, the mean age ± SD was 37.9 ± 14.6, and most were female (60.7%), had at least a college degree (57.6%), private health insurance (56.7%), and usual place of receiving care (70.7%). Majority had no history of cigarette use (81.7%) or alcohol use (91.6%). Regarding HNC symptoms knowledge, only 40-50% knew about most common HNC symptoms: nonhealing ulcers (41%), dysphagia or odynophagia (51.4%), and voice changes (48.6%); while 60.6% knew about swelling or lump in neck/throat. About half of respondents knew of persistent mass or lesion on the tongue (53.3%) and bleeding in the mouth or throat (50.3%) as symptoms of HNC. About a third knew these as HNC symptoms: teeth loosening (31.7%), ill-fitting dentures (25.9%), otalgia (37.8%), and nasal obstruction/congestion (34.9%). For HNC risk factors knowledge, tobacco smoking, chewing, and second-hand smoking were the most common recognized risk factors, identified by 78.9%, 72.8% and 66.8%, respectively. However, less than half knew HPV (40.6%) and Epstein-Barr virus (35.4%) as risk factors.
Conclusion: While there is higher knowledge about tobacco as a risk factor for HNC, knowledge about HPV as a risk factor is very low. Similarly, knowledge about HNC symptoms is suboptimal in the Arab-American community, which could result in late-stage presentation and thus lower survival. Educational programs designed for this community are needed to help close this gap and improve HNC related health outcomes among culturally and ethnically distinct Arab-Americans.

#2223 Cancer risk factors and nativity: Lifestyle and sociodemographic disparities among us-born and non-us-born residents and by length of residence in the US.

L. D. Rolle, M. Lopez-Pentecost, R. Clavon, A. Bhatti, Z. Khan, T. E. Crane;
University of Miami Miller School of Medicine, Miami, FL

Background: Previous studies have found racial/ethnic disparities in cancer and cancer-related risk factors. However, the relationship between US nativity status and cancer risk is not well understood. This study aimed to determine the relationship between cancer risk factors, including lifestyle behaviors, demographic characteristics, and nativity status, among US residents. **Methods:** We used data from the 2010 and 2015 National Health Interview Survey (NHIS). All analyses accounted for the NHIS complex survey design. Our sample consisted of 31,252 US-Born and non-US-born residents. Regression models were employed to assess the association of US nativity with various lifestyle and demographic variables, adjusting for potential confounders such as age, race, sex, education, income, and employment status. **Results:** In our sample, 25,153 (82.73%) were US-born. Among non-US-born respondents (n=6,099), 35.13% have resided in the US for less than 15 years, and 64.87% for greater than 15 years. 80.19% of US-born individuals identified as non-Hispanic White (NHW), followed by non-Hispanic Blacks (NHB) (11.71%), and Hispanics (8.10%). For non-US-born residents, 63.67% identified as Hispanic, followed by NHW (24.21%), and NHB (12.12%). Non-US-born individuals had lower odds of consuming red meat (aOR=0.60, 95% CI: 0.47-0.75), and processed meat (aOR=0.36, 95% CI: 0.31-0.43) compared to their US-born counterparts. Notably, non-US-born individuals had significantly higher odds of never smoking (aOR=1.58, 95% CI: 1.35-1.83), never drinking (aOR=2.45, 95% CI: 2.05-2.93), and consuming grains (aOR=1.45, 95% CI: 1.25-1.68) in comparison to US-born individuals. Conversely, non-US-born individuals had lower odds of meeting physical activity guidelines (aOR=0.77, 95% CI: 0.59-0.99), and consuming fruits (aOR=0.86, 95% CI: 0.74-0.99), and consuming vegetables (aOR=0.83, 95% CI: 0.71-0.97). Additionally, non-US-born respondents had higher odds of being overweight/obese compared to normal weight (aOR=1.36, 95% CI: 1.16-1.60) compared to US-born respondents. When considering the length of time in the US, non-US-born residents with greater than 15 years of residence had lower odds of being normal weight compared to overweight/obese (aOR=0.78, 95% CI: 0.63-0.97), and never drinking alcohol (aOR=0.73, 95% CI: 0.56-0.93). **Discussion:** These disparities highlight the association of nativity and length of residence on health-related behaviors and outcomes in the United States, and the need for targeted public health interventions considering nativity and residency duration to address these health disparities.

POPULATION SCIENCES: Survivorship Research
Poster Session

#2227 Physical activity at breast cancer diagnosis and incident cardiovascular disease in the Pathways Study.

J. K. Kresovich[1], **A. R. Richards**[1], I. J. Ergas[2], C. A. Laurent[2], R. Cannioto[3], J. S. Rana[2], J. M. Roh[2], C. Thomsen[4], S. Shariff-Marco[5], E. Rillamas-Sun[6], R. K. Cheng[7], S. Yao[3], C. B. Ambrosone[3], L. H. Kushi[2], H. Greenlee[6], M. L. Kwan[2];

[1]H. Lee Moffitt Cancer Center, Tampa, FL, [2]Kaiser Permanente Northern California, Oakland, CA, [3]Roswell Park Cancer Center, Buffalo, NY, [4]Zero Breast Cancer, San Rafael, CA, [5]University of California at San Francisco, San Francisco, CA, [6]Fred Hutchenson Cancer Center, Seattle, WA, [7]University of Washington Medical Center, Seattle, WA

Background: Breast cancer survivors are at increased risk of cardiovascular disease (CVD) compared to women without a history of breast cancer. Although cardiotoxic cancer treatments influence these risks, lifestyles that are associated with both breast cancer and CVD also contribute. With the number of breast cancer survivors expected to increase, a growing need exists to identify modifiable risk factors that protect against the development of CVD after diagnosis. Physical activity at breast cancer diagnosis is associated with lower cancer recurrence and mortality risk. However, associations between physical activity at diagnosis and incident CVD have yet to be investigated in detail.

Methods: The Pathways Study is a prospective cohort study of 4,504 women who were members of Kaiser Permanente Northern California (KPNC) when diagnosed with first primary invasive breast cancer between 2005 and 2013. At enrollment, women self-reported their frequency, duration, and intensity of physical activities during the previous six months using the Arizona Activity Frequency Questionnaire. This information was used to dichotomize the women's physical activity levels by the CDC's Physical Activity Guidelines for Americans (≥ 150 minutes of moderate-to-vigorous physical activity per week vs less). CVD events were obtained from electronic health records as part of the Pathways Heart Study and were defined as post-diagnostic incidence of ischemic heart disease, heart failure, cardiomyopathy, and stroke. Deaths were documented through several sources, including the National Death Index. Women were followed until the first of disenrollment from the KPNC health plan, death, or December 31, 2021. Competing risk Cox regression models were used to estimate associations between meeting CDC physical activity guidelines and CVD.

Results: In this cohort of breast cancer survivors, women who self-reported meeting physical activity guidelines at diagnosis experienced lower rates of post-diagnostic CVD events (8.6% vs 13.1%). After adjustment for socio-demographic factors, meeting physical activity guidelines remained associated with lower risk of CVD (HR: 0.78, 95% CI: 0.61, 0.98); this association appeared to be driven by reduced risk of heart failure (HR: 0.68, 95% CI: 0.50, 0.93) and cardiomyopathy (HR: 0.51, 95% CI: 0.28, 0.92). Approximately 15% of the CVD risk reduction in Pathways Study participants can be attributed to meeting physical activity guidelines (population attributable risk percent: 14.5%, 95% CI: 8%, 21%).

Conclusions: Compared to women who did not meet CDC physical activity guidelines, women who reported meeting guidelines near the time of their breast cancer diagnosis had decreased risk of future CVD, including heart failure and cardiomyopathy. Future studies investigating changes in post-diagnostic physical activity patterns and CVD risk are warranted.

#2228 Long-term trajectories of functional disability in older adults with cancer.

G. E. Nam, E. R. Mayeda, Z.-F. Zhang;
UCLA Jonathan and Karin Fielding School of Public Health, Los Angeles, CA

Background: Older individuals with cancer history have lower risk of developing Alzheimer's disease (AD). Cognitive impairment is associated with lower functioning in Instrumental Activities of Daily Living (IADL) and Activities of Daily Living (ADL). However, little is known about long-term IADL and ADL trajectories among individuals with cancer, hindering understanding of the underlying biological mechanisms between cancer and AD. We investigated the long-term functional disability trajectories of adults with cancer, comparing them with similarly aged individuals without a cancer diagnosis.
Methods: Our study included 16,006 individuals aged 50 and older without a cancer history at baseline from the Health and Retirement Study. Biennial assessments were conducted from 1998 to 2020, including self-reported cancer status, IADL, and ADL. Linear probability models with repeated measures were used to assess IADL and ADL independence probabilities, adjusting for demographic and socioeconomic covariates.
Results: Among 16,006 participants (mean [SD] baseline age, 66.1 [9.9] years; 9,169 [57.3%] female), 3,723 (23.3%) reported a cancer diagnosis during follow-up. Before cancer diagnosis, individuals who later developed cancer had a higher probability of IADL independence and experienced a slower decline in independence compared to their similarly aged counterparts who remained cancer-free. Probability of IADL independence was 0.05 lower immediately after cancer diagnosis compared to the pre-cancer phase, followed by accelerated independence losses relative to the pre-cancer period. After diagnosis, the rate of decline in probability of IADL independence remained slower for individuals with cancer than their cancer-free counterparts, but differences in the rate of decline were smaller than prior to cancer diagnosis. Similar trends were observed for ADL independence.
Conclusions: We observed a decline in both IADL and ADL independence around the time of cancer diagnosis, possibly attributed to treatments. Overall, individuals with cancer experienced a more gradual loss in functional independence compared to individuals who remained cancer-free, consistent with the documented inverse association between cancer and AD.
Funding information: The current research was supported by the National Cancer Institute of the National Institutes of Health (T32CA009142), T32 Training Grants from the NCI/NIH, and the National Institute on Aging (RF1AG059872).

#2229 Clinico-pathologic analysis and survival of patients with breast cancer diagnosed with *de novo* brain metastasis: An NCDB-based analysis.

A. Hijazi[1], M. Mohanna[1], S. Sabbagh[1], M. Herran Montes[1], B. Dominguez[1], K. Sarna[2], Z. Nahleh[1];
[1]Cleveland Clinic Florida Foundation, Weston, FL, [2]Cleveland Clinic Foundation, Weston, FL

Introduction: Patients with breast cancer with brain metastasis (BCBM) have poor survival outcomes. In this study, we aimed to explore the clinico-pathologic and therapeutic factors predicting the survival in de novo BCBM patients using the National Cancer Database (NCDB).
Methods: The NCDB was queried for patients with BC between 2010-2020. Survival analysis with Kaplan-Meier curves and log rank tests were used to find median overall survival (OS) in months (95% CI) across the different variables. A multivariate cox regression model was computed to identify significant predictors of survival. All values in the results were statistically significant at $p<0.05$.
Results: N=9,005 (0.34%) had de novo BM out of 2,610,598 BC patients with a median OS of 10.9 (10.3-11.5). A trend of decreasing median OS was observed with increasing age: highest in the ≤50 group at 18.96 (16.92-20.86) and lowest in the ≥70 group at 4.70 (4.07-5.29), Charlson-Deyo score (CDS): 12.42 (11.76-13.17) in the 0 score and 2.86 (2.17-3.78) in ≥3 score, and number of extracranial metastatic sites (EMS): 13.17 (12.02-14.36) in the 1 site and 7.59 (6.70-8.84) in the ≥3 sites group. The HR(+)/HER2(+) subgroup had the highest median OS at 22.05 (18.73-24.67) compared to the lowest in the HR(-)/HER2(-) group at 5.62 (5.19-6.18). Based on treatment regimen, surgery + whole brain radiation therapy (WBRT), chemotherapy + hormonal therapy + immunotherapy (biologic therapy including anti-HER2), and combination of BM + BC therapy achieved the highest median OS in their respective subgroups of 32.33 (23.98-40.44), 42.35 (35.48-54.14), and 16.30 (15.11-17.38), respectively. Similar trends were found in the BC subgroup analysis with immunotherapy demonstrating a survival benefit when added to systemic therapy.The multivariate cox regression model showed that age, race, ethnicity, insurance, median income, facility type, CDS, BC subtype, metastatic location sites, and treatment combinations received were significantly associated with risk of death. Age ≥70 years, CDS ≥3, ≥3 EMS, and receiving no treatment for either BM or BC had the highest risks of death with Hazard Ratio (95% CI) of 1.53 (1.31-1.79), 1.74 (1.39-2.18), 2.06 (1.78-2.38), and 2.65 (2.36-2.98), respectively. The HR(+)/HER2(+) subgroup had the lowest risk of death at 0.43 (0.38-0.49) and receiving only local treatment for BM increased the risk of death 2.3 (2.00-2.63).
Conclusions: This analysis suggests that treatment of systemic disease is the major factor influencing survival in BCBM patients and surgery + WBRT yields the best survival outcomes. Moreover, anti-HER2 therapy and biologic treatment increased survival when added to systemic therapy. To date, this represents the biggest cohort of de novo BCBM survival analysis which provides critical insights that may guide clinical management.

#2230 Connecting Black men to point of prostate cancer diagnosis (PPCD) support using precision intervention based on Virtual Reality Assistant (ViRA).

F. T. Odedina[1], C. Ngufor[1], A. Merriweather[2], D. Pereira[3], R. Dronca[1], E. Kaninjing[4], K. Ashing[5], S. Rotimi[6], V. Gordon[1], iCCaRE for Black Men Consortium; [1]Mayo Clinic Comprehensive Cancer Center, Jacksonville, FL, [2]American Legion Post 197, Jacksonville, FL, [3]University of Florida, Gainesville, FL, [4]Georgia College, Milledgeville, GA, [5]City of Hope, Duarte, CA, [6]Covenant University, Ota, Nigeria

Background: The point of prostate cancer (CaP) diagnosis (PPCD) instantly leads to a life changing experience for Black men, with diverse emotional reactions that includes fear, denial, overwhelmingness, cancer fatalism etc. Black men diagnosed with CaP expressed several needs at the PPCD, including time to reflect on the diagnosis, being comfortable, emotional support, psycho-oncology support and social determinants of health (SDOH) navigation. Given that Black men are diverse in terms of their needs at the PPCD, precision intervention is needed to support them.

Aim: The aim was to develop, implement, and establish the acceptance and usability of a Virtual Reality Assistant (ViRA) that will provide precision intervention tailored to the needs of Black men at the PPCD. This study is one of the five iCCaRE for Black Men projects focused on survivorship care.

Methodology: The development of the ViRA was guided by CaP survivors through qualitative study. Reflective, analytic, and interpretive memos were used to generate action plans for the development of the ViRA. Based on a comprehensive PPCD ViRA intervention guide created by the team, the ViRA prototype was developed with mobile immersive technologies that integrated SDOH navigation, standard CaP psycho-oncology support and emotional support. The goal was to have the intervention personalized to everyone based on participant-provided information. Alpha testing of the ViRA is ongoing and will be completed on November 20, 2023. Participants are three prostate cancer survivors and three clinicians. The assessments will confirm the accuracy of the ViRA predictions and the functionality of the ViRA.

Results: We developed the ViRA SDOH screening and navigation tool to identify participants' needs and appropriately connect them with relevant support services and resources in their communities. The emotional support intervention was based on four CaP survivors as virtual reality avatars, providing empathetic rapport through self-disclosure and sharing of survivorship stories in different settings (home, clinic, barbershop etc). The psycho-oncology support intervention was developed with the guidance of a psycho-oncologist, with her avatar providing psychoeducation about the PPCD experience, reify and concretize the PPCD experience, and foster hope using the basic tenets of Problem-Solving Therapy. The results of the alpha testing and the modified ViRA will be presented during the conference.

Conclusion: Meeting the needs of Black men at the PPCD requires a personalized and decentralized approach, which would allow Black men to access support anywhere. The presentation will unveil the iCCaRE ViRA, a smart and connected personalized AR-enabled intervention that will deliver SDOH navigation, CaP psycho-oncology support and emotional support tailored to the needs of Black men.

#2231 Impact of sociodemographic and clinical factors on symptom burden in the young adult primary central nervous system tumor population.

Kimberly Reinhart[1], Tricia Kunst[1], Jennifer Reyes[1], Alvina Acquaye-Mallory[1], Ewa Grajkowska[1], Byram H. Ozer[1], Marta Penas-Prado[1], Jing Wu[1], Eric Burton[1], Lisa Boris[2], Marissa Panzer[2], Tina Pillai[1], Lily Polskin[2], Mark R. Gilbert[1], Elizabeth Vera[1], Terri S. Armstrong[1]

[1]Neuro-Oncology Branch, NIH-NCI, Bethesda, MD,[2]Leidos Biomedical Research, Inc., Frederick National Laboratory for Cancer Research, Frederick, MD

Purpose: The goal of this analysis was to provide insight into differences in perceived symptom burden and general health status between young adults (YA; 18-39 years of age) and older adults (OA; ≥ 40 years of age) with primary central nervous system (PCNS) tumors. Determining differences in characteristics that impact symptom burden and general health status in YA will allow for tailored survivorship programs that meet the unique needs of this population.
Methods: Data were retrospectively analyzed from the National Cancer Institute Neuro-Oncology Branch's Natural History Study (NCT02851706 PI: T.S. Armstrong), which is an observational prospective cohort study designed to follow and collect PROs and clinical information on patients diagnosed with PCNS tumors throughout their disease trajectory. Differences in patient-reported outcomes (general health status [EQ-5D-3L], symptom burden [MDASI-BT and MDASI-SP], anxiety/depression [PROMIS], and perceived cognition [Neuro-QOL]) and demographic and clinical data were assessed using chi-square tests, one-way ANOVAs, and Students' t-tests. Linear regression with backward elimination determined which characteristics impacted perceived symptom burden and general health status as evidenced by MDASI-BT and EQ-5D-3L, respectively.
Results: The sample included 271 YA (82% with a primary brain tumor [PBT]; median age 31 [range, 18-39]) and 516 OA (88% with a PBT; median age 54 [range, 40-85]). YA were more likely to be single (P<0.001), employed (P<0.001), and make < $50,000 per year (P=0.014). More YA reported pain (P=0.008), nausea (P<0.001), drowsiness (P=0.043), and vomiting (P=0.001) than OA. More YA presented with vision problems (25% of YA, 16% of OA), whereas more OA presented with cognitive deficits (17% of YA, 25% of OA). Compared to YA, 7% more OA with PBTs and 19% more OA with primary spinal tumors (PST) were diagnosed in outpatient clinics, whereas the majority of YA with PBTs (47%) were diagnosed in an emergency room. Among demographic and clinical characteristics, only Karnofsky Performance Scale score was a predictor of general health status (P<0.001) in YA with PCNS tumors and symptom interference (P=0.014) in YA with PBTs. YA reported more affective, cognitive, neurologic, treatment-related, generalized disease, and gastrointestinal symptom burden than OA, with the affective factor being the most severe among the symptom factors reported. Among individuals with PSTs, 20% more YA reported moderate-severe anxiety (P=0.050) and 32% more YA reported moderate-severe perceived cognitive deficits (P=0.023) than OA.
Conclusion: YA patients were more likely to be single, employed, have a lower income, and report more symptom burden than OA. These findings underscore the need for tailored survivorship programs providing additional psychosocial support and resources to address symptom presentation in YA.

#2232 Association between sleep characteristics and cancer survival: Findings from the UK Biobank study.

J. Che[1], J. Lv[1], K. Pan[1], T. Sun[2], C. Cao[3], S. Li[4], T. Zhang[1], F. Xue[1], **L. Yang**[5];
[1]Shandong University, Jinan, China, [2]CancerControl Alberta-Alberta Health Services, Calgary, China, [3]Dana-Faber Cancer Institute, Boston, MA, [4]Children's Hospitals and Clinics of Minnesota, Minneapolis, MN, [5]CancerControl Alberta-Alberta Health Services, Calgary, AB, Canada

Background
Sleep characteristics have been associated with patient outcomes after cancer. We aimed to appraise the causal relationship of chronotype, sleep duration, insomnia, and snoring with cancer survival.
Methods
This large prospective cohort study enrolled 38350 cancer survivors aged ≥40 years from the UK Biobank between 2004 and 2022. Habitual sleep characteristics were obtained from the self-reported baseline questionnaire, including chronotype, sleep duration, insomnia, and snoring. Cox proportional hazards regression models were applied to evaluate the association between sleep characteristics and cancer survival, then one sample Mendelian randomization (MR) analyses were further used to validate these causal relationships. In particular, restricted cubic splines (RCS) and non-linear MR analyses were applied to assess the possible nonlinear association between sleep duration and cancer survival.
Results
Among 38350 study participants (mean [SD] age, 59.8 [7.3] years; 24150 [63.0%] males; 35534 [92.7%] White individuals), 12671 (33.1%) reported evening preference chronotype; 9050 (23.6%) reported short and 3773 (9.8%) reported long sleep duration;12274 (32.0%) reported snoring; and 30426 (79.4%) reported experiencing insomnia sometimes or usually. During up to 18 years of follow-up, 6274 deaths occurred. Multivariable regression models showed that evening preference (HR = 1.09, 95% CI: 1.03 to 1.15), short (HR = 1.14, 95% CI: 1.07 to 1.21) and long sleep duration (HR = 1.37, 95% CI: 1.28 to 1.48), insomnia (HR = 1.14, 95% CI: 1.09 to 1.21) and snoring (HR = 0.83, 95% CI: 0.78 to 0.87) were associated with death among pan to cancer survivors. Restricted cubic splines suggested nonlinear associations between sleep duration and death after cancer (nonlinear $P < 0.001$). In the one-sample MR, genetically predicted sleep duration (HR = 0.71, 95% CI: 0.56 to 0.90) and snoring (HR = 1.18, 95% CI: 1.05 to 1.34) demonstrated a reversed cancer survival pattern compared to multivariable regressions. A nonlinear U-shape association between sleep duration and cancer survival was observed in restricted cubic spline analyses ($P < 0.001$) but not evident when evaluating by nonlinear MR ($P > 0.05$).
Conclusions
Evening preference chronotype, insomnia, snoring, and short sleep duration are likely to be causally associated with a higher risk of death among cancer survivors, whilst long sleep duration does not appear to be a causal factor.

#2233 Limited adherence to clinical practice guidelines on fertility preservation for patients with early-onset cancer.

S. R. Keller[1], M. A. Lewis[2], A. Rosen[3], H. K. Park[4], R. Babyak[1], J. Feldmann[5], F. Ye[6], R. Agarwal[6], K. K. Ciombor[6], T. M. Geiger[1], C. Eng[6], M. K. Roach[1], D. R. Velez Edwards[1], M. L. Cote[7], R. Viskochil[8], **A. N. Holowatyj**[6];

[1]Vanderbilt University Medical Center, Nashville, TN, [2]Intermountain Healthcare, Murray, UT, [3]American Cancer Society, Atlanta, GA, [4]Providence Saint John's Health Center, Santa Monica, CA, [5]EGFR Lung Resisters Group, Chicago, IL, [6]Vanderbilt-Ingram Cancer Center, Vanderbilt University Medical Center, Nashville, TN, [7]Indiana University Simon Comprehensive Cancer Center, Indianapolis, IN, [8]University of Massachusetts Boston, Boston, MA

Background: ASCO Clinical Practice Guidelines on fertility preservation (FP) recommend that healthcare providers discuss the possibility of infertility—including FP options—for cancer patients of reproductive-age as early as possible before treatment initiation. However, the evaluation of patient perceptions on provider adherence to these FP guidelines is largely undetermined. We sought to assess patient-reported provider adherence to FP guidelines for adults ages 18 to 49 years when diagnosed with a first primary cancer (early-onset).

Patients and Methods: The Reproductive Health After Cancer Diagnosis and Treatment (REACT) Study is a patient-partnered study in cooperation with 23 community partners and patient advocates. Adults with a first primary early-onset cancer were recruited over an 8-week period (October to December 2021). Patient-reported provider adherence to FP guidelines, reproductive health history, sociodemographic, cancer and cancer impact questions were prospectively collected via patient questionnaire using a secure, web-based application. To examine the association of provider non-adherence with patient-level factors, logistic regression models were fitted to estimate odds ratios (OR) and 95% CI.

Results: Among 647 patients diagnosed with early-onset cancer between 2006 and 2021 (mean [SD] age, 36.8 [7.8] years), a total of 376 (58.1%) reported that a healthcare professional involved in their cancer care did not discuss FP options before starting cancer treatment. Patients with thyroid, lung, ovarian and colorectal cancers reported the highest rates of provider non-adherence to FP guidelines (all ≥63% non-adherence). Females with cervical (OR 2.87, 95% CI: 1.11-7.41), colorectal (OR 2.05, 95% CI: 1.15-3.68), lung (OR 15.79, 95% CI:5.66-44.1) and ovarian (OR 10.90, 95% CI: 3.19-37.3) cancers, Hodgkin (OR 4.00, 95% CI: 1.15-13.98) and non-Hodgkin lymphoma (OR 4.65, 95% CI: 1.11-19.47) were more likely to report provider non-adherence to FP guidelines compared to breast cancer patients in models adjusted for diagnosis age and year, self-reported race/ethnicity, marital status and insurance coverage at cancer diagnosis. Similar patterns were observed for male patients with early-onset colorectal and lung cancers compared with testicular cancer patients. No overall or sex-specific associations were observed between patient-reported provider non-adherence and race/ethnicity, insurance coverage or diagnosis year.

Conclusions: Nearly six of every 10 early-onset cancer patients reported that a healthcare professional involved in their cancer care did not discuss FP options prior to cancer treatment. The development of tailored, effective strategies for implementation of clinical practice guidelines on FP and delivery of concordant reproductive healthcare to a growing population of reproductive-age individuals with cancer is needed.

#2234 Cardiovascular disease risk among men with prostate cancer: Differences by prostate cancer aggressiveness.

Caroline Himbert[1], Anna Plym[2], Jane B. Vaselkiv[3], Andreas Pettersson[2], Philip W. Kantoff[4], Lorelei A. Mucci[3], Kenneth J. Mukamal[1], Konrad H. Stosapck[1]

[1]Clinical and Translational Epidemiology Unit, Massachusetts General Hospital, Boston, MA,[2]Clinical Epidemiology Division, Karolinska Institutet, Stockholm, Sweden,[3]Department of Epidemiology, Harvard T.H. Chan School of Public Health, Boston, MA,[4]Convergent Therapeutics Inc., Boston, MA

Background: Cardiovascular disease (CVD) is a major cause of morbidity and mortality among men diagnosed with prostate cancer. We evaluated the extent to which men with prostate cancer develop CVD accounting for potential factors that may contribute to the CVD burden in this population.
Methods: We prospectively followed men diagnosed with prostate cancer and free from CVD (stroke and coronary heart disease, including myocardial infarction, coronary artery bypass graft, and percutaneous coronary intervention) before their cancer diagnosis in the Health Professionals Follow-up Study, between 1986 and 2016. Men were categorized by D'Amico prostate cancer risk groups as low-risk (stage T1-2a, Gleason score ≤6, and PSA at diagnosis ≤10 ng/mL), intermediate-risk (T2b and/or Gleason score 7 and/or PSA >10-20), or high-risk (≥T2c/N1/M1 or Gleason score 8-10 or PSA >20). Incident fatal and non-fatal CVD, defined as coronary heart disease and stroke after cancer diagnosis, were centrally adjudicated. CVD risk factors including smoking, hyperlipidemia, hypertension, diabetes mellitus, body mass index, were self-reported on biennial questionnaires. Deaths due to prostate cancer or other causes were treated as competing events when estimating cumulative incidence and cause-specific hazard ratios (HR).
Results: Among 5,707 prostate cancer patients, 1,912 had low-risk, 2,261 had intermediate-risk, and 1,534 had high-risk cancer. 1,102 CVD events were documented over up to 30 years of follow-up after cancer diagnosis. The 10-year CVD risk was 8.1% for men with low-risk cancer, 8.8% for intermediate-risk, and 10.4% for high-risk cancer. The cause-specific HRs for CVD were 1.18 (95% CI 1.03, 1.36) in intermediate-risk and 1.59 (95% CI 1.36, 1.85) in high-risk prostate cancer, both compared to low-risk prostate cancer. Men with high-risk cancer tended to be older; after age adjustment, the HRs were 1.15 for intermediate-risk (95% CI 1.00, 1.33) and 1.35 for high-risk cancer (1.35, 95% CI 1.16, 1.58). Associations between cancer risk group and CVD were essentially unchanged after further adjustment for CVD risk factors present at cancer diagnosis, primary cancer treatment modality (surgery, radiation, androgen deprivation therapy, watchful waiting/active surveillance), and calendar year of diagnosis.
Discussion: Despite the elevated risk of cancer mortality in men with intermediate-risk and high-risk prostate cancer compared to low-risk prostate cancer, CVD risk remains at least as common over time among these men as among men with low-risk prostate cancer. Incident CVD risk after cancer diagnosis among men with more aggressive cancers, which particularly occur in older men, is not primarily attributable to differences in pre-existing risk factor burden. These findings from a cohort with healthcare access and literacy indicate a need for continued clinical attention to CVD after cancer diagnosis.

#2235 Epigenetic inflammation scores for C-Reactive protein and interleukin-6 associate with adverse cardiometabolic and cardiac outcomes among survivors of childhood cancer.

Q. Dong, Y. Chen, X. Zhang, J. Easton, H. Mulder, E. Walker, G. Neale, K. Shelton, S. B. Dixon, J. Zhang, G. T. Armstrong, M. M. Hudson, K. K. Ness, Z. Wang;
St. Jude Children's Research Hospital, Memphis, TN

Background: Inflammaging, a chronic low-grade inflammation as individuals age, is measured by elevated levels of circulating markers of inflammation (e.g., C-reactive protein [CRP] and interleukin-6 [IL-6]) and is associated with age-related chronic health conditions (CHCs). We aim to evaluate epigenetic inflammation scores (EIS) for CRP and IL-6 and their associations with cardiometabolic and cardiac-based CHCs and epigenetic age acceleration (EAA) in childhood cancer survivors (CCS).
Methods: Among 2,052 CCS (47.2% female; mean [SD] = 33.7 [9.3] years of age at blood draw) from the St Jude Lifetime Cohort, EIS of CRP and IL-6 were calculated as the weighted sum of the DNA methylation (DNAm) levels of CpGs that are associated with circulating levels of CRP or IL-6, where blood DNAm data were generated with Infinium EPIC BeadChip, and weights are regression coefficients from previously published EWAS studies. CHCs with a CTCAE (Common Terminology Criteria for Adverse Events) grade ≥2 were considered except for myocardial infarction (MI) where a minimum CTCAE grade of 3 was applied. Residuals of EIS were calculated by regressing EIS on age at blood draw and sex. A multivariable Cox proportional hazard regression model evaluated the associations between the EIS residuals and each CHC adjusting for sex and cancer treatments. The timeframe was years since age at blood draw. All participants alive at the last follow-up were censored. EAA was calculated as residuals from regressing epigenetic age (both GrimAge and PhenoAge) on age at blood draw. A linear regression model evaluated the association between the EIS residual and EAA adjusting for sex and treatments.
Results: The incidence of cardiometabolic conditions (i.e., after the blood draw) included: abnormal glucose metabolism (AGM, 5.1%), hypertension (HTN, 16.6%), hypercholesterolemia (HCL, 3.9%), hypertriglyceridemia (HTG, 6.0%), and cardiomyopathy (CMP, 9.0%), MI (4.4%), and obesity (24.2%). CRP-EIS and IL6-EIS were correlated (r=0.62). The CRP-EIS residual was significantly associated with increased risk of AGM (Hazard Ratio [95% CI] = 1.33 [1.01-1.75], P=0.04) and CMP (1.44 [1.19-1.74], $P=1.58\times10^{-4}$) and suggestively associated with HTN (1.16 [0.99-1.36], P=0.07) and MI (1.55 [0.94-2.57], P=0.09). IL6-EIS residual was associated with CMP (1.25 [1.04-1.49], P=0.02). In addition, both CRP- and IL6-EIS were positively associated with PhenoAge-EAA (β = 0.53 and 0.50 years per SD increase of EIS) and GrimAge-EAA (β = 0.30 and 0.36 per SD increase of EIS).
Conclusion: The CRP- and IL6-EIS are associated with increased risk of cardiometabolic and cardiac-based CHCs and EAA among CCS, suggesting that EIS may be used as clinical tools to identify survivors at higher risk of such CHCs and inflammation may be targeted for intervention to reduce the burden of CHCs.

#2237 Determinants of time to cancer treatment initiation at a comprehensive cancer center.

N. J. Nonzee[1], M. Razavi[1], W. Dale[1], L. Cai[1], A. Mercurio[1], L. Gaytan[1], D. Lefkowitz[2], C. Kim[1], T. Hernandez[1], S. Morales[1], D. Duque[1], A. I. Tergas[1]; [1]City of Hope, Duarte, CA, [2]University of California, Riverside, Riverside, CA

Background: Delays in treatment initiation adversely impact cancer mortality and survival. To inform potential enhancements and targets for our existing oncology patient navigation program, we examined characteristics associated with timely treatment initiation among patients at a tertiary comprehensive cancer center that serves four diverse counties in Southern California.

Methods: We performed a retrospective analysis of patients newly diagnosed with non-hematological cancers between January 2020 and June 2023. Using electronic medical record data, we used a multivariable Cox proportional model to examine the association between patient demographic and clinical characteristics and time to treatment initiation (time between first encounter and start of definitive treatment) within a clinical benchmark of 3 months. A hazard ratio (HR)>1 indicates shorter (faster) time to treatment initiation while a HR<1 indicates a longer (slower) time.

Results: Our sample included 9,148 patients, who were predominantly <65 years (57%), female (61%), married or with a partner (64%), and retired or unemployed (56%); 50% were non-White. In multivariable analyses, patient's age, primary language, employment status, cancer diagnosis type, and first treatment type were significant determinants of time to treatment initiation. Faster treatment initiation was observed among patients ages >=75 vs <65 years (HR=1.36, 95% CI 1.23 - 1.52). Among the primary languages spoken in our sample (Spanish, Chinese, Korean, Vietnamese, among others), patients who spoke Armenian vs English also had shorter time to treatment (HR=1.64, 95% CI 1.32 - 2.04). By contrast, longer time to treatment initiation was associated with patients who were retired or disabled vs employed full-time (HR=0.85, 95% CI 0.78 - 0.94, and HR=0.70, 95% CI 0.59 - 0.83, respectively) and underwent radiation or oral chemotherapy vs chemo-infusion (HR=0.65, 95% CI 0.57 - 0.74, and HR=0.82, 95% CI 0.76 - 0.89, respectively). With the exception of melanoma, all diagnoses had a longer time to treatment compared with neuro-oncology. In our multivariable model, sex, marital status, race and ethnicity, and receipt of at least one navigation encounter were not significant determinants.

Conclusions: In our study, which overlapped the early stages of the COVID-19 pandemic, findings highlight opportunities to enhance navigation delivery, especially for certain subpopulations, diagnoses, and treatment types with complex scheduling and coordination needs. Future research will explore navigation intensity and other process and clinical outcomes modifiable through navigation.

#2238 Reducing cardiovascular disease risk in cancer survivors: Impact of a 16-week circuit-based interval exercise intervention.

A. J. Normann[1], R. L. Wilson[2], C. N. Christopher[3], M. K. Norris[2], S. Cuomo[4], C. M. Dieli-Conwright[2];
[1]Boston University, Boston, MA, [2]Dana Farber Cancer Institute, Boston, MA, [3]Harvard University, Boston, MA, [4]University of Turin, Turin, Italy

Introduction: Obesity and physical inactivity pose a significant health concern for cancer survivors in developing comorbid conditions such as type 2 diabetes, hypertension, and metabolic syndrome that lead to a heightened risk of cardiovascular disease (CVD). Therefore, regular physical activity plays a central role in reducing the risk of CVD. The Framingham risk score (FRS) is an established assessment of CVD risk that combines six risk factors including age, gender, high-density lipoprotein cholesterol (HDL-C), low-density lipoprotein cholesterol (LDL-C), systolic blood pressure, diabetes, and smoking status. The objective of the study was to investigate the effects of a 16-week circuit, interval-based exercise training intervention on FRS and the 10-year FRS-predicted risk of developing CVD among breast, prostate, and colorectal cancer survivors.

Methods: This single center, pilot randomized controlled trial consisted of 90 sedentary, overweight or obese (BMI > 25.0 kg/m^2) survivors of breast, prostate or colorectal cancers, randomized to exercise (n=60) or usual care (n=30). The 16-week intervention comprised supervised moderate to vigorous intensity aerobic (65-85% of VO2max) and resistance (65-85% of 1-repetition maximum) exercise sessions conducted in a circuit-based interval fashion, occurring three times per week. Blood samples were obtained at baseline and post-intervention time points to measure fasting plasma levels of HDL-C and LDL-C, along with resting systolic blood pressure and diagnosis of diabetes. Paired t-test and repeated measure ANOVA were used to determine between-group differences.

Results: Participants (age 63.2 ± 10.8 years) were diagnosed with breast (35%), prostate (30%), and colorectal (35%) cancers and consisted of 55% female participants, participants had a mean BMI of 34.7±5.9, and 85% were obese. Chemotherapy and/or radiation therapy was completed by 75% of participants. Retention and adherence rates to exercise were high (100% and 92%, respectively). Compared to usual care, circuit, interval-based exercise significantly reduced total FRS (between group mean difference, -12.0 points p<0.001) and 10-year CVD risk (-10.0%; p<0.001).

Conclusions: This study underscores the critical role of circuit-based, interval exercise interventions in mitigating the elevated cardiovascular risk faced by sedentary, overweight, or obese cancer survivors. The significant reduction in FRS components highlights the potential of structured exercise programs to enhance cardiovascular health, thereby reducing the burden of comorbid conditions and CVD risk in cancer survivors.

#2239 Comparative effectiveness of cystoscopy surveillance strategies on mortality in non-muscle invasive bladder cancer: A target trial emulation using real-world data.

E. E. McGee[1], X. Garcia de Albeniz[2], A. Eliassen[1], K. Yim[3], B. A. Dickerman[1], M. A. Preston[3], M. A. Hernan[1];

[1]Harvard T.H. Chan School of Public Health, Boston, MA, [2]RTI Health Solutions, Barcelona, Spain, [3]Brigham and Women's Hospital, Boston, MA

Background: More than 60,000 U.S. adults are diagnosed with non-muscle invasive bladder cancer (NMIBC) each year. These patients are recommended to undergo surveillance via repeated cystoscopies. However, the ideal frequency of post-diagnostic cystoscopy surveillance remains unknown, and efforts are underway to de-escalate surveillance given uncertainty regarding its effect on mortality. We therefore aimed to compare the effectiveness of different post-diagnostic cystoscopy surveillance strategies on bladder cancer specific mortality.

Methods: We used observational data from the Surveillance, Epidemiology, and End Results (SEER)-Medicare linkage to emulate a target trial, i.e., a hypothetical, pragmatic randomized trial that would answer our causal question. Eligible individuals were aged 66 years or older, diagnosed with NMIBC (Ta, Tis, or T1) classified as urothelial carcinoma between January 1, 2000 and December 31, 2017, and had completed their first post-diagnostic cystoscopy. We compared 10-year risks of bladder cancer specific mortality under cystoscopy surveillance every 3, 6, and 12 months separately among individuals at low, intermediate, and high risk. We estimated mortality risks using inverse probability weighted pooled logistic regression.

Results: Among 58,004 eligible individuals, the median age at diagnosis was 77 years (interquartile range: 72, 82) and 75.6% were male. Over the 10 year follow-up period, 4,977 bladder cancer deaths occurred. Among individuals at high risk, the estimated 10-year bladder cancer mortality risks were 24.5% under the 3 month strategy, 26.6% under the 6 month strategy, and 27.3% under the 12 month strategy. Compared with cystoscopy every 3 months, the risk differences were 2.1% (95% confidence interval [CI]: -0.3, 3.8) for cystoscopy every 6 months, and 2.8% (95% CI: 1.0, 4.4) for cystoscopy every 12 months. For patients in the intermediate risk group, 10-year bladder cancer mortality risks were 14.4% under the 3 month strategy, 15.1% under the 6 month strategy, and 15.9% under the 12 month strategy. The risk differences were 0.7% (95% CI: -0.6, 2.0) for 6 vs. 3 months and 1.6% (95% CI: 0.3, 2.7) for 12 vs. 3 months. Among individuals at low risk, these mortality risks were 8.3% under the 3 month strategy, 9.2% under the 6 month strategy, and 9.6% under the 12 month strategy. Risk differences were 1.1% (95% CI: -0.1, 2.5) for 6 vs. 3 months and 1.5% (95% CI: 0.2, 3.0) for 12 vs. 3 months.

Conclusions: We estimated that more frequent cystoscopy may result in clinically meaningful reductions in bladder cancer mortality among high risk patients. Among low and intermediate risk patients, more frequent cystoscopy may result in modest absolute risk reductions. Decision-makers should also consider the clinical and financial burden and risk of complications associated with more frequent surveillance.

#2240 An exploratory study of financial toxicity intervention components preferred by cancer survivors.

M. Huq[1], C. Conley[1], H. Derry-Vick[2], A. Khoudary[2], L. Sorgen[1], O. Billini[2], T. Gunning[3], C. Luck[1], S. Kaushik[1], V. Hurley[1], J. Marshall[4], B. Weinberg[4], A. Tesfaye[4], A. Ip[3], A. Potosky[1], M. D. Schwartz[1],

[1]Georgetown University Lombardi Comprehensive Cancer Center, Washington DC, DC, [2]Hackensack Meridian Health, Nutley, NJ, [3]Hackensack Meridian School of Medicine, Nutley, NJ, [4]Medstar Georgetown University Hospital, Washington DC, DC

Background: Despite growing research on financial toxicity (FT) in cancer survivors, few studies have examined cancer survivors' preferences for FT interventions. Understanding cancer survivors' preferences for specific intervention components may facilitate the development and implementation of such interventions, potentially reducing the financial burden of cancer treatment.

Purpose: The current work is an exploratory study of cancer survivors' FT intervention component preferences.

Methods: Adult survivors (N=105) of colorectal cancer (CRC; n=55) or non-Hodgkin lymphoma (NHL; n=50) from three tertiary care centers self-reported demographic characteristics (gender, race, income, employment status, insurance), clinical characteristics (comorbidities), psychosocial characteristics (PROMIS Global Health scale for mental health, Brief Health Literacy Screen scale, eHealth Literacy Scale), financial impact of cancer (the 11-item comprehensive score for financial toxicity COST scale, and life-altering and care-altering coping strategy scales), and preferences for FT intervention components. Intervention preferences were assessed through survey items on intervention timing and specific content. We employed descriptive statistics to assess overall preferences, and unadjusted linear regression and ANOVAs to identify demographic, clinical, psychosocial and financial predictors of intervention preferences.

Results: In terms of timing, 79% of participants favored initiating a FT intervention before treatment compared to during or after treatment. The majority of participants (57%) were interested in at least one FT intervention component. In terms of specific components, participants were most interested in help understanding out-of-pocket costs and insurance (49%), help applying for financial assistance (39%), financial education (32%), and help communicating with the treatment team (32%). Participants were less interested in online tools to manage cancer-related expenses (27%), finance-related stress management (25%), and budgeting (20%). Predictors of overall interest (i.e., number of components endorsed) were: having high FT (B=.413, p=<.001), adopting life-altering coping behaviors (B=.374, p=<.001), using care-altering coping behaviors (B=.241, p=.014), being a non-White survivor (B=.219, p=.024), and having poorer mental health (B=-.280, p=.004).

Conclusions: Cancer survivors may prefer FT interventions offered before treatment, and providing guidance on out-of-pocket costs and insurance. FT interventions may be particularly desired by those who experience greater financial toxicity, life and care-altering costs, are a racial/ethnic minority, or have poorer mental health, suggesting potential priority groups and target outcomes for intervention development.

#2241 Healthcare underutilization, healthcare mistrust, and quality of life among cancer survivors who use cannabis.

S. J. Kim[1], G. D. Abbasabad[1], V. Clark[2], S. Hong[1], V. B. Sheppard[1];
[1]Virginia Commonwealth University - VCU, Richmond, VA, [2]University of Rochester Medical Center, Rochester, NY

Background: An increasing number of states have legalized the use of cannabis and its derivatives. As a result, marijuana use is expected to increase among cancer survivors. Research shows that cancer survivors use cannabis to manage a myriad of cancer-related symptoms, including pain and nausea. Despite this, there is limited evidence on how cannabis use among cancer survivors impacts healthcare utilization, healthcare mistrust, and quality of life among cancer survivors. Environmental scanning is needed to inform clinical oncologic outcomes as well as the benefits and risks of cannabis use among cancer survivors.
Objectives: To examine differences in healthcare utilization, healthcare mistrust, and quality of life between adult cancer survivors who have ever used cannabis and those who have never used it.
Methods: We recruited adults with a history of cancer through Qualtrics online panels for an online survey across all the states with different levels of marijuana laws (e.g., decriminalized and/or medical use only, and fully illegal and/or CBD oil only). We assessed sociodemographic, behavioral, psychological, cancer-related, and treatment-related characteristics, as well as quality of life, healthcare utilization, healthcare mistrust, and cannabis use (e.g., types, duration of use, current/ever use).
Results: Based on a total of 747 respondents, 395 were eligible and enrolled in the survey. Nearly one-fourth of participants were non-White (n=103, 26.1%), and 240 (60.8%) were female. Two hundred and forty participants indicated they had ever used cannabis (240/395, 60.8%). Of these, 35% (n=84) were current users of cannabis. Compared to individuals who never used cannabis, ever users had greater healthcare system mistrust (t(257)=2.58, *p*=.01), underutilized healthcare systems in the last 12 months (e.g., “..had a medical problem but never sought any medical attention about my condition” and “...did not come back for a follow-up appointment that my doctor gave me”) (t(248)=2.83, p=.005), and reported worse physical (t(260)= -3.32, p<.001) and emotional well-being (t(260)= -2.36, p=.02). There was no difference between these two groups (ever users vs. never users) for functional well-being (t(260)= 1.08, p=.28).
Discussion: The present study provides empirical evidence on differences between cancer survivors who ever used and never used cannabis. Compared to never users, ever users of cannabis had greater mistrust of the healthcare system, underutilized healthcare, and reported lower physical and emotional well-being. Further studies are needed to examine how cannabis use impacts the long-term health and wellbeing of cancer survivors.

#2242 Clinical trials knowledge among Hispanic/Latino gastrointestinal cancer survivors in Puerto Rico.

Hilmaris Centeno-Girona[1], Marievelisse Soto-Salgado[1], Mariela Bournigal-Feliciano[1], Sofia F. Contreras-Fernandez[1], Karina Torres-Mojica[1], Victoria Williams[2], Arnethea L. Sutton[2], Katherine Tossas[2], Robert Winn[3], Marcia R. Cruz-Correa[4]

[1]University of Puerto Rico Comprehensive Cancer Center, San Juan, PR,[2]Virginia Commonwealth University, Richmond, VA,[3]VCU Massey Comprehensive Cancer Center, Richmond, VA,[4]School of Medicine, University of Puerto Rico, San Juan, PR

The discovery of innovative cancer prevention and treatment approaches relies on voluntary participation in clinical trials (CTs); however, participation remains low among minorities/ethnic groups. Knowledge of CTs has been reported as a barrier to CT participation. Yet, there is limited understanding regarding CTs knowledge and participation among gastrointestinal (GI) cancer survivors in Puerto Rico (PR). Colorectal cancer is the second leading cause of death in PR, accounting for 13% among men and women. We aimed to describe the knowledge and factors associated with cancer-related CTs among Hispanic/Latino GI cancer survivors in PR. We analyzed preliminary data from an ongoing cross-sectional study targeting Hispanic/Latino GI cancer survivors aged 21+ years in PR. The study employed an interviewer-administered questionnaire to assess participants' awareness, knowledge, and participation in cancer-related CTs, and the social determinants of health (SDoH) associated with CT participation. Descriptive statistics were used to describe the population. Pearson chi-square test or Fisher's exact test were used accordingly to assess significance. A generalized linear model was used to estimate the odds ratios and 95% confidence intervals (CI) for significant variables. As of November 9, 2023, 59 Hispanic/Latino GI cancer survivors had completed the questionnaire. Women accounted for 56% of the sample, and the median age of study participants was 65 years (IQR: 19). Racial identity among participants was primarily white (63%), followed by other races (18%) and African-American (18%). Most participants were in complete or partial remission from cancer (83%). A significant proportion of the respondents reported having at least 12th grade (81%) and an annual income of $20,000 or higher (67%). Most participants (76%) accurately identified the correct definition of a CT. Participants with 12th grade or more had 1.5 (95% CI:1.1-1.9) times the possibility to correctly identify the CT definition compared to to those with less than 12th grade. Similarly, respondents with an annual income equal or higher than $20,000 had 1.4 (95% CI:1.1-1.8) times the possibility to correctly identify the CT definition compared to their counterpart. Furthermore, 93.2% of respondents had a score of at least 80% of correct responses regarding their knowledge of CTs. Although nearly 100% of the respondents knew about CTs, only 20% had participated. Despite a high level of knowledge regarding CTs in PR, a significant gap remains between knowledge and participation. Factors such as education and income might play a role in understanding the CT definition. However, the barriers preventing participation, including SDoH need further exploration. Enhancing participation among Hispanic/Latino GI cancer survivors in PR is essential for advancing cancer research and improving outcomes for this at-risk population.

#2243 A multi-ethnic population-based pilot study of multiple myeloma disparities.

A. M. Rolon[1], A. P. Vang[1], J. Quino[1], A. Estrada[1], E. Stewart[2], R. D. Cress[2], L. Carvajal-Carmona[1], A. Morales Arana[1];
[1]University of California Davis, Davis, CA, [2]Cancer Registry of Greater California, Sacramento, CA

To understand multiple myeloma (MM) disparities we established the Precision MEDicine, EqUity and Disparities Research in MultipLe MyeLomA (MEDULLA) study, a population-based study in California. Our study contacted, via the Cancer Registry of Greater California (CRGC), 100 adult MM patients from four racial/ethnic groups: Non-Hispanic Black (NHB), Non-Hispanic White (NHW), Latinos, and Asians. Data collection included variables reported to the CRGC, a self-administered survey, and biospecimen saliva collection. The survey focused on demographics, risk factors, cancer treatment, family history, quality of life, and social determinants of health. Of the 400 MM patients, we had 95 patients who responded to the survey, giving a response rate of 24%. 44% of those who responded were NHW, 21% NHB, 19% Latinos, and 16% Asians. Those that provided a response tend to be living in a census tract location with lower proportions of poverty ($p=0.0004$), higher proportion of adults ages 25 years or over with a college degree ($p=0.0011$), higher median household income ($p=0.0048$), lower proportion of adults ages 25 years or over without a high school diploma ($p<0.0001$), and a lower proportion of individuals ages 16 or over who are unemployed ($p<0.006$). All respondents also have a lower comorbidity count and expressed being in good health. For minorities, we identified a trend where a higher response rate is seen if they live in an area where median household income is higher ($p=0.0108$). For every 1% increase in poverty rates, NHW living in such neighborhoods were 3% less likely to respond to the survey ($p=0.04$). For every 10% increase in the proportion of individuals having a college degree, response rate increased by 1.17 for minorities in that neighborhood ($p=0.07$). Minorities living in neighborhoods with high proportions of adults without a high school diploma and high unemployment rates are less likely to respond ($p=0.02$ and $p=0.047$, respectively). In conclusion, we found significantly lower participation rates among minority groups, with socio-economic factors affecting response rates. Our findings, therefore, suggest that future studies must develop improved community-focused and culturally tailored strategies to engage and meaningfully understand MM etiology and survivorship in such populations.

#2244 Accelerated aging associated with cancer characteristics and treatments among breast cancer survivors.

C. Wang[1], J. B. De Vis[2], K. Nguyen[1], B. Jia[1], M. Alford[1], A. Chakravarthy[2], X.-O. Shu[1];
[1]Vanderbilt University, Nashville, TN, [2]Vanderbilt University Medical Center, Nashville, TN

There are currently approximately four million breast cancer (BC) survivors in the US. BC survivors may experience accelerated aging, with greater physical dysfunction and cognitive decline than cancer-free women, potentially due to the detrimental effects of BC and/or its treatments (Tx). However, the aging trajectory after BC diagnosis has not been fully elucidated. A biological age measure, PhenoAge acceleration (PAA), derived from chronological age and nine clinical blood chemistry biomarkers, has been associated with aging-related health outcomes and mortality in the general population. Our study aims to evaluate PAA among BC patients by clinical characteristics, cancer Tx, and medications (chemotherapy and endocrine therapy drugs). The study included 1264 BC patients (age 54.7±11.7) recruited at Vanderbilt University Medical Center in 2004-2021. BC-related information and lab test results were obtained from the tumor registry and electronic health records. The differences in PAA (ΔPAA) by BC stage, grade, subtype, Tx, and medications at multiple time points were evaluated using linear mixed models, with the time interval between diagnosis and PAA assessments as a natural spline, and its interaction with the exposures under study as covariates. Associations of PAA with Tx and medications were estimated with adjustment for other Tx and medications. At 10 years post-diagnosis, stage III/IV (vs 0) and intermediate- and high- (vs low-) grade BC were associated with a higher PAA of 4.48 (p<0.001), 1.26 (p=0.03), and 1.95 (p=0.001), respectively; triple-negative (vs hormone receptor+/Her2-) BC was associated with a lower PAA (ΔPAA=-1.96, p=0.004). Compared with surgery, alone or with radiotherapy, surgery plus chemotherapy was associated with a higher PAA at 1 year (ΔPAA ranging from 1.96, p=0.03 to 4.61, p<0.001), while surgery plus endocrine therapy was associated with a higher PAA at 10 years post-diagnosis (ΔPAA ranging from 1.70, p=0.04 to 2.75, p=0.006). The associations of PAA with most chemotherapy agents diminished over time, reverting to negative or null at 10 years. Antimetabolites, on the other hand, were associated with an increased PAA at 2 years (ΔPAA=2.62, p<0.001) which increased further at 10 years post-diagnosis (ΔPAA=7.26, p<0.001). Endocrine therapy and PAA association at 10 years post-diagnosis was likely driven by aromatase inhibitors (AI) (ΔPAA=1.53, p<0.001). Selective estrogen receptor modulators were inversely associated with PAA at year 10 (ΔPAA=-1.03, p=0.01). Additional adjustment for BC stage, grade, and subtype did not materially change the results for Tx and medications. Our study found that BC patients had accelerated aging up to 10 years post-diagnosis, especially those with stage III/IV and high/intermediate-grade BC. The aging trajectory varied by cancer Tx and medications; antimetabolites and AI might accelerate aging in long term BC survivors.

#2245 Awareness and participation in cancer-related clinical trials among gastrointestinal cancer survivors.

Mariela Bournigal-Feliciano[1], Marievelisse Soto-Salgado[1], Hilmaris Centeno-Girona[1], Sofia Contreras-Fernandez[1], Karina Torres-Mojica[1], Virginia Williams[2], Arnethea L. Sutton[2], Katherine Tossas[2], Robert Winn[3], Marcia Cruz-Correa[4]

[1]University of Puerto Rico Comprehensive Cancer Center, San Juan, PR,[2]Virginia Commonwealth University, Richmond, VA,[3]Massey Cancer Center, Richmond, VA,[4]School of Medicine, University of Puerto Rico, San Juan, PR

Despite significant advances in cancer prevention, early detection, and treatment, there is a persistent disparity in cancer outcomes between diverse racial/ethnic groups and medically underserved populations in the United States (US). The underrepresentation of non-white racial/ethnic groups in clinical trials (CTs) poses a critical challenge to cancer research and effective care delivery. The Hispanic/Latino population is one of the fastest-growing ethnic groups in the US and has a high rate of gastrointestinal (GI) cancer. Although Hispanics/Latinos comprise 18.5% of the US population, they have participation rates of only 1% in CTs. We aimed to describe the awareness and participation of Hispanic/Latino GI cancer survivors in cancer-related CTs. We analyzed preliminary data from an ongoing cross-sectional study that examines the social determinants of health (SDOH) associated with participation in cancer-related CTs among GI cancer survivors. As of November 7, 2023, 57 individuals aged ≥ 21 years responded to a survey assessing their awareness and participation in CTs, and other SDOH domains. Descriptive statistics were used to describe the population, including frequencies, percentages, mean, and standard deviation. The participants' mean age was 62.5 ± 12.3 years, and 56.1% were women. Most had more than a high school education (80.6%). Moreover, 59.7% of the participants had state-sponsored health insurance or Medicaid. Twenty-nine (50.9%) of the participants reported having heard about cancer-related CTs; however, only nine (31.0%) indicated that they knew how to participate in a cancer-related CT. Most of the participants had heard about cancer-related CTs from their doctor, nurse, or other health professionals (41.4%), their family/friends (20.7%), or social media/newspapers (20.7%). Furthermore, 13 (44.8%) had been invited to participate and 11 (84.6%) were eligible and participated in cancer-related CTs. Most of the participants who were eligible and participated in cancer-related CTs (90.9%) indicated that they participated because they knew CTs are important for the development of effective cancer treatments. Our preliminary findings show high levels of awareness among Hispanics/Latinos GI cancer survivors towards CTs; however, it is concerning that only a minority of those who were aware of CTs knew how to participate in them. More efforts are needed to assess the factors and SDOH that impact participation in cancer-related CTs among this population. Additionally, we will continue to recruit participants to assess the relationship between adverse SDOH and their willingness to participate in cancer-related CTs.

#2246 The impact of a waitlist control group on physical activity level in the activity after cancer treatment exercise oncology randomized pilot study.

R. Cannioto[1], E. Davis[1], K. Hulme[1], C.-C. Hong[1], C. DeNysschen[2], T. O'Connor[3], C. Ambrosone[1];
[1]Roswell Park Comprehensive Cancer Center, Buffalo, NY, [2]Buffalo State University, Buffalo, NY, [3]Moffitt Comprehensive Cancer Center, Tampa, FL

Background: In randomized clinical trials, control conditions such as blinding are essential for mitigating threats to validity. In exercise oncology trials, researchers are unable to blind participants to randomization, which may confer unintended consequences (i.e., crossover or dropout) that may threaten validity. Despite prior suggestions that a waitlist control is optimal for lessening these consequences, to date there is little agreement concerning control conditions in exercise oncology. Further, the use of a waitlist control is complicated by concerns regarding the ethical implications of instructing participants to delay healthy behavior change. Herein, we leveraged data from the Activity after Cancer Treatment (ACT) study to evaluate the impact of randomization to a waitlist control group on objectively assessed physical activity (PA) levels in breast cancer (BC) survivors.
Methods: The ACT Study (PI: Ambrosone) was a 12-week, four-arm pilot study at Roswell Park Comprehensive Cancer Center. Participants included 37 BC survivors who were randomized to either a waitlist control group (n=10), or one of three exercise interventions of varying intensities including home-based walking (n=9), home-based Zumba (n=9), or a supervised high-intensity interval training treadmill protocol (n=9) delivered by study personnel at Roswell Park Comprehensive Cancer Center. The waitlist group was asked to maintain their usual PA during the 12-week intervention. All participants received weekly phone calls to optimize engagement and ensure Fitbit data were properly synced. For the current analysis, the primary analytic exposure was randomization assignment (control or active intervention); the analytic outcomes included steps/day, moderate-to-vigorous PA (MVPA) minutes/week and total active minutes/week as measured by the Fitbit Charge 2. ANOVA was used to assess mean group differences in steps and active minutes.
Results: At study conclusion, the control group accumulated significantly fewer steps/day [6,087 (±1,353)] than the active intervention groups [8,729 (±2,585), p=0.0003]. The control group also accumulated significantly fewer MVPA minutes/week [146.2 (±114.9) vs. 264.1 (±192.3), p=0.045] and total active minutes/week [1,478 (±291.0) vs. 1,976.8 (±658.6), p=0.003] in comparison to the active intervention groups, respectively.
Conclusions: BC survivors randomized to active intervention accumulated significantly more steps, MVPA and total active minutes than the waitlist group. Although the waitlist was effective for minimizing PA relative to the active arms, waitlisted participants exceeded the national step average of 4800 steps/day by 1200 steps and nearly met the minimum PA recommendation of 150 minutes of MVPA/week, potentially assuaging ethical or public health concerns regarding the delay of health-seeking behavior.

#2247 Cellular senescence as a potential mechanism underlying differences in chemoresistance between lung cancer cell lines derived from African-American and Caucasian patients.

N. Semenova, C. C. Robertson, J. S. Yakisich, R. R. Ayscue, A. K. V. Iyer, N. Azad;
Hampton University, Hampton, VA

Lung cancer remains the leading cause of cancer-related deaths world-wide. Statistical data reveals significant difference in both lung cancer incidence and death rate between African-American (AA) and Caucasian (CA) populations in the United States. Although these disparities can be partially attributed to socio-economical reasons, the biological mechanisms underlying them are poorly understood. In this study, we compared the chemoresistance of cell lines derived from tumor tissues obtained from AA patients (H23, H292) versus CA patients (A549, H460). The cell lines were treated with FDA-approved anti-cancer drugs as well as with cardenolide analogues previously reported by our group to have anti-cancer properties. Irrespectively of drug class, cellular senescence appeared to develop more abundantly in cells derived from AA patients. However, AA-derived cell lines manifested higher drug resistance in comparison to CA-derived ones, especially to cardenolide analogues. Recovery experiments in drug-free media revealed faster and more efficient re-growth after long-term (2 weeks) drug treatment in AA-derived cell lines. Taken together, the data provides a potential role for cellular senescence as mechanism of the differential chemoresistance observed between AA and CA lung cancer cell lines, revealing new potential targets for anti-cancer therapy.

#2248 Diminished survival in patients with pancreatic ductal adenocarcinoma is linked with residence in redlined neighborhoods.

V. Vudatha, D. Freudenberger, C. Liu, L. Fernandez, J. Trevino;
Virginia Commonwealth University, Richmond, VA

Redlining refers to the practice of classifying neighborhoods with racial minorities and low-income residents as “hazardous” for investors. This discriminatory practice by the Home Owners’ Loan Corporation (HOLC) has been shown to impact patient cancer incidence and outcomes in breast, lung, cervical, and colorectal cancers. In this study, we evaluate the impact of HOLC status on pancreatic ductal adenocarcinoma (PDAC) outcomes in Virginia. The Virginia Department of Health Cancer Registry was queried for adult patients diagnosed with pancreatic ductal adenocarcinoma from 2009-2018. The HOLC grade (A: best, B: still desirable, C: definitely declining, D: hazardous) of each patient’s address was determined using the University of Richmond Inequality map. Patient demographics, treatment, and survival data were compared by HOLC Grade via descriptive statistics, bivariate and multivariate analysis. 394 patients were identified (A: 24 (6.1%), B: 54 (13.7%), C: 198 (50.3%), D: 118 (29.9%)). There was no association between patient age, sex, insurance status, receipt of therapy, or smoking history and HOLC status. Patient race was significantly associated with HOLC status with more Black patients living in areas with worse HOLC grades compared to White patients ($p<0.001$). Survival analysis demonstrated that lack of surgery and chemotherapy ($p<0.0001$), metastatic disease ($p<0.0001$), and residential status in areas of HOLC grade D ($p=0.012$) were associated with worse survival. Based on Cox regression analysis, patients who lived in areas with HOLC grade B (adjusted HR 0.70; CI 0.49-0.98) and C (adjusted HR 0.74; CI 0.58-0.95) had improved survival compared to those living in areas with HOLC grade D. Additionally, age greater than 65, metastatic disease, and lack of treatment were associated with worse survival. Residence in a redlined neighborhoods can play a significant role in pancreatic ductal adenocarcinoma outcomes. Location in a “hazardous” area in Virginia is associated with worse survival in PDAC patients. Disparities in socioeconomics, housing, education, and food accessibility in these areas likely play a role in shaping these outcomes. Future studies are warranted to further investigate this disparity in care.

#2249 Clinical outcomes of discontinuing long-term opioid therapy among older cancer survivors in nursing homes.

Y.-J. Wei[1], A. G. Winterstein[2], S. Schmidt[2], R. B. Fillingim[2], M. Daniels[2], S. T. DeKosky[2], B. Kinder[1], T.-Y. D. Cheng[1];
[1]The Ohio State University, Columbus, OH, [2]University of Florida, Gainesville, FL

Purpose: The purpose of this study is to investigate associations of discontinuing vs continuing long-term opioid therapy (LTOT) with pain, physical function, and depressive symptoms among older cancer survivors who resided in nursing homes. Pain is prevalent and use of LTOT is common among patients with cancer, including those living in nursing homes. The Centers for Disease Control and Prevention (CDC) *Guideline for Prescribing Opioids for Chronic Pain—United States* recommends tapering or discontinuing LTOT for patients with chronic pain when risks outweigh the benefits of LTOT. Despite the guideline explicitly stating that its recommendation does not apply to patients with cancer, doctors including oncologists have been prescribing fewer opioid medications for older patients, raising a question regarding the benefit and risk of discontinuing LTOT for cancer survivors who depend on opioids for pain relief.
Study Design: We conducted a cohort study using a 100% Medicare nursing home sample linked to the Minimum Data Set (MDS) from 2010 to 2021. Participants included older (≥65 years of age) long-term (≥2 years) residents with a diagnosis of cancer who received LTOT for ≥90 days in a 12-month nursing home stay. Residents entered the cohort on the 90th day of the latest LTOT episode. Residents who received palliative or hospice care were excluded. The key exposure was discontinuation of LTOT, defined as no opioid refills for ≥90 consecutive days in 1 year after cohort entry. The primary outcomes were pain (measured using a numerical rating scale or categorical verbal descriptor scale), physical function (9-item activities of daily living scale), and depression (Patient Health Questionnaire-9) from baseline to quarterly assessments during 1-year follow-up after the discontinuation of LTOT.
Results: In total, 53,141 cancer survivors who received LTOT were identified (mean [SD] age, 82.9 [8.7] years; 39,522 [74.4%] female; 46678 [87.8] Whites), consisting of 62,387 patient observations during the 10-year study period. Of 62,387 patient observations, 51,357 residents (82.3%) continued LTOT, and 11,030 (17.6%) discontinued LTOT. Residents who discontinued (vs continued) LTOT had lower odds of worsening pain (adjusted odds ratio [AOR], 0.64, 95% CI, 0.59-0.59, $P < .001$) and depressive symptoms (AOR, 0.92 [95% CI, 0.85-0.99]; $P = .033$), with no difference in physical function (AOR, 0.96 [95% CI, 0.89-1.03]; $P = .226$) during the 1-year follow-up.
Conclusion: Among older nursing home residents with cancer, discontinuing vs continuing LTOT was associated with lower odds of worsening pain and depressive symptoms. Funding source: NIH/NIA R01AG073442.

#2250 Effects of loneliness on medical expenditures among US cancer survivors.

F. Chen[1], R. Nipp[2], X. Han[3], Z. Zheng[3], R. Yabroff[3], C. Jiang[4],

[1]Tsinghua University, Dongcheng District, China, [2]University of Oklahoma College of Medicine, Oklahoma City, OK, [3]American Cancer Society, Atlanta, GA, [4]UT Southwestern Medical Center, Dallas, TX

Background: Social isolation in cancer survivors associates with diminished quality of life and worse survival. However, effects of loneliness on medical expenditure are understudied. We examined associations of loneliness with medical costs, and social/psychological/behavioral determinants of health (SDHs).
Methods: We identified 1,866 cancer survivors from the 2021 Medical Expenditure Panel Survey. One has loneliness if answering 'often' for any of: feel lack companionship/left out/isolated from others. Two-part regression models assessed marginal effect of loneliness to annual total health care expenditure (cost) in cancer survivors, aged 18-64 (young) and ≥65 years (older), adjusting for age, sex, race, region, education, health insurance, comorbid illnesses, family income, unemployment, and activity limitation. Models were sequentially adjusted for every single SDH. Ordinal regression models assessed associations of loneliness with SDHs.
Results: Over one-tenth of young (19%) and older (13%) cancer survivors reported loneliness. Loneliness was associated with higher cost in older cancer survivors (conditional coefficient (CC) 0.46, 0.12-0.81), but not young survivors (-0.14, -0.62-0.36). In both age groups, cancer survivors with loneliness more often reported stress, lack of help, as well as less time talking on the phone and getting together with support persons (Table). In older patients, sequential adjustment for stress, expected help, get-togethers, or church attendance decreased effect of loneliness to cost; among which get-togethers showed the greatest decrease (CC 0.28, -0.03-0.62).
Conclusions: Loneliness was associated with higher total medical expenditure in older US cancer survivors. Findings warrant further study of personal or community support to mitigate loneliness, in an effort to reduce healthcare costs and financial burden in older cancer survivors.

Age (year)	18-64 (648)		≥65 (1223)	
Loneliness	No (505, 81%)	Yes (143, 19%)	No (1046, 87%)	Yes (177, 13%)
Mean Age (years)	56	56	75	74
Female %	64.5	66.4	53.0	59.1
Non-white %	23.1	21.8	15.8	26.4
Federal poverty level < 100%, %	7.4	18.9	8.9	7.2
Comorbidities ≥ 3, %	25.4	44.4	60.4	67.1
Unemployment ≥ 1, %	35.8	45.3	83.3	89.6
< high school %	30.8	33.7	37.7	36.6
Conditional coefficient (95% CI)	Ref	-0.14 (-0.62-0.36)	Ref	0.46 (0.12-0.81)
Odds ratio (95% CI) of loneliness to SDHs				
Stress	Ref	8.42 (5.20-13.63)	Ref	6.82 (4.72-9.87)
Lack of help - family		3.46 (2.32-5.14)		2.61 (1.88-3.60)
Lack of help - friends		3.25 (2.00-5.29)		1.92 (1.36-2.72)
Lack of help - community		2.45 (1.64-3.66)		2.16 (1.58-2.96)
Times of talk on phone		0.55 (0.36-0.85)		0.77 (0.55-1.07)
Times of get together		0.34 (0.21-0.55)		0.38 (0.25-0.58)

#2252 Loneliness, quality of life, and physical and mental health among cancer patients: All of US research program.

H. Lee[1], D. Ng[2], D. Lee[1], A. Jemal[1], F. Islami[1];
[1]American Cancer Society, Atlanta, GA, [2]University of California Irvine, Irvine, CA

Background: Loneliness, as a distressing feeling, occurs with a discrepancy between an individual's social needs and one's social relationship. Cancer patients, particularly, may feel loneliness, when their expected practical and emotional support from family or friend were not met. Loneliness can impair the capacity to self-regulate lifestyle behaviors and induce systemic inflammation through dysregulation of autonomic nervous system and the hypothalamic-pituitary-adrenal axis. While a growing body of literature has found an association between loneliness and physical or mental health, quality of life, morbidity or mortality, few studies have examined this association among cancer patients and effects of loneliness by sociodemographic characteristics.
Method: We used All of US Controlled Tier Dataset v7 (summer 2017-July 1, 2022) which comprised survey and electronic health records data. Study sample included cancer patients aged ≥18 years (N=17,367). Loneliness was measured using the University of California, Los Angeles (UCLA)-3 items loneliness scale, which includes relational connectedness, social connectedness, and self-perceived isolation. Logistic regression models were used to estimate the association between loneliness and self-reported pain, fatigue, fair/poor health physical and mental health status, and quality of life, controlling for various covariates. We stratified the models by age, sex, race/ethnicity, income, education, living arrangement, and marital status.
Results: Lonely cancer patients were more likely to have fair or poor quality of life (OR=3.80; 95% CI=3.33-4.34), severe pain (OR=1.55; 95% CI=1.35-1.79), severe or very severe fatigue (OR=2.41; 95% CI=2.07-2.80), fair or poor physical health (OR=2.26; 95% CI=2.05-2.50), and fair or poor mental health (OR=4.22; 95% CI=3.72-4.80) compared to non-lonely cancer patients, controlling for all other covariates. All stratified models generally showed similar results. However, the association between loneliness and severe pain was stronger in the younger group, whereas the association with mental health was stronger in the older group. The effect of loneliness on mental health was stronger among males (OR=5.42; 95% CI=4.30-6.83) than females (OR=3.84; 95% CI=3.29-4.49; p for difference < 0.05). By living arrangements, the relationship between loneliness and severe fatigue was stronger among cancer patients living alone (OR=3.15; 95% CI=2.33-4.25) than those living with others (OR=2.16; 95% CI=1.81-2.59; p for difference < 0.05).
Conclusions: In this study, lonely cancer patients were more likely to have poor quality of life, poor mental and physical health, and severe pain and fatigue compared to non-lonely patients. These findings underscore the significance of policy and clinical interventions to alleviate negative effect of loneliness on health outcomes among cancer patients.

#2253 Cancer-related follow-up health care utilization and fertility discussion, preservation, and reproductive concerns among diverse adolescent and young adult cancer survivors: A population-based study.

J. Stal[1], K. A. Miller[1], J. E. Milam[2], M. Quinn[1], S. E. Kim[1], R. C. Ceasar[1], D. R. Freyer[3],

[1]University of Southern California, Keck School of Medicine, Los Angeles, CA, [2]University of California, Irvine, Irvine, CA, [3]Children's Hospital Los Angeles, Los Angeles, CA

Purpose: To examine cancer-related follow-up (CRFU) health care utilization associated with fertility experiences among diverse adolescent and young adult (AYA) cancer survivors.

Methods: Project Milestones is an ongoing survey study evaluating life outcomes among AYAs diagnosed with cancer at age 21-39 in Los Angeles (LA) County. AYAs had an initial 5-year survival probability of ≥50% and are currently 3-10 years post-diagnosis. A registry-based recruitment strategy through the SEER-affiliated LA Cancer Surveillance Program was used.

Results: Overall, 1442 AYAs responded (Table 1). Compared to AYAs who did not, AYAs who saw: (1) their treating provider for CRFU were more likely to report a fertility discussion (56.0% vs. 41.2%, $p<.01$); (2) another provider for CRFU were less likely to report a fertility discussion (38.1% vs. 52.0%, $p<.01$); (3) their treating provider for CRFU were more likely to report preserving fertility (14.7% vs. 8.4%, $p<.01$); (4) a primary care provider for CRFU were less likely to report preserving fertility (10.1% vs. 13.6% $p<.05$). Compared with AYAs who reported a CRFU visit 1+ years ago or never, AYAs with a visit <1 year ago: (1) had on average greater reproductive concerns (range 5-25, higher scores reflect greater concern, 13.8 vs. 13.4, $p<.05$); and were more likely to report (2) worry passing on a genetic risk for cancer to their child (55.6% vs. 47.8%, $p<.01$); and (3) caution about having children because they may not be around to raise them (23.6% vs. 16.6%, $p<.01$).

Discussion: Iatrogenic infertility concerns persistent into survivorship, yielding a need to optimize oncofertility care throughout the reproductive lifespan. Receiving CRFU care from the treating provider is related to better outcomes, and higher reproductive concerns among AYAs with a recent visit may reflect greater awareness of risk due to more points of contact with a provider.

Table 1: Sample characteristics - N (%) or M (SD)

		Total	**Hispanic**	**Non-Hispanic**
		1442	**622 (43.1)**	**820 (56.9)**
Age at survey		39.5 (5.8)	39.3 (5.8)	39.6 (5.7)
Female		1007 (69.8)	429 (69.0)	578 (70.5)
White		850 (62.4)	301 (55.0)	549 (67.3)
Had employee-sponsored insurance		909 (63.0)	347 (55.8)	562 (68.5)
Age at diagnosis		31.0 (5.2)	30.8 (5.2)	31.2 (5.1)
Cancer type	Leukemia/Lymphoma	396 (27.5)	173 (27.8)	223 (27.2)
	Reproductive	382 (26.5)	208 (33.4)	174 (21.2)
	Thyroid	184 (12.8)	86 (13.8)	98 (12.0)
	Breast	179 (12.4)	61 (9.8)	118 (14.4)
	Skin	130 (9.0)	21 (3.4)	109 (13.3)
	Colorectal	86 (6.0)	35 (5.6)	51 (6.2)
	Other	85 (5.9)	38 (6.1)	47 (5.7)
Discussed fertility		717 (50.3)	327 (53.4)	390 (48.0)
Preserved fertility		176 (12.3)	48 (7.8)	128 (15.7)
Reproductive Concerns After Cancer (RCAC) score		14.1 (3.9)	14.3 (4.2)	14.0 (3.8)
Last visit with a health care provider for cancer related follow-up care	Within the past year	862 (60.3)	343 (56.2)	519 (63.4)
	1-2 years ago	218 (15.3)	90 (14.8)	128 (15.6)
	More than 2 years ago	303 (21.2)	152 (24.9)	151 (18.4)
	Never	46 (3.2)	25 (4.1)	21 (2.6)
Provider seen for cancer related follow-up care	Same doctor who treated me	885 (61.4)	369 (59.3)	516 (62.9)
	Primary care provider	539 (37.4)	224 (36.0)	315 (38.4)
	Another type of provider	179 (12.4)	65 (10.5)	114 (13.9)
	Cancer survivorship clinic	88 (6.1)	46 (7.4)	42 (5.1)

#2254 A population-based study exploring health care self-efficacy and fertility preservation, family planning, and reproductive concerns among diverse adolescent and young adult cancer survivors.

J. Stal[1], K. A. Miller[1], J. E. Milam[2], M. Quinn[1], S. E. Kim[1], R. C. Ceasar[1], D. R. Freyer[3];
[1]Keck School of Medicine, University of Southern California, Los Angeles, CA, [2]University of California, Irvine, Irvine, CA, [3]Children's Hospital Los Angeles, Los Angeles, CA

Purpose: To examine the relationship between health care self-efficacy (HCSE) and fertility experiences among diverse adolescent and young adult (AYA) cancer survivors.
Methods: Project Milestones is an ongoing cancer-registry derived cohort survey study recruiting AYAs through the SEER-affiliated Los Angeles Cancer Surveillance Program. Respondents were diagnosed with cancers prototypical for AYAs between 21-39 years and had a 5-year survival probability of ≥50% at diagnosis.
Results: Overall, 1442 AYAs responded of which 57.9% reported the highest possible HCSE (*totally confident*; score of 3; lower scores reflect greater HCSE), while 42.1% were *somewhat* or *not at all confident* in some areas (score of 4-9; Table 1). Compared to AYAs with lower HCSE, AYAs with the highest HCSE were more likely to report preserving fertility (13.8% vs. 10.3%, $p<.05$) and were less likely to report highly negative change (11.9% vs. 15.5%, $p<.01$) and more likely to report highly positive change (16.3% vs. 9.4%, $p<.01$) to family planning due to cancer. On average, AYAs with the highest HCSE had lower reproductive concerns (range 5-25, lower scores reflect lower concern; 13.3 vs. 14.2, $p<.01$) and were less likely to report worry about: passing on a genetic cancer risk to their child (49.6% vs. 56.6%; $p<.01$), telling their partner they may be unable to have children (13.8% vs. 21.5%, $p<.01$), their ability to become a biological parent (22.7% vs. 28.0%, $p<.01$), and caution having children because they may not be around to raise them (18.5% vs. 24.1%, $p<.01$) than AYAs with lower HCSE.
Discussion: Greater HCSE was associated with higher rates of preservation, lower impacts to family planning, and lower reproductive concerns in this population-based study. As one quarter of AYAs have suboptimal HCSE, accessible avenues for obtaining fertility care are needed to temper possible impacts of low HCSE on preserving fertility.

Table 1: Sample characteristics - N (%) or M (SD)

		Total	Hispanic	Non-Hispanic
		1442	**622 (43.1)**	**820 (56.9)**
Age at survey		39.5 (5.8)	39.3 (5.8)	39.6 (5.7)
Female		1007 (69.8)	429 (69.0)	578 (70.5)
White		850 (62.4)	301 (55.0)	549 (67.3)
Had employee-sponsored insurance		909 (63.0)	347 (55.8)	562 (68.5)
Age at diagnosis		31.0 (5.2)	30.8 (5.2)	31.2 (5.1)
Discussed fertility		717 (50.3)	327 (53.4)	390 (48.0)
Preserved fertility		176 (12.3)	48 (7.8)	128 (15.7)
Impacts to family planning due to cancer	Highly negative change	202 (14.3)	91 (15.0)	111 (13.7)
	Somewhat negative change	128 (9.0)	50 (8.3)	78 (9.6)
	No change	788 (55.6)	315 (52.1)	472 (58.2)
	Somewhat positive change	111 (7.8)	43 (7.1)	68 (8.4)
	Highly positive change	189 (13.3)	106 (17.5)	83 (10.2)
Reproductive Concerns After Cancer (RCAC) score		14.1 (3.9)	14.3 (4.2)	14.0 (3.8)
HCSE score		3.9 (1.4)	4.0 (1.4)	3.9 (1.3)
Could ask doctor or health care provider about things that concern you?	Totally confident	1088 (75.9)	466 (75.5)	622 (76.1)
	Somewhat confident	303 (21.1)	130 (21.1)	173 (21.2)
	Not at all confident	43 (3.0)	21 (3.4)	22 (2.7)
Could schedule and attend your doctor appointments or decide when you needed care?	Totally confident	1057 (73.8)	454 (73.5)	603 (74.1)
	Somewhat confident	310 (21.7)	130 (21.0)	180 (22.1)
	Not at all confident	65 (4.5)	34 (5.5)	31 (3.8)
Could get the cancer related follow-up care you need over the next 2 years?	Totally confident	1006 (70.6)	410 (67.3)	596 (73.1)
	Somewhat confident	328 (23.0)	149 (24.4)	179 (22.0)
	Not at all confident	90 (6.3)	50 (8.2)	40 (4.9)

#2255 Social support with physical and psychosocial quality of life in individuals with prostate cancer in the Health Professionals Follow-up Study (HPFS).

N. Chen, C. B. McGrath, B. A. Dickerman, R. C. Nethery, L. A. Mucci;
Harvard T.H. Chan School of Public Health, Boston, MA

Introduction: Social support is associated with improved cancer survivorship, but literature on its association with prostate cancer specific physical and psychosocial quality of life (QoL) is lacking. We investigated the associations of social support with physical and psychosocial QoL in individuals with prostate cancer in HPFS. Methods: We included 1,692 men (ages 61-95 years, mean: 71 years) diagnosed with non-metastatic prostate cancer between 2008 and 2016. Social support was measured by the Berkman-Syme Social Network Index (SNI) (a composite measure of marital status, sociability, membership in religious groups or other community organizations: socially isolated, moderately isolated, moderately integrated, socially integrated) and marital status (married, not married). Physical (measured by EPIC-CP: bowel function, urinary incontinence, urinary irritation/obstruction, sexual function, vitality/hormonal function) and psychosocial (memory function and wellbeing) QoL were measured through biennial questionnaires. We fit generalized linear and ordinal mixed effect models for the associations of SNI and marital status with physical and psychosocial QoL, adjusting for age, race, employment status, body mass index, comorbidities, smoking history, and clinical factors. We conducted stratified analyses by baseline age (<70, ≥70), baseline comorbidities (yes, no), primary treatment (active surveillance, radical prostatectomy, radiation), and D'Amico Risk Classification at diagnosis (low, intermediate, high risk). Results: Among those with baseline SNI (N=1,586), 740 were socially integrated, 309 were moderately integrated, 437 were moderately isolated, and 100 were isolated. Among those with baseline marital status (N=1,663), 89% were married. Physical QoL did not differ significantly by SNI. Married individuals (compared to not married) experienced less urinary incontinence (β -0.25, 95% confidence interval [CI]: -0.55, 0.05) and urinary irritation/obstruction (β -0.26, 95% CI: -0.52, 0.00). Those who were socially integrated (compared to isolated) reported better memory function (Odds ratio [OR] 1.47, 95% CI 1.06, 2.03) and wellbeing (OR 1.74, 95% CI 1.31, 2.31). The positive association between social support and QoL was stronger among those with baseline aged <70 years (for vitality/hormonal functioning and memory function), those without comorbidities at baseline (for memory function), those with radiation as primary treatment (for urinary incontinence, vitality/hormonal functioning, memory function, and wellbeing), and those with high risk (for memory function and wellbeing). Conclusion: Prostate cancer survivors with more social support experienced better quality of life, including less urinary incontinence and urinary irritation/obstruction, and better memory function and wellbeing.

#2256 Guideline-based physical activity and physical quality of life among individuals with nonmetastatic prostate cancer: A target trial emulation in the Health Professionals Follow-up Study.

N. Chen, R. C. Nethery, L. A. Mucci, B. A. Dickerman;
Harvard T.H. Chan School of Public Health, Boston, MA

Introduction: Randomized trials have shown that physical activity can improve quality of life (QOL) among individuals with cancer. In the absence of a randomized trial of adequate size and follow-up to comprehensively evaluate this relationship for prostate cancer, we aim to emulate a target trial of guideline-based physical activity strategies and 6-year physical QOL.
Methods: We will use observational data on individuals in the Health Professionals Follow-up Study diagnosed with nonmetastatic prostate cancer between 2010-2016 and free of conditions that could preclude following current physical activity recommendations at baseline (first post-diagnostic questionnaire). The physical activity strategies of interest are (1) engage in ≥150 minutes of moderate activity, or ≥75 minutes of vigorous activity per week, or an equivalent combination (i.e., ≥7.5 metabolic equivalent of task [MET]-hours/week of vigorous or moderate activity) and (2) no physical activity intervention. The outcomes of interest are 6-year mean physical QOL scores (based on EPIC-CP measures of bowel function, urinary incontinence, urinary irritation/obstruction, sexual function, and vitality/hormonal function). We will adjust for baseline and time-varying risk factors using the parametric g-formula.
Conclusion: These findings may help to inform clinical recommendations to improve QOL among individuals with nonmetastatic prostate cancer. Further, the proposed approach will provide a framework for future studies designed to evaluate the effectiveness of any intervention strategies to improve patient-reported outcome measures in cancer survivorship research.

Table 1. Specification and emulation of a target trial using observational data from HPFS

Protocol component	**Target trial specification**	**Target trial emulation**
Eligibility criteria	(1) Individuals diagnosed with non-metastatic prostate cancer between 2010 and 2016; (2) No history of other cancers (Except nonmelanoma skin cancer); (3) No history of conditions that could preclude high levels of physical activity: myocardial infarction, stroke, congestive heart failure, amyotrophic lateral sclerosis, or functional impairment (defined as difficulty climbing a flight of stairs or walking eight blocks due to physical impairment)	Same as for the target trial, except: We required complete data on physical activity, birth date, and other risk factors on the pre-diagnostic questionnaire and the first post-diagnostic (baseline) questionnaire.
Physical activity strategies	Each individual is assigned to one of the following strategies at baseline: (1) No intervention (usual physical activity) (2) Engage in ≥1.25 hours/week of vigorous activity or ≥2.5 hours/week of moderate activity or ≥7.5 MET-hours/week of vigorous or moderate activity (an equivalent combination). Strategies are initiated at baseline and continued over follow-up. Individuals are excused from following the physical activity intervention upon the development of myocardial infarction, stroke, congestive heart failure, amyotrophic lateral sclerosis, cancer metastasis, or functional impairment. Individuals must respond to surveys at every follow-up period to assess time-varying variables.	Same as for the target trial, except: (1) Follow-up periods correspond to the questionnaire cycles in the cohort study. (2) We assumed that each 2-year physical activity questionnaire accurately reflects the individual's (1) average physical activity over the previous 2-year period and (2) intended physical activity that the individual would have reported at the start of the current period under no intervention.
Strategy assignment	Individuals are randomly assigned to a strategy at baseline and are aware of their assigned strategy.	We assumed randomization conditional on the following baseline covariates: age; employment status; primary treatment; stage; Gleason score, and prostate-specifc antigen level at diagnosis; pre-baseline values of body-mass index and physical activity.
Outcomes	6-year mean quality of life scores in the following physical domains: (1) Bowel function, (2) Urinary incontinence, (3) Urinary irritation/obstruction, (4) Sexual function, (5) Vitality/hormonal function. Individuals self-report their physical quality of life on EPIC (The Explanded Prostate Cancer Index Composite) questionnaires at every follow-up period.	Same as for the target trial. Follow-up periods correspond to the questionnaire cycles in the cohort study.
Follow-up	For each eligible individual, follow-up starts at strategy assignment (baseline) and ends upon death, loss to follow-up, or the end of follow up in December 2018, whichever happens first.	Same as for the target trial. Loss to follow-up was defined as questionnaire non-response.
Causal contrasts	Intention-to-treat and per-protocol effect.	Observational analogue of per-protocol effect.
Statistical analysis	Intention-to-treat analysis. Per protocol analysis: Parametric g-formula to compare 6-year physical quality of life under each strategy via mean differences, with adjustment for pre- and post-baseline prognostic factors associated with adherence and loss to follow-up.	Same as for the per-protocol analysis of the target trial.

BIOINFORMATICS / COMPUTATIONAL BIOLOGY / SYSTEMS BIOLOGY / CONVERGENT SCIENCE: Application of Bioinformatics to Cancer Biology 2 Poster Session

#2260 Transcriptomic immuno-oncology investigation of B-cell lymphomas using a novel comparative workflow.

N. Rapier-Sharman, M. T. Told, S. Kim, K. L. O'Neill, B. E. Pickett;
Brigham Young University, Provo, UT

Patients with B-cell lymphoma currently have limited treatment options, often with serious side effects; for example, B-cell lymphoma patients undergoing chemo- and radiation therapies experience poor health from off-target toxicity. Similarly, though CD19 CAR T-cell therapy is very effective, patients suffer lifelong B-cell aplasia as a side effect. Comparing a cancer to an autoimmune disease in the same tissue type may grant us additional insights on the immune dysregulation of the cancer, leading to development of more immune-aware cancer treatments. We introduce a new data-driven comparative workflow for the analysis of immuno-oncology attributes by comparing a cancer and an autoimmune disease in the same tissue type. As an example use case, we compare primary B-cell lymphomas to primary B-cells from systemic lupus erythematosus with the goal of delineating new mechanisms that can be leveraged to treat B-cell lymphomas. Our analysis will utilize bulk RNA-sequencing (RNA-seq) of B-cells for initial discovery, followed by single-cell RNA-sequencing (scRNA-seq) of Peripheral Blood Mononuclear Cells (PBMCs) for validation. Our analytical framework incorporates differential gene analysis, GO Terms, known protein-protein interactions, principal component analysis, and machine learning for biomarker detection. Here, we describe our novel tool in detail and share the results of our lymphoma use case to gain a better understanding of the targetable immune-related attributes of B-cell lymphoma. We expect that this novel tool, along with the results of our B-cell lymphoma use case, will contribute to the continued development of immune-focused treatment options for B-cell lymphoma and other cancers.

#2261 A scalable comparison of tumor immune atlases.

J. Yang, Q. Liu, Y. Shyr;
Vanderbilt University Medical Center, Nashville, TN

Large single-cell atlases can serve as references for the analysis of smaller-scale studies. However, there are strong biases among atlases due to their varying sample sources, conditions, cell type annotation strategies and resolutions. Selecting appropriate atlas for future or smaller-scale studies is complicated due to unclear understanding of atlases, that limits the future or smaller-scale studies take advantage of the wealth of data that such atlases provide. For example, the tumor-infiltrating immune cell atlases including pan-cancer and cancer type-specific atlases provide comprehensive profiling of immune cells, which desperately facilitates future single-cell studies. However, lack of a comprehensive assessment and comparison of tumor immune cell atlases with standardized benchmarks blocked the application of the most appropriate atlas for smaller-scale study. In this study, we compared pan-cancer immune cell atlases including TICA, pan-cancer T cells and pan-cancer blueprint atlases, and cancer-type specific immune cell atlases containing ABTC, HCC and STAD atlases. We quantified the correlations of cell types and observed similar heterogeneity among atlases and unique immune cell populations in TICA as well. Then, we assessed the performance of atlases on accurately annotating immune cell types in the widely studied PBMC datasets—in which cell types were well annotated. Comparative analysis revealed the complementarity within atlases on mapping success, accuracy, clustering, annotatability and stability by benchmarking reference-based populations to reference-free de novo clustering on real immunotherapy datasets. We identified potential indicators of immune response and found that reference-based populations outperformed reference-free clusters in recognizing immunotherapy-related cell states. Our study can be easily extended to future atlases.

#2262 Genomic profiling of leukemic cell lines, responders vs. non-responders to Narazaciclib (HX301 or ON123300), a novel kinase inhibitor with activity against CSF1R and FLT3.

J. Xue[1], T. Yang[2], H. Ke[2], S. Guos[1], **H. Q. Li**[2];
[1]Crown Science, Suzhou, China, [2]Hanx Bio, Hangzhou, China

Acute myeloid leukemia (AML) is an aggressive myeloid leukemia with global annual mortality ~150,000. While standard of care (SOC) of the 1st -line treatment being mainly induction chemotherapy, available targeted therapies cover rather limited patients carrying specific driver mutations (IDH mutations and FLT3-ITR). We previously reported a novel kinase inhibitor, Narazaciclib with strong anti-CSF1R activity (IC_{50} 0.7nM) as well as anti-FLT3 (IC_{50} 7nM), and also thus anti-AML activity for certain AML experimental models, as shown *in vitro* and *in vivo* (AACR Annual Meeeting, 2023). In the present study, we assessed the impact of HX301 on the *in vitro* proliferations of a panel of leukemic cell lines (n = 54), including a panel of AML cell lines (n = 33), that have been parallelly genomic-profiled by whole-exome sequencing and whole-transcriptome sequencing. We then set out to analyze the proliferation data and the genomic data, in attempt to elucidate genes and pathways that may be associated with the treatment responses. The biomarker analysis has been performed on gene expression, mutation and copy number variation levels, and the data been presented using common methodologies, including principal component analysis, differential expression analysis, correlation analysis, Gene Ontology enrichment analysis, gene set variation analysis, somatic gene mutation analysis, and copy number variation analysis, *etc*. Some of the observations have been made: 1) differential expression analysis on all leukemic cell lines shows that 254 genes have been positively associated with the responders; while expression of 191 genes are negatively correlated with AUC, i.e. positively associated with response, as revealed by Spearman correlation analysis; 2) Gene Ontology enrichment analysis revealed these response related genes are mostly involved in myeloid leukocyte activation and defense response; 3) all FLT3-ITD AML lines are responders, presumably due to the FLT3i activity of HX301; 4) CSF1R expression levels seem not correlated to drug responses; 5) pathway analysis on non FLT3-ITD AML lines reveals that STAT5 activation downstream of FLT3 signaling, IL7 pathway and NFKB pathway are significantly associated with better response. Finally, we are also attempted to use statistics learning to reveal genes, as a potential predictive biomarker, that may be correlated to drug response.

#2263 Why does the loss of chromosomes 10 and the gain of 7 co-occur in gliomas?.

N. U. Nair[1], A. A. Schaffer[1], M. E. Gertz[1], K. Cheng[1], A. D. Sahu[2], G. Leor[3], E. D. Shulman[1], K. D. Aldape[1], U. Ben-David[3], E. Ruppin[1];
[1]National Cancer Institute, Bethesda, MD, [2]University of New Mexico, Albuquerque, NM, [3]Tel Aviv University, Tel Aviv-Yafo, Israel

Introduction: Gliomas, including aggressive forms such as glioblastoma (GBM) and lower-grade gliomas (LGG), present formidable challenges for treatment. Since the late 1980's it has been known that loss of chromosome 10 (10 loss) and gain of chromosome 7 (7 gain) often co-occur in GBM. The reasons for this frequently co-occurring event are not very clear, with some prior studies speculating on a few driver genes as culprits. In this study, we aim to study and understand the phenomenon of 10 loss and 7 gain in gliomas in a systematic, chromosome-wide level.
Methods: Our analysis consists of three main analyses, that bring independent sources of evidence to address our research question:
a) Analyzing data from Progenetix, we developed rigorous probabilistic models that elucidate the probability dynamics of 10 loss and 7 gain in gliomas.
b) Next, by analyzing hundreds of genomic and transcriptomic samples from TCGA brain cancer patients, and cell lines, we identified a category of clinically relevant genetic interactions termed 'synthetic rescues'. *Synthetic rescue (DU-SR) interactions* refer to a form of functional interplay in which the detrimental impact on cell fitness caused by the inactivation of a specific gene (termed 'vulnerable gene') is compensated by upregulation of another gene (termed 'rescuer gene'). The enrichment of rescuer genes on 7 for the vulnerable genes on 10 was then tested.
c) Utilizing large-scale *in vitro* essentiality screens via CRISPR technology in central nervous system (CNS) cancer cell lines, we sought to investigate the fitness effects of different possible sequences of chromosomal 10 and 7 loss and gains.
Results: The main results emerging from this three-pronged analysis are as follows:
1) We find that 7 gain after 10 loss is a more likely event than the opposite order of loss of 10 after 7 gain whose probability is explained by a random chance model.
2) We show that loss of 10 is enabled by the cells' ability to readily mitigate its loss, specifically through rescue interactions with genes lying on the amplified 7 chromosome.
3) These findings in the analysis of patients' tumors are further reinforced by an independent investigation in IDH wild-type CNS cancer cell line essentiality screens.
Conclusions: The co-occurrence of 10 loss and 7 gain in gliomas is the most frequent loss-gain co-aneuploidy pair occurring in human cancer. Our analysis presents a new multi-pronged approach to analyze co-occurring aneuploidy events in cancer, showing the long-contemplated chromosomal co-occurrence events in gliomas, a mystery that has persisted for decades, is likely to arise from genetic rescue interactions between many genes that lie on those chromosomes. From a future translational standpoint, it additionally points to key rescuer genes that may be potentially targeted.

#2264 Identifying and analyzing independent clonal populations in single Barrett's esophagus biopsies.

M. Kazachkova, P. He, L. B. Alexandrov;
University of California San Diego - UCSD, La Jolla, CA

Barrett's esophagus (BE) is a non-obligate precursor of esophageal adenocarcinoma (EAC), often measuring multiple centimeters in length and characterized by columnar epithelium replacing normal squamous epithelium in the distal esophagus. Early studies in BE suggested that all cells within a patient's Barrett's segment are progenies of a single founder cell. However, in recent years this previously accepted model of BE as a monoclonal disease has been retired in favor of a multiclonal model with new evidence suggesting that a patient's Barrett's segment can be composed of multiple independent clones with independent founder cells. Nonetheless, single BE samples are still routinely assumed to be monoclonal, leading to independent sets of genomic aberrations erroneously being analyzed as a single set in the case of multiclonal samples. Here, we utilize a previously generated whole-genome sequenced BE dataset and repurpose an established pipeline for detecting subclonal populations to identify BE samples that are comprised of multiple independent clones. Additionally, we present a novel approach for validating multiclonality from sequencing data by phasing pair-end sequencing reads using germline variants. We demonstrate that 20/80 patients have at least one multiclonal sample and that the independent clones contained in these single biopsies can have drastically different genomic profiles. Further, we speculate that these multiclonal samples capture a snapshot of clonal competition and evolution within BE. These findings highlight the importance of accounting for multiclonality when studying BE and provide the first systematic analysis of multiclonal BE samples.

#2265 Distinct alternative splicing patterns in genetic subtypes of diffuse large B-cell lymphoma.

Sanyeowool An[1], Youngil Koh[2], Sung-Soo Yoon[2]

[1]Seoul National University, Seoul, Korea, Republic of,[2]Seoul National University, Seoul National University Hospital, Seoul, Korea, Republic of

Advances in sequencing techniques have made molecular subgrouping of Diffuse Large B-cell Lymphoma (DLBCL) based on DNA cahnges, which has led to the development of Lymphgen classification. By the way, although alternative splicing (AS) in cancer cells contributes to proliferation, invasion and metastasis, and immune escape, their role and association with DLBCL molecular subtypes are unknown. Therefore, we analyzed whole-exome sequencing (WES) and bulk RNA-Seq data paired in the public EGA dataset (EGAD00001003600) to explore the patterns of AS events that differ between Lymphgene subtypes. The WES data of 620 DLBCL samples that passed quality control were aligned to the reference using BWA-MEM, and variants were called with Mutect2. We used the information of copy number variants provided by cBioPortal. The RNA-Seq analysis was performed using the STAR-RSEM pipeline and differential splicing events were detected using rMATS to compare subtypes. Among 620 DLBCL samples, there were 19 MCDs, 95 EZBs, 22 BN2s, and 137 ST2s (50 samples with multiple genetic classes, and 291 samples unclassified). Mutations in spliceosome complex genes (ZRSR2 and SF1) were found in 14 and 27 samples, respectively. In BN2 and MCD subtypes, splicing events with significantly different exon inclusion levels were observed at a high frequency of 29 and 16 occurrences, respectively, compared to other subtypes. (P-value < 0.05). In contrast, retained intron is the only event observed in the EZB subtype (Table 1). Samples with mutations in ZRSR2 and SF1 showed four and two aberrant events, respectively, compared to samples without these mutations. Of note, rMATS detected an alternative 3' splice site event in exon 6 of *CD37* in the MCD. *CD37* is involved in tumorigenesis in leukocytes and has been suggested as a potential biomarker in blood cancer, and its dysregulation may have influenced the poor prognosis of MCD. In summary, molecular subtypes of DLBCL had unique features in terms of alternative splicing. Functional consequences of these selective exon usages for each DLBCL subtype are being warranted.

#2266 Detection of androgen receptor splice variants from clinical sequencing.

S. Hwangbo, S. Lee, S. Kim, H. Yun;
Seoul National University Hospital, Seoul, Korea, Republic of

Background: Androgen receptor splice variant-7 (AR-v7) has been widely studied as a biomarker of resistance to AR-targeted therapy in castration-resistant prostate cancer (CRPC). Various methods have been used to detect AR-v7 in CRPC specimens, including next generation sequencing (NGS) technology. However, NGS technologies applied in clinical sequencing have focused on using blood or fresh-frozen CRPC tissue specimens. There is not yet an AR-v7 detection system tailored to formalin-fixed paraffin-embedded (FFPE) tissue specimens commonly used for clinical sequencing in hospitals.
Methods: In this respect, we propose a novel approach to identify AR-v7 in targeted RNA sequencing (RNA-seq) data derived from FFPE specimens. This approach can identify, in addition to AR-v7, all constitutively active AR splice variants (AR-Vs) that are co-expressed with AR-v7. In short, our two-step approach first gathers soft-clipped or divided reads that are adjacent to the splicing sites of AR-Vs and then yields the number of splitting reads that support the existence of AR-Vs. Next, the algorithm selects the paired-end reads whose one side and the other side are mapped to the preceding and following exons, respectively. The final number of spanning reads are calculated following to the removal of low-quality reads.
Results: We validated the proposed approach using two large-scale, independent RNA-seq datasets of prostate cancer (PC) samples: 111 samples from Seoul National University Hospital (SNUH) and 558 samples from The Cancer Genome Atlas (TCGA) dataset. The majority of both datasets were localized PC tumors, especially in the SNUH dataset, where localized PC accounted for 91% of the total. Overall, our approach successfully identified samples with putative AR-Vs, including AR-v7, AR-v3, and AR-v9. Statistical analyses of 111 SNUH PC patients suggested potential detection threshold in clinical sequencing settings (at least 200 split reads). In the SNUH dataset, the AR-v7 positive group, which included 5 patients (5%) with values above the threshold, shared the following characteristics: higher AR-v7/full length AR expression levels, AR amplification and co-expression with AR-v3/AR-v9. AR-v7 positivity was experimentally validated by Sanger sequencing. The similar pattern was also found in the analysis of TCGA dataset.
Conclusions: These results demonstrate that the detection system can successfully identify AR-v7 positivity not only for metastatic PC but also for patients with localized PC through clinical sequencing. We expect that the further in-depth analyses including larger samples and clinical outcomes can discover clinical applicability of AR-v7.

#2267 Assessment of AlphaMissense and structure-function predictions demonstrates efficient reclassification of genetic variants of unknown pathogenicity in inherited myeloid neoplasms.

A. Kurtovic-Kozaric[1], A. Campara[2], M. Jahibasic[2], A. Mujkic[2], A. Fojnica[3], **M. J. Kiel[1]**;
[1]Genomenon, Inc, Ann Arbor, MI, [2]International Burch University, Sarajevo, Bosnia and Herzegovina, [3]Technical University of Munich, Munich, Germany

Introduction: Classification of genetic variants has significant implications for clinical management. Artificial Intelligence (AI) has the potential to transform classification of genetic variants, such as AlphaMissense, which incorporates structure-function relationships and allele frequencies across large datasets of genetic variants. While this represents a promising new tool, the performance of AlphaMissense has only been compared to known pathogenic and benign variants. Therefore, the discriminatory power for variants of unknown significance (VUS) has yet to be determined. We have performed a comparison of these predictions with variants associated with inherited myeloid neoplasms: 1) to assess the accuracy of these models against VUS; 2) to enhance classification of unpublished VUS by leveraging published information about other variants; and 3) to map the predicted classification onto protein structures to examine spatial patterns.
Methods: For 83 genes associated with inherited myeloid diseases, a systematic literature review for missense variants was performed using the Mastermind Genomic Intelligence Platform and ClinVar. We used Alphamissense to characterize VUS missense variants according to predicted pathogenicity scores as pathogenic, ambiguous, or benign. Known pathogenic (n=1594) and benign (n=501) variants served as controls to evaluate the accuracy of the system. AlphaFold2 structures were visualized for structure-function rendering of reclassified VUS and known pathogenic variants to compare and identify discernible patterns of spatial distribution.
Results: This variant dataset comprised 1594 pathogenic, 501 benign, and 46676 VUS missense variants. Among VUS, AlphaMissense reclassified a majority of VUS missense mutations and established that the system was 88% accurate in predicting pathogenicity. A higher percentage of variants was classified as pathogenic among tumor suppressor genes e.g. DDX41 and RUNX1 (57.1% and 40.5%) compared to the oncogenes, GATA1 and GATA2 (25.7% and 34.9%). Furthermore, 3D models revealed a majority of variants reclassified to pathogenic were located in regions with defined tertiary structure clustered with known pathogenic variants, while benign variants were located at peripheral positions lacking definite structure.
Conclusions: These results demonstrate the discriminatory power of AlphaMissense for VUS pathogenicity prediction for both loss-of-function and gain-of-function disease mechanisms. This work may also have implications for rare or challenging somatic cancer variants and variants in rare diseases. Finally, incorporating information available from empirical and clinical studies for disease-causing variants offers the possibility of significantly enhancing the predictive power of these models.

#2268 CREDAC: Copy number-based reference-free expression deconvolution analysis of cancers.

C. Castignani[1], J. Demeulemeester[2], O. Pich[1], T. Lesluyes[1], R. E. Hynds[3], D. R. Pearce[3], E. Larose Cadieux[1], S. C. Dentro[4], T. Consortium[1], N. Kanu[3], C. Swanton[5], P. Van Loo[6];

[1]The Francis Crick Institute, London, United Kingdom, [2]VIB-KU Leuven Center for Cancer Biology; Department of Oncology, KU Leuven, Leuven, Belgium, [3]University College London Cancer Institute, London, United Kingdom, [4]Wellcome Sanger Institute & European Molecular Biology Laboratory, European Bioinformatics Institute, Hinxton, United Kingdom, [5]The Francis Crick Institute & Universtity College London Cancer Institute, Cancer Research UK Lung Cancer Centre of Excelence, London, United Kingdom, [6]Departments of Genetics and Genomic Medicine, The University of Texas MD Anderson Cancer Center, Houston, TX

Introduction: Analyses of bulk RNA sequencing data are central to most large-scale tumor sequencing studies. Bulk expression data represent population averages and its interpretation is confounded by both normal cell contamination and somatic copy number alterations. Several computational methods to deconvolve have been developed recently. However, these methods often rely on a set of cell-type-specific reference signatures and ignore the effect of copy number changes. Methods: To address these issues, we have developed a method that formalizes the relationship between allele-specific copy number, expression and sample purity to deconvolve the expression profiles of tumor and normal cells from bulk RNA-seq in an unbiased manner. Our method was applied to sequencing data produced by the TRACERx consortium, a longitudinal study with multi-region whole-exome and RNA-seq of non-small-cell lung cancers. A total of 414 primary tumor regions and 140 adjacent normal tissue samples from 140 patients with matched DNA and RNA-seq data were processed. Results: We were able to directly deconvolve a median of ~2,000 genes per sample and indirectly infer tumor and normal expression profiles of ~10,000 genes using an scaled and weighted mean approach. The accuracy of the deconvolution was validated using (1) *in-silico* mixtures of patient-derived tumor and normal cells, (2) pseudo-bulk scRNAseq and (3) in regions with loss of heterogeneity (LOH) directly on the bulk sequencing data, where the total fraction of expression attributed to tumor cells can be computed directly using somatic mutations. CREDAC allows for single sample bulk-level tumor-normal differential expression analysis and revealed a strong and constitutive genome-wide overexpression in cancer compared to admixed normal cells, with a more pronounced overexpression in lung squamous cell carcinoma than lung adenocarcinoma ($p<0.001$). CREDAC adjusts for variations in copy number, thus facilitating the investigation of cancer-specific dosage compensatory responses triggered by aneuploidy. We revealed that a majority of genes (~65%) exhibit proportionality to copy number alterations, while a substantial proportion (~35%) shows anti-scaling or dosage compensation strategies. We show an enrichment of genes involved in cell cycle and expression processes within the dosage compensated group and revealed methylation as a key mechanism driving this compensatory process.

Conclusion: Overall, our results suggest that CREDAC is able to accurately disentangle the expression of tumor and normal cells from bulk RNA-seq without any previous knowledge. It has potential applications in many studies that include matched RNA-seq and copy number data and can provide new insights functional characterization, the taxonomy of cancer, and tumor evolution.

#2269 Dual targeting of the PI3K-AKT pathway in triple-negative breast cancer.

G. Colley, A. Eustace, D. AlSultan;
Dublin City University, Dublin 9, Ireland

PIK3CA mutations occur in ~15% of triple-negative breast cancers (TNBCs) and aberrantly activate the PI3K-AKT pathway, resulting in uncontrolled cell proliferation. Alpelisib is approved for hormone receptor-positive (HR+), HER2-negative BC patients with a PIK3CA mutation; however, not all PIK3CA-mutated (MUT), HR+ patients respond to alpelisib and others acquire resistance following exposure, suggesting adaptive mechanisms of PI3K activation. It has been proven that in TNBC, there exists a cohort of mutated genes which activate PI3K-AKT signaling. We hypothesize that testing alpelisib in combination with repurposed approved drugs, targeting alternative mechanisms of PI3K-AKT pathway activation, may be used to treat a cohort of TNBC patients. TNBC patient genetic data from the MSK (N=168), METABRIC (N=209), and TCGA (N=171) datasets were analyzed using cBioPortal to identify frequently occurring mutations. Differential expression analyses based on mutational status were performed on CCLE cell line (N=705) microarray and TCGA BC patient (N=981) RNA-sequencing data using R. Dysregulated genes were functionally analyzed using DAVID Ontology and those associated with poorer survival in TNBC were identified using KM-Plotter. STRING database was used to investigate protein interactions. The antiproliferative effects of targeted drugs tested alone and in combination in a panel of 6 TNBC cell lines were determined using acid phosphatase assays. Reverse-phase protein array analysis was carried out on protein lysates from cells following 24 hour treatment with drugs used alone and in combination.TP53 is the most frequently mutated gene in TNBC and mutations were associated with significant genetic dysregulation. A comprehensive analysis of upregulated genes in TP53-MUT TNBC led to the identification of 5 potential therapeutic targets - MET, S100A9, LCN2, CA9, TACSTD2, and KLK5 - based on their association with poorer survival in TNBC, protein interactions with TP53 and PIK3CA, and availability of targeted drugs. MET was selected for *in vitro* analysis based on its strong correlation with PI3K-AKT signaling. The presence of a TP53 mutation was associated with decreased antiproliferative effects in TNBC cell lines treated with alpelisib. Treatment with alpelisib in combination with a MET inhibitor, crizotinib, demonstrated greater antiproliferative effects in TP53-MUT/PIK3CA-MUT cell lines when compared to TP53 or PIK3CA MUT only models.TP53 mutations are associated with genetic dysregulation in TNBC and may confer resistance to alpelisib. Targeting upregulated proteins in a cohort of TP53-MUT/PIK3CA-MUT patients may improve sensitivity to alpelisib via dual inhibition of PI3K-AKT pathway activation. Protein analysis will uncover the mechanisms of synergy observed between alpelisib and crizotinib, and the therapeutic potential of the combination will be experimentally investigated *in vivo*.

#2270 UALCAN Mobile, An app for cancer gene expression data analysis.

S. Varambally[1], D. Shimoga Chandrashekar[1], G. Puli[2], S. Karthikeyan[1], U. Manne[1], C. J. Creighton[3], S. Kumar[4];
[1]University of Alabama at Birmingham, Birmingham, AL, [2]Kattech Systems Inc . Full-time, Philadelphia, PA, [3]Baylor College of Medicine, Houston, TX, [4]University Illinois, Illinois, IL

Cancer is a complex disease effecting different organs and a major cause of death and a burden on the society. Multiple molecular alteration occur during cancer initiation and disease progression and metastasis. Recent advances in technology led to generation of large amount of molecular data including transcriptome. These large datasets can be used to analyze and identify sub-class specific cancer biomarkers and targets. However, there is a need for the development user friendly tools for its analysis and dissemination of the large scale cancer molecular data. Earlier, we had developed and upgraded web based comprehensive proteogenomic platform UALCAN (ualcan.path.uab.edu), which allows users to analyze and integrate the disparate data to better understand the gene, proteins, and pathways perturbed in cancer and make discoveries. UALCAN web platform enables intuitive analysis and discovery by cancer research community. In the current study, we describe the development of UALCAN Mobile application (App) that will provide cancer transcriptomic data obtained from The Cancer Genome Atlas (TCGA) project, to evaluate protein-coding gene expression based on various stratification including stage, grade, race, gender and molecular-subtypes across over 30 types of cancers. The UALCAN Mobile app aims at providing large cancer dataset on the go. In order to find causative gene expression changes, identify biomarkers and therapeutic targets, UALCAN Mobile will assist as the data will be easily mobile and transportable with this App. Here, we describe the development of UALCAN Mobile and its utility to the cancer research community. UALCAN Mobile App can be found at both iOS/Apple and Android play store and is free to download and use.

#2271 Conservation and faithful representation of circular extrachromosomal DNA in orthotopic patient-derived medulloblastoma xenografts.

R. Kenkre[1], O. Chapman[1], J. Luebeck[2], V. Bafna[2], R. Wechsler-Reya[3], J. Mesirov[4], L. Chavez[1];

[1]Sanford Burnham Prebys Medical Discovery Institute, San Diego, CA, [2]UC San Diego, San Diego, CA, [3]Columbia University Medical Center, New York City, NY, [4]UC San Diego School of Medicine, San Diego, CA

Background: Extrachromosomal DNA (ecDNA) is a driver of tumor heterogeneity and is associated with poor survival in many different adult and childhood cancer types. Patient-derived xenograft (PDX) models facilitate preclinical drug testing in an in vivo environment that enables analysis of tumor growth and survival and molecular tumor profiling. These models, combined with single-cell profiling, can be used to study intratumoral heterogeneity under therapeutic pressure and the emergence of drug resistance. Here we investigate the abundance and conservation of ecDNA in PDX models with the aim of assessing the faithful representation of ecDNA compared to the tumors from which they are derived.

Methods: Whole-genome sequencing (WGS) was applied to 27 medulloblastoma (MB) PDX models and their tumors of origin using Amplicon Architect, a tool used to reconstruct focally amplified regions of DNA to provide insights into the landscape of cancer genomes. The frequency of ecDNA in these models was also compared to that of ecDNA in the MB patient population. Optical genome mapping enabled accurate and reliable ecDNA sequence reconstructions. Multiome single-cell RNA and ATAC-sequencing of a PDX tumor enabled analysis of ecDNA conservation and intratumoral heterogeneity compared to similar data previously obtained from the primary tumor.

Results: Comparative analyses revealed that ecDNA is largely conserved in PDX models, emphasizing their relevance as faithful models of the primary tumors. In addition, we find that ecDNA is significantly more frequent in MB PDX models (16 out of 27 analyzed patient-derived tumors) as compared to their frequency in the overall patient population (~18% of all medulloblastoma tumors contain ecDNA), suggesting ecDNA as a driver for successful establishment of MB PDX models. Single-cell analysis revealed that ecDNA is omnipresent in almost all PDX tumor cells, while its presence was limited to only ~9% of tumor cells in the primary tumor.

Conclusion: Analysis of ecDNA in medulloblastoma primary tumors and in PDX models revealed that ecDNA is preserved in PDX models. This is an important characteristic that renders patient-derived mouse xenografts as faithful models of their primary tumors. These results emphasize the relevance of PDX models for preclinical in vivo studies aimed at analyzing the role of ecDNA under therapeutic pressure and for analyzing clonal selection along with molecular evolution of ecDNA during the development of therapeutic resistance.

#2272 Unlocking the potential of miRNA sequencing for early detection and monitoring of pancreatic cancer progression and recurrence.

R. N. Fuller, A. Morcos, D. Escalera, N. R. Wall;
Loma Linda Univ. School of Medicine, Loma Linda, CA

Pancreatic cancer (PC) is an elusive and deadly disease. Many patients with PC are diagnosed with metastatic or locally advanced tumors, limiting surgical resection, and increasing the risk of relapse after treatment. Relapse is recorded to be as high as 75% in the first 2 years after clinical intervention, resulting in a mean 5-year survival of 12% in the US, and as low as 2% worldwide. It is vital to develop diagnostic and monitoring techniques for PC. MicroRNAs (miRNAs) are robustly expressed in patient tumors and provide a rich source of biomarkers for disease detection and status. miRNA are short nucleic acid strands that bind to catalytic proteins to guide the regulation of large RNAs within the cellular space. This system is altered in tumors, leading to abhorrent expression of miRNA. Due to significant advancements in sequencing technology, miRNA-seq has become more accurate and affordable in detecting profile changes. To identify biomarkers for PC progression, we developed from the Gemcitabine-sensitive MIA-PaCa-2 (MP2) cell line the Gemcitabine and FOLFIRINOX resistant MP2-GR cell line. MiRNA-seq was conducted on the parental MP2 and resistant MP2-GR cells to identify those miRNAs that were differentially expressed between the cell lines. These miRNAs were analyzed via pathway analysis and gene ontology to find predicted functions followed by annotations from the miRNA Enrichment Analysis and Annotation tool (miEAA) to identify differentially expressed miRNAs associated with PC progression. This comparison indicated several miRNAs related to PC resistance. This dataset was then compared to *The Cancer Genome Atlas* (TCGA), which contains data from over 300 PC patients. The miRNA set was used to predict both PC progression after treatment, and recurrence. We are currently refining this data set to increase its predictive sensitivity and widen our patient data set comparison to further elucidate this approach in a clinical setting.

#2273 Development of a prognostic biomarker for ovarian cancer based on a high-resolution digital pathology platform for spatial statistical analysis of platelets and blood vessels.

J. Ahn[1], W. Carlos-Alcalde[2], M. Vasquez[1], M. Cho[2], V. Afshar-Kharghan[2], S. T. Wong[1];
[1]Houston Methodist Research Institute, Houston, TX, [2]The University of Texas MD Anderson Cancer Center, Houston, TX

Purpose: A third of ovarian cancer patients have elevated platelet counts that are associated with poor prognosis. However, the exact mechanism by which platelets preferentially extravasate into tumor microenvironment is unknown, partly owing to lack of effective tools that can accurately segment and measure platelet counts found in tumor tissues. In this study, we developed a high-resolution digital pathology (DP) platform with whole tissue confocal imaging and deep learning model that can be used to automatically segment out platelets and blood vessels to perform spatial statistics (SA) of platelets with high precision and consistency. We utilized our SADP platform to study an interaction between tumor secreted SDF-1 and CXCR4 on platelets which initiates platelet chemotaxis towards tumor microenvironment.
Methods: A deep learning algorithm to accurately segment out platelets was developed based on the U-Net structure using our original datasets from the murine ovarian cancer model. Tumor-bearing mice were injected with 5 mg/kg of Plerixafor, a CXCR4 inhibitor, daily for 4 weeks. Then, tumor nodules were resected, stained with CD41a and CD31 antibodies, and imaged using a whole slide confocal microscopy. We performed manual annotation of these images to generate the mask dataset and performed further data augmentation to increase the diversity of datasets. We trained our model using 85% of these images and performed validation using the remaining 15%.
Results: Using our SADP platform, the validation dataset achieved pixel-wise accuracy of 98.8%. A receiver operating characteristic (ROC) curve demonstrated an area under the ROC curve (AUC) of 0.99 with high sensitivity and specificity. Intersection over union (IoU) score of 0.765 was obtained. A statistically significant ($p=0.0467$), 7.03% reduction in the platelet density was shown in the Plerixafor-treated mouse ovarian tumor tissues ($n=8$) compared to the control tumor tissues ($n=9$). We also found that platelets are spatially concentrated near blood vessels in the control tumor tissues compared to the Plerixafor-treated tumor tissues ($p=0.0377$).
Conclusions: We developed a SADP platform to segment and quantitate tens of thousands of platelets from whole slide mouse ovarian cancer tissues automatically with high accuracy and consistency and incorporated spatial statistics to understand their spatial relationships and patterns that would not be apparent in non-spatial analyses. Applying the SADP platform, we demonstrated that treatment with Plerixafor leads to overall reduction in platelet infiltration within ovarian murine tumors. Our ongoing effort is to utilize our SADP platform on human tumor tissue images from a whole slide digital scanner to further characterize spatial distribution of platelets as a potential prognostic marker for ovarian cancer.

#2274 Genomic and transcriptomic analyses of chemical hepatocarcinogenesis aggravated by loss of oncoproteins in hepatocytes.

X. Wang, J. Zhang, Y. Liu, S. Zhang, Y. Liang, M. Zong, X. Lin, M. Karin, G. Feng;
University of California San Diego - UCSD, San Diego, CA

Hepatocellular carcinoma (HCC) is one of the most common causes of cancer-related death without effective treatment. Oncogenic drivers, including PTPN11/Shp2, Ikkβ kinase (IKK), c-Met and β-catenin, as well as tumor microenvironment as illustrated by a carcinogen or diethylnitrosamine (DEN)-treated models, have combined contribution to cancer progression that have distinct prevalence in human HCC progression. We previously found that disruption of Ras/Erk by Shp2 deletion combined with deletion of NF-κB unexpectedly dysregulated circadian clock genes which leads to further cancer progression. Except for this, limited reports investigated how various other oncogenic genes aberration would incorporate with DEN to induce HCC. Further, no reports investigated the dynamic evolution of transcriptomic aberration incorporating genetic changes and the differential functional pathways involved in DEN plus oncogene triggered-HCC progression. Thus, we here sought to investigate the context-dependent contribution of PTPN11/Shp2, IKK, c-Met and β-catenin to HCC using hepatocyte-specific deletion models (SKO, IKO, MKO, BKO) combined with DEN treatment. Exome sequencing and RNAseq were used to identify dynamic changes of the genomic and transcriptomic variations of HCC development under the influence of both genetic deletion and DEN-treatment. We found that upregulated epithelial-mesenchymal transition (EMT), cancer metastasis/migration and downregulated fatty-acid and cholesterol metabolism were highly involved across models. Macrophages together with genes including *Spi1*, *Clec7a*, and microRNA networks including *miR-122* and *miR-155* etc. were also deregulated. Specifically, upregulated IL2-STAT5 signaling in DEN-SKO liver tissues, upregulated myogenesis, KRAS signaling and EMT as well as apoptosis in DEN-MKO, downregulated xenobiotic metabolism and bile acid metabolism in DEN-IKO and -BKO were identified to be distinct to oncogenic deletion in relation with HCC development.

#2275 Reducing artifactual somatic variant calls from formalin-fixed paraffin-embedded specimens by using DEEPOMICS FFPE, a bioinformatic approach based on deep neural networks.

D.-h. Heo, I. Kim, H. Seo, S.-G. Kim, M. Kim, J. Park, H. Park, S. Kang, J. Kim, S. Paik, S.-E. Hong;
Theragen Bio Co., Ltd., Seongnam-si, Korea, Republic of

Formalin-fixed, paraffin-embedded (FFPE) tissue specimens are routinely used in pathological diagnosis. However, formalin induced artificial mutations make it challenging to accurately analyze next-generation sequencing data. Existing FFPE filtering tools tend to categorize all low-frequency variants as artifacts, making it difficult to identify true variants with low allele frequencies, compromising analysis of tumors with low tumor cell content. To address this issue, we developed DEEPOMICS-FFPE, an AI model designed to distinguish true variants from artifacts. We gathered paired exome genome sequencing data from both fresh frozen and FFPE samples of 24 tumors from public sources. These data were used to train and validate the model, with a split of 70% for training and 30% for validation. The deep neural network model, comprising three hidden layers, was trained using input features derived from the outputs of the MuTect2 caller. We employed the SHapley Additive exPlanations algorithm to identify relevant features, and then fine-tuned them based on the training outcomes. We assessed the performance of the final DEEPOMICS FFPE model in comparison to existing models (MuTect filter, FFPolish, and SOBDetector) using well-defined test datasets. Our findings revealed 43 distinguishing characteristics for FFPE artifacts. Refining the quantification of these characteristics resulted in improved model performance. DEEPOMICS FFPE successfully filtered out 99.6% of artifacts while retaining 85.2% of true variants, achieving an F1-score of 87.8 in the validation dataset, surpassing the performance of existing tools. Furthermore, the model demonstrated consistent performance even for variants with low allele frequencies, exhibiting a specificity of 0.998, suggesting its capability to identify subclonal variants. Future enhancement of the model will include the ability to use other variant callers and analysis of whole genome sequencing data. This newly developed tool has potential applications in designing capture panels for personalized circulating tumor DNA assays and identifying candidate neoepitopes for personalized vaccine development. DEEPOMICS FFPE is freely accessible for research purposes on the web at http://deepomics.co.kr/ffpe.

#2276 Comprehensive analysis of the genomic landscape of thyroid cancer.

SooHyun Im[1], Jong-Lyul Park[1], Jae-Yoon Kim[1], Chan-Kwon Jung[2], Seon-Young Kim[1]

[1]Korea Research Institute of Bioscience & Biotechnology (KRIBB), Daejeon, Korea, Republic of,[2]Department of Hospital Pathology, College of Medicine,, The Catholic University of Korea, Seoul, Korea, Republic of

Thyroid cancer, the most common endocrine malignancy, has a high incidence worldwide. Meanwhile, the incidence of thyroid cancer ranks first in Korea. To assess the possible influence of ethnicity on the molecular profile of thyroid cancer, we compared the genomic features of South Korean thyroid cancer with European thyroid cancer. In this study, we performed whole genome sequencing profiling (WGS) for 459 Korean thyroid cancer patients, including papillary thyroid carcinoma (PTC, n = 274), noninvasive follicular thyroid neoplasm with papillary-like nuclear features (NIFTP, n =18), follicular thyroid carcinoma (FTC, n = 16), follicular thyroid adenoma (FTA, n = 63), Hürthle cell adenoma (HCA, n = 22), and invasive encapsulated follicular variant papillary thyroid carcinoma (IEFVPTC, n = 19). We assessed the single nucleotide variant (SNV) and insertions and deletions using Mutect2, Varscan2, and Strelka2. For mutation signature and copy number alterations analysis, we used the Maftools and GISTIC2.0 packages, respectively. Our results revealed that most somatic mutations were similar between the Korean thyroid cancer dataset and the cancer genome atlas program (TCGA). However, the Korean cohort (1%) had a much lower NRAS mutation frequency than the TCGA cohort (8%). Mutation signature analysis showed that SBS6 and SBS2 were highly associated with the TCGA and Korean cohort. SBS6 is related to defective DNA mismatch repair, and SBS2 is characterized predominantly by CC > TT doublet base substitutions. In addition, we identified the NIFTP-specific somatic mutations such as KEAP1 and ZFP36L2. This study presents insights into the genomic landscape of Korean thyroid cancer and reveals some similarities and differences with European thyroid cancer at the molecular level.

#2277 Understanding the impact of clonal hematopoiesis on multiple myeloma: Insights from exosomal RNA analysis and survival analysis.

J. Park[1], G. Ryu[1], D. Nachun[2], M. Maurer[2], S. Jaiswal[2], D.-Y. Shin[3], J. Byun[3], J. Hong[3], Y. Koh[3], S.-S. Yoon[3];

[1]Seoul National University College of Medicine, Seoul, Korea, Republic of, [2]Stanford University School of Medicine, Stanford, CA, [3]Seoul National University Hospital, Seoul, Korea, Republic of

Clonal Hematopoiesis of Indeterminate Potential (CHIP) is a trait characterized by the accumulation of somatic mutations in hematopoietic stem cells in certain adults. It has been observed that the presence of CHIP can have significant implications for the development and prognosis of various blood cancers. Multiple myeloma (MM), a cancer involving the abnormal proliferation of malignant plasma cells in the bone marrow, is one such condition. Exosomes, a type of extracellular vesicles, play a role in cell communication by carrying information between cells. Analysis of UK Biobank data confirmed the poor prognosis of multiple myeloma patients with CHIP and identified a potential of paracrine effect on plasma cancer cells. To gain deeper insights into this paracrine effect on plasma cells, we attempted to analyze cell-to-cell interaction, such as the expression of miRNAs in exosomes, through exosome RNA sequencing. In our research, exosomes were extracted from bone marrow samples of 30 multiple myeloma patients, and exosome RNA sequencing was performed. Differential expression of miRNAs was identified. A total of 14 down-regulated miRNAs were identified based on adjusted p value < 0.05, log2 fold change < -1. We found that hsa-let-7f-5p, hsa-let-7a-5p, and hsa-miR-148a-3p, which are mainly miRNAs targeting MAP kinase, were significantly down-regulated in the CHIP cases. A computational tool was used to predict and integrate the target genes and pathways regulated by these DE miRNAs. The results suggested that certain inflammatory and oncogenic pathways including the MAPK signaling pathways, were not effectively suppressed in cases with CHIP (KEGG, $p < 0.005$). In addition, the chemokine signaling pathway and cytokine-cytokine receptor interaction (KEGG, $p < 0.005$) related to the paracrine effect, integrins in angiogenesis (PID, $p < 0.005$) related to poor prognosis and metastasis of cancer were also not adequately inhibited in the CHIP cases. Using UK Biobank data, we called somatic CHIP variants excluding those with VAF < 0.02 and analyzed them against ICD-10 codes. Hazard ratios (HR) were computed through Cox proportional regression with covariates. CHIP presence significantly correlated with MM diagnosis (HR: 1.64, CI: 1.35-2, $p < 0.001$), notably in *TET2* mutation carriers (HR: 2.35, CI: 1.63-3.4, $p < 0.001$). *TET2* mutations intensified MGUS to MM progression (HR: 5.0, CI: 2.27-11.0, $p < 0.001$). CHIP in MM impacted EFS (HR: 1.61, CI: 1.25-2.1, $p < 0.001$), with TET2 mutation carriers facing higher hazards (HR: 1.66, CI: 1.05-2.6, $p = 0.031$). CHIP, especially *TET2* mutations, significantly contribute to adverse MM outcomes and MGUS to MM evolution. Our findings provide insight into how CHIP influences the tumorigenesis and cancer progression of MM.

#2278 Unraveling immune dynamics of CD4+ in non-small cell lung cancer through single-cell analysis and gene expression profiling.

Hyunmin Woo[1], JiHye Yang[1], Siyoung Yang[2], Seong-il Eyun[1]

[1]Chung-Ang University, Seoul, Korea, Republic of,[2]Sungkyunkwan University, Seoul, Korea, Republic of

Non-small cell lung cancer (NSCLC) is a type of epithelial lung cancer other than small cell lung cancer and represents the majority of cases in lung cancer. The immune response against NSCLC relies significantly on the vital role by $CD4^+$ T cells, contributing to the regulation of immune system and the suppression of tumor growth. Various $CD4^+$ T cell subtypes, such as T conventional cells (T_{conv} cells) and T regulatory cells (T_{reg} cells), perform distinct functions within the immune system. T_{conv} cells boost immune responses against specific pathogens, while T_{reg} cells play a role in suppressing immune reactions. Investigating the correlation between T_{conv} cells and T_{reg} cells in NSCLC could serve a valuable biomarker for evaluating the immune status of lung cancer patients. We examine the connection between particular $CD4^+$ T cells in the lung and specific gene expressions associated with NSCLC. Through single-cell analysis, we classified the proportions of T_{reg} cells and T_{conv} cells within $CD4^+$ T cells in both the lungs and spleen of mice. Our discovery revealed that the proportion of T_{conv} cells in the lungs exceeded that in the spleen. From the differential gene expression (DEG) analysis using RNA-Seq data for T_{reg} cells and T_{conv} cells in NSCLC, compared to the control group of Peripheral Blood Mononuclear Cells (PMBC), we identified 1823 genes uniquely expressed in NSCLC T_{reg} cells and 711 genes in T_{conv} cells. Within these genes, we verified the expression of IL2RA and CTLA4, known to be expressed in NSCLC. Additionally, we identified high expression of genes TM4SF1 and KRT6A. By comparing the genes specific to T_{conv} and T_{reg} cells in the lungs with those significantly expressed in NSCLC, we were able to identify 114 co-expressed genes in T_{reg} cells and 71 in T_{conv} cells. We conducted GO and KEGG pathway analyses on these genes and examined the interaction networks among the associated genes. Furthermore, we found receptor interactions between T_{conv} cell subtypes (Th1, Th2, Th17, and Tfh) and T_{reg} cells through cell-cell interaction analysis. We explored the mouse phenotypes associated with these genes. These discoveries unveiled connections within lung-specific gene networks of T_{reg} and T_{conv} cells associated with NSCLC, highlighting candidate genes for targeted therapy in cancer.

#2279 Evaluating the metabolic status of gioma microenvironment at single-cell resolution.

F. P. Carcanholo, L. M. M. Fonseca, R. L. Simoes, S. A. Uyemura, **T. M. Malta**;
University of Sao Paulo, Ribeirao Preto, Brazil

Gliomas are brain tumors with low therapeutic response, markedly heterogeneous, and very proliferative. Mutations in the isocitrate dehydrogenase 1 (IDH1) and 2 (IDH2) genes are present in most lower-grade gliomas and less frequent in high-grade gliomas. The reprogramming of energy metabolism marks cancer to support rapid tumor growth and tumor survival. The remodeling of the epigenome in gliomas with and without IDH1/2 mutations is associated with changes in the energy metabolism, which has implications for the evolution of the tumor and for patient outcomes. Comprehending the metabolic reprogramming of different subtypes of gliomas is crucial to understanding tumor development and for the identification of better treatment targets. In this research, we explored the cell-to-cell metabolic variability using public single-cell RNA-seq (scRNA-seq) data of IDH wild-type (IDHwt) and IDH-mutant (IDHmut) gliomas. We analyzed 13,000+ single cells from four datasets [IDHwt (n=7,930), IDHmut codel (n=3,304), IDHmut non-codel (n=6,333), and IDHwt/K27M mutant (n=4,084)]. Data was processed using Seurat. CopyKat was used to distinguish malignant from non-malignant cells. Known marker genes were used to identify normal cell populations (macrophages, T cells, oligodendrocytes). Finally, ssGSEA was used to create a score of activity of 70 important metabolic pathways extracted from KEGG, for each individual cell. Our exploratory analysis revealed a metabolic heterogeneity among malignant cells even within the same patient. Steroid biosynthesis and valine/leucine/isoleucine biosynthesis are the top contributors to metabolic heterogeneity. Oxidative phosphorylation (OXPHOS), fatty acid metabolism (FA), and tricarboxylic acid cycle (TCA) are among the highest metabolic activities. Comparing the distinct glioma subtypes, IDHmut codel showed the lowest OXPHOS, TCA, and glycolysis/gluconeogenesis (GLYCO) activities, suggesting a potential link between low metabolic activity and better prognosis. Comparing astrocytomas IDHmut and IDHwt we observed lower TCA, GLYCO, and FA activities in mutant tumors. Overall, malignant cells showed higher metabolic activity than non-malignant cells of the same tumor. The metabolic microenvironment of IDHmut differed the most compared to the other subtypes. Immune and normal cells could also be distinguished by their metabolic features. We observed subpopulations of T cells and macrophages presenting distinct metabolic activity which may reflect distinct immune activation stages. Collectively, we covered the heterogeneity in energy metabolism of gliomas with potential prognostic value. Understanding the metabolic status of cells in the tumor microenvironment could shed light on intratumoral heterogeneity and aid in identifying therapeutic vulnerabilities.

#2280 HPV integration identifies emerging oncogenes and carcinogenic mechanisms, potentially indicating tumor recurrences.

S. Li[1], S. Xia[1], M. Lawas[1], T. Qin[1], B. Grab[1], N. D'Silva[1], L. Rozek[2], M. Sartor[1];
[1]University of Michigan, Ann Arbor, MI, [2]Georgetown University, Washington, DC, WA

HPV integration events in Head and neck squamous cell carcinomas (HNSCC) are strongly associated with carcinogenesis and tumor progression. Previous studies have elucidated the mechanisms and structures of HPV-human fusion events, pinpointing potential integration “hotspots” (i.e. genes with nearby HPV integration in recurrent patients). However, none has comprehensively investigated the effects of HPV integration on both HPV and human gene expression, nor assessed the clinical implications of these bidirectional expression changes.

In this study, we conducted bulk RNA sequencing on 67 Formalin-Fixed Paraffin-Embedded Oropharyngeal Squamous Cell Carcinoma (OPSCC) tumor samples from the University of Michigan hospital, and analyzed them in conjunction with bulk and single cell RNA-seq from another >200 HPV(+) HNSCC patients from four previous studies. Among the 117 samples confidently identified as HPV integration positive, we recaptured all previously known integration “hotspot” genes as well as several novel ones that have altered expression in the integrated samples.

Exploring the impact of HPV integration on the expression of human and HPV genes, we found that HPV integration in HNSCC is strongly associated with keratinization, immune response, and the development of HPV(+) HNSCC subtypes. Upon HPV integration, expression of non-oncogenic HPV genes is often lost. We hypothesized that the expression ratio of these potentially HPV immunogenic genes (E1-E5, L1,L2) to the HPV oncogenic genes E6 and E7 (termed the ImmunOnco Score) would predict clinical outcomes. Survival analysis of 70 University of Michigan patients showed low ImmunOnco Score is associated with tumor recurrence.

#2281 A tumor-intrinsic signature involving immunosuppression via MIF-CD74 signaling is associated with overall survival in ICT-treated lung adenocarcinoma.

R. Erbe, M. M. Stein, T. A. Rand, J. Guinney;
Tempus, Chicago, IL

Introduction: Immune checkpoint therapies (ICT) have changed cancer care, yielding robust and durable responses in a subset of patients. Identifying patients who are likely to respond to ICT remains an ongoing challenge. In addition, only a portion of patients with clinical biomarkers respond to therapy. Signatures of RNA expression have been developed to predict response, the majority of which focus on T-cell and cytotoxicity markers, yet have been unable to substantially improve outcome predictions. Here, we present a RNA signature that instead describes tumor-intrinsic immune resistance and a potential mechanism of immunosuppression via tumor signaling on macrophages, derived from single-cell RNA-sequencing (scRNA-seq).
Methods: We performed dimensionality reduction using a Variational Autoencoder (VAE) on 30 scRNA-seq samples from 15 lung adenocarcinoma (LUAD) patients, comprising a total of 183,873 cells from the Cell Ranger pipeline. The VAE model was trained on each sample for 250 iterations, yielding 20 signatures from each patient, for a total of 300 signatures. The relationship of each signature with real-world overall survival (rwOS) across 1,983 bulk RNA-sequenced LUAD patients treated with an FDA approved ICT was assessed via a Cox proportional hazards model with risk set adjustment, using TMB and line of therapy as covariates. The NATMI python package was used to identify putative active ligand-receptor interactions between tumor cells and the immune environment.
Results: Among the VAE encodings, we identified an immune resistance signature significantly associated with decreased rwOS across the patient cohort (HR = 4.2 [2.8-6.3], adjusted p = 4.3e-10). This signature was derived from a small cluster of neoplastic cells (4.4% of cells) in a patient sample that was otherwise dominated by immune cells, including a substantial fraction of cytotoxic CD8 T cells (24.5%). The strongest predicted ligand-receptor interactions were found between the neoplastic cells and macrophages, via the MIF-CD74 interaction, an interaction we found upregulated in multiple single-cell tumor samples. Further, MIF RNA expression alone was significantly associated with rwOS across the 1,983 patient LUAD cohort (HR = 1.5 [1.1-2.1], p = 0.004).
Discussion: MIF-CD74 is a known immunosuppressive interaction and MIF signaling from tumor cells on macrophages has been previously shown to have immunosuppressive effects in a mouse model of melanoma that were largely reversible via MIF-CD74 blockade. Taken together, these results identify a signature of tumor intrinsic immune suppression that can indicate patients likely to experience reduced benefit from ICT. In addition, this signature provides evidence to support blockade of the MIF-CD74 axis as a means to enhance anti-tumor immune responses in LUAD.

#2282 Predictive association of tumor cells hijacked NFATC2 activities with resistance to immune checkpoint inhibition in melanoma patients.

B. Lawal, Y. Wang, P. Lotfinejad, X. Wang;
University of Pittsburgh Medical Center, Pittsburgh, PA

Background: Immune checkpoint blockade (ICB) has emerged as an effective cancer therapy. However, only a small fraction of patients receives benefits whereas a significant subset of patients experienced severe or even lethal autoimmune diseases. Stratifying patients that would benefit from immunotherapy remain a highly unmet clinical need. Dysregulations of transcriptional programs have been implicated in cancer initiation and progression. To date, there is a paucity of studies on the predictive values of transcriptional factors on ICB response based on the most recently emerged ICB clinical trial datasets. We reasoned that cancer cells may hijack key transcriptional programs in hematological cells to evade the attack from immune cells and acquired tolerance to immunotherapy.

Method: Herein, we used an R package singscore/1.14.0 to compute the TFs activity scores based on their validated gene targets (TGs). Leveraging melanoma clinical trial datasets, we analyzed the predictive association of the TF scores with resistance to anti-PD1 ICB. The R package, iGenSig was used to evaluate the potential confounding variables.

Results: Our landscape correlation analysis revealed NFATC2 (Nuclear Factor Of Activated T Cells 2)-TGs as the most significant predictor of anti-PD-1 ICB resistance in melanoma. NFATCT-TGS as a predictor of anti-PD1 resistance is confounded by liver metastasis and achieved AUC range between 0.71 to 0.74 in three datasets (PRJEB23709, GSE160638, and Phs000452). In addition, prior anti-CTLA4 exposure (AUC=0.87 and 0.89) is associated with higher predictive efficacy of NFATC2-TGS than anti-CTLA4 naïve tumor (AUC=0.61 and 0.69) in phs000452 and GSE91061 datasets. Survival analysis revealed that NFATC2 is a better predictor of progressive-free survival (PFS; HR=5.95), and overall survival (OS; HR= 3.28-3.38) in anti-CTLA4 exposed tumor than anti-CTLA4 naïve tumor (PFS: HR=1.92, and OS; HR=1.64-2.17). Finally, NFATC2-TGS show strong inhibitory correlation with B cells and T cells infiltration, but strongly correlated with tumor purity.

Conclusion: We demonstrate that NFATC2 TGS predicts ICB benefits in melanoma patients, and thus may guide the recruitment of melanoma patients for anti-PD1 ICB. Our data provide support to the hypothesis that melanoma acquired NFATC2 transcriptional program to avoid immune cells evasion and acquired tolerance to ICB immunotherapy

#2283 A targeted mutation calling workflow - end to end - from FASTQ to clinical report for single cells.

Adithi Ravikumar Varadarajan[1], Thomas Ragg[2], Jonas Grote[2], Vadim Dechand[1], Steffi Treitschke[1], Clara Chaiban[3], Christoph Klein[3], Zbigniew Czyz[3], Jens Warfsmann[1]

[1]Fraunhofer Institute for Toxicology and Experimental Medicine ITEM, Regensburg, Germany,[2]Quantiom Bioinformatics GmbH & Co. KG, Weingarten, Germany,[3]Experimental Medicine and Therapy Research, University of Regensburg, Regensburg, Germany

Molecular profiling of rare cancer cells derived from liquid biopsy holds promise to monitor systemic cancer progression and guide personalized therapy interventions. However, this necessitates reliable and comprehensive profiling of samples at the single cell level and requires whole genome amplification (WGA), which adds amplification errors and bias to common sequencing errors. Therefore, we established a single-cell mutation calling workflow that can identify clinically actionable somatic mutations in rare single cell DNA with high sensitivity and accuracy. Our workflow is an end-to-end solution which can take FASTQ reads from any Panel Sequencing (PanelSeq) data and gives out single nucleotide variations (SNVs), insertion-deletions (InDels), and copy number variations (CNVs) in single cells alongside with mutation specific information from ClinVar, OncoKB, pathogenicity scores, conservations scores as well as known association to drug response and resistance. We incorporated a Bayesian Neural Network (NN) based Classifier algorithm that assigns a single statistical confidence score to the mutations, enabling prioritization of the mutations in a robust manner. On the training dataset including MDA-MB-453, BT474, BT549 and ZR-75.1 cell lines, the classifier achieved 91% sensitivity and 96% specificity (AUC=0.98), while on the independent test collective including HCC1395/HCC1395BL cell lines it achieved 84% sensitivity and 96% specificity (AUC=0.90). We applied the workflow to patient samples suffering from advanced metastatic Triple Negative Breast Cancer (TNBC) assayed with in-house single-cell Integrated Mutation Profiling of Actionable Cancer Targets (scIMPACT) and single-cell Whole Exome Sequencing (scWES). Using our method, we detected clinically actionable SNVs with pathogenic relevance in primary tumor, metastatic specimens, circulating tumor cells (CTCs) from blood and disseminated cancer cells (DCC) from pleural effusions, as well as the matched CTC-derived *in vivo* models (CDX). Notably, functional *in vitro* drug screens performed on CDX models uncovered susceptibility to approved drug treatments conferred by mutations detected in the samples. In summary, we introduce a novel mutation calling workflow facilitating detection of SNVs, Indels and CNVs in rare single cells with high sensitivity and precision. Confident scores assigned by the NN classifier enables identification of functionally actionable mutations. The workflow was executed in GDPR compliant fashion and follows all data protection standards imposed by the European laws. Accordingly, the method is well suited for molecular profiling, therapeutic target selection and longitudinal monitoring of liquid biopsy specimens in diagnostic environments.

#2285 Mass spectrometry-based proteomics profiling reveals differential proteome composition in tumor and normal tissues, with implications for normalization.

Y. Zheng[1], L. Olita[1], M. Nivens[1], A. Chiang[1], S. Ahuja[1], M. Glover[1], J. Bullen[1], E. Hurt[1], W. Zhong[2];
[1]AstraZeneca US, Gaithersburg, MD, [2]AstraZeneca US, New York, NY

The composition of the proteome varies significantly across different tissues and disease states creating a challenge of how best to compare expression levels of each protein across these tissue types. Traditionally, a median approach to normalization has been used, but this could obscure meaningful biological differences between tissues. Here, we present a quantitative proteomic study analyzing proteome composition across tumor and normal tissues in order to assess normalization methods. Human proteomes covering 7 cancer indications (244 samples) and 12 normal tissue organs (370 samples) were analyzed by data-independent acquisition mass spectrometry. On average, over 8,000 proteins were quantified across the study cohorts. Comparison of proteomes revealed an average of 11.4% higher protein identification in tumors compared to matched normal tissues (6 tumor types all $p<0.003$). Tissue origin strongly influenced proteome composition, most notably in bone marrow, while cancer tissues displayed less proteomic composition variation than normal tissues. Compared to global median normalization, riBAQ and tissue-specific quantile normalization reduced technical variances while maintaining biological differences between tissue types. By revealing tissue-specific proteome signatures as well as systemic proteomic alterations in tumors, this study lays the groundwork for appropriate comparative approaches accounting for tissue origins, and establishes a framework for discovery of tissue-specific biomarkers, which may facilitate the development of novel diagnostic and prognostic tests, and guide therapeutic interventions for cancer.

#2286 Clonal sweep dynamics: A marker of tumor fitness and predictor of clinical outcomes.

L. E. Lara Gonzalez[1], S. Loi[1], A. T. Papenfuss[2], D. L. Goode[1];

[1]Peter MacCallum Cancer Centre, Melbourne, Australia, [2]The Walter and Eliza Hall Institute of Medical Research, Melbourne, Australia

Cancer evolution is a complex process driven by cellular adaptations to environmental pressures. Understanding a tumor's evolutionary path is crucial for tailoring therapeutic strategies based on its genomic profile. We developed a method that estimates tumor 'fitness' (w) by analyzing the time of every clonal sweep. This is quantified by driver copy number or point mutations through analytical solutions derived from the branching process of tumor evolution. The method incorporates tumor size and growth rate, assessed through *in-vivo* BrdU staining, to determine the tumor's age, diversity, and aggressiveness. Using our method in the Yates et al. 2015 multi-region study, we analyzed 303 breast cancer tumors from 45 patients using whole-genome and exome sequencing (WES), focusing on ER+ (N=26) and ER- (N=19) subtypes. A negative correlation was observed between clonal cytoband alterations and fitness (ER+, R=-0.41; P=0.04; ER-, R=-0.72; P<0.001). Expanding the analysis with the METABRIC study (Curtis et al. 2012), clonal cytoband alterations (CA) were linked to survival outcomes for both ER+ and ER- subtypes. Additionally, in the TRACERx NSCLC study (Jamal-Hanjani et al. 2017) of 327 tumors from 100 patients who underwent WES, the median tumor fitness was associated with a higher risk of recurrence or death. Survival analyses are detailed in Table 1 below. Multivariate analysis was adjusted for tumor size, nodal status, and CD8α expression in the breast cancer study, and according to the authors' methodology in the TRACERx study, respectively.

Table 1 Survival Analysis

Study and Endpoint	Parameter	Univariate HR (95% CI)	Multivariate HR (95% CI)
METABRIC: ER- (N=128) on RFS	CA > 3 (Ref: CA ≤ 3)	0.61 (0.40, 0.93), P=0.02	0.49 (0.32, 0.75), P<0.001
METABRIC: ER- (N=128) on OS	CA > 3 (Ref: CA ≤ 3)	0.68 (0.47, 1), P=0.05	0.60 (0.4, 0.88), P=0.01
METABRIC: ER+ (N=458) on RFS	CA > 3 (Ref: CA ≤ 3)	1.61 (1.33, 1.94), P<0.001	1.51 (1.25, 1.82), P<0.001
METABRIC: ER+ (N=458) on OS	CA > 3 (Ref: CA ≤3)	1.44 (1.23, 1.68), P<0.001	1.38 (1.18, 1.61), P<0.001
TRACERx NSCLC (N=43) on RFS	Med. w > 1.031 (Ref: w ≤ 1.031)	3.24 (1.38, 7.62),P=0.007	4.11 (1.12, 15.1), P=0.033

The observed tumor growth rates in both studies align with known doubling times, demonstrating our method's accuracy. This approach successfully identifies tumor profiles linked to worse outcomes in breast and NSCLC cancers. Our findings suggest that analyzing clonal composition in tumors can improve patient stratification, particularly in infiltrated tumors, potentially enhancing immunotherapy response due to increased neoantigen exposure.

BIOINFORMATICS / COMPUTATIONAL BIOLOGY / SYSTEMS BIOLOGY / CONVERGENT SCIENCE: Liquid Biopsy and Precision Oncology Poster Session

#2290 Integration of cell-free DNA end motifs and fragment lengths can improve identification of active genes in liquid biopsies.

C. T. Maansson[1], L. S. Thomsen[1], P. Meldgaard[1], A. L. Nielsen[2], B. S. Sorensen[1];
[1]Aarhus University Hospital, Aarhus N, Denmark, [2]Aarhus University, Aarhus C, Denmark

Multiple studies have shown that the plasma cell-free DNA (cfDNA) from cancer patients differs from healthy individuals in both fragment length and fragment end motifs (FEMs). Yet, there is a lack of understanding regarding how the two factors combined can be associated with cancer and gene transcription. In this study, we evaluated cfDNA fragmentomics in plasma from lung cancer patients (n = 17) and healthy individuals (n = 7) using targeted sequencing (lung cancer: n = 12, healthy: n = 7) and whole-genome sequencing (WGS) (lung cancer: n = 5). A personal gene expression profile was established with H3K36me3 cell-free chromatin immunoprecipitation sequencing (cfChIP-seq). cfChIP-seq isolates nucleosomes with histone marks of active transcription directly from plasma, meaning cfDNA enrichment with cfChIP reflects gene activity in the cells of origin. Short cfDNA fragments were isolated using *in vitro* size-selection. Somatic mutations were identified from input cfDNA through the AVENIO pipeline. The findings were validated in an external public dataset comprising of WGS-cfDNA data from healthy individuals. Cancer patients contain a larger fraction of short (<150bp) cfDNA fragments compared to healthy individuals. Cancer patients also demonstrate an enrichment of distinct FEMs compared to healthy individuals. Investigating the association between gene activity and fragment lengths revealed that genes with high expression display an enrichment of short cfDNA fragments (median = 19.99%, IQR: 16.94% - 27.13%, $P < 0.0001$) compared to genes with low expression. Furthermore, distinct GC-rich FEMs are enriched in active genes. Combining the frequency of short cfDNA fragments with the presence of distinct FEMs results in a further enrichment of the highest expressed genes (median = 37.85%, IQR: 30.10% - 39.49%, $P < 0.0001$). *In vitro* size selection of short cfDNA also results in enrichment of GC-rich FEMs. *In vitro* size-selection can isolate cfDNA representing active genes and *in vitro* size-selection enrichment correlates with the cfChIP-seq enrichment (Spearman's ρ range: 0.499-0.882). This study expands the knowledge regarding cfDNA fragmentomics. We document how cancer patients and healthy individuals have different fragmentomic features. In addition, we shed new light on how gene activity in the cells of origin is associated with cfDNA fragment lengths and FEMs. Together, the results can increase the utility of liquid biopsies by determining gene activity in cancer patients.

#2291 Bravo automation of Agilent Avida targeted enrichment for high-throughput detection of genomic alteration and DNA methylation.

A. Wahba, T. Ho, S. Johns, A. Aravind, H. Wang, N. V. Mehendale, G. P. Amparo, K. Win, M. Gomez, G. Zhao, **D. N. Roberts**;
Agilent Technologies, Inc., Santa Clara, CA

Background: Current genomic and epigenomic profiling of cancer tissue DNA or cfDNA (cell-free DNA) in liquid biopsy relies upon separate, time- and sample-consuming technologies for somatic variant detection or methylation analysis. Here we describe workflow and performance of the Agilent Bravo automated liquid handling platform with the Agilent Avida targeted enrichment solution for next generation sequencing of somatic variants and methylation profiling. This solution can effectively analyze low-input tumor DNA or cfDNA samples. The Avida Duo workflow enables highly sensitive detection of single nucleotide variant (SNV), insertions and deletions (INDEL), copy number variation (CNV) and DNA methylation profiles from a single sample, without any sample splitting. Methods and Results: Panels, reagents, and automated workflows for Avida DNA, Avida Methyl, and Avida Duo Methyl (combined DNA & methylation) kits were developed to accommodate up to 96 samples on the Bravo NGS workstation. The automated solution supports independent single-day workflows for somatic variants or methylation sample preparation. The Avida Duo analysis combines both workflows without sample splitting, streamlining the process and reducing sample consumption. Leveraging a focused cancer hotspot panel, we demonstrate excellent reproducibility and low allele frequency (SNV at sub 1%) variant detection in cfDNA samples and reference standards with as little as 10ng DNA input. We exhibit similar performance with a larger ~300 kb target region tumor profiling panel. Finally, we demonstrate DNA methylation detection in the standalone or combined (“Duo”) workflows across differentially methylated regions (DMRs) with a panel of ~3400 targets. Conclusions: Automation of the Avida targeted enrichment solution with the Bravo NGS workstation enables a sensitive, high-throughput, end-to-end analysis for detection of genomic alterations and DNA methylation changes from a single low-input cfDNA or tumor DNA sample.

#2292 Impact of delayed processing on cfDNA quantity and quality using STRECK cfDNA tubes: Connect Pilot Study.

J. Bess[1], D. Hopkins[1], N. Diaz Mayoral[2], H. Cooley[2], A. de Palatis[2], D. T. Wong[3], S. Weinstein Oshinsky[1], C. Abnet[1], M.-J. Horner[1], A. Black[1], M. Brotzman[1], K. Wyatt[1], L. Sorbara[1], M. Young[1], M. Gaudet[1], N. Wentzensen[1], M. Williams[2], C. Karlovich[2], E. Greenbank[2], D. Elashoff[3], F. Wei[3], F. Li[3];
[1]National Cancer Institute, Rockville, MD, [2]Frederick National Laboratory for Cancer Research, Frederick, MD, [3]University of California Los Angeles, Los Angeles, CA

Interest in cell-free DNA detection for multi-cancer early detection and tumor monitoring is growing.1 Prospective evaluations of liquid biopsy assays are critical, and knowledge gaps in standard collection and preparation practices must be addressed for adequate assay execution.2 The NCI Connect for Cancer Prevention Cohort Study (Connect) aims to study new approaches in early detection. A pilot study was conducted with the STRECK Cell-Free DNA BCT tube to determine the impact of processing time on cfDNA quantity and quality utilizing two complementary quality control assays. 4 STRECK DNA BCT tubes were drawn from 40 donors. Plasma samples were analyzed, with half processed immediately and the other half stored for five days before processing. Two QC assays were performed to compare results at the two processing time points. The Alu EFIRM assay measured Alu element concentration (copies/mL). The Cell-free DNA ScreenTape assay evaluated Qubit DNA concentration (µg/mL) and %cfDNA. Descriptive statistics and paired sample t-tests were performed to compare mean concentrations at the two processing time points, with and without identified samples with cytolysis.

Median, mean, and range were recorded for each assay measure (Table 1). A reduction in cfDNA quantity was observed at the 5-day processing time point. Five 5-day processing samples were identified with high DNA quantity and a high Alu element concentration. The five samples experienced hemolysis and clotting as a result of handling and processing at odds with standard protocol. There was a significant difference between the mean DNA quantities of the processing time points following exclusion of the five samples. There was no change in significance between the mean Alu concentration and %cfDNA following exclusion (Table 2).

Both assays successfully detected samples with high nuclear DNA, a major contaminant for cfDNA assays, and identified a reduction in cfDNA at the 5-day processing time point. Proper handling and processing procedures are necessary to avoid cell lysis and maximize cfDNA quality and yield. This pilot establishes a starting point for future evaluations of liquid biopsy tube types, processing delays, and preanalytical cfDNA quality variables.

#2293 Comparisons of saliva versus plasma cfDNA and exosomal DNA as potential biomarkers for head and neck cancer.

M. Barbirou, A. Miller, D. Baek, A. Hameier, A. Wetzel, A. Linnenbach, K. Nunes, P. Llerena, V. Bar-Ad, A. Luginbuhl, U. M. Outschoorn, R. Myers, J. Curry, C. Wang, H. Yang;
Thomas Jefferson University, Philadelphia, PA

Purpose: Liquid biopsy approaches are revolutionizing cancer monitoring and have been considered potential mediators for therapeutic efficacy in multiple cancers. The investigation of different liquid biopsy biomarkers may lead to a better understanding of the cancers they are designed to detect and facilitate optimal management. This study aimed to identify and compare the epigenomic and genomic profiles of tumor biomarkers in circulation using cell-free DNA (cfDNA) and exosomal DNA (exoDNA) in plasma and saliva samples collected from patients with head and neck squamous cell carcinoma (HNSCC).
Methods: In a prospective trial, we performed whole-genome bisulfite sequencing on paired cfDNA and exoDNA from saliva versus plasma of 16 HNSCC patients. cfDNA was directly extracted from plasma and saliva, while exoDNA was extracted from purified exosomes after characterization. DNAs were then converted by Zymo EZ DNA Methylation-Direct kit and libraries were constructed with xGen™ Methyl-Seq Kit and sequenced on the Illumina NovaSeq platform. Sequencing data analyses were performed using Bismark, GATK, and methylKit for methylation pattern and cfTools for Tumor Fraction Estimation (TFE).
Results: Methylation data demonstrated heterogeneities across sample types. Comparisons of ctDNA as a reference for exoDNA showed 7147 hypermethylated and 9984 hypomethylated regions for plasma samples but showed 131 hypermethylated and 123 hypomethylated regions for saliva samples. Comparisons of plasma as a reference for saliva, 37 hypermethylated and 95 hypomethylated regions were noted in exoDNA, while 117 hypermethylated and 262 hypomethylated regions in ctDNA. The mean level of tumor-derived DNA was above 3%, the lower limit of sensitivity to indicate the presence of tumor cutoff as suggested by the cfTools. There were 3.24%, 3.14%, and 3.14% tumor-derived DNA in plasma cfDNA, plasma exoDNA, and saliva exoDNA, respectively. However, the tumor fraction in saliva cfDNA was below this cutoff (2.88%). A statistically significant ($P < 0.001$) difference in TFE was observed between combined cfDNA and exoDNA data from plasma and saliva, but the difference between combined sample types cfDNA and exoDNA did not reach statistical significance ($P = 0.306$). The linear mixed-effects model for TFE influence between the different groups revealed a significant interaction between sample sources (plasma and saliva) and sample types (cfDNA and exoDNA) ($P = 0.005$), as well as a significant effect of sample source on TFE ($P < 0.001$).
Conclusions: This pilot investigation provides evidence that exoDNA and cfDNA have different molecular profiles in plasma and saliva samples from the same HNSCC patient, and indicates that saliva carries additional tumor markers for HNSCC. These results help to advance our understanding of the potential impact of different liquid biopsy sample types in cancer management.

#2294 Monitoring glioma treatment response through longitudinal analysis of cell-free DNA in cerebrospinal fluid: Insights from a comprehensive study using next-generation sequencing.

R.-C. Cecile[1], **X. Dong**[2], C. Dai[2], W. Mo[2], P. Du[2], S. Jia[2], T. Burns[1];
[1]Mayo Clinic, Rochester, MN, [2]Predicine Inc., Hayward, CA

Background: Assessing treatment response in gliomas with high fidelity remains challenging. Cell-free DNA (cfDNA) is increasingly recognized as a liquid biomarker in plasma and cerebrospinal fluid (CSF), showing promise in optimizing therapeutic regimens for various cancers. While CSF has been explored as a source of cfDNA for gliomas, understanding the dynamics of cfDNA abundance and sequencing changes during treatment and recurrence is essential. Leveraging our biobank of longitudinal CSF specimens obtained through CSF access devices, we aimed to determine the potential utility of CSF cfDNA as a monitoring tool for treatment response in glioma patients.
Materials and methods: Longitudinal CSF specimens were collected through Ommaya reservoirs (NCT04692337) or ventriculoperitoneal shunts (NCT04692324) from patients with brain tumors, including gliomas. cfDNA was extracted from 1-5 mL of CSF based on available sample volumes and quantified using Qubit. Next-Generation sequencing using PredicineCARE or PredicineSCORE low-pass whole genome sequencing (LPWGS) was performed based on the available cfDNA.
Results: CSF collected before versus after resection showed an increase in quantified cfDNA (2.97x, range: 1.58-5.26x), indicating the impact of increased parenchymal disruption and closer contact with CSF. Subsequently, CSF cfDNA decreased during chemoradiation and adjuvant treatment and increased at recurrence, even in patients co-enrolled in immunotherapy trials for IL-7 agonists and pembrolizumab. Notably, copy number burden (CNB) increased at recurrence in three patients with known disease progression and decreased throughout immunotherapy treatment in one patient despite concerns of pseudoprogression. In a patient with a hypermutated glioblastoma, CSF cfDNA revealed over 59 genomic alterations, including MAP2K1, KIT, and PDGFRA. Another patient with a progressing EGFR-amplified GBM showed over 200 new variants in the final sample, with EGFR copy number increasing from 2 to over 30.
Conclusion: Analysis of cfDNA throughout a patient's disease course, encompassing resection and treatment with standard-of-care and experimental therapies, may aid in disease monitoring and treatment response. Further evaluation in a larger patient cohort is needed to determine the sensitivity of changes in mutations, CNB, and cfDNA quantity for glioma disease burden.

#2295 Circulating T cell receptor repertoire analysis improves cancer early detection.

Y. Li[1], M. Nahas[1], D. Stephens[1], K. Froburg[1], E. Hintz[1], D. Champagne[1], A. Lochab[1], M. Brown[1], J. Abhyankar[1], J. Braun[1], M. Dinh[2], M. Fortuno[3], M.-d. Ocon[3], A. Pasquier[3], I. Luque[4], C. W. Seder[5], J. A. Borgia[5], L. Seijo[4], L. M. Montuenga[3], **R. Yelensky**[1];
[1]Serum Detect, Inc., Newton, MA, [2]Rush University, Chicago, IL, [3]Clinica Universidad de Navarra, Pamplona, Spain, [4]Clinica Universidad de Navarra, Madrid, Spain, [5]Rush University Medical Center, Chicago, IL

Background: Cancer screening by liquid biopsy promises to detect cancer early when it can be cured. However, current liquid biopsy approaches based on circulating tumor DNA (ctDNA) detect only a minority of early-stage cancers, because these tumors shed little ctDNA and plasma sample volume is limited. For liquid biopsy to realize its potential for the early detection of cancer, sensitivity for the earliest stage disease must be improved.
Methods: We set out to improve sensitivity of liquid biopsy for cancer early detection by exploiting tumor recognition by T cells through sequencing of the circulating T cell receptor repertoire. Using gDNA extracted from blood buffy coats, we studied a cohort of 451 lung cancer patients (86% with stage I disease) and 525 subjects without cancer, enriched for older individuals with a history of smoking. We performed genomic DNA TCR beta chain sequencing to yield a median of 81,088 TCR clonotypes in cancer patients and 112,588 clonotypes in non-cancer controls. We built a TCR sequence similarity nearest neighbor graph to cluster >68M distinct TCR clonotypes into TCR repertoire functional units (RFUs). The TCR frequencies of RFUs were tested for association with cancer status and significantly associated RFUs were combined using a support vector machine model into a TCR RFU cancer score. This model was evaluated by 10-fold cross-validation (CV) and compared to a ctDNA panel of 237 mutation hotspots in 154 lung cancer driver genes (IDT™) and to a panel of 17 lung cancer related protein biomarkers (Olink®) in 87 subjects.
Results: We identified 177 cancer-associated TCR RFUs at FDR≤0.10, including 83 RFUs that were enriched in cancer samples with a TCR count log2-fold change between 0.05 and 1.31, and 94 that were enriched in controls with a log2-fold change between 0.07 and 0.40. We observed 56 of the 83 cancer-enriched RFUs had decreasing TCR counts with increasing age across the cohort, coupled with higher counts in cancer patients relative to age-matched controls. The TCR RFU cancer score achieved a cross-validated ROC AUC of 0.69 for cancer status prediction, with the AUC for stage I cancers similar to that of stage II-IV (0.69 vs. 0.70). 44% of stage I cancers (test samples of each CV fold) were detected by the TCR model at a specificity of 80%. We saw a substantial gain in sensitivity for stage I cancer when TCR RFUs were added to ctDNA and proteins, with a ~15-20%-point increase seen at the 90% target specificity level typical for cancer screening tests. Likewise, sensitivity increased at the 99% specificity level used in multi-cancer early detection, with 35% of stage I lung cancers detected, which could not be achieved by any analyte alone.
Conclusion: We demonstrate detection of a significant fraction of early lung cancer cases from blood by analyzing the circulating TCR repertoire and show that this signal is complementary to established analytes such as proteins and ctDNA.

#2296 Liquid biopsy of cerebrospinal fluid in breast to brain metastases.

S. N. Shishido[1], A. Marvit[1], S. Priceman[2], J. Portnow[2], P. Kuhn[1];
[1]University of Southern California, Los Angeles, CA, [2]City of Hope, Duarte, CA

Up to 30% of patients with breast cancers will develop brain metastases, and this risk is especially high with HER2-positive cancers. For patients with central nervous system metastases, cerebrospinal fluid (CSF) liquid biopsies are a promising opportunity to monitor disease, inform treatment, and predict prognosis. This study explores the CSF liquid biopsy analytes from 3 patients with central nervous system metastases analyzed with the third generation non-enrichment high-definition single cell assay (HDSCA3.0) workflow. The detection of cellular analytes was compared between the CSF and matched peripheral blood (PB) samples. Circulating tumor cells (CTCs) were detected in the CSF but not the PB and were subsequently molecularly characterized by single cell genomics and targeted multiplexed proteomics to reveal a clonal population of phenotypically heterogeneous cells. There was a lack of concordance between CTCs and cfDNA of the CSF in the copy number alteration profiles. In an extracellular vesicle surface marker analysis of the CSF, there was a high signal among tetraspanin CD9/CD63/CD81, with CD81 signal the highest across all 3 patients. The data indicates that the CSF may be used as a diagnostic or potentially prognostic tool to measure and characterize disease burden.

#2297 Longitudinal monitoring of HPV circulating tumor DNA in cervical cancer.

Preetiparna Parida[1], Krishna Sharan[2], Shirley Lewis[2], **Rama Rao Damerla**[1]

[1]Department of Medical Genetics, Kasturba Medical College Manipal, Manipal Academy of Higher Education, Manipal, India,[2]Department of Radiotherapy and Oncology, Kasturba Medical College Manipal, Manipal Academy of Higher Education, Manipal, India

Introduction

Detecting circulating tumor DNA (ctDNA) in the blood using minimally invasive techniques known as a "liquid biopsy", is gaining tremendous popularity in oncology research. Integration of human papillomavirus (HPV) DNA and the overexpression of the E6 and E7 oncogenes are crucial steps in the development of cervical cancer. We investigated the potential utility of HPV ctDNA as a biomarker for monitoring treatment outcomes in patients with cervical cancer.

Material and Methods

We use droplet digital PCR (ddPCR) to measure the amount of HPV16/18 ctDNA in plasma of cervical cancer patients. The HPV standard GP5+/6+ primers were used to determine HPV positivity in our patients. Specific primers were designed to amplify specifically the E6 oncogene of HPV16 and HPV18. Plasmid constructs were made using the PCR-purified products of HeLa and SiHa cell lines which would act as a positive control for the assay. HPV16 and 18 plasmids were serially diluted and then tested in qPCR as a template using different primer sets. Standard curves were made from the recombinant plasmids. This will serve as a positive control and will also provide a correlation between the sensitivity and specificity of qPCR vs ddPCR.

Results and Discussions

We hypothesize that our dPCR test will be able to detect minute quantities of HPV ctDNA in plasma of cervical cancer patients as ctDNA levels are expected to be decrease as treatment progresses. The assay sensitivity and specificity will be obtained by comparing results to QPCR. The study samples involve a tumor biopsy and a blood sample at the baseline prior to the therapy and serial blood sampling in different stages of treatment and follow-ups. These samples will also serve for treatment monitoring of these patients through ddPCR. Tumor samples are used to confirm the HPV status of patients using HPV-specific GP5+/GP6+ qPCR. We have recruited 75 cervical cancer patients with majority of them being squamous cell carcinoma and stage IIB disease. The qPCR results from tumor biopsy revealed HPV 16 was most prevalent (32/43), followed by HPV18 (6/43) and HPV 33(2/43).

Conclusion

we will now use Qiagen digital PCR system to understand HPV ctDNA levels in our patient cohort. we believe that our comprehensive sample collection after every treatment milestone and thorough follow-up for upto 2 years after diagnosis will allow us to study the utility of this sensitive test in monitoring disease and relapse.

#2298 Optimization of high-volume cell free DNA extraction and end-to-end automation for TSO 500 ctDNA library prep.

N. Prasad, R. Rock, R. Beatty, M. Robinson, D. Wildman, M. Sykes, B. Umylny, T. Halsey;
Discovery Life Sciences, Huntsville, AL

Liquid biopsy such as plasma, has emerged as one of the most valuable sample types for profiling circulating tumor DNA (ctDNA) for screening, response to treatment, and monitoring relapse in oncology patients. Due to the diffuse nature of ctDNA however, both extraction and library preparation must be optimized for the efficient downstream next-generation sequencing (NGS) application. We initially addressed the optimization of quality and quantity of cfDNA recovery from healthy and various oncology patients by evaluating QIAsymphony DSP Circulating DNA Kit and Apostle MiniMax cfDNA isolation kits. Overall, the cfDNA yields from Apostle MiniMax kit were approximately 12X higher. We then optimized high-volume automated cfDNA extraction from 1ml, 3ml and 6ml plasma samples using the Biomek i7 for Apostle MiniMax kit. Colorectal, Gastric and Ovarian cancer gave the highest yield of cfDNA whereas, Esophageal, Lung and Kidney cancers were the lowest cfDNA yielding samples. We then analyzed ctDNA from plasma from healthy donors, colorectal, kidney, Breast, and endometrial cancer patients along with Oncospan and Seraseq ctDNA mutation mix (5-0.5% AF) to evaluate the mutation detection efficacy, repeatability, and reproducibility by targeted NGS using TSO 500ctDNA assay ay 10ng, 20ng, and 30ng inputs. For library preparation batches of 48 samples were prepared using a fully automated processes for the library prep, Hybridization capture and post capture enrichment on the Beckman i5 robot. Libraries were sequenced on NovaSeq 6000 at 600M Paired-end depth. This method demonstrates an overall concordance of inter-run and intra-run accuracy of variant detection to be 90% demonstrating that this method run as described produces highly repeatable and reproducible variant detection to sub-1% allele frequencies. The inter-run, lot-to-lot, and operator-to-operator variability was ≥99%. Down-sample analysis demonstrated high levels of assay performance with sample inputs of 30 ng with ≥96% sample passing Illumina cut-off metrics at 150M PE read depth as compared to Illumina recommended 420M PE reads. Taken together, we provide a high-volume automated solution for cfDNA extraction from plasma samples, additionally these data demonstrate a robust, reproducible, and highly accurate targeted DNA sequencing method that can be used for low allele frequency variant detection in cfDNA.

#2299 More information from limited DNA: simultaneous measurement of genetics, 5hmC and 5mC in cell-free DNA.

T. J. Charlesworth, F. Puddu, R. Crawford, A. Johansson, E. Lleshi, A. Modat, J. Scotcher, M. Wilson, N. Harding, J. Teyssandier, J. Fullgrabe, W. Gosal, P. Creed;
Biomodal, Cambridge, United Kingdom

Liquid biopsy for profiling of cell free DNA (cfDNA) in blood holds huge promise to transform how we experience and manage cancer by early detection and identification of residual disease and subtype. While early work in liquid biopsy focused on the identification of actionable somatic variations at specific loci, the past decade has seen an expansion into non-genetic features, notably methylation. 5-methylcytosine (5-mC) profiles of cancer are differential from non-cancer at many more loci and so provide a stronger signal. Moreover, recent research has suggested that 5-hydroxymethylcytosine (5-hmC) profiles in cfDNA can be a marker for early cancer. However, a standard blood draw yields an average of only 10ng of cfDNA, presenting the dilemma of how to use limited sample to obtain maximum information. Existing methods for measuring methylation using next-generation sequencing cannot distinguish between 5-mC and 5-hmC and are limited in their ability to detect mutations, with approaches that measure both 5-mC and 5-hmC requiring two separate workflows. Hence, to measure complete genetics, 5-mC and 5-hmC using existing technologies requires three separate workflows, each of which require separate DNA input. We will present a technology which sequences at single base resolution the complete genetic sequence of input DNA fragments integrated with the modification status (unmodified, 5-mC or 5-hmC) for each CpG from low nanogram input quantities of DNA. A hairpin construct is used to create a copy of the original DNA strand. Enzymatic conversion followed by next-generation sequencing enables coupled decoding of bases across the original and copy strand, uniquely reporting one of A, C, G, T, 5-mC, or 5-hmC for each position in the input DNA fragment. Using this technology, we generated whole genome 6-letter data (measuring A, C, G, T, 5-mC, and 5-hmC at single-base resolution across the genome) on cell-free DNA extracted from plasma of healthy volunteers and patients with colorectal cancer at various stages of progression. We demonstrate how the technology can be used to compare 5-mC and 5-hmC methylomic profiles, genomics, and fragmentomics, across different stages of colorectal cancer. In particular, we show how disease progression can be marked by changes in 5-mC and 5-hmC across several loci. We propose that the ability to measure 5-mC and 5-hmC at high accuracy and single base resolution, alongside genomic and fragmentomic profiles, from a limited quantity of DNA will enable greater insight into the ctDNA in plasma and help advance the field of liquid biopsy towards fulfilling its promise.

#2300 AI enabled whole exome & transcriptome liquid biopsy addressing MCED, MRD, and therapy selection on a single platform.

J. Abraham[1], V. Domenyuk[1], M. Borderias[2], T. Yoshino[3], E. I. Heath[4], E. Lou[5], S. Liu[6], J. Marshall[6], W. S. El-Deiry[7], A. Shields[4], M. Dietrich[8], Y. Nakamura[3], T. Fujisawa[3], D. D. Halbert[1], D. Sacchetti[2], S. Stahl[2], A. Stark[2], S. Klimov[1], S. Antani[1], C. Nabhan[1], J. Swensen[2], G. Poste[9], M. Oberley[2], M. Radovich[1], G. W. Sledge, Jr.[1], D. Spetzler[2];

[1]Caris Life Sciences, Irving, TX, [2]Caris Life Sciences, Phoenix, AZ, [3]National Cancer Center Hospital East, Chiba, Japan, [4]Karmanos Cancer Institute, Detroit, MI, [5]University of Minnesota, Minneapolis, MN, [6]Lombardi Comprehensive Cancer Center, Washington, D.C., DC, [7]Brown University, Providence, RI, [8]AdventHeath Orlando, Orlando, FL, [9]Arizona State University, Phoenix, AZ

Effective clinical management of cancer patients requires an accurate and early diagnosis, highly sensitive monitoring of minimal residual disease (MRD), and precise therapy selection. There are multiple tests available that attempt to address each of these needs independently with varying degrees of clinical utility. Caris Assure is a proprietary circulating nucleic acid sequencing platform that couples whole exome and transcriptome (WES/WTS) sequencing on white blood cells and plasma with advanced machine learning techniques to satisfy all three testing needs on one platform. This test detects SNVs, INDELs, structural variants, copy number, gene expression, tumor mutational burden (TMB), microsatellite instability (MSI), fragment length, and aneuploidy of both somatic (tumor and clonal hematopoiesis) and germline origin. Caris' extensive database of over 350,000 tissue WES/WTS from solid malignancies was used to train deep learning neural networks to identify the molecular underpinnings of cancer. These networks were then deployed on WES/WTS data from plasma and buffy coat in pursuit of signals that can inform early detection, MRD and therapy selection.

Validation studies were performed to characterize the analytic and clinical performance of Assure on over 3000 patient blood samples. These samples include ~1000 non-cancer patients (controls), ~1700 newly diagnosed patients where blood was collected at surgery (early detection), ~500 early-stage patients during adjuvant therapy at multiple time points (MRD), and ~200 locally advanced/metastatic patients where matched tissue testing was also performed (therapy selection).

For early detection, stratification of blood samples from patients with stage I-IV cancer versus those with no reported cancer resulted in an AUC > 0.99 and included over 30 types of solid tumors. Notably, at 99.5% specificity, the sensitivities for stages I-IV (n= 119, 54, 50, 27) were 73%, 80%, 76%, and 89%. In the MRD setting for high-risk patients, the disease-free survival of patients whose cancers were predicted to recur was significantly shorter (39.6 mo) than those predicted not to recur (93.4 mo) (HR: 5.18, 95%CI: 2.94-9.09, p<.00001). This performance was observed across multiple lineages of cancer including but not limited to breast, colon, lung, and bladder. Lastly, for therapy selection, detection of driver mutations where blood was collected within 30 days of matched tissue demonstrated high concordance with a PPA of 93.8% and PPV of 96.8%. CHIP correction proved to be essential as ~35% percent of patients had CHIP mutations, including KRAS, BRAF, ATM, BRCA1/2, findings that could lead to improper therapy selection.

Herein, we demonstrate for the first time a single liquid biopsy assay that addresses the entire continuum of care in clinical oncology with optimal diagnostic, prognostic, and predictive utility for patients and physicians.

#2302 Innovative blood-based cell-free RNA whole transcriptome sequencing for comprehensive RNA profiling in patient plasma samples and its clinical applications.

F. Liu, Y. Huang, M. Wang, X. Sun, B. Xiang, S. Jia, P. Du, S. Luo;
Predicine, Inc., Hayward, CA

Background: Plasma cell-free RNA (cfRNA) holds promise for non-invasive cancer biomarker discovery, particularly in diseases like prostate cancer where specific biomarkers (AR splicing variants and TMPRSS2:ERG fusion) are detectable at the RNA level. Despite its potential, the technical challenges posed by blood cell-originated cfRNA abundance necessitates the development of robust and reliable assays for non-invasive cancer diagnostics. This study establishes and demonstrates the clinical utility of an innovative protocol for isolating and identifying tumor-originated cfRNA in plasma samples.
Methods: A novel methodology was developed for the simultaneous extraction of cfDNA and cfRNA from a single blood sample tube, enabling whole transcriptome sequencing (WTS) analysis with minimal input as low as 1ng. A proprietary method was developed to selectively deplete blood cell-originated transcripts in the library. An enrichment-based WTS assay was conducted, and a customized RNASeq analysis pipeline was employed to enable expression profiling and cancer biomarker testing from the cfRNA samples.
Results: The developed extraction method yielded substantial amounts of cfDNA and cfRNA from a 4 mL blood sample. Efficient depletion of blood cell-originated transcripts, achieving over 99% removal, enhanced the detection of a broader range of gene expressions in plasma. Implementation of the cfRNA WTS assay across healthy donor and cancer samples demonstrated consistency with documented biomarker status. The assay revealed significant differential clustering between cancer samples and healthy donors, with characteristic cancer genes contributing to the distinction. Reproducibility and analytical sensitivity of the developed cfRNA WTS assay were successfully validated.
Conclusions: This study introduces Predicine's proprietary cfRNA WTS assay, enabling concurrent expression profiling and RNA biomarker detection in plasma samples. Overcoming technical challenges associated with blood cell-originated cfRNA, this assay represents a significant advancement in liquid biopsy-based cancer diagnostics.

#2303 Identifying and stratifying circulating tumor cell cluster subtypes in metastatic breast cancer patients and evaluating their clinical outcomes.

D. L. Adams[1], C. Reduzzi[2], A. Aryasomayajula[3], R. Alpaugh[4], S. Chumsri[5], C.-M. Tang[6], G. Del Priore[7], W. V. Williams[8], M. Cristofanilli[2];
[1]Creatv MicroTech, Inc., Monmouth Junction, NJ, [2]Weill Cornell Medicine, New York, NY, [3]Rutgers University, Piscataway, NJ, [4]Fox Chase Cancer Center, Philadelphia, PA, [5]Mayo Clinic Cancer Center, Jacksonville, FL, [6]Creatv MicroTech, Inc., Potomac, MD, [7]BriaCell Therapeutics Corp, Philadephlia, PA, [8]BriaCell Therapeutics Corp, Philadelphia, PA

Background: Circulating tumor cell clusters (CTCCs) are aggregated groups of tumor cells that detached from primary tumors and circulate the bloodstream. However, while Circulating Tumor Cells (CTCs) are a well studied phenomenon, CTCCs remain relatively unexplored and ill-defined, with only a few descriptive investigations evaluating their clinical utility. Adding to CTCC complexity is that various subtypes exist, including homotypic clusters consisting of a homogenous population of tumor cells and heterotypic CTCCs made of CTCs with immune/stromal white blood cells (WBCs). Furthermore, CTCs can undergo Epithelial-Mesenchymal Transition (EMT), a process characterized by loss of epithelial traits and upregulation of mesenchymal traits, and can form clustered EMTs (CEMTs). Moreover, CTCs can fuse with macrophages forming Tumor Macrophage Hybrid Cells, aka Cancer-Associated Macrophage Like cells (CAMLs) when in circulation. We enumerated all these types of cells and complex aggregates in the peripheral blood of patients with metastatic breast cancer (mBC).
Methods: We enumerated the 6 populations from patient samples enrolled in IRB aproved prospective pilot studies. Whole peripheral blood (7.5mL) was filtered and stained with cytokeratin (CK) & CD45/CD14 to identify CTCs. CTCs were defined as an intact DAPI nuclei and strong filamentous CK. Homotypic CTCCs were defined as ≥2 CTCs attached together. Heterotypic CTCCs were defined as ≥1 CTC attached to ≥1 WBC. EMTs were defined as having DAPI nuclei and weak non-filamentous CK. CEMTS were defined as ≥2 EMTs. CAMLs were defined as having an enlarged polynucleated DAPI, and positive for CD45/CD14 or non-filamentous CK. Median progression free survival (mPFS) and median overall survival (mOS) over 24 months (m) were evaluated.
Results: We evaluated the blood of 79 mBC patients. Single CTCs were found in 57% of patients (n=34/79), homotypic CTCCs 15% (n=12/79), heterotypic CTCCs 66% (n=27/79), EMTs 56% (n=44/79), CEMTs 23% (n=18/79) and CAMLs 97% (n=77/79). Over 24 ms, patierns with detectable heterotypic CTCCs & homotypic CTCCs had the shortest response times at mPFS=2.8 & mOS=5.8 ms, or mPFS=2.1 & mOS=4.3 ms, respectively. This was followed by CTCs mPFS=3.7 & mOS=13.7 ms, EMTs mPFS=4.3 & mOS=14.4 ms, CAMLs mPFS=4.3 & mOS=14.4 ms, and CEMT mPFS=4.7 & mOS=13.2 ms. Additionally, CTCCs were rare in HER2+ patients at 4.4% (n=1/23), but no associations to other hormone statuses were found.
Conclusion: CTCCs appear to represent an array of subtypes with different biological and clinical meanings. Here we enumerated CTCC subtypes in the blood of mBC patients and stratified the various types to clinical outcomes. These data suggest CTCCs are clinically important and further understanding of their biology in the context of tumor pathogenesis is needed.

#2304 Detection of early-disseminated cancer cells with deep learning-enabled holographic imaging.

N. Heller[1], K. Mallery[1], N. Bristow[1], Y. Travadi[2], E. Lee[2], J. Hong[1];
[1]Astrin Biosciences, Inc., St Paul, MN, [2]University of Minnesota, Minneapolis, MN

Recent research increasingly validates the early dissemination of tumor cells in peripheral blood during the nascent stages of cancer, often preceding clinical identification of the primary tumor. This emerging evidence emphasizes the potential of Circulating Tumor Cells (CTCs) as early indicators for cancer. Despite their significance, CTCs are exceptionally rare compared to normal blood cells, which presents a considerable challenge in detection, particularly during early stages of cancer. Traditional detection methods, such as those based on nucleated cell enrichment, antibody labeling and fluorescence imaging, encounter notable limitations when applied in the context of early detection. These limitations arise from the inherent heterogeneity of CTCs, and the multistep process involved in labeling and manual enumeration, compromising cell viability and resulting in cell loss. This loss becomes particularly problematic in the context of early cancer detection scenarios where the tumor burden is extremely low, and any cell loss can significantly impact assay sensitivity. To overcome these challenges, we propose an innovative CTC detection approach employing a deep learning framework combined with holographic imaging. This technique utilizes coherent light to generate holograms from cell samples, capturing detailed 3D morphological and optical properties of individual cells. We developed a custom convolutional neural network designed to facilitate high-throughput cell sorting in real-time. Trained on healthy blood samples and diverse cancer cell lines, the dataset consists of more than 50 million cellular holograms enhanced by proprietary Gaussian annotation and image augmentation strategies. Moreover, by combining the morphological signatures from holography with antigen signatures (e.g. HER2/ER/PR) in real-time, our model demonstrates the ability to detect less than 1 false positive per 1 million nucleated cells, highlighting its potential as a robust tool for targeted early-stage breast cancer detection. Our technology represents highly sensitive alternative to traditional screening methods, with the promise of enhancing patient outcomes.

#2305 Label-free high dimensional single cell morphological profiling of different hematological malignancies by ghost cytometry.

A. Tsubouchi[1], J. J. Miettinen[2], K. Wagatsuma[1], S. Akai[1], Y. An[1], M. Uematsu[1], P. Sergeev[2], D. Tsallos[2], M. J. V. Vaha-Koskela[2], S. Ota[3], C. A. Heckman[2]; [1]ThinkCyte K.K., Tokyo, Japan, [2]University of Helsinki, Institute for Molecular Medicine Finland - FIMM, Helsinki, Finland, [3]The University of Tokyo, Tokyo, Japan

Characterizing the heterogeneity in human leukemias is critical for understanding mechanisms of disease onset, uncovering biomarkers for disease diagnosis, and guiding research into novel treatment approaches. While extensive research focus has been placed on characterizing the molecular heterogeneity in leukemia by modern omics technologies, comparatively less emphasis has been placed on studying the diversity in holistic morphological changes that occur in single cells in the context of disease. Here, we report on a novel approach to understanding and characterizing different hematological malignancies using ghost cytometry, a recently developed high-content flow cytometric method that leverages high-speed, artificial intelligence (AI) driven morphological characterization and analysis of single cells. We performed morphometric profiling on human bone marrow samples from patients with T and B-cell acute lymphoblastic leukemia (ALL, n=5), acute myeloid leukemia (AML, n=5), multiple myeloma (MM, n=5) and healthy bone marrow mononuclear cell (BM-MNC) controls (n=6). Morphological profiles from individual cells were analyzed by unsupervised machine learning (universal manifold approximation and projection, UMAP) and compared within disease subsets and against controls. We identified disease-specific cell populations from a mixture of healthy control and disease samples without any labeling, based on completely label-free information. For validation of the specific cell subsets, we overlaid known cell surface markers (e.g. CD45 for blast cells, CD10/CD19 for B-ALL, CD33/CD34 for AML, CD38/CD138 for MM). The intensity of CD45 was dimmer and disease-specific markers were highly expressed in the disease-specific cell population. We also identified a unique cell subpopulation in the disease-specific cell population that could not be distinguished by existing markers. We also analyzed three human myeloma cell lines (AMO1, KMS, and L363) for comparison to the primary MM samples. In the UMAP analysis using LF-GC data, in all three types of cell lines, Bortezomib-resistant cell lines exhibited different distributions from the control parental cell lines. In addition, we observed distinct morphological profiles between primary myeloma samples and myeloma cell lines.
Here we present a novel cell characterization approach for human hematological diseases that leverages AI-based, label-free, high-speed morphological characterization of single cells. We demonstrate that the approach can be used to identify subtle morphological differences in blast cells from a range of blood cancer subtypes. Application of morphological profiling and AI can be used to identify measurable, disease-related changes in these diseases that have diagnostic, drug screening, and therapeutic monitoring potential.

#2306 A deep learning framework for automated segmentation and analysis of 3D breast cancer spheroid invasion dynamics.

T. Ngo, T.-H. Nguyen, F.-Y. Lin, T.-Y. Tu;
National Cheng Kung University, Tainan, Taiwan

Invasion of neighboring tissues is a cardinal feature of malignancy, notably observed in aggressive cancers like breast cancer, where it can lead to significant morbidity. To explore cancer invasion dynamics, the implementation of a three-dimensional (3D) tumor spheroid invasion assay offers a swift approach to mimicking a tumor micro-region or micro-metastasis. Differential Interference Contrast (DIC) time-lapse imaging was chosen for its fluorescence-free and non-destructive advantages in capturing live spheroid movement. However, the subsequent analysis posed challenges, including out-of-focus cells and a voluminous dataset with diverse microscope planes and time points. Our study introduces a segmentation framework featuring in-focus spatial stacking algorithm and novel training architecture that enabling in-depth automated analysis of 3D spheroid invasion behaviors within a microenvironment. Firstly, the MDA-MB-231 breast cancer spheroids were cultured in a microwell dish and then incorporated into a collagen type I matrix for the 3D spheroid invasion assay. Capturing spheroid invasion dynamics involved acquiring 15 z-plane images (spaced at 20 µm intervals) per timepoint for each spheroid using DIC microscopy at 15-minute intervals over a 28-hour period, employing a 20X objective lens. We refined the Focus Stacking framework into Multiple Slices Blurry Stacking (MSB-Stack) by pre-filtering blurred areas before stacking images. This process produced 6390 slices consolidated into 426 labeled stacked images, highlighting Invasive area, Spheroid core, and Invasive cells post-invasion. We then enhanced Mask R-CNN (Region based-Convolutional Neural Networks) with a weak-to-strong augmentation mechanism, leveraging well-segmented samples from MSB-Stack for training on both fully stacked and blurred images. Blurry Consistency Mask R-CNN (BCMask R-CNN) demonstrates overall improvement across feature extractors, outperforming Mask R-CNN. Using Mean average precision (mAP) as the main metric for instance segmentation and detection, our proposed model achieves 73.0% and 65.2% on mAP @[0.5, 0.95], showcasing robustness. Notably, our best results for mAP @0.5 reach 96.6% and 96.7% on both tasks, underscoring the effectiveness of consistency training in mitigating unclear boundary issues during preprocessing. In conclusion, our proposed method, MSB-Stack, effectively addresses the challenge of unclear boundaries in 3D breast cancer cell DIC microscopy datasets. The integration of weak-to-strong consistency training in our model, BCMask R-CNN, not only mitigates biases but also enhances performance across different backbones, setting the stage for future advancements in cell-tracking tasks and broader migratory analyses.

#2307 State-transition modeling of blood transcriptome predicts disease evolution and treatment response in chronic myeloid leukemia (CML).

D. E. Frankhouser, **R. C. Rockne**, D. Zhao, S. Branciamore, L. Uechi, D. O'Meally, Y.-H. Fu, Y.-H. Kuo, B. Zhang, G. Marcucci;
City of Hope National Medical Center, Duerte, CA

Chronic myeloid leukemia (CML) is initiated and initially maintained by BCR-ABL which is clinically targeted using tyrosine kinase inhibitors (TKIs). Although TKIs can induce long-term remission, they are frequently not curative. Thus, CML is an ideal system to test our hypothesis that transcriptome-based state-transition models accurately predict cancer evolution and treatment response. We collected time-sequential blood samples from tetracycline-off (Tet-Off) BCR-ABL-inducible transgenic mice that recapitulates human chronic phase CML and wild-type controls. From the transcriptome, we constructed a CML state-space and a three-well leukemogenic potential landscape that describes CML state-transition from health to disease. The potential's stable critical points were used to define three distinct disease states. The Early state was characterized by anti-CML genes (n=35) that opposed leukemia progression, whereas an expanding number of pro-CML genes characterized the Transition state (n=357) and Late states (n=1,858). Gene modules that were co-regulated at the unstable points in the potential landscape were identified as the drivers of transition between stable disease states. To investigate CML therapies we used two treatments: silencing of BCR/ABL by readministering Tet (Tet-on, Tet-off [TOTO]) which represented a best-case scenario of disease being cured, and TKI (nilotinib) therapy which represents current clinical practice. TOTO returned the diseased mice transcriptomes to a near health state, without reaching it, suggesting partly irreversible transformation. TKI, however, only reverted the transcriptome to an intermediate disease state, without approaching health, and disease relapse occurred soon after treatment. Finally, using only the earliest time-point as initial conditions, our state-transition models accurately predicted both disease progression and treatment response to both therapies for each individual mouse. In conclusion, these results show state-transition analysis is a valuable approach to gain real time insights into CML development, progression and ongoing treatment response that can also be applied to other type of leukemia and cancers in general. We predicted disease evolution and treatment response in a murine model that recapitulates human disease, supporting this as a potentially valuable approach to time clinical intervention even before phenotypic changes become detectable.

#2308 Semi-automated Ki-67 index assessment using top-k hotspot recommendation in Ki-67 IHC stained WSIs.

H. Yang[1], Y. Hwang[1], Y. Lee[1], K. Jung[2], M. Sung[2], T.-Y. Kwak[1], S. Kim[1], H. Chang[1];
[1]Deep Bio Inc., Seoul, Korea, Republic of, [2]Samsung Medical Center, Seoul, Korea, Republic of

Ki-67 index is commonly used as a breast cancer proliferation marker. However, it is a laborious and time-consuming task for a pathologist to directly measure the Ki-67 index. Recently, automation techniques using machine learning techniques such as deep learning have been proposed. In this study, we propose a top-*k* hotspot recommendation method to help Ki-67 index assessment based on nuclei detection detected by a deep learning model. The dataset included a total of 32 diaminobenzidine-hematoxylin (DAB-H) Ki-67 IHC whole slide images (WSIs) of breast cancer obtained by core biopsy. Each of these WSIs was evaluated by a pathologist using the interval of the Ki-67 index estimate and the scores of 1+, 2+, 3+, and 4+. Additionally, the search area was manually designated to exclude internal control. We developed a Ki-67 index analysis model based on deep learning and image analysis. Nuclei segmentation used the StarDist model. The detected results were filtered based on nucleus size and nucleus eccentricity. The filtering threshold was determined experimentally. To recommend top-*k* hotspots, a coarse search is performed to move the circle region horizontally and vertically in specific units, and the top *k* regions based on Ki-67 index are found among areas containing more than 500 cells. Next, a fine search is performed around the *k* areas in detail. Finally, the top-*k* hotspots and each detected positive and negative cells, count of positive cells and negative cells, and predicted Ki-67 index are provided. It was confirmed that the Ki-67 score estimated for the detected top-1 hotspot and the pathologist's Ki-67 score had a correlation of Pearson correlation coefficient=0.8153, R^2=0.6648. As *k* increased, the top-*k* accuracy was observed to increase from 68.75% when $k = 1$ and 3 to 75.00% when $k = 5$, based on the pathologist's score. When a pathologist reviewed 10 cases where the Ki-67 score differed from the prediction, 6 cases were judged to be worth reexamining considering the proposed hotspot and Ki-67 index, and 2 cases included stromal cells in cell detection. In two cases, the WSI was judged to be blurry. Cell analysis and top-*k* hotspot recommendation using deep learning and image analysis were performed on Ki-67 IHC stained WSIs and compared with the pathologist's Ki-67 score. Through semi-automatic top-*k* hotspot recommendation, the reliability of diagnosis can be increased as an auxiliary test to Ki-67 index assessment.

#2309 3D spatial quantification of lymphocyte infiltration and collagen features in the tumor microenvironment using a novel assay: 3D I/O Pro™.

C. Stoltzfus[1], J. Wilson[1], N. Grant[1], A. Alvarsson[1], A. DeWitt[1], D. Simmons[1], B. Olin[1], B. Phillips[1], L. A. Dillon[2], G. Clifton[2], **N. P. Reder[1]**;
[1]Alpenglow Biosciences, Inc., Seattle, WA, [2]Incendia Therapeutics, Inc., Boston, MA

Background: The composition of the tumor microenvironment (TME) is a major determinant of response to therapy in many solid tumors. To-date, characterization of the TME has been based on limited analysis of thin tissue sections. Here we demonstrate the utility of an end-to-end 3D spatial biology workflow, the 3D I/O Pro™, based on whole tissue imaging, to identify and quantify tumor cells, lymphocytes, and collagen features in human FFPE tissue samples.
Methods: Five human colorectal cancer FFPE blocks were deparaffinized, stained with nuclear (TO-PRO-3) and general protein (eosin) dyes, and cleared using a modified iDISCO protocol. Entire samples were imaged at 2 µm/pixel resolution with a hybrid open-top light-sheet microscope, the 3D*i*™. Regions of interest (ROIs) with a volume of 0.5 mm^3 were re-imaged at 0.33 µm/pixel. Cell nuclei and collagen were segmented and 3D spatial relationships between tumor cells, lymphocytes, and collagen fibers were quantified. Analyses were performed within select ROIs using 3D*a*i™ tools including U-Net, CytoMAP, CT-FIRE, CurveAlign, and custom Python scripts.
Results: The ratio of stromal to tumor parenchymal lymphocytes (lymphocyte infiltration ratio) varied from 1.4 up to 9.1 in 3D volumes and 1 to 25 in 2D virtual sections taken throughout all 5 CRC samples. The ratio of the collagen fibers within 100 µm of the tumor border-oriented perpendicular to the tumor-stromal boundary compared to those oriented parallel to the tumor-stromal boundary was 0.37 in a proof-of-concept evaluation of a 2D virtual section with a lymphocyte infiltration ratio of 12. Qualitatively, areas with perpendicular collagen had more lymphocyte infiltration into the tumor parenchyma than areas with parallel collagen orientation.
Conclusions: We demonstrated that the 3D I/O Pro™ pipeline can quantify lymphocyte density in tumor parenchyma and stroma and analyze collagen features, including orientation, within 3D ROIs in the TME. This workflow allows us to characterize tumors based on many complex spatial relationships and could have broad applicability in research and development of novel cancer therapies that target tumor fibrosis or other features of the TME. In the future, we plan to correlate features from the 3D TME with response to immunotherapy and use these features to refine histologic definitions of immune spatial phenotypes.

#2310 Integrating real-world histopathological and clinicogenomic data from 1799 lung cancer patients by applying unsupervised deep learning.

S. Wu[1], Y. Zhao[2], H. Luo[1], K. Kolahi[1], T. Bui[1], X. Shi[1], A. Shrotre[1], A. Liede[1], X. Zhao[1], J. Samayoa[1], W. Zhao[1];
[1]Abbvie South San Francisco, South San Francisco, CA, [2]Johns Hopkins University, Baltimore, MD

Hematoxylin and eosin (H&E) stained histologic sections contain invaluable information that remains largely untapped because of its complexity. To this end, AI applications employing deep learning (DL) can facilitate the translation of image data to enable human interpretation and yield novel oncological insights that would have otherwise remained imperceptible. DL-based methodologies are multimodal, capable of integrating imaging with clinicogenomic data to furnish a more holistic perspective and affording more accurate predictions in oncology. Here, we developed an unsupervised DL workflow to analyze 1,799 H&E images of lung cancer (NSCLC n = 951; SCLC n = 50; others n = 798) incorporating comprehensive patient-level clinical data (electronic health records [ConcertAI]) integrated with genomics (WES and RNA-seq [Caris Labs]). There are three steps in our approach: (1) image preprocessing and filtering, yielding > 30 million image patches; (2) utilizing pretrained SimCLR models from 57 public oncology histopathology datasets with ResNet-18 as a backbone structure to extract 512-dimensional-feature vectors for each patch; (3) using three unsupervised clustering methods (kmeans, DBSCAN, Leiden clustering) to cluster patches and selected Leiden clustering. We identified 635 primary imaging clusters using an elbow method and generated an image feature matrix by calculating correlations between each patch and cluster centroids; these were aggregated and mapped back to source slides. In this proof-of-concept, distinct image feature patterns characterized SCLC and NSCLC samples. For SCLC, one of the salient features was the presence of hemorrhage, which may be associated with higher rates of fine-needle aspiration biopsy procedure for SCLC compared with NSCLC which was confirmed in the EHR data (p = 0.032). Derived morphological clusters were correlated with tumor-immune genomic features (Tumor Mutational Burden [TMB], Immunologic Constant of Rejection [ICR], and Miracle scores[1]) serving as predictors of response to immune-checkpoint inhibitor therapy. By applying linear models, we detected 11, 96 and 249 significantly associated imaging clusters, respectively, highly enriched with immune cells e.g., plasma cells, macrophages, lymphocytes, and supporting an infiltrated and inflamed tumor-immune microenvironment. In summary, a multimodal, unsupervised deep learning workflow combining H&E imaging with clinicogenomic data was developed to identify histologic feature clusters associated with well-established tumor-immune genomic signatures of NSCLC immune infiltration and molecular phenotypes. These studies demonstrate enormous potential to yield histopathological and translational insights in NSCLC and SCLC that can empower clinicians to make better therapeutic response predictions.

#2311 Precise assessment of cancer cell growth and survival by artificial intelligence.

C. Wong[1], N. Khazamipour[1], S. Alibagi[2], J. Saade[2], D. Golanarian[2], N. Farivar[2], M. Daugaard[1], **N. Al Nakouzi**[1];
[1]Vancouver Prostate Center, Vancouver, BC, Canada, [2]SnapCyte Solutions Inc., Vancouver, BC, Canada

Introduction: Cancer research requires accurate methods for measuring analytical parameters like cell culture confluence, cell count, colony numbers, viability, and motility. These methods must be unbiased and user-independent for reproducible data. Cell analytics involves manual processes (e.g., manual cell counting) or reagent-based approaches (e.g., viability kits). In recent years, semi-automated systems have been introduced that can either count cells, measure cell growth by density tracking, and/or determine cell viability. However, these methods are often time-consuming, require reagents and labeling, and may involve costly instrumentation. Artificial Intelligence (AI) has made strides in clinical and laboratory research, holding promise for swift integration into cancer research. Here, we present the development and validation of SnapCyte™, an AI performing accurate, unbiased, label- and reagent-free cell analytics from basic cell culture images, independent of specialized instrumentation.
Materials and Methods: Cell images were generated using diverse cell lines (MCF7, PC3, Hela, Raji⋯) cultured in various vessels with and without treatments (Taxane, Cisplatin, Heatshock⋯). For the cell count dataset, adherent cells were detached using trypsin, stained with trypan blue and loaded into a standard hemocytometer. Images were acquired using the SnapCyte™ adaptor and diverse microscopes (Leica, Hund, Zeiss, Nikon) and cell phones. Multiple datasets of 500 annotated images each were created, with images masked for confluency or for singular live and dead cells by experienced scientists. Object segmentation utilized the UNet architecture for localizing cells in cell culture images and iterative training was applied to achieve the required accuracy.
Results: After multiple training iterations, SnapCyte™ AI detection models achieved 99% precision for confluency and >95% precision and recall for cell count. SnapCyte™ surpassed standard methods (Crystal Violet, WST1, MTT, Presto blue, CyQuant, Incucyte®, and Bio-Rad TC20 cell counter), displaying high accuracy and smaller standard error variation than reagent-based assays. Compared to IncuCyte® Bio-Rad TC20, SnapCyte™ demonstrated similar accuracy and greater user-independent results. Furthermore, SnapCyte™ acquired data in under 10 minutes, with non-invasive measurements, allowing direct use of cells in downstream assays.
Conclusion: We have developed and validated an AI model for advanced cell analytics. Our data show that the SnapCyte ™ AI is *at par* or better than existing reagent and instrument-based solutions in assessing cell confluency, number, and viability. This technology offers a fast, accurate, and unbiased cell analytics platform that is resistant to user variations, and independent of reagents and costly equipment.

#2312 Integrating spatial multi-omics data with spatial quantitative pharmacology (spQSP) model to simulate human neoadjuvant immunotherapy clinical trial of hepatocellular carcinoma.

Shuming Zhang, Atul Deshpande, Babita K. Verma, Hanwen Wang, Haoyang Mi, Long Yuan, Won Jin Ho, Elizabeth M. Jaffee, Qingfeng Zhu, Robert A. Anders, Mark Yarchoan, Luciane T. Kagohara, Elana J. Fertig, Aleksander S. Popel

Johns Hopkins University School of Medicine, Baltimore, MD

Human clinical trials provided tremendous insights to advance novel systemic therapies and to improve treatment outcomes for cancer patients. The few durable treatment options have led to a critical need to advance new therapeutics in hepatocellular carcinoma (HCC). Recent human clinical trials have demonstrated that new combination of immunotherapeutic regimens provide augmented clinical response in a subset of patients. Computational methods that can simulate tumors from mathematical equations describing cellular and molecular interactions are emerging as promising tools to simulate the impact of therapies entirely *in silico*. To facilitate designing dosing regimens and selecting potential predictive biomarkers, we developed a new computational model to track tumor progression at organ scale while reflecting the spatial heterogeneity in the tumor at cellular and molecular scale in HCC. This computational model is called a spatial quantitative systems pharmacology (spQSP) platform and it is also designed to simulate the effects of combination immunotherapy. The model is first calibrated using clinical outcomes and measured immune cell densities based on recent neoadjuvant HCC clinical trial combining anti-PD-1 immunotherapy and a multitargeted tyrosine kinase inhibitor (TKI) cabozantinib (NCT03299946). Then, we validate the results from the spQSP model by leveraging real-world spatial multi-omics data from the same clinical trial. The model output is compared with spatial data from Imaging Mass Cytometry (IMC). Both IMC data and simulation results suggest closer proximity between CD8 T cell and Arginase 1 (Arg1) positive macrophages among non-responders while the reverse trend was observed for responders. We also compared the model output with Visium spatial transcriptomics analyses of samples from post-treatment tumor resections in the original clinical trial. Both spatial transcriptomic data and simulation results identify the role of spatial patterns of tumor vasculature and TGFβ in tumor and immune cell interactions. To our knowledge, this is the first spatial tumor model for virtual clinical trials at a molecular and cellular scale that is grounded in high-throughput spatial multi-omics data from a human clinical trial.

#2313 Multi-modal deep learning to predict cancer outcomes by integrating radiology and pathology images.

Z. Li, Y. Jiang, **R. Li**;
Stanford University, Palo Alto, CA

Purpose: Cancer patients routinely undergo radiologic and pathologic evaluation for their diagnostic workup. These data modalities represent a valuable and readily available resource for developing new prognostic tools. Given their vast difference in spatial scales, effective methods to integrate the two modalities are currently lacking. Here, we aim to develop a multi-modal approach to integrate radiology and pathology images for predicting outcomes in cancer patients.
Methods: We propose a multi-modal weakly-supervised deep learning framework to integrate radiology and pathology images for survival prediction. We first extract multi-scale features from whole-slide H&E-stained pathology images to characterize cellular and tissue phenotypes as well as spatial cellular organization. We then build a hierarchical co-attention transformer to effectively learn the multi-modal interactions between radiology and pathology image features. Finally, a multimodal risk score is derived by combining complementary information from two images modalities and clinical data for predicting outcome. We evaluate our approach in lung, gastric, and brain cancers with matched radiology and pathology images and clinical data available, each with separate training and external validation cohorts.
Results: The multi-modal deep learning models achieved a reasonably high accuracy for predicting survival outcomes in the external validation cohorts (C-index range: 0.72-0.75 across three cancer types). The multi-modal prognostic models significantly improved upon single-modal approach based on radiology or pathology images or clinical data alone (C-index range: 0.53-0.71, $P<0.01$). The multi-modal deep learning models were significantly associated with disease-free survival and overall survival (hazard ratio range: 3.23-4.46, $P<0.0001$). In multivariable analyses, the models remained an independent prognostic factor ($P<0.01$) after adjusting for clinicopathological variables including cancer stage and tumor differentiation.
Conclusions: The proposed multi-modal deep learning approach outperforms traditional methods for predicting survival outcomes by leveraging routinely available radiology and pathology images. With further independent validation, this may afford a promising approach to improve risk stratification and better inform treatment strategies for cancer patients.

#2315 AI-enabled precision oncology era: Advanced and interactive interpretation of next-gneneration sequencing (NGS) reports.

H. Chen, Z. Xu, L. Chen, M. Wang, P. Zhang, F. Pang, K. Wang;
Shanghai OrigiMed Co., Ltd, Shanghai, China

Background: Next-generation sequencing (NGS) has been widely adopted in clinical practice, but there are still unmet needs among physicians regarding the interpretation and application of NGS reports. These needs include selecting multi-targeted and combination therapies, keeping up with evolving treatment options and clinical trial results, and incorporating personalized medicine based on real clinical cases.
Methods: To address these challenges, we propose using large language model (LLM) to analyze and interpret clinical questions, perform semantic searches in a high-quality database, and provide customized prompts and logical outputs. Our knowledge base includes diagnostic and treatment details for 600+ tumor subtypes, 620,000+ entries, 2,000+ drug details, and 440,000+ clinical trials. The database is updated automatically using a fact engine and medical literature sources. Personalized gene interpretation is incorporated using pretraining, cosine similarity, and context learning prompts.
Results: Our tool, named "SmartMTB", enables personalized interpretation of genomic testing reports for precision oncology. Users input the latest clinical features using a selection-based or question-and-answer approach. The tool identifies the treatment stage and genomic variations, provides information on mutation frequencies, sensitivity and resistance of targeted and immunotherapies, and priority selection strategies for multi-gene mutations. It matches similar clinical cases and provides real-time updates on treatment options and clinical trial literature. It also facilitates patient matching for clinical trials and considers economic factors.
Conclusion: We present a groundbreaking artificial intelligence (AI) tool in cancer care that revolutionizes precision oncology. This AI system, trained on extensive datasets, swiftly and accurately analyzes and interprets complex genomic and clinical data. It enables clinicians to make informed decisions about personalized treatment strategies, significantly improving patient outcomes in cancer therapy.

#2316 A deep Gaussian process (DGP)-based prediction model for immunecheckpoint inhibitor (ICI) response in gastric cancer (GC).

S. Park, M. Kim, C. Hong, T. Hwang;
Mayo Clinic, Jacksonville, FL

Background: Immune checkpoint inhibitors (ICIs) targeting PD-1 or PD-L1 have dramatically improved survival of patients with gastric cancer (GC). However, recent clinical trials, including KEYNOTE-059, KEYNOTE-061, and ATTRACTION-2, show that the objective response rate (ORR) for ICIs is still less than 20% in patients with advanced GC. Therefore, predicting who will respond to ICIs in advance is essential to make better treatment plans for GC patients. There are potential biomarkers to predict ICI response, but most of them can only be applied to a limited population of patients. For example, Kim ST., et al., (PMID: 30013197) show that patients with MSI-high or EBV-positive responded well to ICIs, but these subtypes account for less than 30 percent of GC patients (PMID:25079317). In this study, we propose a prediction model of ICI response using the 32 GC-specific genes that we identified from mutation data (PMID: 26635139) and showed their close association with survival and ICI response in GC (PMID: 35140202; PMID: 36508166). In addition, since the number of available GC-ICI samples is small, we design our prediction model in Bayesian and ensemble learning frameworks which are robust to small sample size problems.

Methods: We collected mRNA sequencing data from GC-ICI treated patients from our institutions and publications (PMID: 30013197; PMID: 35254400; PMID: 33846173). We used 108 samples previously included in our previous work (PMID: 36508166) as the training data and 27 samples (13 responders and 14 non-responders) from (PMID: 3384617) as the test data. We built and trained a classifier to separate responders from non-responders using the expressions of the 32 genes. We proposed to use a Deep Gaussian process (GP) model, a multi-layered extension of a GP that is itself a Bayesian method. We optimized the parameters of each GP model in variational inference. To implement ensemble learning, we trained multiple DGP models with different initializations of the model parameters and data splitting (training/validation sets). For each training run, the best model was selected based on the prediction performance on the validation set, measured by AUC. The final prediction for a test sample was made by combining the prediction results of all the DGP models by taking the average.

Results: We implemented the DGP-based prediction model using PyTorch in Python, and the codes will be publicly available on the GitHub repository (https://github.com/hwanglab/GC_ICI_response_prediction). We achieved a prediction performance of 0.813 AUC on the test data (sensitivity = 0.769 and specificity = 0.714).

Conclusion: We propose the prediction model of ICI response, which can handle small sample size problems in the framework of Bayesian and ensemble learning. The experimental results using the GC-ICI data demonstrate that the 32 genes can be used as predictive markers for ICI response in GC.

#2317 Development and validation of a colorectal cancer prediction model: A nationwide cohort-based study.

S. Hayek;
Tel Aviv University, Tel-Aviv, Israel

Background: Colorectal cancer (CRC) ranks as the third most prevalent cancer globally and is a major cause of cancer-related mortality. Early diagnosis is critical to increase survival rates. While CRC screening has shown significant benefit, adherence remains low, and there is a need for better tools to identify high-risk patients. Risk prediction models were demonstrated to identify such patients.
Aim: To establish an individualized risk prediction model for CRC diagnosis based on Electronic Health Records (EHR).
Methods: This is a retrospective cohort study utilizing EHR data of Clalit Health Services (CHS) members aged 50-74 that were eligible for CRC screening, from January 2013 to January 2019. The model was trained to predict CRC diagnosis within two years using approximately 20,000 EHR features including socio-demographic information, laboratory results and medical history. Model performance, as a complementary screening method, was evaluated.
Results: The study included 2679 subjects with CRC diagnosis and 1,133,713 subjects without CRC diagnosis. The model was trained on subjects from 2013-2017, and performance was validated on subjects from 2019 and a cohort of subjects that underwent fecal occult blood test (FOBT). Incidence values of CRC among subjects in the top 1% risk scores were higher than baseline (2.3% vs. 0.3%; lift 8.38; P-value <0.001). Characteristics of subjects by risk scores percentiles are presented in Table1. Cumulative event probabilities increased with higher model scores, indicating a correlation between predicted and actual risk of CRC diagnosis. Model-based risk stratification among subjects with a positive FOBT, identified subjects with more than twice the risk for CRC compared to FOBT alone.
Conclusions: We developed an individualized risk prediction model for CRC that can be utilized as a complementary decision support tool for healthcare providers to precisely identify patients at high risk for CRC and refer them to confirmatory testing.

#2318 Multimodal machine learning for the automatic classification of recurrent cancers.

P. Krawczuk[1], **Z. Fox**[1], D. Murdock[1], J. Doherty[2], A. Stroupe[3], S. M. Schwartz[4], L. Penberthy[5], E. Hsu[5], S. Negoita[5], V. Petkov[5], H. Hanson[1];
[1]Oak Ridge National Laboratory, Oak Ridge, TN, [2]Huntsman Cancer Institute, Salt Lake City, UT, [3]Rutgers Cancer Institute of New Jersey, New Brunswick, NJ, [4]Fred Hutchinson Cancer Center, Seattle, WA, [5]National Cancer Institute, Washington, DC

The National Cancer Institute's (NCI) Surveillance, Epidemiology, and End Results (SEER) registries maintain and organize cancer incidence information allowing researchers to derive valuable insights into cancer epidemiology. While significant attention has been devoted to identifying cancers either from clinical text or through tabular data collected by SEER registries, there has been less emphasis on integrating these distinct modes of data. In our multimodal deep learning approach, we use longitudinal tabular data from the Consolidated Tumor Case (CTC) database that encompass a patient's past diagnoses. This tabular information can augment clinical text to aid in the classification of pathology reports indicative of recurrent cancers. Four NCI SEER registries (Louisiana, New Jersey, Seattle and Utah) have manually labeled 61,150 pathology reports with one of six categories, which we refine into a four-class classification problem. Each pathology report is identified as either positive for recurrence, negative for recurrence/not disease free, new tumor, or an "other" (no malignancy/uncertain) class. Natural Language Processing techniques can extract meaningful information from clinical pathology reports, aiding in the identification of subtle indicators of recurrence by using relevant context. We use a hierarchical self-attention model (HiSAN) to construct document embeddings and classify the pathology report. To further enhance the predictive accuracy of our modeling approach we fuse the textual information from a pathology report with categorical data about patient's cancer history. For each report, we create a patient context vector that encapsulates tumor-level information from patient's previous cancer(s). The selected CTC records are associated with cancers diagnosed more than 120 days before the date of biospecimen collection stated in the pathology report. The patient context vector is crafted based on diverse categorical features; including cancer staging, patient age, treatment and sites of metastasis at the time of diagnosis. Features are represented using a combination of one-hot encoding and binning. Additionally, we employ patient and feature-level normalization to maintain proportional significance of features for individuals with multiple past diagnoses. We present preliminary results corresponding to different approaches for classifying cancer recurrence; first, we observe that using only the pathology reports as input yields an accuracy of 68%. Secondly, when using only CTC features with an XGBoost model, we achieve an accuracy of 49%. Finally we show that leveraging multiple data modalities, i.e. HiSAN generated pathology report embeddings and CTC data, significantly improves the model's predictive accuracy to 76%. This research demonstrates a promising path forward in enhancing classification of clinical text by incorporating longitudinal patient history data.

#2319 Deep learning-enabled dynamic infiltration and response to NK therapies in solid tumor organoids.

L. Lonini[1], S. Khare[1], T. D. Lopez[1], S. Szydlo[1], M. Streit[1], O. A. Karginova[1], M. K. Flaherty[1], A. Salhaudeen[2], A. Kunert[3], A. Oja[3], K. Sasser[1], M. C. Stumpe[1], C.-S. Ho[1];

[1]Tempus Labs, Chicago, IL, [2]University of Illinois Chicago, Chicago, IL, [3]Sanofi, Amsterdam, Netherlands

Patient-derived organoid co-culture models have become a state of the art platform to evaluate the effectiveness of immunotherapeutic agents in preclinical studies. However, preclinical development as well as quantification of therapeutic potency and resistance require differential labeling of cells with fluorescent dyes or transgenic fluorescent proteins, which may dysregulate the effector cell function or produce undesired cytotoxicity. Deep learning-based image analysis allows the use of brightfield images to co-localize tumor organoids (TOs) with effector cells, and measure TO-specific responses to novel candidate immunotherapies in a label-free manner; this can accelerate their evaluation as therapeutic candidates in cancer patients and shed light on tumor-immune interaction mechanisms.

Here we record multi-day time-lapse confocal microscopy images of TOs co-cultured with NK cells at increasing concentrations of target to effector cells. Two pre-trained U-Net convolutional neural networks are used to separately segment tumor and immune cells from the brightfield channel, and quantify immune cell infiltration over time. TO segmentation masks are registered with a vital dye (caspase 3/7) channel to selectively quantify TO cell death and correlate it with estimated immune cell infiltration across a large cohort of patient-derived TO models (including breast, colorectal, endometrial, gastric, head and neck, liver, lung and pancreatic cancer), at increasing concentrations of 6 different NK cell types (identified as A through F).

We find that the estimated density of infiltrating immune cells is highly correlated with TO death, as quantified by fluorescence intensity of caspase over time (median Pearson's r=0.89, P<0.001). Higher ratios of effector to target cells lead to higher activation of NK cells as measured by infiltrating cell density. Differential infiltration dynamics are observed across TOs and immune cell lines, as peak infiltration density is affected by co-culture time, ratio of target to effector cells, TO line, and NK cell type. These findings highlight that the paired segmentation models are able to measure varying degrees of infiltration across different types of immune cells and TO models.

The approach described here is highly scalable and only requires capturing brightfield images of the assay, therefore eliminating the need to label cells and avoiding phototoxic effects or alteration of the immune cells activity. Time series measurements enable quantification of patterns of immune cell activation, including infiltration, migration and co-localization dynamics, which provide insights into the pharmacokinetics and mechanisms for specific immune therapies. Overall, this methodology enables high throughput screening of many therapeutic candidates across dozens to hundreds of unique TO-models, thereby facilitating targeted precision therapy.

BIOINFORMATICS / COMPUTATIONAL BIOLOGY / SYSTEMS BIOLOGY / CONVERGENT SCIENCE: New Algorithms, Software, and Models Poster Session

#2323 Deciphering RNA degradation: Insights from a comparative analysis of paired fresh frozen/FFPE total RNA-seq.

W. Choi[1], M. Yeon[2], H. Choi[1], D. N. Hayes[1];

[1]University of Tennessee Health Science Center, Memphis, TN, [2]Florida State University, Tallahassee, FL

Background: Fresh frozen (FF) and formalin-fixed paraffin-embedded (FFPE) samples are primary resources for archival tissues in cancer studies. Despite the advantages of easy storage and cost-effectiveness, FFPE samples have the disadvantage of inevitable chemical-induced RNA degradation. Although, in mRNA-seq data, the 3' bias due to the characteristics of the mRNA-seq platform allows the measure of RNA degradation levels, for total RNA-seq and FFPE samples, there is still no clear measure for RNA degradation.

Methods: Our study, utilizing The Cancer Genome Atlas (TCGA) pilot data comprised of 26 paired samples of fresh frozen mRNA-seq [FFM], fresh frozen total RNA-seq [FFT], and FFPE total RNA-seq [PET], investigated RNA degradation patterns in FFPE samples. Upon investigating the read coverage of transcripts in FFPE data, we observed increased noise parameters in selected samples compared to others, suggesting a method for assessment of RNA degradation in FFPE. To measure these noise patterns, we developed a method called windowCV (wCV) utilizing coefficient of variance (CV) along the transcript length. Also, based on reports that membrane-surrounded RNA such as lncRNA and mitochondrial RNA (mtRNA) might be less affected by formalin fixation, we developed the simple measure dividing expression value of other proteins with certain lncRNA or mtRNA inferring the degree of RNA degradation.

Results: We first compared the shape of transcript read coverage from 3 different RNA-seq data and observed 3'bias pattern in FFM which was not observed in FFT and PET. For FFT and PET, we applied wCV and executed hierarchical clustering. We observed that a subset of samples and genes were clustered by high wCV value suggesting notable RNA degradation. To support the hypothesis of RNA degradation, we utilized Trimmed Mean of M values (TMM) expression ratio of paired FFT and PET to determine which samples and genes were associated with underestimation of expression in PET. Interestingly, we observed that PET/FFT TMM ratio showed negative correlation with wCV. Additionally, when we investigated hierarchical clustering result of PET/FFT TMM ratio, we found that lncRNA and mtRNA were less affected by FFPE. We then calculated expression ratio between membrane-surrounded RNA and a set of protein coding genes largely affected by FFPE. As a result, we found that this ratio positively correlated with paired PET/FFT TMM ratio. We conclude that this simple measurement can provide information of FFPE induced underestimated expression with limited transcriptome data as well as RNA degradation.

Conclusion: Our method can provide gene-level CV while avoiding false positive variance signal originating from transcript model and simple way to detect the degree of RNA degradation across FFPE samples.

#2324 Leveraging a comprehensive genomic data library for detecting clonal hematopoiesis in liquid biopsy.

A. Sonnenschein, M. Hasan, S. Hui, B. Tell, H. Nimeiri, J. Freaney, K. Sasser, W. Zhu, C. Lo;
Tempus Labs, Chicago, IL

Background: Clonal Hematopoiesis (CH) is a well established confounder in next-generation sequencing (NGS)-based liquid biopsy cancer diagnostics. Misclassification of CH variants as tumor variants can lead to false positive actionable variant detection, potentially resulting in incorrect interpretation of results and therapy selection. Moreover, CH variants may also interfere with quantitative variant monitoring leading to inaccurate assessment of treatment response. While filtering of CH variants is possible via matched sequencing of white blood cell and plasma DNA, emerging algorithmic approaches may enable a more resource-effective, time-sensitive approach with high precision.

Methods: A random forest classifier was trained and validated on 1321 advanced, pan-solid tumor cancer samples (training n=660, validation n=661) sequenced using both the Tempus xF+ (liquid biopsy) and Tempus xT (solid tumor with matched buffy coat) NGS assays. Variants were labeled as CH or tumor-derived based on solid-tissue results in 39 genes that are known to be associated with CH (e.g., DNMT3A, TET2, TP53). The classifier was trained to classify SNV and indel variants detected via liquid biopsy as circulating-tumor or non-tumor (CH + germline) in origin. Features used by the classifier include the fragment size of reads overlapping each variant, prevalence in solid-tumor samples from the Tempus multimodal database, and variant allele fraction relative to estimated tumor fraction. Model classifications were validated against Tempus xT.

Results: Our training set (n=660 liquid biopsy samples) included 680 pathogenic variants. 50% (n=342/680) were determined to be tumor-derived, while 50% (338/680) are likely due to CH.

Our independent validation (n=661 samples) included 600 pathogenic variants. Model prediction accuracy on these validation set variants was 91.7%, with an ROC-AUC of 0.97. Sensitivity was 88.3% (n=257/291 true positives correctly labeled as non-tumor variants), specificity was 94.8% (n=293/309 true negatives correctly labeled as tumor variants), and precision was 94.1%.

The model ranked “gene” as the most informative feature for variant classification, followed by measurements of fragment distribution and historical prevalence of individual variants within the Tempus Database.

Conclusion: A novel classifier trained on multiple orthogonal bioinformatics features can reliably distinguish CH from tumor-derived variants using only liquid biopsy data with high accuracy, including high sensitivity and high specificity.

#2325 NUWA-ms: A network-based method to infer quantification of missing proteins using multi-cohort proteomics profiles.

Lihua Cao, Yuhao Xie, Jiale Chen, Man Wang, Tingting Zhao, Heli Yang, Yang Du, Yang Yang, Zhaode Bu, Jiafu Ji, **Jianmin Wu**

Peking University Cancer Hospital & Institute, Beijing, China

Although mass spectrometry is powerful for proteomic quantification, the inherent issue of missing values remains a significant challenge. We found a prevalent lack of quantification of valuable proteins (e.g., immune cell markers and drug targets) in published datasets, limiting the functional utilities of quantitative proteomic profiles. This was exemplified by the substantial lack of quantification of immune cell marker, which impede the dissection of tissue-infiltrating immune cells by deconvolution analysis of cancer proteomic profiles. Thus, we introduce a network-based method NUWA-ms for robust abundance inference of missing proteins using multi-cohort proteomic profiles. By evaluating 561 tumors with paired proteomic and transcriptomic profiles, a significant improvement of deconvolution performance was shown with the aid of NUWA-ms. This was further validated by the comparison between scRNA-seq and proteomic analyses of a same gastric cancer tumor tissue. NUWA-ms applications to cancer proteomic profiles facilitated the inference of CD8+ T cell markers and effector proteins, enabling the associations of CD8+ T cell infiltration with MSI status in colorectal cancer and anti-PD-1 therapy response in melanoma. These findings demonstrated the utilities of NUWA-ms in depicting infiltrating lymphocytes in the tumor microenvironment using proteomic profiles. Furthermore, based on the proteomic profiles of six patient-derived tumor organoids (PDOs), NUWA-ms application helped identifying PDOs sensitive to a targeted therapeutic agent including the ones neglected by the raw MS quantification, and aided in revealing the resistant mechanism. Together, NUWA-ms could enable a robust inference of protein abundance, to help identifying protein biomarkers and therapeutic targets for cancer and other complex diseases.

#2326 Integrating single nucleotide variants (SNVs), copy number alterations (CNAs), and structural variants (SVs) into single-cell clonal lineage inference.

N. Bristy, X. Fu, R. Schwartz;
Carnegie Mellon University, Pittsburgh, PA

Background: We extend algorithms for clonal lineage inference (``tumor phylogenetics") from single-cell DNA sequence (scDNA-seq) data to accommodate broader classes of genetic variants, including single nucleotide variants (SNVs), copy number alterations (CNAs), and structural variants (SVs).
Methods: We develop a computational method based on constrained optimization, posing a problem of inferring cellular lineage trees consistent with a given scDNA-seq data set constrained to follow a Dollo parsimony model for SNVs and SVs. We then seek an optimal tree consistent with these constraints so as to optimize for a CNA minimum evolution model balanced against measure of consistency of the different data types with one another relative to the reconstructed set of clones. We pose this problem as an integer linear program (ILP) that we solve heuristically via a coordinate descent algorithm. We tested the resulting method on a combination of synthetic scDNA-seq data and publicly available real data.
Results: Results on synthetic data show the method to be effective at constructing lineage trees under a variety of parameter domains, including variations in noise levels, clone numbers, single cells, and mutation rates. We further show it to yield improved accuracy over widely used prior models that operate on only subsets of these variant types. Application to previously published scDNA-seq data demonstrate the method to be effective at inferring clonal lineage trees incorporating all three variant types. The results further show how the different kinds of variants can contribute in tandem to progression along single cell lineages or to the emergence of clones exhibiting hallmarks of distinct mechanisms of progression.
Conclusion: The results support the effectiveness of our method in resolving accurate trees from scDNA-seq data including diverse variant types, as well as the value of considering these mutation types collectively in developing a comprehensive understanding of how various forms of somatic mutability together shape clonal evolution in cancers.

#2327 MADVAR: An algorithm that improves the relevance of computational biology output, while reducing compute time and space requirements.

G. Silberberg[1], **M. Ritchie**[2];
[1]Champions Oncology, Hackensack, NJ, [2]Corellia AI, Rockville, MD

High-throughput methods implemented in biology research produce a continuously growing array of data input that are used to produce data output with an increasing abundance of features. While growth in the volume and diversity of data input can be highly valuable for studying biological systems, it presents the challenge of managing enormous quantities of features, many of which are not relevant to the specific research question being asked. This excess data input burdens storage and computation of downstream clustering and machine learning tasks. A common approach used to manage this data input relies on filters applied to the features by their variance across the sample set, while applying random cutoffs. Our proprietary algorithm (“MADVAR”) enables the prioritization of variable features from high-throughput continuous data, by automatically finding an optimal cutoff for the distribution of the data. Based on the right-skew nature of biological data distribution, MADVAR finds and excludes the "0 variance peak" using the median of the distributions and the median absolute deviation (MAD). MADVAR enables a faster analysis with a reduced memory requirement, and dramatically improves clustering results with minimal loss of relevant features.

#2328 Next-generation sequencing-based regression algorithm to determine homologous recombination deficiency scores in a pan-cancer cohort.

B. Choi, Y. Choi;
Seoul St. Mary's Hospital, Seoul, Korea, Republic of

Background: Homologous recombination deficiency (HRD) inhibits double strand breaks from being repaired in DNA, leading to cancer cells failing to recover themselves and cell death. Previous studies found that HRD-positive ovarian cancer patients had more significant clinical benefits from poly ADP-ribose polymerase inhibitors (PARPi) treatment. For accurate detection of HRD, next-generation sequencing (whole exome, whole genome) was used to identify large-scale genomic aberrations including telomeric allelic imbalance (HRD-TAI score), loss of heterozygosity profiles (HRD-LOH score), and large-scale state transitions (HRD-LST score). So far, many studies (HRDetect, SigMA, CHORD and shallowHRD) have been conducted to accurately determine HRD in a pan-cancer cohort. As the study progressed, it has been revealed that PARPi is effective when applied to patients with HRD in not only ovarian cancer but also breast cancer, prostate cancer, and pancreatic cancer.
Purpose: To develop an algorithm that accurately predict HRD score in patients with ovarian cancer, breast cancer, prostate cancer, and pancreatic cancer utilizing a machine learning algorithm.
Methods: We used whole-genome sequencing (WGS) data of 710 samples from 309 patients, whole-exome sequencing (WES) data of 4,650 samples from 2,193 patients from the pan-cancer cohort of the TCGA (TCGA-OV, TCGA-BRCA, TCGA-PRAD, and TCGA-PAAD). The HRD-TAI/HRD-LST/HRD-LOH scores were calculated through structural variation analyses. After data cleaning processes, machine-learning models were trained and tested on 228 out of 2,502 samples, and validation was performed on 1,248 out of 2,502 samples from the TCGA dataset.
Results: To assess the performance of the machine-learning regressor, the concordance between predictions and annotations was quantified by calculating the R squared (R;;;^2). As a result of training using machine learning algorithm, we achieved a high R;;;^2 (0.904) with a RMSE (root mean squared error) score (7.649) for a pan-cancer cohort.
Conclusions: Our regressor was robust and accurate when applied to 4 cancer types. Using our systematic pan-cancer analysis, we found novel insights into the mechanisms of HRD across cancer types with potential contribution to clinical practice.
Figure 1. Functional HRR genes can repair DNA breaks, but deficient HRR genes will decrease rates of DNA repair leading to cell death via apoptosis.HRR, Homologous recombination repair; HRD, Homologous recombination deficiency
Figure 2. Receiver operating characteristic (ROC) and under the curve (AUC) values showing the performance of machine-learning algorithm. TPR, true positive rate; FPR, false positive rate

#2329 Cancer region definition using spatial gene expression patterns by super resolution reconstruction algorithm for spatial transcriptomics data.

Jeongbin Park[1], Seungho Cook[1], Dongjoo Lee[1], Jinyeong Choi[1], Seongjin Yoo[1], Hyung-Jun Im[2], Daeseung Lee[1], Hongyoon Choi[1]

[1]Portrai, Inc., Seoul, Republic of Korea, Seoul, Korea, Republic of,[2]Department of Molecular Medicine and Biopharmaceutical Sciences, Graduate School of Convergence Science and Technology, Seoul National University, Seoul, Korea, Republic of

Background: Spatially resolved transcriptomics (ST) has enabled a variety of cancer research on the heterogeneity of tumor microenvironment. However, when identifying cancer boundaries based on ST, the limited resolution of ST such as Visium hinders the accurate identification of cancerous regions. To address these issues, we have developed a novel approach for accurately classifying regions of the tumor by using deep image prior (DIP) algorithm to convert Visium data into high-resolution images.

Methods: We proposed SuperST, which utilizes deep image prior to transform low-resolution ST data into high-resolution images, providing more accurate spatial marker expression patterns. This method was used to define cancer regions by combining with a pre-trained deep learning algorithm that recognizes spatial patterns. ST data of hepatocellular carcinoma (HCC) patients were used to apply SuperST. Firstly, 400 spatially variable genes were identified. SuperST leverages the deep image prior (DIP) algorithm and a U-Net neural network to transform ST data into high-resolution ones without needing ground-truth high-resolution data. The final high-resolution images of gene expression data were used to extract 512-dimensional feature vectors for each gene via a pre-trained convolutional neural network model (VGG16). Subsequently, we apply K-means clustering to these features to identify transcriptionally distinct tissue regions considering spatial information and compared with the human-labeled cancer regions.

Results: The cancer region detection using spatial gene expression data and our algorithm yielded results that substantially align with the human annotations on the H&E images. Furthermore, compared to the cancer definition obtained using the CopyKat and SPACET algorithms, our results were more spatially consistent for cancerous regions as well as providing high-resolution image-level definition of cancer region margin. This indicates that our algorithm better utilizes spatial information and more effectively overcomes the low resolution of ST data.

Conclusion: This research demonstrates the effective application of our SuperST algorithm to the challenging problem of cancer region detection only using spatial gene expression data. It suggests that our algorithm could be utilized for a variety of problems in spatial biology in cancer research.

#2330 CTD2 "Connects the Dots" to capture disease genes in complex networks and its application on the Cancer Genomics Cloud.

V. Petrosyan[1], V. Kovacevic[2], P. Obradovic[3], C. Fisher[4], Z. Worman[4], D. Sain[4], J. DiGiovanna[4], B. Davis-Dusenberry[4], A. Milosavljevic[1];
[1]Baylor College of Medicine, Houston, TX, [2]Persida Bio, Brooklyn, NY, [3]University of Belgrade, Belgrade, Serbia, [4]Velsera, Charlestown, MA

We have developed CTD2 (an algorithm to "Connect the Dots") to capture biological signals and identify candidate genes in complex networks. CTD2 extends the functionality of its predecessor CTD by providing ranked lists of genes that are “guilty by association” and significantly linked to other genes of interest. With the explosion of large scale multi-omics studies in the cancer field, novel approaches are needed to interpret these valuable datasets. Both CTD and CTD2 are information-theoretic algorithms that allow identification of highly connected sets of genes in complex networks without the need for permutation testing. CTD has been previously used to interpret perturbations in different subtypes of breast cancer. Additionally CTD has been used to identify biomarkers of chemotherapy response in Triple Negative Breast Cancer (TNBC) murine PDX models to both platinum and taxane agents. These small multigene biomarkers of response were shown to be informative for the response of both patients and PDXs. CTD2 was developed to expand the utility of the CTD package by also capturing genes that are "guilty by association". These genes are significantly connected to genes of interest (such as disease genes), and are ranked by their connectedness to these informative gene sets. To demonstrate its utility, we investigated if CTD2 could identify known breast cancer genes. Using TCGA breast cancer expression data, we built case/control graphs over 5,000 variable genes for each subtype of breast cancer. Genes previously associated with breast cancer were identified with DisGeNET and split into a training set discovered pre-2015 and test set discovered post-2015. The genes that were discovered pre-2015 that overlapped with our networks (n = 680) were then used as an input for CTD2 along with the case/control graphs. We then ranked the connectedness of all the genes in these graphs to the training set and found that the test set of breast cancer genes that were discovered post-2015 were significantly enriched in these ranked lists.We have shown that CTD2 and CTD can be utilized to discover biologically informative signals in complex networks. Furthermore we have deployed these tools on the Cancer Genomics Cloud to make them easily accessible for users without a bioinformatics background. The democratization of these in silico tools will allow for their adaptation by a wider audience and aid in the interpretation of large multi-omic datasets.

#2331 Uncovering gene co-regulation networks in spatial transcriptomics data.

P. Danaher, D. McGuire, M. Patrick, D. Kroeppler, J. Schmid, J. M. Beechem;
NanoString Technologies, Inc., Seattle, WA

Single-cell spatial transcriptomics measures thousands of genes *in situ* over potentially millions of cells. These rich datasets pose the best problem in genomics: how can an analyst possibly uncover all the biological insights contained within them? Careful analysis can uncover intricate biological relationships, but only if the analyst knows where to look. One useful set of “places to look” is genes sharing spatial correlations, i.e. that tend to be expressed in the same regions as each other. When genes are expressed together in space, it suggests causality, either by one gene acting on another, or by some latent variable impacting all the genes. These causal relationships have only become detectable en masse with the advent of spatial transcriptomics data, making them rich in potential for previously unknown findings. Unfortunately, spatial correlation has largely fallen short of its promise for one reason: genes expressed by the same cell type are usually highly spatially correlated. These trivial correlations overwhelm results driven by interesting biology.

Here we present an algorithm designed to discover spatial correlations arising from causal relationships and not from the cell type landscape. We compute genes’ conditional correlations over space, looking at the residuals of spatial expression after accounting for the cell type landscape.

In a 6,000-plex Spatial Molecular Imaging (SMI) analysis of colon cancer, we find that approximately 80% of the strongest spatial correlations can be attributed to cell type; the remaining 20% suggest underlying causal relationships. 96 distinct modules comprising up to 46 spatially correlated genes were discovered. The expression within these modules is driven by between 1 and 19 different cell types. Notable modules include those related to IFNG signaling, antigen presentation, B-cell chemotaxis and activation, and microenvironmental remodeling. Further, our study delves into the spatial correlations among ligand-receptor pairs, revealing spatial co-regulation in a limited subset of the 555 ligand-receptor pairs examined in the 6,000-plex panel.

This approach enables us to discern spatial correlations that hint at biological causality, thereby beginning to delineate the "spatial interactome" of cancer. Leveraging a growing collection of 6,000-plex CosMx™ SMI cancer datasets that span various cancer types including breast, liver, kidney, lung, color, skin, and pancreatic cancers, we are systematically documenting the spatial dependencies of genes. This includes identifying correlations that are consistent across different tumors, as well as those unique to specific tumors or tumor types. Early observations have highlighted modules of chemokines (CCL3/CCL4/CCL3L, CXCL1/CXCL2/CXCL3), genes indicative of CAF phenotype (FN1 and collagens), and those involved in cell adhesion and collagen formation.

For research use only. Not for use in diagnostic procedures.

#2332 Enhanced analysis of CO-Detection by indEXing (CODEX) imaging through a novel image processing technique utilizing two-dimensional Fourier transform for stitching artifact detection.

Afrooz Jahedi[1], Aliya Khan[2], Kasthuri Kannan[1], Krishna Bhat[1]

[1]The University of Texas MD Anderson Cancer Center, Houston, TX,[2]College of Osteopathic Medicine, Sam Houston State University, Conroe, TX

Objective: The objective of this study is to address the challenge of stitching artifacts in CODEX imaging, which hinders the accurate spatial quantification of positive cell locations—a critical step for reliable spatial analysis in computational pathology.
Methods: Our algorithm applies 2D-FT and inverse transformations to process pathological images. We tested the algorithm on 16 different histology images, each containing 5 or more regions. Within these regions, we evaluated 29 protein markers, culminating in the analysis of over 2800 images.
Results: The algorithm demonstrated a recall rate of over 85 percent, indicating a high likelihood of accurately identifying true positive regions with stitching artifacts. However, the precision varied, suggesting further investigation is needed to understand the variability and improve consistency.
Conclusion: The proposed method significantly improves CODEX imaging reliability by detecting and quantifying stitching artifacts. The method's high recall rates are promising, but the variable precision indicates the necessity for ongoing refinement to ensure consistent diagnostic accuracy across diverse and extensive image sets. Keywords: Computational pathology, Fourier transform, Image stitching, CODEX, Spatial analysis, Diagnostic precision, Recall.

#2333 Methylation based phylogeny and timing in cancer.

N. Guteneva, E. Lichter, **I. Leshchiner**;
Boston University, Boston, MA

Knowing the chronological sequence of genetic alterations during cancer development and progression is crucial for understanding the process of transformation of normal tissue into malignant tumors. This can offer insights into the etiology and intrinsic cellular mechanisms of the process, presenting opportunities for early detection and treatment of initial disease stages, as well as highlight key events as potential therapeutic. Current methods of establishing progression histories of cancers rely either on direct sequencing of premalignant lesions, which are seldom available for tumors or on computational inference timing methods capable of reconstructing the history from primary tumor data. These methods require genome or exome sequencing data from a relatively large cohort of tumors and provide limited resolution due to overall scarcity of somatic mutations. We utilize a different source of genetic information, genome methylation, that also “records” historic information about acquisition and development of mutations. Over 28 million methylated CpG sites exist in the genome with several percent of them differentially methylated (DMS) between tissue types and tumor vs adjacent normal tissue. The several orders of magnitude higher density of distinctly methylated sites provides unprecedented resolution, needs fewer tumors, can be merged with driver mutation data and co-analyzed with “methylation clock” information that allows to establish early development, phylogeny and progression at unprecedented resolution. We developed methods for whole genome bisulfite sequencing (WGBS), reduced representation bisulfite sequencing (RRBS) and Oxford Nanopore Technologies native methylation sequencing data. Somatic DMS sites have distinct properties from somatic point mutations, can appear and disappear in the process of tumor evolution and development allowing for unique configuration of methylated islands. Our tools perform single sample and cohort level “timing”, multi-sample phylogeny reconstruction and cancer population reconstruction by integrating methylation and mutation information from the same sample. These new methods will significantly contribute to our understanding of cancer initiation and progression at a resolution not available previously.

#2334 Computational methods for optimizing marker selection, clonal lineage reconstruction, and longitudinal tracking of clonal dynamics via circulating tumor DNA (ctDNA).

X. Fu[1], Y. Deng[1], Z. Luo[1], W. Laframboise[2], D. Bartlett[3], R. Schwartz[1];
[1]Carnegie Mellon University, Pittsburgh, PA, [2]Allegheny Health Network and Drexel University College of Medicine, Pittsburgh, PA, [3]Allegheny Health Network, Pittsburgh, PA

Background: Technologies for blood-based profiling of tumor DNA (“liquid biopsy”) have offered great prospects for non-invasive early cancer diagnosis, treatment monitoring, and clinical guidance, but further advances in computational models and data analysis to optimize monitoring protocols and develop liquid biopsy as a robust quantitative assay of tumor clonal evolution.
Methods: We propose new computational methods to improve our ability to characterize tumor clonal dynamics from circulating tumor DNA (ctDNA). Our methods address how to apply ctDNA assays most effectively to two distinct questions in profiling tumor clonal dynamics: 1) How to apply longitudinal ctDNA data to refine phylogenetic tree models of clonal evolution, and 2) how to most effectively characterize changes in clonal frequencies that may be indicative of treatment response or tumor progression. We pose these questions computationally in terms of a probabilistic framework for optimally identifying maximum likelihood markers for the preceding tasks and applying measured marker concentrations to their solution. We apply this framework by first evaluating the distribution of plausible clonal lineage models using bootstrap samples over pre-treatment tissue-based genetic variation data, then refining these lineage models and the clonal frequencies we can infer from them over successive longitudinal samples of selected markers.
Results: We tested our method on synthetic data under various model assumptions and showed the method to be effective at refining distribution tree models and clonal frequencies over longitudinal samples so as to minimize measures of tree distance relative to the ground truth. We further apply the methods to a real ovarian cancer case and show their ability to develop and refine a clonal lineage model and assess clonal frequencies.
Conclusion: Our methods show the power of ctDNA assays in conjunction with computational optimization to lead to improved marker selection, clonal lineage reconstruction, and tracking of clonal dynamics, with potential for more precise and quantitative profiling of tumor progression enabling improved clinical decision-making.

#2335 MultiNMF: multiview factorization for joint modeling of spatial multi-omics and histology images.

W. Bowie, S. Wang, B. Strope, **Q. Zhu**;
Baylor College of Medicine, Houston, TX

An increasing number of cancer research studies employ spatially resolved transcriptomics (SRT) to investigate the composition of tumor microenvironment in a cancer type of interest. These studies have defined tumor microenvironment (TME) states and spatial domains based on clustering spatial gene expression patterns in SRT in an unbiased manner, yet a more thorough delineation of TME states requires the incorporation of the tumor's histology image. Here, we develop MultiNMF, a multiview factorization approach that is suitable for cancer research studies where joint profiles of spatial multi-omics and tumor histology images are available. We apply MultiNMF to analyze a set of TNBC SRT primary tumor samples and reveal TME states in the stromal, epithelial, and immune enriched compartments, defined by distinct histomorphological features. We further illustrate the ability of the approach to extend to paired spatial ATAC-seq and histology dataset that is recently published on HER2 breast cancer. MultiNMF thus permits an automated and data-driven decomposition of SRT and spatial ATAC data supported by histomorphological evidence.

Context

In SRT by 10X Visium, the hematoxylin eosin (H&E) staining image is automatically aligned to the slide where the tissue section is mounted. Image patches can be easily extracted from areas under the SRT barcoded spots. For these images, I will apply a pre-trained convolutional neural network (CNN) model to extract high dimensional features from spot images. The image features can be added as a second view after gene expression view for joint analysis under MultiNMF.

Results

MultiNMF can factorize the SRT data into components well-supported by histological evidence. It has identified T-cell infiltrating regions, and EMT-enriched regions with distinct immune and stroma morphological characteristics. The T-cell infiltration neighbors a region that has an appearance of necrosis according to the pathologist evaluation. These domains further demonstrate enrichments of modules with motif enrichment (known as regulons) according to SCENIC analysis. Analysis of spatial ATAC illustrates not only HER2 but also its amplicon amplification. From MultiNMF components of spatial ATAC, we derive regulatory regions for T-cell/B-cell marker genes. Overall, MultiNMF is a novel model that has not been applied to SRT field. It provides an multiomic extension to the traditional NMF.

#2336 A prototype for a machine-learning assisted image analysis tool for preclinical *in vivo* studies.

A. M. Aji[1], T. M. Kierski[1], J. D. Rojas[1], H. Morilak[1], O. J. Kelada[1], K. H. Gessner[2], A. S. Gdowski[2], L. Kim[2], W. Y. Kim[2], R. C. Gessner[1], **T. J. Czernuszewicz[1]**; [1]Revvity, Durham, NC, [2]UNC Chapel Hill, Chapel Hill, NC

The purpose of this study was to build a software tool to test the feasibility of machine-learning (ML) assisted analysis of *in vivo* 3D images in oncology research studies. Conventionally, *in vivo* image segmentations are performed by hand, and are a bottleneck for data analysis, taking time and introducing both inter and intra-user variability. Recently, advances in ML have shown promise in accelerating similar clinical image analysis tasks. Our objective was to work toward making this technology accessible to preclinical cancer researchers. 3D image data across multiple mouse models, organs, modalities, and imaging systems were used. ML segmentation models were trained with user-defined masks on images of mouse bladders (N=134), kidneys (N=131), livers (N=65), and lungs (N=26) from either ultrasound or micro-computed tomography (uCT) scanners. Models were developed using PyTorch / MONAI, hosted in an AWS cloud environment, and served to users via a custom extension for 3D Slicer (www.slicer.org). Performance was assessed as the difference between the human vs. ML organ volumes on a test set unseen by the models during training. Lastly, the functionality of on-the-fly segmentation improvement tools through iterative user feedback was assessed. Results demonstrated that generating segmentations with the prototype ML software took 2-6 seconds per image running on a modern GPU (NVIDIA RTX 3090), compared to 3-7 minutes if performed manually by an expert user (>30x improvement). The Dice scores between the ML generated and human segmentations ranged from 0.81 (liver ultrasound) to 0.84 (bladder ultrasound) but could be improved using ML-based on-the-fly mask improvement tools. Using data from this pilot study, we estimate that the threshold to achieve 90% accuracy on first-pass segmentations is between 200-300 training images, depending on the variance observed in the image data. In summary, the prototype software was able to decrease the manual analysis time across a variety of preclinical *in vivo* image modalities, which is broadly relevant to preclinical oncology research. The next steps for this project will be to extend the platform to additional orthotopic tumor models (e.g. pancreatic, liver, prostate, etc.) and deploy to the field to enable access to this toolset by preclinical imaging scientists across the world.

#2337 Accelerated optical genome mapping analysis with Stratys Compute and Guided Assembly.

D. Senol Cali, T. Anantharaman, M. Muggli, S. Al-Saffar, C. Schoonover, N. Miller;
Bionano Genomics, San Diego, CA

Background

Optical genome maps (OGM) from Bionano enable the detection of genomic structural and copy number variants that cannot be detected by next-generation sequencing (NGS) technologies and are often missed by conventional cytogenetic techniques. Bionano has developed bioinformatics pipelines for calling structural and copy number variants including the Bionano Solve *de novo* assembly pipeline for constitutional analysis and the Rare Variant Analysis (RVA) pipeline for low-allele-fraction cancer applications. Both pipelines are computationally intensive and currently take 5-10 hours on the latest generation of the Bionano Saphyr® Compute which is deployed as a four-node compute cluster and requires significant IT resources.

Methods

To increase throughput and simplify the deployment of the compute resources needed to support the Stratys™ optical genome mapping instrument, Bionano has developed Stratys™ Compute. Stratys Compute improves both compute and analytical performance by adapting compute-intensive stages in the Solve pipeline to run on GPUs and by developing the Guided Assembly pipeline.

Stratys Compute is powered by state-of-the-art NVIDIA RTX 6000 Ada generation cards and CUDA-optimized refinement, alignment, and structural variation detection kernels to accelerate OGM analysis. Stratys Compute is a standalone workstation placed adjacent to Stratys instrument. This will minimize the IT footprint and bypass the integration with the customer site's data center.

We have incorporated these optimizations into the new Guided Assembly pipeline, which aims to combine the low-allele fraction detection capability of the RVA pipeline with the whole genome coverage and ability to detect smaller structural variants enabled by the *de novo* assembly pipeline. The Guided Assembly pipeline uses the reference genome as an initial seed followed by extension, refinement, and structural variant calling. This new analysis method has been evaluated through comparison to previous results from both existing pipelines and standard benchmarking datasets used to estimate structural variant calling performance and is deployed on Stratys Compute for both constitutional and low allele-fraction applications.

Results

Guided Assembly has been adapted to run on GPU hardware in a simplified compute tower that can be deployed to a lab along with the Stratys instrument without the need for a dedicated server room. We found concordance between the guided assembly results and our previous *de novo* and RVA pipeline results. We also found increased sensitivity at low allele fractions for detecting insertion variants smaller than 5 kb and larger than 200 kb while finding equivalent performance for other variant types with the updated methods. The accelerated Guided Assembly for constitutional and low-allele-fraction applications will be available to early access customers in Q4 2023 with full commercial release in Q2 2024.

#2338 Benchmarking long- and short-read somatic structural variation callers using a multi-technology panel of six tumor/normal cell lines.

A. Keskus[1], **A. Bryant**[1], T. Ahmad[1], A. Donmez[1], I. Rodriguez[2], N. Rossi[2], Y. Xie[2], B. Yoo[3], R. Milano[2], H. Lou[4], J. Park[5], J. Gardner[5], B. McNulty[5], K. Miga[5], M. Dean[2], M. Farooqi[3], B. Paten[5], M. Kolmogorov[1];

[1]Center for Cancer Research, National Cancer Institute, Bethesda, MD, [2]Division of Cancer Epidemiology and Genetics, National Cancer Institute, Rockville, MD, [3]Children's Mercy Hospital, Kansas City, MO, [4]Leidos Biomedical Research, Inc., National Laboratory for Cancer Research, Frederick, MD, [5]UC Santa Cruz Genomics Institute, Santa Cruz, CA

Better structural variation (SV) detection could improve cancer diagnosis, treatment and prevention. Yet many cancer genomics studies have only reliably detected single nucleotide variants and small indels due to technological limitations of short-read sequencing. While structural variants can be inferred from discordant short read pairs, as much as 70% of SVs remain undetected because of the mappability difficulties. This is especially true for SVs in regions where GC content is greater than 45% or regions which harbor tandem repeats and segmental duplications.

Advances in long-read sequencing enabled direct observation of SVs with recall and precision over 95% across a larger portion of the genome. To harness this technology, we developed Severus - a long-read SV caller that provides phased detection of both simple germline SVs as well as complex rearrangements commonly found in cancer genomes. Such rearrangements are built into a breakpoint graph to reconstruct derived tumor chromosome structure.

To benchmark Severus and other long-read SV calling methods, we sequenced six tumor/normal cell line pairs using Nanopore, HiFi, short-read and Hi-C sequencing technologies. We combined the calls from multiple tools and technologies to generate benchmarking sets of somatic SV for each tumor cell line, and evaluated short- and long-read tools against this benchmark set.

Current tools for SV merging and comparison (such as truvari) were primarily designed for long indels, rather than breakends that are more common in somatic SVs. Another challenge is that different tools may represent the same variants differently in a VCF output. To enable robust somatic SV outputs comparison, we developed a tool called Minda that translates an input VCF entries into a unified representation, and then compares the calls in either pairwise or multi-tool mode.

As expected, in our benchmarking of cell six tumor cell line pairs, short-read methods had substantially lower recall and precision, compared to long-read methods. Among the long-read methods, Severus consistently had substantially better recall and precision, compared to Sniffles2, nanomonsv and SAVANA. An analysis of publicly available long-read sequencing of a melanoma cell line (for which curated benchmark SV set is available) produced consistent results.

#2339 GPNotebook: A toolkit for identifying cancer-related glycosylation alterations in glycoproteomic analysis.

H. Zhang[1], T. Hoang[2], **Y. Hu**[1];

[1]Johns Hopkins University, Baltimore, MD, [2]University of Maryland at College Park, College Park, MD

This study is dedicated to the development and application of 'GPNotebook', an innovative Python-based data analysis tool, specifically designed to enhance glycopeptide research in cancer studies by enabling the detailed investigation of glycosylation patterns and their correlation with various clinical cancer phenotypes. In our study, we recognize the critical role of protein glycosylation in biological processes and its relevance in cancer. To address the lack of specialized tools for glycoproteomic analysis, we developed GPNotebook, a comprehensive Python package designed for detailed investigation of intact glycopeptides (IGPs). This tool integrates multiple functionalities, including statistical profiling, differential expression analysis, categorization of glycosylation subtypes, and exploration of the interactions between glycosylation and phosphorylation. It also encompasses survival analysis and assessments of glycosylation enzymes. We applied GPNotebook in a research project focused on 10 cancer types collected from Clinical Proteomic Tumor Analysis Consortium (CPTAC) projects to validate its efficacy and demonstrate its wide-ranging capabilities. Through this application, we were able to analyze and interpret complex glycoproteomic data, revealing potential IGPs as biomarkers for cancer detection and differentiation of cancer subtypes. We identified hundreds of cancer-specific IGPs, with several showing promise as early-stage cancer biomarkers. In addition, our analysis revealed unique glycosylation patterns linked to specific molecular subtypes and immune cell distributions in tumor microenvironments. We also clarified the roles of certain glycosylation enzymes across different cancer types, highlighting their potential significance in cancer progression. GPNotebook has proven to be a critical tool in glycopeptide research. Our findings not only enhance the understanding of glycosylation in cancer but also demonstrate GPNotebook's potential in identifying novel biomarkers and providing insights into cancer subtype differentiation. This study positions GPNotebook as a valuable resource for exploring the complex relationships between protein glycosylation and cancer phenotypes.

#2340 STRUMP-I: Structure-based binding prediction of MHC class I.

A. Voshall[1], W. Park[2], E. A. Lee[1], Y. Choi[3],

[1]Boston Children's Hospital and Harvard Medical School, Boston, MA, [2]Samsung Medical Center, Seoul, Korea, Republic of, [3]Chonnam National University Medical School, Gwangju, Korea, Republic of

The presentation of short peptides derived from endogenously expressed proteins within the Major Histocompatability Complex-I (MHC-I), together known as the pMHC, allows the adaptive immune system to monitor the internal functioning of a cell and surveil for foreign or mutated self-proteins. With the rising importance of immunotherapies targeting neoantigens in cancers, the ability to accurately predict which peptides will bind to the diverse population of MHC alleles is critically important. Computational methods for predicting MHC/peptide interactions fall into two broad categories: sequence-based methods that utilize machine learning or deep learning to predict binding from information about the MHC and peptide sequence alone, and structure-based methods that leverage the computed structure and energetics of the pMHC to predict binding. While sequence-based methods have outperformed structure-based methods, their performance varies with the quantity and quality of training data for each MHC allele. The pMHC structure also provides additional insights into downstream analyses, such as predicting the immunogenicity of cancer neoantigens, that cannot be determined from the sequence alone. We developed a STRUMP-I (STRUcture-based pMHC Prediction (for class I)), a novel pMHC binding prediction tool that combines structural modelling with a machine learning-based classifier to discriminate binders from non-binders. STRUMP-I has comparable performance to the state-of-the-art sequence-based methods on data taken from IEDB, the HLAthena training set, TESLA, PRIME, and an in-house cancer neoantigen dataset. However, it generalizes better to alleles with low representation or a lower proportion of positive examples in the training data than the sequence-based methods. Additionally, we demonstrate how STRUMP-I can be used in conjunction with PRIME, a sequence-based immunogenicity prediction method, to use structural information about the peptide to filter out false positive predictions and increase the precision of immunogenicity predictions, increasing the precision by up to 2-fold. Further, on a set of 10 experimentally validated peptides from the in-house cancer neoantigen dataset containing only a single immunogenic peptide, STRUMP-I filtered all false positive predictions and retained only the true positive prediction. By leveraging structural information about the pMHC, STRUMP-I provides robust binding predicting performance across MHC alleles and increases the precision of immunogenicity prediction for neoantigen screening.

#2341 Morph: A feature extraction toolset for spatial transcriptomics.

A. N. Targino da Costa, J. Liu, C.-K. Mo, E. Storrs, A. N. Southard-Smith, R. G. Jayasinghe, J. T. Wang, M. D. Iglesia, M. Wendl, S. Chen, A. Houston, A. Karpova, Y. Li, L. Ding;
Washington University In St. Louis, Saint Louis, MO

Accurately defining spatial characteristics of tumors has been a challenge in cancer research. Specifically, there is still a lack of spatial transcriptomic (ST) bioinformatic methods that infer tumor boundaries, a necessity for tumor microenvironment (TME) analyses, that are fully automated and handle non-rectangular grids (like the one found in Visium). Here we introduce Morph, a toolset that not only addresses these limitations, but also accurately extracts tumor regions, layers surrounding them, and distances related to such regions. Morph was tested on a dataset composed of 117 ST slides across 6 different cancer types, including primary and metastatic tumors. More broadly, Morph is a computationally efficient tool based on mathematical morphology that is designed to work without any approximations on ST slides (that can be composed of spots in a hexagonal lattice) of any resolution. The toolset accepts a variety of input types, such as tumor purity and manual annotation, and can perform a diverse set of morphological operations, such as erosion, dilation, opening and closing, using a number of structuring elements with different shapes and sizes, such as a hexagon of side 1. Moreover, Morph runs quickly (seconds per sample). Its main focus is to unveil the aforementioned features of any spatially distinct tumor region (here defined as microregion) for various downstream analyses, such as spatially-varying copy number variations, cell-type distribution, and tumor-microenvironment interaction. Overall, we developed a spatial transcriptomics toolset that is not limited to any specific technology platform, and that can accurately extract ST features facilitating the discovery of spatial transcriptomic and interaction patterns.

#2342 BARTsc: A transcription factor analysis suite for single-cell omics data.

H. Zhang, J. Wang, Z. Wang, C. Zang;
University of Virginia, Charlottesville, VA

In Eukaryotic cells, the expression of a small set of transcription factors (TFs) is usually sufficient to set up a cell-type-specific gene expression program. The underlying complicated epigenetic mechanisms that explain how cells change their states in response to intra- and extra-cellular signals in different scenarios remain to be fully understood. Importantly, epigenetic regulation of gene expression has been considered a central regulatory mechanism of cell fate determination and cellular plasticity. Insights into it will also profoundly impact our understanding of misregulation of gene expression in diseases such as cancer. However, the functional TFs of many cell types remain unclear, which greatly hinders the study of epigenetic regulatory mechanisms.
The rapid development of single-cell technology is a promising opportunity that enables us to infer functional TFs for different cell types. Some computational methods have been published in this area. However, existing methods have various pitfalls. For instance, some methods use transcription factor binding motifs (TFBMs) as the reference of TF binding, overlooking widespread non-specific binding. Some other methods hold strict criteria for training data and thus can only predict a small number of TFs. To overcome these issues, we propose to leverage publicly available high-quality ChIP-seq data to predict TFs functional in single-cell omics data. Here, we present BARTsc, a comprehensive suite for a series of TF analysis functionalities, including inference of signature TFs of given cell types/clusters, cross-cell-type/cluster TF activity comparative analysis, and TF clustering based on their cross cell-type distributions. The input of BARTsc can be either scRNA-seq, scATAC-seq, or scMultiome data. We demonstrate that BARTsc outperforms several existing tools in both sensitivity and specificity in identifying key cell type regulators in single-cell datasets of well-studied systems. Applying BARTsc to a scRNA-seq dataset for cancer-associated fibroblasts (CAFs), we identified distinct regulatory activities of some TFs in different subtypes of CAFs, but the TF genes are universally expressed in these subtypes. In addition, by time course BARTsc analysis, we identified a list of TFs that may either promote or suppress CAF differentiation, offering a new approach to find potential candidate therapeutic targets.

#2343 Adapting gene set enrichment analysis to single cell data.

A. T. Wenzel, J. Jun, J. P. Mesirov;
UC San Diego, San Diego, CA

Gene Set Enrichment Analysis (GSEA) is a method for quantifying the activation of pathways and processes in gene expression data. GSEA works by ranking genes and testing if genes in annotated gene sets representing molecular pathways are overrepresented at the top or bottom of the ranked list. Standard GSEA assumes a gene-by-sample matrix with samples falling in two phenotype class labels and ranks genes based on correlation of expression and sample class labels. Single sample (ssGSEA) uses a similar approach to enrichment scoring but ranks genes in a single sample based on their expression. There has been recent interest in using the ssGSEA modality to measure pathway activity in individual cells from single cell RNA-sequencing (scRNA-seq) data. However, we have observed that ssGSEA scores in scRNA-seq cells are prone to uncertainty due to the characteristic sparsity of scRNA-seq data. This is because sparse data leads to large groups of tied genes, that is, genes with equal expression and subsequently equivalent positions in the ranked list. Because ssGSEA, which was designed for bulk gene expression technologies which yield much less sparse data, breaks ties arbitrarily, these ties can lead to variability in enrichment scores that is purely algorithmic and not a result of the underlying biology. To address this issue, we performed benchmarking to characterize the stability of scores using different enrichment scoring statistics, normalization methods, and aggregation of similar single cells. We have implemented the best practices identified using this analysis as Single Cell GSEA (scGSEA), a software tool which we will make freely available to researchers as open-source software to enable robust gene set enrichment scoring in scRNA-seq data.

#2344 Federated image quality assessment of prostate MRI scans in a multi-institutional setting.

Mohsen Hariri[1], Prathyush Chirra[1], Malhar Patel[2], Tal Tiano Einat[2], Ittai Dayan[2], Alex Tonetti[2], Yuval Baror[2], Tristan Barrett[3], Nikita Sushentsev[3], Joshua D. Kaggie[3], Shuaiyu Yuan[3], Dufan Wu[4], Baihui Yu[4], Zhiliang Lyu[4], Cheyu Hsu[5], Weichung Wang[6], Smitha Krishnamurthi[7], Satish E. Viswanath[1]

[1]Department of Biomedical Engineering, Case Western Reserve University, Cleveland, OH,[2]Rhino Health, Boston, MA,[3]Department of Radiology, Addenbrooke's Hospital and University of Cambridge, Cambridge, United Kingdom,[4]Department of Radiology, Massachusetts General Hospital and Harvard Medical School, Boston, MA,[5]Division of Radiation Oncology, Department of Oncology, National Taiwan University Hospital, Taipei, Taiwan,[6]Institute of Applied Mathematical Sciences, National Taiwan University, Taipei City, Taiwan,[7]Cleveland Clinic Foundation, Cleveland, OH

Introduction: Reliability of machine and deep learning models on medical images can be compromised by the presence of image artifacts of variability in image acquisition. This is further exacerbated when validating model performance across multiple institutions, where multiple acquisition protocols and scanner equipment may result in significant numbers of outlier scans. We developed a privacy-preserving outlier identification algorithm via federated MR imaging quality evaluation of a distributed multi-institutional cohort of prostate MRI scans.

Methods: This retrospective study utilized T2-weighted prostate MRI scans from 1 public collection (used as a template) and 3 federated institutions. An open-source MR image quality evaluation tool (MRQy) was implemented via Docker within the RhinoHealth Federated Computing Platform (FCP). This enabled remote extraction of 9 specific metadata values and remote computation of 15 quality measurements from each scan, while ensuring confidentiality of patient data by avoiding direct access to patient images and information. Centralized analysis of extracted image quality attributes utilized a rule-based classifier to determine whether individual metadata or measurement values for a given MRI scan fell within or outside predefined bounds: (i) ±20% of template metadata values, (ii) 5th - 95th percentile range of template measurement values. Scans were considered outliers if more than 60% of their image quality attributes fell outside predefined bounds.

Results: In total, 630 MRI scans from 3 institutions were analyzed in a federated manner. 344 MRI scans from 1 public collection formed a benchmark cohort to calibrate the rule-based classifier and determine predefined bounds for outlier detection. Centralized analysis of federated image quality attributes showed marked differences in the number of outliers per institution (3%, 19%, 79% for Institutions 1, 2, 3, respectively). Further analysis of Institution 3 determined significant intensity and resolution differences compared to other institutions, requiring extensive post-processing prior to downstream analysis.

Conclusion: Federated image quality assessment can allow for distributed, privacy preserving analysis of outliers and thus curate multi-institutional cohorts of consistent quality for downstream machine learning tasks. Further analysis of the impact of quality-based curation on federated machine learning applications is currently underway.

#2345 Docking and molecular dynamic simulations of mithramycin against Sp1, Sp3, and survivin.

C. B. Lambring[1], S. K. Behera[2], R. Basha[1];

[1]University of North Texas Health Science Ctr., Fort Worth, TX, [2]Department of Biotechnology, Institute of Pharmaceutical Education and Research, Ahmedabad, India

Purpose: Therapeutic targeting of transcription factors, Specificity protein (Sp)1 and Sp3 and their downstream effectors, such as survivin, are studied in various cancers. Due to role in in poorer cancer prognoses in several cancers their downregulation has been investigated as an effective treatment approach. Mithramycin (Mit) showed innate anti-cancer properties by targeting Sp proteins through GC/GT DNA binding interference. Recent studies have given new insights into further mechanisms of action of Mit, however in-depth binding and mechanistic studies are lacking. Our objective is to investigate Mit's specific binding interactions with Sp1, Sp3, and survivin.

Methods: Protein structures and sequences for Sp1, Sp3, and survivin (ID: P08047, Q02447, and O153392, respectively) were retrieved from UniProtKB database. Experimental predicted structures for Sp1 and Sp3 were obtained from AlphaFold. Sequence lengths of Sp1 and Sp3 were 785 and 781 amino acids (aa), domain regions of Sp1 (619-785) and Sp3 (461-781) were note. Survivin structure was obtained from PDB and was comprised of 142 aa. Co-crystallized compounds were removed during analyses using BIOVIA Discovery Studio 4.5 Visualizer. Prediction of binding sites and docking were performed using CASTp, GHECOM, DEPTH tools, glide, and AutoDock 4.2 software. Energy minimization and Molecular dynamics simulations were performed in the Schrödinger suite.

Results: Binding sites were identified for Sp1, Sp3, and survivin. Simulated docking demonstrated multiple binding complexes and varying binding energies. The most efficient binding was seen with Sp1 and Sp3. RMSF and RMSD simulations revealed stabilization of Sp1-, Sp3-, and survivin-Mit complexes. This shows Mithramycin can potentially inhibit all three proteins, with slightly more stability with Sp1 and Sp3. Radius of gyration (rGyr), H-bond analysis, and solvent accessible surface area (SASA) support docking findings with Mit-protein complexes remaining stable in the binding pocket, forming new H-bonds, and altering hydrophilic and hydrophobic interaction areas.

Conclusion: Our findings warrant further in vitro testing of the ability of Mit to interact with a wider range of oncogenic targets. While we only tested the ability of Mit to interact with Sp1, Sp3 and survivin, similar model can be used to evaluate the interaction with other critical proteins associated with cancer and to further elucidate mechanisms of action. These finding are crucial to understanding base mechanistic abilities and can be useful to test additional agents for their ability to interact with Sp1 or survivin.

#2346 Meningioma molecular classification predict response to surgical resection and adjuvant radiotherapy: An integrated clinicomolecular analysis.

J. Z. Wang[1], A. P. Landry[1], V. Patil[2], A. Ajisebutu[2], C. D. Wilson[3], A. Cohen-Gadol[4], G. Tabatabai[5], S. Chotai[6], J. Barnholtz-Sloan[7], R. Yakubov[2], M. Wilson[2], R. Kaloti[2], A. Rebchuk[8], D. A. Almiron Bonnin[9], E. C. Holland[9], S. Yip[8], F. Sahm[10], K. Aldape[11], The International Consortium on Meningiomas, F. Nassiri[1], G. Zadeh[1];

[1]University of Toronto, Toronto, ON, Canada, [2]University Health Network, Toronto, ON, Canada, [3]Ascension St. John Medical Center, Tulsa, OK, [4]Indiana University, Bloomington, IN, [5]Eberhard Karls University Tubingen, Tubingen, Germany, [6]Vanderbilt University, Nashville, TN, [7]Center for Biomedical Informatics and Information Technology, Bethesda, MD, [8]University of British Columbia, Vancouver, BC, Canada, [9]Fred Hutchinson Cancer Center, Seattle, WA, [10]University Hospital Heidelberg (DKFZ), Heidelberg, Germany, [11]National Cancer Institute, Bethesda, MD

Importance: Meningiomas are the most common primary brain tumor and a heterogeneous disease with a need to study response to surgery and adjuvant RT in the context of contemporary molecular classifications.

Objective: The gold standard for treatment of symptomatic meningiomas has been surgical resection including complete removal of tumor and its surrounding dural margin, although the necessity of different degrees of marginal resection is controversial. Adjuvant radiotherapy (RT) is generally reserved for aggressive or subtotally resected (STR) meningiomas. However, uncertainty exists regarding optimal case selection for RT and response to treatment is variable. We aimed to examine the effects of treatment (surgery/RT), molecular, and clinical factors on meningiomas in the context of molecular classifications.

Design, Setting, and Participants: In this retrospective analysis, a 20-year cohort of 2490 patients with meningiomas were assembled across 10 institutions. Molecular data (DNA methylation, RNA sequencing) was generated for 1645 cases. Propensity score matching (PSM) was performed for key baseline covariates including WHO grade and molecular classifications, mimicking a randomized, molecular pathology informed clinical trial.

Main Outcome and Measures: Progression-free survival (PFS), and overall survival (OS) were assessed based on extent of resection (EOR), Simpson grade, and receipt of adjuvant RT.

Results: Gross total resection (GTR) was associated with improved PFS across all molecular groups. The PFS benefit of GTR was lessened in molecularly-defined proliferative meningiomas (HR 0.69, 95%CI 0.50-0.95), but OS benefit was enhanced (HR 0.52, 95%CI 0.30-0.93). Surgically treating the dural margin (Simpson grade 1/2) was associated with improved PFS compared to removal of tumor alone (Simpson grade 3) particularly for immunogenic (HR 0.16, 95%CI 0.03-0.82) and NF2-wildtype meningiomas (HR 0.24, 95%CI 0.11-0.53). Adjuvant RT was associated with improved PFS across all molecular classifications. Molecular groups could reliably predict response to RT, even when controlling for WHO grade and EOR with immunogenic and NF2-wildtype meningiomas benefitting most while proliferative meningiomas are largely RT-resistant (HR 0.96, 95%CI 0.67-1.37).

Conclusion: This study is the first to investigate interactions between contemporary molecular classifications and response to both surgical resection and adjuvant RT in a large, multi-institutional cohort of molecularly defined, clinically annotated meningioma cases.

#2347 Zuclopenthixol as an inhibitor of glioblastoma-induced neuronal hyperexcitability.

M. B. Negussie, S. Krishna, Y. Wei, C. Nava Gonzales, M. Mehari, S. L. Hervey-Jumper;
UCSF School of Medicine, San Francisco, CA

Introduction
Drug repurposing serves as a promising avenue for glioblastoma treatment, especially as new evidence emerges about the role of neuronal activity dependent tumor proliferation. Structure based drug discovery with virtual screening requires highly accurate 3D information about the target of choice. Recent developments in machine learning based protein structure prediction have allowed for the exploration of chemical space with virtual screening tools not previously accessible via traditional methods. Netrin-G1 (NTNG1) is an axonal guidance molecule implicated in glioblastoma with high functional connectivity to the cortex. In this study, we explore pharmacologic inhibition of NTNG1 with a clinically approved compound.
Methods
We perform protein structure predictions with AlphaFold2, followed by structure relaxation in an explicit solvent environment with NAMD 2.14. A final confirmation of NTNG1 was used as input to an AutoDock Vina based virtual screening platform. Zuclopenthixol (ZP) was chosen from a list of hits for microelectrode array (MEA) experiments in a mouse neuron/ patient-derived tumor cell co-culture environment.
Results
A list of clinically approved compounds were returned from our virtual screen. ZP was chosen for validation studies, as it readily crosses the blood-brain barrier and occupies the entire TSP1 binding site in NTNG1. Preliminary results from MEA studies suggest ZP reduces tumor-mediated hyperexcitability and adequately modulates a protein-protein interaction between NTNG1 and TSP1.
Conclusion
By demonstrating that ZP decreases tumor-mediated hyperexcitability, this study offers evidence for the novel application of ZP to reduce glioblastoma proliferation. Further work will focus on survival analyses in mice treated with ZP and validation of experimental compounds that are structurally similar to ZP.

#2348 A global multiscale map of protein assemblies from integration of protein interactions and images.

L. V. Schaffer[1], M. Hu[1], E. L. Huttlin[2], G. Qian[1], A. Pal[3], N. Soni[3], A. Latham[3], L. Vaites[2], T. Le[4], Y. Qin[1], C. Churas[1], D. Pratt[1], I. Echeverria[3], A. Sali[3], J. Harper[2], S. P. Gygi[2], E. Lundberg[4], T. Ideker[1];

[1]University of California, San Diego, La Jolla, CA, [2]Harvard Medical School, Boston, MA, [3]University of California, San Francisco, San Francisco, CA, [4]Stanford University, Palo Alto, CA

Cells regulate growth and function through a hierarchical structure of subcellular protein assemblies, in which alterations can result in cellular dysfunction leading to disease such as cancer. Much of this structure remains uncharted, resulting in recent efforts to map subcellular organization at different physical scales. Here, we report a global architectural map of human cancer cell protein assemblies spanning 10^{-9} to 10^{-5} nm, based on integration of near-proteome-wide affinity purification mass spectrometry-based protein interactions and immunofluorescent imaging in U-2 OS osteosarcoma cancer cells. The U-2 OS multi-scale integrated cell map places >5000 proteins into 270 distinct subcellular protein assemblies across biological scales, representing approximately half of expressed proteins. There are known organelles and protein complexes recovered in the map, as well as 152 putative assemblies, such as a putative interferon signaling complex consisting of a serine protease and STAT transcription factors. The map also incorporates 128 previously uncharacterized proteins into protein assemblies, such as C18orf21 association with a canonical RNAse complex. Protein subsystems in the U-2 OS map were evaluated for the potential for downstream integrative structural modeling, where available structural data (e.g. crosslinking, Protein Data Bank structures, AlphaFold predictions) are combined in a Bayesian framework to model the physical structures of protein complexes. Using this framework, we created an integrated structural model of new proteins interacting with the Rag-Ragulator complex, which regulates MAPK and mTOR signaling. In summary, the global proteome architecture map provides a resource for cellular biology discovery and the systematic determination of protein functions and structures.

#2349 A phenotypic model for cancer metabolism.

Javier Villela-Castrejon[1], Jason T. George[2], Dongya, Jia[3], Herbert Levine[4], Jose N. Onuchic[5], Benny Abraham Kaipparettu[6]

[1]Center for Translational Cancer Research, Texas A&M University, Houston, TX,[2]Department of Biomedical Engineering, and Department of Translational Medical Sciences, Texas A&M University, Houston, TX,[3]Immunodynamics Group, Laboratory of Integrative Cancer Immunology, Center for Cancer Research, National Cancer Institute (NCI), Bethesda, MD,[4]Center for Theoretical Biological Physics and Depts. of Physics and Bioengineering, Northeastern University, Boston, MA,[5]Center for Theoretical Biological Physics; Dept. of Physics and Astronomy; Dept. of Chemistry, Rice University, Houston, TX,[6]Department of Molecular and Human Genetics, Baylor College of Medicine, Houston, TX

Understanding cancer metabolism is crucial for deciphering various cancer hallmarks, including metastasis and immunosuppression. This study investigated the intricate interplay of catabolic processes involving glucose, fatty acids, and glutamine in cancer cells. Recent evidence highlights the dual reliance of cancer cells on glycolysis and oxidative phosphorylation (OXPHOS), challenging the simplistic Warburg effect. Fatty acids and glutamine also emerged as vital contributors to tumorigenesis. Despite these advances, a comprehensive model encompassing both catabolic and anabolic processes, especially glutamine metabolism, is lacking. A metabolic network model integrates catabolic and anabolic modes for glucose, fatty acids, and glutamine, incorporating genetic regulation involving AMPK, HIF-1, and MYC. Equations capture the temporal dynamics of regulatory proteins (pAMPK and HIF-1) and metabolites (mtROS and noxROS), modeling metabolic flux for glucose and glutamine uptake, fatty acid, acetyl-CoA utilization, and activities of glucose oxidation, glycolysis, and FAO. The regulatory network outlines competition for resources, gene regulation, chemical intermediates, cross-regulation among gene regulators, and regulation of metabolic ingredient uptake. The phenotypic model focusing on AMPK, HIF-1, and MYC reveals metabolic states: OXPHOS (O), glycolysis (W), hybrid (W/O), and low/low, characterized by varying levels of AMPK and HIF-1, influencing pathway activities and anabolic processes. Parameter randomization analysis shows state robustness, especially in MYC overexpressing cancer cells. Analyzing TCGA data reveals differential expression of glutamine metabolism genes. The "W" state exhibits enhanced glutamine uptake, the "O" state heightened glutamine oxidation, and the "W/O" state displays both, aligning with the model's predictions. Bifurcation analyses of AMPK, HIF1, and MYC shed light on state stability and transitions, providing insights into regulatory mechanisms. The low/low phenotype, inactive in both OXPHOS and glycolysis, raises questions about significance and therapy resistance. The study explores this phenotype further, unraveling molecular underpinnings and therapy resistance implications. A deeper understanding could reveal novel therapeutic targets, enhancing comprehension of cancer cell behavior. This study introduces a minimal network model capturing essential features of cancer metabolism, replicating experimental observations of metabolic heterogeneity. The model predicts diverse cancer cell phenotypes based on MYC expression levels, emphasizing the importance of considering both catabolic and anabolic processes.

#2350 Comparison of normalization methods for RT-qPCR microRNA expression in cancer datasets.

H. Treleaven, L. Ludwig, A. Viloria-Petit, R. D. Wood, A. Ali, G. A. Wood;
University of Guelph, Guelph, ON, Canada

Real-time quantitative PCR (RT-qPCR) is a widely used method for quantifying microRNA (miRNA) expression, but its accuracy depends on appropriate normalization. RT-qPCR is susceptible to technical variation from several sources, including sample collection and storage, miRNA quantity/quality, and extraction and amplification efficiencies. Normalization corrects for these factors, theoretically leaving behind only biological variation. With growing interest in miRNAs as biomarkers for the diagnosis and prognosis of various cancers, analyses must be accurate and consistent. Primarily, the comparative Ct method is used, which compares the expression of miRNAs to a reference value. Unfortunately, there is a lack of consistency on what to use as a reference. A standard recommendation is the average of multiple, stable miRNAs referred to as endogenous controls (ECs). Currently, there are no known universally stable miRNAs. Therefore, ECs should be selected on a per-disease and per-sample type basis. Multiple algorithms exist to identify stable ECs, but few studies indicate what, if any, steps were taken to implement them correctly. Also, many studies have used non-ideal reference values such as small nuclear RNAs or a single miRNA. This lack of agreement on protocol often leads to difficulty comparing studies and may produce incorrect results. This work addresses these inconsistencies by making recommendations for the normalization of RT-qPCR miRNA expression. We compared 2 widely used methods for EC selection, NormFinder and GeNorm, and to show how normalization influences results we also used an unstable miRNA. Only miRNAs with expression in all samples were considered as potential ECs. GeNorm is sensitive to correlated genes. Therefore, for any pair or trio of correlated miRNAs 1 was kept. NormFinder performs optimally with 5-10 candidate genes; therefore, we tested the 10 miRNAs with the lowest coefficients of variation (CV). The top 3 stable miRNAs were selected from each algorithm to serve as ECs, and we used their average expression to normalize each sample. For the single miRNA, samples were scaled based on its value. We applied these methods to 3 independent datasets: First, plasma samples from a study on canine osteosarcoma (OSA), including pre-amputation (n=45), post-amputation (n=27), and healthy controls (n=21). Second, tissue samples from a study on canine OSA, including primary tumour (n=42) and lung metastases (n=12). Third, serum samples from a study on canine lymphoma included B-cell (n=24), T-cell (n=16), and healthy controls (n=14). For datasets 1 and 3, NormFinder provided a better reduction in gene-specific CV and a more favourable cumulative distribution of the CV. For dataset 2, there was less initial variability, but NormFinder still had slightly better results. Both algorithms had pros and cons, but NormFinder consistently provides a better reduction in sample variation across datasets.

#2351 Genomics annotation and interpretation in somatic oncology using structured data from a clinical knowledgebase.

Jian Li[1], Lili Niu[1], Shuba krishna[1], Fnu Kinshuk[2], Martin Jones[3], Carlos Hernandez[3], Michael Clark[4], Sandra Balladares[5]

[1]Computational Biology - Research and Early Development, Roche Diagnostics Solutions, Santa Clara, CA,[2]Computational Science & Informatics - SW Engineering, Roche Diagnostics Solutions, Santa Clara, CA,[3]Computational Science & Informatics - Product Management, Roche Diagnostics Solutions, Santa Clara, CA,[4]Clinical Development - Oncology & Genetic SC, Roche Diagnostics Solutions, Santa Clara, CA,[5]Disease Area Life Cycle - Oncology, Roche Diagnostics Solutions, Santa Clara, CA

Accurate and comprehensive interpretation of genomic variants has become a bottleneck in clinical sequencing applications due to the accelerating precision oncology and biomedical information explosion. This motivated us to build Ephesus, a framework enabling curation of predictive, prognostic and diagnostic evidence for clinical biomarkers in cancers. Currently Ephesus is the primary content source for Roche navify Mutation Profiler (nMP).

The Ephesus' data model ensures adherence to best practices in clinical genomic content curation. Variant classification follows the AMP guidelines for somatic variant interpretation. Variant interpretations are derived from international regulatory approvals and clinical practice guidelines (FDA, EMA, TGA, eVIQ, etc.) and recommendations (NCCN, ESMO). The data model is mapped to a set of relational tables. To enforce data integrity and validity, strategies such as data normalization based on standard nomenclatural ontologies, a submit-review-approval workflow, and biological constraints are adopted. Ephesus is deployed as a web application used by curators inside and outside Roche. The UI allows users to conduct edits, filtering, sorting and bulk operations on entities by attributes. In order to minimize manual effort and maximize content coverage, inference rules are applied before ingesting into nMP.

Currently Ephesus is developed for data collection, browsing and summarizing primary entities such as biomarkers, evidence items, genes, variants, variant groups, and drugs. The content from the 2023-Aug snapshot contains 11,596 directly curated biomarker profiles (including biomarker combinations), and 6M+ expanded profiles for 41 major cancer types. To evaluate the clinical reporting value of the curated knowledge, ~160k real cancer patient samples of the AACR GENIE project were queried on Ephesus. Compared with three other major knowledgebases, Ephesus/NMP is observed showing the highest performance.

Table1 Percentage of patients or biomarkers with at least one interpretation from each knowledgebase

	CGI (2022-10-17)	CIVIC(2023-09-01)	ClinVar(2023-09-09)	NMP(2023-08-11)	AACR-Genie-v14.0 Total
patient % with any interpretation	25% (40,545)	46% (73,835)	81% (130,882)	89% (142,905)	160,965
biomarker % (including combos) with any interpretation	0.03% (256)	0.06% (526)	13.26% (122,424)	73.79% (681,128)	923,093

#2352 Development of an AI-based algorithm to quantify eosinophils in H&E images from colorectal cancer (CRC) tissue sections guided by biomarker staining using multiplex immunofluorescence imaging.

A. Hanifi, E. Blain, J. Hargrove, J. Lock, N. Tran, V. Chizhevsky, Q. Au;
NeoGenomics, Aliso Viejo, CA

Background: Eosinophils are innate immune granulocytes that migrate to areas of inflammation to combat against infection and disease. Best known for their detrimental role in asthma and allergic disorders, there is growing interest in the involvement of eosinophils in cancer. Eosinophils are routinely observed in the tumor microenvironment (TME) and, depending on the cancer type, have been shown to drive other immune cells to either suppress or promote tumor growth - In colorectal cancer (CRC), eosinophil infiltration into the TME has been linked to a favorable prognosis. However, the behavior of eosinophils and their effect on associated immune mediators in the TME remains poorly understood. Currently, eosinophils are primarily identified from H&E stained tissue sections based on morphological features by a pathologist, but it can be challenging to reliably and efficiently identify all eosinophils based on morphology alone. Here, we present a novel image analysis workflow that established an AI-based cell classifier which can accurately quantify eosinophils in H&E stained CRC tissue sections by leveraging biomarker staining of eosinophils using multiplex immunofluorescence (mIF) imaging in conjunction with the morphological characteristics of eosinophils observed by H&E.

Methods: CRC tissue sections were labeled with a 5plex panel of eosinophil-specific markers and imaged by mIF using the PhenoImager HT platform (Akoya). Biomarker fluorescence was then quenched, sections stained by H&E, and reimaged using the PhenoImager. mIF and H&E images were then imported into the HALO® platform for algorithm development. Halo AI cell classification of eosinophils was trained on the morphological features of eosinophil staining in H&E images, guided by eosinophil-specific labeling in the 5plex mIF images. H&E staining was also performed on a serial section of each specimen. Morphological identification of eosinophils in H&E images was performed by a pathologist.

Results: Correlation analysis was performed to evaluate the relationship, per high power field (HPF), between manual eosinophil counts by a pathologist and AI algorithm derived eosinophils counts. The results showed the two methods are highly correlated, demonstrating reliable algorithm performance.

Conclusion: The AI-based eosinophil detection algorithm established here enables high-throughput analysis and quantification of eosinophils from H&E stained CRC tissue specimens and facilitates morphology diagnosis.

CLINICAL RESEARCH: Antibodies 1
Poster Session

#2355 SGN-EGFRd2 binding and activity are agnostic to common EGFR extracellular resistance mutations acquired in response to anti-EGFR targeted antibody therapies.

L. Nguyen, C.-S. Wong, S. Wo, B. Grogan, D. Diolaiti, M. Palanca-Wessels, A. Clarke;
Seagen Inc., Bothell, WA

SGN-EGFRd2 is an investigational bispecific antibody comprised of two camelid-derived humanized variable heavy chain only (VHH) domains, one targeting Vγ9Vδ2 (gamma delta) T cells and the other targeting the epidermal growth factor receptor (EGFR). Selective antitumor activity occurs when two conditions are met: 1) the molecule engages both EGFR-expressing tumor cells and gamma delta T cells and 2) butyrophilins, in complex with phosphoantigens (pAgs), are expressed by EGFR-positive tumor cells, resulting in gamma delta T cell directed tumor cell killing by activation, degranulation and secretion of cytolytic molecules. The tumor specific proximity of gamma delta T cells and expression of the butyrophilins/pAgs complex results in the killing of EGFR-expressing tumor cells but not EGFR-expressing normal cells.

EGFR is an oncogenic receptor tyrosine kinase and target of several classes of therapeutic modalities, including antibodies. Two antibodies are currently approved for the treatment of EGFR-expressing, KRAS wild-type metastatic colorectal cancer (mCRC): cetuximab (CET) and panitumumab (PAN). Although these anti-EGFR therapies provide significant survival benefits to patients, the duration of response is transient, and most patients progress and develop secondary resistance [1]. One such escape mechanism is the acquisition of mutations in the extracellular domain (ECD) of EGFR, which prevent binding of therapeutic antibodies [2].

Because SGN-EGFRd2 will be tested on patients previously exposed to anti-EGFR therapeutic antibodies, it is paramount to assess its binding to EGFR ECD mutations identified in antibody resistant mCRC patients. EGFR-negative A2058 cells were transduced to express wild type EGFR and a panel of EGFR ECD resistance mutations (N=16). The binding specificity and kinetics of SGN-EGFRd2 were compared to CET and PAN by flow cytometry on engineered cell lines and biolayer interferometry, respectively. Results indicated SGN-EGFRd2 maintained the ability to bind to all tested EGFR ECD mutants, whereas CET and PAN were unable to bind several ECD mutants, as previously described [3,4]. SGN-EGFRd2 binding to EGFR ECD mutant cell lines induced the production of interferon gamma and expression of cell surface CD107a on gamma delta T cells, confirming functional engagement.

In contrast to current anti-EGFR therapeutic antibodies, SGN-EGFRd2 binding and activity was unaffected by commonly identified EGFR ECD mutations. These findings highlight SGN-EGFRd2 as a novel molecule targeting wild-type EGFR and common EGFR ECD mutations identified in the mCRC setting.

#2356 NAV-006: A next-generation rituximab targeting CD20 for the treatment of B-cell lymphomas immunosuppressed by MUC16/CA125.

L. Grasso, J. Kline, N. C. Nicolaides;
Navrogen, Cheyney, PA

Rituximab is a CD20-targeting antibody that is the standard-of-care for patients with Non-Hodgkin Lymphoma (NHL) cases. Rituximab's mechanism of action includes complement-dependent cytotoxicity (CDC) and antibody-dependent cellular cytotoxicity (ADCC), herein referred to as Humoral Immuno-Oncology (HIO) mechanisms. Recent clinical evidence suggest that high serum levels of the MUC16 (CA125) protein inversely correlate with the effectiveness of rituximab clinical activity in 40-50% of follicular lymphoma (FL) as well as diffuse large B-cell lymphoma patients with newly diagnosed or relapsed/refractory (R/R) disease. In this study we demonstrated that CA125 binds to and suppresses the activity of rituximab, tafasitamab as well as the bispecific mosunetuzumab and glofitamab antibodies, which are approved for treating cases with indolent disease. These therapies have an overall response rate around 50-60%, suggesting the presence of a mechanism that allows lymphoma cells to escape these agents' immune-mediated killing effects. CA125 may facilitate this immunosuppressive mechanism, and in fact, upon binding rituximab, CA125 reduces its affinity for the Fc receptor, CD16a, thus suppressing ADCC. Using a proprietary technology called Block-Removed Immunoglobulin Technology (BRITE) that employs randomized amino acid substitution and HIO effector function screening, we have identified a rituximab variant named NAV-006. NAV-006 is refractory to the immunosuppressive effects mediated by CA125 via its reduced CA125 interaction and increased HIO activity as compared to parent rituximab as well as the other antibodies used to treat R/R FL. In an *in vivo* model of human B-cell lymphoma, NAV-006 showed superior efficacy compared to parent rituximab. These data warrant further investigation of NAV-006 as a next generation anti-CD20 antibody that could improve upon the efficacy of antibody-mediated therapies used to treat NHL patients with high levels of CA125.

#2357 T cell receptor beta chain-directed Tri-specific antibody molecules retarget V-beta T cell subsets to tumors to promote potent and durable antitumor activity.

M. Katragadda, J. Moisan, G. Guntas, M. Sequeria, R. Servattalab, J. Lowry, R. Ruidera, K. Nybakken, E. Gerson, K. Liu, K. Chin, Z. Su, A. Bayliffe; Marengo Therapeutics, Cambridge, MA

Background We have previously shown that novel bifunctional “STAR” antibody-fusion molecules comprising germline β chain TCR-targeting antibodies fused to costimulatory cytokines co-engage the TCR and T cell cytokine receptors, thereby promoting activation and expansion of subsets of T cells expressing distinct germline variable β (Vβ) chain TCRs. Here we describe a new class of T cell engager (TriSTAR) that utilizes a tri-specific format comprising the STAR TCR β chain antibody-IL-2 fusion with an additional Fab arm targeting tumor-associated antigens (TAA). By design, TriSTAR molecules promote the activation and expansion of Vβ T cell subsets that adopt a novel memory phenotype and are subsequently re-targeted to tumors expressing specific TAAs. TriSTAR molecules induce potent and durable anti-tumor activity which in refractory murine solid tumor models appear to be superior to established anti-CD3 T cell engager (TCE) formats.

Methods Using the gp75 (Tryp1) melanoma antigen as a model TAA, gp75-targeting TriSTARs were tested in vivo in the B16F10 syngeneic mouse tumor model, compared with a conventional gp75-targeting CD3 bispecific TCE. Cured mice were re-challenged with tumors to assess the potential of TriSTARs to induce immunological memory responses. The pharmacodynamics and pharmacokinetics of gp75-targeting TriSTARs and anti-CD3 TCEs were assessed in blood and tumor using flow cytometry, NanoString and other immunoassays. This work was further extended to testing human TAA-targeting TriSTARs using in vitro human cytotoxicity assays and a transgenic MC38 model.

Results In the B16F10 murine melanoma model, gp75-targeting TriSTARs induced potent anti-tumor responses that were superior to control constructs and gp75-targeting CD3 TCEs. The superior anti-tumor activity of the gp75-targeting TriSTARs was attributed to a significant increase and accumulation of $CD8^{+}$, $CD25^{+}$ and Granzyme B^{+} T cells in tumors that was due to the expansion of the target Vβ T cell subset. Further immune profiling by flow cytometry and NanoString in tumors and blood isolated from treated B16F10 mice highlighted significant remodeling of tumor-infiltrating lymphocytes (TILs) and other immunological changes associated with immune activation. These observations with murine gp75-targeting TriSTAR molecules were broadly confirmed with TriSTARs targeting human TAAs in both human in vitro studies and human TAA transgenic mouse tumor models.

Conclusions Vβ TCR-targeting TriSTAR molecules represent a new class of T cell engager with the potential to deliver improved anti-tumor activity compared with existing anti-CD3 T cell engagers in immunologically “cold” solid tumors with low levels of T cell infiltration and antigen presentation and may therefore offer a new therapeutic approach for the treatment of patients with refractory solid tumors.

#2358 YH41723 (IMC-202), a Novel TIGITxPD-L1 bispecific antibody, leads to potent anti-tumor immunity through T cell engaging and T/NK cell activation.

Min Hyeok Jee[1], Young Bong Park[1], Byeong-Yun An[1], Hee Ra Jung[1], Eunjung Lee[1], Jun Hwan Kim[1], Ji Eun Park[2], Ji Young Yoon[2], Seung Mi Jeong[2], Yang Kyun Ryu[2], Sung Ho Kim[2], Heung Tae Kim[2], Se-Woong Oh[1], Yeol Hong Kim[1]

[1]Yuhan Corporation R&D Institute, Yongin, Korea, Republic of,[2]ImmuneOncia Therapeutics Inc., Seoul, Korea, Republic of

Immune checkpoint inhibitors (ICIs) have been making innovative advances in current cancer therapy. In particular, the PD-L1/PD-1 blockades changed the paradigm of anti-cancer treatment, showing high efficiency compared to conventional therapy. However, drug resistance has been observed in many patients receiving PD-1/PD-L1 monoclonal antibodies (mAbs), and there are still many limitations in restoring T cell. To overcome this, various ICI targets including T cell immunoreceptor with Ig and ITIM domain (TIGIT) are being studied. TIGIT is a T cell co-inhibitory receptor, highly expressed on regulatory T (Treg) cells and memory T cells and natural killer (NK) cells. In combination with PD-1/PD-L1 inhibition, the activation of CD226 through the blocking of TIGIT/PVR ligation is important for T cell activation. In this study, we demonstrated the synergistic effect that can be obtained by simultaneously blocking of PD-L1 and TIGIT and effect of T cell engager function using TIGITxPD-L1 bispecific antibody (BsAb). We generated an anti-TIGITxPD-L1 BsAb, YH41723 (IMC-202), with Fc-engineering to enhance the effector function. In order to confirm superior efficacy of YH41723 compared to combination of two monoclonal antibodies, PD-L1 mAb+TIGIT mAb, we verified the $CD8^{\pm}$ T cell-mediated tumor killing effect by T cell engager function of YH41723. We also observed strong antibody-dependent cell-mediated cytotoxicity (ADCC) effect of YH41723 against various cancer cell lines. In addition, YH41723 showed superior anti-tumor efficacy than combination treatment in NK cell-mediated tumor killing assay. We further confirmed the significant Treg cell depletion efficacy of YH41723 *in vitro* compared to combination. We tested *in vivo* anti-cancer efficacy of YH41723 in hPD-L1 KI CT26 with BALB/c-H/K-dKO mouse models (B cell-deficient mice). As a result, YH41723 showed superior tumor growth inhibition effect compared with anti-PD-L1 mAb and anti-TIGIT mAb combination. Even, 7 of 8 mice showed complete regression in 30 mg/kg dosing group. 60 days after the last administration, we further performed tumor re-challenge test. The tumor-free state of tumor re-challenged mice was sustained, indicating that the immune memory was generated by YH41723. Taken together, YH41723 showed strong efficacy in NK/T cell activation and Treg depletion *in vitro* and excellent anti-tumor efficacy *in vivo*, supporting that YH41723 as an effective anti-cancer immunotherapy and combination candidate with other ICIs.

#2359 New insights into targeting the CD200R1 pathway in T and NK cells using 23ME-00610 as a single agent or in combination.

M. R. Kumar, S. Duan, S. Yadav, A. Jarret, Z. Yan, J. Fenaux, M. Kinisu, Z. Yi, M. Poggio, P. Collins, A. Symons, L. Riol Blanco, M. Schmidt, S. Majeed, A. Diep, C. Lee;
23andMe, Inc., South San Francisco, CA

23ME-00610 is a monoclonal antibody that is being evaluated as a single agent in a Phase 1/2a clinical trial for advanced solid malignancies (NCT05199272). It binds with high affinity (K_D < 0.1 nM) to CD200R1, a promising immune-oncology (IO) target identified by surveying the 23andMe genetic and health survey database. CD200R1 is an inhibitory receptor that when bound to its ligand CD200, reduces pro-inflammatory cytokine production, and leads to an immunosuppressive tumor environment. To gain further insight into the mechanism of action of 23ME-00610 and its potential for combination therapy, we profiled CD200R1 and other immune inhibitory receptors in human dissociated solid tumor samples using spectral flow cytometry. CD200R1 was broadly expressed across tumor-infiltrating immune cells, including T cells and NK cells, cytotoxic cell types with known antitumor functions. Notably, CD200R1 expression pattern was differentiated from PD-1, which is mostly restricted to T cells, indicating differences in patient populations that could potentially benefit from anti-CD200R1 and anti-PD-1 treatments. The ligand, CD200 was broadly expressed, including on tumor cells and endothelial cells. The differential expression profiles of CD200R1 and PD-1 on immune cells, along with CD200 expression on endothelial cells, suggest that combining 23ME-00610 with other clinically validated immunomodulatory agents could enhance antitumor responses. Follow-up experiments were conducted to validate and extend these findings. In an *in vitro* assay with cancer patient-derived PBMCs, 23ME-00610 promoted higher production of IFNγ, a key functional antitumor cytokine, compared to anti-PD-1 in 9 of 10 donors. Subsequent attempts were made to pinpoint immune cells responsible for 23ME-00610's anti-tumor activity. 23ME-00610 reversed CD200-mediated suppression of chronically stimulated primary T cells and CD200-mediated inhibition of NK cell degranulation, suggesting that 23ME-00610 can mediate tumor cell killing through at least two different cell types. To test the potential of 23ME-00610 to combine with anti-PD-1 to enhance T cell function, an artificial antigen-presenting cell (aAPC) line overexpressing PD-L1 and CD200 was co-cultured with chronically stimulated primary human T cells. Anti-PD-1 and 23ME-00610 each independently enhanced IFNγ secretion levels compared to isotype control, yet their combination resulted in a more than additive effect. Taken together, these data demonstrate that 23ME-00610 can enhance both NK and T cell antitumor effector functions, and 23ME-00610 could synergize with anti-PD-1 to further increase the activity of T cells against cancer cells. The results of this study provide evidence that 23ME-00610 could expand IO treatment options for patients with advanced solid malignancies as a single agent or in combination with other anti-tumor therapeutics.

#2360 ADV101, a first-in-class IL-1RAP ADC demonstrates significant anti-tumor activity in solid tumor models.

R. C. Sainson, L. Demolis, E. De Dreuzy, O. Favre-Bulle, A. Collette, L. Bourhis, S. Reda El Sayed, D. Genin, C. Primus, L. Bouquet, K. Pavletic, C. Ferrand, M. Deschamps, S. Lameynardie, E. Rutjens, J. Hasskarl;
Advesya, Paris, France

Chronic inflammation is intricately linked to cancer development, and the IL-1 cytokine family stands out as pivotal regulators of inflammation. All the pro-inflammatory cytokines within the IL-1 family rely on a single co-receptor called IL-1RAP which therefore emerges as a crucial and central node for modulating these pathways. While healthy tissues, except for the placenta, showed minimal plasma membrane IL-1RAP expression, tumor tissues exhibited high IL-1RAP expression, particularly in Acute myeloid leukaemia, Ewing sarcoma, ovarian cancer, head and neck, and squamous gastric and oesophageal cancers. In addition, elevated IL-1RAP expression in haematological and solid malignancies has also been associated with poor overall survival, making it an attractive target for therapeutic intervention. In this study, we present the development and characterization of an antibody-drug-conjugate (ADC) targeting IL-1RAP for potential anti-tumor applications. Following on from this, an anti-IL-1RAP antibody, ADV58, was generated and confirmed to have the anticipated biophysical, specificity, and functional properties, including low nanomolar affinity (SPR and ELISA), selectivity/specificity to human IL-1RAP, and internalization potential into IL-1RAP-positive tumor cells. In addition, ADV58 bind similarly well to human, cynomolgus and rhesus monkey IL-1RAP antigens but not to rat and mouse. Altogether these properties made ADV58 an ideal candidate for an ADC program. Concurrently, solid tumor cell lines from indications of interest with elevated IL-1RAP expression were identified, laying the groundwork for disease relevant pre-clinical tumor models. Using these models, the anti-tumor potential of ADV101 (ADV58-derived ADC) was assessed in vitro and in vivo in successful proof-of-concept studies by conjugating ADV58 with monomethyl auristatin E (MMAE, DAR of 4) or Deruxtecan (DXd, DAR of 8). Humanisation and conjugation did not compromise binding of the naked antibody, the ADV58-MMAE or the ADV58-DXd ADCs to human and non-human primate IL-1RAP. In vitro, the ADCs selectively killed IL-1RAP-positive tumor cells. In vivo efficacy studies in IL-1RAP-positive subcutaneous xenograft tumor models also demonstrated a significant dose-dependent and IL-1RAP antigen-dependent anti-tumor response for both anti-IL-1RAP ADCs. Altogether the robust preclinical data package supports the continued development of ADV101 as a novel targeted ADC therapeutic strategy for a broad spectrum of cancers.

#2361 A PD1-antibody-attenuated IL-2 fusion protein activates immune cells leading to the inhibition of tumor growth in ex vivo human 3D tumor models.

R. Satchi-Fainaro[1], O. Avramoff[1], A. Katyal[1], E. Yeini[1], A. Krinsky[1], Y. Liubomirski[1], S. Dulberg[1], G. Tiram[1], A. Kaminitz[1], J. Gill[2], J. Pedersen[2], D. Bar-On[2], A. Tamir[2], P. Ayton[2], T. Taura[2], D. Wilson[2], A. Madi[1];

[1]Tel Aviv University, Tel Aviv, Israel, [2]Teva Pharmaceutical Industries Ltd., Tel Aviv, Israel

IL-2 has been prescribed to effectively treat malignancies, mainly melanoma, for decades. Its use has waned in recent years due to significant toxicity and a narrow therapeutic index. To overcome the limitations of systemic administration of IL-2, we have generated a modified IL-2 (IL2Att) with specific substitutions to reduce the binding affinity with the IL-2R. The attenuated cytokine was fused to a high-affinity anti-PD1 antibody that does not block PD-1 binding with its ligands (PD-L1 and PD-L2). The resulting antibody-cytokine fusion, anti-PD1-IL2Att, allows selective delivery of IL-2 to tumor-reactive $PD1^{+}$ T cells, with limited potential to activate $PD1^{-}$ cells. To evaluate the effect of anti-PD1-IL2Att in a human tumor microenvironment (TME), we established a unique human 3D multi-cellular cancer system. This model system includes neoplastic and somatic cells that make up the TME, further supplemented with peripheral blood mononuclear cells (PBMC). We found that the anti-PD1-IL2Att reduced tumor cell survival more effectively in several types of these 3D cancer models (melanoma, glioblastoma, ovarian and colon cancer) than standard immune checkpoint inhibitors pembrolizumab or nivolumab. Combination treatments of anti-PD1-IL2Att with either of these agents resulted in improved immune activation and tumor cell killing. Our findings suggest that tumor-targeted attenuated cytokines such as IL-2 can promote robust tumor killing while minimizing systemic toxicity.

#2362 Preclinical efficacy and safety of M9140, a novel antibody-drug conjugate (ADC) with topoisomerase 1 (TOP1) inhibitor payload targeting carcinoembryonic antigen-related cell adhesion molecule 5 (CEACAM5)-expressing colorectal tumors.

S. Raab-Westphal, F. Hart, W. Sloot, M. Shan, N. Rasche, C. Amendt, J. Anderl;
The Healthcare Business of Merck KGaA, Darmstadt, Germany

Background: M9140 is the first clinical-stage TOP1 inhibitor payload ADC directed against CEACAM5, which is expressed in colorectal cancer (CRC) and other cancer indications. M9140 is composed of a CEACAM5-specific antibody conjugated to eight, highly stable and hydrophilic ß-glucuronide-exatecan linker-payloads. After linker cleavage, the highly potent and membrane permeable TOP1 inhibitor exatecan is released.
Methods: M9140 potency was tested in viability assays using cancer cell lines with different levels of CEACAM5 expression. Potency shift viability assays were conducted using two CRC cell lines, with zosuquidar used as multidrug resistance-1 (MDR-1) inhibitor. The M9140 bystander effect was assessed in co-culture experiments with CEACAM5-negative and -positive cancer cells. Antitumor efficacy and safety were evaluated in patient-derived xenograft (PDX) mouse models and in cynomolgus monkeys, respectively.
Results: M9140 demonstrated specific binding to CEACAM5 and selective killing of target-positive cancer cells with potencies between 0.09 nM and 0.62 nM. A potent bystander effect of M9140 was demonstrated in co-culture experiments indicating the potential to treat tumors with heterogeneous target expression. Unlike other ADC payloads such as monomethyl auristatin E (MMAE) and the maytansine derivative DM4, exatecan potency was not affected by MDR-1 inhibition, indicating that this drug efflux resistance mechanism may not be relevant for exatecan. A single treatment with 10 mg/kg M9140 caused strong antitumor effects in all 14 CRC PDX models tested, with tumor stasis in 10 models and tumor regression in four models as the best response. The TOP1 inhibitor-based ADC M9140 caused strong antitumor efficacy with a tumor volume reduction of 74% and 88% as best response in two CRC PDX models where a maytansine-based CEACAM5 ADC was not effective. In cynomolgus monkeys, M9140 showed dose-dependent hematolymphoid and intestinal effects, consistent with exatecan payload, with no indication of any other toxicities such as interstitial lung disease (ILD) or ocular toxicity.
Conclusions: M9140 demonstrated high potency, strong antitumor activity, and bystander effect in preclinical models. The side effect profile in monkeys was favorable and in line with the expected toxicity of exatecan. Notably, ILD and ocular toxicity, which are known adverse effects of deruxtecan and maytansine-based ADCs respectively, were absent. A first-in-human study to evaluate the safety, tolerability, pharmacokinetics, and preliminary clinical activity of M9140 in advanced solid tumors is ongoing (NCT05464030).

#2363 Enhanced T cell activation and cytotoxicity against AML via targeted anti-CD99-A192 ScFv-ELP nanoparticle treatment.

S. Kadam, A. Ali, M. Pospiech, S. Onyemaechi, Y. Meng, K. Dhuri, A. Mackay, H. Alachkar;
USC - University of Southern California, Los Angeles, CA

CD99 is a transmembrane protein overexpressed in acute myeloid leukemia (AML), presenting a potential novel therapeutic target. Our previously developed anti-CD99-A192, comprising scFv and elastin-like polypeptides (ELPs), showed promising anti-leukemic activity by inducing apoptosis in AML cell lines and prolonging survival in AML xenograft models. Considering CD99's expression and role in T cell activation, we proposed that anti-CD99-A192 could have a dual function: targeting leukemic cells while activating T cells.

Blood samples were obtained from 20 healthy donors, and peripheral blood mononuclear cells (PBMCs) were isolated and stimulated with PHA and IL-2 cytokines to expand T cells for 72-96 hours. Post-expansion, T cells were treated with either anti-CD99-A192 or control anti-A192. Proliferation was evaluated via cell count and cell trace assays. The percentages of $CD4^{\pm}$, $CD8^{\pm}$, and $CD25^{\pm}$ T cells, and the levels of T cell activation markers CD69 and CD38, were quantified by flow cytometry. Cytokine release profiles were assessed by the Proteome Profiler Human Cytokine Array Kit. The cytotoxic impact of the anti-CD99-A192-activated T cells on MV4-11Luc+ AML cells was measured in co-culture apoptosis and luciferase assays. Statistical comparisons utilized paired and unpaired T-tests with Holm-Sidak correction for multiple comparisons, and P value <0.05 was considered significant.

T cells treated with anti-CD99-A192 displayed significant increased proliferation compared with untreated and anti-A192-treated groups at Day 5 (163.3% vs. 97% and 92.4%, p=0.042 and p=0.03, respectively). The percentage of $CD4^{\pm}$, $CD8^{\pm}$, and $CD25^{\pm}$ cells remained unchanged across treated and control groups. Activation marker analysis revealed increase in % $CD38^{\pm}$ cells in the anti-CD99-A192 group compared with the control (58.15% vs. 49.15%, p=0.0028). Among the cytokine panel, significant increases in IL-1β/IL-1F2 (11-fold change, p<0.001, adjusted p=0.006) and TNF-α (12-fold change, p=0.002, adjusted p=0.03) were observed, along with a marked decrease in IL-8 (70% reduction, p<0.001, adjusted p=0.001). GM-CSF (20-fold change, p=0.005, adjusted p=0.071) and IL-16 (2-fold change, p=0.003, adjusted p=0.051) levels also increased, though not significantly after adjustment. Co-culture assays showed greater apoptosis in MV4-11 cells at 18 hours (33.6% vs. 41.13%, p=0.015) and a reduction in viable leukemic cells at 18 hours (10.89% vs. 8.05%, p=0.034) and 48 hours (9.69% vs. 6.54%, p=0.065) in the anti-CD99-A192 compared with the control group, results were also validated by the luciferase assay (~32% reduction, p<0.001).

Anti-CD99-A192 scFv-ELP nanoparticle stimulates T cell proliferation, elevates activation markers, and increases the release of pro-inflammatory cytokines. Anti-CD99-A192 culminates in heightened cytotoxicity against leukemic cells.

#2364 Anti-CADM1 chimeric antigen receptor (CAR) is a novel therapeutic strategy against small cell lung cancer.

S. Katkam, S. Zolov, D. Shield, S. Chuikov, V. Keshamouni;
University of Michigan, Ann arbor, MI

Small cell lung cancer (SCLC) is a highly aggressive form accounting for 15% of all lung cancers. SCLC is characterized by high proliferative rates, early metastasis, and poor prognosis. The median survival is less than 2 years even in patients with early-stage disease and less than a year in patients with metastatic disease which highlights the need for new therapeutic strategies. Cell Adhesion Molecule (CADM) 1 encodes a glycoprotein which belongs to an immunoglobulin superfamily of cell adhesion molecules responsible for epithelial cell adhesion through its homophilic trans-interaction between the adjacent cells. CADM1 is highly expressed on the cell surface of 80% of the SCLC cells, associated with its neuroendocrine features, along with the expression of Neural Cell Adhesion Molecule (NCAM). CADM1 is known to act as tumor promoter through its interactions with actin binding proteins. Consistently, we observed CADM1 expression in H69, H82, and H510 SCLC cell lines as assessed by western immuno blot. More importantly they were all susceptible to NK mediated cytotoxicity when assessed against NK cell line, NK92. We previously demonstrated that CADM1 mediates NK-mediated immune surveillance in non-small cell lung cancer, suggesting that CADM1 could be a potential immunotherapeutic target for SCLC. Here we report the development of an anti-CADM1 chimeric antigen receptor (CAR) specific for T and NK cells engineered with T and NK cell specific adaptor domains. Assessed the specificity of CARs by expressing them in NK92 cells and testing them against CADM1 expressing and CADM1-null A549 cells as targets. Finally, we evaluated the efficacy of anti-CADM1 CAR-T and CAR-NK cells against SCLC targets and observed a robust killing, largely proportionate to the levels of CADM1 expression in them. We are further assessing the efficacy of anti-CADM1 CAR-T and CAR-NK products in inhibiting tumor growth in NSG mice against SCLC xenografts. Together, these observations demonstrate that targeting CADM1 with CAR-T and CAR-NK cells is a potential new therapeutic strategy for SCLC.

#2365 Disrupting IL-11/IL-11R signaling by an efficacious anti-IL-11 antibody 9MW3811 enhances T cell tumor infiltration and synergizes with anti-PD-1 therapies *in vivo*.

S. Wang, Sr.[1], C. Zhang[1], S. Jiao[1], D. Zeng[1], R. Wang[1], M. Wang[2], W. Lu[1], B. Zheng[2], X. Gui, Sr.[2], J. Zhang[2];
[1]Beijing Kohnoor Science and Technology Co.Ltd, Beijing, China, [2]Mabwell (Shanghai) Bioscience Co., Ltd, Shanghai, China

Background: IL-11 is known as an inflammation-related factor, and it has been proved to be a key driver in fibrotic diseases. Besides, the roles of IL-11 in tumor immunopathology were recognized more in-depth and comprehensively in recent years. IL-11 expression is highly and positively correlated with overall survival in various cancer types, including colorectal cancer, hepatocellular carcinoma and lung cancer. It was reported that IL-11 promoted tumor cell growth and metastasis, mediated partly through its direct effects on macrophages, T cells and cancer-associated fibroblasts. All these studies indicated that blocking IL-11 signaling may be a promising therapeutic approach for the treatment of solid tumors. In this report, 9MW3811, a high-affinity IL-11 blocking antibody was developed to test its anti-tumor activity and synergistic effects with anti-PD-1 antibody in mouse tumor models.
Methods: 9MW3811 was generated by mouse hybridoma technology followed by antibody humanization and affinity maturation. Affinity of 9MW3811 was measured by Octet system. Its blocking activity of IL-11/IL11Ra/gp130 protein interaction was detected by ELISA, and the inhibiting effect of IL-11-mediated signaling was assessed with a luciferase reporter cell-based assay. *In vivo* efficacy of 9MW3811 was tested on A549 xenograft and LUSC PDX models. ScRNA-seq data collection and computational analysis were used to investigate immune cell tumor infiltration and differentiation. The synergistic tumor-suppressing effect of 9MW3811 with anti-PD-1 antibody was evaluated in MC38, CT26 and Hepa1-6 syngeneic models.
Results: 9MW3811 showed sub-nanomolar binding affinity to recombinant and membrane bound IL-11 derived from human, mouse, rat and dog. 9MW3811 effectively blocked the formation of IL-11/IL-11R/gp130 protein complex, and inhibited the downstream cell signaling transduction. In the NSCLC A549 xenograft model, as compared with isotype control hIgG, 9MW3811 (2mpk) showed significant tumor growth inhibition (TGI 62%). In two LUSC PDX models, the TGIs for 9MW3811 (10 mpk) were 50% and 28%, respectively. Further, in MC38 and Hepa1-6 syngeneic models, 9MW3811 addition increased the TGI of anti-PD-1 antibody from 45% to 83%, and 34% to 75%, respectively. Interestingly, in an anti-PD-1 non-responsive CT26 model, the combo of 9MW3811/anti-PD-1 antibody exhibited an impressive antitumor activity (TGI 67%). Mechanistic study showed that treatment with 9MW3811 could significantly ameliorate T cell exhaustion, increase CD8+ T cells tumor infiltration and enhance the cytotoxic function of these infiltrated T cells by modulating the expression of a variety of cytokines/chemokines
Conclusion: Our results demonstrated profound antitumor activity of 9MW3811 in different tumor models. 9MW3811 is currently in phase I clinical trials in AU, CN and US.

#2366 Balancing efficacy and toxicity of a fibroblast activation protein dependent tetravalent CD40 agonist antibody for cancer therapy.

s. chen, Y. Lin, X. Zhou, X. Sun, C. Yang, C. Liao;
Jiangsu Hengrui Pharmaceuticals Co., Ltd., Shanghai, China

Background: CD40 agonist antibodies have been found to augment tumor antigen presentation and have shown potential as anti-tumor treatments in human clinical trials. The clinical success of CD40 agonist antibodies has been restricted due to their limited efficacy and on-target, off-tumor toxicity. We hypothesized that toxicity associated with CD40 agonist antibodies could be overcome by activating CD40 specifically through tumor-specific antigens. Additionally, limited efficacy can be improved by rational design of CD40 bispecific antibodies (BsAbs). Herein, we present FAPxCD40, a trivalent CD40 agonist BsAb targeting fibroblast activation protein (FAP) possessing an optimized therapeutic window.
Method: We generated a series of FAPxCD40 bispecific antibodies with 2, 4, and 6 CD40 valences by using a high-affinity anti-FAP antibody and a crosslink-dependent CD40 agonist VHH antibody. These BsAbs were evaluated using multiple immune cell functional assays, including assays for dendritic cell (DC) maturation, B cell maturation, and CMV-reactive T cell recall. The in vivo therapeutic window of the FAPxCD40 bispecifics was compared in CD40 humanized mice with subcutaneously transplanted FAP-positive MC38 tumor xenografts.
Results: We developed FAPxCD40 BsAbs with varying valences, including bivalent FAPxCD40-2, tetravalent FAPxCD40-4, and hexavalent FAPxCD40-6. FAPxCD40-2 showed strict FAP-dependent CD40 agonist activity in both DC and B cell maturation assays, while its CD40 agonist activity upon FAP-crosslinking was modest. FAPxCD40-4 exhibited efficient CD40 agonist activity upon FAP-crosslinking, but however, it also exhibited some undesired FAP-independent CD40 agonist activity. FAPxCD40-6 efficiently clustered CD40 but marginally benefited from FAP binding, making it unsuitable as a choice. In the humanized CD40 mice model, FAPxCD40-2 effectively eliminated systemic toxicity at all tested doses. Its antitumor activity, however, is modest with TGI (tumor growth inhibition) rate of 32.8 % at a dose of 6.96 mpk. Further escalation of the FAPxCD40-2 dosage to 13.92 mpk did not result in enhanced antitumor activity with TGI rate of 46.9 %, indicating that its CD40 agonist activity may have reached a plateau. In contrast, FAPxCD40-4 broke this plateau and induce a promising antitumor response at a dose of 1.3 mpk, resulting in a 92% TGI rate. Furthermore, no liver enzyme upregulation or platelet count decrease was observed under these conditions, indicating an ideal therapeutic window. In addition, during nonclinical toxicology studies conducted on cynomolgus monkeys, it was found that doses of FAPxCD40-4 up to 99 mg/kg administered weekly for a total of four doses were well-tolerated.
Conclusion: Our study demonstrates that FAPxCD40-4, a tetravalent FAPxCD40 BsAb, exhibits efficient CD40 agonist activity with an optimized therapeutic window.

#2367 STING agonist ADU-S100 improves the antitumor response of CLDN18.2/CD3 BiTEs by enhancing stem-like tumor-reactive CD8$^{\pm}$ T cells in pancreatic adenocarcinoma.

T. Zhou, J. Yan, B. Wang, Y. Xie, C. Yang, J. Yu, J. Hao;
National Clinical Research Center for Cancer; Key Laboratory of Cancer Prevention and Therapy, Tianjin Clinical Research Center for Cancer; Tianjin Key Laboratory of Digestive Cancer; Pancreas Center, Tianjin Medical Univ. Cancer Inst. & Hospital, Tianjin, China

Background: Immunotherapy with CLDN18.2/CD3 BiTEs (bispecific T-cell engagers) has shown clinical activity in pancreatic adenocarcinoma. However, only few patients benefit from the treatment, and most responders develop acquired resistance. STING agonists may promote the development of stem-like central memory CD8$^{\pm}$ T cells and enhance antitumor responses. This study aimed to investigate the synergistic effect and related mechanism of STING agonist plus CLDN18.2/CD3 BiTEs regimen.

Methods: Single-cell RNA sequencing and flow cytometry were used to examine the tumor immune landscape in humanized PDX mouse models. By qPCR, western blot and flow cytometry, an orthotopic transplantation mouse model of pancreatic cancer and an *in vitro* tumor-PBMC coculture system were established to reveal the potential molecular mechanism of STING agonist ADU-S100 in optimizing the effects of CLDN18.2/CD3 BiTEs (IBI389).

Results: In PDAC organoids, IBI389 induced potent, specific cytotoxicity, the CLDN18.2 BiTEs significantly engaged human CD3$^{\pm}$ T cells with tumor cells in an organoid-PBMC coculture system *in vitro*, resulting in the formation of the immunological synapse (IS). IBI389 monotherapy significantly suppressed tumor growth and improved survival *in vivo* in hCD3e C57BL/6 and humanized hCD34$^{\pm}$ PDX mouse models. Further, single-cell RNA sequencing and flow cytometry analysis revealed that the intertumoral TCF1$^{\pm}$PD-1$^{\pm}$ stem-like T cells and STING signaling activity of T cells were enriched in the early stage of tumor development and sharply decreased in the late stage during CLDN18.2 BiTEs administration. Furthermore, we discovered that the STING agonist ADU-S100 could significantly induce the enrichment of TCF1$^{\pm}$PD-1$^{\pm}$ stem-like CD8$^{\pm}$ T cells *in vitro* and *in vivo*, increasing IBI389's therapeutic effects. Furthermore, humanized PDX mice that were given the combination of IBI389 and ADU-S100 and survived after complete tumor rejection were rechallenged with PDX tumors. Humanized PDX tumors and hCD3e KPC orthotopic tumors from mice treated with the combination contained increased numbers of TCF1$^{\pm}$PD-1$^{\pm}$ stem-like CD8$^{\pm}$ T cells, CD4$^{\pm}$CD127$^{\pm}$ memory T cells, CD8$^{\pm}$CD127$^{\pm}$ memory T cells, and fewer numbers of CD4$^{\pm}$PD-1$^{\pm}$Tim-3$^{\pm}$ exhausted T cells, CD8$^{\pm}$PD-1$^{\pm}$Tim-3$^{\pm}$ exhausted T cells and CD4$^{\pm}$CD25$^{\pm}$ Treg cells.

Conclusions: Pancreatic tumors appear to evade immune response by inducing immune-suppressive tumor microenvironment development. In mice, the combination of STING agonist ADU-S100 and CLDN18.2 BiTEs increased the proportion of memory and stem-like CD4$^{\pm}$ and CD8$^{\pm}$ T cells while decreasing the proportion of regulatory and exhausted T cells in pancreatic tumors, eradicating all detectable tumors. This data may be utilized to formulate immune-based combination therapies for PDAC.

#2368 Intratumoral delivery of HER-2-CD3hFc mRNA-LNP inhibits ovarian tumor growth..

V. M. Golubovskaya[1], J. Sienkiewicz[1], J. Sun[1], S. Zhang[1], Y. Huang[1], L. Hu[1], H. Zhou[1], H. Harto[1], S. Xu[1], R. Berahovich[1], L. Wu[2];
[1]ProMab Biotechnologies, Inc., Richmond, CA, [2]ProMab Biotechnologies/Forevetek Biotechnology, Richmond, CA

Her-2 is a well-known driver of carcinogenesis that is overexpressed in breast, ovarian and other tumors. Immunotherapy with bispecific antibodies is a promising cancer therapy approach. Her-2 (Herceptin) antibody was used to test bispecific antibody against ovarian cancer cells. First, Her-2-CAR-T cells with Her-2 (4D5) ScFv and 4-1BB costimulatory domain were generated and tested using *in vitro* killing and IFN-gamma assays, and *in vivo* efficacy SKOV-3 xenograft NSG mouse model. Her-2-CAR-T cells killed SKBR-3 breast and SKOV-3 ovarian cancer cells and stopped SKOV-3 xenograft tumor growth. This Her-2-ScFv was used to generate bispecific Her-2 ScFv-CD3-ScFv human Fc antibody using *in vitro* transcribed mRNA. The 5'capped Her-2-CD3-hFc mRNA with 5'UTR, 3'UTR and poly A tail was generated by *in vitro* transcription using DNA template. The mRNA was embedded into lipid nanoparticles (LNP) using microfluidic PreciGenome Flex S NanoGenerator. Western blotting detected >160 kDa bispecific antibody secreted from A1847 and 293 cells transfected with mRNA-LNPs. The bispecific antibody was binding Her-2-positive A1847 ovarian cancer cell lines and T cells by FACS analysis. The Her-2-CD3-hFc bispecific antibody with T cells effectively killed Her-2-positive target cells in a dose-dependent manner in RTCA assay and produced high level of IFN-gamma. Moreover, intratumoral delivery of Her-2-CD3-hFc mRNA-LNP with intravenous injection of T cells completely blocked A1847 xenograft tumor growth. In conclusion, intratumoral delivery of Her-2-CD3 mRNA-LNP blocks ovarian xenograft tumor growth and provides a solid basis for future pre-clinical and clinical studies.

#2369 EVOLVE-105, a differentiated CD20-targeted CD2 co-stimulatory T cell engager engineered for the treatment of B cell malignancies.

X. An, M. Sarkar, S. Martomo, M. Hackett, G. Jin, T. Liang, D. Klaskin, T. Lichter, N. Pels, A. Abulizi, E. Teran, A. Sabrin, O. A. Sergeeva, A. Fearnley, H. Karp, J. Rodriguez, Jr., E. M. Tam, L. Matis, J. S. Fine, J. S. Myers;
EvolveImmune Therapeutics, Inc., Branford, CT

Despite the recent approvals of CD20-targeted CD3 bispecific molecules in follicular lymphoma (Lunsumio™, mosunetuzumab) and diffuse large B cell lymphoma (Columvi™, glofitamab; and Epkinly™, epcoritamab), significant opportunities to improve patient outcomes in these indications remain. Targeted induction of T cell costimulatory receptors (signal 2) as a complement to T cell activation mediated by T cell receptor signal 1 is an attractive strategy to sustain and optimize the redirected T cell effector response to these tumors. Drug combinations of CD3-bispecifics and tumor-targeted costimulatory biologics such as CD19-41BBL and CD19-CD28 costimulatory agonists are promising approaches that have shown preclinical efficacy and are being investigated in the clinic. EVOLVE-105 is a CD20-targeted trispecific T cell engager biotherapeutic with an integrated, affinity-tuned CD3 and a CD2 co-stimulatory agonist. The advantages of physical integration include an increased probability of simultaneous T cell receptor and CD2 receptor engagement on each T cell and a simplified patient management strategy, compared to drug combinations of molecules individually targeting each receptor. EVOLVE-105 displays improved human T cell activation, increased T cell expansion, and tumor cell killing activity without a substantial increase in cytokine release compared to CD20xCD3 bispecifics with matching CD3 affinity which does not supply CD2 costimulation. EVOLVE-105 also displays superior potency compared to the CD20xCD3 clinical benchmarks mosunetuzumab, epcoritamab, and odronextamab. Importantly, the tumor-killing potency of EVOLVE-105 was within two-fold of the activity of glofitamab, while inducing less cytokine release, suggesting its potential to establish an improved therapeutic index. In cynomolgus monkeys, EVOLVE-105 demonstrated favorable tolerability and pharmacokinetics consistent with an attractive clinical developability profile. Sustained, dose-dependent B cell depletion in peripheral blood, lymph nodes, and spleen was observed. Circulating cytokine excursions, including IL-6, IFNγ, and TNFα at efficacious doses were markedly reduced by EVOLVE-105 treatment, in contrast to the circulating levels of cytokines reported for epcoritamab and glofitamab at their efficacious doses. EVOLVE-105 demonstrates favorable biophysical properties conducive to its development as intravenous and subcutaneous formulations. The emerging profile of EVOLVE-105 suggests its potential as a differentiated CD20-targeted immunotherapy capable of providing superior, more durable tumor control with a preferred cytokine release profile, compared to current CD20-targeted T cell engager therapies.

#2370 Revitalizing anti-tumor immunity through PLT012 monoclonal antibody, targeting CD36 for metabolic rewiring in the tumor microenvironment.

Y.-R. Yu[1], S.-F. Tzeng[2], H.-W. Hsiao[3], J. Park[4], L. Kandalaft[5], Y.-H. Lin[1], C.-H. Tsai[2], P.-C. Ho[4];

[1]Pilatus Biosciences SA, Epalinges, Switzerland, [2]Institute of Life Science, National Defense Medical Center, Taipei, Taiwan, [3]Elixiron Immunotherapeutics, Taipei, Taiwan, [4]University of Lausanne, Epalinges, Switzerland, [5]Center for Experimental Therapeutics, Lausanne University Hospital (CHUV), Lausanne, Switzerland

The accumulation of lipid metabolic products in the TME has been extensively documented to exacerbate cancer malignancy by suppressing anti-tumor immunity. This phenomenon is characterized by the induction of immunosuppressive features in various immune cells and the development of exhausted phenotypes in T cells, creating formidable obstacles for effective immunotherapies. Notably, CD36, a fatty acid transporter, has been identified as up-regulated in both malignant cells and various tumor-associated immune cells, including regulatory T cells, tumor-associated macrophages, and CD8+ T cells. This upregulation serves to adjust the metabolic preferences of these cells, enabling adaptation to the lipid-enriched TME. CD36-mediated adaptation not only instigates alterations in metabolic regulations but also significantly influences immune cell properties, contributing to the establishment of an immunosuppressive TME. Consequently, it has been proposed that inhibiting CD36-mediated fatty acid uptake could strategically reshape the host's anti-tumor immunity within the TME, resulting in the reduction of tumor-infiltrating regulatory T cells and the restoration of both survival and functionality in CD8 T cells. These findings underscore the therapeutic potential of anti-CD36 antibodies as a targeted approach to mitigate the immunosuppressive milieu within the TME. Hence, PLT012, a humanized anti-CD36 antibody, was developed via phage display, followed by affinity maturation and developability optimization, and possesses cross-reactivity among species, including murine, non-human primates, and human. Through CryoEM-based structural analysis, we found that PLT012 recognizes the lipid binding domain of CD36 without interfering with the TSP-1 binding site. Moreover, administration of PLT012 significantly reduced oxLDL-mediated M2 macrophage polarization and fatty acid uptake in CD8+ TILs. Notably, HCC-bearing mice treated with PLT012 exhibited a significant reduction in tumor growth with an increased CD8/Treg ratio and CD8 effector functions, consistent with the ex vivo observations of PLT012 treatments in human HCC samples. In addition to murine studies, PLT012 also demonstrated excellent tolerability in NHP studies without any adverse effects. Ongoing studies in translational medicine will further bridge our findings and proposed mechanism of action with clinical observations, highlighting the potential therapeutic outcome in HCC patients particularly. Taken together, these results reveal that blocking CD36-mediated metabolic alterations in Treg and CD8+ TILs with PLT012 treatment can elicit robust tumor growth inhibition and shift the immunosuppressive nature within the TME toward an immunosupportive one. This study further provides the pillar for harnessing immunometabolic targeting in cancer immunotherapy.

#2371 BGB-B167, a first-in-class 4-1BB (CD137)/ CEACAM5 bispecific antibody, exhibits potent in vitro and in vivo anti-tumor activity and superior safety profile in preclinical models.

Z. Li[1], L. Qu[2], X. Chen[2], L. Xue[2], J. Li[1], Q. Liu[2], J. Sun[2], H. Sun[2], Y. Chen[1], Y. Xie[2], W. Wang[2], L. Zhu[2], P. Wang[2], X. Zhou[2], H. Hou[2], J. Chen[2], X. Liu[2], Y. Zhang[2], N. Liu[2], X. Liang[2], S. Zhang[2], X. Tang[2], J. Song[2], T. Zhang[2], X. Song[2], X. Liu[2], K. Li[2], C. Huang[2];

[1]BeiGene (Shanghai) Research & Development Co., Ltd., Shanghai, China, [2]BeiGene Co., Ltd., Beijing, China

4-1BB (CD137) is a key costimulatory immunoreceptor and a promising therapeutic target in cancer. CEACAM5 (CEA) is a well-established tumor associated antigen overexpressed in many cancers, including colorectal, gastric, lung, pancreatic cancer, liver, breast and thyroid cancers. BGB-B167 is a novel immunoglobulin G (IgG)-based bispecific antibody targeting 4-1BB and CEA and is under clinical development for the treatment of advanced or metastatic solid tumors in humans. BGB-B167 binds to its target proteins with high specificity and affinity. Potent and CEA-dependent functional activities were demonstrated using peripheral blood mononuclear cell (PBMC)-based immune cell activation and cytotoxicity assays. In humanized 4-1BB knock-in mice bearing human CEA-expressing tumors, BGB-B167 exhibited potent, dose-associated single-agent efficacy as well as synergistic antitumor activity in combination with anti-PD-1 antibody. BGB-B167 was well tolerated in 1-month repeat-dose toxicology study in cynomolgus monkeys. Here, we describe the characterization of BGB-B167 with regard to preclinical proof-of-concept and basic drug-like properties. The combined dataset provides an overview on the design, mode of action, preclinical pharmacology and safety profile of BGB-B167.

#2372 ATG-102, a novel LILRB4 x CD3 T cell engager, targeting two nonoverlapping epitopes of LILRB4, for the treatment of monocytic AML.

A. Sun[1], M. Gao[2], R. Guo[1], H. Liu[2], Z. Hu[2], E. Zheng[1], H. Yuwen[1], P. Chen[1], J. Mei[3], B. Shan[3], **B. Hou**[3];
[1]Antengene Corporation Co., Ltd., Shanghai, China, [2]Antengene Biologics, Hangzhou, China, [3]Antengene Corporation Co., Ltd., Shaoxing, China

Background: Acute myeloid leukemia (AML) is the most common acute leukemia in adults, and the treatment of AML, especially monocytic AML subtypes still has a poor outcome. T cell engagers (TCE) have been well used for the treatment of hematological malignancies, such as B cell leukemia and multiple myeloma. However, lack of ideal target antigens that only express on AML and leukemic stem cells (LSCs) but not on normal hematopoietic stem cells (HSCs) hampers the development of TCE therapy for AML. Leukocyte immunoglobulin-like receptor B4 (LILRB4), an inhibitory receptor belonging to the LILR family, is highly and restrictedly expressed on monocytic M4/M5 AML subtypes and LSCs, but not on normal HSCs which makes it an ideal target for TCE. Here we report a novel LILRB4 x CD3 bispecific T cell engager based on *AnTenGager*™ platform, ATG-102. It targets two distinct epitopes of LILRB4, inducing potent T cell-dependent cellular cytotoxicity (TDCC) with low CRS, resulting in a potent anti-tumor efficacy *in vitro* and *in vivo*.

Method: ATG-102 was constructed by introducing a high affinity anti-CD3 single chain fragment variable (scFv) to the hinge region of one of the heavy chains of a LILRB4 monoclonal antibody. A scFv targeting another epitope of LILRB4 was connected to the C terminal of the same heavy chain by GSSS linker, enabling a trivalent, dual epitope recognition of LILRB4. ATG-102 was evaluated in a series of preclinical studies for binding epitope and affinity, T cell activation, T cell dependent cytotoxicity (TDCC), and cytokine release. The *in vivo* antitumor efficacy of ATG-102 was evaluated in a humanized PBMCs and THP-1-luciferase cells engrafted NCG mice model.

Results: ATG-102 binds to LILRB4 positive cells with a single-digit nM affinity. It binds to two distinct and nonoverlapping epitopes of LILRB4. ATG-102 showed limited binding capability to CD3+ cells before LILRB4 crosslinking. However, with the presence of LILRB4 positive THP-1 cell, ATG-102 strongly activated primary T cells, upregulating early and later markers of T cell activation, CD69 and CD25, respectively. ATG-102 induced strong TDCC against LILRB4-high expressing THP-1 cells, and it induced more potent TDCC against LILRB4-low expressing MOLM-13 cells than a benchmark antibody. While compared with benchmark, ATG-102 induced significantly lower release of IL-6, which is one of the major cytokines involved in cytokine release syndrome (CRS). In addition, ATG-102 demonstrated more potent *in vivo* anti-tumor efficacy compared with the benchmark antibody at 1 mg/kg and 0.1 mg/kg dose level in PBMC-humanized NCG mice bearing THP-1-luciferase cells.

Conclusion: ATG-102 demonstrates trivalent, dual epitope recognition of LILRB4, conditionally redirects and activates T cells to recognize and kill monocytic AML cells. It demonstrates potent *in vitro* and *in vivo* anti-tumor efficacy with low risk of CRS.

#2373 Functional and specific T-cell engagers against a peptide-MHC tumor target.

Davide Tortora, Peter Bergqvist, Allison Goodman, Ryan Blackler, Nathalie Blamey, Stefania Carrara, Lauren Chong, Gabrielle Conaghan, Cindy-Lee Crichlow, Valentine de Puyraimond, Harveer Dhupar, Patrick Farber, Jessica Fernandes Scortecci, Kate Gibson, Rodrigo Goya, Ahn Lee, Franco Li, Tova Pinsky, Craig Robb, Patrick Rowe, Antonios Samiotakis, Eduardo Solano Salgado, **Raffi Tonikian**, Ping Xiang, Irene Yu, Kelly Bullock, Tara Fernandez, Stephanie K. Masterman, Kush Dalal, Tim Jacobs, Bryan C. Barnhart

AbCellera, Vancouver, BC, Canada

Accessing peptides from intracellular tumor antigens displayed on MHC class I (pMHC) can expand the T-cell engager (TCE) target pool for solid tumor applications. A challenge limiting TCE development for pMHC targets is the identification of rare, high-affinity, and high-specificity pMHC-binders. In this work, we describe TCEs in a 1x1 format with potent tumor-cell killing activity and high specificity for MAGE-A4, a pMHC tumor antigen expressed in multiple cancer types. We identified functional MAGE-A4 x CD3 TCEs with high specificity and affinity to a human MAGE-A4 peptide sequence of 10 amino acids presented on MHC-I (HLA-A:02*01). We strategically selected MAGE-A4-binders with high binding specificity for pMAGE-A4$_{230\text{-}239}$, but not MHC-I or many closely related MHC-restricted peptides. We then paired them with diverse and developable CD3-binders with a range of binding affinities, subunit specificities, and binding kinetic profiles. High-throughput *in vitro* functional characterization of hundreds of these TCEs enabled identification of molecules with optimal T-cell dependent cellular cytotoxicity in MAGE-A4-expressing tumor cell lines, with comparable tumor-killing activity and cytokine release to a clinical-stage TCE in a 2x1 format. Previous studies have highlighted unique challenges associated with pMHC targets, including their potential for cross-reactive binding to pMHCs on healthy tissues, and the absence of pharmacologically relevant species for preclinical toxicity testing. To address these challenges, we have designed and implemented an *in vitro* and *in silico* workflow to identify antibody binding to potential off-target peptides. Using this approach, we selected TCEs with several pMHC binding orientations and high specificity and affinity. These TCEs killed tumor cell lines endogenously expressing MAGE-A4 pMHCs and not isogenic cells with MAGE-A4 knocked out. Results demonstrate that our high-resolution, multiparametric antibody discovery capabilities can identify pMHC-binding antibodies with desired functional and specificity attributes. This approach unlocks the discovery and development of optimal TCEs against complex pMHC antigens.

#2374 Bispecific and trispecific GPRC5D antibodies with potent cell-killing activity against multiple myeloma.

H. Roth, D. Rogers, **I. Sanchez**, B. Tyrell, T. Barnes, A. Snyder, N. Nowgu, K. Doolan, B. J. Doranz, R. Chambers, J. B. Rucker;
Integral Molecular, Philadelphia, PA

Background: GPRC5D is a G protein-coupled receptor that is expressed on multiple myeloma cells but absent from most healthy tissues except for hair follicles. It is an attractive target for anti-tumor modalities including T cell-engaging bispecific antibodies. Recent clinical data demonstrate that combination therapy of T cell-engaging molecules individually targeting GPRC5D and BCMA on tumor cells offers unprecedented therapeutic benefits in relapsed/refractory multiple myeloma patients. A trispecific antibody that simultaneously engages these molecules while activating T cells is expected to provide comparable and additional benefits as a monotherapy.

Methods: Multipass membrane proteins are valuable therapeutic targets but are largely inaccessible for antibody discovery due to structural complexity and high conservation. We developed an antibody discovery platform (MPS) tailored for membrane proteins that utilizes advanced immunization techniques including DNA, mRNA, and Lipoparticles (virus-like particles) and evolutionarily divergent host species.

From the parental antibodies isolated, we engineered panels of GPRC5DxCD3 bispecific and GPRC5DxBCMAxCD3 trispecific antibodies using multiple formats and CD3 arms that encompass different geometries and binding stoichiometries. GPRC5D multispecific antibodies were tested for target specificity using Integral Molecular's Membrane Proteome Array (MPA), and epitope residues were defined using alanine scanning mutagenesis. Both bispecific and trispecific antibodies were tested for in vitro potency and cytokine release using MM.1R and RPMI 8226 multiple myeloma cell lines. In vivo efficacy for a subset of antibodies was determined using xenograft models in PBMC-engrafted mice.

Results: We immunized chickens with GPRC5D to obtain high-titer immune responses and configured resulting antibodies as T cell-engaging bispecific molecules with a CD3 binding arm. A subset of GPRC5DxCD3 bispecific antibodies displayed potent T cell-mediated cytotoxicity with picomolar potency on multiple myeloma cell lines. Antibody specificity profiling showed high specificity binding, and epitope mapping helped to explain why only some GPRC5D antibodies were active as multispecific antibodies.

Bispecific molecules were then re-engineered as trispecific antibodies with additional binding to BCMA, a well-validated multiple myeloma target. GPRC5DxBCMAxCD3 trispecifics showed improved cytotoxic activity against multiple myeloma cells. Both bispecific and trispecific antibodies demonstrated a large window between cell killing and cytokine release. We will present in vivo efficacy data for a panel of bi- and trispecific molecules against MM.1R xenografts in PBMC-engrafted mice.

#2375 23ME-01473, a novel anti-ULBP6/2/5 monoclonal antibody, reinvigorates anti-tumor NK cell function through NKG2D and FcγRIIIa activation.

J. Benjamin, A. Jarret, S. Bharill, S. Yadav, D. Ayupova, C. Hom, Z. Bahrami Dizicheh, I.-L. Chen, A. Diep, S. Shi, C. Bonnans, D. Kellar, G. Fuh, M. Schmidt, **K. Gerrick**, P. Koenig, M. Poggio;
23andme, Inc., South San Francisco, CA

Using genome-wide association studies (GWAS) of the 23andMe genetic and healthy survey database across all phenotypes as part of our unique target discovery platform, we identified immuno-oncology (I/O)-related genetic variants as those with opposing directionality of effects on cancer and immunological phenotypes, which comprise the I/O signature. This I/O signature identified ULBP6 as a potential cancer therapeutic target. ULBP6 is a stress-induced cell surface ligand found on cancer cells, that binds to the activating receptor, NKG2D, on NK and T cells to induce tumor cell killing. However, as a mechanism of immune escape, tumors shed ULBP6 to produce a soluble form that attenuates NKG2D activation and is elevated in cancers. Given that the 2 allelic variants of ULBP6 have the highest binding affinity to NKG2D of all human NKG2D ligands, ULBP6 may be the most immunosuppressive soluble NKG2D ligand and a critical regulator of anti-tumor response. Accordingly, soluble ULBP6 exhibited significant suppression of IFNγ release and detectable cell surface NKG2D expression on healthy donor PBMCs using in vitro cell-based assays. Moreover, the overexpression of human ULBP6 in a genetically modified MC38 murine model resulted in decreased infiltration of NK, NKT, and CD8 T cells in vivo. As such, we developed a novel humanized monoclonal antibody, 23ME-01473, that binds with high affinity to ULBP6, and due to the high sequence homology, to ULBP2 and ULBP5, to block their interaction with NKG2D. By preventing the binding of soluble ULBP6 to NKG2D on PBMCs in vitro, 23ME-01473 restored NKG2D activation as measured by increased detectable cell surface NKG2D expression, IFNγ and granzyme B release, and tumor cell killing by PBMCs. To further leverage the binding of 23ME-01473 to ULBP6/2/5, 23ME-01473 was designed to have an afucosylated Fc domain that enhances its binding affinity to the activating Fc receptor, FcγRIIIa, on NK cells to induce ADCC against tumor cells. The combination of NKG2D and FcγRIIIa activation resulted in synergistic PBMC-mediated IFNγ secretion and enhanced tumor cell killing, compared to activation of either NKG2D or FcγRIIIa. Taken together, these results reveal ULBP6 as a novel cancer therapeutic target, and given the dual activation of NKG2D and FcγRIIIa, suggest the potential of 23ME-01473 to activate NK cells and elicit anti-tumor immunity.

#2376 Mitazalimab, a potent CD40 agonist in combination with FOLFIRINOX demonstrates changes consistent with increased immune activation in TME and peripheral blood in a preclinical pancreatic cancer tumor model.

K. Enell Smith, **D. Gomez Jimenez**, M. Thagesson, A. Nilsson, Y. Pico de Coana, S. Ambarkhane, P. Ellmark;
Alligator Bioscience, Lund, Sweden

Mitazalimab is a human CD40 FcγR-conditional agonistic IgG1 antibody developed for cancer immunotherapy. Immune-excluded tumors, such as pancreatic ductal adenocarcinoma (PDAC), are defined by low infiltration of immune cells. In PDAC, effector $CD8^{\pm}$ T cells are excluded from the tumor by its desmoplastic stroma which surrounds cancer cell islets and hosts immunosuppressive macrophages. CD40 is expressed on key myeloid cell populations and targeting this receptor has a two-fold mode of action. First, mitazalimab activates macrophages, skewing them towards a tumoricidal phenotype that can potentially reverse the suppressive tumor microenvironment found in PDAC and sensitizes the tumor for chemotherapy by stromal degradation. Second, mitazalimab activates antigen-presenting cells, resulting in priming and expansion of tumor-specific T cells with the potential to generate an effective immune response that could provide immunological memory resulting in long term benefits to patients.

Mitazalimab is currently being investigated in a phase 2 study in patients with metastatic PDAC (OPTIMIZE-1) in combination with modified FOLFIRINOX (NCT04888312). The treatment starts with a dose of mitazalimab administered one week prior to chemotherapy in the first cycle to leverage the mode of action and increase the efficacy of the combination therapy. Interim results of the study demonstrated encouraging anti-tumor activity with good durability of responses.

To study the changes induced by mitazalimab and FOLFIRINOX in the tumor microenvironment, we evaluated the combination in human CD40 transgenic mice using the KPCY pancreatic tumor model. Tumor, tumor draining lymph nodes, blood and spleen were analyzed for changes in the immune compartment using multiplex assays at different time points.

The results showed distinct immunophenotypical changes induced by mitazalimab, FOLFIRINOX and the combination. The combination of mitazalimab and FOLFIRINOX resulted in an increased tumoricidal immune profile, including a marked increase in effector $CD8^{\pm}$ T cells compared to the individual therapies.

Overall, these preclinical data support the chosen dosing regimen of mitazalimab and modified FOLFIRINOX in the OPTIMIZE-1study and underline the synergistic potential of this combination for an improved antitumor response.

#2377 HER2-ADC efficacy is rooted in its induction of immunogenic cell death with FcGR activation and a systemic bystander effect.

L.-C. Tsao, X. Ma, J. S. Wang, T. N. Trotter, T. Wang, J.-P. Wei, G.-j. Lei, J. McBane, P. Fan, I. Spasojevic, **Z. C. Hartman**;
Duke University Medical Center, Durham, NC

Background: T-DXd is an antibody-drug conjugate (ADC) targeting HER2 that has demonstrated superior clinical efficacy over previous HER2-targeting agent Trastuzumab emtansine (T-DM1). Notably, T-Dxd is clinically effective in breast cancers (BC) with a range of HER2 expression. While its purported mechanism of action (MOA) involves its cleavable linker leading to bystander killing, it remains unclear how this potential MOA accounts for efficacy in HER2-low cancers or the role FCGR-mediated signaling and immune induction plays in its clinical efficacy.
Method: In vitro studies utilized co-culture, internalization, FCGR activation, ADCP, flow cytometry, and gene expression by QRT-PCR and ELISA assays. Assessments of tumor antigen-specific T cell stimulation involved JEDI T cells. In vivo studies were conducted using in vivo implantation of HER2+ and HER2- cells, PK assessments of T-Dxd/DM1 and therapeutic effects determined using an endogenous HER2 transgenic mouse model that measured HER2-specific adaptive immune responses, in combination with immune checkpoint blockade anti-CD47.
Results: T-Dxd elicited a systemic bystander effect that was only partially dependent on HER2 expression, mediated by specific cathepsins in the extracellular TME. Notably, T-Dxd cytotoxicity induced immunogenic cell death (ICD), while also retaining the ability to engage FCGRs to promote ADCP and innate immune activation. ICD was mediated by secretion of specific Dxd driven DAMPs (HMGB1 and eATP), resulting in TLR4/STING activation. ICD and FCGR activation along with antigen ADCP together elicited myeloid cell activation (CD80, CD40) and antigen presentation, resulting in effective expansion of tumor antigen-specific T cells responses, demonstrated by co-culture assays using EGFP/HER2+ BC cells and CD8+ JEDI T cells. T cell activation required TLR4 and STING pathways while in vivo, T-Dxd anti-tumor responses associated with augmented HER2-specific T and B cell responses. However, T-Dxd also induced CD47 to limit phagocytosis. But, the use of CD47/SIRPa blocking antibodies dramatically enhanced CD8+ T cell expansion in vitro and anti-tumor efficacy in vivo upon T-Dxd treatment.
Conclusion: Our study demonstrates that T-Dxd is cleavable in HER2 negative BC in vivo, which permits more widespread Dxd activity against HER2 low BC. Critically, Dxd elicits ICD, resulting in innate immune stimulation of myeloid cells, which when combined with FCGR activation and ADCP, leads to a striking induction of tumor-specific adaptive immunity. This combination was unique to T-Dxd, which may underlie its clinical superior efficacy. However, T-Dxd activity also elicits suppressive CD47 expression which could be negated using CD47/SIRPA blockade. We found that this combination dramatically enhanced T-Dxd resulted therapeutic efficacy, thus supporting clinical exploration of these combinations.

#2378 The triple-specific antibody KA-3003, targeting PSMA, CD28, and 4-1BB, is developed for the treatment of prostate cancer by enhancing T cell activity within the tumor.

G. Wu, Z. Guo, H. Peng, F. Hao, T. Liu, J. Ning;
Kyinno Biotechnology Co., Ltd, Beijing, China

Immunotherapy, revolutionizing the treatment of advanced solid tumors by blocking PD1 signaling, has encountered a challenge in prostate cancer, exhibiting a low response ratio to anti-PD-1 therapy. Furthermore, cancer immunotherapy using 4-1BB agonists faces limited clinical development due to dose-limiting toxicity. Here, we developed a tri-specific antibody, KA-3003, targeting PSMA, CD28, and 4-1BB, with the goal of enhancing T cell activation in the tumor microenvironment. This antibody was created using our common light chain bispecific antibody discovery platform and nanobody antibody discovery platform with knob-into-hole technology. KA-3003, in IgG1 format, features mutations in the Fc domain to eliminate ADCC, ADCP, and CDC activity. It contains two identical nanobodies at the C-terminal against 4-1BB, while binding to PSMA and CD28 with two Fabs at the N-terminal, sharing an identical light chain. KA-3003 exhibits high affinity for PSMA and relatively lower affinity for CD28 and CD137. In the presence of a low concentration of CD3 antibody to stimulate T cell activation, co-culture of tumor cells expressing PSMA with primary T cells isolated from human PBMC enhances T cell activation and proliferation. In PBMC humanized immunodeficient mouse tumor models, KA-3003 effectively suppresses the growth of 22Rv1 tumors with or without a PD1 antagonist antibody. Additionally, KA-3003 has a half-life of more than five days in the blood of Balb/c mice. Finally, we assessed the developability of this antibody with different treatments such as high concentration, low pH, repeated freezing and thawing, and high temperature. KA-3003 shows neither aggregation nor degradation. In conclusion, the tri-specific antibody KA-3003, developed with our common light chain antibody discovery platform, stands out as a promising pre-clinical candidate drug for the treatment of prostate cancer.

#2379 The bispecific antibody KA-3007 against B7H3 and CD28 enhances T cell activation in solid tumors.

G. Wu, Z. Guo, H. Peng, F. Hao, F. He, J. Ning;
Kyinno Biotechnology Co., Ltd, Beijing, China

Immunotherapy, revolutionizing the treatment of advanced solid tumors by blocking PD1 signaling, faces challenges as most cancers remain unresponsive to anti-PD-1 therapy. CD28, a key immune co-stimulatory receptor on T cells, often lacks ligands expressed on tumor cells. B7H3 is highly expressed in various solid tumors. In this study, we developed a bispecific antibody (BsAb) named KA-3007, targeting B7H3 and human CD28 to activate T cells in the tumor microenvironment. KA-3007, featuring an identical light chain, was developed using our common light chain bispecific antibody discovery platform with knob-into-hole technology. This BsAb is in regular IgG1 format with mutations in the Fc domain to eliminate ADCC, ADCP, and CDC activity. Its two Fabs bind to B7H3 with high affinity and CD28 with relatively low affinity. Co-culturing T cells with tumor cells expressing B7H3 enhances T cell activation. In PBMC humanized immunodeficient mouse tumor models, KA-3007 effectively suppresses the growth of NCI-H292 tumors, with or without a PD1 antagonist antibody. Furthermore, this antibody exhibits a half-life of more than five days in the blood of Balb/c mice. Finally, we assessed the developability of KA-3007 with different treatments such as high concentration, low pH, repeated freezing and thawing, and high temperature, and it shows neither aggregation nor degradation. In conclusion, the BsAb KA-3007, developed with our common light chain antibody discovery platform, emerges as a promising pre-clinical candidate drug for the treatment of solid cancers.

#2380 The bispecific antibody KA-3004, targeting PD-L1 and 4-1BB, is designed to enhance anti-tumor activity.

J. Liang, Z. Guo, H. Peng, F. Hao, T. Liu, J. Ning, **G. Wu**;
Kyinno Biotechnology Co., Ltd, Beijing, China

Checkpoint inhibitors (CPI) have transformed the treatment landscape for advanced solid tumors; however, a majority of cancers still do not respond to immune checkpoint therapy. In this study, we developed a bispecific antibody (BsAb) named KA-3004, targeting PD-L1 and human 4-1BB, with the aim of enhancing the functionality and survival of stimulated CD8+ T cells in the tumor microenvironment. This antibody was designed using our nanobody antibody discovery platform. KA-3004, in IgG1 format, incorporates mutations in the Fc domain to eliminate ADCC, ADCP, and CDC activity. It features two identical nanobodies at the C-terminal against 4-1BB to stimulate 4-1BB signaling in T cells and binds to PD-L1 with two Fabs at the N-terminal. KA-3004 binds to PD-L1 with high affinity, blocking the interaction of PD-1 and PD-L1. It also binds to 4-1BB expressed on 293T cells and activated human T cells. In the presence of a low concentration of CD3 antibody to stimulate T cell activation, co-culture of tumor cells expressing PD-L1 with primary T cells isolated from human PBMC enhances T cell activation and proliferation. In PBMC humanized immunodeficient mouse tumor models, KA-3004 effectively suppresses the growth of NCI-H292 tumors expressing PD-L1. Additionally, KA-3004 has a half-life of more than five days in the blood of Balb/c mice. Finally, we assessed the developability of this antibody with different treatments such as high concentration, low pH, repeated freezing and thawing, and high temperature, and KA-3004 shows neither aggregation nor degradation. In conclusion, the BsAb KA-3004, developed with our nanobody antibody discovery platform, stands out as a promising pre-clinical candidate drug for the treatment of solid cancers.

#2381 The bispecific antibody KA-3001, targeting PSMA and CD28, specifically enhances T cell activation within prostate tumors.

J. Liang, C. Su, H. Peng, F. Hao, T. Liu, J. Ning, **G. Wu**;
Kyinno Biotechnology Co., Ltd, Beijing, China

Immunotherapy, which involves blocking PD-1 signaling, has revolutionized the treatment paradigm for advanced solid tumors. However, prostate cancer exhibits a low response ratio to anti-PD-1 therapy. In this study, we have developed a bispecific antibody (BsAb), KA-3001, targeting PSMA and human CD28, aiming to enhance T cell activation in the tumor microenvironment. KA-3001, in a regular IgG1 format, features an identical light chain and was designed using our common light chain bispecific antibody discovery platform with knob-into-hole technology. Mutations in the Fc domain were introduced to eliminate ADCC, ADCP, and CDC activity. KA-3001's two Fabs demonstrate high affinity for PSMA and relatively low affinity for CD28. In comparison to REGN5678, KA-3001 exhibits significantly stronger binding to PSMA-expressing prostate tumor cells, along with relatively lower CD28 activation, minimizing toxicity while maintaining anti-tumor efficacy. In PBMC humanized immunodeficient mouse tumor models, KA-3001 effectively suppresses the growth of 22Rv1 tumors with or without PD-1 antagonist antibody. Furthermore, KA-3001 has a half-life of more than five days in the blood of Balb/c mice. Finally, we assessed the developability of this antibody through various treatments such as high concentration, low pH, repeated freezing and thawing, and high temperature. The BsAb demonstrates neither aggregation nor degradation. In conclusion, the BsAb KA-3001, developed using our common light chain antibody discovery platform, stands out as a promising pre-clinical candidate drug for the treatment of prostate cancer.

#2382 KY-CLC-mouse: a common light chain bispecific antibody discovery platform.

H. Peng, **G. Wu**, F. Hao, F. He, Y. Gu, J. Ning;
Kyinno Biotechnology Co., Ltd, Beijing, China

Bispecific antibodies (BsAbs) have emerged as a potent therapeutic tool in cancer treatment, gaining increasing centrality in therapeutic applications. However, the development of bispecific antibodies is hindered by the mispairing of light and heavy chains. In response to this challenge, our company developed the KY-CLC-mouse, featuring an identical κ light chain without the expression of the λ light chain. This mouse shows great promise in bispecific antibody development, as the identical κ light chain, modified from a frequently occurring light chain in mice, pairs with multiple heavy chains. The advantages of such a light chain include good solubility and stability, as well as ease of humanization without post-translational modifications in the complementary-determining regions (CDRs). Furthermore, the CDRs were modified to reduce immunogenicity. This KY-CLC-mouse platform has facilitated the identification of antibodies that specifically target over a dozen antigens, such as PD-1, LAG33, MET, PSMA, and CD28, with KD ranging from 0.1 nM to 10 nM. We apply the knob-in-hole technology to assemble bispecific antibodies, targeting two antigens or different epitopes of the same antigen, following their humanization. Prime examples include fully humanized BsAbs PD1xLAG-3, PDL1xEGFR, PSMAxCD28, and EGFRxB7H3. These bispecific antibodies have an identical light chain and were developed with knob-into-hole technology. With different treatments such as high concentration, low pH, repeated freezing and thawing, and high temperature, the BsAbs show neither aggregation nor degradation, suggesting good developability of these antibodies. Additionally, these BsAbs have a half-life of more than five days in the blood of both mice and monkeys. In conclusion, our common light chain KY-CLC-mouse is a powerful bispecific antibody discovery platform.

CLINICAL RESEARCH: Biostatistics in Clinical Trials / Surgical Oncology
Poster Session

#2386 Meta-analysis of efficacy and safety in early-phase clinical trials for refractory colorectal cancer.

Maarten A. Huismans, Lidwien P. Smabers, Niels N. van Nieuwenhuijzen, Monique C. Minnema, Miriam Koopman, Hugo J. G. Snippert, Anne M. May, Jeanine M. L. Roodhart

UMC Utrecht, Utrecht, Netherlands

Introduction: Despite a decade of metastatic colorectal cancer (mCRC) therapeutic innovations, a comprehensive synthesis of patient outcome and risk-benefit assessment of phase 1/2 trials, extending beyond single-center studies, is missing. The aim of this meta-analysis is to assess efficacy, safety, and trends over time for phase 1 and 2 mCRC trials by examining clinical benefit rate (CBR), overall response rate (ORR), grade 3 or higher adverse events (AE), and discontinuation due to AE.
Methods: The protocol and search were preregistered on PROSPERO. We searched PubMed and Embase for publications of phase 1/2 trials between 2010-2022. Reports were screened for inclusion criteria, followed by data-extraction by two researchers. Trials reporting on non-standard therapies for treatment-refractory mCRC or trials reporting specific mCRC efficacy data were included. CBR was defined as the proportion of patients with complete/partial response or stable disease ≥14 weeks. We used logit transformations for pooled effect analysis via a random-effects model, assigning study weights by the inverse variance method. Subgroup analyses were performed for publication year, preselection on molecular traits, and drug class: antiangiogenics, chemotherapy, immunomodulator, targeted therapy, or vaccine. Data are presented with 95% confidence intervals (CI); reported differences had non-overlapping CIs.
Results: The search strategy yielded 4175 unique reports, from which we extracted data for 279 trials. Most trials were phase 1 (63%). ORR was limited to 6% [6-7] in both phase 1 and 2, CBR was higher in phase 2 than in phase 1 trials (36% vs 27%). Trials testing antiangiogenic drugs had the highest CBR (47%) and immunomodulators the highest ORR (8%). Trials with patients preselected on molecular traits had higher CBR compared to other trials (38% vs 28%). We observed an increase in efficacy, especially in phase 2 trials, with a CBR rising from 22% to 42% between trials published in 2010-2012 and 2019-2021. Compared with 2010-2012, trials in 2019-2021 were more often testing immunomodulators (23% vs 4%), performed on molecular preselected populations (38% vs 4%), and including younger patients (median age <60 in 66% vs 44%). The occurrence of grade 3+ AE was 33% [28-38] in both phase 1 and 2. AE led to discontinuation in 12% of phase 1 trial patients, and 7% of phase 2 patients. Grade 3+ AE occurred in 4% of vaccine trial patients, in contrast to 41% in trials on targeted therapies. Occurrence of grade 3+ AE did not change over time.
Conclusion: We found limited ORR and CBR in early phase trials conducted in 2010-2021 for mCRC patients, while noting severe AEs in many patients. However, during this period, clinical benefit rate increased for phase 2 trials, possibly due to evolving study strategies that entail testing new treatment types in a younger, fitter, and stricter preselected study population based on molecular traits.

#2387 Drivers of precision in oncology trials: A landscape analysis of biomarkers and treatments.

M. Schuessler[1], E. Skarga[2], P. Geldsetzer[1], Y. Lu[1], M. Hohberg[3];

[1]Stanford University, Stanford, CA, [2]Heidelberg University, Heidelberg, Germany, [3]University Medical Center Goettingen, Goettingen, Germany

Background: Molecular profiling is powerful to match patients' tumor profile with targeted therapies in oncology. While our understanding of treatments and biomarkers that enhance overall response rates is growing, the level of consistency at which treatment response is assured in biomarker-enriched (BE) cohorts (e.g. immune-checkpoint inhibitors in PD-L1-positive tumors) remains poorly understood. In essence, an optimal biomarker would not only result in high mean survival but also precise, closely clustered response of all patients around this mean. **Objectives**: The primary objective of this study is to develop a method to measure the variability of survival outcomes from published Kaplan-Meier (KM) curves in trials. The secondary objective is to assess whether novel treatments, when given in the presence of predictive biomarkers, improve not only mean survival, but also its precision. This is clinically relevant as higher precision guarantees patients a treatment outcome closer to the mean, thereby providing safeguards against non-response. **Methods**: We conducted a criteria-based search in PubMed and EMBASE to identify all phase-II and -III drug trials on breast cancer and non-small cell lung cancer (NSCLC) published between 2018-2022. We developed an algorithm to derive pseudo-individual patient data (p-IPD) from KM curves. We measured variability of survival outcomes in treatment and control groups using ratios of coefficients of variation (CVRs) derived from log-normal models and restricted mean survival time. This novel computational approach enables comparing the consistency of treatment responses in BE subgroups versus total, i.e. intention-to-treat (ITT), populations in each trial. **Results**: From screening 780 publication records (NSCLC: n = 405; breast cancer: n = 375), we identified 67 biomarker-stratified drug trials (NSCLC: n = 41; breast cancer: n = 26). We successfully constructed p-IPD using KM curves from ITT and BE cohorts for the first 18 trials (NSCLC: n = 10; breast cancer: n = 8) from a total of 11,373 patients (NSCLC: n = 7,547; breast cancer: n = 3,826). The preliminary meta-analysis for overall survival on these first 18 trials shows that BE treatment groups respond more precisely, with a variability reduction from 0.93 [95%-CI: 0.91, 0.96] in the ITT group to 0.86 [0.83, 0.91] in the BE subgroup. This variability reduction varies across treatment, biomarker, and tumor types. Finally, we observe different variability estimates in trials (n = 6) that are stratified by subgroups of different PD-L1 expression. **Conclusion**: This is the first study that presents a viable approach to analyze the variability of biomarker-treatment pairs in oncology at large scale. We find a reduction of treatment variability in breast and lung cancer trials in BE populations. Our work offers an orthogonal approach to measure biomarker utility with the potential to inform biomarker discovery and trial design.

#2388 Artificial neural network based ensemble models for single-arm glioblastoma trials: A new historical control adjustment method.

Wonsuk Yoo[1], Tortsen Ullrich[2], Nader Sanai[1]

[1]Barrow Neurological Institute, Phoenix, AZ,[2]Brown University, Providence, RI

Background: Despite a long history of poor decision making leading to repeated failed phase 3 trials, phase 2 single-arm studies continue to be common in glioblastoma (GBM). With the drawback of inflated false positive rate in current adjustment method for historical control data as concurrent controls, the new statistical methods and validation approach will be needed for adequate covariate adjustment in the GBM single-arm trial data.
Methods: The systematic review was performed to extract the summary-level external data of survival outcomes (mean progression-free survival, mPFS, and PFS at 6 months, PFS6) and prognostic factors (age, gender, extent of resection, KPS, methylation status, and treatment history) from published randomized clinical trials for the standard of care (SOC) treatment in GBM. Four models of the standard, bootstrap aggregating, random subspaces, and random patches models were developed to construct a powerful predictive tool by comprising a series of connections producing survival outputs as a function of prognostic inputs using (1) artificial neural network (ANN) method and (2) linear method (Fig1). The root mean square errors (RMSEs) were calculated to evaluate the model performance using the five-fold cross-validation approach with the effects of ensemble size. The predictive survival outcomes among prognostic factors were calculated to evaluate the relative importance of factors.
Results: We identified 19 Phase 2 and 3 clinical trials in glioblastoma and two survival outcomes and seven prognostic factors (Table1). ANN models have less prediction error and therefore better performance on the test set than linear models. Presumably, the relationships in the data are highly nonlinear, and thus linear models cannot capture these relationships (Table2). Bagging models typically outperform their standard counterparts for both ANNs and linear models. Ensemble methods can capture many trends within the data by manipulation of the training set and are therefore less prone to biases of individual models exacerbated by the small sample size. The previous treatment history and methylation status were the top two influential prognostic factors for both mPFS and PFS6, followed by the extent of resection and mean age (Fig2). With the examination of the ANN parameters of sample size, learning rate, training hyperparameters, it could be observed that there is no clear change in error when increasing sample size beyond 10 (Fig3).
Conclusions: High failure rate of phase 3 glioblastoma trials emphasizes the need for greater reliability of earlier studies in phase 2 single-arm trials. The proposed statistical and epidemiologic approach based on the ensemble-based ANN models will be an effective tool to lead to better decision with phase 2 single-arm trials, which may give better chance to appropriately advance to phase 3 trials with higher predictive power.

#2389 Empowering early drug development in neoadjuvant non-small cell lung cancer studies using an innovative proof-of-concept platform trial design.

Z. Chen, P. A. Dennis, J. Lin;
Sanofi US Services Inc., Cambridge, MA

Several platform trial designs have recently been proposed in oncology. However, developing an efficient one in the neoadjuvant non-small cell lung cancer (NSCLC) is not easy due to the difficulties in patient recruitment and limited relevant data. These obstacles hinder the inclusion of a control arm, thereby losing the ability to make an informed Go/No-Go decision, and to assess prognostic and predictive biomarkers. To overcome these challenges, we have developed an innovative and efficient proof-of-concept platform trial design that aims to empower drug development in early stage of neoadjuvant NSCLC. The proposed platform trial incorporates available experimental agents, allowing for new agents to be added when available. Within the master protocol structure, a small control arm is included, only about 20% of experimental arm size, and is shared by all experimental arms for the analysis purpose. Consequently, the resulting direct comparison with the control arm enables an informed Go/No-Go decision-making, while the total sample size and budget impacts are minimized. The flexibility of Go/No-Go decision-making is further enhanced in a 3-outcome decision-making framework where a consider zone is introduced for physicians to examine the totality of data. Two innovative statistical techniques are incorporated: Bayesian dynamic borrowing for current control, and response-adaptive randomization (RAR). The former helps reduce the sample size, and the latter aims to optimize patient allocation and improve the ability to identify promising agents. Simulation results demonstrate that the direct comparison sharply reduces the false positive rate below 10%, compared to a single-arm design setting. The effective sample size of the control arm is statistically augmented through Bayesian dynamic borrowing. The patient allocation is guided based on the agent's efficacy data with a well-calibrated RAR. The promising agent receives meaningfully more patients than if a fixed-randomization is used, while the variability in patient allocation is decreased. Compared to a traditional design, our innovative design boosts the probability of identifying promising agent by up to 2-fold. To conclude, this research develops an innovative platform trial design to improve the success of drug development in early stage NSCLC. The master protocol structure, inclusion of a small control arm, and dynamic borrowing, increase the plausibility of conducting a trial in the neoadjuvant population. Advanced statistical features optimize the patient allocation and enhance the ability to identify promising drugs. Lastly, the proposed design can be easily applied to other oncology indications with appropriate modifications.

#2390 Longitudinal assessment of circulating tumor DNA in patients with advanced colorectal cancer: A proposed general statistical framework and visualization tool.

C. R. Pretz, J. Liao, L. Drusbosky, A. Das;
Guardant Health, Palo Alto, CA

Background: Understanding how ctDNA levels change over time can act as a surrogate marker for disease progression. Since ctDNA evolution is complicated—exhibiting variability within and between patients—we propose a rigorous and flexible statistical framework that comprehensively represents these types of time-varying biomarkers. We propose employing a hierarchal random effects cubic spline model due to its advantages over traditional longitudinal modeling approaches such as the former's ability to incorporate patient characteristics and create patient-specific results. Visualization of individual patient trajectories may provide clinical utility in precision oncology settings.

Methods: 167 patients with CRC were selected from GuardantINFORM, a real-world database linking genomic and claims data. All patients received chemotherapy and had at least three serial liquid biopsy tests completed via Guardant360. To meet model assumptions, ctDNA levels, measured by maximum variant allele frequency on each test, were transformed into logits. Due to the model's hierarchal structure, an unconditional cubic spline model was fit first, producing an estimated response pattern for the cohort. Next, as patient-level results are of interest, the unconditional model was built upon by fitting a conditional model that incorporated covariates consisting of demographic, health status, and mortality information, which provided numerous patient-level response patterns. The best fitting conditional model was guided by Akaike's information criteria.

Results: Since model parameter estimates are uninterpretable, and because numerous patient-level projections are generated (each covariate value combination produces a unique projection), an R-Shiny application was developed to visually present and compare results in an intuitive interactive fashion. Additionally, to enhance the understanding of patient response patterns, velocity plots, which provides the instantaneous rate of change in ctDNA levels at different time points, are also provided.

Conclusions: We demonstrate that the proposed method can successfully be applied to genomic data to describe and explore complex patient-level temporal ctDNA patterns while accounting for the impact of covariate values have on these patterns. We implemented the proposed methodology as a visualization tool that can be used in a wide variety of settings, ranging from hypothesis testing in clinical trials to patient monitoring. Results from the model can further our basic conceptualization of ctDNA dynamics and enhance our ability to integrate these results into targeted, patient centric, clinical decision-making.

#2391 Towards better prediction of treatment resistance: Directly modeling progression from multiple lesions.

S. Protich[1], M. Stoddard[2], **L. Yuan**[2], D. White[3], D. Bottino[4], A. Chakravarty[2];
[1]PHP Agency Inc, Brentwood, CA, [2]Fractal Therapeutics, Inc., Lexington, MA, [3]Independent Researcher, Atlanta, GA, [4]Takeda Pharmaceuticals, Inc., Cambridge, MA

Late-stage cancers in the clinic present as a set of dispersed tumors, each with distinct growth kinetics. As most patients enrolled in trials of experimental anticancer therapeutics have late-stage malignancies, it is important to understand the impact of data analysis methodologies on the ability to detect treatment effect. In particular, we are interested in the potential risk posed by aggregating individual tumor measurements from multiple-lesion clinical data into a single tumor burden measurement, as this may cause a loss of information. In this work, we use quantitative modeling to assess how analyzing multiple lesions separately versus using an aggregated readout affects tumor response and detection of progression free survival and relapse. To assess the impact of data aggregation, we built a two-population clonal dynamics model consisting of sensitive and resistant tumor cells undergoing growth in the presence or absence of treatment. We performed parameter sweeps to assess the impact of individual model parameters on progression free survival and relapse. We then extended these sweeps to the multi-lesion situation, using nonlinear regression to compare parameter values of aggregated models and the parameter values of the individual models that comprised it. From our simulations, the most influential parameters in determining rebound are the growth rate of the resistant cells and the fraction of these cells, while growth rate of sensitive cells and growth rate inhibition affect effectiveness of treatment. In analyzing the multiple lesion model in different situations, we found that estimates for progression free survival were significantly more sensitive when the lesions were analyzed separately, rather than being aggregated. Our work suggests that aggregating the lesions into a single readout loses impact of individual lesion growth rate inhibitions, impairing early detection as the ability to detect fast growing, small, resistant lesions (despite overall tumor burden decreasing) is lost. Taken together, our findings suggest that data aggregation causes a loss of information. Relapse can be predicted at earlier times when using the multiple lesion model compared to an aggregated model.

#2392 Use of early dynamics of clinical and laboratory parameters to predict resistance in patients with metastatic urothelial carcinoma receiving post-platinum atezolizumab.

Christopher Graser[1], Thomas O. McDonald[1], Guru Sonpavde[2], Franziska Michor[1]

[1]Dana-Farber Cancer Institute, Boston, MA,[2]AdventHealth Cancer Institute, Orlando, FL

Background: Substantial variability exists in outcomes of patients with metastatic urothelial carcinoma (mUC) receiving PD1/PD-L1 inhibitors. Unfortunately, there is an absence of optimal predictive biomarkers of refractory disease. We hypothesized that with a combination of baseline and early-on-treatment (EOT) parameters we can distinguish patients who will respond from those who will have refractory disease. We investigated readily available baseline and EOT variables from the phase 3 clinical trial IMvigor211, which compared atezolizumab, a PD-L1 inhibitor, with chemotherapy (taxane or vinflunine), in patients with mUC who have progressed on platinum-based chemotherapy.

Methods: Of 931 patients in IMvigor211, 902 were evaluable for our analysis. We built logistic regression models for both atezolizumab and chemotherapy to predict the clinical endpoint of risk of treatment failure defined as progressive disease as best response. We used LASSO to select covariates from an array of clinical (e.g. metastatic site, performance status, prior therapy) and laboratory variables (e.g. albumin, hemoglobin, PD-L1 expression) measured before treatment, and EOT 3-6 weeks after starting therapy. Moreover, we used our models to identify clinical features that are differentially associated with outcomes in response to either therapy.

Results: Based on pre-treatment information, our baseline model achieves a predictive accuracy for treatment failure of AUC = 0.69 for both therapies. The strongest baseline predictors are PD-L1 expression, prior treatment with both cisplatin and carboplatin, and the presence of liver metastases. Moreover, higher TNM-stage of the primary tumor is strongly predictive of worse treatment outcomes for atezolizumab but not for chemotherapy. After the first treatment cycle (3 weeks), the predictive accuracy of the model increases to AUC = 0.83 with differences in importance of variables between the atezolizumab- and chemotherapy-treated patients. No variable stood out as a dominant predictor in the EOT model, with 14 variables significant at p=0.05. We found that 66% of patients have a lower predicted risk of treatment failure for atezolizumab than for chemotherapy at baseline. Our EOT model suggests that 36% of patients treated with atezolizumab would benefit from switching to chemotherapy after the first cycle.

Conclusions: Our prediction models employing readily available and affordable EOT clinical and laboratory variables robustly (AUC 0.83) identified patients with early resistance and may inform patient-specific therapeutic decisions. Further validation is required.

#2393 Development of a novel implantable drug-eluting product for the local treatment of pancreatic adenocarcinoma.

M. Lashof-Sullivan[1], L. S. Sloan[1], M. P. Kim[2], **L. Indolfi**[1], C.-W. D. Tzeng[2];
[1]PanTher Therapeutics, Austin, TX, [2]The University of Texas MD Anderson Cancer Center, Houston, TX

Background Local control of non-metastatic pancreatic ductal adenocarcinoma (PDAC) remains a major challenge. Therapies with reduced systemic toxicity are needed as intravenous (IV) infusions are limited by patient tolerance with only small amounts reaching the tumor. PanTher created PTM-101, a novel absorbable drug formulation containing paclitaxel, designed to be locally applied via minimally invasive surgery to provide chemotherapy precisely to the peritumoral area in PDAC.

Methods A study was conducted using 3 cadaveric abdomens to evaluate surgical feasibility of delivering PTM-101 via laparoscopy. Prior to insertion of PTM-101 into the peritoneum, the surgeons prepared each product by suturing a 3-0 Vicryl SH (Ethicon) at four evenly spaced locations around the edge of the flat circular product. A periumbilical 10mm Hasson port was placed to insufflate the abdomen, followed by placement of 3 additional working ports (5mm). The liver capsule was carefully surveyed to exclude metastatic disease. The surgeons opened a window into the lesser sac through the greater omentum, lifting the stomach up from the transverse colon to expose the pancreas. PTM-101 (a 1mm thick and 6cm diameter film) was rolled into a tubular shape, inserted through the cannula, and affixed to the peri-pancreatic fat with existing vicryl stitches.

Results The estimated total operative time from placement of the first trocar to removal of all equipment was 45 minutes, for the 3 procedures. The operations included 25 minutes for entry, port placement, exposure of the simulated pancreatic tumor location and 20 minutes to place and suture PTM-101. PTM-101 was easy to fit through the cannula and was sutured without difficulty to the peri-pancreatic fat that surrounds the capsule of the pancreas. To simulate a tumor with hepatic artery involvement, the implant was sutured towards the hepatoduodenal ligament in one specimen, near the area of the gastroduodenal artery takeoff, proper hepatic artery, and proximal portal vein. PTM-101 covered the entire head/neck area of the simulated tumor locations without requiring disruption of the tumor area or dissection of the tunnel under the pancreatic neck.

Conclusion PTM-101 is flexible and conforms easily to the underlying topography, both in a concave (i.e., with the tumor intact) and convex (i.e., after resection) scenario. Although human anatomy does not allow for PTM-101 to completely wrap around the pancreas, the size and flexibility of the product enables it to “drape” over the edges covering areas near the superior mesenteric vein and artery (SMV/SMA). This placement could hypothetically increase the amount of drug reaching the area behind the pancreas to target tumors which abut or encase the mesoportal vasculature. A decrease in the tumor-vessel interface could downsize pancreatic tumors, with the goal of increasing resection rates and post-resection local control.

#2394 Significance of regional lymph node dissection in patients with clear cell sarcoma and epithelioid sarcoma.

T. Takemori, E. Kobayashi, S. Iwata, K. Ogura, S. Osaki, S. Fukushima, A. Kawai;
Department of Musculoskeletal Oncology and Rehabilitation, National Cancer Center Hospital, Tokyo, Japan

Objective Clear cell sarcoma (CCS) and epithelioid sarcoma (ES) are common as soft-tissue sarcoma subtypes causing lymph node metastasis (LNM), but the role of regional lymph node dissection is still unclear especially in these patients without imaging evidence of LNM. Here we retrospectively investigated the significance of lymph node dissection for patients with CCS and ES. Methods Forty-one patients (CCS: 13, ES: 28) with no distant metastasis other than in the regional lymph nodes were enrolled in this study. Of these 41 patients, those without LNM on imaging findings were categorized into two groups: "with dissection (WD)" group and "no dissection (ND)" group, respectively. Overall survival (OS), lymph node metastatic-free survival (LNMFS), progression-free survival (PFS), and post-operative LNM rate were compared between two groups. Results There were 26 patients who had undergone regional lymph node dissection and 15 patients who had not undergone regional lymph node dissection (ND group). Histopathological examination revealed metastasis to the lymph nodes in 9 of the 26 patients (38.5%). 9 patients were suspected of having LNM based on preoperative imaging findings such as CT or FDG PET/CT. Among the remaining 17 patients (WD group) in whom LNM was not suspected based on preoperative imaging findings, 6 patients (35.3%) had LNM. OS ($p=0.03$), LNMFS ($p<0.01$), and PFS ($p<0.01$) were all significantly better in the WD group. The postoperative LNM rate was significantly lower in the WD group than in the ND group ($p=0.03$), and there were no significant differences in OS, LNMFS, or PFS between the CCS and ES groups in terms of histological type. Discussion Even in cases where LNM was not suspected on preoperative imaging, LNM was present in more than 30% of cases. The possibility of regional LNM should be borne in mind in soft-tissue sarcomas, which frequently present with LNM, regardless of imaging findings. We also suggested that simultaneous dissection of the regional lymph nodes at the time of resection of the primary tumor improves the prognosis. Although ES and CCS are ultra-rare sarcomas, further validation with the accumulation of case series is desirable.

#2395 Camrelizumab combined with apatinib and hepatic artery infusion chemotherapy (HAIC) as conversion therapy for patients with unresectable hepatocellular carcinoma(HCC): A single-arm exploratory clinical study.

L. Zhao, B. Zhang, X. Shi, K. Cui, J. Zhang, J. Zhong, Z. Li, P. Sun, C. Zhang, L. Li;
Shandong Cancer Hospital, Jinan, China

Background: There is still no standard treatment recommendation for hepatocellular carcinoma transformation therapy, and researches are still under exploration.
Methods: This study was a single-arm phase II trial, eligible patients had histologically or cytologically confirmed unresectable HCC, without extrahepatic metastases and multiple diffuse liver lesions. Patients received camrelizumab and apatinib combined with HAIC for 2-8 cycles followed by surgery after evaluation. Primary endpoints were radiographic assessment of conversion rate and radical (R0) resection rate. Secondary endpoints were pathologic complete response rate (pCR) , objective response rate (ORR) by modified RECIST (mRECIST) and RECIST version 1.1(RECIST v1.1) and safety.
Results: Between March 17, 2021 and July 28, 2023, 22 patients were enrolled, including 9 (40.9%) patients with BCLC stage A, 2 (9.1%) patient with B, and 11 (50%) patients with C, 9 (40.9%) patients had tumor thrombus. Patients received treatment of a median of 2 cycles (range: 1-6 cycles). All 22 patients were included in thte safety set, before the first scheduled post-baseline tumor assessment, one patient changed treatment plan because of live function damage, three patients were failed to return to hospital for treatment because of civid-19. At the data cut off on 23 November, All other 18 patients conducted at least one efficacy evaluation, 8(44.4%) of 18 patients had an objective response and 16(88.9%) had disease control according to RECISIT v1.1, 3(16.7%) had a complete response, 9(40.9%) had a partial response and 18(88.9%) had disease control according to m RECIST. 15(68.2%) of 22 patients could undergo surgical resection based on imaging evaluation. 7 patients failed to undergo surgery due to CR (3patients), abnormal liver function(1 patient), immune myocarditis(1 patient), patient rejection(1 patient) waiting for surgery(1 patient). Resection was completed in 8 (44.4%) patients, and the R0 resection rate was 100%. The pCR rate in the surgery population was 25%, and the MPR rate is 37.5%. The most common grade 3 adverse events were increased alanine aminotransferase (36.3%) and decreased lymphocyte count (36.3%). A case of grade 4 immune-associated myocarditis occurred. No grade 5 treatment-related toxicity occurred.
Conclusion: Camrelizumab combined with apatinib and HAIC showed promising activity and manageable toxicity, and might be a potential conversion treatment option for patients with unresectable HCC.

#2396 Tumor treating fields (TTFields) for spinal metastasis: Clinical trial concept for use of conductive implants as waveguides to enhance TTFields strength.

C. E. Tatsui[1], K. W. Carlson[2], C. B. Patel[1];

[1]The University of Texas MD Anderson Cancer Center, Houston, TX, [2]Carlson Research LLC, Concord, MA

Tumor treating fields (TTFields) is a FDA-approved electric fields-based therapy for glioblastoma (GBM) and malignant pleural mesothelioma. We describe a novel approach to increase the strength and therapeutic effect of TTFields at vertebral tumor targets, using spinal implants as electrically-conductive waveguides. In vivo anti-cancer efficacy is achieved with TTFields strength >1 V/cm. If the tumor is surrounded by tissues of lower conductivity (e.g., the skull in the case of GBM), then the TTFields strength reaching the tumor is decreased. Surgical treatment of radiation-refractory spinal metastases is difficult and provides a short-term benefit at the expense of a lengthy recovery. Such resections require bone removal that disrupts the spinal stability, necessitating reconstruction with titanium (Ti) pedicle screw constructs that are electrically conductive. We theorize that astute placement of Ti hardware in the proximate spinal levels post-resection would have a waveguiding effect of electrical current from the surrounding muscle towards the tumor. This would in turn boost TTFields strength achieved around the resection cavity, decreasing the chances of tumor recurrence. Bomzon et al. described a computational model of the distribution of TTFields in a realistic human torso. The simulation demonstrated that a TTFields strength of 3 V/cm can be achieved, which is approximately 3-fold greater than what is achieved in the brain parenchyma in the context of TTFields for GBM. In a more generic simulation using a 0.5 × 100 mm waveguide targeting a tumor deeper in the torso (480 mA), we found 21.8 vs. 61.2 cm^3 volumes achieving ≥ the 1.0 V/cm efficacy floor, without and with the waveguide, respectively, a 2.8-fold increase. At a higher amplitude (550 mA) and stronger TTFields strength threshold of ≥1.5 V/cm, a negligible volume was attained with no waveguide (0.1 cm^3), whereas a volume of 17.6 cm^3 was attained around the tip of the waveguide when present. Based on compelling pre-clinical data, a prospective clinical trial is being designed in which patients with radiation-refractory spinal metastasis from any number of primary sites will undergo resection. Next, primary cultures of their tumor cells will be made and evaluated for the TTFields frequency that maximizes cell death on a per-patient basis. Patients will then undergo postoperative local TTFields therapy ± systemic therapy. The primary endpoint will be safety and efficacy of such an approach, with future aims focusing on local control rates. The application of TTFields as an adjunct to surgery may offer a new therapeutic option for patients with spinal metastasis who would otherwise not be considered surgical candidates. Similarly, waveguides may be used throughout the head and body to increase TTFields efficacy.

#2397 Double lung transplantation (DLT) in patients with stage IVA lung-limited non-small cell lung carcinoma (NSCLC): A case series.

Y. Chae, T. Demir, L.-Y. Chung, C. Moloney, R. Tomic, A. Bharat;
Northwestern Univ. Feinberg School of Medicine, Chicago, IL

Introduction: Despite technological advances and expanded indications in lung transplantation, lung cancer constituted less than 0.1% of the lung transplantation over the past two decades. DLT may offer curative treatment for stage IVA NSCLC patients without extrapulmonary disease. We present a case series of consecutive NSCLC patients who underwent DLT.

Methods: Patients treated with DLT were identified between 09/2021 and 09/2023 at Canning Thoracic Institute of Northwestern University. All patients had enrolled in the DLT registry aimed for lung-limited malignancies (DREAM) study (NCT05671887). Exclusion criteria include: presence of extrapulmonary disease and medical ineligibility for lung transplantation. All patients were followed up with computed tomography and tumor-informed ctDNA assay every 12 weeks.

Results: Five patients with stage IVA NSCLC who underwent DLT were included. Three (60%) patients had invasive mucinous, and two (40%) had invasive non-mucinous adenocarcinoma histology. One of the two invasive non-mucinous patients had acinar, and the other had mixed lepidic, papillary, and acinar histology. Patients were aged 56-70; one (20%) was Asian, four (80%) were White, three (60%) were male, and two (40%) had a history of smoking. No patient had a past medical history of interstitial lung disease (ILD) or chronic obstructive pulmonary disease (COPD). All patients had high oxygen requirements before DLT due to cancer progression. Pre-transplant endobronchial ultrasound and evaluation of bilateral pneumonectomy lungs found no lymph node involvement (pN0). One patient had an epidermal growth factor receptor (EGFR) mutated cancer and but had failed relevant targeted therapy prior to transplant. All patients had disease progression on standard of care treatments with/without clinical trials. The indication for DLT was respiratory failure or refractory cancer for all patients. After DLT, one patient had a recurrence of the disease at 18 months with a 1cm solid nodule and was treated with stereotactic body radiotherapy (SBRT). Both original and recurrent tumors had invasive mucinous adenocarcinoma histology, negative PD-L1 expression, and the same JAK3 c.2174C>T, P725L mutated clone. It suggests that the recurrence likely arose from the original cancer. Transplant rejection did not occur in any of the cases. Following the transplant, there was no requirement for oxygen therapy for any patient. All patients are alive with 25, 15, 6, 3, and 1-month posttransplant follow-up.

Conclusion: Five patients underwent DLT successfully without significant complications. Notably, one patient (25 months post-transplant) experienced cancer recurrence 18 months post-transplant and was effectively treated with SBRT. Ongoing DREAM study will continue to investigate the role of DLT in stage IVA NSCLC patients (especially in pN0).

#2399 Stage-matched prognosis comparison between ypTNM and pTNM stage in pancreatic cancer.

H. Kim, H. Chae, S. Lim, H. Jeong, S. Yoon, S. Shin, I. Han, J. Heo, H. Kim;
Samsung Medical Center, Seoul, Korea, Republic of

Introduction: The prognostic significance of pathological stage in pancreatic cancer is well-established. The 8th American Joint Commission on Cancer (AJCC) TNM staging introduced the ypTNM stage for neoadjuvant treatment (NAT) patients responding to the increased use of NAT. Despite this, there has been no comparative assessment of the prognosis between ypTNM and pTNM stages in pancreatic cancer. This study aimed to evaluate and compare the prognoses between ypTNM and pTNM stages in surgically resected pancreatic cancer.

Method: A cohort of 586 patients who underwent pancreatic cancer surgery at a tertiary center from January 2018 to March 2022 was analyzed. Exclusions comprised those with prior pancreatectomy, suspicious liver metastasis or peritoneal seeding before NAT, those with open biopsy, R2 resection, and distant metastasis during operation, and postoperative mortalities or immediate follow-up losses. Clinicopathologic demographics underwent analysis, and a propensity score-matched (PSM) analysis (1:3) was conducted based on factors influencing overall survival (OS) in multivariate analysis. Subgroup analyses, categorized by stage, compared survival between ypTNM and pTNM stages.

Results: The analysis included 541 patients, with 100 undergoing NAT (ypTNM) and 441 opting for upfront surgery (pTNM). Comparable OS was observed between ypTNM and pTNM patients (median 51.0 vs. 46.0 months, 3-year survival rate (YSR) 68.7% vs 56.3%, $p = 0.094$). Subgroup analysis by stages I (3YSR 76.8% vs 67.5%, $p = 0.577$), II (56.2% vs 53.0%, $p = 0.715$), and III (26.5% vs 28.7%, $p = 0.596$) revealed similar survival between ypTNM and pTNM. Multivariate analysis identified factors such as age >65 (HR 1.651, $p = 0.002$), CA19-9 >150 (HR 1.476, $p = 0.010$), preoperative biliary drainage (HR 1.372, $p = 0.048$), pathologic T2 stage (HR 2.188, $p = 0.002$) and T3, 4 stage (HR 3.178, $p < 0.001$) compared to T0, 1 stage, lymphovascular invasion (HR 2.087, $p < 0.001$), and adjuvant treatment (HR 0.243, $p < 0.001$) associated with OS. After PSM analysis, stages I (3YSR 76.8% vs 71.7%, $p = 0.923$), II (56.2% vs 46.6%, $p = 0.886$), and III (26.5% vs 31.4%, $p = 0.856$) exhibited no significant difference in OS between ypTNM and pTNM stages.

Conclusions: Our study underscores comparable survival outcomes between ypTNM and pTNM stages in surgically resected pancreatic cancer, affirming the applicability of the TNM staging system after NAT. Consistent survival results, even following PSM analysis, highlight the reliability of TNM staging for guiding therapeutic decisions even in patients with NAT.

#2400 Determinants of early recurrence in surgically-resected colon cancer: A multi-omics analysis.

S. Al-Aomar[1], H. Abushukair[1], A. Zaitoun[1], S. Zytoon[2], S. Illeyyan[1], H. Almomani[2], G. Al-Majali[1], A. Hammad[1], K. Obeidat[1], F. Turfah[3], A. Shahait[4], F. Ali[5]; [1]Jordan University of Science & Technology, Irbid, Jordan, [2]Yarmouk University, Irbid, Jordan, [3]Corewell Health, Dearborn, MI, [4]Southern Illinois University, Carbondale, IL, [5]University of Texas Southwestern, Dallas, TX

Introduction: Colon cancer is the third most common cancer worldwide. The mainstay treatment for localized disease is surgical resection, often followed by adjuvant chemotherapy in stage III patients, and stage II patients with high-risk features. Unfortunately, some patients experience early local and/or distant recurrence. Besides classic anatomical/pathological tumor features, insight into the genomic determinants of early recurrence in colon cancer is lacking. Herein, we utilize a multi-omics approach to identify early-recurrence-specific features that could aid in more accurate risk stratification.

Methods: We utilized the Cancer Genomic Atlas Colon Adenocarcinoma (TCGA-COAD) Database. Clinical, histopathological and genomic data were retrieved through the cBioPortal database. Our analysis was limited to patients with stage 2 or 3 (n = 390) disease based on the American Joint Committee on Cancer Code. Early recurrence (ER) was defined as disease relapse/recurrence within 12 months of sample acquisition post-surgery. Accordingly, patients were categorized into the ER and non-early recurrence (NER) groups based on a cut-off point of 12 months of disease-free survival.

Results: The colon cancer ER and NER group included 45 and 345 patients, respectively. Comparable age, sex and race percentages were found between both groups. The ER group had significantly worse overall, progression-free, and disease-specific survival (HR: 0.083 95% CI: 0.031-0.220, HR: 0.035 95% CI: 0.011-0.0109, HR: 0.021 95% CI: 0.006-0.076, respectively). ER patients had a significantly higher proportion of patients with T4 and N2 disease based on the TNM staging system. ER patients had significant (P< 0.05) expression of TRIM46, TRPC4, ELOVL7, CSMD1, BCLAF1, and CD70 mutations, while tumor mutational burden was comparable between both groups (median TMB in ER vs NER: 4.2 vs 3.62, p = 0.28). Differential gene expression analysis revealed 68 genes to be upregulated in the ER group which were found to be enriched in hypoxia and interleukin-11 pathway genes. Genes upregulated in the NER group (n = 49) were enriched in interferon-alpha response and glycolysis/gluconeogenesis pathway genes. Proteomics analysis revealed significantly higher levels of EIF4E, CCNE1, SRSF1, SCD, and PECAM1 proteins in NER patients

.Conclusion: Our results highlight insights into molecular and genomic features unique to colon cancer patients with early recurrence. Understanding such predictors for early recurrence will aid in risk stratification and help in determining patients who would derive the most benefit from adjuvant treatment considerations.

#2401 Changes in skeletal muscle mass after gastrointestinal cancer surgery by body composition.

Y. Maeda, Y. Miyamoto, M. Ohuchi, Y. Hiyoshi, N. Yoshida, H. Baba;
Kumamoto University, Kumamoto, Japan

Background: Previous studies have extensively explored the correlation between preoperative skeletal muscle mass and long-term survival in gastrointestinal cancers. However, investigations into postoperative skeletal muscle mass alterations are limited. In gastrointestinal cancers, factors such as the tumor and surgical interventions can significantly impact dietary intake, nutritional status, and skeletal muscle mass, affecting postoperative body composition. This study aimed to examine these postoperative changes in skeletal muscle mass across different gastrointestinal cancers, including esophageal, gastric, and colorectum.
Methods: This study encompassed 969 patients with Stage I-III esophageal (307 cases), gastric (278 cases), and colorectal (384 cases) cancers who underwent radical resection between 2005 and 2019. Skeletal muscle mass was quantified as the total psoas volume (TPV), measured using Ziostation2® imaging software from preoperative and postoperative CT scans at 1, 2, and 3 years. The study compared postoperative TPV trends across the different cancer types.
Results: The study cohort comprised patients with esophageal (median age 66 years, 85% male), gastric (65 years, 60%), and colorectal cancers (67 years, 55%). Median BMIs were 21.5, 19.4, and 22.6 kg/m^2, and median TPVs were 352.0, 305.8, and 309.5 cm^3 for esophageal, gastric, and colorectal cancers, respectively. Esophageal cancer patients had significantly higher TPV and male predominance, while gastric cancer patients had notably lower BMI. Relative to preoperative TPV, the postoperative TPV at three years was 0.92, 0.91, and 0.96 for esophageal, gastric, and colorectal cancers, respectively. A year-by-year decrease in TPV was observed for each cancer type, with colorectal cancer demonstrating a less pronounced decrease compared to esophageal and gastric cancers ($p<0.01$). Stage-wise analysis revealed no significant differences among the cancer types. Regarding gender, no significant differences were noted between gastric and colorectal cancers, but esophageal cancer showed a more marked decrease in TPV in males compared to females. In recurrent cases, no significant TPV differences were observed in esophageal cancer, while recurrent gastric and colorectal cancers exhibited significant TPV decreases.
Conclusions: The study indicates a general decline in TPV following gastrointestinal cancer surgery, with the extent of reduction varying according to the type of tumor and treatment.

CLINICAL RESEARCH: Circulating Nucleic Acids 2
Poster Session

#2405 Harnessing liquid biopsy and genetic barcoding in evaluating diversity within triple-negative breast cancer.

D. Ceresa[1], **B. Cardinali**[1], A. Daga[1], R. Tasso[2], A. Sciutto[1], I. Appolloni[2], D. Marubbi[2], F. Carli[1], P. Fregatti[1], P. Malatesta[2], L. Del Mastro[1];
[1]IRCCS Ospedale Policlinico San Martino, Genova, Italy, [2]Universita di Genova, Genova, Italy

Introduction: While liquid biopsy shows promise as a non-invasive precision medicine tool, its ability to comprehensively represent the complexity of a tumor or only a subset of its clones remains uncertain. This issue is particularly crucial in the context of triple-negative breast cancer (TNBC), a type of cancer known for its significant heterogeneity. The goal of this study is to examine the clonal diversity within Circulating Biomaterials (CBMs): namely circulating tumor cells (CTCs), extracellular vesicles RNA (evRNA), and circulating tumor DNA (ctDNA), employing genetic barcoding and patient-derived TNBC xenografts.
Methodology: Cells from TNBC patients' resected tumors were tagged with a unique barcode sequence through vector transduction. These barcoded cells were subsequently introduced into immunodeficient mice to form xenografts. When these xenografts grew to a certain size (15mm in diameter), the mice were humanely euthanized, and the tumor tissues as well as CBMs from their blood and plasma were collected. CTCs were isolated through negative enrichment and DEPArray technology; evRNA was extracted using ultracentrifugation and TRIzol™ Plus RNA Purification method; ctDNA was retrieved using the QIAamp DNA Micro Kit. Tumor tissues were processed for RNA and DNA using RNeasy micro kit and Qiamp DNA micro kit, respectively. RNA sequencing of the tumor tissues was carried out using the Lexogen - CORALL Total RNA-Seq Kit and Illumina NextSeq high output reagents.
Results: Analysis of xenografts from four patients showed that ctDNA was the predominant genetic material detected through liquid biopsy. Crucially, clonal analysis using Next Generation Sequencing (NGS) demonstrated that ctDNA provides an accurate reflection of the primary tumor's clonal heterogeneity. The method efficiently identified both main tumor clones and subclones, even those constituting as little as 1% of the tumor, with a 50% detection probability. Transcriptomic analysis of the tumor tissues uncovered a distinct mesenchymal and pro-metastatic signature, more pronounced in tumors with higher ctDNA release. Clonal analysis of CTCs and evRNA is still ongoing.
Conclusions: This investigation affirms the effectiveness of ctDNA analysis in liquid biopsy for identifying subclonal diversity in TNBC. Our results suggest that liquid biopsy via ctDNA is capable of managing TNBC's extensive intra-tumoral heterogeneity, including the identification of smaller subclones. Furthermore, a link was identified between the release of ctDNA and a mesenchymal, prometastatic gene expression pattern in the tumors.

#2406 Circulating tumor DNA as a potential indicator of treatment response in patients with surgically unresectable PDAC.

F. Pittella Silva[1], Y. Kimura[2], M. Motoya[2], T. Nakamura[3], T. Murakami[2], K. Watanabe[3], S.-K. Low[4], Y. Nakamura[4];
[1]University of Brasilia, Brasilia, Brazil, [2]Sapporo Medical University School of Medicine, Sapporo, Japan, [3]Hokkaido University, Sapporo, Japan, [4]Japanese Foundation for Cancer Research, Tokyo, Japan

Pancreatic ductal adenocarcinoma (PDAC) is a highly heterogeneous and extremely aggressive neoplasm. Most patients with PDAC present with symptomatic, surgically unresectable disease at initial diagnosis. Systemic chemotherapy is the standard care for patients diagnosed with unresectable PDAC, despite the dismal survival rate due to disease recurrence. In this context, liquid biopsy based ctDNA monitoring may aid to improve detection accuracy and allow real time disease prognosis. Here we aimed to investigate the utility of ctDNA in longitudinal tumor monitoring to assess treatment response and to predict disease recurrence. We performed targeted NGS sequencing to investigate over 900 mutations (SNVs) and 12 copy number variations (CNVs) in 53 genes, using the Ion S5 Oncomine PanCancer gene panel in 40 PDAC patients with unresectable disease. Serial plasma samples were obtained from patients in the course of 24 months, including samples collected before the first intervention (baseline) as well as within 2 months after initiation of chemotherapy. Patients were followed for a period of up to 2-years from diagnosis through treatment, to death or final follow-up. Genomic DNA from paired plasma-buffy coat samples were sequenced to exclude clonal hematopoiesis. Overall detection of ctDNA alterations in baseline samples was 55% (22/40) with increasingly higher detection rates and mutation loads in advanced disease (88% in stage IV patients). Alterations including SNVs and CNVs were preferentially distributed among 9 genes; mutations in *TP53* (45%), *KRAS* (38%) and *SMAD4* (5%) were most commonly identified. To asses response to chemotherapy, the presence of residual ctDNA after clinical intervention was evaluated by comparing total ctDNA MAF (mutant allele frequency) detected in plasma at diagnosis and within 2 months of chemotherapy. 71% (17/24) of patients who reached progressive disease (PD) had detectable baseline mutations and 79% (19/24) had persistent residual mutations at 2 months of treatment. Conversely, 94% (15/16) of non-PD patients had no detectable ctDNA or had a significant reduction in total MAF after 2 months of chemotherapy. Absence of residual ctDNA after 2 months of chemotherapy was associated with a better OS (p=0.031; HR = 3.48). On the other hand, residual ctDNA after 2 months of chemotherapy was associated with a shorter PFS (p=0.042; HR = 3.28). Our study demonstrates that monitoring ctDNA levels derived from plasma provides valuable insights into the therapeutic response in patients with unresectable PDAC, even in the absence of matched tumor genotyping. We found a significant correlation between increased ctDNA levels following the initiation of treatment and poorer survival outcomes.

#2407 Detection of hotspot *PIK3CA* mutations in primary tumors and plasma-cfDNA of breast cancer patients using a novel highly sensitive CE-IVD kit.

S. Smilkou[1], D. Stergiopoulou[2], E. Tzanikou[2], L. Kaklamanis[3], I. Balgkouranidou[4], H. Linardou[5], F. Zagouri[6], E. Razi[7], S. Kakolyris[4], A. Psyrri[8], C. Papadimitriou[9], I. Koukli[2], **A. Markou**[1], E. Lianidou[1];

[1]National & Kapodistrian University of Athens, Athens, Greece, [2]Pharmassist Ltd, Athens, Greece, [3]Onassis Cardiac Surgery Center, Athens, Greece, [4]University General Hospital of Alexandroupolis, Alexandroupolis, Greece, [5]Metropolitan Hospital, Athens, Greece, [6]Alexandra Hospital, Athens, Greece, [7]Hygeia Hospital, Athens, Greece, [8]Attikon University Hospital, Athens, Greece, [9]Aretaieio University Hospital, Athens, Greece

Introduction: Detection of *PIK3CA* mutations in primary tumors (FFPEs) and liquid biopsy samples is of increasing importance for treatment decisions in breast cancer. Oncolipsy PIK3CA kit (Pharmassist Ltd, Greece) is based on the combination of allele-specific priming, asymmetric PCR, and melting curve analysis. The CE-IVD kit can detect the presence of four PIK3CA hotspot mutations (E542K, E545K, E545Q, H1047R). The aim of the present study was to: a) evaluate the performance of this novel CE-IVD kit both in FFPEs and plasma-cfDNA samples from patients with metastatic breast cancer (MBC) and b) directly compare the derived results using the Oncolipsy *PIK3CA* kit with the cobas® *PIK3CA* mutation test (CE-IVD, Roche Diagnostics, Germany) in identical gDNAs isolated from FFPEs samples.

Patients and methods: We analyzed 42 primary tumors (FFPEs) and 29 plasma-cfDNA samples from patients with estrogen receptor (ER) positive metastatic breast cancer. Genomic DNA was isolated from FFPEs using the QIAamp DNA FFPE Tissue Kit (Qiagen, Hilden, Germany), while cfDNA was extracted from 2.00 mL of plasma using the QIAamp DSP cNA Kit (Qiagen, Hilden, Germany). *PIK3CA* hotspot mutations were detected in the LightCycler® 2.0 (IVD instrument, Roche Diagnostics, Germany) using the highly sensitive Oncolipsy *PIK3CA* kit (analytical sensitivity 0.05%). A direct comparison study was performed using the cobas® *PIK3CA* Mutation Test on the cobas z 480 analyzer (IVD instrument, Roche Diagnostics, Germany).

Results: In primary tumors the E545K mutation was detected in 22/42 (52.4%), the E542K and H1047R mutations were detected in 11/42 (26.2%) and 4/42 (9.5%) of primary tumor samples, respectively, while the E545Q mutation was not detected in any FFPE sample tested. At least one *PIK3CA* mutation was detected in 14/29 (48.3%) plasma-cfDNA samples. More specifically the E545K mutation was detected in 11/29 (38%), the H1047R mutation in 3/29 (10.4%) and the E542K mutation in 2/29 (6.9%) while the E545Q mutation was not detected in any plasma-cfDNA sample tested. In FFPEs, as expected, *PIK3CA* mutation frequency was higher compared to plasma-cfDNA. Direct comparison of the results derived using these two commercially available kits, the Oncolipsy CE-IVD kit and the cobas *PIK3CA* mutation test, using the same gDNA isolated from 42 FFPEs revealed a concordance of 34/42 (81%).

Conclusions: The commercially available Oncolipsy *PIK3CA* CE-IVD kit is highly sensitive and specific for the detection of four *PIK3CA* hotspot mutations in primary tumors and plasma-cfDNA.

Acknowledgement: This study has been financially supported by the European Union and Greek national funds through the Operational Program Competitiveness, Entrepreneurship and Innovation, under the call RESEARCH - CREATE - INNOVATE (project code: T1RCI-02935).

#2408 Comprehensive genomic profiling of ctDNA reveals distinct genomic signatures and therapeutic implications for immunotherapy response in advanced head and neck cancer.

A. Bharde[1], V. Noronha[2], M. Ratnaparkhi[1], V. Patil[3], B. Jadhav[1], S. Prajapati[1], A. Choughule[2], P. Chandrani[2], S. Haldar[4], F. Moubeen[4], N. Menon[2], K. Hariramani[4], M. Basavalingegowda[1], A. Ramesh[1], J. Khandare[1], P. Chaturvedi[2], G. Shafi[5], K. Prabhash[2];
[1]OneCellDx, Pune, India, [2]Tata Memorial Hospital, Homi Bhabha National Institute, Mumbai, India, [3]Tata Memorial Hospital, Mumbai, India, [4]Indxtechnology, Pune, India, [5]OneCellDx, Cupertino, CA

Background: Head and Neck Cancer (HNC) is highly prevalent malignancy in Southeast Asia. We investigated comprehensive genomic profiling (CGP) of ctDNA, aimed to compare genomic landscapes between responders (R) and non-responders (NR) to immunotherapy among advanced HNC patients.
Methods: An observational study, ctDNA was evaluated in 69 advanced HNC patients both at the baseline (BL) and during follow up (FL). OncoIndx® CGP was used to identify patient-specific genomic alterations in the ctDNA cohort. Raw sequence alignment and variant calling were performed using iCare® software. Progression-free survival (PFS) and overall survival (OS) were assessed using Kaplan-Meier statistics.
Results: Total 250 mutations, encompassing pathogenic (P), likely pathogenic (LP), and variants of unknown significance (VUS), were identified at BL. In FL samples a slight decrease in the overall number of mutations was observed. Loss-of-function (LOF) KMT2C, MSH6 mutations, and activating HNF1α mutations were consistently present at comparable frequencies in BL and FL samples, exhibiting ubiquity across immunotherapy R and NR populations (F test, P 0.00063, OR 13). The variants did not demonstrate statistically significant association with PFS and OS. Most prevalent variants at follow-up emerged from tumor suppressor genes TP53, BRIP1, STAT5B, NF1, suggesting their potential role as therapy-resistant variants. PFS and OS were notably lower for patients with TP53 + BRCA pathway variants compared to their wild-type counterparts (median PFS TP53 + BRCA pathway mutated 2.7 months vs wt 9.1 months, HR = 4.1; median OS TP53 + BRCA pathway mutated 4.7 months vs 12.8 months for wt, HR 7.7). Similarly STAT5B carriers compared to the wild-type STAT5B-bearing population. Multivariate analysis further confirmed the independent role of TP53 + BRCA pathway and STAT5B variants as determinants for worst outcome (P 0.006, HR2.5). Population with prevalent TP53 and STAT5B LOF variants exhibited a strong negative correlation with the PD-L1 score compared to the population with their wild-type counterparts (P 0.03). Average scores for genome-wide homologous recombination deficiency (HRD), bTMB, and loss of LOH were low at BL and FL and did not correlate with the PD-L1 score. Interestingly, bTMB was low for the cohort, Tumor fraction (TF) emerged as an independent prognosticator for OS and PFS.
Conclusions: ctDNA revealed distinct genomic signatures in R and NR populations at BL and FL. Significant prevalence of TP53, BRIP1, STAT5B, and NF1 in the NR population suggest a potential role in conferring immunotherapy resistance. Genomic signatures, TMB and TF impacted survival of immunotherapy responders. Integrating CGP into SOC protocol may help in identifying therapy resistance in advanced HNC patients who did not respond to initial treatment.

#2409 Circulating differential methylation allele fraction (DMAF) strongly correlates with circulating tumor DNA (ctDNA) variant allele fraction (VAF).

P. Srinivasan[1], T.-C. Chen[1], E. Haghshenas[1], M. Kordi[1], I. Tunc[1], W. Chan[1], O. S. Solari[1], J. Babiarz[1], Y. Nakamura[2], T. Yoshino[2], A. Aleshin[1], T. Kawli[1], J. G. Reiter[1];

[1]Natera, Inc., Austin, TX, [2]National Cancer Center Hospital East, Kashiwa, Japan

Measurement of ctDNA has been established as a prognostic biomarker of cancer disease burden. Emerging evidence has demonstrated that differential methylation patterns can serve as an accurate biomarker both for cancer detection and for predicting the tissue of origin. While it is important to distinguish cancer-positive from cancer-negative patients, clinical decision making increasingly depends on the exact level of the measured biomarker. To that end, we report on the correlation between ctDNA VAF and DMAF across patients with colorectal cancer (CRC). Pre-surgical plasma samples from patients with CRC (N=70) were sourced from the prospective GALAXY, observational arm of ongoing CIRCULATE-Japan study trial (UMIN000039205). Samples classified as ctDNA-positive by a tumor-informed ctDNA assay (Signatera™) were included in this analysis and ctDNA VAF (%) was calculated. We performed deep methylation sequencing (Illumina Novaseq) across multiple target regions using two independent target sets. DMAF was calculated computationally, which estimates the fraction of differential methylation alleles for circulating cell-free DNA across target regions. Among 70 CRC patients, 68 had positive ctDNA results. Median age at testing was 64.0 years and male individuals represented 55.9% (n=38) of the cohort. Among them, 9 (13.2%) were stage I, 24 (35.3%) were stage II, 22 (32.3%) were stage III, 8 (11.7%) were stage IV, and 5 (7.3%) had unknown staging. The correlation of DMAF with ctDNA VAF was 0.894 (Spearman's Rank Correlation Coefficient) and was independent of disease stage, histology, age, and sex. Among MSS (micro-satellite stable; n=58) and MSI-H (micro-satellite unstable n=10) patients, the DMAF correlation was 0.9 and 0.915, respectively. The correlation between two target sets evaluating DMAF with differing numbers of targeted regions was high (0.89). These data demonstrate that abundance of differential methylation in CRC patients correlates with VAF regardless of clinicopathologic features of patients with CRC. Methylation-based assays are a promising tool for cancer detection and quantifying the disease burden.

#2410 Comparative genomic profiling of unresectable NSCLC patients in the U.S. and China using a globally harmonized liquid biopsy assay platform.

H. Tang[1], C. Jia[1], F. Xie[1], Y. Zhang[1], X. Dong[2], Y. Huang[2], S. Jia[2];
[1]Huidu (Shanghai) Medical Sciences, Ltd., Fengxian District, Shanghai, China, [2]Predicine, Inc., Hayward, CA

Background: Non-Small Cell Lung Cancer (NSCLC), accounting for over 80% of all lung cancers, benefits from targeted therapies based on genetic tests like EGFR, KRAS, ALK, and ERBB2. While prior studies focused on molecular characteristics through tissue biopsies, limited research has explored NSCLC molecular profiles via liquid biopsy, especially across different human races. This study presents a comprehensive genomic profiling analysis of unresectable NSCLC patients in the U.S. and China, using a globally harmonized liquid biopsy assay.
Methods: As part of Predicine's Phoenix Program, a global molecular biomarkers screening initiative, 61 patients in the U.S. and 352 patients in China with unresectable advanced NSCLC were enrolled. All were treatment-naïve or recurred after 1st-line targeted therapies. Blood samples (10ml) were tested using PredicineCARE, an NGS-based liquid biopsy assay, to profile somatic mutations, copy number variations, and gene fusions.
Results: The assay, validated in both regions using the same reference materials, achieved a Limit of Detection (LOD) of 0.25% mutation allele frequency, with a positive predictive value exceeding 99%. Profiling NSCLC patients in the U.S. and China revealed common genes like TP53, CDKN2A, EGFR, KRAS, RB1, and PIK3CA. TP53 and PIK3CA variations showed equivalent prevalence. However, EGFR variations were significantly higher in China ($p<0.05$), while CDKN2A ($p<0.001$), KRAS ($p<0.01$), and RB1 ($p<0.01$) variations were notably higher in the U.S.
Conclusions: This study unveils the mutational landscape of advanced NSCLC through liquid biopsy. Unique prevalence patterns between U.S. and China cohorts suggest novel biomarkers for clinical diagnosis and provide insights for targeted therapy mechanism studies.

#2411 A deep learning-based multimodal ensemble algorithm for lung cancer early detection with cross-ethnic generalizability.

T.-R. Lee[1], J. Ahn[1], J. Lee[1], D. Kim[1], B.-H. Jeong[2], D. Oh[3], M. Wang[4], M. Salmans[4], A. Carson[4], B. Leatham[4], K. Fathe[4], B. Lee[4], C.-S. Ki[1], Y. Park[5], **E.-H. Cho**[1];

[1]GC Genome, Yongin, Korea, Republic of, [2]Division of Pulmonary and Critical Care Medicine, Department of Medicine, Samsung Medical Center, Sungkyunkwan University School of Medicine, Seoul, Korea, Republic of, [3]Department of Radiation Oncology, Samsung Medical Center, Sungkyunkwan University School of Medicine, Seoul, Korea, Republic of, [4]GENECE Health, San Diego, CA, [5]Division of Pulmonary and Critical Care Medicine, Department of Internal Medicine, Seoul National University Hospital, Seoul, Korea, Republic of

Background: Lung cancer is the leading cause of cancer-related mortality worldwide, and early detection is crucial for improving patient outcomes. Cell-free DNA (cfDNA) whole genome sequencing (WGS) is a non-invasive technique that has the potential to detect lung cancer early, but it is challenging to develop accurate and generalizable detection algorithms due to the low abundance of tumor-derived cfDNA in early-stage cancer.
Methods: We developed a novel deep learning-based multimodal ensemble algorithm that combined two independent models: FEMS (fragment end motif frequency and size) and COV (coverage of genome positions). To assess the performance and ethnic generalizability of our algorithm, we evaluated it on three distinct cohorts: a Korean development cohort, a Korean external cohort, and a Caucasian external cohort. The Korean development cohort for model development comprised 236 lung cancer samples (stage I: 30%, stage II: 12%, stage III: 24%, stage IV: 20%, unknown: 14%) and 2205 normal samples. The Korean external cohort for performance evaluation of the model comprised 288 lung cancer samples (stage I: 31%, stage II: 13%, stage III: 26%, stage IV: 19%, unknown: 12%) and 1463 normal samples. And the Caucasian external cohort for confirm the ethnic generalizability consisted of 126 lung cancer samples (stage I: 17%, stage II: 12%, stage III: 37%, stage IV: 32%, unknown: 3%) and 93 normal samples. All data were generated using Novaseq6000 with a minimum of 40 million reads.
Results: Our multimodal ensemble algorithm achieved high sensitivity and specificity in all three cohorts. The Korean development cohort had an overall sensitivity of 94.1% (95% CI: 90.7% to 97%) and specificity of 85%. The Korean external cohort had an overall sensitivity of 90.4% (95% CI: 82.7% to 98.1%) and specificity of 82%. The Caucasian external cohort had an overall sensitivity of 92.1% (95% CI: 87.3% to 96%) and specificity of 82.8%. The Caucasian cohort also had a sensitivity of 80% for early-stage lung cancer.
Conclusion: Our deep learning-based multimodal ensemble algorithm is a promising tool for early lung cancer detection using low-coverage cell-free whole genome sequencing (LC-cfWGS). It performed well on three distinct cohorts, including a Caucasian cohort, suggesting that it is robust and generalizable to different populations. This makes it a potential candidate for clinical implementation.

#2412 Circulating HPV DNA as a potential biomarker to monitor response to the pembrolizumab and vorinostat combination in patients with squamous cell carcinoma of different locations.

E. Jeannot[1], D. Filippini[1], C. Dupain[1], M. Halladjian[1], G. Marret[1], C. Coutzac[2], E. Coquan[3], M. Saint-Ghislain[1], O. Le Saux[2], L. Mazzarella[4], G. Frige[4], E. Guerini-Rocco[5], M. Francisco[6], N. Servant[6], M. Tonini[7], L. Chanas[1], F. Legrand[8], S. Bernhart[9], G. Balogh[9], M. Jimenez[8], I. Bieche[1], T. Filleron[10], B. Cabarrou[10], **C. Le Tourneau**[1], M. Kamal[1];

[1]Institut Curie, Paris, France, [2]Centre Leon Berard, Lyon, France, [3]Centre Francois Baclesse, Caen, France, [4]IEO - Istituto Europeo di Oncologia, Milan, Italy, [5]IEO - Istituto Europeo di Oncologia IRCCS, Milan, Italy, [6]INSERM U900, Paris, France, [7]Luxembourg Institute of Health, Luxembourg, Luxembourg, [8]Unicancer, Paris, France, [9]Universitat Leipzig, Leipzig, Germany, [10]Institut Claudius Regaud, IUCT-Oncopole, Toulouse, France

Background: The PEVOsq basket trial (NCT04357873) evaluated the efficacy of pembrolizumab and vorinostat (P+V) in patients (pts) with advanced squamous cell carcinoma (SCC) of different locationsAmong 112 pts included, 66 were HPV-positive (HPV+). Here we report HPV ctDNA monitoring in these pts.
Methods: ctDNA before treatment (T0) and at first imaging (T1) from HPV+ SCC pts enrolled in the PEVOsq trial were analyzed using digital droplet PCR. Changes in HPV ctDNA levels between T0 and T1 were correlated to tumoral response (RECIST1.1). Landmark survival analyses were performed to study the association with progression free survival (PFS) and overall survival (OS).
Results: Among the 66 HPV+ pts, 47 (71%) had plasma at T0 and T1. Most pts had anal (n=24, 51%) or cervix cancers (n=11, 23%), followed by vulva/vagina (n=8, 17%), penis (n=3, 6%) and head and neck (n=1, 2%) cancers. HPV ctDNA was detected in all 47 pts at baseline. Increasing HPV ctDNA copies at T1 correlated with progressive disease in 8 pts (67%), whereas decreasing HPV ctDNA occured in 6 (100%) and 8 (80%) pts with complete (CR) and partial response (PR), respectively (Table).Increase in HPV ctDNA copies were more frequent in non-responders pts versus responder pts (p=0.03) and was associated with shorter OS (12.1 months vs not reached, p=0.02) and a trend towards shorter PFS (4.3 versus 8.2 months, p=0.06). Taken as a continuous variable, 10% increase in HPV ctDNA between T0 and T1 was associated with higher risk of progression (HR=1.05; 95%CI, 1.02-1.08, p=0.0007) and shorter OS (HR=1.02; 95%CI, 1.01-1.03, p<0.0001) in univariate analysis.
Conclusions: HPV ctDNA was detected at baseline in all pts reliably reflecting HPV detected on tissue. Dynamic changes in HPV ctDNA levels might help monitoring response to treatment in pts with advanced HPV+ cancers.
Table:

Variation in HPV-ctDNA (N=47)	Best response			
	CR N=6	PR N=10	SD N=19	PD N=12
Increase	0	2 (20%)	6 (32%)	8 (67%)
Decrease	6 (100%)	8 (80%)	13 (68%)	4 (33%)

#2413 Mutated *TP53* prevalence in *EGFR*-mutated advanced non-small cell lung cancer patients with brain metastases.

S. Stensgaard[1], I. Z. Eide[2], E. Stensland[2], A. Helland[3], S. Ekman[4], K. H. Hansen[5], S. Cicenas[6], B. Gronberg[7], P. Meldgaard[1], B. S. Sorensen[1], O. Brustugun[2]; [1]Aarhus University Hospital, Aarhus, Denmark, [2]Vestre Viken Hospital Trust, Drammen, Norway, [3]Oslo University Hospital, Oslo, Norway, [4]Karolinska University Hospital, Stockholm, Sweden, [5]Odense University Hospital, Odense, Denmark, [6]Vilnius University Faculty of Medicine, Vilnius, Lithuania, [7]Trondheim University Hospital, Trondheim, Norway

Introduction: Approximately 50% of patients with *EGFR*-mutated advanced non-small cell lung cancer (NSCLC) develops brain metastases (BM), which is associated with a poor prognosis. Mutations in *TP53* are associated with earlier development of resistance to *EGFR* tyrosine kinase inhibitors, but it is unclear whether patients who develops BM have a higher prevalence of *TP53* mutations. Analyses of circulating tumor DNA (ctDNA) in blood have been established as a good alternative to tissue biopsies to assess the genomic landscape of NSCLC. In this study, we aim to analyze ctDNA from patients with advanced *EGFR*-mutated NSCLC to investigate the prevalence of *TP53* mutations in patients with BM, and to explore whether patients with BM exhibit a distinct ctDNA profile compared to patients without.

Materials and Methods: Plasma samples collected before treatment commenced from 97 of the 100 patients with *EGFR*-mutated advanced NSCLC enrolled in the First-line Treatment With Osimertinib in *EGFR*-mutated Non-small Cell Lung Cancer study (The FIOL study: NCT03804580) were analyzed. Patients were split into cohorts with (n=44) and without BM (n=53) at baseline. The cell-free DNA was isolated and sequenced with targeted next-generation sequencing with the AVENIO ctDNA Surveillance Panel (Roche) containing 197 lung cancer-related genes.

Results: Mutations in ctDNA were found in 83 patients (85.6%), with 6 patients with BM having no ctDNA mutations and 8 patients without BM having no ctDNA mutations. Besides *EGFR* mutations, *TP53* was the most frequently mutated gene, with 42 patients (43.3%) harboring *TP53* mutations. There was no significant difference in the prevalence of *TP53* mutations between the cohort with BM (n=23) and the cohort without (n=19), (p=0.15). There was no difference in the number of identified mutations in the two cohorts (BM: median: 2 (range: 0-6), without BM: median: 2 (range: 0-11), p=0.71). Patients with BM had a numerically lower ctDNA level (median: 45.5 mutant molecules/mL), than patients without BM (median: 75.9 mutant molecules/mL), though the difference was not statistically significant (p=0.68).

Conclusion: Prevalence of *TP53* mutations in plasma collected before osimertinib treatment initiation in advanced *EGFR*-mutated NSCLC was similar between patients with and without BM at baseline. Furthermore, there was no difference in the ctDNA profile between these two cohorts. Future experiments will clarify the impact of *TP53* mutations in patients with or without BM.

#2414 Feasibility and clinical utility of blood based NGS in head and neck carcinomas : A single center experience from precision medicine program..

Filippo Gustavo Dall'Olio[1], Damien Vasseur[2], Lea Loriguet[1], Francois Regis Ferrand[1], Antoine Moya-Plana[1], Yungan Tao[3], Mariana Iacob[1], Karim Benihoud[4], Odile CASIRAGHI[5], Catherine Brenner[4], Pierre Busson[4], Philippe Gorphe[1], Santiago Ponce[6], Pierre Blanchard[3], Etienne Rouleau[2], Yohann Loriot[6], Ludovic Lacroix[2], Antoine Italiano[6], Ingrid Breuskin[1], Caroline Even[1]

[1]Head and Neck Oncology, Gustave Roussy, Villejuif, France,[2]Medical Biology and Pathology Department, Gustave Roussy, Villejuif, France,[3]Radiation Oncology, Gustave Roussy, Villejuif, France,[4]Metabolic and Systemic Aspects of Oncogenesis for New Therapeutic Approaches, Gustave Roussy, Villejuif, France,[5]Anatomopathology, Gustave Roussy, Villejuif, France,[6]Drug development, Gustave Roussy, Villejuif, France

Background: While blood-based next-generation sequencing is increasingly integral to clinical practice across various malignancies, the routine assessment of circulating tumor DNA (ctDNA) in head and neck cancer remains underexplored, with limited supportive data.
Methods: This study focused on head and neck cancer patients enrolled in the Gustave Roussy precision medicine program (STING, NCT04932525), undergoing liquid biopsy (LB) with the FoundationOne Liquid CDX panel. The Molecular Tumor Board discussed cases, calculating Tumor Fraction (TF) based on aneuploidy, categorizing it as high or low with a 10% cutoff.
Results: The analysis encompassed 239 LBs from 214 patients with relapsed or metastatic head and neck cancers. Of these, 59 LBs were from 57 patients showing stability or positive response (SD/R), while 180 were from 167 patients at diagnosis or disease progression (BL/PD). Notably, 156 (73%) were male, with a median age of 61 years. Within the cohort, 65% of LBs were from patients with squamous cell carcinomas (SCC), 15% adenoid cystic carcinomas (ACC), and 20% other histologies mainly adenocarcinomas. The anatomical distribution included 59 LBs from salivary gland (SG) cancers, 49 oropharynx (OP), 48 oral cavity (OC), and others including larynx, hypopharynx, sinus and nasopharynx. Among LBs performed at BL/PD, 72% were informative, while only 36% were so at SD/R. The proportion of informative biopsies varied across anatomical sites. For SCC, TP53 mutations were most prevalent (71%), followed by TERT and PIK3CA variants, and FGF19 and FGF3 amplifications. ACCs showed NOTCH1 mutations (6/19, 32%) as the most common, followed by TP53 and various other variants. In the entire cohort, clonal hematopoiesis-related variants were identified, with 40% showing at least one of DNMT3A, CHEK2, or ASXL1. Patients with low TF at BL/PD exhibited significantly improved overall survival (21.6 vs. 7.6 months, HR 0.35, 95% CI 0.23 - 0.53, $p < 0.0001$), consistent across subgroups except for OP.Conclusion: This study demonstrates the feasibility of liquid biopsy in HNSCC and rare head and neck tumors, providing valuable therapeutic and prognostic insights. The findings underscore the potential of liquid biopsy as a valuable tool in clinical decision-making for head and neck cancer patients.

#2415 Resistance to immune checkpoint inhibitor (ICI) therapy in metastatic melanoma is revealed by deep circulating tumor DNA tracking in concert with tumor immune profiling.

C. W. Abbott[1], L. Keller[2], I. Heidrich[3], J. Kott[3], G. Geidel[3], D. J. Smit[3], R. Simon[3], S. Schneider[3], J. Pugh[1], S. M. Boyle[1], R. O. Chen[1], K. Pantel[3], C. Gebhardt[3];

[1]Personalis, Inc., Fremont, CA, [2]IUCT Oncopole, Toulouse, France, [3]University Medical Center Hamburg-Eppendorf, Hamburg, Germany

Monitoring clinically actionable and emerging mutations in circulating tumor DNA (ctDNA) may be crucial for guiding treatment, but adoption has been slow due to the narrow scope and reproducibility of current approaches. Here, we investigate melanoma patients receiving ICI over several years, beginning with extensive tumor mutational and immune profiling followed by deep, whole-exome ctDNA monitoring.Here, 66 plasma samples from 23 advanced stage melanoma patients that were collected throughout ICI treatment (up to 40 months) were profiled using the NeXT Liquid Biopsy® platform (NeXT LB) . NeXT LB monitors exome-wide ctDNA by leveraging a patient's tumor, PBMCs and plasma samples, detecting both tumor-derived and emerging mutations. In addition to ctDNA tracking, we also used the ImmunoID NeXT Platform® to immunologically profile tumor tissue; including gene expression quantification, HLA profiling (typing, mutation, and loss of heterozygosity), T-cell receptor and tumor microenvironment profiling, and neoantigen prediction. ctDNA dynamics and tumor immunity were correlated with clinical outcome. Patients who progressed had lower tumor mutational burden (TMB, Mann-Whitney (MW); p=0.03), and lower neoantigen burden (MW; p=0.04). Responding tumors were enriched for interferon gamma and inflammatory signaling (Wald; adjusted p<0.01) and myeloid dendritic cells (MW; p=0.01), as measured by baseline RNA expression profiling. With an average coverage of 2260X SD +/-157, plasma samples yielded from 4 to 4081 variants. The number of on-treatment tumor variants detected in plasma predicted increased OS hazard (HR=2.95, Wald p=0.03; Kaplan-Meier (KM) p=0.0003) and progression hazard (HR=1.74, Wald p=0.04; KM p=0.0003). Overall, 10% (4277) of all variants were novel mutations observed only in the plasma. Novel variants were less likely to emerge in genes conferring sensitivity to ICI therapy (mixed-model; p<0.001). Dynamic shifts in allelic fraction between baseline and the first available on-treatment timepoint predicted increased OS hazard (HR=3.02, Wald p=0.05) and progression hazard (HR=2.90, Wald p=0.02). In ctDNA clonal phylogenies, 100% of BRAF and NRAS mutations belonged to the dominant clone. By combining immune and ctDNA features, a multivariable model predicted resistance to ICI treatment (log-likelihood p=0.002; c-index=0.89). Using a single liquid biopsy platform, we profiled tumor immunity and tracked existing and emerging ctDNA variants over the course of ICI treatment. We demonstrate that, even though counts of on-treatment ctDNA variants were sufficient for significant survival models, deep profiling of both tumor immunity and ctDNA dynamics provided deeper understanding of ICI resistance. Subsequent studies will determine if ctDNA-guided intervention can improve clinical outcomes.

#2416 Personalized minimal residual disease detection using tumor-derived structural variants in cell-free DNA.

B. R. McDonald[1], **K. L. Dennison**[1], A. L. Schussman[1], S. M. McGregor[1], B. A. Pockaj[2], M. Murtaza[1];
[1]University of Wisconsin-Madison, Madison, WI, [2]Mayo Clinic Arizona, Phoenix, AZ

We demonstrate development and technical validation of a novel approach for analysis of plasma circulating-tumor DNA (ctDNA) for residual disease detection and monitoring that offers improvements over existing technologies. ctDNA in blood can be leveraged to monitor treatment response, detect cancer recurrence, and inform treatment decisions for cancer patients. However, accurate detection and quantification of ctDNA is technically challenging due to low concentration of plasma DNA, especially in the adjuvant setting. Most current assays rely on interrogating multiple patient-specific point mutations to achieve exquisite limits of detection but struggle with polymerase errors, sequencing artifacts and limited conversion of input DNA. To overcome these challenges, we developed an approach called Structural Variant Enrichment and Normalization (SVEN) that targets patient-specific genomic rearrangements to achieve sensitive detection and quantification of plasma ctDNA. This method leverages intrinsic features of tumor-derived structural variants (SVs) to improve enrichment and confidence of detection at low tumor fraction through multiplexed PCR and amplicon-based next generation sequencing. To evaluate the assay, we performed whole genome sequencing of DNA from two breast cancer cell lines, as well as matched FFPE tumor and buffy coat samples from 21 early-stage breast cancer patients. We identified consensus SVs, and designed multiplexed SV-specific primers for each subject. We then conducted PCR amplification of cell-free DNA followed by sequencing, amplicon identification, and quantification. Analytical validation was conducted using 284 replicates of cell line dilutions from 1% to 0.003%, and 5 to 40 ng of input. We developed multiplexed assays targeting 25 and 32 SVs across two cell lines, and 3 - 43 SVs across breast cancer patients (median 23 per patient). 91% and 42% of PCR targets were successfully validated for cell lines and FFPE samples respectively. Cell line dilutions demonstrated a sensitivity of 89% at 0.003% tumor fraction with 10 ng input or more. Tumor fractions measured using SVEN agreed with known values (R^2 = 0.989). Application of validated panels to patient plasma samples and tumor/germline dilutions is ongoing. SVEN is a novel approach for tumor-guided ctDNA detection and quantification with potential relevance for residual disease detection. On-going studies are investigating the performance of this approach for ctDNA detection in patients with early and locally advanced breast cancer treated with neoadjuvant therapy.

#2417 Detection and quantification of site-specific DNA methylation from liquid biopsies as a pharmacodynamic biomarker of OTX-2002, a novel MYC-targeting epigenomic mRNA therapeutic.

J. Chen, W. Senapedis, S. Siecinski, E. Figueroa, A. Katz, S. Mildrum, Y. E. Wang, H. Belaghzal, K. Gallagher, G. Hodgson, C. W. O'Donnell, T. G. McCauley; Omega Therapeutics, Cambridge, MA

Omega Therapeutics has developed a novel platform of programmable epigenomic mRNA medicines capable of modifying chromatin state to specifically tune gene expression at the pre-transcriptional level. Epigenomic controllers (ECs) unlock targets that have been historically considered "undruggable," with one of the most elusive being the *MYC* oncogene. A direct MYC-targeting anti-cancer agent has previously remained intangible, largely due to the absence of a drug binding pocket and tight autoregulation. A clinical trial is underway (MYCHELANGELO, NCT05497453) to investigate pre-transcriptional inhibition of *MYC* with OTX-2002 in patients with hepatocellular carcinoma (HCC). OTX-2002, a first-in-class mRNA therapeutic delivered via lipid nanoparticles (LNP), encodes two proteins that durably modify chromatin, in part, through CpG DNA methylation at the *MYC* locus. Using both liquid and solid biopsy sampling from *in vivo* studies, we investigated whether target engagement for OTX-2002 could be assessed by *MYC* methylation.

Detection of DNA methylation has long held promise as an oncology biomarker given its functional roles in various cancer types and the potential signal afforded by methylated CpGs. Indeed, DNA methylation has been shown to serve as a robust analyte in liquid biopsy-derived multi-cancer early detection (MCED) and minimal residual disease (MRD) tests that have recently been utilized in the clinic. Many of these platforms are founded on complex models that leverage methylation signals across >1 million CpGs that can span tens of megabases of genomic space. We faced a distinct challenge when compared to these MCED/MRD tests in developing a pharmacodynamic methylation assay for OTX-2002 as the target region consists of just a few kilobases. With a tissue specific LNP delivery system, ultra-high sensitivity was required to identify rare ctDNA events from the larger cfDNA population.

To this end, we designed a minimal hybridization/capture panel that targeted ~50 kb of genomic space, effectively allowing for ultra-deep methylation sequencing of *MYC*. When this technique was paired with enzymatic (EM) conversion for methylation detection and supported by an analysis pipeline focused on epiallele identification, this assay was able to detect methylation down to the theoretical limit in a dilution series of control genomic DNA, 1 in 10^4 copies of *MYC*. This degree of sensitivity translated to successful preclinical detection of on-target methylation by OTX-2002 from DNA extracted from plasma samples collected from mice-bearing human HCC xenografts. Overall, we present a non-invasive and exquisitely sensitive method of assessing target engagement and site-specific pharmacodynamic activity of a novel epigenomic medicine that can be directly translated to the clinical setting.

#2418 Copy number variation status of DNA in extracellular vesicles as novel biomarkers of high-grade serous ovarian carcinoma.

R. Uekusa[1], A. Yokoi[1], K. Yoshida[1], J. Matsuazki[2], Y. Yamamoto[3], H. Kajiyama[1];

[1]Nagoya Univ. Graduate School of Medicine, Nagoya, Japan, [2]Keio University Faculty of Pharmacy, Tokyo, Japan, [3]National Cancer Center Research Institute, Tokyo, Japan

Objective: Ovarian cancer is a gynecologic malignancy with a dismal prognosis due to the lack of accurate methods for early diagnosis methods and effective therapies. High-grade serous ovarian carcinoma (HGSOC) is the most common subtype and copy number variations (CNVs) are the dominant genomic events in HGSOC. Extracellular vesicles (EVs) circulate in body fluids and carry pathological genomic information positively. In this study, we evaluated the significance of EV-DNA as novel biomarkers for HGSOC patients.

Methods: A total of 124 samples from HGSOC patients and cell lines were analyzed. EVs were isolated using the ultracentrifuge method. Comprehensive CNV statuses were analyzed by whole genome sequencing (WGS) and SNP array. In reference to the Ovarian Cancer Moon Shot database, 30 dominant CNVs in HGSOC were selected as dominant targets for analysis by droplet digital PCR (ddPCR). For predicting the response to PARP inhibitors, HGSOC patients who were treated with olaparib were collected, and DNA was extracted from FFPE tissue at the time of surgery.

Results: NTA assays and cryo-electron microscopic analyses showed that the EVs were successfully isolated from all samples. Both WGS and SNP arrays detected correlating CNVs in cell-DNA and EV-DNA for cell lines, and in tissue-DNA and EV-DNA in ascites for patients. The CNV status was also accurately measured by ddPCR. Copy numbers of *RAD51*, *BRCA1*, *AKT2*, *CCNE1*, and *MSH6* were significantly higher in malignant tissue than in benign tissue ($p<0.0001$, $p<0.0001$, $p=0.0012$, $p=0.002$. $p=0.0328$, respectively), and were detectable in EV-DNA from ascites. Additionally, the amount of DNA in malignant ascites was significantly higher than in benign ascites ($p=0.016$), and increased DNA in ascites itself suggested the presence of malignancy. Furthermore, EV-DNA more accurately reflected the CNV status of tumor DNA than cell-free DNA in ascites. Regarding the prediction of PARP inhibitor response, the CNV status in EV-DNA from patients who were treated with olaparib, a PARP inhibitor, demonstrated a marked difference between responders and non-responders. The equation calculated based on the combination of six genes (*RB1*, *GABRA6*, *CTNNB1*, *MYC*, *RAD51*, *BARD1*) could predict the response to olaparib (AUC: 1.0). The selected genes were validated in vitro using EV-DNA, and responders could be identified using the prediction equation calculated from CNV status of the selected genes in EV-DNA from ascites.

Conclusion: CNV status of EV-DNA was correctly evaluated and can serve as novel diagnostic and prognostic biomarkers for HGSOC.

#2419 Personalized longitudinal ctDNA monitoring is useful for biomarker in head and neck squamous cell carcinoma.

R. Kogo, T. Manako, T. Nakagawa;
Kyushu University, Fukuoka, Japan

Introduction: There is no established and useful tumor biomarker to evaluate treatment response and predict early locoregional and distant metastatic relapse in head and neck squamous cell carcinoma (HNSCC). Circulating tumor DNA (ctDNA) has a potential for detecting minimal residual diseases (MRDs). However, the absence of specific hotspot mutations in most HNSCCs makes ctDNA-based studies difficult in HNSCC. As a novel biomarker, we investigated whether individualized ctDNA analysis could help monitor and predict treatment response and relapse in HNSCC.
Methods: Thirty-two HNSCC patients were enrolled in this study. Twenty-two patients received radical resection and 10 patients were received radical irradiation as initial curative treatment. We collected tumor tissues and paired PBMCs (peripheral blood mononuclear cells) before treatment. Furthermore, we collected serial plasma samples for ctDNA analysis. To identify tumor specific individualized mutation, we isolated DNA from tumor tissue and PBMC and performed mutation analysis using custom SCC panel with frequent altered 31 genes (all exon coverage). We defined tumor-specific mutated genes per patient with variant allele frequency (VAF) >10 % and total coverage >100 as ctDNA candidate genes and performed ctDNA analysis using dPCR. We generated mutation specific primer-probe for droplet digital PCR (ddPCR), quantified the amount of ctDNA in plasma and compared ctDNA level with clinical data.
Results: For mutation analysis, most frequent mutated gene was *TP53* (21/32, 65.6%). Longitudinal ctDNA was monitored in a total of 24 cases. In 13 cases, ctDNA tested positive again or did not test negative, and all 13 cases had a residual tumor or relapsed after initial treatment. In 11 cases, after initial treatment, ctDNA remained negative and patients were alive without recurrence. Our cohort included 6 patients in whom it was possible to monitor ctDNA during chemotherapy in recurrent metastatic HNSCC cases. ctDNA alterations correlated well with clinical treatment response in four cases, but not in two cases. Patients who remained negative for ctDNA during follow-up after initial treatment (n=11) had a significantly better prognosis than those who reverted to ctDNA positivity (n=13, $P < 0.0001$).
Conclusion: Custom SCC panel is useful to detect more tumor specific mutation in HNSCC patients. Detection of ctDNA using next generation sequencing and digital PCR is promising strategy capable of monitoring in HNSCC patients. However, this method is not useful in all HNSCC, and there is room for improvement in the selection of ctDNA candidate genes.

#2420 Evaluating circulating tumor DNA (ctDNA) as a prognostic biomarker utilizing a tissue-free epigenomic assay in early-stage triple negative breast cancer (TNBC).

F. O. Ademuyiwa[1], C. X. Ma[1], K. Weilbaecher[1], R. Suresh[1], L. Peterson[1], R. Bose[1], N. Bagegni[1], C. E. Rigden[1], A. Frith[1], K. Clifton[1], A. Davis[1], D. Dustin[2], M. Cai[2];

[1]Washington University School of Medicine in St. Louis, Saint Louis, MO, [2]Guardant Health, Palo Alto, CA

Background: ctDNA has shown promise as a prognostic biomarker in early-stage solid tumors. Current breast cancer clinical guidelines do not recommend routine screening for metastatic disease outside of clinical features suggestive of disease recurrence. The detection of ctDNA may be a useful biomarker for the management of early-stage cancer patients to identify patients who are at high risk of recurrence.

Methods: Patients with stage II or III TNBC undergoing neoadjuvant docetaxel and carboplatin chemotherapy on a clinical trial (NCT02124902) followed by surgery were included in this study. Blood samples were prospectively collected prior to, during, and after completion of neoadjuvant chemotherapy, post-surgery, and throughout pre-specified surveillance time points (every 6 months for 5 years). Plasma samples were analyzed using Guardant Reveal powered by Infinity, a tissue-free, multiomic assay that interrogates differentially methylated regions of DNA using an applied bioinformatics filter optimized to detect breast cancer DNA from non-cancerous cell-free DNA and estimate quantitative tumor fraction. Samples were sequenced and resulted blinded to the patients' clinical data.

Results: A total of 120 patients with evaluable plasma samples were included in this study. At baseline prior to chemotherapy, ctDNA was detected in 75% (54/72) of patients. Baseline ctDNA detection was higher in node-positive cancers (100%; 29/29) versus node-negative cancers (58%; 25/43; p<0.0001). ctDNA quantity was higher in node-positive cancers (p<0.0001), and in stage III versus stage II disease (p=0.0179). During surveillance follow-up, the sensitivity for detecting any distant metastatic recurrence was 71% (5/7). Among patients with samples drawn within one year of recurrence, the sensitivity for detecting distant recurrence was 83% (5/6) with a sample-level specificity of 98% (186/190) and a patient-level specificity of 94% (63/67). ctDNA detection prior to recurrence had a median lead time of 5.0 months (range, 4.6-5.6). Notably, the detection of ctDNA during follow-up was associated with worse recurrence-free (HR 23.3, 95% CI 2.70-201, p<0.0001) and distant-recurrence free survival (HR 29.3, 95% CI 1.86-461, p<0.0001).

Conclusions: ctDNA is detected with a tissue-free MRD assay with high sensitivity and specificity for distant recurrence in early-stage TNBC. Furthermore, the presence of ctDNA during follow-up is a prognostic indicator. Additional prospective studies are needed to assess the clinical utility of ctDNA monitoring in early-stage TNBC.

#2421 Targeted and low-pass whole genome sequencing of cerebrospinal fluid circulating tumor DNA for the diagnosis and monitoring of pediatric, adolescent and young adult CNS tumors.

I. Burns[1], L. Nobre[2], Y. Nakano[1], M. Ku[3], M. Johnson[3], J. Sheth[4], L. Negm[4], C. Cacciotti[5], M. Rana[3], R. Yuditskiy[3], A. Bondoc[3], R. Siddaway[3], U. Tabori[1], C. Hawkins[1];

[1]The Hospital for Sick Children, University of Toronto, Toronto, ON, Canada, [2]University of Alberta, Edmonton, AB, Canada, [3]The Hospital for Sick Children, Toronto, ON, Canada, [4]University of Toronto, Toronto, ON, Canada, [5]University of Western Ontario, London, ON, Canada

Molecular analysis of CNS tumors is essential to their diagnosis and guides individualized treatment for patients, but tissue biopsy of primary and/or relapsed lesions to allow for this characterization often carries intolerable risk. The analysis of genetic material in cerebrospinal fluid (CSF), known as liquid biopsy, can allow for minimally invasive tumor identification and diagnosis. Furthermore, liquid biopsy can serve as a more sensitive test for residual disease than imaging or cytologic analyses. We aimed to implement CSF liquid biopsy at Canada's largest pediatric hospital. >150 CSF samples were collected from CNS tumor patients with a median age of 9. The most common tumor types were low-grade gliomas (40%), high-grade gliomas (21%) and medulloblastomas (MB) (17%). The majority were collected via lumbar puncture (46%), external ventricular drain (24%) and intraoperatively (22%). The most frequent collection times were diagnosis (53%) and progression/relapse (28%). Cell-free DNA was extracted, and circulating tumor DNA was analyzed using low-pass whole genome sequencing and a targeted hybridization capture glioma gene panel for select cases. Pathogenic mutations and copy number alterations (CNA) were called using an in-house bioinformatics pipeline. Somatic alterations were detected in 57% of samples from patients with pathologically confirmed CNS tumors. CNAs were identified in 5/7 MB patients at the time of pre-treatment staging lumbar puncture. We also detected CNAs in several MB patients during treatment and at progression/relapse, including a patient with disseminated MB who was mid-induction chemotherapy with 1 suspicious cell in their CSF, highlighting our ability to detect minimal residual disease. Among samples with no previous biopsy, we identified tumor DNA in 29%, often providing diagnostic clarity and guiding management. For example, we identified a targetable FGFR1 N546D missense mutation in a patient with an unbiopsied suprasellar lesion. We also diagnosed recurrent MB in a patient 6 years off treatment with a new ambiguous nodule in their tumor bed by detecting an isochromosome 17q CNA. Overall, our liquid biopsy platform is feasible and can yield clinically impactful results. Next steps include refining our assays to increase their sensitivity and systematically evaluating our platform's efficacy for monitoring response to treatment and tumor surveillance.

#2422 Liquid biopsy approaches for monitoring metastatic pancreatic cancer in immunotherapy treated patients.

C. A. Hruban[1], I. Chen[2], D. C. Bruhm[1], S. Koul[1], J. Yao[1], S. Theile[2], K. Boyapati[1], N. A. Vulpescu[1], A. Annapragada[1], L. Ferreira[1], S. Cristiano[1], Z. H. Foda[1], V. Adleff[1], J. Johansen[2], J. Phallen[1], R. B. Scharpf[1], V. E. Velculescu[1];

[1]Johns Hopkins University School of Medicine, Baltimore, MD, [2]Copenhagen University Hospital - Herlev and Gentofte, Herlev, Denmark

Introduction: Pancreatic cancer has a poor prognosis especially when identified at advanced stages. Globally in 2020, >450,000 people died from the disease. For those with locally advanced or metastatic cancer, the standard of care treatment is chemotherapy. Preliminary studies show that some patients with advanced-stage disease respond to immune checkpoint blockade treatment. Determining response to therapy using imaging techniques can be challenging. There is a clinical unmet need for noninvasive approaches that can provide a real-time assessment of response to therapy in these patients. We evaluated two methods for assessing response to therapy using circulating cell-free DNA (cfDNA) in patients with metastatic pancreatic cancer treated with immune checkpoint inhibition and radiation as part of the CheckPAC study (NCT02866383).

Methods: For all patients with available samples (n=40), we evaluated one pre-treatment blood draw and one on-treatment blood draw (26-65 days after treatment start). We extracted cfDNA from each sample and performed low-coverage 1-2x whole genome sequencing (WGS). We evaluated tumor and matched buffy coat for the 34 patients who had > 10% tumor purity using WGS with at least 60x and 30x coverage, respectively. We compiled the mutated bases in the tumor genome and examined these positions in the cfDNA. We counted the number of mutant observations from cfDNA WGS and divided them by the total number of observations at these bases to calculate whole-genome mutant allele frequency (MAF). We categorized responders based on >30% drop in MAF from baseline. In a tissue independent approach, we detected changes in genome-wide cfDNA fragmentation patterns using the DNA evaluation of fragments for early interception (DELFI) approach. We evaluated survival using DELFI scores of on-treatment samples. Samples were designated DELFI high (above median) or DELFI low (below median.) Log-Rank tests were used to compare survival curves.

Results: For the mutation based approach, molecular responders (n=7) had a median progression free survival (PFS) of 485 days compared to 57 days for non-responders (n=9) (p=0.02). Molecular responders had a median overall survival (OS) of 694 days compared to 200 days for non-responders (p=0.062). Patients with DELFI low scores after therapy (n=14) had a longer median PFS than those with DELFI high scores (n=14) (307 days versus 70 days, respectively) (p=0.013). DELFI low patients also had a longer median OS than DELFI high patients (627 vs 158 days, respectively) (p<0.0001).

Conclusions: These analyses suggest that WGS mutation-based and fragmentation cfDNA approaches can identify individuals with metastatic pancreatic cancer who respond to immune checkpoint inhibition. Incorporation of these molecular methods for evaluation of tumor burden may provide information for patient-physician decision making to improve patient quality of life.

#2423 Linking liquids: cfDNA in urine and plasma as informative allies in metastasized prostate cancer.

T. Moser, A. Eberhard, M. J. Moser, L. Glawitsch, S. Hammer, G. Vlachos, I. Lazzeri, L. Ziegler, E. Bauernhofer, N. Monsberger, J. B. Geigl, T. Bauernhofer, E. Heitzer;
Medical University of Graz, Graz, Austria

Background: Liquid biopsy has become a cornerstone of non-invasive cancer diagnostics. While the major analyte for detecting and monitoring tumors has been blood, examining other body fluids, such as urine or saliva, is increasingly shifting into focus. Urine is a particularly valuable specimen due to its easy accessibility. Particularly in urologic cancers, the sensitivity of liquid biopsy could be improved by proximal sampling. While there is already evidence that cell-free DNA from urine (ucfDNA) can add to the diagnostic sensitivity in renal and bladder cancer, less is known about ucfDNA in prostate cancer patients. In this study, we aimed to determine the presence, levels, and potential clinical applications of ucfDNA in patients with metastatic prostate cancer. Moreover, we compared the findings with information obtained from plasma cell-free DNA (cfDNA).
Methods: Urine was stabilized using a urine collection/stabilization solution under development at PreAnalytiX (QIAGEN/BD Company) or STRECK as preservative. Blood was collected in PAXgene Blood ccfDNA Tubes (PreAnalytiX). Matched blood and urine cfDNA samples from 122 metastatic prostate cancer patients were isolated using the QIAsymphony platform. Tumor fraction and presence of somatic copy number alterations (SCNA) were assessed from shallow whole genome sequencing data using the ichorCNA algorithm.
Results: In 22/122 (18%) of patients SCNAs could be detected in both, urine and blood. Although the copy number profile was highly concordant in those patients, tumor fractions varied between plasma and urines on an individual patient level. In addition, in 52/122 (43%) and 48/122 (39%) patients, tumor-derived DNA was detected only in plasma or urine. Considering the entire cohort, neither the absolute cfDNA concentration nor tumor fraction did significantly differ between urine and plasma samples.
Conclusion: Our data demonstrate that ucfDNA can provide complementary information to blood about prostate tumors, which would be missed by the sole analysis of plasma cfDNA. Taking this into account and adding that urine represents a non-invasive specimen type that can be collected at great ease, ucfDNA holds promise in the clinical management of prostate cancer.

#2424 Detection of prostate cancer in urine by fragment-level DNA methylation analysis.

T. Bedekovics, W. R. Taylor, Z. Sun, S. Baheti, X. Cao, K. N. Burger, K. A. Doering, P. H. Foote, B. Gochanour, D. W. Mahoney, M. T. Gettman, J. B. Kisiel; Mayo Clinic, Rochester, MN

Introduction: Screening for prostate cancer (PCa) with molecular markers is hindered by low tumor allele fraction (TAF) in liquid biopsy samples such as blood or urine. Others have suggested that tumor allele enrichment can be achieved by evaluating fragment-level methylation patterns generated by next generation sequencing (NGS). Here, we test this concept using target capture NGS on cfDNA from prediagnostic collected urine samples to discriminate PCa from otherwise healthy men.

Methods: Buffered urines were collected from 23 patients with biopsy confirmed PCa (Gleason score 6-9) and 24 otherwise healthy age matched cancer-free controls. cfDNA was isolated and enzymatic methyl-seq libraries were prepared and enriched by hybrid capture using probes mapping to 197 differentially methylated regions (DMRs) from a previous PCa/normal tissue marker discovery study in our lab. These DMRs were subsequently vetted independently using a methylome-wide dataset from a cohort of 36 clean and disease control urines to ensure low non-cancer background signal (<1%). Indexed libraries were sequenced at 560X deduplicated coverage and fragment-level CpG methylation information was extracted from individual sample .bam files. Mapped sequencing reads exhibiting concordant methylation were used to derive a quantitative α-score. Reads had to contain at minimum 5 CpGs and have an α-value (% 5mC per read) > 60%. Positivity for the 197 markers required an α-score greater than 6 sigma (σ) above the mean of the control arm. Values were variance-adjusted to ensure equal weighting. Beta (β) analysis (mean % 5mC across all reads) of the data was also performed for comparison.

Results: Of the 197 markers, 187 were positive for one or more PCa patients. Tumor-derived fragments were detected in 22 of 23 cases, which included 8 G-6, 9 G-7, 2 G-8, and 3 G-9 patients. 1 G-7 was missed, however the sequencing coverage for this sample was significantly lower than the others due to poor library enrichment. 2 of the 24 healthy controls were positive, one with extremely high fragment counts. Upon re-review of the full control cohort, this patient had been diagnosed with bladder cancer 2 years after urine collection. The 2nd patient had was diagnosed with lung cancer in a similar timeframe. The other 22 confirmed cancer-free controls had α-scores below the 6σ threshold. Using a co-captured reference gene (*B3GALT6*) to mimic genomic equivalents, the TAFs ranged from 0.015% to 8%. β analysis of the data detected only 13 PCa patients (>6σ) and marker positivity was lower than the fragment-level approach.

Conclusion: Target capture NGS coupled with fragment-level analysis is a rational approach for sensitive and specific detection of low tumor-derived DNA in liquid biopsy samples. For PCa assay in urine, we were able to uncover positivity in cancer patients approaching 1 in 10,000 ctDNA dilution levels. These results warrant further validation studies with this and other cancers.

#2425 Pairwise analysis of plasma cell-free DNA before and after paclitaxel plus ramucirumab treatment in patients with metastatic gastric cancer.

J.-W. Kim[1], D. Kyung[2], W. Ko[2], H.-P. Kim[2], S.-H. Hwang[1], K.-J. Kim[1], J. Lee[3], J. Seo[1], M. Kang[1], E. Jung[1], K. Suh[1], S. Kim[1], J. Kim[1], Y. Kim[1], J. Kim[1], K.-W. Lee[1];

[1]Seoul National University Bundang Hospital, Seongnam, Korea, Republic of, [2]IMBdx, Inc., Seoul, Korea, Republic of, [3]Hankuk University of Foreign Studies, Yongin, Korea, Republic of

Background: Plasma cell-free DNA (cfDNA) analysis has emerged as an appealing alternative to detect somatic mutations. This study compared cfDNA at baseline (baseline-cfDNA) and progressive disease (PD-cfDNA) and tumor tissue DNA (ttDNA) in patients with metastatic gastric cancer who underwent palliative second-line paclitaxel+ramucirumab treatment.

Methods: We conducted targeted sequencing of 106 cancer-related genes using germline DNA, baseline-cfDNA, and PD-cfDNA samples. The results were then compared with conventional cancer panel results using ttDNA.

Results: Of 76 consecutively enrolled patients who received paclitaxel+ramucirumab treatment, 46 patients (27 males; median age 57.5 [range, 32-73] years) with access to all three samples were analyzed along with their ttDNA data. A total of 138, 145, and 80 mutations were detected in baseline-cfDNA, PD-cfDNA, and ttDNA respectively. Combined analysis of baseline-cfDNA and ttDNA revealed that *TP53* (56.5%) was the most frequently mutated gene, followed by *CDH1* (26.1%), *KRAS* (21.7%), and *APC* (13.5%). For the top four genes, the sensitivity and positive predictive value of baseline-cfDNA compared with ttDNA were 71.8% and 51.9%, respectively. Compared with ttDNA alone, 32 patients (70.0%) benefited from baseline-cfDNA in detecting novel mutations. When combined with baseline-cfDNA and PD-cfDNA, novel mutations were discovered in 34 patients (73.9%). Of note, PD-cfDNA analysis detected 9 novel pathogenic mutations in *TP53*, *APC*, *PIK3CA*, *CDH1*, *RNF43*, *CTNNB1*, and *BRCA2* genes in 8 patients (17.4%) after treatment. In baseline-cfDNA, patients with a circulating ttDNA fraction concentration at 110-160 bp of >4.3777 ng/μL had significantly shorter progression-free survival (PFS) (median 3.5 vs. 5.3 months, P=0.016). In addition, maximal variant allele frequency (VAF) values of >0.1045 (median 3.4 vs. 5.2 months, P=0.022) and the sum of VAF values of >0.2071 (median 3.4 vs. 5.2 months, P=0.028) were significantly associated with shorter PFS. In patients with *TP53* mutations, those with *TP53* VAF values of >0.1014 significantly had worse PFS (median 4.6 vs. 6.4 months, P=0.022).

Conclusions: Although cfDNA could not entirely take over the role of ttDNA, cfDNA analysis identified additional somatic mutations that were otherwise missed by ttDNA alone. Moreover, PD-cfDNA analysis detected novel pathogenic mutations that developed during treatment, implicating the clonal evolution of cancer. In addition, baseline cfDNA predicted PFS of patients receiving paclitaxel+ramucirumab therapy.

#2426 Liquid biopsy for a predictive biomarker of resistance to immunotherapy.

A. Sinkoe, J. L. Gulley;
National Cancer Institute, Bethesda, MD

Immunotherapy has become a mainstay for cancer treatment. However, immune editing is a well-known resistance paradigm that limits the efficacy of immunotherapy in many patients. One type of immune editing that occurs in 1/6 of all cancer patients, with prevalence over 40% in some cancer types, is human leukocyte antigen loss of heterozygosity (HLA LOH). Liquid biopsies provide a non-invasive and inexpensive way of guiding treatment decision-making. We have developed a liquid biopsy assay for detecting HLA LOH in cancer patients, with the goal of utilizing the assay for deciding whether immunotherapy is the right course of treatment for a given patient.

The assay was tested utilizing sample sets from cancer patients, where each sample set from a patient included a solid tumor biopsy, a liquid biopsy plasma sample, and PBMC sample for control. Tumor HLA LOH results were used for ground truth, and HLA LOH results from the liquid biopsy sample were compared to those from the tumor sample from the same patient. Whole exome sequencing (WES) was performed on tumor DNA, cell-free DNA (cfDNA) from plasma, and germline DNA from PBMCs, and we ran our novel liquid biopsy HLA LOH detection algorithm on the plasma WES data. Standard copy number variant (CNV) calling tools were utilized for calling HLA LOH from the tumor sequencing data. In both cases - tumor and plasma - germline PBMC DNA was used as control. We tested the liquid biopsy HLA LOH detection method on sample sets from 2 HPV-negative primary head and neck cancer patients, 14 castration-resistant prostate cancer patients, and 27 metastatic breast cancer patients. The samples from the head and neck cancer patients were obtained from patients on clinical trials at NCI, while WES data from prostate cancer patient samples and breast cancer patient samples were downloaded from NCBI Database of Genotypes and Phenotypes (dbGaP) after applying for access to dataset phs001417.v1.p1 (Adalsteinsson, et al., Nature Communications, 2017). The method for liquid biopsy HLA LOH detection utilizes a novel mathematical framework that takes into account biological and experimental variables to generate allele-specific HLA LOH information from sequencing data.

In the first two cohorts tested - the head and neck cancer cohort and the prostate cancer cohort - the method was 100% consistent when comparing liquid biopsy HLA LOH results from our method to CNV calling results from matched tumors (4 true positives and 36 true negatives; 0 false negatives and 0 false positives). In the breast cancer cohort, some false negatives and false positives were observed (6 true positives and 48 true negatives; 5 false negatives and 8 false positives). Experiments are ongoing in a CLIA lab to establish sensitivity, specificity, and limit of detection (LoD) for the assay. Upon improvements and validation of the assay, the goal is to utilize the liquid biopsy HLA LOH detection method in the clinic for treatment selection in the context of immunotherapy.

#2427 The development of a tissue-agnostic genome-wide methylome enrichment MRD assay for applications across the cancer care continuum for head and neck malignancies.

G. Liu[1], J. Min[2], Y. Wang[2], J. Burgener[3], B. Brown[2], K. Budhraja[2], J. Zhang[3], O. Hall[2], S. Shen[3], M. Pienkowski[1], S. Huang[1], L. Ailles[1], K. Rey-McIntyre[1], J. B. Provance[2], E. Sosa[2], C. Frye[2], S. Bratman[2], B. Allen[2], J. T. Jones[2], A. Licon[2], J. Zhang[2], A.-R. Hartman[2], D. D. De Carvalho[3];
[1]University Health Network, Toronto, ON, Canada, [2]Adela, Inc., Foster City, CA, [3]Adela, Inc., Toronto, ON, Canada

Background: Plasma-based tests to quantify circulating cell-free DNA cancer signal have emerged as viable applications across the cancer continuum, from early detection to optimal disease management. Here we demonstrate the feasibility of a tissue-agnostic, genome-wide methylome enrichment platform based on cell-free methylated DNA immunoprecipitation and high throughput sequencing (cfMEDIP-seq) for cancer detection, cancer signal quantification, and prognostication in head and neck cancer (HNC).
Methods: Pre-treatment plasma samples from individuals with newly diagnosed stage I-IV HPV+ or HPV- HNC were analyzed with a bisulfite-free, non-degradative, genome-wide methylome enrichment platform using 5-10 ng of cell-free DNA. For cancer detection, a machine learning classifier used differentially methylated regions to distinguish cancers from non-cancer controls. The area under the receiver operating characteristic curve (AUC) and 95% confidence intervals were calculated. Cancer signals were quantified from average normalized counts across informative methylated regions and a 95% specificity threshold. For prognostication, events were defined as recurrence, progression, or death due to HNC, whichever occurred earliest. Time to event was compared for samples with cancer signal quantities above versus below the threshold. Post-treatment and longitudinal plasma samples from individuals with Stage I-IVB HNC (HPV+ and HPV- included) will be analyzed for recurrence prediction and detection of relapse. More than 100 patients and 300 samples will be analyzed.
Results: For cancer detection, 92 pre-treatment plasma samples from HNC cases were distinguished from 674 controls with an AUC of 0.96 (0.94, 0.98). The AUC was 0.93 (0.86, 1.0) for Stage I, 0.93 (0.83, 1.0) for Stage II, 0.96 (0.94, 0.99) for Stage III, and 0.97 (0.96, 0.99) for Stage IV. For prognostication, 91 pre-treatment samples were included (7 stage I, 16 stage II, 23 stage III, 45 stage IV). Median follow-up time was 50.6 months with 27 events. Likelihood of recurrence or progression was significantly higher in samples with cancer signal above the threshold [hazard ratio 5.4 (95% CI 2.25, 12.95), log-rank P<0.001]. In the upcoming analysis, data will be reported on the ability to predict recurrence and relapse in post-treatment samples.
Conclusions: The cfMeDIP-seq approach demonstrated robust detection of HNC, across all stages and subtypes, and the ability to predict recurrence and progression from pre-treatment samples. We will report training data with cross validation to predict recurrence and relapse using post-treatment and longitudinal sampling. Collectively, data from these studies indicate that genome wide methylome enrichment has multiple use cases across the care continuum for patients with HNC.

#2428 Novel ctDNA technology for early cancer detection by immunoprecipitation of tumor associated ctDNA fragments and analysis by qPCR.

J. Micallef, D. Pamart, J.-V. V. Turatsinze, T. Bygott, B. Berman, B. Cuvelier, M. Herzog;
Volition Ltd, Henderson, NV

Introduction: Current ctDNA methods involve extraction of all plasma cfDNA, next generation sequencing (NGS) and complex bioinformatic analysis. We have developed a novel ctDNA analysis in which classes of tumor derived ctDNA are isolated, with removal of all non-tumor cfDNA of the same sequences, for analysis by qPCR. We now report the results of this analysis on cohorts of patients diagnosed with common solid cancers.
Methods: We developed a chromatin immunoprecipitation (ChIP)/qPCR method for the isolation of cell free plasma CTCF-DNA (cfCTCF-DNA) nucleoproteins that include binding sites selectively occupied in cancer. CfDNA fragments of non-cancer origin that comprise the same CTCF binding site sequences are nucleosome covered and washed away. We performed plasma CTCF ChIP-Seq discovery experiments to identify CTCF gain of occupancy cancer biomarker sequences by analysis of plasma samples taken from cancer patients as well as patients with inflammatory conditions and healthy volunteers. Suitable pan-cancer, or cancer tissue specific, biomarkers were selected as characterized CTCF binding site sequences that were present in the ChIP isolates of cancer patients but absent in isolates from patients without cancer. We then developed qPCR assays for selected CTCF gain of occupancy biomarker sequences. We initially investigated whether CTCF gain of occupancy biomarkers would identify patients with cancer in a small cohort of subjects with acute myeloid leukemia (AML) (n=31), breast (n=10), prostate (n=10), liver (n=10) or colorectal cancer (CRC) (n=13) and 50 control subjects including 15 subjects with an inflammatory condition.
Results: In our small initial experiments, a simple cutoff where a qPCR result exceeding the cutoff was positive, a single qPCR assay detected 19 of 31 AML cases (61%) with 1 false positive result among 50 control samples (98% specificity). Addition of a second qPCR assay to make a 2-member qPCR panel, where a result exceeding cutoff in either or both assays was classified as positive, resulted in the detection of 23 of 31 AML cases (74%) with 2 false positive results (96% specificity). On the same basis a 2-member qPCR panel also detected 58% of solid cancers including 44% of stage I cases. Another 2-member qPCR panel detected 77% of CRC cases at 92% specificity. We now report the results of investigations of larger cohorts of patients with common solid cancers by cancer type, stage and tissue specificity.
Conclusion: Combining the isolation of plasma cfCTCF-DNA nucleoproteins with PCR analysis of cancer associated CTCF gain of occupancy binding site sequences is a novel ctDNA analysis technology that may provide the basis of useful, rapid, low cost, automated liquid biopsy methods. Further clinical studies to ascertain the clinical accuracy of the method are required.

#2429 Longitudinal ctDNA monitoring using a high sensitivity tumor-informed assay in patients with metastatic HR^{+}/HER2^{-} breast cancer receiving endocrine therapy and CDK4/6 inhibitors.

J. Fuentes-Antras[1], M. J. Elliott[1], P. Echelard[1], A. Dou[1], Z. Veitch[1], P. L. Bedard[1], E. Amir[1], M. B. Nadler[1], N. Meti[2], N. Gregorio[1], E. Shah[1], E. Van de Laar[1], C. Yu[1], L. Gates[3], C. Murray[4], C. G. Smith[4], A. Chevalier[3], L. L. Siu[1], H. K. Berman[1], D. W. Cescon[1];

[1]UHN Princess Margaret Cancer Centre, Toronto, ON, Canada, [2]St. Mary's Hospital Center, Montreal, QC, Canada, [3]NeoGenomics, North Carolina, NC, [4]NeoGenomics, Cambridge, United Kingdom

BACKGROUND: ctDNA burden is prognostic and its dynamics during therapy may permit innovative strategies in metastatic breast cancer (mBC). Previous analyses have focused on driver genes, with limited sensitivity to quantify depth of response or detect early molecular progression. To enable sensitive, quantitative ctDNA monitoring, we analyzed samples from a cohort of HR^{+}/HER2^{-} mBC pts treated with endocrine therapy (ET) and CDK4/6 inhibitors (CDKi) using RaDaR, a patient-specific assay that tracks tumor-informed truncal variants independent of driver status with a limit of detection of 0.001%.

METHODS: HR^{+}/HER2^{-} mBC pts receiving standard ET + CDKi were enrolled in a prospective observational cohort from 2018. Plasma samples were collected at baseline (BL), within 30 days (d), and ~q3 months (mo) with radiological scans. RaDaR was performed on all samples for pts with tissue available for WES (as per assay). Clinico-pathological variables were collected. Endpoints were time to treatment failure (TTF) and overall survival (OS).

RESULTS: 51 pts were available for analysis. Median age was 60 years (range 38-88), 63% had visceral disease, and most pts were treated as first (75%) or second (20%) line. RaDaR was successful on 43 pts, with the rest dropping out due to failed WES (1) or panel failure (7). Archival tissue WES was used to design bespoke assays targeting a median 48 (23-52) variants in 248 samples, with a median of 5 samples/pt (2-14) collected over a median follow up of 27.8 (0.9-64.3) mo. ctDNA was detected in 91% (39/43) of BL and 70% (174/248) of all samples, with a median estimated variant allele fraction (eVAF) of 0.05%. Higher BL eVAFs were associated with liver disease (p=0.02) and with shorter TTF (p<0.01 adjusted by age and visceral disease) and OS (p<0.01). 36/39 pts had ≥1 sample with ctDNA decrease from BL, occurring within the first mo of therapy in 77% (24/31) of pts with available early samples. In 13 pts ctDNA became undetectable ('suppressed') at a median time (T) of 157 d (14-343). Among 25 pts with treatment failure (TF), the median T from the last negative/decreasing eVAF to TF was 163 d (0-943). Only 3 pts with TF had prior negative ctDNA, occurring with a median lead T of 198 d (119-595). Among ongoing pts, the median T from the last ctDNA decrease to last follow up was 317 d (163-1508), and from the last negative ctDNA sample was 352 d (163-993).

CONCLUSION: RaDaR enabled sensitive ctDNA monitoring in 91% HR^{+}/HER2^{-} mBC pts on ET + CDK4/6i. ctDNA levels were prognostic and fell rapidly with therapy, but suppression occurred in less than one-third of pts, taking a median of 5.2 mo. Pts with negative/decreasing ctDNA may require less frequent clinical/radiographic tumor evaluations. Highly sensitive ctDNA tracking may inform prognostic assessments, follow up strategies, and innovative interventional trial designs.

#2430 Enhancing urine-based cfDNA detection for prostate cancer diagnosis through increased urine input volume.

Nafiseh Jafari[1], Annika Dorn[2], Jason Saenz[1], Lauren Lee[1], Carlos Hernandez[1], Andrew Dunnigan[1], Mayer Saidian[1]

[1]nRichDX, Irvine, CA,[2]Agilent Technologies, Deutschland GmbH, Germany

Introduction: Cell-free DNA (cfDNA) extracted from urine has created new opportunities in non-invasive cancer diagnostics, particularly for prostate cancer. Detecting cfDNA in urine can be challenging due to its inherently low concentration. Increasing the input volume of urine addresses this limitation, enhancing the sensitivity of cfDNA detection. This study explores the benefit of collecting larger volumes of urine spiked with a TP53 mutation and the corresponding increase in assay sensitivity for early prostate cancer diagnosis and monitoring.

Methods: Pooled urine from healthy donors was collected, preserved, processed, and extracted from 10 mL, 20 mL, 30 mL, 40 mL, and 50 mL inputs (with four replicates each) using the Revolution Max 20 cfDNA Extraction kit. Replicate samples were also extracted using a MagMAX cfDNA Isolation kit from Thermo Fisher Scientific. All samples were spiked with a cfDNA standard containing TP53 R58L mutation. The quantity and quality of extracted cfDNA were determined using the Agilent TapeStation system with the Cell-free DNA ScreenTape assay and qPCR mutation detection assay.

Results: The Revolution Max 20 cfDNA kit consistently delivered a higher yield of cfDNA, demonstrating excellent extraction efficiency and quality, as shown by the Agilent Cell-free DNA ScreenTape assay. Notably, the Revolution Max 20 cfDNA kit exhibited a linear increase in yield as the sample volume grew from 10 mL to 50 mL. The MagMax kit did not provide this yield linearity. Furthermore, both methods successfully maintained the integrity of cfDNA fragmentation, which was confirmed through the Agilent Cell-free DNA ScreenTape assay.

Conclusion: Compared to the MagMax kit, the Revolution Max 20 cfDNA kit outperforms in extracting cfDNA with high efficiency, as shown by the Agilent Cell-free DNA ScreenTape and the qPCR assay. The Revolution Max 20 cfDNA kit offers the unique advantage of accommodating up to 50 mL of urine in a single extraction. As input volume increases, it consistently produces high cfDNA yields while maintaining quality. In contrast, the MagMax kit is limited to an input volume of only 10 mL, necessitating the cumbersome process of dividing a 50 mL urine sample into five separate extractions and pooling the eluates. This scheme resulted in lower yields. The Agilent Cell-free DNA ScreenTape assay is a valuable tool for quickly and accurately assessing the %cfDNA quality metric. Its minimal sample volume requirement makes it an efficient quality control method for determining cfDNA samples before performing downstream testings. The enhanced capability of the Revolution Max 20 kit to yield more significant quantities of high-quality cfDNA from urine samples can profoundly impact liquid biopsy test sensitivity and the early detection of prostate cancer, potentially revolutionizing the diagnostics process.

#2431 Identification of highly expressed exosomal RNAs derived from pancreatic cancer cell lines and exploration of their potential as biomarkers.

Yuhan Rong, Naoki Okubo, Noritoshi Kobayashi, Eriko Katsuta, Yasushi Ichikawa

Yokohama City Univ. Graduate School of Med., Yokohama, Japan

Background: Not all exosomes in the blood of cancer patients originate from cancer cells. This study evaluated the relationships between mRNAs and miRNAs in pancreatic cancer (PC) cell lines and those in exosomes secreted into the supernatant. We aimed to identify candidates for PC biomarkers from cancer-specific exosomal mRNAs and miRNAs.
Materials and Methods: Three PC cell lines were utilized. Exosomes were isolated from the supernatant, and cellular and exosomal mRNAs and miRNAs were extracted. Subsequently, RNA sequencing (RNA-seq) was performed, and the data were analyzed using R software.
Results: In the MIAPaCa-2 cell line, the expression of cellular mRNAs and corresponding exosomal mRNAs showed a strong correlation. In the other two cell lines, a moderate correlation was observed. Across all three cell lines, cellular miRNAs and corresponding exosomal miRNAs exhibited moderate correlation. We focused on RNAs that were lowly expressed in cells but highly expressed in exosomes and conducted differential expression analysis using R. Compared with healthy volunteers in the GEO database, some RNAs showed high expression in the supernatant and low expression in the plasma of healthy volunteers.
Conclusion: We identified three mRNAs and three miRNAs that may serve as promising biomarker candidates for PC.

#2432 Improved liquid biopsy assay performance using sequencing by binding (SBB).

D. Nasko, P. Pham, S. Joshi, K. Kim, N. Pezeshkian, Y. Kim, **A. Sockell**, J. Korlach;
PacBio, Menlo Park, CA

Liquid biopsy is revolutionizing the field of early cancer detection research through non-invasive detection of tumor DNA in the blood. However, existing liquid biopsy assays are limited in their sensitivity for ctDNA detection at low variant allele frequencies (VAFs), with most relying on extreme sequencing depth and computational error correction to separate the true ctDNA signal from background errors. This limitation is particularly problematic in the area of early cancer detection, in which expected ctDNA allele frequencies are extremely low. Novel strategies are therefore needed to help improve liquid biopsy assay sensitivity and reduce per-sample sequencing requirements. Here we describe PacBio's application of the Onso short-read sequencing system to enable detection of ctDNA at low VAFs using the SeraCare Complete ctDNA Mutation Mix reference standard. The Onso system makes use of a novel sequencing by binding (SBB) method to achieve up to 15x greater quality scores, with ≥90% of reads at Q40 or above. We performed targeted capture and sequencing of libraries prepared from the SeraCare reference mix diluted into WT human DNA at the following VAFs: 0.00% (WT), 0.05%, 0.10%, 0.25%, and 0.50%, and compared the sensitivity at each VAF for SBB compared to a competitor method using sequencing by synthesis (SBS) at varying sequencing depths. We observed superior sensitivity for ctDNA detection at low VAFs (0.05%, 0.1%) using SBB at half the sequencing depth compared to SBS, in part due to reduced false positive calling in the WT sample for SBB. Furthermore, SBB was able to achieve comparable sensitivity results to SBS using four-fold less sequencing, and without the use of computational error correction. Finally, combining SBB with computational error-correction methods boosted sensitivity even further, suggesting an additive value for these technologies. Taken together, our results demonstrate the potential of SBB to improve upon existing methods of liquid biopsy and better enable research on early cancer detection.

CLINICAL RESEARCH: Early Detection Biomarkers 2
Poster Session

#2436 In-depth analysis of microRNA signature in breast cancer derived extracellular vesicles: A potential biomarker repository for breast cancer diagnosis.

Jee Ye Kim, Min Woo Kim Kim, Young Kim, Sol Moon, Suji Lee, Hyojung Lee, Joon Ye Kim, Seung Il Kim

Yonsei University College of Medicine, Seoul, Korea, Republic of

Breast cancer remains one of the leading causes of cancer-related mortality among women worldwide. With the rising incidence of breast cancer, early and accurate diagnosis is pivotal in improving survival rates and patient outcomes. Our study addresses to identify vesicles associated with breast cancer in scope of miRNA signature. We focused on isolating breast cancer-derived extracellular vesicles (BEVs) from the bloodstream with immune affinity capture techniques. Then, we analyzed the miRNA profiles of BEVs in plasma samples from 120 breast cancer patients, 46 individuals with benign tumors, and 45 healthy controls. In this study, we analyzed to discover miRNA candidates for diagnosis of breast cancer with The Gene Expression Omnibus (GEO) database and found 379 down-regulated and 584 up-regulated differentially expressed miRNAs (DEMs) in tissue samples across 5 GEO datasets, and 28 down-regulated and 80 up-regulated DEMS in blood samples. Subsequently, we measured the expression levels of these 10 candidate miRNAs in BEVs from breast cancer cells and compared them with EVs from human mammary cells (MCF10a), using our BEV isolation method. The expression profiles of these miRNAs in BEVs were significantly elevated, supporting their potential as surrogate markers for breast cancer diagnosis. When comparing the AUC values of 10 candidate miRNAs through ROC analysis, 5 EV miRNAs (miR-21, miR-106b, miR-181a, miR-484, and miR-1260b) showed a high AUC values above 0.8. Subsequently, we verified a distinct signature of 5 EV miRNAs that effectively differentiate breast cancer patients from normal controls with 57.14% of sensitivity and 95% of specificity. Overall, our study not only complements existing diagnostic methods with high accuracy but also provides a deeper understanding of the molecular aspects of breast cancer, heralding a significant advancement in precision medicine and personalized cancer care.

#2437 Distinct DNA methylation patterns in male urogenital cancers.

G. Yu[1], J. Wang[1], L. Li[1], W. Xie[2], Y. Liu[1], Q. Yang[1], B. Xu[1];

[1]Shanghai Ninth People's Hospital, Shanghai Jiaotong University School of Medicine, Shanghai, China, [2]Burning Rock Biotech, Guangzhou, China

Background: Male urogenital cancers including prostate cancer (PCa), bladder cancer (BLCA) and kidney renal cancer (KIRC), account for 38% of the total number of new male cancers. Previous studies have shown that changes in DNA methylation patterns are associated with the occurrence and progression of these cancers. Here, we performed whole-genome bisulfite methylation sequencing (WGBS) on tissue samples from these cancers to comprehensively characterize the methylation patterns to provide insights into the potential biological functions of methylation and to identify possible early detection biomarkers.
Methods: Tissue samples were collected from patients with PCa, BLCA and KIRC who had not received any treatment prior to surgery from Shanghai Ninth People's Hospital, Shanghai Jiaotong University School of Medicine. Samples with the cancer cells content ≥30% in cancer tissues and no cancer cells in the adjacent tissues was deemed qualified. A total of 43 samples were sequenced by whole-genome bisulfite methylation sequencing (WGBS) with a depth of 30X, including PCa, BLCA, KIRC cancer tissues, and their adjacent cancer tissues.
Results: Distinct methylation patterns were observed in the 3 cancers. By comparing cancer and adjacent tissues, the numbers of differentially methylated sites (DMSs) were 21,195 (31% hyperDMSs and 69% hypoDMSs), 587,010 (23% hyperDMSs and 77% hypoDMSs) and 7,855,162 (5% hyperDMSs and 95% hypoDMSs) in PCa, BLCA and KIRC, respectively. The distribution of hyperDMSs and hypoDMSs across various chromosomes was relatively consistent in KIRC and BLCA. However, in PCa, the hypoDMSs were mainly located on chromosome 8 (5265/14666, 36%). Among the three cancers, only 2-3% of hypoDMSs were located in gene promoter regions, while the proportions of hyperDMSs in gene promoter regions were higher with 4%, 8% and 17% for PCa, BLCA and KIRC, respectively. Among the above DMSs, 1901 DMSs-related genes were shared by PCa, BLCA and KIRC and 251, 4252, 2475 DMSs-related genes were unique in PCa, BLCA and KIRC, respectively. Gene Ontology analysis revealed that the shared DMSs-related genes were enriched in Wnt signaling pathway and positive regulation of MAPK cascade.
Conclusions: Our present study demonstrated the differential methylation patterns in male urogenital cancers, which may provide insights into the potential biological functions of methylation and to identify possible early detection biomarkers.

#2438 A retrospective pilot study to validate the utility of proteomic biomarkers in the blood for diagnosis of breast cancer.

S.-Y. Jung[1], E.-G. Lee[1], J. Han[1], S. Lee[1], S. Shin[1], J. Lee[1], S.-S. Kim[2], Y. Kim[3], D.-Y. Noh[3];

[1]National Cancer Center - Korea, Goyang-si, Korea, Republic of, [2]Manufacturing and Technology Division, Bertis Inc, Yongin-si, Korea, Republic of, [3]CHA Gangnam Medical Center, CHA University School of Medicine, Seoul, Korea, Republic of

Background: Previously, three-protein signature (Mastocheck®, Bertis Inc.) from plasma has been launched to overcome the limitation of low accuracy of mammography. In addition, nine-protein signature from serum was newly developed to improve the accuracy of three-protein signature as a blood-based diagnostic tool. This study aimed to validate the diagnostic utility for breast cancer of nine-protein signature with comparison with three-protein signature.
Methods: A blood-based test using multiple reaction monitoring (MRM) by mass spectrometry to quantify nine proteins (APOC1, CHL1, FN1, VWF, PPBP, CLU, PRDX6, PRG4, and MMP9) in serum and three proteins (APOC1, CHL1, CA1; Mastocheck®) in plasma was investigated using blood of 30 health women and 30 breast cancer patients. Using the cut-off values confirmed by AI-based deep learning model, we evaluated the sensitivity, specificity, and accuracy of nine- and three-protein signature for detecting breast cancer.
Results: Among 60 cases, the sensitivity and specificity of nine-protein signature was 87.9% and 80.7% for diagnosis of breast cancer. These values were 20% and 10% higher than those of three-protein signature, respectively (66.7% of sensitivity and 70.0% of specificity). The accuracy of nine-and three-protein signature was 83.3% and 68.3%.
Conclusion: This study demonstrated that nine-protein signature could be a more accurate and effective tool for detecting breast cancer compare to three-protein signature). For a confirmatory study, we need to perform a large scaled validation study in future. Grants: This research was supported by Bertis, Republic of Korea (grant number: NCC 2341770-1)

#2439 Potential target genes for early stage detection in Hispanic colorectal cancer.

E. V. Caraballo, **C. Zenon-Melendez**, J. Perez-Santiago, M. Cruz-Correa;
University of Puerto Rico Comprehensive Cancer Center, San Juan, Puerto Rico

Background: Colorectal Cancer (CRC) has become the second leading cause of death related to cancer worldwide and the third most common malignancy. CRC tumors are classified into stages to describe the cancer; early (stages I and II) and advanced (stages III and IV). Despite the available screening methods and the scientific efforts in the development of a universal biomarker panel for CRC early detection, there still exists a gap in a reliable non-invasive screening method for the Hispanic community. *We aimed to elucidate the most important pathways along with the differential gene expression in early and advanced CRC stages in a Hispanic population.*

Methods: We examined restrospectively 7 tissue samples from a Puerto Rican Hispanic population recruited throughout the Puerto Rico Familial Colorectal Cancer Registry (PURIFICAR) IRB #A2210207. We evaluated transcriptomic changes in advance tumors (n=4) vs. early tumors (n=3) with their respective normal mucosal tissue as negative control. Extracted RNA was sequenced using the Illumina NextSeq (2 X 75bp). The higher-quality reads were aligned, annotated, and quantified to the human genome (hg38) using STAR and RSEM softwares. Gene expression analysis was performed in R statistical software (packages tximport and DESeq2). We compared significantly expressed genes (adjusted p-value <0.05) between study groups (Tumor Advance [TA] vs. Mucosal Advance [MA] and Tumor Early [TE] vs. Mucosal Early [ME]) using Venny, and we performed enrichment analyses and protein-protein interaction networks using Metascape and STRING database, respectively.

Results: There were 2284 differentially expressed genes (TA vs. MA) and 984 (TE vs. ME), in which 1736 were unique to advance stages, 436 were unique to early stages and 548 were shared in both tumor stages. Significantly impacted biological processes and pathways include: granulocyte chemotaxis, regulation of inflammatory response, positive regulation of apoptotic process, tissue morphogenesis, G alpha signaling events, interleukin-10 signaling, signaling by interleukins. Additionally, physical and functional interaction networks showed 11 major clusters (≥ 5 genes), which contained several gene hubs including LYN (proto-oncogene), IL-1β, IL-1α, TNF, CCL3, CCL4, CXCR1 and CXCR2 (cytokines/ chemokines) among others genes previously reported as CRC biomarkers (DKK1, AQP8, AQP9, CTNNB1, and GNAQ).

Discussion/Conclusions: Differential analysis of early CRC tumor samples shows a deregulation of genes related to the inflammatory response which plays an important role in CRC. Modulation of these genes suggests significant potential targets for early detection of CRC in a Hispanic population. Future studies will be focus on the evaluation of selected target genes as a non-invasive early CRC screening method.

#2440 Cancer driver mutations as quantitative biomarkers of cancer risk interspecies analyses using CarcSeq.

K. L. Harris, B. Gong, B. Parsons, J. Faske, J. Xu;
FDA-NCTR (National Center for Toxicological Research), Jefferson, AR

Unmet needs in cancer risk assessment include the ability to predict rodent life-time tumor responses from short-term exposures and a scientific basis for rodent to human extrapolation. As an approach to address these needs, the use of hotspot cancer driver mutations (CDMs) as biomarkers of cancer risk was integrated with an error-corrected, next generation sequencing (NGS) approach. We have developed and investigated the sensitivity of a high-throughput NGS method capable of detecting a panel of the most prevalent point mutations observed in human oncogenes and tumor suppressor genes. This method, CarcSeq, involves performing multiple, high-fidelity PCR reactions to amplify the most prevalent mutations reported to occur in human tumors, tagging the amplicons with 9 bp unique identifier sequences at each end, constructing libraries using Illumina ChIP Seq kits, sequencing the libraries on an Illumina NextSeq500 platform and generating single-strand consensus sequences (SSCS), bioinformatically, as a means of error-correction. We validated CarcSeq mutant fraction measurements through observations related to known cancer driver tissue-specificities and mutation spectra for normal human breast and lung, ductal carcinoma, and lung adenocarcinoma samples. Performance of a reconstruction experiment established CarcSeq has a sensitivity of 10^{4}. The approach has now been adapted to analyze analogous conserved codons in rat and mouse. For each of the three species, the developed panel includes 13-15 amplicons encompassing known cancer driver genes (e.g., *KRAS*, *PIK3CA*, and *TP53*) encompasses the equivalent of 30 known human hotspot codons and has a combined target sequence length of ~1 kb. Amplicons were generated from DNA isolated from 16-week-old, untreated rodent tissue samples with known differences in spontaneous tumor incidence: female Wistar, Sprague Dawley, and F344 rat mammary samples and male and female $B6C3F_{1}$ and CD-1 mouse lung samples. The rodent panel was optimized to generate ~100,000 SSCS/amplicon. CDMs were observed at conserved codons in young, untreated rodents, and results are consistent with what was expected based on strain differences in spontaneous tumorigenesis.

#2441 Higher levels of LPS in blood plasma as potential novel biomarker for cancer risk in Puerto Rican people living with HIV.

J. Torres Reyes[1], T. L. Shull[2], G. Borges-Velez[1], V. S. Sanchez Gonzalez[1], J. L. Salgado Montilla[1], J. Perez Santiago[1];
[1]UPR - Comprehensive Cancer Center, San Juan, Puerto Rico, [2]Medical Center, Chicago, IL

Background: People living with HIV (PWH) have a significantly higher risk of developing cancers than people without HIV (PWOH), even with suppressive antiretroviral therapy. Puerto Rico (PR) is considered a high-risk group disproportionately affected by HIV and a priority group for cancer prevention strategies. Dysbiosis of the human microbiota can contribute to persistent inflammation by upregulating TGF-β (microbial-induced oncogenesis biomarker), which can promote the translocation of microbial products into the bloodstream, increasing cancer risk at local and distant sites. However, the relationship between TGF-β, and microbial products such as lipopolysaccharide (LPS) and short-chain fatty acids (SCFA) in relation to HIV infection is poorly understood, therefore we aimed to quantify the levels of LPS and SCFA in the blood plasma of PWH vs. PWOH and investigated their relationship with cancer risk measured by TGF-β.
Methods: Blood samples, sociodemographic, and clinical data from 80 adults (50 PWH and 30 PWOH) were collected. PWH were virally suppressed (<50 copies/mL) with a median CD4 count of 699.8 cells/μL. We measured TGF-β, LPS, and soluble CD14 (sCD14, marker of innate immune activation and microbial translocation) using immunoassays. SCFA (acetate, butyrate, and propionate) were measured using gas chromatography followed by mass spectrometry. Differences in the median levels of TGF-β, LPS, and SCFAs were evaluated using a Mann-Whitney test. We assessed the effects of LPS, SCFAs, and HIV infections in relationship with levels of TGF-β using multivariate fixed-effects regression analysis in R-statistical software.
Results: PWH had significantly higher levels of TGF-β (4397 pg/mL vs. 1121 pg/mL, p=0.017), higher levels of LPS (38.97 pg/mL vs. 19.26 pg/mL, p<0.001), higher levels of sCD14 (1326 pg/mL vs. 1137 pg/mL, p=0.007), and significantly lower levels of butyrate (84.5 ng/mL vs. 62.0 ng/mL, p<0.001). Higher levels of TGF-b were associated with higher levels of LPS (rho=0.38, p=0.017) and higher levels of sCD14 (rho=0.27, p=0.016) these relationships remain significant after adjusting for HIV status (p<0.001).
Conclusion: Our findings suggest that microbial products in blood plasma can contribute to higher cancer risk in Puerto Rican PWH and may represent potential novel biomarkers for cancer prevention.

#2442 Blood based novel mRNA genomic test, for screening, early detection, prognosis and monitoring of prostate cancer using a multi-center study.

Y. Hashimoto[1], S. Verma[2], G. Deng[3], D. P. Chauhan[3], S. Nair[4], D. Chakravarty[4], H. Yoshino[5], J. Arima[5], S. Tatarano[5], Y. Liu[6], K. Hatano[6], Y. Shivakumar[7], M. Ghosh[7], K. Raghunath[7], C. Chandran[8], N. Ragavan[8], H. Enokida[5], N. Nonomura[6], K. Balaji[9], S. Rawal[10], A. Tewari[4], R. Dahiya[1], **S. Gupta**[2];
[1]UCSF School of Medicine, San Francisco, CA, [2]Case Western Reserve University and University Hospitals Cleveland Medical Center, Cleveland, OH, [3]Geneverify Inc, Hayward, CA, [4]Tisch Cancer Institute, Icahn School of Medicine at Mount Sinai, New York, NY, [5]Kagoshima University Hospital, Kagoshima, Japan, [6]Osaka University Medical School, Osaka, Japan, [7]HCG Cancer Center Hospital, Bengaluru, India, [8]Apollo Cancer Center Hospital, Chennai, India, [9]University of Florida College of Medicine, Jacksonville, FL, [10]Rajiv Gandhi Cancer Institute & Research Centre, New Delhi, India

Background: Current screening tools, including prostate-specific antigen (PSA) and clinico-pathologic parameters, have limitations in the diagnosis and prognosis of prostate cancer. This study examined whether genomic biomarkers can improve screening and monitoring of prostate cancer.
Methods: We identified a panel of 25 prostate cancer-related genes through rigorous bioinformatics, computational analyses and genetic testing. These tests, developed by Geneverify Inc. (Hayward, CA; U.S. patent # 10801072 and 10822661) were utilized and optimized by qRT-PCR to determine the diagnostic and prognostic ability of prostate cancer using blood and tissues. The log2-fold increase in gene expression was used to assign the risk score to individual patients. ROC (receiver operator characteristic), AUC (area under ROC curve), and calibration curves were generated to display the overall performance and discrimination ability to separate cancer and non-cancer specimens.
Results: A total of 445 prostate cancer patients (135 blood and 310 tissue samples) and 130 normal samples were analyzed in this study. The eligibility criteria were to collect blood and surgical specimens from patients with prostate cancer. The study endpoints were to analyze mRNA genomic profiling and correlate with clinico-pathologic parameters of the patients. In the blood, a 25-panel gene-set separated prostate cancer patients (n=135) from non-cancer (n=30), AUC = 0.906 [sensitivity = 90% and specificity = 91%]. Assessment of tissue specimens from benign (n=100) and cancer patients (n=310) demonstrated similar results with AUC=0.9514 [sensitivity=95% and specificity=94%]. Interestingly, patients with Gleason grades more than 7 showed higher expression of these genes compared to Gleason Grades less than 7, suggesting the prognostic ability of the gene-set. When we compared the gene expression in blood verses tissues, there were similar patterns, suggesting that blood can be used for screening, diagnosis and risk assessment of prostate cancer.
Conclusions: To our knowledge, this is the first study to investigate the role of mRNA-based genomic signatures for screening, early diagnosis and prognosis of prostate cancer using blood samples. Our results suggest that blood mRNA-genomic profiling developed by Geneverify has the ability to diagnose prostate cancer and stratify patients into distinct prognostic groups, which in turn help in making better treatment strategies.

#2443 Improved detection of low frequency mutations in ovarian and endometrial cancers by utilizing a highly accurate sequencing platform.

T. Revil[1], N. Pezeshkian[2], L. Gilbert[1], **A. Sockell**[2], J. Ragoussis[1];
[1]McGill University, Quebec, QC, Canada, [2]PacBio, Menlo Park, CA

Ovarian and endometrial cancers come within the top-4 for incident cancers as well as deaths in North American women. Cure rates have not improved in 30 years as high-grade subtypes continue to be diagnosed in Stage III/IV. Attempts at early diagnosis have failed because high-grade cancer cells exfoliate and metastasize while the primary cancer is small and undetectable by existing tests based on imaging and blood-based tumor markers. DOvEEgene (Detecting Ovarian and Endometrial cancers Early using genomics) is a genomic uterine pap test developed by a McGill team to screen and detect these cancers while they are confined to the gynecologic organs and curable by surgery. The test identifies pathogenic somatic mutations in uterine brush samples. Here we tested the Onso system, a highly accurate sequencing technology from PacBio in order to potentially increase sensitivity while driving down sequencing costs by reducing required sequencing depth vs the current NGS standard. A highly sensitive, error-correcting capture technology (DOvEEgene-SureSelectHS) utilizing duplex error correction sequencing interrogated the exons of 23 genes involved in the development of sporadic and hereditary ovarian and endometrial cancers. We applied a combination of germline gene panel testing on saliva samples with deep duplex sequencing to detect somatic mutations at <0.1% VAF, interrogation of microsatellite loci for instability, and low coverage WGS for copy number analysis of uterine brush samples. We sequenced 20 duplex Illumina sequencing libraries produced using the DovEE assay at PE 100bp mode and compared Onso data in non- duplex sequencing mode as well as duplex sequencing mode to the original Illumina duplex sequencing method. Here, we present this comparison and highlight the benefits of high accuracy sequencing for the detection of very low frequency (<0.1%) somatic mutations. We observed improved mismatch rates for Onso data compared to Illumina, even after duplex error correction was applied. In addition, we found that more individuals are called as displaying microsatellite instablity from the Onso data, which may be due to improved sequencing performance in repetitive regions for Onso. Finally, we observed fewer potential false positive variant calls in the Onso data, highlighting the value of improved sequencing accuracy for rare variant detection.

#2444 Plasma levels of matrix metalloproteinases 8 are significantly increased in patients with colorectal cancer (CRC) and mRNA levels are increased in 71% of tumors vs normal tissue.

Chandana S. K. Herath Mudiyanselage, Anuj R. Sharma, Neil Mitra, Aashutosh Sah, Xiaohong Yan, Pablo Palacios, Vesna Cekic, Richard L. Whelan

Department of Surgery, Lenox Hill Hospital, New York, NY

Introduction: Matrix metalloproteinases 8 (MMP-8) is a member of the MMP protease family mainly involved in degrading extracellular matrix. A variety of cells express MMP-8 and during pathological inflammation neutrophils release IL-1, IL-8, TNF-α, and GM-CSF which triggers MMP-8 secretion. MMP-8 aids tumors in evading immune detection during the development of CRC and also regulates the role of endothelial cell in angiogenesis. Increased MMP-8 tumor expression and serum levels has been noted in hepatocellular cancer and melanoma patients and are associated with adverse outcomes. There is limited data regarding blood levels of MMP-8 in CRC patients. This study compared preoperative (PreOp) plasma MMP-8 levels in patients with CRC and benign colonic pathology (BCP) undergoing bowel resection.

Method: Patients with CRC or BCP who had elective colorectal resection who were enrolled in an IRB approved tissue and data bank for whom preop plasma samples were available were eligible. Data analyzed included demographic, clinical, operative, and final pathology reports. Blood specimens were quickly processed and plasma stored at -80°C. MMP-8 levels in Preop plasma samples were measured via ELISA, in duplicate, and reported as median +95% CI (ng/ml). MMP8 expression was examined in paired CRC and normal mucosal tissue samples from a subset of the CRC patients (n=20) via QRT-PCR. Immunohistochemistry (IHC) was conducted on formalin-preserved tissue sections (tumor/normal pairs) following standard protocols. The concept of MMP8 as CRC diagnostic marker was evaluated by assessing the receiver operating characteristic (ROC) curve and the area under the ROC curve (AUC). The analysis was done with the Mann-Whitney test (significance, $p<0.05$).

Results: 96 CRC patients (74% colon and 26% rectal cancer) and 96 BCP patients (32% adenoma, 64% diverticulitis, 4% other) met entry criteria. The CRC stage distribution was: Stage 1, 26%; Stage 2, 26% Stage 3, 40%; and stage 4, 8%. Median plasma MMP-8 levels were higher in CRC (8.21, CI: 6.92, 10.81) compared to BCP patients (5.59, CI: 4.68, 7.30; $p<0.001$). A non-significant increase in median MMP-8 levels were noted in STG IV vs STG I and STG II and STG III was found (38-89%). IHC validated the expression of MMP-8 in CRC tumors relative to normal colon. Increased expression of MMP-8 was seen in 71% of the tested CRC samples (12/17). The AUC value for the ROC curve was 0.653 (sensitivity 35%, specificity 0.95%).

Conclusion: The median MMP-8 level in CRC patients was found to be 47% higher compared to BCP patients and 89% higher in stage IV vs stage II patients ($p=0.06$). The tumor is the most likely the cause of elevated plasma levels. Increased tumor expression of MMP-8 mRNA was noted in 71% of tumors. The low sensitivity of the ROC curve suggests MMP8 alone has no value as diagnostic factor. Larger studies are justified.

#2445 Peripheral blood immune phenotypes in pancreatic ductal adenocarcinoma.

K. D. Pavelko, J. C. Villasboas, W. R. Taylor, K. A. Doering, J. B. Kisiel, S. Majumder;
Mayo Clinic, Rochester, MN

Introduction: Pancreatic ductal adenocarcinoma (PDAC) is a major cancer killer with a low 5-year survival rate of 12%. Diagnosing PDAC at an early stage is one of the strongest predictors of long-term survival. Therefore, novel methods for early detection of PDAC must be explored. In this pilot study we aimed to compare the peripheral blood immune cell phenotypes in PDAC cases and cancer-free controls.
Method: CyTOF (cytometry by time-of-flight) was used to evaluate peripheral blood mononuclear cells (PBMC) from newly diagnosed treatment naïve patients with PDAC and sex and age matched cancer-free controls using a 29-marker immune phenotyping panel. Multiple analysis approaches including dimensionality reduction using tSNE and clustering using Phenograph were used to evaluate the results. Immune subsets having differential abundance differences were verified by manual gating.
Results: Twenty patients were included in this pilot study (15 PDAC cases; 5 Cancer-free controls). Among the 15 PDAC cases, 5 were early stage (Stage 1-2). Thirty-two unique immune cell clusters were identified using the Phenograph algorithm: 10 unique clusters with properties consistent with monocytes/macrophages, 9 CD4 T cell clusters, 6 CD8 T cell clusters and 4 NK cells clusters. When comparing the case and control groups we noted lower percentages of CD8+CD27+ T-cells in cases. This was further verified by manual gating that confirmed the distribution of CD8+CD27+ T-cells relative to all T-cells were decreased in PDAC patients. In addition, a 57% increase in naïve CD4 T cells was found in case samples compared to controls. A principal component analysis of the clustering results identified two unique clusters of immune profiles that emerged providing a potential peripheral blood immune cell signature that could stratify and differentiate PDAC cases from controls. A $CD14^{+}CD16^{+}CD4^{Lo}CD38^{+}CD45RO^{+}$ population of monocytes was the primary cell population driving this difference.
Conclusion: This study provides early evidence to indicate that a distinct PBMC immune phenotype may differentiate PDAC patients from control subjects. Further analysis in larger sample sets is warranted for in-depth characterization and identification of unique immune based biomarkers for PDAC detection.

#2446 Genomic landscape of longitudinally collected preinvasive airway lesions.

A. Alhendi, L. Kalinke, A. Pennycuick, K. Davies, P. Durrenberger, K. Gowers, K. Grigoriadis, N. McGranahan, S. Janes;
University College London (UCL), London, United Kingdom

Lung carcinoma in situ (CIS) lesions, as precursors to squamous cell carcinoma, exhibit microscopic uniformity while displaying diverse clinical trajectories. Half of these lesions progress to invasive cancer, while the remaining half either regress or remain indolent. Previous genomic profiling efforts have elucidated progression-specific genomic changes against a backdrop of inherent heterogeneity and notable chromosomal instability signatures. Here, we present a novel approach by analyzing longitudinally collected samples of preinvasive airway lesions, encompassing both progressive and indolent trajectories.
Our findings reveal that genomic integrity and cell cycle dynamics constitute key distinctions between progressive and indolent lesions. Notably, a decrease in clonal diversity and an inverse correlation between TCRA-Tcell fraction and genomic instability are observed as lesions approach invasion. Somatic mutations in cancer driver genes *BRAC2*, *CSMD3*, and *MUC16* are found significantly associated with lesion progression. Furthermore, progressive lesions exhibit a higher frequency of copy number changes compared to indolent lesions. Copy number loss in 1p, 3p, 9p, and 17p are found to be significantly associated with lesion progression. Phylogenetic analysis further confirms positive selection for copy number loss in these specific genomic regions, providing insights into the evolutionary trajectory of alterations in progressive lesions. The comprehensive understanding derived from these genomic analyses is anticipated to advance early detection strategies, mitigate overtreatment, and facilitate the development of preventative therapies targeting early clonal events in lung cancer.

#2447 Identification of tumor marker gangliosides for early cancer detection: A mass spectrometry approach.

Rachel Culp-Hill, Collin Hill, Adele Blackler, William Ricketts

AOA Dx, Inc., Boulder, CO

Tumor-marker gangliosides (TMGs) have enormous potential for early-stage cancer detection as diagnostic biomarkers despite being relatively understudied in this context. AOA Dx is focused on the development of a mass spectrometry platform for the quantitation of TMGs in human serum, particularly disialogangliosides GD2 and GD3. The development of a mass spectrometry platform for TMG quantitation may allow for the identification of diagnostic signatures for early-stage cancer detection. Briefly, we monitored fragment moieties characteristic of gangliosides in an untargeted fashion by mass spectrometry. We then identified those differentially altered in cancerous groups compared to normal, and subsequently performed targeted MRM analysis. Through these investigations, we have identified multiple TMGs, specifically multiple types of GD2 and GD3 species characterized by unique lipid tails across different cancer types in human serum from confirmed cancer diagnoses. Other ganglioside classes including GMs and relatively understudied GTs were also identified in this study. Notably, the serum of melanoma and ovarian cancer patients exhibited significantly increased levels of several ganglioside species compared to age-matched healthy serum, highlighting the potential of TMGs as a promising avenue for cancer diagnosis. Further experiments will focus on refining this mass spectrometry method and expand demographic representation to confirm our initial findings and identify additional TMGs of interest. In addition, we intend to apply immune-based platforms such as thin-layer chromatography and ELISA, which have already shown promising results in the detection and quantitation of these compounds. Taken together, AOA Dx is advancing the development of a high-throughput mass spectrometry platform designed for the detection of TMGs, with a primary focus on GD2 and GD3. Our objective is the identification of a diagnostic disease signature for early-stage cancer detection. The validation of this type of diagnostic panel would allow for expedited diagnosis and treatment of cancers currently diagnosed at late stages, ultimately reducing healthcare costs and increasing survival rates. Future research will aim to validate these biomarkers in independent prospective studies.

#2448 Field cancerization proteomic analysis provides a novel class of functional risk biomarkers for non small cell lung cancer.

R. I. Alhammad[1], N. B. Vuong[1], W. Zhou[1], D. Johann Jr[2], B. Birkaya[1], L. Liotta[1], A. Luchini[1];
[1]George Mason University, Manassas, VA, [2]UAMS Medical Center, Little Rock, AR

Lung cancer carcinogenesis is the outcome of a field of premalignant changes that occur in the bronchial tree leading to the overt emergence of the malignant lung cancer (field cancerization). A tissue or blood proteomic signature of these premalignant changes represent a novel concept of risk biomarkers that can predict the probability of future emergence of Lung Cancer. In this study, we analyzed two independent cohorts of non-small cell lung cancer (NSCLC) patients. One cohort consisted of 18 patients who donated blood before and after tumor resection surgery and matched tissue samples (UAMS Medical Center). The second set derived from a longitudinal case-control study of plasma sample collected during the physician health study that were donated at different times prior to the diagnosis of Non-Small Cell Lung Cancer (N=272). We used affinity-enriched mass spectrometry analysis and statistical learning techniques to identify a set of common markers that discriminated plasma cases and controls and were conserved in different bronchial tissue compartments including tumor and adjacent tissue. The tumor microenvironment adjacent to and surrounding cancer cells undergoes to progressive stages of carcinogenesis during field cancerization. We identified 22 proteins involved in cell adhesion, protein folding, immune response, angiogenesis, and cancer proliferation. This is a novel class of functional risk biomarkers to determine the probability of NSCLC onset. In conclusion, our findings shed light on a new class of functional biomarkers that underly tumor pathogenesis mechanisms and can provide hints for new strategies of tumor prevention therapy or lifestyle modification.

#2449 Case report: DETECT-A participants with pre-malignant conditions.

O. A. Choudhry[1], A. Kharge[1], **S. P. Rego**[1], P. Z. Elias[1], A. H. Buchanan[2], A. Lennon[3], N. Papadopoulos[3], F. Diehl[1], T. M. Beer[1];
[1]Exact Sciences Corp., Madison, WI, [2]Geisinger, Danville, PA, [3]Johns Hopkins University, Baltimore, MD

Background: Blood based tests for multi-cancer early detection (MCED) are being developed to facilitate the earlier detection of various cancer types. The Detecting cancers Earlier Through Elective mutation-based blood Collection and Testing (DETECT-A) study evaluated the CancerSEEK MCED test, an early version of the Exact Sciences MCED test in development, in 9,911 women, age 65-75, without previous history of cancer (Lennon et al., Science 2020). The degree to which MCED testing will facilitate detection of precancerous conditions or incidental findings is unclear. Here we focus on DETECT-A participants who had pre-cancerous conditions diagnosed during a diagnostic work-up for a positive CancerSEEK MCED test.
Methods: In a post-hoc analysis, we report on the detection of precancerous conditions consequent to CancerSEEK MCED testing and follow-up. Electronic health records were reviewed for diagnostic procedures performed, details of premalignant and cancer diagnoses, and vital status.
Results: In three individuals, mutations in *PIK3CA*, *TP53*, or *KRAS* genes led to a positive CancerSEEK MCED test result. The prescribed imaging protocol using 2-deoxy-2[fluorine-18] fluoro-D-glucose positron emission tomography-computed tomography (18-FDG PET-CT), revealed a 10.3x9.8x7.8(cm) ovarian mucinous cystadenoma, a 0.8 cm appendiceal mucinous neoplasm, and 3 colonic polyps displaying high-grade dysplasia. All three participants were diagnosed with clinically significant pre-cancerous lesions, subsequently underwent surgical treatment, and remain alive and cancer-free as of February 2023 (Table 1).
Conclusion: The diagnostic evaluation of a positive MCED test may occasionally reveal clinically significant pre-cancerous conditions amenable to interventions. The frequency of such findings and their clinical impact warrants further study.

#2451 Investigation of SIRT6 usefulness as a novel biomarker for oral cancer.

H. Yoshii, A. Shimoda, K. Mitsudo, M. Kioi;
Yokohama City Univ. - Fukuura Campus, Yokohama, Japan

Introduction: SIRT6 is one of the seven human sirtuin genes and is known to function as an onco-suppressor gene in colorectal and ovarian cancers, although it is up-regulated in other cancers. Thus, SIRT6 is considered performing both tumor-suppressing and promoting roles. However, the association of SIRT6 with oral squamous cell carcinoma (OSCC) and its role in OSCC pathogenesis are currently unclear. Currently, SCC or CYFRA are used as a tumor marker to assist in the diagnosis of OSCC in a clinical setting whereas its sensitivity is low. Therefor the development of a novel biomarker for early diagnosis and identification of new therapeutic targets is critical to resolve the pressing clinical issues related to the management of OSCC. This study aimed to investigate the expression and the relevance of SIRT6 in patients with OSCC and its potential as a biomarker for early detection and prognosis prediction.
Materials and Methods: This study enrolled 78 patients with OSCC and 9 patients with carcinoma in situ (CIS) . The OSCC patients had undergone surgery or chemoradiotherapy (51 surgery and 27 chemoradiotherapy). The CIS patients had undergone surgery. Samples were also obtained from 10 patients with oral potentially malignant disorders (OPMDs). Biopsied or surgical resected samples were used for the study. We obtained 21 noncancerous tissues as normal tissues from the adjacent noncancerous tissues after tumor resection. Immunohistochemistry, quantitative real-time RT-PCR, and microarray analyses were performed to determine SIRT6 expression and its association with clinicopathological features in OSCC, CIS, and OPMDs using clinical paraffin embedded specimens.
Results: SIRT6 mRNA levels were higher in OSCC tissues than those in noncancerous tissues ($p<0.05$). And SIRT6 protein expression levels were higher in OSCC, CIS and OPMDs tissues than those in noncancerous tissues ($p<0.05$). SIRT6 expression was predominant in patients aged ≥65 years and significantly correlated with shorten overall survival. In the microarray analysis, some SIRT6-associated genes, such as ANXA2 was significantly up-regulated, and PIGC and RGPD4 were down-regulated in OSCC.
Conclusion: SIRT6 plays a role in tumor homeostasis, leading to a poor prognosis in OSCC. SIRT6 may represent a novel target not only for the treatment, but also as a prognostic marker in OSCC.

#2452 Clinical importance of nicotinamide nucleotide transhydrogenase in obesity-associated colorectal cancer.

S. Jeong[1], S. Park[1], J. An[2], m. Kang[1], S. Nam[1], J. Kim[1];

[1]Gachon University Gil Medical Center, Incheon, Korea, Republic of, [2]Korea University Anam Hospital, Seoul, Korea, Republic of

Background: Obesity is increasing worldwide, and many associated diseases are emerging as global health problems. There is a relationship between body mass and the risk of developing colorectal cancer (CRC). However, predictive biomarkers of survival with body mass remain elusive. Therefore, we aimed to identify novel clinically relevant biomarkers for obesity-associated CRC.

Methods: We searched for biomarker candidates in The Cancer Genome Atlas CRC cohort. We divided the TCGA CRC cohort (n=268) data into 3 groups (healthy weight CRC group [HT], adjacent normal tissue from the HT group [AN]), and obesity CRC group [OT]). Candidates were validated by survival analysis after immunohistochemistry in an independent cohort of 420 patients.

Results: The gene expression levels of NNT, PANK3, PPARGC1B, RTL6, FAM220A, and TMEM9 were associated with survival in overweight and obese patients with CRC from TCGA cohort. These findings were validated using protein expression data from our independent cohort. In our patient cohort, the hazard ratio (HR) of the subgroup of low NNT versus that of high NNT in terms of 5-year event-free survival (EFS) was 2.20 (adjusted for age and sex, 95% CI: 1.01-4.80, $p < 0.05$) among patients of obesity-associated CRC. When both TNM staging and NNT expression were considered, patients of obesity-associated CRC with low NNT expression and advanced stage III-IV cancer had a HR of 21.20 (adjusted for age and sex, 95% CI: 2.88-156.08, $p < 0.01$) compared to those with high NNT expression and early stage I-II cancer. However, when patients of obesity-associated CRC with high NNT expression and advanced stage III-IV cancer were compared to those with high NNT expression and early stage I-II cancer, the former subgroup had a HR of 8.39 (adjusted for age and sex, 95% CI: 1.03-68.39, $p < 0.05$) in terms of the 5-year EFS. Finally, when the 5-year disease-specific survival analysis was performed, the patients of obesity-associated CRC with low NNT expression and advanced stage III-IV cancer were found to have a HR of 14.05 (adjusted for age and sex, 95% CI: 1.89-104.38, P = 0.01) compared to those with high NNT expression and early stage I-II cancer. Furthermore, low NNT expression results in the inactivation of several metabolic pathways, including ROS-related pathways.

Conclusions: NNT is a novel and promising CRC prognostic biomarker for overweight and obese patients. It can provide clinicians with early indicators of patient prognosis and aid in appropriate treatment selection.

#2453 Soluble B7H3 has a potential of novel serum biomaker for colorectal cancer.

A. Koizumi[1], T. Ito[1], K. Kato[2], T. Iwasawa[1], T. Kushida[1], K. Sato[1], C. Okamoto[1];
[1]Juntendo Shizuoka Hospital, Izunokuni City, Japan, [2]Toyo University, Kawagoe, Japan

B7H3 (also known as CD276, an immune checkpoint molecule) is aberrantly over expressed in many types of cancer. Recently, several reports indicate a crucial role for B7H3 in promoting carcinogenesis and metastasis. We investigated whether concentration of the soluble B7H3 could be used as a new prognostic predictor of colorectal cancer by measuring serum level of B7H3. Recently we established a new mAb to B7H3 and developed sandwich ELISA-system detecting human serum B7H3 with high sensitivity and specificity. Measuring the levels of B7H3 in the serum specimens of colorectal cancer donors, we examined the usefulness of B7H3 as a novel biomarker for colorectal cancers. We tested the blood from the 82 donors of colorectal cancers and 9 healthy donors who agreed in writing to this research, just before the operation. The mean value + 2SD in 9 healthy donors was set as the cutoff value. We classified cancer patients into 2 groups with high value of B7H3 and low value of B7H3. We also analyzed the relationships between serum B7H3 levels and disease-free survival (DFS) and overall survival (OS). Serum B7H3 levels were also compared with diagnostic biomarkers such as CEA and CA19-9. B7H3 immunostaining was also performed on tissue samples. The serum levels of B7H3 in patients with colorectal cancer were significantly higher than those of healthy donors. However, there were no correlation between B7H3 and other diagnostic markers CEA and CA19-9. Regarding DFS, the higher value group of serum B7H3 showed a tendency for DFS to decrease in Stage II and III. Regarding OS, there was no significant difference of serum levels of B7H3 in Stage I and IV cases, however, in Stage II and III, OS decreased significantly in the high B7H3 group. In B7H3 immunostaining, the tissue was not sufficiently stained. These data indicate that serum B7-H3 should be useful for novel biomarker for a rationale of disease monitoring and prognosis of colorectal cancer.

CLINICAL RESEARCH: Immunomodulatory Interventions and Mechanisms
Poster Session

#2457 Brain derived endothelial cells as a mediator of cGAS-STING driven anti-tumor efficacy in glioblastoma.
A. Schmidt, S. Remson, P. Vaughn-Beaucaire, J. L. Jimenez-Macias, P. Srinivasan, M. Pinho-Schwermann, S. Lawler;
Legorreta Cancer Center at Brown University, Providence, RI

The median survival time for newly diagnosed patients with glioblastoma (GBM) is 15 months, highlighting the need for improved therapies. Current treatment for newly diagnosed and recurrent GBM consists of tumor resection and chemoradiation therapy. The immunosuppressive tumor microenvironment (TME) is a central obstacle in the treatment of GBM. Lack of NK cell and CD8+ T cell infiltration prevents efficacy with immunotherapies like immune checkpoint blockade (ICB).One approach our lab is pursuing to enhance tumor infiltrating lymphocytes is through harnessing the anti-viral cGAS-STING pathway. Upon cGAS activation by cytosolic double stranded DNA, the TBK1 kinase is phosphorylated, initiating a subsequent type I interferon (IFN) response and the recruitment of immune cells. This pathway is commonly altered in many cancer types to evade immune activation. Our lab has demonstrated survival benefits with STING agonist treatment in immunocompetent GBM mouse models. We have also shown strong STING localization in the vasculature, implicating endothelial cells as a potential treatment target for anti-tumor efficacy. Here we investigated the potential role of tumor vasculature in mediating the effects of STING agonists in GBM therapy.We have shown robust cGAS-STING activation in brain endothelial cell lines through enhanced secretion of CXCL10, IFN-β, and RANTES upon STING agonist treatment *in vitro*. Western blotting also shows pathway activation in response to treatment through increased phospho-TBK1 levels. Activation was further potentiated by manganese.To investigate the effects of STING activation in brain endothelial cells in detail, we performed RNA sequencing. This showed 262 differentially expressed genes in response to pharmacologic cGAS-STING activation, with 183 of these being upregulated. The top gene ontology terms enriched include type I interferon signaling pathway, defense response to virus, and antigen processing and presentation of exogenous peptide antigen via MHC class I, TAP-independent. In addition, gene expression of tight junction protein Claudin 5 was also enhanced. We have also shown increased resistance in response to activation, through transendothelial electrical resistance (TEER) assays. Taken together, these results suggest that cGAS-STING activation in endothelial cells leads to tight junction remodeling in addition to immunomodulatory changes, implicating roles for endothelial cells in barrier function and immune cell interactions respectively. Current research in our lab focuses on elucidating the mechanisms behind these changes. Our goal is to identify beneficial endothelial cell changes which promote anti-tumor immunity in order to inform future treatment strategies. We are currently performing studies aimed at demonstrating that cGAS-STING activation in endothelial cells is critical for the efficacy of STING agonist treatment.

#2458 Targeting the CXCR3 axis in HER2+ breast cancer to enhance anti-tumor immunity.

A. Bhagat, J. Joseph, J. D. Ginzel, C. Rabiola, A. C. Hobeika, J. C. Snyder, H. K. Lyerly, E. J. Crosby;
Duke University, Durham, NC

Breast cancer (BC) is the most frequently diagnosed cancer in women worldwide with more than 2 million new cases in 2020. The efficacy of immunotherapies for BC is limited, with response rates of <10% for anti-PD-1/PDL1 monotherapy in pre-treated triple-negative breast cancer (TNBC) patients and even lower in subtypes that express human epidermal growth factor receptor 2 (HER2+) and/or hormone receptors. Hence, there is an urgent need to improve immune based strategies for BC. One possible approach to enhance response is the application of intratumoral (IT) immunotherapy utilizing IL-12; a potent pro-inflammatory cytokine that is critical in producing an anti-tumor response. However, systemic delivery of IL-12 has substantial toxicity and localized delivery of protein has insufficient residence time. To circumvent these issues, we have previously reported the efficacy of intratumorally injected plasmid IL-12 (pIL-12-EP) followed by electroporation in a TNBC mouse model and in clinical trials. Following pIL-12-EP, treated tumor expressed genes that were associated with increased CD8+ T cell infiltration, activation, trafficking, antigen presentation, and exhaustion. Single-cell RNA sequencing (scRNAseq) of tumor infiltrating immune cells from treated tumors revealed a striking enrichment of the CXCL9/10/11/CXCR3 family. This CXCR3 axis is upregulated in response to IFNγ production and has been studied extensively in melanoma and NSCLC patients as a potential predictive biomarker for responses to immune checkpoint inhibitors but has not been well characterized in BC. We hypothesized that this axis may be the critical component downstream of pIL-12-EP treatment that is responsible for anti-tumor responses and that targeting it will be effective in other molecular subtypes of BC beyond TNBC. We first evaluated the expression of CXCR3 by tumor infiltrating lymphocytes (TILs) in biopsies of human HER2+ BC. Using a single cell resolution spatial transcriptomic Xenium instrument we find not only expression of CXCR3 by TILs, but can also track the distance and gradients of the chemokine ligands CXCL9 and CXCL10 in this tumor microenvironment. Having confirmed the activity of this axis in human HER2+ BC, we used our well-established spontaneous HER2-driven mouse model to compare treatment of HER2+ tumors with pIL-12-EP or pCXCL9-EP intratumorally. We observed tumor growth inhibition in both treatment groups as compared to control treated tumors. Interestingly, the abscopal effect previously seen with pIL-12-EP was not evident for distant tumors in mice treated with pCXCL9-EP. These data suggest that IT CXCL9 therapies may benefit from combination with a systemic immune activator like a vaccine or immunogenic chemotherapy. Ongoing studies will continue to evaluate ways to better target this axis therapeutically and define clinically active combination therapies.

#2459 ADT-030 is a novel dual-acting RAS/β-catenin inhibitor that potentiates antitumor immunity.

M. Y. Gazi[1], O. Okoko[1], X. Wang[1], C. Brandle[1], X. Chen[2], K. Fadlalla[2], A. Keeton[2], Y. Maxuitenko[2], C. Hedrick[1], H. Shi[1], G. Piazza[2], **G. Zhou**[1];
[1]Augusta University Medical Center, Augusta, GA, [2]Auburn University, Auburn, AL

ADT-030 is a novel indene identified from a screening campaign and chemically optimized for drug-like properties that acts as a dual inhibitor of RAS and β-catenin signaling. Here we demonstrate that ADT-030 binds RAS with high affinity and inhibits MAPK/AKT signaling with high potency and selectivity in KRAS mutant cells to inhibit proliferation and induce apoptosis. ADT-030 also inhibits phosphodiesterase 10A (PDE10) that is overexpressed in cancer cells to selectively activate cyclic guanosine monophosphate (cGMP)/protein kinase G (PKG) signaling, which induces phosphorylation and degradation of the oncogenic pool of β-catenin. ADT-030 exhibited cytotoxicity to a variety of murine cancer cell lines *in vitro*, and inhibited tumor growth in syngeneic immunocompetent mice when orally administered. The antitumor activity of ADT-030 was diminished in mice that were immunodeficient or depleted of CD8+ T cells, indicating a critical role of the host immune system. In a metastatic breast tumor mouse model (4T1), ADT-030 not only delayed the growth of the primary tumor but also reduced tumor colonization in the lungs, leading to increased survival. CyTOF and scRNAseq analyses provided a plethora of information revealing the impact of ADT-030 on the immune milieu in the tumor microenvironment. Notably, ADT-030 selectively induced apoptosis of myeloid-derived suppressor cells (MDSCs) while CD8+ T cells were not affected. Consequently, ADT-030 treatment resulted in a marked reduction of MDSCs, which was accompanied by increased tumor infiltration of effector CD8+ T cells. ADT-030 treatment of cancer cells led to immunogenic cell death and enhanced dendritic cell activation. Furthermore, the ability of ADT-030 to augment the antitumor activity of immune checkpoint blockade therapy underlines its potential as a desirable immune-potentiating agent to improve the outcome of cancer immunotherapy. ADT-030 represents a development candidate ready for IND-enabling safety assessment.

#2460 Receptor antibody conjugated engager (RACE): A novel bispecific 4-1BB engager platform for enhanced immuno-oncology therapy.

DaeHee Lee[1], Jihye Yoon[1], Jonggwan Jeong[1], Jeonghyeon Bak[1], KkaBi Son[1], Heechan Kim[1], Seil Jang[1], **Minseok S. Kim**[2]

[1]CTCELLS Inc., Seoul, Korea, Republic of,[2]Daegu Gyeongbuk Institute of Science and Technology (DGIST), Daegu, Korea, Republic of

Background: Traditional immuno-oncology strategies, such as checkpoint blockade therapy, are evolving to immune cell engagers as a smarter strategy. The early successes of Blincyto, a CD3 engager, demonstrated its capacity to activate host pan-T cells irrespective of their TCR-pMHC restriction status. However, this broad activation has been linked to off-target immunotoxicities, thus limiting its therapeutic applicability. In response, targeting immune co-stimulatory receptors like CD28 or 4-1BB has gained attention by their expression being induced on activated immune effector cells, presenting a more targeted approach to cancer therapy.

Methods: We developed RACE, a novel bispecific 4-1BB engager. This platform fuses a 4-1BB ligand (4-1BBL) trimer with antibody F(ab')2 fragments, excluding Fc domains. A Key and lock design on the 4-1BBL trimer interface facilitates asymmetric assembly of 4-1BBL dimer and monomer in the endoplasmic reticulum, achieving over 95% assembly efficiency in mammalian systems.

Results: RACE differs from conventional 4-1BB agonistic antibodies in its ability to form natural hexagonal hyper-clusters of 4-1BB receptors, enhancing NF-κB signal transduction. Unlike first-generation 4-1BB antibodies, which incurred off-tumor hepatotoxicity, RACE selectively activates 4-1BB receptors only in the presence of tumor antigens. Enhanced cytotoxicity requires successful TCR signaling complex formation between T cells and cancer cells. In CT26 and MC38 tumor models, RACE not only induced strong anti-tumor effects without hepatic or systemic toxicities but showed synergistic efficacy with anti-PD-1 antibodies as well.

Conclusion: The novel RACE platform represents a potent as well as safe immuno-oncology strategy, demonstrating significant potential for clinical application.

#2461 Discovery of an orally available and liver-targeted ALPK1 agonist for cancer immunotherapy.

Yupeng Wang[1], Nana Du[1], Xiaona Dong[1], Xuebing Sun[1], Yuan Hong[1], Xiaolong Yang[1], Zhijiang Ji[1], Qianyu Wang[1], Yun Lv[1], Zhichen Shi[1], Yajuan Gao[1], Xiaofu Hou[1], Yaxin Zhang[1], Juan Wang[1], Rui Mao[1], Yinxin Liu[1], Liang Li[1], Jingjin Ding[2], Hexiang Wang[1], Nan Hu[1], Counde O'Yang[1], Zhihong Li[1], Keith Bley[3], Feng Shao[4]

[1]Pyrotech (Beijing) Biotechnology Co., Ltd., Beijing, China,[2]National Laboratory of Biomacromolecules, CAS Center for Excellence in Biomacromolecules, Institute of Biophysics, Chinese Academy of Sciences, Beijing, China,[3]Pyrotech Therapeutics, Inc., Reno, NV,[4]National Institute of Biological Sciences, Beijing, China

Boosting anti-tumor immune responses can be achieved by activating the innate immune system. Despite the ongoing development of numerous STING and TLR agonists for this purpose, none of them have progressed to late-stage clinical evaluation. Alpha protein kinase-1 (ALPK1) is an intracellular innate immune receptor newly identified for its ability to detect ADP-heptose, a metabolite released during the biosynthesis and degradation of lipopolysaccharides (LPS). Since heptose is not naturally present in mammalian cells, the recognition of heptose metabolites by ALPK1 serves as a reliable mechanism to identify bacterial infections. When ADP-heptose binds to ALPK1, it initiates the phosphorylation of TIFA, thereby triggering a cascade of immune responses. Systemic administration with ADP-heptose induces robust ALPK1-dependent cytokine responses in mice. While high doses of ADP-heptose demonstrate anti-tumor effects, its instability and low *in vivo* potency hinder its clinical development. Through a SBDD medicinal chemistry effort, a novel, stable, and potent ADP-heptose analog, designated PTT-936, has been discovered and is progressing into clinical evaluation in cancer patients. PTT-936 exhibits remarkable nanomolar potencies for ALPK1 activation in various cellular assays. Notably, in human PBMCs, PTT-936 induces both concentration-dependent release of cytokines and activation of NK and T cells. Consistent with *in vitro* studies, oral administration of PTT-936 triggered significant cytokine responses in mice at microgram dose levels. However, overt toxicities were observed only at milligram dose levels, indicating a wide therapeutic window for this compound. In syngeneic tumor models, oral administration of PTT-936 induced dose-dependent tumor growth inhibition, which correlated with elevations in several cytokine biomarkers. Mechanistic studies show that PTT-936, working exclusively through the ALPK1 pathway, elicited strong innate and adaptive immune responses, as evidenced by robust cytokine induction and immune cell activation and recruitment. In syngeneic mouse models, the anti-tumor effects of PTT-936 were significantly hindered by either $CD8^+$ T cell depletion or neutralization of select cytokines. Besides monotherapy studies, compelling evidence demonstrates strong synergistic anti-tumor effects when combining PTT-936 with immune checkpoint inhibitors. Intriguingly, PTT-936 exhibits favorable tolerability and a wider therapeutic index compared to certain clinical-stage STING and TLR agonists. Furthermore, PTT-936 does not enhance cytokine elevations induced by checkpoint inhibitors, which have been linked to adverse events (including CRS) observed in clinical combination studies. The dosing frequency of PTT-936 in the upcoming first-in-human clinical trial is carefully designed to prioritize both tolerability and patient compliance.

#2462 Live attenuated Salmonella ZH9 as novel microbial immunotherapy for the treatment of bladder cancer.

N. Glanville[1], O. Oke[1], C. Prevosto[1], A. Sevko[1], A. Scott[1], S. Domingos-Pereira[2], L. Polak[2], D. Nardelli-Haefliger[2], L. Deban[1];
[1]PROKARIUM, London, United Kingdom, [2]Centre Hospitalier Universitaire Vaudois (CHUV), Lausanne, Switzerland

Microbial immunotherapy with Bacillus Calmette-Guérin (BCG) has been the standard-of-care for non-muscle invasive bladder cancer (NMIBC) for over 30 years. Today, global demand for BCG exceeds supply, leaving many patients untreated. BCG is associated with high disease recurrence and presents high treatment burden for patients. There remains therefore significant unmet need for novel therapeutic approaches for NMIBC and we sought to establish the utility of the live-attenuated *Salmonella enterica* Typhi ZH9 as a more effective microbial immunotherapy. Efficacy of ZH9 was established in orthotopic, syngeneic, mouse MB49 tumor models in which animals were treated in the bladder via catheterization, with or without prior subcutaneous immune priming. Immune responses were measured by flow cytometry and Nanostring transcriptomic analyses of bladder tissues. An intravesical dose of ZH9 after orthotopic MB49 tumour inoculation demonstrated significant survival benefit compared to both vehicle control and equivalent colony forming unit (CFU) BCG treatments. Repeat, weekly dosing studies showed a single administration of ZH9 was sufficient for maximum efficacy. To explore the durability of protection, surviving intravesical ZH9 treated animals were rechallenged, demonstrating protection from both bladder and subcutaneous MB49 tumors suggestive of lasting local and systemic anti-tumor immunity. Flow cytometry analysis of bladders showed that intravesical ZH9 treatment resulted in cellular immune response characterised by recruitment of NK cells, CD4+ and CD8+ T cells, and dendritic cells with an activated, cross-presenting phenotype, in all cases of greater magnitude than after treatment with an equivalent dose of BCG. Based on observations that pre-existing immunity to BCG has been associated with improved outcomes to intravesical BCG therapy in NMIBC, we explored whether systemic priming with ZH9 benefits local bladder therapy. Systemic prime with ZH9 followed by a single intravesical dose of ZH9 showed a trend for improved survival and will be explored in the clinical setting. This systemic immune priming effect was associated with enhanced local bladder immune cell infiltrates and the upregulation of more than 150 immune response genes in the bladder compared to intravesical therapy alone. These data form the basis of preclinical package accepted by the FDA for a Phase 1/1b study evaluating the safety, pharmacology, and clinical effect of ZH9 treatment in patients with NMIBC, currently recruiting patients. The investigation includes thorough translational and biomarker studies to delve into the mechanism of action of ZH9 and explore patient stratification approaches. By easing the treatment burden on patients, lowering healthcare costs, and featuring a scalable manufacturing process, ZH9 has the potential to revolutionize the treatment paradigm in NMIBC and reshape the patient journey.

#2463 Targeting CXCR4 impaired T regulatory function through PTEN in renal cancer patients.

Giuseppina Rea[1], Sara Santagata[1], Anna Maria Bello[1], Anna Capiluongo[1], Maria Napolitano[1], Sonia Desicato[1], Alessandra Fragale[2], Crescenzo D'Alterio[1], Anna Maria Trotta[1], Caterina Ierano[1], Luigi Portella[1], Marilena Di Napoli[1], Salvatore Di Maro[3], Florinda Feroce[1], Rosa Azzaro[1], Lucia Gabriele[4], Nicola Longo[5], Sandro Pignata[1], Sisto Perdona[1], Stefania Scala[1]

[1]IRCCS National Cancer Inst. G. Pascale Foundation, Naples NA, Italy,[2]Oncology and Molecular Medicine, Istituto Superiore di Sanit, Roma, Italy,[3]Biological and Pharmaceutical Science and Technology, University of Campania "Luigi Vanvitelli, Naples NA, Italy,[4]Oncology and Molecular Medicine, Istituto Superiore di Sanit, Naples NA, Italy,[5]Reproductive Sciences and Odontostomatology, Urology Unit, University of Naples "Federico II", Naples NA, Italy

Purpose: In Renal Cell Carcinoma (RCC) a crucial role is played by tumor microenvironment (TME). The high presence of T regulatory cells (Tregs) in TME cause a suppressive environment that promotes the tumor growth and its treatments failure. Tregs trafficking is controlled by CXCR4. In RCC, the new CXCR4 antagonist R54 was explored in peripheral blood Tregs isolated from primary RCC patients.

Experimental Design: To investigate the mechanism by which the new CXCR4 antagonist R54 impairs Tregs activity, peripheral blood (PB) Tregs were explored on primary RCC patients. PB-Tregs were isolated from 77 RCC patients and 38 healthy donors-(HD) and CFSE-Tregs suppression assay, IL-35 secretion and Nrp-1+Tregs frequency was conducted. PB-Tregs were analyzed for PTEN, CD25, TGF-β1, FOXP3, DNMT1 expression. PTEN-pAKT signaling was evaluated in the presence of R54 and/or triciribine (TCB), Akt inhibitor. TSDR (Treg-specific Demethylated Region) methylation analysis was conducted.

Result: Ex vivo R54 impaired PB-RCC-Tregs function, reduced IL-35 release and Nrp-1+Tregs. As PTEN and CD25 expression significantly decreased in R54-PB-RCC-Tregs, PTEN signaling was evaluated. While CXCL12 recruited PTEN+CD25+Tregs cells, R54 significantly reduced it in PB-RCC-Tregs. Tregs activation through IL-2/PMA impaired pAKT+Tregs while R54 increased it. The Akt inhibitor, triciribine, prevented the pAKT+Tregs R54 induction. As active Tregs present demethylated Treg-specific region (TSDR), a significant decrease in demethylation rate (DMR) of Foxp3-TSDR was observed in R54 treated PB-RCC-Tregs. As consequence of TSDR modulation, the expression of Tregs regulating genes was evaluated with significant reduction in DNMT1 and FOXP3 expression. Taken together, our findings demonstrated that R54 causes an impairment of peripheral Tregs functionality in primary RCC patients through regulation of PTEN/PI3K/AKT pathway, resulting in impaired Tregs activity.

Conclusion: The CXCR4 antagonist R54 affects Tregs function in primary RCC patients through regulation of PTEN/PI3K/AKT pathway, reduction in TSDR demethylation and Foxp3 and DNMT1 expression. CXCR4 targeting is thus a strategy to inhibit Tregs activity contributing to the CXCR4 function in RCC tumor microenvironment.

#2464 Defective NMD promotes aberrant intron retention in clear cell renal cell carcinoma.

M. Zhou, G. Giri, W. Y. Kim, D. Dominguez;
UNC Chapel Hill, Chapel Hill, NC

Clear cell renal cell carcinoma (ccRCC) is the 8th most common cancer in the United States, constituting 75% of all kidney cancer cases. Clear cell RCC (ccRCC) along with melanoma has traditionally been viewed as an immunotherapy responsive disease with a storied history of immunotherapy treatments including high dose interleukin 2 (IL2), interferon, and allogeneic stem cell transplant. Indeed, RCC was one of the first tumor types to garner FDA approval for PD1 immune checkpoint inhibition (ICI). However, unlike melanoma, most RCC tumors do not have a high tumor mutational burden (TMB) to potentially explain their immunotherapy responsiveness. We and others have sought to explain this unanswered question and have demonstrated that *non-canonical tumor associated antigens* like endogenous retroviruses (ERVs) may in part explain ICI response in RCC. We have noted that ccRCC tumors have the highest level of retained introns (RI) across all TCGA tumors, that RI levels are secondary to suppressed non-sense mediated decay (NMD) activity, and that one can subset ccRCC into RI-high and normal-like tumors. Moreover, we have found that mTOR signaling plays a key role in regulating NMD and intron retention and that mTOR inhibition can promote intron retention. We hypothesized that these aberrantly retained introns could serve as a rich source of highly foreign, tumor associated neoantigens and that of retained intron neoantigens, the ones not observed in normal tissue would be the most immunogenic. We derived a so called “Neo-RI-antigen burden” that represents the burden of retained intron neoantigens not found in normal tissues and demonstrate that the Neo-RI-antigen burden of complete responders is numerically higher than those with partial response or progressive disease in a dataset of immunotherapy treated melanoma patients. Our work suggests the possibility of using NMD-targeting drugs as a potential therapeutic in combination with ICI to enhance the overall treatment response.

#2465 A novel agonist of CD137 as a single agent shows cancer immunoprevention efficacy against various tumor types that is not dependent on the trained immunity.

F. N. Arguc, M. Tarique, V. Ulker, E. S. Yolcu, H. Shirwan;
University of Missouri - Columbia, Columbia, MO

Introduction: We recently demonstrated that pretreatment of mice with SA-4-1BBL, a novel oligomeric form of CD137 agonist, as a single agent prevents the development of various tumor types in mice. The tumor immunoprevention efficacy is long-lasting (>14 weeks) and contingent upon $CD4^{\pm}$ immune cells, NK cells, and IFN-γ, but not CD8+ T and B cells. Trained immunity mediated by previously activated myeloid cells has been shown to have efficacy against cancer. The objective of this study was twofold: i) assess the role of trained immunity and ii) elucidate the mechanistic underlying of cancer immunoprevention.
Study Design: Wild-type C57BL/6 mice and various transgenic ($CD4^{\pm}$ OT-II.$Rag^{+/+}$, $CD4^{\pm}$ OT-II.$Rag^{-/-}$, $CD8^{\pm}$ OT-I/$Rag2^{-/-}$ KO, and $Rag1^{-/-}$) mice on C57BL/6 background were pretreated subcutaneously with SA-4-1BBL or an agonistic Ab that does not have immunoprevention efficacy (3H3) twice two weeks apart. Mice were challenged two weeks later with a cervical cancer cell line (TC-1) and monitored for tumor development. A group of mice was also treated with monophosphoryl lipid A (MPLA), an agonist of TLR4 involved in trained immunity, using the above scheme. Mice treated with saline served as the control throughout all studies. Deep immunophenotyping was conducted to assess immune correlates of cancer immunoprevention.
Results: Pretreatment with SA-4-1BBL prevented tumor growth in wild-type mice (> 60%), whereas all MPLA treated mice developed tumor. SA-4-1BBL did not show tumor immunoprevention efficacy in mice lacking adaptive immune cells ($Rag1^{-/-}$ KO), OT-II cells on $Rag^{-/-}$ or $Rag^{+/+}$ background, and OT-I on $Rag2^{-/-}$ background. Deep immunophenotyping revealed a significant increase in the absolute number of $CD4^{\pm}$ T central memory and $CD4^{\pm}$ T stem cell-like memory cells, NK cells, NKT cells, and various myeloid cells in mice treated with SA-4-1BBL as compared with those treated with the 3H3 Ab or saline treated controls.
Conclusions: These results demonstrate that cancer immunoprevention efficacy of SA-4-1BBL requires a diverse T cell receptor repertoire as OT-II mice on $Rag^{+/+}$ background, restricted to a TCRβ chain, but have all other myeloid and NK cells, do not show efficacy. Furthermore, treatment with MPLA involved in trained immunity has no efficacy. Altogether, these observations do not implicate trained immunity as a mechanism of cancer immunoprevention. Elucidation of the mechanistic basis of SA-4-1BBL immunoprevention may have significant clinical implications.

#2466 tRNA-derived fragments as immunotherapy response targets in head and neck squamous cell carcinoma.

R. Yalamarty[1], D. John[1], A. Do[1], T. Chen[1], M. Ngo[1], P. Gande[1], M. Uzelac[1], W. Li[2], W. M. Ongkeko[1];
[1]University of California San Diego - UCSD, San Diego, CA, [2]University of California San Francisco School of Medicine - UCSF, San Francisco, CA

Background: Despite significant advances in immunotherapy-based treatment options for Head and Neck Squamous Cell Carcinoma (HNSCC), patient prognosis and survival remains poor. To enhance response to immune-based therapies, specific targeting of immunomodulatory pathways has been investigated through co-stimulatory gene targets, the microbiome, and more. An emerging biomolecule is Transfer RNAs (tRNAs), which are a class of RNAs that transport amino acids from the cytoplasm to ribosomes, and synthesize new proteins encoded by mRNA transcripts. tRNA-derived fragments (tRFs) are a category of cleaved, mature tRNA that participate in post-transcriptional regulation and have been implicated in the modulation of cancer and other immune-associated diseases. While tRFs are primarily implicated in diagnostic signatures for various cancers, few studies have investigated their role in modulating the immunotherapy-based response in HNSCC. In this study, we characterized the role of tRFs in modulating immunotherapy gene targets pertinent to HNSCC.
Methods: We extracted tRF read counts from MINTbase 2.0 for 455 primary HNSCC tumor samples and 44 adjacent normals. Differential expression analysis was first performed to identify tRFs implicated in HNSCC tumors, with respect to adjacent normal tissue. Next, these tRFs were associated with immunotherapy target genes and response markers with Spearman's correlation. Further characterization of these tRFs was performed by correlating their abundance to infiltrating immune cells, pathway enrichment of immunotherapy targets, and clinical variables.
Results: Significant differential expression of tRFs were found between HNSCC primary tumor samples and adjacent normal tissue, including 7 tRFs (FDR < 0.05, |log fold change| > 0.5). All were enriched in normal samples. AlaCGC5tRF appeared to be an important regulator of immunotherapy target genes through increased co-expression of PTPN11, STAT3, and PTEN (p-value < 0.05, R > 0) and decreased co-expression of CD58 and TNFRSF14 (p-value < 0.05, R < 0). Immune Checkpoint Inhibitor (ICI) genes were significantly correlated with several tRFs. Among several pertinent tRF markers, AlaCGC5tRF was strongly associated with negatively correlated with infiltrating activated NK cells naïve CD4 T cells (p-value < 0.05, R < 0).
Conclusion: Our study is the most comprehensive to date to characterize the role of tRF elements in modulating HNSCC immunotherapy targets. We found several potential tRF biomarkers that may be indicative of enhanced immunotherapy treatment susceptibility, including AlaCGC5tRF and ArgTCT3tRf. Further studies are needed to investigate how these tRFs may be targeted alongside immunotherapies to enhance response to treatment.

#2467 Enhanced CD8+T-cell infiltration, PD-L1 expression, and T-cell repertoire expansion in patients with metastatic uveal melanoma responding to treatment with RP2 alone or in combination with nivolumab.

P. K. Bommareddy[1], A. Kalbasi[1], K. J. Harrington[2], A. Olsson-Brown[3], T. Y. Chan[3], P. Nenclares[2], I. Leslie[2], M. R. Middleton[4], D. M. Cohan[1], K. Xynos[1], R. Coffin[1], J. J. Sacco[3];

[1]Replimune, Inc., Woburn, MA, [2]The Institute of Cancer Research, London, United Kingdom, [3]The Clatterbridge Cancer Centre and University of Liverpool, Liverpool, United Kingdom, [4]Churchill Hospital and University of Oxford, Oxford, United Kingdom

Background: Metastatic uveal melanoma (MUM), typically an immune-excluded tumor, has few effective treatments and shows limited clinical response to immunotherapy. RP2 is an enhanced-potency oncolytic HSV-1 that expresses GM-CSF, an anti-CTLA-4 antibody-like molecule, and the fusogenic gibbon ape leukemia virus membrane R− glycoprotein (GALV-GP-R−). Here, we present the biomarker data of RP2 monotherapy and RP2 + nivolumab (nivo; anti-PD-1) in patients (pts) with MUM from an ongoing clinical trial (NCT04336241).

Methods: Tumor biopsies and peripheral blood mononuclear cells (PBMCs) were collected pre-treatment and at Day 43 (D43). The tumor microenvironment (TME) was analyzed by immunohistochemistry (IHC). Systemic peripheral anti-tumor immunity was assessed by sequencing the CDR3β region of the T-cell receptor (TCR) using immunoSEQ Assay. HLA typing was obtained from patient history when available. Correlations between baseline tumor PD-L1 and CD8 expression, HLA type, prior treatment with ipilimumab (ipi)/nivo, and HLA status—vs clinical response status—were assessed.

Results: As of August 2022, 17 pts with MUM were enrolled (RP2 monotherapy, n = 3; RP2 + nivo, n = 14). The majority of pts had previously received both anti-PD-1 and anti-CTLA-4 therapy (12/17, 70.6%), and 17.6% had received ≥3 prior lines of therapy. ORR for the 17 pts was 29.4% (5/17; all PRs; RP2 monotherapy, 1/3; RP2 + nivo, 4/14). Eight pts (2 PR, 3 SD, and 3 PD) had evaluable baseline and post-treatment biopsies for IHC, and 13 pts (4 PR, 4 SD, and 5 PD) had evaluable baseline and post-treatment PBMCs for TCR sequencing analyses. Of the 10 patients that achieved clinical benefit (PR/SD), IHC analysis of all available (n = 5, 2 PR, 3SD) paired biopsies demonstrated an increase in intra-tumoral PD-L1 expression, and 4 patients (2 PR, 2 SD) exhibited an increase in CD8+ T-cell infiltration into tumors at D43. No increase in either CD8+ T-cell infiltration or PD-L1 expression was observed at D43 in patients with PD. There was no correlation between HLA-A2*02:01 status or prior treatment with ipi/nivo and response. In addition, TCR sequencing revealed expansion of pre-existing TCRs (including a tumor antigen-specific clone targeting MART-1 in a responding patient) and generation of new T- cell clones, following RP2 + nivo.

Conclusions: Preliminary RP2 + nivo data demonstrated meaningful antitumor activity in pts with MUM. Biomarker data indicated a conversion of the TME from an immune-excluded to an immune-infiltrated phenotype in responding patients following treatment with RP2 + nivo. Furthermore, systemic peripheral T-cell clonal expansion was noted. These results support further clinical development of RP2 + nivo in pts with MUM.

#2468 Phase II study of cryoablation and post-progression immune checkpoint inhibition in metastatic melanoma.

M. J. Mooradian, F. J. Fintelmann, T. J. LaSalle, J. Simon, A. Graur, A. Muzikansky, M. Mino-Kenudson, S. Shalhout, H. L. Kaufman, R. W. Jenkins, D. Lawrence, A. Lawless, T. Sharova, R. N. Uppot, J. Fang, E. M. Blaum, A. L. K. Gonye, I. Gushterova, G. M. Boland, N. Hacohen, M. Sade-Feldman, R. J. Sullivan;

Massachusetts General Hospital, Boston, MA

Introduction: Efforts to overcome resistance to immune checkpoint inhibition (ICI) are paramount, and novel combination strategies are in development. Image-guided percutaneous cryoablation is an established minimally invasive oncologic treatment that has demonstrated immune modulatory effects. We hypothesized that cryoablation may prime the tumor microenvironment (TME) through direct modulation of the tumor, thereby generating an anti-tumor response in ICI refractory tumors.

Methods: In this non-randomized phase II single-center study, subjects with unresectable melanoma progressing on ICI underwent cryoablation of an enlarging metastasis, and ICI was continued for a minimum of two additional cycles. The primary endpoint was safety and feasibility, with objective response rate (ORR) and disease control rate (DCR) in non-ablated lesions a key secondary endpoint. To better understand the inflammatory state of TME as well as factors determining response to cryoablation, we performed immunohistochemistry (PD-L1, CD8+ TIL) as well as single-cell RNA-sequencing (ScRNAseq) on evaluable pre- and post-cryoablation biopsies obtained from metastatic sites of 15 patients.

Results: From May 2018 through July 2020, 17 patients were treated. This regimen was feasible with all patients ongoing cryoablation with no unexpected safety signal. The ORR and DCR was 23.5% (95% CI 6.81-49.9) and 41.2% (95% CI 18.44-67.08), respectively, with four patients experiencing PR and three patients SD. Durable control, defined as tumor control ≥6 months, was achieved in 35%. Median progression-free survival (PFS) was 59 days (95% CI 42, 179) with a 6-month PFS rate of 23.5% (95% CI 7.3%, 44.9%). Median overall survival (OS) was 387 days (95% CI 106, 608) with a 1-year OS rate of 53% (95% CI (27.6%, 73%). Correlative analysis demonstrated pre-ablation tumors were uniformly associated with a “cold” TME, as all samples were PD-L1 negative and the majority had low levels of CD8+ TIL, defined as <5% of tumor cells associated with CD8+ TILs. ScRNAseq revealed no clear trends of cell type composition to predict best response to cryoablation, however an increase in B/plasma cells was seen in patients with disease control, suggesting these cells may play a role in mounting a durable anti-tumor response after cryoablation.

Conclusion: The anti-tumor efficacy of combining cryoablation and post-progression ICI was superior to what would be expected with the use of post-progression ICI alone with an acceptable safety profile. Our data support further study of this novel, synergistic therapeutic approach.

#2469 PROTAC mediated NR4A1 degradation as a novel strategy for cancer immunotherapy.

L. Wang[1], Y. Xiao[1], Y. Luo[2], R. Master[3], J. Mo[4], M.-C. Kim[5], Y. Liu[1], C. Maharjan[1], U. Patel[1], X. Li[6], D. Shaffer[6], G. Kevin[6], H. Zhuang[1], E. Moser[1], K. Smalley[7], D. Zhou[8], G. Zheng[1], W. Zhang[1];

[1]University of Florida, Gainesville, FL, [2]University of Copenhagen, Copenhagen, Denmark, [3]Florida State University, Tallahassee,, FL, [4]Thermo Fisher Scientific, Alachua, FL, [5]Veterinary Diagnostic Laboratory Medicine, Jeju-si, Jeju-do, Korea, Republic of, [6]Sanofi, Cambridge, MA, [7]Moffitt Cancer Center & Research Institute, Tampa, FL, [8]University of Texas Health Science Center at San Antonio, San Antonio, TX

An effective cancer therapy requires both killing cancer cells and targeting tumor-promoting pathways or cell populations within the tumor microenvironment (TME). We purposely search for molecules that are critical for multiple cell types in the TME and identified nuclear receptor subfamily 4 group A member 1 (NR4A1) as one such molecule. NR4A1 has been shown to promote the aggressiveness of cancer cells and maintain the immune suppressive TME. Using genetic and pharmacological approaches, we establish NR4A1 as a valid therapeutic target for cancer therapy. Importantly, we have developed the first-of-its kind proteolysis-targeting chimera (PROTAC, named NR-V04) against NR4A1. NR-V04 effectively degrades NR4A1 within hours of treatment in vitro and sustains for at least 4 days in vivo, exhibiting long-lasting NR4A1-degradation in tumors and an excellent safety profile. NR-V04 leads to robust tumor inhibition and sometimes eradication of established melanoma tumors. At the mechanistic level, we have identified an unexpected novel mechanism via significant induction of tumor-infiltrating (TI) B cells as well as an inhibition of monocytic myeloid derived suppressor cells (m-MDSC), two clinically relevant immune cell populations in human melanomas. Overall, NR-V04-mediated NR4A1 degradation holds promise for enhancing anti-cancer immune responses and offers a new avenue for treating various types of cancer such as melanoma.

#2470 Harnessing cytomegalovirus immunity against pancreatic tumors for immunotherapy.

R. Marrocco[1], J. Patel[2], S. Sun[2], R. Medari[2], K. Gulay[2], E. Lucero-Meza[1], E. Mose[2], A. Lowy[2], C. Benedict[1], **T. Hurtado de Mendoza**[2];
[1]La Jolla Institute for Immunology, La Jolla, CA, [2]UCSD Moores Cancer Center, La Jolla, CA

Immunotherapy has had very limited success in pancreatic cancer, due to its low mutational burden and immunosuppressive microenvironment. Our approach consists in redirecting pre-existing antiviral immunity against pancreatic tumors by delivering viral antigens using the tumor penetrating peptide iRGD .This peptide, targets the tumor vasculature through αv integrins and neuropilin-1, delivering conjugated or co-administered cargo to tumors. Here we used mouse cytomegalovirus (CMV) as an infection model. CMV is a β-herpesvirus that induces a strong T-cell response in mice and humans, comprising >10% of all circulating CD4 and CD8 T cells mostly with effector-memory phenotype. Importantly, human CMV infects over 60% of the world's population rendering it a suitable candidate for translation. Mice latently infected with CMV were orthotopically implanted with KPC pancreatic tumor cells and treated with systemic injections of vehicle or iRGD plus CMV class I and II binding peptides. Another cohort of age matched uninfected mice was used as a control. Tumor growth and mouse weight were monitored twice a week and CMV specific immune responses were measured in spleen and tumor by flow cytometry, using tetramer staining and CMV specific peptide recall. CMV infected mice receiving iRGD + CMV peptides responded to treatment as evidenced by delayed tumor growth associated with increased tumor necrosis and T cell infiltration. In addition, flow cytometry analysis of tumor and spleen showed a significant increase in CMV specific T cells that produced significant amounts of IFN-γ and TNF-α upon CMV peptide recall. Furthermore, tumor regulatory T cells (Treg) were significantly reduced and the CD8/T reg ratio was greatly increased. Survival studies showed a 68% increase in median survival in the treated and infected group. Combining this strategy with anti-PD1 and or anti-IL10R did not significantly improve the benefits of iRGD + CMV therapy alone. Other combinations with chemotherapy and TME remodeling agents are being tested.Taken together, this data shows we can deliver antigens to pancreatic tumors via iRGD and elicit an anti-tumor immune response that results in delayed tumor growth and has a survival benefit. This is a mutation agnostic approach with high translational value, since more than 60% of the population has previous CMV immunity and iRGD in combination with chemotherapy is already in phase II clinical trials for advanced pancreatic cancer.

#2471 State-of-the-art Specific T cell Activating Modulator on ePENDY platform (STAM.eP) activates specific CD8+ T cell by stimulating TCR signal.

K.-g. Hyun[1], S. Kang[1], Y. Kang[1], J. Koo[1], S. Park[1], S. Byun[1], S. Yoon[1], J. Lee[1], H. Lee[1], H. Lee[2], E. Cho[1], C. Lee[1], K.-C. Choi[2], G. Ha[1];
[1]IMBiologics, Suwon-si, Korea, Republic of, [2]Chungbuk National University, Cheongju-si, Korea, Republic of

After decades of research, therapeutic cancer vaccine approach now sheds light on developing efficient cancer therapy treating patients who have resistance to other cancer immunotherapy. However, cancer vaccine approach using conventional modalities such as protein, peptide, and mRNA is considered a powerful cancer treatment only when the patients have healthy immune systems. In addition, dendritic cell (DC) cancer vaccine can be a great alternative therapy, but manufacture of DC vaccines in vitro is a labor-intensive, time- and money-consuming procedure. Here, we developed Specific T cell Activating Modulator (STAM) on our engineered IgM backbone, ePENDY (engineered PENtamer boDY), with high avidity based on multivalent binding sites to overcome the disadvantages of other therapeutic cancer vaccines. STAM on ePENDY (STAM.eP) consists of ten peptide-loaded-HLAs linked to ePENDY to simulate priming signal of CD8+ T cell by TCR cluster and a costimulatory signal molecule is linked to J chain of ePENDY to prevent CD8+ T cell from becoming anergic status. With these features, STAM.eP mimics cognately licensed DC that can present tumor peptide-loaded MHC class I molecule to CD8+ T cell and promote its priming. Thus, one of the greatest advantages of STAM.eP is to be a potential treatment for immunosuppressive cancer patients with DCs that do not respond appropriately. Another advantage is that any tumor specific antigen (TSA), including from intracellular proteins, can be applied to STAM.eP concept to activate specific CD8+ T cells for targeting cancer cells. In this study, we used Human Papillomavirus (HPV) E7-derived peptide which is an oncoprotein associated with cervical and head/neck cancers. We observed that HPV E7-derived peptide loaded STAM.eP, named IMB-401, increases antigen-specific CD8+ T cell population and shows cytotoxicity activity against cancer cells expressing HPV E7 protein in vitro test model. In vivo test model, it was also observed that population of specific CD8+ T cells and memory T cells were increased in the blood and spleens of transgenic mice treated with IMB-401. Furthermore, we confirmed that IMB-401 shows anti-tumor efficacy due to an increase of antigen-specific CD8+ T cell in vivo humanized mouse model. These results suggest that IMB-401 can be a new therapeutic cancer vaccine technology that replaces DC function and is expected to have robust anti-tumor activity in combination with immune checkpoint inhibitors.

#2472 Inhibition of ENPP1 catalyzed ATP and cGAMP hydrolysis and *in vivo* antitumor efficacy of RBS2418 in the Hepa1-6 and GL261-luc syngeneic liver and glioblastoma mouse models.

N. Huang, J. Cheng, R. Hawley, K. Klumpp;
Riboscience LLC, Sunnyvale, CA

Background: ENPP1, a nucleotide pyrophosphatase and phosphodiesterase, has emerged as an important modulator of anti-tumor immune activation, as it regulates the concentrations of cGAMP and ATP in the TME. ENPP1 expression in tumors is common and correlates with a cold tumor phenotype. Its loss has been reported to suppress metastasis, restore immune cell infiltration into the tumor and potentiate the response to immune checkpoint blockade, while, conversely, the overexpression of ENPP1 promoted metastasis and rendered tumors resistant to checkpoint blockade. RBS2418 was designed as a potent and selective inhibitor of ENPP1 and is in clinical development.
Methods: ENPP1 enzyme inhibition was measured in vitro using cGAMP and ATP substrates. Effects of pH and serum and selectivity against related enzymes were evaluated. In vivo efficacy was assessed in Hepa1-6, and GL261-luc syngeneic liver and glioblastoma mouse models. Compound exposures were determined in tumor and blood samples. Cures were confirmed by re-challenge of cured animals with the same cancer cells.
Results: RBS2418 inhibited hydrolysis of cGAMP and ATP in vitro with similar potency (Ki =0.14 and 0.13 nM). Inhibition was also similar in human serum, consistent with low binding affinity to human serum albumin. In humans, oral dosing at doses of 100 mg could inhibit ENPP1 enzyme activity during the full dosing interval. Dosing of RBS2418 was performed in mice to achieve trough concentrations of RBS2418 in tumors and plasma exceeding ENPP1 EC90 levels for the complete dosing interval. In the Hepa1-6 model treatment with RBS2418 for either 2 or 10 days resulted in significant reduction of tumor growth and prolongation of survival as compared to vehicle control. There was no significant difference between the RBS2418 groups. Complete tumor regression was observed in 44% of treated mice across the two treatment groups. These mice were resistant to rechallenge with Hepa1-6 tumor cells. In the GL261-luc model treatment with RBS2418 showed significant reduction of tumor burden and prolongation of survival as compared to vehicle control. The mice that achieved complete tumor regression were resistant to rechallenge with GL261-luc tumor cells.
Conclusions: RBS2418 inhibited ATP and cGAMP hydrolysis by ENPP1 with similar high potency. The pharmacology profile was optimized to achieve low serum protein binding and oral bioavailability in humans. RBS2418 treatment was well tolerated in mice under conditions where tumor and plasma levels exceeding ENPP1 serum EC90 levels were achieved. In the syngeneic mouse models Hepa1-6 and GL261-luc significant tumor growth reductions, complete tumor regression and cures were observed. Resistance to cancer cell rechallenge was consistent with treatment-induced anti-tumor immunity.

#2473 A novel anti-PD-1 and proIL-2 bifunctional fusion protein delivers potent anti-tumor activity via PD-1 checkpoint inhibition and tumor selective IL-2R agonism preferentially on antigen specific T cells.

Z. Li, F. Zhang, Z. Zhang, **H. Zhou**;
Proviva Therapeutics, Inc, Bedford, MA

High-dose IL-2 (HD IL-2) induces complete and durable responses in RCC and melanoma but the treatment is associated with severe toxicities. PD-(L)1 blockade represents a recent breakthrough in immunotherapy with solid tumors, but only 20-30% of patients can benefit from the therapy and most responders eventually develop resistance. In more recent clinical studies with small number of subjects, HD IL-2 has shown promising responses in patients who progressed on anti-PD-1 therapy and combination therapy of HD-IL-2 and PD-1 blockade has resulted in high rate of objective response. In an attempt to maximize the clinical benefit of these immunotherapies to a broader patient population with deeper response and in the meantime to minimize the severe toxicity of HD IL-2, we have generated a novel bifunctional PD-1-proIL-2v fusion protein harnessing the mechanisms of PD-1 blockade and PD-1-cis directed tumor conditional IL-2R activation. PD-1-proIL-2v shows dose dependent inhibition of PD-1 immune checkpoint pathway measured by GM-CSF and IFNγ production in an MLR assay. Protease activated PD-1-proIL-2v, but not the intact drug, stimulates the phosphorylation of STAT5 of NK and T cells, the proliferation of CD8 T cells as well as the cytokine production in human whole blood. The potency of pSTAT5 by protease activated product is enhanced by 10-20 folds on PD-1^{+} T cells than T cells without PD-1. When tested in mouse tumor models resistant to PD-1 blockade, PD1-proIL-2v demonstrated high potency of tumor inhibition at as low as 0.1 mg/kg dose. In contrast, non-targeted proIL-2v at molar equivalent or higher dose showed minimal antitumor effect in either monotherapy or combination with anti-PD-1. Analysis of PD-1-proIL-2v treated mice showed dramatically increased tumor infiltrating CD4^{+} and CD8^{+} T cells, including PD-1^{+}Tcf-1^{+} and PD-1^{+} IL-18Ra^{+}TIM3^{-} CD8^{+} T cells, referred to “stem-like” progenitor effector cells and “fresh” effector cells, respectively. Activation of the IL-2 procytokine in PD-1-proIL-2v was observed in mouse tumor tissues but not in the plasma. In monkey GLP-compliant 4-week repeat-dose toxicity study, PD-1-proIL-2v demonstrated excellent safety profiles without overt irAEs that are characteristic of IL-2. In conclusion, our preclinical data demonstrated that PD-1-proIL-2v effectively stimulated the expansion and reinvigoration of antigen specific T cells in the tumor tissue resulting in strong anti-tumor efficacy while it did not cause significant peripheral toxicity. Phase 1 clinical trial of PD-1-proIL-2v is planned to start in early 2024 to evaluate the safety, pharmacokinetics and anti-tumor activity in advanced solid tumors.

#2474 Antitumoral efficacy of ASKG812, a Smartkine® based bifunctional PD-1-eIL-2 molecule, through enhancing T effector cis agonism.

C. Yu, K. Shanebeck, S. Yu, J. Ruiz, S. Li, S. D. Shi, H. Ma, Y. Lu;
AskGene Pharma Inc., Camarillo, CA

Cytokines are potent molecules, yet their broad application as therapeutics has been significantly hampered due to short PK, severe systemic toxicity, and narrow therapeutic window. To improve the developability of cytokines, AskGene has invented a proprietary cytokine platform (Smartkine®) to achieve its overarching objective of modulating immune reactions at a disease site in a selective and controlled manner. Several antibody-cytokine fusion molecules using the SmartKine® platform have been moving into preclinical and clinical development. ASKG812 is a unique fusion molecule composed of anti-PD-1 antibody and engineered IL-2 (eIL-2). The eIL-2 moiety also comprises a specific mask such that the eIL-2 molecule binding biases towards PD-1$^{\pm}$ T effector cells in a *cis* agonism manner for improved efficacy and therapeutic window. In *ex vivo* human PBMC assays, we demonstrated that ASKG812 significantly reduced activity in PD-1^{-} T and NK cells, and enhanced activity in PD-1$^{\pm}$ T cells judged by levels of pSTAT5, Ki67 and Granzyme B. In a cytotoxicity assay, ASKG812 can efficiently induce PBMC-mediated killing of MDA-MB-231 tumor cells in a dose-dependent manner. Moreover, in both anti-PD-1 therapy responsive and non-responsive syngeneic mouse tumor models, ASKG812 showed robust efficacy; without noticeable toxicity compared to a reference anti-PD-1-IL-2v fusion molecule. In conclusion, these findings provide the basis for the development of this new generation of PD-1 cis-targeted IL-2R agonists with enhanced therapeutic potential for the clinical treatment of cancer.

#2475 MB5029: A novel anti-PD-1 x IL-2v with improved safety profile and enhanced anti-tumor efficacy by selectively targeting activated T cells.

B. Park, H. Bang, S. Kim, S. Kim, S. Cho, S. Kim, M. Kim, Y. Park, J.-E. Park;
Research Institute of MustBio, Seoul, Korea, Republic of

Interleukin-2 (IL-2) offers therapeutic potential for cancer treatment, however, its clinical application is limited due to systemic adverse effects, such as vascular leakage syndrome (VLS). Notably, the high affinity of IL-2 for the IL-2 receptor α (IL-2Rα) activates immune-suppressive Treg cells and endothelial cells, leading to undesired outcomes. To address this challenge, a number of clinical studies are under development including non-α IL-2 variant (IL-2v) drugs and further the anti-PD-1 x IL-2v for targeted delivery of its IL-2v to PD-1 enriched T cells. Nevertheless, concerns about peripheral toxicity have not yet been solved. Thus, here we present MB5029, a novel anti-PD-1 x IL-2v bispecific fusion protein with modulated IL-2R binding affinity to mitigate the peripheral toxicity maintaining the anti-tumor efficacy. MB5029 has unique characteristics with no binding affinity to IL-2Rα and reduced binding affinity to IL-2Rγ, which is widely and highly expressed in various immune cells. MB5029 exhibited strong STAT5 phosphorylation activity under activated conditions but weak activity in the resting conditions, while the anti-PD-1 x IL-2v (non-α) showed strong STAT5 phosphorylation in both resting and activated conditions. In addition, MB5029 strongly induced the expansion of $CD8^{+}$ T cells in the activated conditions but less expansion of $CD8^{+}$ T cells in the resting conditions, in contrast to anti-PD-1 x IL-2v (non-α). The murine surrogate of MB5029 showed remarkable anti-tumor efficacy without body weight loss at the dose range of 1 to 10 mg/kg, whereas anti-muPD-1 x IL-2v (non-α) showed significant body weight loss in several tumor-bearing mice models. Moreover, MB5029 showed 100% complete regression (6/6) at the dose of 5 mg/kg or higher in the MC38 tumor model. The mice with complete response showed no signs of relapse upon tumor re-challenge until day 56, indicating a durable memory response. MB5029 exhibited a comparatively superior safety profile in normal mice. While anti-muPD-1 x IL-2v (non-α) led to significant body weight loss at the dose of 5 mg/kg in normal mice, the murine surrogate of MB5029 was shown to be well-tolerated up to a dose of 30 mg/kg without body weight loss. MB5029 exhibited dose-proportional PK properties and induced expansion of $CD8^{+}$ T cells in a dose-dependent manner in cynomolgus monkeys. MB5029 is shown to be well-tolerated up to 9 mg/kg without severe clinical signs and no significant increase in eosinophil and cytokines in the blood. Overall, MB5029 represents a promising potential as an immunotherapeutic approach, as it has demonstrated both strong efficacy and good tolerability, along with improved safety margins.

#2476 Electroporation-mediated novel albumin-fused Flt3L DNA delivery promotes cDC1-associated anticancer immunity.

M.-H. Hu[1], T.-C. Wu[2], C.-F. Hung[2];

[1]Wan Fang Hospital, Taipei, Taiwan, [2]Johns Hopkins University, Baltimore, MD

Introduction: Dendritic cells (DCs) constitute a distinct type of immune cell found within tumors, serving a central role in mediating tumor antigen-specific immunity against cancer cells. Frequently, DC functions are dysregulated by the immunosuppressive signals present within the tumor microenvironment (TME). Consequently, DC manipulation holds great potential to enhance the cytotoxic T cell response against cancer diseases. The Fms-like tyrosine kinase receptor 3 ligand (Flt3L) is a pluripotent growth factor that regulates the maturation and differentiation of DCs in hematopoiesis. The *in vivo* administration of Flt3L itself is limited by its short serum half-life. To overcome this major drawback, our group developed a novel fusion protein albumin-Flt3L (alb-Flt3L), which is the conjugation of albumin to Flt3L. Our hypothesis is that the Flt3L, which has extended bioavailability, is a feasible therapeutic strategy to overcome these treatment limitations.

Method: A novel alb-Flt3L DNA, a plasmid encoding the alb-Flt3L protein, was administrated for its anti-tumor effect on TC-1 tumor-bearing C57BL/6 mice. For the generation of pcDNA3-albFlt3L, mouse Flt3 ligand was amplified by PCR using cDNA template of pcDNA3-Flt3L[1] and a set of primers, 5′-TTTGAATTCGGGACACCTGACTGTTACTTC-3′ and 5′- AAACTTAAGCTACTGCCTGGGCCGAGGCTCTGG -3′. alb-Flt3L DNA (10ug), Flt3L DNA (10ug) or vehicle control was injected intratumorally followed by electroporation for a total of three times in 5-day intervals. Peripheral blood mononuclear cells and tumor-infiltrated immune cells were isolated after treatment. Flow cytometry was performed for immune cell analysis.

Results: In this current study, the electroporation-mediated delivery of alb-Flt3L DNA demonstrated the ability to induce an anti-tumor immune response. This albumin fusion construct possesses more persistent bioactivity in targeted organs. Furthermore, mice receiving alb-Flt3L DNA treatment presented better tumor control and superior survival. Cellular analysis revealed that alb-Flt3L DNA administration displayed greater systemic DC population. In addition, robust cDC1 expansion, which is associated with superior antigen cross-presentation and cellular immunity against tumors, developed extensively in the tumor, lymph node, and blood. In addition, increased levels of IFN-γ-secreting $CD8^+$ lymphocytes and tumor-infiltrated immune cells were found in correlation to greater cDC1 population.

Conclusion: Our data showcases a novel DC-based immunotherapy using electroporation to administer alb-Flt3L DNA. The treatment effect is revealed by a controlled tumor response, characterized by enhanced DC mobilization and accumulation in both the lymph nodes and TME, coupled with an increase in the expansion of cDC1 subsets and a heightened level of $CD8^+$ T cell activation.

#2477 Selective IL-21 and IFN-alpha immunocytokines engineered using the AlphaSeq platform.

C. Lin, C. Shikany, L. Homad, J. Fint, R. Bansal, D. Goodnight, J. Adamo, D. Van Citters, **R. Swanson**, R. Lopez;
A-Alpha Bio, Seattle, WA

Although cytokine therapies have demonstrated curative effects in some cancer patients, clinical use remains limited due to undesired toxicity profiles accompanying systemic administration. Next generation cytokine approaches include conditional signaling focused on sites of interest, such as the tumor microenvironment or specific immune cell populations. Here, we share a novel approach for generating detuned cytokine therapeutic candidates using the AlphaSeq platform, which involves the re-engineering of yeast agglutination and mating to quantitatively measure protein-protein interactions at a library-on-library scale. Engineering interferon-alpha (IFNα) and interleukin-21 (IL-21), we show how AlphaSeq measures cytokine-receptor interactions and identifies cytokine variants with a broad range of affinities. A saturated mutational library was created for IFNα and IL-21and subsequently screened against a second library consisting of human IFNAR2 or human IL-21R, species orthologs and off-target receptors. AlphaSeq enabled identification of hundreds of detuned IFNα and IL-21 variants against both human and mouse receptors in parallel assays. Cytokine variants with lower affinity than parental IFNα or IL-21 were recombinantly expressed as Fc fusion proteins to orthogonally measure affinity with biolayer interferometry and characterize potency with an in vitro human PBMC phosflow assay, which showed strong correlation with AlphaSeq affinity measurements. Finally, detuned cytokine candidates were fused to anti-CD8 and other localizing antibodies to demonstrate cell population-specific signaling. Candidate molecules showed 1000-fold or greater potency in the targeted cell population than non-targeted populations. Our results show the AlphaSeq platform can accurately quantitate thousands of cytokine variant affinities simultaneously against multiple relevant receptors, enabling the selection of candidate immunocytokine antibody fusion proteins with targeted cell biased signaling. AlphaSeq's rapid, comprehensive affinity determination is being used to develop clinically relevant IFNα and IL-21 therapeutic immunocytokines with accompanying preclinical data.

#2478 Inhibition of CD39 by AB598 increases extracellular ATP resulting in activation of myeloid cells and T cells to enhance anti-tumor immunity.

K. Jin, J. Clor, K. Parashar, R. Fuchs, L. Stetson, S. Cho, M. J. Walters, E. Fernandez-Salas, C. E. Bowman;
Arcus Biosciences Inc., Hayward, CA

Extracellular ATP (eATP) is a potent immunostimulatory signal in the tumor microenvironment (TME), but it is rapidly degraded into AMP and immunosuppressive adenosine. Therefore, ATP metabolism is an attractive anti-tumor target. Several enzymes are involved in the immunosuppressive process used by the TME to convert ATP to AMP and adenosine. Among them, CD39 (gene: *ENTPD1*), an extracellular ATPase, is a promising target. Analyzing mRNA expression from the TCGA, we show that CD39 is consistently expressed at high levels in comparison to the other extracellular ATP-converting enzymes, ENPP1 and TNAP. We further demonstrate that CD39 has greater enzymatic activity at the slightly acidic physiological pH (pH = 6.8) of the TME than either ENPP1 or TNAP. Flow cytometry profiling of dissociated primary human gastric tumors showed that CD39 was highly expressed on both myeloid and lymphoid cells, including several populations of T cells present in the tumors. This is distinct from findings in healthy primary human PBMCs that show high expression of CD39 on myeloid subsets and relatively few subsets of T cells with high CD39 expression. AB598 is a novel, humanized, Fc-silent anti-CD39 therapeutic antibody that potently binds to CD39 and inhibits its enzymatic activity with sub-nanomolar potency. Treatment of dissociated primary human gastric tumor cells with AB598 resulted in a decrease in the rate of ATP degradation, indicating both the effectiveness of AB598 and the relevance of CD39 as a main contributor to the ATPase activity of the TME. Although eATP is low in healthy tissues, high levels of ATP can be released when cancer cells are treated with immunogenic cell death (ICD)-inducing agents, increasing the eATP in the TME, providing a rationale for the combination of ICD-inducing chemotherapy and AB598. Thus, cancer cells were co-cultured with monocyte-derived dendritic cells (moDCs) and treated with chemotherapy and AB598 to preserve the eATP released by dying cancer cells. The increased expression of CD83 and CD86 on moDCs demonstrated that the combination treatment enhanced the maturation of moDCs, compared to single or no treatment. To further elucidate the anti-tumor effects of the combination treatment, autogenous T cells were introduced into this system. AB598 significantly enhanced T cell activation in the presence of chemotherapy. These data demonstrate that using AB598 results in elevated eATP, which boosts immune cell activation to promote anti-tumor immunity.

#2479 Discovery of agonist CD28-specific single domain antibodies from alpaca.

Y. Chen, Y. Ding, X. Liu, Q. Zhu, W. Xin, **H. Liu**, T. Yang, Y. Qiu;
ChemPartner Biologics Co., Ltd., Shanghai, China

Upon immune activation, in addition to the first signal driven by the TCR-peptide/MHC interactions, the costimulatory signals are indispensable to optimal T-cell activation, the absence of which will trigger naive T cells to an anergic state. The CD28-CD80/CD86 pathway is widely known as the most classical and critical costimulatory signal for the initial activation of T cells. Bispecific T-cell engagers targeting CD3e can activate cytotoxic T-cells and have shown remarkable tumor regressions in clinical trials. However, the absence of a costimulatory signal through CD28 results in insufficient T-cell activation and early exhaustion. Combination of both CD3e and CD28 targeting antibodies offers attractive approach to optimally boost T-cell activity. Development of superagonistic CD28-targeting antibody has been paused after TeGenero's TGN1412 Phase 1 trial in 2006 due to life-threatening cytokine release syndrome. Unlike superagonist TGN1412, which activates T cells and induce cytokine storm, tumor targeting antigen and cross-linking dependent CD28 bispecific antibody is supposed to display little or no toxicity. In the present study, we explored Alpaca immunized phage library approach to generate cross-linking dependent agonist CD28 single domain antibody for bispecific antibody development. Alpacas were immunized subsequently with recombinant human CD28 extracellular domain and 293F cells stably expressing human CD28. Serum samples after immunizations showed decent immune response against CD28. At the end of Boost 2 and 3, peripheral blood was collected and phage display libraries were constructed using VHH specific primers. Phage display libraries were panned against recombinant CD28 ECD protein and CHOK1 cells overexpressing CD28. After one round of panning, both protein and cell panning tracks showed robust enrichment in output titer and repeating sequences. Next, 600 clones were randomly picked for screening by the binding to U266B1 cells endogenously expressing CD28. Of the 326 clones showed positive binding to U266B1, 79 unique sequences were identified. Secondary screening by ELISA and FACS using periplasmic extract confirmed 69 unique sequences that bound to both CD28 protein and cells expressing CD28. Seventeen unique sequences were selected for VHH-Fc production. All purified VHH-Fc showed sub-nanomolar affinity by ELISA and bind to primary T cells by flow cytometry. Three VHH-Fc induced IL-2 production in a primary T cells activation assay only when cross-linked and in the presence of CD3 co-stimulation and are suitable for further bispecific T cell engager development.

#2480 Treatment of steroid-refractory immune checkpoint inhibitor-associated myocarditis: A case series of 18 patients.

R. Jayakrishnan, S. Brongiel, D. Luon, S. Halene, J. M. Kwan;
Yale New Haven Hospital, New Haven, CT

Background: Immune checkpoint inhibitors (ICI) have improved survival in various malignancies but are associated with significant immune-related adverse events (irAE). Up to 2% of patients on ICI develop ICI-myocarditis, which is associated with significant mortality. Treatment guidelines for ICI-myocarditis are limited. The initial treatment starts with high dose glucocorticoids, but the subsequent lines of treatment remain ill-defined.
Methods: We retrospectively identified patients at our institution from 2021 onwards who were treated for ICI-myocarditis and who had an inadequate response to steroid treatment (thus steroid refractory). Baseline characteristics, laboratory and imaging data, and outcomes were reviewed.
Results: Of the 34 patients diagnosed with ICI-myocarditis, 18 (53%) were steroid refractory. Amongst the 18, 11 were female and 7 were male, with a mean age of 73. Cancer types included head and neck, thoracic, urologic, gynecologic, and gastrointestinal. Patients had received a median of 2 ICI doses prior to myocarditis presentation. Thirteen (72%) patients had prior or concurrent irAE, most commonly neurologic or neuromuscular such as myasthenia gravis/myositis (44%) or hepatitis (33%). For initial treatment, 14 (41%) patients received a max dose of methylprednisolone 1g/day, while 4 (12%) received smaller doses (less than 500mg/day). Following steroids, the most common next treatment was mycophenolate mofetil (MMF) for 9 (50%), IVIG for 6 (33%), and Abatacept for 3 patients (17%). MMF was most often added and uptitrated to wean steroids, with 8 (44%) patients being able to be tapered off after a median duration of 112 days. IVIG was more commonly used for patients with concomitant neurologic symptoms while Abatacept was more commonly used for patients presenting with grade IV toxicities. The most encountered side effects following steroids were hyperglycemia, weight gain, adrenal insufficiency, and myopathy and following MMF were cytopenias and hypertension. The median survival since myocarditis diagnosis was 412 days. The patient with the longest documented survival of 645 days received IVIG and then MMF following steroids. Two patients with severely immunosuppression-resistant myocarditis responded well to tofacitinib, with one patient living 521 days after diagnosis (after methylprednisolone, IVIG, MMF, Abatacept, Tofacitinib) and one still alive more than 400 days after diagnosis (after methylprednisolone, MMF, Abatacept, IVIG, Infliximab, Tofacitinib).
Conclusion: Steroid-refractory ICI-associated myocarditis can be responsive to other immunosuppression agents. Our case series, one of the largest studies of this population, highlights their effectiveness and the populations they can cater to. Adjunctive treatments for ICI-myocarditis require further study to identify right doses and order of treatment.

CLINICAL RESEARCH: Predictive Biomarkers 1
Poster Session

#2484 Association of artificial intelligence (AI)-based HER2 scoring with clinical outcomes to first-line trastuzumab plus chemotherapy in HER2-positive metastatic gastric cancer (mGC).

M. Kang[1], **Y. Lim**[2], H. Oh[1], J. Lee[1], J. Kim[1], J.-W. Kim[1], S. Song[2], H. Song[2], K.-W. Lee[1];
[1]Seoul National University Bundang Hospital, Seongnam, Korea, Republic of, [2]Lunit, Seoul, Korea, Republic of

Background: Although trastuzumab plus chemotherapy is the treatment of choice for HER2-positive mGC, not all patients respond to the therapy. To date, there is no reliable and efficient biomarker that can predict the response to trastuzumab-based treatment.
Methods: Clinical data and pathology slides from HER2-positive mGC patients treated with first-line trastuzumab and capecitabine/5-fluorouracil plus cisplatin were retrospectively collected. HER2 positivity was confirmed using standard methods with immunohistochemistry (IHC) and/or in situ hybridization. An AI-based model was applied to a single HER2 IHC-stained whole slide image (WSI) of each patient to identify and quantify the tumor cells with HER2 IHC staining intensity categories of 0, 1+, 2+, or 3+ on the slide. The proportion of tumor cells with 3+ staining intensity among total tumor cells (h3 percentage) in each slide was calculated and analyzed in relation to clinical outcomes.
Results: A total of 160 cases were included in this analysis. Overall, the median progression-free survival (PFS) was 9.2 mo, and the overall survival (OS) was 18.9 mo. By standard IHC HER2 grading, 107 (66.9%) 3+ and 53 (33.1%) 2+ cases were included. The median AI-estimated h3 percentage in these patients was 14.8% (range 0 - 99.5%). The patients with their best tumor response of complete (CR) or partial response (PR) (44.4%) exhibited significantly higher h3 percentages (mean h3 percentage 46.6% in CR/PR vs. 29.4% in stable or progressive disease, p = 0.018). The h3 percentage exhibited strong associations as a continuous variable with longer PFS (hazard ratio [HR] 0.94 [95% confidence interval (CI) 0.90 - 0.99] for 10% change of h3 percentages, p = 0.015) or OS (HR 0.93 [95% CI 0.89 - 0.98] for 10% change of h3 percentages, p = 0.004). Notably, patients having a proportion of 3+ tumor cells at ≥ 90% (27/160, 16.9%) showed particularly longer PFS (median PFS 21.4 mo in ≥ 90% vs. 8.5mo in < 90%, p = 0.006) and OS (median OS 40.3 mo in ≥ 90% vs. 16.6 mo in < 90%, p = 0.004).
Conclusion: AI-based models interpreting WSI can provide additive predictive information to HER2-positive mGC patients treated with trastuzumab plus chemotherapy.

#2485 A combined mregDC and Treg signature associates with antitumor efficacy of CCR4 antagonist tivumecirnon FLX475.

Adam Grant[1], Juraj Adamik[1], Jingtao Qiu[1], Jacob Wert[1], Molly Grandcolas[1], Scott Jacobson[1], Rakesh K. Goyal[1], William Ho[1], Shoji Ikeda[1], Marvin Au[1], Damian Trujillo[1], Michael Chisamore[2], Denise de Almeida Nagata[1], Mohsen S. Ghomi[1], Dirk G. Brockstedt[1], Paul D. Kassner[1], **George Katibah**[1]

[1]RAPT Therapeutics, Inc., South San Francisco, CA,[2]Merck & Co., Inc, Rahway, NJ

Cancers evade immune surveillance through multiple mechanisms including the recruitment of immunosuppressive regulatory T cells (Treg). Tivumecirnon (formerly known as FLX475), a small molecule oral CCR4 antagonist under clinical evaluation, blocks the binding of CCR4 to its ligands CCL17 and CCL22 and thereby reduces Treg infiltration into the tumor microenvironment (TME). This relieves Treg-mediated immune suppression resulting in increased antitumor immunity. Our clinical study (NCT03674567) demonstrated that tivumecirnon can block the local accumulation of Treg in the TME and has clinical activity as monotherapy as well as in combination with pembrolizumab. In both mouse and human tumors, we identified a subset of tumor infiltrating dendritic cells (DC) producing high levels of CCL22, previously identified as mregDC, suggesting a potential role in the CCR4-dependent recruitment of Treg.

To study the role of mregDC in the recruitment of Treg, non-clinical studies were performed. CD45+ immune cells from the TME of MB49 tumor bearing mice treated with tivumecirnon or vehicle and were analyzed by flow cytometry, scRNA-seq and CITE-seq. We confirmed that mregDC cells are the primary producer of CCL22 in the TME and that tivumecirnon treatment reduced the number of Treg cells in the TME and increased the percentage of IFN gamma and granzyme B expressing CD4+ T cells.

Based on these findings we interrogated tumor biopsies from patients from our clinical study prior to (n = 33), and after approximately 6 weeks of treatment (n = 22, pre/post-treatment paired samples) with tivumecirnon +/- pembrolizumab. We performed RNAseq and compared to published biopsy data from anti-PD-1 treated patients. We found that higher mregDC + Treg signature levels at baseline significantly ($p < 0.001$) associated with response to tivumecirnon and pembrolizumab therapy. Importantly, analysis of published datasets revealed that higher baseline mregDC and Treg levels are not associated with response to anti-PD-1 monotherapy. Analysis of TCGA gene expression data demonstrated a positive correlation with mregDC and Treg cells across human tumor types, indicating a previously unknown relationship between these cell types. Further application of this mregDC and Treg signature to the TCGA dataset identified a subset of cancer types resistant to prior treatments that could potentially benefit from combinatorial treatment with tivumecirnon. Overall, this study demonstrated that inhibition of the CCR4 pathway using tivumecirnon can disrupt the immunosuppressive mregDC – Treg axis leading to enhanced antitumor activity. Furthermore, the levels of mregDC and Treg may be used as a biomarker for selection of patients more likely to respond to tivumecirnon in combination with anti-PD-1. Additional studies are required to confirm these results

#2486 Dissecting tumor-immune interaction in response and resistance to immune checkpoint blockade in metastatic melanoma.

G. Tarantino[1], Y. He[1], P. Solanky[1], A. Thorner[1], T. Aprati[1], R. Sullivan[2], E. Robitschek[1], T. Blosser[3], X. Zhuang[3], X. Zhuang[3], E. Boblitt[4], A. Frangieh[1], M. Holovatska[1], A. Lawless[2], M. Manos[1], K. Pfaff[1], K. Helvie[1], T. Sharova[2], D. Frederick[4], J. Fahey[2], D. Villamarin[2], S. Farhi[4], S. Rodig[1], B. Johnson[1], A. K. Shalek[4], E. Van Allen[1], S. Hodi[1], G. M. Boland[2], D. Liu[1];

[1]Dana-Farber Cancer Institute, Boston, MA, [2]Massachusetts General Hospital, Boston, MA, [3]Harvard University, Cambridge, MA, [4]Broad Institute of MIT and Harvard, Cambridge, MA

Background: Immune checkpoint blockade (ICB) has revolutionized the treatment and prognosis of various cancers, including melanoma. Nevertheless, intrinsic or acquired resistance is common, and the interactions between tumor-intrinsic features and the microenvironment underlying these resistances remain unclear for most patients.

Methods: In this study, we developed a framework to analyze response and resistance, both intrinsic and acquired, via tumor-intrinsic programs, immune features, and tumor-stromal-immune interactions in a standardized, uniformly processed, and deeply clinically annotated cohort of metastatic melanoma patients (n=61) treated with ICB as part of the NCI funded human tumor atlas network (HTAN) initiative. From the same tumor samples (pre-treatment (n=33) and post-progression (n=28)), we conducted bulk whole-exome sequencing (WES), single-nucleus RNA sequencing, and for a subset of the samples high-resolution spatial imaging (including protein mIHC, CODEX, and transcriptomics MERFISH). Standardized processing and data pipelines allowed for integration of genomic, transcriptomic, and spatial features to elucidate shared tumor and microenvironmental states and their relationships with resistance.

Results: Our preliminary analysis on a subset of 28 samples identified an enrichment of B cells, plasma cells, and T follicular helper-like cells in the tumor microenvironment (TME) of patients sensitive to treatment. The TME of non-responders was predominantly characterized by macrophage/monocyte cell populations. Post-treatment responder samples showed an enrichment of CD4+ T cells. Genomic heterogeneity, assessed through WES, was confirmed as a feature of intrinsic resistance across different ICB treatment settings, while ploidy was associated with treatment response in pre-treatment, ipilimumab-naïve patients treated with PD-1 inhibitors. Comparing the immune compartments of samples with high and low heterogeneity revealed NK cell enrichment in samples with a high proportion of subclonal mutations.

Conclusions and Future Directions: Overall, our work provides a high-resolution understanding of the tumor-stromal-immune interaction in metastatic melanoma, shedding light on the factors contributing to therapy response and resistance, and contributing a repository of data from deeply clinically annotated, multimodally characterized and uniformly processed patient samples. Ongoing spatial analysis will further enhance our understanding of these compartments at a spatial level. The results of our study have the potential to guide more personalized and effective treatment strategies for metastatic melanoma in the future.

#2487 KRAS and TP53 co-mutation predicts benefit of immune checkpoint blockade in lung adenocarcinoma.

Jan Budczies[1], Eva Romanovsky[1], Martina Kirchner[1], Olaf Neumann[1], Miriam Blasi[2], Johannes Schnorbach[2], Rajiv Shah[2], Farastuk Bozorgmehr[2], Rajkumar Savai[3], Thorsten Stiewe[4], Solange Peters[5], Peter Schirmacher[1], Thomas Michael[2], Daniel Kazdal[1], Petros Christopoulos[2], Albrecht Stenzinger[1]

[1]Heidelberg University Hospital (UKHD), Heidelberg, Germany,[2]Thoraxklinik, Heidelberg University Hospital and National Center for Tumor Diseases, Heidelberg, Germany,[3]Institute for Lung Health (ILH), Justus Liebig University, Giessen, Germany,[4]Institute of Molecular Oncology, Member of the German Center for Lung Research (DZL), Philipps-University, Marburg, Germany,[5]Department of Oncology, Centre Hospitalier Universitaire Vaudois (CHUV), Lausanne University, Lausanne, Switzerland

PD-L1 protein expression is the most important predictive biomarker for immune checkpoint inhibition (ICI) in advanced non-small cell lung cancer (NSCLC), but has limited sensitivity and specificity. We analyzed the potential of activating KRAS and pathogenic TP53 mutations to provide additional predictive information. The study cohort included 713 consecutive immunotherapy patients with advanced lung adenocarcinomas of the Thoraxklinik Heidelberg who were negative for actionable EGFR and ALK/RET/ROS1 alterations. Two external cohorts of patients treated with immunotherapy (SU2C-ICI: n=247, MSK-ICI: n=135) and two external cohorts of surgical early stage patients were additionally analyzed (TCGA-LUAD: n=417, MSK-LUAD: n=394). Therapy benefit was assessed stratified by KRAS and TP53 mutations. RNA-Seq data of TCGA were analyzed to reveal the molecular characteristics of KRASmut/TP53mut tumors. Analyzing overall survival, an interaction between KRAS and TP53 mutations was observed in univariate and multivariate analyses (HR=0.56, p=0.0044 and HR=0.53, p=0.0021). KRASmut/TP53muts tumors performed better than tumors not harboring the dual mutation configuration (HR=0.71, CI 0.55-0.92). This observation could be confirmed in the external cohorts of immunotherapy patients (SU2C-ICI: HR=0.54, CI 0.28-1.03 and MSK-ICI: HR=0.35, CI 0.14-0.88), whereas KRASmut/TP53mut was not associated with prolonged survival in the surgical cohorts. Tumor mutational burden, proliferation (measured by TOP2A mRNA expression), and PD-L1 mRNA were significantly higher in TP53mut compared with TP53wt tumors, regardless of KRAS status. Genome-wide mRNA expression analysis revealed 64 genes including the chemokine CX3CL1 (fractalkine) as specific transcriptomic characteristic of KRASmut/TP53mut tumors. In summary, KRAS/TP53 co-mutation predicts ICI benefit in univariate and multivariate survival analyses and is associated with unique molecular tumor features. Further validation studies are warranted. Mutation testing of the two genes can be easily implemented using small gene panels or even single gene analyses.

#2488 The penile cancer tumor microenvironment and immunotherapy response: Results from the PERICLES trial.

T. S. Rafael[1], A. Gil-Jimenez[1], H. M. de Vries[1], I. M. Seignette[1], E. Bekers[1], M. Lopez-Yurda[1], D. Peters[1], E. Hooijberg[1], A. Broeks[1], O. R. Brouwer[1], E. Schaake[1], D. J. Vis[1], T. D. de Gruijl[2], L. F. Wessels[1], M. S. van der Heijden[1];
[1]Netherlands Cancer Institute, Amsterdam, Netherlands, [2]Amsterdam University Medical Center, Amsterdam, Netherlands

Introduction: The phase II PERICLES trial investigated the efficacy of atezolizumab (anti-PD-L1) for advanced penile cancer, with or without radiotherapy. As previously published, durable responses (progression-free at 12 months) were observed in 4 out of 32 enrolled patients. Here, we present the final overall survival (OS) results and an analysis of potential biomarkers for immunotherapy response.

Methods: Preplanned analysis projected that at 27/32 events, the study would have 80% power (2-sided α=0.05) to assess whether the OS for the entire cohort significantly differed from the hypothesized historical median for stage IV patients. Baseline tumor tissue samples were subjected to bulk-RNA sequencing (n=31), fluorescent (n=28) and chromogenic (n=30) multiplex immunohistochemistry. We quantified the densities of $CD3^{+}CD8^{+}$ cytotoxic T-cells, $CD3^{+}CD8^{-}FoxP3^{-}$ T-helper cells, $CD3^{+}CD8^{-}FoxP3^{+}$ regulatory T-cells, $CD68^{+}$ macrophages and $CD20^{+}$ B-cells in both the tumor and stromal compartments and assessed spatial relationships. We also quantified $CD8^{+}PD1^{+}$ (potentially enriched for tumor reactivity) and $CD8^{+}PD1^{-}$ T-cells. Differential expression and gene set enrichment analysis (GSEA) were performed using the hallmarks gene sets.

Results: The median OS for the entire study cohort was 11.3 months (95% CI, 5.5-16.7), which is an improvement compared to the hypothesized historical median of 7.8 months for stage IV patients (one sample log-rank p=0.033). Biomarker analyses showed an increased density of stromal macrophages (p<0.001) and intratumoral cytotoxic T-cells (p=0.035) in durable responders compared to non-responders. Additionally, we observed an increased density of intratumoral $CD8^{+}PD1^{+}$ in durable responders (p<0.001). In contrast, intratumoral $CD8^{+}PD1^{-}$ densities were comparable between durable and non-responders (p=0.057). Patients with a high density of intratumoral $CD8^{+}PD1^{+}$ also had an improved progression-free survival (PFS) (log-rank, p<0.001) and OS (log-rank, p=0.002). Analysis of the spatial relationships in the tumor microenvironment (TME) showed that durable responders had larger distances between cytotoxic T-cells and T-helper cells (p=0.034). GSEA revealed significant (FDR≤5%) up-regulation of IFN-α/γ responses in durable responders. In contrast, non-responders showed up-regulation of epithelial-mesenchymal transition, KRAS signaling and angiogenesis, suggesting potential barriers to an anti-tumor response.

Conclusion: In the final clinical analysis, OS was improved with atezolizumab compared to the historical population of stage IV patients. $CD8^{+}PD1^{+}$ T-cells, a common proxy for tumor-reactive T-cells, and spatial relationships in the TME might serve as biomarkers of durable response to immunotherapy in advanced penile cancer.

#2489 A cell-free DNA methylation biomarker outperforms irRECIST in predicting treatment outcome.

P. Xie[1], M. Innoue[1], P. Siejka-Zielińska[1], R. Amess[1], J. Chang[1], S. Wilding[2], G. Griffiths[2], M. R. Middleton[1], R. P. Owen[1], C. Song[1], X. Lu[1], **B. Schuster-Boeckler[1];**

[1]University of Oxford, Oxford, United Kingdom, [2]Southampton General Hospital, Southampton, United Kingdom

Immune checkpoint inhibitors (ICI) are established as first-line treatment for inoperable esophageal adenocarcinomas (EAC), in combination with chemotherapy (CTX). Unfortunately, response to immunochemotherapy is highly variable, despite most EAC cases featuring a high mutation burden. EAC response to ICI is assessed using radiological criteria such as irRECIST, but its ability to predict long-term survival is poor. Consequently, early recognition of a failing therapy is challenging. More accurate early biomarkers of response to ICI are therefore of critical importance.

Here, we show that a classifier based on epigenetic features in cfDNA taken 4 weeks after treatment initiation accurately predicts treatment benefit after one year. Strikingly, this blood-based biomarker predicts OS better than radiological criteria.

We collected cell free DNA (cfDNA) from patients enrolled in the LUD2015-005 trial, in which ICI was administered for four weeks before adding standard-of-care chemotherapy (ICI+CTX). For each patient, we collected cfDNA, tumor and adjacent normal tissue at diagnosis, before ICI+CTX, during and at the end of treatment, in addition to radiological clinical imaging.

Tissue and cfDNA samples were sequenced using TET-Assisted Pyridine-borane Sequencing (TAPS), a method recently developed in Oxford which provides high-depth, base-resolution DNA methylation information from low-input samples.

Based on tissue data, we identified a genome-wide hypomethylation signature specific to tumor cells. By accounting for sample-to-sample variability in stromal composition, we show that this signature is present in most EACs, allowing us to model the admixture of tumor and normal methylation patterns to quantify the amount of tumor methylation detected (TMD) in cfDNA.

16 patients had increased TMD (TMD-up) after 4 weeks of ICI monotherapy compared to pre-treatment levels, while 15 patients had decreased TMD (TMD-dn). Median OS for the two groups were 37 and 112 weeks, respectively ($p < 0.0001$). We evaluated the radiological response according to irRECIST at similar timepoints. 17 of 32 patients (53.1%) had no definitive evidence of progression nor response and were deemed to have radiologically stable disease. 8 of these patients went on to develop progressive disease within 1 year - all 8 patients belonged to the TMD-up group. Contrastingly, 8 out of 9 patients who had PFI greater than 1 year belonged to TMD-dn. In all 32 patients, TMD predicted radiological disease progression within 1 year with 83.3% sensitivity and 92.3% specificity.

Taken together, we report the discovery of a circulatory biomarker that measures molecular response to ICI in EAC and identifies poor prognosis patients that appear stable from radiological imaging. Furthermore, patients with favorable molecular response were found to have a median OS almost 3 times that of patients with unfavorable molecular response.

#2490 Quantification of tumor fraction and outcomes association in a real-world non-small cell lung cancer (NSCLC) cohort using a tissue agnostic epigenomic circulating tumor DNA (ctDNA) assay.

S. Wienke[1], S. Gordon[1], S. Liang[2], J. Wang[1], R. Barnett[1], K. Chang[1], S. Zhang[1], C. R. Espenschied[1], K. Quinn[1], K. Banks[1];
[1]Guardant Health, Palo Alto, CA, [2]Parker Institute for Cancer Immunotherapy, San Francisco, CA

Background: The validity of ctDNA assays for evaluating molecular response to therapy by measuring changes in variant allele fraction (VAF) while on treatment is well established, but they are prone to limitations such as low ctDNA levels and interference from copy number variation and clonal hematopoeisis (CH), which may be overcome by methylation-based quantification. ctDNA levels may be monitored throughout a patient's (pts) journey to indicate when relapse or progression is present, often sooner than current methods (RECIST). Here we describe the performance of a methylation-based ctDNA assay to quantify ctDNA levels and correlate changes with outcomes in a real-world NSCLC cohort.

Methods: RADIOHEAD is a pan-tumor observational study of 1200 patients on standard of care ICI treatment regimens with plasma samples collected prospectively for retrospective analysis. We randomly selected 241 NSCLC pts that have a combined total of 761 samples (236 baseline, 191 C3D1, and 128 at 6 months post first dose). Samples were analyzed using a commercial NGS assay, which quantifies circulating tumor fraction (cTF) via interrogating thousands of methylation sites from ctDNA, validated with LoB, LoD, LoQ, and linearity studies. Cox proportional hazards (CPH) were used for comparison of real-world progression free survival (rwPFS). Gender, age, disease stage, and blood-assessed tumor mutational burden (bTMB) were included as covariates. Median rwPFS was calculated using Kaplan Meier analysis. rwPFS ordinal groups were defined as PFS event within 3mo, 3-6mo, 6-12mo, and greater than 12mo, and association with early ctDNA changes was assessed with a chi-squared test.

Results: In this cohort, 4, 11, 83 and 142 pts were stage I to IV, respectively (1 unknown). Methylation based detection of ctDNA at baseline or C3D1 was associated with shorter rwPFS (baseline: mPFS 12.7 mo [9.3-19.5] vs NR [16.4-NR]; HR=2.2 [1.3-3.7] p<0.005, C3D1: mPFS 12.4 mo [9.3-16.1] vs NR [19.5-NR] HR= 2.2 [1.3-3.5], p<0.005) independent of stage, gender, or age. Longer rwPFS was associated with >95% reduction in cTF from baseline to C3D1 or low ctDNA at both timepoints (rwPFS <3mo = 12.5%, 3-6 mo = 30.8%, 6-12 = 37.1%, ≥12 mo = 55.3%; N=153, p=0.015). For pts with ctDNA not detected at C3D1, ctDNA detection at 6 months post first dose was strongly associated with shorter rwPFS (mPFS 13.5 mo [9.5-NR] vs. NR [19.5-NR]; HR= 6.2 [1.9-20.1], p<0.005).

Conclusions: These data demonstrate a significant association of ctDNA detection via methylation-based cTF and on-treatment changes in cTF with rwPFS. Furthermore, subsequent cTF detection 6-months on-treatment, without cTF detected early on-treatment was associated with worse outcomes, suggesting the value of serial monitoring to improve identification of patients likely to progress.

#2491 The Oxford Classic can identify HGSOC patients who may benefit from EMT-targeting therapies.

L. Rai[1], A. Ravaggi[2], E. Bignotti[2], R. Hollis[3], J. Nulsen[1], L. Campo[1], A. Easton[1], M. Artibani[1], M. Churchman[3], F. Ferrari[2], C. Yau[1], C. Gourley[3], F. Odicino[2], A. Ahmed[1],

[1]University of Oxford, Oxford, United Kingdom, [2]Istituto di Medicina Molecolare "Angelo Nocivelli", Brescia, Italy, [3]University of Edinburgh, Edinburgh, United Kingdom

Introduction: Despite development of novel targeted therapies such as PARP inhibitors and anti-angiogenic drugs, there is a clear lack of treatment options for High Grade Serous Ovarian Cancer (HGSOC) patients who are Homologous Recombination Repair proficient (50% of cases) and those with intrinsic resistance to these drugs. In this study we demonstrate the ability of the Oxford Classic (OxC)[1,2], a non-genetic classifier, to identify HGSOC patients who may benefit from EMT targeting drugs.

Methods: 139 HGSOC diagnostic tumor tissue (Brescia cohort) underwent RNA sequencing. Scottish cohort[3] was used for external validation and TCGA, AOCS & OVCAD datasets were used for meta-analysis. Deconvolution of tumor RNAseq data, survival analyses, differential gene expression (DGE) analysis, gene pathway analyses in R and tumor immune profiling using CIBERSORT were performed.

Results: Risk stratification of HGSOC using the Oxford Classic Patients with a higher OxC-EMT score had 3.6 times increased risk of death (95%CI: 1.6-8.0; p=2e-03) compared to patients with a lower OxC-EMT score by a multivariable cox regression analysis of Brescia cohort. By Kaplan-Meier survival analyses, a significant difference in overall survival in Brescia cohort (p=9e-06), Scottish cohort (p=2e-03) and a combined set of 1023 cases (p=1e-04), was observed between EMT-low risk patients (OxC-EMT score-0) and EMT-high risk patients (OxC-EMT score>0). Notably, 5-year median survival of EMT-low risk and EMT-high risk group was 50% and 13%, resp. (95%CI: 36.1%-69.3% vs 7.1%-23.5%) in Brescia cohort. Therapeutic options for OxC-EMT-high risk group DGE analysis of EMT-low patients and EMT-very high patients (OxC-EMT score>0.5) identified 404 differentially expressed genes common to the datasets. These included genes related to extracellular matrix organisation (*VCAN, TGFβI*), epithelial cell proliferation (*RUNX2, FABP4, SERPINF1*), cell chemotaxis (*CCL19, DUSP1*), angiogenic factors (*VEGFC, CXCL12*) and transmembrane kinase signalling pathways (*TGFβ1/3, PDGFRα/β, IGFBP4/5/6, Wnt11*). Of note, key EMT transcription factors, *TWIST1/2, SNAI1/2, ZEB1/2,* and stemness marker, *ALDH1A3,* were 2-7 times overexpressed in EMT-very high group. Furthermore, immune modulators, *IL6 and IL10* were significantly upregulated and M2 macrophages were significantly more abundant in EMT-very high patients. Multiplex IHC is currently underway to confirm the abundance of TAMs and CD8-positive TRM in the two risk groups.

Conclusions: 1) The Oxford Classic-based EMT is a robust prognostic biomarker of overall survival in HGSOC, that faithfully represents the complex circuitry of pathways which are a hallmark of Epithelial to Mesenchymal Transition. 2) OxC-EMT risk stratification can identify HGSOC patients who may benefit from EMT-targeting therapies.

Reference: 1) Hu Z. Cancer Cell 2020 2) Hu Z. Clin Cancer Res 2021 3) Hollis R. Clin Cancer Res 2022

#2492 Enhanced patient selection for anti-PD-L1 treatment in metastatic NSCLC with quantitative continuous scoring of PD-L1.

J. Lesniak[1], M. Schick[1], T. Kunzke[1], F. Pollastri[1], J. Vigueras-Guillen[1], H. Hessel[1], S. Haneder[1], P. Sontakke[1], K. DaCosta[1], R. Alleze[1], H. Sade[1], J. Barrett[2], G. Schmidt[1], R. Stewart[3];

[1]AstraZeneca, Munich, Germany, [2]AstraZeneca, Gaithersburg, MD, [3]AstraZeneca, Cambridge, United Kingdom

Background: Anti-PD-L1 therapy has demonstrated clinical activity in patients with metastatic non-small cell lung cancer (mNSCLC). However, only subgroups of patients respond and their identification via PD-L1 as a biomarker remains imperfect. PD-L1 expression is commonly assessed by pathologist tumor cell (TC) scoring of immunohistochemically (IHC) stained tissue. We developed a system for digitally scoring PD-L1 in IHC (PD-L1 QCS), which demonstrated robust scoring across studies [1]. Here, we present a comparison of PD-L1 QCS against manual scoring of PD-L1 (SP263 assay, Ventana) in the MYSTIC clinical trial.

Methods: PD-L1 QCS on digitized whole slide images (WSI) comprises two deep learning models, enabling segmentation of single TCs followed by PD-L1 expression quantification via their optical density (OD). Positive cells are classified based on an OD threshold, allowing robust digital calculation of the TC percentage [1]. The analysis included 502 WSI from the MYSTIC trial (NCT02453282), representing 256 patients treated with anti-PD-L1 therapy and 246 treated with chemotherapy as standard-of-care (SoC) [2]. First, an optimal cut-point was determined by optimization against outcome, classifying patients with ≥0.575% TC as biomarker positive (BM+). Next, the approach was compared against manual TC scoring at 1%, 25% and 50% cut-off.

Results: In durvalumab treated patients, median overall survival (mOS) in the PD-L1 QCS BM+ subgroup (prevalence 54.3%) was 12.1 months longer than in the BM- subgroup (19.9m vs. 7.8m, HR=0.45, CI [0.33, 0.60]). Analogous comparison of subgroups based on manually scored TC proportion at 1% (prev. 75.0%), 25% (prev. 42.6%) or 50% (prev. 29.7%) cut-points yielded a mOS difference of 7.8m (HR=0.52, CI [0.38, 0.72]), 8.3m (HR=0.61, CI [0.45, 0.82]) and 11.0m (HR=0.55, CI [0.40, 0.77]) respectively. Comparing durvalumab treatment against SoC within the PD-L1 QCS BM+ subgroup yielded a HR of 0.62 (CI [0.46, 0.82], log rank p=0.0008, 7.4m mOS delta). In comparison, a HR of 0.69 (CI [0.46,1.02], p=0.0642, 8.4m mOS delta) was obtained for manual TC scoring at 50%.

Conclusion: We compared a computational pathology approach for continuous PD-L1 scoring for the selection of mNSCLC patients for anti-PD-L1 treatment against established manual scoring. Our results suggest that PD-L1 QCS has the potential to identify a larger patient subgroup that retains benefit from anti-PD-L1 treatment and more precisely identifies non-responders.

References: 1. Lesniak, Jan, et al. "Quantitative computational assessment of PD-L1 enables robust patient selection for biomarker-informed anti-PD-L1 treatment of NSCLC patients." *J. Immunother. Cancer,* Vol. 10., 2022. 2. Rizvi NA, et al. "Durvalumab with or without tremelimumab vs standard chemotherapy in first-line treatment of mNSCLC: the MYSTIC phase 3 randomized clinical trial." *JAMA Oncology*. 2020;6.5:661-674.

#2493 Prospective evaluation of predictive biomarkers for Palbociclib (P) and endocrine therapy (ET) benefit in hormone receptor (HR)-positive [+]/human epidermal growth factor receptor 2 (HER2)-negative [-] advanced breast cancer (ABC) patients (pts) from PARSIFAL clinical trial: The transFAL sub-study.

Joan Albanell[1], Angelo Gamez Pozo[2], Carlos L. Arteaga[3], Meritxell Bellet[4], Federico Rojo[1], Abel Gonzalez[1], Beatriz Bellosillo[1], Violeta Serra[4], Petra Gener[5], Jose Antonio Guerrero[5], Laura Lopez-Montero[5], **Mario Mancino**[5], Jose Rodriguez-Morato[5], Leonardo Mina[5], Jose Manuel Perez-Garcia[5], Javier Cortes[5], Antonio Llombart-Cussac[5]

[1]Hospital del Mar Medical Research Institute, Barcelona, Spain,[2]Molecular Pathology Lab, La Paz Hospital Center, IDIPAZ, Madrid, Spain,[3]Harold C. Simmons Comprehensive Cancer Center, UT Southwestern, Dallas, TX,[4]Vall d'Hebron Institute of Oncology, Barcelona, Spain,[5]Medica Scientia Innovation Research (MEDSIR), Barcelona, Spain

BACKGROUND Combining cyclin-dependent kinases 4 and 6 inhibitors (CDK4/6i) with first-line ET is the standard of care for pts with HR[+]/HER2[-] ABC. PARSIFAL was a randomized, open-label, phase II trial that evaluated the efficacy and safety of first line P plus fulvestrant (F) or letrozole (L) in this pts population. Both treatments had comparable efficacy and safety results (JAMAOncol. 2021;7(12):1791-1799). Although multiple CDK4/6i clinical outcomes biomarkers have been reported, the only validated predictive factor for response is HR positivity. TransFAL, a translational study of PARSIFAL, assessed a comprehensive set of biomarkers of sensitivity/resistance to P plus ET.

MATERIALS AND METHODS TransFAL employed a sample biorepository from PARSIFAL comprising formalin-fixed paraffin-embedded (FFPE) tissue and blood samples obtained from pts included in either study arm. Tumor samples (N=33) derived from the primary tumor at initial diagnosis or from primary tumor or metastatic lesions at study entry. Blood samples were obtained at baseline (N=73) and disease progression (N=22). Pts were categorized as sensitive or resistant based on progression-free survival (PFS). CDK4/6 pathway activation was assessed by immunohistochemistry for CDK4, CDK6, Rb, pRb, ER, PgR, and Ki67. Proteins extracted from FFPE slides were analyzed using hierarchical clustering, significance analysis of microarrays, and probabilistic graphical models. RNA expression and circulating tumor DNA (ctDNA) analysis were assessed by next-generation sequencing (NGS) and analysis of panel of 56 genes/gene regions, respectively.

RESULTS A worse median PFS was found in pts with CDK6 positive (≥ 1% positive cells; $p < 0.001$) and high Ki67 (≥ 10% positive cells; $p = 0.013$)at baseline. ctDNA density at baseline was significantly higher for resistant (PFS < 9 months; 17.1 ng/mL) pts compared to sensitive (PFS > 31 months; 11.3 ng/mL) pts ($p < 0.001$). Most pts (83%) presented a genomic alteration detected in ctDNA, TP53 (28%) and PIK3CA (28%) being the most frequently mutated genes. Pts (9%) who harbored ARID1A mutation had lower PFS ($p = 0.052$). ESR1 mutations at progression were numerically higher in the L arm (37.5%) compared to F arm (14.3%); (p=0.31), but numbers were low. Proteomic and RNA analyses did not yield confirmable distinctive expression pattern between resistant/sensitive pts...

CONCLUSIONS High Ki67 levels and CDK6 expression in the tumor and high ctDNA density, but not proteomic or RNA sequencing data, were associated to poor outcome in this analysis of pts treated with CDK4/6i and ET. This data adds to the growing evidence of poor prognosis biomarkers in this setting, highlighting the need of novel strategies for these pts.

#2494 RAS-Bio a unique pan-cancer biobank for RAS-driven tumors.

M. Carter[1], K. D. Brown[1], H. Adderley[1], G. Morrissey[1], L. Woodhouse[1], J. Weaver[1], K. Simpson[2], J. Roebuck[2], J. Rogan[3], J. Mercer[3], A. Chaturvedi[3], D. Wedge[4], C. Jorgensen[2], A. Malliri[2], C. Dive[2], C. R. Lindsay[4];

[1]The Christie NHS Foundation Trust and University of Manchester, Manchester, United Kingdom, [2]Cancer Research UK, Manchester Institute, University of Manchester, Manchester, United Kingdom, [3]The Christie NHS Foundation Trust, Manchester, United Kingdom, [4]University of Manchester, Manchester, United Kingdom

Background: RAS-driven cancers represent a significant unmet clinical need, while breakthroughs in treatments targeting *KRAS*^{G12C} driven-NSCLC have invigorated drug-development for other RAS mutant cancers. Most RAS mutant cancers are not driven by *KRAS*^{G12C}, leaving an enormous amount of work needed to establish the contextual treatment vulnerabilities of cancers driven by different RAS mutant subtypes. RAS-Bio was pioneered within The Cancer Research UK Lung Cancer Centre of Excellence in Manchester. RAS-Bio is a uniquely curated resource of unparalleled clinical, genomic, translational and biological detail. RAS-Bio was established with the aim of generating novel model systems along with clinical observation to facilitate RAS precision medicine breakthroughs.

Method: RAS-Bio recruits patients affected by epithelial cancers with RAS pathway mutations, aiming to i) optimize sample collection & processing protocols (FFPE/fresh/frozen) for multi-omic profiling, ii) validate preclinical hypothesis-generating findings in a clinical cohort, iii) generate novel RAS-mutant organoid, PDX and other models for analyses and drugging experiments, iv) foster academic/industry collaboration using a unique dataset including demographics, pathology/imaging details, treatment types and survival outcomes.

Results: In two years, we have recruited 190 cancer patients with cancers harboring *KRAS*^{G12C} (*n*=71), *KRAS*^{G12D}(17), *KRAS*^{G12V}(23), *KRAS*^{G12A}(8), *KRAS*^{G12S}(2), *KRAS*^{G12F} (3), *KRAS*^{G12R} (1) and *KRAS*^{G12E} (1). A further 20 harboring KRAS codon 13 mutations and 12 *KRAS*^{Q61} cancers and an additional 32 patients with mutations in other key signaling nodes of the MAPK pathway have been recruited. Seventeen PDX models have been attempted; lung cancer (14) and colorectal cancer (3). Four lung cancer cases are currently growing (*KRAS*^{G12C} treatment naïve, *KRAS*^{G12C} inhibitor resistance, *KRAS*^{G12C} inhibitor refractory, *KRAS*^{G13C} treatment naïve) and two colorectal cancer cases (KRAS^{G12C} and KRAS^{G12V}). We will present two deep-dive lung patient cases i) *KRAS*^{G12C} 'OFF' state inhibitor (sotorasib) resistance where multiple tissue samples, CTCs and a successful PDX were derived, and ii) sotorasib resistance where paired biopsies and PDXs were derived pre- and post-treatment. Both cases demonstrate the clinical utility of longitudinal sampling in understanding clinically relevant resistance mechanisms to targeted treatment.

Conclusion: RAS-Bio represents a comprehensive biobank of clinical, pathological, and genomic detail in RAS-mutant lung cancers. Optimizing collaborative potential with academia/industry to facilitate prospective sampling of patients at different timepoints and integrating colorectal and pancreas cancers in our protocol.

#2495 CCL3 predicts an exceptional response to TGFβ inhibition in pancreatic ductal adenocarcinoma by sustaining a basal-like ecotype enriched in LIF-producing macrophages.

S. Pietrobono, M. Bertolini, V. De Vita, E. Scarlato, F. Fazzini, F. Sabbadini, D. Mangiameli, A. Quinzii, S. Casalino, **D. Melisi**;
University of Verona, Verona, Italy

The TGFβ receptor inhibitor galunisertib (GAL) exhibited promising efficacy in patients with pancreatic ductal adenocarcinoma (PDAC) in the randomized phase 2 H9H-MC-JBAJ study. However, the identification of predictive biomarkers remains of unique importance. We used a 279 multi-analyte panel and confirmed CCL3 as the most significant plasma protein for chemoresistance in patients receiving gemcitabine (GEM) [overall survival (mOS) (95%CI), high vs low, 3.6 (2.5-4.0) vs 10.1 (7.2-17.0) months, HR (95%CI)= 3.92 (2.14-7.20); p<0.001]. GAL dramatically reverted this resistance and CCL3 was the most significant predictive marker for the combination of this agent plus GEM [mOS (95%CI), GAL + GEM vs. placebo + GEM, 9.0 (5.5-12.1) vs 3.6 (2.5-4.0) months, HR (95%CI)= 0.39 (0.23-0.68); p<0.001]. We delved into the mechanisms behind this exceptional response in PDAC with this prognostically negative ecotype sustained by CCL3 in 6 different murine PDAC models. Mice bearing high-Ccl3 tumors had a significantly shorter mOS, a higher infiltration of M2-macrophages (TAMs), and a more mesenchymal/basal-like phenotype than did models with undetectable Ccl3.Ccl3 was stably expressed in DT4313 and PAN610, and silenced in RC416 cells. In co-culture models, $DT4313^{Ccl3}$ and $PAN610^{Ccl3}$ had a more mesenchymal phenotype and induced a M2 polarization of RAW264.7 murine TAMs than did controls. Mice bearing $DT4313^{Ccl3}$ or $PAN610^{Ccl3}$ tumors had a significantly shorter mOS, an higher infiltration of M2-polarized TAMs and a more mesenchymal/basal-like phenotype than controls. The expression of Tgfβ1 ligand and the phosphorylation of Smad2 were triggered only in TAMs if co-cultured with Ccl3-high $RC416^{scr}$, $DT4313^{Ccl3}$ or $PAN610^{Ccl3}$ cells. This activation of Tgfβ pathway was blocked by maraviroc, a selective inhibitor of Ccl3-receptor Ccr5. In co-culture, GAL reverted the mesenchymal phenotype of PDAC cells and the M2 polarization of TAMs. By using an 111 different cytokine immunoassay, Leukemia Inhibitory Factor (Lif) was the most significantly factor overexpressed by TAMs if stimulated by Ccl3. GAL suppressed this Lif expression. In mice bearing $DT4313^{Ccl3}$ tumors GEM was ineffective, whereas it prolonged mOS in those with $DT4313^{NTC}$ tumors. Conversely, GAL plus GEM doubled mOS duration vs. GEM, modulated M2- TAMs infiltration, the mesenchymal/basal-like phenotype and plasma Lif only in mice bearing $DT4313^{Ccl3}$ tumors, but not in those with $DT4313^{NTC}$ controls. In summary, we demonstrated that tumor-derived Ccl3 activates an autocrine Tgfβ signaling in TAMs, triggering their M2-phenotype and secretion of Lif. This Tgfβ-Lif axis sustains paracrinally a mesenchymal/basal-like PDAC ecotype resistant to GEM. Inhibition of Tgfβ signaling modulates this poor prognosis ecotype, and explains the exceptional response to GAL in patients with high-CCL3 PDAC.

#2496 Molecular characterization of stage III colon cancer patients with recurrence after adjuvant chemotherapy.

I. Franken[1], S. Ketelaars[2], C. Rubio-Alarcon[2], S. van Nassau[1], S. Schraa[1], G. Meijer[2], M. Sausen[3], M. Koopman[1], G. Vink[4], S. Abeln[5], R. Fijneman[2], J. Roodhart[1], on behalf of the PLCRC-MEDOCC group;

[1]UMC Utrecht, Utrecht, Netherlands, [2]Netherlands Cancer Institute, Amsterdam, Netherlands, [3]Personal Genome Diagnostics (LabCorp), Baltimore, MD, [4]Netherlands Comprehensive Cancer Organisation (IKNL), Utrecht, Netherlands, [5]Utrecht University, Utrecht, Netherlands

Introduction: Patients with stage III colon cancer are routinely treated with resection followed by adjuvant chemotherapy (ACT) with a fluoropyrimidine and oxaliplatin. This one-size-fits-all approach does not account for heterogeneity in tumor biology and fails to cure ~30% of patients, highlighting the urgency for biomarkers to better understand and predict resistance to ACT or to offer alternative targeted treatment.

Aim: To identify molecular characteristics predictive of resistance to standard ACT in stage III colon cancer.

Methods: Patients with resected stage III colon cancer who received ACT (93% CAPOX, 7% CAP) were selected from the Prospective Dutch Colorectal Cancer cohort (PLCRC). RNA exome capture sequencing was performed on resected FFPE tumor tissue to compare differential gene expression, hallmark pathway enrichment, immune cell deconvolution and consensus molecular subtypes (CMS) between patients with versus without recurrence after surgery and ACT. Postsurgery circulating tumor DNA (ctDNA) detected in PLCRC-PROVENC3 (separate abstract) was used to select a subgroup with minimal residual disease (MRD) postsurgery, as sensitivity analysis of patients with recurrence despite ACT (chemoresistant) versus curation by ACT (chemosensitive).

Results: For 264 out of 278 patients (95%), tumor-derived RNA sequencing libraries were of sufficient quality. 67 patients (25%) with recurrence (median after 13 months [IQR 7-23]) were compared to 178 patients with at least 2 year recurrence-free follow-up (median 42 months [IQR 30-53]). A total of 320 genes were differentially expressed between patients with versus without recurrence. Genesets defining epithelial-mesenchymal transition ($p = 0.002$) and angiogenesis ($p < 0.001$) were enriched in the primary tumor of patients with recurrence, in part explained by the estimated larger fraction of stroma (Wilcoxon effect size r 0.18, $p < 0.001$) and cancer-associated fibroblasts (CAFs) (r 0.19, $p = 0.003$). In contrast, the fraction of CD4+ T cells was lower (r 0.14, $p = 0.001$). Consistently, CMS4 was found more frequently in tumors from patients with versus without recurrence (57% versus 34%, $p < 0.001$).

Of the subgroup with ctDNA-based MRD postsurgery (26 out of 171 assessed patients), 19 patients (73%) with recurrence (median after 12 months [IQR 7-17]) were compared to 7 patients without recurrence (minimum follow-up 32 months). This sensitivity analysis showed similar trends in pathways, immune cells and CMS as the main analysis, with a more pronounced effect size for CAFs (r 0.27).

Conclusion: Stage III colon tumors of patients who experience recurrence after resection and ACT are enriched for stroma and CAFs, while displaying less CD4+ T cells. The observed trends are sustained in the patients with MRD postsurgery. These findings may help to better predict resistance to standard ACT and elucidate targets for alternative personalized treatment.

#2497 Extracellular vesicle based ALPPL2 and THBS2 as biomarkers for disease monitoring in patients with pancreatic ductal adenocarcinoma.

K. Halder[1], G. Jameson[2], E. Borazanci[2], W. Lin[1], D. Cridebring[1], D. Von Hoff[1], H. Han[1];
[1]TGen (The Translational Genomics Research Institute), Phoenix, AZ, [2]HonorHealth Research Institute, Scottsdale, AZ

Pancreatic ductal adenocarcinoma (PDAC) remains a formidable challenge in the realm of oncology, characterized by its aggressive nature and resistance to treatment. Several therapeutic regimens have been shown to extend patient survival, but the majority of the patients become refractory to the treatments in a short period of time. Hence, it is critical to monitor a patient's response to treatment in a timely manner so that different treatment regimens can be considered promptly. Currently, CA19-9 is the most common blood-based marker being used to monitor disease burden in patients with PDAC. However, 15-20% of patients with PDAC do not have elevated blood CA19-9 levels. In this study, we sought to determine the utility of two circulating extracellular vesicle (EV) based protein biomarkers, ALPPL2 (Alkaline phosphatase, placental-like 2) and THBS2 (Thrombospondin 2), for disease monitoring in patients with PDAC. We first established and optimized EV assays using the ExoView^{TM} platform for detecting and quantifying the number of ALPPL2^{+} or THBS2^{+} EVs in serum samples. We then determined the concentrations of ALPPL2^{+} or THBS2^{+} EVs in samples from healthy individuals and longitudinal samples from patients with Stage IV PDAC undergone treatment. The longitudinal samples were from 26 patients of which 16 were CA19-9 secretors (defined as >35 U/ml) and 10 were CA19-9 non-secretors (defined as <35 U/ml) that were treated with various regimens for 4-24 months with monthly blood sample collection and CT scans (a total of 305 samples). We found that the concentrations of ALPPL2^{+} and THBS2^{+} EVs are on average 1,737 and 1,113 times higher in PDAC patients than in the healthy controls, respectively. Correlation analysis using the mixed linear model showed that the concentrations of both ALPPL2^{+} and THBS2^{+} EVs significantly correlate with changes in tumor size (based on RECIST measurements) in the longitudinal samples of CA19-9 non-secretors or secretors. In CA19-9 non-secretors the correlation p values are 0.003 and 0.006 for ALPPL2^{+} and THBS2^{+} EVs, respectively, whereas in CA19-9 secretors, the p values are 0.014 and 0.016 for ALPPL2^{+} and THBS2^{+} EVs, respectively. Our data indicates that EV based ALPPL2 and THBS2 could potentially serve as biomarkers for disease monitoring in patients with PDAC. (This work was supported in part by the Dorrance Family Fund and the Flinn Foundation)

#2498 Assessing the clinical value of ctDNA sequencing for initial tumor profiling in metastatic colorectal cancer patients with sufficient tumor tissue.

Y. Cha, B. Kim, D. Lee, H. Yeo, C. Hong, K. Han, B. Kim, H. Chang;
National Cancer Center - Korea, Goyang, Korea, Republic of

Introduction Tumor profiling including RAS, BRAF, HER2, and MSI/MMR status, is required to determine the treatment for patients with metastatic colorectal cancer (mCRC) at the time of diagnosis. While comprehensive tumor profiling using tissue-based next-generation sequencing (NGS) is increasingly adopted for initial profiling in mCRC, the role of circulating tumor DNA (ctDNA) NGS as initial testing in patients with sufficient tumor tissue is not clearly understood. We assessed the clinical value of ctDNA sequencing compared to tumor NGS in patients with newly diagnosed mCRC who have sufficient tumor specimens.
Methods We prospectively enrolled consecutive patients with newly diagnosed mCRC at the National Cancer Center Korea. As per the institutional protocol for mCRC, initial tumor profiling was performed on primary tumor tissue using an in-house NGS panel (NCC PCP ver.3), which included 525 genes. For ctDNA sequencing, patients were evaluated using the AlphaLiquid®100 comprehensive cancer panel (IMBdx, Inc.), which included 118 genes, before the initiation of chemotherapy. Additionally, immunohistochemical (IHC) testing for HER2 and polymerase chain reaction (PCR)/IHC testing for MSI and/or MMR were performed to assess the accuracy of HER2 and MSI/MMR status.
Results A total of 188 patients were enrolled. In 139 eligible patients, 275 potentially actionable mutations were found in 12 selected CRC-related genes (APC, TP53, KRAS, NRAS, BRAF, FBXW7, PIK3CA, ERBB2, SMAD4, NF1, EGFR, MET). Of these, 32% were found both in ctDNA and tissue; 54% were found in ctDNA only; 12% in tissue only, and 2% were discordant. For RAS/BRAF mutations, which are required for anti-EGFR treatment decisions, the concordance rate between ctDNA and tissue NGS was 83.1%, and the concordance was higher in patients with higher ctDNA concentrations. For 9 patients with potentially actionable copy number variations (CNV) in EGFR, HER2, MET, and FGFR1, 3 cases were found by both assays; 4 were found by ctDNA only, and 2 were found by tissue only. ctDNA NGS correctly predicted MSI/MMR status in 2 out of 4 patients with MSI-H/dMMR; in the 2 other patients, the MSI and MMR statuses were different, suggesting potential false positivity. In addition, the fold changes in ctDNA dynamics during treatment significantly correlated with changes in tumor size and CEA levels, as well as with droplet digital PCR copy number fold changes. In a patient with MET amplification, ctDNA NGS identified MET Y1230H as a potential acquired resistance mutation after crizotinib treatment, which responded to cabozantinib but not to capmatinib.
Conclusions Initial tumor profiling using ctDNA NGS yielded outcomes comparable to those of tumor tissue NGS in guiding treatment for patients with newly diagnosed mCRC, thereby suggesting its utility as an initial profiling method in mCRC.

#2499 Window-of-opportunity trial of metastatic pancreatic cancer reveals potential mechanisms of response to targeting RAS signaling.

M. Tsuda, C. Daniel, X. Wang, C. Pelz, H. Zimny, A. Smith, J. Muschler, X. Li, T. Yildiran Ozmen, F. Ozmen, D. Keith, C. Corless, K. Chin, J. Brody, C. Lopez, G. Mills, R. Sears;
OHSU, Portland, OR

KRAS is mutated in ~85% of pancreatic ductal adenocarcinoma (PDAC) patient's tumors, suggesting that it is a key node of PDAC targeted therapy. RAF/MEK/ERK signaling is downstream of KRAS signaling. Preclinical studies targeting MEK showed promises but clinical trials failed to show the benefit compared to Standard-of-Care treatment chemotherapy. To elucidate the mechanism of action and resistance to several targeted therapies including MEK inhibition in human PDAC, we conducted a Window-Of-Opportunity trial for Metastatic pancreatic cancer (WOOM trial). In this trial, metastatic PDAC patients received 10 days of Cobimetinib, a FDA approved MEK inhibitor, therapy and specimens of pre- and post- treatment were obtained by biopsy to evaluate the response to targeted treatment using deep multi-omic analytics including DNA-seq, RNA-seq, multiplex IHC, cyclic IF and Digital Spatial Profiling (DSP). The clinical grade KI67 staining positivity was used as a readout of tumor response. We found three of 15 patient's tumors had significantly decreased KI67 staining positivity after Cobimetinib treatment and defined them as Responsive tumors. Genomic sequence showed that KRAS allelic imbalance and $Kras^{G12R}$ mutations were seen significantly higher frequency in Responsive tumors compared to Non-responsive tumors. RNA-seq analysis showed that these Responsive tumors were more likely to be classical-like subtype compared to Non-responsive tumors. DSP analysis confirmed the downregulation of ERK phosphorylation after treatment in all examined cases consistent with effective target inhibition. Interestingly, MEK phosphorylation was upregulated after treatment paradoxically. This suggests that paradoxical upstream pathway activation including RAF activation could be potential resistance mechanism. MYC protein expression change was significantly correlated with KI67 protein expression change, which suggests MYC downregulation could contribute to action of Cobimetinib. We also found that Cobimetinib treatment increased the immunosuppressive TREM2+ Macrophage population from single cell RNA-seq data. Furthermore, PDX from biopsy recapitulated patient's response to therapy and could be a great tool for testing new therapeutic strategies. Here, we summarize the multi-omics data and discuss potential mechanisms of response and resistance to targeting RAS signaling and related microenvironmental changes.

#2500 Technical feasibility of CRISPR-based functional profiling for solid tumor precision medicine.

K. Hodel[1], A. Varkaris[2], N. Chevalier[2], M. Meyers[1], A. Kehlmann[2], S. Corbel[1], A. Stavridi[3], P. Kilfeather[1], L. Hagmann[1], K. Tran[1], Y. Li[1], C. Schmedt[1], I. Sanidas[2], S. Sampath[1], S. Sampath[1], D. Juric[2];

[1]Function Oncology, Inc., San Diego, CA, [2]Termeer Center for Targeted Therapies, Massachusetts General Hospital, Boston, MA, [3]Beth Israel Deaconess Mexicali Center, Boston, MA

Introduction: Next generation sequencing (NGS) has revolutionized precision oncology by enabling identification of cancer patients harboring actionable mutations who may benefit from corresponding targeted therapies. However, sequencing-based biomarkers are not detected for most patients and imperfectly predict response to therapy even when present. To address this unmet need, we have developed a CRISPR-based diagnostics platform for 'personalized functional genomics', allowing identification of patient-specific therapeutic vulnerabilities irrespective of mutation status. We have previously applied this approach to primary hematologic malignancies, and here report application to solid tumor-derived samples.

Methods: Patient-derived solid tumor samples from several tumor types including breast, ovarian, colon and lung were obtained from 3 sources: fresh tissue (obtained from patients via core biopsy, surgical resection, or malignant fluid sampling), primary Patient-Derived Cell Lines (PDCLs, generated from surgical material and adapted for *ex vivo* culture), and commercially obtained viably frozen dissociated tumor cells (DTCs). Samples were dissociated to single cell suspensions and transduced with a lentivirus encoding Cas9 and an sgRNA library covering a custom targeted oncology gene panel. The panel consists of genes encoding targets of FDA-approved oncology drugs, as well as reference genes. After a short culture period, transduced cells were harvested and relative sgRNA distribution was measured by amplicon NGS. Changes in sgRNA abundance were collapsed into gene-level log2-fold changes, and significantly depleted genes scored as functional dependencies. For select PDCLs, cells were treated with cognate small molecule inhibitors over the course of 4 days. Cell viability was read out using CTG assay and a calculated IC50 lower than 500nM inferred as inhibitor sensitive.

Results: In a double-blind study using primary PDCLs, functional dependencies identified by CRISPR perfectly discriminated alpelisib sensitive (2/2) from resistant samples (6/6). Using fresh primary samples from varying cancer types and specimen sources, we achieve a technical success rate >70%. Among gene dependencies identified, targets of FDA-approved oncology drugs and those under late-stage clinical investigation were both observed including BRAF, CDK4/6, VEGFR1/2 and PARP1/2.

Conclusion: We demonstrate technical proof of concept of the FX platform for CRISPR-based personalized functional genomics. This approach is feasible when applied to primary patient samples from a variety of tumor types and tissue sources, and results are validated by comparison with orthogonal methods. CRISPR-based functional profiling represents a powerful adjunct to traditional genomic profiling, for the first time allowing drug target dependency mapping in a patient-specific and mutation-agnostic manner.

#2501 High mutation burden and ultraviolet light signature in conjunctival squamous cell carcinoma.

B. Esmaeli[1], F. O. Gleber-Netto[1], O. Sagiv[1], C. R. Pickering[2], N. Gross[1], J. Ning[1], M. M. Yeshi[3], J. Mitku[3], M. T. Tetzlaff[4], P. Nagarajan[1];
[1]UT MD Anderson Cancer Center, Houston, TX, [2]Yale University, New Haven, RI, [3]Mekelle University, Mekelle, Ethiopia, [4]UCSF, San Francisco, CA

Purpose: Conjunctival squamous cell carcinoma (conjSCC) is endemic in sub-Saharan Africa and is a major cause of ocular morbidity and mortality. This study aims to evaluate Tumor Mutation Burden (TMB), genomic signature, and histologic characteristics of conjunctival squamous cell carcinoma (conjSCC) in two cohorts of patients; one from the USA and one from Ethiopia.
Methods: Whole exome sequencing data, PD-L1 expression, histologic features, and human papillomavirus (HPV) status were analyzed in conj SCC tumors of 25 patients treated at an Ethiopian (ETH) cancer center and 29 patients treated at a US cancer center. Genomic alterations in conjSCC were compared with SCCs from other anatomic sites using data from The Cancer Genome Atlas (TCGA).
Results: TMB was found to be relatively high in conjunctival SCC (3.01/Mb, log10), was comparable to TMB values associated with cutaneous SCC, and was higher than most other SCC types available in the TCGA database. ETH samples had higher tumor mutational burden compared to the US cohort (3.34 vs 2.73). Solar elastosis was seen in a higher percentage of tumors from Ethiopia compared with the US cohort (78% vs. 10%). HPV status was similar between the cohorts (ETH: 21%, MDA: 28%). PD-L1 positivity defined as > 1% of tumor cells was seen in 33 of 53 tumors (62%). Mutations associated with ultraviolet light (UV) signature were the most frequently encountered signatures in both cohorts (SBS7b: 74% and SBS7a: 72%). UV signatures were more prevalent in the ETH cohort compared with the US cohort.
Conclusions: Conjunctival SCC is associated with a high TMB providing the opportunity for immune checkpoint inhibitor therapy for patients with locally advanced and/or metastatic conjunctival SCC. Clinical trials are needed to assess the efficacy of immune checkpoint inhibitors in patients with conjunctival SCC, particularly in sub-Saharan Africa where this cancer is more frequently seen, and is associated with significant morbidity and mortality.

#2502 Identification of poor responders to trastuzumab-deruxtecan with a multi-modal HER2-status predictor.

K. Nadhamuni, T. Ahmed, M. Carty, B. Terdich, W. L. Hensing, T. Taxter, C. Chao, **R. Pelossof**;
Tempus Labs, Chicago, IL

Trastuzumab deruxtecan (TDXD) is approved for HER2 low or positive metastatic breast cancer. HER2-status is assessed through HER IHC and ERBB2 FISH assays. HER2-status has been shown to be correlated to RNA expression. This study aimed to assess if the addition of DNA to an RNA-based model can improve HER2-status prediction performance. Furthermore, to investigate the relationship between model score and outcomes for TDXD patients according to their overall survival (OS).

Training and test sets of breast cancer samples were collected for HER2 status prediction (n = 1275, n = 397 respectively). HER2 status was reported positive: 11%, 12%, low: 61%, 60%, negative: 28%, 29% for each set respectively. HER2 testing and NGS were performed on samples with the same collection date. A TDXD discovery cohort of 284 patients included patients who received TDXD after RNA/DNA collection and had at least a 30-day follow-up. Metastatic disease was reported for 98% of the TDXD cohort. Receptor status was HR+/HER2- 39%, HR-/HER2- 17%, HR+/HER2+ 16%, HR-/HER2+ 9%, unknown 19%, and HER2-status was negative 11%, low 42%, and positive 27%, unknown 20%. OS was measured from medication start date.

We trained a 12-gene linear model based on RNA expression and DNA copy number to predict HER2-positivity. The genes were selected by stepwise-selection on RNA and DNA features when predicting HER2-positivity using a random forest model. A baseline model consisting only of ERBB2 RNA expression was compared. Setting a HER2-positivity score threshold and allowing for an indeterminate group of 15% of the validation cohort, the RNA-DNA model achieved 91% PPA and 91% PPV in validation, whereas the RNA-only model achieved 83% PPA and 85% PPA. This indicates that the addition of DNA data improved the RNA-only HER2 predictor.

The Concordance index of the RNA-DNA model score and OS for TDXD was 0.64. Characterizing this relationship, we partitioned the TDXD cohort to three equal sized sub-cohorts (33 1/3%) ordered by model score: low, intermediate, and high. Median OS in months for groups was: low 13.6, intermediate 18.5, and high 20.4. High-group patients had significantly better OS on TDXD compared to the low-group (HR = 0.39, log-rank p-value < 0.002). For patients with reported status, HER2-positivity rate in each group respectively was 6%, 16%, 85% (n=78), and HR-positivity in each group was 70%, 68%, 67% (n=156).

Together, these findings indicate that HER2 status prediction improved by adding DNA to an RNA base predictor, and the predicted score was positively correlated with OS for TDXD.

#2503 The role of APOBEC in early stage-*EGFR* mutant non-small cell lung cancer.

H. Jung, J. Lim, Y.-L. Choi, S. Park, J.-M. Sun, M.-J. Ahn, S.-H. Lee;
Samsung Medical Center, seoul, Korea, Republic of

Background: The APOBEC family of zinc-coordinating enzymes converts cytosines to uracils in single-strand DNA. APOBEC plays a crucial role in the mutation process of non-small cell lung cancer (NSCLC) and is essential for both adaptive and innate immune responses. This study aims to evaluate the role of the APOBEC mutation signature in early-stage non-small cell lung cancer (NSCLC).
Methods: We conducted whole-exome sequencing and whole-transcriptome sequencing using fresh tissue or formalin-fixed paraffin-embedded samples from 100 patients diagnosed with pathologic stage II-IIIA non-squamous NSCLC, all of whom underwent complete resection between January 2014 and December 2020 at Samsung Medical Center. This study aimed to assess the impact of APOBEC enrichment on disease-free survival (DFS), progression-free survival (PFS) of EGFR-TKI, and overall survival following recurrence.
Results: Median follow-up duration was 58.2 months (range, 11.3-141.1). Of the patients, 74% were never-smokers, and 52% had stage III disease. Among the 100 patients, 18 (18%) exhibited APOBEC enrichment (≥ 2). The median RFS was 25.2 months (95% CI, 17.3-33.2). Notably, APOBEC enrichment did not show a significant association with DFS (P=0.14). Among the 76 patients who experienced radiological recurrence, 69 received EGFR-TKI as first-line treatment. The median PFS for EGFR-TKI was 22.9 months (95% CI, 13.0-32.8). However, within this group, patients with APOBEC enrichment showed a shorter PFS compared to those without APOBEC enrichment (8.1 months vs. 24.6 months, P=0.014). In multivariate analysis, poor PFS of EGFR-TKI was associated with the type of EGFR mutation (L858R vs. exon 19 deletion, HR=1.9, P=0.04), TP53 mutation (mutation vs. wild type, HR=2.1, P=0.03), and APOBEC enrichment (≥ 2 vs. <2, HR=2.2, P=0.02). Overall survival from the starting EGFR-TKI was 61.1 months and 21.7 months for patients with APOBEC enrichment or patients without APOBEC enrichment, respectively (P=0.027).
Conclusions: APOBEC mutation signature may be presented at initial diagnosis of early-stage *EGFR* mutant NSCLC and it was associated with poor PFS of EGFR-TKI and overall survival.

#2504 Determining tumour homologous recombination repair status in PDX and clinical samples using automated RAD51 scoring.

J. Robertson[1], J. Ashton[1], G. N. Jones[1], G. Mills[2], T. Y. Ozmen[2], M. J. Rames[2], S. Park[2], P. Waring[1], N. Lukashchuk[1], E. Harrington[1];
[1]AstraZeneca, Cambridge, United Kingdom, [2]Oregon Health & Science University, Portland, OR

PARP inhibitors (PARPi) as monotherapy are approved in a wide variety of cancers that show genetic alterations that result in homologous recombination repair (HRR) deficiency. Current genomic scar tests for HRR deficiency (HRD) are predictive of response to PARPi on a population scale but they may fail to provide a real-time functional status of HRR in an individual. RAD51 is a critical DNA repair factor that functions in HRR to safeguard the integrity of the genome and could be a useful patient selection biomarker for PARPi response.During HRR, RAD51 forms filamentous structures to facilitate repair, which can be visualised by direct immunofluorescence (IF) as nuclear foci. Quantification of these RAD51 foci has been shown to be a functional readout of HRR status, however current manual counting of foci is challenging and can result in high inter-observer variability. In order to standardise RAD51 quantification, we aimed to develop an image analysis solution.Tumour samples from patient derived xenograft (PDX) studies and human tissues from commercial sources and clinical trials were co-stained with IF for RAD51 and geminin, as a marker of cells in S/G2 phase of the cell cycle. Manual scoring was performed as reported previously. Visiopharm was used to create and image analysis pipeline in allowing delineate tumour epithelial areas, detection of the geminin positive nuclei and RAD51 foci within these and the quantification of the foci.We have successfully developed an image analysis solution to select geminin positive proliferating tumour cells from PDX and clinical material, then quantify the RAD51 foci within these cells. There is a good correlation with manual scores with a similar accuracy to the manual inter-observer variability (PDX: R^2 = 0.76, F1 = 0.95 [n=34]; breast cancer samples: R^2 = 0.72, F1 = 0.92 [n=33]). Developing and image analysis solution has challenges due to several factors such as pan-nuclear staining of non-focus forming RAD51 being variable across samples, manual scoring using a wider Z-plane, susceptibility of RAD51 to pre-analytical factors and the fact that a duplex IF stain with geminin is required to mark actively replicating cells.The frequent inactivation of HRR is known to sensitise cancer cells to PARP inhibitors, we demonstrate a quantitative functional readout of HRR competency using RAD51 foci staining and an image analysis algorithm. This solution may enable the use of RAD51 foci as a patient selection biomarker for PARP inhibitors by providing an objective, robust and reproducible algorithm for scoring.

#2505 Immune dynamics and response predictors to regorafenib, ipilimumab, and nivolumab (RIN) treatment in chemotherapy resistant microsatellite stable (MSS) metastatic colorectal cancer (mCRC).

Jian Ye[1], Chongkai Wang[2], Colt Egelston[1], Weihua Guo[1], Peter Lee[1], Marwan Fakih[2]

[1]Department of Immuno-Oncology, Beckman Research Institute of The City of Hope, Duarte, CA,[2]Department of Medical Oncology and Therapeutics Research, City of Hope National Medical Center, Duarte, CA

Background: In our previous study, RIN therapy in MSS mCRC patients, excluding those with liver metastases, yielded a notable 36.4% objective response rate. RIN treatment was observed to remodel the local tumor microenvironment by enhancing immune infiltration, especially in responders. Systemic immunity, as assessed through peripheral blood analysis, showed that responders had lower baseline immune activity, which increased markedly post-treatment. Patients with liver metastases demonstrated a reduced CD4/CD8 T cell ratio, indicative of immunosenescence.
Methods: Building on our prior research, we analyzed blood samples from 29 chemotherapy-resistant MSS mCRC patients undergoing RIN therapy, collected at baseline and after two consecutive treatment cycles. Two 28-marker spectral flow cytometry panels were used to assess immune senescence and cytokine production in lymphocytes. Additionally, T cell receptor repertoires and transcriptional profiles were analyzed using RNA sequencing from sorted non-naïve T cells. Results: The study unveiled distinct immunological profiles in MSS mCRC patient responders vs non-responders to RIN treatment. Responders demonstrated increased numbers of newly expanding CD8 T cell clones on-treatment, indicative of an active immune responses. In contrast, non-responders displayed evidence of increased DNA damage in circulating lymphocytes (T, B, and NK cells), as marked by elevated γ-H2AX levels. We also identified divergent cytokine production profiles patterns at baseline: T cells in non-responders demonstrated increased capacity for production of IL-2, IL-10, IL-4/-13, and IL-22, while production of IFN-γ in both T cells and NK cells correlated with improved outcomes. Notably, patients with liver metastases exhibited greater frequencies of senescent T cells, characterized by increased expression of senescence markers (SA-βGal, CD57, Granzyme B/K) and a reduction in CD27 and CD28 in CD4 T cells, along with an accumulation of terminally differentiated CD8 T cells both pre- and post-treatment. Additionally, RNA sequencing revealed an upregulation of FOXO1 related genes in non-naive T cells of responder patients, which is consistent with its important role for this pathway in attenuating senescence and maintenance of stem-like properties in T cells.
Conclusions: The effectiveness of RIN therapy is associated with baseline functional potential of circulating T cells and an on-treatment expansion of T cell clonotypes. Pre-existing and persistent features of senescence and DNA damage in circulating lymphocytes may be a major barrier to RIN treatment efficacy in MSS colorectal cancer and should be validated further in future studies.

#2506 Novel biomarkers that predict response to neoadjuvant chemoradiotherapy in locally advanced rectal cancer.

A. Hasan[1], E. V. Demidova[1], P. Czyzewicz III[1], K. Devarajan[1], M. B. Einarson[1], D. Baldwin[1], E. A. Golemis[2], J. E. Meyer[1], S. Arora[1];
[1]Fox Chase Cancer Center, Philadelphia, PA, [2]Lewis Katz School of Medicine, Temple University, Philadelphia, PA

Background: Neoadjuvant chemoradiotherapy (nCRT) followed by surgery is standard of care for locally advanced rectal cancer (LARC). About 20% patients receiving nCRT alone experience a pathologic complete response (pCR), while up to 25% patients exhibit a poor response. Currently, there is no biomarker to predict response to nCRT. We hypothesized that inherited ability to recognize and repair DNA damage, especially lethal double-strand breaks (DSBs), manifest in lymphocytes, would yield a reproducible test predicting therapeutic response to nCRT.
Methods: Expression of DNA damage response (DDR) proteins was studied using peripheral blood lymphocytes (PBLs) from LARC patients and healthy controls. PBLs from LARC patients collected either before nCRT or after a standard course of ~5.5 weeks of nCRT were assessed by immunofluorescence (IF) for phospho-γH2AX^{Ser139} and by Luminex multi-analyte platform (xMAP) approaches. The xMAP assay was modified from a qualitative to a semi-quantitative assay that measures the following DDR-associated proteins- total ATR, phospho-γH2AX^{Ser139}, total MDM2, phospho-Chk1^{S345}, phospho-Chk2^{T68}, phospho-p53^{S15}, total p21. The analytical performance of the assay was assessed with vendor-provided reference controls and banked PBLs from healthy controls (n=50). LARC patients were segregated by neoadjuvant rectal (NAR) score to determine if tested biomarkers correlated with nCRT response. We used two independent sets of LARC biospecimens for xMAP analysis (set 1, n=48; set 2, n=44).
Results: IF-based assessment: Using PBLs from LARC patients, we found that poor responders (PoR; NAR score>14; n=21) had significantly lower γH2AX foci than complete responders (CR; NAR score<1; n=21) (P<0.0001, logistic regression). No significant difference was observed in positive γH2AX foci from PBLs drawn pre-nCRT versus post-nCRT from the same patient (p=0.4961, n=11, Wilcoxon test). xMAP assay performance: The performance assessment showed linear sample curves, precision with acceptable inter- and intra-assay coefficients of variability, and high reproducibility with ~1% outliers identified in replicates. Clinical associations using xMAP assay: levels of six proteins (ATR, p-γH2AX^{Ser139}, MDM2, p-Chk1^{S345}, p-Chk2^{T68}, p-p53^{S15}) significantly differentiated CRs from PoRs (p-values and False Discovery Rate <= 1e-5). The strongest associations with nCRT response were observed for: ATR, MDM2 and γH2AX.
Conclusion: 1) we standardized an xMAP assay to assess DDRs in human PBLs, and 2) found novel biomarkers that predict response to nCRT in LARC patients using minimally invasive PBL biospecimen. In ongoing work, we are using a larger biospecimen set to establish clinical validity parameters.

#2507 Drivers of immunotherapy response within the CPI3000+ cohort.

K. Thakkar[1], A. Castro[1], D. Qian[1], C. Swanton[2], K. Litchfield[1];

[1]University College London (UCL) Cancer Institute, London, United Kingdom, [2]The Francis Crick Institute, London, United Kingdom

Introduction: Multiple genomic and transcriptomic biomarkers have been associated with response to immune checkpoint (CPI) therapy. These markers include tumor mutational burden (TMB), immune infiltration and HLA loss of heterozygosity. Our previously published meta-analysis of biomarkers included over 1000 patients (CPI1000) across multiple cancer types and demonstrated that clonal TMB and CXCL9 expression were the strongest predictors of response pan-cancer. Biomarkers were combined into a multivariable predictor of response which out-performed TMB in three validation cohorts. However, even with an extensive systematic review, the literature and exploratory biomarkers only accounted for ~60% of the variance explained in CPI response. Approach and Results: Extending the cohort to over 3000 patients from 20 studies, across 11 tumor solid tumor types, we have utilized available genomic and transcriptomic data to further validate the multi-variable predictor of response as well as conduct additional exploratory analysis to uncover the remaining variance explained. The raw data is processed through a robust bioinformatics pipeline and is harmonized across studies. The pipeline developed to process the CPI3000+ cohort will be open-access and available to promote federated learning and collaborations. Firstly, we have expanded the systematic review to include recent biomarkers from literature. The literature review included over 1000 papers, and we identified greater than 200 unique biomarkers which can be quantified and assessed in the CPI3000+ cohort. Data presented on this extensive set of genomic and transcriptomic biomarkers across the cohorts will improve understanding of biomarkers of response to CPI therapy. Second, we will explore novel biomarkers of response including non-classical sources of antigen such as retained introns as well as pathways such as the unfolded protein response. We will also survey the effects of tumor-associated antigens such as those involved in CAR-T cell and vaccine trials in CPI response which was limited in the CPI1000 cohort. We will also be presenting data on emerging checkpoints in late-stage trials across cancer types. Finally, we will be combining the biomarkers into a novel multivariable predictor of response.
Conclusions: Results from this work will highlight the varying determinants of immunotherapy response across solid tumor types, offering insight into tumor intrinsic and extrinsic drivers of immunogenicity. We have shown that sources of tumour antigen are a major group of biomarkers for CPI response, here we expand on this further in a larger cohort as well as identifying novel biomarkers to create an improved multivariable predictor of clinical value.

#2508 EMP2 is a targetable biomarker in GBM tumors resistant to anti-angiogenic therapies.

B. Aguirre, M. Mekonnen, R. Mehta, M. Suresh, A. Chandla, K. Han, I. Yang, M. Wadehra;
UCLA David Geffen School of Medicine, Los Angeles, CA

Background: Glioblastoma (GBM) is characterized as the most aggressive and lethal primary brain tumor. One of the hallmarks of GBM tumor growth and progression lies within the proangiogenic tumor microenvironment. Current anti-angiogenic drugs such as the anti-VEGF antibody take effect by inducing tumor cell starvation, leading to a functional normalization of the tumor vasculature. However, the survival benefits of anti-angiogenic drugs have been very limited. To this end, we hypothesized that the tetraspan Epithelial Membrane Protein-2 (EMP2) may help mediate resistance.
Objective: We hypothesize that Epithelial Membrane Protein-2 may serve as a targetable biomarker for anti-VEGF resistance. We further explored the effectiveness of combination therapy in SB28 and GL261 GBM mouse models using anti-VEGF drug, Aflibercept, with a novel anti-EMP2 monoclonal antibody (mAb).
Results: Tumor tissue was collected prospectively from patients undergoing surgery for suspected glioblastoma and stained for EMP2 and HIF2a using standard immunohistochemistry. Patients had banked tumor tissue both prior to and after bevacizumab treatment with 3 months of clinical and radiologic follow-up available. Bevacizumab treatment increased EMP2 protein expression. This increase in EMP2 correlated with reduced mean survival time post-bevacizumab therapy. Similarly, HIF-2a showed increased expression post-bevacizumab treatment and showed expression in both tumor and stromal cells. Limited animal models exist for anti-VEGF therapy for GBM. To establish syngeneic models, 10 week-old mice were subcutaneously implanted with murine SB28 or GL261 GBM cells. Treatment with either polyclonal sera to VEGF or Aflibercept failed to reduce tumor load or provide a therapeutic benefit. To next investigate if this model could recapitulate the response obtained patients tumors, formalin fixed paraffin embedded tissue was analyzed for both EMP2 and HIF-2a expression. Both markers were significantly upregulated in Aflibercept treated samples compared to the control.To next investigate if combination treatment could produce a significant reduction in tumor load, animals were treated with a combination treatment with Aflibercept and anti-EMP2 mAb. The combination therapy significantly reduced tumor volume and weight in comparison to control-treated tumors. Combination treatment in SB28 tumors resulted in a two fold reduction in tumor load and 50% reduction in tumor weight. Moreover, tumors showed reduced Ki67 expression. Similarly, treated GL261 tumors produced a 2.3 fold reduction in tumor size and ~2.7 fold reduction in tumor weight. Our results suggest that EMP2 can be a promising new target therapeutic target that can be combined with anti-VEGF treatment to potentially increase overall survival in GBM patients.

#2509 Abundant glucocorticoid receptor (GR) expression in human tumors: A tissue microarray study on more more than 18,000 tumors.

C. Tsourlakis, F. Wegener, K. Moller, M. Kluth, C. Hube-Magg, C. Bernreuther, G. Sauter, A. H. Marx, R. Simon, T. Krech, C. Fraune, N. Gorbokon, **M. Lennartz**, S. Minner, F. Viehweger;
University Medical Center Hamburg-Eppendorf, Hamburg, Germany

The glucocorticoid receptor (GR, or GCR) is a nuclear receptor protein for cortisol and other glucocorticoids and regulates the transcription of thousands of genes involved in metabolism, development, stress, and inflammatory response. In cancer, both an oncogenic and a tumor suppressive function of GR has been proposed. To comprehensively evaluate GR expression in normal and tumorous tissues, a tissue microarray containing 18,570 samples from 147 different tumor types and subtypes and 608 samples of 76 different normal tissue types was analyzed by immunohistochemistry (IHC). GR positivity was found in 76.3% of 14,349 interpretable cancers, including 18.5% with weak, 19.6% with moderate, and 38.3% with strong positivity. GR positivity of at least a fraction of tumors was found in all 147 analyzed tumor types and at least one strongly GR positive tumor was found in 136 tumor types. 77 of our 147 tumor entities showed GR positivity of variable intensity in all analyzed cases. 43 further tumor entities showed GR positivity in 80-99.9% of cases. 21 tumor entities had a GR positivity rate between 50 and 80%, including urothelial carcinoma as well as gastric and esophageal adenocarcinoma. Only 6 tumor types had less than 50% GR positive. These included adenomas (21.7-32.5%), adenocarcinomas (17%) and neuroendocrine carcinomas (45.5%) of the colorectum. Reduced GR staining was significantly associated with adverse histopathological and clinical features in several tumor types. Low GR expression was linked to grade progression in pTa ($p<0.0001$) and to nodal metastasis in pT2-4 urothelial carcinoma of the urinary bladder ($p=0.0051$), advanced pT stage ($p=0.0006$) and estrogen receptor positivity ($p=0.0126$) in breast carcinomas of no special type (NST), as well as to high grade ($p\leq0.0076$), advanced pT stage ($p<0.0001$), distant metastasis ($p=0.0081$), and poor overall survival ($p=0.002$) in clear cell renal cell carcinoma. GR expression was unrelated to clinic-pathological parameters in gastric, pancreatic, and colorectal adenocarcinoma as well as in serous high-grade carcinoma of the ovary. In summary, our data demonstrate frequent GR expression across all cancer types. Significant associations between reduced GR expression and unfavorable tumor features in some but not all tumor types suggest that the functional importance of GR regulated genes for cancer progression depends on the cell of tumor origin.

CLINICAL RESEARCH: Predictive Biomarkers 2
Poster Session

#2513 MAGE-A3, MAGE-A4, and PD-L1 protein show co-expression in colon, lung and bladder cancer.
R. Gonzalez, Y. Guo, J. Yom, B. Gilmore, E. Zewdu, X.-A. Han, D. Kong, T. Qu, Q. Ren, X. Hu, R. Zhang, Z. Wu, A. Strom, X. Liu, W. Fu;
OriGene Technologies, Inc., Rockville, MD

PD-L1 programmed death ligand 1/CD274 has been shown to be an excellent immune therapy target for many tumors. Currently, studies have shown PD-L1in combination with other immune therapy targets can improve patient outcomes generating the need for new targets. One candidate is the cancer testis antigen Melanoma Antigen Gene Family (MAGE-A) because these genes have limited expression in normal tissues and high expression in cancer. Clinical trials have already begun targeting MAGE-A3 and MAGE-A4 proteins in multiple tumor types. Protein assessment of individual MAGE-A family members has been challenging due to sequence homology as high as ninety-five percent between members. Previously, with the use of CytoSections two highly specific antibodies for immunohistochemistry to MAGE-A3 (clone OTI1H1) and MAGE-A4 (clone OTI2C1) were found. In this study, the MAGE-A3 and MAGE-A4 antibodies were screened with PD-L1 on colon, lung, and bladder cancers. Results show detection of both MAGE-A3 and MAGE-A4 in 25% of colon; 30% of lung; and 20% of bladder cancers. More than 70% of the lung and bladder cancers were positive for MAGE-A4 but only six of twenty-four colon cancers were positive for MAGE-A4. The results show 60 percent of the positive for MAGEA3 or MAGEA4 in colon, lung, and bladder cancers were also positive for PD-L1. This study suggests that MAGE-A3 and MAGE-A4 have tumor specific expression patterns and a potential to be a co-immunotherapy target with PD-L1.

#2514 Adjuvant chemotherapy drug response-related gene detection using JASPAC01 pancreatic cancer resection cohort.

Y. Okamura[1], T. Otsu[2], M. Hayashi[2], R. Ashida[3], K. Uesaka[3];

[1]Nihon University School of Medicine, Itabashi-ku, Tokyo, Japan, [2]Nagoya University Graduate School of Medicine, Nagoya, Japan, [3]Shizuoka Cancer Center, Sunto-Nagaizumi, Shizuoka, Japan

Background of Purpose: Although various multidisciplinary treatments have been attempted for pancreatic cancer, sufficient improvement in prognosis has not been achieved. It is necessary to establish biomarkers that can predict the malignant potential for each patient and the therapeutic effect of chemotherapy in order to select the optimal treatment for each individual case.This study was designed as a companion study to the phase III comparative study (JASPAC 01 of gemcitabine (GEM) and S-1 therapy as adjuvant chemotherapy after pancreatectomy. Among the 22 candidate biomarker genes that have been reported to be involved in pancreatic cancer treatment prognosis, we focused on E2F transcription factor 7 (E2F7), which is associated with a significantly poor overall survival rate when highly expressed. E2F7 is one of the target proteins of p53 and has been reported to be involved in cell cycle regulation. We examined the possibility of E2F7 expression in pancreatic cancer surgery and the effect of adjuvant chemotherapy.

Patients and Methods: After optimizing the E2F7 imunostaining protocol, we scored E2F7 protein expression using the slides from excised tissues from JASPAC 01 registered cases. We investigated the relationship between malignancy and treatment efficacy using the case cohort treatment allocation information, clinicopathological information, and prognosis data.

Results: Immunostaining was performed on approximately 330 resected pancreatic cancer specimens from 24 facilities nationwide. Of the 311 patients for whom E2F7 protein expression could be scored, 202 patients who completed the assigned treatment were included in the analysis. In 88 cases with high E2F7 expression, no significant difference in clinicopathological factors was observed between the S-1 treatment group and the GEM treatment group, but the S-1 treatment group showed better recurrence-free survival (RFS, P=0.066) and overall survival (OS, P=0.015) were observed. On the other hand, in the 114 patients with low E2F7 expression, there was no significant difference in clinicopathological factors between the two groups (RFS, P=0.168, OS: P=0.276). High E2F7 expression in pancreatic cancer tissues may affect S-1 sensitivity, GEM resistance, or both.

Conclusions: It is considered that high expression E2F7 in pancreatic cancer may affect the therapeutic efficacy of GEM and S-1, which are frequently used in adjuvant chemotherapy for pancreatic cancer.

#2515 Cation transport gene signature predicts overall and progression free survival in bacillus-calmette-guerrin-treated non-muscle invasive bladder cancer in The Cancer Genome Atlas.

L. K. Tran, S. P. Lerner;
Baylor College of Medicine, Houston, TX

Introduction: Bacillus Calmette-Guerrin (BCG) is a commonly used immunotherapy for non-muscle invasive bladder cancer (NMIBC), and there is limited understanding of its *in vivo* mechanisms. *In vitro* studies on patient-derived tumor cells suggest the role of calcium signaling as an effector of immune response. We aimed to elucidate further understanding of important signaling pathways implicated in BCG response using gene expression data. The goal is to identify a gene signature for predicting BCG response and survival post-BCG therapy.

Methods: Gene expression data for the BCG treated NMIBC cohort was downloaded from TCGA. Individual gene expression data analyzed with univariate cox proportional hazard models versus overall survival (OS) and progression-free survival (PFS) independently. The survival outputs were then fed into String DB network analysis. Overlapping genes in the 2 networks were combined into a Z- sum composite score for survival prediction. Correlation analysis was performed for the overlapping genes.

Results: Based on the selection criteria, 35 patients were available for the study. In OS analysis a total of 622 genes were filtered based on HR>2 or <0.5 with adjusted-p <0.05. Network analysis of those significant genes demonstrated significant calcium ion transmembrane transport upregulation in patients with better OS, showing a subnetwork of 16 genes. In the PFS analysis, 500 genes with HR>2 or <0.5 with adjusted-p<0.05 were subjected to network analysis. The main cluster was enriched in cation transmembrane transport upregulated in patients with better PFS, and consisted of a subnetwork of 39 genes. There were 295 shared genes between the genes associated with improved OS and PFS gene sets. A composite score constructed from these 295 genes revealed an optimized cutoff of the lower 70th percentile of expression versus the upper 30th percentile of normalized summed gene expression (HR = 0.192, p = 0.00048 for OS; and HR = 0.171, p < 0.0001 for PFS). Internal correlation reveals 3 sub-clusters of gene expression within our data set.

Conclusion: Similar to *in vitro* studies we report increased cation transport expression *in vivo*, that was significantly associated with improved OS after BCG immunotherapy. Our composite gene signature score was able to identify a poor survival subgroup—about 1/3 of patients—with 5-fold worse PFS and OS following BCG therapy. Increasing calcium signaling may potentiate BCG response in currently poor BCG-responders.

#2516 Influence of pre-treatment nutrition and inflammation on immunotherapy response in non-small cell lung cancer.

L. A. Robinson, Y. Kim, A. Buro, S. R. Hogue, A. Bailey, G. M. DeNicola, C. Pierce, M. Umbarger, D. A. Byrd;
Moffitt Cancer Center, Tampa, FL

Purpose: Immune checkpoint inhibitor therapy (ICI) is effective in non-small-cell lung cancer (NSCLC) but only a minority respond, likely due in part to the gut microbiome. Given the coupling of host nutritional status and gut microbiota composition, we investigated the pre-treatment associations of nutritional status and biomarkers with ICI treatment response and survivals.

Methods: We recruited stage III-IV NSCLC patients. Pre-ICI treatment clinical information and blood samples were obtained. Clinician assessed ICI response and survival data were recorded. The nutritional/inflammatory indicators were compared based on treatment response and survivals. ICI Clinical Benefit was defined as 12-month progression free survival. Pearson Chi-square or Fisher's Exact test was used to compare categorical metrics; non-parametric analysis compared continuous metrics by treatment response. Overall survivals were assessed using multivariable Cox proportional hazards models to estimate associations.

Results: Of the 76 patients recruited, all were ECOG performance status 0 (14.5%) or 1 (85.5%). 36 (47%) had Clinical Benefit with median survival 21.3 mo. vs. 6.6 mo. among the No Clinical Benefit patients ($p<0.01$). Non-responders had significantly more often weight loss, lower serum albumin, elevated red cell distribution index (RDW) and worse scores for Frailty Index, Geriatric Nutritional Risk Index and Mini-Nutritional Assessment (MNA). Non-responders had significantly more inflammation with a higher Systemic Immune Response Index (SIRI) and RDW. Overall survival was negatively correlated with: 1. weight loss; 2. low serum albumin; 3. low serum sodium; 4. high RDW; 5. elevated total neutrophils, total white blood cells, total monocytes, neutrophil to lymphocyte ratio, and monocyte to lymphocyte ratio; 6. adverse MNA and Geriatric Nutritional Risk Index; 7. elevated SIRI and Systemic Immune Inflammation Index (SII). ICI response prediction accuracy using a solely MNA-based model was significantly high in terms of AUROC of 0.85 [95% CI= (0.76, 0.93); $p<0.05$]. In multivariable analysis, the predictor of immunotherapy response and survival was the 6-measure MNA which strongly correlates with weight loss, low serum albumin and depressed Frailty Index.

Conclusions: An adverse nutritional status with accompanying chronic inflammation is strong predictor of non-response to ICI. Since lung cancer patients with depressed pre-treatment nutrition have a low likelihood of an ICI response, they should be promptly referred for dietician consultation for intensive nutritional therapy which may improve their clinical outlook. Considering the negative association of malnutrition/inflammation with response to ICI treatment in NSCLC patients who still qualify as ECOG performance status 0-1 patients, prospective clinical trials should also stratify their results by nutritional status.

#2517 The amplification of TPX2 is a potential biomarker of oxaliplatin-sensitivity of colorectal cancers (CRCs) with CIN phenotype.

Shohei Ueno[1], Taichi Isobe[2], Ryosuke Taguchi[1], Kenji Tsuchihashi[3], Koichi Akashi[1], Eishi Baba[2]

[1]Department of Medicine and Biosystemic Science, Graduate School of Medical Sciences, Kyushu University, Fukuoka, Japan,[2]Department of Oncology and Social Medicine, Graduate School of Medical Sciences, Kyushu University, Fukuoka, Japan,[3]Department of Hematology, Oncology and Cardiovascular Medicine, Kyushu University, Fukuoka, Japan

The amplification of Chr20q11.21 harboring TPX2 gene is the most frequent copy number alteration among the cases of colorectal cancers (CRCs), especially left-sided ones. We retrospectively examined 2828 cases of CRC patients who took cancer-genome panel tests in Japan between June 2019 and November 2022. The time to first-line treatment failure was longer with regimen with oxaliplatin than with those with irinotecan in CRC patients with Chr20q11.21 amplification (12.2 versus 9.2 months, p=0.0481). Oxaliplatin induces double-strand breaks (DSBs) and then cellular apoptosis. A key event of the DNA damage response to DSBs for cellular survival is the extensive phosphorylation of Ser139 of Histone H2AX adjacent to the chromosomal break. TPX2 whose gene resides in Chr20q11.21 has been reported to repress the phosphorylation of H2AX upon ionizing radiation. The purpose of this study is to identify the relationship between the amplification of TPX2 and oxaliplatin sensitivity in human CRCs. The knockdown of TPX2 decreased the oxaliplatin-susceptibility of COLO320 and Caco-2, CIN phenotype CRC cell lines which highly expressed TPX2. However, TPX2 knockdown did not reduce the oxaliplatin sensitivity of HCT-116, an MSI phenotype CRC cell line with low-level of TPX2 expression. The knockdown of TPX2 in CIN phenotype CRC cells, not in the MSI phenotype CRC cells, enhanced the phosphorylation of H2AX upon the DNA-damage induced by oxaliplatin. These findings suggest that amplification of TPX2 contributes to the oxaliplatin-susceptibility of CRCs with CIN phenotype through DNA repair machinery.

#2519 Alteration of tumor immune microenvironment after recurrence and its impact on the efficacy of anti-PD-1 antibody in resected non-small cell lung cancer patients.

Y. Matsumoto, T. Watanabe, M. Mizutani, A. Sugimoto, H. Nagamine, Y. Tani, K. Sawa, T. Tsukioka, H. Kaneda, S. Mitsuoka, N. Nishiyama, T. Kawaguchi; Osaka Metropolitan University, Osaka, Japan

Background: Tumor immune microenvironment (TIME), including programmed death-1 ligand-1 (PD-L1) and CD8-positive tumor-infiltrating lymphocytes (TIL), has been suggested as a potential biomarker to predict the efficacy of anti-PD-1 antibody. Postoperative recurrence in patients with non-small cell lung cancer (NSCLC) is treated with therapeutic strategies similar to those for metastatic disease. However, in postoperative recurrence cases, PD-L1 evaluation is generally based on archival resection specimens, because there is little opportunity for a new biopsy of the recurrent site. Therefore, it remains unclear whether TIME of recurrent lesion is similar to TIME of primary lesion at surgery, and the efficacy of anti-PD-1 antibody for postoperative recurrent NSCLC patients based on TIME status at surgery is unknown.

Materials and Methods: Cohort A included 59 patients with advanced and 25 patients with postoperative recurrence NSCLC who treated with first-line pembrolizumab monotherapy. PD-L1 expression and CD8-TIL were evaluated immunohistochemically in tumor specimens obtained at diagnosis in the advanced cases and at surgery in the postoperative recurrence cases. Tumor proportion score for PD-L1 and the extent of CD8-TIL were evaluated and classified as high or low. TIME was categorized into 4 subclasses, according to the respective PD-L1 and CD8-TIL, as follows: (class I) high/high; (class II) low/low; (class III) high/low; and (class IV) low/high. Progression-free survival (PFS) of pembrolizumab was compared based on TIME. Cohort B consisted of 50 NSCLC patients who underwent radical resection, and whose tumor specimens were obtained from recurrent site. As in cohort A, TIME was assessed for paired resection and recurrent tumor samples.

Results: In cohort A, the median PFS of pembrolizumab for the advanced cases were 25.7 months in class I (n=25), 2.3 months in class II (n=8), 8.0 months in class III (n=20), and 6.5 months in class IV (n=6) (p<0.001), respectively; while those for the postoperative recurrence cases were 9.0 months (n=7), 4.3 months (n=7), 7.6 months (n=6), and 2.5 months (n=5) (p=0.55), respectively. In cohort B, TIME for resected primary lesion were observed in 9 with class I, 20 with class II, 3 with class III and 18 patients with class IV, respectively. The concordance of PD-L1 category (high vs low) between resected primary lesion and recurrent lesion was 88.0%, while that of TIME classification was 54.0%.

Conclusion: TIME classification using tumor specimens just before administration of anti-PD-1 antibody was useful predictive biomarker. However, TIME alterations between resection and postoperative recurrence were observed in many cases, suggesting that TIME based on tumor specimens at surgery may not be useful for predicting the efficacy of anti-PD-1 antibody for postoperative recurrent NSCLC.

#2520 CD133 expression is associated with less DNA repair, better response to chemotherapy, and survival in ER-positive/ER-negative breast cancer.

T. Sato[1], M. Oshi[2], J. Lee[2], A. M. Roy[2], K. Chida[2], I. Endo[3], M. Obayashi[4], K. Takabe[2];
[1]The University of Tokyo Hospital, Tokyo, Japan, [2]Roswell Park Comprehensive Cancer Center, Buffalo, NY, [3]Yokohama City University Graduate School of Medicine, Yokohama, Japan, [4]National Hospital Organization Disaster Medical Center, Tokyo, Japan

Introduction: Cancer stem cells (CSC) constitute only 0.1-1% of all the cells in a bulk tumor, yet they play a crucial role in treatment resistance and relapses. Its role in breast cancer (BC) has been studied but a consensus remains elusive. We focused on gene expression of a CSC marker CD133 and studied its clinical significance in ER-positive/HER2-negative (ER+/HER2-) BC, the most prevalent subtype. We utilized multiple independent large patient cohorts of gene expression and clinical variables for transcriptome analysis.
Methods: A total of 2969 patients from The Cancer Genome Atlas (TCGA, n=1065) and the Molecular Taxonomy of Breast Cancer International Consortium (METABRIC, n=1904) BC cohorts, as well as BC patients who underwent neoadjuvant chemotherapy (NAC; GSE25066, GSE20194, GSE32646 cohorts) were analyzed.
Results: By analyzing SCP1039 and SCP1106 single-cell sequencing cohorts, we found that epithelial cells were the predominant source of CD133 gene expression in the tumor microenvironment. High expression of CD133 in ER+/HER2- BC correlated with elevated gene expressions of the other CSC markers; CD24, NOTCH1, DLL1, and ALDH1A1 (all $p<0.001$), and significantly enriched WNT/β-Catenin, Hedgehog, and Notch signaling (all FDR<0.25), which are all known pathways related with CSC in TCGA and validated in METABRIC cohort. Consistent with CSC phenotype, CD133-high BC was negatively enriched with Hallmark cell proliferation-related gene sets, such as E2F Targets, G2M Checkpoint, MYC Targets V1, Ki67 gene expression and proliferation score (FDR<0.25 and $p<0.001$, respectively) in both cohorts. CD133-high BC was negatively associated with DNA repair genes, such as BRCA1, E2F7 in both cohorts (all $p<0.001$). In agreement, CD133-high BC was associated with less homologous recombination deficiency, lower silent and non-silent mutation rates. Surprisingly, CD133-high BC exhibited a proinflammatory microenvironment, as represented by higher cytolytic activity in the METABRIC and higher lymphocyte infiltrations, TGF-beta response, and TCR richness in TCGA (both $p<0.001$), but less Th1 cells, M1 macrophages and dendritic cell infiltrations consistently in both cohorts. It also enriched signaling pathways related to inflammation and immune responses such as inflammatory response, allograft rejection, TNF-alpha, IL-6, TGF-beta signaling, and complement signaling (all FDR<0.25). CD133-high tumors had better pathological complete response after NAC in GSE25066 cohort and improved Disease-Free Survival and Overall Survival in both TCGA and METABRIC cohorts (all $p<0.05$).
Conclusion: CD133-high ER+/HER2- BC is associated with CSC phenotype, reduced cell proliferation, and impaired DNA repair, but enhanced inflammation, potentially explaining the better response to NAC and favorable patient prognosis.

#2521 New predictive markers for dasatinib responsiveness in triple-negative breast cancer: A biomarker discovery study.

D. Ortega-Alvarez[1], D. Tebar[1], M. Casado[1], E. Castillo[1], C. Guardia[1], D. Olivares-Osuna[1], E. Musulen[1], E. Mereu[1], G. Luengo[2], E. M. Galan-Moya[3], **V. Rodilla**[1];

[1]Josep Carreras Leukaemia Research Institute, Badalona, Spain, [2]Instituto Murciano de Investigacion Biosanitaria (IMIB), Murcia, Spain, [3]Centro Regional de Investigaciones Biomedicas (CRIB), Albacete, Spain

Triple negative breast cancer is the most heterogeneous and aggressive type of breast tumor type and is characterized by the lack of expression of clinical biomarkers (ER, PR, and HER2) and targeted therapies. In this regard, different clinical trials have failed, unable to stratify these patients to find an effective response to specific therapy. This study aimed to identify biomarkers exclusively expressed in the basal mammary compartment that can help us to subclassify the triple-negative breast cancer subtype. Based on computational analysis from single-cell RNA sequencing data, we have identified a list of basal identity-associated genes (BC-markers). Subsequent histological validation confirmed the expression pattern of these markers in a cohort of 50 samples, which has allowed us to stratify triple-negative breast cancer patients into BC-TNBC and luminal-like subtypes. Importantly, the expression of these markers correlated with poorer prognosis in TNBC patients. Functional analysis revealed that *TAGLN* played a significant role in cell proliferation and migration, potentially impacting tumor aggressiveness. Moreover, the expression of these BC-markers is associated with a mesenchymal phenotype which corresponds to the previously described Lehmannn's mesenchymal-like signature. In this study, *TAGLN* appeared to influence dasatinib sensitivity, suggesting its potential as a predictive biomarker for dasatinib response in TNBC patients.

#2522 Predictive value of tumor mutational burden (TMB) in patients with metastatic microsatellite-stable (MSS) colorectal cancer (CRC) given first-line oxaliplatin-based chemotherapy and immune checkpoint blockade (ICB).

A. H. Ree[1], P. A. Bousquet[1], H. L. Nilsen[1], T. Luders[1], S. Wang[1], T. Visnovska[1], D. L. Bordin[1], E. Hoye[2], H. M. Hamre[1], C. Kersten[3], E. Hofsli[4], M. G. Guren[2], H. Sorbye[5], K. Flatmark[2], S. Meltzer[1];

[1]Akershus Univ. Hospital, Lorenskog, Norway, [2]Oslo Univ. Hospital, Oslo, Norway, [3]Sorlandet Hospital, Kristiansand, Norway, [4]St. Olav's Univ. Hospital, Trondheim, Norway, [5]Haukeland Univ. Hospital, Bergen, Norway

Purpose: Most CRC patients harbor primarily non-immunogenic MSS tumor. The randomized METIMMOX trial (NCT03388190) examined if patients with previously untreated, unresectable abdominal metastases from MSS-CRC may achieve therapeutic efficacy from short-course oxaliplatin-based chemotherapy (FLOX) and sequential ICB (nivolumab) repeatedly. Half of study patients assigned to this experimental treatment had significantly extended progression-free survival (PFS) while the other half had shortened PFS, compared to the control-group patients given standard FLOX chemotherapy with median PFS 9.3 months. Here we explored if somatic mutations (mut) unveiled by next-generation sequencing might provide insights into responsiveness to the METIMMOX regimen.

Procedures: Patients had MSS-CRC with infradiaphragmatic metastases deemed unresectable and were eligible for first-line oxaliplatin-based therapy. They were randomly assigned to the control group of FLOX (oxaliplatin, 5-fluorouracil, folinic acid) Q2W or the experimental group of alternating 2 cycles each of FLOX Q2W and nivolumab Q2W, with prespecified break periods. Radiologic response assessment was done every 8 weeks with PFS as the primary endpoint. Diagnostic tumor biopsies and baseline metastasis biopsies were sequenced with the TruSight Oncology 500 assay. TMB was calculated using only coding, non-synonymous single-nucleotide variants and insertions/deletions with variant allele frequency ≥5% and sequencing depth ≥50×, applying the effective panel size as the megabases (Mb) denominator.

Results: Sequencing data were acquired from 20 experimental-group patients with median PFS 7.9 months (minimum 2.0, maximum 41.6). Median TMB was 5.1 mut/Mb (minimum 0.8, maximum 11.8), concordant in patient-paired primary tumor and metastasis specimens. The TMB was associated with treatment outcome; the higher TMB, the better PFS with hazard ratio 0.83 (95% confidence interval (CI) 0.70-0.98; $p = 0.026$, Cox regression) for a PFS event with increasing TMB. TMB cut-off as low as 5.0 mut/Mb distinguished between patient groups ($p = 0.007$, log-rank test) with median PFS 34.9 months (95% CI 10.6-59.2; TMB>5, $n = 10$) and median PFS 4.6 months (95% CI 2.7-6.5; TMB≤5, $n = 10$). In the TMB>5 group, 8/10 were *KRAS*- or *BRAF*-mutant cases. In the TMB≤5 group, 9/10 metastasis specimens were *RAS*/*BRAF*-wildtype cases.

Conclusions: TMB >5 mut/Mb was associated with tumor *KRAS* or *BRAF* driver mutation and remarkably long PFS in first-line treatment of patients with abdominal metastases from MSS-CRC with alternating short-course oxaliplatin-based chemotherapy and ICB.

#2523 Predictive biomarkers for neoadjuvant FLOT4 chemotherapy response in gastroesophageal cancer: Results of multi-omics approach.

A. Al-Fahdi, S. Al Zadjali, I. Al Haddabi, A. Pullanhi, M. Al Jabri, A. Al Yayahee, N. Al Shuaili, N. Al Mahrouqi, M. Al Moundhri;
Sultan Qaboos Comprehensive Cancer Care & Research Centre, Muscat, Oman

Background: The FLOT4 chemotherapy regimen is a standard preoperative treatment for gastroesophageal junction (GEJ) and gastric cancer (GC), yet the response to this treatment is variable. Identification of predictive biomarkers is crucial for optimizing therapeutic strategies. This study aims to identify predictive biomarkers for FLOT4 treatment efficacy using a multi-omics approach.
Methods: We conducted a preliminary differential gene expression analysis in diagnostic tissue pre-treatment and surgical resection post-treatment in six patients (two GEJ and four GC) who all exhibited a partial pathological response (G2) to neoadjuvant FLOT4 chemotherapy. Utilizing DESeq2 for differential gene expression and David pathway analysis for functional insights, we have begun to unravel the complex molecular response to treatment. Upcoming assays include blood gDNA and tumor tissue whole exome sequencing (WES), comprehensive methylation profiling, miRNA characterization, and proteomics via LC-MSMS.
Results: Our preliminary data suggest alterations in gene expression associated with cell adhesion, extracellular matrix interaction, and immune response pathways. Three common genes (*CXCL2*, *CXCL3*, *CXCL1*) were identified among upregulated pathways in GEJ patients, while one common gene (*IL1A*) was observed in GC patients. These findings suggest a complex network of biological processes influenced by FLOT4. In-depth results, including whole-exome sequencing, methylation patterns, and miRNA profiles, will be completed and presented at the conference.
Conclusion: These initial findings propose that changes in gene expression related to cellular architecture and immune response are indicative of a partial response to FLOT4 in both GEJ and GC patients. The identified genes and pathways may serve as potential biomarkers for predicting treatment outcomes.
Future Directions: By the time of the conference, we anticipate including a more extensive patient cohort with complete response or no response to FLOT4, and comparative analyses with a FOLFOX treatment group. The integration of forthcoming WES, methylation, miRNA, and proteomics data will provide a more comprehensive molecular predictive model.
Keywords: FLOT4 chemotherapy, gastroesophageal junction cancer, gastric cancer, predictive biomarkers, differential gene expression.

#2524 Molecular and clinicopathologic landscape of HER2 positive breast cancer: A single institution study.

G. Ardor, Z. M. Coty-Fattal, L. Z. Blanco, Jr., K. Siziopikou;
Northwestern Memorial Hospital, Chicago, IL

Background: Human epidermal growth factor receptor 2 (HER2) is a transmembrane tyrosine kinase that is encoded by the *ERBB2* gene, located on chromosome 17. Expression levels of HER2 are a key pathogenic and treatment-associated factor in breast carcinomas, with HER2 expression reported as per the ASCO/CAP scoring guidelines. Outside the intense focus on the HER2 overexpression few studies currently exist that look at the comprehensive molecular profile of these aggressive tumors .

Design: Our institutional pathology database was searched for patients with breast carcinoma diagnosed between 2009 and 2013 and with HER2 scored as 3+ based on immunohistochemistry, or HER2 2+ with confirmatory positive FISH results. Comprehensive next-generation sequencing (NGS) was performed using the Illumina TruSight Oncology 523 gene panel, and clinicopathologic data were gathered from the institutional electronic health record system. A CoMutation plot was made using the CoMut python library.

Results: The mean age of the patients at time of diagnosis was 56.1±12.7 years. The tumors were overwhelmingly high-grade, with 26/30 being grade 3 and the remaining 4/30 being grade 2 and a mean size of 2.6 cm. All were histologically invasive ductal carcinoma, and 26/30 were scored as HER2 3+ on IHC while 4/30 were HER2 2+ with positive FISH. ER was positive in 30% of cases (9/30), PR was positive in 23.3% (7/30), p53 was positive by IHC in 53.3% (16/30), and the mean Ki-67 proliferative index was 47.1%. 20 of the 30 (66%) cases meeting the inclusion criteria had pathogenic mutations detected by NGS testing. Several distinct molecular subgroups were seen on the CoMutation plot (figure 1). The mean tumor mutational burden (TMB) was 14.1 mutations per megabase. A significant subset of the tumors 70% (14/20) showed *TP53* mutations, and 30% (6/20) show PIK3CA mutations. Of interest, only 1/14 tumors showed a co-occurring homologous recombination repair gene mutation and one tumor (1/20) showed mutations in 2 homologous recombination pathway genes (*FANCA* and *BRCA1*) as well as numerous additional mutations (tumor mutational burden of 65.3 mutations per megabase).

Conclusion: Overall the mean TMB was 14.1 mutations/megabase in this HER2-positive breast cancer study set. Over 2/3 of our HER2-positive breast cancer cases also had *TP53* mutations. In addition, 1/3 had PIK3CA mutations, suggesting that a subset of HER2-positive carcinomas also harbor other potentially actionable mutations which may increase the effectiveness of our existing interventions. Additional studies are needed to further subclassify genetically distinct subsets of HER2-positive breast cancers and to further understand clinical, pathologic and treatment-related differences in this aggressive breast cancer subset.

#2525 A novel splicing factor, SPF45/RBM17, might influence 5-FU resistance of gastric carcinoma.

K. Maruo, M. Yashiro, T. Sakuma, G. Tsujio, y. Fukui, H. Kasashima, K. Maeda;
Koji Maruo (Individual), Osaka, Japan

Background: SPF45/RBM17 was identified as a factor required for splicing of short introns in mRNA precursors transcribed from DNA. SPF45 is also thought to be related to anti-cancer drug resistance, suggesting that the SPF45 molecule has a different resistance mechanism from the conventional mechanism of anticancer drug resistance. In this study, we investigated the relationship between SPF45 expression and anticancer drug sensitivity in gastric cancer.
Materials and Methods: A total of 654 gastric cancer cases were used in this study. SPF45 expression was examined using immunohistochemistry. The correlation between SPF45 expression and clinicopathological factors was evaluated.
Results: Of the 654 gastric cancer cases, 240 were positive for SPF45 expression and 414 were negative for expression. There was no significant difference in age and gender between the two groups, but SPF45-positive cases were significantly more frequent in patients with undifferentiation ($p = 0.004$), lymphatic invasion ($p = 0.013$) and venous invasion ($p < 0.001$). As for anticancer drug therapy, 215 of the 654 patients with gastric cancer who underwent radical surgery were treated with adjuvant chemotherapy and 94 patients with advanced recurrent gastric cancer were treated with chemotherapy. 75 SPF45-positive-patients who received 5FU-based adjuvant chemotherapy (S-1, UFT, 5-DFUR) after surgery had significantly worse recurrence-free survival (RFS) than 140 SPF45-negative-patients ($p=0.027$). 102 SPF45-positive-patients who didn't receive adjuvant chemotherapy was no significantly different in RFS from 203 SPF45-negative-patients. In the 215 patients who received adjuvant chemotherapy, 81 DPD-positive patients had significantly worse RFS than DPD-negative patients ($p=0.043$). In the 305 patients who didn't receive adjuvant chemotherapy, there was no significant difference in RFS between DPD-positive patients and DPD-negative patients ($p=0.880$). SPF45-positive cases were significantly more frequent in patients with DPD expression ($p < 0.001$).In 94 patients with advanced recurrent gastric cancer treated with chemotherapy, there were 42 recurrent patients and 52 stage IV patients. 50 of SPF45-positive patients had significantly worse progression-free survival than 44 of SPF45-negative patients ($p < 0.001$). Regarding overall response, SPF45-positive-patients had worse response rate than SPF45-negative-patients ($p=0.016$). In SPF45 positive group, 20.0% responded (CR in 0% and PR in 20%) and 80.0% did not respond (SD in 52% and PD in 28%). In SPF45 negative group, 42.6% responded (CR in 0% and PR in 42.6%) and 57.4% did not respond (SD in 46.8% and PD in 10.6%)
Conclusion: Our results suggest that the splicing factor SPF45 influences anticancer drugs such as 5-FU resistance in gastric cancer.
Acknowledgments: We thank Kazuhiro Fukumura and Akila Mayeda, Fujita Health University.

#2526 Exploratory study of predicting systemic therapy response by IGRA in advanced stage NSCLC patients.

H. Huang[1], C.-L. Chiang[1], Y.-H. Luo[1], Y.-M. Chen[1], C.-H. Chiu[2];

[1]Taipei Veterans General Hospital, Taipei, Taiwan, [2]Taipei Medical University Hospital, Taipei, Taiwan

Purpose: In this study, we aim to prospectively evaluate how patients' pretreatment PSIG correlated with chemotherapy, immune checkpoint inhibitors (ICI) and epidermal growth factor receptor (EGFR) Tyrosine Kinasae Inhibior (TKI) . Also, to assess the change of PSIG during anti-cancer treatment and the relation with clinical condition.

Materials and Methods: Newly diagnosed advanced stage non-small cell lung cancer patients were enrolled. The inclusion criteria included pathology or cytology-proved stage IV and non-operable stage III non-small cell lung cancer, treatment-naïve, and planned to receive chemotherapy, EGFR-TKI therapy. Or, planned to receive any line of singe agent immunotherapy. We planned to enroll 30 patients in each treatment group (chemotherapy, immunotherapy, EGFR TKI therapy) with and additional control group of stage I NSCLC.Blood sample from each enrolled patient was obtained for INF-γ release assay (IGRA) within 3 days before the initiation of systemic therapy and 8-12 weeks after treatment. The IGRA was performed with QuantiFERON-TB In-Tube (QFT-GIT; Qiagen, Germany) according to the manufacture's instruction. The amount of INF-γ produced in response to PHA is determined by the INF-γ level in the PHA-coated tube minus saline-coated tube, and is termed PHA-stimulated INF-γ (PSIG) level. Patients with PSIG level above 7.06IU were defined had high PSIG level according to our previous study. we also performed our in house INF-γ level by ELISA. Tumor response was assessed mainly by chest CT and brain MRI (if available) according to Response Evaluation Criteria in Solid Tumors (RECST) .

Results: Total 116 patients were enrolled. Demographic distribution was summarized in Table 1. Thirty-five of 116 (30.2%) patients had latent TB infection, while 12 patients (10.3%) had indeterminate OFT test, all due to low mitogen-stimulated INF-γ level. 84 patients had been obtained post-treatment blood test, and the box-plot of in-house INF-γ level were shown in Figure1. For stage I control group, INF-γ level seemed higher after surgery; for chemotherapy and immunotherapy, the INF-γ level also seemed increase among responders (who achieved disease control after treatment). There were no statistically difference of disease control rate between patients with high PSIG level and low PSIG level. Overall survival also showed no statistically difference between 2 PSIV level patient group among advanced stage NSCLC patients.

Conclusions: There were no statistically different of disease control rate in PSIG high and low group. The increased trend of INF-γ level after surgery, immunotherapy and chemotherapy may suggested improving immune function after treatment even in the very early disease stage.

#2527 PD-L1 regulation by Dual Oxygenase 2 (DUOX2), a reactive oxygen species (ROS) producing enzyme in gastric cancers.

F. Carrier, **M. B. Martins**;
Univ. of Maryland Marlene & Stewart Greenebaum Cancer Ctr., Baltimore, MD

Immune checkpoint inhibitors have shown outstanding activities in some cancers, but their efficacy is rather variable with limited long-term response in most patients while others do not respond well or even develop resistances. The oxidative state of the tumor and its microenvironment plays a critical role in this response and highlights the importance of better understanding the role of redox enzymes in response to immunotherapy. In fact, Reactive Oxygen Species (ROS) effectors can either up or down regulate PD-L1 expression depending on their targets and mechanisms of action. Our data indicate that DUOX2, an NADPH enzyme involved in the production of H_2O_2, is expressed in about forty percent of human gastric cancers and is significantly increased in esophageal cancers. Moreover, DUOX2 expression in human gastric and esophageal cancer cells corresponds to down regulation of the immune checkpoint PD-L1. Conversely, down regulation of DUOX2 increases PD-L1, HIF-1α and c-Myc expression in these cells. To better understand the role of DUOX2 in the production of ROS and how it interferes with the expressions of HIF-1α and PD-L1, we also evaluated its effects on the ROS scavenger glutathione (GSH) and the ROS generating Ceramide in cells expressing or not DUOX2. The down regulation of DUOX2 reduced by more than half Ceramide levels and significantly increased GSH levels. This is consistent with the known effect of H_2O_2 on Ceramide generation through sphingomyelin hydrolysis and H_2O_2 inhibitory effect on HIF-1α binding and accumulation of HIF-1α protein. Because HIF-1α is a known regulator of PD-L1, DUOX2 expression on some tumors could thus interfere with PD-L1 expression through generation of H_2O_2. Moreover, because HIF-1α and PD-L1 expression contribute to radio-resistance, DUOX2 expression could sensitize cancer cells to radiation therapy. On the other hand, tumors lacking DUOX2 expression would be expected to be more sensitive to immunotherapy targeting PD-1 and/or PD-L1. DUOX2 expression thus appears to hold significant potential as a valuable biomarker to guide therapeutic decisions regarding radiation or immuno-therapy.

#2528 Genomic and immune microenvironment features influencing chemoimmunotherapy response in gastric cancer with peritoneal metastasis: A retrospective cohort study.

Pengfei Yu[1], Guangyu Ding[1], Xingmao Huang[1], Chenxuan Wang[2], Jingquan Fang[1], Ling Huang[1], Zeyao Ye[1], Qi Xu[3], Xiaoying Wu[2], Junrong Yan[2], Qiuxiang Ou[2], **Haimeng Tang**[2], Yian Du[1], Xiangdong Cheng[1]

[1]Department of Gastric Surgery, Zhejiang Cancer Hospital, Hangzhou Institute of Medicine (HIM), Chinese Academy of Sciences, Hangzhou, China,[2]Nanjing Geneseeq Technology Inc, Nanjing, China,[3]Department of Medical Oncology, Zhejiang Cancer Hospital, Hangzhou Institute of Medicine (HIM), Chinese Academy of Sciences, Hangzhou, China

Background: Patients with peritoneal metastasis (PM) from gastric cancer (GC) exhibit poor prognosis. Chemoimmunotherapy offers promising clinical benefits; however, its efficacy and predictive biomarkers in a conversion therapy setting remain unclear. We aimed to retrospectively evaluate chemoimmunotherapy efficacy in a conversion therapy setting for GC patients with PM and establish a prediction model for assessing clinical benefits.

Methods: A retrospective evaluation of clinical outcomes encompassed 55 GC patients with PM who underwent chemoimmunotherapy in a conversion therapy setting. Baseline PM specimens were collected for genomic and transcriptomic profiling. Clinicopathological factors, gene signatures, and tumor immune microenvironment were evaluated to identify predictive markers and develop a prediction model.

Results: Chemoimmunotherapy achieved a 41.8% objective response rate and 72.4% R0 resection rate in GC patients with PM. Patients with conversion surgery showed better overall survival (OS) than those without the surgery (median OS: not reached vs 7.82m, P<0.0001). Responders to chemoimmunotherapy showed higher *ERBB2* and *ERBB3* mutation frequencies, *CTLA4* and *HLA-DQB1* expression, and CD8+ T cell infiltration, but lower *CDH1* mutation and naïve CD4+ T cell infiltration, compared to non-responders. A prediction model was established integrating CDH1 and ERBB3 mutations, HLA-DQB1 expression, and naïve CD4+ T cell infiltration (AUC=0.918, 95%CI: 0.846-0.991), which were validated using an independent external cohort (AUC=0.785, 95%CI: 0.637-0.933).

Conclusion: Our study comprehensively evaluated clinicopathological, genomic, and immune features and developed a novel prediction model, providing a rational basis for the selection of GC patients with PM for chemoimmunotherapy-involved conversion therapy.

#2529 Comparison of small cell lung cancer transcriptional factor expression by immunohistochemistry, multiplex immunofluorescence, and a targeted RNA expression panel.

H. Ozakinci, A. Alontaga, J. Nguyen, C. Moran Segura, D. Saeed-Vafa, J. Gray, E. Haura, A. Chiappori, T. Boyle;
Moffitt Cancer Center, Tampa, FL

Recent studies have identified distinct molecular subtypes of small cell lung cancer (SCLC) (SCLC-A, SCLC-N, SCLC-P, and SCLC-Y) based on ASCL1, NEUROD1, POU2F3, and YAP1 expression. In this study, we investigated the correlation between immunohistochemistry (IHC), multiplex immunofluorescence (mIF), and RNA Salah Targeted Expression Panel (RNA STEP) for ASCL1, NEUROD1, POU2F3, and YAP1 in formalin-fixed-paraffin-embedded (FFPE) samples from 14 SCLC samples collected under an IRB-approved protocol (MCC19163). For the mIF evaluation, FFPE samples were immunostained using the AKOYA Biosciences OPAL TM 7-Color Automation IHC kit on the BOND RX autostainer. For RNA STEP, nanoString nCounter TagSet chemistry was used to measure gene expression levels of test FFPE samples relative to a reference pooled human normal mRNA control. All three methods demonstrated significant correlation for ASCL1 levels (Table 1). IHC and RNA STEP NEUROD1 results exhibited significant correlation. However, mIF NEUROD1 results did not correlate with the results of other methods likely due to non-specific positivity of the NEUROD1 mIF antibody. No strong correlation was observed between any of the methods for POU2F3 and YAP1. Only 2 of the 14 samples displayed positive POU2F3 protein expression by IHC; one of these also had elevated POU2F3 expression by RNA STEP. Importantly, the sample with the highest POU2F3 protein expression by IHC also had the highest values by mIF and RNA STEP. All samples were negative for YAP1 by IHC and RNA STEP. Notably, ASCL1 staining was primarily observed in CD56+ POU2F3- cells by mIF. These findings highlight the reliability and utility of IHC and RNA STEP in assessing transcriptional factors in SCLC. Also, mIF presents an innovative method for the simultaneous analysis of multiple markers using a single tissue section, enabling the concurrent detection of multiple markers within individual cells.

Table 1. Statistical Significance (p-values) and Correlation Analysis (Spearman's Coefficients)

	IHC vs RNA STEP		***IHC vs mIF***		***RNA STEP vs mIF***	
	p	**r**	**p**	**r**	**p**	**r**
ASCL1	0.021	0.62	<0.0001	0.91	0.010	0.67
NEUROD1	0.002	0.78	0.517	-0.14	0.671	0.12
POU2F3	0.201	0.36	0.422	0.18	0.045	0.55
YAP1	0.299	0.30	0.364	0.20	0.295	0.30

#2530 Advancing ICK assay: Real-time, label-free imaging of lymphocyte subsets.

S. Oh[1], J. Do[1], H.-S. Min[1], D. Ryu[1], W. Park[2];

[1]Tomocube, Inc., Daejeon, Korea, Republic of, [2]Korea Advanced Institute of Science and Technology, Daejeon, Korea, Republic of

Background: Immune Cell Killing (ICK) Assay is pivotal in immunology and clinical research, uncovering the intricate connections between the immune system and diseases. Traditional ICK assays utilizing antibody staining for endpoint data generation pose challenges in capturing dynamic interactions. Moreover, antibody labeling for data quantification may compromise sensitivity, especially with low-affinity antibodies or a limited number of cells. The anticipation of label-free lymphocyte subset classification and real-time effector/target cell interaction analysis in one field of view is expected to provide more valuable insights than traditional ICK assays. Previous studies achieved 70-80% accuracy in image-based lymphocyte subset classification using digital holographic microscopy, light scattering, etc. but the cells' condition during the cell sorting or sample preparation process may affect the lymphocyte subset status, resulting in real morphological discrepancies. Our approach focuses on directly sorting human PBMCs to enable label-free, dynamic interaction analysis of natural immune system responses in one field of view.

Method: In this study, PBMC samples from 6 individuals were separated using standard-density gradient centrifugation and labeled with antibodies. Data were acquired using the Holotomographic Microscope HT-X1 (Tomocube Inc.). We employed Densenet 121 as the deep learning model architecture, considering the trade-off between memory consumption and performance. The cross-entropy loss function was utilized, and the AdamW optimizer was chosen for model parameter optimization. Input data consisted of 3D refractive index (RI) data for individual cells, each of sized (20, 54, 54). Individual cell labeling was performed using staining information.

Results: An overall accuracy of 93.75% in Human PBMC subtype cell classification was achieved. In stage 1, an accuracy of 97.56% was demonstrated in classifying [CD14, CD15, Others]. Among the cells classified as "Others" in stage 2, [CD3, CD19, CD16&CD56] displayed an accuracy of 93.5%. In stage 3, classifying [CD4, CD8] within the CD3 subtype achieved an accuracy of 90.2%. This classification is presumably based on pattern recognition of the chromosomal landscape in holotomography images.

Conclusion: Our research has successfully demonstrated the feasibility of real-time label-free lymphocyte subset classification. This approach enabled the classification of effector cells as live cells in ICK assay and the analysis of effector-target cell dynamic interactions. Further training in the classification of more detailed subtype cells and various cell death types will provide additional insights. The advancement of this technology is expected to play a pivotal role in disease prevention, treatment, vaccine development, medical research, and academic studies.

#2531 rs822336 as a predictive biomarker for anti-PD-1/PD-L1 immunotherapy in advanced NSCLC: Unraveling molecular mechanisms.

G. Polcaro[1], L. Liguori[2], V. Manzo[3], A. Chianese[4], G. Donadio[1], A. Caputo[1], G. Scognamiglio[5], F. Dell'Annunziata[4], M. Langella[3], G. Corbi[6], A. Ottaiano[5], M. Cascella[5], F. Perri[5], M. De Marco[1], J. Dal Col[1], V. Pagliara[1], P. Zeppa[1], A. Filippelli[1], G. Franci[1], F. Dal Piaz[1], V. Conti[1], S. Pepe[1], **F. Sabbatino**[1]; [1]University of Salerno, Baronissi, Italy, [2]University of Naples "Federico II", Napoli, Italy, [3]University Hospital "San Giovanni di Dio e Ruggi d'Aragona", Salerno, Italy, [4]University of Campania "Luigi Vanvitelli", Naples, Italy, [5]Istituto Nazionale Tumori di Napoli, IRCCS "G. Pascale", Naples, Italy, [6]University of Naples "Federico II", Naples, Italy

Efficient predictive biomarkers are needed for immune checkpoint inhibitor (ICI)-based immunotherapy in non-small-cell lung cancer (NSCLC). So far, testing the predictive value of single nucleotide polymorphisms (SNPs) in programmed cell death 1 (PD-1) or its ligand 1 (PD-L1) has shown contrasting results. Here, we aimed to validate the predictive value of PD-L1 SNPs in advanced NSCLC patients treated with ICIs as well as to define the molecular mechanisms underlying the role of identified SNP candidate. rs822336 SNP efficiently predicted response to anti-PD-1/PD-L1-based immunotherapy in advanced NSCLC patients as compared to rs2282055 and rs4143815 SNPs. rs822336 SNP mapped on promoter/enhancer region of PD-L1, differentially affecting the induction of PD-L1 expression in human NSCLC cell lines. The induction of PD-L1 expression by rs822336 SNP was predicted by allele-specificity binding of two identified transcription factors: C/EBPβ and NFIC. As a result, silencing of C/EBPβ and NFIC differentially modulated the induction of PD-L1 expression in human NSCLC cell lines carrying different rs822336 genotypes. In addition, binding microarray validated the allele- specificity binding of C/EBPβ and NFIC to PD-L1 promoter/enhancer region based on rs822336 genotype in human NSCLC cell lines. Lastly, the induction of PD-L1 expression by rs822336 genotype differentially affected the susceptibility to anti-PD-1 monoclonal antibody nivolumab of human NSCLC cell lines co-cultured with HLA class I antigen matched PBMC. These results have clinical relevance since identified rs822336 SNP and the induction of PD-L1 expression as novel biomarkers for predicting ICI-based immunotherapy in NSCLC patients.

#2532 Deciphering multiple protein complexes in BCL2 family to measure apoptotic dependencies in acute myeloid leukemia.

Hongwon Lee[1], Changju Chun[2], Byungsan Choi[1], Saem Hong[1], Yunseo Lee[1], Youngil Koh[3], Tae-Young Yoon[2]

[1]PROTEINA Co., Ltd, Seoul, Korea, Republic of,[2]School of Biological Sciences and Institute for Molecular Biology and Genetics, Seoul National University, Seoul, Korea, Republic of,[3]Department of Internal Medicine, Seoul National University College of Medicine, Seoul National University Hospital, Seoul, Korea, Republic of

The BCL2 protein family controls apoptosis by shifting the dynamic equilibrium state of complex formation. BH3 mimetics disrupt this balance by disturbing the interaction of a specific anti-apoptotic protein, leading to the initiation of apoptosis. However, relying solely on molecular data for the specific anti-apoptotic protein can be challenging due to the functional redundancy within the BCL2 protein family and their complex interaction network. Therefore, comprehensive profiling information considering protein complexes is essential to determine apoptotic dependencies, particularly in a clinical context. In this study, we adapted a Single-molecule Protein Interaction Detection (SPID) platform that can assess levels of protein complexes in a quantitative manner. Out of the 47 metrics included in our Apoptosis Signaling 47 panel, we utilized 22 assays to measure apoptosis dependencies in acute myeloid leukemia (AML) cells obtained from 32 patients. By combining these metrics, we developed a predictive model for the ex vivo response to ABT-199 treatment, focusing on three key biomarkers: BCL2-BAX complex, BCL2-BIM binding potential, and BCLxl-BAK level. From a receiver operating curve (ROC) analysis, the model exhibited high accuracy with a value of 0.94 area under the curve (AUC). We further validated our model by comparing the predicted response to the therapeutic outcomes in 10 AML patients according to the 2017 ELN guidelines, and achieved 100% sensitivity (4 out of 4 identified correctly) and 83.3% specificity (5 out of 6 identified correctly). Overall, our platform provides an effective method to explore apoptosis dependencies in clinical samples based on the information regarding protein complexes within the BCL2 protein family. Three key molecular biomarkers can be translated into a gauge for predicting therapeutic outcomes of BH3 mimetics, suggesting an improvement of precision medicine in AML treatment.

#2533 In-depth multi-omic profiling of immune cells in cancer patients developing immune-related adverse events.

D. Shek[1], B. Gao[2], J. Lai[3], B. Gloss[3], A. Nagrial[4], I. Pires da Silva[5], M. S. Carlino[2], S. A. Read[3], G. Ahlenstiel[1];

[1]Western Sydney University, Sydney, Australia, [2]Blacktown Hospital, Sydney, Australia, [3]Westmead Institute for Medical Research, Sydney, Australia, [4]Westmead Hospital, Sydney, Australia, [5]Melanoma Institute Australia, Sydney, Australia

Background: The clinical efficacy of immune-checkpoint inhibitors is complicated by the risk for immune-related adverse events (irAEs) that can involve any organ systems. To date, (1) we cannot predict irAE risk reliably at patient level and (2) irAEs remain a diagnosis of exclusion as there are no specific clinical or biological markers. The goal of this study was to elucidate intricate transcriptomic and proteomic signatures of immune cells in patients evolving irAEs.

Methods: This pilot trial was conducted as part of a prospective multicenter cohort study (NCT04631731). The study cohort consisted of n=71 patients who were treated with ICIs across Blacktown and Westmead Hospitals, NSW, Australia. Peripheral blood mononuclear cells (PBMCs) were collected from both pre-treatment and after 6-8 weeks post-ICI commencement. Samples were further utilized for RNA sequencing, flow cytometry and Chromium 3' gene expression analysis (10x Genomics).

Results: The median age was 67 years old with the 78% (n=56) of Caucasian origin. The predominant number of patients were treated with dual ICIs. N=21 patients experienced irAEs. Firstly, a differential analysis established a set of genes which were significantly (FDR<0.01) dysregulated between patients with (group A) and without irAEs (group B) and were mostly related to cell cycle and regulation. Notably, phospholipase D signaling pathway was exclusively upregulated in group A and is known to be linked to B cell expansion. Secondly, a cell enrichment analysis within the group A revealed a significant increase of CD4+ and CD8+ T central memory (Tcm) cells upon the toxicity onset as compared to baseline stage. Thirdly, the flow cytometry data established that group A had (1) higher expression of CD27 on CD4+ T cells, a member of Traf-linked tumor necrosis factor receptor family essential for T cells' maturation and (2) lower expression of inhibitory receptor LAG3 (CD223) which is crucial for maintaining homeostasis of immune system through suppression of T cell proliferation. Finally, we sequenced CD45+ cells from n=4 patients from group A and n=4 from group B at both pre- and post-treatment stages. The unsupervised clustering established 17 different clusters in our single cell dataset with cluster 11 was unique only to patients from group A. The differential analysis established that a set of n=62 genes was significantly upregulated ($p<0.05$) in cluster 11. Functional annotation established that B cell activation and proliferation pathways were enriched by those genes further stressing B cells' role in irAEs development.

Conclusions: Our real-world cohort study established significant molecular and cellular differences between patients with and without irAEs. Further research in larger cohorts is imperative to validate the established findings and to elucidate the precise mechanisms contributing to the development of irAEs.

#2534 Single-cell dissection of heterogeneity and dynamics of tumor ecosystem upon immune-checkpoint blockade in hepatocellular carcinoma.

A. S. Cheng[1], Z. Xiong[1], H. Wu[1], J. Cao[1], Z. Liang[1], J. Zhou[1], J.-Y. Sung[2], K. Yip[3], S. Chan[1];

[1]Chinese University of Hong Kong (CUHK), Hong Kong, Hong Kong, [2]Nanyang Technological University, Singapore, Singapore, [3]Burnham Prebys Medical Discovery Institute, La Jolla, CA

Background: Therapy-induced alteration of tumor ecosystem poses a major barrier for cancer regression. As the majority of patients with hepatocellular carcinoma (HCC) develops resistance to immune checkpoint blockade (ICB) therapy, we aimed to characterize heterogeneity and dynamics of multicellular tumor ecosystem following anti-PD-1 treatment using scRNA-seq.

Methods: In a phase II clinical trial of pembrolizumab on advanced hepatitis B virus-related HCC patients (NCT03419481), we performed a comprehensive single-cell transcriptomic profiling of biopsy samples from 26 patients before and during treatment. The composition and distribution of immune aggregates in responsive tumors was characterized by scRNA-seq and spatial transcriptome analyses. The anti-tumor efficacy of combined therapy with anti-PD-1 and inhibition of immunosuppressive macrophage were further determined in RIL-175-derived PD-1-resistant mouse model.

Results: After initial data processing and quality control, we obtained 353,329 high-quality cells that included tumor cells, myeloid cells, lymphoid cells, endothelial cells and fibroblasts. Our analysis revealed that baseline tumor-reactive $CD8^{+}$T cells exhibited a strong association with improved prognosis. Notably, treatment-induced expansion and differentiation of tumor-reactive $CD8^{+}$T cells with memory-like phenotype highly correlated with durable ICB response. Moreover, we observed a co-occurrence pattern of key anti-tumor immune subsets in the tumor microenvironment (TME), which associated with ligand-receptor pair interactions. Spatial transcriptome analysis further validated the presence of immune aggregates in responsive tumors. Importantly, we derived an responsive signature from immune aggregates, which showed a strong association with improved prognosis in pan-cancer ICB datasets. Paired comparisons of pre- and on-treatment macrophage percentages in non-responders revealed a specific expansion of an immunosuppressive macrophage subset. Inhibition of this macrophage subset could overcome ICB resistance by enhancing T cell function in our PD-1 resistant model. We further observed that a tumorous epithelial-mesenchymal transition (EMT) program might contribute to therapeutic resistance via TME remodeling.

Conclusions: Our study suggests that tumor-reactive $CD8^{+}$T cells and immune aggregates may be associated with durable ICB response, while ICB-induced upregulation of immunosuppressive macrophages and EMT^{hi} tumor cells contributed to therapeutic evasion. These findings provide valuable insights for identification of predictive biomarkers and therapeutic strategies for ICB therapy of HCC. This project is supported by the General Research Fund (14119023, 14120621 and 14115820), the Li Ka Shing Foundation, and the CUHK Strategic Seed Funding for Collaborative Research Scheme.

#2535 Development of Claudin 18.2 IHC 14G11 pharmDx as a clinical trial assay for the clinical development of anti-claudin 18.2 monoclonal antibody osemitamab (TST001) in gastric and gastroesophageal junction adenocarcinoma.

H. Alderson[1], K. Lefley[1], L. Fregoso[1], A. Bharadwaj[1], D. Castellanos-McKenney[1], S. Tabuena-Frolli[1], D. Kell[1], X. Yao[2], X. Qian[2], L. Xu[3], C. Germa[3], E. Oroudjev[1];

[1]Agilent Technologies, Inc., Santa Clara, CA, [2]Suzhou Transcenta Therapeutics Co., Limited, Suzhou, China, [3]Transcenta Therapeutics Inc., Princeton, NJ

Clone 14G11 is a mouse anti-Claudin 18.2 monoclonal antibody developed by Transcenta. The antibody was generated against a linear epitope located on the extracellular domain of loop1 and has a binding site that overlaps with the binding site of therapeutic antibody Osemitamab. It was selected to further develop for the detection of Claudin 18.2 expression in human cancer. Agilent Technologies, Inc. is developing Claudin 18.2 IHC 14G11 pharmDx as an immunohistochemical (IHC) assay for the detection of Claudin 18.2 protein in gastric and gastroesophageal junction (GEJ) adenocarcinoma in support of clinical studies conducted by Transcenta Therapeutics. Analytical verification for Claudin 18.2 IHC 14G11 pharmDx included sensitivity, specificity, and precision assessment. Testing was performed on human formalin-fixed, paraffin-embedded (FFPE) gastric and GEJ tissues using Autostainer Link 48 with EnVision FLEX visualization system. Biomarker expression was evaluated using Tumor Proportion Score (TPS). TPS is defined as the percentage of viable invasive tumor cells that exhibit convincing partial or complete membrane staining at any intensity. Sensitivity testing of 102 commercially procured FFPE gastric/GEJ specimens demonstrated a broad dynamic range of Claudin 18.2 positivity that covered TPS from 0% to 100%. Specificity tests confirmed specific targeting of the Claudin 18.2 protein in a variety of normal and abnormal tissues. For laboratory precision testing, which evaluated the assay variability in relation to run, instrument, operator, and reagent lot, ≥ 95% of TPS values were within expected variability limits for each parameter. For observer precision testing, two-sided 95% confidence intervals were ≥ 85% for negative, positive, and overall agreements when assessing two clinical cutoffs. These results demonstrated the Claudin 18.2 IHC 14G11 pharmDx assay can provide reliable and reproducible results in day-to-day testing. Analytical verification testing indicates Claudin 18.2 IHC 14G11 pharmDx is a sensitive, specific, and precise assay for detecting Claudin 18.2 in gastric and GEJ adenocarcinoma. Claudin 18.2 IHC 14G11 pharmDx for Investigational Use Only/for Performance Evaluation Only will be used for patient selection in the upcoming phase III trial of gastric/GEJ adenocarcinoma where applicable ethics committee and regulatory approvals have been granted.

#2536 Multimodal stratification of predictive biomarkers in head and neck cancers: A focus on cytokine-based immunotherapy.

C. Ramos, R. Ruez, S. Delebecq, V. Senechal;
Aliri, Lille, France

Background Immunotherapy, particularly cytokine-based therapy, has been gaining traction in the treatment of head and neck cancers. Cytokines are small proteins that play a crucial role in the immune response to cancer. However, not all patients respond to cytokine-based immunotherapies, and some may experience severe side effects. The ability to predict which patients are most likely to benefit from these therapies could greatly improve the efficacy and tolerability of treatment. In this context, the study of predictive biomarkers, such as the expression of immune checkpoint molecules like PD-L1 and TIGIT, and the profiling of cytokines within the tumor microenvironment, has become crucial. These biomarkers could provide valuable information about the patient's immune response to the tumor and their likelihood of responding to cytokine-based immunotherapies.
Method A multimodal approach to stratify predictive biomarkers in head and neck cancers was used. The methodology was founded on combining metabolic, transcriptomic, and proteomic data to offer a comprehensive understanding of potential biomarkers. The data from different modalities were integrated using bioinformatics and machine learning algorithms. This comprehensive dataset was analyzed to identify multimodal biomarker signatures that could predict patient responses to cytokine-based therapies.
Result Preliminary finding showed significant heterogeneity in the expression of PD-L1, TIGIT, and various cytokines across the tumor microenvironment. This underscored the complexity of head and neck cancers. Certain multimodal biomarker signatures, which included specific patterns of immune checkpoint molecule expression, cytokine profiles, and immune cell infiltration, correlated robustly with patient responses to cytokine-based therapies.
Conclusion Our study demonstrates the considerable potential of a multimodal stratification approach in deciphering the complexity of head and neck cancers and predicting responses to cytokine-based immunotherapies. By integrating metabolomic, transcriptomic, and proteomic data, we identified unique biomarker signatures that strongly correlated with therapy responses. This work underscores the invaluable role of integrated predictive biomarker profiles in enhancing the precision of immunotherapy.

CLINICAL RESEARCH: Real-World Biomarkers
Poster Session

#2541 The landscape of circular extrachromosomal amplification in pediatric cancers.

S. Sridhar[1], **O. S. Chapman**[2], S. Wang[3], A. Dutta[3], J. P. Mesirov[3], L. Chavez[2];
[1]Rady Childrens Hospital San Diego, San Diego, CA, [2]Sanford Burnham Prebys Medical Discovery Institute, San Diego, CA, [3]University of California San Diego, San Diego, CA

Circular extrachromosomal DNA (ecDNA, also known as double minutes, dm) has emerged as a driver of oncogenic copy number amplification, intratumoral heterogeneity, tumor evolution and therapy resistance. We recently screened the whole genomes of 481 medulloblatomas for ecDNA and concluded that medulloblastoma tumors harboring ecDNA are more than twice as likely to progress within 5 years of diagnosis. To evaluate the frequency and clincical impact of ecDNA across the spectrum of childhood cancers, we performed a retrospective analysis of 1671 tumors from 1482 patients across 47 pediatric tumor types from two large cloud pediatric cancer genomics resources, the Children's Brain Tumor Network and St. Jude Cloud. ecDNA was detected in 15 pediatric tumor types, including ETMR (100%, n=4), osteosarcoma (47%, n=57), rhabdomyosarcoma (40%, n=35), neuroblastoma (30%, n=106), high-grade glioma (20%, n=157), and retinoblastoma (19%, n=32). Patients with tumors containing ecDNA had significantly poorer 5-year overall survival. In sequential samples from the same tumor at diagnosis and relapse, we observe evidence of ecDNA evolution including sequence instability and generation of new high-copy ecDNA amplification not detected at initial diagnosis. These results comprise the most detailed survey to date of the landscape of extrachromosomal amplifications across childhood cancers.

#2542 Real-world validation of the PurIST classifier demonstrates enhanced therapy selection for pancreatic ductal adenocarcinoma (PDAC) patients.

S. Wenric[1], J. M. Davison[2], J. Guittar[1], G. M. Mayhew[2], K. Beebe[2], A. Zander[1], S. Hyun[1], K. Beauchamp[1], M. V. Milburn[2], V. Chung[3], T. S. Bekaii-Saab[4], C. M. Perou[5];

[1]Tempus Labs, Chicago, IL, [2]GeneCentric Therapeutics, Durham, NC, [3]City of Hope, Duarte, CA, [4]Mayo Clinic, Phoenix, AZ, [5]University of North Carolina, Chapel Hill, NC

Background: PDAC is a particularly fatal condition lacking established biomarkers for the choice of first-line treatment (1L). The PurIST algorithm is a gene signature (Rashid et al. Clin. Cancer Res., 2020) that categorizes PDAC tumors into basal or classical molecular subtypes and has been previously validated in a patient cohort of advanced PDAC (N=258). In this post-hoc analysis study, we examine whether the PurIST subtypes can distinguish patients likely to respond to FOLFIRINOX (FFX) versus Gemcitabine + nab-paclitaxel (GnP).

Methods: A cohort of de-identified PDAC patients was selected from the Tempus Oncology Database following an IRB-approved protocol. Inclusion criteria required no prior systemic treatment, a surgically unresectable/metastatic status, available RNA-sequencing data from primary or metastatic tissue, and the use of FFX or GnP as 1L systemic therapy with documented outcomes. RNA-sequencing was generated by the CAP/CLIA validated Tempus xR assay. The PurIST gene signature was applied to normalized gene expression values to classify samples into basal or classical subtypes. Univariate and multivariate Cox PH analyzes comparing overall survival (OS) with adjustment for delayed entry, between two common 1L treatment regimens, FFX and GnP, were performed for classical patients with an ECOG performance status of 0 or 1.

Results: Application of the PurIST model to the PDAC cohort (N=258) resulted in 67% (N=173) labeled as classical, 23% (N=59) as basal, and the remainder as no-call. Amongst classical patients, 35% (N=61) had a known ECOG score of 0 or 1 and were retained for subsequent analysis. Within this subset, 37 were treated with FFX and 24 with GnP as 1L, with an overall median OS of 11.4 months (95% CI: 9.5-16.5) and a 12-month survival rate of 47.2%. A univariate Cox PH analysis showed that classical patients treated with FFX had a significantly longer OS time (HR (95% CI) = 2.32 (1.29-4.17)). This result remained significant in a multivariate Cox PH, adjusting for age and ECOG, (HR=2.5 (1.15-5.44)).

Conclusion: In this real-world cohort of advanced PDAC patients, we showed that classical patients with low ECOG scores had superior OS with 1L FFX treatment compared to 1L GnP. These findings demonstrate the potential for PurIST to aid in optimal treatment selection for patients with advanced PDAC.

#2543 Evaluating biomarkers of immunotherapy response in a real-world metastatic NSCLC cohort.

K. C. Chua, A. Saadatpour, A. Chen, A. Hasan, B. Huang, S. Bates;
Interventional Oncology at Johnson & Johnson, New Brunswick, NJ

Background: Non-small cell lung cancer (NSCLC) is the leading cause of global cancer deaths, since a large proportion of cases are initially diagnosed at advanced stages. Therapeutic developments have shifted first-line (1L) therapy in the metastatic setting to immunotherapy (IO)-based regimens, albeit with heterogeneity in response. Patients harboring KEAP1 and STK11 mutations have been reported to exhibit both poorer outcomes and IO treatment resistance. Recent work suggests gene expression signatures which characterize mutant phenotypes may better identify those with compromised IO response. Leveraging a molecular real-world dataset of metastatic NSCLC patients treated with 1L IO, we aimed to evaluate gene expression signatures representing KEAP1 and STK11-mutated phenotypes and their impact on real-world outcomes.
Methods: Metastatic NSCLC patients who received 1L anti-PD(L)1 as a monotherapy or in combination were identified from the multimodal real-world database of Tempus Labs, Inc. All patients in the analytical cohort had tissue biopsies sequenced on Tempus targeted DNA and whole transcriptome RNA assays within 90 days prior to the start of the 1L IO regimen. Patients were negative for actionable mutations with record duration of at least 30 days from 1L initiation. KEAP1 and STK11 mutants were identified with likely pathogenic and/or pathogenic mutations as annotated by Tempus bioinformatic pipelines. Gene expression signatures related to these mutations were obtained from recently published literature. Evaluation of mutations or signatures as genomic markers for IO non-response were conducted using real-world progression-free survival (rwPFS) and overall survival (rwOS).
Results: A total of 332 patients were included in the study (45% IO monotherapy, 55% IO combination therapy). Previously validated biomarkers, including tumor mutation burden, T-cell inflamed GEP signature, and PD(L)1 expression, were associated with prolonged rwPFS. KEAP1 mutations were observed in 9% of analytical cohort with a higher proportion in non-squamous (11%) compared with squamous (4%) samples. For STK11, 10% were identified as mutants with a similar histology distribution (12% vs. 3%). Neither KEAP1 mutations nor related gene signatures evaluated in this study were significantly associated with real-world survival outcomes. Patients harboring STK11 mutations trended towards poor outcomes; furthermore, those with higher STK11 inactivation signature score were associated with shorter rwPFS and rwOS.
Conclusions: STK11 inactivation phenotype described by a gene expression signature was able to distinguish patients with significantly poorer survival outcomes. This finding would need validation in independent cohorts. This real-world cohort study adds supporting evidence for the utility of gene expression signatures encompassing mutant phenotypes for patient stratification.

#2545 *KRAS* co-mutational landscape dictates treatment outcomes in pancreatic cancer (PC) patients.

P. Ghosh, R. George, N. Singh, S. Agrawal;
ConcertAI, Bengaluru, India

Background: *KRAS* is commonly mutated in PC patients, with a prevalence of ~80%. A holistic understanding of the landscape of *KRAS* mutations, co-occurring mutations (co-mutations) in other driver genes, and their impact on patient outcomes treated with current standard-of-care (SoC) therapies may inform better treatment decisions.

Methods: In this study, we use a real-world clinico-genomics PC database (ConcertAI's Genome360™ PC dataset; N=1302) to:1.Examine the distribution of *KRAS* mutations.2.Identify the genes most frequently co-mutated with *KRAS*, both positively and negatively, based on their odds ratios.3.Evaluate patient outcomes (overall survival (OS) and progression-free survival (PFS)) for the two most common first-line SoC therapies (FOLFIRINOX: folinic acid, fluorouracil, irinotecan hydrochloride, oxaliplatin, and GEMPAC: gemcitabine, paclitaxel) stratified by the mutational status of *KRAS* and *TP53*.

Results: The top 5 most observed *KRAS* mutations and the top 3 positively (OR>1) and negatively (OR<1) *KRAS* co-mutated genes are shown in Table 1. 80%, 71%, and 65% of PC patients had pathogenic mutations in *KRAS*, *TP53*, and both genes, respectively. In the entire cohort, FOLFIRINOX (n=327, OS/PFS=1.26/0.58 years) was more effective (p-value<0.05) than GEMPAC (n=305, OS/PFS=0.79/0.44 years). However, the underlying genetic makeup (mutational status of *KRAS* and *TP53*) significantly affects these outcomes (Table 1). The $KRAS^{+}/TP53^{-}$ (pathogenic mutations in *KRAS*, but not in *TP53*) cohort has the worst prognosis, and the advantage of FOLFIRINOX as the treatment of choice is not observed in this cohort.

Conclusions: This study provides insights into the genetic makeup of patients with *KRAS* mutations and how co-mutation with *TP53* affects outcomes of SoC treatments. It highlights the need for comprehensive genetic profiling to make better therapy decisions.

Table 1: Evaluation of *KRAS* mutational landscape in PC and its impact on treatment outcomes.

Top 5 *KRAS* mutations	***KRAS* mutations**	**G12D**	**G12V**	**G12R**	**Q61H**	**Q61R**
	% PC patients tested positive	42.51	32.52	14.33	4.62	1.79
Top 3 positively and negatively co-mutated genes with *KRAS*	***KRAS* co-mutated genes**	**Positive association**			**Negative association**	
		TP53	***CDKN2A***	***SMAD4***	***BRAF***	***TERT***	***PTEN***
	Odds Ratio	8.56	6.93	6.66	0.05	0.27	0.32
Treatment outcomes for various genetic states of *KRAS* and *TP53*	**Mutational status**	**OS (years)**			**PFS (years)**	
		FOLFIRINOX	**GEMPAC**		**FOLFIRINOX**	**GEMPAC**
	$KRAS^{+}$ $TP53^{+}$ (850)	1.13 (196)	0.68 (188)		0.58 (196)	0.39 (188)
	$KRAS^{-}$ $TP53^{-}$ (155)	2.08 (40)	1.11 (27)		0.66 (40)	0.51 (27)
	$KRAS^{+}$ $TP53^{-}$ (190)	0.77 (33)	0.93 (37)		0.51 (33)	0.33 (37)
	$KRAS^{-}$ $TP53^{+}$ (81)	2.14 (15)	0.84 (24)		0.54 (15)	0.4 (24)

#2546 Identifying co-mutational signatures in *STK11* mutated advanced non-small cell lung cancer (aNSCLC) patients that help overcome poor response to immune checkpoint inhibitors (ICI's).

N. Singh, S. Agrawal;
ConcertAI, Bengaluru, India

Background: ICIs, either alone or in combination with chemotherapy, have become the primary treatment options for aNSCLC patients without any targetable mutations. However, not all patients benefit similarly from these therapies even after selection based on the currently approved biomarker PD-L1 expression. Previous studies have shown that mutations in certain genes like *STK11* and *KEAP1* may predict non-response to these therapies. Mutations in *STK11* occur in 25-30% of aNSCLC patients. We have used a real-world clinico-genomics dataset to investigate how this *STK11*+ aNSCLC patient population responds to ICIs in the context of other underlying co-mutations and whether some beneficial co-mutations may help patients overcome resistance due to their *STK11* status.

Methods: The ConcertAI Genome360™ NSCLC dataset (N=14193) was used in this retrospective study. aNSCLC patients who tested positive for *STK11* mutations and received ICIs were considered (N=377). Based on their response to ICIs, the patients were divided into responder (N= 192) and non-responder (N=185) cohorts. Other genes with pathogenic mutations, fusions, and copy number changes were identified in both cohorts, and enrichment analysis was performed to identify co-mutations significantly enriched in one cohort vs the other. Once significant co-mutations were identified, pathway analysis was performed, taking into account the immune signaling network to help rationalise and validate the results.

Results: One potential mechanism by which STK11 mutations influence the response to ICIs is through downregulation of the cGas-Sting pathway, which has been shown to play an important role in ICI response. Our co-mutational analysis also strongly supported this theory. We found that additional mutations that can nullify the effect of *STK11* mutations on the cGas-Sting pathway led to a positive response (p=0.002) within the *STK11*+ cohort. Two such co-mutational signatures in responder patients identified were co-mutations in *STK11*/*SMARCA4*/*TP53* (no *KEAP1*) (p-value = 0.003) and *SKT11*/*KRAS*/*RBM10* (p-value = 0.04). Additionally, co-mutations in the DNA damage pathway genes (*ATM*, *BRCA1*, *BRIP1*, *PALB2*, *STAG2*) (p-value = 0.001) were also predictive of response to ICIs in the *STK11*+ cohort.

Conclusion: By leveraging a real-world clinico-genomics dataset linking the tumor genomic profiles with patient response to ICIs, we have been able to perform a comprehensive co-mutational analysis of *STK11*+ aNSCLC patients to tease out the interplay of various biomarkers and signaling pathways that determine response to ICIs. Even though 25-30% aNSCLC patients are *STK11*+, we find that ~23% of these patients could still benefit from ICI treatment due to the presence of other co-mutations.

#2547 *KRAS* Q61 mutations in patients with gastrointestinal malignancies and association with real-world clinical outcomes.

M. Yousef, A. Yousef, S. Chowdhury, M. Fanaeian, M. Knafl, P. M. Roy, A. Pillai, M. Zeineddine, F. Zeineddine, J. Peterson, B. G. Smaglo, R. A. Wolff, S. Pant, M. S. Lee, J. A. Willis, M. Overman, E. B. Ludmir, M. W. Hurd, J. Shen, D. Zhao;
The University of Texas MD Anderson Cancer Center, Houston, TX

Introduction: Gene-wide *KRAS* mutation has been associated with worse outcomes in multiple malignancies with newer data suggesting differential impact based on specific allele. Mutation at codon Q61 is relatively infrequent with clinical significance not well understood. Here we aim to investigate the clinical significance of $KRAS^{Q61}$ mutation in gastrointestinal (GI) malignancies.
Methods: The Foundry software platform was used to retrospectively query electronic health records to identify patients diagnosed with colorectal (CRC), pancreatic (PDAC), appendiceal (AA), cholangiocarcinoma (CC) and gastroesophageal carcinoma who underwent clinical testing for *KRAS* mutations in our institution between 2002-2023; clinical, molecular, and overall survival (OS) data were collected.
Results: *KRAS* mutation was tested in 9,088 patients with CRC, PDAC, CC, AA, and gastroesophageal carcinoma. Incidence of *KRAS* mutation was 47% (n= 3,181) for patient with CRC, 82% for PDAC (n= 579), 16% for CC (n= 76), 51% for AA (n= 236), and 7% for gastroesophageal carcinoma (n= 43). $KRAS^{Q61}$ mutation was in 5% (n=218) of patients with *KRAS* mutation (n= 4,115). Overall frequency of $KRAS^{Q61}$ was 2% (n= 156) for CRC, 5% (n= 36) for PDAC, 3% (n= 12) for CC, 2% (n= 10) for AA and 1% (n= 4) for gastroesophageal carcinoma. $KRAS^{Q61}$ fraction of *KRAS* mutations was 5% for CRC, 6% for PDAC, 16% for CC, 4% for AA, 9% for gastroesophageal carcinoma. $KRAS^{Q61H}$ was the most frequent $KRAS^{Q61}$ mutation among all tumor types, 57%, 61%, 60%, 50% out of $KRAS^{Q61}$ for CRC, PDAC, AA, and gastroesophageal carcinoma respectively; followed by $KRAS^{Q61L}$ (20%) for CRC, but $KRAS^{Q61R}$ for PDAC (25%), AA (20%), and gastroesophageal (25%); Patients with CC showed exclusively $KRAS^{Q61H}$ mutations. Compared to patients with *KRAS* wildtype, patients with $KRAS^{Q61}$ mutations had worse OS in PDAC (median OS=20 vs 37 months, HR=1.9, 95%CI=1.2-3, p=0.006), while (55 vs 63 months, HR=1.2, 95%CI=0.98-1.5, p=0.076) for CRC, (29 vs 25 months, HR=1.3, 95%CI=0.64-2.6, p=0.47) for CC, and (33 vs 52 months, HR=1.1, 95%CI=0.5-2.6, p=0.75) for AA. Compared to other *KRAS* mutations, $KRAS^{Q61}$ median OS was (55 vs 53 months, HR=1, 95%CI=0.81-1.3, p=0.96) for patients with CRC, (20 vs 26 months, HR=1.4, 95%CI=0.91-2.1, p=0.1) for PDAC, (25 vs 28 months, HR=1.1, 95%CI=0.54-2.5, p=0.72) for CC, (33 vs 78 months, HR=1.6, 95%CI=0.72-3.7, p=0.24) for AA.
Conclusion: $KRAS^{Q61}$ mutations frequency varied from 1% to 5% across different GI malignancies, with highest frequency in PDAC and CC. $KRAS^{Q61}$ mutations had worse OS in patients with PDAC which may suggest different co-mutations rather than specific $KRAS^{Q61}$ activity difference. Further allele specific analysis of $KRAS^{Q61}$ and co-mutations landscape is underway.

#2548 Retrospective prediction of clinical response to standard-of-care therapies in acute myeloid leukemia by an *ex vivo* drug sensitivity assay using cryopreserved primary samples.

L. Patil[1], C. J. Gu[1], W. Anderson[1], N. Long[2], K. Johnson[2], C. Tognon[2], M. D. Lacher[1];
[1]Notable Labs, Foster City, CA, [2]Oregon Health & Science University, Portland, OR

Background: Assessing drug efficacy in primary acute myeloid leukemia (AML) patient cells is crucial for pinpointing drug targets and rationally selecting therapies for patients. We have previously shown that our flow cytometry-based predictive precision medicine platform (PPMP) predicts patient outcomes for standard-of-care (SOC) AML treatments using fresh blood or bone marrow samples with high precision. Here, we wanted to test the feasibility and efficacy of the PPMP on cryopreserved patient-derived leukemic samples. However, cryopreserved leukemic samples are known for exhibiting low viability and cell recovery, rendering their practical utilization often challenging. In this study, we adapt an existing methodology for cryopreservation for patient-derived leukemic cells to investigate the potential of cryopreserved samples as an alternative to fresh samples for ex vivo prediction of treatment outcomes on our PPMP.
Methods: We screened freshly isolated white blood cells from AML patients on the PPMP to assess their response to multiple SOC single agents and combinations. The assay was also run without drug treatments immediately after receiving the fresh sample (≤ 2 days from draw) to establish a phenotype baseline. The cryopreserved samples were processed using a similar protocol, with post-thaw culture times of either 24 or 48 hours in two types of cytokine-containing media. A comparative analysis between untreated fresh and cryopreserved samples determined the optimal post-thaw culture time for cryopreserved samples. Once culture time was optimized, we screened cryopreserved samples on the PPMP with identical SOC drug conditions as the fresh samples and compared the response of leukemic blasts to drug treatment as well as impacts on other phenotypic markers.
Results: Based on our preliminary data, we found that culturing cryopreserved cells for 24 hours post-thaw was sufficient to maintain a minimum cell viability of 80% while closely maintaining a phenotype that recapitulated that of the corresponding fresh samples. In response to drug treatments within the ex vivo assays, preliminary data support a correlation (Decitabine single agent, R^2=0.81) between the response profiles of cryopreserved and fresh patient samples as gauged from AUC calculations.
Conclusion: While the preferred method for screening is to use fresh patient samples, many practical constraints make it challenging or unfeasible. The ability of Notable Lab's high-throughput platform to use cryopreserved samples opens the doors to enhanced retrospective studies leveraging clinically annotated data from biobanks or clinical trials. These retrospective studies provide a substantial reduction in the time needed to conclude such investigations.

#2549 Activity-regulated cytoskeleton-associated protein (ARC) gene expression is associated with high infiltration of stromal cells and immune cells, but with less cancer cell proliferation and better overall survival in ER-positive/HER2-negative breast cancers.

G. Yee[1], R. Wu[1], T. Ishikawa[2], K. Takabe[1];

[1]Roswell Park Comprehensive Cancer Center, Buffalo, NY, [2]Tokyo Medical University, Tokyo, Japan

Introduction: Recently peritumoral lidocaine infiltration prior to removal was reported to be associated with better survival in early-stage breast cancer (BC). This led us to hypothesize that innervation to the tumor affects its biology and patient survival. Activity-regulated cytoskeleton-associated protein (ARC) gene expression is known to be regulated by neuronal activity. Therefore, we studied the clinical relevance of ARC gene expression as a surrogate of neuronal activity in BC. **Methods:** Sweden Cancerome Analysis Network-Breast (SCAN-B (GSE96058), n=3273) cohort was analyzed, and the results were validated using The Cancer Genome Atlas (TCGA, n=1069). **Results:** ER+/HER2- and Luminal A type cancers expressed significantly higher ARC compared to the other subtypes in both cohorts ($p<0.005$). In the tumor microenvironment, the stromal cells (fibroblasts, endothelial cells and adipocytes) were all found to be significantly infiltrated in high ARC BC ($p<0.01$). Multiple immune cells were significantly infiltrated in high ARC BC, including CD8, CD4 memory cells, helper type II T cells, regulatory T cells, M1 and M2 macrophages, dendritic cells and B cells (all $p<0.03$ in both cohorts). In terms of cancer characteristics, there was no difference in silent or nonsilent mutations, single nucleotide variant or indel neoantigens between tumors with low or high ARC expression. However, high ARC BC was significantly associated with less homologous recombination deficiency, intratumor heterogeneity and fraction altered mutation rate compared to low ARC BC in TCGA ($p<0.001$). High ARC expression was significantly associated with smaller tumor size ($p<0.001$) and without lymph node metastasis in the SCAN-B cohort ($p<0.02$), and less Stage IV disease in the TCGA cohort ($p<0.02$); however, these results were not validated by the other. High ARC BC was significantly associated with lower Nottingham histologic grade and lower MKi67 expression in both cohorts ($p<0.001$). Cell proliferation-related gene sets in the Hallmark collection (E2F targets, G2M checkpoint, and MTORC1 signaling) were significantly less enriched to high ARC BC consistently in both cohorts. Overall survival (OS) was significantly better in high ARC BC in the ER+/HER2- subtype consistently in both cohorts ($p<0.01$) and when including all subtypes in the SCAN-B cohort ($p<0.001$); however this was not validated in TCGA. No significant difference in OS was found between low and high ARC gene expression in triple negative BC in either cohort. **Conclusion:** ARC gene expression as a surrogate of neuronal activity in BC was associated with high infiltration of stromal cells and immune cells but with less cancer cell proliferation and better overall survival, particularly in the ER+/HER2- subtype.

#2550 Investigating glutathione peroxidases as potential prognostic factors in uterine corpus endometrial cancer.

A. Dukesherer, **C. A. Davison-Versagli**;
Saint Mary's College, Notre Dame, IN

Introduction: Uterine corpus endometrial cancer (UCEC) is one of the deadliest women's reproductive cancers in the United States, and mortality rates have not improved in the last 30 years due to poor prognostic methodologies. Altered expression patterns of Glutathione Peroxidases (GPX1-8) have been connected to the outcome of many cancers. Still, GPX expression patterns and their use as prognostic biomarkers in UCEC have yet to be explored. This project aimed to evaluate the potential utility of GPX1-8 as prognostic biomarkers for UCEC.

Methods: To identify GPX1-8 expression alterations in UCEC tumors, the UCEC tissue samples (n=543) from the Cancer Genome Atlas Database (TCGA) dataset were analyzed using the University of Alabama at Birmingham Cancer Data Analysis portal (UALCAN) software to statistically compare mRNA levels between UCEC tumor samples and non-tumorigenic uterine tissue. To determine the impacts of GPX1-8 expression on overall survival (OS) and relapse-free survival (RFS), the UCEC TCGA dataset was analyzed using the pan-cancer RNA seq platform using Kaplan-Meier Plotter (KM plotter). The patient cohort was split into groups according to high GPX expression status and low GPX expression status using the trichotomization function in KM plotter. Hazard ratio (HR), 95% confidence interval (95% CI), and log-rank P value were calculated using the KM plotter platform.

Results: GPX1, GPX2, GPX4, GPX7, and GPX8 were differentially expressed in UCEC tumor tissue compared to non-cancerous uterine tissue. However, unfavorable OS in patients associated with low GPX4 expression in UCEC tumor samples (P=0.0043, HR=0.39, 95% CI=0.2-0.76) only. Unfavorable RFS in UCEC patients only correlated with low GPX1 expression (P=0.019, HR=0.43, 95% CI=0.21-0.89) or high GPX6 expression (P=0.0032, HR=2.37, 95% CI=1.31-4.27) in UCEC tumor samples.

Conclusion: Low GPX1 and GPX4 expression and high GPX6 expression may be novel unfavorable UCEC prognostic markers.

#2551 Harness the power of real-world-data for oncology target and biomarker research: A case study by applying clinic-genomics data for 2,659 lung cancer patients and beyond.

S. Wu, W. Zhao, C. Choi, M. Cai, P. Ansell, A. Liede, R. Chen, X. Zhao, J. Samayoa;
Abbvie, South San Francisco, CA

Randomized controlled trials (RCTs) are the gold standard for evaluating drug safety and efficacy in controlled settings, but they have limited generalizability due to their focus on selective and homogeneous populations. Real-world-data (RWD), collected from larger and more varied patient populations, can address inherent limitations of RCTs and aid in clinical trial design and drug approval. However, with the challenges of RWD, unlocking its full potential for tumor target and biomarker identification and validation demands innovative analytical approaches. Here we present RWD analyses of ConcertAI® electronic health records (EHR) linked with Caris Lab data for 2,659 lung cancer patients. Comprehensive genomics analyses incorporate WES and RNA-seq data, coupled with rich clinical EHR data. By integrating clinical and genomics data, we showcase the potential of harnessing RWD as follows: (1) we investigated genomic alterations across five histology groups (adenocarcinoma, squamous, large cell, small cell lung cancer [SCLC], neuroendocrine [NE] lung cancer). Notably, TP53 and LRP1B mutations were prevalent across all groups. LRP1B mutations correlated with higher tumor mutation burden, indicative of a favorable response to immunotherapy. Biallelic TP53 and RB1 inactivation was predominant in SCLC and NE lung tumors. The five histological groups exhibit distinct expression profiles, reflecting tumor intrinsic characteristics. Most immune gene signature scores were significantly lower in SCLC and NE tumors, aligned with that they are cold tumors with immune resistance, except CD56-centered NK and neuroendocrine gene signatures; (2) we analyzed patient treatment patterns and persistence by line of therapy. Among the 206 NSCLC patients with clinically actionable EGFR mutations, 143 received targeted therapy during their treatment courses (69.4%). Time to treatment discontinuation (TTD) was used as a surrogate clinical outcome endpoint. TTD was significantly longer when TKI was the first line treatment compared to later lines ($p = 0.01$), while the trend is opposite for ICI where TTD is significantly shorter in the 1st line setting ($p = 0.025$); (3) we highlight the unique potential of leveraging H&E imaging modality in such RWD. In summary, we successfully identified unique molecular signatures among various lung cancer histological groups, pinpointed distinct subpopulations within lung adenocarcinoma and squamous tumors linked to their immune phenotypes, and investigated the different patient treatment patterns and outcomes, facilitating personalized medicine. In the broader context of our work, we have developed a framework for harnessing various data modalities (clinical, multi-omics, imaging) within AbbVie's oncology RWD realm, enhancing the discovery and validation of new oncology targets and biomarkers.

#2552 Real-world analysis of biomarker testing and use of targeted therapies in metastatic non-small cell lung cancer (mNSCLC) in the United States (US).

M. J. Dennis[1], D. Abrahami[2], M. Vieira[2], D. Benjumea[3], M. Boyd[3], A. Shao[3], K. Duncan[2], J. Kelton[2], **S. P. Patel**[4];
[1]Dana-Farber Cancer Institute, Boston, MA, [2]Pfizer, Inc., New York, NY, [3]Genesis Research Group, Hoboken, NJ, [4]University of California - San Diego, San Diego, CA

Background: Between 1998 and 2022, over 40% of new oncology drugs approved by the US FDA were precision therapies. In nonsquamous mNSCLC, detecting biomarkers where targeted therapies exist (EGFR, ALK, ROS1, BRAF V600E variant, MET exon 14 skipping variant, RET and PD-L1) has become essential for adequate clinical care. This study investigated real-world use of these biomarker tests, their characteristics, and associated use of targeted therapies in mNSCLC patients in the US.
Methods: Adults ≥18 years old with stage IV mNSCLC from the nationwide Flatiron Health electronic health record-derived de identified database (01/2011 - 04/2023). The proportion of patients receiving biomarker tests, timing, characteristics, test type (single, multiple or next-generation sequencing), and proportion of patients receiving guideline recommended associated targeted therapies (i.e. actionable treatment) was assessed. Actionable treatment was defined in study years where at least one actionable therapy was FDA approved (biomarker, therapy, date: ALK, crizotinib, Aug 2011; BRAF V600E, dabrafenib+trametinib, Jul 2015; EGFR, afatinib, Jul 2013; MET exon 14 skipping, capmatinib, May 2020; PD-L1, pembrolizumab, Oct 2015; RET, pralsetinib, Sep 2020; ROS-1, crizotinib, Mar 2016).
Results: In 42,037 patients with mNSCLC, the proportion of patients receiving each test were: ALK: 71.6%, BRAF: 48.8%, EGFR: 74.9%, MET: 41.4%, PD-L1: 49.3%, RET: 42.3%, and ROS1: 54.2%. Median (Q1, Q3) time from mNSCLC diagnosis to first biomarker result was 21 (12, 37) days. Tissue was the most common sample type for biomarker testing, although sampling by blood has increased in recent years. Multiple testing methods were more common in ALK and PD-L1 (48.1% and 50.3%, respectively) and next generation sequencing was more common in the other biomarkers (BRAF: 77.7%, EGFR: 57.1%, MET: 74.1%, RET: 70.7%, ROS1: 54.0%). Testing rates increased from 2011 through 2023 for each biomarker, with the highest rates in 2023: ALK (87.7%), BRAF (85.2%), EGFR (88.7%), MET (85.7%), PDL1 (78.7%), RET (84.8%), and ROS1 (86.9%). Testing rates were similar when timing was restricted to a 1-year window from mNSCLC diagnosis. Receipt of actionable treatment varied by biomarker, in order of increasing frequency: RET+ (23.0%), MET+ (34.0%), BRAF+ (42.7%), PDL1+ (56.3%), ROS1+ (59.8%), EGFR+ (70.6%), and ALK+ (89.0%). Generally, across all biomarkers, receipt of actionable therapy increased in more recent years.
Conclusion: Current real-world biomarker testing rates and use of actionable treatments may reflect increased adoption of clinical guideline recommendations. Despite increased testing, use of actionable therapy remains low for certain biomarkers. Further improvements in the implementation of robust biomarker testing to use appropriate therapies are needed, which can lead to better patient outcomes.

#2553 Functional precision medicine as a valid tool in glioblastoma clinical practice.

N.-G. Her[1], A. Woehrer[2], G. Lee[1], S. Hyun[1], J. Ahn[1], J. Kang[1], R. Hwang[1], A. El-Heliebi[2], B. Prietl[2], S. Stanzer[2], T. R. Pieber[2], **D.-H. Nam**[1];
[1]Aimed Bio Inc., Seoul, Korea, Republic of, [2]Center for Biomarker Research in Medicine (CBmed), Graz, Austria

Background: Glioblastoma remains a formidable therapeutic challenge, necessitating innovative strategies such as functional precision medicine (FPM). FPM offers personalized treatment by utilizing high-throughput screening of 10-100 compounds on patient-derived tumor cells (PDCs), assessing both efficacy and relative sensitivity, with results reported to the molecular tumor board within 2 weeks. The focus of this study is the cross-laboratory validity of this approach in glioblastoma, an essential step towards confirming FPM's consistency and potential as a game-changing tool in personalized cancer treatment.
Methods: Patient-derived tumor cells from glioblastoma cases were cultured for 3-7 days followed by automated high-throughput screening. The drug library contained ~80 compounds, including specific numbers of cytotoxic and targeted drugs. Drug response curves informed the calculation of sensitivity scores, which were compared to the AimedBio reference library to identify potentially effective drug candidates for a given patient. Additionally, corresponding tumor tissues were analyzed through panel sequencing of 50 glioma-related genes.
Results: A total of >50 patients with glioblastoma were included, with subgroups from CBmed, Austria, and AimedBio, South Korea. PDC cultures were successful in over 90% of cases, and informative high-throughput drug screening results were obtained. Integration of drug response with genetic tumor profiles yielded testable treatment candidates. Additionally, transcontinental shipping and re-screening of PDCs yielded comparable results, affirming the robustness of the method.
Conclusion: This study establishes and validates high-throughput drug screening platforms specifically tailored for functional precision medicine, utilizing glioblastoma as a model. The findings reveal a high degree of validity in the drug screening results, reinforced by the excellent performance of both technical and biological replicates. Such success not only lays a solid foundation for further academic and pharmaceutical collaborations but also opens the path for regulatory approval, bringing the platforms one step closer to clinical implementation. Funding: K1 COMET Competence Centre CBmed, funded by the Federal Ministry of Transport, Innovation and Technology; the Federal Ministry of Science, Research and Economy, Land Steiermark (Dep. 12, Business and Innovation), the Styrian Business Promotion Agency (SFG), and the Vienna Business Agency. COMET is executed by the Austrian Research Promotion Agency (FFG).

#2554 Development/validation of a molecular and clinical evidence-based algorithm for selecting optimal precision therapeutic strategy for cancer patients - continuous study.

Y. Sun, T. Meissner, R. Elsey, C. Hattum, C. Williams;
Avera Cancer Institute, Sioux Falls, SD

Background: The integration of genotyping and genomics in clinical practice has brought about significant advancements in precision oncology. However, a persistent challenge for treating oncologists lies in selecting the most effective patient-specific therapeutic strategy due to the molecular rationale, disease relevance, and patient-specific issues. To address this challenge, we have developed an algorithm that incorporates both molecular and clinical evidence-based criteria to rank therapeutic strategies in order to deliver optimal care and improve outcomes in patients with malignancy. The purpose of this part of our studies was to evaluate the effectiveness and accuracy of our novel algorithm.

Methods: History of present illness and comprehensive genomic profiling results of 306 patients with malignant tumors were reviewed by Avera Molecular Tumor Board (MTB) from June 2021 to February 2023. Therapeutic recommendations were provided with the Matching Score that we used in the I-PREDICT study based on molecular matching only as well as with the Ranking Score calculated by our novel algorithm with the criteria not only focusing on molecular matching, but also including disease relevance, patient-specific clinical considerations and treatment availability as weighting factors (Cohort 2). The other 50 patients with previously treated solid tumors reviewed by MTB (before 2018) and treatment recommendations provided with Matching Score only, were used as a control group (Cohort 1). The matching rates from recommendations and treatment outcomes of the patients were then assessed.

Results: In Cohort 1, of the 50 patients, 33 patients (66%) received matched therapeutic plans recommended by our MTB. The other 17 patients were not on a matched plan from the MTB. At 12 weeks, 12 patients (36.4% of 33 patients) remained progression free, including 8 patients (24.2%) who were progression free at 6 months. The other 21 patients (63.6% of 33 patients) could not be assessed due to treatment termination per drug toxicity or death before the follow-up time point. The median PFS/overall survival (OS) for patients with a Matching Score > 50% (N = 17) were 7.5/10.5 months, whereas with Matching Score ≤ 50% (N = 16) were 3/7.35 months. In Cohort2, of the 306 patients, 130 (42.5 %) patients have initiated matched therapeutic plans and follow-up is ongoing. Updated results will be presented at the meeting.

Conclusion: Our novel molecular and clinical evidence-based algorithm may be used to support oncologists' decision-making to utilize the most clinically appropriate and effective therapeutic options to benefit patients. Further validation studies and development of a user-friendly computational ranking platform based on the algorithm are planned in order.

#2555 Real-world data analysis of comprehensive genomic profiling using plasma samples from non-small cell lung cancer patients.

M. Morishita, K. Fujii, M. Ueki, H. Ikushima, H. Isago, K. Watanabe, K. Oda, H. Kage;
The University of Tokyo Hospital, Tokyo, Japan

Introduction: Comprehensive genomic profiling (CGP) tests which use plasma samples can detect driver mutations and are recommended when tissue samples are unavailable. Multiple studies have shown that plasma CGP tests can result in genomically matched treatment for cancer patients, especially in gastrointestinal cancer. However, data for non-small cell lung cancer (NSCLC) remain limited.
Methods: We searched the database of the Center for Cancer Genomics and Advanced Therapeutics (C-CAT), which comprised 99.7% of the CGP data under insurance coverage in Japan. NSCLC patients analyzed with FoundationOne Liquid CDx (F1LCDx) between August 1 2021 to July 31 2023 were included, all of whom were previously treated.
Result: 694 patients with NSCLC underwent liquid biopsy. Among them, 572 cases were adenocarcinoma, and 71 were squamous cell carcinoma. The median age was 68 years (range: 24-93), and 423 patients were male. Pathogenic or likely pathogenic *EGFR* mutations, *ALK* rearrangements, *ROS1* rearrangements, *MET* exon 14 skipping mutations, *BRAF* V600E, *RET* fusions, *ERBB2* mutations, and *KRAS* G12C were detected in 174 cases (25.1%), 18 cases (2.6%), 2 cases (0.3%), 9 cases (1.3%), 3 cases (0.4%), 7 cases (1.0%), 26 cases (3.7%) and 17 cases (2.4%), respectively. Among the 499 patients without known driver mutations, driver mutations were detected by F1LCDx in 60 patients (12.0%). The detection rate of each driver oncogene is shown in Table 1. Conversely, among the 174, 20, 9 and 3 patients with known *EGFR*, *ALK*, *ROS1*, or BRAF V600E alterations, F1LCDx showed false negative results in 48 (27.6%), 10(50.0%), 8 (88.9%), and 3 cases (100%) (*EGFR/BRAF* vs. *ALK/ROS1*, p = 0.001), respectively.
Conclusion: In patients without known driver oncogenes, mutations associated with approved therapeutic implications were detected in 12.0%. The detection of gene rearrangements using liquid biopsy may be limited compared with genetic mutations.

Genomic profiling detected by FoundationOne Liquid CDx

Cases (%)	EGFR, known	EGFR, unknown	ALK, known	ALK, unknown	ROS1, known	ROS1, unknown	BRAF V600E, known	BRAF V600E, unknown
Detected by F1LCDx	126 (72.4)	48 (9.2)	10 (50.0)	8 (1.2)	1 (11.1)	1 (0.15)	0	3 (0.43)
Undetected by F1LCDx	48 (27.6)	472 (90.8)	10 (50.0)	666 (98.8)	8 (88.9)	684 (99.9)	3 (100)	688 (99.6)
Total	174	520	20	674	9	685	3	691

#2556 Longitudinal analyses of clinical sequencing data provide novel insights into the evolutionary dynamics of lung adenocarcinoma.

B. Mastrogiacomo, E. G. Dunne, C. N. Fick, J. Nguyen, J. Hathwar, M. Lankadasari, Y. Liu, S.-R. Yang, J. Chang, W. K. Chatila, N. Schultz, D. R. Jones, F. Sanchez-Vega;
Memorial Sloan Kettering Cancer Center, New York, NY

Background: Tumor heterogeneity plays a crucial role in disease progression, metastasis and treatment response in lung adenocarcinoma (LUAD). Limited availability of multiple molecularly profiled samples from the same patients poses a challenge to validate models of tumor evolution using real-world data. We investigated genomic changes in a large cohort of patients with clinically directed DNA sequencing of multiple LUAD samples.
Methods: We analyzed longitudinal genomic data from 524 patients with at least two LUAD samples sequenced with MSK-IMPACT- a targeted panel that identifies somatic mutations, copy number alterations and gene fusions in 341-505 genes. Our analysis of 1084 tumors (634 primaries [P] and 450 metastases [M]) included 189 matched P-P pairs, 99 M-M pairs and 271 P-M pairs. Pairs were required to share an identical somatic mutation to confirm relatedness. Additional criteria included: excision of primary tumor prior to excision of the metastasis in P-M pairs collected over 90 days apart and collection of M-M pairs from the same anatomic site. Intra-pulmonary metastases were removed from P-P pairs.
Results: Tumor mutational burden was correlated in paired specimens from the same patient, irrespectively of P-P (R= 0.75, p<0.001; Spearman correlation), P-M (R=0.72, p<0.001) or M-M (R=0.6, p<0.001) status. Chromosomal instability, measured as the fraction of genome altered by copy number changes (FGA), was also correlated in P-P (R=0.69, p<0.001) and M-M (R=0.57, p<0.001) pairs, but tended to increase in metastases with respect to matched primaries (median 0.58 vs. 0.72, p<0.001; Wilcoxon test). In M-M pairs, changes in FGA differed by anatomic site. Liver pairs had the strongest correlation (n=17 pairs, R=0.86, p <0.01), whereas brain pairs had the weakest (n=35 pairs, R=0.085, p=0.71). Most somatic mutations were shared between paired samples (P-P: 639/1055, 60%, P-M: 1563/2877, 54%, M-M: 550/958, 57%), including those in LUAD drivers- *TP53*, *KRAS*, and *EGFR*. Conversely, most oncogenic copy number alterations - including *CDKN2A* deletions and *MET* amplifications - were private to one specimen (P-P: 183/276, 66%, P-M: 880/1148, 76%, M-M: 430/601, 71%), most often in the later sample (P-P: 113/183, 61%, P-M: 636/880, 72%, M-M: 212/430, 49%). Clinically targetable alterations (OncoKB Level 1) tended to be shared by tumor pairs from the same patient (93% shared vs. 6% private in P-P, p<0.01; 85% vs. 14% in P-M, p<0.01; 78% vs. 21% in M-M, p <0.01).
Conclusions: In LUAD, metastatic specimens exhibit increased chromosomal instability in relation to their matched primaries. This translates into unique copy number alterations detected only in the metastasis. By contrast, driver mutations - which account for most of the clinically targetable alterations with currently approved FDA drugs - are more often shared between paired samples from the same patient.

#2558 Molecularly matched targeted therapies benefit high risk pediatric cancer patients.

A. Tao, J. Pavisic, J. A. Oberg;
Vagelos College of Physicians and Surgeons, Columbia University, New York, NY

Introduction: Genomic technologies have the potential to transform the paradigm for diagnosing and treating children with cancer. Although druggable alterations are identified in a large fraction of pediatric cancer patients, the extent to which point-of-care genomic testing directly impacts therapeutic outcomes of individual patients in real-world settings is less well-known. A review of patients sequenced through the Precision in Pediatric Sequencing (PIPseq) program at Columbia University Irving Medical Center (CUIMC) was conducted to describe outcomes of patients treated with a molecularly matched targeted therapy (MTT).
Methods: Matched tumor-normal whole exome and tumor transcriptome sequencing was conducted in a CLIA-certified laboratory at CUIMC between January 2013 and March 2023 on samples from 373 high risk pediatric cancer patients including those with <50% survival, rare cancers lacking standard therapies, and relapsed/refractory disease. All cases were reviewed at a multi-disciplinary molecular tumor board and reports were transmitted to the electronic health record (EHR). EHR data were reviewed to identify patients who received a MTT. Tumor-specific response and progression-free survival (PFS) among the MTT cohort were investigated. Clinical benefit was further assessed using the Growth Modulation Index (GMI) whereby patients served as their own control. GMI is the ratio of PFS on the MTT therapy to the PFS on the most recent prior therapy. A ratio of >/=1.3 indicates meaningful clinical activity.
Results: Thirty pediatric patients (solid tumors, n=5; CNS tumors, n=15; hematologic malignancies, n=10) received a MTT. Median age at sequencing was 11 years, range 10 months-23 years. Median time to MTT from sequencing was 4.5 months, range 7 days to 19.2 months. Best overall response included 7 complete responses (23%), 6 partial responses (20%), 5 with stable disease (17%), 10 with progressive disease (33%), and 2 indeterminate due to early death or lack of follow-up during therapy (7%). GMI was calculated for 19/30 patients (63%); median GMI=1.1. 11 patients were excluded due to lack of prior therapy, early death, insufficient follow-up, or lack of progression between prior and targeted therapies. GMI ratios indicated clinical benefit from MTT for 12/19 patients (63%), median GMI=1.5.
Conclusions: Clinical comprehensive molecular profiling for pediatric patients with high risk cancers identified patients who are candidates for MTT. Overall, MTT led to stable disease, partial or complete response, for 60% of patients. Utilizing GMI ratios as an indicator of clinical benefit for select patients provided additional information beyond traditional endpoints. Twelve patients with GMI >/=1.3 experienced improved PFS compared to their most recent prior therapy. These results demonstrate real-world clinical benefit from MTT, supporting molecular profiling of pediatric high risk tumors.

#2559 Genotype-phenotype associations in von hippel-lindau syndrome: Implications for screening.

N. Murray, C. Leavitt, N. Shepard, Z. Gonzales, J. Li, B. O'Neil, C. Dechet, B. Schmidt, B. L. Maughan, K. Pauley, A. Naumer, W. Kohlmann, **A. Sanchez**; University of Utah Huntsman Cancer Institute, Salt Lake City, UT

Introduction and Objectives: Von Hippel-Lindau (VHL) is an autosomal dominant genetic disease. The type of *VHL* alteration has been shown to impact downstream VHL expression and clinical phenotype. However, current screening practices do not differ based on VHL genetic subtype. We aim to define the genotype-phenotype association among an institutional cohort of VHL patients.

Methods: We conducted a retrospective cohort study of 69 patients (27 families) with von Hippel-Lindau at the Huntsman Cancer Institute from 1998-2023. 55% (38/69) patients have documented VHL variants for review. We evaluated the association of VHL type with risk of pheochromocytoma (Pheo), renal cancer (RCC), and hemangioblastoma (HB). *t* test and Fisher's exact test were used to assess differences in clinicopathologic characteristics by VHL Type. P-value < 0.05 was considered significant.

Results: We identified 24 unique *VHL* alterations among 38 patients. 66% (25/38) of patients had missense mutations, 10% (4/38) nonsense mutations, 21% (8/38) splice mutations, and 3% (1/38) deletion/duplication (Table 1). The median age at VHL diagnosis was 31 years old (range 4-76). VHL Type 2 was more common, 87% (33/38). All VHL Type 1 patients (5/5) developed RCC and HB. No patients with VHL Type 1 developed PheoPara. Of the VHL Type 2 patients, 39% (13/33) have not developed any VHL-associated clinical manifestations. Of the 33 patients diagnosed with VHL Type 2, 18% (6/33) were diagnosed with PheoPara, 30% (10/33) with RCC, and 48% (16/33) with HB.

Conclusion: VHL type 2 comprised the majority of VHL diagnoses in our cohort with a notable absence of PheoPara phenotype. VHL Type 1 had higher penetrance and a higher prevalence for RCC and hemangioblastoma. With validation in larger cohorts, this cohort supports utilizing VHL genetic subtypes to personalize surveillance. Additional VHL testing for the remainder of the cohort is ongoing.

Clinicopathologic characteristics of von Hippel-Lindau Syndrome cohort with known genetic mutations

	All (n=38)	Type 1 (n=5)	Type 2 (n=33)	p-value
AgeMean (Median)	33.1 (31)	42 (28)	31.7 (31)	0.38
White, n (%)	92% (n=35)	5 (100%)	30 (91%)	1
Hispanic, n (%)	8% (n=3)	-	3 (9%)	1
VHL alteration, n (%)				-
Missense	25 (66%)	-	25 (76%)	
Nonsense	4 (10%)	4 (80%)	-	
Splice site	8 (21%)	-	8 (24%)	
Deletion/Duplication	1 (3%)	1 (20%)	-	
Penetrance, n (%)	25 (66%)	5 (100%)	20 (61%)	0.14
Phenotype, n (%)				
PheoPara	6 (16%)	-	6 (18%)	0.57
RCC	15 (39%)	5 (100%)	10 (30%)	0.006
Hemangioblastoma	21 (55%)	5 (100%)	16 (48%)	0.26

#2560 Genomic biomarkers of survival in patients (pts) with metastatic castrate-sensitive prostate cancer (mCSPC) undergoing androgen deprivation therapy (ADT) intensification (ADTi).

A. Narang, G. Gebrael, C. Hage Chehade, N. Sayegh, Y. Jo, B. Chigarira, N. Tripathi, A. Srivastava, C. Tandar, B. L. Maughan, U. Swami, N. Agarwal; Huntsman Cancer Institute, University of Utah, Salt Lake City, UT

Background: ADTi with androgen receptor pathway inhibitors (ARPI) with or without docetaxel improves survival outcomes in pts with mCSPC. Even with ADTi, 20% of these pts progress within a year and experience poor overall survival (OS). Identifying baseline genomic biomarkers predicting poor survival outcomes in pts receiving ADTi remains an unmet need.

Methods: In this IRB-approved retrospective study, pts with a new diagnosis of mCSPC who underwent comprehensive genomic profiling of primary prostate tissue or metastatic site or cell-free DNA and treated with ADTi (ADT with ARPI or docetaxel) were included. Genomic alterations with an incidence > 5% were included in the analysis. Study endpoints: progression-free survival (PFS) was defined from the start of therapy for mCSPC to progression (per PCWG-2) or death from any cause. OS was defined from the start of therapy for mCSPC to the date of death from any cause or censored at the last follow-up. A multivariable analysis using the Cox proportional hazards model was used, adjusting for age at mCSPC diagnosis, disease volume (high vs. low), Gleason score (≥ 8 vs. < 8), Log_2PSA at baseline, and initial timing of metastasis (de novo vs. non de novo). A subgroup analysis by intensification treatment received (ARPI vs. docetaxel) was also performed. Missing baseline characteristics such as volume of disease, Gleason score, and Log_2PSA were multiply imputed on 50 chained equations using “mice” package in R. All the analyses were done using R version 4.3.1.

Results: A total of 289 pts were included in the study. The baseline characteristics of the cohort will be presented in the meeting. The alterations included in the analysis were *TP53* (31.8%), *TMPRSS2* (30.4%), *PTEN* (17%), *APC* (10.4%), *SPOP* (9%), *RB1* (6.2%), *BRCA2* (5.2%), and *CDK12* (5.2%). In the multivariable analysis, *TP53* (HR 1.87, 95% CI 1.29-2.72, p = 0.001), *RB1* (HR 2.56, 95% CI 1.45-4.53, p = 0.001), *PTEN* (HR 1.77, 95% CI 1.15-2.72, p = 0.009), and *BRCA2* (HR 2.68, 95% CI 1.47-4.89, p = 0.002) were associated with significantly shorter PFS while *TP53* (HR 1.78, 95% CI 1.1-2.88, p = 0.019), *RB1* (HR 4.78, 95% CI 2.53-9.02, p < 0.001), and *PTEN* (HR 2.37, 95% CI 1.37-4.1, p = 0.003) were associated with significantly worse OS. Results of the subgroup analysis by intensification treatment (ARPI vs. docetaxel) will also be presented in the meeting.

Conclusions: In this real-world study, we identified genomic biomarkers that could be associated with shorter PFS and OS in pts with mCSPC treated with ADTi. Upon external validation, these results may aid in developing a clinical-genomic risk stratification model, patient counseling, and treatment selection.

#2563 Understanding the new subgroup- Her 2 low breast cancer.

R. Kulkarni, M. A. Shahid, O. Hinojosa Castro, K. Patel, C.-H. Lin, C. Rose, V. Dabak;
Henry Ford Health System, Detroit, MI

Introduction: Outcomes have greatly improved for patients with HER2+ breast cancer. Recently, tumors with IHC 1+ or 2+/negative FISH have been classified as 'HER2-low'. The development of novel HER2 agents has shown clinical benefit in this subset of patients. Information on the clinical characteristics of these patients which could be prognostic, and which could impact therapeutic options is limited.
Methods: This was an IRB-approved study. Relevant patient demographics, disease characteristics, and treatment details of patients with metastatic breast cancer seen at our center from 2018 to 2021 were collected by chart review. All data analyses were performed using R version 4.3.1, and a p-value ≤ 0.05 was considered statistically significant.
Results: A total of 102 patients with metastatic breast cancer were included. Patients were divided as HER2+, HER-, HER2 low ER+ and HER2 low ER -. 66.6% of patients had HER2 low disease. Patients with HER2 low ER- disease were more likely to have tumors that were of higher grade (grade 3, 71.4%, p=0.003), higher mean Ki67 (60%, p<0.001), and of ductal histology (100%, p=0.006). There was a statistically significant difference in PFS among the four groups (p=0.001). Median survival was longer in patients with HER2 low ER+ compared to the HER2- group. (1.42 vs 0.58, p<0.001, Table 1). Amongst HER2 low ER+ patients, there was a significant PFS difference in those treated with CDK4/6 inhibitors compared to chemotherapy (2.83 vs. 0.67, p=0.009). We found no difference in PFS between patients who were HER2 1+ ER+ and HER2 2+ ER+. In multivariate analysis, there was no significant association of race, grade, menopausal status, Ki67, histologic subtype, and metastatic sites with PFS.
Conclusion: In this small single-center retrospective study, patients with metastatic HER2 low ER- breast cancer had higher-grade tumors. HER2 low ER+ patients had a better PFS compared to HER2- patients. This seems to suggest that the HER2 low group may have some inherent biologic differences. Larger studies are needed.

Table 1: PFS Summary

Group	Total number	Progression/Death	Median Survival
HER2-	13	13	0.58
HER2 low ER-	14	11	0.88
HER2 low ER+	54	32	2.42
HER2+	20	12	1.08

#2564 Circulating monocytes decrease significantly following disease-directed therapy and may reflect disease expansion in Langerhans cell histiocytosis.

H. Ali, S. Reynolds, S. Wilcox, N. Chipalkatti, A. Ahmed;
University of Michigan, Ann Arbor, MI

Introduction: Langerhans Cell Histiocytosis (LCH) is a rare disorder characterized by clonal hematopoietic cell expansion forming eosinophilic granulomas. Treatment approaches vary based on disease severity. Despite established therapies, assessing treatment response, particularly regarding peripheral blood monocytes, lacks comprehensive markers.

Methods: We studied 76 LCH patients, collecting data on demographics, diagnostic methods, and treatment responses. Peripheral blood absolute monocyte counts were analyzed at key time points, including disease onset, progression, and post-therapy reinstatement, using statistical tests for comparison.

Results: Analyzing data from 76 patients (average age: 38), we found diverse disease presentations, with common imaging modalities being CT (37), PET (29), and MRI (22). Complete responses were observed in 17 of 49 patients, with 11 undergoing local therapy. Conversely, 5 patients with pulmonary LCH and chronic tobacco use showed persistent progression. Notably, peripheral blood monocyte counts did not differ between initial and latest assessments, but on disease progression, the mean count (0.94 K/μL) significantly exceeded that following therapy reinstatement (0.31, p=0.000794).

Results: Analyzing data from 76 patients (average age: 38), we found diverse disease presentations, with common imaging modalities being CT (37), PET (29), and MRI (22). Complete responses were observed in 17 of 49 patients, with 11 undergoing local therapy. Conversely, 5 patients with pulmonary LCH and chronic tobacco use showed persistent progression. Notably, peripheral blood monocyte counts did not differ between initial and latest assessments, but on disease progression, the mean count (0.94 K/μL) significantly exceeded that following therapy reinstatement (0.31, p=0.000794).

Discussion: LCH is proposed to result from dysregulated hematopoiesis, leading to sequential somatic mutations during monocyte differentiation leading to clonal expansion of CD1A and CD207+ histiocytes. Our finding of increased monocyte count during disease progression may suggest elevated circulating LCH or heightened monocyte production for subsequent differentiation, potentially contributing to MHC Class 1 upregulation. This phenomena mirrors published findings from our own group in patients with Rosai Dorfman and Erdheim Chester Disease. To further elucidate the molecular underpinnings of LCH and explore the etiology of this monocyte trend, genetic sequencing analysis is in progress. Ultimately, monitoring peripheral blood monocyte dynamics could offer valuable insights into LCH progression and treatment response.

#2565 Vitamin D deficiency and outcomes in prostate cancer patients: A real-world database.

L. L. Hart[1], J. Reeves[2], S. Garofalo[2], W. Amick[3];

[1]Atrium Health-Wake Forest Baptist Comprehensive Cancer Ctr., Fort Myers, FL, [2]Florida Cancer Specialists, Fort Myers, FL, [3]Immunonutrition, Inc, Miami, FL

Introduction: Vitamin D is essential for many bodily functions, including bone health and the prevention of osteoporosis and rickets. In recent years, the importance of vitamin D metabolism in immune system regulation and cancer prevention has been studied with increased focus. With the advent of cancer immunotherapies this has become more important. Multiple recent publications document that vitamin D deficiency is prevalent in cancer patients. This has also been observed specifically in prostate cancer patients, with a high percentage of these deficient patients being of African- American ancestry. It has been theorized that high levels of vitamin D deficiency among African American prostate cancer patients could contribute to worse cancer outcomes and increased health disparities. However, routine vitamin D testing has not been commonly performed in the oncologic community. We hypothesized that deficient levels of vitamin D could lead to inferior prostate cancer outcomes in men with a wide range of ethnic and socio-economic backgrounds. In this project we recorded vitamin D levels in prostate cancer patients at a large community oncology group and evaluated them by stage, pathologic data, survival, race/ethnicity, and other clinical features.

Methods: This study is a retrospective, observational study of the data from the electronic medical records of patients with prostate cancer who received vitamin D level testing at Florida Cancer Specialists & Research Institute from 2008- 2023, throughout the state of Florida. All data used in this study will constitute secondary data, it will have been collected originally for clinical use in the general oncology practice setting. No date parameters or patient limits will be applied to this study, and all eligible patients are included.

Results: 451 patients with prostate cancer had determination of vitamin D levels, out of a total of 27,772 prostate cancer patients in the database. 38% of the prostate cancer patients analyzed had low 25-OH vitamin D levels (<32 ng/ml). Patients with low vitamin D levels had an average Gleason score of 7.46. Patients with low vitamin D levels who died had an average survival of 144 months. Patients with low vitamin D levels who presented with localized disease had a 35% chance of eventually developing castrate-resistant disease. 45% of the low vitamin D group developed metastatic disease during their course of treatment. Further comparisons of vitamin D levels with pathologic data, survival/longevity, race/ethnicity, and clinical course will be evaluated and presented.

#2566 Molecular characteristic profile in early colorectal cancer with V600E and non-V600E BRAF mutations.

Z. Quan An;
Xiangtan Central Hospital, Xiangtan, China

Background: The BRAF V600E mutation in colorectal cancer (CRC) is a significant indicator of poor prognosis, especially in tumors exhibiting microsatellite instability (MSI). It is more common on the right side of the colon but can occur anywhere within the colon. Although other BRAF mutations existed, current research primarily focused on BRAF V600E. Most clinical data sets were centered on advanced colorectal cancer. There was limited understanding of the molecular characteristics of early-stage colorectal cancer patients with BRAF mutations, which impacted postoperative prognosis management, including refining adjuvant therapy regimens. Therefore, we analyzed the molecular characteristics of early-stage CRC surgical patients.
Methods: Tumor tissue from 767 early-stage CRC patients diagnosed between 2021 to 2022 in China were analyzed using NGS (panel on 733 gene) to validate the mutation characteristics. Tumor specimens were tested for the BRAF mutation and MSI status.
Result: Among 767 early CRC cases tested, BRAF mutations accounted for 6.52% (50/767), with 62% (31/50) being BRAF V600E, followed by 14% (7/50) for BRAF D594G. Notably, there were two cases of fusion variations, TRIM24-BRAF, and one case of BRAF copy gain. Among the BRAF mutation population, 11 cases were MSI-H, with 8 of them being BRAF V600E/MSI-H. Only one MSH-H patient had a germline mutation in the MLH1 gene, with a concurrent mutation in BRAF K601T.Interestingly, when comparing the mutation profiles of the BRAF V600E population with those of the non-V600E BRAF mutation population, we found distinct co-mutated genes despite both being BRAF mutations. In the BRAF V600E group, the top three frequently mutated genes were TP53 (52%), RNF43 (32%), and SMAD4 (32%). Additionally, the BRAF V600E/MSI-H subgroup presented a distinct
mutation profile, with minimal occurrences of TP53 and SMAD4 mutations. In the non-V600E BRAF mutation group, the top three frequently mutated genes were TP53 (84%), APC (63%), and KRAS (32%).
Conclusions: In examining the mutation profile characteristics of early colorectal cancer with BRAF mutations, the proportion of BRAF V600E/MSI-H appeared to have been lower than that reported in advanced cases. Furthermore, in terms of the frequency of co-mutated genes, it seemed that BRAF V600E had exhibited a higher malignant driving mutation effect as a single gene, while non-V600E mutations had required more cooperative tumor suppressor genes or oncogenes. Analyzing the molecular characteristics of early colorectal cancer patients with V600E and non-V600E BRAF mutations could help improve postoperative management and further our understanding of tumor progression.

#2567 An analysis of proviral insertion site of Moloney murine leukemia virus, PIM1, kinase expression and clinical outcomes in renal cell carcinoma.

S. L. Holder[1], G. Lagos[1], B. A. Carneiro[1], A. Mega[1], A. De Souza[1], R. R. McKay[2], A. Elliott[3], C. Nabhan[3], S. L. Graff[1];
[1]Legorreta Cancer Center and Warren Alpert Medical School at Brown University, Providence, RI, [2]Moores Cancer Center - UC San Diego Health, La Jolla, CA, [3]Caris Life Sciences, Irving, TX

Background: Wild-type Proviral Insertion Site of Moloney Murine Leukemia Virus 1 Kinase (PIM1) is a constitutively active serine/threonine kinase that inhibits apoptosis and promotes cell cycle progression, proliferation, angiogenesis, invasion, and migration. Due to constitutive activation, PIM1 is regulated at transcription and degradation. We have previously shown PIM1 protein levels are elevated in clear cell renal cell carcinoma (ccRCC) compared to normal kidney and that PIM1 inhibition induces tumor regression in pre-clinical models. Current approved therapies for ccRCC do not inhibit PIM1. We hypothesized that high PIM1 expression will adversely affect clinical outcomes in ccRCC.
Methods: Whole transcriptome sequencing (WTS) data in the Caris Life Sciences database were examined for PIM1expression and overall survival (OS; defined as time from diagnosis to last contact or death). We assessed PIM1 in primary and metastatic ccRCC, and the impact on survival in ccRCC and papillary RCC. Differentially expressed genes (DEGs) associated with high PIM1 were also determined.
Results: PIM1, in the highest quintile, was associated with a shorter OS (869 vs 1738 days; HR 2.629; CI 1.495 - 4.611; p<0.001; N=147) in ccRCC. PIM1 is enriched in metastatic (median 7.62 transcripts per million (TPM), CI 6.35 - 9.26) vs primary (median 5.07 TPM; CI 4.28 - 6.45; p=0.0025) RCC. Upregulated DEGs associated with high PIM1 are involved in the extracellular matrix. IL-6 expression, known to correlate with worse outcomes, was 6.5-fold higher in PIM1 high vs PIM1 low (13.2 vs 2.1 TPM, p<0.0001) RCC. High PIM1 was associated with poor survival following checkpoint inhibition (HR 3.714, 95% CI 1.339 - 10.303, p=0.007) and a trend towards poorer survival following mTOR inhibition and VEGF inhibition. PIM1 did not affect survival in papillary RCC.
Conclusions: Real-word data show that high PIM1 correlates with poorer survival in ccRCC but not in papillary RCC. This effect likely persists independent of treatment received. PIM1 enrichment in metastatic ccRCC, and associated DEGs, suggest that PIM1 influences the extracellular matrix to promote metastases. The correlation between IL-6expression and PIM1 supports our prior data that an IL-6/JAK/STAT/PIM1 pathway is involved in ccRCC.

#2568 High infiltration of neurons was associated with lower cell proliferation and less immune response but not with response to treatments or survival in estrogen receptor-positive breast cancer.

K. Chida[1], M. Oshi[2], A. M. Roy[1], J. Arima[1], P. Sharma[1], I. Endo[2], K. Hakamada[3], K. Takabe[1];
[1]Roswell Park Comprehensive Cancer Center, Buffalo, NY, [2]Yokohama City University Graduate School of Medicine, Yokohama, Japan, [3]Hirosaki University Graduate School of Medicine, Hirosaki, Japan

Introduction: Psychological stress aggravates cancer cell biology which leads to cancer progression and metastasis through its influence on the sympathetic nervous system. Recently, infiltration of a local anesthetic lidocaine around a tumor prior to its removal was reported to lead to better survival in early-stage breast cancer (BC). Therefore, we hypothesized that neuron infiltration within the bulk tumor of BC could be associated with cancer aggressiveness and worse survival.
Methods: A total of 5755 BC patients from five independent cohorts, including METABRIC (*n*=1903), SCAN-B (*n*=3273), GSE25066 (*n*=508), and ISPY2 (GSE173839; *n*=105), which have both clinical and transcriptomic data, were included in the study. The fraction of neuron infiltration was calculated using the xCell algorithm.
Results: High neuron infiltration in BC was not associated with survival in either the METABRIC or SCAN-B cohorts. BC with high neuron infiltration had high expressions of neurotransmitter receptors: adrenergic receptor α1B and 2A, dopamine receptor D2, muscarinic acetylcholine receptor M3 and M4, and TAC1, which encodes TACR1, the receptor for substance P, but had lower expression of adrenergic receptor β2 and cholinergic acetylcholine receptor 1 and 10. Further, levels of neuron infiltration were highest in estrogen receptor-positive/HER2-negative (ER+/HER2-) among the subtypes and lower in tumors with lymph node metastasis, but was not associated with tumor size. Neuron infiltration was associated with higher AJCC staging in METABRIC, which was not validated in SCAN-B cohort. High neuron infiltration in BC was associated with reduced homologous recombination defects, mutation rate, and SNV neoantigen, and with less cell proliferation, evidenced by lower Nottingham histological grade and Ki67 gene expression, as well as less enrichment of Hallmark cell proliferation-related gene sets: E2F targets, G2M checkpoint, and Mitotic spindle. Despite its association with less cell proliferation, BC with high neuron infiltration was not associated with pathological complete response (pCR) in the GSE25066 cohort. High neuron infiltration in BC was associated with higher infiltration of lymph endovascular cells as well as less immune cell infiltration; CD8, CD4 memory, T-helper 1 and 2, dendritic cells, M1 and M2 macrophages, regulatory T cells, and B cells, lower cytolytic activity, and immune response; interferon-alpha and interferon-gamma and IL2 stat signaling. Despite this association, BC with high neuron infiltration was not associated with pCR after immunotherapy in the ISPY2 clinical trial cohort.
Conclusion: BC with high infiltration of neurons was associated with lower cell proliferation and less immune response but not with response to systemic therapies or patient survival in ER+/HER2- subtype.

#2569 VEGFA gene expression is associated with cell proliferation, less immune cell infiltration, and worse survival, but better response to chemotherapy and immunotherapy.

P. Sharma[1], K. Chida[1], K. Hakamada[2], K. Takabe[1];

[1]Roswell Park Comprehensive Cancer Center, Buffalo, NY, [2]Hirosaki University Graduate School of Medicine, Hirosaki, Japan

Introduction: Vascular endothelial growth factor-A (VEGFA) is a well-known factor that induces angiogenesis, one of the hallmarks of cancer, which generates new blood vessels in the tumor microenvironment (TME) and provides conduit for cancer to metastasize. Interestingly, an anti-VEGFA drug (Avastin) failed to show benefit in clinical trials for breast cancer (BC). In this study we investigated the clinical relevance of VEGFA gene expression in BC. **Methods:** A total of 7336 BC patients from eight independent cohorts, TCGA (n= 1073), METABRIC (n= 1903), SCAN-B (GSE96058, n= 3069), GSE20194 (n=278), GSE34138 (n=178), GSE163882 (n=222), GSE25066 (n=508), and ISPY2 (GSE173839, n= 105) were analyzed. These cohorts were divided into high and low VEGFA gene expression groups using the median. **Results:** High VEGFA expression in BC was associated with worse overall survival in SCAN-B cohort which was validated in METABRIC cohort with overall, disease-specific, and disease-free survival (all $p<0.02$). VEGFA expression was higher in Triple Negative BC (TNBC) but was lower in BC with lymph node metastasis. High VEGFA BC was associated with significantly high intratumoral heterogeneity, homologous recombination defect, silent and non-silent mutations, and SNV neoantigens in TCGA, and was also associated with higher cell proliferation, evidenced by higher Nottingham histological grade, higher Ki67 gene expression, and enrichment of all the Hallmark cell proliferation-related gene sets: Mitotic spindle, G2M Checkpoint, E2F Targets, MYC Targets v1 and v2, and mTorC1 signaling, consistently, in SCAN-B, METABRIC, and TCGA cohorts. Reflecting its enhanced growth, high VEGFA expression was associated with less infiltration of fibroblasts and adipocytes (all $p<0.05$). Surprisingly, VEGFA expression did not enrich angiogenesis gene set in any of the cohorts, nor was related with infiltrations of blood or lymphatic vascular endothelial cells, besides pericytes. But high VEGFA BC was associated with significantly less infiltrations of anti-cancer immune cells; CD8, CD4, and dendritic cells were all significantly less, and T helper type 1 cells and regulatory T cells were significantly higher consistently in SCAN-B, METABRIC, and TCGA cohorts. VEGFA expression was significantly higher in BC that achieved pathological complete response after Anthracycline and Taxane based neoadjuvant therapy in both ER+/HER2- and TNBC subtypes in the GSE25066 cohort, and after immunotherapy in ER+/HER2- subtype, but not TNBC, in the ISPY2 clinical trial cohort. This was not validated in GSE20194, GSE34138, GSE163882 cohorts. **Conclusion:** Our research indicates that high VEGFA BC is associated with high cell proliferation, less immune cell infiltration, and worse survival, but better response to Anthracycline and Taxane based chemotherapy, and immunotherapy.

#2570 Gastric cancer with high neuron infiltration was associated with enhanced epithelial-to-mesenchymal transition, angiogenesis and poor clinical outcomes.

K. Chida[1], M. Oshi[2], A. M. Roy[1], J. Arima[1], P. Sharma[1], G. K. Mann[1], I. Endo[2], K. Hakamada[3], K. Takabe[1];
[1]Roswell Park Comprehensive Cancer Center, Buffalo, NY, [2]Yokohama City University Graduate School of Medicine, Yokohama, Japan, [3]Hirosaki University Graduate School of Medicine, Hirosaki, Japan

Introduction: Neurons within the tumor microenvironment of gastric cancer (GC), as identified through immunohistochemistry, have been reported to be associated with worse overall survival (OS) of GC patients. However, histology-based analyses have limitations in quantifying nerve cells and investigating the underlying biology. Thus, we aim to study the clinical significance of intratumoral nerve cells in GC using computational deconvolution of transcriptomes from bulk tumors.
Methods: Total of 807 GC patients from two independent cohorts (TCGA; n = 375, GSE84437; n = 432) were included, encompassing both clinical and transcriptomic profiles. The neuron infiltration fraction was determined using the xCell algorithm.
Results: GC with high neuron infiltration was associated with high expressions of neurotransmitter receptors; beta-adrenaline, dopamine, muscarinic acetylcholine, and neurokinin receptors in TCGA cohort (all $p < 0.02$). It was associated with reduced mutation rate and increased intratumoral heterogeneity (all $p \leq 0.002$), as well as less immune response; interferon-alpha and interferon-gamma, and with low infiltration of immune cells; CD4 memory, T-helper 1, M1 and M2 macrophages, and NK cells (all $p \leq 0.02$). Further, neuron highly infiltrated GC enriched Epithelial-to-Mesenchymal Transition and Angiogenesis gene sets and had higher lymphatic and microvessel endothelial cells and pericyte infiltrations (all $p \leq 0.001$). Conversely, GC with high neuron infiltration showed an inverse relationship with cell proliferation-related gene sets; E2F Targets, G2M Checkpoint, and MYC Targets v1 and v2, and had lower Ki67 gene expression (FDR < 0.25 and $p < 0.001$, respectively). High neuron infiltration in GC was associated with worse patient OS in TCGA cohort, which was validated in GSE84437 cohort (both $p < 0.05$). It was an independent prognostic factor of OS in both univariate and multivariate Cox-regression analysis in the TCGA cohort (hazard ratio [HR]: 1.46; 95% confidence interval [CI]: 1.01 to 2.12; $p = 0.045$ and [HR]:1.54; 95% CI: 1.05 to 2.26; $p = 0.026$).
Conclusion: Our research indicates that high infiltration of neurons in GC correlates with high expressions of neurotransmitter receptors, high intratumoral heterogeneity, less immune response and immune cell infiltrations, and less cell proliferation. It enriched EMT and angiogenesis which may explain its association with worse patient survival.

CLINICAL RESEARCH: Translational Research: Imaging and Radiomics
Poster Session

#2574 The effect of epidermal growth factor expression in detecting oropharyngeal tumors during fluorescence-guided robotic surgery.
L. Stone, S. M. Rao, M. L. Gonzalez, D. Lin, H. Jeyarajan, C. M. Thomas, J. Warram;
University of Alabama at Birmingham, Birmingham, AL

Intro: Oropharyngeal squamous cell carcinoma (OPSCC) has been shown to overexpress epidermal growth factor receptor (EGFR), making it a targetable biomarker for fluorescently labeled monoclonal antibodies such as panitumumab-IRDye800, which can be used during fluorescence-guided trans oral robotic surgery (TORS). Although antibody-based fluorescence-guided surgery is being evaluated in several late-stage trials, the use of intraoperative fluorescence imaging for TORS has not been thoroughly explored. We observed that the bi-polar cautery tool[AHM(1] of the TORS robot was auto-florescent and would appear dimmer in the presence of fluorescence from surgically exposed tumor. We aim to characterize the florescence contrast of the tool and tumor to create a rapid qualitative assessment on tumor presence.
Methods: During a phase 2 clinical trial evaluating panitmumab-IRDye800 fluorescence-guided TORS of OPSCC, consenting patients (n=12) with biopsy-confirmed OPSCC received 50mg panitumumab-IRDye800 48 hours prior to surgery. Intraoperative fluorescence images were acquired using the onboard fluorescence camera of the Da Vinci Xi robot and post-operation fluorescence exams were conducted by the Pearl and Odyssey Systems (Li-Cor)[BK2] . For each patient, 3 intraoperative views (pre, mid and late resection) showing pathology-confirmed tumor, normal mucosa, and the tool were taken, and several frames from each view were analyzed via ImageJ to calculate mean fluorescence intensity (MFI) in regions of interest. The MFI of tumor and normal muscoa was normalized with MFI of the tool to obtain a standard fluorescence ratio (SFR) per patient[BK3] . A paired t-test was used to compare differences in MFI between the tumor and tool or normal mucosa.
Results: The MFI for each time point was graphed for the tool, tumor and normal mucosa. Significant differences were found between tumor and mucosa and tumor and tool for every time point. Tumor/tool SFRs per patient ranged from 2.1 to 60.9, while normal/tool SFRs ranged from 0.4 to 3.1. Receiver operator characteristics curve analyses of tissue-to-tool SFR data showed a sensitivity of 90.9% and a specificity of 96% to identify the presence of tumor.
Conclusion: The auto-fluorescent properties of the bipolar cautery tool of the Da Vinci Xi robot can be used for qualitative assessments of tumor presence during fluorescence-guided TORS. Bright fluorescence from the tool relative to surrounding tissue suggests the lack of carcinoma presence, which could confirm the surgeon's complete resection of OPSCC.

#2575 GD2 targeted dual-labeled intraoperative molecular imaging probe for neuroblastoma.

R. E. Sever[1], L. T. Rosenblum[2], **K. C. Stanley**[2], D. M. Menendez[3], W. B. Edwards[3], M. M. Malek[2], G. Kohanbash[1];
[1]University of Pittsburgh, Pittsburgh, PA, [2]University of Pittsburgh School of Medicine, Pittsburgh, PA, [3]University of Missouri, Columbia, MO

Neuroblastoma (NB) is the most common pediatric extracranial solid tumor, with a 5-year survival rate under 50% for those with high-risk disease. Complete surgical resection is essential for these patients and is associated with improved outcomes. However, NB resection presents significant technical challenges due to encasement of vital structures that must be preserved, as well as remote deposits of disease. The current approach to find and safely resect tumor depends on the surgeon's eyes and hands alone. Fluorescence tracers allow enhanced tumor visualization, but most are not molecularly targeted which leads to poor tumor to background signal. Further, fluorescent signal does not penetrate more than a few millimeters, a limitation that can be overcome by inclusion of a radiotracer. We, therefore, generated and evaluated a dual radio and fluorescent antibody-based probe targeting the GD2 tumor antigen to improve the identification of NB with widely available intraoperative handheld instruments. We generated an intraoperative probe (^{111}In-αGD2-IRDye800CW) with retained affinity and stability. *In vivo*- Nu/j mice were injected with SK-N-BE(2) NB cells. After tumors grew for five weeks, mice were given tail vein injections of the probe. Gamma and optical biodistribution studies were performed to determine the specificity of binding and tumor to background signal four- and six-days post probe injection. Probe uptake was compared to an isotype. Gross dissections and surgeries aimed at improving completeness of resection were performed using a handheld fluorescent camera (SPY-PHI) and a gamma probe (Neoprobe). The handheld gamma probe detected xenografts with great sensitivity (average *in vivo* 818 cps of In^{111} in tumor region versus 34.8 cps in the tail). The fluorescent imaging showed high specific binding to the tumor region. Gamma biodistribution results indicated high accumulation within tumor (13.5 %ID/g) with lower accumulation in blood (3.49 %ID/g) and muscle (0.45 %ID/g). Uptake of the probe greatly exceeded isotype control antibody on days 4 and 6 post-agent injection, for both gamma and optical biodistributions. Initial tumor resection using ^{111}In-DTPA-aGD2-IRDye800CW in an NB bearing mouse identified residual disease left behind when resection was performed using white light alone; the residual disease was then removed, guided by fluorescence imaging. Our dual-labeled probe demonstrated antigen specificity and allowed for the sensitive detection and visualization of NB *in vivo* with widely available intraoperative tools. This targeted probe could provide a means to improve surgical NB resection, by enabling localization of the all regions of tumor using radio-guidance, followed by clear definition of tumor margins with fluorescent signal, to maximize preservation of vital tissues. Ultimately, we believe this approach can improve safety, extent of NB resection, and patient outcomes.

#2576 Radiomic features of intrathoracic lesions can predict the mixed response in non-small cell lung cancer treated with immunotherapy.

M. Yadav[1], J. Lee[2], **P. Kim**[3], M. J. A. Chuchuca[1], T. Um[1], L.-Y. Chung[1], Y. S. Velichko[1], Y. Chae[1];

[1]Feinberg School of Medicine, Northwestern University, Chicago, IL, [2]School of Medicine, Kyungpook National University, Daegu, Korea, Republic of, [3]The University of Texas at Austin, Austin, TX

Background: Although immunotherapy has emerged as a promising treatment for lung cancer, the decision to continue immunotherapy becomes challenging when mixed response (MR) occurs. This study is aimed to evaluate whether radiomic features from pre-treatment intrathoracic images can predict MR.
Methods: 127 consecutive patients with NSCLC who received first line systemic treatment containing immunotherapy were included in this study. Chest CT scans were obtained at baseline and 1-3 times from 11 different CT scanners and harmonization method was applied to minimize scanner-related bias. The durable response of intrathoracic lesions (n=266) at least 24 weeks was evaluated based on RECIST 1.1 and irRECIST. MR was defined as the simultaneous presence of at least one lesion that increased and decreased in a single patient during immunotherapy and two different criteria of MR for the change of tumor lesions were applied: Definition-A (MR-A), Δ [baseline - first follow-up] ≥ 5 mm; Definition-B (MR-B), any change of Δ [baseline - first follow-up]. All intrathoracic lesions were identified and segmented by four different physicians. Radiomic features, including morphological, intensity, GLCM, GLRLM, GLSZM, and NGTDM, were extracted using LIFEX software (IMIV/CEA, Orsay, France). Confusion matrix was used to assess tumor responses, and area under the curve (AUC) for intrathoracic lesions was calculated.
Results: Tumor responses based on irRECIST were CR (n=1, 0.8%), PR (n=33, 26.0%), SD (n=55, 43.3%), and PD (n=39, 30.7%). There were 10 cases (7.9%) of MR-A and 25 cases (19.7%) of MR-B. While the median progression-free survival (PFS) and overall survival (OS) in MR-A group were 22.9 (range, 0.5-50.6) and 23.5 (range, 1.1-42.2) months, those in MR-B group were 2.0 (range, 0.5-50.6) and 3.3 (range, 0.7-49.0) months respectively. While the overall sensitivity (SN) and specificity (SP) for MR-A in intrathoracic lesions were 0.55 and 0.87, those for MR-B were 0.52 and 0.71, respectively. The AUC for MR-A and MR-B were 0.71 and 0.62 respectively, and the AUC for durable response was 0.56. In the SD group, median PFS and OS were 3.3 (1.4-18.9) and 6.1 (4.8-26.2) in the MR-A group and 9.7 (0.7-18.9) and 23.9 (0.7-26.2) respectively in the MR-B group. Median PFS and OS were 18.2 (0.5-65.2) and 23.9 (0.9-55.3) respectively in the non-MR-A group and 18.2 (0.5-65.2) and 23.9 (0.9-55.3) respectively in the non-MR-B group. In the PD group, median PFS and OS were 23.5 (0.5-41.3) and 24.7 (1.1-42.2) respectively in the MR-A group and 5.1 (0.5-41.3) and 11.5 (1.1-49.0) respectively in the MR-B group. Median PFS and OS were 20.3 (0.7-71.4) and 37.1 (1.0-72.9) respectively in the non-MR-A group and 20.3 (0.7-71.4) and 37.1 (1.0-72.9) respectively in the non-MR-B group.
Conclusion: The radiomic features in NSCLC patients who received immunotherapy may help predict MR in NSCLC patients treated with immunotherapy.

#2577 Analyzing specific and nonspecific tissue uptake of antibodies by SPECT imaging and non-linear compartmental modeling.

N. Cho, P. Spinosa, D. Mandikian, G. Del Rosario, S.-F. Yu, J. Ho, G. Ferl, C. A. Boswell;
Genentech, South San Francisco, CA

Understanding the mechanisms driving specific target engagement versus off-target nonspecific cellular uptake of antibodies can help inform design and/or delivery strategies that maximize therapeutic indices. Receptor binding kinetics, rates of receptor-mediated internalization and nonspecific pinocytosis are often measured through *in vitro* cell culture models, but there have been fewer efforts to collectively measure these cellular parameters *in vivo*. Single photon emission computed tomography (SPECT) imaging is a powerful method of estimating these parameters by quantifying both free/bound (intact) and internalized/catabolized antibody using non-residualizing halogen labels and residualizing radiometal-chelates, respectively. Modeling longitudinal *in vivo* imaging data of non-residualizing antibody can inform receptor occupancy (RO), while residualizing tracer kinetics can provide additional insights into catabolism due to pinocytosis and receptor-mediated internalization in the intracellular spaces. Here, we describe SPECT imaging of tumor-targeting trastuzumab (anti-HER2) and non-targeting anti-glycoprotein D (anti-gD) antibody, each labeled with non-residualizing ([^{125}I]SIB) and residualizing radiometal-chelate (^{111}In-DOTA) radionuclides in HER2^{+} xenograft-bearing mice. A non-linear compartmental model was fitted to SPECT imaging data to characterize RO of 10 mg/kg of anti-HER2 out to 7 days post dosing as well as to estimate rate constants of pinocytosis and receptor-mediated internalization of anti-HER2 in tumor. Longitudinal SPECT imaging demonstrated statistically significant differences in tumor drug exposure between ^{125}I- and ^{111}In-labeled anti-HER2 relative to anti-gD ($p < 0.01$). Tracer kinetics of anti-HER2 and associated RO simulations in tumor showed rapid extravasation from blood to tumor with peak RO of 25% at 13 hours post administration followed by a reduction in RO, reaching ~10% by day 7. Simulations for free, bound and catabolized tracer kinetics from our fitted model showed that anti-HER2 in the tumor interstitium was primarily receptor-bound with minimal pinocytosis of unbound anti-HER2 as well as gradual receptor-mediated catabolism, reaching a peak concentration of 113 µg/mL 7 days post dosing. Rate constants of nonspecific pinocytosis and HER2-mediated receptor internalization were estimated to be 0.0145 and 0.036 hours^{-1}, respectively. Our model allowed us to successfully capture anti-HER2 antibody receptor binding and specific and nonspecific internalization over time *in vivo*. These data and analyses demonstrate the power of SPECT imaging using both non-residualizing and residualizing radiolabels combined with compartmental modeling to better characterize the different biological states (free, bound, and catabolized) of antibody within interstitial and intracellular compartments.

#2579 A nectin-4 PET radiotracer for pharmacodynamic evaluation of enfortumab vedotin (EV) therapy in urothelial carcinoma.

A. Mishra, A. K. Sharma, K. Gupta, B. A. Johnson III, D. J. McConkey, J. Hoffman-Censits, S. Nimmagadda;
Johns Hopkins University, Baltimore, MD

Introduction: Enfortumab vedotin (EV), an antibody-drug conjugate targeting nectin-4, offers hope for urothelial carcinoma patients (UC) but prolonged use leads to treatment-related toxicities often necessitating dose adjustments. How EV engages nectin-4 at the tumor and its relevance to efficacy is unknown. To understand the pharmacodynamics (target engagement) of EV at the tumor across FDA approved dosing levels, we developed a nectin-4 specific peptide-based radiotracer, [^{68}Ga]AJ647, for positron emission tomography (PET) imaging.

Methods: Six UC cell lines of luminal (HT-1376, UC-14, RT-112) and basal (UC-9, SCaBER, T24) morphological type were selected for in vitro and in vivo testing of [^{68}Ga]AJ647 and nectin-4 target engagement by EV. Cell uptake and competitive binding assays were conducted to test [^{68}Ga]AJ647 specificity for nectin-4 in the presence or absence of EV. Flow cytometry derived receptor density was used to correlate [^{68}Ga]AJ647 uptake in cells with nectin-4 expression. Pharmacokinetics, biodistribution and specificity of [^{68}Ga]AJ647 for nectin-4 expression was evaluated in six xenograft models by PET imaging and biodistribution studies. Target engagement by EV was quantified by measuring unoccupied nectin-4 levels by [^{68}Ga]AJ647-PET in HT-1376 xenografts at different doses (15, 9, and 6 mg/kg) and time (1, 3, and 6 days).

Results: [^{68}Ga]AJ647 was generated in 20-30% radiochemical yield with >95% purity. In vitro assays showed distinctive uptake in cell lines (HT-1376 > UC-14 > RT-112; UC-9 > SCaBER > T24) that correlated with nectin-4 density (R^2=0.85). PET and biodistribution studies showed tractable pharmacokinetics of [^{68}Ga]AJ647 enabling high contrast images in 60 min and exhibiting nectin-4 dependent uptake in all the six xenografts. Uptake of [^{68}Ga]AJ647 in UC cells reduced in a dose dependent manner in the presence of EV, indicating that [^{68}Ga]AJ647 measures unoccupied nectin-4, and paving the way for EV target engagement evaluation. For target engagement evaluation, [^{68}Ga]AJ647 accumulation in HT-1376 tumors in saline treated mice was assumed as 100% unoccupied nectin-4 levels. In mice treated with EV for 24 hrs (n=3-5), unoccupied nectin-4 levels were 21.1±11.6, 23.2±14.5, and 24.3±18.8 for 15, 9, and 6 mg/kg doses, respectively. Whereas on day 6, unoccupied nectin-4 levels showed significant differences at 29.5±15.8, 64.2±21.0, and 89.5±18.9 for 15, 9, and 6 mg/kg dose, respectively. These data indicate that FDA approved doses of EV show higher target engagement at 24 h but a dramatic reduction at lower doses over time.

Conclusion: [^{68}Ga]AJ647-PET quantifies variable nectin-4 expression in tumors. Furthermore, [^{68}Ga]AJ647-PET quantifies EV therapy induced pharmacodynamics at the tumor. Such real-time ADC target engagement assessment could inform patient selection and dosing strategies to enhance efficacy and minimize toxicities.

#2580 Targeting chromatin in ovarian cancer stem cells.

Y. Wang[1], J. Frederick[2], Y. Zhang[1], E. T. Bartom[1], G. Bauer[2], E. Tanner[1], V. Backman[2], D. Matei[1];
[1]Northwestern University - Chicago, Chicago, IL, [2]Northwestern University - Chicago, Evanston, IL

The dynamic organization of chromatin, governed by epigenetic modifiers, critically regulates cell plasticity and determines cell fate in both normal and malignant stem cells. We hypothesized that chromatin architecture plays a role in regulating transcriptional heterogeneity in ovarian cancer stem cells (OCSCs) to maintain stemness and chemoresistance. PWS microscopy showed that ALDH+ OCSCs derived displayed higher nuclear fractal dimension D signals ($P<0.05$) than ALDH- non-OCSCs, indicating that chromatin in OCSCs possesses higher packing compared to non-OCSCs. Cut & TAG Sequencing showed that of the 3606-histone repressive H3K27m3 enriched regions ($P<0.05$, fold change >2), 3208 were detected in OCSCs while 398 peaks were present in non-OCSCs, consistent with findings supporting high D features in OCSCs. The active mark H3K4me3 was enriched at the promoter of stemness-associated genes, including SOX2, ALDH1A3, and FZD7 in OCSCs; and the repressive histone mark H3K27me3 was enriched at the promoter of the epithelial cell marker CDH1 in OCSCs. These results support that the chromatin of OCSCs contains open genomic regions, corresponding to stemness-associated genes and repressed regions associated with genes related to differentiation. RNA sequencing indicated that the coefficient of variance (COV) reflecting transcriptional heterogeneity in OCSCs was higher than in non-OCSCs at baseline. In response to platinum, genes with low baseline expression in OCSCs were most upregulated, supporting increased transcriptional heterogeneity in response to chemotherapy. Inhibitors of epigenetic modifiers (DNMTi, EZH2i, and Dot1Li) induced chromatin re-organization in OCSCs and promoted OCSCs transition toward differentiation, supporting that stemness-associated chromatin structure is targetable. We demonstrated that a Dot1L inhibitor (Dot1Li) targeted OCSCs by decreasing chromatin packing D, resulting in decreased transcriptional heterogeneity. In conclusion, OCSCs harbor highly packed chromatin, contributing to chemoresistance and cell plasticity. Epigenetic modifiers (such as Dot1Li) inhibit stemness by regulating chromatin organization and transcriptional malleability.

#2581 Measuring interstitial fluid flow to predict and optimize spatial CAR-T dynamics in the clinic.

R. T. Woodall[1], C. Esparza[2], C. C. Brown[1], J. M. Munson[2], R. C. Rockne[1];
[1]Beckman Research Institute of The City of Hope, Duarte, CA, [2]Fralin Biomedical Research Institute, Roanoke, VA

Interstitial fluid flow dynamics in brain tumors are known to be an important indicator for tumor invasion into healthy tissue, as cancerous cells follow the interstitial flow towards tumor-stimulating chemokines. These flow gradients not only carry tumor-stimulating chemokines, but also carry cytokines secreted by immune response. CAR-T cells are known to also depend highly on the cytokines present in the CSF and serum. For these reasons, we have developed a novel method, Localized Convolutional Function Regression (LCFR) for measuring interstitial fluid flow, perfusion, and diffusion using dynamic contrast-enhanced MRI. LCFR works by applying the known physics of contrast agent transport, and fitting the observed contrast agent dynamics to the known physics. From LCFR, we can recover standard Tofts-Kety perfusion dynamics, including Ktrans and Vp, and also recover the underlying flow field and diffusivity. These new measurements allow for the prediction of where tumors invade, and allow for us to model how CAR-T cells move within a tumor. In a case study, we model the spatial distribution of CAR-T cells and glioblastoma cells over time, assuming that the fluid velocity field drives CAR-T spread throughout the tumor. Using multiple delivery locations, we identify the optimal catheter placement to optimally distribute CAR-T cells through the tumor, improving the 50% kill rate of simulated tumor cells by over 25% from a naive delivery strategy. Further, we collect longitudinal cytokine levels from patients undergoing CAR-T therapy, allowing us to understand how interstitial flow, CAR-T dynamics, and tumor dynamics interact with each other. We report a case study wherein a patient is longitudinally followed through their treatment with CAR-Ts. Perfusion imaging reveals that the patient experienced a steady increase in perfusion and decrease in fluid leakage into surrounding tissue. VEGF and IL12 levels are observed to increase as tumor volume increases. To better understand this patient's dynamics, we use the fluid velocity field measured by LCFR to simulate the development of CAR-T cells within the tumor, using the cytokine profile as a surrogate measurement of CAR-T population. These results demonstrate the importance of fluid flow and cytokines in understanding how brain tumors develop and respond to treatment.

#2582 Intra- and peri-tumoral radiomic features are predictive of pathologic response to multiple neoadjuvant therapy regimen in rectal cancers via pre-treatment MRI.

Leo Bao[1], **Thomas DeSilvio**[1], Benjamin N. Parker[1], Mohsen Hariri[1], Prathyush Chirra[1], Murad Labbad[1], Stephen Tang[1], Gregory M. O'Connor[2], Emily Steinhagen[2], Jennifer L. Miller-Ocuin[2], Amit Gupta[2], Eric L. Marderstein[3], Aaron Carroll[4], Marka Crittenden[4], Michael J. Gough[4], Smitha Krishnamurthi[5], Kristina H. Young[4], Satish E. Viswanath[1]

[1]Case Western Reserve University, Cleveland, OH,[2]University Hospitals Cleveland Medical Center, Cleveland, OH,[3]Louis Stokes Cleveland Veterans Affairs Medical Center, Cleveland, OH,[4]Providence Cancer Institute, Portland, OR,[5]Cleveland Clinic Foundation, Cleveland, OH

Introduction: Rectal cancers undergo neoadjuvant chemoradiation prior to resection, with increasing evidence that neoadjuvant chemotherapy or immunotherapy can boost clinical or pathologic response rates. However, baseline clinical tumor staging and carcinoembryonic antigen levels are limited for identifying which patients will most benefit from a multimodal neoadjuvant regimen, and which will not. We evaluated whether radiomics (computational features from radiographic images) from pretreatment MRI could identify which rectal cancer patients will achieve clinical or pathologic response to different neoadjuvant treatment regimens.

Methods: MRI scans were retrospectively obtained from 3 different institutions for rectal cancer patients who had either undergone neoadjuvant chemoradiation or an experimental immunotherapy + chemoradiation. After pre-processing all MRI scans, tumor was manually delineated with an automated annotation of a 10 mm peritumor region. 916 radiomic features were extracted from two planes of acquisition (axial, coronal) and two ROIs (tumor, peritumor). 5 top-ranked radiomic features were identified from each region and plane via multi-stage mutual information feature selection to train a linear discriminant machine classifier to assign a predicted likelihood of achieving complete response to each patient. Model performance was validated via ROC analysis against response groups defined via (i) tumor regression grade indicating no tumor present on surgical pathology, and (ii) 1-year clinical complete response for patients who underwent non-operative management. Clinical variables (CEA, clinical stage) were statistically compared between response groups.

Results: Training cohort comprised 64 patients who underwent chemoradiation alone (2 institutions, median age 61 yrs, M:F:MtF = 36:27:1). Validation cohort included 37 patients who underwent experimental TGFß inhibitor therapy prior to chemotherapy + chemoradiation (1 institution, median age 51 yrs, M:F = 25:12). Area under the ROC curve for multi-plane tumor+peritumor radiomic features (0.765 ± 0.054) was significantly higher for distinguishing complete response vs non/partial response compared to tumor (AUC = 0.635 ± 0.057, $p < 0.0001$) or peritumor (AUC = 0.612 ± 0.064, $p < 0.0001$). In holdout validation, performance was maintained with AUCs of 0.742 (tumor) 0.596 (peritumor), and 0.700 (all), respectively. Baseline CEA levels (p=0.3385) and cT stage (p=0.3386) were found to lack statistical significance as a predictor of response.

Conclusion: Radiomic features from tumor and peritumor regions on pre-treatment MRI scans in rectal cancer patients may enable robust and accurate identification of pathologic or near-complete response after multiple neoadjuvant treatment regimen, while outperforming baseline clinical variables.

#2583 [^{68}Ga]Ga-RYZ-GPC3: A glypican-3 targeted diagnostic radiopharmaceutical for hepatocellular carcinoma molecular imaging.

A. J. Braat[1], A. J. Poot[1], C. Lapa[2], M. G. Lam[1], W. A. Weber[3], A. Karmann[4], Y. Yuan[4], J. Rearden[4], K. Song[4], R. A. Bundschuh[2];
[1]UMC Utrecht, Utrecht, Netherlands, [2]University Augsburg, Augsburg, Germany, [3]Technische Universitat Munchen, Munchen, Germany, [4]Rayzebio, San Diego, CA

Introduction & Purpose: Hepatocellular carcinoma (HCC) is the most common type of liver cancer. To date, the imaging of HCC is difficult, insufficient for disease staging and barely improved over the past decades. Glypican-3 (GPC3) is a cell-surface receptor highly expressed by HCC and of diagnostic and prognostic value. GPC3 has been reported as potential target for diagnosis and treatment of HCC for nuclear theranostics. RYZ-GPC3 is a DOTA modified macrocyclic peptide with high affinity for GPC3, which may allow PET imaging or nuclear therapy. Here we report the first clinical results of [^{68}Ga]Ga-RYZ-GPC3 PET-imaging in patients with known or suspected HCC.

Methods: [^{68}Ga]Ga-RYZ-GPC3 was obtained upon labeling the peptide precursor with ^{68}Ga from a ^{68}Ge/^{68}Ga-generator and heating till 90^{0}C for 10 min followed by sterile filtration. After administration of 2 MBq/kg [^{68}Ga]Ga-RYZ-GPC3, a 60 min dynamic PET scan was acquired or multiple static PET/CT were acquired at 20 min, 1, 2 and 4 hours. Besides qualitative interpretation, standardized uptake values (SUV_{max}, SUV_{mean}) were measured in various compartments; HCC lesions, healthy liver (HL), kidneys, blood pool activity in the left ventricle (BP) and gastric fundus. Additionally, tumor-to-healthy liver ratios (TLR) were calculated: $SUV_{mean,HCC}$ divided by $SUV_{mean,HL}$.

Results: Radiolabeling to obtain [^{68}Ga]Ga-RYZ-GPC3 was near quantitative, making the production highly reliable. Eleven patients (4 patients dynamic; 7 patients static protocol) were scanned. One patient did not have an HCC. Another patient had a concurrent metastatic prostate adenocarcinoma, which did not show uptake, both qualitatively and quantitatively. All HCC lesions showed uptake in qualitative assessment, even in immunohistochemistry confirmed GPC3-negative HCC lesions (3 lesions). In 23 HCC lesions, including the aforementioned GPC3-negative lesions, mean SUV_{max} was 17.9 (range 2.7-95.3) and mean SUV_{mean} was 10.2 (range 1.0-49.2) at 60 minutes. Uptake in HL and BP decrease over time and become negligible 45 minutes after administration (SUV_{mean} ≤1.5). The opposite occurs for HCC and TLR, which continuously increase up to 4 hours after administration (TLR 4.4 to 19.2, at 18 minutes and 4 hours respectively). In individual lesion analysis, TLR was the highest at 60 or 120 minutes post-injection scans. Uptake in the gastric fundus, gradually increases in the first hour, and decreases gradually afterwards (SUV_{mean} from 4.0 to 12.7, back to 10.1).

Conclusions: [^{68}Ga]Ga-RYZ-GPC3 is the first peptide based PET tracer that allows the high quality molecular imaging of HCC. Thereby [^{68}Ga]Ga-RYZ-GPC3 is suitable for the selective diagnosis of HCC. In addition, based on the biodistribution and in vivo dynamics on these diagnostic images, RYZ-GPC3 is very likely to hold therapeutic potential upon labeling with a therapeutic isotope (e.g ^{177}Lu or ^{225}Ac).

#2584 Decoding colon cancer recurrence: Unveiling accurate predictions with attention-guided deep neural networks on histopathological whole slide images.

Mohammad K. Alexanderani, Mohamed Omar, Matthew Greenblatt, Luigi Marchionni

Weill Cornell Medicine, New York, NY

Background: Up to 40% of colon cancer patients are at high risk of cancer recurrence, yet accurate and timely prediction tools are lacking. Leveraging whole slide images (WSIs) and deep learning models, we aimed to develop precise algorithm for prediction of colon cancer recurrence. Thus, enables risk stratification for optimized therapeutic interventions and improved health outcomes.

Design: We designed an attention-based deep learning model for predicting colon cancer recurrence on paraffin-embedded, hematoxylin and eosin-stained colon tissue biopsies of digital slides. The WSIs were downloaded from the TCGA dataset, and preprocessed for color normalization, tissue segmentation, tilling, and histopathological features extraction. The entire dataset was then labeled based on cancer recurrence status, and divided into training (70%), validation (15%), and testing sets (15%). The model's performance was then evaluated by standard evaluation metrics, including receiver operating characteristic Area Under the Curve (AUC) and accuracy, on the training, validation, and testing datasets, where interpretability attention heatmaps were applied to gain insights into specific histological features and patterns involved in the model's decision-making process. The study is supported by the NIH-NCI-T32 for Next Generation Pathologists Program at our institution.

Results: A total of 350 WSIs were included and labeled into two classes: post-therapeutic colon cancer recurrence and no recurrence. The tissue segmentation process involved converting RGB images to HSV color space, applying a median blur filter (kernel size: 7), and performing thresholding using Otsu's method. The extracted features were utilized to train and construct a Clustering-constrained Attention Multiple Instance Learning (CLAM) model. The model demonstrated consistent performance across the validation and testing datasets, achieving an AUC of 0.85 with an accuracy of 0.83 on the validation set, and an identical AUC of 0.85 with an accuracy of 0.83 on the testing set, indicating the model's robust ability to identify patients at risk of cancer recurrence.

Conclusion: The study demonstrates the strong performance of our deep learning model in accurately identifying patients at risk for colon cancer recurrence based on H&E WSIs. This capability paves the way for optimizing therapeutic interventions and implementing effective surveillance strategies. Consequently, highlighting the crucial role of pathologists in collaborating with the oncologist for optimizing the management of colon cancer care in the era of personalized medicine.

#2585 First in human study with a novel peptide binder to glypican-3, demonstrates high specificity as a PET imaging agent in patients with hepatocellular carcinoma.

C. Bal[1], S. Ballal[1], K. Kallur[2], A. Karmann[3], Y. Yuan[3], J. Rearden[3], K. Shah[3], C. Lorenz[3], S. Moran[3], K. Song[3], I. Sen[4];
[1]All India Institute of Medical Sciences, New Dehli, India, [2]HCG, Bangalore, India, [3]RayzeBio, San Diego, CA, [4]Fortis, New Dehli, India

Introduction: Hepatocellular carcinoma (HCC) is the most common primary liver malignancy. The American Association for the Study of Liver Disease recommends surveillance for high-risk individuals with abdominal ultrasound, triple phase contrast CT or MRI. However, these imaging techniques have limited sensitivity in classifying lesions smaller than 2 centimeters. The use of [^{18}F]FDG Positron Emission Tomography (PET) is constrained due to insufficient uptake by HCC lesions over background liver uptake. Hence, there is an urgent need for more precise radiotracers for HCC. This study introduces the development of a novel radiotracer that binds to glypican-3 (GPC3), a cell membrane-anchored oncofetal protein overexpressed in HCC with minimal normal tissue expression.

Methods: [^{68}Ga]Ga-RYZ-GPC3 is composed of a small macrocyclic peptide binder with high affinity to GPC3 linked with a tetraxetan moiety capable of chelating a variety of radioisotopes including positron-emitting ^{68}Ga and other radiometals. The unlabeled binder to GPC3 was synthesized by the sponsor and provided to three imaging centers in India as part of investigator-initiated trials reviewed and approved by each site's institutional review board and ethics committee. Labeling with ^{68}Ga and quality checks of the product was performed locally at each center. Patients with high clinical suspicion or with confirmed HCC who gave informed consent received injections of 1.5-5.5 mCi of [^{68}Ga]Ga-RYZ-GPC3 and underwent PET-CT scanning at predetermined intervals. Some patients underwent companion [^{18}F]FDG PET-CT scans in accordance with local guidelines.

Results: A total of 64 patients underwent [^{68}Ga]Ga-RYZ-GPC3 PET-CT scans. The median age within the cohort was 61 (41-83), 22% were female. Liver cirrhosis was present in 72% of patients, attributed to hepatitis B, hepatitis C or NASH in 17%, 13% and 20% of cases. Notably, 92% of patients exhibited at least one positive lesion on [^{68}Ga]Ga-RYZ-GPC3 scans. The median SUVmax of GPC3-avid liver lesions was 15.5 (range 1.1 to 137.0) while the median liver SUVmean was 1.6 (0.3-7.9). Physiologic uptake was predominantly observed in the kidneys, the primary route of clearance, with a median SUVmean of 10.9 (2.2-20.7). Additionally, 20 patients underwent [^{18}F]FDG PET-CT scan for comparison. The median SUVmax of lesions on ^{68}Ga-RYZ-GPC3 vs [^{18}F]FDG PET was 11.0 (1.1-137.0) vs 3.8 (1.2-12.2).

Conclusion: Early human imaging results in patients with HCC indicate that [^{68}Ga]Ga-RYZ-GPC3 has high tumor lesion specificity compared to normal liverand demonstrates the potential of [^{68}Ga]Ga-RYZ-GPC3 to improve detection of HCC over conventional [^{18}F]FDG PET-CT. In addition, the binder could be complexed with a therapeutic radioisotope as a novel targeted therapeutic option for HCC. Further investigation of this first-in-class binder to HCC is warranted.

#2586 Heterogeneous enhancement pattern of Gd-EOB-DTPA-enhanced MRI predicts vessels encapsulating tumor clusters (VETC)-positive hepatocellular carcinoma.

K. Matsuda[1], A. Ueno[2], J. Tsuzaki[1], Y. Kurebayashi[1], K. Yamazaki[1], M. Tamura[1], M. Jinzaki[1], Y. Abe[1], Y. Hasegawa[1], M. Kitago[1], M. Sakamoto[1];
[1]Keio University School of Medicine, Tokyo, Japan, [2]Keio University Hospital, Tokyo, Japan

Background: Vessels encapsulating tumor clusters (VETC) pattern is known as a distinct hepatocellular carcinoma (HCC) vascularization that correlates with angiogenic status, lower lymphocytic infiltration, and higher recurrence rates. Despite the molecular and clinical significance of VETC$^{\pm}$ HCC, its characteristics on radiological imaging have not been clearly elucidated. We aimed to characterize VETC$^{\pm}$ HCC on gadolinium-ethoxybenzyl-diethylene-triamine-pentaacetic acid-enhanced MR imaging (EOB-MRI) and provide pathological evidence.

Method: We studied 204 surgically resected HCCs with preoperative EOB-MRI. VETC$^{\pm}$ HCC was defined as ≥1% VETC occupied area evaluated by CD34 immunostaining. The visual pattern classification of the arterial and hepatobiliary phase images is shown in Table 1. To investigate the relationships between imaging patterns and VETC$^{\pm}$ HCC, we evaluated immunohistochemical expression of h-caldesmon$^{\pm}$ arterial vessel density (AVD) and OATP1B3.

Result: In the arterial phase, VETC$^{\pm}$ HCCs showed heterogeneous hypervascular pattern and homogeneous hypovascular pattern. Accordingly, VETC$^{\pm}$ HCCs had lower AVD than VETC^{-} HCCs, as well, VETC regions had lower AVD than other regions within the same tumor. In the hepatobiliary phase, VETC$^{\pm}$ HCCs were observed more frequently in heterogeneous hyperintense pattern (36%) compared to homogeneous hyperintense pattern (5%). Hyperintensity in the hepatobiliary phase was correlated with high expression of OATP1B3. Among tumors with high OATP1B3 expression, VETC regions showed decreased expression of OATP1B3.

Conclusion: VETC$^{\pm}$ HCC showed reduced vascularity and heterogeneous hyperintensity in the hepatobiliary phase of EOB-MRI. These findings were explained by locally reduced AVD and downregulated OATP1B3 expression in the VETC regions. The potency to predict VETC$^{\pm}$ HCCs by radiological findings could improve HCC treatment strategy.

Relationship between enhancement patterns and VETC+ HCC in arterial and hepatobiliary phase

Arterial phase					
	Hypervascular/Homogeneous	Hypervascular/Heterogeneous	Hypovascular/Homogeneous	Hypovascular/Heterogeneous	Rim-like
Number of tumors	68	103	8	15	11
VETC^{+} HCC (%)	6 (9%)	32 (31%)	3 (37%)	3 (20%)	1 (9%)
Hepatobiliary phase					
	Hyperintense/Homogeneous	Hyperintense/Heterogeneous	Hypointense/Homogeneous	Hypointense/Heterogeneous	
Number of tumors	21	39	115	31	
VETC^{+} HCC (%)	1 (5%)	14 (36%)	23 (20%)	8 (26%)	

#2587 Evaluating the potential of radiomics features to predict outcome to an antibody-drug conjugate therapy in non-small cell lung cancer patients.

A. W. Chen[1], **L. K. Brady**[2], E. A. Cohen[1], W. C. Mankowski[1], L. Roshkovan[1], M. Qutaish[2], S. Katz[1], P. G. Castro[3], N. Pencheva[3], M. Jure-Kunkel[3], B. W. Higgs[2], D. Kontos[1];

[1]Perelman School of Medicine, University of Pennsylvania, Philadelphia, PA, [2]Genmab, Princeton, NJ, [3]Genmab B.V., Utrecht, Netherlands

This study evaluated radiomics, a non-invasive biomarker, for assessment of tumor heterogeneity in non-small cell lung cancer (NSCLC) patients treated with an AXL-targeting antibody-drug conjugate (ADC), enapotamab vedotin (EnaV), through analyzing baseline and post-treatment radiomic features from CT images for predicting outcome.

Clinical development of EnaV was discontinued in 2020 due to low response rates unimproved by dose optimization and/or predictive biomarkers. Study data included CT images, target expression and clinical data from 77 advanced NSCLC patients treated at 1.0 mg/kg (3Q4W), 1.8 mg/kg (Q3W), or 2.2 mg/kg EnaV (1Q3W) in the first in human phase I/II study assessing safety and preliminary efficacy of EnaV (NCT02988817). Radiologist-segmented tumors were examined using the cancer imaging phenomics tooklit CaPTk[1], deriving 225 radiomic features from 77 baseline and 50 Cycle 2 post-treatment CT images. Batch effects were balanced using nested ComBat[2], and radiomic feature dimensionality was reduced in two stages: clustering features with ≥80% similarity followed by principal component analysis (PCA). Radiomic PC1 was utilized in statistical models to assess overall and progression-free survival (OS, PFS), overall response rate (ORR), and disease control rate (DCR). Both baseline and delta radiomic PC1 were evaluated for correlation with biomarker and clinical activity, independently and with soluble or tumoral AXL expression.

Baseline radiomic PC1 significantly predicted DCR: confirmed (p=0.03), and unconfirmed (p=0.03). Baseline tumor membrane AXL predicted ORR for this NSCLC subset: confirmed (p=0.03) or unconfirmed (p=0.02). Delta analysis showed delta PC1 predicted unconfirmed (p=0.03) and confirmed (p=0.03) DCR and remained predictive for DCR with soluble AXL (p=0.04). No association was found between baseline and delta radiomics with OS or PFS.

Baseline and delta radiomic signatures showed potential in predicting NSCLC response. Preliminary findings suggest that radiomics combined with target expression predicted DCR, an early clinical activity indicator, although they did not predict OS or PFS. These outcomes pertain to a NSCLC subset and might not apply to other tumor types. Tumoral AXL expression did not linearly correlate with EnaV activity in a patient-derived soft tissue sarcoma model[3], possibly due to AXL expression in both tumor cells and myeloid-derived suppressor cells, or the presence of tumor-intrinsic MMAE resistance[4], implying the AXL expression and EnaV activity relationship is contingent on the tumor microenvironment[5]. Further validation in larger cohorts is planned.

[1] Davatzikos C, et al. J Med. Imaging 2018

[2] Horng H, et al. Sci. Reports 2022

[3] Van Renterghem B, et al. Int J Mol Sci. 2022

[4] Holtzhausen A, et al. Cancer Immunol Res 2019

[5] Boshuizen J, et al. Cancer Res. 2021

#2588 Bioengineering of site-specific antibody labeling from basic research to spatial omics platforms.

K. Tao[1], M. J. Rames[1], M. Dai[1], G. Sener[1], S. Olson[1], S. Ranganathan[1], S. Ozdemir[1], A. Oken[2], M. Brasino[1], R. Armstrong[1], Y.-J. Chiu[1], E. Eksi[1], B. Branchaud[1], S. Esener[1];

[1]Knight Cancer Institute, Oregon Health & Science University, Portland, OR, [2]Oregon Health & Science University, Portland, OR

Over the last few years, spatial multi-omics platforms have emerged as a powerful tool for characterizing cancer biology in multiple dimensions. Notably, these systems typically rely on multiplex immunolabeling. Conventionally, multiplexing is accomplished through carefully selecting primary antibodies from different animal species, and in combination with their corresponding polyclonal secondary antibodies. However, given the practical complication related to the species availability of primary antibodies, the multiplexing labeling is still under constraint due to the necessity for matched secondary species labels and the availability. For decades, non-specific labeling of primary antibodies through amine- or thiol-reactive chemistries was widely performed. Evolving research and commercial products have sought to overcome this antibody-based multiplexing limitations by developing enzymatic reaction-directed chemical reaction or antibody targeting proteins that could contain affinity to the Fc or Fab regions of antibodies. However, these methods mentioned above have substantive limitations and side-effects on affinity, conjugation number, buffer incompatibilities, storage incompatibilities, insufficient conjugation, and uncontrolled stoichiometric labeling. Herein, we introduce an efficient, sustainable, reproducible site-specific antibody covalent labeling strategy through engineering anti-IgG secondary nanobodies. These infer the stability, high-affinity of species specific and easy-to-produce IgG binders with the permanence of controlled activation for proximity-driven intermolecular covalent conjugation, with a promise for efficient multiplexity. This labeling technology addresses antibody labeling challenges through currently available approaches, and would substantially enhance multiplexity in a wide variety of research and clinical settings.

#2589 Novel workflow to generate natural killer cell sensitivity prediction model based on the epithelial mesenchymal transition related reprogramming at a single cell resolution.

Y. Zou, H. Ball, C. Harris, N. Ramnath, V. Keshamouni, S. Nagrath;
University of Michigan, Ann Arbor, MI

Single cell technology allows us to examine cell heterogeneity and identify rare cell populations; however, the high cost of single cell RNAseq limits its adoption into clinical and research environments. As an inexpensive alternative, immunofluorescent assays analyzing cell morphologies have been used in high content screening to examine cell phenotype and response to external stresses. Natural Killer cells (NK) are the bodies first line of defense and gained traction as a potential target in treating cancer. A study showed that cancer cells undergoing the process epithelial mesenchymal transition (EMT) increase their vulnerability to NK mediated cytotoxicity. We hypothesize that the EM morphology change can be correlated with NK sensitivity. Our goal is to develop an image-based, cost-effective, and efficient workflow capable of extracting cancer cell morphological features to predict its NK sensitivity at the single-cell level. To optimize this workflow, we use A549 cell line cells treated with transforming growth factor- β (TGF-β) as a representative models of cells with various EM phenotypes as NK sensitivities. We utilized a Cell Painting inspired novel image based live cell cytotoxicity assay. To capture cell morphological features, we optimized an organelle specific and live cell compatible staining panel that targets the nucleus, nucleic acid, cell membrane, F-actin, and mitochondria. The cell viability is assessed by Propidium Iodide, which stains dead cell nuclei. Our image analysis pipeline can extract the morphological features and track the cells of interest during the experiment and assess their viability. Subsequently, the morphology and viability data will be processed by a classification algorithm that could discern morphological features of cancer cells that indicate high NK vulnerability. We started with treating A549 cells with 5ng/mL TGF-β for 0, 24, 48, and 72 hours, and successfully applied the organelle staining panel. We observed distinct cell morphologies at each timepoint of TGF-β treatment, with cells shifting from a cobblestone (no TGF-β) to a spindle-like (72 hours TGF-β) morphology. Notably, the F-actin signal was significantly overexpressed in the 72 hours TGF-β treated A549 cells. A CellProfiler based preliminary image analysis pipeline was established for cell segmentation, cell features extraction, and cell viability tracking with quality control filters. Further optimization for cell segmentation, viability tracking, and classification algorithms will be needed to enhance the robustness of the workflow. Our established workflow demonstrates the feasibility of live cell functional assay with organelle staining. This workflow could be adopted to correlate and predict single tumor cell susceptibility to cytotoxic immune cells, with the goal of developing a therapeutic index.

#2590 Automating 6-plex chromogenic multiplexing with BOND RX.

D. Talia, S. Lindsay, S. Ketting, R. Williamson, D. Cockfield;
Leica Biosystems, Deer Park, IL

Multiplex staining using a sequential approach provides a means of visualizing multiple targets in a single biopsy section, further evaluation paired with digital imaging provides a deeper analysis into the spatial relationship at a cellular level. Leica Biosystems enables researchers to complete proof of concept for sequential multiplex staining methods, on board the BOND RX system. Thus, paired with a compatible reagent workflow and a digital slide imaging offering (Aperio GT 450/Aperio AT2) enhances the possibilities for analysis. As with any assay there is a requirement for user optimization, in particular, marker/chromogen layer selection and the pertinent use of an elution step. Such elution step is specifically important within a sequential stain utilizing the same detection reagents on subsequent layers. The results from the multiple staining rounds show a successful 6-plex fully automated stain, possible without the removal and reapplication of the slide onto the BOND system between staining layers. The marker combinations chosen demonstrate compatibility of different host species (Rabbit & Mouse), cellular compartments and isotypes which are provided by Leica Biosystems as BOND Ready to Use reagents. Overall, chromogenic multiplexing provides a stained image which enables color separation, due to the assignment of each chromogen to a marker with an individual cell type and cellular compartment. Finally, the process outlined avoids the risk of signal quenching commonly associated with fluorescent offerings and negates the requirement for specialized equipment due to the enablement of brightfield primary analysis.

#2591 Nonclinical ocular toxicity of a maytansinoid payload-antibody drug conjugate: Ocular tissue distribution, lesion pathogenesis, and mitigation.

A. Warbington[1], O. Ab[1], S. Lakshmikanthan[1], S. Dalton[2], P. Miller[3], E. Stevens[2], P. Zweidler-McKay[1], G. Lytle[1];
[1]ImmunoGen Inc., Waltham, MA, [2]Labcorp Early Development Laboratories, Madison, WI, [3]Ocular Services On Demand, Madison, WI

Background: Antibody-drug conjugates (ADCs) have emerged as a compelling therapeutic modality in oncology with several recent regulatory approvals. However, on and off-target toxicities require further evaluation. Corneal microcyst-like epithelial changes (MECs) are a well-known off-target class effect of ADCs with microtubulin-acting payloads, with varying degrees of severity. Manifestation of MECs is generally unrelated to antibody target and occurs in the absence of corneal target expression.
Methods: An ocular toxicology model in Dutch belted rabbits was established using a humanized monoclonal antibody not cross-reactive in rabbits conjugated through an SPDB linker to the maytansinoid drug, DM4. Radiolabeled ADC was administered once and tissues were collected for radioanalysis at multiple time points to evaluate the contribution of ADC exposure and ocular tissue distribution to corneal toxicity. Non-radiolabeled ADC was administered once or twice to evaluate onset and characterization of MECs using slit lamp microscopy and histopathology. Furthermore, potential prophylactic methods for reducing MECs were evaluated.
Results: The drug radioactivity was measured over 14 days and was widely distributed with elimination from most ocular tissues (except cornea) similar to blood/plasma elimination ($T_{1/2}$ of 4.5-7.5 days). In contrast, the corneal layers had an apparent absorption phase followed by a relatively stable concentration plateau through 14 days. Furthermore, preferential distribution to the corneal epithelium was evident by high tissue-to-plasma ratio (1.6 vs <0.5 for other ocular tissues, including other corneal layers). Generally, MECs increased in frequency (number of eyes affected) and decreased in time to onset with increasing dose. Ophthalmic observations of MECs began in the perilimbal cornea with axial migration over time and were reflected by the histopathologic findings in the corneal epithelium of single cell necrosis, increased mitosis, mononuclear cell infiltration, and/or atrophy. A topical ophthalmic vasoconstrictor (brimonidine tartrate 0.2%) delayed the onset of MECs compared to controls (8% vs. 67% of eyes at 7 days; 33% vs. 100% at 10 days) and mitigated severity of some histopathological findings (reduced or absent corneal epithelial atrophy, punctate erosion, pigment, and/or mononuclear cell infiltration). In contrast, corticosteroid administration (prednisolone acetate 1%) did not reduce MECs clinically but did reduce the histologic incidence and severity of corneal pigment and mononuclear cellular infiltration.
Conclusion: Collectively, this rabbit model reproduces the MECs associated with maytansinoid ADCs, demonstrates selective long-term corneal epithelium exposure, and provides data to support clinical testing of vasoconstrictor drops as ocular prophylaxis.

#2592 New technologies and capabilities supporting the development of novel molecular radiotherapy agents.

S. Belderbos[1], C. Mothes[1], C. Bernhard[2], F. Denat[2], P. Adumeau[1], M. Chevalier[3], J. Llop[3], A. Kownacka[1], C. Tihansky[4], M. Ruch[2], M. Claron[2], M. Moreau[2], **C. Berthet**[1], E. Koumarianou[1];

[1]Oncodesign Services, Dijon, France, [2]ICMUB Institut de Chimie Moleculaire de l'Universite de Bourgogne, Dijon, France, [3]CIC Biomagune, Donostia, Spain, [4]ImaginAb, Bracknell, United Kingdom

At Oncodesign-Services we aim to provide cutting-edge technologies and products to support the development of radiopharmaceuticals for theranostics.
Starting from the optimization of lead compounds, the site-specific bioconjugation chemistry of a bifunctional chelator to large biological compounds, such as antibodies, can preserve the biological profile and the reliable batch production. Thanks to new technologies we can conjugate a variety of payloads (cytotoxins, radioactive chelates, fluorescent dyes) on antibodies at targeted lysine residues of the Fc region, independent of Fc glycosylation.
Moreover, we aim to use relevant models for valuable translational results. In line with this, we established tumor spheroids to finely monitor the diffusion and subcellular distribution of novel fluorescent and radioactive probes in a 3D environment.
Furthermore, we are currently generating two animal tumor models for optimal target expression levels and recapitulation of the human tumor microenvironment. Our first model is a PSMA+ expressing tumour model, in a non radiosensitive rodent strain allowing improved assessment of novel radiopharmaceuticals. Our second tumor model is under development to assess novel FAPI tracers.
Finally, we present in partnership with *ImaginAb* ^{89}Zr Crefmirlimab Berdoxam, a minibody (human and murine analog) with high affinity to the CD8α glycoprotein, a valuable PET imaging tool for preclinical tracking and assessment of CD8 cells. This PET imaging can be used to evaluate immunoresponse following treatment, autoimmune, inflammatory and/or infectious diseases models.
To conclude, our continuous efforts aim at expanding our service portfolio to fulfil the needs of our various projects, as presented herein. Our experience and expertise allow us to suggest alternatives based on the latest technological progresses to facilitate and expedite the drug discovery progress from bench to bedside.

#2593 Spatial multi-omics profiling of tumor cell phenotypes in primary cutaneous melanoma at single-cell resolution.

T. Vallius[1], E. Novikov[1], A. Nirmal Johnson[2], S. Yingxiao[3], R. Pelletier[1], S. Pant[1], Z. Maliga[1], A. Chen[1], C. Yapp[1], S. Chan[3], C. Lian[2], G. F. Murphy[2], S. Santagata[1], P. Sorger[1];

[1]Harvard Medical School, Boston, MA, [2]Brigham and Women's Hospital, Boston, MA, [3]Dana-Farber Cancer Institute, Boston, MA

Primary cutaneous melanomas develop in stages from melanoma precursor cells that may progress to melanoma *in situ* (MIS) and eventually to invasive disease. Molecular changes, such as tumor cell state switches from melanocytic to undifferentiated and neural-crest-like phenotypes, have been associated with the development of melanoma metastases and therapeutic resistance. However, it is unknown whether cell states or gene expression changes enriched in advanced tumors exist at the premalignant stage and if they can elicit tumor-infiltrating lymphocytes (TILs). To address this gap, we analyzed a cohort of clinical samples from 43 patients with primary cutaneous melanoma using whole-slide cyclic multiplex immunofluorescence imaging (CyCIF), morphology-guided micro-regional RNA sequencing, and high-resolution 3D imaging. Each specimen contained multiple histologically-distinct regions representing a progression axis from normal to precursor to melanoma *in situ* to invasion. Subsequently, we examined the molecular profiles of both atypical melanocytes and tumor cells, and the gene expression and tumor microenvironmental (TME) changes that occurred during these progression stages. We identified major intra- and inter-specimen heterogeneity in the tumor intrinsic and extrinsic features across progression stages. Multiple tumor samples contained regions where publicly available gene signatures linked to both melanocytic and undifferentiated cell phenotypes were enriched. CyCIF analysis confirmed that various tumor cell phenotypes can coexist in close proximity to each other in early-stage untreated melanomas, and that the majority of undifferentiated tumor cells were located within regions of dermal invasion. Moreover, the cellular neighborhoods around undifferentiated tumor cells had a higher proportion of CD8+ T cells and cells of myeloid lineage compared to the neighborhoods around melanocytic tumor cell phenotypes. When assessing the localization and abundance of various tumor cell phenotypes, the levels of spatial and regional heterogeneity increased proportionally along normal to premalignant to malignant progression. Furthermore, the regional entropy of tumor cell phenotypes decreased along tumor depth in the majority (63%) of the samples, and even the melanoma *in situ* regions showed varying levels of spatial heterogeneity. Our in-depth multimodal molecular analyses highlight the presence of spatial heterogeneity among tumor cell phenotypes as well as the organization of early-stage primary melanomas, and are suggestive of tumor cell adaptation to the local environment.

#2594 AI-powered radiomics model predicts immune checkpoint inhibitor-related pneumonitis (CIP) in advanced NSCLC patients.

S. Lee[1], A. Hiremath[2], J. Lee[1], P. Kim[3], K. Zhang[2], S. Lee[4], M. Yadav[5], M. J. A. Chuchuca[5], T. Um[5], M. Nam[6], L.-Y. Chung[5], H. Kim[5], J. Yu[7], T. Djunadi[8], L. Kim[9], Y. Oh[10], S. Yoon[5], Z. Shah[11], Y. Kim[5], I. Hong[12], G. Kang[12], J. Jang[12], A. Cho[12], S. Lee[13], C. Nam[12], T. Hong[12], Y. Velichko[5], V. Velcheti[14], A. Madabhushi[2], N. Braman[2], Y. Chae[5],

[1]Kyungpook National Univeristy, Daegu, Korea, Republic of, [2]Picture Health, Cleveland, OH, [3]The University of Texas at Austin, Austin, TX, [4]School Of Medicine at UCI, Irvine, CA, [5]Feinberg School Of Medicine, Northwestern University, Chicago, IL, [6]Lincoln Medical Center, Bronx, NY, [7]Dignity Health - St. Rose Dominican Hospital, Henderson, NV, [8]Richmond University Medical Center, Staten Island, NY, [9]Ascension Saint Francis, Evanston, IL, [10]John H. Stroger, Jr. Hospital of Cook County, Chicago, IL, [11]Roswell Park Comprehensive Cancer Center, Buffalo, NY, [12]Northwestern University, Evanston, IL, [13]Johns Hopkins Bloomberg School of Public Health, Baltimore, MD, [14]Laura and Isaac Perlmutter Cancer Center, New York University Langone Health, New York, NY

Background: With the escalating integration of immunotherapy in the management of advanced non-small cell lung cancer (NSCLC), the emergence of adverse events, particularly immune checkpoint inhibitor-related pneumonitis (CIP), poses important challenges. CIP is not uncommon and can be life-threatening. It often necessitates the discontinuation of immunotherapy, even in patients with an otherwise favorable response. Prevention, early detection and early management of CIP can enhance patient outcomes, yet no such predictive models have been established. This study investigates the use of Artificial Intelligence (AI) algorithms in analyzing radiomic features for the prediction of CIP in NSCLC patients receiving immunotherapy.

Methods: A cohort of 105 stage III-IV NSCLC patients receiving immunotherapy was examined. Half of the patients were randomly split to a training set, while the remaining half were reserved for algorithm testing. The manual segmentation was performed by three physicians annotating in consensus using LIFEx software v7.3.0 (IMIV/CEA, Orsay, France). The Picture Health Px platform was utilized to perform an AI-powered deep phenotyping of the tumor and its surrounding habitat. A number of interpretable feature measures were extracted from baseline CT scans, which were in turn used to train a deep learning classifier for the detection of pneumonitis. Weighting techniques were applied to compensate for the imbalance of pneumonitis cases.

Results: Among the 105 patients, 63 (60.0%) received immunotherapy-only regimen and 42 (40.0%) received combination immunochemotherapy. 18 (17.1%) patients had pneumonitis events. Within this subset, 10 (55.6%) had CIP. Among the CIP group, six patients (60.0%) had grade 1 pneumonitis, three patients (30.0%) had grade 2 pneumonitis, and one patient (10.0%) had grade 3 pneumonitis, and none had grade 4 or grade 5 pneumonitis. Within the training set (n=51), the cross-validated area under the ROC curve (AUC) was 0.71 (95% CI: 0.68-0.74). When applied to the test set, the model predicted pneumonitis with AUC=0.63. Across the two datasets, the model correctly identified 4/6 (66.7%) grade 1 pneumonitis events and 2/3 (66.7%) grade 2 pneumonitis events, but misclassified the only available grade 3 event.

Conclusion: The utilization of CT-based radiomic features demonstrates promise in predicting CIP in NSCLC patients undergoing immunotherapy. This approach holds potential for enhancing the identification and management of CIP, among NSCLC patients treated with immunotherapy.

#2595 Accelerated and precise tumor segmentation in NSCLC: A comparative analysis of automated ClickSeg and manual annotation for radiomics.

Seyoung Lee[1], Kai Zhang[2], Jeeyeon Lee[1], Peter Haseok Kim[3], Amogh Hiremath[2], Salie Lee[4], Monica Yadav[5], Maria J. A. Chuchuca[5], Taegyu Um[5], Myungwoo Nam[6], Liam Il-Young Chung[5], Hye Sung Kim[5], Jisang Yu[7], Trie Arni Djunadi[8], Leeseul Kim[9], Youjin Oh[10], Sungmi Yoon[5], Zunairah Shah[11], Yuchan Kim[5], Ilene Hong[12], Grace Kang[12], Jessica Jang[12], Amy Cho[12], Soowon Lee[13], Cecilia Nam[14], Timothy Hong[12], Yuri S. Velichko[5], Anant Madabhushi[2], Nathaniel Braman[2], Young Kwang Chae[5]

[1]Kyungpook National Univeristy, Daegu, Korea, Republic of,[2]Picture Health, Cleveland, OH,[3]The University of Texas at Austin, Austin, TX,[4]School Of Medicine at UCI, Irvine, CA,[5]Feinberg School Of Medicine, Northwestern University, Chicago, IL,[6]Lincoln Medical Center, Bronx, NY,[7]Dignity Health - St. Rose Dominican Hospital, Henderson, NV,[8]Richmond University Medical Center, Staten Island, NY,[9]Ascension Saint Francis, Evanston, IL,[10]John H. Stroger, Jr. Hospital of Cook County, Chicago, IL,[11]Roswell Park Comprehensive Cancer Center, Buffalo, NY,[12]Northwestern University, Evanston, IL,[13]Johns Hopkins Bloomberg School of Public Health, Baltimore, MD,[14]Northwestern University, Chicago, IL

Background: Radiomics models utilizing artificial intelligence are being explored as a potential biomarker in the field of oncology. Radiomics analysis requires segmentations of radiographic imaging. However, manual segmentation is a labor-intensive process that is time consuming, and acts as a major rate-limiting step. Thus the development of automated segmentation tools presents an opportunity for innovation in regards to efficiency and precision. Our study aims to explore the feasibility of autosegmentation in comparison with manual segmentation.
Methods: A cohort of 105 stage III-IV non-small cell lung cancer patients receiving immunotherapy was examined, with a total of 168 lesions. We conducted a comprehensive comparative analysis of manual versus automated segmentation in time efficiency and segmentation quality, utilizing CT scans from the patients. Manual segmentation was performed by three physicians annotating in consensus using LIFEx software v7.3.0 (IMIV/CEA, Orsay, France). For a subset of randomly selected patients, annotation time was recorded as a reference point for the automated segmentation. In addition, automated segmentation was performed on all 168 lesions using ClickSeg from PictureHealth, a click-based interactive segmentation algorithm optimized for NSCLC lesions. Segmentation quality was evaluated using the Dice similarity coefficient to measure the concordance between ClickSeg outputs and consensus expert annotations.
Results: Average manual annotation time of the tumor region was 15min 34sec, and ranged from 1min 2sec to 53min 12sec. . Average prediction time for the automated segmentation model was 1.94 seconds, and ranged from 0.71 seconds to 4.39 seconds. The median Dice coefficient, reflecting segmentation accuracy, was 0.72, highlighting the robust performance of the automated method.
Conclusion: Our study demonstrates the efficient and accurate nature of automated segmentation supporting its potential integration into routine radiomic analysis procedures, streamlining the assessment of treatment response and ultimately improving patient care.

: Advocates Poster Session 2
Poster Session

#ADV021 Angelmira's Center for Women with Advanced Cancer.

Maricarmen Delia Planas-Silva

Angelmira's Center for Women with Advanced Cancer, Houston, TX

The poster will cover the following items: 1. We will present the background about AC4WAC. 2. We will explain the four programs AC4WAC and how they relate to cancer or cancer research. 3. We will share some of our data on those we serve. 4. We will comment on future goals. 5. We will provide contact information.

#ADV022 Disparities in Breast Cancer or Social Determinants of Health.

Marshelle Harris

Patient Advocate, Gardendale, AL

This poster will provide information on establishing a Health and Wellness Program for your individual needs that help you advocate for your own health and wellness with confidence so that you can navigate through the healthcare system with confidence.

#ADV023 THE CANCER HEALTH FUND - Giving Hope to the Nigerian Cancer Patient.

Mary-Gloria A. Orji

Patient Advocate, Abuja, Nigeria

The poster reflects on a true life story of a middle aged cancer patient named Alice [Pseudonym] who shared her cancer treatment journey with me and how the Cancer Health Fund {CHF}, a fund set aside for indigent cancer patients to enable them access care without having to pay for treatment, enabled her to continue with her treatments. Her story is typical of what a Nigerian Cancer patient faces. The stigma is very apparent especially from close relatives.. This leads to most patients not wanting to go to the hospital for care due to lack of funds and due to stigma associated with being diagnosed with cancer in my country. This, in effect, leads to late presentation, hence the very high morbidity recorded in the country. The fund was part of a 2 years advocacy by the Health Federation of Nigeria {HFN} and myself, as a cancer patient advocate, to the legislators to have it appropriated in the national budget and this, when it came to fruition was a great relief for many cancer patients who could access treatments even when they cannot afford it. Currently there are plans underway by the Nigerian government to have the funds expanded to other chronic diseases.

#ADV024 Patients First: Leveraging Investor Influence for Patient-Centric Pharmaceutical Research and Clinical Trials.

Mike Herman

Patient Advocate, Toronto, ON, Canada

The pharmaceutical industry often grapples with the tension between profit motives and patient-centricity. This abstract delves into the potential of the influence of investors in reshaping this dynamic to prioritize patients' needs and viewpoints. By leveraging investor power, all stakeholders can drive a transformative shift towards patient-focused practices, thereby enhancing study design, speed of approval, and ensuring patient-centric outcomes. This presentation explores strategies to align investor interests with patient welfare, while maximizing return on investment (ROI). While seeking successful instances of investor-driven improvements in pharmaceutical research and clinical trials, our analysis revealed a gap. This prompts reflection on whether we are asking the right questions. This discussion aims to inspire collaborative efforts among investors, pharmaceutical industry leaders, and patient advocates to ensure patients remain central to medical innovation.

#ADV025 Uncovered: The breast cancer journey of a Black woman from advocacy to awareness to action.

Michelle Audoin

Patient Advocate, Toronto, ON, Canada

This poster will provide a summary description of Uncovered: A Breast Recognition Project, which I created in 2020, in collaboration with Rethink Breast Cancer. It will focus on the Wish List action items of the 2021 edition of Uncovered, which have served as my guide and catalyst for growth as a patient advocate and partner. It will describe my journey from advocating for my own personal needs to be met to how education has empowered my growth as a patient advocate, by moving beyond awareness campaigns, to becoming an informed and engaged patient partner who is taking action to drive systemic change in breast cancer from early detection to survivorship, with a focus on equity, diversity, and inclusion. The purpose of the poster will not only be to describe my journey, but it will also serve as an inspiration for Black women and other underserved groups to engage more in cancer research and trials as partners.

#ADV026 AACR Cancer Disparities Progress Report shows us the gap of Health Equity for Racial and Ethnic Minorities and Other Underserved Populations.

Naomi Sakurai

CSR Project, NPO, Tokyo, Japan

Medical treatment including hormonal therapy and chemotherapy is critical to cure breast cancer. However, many breast cancer patients are also suffering from the side effects and financial burden.In order to highlight the current situation regarding side effects, employment conditions and financial burden, we conducted a web survey with 150 breast cancer patients (100 patients : early stage breast cancer, 50 patients : metastatic breast cancer).Our survey found that metastatic breast cancer patients, compared to early-stage breast cancer patients, are more affected by side effects such as fatigue, hair loss, symptoms and changes in skin color, pain and depression. In addition, we found that 54% of metastatic breast cancer patients are not able to return to work and 96% of breast cancer patients had financial toxicity on 'COST scores'. Return to Work is very critical both to continue medical treatment and keep patients' quality of life (QOL).Medical professionals should be more concerned about the side effects of treatment and how they affect the patients' daily lives. They should also be aware that social environmental factors play a very important role in maintaining health and treatment adherence, and look for ways to improve them.

#ADV027 What advocacy looks like in Rural and Frontier Communities: Cancer Advocacy in Indian Country.

Nathan Begaye

Huntsmans Cancer Institute, Salt Lake City, UT

It is the work of Huntsman Cancer Institute to understand cancer from its beginnings. To use that knowledge in the creation and improvement of cancer treatments to relieve the suffering of cancer patients. To also provide education about cancer risk, prevention, and care. The American Indian (AI) Program (AIP) in the Office of Community Outreach and Engagement at Huntsman Cancer Institute at the University of Utah seeks to reduce the impact of cancer in tribal communities through; (1) culturally tailored educational cancer outreach, (2) advocate for equitable access to clinical care for rural, frontier and AI patients from prevention to palliation, including access to clinical trials and cancer research, (3) to provide in-reach for clinicians and principal investigators about best practices in working with rural, frontier and AI persons and communities. The AIP centers it's advocacy in the rural and frontier Rocky Mountain West, knowing that it takes commitment, communication and consistency to build trust. Which involves engaging with community members and leaders where they gather and on their terms. To develop bidirectional relationships that facilitate connection and communication about their needs, resources and experience in accessing cancer related services. It is AIP's approach in working with rural, frontier and AI patients, survivors and their caregivers to be culturally informed. Understanding as best we can their lived reality, and considering the barriers they face in accessing treatment and care.

#ADV028 Ways to reduce breast cancer risk.

Nicole Stromer

Breast Cancer Options, New York, NY

Patient advocates serve a critical role in educating the public about various factors that can influence and reduce breast cancer risk. This poster will describe this role and the impact patient advocates can have.

#ADV029 Increasing Early Onset Colorectal Cancer Awareness and Screening in Young Adults in African American Communities.

Paulette Duggins

Patient Advocate, Winston Salem, NC

This poster will present the following: 1. The Mission of the Angelic Warrior Foundation (To increase Colorectal Cancer Awareness and provide support to patients, caregivers, and families). 2. Identify the cancer focus and the significance of the problem—The cancer focus is Colorectal Cancer Awareness with emphasis on Early Onset Colorectal Cancer (CRC). According to the American Cancer Society, “In 2023 an estimated 153,020 people will be diagnosed with CRC, 52,550 of them will die from CRC and 3,750 of them will be younger than age 50.”. 3. An overview of AWF’s Early Onset CRC Awareness Initiative—This initiative will address the need for increased CRC awareness and screening, especially among younger, Black and African American individuals, by building partnerships with Universities and Churches to plan and implement an evidence-based intervention focused on increasing CRC awareness.

#ADV030 Advancing Pediatric Oncology Research Through Collaboration: A Survivor/Clinician/Scientist Tri-Lens Perspective.

Rachel Hamilton

Patient Advocate, Markham, ON, Canada

Introduction: Cancer is the leading cause of death in children globally, with over 400,000 cases diagnosed annually. Although the overall outlook on pediatric cancer has drastically improved over the last half-century, survival rates remain poor for some cancer types, indicating the need for new treatment advances and continued research to improve treatment efficacy. Discussion: Advancing pediatric oncology research requires collaboration with multiple stakeholders to urgently drive new trials with the goal of creating new therapies to cure more patients. My unique tri-lens as a childhood cancer survivor, pediatric oncology registered nurse, and a pediatric cancer researcher allows me to apply the viewpoints from each facet of my identity, and understand where gaps may arise if partnership is not engaged. Supporting collaboration by involving all invested parties in pediatric cancer research, including patients, clinical staff, researchers, parents/caregivers, advocates and policy-makers, will encourage the implementation, and overall success of the science.Reflections: Each invested group involved in pediatric oncology research brings a wealth of knowledge and value, thus it is imperative to learn from each other to improve our practices. It is of utmost importance to include the patient and family, as equals, in all phases of research, in order to ensure research is done with, and not to participants. Together, with devoted parties pushing the science forward collaboratively, there is hope for progress.

#ADV031 Striving to Hold Accountability in Research Equity.

Rachel Hirschey

Patient Advocate, Durham, NC

This poster will present the following about Striving to Hold Accountability in Research Equity (SHARE): 1. Mission (To reduce cancer disparities in African American and Black communities by informing research and program development. SHARE identifies community needs, promotes evidence-based interventions and information, raises awareness about health disparities in communities, and educates researchers.), 2. Core Values (dignity, humility, openness, representation, transparency, honesty, service and accountability), member profiles, community partners and 2023 impact report.

#ADV032 Making the cancer journey easier and safer for patients and caregivers..

Robert Blomquist

CAREBOX PROGRAM, TX

The poster will describe the CareBOX process and how this model can be replicated in other cities and communities. Patients Apply: We have removed barriers and made a simple process for patients to apply. Visit the Get a CareBOX page to see just how easy it is. Customized CareBOXes: We have curated a list of 40 care supplies patients can choose from to meet their needs. They can replenish their CareBOXes every three months. Packaged with Love: Once wishlists are submitted our team of staff and volunteers get busy packing.

#ADV033 Empowered Choices: Transforming Breast Cancer Care through Patient-Friendly Online Clinical Trial Matching.

Sabrina Mayhew

Patient Advocate, Markham, MI

Breast cancer patients often find it challenging to navigate the landscape of clinical trials. For patients seeking information and participation in trials, BCT (breastcancertrials.org) and MTS (metastatic trial search) are important resources to assist patients with the complexity of trial matching. Recognizing the need for personalized support, this investigation aims to address the complexities in trial eligibility, and the need for breast cancer navigator assistance to optimize the trial search process.

#ADV034 Helping Older Breast Cancer Patients Navigate Cancer Care.

Sophia Turner

Patient Advocate, London, United Kingdom

Patients over the age of 70 are less likely to be offered the same treatment opportunities as younger patients (real world data supports). This poster will discuss guidelines for older patients that I have developed and mechanisms that I have used to distribute to this group (materials embedded). Issues that arise when accessing this population (timely, paper-based, confidence). Survey results of patient response to guidelines (graphs of patient response). Further enabling patients of 70 and over to receive the best care for their breast cancer, regardless of age.

#ADV035 Co-creation of a patient engagement strategy in cancer research funding.

Suzanne Bays

Patient Advocate, Piedmont, QC, Canada

As research teams, networks, and institutes, and health, medical, and scientific communities begin to build consensus on the benefits of patient engagement in cancer research, research funders are increasingly looking to meaningfully incorporate patient partnership within funding processes and research requirements. The Canadian Cancer Society (CCS), the largest non-profit cancer research funder in Canada, set out to co-create a patient engagement in cancer research strategy with patients, survivors, caregivers and researchers. The goal of this strategy was to meaningfully and systematically engage with patients in research funding and research activities.

#ADV036 “Ask Me!”: Transforming Patient Communication to Improve Enrollment and Adherence in Clinical Trials and Cancer Care.

Tambre Leighn

Patient Advocate, Rincon, Puerto Rico

This poster presentation delves into the pivotal role of effective communication in healthcare, specifically in the context of cancer research and cancer care. Challenging the traditional view that considers communication skills to be soft skills, this presentation highlights the pivotal role of mastering effective communication and positions these skills as the new hard skills essential for revolutionizing patient communication.

• Only at 6.3% of all oncology patients participate in cancer treatment clinical trials • Less than one quarter of patients have had their doctor or nurse suggest a clinical trial • Poor communication can result negative outcomes, such as decreased adherence to treatment, patient dissatisfaction, and inefficient use of resources • There is a 19% higher risk of nonadherence among patients whose physician communicates poorly

The poster includes real life examples of poor communication received by patients along with tips and strategies for how to better address these scenarios. The poster also discusses barriers and perceptions that impede communication, negatively impacting clinical trial enrollment and adherence. Too many patients continue to share experiences online and during speaking engagements about harmful and, sometimes, life threatening communication breakdowns. Stories about being ignored only to be later diagnosed with advanced stage cancers, side effects being deemed ‘normal’ or ‘tolerable’ with no interventions being provided, and patients not being asked to participate in clinical trials are still too common, particularly for diverse populations.

Drawing on her professional training in communication and coaching, this poster session by patient advocate, Tambre Leighn, promises to be interactive with tangible tips and takeaways that can be put into practice with relative ease.

This poster encourages researchers and clinicians to ask patients more often while highlighting the transformative power of advanced communication skills in cancer research and care. The “Ask Me!” approach paves the way for a more empathetic, effective, efficient, and patient-centered approach to communication in cancer research and cancer care.

#ADV037 Growth of Collaborative Partnerships: An Advocate's Aspiration for Improved. Global Approaches to Cancer Research.

Vivian Simbul Sim

Patient Advocate, Toronto, ON, Canada

I was diagnosed with breast cancer in 2011 and had a lumpectomy followed by radiation in 2012 at Sunnybrook Health Sciences Centre in Toronto. Like other people who have had a cancer diagnosis, I continue to ask:• How did I get cancer in the first place?• Is it still there?• Will it recur? And if so, will it spread?• How will my loved ones be affected?

#ADV039 KARMANOS CANCER INSTITUTE, OFFICE of CANCER HEALTH EQUITY & COMMUNITY ENGAGEMENT.

William Winkler

Patient Advocate, Canton, MI

Our poster will describe, through the 15 Karmanos sites, our statewide effort to educate and facilitate the formation of local Cancer Action Councils in an attempt to gain input from cancer survivors. Our purpose is to educate, especially populations of color that have been marginalized, thus increasing enhanced involvement in their treatment and possibly more engagement with clinical trials.

#ADV039 Designing a Culturally Tailored Educational Tool to Improve Engagement of African Americans in Clinical Trials.

Yvonne McLean Florence

Patient Advocate, Yeadon, PA

This poster highlights the perceptions of African Americansurvivors and caregivers about participation in clinical trials.

SURVIVORSHIP: Advocates Poster Session 1
Poster Session

#ADV001 Portraits of Resilience: Exploring the Lung Cancer Diagnosis Journey among BIPOC Young Women through Narrative Inquiry.

Aurora Lucas

Patient Advocate, Romeoville, IL

This qualitative study delves into the lived experiences of BIPOC (Black, Indigenous, and People of Color) young women who have been diagnosed with lung cancer. Utilizing a methodological approach grounded in portraiture and narrative inquiry, the research seeks to illuminate the multifaceted dimensions of their journey from diagnosis onwards. Through in-depth interviews, the study captures the nuanced narratives, perspectives, and coping mechanisms of these resilient individuals. By employing portraiture, the research aims to create rich, contextualized portrayals of their experiences, highlighting their agency, challenges, and triumphs in navigating the complexities of lung cancer diagnosis as BIPOC young women. This exploration not only contributes to a deeper understanding of the psychosocial aspects of lung cancer within this demographic but also underscores the importance of amplifying their voices within healthcare discourse and policy-making.

#ADV002 Patient Cancer Identification Begins with Primary Care.

Cathy Nobil-Dutton

Patient Advocate, Glenside, PA

Primary care physicians (PCP) are on the front line of identifying possible genetic links that may indicate a predisposition for a hereditary cancer. A PCP's relationship with their patient is an ongoing one and it is at this entry point that possible risk factors can be noted and testing recommended. Educating PCPs about the possible genetic factors and how to take a thorough family history could result in lifesaving early interventions for their patients.

#ADV003 AYA Can: Canadian Cancer Advocacy - A Pan-Canadian Patient Led Organization for Adolescents and Young Adults.

Chantale Thurston

AYA CAN - Canadian Cancer Advocacy, Winnipeg, MB, Canada

This poster outlines the establishment of a peer-led advocacy charity, AYA Can, in Canada dedicated to adolescents and young adults (AYAs) affected by cancer. The charity's vision is to advocate for an equitable and integrative system of care, incorporating patient perspectives into policy, research and care practices. It aims to amplify AYA research, particularly in integrative oncology and precision medicine, improving care quality. Through fostering interdisciplinary collaboration, the organization seeks to advance the field of AYA oncology and ultimately enhance the quality of life and survivorship outcomes for young cancer patients across Canada.

#ADV004 Patient Advocate Perspective: Conversation in Cancer Care.

Christina Sisti

Patient Advocate, Bradenton, FL

The poster will highlight how conversations can begin between researchers and patient advocates. The poster will have tips about including patient advocates in research. And ways to decrease inaccessibility to patient advocacy opportunities and care.

#ADV005 More Than a Token: A BIPOC's Experience with Patient Engagement.

Clare Cruickshank

Patient Advocate, Hamilton, ON, Canada

This poster focuses on the author's experiences providing a patient perspective in research, and provides suggestions for improving engagement along IAP2's spectrum of participation.

#ADV006 Expanding Outreach to Uterine Cancer Survivors.

Davida Pantuso

Kent State University, Barberton, OH

Uterine cancer is the most common gynecologic cancer, and the fourth most common cancer among women in the United States. Unlike most cancers, incidence and mortality rates are increasing. Despite these concerns, a silence about uterine cancer exists and resources remain limited. This poster will highlight how SHARE Cancer Support is committed to expanding awareness and resources to uterine cancer patients and survivors, especially for Black Women - a population that is particularly impacted.

#ADV007 The Amy Krouse Rosenthal Foundation: Spearheading Innovative Research for the Early Detection of Ovarian Cancer.

Deborah Binder

Patient Advocate, Barberton, OH

Ovarian cancer is the 5th leading cause of cancer-related deaths in women. Research shows that, if ovarian cancer is found before the cancer has spread outside the ovary, the 5-year relative survival rate is 92%. However, only 15% of all ovarian cancers are found at this early stage. Because we know that early detection exponentially increases a woman's survival rate, the Amy Krouse Rosenthal (AKR) Foundation focuses on early detection research, education and awareness. Among the Foundation’s programs and efforts, we are proud to provide grant funding for groundbreaking ovarian cancer early detection research.

#ADV008 Advocacy: A Cancer Survivor's Holistic Approach to Community Wellness.

Deirdre F. Lea

Patient Advocate, Burlington, NC

This poster will provide an overview of the establishment and growth of the Cancer Support Ministry and Health Fair at Jeffries Cross Baptist Church (JCBC). It will detail the community-driven initiatives that focus on delivering cancer prevention and awareness services. Additionally, the poster will highlight the community-initiated partnerships with health services and academic entities to support the health fair which provides a holistic approach to wellness. Healthcare professionals attend to offer blood pressure screenings, flu and COVID-19- vaccines, as well as educate attendees about cancer, mindfulness, diet, physical activity, insurance benefits, mental health, substance abuse, and oral health. We also offer a farmer's market with fresh produce from local farmers and a food truck offering healthy food options such as fresh salads, fruits and veggies, and hibiscus power drinks. We believe these offerings bring the wellness approach full circle; from educating attendees on how to live a healthy life to providing foods, mindfulness activities, and preventive measures to help our church members and community live longer, healthier lives.

#ADV009 Advocacy: A Cancer Survivor’s Holistic Approach to Community Wellness.

Don Desserud

Patient Advocate, Cornwall, PE, Canada

Proper communication with patients is recognized as an important skill for health-care providers. However, good communication with patients is more than simply speaking slowly or simply: communication with patients is teaching. Whenever a health-care provider tells patients something they do not know, they are teaching. What, however, is the appropriate teaching technique for dealing with patients who are frightened and who have just had their world turned upside down? We need to develop a unique teaching methodology for patients with life-threatening diseases, which I am calling kamnagogy, or teaching the sick. I am looking for research partners to help me design this method.

#ADV010 Caregivers have experience too!.

Don Wood

Patient Advocate, Calgary, AB, Canada

This poster describes becoming a caregiver when you never wanted to be one (due to a cancer diagnosis) and how I turned that into a career in patient engagement in cancer research. How I used my lived experience to gain experience so that I was able to work in the cancer research space and add value as a caregiver with lived experience. This poster is also an opportunity to coach and mentor other patient advocates and researchers as to how to engage caregivers in their projects and work.

#ADV011 Struggle with Diagnosis and Pandemic Across State Lines: A Case For Point of Care.

Donna Short

Patient Advocate, Brookfield, CT

Two weeks into the shutdown due to Covid, I was diagnosed with breast cancer. I struggled to receive treatment but ultimately navigated those waters and was able to access care. Then, I struggled as a cancer patient to receive expedited access to Covid shots because I lived in one state but was being treated in another. It is time for State Guidelines for care to be dissolved and replaced with guidelines due to point of care. We are a mobile society and live and work beyond state borders and our care should reflect this.

#ADV012 The State of Mental Health Supports for the Cancer Community.

Ethan Schilling

Patient Advocate, Waynesville, NC

This poster will present an overview of best practices in the mental health support of cancer patients and survivors. The most effective evidence-based treatments will be presented as well as current barriers that exist to treatment. Finally, implications and future directions for mental health research in the cancer space will be discussed.

#ADV013 Surgery for Invasive Lobular Carcinoma: A Patient Experience Survey from the Lobular Breast Cancer Alliance.

Gitte Joergensen

Patient Advocate, Coventry, CT

The Lobular Breast Cancer Alliance (LBCA) is a nonprofit, patient advocacy organization committed to raising awareness and promoting research into invasive lobular carcinoma (ILC). While ILC accounts for 15% of breast cancers, knowledge about ILC remains limited. ILC's hallmark is a lack of E-cadherin, which results in non-cohesive formation and impacts the accuracy of imaging tests and staging. Consequently, patients with ILC have higher rates of positive surgical margins, mastectomies, and axillary lymph node (LN) dissections. To understand the surgery experience of individuals with ILC, LBCA conducted an anonymous online survey from 6/21-7/2/23, distributed via the LBCA newsletter, social media, and partner organizations. Questions addressed pre-operative imaging, type of surgery, surgical margins, LN status, decision-making about, and patient experience with surgery. Analyses were limited to those respondents who had surgery. Study limitations include potential recall and selection bias. Results 1,482 individuals with a diagnosis of ILC completed the survey and 1,426 had undergone surgery. 76% were from North America, 11% from England, and 4% from Australia. The average age at diagnosis was 56 (range 31-86). At diagnosis, 38% were clinically stage 1; 37% stage 2; 17% stage 3; and 4% de novo metastatic. 75% had a mammogram that indicated dense breasts. Of 1,426 surgery respondents (SR), 95% reported that ILC was identified in only one breast at diagnosis. 80% had a pre-surgical MRI. MRI revealed larger tumors than seen on other imaging for 43% and revealed previously unseen contralateral ILC for 3%. 375 (26%) of SRs were diagnosed with ipsilateral disease and had a pre-surgical MRI that did not reveal new information about their ILC. Of these, post-surgical pathology reports indicated 16% had additional ipsilateral foci, 2% had contralateral disease, and 40% had larger tumors than seen on pre-surgical imaging. 614 (43%) of SRs had one or more lumpectomy (L), 560 (39%) of SRs had a double mastectomy (DM), and 451 (32%) of SRs had a single mastectomy (SM). 123 (20%) of SRs who had one or more Ls, had a subsequent SM or DM. For those undergoing L (614), reasons for this choice included: a recommendation from their care team (83%), wanting to keep their breast (25%), thinking it was better for their overall survival (OS) (14%), and 13% indicated they wanted breasts but did not want reconstruction. Of the 560 women who had a DM, 60% indicated that they thought a DM would improve their OS, 50% were concerned about the risk of local recurrence, 47% doubted that imaging would detect future ILC tumors and 45% noted concern that ILC is more likely to be bilateral. Of note, only 9% had ILC or ILC and another invasive breast cancer in both breasts at initial diagnosis and 31% who had a pre-surgical MRI changed their initial surgical treatment plan. Post-surgery, pathology for the DM group revealed larger tumors than seen on imaging (57%), and 6% had tumors found in a second breast that were not seen on imaging. For those 451 who had an SM, reasons for this choice included: 75% said it was what their care team recommended, 35% thought it would improve OS, 20% feared risk for local recurrence, and 15% doubted imaging would detect future ILC. Of 614 respondents who had L, 33% had positive margins at first surgery. Of those, 17% reported multiple Ls and M; and 24% reported clear margins were never achieved. Of the 1011 SM or DMs reported, 10% did not achieve clear margins after these surgeries. Conclusion The survey demonstrates the experience of a large cohort of women with ILC, reporting high rates of uncertainty about the accuracy of imaging, high rates of repeat surgery, bilateral mastectomies, and positive margins. Patients are factoring concerns about the potential extent of disease and future recurrence in their surgical decision-making. These results support the need for improved pre-operative staging and imaging modalities specific to ILC.

#ADV014 The NC Minority Prostate Cancer Awareness Action Team.

John L. Milner

Patient Advocate, Garner, NC

This poster will provide an overview of the NC Minority Prostate Cancer Awareness Action Team. It will detail our mission: “Promoting education, awareness, advocacy, best practices treatment, and support services to the residents of North Carolina with an emphasis on African-American, Hispanic/Latino, and Native American residents.” and vision: “Carrying the Sword Against Prostate Cancer for the Next Generation.” It will include an overview of our leadership, membership, partnerships, programs, events, and large-scale screenings for men.

#ADV015 iCCaRE Engagement with Black Faith-Based Organization Leveraging Their Use of Communication Technology to Remedy Disparities in Cancer Literacy, Screening, and Clinical and Biospecimen Studies Participation.

John McCall

D'Veal Family and Youth Services, Pasadena, CA

Faith-based organizations have a longstanding role as essential pillars of community health in predominately Black communities, filling in gaps for inequitable public health infrastructure. The COVID-19 pandemic highlighted the significance of faith-based organizations (e.g., churches) as trusted members in reaching the Black community for COVID-19 testing and vaccination. Additionally, in response to the COVID-19 social distancing guidelines, faith-based organizations including Black churches mastered the importance of communication technology platforms to maintain their congregation. The COVID-19 pandemic also had a significant impact on cancer prevention and control -- leading to 9.4 million undone cancer screenings specifically for breast, colorectal and prostate cancer. Specifically, Black men experience the highest incidence of prostate cancer among ethnic men, and studies repeatedly show that Black men are less likely to be screened for early detection. Therefore, recognizing Black faith-based organizations' status, credibility and effectiveness in engaging the Black community, as well as our proficiency in using communication technology, we are leveraging our status and communication capacity for disseminating health information focusing on cancer literacy and screening guidelines towards enhancing the health and well-being of Black communities.

#ADV016 Colontown - A Paltown Community A Wildly Supportive Colorectal Cancer Community.

Keith Hollingsworth

Patient Advocate, Lafayette, IN

COLONTOWN under the 503c umbrella of PALTOWN, empowers proactive colorectal cancer patients and caregivers with educational tools and relevant peer-to-peer support.

•Colorectal cancer is now the #1 killer of men and #2 killer of women under 50, with an expected 152,810 new cases in the US in 2024.•COLONTOWN is currently home to 10,000+ patients and caregivers. A large makeup of our “population” consists of those under the age of 60 (85%) as well as many considered late stage III or IV (81%).•Every program available in COLONTOWN has been created in response to a specific need expressed by patients or caregivers.

This poster highlights several of our key programs. These resources are all available to our members at no charge, and aim to empower, educate, and ultimately put the patient and caregiver in the driver’s seat with their medical team.

#ADV017 Cancer Doesn’t Know Age.

Kirsten Efremov

Patient Advocate, Brampton, ON, Canada

In pediatric oncology the most common cancers are leukemia, lymphoma and central nervous system (CNS) cancers. In those 60 years and older it is common to see breast, lung and colon cancers. The adolescent and young adult (AYA) population has a mix of both, but that population often hears, “you're too young to get cancer”, so their diagnosis is delayed. AYA’s are being diagnosed with cancer and it is not often in a timely manner. Anecdotally, diagnosis is delayed due to dismissal of symptoms and for the patient to lose weight, seek mental health help or blame it on their sexual orientation. However, the data shows that AYA’s are being diagnosed with a mix of both common pediatric and older adult cancers and the incidence of cancer in this population is increasing. Cancer doesn’t know age. There are cases of children with breast, colon and lung cancers and older adults with leukemia, lymphoma and CNS cancers. Person-centered health care is now, and the concept of “you are too young for cancer” and defining cancer by age is gone by the wayside. Cancer doesn’t know age, nor does it care.

#ADV018 My Walk With Cancer - And Why Faith, Spirituality And Its Leaders Should Be In A Clinician's Toolbox.

Linda Kitts

Patient Advocate, Burlington, NJ

This poster will describe my experience with cancer and how my journey was impacted by the following:• A positive, faith-filled attitude goes far in beating cancer.• I gave a talk to "Women of Faith", speaking of grace and blessings God has given to me through cancer. o Because of my new, faith-filled attitude, positive experiences far outweigh the negatives.• I am passionate about spreading positive, encouraging messages, and speaking freely to others about how, despite dreadful illness, good can come from it.• The quality of life is greatly enhanced with a positive attitude.

#ADV019 Multilevel Educational Strategies and Support for the Cholangiocarcinoma Patient Population.

Lourdes Rocha-Nussbaum

Patient Advocate, Golden, CO

Cholangiocarcinoma is a cancer that starts in the bile ducts. It can be diagnosed as cancerous cells located in the bile ducts that branch inside the liver (intrahepatic), or outside of the liver (distal), or where the right and left bile ducts join and leave the liver (perihilar). The Cholangiocarcinoma Foundation (CCF) has partnered with Komodo Health to gather data on the number of newly diagnosed patients in the United States to help CCF identify potential needs and gaps for support that can be addressed. Since cholangiocarcinoma is a rare cancer, it is important for patients to find information that can help them navigate their diagnosis, as well as have resources that support them through their cancer journey. Incorporating different strategies to provide education and support has been an important effort led by CCF.

#ADV020 Vaping and Gastric Cancer Risk - Is There a Link?.

Mahathi Vojjala

Patient Advocate, Marina del Rey, CA

This poster will present findings from my dissertation titled "The Relationship between Electronic Cigarettes and Risk Factors for Gastric Cancer in US Adults: Secondary Data Analysis using the PATH Study, Wave 1 and 5." The dissertation aims to: 1) Explore the association between e-cigarette, cigarette, dual user, and nonuser groups and gastric ulcers, cancer diagnoses, gastrointestinal bleeding, and other GI cancer-related issues using PATH Wave 5 data. 2) Characterize biomarkers of harm/outcome in PATH Wave 1, evaluating trends across tobacco-user groups and demographic correlates (race and sex) using cross-sectional data from Wave 1 of the PATH Restricted Use Files. 3) Determine the overall effect of e-cigarette and oral tobacco use specificity on H. pylori or gastric cancer risk in adults through a meta-analysis. I will also discuss my advocacy work with Hope for Stomach Cancer, highlighting my learning experiences and contributions to their campaigns and patient support initiatives.

IMMUNOLOGY: Antibody-Drug Conjugates
Poster Session

#2599 Trastuzumab deruxtecan reprograms immune response by stimulating cGAS-STING pathway in gastric cancer cells.
K.-S. Oh, A.-R. Nam, J.-H. Bang, Y. Jeong, S. Choo, H. Kim, S. Lee, J.-M. Kim, J. Yoon, T.-Y. Kim, D.-Y. Oh;
SNU Medicine, Seoul, Korea, Republic of

Background: The combination approach of antibody-drug conjugates and immune checkpoint inhibitors (ICIs) is being tested to enhance efficacy and overcome resistance in solid tumors. Although trastuzumab deruxtecan (T-DXd) is approved in HER2-positive gastric cancer (GC), its impact on the GC immune microenvironment remains elusive. This study explores how T-DXd modulates the immune response, providing essential insights on the development of T-DXd and immunotherapy combinations.
Methods: Comet assays and immunofluorescence assessed DNA damage. RNA-seq delineated the impact of T-DXd on GC cells (NCI-N87 and SNU-484). In vivo complex of enzyme assays and immunostaining of topoisomerase 1-DNA covalent cleavage complex (TOP1cc) were used to determine the action mechanism of T-DXd. RT-qPCR, and ELISA measured cGAS-STING cytosolic dsDNA sensing pathway activation. Further validation included cGAS knockdown and 2'3'-cGAMP addition to confirm the role of cGAS in T-DXd-induced promotion of inflammatory response. In coculture experiments, we utilized THP-1-derived dendritic cells (TDDCs) and PBMCs from healthy donors to prove the effect of T-DXd on immune cells. FACS analyses probed the activation markers of TDDCs and $CD8^+$ T cells.
Results: T-DXd-induced DNA damage upregulated PD-L1 expression in GC cells in an IRF1-dependent manner. RNA-seq revealed gene signatures associated with increased antitumor immune response, including proinflammatory response and type-I IFN, following T-DXd treatment. Mechanistically, T-DXd co-localized TOP1cc with γ-H2AX-positive micronuclei, activating the cGAS-STING pathway and triggering a robust IFN-I response. Knockdown of cGAS in cancer cells abolished the T-DXd-induced IFN-I response. T-DXd enhanced HLA-DR and CD86 expression in TDDCs, particularly when cocultured with GC cells. The physical interaction between cancer cells and TDDCs, along with the presence of cGAS in cancer cells, was found to be essential for the upregulation of dendritic cell (DC) activation marker by T-DXd. Furthermore, T-DXd elevated CD69, Granzyme B, and IFNG expression in $CD8^+$ T cells exclusively under coculture setting with NCI-N87.
Conclusion: T-DXd exerts immunostimulatory effects in GC cells through the activation of the cGAS-STING pathway, leading to a reprogramming of DC and $CD8^+$ T cell phenotypes. This provides a molecular rationale for combining T-DXd with ICIs for the treatment of patients with HER2-positive tumors.

#2600 Novel dual TOP1i ADC inducing superior tumour growth inhibition at low-drug load vs. trastuzumab deruxtecan.

P. Spycher, R. Fay, R. Bertrand, P. Probst, R. Stark, R. Santimaria, P. Maurhofer, L. Kallenberger, E. Renard, B. Schlereth, D. Grabulovski, I. Attinger-Toller; Araris Biotech AG, Au ZH, Switzerland

The Araris' site-specific and one-step conjugation technology aims at generating stable, safe and highly potent ADCs without the need for antibody engineering prior to payload conjugation. Here, we generated an anti-HER2 ADC using two different Topoisomerase-1 inhibitors (TOP1i) as payloads that shows superior anti-tumor efficacy compared to trastuzumab deruxtecan (T-DXd) in head-to-head in vivo studies.

For proof-of concept and comparison to T-DXd, trastuzumab was used as the targeting antibody. The Araris ADC was designed to combine two features in one ADC to maximize tumor-specific activity by using two different exatecan-based payloads: one that is able to exert bystander activity to address tumor heterogeneity and low-target expression and one that accumulates in cancer cells (no bystander activity) to achieve greater potency.

We found that the ADC was well-defined with a drug to antibody ratio (DAR) of 4 (2+2), as expected and no signs of aggregation under stressed conditions (40°C) during a period of 14 days. In in-vitro assays on target positive cell-lines, the ADC demonstrated taget-specific cell-cytotoxicity in the low nM-range similarly to T-DXd. Importantly, the non-bystander exatecan showed an increased intracellular concentration (up to 4x) and the bystander capable exatecan demonstrated high bystander activity in co-cultured, target-negative cell lines. In mouse pharmacokinetic studies, the ADC showed excellent stability in circulation with no signs of payload loss or linker-cleavage with a PK profile comparable to the unconjugated trastuzumab antibody which is key for a maximal and tumor-specific payload delivery.

Finally, a head-to-head study vs T-DXd was done in a challenging, medium HER2-expressing breast cancer model (JIMT-1), known to be resistant against the FDA-approved ADC T-DM1 (trastuzumab emtansine) and for T-DXd only showing limited activity (Ogitani et al., 2016). Impressively, it was found that the dual-TOP1i DAR4 Araris ADC showed superior anti-tumor efficacy compared to the payload-dose-adjusted T-DXd (DAR8). Using published doses for T-DXd, the Araris ADC was administered at ADC doses of 2x10mg/kg on days 1 and 8, resulting in superior anti-tumor activity and tumor eradication compared to T-DXd lasting for more than 47 days. T-DXd dosed at 2x5mg/kg (same payload dose) on days 1 and 8, only showed a very limited tumor growth inhibition with tumor regrowth occurring in all animals already at around 21 days.

We here show first encouraging results on a novel concept of combining TOP1i payloads that have two different features in one ADC to maximize efficacy. We believe that this concept in combination with a stable payload attachment at low DAR and an excellent exposure may help to develop ADCs with an improved therapeutic index for various solid tumor indications.

#2601 Potent antitumor activity of anti-HER2 antibody-topoisomerase I inhibitor conjugate based on self-immolative dendritic dimeric-linker.

Y. Liubomirski[1], G. Tiram[1], A. Scomparin[1], S. Gnaim[1], S. Das[1], S. Gholap[1], L. Ge[1], E. Yeini[1], O. Shelef[1], A. Zauberman[2], N. Berger[2], D. Kalimi[2], M. Toister-Achituv[2], C. Schroter[3], S. Dickgiesser[3], J. Tonillo[3], M. Shan[3], C. Deutsch[3], S. Sweeney-Lasch[3], D. Shabat[1], **R. Satchi-Fainaro[1]**;
[1]Tel Aviv University, Tel Aviv, Israel, [2]Merck KGaA, Yavne, Israel, [3]Merck KGaA, Darmstadt, Germany

Antibody-drug conjugates (ADCs) are a rapidly expanding class of anticancer therapeutics, with 14 ADCs already approved worldwide. We developed unique linker technologies for the bioconjugation of drug molecules with controlled-release applications. We synthesized cathepsin-cleavable ADCs using a dimeric prodrug system based on a self-immolative dendritic scaffold, resulting in a high drug-antibody ratio (DAR) with the potential to reach 16 payloads due to its dendritic structure, increased stability in the circulation and efficient release profile of a highly cytotoxic payload at the targeted site. Using our novel cleavable linker technologies, we conjugated the anti-human epidermal growth factor receptor 2 (anti-HER2) antibody, trastuzumab, with topoisomerase I inhibitors, exatecan or belotecan. The newly synthesized ADCs were tested in vitro on mammary carcinoma cells overexpressing human HER2, demonstrating a substantial inhibitory effect on the proliferation of HER2-positive cells. Importantly, a single dose of our trastuzumab-based ADCs administered in vivo to mice bearing HER2-positive tumors, showed a dose-dependent inhibition of tumor growth and survival benefit, with the most potent antitumor effects observed at 10 mg/kg, which resulted in complete tumor regression and survival of 100% of the mice. Overall, our novel dendritic technologies using the protease-cleavable Val-Cit linker present an opportunity for the development of highly selective and potent controlled-released therapeutic payloads. This strategy could potentially lead to the development of novel and effective ADC technologies for patients diagnosed with HER2-positive cancers. Moreover, our proposed ADC linker technology can be implemented in additional medical conditions such as other malignancies as well as autoimmune diseases that overexpress targets, other than HER2.

#2602 Near-infrared light-triggered pyroptosis boosts anti-tumor immunity via a novel antibody-drug conjugate.

F. Chen[1], X.-F. Tian[2], Y. Lu[1], P. Guo[1], W.-H. Tan[1];

[1]Hangzhou Institute of Medicine (HIM), Chinese Academy of Sciences, Hangzhou, China, [2]Institute of Molecular Medicine, Hangzhou Institute for Advanced Study (UCAS), Hangzhou, China

Background: Cancer remains a significant health challenge, driving advancements in therapies. Despite progress in chemotherapy and radiotherapy, the quest for more precise, immunostimulatory interventions continues. Photodynamic therapy (PDT)/photothermal therapy (PTT) has utilized various photosensitizers to induce programmed cell death in tumors. The mechanism of action (MoA) solely relies on apoptosis. Among these, indocyanine green (ICG), a clinically approved photosensitizer, has shown efficacy in PDT/PTT. Meanwhile, pyroptosis, a newly discovered programmed cell death, holds promise in boosting anti-tumor immunity by generating pro-inflammatory factors. However, there remains a lack of therapeutic agents for facilitating precise and controllable pyroptosis of cancer cells.

Methods: In this study, ICAM1-ICG was developed as a novel near-infrared (NIR) pyroptosis agent for anaplastic thyroid carcinoma (ATC). The *in vitro* cytotoxicity on ATC cells under NIR light was determined by flow cytometry. Morphological changes were confirmed under both light microscopy and transmission electron microscopy (TEM). Western blot evaluated the impact of ICAM1-ICG under NIR light on pyroptosis-related proteins. Considering that the NIR radiation product of ICG is mainly reactive oxygen species (ROS), we next investigated the role of ROS in ICAM1-ICG-mediated pyroptosis using the ROS scavenger n-acetyl-l-cysteine (NAC). Anti-tumor activity and biosafety were determined using animal models with different immune backgrounds. In addition, we assessed its impact on the anti-tumor immune response through RNA-seq and evaluated the synergistic effect of NIR-pyroptosis and PD-1 combination therapy.

Results: ICAM1-ICG exhibits a NIR light dose-dependent cytotoxicity on ATC cells under a serial dose of NIR light irradiation, along with pyroptosis-like morphological changes that are directly visualized under both microscopy and TEM. Western blot further revealed that ICAM1-ICG can induce tumor-specific pyroptosis under NIR light, evidenced by NLRP1 activation, Caspase1 tetramer formation, and GSDMD cleavage, indicating that ICAM1-ICG induces tumor-specific pyroptosis under NIR light through a ROS/NLRP1/Caspase1/GSDMD signaling cascade by using NAC. Animal models' dates validated the anti-tumor efficacy of NIR-pyroptosis and enhanced anti-tumor immune responses. Additionally, NIR-pyroptosis synergizes with PD-1 immunotherapy to boost anti-tumor immunity in naïve and immune-rechallenged tumor models.

Conclusions: Overall, we discovered that antibody-conjugated ICG can work as a novel tumor-specific NIR-pyroptosis agent and explored its potential in boosting anti-tumor immunity, providing a viable approach for the clinical translation of pyroptosis-based therapy.

#2603 Targeting chemo-resistant ovarian cancer with a first-in-class, first-in-human immune-oncology agents containing granzyme B.

A. Alvarez-Cienfuegos, L. H. Cheung, K. A. Mohamedali, M. G. Rosenblum;
UT MD Anderson Cancer Center, Houston, TX

Ovarian cancer (OC) is the fifth leading cause of cancer-related mortality in women. The current standard of care consists of debulking surgery with platinum-taxane maintenance chemotherapy. However, OC will recur in most patients, resulting in a five-year survival rate of 45%. In the past decades, there have been several developments in front-line maintenance therapy including bevacizumab or PARP inhibitors. While these therapies have shown effectiveness in prolonging progression free survival, this has not translated into improvements in overall survival. It is, therefore, essential to develop more effective maintenance therapies and most of the current efforts are focused on targeted approaches and immune therapeutics. Though immunotherapeutic strategies have induced durable responses in patients with melanoma, lung cancer, and other malignancies, the OC response to immunotherapy is limited as there is a significant subset of patients who do not respond. Our laboratory has developed several fully human granzyme B (GrB) based fusion proteins against key OC targets including folate receptor 1 (GrB-Fc-mov018) and fibroblast growth factor-inducible 14 (GrB-Fc-IT4) which retain high specificity of the targeting agent, combined with the GrB specific activity, a pro-apoptotic mechanism of action, and a robust in vivo efficacy. We assessed the *in vitro* cytotoxicity of GrB-based constructs against a panel of OC cell lines sensitive (OVCAR8, SKOV3, A2780, HeyA8) or resistant (SKOV3-TX, A2780/Cl-16, HeyA8-MDR) to common chemotherapeutic agents. SKOV3-TX cells were >10 fold more resistant to Paclitaxel than the parental SKOV3 cells while A2780/Cl-16 were 11-fold more resistant to Cisplatin than the parental A2780 cells. In contrast, none of the chemo-resistant cell lines showed resistance to the GrB-based constructs and the IC_{50} values observed were similar to those of the parental cell lines in the low nanomolar range (≤50 nM). Moreover, target expression analysis did not show significant differences between parental and chemo-resistant cell lines. A pilot *in vivo* efficacy study of GrB-Fc-IT4 and GrB-Fc-mov018 against a subcutaneous, established ovarian tumor (OVCAR8) xenograft showed promising growth inhibition of established tumors compared to vehicle controls. *In vivo* studies evaluating the response to different treatments of mice bearing chemo-resistant ovarian tumors are ongoing. Our results suggest that the mechanism of resistance developed to conventionally used chemotherapeutic agents such as Paclitaxel, Doxorubicin, Cisplatin or Mitomycin do not confer resistance to GrB-based constructs. Hence, we speculate that GrB-based constructs could be an effective therapy in OC patients with immune-excluded tumors that have developed resistance to conventional treatment. Research conducted, in part, by the Clayton Foundation for Research.

#2605 STX-1, a potent first-in-class ADC directed against DPP4 (CD26) as a biomarker of senescent tumor cells.

E. Angevin[1], V. Lelarge[2], R. Capelle[2], J. Choeur[2], T. Mathieu[2], B. Le Calve[2];
[1]Gustave Roussy, Villejuif, France, [2]Starkage Therapeutics, Lille, France

Dipeptidyl Peptidase 4 (DPP4/CD26) is a membrane glycoprotein involved in particular chemotactic and inflammatory responses, via its N-terminal protein cleavage enzymatic activities. DPP4 expression is found in various cell types, in certain subsets of lymphocytes and frequently overexpressed in primary tumors and metastases where its role remains still poorly understood. Recently, DPP4 was identified as a novel biomarker of senescent cells. In cancers, the harmful effect of senescent tumor cells is well recognized and mediated by the local production of pro-inflammatory cytokines, soluble immunosuppressive factors and metalloproteinases, called 'SASP' phenotype which could be induced by many chemotherapy and radiation regimens. This deleterious microenvironment promotes tumor growth, invasion and neoangiogenesis which can lead to treatment resistance, relapses and poor prognosis in many cancers, especially at advanced stages. STX-1 is a leading first-in-class ADC platform based on a proprietary anti-DPP4 mAb generated after a screen between normal and senescence-induced cells identifying DPP4 as a candidate for cancer targeting. Other biomarkers of interest were also identified as being selectively expressed for further preclinical evaluation. This IgG1/k mAb has potent *in vitro* activities on DPP4+ cells : i) in a bleomycin-induced senescent fibroblasts model; ii) on DPP4-expressing and chemotherapy- or radiotherapy-induced senescent human tumor cell lines with overexpression of DPP4; iii) binding of the mAb to its target results in its internalization into the endolysosomal compartment of cells. The first formulations of STX-1 are undergoing preclinical evaluation *in vitro* and *in vivo* and consist of a classical maleimide-based conjugation, an enzymatically cleavable cathepsin-dipeptide linker comprising a self-immolative spacer and either inhibitor of tubulin (MMAE/DAR4) or topoisomerase I inhibitor (exatecan/DAR8) payloads. Plasma stability and affinity, dose-response potency and permeability bystander activity on human tumor cell lines were evaluated *in vitro*. Preliminary efficacy is demonstrated *in vivo* on tumor xenograft models with various DPP4 expressions (constitutive or chemo/radio-induced to senescence) based on a 21-28 days weekly infusion schedule (3 or 5 µg/kg). The indications selected for further therapeutic development are prostate, liver and colorectal carcinoma models. Data on antitumor efficacy, tolerability and pharmacokinetics will be presented. Further studies will include optimization of the best STX-1 formulation, NHP studies and GMP scale-up with planned IND submission expected in Q3-2024. Exploiting the targeting of senescent cells in cancer based on selected biomarkers such as DPP4 constitutes a new therapeutic avenue to counteract tumor dormancy, recurrences and resistance to conventional chemo/radiotherapies.

#2606 Targeting mesothelin on tumor cells with a novel, completely human fusion construct delivering the serine protease granzyme B.

K. A. Mohamedali[1], L. H. Cheung[1], M. G. Iurascu[1], L. R. DePalatis[2], C. Thuning-Roberson[2], M. G. Rosenblum[1];
[1]UT M.D. Anderson Cancer Center, Houston, TX, [2]H2Biologics, Bolton, MA

Mesothelin is a cell-surface antigen identified as an excellent cancer-associated target upregulated on numerous tumors, including pancreatic and ovarian cancers, as well as mesotheliomas and lung cancers. Granzyme B is a highly cytotoxic serine protease nominally delivered by immune effector cells to target cells, resulting in induction of cell death pathways that are both caspase-dependent and -independent. We developed a fusion protein (GrB-Fc-SD1) composed of GrB and containing SD1, a novel human single-domain antibody that uniquely targets Region III of the mesothelin glycoprotein. The SD1 and GrB domains are tethered by a human IgG heavy chain fragment which enables dimerization. The fusion protein was transiently expressed in HEK-293E cells in serum-free conditions with a final yield of 5 mg/L. Western blot analysis confirmed the expression of this construct as a homodimer. The GrB enzymatic activity in GrB-Fc-SD1 was similar to that of commercially available human granzyme B. ELISA studies confirmed the specific recognition of the SD1 antibody to mesothelin extra-cellular domain. Biacore analysis confirmed binding of GrB-Fc-SD1 with a dissociation constant between 10^{-7} and 10^{-8} M. *In vitro* cytotoxicity against a limited panel of lung, pancreatic and ovarian cancer cell lines expressing surface mesothelin indicate cytotoxicity in the nanomolar range, while cytotoxicity against mesothelin-negative cells was at micromolar levels. *Ex vivo* serum stability studies showed excellent stability of GrB-Fc-SD1 at both 4°C and -20°C over ninety days and a half-life of approximately three days at elevated temperatures (37°C). *In vivo* efficacy studies against Capan-2 xenografts in nude mice using both weekly x 5 and QOD x 5 doses of GrB-Fc-SD1 (130 mg/mg total dose, delivered IP) indicated highly significant efficacy in both dose regimens, with $p < 0.001$ compared to vehicle-treated mice. Mouse body weights were not impacted at the efficacy doses used in this study, indicating that this dose was non-toxic. Histopathology studies revealed a significant decrease in the percentage of Ki-67+ nuclei in treated tumors compared to controls. These data warrant continued investigation of the protein as a therapeutic candidate. Research supported by H2Biologics. Research conducted, in part, by the Clayton Foundation for Research.

#2607 Dual payload immunochemotherapy to treat CD276 positive cancers.

Zhuoxin "Zora" Zhou[1], Jiashuai Zhang[2], Lufang Zhou[3], **Xiaoguang "Margaret" Liu**[4]

[1]Chemical and Biomolecular Engineering, The Ohio State University, Columbus, OH,[2]Biomedical Engineering, The Ohio State University, Columbus, OH,[3]Surgery and Biomedical Engineering, The Ohio State University, Columbus, OH,[4]The Ohio State University, Columbus, OH

The Cancer Genome Atlas (TCGA) dataset showed higher level of CD276 (B7-H3) transcript in multiple cancers, including triple-negative breast cancers (TNBCs), non-small cell lung cancers (NSCLCs) and other cancers, than normal tissues. Our immunohistochemistry staining of hundreds of patient tissue microarrays confirmed the high expression of CD276 surface receptor in >60% of TNBC and >70% of NSCLC while minimal or low expression in 33 normal organs or tissues. This study aims to develop and evaluate a novel treatment strategy, i.e. anti-CD276 mAb-dual payloads conjugate (DualADC), as immune-chemotherapy to treat CD276-positive TNBCs and NSCLCs. First, a new CD276-targeting monoclonal antibody (mAb) capable of delivering payloads and upregulating tumoral immunity was developed and engineered. Then, a new platform to concurrently conjugate both traditional cytotoxic payload and immunoregulating regent with one CD276 mAb (DualADC) was established. Our evaluations showed that this targeted therapy effectively killed multiple subtypes of TNBC and NSCLC, significantly upregulated immune functions in tumor microenvironment, and reduced tumor burden by up to 90-100% in seven animal models (including patient-derived xenograft). The post-treatment analysis using single-cell RNA sequencing, Luminex multiplex cytokine assay, whole blood, histology and histopathology analysis demonstrated an integrated anti-cancer mechanisms and minimal systematic toxicity. Altogether, our study suggested that the 276-DualADC could provide a promising targeted chemo-immunotherapy for CD276-postive cancer patients. In future, translational investigations will be performed to determine the toxicology, optimal dose, and treatment strategy, and the combination with other therapy will also be evaluated.

#2608 Hu2G10 antibody-drug conjugates selectively target cleaved-activated Trop-2 in cancer cells and show therapeutic efficacy against multiple human cancers.

S. Alberti[1], M. Trerotola[2], A. Moschella[1], R. Giavazzi[3], E. Guerra[2];
[1]University of Messina, Messina, Italy, [2]University of Chieti-Pescara, Chieti, Italy, [3]Istituto di Ricerche Farmacologiche Mario Negri IRCCS, Milano, Italy

Trop-2 is a transmembrane calcium signal transducer which activates growth-signaling networks that converge on Akt, ERK, Cyclin D1, NFkB (1). Trop-2 cleavage by ADAM10 was shown to be an activator switch for induction of cancer growth and metastatic diffusion (2). We devised a strategy to obtain monoclonal antibodies (mAb) capable of recognizing ADAM10-exposed sites in cancer cells. We succeeded at obtaining mAb that efficiently bound Trop-2 expressing cancer cells and were able to inhibit cell growth *in vitro*. We humanized the 2G10 mAb as the IgG1/k Hu2G10 antibody. Hu2G10 binds cancer-specific, cleaved/activated Trop-2 with K_d 10^{-12} M. On the other hand, it binds uncleaved/wtTrop-2 in normal cells with K_d $3.16x10^{-8}$ M, thus promising an unprecedented therapeutic index in patients. Antibody-drug conjugates (ADC) of Hu2G10 were obtained using stable linkers, multiple conjugation chemistries and different payloads, among them topoisomerase I inhibitors, bleomycin, RNA polymerase inhibitor, MMAE and calicheamicin. Hu2G10-ADC selectively killed Trop-2-expressing cells *in vitro.* Dose-response curves were obtained for the BxPC-3 pancreatic cancer, DU-145 prostate cancer, HT29 colon cancer cell lines and KM12SM/Trop2 colon cancer transfectants, reaching EC_{50} values as low as $5.05\ x10^{-10}$ M. Hu2G10-ADC drove high anticancer effectiveness on cell- and patient-derived xenografts from colon, pancreas, prostate and ovarian cancer. Effectiveness followed a gradient of payload potency, with correspondingly high therapeutic indexes. Consistently, neither detectable toxic effects nor weight loss were observed in any subgroup of treated xenotransplant-bearing mice. Taken together these findings candidate anti-Trop-2 Hu2G10-ADC for best-in-class anticancer therapy. (1) E. Guerra et al., The Trop-2 signaling network in cancer growth. Oncogene 32, 1594-1600 (2013).(2) M. Trerotola *et al.*, Trop-2 cleavage by ADAM10 is an activator switch for cancer growth and metastasis. *Neoplasia* 23, 415-428 (2021).

#2609 Vesicular LGALS3BP is a neuroblastoma biomarker and a therapeutic target for combination therapy with antibody-drug conjugate and checkpoint inhibitors.

G. Sala[1], E. Capone[1], I. Cela[1], G. Lovato[1], A. Lamolinara[1], M. Iezzi[1], C. Rossi[1], V. De Laurenzi[1], R. Ippoliti[2], S. Iacobelli[3],
[1]University of Chieti-Pescara, Chieti, Italy, [2]University of l'Aquila, University of L'Aquila, Italy, [3]Mediapharma srl, Chieti, Italy

We have recently shown that targeting circulating LGALS3BP with a maytansinoid-based non-internalizing antibody-drug conjugate (ADC) resulted in tumor eradication of high-risk NMYC-amplified neuroblastoma patient-derived xenografts. LGALS3BP is a high molecular weight, hyperglycosylated and secreted protein which is enriched at the surface of cancer-derived extracellular vesicles (EVs). Here, using a neuroblastoma pseudometastatic preclinical model, we extended our previous work demonstrating that EVs-associated LGALS3BP strictly correlates with disease progression and dissemination. Moreover, to investigate whether LGALS3BP ADC, named 1959sss/DM4, possesses immune-modulating properties, we analyzed DM4 ability to induce immunogenic cell death (ICD). Interestingly, using NXS2 murine neuroblastoma cells, we found that DM4 induced a time-dependent surface expression of three different ICD marker, i.e. calreticulin, HSP70 and HSP90. As it was recently demonstrated that to limit immune surveillance NXS2 cells increase PD-L1 expression in response to IFNγ production in the tumor immune infiltrate, we evaluated potential synergism between LGALS3BP targeting ADC and an anti-PD1 immune check-point inhibitor. To this aim, we genetically manipulated NXS2 cells which resulted nearly negative for murine LGALS3BP expression. Therefore, using a lentivirus-based gene transduction system, we obtained NXS2 cells producing large amounts of vesicular human LGALS3BP. Of note, the vesicular LGALS3BP could be quantified by ELISA and imaged by confocal microscopy using 1959 antibody. Strikingly, while single agent treatment showed a limited antitumor activity in NXS2-LGALS3BP syngeneic model, the LGALS3BP ADC/anti-PD1 combination resulted in a marked inhibition of tumor growth, which was followed by a prolonged survival. In conclusion, our findings establish that vesicular LGALS3BP is a potential biomarker for liquid biopsy and reveals this protein as a suitable target for therapeutic strategy that combines 1959sss/DM4 ADC with immune checkpoint blockade for the treatment of LGALS3BP expressing neuroblastoma.

#2610 Discovery of AM E3: A novel α-TLSPR monoclonal antibody for the ADC treatment of CRLF2-rearranged Ph-like B-ALL.

C. Dall'Armi, V. Di Biasio, C. Paolini, D. Natale, F. Scalabri, A. Missineo, N. Alaimo, M. Nuzzo, A. Demartis, P. Di Pasquale, R. Benoni, F. Caretti, E. Beghetto, F. Colaceci, R. Sasso, V. Pucci, A. Carugo, L. Tomei, C. Toniatti;
IRBM S.p.A., Pomezia, Italy

Background: Patients affected by Ph-like B-cell acute lymphoblastic leukemia (B-ALL) have a high mortality rate and elevated levels of disease relapse upon chemotherapy treatment. More than 60% of Ph-like B-ALL is characterized by genomic rearrangements resulting in high expression level of the CRLF2/TLSPR receptor on the cell surface. While significant advances have been made in developing targeted agents for B-ALL treatment, the CRLF2-rearranged subpopulation is in complete absence of selective and effective therapies. Here, we report the identification of α-TLSPR monoclonal antibodies with therapeutic potential and the preclinical validation of AM E3 as an Antibody-Drug Conjugate (ADC) for the treatment of CRLF2-rearranged Ph-like B-ALL.
Material and Methods: Leveraging a high-complex phage display platform we have first identified several fully human α-TLSPR monoclonal antibodies with single-digit nanomolar affinity for the target. Among them, AM E3 emerged as suitable for ADC development due to its rapid internalization by CRLF2-expressing cells. As a proof of concept, upon conjugation with the cytotoxic payload tesirine (SG3249) AM E3 was validated for anti-tumor response in both CRLF2-rearranged *in vitro* cell lines and *in vivo* xenograft models. Further, since human/mouse CRLF2 homology is low (<35%), we have also developed an ADC surrogate against murine TLSPR to establish a therapeutic window for the ADC therapy in CRLF2-rearranged preclinical models.
Results: ADC AM E3 demonstrated strong cytotoxicity (EC_{50}=40pM) on cell lines derived from hCRLF2-rearranged B-ALL patients. In xenograft models a single injection of ADC AM E3 (0.7mg/Kg) showed antitumoral activity proportional to hCRLF2/TSLPR receptor density at the cell surface. Moreover, ADC AM E3 treatment reduces tumor growth and disease burden of hCRLF2-rearranged B-ALL orthotopic xenografts and extends survival over standard induction therapy. ADC surrogate mB4 AM23, which retains similar properties as the human ADC AM E3, reduces tumor growth and is well tolerated in xenograft models engineered to express mCRLF2/TSLPR.
Conclusions: AM E3 is a novel α-TLSPR mAb with ideal features for the development of a first-in-class ADC therapy. α-TLSPR ADC demonstrated *in vitro* and *in vivo* efficacy as a monotherapy for the treatment of CRLF2/TLSPR rearranged Ph-like B-ALLs and proven to be well-tolerated in surrogate animal studies.

#2611 Non-specific elimination of tumor-associated neutrophils by antibody-drug conjugates boosts anti-tumor immunity for PD-1 immunotherapy.

S. Yao[1], L. Sun[2], X. Zhu[2], H. Xie[3], T. Yang[4], P. Guo[4], H. Tang[2], T. Zhu[2];

[1]School of Materials Science and Engineering, Tianjin University, Tianjin, China, [2]Zhejiang Cancer Hospital, Hangzhou, China, [3]Postgraduate Training Base Alliance of Wenzhou Medical University (Zhejiang Cancer Hospital), Wenzhou, China, [4]Hangzhou Institute of Medicine (HIM), Chinese Academy of Sciences, Hangzhou, China

Background: Antibody-drug conjugates (ADCs) play a key role in targeted therapy of solid tumors. However, few studies have examined the impact of ADCs on the tumor microenvironment (TME), particularly on innate immune cells. To elucidate this, this study focuses on investigating the comprehensive impacts of ICAM1-DXd on the tumor microenvironment, especially on tumor-associated neutrophils (TAN) and its synergistic effect with PD-1 immunotherapy.
Methods: Firstly, the efficacy and prognosis of ICAM1-DXd, a potent ADC for cervical cancer, were determined in pre-clinical tumor models, providing crucial transcriptomic and biological function information by using RNA-seq. Then, pathological studies were performed to evaluate the abundance and location of TAN (Ly6G+/MPO+) in TME post-ADC treatment. The interaction between TAN and ICAM1-DXd and subsequent impacts on adaptive immune cells (e.g., CD8+ cells) was examined by flow cytometry (FACS), confocal fluorescent imaging, and western blot techniques (WB). Eventually, the synergistic effect of ICAM1-DXd and PD-1 monoclonal antibody were investigated in an immunocompetent animal model.
Results: ICAM1-DXd potently inhibits cervical tumor growth in preclinical models, and RNA-seq analysis revealed that ICAM1-DXd treatment induces a strong down-regulation of neutrophil activation, especially for Ly6G+/MPO+ TANs, a subtype with pro-tumor function. IHC and FACS results confirmed that pro-tumor TANs were efficiently eliminated in TME by ICAM1-DXd treatment via non-specific phagocytosis in comparison with peripheral blood neutrophils. ICAM1-DXd-phagocytised TANs also elicit a strong bystander killing effect by cleaving the quadra peptide linker of ICAM1-DXD by cathepsin B. This ADC-mediated TAN elimination effectively ameliorates immunosuppressive TME and works in synergy with PD-1 immunotherapy in preclinical models.
Conclusion: In preclinical models of cervical cancer, ICAM1-DXd not only directly ablates cancer cells via antigen recognition but also non-specifically kills tumor-promoting TANs, resulting in an improved tumor immune microenvironment, providing a shred of mechanistic evidence supporting ADC and PD-1 combination therapy.

#2613 Treatment of solid tumors with antibody drug conjugates targeting aberrant O-glycoproteins.

A. C. W. Groen[1], N. Shrestha[1], B. Klebanov[1], B. Yu[2], B. Lee[2], C.-W. Chung[2], C. Park[2], M. K. M. Aasted[3], S. Dabelsteen[3], H. H. Wandall[3];
[1]GO Therapeutics, Natick, MA, [2]LegoChem Biosciences, Daejeon, Korea, Democratic People's Republic of, [3]University of Copenhagen, Kobenhavn, Denmark

The lack of antibodies with sufficient cancer selectivity is currently limiting the treatment of solid tumors by immunotherapies. Many solid tumors display aberrant glycosylation that results in the expression of tumor-associated carbohydrate antigens (TACAs) distinct from healthy tissues. Targeting aberrantly glycosylated glycopeptide epitopes provides the cancer selectivity needed for immunotherapy of solid tumors. However, only a few such glycopeptide epitopes have been targeted to date. We have developed a strategy to predict, design, and produce cancer-specific antibodies targeting novel O-glycoprotein epitopes with exquisite cancer specificity. Our mAbs avoid on-target off-tumor toxicity due to the specificity of aberrant glycosylation, and cover a broad range of cancer indications, including breast, lung, colon, pancreatic, and ovarian cancer. Additionally, our antibodies can be used as an IHC companion diagnostic and can be functionalized across a number of modalities, including next-generation CAR-T, T-cell bispecifics, and antibody-drug-conjugates (ADCs).Here, we present two novel antibodies, GO-08 and GO-013, selectively targeting cancer-specific Tn-glycosylated proteins in a site-specific manner with low nanomolar affinities. GO-008 and GO-013 were collectively shown to be highly cancer-selective by immunohistochemistry of sections from a large array of different squamous and adenocarcinomas, including triple-negative breast cancer, lung cancer, gastric cancer, ovarian cancer, pancreatic, and colorectal cancer. The two antibodies were functionalized utilizing ConjuAll™ technology, conjugating the microtubule disrupting payload MMAE via a site-specific beta-glucuronidase cleavable linker. ConjuAll™ functions as a plasma stable, tumor labile linkage, and due to the minimal expression pattern of beta-glucuronidase in healthy tissues, reduces both off- and on-target toxicity due to the minimization of release of free payload in non-tumor tissues. The ADCs based on GO-08 and GO-013 (LCB45A and LCB22A) demonstrated target-specific cytotoxicity invitro and in vivo with tumor elimination in breast and lung PDX models. GO-013 conjugated to MMAE (LCB22A) was well tolerated in cynomolgus monkey toxicity studies. Moreover, the ADCs selectively kill target cells in a human mixed organotypic cancer model without affecting healthy cells, indicating tolerability and safety. The combination of specificity of TACA targeting to differentiate ADC binding from healthy tissue and ConjuAll's tumor selective payload release promises to enable an excellent anti-cancer therapy.

#2614 GlycoConnect™ ADC toolbox expansion with high DAR technology.

L. Lelieveldt, E. Post, M. Nassiet, V. Hendriks, M. Verhagen, R. van Geel, S. van Berkel, F. van Delft;
Synaffix - A Lonza company, Oss, Netherlands

Recently topoisomerase 1 inhibitors have gained significant traction as a cytotoxic payload for ADCs based on the clinical success of camptothecin-based ADCs Enhertu® (DXd) and Trodelvy® (SN-38). In contrast to the majority of other approved ADCs, both Enhertu® and Trodelvy® are feature an average of 7-8 payloads per antibody. Obviously, such a high drug-to-antibody ratio (DAR) effectively delivers more drug to the tumor per internalization event, which is key in driving the clinical success.

Previously, we have shown that the native glycan of monoclonal antibodies is a privileged site for attachment of cytotoxic payloads[1], for the generation of site-specific and stable ADCs with DARs varying from 1-6, while the therapeutic index is further elevated by a highly polar spacer technology (HydraSpace™)[2]. The success of GlycoConnect™/HydraSpace™ ADCs is further driven by the use of exatecan as a potent and highly cell-permeable payload (SYNtecan E™).

Here we show that GlycoConnect™ technology can be readily extended to generate efficacious and safe DAR8 ADCs. We have developed a modular, non-genetic method, involving three simple process steps from any antibody: (a) enzymatic glycan remodeling, (b) strain-promoted azide-alkyne cycloaddition of a bifunctional, branched spacer comprising one strained alkyne and two orthogonal click tags (e.g. tetrazines), and (c) inverse electron-demand Diels-Alder cycloaddition with a branched linker-drug construct based on BCN and a two cytotoxic payloads. The resulting conjugates, with DAR 6 or 8, are rapidly generated with high homogeneity and with good stability. In addition, HIC profiles of the resulting ADCs indicate small relative retention time as an indication of good PK profile. Excellent in vivo tolerability is demonstrated, while efficacy studies in mice xenograft models show that the DAR8 technology clearly out-performs currently marketed ADCs (including Enhertu®).

[1] (a) van Geel *et al.* Chemoenzymatic Conjugation of Toxic Payloads to the Globally Conserved N-Glycan of Native mAbs Provides Homogeneous and Highly Efficacious Antibody−Drug Conjugates. *Bioconj. Chem.* 2015, *26*, 2233-2242. (b) Wijdeven *et al.* Enzymatic glycan remodeling-metal free click (GlycoConnect™) provides homogenous antibody-drug conjugates with improved stability and therapeutic index without sequence engineering. *MAbs* 2022, DOI: 10.1080/19420862.2022.2078466. [2] Verkade *et al.* A Polar Sulfamide Spacer Significantly Enhances the Manufacturability, Stability, and Therapeutic Index of Antibody-Drug Conjugates. *Antibodies* 2018, *7*, 12, doi:10.3390/antib7010012.

#2615 Preclinical development of a next generation antibody drug conjugate (ADC) targeting cMET for treatment of solid tumors.

L. Xiao[1], W. Lian[1], S. Song[1], Q. Liu[1], Q. Zong[1], S. Stann[2], J. Cai[1], T. Xue[1];
[1]MediLink Therapeutics (Suzhou) Co., Ltd., Suzhou, China, [2]MediLink Therapeutics USA, INC., Boston, MA

cMET (mesenchymal-epithelial transition factor), which belongs to the MET family, is a type of receptor tyrosine kinase that is expressed on the surfaces of various epithelial cells. The elevation of cMET can promote the development and progression of multiple cancers. cMET- ADCs have shown promising clinical activity with highest cMET levels, indicating tumor cMET levels may be limited for efficacy. YL211, a novel cMET-ADC was developed by leveraging on MediLink's tumor microenvironment activable linker-payload platform (TMALIN platform), which could release the payload both in the tumor cell and in the tumor microenvironment. YL211 is comprised of an anti-cMET humanized monoclonal antibody conjugated to a novel topoisomerase 1 inhibitor *via* a protease-cleavable linker. The novel linker-payload and site-specific conjugation of YL211 results in a homogeneous product with a DAR (Drug-to-Antibody Ratio) of 8. Furthermore, the advancement in linker-payload design has facilitated the development of more hydrophilic ADCs, which exhibit minimal impact on the antibody's characteristics while being less prone to aggregation and showcasing lower systematic clearance. Along with release of the payload in the tumor microenvironment extracellularly, upon binding to cMET on tumor cell surfaces, the antigen-ADC complexes are internalized to lysosomal vesicles and subsequently release the toxic payload. The cytotoxic features drive cell cycle arrest, apoptosis, elevation of PARP/caspase 7 expression, as well as cell death and bystander effect. These findings translated in vivo where YL211 showed superior efficacy in causing tumor regressions and good tolerability in both cell lines and patient-derived xenograft (CDX and PDX) mouse models with both low to high cMET expression levels (H358, CR5088, *ect.*). The *in vivo* pharmacokinetics in monkeys showed that YL211 is highly stable with less than 0.1% (molar ratio) payload released in circulation. GLP safety evaluations demonstrated good safety profiles and no off-target toxicity in monkeys. These non-clinical data suggest the stability of the linker in circulation as well as efficient release of the payload in tumors with improved therapeutic window. Taken together, preclinical data suggest that YL211 could be a promising treatment strategy for cMET positive cancer patients.

#2616 BCG033, a novel bispecific antibody-drug conjugate targeting PTK7 and TROP2, demonstrates preclinical efficacy against triple-negative breast cancer and other solid tumor xenografts.

S. Yao, C. Shang, G. An, **C. Guo**, W. An, Y. Yang;
Biocytogen Pharmaceuticals (Beijing) Co., Ltd., Beijing, China

Metastatic triple-negative breast cancer (TNBC) patients have poor overall survival, highlighting the need for novel treatments. Although the TROP2-targeting ADC sacituzumab govitecan recently received accelerated approval from the FDA for the treatment of patients with metastatic TNBC, the on-target toxicity of this single-target agent has limited clinical efficacy. We sought to improve the specificity and efficacy of future TNBC-targeted therapies by generating a bispecific antibody-drug conjugate (bsADC) targeting TROP2 and PTK7, another tumor-associated antigen (TAA) that is highly expressed in TNBC and correlates with poor prognosis and metastatic disease.

We previously generated fully human antibodies targeting PTK7 and TROP2 from Biocytogen's fully human, common light chain antibody transgenic RenLite® mice, which were selected such that their monovalent antibodies exhibited reduced internalization profiles for improved tumor selectivity. These antibodies were then constructed into a bispecific antibody targeting PTK7×TROP2, which demonstrated reactivity to human and cynomolgus monkey antigens and binding to multiple cancer cell lines, including TNBC, with high affinity. PTK7×TROP2 bsAb also showed enhanced internalization *in vitro* compared with parental monovalent antibodies. Next, the PTK7 x TROP2 bsAb was conjugated to vcMMAE with a drug-to-antibody ratio (DAR) of 4 to generate a bsADC (BCG033). BCG033-vcMMAE demonstrated superior activity to benchmark and parental ADCs in a cell line-derived xenograft (CDX) TNBC model with low PTK7 expression. Here, we demonstrate that BCG033-vcMMAE ADCs also exhibited superior efficacy to benchmark ADCs in PDX models, including TNBC xenografts and NSCLC xenografts. We next tested the efficacy of the PTK7 x TROP2 bsAb conjugated to BLD1102, Biocytogen's novel, proprietary linker/payload composed of a DNA Topo I inhibitor payload and a highly hydrophilic protease-cleavable linker, with a DAR of 8. BCG033-BLD1102 showed potent activity in a colorectal cancer PDX model in which benchmark ADCs were inactive, even at high doses.

In summary, BCG033 conjugates demonstrate promising preclinical efficacy *in vivo*, which ultimately could provide a new treatment option for TNBC and other solid tumors expressing PTK7 and TROP2.

#2617 BCG022, a novel HER3×MET bispecific antibody-drug conjugate (bsADC), demonstrates promising anti-tumor efficacy.

Z. Li, C. Shang, Z. Han, G. An, **C. Guo**, W. An, Y. Yang;
Biocytogen Pharmaceuticals (Beijing) Co., Ltd., Beijing, China

HER3 and MET expression act as bypass resistance mechanisms, conferring resistance to multiple therapeutic agents, such as EGFR TKI treatment. HER3 and MET are also co-expressed at high prevalence in multiple tumor types, including gastric, colorectal, breast, and non-small-cell lung cancer (NSCLC). In addition, HER3 and MET are frequently overexpressed in liver metastases from patients with colorectal cancer, indicating that targeting both targets may provide clinical benefit.

We previously reported generation of a fully human bispecific antibody (bsAb) targeting HER3 and MET using RenLite® mice, which contain the full human heavy chain variable domain with a common human kappa light chain to facilitate bispecific antibody assembly. This bsAb demonstrated reactivity to human and cynomolgus monkey antigens and binding to multiple cancer cell lines, including NSCLC, gastric, colorectal, and hepatocellular cancer cell lines. The bsAb also showed enhanced internalization activity compared to parental monovalent antibodies in the NUGC-4 cell line expressing HER3 and MET.

Here, we evaluated the efficacy of the bsAb when conjugated to two distinct payloads: vcMMAE and BLD1102, Biocytogen's novel, proprietary linker/payload system composed of a DNA Topo I inhibitor payload (BCPT02) and a highly hydrophilic protease-cleavable linker. The *in vivo* efficacy of BCG022-vcMMAE and BCG022-BLD1102 was evaluated in cell-derived NSCLC and gastric cancer xenografts, and in patient-derived gastric and pancreatic xenograft models. Both demonstrated strong anti-tumor activity, with efficacy greater than or comparable to benchmark ADCs. Taken together, these promising preclinical results suggest that the BCG022 bsADC could be a novel treatment for HER3 and MET co-expressing tumors.

#2618 BCG017, a bispecific ADC targeting PTK7 and EGFR exhibits anti-tumor efficacy in PDX models.

S. Yao, C. Shang, Z. Li, G. An, **C. Guo**, W. An, Y. Yang;
Biocytogen Pharmaceuticals (Beijing) Co., Ltd., Beijing, China

EGFR is a favored target in various cancer therapies. However, EGFR-based treatments have been challenged by drug resistance and cytotoxicity. Targeting EGFR with an antibody-drug conjugate (ADC) is a promising new therapeutic strategy to address the drug resistance, due to the potent killing effects of the payload. Furthermore, we hypothesized that development of a bispecific ADC (bsADC) targeting EGFR and another tumor-associated antigen (TAA) might improve the tumor selectivity, thereby limiting the on-target off-tumor toxicity. One such TAA candidate is PTK7, which belongs to the same receptor tyrosine kinase family as EGFR, and is co-expressed with EGFR in multiple types of solid tumors, including lung, esophageal, head and neck, and colon cancers. Herein, we developed a fully human anti-human PTK7 EGFR bsAb using our proprietary common light chain RenLite® mouse platform and knobs-into-holes technology. The anti-PTK7 EGFR bsAb demonstrates good purity by SEC-HPLC, and can cross-react with human and cynomolgus monkey antigens with favorable affinity. The PTK7 x EGFR bsAb demonstrated higher binding to various types of cancer cell lines, as well as enhanced internalization *in vitro* compared with PTK7 parental antibody. Next, the bsAb was conjugated with monomethyl auristatin E (MMAE) to generate an anti-PTK7 x EGFR bsADC, BCG017, with a drug-to-antibody ratio of approximately 4. BCG017 demonstrated superior anti-tumor activity compared to benchmarks and its PTK7 parental ADC in cell-derived non-small-cell lung cancer (NSCLC) xenografts, and showed enhanced anti-tumoractivity when compared to benchmark ADCs and parental ADCs in patient-derived breast and pancreatic ductal adenocarcinoma xenograft models. These results suggest that BCG017 have the potential to be a novel therapeutic alternative for PTK7 and EGFR co-expressing tumors.

#2619 A novel EGFR×HER3-targeting bispecific antibody drug-conjugate, BCG019, demonstrates robust anti-tumor efficacy in preclinical evaluation.

Z. Li, C. Shang, G. An, **C. Guo**, W. An, Y. Yang;
Biocytogen Pharmaceuticals (Beijing) Co., Ltd., Beijing, China

EGFR and HER3 are receptor tyrosine kinases that are highly expressed in multiple epithelial tumors. EGFR point mutations and small insertions within the kinase domain are common in lung cancer. HER3 is overexpressed in patients who are resistant to EGFR-TKI therapy, and is one of the common resistance mechanisms of EGFR and HER2-targeted therapy. We hypothesize that simultaneous targeting of EGFR and HER3 with a bispecific ADC will have the potential to overcome the resistance caused by HER3 after EGFR-targeted therapy and obtain better efficacy than the combination of EGFR monotherapy and HER3 monotherapy.

We first generated fully human bispecific antibodies (bsAbs) targeting EGFR and HER3 using RenLite® mice, which contain the full human heavy chain variable domain with a common human kappa light chain to facilitate bispecific antibody assembly. The anti-EGFR×HER3 bsAb demonstrated reactivity to human and cynomolgus monkey antigens and binding to multiple cancer cell lines, including NSCLC, gastric, pancreatic, colorectal, and breast cancer cell lines. The anti-EGFR×HER3 bsAb also showed high internalization activity in cell lines expressing EGFR and HER3.

The anti-EGFR×HER3 bsAb was then conjugated with vc-MMAE (valine-citrulline-monomethyl auristatin E) for proof-of-concept studies, as well as BLD1102, Biocytogen's novel, proprietary linker/payload system composed of a DNA Topo I inhibitor payload (BCPT02) and highly hydrophilic protease-cleavable linker, to generate EGFR- and HER3-targeting bispecific ADC candidates BCG019. *In vivo* efficacy of the bsADC candidates were evaluated in cell-derived NSCLC and gastric cancer xenografts and in patient-derived gastric and colorectal xenograft models. Both bsADCs showed superior anti-tumor activity when compared to benchmark ADCs. Collectively, these results suggest that our novel anti-EGFR×HER3 bsADC has therapeutic potential for EGFR and HER3 co-expressing tumors.

#2620 BCG016, a first-in-class bispecific antibody-drug conjugate targeting 5T4 and MUC1, demonstrates potent preclinical anti-tumor activity.

Z. Han, C. Shang, Y. Zhang, G. An, **C. Guo**, W. An, Y. Yang;
Biocytogen Pharmaceuticals (Beijing) Co., Ltd., Beijing, China

5T4 is a highly expressed tumor-associated antigen associated with adverse clinical outcomes in solid tumors, and is an attractive therapeutic target due to low expression on normal adult tissues. While several therapeutic agents targeting 5T4 antigen are currently being evaluated in human clinical trials, none have yet entered the market. Another target, MUC1, is currently under clinical investigation, with most drugs in clinical trials showing limited efficacy due to shedding of the target antigen MUC1-N. 5T4 and MUC1 are commonly co-expressed in various solid tumors, including lung, breast, colorectal and pancreatic cancers, suggesting that targeting both antigens with a single drug could be a promising therapeutic strategy.

We previously identified and evaluated antibodies targeting human 5T4 and MUC1-C (cleaved MUC1) using RenLite® fully human common light chain mice. Here, selected antibodies were constructed into 5T4×MUC1 bispecific antibodies (bsAb). The 5T4-MUC1 bsAb demonstrated high avidity in multiple human tumor cell lines by flow cytometry. Notably, the parental 5T4 antibody also binds strongly to many tumor cell lines. Internalization assays demonstrate that the internalization of 5T4-MUC1 bsAb in breast cancer cells was enhanced compared to the parental anti-5T4 and anti-MUC1 monoclonal antibodies, as measured by Incucyte® live cell imaging. Subsequently, the 5T4-MUC1 bsAb was then conjugated with monomethyl auristatin E (MMAE) to generate 5T4 x MUC1 bsADC (BCG016). Cytotoxicity assays indicate that BCG016 improved tumor cell killing *in vitro* compared to benchmark ADCs, and *in vivo* efficacy studies showed superior anti-tumor efficacy of BCG016 in patient-derived NSCLC xenografts compared to benchmark ADCs and parental ADC combination therapy.
In summary, we have generated a novel bispecific ADC targeting 5T4 and the cleaved MUC1-C protein, which remains membrane-bound on tumor cells. The 5T4-MUC1 bsADC showed superior anti-tumor efficacy in PDX models and has the potential to be a novel therapeutic for 5T4 and MUC1 co-expressing tumors.

#2621 Preclinical Efficacy of DM002, a bispecific HER3×MUC1 antibody-drug conjugate with a novel DNA topoisomerase I inhibitor, in solid tumor models.

Y. Zhang[1], C. Shang[1], N. Wang[2], G. An[1], **C. Guo**[1], W. An[1], Y. Yang[1];
[1]Biocytogen Pharmaceuticals (Beijing) Co., Ltd., Beijing, China, [2]Doma Biopharmaceutical (Suzhou) Co., Ltd., Suzhou, China

MUC1 is a known tumor-associated antigen (TAA), but previous anti-MUC1 agents have shown limited clinical efficacy due to neutralization by the soluble N-terminal autoproteolytic product of MUC1. More recently, HER3-targeted ADCs, such as Patritumab deruxtecan, have shown encouraging early clinical activity in a variety of tumors. However, the majority of patients did not exhibit response to paritumab deruxtecan treatment. Therefore, improved therapies targeting these TAAs are needed.

As HER3 and MUC1 are co-expressed in a wide range of cancer types, we hypothesized that simultaneous targeting of HER3 and MUC1 with a bispecific antibody-drug conjugate (bsADC) could potentially lead to increased efficacy, reduced resistance and improved safety in the clinical setting. We generated an anti-HER3×MUC1 bispecific antibody using the fully human common light chain antibody transgenic mice (RenLite®).

The HER3×MUC1 bsAb showed improved cell binding and internalization *in vitro* compared to the parental mAb, suggesting synergy between the two arms. We then conjugated the HER3xMUC1 bsAb with vcMMAE for proof-of-concept studies, or with our novel DNA topoisomerase I inhibitor linker/payload conjugates (BLD1102) to make DM002-BLD1102 bsADC. Both bsADCs potently inhibited the growth of HER3+MUC1+ PDX tumors. DM002-vcMMAE also showed greater *in vivo* efficacy than its parental mAb ADCs, consistent with their *in vitro* internalization activity. DM002-BLD1102 also showed strong anti-tumor activity in DM002-vcMMAE resistant PDX models, suggesting the superiority of this new DNA topoisomerase I inhibitor linker/payload over the classical vcMMAE linker/payload. In conclusion, the HER3×MUC1 bsAb is a promising agent for the treatment of HER3 and MUC1 positive tumors.

#2622 TUB-040, a novel Napi2b-targeting ADC built with ethynylphosphonamidate conjugation chemistry, demonstrates high and long-lasting anti-tumor efficacy via Topoisomerase-I inhibition and excellent tolerability predictive of a wide therapeutic window in humans.

S. Schmitt, I. Mai, P. Machui, S. Herterich, D. Hauswald, P. Ochtrop, P. Cyprys, I. Kozlowska, A. Kitowski, M. Gerlach, O. Marcq, P. A. Trail, D. Schumacher, M.-A. Kasper, G. Fingerle-Rowson, B. Hock, **J. Helma-Smets**, A. M. Vogl;
Tubulis GmbH, Planegg, Germany

TUB-040 is a novel Antibody-Drug Conjugate (ADC) targeting Napi2b, a highly overexpressed target in ovarian cancer and lung adenocarcinoma. Napi2b is a member of the solute-carrier transporter family with eight transmembrane domains and an antibody-accessible extracellular loop, that regulates sodium-dependent phosphate homeostasis. Ethynylphosphonamidate conjugation chemistry was used to build TUB-040 with a homogenous DAR (drug-antibody-ratio) of 8 and the Topoisomerase I inhibitor Exatecan as payload, which is connected to a humanized, Fc-silenced IgG1 antibody targeting Napi2b using a cleavable linker system. *In vitro*, TUB-040 is characterized by sub-nanomolar affinity and specific binding to Napi2b, efficient target-mediated internalization and high cytotoxicity towards Napi2b-expressing ovarian and lung cancer cell lines as well as bystander activity against co-cultured target-negative cells. TUB-040 induces DNA damage and apoptosis in a dose-dependent fashion as well as markers of immunogenic cell death. In addition, no unspecific uptake and cytotoxicity in healthy, target-negative human cells could be detected, reducing the risk of target-independent toxicities. Pharmacokinetic analysis showed that - in contrast to maleimide-conjugated ADCs - TUB-040 is highly stable - and does not lose or transfer its linker-payload to serum proteins during blood circulation, thus enabling most efficient and continued delivery of Exatecan to the tumor. Across a variety of cell line derived xenograft (CDX) and patient derived xenograft (PDX) models of ovarian and non-small cell lung cancer, including models with low target expression, single dose administration of TUB-040 results in long-lasting tumor growth inhibition with high complete remission rates *in vivo*. The minimally effective dose (MED) leading to complete remission is 1 mg/kg. Preliminary repeat-dose toxicological assessment of TUB-040 in the pharmacologically relevant species cynomolgus monkey demonstrated that TUB-040 is well tolerated with no signs of lung toxicity and thrombocytopenia. Allometric scaling and PK/PD modelling predicts a human serum half-life greater 10 days and a therapeutic index in humans up to 55. Based on these results, TUB-040, designed with differentiating technology for optimal efficacy and tolerability, is ready for testing in clinical trials.

#2623 Enabling 5T4 for targeted cancer therapy: TUB-030, a novel ADC built with ethynylphosphonamidate conjugation chemistry, shows long-lasting anti-tumor activity via Topoisomerase-I inhibition with an optimized therapeutic index.

S. Schmitt, I. Mai, P. Machui, S. Herterich, D. Hauswald, P. Ochtrop, P. Cyprys, I. Kozlowska, A. Kitowski, M. Gerlach, O. Marcq, P. A. Trail, D. Schumacher, M.-A. Kasper, G. Fingerle-Rowson, B. Hock, **J. Helma-Smets**, A. M. Vogl;
Tubulis GmbH, Planegg, Germany

TUB-030 is a novel Antibody-Drug Conjugate (ADC) targeting the oncofetal 5T4 antigen, a glycoprotein, that is functionally involved in regulation of the Wnt signalling pathway and promoting cellular motility and adhesion. Immunohistochemical analysis identified 5T4 overexpressed in many types of cancers, including bladder, lung, breast, stomach, esophagus, head and neck, colon, and ovarian. Analysis in fresh frozen healthy human tissue with the therapeutic mAb candidate of TUB-030 revealed limited cross reactivity. Ethynylphosphonamidate conjugation chemistry was used to build TUB-030 with a homogenous DAR (drug-antibody-ratio) of 8 and the Topoisomerase I inhibitor Exatecan as payload, which is connected to a humanized, Fc-silenced IgG1 antibody targeting 5T4 using a cleavable linker system. Overall, TUB-030 contrasts previous ADC designs targeting 5T4, implementing several layers of differentiation in terms of antibody, payload and conjugation technology. In vitro, TUB-030 is characterized by sub-nanomolar affinity to 5T4, efficient target-mediated internalization and strong cytotoxicity towards cancer cells from different tumor indications with a broad range of 5T4 expression levels. Differently to previous 5T4-targeting ADCs, TUB-030 has efficient bystander activity against co-cultured target-negative cells, which facilitates targeting of tumors with heterogenous 5T4 expression. Pharmacokinetic analysis showed that TUB-030 is highly stable - and does not lose or transfer its linker-payload to serum proteins during blood circulation and antibody-like clearance profile contrasting maleimide-conjugated ADCs and enabling most efficient and continued delivery of Exatecan to the tumor site. Single-dose treatment with TUB-030 results in long-lasting tumor regression with high complete remission rates across a variety of both cell-line derived xenograft (CDX) and patient-derived xenograft (PDX) cancer models of multiple tumor indications in vivo, including models with low target expression. Preliminary repeat-dose toxicological assessment of TUB-030 in a pharmacologically relevant non-human primate species demonstrated that TUB-030 is well tolerated. The preclinical results underline that TUB-030 with novel ADC technology has the potential to enable 5T4 as a therapeutic target and provide treatment options in numerous solid cancer indications with high unmet medical need supporting further development towards the clinic.

IMMUNOLOGY: Epigenetic Regulation of Tumor Immunity
Poster Session

#2627 PanCancer epigenetic regulators of lymphocyte activation states.
A. Karpova, N. V. Terekhanova, S. Chen, R. G. Jayasinghe, A. Houston, W. Caravan, R. C. Fields, L. Ding;
Washington University in St Louis, St. Louis, MO

Several immune cell types have been successfully targeted for immunomodulatory therapy; however, the efficacies of such therapies are hindered by incompatible immune cell activation states. CD8+ T-cell exhaustion is one of the most studied T-cell states in the context of cancer and was shown to limit checkpoint blockade efficacy. Although CD8+ T-cell exhaustion studies in mice showed this state is tightly regulated by chromatin accessibility of cis-regulatory elements (CREs) and transcription factor activation, the exploration of these mechanisms, their prevalence, and their specificity in human cancers remains limited. In addition, chromatin accessibility signatures of other lymphocyte (CD4+ and NK) states frequently found in solid tumors have not been carefully characterized in a pan-cancer setting. Here we introduce the first single-nuclei atlas of pan-cancer and disease-specific cis- and trans-regulatory elements in tumor infiltrating lymphocytes. We profiled ~140K T-cell and NK cell nuclei with snATAC-seq and snRNA-seq from 227 tumor and normal samples from eleven cancer types. We distinguished two major subpopulations among exhausted CD8+ T-cells: GZMK expressing (CD8+ GZMK+ Tex) and ITGAE+ tissue-resident (CD8+ Trm ex). CD8+ GZMK+ Tex was enriched in clear cell renal cell carcinoma, while CD8+ Trm ex was found in all other cancers. Both exhausted groups featured high motif accessibility and expression of NR4A1, NFATC2, and NFKB2 transcription factors (previously reported to regulate exhaustion), but differed in EOMES motif accessibility and gene expression. We have identified other lymphocyte subpopulations showing exhaustion signatures, including CD4+ follicular helpers (CD4+ Tfh), CD4+ regulatory cells (CD4+ Tregs), and weakly cytotoxic tissue-resident NK cells (trNK weak). All these subpopulations showed increased expression and motif accessibility of the NR4A1 transcription factor, highlighting its role in regulating dysfunctional states not only in CD8+ T-cells, but also in CD4+ and NK cells. Additionally, CD4+ Tfh and Tregs showed enhanced activity of NFKB1, NFKB2, and POU2F2, and trNK weak cells had increased activity of NR4A2 and NR2F2. To put our results into clinical perspective, we have collected cohorts of renal cancer, melanoma and triple-negative breast tumors treated with immunotherapy in clinical trial settings, and showed elevated GZMK expression in exhausted T-cells in responders compared to non-responders.

#2628 Generation of multi-antigen specific T cells for ovarian cancer using Prussian Blue nanoparticles and photothermal therapy.

E. E. Grundy[1], A. Lee[1], S. Chin[1], M. Hadley[1], D. Schmidt[1], L. Wang[1], O. Cox[1], K. Omar[1], C. M. Bollard[2], R. Fernandes[1], K. B. Chiappinelli[1];
[1]The George Washington University, Washington, DC, [2]Children's National Hospital, Washington, DC

The immunosuppressive nature of ovarian cancer (OC) allows these tumors to evade the immune system, contributing to late-stage diagnoses and poor clinical outcomes for patients. However, a higher number of tumor-infiltrating lymphocytes is associated with improved clinical outcomes in OC. One type of lymphocyte, the T cell, can traffic to the tumor and kill tumor cells. We have shown that treating tumor cells with Prussian Blue nanoparticles and photothermal therapy (PBNP-PTT) results in immunogenic cell death, a form of cell death that is visible to the immune system, including T cells. PBNP-PTT-treated tumor cells were then used to expand tumor-specific T cells from partially genetically matched healthy donors against breast and brain cancer cell lines. These expanded T cells were better able to recognize and kill the target tumor cell lines than bulk unexpanded T cells from the same donors. Hence, we hypothesized that using PBNP-PTT-treated OC cells would allow us to expand a polyclonal tumor-specific T cell product that is cytolytic against OC cells *in vitro* and *in vivo*.We first evaluated whether multi-antigen OC-specific T cells could be expanded from partially genetically matched healthy donors and confirmed that PBNP-PTT elicited immunogenic cell death in the HLA-A*02:01 human OC cell lines Hey and TykNu. Using our established *in vitro* T cell expansion protocol, we then successfully expanded T cells from multiple HLA-A*02:01 healthy donors (n=3) against these cell lines. Functional analyses—including interferon-gamma ELISPOT, multi-color flow cytometry, and cytotoxicity assays—demonstrated that the expanded T cells had enhanced anti-tumor responses against OC cell lines compared to bulk unexpanded T cells derived from the same donors. Current work is expanding this approach to a syngeneic murine setting in C57BL/6J mice. Moreover, we will evaluate HLA-matched T cells and tumor cells from patients with OC *ex vivo*. Collectively, these efforts serve as a novel approach towards a curative immunotherapy for OC.

#2629 N6AMT1-mediated DNA 6mA modification in DNA repetitive elements LINE-1 dynamically regulates the IFN signal pathway in colorectal cancer.

Z. Yuan, X. Liu, X. Wang, Y. Luo, **H. Yu**;
The Sixth Affiliated Hospital of Sun Yat-sen University, Guangzhou, China

Background: DNA N^6-methyldeoxyadenosine (6mA) modification is the most prevalent DNA modification in prokaryotes, like bacteria, which participates in the host defense system. However, the presence and function of DNA 6mA in eukaryotes remains elusive. Many studies have reported that DNA 6mA modification is distributed across the genome and regulates transcription and the activity of transposable elements, in which the DNA 6mA methyltransferases and demethylases are involved, including the methyltransferase N6AMT1. LINE-1 is a genome-wide DNA repetitive element that acts as a diagnostic and prognostic biomarker for colorectal cancer. Therefore, we aimed to map the DNA 6mA in LINE-1 and investigate its role in the colorectal cancer (CRC) development.
Methods: The restriction-enzyme-digestion assay followed by quantitative PCR (6mA-RE-qPCR) was used to evaluate the LINE-1 DNA 6mA levels in the tumor and normal tissues. The DNA Nanopore sequencing was utilized to determine DNA 6mA and 5mC modifications. After the knockdown of N6AMT1, the dynamic changes of LINE-1 DNA 6mA methylation and RNA transcription under various stresses were determined by 6mA-RE-qPCR and qPCR, and the subsequent RNA-seq was performed to explore the downstream regulated pathways.
Results: The DNA 6mA methylation in LINE-1 is highly variant in the tumor and normal tissues, and it was significantly less prevalent in tumor tissues. The genomic distribution of LINE-1 DNA 6mA is significantly different from that of LINE-1 5mC. The LINE-1 DNA 6mA methylation and RNA transcription levels were dynamically changed in response to various stimuli, including 5-FU and H_2O_2. Knockdown of N6AMT1 downregulated LINE-1 DNA 6mA methylation and RNA transcription, promoted the proliferation, migration and invasion of CRC cells in vitro, and suppressed the IFN-gamma pathway. The co-culture assay showed N6AMT1 facilitated chemotaxis of macrophages and cytotoxicity of T cells via the IFN-gamma signal pathway.
Conclusions: The heterogeneity of DNA 6mA methylation in LINE-1 and its dynamic change in response to stimuli indicate a biological role of LINE-1 6mA methylation in the primary and adaptive tumor heterogeneities, which provides a novel insight into cancer development. The N6AMT1-mediated DNA 6mA modification in LINE-1 regulates CRC development through the IFN-gamma pathway.
Keywords: N6AMT1, LINE-1, DNA 6mA methylation, colorectal cancer

#2630 Identifying most promising combination therapies for immune suppressive breast cancer using a combined in vitro/ in vivo approach.

H. Silberzahn, M. Bleisch, A. Lohr, V. Knauff, K. Lashuk, **J. B. Schueler**;
Charles River Laboratories, Inc., Freiburg, Germany

Combining epigenetic therapy with immunotherapy is a promising strategy to address the complexities of cancer biology. However, it's important to note that the field is still evolving, and more research is needed to understand the optimal combinations, timing, and patient populations that will benefit the most from these approaches. We evaluated a combination of two different checkpoint inhibitor therapies (anti-CTLA4 and anti-PD1) with two different hypomethylating agents (5-azacytidine, AZA and Decitabine, DEC) in vitro and in vivo using a mouse breast cancer cell line 4T1 known to be resistant towards checkpoint inhibition (CPi). Beside tumor cell killing and tumor volume measurement, cytokine expression and immune cell phenotyping was determined. In a co-culture assay with autologous T cells and 4T1 cells, antitumor efficacy weas increased in all combination arms using AZA but not in combination with DEC. The combination of AZA with anti-CTLA4 was significantly better than the respective monotherapies (oneway ANOVA, $p< 0.001$). This effect was observed as well in the combination with anti-PD1 and AZA, however it was less pronounced (oneway ANOVA, $p< 0.01$). Of note, AZA restored the CTLA4 expression on CD8+ T cells in vitro, which was reduced by co-culture with tumor cells alone. In the follow-up in vivo experiment we focus on the combination of both CPi with AZA on different treatment schedules in the combination arms. The combination of anti-CTLA4 and AZA in a staggered treatment schedule displayed significant efficacy compared to control (oneway ANOVA, $p< 0.05$). The implantation of 4T1 reduced the number of T cells in bone marrow (BM), peripheral blood (PB) and spleen of the mice, confirming the immune-suppressive nature of the breast cancer line. This effect was restored under treatment with AZA in monotherapy and combination with CPi. Interestingly AZA reduced the number of immunosuppressive MDSC in BM, spleen and in tumor tissue. Vice versa NK cells were increased in BM, spleen and tumor tissue under treatment with AZA. AZA reduced the number of circulation tumor cells in PB and increased as already shown in vitro the percentage of CD8/CTLA4++ in PB. The PCA analysis of 36 mouse cytokines in vivo displayed two main clusters separated mainly by the presence of absence of AZA in the treatment arms. The combination arms which displayed the highest efficacy showed an increase in CXCL1, G-CSF, IL-6, LIF, M-CSF, MCP-1 (CCL2) and MCP-3 (CCL7) and a decrease of IFN-gamma, CXCL2. This is in line with the more inflammatory pattern of the tumor infiltrating lymphocytes in those groups. In summary, we have strong evidence that AZA influences the immune landscape of breast cancer towards a more inflammatory subtype. The combination with CPi was superior to the monotherapy. In addition, our data indicate that the treatment schedule of the combination might have a crucial influence on efficacy.

#2631 HMGA1 chromatin regulators drive immune evasion in myeloproliferative neoplasms by repressing gene networks involved in antigen presentation.

A.-A. Supreme, L. M. Resar, J. Kim, B. West, M. Antopia, H. Woo, K. Reddy, J.-H. Kim, L. Cope, J. Spivak, A. Moliterno;
Johns Hopkins University School of Medicine, Baltimore, MD

Myeloproliferative neoplasms (MPN) are clonal hematopoietic stem cell disorders caused by hyperactive JAK/STAT signaling and increased risk of transformation to acute myeloid leukemia (AML). However, targetable mechanisms driving progression remain elusive and therapies are ineffective after leukemia develops. We discovered that HMGA1 chromatin regulators are required for leukemogenesis in *JAK2*^{V617F} models of MPN AML by dysregulating transcriptional networks involved in proliferation and cell fate (Li et al, *Blood* 2022). Multi-omics analyses also showed that HMGA1 represses gene networks involved in interferon γ signaling in *JAK2*^{V617F} AML cells, a pathway that drives immune escape in solid tumors. We therefore sought to test whether HMGA1 drives immune evasion during leukemic transformation in MPN. Integrating RNA/ChIP/ATACseq in *JAK2*^{V617F} AML cells revealed that HMGA1 represses transcriptional networks involved in antigen presentation, including genes encoding major histocompatibility complex (MHC) class I and II proteins. Silencing *HMGA1* via CRISPR or shRNA results in up-regulation of MHC genes, with greatest induction of MHC class II (MHC II) genes (*HLA-DRA, DRB1, DPA1, DPB1*). Further, HMGA1 depletion increases protein levels of MHC II. To determine how HMGA1 represses MHCII genes, we examined genome architecture at the MHC II loci. We found that HMGA1 recruits repressive histone marks to regulatory regions for MHC II genes which preclude binding by CTCF, a chromatin regulator involved in genome organization, and CIITA, a transcription factor that activates MHC II genes. HMGA1 depletion enhances chromatin accessibility at critical enhancers (super enhancers) involved in MHC II expression, which allows CIITA and CTCF to activate MHC II genes. Because the histone acetylase inhibitor, entinostat, induces MHC II genes in solid tumors, we assessed MHC II with entinostat and HMGA1 depletion. *HMGA1* silencing enhances up-regulation of MHC II by entinostat. To test the functional significance of HMGA1 in immune evasion, we performed co-culture experiments with T cells and *JAK2*^{V617F} AML cells which showed that *HMGA1* silencing in AML cells activates T cells, resulting in cytotoxic T cell killing of *JAK2*^{V617F} AML cells. To examine the relevance of this pathway in patients, we interrogated RNAseq from peripheral blood mononuclear cells and found that *HMGA1* overexpression is associated with repression in MHC II genes in about 30% of MPN patients after progression to AML. Together, these data define a new mechanism of gene repression by HMGA1 through chromatin compaction and repressive histone marks that preclude CIITA and CTCF binding to the MHC II loci. Both HMGA1 depletion and entinostat up-regulate MHCII genes, thus illuminating HMGA1 as a potential therapeutic target to stimulate an immune attack and prevent MPN progression.

#2632 A new paradigm for brain tumors treatment: Guadecitabine as a fundamental player to improve tumor immune response.

M. Lofiego[1], F. Piazzini[1], F. Caruso[2], F. Marzani[1], L. Solmonese[1], E. Bello[1], F. Celesti[1], M. Costa[2], T. Noviello[3], R. Mortarini[4], A. Anichini[4], M. Ceccarelli[3], S. Coral[1], A. Di Giacomo[1], M. Maio[1], A. Covre[1];

[1]University of Siena, Siena, Italy, [2]BIOGEM Institute of Molecular Biology and Genetics, Ariano Irpino, Italy, [3]University of Miami, Miami, FL, [4]Fondazione IRCCS Istituto Nazionale dei Tumori, Milan, Italy

Background: Glioblastoma multiforme (GBM) is a highly aggressive primary brain tumor refractory to standard treatments and to immunotherapy with immune-checkpoint inhibitors (ICI) (PMID: 35626018). Interestingly, melanoma brain metastases (MM-BM), sharing the same niche as GBM, often respond to current ICI immunotherapies (PMID: 36521332). The role of epigenetic modifications in regulating GBM cellular proliferation, invasion, and prognosis, as well as their impact on the cross-talk between GBM and immune cells in the tumor milieu, has become evident (PMID: 34361090). Consequently, manipulating the epigenome has emerged as a therapeutic opportunity in GBM.

Methods: Microarray transcriptional and methylation profiles, followed by gene set enrichment and IPA analyses, were conducted to study the differences in constitutive expression profiles between GBM and MM-BM cells compared to extracranial MM cells. Additionally, the modulatory effects of the DNA hypomethylating agent (DHA) guadecitabine on different tumor cells were investigated. The prognostic relevance of DHA-modulated genes was assessed through Cox analysis in a TCGA GBM patients' cohort.

Results: The most notable differences between constitutive GBM and MM-BM cells lie in the enrichment of biological processes associated with tumor growth, invasion, and extravasation, as well as the inhibition of MHC class II antigen processing/presentation in GBM cells. Guadecitabine treatment appeared to shrink these differences, shifting the phenotype of GBM cells towards the more immunogenic MM-BM profile. This was achieved through promoter hypomethylation and subsequent up-regulation of genes mainly associated with the activation, proliferation, and migration of T and B cells, along with MHC class II antigen processing/presentation. Among DHA-modulated genes in GBM, 7.6% exhibited significant prognostic relevance. Moreover, a substantial set of immune-related upstream regulators (URs) were commonly modulated by DHA in GBM, MM-BM, and/or MM cells: DHA-activated URs enriched biological processes mainly involved in the regulation of cytokines and chemokines production, inflammatory response, and Type I/II/III IFN-mediated signaling. DHA-inhibited URs were associated with metabolic and proliferative pathways.

Conclusions: Epigenetic remodeling of GBM by DHA represents a promising strategy to enhance the efficacy of cancer immunotherapy, supporting the rationale for developing new combinatorial approaches for the treatment of brain malignancies.

#2634 CRISPR *in vivo* screen utilizing removable Cas9 system to identify epigenetic immune response modulators in antigen-sensitive mouse syngeneic models.

Y. He, Y. Liu, X. Wang, X. Li, W. Dong, T. Hao, C. Zhu, W. Zhou, Z. Peng;
Oncology & Immunology Unit, WuXi Biology, WuXi AppTec, Shanghai, China

The application of CRISPR-Cas9 screen in tumor immunology research has promoted the discovery of potential therapeutic targets and provided a deeper understanding of the mechanisms of immunotherapy resistance. Mouse syngeneic tumor model based CRISPR *in vivo* screen revealed significant features of immunotherapy by better approaching the tumor immune interaction. However, the immunogenicity of CRISPR-Cas9 has been widely observed in a variety of syngeneic models, which greatly limited for the application of CRISPR *in vivo* screen. Herein, we used two strategies for cancer cell gene editing, Cas9 protein electroporation and loxP-flanked Cas9 with Cre recombinase, to reduce the immunogenicity of CRISPR-Cas9 in CT26 subcutaneous and Renca orthotropic syngeneic models. Encouragingly, we found out that compared with constitutive Cas9-expressing All-In-One based cell pool models, both CT26 subcutaneous model and Renca orthotropic model showed a parental cell tumor comparable growth kinetics and immune checkpoint blockade ICB response by PD-1 antibody treatment. Further immuno-profiling of tumor immune microenvironment indicated limited changes from the parental cell model, which helped the data interpretation of *in vivo* screen outcome. We then performed a CRISPR *in vivo* screen by using a focused library against mouse epigenetic regulators in these two models and will discuss the hits from the screen in future.

#2635 An epigenetic regulation targeting inhibitory receptors and attenuates CD8 T cell exhaustion in breast cancer.

Y.-Z. Lin[1], W.-R. Wu[1], F.-C. Chung[1], Y.-C. Shen[2], C.-C. Lee[2], H.-W. Li[1], G.-J. Lin[1], W.-C. Cheng[1], S.-C. Wang[1];
[1]China Medical University, Taichung City, Taiwan, [2]China Medical University Hospital, Taichung City, Taiwan

T cell exhaustion is a state of dysfunctional T cell response characterized by prolonged antigen exposure and diminished effector functions, a significant cause of tumor tolerance, and poor response to immune checkpoint blockade (ICB) therapy. T cell exhaustion is a highly dynamic process involved with a network of genetic and epigenetic regulation that program the T cell functions. Epigenetic regulation by microRNAs targets multiple genes involved in T cell function and is expected to be a major contributor to the functional programming of tumor-associated T cells. However, the underlying causal mechanisms remain to be determined. Here, we show that the microRNA miR-379-5p is a critical epigenetic regulator for promoting T cell function and suppressing exhaustion induced by chronic stimulation. The microRNA is identified by integrating bioinformatic interrogation of the miRNA databases cross-referencing with the TCGA database for genes involved in T cell functioning and their correlation with clinical outcomes, coupled with molecular profiling of miRNAs in experimental T exhaustion. Notably, the expression levels of miR-379-5p in tumor tissues, which encompass cancer cells and the surrounding stromal components, including immune cells, are closely associated with favorable prognosis of various cancer types. Further molecular and cellular characterization of miR-379-5p entailing cell culture, animal models, and patient-derived tumor organoids shows that it exerts suppressive effects by targeting specific sequences in the 3' untranslated region (UTR) of critical immune checkpoint genes in T cells, thereby enhances the effector functions of cytotoxic T cells for tumor clearance. Ectopic expression of miR-379-5p shifts the evolution of primary T cells toward memory-like effector cells while silencing miR-379-5p induces exhaustion and abrogates the cytotoxic activity of primary T cells. We further demonstrate that transcriptional downregulation of miR-379-5p in T cells by a nuclear receptor transcription factor which is responsible for initiating the exhausting process impairs the tumor suppression function of T cells. Our studies indicate that miR-379-5p can function as a tumor suppressor by protecting T cells from exhaustion and bears the potential for developing novel strategies to improve the response to ICB therapy in breast cancer.

#2636 Epigenetic landscape of CD8+ T cell exhaustion and tissue residency in HPV-negative head and neck squamous cell carcinoma.

M. K. Luff, M. Craviero, M. Dar, K. McKinnon, A. Kaskas, C. T. Allen, V. Saloura;
National Institutes of Health, Bethesda, MD

Background Head and neck cancer is the 8th most common cancer worldwide. Human Papilloma Virus (HPV)-negative head and neck squamous cell carcinoma (HNSCC) overall survival rates remain low (25-40%) despite advances in treatments. CD8+ T cell differentiation into activated/cytotoxic (CTL), exhausted (T_{EX}) and tissue-resident memory (T_{RM}) phenotypes is a major determinant of successful cancer immunotherapy, which relies on the ability of CD8+ T cells to detect and eliminate cancer cells. Recent evidence suggests the importance of epigenetic regulation in the development of CD8+ T cell exhaustion and tissue residency; yet the epigenetic mechanisms that govern the transition between CTL, T_{EX}, and T_{RM} CD8+ T cell states remain unclear. This study investigates the epigenetic modifications associated with CTL, T_{EX}, and T_{RM} states using CD8+ T cells from healthy donors and HPV-negative HNSCC tumors.
Methods An *in vitro* human CD8+ T cell stimulation assay using healthy donor cells was utilized to generate CTL, T_{EX} and T_{RM} phenotypes. Naïve T cells underwent CD3/28, TCR-independent stimulation for 9 days to promote CTL (3 days) and T_{EX} (9 days) phenotypes, and TGF-β exposure (days 3-9) occurred to induce a T_{RM} phenotype. Flow cytometry to confirm expression of cell-surface and intracellular markers for each phenotype is ongoing. Genome-wide mapping for activating (H3K4me1, H3K4me3) and repressive (H3K9me3, H3K27me3, H4K20me3) histone marks with CUT&Tag assays will be pursued for each of the *in vitro* CTL, T_{EX} and T_{RM} states, along with RNA-seq. CUT&Tag and RNA-seq will also characterize the epigenetic profiles of CD8+ T cells from single-cell suspensions generated from HPV-negative HNSCC tumors (n=5). Findings will be correlated with results from our *in vitro* T cell states.
Results Preliminary flow cytometry confirmed increased expression of CD25, PD-1, Tim3 after 9 days of *in vitro* stimulation, supporting the induction of a CD8+ T_{EX} phenotype. CD103 was also highly expressed in CD8+ T cells exposed to TGF-β, supporting the induction of the CD8+ T_{RM} phenotype. Validation of the CTL state is ongoing. Phenotypic validation of cell states with flow cytometry (18 cell surface and intracellular markers) is ongoing. Feasibility of genome-wide mapping for activating and repressive histone marks with CUT&Tag on naïve CD8+ T cells has been confirmed.
Conclusion This study investigates epigenetic changes that characterize the transition between CTL, T_{EX}, and T_{RM} states of CD8+ T cells using healthy donor cells through an *in vitro* assay and CD8+ T cells isolated from HPV-negative HNSCC tumors. Understanding the epigenetic profile of T cell states can help determine the major epigenetic regulators that lead to exhaustion and tissue residency, paving the way for improved T cell-based immunotherapies. Future experiments aim to validate our findings using TCR-specific *in vitro* and *in vivo* models.

#2637 Super-enhancer-related m6A modification promotes immune escape in hepatocellular carcinoma associated with metabolic dysfunction-associated fatty liver disease via CCL4 signaling pathway inhibition.

L. Xu;
Peking University Shenzhen Hospital, Shenzhen, China

The incidence and mortality rates of hepatocellular carcinoma caused by metabolic dysfunction-associated fatty liver disease (MAFLD) have been increasing in recent decades, emphasizing the urgent need for new therapeutic approaches. Emerging evidence suggests that approximately 80% of super-enhancer RNAs (seRNAs) undergo selective m6A modifications. seRNA and m6A modifications have been implicated in the progression of various cancers, making them potential targets for therapeutic intervention. Based on our previous research, we hypothesize that the lack of m6A modification on the super-enhancer of CCL4 may contribute to the reduced expression of the CCL4 gene in HCC.To validate our hypothesis, we employ nano-chromatin immunoprecipitation combined with high-throughput sequencing (nano-ChIP-seq), m6A-seq (m6A-seq), single-cell RNA sequencing (scRNA-seq) on multiple models including clinical samples, cell lines, and mouse models. Interestingly, we have made a significant discovery that overexpression of CCL4 in tumor cells enhances the infiltration of CD8+ T cells, which are crucial for anti-tumor immune responses. In contrast, normal tissue cells undergo m6A modification on the CCL4 seRNAs, while this modification is notably absent in cancerous tissue. Consequently, the reduced expression of CCL4 could impair the tumor-killing capabilities of CD8+ T cells and facilitate immune evasion by the tumor.Furthermore, our results shed light on the underlying molecular mechanisms involving super-enhancers and m6A modifications in the regulation of immune escape in MAFLD HCC. We identify the specific super-enhancer and downstream regulatory genes influenced by m6A modification in MAFLD-associated HCC, providing valuable insights and novel targets for the treatment of this condition.

#2638 Sensitizing immunotherapy-refractory prostate cancer to immune checkpoint blockade therapy with optimized ketogenic diet regimens.

S. Murphy, S. Rahmy, D. Gan, J. Li, **X. Lu**, X. Lu;
University of Notre Dame, South Bend, IN

The purpose of this study is to investigate strategies for enhancing immune checkpoint blockade (ICB) therapy in prostate cancer (PCa).
To achieve this, we established a series of ICB-resistant PCa cell lines derived from a previously sensitive cell line, which originated from a murine model of metastatic PCa. Notably, we observed a reduction in major histocompatibility complex (MHC) class I protein levels in the resistant sublines.
Our study demonstrated synergistic efficacy through the combination of anti-PD1 and anti-CTLA4 antibodies with histone deacetylase inhibitor (HDACi) vorinostat, a cyclic ketogenic diet (CKD), or β-hydroxybutyrate (BHB) supplementation. Importantly, these interventions significantly delayed PCa tumor progression. Furthermore, our analysis revealed that the effects of these interventions were contingent on both BHB and adaptive immunity. In-depth single-cell transcriptomic and proteomic profiling unveiled mechanisms involving cancer-cell-intrinsic changes (upregulated MHC class I molecules) and extrinsic factors, including CD8+ T cell chemoattraction, M1/M2 macrophage rebalancing, monocyte differentiation toward antigen-presenting cells, and reduced neutrophil presence.
In conclusion, our findings provide valuable insights into the potential clinical utility of combining HDACi and optimized ketogenic diet regimens to enhance ICB therapy for PCa.

#2639 Combined therapy targeting AR and EZH2 restrains the growth of castration resistant prostate cancer by enhancing antitumor T cell response.

I. Fischetti[1], B. Laura[1], R. Sulsenti[1], V. Cancila[2], C. Enriquez[1], R. Ferri[1], M. Bregni[3], F. Crivelli[3], C. Tripodo[2], M. P. Colombo[1], **E. Jachetti**[1];
[1]Fondazione IRCCS Istituto Nazionale dei Tumori, Milan, Italy, [2]University of Palermo, Palermo, Italy, [3]ASST Valle Olona, Busto Arsizio, Italy

Castration resistant prostate cancer (CRPC) is a fatal disease. Androgen receptor pathway inhibitors, like enzalutamide, are initially effective but resistance eventually occurs, often associated to the emergence of aggressive neuroendocrine variants (NEPC). Even immunotherapy induced limited results in prostate cancer, governed by an immunosuppressive microenvironment. Therefore, effective therapies are needed. We here investigate in preclinical models a new approach aimed to revert castration resistance and simultaneously turn the immune milieu from “cold” to “hot”, through the combination between enzalutamide and the drug GSK-126, which inhibits the epigenetic modulator EZH2. We show that enzalutamide and GSK-126 can synergize to restrain the growth of CRPC *in vitro* and *in vivo.* Moreover, this therapeutic combination efficiently reduced NEPC differentiation, in both subcutaneous and autochthonous *in vivo* models, increasing the rate of cured mice with regressed lesions. The antitumor efficacy observed in immunocompetent mice bearing subcutaneous syngeneic CRPC tumors was lost in immunodeficient mice, indicating a contribution of immune cells. Additional experiments in the TRAMP spontaneous mouse model revealed that the combination of enzalutamide and GSK-126 significantly induced cytotoxic activity and IFNγ production by tumor-specific $CD8^+$ T cells, otherwise tolerant, and increased IL-17 production by $CD4^+$ T cells. The two drugs did not directly modulate T cell activity *in vitro*, suggesting the importance of microenvironment accomplices in triggering these effects. These results promote the combined use of enzalutamide and GSK-126 to restrain CRPC growth and NEPC differentiation, and, simultaneously, to awake antitumor T cell response, opening new possibilities for immunotherapy in prostate cancer.

#2640 HBI-2375, a first-in-class IND ready selective MLL1-WDR5 inhibitor, retains desirable preclinical characteristics in solid tumors and in leukemias to be pursued in clinical studies.

F. Shojaei, C. Fang, J. M. Ricono, M. Gillings;
HUYA Bioscience International, San Diego, CA

MLL1 (mixed lineage leukemia1) interaction with WDR5 (WD repeat domain 5) is critical for its histone methyl transferase (HMT) activity leading to transcriptional regulation of gene expression. MLL1 dysregulation such as its translocation at chromosome 11q23 results in generation of MLL1 fusion genes and leukemia development. Additionally, recent studies indicated a role for MLL1-WDR5 interaction in solid tumors progression via directly affecting cancer cells or by suppression of tumor immunity. Therefore, MLL1-WDR5 interaction is an important target in the discovery of anti-cancer drugs for both leukemia and solid tumors. We recently identified HBI-2375 as a selective inhibitor of MLL1-WDR5 interaction. HBI-2375 showed potent inhibition of WDR5 (IC50: 4.48nM) in biochemical assay and inhibited MV4-11 cellular proliferation (average IC50: 3.17μM) in CTG assays. In addition, HBI-2375 was stable in liver S9 and whole blood, with moderate to high plasma protein binding rates in multiple species, and acceptable hERG (IC50: 17μM). Furthermore, HBI-2375 displayed reasonable oral PK properties (C_{max}, $T_{1/2}$, AUC, and F%) in mouse, rat and dog and showed good safety profile in GLP tox studies. In pharmacology studies HBI-2375 showed significant dose dependent anti-tumor activity in MV4-11 AML model along with reduction in methylation of H3K4 in the tumors harvested from the treated animals demonstrating the targeted disruption of HMT activity in cancer cells by HBI-2375. Furthermore HBI-2375 in combination with PD-1 mAb significantly inhibited tumor growth in MC38, colorectal tumor model, and in 3LL lung carcinoma syngeneic tumor models. Flow cytometry and IHC showed significant increase in the infiltration of CD8+ CTLs in the combination group further providing immune-driven mechanisms for greater efficacy of combination therapy. Gene expression analysis also identified genes that are involved in promoting immune system activity in the combination group. Tissue distribution studies also showed greater accumulation of HBI-2375 in brain tissue indicative of a potential to target glioma and glioblastoma in clinical studies. Therefore, HBI-2375 represents a first-in-class MLL1-WDR5 inhibitor with promising characteristics for future testing in the clinic.

#2641 Transcriptional reprogramming of Ewing tumors: gains and losses noted when utilizing immunocompetent in vivo models.

J. D. Daley[1], E. Mukherjee[1], A. C. Tufino[1], R. Bao[2], K. M. Bailey[1];
[1]UPMC Children's Hospital of Pittsburgh/University of Pittsburgh, Pittsburgh, PA, [2]UPMC Hillman Cancer Center, Pittsburgh, PA

Objective: Ewing sarcoma is an aggressive cancer most frequently diagnosed in adolescents and young adults. Currently, there is a limited understanding of the immunobiology of Ewing sarcoma, including limited pre-clinical studies of immunotherapeutic interventions. This, in part, is due to the historical lack of an immuno-competent murine model. Here, we utilize an immunocompetent, humanized mouse model to investigate the Ewing tumor immune microenvironment. Specifically, we sought to determine the transcriptional differences that occur when comparing human Ewing tumors established in a humanized backdrop versus those developed in an NSG (immuno-deficient) model.
Methods: Human Ewing cell lines (A673, TC32, TC71) and PDX (PSaRC219) were injected orthotopically into humanized or NSG mice. After ~3 weeks, bulk RNA sequencing was performed on tumors utilizing an Illumina Next Generation Sequencer. Tumor single-cell suspensions underwent immunophenotyping by flow cytometry (CyTek Aurora) for the following human markers: CD45, CD3, CD4, CD8, CD56, CD14, CD16, etc.. Peripheral blood was collected, PBMCs isolated, and immunophenotyping was again performed to determine peripheral blood immune cell populations.
Results: Ewing tumors established in humanized mice demonstrate infiltration of human CD45+ cells as well as immune cell sub-populations (CD3+, CD14+, CD56+ cells). Bulk RNA sequencing analysis utilizing unsupervised hierarchal clustering revealed that the transcriptional profile of Ewing tumors generated in humanized vs NSG mice cluster distinctly. Pathway analysis of differentially expressed genes ($p < 0.05$) in Ewing tumors developed in humanized versus NSG mice demonstrates upregulation of pathways including extracellular matrix remodeling, collagen biosynthesis, and Wnt signaling. Notably, transcripts known to be specific to TGFBeta-dependent signaling in Ewing tumors are upregulated in the immune competent model, including *TGFB1*, *FBLN5*, and *COLEC12*.
Conclusion: This work demonstrates the Ewing tumor transcriptional remodeling that occurs when tumors are developed in an immunocompetent *in vivo* backdrop. Upregulation of several pro-metastatic pathways were noted. Ongoing work focuses on testing drug response differences between Ewing tumors developed in humanized versus NSG backdrops and pursuing immunocompetent Ewing models as a component of preclinical agent testing.

#2642 *KEAP1* mutation in lung cancer cells leads to increased immunosuppressive capability.

C. J. Occhiuto[1], K. T. Liby[2];
[1]Michigan State University, East Lansing, MI, [2]Indiana University, Indianapolis, IN

Considerable advances have been made in lung cancer therapies, but there is still an unmet clinical need to improve survival for lung cancer patients. Immunotherapies have improved survival, although only 20-30% of patients respond to these treatments. Interestingly, cancers with mutations in *KEAP1*, the negative regulator of the NRF2 cytoprotective pathway, are resistant to immune checkpoint inhibition and correlate with decreased immune cell infiltration. NRF2 is known for promoting an anti-inflammatory phenotype when activated in immune cells, but the study of NRF2 activation in cancer cells has not been adequately assessed. The overall objective of this study is to determine how lung cancer cells with constitutive NRF2 activity interact with the immune microenvironment to promote cancer progression and metastasis. To assess this, we generated CRISPR-edited mouse lung cancer cell lines (Lewis Lung Carcinoma/LL2) with knockouts (KO) of the *KEAP1* and *NFE2L2* genes. The transcriptomic profiles of 3 *KEAP1* KO and 1 *NRF2* KO cell lines were compared to the parental wildtype (WT) line using RNA-sequencing. On unsupervised hierarchical clustering of differentially expressed genes, the 3 *KEAP1* KO cell lines clustered together and the *NRF2* KO clustered with WT cells. Importantly, canonical NRF2 pathway-related genes were significantly increased in *KEAP1* KO clones, but the same genes were either decreased or similar to WT in the *NRF2* KO clone. We then used flow cytometry to evaluate immunosuppressive surface markers known to suppress T cell function when expressed on cancer cells. Importantly, PD-L1, CD155, CD80, and CD86 were increased in the *KEAP1* KO lines compared to WT, but not in the *NRF2* KO clone. In addition, the cytokine release profile was differentially regulated in the *KEAP1* KO clones in a manner that could alter T cell recruitment and function. These results were also consistent with gene expression in the sequencing dataset. Finally, using an orthotopic allograft model, we completed a preliminary immunophenotyping study of lung tumors for WT, *KEAP1* KO, and *NRF2* KO cell lines. The activation status of $CD8^+$ T cells and the ratio of $CD8^+/CD4^+CD25^+$ T cells (a prognostic marker) were decreased in *KEAP1* KO tumors. Taken together, these data suggest cancers with *KEAP1* mutations may increase tumor growth through suppression of T cells.

IMMUNOLOGY: Immune Checkpoints and Inhibitory Molecules 2
Poster Session

#2647 Topical corticosteroids stimulate T cell-dependent melanoma growth control.

C. H. Earnshaw[1], S.-C. Chiang[1], A. Moeini[1], M. Koufaki[1], E. Bonavita[1], L. Nebot-Bral[1], M. Russo[1], C. Bell[1], T. Bigirumurame[2], J. Nsengimana[2], J. Newton-Bishop[3], C. E. M. Griffiths[4], S. Zelenay[1];
[1]Cancer Research UK Manchester Institute, Manchester, United Kingdom, [2]Population Health Sciences Institute, Newcastle University, Newcastle, United Kingdom, [3]University of Leeds, Leeds, United Kingdom, [4]University of Manchester, Manchester, United Kingdom

Melanoma is the deadliest form of skin cancer. Treatment with immune checkpoint blockade (ICB) has transformed outcomes. However, half of melanoma patients do not derive long-term benefit. Side-effects of ICB are frequent, and typically managed by systemic or topical treatment with corticosteroids, widely known for their immunosuppressive effects. However, clinical data is contradictory as to the effect on prognosis of patients receiving ICB that also receive corticosteroids, with some studies suggesting a negative effect of steroid use, and others suggesting no effect or even positive outcomes with steroid use. Additionally, our lab recently showed that combining corticosteroids with ICB improves treatment responses in certain preclinical cancer models. Thus, understanding the role of corticosteroids in cancer progression, and their effect on the tumor immune microenvironment, is critical.
In an intradermal murine melanoma model unresponsive to ICB, we found that topical corticosteroid treatment significantly impairs tumor growth. After just two doses, glucocorticoid-treated tumors shrank, whereas control-treated tumors doubled in volume. Intriguingly, this effect was lost in *Rag1*$^{-/-}$ mice (deficient in B and T cells) or in mice depleted of CD8^{+} T cells, uncovering a key role for T cells in corticosteroid-induced tumor growth control. Genetic ablation of the glucocorticoid receptor in tumor cells abrogated this effect, suggesting corticosteroids act directly on tumor cells to stimulate anti-tumor immunity. Analysis of TCGA RNA sequencing data showed melanoma patients with high glucocorticoid receptor expression have better overall survival than those with low expression, a finding repeated in a large, independent cohort of primary melanoma specimens of the Leeds Melanoma Cohort (n=703). Through cellular and molecular profiling using multiparametric flow cytometry and whole exome RNA sequencing, we have identified promising candidate pathways that might underlie the immune-dependent tumor control induced by steroids.
Steroids induce tumor control in other, but not all, melanoma and non-melanoma tumor models studied, suggesting this may be a conserved immune-evasive pathway in a subset of tumors. Ongoing work aims to characterize the molecular and cellular effects of topical corticosteroid treatment, and to investigate their relevance in human melanoma. Given the widespread use of corticosteroids in patients receiving ICB, these unexpected findings may have significant clinical impact.

#2648 CD155 regulates cell growth and immune evasion in diffuse midline glioma.

T. Tzaridis[1], T. Eisemann[1], A. F. Andrade[2], J. L. Hope[3], O. Becher[4], N. Jabado[2], L. M. Bradley[1], P. Adams[1], R. Wechsler-Reya[5];
[1]Sanford Burnham Prebys Med. Discovery Inst., La Jolla / San Diego, CA, [2]Department of Human Genetics, Department of Paediatrics of the McGill University and Research Institute of the McGill University Health Center, Montreal, QC, Canada, [3]Department of Microbiology & Immunology, Drexler University College of Medicine, Philadelphia, PA, [4]Jack Martin Division of Pediatric Hematology-Oncology, Mount Sinai Kravis Children's Hospital, Icahn School of Medicine at Mount Sinai, New York, NY, [5]Department of Neurology and Herbert Irving Comprehensive Cancer Center, Columbia University Medical Center, New York, NY

There is an unmet need for effective treatment strategies for diffuse midline glioma (DMG), a devastating brain tumour arising in children and young adults. While immunotherapy is emerging as a powerful approach for treatment of other cancers, clinical trials with immune checkpoint inhibitors have failed to show a survival benefit for DMG patients. In this study, we analysed the expression of known immune checkpoint molecules on the surface of human and murine DMG cells by flow cytometry and identified CD155 and B7-H3 as the most highly expressed checkpoint molecules, with minimal expression of others, including PD-L1 and PD-L2. These findings were confirmed in primary patient samples from pediatric brain tumours (gliomas, medulloblastomas and ependymomas). To test whether CD155 regulates susceptibility to CD8+ T cell killing, we cultured murine DMG cells expressing ovalbumin (OVA) with CD8+ T cells from OT-I mice, which express T cell receptors specific for OVA. shRNA mediated silencing of CD155 led to a strong increase in T cell-mediated killing. *In vivo*, adoptive transfer of OT-I T cells into OVA-positive DMG-bearing immuno-compromised mice resulted in delayed tumour growth, and this effect was enhanced when tumours lacked CD155. Strikingly, CD155-deficient DMG cells failed to grow at all in immuno-competent mice, and depletion of CD8 T cells allowed these tumours to grow, highlighting a role for CD8 T cells in rejection of CD155-deficient cells. In addition to its effects on susceptibility to T cells, CD155 also exerted cell-autonomous effects on tumour cells: silencing of CD155 led to induction of apoptosis of DMG cells *in vitro* and to delayed tumour *growth in vivo*, even in immune-compromised mice. These studies demonstrate that CD155 functions as an immune checkpoint and as a regulator of tumour cell survival in DMG, and suggest that targeting CD155 could be a valuable double-pronged therapeutic strategy for this devastating disease.

#2649 A new role for the aryl hydrocarbon receptor (AhR) as a proximal mediator of immune checkpoints (PD-L1/2 and IDO1) in non-small cell lung cancer: Insights into an interferon-induced, LncRNA-and JAK/STAT-mediated signaling pathway.

B. Lara[1], M. Snyder[2], Z. Wang[1], J. Fimbres[1], E. Yang[3], D. H. Sherr[1];

[1]Boston University School of Public Health, Boston, MA, [2]Boston University School of Medicine, Boston, MA, [3]Boston University, Boston, MA

Non-small cell lung cancer (NSCLC) is the second most common cancer and accounts for ~127,000 deaths/year in the U.S. Its current ~30% five-year survival rate is an improvement from a decade ago thanks in part to the introduction of immune checkpoint inhibitors including PD1- and PD-L1-specific monoclonal antibodies. While PD-1/PD-L1-targeted immunotherapy is effective in many cases, not all patients respond and complete remissions still only occur in a minority of patients. Therefore, a greater understanding of immune checkpoint regulation in human NSCLC is needed. Here, we investigated a novel role for the aryl hydrocarbon receptor (AhR), an environmental carcinogen receptor previously associated with smoking-induced lung cancers, in the regulation of immune checkpoints PD-L1, PD-L2, and IDO1. Computational analyses of existing databases for protein-protein interactions linked to the AhR signaling pathway suggested crosstalk between the AhR, type I and type II Interferon (IFN), and JAK/STAT signaling pathways. AhR deletion from human lung A549 adenocarcinoma cells significantly reduced expression of *JAK2*, *STAT1*, *STAT2*, and the JAK/STAT signaling targets *IRF1* and *IRF9*. Type II IFNγ significantly increased expression of those genes as well as the immune checkpoints IDO1, PD-L1, and PD-L2 in an AhR-dependent fashion. Interestingly, AhR deletion also eliminated IFNγ-mediated induction of a recently described long non-coding RNA, *INCR1*, which is encoded across the *CD274*/*CD273* locus, and which facilitates *JAK2*, *CD274*/*PD-L1*, and *IDO1* translation. Concomitantly, AhR knockout increased baseline expression of an RNA-binding protein, HNRNPH1, known to sequester *JAK2* and *CD274* mRNA thereby reducing IDO, PD-L1 and PD-L2 expression. Similarly, the AhR was shown to regulate Type I IFNα-mediated induction of *STAT1*, *STAT2*, *CD274*/*PD-L1*, and *CD273*/*PD-L2*. The data indicate that IFN induction of key immune checkpoints in lung adenocarcinoma cells is dependent on the AhR through its control of a conventional JAK/STAT pathway and an unconventional lncRNA (*INCR1*) and RNA-binding protein (HNRNPH1) pathway.

#2650 IGFBP2 assists EGFRvIII-positive glioblastoma to evade immune elimination.

Jikang Fan[1], Xisen Wang[1], Tao Li[1], Xuejun Yang[2], Wei Zhang[3]

[1]Tianjin Medical University General Hospital, Tianjin, China,[2]Department of Neurosurgery, Beijing Tsinghua Changgung Hospital, Beijing, China,[3]Departments of Cancer Biology, Wake Forest School of Medicine, Winston-Salem, NC

In recent years, immunotherapy has achieved significant success in the treatment of a variety of cancer types, including melanoma, non-small cell lung cancer, and colorectal cancer. However, in stark contrast, patients with glioblastoma (GBM) show remarkably poor responses to immunotherapy, failing to derive any therapeutic benefit. Thus, an understanding of the immunosuppressive microenvironment of GBM, which is considered an immunotherapy-cold tumor, is of paramount importance. One common and distinctive genetic mutation found in gliomas is that of EGFRvIII, which is linked with enhanced cell proliferation, invasion, migration, and angiogenesis in GBM. Intriguingly, we found that this mutation induced a significantly more severe immunosuppressive microenvironment compared with wild-type EGFR. To unravel the mechanisms underlying EGFRvIII mutation-induced immunosuppression in GBM, we posited that the mutant variant secretes an array of immunosuppression-related proteins into the glioma microenvironment. To investigate this, we conducted proteomic analysis of conditioned media from EGFRvIII mutant cell lines and discovered significant changes in the expression of insulin-like growth factor-binding protein-2 (IGFBP2), a well-documented oncogenic protein. Although IGFBP2 is known to be upregulated in various tumor types and is associated with malignant behaviors such as proliferation and invasion in gliomas, its role in glioma immunology remains largely unexplored. In line with our earlier bioinformatic analyses, our study revealed significant enrichment of IGFBP2 in pathways related to immunosuppression in GBM. Thus, in the present investigation, we analyzed the mechanisms by which IGFBP2 induces an immunosuppressive microenvironment. Using co-culture models, we found that IGFBP2-overexpressing glioma cells as well as glioma cells treated with exogenous IGFBP2 recruited immune cells through binding to integrin αvβ5. Furthermore, we demonstrated that IGFBP2 promoted the secretion of the classical macrophage polarization factor IL-10 by phosphorylation of STAT3. These findings indicate the significant influence of IGFBP2 in steering glioma-associated macrophages toward a pro-tumor M2-like phenotype. We also observed that IGFBP2 upregulated the expression of PD-L1 on tumor cell surfaces. These results were verified in animal experiments. Intriguingly, our preliminary data indicated that exogenous IGFBP2 translocated to the cell nucleus within hours, and immunoprecipitation assays confirmed its interaction with STAT3 *in vitro*. These findings collectively underscore the pivotal role of IGFBP2 in the creation of the immunosuppressive microenvironment induced by EGFRvIII mutation. Consequently, targeting IGFBP2 holds great promise for advancing immunotherapeutic approaches in EGFRvIII-mutant glioblastomas, offering an exciting avenue for potential treatments of GBM.

#2651 A selective HPK1 inhibitor FB849 reprograms intratumoral immune cells and elicits strong anti-cancer immunity.

H. Kim[1], S. Lim[1], A. Park[1], J. Lee[1], J. Kim[1], S. Jeon[2], Y. Lee[2], E.-C. Shin[2], S. Kim[1];

[1]1STBiotherapeutics, Yongin-si, Gyeongido, Korea, Republic of, [2]Korea Advanced Institute of Science and Technology, Daejeon, Korea, Republic of

Hematopoietic progenitor kinase 1 (HPK1) is a negative regulator of immune cells and suppresses the immune function of a wide range of cells, including T cells, B cells, and dendritic cells (DCs). Recent studies have shown that HPK1 is correlated with increased T cell exhaustion, one of hallmark phenomena for acquired resistance to immune checkpoint inhibitors (ICIs), that is a major obstacle in the current immunotherapy regimen with an increasing need of novel agent to overcome it. We have discovered FB849, a highly potent, highly selective, and orally available HPK1 inhibitor especially with an excellent selectivity over key immune-related off target kinases. FB849 confers the activation of various human primary immune cells such as T cells, B cells, and DCs *in vitro.* FB849 elicited robust anti-cancer efficacy in syngeneic mouse models including MC38 and CT26 both as a monotherapy and in combination with a PD-1 antagonist. A dramatic synergistic efficacy with FB849 and PD-1 combination was observed in EMT6. Durable effects possibly through immunological memory were also confirmed in CT26. Under a CD8+ T cell depletion condition *in vivo*, FB849 still maintained monotherapy efficacy, demonstrating its anti-cancer immunity through CD8+ T cell-independent pathway possibly via efficacy through myeloid lineage. FB849 significantly reduced the LAG3+ and PD-1+ exhausted T cells and CD25+ FoxP3+ regulatory T cells, simultaneously depleted tumor associated macrophages (TAMs), and modulated dendritic cell population in the syngeneic tumors. To better understand how FB849's effects on human cancer, FB849 was evaluated in isolated TILs (tumor-infiltrating lymphocytes) from patients with renal cell carcinoma and other cancer types. CD8+ T cells from a RCC patient was highly activated evidenced by the increased cell proliferation and the enhanced cytokine secretion by *ex vivo* treatment of FB849 alone or by the combination with PD-1 antagonist. Similar phenomena were observed in gastric cancer, hepatocellular carcinoma, colorectal cancer, and head and neck cancer. FB849 treatment resulted in the activation of not only stem-like T cells but also in the partial reinvigoration of terminally differentiated T cells from a RCC patient. These data from patient TIL's together with mouse TIL's pinpoint unprecedented anti-tumor mechanism by FB849 through modulation of exhausted T cells as well as myeloid cells. Altogether, this study supports the planned clinical development of FB849 as a promising immuno-oncology agent as a monotherapy in the selected cancer types and as post-ICI combination with a PD-1 antagonist.

#2652 NDI-101150 is a potent and highly selective HPK1 inhibitor that both synergizes with and differentiates from anti-PD1 immune checkpoint blockade.

D. Ciccone, F.-S. Kuo, S. Daigle, N. Kaila, G. Yau, M. Carlson, D. Levasseur, B. Srivastava, F. G. Basile, C. Loh;
Nimbus Therapeutics, Boston, MA

Introduction HPK1 is a member of the MAP4K family of protein serine/threonine kinases that negatively regulates activation signals in multiple immune cells and is an attractive therapeutic target for many cancers. Using structure-based drug design, we developed a highly selective HPK1 inhibitor, NDI-101150, with nanomolar potency and physiochemical properties suitable for once daily oral administration.

Methods & Results HPK1 inhibition with NDI-101150 has a differentiated pharmacology profile when compared directly to PD1 blockade. NDI-101150 was able to overcome the immunosuppressive effects of prostaglandin E2, adenosine, and TGF-β on human T cell activation. HPK1 inhibition also directly limited the suppressive capacity of T regulatory cells. In contrast, anti-PD1 treatment was not able to overcome the immunosuppressive activity associated with any of these mechanisms. In vivo, HPK1 inhibition significantly enhanced the production of antigen-specific antibodies in response to immunization with both T-dependent and T-independent antigens, while anti-PD1 treatment had minimal to no effects on antibody production. In the EMT-6 syngeneic model, 7/10 mice receiving NDI-101150 exhibited complete tumor regressions, compared to only 1/10 from an anti-PD1 cohort. Furthermore, NDI-101150 established a robust and durable immune memory response as 100% of treated mice showed complete rejection of tumor growth upon subsequent re-challenge. HPK1 inhibition with NDI-101150 also shows robust synergy with PD1 blockade in vitro and in vivo. Both NDI-101150 and anti-PD1 were able to reinvigorate exhausted human T cells, restoring cytokine production and proliferative effects in mixed lymphocyte reactions. Further, in combination HPK1 inhibition and PD1 blockade synergized to enhance the activity of exhausted human T cells to an extent exceeding that observed with naïve human T cells in similar experiments. In vivo, while NDI-101150 or anti-PD1 treatments alone induced tumor growth inhibition in the murine CT-26 syngeneic tumor model, NDI-101150 and anti-PD1 in combination mediated complete tumor regressions in several mice. Furthermore, NDI-101150 seemed to induce a durable immune memory response as evidenced by the combination-treated animals showing complete rejection of tumor growth upon subsequent re-challenge, without any further dosing of NDI-101150.

Conclusions Pharmacological inhibition of HPK1 with NDI-101150 represents a powerful system-wide immunomodulatory approach with the potential to enhance anti-tumor immunity in patients failing to respond to currently approved immune checkpoint therapies or in combination with immune checkpoint blockade therapies. NDI-101150 is currently being tested in a Phase 1/2 trial (NCT05128487) in patients with advanced solid tumors.

#2653 Integrative analysis of proteomic alterations in human PBMC's treated by HPK1 inhibitor FB849 reveals enriched pathways from various immune cells leading to potential novel biomarker discovery.

S. Lim, S. Jin, A. Park, H. Kim, S. Kim, J. Kim, J. Lee;
1ST Biotherapeutics, Inc., Gyeonggi-do, Korea, Republic of

HPK1, also known as MAP4K1, is a critical signaling kinase molecule as a negative feedback loop in various immune cells. Despite the advancement of multiple clinical programs for therapeutic inhibition of HPK1, there is an urgent need to understand HPK1 biology in genome-wide signaling networks not only from lymphocytes but also from monocytes. FB849 is designed as a potent and highly selective inhibitor of HPK1 and is currently in phase I clinical trial with advanced cancer patients (NCT05761223). We aim to generate proteomic and phosphoproteomic profiles to reveal modes of action of FB849 in the broad spectrum of cancer immunity. Human PBMCs were treated with FB849 under conditions with or without CD3/CD28 stimulation. Utilizing an antibody array comprising 1,930 antibodies, the expression of 1,438 distinct proteins was assessed. The antibody arrays in human PBMCs identified a total of 85 and 33 phospho-proteins showing differential expression in response to FB849 treatment compared to the control in the presence or absence of CD3/CD28 stimulations, respectively (fold change > 2, adj. p-value < 0.01). KEGG pathway enrichment analysis demonstrated that the differentially expressed proteins by FB849 in the presence of CD3/CD28 stimulation were significantly enriched in immune-related biological processes, including 'pathways in cancer', 'PI3K-Akt signaling pathway', 'Focal adhesion', 'cytokine-cytokine receptor interaction', 'MAPK signaling pathway', 'JAK-STAT signaling pathway', and 'Th1 and Th2 cell differentiation'. Reactome biology pathway analysis also showed significant enrichment in 'immune system', 'homeostasis', and 'cytokine signaling in immune cells'. In addition, we performed LC-MS/MS-based phosphoproteomics in PBMC samples pooled from CT26 mouse syngeneic models treated with 25mg/kg and 50mg/kg of FB849 and its derivative. The proteomics identified 1239 unique phosphorylated proteins and 915 distinct phosphorylation proteins, while 68 and 39 phosphorylated proteins were identified as differentially expressed proteins in FB849 or its derivative treated groups compared with control groups, respectively. The several phosphoproteins exhibited consistent decreases or increases in both FB849 and its derivative. Together, this work reveals genome-wide alterations in the proteomic and phosphoproteomic landscape by FB849 in both mouse PBMC's and human PBMC's with clear pathway enrichment potentially from various immune cell lineages. Further exploration of the differential expression of each protein and/or phosphoproteins especially in T cell-, B cell-, and monocyte-enriched biomarkers which link to HPK1-relevant signal transduction is needed to find out their clinical implication and to highlight new understanding of HPK1 signaling network in cancer immunity.

#2654 HPK1 inhibits CD8+ T cell effector gene expression following T cell activation.

R. Y. Ames, R. Zhao, P. Mace, A. Grant, G. Xie, H. Milestone, M. Grandcolas, E. Fang, N. Kiosea, S. Wong, M. Brovarney, S. Jacobson, D. Nebalasca, J. Arguello, B. Gomez, H. Kandala, M. Y. M. Ko, L. Nguyen, O. Robles, G. Shibuya, A. A. Shakhmin, P. Tivitmahaisoon, V.-A. Vu, A. Younai, M. Zibinsky, B. Subramanyam, D. Poon, M. Sabouri Ghomi, D. J. Wustrow, P. D. Kassner, G. E. Katibah, D. G. Brockstedt;
RAPT Therapeutics, Inc., South San Francisco, CA

Hematopoietic progenitor kinase 1 (HPK1) has been shown to act as a negative regulator of T cell receptor signaling and of subsequent effector T cell function. Inhibiting HPK1 to enhance T cell activity has emerged as a promising strategy for cancer immunotherapy. Upon T cell receptor engagement, the kinase domain of HPK1 is activated and targets components of the T cell receptor (TCR) signaling pathway for degradation, including SLP76. However, the molecular events connecting HPK1 kinase activity to observed T cell functions downstream of proximal TCR signaling are not well understood. Through transcriptional profiling of HPK1-kinase-dead (HPK1-KD) versus wild-type CD8+ T cells following an acute, attenuated Listeria monocytogenes infection, we observed increased expression of many genes associated with T cell activation and effector function, including changes in expression of several key transcription factors and their targets. Upon activation, HPK1-KD T cells, as well as T cells treated with our small-molecule HPK1 inhibitor, produce higher levels of a wide range of effector cytokines in vitro and in vivo. Treatment of mice with the HPK1 inhibitor also inhibited tumor growth in several syngeneic tumor models. These data expand our understanding of the role of HPK1 in inhibiting CD8+ T cell effector programs, and, importantly, the impact of HPK1 inhibitors on T cell function.

#2655 Unexpected role of the NuRD component, Chd4, in Foxp3+ Treg cells and its relevance to tumor immunotherapy.

W. W. Hancock[1], L. Wang[2], M. Minisini[3], E. di Giorgio[3], I. Babic[4], E. Nurmemmedov[4];
[1]University of Pennsylvania, Philadelphia, PA, [2]Children's Hospital of Philadelphia, Philadelphia, PA, [3]University of Udine, Udine, Italy, [4]Nerd Bio, LLC, San Diego, CA

We are investigating basic questions like why do Foxp3+ T-regulatory (Treg) cells have at least 3 nuclear complexes involving Hdac1 and Hdac2 (CoREST, Sin3, NuRD), and how can the inhibitory effects of Foxp3+ Tregs on host anti-tumor immune responses be targeted therapeutically? Here, we report on the immune functions of chromodomain-helicase-DNA-binding protein 4 (Chd4), a key enzyme of the nucleosome remodeling and deacetylase complex (NuRD) complex. TCGA analysis showed increased Chd4 expression and Foxp3+ Tregs within lung tumors, leading us to assess the effects of conditional gene deletion within Foxp3+ murine Tregs. Chd4 knockout led to systemic autoimmunity and death of mice within 3 weeks of life and RNAseq studies showed Chd4 loss led to derepression of ~1400 genes and repression of >700 further genes resulting in a Treg signature markedly different from conditional deletion of Hdac1, Hdac2 or Mbd2 in Treg cells. Chd4 is an intrinsically disordered therapeutic target without a defined structure outside its physiological cell environment. To date, no specific inhibitors targeting Chd4 have been developed. We have identified Ch41, a novel and potent inhibitor of Chd4, using a novel cellular target engagement platform. Transcriptomic and mass-spec investigations showed that Ch41 impaired thymic Treg function and iTreg development, led to decreased CNS2 demethylation within the Foxp3 locus, and significantly impaired growth of lung tumors and hepatocellular carcinomas in immunocompetent but not in immunodeficient C57BL/6 mice ($p<0.01$). Following Chd4 inhibitor therapy, intratumoral conventional T cells had increased activation and cytokine production (IL-2, IFN-g) compared to intratumoral T cells in control tumor-bearing mice but, perhaps unexpectedly, treated mice did not show histologic or biochemical evidence of autoimmunity. We conclude that while tumor associated Tregs have unique properties that include their increased suppressive activity compared to non-tumor associated Treg cells, they are also more susceptible than the latter and conventional T cells to newly developed therapeutic interventions, including targeting of the Chd4 chromodomain of the NuRD complex.

#2656 The selective IKZF2 molecular glue degrader, PVTX-405, counters Treg immune suppression,shows significant tumor growth delay as single agent and synergistic response with immune checkpoint therapies (ICTs).

H. D. Dhruv[1], D. McEachern[2], L. Bai[2], X. Zhang[1], Z. Chen[2], R. Nagilla[1], E. Behshad[1], B. Han[1], P. Orth[1], R. Rej[2], P. Kirchhoff[2], N. Shin[1], L. Jolivette[1], C. Strickland[1], Z. Sui[1], S. Priestley[1], S. Wang[2], H. Mohammad[1];

[1]SK Life Science Labs, King of Prussia, PA, [2]University of Michigan, Ann Arbor, MI

Immunosuppressive regulatory T-cells (Tregs) are key modulators of tumor immune evasion and resistance to immune checkpoint therapies (ICTs). IKZF2 (Helios) is a transcription factor that is selectively expressed by Treg and has been shown to be essential for maintaining function and stability of Tregs in the face of inflammatory conditions that include autoimmune disease as well as cancer. Here we describe the discovery of PVTX-405, a potent and selective IKZF2 molecular glue degrader (DC_{50}=6.3 nM). Our molecular glue degrader promotes a productive ternary complex with the E3 ubiquitin ligase substrate receptor cereblon (CRBN) to selectively degrade IKZF2 while sparing other CRBN neosubstrates (IKZF1/3, GSPT1, CK1a). PVTX-405 demonstrates rapid and selective degradation of IKZF2 in Jurkat cells *in vitro,* human PBMC derived Tregs *ex vivo,* and in cynomolgus monkeys *in vivo*. Degradation of IKZF2 in Jurkat cells leads to dose dependent increase in production of inflammatory cytokine IL-2. In *ex vivo* co-cultures of Tregs and effector T-cells, PVTX-405 reduces the suppressive activity of Tregs. To determine whether the relief of Treg suppressive activity observed *in vitro* and *ex vivo* can translate to anti-tumor activity *in vivo* we utilized $CRBN^{I391V}$(humanized CRBN) mice. We developed a novel MC38 syngeneic tumor model to test both monotherapy and combination efficacy in an immune-competent setting. Once daily oral administration of PVTX-405 as single agent significantly delays the growth of MC38 tumors. Further, *in vivo* treatment of PVTX-405 in combination with ICTs, anti-PD1 or anti-LAG3, significantly increased animal survival and led to durable tumor regressions compared to ICTs alone. Together, these results demonstrate a strong synergy between ICTs and Treg destabilization through pharmacological degradation of IKZF2 and represent a promising combination strategy for treatment of cancer.

#2657 Immune checkpoint therapy as a treatment option for non-muscle invasive bladder cancer.

S. Benmerzoug, K. Louche, T. Angles, N. Serhan, F. Dol-Gleizes, P. Lejeune, S. Chabot;
Evotec France SAS, Toulouse, France

Bladder cancer (BCa) is one of the most common malignancies with more than 500,000 new cases diagnosed each year. Intravesical instillations of Bacillus Calmette-Guérin (BCG) is the gold-standard treatment for non-muscle invasive BCa (NMIBC) patients despite significant side effects and high rates of refractory disease and/or recurrence. Indeed, treatment failure occurs in ~40% of cases emphasizing the urgent need to evaluate alternative and/or complementary new therapies including immunotherapies. Recently, the use of immune checkpoint inhibitor (ICI) anti-PD-1 therapy has been approved for the treatment of BCG-unresponsive NMIBC patients. Here, we investigated whether targeting PD-1 or CTLA-4 can boost anti-tumor immunity in the orthotopic murine MB49 BCa model. To this purpose, $2.5x10^5$ luciferase-expressing MB49 cells (MB49-Luc) have been instilled into the preconditioned bladder of female C57Bl/6 mice by intra-urethral catheterization. *In vivo* tumor growth has been monitored three times a week using the IVIS spectrum *in vivo* imaging system. All the inoculated mice showed a luciferase signal at day 3 post-bladder tumor inoculation, demonstrating 100% of tumor uptake. Based on the *in vivo* bioluminescence, a randomization has been performed before ICI treatment consisting of anti-CTLA-4 (10 µg/mouse; q3dx4, intraperitoneal) or anti-PD-1 (100 µg/mouse, q3dx4, intraperitoneal). Our data indicate that ICI treatments significantly decreased the *in vivo* bioluminescence, indicating reduced tumor growth. Furthermore, anti-CTLA-4 and anti-PD-1 administration resulted in a significant long term anti-tumor activity, with ~90% and ~70% overall survival of anti-CTLA-4 and anti-PD-1 treated mice, respectively, while isotype control mice displayed ~10% survival by day 74 post-MB49-Luc cells inoculation. To investigate the potential development of systemic adaptive anti-tumor immunity elicited by ICI treatment, remaining ICI-treated mice and newly onboarded non-treated control mice have been (re)-challenged with MB49 tumor cells subcutaneously (s.c.). While all the control mice showed tumor outgrowth and needed to be sacrificed due to humane endpoint by the day 32 post-s.c. challenge, rechallenged ICI-treated mice showed potent abscopal effect and displayed no tumor engraftment with 100% overall survival. Altogether, these findings demonstrate that systemic ICI immunotherapies such as PD-1 and CTLA-4 elicit potent anti-tumor activity and induce protective anti-tumor immune memory. ICI might present an alternative or a complementary treatment to BCG therapy for NMIBC patients.

#2658 The circadian clock modulates cancer immune checkpoint therapy through immune cell trafficking.

J. N. Lichterman, T. Srinivasan, W. Li, P. Sabaeifard, L. A. Coughlin, N. Poulides, L. V. Hooper, A. Y. Koh;
UT Southwestern Medical Center, Dallas, TX

Immune checkpoint inhibitor therapy (ICT) can provide durable remissions for cancer patients with previously incurable malignancies. However, ICT is ineffective for many cancer types, and even those who initially respond may develop ICT resistance and succumb to their cancer. Tumor cell extrinsic factors, termed host factors, have recently emerged as key mediators and biomarkers of ICT response. One intriguing host factor that may influence ICT response is the circadian clock, an evolutionarily conserved transcriptional-translational feedback loop that allows mammalian organisms to adapt to environmental exposures (e.g. light). However, whether “the clock” modulates the ICT anti-tumor immune response is unknown.

Utilizing preclinical mouse models of cancer immunotherapy, we found that ICT efficacy is time-of-day dependent. ICT was most efficacious if ICT was administered at two hours after first light exposure (Zeitgeber time 2, ZT2) and least efficacious at ZT18. Utilizing flow cytometry, bulk cytokine analysis, and single cell RNA sequencing, we characterized the anti-tumor immune response after administering ICT at ZT2 and ZT18. There was an increase in effector granzyme B- and interferon-*γ* producing CD8+ T-cells in the tumor at ZT2 versus ZT18. This was accompanied by an increase in CD11c+ dendritic cells (DCs) and intratumoral chemokines (e.g. CXCL10) that promote DC/T-cell migration into the tumor microenvironment, and leads to enhanced DC-T-cell priming and anti-tumor immunity. Interestingly, these time-of-day dependent differences in tumor immune cell infiltration were present prior to the administration of ICT. To interrogate the role of the clock in mediating these time-of-day dependent differences, we characterized the response to ICT in mice that lack the core clock gene, BMAL1. Loss of BMAL1 in DCs (BMAL1fl/fl crossed with CD11c-cre) attenuated ICT efficacy, abrogated time-of-day dependent differences in ICT efficacy and dampened anti-tumor immunity. These findings highlight a role for a novel host factor, the circadian clock, in mediating the efficacy of cancer immune checkpoint therapy.

#2659 Therapeutic administration of an engineered sphingosine-1-phosphate lyase improves T cell trafficking to tumors and enhances antitumor response.

A. Araujo, M. Rodnick-Smith, R. Al-Khaledy, G. Georgiou, **M. Badeaux**, E. Stone;
The University of Texas At Austin, Austin, TX

Introduction: Immunotherapy has revolutionized the landscape of cancer treatment; however, to date, only limited aspects of the tumor-immune interaction have been exploited successfully, e.g., relief of immune checkpoints, increase of tumor-associated antigen presentation. Although it is well-known that trafficking and entry of T cells from the circulation into tumors is often impaired, leading to an immune “cold”, checkpoint inhibitor-refractory state, there are no available therapies that address this important aspect of antitumor immunity.

Sphingosine-1-phosphate (S1P) is a pleiotropic, bioactive lipid that has been shown to regulate lymphocyte egress from lymph nodes through its interaction with one of its several receptors, S1P1. Clinically, tumor expression levels of the sphingosine-1-phosphate-producing enzyme sphingosine kinase 1 (SPHK1) strongly and negatively correlates with survival of melanoma patients after immune checkpoint inhibitor (ICI) therapy, and pre-clinically correlates with reduced tumor infiltrating lymphocytes (TILs). We therefore hypothesize that aberrant S1P signaling in tumors and in their draining lymph nodes (TDLN) causes immune exclusion by impeding lymphocyte egress from the TDLN, ultimately restricting immune cell infiltration of tumors.

Methods: We tested the therapeutic efficacy of an engineered S1P-degrading enzyme, S1P lyase (S1PL), on established (~100mm^3) syngeneic B16, CT26, and MC38 murine tumors. Using flow cytometry, we performed immune profiling of systemic, TDLN, and intratumoral T cell populations, assessing both activation status and expression of the S1P1 receptor.

Results: Treatment of tumor-bearing animals with S1PL depleted systemic S1P, and dramatically increased both trafficking of lymphocytes out of TDLNs and T cell infiltration of tumors relative to control-treated animals. Mice treated with S1PL evinced a higher proportion of S1P1+ circulating and intratumoral T cells relative to control-treated mice, suggesting that the increase in liberation of T cells from the TDLN was effected through the S1P/S1P1 axis. This increased lymphocyte trafficking correlated with strong inhibition of tumor growth when S1PL was administered as a single agent.

Conclusions: Therapeutic administration of S1PL may represent an attractive strategy for modulating lymphocyte trafficking to improve the efficacy of therapies that rely on the adaptive immune system to exert antitumor activity. This approach may be particularly potent in settings wherein tumor-mediated immune exclusion is a dominant method of immune escape.

#2660 CXCL9/10 is critical for immunotherapeutic efficacy by recruiting and activating T lymphocytes in tumor microenvironment.

C.-C. Cheng[1], J. Chang[2], Z.-L. Sie[1], A.-S. Ho[3], C.-L. Peng[4], C.-C. Chang[5];

[1]Chang Gung University, Taoyuan City, Taiwan, [2]Taipei Medical University, Taipei City, Taiwan, [3]Cheng Hsin General Hospital, Taipei City, Taiwan, [4]National Atomic Research Institute, Taoyuan City, Taiwan, [5]Taipei Medical University Hospital, Taipei City, Taiwan

Background: Tumor immunotherapies targeting PD-(L)1 exhibit anti-tumor efficacy in only about 20% of patients with a variety of cancers. Literature has demonstrated that “hot tumor” which contains high T lymphocytes in tumor microenvironment exhibits a better response to immunotherapies than “cold tumor”. Therefore, we hypothesize that T lymphocyte-recruited factors play the roles determining the immunotherapeutic efficacy, including CXCL9, 10, and 11, which are located in human chromosome 4 with consistent co-expression and protein structure.

Aims: The aim of this study is to investigate whether CXCL9/10 is critical in determining the anti-PD-(L)1 immunotherapeutic efficacy.

Methods: GEPIA, cBioPortal, and Kaplan-Meier Plotter were used to investigate the gene expression, co-expression, and immunotherapeutic association for CD274 (PD-L1), ICAM1, and CXCL9/10 in lung, colon, and liver cancers. qPCR and flow cytometry were used to detect the gene expression in tumor cells and T lymphocytes, particularly comparing the differences between LL/2 and CT26 cells whereas LL/2 is immunotherapy-resistant and CT26 is immunotherapy-sensitive. CD8+ T cell transwell assay and qPCR were used to measure the function of CXCL10 on CD8+ T cell migration and activation, whereas IFNγ and IL-2 as the activation markers.

Results: We found that CXCL9/10 overexpressed in a variety of tumors, including lung, colon, and liver tumors with a correlation with PD-L1. However, PD-L1 was not overexpressed in most tumors. High PD-L1 and CXCL10 are basically associated with better survival rates in tumor patients receiving immunotherapies. Correlation analysis revealed that IRF-1 and STAT1 were correlated with PD-L1 and CXCL10 expression in lung cancer. Since literature has indicated that LL/2-derived syngeneic tumor exhibits immunotherapy-resistant and CT26 exhibits immunotherapy-sensitive, we further compared the gene expression between them. We found that IFNA, IFNG, CXCL10, and PD-L1 all expressed higher levels in CT26 cells than LL/2. Moreover, we found that T lymphocytes specifically expressed high CXCR3, a receptor of CXCL9/10, including CD4+ T and CD8+ T cells by flow cytometry. As expected, CD8+ T cells can be recruited in a transwell assay by IFNα and CXCL9. In addition, we found that IFNα induced CXCL10 expression in monocytes and CXCL10 increased activation markers IFNγ and IL-2 in CD4+ T and CD8+ T cells.

Conclusions: This study revealed that CXCL9/10 expression is correlated with PD-L1 in tumors, resulting in better immunotherapeutic efficacy. The evidence demonstrated that CT26 intrinsically exhibited higher IFNs and CXCL9/10 compared to LL/2. Therefore, CXCL9/10 potentially recruits and activates CD8+ T cells to tumor microenvironment, transferring “cold tumor” to “hot tumor”. This study indicates that CXCL9/10 is critical for immunotherapeutic efficacy.

#2662 Deciphering the cellular and molecular determinants of immunotherapy resistance in NASH-associated hepatocellular carcinoma by single-cell analysis.

L. Zhang, Y. Zhang, W. Tang, Z. Xiong, X. Liu, Z. Liang, Y. Tsang, W. Yang, X. Long, A. S. Cheng;
The Chinese University of Hong Kong, Shatin, Hong Kong

Introduction: Non-alcoholic steatohepatitis (NASH) has emerged as a prominent risk and the most rapidly increasing aetiology of hepatocellular carcinoma (HCC). Despite the effectiveness of immune checkpoint blockade (ICB), like anti-programmed cell death-ligand 1 (anti-PD-L1) antibodies, in a subset of HCC patients, NASH has been shown to impair the anti-tumor immunity in ICB-treated HCC. We aim to elucidate the mechanisms responsible for ICB resistance in NASH-HCC at single-cell resolution.
Methods: Orthotopic NASH-HCC mouse models were generated by orthotopically injecting liver cancer cell line into NASH liver induced by methionine-and choline-deficient diet (MCD) or choline-deficient, L-amino acid-defined, high-fat diet (CDAHFD). Multi-color flow cytometry and single-cell RNA-sequencing (scRNA-seq) were utilized to dissect the liver and tumor immune microenvironment upon anti-PD-L1 treatment.
Results: Anti-PD-L1 treatment failed to alleviate tumor burden in NASH mice, indicating that orthotopic NASH-HCC mouse models were resistant to ICB therapy. Compared to the control liver, multi-color flow cytometry demonstrated that $CD11b^{+}F4/80^{+}CD206^{+}$M2 macrophages accumulated in NASH liver and further increased in liver and tumor upon anti-PD-L1 treatment. Tumor-infiltrating M2 macrophages exhibited the most significant and robust correlation with tumor weight among all immune cell types. Moreover, PD-1 expression on tumor-infiltrating $CD8^{+}$ T cells positively correlated with tumor weight and intratumoral M2 macrophages. Furthermore, scRNA-seq analysis identified a NASH-specific tumor-infiltrating monocyte subcluster, which may differentiate into an ‘M2-like’ macrophage subtype upon anti-PD-L1 treatment as demonstrated by cell trajectory analysis.
Conclusion: Our study provides insights into the significance of monocyte/macrophage reprogramming in ICB resistance in NASH-HCC. Further investigation is conducted to identify the molecular mechanisms during monocyte-macrophage differentiation and explore potential targeted strategies to overcome ICB resistance in NASH-HCC.
Acknowledgment: This study is supported by the General Research Fund (14120621 and 14119023), the Collaborative Research Fund (C4045-18W), the Li Ka Shing Foundation and CUHK Strategic Seed Funding for Collaborative Research Scheme.
Keywords: hepatocellular carcinoma, single-cell RNA-sequencing, anti-PD-L1, macrophages.

#2663 Determining the role of tumor mutational burden in a pre-clinical model of glioblastoma.

K. Breen, T. Haynes, M. Watanabe, M. Gilbert;
NIH-NCI, Bethesda, MD

Despite advances in care in many cancer types, patients with glioblastoma (GBM) have a grim prognosis of 15 to 21 months and unchanged standard therapy since 2005. These tumors have a profoundly immunosuppressive tumor immune microenvironment. Immunotherapy, including the checkpoint inhibitors (ICIs) targeting PD-1 and CTLA-4, has transformed the treatment of many cancers but has failed in trials of both newly diagnosed and recurrent GBM. Tumor mutational burden (TMB) has been proposed as a predictor of response to ICI treatment, presumably through an increase in neoantigens that can be recognized by cytotoxic CD8+ T cells leading to tumor rejection. GBM typically has a low TMB, a feature speculated as a contributor to poor response to ICI treatment. However, cases with an extremely high TMB (i.e., patients with the biallelic mismatch repair deficiency syndrome) do show response to immunotherapy. To begin to investigate the impact of mutational burden on immune response in GBM, we created a murine syngeneic tumor model using CRISPR-Cas9 to knockout (KO) the mismatch repair protein Msh2, the lynchpin to mismatch recognition, in the SB28 GBM model that has a low TMB (108 mutations) at baseline. Msh2 KO increased the TMB from 2 to 12-fold depending on single cell sorted clone, resulting in between 150 and 200 predicted strong MHC-I binding neoantigens estimated by the NetMHC algorithm. Preliminary studies have demonstrated that in vitro proliferation is similar amongst low TMB and high TMB SB28 clones. Flank implantation of high TMB SB28 clones revealed slower growth compared to the low TMB SB28 tumors. Furthermore, treatment with ICIs did provide a survival advantage in this flank model. However, no survival advantage was noted when the high TMB clones were implanted intracranially either with or without ICI treatment. These results suggested that either there is poor immune cell trafficking to the intracranial tumors, or a robust immune response was causing increased intracranial pressure that is prematurely causing death. Use of dexamethasone starting at day 11 to control cerebral edema has shown some survival improvement with ICI treatment, supporting that an inflammatory response is at least partially responsible for the lack of improved survival in early studies. We are currently evaluating CD4+ and CD8+ T cell clonality, earlier timepoints to evaluate the immune infiltrate and anti-tumor immune response, and alterations in chemokines/cytokines in the tumor microenvironment. By creating high mutation burden clones from a GBM with a low mutational burden, we will be able to interrogate potential mechanisms of heightened immunogenicity that has been reported in other cancers.

#2664 Targeting PD-L1/CMTM6 in myeloid cells results in elevated release of CCL2 to improve CD8 T cell-mediated antitumor response.

M. A. Hsu[1], X. Liu[1], Y. Li[1], W. Barham[2], K. Pavelko[1], J. Hirdler[1], F. Lucien[1], H. Dong[1];
[1]Mayo Clinic, Rochester, MN, [2]Vanderbilt University, Nashville, TN

Background: Although targeting myeloid cells has become one of the next generation targets for cancer immunotherapy, there is a lack of therapeutic tools to specifically target these cells. Our group has developed a novel humanized PD-L1-targeting antibody, H1A, that induces PD-L1 degradation via blockade of PD-L1 and CMTM6, therefore limiting PD-L1 intrinsic signaling while also preventing interactions with PD-1. In the immune cell compartment, CMTM6 expression is restricted to myeloid cells, making these cells the primary target of H1A. Recently, we unexpectedly found that targeting intrinsic PD-L1 in myeloid cells via H1A resulted in increased release of CCL2 from myeloid cells. In this study, we examined the role of CCL2/CCR2 signaling in CD8 T cell function using human peripheral blood-derived immune cells and evaluated the therapeutic potential of H1A antibody using our humanized PD-L1/PD-1 mouse model.
Methods: Human PBMCs derived from healthy donors were treated with H1A or Atezolizumab, a blocking PD-L1 antibody, followed by mass cytometry and flow cytometry to evaluate immune cell phenotype and functional states. PD-L1 expressing myeloid cells isolated from human PBMCs were treated with H1A or Atezolizumab and assessed for CCL2 secretion using multiplex immunoassays. CCL2 production and transcription were confirmed by flow cytometry and single-cell RNA-sequencing. CCR2 blockade was used on human PBMCs to evaluate the effects of CCL2/CCR2 signaling on T cell function alongside H1A treatment. Finally, in vivo antitumor activity of H1A and Atezolizumab were compared in two humanized PD-L1 tumor models.
Results: H1A reduced the frequency of regulatory T cells and increased effector T cells, in whole PBMCs upon global T cell activation with anti-CD3/CD28. H1A enhanced the secretion and production of CCL2 from myeloid cells, which was confirmed at a transcript level. CCR2 blockade diminished CD8 T cells' ability to differentiate into effector cells in H1A treated PBMCs. H1A demonstrated comparable therapeutic effects with Atezolizumab in treatment of immunogenic and ICI-responsive mouse tumor MC38, which is CD8 T cell-dependent, but showed superior therapeutic effects in treatment of ICI-insensitive mouse tumor E0771 compared to Atezolizumab. Both treatments elicited durable memory specific immune responses upon E0771 tumor rechallenge.
Conclusion: H1A demonstrated a superior antitumor activity compared to Atezolizumab in our preclinical models via a new mechanism by which H1A caused degradation of intrinsic PD-L1 in myeloid cells. This causes more release of CCL2 to improve T cell function via CCR2 upon T cell activation. Thus, H1A is emerging as a new immunotherapy tool to target PD-L1/CMTM6 in myeloid cells for treatment of cancers that are refractory to current immune checkpoint inhibitor therapy.

#2665 Fc silencing of commonly used surrogate anti-PD-1 RMP1.14 increases its therapeutic profile in MC38 syngeneic model.

E. Morgado, L. Pouyet, O. Deas, F. Romagne;
Janvier Group, Le Genest Saint Isle, France

Introduction: Anti-PD1 treatment has become a backbone treatment in several cancers such as melanoma and lung carcinoma. Adding new drugs to PD-1 requires careful evaluation of combination treatments in preclinical models to evaluate efficacy and tolerability. Syngeneic tumor model remains one of the best way of preclinical evaluation of combinations, as such evaluation requires fully immune competent animals to correctly assess both the PD-1 contribution and the added value or synergistic effect of new drugs in the combination. Anti mouse PD-1 such as RMP1.14, a rat IgG2a, is widely used in these models as anti-PD-1 mAb surrogate for such studies. Although RMP1.14 demonstrated efficacy in several models such as MC38, and CT26, it may not fully recapitulate the use of blocking mAb in the human as it may be immunogenic in mice and may retain some agonist activity due to its rat isotype. Here, we demonstrate that engineering this antibody with a mice Fc silent backbone increases its activity in MC38 model.
Methods: VH/VL from RMP1.14 rat IgG2a (mPD1) were sequenced and engineered with a mouse Fc silent IgG1 backbone (N297Q) and produced in CHO. Both antibodies (mPD-1: rat IgG2a ; and MOS2-mPD-1: Fc silent mouse IgG1) were purified on protein A using standard procedures. MC38 (1million cells) were injected subcutaneously in C57BL/6 mice, and randomized when tumor volume reached 100mm^3. Dose effect of mPD-1 and MOS2-mPD-1 and their corresponding isotype controls were tested in this MC38 model at doses of 0.5 ; 1.25 ; 2.5 and 12.5 mg/kg at day 0, day 3, and day 7 post randomization (8 mice per group). Treatment route effect was tested in the same model by comparing intraperitoneal and intravenous injections in an additional experiment using both antibodies at 1.25 mg/kg and 12.5 mg/kg doses.
Results: Both mPD-1 and MOS2-mPD-1 demonstrated efficacy in survival in MC38 model at all tested doses ($p<0,05$ Mantel-Cox test) compared to their isotype controls. MOS2-mPD-1 demonstrated increased efficacy in terms of complete responses in the above escalated doses (CR of 12.5, 12.5, 12.5 and 37.5 % and 0, 75, 50 and 62.5 % for mPD-1 and MOS2-mPD-1 respectively). Tumor volumes and survival were also always lower in the MOS2-mPD-1 groups compared to dose corresponding mPD-1 groups and were statistically different in two independent experiments at medium doses ($P<0,05$ Dunn's test performed at 1.25mg/kg at day 27, and Mantel-Cox test). IP and IV routes were equivalent in efficacy at the tested doses.
Conclusion: Mouse Fc engineered surrogate have significantly different behavior in mice models compared to the commonly used surrogates usually from rat origin. These new formatted antibodies should better mimick the efficacy and tolerability of antibodies used in human, and should be preferred when new combinations of treatments are tested.

#2666 Genetic ablation of B2M leads to resistance to PD-1/PD-L1 blockade *in vivo*.

Y. Zhang, H. Ma, B. Han, Y. Li, P. Yang, Z. Li, D. Feng, L. Ci, R. Sun, **D. X. He**;
Shanghai Model Organisms Center, Inc., Shanghai, China

Immune checkpoint inhibitors (ICIs) has revolutionized the treatment landscape of various cancers by reinvigorating the exhausted T cells in patients. However, the therapeutic efficacy is largely confined due to the primary or acquired resistance to anti-PD-1 (L1) therapy in many patients. Recently, the mechanisms of resistance to ICIs has been extensively elucidated from different aspects and emerging sequencing data from clinical samples has pointed to IFN-γ signaling defects and antigen presentation loss in patients who are resistant to PD-1(L1) blockade. The loss-of-function mutations in JAK1 and JAK2 results in lack of response to IFN-γ signaling and incapacity to upregulate PD-L1 and MHC-I, which subsequently leads to noninflammatory TMEs and resistance to anti-PD-1/PD-L1. The loss-of-function of B2M is likely a common resistance mechanism that the intratumoral cytotoxic CD8+ T cells are failed to be boosted owing to antigen presentation loss. In order to obtain higher clinical benefits in various cancers, it's appealing and urgent to develop mechanism-based strategies to overcome resistance to ICI-based immunotherapy. To this end, we developed a genetically acquired resistant tumor model with B2M mutations in syngenic MC38 tumor cells using CRISPR/Cas9 technology, which is 'hot' tumor to PD-1/PD-L1 blockade. The expression of B2M was detected by western blotting and flow cytometry. Mouse *B2M*-knockout MC38 tumors became resistant to PD-1/PD-L1 blockade in vivo. Notably, we found a remarkable increase of CD8+ T cell infiltration in B2m-KO MC38 tumors in comparison to parental MC38 tumors upon anti-PD-1 treatment, which further explains that antigen presentation loss results in inactivation of cytotoxic CD8+ T cells within the tumor microenvironments (TMEs), subsequently leading to resistance and poor survival to ICI therapy.In summary, our data consistently indicated the importance of MHC-I expression in T cell activation in the TMEs and the possibility to dig out the pathway involved in MHC-I expression independent of IFN-γ signaling by CRISPR-based screening to overcome MHC-I deficiency-induced resistance in the future. In addition, it's possible to leverage the cytotoxic NK cells and CD4+ T cells in antitumor immunity against MHC-II+ tumors even with the loss of MHC-I molecules. For example, high dose of IL-2RB-biased IL-2 agonist preferentially binding to the dimeric IL-2R can stimulate Teff and NK cells independent of immune checkpoint expression. Likewise, cytokine modified anti-PD-1 fusion formulation like anti-PD-1-IL-2 mutein and anti-PD-1-IL-15 mutein are promising to overcome the resistance. Furthermore, it has been suggested that the resistance due to genetic mutations of MHC-I could be overcome by combining NF-B targeted therapies.

#2667 Mucin 5AC inhibition via intratracheal RNAi delivery as an effective alternative strategy for prevention and treatment of Kras mutant lung cancer.

M. Zarghooni[1], M. T. Grimaldo[2], A. Krishna[2], M. J. Clowers[2], L. Phan[1], Y. H. Rezai[1], A. Gaitonde[1], C. Rodriguez Reyna[1], W. Velasco Torrez[1], E. Bush[3], S. Javad Moghaddam[1];

[1]Department of Pulmonary Medicine, The University of Texas MD Anderson Cancer Center, Houston, TX, [2]The University of Texas MD Anderson Cancer Center UTHealth Houston Graduate School of Biomedical Sciences, Houston, TX, [3]Arrowhead Pharmaceuticals, Pasadena, CA

Lung cancer, including lung adenocarcinoma (LUAD), is the leading cause of cancer-related deaths in the United States. *KRAS* mutations are the most prevalent oncogenic driver alteration in human LUAD. We have previously shown that high expression of Mucin 5 AC (MUC5AC), a main airway secretory mucin, is significantly associated with poor prognosis. Mucins are essential for mucociliary clearance and the maintenance of airway homeostasis, however, their overproduction could negatively affect the lung immune microenvironment and has been shown to promote airway diseases such as chronic obstructive pulmonary disease (COPD) and lung cancer. Previously, we have shown that genetic deletion of MUC5AC in a murine model of K-ras mutant lung adenocarcinoma (KM-LUAD) impedes tumor development and reduces pro-tumor inflammatory and immune phenotypes. These findings indicate that MUC5AC is a potential druggable target against KM-LUAD. In this study, we sought a translational approach and inhibited MUC5AC in our K-ras^{G12D} mutant mouse model of LUAD via RNA interference (RNAi). Six-week-old mice were given RNAi (5mg/kg) or vehicle (saline) via biweekly intratracheal administration for 8 weeks. This approach led to a significant decrease in tumor burden (40%) and a trending increase in total white blood cell counts, predominantly macrophages in the lung tumor microenvironment which was associated with phenotypic changes in macrophages characterized by reduced expression of *Fizz1*, and M2 pro-tumor macrophage marker. Additionally, RNAi-treated mice had reduced expression of *Siglec-E*, a mucin receptor and known inhibitor of the TLR4 endocytosis and promoter of NF-κB signaling, as well as a significant decrease in *IL-6*, a product of the NF-κB pathway and promoter of STAT3 signaling which we have previously shown to have an essential role in promotion of KM-LUAD. In summary, these findings elucidate a potential mechanism by which MUC5AC protects tumor cells from apoptosis and immune-mediated cytotoxic activity but also highlights how MUC5AC RNAi is an effective indirect preventive and therapeutic strategy in high-risk individuals (smokers with COPD) and patients with early stage KM-LUAD, respectively.

#2668 CBO421: A novel drug Fc-conjugate to prevent tumor immune evasion via the CD73/adenosine pathway.

A. Almaguer, D. Zuill, S. Dohrmann, J. Levin, N. Dedeic, E. Abelovski, J. Fortier, Q. Zhao, M. Hernandez, K. Amundson, M. Moniz, H. Chen, D. Panickar, T. Lam, T. Brady, A. Borchardt, G. Hough, J. B. Locke, J. N. Cole, L. W. Tari;
Cidara Therapeutics, San Diego, CA

Background

CD73 (5'-nucleotidase or NT5E) is a cell surface enzyme responsible for the rate limiting step in adenosine production; the conversion of adenosine monophosphate (AMP) into adenosine. Adenosine contributes to immune evasion by solid tumors by concentrating immunosuppressive adenosine in the tumor microenvironment. CBO421, a Drug Fc-Conjugate (DFC), comprises a novel small molecule CD73 inhibitor stably conjugated to an immune-silent human IgG1 Fc, combining the strengths of small molecule inhibitors and CD73-targeting monoclonal antibodies (mAbs) for potential best-in-class efficacy.

Methods

CBO421's binding affinity to human CD73 and Fc receptors was assessed by surface plasmon resonance. Antibody-dependent cellular cytotoxicity (ADCC) was evaluated using a commercial kit. Immunophenotyping and binding to cancer cells was measured by flow cytometry. Inhibition of soluble and membrane-bound CD73 on human PBMCs and mouse cancer cells was determined by measuring free phosphate levels. Functional activity was measured using PBMC rescue assays. *In vivo* efficacy of CBO421 monotherapy was evaluated in a syngeneic mouse model.

Results

CBO421 exhibited a binding affinity to human CD73 (K_D = 0.8 nM) that was comparable to or greater to the affinity observed with small molecule inhibitors (AB680, OP-5244) and CD73-targeting mAbs (oleclumab, mupadolimab biosimilars). As expected, human FcRn binding of CBO421 was comparable to the unconjugated Fc and the full-length wild-type IgG1 control mAb. CBO421 binding to human Fc gamma receptors and ADCC activity was significantly reduced or abolished compared to the control mAb, such that it poses a minimal risk for undesired autoimmune activity. CBO421 potently inhibited soluble CD73 and CD73 expressed on human MDA-MB-231 and mouse EMT6 cancer cells. Immunophenotyping revealed that CD73 expression was primarily observed on $CD8^{\pm}$ T and B cells from human PBMCs. In functional PBMC rescue assays, CBO421 demonstrated potent reactivation of AMP- or ATP-suppressed $CD4^{\pm}$ or $CD8^{\pm}$ T cells at levels comparable to small molecule inhibitors and greater than anti-CD73 mAb comparators. CBO421 monotherapy demonstrated a dose-dependent reduction in tumor volume in a syngeneic mouse model using MC38, a colorectal cancer cell line.

Conclusions

CBO421 exhibited strong binding and potent inhibition of both soluble and membrane-bound CD73, differentiating it from mAb CD73 inhibitors. The proprietary immune-silent Fc of CBO421 did not affect FcRn binding but substantially reduced Fc gamma receptor binding, leading to the elimination of ADCC activity to prevent undesired immune cell depletion in host tissues. CBO421 demonstrated high potency in functional cell-based assays and robust antitumor efficacy in a syngeneic mouse model. Currently, CBO421 is being advanced as a clinical development candidate for the treatment of solid cancers.

#2670 Development of novel anti-SIRPα/β dual antibody with single-agent phagocytosis activity.

Subhra Prakash Chakrabarty, Sandeep Sadashiv Patil, Sunaina Singh Rajput, Amrita Mukerji, Sandhya Aurumugam, Pooja Balu Gade, Sidhesha S, Anup Kumar Patra, Shivaranjini C, Vaishnavi Shivaji Khamkar, Lavanya P, Lakshmeesha K N, Ujjwal Kapoor, Jagadeesh R, Jwala Nagaraj, Vijaya Shankar Nataraj, Kavitha Nellore, Thomas Antony, Susanta Samajdar, Murali Ramachandra

Aurigene Oncology Limited, Bengaluru, India

Signal-regulatory protein alpha (SIRPα) is an inhibitory receptor expressed on macrophages that interacts with CD47, resulting a "don't eat me" signal on cancer cells. This interaction suppresses macrophage dependent phagocytosis and contributes to the evasion of host immune system. Consequently, the SIRPα-CD47 axis has become a well sought after and established therapeutic angle to treat cancer. While CD47-targeting agents have shown promise in clinical trials, the ubiquitous expression of CD47 raises the concerns about hematologic toxicity, including anaemia and thrombocytopenia, hindering the development of CD47-targeting therapies. This has prompted exploration of another end of the axis i.e., targeting SIRPα. Moreover, targeting SIRPβ protein, expressed on myleoid cells, via agonistic approach would generate ITAM-mediated activating signal through DAP12 protein contributing to cancer cell death. Considering the limited expression of SIRPα and β, a dual antibody capable of blocking the CD47-SIRPα pathway and activating SIRPβ downstream signaling may result in a desirable efficacy and safety profile. In this study, we present novel anti-SIRP α/β dual antibody clones discovered from a proprietary human antibody discovery platform consisting of a large human antibody library, along with *in vitro* and *in silico* screening technologies. The platform was explored against native SIRPα/β antigens to identify novel human antibody clones based on affinity-based epitope coverage. Subsequently, antibody clones were produced and evaluated for preclinical functional relevance. Novel full-length SIRPα/β dual antibody clones demonstrated high affinity binding to soluble human SIRPα and SIRPβ proteins as well as these receptors expressed on CHO-K1 cells and macrophages. The antibody clones effectively disrupted CD47-SIRPα interaction in biochemical assays and significantly enhanced activation of macrophages as observed by increased cytokine release. Most importantly, the dual antibody clones demonstrated potent *in vitro* single-agent phagocytosis activity against tumor cells. In summary, the novel SIRPα/β dual antibodies activating macrophage mediated phagocytosis of tumor cells without the need for tumor opsonizing antibodies or agents capable of inducing “eat-me-signals” highlight their potential as a single-agent therapy. These findings prompt us to continue the development of the anti-SIRP α/β dual antibody for use in cancer therapy.

#2671 Sustained inhibition of CSF1R signaling effectively augments antitumor immune responses through inhibiting tumor-associated macrophages.

T. Sato[1], D. Sugiyama[1], Y. Kojima[2], S. Hattori[1], K. Sone[1], T. Ishikawa[1], Y. Ishikawa[1], T. Kato[1], H. Kiyoi[1], H. Nishikawa[1];
[1]Nagoya Univ. Graduate School of Medicine, Nagoya, Japan, [2]National Cancer Center, Tokyo, Japan

Tumor-associated macrophages (TAMs) are one of the key immunosuppressive components in the tumor microenvironment (TME) and contribute to tumor development, progression, and resistance to cancer immunotherapy. Several reagents targeting TAMs have been tested in preclinical and clinical studies, but they have had limited success. Here, we show that a novel reagent, FF-10101, exhibits a sustained inhibitory effect against colony stimulating factor 1 receptor by forming a covalent bond and reduces immunosuppressive TAMs in the TME, which leads to strong antitumor immunity. In preclinical animal models, FF-10101 treatment significantly reduced immunosuppressive TAMs and increased antitumor TAMs in the TME. In addition, tumor antigen-specific $CD8^+$ T cells were increased; consequently, tumor growth was significantly inhibited. Moreover, combination treatment with an anti-PD-1 antibody and FF-10101 exhibited a far stronger antitumor effect than either treatment alone. In human cancer specimens, FF-10101 treatment reduced PD-L1 expression on TAMs, as observed in animal models. Thus, FF-10101 acts as an immunomodulatory agent that can reduce immunosuppressive TAMs and augment tumor antigen-specific T cell responses, thereby generating an immunostimulatory TME. We propose that FF-10101 is a potential candidate for successful combination cancer immunotherapy with immune checkpoint inhibitors, such as PD-1/PD-L1 blockade.

#2672 GD3 synthase (ST8SIA1) is a key immunomodulator in GD2^{+} breast cancer cells.

B. Oderinde, V. Anand, M. Siddiqui, A. Tyagi, B. Jenny, V. Battula;
UT MD Anderson Cancer Center, Houston, TX

Background: Gangliosides are acidic glycosphingolipids involved in cell adhesion, proliferation, and modulation of signal transduction pathways. It has been reported that tumor-shed gangliosides influence the activity of immune cells, including macrophages, NK cells, and T cells. GD3 synthase (GD3S) is the key enzyme that regulates the biosynthesis of the b and c-series gangliosides, particularly GD3 and GD2, and studies have shown that GD3S is upregulated in most tumors and plays a role in tumor progression. Similarly, we have found GD3S to be significantly upregulated in GD2^{+} breast cancer stem cells (BCSC) compared to GD2^{-} cells, and the knockdown of this gene prevented tumor formation in mice. Here, we hypothesize that GD3 synthase has an immunomodulatory function in breast cancer (BC) cells through the upregulation of GD2.

Methods: We stably overexpressed GD3S in BT549 and MCF-7 breast cancer cell lines by lentiviral transfection and performed CRISPR-Cas9 knockout of GD3S in BT549 and SUM 159 cell lines. We examined the effect of GD3 synthase on macrophage-mediated phagocytosis, NK cell-mediated killing, and T-cell cytotoxicity of BC cells using the live cell imaging system, IncuCyte®. Naxitamab is a US FDA-approved fully humanized anti-GD2 monoclonal antibody for the treatment of neuroblastoma. We evaluated the effects of naxitamab in GD2^{+} BC cell lines (HCC1395, Hs578T) using the Incucyte, and also examined its effect on in vivo tumor growth using TNBC PDX models.

Results: We observed a highly significant decrease in macrophage-mediated phagocytosis ($p<0.005$; $p<0.0001$) and NK-mediated killing ($p<0.0001$; $p<0.0001$) in BT549 and MCF-7 cell overexpressing GD3S compared to the control cells. Interestingly, we observed a significant increase in phagocytosis in GD3S knockout BT549 and SUM 159 cells ($p<0.05$; $p<0.005$) compared to their wild-type counterparts. Moreover, the knockout of GD3S enhanced NK cell-mediated apoptosis in BT549 cells ($p<0.001$) and T cell killing in BT549 and SUM 159 cells ($p<0.0001$; $p<0.0001$). Finally, we found that naxitamab dose-dependently enhances macrophage-mediated phagocytosis and NK cell-mediated apoptosis in HCC1395 and Hs578T BC cells, with 20µg/ml being the most effective concentration in comparison to IgG control ($p<0.0001$; $p<0.0001$). In addition, we observed a reduction in tumor volume in naxitamab-treated mice compared to IgG control ($p<0.05$)

Conclusion: GD3 synthase regulates macrophage-mediated phagocytosis, NK cell-induced apoptosis, and T-cell cytotoxicity in BC cells. Naxitamab enhances immune cell killing of breast cancer cells with high GD2 expression. Furthermore, naxitamab inhibited tumor growth in GD2^{+} TNBC PDX models.

#2673 Copper chelation overcomes the immunosuppressive neuroblastoma microenvironment to potentiate anti-GD2 antibody therapy.

J. R. C. Rouaen[1], A. Salerno[1], F. Luciani[2], J. Murray[1], T. Shai-Hee[1], N. Tedla[2], M. Haber[1], T. N. Trahair[1], O. Vittorio[2];
[1]Children's Cancer Institute Australia, Sydney, Australia, [2]University of New South Wales, Sydney, Australia

Neuroblastoma is the most frequent extra-cranial pediatric cancer with high-risk disease possessing a dismal five-year survival rate <50%. Antibody-based therapies targeting the surface disialoganglioside GD2 have shown promising anti-tumor activity in patients however efficacy is strongly hampered by immunosuppressive mechanisms present in the tumor microenvironment. Neuroblastomas typically feature low mutational burdens, limited major histocompatibility complex class I expression, increased immune checkpoint markers, sparse immune infiltration, and soluble mediators which drastically limit anti-tumor immunity. Given the emerging link between elevated copper levels and tumoral immune evasion, we explored copper chelation as a therapeutic strategy using the agents tetraethylenepentamine (TEPA) and the clinically approved analogue triethylenetetramine (TETA). Using the immunocompetent TH-MYCN model, we performed single-cell RNA sequencing supported by OPAL multiplex immunohistochemistry and cytokine profiling of resected tumors to assess cellular and molecular changes occurring after one week of TEPA treatment. Therapy was observed to successfully deplete intratumoral copper and reinvigorate anti-tumor immunity with increased infiltration and activity of pro-inflammatory immune cells, and was specifically found to induce egress and N1-polarisation of neutrophils. Further mechanistic studies in vitro revealed the sequestration of copper by neuroblastoma cells attenuated neutrophil function, which could be successfully reversed upon TEPA treatment. Findings propose a novel mechanism of immune evasion, highlighting copper chelation as a therapeutic strategy to counteract immunosuppression. Using the TH-MYCN model, TEPA was employed as a priming agent to effectively potentiate anti-GD2 antibody therapy and achieve durable tumor control. Importantly, this was associated with increased Fc-receptor-bearing natural killer and myeloid cells, which elicit tumor clearance via antibody-dependent cellular cytotoxicity. Currently indicated for the treatment of copper overload disorder Wilson's disease, TETA was evaluated for potential repurposing as a novel immunomodulatory agent. Using the syngeneic NXS2 model, TETA exhibited an exceptional safety profile and combination therapy achieved durable tumor control with no relapses occurring after treatment cessation. This result was similarly associated with the infiltration of pro-inflammatory immune cells, including N1 neutrophils. Collectively, this study credentials copper chelation as a non-toxic strategy to disrupt the immunosuppressive tumor microenvironment and reinvigorate anti-tumour immunity. Findings provide crucial translational evidence for repurposing TETA to potentiate anti-GD2 antibody therapy and improve neuroblastoma patient responses.

#2675 A new dual-targeting anti-immune checkpoint therapeutic approach for the treatment of “hot” and “cold” tumors.

M. M. Moutuou[1], N. DeLuce[2], E. Creton[2], H. Lucchi[2], J. Accolas[1], A. Savatier[1], **M. Leonetti**[1];
[1]CEA, Saclay, France, [2]Blue Bees Therapeutics, Parc Club-Orsay Universite, Orsay, France

Anti-Immune Checkpoint (ICP) antibody approaches provided a major breakthrough in the field of cancer therapy. However, their efficiency is mainly restricted to patients with “hot” tumors characteristics, which limits the breadth of their use. To tackle this limit, we developed a new strategy aimed at amplifying anti-ICP antibody ability to activate immune cells. This approach is based on antibodies engineered to make them able to target both an ICP receptor and a co-receptor often involved in receptor-mediated activation, namely Heparan Sulfate Proteoglycan.
The dually-targeting engineered anti-ICP antibodies were produced in eukaryotic cells. They were purified to homogeneity using two chromatographic steps and remain stable for months in frozen conditions. A first engineered antibody-derived construct was assessed for its ability to impact immune cell activation and tumor-growth. It is able to stimulate subsets of immune cells from mouse splenocytes as well as from human peripheral mononuclear cells, *in vitro*. In addition, its injection in healthy mice triggers activation of T-cells. Last, in mice previously implanted with different types of cancer cells it impacts growth of “hot” as well as “cold” tumors. Immune profiling in a “cold” cancer model shows that the treatment decreases the proportion of MDSCs and increase that of $CD8^{+}$ T-cells and NK-cells in tumor microenvironment making it close of that found in “hot” tumors. Altogether, our data indicate that our first engineered antibody-derived construct presents an attractive immunotherapeutic potential for a large variety of cancers paving the way for its evaluation in clinical phases.

IMMUNOLOGY: Innate Immunity in Cancer
Poster Session

#2679 Myeloid olfactory receptors in melanoma.
E. M. Benson, K. Ley, M. Orecchioni, C. C. Hedrick;
Immunology Center of Georgia, Augusta, GA

Olfactory receptors are commonly found in the nasal cavity and function to detectodorants. However, very recent studies have determined that innate immune cells,including monocytes and macrophages, express olfactory receptors. OLFR2 (OR6A2 inhumans), was recently linked to atherosclerosis development through interaction with itsligand, octanal. Increased levels of octanal are considered as a risk factor foratherosclerosis. Conversely, octanal levels are associated with lower cancer incidence,suggesting that OLFR2 may play a protective role in cancer. Indeed, data from TheCancer Genome Atlas for liver and brain cancers show that OLFR2 expression isassociated with increased patient survival. Here, we utilized an orthotopic melanomamouse model using B16 cancer cells in C57/BL6 mice that had been transplanted witheither wild type or OLFR2 knockout bone marrow to directly test the role of OLFR2 onimmune cells in regulating tumor growth. We found that hematopoietic deletion of OLFR2exacerbated melanoma tumor growth in these mice; again, supporting the notion thatOLFR2 is anti-tumoral. The OLFR2+ cells present in the tumor were myeloid cells.Monocytes, non-classical monocytes specifically, function to detect cancer cells in tumorseeding sites, and recruit NK cells for tumor cell destruction. OLFR2-deficientmacrophages were found to migrate less to tumor cells in an in vitro assay, suggestingthat OLFR2 is involved in the sensing of newly seeding tumor cells, likely through sensingoctanal. Studies are ongoing to determine the exact functions of OLFR2+ monocytes andmacrophages in the tumor microenvironment. OLFR2 may be one of several olfactoryreceptors that is utilized by myeloid cells as a defense mechanism for detection of newlyseeding or metastatic tumor cells. As olfactory receptors are easily druggable targets,understanding their role in cancer prevention could lead to emerging newimmunotherapies for cancer.

#2680 Knockout on enhancer of zeste homolog 2 in triple-negative breast cancer model alters immune signaling and decreases tumor progression and lung metastasis.

L. Monterroza[1], M. Parrilla[2], S. Samaranayake[1], D. Rivera[1], B. Dobosh[1], P. Selvaraj[1], R. Tirouvanziam[1];
[1]Emory University, Atlanta, GA, [2]Georgia State University, Atlanta, GA

Triple-negative breast cancer (TNBC) is an aggressive and highly metastatic subtype of breast cancer. Lack of known targets, patient-to-patient variations of target antigens and resistance to immune checkpoint inhibitors make TNBC one of the most challenging cancers to treat. TNBC is enriched in tumor-infiltrating neutrophils (TINs). TINs are key contributors to pro-tumorigenic processes linked to “immunologically cold” tumors, in part by preventing recruitment of T-lymphocytes (TILs). Prior studies identified the Enhancer of zeste homolog 2 (EZH2) as a prominent methyltransferase expressed in primary and metastatic TNBC cells. EZH2 is an upstream regulator of the stimulator of interferon genes (STING), a critical innate sensor mediating anti-tumor responses that is inhibited in cold tumors. To date, EZH2/STING signaling in TINs is relatively unknown. Here, we hypothesized that EZH2 inhibition and subsequent STING activation could exert anti-tumor activity by modulating TINs. We derived EZH2-knockout (KO) and EZH2-overexpressed (OX) cell lines from the well-established 4T1 TNBC mouse cell line. We demonstrate a 10-fold decrease in lung metastasis and significant reduction of 4T1 EZH2 KO tumor growth compared to the parent 4T1 cell line. Concomitantly, the TIN:TIL ratio was significantly reduced in 4T1 EZH2 KO vs. control tumors. Overexpression of EZH2 in 4T1 TNBC cells did not affect the primary tumor growth or lung metastasis. A therapeutic study using the repeated injection of the STING agonist MSA-2 after tumor engraftment in vivo also demonstrated a decrease in lung metastasis and tumor growth in MSA-2 vs. vehicle injection with both 4T1 parent and EZH2 KO cell lines. Together, our findings suggest a key role for STING pathway modulation and TIN/TIL poise in primary TNBC progression and lung metastasis.

#2681 Blockade of SIRPα in glioblastoma cells inhibits mitochondrial fatty acid β-oxidation and increase immune cell mediated cytotoxicity.

Y.-T. Tsai, G. Lesser, D. Soto-Pantoja;
Wake Forest University School of Medicine, Winston Salem, NC

Glioblastoma (GBM) is the most malignant brain tumor with limited immunotherapeutic options, likely due to significant GBM-associated systemic and intra-tumoral immunosuppression. The binding of SIRPα on myeloid cells to CD47 on cancer cells restricts immuno-phagocytosis against cancer cells. However, less attention has been given to SIRPα is also expressed in cancer cells, and the role of SIRPα on cancer cells is still unclear. Immunohistochemistry (IHC) staining was used to examine the expression of SIRPα in normal brain tissues and GBM. A single-cell database on the Broad Institute Portal was utilized to analyze the SIRPα expression in different cell types. SIRPα antisense morpholino was applied for gene knockdown. Established stable SIRPα overexpressed GBM cell lines were used to examine the mitochondrial function through the Seahorse Mito Stress test. In vitro, immune cell-mediated cytotoxicity was measured by Agilent xCELLigence Real-Time Cell Analysis. Patient biopsies show a 2-fold increase in SIRPα expression in GBM tumors compared to the normal adjacent ($n=14-21$; $p < 0.01$). Single-cell RNA-seq data on GBM tumors shows that SIRPα is expressed not only in the myeloid compartment but also in malignant cells. Studies have shown that mitochondrial function and fatty acid β-oxidation (FAO) play a critical role in GBM progression. Respirometry data revealed that blocking SIRPα in murine GBM cell line (CT2A) decreases mitochondrial ATP production. Seahorse Mito Stress test combined with fuel inhibitors showed that SIRPα expression mainly affects the usage of FAO (approximately 50%). In addition, stably, the GFP-tagged SIRPα overexpressed GBM cell line showed an increase of mitochondrial respiration with enhanced FAO ratio compared to the GFP control cell line. These suggested that SIRPα regulates mitochondrial FAO. Studies have shown that tumor-intrinsic FAO confers cell resistance to immune cell-mediated cytotoxicity. Interestingly, by coculturing with microglia, the innate immune population in the brain, our data showed that SIRPα blockade on GBM enhanced microglia-mediated cytotoxicity. Our data showed that targeting SIRPα on GBM may be a prospective therapeutic option by inhibiting FAO in mitochondria and increasing immune cell-mediated cytotoxicity.

#2684 Pan-cancer neutrophil profiling illuminates anti-tumor antigen-presenting potency.

Y. C. Wu, J. Ma, Q. Gao;
Fudan University, Shanghai, China

Neutrophils, the most abundant and efficient defenders against pathogens, exert opposing functions across cancer types. However, given their short half-life and fragile proliferation, it remains challenging to explore how neutrophils adapt to specific fates in cancer. Here we generated and integrated single-cell neutrophil transcriptomes from 17 cancer types (225 samples, 143 patients). Neutrophils exhibited extraordinary complexity, with 10 distinct cell states along differentiation paths including inflammation, angiogenesis, and antigen presentation. Notably, the antigen-presenting program was associated with favorable survival in most cancers and could be evoked by leucine metabolism and subsequent histone H3K27ac modification. These neutrophils could further invoke both (neo)antigen-specific and antigen-independent T-cell responses. Neutrophil delivery or leucine diet fine-tuned the immune balance to boost anti-PD-1 therapy in various murine cancers. In summary, these data not only unravel the neutrophil divergence across cancers, but also offer therapeutic opportunities such as antigen-presenting neutrophil delivery.

#2685 Activated phenotype of intraepithelial type 1 innate lymphoid cells is enriched in HPV-positive head and neck cancers.

H. Takahashi[1], S. ida[2], H. Tada[2], K. Chikamatsu[2];

[1]Ai Komagata Clinic, Maebashi, Japan, [2]Gunma Univ. Grad. School of Medicine, Maebashi, Japan

Innate lymphoid cells (ILCs) and natural killer (NK) cells are a heterogeneous family of innate immune cells that regulate inflammation, immune tolerance and tissue homeostasis in infection, chronic inflammation, metabolic diseases and cancer. The ILC family lacks the expression of antigen-specific receptors and demonstrate effector function by generating cytokines and secreted proteins. In tumor microenvironment, ILCs play a dual role including both tumor regression and tumor promotion, suggesting their diverse phenotypes and functional states. Among the ILC family, ILC1s and NK cells share some features, including the expression of the transcription factor T-bet and the ability to produce IFN-γ. In the present study, we analyzed single-cell RNA sequencing (scRNAseq) data to investigate the landscape and functional status of ILC families in patients with head and neck squamous cell carcinoma (HNSCC). The GSE164690 dataset, including pre-processed scRNAseq data and clinical data, was obtained from Gene Expression Omnibus. A total of 17 pairs of tumor-derived CD45-positive cells and peripheral blood lymphocytes, consisting of 6 HPV-positive HNSCCs and 11 HPV-negative HNSCCs, were analyzed using the Seurat v4 R package. After quality control, a total of 95,809 cells were obtained and clustered into 16 immune cell clusters. Next, a total of 7,278 NK cells were extracted and sub-clustered into 11 clusters. To characterize the 11 clusters, the abundances of NK subsets were estimated by CIBERSORTx. This approach identified eight NK cell clusters, two intraepithelial ILC1 (ieILC1) clusters, and one ieILC1-NK-intermediate (ieILC1-NK-int) cluster. Single-sample GSEA (ssGSEA) analysis was performed to further characterize each subset. ieILC1 clusters expressed tissue-resident markers *ITGA1*, *CD69*, and *CXCR6*, whereas ieILC1-NK-int cluster expressed ILC1 markers *CCR7*, *IL7R*, and *SELL*. Principle component analysis (PCA) based on ssGSEA indicated that ieILC1 clusters and ieILC1-NK-int showed the different PCA distribution from NK clusters. Inflammation and effector function-related pathways, including inflammatory response, interferon-gamma response, and interferon-alpha response, were enriched in ieILC1 clusters compared with the others. Among ieILC1 clusters, several pathways, including hypoxia, TNFA signaling via NFKB, allograft rejection, TGF beta signaling, were more enriched in ieILC1-1 than in ieILC1-2, suggesting that ieILC1-1 is the most immunologically active phenotype among NK subclusters. Of note, ieILC1-2 mainly comprised cells isolated from HPV-negative tumors, whereas ieILC1-1 mainly comprised cells isolated from HPV-positive tumors. In conclusion, we have demonstrated the diverse landscape of NK and ieILC1 cells in patients with HNSCC. Further characterization of the ILC family would lead to a novel therapeutic approach against HNSCC.

#2686 Glycolysis-stimulated lactate production by tumor-associated macrophages promotes their M2-like phenotype.

K. Kurylowicz[1], K. Chakraborty[1], C. Cui[1], G. Davanzo[2], G. Zhou[1], X. Tang[1], K. Q. Schoenfelt[1], N. Pulliam[3], C. A. Reardon[1], S. Kulkarni[3], T. Vaisar[4], P. M. Moraes-Vieira[2], Y. Zhao[1], L. Becker[1];

[1]The University of Chicago, Chicago, IL, [2]University of Campinas, Campinas, Brazil, [3]Northwestern University, Chicago, IL, [4]University of Washington, Seattle, WA

Tumor-associated macrophages (TAMs) are the predominant immune cells within the tumor microenvironment (TME), and their phenotypic modulation is influenced by environmental cues in the TME. In early tumors, TAMs adopt a pro-inflammatory M1-like phenotype, characterized by the secretion of immunogenic cytokines and the ability to kill cancer cells, thus opposing tumorigenesis. However, as tumors progress, TAMs mainly transition to an anti-inflammatory M2-like phenotype, promoting angiogenesis, suppressing anti-tumor immunity, and supporting metastasis. Importantly, a high M2-like/M1-like TAM ratio correlates with poor survival and decreased treatment responses.Despite the significance of TAMs, the molecular mechanisms driving their pro-tumorigenic M2-like phenotype remain unclear. One potential mechanism is metabolic reprogramming, where, traditionally, M1 macrophages favor glycolysis, and M2 macrophages rely on oxidative phosphorylation. However, this paradigm is primarily derived from in vitro experiments using well-defined polarization cocktails, which may not accurately replicate the complex TME. For instance, while in *in vitro* experiments IL4 and IL13 can induce oxidative phosphorylation and an M2-like phenotype, these cytokines do not seem essential for M2-like TAM polarization *in vivo*.Our studies reveal that, relative to M1-like TAMs, M2-like TAMs exhibit heightened glycolysis, intracellular lactate accumulation, and increased histone lysine lactylation - an epigenetic mark directly stimulated by lactate. Importantly, we demonstrate that TAM glycolysis and the M2-like phenotype are positively associated with hypoxia within a single tumor (GEM model and human tumors) and across various tumor types (syngeneic models). Inhibition of glycolysis-stimulated lactate production in TAMs through myeloid cell-specific deletion of lactate dehydrogenase A (mLdha-/-) reduces the M2-like:M1-like TAM ratio. This intervention increases tumor-infiltrating CD8+ T cells and reduces tumor growth in pre-clinical models, particularly in highly hypoxic environments. Moreover, to exclude the role of cancer cell-derived lactate on TAMs' phenotypic changes, we reduced glycolysis in cancer cells by deleting pyruvate kinase muscle isozyme M2 (PKM2). This resulted in decreased lactate production and suppressed tumor growth. However, the M2/M1 ratio remained unaffected, suggesting that the intrinsic lactate production by TAMs is crucial for their phenotype modulation.Our findings underscore the pivotal role of hypoxia-induced glycolysis and lactate production in TAMs, shaping their M2-like phenotype and impacting tumor progression. This understanding not only advances our knowledge of macrophage metabolism and phenotype dynamics in the context of cancer but also in other diseases.

#2687 NK cell plasticity in SCLC is linked to tumor transcriptional diversity.

J. Malin, S. Zhuang, A. K. Sharma, J. Clara, A. Thomas;
NIH-NCI, Bethesda, MD

Natural Killer (NK) cells are innate lymphoid cells that are pivotal in the body's response to cancer. To harness their cytotoxicity in clinical interventions, it is critical to understand their biology, which is highly tissue- and tumor-specific. In Small Cell Lung Cancer (SCLC), reports have described widely divergent levels of NK activity in neuroendocrine (NE) and non-neuroendocrine (non-NE) subtypes. Diminished self-antigen presentation by MHC-I is a classic trigger of NK cell activity but, counter-intuitively, NK cells exhibit reduced cytotoxicity in MHC-I downregulated NE SCLC.

To explore potential causes for depressed NK activity in NE SCLC relative to non-NE, we applied scRNA-Seq to 45 SCLC patient biopsies and rapid autopsies, and identified 4000 NK cells based on gene expression signature. There was a notable dip in NK cell infiltration in NE tumors compared to non-NE tumors. Tumor cell-surface ligands recognized by activating and, unexpectedly, inhibitory NK cell receptors were generally both more highly expressed in non-NE tumors. While inhibitory NK receptors were comparable in NE and non-NE tumors, activating NK receptors were expressed significantly, though modestly, higher in non-NE. We observed tumor site-specific gene expression patterns in NK cells from different metastatic sites. Overall, there were a remarkably high number of differentially expressed genes (>1k) between NK cells from NE and non-NE tumors, even after controlling for tumor site. Together, our work suggests that NK cell plasticity is manifest at the level of SCLC transcriptional subtypes.

#2688 Age-associated changes in macrophage function and phenotype affects cancer development, and the efficacy of macrophage targeted anticancer therapies in murine melanoma model.

M. Suresh, X. Li, S. Noonepalle, N. Gajendran, M. Durr, D. Quiceno-Torres, K. Tan, A. Villagra;
Georgetown Lombardi Comprehensive Cancer Ctr., Washington, DC

Introduction: Aging of the immune system is a critical risk factor for chronic diseases, including cancer. Globally, cancer incidence is higher between 45 to 75 years of age and declines thereafter. However, the implications of aging in cancer are understudied, and aged populations are underrepresented, both in preclinical and clinical studies. The role of macrophages in cancer progression has gained attention as a tool and target for anticancer therapies. Tumor-associated macrophages (TAMs) mainly exhibit an anti-inflammatory M2 phenotype, promote an immunosuppressive tumor microenvironment (TME), and contribute to developing resistance against immunotherapies. Therefore, several strategies targeting the phenotype and function of TAMs are being explored, including inhibitors of histone deacetylases (HDACis), adoptive macrophage cell therapy, and CAR macrophages. Studies from our group have shown that ultra-specific HDAC6is can switch macrophages from anti-inflammatory, M2, to pro-inflammatory and antitumoral M1 phenotype with minimal cytotoxicity to cancer cells. However, it is unknown if age-related changes in macrophages affect such therapeutic strategies and the TME.
Objective: To characterize the changes in macrophage function and phenotype with aging and study its implications on the TME and the efficacy of macrophage-based anticancer therapies.
Methods: Wildtype mice of ages 6-8 WKS, 3-6 MO, 10-12 MO, and 20-24 MO were injected with SM1 melanoma cells to study tumor growth kinetics. Bone marrow-derived macrophages (BMDMs) isolated from tumor-bearing and healthy mice were polarized to M1 and M2 phenotype treated with HDAC6i to study age-associated changes in phagocytic activity, antigen presentation, and gene expression. Pathways associated with macrophage polarization were examined by flow cytometry, qRT-PCR, western blot, and single-cell proteomics. Immune cells in TME were characterized in flow cytometry and single-cell RNA and secretome analyses.
Results: Tumor growth in SM1 murine melanoma model was significantly slower in older mice when compared to younger mice. Aged macrophages demonstrated significant defect in polarization to M1 and M2 phenotypes that was more pronounced in BMDMs from tumor-bearing mice. Tumor-associated macrophages showed inefficient monocyte-to-macrophage transition, as also reflected in the single-cell secretome analysis. The ability of HDAC6i to enhance macrophage function was reduced among older mice.
Conclusions: The functional and phenotypic characteristics of macrophages change with age and can significantly affect tumor growth and the effectiveness of macrophage-targeted anticancer therapies. Our study highlights the importance of studying aging in macrophages and better representation of aged populations in preclinical and clinical studies.

#2689 Mass cytometry analysis of CXCR3 expression in tumor-infiltrated myeloid cells as a predictive biomarker For immunotherapy response.

G. A. Valentin-Guillama, N. Chatterjee, A. Alimadadi, C. C. Hedrick;
Augusta University, Augusta, GA

Monocytes have emerged as important regulators of cancer progression. We have recently found that $CXCR3^{\pm}$ circulating monocytes in humans are associated with better response to immunotherapy. Here, we aimed to study the functions and heterogeneity of $CXCR3^{\pm}$ monocytes in two different triple negative breast cancer (TNBC) tumors in mice, using either AT3 or EO771 tumor cell lines. AT-3 tumors exhibit higher resistance to anti-PD-1 and anti-CTLA-4 therapy in C57BL/6 breast cancer mouse models compared to EO771 tumors. We evaluated 36 surface protein markers on tumor-infiltrated myeloid cells in tumors isolated from each model using CyTOF mass cytometry. Analysis of monocytes, macrophages and dendritic cells in the tumors using unsupervised clustering identified 13 cell subsets. Significant differences were discovered between the two tumor types in frequencies of nine of 13 identified subsets. However, 3 of these subsets displayed relatively high expression of CXCR3 in EO771 tumors when compared to AT-3 tumors. The significant CXCR3 positive subsets were identified as $CXCR3^{\pm}$ early macrophages, $CXCR3^{\pm}$ $Ly6C^{+}CD11b^{lo}$ classical monocytes and $Trem2^{\pm}$ $CXCR3^{\pm}$ dendritic cells. We observed higher expression of CXCR4, Trem2, and CCR1 in $CXCR3^{\pm}$ myeloid cells when compared to their $CXCR3^{-}$ counterparts in both tumor models. To elucidate the role of these $CXCR3^{\pm}$ cells, we performed low-input bulk RNA sequencing of $CD115^{+}/CD11b^{+}$ cells from blood and spleen of EO771 tumor bearing mice with a wild type or $CXCR3^{KO}$ genotype. Ingenuity Pathway Analysis (IPA) of the differentially expressed genes suggests a significant inhibition of the IL-10 signaling pathway of $CXCR3^{KO}$ cells. These differentially expressed markers and genes suggest a functional importance in this subset in migration to the tumor and antigen presentation, both of which are anti-tumoral functions. Ongoing studies are aimed towards understanding the role of $CXCR3^{\pm}$ myeloid cells in regulating response to immunotherapies.

#2690 The role of PCNA tyrosine phosphorylation in evading innate immune surveillance.

C.-C. Lee[1], W.-R. Wu[2], Y.-C. Shen[1], F.-C. Chung[2], Y.-L. Wang[1], Y.-Z. Lin[2], C.-H. Lu[3], W.-C. Cheng[2], H. Chang[1], L.-C. Liu[1], J.-A. Liang[1], C.-F. Chiu[1], M.-C. Hung[2], S.-C. Wang[2];

[1]China Medical University Hospital, Taichung, Taiwan, [2]China Medical University, Taichung, Taiwan, [3]National Yang-Ming Chiao Tung University, Taipei, Taiwan

Cancer cells are continually exposed to intrinsic and extrinsic proliferative stresses that can send the genome stability awry. The aberrant DNA metabolism, evolving through deregulated replicative growth in cancer cells, is increasingly recognized as a major mechanism bridging the crosstalk between the immune microenvironment and tumor tissue, thereby either promoting or suppressing tumor progression. However, the triggering and regulation of these mechanisms remain largely unknown. Proliferating cell nuclear antigen (PCNA) and its homologs are the evolutionarily conserved central components of the DNA replication machinery. In eukaryotic cells, PCNA forms homotrimeric rings encircling the DNA double helix to coordinate the complex processes of DNA replication and damage repair, directed at least in part by differential post-translational modifications of the PCNA protein. In cancer cells, growth signal-stimulated phosphorylation at tyrosine 211 of PCNA (pY211-PCNA) is known to play an important function for active proliferation. Here, we demonstrate that inhibition of pY211 disrupts the processivity of replication forks. This disruption triggers single-stranded DNA (ssDNA) production catalyzed by the MRE11 nuclease, activating the cGAS-STING axis to launch an anti-tumor immune response by natural killer (NK) cells. We further show that the pY211 regulates site-specific post-translational modifications of MRE11, and loss of pY211 promotes the endonuclease mode of MRE11. This causes ssDNA generation in the cytosol, subsequently inducing type I interferon-activated cytotoxicity by NK cells and fostering an anti-tumor immunity that abrogates distant metastasis. Mechanistically, the pY211 determines the recruitment of the writer or eraser of the modification on MRE11, thus tuning the nucleolytic modes of MRE11 and, consequently, ssDNA generation. Therapeutic measures promoting MRE11-dependent ssDNA enhance the response of triple-negative breast cancer to cytotoxic killing mediated by endogenous or allogenic NK cells in mice. In breast cancer patients, the level of cytosolic ssDNA is inversely correlated with the expression of the eraser and pY211-PCNA, which is associated with poor overall survival in cancer patients. Our studies shed new light on the shaping of the tumor immune microenvironment and demonstrate the potential to develop therapeutic approaches that proactively leverage genomic instability and immune activation to target malignant tumors.

#2691 Mapping the landscape of innate immune pattern recognition receptors in pancreatic cancer.

B. Kashgari[1], L. McLeod[1], L. J. Gearing[1], D. Croagh[2], **B. J. Jenkins**[3];
[1]Hudson Institute of Medical Research, Melbourne, Australia, [2]Monash University, Melbourne, Australia, [3]University of Adelaide, Adelaide, Australia

Pancreatic ductal adenocarcinoma (PDAC) accounts for 90% of all pancreatic cancer cases, and is among the most aggressive and lethal malignancies worldwide. PDAC is driven by genetic alterations in the pancreatic epithelium (e.g. *KRAS*, *TRP53*) coupled with a dysregulated innate immune response, the latter leading to an inflammatory tumor microenvironment enriched in innate immune cells (e.g. macrophages). However, immune-based treatment regimens for PDAC patients have primarily focused on immunotherapy with adaptive immune checkpoint inhibitors (e.g. PD-1) which disappointingly have yielded minimal clinical benefit. Thus, there is an unmet clinical need to identity disease-associated innate immune regulators as therapeutic targets in PDAC. Innate immune responses depend on a series of cell surface, endosomal and cytosolic pattern recognition receptors (PRRs) that are expressed in immune and non-immune cells. PRRs are classified into several structurally and functionally conserved subfamilies, including Toll-like receptors (TLRs), Absent in melanoma 2 (AIM2)-like receptors (ALRs), and Nod-like receptors (NLRs). A subset of NLRs and AIM2 are also well documented for their formation of multiprotein complexes called 'inflammasomes' - comprising the adaptor ASC and Caspase-1 - which direct the maturation and release of bioactive pro-inflammatory cytokines, IL-18 and IL-1β. However, the role of these critical innate immune regulators in PDAC has been underexplored, and is virtually unknown. By coupling endoscopic ultrasound-guided fine needle aspiration (EUS FNA) to capture tumor biopsies from all stages of PDAC, with whole transcriptome profiling of PDAC patient primary tumors, we reveal specific enrichment of the innate immune TLR2 and ASC inflammasome molecular pathways. Augmented TLR2 and ASC expression was prognostic for low survival, and a "TLR2 activation" signature was also predictive for chemoresistance. Antibody-mediated anti-TLR2 therapy suppressed tumor growth in human PDAC tumor xenografts (patient and cell line) in both immunocompromised and 'humanized' mice. With respect to ASC, using the genetically engineered KPC PDAC mouse model, we show that Caspase-1 activation, a read-out for inflammasome activation, is upregulated in pancreatic tumors. Moreover, genetic ablation of ASC in KPC mice markedly suppressed the development of pancreatic tumors, which was associated with significant reductions in levels of both Caspase-1 activation and inflammation. Transcriptome profiling further identified unique downstream molecular networks associated with a range of oncogenic cellular processes. Taken together, our results support innate immune TLR2- and ASC inflammasome-based therapeutic targeting in PDAC, with further clinical utility that ASC inflammasome and TLR2 activation is prognostic, with TLR2 also predictive for chemoresponsiveness.

#2692 ELK3 is a key regulator as the response of natural killer cell therapy in triple-negative breast cancer.

H.-Y. Jung, Y. Lee;
Korea Institute of Radiological & Medical Sciences (KIRAMS), Seoul, Korea, Republic of

Triple-negative breast cancer (TNBC) is the most challenging subtype of breast cancer because of its aggressive behavior and the limited therapeutic strategies available. In the last decade, immunotherapy has become a promising treatment to prolong survival in advanced solid cancers including TNBC. However, the efficacy of immunotherapy in solid cancers remains limited because solid tumors contain few tumor-infiltrating lymphocytes. Here, we show that targeting an ETS transcription factor ELK3 (ELK3) enhances the response of nature killer (NK) cells through intracellular and extracellular signaling. In extracellular signaling, ELK3 depletion increases CXCL16 expression level and promotes NK cell cytotoxicity through CXCL16-mediated NK cell recruitment in TNBC. In intracellular signaling, ELK3 depletion controls mitochondrial fission-fusion status to induce NK cell-mediated cell death. In silico analysis showed that ELK3 is negatively correlated with CXCL16 or MID51 expression in breast cancer patient samples. Low expression of ELK3 and high expression of CXCL16 or MID51 were associated with a better prognosis. Low expression of ELK3 and high expression of CXCL16 or MID51 were associated with increased expression of NK cell-related genes. Our findings demonstrate that ELK3-CXCL16 axis controls NK cell recruitment to target cancer cells and ELK2-MID51 axis triggers mitochondrial dysfunction-mediated apoptosis during NK cell therapy, suggesting that targeting the ELK3 gene could be an adjuvant strategy for increasing the efficacy of immunotherapy in TNBC

#2693 MicroRNA manipulation of macrophage polarization in DLBCL to augment antibody immunotherapy.

J. Longley, R. Foxall, S. Thirdborough, S. Beers, M. Cragg;
University of Southampton, School of Medicine, Southampton, United Kingdom

Background: CD163 positive tumor associated macrophages (TAM), have been associated with poor response to immunochemotherapy in DLBCL. Targeting these TAMs to reverse immunosuppression is one approach for improving treatment response rates. MicroRNAs have the potential to modify hundreds of genes by interacting with multiple mRNA targets, thereby altering the global transcriptional profile of cells. Manipulation of microRNAs may prove an effective means of switching the transcriptomic profiles of TAMs to more activated, anti-tumor states resulting in the reversal of immune resistance and enhancement of treatment efficacy.

Methods: MicroRNAs differentially expressed in DLBCL and associated with poor response were identified using whole gene correlated network analysis of DLBCL datasets. Peripheral blood mononuclear cells (PBMCs) were obtained from normal blood donors and differentiated into macrophages following cell culture with MCSF. Macrophages were polarized using immunosuppressive (IL4 + IL13) or immunostimulating (LPS + IFNγ) cytokines and microRNA expression measured using RT-qPCR. To assess antibody dependent cellular phagocytosis (ADCP), macrophages were generated and polarized as above and transfected with microRNA inhibitors (Thermofisher) prior to co-incubation with target cells. Human Chronic Lymphocytic Leukemia (CLL) cells were labelled with CSFE and used as target cells with Rituximab as the ADCP-inducing monoclonal antibody (mAb) and Herceptin as an isotype control. The percentage of Fc gamma receptor IIIA (FcγRIIIA)-expressing macrophages taking up target cells was determined using flow cytometry and analyzed using Flowjo software. Diagnostic biopsies from patients were then analyzed for microRNA 142-5p and CD206 expression using miRNAScope assays and immunohistochemistry.

Results: There was significant upregulation of microRNA 142-5p in macrophages polarized with IL4 plus IL13 compared to macrophages polarized with LPS plus IFNγ and non-polarized macrophages. Inhibition of microRNA 142-5p in IL4 plus IL13 polarized macrophages led to a significant increase in FcγRIIIA, CD40 and CD47 expression resulting in enhanced phagocytosis of CLL cells opsonized with Rituximab plus anti-CD47 mAb when compared with controls. High microRNA 142-5p expression in combination with high CD206 expression predicted poor response to immunochemotherapy in 38 treatment naïve human DLBCL samples (median PFS 12 months v NR p=0.0096).

Discussion: Transfection of a microRNA 142-5p inhibitor can repolarize immunosuppressive macrophages to a more anti-tumor phenotype leading to enhanced ADCP. CD206 positive TAM infiltration in combination with high microRNA 142-5p expression predicted poor outcome following treatment with immunochemotherapy in DLBCL. It may be possible to use microRNA directed therapies targeting the tumor microenvironment to enhance treatment efficacy.

#2694 The role of innate lymphoid cells and innate like T cells in hepatocellular carcinoma.

P. Huang, B. Ruf, R. Trehan, D. Soika, C. Ma, T. F. Greten, F. Korangy;
National Cancer Inst. - Bethesda Campus, Bethesda, MD

The major focus of cancer immunotherapy has been on conventional T cells due to their unique recognition of specific peptide antigens. Despite advances in the cancer immunotherapy field, including the use of atezolizumab and bevacizumab as first-line therapy for unresectable hepatocellular carcinoma (HCC), the overall mortality rate of HCC continues to rise. Innate lymphoid cells (ILC) and innate-like T cells (ILTC) are broadly categorized within the innate lymphoid population as playing an important role in inflammation, tissue repair and immune tolerance. Their ability to react rapidly to stimulants in their local tissue environment as well as to recruit and activate a variety of other immune cells makes these cells attractive targets for anti-tumor therapy. However, previous studies looking at ILCs and ILTCs in cancer have revealed both pro- and anti-tumor functions. Furthermore, the complex interplay between these cell populations in the tumor microenvironment is not well understood, particularly over the natural course of tumor development. In this study, we aim to better elucidate the role of ILC and ILTC populations in HCC progression in terms of both their kinetics and role as potential therapeutic targets. We performed hydrodynamic tail vein injections in mice with two different plasmid combinations to alter expression of commonly mutated oncogenes and tumor suppressors in human HCC (MYC;TP53 and MYC;CTNNB1). Histologic analysis of the livers was performed to determine appropriate time points to assess ILC and ILTC populations. We then designed a comprehensive 29-plex spectral flow panel to assess broad kinetic changes in the frequency of ILC, ILTC, and conventional T cell populations. We show that in early time points (4-7 days post-injection) when neoplastic transformation of hepatocytes has already occurred, mucosal-associated invariant T (MAIT) cells, group 1 ILCs, ILC2s, and ILC3s expand in frequency for both tumor models. Cytokine analysis shows a generalized decreased trend across timepoints in effector cytokine production in MAITs and group 1 ILCs, suggesting gradual dysfunction over time. Taken together, these preliminary findings show that ILC and ILTC populations expand early during tumor progression but gradually decrease in functionality with tumor progression.

#2695 A higher percentage of M2 macrophages in non-tumor part predict the tumor recurrence in patients with hepatocellular carcinoma after surgical resection.

P.-T. Lin[1], W.-T. Ku[2], T.-H. Wu[1], C.-H. Wu[1], C.-K. Yang[1], W. Teng[1], Y.-C. Lin[1], C.-Y. Lin[1];
[1]Chang Gung Memorial Hospital - Taoyuan Branch, Taoyuan, Taiwan, [2]Chang Gung University, Taoyuan, Taiwan

The primary hurdle in improving outcomes for hepatocellular carcinoma (HCC) patients after curative treatment is the high early recurrence rate. The existing literature indicates the presence of type 2 macrophages (M2), renowned for their immunosuppressive capabilities, has been implicated in creating a microenvironment conducive to tumor growth and recurrence. However, the intricate interplay involving M2 macrophages and the recurrence of HCC is underexplored. Therefore, we conducted an analysis involving HCC patients who underwent hepatectomy at our hospital between 2013 and 2017. We collected samples from both the tumor and non-tumor regions and subjected them to bulk RNA sequencing for comprehensive molecular profiling. The proportion of immune cells was calculated by CIBERSORTx.In our study, we enrolled fifty patients, with sixty percent presenting with cirrhosis and seventy-three percent having viral hepatitis. Twenty-three patients experienced tumor recurrence, with a median time to recurrence of 12.6 months. First, we found no correlation between five TIMR subtypes defined by TIMELASER (Xue R, Nature, 2022) and recurrence. However, as for the proportions of immune cell, a significantly lower NK/Treg ratio (p= 0.0163) and high within the resected tumor section in recurrent group was found. On the other hand, the ratio of M2 macrophages to total macrophages (M2/M) was significantly higher within the non-tumor region in patients experiencing tumor recurrence after hepatectomy (p=0.0357). Furthermore, the expression of the ACGT2 gene in non-tumor part, which strongly correlates with Treg function, was significantly higher (p=0.0056) in recurrent group. In addition, the innate T cells score was increased in non-tumor pat in recurrent group but with borderline significance (p=0.0628). However, in multivariable analysis, only a higher M2/M ratio within the non-tumor region (HR 3.756, p=0.0072) were identified as independent risk factors for tumor recurrence. We also found that patients with a higher M2/M ratio had a lower percentage of cirrhotic patients (p=0.0049) and less association with TIME-IA (immune activation) subtype of HCC by TIMELASER classification (p=0.0030). In conclusion, a higher M2/M ratio within the non-tumor region predict the tumor recurrence in patients with hepatocellular carcinoma.

#2696 Tumor organoid and immune cells co-cultures to study myeloid cells-targeting immunotherapy.

L. Spagnuolo, F. Morales-Rodriguez, A. Merenda, C. Oyarce, F. Pourfarzad, R. G. J. Vries, S. F. Boj;
HUB Organoids B.V., Utrecht, Netherlands

Cancer immunotherapy is one of the main pillars of oncology treatment due to the clinical success of approaches that enhance anti-tumoral T cell responses. Nonetheless, many patients do not benefit from these approaches, highlighting the need to develop novel immunomodulatory strategies. Exploiting the anti-tumor capacity of innate immune cells is a promising approach that can overcome specific limitations of T cell-targeting therapies and complement existing immunotherapies. Still, promising therapeutic developments face hurdles in translating preclinical findings into treatment since conventional 2D cancer models hold low clinical predictive value. HUB developed an innovative alternative, building on the discovery that adult stem cells proliferate and organize into three-dimensional organotypic structures. Patient-specific organoids are generated from healthy and disease tissues and recapitulate complex characteristics of the original parental tissue, including molecular heterogeneity and morphological and functional traits. To assess the efficacy of therapies that engage innate immune cells, we developed an assay in which organoids derived from colorectal (CRC) or breast cancer patients are co-cultured with PBMC-derived macrophages or monocytes to evaluate the cytotoxic potential of exogenously activated myeloid cells. We tested the ability of macrophages to phagocyte human CRC organoid cells in response to anti-CD47 antibody. The pro-phagocytic function of anti-CD47 was detected by several methods (i.e., flow cytometry, imaging), indicating the platform's suitability to evaluate ADCP-modulating compounds.
Moreover, to assess whether our PBMC-organoids co-culture platform is suited to detect monocyte-mediated effects, Lipopolysaccharide (LPS) plus IFN-γ were used to activate monocytes in the co-culture assays. We observed an increase in cytokines secretion (i.e., CXCL10), immune cell activation and organoid killing, indicating that our assay allows the detection of monocyte activation through different types of readouts. In summary, our organoid-immune cell co-culture platform allows to study the response of tumor organoids to innate immune cells, holding significant value for the preclinical development of immunotherapies based on innate immune cells.

#2697 Simultaneous activation of innate immune suppressive components impairs antitumor efficacy of immunotherapy against the innate immune system.

H. Nishinakamura[1], S. Shinya[2], T. Irie[3], S. Sakihama[4], T. Ioroi[1], T. Naito[3], K. Watanabe[1], D. Sugiyama[5], M. Tamiya[6], T. Yoshida[1], T. Hase[5], T. Yoshida[7], K. Karube[5], Y. Maeda[1], S. Koyama[3], H. Nishikawa[1];

[1]National Cancer Center Japan, Tokyo, Japan, [2]Discovery Research Alliance, Ono Pharma USA, Inc., Massachusetts, MA, [3]National Cancer Center Japan, Chiba, Japan, [4]Graduate School of Health Sciences, University of the Ryukyus, Nishihara, Japan, [5]Nagoya University Graduate School of Medicine, Nagoya, Japan, [6]Osaka International Cancer Institute, Osaka, Japan, [7]Ono Pharmaceutical Co., Ltd., Osaka, Japan

Cancer immunotherapy has shown noticeable clinical efficacy in many cancer types, while clinical benefits are only observed in 20-40% of treated patients. Therefore, combination cancer immunotherapy targeting multiple factors that limit antitumor immunity has been tested in the clinic. Accumulating evidence reveals that cancers that harbor limited immune cell infiltration (so-called immunologically cold tumors) respond poorly to current immunotherapy. Preclinical studies using animal models have shown that activation of innate immunity by TLR agonists or STING agonists can successfully remodel the TME to effectively induce antitumor immunity in those immunologically cold tumors. However, unexpectedly, all TLR agonists and STING agonists tested have not shown clinical efficacy in combination with immune checkpoint blockade therapy, including PD-1/PD-L1 blockade therapy. Hence, we addressed the mechanism(s) why stimulators of innate immunity failed to elicit effective antitumor immunity in cancer patients. We then employed OK-432, which reportedly stimulates TLR-2, TLR-4, and/or TLR-9, as OK-432 is widely used in Japan in the clinic. In vitro OK-432 treatment accelerated the maturation DCs, and efficiently induced CD8+ T cells in humans. However, the combination treatment with anti-PD-1 mAb and OK-432 failed to augment antitumor immunity in animal models using anti-PD-1 mAb monotherapy-resistant tumors; the data mirrors the failure of clinical trials of combination therapy with immune checkpoint blockade and TLR agonists or STING agonists in humans. Therefore, using the animal models, we explored the acquired resistance mechanism developed after combination treatment. While OK-432 treatment effectively stimulated DCs, innate immune suppressive cells, such as MDSCs, were concurrently accumulated in the TME. The accumulation of PMN-MDSCs after OK-432 treatment was induced in a CXCL1-CXCR2-dependent fashion. Accordingly, triple combination treatment with a PMN-MDSC inhibitor along with OK-432 and anti-PD-1 mAb attenuated the accumulation of PMN-MDSCs in the TME and improved the antitumor effect of the combination treatment. Taken together, we propose that successful combination treatment stimulating innate immunity against immunogenically cold cancers requires controlling the unwanted co-activation of innate immune suppressive cells. This study clearly demonstrates the mechanism of acquired resistance after administration of reagents that activate innate immunity, such as TLR agonists or STING agonists, and provides the basis for future successful combination therapy.

#2698 TCF-1 is a critical regulator of intraepithelial lymphocytes in colorectal carcinoma.

M. H. Yakou[1], S. Ghilas[1], K. Tran[1], Y. Liao[1], S. Afshar-Sterle[1], A. Kumari[1], K. Schmid[1], C. Dijkstra[1], C. Inguanti[1], S. Ostrouska[1], J. Wilcox[1], M. Smith[2], P. Parathan[1], A. Allam[1], H.-H. Xue[3], G. T. Belz[4], J. M. Mariadason[1], A. Behren[1], G. R. Drummond[5], R. Ruscher[2], D. S. Williams[1], B. Pal[1], W. Shi[1], M. Ernst[1], D. Raghu[1], L. A. Mielke[1];

[1]Olivia Newton-John Cancer Research Institute, Heidelberg, Australia, [2]Australian Institute of Tropical Health and Medicine, Cairns, Australia, [3]Center for Discovery and Innovation, Hackensack University Medical Center, Nutley, NJ, [4]University of Queensland Frazer Institute, Woolloongabba, Australia, [5]La Trobe University, Bundoora, Australia

Tissue-resident immune cells reside within the gastrointestinal tract known as intraepithelial lymphocytes (T-IELs), including αβ and γδ T-IELs. This unique population of T cells constantly survey and are critical in maintaining the gastrointestinal epithelium. We show that T-IELs in various regions of the gastrointestinal tract have distinct features. T-IELs in the small intestine exhibit high expression of cytotoxic molecules important for cancer defense while colon T-IELs are distinctively regulated by the transcription factor, *TCF-7*/TCF-1, which suppresses their effector and cytotoxic properties, including reduced expression of granzymes, and their abundance is dependent on the microbiome. Targeted deletion of TCF-1 in γδ T-IELs using pre-clinical mouse models resulted in a distinct effector profile and reduced colon tumor burden. Furthermore, TCF-1 expression was significantly reduced in γδ T-IELs present in human colorectal cancers compared with normal healthy colon, strongly correlating with an enhanced γδ T-IEL effector phenotype and improved patient survival. Further investigation aims to elucidate diverse mechanisms by which TCF-1 controls tissue-specific anti-tumor immunity and uncover the important factors controlling TCF-1 expression. Our study underscores the necessity to consider tumor and organ microenvironment-specific factors in optimizing immunotherapy, advancing our understanding of T cell function in the colon to pave the way for innovative CRC treatments.

#2699 Application of whole genome loss of function CRISPR screen in primary natural killer cells.

M. Sheffer, I. E. Kaplan, E. Bobilev, Y. Z. Abdulhamid, R. Romee;
Dana-Farber Cancer Institute, Boston, MA

Natural killer cells (NKs) are cytotoxic lymphocytes of the innate immune system, operating against infections and cancer. NKs act in an antigen independent manner, preventing graft versus host disease in allogeneic settings. NKs can be isolated from healthy donors, activated, expanded and safely administered to cancer patients. Although NKs are highly cytotoxic against cancer cells *in vitro*, they lose viability and functionality in the suppressive tumor microenvironment (TME).

Until recently, viral transduction of primary NKs was considered a technical hurdle. The latest progress using Baboon Lentiviral (BaLV) pseudotyping substantially increased transduction rates and facilitated the use of chimeric antigen receptor (CAR) NKs for cancer immunotherapies. Due to this challenge, most genetic manipulations were performed in single genes with limited capabilities. Large-scale functional manipulation of NKs using CRISPR-cas9 editing was not implemented, leaving a gap in our understanding of NK suppression.

We generated a whole genome library of 55,548 guide RNAs (gdRNAs, 4 per gene), targeting 13,749 genes that were determined to be expressed in NKs and 138 (10%) olfactory receptor genes that are not expressed in NKs as control gdRNAs. The gdRNA plasmid was optimized based on our CAR-NK backbone, to express the gdRNA scaffold under U6 promotor and GFP under EF1α promotor. The library plasmids were sequenced and their gaussian distribution was verified, with high representation of all the different gdRNAs.

Primary NKs were isolated from 3 healthy donors and transduced at 25% transduction rates using our optimized BaLV system. After a week expansion *in vitro*, NKs were electroporated with protein cas9-RFP using the maxCyte electroporator. RFP levels at 6 hours after electroporation were at least 80%.

The cells were profiled after electroporation for cytotoxicity and for functionality against the K562 target cell line. IFNγ production and degranulation (CD107a) were similar before and after electroporation. Genomic DNA was extracted from the transduced NKs and the gdRNA barcodes were amplified by PCR and sequenced. The distribution of the gdRNA barcodes after sequencing exhibited high representation of almost all gdRNAs, with minimal loss of gdRNAs. Several gene knockouts were identified as important for survival/proliferation of NKs and are being validated using single gdRNAs *in vitro* and *in vivo*.

NK cell immunotherapy is a promising approach for cancer treatment. Although recent clinical trials with CAR-NK present exciting results, many solid tumors do not benefit from NK immunotherapies due to the inactivation of NKs in the immune-suppressive TME. Here, we successfully implemented an unbiased genome wide loss-of-function CRISPR screen as an effective and informative method to identify novel candidates for NK cell suppression.

#2700 Therapeutic IL-33 enhances the antigen presentation function of ILC2s to exert anti-tumor immune activity.

J. Liu, Z. Feng, H. Wei, C. Li, X. Li, W. Chen, Y. Ke, M. Wang, L. Liu, C. Zheng, Q. Liu;
Southern University of Science and Technology, Shenzhen, China

IL-33 regulates the function of ILC2s through ST2. However, the role of IL-33, especially exogenous IL-33, on ILC2s in tumors is controversial depending on the cytokines they secrete. Here we report that exogenous, but not endogenous, IL-33 significantly inhibits the progression of a variety of mouse solid tumors, including melanoma, colorectal cancer, lung adenoma, and breast cancer. By inoculating tumor cells in *Il1rl1*$^{-/-}$ and NSG mice, we found that the tumor-suppressive effect of IL-33 on tumors was dependent on the expression of ST2 receptors and the presence of lymphocytes. Regarding tumor-infiltrating immune cells, exogenous IL-33 significantly increases the proportions of ST2^{+} Tregs (1.10 ± 0.20% vs. 1.74 ± 0.36%), eosinophils (6.00 ± 1.33% vs. 22.73 ± 6.51%), Granzyme B^{+} CD8^{+} T cells (4.32 ± 2.77% vs. 11.53 ± 6.81%), and bulk ILC2s (0.08 ± 0.04% vs. 5.31 ± 1.33%) and IA/IE^{+} ILC2s (0.02 ± 0.01% vs. 3.67 ± 1.03%) . In draining lymph nodes, IL-33 also significantly increases the proportions of ILC2s (0.03 ± 0.02‰ vs. 6.37 ± 1.71‰) and IA/IE^{+} ILC2s (0.003 ± 0.003‰ vs. 4.38 ± 1.21‰). Importantly, single-cell transcriptomic analysis on tumor-infiltrating ILC2s highlights the expression of genes related with antigen processing and presentation including *H2-K1*, *H2-Q7*, *B2m*, *Hspa1a*, *Hspa1b*, *Creb1*, *Hspa4*, *Tap1* and *Tap2*. We testified this finding by DQ-OVA experiment and found that IL-33 could promote ILC2s to up-take and process exogenous antigens (17.78 ± 0.75 fold vs. 22.02 ± 0.75 fold). The antigen presentation function of ILC2s was further established by mixed lymphocyte culture where BALB/c ILC2s potently stimulated C57BL/6 CD8^{+} T cell proliferation, which was further augmented by IL-33 treatment. Taken together, our data demonstrate an anti-tumor function of therapeutic IL-33 that elevates the number and antigen presentation function of ILC2s.

#2701 EREG reprograms M2-tumor-associated macrophage and suppresses colorectal cancer cell proliferation and migration.

A.-R. Yu, S. Kim, Y. Jeong, H. Hong, Y. Shin, **Y. Cho**;
Samsung Medical Center, Seoul, Korea, Republic of

Colorectal cancer (CRC) represents a common malignancy within the digestive system, linked to significant morbidity and mortality rates. Tumors exert diverse effects on immune modulation, facilitating progression and metastasis. Amid the abundant immune cell populace within the tumor microenvironment (TME), tumor-associated macrophages (TAMs) play a pivotal role. M2-type TAMs actively foster tumor growth and engage in immune suppression by fostering angiogenesis and tissue restructuring. In a previous study, we analyzed single-cell RNA-sequencing (scRNA-seq) data derived from colorectal cancer patients. We observed an enrichment of the secreted phosphoprotein 1 (SPP1)+ macrophage fraction in both the tumor core and border when compared to normal tissues. Additionally, epiregulin (EREG), an epidermal growth factor receptor (EGFR) ligand, was found to be upregulated in SPP1+ macrophages, correlating with tumor growth and metastatic tendencies. Research on EREG is important because it has been found to play a significant role in cancer progression, including colorectal cancer. Understanding the mechanisms by which EREG contributes to tumor growth and metastasis can provide valuable insights into the development of targeted therapies for cancer treatment. Our hypothesis centered around the impact of EREG from TAMs on tumor progression. To identify TAM-specific EREG and its functional significance, we isolated tumor-associated macrophages from CT26 (mouse colorectal carcinoma)-bearing tumors and cultured them with conditioned and normal mediums. Subsequently, we examined EREG expression at the gene level using quantitative PCR. Our findings indicated significantly higher levels of EREG in the conditioned medium compared to the normal medium, suggesting an association between EREG and cancer cells. Remarkably, our investigation also confirmed that EREG has the capacity to reshape macrophage signatures. Notably, the surface marker CD206, characteristic of M2 macrophages, exhibited a significant decrease, while iNOS, a marker for M1 macrophages, showed an increase upon EREG depletion. We evaluated the interaction between CT26 cancer cells and TAMs using indirect co-culture methods. EREG-depleted TAMs were plated in the top chamber, while CT26 colorectal cancer cells were seeded at the bottom. Our results validated that knocking down EREG in TAMs not only hindered the proliferation of cancer cells but also affected the behavior of TAMs. Additionally, the reduced EREG expression in TAMs hindered the migration of cancer cells. These findings strongly suggest that targeting EREG could effectively restrain the growth and metastasis of colorectal cancer cells by reprogramming macrophage polarization in the TME. Consequently, this indicates its potential as a promising therapeutic target in colorectal cancer.

#2702 Hyperprogression due to myeloid mimicry in renal medullary carcinoma treated with nivolumab plus ipilimumab.

M. Soeung[1], **X. Yan**[1], L. Zhang[1], L. Perelli[1], J. Chen[1], B. Slack Tidwell[1], H. Khan[1], C. N. Le[1], T. N. A. Lam[1], N. Bhattacharya[1], R. Shah[1], I.-L. Ho[1], Z. Chen[1], S. R. K. Lundgren[1], N. Feng[1], C. Zanca[1], M. Karki[1], N. Millward[1], R. He[1], R. A. Sheth[1], B. K. Tharakeswara[1], P. Rao[1], N. C. Daw[1], D. N. Tripathi[2], C. L. Walker[2], G. Han[1], Y. Chu[1], R. Wang[1], M. Dang[1], E. Dai[1], F. Peng[1], Y. Liu[1], A. S. Jadhav[1], W. Lang[1], C. A. Arrechedera[1], L. Campos Clemente[1], E. R. Parra-Cuentas[1], H. Lu[1], C. Haymaker[1], I. I. Wistuba[1], A. Futreal[1], T. Heffernan[1], A. Viale[1], G. F. Draetta[1], N. M. Tannir[1], J. Gao[1], L. Wang[1], G. Genovese[1], P. Msaouel[1];
[1]UT MD Anderson Cancer Center, Houston, TX, [2]Baylor college of Medicine, Houston, TX

Renal medullary carcinoma (RMC) is a rare but highly aggressive SMARCB1-deficient kidney cancer that mainly afflicts young individuals of African descent and has few treatment options. Despite the advancements in immune checkpoint therapy (ICT) for other kidney cancers, its efficacy against RMC remains elusive. The majority of RMC patients treated with ICT have experienced aggressively progressive disease as the best response. This hyperprogression was confirmed in our prospective clinical trial of nivolumab plus ipilimumab specifically designed for RMC patients (ClinicalTrials.gov identifier: NCT03274258). To elucidate the mechanisms of resistance to ICT in RMC, we generated high-quality single-cell RNA sequencing data on 23,880 cells from 7 patients at baseline and 2 patients exhibiting hyperprogression after ICT intervention. Our analysis revealed that RMC tumor cells undergo a distinct transcriptional reconfiguration following ICT therapy. This reconfiguration is manifested by upregulation of S100A9 and activation of the MEK/ERK pathway, indicating that RMC tumor cells adopt myeloid-affiliated transcriptional circuits, potentially promoting cell proliferation and leading to hyperprogression. Using a mouse model of RMC, we further demonstrated in a controlled setting that ICT causes hyperprogressive disease via activation of MEK/ERK pathway and an increase of S100A9 positive tumor cells. This process can be reversed by inhibiting master regulators of this “myeloid mimicry” mechanism, such as the CEBPB/p300 complex in our mouse model of RMC, thus restoring sensitivity to ICT. These findings provide novel insights into RMC resistance to ICT and suggest valuable directions for the development of therapeutic strategies.

#2703 Targeting STING pathway as a therapeutic strategy against β-catenin driven immune escape and resistance to anti-PD1 therapy in hepatocellular carcinoma..

Qingmei Zhang[1], Jiacheng Bi[2], Oscar Wai-Ho Yeung[1], Tao Ding[1], Wing-Lim Chan[3], yueqin Zhu[1], Jiang Liu[1], Kevin Tak-Pan Ng[1], Kwan Man[1]

[1]Surgery, The University of Hong Kong, Hong Kong, Hong Kong,[2]The CAS Key Laboratory of Quantitative Engineering Biology, Shenzhen Institute of Synthetic Biology, Shenzhen Institute of Advanced Technology, Chinese Academy of Sciences, Shenzhen, China, Shen Zhen, China,[3]School of Biomedical Sciences, The University of Hong Kong, Hong Kong, Hong Kong

β-catenin mutation occurs in around 40% of hepatocellular carcinoma(HCC); yet no precision therapies are available to treat this tumor subset. Immune checkpoint inhibitors (ICIs) are now widely used for the treatment of patients with advanced HCC. Unfortunately, preliminary evidence showed that β-catenin mutation drives resistance to anti-PD1 immunotherapy in HCC. In this study, we studied the molecular mechanisms underlying β-catenin mutation during HCC pathogenesis to develop novel therapeutics targeting β-Catenin-driven HCC. Firstly, three HCC cohorts were examined, including 70 untreated, 20 treated patients with nivolumab, and patients from a public TCGA database. By single-cell RNA sequencing analysis, we identified that anti-PD-1 treatment displayed effectiveness with the increase of CD27+CD8+ T-cell infiltration, correlating to improved prognosis with longer progression-free survival (PFS) and OS. Importantly, multiplex IHC staining showed that β-catenin activation is associated with significantly reduced CD8+CD27+ T cell infiltration in tumors (n=70), demonstrating that β-catenin promoted immune escape and resistance to anti-PD-1 treatment involved defective cytotoxic T-cell activity. Subsequently, we found that the interaction of β-Catenin with sirtuin 1 (SIRT1) mediated suppression of IRF3/IRF7 activity, resulting in inhibition of Type I interferon (IFN-I) production. However, by CRISPRi screening, we found that disruption of β-catenin-SIRT1 interaction via STING caused persistent high-level IFN-I response which increased the transcription of T-cell costimulatory molecule CD27 via IL10/STAT3/BATF signaling on infiltrated CD8+ T cells. This effect was also confirmed in the STING null mice, emphasizing that STING signaling is a therapeutic target to overcome β-catenin driven immune escape. Further, using hydrodynamic tail-vein injection murine HCC models, we found that the STING agonist inhibited β-catenin-SIRT1 activity, restored IFN signaling to rescue T-cell cytotoxic capacities, and enhanced the anti-PD-1 therapy efficacy. In conclusion, we demonstrated that STING reprogrammed β-Catenin mutated the HCC tumor microenvironment and a combination of STING and anti-PD-1 treatment represents an effective novel therapeutic strategy for HCC patients with β-Catenin mutation.

#2704 cGAS-STING drives myeloid inflammation in chromosomally unstable esophageal cancer.

B. Beernaert, E. Erdal, R. Clark, T. Liu, E. M. Hammond, E. E. Parkes;
University of Oxford, Oxford, United Kingdom

Esophageal adenocarcinoma (EAC) is an aggressive disease characterized by chromosomal instability (CIN), whereby cells continuously acquire chromosomal abnormalities that promote therapeutic resistance, immune evasion and metastasis. CIN in cancers also fuels the misplacement of genomic DNA in the form of structural abnormalities of the nucleus, such as micronuclei (MN), that lead to chronic activation of the cytosolic DNA sensing cGAS-STING pathway. However, how chronic cGAS-STING pathway activation is tolerated and shapes the tumor landscape of CIN^{high} EAC cancers is poorly understood. Using publicly available RNA-seq and genome sequencing data of EAC tumours and esophageal cancer cell lines as well as a panel of EAC cell lines, we demonstrate that the core cGAS-STING pathway machinery is rarely inactivated in EAC despite high levels of baseline CIN and aneuploidy. Through transcriptomic profiling of an isogenic EAC precursor cell line model of variable CIN and $cGAS^{KO/WT}$ EAC cell lines we show that both chronic and transient CIN-driven cGAS-STING activation converge on the expression of CXCR1/2 ligands and other pro-inflammatory cytokines and chemokines rather than typical anti-tumor type I interferon signalling in EAC cells. Indeed, a novel transcriptional signature of $cGAS^{+}$ micronuclear burden-correlated genes correlates with orthogonal measures of CIN in EAC tumours and esophagogastric cancer cell lines and is associated with an enrichment in myeloid-derived cells as well as poor prognosis. Correspondingly, using multiplexed immunofluorescence (IF) we find that a high preponderance of $cGAS^{+}MN$ and STING expression in human EAC samples is associated with decreased tumor purity, increased myeloid cell and macrophage infiltration, and increased peripheral blood neutrophil counts, indicative of tumor-promoting myeloid inflammation. Ongoing multiplexed IF and single-nuclei RNAseq analysis of $cGAS^{+}MN^{high}$ and $cGAS^{+}MN^{low}$ EAC tumors will further help characterise the components that comprise the CIN-EAC tumor microenvironment (TME) and the CIN- and cGAS-STING-dependent cell-cell interactions that govern it. Taken together, our findings provide an explanation for the observed maintenance of cGAS and STING in EAC and identify disruption of cGAS-STING-dependent myeloid cell inflammation and recruitment as a potential therapeutic target for CIN^{high} EAC.

#2705 Hyaluronic acid impairs NK killing towards breast tumor spheroids despite elevated cytotoxicity.

B. C. H. Cheung[1], A. T. Li[1], J. E. Segall[2], M. Wu[1];
[1]Cornell University, Ithaca, NY, [2]Albert Einstein College of Medicine, Bronx, NY

The tumor microenvironment (TME) is often regarded as a critical component in tumor progression and metastasis. Among the main structural components of the TME, such as collagen and glycosaminoglycans (GAGs), hyaluronic acid (HA) is highly elevated in the breast TME, and is associated with poor prognosis. In recent years, immunotherapy has gained tremendous success in the battle against hematological cancers. Yet, solid tumors have remained a significant clinical challenge for immunotherapy due to the physical constraints they impose on immune cells. Mechanically, our previous work has shown that the abundance of high molecular weight (HMW) HA significantly reduces matrix pore sizes and softens the collagen and HA cogel, and impairs breast tumor invasion. However, it is still unclear how modulating tumor invasion through the mechanics of the TME may correlate with the efficacy of immunotherapy. In this study, we aim to investigate the effect of HMW HA on natural killer (NK) cell-based immunotherapy using a tumor spheroid model (GFP-labeled MCF-7). We introduced NK-92 MI cells into tumor spheroid embedded collagen gels with or without HA, and followed spheroid-NK cell interactions through live cell imaging. Preliminary data shows that while tumor spheroids were still able to invade in the collagen only gel, they underwent apoptosis in the presence of NK cells. More importantly, the presence of HA within the ECM reduced NK cells' ability to kill tumor spheroids. Specifically, when surrounded by NK cells, tumor spheroids remained intact and viable in the collagen-HA cogel, while they underwent apoptosis in collagen only gels. In a parallel experiment, multicolor flow cytometry data showed that HA increased NK activation and certain cytotoxic markers (interferon-gamma, perforin, and granzyme-B), despite the fact that spheroids appeared to be more resistant towards NK cells in the presence of HA. Taken together, we speculate that the presence of HMW HA in the TME may protect solid tumors from immune attacks by modulating the mechanical environment.

#2706 Identification and characterization of cancer-associated polymorphonuclear cell subsets in mice.

Marco A. De Velasco, Yurie Kura, Kazuko Sakai, Takashi Kikuchi, Yasunori Mori, Takafumi Minami, Kazuhiro Yoshimura, Kazutoshi Fujita, Kazuto Nishio, Hirotsugu Uemura

Kindai University Faculty of Medicine, Osaka-Sayama, Japan

Background: Neutrophils are the main type of polymorphonuclear cells (PMN) and comprise most immune cells in the body. PMN cells are upregulated in cancer and accumulate in the tumors. Tumor-associated PMNs comprise a heterogeneous population consisting of immunologically active mature neutrophils and immature polymorphonuclear myeloid-derived suppressor cells (PMN-MDSCs). The phenotype of these cells evolves with disease progression and is implicated in modulating immune response. However, there is yet to be a consensus to define PMN populations in tumors and blood.
Methods: Here, we used single-cell RNA-seq, bulk RNA sequencing, flow cytometry, and immunohistochemistry (IHC) analysis to characterize cancer-associated PMN-MDSCs in tumor-bearing mice.
Results: Single-cell RNA-seq data from lung tumors and healthy individuals revealed five metaclusters (MC): MCA, MCB, MCC, MCD, and MCE. MCA and MCB made up 34.4 and 65.1% of PMNs in healthy tissues, respectively. MCA, MCB, MCC, MCD, and MCE comprised 3.8%, 23.5% 3.3% 14.6%, and 54.7% of PMNs in tumors, respectively. Genes enriched in MCA and MCE were associated with MDSCs and myeloid progenitor cells. MCB and MCC were associated with inflammatory responses mediated by TNF-alpha signaling and neutrophil degranulation. MCD was associated with a CD33 myeloid cell phenotype and had high expression levels of *CD274*, *Pdcd1lg2*, *Havcr2*, and *Tigit* genes. Cells from MCE were associated with protein translation signatures and had elevated levels of *Nt5e*. Gene expression signatures from single-cell RNA-seq data were compared with bulk transcriptomic data from healthy mouse prostates and *Pten*-null prostate tumors characterized by high PMN cell infiltration. Gene set enrichment analysis showed enrichments after androgen deprivation therapy and Cluster MCE was associated with castration-resistant tumors. Flow cytometric and IHC analysis confirmed the enrichment of PMN cells expressing elevated levels of proteins identified from gene expression analysis including CD73, PD-L1, and PD-L2.
Conclusion: This study offers further insights into the distinct subsets of PMN-MDSCs present in tumors.

IMMUNOLOGY: Single Target and Bispecific Antibodies
Poster Session

#2710 Combination CXCR4 and PD-1 blockade increases T cell infiltration and effector function in fibrolamellar carcinoma (FLC).

L. K. Dickerson[1], R. van den Bijgaart[2], X. Jiang[1], S. K. Daniel[3], J. A. Carter[1], A. Farghli[4], K. M. Sullivan[5], Y. Liu[1], H. L. Kenerson[1], R. S. Yeung[1], T. S. Kim[1], I. N. Crispe[1], P. Sethupathy[4], K. C. Barry[2], V. G. Pillarisetty[1];

[1]University of Washington, Seattle, WA, [2]Fred Hutchinson Cancer Center, Seattle, WA, [3]Stanford University, Stanford, CA, [4]Cornell University College of Veterinary Medicine, Ithica, NY, [5]City of Hope Medical Center, Duarte, CA

Introduction: Fibrolamellar carcinoma (FLC), a rare liver cancer affecting young patients without cirrhosis, has a poor prognosis and few systemic therapy options. Current evidence implicates an immunosuppressive tumor microenvironment (TME), including our preliminary data suggesting preferential localization of T cells in stromal bands. We hypothesized that dual blockade of C-X-C chemokine receptor type 4 (CXCR4) and programmed cell death protein (PD-1) would enhance T cell infiltration and activation, respectively, and thereby increase tumor killing.

Methods: Flow cytometry and single-nuclear RNA sequencing (snRNA-seq) were used to analyze immune cells and evaluate gene expression, respectively, in patient-derived FLC and non-tumor liver (NTL). Immunohistochemistry (IHC) was used to assess $CD3^{\pm}$ T cell localization in relation to CXCL12, the chemokine ligand of CXCR4. Tumor slice cultures (TSCs) from fresh FLC resection specimens (n=11) were treated with control (IgG1), a small molecule CXCR4 inhibitor (AMD3100), anti-PD-1 blocking antibody (αPD-1), or combination CXCR4 and PD-1 blockade (AMD3100/αPD-1). IHC, RNA expression (Nanostring), and live microscopy were used to evaluate T cell mobilization and function.

Results: Flow cytometry analysis demonstrated fewer $CD45^{\pm}$ cells (16% vs 54% of live cells, p=0.01) and heterogenous PD-1 expression on T cells in FLC compared with NTL. SnRNA-seq analysis showed that CXCR4 expression is upregulated in FLC lymphocyte and macrophage populations relative to NTL (15% vs 10% and 20% vs 5% expressed), and CXCL12 is expressed primarily in stellate cells. $CD3^{\pm}$ T cells colocalized with CXCL12 in the FLC stroma on IHC. Multiplex IHC of treated TSCs revealed more T cells in the carcinoma ($CK7^{\pm}$) than the stromal ($SMA^{\pm}$) compartment after AMD3100 compared with IgG1 (63% vs 34% T cells in $CK7^{\pm}$ compartment, p=0.05). Nanostring indicated upregulation of effector pathways (apoptosis, cytotoxicity, lymphocyte activation) after AMD3100/αPD-1 compared with IgG1. Time-lapse live microscopy revealed a greater percentage of apoptotic carcinoma cells ($SR\text{-}FLICA^{\pm}CK7^{\pm}$) colocalized with $CD3^{\pm}$ T cells (37% vs 18%, p=0.005) and longer $CD3^{\pm}$ T cell track length (27 vs 22 μm, p=0.03) after AMD3100/αPD-1 than before treatment. Cleaved caspase-3 (CC3) IHC demonstrated significantly increased tumor apoptosis after AMD3100/αPD-1 compared with IgG1 and monotherapy (53% vs 32% (IgG1), 39% (AMD3100), and 42% (αPD-1) $CC3^{\pm}$ cells, p=0.002, p=0.03, p=0.04).

Conclusion: The CXCR4/CXCL12 axis mediates T cell exclusion in the FLC TME. Combination CXCR4 and PD-1 blockade overcomes immunosuppression in FLC by mobilizing T cells into the carcinoma compartment and activating their effector function, with resultant tumor apoptosis. These findings support consideration of clinical trials testing drugs targeting CXCR4 and PD-1 in FLC.

#2711 A novel bispecific antibody to reprogram the immune suppressive GBM TME.

T. Wong[1], J.-S. Leu[1], X. Fan[2], R. Kang[1], N. Abdelfattah[1], F. Leonard[1], N. Zhang[2], K. Yun[1];
[1]Houston Methodist Research Institute, Houston, TX, [2]Texas Therapeutics Institute, Brown Foundation Institute of Molecular Medicine, The University of Texas Health Science Center at Houston, Houston, TX

GBM (glioblastoma) is the most common and aggressive primary brain tumor in adults. Immunotherapy is an emerging and promising treatment modality for GBM. Unfortunately, most immunotherapy trials have provided only modest benefit to GBM patients thus far. A significant barrier that limits efficacy of immunotherapy in GBM is the paucity of tumor infiltrating lymphocytes and abundance of immune suppressive myeloid cells. A critical step in enhancing the efficacy of immunotherapy for GBM requires approaches that enhance T cell infiltration and reprogram the myeloid cells to a more pro-inflammatory state. S100A4 is a major regulator of stemness, epithelial-mesenchymal transition, and immunosuppression in glioma stem cells and a critical regulator of immune suppressive myeloid and T cell phenotypes in GBM. Targeting S100A4 in either glioma cells or stromal cells is sufficient to reprogram the tumor immune landscape and extend survival of glioma bearing mice, indicating that S100A4 is a promising immunotherapy target. Since S100A4 has both intracellular and extracellular function as well as cytokine-like function, we developed a S100A4 blocking antibody. While the anti-S100A4 antibody blocks breast cancer metastasis efficiently, it did not cross the BBB. Hence, we generated a bispecific S100A4-TfR antibody (BsA) that allows robust BBB penetration. Using ELISA, confocal immunofluorescent microscopy, and multiplexed flow cytometry, our preliminary results suggest that systemic administration of the S100A4-TfR BsA results in accumulation of BsA in the brain and glioma tissue, increased T cell infiltration and immune remodeling. Furthermore, the BsA is taken up by glioma cells and accumulates intracellularly, which is correlated with decreased nuclear SOX2 expression. These results suggest that S100A4-TfR BsA is a promising agent to treat GBM to reprogram the GBM immune landscape and reduce stemness. We are currently performing single cell RNA-sequencing to elucidate molecular and cellular changes induced by the bispecific antibody treatment in different cell types and performing long term survival analyses to evaluate its therapeutic potential.

#2712 Development of GB268, a tri-specific antibody targeting PD-1/CTLA-4/VEGF, with enhanced anti-tumor efficacy and reduced toxicity in pre-clinical studies.

Q. Du, Y. Lv, J. Xu, F. Peng, H. Cao, X. Yang, Z. Qian, X. Li, Y. Cao, Q. Ding, Y. Tan, **S. Han**;
Genor Biopharma Co. Ltd., Shanghai, China

Background: Immunotherapy using immune checkpoint modulators such as anti-PD1/PD-L1 have been widely used in cancer therapy. Combination of checkpoint inhibition using anti-PD1 and anti-CTLA4 has improved therapeutic efficacy but is also accompanied by severe immune related adverse events (irAEs) which limited their clinical use. Bi-specific antibody targeting PD-1/CTLA-4 such as cadonilimab has shown improved clinical benefits with reduced irAEs in cervical cancer. Vascular endothelial growth factor (VEGF) is overexpressed in various solid tumors and anti-VEGF agents inhibit neovascularization and shrink tumor with time. Combined application of bevacizumab and PD-1/PD-L1 blockade displays durable and improved anti-tumor effects. We have recently developed a novel tri-specific antibody GB268, specifically targeting PD-1, CTLA-4 and VEGF with fine-tuned activity & potency for each arm to simultaneously block PD-1/CTLA-4 mediated immune-suppression and VEGF mediated tumor angiogenesis.
Methods: GB268 is a hexavalent antibody with symmetrical structure, composed of anti-PD-1 VHH antibody, anti-CTLA-4 VHH antibody, and anti-VEGF conventional antibody. The Fc part is silenced by introducing L234A/L235A mutations. Comprehensive in vitro and in vivo characterization of GB268 have been carried out. Along with in vivo efficacy studies, toxicity has also been evaluated with a murine arthritis model in hPD1/hCTLA4 double-KI mice to assess immune related AEs.
Results: GB268 specifically bound to PD-1, VEGF, and CTLA-4 with high affinity and completely blocked PD-1 and VEGF pathways in reporter systems. To reduce the CTLA4 inhibition-induced AEs, the CTLA-4 arm was intentionally designed to only partially block the interaction of CTLA4 to its ligands CD80/CD86, and furthermore, the blockade of CTLA-4 was highly dependent on PD-1 expression. GB268 displayed robust anti-tumor efficacy with attenuated toxicity in murine models. In multiple PBMC-humanized models including A375 melanoma model, HT29 colorectal cancer model, and NCI-H460 NSCLC model, etc., GB268 exhibited significantly better anti-tumor efficacy, compared to PD-1/CTLA-4 bsAb and PD-1/VEGF bsAb, or in the combination of monoclonal antibodies to PD-1, CTLA-4 or VEGF. In arthritis induction model using hPD1/hCTLA4 double KI mice, GB268 had improved tolerance than cadonilimab and at least 20-fold better safety profile than ipilimumab combined with nivolumab.
Conclusions: GB268 is a first-in-class anti-PD-1/CTLA-4/VEGF tri-specific antibody with innovative design. Preclinical data demonstrated GB268 is very effective in provoking anti-tumor responses. At the meantime, immune-related AEs is alleviated. Thus, GB268 may emerge as a promising novel therapeutics for cancer treatment.

#2713 Novel anti-PD-L1-IL-15 diabody immunocytokine in combination with radiation therapy improves response rates in immune-resistant murine head and neck cancer.

Abhay R. Sheeri, Robert S. Edinger, Harikrishnan Rajkumar, Ravi B. Patel

Radiation Oncology, University of Pittsburgh, Pittsburgh, PA

Purpose: The purpose of this study was to develop a new anti-programmed death-ligand 1 (αPD-L1) interleukin-15 (IL-15) diabody (Db) immunocytokine to improve the efficacy of combination radiation therapy (RT) and immune checkpoint inhibition (ICI) treatment in head and neck cancer.
Background ICI has revolutionized cancer care by increasing survival in patients with metastatic cancer, yet many patients with poorly immunogenic tumors have limited response to this therapy. To improve the efficacy of ICI, we developed a new immunocytokine combining an αPD-L1 Db with an effector immune cell agonist, IL-15. We hypothesized that our αPD-L1-IL-15 Db construct in combination with immunostimulatory radiation will lead to improved tumor responses and survival from ICI-resistant tumors.
Methods: Production in-vitro: αPD-L1-IL-15 Db construct was transfected into Expi-CHO™ cells and isolated with HiTrap™ Protein L affinity column. The molecular weight was confirmed via SDS-PAGE, and surface plasmon resonance sensorgram kinetics revealed high affinity of the immunocytokine to mouse isoform PD-L1 (K_D < 10 nM). Splenocyte proliferation and HEK-Blue™ reporter assays showed the IL-15 component to be functionally active. Testing in-vivo: 80-100 mm^3 mouse oral carcinoma-2 (MOC-2) tumors were established in C57BL/6 mice. Groups of 6 mice with tumors were treated with rat IgG isotype control, αPD-L1 Db, and αPD-L1-IL-15 Db w/wo 8 Gy of tumor-localized beam RT to upregulate PD-L1. Mice were tracked for tumor growth via tumor measurements and overall survival until the tumor burden endpoint was reached.
Results: We found αPD-L1 Db w/wo RT had an insignificant impact on survival or tumor growth delay in this tumor model in comparison to IgG w/wo RT. However, αPD-L1-IL-15 Db significantly improved survival compared to αPD-L1 Db treatment ($p = 0.004$) and IgG ($p = 0.0013$) in the presence of RT. We also saw significantly increased mean tumor growth delay with αPD-L1-IL-15 Db treatment compared to αPD-L1 Db ($p = 0.0164$) and IgG ($p = 0.0252$), on days 25 and 18 respectively, in the presence of RT. However, in the absence of RT, αPD-L1-IL-15 Db yielded no significant difference in mean tumor growth delay or survival when compared to IgG and αPD-L1 Db w/o RT.
Conclusion: Our results demonstrate that our αPD-L1-IL-15 Db immunocytokine with RT significantly improved tumor response and increased survival in aggressive, ICI-resistant mouse oral carcinoma, as compared to αPD-L1 Db with RT. However, this observation no longer persisted in the absence of RT. Hence, this suggests a synergy between radiation therapy and ICI-cytokine therapy in immunotherapy-resistant tumors. Further correlative and mechanistic tumor microenvironment profiling studies are underway to further elucidate mechanisms of immune activation with our combination of αPD-L1-IL-15 Db and radiation treatment.

#2714 Developing an mRNA encoded therapeutic antibody platform to simplify manufacturing and reduce time to clinic.

Roxana Redis[1], Dan Rocca[2], Rachel Pooley[3], Matthew Benson[3], Namrata Jayanth[1], Eva Oswald[4], Alexander Hale[1], **Louise Brackenbury**[2], Maxim Mashric[5], Christian Cobaugh[5], Michael Shaw[5], Justin Bryans[3]

[1]Charles River Laboratories, Leiden, Netherlands,[2]Charles River Laboratories, Bristol, United Kingdom,[3]Charles River Laboratories, Cambridge, United Kingdom,[4]Charles River Laboratories, Freiburg, Germany,[5]Vernal Biosciences, Colchester, VT

The manufacturing of therapeutic antibodies requires expensive production, often challenging purification, lengthy stability optimization and complex protein characterization that despite continual improvement, keeps the cost of treatment in the clinic high. Alternatively, leveraging gene-based approaches such as mRNA to express therapeutics circumvents many of the manufacturing challenges and instead rely on *in situ* production of antibodies within a patient, improving the developability and cost of sophisticated, disease-modifying antibodies. Crucially, recent work demonstrates that therapeutic antibodies translated *in vivo* from mRNA can be readily detected within hours following infusion into pre-clinical models and can persist up to several days or weeks. Peak levels of circulating mRNA-encoded antibodies are comparable to infused recombinant equivalents dosed to patients and have been shown to be within favorable therapeutic ranges in phase I trials. Here we outline an mRNA-LNP based platform to encode and deliver therapeutic antibodies *in vivo* that can overcome costly and challenging manufacturing and that demonstrates both robust PK/PD kinetics and potency. We describe how to effectively encode a standard-of-care anti-HER2 antibody - Trastuzumab - using LNP-encapsulated modified mRNA and validate using *in vitro* as well as *in vivo* efficacy models. Initial *in vitro* characterization of mRNA encoded antibodies demonstrates robust translation in producer cell lines, reproducible expression kinetics, retention of antigen specificity and HC:LC integrity when analyzed by ELISA and WB. To evaluate whether Trastuzumab-encoding mRNA-produced protein is detectable *in vivo*, antibody levels were measured in mouse serum after IV administration of a single dose of mRNA formulated LNPs. Peak plasma concentrations of mRNA-encoded trastuzumab were benchmarked against circulating recombinant Trastuzumab in parallel groups, and pharmacokinetics interrogated. Of note, the majority of mRNA encoded antibody was likely produced in the liver as shown by bioluminescence imaging. To demonstrate the efficacy of the platform, the potency of mRNA-encoded Trastuzumab isolated from producer cell lines will be assessed using *in vitro* cytotoxicity assays with human PBMCs and HER2+ tumor lines to dissect ADCC or direct tumor growth inhibition. Additionally, to determine whether mRNA-encoded Trastuzumab is able to retain anti-tumor activity *in vivo*, a mouse tumor xenograft model will be established and the mRNA antibody-dependent effects on tumor volume, growth and morbidity-free survival will be examined. Overall, the data demonstrate that mRNA-encoded therapeutic antibodies could provide an effective, alternate strategy for solid tumor treatment and may unlock a strategy to deliver lead biologics at reduced cost and with improved developability.

#2715 Preclinical characterization of SM2248: A dual-action bispecific antibody enhancing immunotherapy for solid tumors.

X. Liu, H. Zhou, S. Lu, H. Geng, W. Song, S. Xie, Y. Wei, X. Zhang, S. Yang, S. Zhou, **Y. Liang**;
Beijing StarMab BioMed Technology, Ltd., Beijing, China

Background: Innate immune cells, such as macrophages and myeloid-derived suppressor cells (MDSCs), dominate the immune landscape within "cold" solid tumors, which typically exhibit poor responses to immune checkpoint inhibitors (ICIs). The dearth of tumor-infiltrating T cells and the prevailing immunosuppressive microenvironment contribute to this ineffectiveness. To bolster immunotherapy against such tumors, we developed SM2248, a bispecific VHH antibody. SM2248 simultaneously obstructs the CD47-SIRPα phagocytosis checkpoint pathway and conditionally activates CD40 on tumor-infiltrating innate immune cells. CD47/SIRPa blockade enhances macrophage and dendritic cell (DC) phagocytosis and cross-presentation of antigens to cytotoxic T cells. CD40 activation fosters DC licensing, reprograms macrophages, and guides MDSC differentiation towards DCs and macrophages. The combined action of CD47 blockade and CD40 stimulation remodels the tumor microenvironment, fostering T cells infiltration and activation.
Methods: SM2248 was developed by fusing a highly selective CD47-blocking VHH module - minimizing binding to human erythrocytes and platelets, with a conditional CD40 agonistic VHH module - selectively activating immune cells upon CD47 engagement, incorporated into an inactivated IgG1 Fc backbone. The specificity and affinity of SM2248 binding to human CD47 and CD40 were assessed via ELISA and flow cytometry assays. CD47 and SIRPα interaction blockade was confirmed through a competitive ligand binding assay. Target-dependent CD40 activation was evaluated via a CD40-NFκB-Luc reporter assay. In vivo anti-tumor efficacy was determined using a syngeneic transplantation model of MC38-hCD47 cancer cells in B-hCD40 humanized mice. Binding to erythrocytes and platelets, compared with magrolimab, was assessed using flow cytometry. Hemolysis toxicity was evaluated through an in vitro erythrocyte lysis assay.
Results: SM2248 effectively inhibits cell surface CD47-SIRPα interaction at nanomolar concentrations and activates CD40-NF-κB-luciferase reporters at picomolar concentrations in a target-dependent manner. In contrast to the CD47 monoclonal antibody magrolimab, SM2248 does not bind to human erythrocytes or platelets and does not induce hemolysis. In murine syngeneic tumor models, SM2248 completely halts the growth of MC38-hCD47 tumors in humanized B-hCD40 mice and does not induce dose-dependent hepatotoxicity at doses up to 10 mg/kg.
Conclusions: SM2248, a humanized bispecific tetravalent VHH antibody targeting CD47 and CD40, exhibits promising in vivo efficacy and a favorable safety profile in preclinical studies, offering the potential for enhancing immunotherapy in solid tumors.

#2716 The O-glycan epitope targeting anti-human carcinoma monoclonal antibody (mAb) NEO-201 can also target human regulatory T cells (Tregs).

A. Tanaka[1], M. Fantini[2], P. M. Arlen[2], C. M. Annunziata[3], K. Y. Tsang[2], S. Sakaguchi[1];
[1]Frontier Research Center, Osaka University, Osaka, Japan, [2]Precision Biologics, Inc., Bethesda, MD, [3]National Cancer Institute, National Institutes of Health, Bethesda, MD

Introduction:NEO-201 is a humanized IgG1 mAb that targets Core 1 and/or extended Core 1 O-glycans expressed by several human solid and blood tumors, as well as neutrophils, but it does not bind to most normal tissues and human immune cell subsets (B cells, $CD4^{\pm}$ T cells, $CD8^{\pm}$ T cells, NK cells, monocytes). Functional analysis revealed that NEO-201 mediates the killing of its target cells through ADCC and CDC. Previous study has shown that approximately 4.6% of $CD4^{\pm}$ T cells express NEO-201 target antigen and that those $CD4^{\pm}$ T cells have Tregs phenotype. In addition, in a recent published phase 1 study we observed that NEO-201 binds to $CD4^{\pm}$/ $CD25^{\pm}$/, $CD127^{-}$/, $Foxp3^{\pm}$/, $CD15s^{\pm}$ cells from peripheral blood mononuclear cells (PBMCs) from cancer patients with solid tumors. The purpose of this study was to further characterize the phenotype of the specific subset of $CD4^{\pm}$ T cells expressing the NEO-201 target antigen.
Experimental Design: Human PBMCs were obtained from 7 healthy donors (HD) collected at Osaka University and 6 cancer patients from our ongoing phase II clinical trial (Clinical Trial NCT03476681) evaluating the efficiency of the combination of NEO-201 with pembrolizumab in adults with solid tumors resistant to checkpoint inhibitors. Phenotypic analysis was performed by flow cytometry using NEO-201 and antibodies CD3, CD4, CD25, CD45RA, FoxP3, and CD15s. The same gating strategy was applied for both normal donors and patients to evaluate which fraction of $CD4^{\pm}$ T cells is recognized by NEO-201. Fraction (Fr) 1 is naïve Treg, Fr II is effector Treg, Fr III is non-Treg, Fr IV is effector CD4 T cells and Fr V is naïve CD4 T cells.
Results: Flow cytometry analysis of PBMCs revealed that NEO-201 recognizes naïve Tregs (nTregs: $CD3^{\pm}$/$CD4^{\pm}$/$CD45RA^{\pm}$/$Foxp3^{low}$ cells) while it does not bind to effector Tregs (eTregs: $CD3^{\pm}$/$CD4^{\pm}$/$CD45RA^{-}$/$Foxp3^{high}$ cells) in both HD and cancer patients. The % of nTregs in cancer patients was higher than HD. Preliminary results from the ongoing Phase II clinical trial showed that subjects with durable SD had a reduction of circulating nTregs after treatment with NEO-201 compared to baseline levels.
Conclusions: NEO-201 binds to human Tregs with significantly higher % of binding to Fr I and a greater % of Tregs expressing NEO-201 target antigen in cancer patients compared to HD. It is conceivable that naïve Tregs in cancer patients express high levels of Core 1 O-glycans. Furthermore, when subjected to TCR stimulation, naïve Tregs undergo proliferation and differentiate into eTregs. eTregs can then infiltrate into tumor microenvironment (TME). These data suggest that depletion of circulating nTregs in cancer patients after NEO-201 treatment may prevent the differentiation of nTregs into eTregs and their accumulation in the TME. This study suggests the potential use of NEO-201 to reduce the Treg-mediated suppression of anticancer immunity.

#2717 Bifunctional fusion protein PDL1sFv/MICAe for cancer immunotherapy.

J. Li, Y. Wei;
Clemson University, Clemson, SC

Many cancer cells upregulate the expression of programmed death ligand 1 (PD-L1) to surpass T-cell mediated immune response. Immune checkpoint blockers targeting PD-L1 or its receptor PD1 have been shown to suppress the inhibitory signals and enhance T cell function. As a new immunotherapy, immune checkpoint blockers have been used to treat multiple cancers. However, most clinically available blockers only engage with one type of immune cell: the T cells. Natural killer (NK) cells, on the other hand, play a significant role in anti-cancer immune responses. It will represent an advancement in anti-cancer immunotherapy if NK cells are engaged with immune checkpoint blockers. In this study, we designed a unique bifunctional fusion gene, *PDL1sFv/MICAe*, consisting of the variable regions of an anti-PD-L1 antibody and the extracellular domain of stress protein MICA and hypothesized that fusion protein PDL1sFv/MICAe will simultaneously bind to PD-L1 on tumor cells to block the inhibitory signal and extend T cells activity, and to NKG2D to activate NK Cells. cDNA sequence of fusion gene *PDL1sFv/MICAe* was designed based on the variable region of an established clinically used antibody, Atezolizumab, and the extracellular domain of *MICA* with linkers in between. After a computational confirmation of its structure and binding affinities, the fusion gene was synthesized and cloned into an expressing vector, and the fusion protein was produced for evaluation. Western blotting and fluorescent microscopic analyses confirmed that the protein binds to PD-L1 of human tumor cells, including MCF7 and MDAMB231, and NKG2D of KHYG1 cells. Preliminary results also show that the fusion protein enhances NK cell cytotoxicity against tumor cells. Studies on confirming the fusion protein's activities on other tumor cells, NK cell IFN-γ production, T cell function, etc., are underway. In summary, fusion protein PDL1sFv/MICAe represents an improved version of the immune checkpoint blockers and could treat cancer patients quickly and effectively.

#2718 A novel TROP2-targeted immune stimulating antibody conjugate (ISAC) with potent anti-tumoral activtiy and accpetable safety.

Ye Chen[1], Fei You[2], Chenchen Zhu[1], Yao Xiong[1], Li Li[1], Nana Luo[1], Shuaixiang Zhou[1], Fushuai Wang[1], Chenyang Xu[1], Fan Fei[1], Chang Li[1], Jianglu Wang[1], Jinling Xu[1], **Huizhong Xiong**[1]

[1]Innovent Biologics, Suzhou, China, [2]Innovent Biologics, Rockville, MD

Immune stimulating antibody conjugates (ISACs) are a unique class of ADC in which antibodies recognizing tumor antigens are conjugated with immune agonists. ISACs target tumor tissue and specifically activate intra-tumoral myeloid cells, unleashing downstream immune response. Like the other immune agonists, balance between efficacy and safety remains a challenge for ISACs.

Here we describe a potential first-in-class TROP2 ISAC with rationally selected antibody and TLR7/8 agonist linker-payload. The anti-TROP2 antibody elicited robust ADCP of TROP2+ tumor cells by macrophages. *In-vitro,* TROP2 ISAC mildly activated myeloid cells only in the presence of TROP2+ tumor cells. *In-vivo,* the molecule potently suppressed tumor growth in different TROP2+ xenograft tumors, and effectively enhanced killing of an ADC. In terms of safety, the ISAC was tolerated in both WT and hTROP2KI mice, and, importantly, in monkeys. Taken together, our data demonstrate a novel TROP2 ISAC with outstanding efficacy and manageable safety profile, which may benefit patients with TROP2+ tumors.

#2719 Papiliximab, a bispecific nanobody targeting CD47 and PDL1 retards tumor growth without hemolysis.

B. Baek[1], M. Kim[2], J. Kim[1], I. Jang[1], S. Kim[1], J. Kim[1], S. Lee[1], **H. Kim**[1], S.-Y. Seong[2];
[1]Shaperon Inc., Seoul, Korea, Republic of, [2]Seoul National University, Hongcheon, Korea, Republic of

Cancer cells are known to express immune checkpoint proteins, enabling them to evade immune surveillance. In response, anti-cancer therapies targeting these proteins have been developed. While immune checkpoint inhibitors targeting PD-L1 have been clinically approved, their effectiveness as standalone therapies is limited, with only a 20% response rate. To improve responsiveness, bispecific monoclonal antibodies (MoAbs) targeting both CD47 and PD-L1 have been developed. These bispecific antibodies activate both the innate (by blocking CD47) and adaptive (by blocking PD-L1) immune systems simultaneously. However, conventional antibodies targeting CD47 have been dropped during development due to the risk of hemolysis. In this study, we developed a bispecific single-domain antibody (nanobody, Nb) that targets both CD47 and PD-L1 with a minimal hemagglutination risk. Using phage display libraries from alpacas immunized with recombinant antigens, we screened for an anti-CD47 Nb and an anti-PD-L1 Nb. The affinities (Kd) of these Nbs for their antigens were 7.0×10^{-9} and 9.7×10^{-9}, respectively. To maximize affinity for both antigens, a bispecific antibody (Papiliximab) was designed to tandemly array anti-CD47 and PD-L1 Nbs with the Fc region of IgG4. Papiliximab has a lower affinity for RBC (up to 3 μM) than conventional anti-CD47 MoAbs reported earlier. Papiliximab successfully inhibited interactions between CD47/SIRP-α and PD-L1/PD-1, with IC_{50} values of 7.09 nM and 2.67 nM, respectively. Papiliximab induced the expression of IFN-γ by inhibiting the PD-L1/PD-1 interaction in the PBMC-based MLR (Mixed Lymphocyte reaction) assay. In addition, Papiliximab demonstrated the induction of a phagocytosis effect through CD47 blocking and its IgG4 Fc domain. Therefore, Papiliximab is a multifunctional hybrid bispecific antibody that modulates both innate and acquired immunity. Papiliximab exhibited no cross-reactivity with mouse antigens, but did with cynomolgus antigens. We tested its efficacy on the growth of human B cell lymphoma (Raji cells) and human breast cancer (MDA-MB-231 cells) in humanized NSG mice. Papiliximab was more effective in inhibiting tumor growth than mono-specific Abs and Nbs for PD-L1 or CD47, and their combination. These observations suggest that Papiliximab might be able to improve clinical remission more effectively than the combination of monotherapies without the risk of anemia associated with anti-CD47 MoAbs. We are now working to elucidate the mechanisms behind Papiliximab's superior efficacy and safety compared to the combination of monotherapies.

#2720 Engineering sweeping antibodies for the clearance of tumor-derived, pro-tumorigenic cytokines.

J. M. Baker, N. J. Singh, T. Luetkens;
University of Maryland, Baltimore, Baltimore, MD

Soluble, tumor-derived, pro-tumorigenic (STP) cytokines have been shown to contribute to cancer cell proliferation and drug resistance. But therapeutic targeting of STP cytokines by monoclonal antibodies is limited by high concentrations and persistent production of antigen. We hypothesize that the ability of sweeping antibodies (swAbs) to actively clear soluble antigens will overcome these limitations. SwAbs differ from conventional antibodies via (1) pH-dependent binding of antigen, and (2) increased binding to the neonatal Fc receptor (FcRn). SwAbs facilitate clearance of soluble antigens by releasing antigen in the low pH environment of FcRn-expressing cells. SwAbs are then recycled via FcRn for repeated clearance of antigen.We are developing swAbs against four STP cytokines contributing to cancer cell proliferation, survival, migration or intra-tumoral angiogenesis: hepatocyte growth factor (HGF), vascular endothelial growth factor (VEGF), transforming growth factor-β (TGF-β) and interleukin 16 (IL-16). We selected four existing neutralizing antibodies against these cytokines with available crystal structures and generated a second antibody targeting interleukin 16 with high affinity (clone 3B6; K_D = 13 nM) *de novo* using phage display. We are using bio-layer interferometry and custom recycling/clearance assays for antibody characterization and pre-clinical validation. To introduce pH dependency into the four antibodies with crystal structures, we performed targeted histidine mutagenesis of residues at the interface with the respective target antigens. For the *de novo*-generated interleukin-16 antibody, we performed an unbiased histidine scanning approach by mutating residues across all six complementarity-determining regions (CDRs), which resulted in slight increases in pH sensitivity. We then performed a second round of mutagenesis of the most pH-sensitive 3B6 variants by replacing additional residues considered developability liabilities with histidine residues. We found that this approach significantly increased expression and affinity at pH 7 of the resulting 3B6 variants but only modestly increased pH sensitivity. In contrast, replacing a single residue in the heavy CDR1 in clone 14.1, a pre-clinical anti-IL-16 antibody, resulted in substantially increased pH sensitivity ($K_{D(pH=7)}$ = 2 nM; $K_{D(pH<6)}$ = n.b.). We are currently performing pH-sensitivity screenings for the three additional STP-specific antibodies. Our findings indicate that the ability to introduce pH sensitivity is largely dependent on the parental antibody and that some antibodies may not be amenable to this process. In addition, we show that histidine mutagenesis can be an effective approach to enhance expressibility and binding, while also increasing pH sensitivity. This project will answer the question whether anti-STP cytokine swAbs are an effective approach to treat patients with cancer.

#2721 FF01: a novel humanized heavy chain antibody targeting endogenous retroviruses with anti-lymphoma activity.

F. Spriano[1], L. Cascione[1], J. Sgrignani[2], N. Bendik[1], S. Napoli[1], G. Sartori[1], E. Cannas[1], T. Gongo[2], A. J. Arribas[1], D. Rossi[1], D. F. Robbiani[2], A. Cavalli[2], F. Bertoni[1];

[1]Institute of Oncology Research, Faculty of Biomedical Sciences, USI, Bellinzona, Switzerland, [2]Institute for Research in Biomedicine, USI, Bellinzona, Switzerland

Background: Human endogenous retroviruses (HERVs) are transposable elements (TE) derived from retrovirus infections that occurred millions of years ago. Despite constituting 8% of our genome, their biological role still needs to be explored. HERV-K (HML-2), a subgroup of HERVs, represents the most recent retroviruses integrated into the human germline DNA. Members of the HML-2 subgroup retain complete ORF with coding potential and have garnered the most attention in disease-related studies. HERVs exhibit physiological expression in embryonic stem cells but are heavily methylated and remain almost silent in normal adult tissues. Although the mechanisms underlying HERV-K contribution to tumor cell growth and survival remain poorly understood, aberrant expression of HERVs has been demonstrated in various human tumor tissues and lymphoma. These findings led us to explore HERV-K as a potential therapeutic target in B cell lymphomas

.Methods: RNA data were analyzed with Telescope. Validations were performed by qPCR, Western blot, flow cytometry, and ELISA. Env structure was obtained with AlphaFold and peptides were purchased from GeneScript. Antibody-dependent cellular cytotoxicity (ADCC) was performed with the ADCC Reporter Bioassay (Promega). Internalization was assessed using the Incucyte Fabfluor-pH Antibody labeling reagents.

Results: We assessed the TE expression in RNA-seq datasets of diffuse large B cell lymphoma (DLBCL) and B cells from healthy individuals. An MDS plot showed that TEs could separate neoplastic from healthy samples, demonstrating that tumoral and normal specimens have distinct TE and HERV expression profiles. Focusing on tumor samples, DLBCLs were divided into four clusters with different prognoses. Similar results were obtained in a 47 B-cell lymphoma cell line panel. Focusing on the HML-2 family in lymphoma patients, we identified many of them upregulated in tumors. We validated RNA and protein expression of the HML-2 envelope (env) in seventeen lymphoma cell lines, and in two of them, we also proved the protein surface expression. Env-specific siRNA reduced env expression determined a decrease in cell proliferation, suggesting a contribution to lymphoma cell growth. In silico examination of the env identified four linear regions with potential for antibody binding, and peptides covering them were synthesized. We screened 150 lymphoma patients' serum samples for IgG antibodies binding to the peptides, and all peptides showed positive hits. We used a phage display screen to obtain one nanobody, FF01, binding one peptide. FF01 induced ADCC in the cell line with high surface env expression and not in a negative one. FF01 was internalized in an expressing cell, proving the principle for using it as a component of an antibody-drug conjugate.

Conclusions: Our data demonstrate that HERVs are in DLBCL patients and propose FF01 as a new candidate to target HERV Env+ lymphomas.

#2722 CTN001, a first Twin Fc-immune cell engager, with a superior potency against Her2+ and Her2-low cancers by engaging multiple Fc-mediated mechanisms.

D. Lee, S. Yoon, J. Bae, M. Kim, K.-J. Lee, E. Kim, H. Park, E. S. Choi, G.-H. Yang;
Centenaire Biosciences Inc., Seongnam-si, Korea, Republic of

Many therapeutic monoclonal antibodies mediate the immune effector functions through the engagement of their fragment crystallizable (Fc) domain and Fcγ receptors on the immune cells. However, these functions are limited due to the low affinity of their interactions and the requirement of abundancy of antigens for the avidity effects. Recently, mutation-based Fc engineered antibodies showed their enhanced immune effector functions mostly through the NK cell-mediated ADCC. To overcome the limited improvement of current Fc engineering, we developed an innovated platform, Twin Fc-Immune Cell Engager (Twin Fc-ICE) composed of a single Fab domain and two Fc domain with drug-like properties. Here we demonstrated the superior efficacy of CTN001, a first Twin Fc-ICE, in *in vitro* and *in vivo* Her2+ tumor models. CTN001 bound to various types of Fcγ receptor-expressing immune cells with stronger affinity, supported by its better *in vitro* affinity to all types of Fcγ receptors than wild type and Fc-engineered antibodies. To evaluate the pharmacological efficacies, CTN001 was tested for its functions of *in vitro* antibody-dependent cellular cytotoxicity (ADCC), antibody-dependent cellular phagocytosis (ADCP) and complement-dependent cytotoxicity (CDC) and *in vivo* efficacy with Her2+ xenograft models. In Her2+ models, both CTN001 and trastuzumab induced ADCC-mediated effects, but CTN001 showed better anti-tumor cytotoxicity through ADCP and CDC than trastuzumab. Importantly, CTN001 also showed cytotoxic effects on Her2-low tumor cells. Consistently, CTN001 showed better anti-tumor efficacy than trastuzumab or its combination with pertuzumab in Her2+ tumor xenograft model and, surprisingly, even in Her2-low or resistant models. These results suggest that CTN001 can provide new therapeutic options for treating Her2-low patients differentiated from antibody-drug conjugates (ADCs), and that the Twin Fc-ICE can be an innovative platform to overcome limitations of existing therapeutics.

#2724 BCG020, a novel bispecific antibody targeting EGFR and CD70, is effective against EGFR and CD70 high expressed tumors.

Y. Yang, X. Sun, Z. Li, Y. Yan, L. Xu, X. Wu, L. Du, Y. Zhu, **C. Guo**, W. An;
Biocytogen Pharmaceuticals (Beijing) Co., Ltd., Beijing, China

The epidermal growth factor receptor (EGFR) is highly expressed across a wide range of different cancers, and is a known driver of cancer growth; EGFR upregulation is frequently associated with adverse prognosis. Many patients undergoing EGFR-TKI (tyrosine kinase inhibitors) treatment will acquire resistance, which can be accompanied by increased expression of CD70 in some cancers. Simultaneous engagement of both EGFR and CD70 with a bispecific antibody (bsAb) is a potential strategy to overcome such resistance and achieve greater efficacy. To explore this strategy, we developed a novel IgG1 bsAb, BCG020, targeting EGFR and CD70. The parental EGFR antibody and CD70 antibody were developed from fully human common light chain antibody mice (RenLite®). When compared to EGFR benchmarks, the parental EGFR antibody exhibits similar affinity to both human and cynomolgus monkey EGFR, similar internalization activity in EGFR+ tumor cell lines, and superior blocking activity of EGF to EGFR *in vitro*. Furthermore, the EGFR parental antibody demonstrates good stability. The parental CD70 antibody exhibits high affinity to both human and monkey CD70, with superior internalization activity to benchmark antibody in CD70+ tumor cell lines, as well as superior blockade of CD70-induced signaling of CD27-Luc when compared to benchmark antibodies. When assembled into a bsAb, BCG020 exhitibs the same high affinity as both parental antibodies, with higher internalization activity than parental antibodies and benchmark antibodies. To evaluate the efficacy of BCG020 *in vivo*, we established cell line-derived xenograft (CDX) models in immunodeficient (B-NDG) mice. We observed that BCG020 treatment (10 mg/kg) potently inhibited growth of EGFR+CD70+ tumors. Taken together, these data indicate that BCG020 is a first-in-class bispecific antibody with potential to treat solid tumors with high expression of EGFR and CD70.

#2726 A novel trispecific antibody HC010 targeting PD-1/CTLA-4/VEGF for the potential treatment in anti-PD-1 antibody resistant NSCLC patients.

D. Jiang, Y. Xi, C. Xu, X. Wang, Q. Yin, Z. Li, **T. Yang**;
HC Biopharma Inc., Shanghai, China

Background and Aim: Immune checkpoint inhibitors (anti-PD-1 /CTLA-4 antibody) have been approved and widely used for the first line treatment of non-small cell lung cancer (NSCLC). However, most patients are experiencing resistant to PD-1 blockade. In recent clinical trials, anti-VEGF antibody has shown to improve the clinical outcomes of anti-PD-1 antibodies and overcome resistance to checkpoint blockade. We developed a PD-1/CTLA-4/VEGF trispecific antibody (HC010) by site-specifically fusing anti-PD-1 scFv and anti-CTLA-4 nanobody to the defined site of anti-VEGF antibody. The aim of this study was to evaluate the potential use of HC010 for treatment of anti-PD-1 antibody resistant NSCLC patients.
Method: Humanized mice were established in NCG mice by reconstituting human PBMC before inoculating the PDX tissue, which was derived from a NSCLC patient treated with two cycles of an anti-PD-1 antibody sintilimab. When tumors were approx. 170mm3, mice were dosed with HC010 twice weekly for 3 weeks. Pembrolizumab, sintilimab and a Standard of Care (SoC) agent docetaxel were included as reference. For IHC analysis, tumor samples were harvested 24h post final dose and fixed with 10% NFB overnight and subsequently stained with CD31 and CD8 to explore the change in tumor microenvironment after HC010 treatment. For preclinical toxicity assessment, HC010 was intravenously administered once weekly for four weeks in naïve cynomolgus monkeys and immunogenicity/local tolerance/clinical pathology were evaluated during the dosing and recovery phase.
Results: HC010 showed a significant tumor inhibition (TGI=81%) when compared with the vehicle control. Pembrolizumab and sintilimab alone exhibited limited anti-tumor effect. Docetaxel only showed a partial response during the dosing phase. By analyzing tumor samples, there was a significant increase in CD8+ positive T cells in HC010 treated tumors in contrast to the vehicle group and pembrolizumab/sintilimab treated groups, suggesting that HC010 can significantly improve CD8+ T cell infiltration. Expression of CD31 as an angiogenic and vasculogenic marker, was significantly reduced in HC010 treated tumors. In the toxicity study, HC010 at selected doses showed no obvious toxicity in cynomolgus monkeys.
Conclusion: Our trispecific antibody HC010 targeting PD-1/CTLA-4/VEGF showed a superior anti-tumor effect in a sintilimab resistant PDX animal model when compared with pembrolizumab and sintilimab as well as SoC. By analyzing tumor microenvironment , HC010 overcame acquired resistance by modulating tumor microenvironment such as increase in intra-tumoral cytotoxic T cell infiltration and normalization of blood vessels. Together with preclinical efficacy and safety data, HC010 showed potential benefits in treatment of anti-PD-1 antibody resistant NSCLC patients.

#2727 Pre-clinical development of a novel anti-GPRC5D inducing potent anti-tumor effect through enhanced antibody-dependent cell-mediated cytotoxicity (ADCC) for multiple myeloma.

H. Bonnevaux, E. Remy, T. Pizette, S. Bouvier, K. Desrumeaux, L. Bassinet, C. Nicolazzi, P. Rettman, Z. Klippel, M. Meloni, M. Chiron, A. Virone-Oddos; Sanofi-Aventis, Vitry-sur-seine, France

Multiple myeloma (MM), characterized by clonal accumulation of malignant plasma cells in the bone marrow, is the second most prevalent hematopoietic malignancy. Despite emerging therapies, MM remains an incurable disease with a 5-year overall survival of 56% for relapsed and/or refractory disease (RRMM) patients. Thus, innovative approaches that would be safe and potent are required. GPRC5D (G Protein-Coupled Receptor Class C Group 5 Member D) is an orphan GPCR protein involved in keratin synthesis with limited expression in healthy tissues. GPRC5D is expressed at very high prevalence among MM patients and its expression on tumor cells is maintained after treatments with standard of care agents such as anti-CD38, or BCMA-targeting therapies. The ability of NK cells to kill tumor cells leaving other cells unharmed and to induce minimal pro-inflammatory cytokine release as compared to T cell-based therapies, makes NK cells ideal immune cells for a safe and efficacious therapeutic approach. Like Sarclisa®, other therapies engaging NK cells and mediating tumor cell killing through antibody-dependent cell-mediated cytotoxicity (ADCC) mechanism have demonstrated their efficacy in clinic. Here we report the design, preclinical characterization, and development of a novel anti-GPRC5D antibody inducing potent cytotoxic activity against MM cells. SAR446523 is an IgG1-based antibody with an engineered Fc domain for enhanced ADCC function and targeting human GPRC5D on tumoral plasma cells. SAR446523 demonstrated high affinity for GPRC5D target and increased affinity for both high and low affinity FCGR3A-158V and 158F variants of CD16a receptor. The ability of SAR446523 to induce ADCC *in vitro* was assessed in a panel of MM cell lines exhibiting low, medium, and high GPRC5D expression. SAR446523 induced strong potency against all tested cell lines (picomolar range), regardless of the levels of GPRC5D. In addition, SAR446523 induced higher cytotoxic activity compared to a clinical benchmark compound. This anti-tumor activity was associated with very low IL-6, TNFa and IFNg pro-inflammatory cytokine release, much lower compared to a CD3xGPRC5D T-cell engager in *in vitro* assay using human peripheral blood mononuclear cells (PBMC) in presence of GPRC5D positive cells. In addition, the *in vivo* anti-tumor activity of SAR446523 was investigated in a NK humanized NOG huIL15 transgenic mouse model bearing disseminated MM cells. SAR446523 led to a robust antitumoral efficacy with a significant improved mouse survival. These data demonstrating potent anti-tumor activity and favorable safety profile of this novel anti-GPRC5D antibody suggest that SAR446523 may be a promising therapy for patients with RRMM and provide consistent support for clinical development.

#2728 Discovery of a multispecific CD73/PD-1 targeting drug Fc-conjugate (DFC), which improves tumor reduction compared to PD-1 monotherapy in a humanized mouse model.

J. Levin, S. Dohrmann, N. Dedeic, A. Almaguer, D. Zuill, E. Abelovski, J. N. Cole, J. B. Locke, J. Fortier, Q. Zhao, M. Hernandez, K. Amundson, M. Moniz, H. Chen, D. Panickar, T. Lam, T. Brady, A. Borchardt, G. Hough, L. W. Tari;
Cidara Therapeutics, Inc., San Diego, CA

Background: The approval of immune checkpoint therapies has revolutionized cancer treatment and established immuno-therapy as an additional treatment option. However, while anti-PD-(L)1 therapies have demonstrated durable responses, only a small subset of patients respond. One mechanism of tumor escape is via the release of immunosuppressive metabolites such as adenosine. CD73, an extracellular enzyme expressed on immune cells and some tumors, catalyzes the conversion of AMP to adenosine, the rate limiting step in adenosine production. As a strategy to improve response rates we developed a first in class CD73/PD-1 targeting DFC, comprised of a multivalent conjugate of a small molecule CD73 inhibitor stably linked to a proprietary human IgG1 Fc-fusion with a PD-1 inhibitor peptide. This multispecific DFC has the potential for differentiation and increased therapeutic potency compared to approved PD-(L)1 inhibitors.

Methods: Binding of CD73/PD-1-001 to biotinylated hPD-1 was determined using ELISA and to human $CD8^{\pm}$ T cells by flow cytometry. CD73 inhibition was measured in cell-free and cell-based assays. Efficacy was determined in a humanized mouse model optimized for PD-1 activity against a transgenic MC-38 colon cell line expressing hPD-L1 (Genoway, France). Tumor volumes were recorded and statistical analysis was conducted by t-test (Mann-Whitney) or two-way ANOVA.

Results: In vitro, CD73/PD-1-001 demonstrated potent activity against both checkpoint targets. CD73/PD-1-001 bound to hPD-1 with an IC_{50} of < 1 nM and demonstrated functional inhibition of CD73 with an EC_{50} of <10 nM, which is on par with respective single agent molecules. Importantly, addition of the CD73 targeting moiety resulted in no significant loss in PD-1 binding relative to PD-1-001, a DFC containing only the PD-l inhibitor peptide. Efficacy was determined in a humanized mouse model against a transgenic MC-38 cell line. Both CD73/PD-1-001 and PD-1-001 DFCs were highly potent in this model with tumor growth inhibition (TGI) of >70% at dose concentrations of 3 mg/kg or greater ($p \leq 0.01$). However, at the lowest test concentration of 1 mg/kg, only CD73/PD-1-001 retained significant potency with a TGI of 56.0 % ($p \leq 0.05$). Tumor reduction in the 1 mg/kg PD-1-001 group did not reach statistical significance (36.5%, $p > 0.05$).

Conclusions: This work demonstrates that a multispecific CD73/PD-1 targeting DFC, is a potent inhibitor of tumor growth in a humanized mouse model. Furthermore, CD73/PD-1-001 was more potent than PD-1 monotherapy, demonstrating the therapeutic benefit of targeting two important checkpoints with a single agent molecule. Collectively, preclinical testing of a CD73/PD-1 DFC has validated the benefits of targeting the PD-(L)1 axis in combination with adenosine suppression, resulting in improved anti-tumor effects.

#2729 Discovery and characterization of LILRB2XPD-L1 bispecific antibody SPX-303.

A. Haight[1], Q. Chen[1], B. William[1], D.-D. Nguyen[1], R. Cai[1], J. Ma[1], M. White[1], J. Jin[1], J. Shen[1], M. Siekierzycki[1], V. Hall[1], H. Jin[1], R. Meier[1], J. Moser[2]; [1]Sparx Biopharmaceutical Corp, Mount Prospect, IL, [2]HonorHealth Research Institute, Scottsdale, AZ

The advent of immunotherapy has led to deep and sometimes durable remissions in certain cancers. However, the variable response rates and development of resistance mechanisms pose significant challenges to the current therapies. The immunosuppressive nature in the tumor microenvironment (TME) can drive many of these observations. Reversing this immunosuppression is a promising avenue for enhancing and broadening the applicability of IO therapies. Macrophages are critically modulated by LILRB2, a pivotal receptor in their maturation and polarization to the M2 immunosupressive phenotype. We report the discovery and development of a novel anti-LILRB2/PD-L1 bispecific antibody, SPX-303, designed using an anti-LILRB2 IgG4 derived from a mouse hybridoma screen and linked with an anti-PD-L1 epitope. SPX-303 demonstrates sub-nanomolar binding affinity to both LILRB2 and PD-L1 targets, effectively blocking the interaction between LILRB2 and its ligand, as well as inhibiting PD-1 binding to PD-L1. In *in vitro* functional assays, SPX-303 exhibits effects comparable to the parental monomeric anti-LILRB2 (SPX-104) in redirecting macrophage polarization from M2 to M1 stage, as observed in both cultured PBMC and human monocyte-derived macrophage (HMDM) models. Furthermore, SPX-303 demonstrates a synergistic effect in inducing T cell activation in the autologous mixed lymphocyte reaction assay (auto-MLR), surpassing the effects of the anti-LILRB2 epitope (SPX-104) and the anti-PDL1 fragment (single-domain anti-PDL1) alone or in combination. *In vivo* experiments reveal that SPX-303 significantly inhibits tumor growth. Collectively, these results support SPX-303 as a novel therapeutic antibody that effectively enhances anti-cancer immunity in the treatment of advanced solid tumors. The pre-clinical data as well as the clinical plan of SPX-303 will be presented.

#2730 Beyond antibodies and CAR-T: Topologically-engineered, super-dimeric antibody-like molecules with dual Fc domains for trispecific, bivalent targeting of CD19, CD20, and Fcgamma receptors.

D. J. Capon, N. L. S. Chan, L. Troitskaya, M. Fomin, U. Edman, B. Frank, B. Z. Capon, B. Law, S. J. Chapin, G. M. Lewis, M. L. Gefter, J. Punnonen; Hinge Bio, Inc., Burlingame, CA

Background: Depletion of B cells has resulted in major therapeutic benefits in autoimmune diseases and hematological malignancies. Several FDA-approved B cell-depleting antibody-based therapies are available, including antibody-drug conjugates, T cell engagers, CAR-T cells, and antibody variants with enhanced effector functions through Fc engineering. However, a significant unmet need remains in both oncology and autoimmune disease. All currently approved B cell-depleting therapies target a single B cell antigen, increasing potential for incomplete depletion and emergence of escape mutants that give rise to relapse and treatment failure.

Methods: Here we describe trispecific antibody-like molecules generated using GEM-DIMER technology. In addition to bivalent target binding of both CD19 and CD20, the GEM-DIMER candidates are designed to have two Fc domains to enable powerful effector functions via cooperative binding of Fcgamma receptors. The approach is based on incorporation of a super-dimerization domain into the hinge region of an immunoglobulin heavy chain, enabling the combination of all of the components of two IgG antibodies into a single molecule. Using this approach, we generated GEM-DIMER candidates from rituximab and FMC63, the parental anti-CD19 antibody for anti-CD19 scFv used in approved CAR-T cell therapies.

Results: CD19/CD20-targeting GEM-DIMER molecules demonstrated binding to both CD19 and CD20 with affinities comparable to the individual parent antibodies. Importantly, CD19/CD20-targeting GEM-DIMER molecules demonstrated robust depletion of human B cells in overnight cultures of whole blood. Moreover, antibody-dependent cellular cytotoxicity (ADCC) was demonstrated in co-cultures of the human B cell lymphoma cell line Raji and human peripheral blood mononuclear cells (PBMC). As expected, due to the presence of dual Fc domains, CD19/CD20-targeting GEM-DIMER molecules exhibited enhanced binding to Fcgamma receptors, further explaining the robust effector functions observed.

Conclusions: CD19/CD20-targeting GEM-DIMER molecules are promising candidates to provide efficient depletion of both CD19+ and CD20+ cells, providing potential for broad and deep depletion of B cells with reduced risk of emergence of antigen escape variants. These data support the advancement of CD19/CD20-targeting GEM-DIMER molecules in multiple indications where depletion of CD19+ and/or CD20+ B cells is needed. Preparations for clinical investigation are ongoing.

#2731 CCR5-001, a novel drug Fc-conjugate (DFC) targeting CCR5, demonstrates potent efficacy in a colorectal cancer mouse model.

S. Dohrmann, J. Levin, N. Dedeic, A. Almaguer, D. Zuill, E. Abelovski, J. B. Locke, J. Fortier, M. Hernandez, Q. Zhao, K. Amundson, M. Moniz, H. Chen, D. Panickar, T. Lam, G. Hough, T. P. Brady, A. Borchardt, J. N. Cole, L. W. Tari;
Cidara Therapeutics, San Diego, CA

Background The approval of immune checkpoint inhibitors (ICI) such as PD-(L)1 inhibitors has revolutionized cancer therapy and established a role for immune effector cells, most notably $CD8^+$ T cells, in tumor control and destruction. While anti-PD-(L)1 therapy has demonstrated durable responses, only a small subset of patients benefit and respond to therapy. CCR5 is expressed on multiple immune cells (e.g. myeloid-derived suppressor cells) and CCR5-dependent migration of these cells contribute to an immune-suppressive tumor microenvironment (TME) thereby limiting response to ICI therapy. In addition, expression of CCR5 on cancer cells has been linked to increased metastasis and resistance to ICI therapy. Upregulation of CCL5/CCR5 has been associated with poor outcomes in multiple solid tumor indications, including colorectal cancer (CRC). Therefore, targeting CCR5 has the potential to increase response rates to ICI therapy and improve outcomes. Herein, we describe a first-in-class CCR5 targeting DFC, CCR5-001, a multivalent conjugate of a potent, small molecule CCR5 antagonist conjugated to an immune-silent proprietary human IgG1 Fc. This CCR5 targeting DFC has the potential to improve responses to ICI therapy by preventing pro-tumorigenic reprogramming of the TME induced by CCL5/CCR5 expressing tumor and myeloid cells.

Methods Binding of CCR5-001 to hCCR5 was measured by surface plasmon resonance (SPR) and to $CCR5^+$ PathHunter cells (DiscoverX) by flow cytometry. Functional activity was determined in $CCR5^+$ PathHunter β-arrestin assay with CCL3 to induce CCR5 signaling according to manufacturer's instructions. Efficacy was determined in an immune-competent syngeneic mouse model using the CRC cell line, MC38. CCR5-001 was dosed at 20 mg/kg twice per week for two weeks. Tumor volumes were recorded and statistical analysis was conducted by t-test (Mann-Whitney) or two-way ANOVA in Prism.

Results CCR5-001 displayed a KD of 4.2 nM to immobilized hCCR5 by SPR and IC_{50} of 0.63-0.98 nM for binding to engineered $CCR5^+$ PathHunter cells. This high affinity binding translated to potent functional inhibition of CCL3-induced CCR5 signaling with an IC_{50} of 12.7 nM in $CCR5^+$ cell-based assay. CCR5-001 demonstrated potent, statistically significant ($p = 0.0052$) tumor growth inhibition of 76% by day 13 in a syngeneic mouse model.

Conclusions CCR5-001 demonstrated potent CCR5 binding and functional inhibition of CCR5 signaling in cell-based assays. The *in vitro* activity translated to robust efficacy as a monotherapy in a syngeneic mouse model. Based on these results and other emerging data, CCR5-001 represents an exciting new avenue for targeting CCR5 with DFCs in solid cancers where the pathology is driven by the CCR5/CCL5 axis.

#2732 NB203: A Novel therapeutic bispecific antibody targeting CEACAM1/VEGF for tumor immunity and angiogenesis modulation in the tumor microenvironment.

J. Dong, B. Wang, D. Wang, J. Ni, T. Bu, H. Wang, B. Nayak, B. Wang, X. Dong, **Y. Zhang**;
NeoLogics Bioscience Co. Ltd., Suzhou, China

The carcinoembryonic antigen cell adhesion molecule 1 (CEACAM1) is detected on leukocytes, epithelia and endothelia, and involved in cell adhesion through homophilic or heterophilic binding. In various gastrointestinal cancers, NSCLC (non-small cell lung cancer), and melanoma, CEACAM1 is highly expressed on tumor cells and tumor stroma, with its levels increasing as the disease progresses. Notably, CEACAM1 has been found to dampen T and NK cell functions while promoting tumor angiogenesis and metastasis. In this study, we present NB203, a novel CEACAM1/VEGF bispecific antibody developed using Neologics CEACAM-*plus*, a bifunctional molecule engineering platform designed to target and modulate the tumor microenvironment (TME). NB203 effectively accumulated in the TME and hindered the homophilic or heterophilic interactions of CEACAM1. It demonstrated a significant enhancement in T cell activities and NK cell-mediated killing of CEACAM1-expressing tumor cells, and the inhibition of tumor cell migration and polyploidy through macrophages. More importantly, NB203 was specifically designed to impede tumor angiogenesis. It exhibited an increased binding capacity to both CEACAM1 and VEGF in pro-angiogenic TME, and undermined intratumoral vessel maturation by blocking VEGF and negatively regulating myeloid cell-dependent tumor angiogenesis. In summary, our preclinical data indicate that NB203 exhibits effective anti-tumor activity by mediating NK and cytotoxic T cell activities, improving the immune-suppressive TME, and suppressing tumor angiogenesis. The use of NB203 holds promise in overcoming resistance to anti-VEGF therapy and substantially improving the safety of therapeutic targeting of angiogenesis in cancer treatment.

#2733 NB202: A bispecific anti-PD1/TIM-3 antibody for cancer immunotherapy.

J. Dong, **Y. Zhang**, B. Wang, D. Wang, T. Bu, J. Ni, B. Nayak, X. Dong;
NeoLogics Bioscience Co. Ltd., Suzhou, China

Despite the remarkable efficacy of PD-(L)1 therapy, a significant proportion of cancer patients fail to respond or develop resistance over time. Co-expression of T-cell immunoglobulin and mucin domain containing-3 (TIM-3) with PD-1 on primed T cells has been observed in patients exhibiting resistance to PD-1 blockade. Moreover, TIM-3 is also expressed on other immune cells, including NK and DC, and plays a negative regulatory role in these immune cells. Therefore, the dual blockade of PD-1 and TIM-3 holds potential for enhanced clinical benefits. NB202 is a bispecific anti-PD1/TIM-3 antibody that has been designed to optimize the therapeutic response of anti-PD1 therapy by maximizing TIM-3 blockade on antigen-experienced T cells, enhancing NK cell activity, and improving antigen presentation ability of antigen-presenting cells (APC). NB202 has demonstrated high affinity binding to human TIM3 and PD-1 in the low nanomolar range. Moreover, it can simultaneously bind to TIM-3 and PD-1 receptors through a trans-manner, suggesting its potent capacity to enhance the interaction between T cells and dendritic cells (DCs). In classic MLR (mixed lymphocyte reaction) and T cell stimulation assays, NB202 has exhibited superior efficacy compared to the combination of anti-PD1 mAb and anti-TIM3 monoclonal antibodies as it significantly enhances the secretion level of interferon-gamma (IFN-gamma), and particularly interleukin-2 (IL-2). Moreover, in an anti-PD1 resistant mouse model, NB202 has shown promising efficacy results.

#2734 RC148, a novel bispecific antibody targeting PD-1 and VEGF for cancer immunotherapy.

Jianmin Fang[1], **Dong Li**[2], Kaiyue Wu[2], Sisi Wang[2], Du Li[2], Guorui Zhao[1], Shenjun Li[1], Jing Jiang[1]

[1]RemeGen Co., Ltd., Shandong, China,[2]Shanghai RemeGen Biotechnology Co., Ltd., Shanghai, China

Vascular endothelial growth factor (VEGF) is one of the most important pro-angiogenic factors in modulating tumor microenvironment (TME), and the concentration of VEGF in TME is significantly higher than that of peripheral. Inhibiting VEGF can improve immunotherapy efficacy by modulating the TME, preventing angiogenesis and regulating immune cell populations. Combined anti-VEGF and anti-Programmed cell death protein 1 (PD-1)/Programmed cell death ligand (PD-L1) therapies have exerted potent antitumor effect in preclinic and clinic studies. Therefore, we developed a novel humanized IgG1 silenced bispecific antibody RC148 to target VEGF and PD-1. RC148 allows dimeric VEGF crosslinking and gradually enhances PD-1 binding activity, potentially reduces systemic toxicity of anti-VEGF therapy and enhances antitumor potency via VEGF trigged enrichment in tumor areas. In preclinical studies, RC148 blocks the binding of VEGF to VEGFR and PD-1 to PD-L1, prevents the growth and migration of human umbilical vein endothelial cells, enables efficient T cell activation, exhibited synergistic antitumor effects in rodent models and showed safety profiles in non-human primate studies.

#2735 High affinity and potent anti-tumor efficacy of Nivo813, an anti-PD-1/ALK-1 bispecific antibody, in pre-clinical studies for solid tumors.

Qingqing Zhou[1], **Rong Tang**[1], Lanfang Zhuang[2], Jianyu Huang[1], Jiang Qian[1], Zhihua Ren[1], Youzhi Tong[1]

[1]Kintor Pharmaceutical Limited, Suzhou, China,[2]Kintor Pharmaceutical (Guangdong) Co., Ltd., Zhuhai, China

Background: The activin-like kinase receptor 1 (ALK-1, encoded by ACVRL1) is a member of the transforming growth factor β (TGF-β) superfamily. Combination treatment using anti-PD-1/PD-L1 agents with anti-angiogenetic reagents might bring additional benefits, such as establishing a favorable TME leading to better responses towards immunotherapy. In the phase II clinical trial (NCT03893695) of combination therapy of ALK-1 (GT90001) and Nivolumab for the second line therapy in patients with metastatic hepatocellular carcinoma (“HCC”) in Taiwan, among the 20 evaluable patients, the overall response rate is 40%, and the side effects were well tolerated and manageable. Nowadays, the combination of GT90001 and nivolumab shows a remarkable long-tail effect, since 7 patients are still alive as of March 30, 2023, 6 of them had received no further systematic anti-tumor therapy after trial completion. Among them, 4 patients are still on progression free status. Our pre-clinical data demonstrated that Nivo813 has improved cell-binding potency and potent anti-tumor effects, lighting up its potential capacity as a therapeutic drug in the treatment of human cancers.

Methods: The antigen binding activity of Nivo813 with PD-1 and ALK-1 were assessed by ELISA, Fortebio and flow cytometry. Endothelial cell tube formation assay was performed to identify the anti-angiogenesis function of Nivo813. The anti-tumor activity of Nivo813 was investigated in PBMC implanted with MDA-MB-231 breast cancer cells.

Results:Nivo813 could specifically bind to human PD-1 and ALK-1 with high affinity. Intriguingly, Nivo813 was found to have much higher affinity (40-fold, nM) to cell surface PD-1 than that of nivolumab. Meanwhile, Nivo813 exhibited dose-dependent anti-angiogenesis activity in vitro. Nivo813 demonstrated greater anti-tumor efficacy compared to nivolumab in mice model.

Conclusions: Nivo813, a dual-blocking anti-PD-1/ALK-1 bispecific antibody, shows improved binding potency to cell surface PD-1 and ALK-1 simultaneously, and displays dose-dependent anti-angiogenesis in vitro and great anti-tumor efficacy in vivo, supporting its clinical potentials for the treatment of human cancers.

#2736 Ligand-independent targeting of tumor cells for antibody-dependent cell-mediated cytotoxicity.

M. L. Aliru, N. R. Sultanpuram, K. Au, T. Zhang, A. Z. Wang;
University of Texas Southwestern Medical Center, Dallas, TX

Introduction: Biological targeting is a key concept in cancer treatment utilized by most therapeutics. Targeted agents that selectively treat diseased tissues while reducing off-target effects to normal tissues are widely used for cancer therapies. However, key hurdles include: (i) a limited number of tumor-specific biomarkers expressed in sufficiently high levels for targeted therapy, (ii) lack of specific biomarkers amenable to targeting, and (iii) current technologies rely on largely protein-based targeting ligands limiting the applications of these therapies due to final conjugates with low payloads. We developed a novel method for tumor-specific delivery by combining metabolic glycoengineering and nanomedicine to engineer targetable chemical groups on cancer cells and enable directed treatments. We hypothesize that increased Fc fragments on the surface of tumor cells can enable antibody-dependent cell mediated cytotoxicity (ADCC) response to tumor cells, providing innate immunotherapy.

Materials/Methods: We formulated nanoparticles (NPs) using polyethylene glycol-ply lactic acid-co-glycolic acid (PEG-PLGA). Using the Dolomite microfluidic device, we formed NPs by nanoprecipitation of PEG-PLGA with tetraacetylated N-azidoacetyl-D-mannosamine (Ac_4ManNAz), a sialic acid analogue containing a click chemistry group. We targeted this reactive group by functionalizing the Fc fragment with dibenzylcyclooctyne (DBCO). We characterized the NPs using dynamic light scattering (DLS), charge measurements and transmission electron microscopy (TEM). We evaluated toxicity using a cell viability assay and assessed preliminary efficacy with a tumor growth delay study.

Results: NP characterization revealed a size of 30-40 nm via DLS, congruent with TEM imaging. Charge measurements ranged from -4 to +4 mV. Toxicity studies revealed no differences in cell viability amongst different treatment groups. Preliminary efficacy studies demonstrated improved tumor growth delay in the cohort of mice treated with a combination of NPs and Fc-DBCO conjugate, as well as a survival benefit. Median OS was 31.5 days for the control groups vs 57.5 days for the combination treated group ($p = 0.0067$).

Conclusion: There is growing interest in harnessing the power of the innate immune response to shape anti-tumor immunity. This is because clinical data demonstrates tumor cells can evade the adaptive immune system through mutations as well as downregulate MHC receptors. One of the most effective innate immune responses is ADCC. To this end, we developed a novel method for tumor-specific delivery of Fc fragments to enhance ADCC. While this data reveals improved tumor growth delay and a survival benefit, the sample size is limited, and a larger study is needed to evaluate the potential benefits of this strategy. Furthermore, correlative studies are needed to identify the mechanism for treatment response.

#2737 LIS22, a first in class polyclonal antibody immunotherapy in T cell blood cancers.

C. Ciron, F. Shneiker, O. Dauphouy, J. Rousse, P.-J. Royer, G. Evanno, O. Duvaux, **F. Bassissi**;
Xenothera, Nantes, France

Background: Several approaches such as antibody drug conjugate (ADC), chimeric antigen receptor T cells (CAR-T) and recently bispecific antibodies are being introduced as innovative weapon in B-Cell lymphoma treatment. In the opposite, very limited therapeutic options are available for the treatment of rare refractory T cell malignancies such as PTCL. The 5-year survival rate of PTCL is lower than 30% according to the recent clinical data. Developing new effective treatment strategies for PTCL is an urgent problem. LIS22, is a first in class glyco-humanized polyclonal antibody (GH-pAb), targeting multiple tumor-associated antigens simultaneously. In this study, we characterized the safety and efficacy of LIS22 in preclinical models of T cell malignancies.
Material and Methods: LIS22 ability to induce Antibody-Dependent Cell Cytotoxicity (ADCC), Antibody-Dependent Cellular Phagocytosis (ADCP), Complement Dependent Cytotoxicity (CDC), and apoptosis was tested in a panel of hematologic malignancy cell lines and peripheral blood mononuclear cell (PBMC). To assess the targeting and recognition of LIS22 in PTCL patients, we evaluated the immunolabelling of LIS22 on patients' biopsies (n=119) using tissue microarray. LIS22 efficacy in vivo were evaluated in NMRI nude mice and SRG rats using T1301 and Jurkat cancer cell lines. Pharmacokinetics and safety of this drug were assessed in cynomolgus monkeys after single and repeated IV dosing up to 50mg/kg.
Results: LIS22 acts via several mechanisms, at 30µg/ml, it induced cytotoxicity via CDC (in 70%), ADCP (in 49%), ADCC (in 41%) and apoptosis (in 30%) of HPB-ALL human T blood cancer cell line but not in PBMC. LIS22 showed a potent in vitro antitumor activity in a panel of hematologic malignancy cell lines, it induced specific tumor cell CDC (EC50=41.4±28.9µg/mL). In both CDC and apoptosis cytotoxicity assays, LIS22 displayed a significantly higher potency on T cell blood cancers and no toxicity on healthy blood cells compared to PTCL clinically active drug Alemtuzumab (Anti-CD52). It was able to kill up to 100% of the cancer cells without affecting PBMC. In immunolabeling assay, LIS22 demonstrated cross-reaction to PTCL patient biopsy (staining up to 93%). In vivo efficacy studies in different mice and rat xenograft models, LIS22 induced a significant reduction of tumor growth up to 90% across several tested tumors. LIS22 was also characterized by high tolerance profile and satisfactory exposure in monkeys after repeated dosing (up to 250mg/kg of cumulative dose).
Conclusion: LIS22 appeared as a novel and promising cancer immunotherapy against T Cell hematologic malignancies. It has already been administered to human in another indication and showed a satisfactory PK and safety profile (no signs of immunotoxicity or systemic cytokine release). LIS22 is now ready to enter Phase I/II in the coming months for the treatment of peripheral T cell lymphoma (PTCL).

#2738 XON7, a new Glyco-Humanized Polyclonal Antibody, first in class immunotherapy against several solid tumors.

C. Ciron, G. Evanno, P. Morice, P.-J. Royer, F. Shneiker, O. Duvaux, B. Vanhove, **F. Bassissi**;
Xenothera, Nantes, France

Introduction: Cancer immunotherapy has recently generated much excitement after the success of the immunomodulating anti-CTLA-4 and anti-PD-1 antibodies against various types of cancers. However, for many cancers, there is still a lack of effective treatment that can result in long-term cancer-free survival and lower metastatic and relapse risks. The emergence of cancer resistance could be minimized by drug combination or by multi-targeting of tumor cells. Polyclonal antibodies can target several tumor-associated antigens simultaneously and would be more efficient than a conventional mAbs. Here we evaluate the safety and efficacy of XON7, a first in class glyco-humanized polyclonal antibody (GH-pAb), in cancer preclinical models.
Material and Methods: XON7 ability to induce Complement Dependent Cytotoxicity (CDC) and apoptosis was tested in a panel of cancer cell lines and PBMC. XON7 was also evaluated in sphere formation assay to predict its effects on cancer resistant. Specific binding to human tumors and healthy tissues was assessed by immunochemistry on tissue micro-array. Cross-cancer activity was evaluated on biopsies from patients with solid tumor such as CRC, NSCLC, osteosarcoma, and breast cancers. In vivo XON7 efficacy was evaluated in NMRI nude mice using A549: NSCLC, HCT-116: colon cancer, LNCaP: prostate cancer and MDA-MB-231: breast cancer cells. A human NSCLC chorio-allantoic membrane (CAM) model was used to evaluate the efficacy of XON7 + anti PD-1 on tumor growth and metastasis. Pharmacokinetics and safety of this drug were assessed in marmoset after single and repeated IV dosing up to 60mg/kg.
Results: XON7 showed a potent in vitro antitumor activity in a panel of cancer cell lines, it induced specific tumor cell CDC (EC50=50ug/mL) and apoptosis (IC50= 100ug/mL). it was able to kill up to 100% of the cancer cells without affecting PBMC. In addition, it induced a striking decrease of tumor sphere formation in HCT116, A549 and MDA-MB-231 cancer cell lines. XON7 showed preferential recognition of tumor cells as compared to normal cells, it demonstrated cross-reaction to tumor patient biopsy without staining of the healthy tissues. In vitro XON7 potency was translated into in vivo efficacy in different mice xenograft models. XON7 induced a significant reduction of tumor growth ranging from 40 to 90% across several tested tumors. Furthermore, it showed, significant increase of anti-tumor response rate and decrease of metastasis when it is associated with anti PD-1 in vivo CAM model (>90%, p=0.001). XON7 was also characterized by high tolerance and satisfactory exposure in marmoset.
Conclusion: Based on its safe toxicity profile and potent activity, XON7 appeared as a novel and promising cancer immunotherapy to fight against recurrent solid tumor, it is now aimed to reach clinical development, FIH in patients is planned to start before the end of 2023.

#2739 XON27, a novel and potent immunotherapy against hematologic malignancies.

C. Ciron, P. Morice, F. Shneiker, O. Duvaux, **F. Bassissi**;
Xenothera, Nantes, France

Background: Over the past decades, intensive research has led to the development of innovative therapies (monoclonal and bispecific antibodies, CAR T cells) that have increased the survival rate of patients with multiple myeloma (MM) and B cell lymphoma. However, despite this progress, the majority of patients relapse and become refractory due to the development of resistance. Polyclonal antibodies, with their ability to target multiple antigens, can counteract this resistance. Here we evaluate the safety and efficacy of XON27, a first-in-class glyco-humanized polyclonal antibody (GH-pAb), in MM and other blood cancers.
Material and Methods: The ability of XON27 to induce antibody-dependent cellular phagocytosis (ADCP), complement-dependent cytotoxicity (CDC) and apoptosis was tested in a panel of hematological malignancy cells and peripheral blood mononuclear cells (PBMC). Specific binding to human blood cancers was assessed using tissue microarrays. To study resistance mechanisms, MM cell lines were cocultured with macrophages in the presence or absence of XON27 and macrophage. To study relapse mechanisms and tumorigenicity, repeated in vitro administration of XON27 was evaluated in KMS-12-BM. The in vivo efficacy of XON27 was evaluated in KMS-12-BM NMRI nude mice model. Pharmacokinetics and safety of this drug were assessed in non-human primate after repeated IV dosing up to 60mg/kg.Results: XON27 induces potent and specific cytotoxicity in several blood malignancy cell lines including human MM cells via multiple mechanisms: CDC (EC50=35.84 ug/ml), apoptosis (IC50=100 ug/ml) and ADCP (up to 40% of cell death at 50 ug/ml). The cytotoxicity induced by XON27 in the KMS-12-BM was significantly more potent compared to daratumumab (anti-CD38) in both CDC and apoptosis assays, XON27 was able to kill up to 100% of cancer cells without affecting PBMC. XON27 showed cross-reactivity with blood cancer patient biopsies without staining healthy tissue. In addition, repeated administrations of XON27 demonstrate its ability to effectively kill tumor cells after each administration. No resistance is induced after repeated treatments. Interestingly, XON27 blocked the proliferation of residual tumor cells for up to 45 days after the second treatment at 50 ug/ml compared to the control condition, demonstrating sustainable effect of XON27 on tumorigenicity. The in vitro efficacy of XON27 was translated into in vivo efficacy in a murine MM xenograft model. It induced a significant reduction in tumor growth of up to 75%. XON27 was also characterized by a high tolerability profile and satisfactory exposure in primates.
Conclusion: Although many therapeutic advances have been made in the field of blood cancers, myeloma remains an incurable disease with a real need for new innovative therapies. XON27 represents a promising and selective immunotherapy which may provide an effective and safe treatment against refractory myeloma.

TUMOR BIOLOGY: Biomarkers and Expression Differences in Metastatic Progression
Poster Session

#2743 Molecular characterization and prognostic evaluation of disseminated cancer cell subpopulations detected in bone marrow of non-small cell lung cancer patients.

Daniel Spitzl[1], Tobias Mederer[1], Julius Zank[1], Severin Gutter[1], Michael Ried[2], Hans-Stefan Hofmann[3], Christoph A. Klein[1]

[1]Chair of Experimental Medicine and Therapy Research, University of Regensburg, Regensburg, Germany,[2]Department of Thoracic Surgery, University Hospital Regensburg, Regensburg, Germany,[3]Department of Thoracic Surgery, Krankenhaus Barmherzige Bruder Regensburg, Regensburg, Germany

Introduction: Disseminated cancer cells (DCC) can be detected years before metastatic manifestation in bone marrow of lung cancer patients. Although a consensus protocol has been established, the impact of markers and methods for DCC detection are still not settled. We recently found that $EpCAM^{\pm}$ DCC detected by immunofluorescence (IF) outperform the classical immunocytologic (IC) detection by cytokeratin (CK) antibodies regarding prognostic impact. However, it remained unclear whether this difference resulted from biological traits associated with $EpCAM^{\pm}$ *vs* $CK^{\pm}$ DCC or from methodological reasons. We therefore performed a side-by-side comparison of IC *vs* IF for CK and EpCAM.

Methods: We prospectively collected bone marrow (BM) aspirates from 56 non-metastasized NSCLC patients that underwent tumor resection with curative intention. After density gradient centrifugation, we analyzed the mononucleated cells by (i) IC using the anti-CK antibody A45-B/B3 and (ii) by IF using the anti-CK antibody A45-B/B3 and the anti-EpCAM antibody HEA-125. IF signals were captured and objectively quantified using ImageJ, whereas IC was evaluated by two independent observers. Marker-positive cells were isolated and subjected to Whole Genome Amplification (WGA) and whole genome sequencing for assessment of copy number alterations (CNA). Survival analysis was performed for progression-free survival (PFS), tumor-specific survival (TSS) and overall-survival (OS) after a median follow-up time of 72.5, 78.7, 78.7 months, respectively.

Results: IC and IF revealed the presence of $CK^{\pm}$ DCCs in 37.5% and 41.1% of cases, respectively (P=0.34). IF identified $EpCAM^{\pm}$ DCCs in 55.4% of patients, resulting in a 63.8% DCC-positivity rate found by IF, when combined with CK. The average number of DCCs per million MNC, the DCC density (DCCD), was 0.92, 0.93 and 1.44 for CK_{IC} and CK_{IF} and for $EpCAM_{IF}$, respectively. No association was found between $CK_{IC}^{\pm}$ DCCs and PFS, TSS or OS. In contrast, detection of $EpCAM_{IF}^{\pm}$ and/or $CK_{IF}^{\pm}$ DCCs showed a trend towards reduced PFS (P=0.055), TSS (P=0.225) and OS (P=0.155). Subgroup analysis revealed that both $EpCAM_{IF}^{\pm}$ and $CK_{IF}^{\pm}$ cells were correlated with worse PFS (P=0.016 and P=0.040, respectively) and TSS (P=0.033 and P=0.008, respectively). CK_{IF}-positivity was also associated with worse OS (P=0.014), whereas EpCAM was not. $CK_{IF}^{\pm}$ DCCs remained an independent prognostic variable for TSS and OS upon multivariate testing (hazard ratio: 6.45 and 3.31, respectively), while $EpCAM_{IF}^{\pm}$ was not. The IF-marker-defined cell phenotypes exhibited comparable frequencies and distributions of CNAs across the entire genome (~50% of cells).

Conclusions: Detection of $CK^{\pm}$ DCC by quantified IF analysis apparently outperforms CK detection by IC in survival analysis. The impact of CK and EpCAM expression levels on outcome are under investigation.

#2744 Exploring the role of the MSLN/MUC16 interaction in cancer progression via the in situ proximity ligation technique.

S. Bodbin, **D. Raykova**, A. Zieba-Wicher;
Navinci Diagnostics AB, Uppsala, Sweden

Introduction: Mesothelin (MSLN) is a glycoprotein present on the surface of mesothelial cells, sometimes used as a tumor marker. Its overexpression in various cancers, including mesothelioma, ovarian, pancreatic, and lung, is linked to increased tumor aggressiveness, evasion of apoptosis, metastasis, and resistance to treatments. Mucin16 (MUC16) belongs to a family of proteins that play a crucial role in cell adhesion, signaling, and immune responses. In cancer, alterations in mucin expression and structure may contribute to tumor progression and metastasis by enhancing cell survival and immune evasion. Mesothelin is known to interact with mucins, influencing tumor cell behavior and metastatic potential. More specifically, the MSLN/MUC16 interaction facilitates tumor cell invasion and peritoneal spread in ovarian cancer. However, reliable molecular tools to study protein interactions have been scarce. Here, we relied on the Naveni® *in situ* proximity ligation technology to identify MSLN/MUC16 in various cancer samples. The method detects proteins located within interaction range (<40 nm) by means of antibodies conjugated to oligonucleotides that create amplified fluorescent signal. Since the technique does not compromise the structural integrity of tissues, communication between proteins can be studied in their native environment.

Materials & Methods: Human FFPE tissue microarrays (TMA) with ovarian primary carcinoma and matched metastatic cancer (80 cores) and ovarian cancer tissue with normal tissue (100 cores) were deparaffinized and subjected to standard heat-induced antigen retrieval and blocking. Staining against the MSLN/MUC16 interaction was performed with the NaveniFlex Tissue MR Atto647N kit (Navinci Diagnostics). Co-staining antibodies against pan-Cytokeratin and Ki67 were included in the detection mix. Immunofluorescence (IF), using the same MSLN and MUC1 primary antibodies, was completed on an additional slide of each TMA, and then secondary antibodies conjugated to Alexa Fluor™ 488 and 594 were used for detection. Imaging was performed on an Olympus scanner VS200.

Results & Discussion: In this study, we showed that the interaction is abundant in ovarian cancer, with a distinguishable difference in the signal presence between cancerous and normal adjacent tissue. Furthermore, the additional tumor marker co-stainings give insights into the tumor invasion and growth. When comparing the Naveni® signal of MSLN/MUC16 against IF staining of each, the Naveni® signal shows true interactions, as opposed to expression patterns. Understanding the roles of mesothelin and mucin in cancer, both individually and in interaction, is crucial for developing targeted therapies and diagnostic tools. Further research on their interaction and specific molecular pathways triggered by it is essential for devising effective strategies to combat cancer progression.

#2745 Sequential tracking of PD-L1 expression on circulating epithelial tumor cells (CETCs) in men with primary non-metastatic prostate cancer.

D. Schott, M. Pizon, U. Pachmann, K. Pachmann, M. Maurer;
Laboratory Dr. Pachmann, Bayreuth, Germany

Background: Radiotherapy (RT) is an essential component of multimodality therapy in the primary or postoperative treatment of prostate cancer with curative intent by preventing local recurrence and distant metastases, indicating its impact on residual occult tumor, such as circulating tumor cells. Immunogenic changes in cancer cells induced by RT can lead to adaptive up-regulation of PD-L1 expression. As immune checkpoint inhibition plays an increasingly important role in prostate cancer, radiogenic PD-L1 upregulation may be of therapeutic importance. The aim of this study was to determine PD-L1 status on CETCs before and during RT.

Methods: Peripheral blood samples were collected from 52 primary non-metastatic prostate cancer patients. CETCs were enumerated and analyzed for PDL-L1 expression prior to (baseline), 3 and 6 weeks after the start of RT using fluorescence scanning microscopy.

Results: PD-L1 expression was detectable in CETCs and localized in the membrane and/or cytoplasm. We found a correlation between PD-L1 status in CETCs and aggressiveness of cancer disease prior to RT. The frequency of PD-L1 positive CETCs depended on the grading and Gleason score of the primary tumor. Patients with a high Gleason score and G3 tumors had significantly more PD-L1 positive CETCs compared to patients with a low Gleason Score and G1 tumors. Moreover, patients in stage I/II had significantly less PD-L1 positive CETCs compared to patients in stage III/IV (mean 54.25 vs. mean 69.65; $p<0.05$). A higher number of PD-L1 positive CETCs were detected in patients who had radical prostatectomy before start of RT than in those who had no surgical intervention (mean 66.24 vs. mean 47.46; $p<0.01$). Interestingly, the fraction of PD-L1 positive CETCs decreased significantly during RT only in patients with G3 tumors and a high Gleason Score.

Conclusion: Our results indicated that PD-L1 in CETCs is closely related to the aggressiveness of the primary tumor and may be a co-factor associated with the progression of prostate cancer. PD-1/PD-L1 blockade combined with RT represents a novel and promising treatment strategy that could contribute to improve the treatment efficacy of prostate cancer.

#2746 MAGE-A3 co-expression with IDH1-R132H and IL-1β in colon cancer.

Andy /Xi Han[1], Rachel Gonzalez[1], Jina Yom[1], Zhaoying Guo[1], Bailey Gilmore[1], Eden Zewdu[1], Tianli Qu[1], Hailey /YiChen Guo[1], Qi Ren[2], Xiaomin Hu[2], Ranran Zhang[2], Zhaohui Wu[2], Xuan Liu[1], Wei Fu[1]

[1]OriGene Technologies, Inc., Rockville, MD,[2]OriGene Wuxi Biotechnology Co., Ltd., Binhu District Wuxi, China

Colorectal cancer (CRC) remains a significant cause of cancer death worldwide with an estimated 52,000 deaths in 2023. Over the past few decades, the incidence rate of CRC in individuals younger than 50 has been steadily increasing. Currently, diagnostic biomarkers play an important role in the detection and treatment of CRC. MAGE-A3 has been shown to be expressed in many tumor types, including colon cancer by RNA expression. Due to their high sequence homology, members of the MAGEA family have been difficult to evaluate and screen for their protein expression. However, in a previous study, highly specific antibodies were identified using CytoSections for MAGE-A3 immunohistochemistry. IL-1β is a cytokine that induces inflammatory responses and when localized to the nucleus in colon cancer cells it can promote stemness. IL-1β expression has been shown to be increased in wildtype IDH1 positive glioblastoma. However, the relationship between IL-1β and IDH1 has not been studied in colon cancer. In this study, the difference in the expression of MAGE-A3, IL-1β, and wildtype IDH1 compared to mutant IDH1-R132H in colon cancer tissues was evaluated. The results show that IL-1β, wildtype IDH1, and MAGE-A3 were co-expressed in 27 of the 38 colon cancer tumors. However, IDH1-R132H expression was only seen in 20% of the tumors. This study suggests that MAGE-A3, IL-1β, and IDH1 are candidate biomarkers for immunotherapy due to their high expression in colon cancer tissues.

#2747 Chaperonin-containing TCP-1 promotes the release of exosomes from prostate and breast cancer cells.

A. R. Khaled[1], L. Truong[1], C. Frank[1], C. Dang[1], J. Velazquez[1], P. Gopalan[2], S. Litherland[1];
[1]University of Central Florida, Orlando, FL, [2]Orlando VA Healthcare System, Orlando, FL

Coping with cancer recurrence and assessing metastatic risk are challenges for cancer patients that could be addressed with an effective diagnostic predictor. Exosomes, a subpopulation of extracellular vesicles released by tumor cells, can promote distal metastatic site development and could have promising diagnostic applications. However, the mechanisms controlling exosome secretion by cancer cells remain to be determined, which impedes clinical development. The actions of protein-folding chaperones could facilitate tumor exosome formation, payload loading, and extracellular release. Protein folding complexes link the expression of tumor-promoting oncogenes with the proteins driving oncogenic cancer behavior. Of these, the eukaryotic type II chaperonin, Chaperonin-Containing TCP-1 (CCT), folds many of the oncoproteins (e.g., KRAS, MYC, CDKs, STAT3, etc.) responsible for cancer growth and invasion. CCT is a complex machine composed of eight subunits, each encoded by a unique gene (cct1-8), which folds proteins in an ATP-dependent fashion. We and others showed that CCT is upregulated in breast, lung, and prostate cancer cells as well as neuroblastoma, leading to alterations in apoptosis, migration, cell morphology, and proliferation. Using T47D breast cancer and PC3 and 22rV1 prostate cancer cells, we exogenously expressed or depleted the second subunit of the CCT complex (CCT2). With these cells, we isolated exosomes from culture media by membrane-based affinity binding and examined exosomal RNA and protein content. In exosomes from prostate and breast cancer cells, we found abundant CCT2 subunit mRNA and protein in CD63+ exosomes ranging from 50 to 120 microns in size. When CCT2 was exogenously expressed in breast and prostate cancer cells, CCT2 mRNA and protein were higher in exosomes than other CCT subunits, and CCT2 was randomly distributed throughout the size range of exosomes. Of interest, an increase in CD63+ small exosomes (50-75 microns) was evident in cancer cells exogenously expressing CCT2 compared to mock-transfected and parental controls, suggesting a role for CCT2 in the exosomal secretory pathway. FACS-sorted CD63+ exosomes subjected to mass spectrometry yielded distinct protein content based on CCT2 expression. These findings are the first report of CCT2 driving exosome secretion in cancer cells and suggest that exosomes containing CCT2 RNA and protein are associated with metastatic potential. Exosomal CCT2 thus represents a promising diagnostic indicator for a liquid biopsy approach to monitor cancer recurrence and metastasis.

#2748 Single cell biomechanical profiling of the metastatic potential of MDA-MB-231 cells.

Zeina Habli[1], Ahmad Zantout[2], Nadine Al Hajj[3], Raya Saab[4], Marwan El-Sabban[3], Massoud L. Khraiche[1]

[1]Neural Engineering and Nanobiosensors Group, Biomedical Engineering Program, American University of Beirut, Beirut, Lebanon,[2]Biomedical Engineering Program, American University of Beirut, Beirut, Lebanon,[3]Department of Anatomy, Cell Biology, and Physiological Sciences, Faculty of Medicine, American University of Beirut, Beirut, Lebanon,[4]Department of Pediatrics, Stanford, Palo Alto, CA

Cancer metastasis is a multistep complex process accompanied by changes in the mechanical properties of cancer cells, such as adhesion, viscoelasticity, deformability, and motility. Connexin 43 (Cx43), a gap junction protein with a putative tumor suppressor function, plays a pivotal role in Epithelial to Mesenchymal transition (EMT). It affects cell motility indicators and promotes cytoskeleton reorganization and, ultimately, metastasis when downregulated, corroborating resistance to chemotherapy. The lack of universal markers that can predict the metastatic ability of cancer cells necessitates the evaluation of parameters, such as cell adhesion, viscoelasticity, and stiffness, to serve as unique biophysical metrics that predict cancer cell metastatic potential and elucidate how metastasis and cell mechanics are coupled. Therefore, we utilized fluidic-based single-cell force spectroscopy (SCFS) and Quartz Crystal Microbalance with Dissipation Monitoring (QCM-D) to measure the mechanical properties of single cancer cells with different metastatic potential. To explore the relationship between cell mechanics and metastatic cell behavior, we quantitatively demonstrate the progression of cancer cell biomechanics across different metastatic states using MDA-MB-231 breast cancer cells with varying connexin 43 (Cx43) expression as a model of cells with varying metastatic potential. We measured, at a single-cell level and in real-time, the adhesion and viscoelastic properties of MDA-MB-231 cells and their response to chemotherapy. Our data show that cells with higher metastatic potential (down-regulated Cx43 expression) exhibited a softer, less adherent, and more viscoelastic phenotype, consistent with their metastatic state when in clusters compared to cells at the lower spectrum of metastatic potential (up-regulated Cx43 expression). These mechanical biomarkers are significantly absent in single cells outside of a cluster. Of particular interest, we also observed significant cellular stiffening upon treatment with docetaxel (DTX), a chemotherapeutic agent that targets microtubules, with a rapid and profound response of highly aggressive cells when compared to cells with attenuated metastatic potential. Such treatment schemes could render cancer cells less deformable, potentially impeding their ability to invade and metastasize to other tissues. Our study demonstrates a unique quantitative metric that unfolds biomechanical markers for discerning the metastatic state of cancer cells. Our data represents a stepping stone to understanding how mechanical changes in cancer cells may determine how cancer progresses and responds to chemotherapeutic agents and may provide novel modalities to inhibit metastasis.

#2749 DHX36 may promote the growth and metastasis of lung cancer.

T. Li, N. Luo, J. Fu, C. Wei, **J. Fu**;
Southwest Medical University, Luzhou, China

Introduction: Helicase is a kind of protein molecular motor that widely exists in eukaryotic cells, viruses and bacterial cells, and participates in DNA replication, transcription and other life activities. DHX36, a kind of helicase, is a new homologous gene of human DNA/RNA helicase cloned by our laboratory by homologous molecular cloning which used the sequence of the maleless gene (mle) of Drosophila. Studies have shown that DHX36 upregulates the expression of proto oncogene and promotes the occurrence of cancer. At present, there are few studies on DHX36 in lung cancer. This study aims to clarify the relationship between DHX36 and lung cancer and provide a new molecular target for the diagnosis, treatment and prognosis of lung cancer.
Methods: Twenty-eight pairs of clinical tumor samples from lung adenocarcinoma and adjacent tissues were collected, and the protein expression of DHX36 in different tissues was detected by western blot. Correlation between DHX36 expression and survival prognosis of lung cancer patients was analyzed by online database. Over-expression of DHX36 in A549 and H460 cells and knockdown of DHX36 in A549 and H1975 cell lines, then the migration, invasion and growth index of cells were analyzed by real-time cell analyzer. After DHX36 stable knock-down cell line was established in H1975 cells, they were injected into nude mice by subcutaneous injection and tail vein injection respectively at the same time as the control cells, and the growth of subcutaneous tumors and the metastasis of lung tissues in nude mice were recorded and collected respectively. The tissues were analyzed by histology, immunohistochemistry, and western blot.
Results: In 28 pairs of clinical lung cancer tumor samples, we found that DHX36 was higher in cancer tissues than in adjacent tissues in 23 pairs, which indicated that DHX36 might be a kind of proto oncogene to promote the occurrence and development of lung cancer. Bioinformatics analysis revealed that the high expression of DHX36 was related to the low survival of lung cancer patients. The results of RTCA showed that the abilities of growth, invasion and migration of cells in the over-expressed DHX36 groups were higher than those in the control groups. After DHX36 was knocked down, the growth, invasion and invasion of lung cancer cells were inhibited.
Conclusion: DHX36 is expected to be a new molecular target of lung cancer. Next, we will knock out DHX36 in lung cancer cells to observe the tumor growth and lung metastasis in mice.

#2750 Leveraging machine-learning approaches to dissect drivers of clinical metastatic dynamics in lung adenocarcinoma.

Tyler Aprati[1], Michael Manos[1], Giuseppe Tarantino[1], Marc Glettig[1], Maryclare Griffin[2], Alexander Gusev[1], Kenneth Kehl[1], David Liu[1]

[1]Dana-Farber Cancer Institute, Boston, MA,[2]University of Massachusetts Amherst, Amherst, MA

Background: Non-small cell lung cancer (NSCLC) survival is closely linked to metastatic progression. 5-year survival rates drop from >65% when localized to ~9% when distant metastases occur. Despite this impact on mortality, drivers of overall metastasis and site-specific organotropism are not well understood in NSCLC. To investigate these questions, we focused on Lung adenocarcinoma (LUAD), the most common subtype of NSCLC. Although previous efforts have been made to examine LUAD organotropism, we sought to expand upon longitudinal modeling approaches and explore associations in an independent large clinical and genomic annotated cohort.

Methods: Using the artificial intelligence model from (Kehl et al. 2021), we annotated a clinico-genomic cohort of 2777 patients with lung adenocarcinoma, resulting in 59,177 annotated imaging reports. This resulted in time to metastatic site annotations for each patient, with median of 2 years follow up. Metastatic sites included brain, bone, adrenal, liver, lymph node, and mesentery. All patients were evaluated at the Dana-Farber Cancer Institute, and each patient had at least one tumor biopsy sequenced with targeted panel sequencing of 400+ cancer related genes. To infer genomic and clinical correlates of site-specific metastasis, we performed cause-specific and Fine-Gray hazard modeling in this cohort. We used the recurrent event Andersen-Gill model to infer predictors of longitudinal metastasis rates.

Results: Site-specific analyses yielded genes whose mutant status were significantly associated with a change in risk and/or rate of certain metastatic sites. We found that NOTCH1 is significantly associated with an increased rate and risk of brain metastases (HR=2.46, P<0.001). SETD2 is associated with decreased incidence of brain (HR=0.42, P<0.001). SMARCA4 is significantly associated with increased incidence and rate of adrenal metastasis (HR=1.64, P<0.01), while NF1 is significantly associated with decreased rate of adrenal metastasis (HR=0.72, P<0.01). In a multivariable model, Female patients and younger patients had a lower rate of new metastatic sites. As previously seen, TP53 and SMARCA4 mutations associated with higher rates of new metastatic sites (HR=1.17, P<0.001; HR=1.36, P<0.001 respectively), and SETD2 is associated with a lower rate of new metastatic sites (HR=0.71, P<0.001).

Conclusions: By using time-to-event analysis with longitudinal metastatic annotations, we identify potential drivers of overall metastasis and site-specific organotropism in LUAD patients. Identification of new associations and concordance of our results with previous studies also supports the utility of artificial-intelligence-annotated datasets, allowing for larger cohorts without the need for manual annotation.

#2751 Functional assessment of STK11 C-terminal domain variants.

G. Nandagopal, S. Lenahan, H. Ross, H. Sarausky, D. Seward, P. Deming;
University of Vermont, Burlington, VT

STK11 mutations in KRAS-driven lung adenocarcinomas (LUADs) are associated with aggressive tumor phenotypes characterized by increased risk of metastasis and lower overall and progression free survival. STK11 is a serine-threonine kinase that is comprised of an N-terminal domain containing a nuclear localization signal, a kinase domain, and a C-terminal domain (CTD). In LUAD, STK11 loss of function impacts many aspects of coordinated cell motility and promotes alterations characteristic of metastasis including cell polarity and adhesion. Both kinase activity and subcellular localization are important for STK11 tumor suppressor function. Our objective was to develop a reliable method to identify pathogenic STK11 mutations. Using archival data from the University of Vermont Medical Center, we identified 28 STK11 missense variants that had not yet been functionally characterized. We evaluated the functional impact of these variants on STK11 kinase activity through detection of autophosphorylation using an in-vitro kinase assay, as well as their ability to induce p53 activity through a luciferase reporter. Of the variants studied, 5 were CTD mutations. These variants retained kinase activity and the ability to bind STK11's partners STRAD-alpha and MO25 in co-immunoprecipitation assays. Although the CTD of STK11 has no catalytic activity, it is thought to be integral for translocation to the cytoplasm where it can colocalize with actin and the cell membrane. STK11 dependent regulation of directional migration requires both proper localization to the actin cytoskeleton and kinase activity. Moreover, it has been reported that the C-terminal polybasic motif of STK11 (aa403-426), consisting of 3 Lysine and 5 Arginine residues is key for its localization and activation of AMPK at the plasma membrane. Therefore, when ascertaining functional status of STK11 in vivo, it is important to consider kinase independent STK11 functions. In LUAD cell lines, we show through immunofluorescent microscopy that expression of a truncated construct encoding STK11 with a CTD deletion results in nuclear sequestration. Additionally, point mutants in 3 of the polybasic motif residues (R409W, K416E and K423E) retain kinase activity and STRAD-alpha binding, but also lead to nuclear sequestration - highlighting the importance of a multipronged approach when assessing STK11 function. Future studies will assess the ability of these C-terminal domain mutants to phosphorylate cytoplasmic substrates, and their impact on cell migration and invasion. Additionally, we will utilize the TurboID proximity ligation system to assess the effect of C-terminal domain point mutations on binding partner accessibility.

#2752 ICA1 promotes prostate cancer progression and metastasis via AR down-regulation.

F. Wang, Y. He, X. Huang, M. Chang, X. Zhang, X. Li, X. Ye, **Y. Lu**;
Southern University of Science and Technology, China, Shenzhen, China

Cancer metastasis, one of the main characteristics in malignancy, contributes to high mortality in cancer patients. Prostate cancer (PCa) is the most common cancer among men and the second leading cause of cancer-related death in Europe and the United States. In China, its incidence has been dramatically increased over past years. However, the mechanism of PCa progression and metastasis remains unclear. The androgen receptor (AR) has been demonstrated to play an important role in PCa progression and metastasis. We have previously established mouse models of PCa bone metastasis and PCa lung metastasis. We have obtained cell clones with bone-specific or lung-specific metastatic capability. By transcriptomic analysis of highly metastatic cell clones and their parental cells, we found a gene group including islet cell autoantigen 1 (ICA1) that are highly expressed in both metastatic cell clones. We further compared these results with RNA array data in clinical samples. Data comparison and correlation analysis showed that ICA1 was negatively correlated with AR expression. Survival analysis of PCa and lung cancer patients showed higher expression of ICA1 but with shorter overall survival. Down-regulation of ICA1 expression in highly metastatic tumor cells significantly inhibited cell growth, colony formation, migration, and invasion. ICA1 overexpression in parental RM1 cells apparently increased cell growth, migration, and metastasis. Interestingly, down-regulation of ICA1 also significantly activated AMPK/mTOR signaling pathway. These findings are anticipated to shed light on the novel pathogenic mechanism underlying PCa and propose a compelling theoretical basis for the application of ICA1 in PCa. This work supported by the NSFC projects (81972420, 81972766, 82173336), as well as grants from the Science and Technology Project of Shenzhen (JCYJ20210324104214040, JCYJ20190809161811237).Keywords: prostate cancer, metastasis, ICA1, androgen receptor

#2753 Muc4 is a biomarker of metastasis in TNBC and its downregulation by blocking soluble TNF prevents metastasis in combination with immunotherapy.

F. L. Mauro[1], S. Bruni[1], A. Dupont[2], G. Inurrigarro[2], S. Figurelli[3], S. Barchuk[3], D. Lopez Della Vecchia[3], R. Cordo Russo[1], E. Gil Deza[4], M. Mercogliano[1], R. Schillaci[1];

[1]IBYME-CONICET (Institute of Biology and Experimental Medicine), Buenos Aires, Argentina, [2]Sanatorio Mater Dei, Buenos Aires, Argentina, [3]Hospital Juan A. Fernandez, Buenos Aires, Argentina, [4]Instituto Oncologico Henry Moore, Buenos Aires, Argentina

Triple negative breast cancer (TNBC) accounts for about 10-15% of all breast cancers and has the worst survival rate. Immunotherapy is a new treatment option but resistance is frequent. We have demonstrated that TNF induces trastuzumab resistance through mucin 4 (MUC4) upregulation and it is an independent biomarker of poor response to therapy in HER2+ breast cancer. MUC4 is a transmembrane glycoprotein involved in metastasis (MTS) dissemination. Here, we evaluated the impact of the axis TNF/MUC4 on the invasive capacity of TNBC cell lines and in a preclinical model of spontaneous MTS. Finally, we assessed the clinical impact of MUC4 expression in TNBC patients. TNF blockade was achieved with etanercept (E), which blocks the soluble (sTNF) and transmembrane isoform of TNF, or with the dominant negative protein INB03 (DN) which neutralizes only sTNF. BT-549 and MDA-MB-231 human TNBC cell lines treated with E or DN exhibit a decrease in MUC4 expression. To assess the impact of TNF blockade on tumor cells and its effect on the tumor microenvironment, we collected conditioned media (CM) from MDA-MB-231 and BT-549 cells treated with E or DN which were used to evaluate the invasive capacity of the TNBC cell lines. The invasion of BT-549 and MDA-MB-231 was impaired with CM-Eta ($p \leq 0.01$) and CM-DN ($p \leq 0.01$ and $p \leq 0.05$, respectively). Female BALB/c mice bearing the TNBC LMM3 tumors were treated with IgG, DN, anti-PD-1 antibodies or DN+anti-PD-1 for two weeks. After the treatments we performed surgery to remove the primary tumor and the animals were sacrificed 2 weeks later. No effect on tumor growth was observed. However, the DN+anti-PD-1 group was the only one with less of 3 MTS per lung ($p \leq 0.05$). We obtained tumor extracts and found that the tumors of the animals treated with DN or DN+anti-PD-1 had decreased MUC4 expression measured by Western blot. We determined the presence of TILs by H & E and the expression of MUC4, Ki67, PD-L1 (SP142), androgen receptor (AR) and cytokeratin 5 by immunohistochemistry in a cohort of 56 early TNBC patients. MUC4 expression was inversely correlated with TILs presence ($p=0.0003$). Since TILs are associated with good prognosis, we evaluated the effect of BT-549-CM and MDA-MB-231-CM on T cell migration. CM-DN from both cell lines increased T cell migration compared to control CM ($p \leq 0.01$). MUC4 expression was inversely correlated with Ki67 ($\geq 30\%$, $p=0.036$), PD-L1 ($p=0.001$) and AR ($p=0.047$) in our cohort. Moreover, MUC4 proved to be an independent predictor of poor overall survival ($p=0.02$), and is associated with a higher MTS risk ($p=0.005$). MUC4 is associated with poorly-infiltrated TNBC, and sTNF blockade downregulates its expression decreasing MTS when combined with anti-PD-1. We propose the TNF as a new target for the treatment of TNBC, and MUC4 as a predictive biomarker to guide a combined treatment of TNF blockers with immunotherapy.

#2754 Uncovering the role of TEADs in treatment induced small cell or neuroendocrine prostate cancer.

L. G. Brown[1], I. M. Coleman[2], T. L. H. Chu[2], D. W. Lin[1], J. K. Lee[2], E. Sayar[2], L. D. True[1], R. Dumpit[2], E. Corey[1], P. S. Nelson[2], M. C. Haffner[2], **C. Morrissey**[1]; [1]University of Washington, Seattle, WA, [2]Fred Hutchinson Cancer Center, Seattle, WA

Study Purpose: Determine the role of the transcription factor TEAD1 in promoting the neuroendocrine phenotype in castration-resistant prostate cancer (CRPC).
Experimental Procedures: We quantitated YAP-pathway associated transcripts, protein abundance, and splicing events in androgen receptor (AR) positive prostate adenocarcinoma (ARPC) and small cell or neuroendocrine prostate cancer (SCNPC) using RNAseq, scRNAseq, qPCR, immunohistochemistry (IHC), CpG methylation, and western blot analyses on patient samples, patient-derived xenograft (PDX) models, and cell lines. In addition, we tested the impact of the pharmacological inhibition and knockdown of proteins and genes associated with TEAD1 activity in ARPC and SCNPC cell lines on TEAD1 expression, cell number, and tumor cell differentiation.
Results: Transcriptomic analyses revealed a decrease in YAP1, TAZ, LATS2, and TEAD2 and an increase in LATS1, TEAD1 and RBFOX2 transcript levels in SCNPCs compared to ARPCs in SU2C, rapid autopsy metastases, and PDX models. Similar results were observed in ARPC and SCNPC cancer cell lines, in the transplantable LTL331 prostate cancer transdifferentiation model, and scRNAseq of liver CRPC metastases from patients. The decrease in YAP1, TEAD2 and LATS2 expression correlates with increased methylation and the increase in TEAD1 correlates with decreased methylation in SCNPC PDX models, suggesting epigenetic control. The changes in YAP and YAP-associated proteins (most importantly TEAD1) at the epigenetic and transcriptional level were confirmed by IHC analysis comparing ARPC to SCNPC PDX models. Of the four TEAD proteins, TEAD1 expression was increased, with a concomitant decrease in TEAD2 and TEAD3, whereas low levels of TEAD4 transcript are maintained in the SCNPC phenotype. Notably, RBFOX2 was increased in the SCNPC datasets. RBFOX2 is a pre-RNA splicing regulator that promotes the inclusion of exon 6 in TEAD1 mRNAs associated with increased TEAD1 activity. The RBFOX2 spliced TEAD1 was observed in the SCNPC PDX models, while not detected in the ARPC PDX models.
Conclusions: The conversion of ARPC to SCNPC involves the loss of transcriptional regulators: AR, YAP, and REST inactivation in SCNPC. It also involves the expression of ASCL1 or NEUROD1, well described master regulators that are implicated in the conversion to and maintenance of the SCNPC phenotype. Our work suggests TEAD1 is another transcriptional regulator in SCNPC that warrants further investigation.

#2755 Characterizing breast cancer cells following immune pruning in mice.

S. McElduff, D. Bronder, M. Duran, S. Bakhoum;
Memorial Sloan Kettering Cancer Center, New York, NY

In cancer patients, metastasis is the leading cause of death. Indeed, primary tumors which are diagnosed early and treated in a timely manner have the highest rate of success. In contrast, metastatic disease and late diagnosis of tumors portend poor outcomes. Thus, understanding the underlying biology and developing novel therapeutic approaches for metastatic cancers is pivotal. Most cancer-based mutational characteristics are tissue-dependent, and cancers with higher mutational load are generally more susceptible to immunotherapy. We observed that poorly metastatic, murine breast cancer cells established a clear phenotypic difference in lung metastasis formation assays. Upon injection of these cells into immune-proficient mice, few, large metastases developed, whereas in immuno-deficient mice, many small metastases grew instead. To determine the molecular features which enable escape under immune editing, we designed the following workflow. We intravenously injected immune-proficient and immune-deficient mice with our poorly metastatic, murine breast cancer cells. As expected, cells readily engrafted in the lungs, causing a significant reduction in survival of immune-deficient mice. Furthermore, liver metastases were observed only in immune-deficient mice. Upon euthanasia, we resected and dissociated both organs. To isolate the tumor cells from these samples, we flow-sorted and subjected them to next-generation sequencing. To elucidate the epigenomic, genomic, and transcriptomic differences between metastases of each background, we performed ATAC, WGS, and RNAseq, respectively. By dissecting the evolutionary mechanisms which allow cancer cells to evade immune detection in metastasis, we can develop targeted immunotherapy strategies to diminish the spread (and lethality) of metastatic cancers. In the future, we plan to examine the descriptive discrepancies between the tissues reared with and without immune pruning in order to put forward innovative therapeutic strategies.

#2756 Single cell analysis reveals treatment response-associated plastic cell state and lineage switching in aggressive variant prostate cancer.

Shuai Guo[1], Elavarasan Subramani[2], Daniel E. Frigo[2], Patrick G. Pilie[3], Sangeeta Goswami[3], Rama Soundararajan[4], Ana Aparicio[3], Wenyi Wang[1]

[1]Department of Bioinformatics and Computational Biology, UT MD Anderson Cancer Center, Houston, TX,[2]Department of Cancer Systems Imaging, UT MD Anderson Cancer Center, Houston, TX,[3]Department of Genitourinary Medical Oncology, UT MD Anderson Cancer Center, Houston, TX,[4]Department of Translational Molecular Pathology, UT MD Anderson Cancer Center, Houston, TX

Prostate cancer (PCa) is a common malignancy in men over 65, ranking as the second leading cause of cancer-related deaths among men in the United States. While most prostate cancers respond to androgen receptor (AR) targeting therapies, Aggressive Variant Prostate Cancers (AVPCs), characterized by RB1, Tp53, and/or PTEN alterations, do not. AVPCs exhibit lineage plasticity in preclinical models, enabling the expression of non-prostate epithelial lineage markers to adapt to therapeutic pressures. However, a measurable definition of lineage plasticity as a potential therapeutic target for clinical trials is currently lacking. To arrive at said definition, we perform single-nuclei RNA sequencing (snRNA-seq) on lymph node metastases from twelve AVPC patients with matched sample pairs of both pre- and post-treatment. Additionally, we include snRNA-seq data from eight non-AVPC patients as a baseline. Expanding upon our prior establishment of tumor-specific total mRNA expression (TmS) as an indicator of tumor cell lineage plasticity (*Nature Biotechnology*, PMID: 35697807), we employ unique molecular identifier (UMI) counts from individual cells to quantify this plasticity. We reveal a distinct cluster of tumor cells with notably high UMI counts in resistant samples, indicative of a less differentiated state and increased transcriptional diversity. This high-UMI cluster is marked by significant enrichment in pathways associated with epithelial-mesenchymal transition (EMT), stemness, one-carbon metabolism, and arginine metabolism pathways. Concurrently, there is a reduction in activity within the androgen receptor (AR) and DNA damage repair pathways. These characteristics suggest an enhanced capacity for lineage switching in AVPC tumor cells, potentially contributing to evasion from targeted therapies. Moreover, immune components within resistant samples consistently display lower UMI counts, indicating a diminished propensity for lineage plasticity. In conclusion, we present a better understanding of lineage switching in therapeutic resistance in AVPCs, paving the way for novel treatment strategies in PCa management.

#2757 Investigating regulatory drivers of prostate cancer metastasis in circulating tumor cells.

A. Zheng[1], A. Obradovic[2], K. Ronaldson-Bouchard[1], G. Vunjak-Novakovic[1], A. Califano[2], P. A. Sims[2], C. Abate-Shen[2], A. Giacobbe[2];
[1]Columbia University, New York, NY, [2]Columbia University Irving Medical Center, New York, NY

Prostate cancer is the most common cancer in men and the second-leading cause of death. Most prostate cancer deaths are due to metastasis, particularly to the bone. Metastasis occurs when cells from the primary tumor travel through the blood as circulating tumor cells (CTCs) and settle in metastatic sites. CTCs are difficult to collect from patients, and understanding the relationships between CTCs and the tumor phenotypes of origin could reveal mechanisms of cancer metastasis. Hence, we utilized several genetically engineered mouse models (GEMMs) of metastatic prostate cancer to evaluate tumor phenotypes and CTCs. We compared the tumor phenotypes of several GEMMs of metastatic prostate cancer and identified a level of heterogeneity among tumors, particularly focusing on a GEMM that demonstrated severe metastasis, especially to the bone. Next, we analyzed CTCs from this GEMM and focused our analysis on transcriptional states that are regulated by proteins called master regulators (MRs). MRs control the expression of groups of genes called regulons, and pharmacologically inhibiting these MRs may lead to reversal of cancer phenotypes. We hypothesized that these MRs may be mechanistic drivers of CTC cell state in prostate cancer metastasis. We investigated MRs enriched in CTCs from mice and screened and validated Lap2, the lamina-associated polypeptide 2 protein, as a regulatory driver in mice with metastatic prostate cancer. Analysis of bulk RNA-seq profiles from primary and metastatic prostate samples in The Cancer Genome Atlas and Stand Up to Cancer cohorts, respectively, revealed that the regulon-based activity of Lap2 was significantly higher in the latter group. Moreover, analysis of single-cell RNA-seq profiles of CTCs isolated from prostate cancer patients confirmed aberrant Lap2 activity. Finally, the role of Lap2 was assessed in human tissue from an engineered multi-organ-on-a-chip model of metastasis. Silencing of Lap2 production in cells dissociated from mouse CTC-derived organoids inhibited extravasation to the bone in the model, suggesting a critical role for Lap2 in metastasis. Our findings illustrate the unique transcriptional profile of prostate cancer CTCs associated with their metastatic potential. We identified Lap2 as a novel driver of CTC dissemination and metastasis in mice and validated its activity in human prostate cancer, which can aid future therapies to prevent metastatic progression in patients.

#2758 Stemness subtype gastric cancer accelerate hematogenous metastasis.

Seungho Lee[1], Jaeun Yoo[2], Seungbok Lee[3], Hyun Myong Kim[4], Kyoungyun Jeong[4], Yie-Ri Yoo[4], Ji-Yeon Shin[4], Kyoung Un Park[5], Hye Seung Lee[6], Seong-Ho Kong[1], Do Joong Park[1], Hyuk-Joon Lee[1], Han-Kwang Yang[1]

[1]Department of Surgery, Seoul National University Hospital, Jongro-gu, Korea, Republic of,[2]Cancer Research Institute, Seoul National University, Jongro-gu, Korea, Republic of,[3]Department of Genomic Medicine, Seoul National University Hospital, Jongro-gu, Korea, Republic of,[4]Cancer Research Institute, Seoul National University Hospital, Jongro-gu, Korea, Republic of,[5]Department of Laboratory Medicine, Seoul National University Bundang Hospital, Seongnam, Korea, Republic of,[6]Department of Pathology, Seoul National University Hospital, Jongro-gu, Korea, Republic of

Oncogenic progression and metastasis correlate with the acquisition of stem cell-like characteristics and the loss of differentiated phenotype. Poorly differentiated primary tumors often lead to unfavorable oncologic outcomes due to a heightened likelihood of metastasis to distant organs across various cancers. However, the relationship between stemness traits and metastasis in gastric cancer (GC) remains insufficiently explored. In this investigation, we analyzed bulk RNA-sequencing from microdissected primary tumor specimens and clinical data to pinpoint molecular subtypes linked to distant organ metastasis. Transcriptomic data from patient-derived xenograft (PDX) samples and available single-cell RNA datasets validated our bulk RNAseq findings. Comprehensive analysis highlighted the molecular traits of GC tied to hematogenous metastasis. Microdissection of primary tumor FFPE samples facilitated bulk RNA sequencing, encompassing samples from 33 metastatic and 31 metastasis-free patients, with 8 paired normal samples. Most samples contained less than 10% of tumor microenvironment (TME) components like fibroblasts, endothelial cells, and immune cells. Using non-negative matrix factorization (NMF) clustering, we achieved unsupervised subtyping of the gastric cancer gene expression matrix. Permutation tests based on subsampling indicated consistent high-level cophenetic coefficients at k=2, suggesting robust bifurcation of transcriptomic data into two clusters. One showed augmented stemness traits while the other emphasized differentiated mucosal genes, labeled as stemness and differentiated subtypes, respectively. GSEA highlighted a significant boost in the Hallmark angiogenesis score in the stemness subtype, not attributed to endothelial cell infiltration as verified by CIBERSORTx. This subtype also exhibited a marked decrease in hematogenous metastasis-free survival (HMFS) ($p=0.008$, log-rank test). Further, PDX samples were scrutinized. Post classification of the PDX graft expression matrix via logistic regression, we examined the endothelial cell fraction, determined by CIBERSORTx. Stemness subtype PDX grafts revealed a significant elevation in the host (mouse) endothelial cell fraction ($p<0.05$). In addition, stemness PDX patient showed significant decreased HMFS ($p = 0.03$). We also categorized the pseudobulk expression matrix of malignant cells into stemness or differentiated subtypes using GSE183904 scRNA cohort. scRNA sample analysis consistently presented an elevated endothelial cell fraction in the stemness GC subtype. The outcomes suggest a propensity for angiogenesis in the TME of the stemness subtype of GC. In conclusion, our findings demonstrate that the stemness subtype of GC accelerates hematogenous metastasis, as evidenced through clinical data, bulk RNAseq, PDX, and scRNAseq data.

#2759 Transcriptional intra-tumoral heterogeneity of putative therapeutic targets in colorectal cancer peritoneal metastases.

J. J. Zhao[1], J. C. Ong[2], D. K. Chia[3], M. C. Teo[2], Q. Tan[2], G. Ng[2], J. W. Tan[2], H. Ma[4], X. Ong[4], S. Tay[4], P. Tan[4], R. Sundar[1];
[1]National University Cancer Institute, Singapore, Singapore, [2]Division of Surgery and Surgical Oncology, National Cancer Centre Singapore, Singapore, Singapore, [3]University Surgical Cluster, National University Health System, Singapore, Singapore, [4]Duke-NUS Medical School, Singapore, Singapore

Background: The poor prognosis of peritoneal metastasis (PM) in colorectal cancer (CRC) is typically attributed to, and characterized by, resistance to systemic chemotherapy and immunotherapy. The evolutionarily conserved plasma-peritoneal barrier as well as reduced tumor tissue vascularity contributes to poorer responses to systemically administered antineoplastic therapy. Beyond these, we sought to understand transcriptomic variations of important therapeutic targets implicated in peritoneal organotropism and by extension, resistance to systemic regimens in CRC PM.
Methodology: FFPE tissue samples from CRC patients were collected during oncological surgical resection of the synchronous PM (cytoreductive surgery [CRS] with or without hyperthermic intra-peritoneal chemotherapy [HIPEC]), or exploratory laparotomy for palliative surgery, with the majority of patients receiving systemic therapy prior to surgery. Samples were sequenced with whole transcriptomic sequencing. Paired and unpaired T-tests between PT and PM samples were undertaken with log2(fragments per kilobase of exon per million mapped [FPKM]) gene expression values.
Results: Fifty-six (22 primary tumor [PT], 34 peritoneal metastases [PM]) samples from 35 patients, comprising 21 paired PT-PM samples, were included in this analysis. TEAD1 (unpaired T-test, p=0.087; paired T-test, p=0.041), FGFR1 (unpaired T-test, p=0.003; paired T-test, p<0.001), PIK3CA (unpaired T-test, p=0.034; paired T-test, p=0.003), SMAD4 (unpaired T-test, p=0.095; paired T-test, p=0.010), and HAVCR2 (unpaired T-test, p=0.009; paired T-test, p=0.007) were found to be upregulated in the PM. Conversely, MET was found to be downregulated in PM samples (unpaired T-test, p=0.004; paired T-test, p=0.002). There were no significant differences in gene expression profiles of BRAF, RHOA, CD274, CTLA4, PDCD1 and TIGIT between PT-PM (all p>0.05).
Conclusion: Through CRC PT-PM comparisons, we identify potential therapeutic targets implicated in transcoelomic metastasis and provide rationale for development of immunotherapeutic biology and drug discovery for CRC PM. These findings underscore an exigent need to develop intra-peritoneal therapeutic strategies to overcome resistance to systemic regimens.

#2760 Novel GPCR recombinant monoclonal antibodies for cancer biology research.

A. Ball, Y. Hsieh, C. Huang, S. Huang, S. Wu, Y. Chang, J. Liu, P. Peng, C. Lin;
GeneTex, Inc., Irvine, CA

Recombinant technology is becoming the preferred production mechanism for creation of antibody reagents used in academic and clinical cancer biology research. Recombinant antibodies (rAbs) are superior to standard polyclonal and hybridoma-generated monoclonal reagents as they offer reproducible performance and consistent, scalable supply. A major focus of antibody manufacturers is to leverage rAb production strategies to generate antibodies against challenging targets for which there are few, if any, reliable antibodies. G-protein coupled receptors (GPCRs) are encoded by more than 820 human genes and represent the largest membrane protein superfamily in the genome. These seven-pass transmembrane domain receptors are involved in a multitude of physiological and pathophysiological processes related to various chronic diseases, including an array of malignancies. Perhaps 30-40% of all therapeutics are directed against GPCR activity, and ~350 of the non-olfactory GPCRs are thought to be potential candidates for drug development. However, for a slew of technical reasons, the development and validation of high-quality antibodies against GPCRs has proven difficult. In an effort to facilitate further research into GPCRs, GeneTex is combining its recombinant antibody production platform with enhanced validation techniques to make specific monoclonal antibodies against GPCRs with direct relevance to cancer and other diseases. GeneTex's rAb production protocol employs a multi-parameter fluorescence-activated single cell sorting (FACS)-based methodology to identify and select antigen-specific IgG+ memory B cells from an immunized rabbit (Starkie *et al.*, 2016). The heavy and light chain variable region genes from single cells are amplified, cloned, and co-expressed in mammalian cells to generate a monoclonal IgG. Application-specific testing is performed in conjunction with knockout/knockdown (KO/KD), differential expression comparison in cells and tissues, cell fraction enrichment (i.e., membrane extracts versus whole cell extracts), and other methodologies. Antibodies directed against extracellular GPCR domains are validated for specificity using GPCR arrays (CDI Labs, Baltimore, MD). This workflow has resulted in the production of specific antibodies for a number of GPCRs studied by cancer biologists. These include novel recombinant monoclonal antibodies to the dopamine D2 receptor (DRD2), retinoic acid-induced protein 3 (RAI3), CXC motif chemokine receptor 2 (CXCR2), CXCR4, and CXCR7. All of these antibodies were validated for at least two applications, while the specificity of three (i.e., RAI3, CXCR4, and CXCR7) is supported by KO/KD data. GPCR array data argues for the specificity of the other two antibodies (i.e., DRD2 and CXCR2). This same production/validation approach will be applied as GeneTex targets the remaining GPCRs.

#2761 Activating RET mutations promotes osteoblastic bone metastasis by inhibiting osteoclastogenesis and stimulating osteoblast activity via regulation of osteoprotegerin.

R. Bagheri-Yarmand, J. L. Kidd, G. M. Pagnotti, T. Trivedi, L. Guerra, X. Wan, J. Song, S.-H. Lin, T. Guise;
UT MD Anderson Cancer Center, Houston, TX

Bone metastases (BM) are a source of increased mortality and significant morbidity in patients with medullary thyroid cancer (MTC), with ~50% survival at five years post-diagnosis. MTC causes osteoblastic, osteolytic, or mixed lesions, yet the underlying mechanisms are unknown. The *RET* proto-oncogene encodes a transmembrane tyrosine kinase receptor and is the driver oncogene in ~60% of MTC cases where a germline or somatic activating mutation results in ligand-independent constitutive activation of the receptor. However, the role of RET mutations in the genesis of bone metastasis lesions is unknown. We show that activating *RET* mutations promotes an osteoblastic phenotype in mice implanted with patient-derived MTC cells by increasing bone formation and decreasing bone resorption. We found that the radiographic appearance of osteoblastic lesions differed between the types of RET mutations (C634W and M918T). MTC cells with RET^{C634W} mutation showed a four-fold increase in bone mineral density, trabecular bone volume, number, and thickness with a decreased number of osteoblasts compared to the non-tumor-bearing femur. TRAP staining revealed that osteoclast numbers per long bone were reduced in the injected femur compared to the control. In contrast, the MTC-RET^{M918T} mutation showed an increased cortical thickness and porosity with reduced medullary area and increased bone formation rate compared to the non-tumor bearing femur. MTC cells formed tumors with extensive mineralized tissue, composed of bone matrix surrounded by osteoblast-like cells and osteoid. The knockdown of RET in the MTC-RET^{M918T} model significantly reduced cortical thickness and increased the number of osteoclasts per bone surface. We observed increased osteoprotegerin (OPG) expression in MTC-bearing femurs compared to controls, suggesting decreased bone resorption. The factors secreted by MTC cells, including OPG, inhibited osteoclast formation from primary bone marrow cells and Raw264 cells. In addition, RET knockdown by shRNA in MTC cells decreased OPG expression. Moreover, the MTC-conditioned media (CM) increased osteoblast differentiation and mineralization of the primary culture of pre-osteoblasts isolated from calvarial bone, long bones, and MC3T3 cells. The conditioned media of RET-depleted cells inhibits osteoblast differentiation and mineralization. The expression of alkaline phosphatase, osteocalcin, OPG, and osterix increased in pre-osteoblast incubated with MTC-CM. Compared to primary non-metastatic tumors, the OPG expression increases in tissues of sporadic MTC bone metastases harboring RET^{M918T} mutation. These results suggest that MTC with RET-activating mutations induces osteoblastic bone metastasis due to decreased bone resorption and increased bone formation.

#2762 Spatial proteomics of lung adenocarcinoma mouse models with divergent propensities for metastasis.

P. Ramkissoon, N. Mitchell-Hutchinson, J. Wells, R. Maser, T. Stodola, B. Hoffmann, A. Marchini, E. Bechtel, R. Doty, C. J. Bult;
The Jackson Laboratory, Bar Harbor, ME

Introduction: Lung cancer is the leading cause of cancer deaths worldwide with most deaths attributed to metastasis. Metastases in existing mouse models of lung adenocarcinoma (LUAD) is sporadic and often requires several months of aging. These factors limit these models for basic and pre-clinical research aimed at identifying mechanisms of metastatic disease. We have recently developed two novel mouse models of LUAD that feature constitutively active *Kras*, loss of *Trp53* function and truncated *Dicer1* in different cell types. The observed survival and metastatic phenotypes of the models are dependent on the cell type in which the genetic alterations are made. We applied spatial proteomics and metabolomics to investigate molecular drivers underlying the phenotypic differences in our models.

Methods and Results: Mouse models were generated by adding mutations in *Dicer1*, an RNAse III enzyme within the microRNA (miRNA) biosynthesis pathway, to a mouse model of *Kras*-driven LUAD. For both models, tumorigenesis was induced by conditional expression of an oncogenic allele of *Kras*, deletion of both alleles of *Trp53* and deletion of one allele of *Dicer1* in one cell type and the expression of a truncated *Dicer1* allele in a different cell type. Mice expressing $Kras^{G12D}$ and deleted *Trp53* in club cells without *Dicer1* truncation have a reported median survival of 28.6 weeks after tumor induction. We observed accelerated development of LUAD and lymph node metastasis (12.1 weeks) only when we induced tumorigenesis in club cells and truncate *Dicer1* in alveolar type II (ATII) cells. Induction of tumorigenesis in ATII cells and truncation of *Dicer1* in club cells did not accelerate tumorigenesis or lead to detectable metastasis. Prelminary spatial proteomic analysis revealed significant upregulation of proteins associated with mitochondrial respiratory chain complex I in the tumors of both models which is consistent with processes of bioenergetic adaptation of tumor cells to hypoxic conditions. Gene Ontology annotation term enrichment revealed that the tumors of the two models have distinctive molecular function profiles. Both models show significant disruption of amino acid metabolism but only the model with increased metastatic potential showed apparent disruption in metabolites associated with steroidogenesis.

Conclusions: Through cell type specific truncation/deletion of *Dicer1* we have generated a mouse model that rapidly develops *Kras*/*Trp53* driven LUAD and metastatic disease. Our findings suggest that tumorigenesis and metastasis are influenced by miRNA-mediated communication between different cell types. Additional studies are underway to link miRNA expression in these models to the results reported here for spatial proteomics and metabolomics. We will continue to develop this model to investigate the molecular mechanisms underlying metastasis.

#2763 A specific ribomethylome pattern in lung cancer is associated with increased risk of metastasis.

C. Pauli[1], D. Heid[1], C. Rohde[1], N. Krall[1], S. Delaunay[2], M. Kienhoefer[1], C. Tischer[3], M. Allgauer[1], M. Blank[1], F. Zhou[1], M. Kardorff[1], M. Thomas[4], H. Winter[4], S. Sandmann[5], M. Kriegsmann[1], M. Schneider[6], T. Muley[6], A. Brobeil[1], N. Baumer[5], S. Baumer[5], S. Raffel[1], A. Stenzinger[1], P. Schirmacher[1], J. Lu[1], J. Zaugg[3], M. Frye[2], C. Muller-Tidow[1];

[1]Heidelberg University Hospital (UKHD), Heidelberg, Germany, [2]DKFZ Heidelberg, Heidelberg, Germany, [3]European Molecular Biology Laboratory, Heidelberg, Germany, [4]Thoraxklinik, Heidelberg University Hospital (UKHD), Heidelberg, Germany, [5]University Hospital of Muenster, Muenster, Germany, [6]Thoraxklinik, Heidelberg University Hospital, Heidelberg, Germany

Non-coding RNAs drive cancer phenotypes and are associated with patients' outcome. SnoRNAs are required for the 2'-O-methylation (2'-O-Me) and pseudouridylation of ribosomal RNA (rRNA) thus being essential for ribosomal biogenesis and function. So far, the role of rRNA methylation (ribomethylation) for non-small cell lung cancer (NSCLC) pathogenesis is unknown. To investigate the role of ribomethylation we included samples from 92 patients with lung adenocarcinoma (pathological stage IA to IIB) for comprehensive multi-omics profiling. Amongst transcriptomics, small RNA sequencing, proteomics, and whole exome sequencing, ribomethylation as epitranscriptomic dimension was analyzed using RiboMethSeq. We focused the analysis on complete tumor resection samples. Here 47 out of 106 2'-O-Me sites were fully methylated in all tumor samples suggesting a crucial role for methylation at this position. Surprisingly, 59 sites had a dynamic methylation pattern. By combining ribomethylation sequencing data of dynamic sites with whole-exome-sequencing as well as transcriptome and proteome analyses using a multi-omics factor analysis (MOFA), we discovered a 2'-O-Me signature in a subset of NSCLC patients with a high risk of metastasis and poor prognosis. We termed the patient subset, with underlying ribomethylation signature, epitranscriptomic pro-metastatic phenotype (EPROMET). This phenotype was not associated with genetic mutations as analyzed by exome sequencing. Analysis of gene sets in both transcriptomics and proteomics showed an upregulation of secreted and extracellular matrix proteins in EPROMET patients. Alongside, the ribomethylation site with major contribution to the EPROMET signature; 18S-Um799, mediated through SNORD105/105B, was found to be the most dynamic within the dataset. It also showed the largest difference between EPROMET and non-EPROMET patients. For functional validation, lung cancer cell lines with knockout of snoRNAs contributing to EPROMET signature were generated using CRISPR/Cas9. Lung cancer cells lacking the corresponding rRNA modifications migrated slower *in vitro,* failed to grow at a distant site *in vivo* and were impaired in metastasis. Functionally, it was shown that the modulated ribomethylation signature effected translation of secreted proteins by altered mRNA binding to ribosomes. This study indicates the presence of a ribomethylome-associated phenotype of NSCLC related to metastasis and poor prognosis. Altered ribomethylation affects the ribosome function towards differential expression patterns of secreted proteins. Taken together, an epitranscriptomic pattern of 2'-O-Me is associated with invasion/migration properties of NSCLC cells and with development of metastasis. The ribomethylome may present a suitable biomarker and a potential therapeutic target.

#2764 Ubiquitin-specific peptidase 22 controls integrin-dependent cancer cell stemness & metastasis.

Q. Gao[1], K. Liu[1], Y. Jia[1], J. Wei[1], S. M. Chaudhuri[1], S. Wang[1], A. Tang[1], N. L. Mani[1], R. Iyer[1], Y. Cheng[1], B. Gao[1], W. Lu[1], Z. Sun[2], H. Liu[1], D. Fang[1]; [1]Northwestern University - Chicago, Chicago, IL, [2]Dalian Medical University-Dalian, Dalian, China

Integrins play critical roles in connecting the extracellular matrix and actin skeleton for cell adhesion, migration, signal transduction, and gene transcription. While the upregulation of integrins is thought to promote cancer stemness and metastasis, the mechanisms underlying their upregulation in cancer stem cells (CSCs) remain poorly understood. Herein, we show that the death from cancer signature gene, USP22, is essential in maintaining breast cancer cell stemness by promoting the transcription of a group of integrin family members, in particular, integrin β1 (*ITGB1*). Both genetic and pharmacological inhibition of USP22 largely impaired breast cancer stem cell self-renewal and prevented their metastasis. Reconstitution of Integrin β1 partially rescued USP22-null breast cancer stemness and their metastasis. At the molecular level, USP22 functions as a bona fide deubiquitinase to protect the proteasomal degradation of the forkhead box M1 (FoxM1), a transcription factor for tumoral *ITGB1* gene transcription. Importantly, unbiased analysis of the TCGA database revealed a strong positive correlation between USP22 and *ITGB1* in more than 90% of human cancer types, implying that USP22 functions as a key factor in maintaining stemness across a broad spectrum of human cancer types possibly through regulating *ITGB1*. To support this notion, immunohistochemistry staining detected a positive correlation among USP22, FoxM1 and integrin β1 in human breast cancers. Collectively, our study identifies the USP22-FoxM1-integrin β1 signaling axis as critical for cancer stemness and offers a potential target for antitumor therapy.

#2765 Novel WNT-RIP1-GDF15 pathway promotes migration and invasion of colorectal cancer cells.

A.-R. Kang, D. Kim, **J. Park**;
Korea Institute of Radiological & Medical Sciences (KIRAMS), Seoul, Korea, Republic of

Growth-differentiation factor 15 (GDF15) is a member of the transforming growth factor β (TGF-β) family protein, also known as NSAID-activated gene 1 (NAG-1) or macrophage inhibitory cytokine 1 (MIC-1), and is a major cause of cancer cachexia, cardiovascular disease, and various inflammatory diseases. Roles of GDF15 as major inflammatory response factor also have been demonstrated in animal models, and it has also showed various malignant functions such as regulating metabolism, promoting metastasis by inducing EMT in cancer. Here, we revealed a novel potential role for RIP1 in colorectal cancer (CRC) in enhancing metastasis by controlling WNT-RIP1-GDF15 signaling. We showed that WNT3A treatment increased the expression of GDF15 and GFRAL. Immunohistochemical analysis of human CRC tissue arrays consisting of primary cancer and metastatic cancer also confirmed that the expression of GDF15 and GFRAL was increased in metastatic cancer. Human XL cytokine assay, western blot, and ELISA results confirmed that GDF15 expression was reduced in cell lines in which RIP1 was knocked down. Reduction of GDF15 expression and secretion by RIP1 knockdown showed suppression of EMT induction resulting to decrease of migration and invasion of CRC cells. Taken together, these results suggest a novel EMT-enhancing role for RIP1 in the WNT pathway and suggest a novel WNT-RIP1-GDF15 pathway contributing to CRC malignancy by promoting EMT.

#2767 Exploring ADAR1 dependencies in breast cancer brain-metastases.

T. Sposito, E. E. Klacking, A. W. Ruiz, J. Pham, C. Jamieson;
University of California San Diego - UCSD, La Jolla, CA

Background: Adenosine deaminase acting on double-stranded RNA (ADAR1) is a recognized driver of epitranscriptomic (post-transcriptional) remodeling and tumor progression. Changes in amino acid sequence, mRNA splicing, and/or polyadenylation sites are only some of the adenosine-to-inosine (A-to-I) RNA editing effects. Under physiological conditions, ADAR1 activity prevents autoinflammation by inhibiting the accumulation of endogenous immunostimulatory double-stranded RNA and by suppressing the Z-RNA sensor ZBP1. Such mechanisms are exploited by cancer cells to desensitize tumor response to therapies, therefore augmenting aggressiveness. Approximately 10 to 20% of patients diagnosed with breast cancer (BC) will develop metastatic disease, which remains the leading cause of death in individuals with BC. We have hypothesized that ADAR1 and its interferon-inducible p150 isoform, play a pivotal role in promoting BC metastases since high levels of ADAR1 are associated with a worse prognosis in patients with high grade BC, especially in the triple-negative BC subgroup (TNBC), which is the most likely to develop brain metastases.

Methods: We established a humanized mouse model of breast cancer brain metastases (BC-BrM) using neonatal intracerebroventricular inoculation of MDA-MD-231 TNBC cells and primary patient derived metastatic cells in $Rag2^{-/-}\gamma c^{-/-}$ mice. Before implantation, MDA-MD-231 cells were transduced with a nanoluc-GFP reporter for tracing ADAR1 enzymatic activity in the brain metastatic niche. Lentiviral shRNA knockdown vectors targeting ADAR1, combined with over-expression vectors of full-length ADAR1 or the p150 deleted isoform were adopted to detect editing changes in the metastatic model through RNA-sequencing of BC-BrM.

Results: BrM derived from MDA-MD-231 implants display upregulation of ADAR1 p150 and activation of the WNT/β-catenin pathway compared to the non-implanted cell lines. Upon shRNA knockdown of ADAR1, decreased expression of BC stem cell markers was detected via FACS in MDA-MD-231 ADAR1 knocked-down versus control BC-BrM isolated cells. We are now exploring molecular pathways affected by ADAR1 loss/overexpression in establishing BrM.

Future Directions: We have developed a biorepository of primary patient-derived metastatic breast cancer samples and have begun the process of tracking metastatic kinetics and ADAR1 activation with the ADAR1 reporter in an orthotopic mouse model. Overall, this study will provide new insights into the molecular role of ADAR1 deaminase activity in establishing and maintaining metastatic niches.

#2768 Ribosome biogenesis score: Prognostic insights and drug responses in cancer.

A. R. Elhamamsy, R. S. Samant, L. A. Shevde;
University of Alabama at Birmingham, Birmingham, AL

Ribosome biogenesis, a crucial cellular process responsible for creating the cellular machinery required for protein synthesis, is vital for cell growth and proliferation. Cancer cells have dysregulated ribosome biogenesis, which contributes to uncontrolled cell growth and proliferation. Aberrant ribosome biogenesis not only drives the increased need for protein synthesis in rapidly developing cancer cells, but it also orchestrates tumor-related signaling cascades. We developed a robust scoring method for ribosome biogenesis and applied it to a broad range of TCGA tumor samples. By categorizing TCGA samples into distinct groups based on their ribosome biogenesis scores, we unveil significant prognostic associations in various cancer types. We used the scoring method and compared the scores with ssGSEA analysis using different ribosome biogenesis signatures in several databases to confirm these predictions. Furthermore, our research goes beyond predictive implications, delving into the biochemical complexities of ribosome biogenesis's impact on drug responses and resistance. This thorough investigation sheds light on the molecular complexities of ribosome biogenesis in tumors, providing useful insights with potential implications for refining strategies for cancer therapy.

#2769 Long non coding RNA H19/cell adhesion molecules circuitry as novel target and diagnostic tool for metastatic prostate cancer.

V. Pecci[1], A. Aiello[2], S. De Martino[2], C. Ripoli[1], D. Rotili[3], F. Pierconti[1], F. Pinto[4], C. Grassi[1], C. Gaetano[5], A. Pontecorvi[1], L. Strigari[6], A. Farsetti[2], S. Nanni[1]; [1]Universita' Cattolica del Sacro Cuore, Roma, Italy, [2]Consiglio Nazionale delle Ricerche, Roma, Italy, [3]Universita Sapienza, Roma, Italy, [4]Fondazione "Policlinico Universitario A. Gemelli IRCCS, Roma, Italy, [5]Istituti Clinici Scientifici Maugeri, Pavia, Italy, [6]S. Orsola Malpighi University, Bologna, Italy

In the complex tumor biology of prostate cancer (PCa), we previously contributed by demonstrating that estrogen receptor and hypoxia signaling promoted transcription of progression-associated genes. Notably, combined treatment, estrogens plus hypoxia, caused a significant down regulation of the long noncoding RNA H19, one of the most sensitive to these pro-tumoral stimuli. Mechanistically, H19 acts as transcriptional repressor: H19 over-expression decreases E-cadherin (CDH1) level causing epithelial-to-mesenchymal transition whereas H19 reduction promotes the expression of E-cadherin and β4 integrin (ITGB4) switching the tumor dissemination program toward an alternative mechanism, specifically the cohesive metastatic phenotype. We focused on this H19/cell adhesion molecules circuitry by investigating its role as: 1.Novel prognostic biomarker at the time of biopsies. eNOS, HIF2a and β4 integrin expression was evaluated by immunohistochemistry, H19 and CDH1 transcripts by Droplet Digital PCR on FFPE-biopsies in a retrospective cohort of PCa patients [n = 30; Gleason score GS≤ 7(3+4) n= 17, GS ≥7(4+3) n= 13; biochemical, local, or metastatic recurrence defining disease progression (n=8/30; time of recurrence: range 2-6 years)]. Importantly, multivariate analysis of combined biomarkers, named “Bioscore”, defined by the presence of at least 3 among HIF-2α, eNOS, CDH1, β4 integrin ≥cut off or H19≤cut off revealed its prognostic value for progression and Progression-Free Survival determined using the ROC analysis (p=0.003) and Kaplan Meier curve (p= 0.005), respectively. 2.Master regulator of metastatic program in vivo and ex vivo PCa experimental models. Upon H19 silencing, mimicking combined estrogens plus hypoxia treatment, luciferase-positive PC-3 and 22Rv1 cells led to increased E-cadherin and β4 integrin expression, enhanced tumor growth and metastasis formation at bone, lung, and liver in PCa mouse models. Further, treatment with H3K27 demethylase inhibitor, GSK-J4, rescued cell adhesion molecules expression by modulating H3K27me3 level at gene promoters, reduced metastasis number and size, and induced cell death in PCa-derived Organotypic Slice Cultures. Additionally, treatment with JQ1 and dBET6 BET protein family inhibitors) markedly reduced both E-cadherin and β4 integrin levels, cell proliferation and in vivo tumor growth. Intriguingly, H19 silencing increased BRD3 and BRD4 levels, implicating H19 in BRD transcription. Overall, this research enhances our understanding of the molecular mechanisms driving aggressive prostate cancer phenotypes, providing a foundation for new diagnostic and therapeutic strategies in prostate cancer management.

#2770 A novel MIRO2/MYO9B/RhoA signaling axis controls tumor cell invasion and metastasis.

Dillon P. Boulton[1], Connor J. Hughes[1], Valentina Vaira[2], Ajita Jindal[3], Masoom Raza[1], Stephen Connor Purdy[1], Shilpa Sant[4], Heide L. Ford[1], M. Cecilia Caino[1]

[1]University of Colorado Anschutz Medical Campus, Aurora, CO,[2]Universita degli Studi di Milano, Milan, Italy,[3]University of Pittsburgh, Pittsburgh, PA,[4]University of Illinois Chicago, Chicago, IL

Metastasis of cancer cells to vital organs remains the leading cause of cancer related deaths, emphasizing a strong need for actionable targets in advanced stage cancer. To address this, we study novel dysregulated mitochondrial signaling mechanisms that cells utilize to metastasize. Here, we focus on how outer mitochondrial membrane protein—Mitochondrial Rho GTPase 2 (MIRO2)—promotes tumor cell invasion and metastasis. Our previous work identified higher MIRO2 mRNA expression in cancer vs. normal patient samples in a multitude of cancer types, which correlated with worse patient outcomes. Furthermore, we demonstrated that MIRO2 was critical for prostate cancer cell growth and survival *in vitro* and *in vivo*. However, it remains unknown if MIRO2 only affects primary tumor growth or if this protein is important throughout tumor progression. Using siRNA mediated knockdown (KD) of MIRO2 we find MIRO2 KD ubiquitously reduces tumor cell invasion in breast, melanoma, pancreatic, and prostate cancer cells. Utilizing metastatic prostate and breast cancer models, we demonstrate that mice injected with MIRO2 shRNA cells have significantly lower metastatic burden compared to mice injected with control shRNA cells. To determine the mechanism that MIRO2 controls invasion and metastasis, we looked at which of the top protein-binding partners for MIRO2 may regulate tumor cell invasion. Of our top hits, we found that depletion of atypical myosin IXB (MYO9B) by siRNA most significantly reduced tumor cell invasion and phenocopied MIRO2 depletion. MYO9B has a well-defined role in controlling cell motility via inactivation of RhoA. Excitingly, we have found 1) MIRO2 KD results in increased active RhoA, phenocopying MYO9B KD, 2) dual ablation of MIRO2 and RhoA fully rescues tumor cell invasion, and 3) MIRO2 is required for MYO9B driven invasion. Taken together, we propose a novel signaling mechanism by which MIRO2 broadly promotes invasion and metastasis through MYO9B dependent inactivation of RhoA.

#2771 Increased mtDNA copy number via EPOR signaling: A potential mechanism for metastatic dissemination in head and neck squamous cell carcinoma.

A. Chauhan[1], G. S. Boora[1], S. Ghosh[2], S. K. Patra[2], R. K. Verma[1], J. Bakshi[1], D. Chatterjee[1], R. Srinivasan[1], S. Ghoshal[1], A. Maitra[2], A. Pal[1];
[1]Postgraduate Institute of Medical Education & Research (PGIMER), Chandigarh, India, [2]National Institute of Biomedical Genomics, Kalyani, Kolkata, India

Introduction: Head and Neck Squamous cell carcinoma (HNSCC) is characterized by high degree of invasion, locoregional metastasis, relapse which leads to overall poor prognosis. The molecular mechanism responsible for aggressiveness is poorly understood. A better understanding of molecular pathways involved shall precede the identification of newer diagnostic tools and therapeutic targets. We explored EPOR signaling pathway in Circulating tumor cells (CTCs) and HNSCC cell lines.

Methods and Results: By using a validated in-house CTC isolation protocol, which addresses various drawbacks of currently available techniques and isolates CTCs suitable for various downstream molecular analysis, we isolated CTCs from HNSCC patients. The whole transcriptome analysis was performed from CTCs using ultra-low cell number RNA sequencing and corresponding primary tumors in 24 paired samples. We found a significant transcriptomic heterogeneity in CTCs, which are associated with overall disease outcome in HNSCC patients. To explore the plausible molecular pathways, we also identified 521 differentially expressed genes in CTCs with respect to primary tumors and various canonical pathways including oxidative phosphorylation, TCA cycle, cytokine-cytokine receptor interaction signaling, and ECM receptor interaction were enriched in CTC samples. Overexpression of erythropoietin receptor (EPOR) along with various genes encoded by mitochondrial genome and genes involved in maintenance of mtDNA in CTCs as compared to primary tumors was an important finding from our data. When analyzed in depth, there was a significant positive correlation between various genes involved in mtDNA maintenance (ABAT, NT5M) and encoded by mitochondrial genome (MT-ND1, MT-ND2, MT-ND4, MT-ND5, MT-ND6, MT-CO1, MT-CO2, MT-ATP6, MT-CYTB) with EPOR expression in our RNA seq data which is also substantiated by analyzing TCGA data. We confirmed these findings experimentally in HNSCC cell lines Cal 27 and FaDu. It was also observed that metastatic cell line FaDu has significantly higher mtDNA content as compared to non-metastatic cell line Cal 27, which was correlated with EPOR expression. Treatment with low dose Erythropoietin (0.1IU/mL) which a natural ligand for EPOR, enhanced mtDNA content in both the cell lines at low doses and boosted the metastatic capability while minimal effect on cell proliferation was observed.

Conclusion: EPOR signaling might promote the metastatic ability of cancer cells and may act as a potential target for cancer dissemination and metastasis.

#2772 Mechanisms linking STK11 loss with metastatic potential in KRAS-mutated lung adenocarcinoma.

C. M. Royer, L. K. Bialek, H. M. Sarausky, S. M. Prior, G. Nandagopal, P. B. Deming, D. J. Seward, M. N. Scheiber;
University of Vermont, Burlington, VT

Metastasis is one of the major determinants of worsened patient prognosis and occurs in roughly 50% of lung adenocarcinoma (LUAD) patients at the time of diagnosis. Late-stage diagnosis of LUAD often results in the accumulation of a wide range of mutations in tumor cells, with altered *KRAS* being the most frequently encountered oncogenic driver. Co-mutation of the tumor suppressor *STK11* is also common and occurs in 10-15% of KRAS-driven LUAD. Retrospective patient studies have demonstrated that concurrent oncogenic *KRAS* and *STK11* loss-of-function mutations are associated with metastatic disease, poorer patient survival, and inferior therapy response. The purpose of this study was to identify molecular mechanisms by which STK11 loss results in a greater metastatic potential in *KRAS*-driven LUAD in hopes of exploiting that knowledge to improve patient outcomes. For our studies, we utilized the *KRAS*-mutated, STK11-intact human LUAD cell line NCI-H2009. Both parental and ΔSTK11 (generated by CRISPR/Cas9) H2009 cells were seeded in Transwell® inserts coated with fibronectin. As expected, H2009 ΔSTK11 cells displayed a 1.6-fold increase in trans-well migration compared to the parental line (SEM 14393 ± 877.3 cells, n=6; $p<0.0001$). To assess the invasive properties of parental and ΔSTK11 cells in a three-dimensional environment, spheroids generated by hanging drop culture were embedded in Matrigel and imaged by light microscopy at zero and 24-hours post-embedding. Analysis demonstrates a 2.4-fold increase in invasion in ΔSTK11 cells compared to parental cells (SEM 0.03 ± 0.01 mm^2, n=19-21; $p<0.0001$). Three-dimensional LUAD spheroids have been reported to more closely recapitulate *in-vivo* tumor transcriptomes compared to two-dimensional monolayer cultures. qRT-PCR analyses of our spheroids demonstrate that loss of *STK11* promotes a significant increase in the expression of lung cancer stem cell markers CXCR4, NANOG, CD44, and OCT4 (n=3-6; $p<0.002$). These markers are known to support stem cell maintenance, chemoresistance, as well as metastatic potential, suggesting a mechanistic link between STK11 and their transcriptional regulation. To assess the impact of *STK11* loss on early and late-stage metastasis *in-vivo*, we will use an embryonic zebrafish xenograft model. Zebrafish represent a tractable metastasis model due to the number of conserved human homologs - most notable being the CXCR4/CXCL12 axis which models cross-communication between zebrafish endothelium and cognate human tumor ligands. Current and future studies focus on investigating the role of STK11 in regulating stem cell markers; thereby identifying potentially novel therapeutic targets for *STK11* and *KRAS* co-mutated LUAD patients.

TUMOR BIOLOGY: Cancer Stem Cells and Their Microenvironment
Poster Session

#2776 Exploring the differences between brain tumor initiating cell extracellular vesicles and secreted factors that influence the tumor microenvironment.

M. Russo, M. Ulloa Navas, E. Norton-Ramos, A. Quinones Hinojosa, H. Guerrero Cazares;
Mayo Clinic Florida, Jacksonville, FL

Glioblastoma (GBM) is the most common and lethal primary brain tumor in adults. Within the tumor, there is a subtype of cells deemed brain tumor initiating cells (BTICs), which contribute to tumor progression, therapy resistance, and tumoral heterogeneity. The tumor microenvironment, surrounding tumors, contains an ecosystem of cells in which BTICs can interact with and further promote tumor progression. In the lateral wall of the lateral ventricles, the neurogenic niche of the subventricular zone (SVZ), contains neural progenitor cells (NPCs) that self-renew and generate highly migratory neuroblasts. Interestingly, GBM tumors proximal to the SVZ are more proliferative, migratory, and negatively impact the survival of patients. We have previously observed that the presence of GBM induces reciprocal changes to the SVZ altering its neurogenic capacity and resulting in a more proliferative tumor. BTICs share similar self-renewal capacity to NPCs and may exert intercellular communication resulting in increased malignancy features. The mechanisms of intercellular communication, present in the SVZ include paracrine, autocrine, direct cell contact, gap junctions, nanotubes, and more recently extracellular vesicles (EVs). However, the exact mechanisms of how BTICs communicate with NPCs is not well understood. EVs are a heterogenous group of cell-derived membranous structures that serve as means of intercellular communication, allowing for cells to exchange proteins, lipids, RNA, and other genetic material. Cancer cells release higher amounts of EVs than non-malignant cells, and these EVs help communicate with other nearby cells, leading to promotion of tumorigenesis. We have observed that BTICs-derived EVs increase the proliferation of human NPCs, while altering their morphology and expression of stem cell markers. These effects are not observed when NPCs are treated with vesicle-free BTIC-derived secreted factors. To investigate the distinctions between BTIC secreted factors and protein cargo contained in BTIC-EVs, we employ the proximity protein labelling system, TurboID, and express this system in BTIC-EVs. The overarching goal of this project is to characterize BTIC-derived EV cargo to identify proteins that modify the GBM tumor microenvironment. **We hypothesize that the phenotype of non-cancer NPCs is altered by distinct protein cargo contained in BTIC-derived EVs.** The results of these experiments will help us to elucidate what BTIC-specific EV cargo impacts the tumor microenvironment, with the potential of revealing therapeutic targets for GBM.

#2777 A unique sub-population of PDGFRB+ glioma-associated mesenchymal stem cells constitute the perivascular niche in murine glioblastoma.

M. F. Zaman, S. K. Singh, A. Hossain, L. M. Phillips, J. Gumin, D. Ledbetter, B. Milutinovic;
The University of Texas MD Anderson Cancer Center, Houston, TX

Microvascular proliferation (MVP) and spatial heterogeneity are defining histological features of glioblastoma (GBM). Using *ex vivo* culture method to analyze human GBMs we have previously identified mesenchymal stem cell (MSC)-like cells, called glioma-associated-MSCs (GA-MSCs) in the heterogenous tumor-microenvironment (TME) of GBMs. Like pericytes, fibroblastic cells and smooth muscle cells (SMCs), these GA-MSCs reside in the perivascular niche (PVN) within GBM, and their presence correlates with MVP, decrease in immune cell counts, and poor prognosis. However, the impact of GA-MSCs on the TME remains correlative, and to date, a causative role of GA-MSCs in MVP and immune evasion has not been established *in vivo*. We hypothesize that recruited GA-MSCs promote MVP and enhance immune evasion in the GBM-TME. To begin to address this hypothesis, we first identified and characterized GA-MSCs at single-cell resolution in an immunocompetent murine GBM model. We sorted tumor, immune, and non-tumor-non-immune (NTNI) cells from GFP-labelled GSC005 tumors in C57Bl/6 mice and performed scRNA-seq. Tumor cells (GFP^+ cells) clustered together into 13 distinct cell states. Of the immune cells ($CD45^+$), the most abundant cell types were microglia (33.9%), macrophages (31.9%), T cells (10.3%), dendritic cells (7.5%) and B cells (1.4%), mimicking human GBM. In the NTNI compartment, we identified 17 clusters, which mapped to endothelial cells, oligodendrocytes, astrocytes and other cell types. Interestingly, there were 4 distinct cell clusters that exclusively expressed platelet-derived growth factor receptor beta (PDGFRB). Three of these clusters mapped to pericytes, SMCs and fibroblastic cells. The fourth cluster expressed both adipose tissue and bone marrow MSC markers, identifying for the first time, GA-MSCs in murine GBM. Next, to define the spatial organization of GA-MSCs and their relationship to immune cells in the GBM TME, we conducted spatial proteomics. GA-MSC counts were significantly higher in the PVN compared with the avascular niche (AN) ($p= 0.009$) and GA-MSCs were absent in contralateral non-tumor regions. Interestingly, GA-MSCs co-localized with SMCs, fibroblastic cells and pericytes as well as pro-tumorigenic macrophages/microglia ($Iba1^+/CD163^+$) in the PVN indicating potential interactions between these cell populations. In conclusion, we have identified for the first time, MSC-like cells in the PVN of murine GBM. Our results suggest that these GA-MSCs are recruited to the TME where they may promote MVP, a hallmark of GBM, and interact with immunosuppressive immune cells. Building on these observations, future experiments will investigate the extent to which GA-MSCs drive MVP formation and immune evasion in GBM.

#2778 Influence of the differentiation strategy on the phenotypic and genotypic features of iPSC derived NK cells.

M. Huyghe, C. Desterke, J. Imeri, N. Belliard, **A. G. Turhan**, A. Bennaceur Griscelli, F. Griscelli;
INSERM U1310, Villejuif, France

The iPSC-derived NK (iNK) cells offer new perspectives to produce large-scale of homogeneous immunotherapeutic cellular products and open the way towards manufacturing off-the-shelf cancer immunotherapies. Numerous strategies and protocols of differentiation of iPSCs toward NK lineage have been published in the last decade. Nevertheless, the embryological development of the NK cells and the impact of the differentiation strategy on the activity of the NK cells are still not clearly understood. Furthermore, very few studies have compared different NK differentiation strategies from iPSC. this study, we compared two previously reported protocols for NK cell generation from the same iPSC line, one feeder-based and the other feeder-free. In the first protocol, 3D hematopoietic differentiation was followed by lymphoid differentiation, using an OP9 DLL4 expressing feeder cell line. The second protocol employed a clinical-grade approach, utilizing the “spin embryoid body” method to generate primitive hematopoietic progenitors. Subsequently, these progenitors were differentiated towards the NK lineage in a feeder-free environment. Hematopoietic progenitors produced by these protocols have distinct phenotypes, suggesting variations in their maturity levels. Furthermore, the protocols have different kinetics of differentiation revealed by CD56 and CD7 phenotypes. Although, both protocols were able to efficiently generate functional and mature NK cells, characterized by the expression of activating and maturity ligands but with a distinct transcriptomic profile. iNK cells generated using feeders exhibit a more pronounced inflammatory profile with the expression of hallmark NFKB and STAT3 signaling pathways. In contrast, feeder-free iNK cells have a more proliferative profile as evidenced by increased expression of cell cycle factors such as E2F or Myc. Feeder-based iNK cells exhibit increased expression of transcription factors involved in NK cell differentiation, such as GATA2, STAT1, and IRF1. These transcriptional variances are reinforced by superior functionality observed in feeder-based NK cells compared to feeder-free NK cells, evidenced by increased degranulation (p-value < 0.0001) and cytotoxicity (p-value = 0.0004) at a 1:2 (effector-to-target) ratio against the K562 cell line. Our findings indicate that, despite the advantages of the feeder-free strategy, the feeder-based protocol remains more efficient and produces iPSC-derived NK cells with an enhanced cytotoxic profile in vitro. Our comprehensive transcriptional analysis offers significant insights into the biological and functional properties of iNK cells. This information has the potential to oncover novel mechanisms for NK differentiation strategies from iPSCs.

#2779 The significance of TIMP-1 and hypoxia in cancer stemness: A synergistic role in chemoresistance.

I. Thirusenthilarasan[1], W. Xiao[2], M. V. Rojiani[1];
[1]Penn State University, Hershey, PA, [2]Augusta University, Augusta, GA

Chemotherapeutic resistance in non-small-cell lung cancer (NSCLC) poses a formidable clinical challenge. Numerous studies have highlighted the critical role of tissue inhibitor of matrix metalloproteinase-1 (TIMP-1) in tumorigenesis and, increasingly, in the development of chemoresistance. We have studied multiple aspects of the MMP-independent, tumor-promoting function of TIMP1 in human NSCLC. Our recent studies have found a pivotal role for TIMP1 in chemoresistance. In order to gain an enhanced comprehension of the mechanisms underpinning TIMP-1-mediated chemoresistance, we have sought to determine the contribution of CSCs and hypoxia. TIMP-1 plays a role in propagating stemness, although relatively unexplored in the context of CSCs within NSCLC. A second crucial factor in the development of chemoresistance in NSCLC is the interplay between intratumoral hypoxia and CSCs. As the tumor grows, metabolic demand for oxygen increases and hypoxic regions are seen in areas furthest from the blood vessels. We have shown TIMP1 levels to increase under experimentally-induced hypoxia. In the present study, we cultured NSCLC cell lines and their TIMP1 KD clones in an assay with serum-free media and found a significant decrease in spheroid size in TIMP1 KD clones. Postulating a reduction in CSC population in KD clones, we determined the NSCLC CSC markers CD133 and ALDH's expression in the NT and KD TIMP1 clones. Flow cytometry results showed that $CD133^{pos}$ and $ALDH^{high}$ populations were significantly decreased in TIMP1 KD clones relative to NT clones. Moreover, KD clone of TIMP1 showed a decrease in the levels of CSC-specific Transcription factors Oct 4A and Nanog. Taken together, our findings confirm that reduction in TIMP1 expression negatively impacts CSC populations. Furthermore, we determined the mRNA levels of CD44, another CSC marker also expressed in lung cancer is upregulated under hypoxia (1% O_2) in both the NT and KD clones of TIMP1. Thus, we postulate that TIMP1 enhances chemoresistance by promoting CSC propagation within a hypoxic tumor microenvironment.

#2780 Induced pluripotent stem cell (iPSC) based vaccines potentializes anti-CTLA4 immune response in a murine lung carcinoma model.

F. Griscelli, D. Chaker, N. Oudrhiri, C. Desterke, **A. G. Turhan**, A. Bennaceur Griscelli;
INSERM U1310 Universite Paris Saclay, Villejuif, France

Despite the development of new immunotherapy strategies, lung cancer remains the leading cause of cancer-related deaths. One of the reasons is attributed to the persistence of cancer stem cells (CSCs) within the tumor, contributing to drug resistance, dormancy and metastatic spread. To eradicate CSCs, iPSC-based vaccination represents a novel approach based on the paradigm that CSCs and iPSCs share common tumor associated antigens (TAAs) with the ability to elicit a strong anti-tumor immune response.We previously showed that induced allogeneic pluripotent stem cells (miPSCs), combined with a histone deacetylase inhibitor (HDACi), induced a major reduction of tumor growth and metastatic spread to lungs in an aggressive triple negative breast cancer model (4T1) in syngeneic mice. We report here the use of the same protocol in a lung carcinoma model using LLC1 cell line in combination with an anti-CTLA4 antibody. We compared the effectiveness of allogenic miPSCs treatment alone or with an anti-CTLA4 mouse antibody on mice-bearing LLC1-Luc tumors (mean+se: 17,5+0,6 mm^3). Five mice received 5 subcutaneous (SC) injection of $2x10^6$ miPSCs, 5 mice received 3 intraperitoneal injections of anti-CTLA4 antibody at 5mg/kg and 5 mice were treated with the combinatory regimen (miPSCs and anti- CTLA4) with the same doses. In addition, all treated mice received a HDACi in the drink water throughout the experience.After 24 days, all tumor volumes from the 3 groups were significantly reduced compared to the control mice receiving only PBS. We obtained a reduction of 72% (p=0.007) and 74% (p=0.009) respectively for the mice treated solely with miPSCs or anti-CTLA4. An important synergic effect was obtained for the mice treated with miPSCs and anti- CTLA4 with a reduction of the tumor size by 92% (p=0.005) compared to the control mice. We also found a significant inhibition of metastatic spread to lungs for the 3 groups that was more pronounced in mice receiving the combination treatment with a significant reduction of 91 % compared to the control group. All these therapeutic effects were correlated with a significant increase of CD4+ and CD8+ cells that was more pronounced in mice receiving the combinatory regimen.We also have performed single-cell RNA sequencing analysis (10x Genomics) of LLC1 tumors treated with miPSCs and anti- CTLA4 compared to mice treated with monotherapy and untreated mice. T-distributed stochastic neighbor embedding plot reveals distinct clusters of stromal and immune cells across tumors with a significant upregulation of CD8+ and CD4+ T cells in mice receiving the combinatory regimen.Overall, these results demonstrate for the first time the clinical relevance of using an off-the-shelf allogeneic iPSC-based vaccine combined with an anti-CTLA4 antibody as a new anti-cancer immunotherapy strategy against aggressive non-small cell lung cancer (NSCLC) with metastatic potential.

#2781 GBM cells mimic regulatory T cell function to protect the CSC pool from immune surveillance in recurrent GBM.

H. Lopez-Bertoni[1], S. Sall[2], H. Khela[2], J. Korleski[2], K. Luly[1], M. Johnson[2], B. Lal[2], A. Johnson[1], S. Tzeng[1], J. Green[1], J. Laterra[1];
[1]Johns Hopkins School of Medicine, Baltimore, MD, [2]Hugo W Moser Institute at Kennedy Krieger, Baltimore, MD

Glioblastoma (GBM) is the most lethal and aggressive form of brain cancer, with incredibly high recurrence rates and virtually no long-term survival. Despite our growing understanding of GBM at the molecular level, we still don't fully comprehend the molecular mechanisms driving recurrence in GBM. Current knowledge indicates that Glioma Stem Cells (GSCs) drive a resistant cell phenotype in GBM. Understanding the molecular events coordinated by GSCs leading to therapy-resistance can provide key advancements on how we treat recurrent GBM (rGBM). Mechanisms of GSC immune escape are considered fundamental to clinical GBM growth and recurrence. The cross talk between cancer cells and the immune system is now classified as a hallmark of cancer. The current dogma is that cancer cells, including GSCs, influence recruitment of immune-suppressive cell subsets to tumor tissue, *however how subsets of GSCs mimic this immune-suppressive effect within the tumor microenvironment remains to be elucidated.* Single-cell RNA sequencing analysis of GBM neurospheres revealed a previously unrecognized Oct4/Sox2^{high}/FOXP3^{-} cell subpopulation with high expression of TGFβ1, CD39, CD73, PD-L1, and Galectin-1, a gene expression fingerprint typically associated with regulatory T cell (Tregs) and their immune suppressive functions within the tumor microenvironment. Bioinformatics analysis of public databases shows that the above-mentioned genes are enriched in the mesenchymal GBM subtype and highly correlated with TGFβ type II receptor (TGFBR2) expression in clinical GBM. Mechanistically, we show that blocking TGFBR2 or XBP1 signaling, key intermediary of this process, counteracts the immune-suppressive phenotype of rGBM cells by restoring CD4 and CD8 tumor killing capacity and reversing exhaustion in co-culture experiments. siRNA-mediated knock-down of TGFBR2 in rGBM cells also decreased CD206 expression and reduced release of anti-inflammatory chemokines in THP1 cells. By combining miRNA-based network analysis and advanced nanoparticle formulation for miRNA delivery we show that miR-16/124-3p effectively target all nodes of this immunosuppressive axis successfully blocking the immunosuppressive nature of rGBM cells. This research provides the first description of such neoplastic cells in any malignancy and has high potential translational impact since targeting these tumor cell subsets and their immunosuppressive mechanisms may be critical to the successful development of GBM immunotherapies.

#2782 Characterization of quiescence-associated secretory profile (QuASP) in cancer: A novel defining feature and therapeutic target.

Q. Jiang[1], S. Panesso- Gomez[1], D. Natesan[1], M. L. MacDonald[2], R. J. Buckanovich[3];
[1]Magee-Womens Research Inst. & Foundation, Pittsburgh, PA, [2]University of Pittsburgh, Pittsburgh, PA, [3]Magee-Womens Research Inst. & Foundation, UPMC Hillman Cancer Center, Pittsburgh, PA

Senescent cells have a unique senescence-associated secretory profile (SASP) and understanding SASP has contributed to numerous advances in knowledge on aging and cancer biology. Quiescence, which is an important yet poorly understood mechanism for chemoresistance, is related but distinct from senescence. Quiescence shares a non-proliferative feature with senescence but is a reversible state in which quiescent cells can reenter the cell cycle. We hypothesized that, analogous to senescent cells, quiescent cells have a distinct quiescence-associated secretory profile (QuASP) and that defining the QuASP will uncover new genes and pathways associated with cancer cell viability and therapeutic resistance. Indeed, suggesting quiescent cells have a unique and biologically important secretome, we found that tumor conditioned medium (TCM) from quiescent ovarian cancer cells (qOvCa) vs. TCM from proliferating cancer cells increased chemoresistance. Similarly, TCM from quiescent cancer cells vs. TCM from proliferating cancer cells suppressed T cell proliferation and INF-gamma/Granzyme B secretion, suggesting a QuASP immunosuppressive effect. RNASeq analysis of qOvCa cells revealed the secreted factor Follistatin (FST) is upregulated in qOvCa and acted as a paracrine pattern to induce chemoresistance. Furthermore, FST was found to be upregulated in peritumoral fluid following chemotherapy and FST levels in patients with OvCa predicted poor prognosis. To identify additional QuASP factors, we used an ER-BIOID labeled system and LC-MS/MS to characterize the secreted proteins from qOvCa induced by serum starvation compared with normal cells in three OvCa cell lines (PT412, PT340, HEY1). Quiescent OvCa cells indeed have a secretome that is highly unique from proliferating cells, with 137/577 upregulated proteins (LFC>1) and 65/577 downregulated proteins (LFC<-1 or no detection in quiescence). Several proteins identified as upregulated have been linked to immunosuppression and/or chemoresistance, oncogenesis and cell cycle were selected for validation and further analysis (CLU, VGF, SERPINE1). In conclusion, we find quiescent cells have a unique quiescence associated secretory profile and that the QuASP induces chemoresistance and immunosuppression. As such, this study has important implications for cancer therapy.

#2783 The exosomes from cord blood stem cells, containing novel miRNAs, induce apoptosis in melanoma cells and enhance T cell anticancer function.

M. Mojgan Najafzadeh[1], A. Baumgartner[2], S. Jafarinejad[1], Z. Karimi[1], M. Isreb[1], P. Akhbari[3], N. Ghaderi[4], F. Sefat[1], S. Heidari Keshel[5], P. Naeem[1], R. Ghaderi[6], J. E. Gomez[1], D. Anderson[1], A. Wright[4];

[1]University of Bradford, Bradford, United Kingdom, [2]York St John University, York, United Kingdom, [3]University of Exeter, Exeter, United Kingdom, [4]Bradford Teaching Hospitals NHS Foundation Trust, Bradford, United Kingdom, [5]Shahid Beheshti University, Tehran, Iran, Islamic Republic of, [6]Imperial College London, London, United Kingdom

Regulatory T (Treg) cells expressing FOXP3 play a critical role in suppressing immune responses against anti-tumor immune responses. However, their presence in tumor tissues is often associated with poor prognosis. Cord blood stem cell-derived exosome vesicles (CBSC-EV) constitute a valuable source of lipids, microRNAs, and proteins, that are essential for cell-to-cell communication and provide therapeutic benefits.

This study aimed to investigate the contents of CBSC-EV, identifying several known miRNAs (from *Let7* and *Let5* families) and two unknown miRNAs. Healthy lymphocytes, fibroblasts, and CHL1 amelanotic melanoma cell lines were transfected with these two novel miRNA inhibitors, and the changes before and after treatment compared to CBSC-EV and H_2O_2 were examined. Following treatment, the cells underwent a 24-hour incubation period, during which the level of cytotoxicity was assessed using CCK8, and the degree of DNA damage incurred was quantified with the Fast Microplate DNA damage assay. To further investigate the effects of treatment, RNA sequencing was conducted on both healthy and cancerous cells. The results demonstrated that CBSC-EV and novel miRNAs induced cytotoxicity in cancer cells, while in healthy cells, the DNA damage was repaired and cell viability was significantly increased ($p<0.001$). RNA sequencing revealed that following treatment with CBSC-EV and both CBSC-EV+N1 and N2 inhibitors in malignant melanoma cells, the expression of genes involved in the cytokine-mediated signaling pathway, cytokine-cytokine interaction, and cytokine activity were enhanced. In healthy cells treated with CBSC-EV and novel miRNA inhibitor transfection, the MT-CO1 gene was upregulated, contributing to cytochrome-c oxidase activity.

This study presents evidence of the potential use of novel miRNAs as genetic material for cancer therapeutics in the future. Additionally, the findings suggest that these miRNAs could be used as an immune system modulator against melanoma. These findings demonstrate that miRNAs can effectively suppress resistance to anticancer cytotoxic therapy, which is a common feature of cancer cells. This suggests that miRNAs can potentially enhance current cancer therapies.

#2784 Fatty acid synthase enhances stem-like properties of normal intestinal and colorectal cancer cells via an increase in notum expression and secretion.

C. O. Kelson, J. Weber Tessmann, D. He, C. Wang, Y. Zaytseva;
University of Kentucky, Lexington, KY

Introduction: Overexpression of lipogenic enzymes has been associated with a poor clinical outcome in colorectal cancer (CRC). Fatty acid synthase (FASN) synthesizes palmitate which can be utilized for post-translational modifications of various proteins. Notum, a palmitoleoyl-protein, prevents the downstream activation of Wnt signaling by de-palmitoylating Wnt ligands. Notum is also a CRC stem cell marker, and its expression correlates with poor prognosis in CRC. We found that upregulation of FASN is associated with an increase in Notum expression in mouse adenoma tissues. Therefore, the purpose of this study is to elucidate the mechanisms and contribution of FASN/Notum axis in CRC.

Methods: Adenoma and normal intestinal organoids, established from Apc^{Min}/VillinCre-ERT2 and Apc/VillinCre-ERT2 mouse models with hetero- and homozygous deletion of FASN. 4-hydroxytamoxifen (4-OHT) and TVB-3664 (FASN inhibitor) treatments were used to assess the effect of FASN deletion/inhibition on organoid growth and viability. LIVE/DEAD™ Viability/Cytotoxicity and Cell Titer-Glo® 3D Cell Viability Assays were used for quantitative analysis of growth. Human NOTUM/Protein notum homolog ELISA Kit was used to analyze Notum secretion. CRC cells, NTC and FASN shRNA, and control and FASN overexpression, were used for Notum analysis.

Results: The TCGA data analysis shows that Notum is significantly upregulated in CRC and its expression correlates with expression of FASN in tumor tissue. Utilizing qRT-PCR and Western blot analyses, we show that downregulation of FASN leads to a decrease in expressions of active β-catenin, Notum, and other stem cell markers in transgenic mouse models. Moreover, 4-OHT-mediated inhibition of FASN results in decrease viability and size in Apc^{Min}/ FASN/VillinCre-ERT2 and Apc/FASN/VillinCre-ERT2 organoids. Consistently, shRNA-mediated deletion of FASN decreases expression of Notum in CRC cells. In contrast, overexpression of FASN increases the expression levels of active and total β-catenin, Notum, and other stem cell markers in SW480 cells. We show that normal epithelial cells exposed to CRC cell medium exhibit stem-like phenotype which is reduced when cells are exposed to medium collected from Notum shRNA knockdown cells. Moreover, the addition of recombinant Notum restores this phenotype.

Conclusion: In summary, downregulation of FASN leads to a decrease in expression of Notum and is associated with morphological changes and significant decrease in viability in organoid models. Conversely, FASN overexpression upregulates Notum expression suggesting a potential cross talk between *de novo* lipid synthesis and Notum. Delineating the role of FASN regulation of stem-like properties via upregulation of β-catenin signaling and expression of Notum and other stem cell markers will provide the rationale for targeting the FASN/Notum axis in CRC.

#2785 Beyond the role of transcobalamin 1 (TCN1) as a vitamin B12-binding protein in hepatocellular carcinoma.

G. Muliawan, C. Leung, T. Lee;
Hong Kong Polytechnic University, Hong Kong, Hong Kong

Hepatocellular carcinoma (HCC) is a common form of primary liver cancer and is associated with poor prognosis. Although sorafenib and lenvatinib have shown promising results in HCC treatment, their clinical benefits for patients have been limited owing to drug resistance and tumor relapse. This may be associated with the presence of tumor-initiating cells (T-ICs), which require further investigation to identify the key pathways or molecules involved in their regulation. Through *in vitro* enrichment of liver T-IC populations via a series of sphere passages under treatment with chemotherapeutic drugs, subsequent bulk RNA sequencing analysis identified a vitamin B-12 binding protein, transcobalamin 1 (TCN1), as the most upregulated molecule in such enriched T-IC populations. This result was consistent with the enrichment profiles of the stem cell signature in $TCN1^{High}$ HCC samples in the clinical dataset.
TCN1 is a secretory protein expressed at high levels in salivary glands and glandular cells; however, its function beyond its native role as a vitamin B12-binding protein in the regulation of T-ICs is unclear. Using lentiviral shRNA overexpression and knockdown approaches, we identified a critical role for TCN1 in regulating the properties of T-ICs, including self-renewal, invasiveness, tumorigenicity, and drug resistance, through *in vitro* and *in vivo* assays. Clinically, we also observed a substantial increase in TCN1 mRNA signatures in HCC samples, which was associated with poor prognosis of HCC patients. By analyzing the TCGA-LIHC dataset with confirmation by immunoprecipitation, we report, for the first time, that TCN1 directly interacts with integrin subunit alpha 3 (ITGA3), thereby regulating the Notch signaling pathway. Furthermore, ELISA results revealed the presence of the secretory form of TCN1 in HCC cells, which exerts a T-IC-enhancing effect on HCC cells via autocrine regulation.
In conclusion, our study provides novel insights into how TCN1 functions in HCC via a non-canonical mechanism, which goes beyond its conventional role as a vitamin B12-binding protein and uncovers a potential novel therapeutic target for HCC.

#2786 Seizure related 6 homolog (SEZ6), a cancer stem cell-specific secreted protein, is a novel GBM therapeutic target.

A. Mukherjee, S. Sengupta, A. Chowdhury, A. Srivastava, K. Somasundaram;
Indian Institute of Science, Bengaluru, India

Cancer Stem Cells (CSCs) are known to initiate a tumor, resist chemotherapy and radiotherapy, and also cause tumor recurrence. A deeper understanding of CSC biology is needed for a more effective therapeutic response. An integrative study of regulated transcriptome of human patient-derived Glioma Stem-like Cells (GSCs) using Gene Ontology (GO) analysis and Gene Set Enrichment Analysis (GSEA) identified a potential role for GSC in tumor angiogenesis. We chose Seizure Related 6 Homolog (SEZ6), one of the Wnt target genes, for further study, as its downregulation inhibited the potential of GSCs to induce angiogenesis without impacting GSC growth. SEZ6, a transmembrane protein, is shed upon cleavage by Beta-site APP cleaving enzyme 1 (BACE 1) and is known to be involved in normal neuronal functions; however, its role in cancer has not been studied yet.

SEZ6 silencing inhibited GSC-initiated tumor growth in an intracranial orthotopic mouse model due to reduced tumor angiogenesis and increased the mouse survival. Pre-treatment with a pharmacological inhibitor of BACE1 (BACE1i) prevented SEZ6 shedding from GSCs and inhibited the ability of the GSC-secretome to induce angiogenesis. Further investigations are ongoing to establish the use of BACE1i or BACE1-silencing as a novel therapeutic strategy to inhibit SEZ6-mediated tumor angiogenesis.

We also carried out a protein array-based investigation, which revealed that SEZ6 induced IL8 in endothelial cells to induce angiogenesis. Additional investigation showed that SEZ6 activated the TGFβ pathway in endothelial cells to induce IL8. SEZ6 interacted with TGFβRII as seen by confocal microscopy and co-immunoprecipitation. Generation of various deletion mutants of SEZ6 revealed that three Sushi [also known as complement control protein (CCP) module or the short consensus repeat (SCR)] domains, 3, 4, and 5, interacted with TGFβRII. Molecular docking and dynamic simulation studies identified Sushi-3 domain as the mediator of the interaction between SEZ6 and TGFβRII extracellular domain. Based on the above results, experiments are underway to design specific inhibitors of this interaction. We are also developing an improved BACE1 inhibitor that would inhibit the shedding of SEZ6 into the extracellular milieu to inhibit SEZ6 functions.

Thus, this study establishes that GSC-secreted SEZ6 activates the TGFβ pathway in endothelial cells to induce tumor angiogenesis and proposes a novel therapeutic target.

#2787 Heme oxygenase 1 pulls the brake on stemness-induced properties by prostate cancer-bone crosstalk.

A. A. Sabater[1], I. Achinelli[2], P. Sanchis[1], N. Anselmino[3], J. Bizzotto[1], G. Pascual[2], R. Seniuk[2], J. Cotignola[2], E. Vazquez[2], G. Gueron[2], A. Toro[2]; [1]CONICET - IQUIBICEN; Universidad Argentina de la Empresa (UADE), Instituto de Tecnologia (INTEC), CABA, Argentina, [2]CONICET - IQUIBICEN, CABA, Argentina, [3]Department of Genitourinary Medical Oncology and the David H. Koch Center for Applied Research of Genitourinary Cancers, The University of Texas MD Anderson Cancer Center, Houston, TX

Prostate cancer (PCa) is the second most diagnosed cancer in men globally, and it is positioned as the fifth leading cause of cancer-related death in males. PCa aggressiveness and mortality is intricately linked to the metastatic disease, which is propelled by PCa stem cells (PCSCs). We have previously showcased the strong antitumoral role heme oxygenase-1 (HO-1) exerts in PCa. However, little is known about the association of HO-1 with the stemness capacity of PCa cells. In this work, we first performed clonogenic assays in PCa cells (PC3 and C4-2B) to assess colony formation, which evidenced a reduction on the stem-like properties of tumor cells treated with hemin (FDA approved drug and specific HO-1 inducer and activator). Next, we employed an indirect co-culture system of PCa cells (PC3) grown with bone progenitors (MC3T3) to emulate the dynamic PCa-bone crosstalk. PC3 cells were pre-treated or not with hemin. We performed comprehensive RNA-seq analyses and assessed the transcriptome of PC3 cells focusing on genes associated with stemness (*CD44, CD133* and other pluripotency markers), metastasis and a stem-like signature previously identified by our group (*ADAM15*, *BCL2L1*, *LTBR*, *MBNL2*, *SPINT1*). PC3 cells that were co-cultured with MC3T3 displayed upregulated PCSC and pluripotency markers, as well as *BCL2L1* and *LTBR*, when compared with PC3 cells cultured alone. Intriguingly, pre-treatment of PC3 cells with hemin prior to the co-culture impaired the upregulation of these genes, including the PCSC marker *CD44*, underscoring the protective effect of HO-1 induction against the pro-stemness effect triggered by bone progenitors secreted factors. Furthermore, we extended our analysis using PCa patients' survival and transcriptomic publicly available data (TCGA-PRAD (n=565), SU2C-PRAD (n=444), FHCRC-PRAD (n=176)), which revealed that *ADAM15, BCL2L1, LTBR and SPINT1* expression was higher in bone metastases *vs*. primary PCa ($p<0.001$). Moreover, *POU5F1, ALDH1L2, ADAM15, BCL2L1, LTBR* and *SPINT1* presented higher expression in bone metastases *vs*. other sites of metastasis ($p<0.01$). We also performed multiple survival analyses including progression-free, metastasis-free, biochemical relapse-free and overall survival (TCGA-PRAD, GSE116918, GSE70770) which revealed that *CD44* expression is associated with increased risk of metastasis ($p<0.05$), while patients with high expression of *SOX2*, *ALDH1B1* and *ALDH1L2* showed shorter times to biochemical relapse ($p<0.05$) Altogether, HO-1 expression modulates stemness and metastasis-related genes in PCa cells, steering tumor cells towards a more differentiated state and counteracting the pro-stemness effect inherent to the communication with bone progenitors. These findings support the antitumoral role of HO-1 in PCa and underscores *CD44* as an HO-1-modulated compelling candidate for further investigations.

#2788 Immunological targeting of integrin β1^{high}/β3^{high} melanoma.

Feng Wang[1], Ying Xin[2], James J. Moon[3], Alfred E. Chang[1], Max Wicha[2], Qiao Li[1]

[1]Department of Surgery, University of Michigan, Ann Arbor, MI,[2]Department of Internal Medicine, University of Michigan, Ann Arbor, MI,[3]Department of Pharmaceutical Sciences, University of Michigan, Ann Arbor, MI

We previously reported two integrin β4 (ITGB4)-targeted immunologic strategies, e.g., ITGB4 protein-pulsed dendritic cells (ITGB4-DC) for vaccination and adoptive transfer of anti-CD3/anti-ITGB4 bispecific antibody (ITGB4 BiAb)-armed tumor draining lymph node (TDLN) T cells. Both immunotherapies significantly demonstrated efficacy in inhibiting local tumor growth and lung metastases. We found these therapeutic efficacies were closely associated with the T cell as well as humoral anti-integrin β4^{high} cancer stem cells (CSCs) in breast (4T1) and head and neck squamous cell carcinoma (SCC7) tumor models. Recently, we further found that integrin subunits β1 (ITGB1) and β3 (ITGB3) are expressed at significantly high level in melanoma cells. In culture cell lines, integrin β1 and β3 are highly expressed on approximately 98% and 95% of the two mouse melanoma cell lines F10 and D5. We confirmed the expression of these two integrin subunits in newly harvested fresh melanoma tumors *in vivo*, which is very similar to the findings in cell lines. We then assessed ITGB1 and/or ITGB3-pulsed dendritic cell (DC) vaccines using F10 mouse model and demonstrated that ITGB1-DC or ITGB3-DC vaccine both exhibited significant antitumor efficacy inhibiting tumor growth, and ITGB1-DC + ITGB3-DC showed an additive/synergistic anti-tumor effect. Notably, we found that ITGB1 and ITGB3 loaded on separate DCs demonstrated more potent antitumor efficacy than loaded on the same DCs as vaccine. In addition, anti-PD-L1 significantly augmented the antitumor efficacy of ITGB1-DC/ITGB3-DC vaccine to inhibit tumor growth. Considering the crucial role of CSCs in tumor initiation, progression, metastasis, and recurrence, we further evaluated the expression of ITGB1 and ITGB3 on F10 and D5 ALDH^{high} CSCs. We detected significantly higher expression of ITGB1 on ALDH^{high} F10 CSCs (83.3%) and ALDH^{high} D5 CSCs (87.1%) *vs*. ALDH^{low} F10 non-CSCs (0.2%) and ALDH^{low} D5 non-CSCs (2.0%), suggesting that ITGB1 and ITGB3-targeted vaccine-conferred anti-melanoma effects may have significantly involved targeting of ITGB1^{high}/ITGB3^{high} melanoma CSCs. Furthermore, recent studies suggested that bone marrow (BM)-DCs expressing dysfunctional integrin β2 (ITGB2) exhibited more potent antigen presentation function than WT BM-DCs. We found that ITGB2 highly (63.3%) expressed on the surface of BM-DC, but not on F10 or D5 tumor cells. On-going experiments include the investigation of experimental evidence to verify that ITGB1 and ITGB3-targeted vaccines have induced targeting of ITGB1^{high}/ITGB3^{high} melanoma CSCs; and both the cellular and humoral mechanisms underlining the anti- ITGB1^{high}/ITGB3^{high} melanoma CSC immunity. At the same time, generation and use of ITGB2 deficient DCs for the vaccine preparation to improve the efficacy of DC vaccine targeting integrin ITGB1^{high}/ITGB3^{high} melanoma and melanoma CSCs warranty further investigation.

#2789 NCAPG promotes triple-negative breast cancer stemness by a positive feedback loop with HIF-1α.

H. Zhang[1], P. Xie[2], R. An[2];

[1]The First Affiliated Hospital of Xi'an Jiaotong University, Xi'an, China, [2]Xi'an Jiaotong University, Xi'an, China

Objective: Triple-negative breast cancer (TNBC) is life-threatening because of limited therapies and lack of effective therapeutic targets. NCAPG, an oncogenic marker, might be served as a new target for TNBC treatment. Here, we aimed to elucidate the role of NCAPG played in TNBC and the underlying mechanism.
Design: GEO data was used to investigate the potential targets for TNBC. Patient samples and TCGA data were used to demonstrate the clinical significance. Cell migration, self-renewal ability, chemoresistance and expression of pluripotency factors were tested to detect the stemness of TNBC cells. Immunoprecipitation, ubiquitination assay and chromatin immunoprecipitation assay were utilized to investigate the mutual regulation mechanism of NCAPG and HIF-1α.
Results: NCAPG was significantly overexpressed in TNBC compared with other subtypes of breast cancer and was positively correlated with poor overall survival. Elevated NCAPG expression could enhance cancer stem-like cell properties of TNBC cells. Mechanically, NCAPG positively regulated HIF-1α protein stability by interacting with HIF-1α and competitively abrogating the E3 ligase FBXW7-mediated ubiquitination and degradation towards HIF-1α. NCAPG, as a direct target gene of HIF-1α, could be in turn transcriptionally upregulated by HIF-1α.
Conclusion: NCAPG promotes TNBC stemness by a HIF-1α/NCAPG positive feedback loop. NCAPG is a promising target for TNBC treatment.

#2790 Hematopoietic stem cells tropism and conditioned media for targeting the triple negative breast cancer stem cells and associated mechanism: An in vitro study.

S. Mallick, S. Shenoy P, B. Bose;
Yenepoya University, Mangaluru, India

Triple-negative breast cancers are the most challenging to treat with targeted therapy because of their non-expression of cell surface receptors, unlike other types of breast cancer. However, conventional therapies such as chemotherapy, radiotherapy, and surgery are standard treatment modalities. Moreover, drug encapsulation strategies to deliver drugs at the targeted site have been sought-after alternatives. Hematopoietic Stem Cells (HSCs) have unique features to migrate towards inflammatory sites and other body organs during any injuries and release various cytokines, which lead to interaction with molecular pathways and results in reduced inflammation and tissue injuries. From this characteristic, we have hypothesized that hematopoietic stem cells can show tumor tropism and modulate the metabolic alteration in cancer and cancer stem cells, mainly focusing on Triple Negative Breast Cancer Stem Cells (TNBC CSCs). In this study, we have sorted both cancer stem cells and hematopoietic stem cells from TNBC and hematological cell lines, respectively. Sorted HSCs were cultured in specific conditions to prepare conditioned media. Then, both cell' types were used for co-cultured assay and conditioned media cultured with TNBC-CSCs were performed. Metabolomics studies were performed to decipher the molecular interactions and TNBC-CSCs metabolic alterations. The result indicates that the HSCs are showing positive tropism towards TNBC stem cells. Furthermore, HSCs-derived conditioned media (CM) interact with the cell cycle pathway by downregulating the CDK genes and causing DNA breakage in the TNBC-CSCs. Moreover, the Metabolomics studies further confirmed that HSCs CM-derived cytokines interact with various pathways, dysregulating the TNBC-CSCs proliferation and altering the metabolic activities.

#2791 Establishment of immortalized endometrial cell lines using Sendai virus.

K. Hikino, H. Komatsu, G. Hichiwa, K. Kazuki, Y. Kazuki, H. Kugoh, M. Okawa, Y. Ida, M. Hosokawa, M. Sawada, A. Kudoh, S. Sato, F. Taniguchi;
Tottori University School of Medicine, Yonago City, Japan

Objective: To establish endometrial immortalized cell lines using the Sendai virus and analyze their characteristics.
Methods: The study included patients with benign ovarian tumors and endometrioid carcinoma who had regular menstrual cycles. Endometrial cells were collected and separated into epithelial and non-epithelial cells using flowcytometry (FCM) (CD326 (EpCAM) antibody). Furthermore, the isolated cells were infected with Sendai virus carrying three immortalization genes (Bmi-1, hTERT, and SV40T) to create immortalized cell lines. The cells were characterized as epithelial cells by immunocytochemistry (ICC), and receptor expression was assessed by reverse transcription PCR (RT-PCR) and ICC. Non-epithelial cells from the patients with endometrial carcinoma were evaluated using ICC.
Results: The immortalized cell lines were capable of more than 20 passages. Immortalized endometrial epithelial cells tested positive for anti-Keratin antibodies and negative for anti-Vimentin antibodies by ICC. Additionally, FCM detected these cells as positive for anti-EpCAM antibody, confirming that they were epithelial cells. RT-PCR confirmed mRNA expression of estrogen α-receptor and progesterone receptor after 20 passages and ICC confirmed protein expression of them after 10 passages, establishing an endometrial epithelial immortalized cell line. Non-epithelial cells isolated from patients with endometrial carcinoma tested positive for anti-α-smooth muscle actin and anti-Vimentin antibodies by ICC, indicating their characterization as cancer-associated fibroblasts.
Conclusion: We successfully established an immortalized cell line of endometrial epithelial cells using Sendai virus and generated cancer-associated fibroblasts.

TUMOR BIOLOGY: Microbiome and Cancer
Poster Session

#2794 Consumption of dietary fiber correlates with a significant increase in a-diversity in the intestinal Microbiome of allo-HCT recipients and with lower GVHD-lethality in pre-clinical models.

Jenny Paredes[1], Anqi Dai[1], Ruben J. Faustino Ramos[1], Peter Adintori[1], Teng Fei[1], Chi Nguyen[1], Harold Elias[1], Kristen Victor[1], Romina Ghale[1], Charlotte Pohl[1], Ana Gradissimo[1], Justin Cross[1], Oriana Miltiadous[1], Jonathan Peled[1], Marina Burgos da Silva[1], Marcel RM van den Brink[2]

[1]Memorial Sloan Kettering Cancer Center, New York, NY, [2]City of Hope Los Angeles, Los Angeles, CA

Background: Graft-versus-host disease (GVHD) is associated with a decrease in intestinal microbiota and beneficial short-chain fatty acids (SCFAs). Dietary fiber can modulate the intestinal microbiome and SCFA production which effect intestinal epithelium health and immunity. Therefore, we hypothesized that a high-fiber diet in recipients of an allogeneic hematopoietic cell transplantation (allo-HCT) could result in an increase of beneficial commensals, concentrations of SCFAs, and decreased risk of GVHD.

Methods: We evaluated dietary data and fecal samples of allo-HCT patients receiving unmodified grafts (n=95) at MSKCC (day -10 to day +30 relative to allo-HCT) and correlated microbial α-diversity (16s rRNA, n=568 samples) with fiber intake and acute GVHD in No-GVHD (n=30), Non-LGI-GVHD (GVHD except lower gastrointestinal tract, n=41), and LGI-GVHD patients (lower gastrointestinal tract GVHD, n=24).We tested concentrations of cellulose fiber (0%, 6%, 12% and 40%) in a GVHD mouse model (C57BL/6J into BALB/c) to assess survival, microbial composition (shotgun sequencing n=180; n=30 per group), cecal SCFAs concentrations (GC-MS n=24, n=8 per group), and lastly, T cell subsets (Th1/Th17/Tregs) and colonic epithelial MHC-II expression (flow cytometry n=54, n=18 per group).

Results: In allo-HCT patients, fiber intake correlated positively with microbial α-diversity (R=0.3, p=0.04), especially in the LGI-GVHD group (p=0.007). Additionally, patients with high fiber intake had higher microbial α-diversity compared to the low fiber cohort (p<0.0001).GVHD mice receiving a fiber-rich diet (12%), compared to 0% and 6%, had a higher microbial α-diversity (p=0.01); reduced GVHD lethality (p=0.02); and a decrease in the *Enterococcus sp.* (p=0.004) and *Akkermansia sp.* (p=0.01) abundance; taxa which are associated with worse overall survival and increased risk of lethal GVHD. In contrast, compared to 12%, the 40% fiber diet resulted in worse survival (p=0.002), lower α-diversity (p=0.05) and a higher abundance of *Bifidobacterium sp.* (p<0.0001).Cecal butyrate in GVHD mice was higher in response to the 12% vs. the 0% (p=0.01) and 6% (p=0.05) fiber diets. Mice treated with12% fiber displayed higher number of Tregs (CD4+CD25+FOXP3+), than those with 0% (p=0.001) and 6% (p=0.02); and a lower expression of MHC-II in epithelial cells (EpCAM+CD45-) vs. 0% fiber (p=0.02).

Conclusions: We demonstrated that a higher fiber intake in allo-HCT patients is associated with an increase in α-diversity; especially in LGI-GVHD patients. In a pre-clinical GVHD-model, optimal fiber consumption (12% cellulose) leads to an increase in α-diversity, a decrease in pathogen relative abundance, increased T-regulatory cells, and a decrease in GVHD lethality. These results suggest that dietary fiber could be utilized to prevent GVHD.

#2795 An investigation to identify the phylogeny of bacterial communities in the pancreatic cancer microbiome by 16SrDNA sequencing and bioinformatic analysis.

H. N. Banerjee[1], C. Hunter[1], N. BANERJEE[1], K. Perry[1], K. Dia[1], A. Banerjee[1], S. Bhattacharya[2], H. Rachamala[3], E. Wang[3], S. Dutta[3];
[1]Elizabeth City State University under University of North Carolina, Elizabeth City, NC, [2]Mayo Clinic, Jacksonville, NC, [3]Mayo Clinic, Jacksonville, FL

The microbiome refers to the diverse community of microorganisms, including bacteria, viruses, fungi, and other microbes, that inhabit various parts of the human body, such as the skin, mouth, gut, and other mucosal surfaces. The role of the microbiome in cancer is a complex and evolving area of research. While much is still being learned, there is evidence suggesting that the microbiome can influence cancer development and progression in several ways. Some bacteria within the microbiome can produce substances that may be either carcinogenic or protective against cancer. For instance, the conversion of certain dietary components by gut bacteria can produce metabolites that may either promote or inhibit cancer development. Different cancers may be associated with specific alterations in the microbiome, for example, the gut microbiome has been extensively studied in relation to colorectal cancer, with certain bacterial species potentially contributing to the development of this cancer. However, the role of microbiome in Pancreatic cancer is still not extensively studied, henceforth, we did a preliminary study to identify novel bacterial communities around pancreatic cancer microbiome by 16SrDNA sequencing in human pancreatic cancer xenograft model mice. Isolating total genomic DNA from the pancreatic model mice feces, 16SrDNA PCR was done using specific primers and the amplicon obtained as PCR product was confirmed by standard DNA gel electrophoresis with a 1 kb standard ladder to be 1.5kb in size universal for all bacterial 16SrDNA. The amplicon was then sent for Next Generation Sequencing at Zymo Research Corporation (CA). The resultant DNA sequences were analyzed by bioinformatics studies and their phylogeny identified by comparing with 16SrDNA data base. Differential abundance of the bacteria's of the genera Lachnoclostridium, Robinsoniella, Alistipes, Akkermansia and Lactobacillus were observed analyzing the data along with other bacterial communities. We are currently continuing the project to identify more bacterial communities of significance in the pancreatic cancer microbiome and investigating the role and significance of these bacterial communities in pancreatic cancer tumor microenvironment. Acknowledgement This study was done by a joint collaboration between scientists and students of Elizabeth City State University (ECSU) campus of the University of North Carolina Systems and Mayo Clinic, Jacksonville. This research is supported by the NIH-NIGMS grant#T34GM100831-10 to Dr. H. Banerjee and a University of North Carolina General Administration Grant to Dr. Colby Hunter at ECSU.

#2796 Colibactin mutation signatures are associated with younger age of onset in colorectal cancer.

S. Gerstberger[1], M. Lumish[2], S. Hartner[3], F. Shah[1], S. Choi[1], A. Luthra[1], Q. Jiang[1], H. Woo[1], A. Mahmoud[1], H. Walch[1], S. Asawa[4], M. Donoghue[1], A. Cercek[1], R. Yaeger[1], A. McPherson[1], F. Sanchez-Vega[1], K. Ganesh[1];

[1]Memorial Sloan Kettering Cancer Center, New York, NY, [2]Department of Hematology and Oncology, University Hospitals Cleveland Medical Center, Cleveland, OH, [3]McGill University, Montreal, QC, Canada, [4]ETH Zurich, Zurich, Switzerland

Escherichia coli (E. coli) strains carrying the polyketide synthase (pks) island produce the genotoxin colibactin associated with pathogenesis of colorectal cancer (CRC). Colibactin binds directly to DNA, causing alkylating damage leading to double stranded DNA breaks. Colibactin mutagenesis results in mutations in hexameric A-T rich DNA motifs that can be identified by whole genome sequencing (WGS) as mutation signatures SBS28 and SBS88 (SBS-pks). Since WGS is not routinely used clinically, we developed an approach to specifically identify SBS-pks using a clinical targeted exon capture assay, MSK-IMPACT. In an institutional pan-cancer clinical cohort of 78,905 tumors we identified 15,967 samples with > 20 mutations detected by MSK-IMPACT. We identified 150/1,884 samples with microsatellite stable CRC with >10% mutations attributable to SBS-pks. Examining clinicopathologic and genomic features of SBS-pks+ compared to SBS-pks- CRC tumors, we found that SBS-pks+ signatures are significantly enriched in younger age of onset compared to SBS-pks- CRC patients (median age 55 vs median age 59, p= 0.0028). SBS-pks+ CRC exhibit similar driver mutations and tumor mutational burden (TMB) compared to SBS-pks- CRC but are associated with increased fraction of genome altered (FGA). To mechanistically investigate colibactin-associated damage we developed a novel long-term human colon organoid-microbe co-culture model system that takes advantage of reversal of polarity in suspension culture. WGS of human CRC organoids co-cultured for three months with pks+ and delta-pks E. coli NC101 confirmed induction of pks+ specific SBS-pks signatures, validating the model. Leveraging this model and a biobank of normal colon organoids from donors aged </> 50 years, we are investigating the molecular mechanisms underlying the association of SBS-pks with younger age of onset CRC.

#2797 *Fusobacterium nucleatum* antigens drive tumor-associated macrophage-like cells in an engineered oral squamous cell carcinoma on-a-chip.

M. G. C. Sousa, Sr.[1], A. Athirasala[1], M. A. Fraga[1], D. Higashi[2], J. Merrit, Sr.[2], L. Bertassoni, Sr.[1];
[1]Knight Cancer Institute, Oregon Health & Science University, Portland, OR, [2]Oregon Health and Science University, Portland, OR

Oral squamous cell carcinoma (OSCC) is the sixth most prevalent cancer, representing 90% of all head and neck cancers. Oral cancers are expected to cause 11000 deaths in the US in 2023. OSCC comprises a complex microenvironment involving a 3D collagenous matrix, innate and adaptative immune cells, fibroblasts, and opportunistic microorganisms. *Fusobacterium nucleatum,* for instance, is related to OSCC development in different aspects, such as inducing epithelial-to-mesenchymal transition and coordinating the immunological response in the tumor microenvironment (TME). Although some advances were achieved in understanding the OSCC TME, there is an urge to develop advanced *in vitro* models to investigate the immunosuppressive role of opportunistic microorganisms in OSCCs. Offering a promising avenue for studying OSCCs, organs-on-a-chip serve as microphysiological platforms that closely emulate the complexities of biological tissues within the highly controllable microfluidic, cellular communication, and extracellular matrix. Here, we developed an OSCC on-a-chip to understand the immunomodulatory profile of *F. nucleatum* on macrophages in the TME. We cultivated oral squamous carcinoma cells in 3D in a collagen matrix (2.5 mg/mL) in a microfluidic device that has a central chamber (1mm in width) and two lateral channels connected by triangular pillars (space between pillars of 115 µm). Our tested groups were collagen matrix containing OSCC (5.10^5 cells/mL) in the presence or absence of heat-killed antigens (1.10^6 CFUs/mL) from *F. nucleatum* (ATCC 23726). *F. nucleatum* cells were integrated with collagen gels and oral squamous carcinoma cells for three days. On the fourth day, we added 2.10^3 THP-1 derived macrophages (differentiated with PMA 100 ng/mL) in the lateral channel to evaluate their chemoattraction to the 3D matrix in the presence or absence of *F. nucleatum* for 48 hours. We noticed a significantly higher number of macrophages invading the 3D matrices that had heat-killed antigens when compared to the groups containing just OSSCs. By immunofluorescence, we stained the cells with markers for M1 (CD86) and M2 (CD163) and observed a significantly lower number of CD86 and a higher number of CD163-positive cells in the *F. nucleatum* stimulated group. When cytokines and chemokines were measured from these chips by Luminex assay, we found that the presence of heat-killed bacteria upregulated TNF-α, MCP-1, IL-6, VEGF, and CCL5 significantly, showing that the presence of *F.nucleatum* might stimulate tumor-associated macrophages-like cells. These results enable us to understand how the early interactions between opportunistic microorganisms and the immune system modulate the suppression responses in the tumor microenvironment.

#2798 Oral fungal infection tweaks the innate immune tumor microenvironment promoting.

X. Li[1], N.-Y. Song[2], A. K. Singh[1], J. Badger[3], C. Jiang[4], F. Zhu[1], D. Tross[1], Y. Zhao[5], B. Tran[5], Y. Hu[1];
[1]National Cancer Institute, Frederick, MD, [2]Yonsei University College of Dentistry, Seoul, Korea, Republic of, [3]National Cancer Institute, Bethesda, MD, [4]National Heart, Lung, and Blood Institute, Bethesda, MD, [5]Leidos Biomedical Research Inc, Frederick, MD

It is yet unknown how a fungus and tumor interplay impairs innate immunity, modulating tumorigenesis. Here, we found that oral infection with *Cladosporium cladosporioides* of mice with *Ikka* deficiency in epithelial stem cells enhanced STAT3-dependent oral squamous cell carcinoma (SCC) development and fungal colonization. In wild-type mice infection was cleared up, suggesting a synergic tumor-fungus loop involved in the accelerated carcinogenesis. *C. cladosporioides*-mediated EGFR activation stimulated intratumor STAT3-led pathways to generate an acidic oral milieu, which disrupted bacterial compositions and suppressed neutrophil's ROS but increased *Il1b* expression, dampening neutrophil's fungitoxicity and allowing oral fungal and bacterial overgrowth. In addition, fungus-induced IL-1β/IL-17A augmented STAT3 activity in SCC cells, contributing to local and distal carcinogenesis. Significantly, fungal signals were greater in human head and neck SCCs (HNSCCs) and SCC-adjacent tissues than in healthy controls and were co-localized with *IL1B*-expressing neutrophils in HNSCCs. These similar traits of oncogenic pathways, microbiota dysbiosis, and defective neutrophils in HNSCC patients with poor survival highlight the importance of increased fungal infection for human malignant development and therapy.

#2799 Intestinal *Akkermansia muciniphila* complements the therapeutic efficacy of PD1 therapy by reshaping the immunosuppressive microenvironment in nonalcoholic fatty liver disease (NAFLD)-induced hepatocellular carcinoma.

Xueqian Wu, Fan Ying, Katherine Po Sin Chung, Carmen Oi Ning Leung, Terence Kin Wah Lee

Applied Biology and Chemical Technology, Hong Kong Polytechnic University, Hong Kong, Hong Kong

Objectives: Nonalcoholic fatty liver disease (NAFLD)-induced hepatocellular carcinoma (HCC) is an emerging malignancy in the developed world. However, immune checkpoint inhibitors (ICIs) are ineffective for patients with this disease. Advances in research have shown that gut-liver communication contributes to NAFLD progression. Therefore, identifying a key gut microbiota for predicting ICIs response and an effective combinatorial strategy is urgently needed.
Design: 16S rRNA sequencing was employed to identify key gut microbiota crucial in developing the mouse NAFLD-induced HCC model. The *in vivo* roles of *Akkermansia muciniphila* (*Akk*) were evaluated by immunofluorescence staining, qPCR, mass spectrometry analysis, ELISA assay, and single-cell RNA sequencing (scRNA-seq) coupled with immune profiling analysis. The clinical and therapeutic value of *Akk* alone in combination with PD1 treatment was investigated.
Results: *Akk* was decreased from healthy to HCC tissues during HCC tumor development, and daily administration of *Akk* not only ameliorates liver steatosis and cholesterol biosynthesis but could effectively attenuate the development of NAFLD-induced HCC. *Akk* repairs the intestinal lining, with a concurrent decrease in the serum concentration of *lipopolysaccharide* (LPS) and bile acid metabolites. Using scRNA-seq coupled with immune profiling analyses, we found that *Akk* suppressed the populations of immunosuppressive cells, including monocytic myeloid-derived suppressor cells (m-MDSCs) and M2 macrophages, by suppressing the differentiation of these cells from monocytes, which leads to T cell proliferation and activation. Consistent with this finding, *Akk* administration, combined with PD1 treatment, exerted a maximal growth-suppressive effect, accompanied by increased infiltration and activation of T cells. Clinically, the fecal level of *Akk* in HCC patients was decreased in NAFLD-induced HCC patients and serves as a potential biomarker for predicting PD1 response in HCC patients.
Conclusions: *Akk* regulates the immune tumor environment by regulating two key immune suppressive cells via regulation of the LPS flux to develop NALFD-induced HCC. This finding provides a solid therapeutic basis for a rational combination with PD1 for the treatment of this deadly disease. Interestingly, *Akk* may serve as a predictive biomarker for PD1 response in HCC patients.

#2800 Shotgun metagenomics of COPD-associated lung cancer tissue microbiome.

Atsushi Matsuoka[1], Kazuhiko Shien[2], Shuta Tomida[3], Daisuke Mizuno[1], Masayoshi Ohki[1], Ryo Yoshichika[1], Tomohiro Higashihara[1], Naohiro Hayashi[1], Fumiaki Mukohara[1], Mao Yoshikawa[1], Ken Suzawa[2], Hiromasa Yamamoto[2], Shinichi Toyooka[1]

[1]Thoracic, Breast and Endocrinological Surgery, Okayama University Graduate School of Medicine, Dentistry and Pharmaceutical Sciences, Okayama, Japan,[2]Thoracic, Breast and Endocrinological Surgery, Okayama University Hospital, Okayama, Japan,[3]Center for Comprehensive Genomic Medicine, Okayama University Hospital, Okayama, Japan

The gut microbiome plays a crucial role in the development of multiple chronic diseases. Several solid tumors including lung cancer are also implicated in the gut microbiome in cancer initiation and progression, possibly affecting signaling pathways in the tumor microenvironment. However, the microbiome in the peripheral lung tissue is unexplored and their relationship to the lung tumor microenvironment is still unknown. Thus, to explore the relationship between the microbiome and the tumor microenvironment of lung cancer, we performed shotgun metagenomic sequencing of the lung cancer tissue, especially in lung cancer patients accompanied by chronic obstructive pulmonary disease (COPD). We confirmed the presence of a diverse microbiome in peripheral lung cancer tissue. Next, we focused on individual species. We observed significant differences in the relative abundance of several species between COPD and non-COPD patients, and cancer and non-cancer tissue. Then, we focused on the metagenomic diversity between samples. The number of species in COPD patients and cancer tissue were decreased. And the bacterial total abundance in each sample were observed similar trend. On the other hand, alpha diversity in each sample were showed different trend to them. In the analysis of beta diversity using Principal Coordinate Analysis (PCoA), clusters were formed in each group. These findings suggest that microbiome imbalance known as dysbiosis in the peripheral lung tissue may affect the tumor microenvironment resulting in cancer progression.

#2801 Identifying gut microbial determinants of clonal hematopoiesis of indeterminate potential (CHIP) in immunotherapy treated melanoma patients..

E. A. Fallon[1], S. Urrutia[1], R. Ayabe[1], M. Chelvanambi[1], A. Damania[1], S. Johnson[1], T. Tanaka[1], Z. Li[1], Y. Seo[1], S. Cass[2], M. C. Wong[1], N. Ajami[1], J. Wargo[1], K. Takahashi[1];

[1]The University of Texas MD Anderson Cancer Center, Houston, TX, [2]University of Texas Medical Branch, Galveston, TX

INTRO: Clonal hematopoiesis (CH) of indeterminate potential (CHIP) is associated with poor outcomes in those with non-hematologic cancers. CH mutated macrophages and neutrophils have increased capacity to home to peripheral tissues, driving local inflammation; they are also implicated in immunotherapy related toxicity. The relationship between CH and the microbiome in those treated with immunotherapy is not well understood.

RESULTS: 35 patients with stage IV melanoma treated with upfront immunotherapy; treatment and cohort characteristics are below (Table 1). We performed error corrected duplex sequencing on peripheral blood mononuclear cells using a panel previously validated for CH mutations. With a cutoff of 0.5% variant allele frequency (VAF), among 10 CHIP positive patients, we found mutations in TET2 (8/10), DNMT3A (7/10), PPM1D (2/10), and JAK2 (1/10). There was no difference in either survival or response based on CHIP status (Log-Rank Chi-Square p=0.44); however, CHIP positivity was associated with greater microbiome richness as measured by alpha diversity (p=0.0012 Shannon diversity) and distinct structural/compositional diversity vs CHIP negative patients as measured by beta diversity (p=0.032, R-Squared= 0.045). We inferred KEGG pathway activity from whole genome sequencing and identified that CHIP positive patients were enriched for exopolysaccharide biosynthesis while CHIP negative patients had higher expression of nucleotide sugars biosynthesis and amino acid metabolism pathways.

DISCUSSION: In patients treated with immunotherapy for melanoma, microbiome diversity signatures correlate with presence of CHIP. The analysis suggests that there are distinct taxonomic and functional features defining CHIP positivity. The effect of these cells in the tumor microenvironment and their role in immunotherapy response requires further exploration.

#2802 *Enterococcus faecalis*-derived X facilitates pancreatic tumor by regulating immune microenvironment.

B. Wang, C. Yang, Y. Xie, T. Zhou, J. Yu, J. Hao;
Pancreas Center, Tianjin Medical University Cancer Institute and Hospital, National Clinical Research Center for Cancer; Tianjin Key Laboratory of Digestive Cancer; Tianjin's Clinical Research Center for Cancer, Tianjin, China

Previous research in human samples has found a link between the intratumoral microbiome and the development and progression of pancreatic cancer. Nevertheless, the bacterial strains that may have an effect, and the underlying mechanisms, are largely unknown. To identify potential bacterial species, microbiome sequencing was performed on fecal and tumor samples obtained from KPC mice and patients with pancreatic tumors in this study. To identify metabolites associated with bacteria, untargeted metabolomics were analyzed on serum and tumor samples. Furthermore, advanced and high-throughput techniques, such as single-cell RNA sequencing, tumor organoids, engineered bacteria and germ-free mouse models, were used to elucidate the specific influence on the immune microenvironment of pancreatic tumors. Our findings reveal an increased abundance of *Enterococcus faecalis* (*E. faecalis*) in the gut during the development of pancreatic cancer, accompanied by its accumulation in the tumor. Patient-derived *E. faecalis* strain and its metabolite X, facilitated pancreatic tumor growth, reduced the recruitment of $CD8^{\pm}$T cells, and caused their dysfunction in the tumor, relying heavily on *E. faecalis* intratumoral colonization. We found that X inhibits the production of anti-tumor chemokines like CCL21 and CCL8 in tumor cells, reducing peripheral $CD8^{\pm}$ T cell infiltration into the tumor. Furthermore, X was found to inhibit glycolysis and compromise the function of tumor-infiltrating $CD8^{\pm}$ T cells by decreasing the activity of lactate dehydrogenase (LDH) in $CD8^{\pm}$ T cells. Additionally, oral doxycycline, an antibiotic that targets intratumoral *E. faecalis*, effectively enhanced the therapeutic effect of gemcitabine in pancreatic cancer. Finally, we present evidence that X may predicts efficacy and survival in pancreatic cancer patients. Together, our findings provide new insights into the role of *E. faecalis* in mediating the immune environment of pancreatic tumors, highlighting *E. faecalis* and X as potential therapeutic targets for pancreatic cancer patients.

#2803 Identification of microbiome and predictive immune biomarkers in patients with advanced non-small lung cancer treated with pembrolizumab with or without chemotherapy.

J. Lee[1], S.-J. Choi[1], G.-T. Lee[1], J. Yang[2], H.-S. Oh[2], A. Min[2], B.-E. Kwon[2], S.-s. Kang[3], S. Baek[1], D. Kim[1], J. Kim[1], S. Lim[1], M. Hong[1], K.-H. Pyo[1], B. Cho[1]; [1]Yonsei University College of Medicine, Seoul City, Korea, Republic of, [2]CJ Bioscience Inc., Seoul City, Korea, Republic of, [3]JEUK Institute for Cancer Research,JEUK Co., Ltd., Gumi City, Korea, Republic of

Background: Recent studies have shown that gut microbiota modulates antitumor immunity, and affect clinical efficacy of immune checkpoint inhibitors, including anti-programmed death-1 (PD-1) and programmed death-ligand 1 (PD-L1) inhibitors. We aimed to explore the metagenomic profiles of previously untreated, treatment naïve, stage IV non-small cell lung cancer (NSCLC) treated with pembrolizumab, an anti-PD1 agent with or without platinum-based chemotherapy and identify distinct ecological niche between responder and non-responder groups.

Methods: We performed metagenome sequencing, whole exome sequencing (WES), and RNA sequencing (RNA-seq) on 50 patients with stage IV NSCLC, including adenocarcinoma (N=31) and squamous cell carcinoma (N=22). We employed Dirichlet Multinomial Mixtures (DMM) community typing to cluster microbial community profiling data at the genus level and analyzed the changes in microbial composition and diversity between enterotype 1 (E1, N=27) and enterotype 2 (E2, N=23). Mutation landscape including genomic alterations in relation to immune response was analyzed between responders and non-responders using WES data. Differentially expressed genes (DEGs), Gene Set Enrichment Analysis (GSEA), and immune deconvolution analysis were carried out using RNA-seq data to analyze molecular profiling of two enterotypes between the responder (N=15) and non-responder (N=35) groups.

Results: The two enterotypes exhibited distinct microbial abundances and alpha diversity indices. Abundances of members of *Bacteroidaceae* (P=0.011) and *Oscillospiraceae* (P<0.001) were higher in E2 members, and enrichment of *Lactobacillaceae* (P=0.006) and *Bifidobacteriaceae* (P=0.041) were higher in E1. Compared to E1, the number of observed bacterial species (P<0.001) and Shannon index (P<0.001) was significantly higher in E2, indicating a healthier gut environment. The proportion of responders was higher in E2 than in E1 cluster. Comparison between responders and non-responder groups within each enterotype revealed that *Lactobacillaceae* showed an association with the response in E2 cluster. Mutation landscape revealed *TP53* mutation as the most common mutation, more frequently observed in the E2 (100%) than in the E1 (56%) cluster.

Conclusion: We explored the association between the gut microbiome and clinical response to pembrolizumab with or without combination with chemotherapy and found that E2 cluster enriched with *Lactobacillaceae* is associated with treatment response. Further analysis with larger cohort is ongoing.

#2804 Comparative analysis of microbial diversity and abundance in colorectal cancer patients before and after surgery.

H. Park[1], M. Kim[2], J. Park[2], S.-Y. Jeong[2], A. Shin[1], S.-Y. Cho[3], E. Jung[4], D. Suh[4], S. Lee[4], Y. Park[4];

[1]Seoul National University College of Medicine, Seoul, Korea, Republic of, [2]Seoul National University Hospital, Seoul, Korea, Republic of, [3]Seoul National University, Seoul, Korea, Republic of, [4]HEM Pharma Inc., Suwon, Korea, Republic of

Background: Previous studies have indicated differing patterns of the microbiome in colorectal cancer (CRC) patients compared to healthy individuals. Yet, the changes in microbial features of CRC patients before and after surgery remain underexplored. This study aims to investigate the impact of surgical intervention on the gut microbial diversity and abundance at the patient level.

Methods: This hospital-based study analyzed data from 36 CRC patients who underwent CRC surgery at the Department of Surgery, Seoul National University Hospital between January 2020 and May 2022. Fecal samples from these patients were collected twice, both before surgery and during the post-surgery follow-up period. DNA extraction from stool specimens was performed using the MAG-Bind Universal Pathogen kit. This was followed by amplification and sequencing of the 16S rRNA gene V3-V4 region, with subsequent bioinformatics analyses conducted using QIIME 2. To compare the alpha diversity indices of patients before and after surgery, we employed both the paired t-test and the Wilcoxon signed-rank test.

Results: Out of the 36 patients, 21 were male and 15 were female, with a mean age of 63.8 years. The average duration between surgery and post-surgery fecal sample collection was 2.3 years. Post-surgery, the alpha diversity indices decreased compared to pre-surgery, but the differences were not significant, except for Faith's PD. At the phylum level, *Firmicutes* and *Actinobacteriota,* both recognized as beneficial bacteria, increased in abundance after surgery, while *Bacteriodota,* typically considered harmful, significantly decreased. At the genus level, variations in microbial abundance also showed an increase in *Blautia*, *Bifidobacterium*, and *Collinsella*, and a decrease in *Enterococcus*, *Romboutsia*, and *Faecalibacterium*. The rise in *Bifidobacterium* abundance following surgery suggests a gut environment altered by the surgery to favor beneficial bacteria. However, a specific species decline in *Bifidobacterium adolescentis* was observed, highlighting that CRC surgery may have distinct impacts on different bacterial species.

Conclusions: Our study indicates a slight decline in gut microbiome diversity following surgery. At the phylum level, there was an observed increase in beneficial bacteria and a decrease in harmful bacteria post-surgery, suggesting potential health improvements in CRC patients. Further research, particularly with a larger sample size and encompassing a broader range of bacteria, is needed to better understand the patterns and implications of microbiome variation in relation to surgical outcomes. Such insights could be pivotal in optimizing patient care and recovery strategies post-surgery.

#2805 Shotgun sequencing of serial fecal microbiome samples in patients with colorectal cancer reveals distinct bacterial species and metabolic pathways associated with tumor sidedness and age at diagnosis.

M. Lumish, N. Waters, J. Leinwand, A. Saxena, A. Dai, T. Fei, M. Fox, A. Chavez, J. Bermeo, D. Ismailgeci, E. Benitez, C. Cowley, J. Garcia-Aguilar, M. Weiser, A. Cercek, L. A. Diaz, M. van den Brink, J. Peled, K. Ganesh;
Memorial Sloan Kettering Cancer Center, New York, NY

Background: The incidence of early onset (EO) colorectal cancer (CRC) (age <50) is rising with a left-sided predominance. Response to chemotherapy and anti-EGFR therapies differ in left- and right-sided colon cancers after accounting for genomic differences. The intestinal microbiome may contribute to CRC pathogenesis and response to therapy; how organisms drive metastasis and treatment resistance is not known.
Purpose: To define the microbiome contribution to EO-CRC and response to treatment by analyzing longitudinal samples from previously untreated patients with CRC.
Methods: We designed a prospective biospecimen collection platform and selected patients with previously untreated CRC. We collected stool, biopsy or surgical tissue, and peripheral blood mononuclear cells at baseline and serially throughout treatment. Stool samples were analyzed using shotgun sequencing. Alpha diversity was calculated using the inverse Simpson index and compared between groups using the Wilcoxon signed-rank test. Beta diversity was analyzed using the Bray-Curtis dissimilarity matrix and compared using PERMANOVA. Multivariate associations between species abundance, metabolic pathway abundance and clinical covariates were performed using MaAsLin2 R package.
Results: We analyzed a total of 132 stool samples from 65 patients with CRC including up to 5 samples from a single patient over time. Mean alpha diversity did not differ significantly by primary site, stage or age at diagnosis. Beta diversity was significantly different between samples from right- compared with left-sided CRC (P=.011) and pre- and post-surgery (P=.001). Beta diversity also differed significantly by diagnosis age (<50 vs. > 50) (P=.001 all samples, P=.032 baseline samples). When CRC baseline samples were examined at the species level, *Blautia glucerasea* was associated with right-sided primary (P<.001, Q=.1). Considering non-metastatic cases, recurrence was associated with increased *Enteroscipio rubneri, Actinomyces oral taxon 448, Bacteroidales sp.* and *Lancefieldella parvula* (P<.01, Q>0.1). We further investigated metabolic pathway associations. The superpathway of L-threonine metabolism was significantly increased in samples from patients with right-sided colon cancer at baseline (P<.001, Q=.03). Considering samples across all time points, right-sided colon cancer was associated with increased abundance of pathways associated with propanoate degradation, L-threonine metabolism, yeast NADPH production, and hydroxyphenylacetate degradation (all P<.001, Q<.05).
Conclusions: The functional effects of the intestinal microbiome may underlie the distinct biology of right-sided colon cancer. Composition of the intestinal microbiome differs by age at diagnosis. Updated recurrence data will be presented.

#2806 A single dose of perioperative cefazolin disrupts the gut microbiome and immunity in patients (pts) with early-stage melanoma.

E. Fernandez, S. Cass, Y. D. Seo, A. V. Damania, X. Meng, P. V. Sahasrabhojane, J. Liu, W. Liu, Y. Chen, R. L. Bassett, Jr., S. Shelburne, H.-Y. Chang, K. R. Somaiya, K. S. Mungovan, J. C. Malke, B. Matejka, S. B. Fisher, A. Lucci, J. E. Lee, M. I. Ross, J. E. Gershenwald, P. Sharma, N. J. Ajami, C. L. Roland, J. A. Wargo, E. Z. Keung;
UT MD Anderson Cancer Center, Houston, TX

Background: Perioperative antibiotic prophylaxis is routinely utilized to reduce surgical site infections (SSIs). However, the rate of SSIs following a clean surgical procedure is <3%. Overuse of antibiotics is associated with potential adverse effects, including disruption of the composition and function of the native gut microbiota. Numerous studies have shown a negative impact of antibiotics on response and survival in patients with cancer treated with immune checkpoint blockade. The primary objective of this study was to determine the impact of a single dose of perioperative cefazolin on the gut microbiome and immunity. Methods: In this pilot trial (NCT04875728), 22 eligible pts diagnosed with clinical stage I or II melanoma undergoing wide excision with or without sentinel lymph node biopsy were enrolled between October 2021 and January 2023. Pts were randomized 1:1 to receive a single dose of cefazolin as standard-of-care (ABX, n=11) or no antibiotics (No ABX, n=11) at the time of surgery. Stool samples were collected before surgery, on post-operative day (POD) 14 and POD90 for metagenomic sequencing (WMS). Bulk RNA-sequencing of peripheral blood mononuclear cells (PBMCs) collected at the same timepoints was performed and data processed using DESeq2, log-transformed, and standardized for subsequent analysis. Immune pathway enrichment scores were calculated using GSVA for each sample with gene lists from 3 immune pathways (ADAPTIVE_IMMUNE_SYSTEM, INNATE_IMMUNE_SYSTEM, and CYTOKINE_SIGNALING_IN_IMMUNE_SYSTEM) from REACTOME (https://reactome.org) and immune cell gene signatures from Danaher P et al, 2017. Results: Treatment with a single dose of perioperative cefazolin was associated with a decrease in the alpha diversity of the gut microbiome 2 weeks postoperatively in pts who received perioperative cefazolin versus those who did not receive antibiotics (p=0.057, R2=0.0526); this persisted to POD90 (p=0.021, R2=0.0948). WMS showed prominent and persistent decreases in Akkermansia muciniphila (POD14: Log2FC=-8.38, q<0.001) and Alistipes communis (POD90: Log2FC=-4.47, q<0.001) in the ABX group compared to No ABX, respectively. RNA-seq analysis of PBMCs from pts revealed differences in immune subsets at POD90 between ABX and No ABX groups including decreased IFN-γ signatures (p=0.02) in pts who received perioperative cefazolin. Conclusions: Perioperative antibiotic prophylaxis is associated with profound and persistent reduction in microbiome diversity and composition, particularly of bacterial species associated with protective metabolic and inflammatory effects. Further studies will seek to assess the functional impact of this reduction on the immune response in a murine model, evaluate the generalizability of our findings across broader cohorts of patients undergoing surgery, and apply these findings to guide clinical management decisions.

#2807 Distinctive microbiome signatures in colorectal cancer: A comparative metagenomic analysis.

Z. Chen[1], B. Nie[2], B. Luo[1], Z. Wang[1], **X. Wang**[3],

[1]Shanghai Municipal Hospital of Traditional Chinese Medicine, Shanghai University of Traditional Chinese Medicine, Shanghai, China, [2]Nanjing University of Traditional Chinese Medicine, Nanjing, China, [3]University of California, San Diego, San Diego, CA

The human gut microbiome is increasingly recognized for its role in colorectal cancer (CRC) pathogenesis. This study aims to delineate the microbiome characteristics of CRC patients compared to healthy individuals, using a comprehensive metagenomic approach.

We utilized a cohort of 80 CRC patients and an equal number of matched healthy controls. Fecal samples were collected and subjected to in-depth metagenomic sequencing, targeting both structural and functional profiles of the microbiome. Data analysis involved advanced bioinformatics techniques. Key observations were subsequently validated in an independent cohort to bolster the findings.

Our analysis revealed significant alterations in the microbiome composition of CRC patients versus healthy individuals. Notably, there was an increased prevalence of pathogenic bacteria, such as Bacteroides Vulgatus in CRC patients. These bacteria are implicated in promoting inflammation and carcinogenesis. Conversely, there was a noticeable depletion of beneficial microbes like Lactobacillus in the CRC group. Functionally, the microbiome in CRC patients was characterized by enriched pathways related to DNA repair, cell cycle control, and metabolism pathways like Citrate cycle and Galactose metabolism. Validation in an independent cohort confirmed these distinctive microbiomic patterns.

Our study provides compelling evidence of altered microbiome landscapes in CRC patients, highlighting potential roles in disease development and progression. These findings pave the way for further investigation into microbiome-based diagnostics and therapeutic interventions in colorectal cancer.

#2808 Levels of isobutyric acid from gut butyrate-producing taxa are associated to Delta-24-RGDOX efficacy against malignant glioma.

N. M. Melendez-Vazquez[1], X. Fan[2], J. Fueyo[2], C. Gomez-Manzano[2], F. Godoy-Vitorino[1];
[1]University of Puerto Rico - Medical Sciences Campus, San Juan, PR, [2]The University of Texas MD Anderson Cancer Center, Houston, TX

Glioblastoma (GBM) is the most aggressive malignant primary brain tumor worldwide. Current standard-of-care treatments allow for a median survival of 12 to 18 months. GBM has a poor survival prognosis, observing less than 6% of patients surviving 5 years post-diagnosis. Among recent treatment advancements, the oncolytic adenovirus Delta-24-RGDOX armed with the T-cell activator OX40L is promising. Studies have unveiled a relationship between the gut microbiome and high levels of short-chain fatty acids (SCFA), such as isobutyric and propionic acid, to immunotherapy response. Changes in the gut microbiome and metabolome associated to viroimmunotherapy efficacy remain unclear. Here, we assessed the gut microbial changes in addition to isobutyric and propionic acid levels regarding viroimmunotherapy efficacy. Immunocompetent C57BL/6 mice were intracranially implanted GL261-5 GBM cells and received intratumoral injections of PBS (control) or Delta-24-RGDOX. A naïve group with no tumor nor treatment was also included. Fecal pellets were collected at three different time points: (1) before tumor implantation, (2) before treatment, and (3) 14 days after the first dose of treatment. Genomic DNA was isolated with the QIAGEN DNeasy Powersoil Pro Kit from fecal pellets (n=75), followed by sequencing with the Illumina platform of the 16S ribosomal RNA V4 region. Quality assessment of the sequences was executed in QIITA. Bacterial community analysis with a sequencing depth of 1,470 reads, while using the taxonomic database SILVA, was followed downstream with QIIME2 and R. Metabolic profiling of SCFA of the fecal pellets was performed through Gas Chromatography. Results showed significant differences in bacterial community structure of viroimmunotherapy-treated mice with survival of >100 days compared to controls (ANOSIM p-value=0.006). Alpha diversity metrics showed significant differences in richness between the naive and tumor-implanted mice of the PBS (KW p-value=0.049) and Delta-24-RGDOX (KW p-value=0.019) groups, highlighting that tumor presence alters the gut microbiota. Additionally, viroimmunotherapy-treated mice with survival of >100 days had a significant increase of *Lactobacillus* and the butyrate-producing bacterias *Erysipelatoclostridium* and *Ruminococcaceae*. Also, we found significantly higher levels of isobutyric acid and lower levels of propionic acid in viroimmunotherapy-treated mice with survival of >100 days (p-value<0.05). These findings suggest that butyrate-producing bacteria coupled with higher levels of isobutyric acid may be important in the efficacy of Delta-24-RGDOX. This highlights the microbial and metabolic changes associated with oncolytic viral therapy efficacy. *Sponsored by an award within The University of Puerto Rico/UT MD Anderson Cancer Center Partnership for Excellence in Cancer Research Grant (2U54CA096297-17).*

#2809 Bifidobacterium species BB_003 identified through metatranscriptomic analysis with experimentally validated antitumor actions.

Kyungchan Min[1], Xuan-Mei Piao[2], Young Joon Byun[2], Chuang-Ming Zheng[2], Seon-Kyu Kim[3], Seong-Hwan Park[3], Sungmin Moon[4], Kyeong Kim[4], Ho Won Kang[5], Won Tae Kim[5], Seok Joong Yun[5], Hansoo Park[1]

[1]Gwangju Institute of Science and Technology, Gwangju, Korea, Republic of,[2]College of Medicine, Chungbuk National University, Cheongju, Korea, Republic of,[3]Department of Bioscience, University of Science and Technology, Daejeon, Korea, Republic of,[4]Department of Urology, Chungbuk National University Hospital, Cheongju, Korea, Republic of,[5]Department of Urology, Chungbuk National University College of Medicine, Cheongju, Korea, Republic of

Introduction & Objectives: A host's microbiome influences both gene expression and phenotype. Whole transcriptome sequencing (WTS) provides information about the microbiome in addition to gene expression. This research probes the correlation between microbial abundance, host gene transcription, and therapeutic efficacy, pinpointing a beneficial microbial strain and its mechanism of action.
Materials & Methods: Bladder tissue biopsies from NMIBC patients underwent WTS and subsequent bioinformatic analysis. After in silico evaluation, in vitro assays including WST, quantitative PCR, and immune cell profiling were performed on mouse splenocytes. These assays were followed by in vivo assessment in both subcutaneous and orthotopic murine tumor models.
Results: Among 59 biopsies, non-recurrence correlated with heightened presence of Lactococcus species LC_001 and Bifidobacterium species BB_003. Notably, BB_003 was associated with an extended recurrence-free survival (RFS). Gene set enrichment analysis (GSEA) implicated BB_003 in mediating a pro-inflammatory cascade, accentuating macrophages and interferons. In vitro WST assays showed the antitumor potential of BB_003_β, characterized by upregulated pro-inflammatory gene transcription. This strain increased effector CD8 T cells and M2 macrophages. In vivo, direct live BB_003_β introduction into subcutaneous tumors curtailed tumor proliferation. An increase in effector CD8 T cell populations within tumors and elevated cDC1 and M1 macrophage counts in tumor-draining lymph nodes were observed. Intravesical administration of live bacteria markedly decreased bladder weight, amplifying interferon alpha and beta gene expressions compared to controls.
Conclusions: According to this study, BB_003_β inhibits tumor growth and is involved in immune response. Our study confirmed the antitumor properties of BB_003_β and suggested that cytokine and immune cell stimulation play a key role in its mechanism of action. Augmented insights warrant further exploration, particularly in synergy with intravesical BCG treatment.

#2810 Intracellular tumor microbiota promotes metastasis and drives an immunosuppressive phenotype in ovarian cancer.

A. Kumar, N. M. Bardhan, A. M. Belcher;
Massachusetts Institute of Technology (MIT), Cambridge, MA

Background: The tumor microenvironment has immense potential to change a patient's prognosis and therapeutic response. One of the emerging components of interest in the tumor microenvironment is the presence of intracellular microbes. Numerous studies have focused on colon and pancreatic cancer because of their proximity to the commensals in the gut. The female reproductive system is another site in our body where the rich vaginal microbiome has the potential to affect nearby organs and impact diseases. However, there is still little investigation done to understand the impact of microbes on Ovarian Cancer (OC).
Objective: To understand the role of the microbiome in OC metastasis, to develop new therapies to target the tumor microbiome
Methods: We used a co-culture study, the parameters of which were optimized to study the infection of microbes in different cell lines. Using a wide array proteome profiler, we looked for cytokines and chemokines to understand changes in signaling post-infection. Protein levels in the conditioned media using ELISA. Changes in actin, paxillin, and LC3B (autophagy marker) were monitored using immunofluorescence microscopy and western blots. Migration was studied by using transwell assay and spheroid cultures.
Results: We have identified two species of bacteria preferentially enriched in human ovarian tumors based on recent findings in the literature. We have demonstrated that these microbes are better at infecting OC cells in vitro over non-specific bacteria, can reside intracellularly, and are metabolically active. Upon infection, this intracellular uptake drives the release of pro-inflammatory cytokines and chemokine signaling by cancer and normal ovarian surface cells. We have also observed increased autophagy, changes in the actin cytoskeleton and reduced Paxillin foci on cancer cells infected with OC-associated microbes. This has led to increased migration in them; however, inactivated microbes did not change their migratory behavior. The infection also caused individual tumor cells to form more numerous and larger colonies when seeded into soft agar, suggesting an effect on cancer cell migration. Furthermore, we have shown that these microbes also elicit a more robust reaction in immune cells like Dendritic cells and macrophages, causing them to secrete chemokines like CCL 2,3,4,5, which also cause the cancer cells to migrate and have the potential to recruit neutrophils to drive the tumor microenvironment towards an immunosuppressive phenotype.
Conclusion: Most ovarian cancer patients are diagnosed at Stage III/IV, where cancer has metastasized, and is unresponsive to immunotherapy as the cancer is considered "cold". Through functional studies, we were able to gain insights into the role of the microbiome, which is associated with the clinical outcomes of OC, hoping to potentiate the existing therapies by probing the tumor microbiome.

TUMOR BIOLOGY: Modeling Cancer in Mice
Poster Session

#1130 Leveraging the IVIS imaging technologies for drug potency testing in orthotopic and metastatic tumor models.
J. Huang, J. Jin, H. Duan, X. Yang, W. Jin, Y. Zhang, L. Zhang, G. Xu, L. Xie, W. Li;
Pharmaron, Inc., Beijing, China

Assessing anti-tumor drug potency is significantly enhanced using orthotopic and metastasis mouse tumor models. These models imitate the tumor's native environment, biological complexities, and challenges of drug delivery via blood perfusion, thereby providing a high predictive value for clinical outcomes. In this poster, we demonstrate how the IVIS optical imaging technology is employed to determine the effects of two drugs on two tumor models: •The KRAS (G12C) inhibitor, AMG510, was evaluated on the luciferase-expressing Miapaca-2 pancreatic orthotopic model •The third-generation EGFR inhibitor, AZD9291, was tested on the luciferase-expressing NIC-H1975 intracranial metastatic model Both drugs showed significant anti-tumor activity. In addition to potency testing, each drug was administered in single doses for pharmacodynamic analysis, evaluating pERK/ERK and DUSP6 levels. The pERK levels decreased after treatment, which is in line with the mechanism of action of the inhibitors. Our research illustrates that IVIS imaging offers a robust method for monitoring anti-tumor activity of drugs in orthotopic and metastatic tumor models, empowering scientists to assess new drug candidates by using biologically relevant animal models.

#2814 Rectal implantation paves the path to evaluate the metabolic machinery responsible for CRC metastasis.

Said M. Afify, Chen Shen, Siva B. Merugu, Daniel T. Wynn, Anmada Nayak, Wenhui Lu, Ricardo M. Calderin, Evan Pannkuk, Sung H. Hong, Nagi G. Ayad, David J. Robbins

Department of Oncology, Lombardi Comprehensive Cancer Center, Georgetown University, Washington, DC

Introduction: Colorectal carcinoma patients die most often from distant metastases in liver and lung. It is crucial to develop metastatic models for the CRC in order to better understand the process, which will help in treatment.
Method: Using orthotropic transplantation techniques, we tried to test whether rectal implantation could produce spontaneous metastases in-vivo mimicking colorectal cancer. The rectum was injected orthotopically with 0.2 X 106 HCT116 cells. In order to confirm metastasis, histopathological examinations were performed. Further, we generated cancer organoids to evaluate population susceptibility to CRC metastasis and metabolic mechanisms responsible for metastasis process.
Results: We found that rectal implantation was an effective method for simulating CRC cancer metastasis using H&E staining and immunohistochemistry. In less than four weeks after the implant, HCT116 spontaneously metastasized to the liver, lungs, and D lymph node. When compared with cancer organoids derived from primary tumors, liver and lung metastases organoids proliferated more often, were more aggressive, and displayed distinct characteristics. Using non-targeting metabolomic analysis, it was found that metastases derived organoids and primary tumors derived organoids were distinguished by novel metabolites.
Conclusion: By implantation in the rectal cavity, we can evaluate the metabolic machinery that leads to CRC metastasis. In the future, implantation of patient-derived samples will become increasingly important.

#2815 Immunotherapy development landscape for bone metastasis - need of predictive preclinical efficacy evaluation for de-risking clinical development.

T. E. Kahkonen[1], J. M. Halleen[2], G. MacRitchie[3], R. M. Andersson[3], J. Bernoulli[4];
[1]OncoBone Ltd, Aura, Finland, [2]OncoBone Ltd, Kiviniemi, Finland, [3]BioSeeker Group AB, Stockholm, Sweden, [4]University of Turku, Institute of Biomedicine, Turku, Finland

Most cancer deaths are due to metastases, and bone metastases are challenge especially in breast and prostate cancer, being developed in 70-90% of advanced-stage patients. Bone metastases remain incurable causing high mortality, skeletal-related effects and decreased quality of life. Currently used immunotherapies are ineffective in bone metastases. This creates a need to improve understanding immune microenvironment in bone metastases, namely interactions between tumor, immune and bone cells according to the osteoimmuno-oncology (OIO) concept, and ultimately to develop immunotherapies that primarily target bone metastases.

We used 1stOncology database, a cancer drug development resource to identify novel immunotherapies in development for breast and prostate cancer bone metastasis. Twenty-four immunotherapies that included evaluation of effects on bone metastasis were identified. Efficacy of only three of the identified therapies had been evaluated in preclinical bone metastasis models, one reason being that such models have not been commonly available. The use of clinically relevant and predictive preclinical bone metastasis models would significantly de-risk decision making when moving to clinical development in bone metastasizing cancers.

To support predictive preclinical evaluation of immunotherapies for bone metastatic cancers, we describe a preclinical bone metastasis technology platform for evaluating efficacy of immunotherapies. The platform utilizes tumors growing in bone microenvironment, mimicking growth of bone metastases in patients, and generates tumor-induced bone effects in a cancer-type specific manner. Syngeneic and/or humanized mouse models with tumor and immune cells of the same species are needed for development of immunotherapies, allowing interactions of tumor and immune cells in the bone metastatic microenvironment to support mode-of-action studies. The platform is clinically predictive, as demonstrated with observed effects that align with clinical findings. As an example, anti-PD-1 antibody had no effects on breast and prostate cancer bone metastases, predicting recent clinical findings that demonstrate lack of efficacy in clinical prostate cancer trials.

We conclude that tumor microenvironment in bone metastases has unique characteristics and is understudied as a potential primary cause of lack of efficacy of many immunotherapies, especially in breast and prostate cancer. It is prime time to focus on bone metastases by increasing understanding of the immune landscape in the bone tumor microenvironment according to the OIO concept. The biologically relevant and clinically predictive preclinical bone metastasis technology platform should be routinely used to study the mechanism-of-action and efficacy of therapies before entering clinical development in bone metastasizing cancers.

#2816 Comparison of MB-49_luc bladder carcinoma cell clones in the orthotopic superficial bladder tumor model in C57BL/6 female mice.

M. McArthur, **M. Tran**, A. Koznecki, H. Ketteringham, C. Silvio, S. Wenzel, C. Davis, S. Nadaraia-Hoke, C. Holding, L. Salem, V. Caruso, B. Hoerner, M. Spencer, M. Josey, A. Tannu;
Reaction Biology Corporation, Hummelstown, PA

In preclinical research, cell inoculation via bladder wall injection is a standard for studying invasive bladder cancer into the bladder muscle wall. However, a subset of patients presents with non-muscle invasive (superficial) disease. The standard of care for these patients is excision coupled with BCG treatment via catheterization. There is a need to further establish mouse models of cell inoculation via bladder catheterization for early drug development. While the injection places cells into the bladder wall, catheterization coats the inside of the bladder by first instilling Poly-L-Lysine. After instilling Poly-L-Lysine, instillation of luciferase-tagged cell suspension occurs.
MB49-luc cell lines were generated to determine the optimal cell lines for use in analyzing treatments for superficial bladder carcinoma. MB49-luc cells display varying degrees of luciferase activity and growth *in vitro.* A subset of cell lines were selected for further analysis *in vivo,* via bioluminescent imaging, survival analysis, flow cytometry and necropsy. The data provides a preclinical reference for the selection of a cell line for analysis of new drug candidates in C57BL/6 female mice inoculated via bladder catheterization.

#2817 Establishment of KRAS G12C mutant brain metastasis models for pre-clinical evaluation of KRAS G12C targeted anticancer therapy.

Q. Chen, G. Wang, Y. Yin;
Shanghai ChemPartner Co., Ltd., Shanghai, China

KRAS is one of the most frequently mutated oncogenes in cancers, especially in lung cancer. Clinical research has shown that about 14% of non-small-cell lung cancers (NSCLCs) carry the KRASG12C mutation, and brain metastases are a relatively common occurrence in KRASG12C-mutated NSCLC. Approximately 30% of patients with KRASG12C mutations develop brain metastases, and those with KRAS-mutated NSCLC and untreated brain metastases have limited treatment options and poor clinical outcomes. AMG510 (Sotorasib) is a small molecule inhibitor of KRASG12C that specifically binds to inactive GDP-bound KRASG12C, preventing its oncogenic signaling. It has been approved for NSCLC by the FDA. Recent clinical studies have shown that Sotorasib exhibits some activity against KRASG12C NSCLC brain metastasis. To evaluate the in vivo activity of AMG510 for NSCLC brain metastasis treatment and provide insights for the preclinical development of new KRAS targeted inhibitors, we established advanced orthotopic models, including intracranial, intracarotid, and intracardiac metastatic models, using the NCI-H358-luc cell line, which harbors the KRASG12C mutation. We validated these models with AMG510 as a single agent or in combination with radiation, which is commonly used in brain tumor therapeutic strategies, to reveal the efficacy and brain concentration of AMG510 in KRASG12C brain metastasis models. Tumor growth and metastasis incidences were assessed using bioluminescence imaging (BLI). All animal studies were performed in an AAALAC accredited facility and aligned with animal welfare regulations. Our preliminary results reveal that AMG510 could penetrate the blood-brain barrier (BBB) and show therapeutic activity for KRASG12C brain metastatic tumors. These models represent powerful tools for clinically relevant assessment of the efficacy of novel KRAS G12C inhibitors and can be expanded for other KRAS mutations-associated brain metastasis or inhibitors.

#2818 Investigating the role of TNIK in the pathogenesis of lung squamous cell carcinoma.

J. Chang[1], D. Dutta Chowdhury[1], D. N. Council[1], T. Nguyen[2], S. Jagtap[1], A. Chan[1], M. Ajmal Khan[1], N. Connis[3], P. Torres-Ayuso[4], J. Brognard[5], M. Rezaee[3], A. Lafargue[1], C. Hann[3], P. T. Tran[1],

[1]University of Maryland, Baltimore, Baltimore, MD, [2]Johns Hopkins Bloomberg School of Public Health, Baltimore, MD, [3]Johns Hopkins School of Medicine, Baltimore, MD, [4]Temple University Lewis Katz School of Medicine, Philadelphia, PA, [5]National Cancer Institute, Frederick, MD

Lung squamous cell carcinoma (LSCC) is the second most prevalent type of lung cancer with no FDA-approved targeted therapies. Platinum-based chemotherapy and immunotherapy remain the cornerstone of current treatments for advanced LSCC, and the 5-year survival rate is less than 10%. Despite abundant knowledge of the mutational landscape of LSCC, there is a paucity of effective targeted therapies. Amplification of chromosome 3q26 is the most common genomic alteration in LSCC and this leads to the overexpression of oncogenic kinases like TNIK. *TNIK* amplification occurs in approximately 50% of LSCC cases and is associated with tumorigenesis and therapy resistance in other cancers. Recent studies showed that TNIK maintains the survival of LSCC cells and drives LSCC progression. Furthermore, inhibiting the kinase eradicates tumor growth in TNIK-high preclinical models. These findings highlight the potential of TNIK as a therapeutic target in a subset of LSCC patients with 3q amplification. However, one major limitation of previous studies is the lack of animal models with squamous histology and patient-relevant genotypes. Therefore, we have created a novel conditional TNIK-overexpressing genetically engineered mouse model (GEMM) to better understand the roles of TNIK in tumor progression and therapy resistance in LSCC and elucidate mechanisms underlying LSCC pathogenesis. We are also producing a novel TNIK-overexpressing LSCC GEMM based on the simultaneous activation of $Kras^{G12D}$ and deletion of *Fbxw7* (KF model). We will present validation studies such as histological and molecular profiling of our conditional TNIK GEMM and initial data on the TNIK overexpressing LSCC transgenic mouse model (KF (LSCC control) vs KF-TNIK (LSCC-TNIK)).

#2819 Novel drug resistant CDX models for anti-cancer drugs discovery.

Hai-Ting Dai, Tie-Jun Bing, Zhi-Da An, Jie Yang, Tian-Yu Pang, Jia-Wei Gao, Yun-Yi Bo, **Wen-Jen Yu**

ICE Bioscience Inc., Beijing, China

Oncogene BRAF is located on chromosome 7q34, consisting of 766 amino acids and 22 exons, encoding a serine/threonine protein kinase belonging to the RAF family and plays a critical role in the MAPK signaling pathway. The mutation of BRAF was documented in nearly 8% of all human cancers including melanoma (60%), thyroid (60%), and lung adenocarcinoma (10%). The most common mutation of BRAF is V600E (Class I), which was found in more than 70% in these cancers. Despite the clinical success of approved small molecule inhibitors of BRAF V600E (vemurafenib, dabrafenib and encorafenib), this remains an area of unmet medical need because of primary or acquired drug resistance. The construction of BRAF drug-resistant cell lines plays a pivotal role in cancer research. It serves as a crucial tool for discovery of the mechanisms of drug resistance. In this study, we have developed a systematic approach for constructing drug-resistant cell lines, inducing resistance through the gradual escalation of drug concentrations. The validation of drug resistance involves morphological recordings of parent and drug-resistant cell lines, drug resistance index in vitro through IC50 measurements and in vivo through the inhibition of tumor growth (TGI) which compare to those in the parental cell line. We successfully established Vemurafenib and Dabrafenib resistant A375 cell lines (A375 Vemurafenib R, A375 Dabrafenib R) with 21 and 31.5 folds of resistance index, respectively. The in vivo drug resistance efficacy was also tested by implanting Vemurafenib resistant cells subcutaneously into NOD-SCID mice and showed that A375 Vemurafenib R exhibited robust tolerance to 50 mg/kg Vemurafenib treatment (P.O.21 days, 50mpk, TGI=17.4%), whereas the parental cells were nearly completely inhibited (P.O.21 days, 50mpk, TGI=92.3%). In addition, single-cell sequencing of A375 Vemurafenib R revealed significant gene expression differences in the MAPK and EGFR signaling pathways, aiding in the identification of new targets, and signaling pathways associated with drug resistance, thereby providing potential targets for new drug development.

#2820 The effect of *Pten* haploinsufficiency on genomic and transcriptomic profiles in combined genetically-engineered mouse models for colonic neoplasia based on *Apc* inactivation.

H. Sada[1], H. Niitsu[2], H. Nakahara[3], N. Sakamoto[4], H. Tashiro[1], H. Ohdan[4], T. Hinoi[3];
[1]Kure Medical Ctr. & Chugoku Cancer Ctr., Kure, Japan, [2]Aichi Cancer Center Research Institute, Nagoya, Japan, [3]Hiroshima University Hospital, Hiroshima, Japan, [4]Hiroshima University, Hiroshima, Japan

Background and Aim: We have reported genetically-engineered mouse models for colonic neoplasia by using our novel *CDX2P-Cre* mice, in which Cre is restrictedly expressed in colonic epithelial cells. Although colonic tumors are generated in *CDX2P-Cre;Apc*$^{flox/+}$ (*CPC;Apc*) mice with highly penetrant rate, greater number and deeper invasion of colonic tumors were observed in *CDX2P-Cre;Apc*$^{flox/+}$*;Pten*$^{flox/+}$ (*CPC;Apc+Pten*), possibly resulting from haploinsufficiency of *Pten* gene. We have also confirmed shorter lifespan in *CPC;Apc+Pten* than that in *CPC;Apc* (AACR Annual Meeting 2018). Here, we test if these phenotypes come from one copy loss of *Pten* itself or secondary genetic and/or transcriptomic alterations induced by *Pten* loss by using whole genome sequence (WGS) and RNA sequence from macroscopically-dissected colonic tumors (bulk RNA-seq).
Methods: WGS for five tumors and five livers as counterpart controls in each mouse model was performed by DNBSEQ platforms. Bulk RNA-seq was performed for three tumors in each model.
Results: In the analysis using B-allele frequency, copy-neutral LOH occurred in chromosome 18 including *Apc* loci specifically in colonic neoplasia in both *CPC;Apc* and *CPC;Apc+Pten* mice. In contrast, LOH was not observed in chromosome 19 including *Pten* loci in *CPC;Apc+Pten* mice. We also confirmed remarkably decreased coverage of reads in reference mapping in *Apc* locus, and there was a slight decrease of coverage in *Pten* locus. There were no additional driver gene mutations in *CPC;Apc* or *CPC;Apc+Pten* in WGS. All these results suggested just one copy loss of *Pten* resulting in aggressive tumor phenotype in *CPC;Apc+Pten* mice. In RNA-seq and subsequent GSEA comparing colonic tumors in *CPC;Apc+Pten* with those in *CPC;Apc* revealed upregulation of some signal pathways including mTORC1. Supporting this observation, number of colon tumors, especially adenocarcinomas, were decreased by rapamycin administration to *CPC;Apc+Pten*. Similarly, rapamycin was more effective in tumorids from *CPC;Apc+Pten* those from *CPC;Apc*.
Conclusion: WGS reveals one copy loss of *Pten* locus is the only genetic alteration *in CPC;Apc+Pten* when compared with *CPC;Apc*. One copy loss of *Pten* is sufficient to upregulate mTORC1 pathway in a *CPC;Apc+Pten* mouse model, resulting in promotion of tumor formation and invasion.

#2821 Development of therapeutic monoclonal antibodies against DKK1 peptide-HLA-A2 complex to treat human cancers.

J. Qian, W. Qiang, L. Xiao, W. Xiong, M. Xian, C. Zhang, Y. Li, Q. Yi;
The Houston Methodist Research Institute, Houston, TX

Immunotherapy is a promising option for cancer treatment. Targeted immunotherapy with monoclonal antibodies (mAbs) is an effective and safe method for the treatment of malignancies. In recent years, efforts have been made to identify potential therapeutic mAbs by defining alternative or novel target antigens. We reported that Dickkopf-1 (DKK1) is a good target for immunotherapy of human cancers based on its wide expression in different cancers but not in normal tissues. As DKK1 is a secreted protein, mAbs directly binding to DKK1 may have limited effects on cancer cells in vivo. Our previous studies demonstrated that DKK1 peptide (such as P20 and P66v, which bind with HLA-A*0201 (HLA-A2) molecule) specific cytotoxic T cells specifically kill myeloma and other cancer cells that express DKK1 and HLA-A2, but not HLA-A2$^{\pm}$ normal cells, indicating that DKK1$^{\pm}$ tumor cells naturally express these peptides, in the context of HLA-A2 molecules, on their surface. To develop cancer therapeutic antibodies, DKK1 peptide P20-HLA-A2 monomer was synthesized and used to immunize mice. Hybridomas secreting mAbs recognizing cell surface-expressed DKKl P20-HLA-A2 complex (DKK1-A2) were obtained and analyzed. In this study, we generated novel (DKK1-A2) mAbs recognizing DKK1 (P20) peptide in the context of human HLA-A*0201 (HLA-A2) molecules (DKK1-A2 complexes) that are naturally expressed by HLA-A2$^{\pm}$DKK1$^{\pm}$ cancer cells. These mAbs bound to HLA-A2$^{\pm}$DKK1$^{\pm}$ hematologic (myeloma, lymphoma, and leukemia) and solid (breast, pancreatic, and prostate) cancer cells and directly induced apoptosis in the cancer cells by activating the caspase-9 cascade. DKK1-A2 mAbs also effectively lysed cancer cells in vitro by mediating CDC and ADCC activities. Furthermore, DKK1-A2 mAbs were therapeutic against established hematologic and solid cancers in their xenograft mouse models. To enhance the therapeutic efficacy of DKK1-A2 mAbs, we investigated the effect of combination treatment of DKK1-A2 mAbs with lenalidomide. Our results showed that there is an additive therapeutic effect between DKK1-A2 mAbs and lenalidomide in vivo, underscoring a potential clinical development strategy for combining DKK1-A2 mAb with lenalidomide to treat cancer patients. As DKK1 is not detected in most human tissues, DKK1-A2 mAbs did not bind to or kill HLA-A2$^{\pm}$ blood cells in vitro nor caused tissue damage in vivo in tumor-free or tumor-bearing HLA-A2-transgenic mice. Thus, our study suggests that DKK1-A2 mAbs may be a promising therapeutic agent to treat human cancers and warrants further preclinic studies to determine their translatability to clinic.

#2822 Heterogeneity of CD56+ circulating tumor cells and derived xenografts and response to treatment in small cell lung cancer.

L. Martinetti[1], **P. Montagne**[2], M. Davilma[1], U. Jarry[2], A. Chatziioannou[3], M. Aubry[1], C. Ricordel[4], R. Pedeux[1];

[1]OSS (Oncogenesis Stress Signaling), UMR_S 1242, CLCC Eugene Marquis, Univ Rennes 1, Rennes, France, [2]Biotrial, Rennes, France, [3]Centre of Systems Biology, Biomedical Research Foundation of the Academy of Athens, Athens, Greece, [4]OSS (Oncogenesis Stress Signaling), UMR_S 1242, CLCC Eugene Marquis, Univ Rennes 1; CHU Rennes Service de Pneumologie, Rennes, France

Small cell lung cancer (SCLC) represents the most aggressive subtype of lung cancer, comprising 15% of all cases. Clinical advancements in SCLC have been hindered by slow progress, attributed to significant tumor heterogeneity and early metastasis. The majority of patients experience relapse within a few months post-treatment, with 20% exhibiting chemorefractory characteristics. Recent identification of molecular subtypes in SCLC, dependent on predominant transcription factors ASCL1, NEUROD1, and POU2F3, has opened avenues for potential therapeutic targets. Preliminary studies on these transcriptomic subtypes suggest distinct therapeutic susceptibilities, and intriguingly, chemotherapy may induce alterations in transcriptomic subtypes.In the context of SCLC, diagnosis reveals a substantial presence of circulating tumor cells (CTCs) in the patient's bloodstream, which can be efficiently isolated. A previously published method allowed us to isolate CD56+ CTCs with high specificity (Ricordel et al., 2023). Our overarching hypothesis posits a connection between chemosensitivity and the heterogeneity of CTCs, leading us to seek bioclinical markers predictive of chemotherapy response. The clinical study, named CTC-CPC, is a monocentric prospective non-interventional investigation involving treatment-naïve SCLC patients. Blood samples were collected at the time of diagnosis for subsequent analysis. In our study, whole exome sequencing data from isolated CD56+ CTCs of 22 SCLC patients were analyzed. Various methods were employed to characterize inter-tumoral heterogeneity, including the identification of genetic alterations (SSMs and Indels), mutational signatures, and disrupted pathways. Prominently affected pathways included ECM organization, axon guidance, Rho GTPases, and Wnt signaling. Additionally, we unveiled substantial intra-tumoral heterogeneity using PhyloWGS, a technique for reconstructing subclonal composition and evolution from tumor sample sequencing. To further explore the impact of treatment, we aimed to clarify the expression of ASCL1, NEUROD1, and POU2F3 transcription markers in xenografts generated from patient CTCs at the time of diagnosis. Immunohistochemical studies were performed to identify potential changes in molecular subtypes at the protein level. The molecular subtypes of the four CDX we generated were characterized, revealing heterogeneity in the intratumoral expression of transcription markers for some xenografts. Subsequently, CTC-derived xenografts were subjected to chemotherapy, with observations indicating a change in the number of cells positive for ASCL1 and NEUROD1 after treatment, particularly in the CEM51.01 line treated with carboplatin, suggesting a potential modification in the tumor subtype induced by the treatment

#2823 Development of an *in vitro* blood-brain barrier model of CCR7/CCL19 induced invasion of the central nervous system.

A. Rodriguez, C. I. Cardona, C. A. Bill, C. M. Vines;
The University of Texas at El Paso, El Paso, TX

Pediatric T-cell acute lymphoblastic leukemia (T-ALL), an aggressive hematological malignancy, is characterized by abnormal thymocyte proliferation, frequently with mutations of the Notch-1 gene and has an overall 10-year survival rate of ~27%. A marker of poor prognosis is the presence of T-ALL within the central nervous system (CNS), which is treated with intrathecal chemotherapy and cranial irradiation; two toxic treatments with high morbidities. Gene-expression profiling of Notch-1-induced adhesion regulators showed that C-C chemokine receptor 7 (CCR7) was highly expressed and was associated with leukemic T-cell invasion of the CNS. Normal functions of CCR7 include lymph node homing and immune cell trafficking in response to CCR7 ligands, CC-chemokine ligand 19 (CCL19) or CCL21. In several studies CCL19 has been linked to T-cell invasion of the CNS across the blood-brain barrier (BBB). We hypothesize that antagonizing CCR7 binding to CCL19 will block migration of T-ALL into the CNS and thereby alleviate the need for toxic therapies. To test our hypothesis, we are using receptor internalization assays, calcium mobilization assays, transwell migration assays and an *in vitro* model of an intact human BBB. We have used flow cytometry-based CCR7 internalization assays ± CCR7 antagonist and found that we can completely block CCL19-induced receptor internalization in human CCR7-expressing CCRF-CEM, and HuT-78 T-ALL cells, and chemotaxis via β1 integrins across a fibronectin-coated transwell membrane. Our BBB employs HBEC-5i, human cerebral microvascular endothelial cells, in transwell chambers coated with gelatin and fibronectin for the adhesion of endothelial cells. HBEC-5i cells are a suitable cell line to make a 3D model of the BBB, as they form an endothelial monolayer with tight junctions (TJ), which is crucial to maintaining the integrity and inhibiting permeability of the BBB. We are establishing a transwell migration assay to assess the migration of CCRF-CEM T-ALL cells across the HBEC-5i cell monolayer. The integrity of the HBEC-5i cell monolayer is assessed by trans-epithelial electrical resistance (TEER), which measures the electrical resistance across the HBEC-5i monolayer, a measure of TJ integrity. Using TEER measurements, we observe that HBEC-5i form a monolayer that reaches an intact monolayer functioning with TJs over 72-96 hours. We are using this model system to investigate the migration of CCR7-expressing CCRF-CEM cells through the BBB ± CCL19. Subsequently, we will add the CCL19 antagonist (CCL197-77) to determine if inhibiting CCR7 is sufficient to eliminate migration of the CCRF-CEM cells through the BBB. If successful, this model will allow us to test the contribution of CCR7 signaling to integrins, the contribution of other immune cell types and the overall molecular mechanisms that mediate invasion of the CNS in a 3-D model of the BBB.

#2824 Establishing prostate cancer models for orthotopic and bone metastatic growth using the 22Rv1cell line.

J. Zdrojewska, **K. Fagerlund**, J. H. E. Maki-Jouppila, M. I. Suominen;
Pharmatest Services Ltd., Turku, Finland

Prostate cancer is the second most common cancer in men with new cases diagnosed in 1.4 million men each year. Luckily the 5-year survival rates in developed countries are high reaching over 90%. However, approximately one third will develop a metastatic disease. In metastatic patients, prostate cancer almost always progresses despite the androgen deprivation therapy and is then referred to as “castration-resistant (mCRPC)”. Bone is involved in 80% of patients with metastasis, and the bone lesions are typically osteoblastic. The 22Rv1 human prostate carcinoma cell line is androgen sensitive and shown to express androgen receptor (AR). They also express low levels of prostate-specific membrane antigen (PSMA). The aim of this study was to establish orthotopic and intratibial preclinical in vivo prostate cancer models that can be used in drug development when targeting cancer cells and their local environment. Male athymic nude mice (5-6 weeks old) and NOG mice (over 20 weeks old) were used in the study. 2.5×10^5 22Rv1 cells (ATCC) were inoculated orthotopically into the prostate of NOG mice, and 5×10^5 cells were inoculated intratibially into the bone marrow cavity of athymic nude mice. Tumor growth was followed by PSA measurements every second week using Human PSA ELISA assay. In addition, in the intratibial model, tumor-induced bone changes were monitored by X-ray imaging of the hind limbs. Prostates and hind limbs were collected at sacrifice, fixed in 10% NBF, and processed to paraffin blocks for further histological analysis. Sections of prostate were stained with hematoxylin-eosin (HE) and AR. Tumor-bearing and contralateral (healthy) tibias were stained with HE - OrangeG, MGT, TRAP, and AR. The observed tumor take rate was 92% in the orthotopic and 100% in the intratibial models. Confirmed by IHC, tumors formed in both the orthotopic and intratibial models expressed AR. 22Rv1 cells formed osteoblastic - lytic mixed bone lesions in the intratibial model. Based on lesion areas, randomization of the tumor bearing mice in the intratibial model can be done after 2 weeks from cancer cell inoculation. Taken together, the 22Rv1 prostate cancer models are relatively fast growing, express AR and present good take rates. Furthermore, the intratibial model represents robust tumor-induced changes in bone with strong osteoblastic component. Thus, these models have several advantages in efficacy studies of novel drug candidates for prostate cancer.

#2825 Experimental hyperthermic intraperitoneal chemotherapy in mice: Establishment of a novel ovarian cancer xenograft model.

K. Fleten, Y. Andersson, E. Lovstakken, T. M. Herud, S. Waagene, K. Flatmark;
Oslo University Hospital, Oslo, Norway

Introduction: The peritoneum is a common metastatic site for several abdominal cancers, including ovarian and colorectal cancer. Peritoneal metastasis is associated with poor prognosis and poor response to therapy. A potentially curative treatment is cytoreductive surgery (CRS) to remove all visible tumor tissue, followed by perfusion with hyperthermic intraperitoneal chemotherapy (HIPEC) to eliminate small residual tumors and free-floating tumor cells. Hyperthermia can enhance the cytotoxic effect of the drug, inhibit DNA repair and activate the immune system. At the current time, there is no standardized protocol for performing HIPEC, and there is a large variation regarding key parameters, such as choice of drug, drug concentration, treatment duration, carrier solution, volume and temperature. The impact of these parameters is unknown, and in vivo models can be a helpful tool to better understand some of these parameters to improve this treatment strategy.
Methods: HIPEC was established in a murine xenograft model of ovarian cancer to evaluate the response to intraperitoneal perfusion of cisplatin and mitomycin C for 30 min at 41.5°C (HIPEC) and 37°C (NIPEC) compared to no treatment or intraperitoneal perfusion with saline at 41.5°C. The luciferase transfected B76 ovarian cancer cell line was injected intraperitoneally and treatment was performed on day 4 when the tumors were < 2 mm. Treatment efficacy was assessed by weekly luminescence measurement, tumor weight at an early time point (day 17), and overall survival.
Results: Intraperitoneal perfusion with cisplatin or mitomycin C significantly inhibited tumor growth as assessed by luminescence, tumor weight on day 17, as well as increased overall survival of the mice compared to control treatment from 25-27 days to 36 days for cisplatin and 37 days for mitomycin C. No significant differences in tumor growth or survival were observed by the addition of hyperthermia. However, a slight reduction of tumor weight at day 17 was observed in the HIPEC groups.
Conclusion: We have established a functional closed HIPEC model in mice bearing peritoneal metastases from the B76 ovarian cancer cell line which accurately mimics many features of the procedure in patients. Intraperitoneal perfusion of both cisplatin and mitomycin C efficaciously inhibited tumor growth and improved overall survival of the mice. Addition of hyperthermia caused an additional modest, temporary growth inhibition which did not translate into improved long-term outcome.

#2826 Examples of translational preclinical models to mimic cancer drug resistance.

M. Hillairet de Boisferon, N. Hoffmann, E. Rajon, I. Benzaid;
Oncodesign Services, Dijon Cedex, France

Drug resistance is becoming a major obstacle when treating patients with cancer. Cancer is characterized by an uncontrolled growth of abnormal cells with permanent genome alterations, which lead to severe mutations including resistance mechanisms. Mutations can occur in different resistance pathways, such as inhibition of drug transport, DNA damage repair, drug efflux, EMT (epithelial-mesenchymal transition), drug target alteration and cell death inhibition.
Resistance mechanisms are now well studied in vitro, based on mutated cell lines for specific resistance pathways. There is however a gap in our knowledge of resistance mechanisms observed in patient tumor cells. We are challenged to discover cancer resistance treatments in patients and need predictive models of clinical situations. Animal tumor models are the best translational tools to study cancer drug resistance, especially when they closely mimic human pathologies. Such models can bridge the gap between our understanding of cancer resistance in vitro and in tumor patients. In this poster we show different pre-clinical experiments, simulating clinical translational approaches, that led to novel and unique tumor resistant models.
Patient Derived Xenograft (PDX) models: Using our breast cancer PDX collection we showed that after repeated treatment with a spindle poison, tumor-bearing mice started to develop resistance and continued tumor growth under drug pressure. Following this successful approach, we initiated the development of a novel ER2-expressing PDX breast tumor model, resistant to hormone therapy by repeated Fulvestrant treatment. Using our colon cancer PDX collection we were able to recapitulate clinical situations by correlating PDX molecular profiles and drug sensitivity. We confirmed the key role of a *KRAS* mutation in cetuximab resistance.
Syngeneic model: In this model, animals were dosed with anti-PDL1 as first line of treatment. All animals were then defined as initial responders or non-responders at the end of the dosing schedule. Following this, a new treatment protocol was initiated with a Tyrosine Kinase inhibitor to study the effect of second line drug treatment in responder and non-responder arms.
Human model: In this experiment, we performed a first line Avastin treatment on human colon carcinoma tumor-bearing mice. A tumor resistance to Avastin was observed. During the second line of treatment with a tyrosine kinase inhibitor, we observed an antitumor activity on Avastin resistant animals.
In each of these case studies, we developed a novel tumor-resistant mechanism model. In some tumor models, we showed the added value of treating animals with new drugs as second line treatment, after establishing resistance to the first line standard of care treatment.

#2827 Characterization of acute myeloid leukemia PDX models with hotspot gene mutations for therapeutic evaluation.

Q. Liu, J. Wang, J. Liu, L. Zhang, L. Bourre, **J. Wang**;
Crown Bioscience, Inc., San Diego, CA

Introduction: Acute myeloid leukemia (AML) is the most common acute type of leukemia in adults characterized by chromosomal abnormalities and gene mutations. While inhibitors have shown promise targeting FLT3 mutations, resistance to these inhibitors can emerge. Similarly, inhibitors targeting IDH1 and IDH2 mutations showed promise, yet the emergence of drug resistance poses a significant challenge. In this study, a panel of AML PDX models with multiple gene alterations was established to support the development of new therapies.

Methods: The systemic AML PDX models were established using patients' peripheral blood (PB) or bone morrow (BM) injected intravenously and expanded *in vivo* by using splenic tumor cells. One AML PDX model derived from patient skin was established subcutaneously. Expression of human CD45+ in PB cells for systemic models or tumor volume for the subcutaneous model was used to monitor the tumor burden. Leukemic loads (hCD45+ cells) were measured in PB, spleen (SP), and BM. Tumors were categorized following tumor immunophenotyping, histology, and RNA sequencing/Whole Exome Sequencing. For *in vivo* efficacy studies, animals were grouped 3-5 weeks after systemic tumor cells inoculation and treated with AC220 (1, 2 or 10 mg/kg, p.o., QD), Cytarabine (Ara-c, 2mg/kg, i.p., QD), 5-azacytidine (2mg/kg, i.p., QD), Sorafenib (10mg/kg, i.p., QD) and Gilteritinib (10 or 30mg/kg, p.o., QD).

Results: Nine systemic and one subcutaneous AML PDX models carrying hotspot mutations (e.i. FLT3-ITD or TKD, IDH1-R132H and IDH2-R140Q) were established, showing comparable features to the clinic. Systemic AM8231 PDX model harboring FLT3-ITD mutation treated with AC220, a type II FLT3i, showed significant tumor burden reduction in PB at different time points and in SP and BM at termination, as well as a survival increase. Similarly in systemic model AM7577 with FLT3-ITD mutation treated with AC220, significant tumor burden reduction in PB was observed. Whereas using systemic model AM9626 (model with Sorafenib pretreatment history) with coexisting-FLT3-ITD/D835H TKD mutation, no significant efficacy was observed with AC220i, suggesting a FLT3-TKD mediated resistance mechanism. To overcome the resistance, Gilteritinib, a type I FLT3i, was tested in AM9626 and showed significant reduction of hCD45+ cells in PB compared to the control group, even at a lowest dose. As model AM9626 PDX also carries IDH1 mutation, the level of serum 2-HG correlated with the tumor burden. The functional effect of IDH1 inhibitor on the tumor inhibition and 2-HG level is under investigation.

Conclusion: The results presented in this study showed the establishment of a panel of AML PDX models, including different subtypes and genomic features reflecting the clinic. Those models will support the preclinical evaluation of new treatments or combination modalities as well as a better understanding of drug resistance mechanisms.

#2828 Combining neratinib with trastuzumab deruxtecan to treat HER2;TP53 co-mutated breast cancers.

X. Cheng, M. Highkin, J. Hsia, J. L. Prior, I. S. Hagemann, R. Bose;
Washington University in St. Louis, St. Louis, MO

In metastatic breast cancer, *HER2* activating mutations frequently co-occur with mutations in the *TP53* gene and patients with these two co-occuring mutations have a lower response rate to neratinib. In order to address this clinical problem, we bred HER2 activating mutant transgenic mice with two different alleles of TP53. We used mice with the TP53 R172H mutation, which is the murine homolog of the human hotspot TP53 R175H mutation, and mice with TP53flox/flox allele, which mimics TP53 truncating mutations seen in human breast cancers.

Abbreviation	Genotype	Median tumor formation (weeks)	Neratinib IC50 (nM)	Neratinib +T-DXd
H	$HER2^{V777L}$	28	10	Not determined
$H53^{null}$	$HER2^{V777L}$;$TP53^{flox/flox}$	10	240	Synergy
$H53^{172/WT}$	$HER2^{V777L}$;$TP53^{R172H/WT}$	11	100	Synergy
$H53^{172/null}$	$HER2^{V777L}$;$TP53^{R172H/flox}$	6	150	Synergy

All three H53 genotypes ($H53^{null}$, $H53^{172/WT}$, and $H53^{172/null}$) developed breast cancers faster than H mice, with $H53^{172/null}$ mice developing breast tumors the fastest, at just 6 weeks after adenoviral-Cre injection into the mammary fat pad. We developed organoids from these murine breast cancers and found that all H53 genotype organoids were less sensitive to neratinib compared to H, however, neratinib was able to synergize with trastuzumab deruxtecan (T-DXd), likely through neratinib mediated increased internalization of T-DXd. Prior literature studies suggest TP53 mutant cancer cells may have therapeutic vulnerabilities to the topoisomerase 1 (Top1) inhibitors. Organoids from all three H53 genotypes were sensitive to the Top1 inhibitor, exatecan. $H53^{172/WT}$ behaved like H organoids with G1 phase cell cycle arrest and induction of p21 expression after exatecan treatment. In contrast, $H53^{null}$ and $H53^{172/null}$ failed to induce p21 and arrested at late-S/G2 phase. Additional animal experiments with these H53 genotypes are in progress and results will be presented at the AACR Annual Meeting.

#2829 Strategies to overcome challenges in randomization and grouping methodologies in *in vivo* studies using the power of animal study workflow software.

Raghu Ramachandra

Sanford Burnham Prebys Medical Discovery Institute, La Jolla, CA

Preclinical research in Oncology requires using a wide variety of animal models. Robust, clinically relevant distribution methods including randomized and non-random methods appropriate to the model are essential to ensure unbiased group assignments and reliable experimental outcomes. This presentation will explore flaws and inconveniences in prevalent randomization methods and strategies to overcome them using animal study workflow software and demonstrate the power of each with unique examples. Strategies for randomizing individual animals into groups and randomizing mouse cages into groups will be explored. Strategies for exclusion criteria, robust documentation, multi-parameter randomization, re-randomization, and clinical relevance of these strategies will be discussed. Standardization and automation of distribution methods help improve process integrity, research quality, and reproducibility.

#2830 Intravital multiphoton microscopy of bone metastatic renal cell carcinoma.

S. Maksimovic[1], N. Boscolo[1], S. Barrios[1], A. Mikos[2], M. T. Campbell[1], E. Dondossola[1];
[1]UT MD Anderson Cancer Center, Houston, TX, [2]Rice University, Houston, TX

Clear cell renal carcinoma (ccRCC) represents 80% of renal neoplasms, with bone as a major site for distant spread (35-40% of patients). These secondary lesions cause a variety of skeletal-related complications, including pain, spinal cord compression, hypercalcemia, mobility issues and fractures, posing a significant negative impact on patient quality of life and survival. Furthermore, bone is well-known as a site of therapy resistance, which confers to patients treated with systemic therapies significantly worse time-to-treatment failure and progression-free and overall survival compared to those without bone metastases. Because of the complexity of the bone microenvironment and the paucity of suitable models, preclinical investigation of bone metastasis and therapy response is challenging. Preclinical models of bone metastasis that integrate tissue engineering and advanced imaging techniques can facilitate the study of the mechanism of tumor progression and therapy response. We recently developed a window model amenable to intravital multiphoton microscopy (MPM) to longitudinally monitor human ccRCC lesions in tissue engineered bone constructs (TEBCs) in immunodeficient mice. TEBCs were generated by functionalizing polymeric polycaprolactone scaffolds with bone morphogenetic protein 7. Human ccRCC lesions, after implantation into the bone cavity, were longitudinally monitored for growth and niche development, using multi-parameter recording of collagen/bone matrix (SHG), bone surface (THG), blood vessels/stromal phagocytes (fluorescent dextran), and tumor cells (GFP). However, this model lacked key components of the immune system (including B and T-cells), which are of major interest in the study of tumor progression and (immune) therapy response. Therefore, we developed a tissue-engineered preclinical model that incorporate species-specific interactions between cancer and bone stromal cells, and account for an intact immune system. To this purpose, we optimized TEBC formation in C57BL/6 fluorescent reporter mice (Sp7-mCherry, osteoblasts; Trap-td-Tomato, osteoclasts; GFP, immune cells, αSMA-RFP fibroblasts; and Flk1-GFP, blood vessels), coupled to detection by intravital or *ex vivo* multiphoton microscopy analysis, to monitor the evolution and fate of the TEBC. Interestingly, the bone marrow in the core of the TEBC was replaced by a desmoplastic tissue with features like the foreign body response, including foreign body giant cells, which was not present in immunodeficient mice. By applying dual color GFP/αSMA-RFP mice, which expressed red fluorescence in activated fibroblasts, we confirmed the fibrotic nature of this core. To avoid its formation, we generated scaffold-free ossicle, by direct implantation of BMP7 and VEGF in the subcutaneous tissue. To conclude, we established a protocol for generating ectopic ossicles in immunocompetent mice.

#2831 Development and application of the NCG-hIL2 mouse model: A humanized platform for enhanced NK cell evaluation in ADCC efficacy testing.

Y. Fang, H. Sun, H. Wang, J. Xing, J. Fan, J. Zhao, X. Gao, C. Ju;
Gempharmatech Co., Ltd., Nanjing, China

Natural Killer (NK) cells play a pivotal role in immune surveillance and antitumor responses, making them valuable targets in cancer immunotherapy. The assessment of therapeutic antibodies' efficacy, particularly in the context of Antibody-Dependent Cell-Mediated Cytotoxicity (ADCC), necessitates models that faithfully recapitulate human NK cell responses. Here, we introduce the NCG-hIL2 mouse model, designed to address these requirements and advance our understanding of NK cell development.

The NCG-hIL2 mouse model was engineered to express human Interleukin-2 (IL2) cytokine, a critical factor in NK cell development and activation. This humanized platform allows for the robust reconstitution of human NK cells through the transplantation of peripheral blood mononuclear cells (PBMCs) or hematopoietic stem cells (HSCs).

In this study, we validate the NCG-hIL2 model's exceptional capability in supporting the reconstitution of human NK cells, highlighting the indispensable role of IL2 in NK cell development. Moreover, we demonstrate its utility in the evaluation of therapeutic antibodies, specifically Trastuzumab and the ADCC-enhanced Margetuximab, in the context of ADCC efficacy testing. Our findings reveal that the NCG-hIL2 model provides a unique advantage for assessing the impact of IL2 on NK cell development, thus facilitating a deeper understanding of the complex interplay between NK cells and therapeutic antibodies.

The NCG-hIL2 mouse model serves as a valuable tool for studying NK cell development and evaluating the efficacy of immunotherapies, particularly in ADCC. By reconstituting human NK cells and leveraging the role of IL2, this model offers an enhanced platform for preclinical evaluation of therapeutic antibodies, ultimately advancing our ability to harness NK cell-mediated antitumor responses. It is poised to contribute significantly to the field of cancer immunotherapy and drug development.

#2832 Mouse models advancing cancer research - The Jackson Laboratory.

J. Beckwith, J. Merriam, A. Valenzuela, D. Pomerleau, J. Kelmenson;
The Jackson Laboratory, Bar Harbor, ME

Genetically defined mice are a cornerstone of cancer research. The Jackson Laboratory (JAX) offers more than 13,500 unique mouse lines to the scientific community, many useful in advancing cancer research. Available are mouse models for specific cancers, xenograft recipients, immunodeficient platforms for PDX studies and multi-purpose tool strains having CRISPR/Cas9 utility, conditional/inducible expression (Cre-lox, FLP-frt, Tet-On/-Off), optogenetic function and calcium-sensing technologies. This poster will highlight some recently added models, more than 100 of which have cancer research applications. The portfolio of strains useful for transplantation/engraftment and “humanized” mouse research continues to expand and complement the NSG (NOD scid IL2rγc-/-) model as ideal tools for engraftment with a wide range of malignant or non-malignant human or mouse tissues. Fluorescent protein-expressing strains include Traffic Light Reporters for tracking of DNA repair pathways, Gene Editing Reporters for detection of homology directed repair (HDR) and non-homologous end joining (NHEJ) repair events, as well as several CRISPR Editing, Bxb1 Integrase Editing, Base Editor and Prime Editor tools. For example, the Rosa26^{PE2} mouse has Cre-inducible expression of a prime editor enzyme and a fluorescent reporter, allowing viral delivery of prime editing guide RNAs to introduce cancer mutations into the genome. Recently added CRISPR Array Repair Lineage Tracing (CARLIN and DARLIN) component strains allow researchers to achieve high barcode diversity in targeted cell populations. In addition to safeguarding each strain by cryopreservation, JAX has a comprehensive genetic quality control program that confirms mutation identity and genetic background, and screens for unwanted alleles (such as stray GFP, Cre, neo, etc.). Search the comprehensive collection of innovative mouse models using our improved JAX Mouse Search site (mice.jax.org). This resource includes models created by many generous donating institutions. Researchers are encouraged to donate their mouse lines via a very short Strain Submission form (jax.org/donate-a-mouse). Please also visit the JAX Oncology webpage for cancer research related strains and resources (jax.org/jax-mice-and-services/solutions-by-therapeutic-area/oncology). JAX is supported by the NIH, The Howard Hughes Medical Institute and other private charitable foundations.

#2833 Validating cancer biomarker expression on mouse cell-derived xenograft models of human cancer.

M. Huang, A. E. Wiggins, D. Marroquin, M. Liu, L. Tsai;
HD Biosciences, Inc.,a WuXi AppTec company, San Diego, CA

Background and Objective: The target antigen expression level is critical for the potency of immune therapies like ADC, mRNA-LNP, and CAR-T. Selecting an appropriate cancer model remains a challenge to the pre-clinical drug testing. HD Biosciences offers over 1000 cell lines and 150 CDX mouse models of human cancers. Furthermore, we have validated the expression of three therapeutic targets Nectin-4, Trop2, and PD-L1 in various CDX tumor tissues. This poster will highlight some recently established models as well as the antigen validation result. Our study provides a reference that guides the model selection of efficacy studies targeting Nectin-4, Trop2, or PD-L1. In addition, we offer a platform to validate the expression of target antigens in CDX mouse models covering numerous cancer types.

Method and Result: Biomarker surface expression of Nectin-4, Trop2, and PD-L1 on xenograft tumors was validated by IHC staining and FACS analysis. We highlight these models with high expression of each marker. These models are available to support further efficacy studies of anti-cancer drugs targeting the marker. We also analyzed the biomarker surface expression in vitro using cell pellets via FACS analysis to compare with the in vivo expression level. Hence, the biomarker gene expression level was confirmed by FACS. Interestingly, the result indicates biomarker expression in mouse tumor tissues is often inconsistent with in vitro cell expression. For example, the A375 CDX model on humanized immunodeficient mice is commonly used for anti-PD-1/PD-L1 drug efficacy tests. However, the surface expression of PD-L1 is only detected in the A375 tumor tissues and is undetectable in the A375 cell pellet. This finding could explain the inconsistency of in vitro and in vivo drug test results. The in vivo CDX model-based biomarker would better predict the drug's efficacy, as the model better mimics the clinical situation of tumor burden in patients.

Conclusion: In vitro gene expression and protein expression of cell surface biomarkers may not be relevant to the in vivo tumor surface expression level, resulting in inconsistent efficacy data in vitro and in vivo. Thus, validating targeted biomarkers in vivo is crucial for choosing the best cancer tumor model with high target expression for drug efficacy validation. HD Biosciences provides validated 150 CDX models expressing Nectin-4, Trop2, and PD-L1 and have in vivo capability for target validation and drug efficacy study.

#2834 Establishment of orthotopic high grade glioma xenograft model using zebrafish embryos.

E. Winter da Silva[1], A. De Loose[2], Y. Chernyavskaya[1], A. Rodriguez[2], J. Blackburn[1];
[1]University of Kentucky, Lexington, KY, [2]University of Arkansas for Medical Sciences, Little Rock, AR

High grade glioma (HGG) is the most common malignant brain tumor in adults. These tumors represent a lethal group of brain tumors characterized by a remarkable level of genetic, epigenetic, and environmental heterogeneity, which can significantly affect therapy response and patient outcomes. Patient-derived xenograft (PDX) models of glioma are a central tool for neuro-oncology research and drug development, enabling the detection of patient-specific differences in growth and drug response. Mouse xenografts of HGG are well-established, but the time required to generate these models is not practical for integration into clinical paradigms. Patient derived organoids cannot mimic the physiologic aspects of an in vivo system, such as the blood-brain barrier or metabolism of drugs, which can affect how tumor cells respond to treatment. In this context, zebrafish are emerging as a time-efficient and cost-effective *in vivo* model. We investigated a rapid zebrafish-based PDX model that can recapitulate key aspects of different gliomas and enable treatment response evaluation within 8 days. We engrafted one GBM cell line (U-87), two patient-derived glioblastoma (GBM) cells, and one patient-derived IDH mutant grade 4 astrocytoma into the midbrain region of 2-day-old zebrafish embryos. Survival of transplanted larvae were monitored over 8 days post-transplantation and the engraftment was analyzed. Therapy response was evaluated through tumor size. One day post-transplantation, animals received 10 and 25 Gy radiation with or without 50 and 100 μM of temozolomide, a common GBM therapeutic, and tumor size was measured after 3 days by imaging. Results showed that GBM and astrocytoma cells had 100% and 80% of engraftment, respectively. GBM cell induced a median survival of 7 days in transplanted animals while 87 % of astrocytoma-injected animals were alive 8 days post transplantation. GBMs also varied in their drug and radiation response. Although both samples were classified as high-grade GBM and MGMT unmethylated, PDX derived from a younger patient with no alterations in PTEN and MDM2 genes responded better to temozolomide and radiation . Tumor responsiveness to therapy is often a combination of genetic and non-genetic factors that are difficult to clinicians to predict. By combining tumor-specific models and drug testing, a patient's treatment plan could be tailored based on the sensitivity of each sub-clone to targeted therapeutics. In conclusion, we showed that the zebrafish-based PDX model provides a novel, high throughput avenue to assess the impact of tumor heterogeneity on drug response.

#2835 Comparison of xenograft and syngeneic cancer cachexia models for preclinical drug testing.

K. Draheim, D. Gietl, K. Shinn, W. Durham, F. Zhao, C. Thompson, A. Baldwin, G. Harris, C. Hall, **P. Fadden**, A. Avrutskaya;
Charles River Laboratories, Inc., Durham, NC

Cancer cachexia is a wasting syndrome characterized primarily by loss of skeletal muscle and adipose tissue mass and contributes greatly to overall cancer-related mortality (for recent review see Argiles 2023). An estimated 25-75% of cancer patients develop cachexia which leads to impacts on therapeutic tolerability, well-being, and eventually overall survival (Bossi 2021). Some preclinical mouse and rat cancer models manifest cachexia as they progress. In this study we established a syngeneic (immune competent) and a xenograft (immune incompetent) tumor model of cachexia with the intention of comparing the models with respect to typical study endpoints and to provide a platform for testing novel therapeutic agents aimed at inhibiting or reversing the effects of cachexia. The Colon26 syngeneic mouse colon adenocarcinoma model was reported as an experimental cancer cachexia model by Tanaka, et. al. in 1990. The model was developed in male BALB/c × DBA/2 F1 (first generation cross) mice. We typically implant Colon26 in female BALB/c mice for preclinical drug testing of anticancer agents and noticed a strong tendency for mice bearing Colon26 tumors to develop signs of cachexia on study, but not always consistently. A review of the literature showed there are clear gender differences with male cancer patients having higher prevalence of cachexia and greater muscle loss compared with female patients (Zhong 2020). Based on this we implanted Colon26 tumors in male BALB/c mice to establish the cachexia model. The HT1080 human fibrosarcoma model HT1080 was characterized as a cachexic model by Bernardo, et. al. in female severe combined immunodeficiency disease (SCID) mice. We developed the HT1080 model in male SCID mice based on the literature and previous experience. Both models were characterized by multiple endpoints including overall body weight loss, skeletal muscle weight loss, reduction of adipose tissue, and cardiac muscle loss, as well as tracking a broad panel of relevant cytokine levels at study endpoint. Both models generate robust wasting of skeletal muscle and adipose tissue providing an opportunity to assess novel anti-cachexia therapies.

#2836 Assessment of therapeutic antibody efficacy without the interference of murine Fc receptors allows for investigation of human antibody-dependent cellular cytotoxicity mediated by NK cells in the FcResolv™ hIL-15 NOG mouse model.

S. Rhein[1], M. Stecklum[1], M. Buczek[2], J. Richardson[2], **J. Hoffmann[1]**;
[1]Experimental Pharmacology and Oncology Berlin-Buch GmbH, Berlin, Germany, [2]Taconic Biosciences, Rensselaer, NY

Targeted antibody therapy is applied to treat various cancer types. In addition to the primary mode of action (MOA), which involves direct binding to the tumor antigen, indirect MOA acting through the constant region (Fc) of the antibody can enhance anti-tumor efficacy. Indirect mechanisms engage the innate immune system, mediated by both the complement system (complement-dependent cytotoxicity (CDC)) and immune cells (antibody-dependent cellular phagocytosis (ADCP) and antibody-dependent cellular cytotoxicity (ADCC)). These indirect mechanisms can complicate the evaluation and accurate assessment of antibody-induced ADCC by human NK cells in current mouse models. In immune-deficient mouse strains (e.g. NOG), false positives and/or negatives may occur due to interactions with murine Fc receptors. These can either result in anti-tumor responses via activation of the murine innate immune system or can interfere with the human-targeted therapy's primary MOA. To study the response to anti-cancer antibodies without the interference of these murine Fc receptor interactions and to investigate ADCC mediated by human NK cells, a novel mouse model deficient in Fc receptors and expressing human IL-15 (FcResolv™ hIL-15 NOG) was employed for testing antibody therapies. Methods: Patient-derived xenograft (PDX) tumor models were transplanted into hIL-15 NOG and FcResolv™ hIL-15 NOG mice. A human head and neck squamous cell carcinoma and a lung adenocarcinoma PDX model were both treated with cetuximab. Treatment with pertuzumab and trastuzumab was applied in a breast ductal carcinoma PDX model. Rituximab treatment was tested in two diffuse large B cell lymphoma PDX models. Based on growth kinetics, the lung cancer PDX model was chosen for further testing of ADCC in the NK cell-humanized FcResolv™ hIL-15 NOG mouse. Results and Conclusion: There was no difference in percent tumor growth inhibition between the FcResolv™ hIL-15 NOG and hIL-15 NOG mice with regards to cetuximab treatment in the lung and head and neck cancer or for trastuzumab treatment of breast ductal carcinoma. However, pertuzumab treatment revealed a false positive efficacy, with the false positive effect more pronounced in hIL-15 NOG mice than in FcResolv™ hIL-15 NOG mice. In one of the lymphoma models, a false negative result was observed. Here, rituximab did not show notable tumor inhibition in the hIL-15 NOG mice but did in the FcResolv™ hIL-15 NOG mice. These results demonstrate that FcResolv™ hIL-15 NOG mice serve as a suitable mouse model for a more accurate assessment of the therapeutic efficacy of anti-tumor antibodies. Additionally, evaluation of human-mediated ADCC of therapeutic antibodies in NK cell-humanized FcResolv™ hIL-15 NOG allows detection of effects specifically mediated by human NK cells.

#2837 Conservation of JAK-STAT signaling in canine lymphocytes responding to human IL-6, IL-7, and IL-1 alpha.

K. Fung, M. L. Breiner, J. B. Mitchell II, R. E. Parchment;
FNLCR, Frederick, MD

Dogs share physiological similarities with humans, positioning them as valuable models for studying the efficacy and safety of drugs and their underlying mechanisms of action. The JAK-STAT pathway, a highly conserved signaling pathway across species, including humans and dogs, presents an opportunity to investigate the therapeutic potential of cytokines that utilize this pathway.

In this study, we aimed to evaluate the functional activity of three canine cytokines on canine cells. To assess stimulation of the JAK/STAT pathway, we used a flow cytometry assay that measures phospho-STAT in activated canine or human lymphocytes in whole blood specimens. Testing of commercially available human and canine IL-6 proteins revealed that canine lymphocytes respond poorly to most canine IL-6 products, whereas all recombinant human IL-6 products stimulated STAT phosphorylation in canine lymphocytes, despite sharing low sequence similarity with canine IL-6. In human T cells, both canine IL-6 and human IL-6 stimulated STAT phosphorylation, demonstrating biological activity from the canine IL-6 products. Several JAK inhibitors inhibited cytokine-induced STAT phosphorylation in both canine and human CD4 T-cells, consistent with JAK inhibition, but targeting the IL-6 receptor with tocilizumab only blocked IL-6-induced STAT phosphorylation in human but not canine CD4 T-cells in whole blood. These findings demonstrate the potential of our assay system to assess cross-species cytokine reactivity, determine if JAK/STAT inhibitors used clinically might be useful in treating inflammatory conditions in dogs, and identify novel canine-specific inhibitors.

Additionally, we explored the induction of IL-8 by human and canine IL-1 alpha in IL-1 alpha sensitive human cells. Human IL-1 alpha failed to stimulate a canine IL-1 alpha sensitive cell line, suggesting species-specific differences in IL-1 alpha activity. Furthermore, we discovered that canine IL-7 and human IL-7 are species-specific.

In summary, this proof-of-concept study highlights the capability to assess the activation of STATs and pathway inhibition by JAK inhibitors in canine whole blood using flow cytometry. We confirmed that human IL-6 stimulates JAK/STAT signaling in canine CD4 T-cells. Our results also revealed significant differences in species cross-reactivity of human IL-6, IL-7, and IL-1 alpha, underscoring the importance of species-specific investigations. Leveraging the similarities and differences between canine and human cytokines targeting the JAK-STAT pathway can enhance drug development efforts and contribute to the advancement of safer and more effective therapies for both humans and pet dogs with similar diseases. This study was funded by NCI Contract No. 75N91019D00024.

#2838 ZNFX1 is a master regulator and tumor suppressor in epigenetically induced pathogen mimicry, mitochondrial dysfunction and STING-dependent signaling in cancer.

L. Stojanovic[1], R. Abbotts[1], K. Tripathi[1], C. M. Coon[2], S. Liu[3], J. Wan[3], M. Topper[4], S. Baylin[4], K. Nephew[2], F. Rassool[1];
[1]University of Maryland, Baltimore, Baltimore, MD, [2]Indiana University Melvin and Bren Simon Comprehensive Cancer Center, Bloomington, IN, [3]Indiana University, Bloomington, IN, [4]Johns Hopkins University, Baltimore, MD

Immunomodulatory agents are an important recent advance in cancer therapy, but utility is often limited by tumor immune evasion mechanisms. Strategic therapeutic activation of intracellular antiviral immune responses offers an opportunity to reverse immune evasion mechanisms and improve treatment outcomes. Anti-cancer agents such as, DNA methyltransferase inhibitors (DNMTis) induce re-expression of endogenous retroviruses (ERVs), leading to cytosolic double-stranded RNA (dsRNA) accumulation that activates interferon/inflammasome signaling. Moreover, poly (ADP ribose) polymerase inhibitors (PARPi) increase cytosolic dsDNA, activating stimulator of interferon (IFN) genes (STING). We reported that DNMTis in combination with PARPis induce STING-dependent signaling in a process termed pathogen mimicry response (PMR). Mitochondria (mt) are an important gateway for antiviral inflammasome signaling, but are not fully understood in cancer. Our studies of the little-known gene, NFX1-type zinc finger-containing 1 (ZNFX1), show that it acts as a master nucleic acid (dsRNA/DNA) sensor for mt gateway function. Bioinformatics analysis in primary ovarian tumors from TCGA and clinical trial RNAseq datasets, shows that increased ZNFX1 expression tracks with tumor stage and grade but inversely correlates with a mt dysfunction signature. **I**n studies of high-grade and endometrial serous carcinoma (OC) cell lines (N=3), transfection of dsRNA/DNA mimics or DNMTi azacytidine (AZA) and PARPi (talazoparib [TAL]) treatments induce increased ZNFX1 expression and binding to mt antiviral protein (MAVs) localized on the mt outer membrane. Functional studies of mt dysfunction in OC cells, show that dsRNA/DNA as well as above viral mimicry drugs increase mt reactive oxygen species (ROS) as measured by mitosox flow cytometry. AZA and TAL treatments also increase fragmented mtDNA and oxidative mtDNA base damage, as measured by long range PCR and 8-oxoguanine (8-oxoG) ELISA assays. These drug treatments also increase release of mtDNA into the cytosol, resulting in STING-dependent inflammasome signaling and cytokine release. Notably, ZNFX1 knockout (KO) attenuates these dynamics, including in bioinformatics of RNA seq data, thus defining this gene as essential for IFN/inflammasome signaling induced by mtDNA damage. Further pathway analysis of ZNFX1 KO vs wild-type (WT) RNAseq data suggest increased proliferation and epithelial to mesenchymal transition (EMT) that was validated by in vitro and in vivo assays. Not only is ZNFX1 a master regular of the above mt dynamics, but it is a tumor suppressor in OC. Abrogating ZNFX1 expression in OC cells triggers increased cell proliferation, invasive capacity and, in-vivo, increased tumor growth. This work then suggests novel approaches to improve immune therapy responses in OC through manipulating ZNFX1.

#2839 The mouse models of human cancer database (MMHCdb).

D. A. Begley, D. M. Krupke, E. Jocoy, S. B. Neuhauser, **C. J. Bult**;
The Jackson Laboratory, Bar Harbor, ME

The laboratory mouse plays a pivotal role as an experimental system for investigations into the genetic and genomic basis of cancer susceptibility, initiation, and progression and for preclinical research on novel treatment strategies for cancer. Advances in mouse models include humanized mice, transplant compliant mouse strains, and panels of genetically diverse mice (e.g., Diversity Outbred and Collaborative Cross). The distributed and heterogenous nature of information about these model systems presents a significant challenge to finding and aggregating information about mouse models and to identifying the most relevant models for a particular research question. The Mouse Models of Human Cancer database (http://tumor.informatics.jax.org) is an expertly curated FAIR-compliant knowledgebase that applies community annotation standards and nomenclature standards for genes, alleles, and strains to support accurate and comprehensive search results for mouse models of human cancer. The data in MMHCdb are curated from peer-reviewed scientific publications and direct data submissions from individual investigators and large-scale programs. A primary focus of the resource is to reflect the impact that genetic background has on the cancer-related characteristics of mouse models. The database includes information on spontaneous and genetically engineered cancer models as well as Patient Derived Xenografts and diversity panels. The database supports faceted searching for models by multiple criteria including, tumor type, genetic background of the mouse model, somatic mutations, and publication. Model descriptions include summaries of observed frequencies of tumors observed in the model and histopathology images. Information in MMHCdb is linked to cancer model data from other bioinformatics resources including the Patient Derived Cancer Models database (PDCM), PathBase, the Gene Expression Omnibus (GEO), and ArrayExpress.

MMHCdb is supported by NCI R01 CA089713

#2840 Development, characterization, and validation of a systemic human mantle cell lymphoma model utilizing luciferase expressing Jeko-1 tumor cells.

D. Harris, A. Wong, E. Rainbolt, N. Westrick, J. Avery, J. Kolb, A. Vunnava, Z. Ward, C. Hall, **B. John**;
Charles River Laboratories, Inc., Durham, NC

Mantle cell lymphoma (MCL) is an aggressive subtype of B-cell non-Hodgkin lymphoma that is clinically and biologically heterogenous. MCL murine models are scarce and reliable *in vivo* models are necessary for pre-clinical testing and identification of improved novel therapeutics. To address this need, we established and characterized a human MCL *in vivo* model by systemic implantation of the luciferase-expressing Jeko-1 cell line (Jeko-1-luc) into immunodeficient NCG mice. Tumor growth kinetics was evaluated by testing multiple cell inoculums, and disease progression was monitored by *in vivo* serial bioimaging, three-dimensional optical imaging (3D), and *ex-vivo* endpoint analyses. Jeko-1-luc tumor growth profile revealed moderate latency with a median survival of 40 days post implant. Subsequently, we utilized 3D optical imaging and *ex-vivo* imaging that confirmed the localization of tumor growth predominantly in lungs, spleen, and skeletal regions. Additionally, we determined the surface expression of selected B-cell lineage markers including CD19, CD20, and CD22. Next, we evaluated the efficacy and effect on survival in response to various standard of care agents including Vincristine, Rituximab, Palbociclib, Temsirolimus, and Cyclophosphamide. The quantification of tumor burden by *in vivo* and *ex-vivo* bioluminescent imaging demonstrated that the highest therapeutic activity and overall survival was achieved by Palbociclib and Vincristine. Flow cytometric analyses further demonstrated that tumor cells obtained from blood and selected tissues including spleen and bone marrow showed reduced tumor burden in treatment groups relative to the control group. Taken together, these results illustrate the translational value of the Jeko-1-luc model and provides a platform for evaluating novel treatment modalities for mantle cell lymphoma.

#2841 Development and validation of a systemic human multiple myeloma model utilizing luciferase expressing MM1.S tumor cells.

B. John, C. Currie, N. Westrick, T. Rowe, A. Wong, E. Rainbolt, Z. Ward, C. Hall, D. Harris;
Charles River Laboratories, Inc., Durham, NC

Multiple Myeloma (MM) is a complex hematologic malignancy characterized by clonal proliferation of transformed plasma cells leading to overproduction of monoclonal immunoglobulins and subsequently end-stage organ damage. Despite therapeutic advances, MM is an incurable disease with poor prognosis in high-risk patients, and thus relevant preclinical models are necessary to develop novel treatment strategies. We developed a Multiple Myeloma *in vivo* model by systemic implantation of the luciferase-expressing glucocorticoid sensitive tumor cell line MM1.S (MM1.S-Luc) into immunodeficient NCG mice. First, we generated a MM1.S-Luc monoclonal cell line from a polyclonal pool of stable luciferase-expressing cells by limiting dilution. Single cells from the stable pool were expanded under selective pressure and four MM1.S-Luc monoclonal lines were selected based on *in vitro* growth properties and bioluminescence intensity. Next, we determined the *in vivo* tumor growth profile by testing the monoclonal lines at two different cell inoculums, and disease progression was monitored by *in vivo* serial bioimaging. MM1.S-Luc tumor growth kinetics revealed a long latency and based on our *in vivo* imaging results, the tumor preferentially localized to the long bones, lungs, and mandible. For validation of the MM1.S-Luc *in vivo* model, we determined the efficacy and survival benefit in response to various clinically relevant standard of care agents including Dexamethasone, Daratumumab, Cyclophosphamide, Vincristine, Panobinostat, and Bortezomib. The quantification of tumor burden by bioluminescent imaging showed reduced tumor burden and prolonged survival with Panobinostat and Cyclophosphamide. In summary, we have developed a systemic MM1.S-Luc model that recapitulates the disease dissemination and invasiveness of multiple myeloma for evaluating novel therapeutic approaches to treatment.

TUMOR BIOLOGY: Pediatric Cancer Genomics and Epigenomics
Poster Session

#2845 Novel genetic risk loci for B-cell acute lymphoblastic leukemia in African American children: Findings from the Admixture and Risk of Acute Leukemia (ADMIRAL) Study.

C. Im[1], A. Raduski[1], L. J. Mills[1], R. A. Johnson[1], A. DeWan[2], X. Ma[2], J. L. Wiemels[3], C. Metayer[4], J. J. Yang[5], H. H. Nelson[1], T. Yang[1], S. Basu[1], L. M. Turcotte[1], N. Pankratz[1], M. E. Scheurer[6], L. G. Spector[1];
[1]University of Minnesota, Minneapolis, MN, [2]Yale University, New Haven, CT, [3]University of Southern California, Los Angeles, CA, [4]University of California, Berkeley, Berkeley, CA, [5]St. Jude Children's Research Hospital, Memphis, TN, [6]Baylor College of Medicine/Texas Children's Hospital, Houston, TX

Background: Racial and ethnic disparities in incidence and outcomes for childhood B-cell acute lymphoblastic leukemia (B-ALL) are well established. While genome-wide association studies (GWASs) among children of European (EUR) genetic ancestry have identified robust risk loci, comparable studies in children of African (AFR) genetic ancestry do not exist. Here we report on results from the first GWAS of B-ALL exclusive to AFR children.
Methods: A total of 840 AFR cases (diagnosis age <21y) and 3360 sex-/ancestry-matched controls (from ADMIRAL and ZOE 2.0, a childhood caries study) were evaluated. We used 656 cases from the Children's Oncology Group (COG) ALL frontline trials for discovery and 184 non-COG cases for replication. Samples were genotyped with the Illumina Global Diversity Array and imputed with the TOPMed reference panel. Ancestry was ascertained with RFMix-inferred global ancestry values and principal components analysis. Logistic regression models adjusted for cryptic population substructure evaluated variant risk associations. Discovery and replication results were meta-analyzed using an inverse variance-weighted fixed effects model.
Results: We identified 7 genome-wide significant (GWS, $P<5x10^{-8}$) variants, including 2 novel B-ALL risk loci with replication evidence ($P<0.05$) and striking per allele effect sizes: *CNTN4* (meta-analysis odds ratio [OR]=2.09, $P=1.4x10^{-11}$) and *FAM174A* (OR=2.94, $P=1.2x10^{-15}$). Established B-ALL EUR risk loci were corroborated in these data (*ARIDB*5, *IKZF1*; $P<5x10^{-8}$). Five additional novel loci were GWS after meta-analysis including at *SLC37A4* (OR=2.02, $P=1.1x10^{-8}$) and *CBWD1* (OR=2.69, $P=2.7x10^{-9}$), with suggestive associations in discovery data ($P<5x10^{-6}$) and nominal replication ($P<0.05$). Notably, all novel risk alleles were low-frequency in reference AFR populations and AFR-specific (minor allele frequencies of 2-9% in 1000 Genomes AFR and <0.1% in non-AFR). Top variants had relevant *in silico* annotations; variants at *CNTN4* and *SLC37A4* had high predicted functional probability (>0.8, RegulomeDb). For example, annotations for a top *CNTN4* signal suggest a potential leukemogenesis mechanism, overlapping a ChIP-seq peak for CEBPA in transdifferentiated B cells. In our replication data, a polygenic risk score (PRS) with 5 novel AFR-specific GWS variants from discovery had an appreciably stronger B-ALL risk association (top 25% vs rest: OR=2.03, $P=1.2x10^{-4}$) compared to a published B-ALL PRS from a GWAS in EUR children (top 25% vs rest: OR=1.59, P=0.014).
Conclusions: Despite the modest number of AFR B-ALL cases, we successfully detected and replicated genotype risk associations with considerable effect sizes. These results demonstrate the critical importance of increasing diversity in genomic studies of childhood ALL to promote discovery and reduce disparities.

#2846 Investigation of mechanisms that result in health disparity for Hispanic/Latino patients with B acute lymphoblastic leukemia.

J. W. Schramm, B. He, Y. Ding, C. Singh, D. Bogush, K. Dovat, D. Bastihalli Tukaramrao, R. Bhalodia, S. Dovat;
Penn State Health Milton S. Hershey Med. Ctr., Hershey, PA

Although social determinants of health have a large impact on health disparity, biologic vulnerabilities - particularly in cancers that impact at-risk populations are important. Amongst children with Acute Lymphoblastic Leukemia (ALL), the Hispanic/Latino (H/L) population is vulnerable given since the risk of developing ALL is 1.2-1.75 that of Non-Hispanic White children. After corrections for socioeconomic impacts, the mortality for H/L children is 40% higher than NHW. H/L children have a higher rate of high-risk genetic variations: 2-fold rate of heterozygous IKZF1 deletion (IKZF1-del) and a 4-fold rate of CRLF2 translocation. IKZF1 deletion and CRLF2 translocations are associated increased risk of relapse and chemotherapy resistance in B ALL. IKZF1 is an important transcriptional factor and epigenetic regulator that affects global gene transcription in hematopoietic cells. Simultaneous IKZF1-del and CRLF2 translocation represented 94% of H/L children with CRLF2 translocation. Although only 49% of all H/L patients with IKZF1-del had a CRLF2 translocation. Transcriptomics were analyzed for 42 H/L and 18 NHW patient samples using RNAseq. Gene expression from H/L patients was compared to expression in NHW patients and differentially expressed genes were analyzed. Gene set enrichment analysis (GSEA) revealed downregulation of processes responsible for genome maintenance including DNA replication, DNA templated transcription elongation, double strand break repair, and recombinational repair. Ingenuity pathway analysis (IPA) revealed upregulated pathways in stress related translation, histone deacetylases, interferon, and FLT3 signaling compared to NWH. H/L specimens resulted in decreased expression for FGF pathways, ceramide, and FAK signaling. We performed the same analysis in H/L and NHW with wildtype IKZF1 to compare these two population without high risk structural variants. GSEA analysis showed downregulated Intra S DNA Damage checkpoint signaling, DNA replication checkpoint signaling, glutamine amino acid synthesis, and aspartate amino acid synthesis. IPA showed upregulated interferon, histone deacetylases, TREM1 signaling, and Tec Kinase signaling. IPA showed downregulated Ephrin and CDK5 signaling. DNA methylation patterns were compared between 8 H/L and 8 NWH B ALL samples which showed differential methylation patterns affecting multiple cancer relevant genes.In conclusion, these data represent biologic vulnerability in H/L patients with B ALL in comparison to NWH regardless of high-risk genetic variants. H/L B-ALL shows deregulated maintenance of the genome via replication and repair pathways as well as potential vulnerabilities related to regulation of glutamate/aspartate synthesis. These findings give insight into potential mechanisms that can explain increased frequency of high-risk genetic variants in H/L B ALL.

#2847 Study of spatial and temporal epigenetic heterogeneity in neuroblastoma suggests role of H3K27me3-mediated repression.

C. Butterworth[1], A. Saint-Charles[1], Y. Iddir[1], J. Bhalshankar[1], A. Bellini[1], C. Bobin[1], E. Wecht[2], Y.-G. Park[2], C. Louis[1], V. Raynal[1], D. Plantaz[3], H. Sartelet[4], V. Combaret[5], G. Pierron[1], I. Janoueix-Lerosey[1], K.-O. Henrich[2], O. Delattre[1], F. Westermann[2], G. Schleiermacher[1];
[1]Institut Curie, Paris, France, [2]DKFZ, German Cancer Research Center, Heidelberg, Germany, [3]CHU Grenoble, Grenoble, France, [4]CHU Nancy, Nancy, France, [5]Centre Leon-Berard, Lyon, France

Introduction: Trimethylation of Histone 3 Lysine 27 (H3K27) is widely understood to be a mark associated with gene repression and linked to gene silencing during development. Neuroblastoma, a developmental pediatric extracranial solid malignancy, has a relatively silent mutational landscape. Therefore, epigenetic modifications, including H3K27me3 mediated repression, could explain underlying developmental origins and the wide clinical heterogeneity observed. While previous studies have focused on the role of distinct super enhancer histone marks and their core regulatory circuits, less is understood about repressive control. We aimed to therefore investigate the role of H3K27me3-mediated repression in Neuroblastoma patients.
Methods: Genome-wide H3K27me3 ChIP-Seq profiles were obtained from 48 diagnostic tissue biopsies covering all clinical and molecular patient subgroups. Transcriptome sequencing, ChIP-Seq of additional histone marks and WES/WGS was also performed on the same samples and on a panel of Neuroblastoma cell line models, with multiomics integrative analysis to validate findings. HMCAN, deepTools, DiffBind and ROSE packages were used to analyze the ChIP-seq data.
Results: A comparison of H3K27me3 regions across all patient ChIP-Seq profiles, identified commonly repressed genes specific to Neuroblastoma. These genes are enriched in development and differentiation pathways, with significantly lower RNA expression levels than other publicly available pediatric tumor datasets. When compared to publicly available single cell RNAseq of the healthy adrenal medulla, we can further highlight a potential role of H3K27me3-mediated repression in regulating cell lineage commitment and differentiation ability. In addition, we identified that patient samples cluster into their clinical subgroups based on H3K27me3 patterns and differentially repressed genes, specifically between *MYCN*-amplified and non-amplified high-risk groups. A CRISPR screen to further validate the functional role of these repressed genes is being carried out.
Conclusions: To our knowledge, this study shows for the first time that understanding of H3K27me3 mediated repression in Neuroblastoma, can uncover new insights into both disease development and clinical subclassifications. This knowledge will be important when considering future potential novel treatment options.

#2848 MYC and TGFβ promote group 3 medulloblastoma tumor resistance through deregulation of Polycomb targets.

Z. A. Qadeer[1], S. Westelman[1], M. O. Johnson[1], E. Hou[1], S. Grele[1], K. Smith[2], L. Hendrikse[3], L. Wang[1], S. Husain[1], M. Beytagh[1], C. Schmidt[1], M. Huang[4], M. D. Taylor[5], P. Northcott[2], W. A. Weiss[1];

[1]UCSF - University of California San Francisco, San Francisco, CA, [2]St. Jude's Children, Memphis, TN, [3]Hospital for Sick Children, Toronto, ON, Canada, [4]Children's Hospital of Los Angeles, Los Angeles, CA, [5]Texas Children's Hospital, Houston, TX

Medulloblastoma (MB) is one of the most prevalent malignant brain tumors in children, with tremendous cognitive and neuroendocrine disability among survivors. Group 3 (G3) MBs have poor overall survival at <50%, few recurrent mutations, higher frequency of metastasis, and no targeted therapies. Amplification of *MYC* and activation of TGFβ signaling are frequent in G3MB. Remarkably, some MB tumors have no reported mutations, suggesting roles for epigenetic mechanisms in driving disease. We hypothesize that the TGFβ pathway and MYC contribute to the intrinsic resistance of G3MB through deregulation of key genes and pathways. We previously established humanized models for SHHMB by introducing MYCN or *PTCH1* deletions into neuroepithelial stem cells (NESC) derived from normal human induced pluripotent stem cells (hIPSCs). In this study, we transduced NESCs with TGFb effectors activated in G3MB alone and/or in combination with MYC, prioritizing combinations observed in patients. Excitingly, both MYC and TGFβ effectors drove tumor formation *in vivo* with the combination of TGFβ effectors with MYC leading to more aggressive tumors. Moreover, they clustered with human G3/G4MB samples, indicating they phenocopy the relevant tumor of interest. We next found that NESCs expressing MYC with either TGFβR1 or TGFβ1 showed resistance to clinical TGFβR1 inhibitors, compared to cells driven by either TGFβR1 or TGFβ1 alone. To decipher mechanisms of resistance, we integrated CUT&RUN to probe for MYC genomic localization and relevant histone PTMs with RNA-seq analysis and discovered a subset of genes upregulated in MYC and TGFb-driven lines that are targets of the histone demethylase KDM2B. Loss of function mutations in *KDM2B* occur in G3MB patients, indicating that KDM2B deregulated genes are critical in G3MB. We postulate that epigenetic remodeling via MYC and recruitment of other MYC-interacting cofactors to PRC targets culminates in transcriptional changes that lead to aggressive disease. Work from others suggests that PRC-mediated chromatin regulation is critical in many adult and pediatric brain tumors. Overall, our studies provide important insight on identifying new therapeutic avenues for patients with *MYC* and TGFβ driven G3MB.

#2849 Palbociclib as a novel therapeutic for desmoplastic small round cell tumor.

J. W. Magrath, S. Sampath, D. A. Flinchum, A. B. Hartono, I. N. Goldberg, J. R. Boehling, S. D. Savkovic, S. B. Lee;
Tulane University School of Medicine, New Orleans, LA

Desmoplastic small round cell tumor (DSRCT) is an aggressive, pediatric cancer caused by the EWSR1-WT1 fusion oncoprotein. Targeted therapies are lacking and the current standard of care, multimodal therapy, is insufficient, leading to a 5-year survival rate of less than 25%. While the EWSR1-WT1 oncoprotein is critical to growth *in vitro*, its importance has yet to be examined *in vivo*. Further, the set of EWSR1-WT1 downstream targets critical to oncogenesis and the mechanism by which the two EWSR1-WT1 isoforms regulate them remain underinvestigated. Here we generate a toolkit of DSRCT cell lines that deplete EWSR1-WT1 in a doxycycline (dox)-inducible manner. This toolkit enabled us to establish the essentiality of EWSR1-WT1 not only *in vitro* but also for the first time *in vivo*. Using this toolkit, we performed RNA sequencing on four DSRCT cell lines and established the most comprehensive analysis of EWSR1-WT1 downstream targets to date. We discovered novel mechanistic insights into EWSR1-WT1 functionality including the uniqueness of its transcriptional alterations as compared to native WT1, the direct role of EWSR1-WT1 binding in gene upregulation, and the dominant role of the E-KTS isoform in transcription. Given the rarity of DSRCT, we focused on downstream targets with existing inhibitors and perform a drug screen that identified the CDK4/6 inhibitor palbociclib as a novel DSRCT therapeutic. We found that the E-KTS isoform of EWSR1-WT1 binds to the CCND1 promoter, leads to CCND1 expression, and stimulates DSRCT growth through the CCND-CDK4/6-RB axis. Palbociclib treatment conversely reduced DSRCT growth by preventing retinoblastoma phosphorylation and blocking the transition from G1 to S phase. Palbociclib treatment was effective not only *in vitro* but also *in vivo* where it significantly reduced tumor growth in two xenograft models of DSRCT. Given these novel findings and palbociclib's previous approval by the FDA for the treatment of breast cancer, we advance palbociclib as an exciting DSRCT therapy that warrants urgent clinical investigation.

#2850 Noncoding regulatory mutations as driving event for the oncogenic core regulatory circuitries of neuroblastoma.

M. Capasso[1], V. Aievola[1], V. Lasorsa[2], A. Montella[1], F. Bonfiglio[1], M. Avitabile[1], T. Maiorino[1], M. Tirelli[3], G. D'Alterio[3], M. Fischer[4], F. Westermann[5], A. Iolascon[1];

[1]University of Naples Federico II, Naples, Italy, [2]CEINGE Biotecnologie Avanzate Franco Salvatore scarl, Naples, Italy, [3]University of Milan, Milan, Italy, [4]University of Cologne, Cologne, Germany, [5]Hopp-Children's Cancer Center at the NCT Heidelberg (KiTZ), Heidelberg, Germany

Background and Aim: Neuroblastoma (NB) is the most aggressive solid tumor of infancy and arises from neural-crest-derived progenitor cells. It is composed by cell types reflecting developmental stages of the adrenergic lineage: mesenchymal (MES) and adrenergic (ADRN) cell types. These cell identities result from the activity of NB specific Core Regulatory Circuitries (CRCs), transcription factor (TF) sets that co-occupy regulatory regions together impacting the expression of their own genes and those of lineage-specific ones governing cell state transitions and cellular identities. Our hypothesis is that noncoding somatic single nucleotide variants (SNVs) located in NB CRCs TF binding sites (TFBSs) underlie NB CRCs activity, affecting cellular differentiation and promoting tumor onset. We aim to investigate such pattern of regulatory elements and identify putative driver SNVs, exploring their role and characterizing their action mechanism.
Methods: Transcriptionally active TFBSs (aTFBSs) bound by ADRN CRC TFs (GATA3, HAND2, ISL1, TBX2, MYCN, PHOX2B, ASCL1 and LMO1) were identified integrating 27 ChIP-seq and 11 ATAC-seq experiments in 6 NB ADRN cell lines (SKNBE2C, Kelly, NGP, COGN415, LAN5 and NB1643). In particular, aTFBSs were defined as ChIP-seq peaks overlapping ATAC-seq signals in the same cell line. SNVs from 317 NB whole genomes were mapped on aTFBSs and the enrichment of mutations in core regions respect to flanking ones was tested using Fisher test. Observed mutation rate in aTFBSs was compared with background mutation rate due to local sequence context. SNVs in mutated aTFBSs were selected and their impact on TF binding affinity was evaluated with FABIAN-variant and motifbreakR tools. aTFBSs target-genes were identified through promoter capture HiC (CHiC) in ADRN NB cells (SKNBE2C and SHSY5Y).
Results: We found a significant (FDR < 0.05) mutation enrichment in aTFBSs of ISL1, PHOX2B, TBX2, GATA3 and MYCN, suggesting a common somatic mutation burden for a subset of ADRN CRC TFBSs in ADRN NB cells. Starting from 839 SNVs falling in significantly mutated aTFBSs, we selected 269 mutations impacting the binding of ADRN CRC TFs. This mutations subset mapped in aTFBSs interacting with genes that significantly enriched pathways involved in neuronal development and migration (FDR < 0.05), thus suggesting their possible role in affecting cell identity definition. As an example, chr6:137753475:G>T mapped in aTFBSs interacting with the promoter of *OLIG3*, which takes part in neuronal differentiation. Interestingly, chr6:137753475:G>T was predicted to break the binding to ISL1 (FABIAN score: -0.24), a key regulator of ADRN CRC.
Conclusions: These results demonstrate that somatic noncoding SNVs can act synergistically to promote NB onset, affecting CRCs activity and, in turn, the normal cell identity definition.

#2851 Characterization of neogenes in desmoplastic small round cell tumors.

D. Truong[1], J. Magrath[2], S. Lee[2], J. Ludwig[1];
[1]UT MD Anderson Cancer Center, Houston, TX, [2]Tulane University School of Medicine, New Orleans, LA

Desmoplastic Small Round Cell Tumor (DSRCT) is a rare, soft tissue sarcoma caused by the EWS::WT1 fusion protein (FP). The FP acts as an aberrant transcription factor with oncogenic properties. Recently, oncogenic chimeric transcription factors (OCTF), such as EWS::WT1, were discovered to induce the expression of novel transcripts in otherwise silent genomic regions. These neogenes (NGs) are highly specific to each OCTF and not detected in normal tissue. 37 NGs were found to be associated with the EWS::WT1 FP.We explored the NGs to characterize their expression and regulation in a cohort of MD Anderson Cancer Center patients. We annotated and counted the NGs from the bulk RNA-seq data of 37 specimens. After fusion detection, only 22/37 specimens harbored the EWS::WT1 FP. We found that only the same 22 specimens robustly expressed DSRCT-specific NGs. Interestingly the NGs were heterogeneously expressed, suggesting that there may be patient-specific differences. Single-nucleus RNA-sequencing (snRNA-seq) of Ewing sarcoma (ES), CIC::DUX4 sarcoma (CDS), DSRCT, and osteosarcoma revealed that only the three sarcomas driven by an OCTF robustly expressed NGs. Notably, the DSRCT-specific NGs were only expressed in DSRCT. Similarly, ES and CDS only expressed their subtype-specific NGs. Given the robust expression of the DSRCT-specific NGs in DSRCT, we asked if the EWS::WT1 FP regulated the expression of the NGs. Knockdown (KD) of the EWS::WT1 FP in four DSRCT cell lines showed a consistent reduction in DSRCT-specific NGs. While there was variability in NG expression and EWS::WT1 FP KD sensitivity, we identified seven NGs decreased by at least 75% in all four cell lines and an additional eight NGs with 75% reduction across three cell lines. BOD-DSRCT and SK-DSRCT2 had the largest number of NGs reduced after KD, with 25/37 and 20/37 NGs with 75% expression reduction, respectively. EWS::WT1 FP has two known isoforms generated by alternative splicing in the WT1 domain that includes or excludes three amino acids, lysine, threonine, and serine (KTS) between zinc fingers 3 and 4, producing E+KTS and E-KTS isoforms. By transducing one or both isoforms into the mesothelial cell line LP9, we found 3/37 NGs were induced by the E+KTS isoform and 17/37 were induced by the E-KTS isoform, suggesting that the E-KTS isoform is primarily responsible for NG expression. Current work is underway investigating the relationship between EWS::WT1 FP binding and NG expression and the potential for NG to produce novel peptides that could serve as DSRCT immunotherapy targets.

#2852 Novel combination therapy with a KAT6A/B inhibitor together with retinoids induces irreversible differentiation of neuroblastoma cells.

N. Weichert-Leahey[1], A. Berezovskaya[1], M. Zimmerman[1], B. J. Abraham[2], A. W. Durbin[3], A. Look[1];
[1]Dana-Farber Cancer Institute, Boston, MA, [2]St. Jude Children's Research Hospital, Memphis, TN, [3]St. Jude Children's Research Hospital, Memphis, MA

Neuroblastoma is a pediatric tumor of the peripheral sympathetic nervous system derived from migratory neural crest cells that have committed to become sympathetic neuroblasts, but their definitive differentiation is blocked. Neuroblastoma cell identity depends on the adrenergic core regulatory circuit (CRC) of transcription factors that collaborate with MYCN to drive cell proliferation and the oncogenic gene expression program. Retinoic acid is used as differentiation therapy for patients with high-risk neuroblastoma, with the goal to block proliferation and drive sympathetic neuronal differentiation. We recently showed that retinoic acid re-organizes the enhancer landscape of neuroblastoma and promotes a new retino-sympathetic cell state characterized by MYCN downregulation, proliferative arrest, and sympathetic neuronal differentiation. However, the effects of retinoic acid on epigenetic rewiring of the adrenergic CRC and suppression of MYCN expression are reversible *in vitro* and *in vivo*, leading to tumor re-growth when the retinoic acid is withdrawn. Therefore, we sought to determine if retinoid-induced differentiation can be forced to progress to irreversible neuronal maturation by the addition of inhibitors of epigenetic modifying enzymes. Here, we conducted a drug screen of epigenetic modifying drugs alone and in combination with retinoic acid to determine their effects on neuroblastoma cell growth and differentiation. In this screen, we found that an inhibitor of the histone H3K23 acetyltransferases KAT6A/B, PF-9363, synergistically inhibits neuroblastoma cell growth in combination with retinoic acid. Moreover, retinoid-resistant neuroblastoma cell lines can be sensitized to retinoic acid when combined with a KAT6 inhibitor. Importantly, this combination treatment renders the differentiated cell state irreversible, such that it is maintained after retinoic acid is withdrawn, with continued suppression of the adrenergic CRC and MYCN expression. In conclusion, the retino-sympathetic differentiated cell state induced by retinoic acid in neuroblastoma becomes irreversible when the cells are also treated with an inhibitor of the KAT6A/B histone H3K23 acetyltransferases, implicating the essential role of these enzymes in restoring the proliferative immature progenitor phenotype in adrenergic neuroblastoma cells.

#2853 Comparison of methods for detection of hemispheric gliomas of infancy and their characteristic oncogenic tyrosine kinase gene fusions.

T. Pietsch[1], G. Gielen[1], A. Waha[1], E. Dorner[1], V. Dreschmann[1], C. Kramm[2], C. Vokuhl[1];

[1]University of Bonn Medical Center, Bonn, Germany, [2]University of Gottingen Medical Center, Gottingen, Germany

Introduction High grade hemispheric gliomas in infancy (IHG) are characterized by a more favorable outcome compared to high grade gliomas in older children. We have shown in previous studies that these tumors are characterized by a stable genome. The occurrence of tyrosine kinase gene fusions in high-grade hemispheric gliomas of infancy may represent therapeutic targets.

Methods: 33 high-grade hemispheric gliomas occurring in children younger than three years were retrieved from the archives of the Brain Tumor Reference Center, Institute of Neuropathology, University of Bonn. DNA and RNA were extracted from FFPE tumor samples. Methylation-based classification was done by hybridization to Illumina methylation arrays and subsequent use of the Heidelberg brain tumor classifier versions v11b4, v12.5 and v12.8. In addition UMAP plots were used to visualize similarities of methylation profiles. Gene fusions were identified on the DNA level by FISH using break-apart probes for *ALK, NTRK1, -2, -3, ROS1* and *MET* and Molecular Inversion Probe (MIP) methodology. On the RNA level, fusion transcripts were detected by targeted RNA sequencing as well as Nanostring assay with fusion-specific probes.

Results: 32 IHG occurred in the first year of life, one at the age of two years. 23/33 IHG were classified as such by methylation arrays; 6 further cases could be annotated to the IHG group by UMAP plots. 18/33 cases (54.5 %) showed fusions of *ALK* to different partners; all occurred in the first year of life. Fusions of *ROS1* were found in 4, *MET* in 2, *NTRK1* and *-3* in 7 cases. 2 cases showed no fusions. The different methods for fusion detection led to comparable results. Only recurrent fusions with known fusion partners were detectable with Nanostring probes designed for the fusion sequence, and library construction for targeted RNA sequencing was not successful in a fraction of cases. Break-apart FISH led to reliable results on the next day, and MIP technology represented the most sensitive method for analysis of FFPE samples.

Conclusions: Gene fusions involving the tyrosine kinase genes *ALK, MET, ROS1* and *NTRK1* and *-3* occurred in 93 % of high grade hemispheric gliomas of infancy; the most frequent were *ALK* fusions occurring in children younger than 1 year. DNA-based MIP technology represented the most robust and sensitive assay. A combination of RNA- and DNA-based methods to detect these fusions with high reliability is recommended.

#2854 Delineating mediators of oncogenesis in *FOXR2*-expressing cancers.

J. W. Tsai[1], M. Coppola[1], P. Arounleut[2], J. B. Collins[3], P. Hart[4], H. Keshishian[4], D. T. W. Jones[5], P. Bandopadhayay[3], T. N. Phoenix[2];
[1]Children's Hospital Los Angeles, Los Angeles, CA, [2]University of Cincinnati, Cincinnati, OH, [3]Dana-Farber Cancer Institute, Boston, MA, [4]Broad Institute of MIT and Harvard, Cambridge, MA, [5]German Cancer Research Center, Heidelberg, Germany

Background: Pediatric brain tumors are associated with the highest rates of morbidity and mortality of all childhood cancers. Diffuse midline gliomas (DMGs) are universally fatal pediatric tumors with a median survival of less than one year. DMGs are thought to arise from stalled developmental programs in the context of histone mutations (*H3* K27M) which are thought to be a critical initiating event. However, these histone mutations alone are insufficient for gliomagenesis and cooperate with other alterations, including mutations in the *TP53* pathway (TP53, PPM1D), growth factor receptor pathway activation (PDGFRA, EGFR, PIK3CA), and MYC amplifications (MYC, MYC-N) to induce tumor formation. There is a high degree of genetic heterogeneity amongst DMGs, and other alterations are also critical to DMG pathogenesis. This work is focused on Forkhead Box R2 (FOXR2), a forkhead family TF that we have found to be aberrantly expressed in many cancers, including DMGs. Expression of FOXR2 is sufficient to enhance glioma formation, and we have shown that regulation of FOXR2 occurs through a previously unrecognized epigenetic mechanism. Expression of FOXR2 is regulated by novel promoters, and we have demonstrated that these promoters are necessary for FOXR2 expression in several cancer lineages using CRISPR interference technology, including DMGs, melanoma, neuroblastoma, and non-small cell lung cancers.
Methods: We applied an integrative approach using transcriptomics, epigenetics, proteomics, *in vitro* cancer models, and *in vivo* mouse models to systematically evaluate how FOXR2 mediates gliomagenesis.
Results: We have found that FOXR2 is activated across multiple cancer lineages, including DMGs. FOXR2 is required for proliferation *in vitro*, and it is sufficient to enhance gliomagenesis using an *in utero* electroporation *in vivo* mouse model. FOXR2 enhances MYC protein stability, even in the presence of cycloheximide. However, FOXR2 also exerts its oncogenic effects through MYC independent functions. FOXR2 is highly enriched at E26-transformation (ETS) motifs and specifically activates ETS transcriptional gene sets. To determine protein-protein interactions of FOXR2, we have performed immunoprecipitation and mass spectrometry to identify FOXR2 protein interactors. Moreover, we have performed both proteomic and phospho-proteomic analyses of *FOXR2*-expressing human neural stem cells. These proteomic studies have allowed us to identify proteins and phospho-sites that are highly enriched in FOXR2-expressing cells, and that could be potential therapeutic targets in FOXR2-expressing cancers.
Conclusion: Taken together, this study elucidates how FOXR2 protein interactors mediate oncogenesis in FOXR2-expressing diffuse midline gliomas. These studies proposed here have broad applicability across a range of cancers as FOXR2 is aberrantly expressed in 8% of all cancers.

#2855 ETS1, a target gene of the EWSR1::FLI1 fusion oncoprotein, regulates the expression of the focal adhesion protein TENSIN3.

V. J. Ebegboni, T. L. Jones, T. Brownmiller, E. Pehrsson, P. Zhao, S. Sundara Rajan, N. J. Caplen;
National Cancer Institute, Bethesda, MD

Ewing sarcoma (EWS) is an aggressive bone and soft tissue tumor that affects children and young adults. Ewing sarcomas harbor few mutations beyond the chromosomal translocation that initiates disease, and the mechanistic basis for the metastasis of these tumors remains poorly understood. The epigenome of EWS cells reflects the regulatory state of genes associated with the DNA binding activity of the fusion oncoproteins EWSR1::FLI1 or EWSR1::ERG. In this study, we examined the EWSR1::FLI1/ERG's repression of transcription factor genes, particularly those encoding transcriptional regulators of cell differentiation. To examine EWSR1::FLI1/ERG's regulation of gene expression, we assayed DNA binding using ChIP-seq or CUT&RUN, RNA using RNA-sequencing (RNA-seq) or qRT-PCR, and protein using immunoblotting or immunofluorescence. We depleted the expression of EWSR1::FLI1/ERG proteins using RNAi and overexpressed ETS1 using a full-length cDNA or CRISPR activation.RNA-seq analysis of control and *EWSR1::FLI1*-silenced TC-32, TC-71, and A673 EWS cells identified 67 genes encoding proteins with DNA binding activity that exhibited significant increases in expression following depletion of EWSR1::FLI1. Comparison of the expression of these 67 transcription factor genes in EWS cell lines (n=41) and tumors (n=79) showed 37 expressed at a wider range in tumors relative to cell lines ($p < 0.01$). This more variable expression in EWS tumors suggests that one or more of these transcription factors could exert a phenotypic effect. Focusing on one of the EWSR1::FLI1-repressed target genes, *ETS1*, we detected EWSR1::FLI1 binding and an H3K27me3 repressive mark at this locus. Depletion of EWSR1::FLI1 results in ETS1's binding of promoter regions. Analysis of EWS cells in which we profiled ETS1 binding and assessed the effects of ectopically expressed ETS1 defined 265 genes as positively regulated by ETS1 of which 103 also exhibited an increase in expression following depletion of EWSR1::FLI1. Of these 103 genes, we focused on ETS1's regulation of TNS3, as assessment of multiple EWS tumor expression profiles, showed positive correlation of *ETS1* and *TNS3* expression. *TNS3* encodes TENSIN3, a focal adhesion protein that regulates cytoskeletal reorganization and contributes to cell migration by connecting the cytoplasmic tail of integrins to the actin cytoskeleton. EWS cell lines (SK-N-MC (*EWSR1::FLI1*) and ES-5838 (*EWSR1::ERG*), in which we activated *ETS1* expression (CRISPRa) exhibited a migratory phenotype and increased TNS3 expression. Critically, the activated ETS1 EWS cell lines show TNS3 accumulation at leading cell edges, with F-actin cytoskeletal reorganization, a phenotype associated with cell migration. Our study demonstrates that EWS cells expressing ETS1 exhibit a more migratory phenotype, which, has the potential to promote the dissemination of cells and, thus, metastasis.

#2856 Multi-omics approaches for biomarker discovery and target therapy in pediatric germ cell tumors.

A. Souza Peres[1], I. Vieira Cardoso[1], J. Soares Galvao[1], A. Santarosa Vieira[1], M. Nunes Rosa[1], I. Tosi[1], D. Antunes Moreno[1], A. Laus[1], A. van Helvoort Lengert[1], S. Aparecida Teixeira[1], A. Feijo Evangelista[1], R. Manuel Reis[2], L. Lopes[3], **M. Tomazini Pinto**[1];

[1]Barretos Cancer Hospital, Barretos, Brazil, [2]University of Minho, Braga, Portugal, [3]Barretos Children's Cancer Hospital, Barretos, Brazil

Pediatric germ cell tumors (GCT) are rare and heterogeneous, presenting various histologies. There are no specific markers for diagnosing GCT, and 30% of patients are resistant to standard cisplatin-based chemotherapy, which can be related to epithelial-mesenchymal transition (EMT). Therefore, this study aims to elucidate markers for classifying GCTs, evaluate the molecular mechanisms related to drug resistance, and search for new therapeutic approaches. The expression of miRNAs was assessed for 42 GCT-pediatric patients through miRNA Panel - Nanostring technology. Whole Exome Sequencing (WES) was performed for 16 GCT-pediatric patients to assess somatic mutations. *In silico* analysis of epithelial-mesenchymal transition (EMT) markers was performed using the cBioPortal database. The expression of EMT markers was evaluated *in vitro* in parental and cisplatin-resistant models (NTERA-2R). Xenograft model-derived NTERA-2R was established and EMT markers were also assessed. We identified specific miRNA expression signatures for each histology, including 34 miRNAs for dysgerminomas, 13 for embryonal carcinomas, 25 for yolk sac tumors, and one for immature teratoma. We identified 26 miRNAs that were commonly expressed in malignant tumors, with six miRNAs (miR-302a-3p, miR-302b-3p, miR-371a-5p, miR-372-3p, miR-373-3p, miR-367-3p) showing significant overexpression. MiR-302b-3p had a significant association with all the evaluated clinical features. WES analysis showed that Single Base Substitution signature 39 was observed in 68.75% of samples and SBS22 in 12.5%. Copy number alterations were identified in 4, 7, 8, 10, 12, 21, and 22 chromosomes, with amplification of *CDKN1B*, *KRAS*, *CCND2*, *ETV6*, and *KDM5A* genes and deletions of *KIT* and *PTEN* genes. Somatic mutations in *NYAP2, RHBDF2*, *MTOR*, *KIT*, *ATM*, *KRAS*, and *PIK3CA* were frequent among the samples. *KIT* (Asp816Val, Ala829Pro) and *KRAS* (Gln61Leu) mutations were classified with potential clinical significance and were validated. *In silico* analysis showed that different histologies had distinct expression profiles for EMT markers. Patients with $SNAIL^{low}SLUG^{low}$ expression had higher PFS than those with $SNAIL^{high}SLUG^{high}$ (p=0.006). The median PFS of patients with $SLUG^{low}$ was 46.4 months, while $SLUG^{high}$ was 28.0 months (p=0.022). *In vitro* analysis using NTERA-2R showed overexpression of EMT markers. The same result was obtained in the xenograft model derived from NTERA-2R. Our study offers vital insights into pediatric GCTs' molecular landscape, using *in silico*, *in vitro*, *in vivo* analyses, and genetic assessments, highlighting three points: 1) The miRNA signatures for each histology may have robust diagnostic and prognostic potential, besides clinical implications as biomarkers. 2) *KIT* and *KRAS* genes are possible therapeutic targets of pediatric GCTs. 3) EMT is related to cisplatin resistance and SLUG is a potential molecular target.

#2857 Perspectives from a systematic review of kinase fusion oncogenes and access to corresponding kinase inhibitor clinical trials in pediatric, adolescent, and young adult solid malignancies.

L. Lazo de la Vega[1], S. K. Eder[2], E. Sukharevsky[1], Z. A. Kahn[1], M. O'Connell[1], F. Wachter[1], E. P. Anderson[3], M. C. Trissal[1], J. J. LaBelle[1], K. Carpenter[4], L. Kager[2], M. G. Filbin[1], K. A. Janeway[1];

[1]Dana-Farber Cancer Institute, Boston, MA, [2]St. Anna Children's Cancer Research Institute, Vienna, Austria, [3]Massachusetts General Hospital, Boston, MA, [4]Boston Children's Hospital, Boston, MA

Oncogenic kinase fusions (KFs) have been reported in pediatric, adolescent, and young adult (P-AYA) brain tumors, sarcomas, and rare solid malignancies. Molecularly targeted therapy (MTT) matched to KFs generally produce objective responses even in advanced P-AYA malignancies. KFs occur across a broad age range of P-AYA cancer diagnoses (dx) so data on KF prevalence and the relationship between KFs and clinical characteristics including response and resistance to MTT is distributed across many studies. To address resulting knowledge gaps, we conducted a systematic review of KFs reported in P-AYA cancers and assessed the availability of clinical trials (CTs) for P-AYA patients with KF malignancies. A systematic literature search was conducted with PubMed using publication date 2013-2022, search terms for dx, age, and gene names of interest (BRAF, RAF1, NTRK1-3, ALK, FGFR1-4, MET, RET, ROS1). Known P-AYA cancer sequencing studies were also reviewed. Papers were included if they reported ≥1 patient <18 yo with a KF cancer of any type or ≤30 yo with a KF P-AYA cancer dx. Data abstracted included paper type, KF gene and partner, dx, fusion breakpoints, age, stage, MTT received, response to MTT, and CT enrollment. Clinicaltrials.gov was queried for interventional CTs in the U.S. assessing relevant MTTs. We identified 531 studies (299 case reports/series; 119 P-AYA sequencing studies) reporting 4,329 patients with a KF P-AYA solid tumor. Brain tumors had, in decreasing order of frequency, BRAF, NTRK, FGFR, ALK, ROS1, RAF1, MET, and RET fusions. Dx in which KFs were reported were LGG (n=2451), HGG (n=298), embryonal tumors (n=16), ependymomas (n=8), meningioma (n=1), and other (n=16). Extracranial solid tumors (EST) had, in decreasing order of frequency, NTRK, RET, ALK, BRAF, ROS1, MET, FGFR, and RAF1 fusions. Dx in which KFs were reported were thyroid cancer (n=607), sarcoma (n=546), melanoma and spitz tumor (n=183), renal tumor (n=90), carcinoma (n=57), rhabdomyosarcoma (n=12), neuroblastoma (n=11), osteosarcoma (n=9), and other (n=24). As of Aug 23, 2023, 476 CTs were assessing 65 inhibitors relevant for these KFs, of which only 20 are currently FDA-approved. Patients <18 yo were only eligible for 16% of CTs. RET (47%), RAF/BRAF (33%), and NTRK (32%) inhibitors had the highest percent of CTs enrolling patients <18 yo while ERK (4%) and FGFR (6%) inhibitors had the least. Notably, while 467 P-AYA patients identified in our review were <18 yo and had an ALK- or ROS1-fusion positive tumor, only 24% of ALK or ROS1 inhibitor CTs allowed enrollment of patients <18 yo. To our knowledge, this is the first systematic review of KFs in P-AYA solid tumors. Oncogenic KFs are common and occur across P-AYA solid and brain tumor dx demonstrating a need for CTs of relevant MTTs including patients <18 yo, particularly for drugs targeting ALK, ROS1, and FGFR.

#2858 Phenotypic screens identify genetic regulators of nanoparticle delivery to pediatric brain tumors.

M. Coppola[1], J. Kenny-Serrano[2], J. G. Doench[3], P. Hammond[4], P. Bandopadhayay[2], J. W. Tsai[1], J. Straehla[5];
[1]Children's Hospital Los Angeles, Los Angeles, CA, [2]Dana-Farber Cancer Institute, Boston, MA, [3]Broad Institute of MIT and Harvard, Cambridge, MA, [4]Massachusetts Institute of Technology, Cambridge, MA, [5]Koch Institute for Integrative Cancer Research, Cambridge, MA

Pediatric central nervous system tumors are the leading cause of cancer death in children. Diffuse midline glioma (DMG) is a universally fatal pediatric brain tumor and despite many clinical trials over the past decades, less than 10% of patients are long-term survivors. The clinical standard of care is radiotherapy, however it only provides limited symptom relief. There is a clear need to develop creative treatment strategies for patients with DMG. Nanomedicine has the potential to address this challenge, allowing the encapsulation of difficult to deliver therapeutic cargoes, and selectively targeting them to tumors while crossing innate biological barriers. However, a deep understanding of disease-specific nano-bio interactions is crucial to leverage the full potential of these therapies.
To functionally validate the role of candidate biomarkers in nanoparticle delivery to DMGs, we performed pooled genetic perturbation screens using a flow based phenotypic output. We developed a lentiviral all-in-one CRISPR/Cas9 knock-out library paired with fluorescence-activated cell sorting to probe the functional impact of 700 genes on the delivery of nanoparticles to DMG. Layer-by-layer electrostatic assembly was used to generate liposomal nanoparticles with a polymer surface coating of hyaluronic acid. Two patient-derived neurosphere models of DMG were transduced with the pooled all-in-one CRISPR/Cas9 library. Following antibiotic selection, cells were incubated with hyaluronic acid or polymeric nanoparticles for 4 or 24 hours and sorted into populations based on nanoparticle affinity. A dynamic cell-sorting strategy was optimized to separate cells infected with inert DNA barcodes based on their degree of nanoparticle-association. DNA was isolated from sorted cells and subjected to next generation sequencing. The enrichment of each single guide was determined relative to matched controls. We found strong agreement between biologic replicates, and determined which genes, when knocked down, shifted nanoparticle uptake into DMG cells.
Our pooled phenotypic screen revealed strong biologic regulators of nanoparticle uptake. These can be categorized as formulation dependent and independent, as well as time-dependent. We identified several negative regulators of nanoparticle uptake including members of the mitogen-activated protein kinase (MAPK) and mammalian target of rapamycin (mTOR) pathways. The top target genes are currently being validated in DMG and human neural stem cell models. In ongoing work, we are leveraging genetic and chemical inhibition to sensitize DMG cells to nanoparticle therapeutics. We plan to leverage our screening technique to develop novel combination therapy approaches that could be implemented across multiple administration routes (intravenous, intraventricular, or intratumoral) to enhance the use of nanomedicine for DMG and other pediatric brain tumors.

#2859 The Single-cell Pediatric Cancer Atlas: Open-source data and tools for single-cell transcriptomics of pediatric tumors.

A. G. Hawkins[1], J. A. Shapiro[1], S. J. Spielman[1], D. S. Mejia[1], D. Venkatesh Prasad[1], N. Ichihara[1], A. Yakovets[1], K. G. Wheeler[2], C. J. Bethell[3], S. M. Foltz[4], J. O'Malley[1], C. S. Greene[5], J. N. Taroni[1];

[1]Alex's Lemonade Stand Foundation, Bala Cynwyd, PA, [2]Reify Health, Boston, MA, [3]UTHealth Houston Graduate School of Biomedical Sciences, Houston, TX, [4]Children's Hospital of Philadelphia, Philadelphia, PA, [5]University of Colorado Anschutz Medical Campus, Aurora, CO

The Single-cell Pediatric Cancer Atlas (ScPCA) Portal (https://scpca.alexslemonade.org/), developed and maintained by the Childhood Cancer Data Lab, is an open-source data resource for single-cell and single-nuclei RNA sequencing data of pediatric tumors. Originally comprised of data from 10 projects funded by Alex's Lemonade Stand Foundation, the Portal currently contains summarized gene expression data for over 500 samples from a diverse set of over 50 types of cancers and is growing to include community-contributed datasets. In addition to gene expression data from single-cell and single-nuclei RNA sequencing, the Portal holds data obtained from bulk RNA sequencing, spatial transcriptomics, and feature barcoding methods, such as CITE-seq and cell hashing.

ScPCA data are available for download in formats ready for downstream analysis, such as SingleCellExperiment or AnnData objects. Objects include raw counts and normalized gene expression data, PCA and UMAP coordinates, unsupervised clustering assignments, and cell type annotations. Additionally, all downloads include two summary reports for each library. The quality control report is a general overview, including processing information, summary statistics, and general visualizations of cell metrics. The cell type annotation report includes an overview of cell type annotation, comparisons among cell type annotation methods, and diagnostic plots to assess annotation quality. Comprehensive documentation about data processing and the contents of files on the portal, including a guide to getting started working with an ScPCA dataset, can be found at scpca.readthedocs.io.

All data on the Portal were uniformly processed using scpca-nf, a Nextflow-based open-source pipeline developed by the Childhood Cancer Data Lab. The scpca-nf workflow uses alevin-fry for fast and efficient processing of all data currently available on the portal, including single-cell RNA-seq data and any associated CITE-seq or cell hash data, spatial transcriptomics data, and bulk RNA sequencing. The workflow and associated documentation are freely available at https://github.com/AlexsLemonade/scpca-nf, allowing researchers to leverage this pipeline for their own datasets.

Providing an open-source workflow has allowed researchers to process their own single-cell or single-nuclei datasets for their own research. Furthermore, any data sets processed with scpca-nf are then eligible for inclusion on the ScPCA Portal. The continuous growth of the ScPCA Portal will help pediatric cancer researchers spend less time finding and processing data and more time answering their pressing research questions.

#2860 High-resolution mapping of oncogenic structural changes in osteosarcoma.

A. S. Clugston[1], S. Leung[1], E. Fuentes[1], L. Sayles[1], M. Ostrowski[2], C. Wu[2], C. Curtis[3], Z. Ma[4], Y. Zhao[3], G. K. Marinov[3], V. Ramani[2], M. Breese[1], A. Sweet-Cordero[1];

[1]UCSF - University of California San Francisco, San Francisco, CA, [2]Gladstone Institute for Data Science & Biotechnology, San Francisco, CA, [3]Stanford University School of Medicine, Stanford, CA, [4]Stanford Cancer Institute, Stanford, CA

We have leveraged long-read and spatial sequencing modalities to identify cancer-specific oncogenic alterations for treatment of osteosarcomas. Osteosarcoma is archetypal of cancers driven by aneuploidy and structural rearrangement rather than point mutations. The functional consequences of many SVs stem from their effect on multidimensional genome organization. SVs can enable enhancer hijacking, alter boundaries of topologically associated domains (TADs), and move gene loci to different regulatory compartments to affect gene expression. SVs can also lead to the formation of extrachromosomal DNA amplicons (ecDNA), which can be megabases in size and can incorporate both genes and regulatory elements to result in substantial increases in gene transcription and intratumor heterogeneity. Complex SVs may have profound implications for prognosis and treatment in OS and other cancers yet they remain poorly understood. By incorporating long-read optical genome mapping (OGM) and chromatin conformation capture sequencing (HiC), we studied SVs in osteosarcoma with the goal of elucidating their contribution to cancer development.

We used a unique panel of 11 OS patient-derived xenograft (PDX) cell lines which have been previously characterized regarding response to targeted therapies as well as genomically via whole genome (WGS), RNA (RNA-seq), and chromatin accessibility (ATAC-seq) sequencing. To understand the complex genomic reorganization that occurs in osteosarcoma, we integrated OGM and WGS data for all 11 cell lines to describe detailed genome-wide SVs including ecDNA formation. PDX lines assayed using OGM exhibited between 106 and 704 translocations each (versus zero detected in germline controls) and we identified dozens of potential ecDNA amplicons, including one amplicon which may explain exceptionally high expression of YAP1 and BIRC3 transcripts. Further, we used HiC to describe the topological environment resulting from these SVs and observed potential enhancer hijacking events affecting dozens of known oncogenes including MYC and CDK4. HiC interaction maps among six cell lines reveal genomic compartments and TAD boundaries in detail, with 4,167 unique TAD boundaries identified among six cell lines using 50kb genomic bins. Despite the observed complexity of these genomes, we note that 71% of TAD boundaries are consistent in at least four of the six HiC assayed cell lines, and 44% are present in all six lines. Changing TAD boundaries are associated with numerous SVs and/or copy number discrepancies, and are associated with genomic regions that contain genes with dysregulated RNA transcript levels. Overall, OGM and HiC modalities add considerably to our ability to detect oncogenic SVs and the genes they affect.

#2861 Rhabdomyosarcoma fusion-oncogene alters the chromatin landscape to initially drive a neural signature *in vivo*.

J. Kucinski, C. Taslim, A. Tallan, M. Cannon, K. Silvius, B. Stanton, G. Kendall;
Nationwide Children's Hospital, Columbus, OH

Fusion-positive rhabdomyosarcoma is an aggressive pediatric cancer lacking curative therapies, and outcomes for children with this disease have not improved in decades. The chimeric transcription factor PAX3::FOXO1 is the most common and lethal driver of fusion-positive rhabdomyosarcoma, and it consists of the DNA binding domains of PAX3 fused to the transactivation domain of FOXO1. Despite its well-established essentiality for tumorigenesis, how PAX3::FOXO1 initially generates a tumorigenic cell state has been challenging to study due to the lack of in vivo models expressing the fusion-oncogene at accessible early developmental time points. Here, we developed a novel zebrafish mRNA injection model that ubiquitously expresses PAX3::FOXO1 during gastrulation representing all three germ layers. Using this high-throughput model, we used ChIP-seq to identify initial in vivo PAX3::FOXO1 binding sites and targets. PAX3::FOXO1 has pioneering activity, where it can utilize partial-motif recognition to bind to inaccessible chromatin and alter chromatin structure. With biochemical and 2D chromatin sequencing approaches in our model, we find evidence for in vivo PAX3::FOXO1 pioneering activity. PAX3::FOXO1 consists of two DNA binding domains, a paired and homeobox domain, and we demonstrate a new mode of pioneering activity driven by its homeobox domain given a strong enrichment of homeobox-related motifs at PAX3::FOXO1 binding sites. PAX3::FOXO1 activity in developing zebrafish embryos results in an arrested development phenotype and transcriptional signatures enriched for pathways such as an inhibition of segmentation and myogenic development. Critically, we find that PAX3::FOXO1 directly activates neural-related gene targets by increasing chromatin accessibility and re-distribution of the active histone mark H3K27Ac to these loci. These discoveries are particularly striking because rhabdomyosarcoma is traditionally associated with skeletal muscle characteristics. With our findings, we hypothesize neural gene activation is a critical mechanism for fusion-positive rhabdomyosarcoma tumor initiation and could be a critical pathway across various stages of rhabdomyosarcoma tumorigenesis. This hypothesis agrees with our previous discovery of a novel PAX3::FOXO1 cooperating neural transcription factor, HES3, which we find is directly activated by PAX3::FOXO1 in our mRNA injection model. Our long-term goal is to utilize this versatile model to functionally evaluate cooperation between PAX3::FOXO1 and both canonical rhabdomyosarcoma and neural transcription factors. Our approach will employ a cross-species comparative analysis across this injection model, our zebrafish tumor models, other model systems, and patient data. This work will identify conserved targets and mechanisms of PAX3::FOXO1 tumorigenesis that could become new therapeutic vulnerabilities.

#2862 Evolution of clinically relevant variants in advanced pediatric sarcomas.

H. Y. Comeau[1], L. Lazo De La Vega[1], A. J. Church[2], L. D. Maese[3], N. Pinto[4], M. E. Macy[5], M. A. Applebaum[6], A. J. Sabnis[7], A. Kim[8], S. I. Colace[9], F. Dela Cruz, Jr.[10], S. G. DuBois[1], N. B. Collins[1], K. A. Janeway[1];

[1]Dana-Farber/Boston Children's Cancer and Blood Disorders Center, Boston, MA, [2]Boston Children's Hospital, Boston, MA, [3]University of Utah/Primary Children's Hospital, Salt Lake City, UT, [4]University of Washington/Seattle Children's Hospital, Seattle, WA, [5]University of Colorado/Children's Hospital Colorado, Aurora, CO, [6]University of Chicago/Comer Children's Hospital, Chicago, IL, [7]University of California San Francisco/Benioff Children's Hospital, San Francisco, CA, [8]George Washington University/Children's National Hospital, Washington, DC, [9]The Ohio State University/Nationwide Children's Hospital, Columbus, OH, [10]Memorial Sloan Kettering Cancer Center, New York, NY

Objective Few pediatric sarcoma studies have investigated how gene alterations detected by targeted sequencing change in the same patient over time. We leveraged targeted somatic DNA next-generation sequencing (NGS) data from a large cohort of young patients with osteosarcoma (OS), Ewing sarcoma (EWS), or rhabdomyosarcoma (RMS) to identify changes in known oncogenic variants with the aim of addressing the clinical utility of resequencing at recurrence.
Methods The iCat2/GAIN Consortium Study is a cohort study involving 13 US institutions evaluating outcomes after receipt of matched targeted therapy (MTT) in young patients with advanced extra-cranial solid tumors. Tumors are sequenced using OncoPanel, a targeted DNA NGS test performed in a CLIA/CAP certified laboratory assessing single nucleotide variants (SNV), copy number variants (CNV) and structural variants (SV) in up to 447 cancer genes and rearrangements in up to 60 cancer genes. In 2 cases, similar targeted NGS tests were performed. For OS, EWS, or RMS patients with at least 2 OncoPanels from different timepoints (initial diagnosis or relapse) and/or tumor sites (metastatic or primary), we assessed oncogenic variants in genes previously known to be recurrently altered in the respective diagnosis. For each variant, we assigned patterns of change as emergence, disappearance, or persistence.
Results Of 784 iCat2/GAIN patients, there were 157, 107, and 100 patients with OS, EWS, and RMS respectively. The analytic cohort consisted of 34, 20, and 15 OS, EWS, and RMS patients respectively with at least 2 tumor sequenced samples. The median number of sequenced samples per patient was 2 (range 2 to 6). In EWS, 9 (45%) patients had an oncogenic variant (other than an expected fusion) in at least one sample. In 4 patients, the predominant pattern of change was emergence. Specifically, a new pathogenic SNV in STAG2 (N=1) or TP53 (N=3) were observed. In OS, all 34 patients had an oncogenic variant in at least one sample. In RMS, 12 (80%) patients had an oncogenic variant in at least one sample. There was no predominant pattern of change in OS and RMS. In OS, 41% percent of variants persisted in all samples; 32% of variants disappeared in subsequent samples; 22% of variants emerged in subsequent samples; 5% of variants were variably present over time. Interestingly, while TP53 was most often persistent over time, there were also 7 cases with emergence of TP53 variants and 8 cases with disappearance of TP53 variants. In RMS, 26% percent of variants persisted in all samples; 31% of variants disappeared in subsequent samples; 43% of variants emerged in subsequent samples. Interestingly, in three cases there was emergence of a new variant activating the RAF/MAPK or AKT pathway.
Conclusion Pediatric sarcomas display a range of genomic changes over time. Given the observed changes in oncogenic alterations, there may be utility to repeat sequencing of relapsed tumor biopsies to understand these changes.

#2863 *CDKN1A* prevents IR-induced apoptosis in rhabdomyosarcoma tumor via repressing the pro-apoptotic factor NOXA in a novel apoptotic regulatory axis.

P. S. Modi, M. Ignatius, L. Wang, P. Sreenivas;
UTHSA, San Antonio, TX

Rhabdomyosarcoma (RMS) is a tumor of the muscle and is the most common soft tissue cancer in children and teens, with approximately 400 to 500 new cases every year in the United States. While we have a good understanding of the interplay between pro- and anti-apoptotic regulators, much remains to be learned about how the decision to trigger apoptosis or not is controlled at the transcriptional level in RMS tumors. We strive to elucidate how pathways that drive apoptosis avoidance are epi-genetically pre-programmed in cells. We have discovered that SNAI2, a transcriptional repressor, acts as a master switch to either activate or dampen apoptosis in response to ionizing radiation (IR). While elevated SNAI2 results in transcriptional repression of the pro-apoptotic factor *BIM* and protection from apoptosis post-IR, a small number of SNAI2 null cells survive radiation to reproliferate in vivo, revealing the existence of hitherto unappreciated mechanisms that support the survival of irradiated cells. Hence, we hypothesized that there are additional genes or pathways in cells lacking SNAI2 that are co-opted to drive relapse disease. We have identified that CDKN1A or p21 expression is robustly increased in SNAI2 null cells. *CDKN1A* is thought to be a tumor suppressor. However, our preliminary data indicate that *CDKN1A* is an oncogene, and in RMS patients, high tumor expression is associated with poor outcomes. We found that *CDKN1A* expression in combination with SNAI2 can predict resistance to radiation across RMS cell lines. We next developed control RD, Rh30, and Rh18 cells, either *CDKN1A* or both *CDKN1A* and *SNAI2* ablated using CRISPR/Cas9 reagents with control cells expressing control gRNAs. Ablation of *CDKN1A*, while not affecting proliferation, led to a significant increase in apoptosis post-radiation, and this effect was increased in *SNAI2/CDKN1A* double knockout cells. Further, in colony-forming assays, we find that double-ablated cells form significantly fewer colonies than control and single knockout cells. Loss of *CDKN1A, SNAI2, or CDKN1A/SNAI2* led to a G2/M cell cycle block, indicating that the cell cycle effects of p21 might not be responsible for the phenotypes observed. Ongoing xenograft experiments have determined the effect we observe *in vitro* will also translate *in vivo*. Given that SNAI2 and *CDKN1A* are heterogeneously expressed, respectively, we will interrogate CDKN1A for its role in protecting differentiated cells from apoptosis. We will determine if *CDKN1A* prevents apoptosis by repressing the pro-apoptotic factor NOXA in a novel apoptotic regulatory axis specific to differentiated cells. Our study will show that critical primary and alternative apoptosis resistance mechanisms are epi-genetically pre-programmed in cells by SNAI2.

#2864 Transcriptional repressor REST controls autophagy in Sonic Hedgehog medulloblastoma through the VHL-HIF1α axis..

A. Singh, D. Cheng, J. Swaminathan, Y. Zheng, N. Gordon, V. Gopalakrishnan;
UT MD Anderson Cancer Center, Houston, TX

Introduction: Medulloblastoma (MB) is the most common malignant brain tumor in children. It is categorized into four molecular subgroups, each with unique genetic and epigenetic alterations, molecular signatures, and differences in clinical features and treatment responses. Targeted therapy for MB has failed in the clinic, prompting new studies of mechanisms involved in MB tumorigenesis and progression.
Experimental Procedure: The transcriptomic information of the MB patients was obtained from the publicly available RNAseq datasets and was analyzed for differential expression and clustering analysis. Patient-derived orthotopic xenografts of medulloblastoma tumors with high- and low-REST expression were histologically and biochemically studied for autophagy markers. Furthermore, the SHH-MB cell lines were studied to get a mechanistic understanding of the REST-driven autophagy in this MB subgroup.
Summary: Our data showed that autophagy, a process responsible for cellular recycling, and genes associated with this pathway exhibit distinctive expression patterns in human MB subgroups. Specifically, we demonstrate that autophagy is induced in one of the MB subgroups (Sonic Hedgehog-SHH) in response to elevated expression of the RE1-silencing transcription factor (REST), a transcriptional repressor and a canonical regulator of neuronal differentiation genes. REST is also a driver of SHH-MB metastasis. Pharmacological inhibition of autophagy decreases MB cell growth, suggesting it is a pro-survival pathway in REST-driven SHH MBs. In mechanistic studies, we found REST-dependent autophagy induction to involve upregulation of the hypoxia-inducible factor 1-alpha (HIF1α) due to REST-mediated silencing of the von Hippel-Lindau (VHL) gene. The VHL gene product promotes HIF1α ubiquitination and proteasomal degradation, and its loss in SHH-MBs with elevated REST expression drives HIF1α stabilization and nuclear localization to activate target autophagy-related genes.
Conclusion: Our work is the first to link VHL to MB pathology. VHL loss of function in cancers has been mainly attributed to mutational events. Here, we report a novel mechanism of VHL loss, namely its epigenetic silencing by REST. Our findings provide the foundation for future pre-clinical investigations to examine the feasibility of autophagy blockade as a therapeutic strategy for REST-driven SHH MBs.

#2865 Efficacy of MDM2 and epigenetic inhibitors treatments for neuroblastoma.

T. Momenah[1], U. Natarajan[2], S. Jaganathan[2], A. Rathinavelu[3];

[1]Nova Southeastern University, Barry & Judy Silverman College of Pharmacy, Fort Lauderdale, FL, [2]Nova Southeastern University,Barry & Judy Silverman College of Pharmacy, Fort Lauderdale, FL, [3]Nova Southeastern University,, Fort Lauderdale, FL

Pediatric Neuroblastoma (NB) is one of the most prevalent solid tumors in children that arise from embryonic neural crest cells and poses a significant challenge in the field of oncology. There are about 700 to 800 new cases of neuroblastoma diagnosed each year in the United States, and accounts for approximately 15% of all childhood cancer mortalities. Since this malignancy predominantly affects infants and young children, it is imperative to decipher the underlying molecular factors driving its pathogenesis. The novel molecular therapeutic approach includes the use of epigenetic modifiers as drugs. This approach aims to reverse significant epigenetic events underlying cancer pathogenesis, particularly abnormalities in histone modifications and DNA methylation. The reduction of both DNA and histone methylation levels leads to the reactivation of tumor suppressor genes and inhibits cancer cell proliferation and cell growth. In this study, we used selective and reversible small molecule agents such as MDM2 inhibitor (RG7388) and epigenetic modifiers (CM272 and SAHA) to block cell proliferation by inducing cell cycle arrest via enforcing Epigenetic alterations. Our initial experiments were designed to understand the effects of RG7388, CM272, and SAHA treatments on NB and their impact on cell cycle progression. It was hypothesized that the decrease in DNA methylation and increase in histone modification-augment p21 expression *via* the use of MDM2 inhibitors and epigenetic modifiers. To test this hypothesis, the NB cells (SK-N-SK and IMR-32) were treated with RG7388, CM272, and SAHA for 24 hours. The extent of Cell death was determined for NB cells by using the Trypan Blue Dye Exclusion (TBDE) method, and CellTiter-Glo® Luminescent Cell Viability Assay. Induction of apoptosis was determined by using the Immunofluorescence staining method with DEVD-*amc* substrate. The results of our study suggested that RG7388, CM272, and SAHA were able to induce cell death in the SK-N-SH cells following 24-hour treatment. Furthermore, we analyzed the levels of Tumor suppressor (p53), cell cycle arrest (p21, p27, AurkB, CDC25A, CyclinD) cell death (Bax, Bcl2, LC3, Beclin, PARP, Cleaved PARP, RIP1, RIP3, MLKL, p-AKT), and Epigenetic biomarker (DNMT1, DNMT3A, DNMT3B, acetyl histoneH3, H4, and H2b) protein expression levels using western blot analysis. The results showed significant elevation of p53, p21, p27, and acetylation of histone family biomarkers after treatment when compared with the control group. In summary, our results indicate that RG7388, CM272, and SAHA treatments can effectively induce cellular responses and prevent cell growth and progression by enforcing epigenetic changes in the NB cells. (This research was supported by the National Pediatric Cancer Foundation, Tampa, Florida, and the Royal Dames of Cancer Research Inc. of Ft. Lauderdale, Florida)

#2866 *NAPRT*silencing in rhabdomyosarcoma confers therapeutic vulnerabilities to NAD^+depletion.

S. J. Zhao[1], K. J. Noronha[1], P. Bhardwaj[1], K. N. Lucas[1], R. K. Sundaram[1], C. D. Heer[1], R. Morotti[1], J. Spurrier[2], M. Raponi[2], R. S. Bindra[1], **J. C. Vasquez**[1]; [1]Yale School of Medicine, New Haven, CT, [2]Alphina Therapeutics, New Haven, CT

Rhabdomyosarcoma (RMS) is the most common soft tissue sarcoma among children, and new treatments are needed to improve survival. Cells primarily synthesize nicotinamide adenine dinucleotide (NAD) through the Preiss-Handler and Salvage pathways driven by nicotinic acid phosphoribosyltransferase (NAPRT) and nicotinamide phosphoribosyltransferase (NAMPT), respectively. NAMPT inhibitors (NAMPTi) have been tested in clinical trials, but their efficacy has been limited by (a) lack of appropriate biomarkers for patient selection, and (b) significant dose-limiting toxicities (DLTs), including myelosuppression and retinal toxicity, although the latter has been described only in preclinical studies. Previous work from our group indicates that loss of NAPRT expression by tumor-specific promoter CpG island methylation may provide a novel biomarker for sensitivity to NAMPTi in a variety of tumors. Here, we sought to determine if RMS harbors NAPRT silencing that confers a synthetic lethal interaction with NAMPTi. We probed methylation data within the Cancer Dependency Map (DepMap) and found a high frequency of NAPRT gene promoter hypermethylation in RMS models. Predicted NAPRT silencing was confirmed at the protein level by western blot in a panel of RMS cell lines. In vitro growth delay assays demonstrated that NAPRT-silenced cells are exquisitely sensitive to NAMPTi even in the presence of nicotinic acid (NA) supplementation, while NAPRT-expressing cells were completely rescued. This sensitivity to NAMPTi was further mirrored by changes in NAD levels. In vivo, NAMPTi induced significant tumor regression in a NAPRT-silenced RMS xenograft model. To further establish the translational relevance, NAPRT protein expression in a TMA of 51 human RMS tumors was assessed via IHC staining using a newly validated NAPRT monoclonal antibody (4A5D7). Based on a semi-quantitative scoring system accounting for the percentage of positive tumor cells and staining intensity, 28% of RMS samples demonstrated loss of NAPRT protein expression. Overall, these data suggest that NAPRT loss may serve as a therapeutic target in RMS by inducing a synthetic lethal interaction with NAD^+ depleting agents. Future studies in patient-derived xenograft (PDX) models will determine the optimal cut-off of NAPRT expression that portends NAMPTi sensitivity, paving the way for the development of biomarker-driven clinical trials in RMS. Ongoing studies will also evaluate the efficacy of combining NAMPTi with existing cytotoxic and DNA damaging chemotherapy in these difficult-to-treat tumors.

TUMOR BIOLOGY: Radiation Science
Poster Session

#2870 Analysis of cancer cells response to radiotherapy activated NBTXR3 nanoparticles.
J. Da Silva, C. Bienassis, **S. Paris**;
Nanobiotix, Paris, France

In 2011, NBTXR3 emerged as the first-in-class radioenhancer used in clinical practice for treating patients with locally advanced soft tissue sarcoma (LA-STS). NBTXR3 became the first radioenhancer to receive CE mark approval after successfully completing a phase II/III clinical study for LA-STS with a doubling of the pCR rate in the NBTXR3 arm compared with the control arm. NBTXR3 nanoparticles consist of a functionalized core of hafnium oxide, a high atomic number element, specifically designed to amplify the effects of radiotherapy (RT) within cells without additional side effects on healthy tissues. Leveraging this physical mechanism, RT-activated NBTXR3 (NBTXR3+RT) has demonstrated superior efficacy in destroying tumor cells and controlling tumor growth in numerous preclinical models and in human, surpassing the effects of RT alone, while maintaining a favorable safety profile. Preclinical studies have revealed that the benefits of NBTXR3 extend beyond mere radioenhancement and improved cancer cell destruction. Specifically, NBTXR3 has been reported to possess immunomodulatory properties through 1) improved induction of DNA damage, leading to better activation of the cGAS-STING pathway, 2) promotion of immunogenic cell death, 3) enhancement of immunopeptidome presentation, 4) generation of an antitumor immune response leading to the production of an abscopal effect mediated by CD8+ cytotoxic lymphocytes. Notably, a series of recent studies using a two-tumor mouse model of anti-PD1-resistant lung cancer that the addition of NBTXR3 significantly improved the efficacy of various treatment regimens (RT+anti-PD1 and combinations with other check-point inhibitors) in terms of tumor growth, abscopal effect, and survival. It has been demonstrated that same benefits can be achieved when NBTXR3 was combined with proton therapy. Moreover, all these studies (X-ray and proton) reported a robust activation of the antitumor immune response, restoration of the effectiveness of anti-PD1 therapy, and the induction of memory response in cured mice. However, our understanding of the biological events leading to these effects remains limited. To address this question, we conducted a series of in vitro studies that employed cytometry, microscopy, and RNA sequencing on various cancer models, both human and murine. We reported that NBTXR3 nanoparticles primarily accumulate within lysosomes following their uptake by tumor cells, leading to the activation of genes associated with the biogenesis, structure, and contents of these organelles. Upon activation by RT, NBTXR3 within lysosomes induces lysosomal membrane permeabilization (LMP), resulting in an increase in lipid peroxidation, inducing regulation of fatty acid oxidation genes, and impacting mitochondrial genes expression, such as respirasome. These findings provide a deeper insight into the early biological effects of NBTXR3+RT in comparison to RT alone.

#2871 Co-targeting asparagine and glutamine metabolism is a viable treatment strategy for PI3K/PTEN mutated cervical cancer.

Nishanth Noel Gabriel, Naoshad Muhammad, Kevin Cho, Kay Jayachandran, Jin Zhang, Gary Patti, Julie Schwarz

Washington University in St. Louis, St. Louis, MO

Purpose Statement: Alterations in the PI3K/AKT signaling pathway are common in cervical cancer. The most commonly observed mutations are in *PIK3CA* (26%) and *PTEN* (8%). However, the biological and metabolic implications of acquiring these mutations in the cervical cancer genome are poorly characterized.
Materials/Methods: Isogenic cell lines with *PIK3CA E545K* and *PTEN* null mutations were generated using Crispr/CAS9. Cell viability and clonogenic cell survival assays were performed in the presence and absence of inhibitors of glutamine and asparagine metabolism. Glucose and glutamine metabolism was evaluated by stable isotope labeling with U13C glucose and13C5 glutamine in presence of glutamine antagonist DON. RNA-seq was employed to evaluate transcriptomic alterations.
Results: Introduction of the PIK3CA E545K mutation and PTEN mutation in cervical tumor cells leads to an increase in AKT signaling compared to the parental (wild-type) cells. Notably, RNASeq and mass spectrometric analysis of both the tumor cells and their culture media revealed heightened dependencies on glucose and glutamine in the tumor cells carrying the PIK3CA E545K and PTEN mutations as compared to the wild-type cells. Treatment with glutamine antagonists (DON, JHU-083) and GLS inhibitors (CB-839 and IACS-6274), resulted in reduced cell viability and clonogenic survival in tumor cells with PI3K/PTEN mutation compared to wild-type. Additionally, we observed a metabolic reliance on the amino acid asparagine in tumors with PI3K/PTEN alterations when treated with DON. Asparaginase in combination with DON effectively inhibited the proliferation of human and mouse cell lines derived from primary tumors with PTEN mutations. Furthermore, the incorporation of a glutamine antagonist and asparaginase into conventional chemoirradiation further enhanced the therapeutic efficacy in cervical tumors with PI3K/PTEN alterations which are otherwise treatment resistant.
Conclusions: Orthogonal evaluations using glutamine agonists, GLS inhibitors, and mass spectrometric point to a significant role played by *PI3K/PTEN* mutations in altering cervix tumor cell metabolism towards a more glutamine dependent phenotype. This study suggests a potential strategy for improving the treatment of PI3K-AKT-altered cervical tumors by targeting glutamine and asparagine metabolism in combination with standard therapies. These treatment strategies are currently being evaluated *in vivo* using a patient derived xenograft model with *PIK3CA E545K* mutation as well as an immunocompetent cervical tumor model in mice with *PTEN* deletion.

#2872 GLUT3 promotes metabolic plasticity that drives radiation resistance in glioblastoma.

L. Abdulrahman, J. Bailleul, H. Hoang, A. Tang, E. Vlashi;
UCLA - University of California Los Angeles, Los Angeles, CA

Glioblastomas (GBM) are the most common and malignant brain tumors in adults. While radiation therapy (RT) offers a significant advantage for GBM patients, improving long-term survival remains elusive largely due to the remarkable resistant nature of these tumors. We have shown that metabolic plasticity, especially rewiring of glucose metabolism, promotes radiation survival in GBM. In this study, we investigate the role of glucose transporter 3 (GLUT3) translocation to the cell surface in radiation resistance of GBM. The effect of radiation on GLUT3 total protein levels was determined in patient-derived gliomaspheres via westerns blots, while cellular localization of GLUT3 was determined via immunofluorescence, flow cytometry and cell fractionation assays. The role of the AMPK and αvβ3 integrin in the radiation-induced GLUT3 translocation to the cell membrane was probed via small molecule inhibitors and activators. To determine the role of GLUT3 in radiation survival, GLUT3 levels were knocked down via siRNA and shRNA, followed by functional *in vitro* and *in vivo* assays. We provide evidence that irradiated gliomaspheres translocate GLUT3 to the plasma membrane, in a radiation-induced oxidative stress-dependent manner, effectively increasing their glucose uptake and promoting radiation survival. Our data also suggest that GLUT3 translocation to the cell surface contributes to RT resistance. AMPK and αvβ3 integrin are linked to radiation-induced translocation of GLUT3 to the cell membrane, suggesting that targeting these pathways is a potential approach to sensitize GBM tumors to radiation therapy.

#2873 Radiation therapy promotes polyunsaturated fatty acid mediated ferroptosis in cervical cancer: Role of AMPK/xCT/GPX4 axis.

N. Muhammad, N. Gabriel, L. M. Bengtsson, T. McKinnish, N. Msengi, K. Cho, G. Patti, J. K. Schwarz;
Washington University School of Medicine in St. Louis, St. Louis, MO

Purpose: Previously, we found that mono-and di-unsaturated fatty acids can sensitize cervical cancer to radiotherapy (RT) through a p53 dependent apoptotic mechanism that is distinct from ferroptosis (Muhammad et al., *Cancer Res.* 2022; 82: 4515-27). Polyunsaturated fatty acids (PUFAs) enhance therapeutic response in preclinical tumor models by increasing lipid peroxidation (L-ROS) and induction of ferroptosis. Ferroptosis is a form of cell death that requires abundant cytosolic labile iron to promote membrane lipid peroxidation. The objective of the present study is to test whether the combination of RT + PUFAs promotes cell death via increased membrane lipid peroxidation and ferroptosis in cervical cancer, and to determine the impact of RT + PUFAs on cervix tumor cell metabolism and mitochondrial function.

Experimental Procedures: Cell viability and clonogenic cell survival assays were performed using 8 human cervical cancer cell lines including normal cervix epithelial controls incubated with PUFAs (EPA, DHA and AA), before and after RT. Western blotting, siRNA-mediated knockdown, pharmacologic inhibition and activation were performed to determine whether ferroptosis dependent signals were mediating PUFA-induced RT sensitivity. Oxidative stress parameters were quantified using mass spectrometry and fluorometric dyes. Flow cytometry was used to quantify total cell ROS, lipid ROS, mitochondrial ROS and labile iron pool. Mitochondrial morphology and function were characterized using microscopy and the Seahorse assay.

Summary: PUFAs + RT increased total ROS and LROS accumulation followed by a ferroptotic tumor cell death, which was iron-dependent and could be prevented by the addition of iron chelator and lipophilic antioxidants, Ferrostatin-1 and Liproxstatin-1. GPX4, a thiol dependent enzyme that eliminates lipid peroxides, and the cystine-glutamate antiporter (xCT) a key source of cystine for reduced glutathione (GSH) synthesis, were downregulated in response to PUFAs + RT. PUFAs + RT induced increased mitochondrial ROS and subsequent metabolic dysfunction. Mechanistically, the expression of AMPK, a key regulator of metabolic/energy homeostasis and mitochondrial biogenesis, was upregulated by PUFAs + RT. Pharmacological activation and inhibition of AMPK further enhanced and abrogated the effect of PUFA + RT, respectively.

Conclusions: PUFAs modify the RT sensitivity of cervical cancer cells by inducing cell death through ferroptosis and mitochondrial dysfunction via AMPK activation. In vivo experiments are ongoing in immunocompromised and immunodeficient mouse tumor models to confirm this finding and determine the impact of PUFAs on RT induced tumor cell death and anti-tumor immunity.

#2874 Cancer metabolism in radiation resistance: Complementary roles of O-GlcNAc transferase and PARP1.

E. E. Efimova, S. Averbek, D. J. Wolfgeher, D. Wu, Y. Liu, **S. J. Kron**;
University of Chicago, Chicago, IL

The efficacy of image-guided radiotherapy (RT) has been linked to directing increased chromosomal double strand breaks (DSBs) to tumor cells while sparing surrounding normal tissue. DSBs can block cell cycle progression and promote mitotic catastrophe, cell death and senescence. End processing of persistent DSBs releases single strand DNA (ssDNA), driving cGAS/STING signaling and anti-tumor immune response. DSB repair, whether by non-homologous end-joining (NHEJ) or homologous recombination (HR), is a resistance mechanism, supporting cell survival, repopulation and immune evasion. Decades of effort to block DSB repair to enhance benefits of RT has yet to produce approved agents. Toxicity due to lack of cancer specificity may prevent the current generation of targeted agents from reaching the clinic. An answer may come from examining cancer metabolic reprogramming as a determinant of intrinsic radiation resistance. Along with other glucose metabolites, the Warburg effect increases N-acetyl glucosamine (GlcNAc) biosynthesis, which not only supports N-glycosylation but also modification of nucleocytoplasmic proteins by O-GlcNAc transferase (OGT). OGT-dependent O-GlcNAcylation confers radiation resistance, in part by accelerating DSB repair. OGT regulates γH2AX, 53BP1 and BRCA1 foci kinetics and suppresses ssDNA formation at DSB ends, limiting HR but favoring NHEJ for S/G2 DSB repair. Blocking OGT induces radiation sensitization *in vitro* and *in vivo*. In cells, OGT inhibition results in hyperresection, persistent RPA and RAD51 foci and accumulation of cytosolic DNA. One mediator may be the histone methyltransferase EZH2, which is rapidly recruited to deposit H3K27me3 at DSBs, promoting NHEJ repair. Irradiation of EZH2 KO cells results in hyperresection that cannot be suppressed by O-GlcNAcylation. Cancer cells may also accumulate NAD+, a substrate for PARP1 incorporated into poly-ADP-ribose to initiate DSB repair. Much like OGT inhibition, blocking PARP1 induces hyperresection and shifts repair toward HR and away from NHEJ. Importantly, increasing O-GlcNAcylation can suppress ssDNA formation even in PARP1 KO cells. In turn, inhibiting PARP1 enhances hyperesection in EZH2 KO cells, leading to a marked increase in cytosolic ssDNA. Our data assign complementary roles for EZH2 and PARP1 in DSB repair pathway choice by independently limiting 5' end resection. This directs DSBs to rapid, imprecise repair by NHEJ over slow and precise repair by HR. An implication is that PARP inhibitor resistance due to the Warburg effect may be mediated by EZH2. Driving hyperresection by targeting O-GlcNAcylation or H3K27 trimethylation along with PARP inhibition may saturate the capacity of HR and produce irreversible damage in cancer cells. Targeting impacts of metabolic reprogramming on DSB repair may not only enhance the therapeutic index of radiation but also sharpen synthetic lethality with HR deficiency.

#2875 Resistance to conventional chemo and radiotherapy associated with increased DNA repair and stem cell-like phenotype in head and neck squamous cell carcinoma expressing HPV E5.

S. Roy, S. Miyauchi, R. Jones, S. Kim, **A. B. Sharabi**;
UCSD Moores Cancer Center, La Jolla, CA

Human papillomavirus-associated head and neck squamous cell carcinoma (HPV+ HNSCC) is one of the fastest-rising cancers in the US. While HPV+ HNSCC patients exhibit better responses to chemoradiation compared to HPV- HNSCC patients, a subset of HPV+ patients do not respond as well and develop recurrent/refractory disease. In this study, we investigated the potential role of HPV E5 in promoting resistance to conventional chemo- and radiotherapy, and the underlying molecular mechanisms. HPV E5 is a small hydrophobic viral oncoprotein with multiple functions including regulation of tumor cell differentiation and apoptosis, modulation of H+ ATPase responsible for acidification of late endosomes, and immune modulation. To test the impact of HPV E5 on therapeutic resistance, we generated HNSCC cell lines and normal keratinocytes expressing HPV16 E5. Upon treatment with radiation (2Gy, 4Gy, 8Gy) and/or cisplatin, HNSCC cells and keratinocytes expressing HPV 16 E5 had increased cell viability, decreased apoptosis, and increased colony-forming capacity compared to empty vector (EV) control lines. Specifically, treatment with 4Gy radiation, 4μM cisplatin, or the combination led to a ~2-fold decrease in % of apoptotic cells in HPV16 E5-expressing HNSCC cells compared to EV and HPV16 E6/E7 HNSCC cells ($p < 0.05$). Examination of DNA damage response and repair pathways indicated that while HPV16 E5 HNSCC cells initially had increased phosphorylation of H2AX 6 hours post treatment, at 24 hours post treatment H2AX phosphorylation in HPV16 E5 cells was significantly decreased compared to EV or HPV16 E6/E7 HNSCC cells. These findings indicate increased DNA repair capacity of HPV16 E5 HNSCC cells. To identify mechanisms underlying this phenotype, we performed RNA-seq and observed enhanced signaling pathways associated with epithelial development and increased expression of stem cell markers in HPV16 E5 HNSCC cells compared to EV control lines. Functionally, we observed a ~2.5-fold increase in sphere-forming capacity and increased expression of markers associated with stem cell phenotype in HPV16 E5 HNSCC cells compared to EV and HPV E6/E7 HNSCC cells. To determine whether these findings translated clinically, 18 HPV+ HNSCC patients from the GSE74927 dataset were grouped according to median expression level of HPV E5 (High vs Low). In support of our hypothesis, HPV E5-High patients exhibited enrichment of pathways associated with extrinsic apoptotic signaling, pluripotency of stem cells, and positive regulation of DNA repair. Taken together these results identify HPV E5 as a potential mediator of resistance to conventional radiation and chemotherapy in HNSCC and suggest that patient tumors expressing HPV E5 may have increased DNA repair capacity and cell survival after cytotoxic therapies.

#2876 Spatial immune cell atlas predicts the sensitivity to neoadjuvant PD-1 blockade treatment combined with radiotherapy in resectable esophageal squamous cell carcinoma.

X. Yin[1], K. Xu[2], S. Zheng[2], B. Li[3],

[1]The Affiliated Hospital of Qingdao University,, Qingdao, China, [2]The Second Affiliated Hospital, Zhejiang University School of Medicine, Hangzhou, China, [3]Shandong Cancer Hospital and Institute, Shandong First Medical University and Shandong Academy of Medical Sciences, Jinan, China

Combination of radiotherapy and immunotherapy in neoadjuvant treatment seems a promising approach in resectable esophageal squamous cell squamous (ESCC). The clinical study of radiotherapy combined with PD-1 blockade therapy for neoadjuvant treatment of resectable ESCC shows good result. In order to investigate the underlying mechanism of the effectiveness of radiotherapy combined with immunotherapy in ESCC, we collected the pre and post neoadjuvant therapy samples from 5 responders and 5 non-responders ESCC patients and performed multiplexed tissue imaging using 28 markers. Using the detection measurements exported from QuPath, we performed the unsupervised clustering with Seurat and defined 20 cell types. Scimap was used to calculate the distance between different cell types. We found that CD4+ T, CD8+ T, cytotoxic CD8+ T cells and M1 macrophages showed an increase after treatment in both responders and non-responders. Tregs were decreased after neoadjuvant treatment in responder while there was no significant decrease in non-responder. And the distance between Tregs and cancer cells were increased in responders. Collectively, we provide an approach for investigating the underlying mechanism of the sensitivity to neoadjuvant PD-1 blockade treatment combined with radiotherapy in resectable ESCC using spatial multiplexed imaging.

#2877 Enhancing diagnostic precision in peritoneal cancer metastasis: Photodynamic diagnosis-guided laparoscopy in a rabbit model.

H.-I. Kim[1], A. Rivera-Piza[1], S. Lee[2];

[1]Yonsei University Health System, Seoul, Korea, Republic of, [2]CHA Bundang Medical Center, Bundang, Korea, Republic of

Introduction: Precise diagnostic workup is crucial for developing effective treatment strategies in cancer patients. Peritoneal carcinomatosis, often missed in preoperative CT scans and conventional laparoscopy, poses diagnostic challenges. This study aimed to assess the diagnostic accuracy of staging laparoscopy using photodynamic diagnosis (PDD) with the photosensitizer phonozen activated at 405 nm in a rabbit model of peritoneal carcinomatosis.
Methods: Female New Zealand white rabbits (16-20 weeks old) were utilized to establish the model through peritoneal inoculation of VX2 sarcoma cells, resulting in distinct solid-tumor nodules for laparoscopic evaluation. A customized dual-emission laparoscope, capable of both white-light and 405 nm blue-light, was employed for PDD. To minimize blue-light background interference, a 550 nm long-pass filter was placed between the laparoscope and the video camera, optimizing the process. The PDD-enhanced diagnostic laparoscopy comprised a tripartite approach: 1) initial peritoneal cavity exploration under white-light and labeling of suspect nodules, followed by 2) utilization of blue light with the long-pass filter to identify red-light emissions from distinctly labeled tumor cells, and 3) open laparotomy served to palpate the peritoneal surface and identify additional or missed tumor nodules.
Results: Analysis of data from 12 rabbits with 267 tumor nodules revealed that sensitivity and specificity of diagnostic laparoscopy for detecting tumor nodules increased from 84.9% and 18.8% with white light alone to 90.8% and 25.0% when aided by PDD, respectively. These findings underscore the substantial improvement in diagnostic accuracy achievable by combining the rabbit model of peritoneal carcinomatosis with PDD in laparoscopic procedures.
Conclusion: The heightened sensitivity and specificity observed in this study hold significant promise for positively impacting clinical practice, providing a more accurate and effective approach to the diagnosis and management of peritoneal carcinomatosis.

#2878 Hyperthermia increases the efficacy of aminolevulinic acid-mediated photodynamic therapy in human osteosarcoma cells.

P. J. Baugher;
Pacific Univ., Forest Grove, OR

Osteosarcoma is a malignant osteoid tumor that arises from mesenchymal cells exhibiting osteoblastic differentiation. Common treatments for this neoplasm include limb-salvage surgery and/or amputation of the affected limb, either of which can substantially decrease quality of life. Therefore, other, less invasive treatments should be explored. Photodynamic therapy (PDT) represents a more targeted, less invasive treatment possibility for osteosarcoma. Previous data from my laboratory demonstrated that aminolevulinic acid-mediated photodynamic therapy (ALA-PDT) can be used to induce significant cell death in human osteosarcoma MG-63 cells *in vitro*. However, delivering high doses of drugs to deep osteosarcoma tumors could prove difficult, so we aim to explore the use of combination therapies to increase the efficacy of ALA-PDT in human osteosarcoma cells. Previous studies have shown that hyperthermia (increased temperature) can induce cell death in cancer cells. Furthermore, data suggest that combining PDT with hyperthermia can induce cell death in cancer cells synergistically by activating differential death-inducing pathways. However, hyperthermia in combination with ALA-PDT has not been explored in human osteosarcoma. Therefore, we aim to investigate the possibility that hyperthermia in combination with ALA-PDT can increase cell death in human osteosarcoma cells compared to ALA-PDT alone. Data from our lab show that compared to normal body temperature (37°C), cell death in MG-63 human osteosarcoma cells was not significantly increased by mild hyperthermia alone (40°C and 43°C respectively), while moderate hyperthermic temperatures alone (46°C and 49°C) did significantly increase cell death. We also found that at moderately hyperthermic temperatures, ALA-PDT does not increase cell death any further compared to moderate hyperthermia alone. Furthermore, we found that at the mildly hyperthermic temperature of 40°C, cell death was not significantly increased any further by ALA-PDT compared to ALA-PDT alone. However, our data do show that at a temperature of 43°C, hyperthermia plus ALA-PDT increased cell death compared to ALA-PDT alone. Therefore, our data suggest that inducing mild hyperthermia could increase the efficacy of ALA-PDT in human osteosarcoma cells.

#2879 Spatiotemporal fractionation: An innovative concept of fractionated radiotherapy.

I. Vetrugno[1], I. Telarovic[1], N. Torelli[2], J. Unkelbach[1], M. Pruschy[1];
[1]Universitat Zurich, Zurich, Switzerland, [2]University Hospital Zurich, Zurich, Switzerland

Impressive outcomes in therapeutic radiation oncology have been achieved in the past decade through the development of advanced computer technology and imaging methods, such as intensity modulated radiotherapy. Ideally, radiotherapy treatment delivers a high dose to the tumor while sparing the surrounding healthy tissues and organs at risk from radiation damage. Spatiotemporal Fractionated Radiotherapy has emerged as an innovative technique that delivers different dose distributions to different parts of the tumor in order to achieve high doses to the target while ensuring a low dose-bath in the surrounding normal tissue. Spatiotemporally fractionated regimens showed *in silico* up to 10 - 15% sparing of normal tissue from radiation damage, while ensuring isoeffective tumor control compared to conventionally fractionated regimens. However, prior to advancing spatiotemporal fractionation to the clinical level, it is important to probe the validity of the main assumption of spatiotemporal fractionation derived from the Biologically Effective Dose (BED) model: two different fractionation schemes that implement a high and a low dose will lead to equivalent clinical effects, regardless of dose-treatment sequence. A tumor growth delay study was performed in a subcutaneous immunocompetent murine tumor model (MC38-tumor cell derived) receiving two different fractionation regimens. Particularly, tumors belonging to the two treatment groups received the same dose combination - a high (12 Gy) and a low (6 Gy) dose fraction separated by 72 hours - with the doses delivered in opposite order in the two treatment groups. The same experimental outline was performed in a subcutaneous immunodeficient murine tumor model derived from the same tumor cells. Tumors were also characterized by immunophenotyping analysis seven days after first irradiation. Even though the two regimens deliver the same physical dose to the tumor - and would be considered equivalent according to the BED model - different tumor growth delays were observed in a time window of 30 days after first irradiation depending on the treatment group. Such differences were observed in the immunocompetent model but not in the immunodeficient model. The immunophenotyping results showed immunostimulatory vs immunosuppressive phenotypes of the tumor microenvironment depending on the order of the treatment doses. An additional tumor growth delay study including immune checkpoint inhibitors confirmed the fundamental role of the immune system with the differential efficacy outcomes of the two regimens. Overall, these intriguing results suggest that a differential radiotherapy-induced immune response to different doses of ionizing radiation plays an important role in the treatment outcome and asks for re-evaluation of the BED model taking scheduling-dependent parameters into consideration.

#2880 Radiation induces myofibroblast differentiation of pericytes.

T. Yamazaki, K. R. Jordan, M. R. Crittenden, M. J. Gough, K. H. Young;
Providence Cancer Institute, Portland, OR

Radiation not only kills cancer cells directly through DNA damage, but also indirectly by inducing vascular changes. Endothelial cells (ECs) in small blood vessels and capillaries connect with pericytes, a type of mural cells which are important for vascular stability and structure. Effects of radiation on tumor vasculature are critical for the therapeutic efficacy, however, its impacts on pericytes remain largely unknown. In this study, we focused on the effect of radiation on pericytes and sought to elucidate the mechanism by which radiation affects pericytes. We show 20Gy for C3H10T1/2 (10T1/2) mouse embryonic mesenchymal pericyte precursor cells and 10Gy for human pericytes from placenta (hPC-PL) cells induces pericyte differentiation and activation of adhesion molecules. Radiation enhanced lymphocyte adhesion and decreased permeability in co-culture of ECs and pericytes primarily through endothelial cells, not via pericytes. Furthermore, radiation promoted transdifferentiation of pericytes into myofibroblasts. Supernatant from irradiated cells in combination with a TGFβ inhibitor showed that TGFβ signaling is involved in pericyte differentiation by radiation but not all pericyte marker genes are regulated by TGFβ. Therefore, we performed phospho-kinase array analysis and revealed Akt signaling pathway activation 10 minutes following radiation, which was verified by the phosphorylation of GSK3β and PRAS40. Along with this, generation of intracellular reactive oxygen species (ROS) occurs as early as 5 min following radiation. Inhibitors of Akt and ROS suppress the expression of myofibroblast markers increased by radiation.

To investigate whether radiation induces pericyte differentiation into myofibroblast in tumors, we employed NG2DsRedBAC (NG2DsRed) transgenic mice where DsRed is expressed under the control of NG2 promoter to trace pericytes. The endogenous expression of DsRed was detected in pericytes in the tumors implanted to NG2DsRed mice. Flow cytometry analysis of tumors harvested 7 days after radiation shows radiation increased vimentin^{+} cells and decreased DsRed^{+} cells, which indicates radiation induced pericyte differentiation into myofibroblast. In conclusion, radiation promotes pericyte maturation and transdifferentiation into myofibroblast via Akt signaling. Further study using Akt inhibitor with radiation to tumor-bearing N2DsRed mice will be warranted.

#2881 Comparing the effects of proton and photon therapy on promoting cancer aggressiveness in ovarian cancer and glioblastoma.

Y. Jung[1], A. Morcos[2], A. Keniston[1], A. Antonissen[1], S. Asariah[3], A. Bertucci[4], M. Vazquez[4], J. Unternaehrer[2];
[1]California State University, San Bernadino, San Bernardino, CA, [2]Loma Linda University, Loma Linda, CA, [3]California Baptist University, Riverside, CA, [4]Canadian Nuclear Laboratories, Chalk River, ON, Canada

Ovarian cancer is the 12th most common cancer among women in the United States and the 5th leading cause of cancer-related death for women. About 80% of the patients are diagnosed at stages III or IV, classified as High-Grade Serous Ovarian Cancer (HGSOC). HGSOC is highly aggressive, exhibiting an 80% recurrence rate within 24 months after cancer treatment. Brain and nervous system cancer ranks as the 10th leading cause of cancer-related death in the U.S., with Glioblastoma Multiforme (GBM) accounting for 47.7% of all brain cancer cases. GBM is the most aggressive primary brain cancer, with a 90% recurrence rate and a 4% 2-year survival rate. Patients with these cancers encounter limited treatment options, and the recurrence of cancer exacerbates these challenges. Therefore, a deeper understanding of the factors contributing to cancer treatment-induced aggressiveness is greatly needed. In our study, we first examined the treatment efficacy of proton and photon radiation by conducting apoptosis assays. Our findings demonstrate that proton radiation is significantly more effective at eliminating both HGSOC and GBM cells compared to photon radiation. Subsequently, we assessed the level of cancer aggressiveness in the surviving cells after radiation exposure by measuring stemness and epithelial-mesenchymal transition (EMT) levels. While proton radiation proved to be more effective in eliminating a greater number of cancer cells, we hypothesize that both proton and photon irradiation promote cancer aggressiveness in the surviving cells of HGSOC and GBM. To assess the stemness and EMT level of cancer cells following radiation, we integrated a SORE6-GFP reporter to identify the cancer stem cell population expressing SOX2/OCT4 and a 3' UTR-ZEB1-GFP reporter to detect the cell population with mesenchymal traits. Cells transduced with the reporters were treated with 0, 1, 2, 4, and 8 Gy of 250 MeV proton and 6 MeV photon beams, and at 72 hours post-radiation, GFP levels were measured via flow cytometry. Our data demonstrated a dose-dependent increase in stemness and EMT levels in live cells after both types of radiation. Furthermore, cancer cells exposed to radiation were harvested at 72 hours and 240 hours post-radiation for RT-qPCR analysis. Our preliminary data indicate an upregulation of stemness genes including POU5F1 and SOX2, as well as EMT transcription factor genes ZEB1, SNAI1, and TWIST1 in response to both types of radiation in most cell lines. These findings indicate that both proton and photon radiation therapies promote cancer aggressiveness in the surviving cancer cells.

#2882 Investigating mechanisms of radioresistance in TYK2 knockout head and neck cancer cells.

N. M. Constante, V. Kelley, J. Contessa;
Yale University, New Haven, CT

Radiation therapy is the primary form of treatment of head and neck squamous cell carcinoma (HNSCC). However, more than half of patients experience disease progression with standard of care treatment. To investigate novel therapeutic targets, a CRISPR screen was done to identify genes that are associated with radioresistance. The screening results indicated that JAK1 and TYK2 knockout (KO) resulted in radioresistance in HNSCC. Preliminary data suggests that loss of JAK1 causes an enhanced G2/M arrest phenotype and enhanced genome stability that contribute to radioresistance. To investigate whether TYK2 KO caused changes to the cell cycle and genome stability as observed in JAK1 KO, Western blots, cell cycle assays, and micronuclei staining experiments were performed. Cal27, a HNSCC cell line, was used. Cal27 cells were transduced with a non-targeting control (NT2) guide RNA (gRNA) or two different gRNAs targeting TYK2 to generate TYK2 KO cells. Western Blot analysis was performed to determine changes in signaling upon TYK2 KO. Additional conditions included radiation and treatments with Interferon gamma, Interferon alpha and Interleukin-6 to activate the canonical JAK-STAT pathways. Overall, there were minimal changes in downstream signaling between the treatments and the knockouts. Cell cycle analysis via flow cytometry revealed no changes between the NT2 and TYK2 KO cells, potentially corroborating signaling results. Forty percent of TYK2 KO cells were arrested at the G2/M checkpoint at 8 hrs and 24 hrs after radiation treatment, but twenty percent returned to the G1 phase at 24 hrs. This indicates that loss of TYK2 is not responsible for cell cycle arrest. Lastly, micronuclei formation was observed to measure genomic instability. Twenty thousand Cal27 NT2 and TYK2 KO cells were seeded. They were allowed to incubate for 48 hrs before treatment with 4 Gy. Micronuclei staining revealed minimal differences between NT2 and TYK2 KO cell lines, although there were significant differences between the control and the radiation groups. Overall, radioresistance by TYK2 KO is not caused by changes in cell cycle or genomic instability as demonstrated with JAK1 KO. To understand how TYK2 is causing radioresistance in HNSCC, next steps would be to see if there are changes in proliferation. If MTT assays demonstrate significant changes, downstream signaling in growth pathways will be measured. If there is no increased proliferation, we will examine changes in DNA damage repair.

#2883 HDAC6 mediates the radioresistance of NSCLC through LSD1, independent of its own deacetylation activity.

S. Ha[1], H. Kim[1], H. Lee[1], S. Choi[1], H.-y. Lee[2], W.-Y. Kim[1];

[1]Sookmyung Women's University, College of Pharmacy, Seoul, Korea, Republic of, [2]Seoul National University, Seoul, Korea, Republic of

Resistance to radiation therapy significantly affects the prognosis of solid tumors. Histone deacetylase 6 (HDAC6) is a stress-responsive lysine deacetylase that has emerged as a promising target for cancer therapy, with numerous clinical trials investigating interventions to modulate its activity. While HDAC6 appears to be linked to responses to DNA-damaging therapeutics, the reported responses and underlying mechanisms remain intriguing and varied. In this study, we elucidate a novel mechanism of radioresistance mediated by HDAC6 in non-small cell lung cancer (NSCLC). We classified nine NSCLC cell lines into three groups based on their radioresistance using survival assays and correlated this resistance with the induced expression of six deacetylases. We conducted gain-of-function experiments (GOF) using plasmid transfection and loss-of-function experiments (LOF) employing inhibitors or RNAi. Furthermore, we quantified the repair of damaged dsDNA through FACS-based GFP assays and assessed the mechanism of homologous recombination repair (HRR) end-resection via single-strand quantitative PCR. Co-immunoprecipitation assays, cancer stem cell enrichment, DNA damage-induced senescence assays, reverse-phase protein assays (RPPA), and RNA sequencing were also performed to investigate gene expression changes resulting from the loss of HDAC6. Our findings revealed that HDAC6 induction by radiation is strongly correlated with NSCLC resistance to radiation leading to CSC survival and escape from radiation led senescence LOF of HDAC6 through RNAi or inhibitors suppressed resistance, while GOF achieved through wild-type or deacetylase activity-deficient mutant transfection, induced resistance. Importantly, this resistance mechanism was independent of deacetylation activity. RNAi-mediated loss of HDAC6 reduced both HRR and non-homologous end-joining, whereas pharmacological inhibition of HDAC6 activity did not. Notably, DNA end-resection, a critical step in HRR, was decreased by RNA interference but not affected by the inhibitors. RPPA assays demonstrated that Histone demethylase 1A (LSD1/KDM1A) levels decreased significantly upon HDAC6 RNA interference but remained unaffected by pharmacological intervention. Loss of LSD1 alone resulted in decreased HRR and end-resection, likely mediated through HDAC6-induced ubiquitination. Moreover, overexpression of LSD1 rescued the HDAC6 loss-induced sensitization of NSCLCs. In summary, our study unveils a novel mechanism by which HDAC6 mediates HRR after radiation through the stabilization of LSD1. This mechanism operates independently of deacetylase activity. Therefore, our findings suggest that interventions targeting both deacetylation and non-deacetylation roles of HDAC6 should be considered to overcome HDAC6-derived radioresistance in NSCLCs and enhances the radiation therapy efficacy.

#2884 Resistance to pan-FGFR inhibition is determined by the EMT phenotype associating with clinical outcome in HNSCC.

F. Broghammer[1], M. Gouda[2], I. Korovina[3], C. Brunner[4], R. P. Coppes[5], O. Gires[2], M. Seifert[1], **N. Cordes**[3];
[1]Technische Universitat Dresden, Dresden, Germany, [2]Ludwigs-Maximilians-University University Hospital, Munich, Germany, [3]Helmholtz Center Dresden - Rossendorf, Dresden, Germany, [4]Ulm University Medical Center, Ulm, Germany, [5]University of Groningen, Groningen, Netherlands

Receptor tyrosine kinases (RTK) and integrins coalesce at focal adhesions. These cell membrane areas serve as huge signaling hubs critically contributing to central aspects of cancer cell survival and therapy resistance. Despite the fact that these receptors mutually interact, co-dependencies between these receptors and associated therapeutically exploitable vulnerabilities remain largely unclear in HPV-negative head and neck squamous cell carcinoma (HNSCC). Here, we evaluated the cytotoxic and radiochemosensitizing potential of targeting 10 RTK and β1 integrin in up to 20 different 3D matrix grown HNSCC cell models. RNA sequencing and protein-based biochemical assays were performed for molecular and pathway characterization. Bioinformatically identified transcriptomic signatures were applied to patient cohorts to show clinical relevance. Our observations demonstrate that fibroblast growth factor receptors (FGFR 1-4) present with the strongest cytotoxic and radiosensitizing potential, both as monotherapy and in combination with β1 integrin inhibition, surpassing the efficacy of the other investigated RTK. Pharmacological pan-FGFR inhibition elicited a variable response spectrum ranging from cytotoxicity/radiochemosensitization to resistance/radioprotection. Transcriptomic characterization revealed an association of these contrasting responses to FGFR inhibition with a mesenchymal-to-epithelial transition (MET) for sensitive cell models and a partial epithelial-to-mesenchymal transition (EMT) for resistant cell models. Accordingly, deactivation of EMT associated kinases like EGFR, PKC and PAK proved effective in diminishing the adaptive FGFR-driven resistance. Importantly, the translation of the adaptive resistance profiles to HNSCC patient cohorts showed its prognostic value and provided conclusive validation of the presence of EMT-related vulnerabilities that can be strategically used for therapeutic intervention. In conclusion, our study demonstrates that pan-FGFR inhibition induces both a highly beneficial radiochemosensitizing and a detrimental radioprotective effect in HNSCC cell models. Adaptive EMT-associated resistance appears to be of clinical importance, and we provide effective molecular approaches to exploit this therapeutically.

#2885 O-carborane-entrapped polymeric Micelles for Proton Boron Capture Therapy.

Q.-X. Teng[1], G. Zhang[1], H. Chen[1], F. Mendes[2], N. Sahoo[1], C. Fernandes[2], A. Paulo[2], C. Li[1];
[1]UT MD Anderson Cancer Center, Houston, TX, [2]University of Lisboa, Lisbon, Portugal

Introduction: Proton boron capture therapy (PBCT) has the potential to enhance the biological effectiveness of proton therapy, based on proton-boron fusion reactions ($^{11}B + p \rightarrow 3\alpha + 8.7$ MeV), which produce 3 α particles. In this study, we formulated *o*-carborane, a high boron content cage-like compound, into a polymeric micelle (M-carb) as a delivery tool to achieve effective delivery of the boronated compound to cancer cells and validated the enhancement of the biological effectiveness of proton therapy promoted by the uptake of *o*-carborane-entrapped in the micelle.
Methods: *O*-carborane was effectively entrapped into an amphiphilic block copolymer to yield a stable polymeric micelle. The size and surface charge of the resulting M-carb were characterized by dynamic light scattering (DLS) and the uptake of M-carb in MIA PaCa-2 pancreatic cancer cells was measured by inductively coupled plasma mass spectrometry (ICP-MS). A colony formation assay was employed to assess the impact of M-carb on the survival of MIA PaCa-2 cells irradiated with a proton beam at the entrance and distal Spread-Out Bragg Peak (SOBP) positions at doses ranging from 0, 2, 5, and 8 Gy. The γH2AX foci were quantified by immunofluorescence to assess treatment-induced DNA double-strand breaks. Boron phenylalanine (BPA) was used as a control boron-carrying agent.
Results: *O*-carborane-entrapped polymeric micelles (M-carb) had a diameter of about 60 nm and a relatively narrow size distribution (polydispersity index ~0.15) and possessed a slight negative charge. After 6 h incubated with M-carb at an equivalent concentration of 200 μM boron, MIA PaCa-2 cells were found to have taken up ~45 ng ^{11}Boron per million cells. The colony formation assay demonstrated a significant decrease in the survival rate of MIA PaCa-2 cells after 8 Gy proton irradiation in the presence of 40 ppm of boron (corresponding to 4.61 μM BPA or 0.46 μM carborane) compared to irradiation treatment alone ($p<0.05$). At 8 Gy, the survival rates were 0.10, 0.07, and 0.04 for the following irradiation conditions: i) irradiation alone; ii) in the presence of BPA; in the presence of M-carb. At 2 and 5 Gy, these survival rate values were 0.78, 0.69, and 0.69 and 0.33, 0.19, and 0.16, respectively. Importantly, M-carb alone at the concentration used in proton irradiation experiments displayed no cytotoxicity. Immunofluorescence assays revealed that at both 2 Gy and 5 Gy, BPA and M-carb significantly increased γH2AX foci compared to irradiation alone ($p<0.0001$).
Conclusion: M-carb was efficiently taken up by MIA PaCa-2 cells. PBCT mediated by M-carb or BPA enhanced the relative biological effectiveness of proton therapy with consequent improvement of its cell-killing efficacy in pancreatic cancer cells. This approach holds promise for advancing proton therapy as a new treatment modality for pancreatic cancer.

#2886 Osteoclast and neuronal cross-talk as a mechanism for chest-wall pain caused by thoracic radiosurgery for lung cancer.

S. Park, M. Peters, J. Moore, K. Reno, M. Farris, C. Peters, J. Willey;
Wake Forest University, Winston-Salem, NC

Radiation therapy (RT)-induced chest wall pain (CWP) is a severe complication after thoracic stereotactic body radiation therapy (SBRT) for lung tumors; with increased survivorship, ~30% of patients develop severe CWP. The causes of CWP are unknown, but could involve: 1] damage to intercostal peripheral nerves; 2] bone loss from affected osteoclast activity, or 3] both (secreted factors from activated osteoclasts can affect nerves). This study tested the potential for radiation to affect osteoclasts and/or sensory neurons to induce pain. Mature osteoclasts differentiated from RAW264.7 cells plated on Osteoassay surfaces were exposed to an acute 10 Gy Cs137 γ-rays and bone resorption was assessed. We collected conditioned media (CM) from these cells at 48h and applied to cultured primary mouse dorsal root ganglia neurons (irradiated and non-irradiated neuron), assessing neurite growth and pain-associated marker (CGRP, SP) expression through immunohistochemistry and RT-qPCR. Risedronate (50μM), an anti-resorptive agent, was administered pre-radiation to inhibit osteoclast activity. Unpaired t-tests were utilized for statistical analyses (α=0.05). Osteoclast resorption activity was increased by 48h after irradiation. These irradiated, activated osteoclasts exhibited increased mRNA expression of differentiation (RANK) and activity (CTSK, MMP9) markers. Neurons treated with CM from irradiated osteoclasts exhibited elevated levels of CGRP (+38.5%) and SP (+29.5%) compared to cells treated with CM from non-irradiated cells. Consistently, in co-cultures of osteoclasts and neurons exposed to radiation, irradiated neurons exhibited significantly increased neuropeptide levels. Risedronate not only reduced osteoclast activity but also inhibited neuropeptide expression in irradiated neurons within these co-cultures. Moreover, neuropeptide levels were similar between directly irradiated neurons and non-irradiated neurons. However, irradiated neurons exposed to CM from either irradiated or non-irradiated osteoclasts showed a marked 4-fold increase in neuropeptide levels vs neurons that were non-irradiated and then received osteoclast CM. Our findings indicate that radiation activates osteoclasts and leads to direct bone loss *in vitro* and signaling between irradiated osteoclasts and non-irradiated neurons increases pain responses. Importantly, this response is enhanced when neurons were also previously irradiated. During SBRT, intercostal nerves may be influenced by adjacent irradiated osteoclasts, increasing expression of pain-related neuropeptides as the osteoclasts break down bone, thus enhancing the risk of CWP as treatment progresses across time. Understanding these interactions could reveal potential targets for preventing CWP, allowing higher tumor radiation doses with less toxicity. Support: The Milton Raben Foundation.

#2887 Impact of ionizing radiation on the energy metabolism of normal and tumor cells in the brain.

Marvin Kreuzer[1], Pascal Imseng[2], Matthias Wyss[2], Thomas Look[3], Tobias Weiss[3], Bruno Weber[2], Martin Pruschy[1]

[1]Department of Radiation Oncology, University Hospital Zurich, Zurich, Switzerland,[2]Institute of Pharmacology and Toxicology, University of Zurich, Zurich, Switzerland,[3]Department of Neurology, Clinical Neuroscience Center, University Hospital Zurich, Zurich, Switzerland

This study aims to analyze irradiation-induced metabolic alterations in glioblastoma cells and astrocytes to enhance understanding of cellular responses and facilitate the development of more effective radiotherapeutic strategies. Metabolic reprogramming of tumor cells is considered one of the hallmarks of cancer. Studies have shown that abnormal activation of oncogenes and cancer-related signaling pathways, as well as the inactivation of tumor suppressor genes can induce metabolic reprogramming. These metabolic aberrations facilitate rapid proliferation, continuous growth, invasion, metastasis, and immune evasion. Following the application of radiotherapy, the activity of several metabolic pathways significantly changes, potentially leading to the development of radioresistance. However, a differential effect of ionizing radiation on tumor and normal cells is not well understood. Hence, quantifying irradiation-induced metabolic changes in glioblastoma cells and astrocytes is of high importance. We have developed a novel approach to measure dynamic metabolite changes upon irradiation, in vivo, in situ, and in real-time. This tool combines imaging of recently developed fluorescent biosensors via 2-photon microscopy and millimeter-scaled irradiation. Murine glioblastoma cells and astrocytes were generated with stable expression of biosensors for the quantification of intracellular concentrations of various metabolites, including lactate. Cytosolic concentrations of lactate depend on the balance between glycolytic production, mitochondrial consumption of pyruvate and lactate, and the exchange with the extracellular lactate pool via monocarboxylate transporters. Many cancer cells are characterized by an excessive conversion of glucose to lactate even under normoxic conditions. We quantified this so-called Warburg Effect in glioblastoma cells and astrocytes as the ratio between basal lactate production and the lactate increase after OXPHOS inhibition and determined irradiation-induced metabolic changes on the single-cell level. Complementarily, we used metabolomics and Seahorse analyses before and after irradiation. Our data indicate that irradiation increases oxygen consumption in glioblastoma cells but not in astrocytes. Also, we established an orthotopic glioblastoma mouse model via injection of sensor-expressing tumor cells for *in vivo* measurements of metabolite changes during and after irradiation. These data are expected to significantly advance the understanding of the cellular response to irradiation on a molecular level in situ and in real-time. This knowledge will help to develop combination treatments and increase the efficiency of radiotherapy.

#2888 Sensitization of radiation resistant colon cancer - The oxygenated microbubble hydrogel approach.

A. Jose, C. H. Chong, J. Jaiswal, Z. Wu, S. S. Thakur;
University of Auckland, Auckland, New Zealand

Background: Hypoxia, a state of reduced oxygen that develops within the tumor due to its irregular vasculature, could result in treatment resistance. Mounting evidence suggests that reoxygenation of the tumor could improve outcomes of conventional cancer therapies. Our approach combats hypoxia using oxygenated lipid microbubbles (OMB) loaded in a temperature sensitive gel. The OMB would carry the oxygen while the gel would sustain its release into the tumor microenvironment.
Objectives: To formulate an oxygen loaded MB dispersed in a temperature sensitive poloxamer hydrogel for intratumoral administration.
Methods: OMB were generated by first preparing a liposomal mixture DSPC:DSPE-PEG2000, which was dispersed in a thermosensitive poloxamer hydrogel (P407:P188). This was pressurized with oxygen and vortexed in a gas-tight vial. Characterizations included OMB size distribution, injectability, thermosensitivity, oxygen loading and release, and the impact of the formulation on efficacy of radiotherapy against a colon cancer cell line (HCT116) was evaluated.
Results: DSPC:DSPE-PEG2000 liposomes at a molar ratio of 94:6 dispersed in P407:P188 (21:6.5 %w/w) generated OMB with a size distribution in the acceptable range of 0.8-8 µm. Formulations were within the established limits of injectability (F<38N) at room temperature, and gelled near physiological temperatures enabling a sustained release of oxygen. . The formulation co-treatment enhanced radiotherapy significantly as evidenced by the remarkable reductions of clonogenic survival rates in both hypoxic and normoxic HCT116 cells (reduction by 78% vs 68% compared to just their respective radiated controls; $p<0.0001$ for both cases).
Conclusion: Reoxygenation with a newly developed OMB hydrogel formulation effectively sensitized HCT116 to radiotherapy *in vitro*. Studies are underway to explore the importance of reoxygenation rate and extent for optimal tumor sensitization.

#2889 Cartilage oligomeric matrix protein as a potential biomarker and therapeutic target of radiation resistance in NSCLC.

K. E. Reno, S. H. Park, M. K. Farris, R. T. Hughes, J. E. Moore, C. M. Patel, J. S. Willey;
Wake Forest University School of Medicine, Winston Salem, NC

Despite recent advances in lung cancer treatment, the survival rate of non-small cell lung cancer (NSCLC) is ~57% largely due to treatment resistance. Cartilage Oligomeric Matrix Protein (COMP) has previously been implicated in promoting metastasis and is associated with poor survival outcomes in breast, prostate and colorectal cancers. Patients with prostate cancer and osteoarthritis (a condition characterized by elevated circulating COMP) had both increased tumor COMP expression and rate of metastasis. Additionally, elevated COMP expression, among others, was observed in a study that investigated the gene expression of invasive NSCLC cell lines, though association with COMP was not further studied. Therefore, COMP could potentially increase the metastatic potential for NSCLC and thus serve as a therapeutic target to reduce tumor aggressiveness. We performed proliferation and migration assays on NSCLC cell lines, A549 and NCI-H1975, treated with 2 µg/mL COMP to identify COMP's role in NSCLC progression. Plated cells in monolayer were treated with either COMP (2µg/mL) or PBS (control), and then within each group received either: 1] one of two different inhibitors of COMP signaling (either the α_v integrin antagonist cilengitide (1µM), or the Src inhibitor PP2 (1µM)), or 2] no additional treatment. Replicates from each group then received 2Gy Cs137 γ-radiation, or no irradiation. Proliferation and migration were monitored via the IncuCyte ZOOM live-cell imaging system over a 48hr interval. Radiation alone reduced both proliferation (-22%, $p<0.0001$) and migration (-40%, $p<0.01$) of A549 cells. However, exogenous COMP treatment attenuated the effects of radiation, maintaining both A549 proliferation (19% vs irradiated control, $p<0.05$) and migration (91% vs irradiated control, $p<0.0001$). While the overall pattern for NCI-H1975 cells with/without COMP treatment was similar, the magnitude of the responses was reduced vs A549 cells and non-significant. In contrast, radiation resistance with COMP treatment was abrogated by exogenous treatment of both COMP inhibitors. Cilengitide treatment resulted in lower proliferation rates of the COMP treated, irradiated A549 (-16%, $p<0.05$) and NCI-H1975 cell lines (-58%, $p<0.0001$) vs COMP treatment alone, while PP2 reduced proliferation and migration rates for both irradiated and non-irradiated COMP treated cell lines ($p<0.0001$). PP2 treatment alone did not reduce migration rates of either irradiated control cell lines. In conclusion, COMP serves to radioprotect NSCLC in an undetermined manner, and could serve as both a prognostic biomarker for and therapeutic target against radiation resistance in patients with NSCLC. Support: Milton Raben Foundation

TUMOR BIOLOGY: The Tumor Microenvironment as a Drug Target
Poster Session

#2893 Inhibition of ADAMTS4 and 5 to regulate the tumor microenvironment.
C. Lee, S. Kim, S. Kim, Y. Kim, S. Lee, S. Ha, Y. Lee, J. Yang;
Cellus, Seoul, Korea, Republic of

Background: Triple-negative breast cancer accounts for approximately 10~15% of all breast cancers and is characterized by the absence of ER, PR, and HER2 receptors, making targeted therapies challenging due to the lack of biomarkers. ADAMTSs (ADAM metallopeptidase with thrombospondin) are complex extracellular proteases known for their roles in facilitating cancer cell proliferation and safeguarding tumor functions. This enzyme is secreted by cancer cells and various immune cells, influencing the tumor microenvironment. ADAMTSs modulate cellular adhesion, migration, proliferation, and vascular development by cleaving components of the extracellular matrix and regulatory factors such as chemokines and cytokines. Our aim is to positively manipulate the tumor microenvironment of triple-negative breast cancer by inhibiting ADAMTSs, presenting a new strategy for treating this challenging type of breast cancer that lacks targeted therapeutic options.
Results: To confirm the anticancer effects of a protease inhibitor concurrently targeting ADAMTS4 and 5, a co-culture of triple-negative breast cancer cells (MDA-MB-157) and THP-1 was established to artificially create a tumor microenvironment. Subsequently, a wound healing assay was conducted, revealing that treatment with the ADAMTS4 and 5 dual inhibitor effectively inhibited cancer cell migration. This observed anticancer effect is attributed to the inhibition of CXCL16 secretion by the ADAMTS4 and 5 dual inhibitor. To verify the anti-tumor mechanisms of ADAMTS4 and 5, MDA-MB-157 cells, a triple-negative breast cancer cell line, were treated with IFNγ and TNFα to promote CXCL16 secretion artificially. Upon treatment with varying concentrations of the ADAMTS4,5 dual inhibitor, it was confirmed that the secretion of CXCL16 was inhibited in a dose-dependent manner. In a mouse model with transplanted 4T1 breast cancer cells, treatment with the ADAMTS4,5 dual inhibitor resulted in the suppression of CXCL16 secretion, leading to an increase in M1 macrophages. Additionally, it was observed that the inhibitor induced $CD8^{+}$ T cell activation. These regulation and changes of immune cells through inhibition of ADAMTS4 and 5 control the TME to resist tumor cells.
Conclusion: ADAMTSs are known as protein-degrading enzymes responsible for the degradation, modification, and regulation of proteins. Recent research has revealed that ADAMTSs play a crucial role in the proliferation and survival of cancer. Activation of ADAMTS4 and 5 has been shown to promote the secretion of CXCL16, leading to the differentiation of macrophages into tumor-associated macrophages. Specifically, ADAMTS4 and 5 convert membrane-bound CXCL16 into a soluble form, exacerbating the tumor microenvironment of triple-negative breast cancer. Therefore, inhibiting ADAM4,5 is intended to change or maintain TME in a suitable state for anti-cancer therapy, which could lead to a new strategy for anti-cancer therapy.

#2894 Targeting NOS2 and the tumor microenvironment in endometrioid ovarian cancer: Implications for treatment and survival.

G. Melone[1], M. Li[1], I. Uzair[1], M. Chervo[1], K. Ortega[1], W. Qian[1], J. Zhou[1], L. Guzman[1], S. Hynes[2], S. Glynn[2], C. Thomas[1], P. Matre[1], L. Francis[3], J. Chang[1];
[1]Houston Methodist Research Institute, Houston, TX, [2]University of Galway, Galway, Ireland, [3]Swansea University, Swansea, United Kingdom

Purpose of the study: The final aim of the study is to disrupt the deleterious effect of the tumor microenvironment by targeting inducible Nitric Oxide Synthase 2 (NOS2). NOS2 has a role in cancer cell proliferation and immune cells inactivation. It is upregulated by cytokines released from the tumor proinflammatory environment and the adipose tissue. By targeting and reverting NOS2 functions, we want to develop a therapeutic modality that inhibits endometrioid ovarian cancer (EOC) progression and reactivates the immune response in the ovarian cancer tumor microenvironment (OC-TME).
Experimental procedures: We analyzed ovarian cancer patients' cohorts using TNMPlot, Kaplan-Meier Plotter and The Human Protein Atlas. We simulated the tumor proinflammatory microenvironment by administering Interferon-gamma (IFN-Y, 25 ng/mL), Interleukin 1 Beta (IL1-β, 10 ng/mL), Tumor Necrosis Factor-alpha (TNF-α, 10 ng/mL) on A2780 EOC human cell line. We also administered conditioned media (CM) from breast fat adipose tissue to assess the influence of lipid components on cytokines release. After upregulating NOS2, we tested the efficacy of Cisplatin in combination with L-NMMA, a NOS2 inhibitor, on A2780 cells through proliferation assays using RealTime-Glo™ MT Cell Viability Assay (Promega®). In addition, to assess the immune landscape in ovarian cancer, we developed a syngeneic model administering ID8 cells (murine OC cell line) through intraperitoneal injection (IP) in C57BL/6 mice.
Results: The findings indicated higher NOS2 RNA expression levels in tumors than in normal samples according to TNMPlot ($p = 6.84e-01$). KMPlotter analysis revealed that patients with high NOS2 expression treated with Cisplatin had a significantly shorter survival rate (10.64 months) compared to those with lower NOS2 expression (25 months, $p = 0.0088$). Patients untreated with Cisplatin and exhibiting high NOS2 expression also showed lower survival rates (11 months) than those with lower NOS2 expression (34 months, $p = 0.056$). Furthermore, cytokine treatments increased NOS2 protein levels in A2780 cells after 48 hours, and CM similarly elevated NOS2 protein levels. Subsequent administration of Cisplatin and Cisplatin + L-NMMA to cytokine-treated A2780 cells notably reduced cell proliferation by 85% and 89%, respectively.
Conclusion: Taken together, our results showed the importance of a proinflammatory environment and adipose tissue in NOS2 upregulation. These findings show a potential correlation between endometriosis, obesity, and endometrioid ovarian cancer. With the development of an in vivo and in vitro model, we can gain a better understanding of the role of NOS2 in immune inactivation as well as in cell proliferation in EOC.

#2895 ILRAP blockade mediates anti-fibrotic effects in pancreatic cancer-associated fibroblasts.

N. I. Nissen[1], N. Hansen[2], E. Jaensson Gyllenback[3], C. R. Millrud[3], M. Jaras[2], D. Liberg[3], M. A. Karsdal[1], **N. Willumsen**[1];
[1]Nordic Bioscience, Herlev, Denmark, [2]Lund University, Lund, Sweden, [3]Cantargia, Lund, Sweden

Introduction: Pancreatic cancer (PDAC) patients have poor prognosis partly due to excessive activity of cancer-associated fibroblasts (CAFs). CAFs drive the fibrosis that causes excessive type III collagen and extracellular matrix deposition that in turn reduces drug response resulting in poor survival. In support, high levels of the type III collagen serum biomarker PRO-C3 correlates with poor survival in PDAC. TGF-β is thought to be the main driver of PRO-C3 and tumor fibrosis. Cytokines such as Interleukin 1 (IL-1) play a key role in the pancreatic tumor microenvironment and may play a role in tumor fibrosis as well. In this study, we first investigated the potential of IL-1 in activating fibroblasts to drive fibrosis and produce PRO-C3. Subsequently, we established a co-culture of pancreatic cancer cells and pancreatic CAFs to investigate the anti-fibrotic properties of nadunolimab, an antibody that blocks IL-1 signaling by targeting IL-1 Receptor Accessory Protein (IL1RAP). Nadunolimab is currently in phase I/IIa clinical development for treatment of pancreatic cancer (CANFOUR, NCT03267316). Methods: Human primary pancreatic cancer-associated fibroblasts (CAFs) were cultured in Ficoll-media (Scar-in-a-jar, SiaJ) supplemented with TGF-β, IL-1α or IL-1β. The fibrotic activity of the fibroblasts was investigated by measuring the formation of type III collagen (PRO-C3) at days 3, 6, 9 and 12. Then, pancreatic cancer cells (BxPc3) and pancreatic CAFs were cultured either alone or in a co-culture. Nadunolimab or isotype control were added at the start of these cultures and supernatants were collected after three days. The level of PRO-C3 was measured by ELISA. Results: Both IL-1α or IL-1β were equipotent to TGF-β in inducing PRO-C3 in the SiaJ monoculture, indicating that IL-1 is pro-fibrotic. In addition, when cancer cells and CAFs were co-cultured, PRO-C3 levels increased compared to single-cell cultures (1.5-6-fold). When co-cultures were treated with nadunolimab, the induction of PRO-C3 was blocked to levels similar to monocultures, whereas the isotype control had no effect on PRO-C3 levels. Conclusion: IL-1 activated fibroblasts and induced type III collagen formation (PRO-C3), suggesting that IL-1 is a driver of tumor fibrosis. In support, pancreatic tumor cells induced collagen type III formation (PRO-C3) in pancreatic CAFs and blockade of IL1RAP with nadunolimab inhibited this collagen formation. Thus, nadunolimab may have anti-fibrotic properties and PRO-C3 could potentially be used for prognostic/predictive enrichment and as a pharmacodynamic marker in future studies evaluating anti-IL-1 modalities in PDAC.

#2896 Elucidating the role of transglutaminase 2 (TGM2) in pancreatic ductal adenocarcinoma pathogenesis and its therapeutic implications.

P. Wright, A. Atfi;
Virginia Commonwealth University - VCU, Richmond, VA

Pancreatic cancer remains one of the deadliest malignancies, with limited therapeutic options and a poor prognosis due to delayed symptom presentation and disease detection. Pancreatic ductal adenocarcinoma (PDAC) has a 5-year survival rate of less than 8%, predominantly attributed to oncogenic KRAS mutations and loss-of-function mutations in TP53, SMAD4, and P16. Our lab is interested in studying Transglutaminase 2 (TGM2), a multifunctional enzyme involved in protein cross-linking and cellular signaling, because it is highly correlated with cancer cell survival, malignancy, metastasis, and treatment resistance. Clinically, overexpression of TGM2 is associated with poorer survival in patients with Pancreatic Ductal Adenocarcinoma so it is imperative to understand the mechanism of its action in disease progression. To elucidate the role of TGM2 in PDAC, we studied the targeted deletion of TGM2 in the context of a mouse model of PDAC and saw a significant reduction in PDAC incidence and precursor lesion formation, suggesting that TGM2 has a role in the tumor microenvironment. Using single cell sequencing, we found TGM2 levels to be elevated in certain cell populations, specifically endothelial cells and cancer cells. We discovered high TGM2 levels in TIE2-GFP mouse vessels and subsequently found high TGM2 levels in patient tumor vasculature. Further studies aim to conditionally ablate TGM2 in endothelial cells to assess its mechanistic involvement in PDAC initiation and progression. Additionally, we are studying concurrent conditional TGM2 and SMAD4 deletions in mice to investigate pancreatic cancer precursor lesion formation and are further evaluating the protective mechanisms of a TGM2 deletion in a more aggressive mouse model of PDAC. Our preliminary findings substantiate TGM2 as a critical player in PDAC pathogenesis, opening avenues for targeted therapeutics to ultimately improve patient prognosis.

#2897 Cancer associated fibroblasts targeted photoimmunotherapy improves drug delivery.

S. Nishimura[1], K. Noma[1], T. Matsumoto[1], T. Takahashi[1], Y. Takeda[1], H. Matsumoto[1], T. Kunitomo[1], K. Kawasaki[1], H. Kashima[1], T. Kato[1], S. Kikuchi[1], T. Ohara[1], H. Tazawa[2], T. Fujiwara[1];

[1]Okayama Univ. Graduate School of Med., Okayama, Japan, [2]Okayama Univ., Okayama, Japan

Introduction: Desmoplasia is often associated with adverse outcomes in cancer, particularly in esophageal cancers characterized by stroma-rich environments and poor prognoses. The dense extracellular matrix (ECM) within the stroma hinders effective drug delivery, primarily due to elevated interstitial pressure. Cancer-associated fibroblasts (CAFs) of the tumor microenvironment deteriorate this issue by promoting cancer proliferation and ECM production. We have developed a photoimmunotherapy targeting these CAFs via fibroblast activation protein (FAP-PIT), which has demonstrated notable antitumor efficacy in CAF-rich tumors that are typically chemoresistant. This study explores the potential of FAP-PIT to enhance drug delivery in CAF-rich tumors.

Methods: We have conjugated Sibrotuzumab, a clinically-trialed FAP antibody with the photosensitizer IR700DX for application in FAP-PIT. We compared the protein expression levels of ECM components—collagen I (Col I) and hyaluronic acid (HA)—between CAFs and normal fibroblasts (NFs) in vitro. Spheroid models, both CAF-poor (solely cancer cells) and CAF-rich (cancer cells plus fibroblasts), were employed to assess drug uptake. Additionally, 140 esophageal cancer cases from 2008 to 2010 were retrospectively analyzed. In vivo, we induced bilateral subcutaneous tumors to apply FAP-PIT, monitoring drug uptake using in vivo imaging systems (IVIS) and immunohistochemistry (IHC).

Results: Initially, we determined how significantly CAFs impede the drug delivery. In vitro, CAFs secreted higher levels of Col I and HA compared to NFs. Clinically, the expression of Col I and HA consistently showed a positive correlation with α-smooth muscle actin (αSMA) and FAP. CAF-rich spheroids exhibited significantly reduced uptake of fluorescently labeled chemotherapy compared to CAF-poor spheroids. Conversely, FAP-PIT enhanced drug penetration in CAF-rich spheroids through CAFs depletion and ECM remodeling. In vivo studies further demonstrated that FAP-PIT significantly increased Panitumumab and nab-Paclitaxel accumulation in CAF-rich tumors, leading to superior antitumor efficacy. IHC analysis validated the significant reduction of CAFs and Col I.

Conclusion: The ECM, including CAFs, poses a barrier to drug delivery. Our findings indicate that FAP-PIT can effectively enhance drug penetration in CAF-rich tumors, presenting a novel therapeutic strategy to overcome drug resistance.

#2898 Development of the lipid kinase PIKfyve PROTAC degrader against neuroendocrine prostate cancer.

Y. Qiao[1], C. Li[2], Y. Zheng[1], X. Jiang[1], S. N. Yee[1], C. Cheng[1], Y. Bao[1], Y. Zhang[1], Y. Wang[3], Z. Wang[2], K. Ding[2], A. Chinnaiyan[1];
[1]University of Michigan Medical School, Ann Arbor, MI, [2]Shanghai Institute of Organic Chemistry, Chinese Academy of Sciences, Shanghai, China, [3]The Vancouver Prostate Centre, The University of British Columbia, Vancouver, BC, Canada

Therapies targeting the androgen receptor (AR) as the main driver of prostate cancer (PCa) can lead to various mechanisms of resistance and promote progression to castration-resistant PCa (CRPC), which has a median survival of only 13-23 months. Amongst recurrent CRPC, 17%-30% of patients develop neuroendocrine prostate cancer (NEPC), which is a PCa subtype characterized by a unique histology. NEPC exhibits a loss of AR signaling during neuroendocrine transdifferentiation which results in resistance to AR-targeted therapies and gain of cell characteristics resembling poorly differentiated neuroendocrine tumors. Despite advances in the understanding of NEPC development, treatment options remain limited, with platinum-based chemotherapy as the first-line treatment for both de novo and treatment-induced NEPC. However, response to first-line chemotherapy in NEPC is short, with a median survival of only seven months. The poor prognosis of NEPC is attributed in part to late diagnosis and a lack of effective therapeutic agents. Our previous work demonstrated that NEPC and AR-negative PCa exhibit higher dependency on the lipid kinase PIKfyve than AR-positive CRPC. Thus, development of PIKfyve inhibitory therapies targeting the emergent vulnerabilities of NEPC or AR-negative forms of PCa is a promising approach.
Using a proteolysis targeting chimera (PROTAC) technology, we designed a class of PIKfyve specific degrader. The *in vitro* degradation efficiency were determined by immunoblotting, and DC50s (degradation concentration at 50%) were calculated for top candidates. Pharmacokinetic and pharmacodynamic were evaluated for *in vivo* study. In summary, we have developed a class of PIKfyve specific degrader using the E3 ligase von Hippel-Lindau (VHL) as a ligand via a diverse set of linkers. Mechanistic studies revealed that it induced PIKfyve degradation in a VHL- and proteasome-dependent manner.

#2899 Combined inhibition of RAF, MEK and FAK increases PDAC responsiveness to cytotoxic- and immune therapy.

X. Liu[1], J. Baer[1], B. Knolhoff[1], G. Hogg[1], F. Ahmad[1], S. Coma[2], J. Pachter[2], K. Lim[1], D. DeNardo[1];
[1]Washington University in St. Louis, Saint Louis, MO, [2]Verastem Oncology, Needham, MA

Pancreatic ductal adenocarcinoma (PDAC) is a highly lethal malignancy with poor response rate to therapy. An immune suppressive tumor microenvironment (TME) and oncogenic mutations in KRAS have been implicated as drivers of resistance to both conventional and immune therapies. As such, targeting RAS/MAPK signaling is an attractive strategy. However, RAS/MAPK inhibition has not yet shown clinical efficacy for PDAC, likely due to rapid acquisition of resistance in PDAC cells. Tumor intrinsic mechanisms of resistance to RAS/MAPK have been studied, however, the unique PDAC TME may also be a key driver in resistance. Previous studies have shown that FAK inhibition can reprogram the PDAC TME and delay PDAC progression in animal models. Herein, we found that long-term FAK inhibitor treatment led to hyperactivation of the RAS/MAPK pathway in both genetically engineered mouse models and in post-treatment PDAC tissues from FAK inhibitor clinical trials. Concomitant inhibition of both FAK (VS-4718) and RAF/MEK (avutometinib) signaling dramatically suppressed tumor growth, leading to increased survival across multiple PDAC mouse models. The mechanisms of synergy include both changes in tumor-intrinsic signaling and modulation of tumor/stroma interactions that drive avutometinib resistance. In the TME, we found that cancer associated fibroblasts (CAFs) can impair the downregulation of cMyc by RAF/MEK inhibition in PDAC cells. This resulted in de-novo resistance to RAF/MEK inhibition in fibrotic conditions. By contrast, FAK inhibitors reprogramed CAFs to suppress the production of key growth factors, including FGF1, that drove resistance to RAF/MEK inhibition. While combined FAK and RAF/MEK inhibition only led to disease stasis, the addition of chemotherapy to the combination led to tumor regression and improved long-term survival in PDAC mouse models. Analysis of tumor immunity showed that the combination of FAK and RAF/MEK inhibition improved anti-tumor immunity and improved priming of T cell responses, which was further improved with the addition of chemotherapy. These findings led to testing of FAK (defactinib) plus RAF/MEK (avutometinib) inhibition in combination with gemcitabine and nab-paclitaxel in advanced front-line pancreatic cancer patients (RAMP 205; NCT05669482). Finally, we tested whether addition of immunotherapy could enhance the efficacy of FAKi + RAF/MEKi + chemotherapy and found that addition of either PD-1 or CTLA4/PD-1 blockade led to long term disease control in PDAC animal models. Together, these studies identified FAK inhibition as a novel approach to overcome both tumor intrinsic and stromal-derived resistance to RAS/MAPK inhibition and showed that this combination can be exploited to increase the efficacy of cytotoxic and immunotherapy approaches.

#2900 BRAFi-induced epigenetic switch drives the reprogramming of resistant cancer-associated fibroblasts.

Y. Xiao, L. Zhou, Y. Zhang;
University of Cincinnati, Cincinnati, OH

Cancer-associated fibroblasts (CAFs) are a potential target for optimizing therapeutic strategies against melanoma. However, a major unknown still exists in CAFs, which is how CAFs maintain and even reinforce their functions in drug therapy and influence melanoma cell drug sensitivity. Yes-associated protein 1 (YAP1) is the master regulator that shuttles between the cytoplasm and nucleus in CAFs. Apparently, proteins associated with nuclear YAP1 in CAFs when treated with BRAF inhibitor (BRAFi) can potentially influence tumor drug response. Here we unveil that CAFs require the YAP1 function to proliferate, migrate, remodel the cytoskeletal machinery and matrix, and promote cancer cell invasion. Ablating YAP1 in CAFs increases the response of BRAF-mutant melanoma cells to BRAFi and MEK inhibitor (MEKi) *in vivo* and *in vitro*. Using an approach termed RIME (Rapid Immunoprecipitation Mass Spectrometry), we purified nuclear YAP1 and identified protein arginine methyl transferase 1 (PRMT1) as a major YAP1 binding partner in BRAFi-treated CAFs. Binding PRMT1 to YAP1 was confirmed by Co-immunoprecipitation and proximity ligation assay, and YAP1 deficiency in CAFs diminishes the nuclear accumulation of PRMT1, suggesting BRAFi-induced nuclear translocation of PRMT1 in CAFs requires the formation of YAP1 and PRMT1 complex. Silencing PRMT1 expression in CAFs not only deprives them of their ability to proliferate and to induce BRAF mutant melanoma cell resistance to BRAFi and MEKi. PRMT1 is a type I R-methyltransferase that mediates arginine methylation in human cells, which was known to be recruited to chromatin and exert its enzymatic activity to methylate Arg3 of histone H4 (H4R3). Using Histone H4 Modification Multiple Assay, we observed a global increase in Histone H4 methylation, especially H4R3 methylation, in CAFs in response to BRAFi stimulation, suggesting increased chromatin unfolding and accessibility and transcription activation. When YAP1 or PRMT1 expression was silenced, H4R3 methylation was notably suppressed, indicating BRAFi-induced H4R3 methylation was indeed driven by the YAP1 and PRMT1 signaling axis. In conclusion, our data disclose a novel BRAFi-induced YAP1-PRMT1-mediated epigenetic mechanism that reprograms CAFs through H4R3 methylation-directed transcriptional activation to reinforce their drug-resistant functions and modulate melanoma cell drug sensitivity. Moreover, the discovery of PRMT1 as a key player in the intricate molecular mechanisms that govern epigenetic regulation in CAFs in response to BRAFi treatment suggest PRMT1 as a potential CAF target in cancer therapy.

#2901 The apoptotic peptide TB511 targets activated CD18 and suppresses solid tumor progression.

Ilsoeb Choi[1], Ik-Hwan Han[1], Soyoung Kim[1], Juwon Yang[2], Hye Yeon Kim[1], Daehwan Park[1], Hongseo Choi[3], Jeongyoon Choi[3], Heekyung Lee[3], Jin Sun Shin[3], Jinho Kim[2], Jihwan Moon[2], Hyunsu Bae[1]

[1]Department of Physiology, College of Korean Medicine, Kyung Hee University, Seoul, Korea, Republic of,[2]Department of Korean Medicine, College of Korean Medicine, Kyung Hee University, Seoul, Korea, Republic of,[3]R&D Center, Twinpig Biolab Inc., Seoul, Korea, Republic of

Tumor-associated macrophages (TAMs) primarily exist in the M2-like phenotype in the tumor microenvironment (TME). M2-TAMs contribute to tumor progression by establishing an immunosuppressive environment. However, TAM targeting is hindered, mainly owing to a lack of specific biomarkers for M2-TAMs. Herein, we verified that TB511, a fusion peptide comprising a TAM-targeting peptide and the pro-apoptotic peptide dKLA, could preferentially bind to active CD18 in M2-TAMs, inducing apoptosis; it was less toxic to other tissue-resident macrophage lineages. TB511 suppressed tumor progression in various cancer models and humanized mouse models. Removal of M2-TAMs by TB511 significantly increased the infiltration of tumor-killing cells, such as granzyme B-positive $CD8^+$ T cells and natural killer cells, in the TME. Collectively, our findings suggest that targeting CD18 in M2-TAMs using peptide drugs is a potential strategy for immunotherapy in various tumors, including non-small cell lung cancer, colorectal cancer, hepatocellular carcinoma, renal cell carcinoma, and prostate cancer.

#2902 CA-4948 (emavusertib) improves treatment response of preclinical metastatic brain melanoma to anti-PD-1 immune checkpoint blockade.

Christina A. von Roemeling[1], Bently P. Doonan[1], Amanda M. Acevedo[1], Jeet A. Patel[1], Savannah L. Carpenter[1], Alisha Bhatia[1], Reinhard W. von Roemeling[2], Jamison Hoffman[2], **Maureen Lane**[2], Duane A. Mitchell[1]

[1]University of Florida College of Medicine, Gainesville, FL,[2]Curis, Inc., Lexington, MA

Background: Although recent advances in immunotherapy for metastatic melanoma have transformed the treatment paradigm for a disease that once carried a grim prognosis, nearly 50% of patients fail to reach a complete response to immune checkpoint blockade (ICB) due to multiple mechanisms of tumor-induced immune resistance. These challenges are amplified in the CNS tumor microenvironment (TME) where metastatic brain melanoma (MBM) demonstrates diminished clinical benefit to ICB treatment. A deeper understanding of these mechanisms are required to improve therapeutic response to ICB for these patients. Our group has previously identified that aberrant activation of the myddosomal cascade through downstream interleukin (IL)-1 receptor-associated kinase (IRAK-4) signaling results in chronic stimulation of MAPK and NF-κB in MBM. Further investigation reveals myddosome signaling emanates in large part from the TME, resulting in reflexive immune suppression. CA-4948 (emavusertib), a small molecule inhibitor of IRAK-4, is capable of reaching therapeutic dose levels in the brain where it demonstrates on-target inhibition of this pathway. These data highlight a unique therapeutic opportunity where selective inhibition of immune-suppressive signaling via targeted IRAK-4 blockade may sensitize MBM to anti-PD-1 ICB.

Methods Multispectral imaging of patient MBM samples were analyzed for myddosome expression in the TME. Melanoma preclinical models, including both primary site (cutaneous) and metastatic brain disease, were evaluated for tumor burden and survival in response to CA-4948 treatment alone and in combination with anti-PD-1 ICB. Immunological responses of tumor to treatment were evaluated in two transgenic reporter models, $CCR2^{RFP}CX3CR1^{GFP}$ and $IFN\gamma^{IRES\text{-}EYFP}$, to determine both the distribution and activation of infiltrating immune cells. Tumor-associated myeloid cells were assessed for phenotypic markers by multiparameter flow cytometry.

Results Myddosome signaling was found to be elevated in tumor-associated immune cells in patient MBM specimens. Treatment of preclinical melanoma with CA-4948 combined with anti-PD-1 ICB resulted in significantly reduced tumor growth and improved survival in three independent models. CA-4948 treatment was associated with reduced tumor recruitment of peripherally derived tumor-associated macrophages, as well as increased lymphocyte infiltration and improved pro-inflammatory signaling measured by increased IFNγ expression in the combinatorial setting.

Conclusion Targeted inhibition of IRAK-4 with CA-4948 improves immune surveillance and activation in preclinical models when combined with anti-PD-1 ICB, resulting in reduced tumor growth and increased survival. Thus, CA-4948 may be an effective adjuvant treatment strategy alongside anti-PD-1 ICB for the treatment of metastatic melanoma.

#2903 CTHRC1 induces PSCs (pancreatic stellate cells) into myCAFs (myofibroblast-like cancer-associated fibroblasts).

J. Lee[1], M. Kang[1], F. Jiang[1], K. Ryu[1], J. Kim[2], Y.-Y. Park[1], S. Koh[2];

[1]Prestige BioPharma IDC Co., Ltd., Busan, Korea, Republic of, [2]Department of Biomedical Sciences, Dong-A University, Busan, Korea, Republic of

Collagen triple helix repeat containing-1 (CTHRC1) is a secreted protein that contributes to the progression of various cancers, including pancreatic cancer. The higher expression of CTHRC1 in tumor tissues is associated with poorer survival outcomes. However, its specific roles in tumor extracellular matrix (ECM) remodeling remain unclear. Our study aims to investigate the influences of CTHRC1 on pancreatic stellate cells (PSCs), a main source of ECM production in pancreatic cancer. The analyses of the publicly available pancreatic cancer patient data revealed that CTHRC1 is mainly expressed in cancer stroma and highly correlated with ECM-related genes. An in vitro study showed that more than 40% of these genes can be upregulated by CTHRC1. CTHRC1 specifically activated PSC into myofibroblast-like cancer-associated fibroblasts (myCAFs), which are characterized by a significantly upregulated POSTN gene expression. Periostin (coded by the POSTN gene) has a central role in the CTHRC1-PSCs-cancer metastasis axis. Furthermore, CTHRC1 promoted pancreatic cancer cell proliferation through PSC activation to a greater extent than via direct stimulation. Proof-of-concept experiments showed that the long-term (4-week) inhibition of CTHRC1 led to significant tumor suppression and ECM reduction, and also resulted in an unexpected shift in the CAF subtype from myCAFs to inflammatory CAFs (iCAFs). PSC activation was demonstrated to be the key molecular mechanism responsible for the tumor-promoting effects of CTHRC1, and CTHRC1 has a critical role in CAF subtype differentiation and tumor microenvironment (TME) remodeling. The inhibition of CTHRC1 as a therapeutic strategy for the treatment of pancreatic cancer warrants further investigation.

#2904 Small molecule inhibitor targeting DDR represents a novel therapeutic strategy for the treatment of pancreatic ductal adenocarcinoma (PDAC).

T. Do[1], J. Prochnau[1], P. P. Venkata[1], S. Khan[1], S. Timilsina[1], D. Singh[1], D. Medina[1], R. Amaradhi[2], D. Zhou[1], M. Hart[3], S. McHardy[2], M. Rao[1];
[1]UT Health Science Center at San Antonio, San Antonio, TX, [2]UT San Antonio, San Antonio, TX, [3]University of Oklahoma Health Sciences Center, Oklahoma City, OK

Background: Pancreatic ductal adenocarcinoma (PDAC) is ranked as the second leading cause of cancer-related mortality with a 5-year survival rate of merely 12%. The complexity of PDAC lies in its intrinsic resistance to treatment, attributable to the desmoplastic tumor microenvironment, characterized by an abundance of tumor-promoting extracellular matrix (ECM) and stromal cells. We hypothesize that Discoidin Domain Receptors (DDR), members of the receptor tyrosine kinase family known for their affinity to fibrillar collagens within the ECM, play an important role in promoting PDAC growth and progression. While several drugs targeting DDR proteins have been developed, no inhibitors to DDR proteins are specific or approved for PDAC treatment, thus necessitating the development of novel therapeutic interventions.

Methods. A comprehensive high-throughput screening approach employing small molecule inhibitors was executed to identify authentic inhibitors targeting DDR. Subsequently, a rigorous evaluation of specificity of these small molecules was conducted through structural activity relationship (SAR) analyses and reference-based assessments. The efficacy of candidate inhibitors was assessed through functional assays, while mechanistic insights were gleaned using a multifaceted approach, including RNA-seq, real-time PCR, western blot analysis, in vivo experimentation, and Phospho-Receptor Tyrosine Kinase (RTK) profiling to discern any unintended off-target effects.

Results: Using an unbiased screening approach, we identified 13 inhibitors that specifically target DDR. SAR studies and cellular thermal shift assay validated CIDD-0108633 (8633) as a bona fide DDR2 inhibitor. Functional assays and RNA-seq analyses demonstrated 8633's capacity to inhibit PDAC growth, metastatic potential, and expression of DNA replication, cell-cycle, and DNA damage repair genes. Combination therapy of 8633 with gemcitabine synergistically reduced PDAC cell viability and metastatic potential. Mechanistic studies revealed the role of ABC transporters in mediating gemcitabine resistance. RTK profiling shows moderate kinase selectivity. *In vivo* studies affirmed its antitumor effects.

Conclusions: The results indicate that the selective inhibition of DDR with small molecule inhibitors suppresses PDAC cell growth and progression, implying that DDR inhibitors have the potential to be developed as safe and efficacious therapeutics for the treatment of pancreatic cancers.

#2905 Spatial analysis of neuropilin 2 expression in the microenvironment of melanoma.

A. Dimou[1], R. M. Moore[1], C. Ward[2], A. Leontovich[1], R. Guo[1], C. Wang[1], S. Suman[1], B. Dicke[1], J. M. Schimke[1], N. A. Stueven[1], C. A. Atherton[1], W. Nevala[1], S. N. Markovic[1];

[1]Mayo Clinic, Rochester, MN, [2]University of Minnesota, Minneapolis, MN

Background: Neuropilin 2 (NRP2) is a co-receptor that enhances signaling of growth factor and cytokine receptors and is expressed in tumor and microenvironment (TME) cells in melanoma and other tumors. Neuropilin 2 expression in tumor cells is associated with more aggressive tumors. Expression in tumor associated macrophages enhances efferocytosis and immunologically silent tumor cell death.

Methods: Whole excisional lymph node biopsies were obtained from 10 treatment naïve patients with metastatic cutaneous melanoma who subsequently received anti-PD1 treatment. A single 5mm formalin-fixed paraffin embedded tissue section was used to assess a panel of 39 analytes by cyclic multiplex immunofluorescence (MxIF). Fields of view (~1mm2, n=288) were selected from pathologist-annotated regions of the tumor core, tumor-immune interface and adjacent lymphoid tissue. Pixel-based single cell segmentation and a supervised classifier approach was applied to resolve 12 distinct tumor, stromal and immune cell phenotypes and functional states (NRP2 positive or negative) in 1.5 million cells.

Results: Tumor recurrence was observed in 6 patients (relapsed) , whereas 4 patients were recurrence-free (non-relapsed) during follow up. Among the different cell types, NRP2 expression was more frequent in macrophages (44%), tumor cells (40%), dendritic cells (40%), followed by Tregs (31%) and T helper cells (29%), and less frequent in neutrophils (24%), cytotoxic T cells (23%) and B cells (15%). In colocalization permutation analysis, NRP2 expressing macrophages clustered away from tumor cells in non-relapsed patients while a random spatial distribution of NRP2 expressing macrophages with respect to tumor cells was observed in relapsed patients. In comparing the odds of tumor cell interactions with NRP2-expressing macrophages to those with NRP2 non-expressing macrophages, we found in the tumor:stromal interface (10% tumor cells) that cells from both non-relapsed and relapsed patients were more likely to interact with NRP2 non-expressing macrophages (OR = 0.73, 95% CI = [0.71, 0.75] and OR = 0.56, 95% CI = [0.55, 0.58] for non-relapsed and relapsed patients, respectively). However, in the tumor core (90% tumor cells), tumor cells from relapsed patients had significantly higher odds of interacting with NRP2 expressing macrophages, (OR = 1.15, 95% CI = [1.12, 1.18]), and this was not seen for non-relapsed patients (OR = 0.68, 95% CI = [0.66, 0.71]). In FOVs dominated by tumor cells (75% tumor), tumor cells from relapsed patients had 4.97 times the odds of expressing NRP2 compared to tumor cells from non-relapsed patients (95% CI = [2.23, 11.09], p = 0.0001).

Conclusions: These spatial analytics suggest complex interactions among NRP2 expression in tumor and TME of melanoma determining risk for relapse with anti-PD1 treatment.

#2906 Inducing and disabling COX-2 S-nitrosylation to investigate its role in breast cancer progression.

R. J. Hoffmann, A. Bensen, E. de Wilde, J. E. Korkola, P. Schedin;
OHSU, Portland, OR

Background: We aim to assess the effect of S-nitrosylation of COX-2 on tumor attributes in models of early breast cancer. COX-2 is involved in tumor progression in many solid cancers. It is a known oncogene in murine breast cancer models, and targetable by NSAIDs. In women, its clinical correlation to breast cancer progression as well as its efficacy as a therapeutic target have yielded mixed results. These incongruities may be due, in part, to a post-translational modification, as COX-2 undergoes S-nitrosylation on Cys-526. Commercially-available antibodies selectively bind to either the S-nitrosylated (SNO-COX-2) or non-nitrosylated (nCOX-2) forms, and immunohistochemical staining of human tissue reveals that the two forms of COX-2 localize to different cellular sites in normal breast tissue and have opposite associations with breast cancer progression (PMID 33298921).
Hypothesis: S-Nitrosylated and non-nitrosylated COX-2 have distinct roles in cancer progression.
Approach: MCF10DCIS.com is a human breast cancer cell line chosen due to its ability to form DCIS-like (“stage 0”) lesions in culture and xenografting, which can progress to invasion when induced by signals from the tumor microenvironment (TME).
Approach 1: Detect extracellular matrix (ECM) and ligand factors that upregulate SNO-COX-2, independently or in ECM/ligand pairs. We utilized a 2D microenvironment microarray (MEMA) and tested 357 TME conditions.
Approach 2: Validate TME conditions in 3D culture.
Approach 3: Develop a mutant MCF10DCIS.com line in which COX-2 cannot be S-nitrosylated by inducing a single disabling missense mutation at Cys-526 via CRISPR.
Results: The MEMA revealed several conditions in which SNO-COX-2 was upregulated, including fibular collagens and SSP1. In 3D culture, increased SNO-COX-2 was associated with the presence of markers for EMT and an invasive growth phenotype, whereas nCOX-2 was not. Following CRISPR transformation, 59 individual MCF10DCIS.com clones were isolated and the target site of each sequenced. We identified 10 heterozygotic clones with the desired mutation, including a classical heterozygote that also retained the WT allele.
Ongoing: Current studies include a second round of CRISPR to produce a homozygous mutant cell line as well as validation of the mutant protein. The resulting cell lines will model the loss of COX-2 S-nitrosylation in breast cancer cells while retaining otherwise-functional COX-2.

#2907 Therapeutic targeting miR-146a and miR-21 induce malignant cell death and regulate CD8$^{\pm}$ T-cell function in mycosis fungoides with large-cell transformation.

Z. Han, P. Swiderski, X. Wu, Y.-C. Yuan, J. Wu, C. Su, H. Qin, S. T. Rosen, C. Querfeld;
City of Hope, Duarte, CA

Large cell transformation of mycosis fungoides (LCT-MF) occurs in 20-50% of advanced MF and is associated with an aggressive clinical course and poor survival not to overcome by any standard treatment regimen. We have previously identified a distinct miRNA expression profile in LCT-MF from that of non-transformed MF with significant upregulation of miR-21 and miR-146a. Our analyses demonstrated the involvement of genes for immune checkpoint pathways such as ICOS-ICOSL and PD1-PDL1 signaling (Di Raimondo C et al. Cancers 2021). Here, we aimed to investigate the efficacy of antagomiR-146a and -21 (amiR-146a, and -21) on the tumor growth and CD8$^{\pm}$ tumor infiltrating lymphocyte exhaustion in LCT-MF. The amiR-146a, and -21 were synthesized in our DNA/RNA Synthesis Core by linking CpG-D19. *In vitro*, CTCL cell lines (Myla and HH) were treated with amiR-146a and -21, the cell viability was assessed by the 2,5-diphenyl-2H-tetrazolium bromide assay and cell apoptosis was evaluated using apoptosis assay. We found that amiR-146a, and -21 synergistically inhibited the proliferation of MyLa and HH cells due to the activation of apoptosis through Caspase3/7 pathways and inducing cell cycle arrest by blocking STAT3/ CDK1/Cyclin B1 pathway. Our RNA-seq data indicated that the exhausted CD8$^{\pm}$ T cells express elevated amounts of STAT3, IRF4, and BATF in LCT-MF compared with non-LCT MF. To evaluate the functional importance of amiR-146a, and -21 on CD8$^{\pm}$ T cell exhaustion, we induced an exhausted state of CD8$^{\pm}$ T cells with high level of immune checkpoints and dysfunctional cytokine production by continues anti-CD3/DC28 beads and culture supernatant (MyLa or HH cell) exposure. Our data revealed that amiR-146a and -21 attenuated the CD8$^{\pm}$ T cell exhaustion by blockade of immune checkpoints and STAT3/IRF4/BATF pathway to trigger the cytotoxic immune response. Collectively, the findings of our study suggest that targeting miR-146a and -21 is a promising and novel therapeutic strategy for LCT-MF.

#2908 EDB^{+}FN is an attractive therapeutic target in oncology: Insights from protein expression analysis of solid tumors.

S. Lewandowski, L. Diao, A. Quigley, M. Crochiere, J. Pinkas;
Pyxis Oncology, Boston, MA

Stroma plays a major role in the initiation, growth, survival, and drug-resistance of solid tumors, yet few therapeutics specifically target tumor-associated stroma. Extra-domain-B fibronectin (EDB^{+}FN) is an oncofetal splice variant of fibronectin upregulated in solid tumor stroma, which is associated with tumor growth, angiogenesis, and metastases. Here we developed an immunohistochemistry (IHC) assay to assess EDB^{+}FN protein expression in the stroma of tumor and normal tissues to characterize the potential of EDB^{+}FN as a therapeutic target for solid tumors with high unmet need. We validated a primary detection antibody and titrated assay conditions to achieve specificity and a broad dynamic range of EDB^{+}FN expression levels across indications, including thyroid cancer, head and neck squamous cell carcinoma, hepatocellular carcinoma, soft tissue sarcoma, pancreatic cancer, non-small cell lung cancer, ovarian cancer, and renal cancer. Considering the stroma-specific expression pattern of EDB^{+}FN, we developed a scoring algorithm weighting both the intensity and distribution of EDB^{+}FN expression specifically in the stroma compartment and separately in tumor cells. Using this assay and scoring approach, we screened more than 200 tumor samples from 10 solid tumor indications and found EDB^{+}FN to be highly differentially expressed in tumor-associated stroma with little to no expression on tumor cells and trace to undetectable levels in healthy tissue. EDB^{+}FN was expressed across the indications evaluated with a wide range of expression both within and between indications. Stromal EDB^{+}FN expression was not correlated with stromal density, which also varied widely within and across indications. In parallel, we developed an algorithm using digital pathology to approximate pathologist scoring of stromal density and EDB^{+}FN expression, allowing streamlined screening of preclinical samples for in vivo studies and indication selection. The disease-specific expression pattern of EDB^{+}FN and high incidence of expression across indications make EDB^{+}FN an ideal target for high-unmet-need solid tumors. The specificity and dynamic range of our IHC assay for detection of EDB^{+}FN protein expression position it as a robust potential biomarker assay for EDB^{+}FN-targeting therapeutics.

#2909 ST101, a clinical CEBPβ antagonist peptide, promotes an immune-active tumor microenvironment by multiple cellular mechanisms.

C. Scuoppo, J. Diehl, R. Ramirez, M. Koester, E. Gallagher, S. Leong, J. Gonzales, K. Mendelson, Z. Mattes, L. Ghamsari, G. Merutka, A. Vainstein-Haras, B. J. Kappel, **J. A. Rotolo**;
Sapience Therapeutics, Inc., Tarrytown, NY

CCAAT/Enhancer Binding Protein β (C/EBPβ) is a transcription factor that is an established driver of cellular transformation in several cancer types with poor prognosis, including glioblastoma (GBM), triple negative breast cancer (TNBC) and non-small cell lung cancer (NSCLC). These cancers' growth is often supported by an immunosuppressive (IS) tumor microenvironment (TME), characterized by high expression of TAMs, MDSCs, Tregs, and in the case of GBM, IS microglia. In addition to its cell-autonomous role of promoting survival and proliferation in cancer cells, C/EBPβ is also critical for IS M2 macrophage polarization, while its role in other TME populations is less understood. ST101 is a peptide antagonist of C/EBPβ that is being evaluated in a Phase 2 clinical study in patients with recurrent and newly diagnosed glioblastoma (NCT04478279). Here we explored the impact of ST101 on IS TME cell populations and on activation of cytotoxic T-cells in macrophage co-culture systems. ST101 increased the M1:M2 ratio up to 40-fold in hPBMC-derived macrophages cultured under conditions that typically drive M2 polarization. Further, ST101 promoted M2 repolarization to the M1 cell type, demonstrating that C/EBPβ is required for maintenance of the M2 program. When added to co-cultures of T cells with M2 macrophages, ST101 induced a 3-4-fold increase in intracellular IFN-γ staining indicating enhanced T cell activation. Notably, in M1 cultures ST101 further enhanced expression of the immune activity marker CD80 and T cell activation. Similar to its effect on M2 repolarization, ST101 induced activation of iPs-derived IS human microglia cultures toward an M1-like program. ST101 also impacted IS cell populations in vivo, as demonstrated in an orthotopic TNBC model in which ST101 exposure was associated with a reduction of the TAM fraction, increased intratumoral M1/M2 ratios, reduction of Tregs, increase of CD8:Treg fraction, and enhanced activity in combination with anti-PD-1. Similar observations were observed in clinical samples, where following ST101 exposure a significant decrease in expression of factors involved in M2 polarization, including CD209, SIGLEC5, and IL-24, and T cell suppression, including FoxP3 and inhibitory KIR proteins, were observed. Gene expression analysis suggests that ST101 induced a decrease in the intratumoral Treg:TIL ratio, indicating a shift towards a more immune-active TME. Overall, these results provide novel evidence for the contribution of C/EBPβ to the expression of multiple IS cancer-associated cell types and support the use of ST101 to antagonize C/EBPβ and promote an immune-active TME. Further, these data provide rational for evaluating the clinical impact of ST101 in combinations with immune checkpoint inhibitors.

#2910 Targeting thioredoxin reductase 1 (TrxR1) suppresses TAZ-driven glioblastoma progression.

M. Tang[1], K. Dirks[2], S. Kim[1], J. Thorpe[1], W. Li[1];
[1]Penn State College of Medicine, Hershey, PA, [2]Colorado State University, Fort Collins, CO

Glioblastoma (GBM) is the most common and aggressive primary brain malignancy in adults. Poor outcomes for traditional treatments demand targeted therapies based on identified mechanisms that drive tumor development and sustain its malignancy. Molecular pathology studies have classified GBM into subtypes differing in treatment responses and survival rates. Among these subtypes, the mesenchymal (MES) group is associated with the worst prognosis. The Hippo pathway transcriptional co-activator with PDZ-binding motif (TAZ) is one of the three transcriptional regulators that drive the GBM MES gene expression program. Studies from our lab and others have previously shown that TAZ activation is able to promote GBM MES differentiation and progression. Therefore, finding vulnerabilities of TAZ-driven tumors may help to develop targeted therapeutic methods for MES GBM. In an orthotopic GBM mouse model, we found that TAZ-driven tumors show increased expression of thioredoxin reductase 1 (TrxR1), which is responsible for catalyzing the reduction of thioredoxin and maintaining the cellular redox balance. In searching for the cause of increased expression of TrxR1, we found that glucose deprivation can induce TrxR1 expression, suggesting TrxR1 may be an adaptive mechanism for tumor cells to survive in glucose deprivation conditions. Indeed, either depleting TrxR1 genetically or inhibiting TrxR1 pharmacologically can promote tumor cell death under glucose deprivation. Furthermore, knockout TrxR1 in a TAZ-driven mouse GBM model significantly decelerated tumor progression. Collectively, our studies revealed that inhibition of the Trx redox system under glucose deprivation conditions leads to a synergistic cell death induction in GBM cells, therefore making targeting TrxR1 a potential therapeutic strategy for TAZ-driven MES GBM.

#2911 Prevalence of potential antibody drug conjugate targets and co-expression with PD-L1 in breast cancer and lung cancer patients with clinical response information.

M. Cumberbatch[1], W. Kim[2], M. Bhagat[1], J. Cogswell[1];
[1]TriStar Technology Group LLC, Washington DC, DC, [2]Seoul National University Medical College, Seoul, Korea, Republic of

Breast and non-small cell lung cancer (NSCLC) are two of the most important diseases for antibody drug conjugate (ADC) development. ADCs targeting HER2 and TROP2 are currently approved in select breast and lung subgroups with ADC's to many other tumor targets currently in clinical development. Based on TCGA mRNA expression data, ADC tumor targets currently under investigation for treatment of solid tumors have variable overlap in breast and lung cancers, however little is known about the overlap of ADC targets with PD-L1 which is a predictive biomarker in TNBC and for pembrolizumab monotherapy. In the current study, the prevalence and co-expression of ADC targets (HER2, TROP2, Nectin-4, B7-H3, B7-H4, HER3, FOLR1) were investigated in the context of PD-L1 status and clinical response data for standard-of-care (SOC) and immunotherapy, in breast and NSCLC cancer subtypes. Tissue microarrays (TMAs) comprising treatment naïve tumor samples (1mm cores) and including TNBC (26 patients), ER+ BC (90 patients), and NSCLC (adeno & squamous subtypes; 146 patients), all with full clinical follow-up information, were examined by immunohistochemistry (IHC) in serial sections for each ADC target and PD-L1, applying widely used and well optimized IHC assays on the Ventana and Dako Link 48 platforms. Established scoring methods were employed for analysis of PD-L1 and HER2, except for the addition of an exploratory ultra-low score for HER2. All other ADC targets were scored by digital image analysis to deliver percentage positive tumor expression at high (3+), moderate (2+), weak (1+) and negative (0) intensities. Taken together, this analysis revealed variable prevalence for each target in breast and lung cancer histologies by subtype, including differing overlap between ADC targets within tumor indications. In addition, prevalence of each ADC target in breast cancer characterized by HR status and HER2 subgroups (HER2-positive, low, ultra-low, negative) indicated potential opportunities for ADC clinical development in these subgroups. Co-prevalence of the selected ADC targets with PD-L1 CPS>10 (predictive for Pembrolizumab response in TNBC) and PD-L1 CPS categories of interest for NSCLC revealed patterns of expression in support of combination therapies. Furthermore, expression and co-prevalence data for each ADC target +/- PD-L1 was characterized in association with response to immunotherapy or other SOC. In summary, these data provide better understanding of which breast and lung cancer subtypes express the selected ADC targets uniquely and competitively which may be key to future clinical and diagnostic development.

#2912 SFRP2 and CD38 colocalize in triple negative breast cancer microenvironment.

L. Hsu, P. Nasarre, R. Mukherjee, E. Hilliard, M. Romeo, E. O'Quinn, W. Christians, N. Klauber DeMore;
The Medical University of South Carolina, Charleston, SC

Introduction: A promising target for breast cancer is secreted frizzled-related protein 2 (SFRP2), and a humanized monoclonal antibody to SFRP2 (hSFRP2 mAb) inhibits primary triple negative breast cancer (TNBC) in vivo. CD38 is a known cause of PD-1 inhibitor resistance in some tumors, and in metastatic osteosarcoma hSFRP2 mAb overcomes PD-1 mAb resistance by reducing CD38 in tumor infiltrating lymphocytes (TILs). Could this phenomenon be replicated in TNBC? This is unknown as the expression of CD38 in TNBC has not been studied. This study will establish the presence of SFRP2 and CD38 in the TNBC microenvironment.

Methods: Immunohistochemistry (IHC) was performed on an 88 core human TNBC tissue microarray (TMA) with antibodies to SFRP2 and CD38. Spatial analysis software was used to determine percent positivity. Each core was categorized using the scoring system for the estrogen receptor in breast cancer (<1% negative, 1-10% low positive, and >10% positive). Multiplex IHC was performed on 4 human triple TNBCs sections. Tissues were stained with antibodies to CD38, CD68 (macrophage), CD3 (T-cell), CD19 (B-cell), CytoKeratin (tumor), and SFRP2. Percent positivity of each marker was analyzed with a software package. For flow cytometry of tumor associated macrophages (TAMs), 1 million EO771 cells were injected into the mammary fat pad of female C57/BL6 mice. After 4 weeks tumors were extracted and a cell suspension was incubated in a mastermix with antibodies to SFRP2, CD38, PD1, CD11B and F480. Cells were fixed and conjugated to a fluorochrome secondary antibody. TAM gated cells were analyzed for the presence of SFRP2 and CD38.

Results: For the TNBC TMA, 83 cores were positive and 4 cores were low positive for SFRP2, 1 not evaluable; 87 cores were positive and 1 low positive for CD38. For multiplex IHC there was a total of 1,753,544 individual cells in all 4 human TNBC tumors that were stained. 94% of cells stained positive for SFRP2, and 65% stained positive for CD38. Of the cells that were positive for SFRP2, 70% were also positive for CD38, 15% were positive for CD68, 1% were positive for CD19, 77% were positive for CytoKeratin, and 10% were positive for CD3. Of the cells that were CD38 positive, 99% were also positive for SFRP2, 15% were positive for CD68, 1% were positive for CD19, 81% were positive for CytoKeratin, and 9% were positive for CD3. Flow cytometry analysis of TAMs confirmed the presence of SFRP2, CD38 on TAMs. TAMs that were negative for PD1 and CD38 (pro-inflammatory) had a 56% reduction in SFRP2 compared to TAMs that were double positive for PD1 and CD38 (anti-inflammatory).

Conclusion: SFRP2 and CD38 are prevalent in human TNBC and colocalize in the TNBC microenvironment in tumor cells, TAMs and TILs, but not B-cells. The presence and co-localization of SFRP2 and CD38 in TAMs was confirmed with flow cytometry. This confirms that SFRP2 is a therapeutic target in TNBC and provides a mechanistic rational for combination therapy with PD-1 inhibitor.

#2913 Co-expression of extracellular matrix enzymes heparanase or PH-20 augments the anti-tumor efficacy of folate receptor 1-targeting CAR T cells in an ovarian cancer model.

B. L. Steimle, P. Hu, N. Tran, J.-J. Lee, K. Baysac, K. Luo, X. Wang, G. Liang, S. Nurmukhambetova, T. Tran, P. Dash, D. Schneider;
Lentigen Technology Inc., a Miltenyi Biotec Company, Gaithersburg, MD

Introduction: The tumor extracellular matrix (ECM) is a physical barrier which obstructs trafficking of CAR T cells to tumors. We hypothesize that co-expressing ECM remodeling/degrading enzymes heparanase (HPSE) or PH-20 with a CAR directed against folate receptor 1 (FolR1) will overcome the physical tumor microenvironment barrier and improve anti-tumor efficacy of anti-FolR1 CAR in a human ovarian cancer model.

Methods: ECM CARs were constructed by combining anti-FolR1 ScFv with a CD8 hinge and transmembrane domain, 4-1BB, and CD3ζ endodomains, followed by a P2A element and full-length HPSE or GPI-anchored PH-20 sequence. CAR T cells were prepared from CD4+ and CD8+ T cells of healthy donors by lentiviral transduction. CAR expression was evaluated by flow cytometry; HPSE and PH-20 expression were measured via ELISA and Western blotting, respectively. CAR-mediated killing and cytokine release were observed in overnight co-culture assays with FolR1-expressing tumor cells. ECM CARs' migration through Cultrex™ and sodium hyaluronate matrices were assessed for HPSE and PH-20 function, respectively. ECM CARs' efficacy was evaluated *in vivo* using a FolR1-expressing subcutaneous OV90 ovarian cancer xenograft model in NOD SCID Gamma (NSG) mice, and representative OV90 tumors were harvested at day 7 post-CAR T treatment for immunohistochemical staining.

Results: FolR1 expression was confirmed in ovarian cancer cell lines and substrates targeted by HPSE (perlecan, glypican 3, CD138) and PH-20 (hyaluronan) were detected by immunofluorescence in human ovarian tumors' sections. Lentiviral transduced primary T cells yielded robust expression of FolR1 CAR and ECM enzymes. Anti-FolR1 CAR and ECM CARs secreted pro-inflammatory cytokines IL-2, TNFα, IFNɣ and lysed OVCAR3 tumor cells with similar efficacy. ECM CARs with HPSE or PH-20 exhibited enhanced migration through ECM-rich matrices as compared to anti-FolR1 CAR alone. *In vivo*, all anti-FolR1 CAR T cells rejected OV90 tumors and extended survival compared to tumor alone or untransduced T cells (UTD). However, ECM CARs co-expressing HPSE or PH-20 accelerated tumor regression as compared to anti-FolR1 CAR alone. Tumor histology revealed CAR T cell infiltration (CD3+, CD8+) in mice treated with anti-FolR1 CARs but not UTD, indicating that anti-FolR1 CARs can effectively infiltrate OV90 tumors. Imaging studies are underway to evaluate the function of ECM CARs in the tumor microenvironment.

Conclusions: The anti-FolR1 CARs boosted with ECM enzymes HPSE or PH-20 demonstrated specific lysis of FolR1-expressing cell lines, improved penetration through ECM-rich matrices *in vitro*, and accelerated tumor regression in an ovarian cancer model *in vivo*. Therefore, ECM CARs may help improve clinical outcomes in patients with ovarian tumors.

#2914 AI/ML-driven discovery of CTHRC1, collagen triple helix repeat-containing 1, a novel proteoglycan for stroma + tumor targeting and delivery of 4-1BB costimulation.

Christopher Harvey[1], Elizabeth Koch[2], Amanda Hanson[1], Lindsey Rice[1], Amy Berkley[2], Kerry White[1], Reza Saberianfar[2], Nikolai Suslov[1], Sam Cooper[2], **Michael Briskin**[1]

[1]Phenomic AI, Waltham, MA,[2]Phenomic AI, Toronto, ON, Canada

Background: While checkpoint inhibitors have demonstrated efficacy in a number of solid tumor indications, those with high stromal presence have been difficult to treat with minimal objective responses observed. Phenomic has developed a proprietary machine learning/artificial intelligence platform to identify novel stromal targets with superior expression profiles that enable selective targeting of immune activating agents that will relieve these immunosuppressive barriers in difficult to treat indications.

Methods: Using our single cell RNA Atlas, we assessed cancer-associated fibroblasts (CAFs) in several solid tumor indications for identification of novel targets, including proteoglycans. Our Atlas was also used to identify immune activating payloads whose cognate receptors were present in indications of interest. Antibodies were generated, and lead clones who demonstrated potent ligand binding and cell staining were used to generate fusion proteins to immune activating ligands. Efficacy and PD were assessed in multiple syngeneic tumor models.

Results: Bioinformatic analysis identified a unique subset of pathogenic CAFs, which are TGF beta responsive, secrete several ECM proteins, and their presence tracks with poor outcome and resistance to immunotherapy in several solid tumor types. CTHRC1 was identified as a novel matrix protein highly expressed in this CAF subtype as well as tumor epithelium and is highly selective in a range of tumor types such as ovarian cancer, triple negative breast cancer, and pancreatic ductal adenocarcinoma. While secreted, CTHRC1 is complexed on the cell surface and affords the opportunity to drug this target in a variety of ways. We identified an absence of 4-1BBL expression across indications of interest, and fusion proteins were generated to deliver 4-1BBL via CTHRC1 targeting. In checkpoint-resistant tumor models, we observed significant increases in CD8 T cells and robust anti-tumor activity with anti-CTHRC1-targeted 4-1BBL. Biodistribution studies were conducted using our targeting mAb and demonstrate uptake only in sites of primary and metastatic tumors, even at doses 20-fold higher than those that achieve maximal therapeutic activity, suggesting the potential to minimize the toxicity that has been observed with other 4-1BB agonists.

Conclusions: We have identified CTHRC1 as a novel proteoglycan expressed by both pathogenic CAFs and tumor cells that is highly selective for tumors, enabling the therapeutic targeting of immune activating payloads with the potential for safely delivering payloads while limiting toxicity. Given the specificity and selectivity afforded by CTHRC1 expression, ADC and CD3 engager approaches are also being pursued. These data represent novel approaches aimed at breaking down stromal barriers in tumors previously unresponsive to immunotherapies.

#2915 Targeting complement factor H renders STK11-mutant lung adenocarcinoma sensitive to anti-PD-1 therapy in mice.

S. Suzuki[1], A. Khan[1], T. Giridharan[1], C. Ting[1], R. Bushey[2], E. Gottlin[2], M. Campa[2], E. F. Patz[2], E. H. Yau[1], B. Segal[1];
[1]Roswell Park Comprehensive Cancer Center, Buffalo, NY, [2]Duke University Medical Center, Durham, NC

STK11 mutations occurs in 15-20% of lung adenocarcinoma (LUAD) and is associated with KRAS mutations, poor survival and resistance to immune checkpoint inhibitors (ICI). We observed tumor cell lines and primary human STK11-mutant LUAD upregulates of expression of C3 and complement factor H (FH). Deletion of C3 in STK11 knock-out tumor cells resulted in reduced FH expression. FH is a co-factor of Factor I, which converts C3b to proteolytically inactive iC3b thereby limiting activation of the alternative pathway (AP) C3 convertase. FH binds to proteoaminoglycans on the cell membrane and protects cells from AP complement-dependent cytotoxicity. With increased C3 generation by STK11-mutant tumor cells, we reasoned that systemic or tumor-derived FH protects tumor cells from complement attack. We hypothesized that tumor-derived C3 would promote STK11-mutant LUAD growth in immune intact mice by promoting immune evasion and would drive ICI resistance. Based on the expected tumor-protective effects of FH, we also hypothesized that anti-FH antibodies would control tumor growth and render tumor more sensitive to ICI. We evaluated growth of subcutaneously administered CMT167-STK11KO with and without C3 deletion (CMT167-STK11KO is murine $KRAS^{G12V}$ LUAD with CRISPR/Cas9 deletion of STK11). Deletion of C3 in CMT167-STK11KO (CMT167-STK11KO/C3KO) resulted in dramatic inhibition of tumor growth and in sensitivity to anti-PD-1 therapy *in vivo*. In contrast, deletion of C3 in STK11-KO tumors had no effect on tumor growth in nude mice or following CD8 depletion in WT mice. These findings support a role of tumor-derived C3 in evasion of T cell anti-tumor immunity and as an obstacle to anti-PD-1 therapy. GT103 is a therapeutic antibody that binds tumor cell-attached CFH, causes complement activation, kills tumor cells, initiates a shift from a pro- to an anti-tumor immune microenvironment, and is currently being evaluated in a Phase 1b-2 clinical trial in combination with pembrolizumab (NCT05617313). We observed that single agent GT103 or anti-PD-1 has limited efficacy in CMT167-STK11KO tumor in WT mice. However, the combination of GT103 and anti-PD-1 was very effective in limiting tumor growth. Our results support a role of tumor-derived C3 in suppressing CD8 T-cell immunity and in driving ICI resistance and that the addition of GT103 renders STK11-KO tumors sensitive to anti-PD-1 in mice. These studies establish rationale for evaluating this combination in patients with STK11-mutant LUAD.

#2916 Discoidin domain receptor 1 (DDR1) expression is associated with degree of immune exclusion across epithelial tumors.

X. Sher[1], F. D. Gootkind[1], T. Schurpf[1], F. Peyraud[2], J.-P. Guegan[3], A. Italiano[2], G. T. Clifton[1], **L. A. Dillon**[1];
[1]Incendia Therapeutics, Boston, MA, [2]Institut Bergonie, Bordeaux, France, [3]Explicyte Immuno-Oncology, Bordeaux, France

Background: Discoidin domain receptor 1 (DDR1) is highly expressed in epithelial cancers and has been implicated in tumor growth, invasion, and lack of response to therapy. DDR1 contributes to immune exclusion by promoting tumor collagen alignment in *in vivo* models. However, it is unclear how DDR1 expression impacts immune cell infiltration in human tumors. A first-in-human trial of PRTH-101, a DDR1-targeted therapeutic antibody, is underway. Establishing a correlation between DDR1 expression and immune infiltration in the tumor microenvironment (TME) will shed light on the role of DDR1 in the TME and inform indication and patient selection strategies for DDR1-targeted therapies.

Methods: Adjacent formalin fixed paraffin embedded slides from colorectal (CRC), non-small cell lung (NSCLC), ovarian (OC), pancreatic (PDAC), and triple-negative breast cancers (TNBC) were stained by H&E and a multiplex immunofluorescence (mIF) panel containing DDR1 and immune cell markers CD8 and CD45. Tumor-stromal segmentation and cell identification was done from H&E using AI-powered models developed by PathAI (PathExplore™) or from mIF by image analysis using QuPath. *DDR1* mRNA expression was measured by bulk RNA-sequencing, while DDR1 protein expression was measured by mIF. Immune Exclusion Scores (IESs) were calculated for each tumor based on lymphocyte density (from H&E), CD8+ T cell density (from mIF), or CD45+ cell density (from mIF). Each IES is the orthogonal distance between the coordinate of immune cell density in tumor epithelium and stroma, and the regression line representing equal density in epithelium and stroma. Correlations between lymphocyte, CD8, and CD45 IESs and DDR1 mRNA or protein expression levels were evaluated.

Results: Both DDR1 mRNA and protein expression levels were significantly correlated with all Immune Exclusion Scores (IESs) measured by the distribution of lymphocytes (H&E), CD8+, or CD45+ cells (mIF) in tumor epithelium and stroma (R: 0.31-0.55, adjusted p: <0.001-0.01) at a pan-cancer level. While the degree of the correlation varied between tumor indications by IES immune cell type, pancreatic cancer exhibited the strongest correlation between the lymphocyte-based IES and DDR1 mRNA and protein expression (R: 0.48-0.54, adjusted p: 0.04-0.07). *DDR1* mRNA was also moderately correlated with lymphocyte IES in NSCLC and TNBC (R: 0.37-0.48, adjusted p: 0.12-0.14).

Conclusions: We developed a continuous scoring method to quantify the degree of immune exclusion in tumors based on the spatial distributions of lymphocytes, CD8+ T cells, and CD45+ immune cells from H&E and mIF images. DDR1 mRNA and protein expression are correlated with immune exclusion at both the pan-cancer and specific indication level. This adds additional insight into the role of DDR1 in human cancers and may be useful in selecting indications and stratifying patients for DDR1-targeted therapies.

#2917 Purifying cancer-associated fibroblasts (CAFs) from glioblastoma and defining their role in therapeutic resistance.

A. Sati, A. Mathur, M. Lad, A. Saha, M. K. Aghi;
University of California San Francisco, San Francisco, CA

Glioblastoma (GBM), a challenging brain tumor, necessitates the development of new therapies due to poor patient prognoses, with a median survival of 14-16 months. Standard of care, as established almost 20 years ago, remains to be surgical resection followed by chemotherapy and radiation and till date there is no defined standard of care for recurrent GBM, highlighting the urgent need for the development of novel therapies. Recent studies have implicated the tumor microenvironment in these poor prognoses. While cancer associated fibroblasts (CAFs) are a key cellular component of the microenvironment of many systemic tumors, their presence in GBM had been doubted until we recently developed intriguing data identifying cells in GBM that express fibroblast markers, have fibroblast-like morphology, and, most importantly, transcriptomically resemble CAFs from systemic cancers rather than other stromal cells that express similar surface markers such as pericytes (Jain et al. 2023). Similar to other solid cancers, GBM CAFs increase tumor growth and drive immunosuppression. The role of CAFs in regulating these processes could have significant implications in response to standard of care therapy as well as novel immunotherapies. While our initial CAF isolation had just 50% purity, we have developed a novel flow-sorting algorithm for CAF enrichment driven by our bioinformatic data. Through this protocol, we have successfully established, the first of its kind, a biobank of patient derived GBM CAFs with greater than 90% purity. These CAFs are now being utilized to investigate their contribution in conferring resistance to chemotherapy (Temozolomide) and radiotherapy. The CAFs are also being assessed for their role in suppressing T cell function and resistance to immunotherapies. In parallel, the origin of GBM CAFs and their development trajectory is being analyzed to find molecular markers to specifically target CAFs in the GBM microenvironment. The work put together will provide insight on mechanisms employed by CAFs in altering the GBM microenvironment and a basis for developing novel combination approaches, alleviating therapeutic resistance caused due to the presence of CAFs in the GBM microenvironment. The results of this study have the potential to significantly attenuate therapeutic resistance in GBM and provide much needed treatment options and improvement in survival, for what remains one of the most dismal diagnoses in the clinic.

#2918 Potential for a novel therapeutic target: Effects of lactate & lactylation in expression of key regulatory cancer proteins.

Christos P. Costeas[1], Connor Purcell[2], Wafik S. El-Deiry[3]

[1]Warren Alpert Medical School, Legorreta Cancer Center at Brown University, Providence, RI,[2]Legorreta Cancer Center at Brown University, Providence, RI,[3]Pathology and Laboratory Medicine, Legorreta Cancer Center at Brown University, Warren Alpert Medical School, Providence, RI

The purpose of our study is to investigate the immunologic, metastatic, and gene regulation effects of lactate in the context of cancer in normoxic and hypoxic conditions to identify novel biomarkers and potential therapeutic targets. We aim to modify the in-vitro cancer microenvironment to show how lactate and lactylation can be exploited using existing cancer treatments. While hyperlactatemia is defined as lactate levels between 2 mmol/L and 4 mmol/L (Foucher et al 2023), tumor biopsies have demonstrated extracellular concentrations as high as 40 mM (Pérez-Tomás et al 2020). Through CTG viability assays we identified lactate concentrations that PANC1 cells can survive, which are in agreement with the in-vivo findings of Brizel et al (2001). We observed pancreatic cancer cells achieving over 50% viability for 5 days at 50 mM lactate concentrations while at 30 mM on day 5 they proliferated past their initial plating numbers. Furthermore, Brizel et al (2001) found that patients with high tumor lactate concentrations had a significantly higher incidence of metastatic relapse. Through our scratch assay, we show qualitative evidence of increased mobility and inferred migration potential of PANC1 at 7.5mM [lactate] compared to the absence of lactate. We have also observed increased migration at higher lactate concentrations for which we are pursuing quantitative measurements to evaluate significance. Migration experiments will be followed by the investigation of gene regulation (eg. mRNA seq, lactylation profile) involved in the observed increased mobility. Lactate has been shown to affect immune regulation, namely suppression of iNKT (Fu et al, 2020), macrophages (Yang et al, 2020), dendritic cell differentiation and antigen recognition/presentation (Wang et al, 2022), however not much is known about its effect on NK cells and their cytokine expression. Through NK92MI/PANC1 cocultures we show the effects of lactate concentration on the killing ability of NK cells (in the works). And plan on investigating the cytokine profile leading to the phenotypic killing differences. Lastly, via lactate-titrated incubation of PANC1 cells in normoxia we have demonstrated a positive correlation of HIF1a expression, pan-lactyllysine lactylation, and microenvironment lactate concentration. We speculate HIF1a inhibition post-lactate-sensitization may induce cancer killing and we will investigate this theory in normoxia and hypoxia using existing treatment options.

#2919 Targeting regulatory T cells to boost immunity against melanoma.

W. Miao[1], Y. J. Jin[1], V. Jain[2], S. Gregory[2], J. Y. Zhang[1];
[1]Duke University Medical Center, Durham, NC, [2]Duke university, Durham, NC

Tumor-infiltrated regulatory T-cells (Treg) restrict the function of effector T-cells and thereby promote tumor growth. Disrupting the immunosuppression of Treg cells presents an attractive strategy for cancer immunotherapy; However, the risk of autoimmunity, resulting from systemic Treg depletion, limits its therapeutic effectiveness. Here, we show that genetic depletion of Ube2n in Treg cells inhibits tumor growth which is correlated with a markedly enhanced infiltration of cytotoxic immune cells. Notably, the deletion of Ube2n in a fraction of Treg cells was sufficient to produce a long-lasting anti-tumor effect, without apparent systemic autoimmune responses. The antitumor effect persists following adoptive T-cell transfer to an otherwise immunodeficient mouse tumor model. Through flow cytometry, immunostaining and T-cell targeted single-cell sequencing analyses, we demonstrate that the loss of Ube2n dampens Treg suppressive function, as indicated by markedly increased numbers of cytotoxic CD8 T-cells in the tumor microenvironment (TME). Further, differentially expressed genes analyses show a downregulation of Mki67 and an upregulation of Ifng in Ube2n deficient Tregs, concomitant with amplification and activation of effector T-cells. Our findings uncover a hitherto unexplored role of Ube2n in orchestrating the differentiation and functions of Treg in TME, highlighting the therapeutic potential of targeting this pathway to enhance and reprogram anti-tumor immunity.

#2920 *In vitro* assays for investigating the effects of cancer therapeutics on bone.

J. H. E. Maki-Jouppila, M. Ristola, J. Rissanen, **K. Fagerlund**;
Pharmatest Services Ltd., Turku, Finland

Bone microenvironment is an important factor in regulating bone metastasis. When cancer cells home to bone they secrete factors that stimulate osteoclast activity leading to increased bone resorption. Stimulatory factors released from the resorbed bone matrix in turn promote proliferation of cancer cells and this process, referred as the vicious cycle, often leads to osteolytic lesions in bone when osteoclastic bone resorption exceeds osteoblastic bone formation. The vicious cycle observed in osteolytic disease occurs also in osteoblastic metastases, and in addition cancer cells produce osteoblast-stimulating factors. Cancers with bone metastases often include both osteolytic and osteoblastic lesions. Our aim was to establish *in vitro* cell culture models to study the effects of cancer therapeutics on osteoblast and osteoclast differentiation and activity. In the osteoclast differentiation assay, human osteoclast precursor cells (Lonza) were cultured on bovine bone slices for 7 days. Denosumab was added in the cultures at day 0, and tartrate-resistant acid phosphatase isoform 5b (TRACP 5b) activity was measured from the culture medium collected at day 7. Osteoclast activity was studied by allowing osteoclasts resorb bone after 7 days' maturation period for additional 3 days in the presence of odanacatib. The amount of C-terminal cross-linked telopeptides of type I collagen (CTX-I) was measured in the culture medium collected at day 10 to quantitate osteoclast activity. Denosumab and odanacatib showed strong concentration dependent inhibition of osteoclast differentiation and activity, respectively. A mouse osteoblast progenitor cell line KS483 (Pharmatest Services) was used to study differentiation and activity of osteoblasts with test compounds bone morphogenetic protein 2 (BMP-2) and estradiol (E2). In the osteoblast differentiation assay, the activity of cellular alkaline phosphatase (ALP), a marker of osteoblast differentiation, was measured at day 8. In the osteoblast activity assay, the cells were cultured for 13 days. N-terminal propeptide of type I procollagen (PINP) secreted into the culture medium was determined at day 11 to indicate the effects on organic bone formation and calcium deposition was determined at the end of the study as a marker of inorganic bone formation. BMP-2 and E2 stimulated osteoblast differentiation and activity indicated by the increase in ALP activity, PINP and calcium levels. We conclude that these culture systems can be used for studying the effects of cancer therapeutics and identifying new potential compounds affecting the disease process of bone metastases with different mechanisms of action.

#2921 Extended treatment with IAP inhibitor xevinapant post radiotherapy improves therapeutic efficacy and promotes antitumor immunity in preclinical models.

T.-L. Yeung[1], F. Jiang[1], H. Huang[1], H. Yu[1], L.-Y. Chiu[1], M. Bonnemaison[1], B. Marelli[1], R. Ferretti[1], R. Lindemann[2], C. Esdar[2];
[1]EMD Serono, Billerica, MA, [2]The Healthcare Business of Merck KGaA, Darmstadt, Germany

Background: Xevinapant is a first-in-class, oral IAP (inhibitor of apoptosis protein) inhibitor designed to restore cancer cell sensitivity to apoptosis induced by radiotherapy (RT) and chemotherapy. In a randomized phase 2 study of patients with unresected locally advanced squamous cell carcinoma of the head and neck, xevinapant + chemoradiotherapy (CRT) significantly improved locoregional control at 18 months, 3-year progression-free survival and nearly doubled 5-year overall survival vs. placebo + CRT (53% vs. 28%). Two phase 3 trials, in which patients receive 6 cycles of xevinapant or placebo monotherapy (3 cycles in combination with standard-of-care (C)RT followed by 3 cycles of monotherapy), are ongoing. Based on the roles of IAPs in apoptosis and tumor immunity, continual dosing of xevinapant post RT may deliver additional therapeutic benefit through modulation of multiple tumor microenvironment (TME) compartments. Methods: The impact on antitumor efficacy of xevinapant dosing duration was evaluated in A1419 (head and neck), LLC (lung) and MC38 (colorectal) syngeneic tumor-bearing mice treated with vehicle control, RT alone (3.6Gy, QD, 5 days), or RT + xevinapant (100 mg/kg, QD, 1, 2, or 4 weeks). To assess treatment-mediated TME modulation in MC38 tumors, RNAseq and FACS-based immune profiling was performed, followed by functional validation with ex vivo ELISpot assays, in vitro immunogenic cell death assays, T cell activation assays, and macrophage polarization and viability assays. To evaluate the effect of xevinapant on RT-induced cancer associated fibroblast (CAF) activation and CAF-modulated immune phenotype, activation assay and cytokine profiling was performed. Results: In the tumor models tested, RT in combination with extended xevinapant dosing markedly improved efficacy and prolonged survival compared to treatment arms of RT with shorter xevinapant dosing durations, RT alone, and vehicle control. RNAseq and FACS analyses suggested a TME with enhanced antitumor immunity, while ELISpot and in vitro T cell assays confirmed that extended xevinapant dosing promoted antigen-specific T cell response and T cell activation. Furthermore, macrophage polarization and viability assays suggested that xevinapant reduced the viability of M2 macrophages which may have contributed to the increased M1:M2 macrophage ratio and the improved antitumor immune response observed in vivo. In addition, via the suppression of RT-mediated CAF activation, xevinapant may promote M1 polarization of macrophages and recruitment of T cells by upregulating GM-CSF and CXCL10 in CAFs. Conclusions: Extended dosing of xevinapant post concurrent RT improved antitumor efficacy and prolonged survival of tumor-bearing mice. Mechanistic investigation suggested that such benefit may be, in part, modulated by xevinapant enhanced antitumor immunity.

#2922 Sensory innervation as a novel driver of ovarian cancer progression.

M. Knarr[1], K. Cummins[1], D. Racordon[1], H. Reavis[1], T. Lippert[1], R. Hausler[1], P. Rawat[1], S. Ryu[2], J. Moon[2], D. Hoon[2], R. Greenberg[1], P. Vermeer[3], R. Drapkin[1],

[1]Perelman School of Med. Univ. of Pennsylvania, Philadelphia, PA, [2]Saint John's Cancer Institute, Santa Monica, CA, [3]Sanford Research Institute, Sioux Falls, SD

One of the main challenges currently faced in ovarian cancer treatment is that the primary platinum/taxane therapy used to treat patients does not meaningfully extend survival. The overall survival for ovarian cancer patients with advanced disease is less than 30% with most patients recurring within 5 years of initial therapy. Once resistant disease develops there are few second line therapy options, which inevitably leads to disease progression. Thus, there is a critical need to identify new therapies that can overcome ovarian cancer chemoresistance and produce meaningful increases in patient survival. In recent years, new efforts have focused on targeting the tumor microenvironment (TME), the complex mixture of non-cancer cells that surround and support the cancer cells within the tumor. Different strategies have evolved to target the TME, such as immune checkpoint inhibitors or angiogenesis inhibitors. However, these TME targeting therapies have limited effect when used to treat ovarian cancer patients. Most ovarian tumors have a microenvironment that is highly immunosuppressive and do not respond or are resistant to angiogenesis inhibitors. Thus, new TME targeting therapies must be developed that can induce a therapeutic effect in ovarian tumors and can be used to treat most ovarian cancer patients. A novel TME component ripe for therapeutic targeting are the nerve fibers that infiltrate tumors in a process termed tumor innervation. Recent studies in several cancers have shown that tumor innervation can promote tumor growth/metastasis. However, in ovarian cancer the role of innervation in promoting cancer progression remains undefined. Here we show that Transient Receptor Potential cation channel subfamily V member 1 (TRPV1)+ sensory innervation plays a significant role in driving ovarian cancer growth and metastasis. Analysis of patient samples shows that sensory nerve fiber innervation is much higher in ovarian tumors vs benign reproductive tissue. In addition, ablation of TRPV1 sensory nerve fibers in vivo causes reduced tumor burden and prolongs survival in a syngeneic mouse model of ovarian cancer metastasis. Taken together, our results establish TRPV1+ sensory innervation as a novel driver of ovarian cancer growth/metastasis and a potential therapeutic target for ovarian cancer treatment.

MOLECULAR/CELLULAR BIOLOGY AND GENETICS: Advances in Genomic Sequencing Platforms, Methodologies, and Interpretation 2
Poster Session

#2926 The effect of cancer research autopsy parameters on DNA and RNA sequencing quality.

P. Fessas[1], S. Hessey[1], C. Richard[1], C. Naceur-Lombardelli[1], S. Ward[1], D. A. Moore[1], K. Nowakowska[2], B. Trujillo[2], I. Lobon[3], S. T. C. Shepherd[3], F. Byrne[3], S. Turajlic[3], G. Attard[2], C. Swanton[4], M. Jamal-Hanjani[1];

[1]University College London Cancer Institute, London, United Kingdom, [2]University College London, London, United Kingdom, [3]The Francis Crick Institute, London, United Kingdom, [4]Cancer Evolution and Genome Instability Laboratory, London, United Kingdom

Background: Cancer research autopsy genomic studies offer insight into the metastatic cancer landscape but come with complexities that relate to the sampling and processing of post-mortem tissue. Clarifying the effect of autopsy variables on pre- and post-sequencing quality control (QC) is an unmet need that may inform tissue collection strategies.

Methods: The effect of age, sex, post-mortem interval (PMI), and sample type (primary, metastatic, or normal) on pre-sequencing QC (nucleic acid concentration and integrity) was examined in 2678 samples (88.6% metastatic, 8.0% primary, 3.4% normal) from 83 patients with melanoma, lung, renal, or prostate cancer in the PEACE study. In the lung cohort, 160 surgical samples were also included through the TRACERx study, allowing surgery-autopsy tissue comparisons. Post-sequencing QC metrics were evaluated for lung samples that underwent DNA (n=522) or RNA (n=366) sequencing.

Results: RNA concentration and RIN were greater in surgical samples than those collected at autopsy. Across cohorts, metastatic autopsy samples had greater nucleic acid concentrations than primary or normal autopsy samples, but not integrity. DNA and RNA concentration and integrity differed significantly between primary tumor types. When comparing samples of different metastatic sites from the whole cohort, concentration was lowest in bone (DNA) or the digestive tract (RNA), while integrity was greatest in the brain and lowest in the digestive tract (DIN, RIN). Although autopsy variables like age, sex and PMI correlated with pre-sequencing QC metrics in univariate analysis, they were not found to significantly correlate with these metrics in multivariate analysis, which identified that only primary cancer type and metastatic site were independent determinants of concentration and integrity. Similarly, for post-DNA (whole exome) sequencing QC, only the metastatic site was found to independently influence sequencing QC metrics like total number of sequences, average sequence length, and FastQC score. For RNA sequencing, only the metastatic site was found to influence sequencing QC metrics like total number of sequences, percentage of non-duplicated sequences, one hit-one genome percentage, and the alignment percentage on the human genome.

Discussion: The lack of influence of PMI on QC in the largest QC-focused autopsy cancer study to date suggests that quality tissue can be obtained from non-rapid autopsy programs, which are more feasible and less resource-intensive than rapid programs.

#2927 Optimization of sample preparation for single-cell RNA-sequencing using accumulated collection of preclinical and clinical specimens.

K. Lim[1], J. Lee[2], K.-H. Pyo[3], B. Cho[4];

[1]JEUK Institute for Cancer Research, JEUK Co., Ltd, Gumi, Korea, Republic of, [2]Department of Research Support, Yonsei Biomedical Research Institute, Yonsei University College of Medicine, Seoul, Korea, Republic of, [3]Yonsei New Il Han Institute for Integrative Lung Cancer Research, Yonsei University College of Medicine, Seoul, Korea, Republic of, [4]Division of Medical Oncology, Department of Internal Medicine and Yonsei Cancer Center, Severance Hospital, Yonsei University College of Medicine, Seoul, Korea, Republic of

Background: The heterogeneity of tumors became apparent with the introduction of single-cell RNA-sequencing technology, enabling the discovery of rare and novel cell types that were not attainable with bulk RNA-sequencing. Numerous papers have been published, and the data from single-cell RNA-sequencing are publicly available. While current literatures provide detailed guidance on effectively analyzing single-cell RNA sequencing data, documentation for sample preparations is less frequently reported in easily accessible protocols. Additionally, researchers hold diverse opinions on sample handling and practical information is scattered across multiple sources.

Method: A total of 233 cases were included in the study, comprising 150 cases of clinical and 83 cases of preclinical samples. Among the 150 clinical samples, 58 were freshly obtained (32 biopsies and 26 surgical resections), and 92 were frozen. Of the 83 preclinical samples, 70 were fresh, and 13 were frozen. Sample preparations for 10X Genomics Chromium single-cell RNA-sequencing were carried out using the methods of 'Red blood cell lysis', 'Straining', and 'Dead cell removal using magnetic beads' with clinical specimens. Each method was applied based on specific situations involving the presence of red blood cells, cell aggregates, dead cells and debris.

Results: There was a variation in the usage of red blood cell lysis, straining, and dead cell removal methods across different sample types. Specifically, 40.6% of clinical biopsy samples were primarily conducted with red blood cell lysis and/or straining without the removal of dead cells. Whereas, 96.2% of clinical surgical resections and 100% of clinical frozen samples predominantly utilized dead cell removal. The frequency of a double application of dead cell removal was higher in frozen samples, at 34.8% due to low viability as expected. For surgical resections, in comparison, only 15.4% required a second round of dead cell removal. In preclinical samples, both fresh and frozen, removal of dead cells was essential and implemented in 100% of cases. Among these, 62.9% of the fresh preclinical samples and 76.9% of the frozen preclinical samples underwent a second round of dead cell removal.

Conclusions: The utilization of the methods red blood cell lysis, straining, and dead cell removal proved to be adequate in meeting the stipulated criteria of the 10x Genomics guidelines, demonstrating efficiency in terms of time. We have outlined a workflow for each sample type, accompanied by images illustrating pre- and post-conditions for plausible occurrences. Additionally, approximate cell numbers required, or percentages of cell loss are provided for each situation. We anticipate that this protocol will be beneficial for those new to the field, enabling them to generate samples for single-cell RNA-sequencing independently.

#2928 Solving the cancer mutation conundrum: A single cell, massively parallel approach for cancer mutation discovery, genome modelling and functional characterization.

S. M. Grimes, H. Kim, S. Roy, A. Sathe, B. T. Lau, **H. P. Ji**;
Stanford University, Stanford, CA

Large scale genomic studies are cataloguing tens of thousands of cancer mutations across a wide spectrum of tumor types. Conventional DNA sequencing methods have limitations in terms of identify mutations at high resolution among single cells. Moreover, determining cancer mutations' phenotype and function remains an enormous challenge - most mutations are assigned to the category of variants of unknown significance. In-silico functional predictions of cancer mutations are frequently used as a stopgap solution. However, these computational methods lack the ability to make refined biological and functional predictions. We demonstrated a new single cell experimental strategy that accelerates the discovery of cancer mutations and their characterization. This genomic technology framework does the following: (1) identify disease-related mutations at the resolution of individual cells from tumors or cell lines; (2) genome engineer these candidate mutations into cellular experimental systems for further biological characterization. First, we developed a single cell approach to identify cancer somatic mutations and even gene fusion rearrangements found in coding regions of mRNAs. Primary tumors are processed into single cell RNA-seq libraries and analyzed with nanopore long read sequencing. Across thousands of cells from primary tumors, we identified single cell mutations from the nanopore long reads that covered cancer gene transcripts. This approach allows us to even identify cancer rearrangements at single cell resolution. Next, we used short-read single cell transcriptomes to characterize the cell type and determine the gene expression characteristics of those cells with mutations. For single cell phenotypic studies, we developed a highly multiplexed technology using CRISPR base editors to directly engineer hundreds of mutations into their original genes among single cells and determine their transcriptional phenotype. Among specific individual cells, nanopore-based long-read sequencing identifies these modelled mutations directly from a target's transcript sequence. Then, we integrate this single cell mutation data with the short-read transcriptome profile from the same individual cell. Therefore, we determine both the genotype and phenotype of a given engineered mutation from an individual cell. In summary, our work demonstrates a new, direct and highly scalable method for identifying, modelling and functionally assessing cancer mutation phenotype at single cell resolution. This approach enables the broader assessment of cancer mutations impact on tumor biology and clinical ramifications.

#2929 Multiplexed somatic genome editing to model and investigate advanced colorectal cancer.

M. Mastel[1], R. Jackstadt[1], J. Meier[2], G. Diamante[1];

[1]DKFZ German Cancer Research Center, Heidelberg, Germany, [2]Heidelberg Institute for Stem Cell Technologies and Experimental Medicine, Heidelberg, Germany

Colorectal cancer (CRC) is among the deadliest cancers worldwide, with advanced CRC being the leading cause of death. For the development of novel therapy options, it is crucial to investigate mechanisms of advanced CRC in a bona fide way. However, little is known about the impact of distinct genomic alterations on cancer progression. The assessment of the function and role of the putative drivers in tumor progression via sequencing data remains challenging, due to the complexity and possible combinations of the candidates. Hence, genetically engineered mouse models (GEMMs) represent the mainstay for the investigation of the role of oncogenes and tumor suppressor genes in cancer progression. However, particularly in CRC, they are limited by imprecise modeling of cancer-associated changes, challenging scalability, and development of tumors in anatomically incorrect places. To tackle these issues, we developed SOmatic CRISPR-mediated genome Alterations of Tumor suppressors with Exploratory single cell Sequencing (SOCRATES) to analyze advanced CRC. We multiplexed CRISPR-Cas systems, packaged them into lentiviral particles, and delivered them to enterocytes via colonoscopy-guided submucosal injection. With this innovative approach, SOCRATES enables rapid and direct *in vivo* genome engineering for the modeling of advanced CRC with distinct mutational patterns and the investigation of the cancer cell states and tumor microenvironment (TME) upon editing the genes of interest. Similar to the Greek philosopher Socrates, who established a form of argumentized dialogue between individuals, SOCRATES facilitates the understanding of previously undiscovered communication between cancer cells and TME. We analyzed the influence of the most recurrent tumor suppressor mutations (*Fbxw7, Ptprt, Arid1a, Atrx, Atm, Smad4, Pten*) on the cancer cell state and TME in advanced CRC. Further, we created a TS-TME interaction atlas and revealed novel mechanistic insights into how the TS mutations rewire cell states and cell-cell communications. With this generated knowledge, SOCRATES will contribute to our understanding of complex tumor ecosystems and foster the improvement of diagnostic and therapeutic approaches.

#2930 Recovery of limited viable cells from low-quality precious samples for scRNA-seq.

Camila Egidio, Dinesh Bhosale, Lanxin Shen, Susana Jett, Amir Malek, Teddy de Groot, Suzanne Weaver, Gang Sun, **Josh Mahlios**, Kevin Travers, Geoff Facer

LevitasBio, Menlo Park, CA

Biomarker discovery is a critical milestone in pursuing personalized and targeted cancer treatments, yet it faces formidable challenges hindering success rates. Limited access to high-quality samples restricts in-depth biological investigation, with scarce and compromised viable cells acting as barriers to progress. Levitation Technology™ addresses these challenges by significantly improving sample quality and preserving maximum viable cells for single-cell RNA sequencing (scRNA-seq). This innovative approach overcomes limitations in sample quality and availability and heralds a new era of possibilities, propelling significant advancements in biomarker discovery for personalized cancer treatment.

To assess the performance of Levitation Technology using the LeviCell® 1.0 system, 105 cryopreserved samples derived from diseased human tissues were processed by Discovery Life Sciences™. This diverse sample set covered 20 disease indications, including 17 types of cancer. A staggering 70% of the samples (n=74) exhibited cell viability ranging between 14-69%, underscoring the need for enhanced viability for effective scRNA-seq analysis. Notably, 45 of these samples presented fewer than 500,000 cells, a scenario marked by low quality and limited viable cells. Traditional methods fail to recover viable cells from such samples without considerable or complete viable cell loss. After processing the samples with the LeviCell 1.0 system, all samples had improved quality, with an impressive 90% of the most difficult samples (n=40) presenting a viability increase to 70-94%, meeting the minimum quality criteria for scRNA-seq. A notable success story was a particular breast cancer sample with only 31,000 cells and 14% viability. Processing with the LeviCell 1.0 system yielded 13,300 viable cells and a substantial 4.5-fold increase in viability to 64%. Such enhancements in sample quality translate into significant improvements in scRNA-seq data quality, enabling more single-cell data extraction from each invaluable sample.

Levitation Technology represents a paradigm shift in sample processing, rescuing even the most challenging samples. This groundbreaking technology maximizes the retention of viable cells while efficiently eliminating dead cells and debris, factors that have traditionally compromised scRNA-seq data quality. By revolutionizing this aspect of sample preparation, Levitation Technology opens up unparalleled opportunities to explore deeper into disease biology, providing a leap forward in biomarker discovery.

#2931 Utilizing an extracellular matrix-embedded 3D tumor model of NSCLC to identify novel cancer dependencies via genome-scale CRISPR screen.

Pranay Agarwal, Soon Youn Choi, Xin Liu, Jina Song, Maya Tureez, Un Jae Baek, Aashka Mehta, Kyuho Han, Hong-Pyo Lee

MEDiC Life Sciences Inc., Mountain View, CA

INTRODUCTION: Non-small cell lung cancer (NSCLC) is a prevalent and deadly cancer type. Despite advances in targeted therapies in NSCLC, one-third of adenocarcinomas lack actionable oncogenes, limiting targeted therapy options. To address these challenges, CRISPR screening has emerged as a tool to unveil cancer dependencies. However, current genome-scale studies rely heavily on 2D monolayer cancer models that fail to replicate in vivo tumor biology due to altered gene/protein expressions, absence of cell-extracellular matrix (ECM) signaling, and rewired metabolic pathways. To overcome these limitations, we developed a high-throughput 3D extracellular matrix (ECM) based hydrogel culture platform suitable for conducting genome-scale CRISPR screening. Leveraging this platform, we performed genome-wide CRISPR loss of function screens in 3D tumor models in ECM (3D-ECM). These results were compared with the screening outcomes from 3D cultured cells lacking an extracellular matrix (3D-spheroids) and traditional 2D monolayer (2D-monolayer) cells to identify new genes that might be crucial in driving NSCLC tumor cells.

METHODS: Three NSCLC cell lines (NCI-H358, PC-9, and EKVX) were utilized for CRISPR screens. A genome-wide CRISPR library containing 60,000 sgRNAs targeting 20,000 genes was prepared. To create genome-scale 3D tumor models in ECM, cells were encapsulated in sub-millimeter microcapsules made of alginate and an extracellular matrix protein-hydrogel mix. Encapsulated cells were cultured for up to 4 weeks. 3D-spheroids were cultured on ultra-low attachment plates in viscous growth media and split every 3-4 days over 4 weeks.

RESULTS: Cancer cells' proliferation and metabolic activity notably increased in 3D-ECM compared to 3D-spheroids. The CRISPR screens in 3D-spheroids and 3D-ECM revealed numerous positive growth phenotypes in contrast to the conventional 2D monolayer culture model. Specifically, we found 79 additional genes exhibiting positive-growth phenotype in 3D-ECM. Moreover, prominent oncogenic drivers, such as KRAS and EGFR were ranked considerably higher in both 3D-ECM and 3D-Spheroids compared to the 2D-monolayer. Interestingly, the pathway-enrichment analysis revealed that Notch signaling (CREBBP, EP300, APH1A), FoxO signaling (STK11, TGFBR2, MAPK14), and Citrate cycle signaling (MDH2, SDHC, PDHA1) were enriched in 3D-ECM when compared to 3D-spheroids.

CONCLUSION: Our results reveal significant distinctions between the 2D monolayer model, the 3D spheroid model lacking extracellular matrix, and the 3D tumor model incorporating ECM. These differences underscore the importance of conducting CRISPR screens with 3D tumor models within the extracellular matrix to unveil novel cancer dependencies.

#2932 Computational discovery of paralog dependencies drives target identification in lung cancer.

S. O'Brien, A. H. Berger;
Fred Hutchinson Cancer Center, Seattle, WA

Lung cancer is the leading cause of cancer-related death in the United States, and worldwide, with the 5-year survival rate of non-small cell lung cancer at 24%. Treatment options are limited, and even in cancers that harbor druggable biomarkers, resistance is near-universal. Identifying novel treatment strategies is essential to improve the outcomes of patients with lung cancer and provide secondary strategies for those who acquire resistance to first-line therapeutics. Identifying targeted therapies based on the genotype or expression pattern of cancers is an ongoing endeavor. In lung cancer, treatment of patients that harbor activating mutations in EGFR with specific EGFR inhibitors has improved progression-free survival rates and extended the lifespan of patients diagnosed with this aggressive cancer, demonstrating the utility of targeted therapies based genetic-based vulnerabilities, or synthetic lethal interactions. A rich source of synthetic lethal genetic interactions are paralogous genes. Paralogs result from gene duplication events through evolutionary history, and many paralogs share both sequence homology and functional redundancy. Co-targeting of some paralogous genes induces a fitness defect that is synergistic compared to individual paralog loss alone. Nearly 70% of genes in the human genome are considered paralogs, and until recent efforts from the Berger lab and others, this buffering effect has caused them to be under-represented in lethality studies. Identifying frequently-inactivated paralog genes in lung cancer will provide a platform to identify new vulnerabilities in lung cancer and other cancer types that share mutational backgrounds. To identify patterns of mutation and expression of paralog genes in lung cancer, we have accessed publicly available data sets for both cell line and patient tumor samples. Using TCGA and CCLE data sources, and a set of 1030 paralog pairs identified previously by the Berger lab as potential drug targets, we have identified paralog genes that harbor high mutational frequencies in lung cancer. Using these candidates, we next asked whether genetic inactivation or transcriptional repression of one paralog influences the essentiality of its paired gene using CERES scores generated by the Cancer Dependency Map. Preliminary results identifies several paralog pairs with distinct dependency profiles in cell lines for which expression of one paralog is lost, including *MAGOH/MAGOHB* and *TLK1/TLK2*. Further work to characterize these dependencies in relevant cell line models is ongoing. Additionally, the druggability of these targets will be tested using targeted degradation using the dTAG system. This work will uncover a new set of paralog synthetic lethality targets, and further validate the utility of targeting known synthetic lethal paralogs for the treatment of highly lethal lung cancer.

#2933 Use of artificial intelligence to facilitate reporting of comprehensive genomic profiling tests.

H. Kage[1], T. Aoki[2], A. Shinozaki-Ushiku[1], K. Watanabe[1], N. Akiyama[1], H. Isago[1], M. Ogawa[1], K. Ishigaki[1], H. Kobayashi[1], T. Miyagawa[1], J. Omatsu[1], Y. Saito[1], K. Sasaki[1], Y. Sato[1], Y. Sato[1], N. Suzuki[1], S. Tanaka[1], M. Kato[1], M. Tanabe[1], K. Tatsuno[3], T. Ushiku[1], K. Nishimura[2], H. Aburatani[3], K. Oda[1];
[1]The University of Tokyo Hospital, Tokyo, Japan, [2]Xcoo, Inc., Tokyo, Japan, [3]The University of Tokyo, Tokyo, Japan

Background: Comprehensive genomic profiling (CGP) tests have been nationally reimbursed in Japan since 2019, and all test results must be discussed by molecular tumor boards (MTBs). More than 60,000 patients have taken the CGP tests at over 200 government-designated hospitals by November 2023. Streamlining decision-making by MTBs and standardizing interpretation of test results is important. We evaluated the performance of Chrovis, an annotation algorithm for reporting CGP tests.
Methods: We retrospectively reviewed the reporting process of all approved CGP tests done at The University of Tokyo Hospital and its 12 affiliated hospitals between December 2019 and November 2023. Chrovis referenced several public knowledge databases and used natural language processing to annotate each genetic variant and generated reports using the automated program. The MTB reviewed all reports with the addition of clinical information and made any necessary changes Recommendations on disclosure of germline findings were made in accordance with the national guideline.
Results: Among the 2,819 Chrovis reports created, 1,927 were tumor-only FoundationOne CDx (F1CDx), 483 were tumor/normal paired NCC Oncopanel (NOP), and 409 were FoundationOne Liquid CDx (F1Liquid) panels. Among them, 603 changes in 496 reports (17.6% of all reports) were made by the MTB. The most common type of change was germline disclosure with 208 changes (7.4%), followed by clinical trial information (196 changes, 7.0%) and pathogenicity (107 changes, 3.8%). Gene alterations that led to most changes in germline disclosure were *TP53*, *SMAD4, CDKN2A, TERT*, and *NF2* (42, 22, 16, 13, and 13 changes, respectively). Changes in clinical trial information were frequently observed in *TP53*, *NF1*, *BRAF*, *ERBB2*, and *KRAS* (25, 20, 19, 16, and 16 changes, respectively). F1CDx required the greatest number of changes (404/1927, 21.0%) followed by F1Liquid (53/409, 13.0%) and NOP (39/483, 8.1%) ($p < 0.001$). Changes to germline disclosure were made in 9.1% of F1CDx reports, 5.4% of F1Liquid reports, and 2.1% of NOP reports ($p < 0.001$). Changes to clinical trial information were made in 8.3%, 4.4%, and 3.9%, respectively ($p < 0.001$).
Conclusions: Chrovis-generated CGP reports did not require any changes in 82%s, suggesting that artificial intelligence reporting may lessen the burden of MTBs while contributing to its standardization. Recommendation for germline disclosure requires manual supervision, and improvements in clinical trial databases are required to correctly recommend genomically matched trials to patients.

#2934 Somatic variant workflow with HiFi sequencing provides new insights in highly challenging cancer cases.

K. Chua[1], I. McLaughlin[1], O. Hofmann[2], K. P. Stewart[2], P. Baybayan[1], J. Bibliowicz[1], S. Grimmond[2], Z. Kronenberg[1], M. A. Eberle[1];
[1]PacBio, Menlo Park, CA, [2]University of Melbourne, Melbourne, Australia

Tumor evolution is a highly heterogeneous process where multiple oncogenic pathways can lead to host defense evasion. Advancements in genome sequencing are allowing us to better understand these processes and their impact. However, critical genomic variations that could be pivotal to the development of tumors may have remained undetected due to technological constraints of short-read sequencing. PacBio HiFi sequencing generates accurate (>99.9%) long reads (>15 kb) with native 5-methylcytosine information that can comprehensively delineate many variations, including ones which were previously inaccessible with short-read sequencing. Unlike standard whole-genome analysis, cancer variant calling must account for somatic variation, where the assumptions of a diploid genome are violated. We have developed and optimized a bioinformatics workflow for somatic variant detection with HiFi sequence data. To validate this pipeline, we sequenced two well-studied cancer cell lines (COLO829, HCC1395) to 60-fold depth and their matched normal lymphoblast cells (40-fold to 60-fold depth) and called all classes of variations (SNVs, INDELS, and structural variants). Next, we compared our calls against the Valle-Inclan (structural variants) and SEQC2 (small variants : SNV/INDEL) datasets. We achieved 92% F1 score for small variants across all variant allele frequencies (VAF) in the HCC1395 experiment. We observed a maintained accuracy (F1=91%) even at lower variant frequencies (10-20), highlighting the ability of HiFi sequencing to detect subclonal mutations. The workflow calls structural variants with high sensitivity, capturing 57/62 (92%) of all previously validated SVs in COLO829 at all VAF. Lastly, we applied our pipeline to five diverse tumor samples that exhibit complex oncogenic phenotypes including homologous recombination deficiency (HRD) and high genomic instability, e.g. unresolved rearrangement breakpoints in repetitive regions and unknown oncogenic drivers when prior sequencing efforts did not provide full clarity as to the molecular drivers of tumorigenesis. Notably, we were able to identify and phase 5mC methylation of promoters together with large-scale structural variants in cancer genes involved in HRD. Taken together, we demonstrated the high accuracy of HiFi reads in resolving somatic variants and its potential to provide novel insights in complex cancer samples. The ability for long reads to resolve complex genomics aberrations and epigenetic markers that underly the tumorigenesis process will become indispensable in the realm of precision oncology.

#2935 NGS panel customization for comprehensive genomic profiling.

M. Ruvolo, A. Khare, N. Matcha-Balaguruvappa, K. Wilkins, L. Forsmark, S. Gupta;
Agilent Technologies, Santa Clara, CA

Introduction: We have developed a custom SureSelect Cancer design pipeline for the creation of target enrichment gene panels for comprehensive profiling of single nucleotide variations (SNP/INDEL), gene-level copy number variations (CNV), and DNA translocations (TL) as well as content for measuring of microsatellite instability (MSI) and tumor mutational burden (TMB).

Methods: The performance of individual probes was measured for the 679-gene SureSelect Cancer CGP panel and the information used to generate a reference database. When creating a new design, the gene list is cross-referenced with the database and when applicable, the probe information is applied to the new design. If genes are included in the custom design that are not present in the database, a second design algorithm selects the optimal probe based on its sequence characteristics (% GC, homology, etc.). Content is selected based on the biomarker to be measured and can be defined based on gene name (SNV/indel and CNV) or genomic coordinates (SNV/indel, TL). Pre-defined content for MSI measurement can be added to any design to cover 288 microsatellite sites. The performance of these sites in determining MSI status was demonstrated by comparing to the MSI-PCR reference method. To assess the performance of the design methodology, designs of various sizes (50 to 650+ genes) and content type were generated and assayed on reference samples and FFPE with known biomarkers. Sequencing metrics were evaluated for capture specificity and coverage of the target regions.

Results: The design methodology allowed for sub-selection of content present in the 679-gene SureSelect Cancer CGP assay as well as addition of de-novo content. The design algorithm uses empirical data on probe performance to provide robust and reproducible results for the range of supported design sizes. Biomarkers were reliably detected with SNV detection down to 1% allele frequency, detection of gene amplifications and translocations concordant with FISH, and MSI and TMB determination concordant with PCR and Exome sequencing respectively. The design workspace was implemented in the SureDesign platform, providing a web-based interface for creating the designs.

Conclusions: We demonstrated full customization capability of the SureSelect Cancer target enrichment platform that pairs user-defined content with an optimized probe design methodology to enable the sensitive detection of the common types of DNA alterations found in FFPE samples.

#2936 Nanopore adaptive sampling detects nucleotide variants and improves large scale rearrangement characterization for diagnosis of cancer predisposition.

S. Chevrier[1], C. Richard[1], M. Mille[2], D. Bertrand[2], M. Blum[2], N. Philippe[2], **R. Boidot**[1];
[1]Ctr. Georges-Francois Leclerc, Dijon, France, [2]SeqOne Genomics, Montpellier, France

Molecular diagnosis has become highly significant for patient management. Facing new challenges to generate more comprehensive data in reduced time and cost, we tested Nanopore (ONT) adaptive sampling to analyze a gene panel for germline predisposition to cancer.
We tested 30 clinical germline samples carrying known alterations on BRCA1, BRCA2, PALB2 and MLH1 genes to detect large scale rearrangements (LSR) and single nucleotide variants (SNV). We used adaptive sampling to enrich the full sequence (from promoters to 3'UTR) of 152 cancer predisposition genes on ONT R10.4.1 MinION flowcells and the Q20 chemistry. The analysis was performed using the long-read bioinformatics pipeline developed by SeqOne Genomics. We observed a mean enrichment of 7.85 (3.91-9.85) and a mean coverage on target genes of 14.73X (4.71-35).
In our cohort, 11 samples had LSR that were all detected with ONT sequencing. In addition to perfectly detect the locus of the LSR (starts and stops always in intronic regions), we discovered that a known MLPA amplification of exon 13 in the BRCA1 gene was in fact an amplification of both exons 12 and 13. This 2-exon duplication was also confirmed on a patient's relative, originally diagnosed with an exon 13 duplication as well. Another LSR was a total deletion of the BRCA1 gene. ONT sequencing highlighted this complete deletion of BRCA1 was the consequence of a large deletion of almost 140 kbp carrying 5 different genes (BRCA1, IFI35, NBR2, RND2, and VAT1).
ONT sequencing was also able to detect all class-5 SNVs (point mutations and small indel) present in 16 patient samples at low coverage (between 6 and 27X). We faced bioinformatics detection issues for 3 mutations located in homopolymer regions using standard pipelines. These were all confirmed correctly when visualizing the raw data.
As we analyzed complete genes and more genes than with short read sequencing, we detected novel unknown variants. To check the reliability of those novel variant by ONT, we wondered whether we could confirm results obtained at a low coverage (10X) with average quality (Phread score >/= 15). For that we randomly selected 8 new variants we analyzed by Sanger sequencing, and all of these were confirmed, suggesting that variants detected with ONT, even at a 10X coverage and a Phread score higher than 15, could be considered as real variants.
In conclusion, we showed that ONT adaptive sampling sequencing is suitable for the analysis of germline alterations. It improves the characterization of LSR and is able to detect SNV even at low coverage. Nevertheless, an improvement of bioinformatics detection of variants located in homopolymer regions should be considered. A larger comparison study between ONT adaptive sampling and short read sequencings should be performed on hundreds of samples to adapt international guidelines to third generation sequencing for germline diagnosis.

#2937 Accurate detection of human papillomavirus breakpoints in cervical cancers using a novel library preparation strategy for nanopore sequencing technology.

P. Parida[1], N. Mukherjee[2], A. Singh[2], A. Singh[3], K. Sharan[1], M. Rao[4], S. Lewis[1], S. Radhakrishnan[2], R. R. Damerla[1];
[1]Kasturba Medical College, Manipal, Manipal Academy of Higher Education, Manipal, India, [2]National Centre for Biological Sciences, Tata Institute of Fundamental Research, Bengaluru, India, [3]Manipal School of Life Sciences, Manipal Academy of Higher Education, Manipal, India, [4]Manipal College of Pharmaceutical Sciences, Manipal Academy of Higher Education, Manipal, India

Introduction: Integration of human papillomavirus (HPV) DNA into the human genome is considered as a key event in cervical carcinogenesis. Different methods have been employed in exploring HPV integration sites, such as APOT, DIPS-PCR, and NGS. However, these methods have their drawbacks. APOT heavily relies on the quality of the sample due to its dependence on RNA, while DIPS-PCR mostly identifies known sites and has limited capability in uncovering new integration sites. Although the detection sensitivity of virus infection status increased significantly through the Illumina sequencing platform, there were still disadvantages remain for further improvement, including the detection accuracy and the complex integrated genome structure identification, etc. Also, it requires large amounts of sequencing data, and thus is not applicable in clinical usage, which requires fast and accurate results. Therefore, the development of a new method for HPV integration detection with high accuracy and prompt reporting capacity is crucial for future clinical application.
Methods: We established a novel library preparation strategy for the detection of HPV integration in the human genome using Oxford Nanopore sequencing. Using this novel technology, Nanopore libraries were prepared from HPV positive cell lines HeLa and SiHa followed by sequencing on the Oxford Nanopore. We also determined HPV integration sites in five patients with cervical cancer patients with HPV positive tumors using Ilumina WGS. HPV integrations and breakpoints in human genome from both Nanopore and Ilumina WGS were extracted using Minimap and ViFi tool respectively. All HPV integration sites from cell lines and patient samples were validated using Sanger sequencing.
Results: The novel library preparation approach for detection of HPV integrations with Nanopore sequencing technology were sensitive and efficient in detection of commonly reported HPV breakpoints in HPV positive cell lines HeLa and SiHa. Additionally, we applied this method to clinical samples from five patients subjected to Whole Genome Sequencing, consistently yielding concordant results.
Conclusion: Our Nanopore based assay for detecting HPV integrations without the need for WGS demonstrated high efficacy. These data highlight the sensitivity and efficiency of this methodology in detecting HPV integrations events, emphasizing its potential as a reliable diagnostic tool in understanding pathophysiology of HPV-related malignancies and its use as prognostic markers in clinical settings.

#2938 Comprehensive genomic profiling of solid tumor patients with the OncoDEEP assay for broad analysis in clinical diagnostics.

E.-J. M. Speel[1], P.-J. Volders[2], J. Van der Meulen[3], A. De Cock[3], S. Vermeire[4], J. Van Huysse[4], M. De Barsy[5], G. Beniuga[5], W. de Leng[6], A. Jansen[6], S. Thijssen[1], **H. Dubbink**[7], Z. Ozgur[8], W. van Ijcken[8], B. Maes[2], G. Froyen[2];

[1]Maastricht University Medical Center, Maastricht, Netherlands, [2]Jessa Hospital, Hasselt, Belgium, [3]Ghent University Hospital, Ghent, Belgium, [4]AZ Sint-Jan Brugge AV, Bruges, Belgium, [5]Institute of Pathology and Genetics (IPG), Gosselies, Belgium, [6]University Medical Center Utrecht, Utrecht, Netherlands, [7]Erasmus MC Cancer Institute, Rotterdam, Netherlands, [8]Erasmus University Medical Center, Rotterdam, Netherlands

Somatic multi-gene analysis by Next Generation Sequencing (NGS) becomes standardly integrated in medical oncology for clinical decision making. However, with the fast-growing number of recommended and required genomic biomarkers, small panels have become vastly insufficient for most tumor types. Comprehensive Genomic Profiling (CGP) is amenable to screen for single nucleotide variants (SNVs) and subtle insertions and deletions (indels) in several hundreds of genes. Moreover, it provides information on copy number variations (CNVs) and gene fusions of the most relevant genes for optimal patient management. Currently, most comprehensive panels also allow for screening of tumor-agnostic genomic biomarkers, including microsatellite instability (MSI), tumor mutation burden (TMB) and homologous recombination deficiency (HRD), which are implemented as prognostic and therapeutic signatures in a wide variety of solid tumors. So far, only a handful of CGP assays have been validated for their diagnostic utility in routine laboratory practice for the care of cancer patients. In this study we report on an extensive multicentric analysis across multiple centers in Belgium and The Netherlands comparing the novel OncoDEEP CGP assay (OncoDNA) with the diagnostically validated TSO500 assay (Illumina). We describe the technical differences between both assays as well as their outcome and shortcomings. Detection of clinically relevant SNVs, indels and CNVs was very similar and differences were often due to assay-specific settings. Similarly, TMB, MSI and HRD data were concordant for most samples but those with scores close to the cut-offs could deviate. For fusion detection, concordance was found for the limited number of 11 clinically-actionable driver genes covered by the OncoDEEP kit. The uniformity of coverage was much higher with the OncoDEEP assay thereby allowing to pool 2- to 3-times more samples per NGS run. For the diagnostic implementation of the OncoDEEP assay we then performed an extensive validation with clinical samples representing a wide variety of solid tumor types, as well as reference samples. All performance metrics passed the validation criteria. In conclusion, the OncoDEEP kit can be used for reliable diagnostic comprehensive profiling of solid tumors, but currently, extensive fusion analysis requires an additional screening method.

#2939 Harnessing *in vivo* CRISPR screen to uncover metabolic dependencies during cancer progression.

S. Ng[1], Z. Wu[1], J. A. Lidster[2], W. Tam[1];

[1]Genome Institute of Singapore, Singapore, Singapore, [2]Cancer Science Institute of Singapore, Singapore, Singapore

Triple-negative breast cancer (TNBC) is the most aggressive subtype of breast cancer, with the worst prognosis and limited treatment options. TNBC cells undergo metabolic reprogramming in response to nutrient limitations and changes in the tumor microenvironment throughout cancer progression. In the early stages, tumor cells are found to prioritize nutrient uptake and biosynthesis, but as they grow, intensified competition for nutrients fosters the emergence of subpopulations of cancer cells that excel in utilizing specific nutrients. The substantial metabolic pathways and genes that regulate each phase of cancer progression remain poorly understood. To address this, we have developed a stable integration, site-specific, and inducible CRISPR-Cas9 system that allows for temporal control of genetic perturbation. We conducted an unbiased *in vivo* loss-of-function CRISPR screen aimed at identifying metabolic vulnerabilities at different phases of cancer progression of TNBC. The inducible CRISPR system was activated only at the desired study period of each phase, thus capable of uncovering metabolic dependencies for TNBC proliferation at each distinct phase of cancer progression. As many large-scale CRISPR screens have previously been performed to identify gene dependencies for cancer progression *in vitro*, our CRISPR screen could address the shortcomings of *in vitro* screens by identifying novel essential metabolic genes that are significantly important for cancer growth *in vivo*. Preliminary data from our CRISPR screen revealed different pathways to be significantly important for tumor growth and proliferation at different phases of TNBC progression. For example, we find that ferroptosis is altered during the early lag phase of TNBC cancer progression, whereas, at the later stage of cancer progression, metastatic tumors upregulate serine metabolism, suggesting that secondary tumors could have distinct metabolism from the primary sites. Altogether, the findings from this study could provide valuable insights into stepwise metabolic dependencies arising from microenvironmental limitations and identify potential therapeutic targets at each phase of cancer progression. Moreover, our CRISPR-Cas9 model holds promise for dissecting the complex mechanisms of other cancer progressions.

#2940 A comparative analysis of library preparation technologies for RNA sequencing from FFPE samples.

J. Pavlica, T. Sanders, D. Gelagay, K. Reed, T. Harrison, **G. Corbet**, J. Haimes, A. Hanek, K. Giorda, B. Kudlow;
Watchmaker Genomics, Inc., Boulder, CO

Formalin-fixed, paraffin-embedded (FFPE) samples are an invaluable resource in the oncology space, providing access to a vast library of archived diseased tissue samples paired with relevant donor information. Despite the broad utility of these samples, RNA extracted from FFPE tissue is typically difficult to process due to the presence of residual crosslinks and its degraded nature. Further, these samples often vary widely in performance, as the fixation process, block age, block storage, and extraction method can impart large impacts on resulting template quality. As a result, robust and reproducible RNA sequencing from FFPE-derived RNA remains a challenge with unpredictable and high failure rates. We evaluated four commercially available WTA solutions to determine which performed best with this challenging sample type with respect to library complexity, inter-input and intra-sample concordance, and overall reproducibility. Matched fresh frozen and FFPE liver samples were used such that the fresh frozen data set serves as a comparative truth set for the FFPE data. RNA-Seq libraries were prepared from each sample at both 10 ng and 100 ng inputs. The higher input serves as a control while the lower input reflects achievable inputs from very challenging FFPE samples. For 10 ng FFPE-derived RNA, the Watchmaker RNA Library Prep Kit with Polaris Depletion detects more unique genes than other chemistries and has a much higher percentage of genes that overlap with the fresh frozen control libraries. Additionally, differential expression analysis between 10 ng and 100 ng FFPE libraries demonstrates that the Watchmaker solution better preserves the gene expression profile at low inputs, as fewer differentially expressed genes are identified.

The Watchmaker chemistry includes a number of features aimed at improving library complexity, including a novel FFPE decrosslinking step, a reverse transcriptase specifically engineered to improve conversion of RNA to cDNA, and fewer bead purification steps to prevent sample loss. The concordance between FF and FFPE samples at variable input masses observed when using the Watchmaker solution promotes a higher degree of confidence when making decisions based on lower quantity and quality samples and enables researchers to access more meaningful biological information.

#2941 A novel gene signature predicting fibroblast composition in the TME allows for an improved selection of patient-derived xenograft (PDX) models for preclinical studies.

Mara Gilardi, Gilad Silberberg, Hsiu-Wen Tsai, **Stefano Cairo**, Clare Killick-Cole, Michael Ritchie

Champions Oncology, Inc. (Hackensack, NJ), Hackensack, NJ

The Tumor MicroEnvironment (TME) plays a pivotal role in driving tumor progression, metastasis, and therapeutic resistance through diverse mechanisms. Notably, the TME influences the response to therapy by regulating immune surveillance evasion in tumor cells. Fibroblasts can play a significant role in resistance to therapy. In the context of cancer cancer-associated fibroblasts (CAFs) in the TME have been associated with resistance to various therapeutic approaches. CAFs can contribute to therapy resistance through multiple mechanisms, including extracellular matrix remodeling, immune modulation, angiogenesis and paracrine signaling. Understanding the intricate interactions between fibroblasts and cancer cells is crucial for developing more effective therapeutic strategies and overcoming resistance in cancer treatment. In the pre-clinical stages of therapy testing, the use of clinically and biologically relevant models is essential. However, current preclinical tumor models often lack a comprehensive characterization of the TME. To address this limitation, Champions Oncology utilized transcriptomic data from its exclusive TumorGraft models bank to develop a signature predicting TME composition. Validation involved confirming the predicted TME composition through histological analysis of Patient-Derived Xenograft (PDX) models grown in humanized mice. In an immune-competent host, the Tumor Microenvironment (TME) of the model more accurately replicates the conditions observed in cancer patients. PDX) models are recognized as accurate and clinically relevant for pre-clinical studies. Consequently, Champions Oncology built its pre-clinical research on a deeply characterized PDX bank, employing multi-omic datasets, including WES ,RNAseq, proteomics, phospho-proteomics, kinase activity, and patient treatment history. To identify molecular signatures predictive of fibroblast presence, Champions analyzed the data with xCell^{3} computational method. Concurrently, mice were humanized, and high and low infiltration predicted PDXs models were implanted. Tissues were collected and stained for fibroblast populations. Immunohistochemistry analyses confirmed a strong correlation between the infiltration predicted by the molecular signature and positive staining. The application of this method to Champions' model bank provided a comprehensive understanding of the TME profile, culminating in the definition of a gene signature predictive of fibroblast infiltration. Histological analysis validated the computational findings, creating a TME atlas of the PDX bank. This data support the use of the pre-defined molecular signature, facilitating the pairing of ideal model systems with appropriate humanized hosts for future preclinical studies.

#2942 Deciphering histological subtype-associated cellular and molecular characteristics of lung adenocarcinoma using single-cell RNA sequencing and spatial transcriptomics.

J. Lee[1], J. Jeong[2], M. Hong[2], H.-G. Kang[2], J. Choi[2], J. Kim[1], Y. Choi[1], J. Kim[1], **S. Lee**[2];
[1]POSTECH, Pohang, Korea, Republic of, [2]Kyungpook National Univ. School of Med, Daegu, Korea, Republic of

Lung adenocarcinoma (LUAD) is the most frequently observed subtype found in non-small cell lung cancer (NSCLC). Despite its high prevalence, the molecular and histological heterogeneity in LUAD pose a significant challenge for providing effective patient care and aiming to reduce the high mortality rate. The histopathological classification proposed by WHO in 2015 describes five histologic patterns of lung adenocarcinoma (lepidic, acinar, papillary, micropapillary, and solid), and it has been shown that the existence of high-grade subtypes (micropapillary and solid) is associated with poorer survival outcomes. Nevertheless, the specific cellular and molecular mechanisms responsible for these clinical outcome differences based on distinct histological patterns remain unclear. Here, we conducted single-cell RNA sequencing (scRNA-seq) to unveil insights into the tumor microenvironment (TME) and identify cancer cell biomarkers associated with distinct histological patterns. Our study involved 18 specimens from primary LUAD patients who underwent surgical resection, all of whom were previously untreated. These specimens were classified into three groups: acinar/papillary (A/P), micropapillary (MP), and solid. Remarkably, patients with solid-type tumors showed a notable enrichment of CD8+ T cell exhaustion, alongside a significant abundance of GPNMB-high macrophages in the myeloid compartment. Additionally, macrophages from the solid-type demonstrated cholesterol-efflux activation, particularly in alveolar macrophages. It is well-known that cholesterol efflux-activated macrophages display a tumor-associated macrophage phenotype, contributing to immunosuppression in the TME. In contrast, the A/P group exhibited a higher enrichment of mast cells compared to the solid-type. This suggests that the solid-type tumor landscape is more immunosuppressive than the A/P group. In the context of cancer cells, we identified that A/P cancer cells displayed a well-differentiated pattern with a high alveolar epithelial type II cell (AT2) signature. In contrast, solid-type cancer cells showed poorly differentiated states, coupled with a significant activation of the epithelial-mesenchymal transition (EMT) process. Remarkably, even within A/P patients, those with a small portion of solid patterns in the tumor tissue showed higher clonal complexity compared to patients without any solid pattern. Furthermore, we found that cancer cell plasticity can be regulated by cell-cell interactions in the TME. Collectively, this study unveils the relationship between histological patterns and the TME, encompassing distinct immune responses and molecular characteristics of cancer cells in LUAD. These findings provide valuable insights for potential targeted therapeutic strategies.

#2943 Investigation of microsatellite instability in RNA compared to DNA, using microsatellite targeted, anchored multiplex PCR and NGS.

R. Rogge, T. Patterson, A. Navetta, D. Legare;
Integrated DNA Technologies, Inc., Boulder, CO

MSI measurements are typically made on DNA, but it would be useful to make similar measurements from RNA or total nucleic acid inputs (TNA), so that MSI determinations could be made in parallel to interrogation of the RNA. Doing so requires characterizations of microsatellite lengths from those which are transcribed and untranscribed, because both will be detected following cDNA creation. Microsatellite instability (MSI) occurs when small unit repeats of DNA undergo incorrect replication resulting in the growth or contraction of the number of repeats in the newly synthesized DNA. This accumulation of errors at microsatellite DNA is usually mitigated by the mismatch repair (MMR) pathway which can correct these errors. MSI is of interest because it serves as a phenotypic readout of the status of the MMR machinery, and MSI status can correlate to tumor progression and response to agents that regulate these cellular mechanisms. We investigated the status of microsatellites using Anchored Multiplex PCR (AMP™) targeted panels (RUO) and compared results from TNA inputs using an AMP MSI module and both VARIANT*Plex*™ chemistry to interrogate DNA, and FUSION*Plex*™ chemistry to interrogate both RNA + DNA. Our results indicate differences in the diversity of lengths of microsatellites present in RNA, and the resulting stability calls which would be made at those sites. Microsatellite length diversity was highly dependent on the genomic context of the microsatellite. Microsatellites located within transcripts showed increased length diversity when examining the RNA + DNA results compared to DNA alone. Microsatellites located in intergenic regions, which are unlikely to be transcribed, showed no increase in diversity of lengths when comparing the RNA + DNA results to DNA alone. While these results suggest that MSI determinations could be made from RNA or RNA + DNA NGS data, the unique behavior of microsatellites in RNA is likely to require additional investigations and unique data analysis techniques to correctly categorize microsatellites as stable or unstable.

#2944 A high-throughput screening system for identifying therapeutic targets in immuno-oncology.

Dippal Parikh, Soon Youn Choi, Ki Eun Pyo, Hong-Pyo Lee, Kyuho Han

MEDiC Life Sciences Inc., Mountain View, CA

INTRODUCTION: Over the last decade, cancer immunotherapy has revolutionized cancer treatment. However, more than half of patients don't respond, and responders often lack lasting effects. Understanding how genetic variants in cancer cells influence their interaction with immune cells, especially T cells, is crucial to uncover underlying mechanisms. Genetic screens are powerful for uncovering responsible genes for various phenotypes, but challenges in obtaining ample samples to set up a proper immune and cancer co-culture system have limited their use for identifying immune modulators in cancer: primary mouse T cells expressing CD3 against a specific antigen (typically albumin) need to be extracted from transgenic mice and only syngeneic mouse cancer cell lines that match these T cells can be paired, restricting the utilization of human T cells and human cancer cells for this co-culture screening setup.
METHODS: Here, we present a highly scalable co-culture system that enables genome-wide CRISPR screens on a pair of human primary T cells and any allogeneic human cancer cell lines. This system utilizes the expression of a membrane-targeted protein in mammalian cells, named as ImBridge, which directly engages and activates CD3+ immune cells. This mechanism bypasses the need for matched MHC on target cancer cells.
RESULTS: We validated activation of CD3+ immune cells and selective cancer cell cytotoxicity by ImBridge. A genome-scale CRISPR screen utilizing the co-culture system unveiled known immune-oncology targets including PD-L1 and PTPN2 and revealed MEDiC_01 as a novel therapeutic target. Genetic loss of MEDiC_01 in cancer cells significantly sensitized them to cytotoxic cells, effectively eliminating cancers in the presence of human PBMCs.
CONCLUSION: We demonstrated a scalable and efficient approach for conducting high-throughput functional screens to uncover genes that modulate interactions between effector T cells and target cancer cells. This can facilitate the identification of new immuno-oncology therapeutic targets, insights into underlying mechanisms, and genetic factors influencing immune susceptibility and evasion.

#2945 Using pooled minimal genome-wide sgRNA libraries to drive oncology drug discovery.

S. Lukasiak[1], A. Kalinka[2], N. Gupta[2], K. Saeed[2], A. Papadopoulos[1], U. McDermott[1], G. J. Hannon[3], D. Ross-Thriepland[1], **D. Walter**[2];
[1]AstraZeneca, Cambridge, United Kingdom, [2]Cancer Research Horizons, Cambridge, United Kingdom, [3]Cancer Research UK Cambridge Institute, Cambridge, United Kingdom

The emergence of CRISPR technologies has enabled rapid and precise gene editing opportunities. The Functional Genomics Centre (FGC) - a joint venture between Cancer Research UK's (CRUK) drug discovery engine, Cancer Research Horizons, and AstraZeneca has been launched to better utilize and improve the CRISPR technology within cancer research. The FGC leverages the strengths of both CRUK's and AstraZeneca's world-class oncology research and drug discovery experience, with the potential to drive scientific innovation in how new drug targets are identified and validated, and uniquely democratize access to the latest cutting-edge research tools and expertise for many thousands of scientists and clinicians funded by CRUK.
Here, we will showcase how the FGC is leading the development and refinement of functional genomics technologies. Through independent evaluation of publicly available CRISPR tools and leveraging this data we have designed optimized, minimal genome-wide CRISPR libraries. These libraries permit a reduction of the experimental scale of CRISPR screens by 50% and enable our Target Discovery platform to impact more projects, faster, at a lower cost and importantly - more sustainably.

#2946 Characterizing the genomic landscapes of breast and lung tumors using cost-effective whole genome sequencing.

H. Benjamin[1], I. Soifer[1], D. Shem-Tov[1], M. Levy[1], I. Tuncay[2], B.-L. Oh[2], J.-Y. Shin[2], Y. Ju[2], S. Lee[2], O. Barad[1], D. Lipson[1];
[1]Ultima Genomics, Fremont, CA, [2]Genome Insight Inc., San Diego, CA

Whole Genome Sequencing (WGS) has emerged as a pivotal tool for unraveling the intricate genomic alterations underlying cancer, enabling the detection of a broad spectrum of somatic changes in cancer genomes, including single nucleotide variants, insertions, deletions, copy number variations, and structural rearrangements. Characterizing somatic variants across the entire genome significantly benefits from novel cost-efficient sequencing platforms, such as UG100. In the current study, we aim to demonstrate the utility of UG100 WGS in characterizing the landscape of somatic events in breast and lung cancer.
Over 35 tumor-normal cancer sample pairs were profiled using UG100 WGS (mean tumor coverage: >100x; normal: >50x). Variant calling was done using a somatic deep-variant algorithm, optimized to UG100 data. Results were compared to Illumina sequencing and high concordance was observed, with over 97% of SNVs and over 93% of indels detected by Illumina identified also by UG100. UG100 sequencing was deeper and allowed for identification of a larger number of genomic variations, including known driver events in cancer-related genes. The somatic mutational signatures by UG100 were concordant with the Illumina platform, with a cosine similarity higher than 99%. Copy number variation and structural variation analysis was performed on all sample pairs, revealing a wide range of genomic aberrations.
The integration of genetic sequencing into routine clinical oncology practices has proven instrumental in identifying actionable mutations, predicting treatment responses, and monitoring minimal residual disease. Moving from targeted sequencing to WGS provides a more comprehensive and unbiased assessment of the entire genome, uncovering rare or unexpected mutations that might be missed by targeted approaches. WGS allows for the simultaneous evaluation of both coding and non-coding regions of the genome, providing a deeper understanding of the regulatory elements influencing gene expression. This broader scope enhances our understanding of cancer biology and contributes to a more accurate assessment of the tumor's functional landscape.

#2948 Unveiling hidden genomic diversity: Exploring epigenetic potential and gene expression in African Pan Genome contig sequences.

R. Martini[1], K. Founta[2], S. Maurice[3], J. White[1], O. Balogun[4], N. Chambwe[2], M. Davis[1];

[1]Morehouse School of Medicine, Atlanta, GA, [2]Northwell Health, Hempstead, NY, [3]City College of New York, New York, NY, [4]Weill Cornell Medical College, New York, NY

An important consideration when studying cancer in diverse populations is the representativeness of the reference genome. Cancer genomics findings are largely based upon alignments to GRCh37 and GRCh38 references, and with the recent release of the telomere-to-telomere (T2T) and the Human Pangenome Reference Consortium references, analyses of sequences distinct from previous references in the cancer context provide exciting opportunities to identify novel targets that may be linked to cancer outcomes. Because GRCh38 and T2T are overwhelmingly Eurocentric, the question remains if these references have applicability outside the ancestral populations that comprise them. Prior to T2T and pangenome, whole genome sequencing of 910 individuals of African descent revealed 296.5 million distinct base pairs, which were assembled into 125,715 African Pan Genome (APG) contigs. These unique sequences represent African ancestry novel genomic sequences whose function was unclear. Here we present provisional efforts to determine the function of APG contigs, and whether they are represented in newer references. To determine the epigenetic potential of the 125,715 APG contigs, we used Emboss Cpgplot to predict CpG islands. We identified 8,353 potential CpG islands, where 6,352 contigs had at least 1 predicted CpG island, and 1 contig had 9. There was weak correlation between contig length, GC content and number of predicted CpG islands suggesting that these sequences represented potentially functional regions. Using unmapped transcriptomic reads from our published African ancestry triple negative breast cancer cohort, we sought to determine the expression potential of these contigs. Unmapped reads mapped to ~9% of the contigs, where ~1100 APG contigs had both predicted CpG islands and alignment of the unmapped transcriptomic reads. This strongly suggests that these APG contigs contain African ancestry-specific regulatory regions and functional gene coding sequences. Preliminary BLASTn queries of contigs with regulatory potential revealed that these sequences may be present in T2T. Mapping to T2T and visualization of expression and CpG islands showed that our predictions matched novel T2T sequences. We anticipated some contigs would map to T2T given one- or two-end placement in GRCh38 and wanted to determine if any of the ~1100 contigs mapped to T2T. Initial analysis of this contig subset shows ~15% fail to map to T2T, indicating that T2T may still fail to capture diversity across ancestry groups. These sequences represent previously unstudied expression and epigenetic potential not captured in the reference genome, and we are working to evaluate all 125,715 sequences. Capturing the diversity across the genome remains extremely important to contextualize these findings and build resources to continue moving precision medicine approaches forward across diverse ancestry groups.

#2949 A flexible and efficient approach for single-cell CRISPR perturbation screens combined with targeted RNA-seq expression analysis.

D. Tedesco, T. Liu, M. Makhanov, D. Hu, **N. Isachenko**, P. Diehl, A. Chenchik;
Cellecta, Inc., Mountain View, CA

This study presents a novel approach for performing 10X platform-based targeted single-cell RNA-seq analysis in combination with CRISPR perturbation screens. For the analysis, we constructed a custom sgRNA library focused on a small subset of genes associated with the TNFα response (i.e., NFκB pathway). We compared analysis of two targeted gene expression panels—the first, targeting all protein-coding genes (genome-wide) and the other, targeting a selected set of genes representing key hubs in signaling pathway modules. Narrowing down the analyzed gene set enhanced the efficiency of single-cell RNA-seq by reducing the associated next-generation sequencing (NGS) depth required for readout, and significantly streamlining data analysis. Comparing the analysis of the expression panels targeting all protein-coding genes with the smaller pathway-targeted set, we were able to assess the general flexibility of the novel approach for single-cell CRISPR perturbation screens. We evaluated the specific tradeoffs with regard to the size of the CRISPR library, the size of the panel of genes targeted for expression analysis, and NGS sequencing depth. This flexible, targeted approach not only refines the precision of RNA-seq but also provides a more cost-effective solution for comprehensive genomic analyses.

#2950 CRISPR/saCas9 and CRISPR/spCas9 systems for combinatorial genetic screens (CRISPR-KO, CRISPRa, CRISPRi).

N. Isachenko, G. Aleksanyan, P. Diehl, D. Tedesco;
Cellecta, Inc., Mountain View, CA

This study explores the utilization of orthogonal CRISPR-based gene editing/modulation systems for combinatorial genetic screens using CRISPR knockout (CRISPR-KO), CRISPR activation (CRISPRa), and CRISPR interference (CRISPRi) functionalities. *S. aureus* (sa)Cas9 is an alternative nuclease to *S. pyogenes* (sp)Cas9 in scenarios where the latter cannot be used, or when multiple independent CRISPR systems need to be simultaneously expressed in the same cell. In this study we set out to explore the feasibility of utilizing different combinations of saCas9 and spCas9 CRISPR systems to achieve the simultaneous inactivation (via CRISPR-KO or CRISPRi) and transactivation (via CRISPRa) of different target genes in the same host cell. For this purpose, a complete set of tools for CRISPR/saCas9 gene editing and gene modulation was developed, compatible with CRISPR/spCas9 co-expression. Specifically, we developed and validated optimized saCas9 and sg(sa)RNA lentiviral and AAV vectors, dual expression (sp)/(sa)sgRNA lentiviral library vectors, as well as (sa)CRISPR-KO, (sa)CRISPRi, (sa)CRISPRa fluorescence-based activity kits for the functional validation of saCas9 expressing cell lines. Results demonstrating the feasibility of the orthogonal screens will be presented, with different combinations of CRISPR-KO, CRISPRa, and CRISPRi systems in multiple cell lines.

MOLECULAR/CELLULAR BIOLOGY AND GENETICS: Cellular Stress Responses 2
Poster Session

#2954 Androgen deprivation therapy (ADT) and senescence-associated secretory phenotype (SASP) *in vitro*: Correlation with SASP in tumor specimens as well as in the serum of patients after ADT.

M. Schwermann[1], M. Hadfield[2], S. Lu[2], P. Srinivasan[1], V. Tajiknia[1], W. MacDonald[1], A. George[3], S. Zhang[1], L. Zhang[1], K. S. Meza[1], A. De Souza[2], D. Golijanin[2], E. Hyams[2], G. Lagos[2], S. Holder[2], A. Mega[2], J. Sedivy[1], H. Safran[2], W. El-Deiry[2], B. Carneiro[2];
[1]Legorreta Cancer Center at Brown University, Providence, RI, [2]Legorreta Cancer Center and Lifespan Cancer Institute at Brown University, Providence, RI, [3]Yale School of Medicine, New Haven, CT

Introduction: Androgen Deprivation Therapy (ADT) is a highly effective treatment for prostate cancer. However, resistance to ADT develops in most patients, leading to a lethal state of castration-resistant prostate cancer (CRPC). Senescent prostate cancer (SPC) cells can arise after ADT and contribute to therapy resistance. SPCs can restore replicative function and alter the tumor microenvironment through pro-tumorigenic senescence-associated secretory phenotype (SASP). We aimed to characterize changes in SASP in prostate cancer cell lines and serum samples from patients receiving ADT.
Methods: SASP factors (Luminex 100/200 System, xMAP Instruments) were analyzed in patients undergoing ADT. To correlate SASP with the sensitivity to ADT, we sought to evaluate the regulation of SASP in vitro using PCa cell lines. The PC3 (AR resistant) and LNCaP (AR sensitive) cell lines were used in the experiments. We performed an analysis of archival tumor tissue (paired) from 18 patients with or without alterations in DNA repair genes (BRCA1, BRCA2, and CDK12). We performed immunohistochemical (IHC) staining of known SASP markers, such as P16, uPAR, gamma-H2AX, and Lamin B1.
Results: In a cohort of patients (n=8) with pre and post-ADT matched status, we demonstrate increased levels of SASP factors such as IL-6 (pre-ADT: 1.54±0.24 pg/ml, post-ADT: 5.23±1.3 pg/ml p=0.001), IL-7 (pre-ADT: 3.11±0.6 pg/ml, post-ADT: 13.5±2.7 pg/ml p=0.01), IL-1 alpha (pre-ADT: 1.06±0.3 pg/ml, post-ADT: 15.3±3.5 pg/ml p=0.001), IL-15 (pre-ADT: 15.6±3.1 pg/ml, post-ADT: 37.1±4.8 pg/ml p=0.002), MIF (pre-ADT: 1036±67.6pg/ml, post-ADT: 2362±55.5 pg/ml p=0.003), and IL-15 (pre-ADT: 5±2.1 pg/ml, post-ADT: 37.5±5.1 pg/ml p=0.002). In vitro, the AR-responsive LNCaP cell line, exposed to AR blockade, showed similar findings in upregulating IL-6, IL-7, and IL-15 but not the PC3 cell line. We also demonstrate measurable differences between the expression of u-PAR, gamma-2AX, p16, and loss of Lamin B1 expression in tumor specimens from patients with advanced castration-resistant prostate cancer (n=18). The expression of p16 was significantly upregulated post-treatment irrespective of DDR status (p=0.0417). Other SASP factors showed a trend in upregulation but were insignificant (u-PAR p=0.056, gamma-H2AX p=0.62, Lamin B1 p=0.72)
Conclusion: These results provide evidence of systemic increases in SASP-related cytokines following treatment with ADT. The in vitro results suggest that secretion of SASP is promoted by an AR-mediated mechanism. Preliminary results from tumor specimens suggest increased senescence marker p16 expression induced by therapy. Ongoing experiments are further characterizing the senescence markers in prostate tumor specimens and correlated to treatment effect.

#2955 HPV E6* and senescence-related gene expression in cervical cancer.

Louise Medina Bengtsson[1], Matthew Inkman[1], Naoshad Muhammad[1], Leahan Castillo[1], Naomi Msengi[1], Tyler McKinnish[2], Nishanth Gabriel[1], Jin Zhang[1], Julie Schwarz[1]

[1]Department of Radiation Oncology, Washington University In St. Louis, St. Louis, MO,[2]Department of Obstetrics and Gynecology, Washington University In St. Louis, St. Louis, MO

Previous work in our lab found that increased expression of the E6* variant of the HPV E6 viral protein was significantly correlated with worse response to standard-of-care chemoradiation (CRT) and progression-free survival, independently of HPV genotype. *In vitro* validation showed that overexpression of E6* induces senescence in an HPV 16-positive cervical cancer cell line. Given these findings, we hypothesized that increased E6* expression mediates resistance to CRT by inducing a reversible state of tumor cell senescence. We created a senescence score using ten genes that have been consistently reported in the literature as associated with senescence. Using an institutional cohort of 68 patients with cervical cancer with prospectively collected clinical outcome data, we performed bulk RNA sequencing to assess senescence scores before CRT and determine whether there is an association between senescence scores and E6* expression. Using a second institutional cohort of 35 patients with cervical cancer treated with CRT with pre and posttreatment tumor biopsies, we performed bulk RNA sequencing to evaluate the same relationship and determine whether expression of senescence-related genes was affected by CRT. Nine cervical cancer cell lines stratified into low- and high-E6* expression groups will be assessed regarding their senescence score, beta-galactosidase staining, and SASP expression before and after CRT. In our first cohort, there was no correlation between E6*:E6 expression ratio and senescence score, regardless of HPV genotype. In our second cohort, CRT increased senescence score in CRT-treated samples ($p < 0.01$), but $p16^{INK4a}$ expression significantly decreased compared to pre-treatment samples ($p < 0.01$). Increased senescence score was not associated with cancer recurrence. There was no significant difference in senescence scores between different HPV genotypes before therapy. Tumors that were positive for HPV 16 or HPV 18 had significantly lower senescence scores compared to HPV negative tumors ($p = 0.037$ and $p = 0.038$, respectively) after CRT. Among HPV 16-positive tumors ($n = 12$), there was no correlation between E6*:E6 expression ratio and senescence score before or after CRT. We found no association between senescence score and E6* expression, and between senescence score and cancer recurrence after CRT in our dataset. Additionally, our results suggest that $p16^{INK4a}$ might not be an appropriate senescence marker in tumors that have intrinsically high $p16^{INK4a}$ expression, such as in cervical cancer, reinforcing the need for a cervical cancer-specific senescence signature. We are currently testing beta-galactosidase and SASP expression *in vitro* and *in vivo* before and after CRT.

#2956 Chemotherapy-induced adipocyte senescence triggers bone loss through osteoclast activation.

G. K. Raut, T. Malachowski, T. Holt, R. Oliveira, X. Luo, D. Faget, Q. Ren, S. Stewart;
Washington University School of Medicine in St. Louis, St. Louis, MO

Despite breakthroughs in cancer treatment, chemotherapy-induced osteo-toxicity is a major problem that compromises the quality of life and overall survival of cancer patients regardless of cancer type. Recently we demonstrated that chemotherapy-induced senescence drives bone loss by both limiting mineralization of new bone and increasing bone resorption. However, the underlying mechanism of action remains elusive. Therefore, it is critical that we understand the mechanisms that drive these toxicities and develop approaches to mitigate their severity. To establish whether senescent bone resident cells or systemic responses to chemotherapy drove therapy-induced bone loss, we used a vertebral body transplant (vossicle) model. Using this approach, we found that the specific elimination of senescent cells in L4 and L5 donor vossicles (*INK-ATTAC*) implanted into wildtype mice, protects from chemotherapy-induced bone loss within the vossicles but not the femur of the recipient mice. This demonstrated that chemotherapy-induced senescence in resident bone cells is responsible for bone loss. To determine which bone resident cell(s) underwent senescence in response to chemotherapy and how their gene expression was impacted, we used the p16-Cre^{ERT2}-tdTomato mouse model and found that chemotherapy triggers senescence in bone marrow adipocytes. Subsequently, we observed that postnatal fat ablation in adipoqCre-inducible DTR transgenic mice (iDTR^{ADQ}) prevented chemotherapy-induced bone loss, indicating senescent adipocytes trigger bone loss. Furthermore, we observed chemotherapy-induced bone loss is attributed to RANKL-mediated high osteoclasts activity. Collectively, our data demonstrate that chemotherapy causes senescence in marrow adipocytes which in turn triggers bone loss via RANKL-mediated osteoclasts activation and bone loss can be protected by eliminating senescent cells.

#2957 Senescence of stromal, endothelial, and myeloid cells in the tumor microenvironment has distinct effects on cancer progression.

J. Rupert, Z. Gao, Y. Yu, **M. Kolonin**;
University of Texas at Houston, Houston, TX

Accumulation of senescent cells, undermining the function of vital organs, is a culprit of aging. The effects of senescence in different types of cells on tumor growth and metastasis remain incompletely characterized. Cell senescence has been shown to result from inactivation of Telomerase (TERT), an enzyme that maintains telomere length and has obscure roles in regulating gene expression and supporting mitochondrial function. As we reported previously, knockout (KO) of *Tert* gene in mesenchymal stromal cells (MSC) of *Pdgfra+* or *Pdgfrb+* lineages leads to premature replicative stromal cell senescence in adipose tissue. To assess the effect of senescence in endothelial and myeloid cells, we also created mice with *Tert* KO driven by the *Tie2e* promoter or the *LysM* promoter, respectively. Here, to investigate the effect of these three KOs on cancer, we used syngeneic graft models of breast, prostate, and pancreatic carcinoma. Overall, *Tert* KO in cells of *Pdgfra+*, *Pdgfrb+*, *Tie2e+*, or *LysM+* lineage had a suppressive effect on tumor growth. The strongest tumor suppression effect of *Tert* KO was observed in female mice orthotopically grafted with E0771 breast cancer cells. Intermediate suppressive effects of *Tert* KO were observed in mice orthotopically grafted with KPC pancreatic ductal adenocarcinoma cells, whereas the effect on RM1 prostate cancer cells grafts in male mice was the least significant. MSC *Tert* KO and myeloid *Tert* KO also suppressed the growth of breast and prostate cells grafts. Importantly, spontaneous metastases to the liver were induced by *Tie2e-Tert* KO in all mice with pancreatic KPC grafts. Analysis of adipose tissue in this endothelial senescence model revealed vasculature abnormality, leakiness, and tissue hypoxia, which provides a mechanistic explanation for increased tumor dissemination. In contrast, *LysM-Tert* KO did not promote KPC metastases, consistent with the lack of contribution of myeloid cells to the vasculature. *Pdgfrb-Tert* KO in the KPC model resulted in liver metastases observed for some but not all mice, consistent with the role of MSC in supporting vascular integrity. To test an independent model of replicative MSC senescence, we exhausted their pool by several cycles of ganciclovir treatment in mice expressing thymidine kinase under the control of *Pdgfrb* promoter. Upon KPC grafting in this model, reduced primary pancreatic tumor growth was also observed and liver metastases were also induced. We conclude that senescence of distinct cells in the tumor microenvironment affects early and late stages of cancer progression differently. Specifically, our data indicate that vascular cell senescence suppresses tumor growth but promotes metastases. These findings are important to consider as new approaches designed to mitigate cell senescence are investigated in the context of cancer.

#2958 Melphalan-treated multiple myeloma cells exhibit a senescent-like dormancy phenotype.

A. J. Guilatco[1], M. Diaz-del-Castillo[2], G. Alvares Borges[1], N. I. Sannuli[1], M. L. Ritting[1], S. M. M. Aalam[1], N. Kannan[1], T. Tchkonia[1], J. L. Kirkland[1], Y. Lin[1], T. Kourelis[1], M. T. Drake[1], T. L. Andersen[2], M. Weivoda[1];

[1]Mayo Clinic, Rochester, MN, [2]Aarhus University Hospital, Aarhus, Denmark

Multiple myeloma (MM) is an incurable plasma cell (PC) cancer in which all patients are expected to relapse. Cytotoxic agents such as high-dose melphalan (HDM), which is used as a myeloablative agent prior to autologous stem cell transplant (ASCT) in MM, drive therapy-induced senescence (TIS) in non-cancerous tissues. We hypothesized that HDM similarly activates TIS pathways in surviving MM cells and this response may correlate with patient outcomes post-ASCT. To test this, we developed an *in vitro* model in which 5TGM1 mouse MM cells are cultured with 10uM melphalan (HDM) or vehicle (Veh) for 6 hours, followed by co-culture in normal media with primary mouse bone marrow stromal cells. Cultures were maintained for 10 days and imaged to quantify cumulative population doublings (CPDs). 5TGM1 were then isolated by FACS to measure telomere-associated DNA damage foci (TAFs), sensitivity to senolytic drugs, and senescence gene expression (RT-qPCR and scRNA-seq). To translate these studies, scRNA-seq was used to analyze CD138+ PCs from MM patient bone marrow post-ASCT. Additionally, longitudinal bone biopsies from MM patients at diagnosis and post-ASCT were stained for CD138+ PCs; PC burden was quantified using artificial intelligence assisted histology (HALO). HDM-5TGM1 exhibited stable growth arrest (decreased CPDs) and sustained DNA damage (increased TAFs) compared to Veh-5TGM1. HDM-5TGM1 were also significantly more sensitive to senolytic ablation (Dasatinib+Quercetin or Fisetin). HDM-5TGM1 showed increased senescence (*Cdkn1a, Cdkn1c, Glb1)*, anti-apoptosis (*Bcl2l1)*, and senescence associated secretory phenotype (*Ccl5, Icam1, Mmp13*) genes, as well as myeloid markers found to be increased in MM dormancy (*Axl, Fcer1g, Mpeg1*). Analysis by scRNA-seq revealed that HDM-5TGM1 were G0/G1 arrested, and gene set enrichment analysis (GSEA) confirmed upregulation of senescence pathways with downregulation of DNA replication and cell cycle pathways. Consistent with RT-qPCR results, these cells exhibited myeloid gene expression. Analysis of patient CD138+ PCs post-ASCT by scRNA-seq also revealed a myeloid-like cluster. Of interest, of the 491 genes upregulated in this cluster, 268 were also upregulated in HDM-5TGM1. CD138+ PCs could also be detected in patient bone biopsies post-ASCT, although PC burden was significantly reduced post-ASCT. Surprisingly, the percent reduction in PC burden post-ASCT was greater in relapsed (≤3 years) vs non-relapsed patients. Further, in relapsed patients, PC burden post-ASCT positively correlated with time in remission. Altogether, these findings demonstrate that HDM can induce senescence features and a myeloid-dormancy signature in surviving MM cells. This phenotype is associated with longer durable response, suggesting that activation of TIS may be a strategy to extend PFS. Further, senolytic therapy may be a novel approach to eliminate dormant MM cells and prevent relapse.

#2959 Signatures of therapy-induced senescence in glioblastoma-derived extracellular vesicles.

V. DeLuca, P. Digumarti, K. Garcia-Mansfield, P. Pirrotte, M. E. Berens;
TGen (The Translational Genomics Research Institute), Phoenix, AZ

The recalcitrant nature of glioblastoma (GBM) may be due, in part, to the promotion of therapy-induced senescence (TIS) by standard of care treatments. TIS is a prolonged growth arrest associated with epigenetic, metabolic, and biochemical alterations, as well as a robust secretory phenotype. Despite an initial period of tumor stasis due to the loss of cell proliferation, TIS is associated with the development of stemness, increased drug resistance, and immune suppression. Our preliminary data demonstrate the prominent induction of TIS in GBM tumor cells and astrocytes following standard of care therapies for GBM in vitro. However, studies of TIS in GBM patients have been limited due to i) the impracticality of receiving multiple GBM biopsies post-treatment but prior to recurrence and ii) the lack of robust detection methods for TIS even with appropriate biopsy. These challenges argue the need for novel methods to survey TIS in patients. Extracellular vesicles (EVs) are small membrane-bound particles that readily cross the blood brain barrier, and convey information about originating cell identity and cell state through their cargo content. We hypothesize that TIS in host and tumor cells drives the elaboration of senescence-associated EVs (senEVs) with quantifiable senescence protein cargo signatures, and consequently, that EVs can serve as a liquid biopsy for senescence in patients. In a preliminary experiment, two patient derived xenografts grown as short-term in vitro cultures were exposed to 6GY irradiation, with supernatant collected prior to radiation (D0), at peak senescence (D7), and at late senescence (D10). EVs were isolated and subjected to unbiased mass spectrometry. Following unsupervised clustering, EVs were grouped by treatment rather than by cell line. Approximately 6000 proteins were identified across the entire data set, with 105 proteins unique to D7 samples, 162 proteins unique to D10 samples, and 688 proteins exclusive to D7 and D10 samples. Further, proteins from two established senescence gene sets were identified as unique to the D7 and/or D10 conditions. Current work to more robustly identify enrichment of senescence gene sets in EV cargo post-irradiation is underway. We have also established shRNA knockdown cell lines with abrogated TIS to equip validation studies of the TIS-EV cargo relationship. We anticipate that these studies will aid in the development of EVs as a novel reporter of senescence in the clinic.

#2960 Deciphering the role of miRNA146-a and its crosstalk with cellular redox state in senescence escape in breast cancer cells.

S. Pervaiz, A. Q. X. Liew, M.-V. Clement;
National University of Singapore (NUS), Singapore, Singapore

Senescence serves as a double-edged sword in cancer as studies revealed that senescence exhibits both tumor-suppressing and tumor-promoting effects. A subpopulation of cancer cells that enters senescence can evade senescence to proliferate, thereby resulting in tumor regrowth, which has been associated with chemoresistance and tumor aggressiveness. Unlike senescent cells, the senescence-escaped cells harbor low levels of reactive oxygen species (ROS), however, the mechanism(s) underlying this redox dichotomy in senescence and senescence evasion remains elusive. In this regard, recent reports have highlighted the pivotal role of miRNAs in regulating cellular senescence. To that end, miR-146a has been reported as a biomarker of senescence probably via modulating pro-inflammatory and antioxidant pathways. We set up a model of doxorubicin-induced senescence in MDA-MB-231 breast carcinoma cells to study the role and involvement of miRNA146a in senescence induction and its regulation. Senescence induction was confirmed by upregulation of p21, increase in senescence-associated beta galactosidase and C_{12}FDG staining, as well as propidium iodide positivity. We show that, following the initial phase of apoptotic cell death, as evidenced by increased γH2AX and cleaved caspase 3, a population of senescent cells escaped growth arrest to re-enter cell cycle and proliferate. Senescence-escaped cells harbored lower ROS levels compared to senescent cells, which correlated with upregulation of antioxidant enzymes such as MnSOD and CuZnSOD as well as increased transcription of *NRF2* and *NQO1*. Our results also provide evidence for a novel senescence associated redox state, which implicates intracellular peroxynitrite as a driver of cellular senescence. Interestingly, in our model system, p21 upregulation was not associated with intracellular ROS accumulation, which was reported in earlier findings. Interestingly, these changes coincided with a significant increase in *miR-146* expression (during senescence), which was previously shown to downregulate ROS in other model systems. While modulating *miR-146a* did not seem to change ROS levels upon doxorubicin-induced senescence in MDA-MB231 cells, the precise crosstalk between cellular ROS, *miR146-a* and senescence evasion is currently being pursued.

#2961 Investigating the role of aging and treatment-induced senescence in the metastatic liver cancer tumor microenvironment.

K. Gallant, A. Karpova, X. Li, M. Iglesia, A. Houston, D. Rapp, C.-W. Peng, C. Liu, J. Herdon, F. Chen, R. Fields, L. Ding;
Washington University In St. Louis, St. Louis, MO

Liver senescence, marked by the progressive decline in hepatic cell function and regenerative capacity, plays a vital role in the context of aging, chronic liver diseases, and cancer progression, particularly when influenced by anti-cancer therapies. This study is designed to extensively characterize liver senescence under two specific conditions: replicative aging and therapy-induced changes. We examined liver samples from 20 individuals, covering a wide age range (young, <40 years; old, >60 years), and 16 cases of colorectal cancer (CRC) liver metastasis (ages 37-66). Our integrative approach melds single-nucleus RNA-sequencing (snRNA-seq) and ATAC-sequencing (snATAC-seq) to investigate the transcriptomic and epigenetic landscapes across a spectrum of liver cell types, including hepatocytes, cholangiocytes, stellate cells, liver sinusoidal endothelial cells, and diverse immune cells. Key findings include an upregulation of senescence markers such as *CDKN1A*, *CDKN2A*, and *HMGB1*, particularly in specific hepatocytes from older individuals and various cell types in the CRC liver metastasis group. Furthermore, we noted a distinctive senescence-associated secretory phenotype (SASP) across multiple immune cell types in our treated CRC liver metastasis group and upregulation of treatment-induced senescence gene signatures, such as SenCan. Moreover, hepatic stellate cells from older subjects exhibited augmented senescence-related gene signatures (SenSig) and transcription factors (SenMayo), with myofibroblast-like and FAP+ stellate cells showing a marked senescence phenotype, evidenced by elevated SASP molecule expression (*CCL2*, *SERPINE1*, *GLB1*, *IGFBP7*, *IGFBP3*).Incorporating advanced high-resolution imaging techniques, our study delves into the detailed morphological characteristics and spatial distribution of senescence markers within the liver in the setting of replicative aging and treatment-induced senescence. This study sheds light on the heterogeneity and intricacies of senescence-associated gene expression within liver cell populations. By combining comprehensive multiomic data with advanced high-resolution spatial profiling, we aim to decipher unique senescence phenotypes in the context of both replicative and treatment-induced senescence. Our work highlights the significance of cellular senescence in liver pathologies and cancer progression, suggesting new directions for therapeutic interventions that target these complex dynamics.

#2962 Chemotherapy induced senescence drives peripheral neuropathy.

T. Malachowski, G. Kumar Raut, X. Luo, S. Mullick Bagchi, S. Stewart;
Washington University in St. Louis, Saint Louis, MO

Chemotherapy is a mainstay of cancer therapy. Unfortunately, while chemotherapy can profoundly impact disease free survival, it is often accompanied with devastating side effects including hair loss, bone loss, cognitive impairment (referred to as "brain fog"), and peripheral neuropathies. While many of these side effects may subside after the completion of chemotherapy, some persist for a lifetime, substantially compromising the quality of life for survivors. Particularly insidious is chemotherapy-induced peripheral neuropathy (CIPN), which can impair a patient's ability to care for themselves. Shockingly, in over 30% of patients, CIPN persists even after the cessation of chemotherapy, subjecting them to a lifetime of numbness and/or pain. Paclitaxel (PTX), a common treatment for breast cancer, induces CIPN in 61-92% of patients depending on the administered dose. Unfortunately, there are currently no preventative or curative measures for CIPN resulting in side effects that persist for months or even years after the cessation of chemotherapy. Considering chemotherapy can trigger cellular senescence, leading to the release of a diverse array of factors collectively known as the senescence-associated secretory phenotype (SASP) that are capable of negatively influencing neighboring cells. To determine if senescence played a role in CIPN we treated with PTX and found that animals displayed reduced axon innervation in the paws and diminished paw withdrawal responses during the von Frey assay, characteristic symptoms of CIPN. To determine if senescent drove PTX-induced CIPN, we utilized the INKATTAC (INK) mouse, a model in which a p16INK4a promoter drives an inducible suicide transgene to eliminate p16+ senescent cells following treatment with AP20187 (AP). Employing the INK mouse, we successfully prevented CIPN by eliminating PTX-induced senescent cells. Furthermore, through bone marrow (BM) transplant studies using BM from INK mice into wildtype recipients, we failed to prevent CIPN. This result establishes that senescent immune cells, do not contribute to CIPN. In an independent approach, we found that senolytic drugs (kill senescent cells), such as dasatinib and quercetin (DQ) or ABT737 (ABT), effectively prevented and reversed CIPN in mice. Additionally, since the p38MAPK pathway has been shown to regulate SASP mRNA stability, we treated with p38 and MK2 inhibitors and found that inhibition prevented CIPN in mice. To address the mechanism behind CIPN we have carried out single cell RNA sequencing (scRNA-seq) to identify the cell population senescing in response to chemotherapy. These analyses will allow us to understand the mechanisms that drive CIPN and may lead to new treatments for patients suffering from CIPN.

#2963 Dihydromyricetin is a senomorphic agent to promote therapeutic outcome of age-related conditions including cancer and Alzheimer's disease.

Q. Xu, Z. Li, Z. Jiang, J. Campisi, **Y. Sun**;
Chinese Academy of Sciences, Shanghai, China

Aging is characterized by a progressive decline of organ function and gradual rise of susceptibility to multiple chronic disorders, with cancer being a primary cause of human morbidity and mortality worldwide. Cellular senescence represents a state of permanent cell cycle arrest and contributes to chronological aging and age-related diseases including Alzheimer's disease (AD), mainly through development of a distinct secretome termed the senescence-associated secretory phenotype (SASP). By screening a natural medicinal agent library, we noticed Rattan tea extract (RTE) has a prominent antiaging potential, wherein dihydromyricetin (DMY), the most abundant natural flavonoid in RTE, played a central role in suppressing the SASP expression of senescent cells. DMY enhanced total antioxidant capacity (T-AOC), increased catalase (CAT) and glutathione peroxidase (GSH-Px) activity, upregulated the expression of HO-1, NQO1, nuclear Nrf2 and phospho-ERK (p-ERK), but decreased malondialdehyde (MDA) level in senescent cells. Furthermore, DMY regulates PI3K/Akt/mTOR signaling pathway, NLRP3 inflammasome formation, the NF-κB complex activity and ER stress-response, each responsible for a full spectrum SASP development. Transcriptomic profiling suggested that DMY can dampen the genome-wide upregulation of pro-inflammatory factors produced by senescent cells, resulting in abrogated progression of cancer malignancy including elevated proliferation, migration, invasion and chemoresistance. Importantly, combination of DMY with classic chemotherapy significantly enhanced therapeutic efficacy, causing remarkable tumor regression and extending posttreatment survival. Alzheimer's disease (AD) is marked by the presence of amyloid plaques, neurofibrillary tangles, damaged neuronal macromolecules and redox sensitive ions. We found that DMY restrains inflammatory injury in microglial cells, reduces their apoptosis and inflammation, and inhibits TLR4 and MD2 expression. Results of small molecule-protein docking and pull-down assays indicated that DMY binds MD2 to suppress the formation of TLR4 complex. In AD mice, DMY improved the cognitive disorder of animals, suppressed inflammatory injury in brain and reduced TLR4 expression. Together, DMY represents a valid natural candidate that has senomorphic activity and can be applied for treatment of malignancies or neurodegenerative disorders such as AD, pathologies that frequently arise in late life of humans.

#2964 Glutathione S-transferase omega 2 (GSTO2) suppresses the acquisition of the senescent tumor cells phenotype in lung adenocarcinoma.

H. Hatano[1], R. Sumiya[1], T. Hagiwara[1], H. Suzuki[2], K. Yamada[1], N. Kokudo[1], Y. Kawamura[1];
[1]National Center for Global Health and Medicine, Tokyo, Japan, [2]Sapporo Medical University, Hokkaido, Japan

Cellular senescence is a phenomenon characterized by the cell cycle arrest and the induction of inflammatory responses, and is known to contribute to the development and progression of various diseases. In cancerous tissues, some cancer cells acquire the senescent traits, which are referred to as senescent tumor cells (STCs) and contribute to tumor invasion and metastasis. We have previously demonstrated that the expression of glutathione S-transferase omega 2 (GSTO2), which regulates the glutathione redox balance, is exclusively expressed in cells with regenerative ability such as airway basal cells, Clara cells, and type II alveolar cells in the lungs. Contrastingly, the expression of GSTO2 was completely lost in squamous cell carcinoma of the lung (***Cancer Science***, 2022); however, we found that some of lung adenocarcinoma expressed GSTO2. In this study, we aimed to clarify the significance of GSTO2 in lung adenocarcinoma, especially in the regulation of senescence and STCs. To examine whether GSTO2 expression affects senescence marker expression, we prepared GSTO2-transfected and mock-transfected lung adenocarcinoma cell line PC-9. Forced GSTO2 expression resulted in significantly reduced expression of senescence markers, such as p21, p53, and p16. We performed double staining for GSTO2 with p16 and confirmed the inverse correlation between them in lung adenocarcinoma tissues, where GSTO2-positive cells tended to express lower p16 level compared with GSTO2-negative cells. Furthermore, GSTO2-transfected PC-9 cells showed lower expression of senescence-associated secretory phenotype factors, such as IL-6, TNFα, and IL-1β than mock-transfected cells. These results suggest that GSTO2 suppresses senescence in lung adenocarcinoma cells. We next examined whether GSTO2 expression affects tumor cell growth because senescence is involved in the cell cycle arrest. Expectedly, MTT assay revealed that GSTO2 overexpression in PC-9 cells significantly promoted cell growth compared with the mock transfected cells. Contrastingly, the scratching assay showed that the cell migration of GSTO2-transfected PC-9 cells was significantly delayed compared with that of the mock-transfected cells. In conclusion, we demonstrated that GSTO2 regulates senescence, resulting in the suppression of cell migration. The expression of GSTO2 in lung adenocarcinoma may contribute to the inhibition of the emergence of STCs, being a cause of invasion and resistance to radiotherapy and chemotherapy.

#2965 *GADD45B* as a mechanism for enhanced treatment response with the combination of copanlisib and romidepsin in colorectal cancer.

K. Maduscha, A. Schmitz, R. DeStefanis, C. Pasch, D. Deming;
University of Wisconsin - Madison, Madison, WI

Background: Treatment options for molecular subtypes of colorectal cancer (CRC) are urgently needed, including for *PIK3CA* mutant CRC. Previous work in our lab demonstrated enhanced activity of copanlisib in combination with romidepsin in *PIK3CA* mutant CRC models. Here we investigate the induction of *GADD45B* as a mechanism of the enhanced induction of apoptosis seen with this treatment strategy.

Methods: RNA sequencing was done on the CRC 2D cell line, SW48PK (Horizon Discovery, SW48 PIK3CA$^{H1047R/+}$ mutation) as well as *PIK3CA* mutant and wild-type patient derived cancer organoids (PDCOs) through the UW Biotechnology Center. All lines were treated with copanlisib, romidepsin, or combination and were compared with untreated controls. *GADD45B* gene expression was also confirmed on SW48PK, *PIK3CA* mutant, wild type, and *PIK3CA* and *KRAS* mutant PDCOs using RT-qPCR.

Results: RNA sequencing determined that there was an increase of *GADD45B* expression in the SW48PK 2D cell line as well as in *PIK3CA* mutant and wild-type PDCOs treated with the combination compared to untreated controls (average log2 fold change= 1.83). A significant increase in *GADD45B* expression was seen in the SW48PK combination treatment group compared to the control group at 6 hours (combination median fold change= 2.7, p= 0.045) and 24 hours (4.1, p< 0.001). For *PIK3CA* mutant PDCOs treated with the combination, there was significant increase in *GADD45B* expression at 6 hours (9.45, p= 0.005) and 24 hours (14.7, p= 0.002) compared to untreated control. In wild type PDCOs, there was a significant increase in *GADD45B* expression in the combination compared to untreated control at 6 hours (32.95, p=0.004) but not after 24 hours (2.6, p= 0.42). For KRAS mutant PDCOs, there was a significant increase in *GADD45B* expression in combination treated cells at 6 (9.9, p= 0.001) and 24 hours (3.3, p= 0.047), however, this increase was less than *PIK3CA* mutant PDCOs at 24 hours (3.3 vs 14.7).

Conclusions: Copanlisib in combination with romidepsin increases *GADD45B* expression in PDCOs and SW48PK. Further studies will determine if *GADD45B* is required for this treatment response.

#2966 Senescent cancer cell vaccines induce cytotoxic T cell responses targeting primary tumors and disseminated tumor cells.

Y. Liu, J. Pagacz, D. J. Wolfgeher, S. J. Kron;
University of Chicago, Chicago, IL

Diverse conventional cancer therapies, including genotoxic agents and cell cycle or cell division-targeting drugs, can trigger cancer cell senescence. Senescent cells (SnCs) induced by cancer therapy often display unrepaired chromosomal damage but persist indefinitely. SnCs remain metabolically active and display distinct alterations in transcription, secretion, and membrane protein expression/presentation. While initially viewed as a favorable outcome and likely tumor-suppressive mechanism, therapy-induced senescence has more recently been recognized as contributing to resistance, recurrence and metastasis. Adverse effects may be mediated in part by release of inflammatory mediators as components of the senescence-associated secretory phenotype (SASP). Recent studies have argued for reconsidering the potential benefits of therapy-induced senescence, especially in modulating the tumor microenvironment to potentiate anti-tumor immunity and potentiate immunotherapy. We have explored the potential for SnCs to serve as vaccines, building upon prior findings where we demonstrated the immunogenic senescence triggered by the combination of ionizing radiation (IR) and the PARP1/2 inhibitor veliparib. We find that SnCs are avidly taken up by type I conventional, CD11c+/CD103+ dendritic cells (DCs), promoting their activation and maturation. Thereby, SnCs promote DC function in T cell priming and stimulation. The capacity of SnCs to activate DCs depends on how the SnCs are formed, with our results confirming IR+veliparib induces high immunogenicity and implicating a distinct SASP in these effects. On the other hand, blocking STING signaling limits SnC activation of DCs. In vivo experiments with the murine tumor models CT26 and 4T1 suggest that both SnCs and SnC-pulsed DCs serve as effective anti-tumor vaccines. They not only confer protective immunity against tumor engraftment but also act as therapeutic vaccines, inhibiting both primary and disseminated tumor growth, and synergize with radiotherapy and immune checkpoint blockade. While direct administration of tumor-derived SnCs to patients may raise safety concerns, pulsing autologous DCs with tumor SnCs may help drive anti-tumor immune response, offering a promising path toward personalized cancer immunotherapy.

#2967 The mammalian 8-oxo-dGTPase, MTH1, as a novel targetable vulnerability in pancreatic ductal adenocarcinoma.

B. Mateo-Victoriano[1], L. Zhang[1], J. Samaranayake[1], Z. McGaughey[1], C. Due[1], C. Troccoli[1], M. G. Mohsen[2], N. Nagathihalli[1], O. G. McDonald[1], M. VanSaun[1], E. T. Kool[2], P. Rai[1];

[1]University of Miami Miller School of Medicine, Miami, FL, [2]Stanford University, Stanford, CA

Pancreatic ductal adenocarcinoma (PDAC) is an aggressive KRAS-driven cancer that remains one of the most lethal of all human malignancies. Oncogenic KRAS relies on elevated reactive oxygen species (ROS) to support pro-tumorigenic signaling. However, these elevated ROS levels can also evoke tumor suppressive oxidative stress; thus KRAS-driven cancers must evolve protective redox adaptations to mitigate ROS-induced anti-tumor consequences. Here we report a unique adaptation centered on redox maintenance of nucleotide pool integrity, that supports aggressive PDAC tumorigenesis. MTH1 is the main mammalian 8-oxodGTPase that is known to be elevated in various RAS-driven cancers including PDAC. We have previously shown MTH1 is critical for ROS-mediated oncogenic signaling, and promotes escape from oncogene-induced senescence. We therefore hypothesized that MTH1 provides important redox support for aggressive PDAC tumor growth. Consistent with this, we found that elevated MTH1 expression was strongly correlated with poor disease-free survival in PDAC patients. These findings extended to KRAS-driven PDAC cell lines: highly proliferative human PDAC cells strongly expressed MTH1 ($MTH1^{high}$), and MTH1 deletion was selectively anti-tumorigenic against $MTH1^{high}$ cells. Furthermore, introduction of MTH1-null backgrounds into gold standard genetically engineered PDAC mouse models selectively decreased 8-oxodGTPase activity levels and slowed PDAC growth in aggressive, short latency $Ptf1a^{cre/+}$;LSL-$Kras^{G12D/+}$;$Tgfbr2^{flox/flox}$ (PKT) mice, but with no effect in longer latency $Pdx1^{Cre}$; LSL- $Kras^{G12D/+}$; LSL-$Trp53^{R172H/+}$ (KPC) mice. These selective anti-tumorigenic effects were accompanied by a reduction in circulating immunosuppressive cytokines in PKT mice, further suggesting that MTH1 potentially supports aggressive tumorigenesis through induction of systemic immunosuppression. Consistent with this, pancreatic-restricted MTH1 conditional deletion fully rescued PDAC growth in PKT mice. Our findings here thus suggest that MTH1-dependent redox protection of the nucleotide pool represents a unique TME adaptation that supports aggressive PDAC tumorigenesis. Further studies will investigate whether this adaptation is maintained through symbiotic tumor/stroma or tumor/immune cell crosstalk, as observed for other KRAS-driven traits. Ultimately, interventions designed to target MTH1-dependent protection of the nucleotide pool could hold promise as novel therapeutic strategies for this untreatable disease.

#2968 TWIST1-induced suppression of oncogene-induced senescence in non-small cell lung cancer requires the transactivation domain of TWIST1.

A. M. Lafargue[1], H. Wang[2], S. T. Chettiar[3], R. P. Gajula[3], A. C. Shetty[1], Y. Song[1], B. W. Simons[3], T. Nguyen[1], C. Lam[3], F. A. Carrieri[3], C. Smack[3], N. Connis[3], D. Chowdhury[1], J. Chang[1], D. Council[1], K. Nugent[3], I. Siddiqui[3], K. Taparra[3], M. Rezaee[3], N. Zachara[3], Z. S. Morris[4], C. McFarland[5], S. Abdulkadir[6], C. L. Hann[3], P. T. Tran[1];

[1]University of Maryland Baltimore, School of Medicine, Baltimore, MD, [2]GenoImmune Therapeutics, Wuhan, China, [3]Johns Hopkins University, School of Medicine, Baltimore, MD, [4]University of Wisconsin School of Medicine and Public Health, Madison, WI, [5]Case Western Reserve University, School of Medicine, Cleveland, OH, [6]Northwestern University Feinberg School of Medicine, Chicago, IL

Non-small cell lung carcinoma (NSCLC) is a major cause of cancer mortality. High expression of the epithelial-to-mesenchymal transition transcription factor TWIST1 is strongly associated with metastatic cancers and treatment resistance. Additionally, TWIST1 can upregulate O-GlcNAcylation which (1) is required to suppress fail-safe programs such as oncogene ($KRas^{G12D}$)-induced senescence (OIS) to accelerate tumorigenesis in primary NSCLC tumors, and (2) is a potential modulator of DNA repair/radiation response. To decipher the domains and transcriptional targets required for tumorigenicity and radioresistance, we created a novel genetically engineered mouse model (GEMM) allowing tetracycline-inducible expression in the lung epithelium (via lung specific CCSP-reverse tetracycline transactivator (C)) of $KRas^{G12D}$ (R) with $Twist1^{wt}$ (T) or with $Twist1^{F191G}$ transactivation-null mutant (F). CRT mice had shorter tumor-free survival and more aggressive tumors compared to CR/CRF mice indicating that the *Twist1* transactivation domain is required for *Twist1*-dependent tumorigenesis acceleration. Also, $Twist1^{wt}$ expression promoted radioresistance in cell lines and GEMMs. Contrary to CRT, CRF showed a progressive loss of $Twist1^{F191G}$ expression over time suggesting no functionality/no selective advantage. CRT lung tumors had higher proliferation (Ki67) and lower cell-cycle arrest (p16) compared to CR/CRF suggesting that the transactivation domain of *Twist1* is important for the suppression of OIS. Supporting these data, we observed in non-cancer Human Bronchial Epithelial Cell (HBEC) that the co-expression of human $TWIST1^{wt}$ (HBEC-$TWIST1^{wt}$) could suppress $HRas^{G12V}$-induced senescence while the transactivation-null $TWIST1^{F187G}$ mutant (HBEC-$TWIST1^{F187G}$) could not. Additionally, HBEC expressing $HRas^{G12V}$-$TWIST1^{wt}$ had enhanced tumorigenic/invasive programs. Interestingly, we observed that the inhibition of O-GlcNAcylation rescued OIS in HBEC-$HRas^{G12V}$-$TWIST1^{wt}$ while the stimulation of O-GlcNAcylation in HBEC-$HRas^{G12V}$-$TWIST1^{F187G}$ suppressed OIS. Furthermore, $TWIST1^{wt}$ expression with $HRas^{G12V}$ modulated MYC downstream targets and the inhibition of MYC activity using the novel MYC inhibitor MYCi975 in HBEC-$HRas^{G12V}$-$TWIST1^{wt}$ also rescued OIS induction. Altogether, these results suggest that TWIST1 may suppress OIS via MYC signaling and nominate MYCi975 as a means to activate latent OIS programs. In this context, MYC inhibiting strategies could serve as a therapeutic sensitizer for TWIST1-positive NSCLC. This work and our future studies on TWIST1 toward the control of OIS, O-GlcNAcylation and of mechanisms of radioresistance may help to identify new potential NSCLC therapeutic strategies.

#2969 Targeting novel senescence markers by conditionally active biologics eliminates senescence-associated secretory phenotype in *in vitro* and *in vivo* models.

J. Chen, J. Wang, H. Liu, C. Chang, W. J. Boyle, J. M. Short;
BioAtla, San Diego, CA

Clearing senescent cells has been shown to have promising effects against cancer and age-related pathologies in preclinical models as well as early human clinical trials. However, current senescent cell elimination strategies are focused on targets that do not distinguish between hyper-inflamed or SASP senescent cells versus relatively non-inflamed senescent cells. The use of senolytics in the clinic is still limited due to their cytotoxicity to either normal cells or potentially beneficial senescent cells. A more effective senescence cell targeted approach is needed to reduce side effects and increase the efficiency of senescence cell removal or reduction.

Conditionally Active Biologics (CAB) technology is a proprietary platform unique in its ability to be selectively active in the context of diseased tissues, but not normal tissues. The aberrant accumulation of senescent cells in aged and cancerous tissue triggers inflammatory signaling through a senescence-associated secretory phenotype (SASP), promoting aging and tumor progression. Since our CAB technology is currently being tested as a cancer therapy by targeting cell surface markers such as AXL, ROR2, and CTLA4 in clinical studies, we explored whether CAB technology allows selective removal of senescent cells in SASP-associated microenvironments.

In our previous report, we demonstrated several novel senescence-specific surface antigens upregulated in senescent cells (1). CAB antibodies targeting these senescence markers have no or very low binding to the target antigen on senescence cells in physiological, alkaline conditions, but have strong binding in glycolytic, acidic SASP conditions in *in vitro* binding assays. In *in vitro* antibody-dependent cell-mediated cytotoxicity assays, CAB antibodies were more potent against senescent cells compared to proliferating cells and displayed high selectivity for the glycolytic, acidic condition. To study whether CAB antibody reduces senescent cell occurrence *in vivo*, we developed a unilateral ureteral obstruction (UUO) mouse model to induce senescent cells, fibrosis, and inflammation in mouse kidney. The mice treated with CAB antibodies had a significant reduction of senescent cells and inflammatory cells infiltrated in the renal cortex, compared to the mice treated with benchmark and isotype antibodies in UUO kidneys. Thus, the CAB antibody-based therapeutic is a promising strategy for senescent cell removal in an inflammatory microenvironment. In conclusion, CAB technology provides a new generation of biologics with an increased safety margin and therapeutic index targeting SASP, acidic senescence cells in cancer and age-related diseases.

(1). Chen J, Wang J, Liu H, Chang C, Boyle WJ, and Short JM. Abstract 4795: Conditionally active biologics eliminates senescence cells in cancer and aging. Cancer Res (2023) 83.

#2970 Anti-diabetic drug, semaglutide, prevents doxorubicin-induced endothelial cell toxicity.

S. Bakhit, C. Amaefuna, K. Ramana;
Noorda College of Osteopathic Medicine, LLC, Provo, UT

Doxorubicin (Dox) is part of the anthracycline drug family and is known for its broad and effective use as a chemotherapeutic agent. It is commonly used to treat solid tumors and malignancies such as leukemia, breast, lung, and ovarian cancers. Unfortunately, its use in treating advanced cancers is limited due to its cardiotoxic side effects. Therefore, various adjuvant approaches are required to increase Dox's efficacy and to reduce unwanted toxicities including cardiotoxicity. Semaglutideis a glucagon-like peptide-1 (GLP-1) receptor agonist commonly used to treat type-2 diabetes. In his study, the effect of Semaglutide in preventing Dox-induced endothelial cell toxicity was investigated. Our data indicate that Semaglutide prevents Dox-induced cell death in human umbilical vein endothelial cells (HUVEC) in a dose- and time-dependent manner. Similarly, live and dead cell staining assay also confirms Semaglutide prevents Dox-induced endothelial cell death. Semaglutide also prevented the Dox-induced apoptosis of HUVECs. It also prevented the Dox-induced reactive oxygen species and activation of caspase-3. Further, Semaglutide regulated the expression of various anti- and pro-apoptotic and inflammatory factors induced by Dox. Inconclusion, our current results suggests that the anti-diabetic drug, Semaglutide, could prevent Dox-induced endothelial cell death by regulating the expression of various pro-apoptotic, anti-apoptotic and inflammatory markers. Thus, our data indicate that Semaglutide could be used as a potential adjuvant drug to reduce the adverse effects of anthracycline chemotherapeutic drugs.

#2971 A cytosolic growth factor receptor serves as a convergent core of condensates for anabolic activity in cancer and senescence.

T. Kim, **H. Choi**, T. Yoon, C. Kang;
Seoul National University, Seoul, Korea, Republic of

Anabolic activity, driven by growth factor signaling, is essential for cellular activities, including cell growth, proliferation, and protein synthesis. Dysregulation of growth factor signaling has been implicated in numerous human pathological conditions, including cancer and aging. Interestingly, cancer cells and senescent cells - two completely different cell fates - are reported to have an increased anabolic activity. Here, we show endosomal condensation of a growth factor receptor as a molecular switch for such anabolic enhancement. Endosomal condensates of a growth factor receptor (ecGFR) exhibit liquid-liquid phase separation (LLPS), acting as a signaling hub locked in the 'ON' state by preventing their lysosomal degradation. Furthermore, we identify a regulatory circuit that operates in both cancer and senescence to facilitate the formation of ecGFR and its physicochemical properties. Pharmacological and genetic resolution of ecGFR corrects aberrant anabolism in cancer and senescence, thereby suppressing cancer growth and senescence-associated hyperinflammation *in vitro* as well as *in vivo*. Thus, our study provides a convergent anabolic core between cancer and senescence that could be exploited as a therapeutic vulnerability for human pathological conditions associated with aberrant anabolism.

#2972 Senescent macrophages drive tumorigenesis by limiting antitumor immunity.

L. I. Prieto;
Mayo Clinic, Rochester, MN

A big challenge in oncology is tumor heterogeneity, as the same type of tumor can manifest differently across patients. Our current cancer therapies focus on targeting malignant cells without considering how the tumor microenvironment influence tumorigenesis or changes in response to treatment. Therefore, identifying effective therapies that restrict tumor growth and progression while restoring optimal tissue and organ function is imperative. Here, we propose a potential strategy to delay the frequency of lung tumorigenesis and reduce progression by selectively targeting tumor-promoting senescent cells that arise with advancing age, prolonging antitumor immunity.

Using lung tumor-prone mice, we found that senescent cells, specifically senescent alveolar macrophages, accumulate early in hyperplastic lesions. Mechanistically, these macrophages upregulate the cell cycle regulator $p16^{Ink4a}$; express the cell surface protein CXCR1; they are distinct from other established subsets; are sensitive to senolytic interventions; have a tumor-promoting secretome, including SPP1; and express immunosuppressive factors that modulate the antitumor immune response. Selective clearance of senescent macrophages attenuates adenoma development, indicating they, at least in part, promote tumorigenesis. Importantly, we observed alveolar macrophages with these properties accumulating in treatment-naive human early-stage lung adenocarcinoma *in situ,* indicating that the cellular senescence program in macrophages is a conserved etiology. We also found that senescent alveolar macrophages accumulate in otherwise naturally aged normal mouse lungs and their persistence correlates with increased inflammation. Collectively, our findings suggest that targeting senescent macrophages may constitute a potential therapeutic intervention to postpone or attenuate lung cancer during the early stages of the disease.

#2973 Analysis of NBTXR3 nanoparticles recapture after release by dying cells.

J. Da silva, C. Bienassis, S. Paris;
Nanobiotix, Paris, France

In 2011, NBTXR3 emerged as the pioneering radioenhancer used in clinical practice to treat patients with locally advanced soft tissue sarcoma (LA-STS). Following the successful completion of a phase II/III clinical study for LA-STS, with a doubling of the pCR rate in the NBTXR3 arm compared with the control arm. NBTXR3 became the first radioenhancer to receive CE mark approval. NBTXR3 nanoparticles are composed of a functionalized core made of hafnium oxide, a high atomic number element. They were designed to enhance the effects of radiotherapy (RT) within cells without causing additional side effects on healthy tissues. Exploiting this physical mechanism, radiation-activated NBTXR3 (NBTXR3+RT) has exhibited superior efficacy in eradicating tumor cells and managing tumor growth in various preclinical models and in human studies. It surpasses the effects of RT alone while maintaining a favorable safety profile. Recent preclinical investigations have uncovered that the advantages of NBTXR3 go beyond mere radioenhancement and improved cancer cell destruction. Notably, NBTXR3 has been reported to possess immunomodulatory properties through several mechanisms, including 1) improved induction of DNA damage, leading to enhanced activation of the cGAS-STING pathway, 2) promotion of immunogenic cell death, 3) enhancement of immunopeptidome presentation, 4) generation of an antitumor immune response that results in the production of an abscopal effect mediated by CD8+ cytotoxic lymphocytes. Significantly, a series of recent studies using a two-tumor mouse model of anti-PD1-resistant lung cancer demonstrated that the addition of NBTXR3 significantly improved the efficacy of various treatment regimens (combinations of RT plus anti-PD1 and other checkpoint inhibitors) in terms of tumor growth, abscopal effect, and overall survival. Furthermore, similar benefits can be achieved when NBTXR3 is combined with proton therapy (PBT). Moreover, all these studies (both X-ray and PBT) reported a robust activation of the antitumor immune response, the restoration of the effectiveness of anti-PD1 therapy, and the induction of a memory response in cured mice. But our knowledge of the underlying biological processes that lead to these effects remains rather limited. For example, no information is available about the fate of these nanoparticles once they are injected into a tumor or when they are released by dying cancer cells. To gain a better understanding of these issues, we conducted a series of in vitro and in vivo experiments. We demonstrate that the endocytosis occurs similarly both in vivo and in vitro, at the level of tumor cells. Furthermore, we demonstrate in vitro that nanoparticles taken up by these tumor cells and subsequently released upon their death can be reinternalized by other tumor cells, thus facilitating their destruction by RT. These initial findings provide a deeper insight into the behavior of NBTXR3.

#2975 Vitamin D receptor signaling limits DNA damage at early stage of prostate tumorigenesis and prevents tumor aggressiveness.

K. Len[1], J. Gantzer[1], N. Le May[2], C. Thibault-Carpentier[1], D. Metzger[1], G. Laverny[1];
[1]IGBMC -CNRS UMR7104 - INSERM U1258 - Univ. of Strasbourg, Illkirch, France, [2]CRBS - INSERM U1112, Strasbourg, France

Prostate cancer (PCa) is the most common visceral neoplasm and the second leading cause of cancer-related deaths in male of western societies. Low circulating vitamin D levels and reduced expression of its receptor (VDR) correlate with PCa risk and severity, but the clinical use of vitamin D is limited by its pro-calcemic activities. To characterize the role of VDR in PCa, PTEN$^{(i)pe-/-}$ mice, that recapitulate the human disease and in which the tumor suppressor gene PTEN is selectively inactivated in prostatic epithelial cells (PECs) at adulthood, were compared to PTEN/VDR$^{(i)pe-/-}$ mice in which PECs are PTEN and VDR-deficient. Histological analysis showed that prostatic intraepithelial neoplasia (PIN) are formed between 1-3 months after gene inactivation (AGI). Importantly, VDR-deficiency increased by 2-fold the PECs proliferation rate as early as 1-month AGI. At this stage, RNA-seq and immunohistochemistry analysis revealed the presence of oxidative DNA damage selectively in VDR-deficient PINs. Moreover, a 4-week supplementation with the antioxidant N-acetyl cysteine reduced oxidative DNA damage in PTEN/VDR$^{(i)pe-/-}$ prostates, and normalized the number of Ki-67+ cells to the levels of PTEN$^{(i)pe-/-}$ ones. After 3 months AGI, both PTEN$^{(i)pe-/-}$ and PTEN/VDR$^{(i)pe-/-}$ tumors entered in a latency phase characterized by cellular senescence. However, the prostate weight in PTEN/VDR$^{(i)pe-/-}$ mice was 2-fold higher than in PTEN$^{(i)pe-/-}$ mice 12 months AGI. In addition, tumors of PTEN$^{(i)pe-/-}$ were mostly composed of non-invasive PIN-like adenocarcinoma, whereas invasive adenocarcinoma, sarcomatoid and squamous-cell carcinoma were observed in those of PTEN/VDR$^{(i)pe-/-}$ mice. Using single cell and spatial transcriptomics, we unraveled the presence of epithelial cells with epithelial-mesenchymal transition (EMT) hallmarks in PTEN/VDR$^{(i)pe-/-}$ prostate 10 months AGI. In addition, immunophenotyping revealed a higher infiltration of neutrophils, also termed as myeloid-derived suppressive cells and implicated in EMT and metastasis dissemination, in PTEN/VDR$^{(i)pe-/-}$ prostates compared to PTEN$^{(i)pe-/-}$ ones. Moreover, pan-cytokeratin-positive micro-metastasis were detected in lymph nodes and livers of PTEN/VDR$^{(i)pe-/-}$ mice, but not in those of PTEN$^{(i)pe-/-}$ mice, demonstrating that VDR-deficiency in PECs promotes aggressive PCa. Thus, VDR signaling exerts a protective role on PTEN-deficient PECs by limiting the oxidative-stress and proliferation during PINs initiation, and prevents PCa progression.

#2976 The potential use of butyrate and propionate to inhibit oncogenic phenotypes in oral squamous cell carcinoma and triple negative breast cancer.

A. J. Amaral Maisonet;
University of Puerto Rico Comprehensive Cancer Center, San Juan, Puerto Rico

Background
Oral squamous cell carcinoma (OSCC) and triple-negative breast cancer (TNBC) are aggressive cancers with low survival rates, particularly in Hispanics. Since the underpinning mechanisms of oncogenesis for both OSCC and TNBC are multifactorial, the development of novel targeted therapies is limited. The tumor microbiome has been shown to modulate the microenvironment. The microbial product short-chain fatty acids (SCFA) may represent a putative target for treatment as they can potentially inhibit cell growth, proliferation, migration, and induce morphologic changes in cancer cells. We evaluated the impact of the SCFAs butyrate, acetate, and propionate on the oncogenic phenotypes of OECM-1 and MDA-231 cell line models for OSCC and TNBC respectively.
Methods
OECM-1 and MDA-231 cell lines were cultured in RPMI-1640 medium supplemented with 10% FBS. Cytotoxicity was determined using an alamarBlue assay by treating the cells with SCFA in a series of 7 concentrations starting at 125 mM (1:2 dilution factor) for 24, 48, and 72 hours (h). Proliferation quantification was performed using trypan blue dye after treatment with SCFA for 24h, 48h and 72h. Migration and invasion were measured after treatment for 24h with SCFAs. Comparative analysis of our results was performed using GraphPad Prism v10.
Results
Higher concentrations of all SCFA decreased cell viability in OSCC and TNBC at all time points. In OECM-1 cells, the average inhibitory concentration of 50% (IC50) was 3mM for butyrate, 382mM for acetate, and 64mM for propionate while in MDA-MB-231 cells, the average IC50 was 4.3mM for butyrate, 462mM for acetate, and 20mM for propionate. Both OECM-1 and MDA-MB-231 cells treated with butyrate and propionate at 5mM resulted in a slower migration after 24h of treatment. Additionally, there was a significant reduction of cell number and proliferation rate after 48h and 72h of butyrate treatment at the concentrations 1mM ($p=0.0425$) and 5mM ($p=0.0007$) in OSCC.
Conclusions
Our results show that butyrate and propionate can reduce oncogenic phenotypes in OSCC and TNBC and may represent a potential target for the development of alternative treatment strategies for both cancers. Future work includes measuring the impact of these SCFA in epithelial-mesenchymal transition, loss of adhesion, and cell death.

#2977 Novel HSP90 inhibitors with senolytic activity for a targeted therapy in a hormone-induced breast cancer senescence model.

L. Cis[1], M. Gottardi Zamperla[2], V. Barbi[3], P. Cigala Fulgosi[3], S. De Martino[1], A. Aiello[4], S. Nanni[1], C. Cencioni[4], D. Pirolli[5], P. Tabarelli De Fatis[3], G. Ivaldi[3], M. Malavolta[6], C. Steinkuhler[7], M. De Rosa[5], A. Farsetti[4], S. Atlante[4], C. Gaetano[3];

[1]Universita Cattolica del Sacro Cuore, Roma, Italy, [2]stituti Clinici Scientifici Maugeri Spa Societa Benefit, Pavia, Italy, [3]Istituti Clinici Scientifici Maugeri Spa Societa Benefit, Pavia, Italy, [4]CNR-Istituto di analisi dei sistemi ed informatica, Roma, Italy, [5]CNR-Istituto di Scienze e Tecnologie Chimiche, Roma, Italy, [6]Istituto nazionale per il ricovero e la cura dell'anziano IRCCS, Pavia, Italy, [7]Italfarmaco Group, Cinisello Balsamo, Italy

Background: The research into senescent cells, particularly their accumulation and contribution to aging and age-related diseases, has gained significant momentum in recent years. This interest is primarily driven by findings in mouse models, where the excessive buildup of senescent cells is linked to various age-related pathologies. Consequently, there has been a concerted effort in the scientific community to identify and develop senolytics. A notable development in this field is the identification of senolytics within the class of HSP90 inhibitors. These inhibitors, initially investigated for their potential in cancer therapy, have been repurposed due to their high selectivity for senescent cells. Our research has led to new compounds with mild inhibitory activity against HSP90α in response to these challenges. These compounds stand out for their lack of toxic side effects and their demonstrated senolytic activity across multiple cellular models.
Objective: The primary objective of this research is to identify and characterize innovative HSP90 inhibitors that exhibit senolytic properties, specifically in the context of hormone-driven cancers.
Methods and Results: Utilizing a structure-based virtual screening technique, we identified several compounds displaying strong affinity and predicted inhibitory activity against the target protein, HSP90α. Among these, two inhibitors designated K4 and K5, demonstrated notable senolytic activity in vitro without inducing cytotoxic effects in non-senescent cells. These compounds were tested for their efficacy in senolytic activity and displayed half-maximal inhibitory concentrations (IC50) of 155 nM and 111 nM, respectively. The experimental model for this study was the MCF7 cell line, which was treated with 4-Hydroxytamoxifen (Tam, 10uM for 96 hours) to induce a state of senescence. Subsequent growth curve analyses and beta-galactosidase assays established that Tam treatment effectively halted cell proliferation and induced a senescence state in about 40% of the cell population compared to the ethanol control. When treated with K4 and K5 (10 uM for an additional 96 hours), a significant reduction in the senescent cell population was observed, with K5 showing a particularly pronounced increase in the mortality rate of these cells (up to 2.5-fold compared to the DMSO control). Western blot analysis supported these results, suggesting the effectiveness of K5 combined with Tam in inhibiting proliferation and inducing cell death in MCF7 cells.
Conclusion: Our findings propose a novel therapeutic approach for hormone-dependent breast cancer, combining the dual roles of tamoxifen and HSP90 inhibitors to target senescent cancer cells. This strategy could reduce tumor recurrence and contribute to the advancement of cancer treatment methods.

#2978 Extracellular ATP induced senescence in human lung cancer cells.

R. A. Ward, A. Hunt, N. Anderson, X. Chen;
Ohio University, Athens, OH

In tumors, extracellular ATP (eATP) concentrations are 1,000 to 10,000 times higher than is found in normal tissues and eATP is up taken through macropinocytosis leading to a large increase in intracellular ATP levels. eATP is also linked to the TGF-β signaling pathway as exocytosis of ATP is induced that is then used in an autocrine fashion activating the P2X7 purinergic receptor[1]. Through these mechanisms, eATP has also been recently shown to induce EMT, CSC formation, and drug resistance[1]. One of the mechanisms through which these processes may be induced is a senescent cell precursor[2]. Senescence is a generally irreversible epigenetically controlled process characterized by a complete exit from the cell cycle in response to either DNA damage, stressful conditions, or aging. Recent mounting evidence has shown that senescence can be a cancer promoting mechanism by entering this state in response to stress such as during chemotherapy, but they can utilize it to enhance their malignant capabilities, including the ability to escape their senescent state with heightened stem cell characteristics, which can lead to a higher chance of relapse after treatment[2]. Senescent cells have recently been named a hallmark of cancer[3]. This study shows the time dependent induction of a senescent like state in human lung cancer A549 cells after only 2 hours of treatment with 0.5mM eATP, the concentration found in the tumor microenvironment, through analysis of transcriptional markers using total polyA RNAseq as well as chromogenic and flow cytometric assays for senescence associated beta-galactosidase activity. Additionally, inhibitors of macropinocytosis and purinergic receptors have been used to gain insight into the mechanisms of action that this pathway takes. This demonstrates a novel use of ATP within the tumor microenvironment for aiding in cancer progression and drug resistance. After EMT, CSC formation, and drug resistance, senescence is added to the long list of eATP mediated cancer promoting processes.

1. Song J, Qian Y, Evers M, Nielsen CM, Chen X. Cancer Stem Cell Formation Induced and Regulated by Extracellular ATP and Stanniocalcin-1 in Human Lung Cancer Cells and Tumors. *IJMS*. 2022;23(23):14770. doi:10.3390/ijms232314770 2. Zhang D, Monteiro MJ, Liu J, Gu W. Mechanisms of cancer stem cell senescence: Current understanding and future perspectives. *Clin Exp Pharma Physio*. 2021;48(9):1185-1202. doi:10.1111/1440-1681.13528 3. Hanahan D. Hallmarks of Cancer: New Dimensions. *Cancer Discovery*. 2022;12(1):31-46. doi:10.1158/2159-8290.CD-21-1059

#2979 Pancreatic cancer cells upregulate LPAR4 in response to isolation stress to create a fibronectin-rich extracellular matrix niche and promote tumor initiation.

C. Wu, T. Rakhshandehroo, H. I. Wettersten, A. Campos, T. Schalscha, S. Jain, Z. Yu, J. Tan, E. Mose, B. G. Childers, A. M. Lowy, S. M. Weis, D. A. Cheresh; UC San Diego, San Diego, CA

Tumor initiation is an inefficient process in which tumor cells must develop cell-autonomous mechanisms to survive harsh microenvironments, establish colonies, and thereby overcome “isolation stress.” We report that pancreatic cancer cells transiently upregulate lysophosphatidic acid receptor 4 (LPAR4), a G-protein coupled receptor, in response to microenvironmental stress or chemotherapy, which promotes stress tolerance, drug resistance, and tumor initiation. Even without exogenous LPA, LPAR4 drives the expression of a subset of extracellular matrix (ECM) genes via an AKT/CREB axis, including fibronectin and versican, which are established drivers of cancer stemness. The upregulation of fibronectin is indispensable for LPAR4-induced tumor initiation in vivo and anchorage-independent growth in vitro. Furthermore, the ligation of this fibronectin-containing ECM created by LPAR4-positive cells via integrins α5β1 or αvβ3 can transfer cancer stemness and stress tolerance to LPAR4-negative cells by activating Yes-associated protein 1 (YAP). Our findings reveal that in response to isolation stress, pancreatic tumor cells that upregulate LPAR4 can autonomously generate a fibronectin-enriched ECM niche and thereby initiate tumor formation.

#2980 Exploiting the selenoproteome in uveal melanoma.

A. Sanders, C. Cunanan, E. Hartsough;
Drexel University College of Medicine, Philadelphia, PA

Uveal melanoma (UM) is a common intraocular malignancy arising from GNAQ/GNA11 mutations in uveal tract melanocytes. Although primary UM is treatable by radiation and enucleation, half of patients will develop liver metastasis. Unfortunately, patients with metastatic UM have a poor prognosis of approximately one-year - underscoring metastatic UM as one of the deadliest cancers. A strong prognostic indicator for UM liver metastases is a deletion or inactivation of the deubiquitinase BAP1, yet its specific role in disease progression is unclear. Intriguingly, upon BAP1 loss of function, the cysteine importer SLC7A11 is up regulated. Imported cysteine can be converted into glutathione serving as a cofactor for antioxidant enzymes like GPX4, a selenoprotein (SeP). SePs are a protein family characterized by having at least one selenocysteine - a selenium (Se) containing amino acid. Interestingly, the liver serves as a major hub for Se transport via Selenoprotein P (SEPP). The selenocysteine rich SEPP is secreted by hepatocytes and catabolized in recipient cells facilitating synthesis of de novo SeP. Here we hypothesize that mutant BAP1 UM utilizes the liver's Se rich microenvironment to augment selenoproteome expression to stave off oxidative stress. Using publicly available datasets, we found patients with mutant BAP1 UM have increased expression of antioxidants proteins and genes associated with SeP expression. In a panel of BAP1 expressing and deficient UM cells, we found that BAP1 deficient cells have increased expression of SePs, suggesting a predisposition to resist oxidative stress. In the presence of exogenous Se, UM cell lines upregulate SeP expression indicating the importance of selenium availability for SeP expression. In addition, a hepatocyte cell line, and an ex vivo liver slice co-culture model was used to confirm that SEPP was produced in the liver slices and was associated with increased SeP expression in UM cells. Furthermore, we found that BAP1 null UM cells were more susceptible to GPX4 inhibition compared to wild type cells, suggesting a reliance on SeP expression. Taken together, these findings suggest that the liver associated selenoproteome expression may underpin an oxidative stress-associated therapeutic vulnerability in UM liver metastases.

MOLECULAR/CELLULAR BIOLOGY AND GENETICS: microRNA- and Other Non-coding RNA-Based Translational Medicine
Poster Session

#2984 Prostate cancer associated glycosylated RNAs: Who are you and where are you hiding?.
S. McGuire, E. Jones, S. Moen, A. Esquela-Kerscher;
Eastern Virginia Medical School, Norfolk, VA

Glycosylated RNA (glycoRNA) is an emerging field. Carbohydrate modifications are vital for biomolecule (proteins and lipids) stability, transport, and localization. Glycosylation influences cell functions like differentiation, apoptosis, and immune response, potentially impacting human disease. The Bertozzi lab initially discovered that RNAs can carry sugar modifications when they metabolically labeled mammalian cultured cells using bioorthogonal chemistry methods normally employed for glycosylated protein and lipid enrichment. Our lab wanted to investigate the translational potential of glycoRNAs and determine if these modifications could be developed as novel clinical targets for aggressive prostate cancer. (PCa). As advanced forms of PCa often lead to poor prognoses, it is imperative that better screening biomarkers and therapeutic treatment options are developed to increase patient survivorship. We predicted that glycoRNA expression would correlate with malignancy, metastatic status, and hormone sensitivity in prostate cells. Our lab used the sialic acid metabolic precursor Ac4ManNAz and click chemistry to label a panel of human prostate cancer cell lines representing the spectrum of prostate disease followed by rigorous RNA isolation procedures and northern blot analysis. We found that human prostate cell lines with no (RWPE-1) or low malignancy (LNCaP) expressed higher levels of glycoRNA belonging to the small <200 nt (but not large) noncoding RNA class compared to aggressive, metastatic PCa cell lines. Our glycosidase studies and lectin northern blot analysis indicated that RNA carries both N-linked and O-linked modifications. Based on these findings, we hypothesized that glycosylated RNA plays an important role in maintaining prostate homeostasis and in cancer protection. To better profile these glycoRNAs, we aimed to: 1) Test a wider range of metabolic labeling regents to characterize the glycoRNA populations using a panel of human prostate cell lines; 2) Perform cellular fractionation studies to determine localization of glycoRNA in prostate cells; and 3) Explore glycoRNAs in a genetic animal model. These studies focused on LNCaP PCa cell lines, which express high levels of glycoRNA. We found that small glycoRNA expression was noted when LNCaP cells were metabolically labeled with Ac_4GalNAz (predominantly O-linked) and Ac_4ManNAz (predominantly N-linked), verifying glycoRNA heterogeneity. Cellular fractionation studies indicated glycoRNA localization was enriched in the membrane fraction of LNCaP cells using these metabolic labels. Furthermore, we verified that *C. elegans* grown on Ac_4GalNAz plates expressed small glycoRNA, indicating biological conservation. We are now characterizing these glycoRNAs using RNA sequencing and LC-MS/MS glycomics. Our findings will provide novel insights into cancer-associated glycoRNA, leading to improved clinical tools for PCa.

#2985 RXR agonist, 9cUAB30 impacts epigenetic regulations to achieve chemoprevention of UVB-induced Skin cancer by altering global miRNA profiling.

M. P. Kashyap, R. Sinha, C. A. Elmets, V. R. Atigadda, M. Athar;
University of Alabama at Birmingham, Birmingham, AL

Basal cell carcinoma (BCCs) and Squamous cell carcinoma (SCCs) are the most common skin neoplasms in the Caucasian population. UVB is considered as the most important etiologic factor for these cancers. The molecular mechanism regulating pathogenesis of these neoplasms is not well defined. Similar to humans Ptch$^{+/-}$/SKH-1 mice develop both BCCs and SCCs, following chronic UVB-irradiation. We used TaqMan-based Open Array platform containing 796 miRNAs (miRs) to profile miRs associated with BCCs and SCCs. Pathway enrichment analysis was performed using miRPathDB databases at https://mpd.bioinf.uni-sb.de/. 81 miRNAs were differentially expressed in BCCs, of which 54 miRs had cumulative frequency of greater than 1 (FC>1) and 78 miRs were differentially expressed in SCCs, out of which 20 miRs had FC>1. miR-721 was highly induced (123.75 fold, P<0.0430) in BCCs followed by miR-2182, miR-21, miR-451, miR-124a, and miR-685 while downmodulated miRs includes miR-1, miR-133a, miR-133b, and miR-196b. Likewise, miR-21 had maximum fold induction (45.94, P<0.007) in SCCs followed by miR-2182, miR-685, miR-1938, miR-2138, and miR-451 while miR-196b, miR196c, and miR-1 were downmodulated. Kegg pathways analysis revealed that altered miRs belong to Hepatitis B, HIF-1, FoxO, chemokine, adipocytokine, NFκB, cholinergic and TLR signaling pathways. WikiPathway database showed alterations in miRs associated with neovascularization process, Notch Signaling, Pregnane X receptor, α6β4, and BDNF-TrkB signaling. To further investigate the importance of pathways associated with tumor progression, we profiled miRs in residual BCCs and SCCs procured from UAB30 treatment groups. The chemopreventive agent UAB30 is an RXR agonist. In BCCs, UAB30 treatment significantly downmodulated UVB-upregulated miRs. These miRs includes miR-210, miR-546, miR-324-3p, miR-706 and miR-1898. However, UAB30 treatment significantly upregulates miR-380-5p which was downmodulated by UVB-alone. These miRs were involved in immune regulation, Fanconi anemia pathways, FoxO signaling, prostate cancer and p53 signaling. In SCCs, UAB30 treatment significantly reversed the expression of various miRs which were downmodulated by UVB. These miRs were miR-24, miR-26a, miR-30c, miR-328, miR-30b, miR-495 and miR-2100. The expression of miR-21a-3p was downmodulated by UAB30 in SCCs of UVB-exposed group relative to SCCs of untreated but UVB-exposed group. These miRs belong to pathways involved in cell cycle progression, p53 signaling, viral carcinogenesis, Hepatitis B, Melanoma, Prostate cancer, FoxO and PI3K-AKT signaling. In summary, this profiling of miRs in UVB-induced BCC and SCC represents the underlying epigenetic mechanisms that regulate various signaling pathways in these cancers. Our data also show the critical role of miRs responsive to UAB30 treatment in cancer chemoprevention.

#2986 Germline signatures predicting toxicity and response to CTLA4 inhibitors.

J. B. Weidhaas[1], K. McGreevy[1], N. Marco[2], N. Sundahl[3], C. R. Cabanski[4], C. Spencer[4], P. Ost[5], D. Telesca[1];
[1]UCLA David Geffen School of Medicine, Los Angeles, CA, [2]Duke University, Durham, NC, [3]AZ Groeninge, Kortrijk, Belgium, [4]Parker Institute for Cancer Immunotherapy, San Francisco, CA, [5]Ghent University, Ghent, Belgium

Background: Because germline microRNA-based variants predict toxicity risk to anti-PD-1/PDL-1 treatment, and CTLA4 inhibitors are often used in combination with them, we wanted to see if we could also predict toxicity and/or response to anti-CTLA4 therapy.
Methods: The study included 69 patients from 3 institutions treated with anti-CTLA4 therapy alone. Patients were 23-89 years old with median age of 62. “Toxicity” was defined as grade 3 or higher toxicity and “Response” as a complete response, partial response, or stable disease. A panel of previously tested variants (n=139), age, sex and cycles of anti-CTLA4 were used to predict endpoints of interest. To balance model dimensionality we pre-screened variants and included them if they were marginally associated with our outcomes of interest via Fisher’s Exact Test or Jonckheere-Terpstra Test at a p-value threshold of < 0.2. We fit Elastic Net (EN), Random Forest (RF), and Boosted Tree (BT) models with up-sampling to predict outcomes of interest. Leave-one-out cross validation (LOOCV) was used to evaluate model performance, and the model with the highest LOOCV AUC (between all EN, RF, and BT) was chosen as the final model and re-fit using all observations. We also performed a stratified gene ontology (GO) analysis to assess biological differences between variants involved in the signatures. Our GO analysis compared gene clusters across groupings with an adjusted p-value cutoff of 0.05 against a universal genomic background.
Results: 15 patients had toxicity and 21 patients had a response, with 27/139 and 25/139 variants marginally associated with these endpoints, respectively. Our toxicity model had a LOOCV AUC of 0.811 with the top variables being age, TNNT2_rs3729843, REV3L_rs465646, miR34b_c_rs4938723, and XRCC3_rs861539. Our response model had an LOOCV AUC of 0.716 with top variants being IL2RA_rs2476491, REV3L_rs465646, and IL10RB_rs2834167. Including anti-CTLA4 cycles improved the prediction accuracy for Response with an AUC 0.764. GO analysis revealed 117 pathways enriched in both the Toxicity and Response signatures, which were predominantly involved in pri-miRNA transcriptional regulation. Top GO terms in the Response signature (333 unique) were related to apoptosis and cell death. Top GO terms in the Toxicity signature (425 unique) were related to DNA replication and cellular signaling and response, including the interleukin-35-mediated signaling pathway.
Conclusion: We identified germline signatures predicting toxicity and response following anti-CTLA4 therapy. These signatures differed from each other as well as from a previously identified signature of toxicity to anti-PD1/PDL-1 therapy, and GO analysis identified plausible underlying signaling pathways. Our findings continue to validate the potential of these variants to predict meaningful endpoints in cancer therapy, and thus further research in larger and more diverse cohorts is warranted.

#2987 microRNA (miRNA) a putative biomarker to better define the molecular apocrine breast cancer (MABC) subtype.

G. Chamandi[1], A. Borgel[2], A. Kurdi[1], P. Khoueiry[1], L. Teixeira[3], M. Le Bras[2], J. Lehamnn[2], **R. Nasr**[1];
[1]American University of Beirut, Beirut, Lebanon, [2]INSERM U976, HIPI, Paris, France, [3]St. Louis Hospital Paris, Paris, France

Background: Breast cancer (BC), is a highly heterogeneous disease, divided into molecular subtypes based on gene expression and clinical outcomes. Transcriptomics profiling depicted a subtype that has luminal expression profile but lacks estrogen receptor (ER), progesterone receptor expression with an overlapping expression of HER-2; yet it overexpresses androgen receptor (AR). This subtype was referred to as MABC and constitutes 8-14% of all BC types. At present MABC is often misdiagnosed with triple negative BC (TNBC). Its improper diagnosis demands the adoption of complementary tools; miRNA, key players in BC tumorigenic processes, hold promise in defining MABC.
Methods: 539 BC microarray data were downloaded from The Cancer Genome Atlas (TCGA-BRCA) (PMID: 25691825) using TCGA biolinks R/Bioconductor package (PMID:267704973). Cases with available miRNA data were retained and classified using citbcmst R package (PMID: 21785460). Differential expression analysis identified deregulated miRNAs using DEseq2. The validation set consists of 111 ER-neg samples (68 MABC, and 43 TN samples) with an average age at diagnosis 58.51 years and a median follow-up=78.5 months. MABC tumors were characterized apart of TNBC by the molecular signature (AR, FOXA1 and AR-related genes, PMID: 25516281) on fresh tissue sections. Using miRCURY LNA™ miRNA PCR assay, miRNA profiling was done for a panel of differentially expressed miRNAs. Non tumorigenic (MCF-10A) and BC Cellular models MABC (MDA-MB-453) and TNBC (MDA-MB-231) were used to investigate the invasive potential of MABC.
Results: TCGA data analysis indicated MABC as a separate entity based on gene signature. MiRNA-seq data analysis depicted a set of 6 significantly deregulated miRNA with absolute value of log2 fold change> 1 and P-adjusted value <0.05 between MABC and TNBC. We validated, by miRNA profiling, significant upregulation of miR-2115-3p and miR-187-3p in MABC compared to TNBC. These miRNAs significantly differentiate MABC patients from TNBC patients where the combined miRNA panel of miR-2115-3p and miR-187-3p had an area under the curve of 0.904 ±0.28 (P<0.0001 and 95% CI: 0.850-0.958) and sensitivity, specificity, and a diagnostic accuracy of 90.41%, 81.1%, and 86.5% respectively. Preliminary data, showed that non-tumorigenic/non-invasive MCF-10A had a significant increase in its invasive ability upon transfection with miR-187-3p mimic (P<0.05). Similarly, the invasive cell line MDA-MB-231 showed a significant increase in invasion upon transfection with miR-187-3p mimic (P<0.05). On the other hand, only miR-187-3p inhibitor significantly decreased the invasive potential of MDA-MB-453 cells (P<0.05).
Conclusion: MABC has a unique signature of miRNA as compared to TNBC. miR-2115-3p, and miR-187-3p could be potential diagnostic biomarkers for MABC. The invasive potential of MABC could be attributed to miR-187-3p activity.

#2988 TUG1 exosomal lncRNA sponges let-7 miRNA family members and advances prostate cancer.

R. M. Marima[1], M. Mbeje[1], J. Kandhavelu[2], C. Penny[3], Z. Dlamini[1];

[1]University of Pretoria, Pretoria, South Africa, [2]Georgetown University Medical Center, Washington, WA, [3]University of the Witwatersrand, Johannesburg, South Africa

Exosomal long-non coding RNAs (lncRNAs) play an important role in cancer progression and have potential prognostic biomarker potential in several cancers including prostate cancer (PCa). Taurine-upregulated gene 1 (TUG1) is an oncogenic lncRNA overexpressed in PCa. This exosomal lncRNA has been reported to promote PCa migration, invasion and Epithelial-Mesenchymal Transition (EMT). However, TUG1 PCa prognostic mechanisms remain to be elucidated. This study aimed to profile differentially expressed lncRNAs in PCa high-grade tumor cells (PC-3) cells compared to low-grade PCa tumor cells (LNCaP). This was achieved by using a 384-well plate of PCa lncRNA gene panel. A human lncRNA database, LncSEA and other bioinformatics tools were used for annotation and enrichment analysis. RT-qPCR was used to confirm the gene array data. Up or down-regulation of ±2 and $p < 0.05$ were considered significant. Forty two (42%) percent and 14% of lncRNAs were shown to be up and downregulated, respectively. Notably, TUG1 was shown to be upregulated in PC-3 cells from PCR array and RT-qPCR results. Bioinformatics analysis revealed that TUG1 is involved in several cancer hallmarks including apoptosis evasion, migration, invasion and EMT. Furthermore, lncRNA/miRNA complexes regulate a series of oncogenic signaling pathways and this study demonstrated that TUG1 sponges the let-7 miRNA family members (a highly conserved tumor suppressor miRNA family) and promotes PCa progression. Precise mechanisms of TUG1/ let-7 axis in PCa prognosis need to be largely elucidated as this may hold potential to understanding lncRNA/miRNA-mediated PCa progression and thus be targeted for novel therapeutics.

#2989 MicroRNA profiling in human samples and cell lines uncovers eight key players in the cisplain resistance of HGSOC.

M. Rivera-Serrano[1], M. Flores[2], J. Rolon[2], V. Reyes[2], F. Valiyeva[1], P. E. Vivas-Mejia[1];
[1]UPR - Comprehensive Cancer Center, San Juan, PR, [2]UPR Medical Sciences Campus, San Juan, PR

Metastasis and drug resistance remain significant contributors to cancer-related mortality globally. In ovarian cancer, a substantial 70% of cases develop resistance to the front-line therapy, cisplatin. Despite numerous proposed mechanisms for cisplatin resistance, the complete molecular events leading to this phenomenon in ovarian cancer remain incompletely understood. Mounting evidence suggests that dysregulation of microRNAs (miRNAs) plays a pivotal role in carcinogenesis, including the development of drug resistance. While various miRNAs have been identified in ovarian cancer samples and cell lines, few studies have compared miRNA expression in human paraffin ovarian samples and cisplatin-resistant high-grade serous ovarian cancer (HGSOC), the most prevalent and malignant of gynecological malignancies. This study aimed to identify key miRNAs implicated in cisplatin resistance. We performed miRNA expression profiles in RNA isolated from human paraffin ovarian tumors and ovarian cancers cell lines. Eight miRNAs were commonly increased in paraffin samples and cisplatin resistant ovarian cancer cells. Targeting these miRNAs with inhibitors significantly reduced cell proliferation by more than 50% for miR-203a, miR-96-5p, miR-10a-5p, miR-141-3p, miR-200c-3p, and miR-182-5p, and to a lesser extent, miR-296-5p and miR-1206. Inhibitors demonstrated a reduction in cell migration for all targets except miR-200c-3p and miR-10a-5p. Analysis of online databases, literature reports, and molecular pathway construction revealed that these eight miRNAs regulate key molecular pathways associated with cell proliferation, primarily through PTEN regulation in cisplatin-resistant HGSOC cells. Interrogation of the KM plotter patient database revealed that high expression of miR-1206, miR-10a, miR-141, and miR-96 correlates with a poor prognosis in ovarian cancer patients. These findings position these eight miRNAs as potential therapeutic targets and markers for cisplatin response in ovarian cancer therapy.

#2990 Differential micro-RNA expression in circulating exosomes of pancreatic ductal adenocarcinoma patients.

R. Kaur, S. Bhoriwal, P. K. Gautam;
All India Institute of Medical Sciences (AIIMS) New Delhi, New Delhi, India

Pancreatic ductal Adenocarcinoma (PDAC) is a highly lethal solid tumor with 5-year survival rate of 5-8%. Extracellular vesicles like exosomes circulating in the blood are crucial mediators of intracellular communication, immunomodulation and tumor progression. The microRNAs being the major cargo of exosomes, are the primary carriers of intracellular information. The role of exosomal-miRNA (exoMIR's) in regulating the pathogenesis of tumors is well-established in oncology but its potential is still unexplored. To the best of our knowledge no study has yet explored the contrasting exoMIR expression in cancer patients before and after their surgery. In this study, differential exoMIR's profile of three pancreatic ductal adenocarcinoma patients at three stages: pre-surgery, post-surgery, and follow-up was established using small RNA sequencing on the Illumina platform. In blood samples taken before and after surgery total of 181, 201 and 201 microRNAs were dysregulated in circulating exosomes of three different patients viz. P_1, P_9 & P_11 (Patient identifiers) respectively. Out of the total dysregulated microRNAs in post-op samples 76 were upregulated and 105 downregulated in P_1, 95 upregulated and 106 downregulated in P_9 & 69 upregulated and 132 downregulated in P_11 as compared to their Pre surgery samples. Further, when exoMIR's of post-op samples were compared to that of follow-up samples after 6 months of surgery their expression profile changed notably such that a total of 184, 157 & 190 microRNAs dysregulated in follow-up of P_1, P_9 and P_11 respectively. Out of the total dysregulated microRNAs in follow up samples 93 were upregulated and 91 downregulated in P_1, 69 upregulated and 88 downregulated in P_9 & 96 upregulated and 94 downregulated in P_11 as compared to their post-op samples. On Venn diagram analysis 27 microRNAs were found to be commonly dysregulated in all 3 patients before surgery and 22 common micro RNAs were again dysregulated even after 6 months of surgery. Bioinformatic analysis of these
differentially expressed miRNAs and their respective protein targets revealed that their role in oncogenic molecular pathways is very prominent, thus highlighting their potential use in cancer therapeutics, diagnostics as well as prognosis.

#2991 Global analysis of miR-210 and miR-21 dysregulation and direct targeting in thyroid cancer during hypoxia.

B. H. Powell[1], W. T. Mills IV[1], A. Turchinovich[2], Y. Wang[1], M. A. Zeiger[3], C. B. Umbricht[1], M. K. Meffert[1], K. W. Witwer[1];
[1]Johns Hopkins University, Baltimore, MD, [2]SciBerg e.Kfm, Mannheim, Germany, [3]National Cancer Institute, National Institutes of Health, Bethesda, MD

Introduction: Hypoxia is frequent in solid tumors and stabilizes Hypoxia Inducible Factor-1 (HIF-1). HIF-1, in turn, activates several cellular pathways that promote tumor growth and resistance to chemotherapy. MicroRNA (miRNA) miR-210 is a direct HIF-1 target. HIF-1 binds to a Hypoxia-Response Element (HRE) in the miR-210 promoter, up-regulating its expression. miR-21 is the most widely reported oncogenic miRNA in cancer. miRNAs complexed with Argonaute-2 (AGO2) bind target mRNAs to inhibit translation. Given that a single miRNA can have hundreds of predicted mRNA targets, we sought to identify mRNA targets of miR-210 and miR-21. Identifying dysregulated target genes of miR-210 and miR-21 may highlight new therapeutic targets.
Methods: The SW1736 (anaplastic thyroid cancer) cell line was cultured at 2% (hypoxic) or atmospheric (normoxic) O_2 for 24 or 48hrs. HIF-1α accumulation relative to normoxia was analyzed by Western blot. miR-210-3p expression was measured relative to normoxia by RT-qPCR. Small and total RNA-sequencing was performed to identify additional differentially expressed miRNAs and mRNAs in hypoxia after 48hrs. To identify direct miRNA targets, SW1736 cells were cross-linked by UV irradiation after 48hrs of normoxic or hypoxic conditions. AGO2 covalently cross-linked to miRNA and target mRNAs were purified by immunoprecipitation after DNA and RNA digestion. miRNA and target mRNAs protected by AGO2 were ligated to generate chimeric miRNA:mRNA molecules followed by sequencing. miRNA:mRNA chimeras were analyzed using the SCRAP bioinformatic pipeline.
Results: miR-210-3p expression was up-regulated by ~11-fold at 24hrs and ~19-fold at 48hrs, which was consistent with increased HIF-1α protein levels assessed by Western blot. miR-210-3p and HIF-1α levels were highest after 48hr of hypoxia relative to normoxia. Small RNA-seq showed that miR-210-3p was the only miRNA significantly up-regulated (>2-fold) in hypoxia (48hr) in SW1736. Further, miRNA:mRNA chimeric sequencing results confirmed that miRNAs primarily interacted with the 3'UTRs and coding sequences of mRNA. miR-210-3p was most abundant in hypoxia and found in chimeras with HIF-1α mRNA as well as some oncogenic and tumor suppressor transcripts involved in metabolism and mRNA processing. miR-21-5p was the most abundant chimera miRNA in both normoxia and hypoxia and was primarily bound to tumor suppressor mRNAs associated with cell cycle arrest, TGFB signaling, and inhibition of tumor invasion and migration.
Conclusions: miR-210-3p and miR-21-5p elevated levels and interactions indicate hypoxia and malignancy in solid tumors including breast, thyroid, prostate, and lung. Further analysis of other miRNA:mRNA interactions and functional validation may aid in identifying novel therapies for solid tumors.

#2992 miR-200-mediated inactivation of cancer-associated fibroblasts attenuates lung cancer invasion and metastasis.

I. Cheon, S. Lee, Y.-H. Ahn;
Ewha Womans University College of Medicine, Seoul, Korea, Republic of

Cancer-associated fibroblasts (CAFs) play a crucial role in the tumor microenvironment and contribute to the development and progression of lung cancer. We aimed to elucidate whether miRNA-200 (miR-200), which is recognized for its ability to suppress EMT, prevents CAFs from promoting cancer progression. Inactivation of CAFs mediated by miR-200 suppressed lung cancer cell invasion, migration, tumorigenesis, and metastasis. Additionally, miR-200 attenuated the ability of CAFs to facilitate the aggressiveness of lung cancer cells, encourage M2 polarization of macrophages, and increase the angiogenic sprouting of vascular endothelial cells. NRP2, known as a co-receptor of VEGFR, was identified as a target of miR-200, mediating the functional activity of miR-200 in CAFs. NRP2-VEGFR signaling promoted the secretion of VEGFD and PTN from CAFs to activate cancer cell migration and invasion. Based on these findings, we suggest that miR-200 impedes cancer progression and metastasis by remodeling CAFs, and that miR-200 and NRP2 are potential therapeutic targets in the treatment of lung cancer.

#2993 TmiS: A prognostic indicator for prostate cancer survival based on total tumor cell miRNA levels.

M. Montierth[1], K. Nemeth[2], G. A. Calin[2], W. Wang[2];

[1]Baylor College of Medicine, Houston, TX, [2]University of Texas MD Anderson Cancer Center, Houston, TX

Background: MicroRNAs (miRNAs) are small noncoding RNAs that bind mRNA and inhibit translation or encourage degradation. MiRNAs play a significant regulatory role, with approximately 60% of protein-coding genes harboring miRNA binding sites. MiRNA dysregulation is associated with tumor onset, growth, and metastasis. These important regulatory RNAs have been studied as potential cancer biomarkers, yet the widespread adoption of any miRNA signature has been hindered by the variable nature of miRNA targeting, which is highly context specific. Total tumor cell mRNA content, or TmS, has been shown to have potential as a pan-cancer prognostic indicator. Here we expand the TmS framework using deconvolved miRNA expression to calculate TmiS, an estimate of total tumor-cell miRNA content and investigate the utility of TmiS as a prognostic marker in prostate cancer.

Methods: Whole exome sequencing and miRNA sequencing, along with clinical annotations were downloaded for prostate cancer patient samples from The Cancer Genome Atlas (TCGA). Sample purity and ploidy were estimated from exomes using ASACT and ABSOLUTE. Tumor miRNA proportion was estimated using our previously developed miRNA deconvolution method DeMixMir, and TmiS, the total miRNA content per haploid genome per tumor cell, was calculated for each sample. Patients were separated by Gleason category and were binarized into High-TmiS and Low-TmiS within samples with Gleason 7 and Gleason 8+ scores separately.

Results: We find Low-TmiS patients to have significantly better prognosis in both Gleason 7 ($P = 0.04$) and Gleason 8+ ($P = 0.01$) prostate cancer. We confirm that TmiS is indeed an aggregate measure of total miRNA levels, with no strong correlations observed with any one miRNA. We identify differentially expressed miRNAs and mRNAs between high and low TmiS, and find distinct enriched pathways between Gleason 7 and Gleason 8+ samples, and that several of the differentially expressed miRNAs are well-characterized cancer-related transcripts.

Conclusions: In spite of their important regulatory function, the variable and context specific nature of miRNA targeting has been a barrier to their implementation as a robust biomarker. We find TmiS to be a measure of total miRNA dysregulation, and that patients with high total miRNA content show poorer survival within prostate samples graded at Gleason 7 (as well as Gleason 8+), which has been a challenging group for further risk classification. In summary, while the consequences of miRNA dysregulation are subtype specific, we find that by measuring total tumor cell miRNA, TmiS has potential as a robust prognostic indicator independent cellular context.

#2994 MIR99AHG promotes ERα expression and ER-positive breast cancer cells proliferation via activating Hippo signaling.

Wende Wang[1], Danping Lin[1], Ziyang Lin[1], Yangyang Yan[1], Yusen Qin[1], Yuanke Liang[2], Haoyu Lin[2], De Zeng[1]

[1]Department of Breast Medical Oncology, Cancer Hospital of Shantou University Medical College, Shantou, China,[2]Department of Breast and Thyroid Surgery, The First Affiliated Hospital of Shantou University Medical College, Shantou, China

Background: Estrogen receptor (ER) positive breast cancer is the most common subtype of breast cancer. Elucidation of the regulatory network in estrogen receptor pathway is critical to develop and deliver potent targeted therapy for ER-positive breast cancer. The Mir-99a-let-7c cluster host gene MIR99AHG is a long non-coding RNA involving in a variety of tumor formation and disease progression processes. However, the biological functions of MIR99AHG in ER-positive breast cancer have not been reported.

Methods: The Western-blot, qRT-PCR, Immunofluorescence and fluorescence in-situ hybridization were used to identify potential target genes and regulatory pathway of estrogen receptor α (ERa), which is a key proliferative driver of ER-positive breast cancer cells. The cell proliferation assay, clone formation assay, xenograft tumor model and rescue assay were used to investigate the effect of differential expression of MIR99AHG on the proliferative capacity of ER-positive breast cancer cells MCF7 and T47D. In addition, correlation analysis was performed to verify the relation of the expression of MIR99AHG, LATS1, LATS2, CYR61, CTGF and ESR1 from The Cancer Genome Atlas (TCGA) and Gene Expression Omnibus (GEO) cohorts. And survival analysis was used to predict the prognostic impact of MIR99AHG in breast cancer patients.

Results: MIR99AHG expression was significantly higher in ER-positive breast cancer cells MCF7 and T47D than in ER-negative breast cancer cells SKBR3, MDA-MB-231 and BT549. The high expression of MIR99AHG predicted poor prognosis in ER-positive breast cancer patients. *In vitro* and *in vivo* assays demonstrated that MIR99AHG positively regulated the proliferation of MCF7 and T47D cells. Importantly, the Hippo signaling was identified to be down-stream mediators of MIR99AHG in modulating ERα transcription. Furthermore, XMU-MP-1, which targets the Hippo signaling upstream kinase MST1/2, was able to reverse the effect of MIR99AHG on MCF7 cell proliferation.

Conclusions: MIR99AHG up-regulates ERα expression and promotes proliferation in ER-positive breast cancer cells through activating Hippo signaling pathway. Targeting MIR99AHG/Hippo pathway is a potential strategy for the treatment of ER-positive breast cancer.

#2995 The ectopic expression of miR-380-5p interferes with the aggressive traits of diffuse malignant peritoneal mesothelima cells.

Stefano Percio, Lorenzo Di Pietro, Eisa Naghshineh, Marcello Deraco, Nadia Zaffaroni, **Marco Folini**

Fondazione IRCCS Istituto Nazionale dei Tumori, Milan, Italy

Telomerase activity (TA) and the alternative lengthening of telomere (ALT) pathway are two telomere maintenance mechanisms (TMM) yet identified in human cancers. Although the activation of either TMM seems to be equivalent in supporting tumor cell immortalization (a hallmark of cancer), the contribution of TA and ALT to tumor progression and aggressiveness may be different. Mounting evidence suggests that cancer cell aggressiveness could be associated with a TA↔ALT shift that would allow the acquisition of distinct aggressive traits. We previously showed that an ALT-like phenotype emerged in diffuse malignant peritoneal mesothelioma (DMPM) cells upon miR-380-5p-dependent inhibition of TA (*Cimino-Reale G, et al. J Hematol Oncol. 2017*). To analyze the transcriptomic changes associated with the emergence of such a phenotype, gene expression profiling was carried out. Results showed that 3331 genes were differentially expressed (FDR<0.05, adjusted for multiple hypothesis testing) in miR-380-5p- *vs.* preNeg-transfected DMPM cells, out of which 1673 genes were up-regulated and 1658 genes down-regulated. To get biological meaning about the molecular events occurring upon miR-380-5p reconstitution, Gene Set Enrichment Analysis was performed. Results showed a positive enrichment of 188 gene sets, restricted for an FDR < 0.05, out of which signatures related to DNA replication, DNA recombination and telomere maintenance via recombination were present. Conversely, only 1 gene set (GO: positive regulation of blood vessel endothelial cell migration) was negatively enriched at significant level. Notably, among the leading edge genes, *PTGS2*, which encodes for cyclooxygenase-2 (COX-2) and represents a predicted target of miR-380-5p (miRWalk), was the most significantly down-regulated gene (FDR< 0.000001; log(fold-change): -2.15). Notably, a complete abrogation of *PTGS2* expression levels and COX-2 protein amounts was observed in miR-380-5p- compared to preNeg-transfected cells upon validation by qRT-PCR and western blotting, respectively. This evidence was paralleled by reduced amounts of phospho-FAK (focal adhesion kinase) and impaired migrating/invading capabilities of cells ectopically expressing miR-380-5p. Moreover, a reduction of Vimentin and a slight increase in P-Cadherin protein levels were also observed in cells ectopically expressing miR-380-5p, likely indicating the occurrence of a reverse-EMT program. Finally, a pronounced increase in the sensitivity to Cisplatin and Doxorubicin was also appreciable in miR-380-5p- *vs.* preNeg-transfected cells, suggesting that miRNA-mediated induction of a reverse-EMT may, at least in part, contribute to improve the response of DMPM cells to chemotherapeutic drugs.

#2997 Identification of novel long non-coding RNAs in mantle cell lymphoma patients.

A. LaFerlita, S. Singh, A. Sircar, R. Baiocchi, N. Muthusamy, L. Alinari, N. Epperla, L. Sehgal;
The Ohio State University Wexner Medical Ctr., Columbus, OH

Mantle Cell Lymphoma (MCL) is a rare and incurable type of B-cell non-Hodgkin lymphoma that affects about 4,000 people per year in the United States. Despite intense research to identify novel therapeutic approaches, the median progression-free survival after first-line treatment is four years. For this reason, the discovery of novel therapeutic targets remains crucial. Over half of the human genome is actively transcribed as non-coding RNAs. Among them, the non-coding RNAs that are longer than 200 nucleotides are named long non-coding RNAs (lncRNAs). lncRNAs have been shown to play essential roles in several human diseases, including cancer, by modulating cell cycle, immune response, or stemness through their interactions with DNA, protein, and RNA. For this reason, we decided to perform an RNA sequencing (RNA-Seq) profiling to identify the dysregulated lncRNAs in MCL. In more detail, we performed RNA-Seq in a cohort of 18 MCL patients compared to normal B-cells from the peripheral blood of healthy donors (HD). Reads were first trimmed for quality filtering, and adapters were removed using Trim Galore. Trimmed reads were mapped to the human genome (HG38 assembly) using HISAT 2. All the reads mapped inside the genomic coordinates of lncRNAs, reported in the GTF annotation file of GENCODE v43, were counted by featureCounts. Differential expression analysis between MCL samples vs HD was performed by LIMMA. To validate the results obtained from our internal MCL cohort, we also downloaded publicly available RNA-Seq data of 16 MCL patients and analyzed them using the previously described pipeline. Our analyses revealed several dysregulations in lncRNA expression occurring in MCL. Precisely, we identified 385 upregulated and 387 downregulated lncRNAs ($|log2FC| > 0.58$ and adjusted p-value < 0.05) in our internal MCL cohort, and 63% of them were also confirmed in the external cohort. Notably, the lncRNA called MALAT1 showed the highest significant upregulation in both cohorts, reinforcing this lncRNA's pivotal role in cancer development. To study the potential involvement of MALAT1 in MCL, we compared the MCL samples with higher MALAT1 expression (upper quartile) against those with lower expression (lower quartile) in both cohorts. The identified differentially expressed genes were used as input for a mechanistic network-based topological pathway analysis using MITHrIL. The analysis revealed that the KEGG pathway "Cell Cycle" was among the top upregulated pathways in MCL samples with high MALAT1 expression, suggesting the relevance of this lncRNA in promoting cellular proliferation, as also reported in the literature for other tumor types. In conclusion, our is the first study to describe the novel dysregulation signature of lncRNAs in MCL in two independent cohorts.

#2998 Regulation of epidermal growth factor receptor signaling by BRCA1-microRNA 146a network.

E. Kumaraswamy[1], R. M. Koren Shimak[1], S. Gunewardena[2], K. L. Wendt[3], D. Alexander[2], S. L. Hembruff[1], R. A. Jensen[1];
[1]The University of Kansas Cancer Center, Kansas City, KS, [2]University of Kansas Medical Center, Kansas City, KS, [3]The University of Oklahoma, Norman, OK

Inherited defects in the breast cancer susceptibility gene, BRCA1 are associated with an increased risk for hereditary breast, ovarian, and other cancers. BRCA1-associated basal like breast cancers (BLBCs) are high-grade ductal carcinomas that do not express ER, PR or HER2, but frequently overexpress epidermal growth factor receptor (EGFR/ErbB1/HER1). The EGFR-driven signaling network plays a pivotal role in BLBC pathogenesis. EGFR overexpression is associated with tumor progression and metastasis, resistance to radiation and chemotherapy, and poor prognosis. Growth factor receptors are regulated by multiple miRNAs, each having many targets, coordinately controlling the complex pathways of downstream signaling. We have previously reported a post-transcriptional mechanism by which BRCA1 regulates EGFR expression through the induction of miR-146a and provided a rationale for the development of miR-146a based therapeutic strategies. In addition, we have shown that BRCA1 also exerts regulatory control over dozens of important miRNAs that appear to play a critical role in breast neoplasia. From TCGA analysis, we show that low expression of these miRNAs is associated with distinctively poor overall survival of TNBC patients. Using miR-146a loss or gain of function experiments *in vitro*, we show that BRCA1 and miR-146a regulate EGFR signaling, stemness, epithelial-to-mesenchymal transition (EMT), extracellular matrix (ECM) remodeling and chemoresistance. Using *in vivo* mouse models, we demonstrate that miR-146a overexpression delays tumor formation leading to better overall survival. BLBC unlike the other subtypes, lacks targeted therapy approaches making cytotoxic chemotherapy essentially the only option for treatment. Though EGFR inhibitors have been used to treat other cancers, clinical trials for breast cancer have so far been unsuccessful due to poor response rates. Since one miRNA can target multiple genes and regulate multiple signaling pathways, our study provides evidence to suggest that restoring miR-146a could suppress EGFR-RAS-MEK signaling and the other compensatory pathways, providing a targeted therapeutic option for BRCA1 associated BLBC.

#2999 Evaluation of microRNA expression in metastatic and non-metastatic salivary gland mucoepidermoid carcinoma.

M. E. S. Trevizani[1], K. K. Oliveira[1], F. A. Marchi[2], D. Bizinelli[2], F. V. Mariano[3], C. P. Nagano[2], F. A. Costa[1], C. A. L. Pinto[1], L. P. Kowalski[1], S. V. Lourenco[2], **C. M. Coutinho-Camillo**[1];

[1]A.C.Camargo Cancer Center, Sao Paulo, Brazil, [2]University of Sao Paulo, Sao Paulo, Brazil, [3]Unicamp, Sao Paulo, Brazil

Salivary gland tumors are a heterogeneous group of lesions, being mucoepidermoid carcinoma (MEC) the malignant neoplasm with the highest incidence, occurring mainly in the parotid gland. Characterization of its histological grade (high, intermediate, and low) is important for determining patient prognosis. Metastasis is more common high-grade tumors and can occur at regional lymph nodes or distant sites. Although the mechanisms underlying the metastatic process are largely unknown, large-scale microRNA expression profiling studies of human cancers have demonstrated that dysregulation of miRNA is frequently associated with many cancer types. The aim of this study is to validate the use of microRNA expression for the discrimination of the metastatic potential of MEC samples. Using Real Time RT-PCR (qPCR) we have analyzed the expression of 384 miRNAs and controls in 4 non-metastatic MECs, 3 MECs with lymph node metastasis, 3 MECs with distant metastasis, and 2 non-neoplastic human salivary gland samples. Comparing the expression among these groups we identified 45 differentially expressed miRNAs that may be related with the metastatic potential of these tumors. To validate the microRNA expression associated with the metastatic potential, we selected 7 out of the 45 differentially expressed microRNAs and 7 MEC samples from the different groups of samples. Considering the 7 microRNAs evaluated, we validated that the expression of miR-191 was increased in non-neoplastic samples when compared to MECs with lymph node metastasis and the expression of miR-494 was increased in non-neoplastic samples when compared to MECs with distant metastasis, suggesting that loss of these microRNAs might be involved in the development of metastasis in mucoepidermoid carcinoma. The determination of a miRNA expression profile could provide a better understanding of the molecular basis of MEC and facilitate the determination of diagnosis and prognosis of patients.

MOLECULAR/CELLULAR BIOLOGY AND GENETICS: New Insights into Tumor Suppressor Genes
Poster Session

#3003 Exon skipping for the tumor suppressor Annexin A7 promotes EGFR signaling in stem-like brain tumor initiating cells through receptor recycling.

Aran Merati, Sindhu Nair, Rajani Rajbhandari, Nicholas Johnson, Markus Bredel

Radiation Oncology, University of Alabama - Birmingham, Birmingham, AL

Background: Glioblastoma (GBM) is one of the most lethal forms of cancer. The majority of GBMs express aberrant receptor tyrosine kinase (RTK) activity, which upon activation, are canonically endocytosed and degraded. This process is disrupted in GBM to promote receptor recycling resulting in hyperactive RTK signaling. We demonstrated that the alternative splicing of the tumor suppressor Annexin A7 (ANXA7) supports the impaired endosomal trafficking of RTKs to favor recycling in GBM. Exon six of ANXA7 can be alternatively spliced to yield two distinct protein isoforms through its inclusion (I1) or exclusion (I2).
Methods: We investigated ANXA7 isoform differences for epidermal growth factor receptor (EGFR) trafficking fates first in U251 malignant glioma followed by stem-like brain tumor initiating cells (BTICs) originating from patient-derived xenografts (PDXs). U251s and primary BTICs (JX14) were transduced with lentivirus to overexpress ANXA7 and GFP for enrichment by flow cytometry. JX14 empty vector (EV; I2 only) and I1 (I2 and I1 expressing) cells were plated onto Geltrex and ligand starved overnight in serum-free media to maintain BTICs. We assessed EGFR protein levels following EGF stimulation in a time dependent manner. Immunofluorescence experiments were conducted to measure EGFR-ANXA7 colocalization (Pearson) with markers of the endocytic pathway, which included the early endosomes (EEA1), recycling endosomes (Rab4/Rab11), and lysosomes (LAMP1). EV and I1 cells were also incubated with siRNA targeting both ANXA7 isoforms to determine the impact of ANXA7 loss on endosomal EGFR trafficking.
Results: Interestingly, we found drastic differences in endosomal EGFR trafficking in I1 expressing cells. EGFR colocalized with EEA1 in both EV and I1 cells (R^2=0.01336, P>0.6275). In EV cells, EGFR was recycled via fast/slow recycling endosomes demonstrated by Rab4/Rab11 colocalization while I1 did not (Rab11: R^2=0.9267, P<0.0001). Immunoblotting revealed a significant reduction in EGFR protein in I1 cells only. Furthermore, I1 cells and not EV preferentially degraded EGFR as seen by LAMP1 colocalization (R^2=0.9398, P<0.0001). ANXA7 siRNA in EV cells did not alter EGFR trafficking, which implicates I2 as nonfunctional. On the other hand, ANXA7 KD in I1 cells impaired EGFR sorting via a 40% increase (P<0.0010) in total EGFR protein and a 40% reduction (P<0.0001) in colocalization with EEA1. Loss of I1 also shifted the degradation of EGFR back towards recycling.
Conclusion: GBMs express I2, which supports EGFR hyperactivity by favoring receptor recycling. I1 overexpression significantly reduced EGFR signaling by promoting degradation. I1-induced reduction in EGFR signaling suggests a new therapeutic vulnerability for BTICs by potentially reducing tumorigenicity or improving the efficacy of EGFR inhibition.

#3005 *Low-density lipoprotein receptor-related protein 1B* (*LRP1B*) depletion promotes tumorigenicity by modulating fibroblasts in the tumor microenvironment in esophageal squamous cell carcinoma.

K. Xu, J.-y. KO, V. Yu, M. L. LUNG;
University of Hong Kong, The - Li Ka Shing Faculty of Medicine, Hong Kong, Hong Kong

Background: Esophageal squamous cell carcinoma (ESCC) is widespread worldwide with a poor survival rate. Tumor cells shedding from tumor tissues traveling to other organs through the blood circulatory system are called circulating tumor cells (CTCs). The CTCs in the blood of ESCC patients were enriched and then subjected to CTC mutational profiling by target sequencing. Our results suggested that CTC mutations in *low-density lipoprotein receptor-related protein 1B* (*LRP1B*) may have a potential prognostic role for ESCC. *LRP1B* belongs to the low-density receptor (LDLR) family with diverse roles in cellular functions and development, but the function of *LRP1B* in ESCC remains unclear. Therefore, this study aims to do a functional characterization of *LRP1B*.
Methods: The CRISPR cas9 system was used to functionally knock down the candidate gene in ESCC cell lines with the highest endogenous level of *LRP1B*. The *in vitro* cell proliferation rate and viability were measured by MTT assay, colony formation assay, and wound healing assay. The *in vivo* tumorigenicity assay was performed to evaluate the tumor suppressive effect by subcutaneous injection. To examine the clinical relevance of *LRP1B*, we also performed immunohistochemistry (IHC) in tumor tissue microarray (TMA).
Results: The reduction or loss of *LRP1B* mRNA was demonstrated in 60% of a panel of 15 ESCC cell lines. The depletion of *LRP1B* did not influence cell proliferation, cell clonogenic ability, or cell migration in ECSS cell lines. However, *LRP1B* depletion significantly promoted the growth of tumors in mouse xenograft models. Therefore, we hypothesize that *LRP1B* may be involved in modulating the tumor microenvironment (TME) by impacting various stromal components leading to an immuno-suppressive TME. We utilized RT-qPCR to investigate markers of various stromal components and observed that fibroblast markers (*acta2*, *pdgfrb*, and *vimentin*) had significantly higher expression levels after *LRP1B* downregulation in ESCC cell-derived mouse xenografts. The higher level of fibroblast cells was then verified by IHC staining. Further molecular mechanistic studies are underway and are expected to provide novel therapeutic insights by targeting the *LRP1B* genes. The *LRP1B* ESCC TMA data analysis is underway and statistical analysis will be presented.
Conclusions: *LRP1B* plays a tumor-suppressive role in ESCC by modulating the tumor-associated fibroblasts in the TME.
Acknowledgements: TBRS grant T12-701/17R and HMRF grant 05160926 to MLL

#3006 Morphogen-driven regulation of nuclear shape and its implication for colorectal cancer.

M. A. El Gendi, S. Herve, S. Gautam, Y. A. Miroshnikova;
NIH, National Institute of Diabetes and Digestive and Kidney Diseases (NIDDK), Bethesda, MD

Colorectal cancer (CRC) is the second leading cause of cancer-related deaths worldwide despite improved rates of early detection and development of targeted treatments. Dysregulation of nuclear shape and the emergence of aberrant chromatin architecture correlate with cancer onset and progression, including CRC. Both extrinsic and intrinsic factors, most critically cytoskeletal and nucleoskeletal organization, chromatin architecture, and metabolic signaling, impact nuclear shape. Yet, what precisely determines nuclear shape in health and disease and how it is linked to cell fate and function remains a fundamental open question. In the case of over 75% of CRC cases, the first transformative genetic event is the loss of function in the tumor suppressor gene, adenomatous polyposis coli (APC). Mechanistically, perturbed APC signaling leads to aberrant activation of Wnt/beta-catenin signaling. This pathway is essential for intestinal homeostasis, as is the regulation of proper nuclear shape and function. Here, we aim to decipher the crosstalk between Wnt gradients and nuclear shape regulation in non-transformed and APC-mutated epithelial cells in vitro, as well as in WT and APC-mutant mouse colon tissues. The long-term goal of this work is to test whether a mechanistic link exists between Wnt-driven cellular transformation and the emergence of aberrant nuclear shape and function.

#3007 AZGP1 inhibits angiogenesis in prostate cancer.

R. Wen, G. Wen, Z. Qiu, E. Peterson, F. Marques, A. Bermudez, J. Pollack, H. Zhao, S. Pitteri, J. Brooks;
Stanford University, Stanford, CA

AZGP1 is involved in various biological processes, including lipid metabolism, regulation of cell proliferation, migration and invasion, and immune response. The loss of AZGP1 is associated with worse clinical outcomes, and AZGP1 has been indicated as a potential biomarker for prostate cancer. However, the underlying mechanisms of AZGP1 function in prostate cancer are unknown. This study reports AZGP1's pivotal involvement in angiogenesis within the prostate cancer tumor environment. Neither knockout nor overexpression of AZGP1 affects *in vitro* prostate cancer cell proliferation, migration, or invasion. Morphologically, AZGP1-deficient mouse prostates appear normal, but exhibit increased fibroblast growth in periglandular stroma after 6 months. The overexpression of AZGP1 does not impact the growth of PC3 and DU145 tumors; instead, these tumors significantly reduced microvessel density, suggesting AZGP1 exhibits anti-angiogenic properties. Proteomic profiling shows distinct profile of angiogenesis-related proteins between PC3-AZGP1-OV and PC3 control cells, featuring proteins like PDCD6 and MMP9. This study provides insights into the anti-angiogenic attributes of AZGP1 in prostate cancer, underscoring its potential as a therapeutic target for prostate cancer.

#3008 Loss of Rab25 accompanied by NRAS activation cooperatively mediates the tumorigenic transformation in melanoma.

S. Kandel[1], K. Rao[2];

[1]Southern Illinois University School of Medicine, Springfield, IL, [2]Simmons Cancer Institute and Southern Illinois University School of Medicine, Springfield, IL

Background: Ras oncogene activation is a common and often essential event in cancer development, including melanoma. Ras mutation is present in 20-30% of melanomas and remains an undrugged target. NRAS mutation is the most frequent Ras isoform activated in melanoma, with more than 80% cases of Q61 substitutions, and is closely associated with tumor aggressiveness. Rab25 is a ubiquitously expressed small GTPase protein with a context-dependent role in cancer pathophysiology. Its role remains undiscovered in the case of melanoma. Rab25 deep deletion can be seen in portions of melanoma in databases such as the Cancer Genome Atlas and Cbioportal. Interestingly, Rab25 has a consensus sequence homologous with the binding site of Q61 mutant Ras. We propose that the loss of Rab25 in melanocytes accompanied by Ras oncogenic activation are significant events in melanoma development, and restoration of Rab25 can potentially inhibit constitutively activated N-RAS; Rab25 serves as a tumor suppressor in melanoma genesis.

Objectives: To discover the role of Rab25 in melanoma, we studied Rab25 expression via mRNA and protein levels in different melanoma cell lines and screened biopsy-proven melanoma samples through immunohistochemistry in 61 different melanoma sections. Further, to see the tumor suppressive mechanism of Rab25 in vitro, we transduced selected cell lines Rab25.

Results: There is an 87% and 62.7% reduction in Rab25 mRNA level in NRASQ61R(SKMEL-2) and NRASQ61L type (WM1366) melanoma cell lines, respectively, also reflected in Rab25 protein level, and statistically significant at p-value <0.005, using student's T-test. Further, Rab25, prominent in adjacent normal tissues, was significantly lost in biopsy-proven melanoma tissues, with an H-score ranging from 13.28 to 91.77% and 0.00 to-11.24 % for normal skin tissue and melanoma section, respectively, and a negative correlation of -0.350, indicating a promising association of Rab25 loss with the progression of melanoma.

Conclusion: There is a loss of Rab25 in NRAS mutant melanoma with cancer progression. We saw a significant increase in Rab25 expression among the transduced sublines of NRAS mutant melanoma cell lines at the mRNA level, which will be further assessed through western blotting, cell proliferation assay, trans well migration assay, soft-agar colony formation assay to confirm NRAS mutant melanoma cell behavior. We will attempt to deliver a liposomally encapsulated six-peptide sequence to therapeutically inhibit the mutant NRAS.

#3009 ATRX loss blocks the differentiation of mesenchymal stem cells and promotes undifferentiated sarcoma development.

Y. Cai, J. Yao, D. N. Pan, Y. Jin, J. M. You, W. Yao, H. Ying;
UT MD Anderson Cancer Center, Houston, TX

Soft tissue sarcomas (STSs) are a collection of rare tumor types originated from the mesenchymal tissues. Among the over 70 histological subtypes of STS, undifferentiated sarcoma (US), which lacks any discernible morphological features of differentiated tissues, accounts for over 20% of all STSs and is correlated with high tumor grade and poor prognosis. Recent genomic profiling in US has identified p53 and ATRX among the most frequently mutated or deleted genes. ATRX is a SWI/SNF2 type of chromatin remodeling factor which functions in a histone variant H3.3-specific chaperone complex to orchestrates replication-independent nucleosome assembly at repetitive heterochromatic DNA regions including telomeres. Loss-of-function mutations occur frequently in many tumor types and is associated with the development of alternative lengthening of telomere (ALT). However, how loss of ATRX function may contribute to tumorigenesis is largely unknown. Here, we demonstrated that ATRX is required for the terminal differentiation of mouse mesenchymal stem cells (MSCs) into multiple lineages, such as adipocytes and osteocytes. Targeted deletion of Atrx in mouse MSCs, but not terminally differentiated mesenchymal lineage cells, accelerated sarcoma initiation induced by loss of p53 and significantly shortened the overall survival. Atrx-deficient tumors express high level of MSC markers such as CD44 and CD29 and exhibit pathological features highly reminiscent of human high-grade US. Transcriptomic analysis indicates that Atrx deficiency is associated with enhanced proliferation. Together, our data indicates that ATRX deficiency contributes to undifferentiated sarcoma development by inhibiting mesenchymal stem cell differentiation.

#3011 The loss of an orphan nuclear receptor NR2E3 augments Wnt/β-Catenin signaling via epigenetic dysregulation that links to the Sp1-β catenin-p300 interactions in hepatocellular carcinoma.

Y.-K. Leung[1], S.-G. Lee[2], J. Wang[3], S.-M. Ho[1], N. Rusch[1], C. Park[2], **K. Kim[1]**;

[1]University of Arkansas for Medical Sciences, Little Rock, AR, [2]Chonnam National University, Gwangju, Korea, Republic of, [3]University of Cincinnati, Cincinnati, OH

Hepatocellular carcinoma (HCC) stands as the fourth leading cause of global cancer-related mortality due to late-stage detection, tumor heterogeneity, and drug resistance. The pivotal role of epigenetic factors in HCC development and progression necessitates the identification of critical epigenetic regulators. The orphan nuclear receptor NR2E3 (Nuclear receptor subfamily 2 group E, Member 3), primarily associated with retinal development, has emerged as a potential tumor suppressor. Earlier studies showed that the loss of NR2E3 leads to epigenetic repression of the estrogen receptor α (ER) through the involvement of Lysine Specific histone Demethylase 1 (LSD1). NR2E3 also forms a transcriptional complex with Sp1, governing the aryl hydrocarbon receptor (AHR) expression, a crucial factor in liver xenobiotic metabolism. In vivo, NR2E3 ablation results in p53 inactivation and severe liver injuries when exposed to liver toxicants, highlighting its role in activating p53. Nonetheless, the precise tumor suppressive and epigenetic role of NR2E3 in HCC remains unclear. HCC patients expressing low NR2E3 exhibit unfavorable clinical outcomes, aligning with heightened activation of the Wnt/β-catenin signaling pathway. The murine HCC models utilizing NR2E3 knockout mice show accelerated liver tumor formation and progression accompanied by enhanced activation of the Wnt/β-catenin signaling pathway and inactivation of the p53 signaling pathway. At a cellular level, losing NR2E3 increases the acquisition of aggressive cancer cell phenotype and tumorigenicity and upregulates vital genes in the Wnt/β-catenin pathway with enhanced chromatin accessibility. This event is mediated through the increased formation of active transcription complex involving Sp1, β-catenin, and p300, a histone acetyltransferase, on the promoters of target genes. Correspondingly, treatment of p300 inhibitor C646 decreased the expression of critical genes in the Wnt/β-catenin signaling pathway. These findings demonstrate that the loss of NR2E3 promotes Wnt/β-catenin signaling activation at cellular, organismal, and clinical levels. In summary, NR2E3 is a novel tumor suppressor that maintains epigenetic homeostasis, thereby preventing activation of Wnt/β-catenin signaling that promotes HCC formation.

#3012 Characterizing the functional significance of "variant of uncertain significance" of the tumour suppressor *CDH1*.

J. Wen[1], A. Singh[1], D. Nguyen[2], K. Meier-Ross[3], B. Martin[1], V. Khan[1], K. Dhami[4], J. Chao[1];

[1]University of Toronto, Toronto, ON, Canada, [2]Queen's University, Kingston, ON, Canada, [3]University of Ottawa, Ottawa, ON, Canada, [4]McMaster University, Hamilton, ON, Canada

We aim to develop a new approach to systematically characterize the functional significance of “variant of uncertain significance (VUS),” focusing on the tumor suppressor gene *CDH1*. Genetic testing is a powerful clinical tool for identifying individuals at risk of developing inherited or familial cancers. If a potential cancer-causing genetic variant (mutation) is found, clinicians can begin managing the patient’s risk early by initiating surveillance or prophylactic treatment. For an aggressive form of inherited stomach cancer called hereditary diffuse gastric cancer (HDGC), the most commonly mutated gene is *CDH1*, which encodes the tumor suppressor E-Cadherin. However, due to insufficient clinical evidence, over 50% of all publicly reported *CDH1* variants either have conflicting interpretations or cannot be classified, thus are not actionable. Consequently, almost 1 in 2 patients who undergo genetic testing for HDGC will not have a definitive test result and cannot benefit from early screening, causing strain on the healthcare system and psychological burden for the patients. To overcome this challenge, we developed a single-cell screening system to accurately classify *CDH1* variants using a combination of functional assays, machine learning, and deep learning. Our hypothesis, now supported by preliminary data, is that pathogenic variants will disrupt normal E-Cadherin’s ability to control its signaling partner beta-catenin. Thus, loss-of-function (LoF) *CDH1* variants would cause protein mislocalization and altered signaling which lead to abnormal proliferation, an early indicator for carcinogenesis. We express *CDH1* variants in human cell lines and use multiplexed high-content imaging to visualize E-Cadherin and beta-catenin. Next, our deep learning pipeline extracts single-cell phenotypic profiles, and our classifier then classifies variants as functional or LoF. Initial analysis of prioritized variants show that our pipeline can accurately separate clinically pathogenic and benign variants based on their functional status as predicted by our pipeline. The outcomes of this project will contribute to a systematic approach to reclassify VUS.

#3013 Alzheimer's-linked gene BIN1: Unraveling its unexpected role as a tumor suppressor in prostate cancer and influence on androgen receptor signaling.

C. McColl[1], D. Skapura[1], E. Ruiz Echartea[1], J. Deng[1], A. Rusin[1], J. Shin[1], A. Tyryshkin[1], C. Davis[2], E. Ehil[2], S. Kaochar[1];
[1]Baylor College of Medicine, Houston, TX, [2]Avera Institute for Human Genetics, Sioux Falls, SD

Androgen-receptor signaling inhibitors (ARSI) have been shown to significantly alter the natural history of castration-resistant PCa (CRPC). Unfortunately, resistance to ARSIs is inevitable. Unraveling the underlying mechanisms to identify potential therapeutic interventions to treat these lethal tumors has become a critical challenge in the post-ARSI era. Recent genomic sequencing has revealed a subclass of PCa harboring deletion of bridging integrator-1 (BIN1) and is associated with increased AR activity. Notably, BIN1 deletion frequently co-occurs with SPOP mutation and deletion of SPOPL, collectively suggesting BIN1 may function as tumor suppressor. To elucidate the role of BIN1 in prostate cells, we generated a prostate-specific BIN1 knockout murine model (PB-CreBIN1$^{FL/FL}$). This model revealed increased prostate mass at 6 months of age, accompanied by increased cell proliferation. We next crossed this strain to SPOP mutant (SPOP^{F133V}) model to generate a prostate specific BIN1 knockout, SPOP mutant model (PB-CreSPOP^{F133V}BIN1$^{FL/FL}$) and found increased proliferation and greater prostate mass compared to animals harboring SPOP mutation or BIN1 deletion alone. Next, we generated a doxycycline inducible BIN1 overexpressing PCa model (22Rv1BINOE) to evaluate AR signaling in vitro. We found that overexpression of BIN1 modestly reduced prostate cancer cell proliferation but profoundly suppressed androgen receptor protein level. To evaluate the transcriptional activity of AR and ARv7, we also utilized a luciferase reporter system harboring ARE consensus sequences found in the *KLK3* gene (AR-FL target) promoter or in the *EDN2* gene (ARv7 target) promoter, respectively. These reporter assays illustrated suppression of both AR-FL and AR-v7 driven gene transcriptional program upon BIN1 overexpression. Co-expression of both BIN1 and SPOPwt showed a synergistic knockdown of AR activity, while SPOPmut did not show this effect. These observations were further confirmed using global RNAseq. The RNAseq analysis also showed downregulation of several AR pathways as well as gene sets associated with cancer progression and metastasis. Interestingly, the RNAseq data showed downregulation of genes that are normally upregulated after SPOP mutation, further suggesting a synergistic role between SPOP and BIN1.

#3014 Exploring the correlation between oncogenic viruses and BRCA1/2gene mutations in Egyptian breast cancer patients.

S. Loutfy, Sr.[1], R. A. Al Najar[1], S. ElSayed[1], N. Abdel Fattah[1], A. Abdel-Samie Gaber[1], T. Hashem[1], W. S. Khalaf[2], A. F. Basyony[3], A. El-Sharif[2], S. M. Radwan[2], **M. Eltokhy**[4],

[1]National Cancer Institute, Cairo University, Cairo, Egypt, [2]Faculty of Pharmacy (Girls), Al-Azhar University, Cairo, Egypt, [3]Faculty of Pharmacy, Egyptian Russian University, Cairo, Egypt, [4]Texas Tech Health Science Center, USA, TX

Background: Recognizing the complexity of viral carcinogenesis and its perspectives, we aimed to investigate one of the key genetic factors associated with breast cancer development, BRCA1,2 mutations, and its association with the presence of some oncogenic viruses like HPV, MMTV, and EBV DNAs in both blood and tissues of breast cancer (BC) patients, hoping to provide new insights on role of oncogenic viruses in cancer development.

Patients and Methods: This study was conducted on 84 tissues and blood samples from Egyptian BC women and 50 blood samples from controls without known oncological disease. All samples were tested for the presence of viral DNAs, using real-time PCR assay. Fifty-five BC patients were investigated for the presence of mutations in exons 6 and 9 of BRCA1, and exons 11, 14, and 27 of BRCA2 using a high-resolution melting (HRM) assay. Results were correlated with the clinicopathological characteristics of BC. Results. HPV, MMTV, and EBV DNAs were detected in 30(35.7%), 19(22.6%), and 23 (27.3%) of tissues obtained from 84 BC patients, respectively, and into 16 (19%), 14 (16.7%) and 0 (0%) of blood from the same patients, respectively. On the other hand, these viruses were detected in 0 (0%), 7 (14%), and 0 (0%) of blood specimens obtained from 50 normal controls, respectively. Among 55 BC patients, mutations were detected in 37 (67%) of the tested exons of BRCA1/2 genes in the blood of BC patients, divided as 7 (12.7%) for exons 6 and 9 of BRCA1 gene, and into 11 (20%), 3 (5.5%), and 9 (16.4%) for exons 11, 14 and 27 of BRCA2 gene. Our previous investigation based on NGS showed that pathogenic mutations were (G509A:p.R170Q and c.C1471T:p.Q491X) for exons 6, 9 of BRCA1, respectively, and were (cT4001A: p.L1334X, c.7231delA: p.T2412Lfs and c.T9861A: p.C3287x) for exons 11, 14 and 27 of BRCA2, respectively. Further analysis showed that half of the patients with positive HPV DNA in tissues had mutations in the tested exons of BRCA1/2 genes. In contrast, none of the patients with MMTV DNA (15/55 (27%)) in their tissues had mutations in exons 6 and 9 of BRCA1 and only one patient had a mutation in exons 11 of BRCA2. Regarding EBV, 35% of positive patients had mutations in the tested exons of the BRCA1 gene and 21% in the tested exons of BRCA2 gene. Results were not affected by clinicopathological parameters.

Conclusion: MMTV DNA followed HPV, and then EBV DNAs were detected in more than 80% of our BC patients. HPV was the most frequent virus among BC patients showed to be associated with BRCA1/2 mutations in the tested exons. Sequencing analysis is in progress. Understanding this association will provide a relevant implication for developing novel, and personalized therapeutic options for treatment of oncogenic viruses.

#3015 HD-PTP mediates tumor suppression via modulation of anti-tumor immunity.

Chenxu Guo, Sheng Sun, Nayana Thimmiah, Agustina Maccio, Siang Koh, Leif Ellisen

Mass General Cancer Center, Boston, MA

The role of circulating extracellular vesicles in cancer biology is an area of intense research interest. Here, we reveal a tumor suppressor mechanism of HD-PTP (His Domain Protein Tyrosine Phosphatase, encoded by PTPN23), a protein associated with ESCRT (endosomal sorting complex required for transport), a complex that controls endosome sorting and exosome secretion. While loss of HD-PTP is known to be tumorigenic in mice and is frequently observed in human cancers including Triple Negative Breast Cancer (TNBC), the relevant pathways have remained obscure. We find that inhibition of HD-PTP *in vivo* promotes tumor progression selectively in a syngeneic, immune-competent TNBC model but not in a matched immune-deficient model. Through systematic profiling of the exosomal proteome in HD-PTP proficient and deficient cells, we identify PD-L1 as a key exosomal cargo selectively enriched due to loss of HD-PTP. Mechanistically, we show that inhibition of HD-PTP results in PD-L1 stabilization, its co-localization with the exosomal marker CD63, the enrichment of endosomal PD-L1 and subsequent increase in ExoPD-L1 release. Exosomes produced post HD-PTP loss inhibits antigen-dependent T cell activity *in vitro*, and HD-PTP inhibition in a syngeneic TNBC model promotes non-cell-autonomous, exosome- and PD-L1-dependent tumor progression, associated with reduced T cell infiltration and altered macrophage polarization. Consistent with these findings, low HD-PTP levels in human solid tumors are associated with decreased tumor infiltrating lymphocytes, poor response to immune checkpoint inhibition and inferior overall survival. Taken together, our studies unveil a novel tumor suppressor pathway controlling PD-L1 trafficking and ExoPD-L1 secretion, highlighting the critical roles of HD-PTP and ESCRT in anti-tumor immunity.

#3016 MCPIP1 endoribonuclease protects from liver fibrosis and regulates hepatocellular development.

K. Miekus[1], O. Kwapisz[1], P. Marona[1], J. Gorka[1], J. Kotlinowski[1], E. Pospiech[2], J. Jura[1];

[1]Jagiellonian University, Faculty of Biochemistry, Biophysics and Biotechnology, Krakow, Poland, [2]Human Genome Variation Research Group, Malopolska Centre of Biotechnology, Jagiellonian University, Krakow, Poland

Introduction: MCPIP1 (Monocyte Chemotactic Protein-1 Induced Protein), also known as Regnase-1, belongs to the CCCH zinc finger protein family, featuring a PilT N-terminus (PIN) domain-like RNase domain. Utilizing its intrinsic endonuclease activity, MCPIP1 functions as a precise modulator of cytokines, exhibiting an anti-inflammatory effect through the targeted degradation of specific mRNA transcripts. While recent studies have highlighted MCPIP1 as a potential tumor suppressor with decreased levels in breast cancer and clear cell renal cell carcinoma, its role in hepatocellular carcinoma (HCC) development remains unexplored.

Material and Methods: To investigate the role of MCPIP1 in HCC development, we used tissue-specific knockout mice with the deletion of Mcpip1 in hepatocytes. HCC was induced by administering diethylnitrosamine (DEN) to two-week-old mice. We conducted a comprehensive analysis, including the assessment of EMT and fibrosis markers, proinflammatory cytokines, and immune cell infiltration, using Western blot (WB), mass spectrometry, quantitative PCR (qPCR), and multiple immunohistochemistry (IHC) stainings. To identify differences between the wild-type (wt) and Mcpip1 knockout (KO) mice groups more effectively, hepatocytes were isolated using the perfusion method, and RNA-Seq analysis was performed.

Results and Discussion: The tissue-specific knockout of Mcpip1 in the liver has notable molecular consequences. Transcriptomic profiling revealed an upregulation of transcripts integral to tumor development, including Cxcr4, Met, Cxcl12, Hgf, and Src, alongside factors characteristically associated with cancer stem cells, Myc, Klf4, and CD133. The absence of MCPIP1 triggered immune cell activation in the liver, as evidenced by an augmented expression of markers specific to myeloid and lymphoid cell populations, indicative of an intensified immunological response. IHC examination of liver tissue from Mcpip1-deficient mice revealed significant fibrotic alterations, characterized by increased collagen deposition, and enhanced expression of alpha-smooth muscle actin (αSMA). The lack of Mcpip1 influences the increased levels of vimentin, fibronectin, and connective tissue growth factor (cTGF), indicating enhanced tissue remodeling.

Conclusions: MCPIP1, recognized for its anti-inflammatory functions, appears to function as a potential tumor suppressor in HCC development. The lack of MCPIP1 results in the upregulation of transcripts linked to tumorigenesis, immune cell activation, and notable fibrotic changes, highlighting its involvement in the complex molecular dynamics of HCC progression.

This study was supported by National Science Center grants no. 2017/26/E/NZ5/00691, 2021/41/N/NZ4/04187.

#3017 Lack of MCPIP1 enzymatic activity leads to neoplastic transformation of normal kidney cells.

P. Marona[1], I. Piasecka[1], J. Gorka[1], O. Kwapisz[1], R. Myrczek[1], E. Pospiech[2], J. Jura[1], K. Miekus[1];
[1]Jagiellonian University, Faculty of Biochemistry, Biophysics and Biotechnology, Krakow, Poland, [2]Jagiellonian University, Malopolska Center of Biotechnology, Krakow, Poland

Introduction: The MCPIP1 protein (Monocyte Chemotactic Protein-1 Induced Protein) is involved in the negative regulation of inflammation due to its RNase activity. A growing number of publications suggest that the MCPIP1 protein may influence the development of cancer by regulation of factors involved in angiogenesis, proliferation and cell death. We believe, that MCPIP1 may be a potential tumor suppressor. Our recent results show that lack of enzymatic activity of MCPIP1 leads to increased tumor growth, angiogenesis and metastasis. The main aim of our research is to study the importance of MCPIP1 for neoplastic transformation of normal, epithelial kidney cells, as well as acquirement of stemness features.
Material and Methods: To examine the effect of MCPIP1 in normal epithelial cell lines TCMK-1, RPTEC-Tert1 and HK-2 were transduced to overexpress mutated, inactive form of MCPIP1 (pLIX D141N) with proper control (pLIX PURO). We analyzed cells clonogenicity, as well as the levels of CSCs markers by western blot, NGS and qPCR. Next, cells were injected subcutaneously into NOD-SCID mice to check if mutation of MCPIP1 will induce tumor growth *in vivo*. Mice blood was analyzed for the presence of circulating tumor cells (CTCs), and secretion of cytokines by Proteome Profiler assay. Tumors were evaluated by multiple IHC stainings, as well as western blot and qPCR.
Results and Discussion: We have shown that the mutation of MCPIP1 increases the clonogenicity of kidney cells. Moreover, pLIX D141N cells were characterized by higher levels of the c-Met receptor, vimentin, Twist, CD44 and c-Myc, which are the markers of epithelial to mesenchymal transition and cancer stemness. The obtained results suggest that the loss of the MCPIP1 protein causes the acquisition of the characteristics of neoplastic cells. Next, we checked whether MCPIP1 mutation in normal cells predisposes them to proliferate when administered to mice. We found that, D141N mutation caused the growth of large tumors with higher expression of Cd44, Klf4 and Myc and number of CTCs, while the control cells injected into mice developed only local fibrosis with high expression of aSMA. pLIX D141N tumors secreted CXCL16 into mice plasma, and were characterized by increased phosphorylation of c-Met, Src kinase and c-Myc.
Conclusions: We believe that the MCPIP1 protein may be a marker of tumor initiation and play a key role in neoplastic transformation by regulating the changes in cell phenotype and levels of CSCs markers.
This study was supported by National Science Center grants no. 2022/47/B/NZ5/02724, 2022/45/B/NZ5/01973 and MNS 15/2021.

#3018 Transcriptional dysregulation in germline *TP53*-driven breast cancers.

N. Boruah, R. Moses, R. Hausler, H. Desai, A. Le, G. Kelly, A. Raghavakaimal, M. Narasimhamurthy, A. Nayak, A. J. Levine, K. N. Maxwell; University of Pennsylvania, Philadelphia, PA

Background: Pathogenic germline variants (PGVs) in *TP53* is associated with multicancer risk syndrome known as Li-Fraumeni Syndrome (LFS) and females have 80-90% risk of breast cancer at very early age compared to sporadic breast cancers. The mechanism of p53 tumor suppression relies on its function as a transcriptional activator; however, there is little data on the specific transcriptional defects in human breast tumors driven by germline mutant p53.
Methods: To investigate the specific transcriptional defects due to *TP53* PGVs in human breast, we performed bulk RNA-seq on invasive ductal carcinoma (IDC), ductal carcinoma in situ (DCIS) and surrounding and contralateral normal breast tissue in LFSBC compared to non-LFS sporadic BC. We also compared our results to breast tumors from The Cancer Genome Atlas (TCGA) with and without acquired *TP53* mutations.
Results: Our RNA-seq analysis revealed significant changes in the expression of key pathways in LFSBC compared to non-LFS breast cancer. Notably, cancer hallmark pathways such as apoptosis and reactive oxygen species were downregulated, while androgen response and cholesterol homeostasis pathways were upregulated in LFSBC compared to non-LFSBC. Expression of downstream targets of p53 such as *BAX*, tumor suppressors such as *CDKN1A* (p21) and *BTG2*, were significantly down in LFSBC suggesting impaired transcriptional activity of mutated *TP53* in LFS patients. We also observed downregulation of cell cycle regulators in LFS breast tumors compared to their surrounding and contralateral tissues. Although, there were no significant transcriptional differences as the tumor progressed from LFS DCIS to IDC, indicating that the damage caused by the mutated p53 had already occurred at the early stage. Additionally, we also investigated the immune cell composition in LFS-BC and non-LFSBC. LFSBC exhibited a higher relative proportion of CD4+ T cells, CD20+ B cells, NK cells, macrophages and monocytes compared to all sporadic non-LFSBC subtypes (TCGA) and age matched non-LFSBC. This providing novel insights into the immune landscape associated with LFS-driven breast cancer.
Conclusion: Our findings suggest that breast tissues with an inherited *TP53* mutation undergo a defective transcriptional state, shifting away from apoptosis, and experiencing dysregulation of cell cycle at an early stage as DCIS, potentially contributing to the early onset of LFS breast cancer. The preliminary analysis of immune repertoire in LFSBC opens avenues for deeper investigations into spatial transcriptomic profiles of germline *TP53*-mutated breast tumors also the immune cells. Overall, this study provides valuable insights into the *TP53* mutation driven breast cancers in humans.

#3019 Dissecting *in vivo* functions of R-Loops in *Brca1*-associated DNA replication stress and mammary tumorigenesis.

H.-C. Chiang, L. Qi, Y. Hu, R. Li;
The George Washington University, Washington, DC

Germ-line *BRCA1* mutations are associated with a significantly increased incidence of breast cancer in women. Although *BRCA1*-associated breast tumors are basal-like and estrogen receptor α negative (ERα^{-}), they originate from luminal progenitor cells. At the molecular level, BRCA1 is best known for its roles in resolution of DNA replication stress and promotion of homologous recombination (HR)-based double strand break (DSB) repair. In addition, BRCA1 is implicated in reduction of R-loops, a DNA-RNA hybrid structure and transcriptional byproduct associated with genome instability and transcriptional regulation. Our published findings suggest that BRCA1-dependent R-loop mitigation contributes to luminal cell-specific transcription and differentiation (Zhang et al, 2017, *Nature Communications*, 8:15908), which could in turn suppress *Brca1*-associated tumorigenesis. Using cell type-specific mouse genetics, we investigate a direct impact of R-loop removal on *Brca1*-associated mammary epithelial tumor formation. R-loop formation in mammary epithelial cells is efficiently reduced by over-expression of RNase H1, an R-loop-specific ribonuclease. R-loop removal does not affect mammary duct development or function. However, it drastically increases γH_2AX foci in proliferating BRCA1-deficient epithelial cells without external DNA damage. This suggests a role of R-loops in attenuating elevated DNA replication stress caused by the loss of *Brca1*. While R-loop removal does not appear to affect the overall *Brca1*-associated mammary tumor incidence, it promotes cell differentiation from ERα^{-} luminal progenitor cells to ERα^{+} mature luminal cells. Accordingly, unlike their counterparts, a significant percentage of *Brca1*-associated mammary tumors with RNase H1 overexpression tend to be ERα^{+}. Thus, our findings provide *in vivo* evidence for a previously unappreciated role of R-loop dynamics on *Brca1*-associated DNA replication stress and tumor development in mammary epithelium.

#3022 GPR109A activation limits cell growth by inducing p53 and its targets in human colon cancer cells.

M. Thangaraju[1], N. N. Thangaraju[2], L. Gilstrap[1], M. Chimenti[1], T. Patel[1], S. Sivaprakasam[3], N. Patel[1], S. Manicassamy[1], P. D. Prasad[1], V. Ganapathy[3]; [1]Augusta University, Augusta, GA, [2]Mercer University, Augusta, GA, [3]Texas Tech University Health Science Center, Lubbock, TX

Chemical carcinogens or xenobiotics present in the diet play a significant role in colon cancer (CC) formation. p53, a tumor suppressor and multi-functional protein, provides an important barrier against the initiation and maintenance of CC. p53 mutation or inactivation is observed in about 60% of CCs and about 90% of all cancers. Therefore, therapeutic avenues that will rejuvenate wild-type p53 or target mutant p53 should have a significant impact on the prevention and treatment of CC. GPR109A, a G-protein coupled receptor for the FDA-approved lipid-lowering drug Niacin (NA), bacterial metabolite Butyrate (BTR), and ketone body β-hydroxybutyrate (BHB), functions as a novel tumor suppressor in the colon by providing the molecular link between colonic bacteria and p53 function. GPR109A activation limits cAMP by inhibiting adenylate cyclase (AC), which induces RAS and its downstream growth-promoting signaling. cAMP also enhances the binding of MDM2 to p53 and induces the proteasomal degradation of p53. p53 is an NAD^{+}-dependent molecule and deficiency of NA, the precursor of NAD^{+}, impairs p53 function. We tested the role of GPR109A and its agonists (NA, BTR, and BHB) in normal immortalized colon epithelial cell lines (CCD33 and CCD81) and various CC lines such as HCT116-$p53^{+/+}$, HCT116-$p53^{-/-}$, DLD1 (p53 point mutation), VACO4A (p53 insertion mutation), and SW498 (p53 deletion) and measured cell proliferation, cell cycle, apoptosis, and analyzed the expression of GPR109A and p53 (total, phosphorylated, and acetylated), MDM2, p21, Bax, and Puma in the presence and absence of GPR109109 agonists. We found that GPR109A expression is significantly reduced in CC cell lines, especially in p53 mutant cell lines, when compared to normal immortalized colonic epithelial cell lines. Treatment of CC cell lines with GPR109A agonists-induced apoptosis in wild-type p53 expressing CC by activating p53 and its targets. However, some lesser extent in p53 mutant or p53 null cell lines. Lentiviral-mediated GPR109A expression in CC cell lines itself induced apoptosis in both wild-type and mutant p53 expressing CC cell lines and GPR109A agonists treatment induced further. Interestingly, GPR109A agonists BTR and BHB significantly increased apoptosis in p53 mutant and p53 null CC cell lines in a p53-independent manner. Overall, our results provide evidence that GPR109A activation can be used as an effective therapeutic strategy for the treatment of CC.

#3023 Master corepressor inactivation through oncogene suppressor RAI2 mediated polymerization.

N. Goradia[1], S. Werner[2], E. Mullapudi[1], G. von Amsberg[2], **K. Pantel**[2], M. Wilmanns[1];
[1]European Molecular Biology Laboratory, Hamburg, Germany, [2]University Medical Center Hamburg-Eppendorf, Hamburg, Germany

Imbalanced transcription of a large number of genes can be caused at various levels, ranging from alterations in individual transcription factors to dysfunctional corepressor and coactivator complexes [1]. C-terminal binding proteins (CtBPs) are ubiquitous master transcriptional coregulators associated with the Polycomb Repressive Complex 2 (PRC2), with essential functions in the development and oncogenesis of various tumor entities, including breast cancer and prostate cancer (PC) [2,3]. As CtBPs bind to short linear PxDLS-like sequence motifs (SLiMs), the presence of such motifs in tandem on the putative metastasis suppressor RAI2 [4] suggested a previously undiscovered dual interaction with CtBPs. Here, we show that RAI2 induces CtBP polymerization through well-ordered filaments of stacked tetrameric CtBP layers, as illustrated by a high-resolution single particle cryo electron microscopy structure. These filaments are mirrored by RAI2-mediated CtBP nuclear foci and relief of CtBP corepressor function in RAI2-expressing cancer cells. Analyses of a diverse PC patient cohort revealed a substantial decrease in RAI2 in the aggressive subtypes, suggesting a pivotal role of RAI2 in the transition to androgen receptor signaling-independent progression. Taken together, our data demonstrate a previously unknown mechanism of multivalent short linear sequence motif-induced polymerization. As RAI2-like SLiM motifs are found in a wide range of organisms, including pathogenic viruses, our findings serve as a paradigm for diverse functional effects through multivalent interaction-mediated polymerization by disordered proteins in healthy and diseased conditions. The specific properties of these repeated interactions open up new therapeutic opportunities.

References

[1] Lee, T.I. & Young, R.A. Transcriptional regulation and its misregulation in disease. Cell 152, 1237-51 (2013).
[2] Di, L.J. et al. Genome-wide profiles of CtBP link metabolism with genome stability and epithelial reprogramming in breast cancer. Nat Commun 4, 1449 (2013).
[3] Wang, R. et al. Role of transcriptional corepressor CtBP1 in prostate cancer progression. Neoplasia 14, 905-14 (2012).
[4] Werner, S. et al. Suppression of early hematogenous dissemination of human breast cancer cells to bone marrow by retinoic Acid-induced 2. Cancer Discov 5, 506-19 (2015).

#3024 HIF1A and HIF2A differentially contribute to early and adaptive changes following *in vivo Vhl* inactivation in the kidney.

S. Kurlekar, J. Lima, A. B. Barros, N. Masson, S. Zhai, C. W. Pugh, J. Adam, P. J. Ratcliffe;
University of Oxford, Oxford, United Kingdom

The von Hippel Lindau (VHL) tumor suppressor gene is a classical tumor suppressor whose biallelic inactivation is a truncal event in clear cell renal cell carcinoma (ccRCC) evolution. VHL is best characterized as the recognition component of an E3 ubiquitin ligase complex that targets hypoxia inducible transcription factors (HIF1A and HIF2A) for conditional oxygen-dependent degradation. HIF activation following VHL inactivation is an early event in ccRCC progression. While the functions of HIF1A and HIF2A in ccRCC biology and progression have been studied, those in VHL-null non-neoplastic cells of the renal tubular epithelium (RTE) and their contribution to tumorigenesis have not been fully explored. Here, using a combination of lineage marking and single-cell RNA sequencing (scRNA-seq), we provide the first description of HIF1A- and/or HIF2A-dependent and -independent consequences of *in vivo Vhl* inactivation in the RTE with single-cell resolution. We have previously reported on the development of a novel mouse model designed to mark and track cells that have undergone Vhl inactivation in vivo. Using this model, we have shown that Vhl inactivation has extensive, cell-type specific effects on gene expression in cells of the RTE within 3 weeks of recombination. Furthermore, we have shown that over a course of 4-8 months after Vhl inactivation, Vhl-null cells undergo specific adaptive changes in gene expression that encompass genes not regulated early after Vhl inactivation. In the work reported here, we have coupled this mouse model to a tamoxifen-inducible RTE-specific Pax8-CreERT2 and conditional alleles for Hif1a and/or Epas1 (codes for HIF2A). We have analyzed ‘marked’ recombined cells at early (1-3 weeks) or late (4-8 months) timepoints after recombination and compared these cells to time-matched Vhl-null cells using immunohistochemistry, in situ RNA hybridization and scRNA-seq. We found that though both HIF isoforms were present in Vhl-null cells at the early timepoint, expression of genes regulated early after Vhl inactivation was affected more by Hif1a inactivation than Epas1 inactivation. In contrast, expression of genes that are regulated in Vhl-null cells over time was drastically impacted by Epas1 deletion but was unaffected by Hif1a deletion. Interestingly, most of these Epas1-dependent, time-dependent changes in Vhl-null cells involved genes that have not been identified as direct transcriptional targets of HIF. Collectively, our work suggests that HIF1A and HIF2A have temporally distinct contributions to gene expression in Vhl-null cells in the RTE. We are currently analyzing the cell-type specificity of these contributions and ascertaining their relevance to the adoption of ccRCC-associated gene expression profiles.

#3025 Germline p53 R181 variants and DNA binding cooperativity in tumorigenesis.

R. Moses[1], R. Hausler[1], G. Kelly[1], A. Indeglia[2], S. Miller[3], J. Karanicolas[3], M. Murphy[2], K. Maxwell[1];
[1]University of Pennsylvania, Philadelphia, PA, [2]Wistar Institute, Philadelphia, PA, [3]Fox Chase Cancer Center, Philadelphia, PA

TP53 is the most frequently mutated gene in cancer, and its encoded protein p53 has many tumor-suppressive functions. There are several different classes of mutant p53 acquired in human cancer and inherited in cancer-prone families with Li-Fraumeni Syndrome, where individuals have an 80-90% increased risk of cancer. These include structural mutations that are generally (e.g R175H) or locally (e.g Y220C) misfolded, DNA contact mutations (e.g R273H); and oligomerization mutations (A347D). Cooperativity mutations affect binding of the p53 tetramer to DNA via disruption of a salt bridge formed by the negatively charged glutamic acid (E) 180 residue of one p53 monomer and the positively charged arginine (R) 181 residue of another. p53 “cooperativity” mutations at the R181 residue (R181H and R181C) have been increasingly identified in cancer-prone families undergoing genetic testing; however, the mechanism by which these variants disrupt p53 tumor suppression in humans is not understood. We show that the purified DNA binding domains of p53 variants R181H and R181C bind less cooperatively to the p53 binding site in the *CDKN1A* (p21) promoter, despite retaining wild-type levels of structural stability. RNA-sequencing of CRISPR knock-in colorectal and breast cancer cell lines shows reduced ability of R181H and R181C to transactivate a curated set of ~300 known p53 target genes. Upon treatment with p53 activating molecule Nutlin-3a, the R181-mutant cells fail to cell cycle arrest in the G1 phase and maintain high proliferative rates. Interestingly, we observe some residual apoptotic activity in R181H and R181C mutant cells treated with DNA-damaging agent 5-fluorouracil, despite losing the transactivation of proapoptotic p53 targets; this suggests that these mutants retain the p53 transcription-independent mechanism of apoptosis which is observed in other p53 variants such as P47S and A347D. These studies will define the pathogenicity of R181 variants and guide therapeutic intervention for patients that harbor these p53 mutations.

#3026 STK11 negatively regulates NFKB signaling in KRAS-driven lung adenocarcinoma.

David Joseph Seward[1], Sean Lenahan[2], Allison Racela[1], Israel Odekunle[1]

[1]Pathology and Laboratory Medicine, University of Vermont Medical Center, Burlington, VT,[2]Dana-Farber Cancer Institute, Boston, MA

In the US, more people die each year from lung cancer than breast, colorectal, and prostate cancers combined. Despite advances in lung cancer detection and treatment, the overall prognosis for patients remains poor. Patients whose lung tumors harbor druggable mutations often experience initial responses with targeted therapies, but acquisition of therapy resistance results in 5-year survival rates that have remained near ~20%. Immune check-point inhibitors (ICI) promise to improve outcomes in patients with lung cancer by targeting mechanisms of immune evasion. Drugs that disrupt PD-L1-mediated immune evasion, including pembrolizumab and nivolumab, have revolutionized treatment for some cancers. Unfortunately, only ~30% of lung adenocarcinomas (LUADs) respond to anti-PD-1 therapy and we cannot reliably identify this group prior to treatment. This underscores the need to discriminate which patients will respond to ICI therapies, while simultaneously highlighting the ~70% non-responder rate. To that end, recent clinical studies have linked anti-PD-1 therapy resistance with Serine/Threonine Kinase 11 (STK11) loss of function (LoF). STK11 operates in a heterotrimeric complex with the pseudo-kinase STRADα and the scaffolding protein MO25 where it regulates numerous intracellular signaling networks impacting metabolism, proliferation, transcription, and cell morphology. Why STK11 LoF correlates with anti-PD-1 resistance in the context of KRAS-driven LUAD remains unknown and represents a critical question in lung oncology. As an initial approach to understand this phenomenon, we knocked-out STK11 in multiple KRAS-driven, STK11-competent human LUAD cell lines and performed whole transcriptome analyses to identify STK11-loss-dependent differential gene expression profiles. We assert the transcriptional mediators downstream of STK11 governing the changes we report represent therapeutic targets whose antagonism may restore anti-PD-1 efficacy. Supporting this rationale, our data has identified STK11-loss-dependent activation of the NFκ-B transcriptional network. NFκB is a master transcription factor that regulates numerous cytokines, but whether and/or how STK11 directs NFκB activity remains largely unaddressed. We highlight NFκB activation as a potential mechanistic link between STK11 loss and tumor-intrinsic cytokine upregulation. We speculate that STK11 normally acts as a key player in the negative feedback loop limiting NFκB activity. When STK11 is lost, that activity continues unabated. In summary, we propose STK11 loss drives anti-PD-1 therapy resistance by generating an altered tumor immune microenvironment via constitutive activation of NFκB-mediated cytokine production. In future we intend to assess strategies for reversing anti-PD-1 therapy resistance via disruption of the NFκB transcriptional axis in KRAS-driven LUAD lacking STK11.

#3027 p53 aggregation promotes transformation from non-malignant lesions to high-grade serous ovarian carcinomas.

S. Sartini, L. Omholt, N. A. Moatamed, A. Soragni;
UCLA - University of California Los Angeles, Los Angeles, CA

High-Grade Serous Ovarian Cancer (HGSOC) is the most common and aggressive gynecological malignancy. It is typically diagnosed in late stages due to lack of diagnostic tests and current therapies available are not efficacious when the tumor is advanced. HGSOC is characterized by ubiquitous loss of functional p53 tumor suppressor protein function, largely due to point mutations that arise very early in carcinogenesis. P53 mutations are detected in pre-neoplastic cells of the fallopian tube mucosa, called p53 signature, and in early precursor lesions called serous tubal intraepithelial carcinoma (STIC). Some mutations promote the misfolding and aggregation of p53, transforming the protein into a cancer-promoting oncogene. Here, we hypothesize that the transition from folded, soluble to aggregated mutant p53 underlies the transformation from a pre-neoplastic lesion (p53 signature, STILs), to STICs and eventually HGSOC. We first set to determine the proportion of cells carrying soluble vs misfolded mutant p53 in fallopian tube tissues collected from n=10 patients undergoing salpingo-oophorectomy. We performed conformation-sensitive staining and quantification of folded and unfolded p53 cases and demonstrated that p53 misfolding, a mandatory precursor to aggregation, is present in STICs and HGSOCs, but notably absent from p53 signatures and surrounding healthy tissue. To better characterize the role of aggregated p53 in the progression of HGSOC, we took advantage of primary human fallopian tube secretory epithelial cells (FTSEC) that mimic early and more advanced stages of carcinogenesis. We utilize the FTSEC cells line FT282, immortalized by introducing hTERT and the aggregation-prone mutant $TP53^{R175H}$ that is found in p53 signature lesions and STILs, as well as the FT282-CCNE1, derived from FT282 cell line with overexpression of CCNE1, representing a more malignant phenotype.We used these models to investigate p53 aggregation, characterize the mutant p53 interactome and test the efficacy of ReACp53, a p53 aggregation-targeting peptide we developed. Our results demonstrated that p53 aggregation is more severe in the FT282-CCNE1 line, with a higher susceptibility to ReACp53 compared to the FT282 cells. Overall, our results demonstrated that aggregation of mutant p53 is a structural defect that can distinguish between pre-malignant and malignant HGSOC lesions and can potentially be targeted, offering a potential window for early intervention in halting ovarian cancer progression.

MOLECULAR/CELLULAR BIOLOGY AND GENETICS: Oncogenic Transcription Factors
Poster Session

#3031 Overcoming drug resistance in cancer: A paradigm shift with FoxM1 targeting.
M. Pettersson, S. Bae, K.-k. Cho, H.-y. Yun, H.-S. Park;
Promedigen, Daejeon, Korea, Republic of

In cancer treatment, overcoming drug resistance remains a formidable challenge. The oncogenic transcription factor FoxM1 is widely recognized for its crucial role in promoting drug resistance to various chemotherapeutic and target therapies. Its involvement is attributed to pivotal pathways, encompassing cell cycle progression, angiogenesis, and metastasis. Despite its prominent role in tumor drug resistance, achieving modulation of FoxM1 using small molecule therapeutics has proven elusive. 5-fluorouracil (5-FU), a commonly used chemotherapeutic agent, is known to induce a significant upregulation of FoxM1. In this study, we demonstrate that our novel compound A3 leads to a robust dose-dependent reduction of FoxM1 driven by 5-FU in HT-29 colorectal cancer cells. Notably, exposure of 5-FU-treated HT-29 cells to A3 was shown to promote apoptosis via pro-apoptotic factors, including PUMA. The mechanism of action was further elucidated through a comprehensive analysis of cell signaling molecules. This study presents an innovative approach using small molecule modulators to control FoxM1 levels, providing profound insights for potential therapeutic interventions in cancer treatment.

#3032 Generation of a FOXC2-deficient melanoma cell line using CRISPR-Cas9 gene editing.

D. M. Clark, P. D. Conde, K. M. Hargadon;
Hampden-Sydney College, Hampden-Sydney, VA

Melanoma, a cancer derived from pigment-producing melanocytes of the skin, is a highly aggressive cancer characterized by rapid growth and metastasis. FOXC2 is a forkhead box transcription factor family member that is often dysregulated in various cancers, including melanoma, where its expression correlates with metastatic progression and drug resistance. To gain insight into the oncogenic activity of FOXC2 in melanoma, we have employed CRISPR-Cas9 gene editing technology to generate a novel FOXC2-deficient B16-F10 murine melanoma cell line. This model will be a useful tool for studying the tumor-promoting functions of FOXC2.

#3033 Oncogenic ETS transcription factors avoid repression by EZH2 and FOXO1 in prostate cancer and Ewing sarcoma .

N. F. Downing, K. M. Mills, P. C. Hollenhorst;
Indiana University Bloomington, Bloomington, IN

ETS transcription factors play roles throughout development, aiding in hematopoiesis, blood vessel formation and cell fate. The ETS family is composed of 28 members, all of which share an ETS DNA-binding domain. Chromosomal rearrangements that lead to the overexpression of specific ETS promote oncogenic transformation and tumor development. More than half of prostate tumors are driven by aberrant expression of an ETS protein. Our lab has demonstrated that oncogenic ETS form essential interactions with a ubiquitous RNA-binding protein, EWS, to promote prostate tumorigenesis. A similar mechanism exists in Ewing sarcoma (ES). ES tumors are driven by the expression EWS/ETS fusion proteins. This project focuses on the similarities and differences between oncogenic ETS in prostate cancer and EWS/ETS fusions in Ewing sarcoma.

We compared biological functions of the most common oncogenic ETS in prostate cancer, ERG, and the most common fusion in ES, EWS/FLI1. Both ERG and EWS/FLI1 promoted migration and clonogenic survival in normal prostate epithelial cell lines, RWPE1 and PNT2. These data suggest that the EWS-ERG complex and EWS/FLI1 fusion protein can function similarly in prostate cells. Knockdown of endogenous EWS/FLI1 in the ES cell line, A673, reduced anchorage-independent colony formation in soft agar. Rescue with exogenous EWS/FLI1 or EWS/ERG restored colony formation relative to control. Wildtype ERG was unable to rescue colony formation in A673. This suggests that ERG and EWS/FLI1 function differently in A673 cells. Pulldown assays from A673 lysates reveal that ERG interacts with EZH2 and FOXO1. Our lab has established that ERG acts as a transcriptional repressor through the formation of an ERG-EZH2-PRC2 complex. Others demonstrate that FOXO1 represses ERG activity by reducing its recruitment to the target sites. Both the N-terminal truncation of ERG and phosphorylation of ERG at S96 disrupted these interactions and rescued anchorage independent growth in A673 ES cells. These data suggest that EWS/ETS fusions avoid transcriptional repression in Ewing tumors due to loss of the N-terminus of the ETS protein.

#3034 Krüppel-like factors in regulation of gastric cancer progression.

S. Kakkat[1], P. Suman[1], S. Goswami[1], S. Basu[2], M. J. Heslin[1], E. A. Turbat-Herrera[1], V. Ramirez Alcantara[1], C. Sarkar[1], D. Chakroborty[1];
[1]University of South Alabama, Mobile, AL, [2]The Ohio State University, Columbus, OH

Introduction: Gastric cancer (GC) is the third leading cause of cancer-associated mortality and the fifth most frequently diagnosed cancer worldwide. The development and progression of GC is a complicated multistage process subjected to dynamic changes in gene regulation. Investigating the effects of these changes is therefore critical for improving our knowledge about GC initiation and progression. Krüppel-like factors (KLFs) are evolutionarily conserved zinc finger-containing transcription factors with altered expressions and diverse regulatory functions in GC. We previously reported that there is loss of KLF4 in GC. Here we report that KLF4 is a crucial regulator of KLF5 expression and vice versa and together they regulate GC cell behavior.
Methods: The Cancer Genome Atlas (TCGA) and pan cancer data of differential expressions of KLFs in GC was analyzed. TCGA RNAseq and clinical data for the differential expression status of KLF genes in normal and cancerous tissues and the clinicopathological association was accessed from the UALCAN web portal. The expressions of KLF4 and KLF5 in human normal stomach and GC and orthotopic xenografts were detected by immunohistochemistry (IHC). KLF4, KLF5 cross regulation was evaluated by gene manipulation of each gene individually and checking the expression of the other factor in GC cells. The effect of KLFs on GC cell proliferation, migration, and invasion was determined by Ki67 staining of tissues, PrestoBlue cell viability assay, scratch wound and transwell cell invasion assays.
Results and Conclusion: Our results indicated that not only KLF4 and KLF5 have contrasting expressions and effects in GC but also these two factors cross regulate each other. While lower expressions of KLF4 was found in human GC and orthotopic xenografts, increased expression of KLF5 was found in both human GC tissue and orthotopic xenografts. KLF4 silencing and CRISPR /Cas9 knockdown in human GC cells resulted in increased expression of KLF5 which was associated with increased GC cell proliferation and invasiveness. Interestingly, KLF5 knockdown by CRISPR / Cas9 in human GC cells on the other hand resulted in increased expression of KLF4, which was associated with decreased GC cell growth. Our data therefore suggests that the differential expressions of KLF4 and KLF5 might serve as valuable prognostic markers in GC.

#3035 Bridging the gap: Exploring the roles of ETS- coactivator interactions in promoting prostate cancer .

K. M. Mills, N. Downing, S. Metcalf, P. Hollenhorst;
Indiana University Bloomington, Bloomington, IN

The ETS family of transcription factors is comprised of 28 members that all share a common C- terminal DNA-binding domain. ETS play essential roles in developmental processes, such as stem cell maintenance, blood vessel formation, and cellular fate. While absent in the normal prostate, four members of the ETS family become expressed in prostate tumors: ETV1, ETV4, ETV5 and ERG. Our lab has previously classified these proteins as oncogenic ETS for their ability to promote cellular migration in normal prostate epithelial RWPE1 cells. Transcription factors may need to interact with additional proteins to serve oncogenic roles. My research explores the interactions between 1) ETV1 and EWS, as well as 2) ERG and p53. Our lab has established that ETV1, ETV4 and ETV5 form essential interactions with EWS, a transcriptional coactivator that promotes ETS activity. In prostate tumors, chromosomal rearrangements result in the N-terminal truncations of ETV1, ETV4 and ETV5. I hypothesize that the EWS interaction domain is retained and that these truncated ETVs will remain oncogenic. Pulldown assays using purified full-length and truncated ETV1 suggests EWS interacts with both N-terminal and C-terminal portions ETV1. I am attempting to express truncated ETV1, ETV4 and ETV5 in RWPE1 cells. Upon stable expression, I will evaluate their interactions with EWS and their ability to promote migration in vitro. To identify putative proteins that bridge EWS to ETV1, immunoprecipitation mass spectrometry will be used. Mutations in p53, a tumor suppressor protein, promote oncogenesis and occur in nearly half of all cancer cases. We hypothesize that mutant p53 interacts with ETS to promote its recruitment to new genomic sites. Previous studies demonstrate that mutant p53 binds ETS2 at a higher affinity than wildtype p53 and we have expanded this list of interacting ETS to include ERG. We seek to explore whether ERG and mutant p53 cooperate to promote oncogenic phenotypes. I successfully cloned wildtype p53, mutant p53 (R248W) and double-mutant p53 (R248W, T81A) into a retroviral backbone. I then transduced RWPE1-Vector and RWPE1-ERG expressing cells to express these constructs. Although additional replicates are needed, it appears that mutant p53 promotes colony formation in both cell types relative to wildtype p53. I plan to validate these observations and generate an appropriate negative control cell line before extending into a mouse model. Through the continuation of this work, I will provide critical insight into the molecular mechanisms by which a subset of ETS factors achieve oncogenic function. We address the contributions of DNA-binding specificity and coactivator interactions in promoting the phenotypes associated with prostate cancer.

#3036 Sensitivity of ONC201/TIC10 cancer therapeutic on neuroendocrine prostate cancer (NEPC) and neuroendocrine differentiation (NED).

E. C. Ding, M. Pinho-Schwermann, S. Zhang, C. Purcell, W. S. El-Deiry;
Legorreta Cancer Center at Brown University, Providence, RI

Although androgen deprivation therapy and androgen receptor (AR) blockade are highly effective therapies for metastatic prostate cancer (PCa), most patients develop resistance, leading to castration-resistant prostate cancer (CRPC). A subset of CRPC shows neuroendocrine prostate cancer (NEPC) features, which are associated with poor prognosis and limited therapeutic strategies. NEPC is characterized by oncogenic driver activation and epigenetic changes, partly controlled by transcription factors like BRN2 and SOX2. AR has been shown to suppress BRN2 transcription, which is required for NEPC, and BRN2-dependent regulation of the NEPC marker SOX2 (Bishop et al., 2017). Dordaviprone (ONC201/TIC10) is a first-in-class small molecule that antagonizes DRD2, induces tumor necrosis factor-related apoptosis-inducing ligand (TRAIL), and activates the integrated stress response (ISR). Neuroendocrine tumors express significant DRD2 levels, suggesting ONC201 as a potential therapeutic strategy in NEPC or when drivers for disease progression are overexpressed (OE). PCa cell lines PC3, DU145, LNCaP, and 22RV1 are ONC201 sensitive, with IC50=2.87 μM, 3.18 μM, 1.31 μM, and 1.16 μM, respectively (Ding et al., 2023). To characterize the association of BRN2/SOX2 dysregulation with ONC201 sensitivity, we transiently OE BRN2/SOX2 in PCa. We hypothesized that markers of neuroendocrine differentiation (NED), activation of the ISR, TRAIL, and ClpP and dopamine receptor expression contribute to NEPC cell death and sensitivity to ONC201. We performed CellTiter-Glo experiments to assess viability after 96 hours ± BRN2 OE. DU145 cells with BRN2 OE increased their sensitivity to ONC201 (IC50=2.75 μM) compared to empty vector (IC50=3.03 μM). Colony formation assays were conducted in PCa and analyzed 7 days after ONC201 treatment to show ONC201 effect on PCa cell lines. DU145 was treated at 0.5, 1, and 2 μM of ONC201. There were 95 ± 3.22 colonies for the control group, 83 ± 5.22 colonies with 0.5 μM, 74 ± 3.64 colonies with 1 μM, and 8 ± 2.03 colonies with 2 μM ONC201. DU145 showed a significant reduction in colony-forming ability when treated with 1 and 2 uM ONC201 compared to the control, with P values of <0.05 and <0.0001, respectively. We OE BRN2 and observed changes in NED markers and ISR pathway. In PC3, FoxO1 and ATF4 levels increased. In DU145, FoxO1, ENO2, PGP9.5, CgA, and ATF4 levels decreased. We reveal that DU145 OE at 48 hours does not result in greater expression of NEPC markers. BRN2 OE significantly increased PCa cell sensitivity to ONC201 and was evident without an increase in common phenotypical markers used for NEPC assessment (FoxO1, ENO2, PGP9.5, CgA). Expression change was not shown when PCa had an integral AR pathway. Ongoing efforts are observing ONC201 treatment effects on NED markers and the TRAIL pathway due to BRN2 OE and showing increased sensitivity of PCa to ONC201 with BRN2 OE.

#3037 Sex-specific differences in *Yap1* and *Cd276* function and expression regulate medulloblastoma progression and immune evasion.

N. Abdelfattah[1], S. Natarajan[2], H. Tran[1], J. Maldonado[1], R. McMinimy[3], H. Borland[4], S.-h. Chen[1], F. Camargo[5], J. Olson[6], J. George[7], K. Yun[1];
[1]Houston Methodist Research Institute, Houston, TX, [2]The Jackson Laboratory for Mammalian Genomics, Bar Harbor, ME, [3]Jackson Laboratory for Genomic Medicine, Bar Harbor, ME, [4]Texas A&M University, College of Liberal Arts, College Station, TX, [5]Harvard Department of Stem Cell and Regenerative Medicine, Boston, MA, [6]Fred-Hutch, University of Washington School of Medicine, Seattle, WA, [7]Jackson Laboratory for Genomic Medicine, Farmington, CT

Unveiling the molecular mechanisms underlying sex-specific differences in cancer initiation, progression and treatment outcomes will provide novel insights that will advance cancer research and clinical care. This study highlights an unexpected, sex-biased role of the oncogene *Yap1* in SHH medulloblastoma (MB). We discovered that *Yap1* deletion in *SmoM2*-driven SHH MB significantly prolongs survival in male but not female mice. Using an integrated multi-omics approach, we show that YAP1 promotes cancer stem cell maintenance through concurrent transcriptional activation of stemness genes, such as *Sox2,* and repression of differentiation genes such as *NeuroD1* and *Zic1*/2. Interestingly, while *Yap1* is essential for maintaining cancer stem cells in both sexes, it plays a more critical role in immune evasion in males. Specifically, YAP1 regulates the expression of an immune checkpoint molecule *Cd276* to suppress T cell function. Blocking CD276 or deleting *Yap1* is sufficient to significantly reverse T cell suppression in males but not females. Furthermore, YAP1 direct targets of transcriptional regulation, including CD276, predicts survival in male but not female patients across multiple human cancers, suggesting that our findings have broader implications beyond medulloblastomas and is conserved across species. This study provides compelling evidence for male-biased susceptibility to *Yap1* inhibition and uncovers the YAP1-CD276 axis as a sexually diverse pathway in T cell suppression in tumors.

#3038 PPARδ promotes gastric adenocarcinoma carcinogenesis by enhancing ZBP1-induced necroptosis and inflammation and fostering gastric tumor immunosuppressive microenvironment.

Y. Liu[1], D. Wei[1], L. Wang[1], J. C. Yao[1], I. Shureiqi[2], X. Zuo[1];

[1]University of Texas MD Anderson Cancer Center, Houston, TX, [2]University of Michigan, Ann Arbor, MI

Overexpression of peroxisome proliferator-activated receptor delta (PPARδ) in villin-positive gastric progenitor cells (VGPCs) has been demonstrated to spontaneously induce gastric adenocarcinoma (GAC) in mice. PPARδ is upregulated in human GAC tissues, and its expression level is positively associated with human GAC grades and stages. However, the potential for targeting this tumorigenic effect of PPARδ, along with the underlying molecular mechanisms, remains elusive. In this study, we investigated the impact of PPARδ genetic deletion/loss of function in VGPCs on *Helicobacter felis* (*H. felis*)-induced GAC carcinogenesis by orally exposing the mice carrying wild-type (WT) PPARδ or genetically deleted PPARδ in VGPCs to *H. felis* infection. We also examined the effect of PPARδ inhibition by its specific antagonist, GSK3787, on PPARδ-induced GAC carcinogenesis in mice. Furthermore, we conducted RNA-seq for transcriptomic profiling analysis and validated the results through quantitative reverse transcription-polymerase chain reaction (qRT-PCR) on the gastric tissues of those mice and the mice with WT PPARδ or PPARδ overexpression in VGPCs at ages 10, 25 and 55 weeks. We found that 1) PPARδ genetic deletion in VGPCs significantly inhibited *H. felis*-induced gastric chronic inflammation and GAC carcinogenesis; GSK3787 significantly suppressed PPARδ-induced GAC carcinogenesis in mice; 2) PPARδ overexpression in VGPCs significantly enhanced while PPARδ genetic deletion in VGPCs significantly inhibited ZBP1-induced necroptosis and the related inflammatory signaling pathways such as interferon-gamma signaling, IL6-JAK-STAT3 signaling, and IL2-STAT5 signaling evidenced by gene set enrichment analysis of RNA-seq data, which were further validated by qRT-PCR; and 3) PPARδ overexpression in VGPCs markedly increased the expression of CCL20 in gastric epithelial cells of the mice before (age 10 weeks) and after GAC initiation and progression (age 25 weeks-early stage GAC and age 55 weeks-late stage GAC), and gastric infiltrations of $CCR6^{+}$ myeloid-derived suppressor cells and $CCR6^{+}$ tumor-associated macrophages, thereby creating a gastric tumor immunosuppressive microenvironment. In contrast, PPARδ genetic deletion in VGPCs or the administration of GSK3787 diet significantly reversed this PPARδ-induced immune suppression in mice. In conclusion, our findings highlight the pivotal role of PPARδ in VGPCs as a key host factor in GAC carcinogenesis, especially in individuals exposed to chronic *H. pylori* infection that could lead to an upregulation of PPARδ expression. This suggests that targeting PPARδ signaling could be a novel therapeutic approach for GAC prevention and therapy.

#3039 Pan cancer therapeutic inhibition of oncogenic c-MYC by the engineered destabilized 3'UTR of c-MYC.

C. U. Awah;
UTR Therapeutics Inc, New York, NY

c-MYC is a master transcription factor that is over expressed in more than 70% of human cancers. There is no clinically approved direct inhibitor of c-MYC. Recently, we reported the development of the engineered destabilized 3'UTR of MYC constructs which is a novel mRNA overwriting technology through which we directly destabilized and degraded c-MYC. Here we report that we have extended this technology in directly targeting and degrading c-MYC in multiple ethnically diverse triple negative breast cancer cell lines, ovarian cancers, neuroendocrine prostate cancers and pancreatic cancers. The constructs are specific, titratable, and directly engaged the c-MYC target validated by RNA transcript technologies. We have performed head-to-head IC50 dose dependent titration comparison with the engineered destabilized 3'UTR of c-MYC constructs and chemotherapies (DNA damaging agents, microtubules inhibiting drugs, alkylating agents) as well as immune checkpoint inhibitor. We found evidence that suggests that the engineered destabilized 3'UTR of c-MYC is likely to be superior to these therapies in pan cancers driven by c-MYC.

#3040 Tumor-specific super-enhancer drives overexpression of *EVI1* in ovarian cancer.

Leonie Smeenk[1], Sabrina Kruse[2], Roger Mulet-Lazaro[1], Ingrid Boere[3], John Martens[3], Stefan Groschel[4], Claudia Scholl[5], Stefan Frohling[2], Ruud Delwel[1]

[1]Hematology, Erasmus MC Cancer Institute and Oncode Institute, Rotterdam, Netherlands,[2]Translational Medical Oncology, German Cancer Research Center (DKFZ), Heidelberg, Germany,[3]Medical Oncology, Erasmus MC Cancer Institute, Rotterdam, Netherlands,[4]Oncology Center Worms, Worms, Germany,[5]Applied Functional Genomics, German Cancer Research Center (DKFZ), Heidelberg, Germany

Epithelial ovarian cancer (OC) is typically diagnosed at a late stage and, despite treatment with cytoreductive surgery and chemotherapy, 70-80% of patients relapse and eventually die due to the disease. Major challenges to improve patient outcomes are to overcome therapy resistance and to individually tailor therapy. Uncovering the molecular drivers of OC, especially in the most common subgroup high-grade serous (HGS), will help develop novel therapeutic strategies to meet these challenges.

Using the Cancer Genome Atlas (TCGA) data, we observed that a locus in 3q26.2, near the *EVI1* oncogene, was the most significantly amplified region in HGS OC, occurring in more than 80% of those tumors. We validated these findings in an OC dataset from the Hartwig Medical Foundation and in OC cell lines from the DepMap database. Furthermore, HGS OC had the highest mean copy number of the 3q26.2 locus co-occurring with high mean *EVI1* expression among all tumor entities in the pan-cancer TCGA dataset. These *EVI1* expression levels are significantly higher than in normal fallopian tube, from which HGS OC most likely arises. *EVI1* overexpression promotes leukemogenesis in 3q26-rearranged acute myeloid leukemia (AML), as a result of chromosomal translocations that enable hijacking of hyperactive enhancers. Here, we hypothesize that *EVI1* also plays a crucial role in OC development, but that its aberrant expression in this disease is driven by the amplification of yet undiscovered regulatory elements near *EVI1*.

We showed that EVI1-positive OC cell lines, of which the majority are HGS, are EVI1-dependent and harbor a ~200 kb amplified region near *EVI1*. This region interacts with the *EVI1* promoter (4C-Seq), is characterized by open chromatin (ATAC-Seq), and shows high levels of H3K27 acetylation (H3K27ac ChIP-Seq), suggesting the presence of an active enhancer. Furthermore, based upon H3K27ac signal, we identified within this region a super-enhancer of approximately 65 kb. In OC cell lines without detectable *EVI1* levels or cell lines from other cancer subtypes, such as breast and colon cancer, this location had no active enhancer and did not loop to the *EVI1* promoter.

Altogether, these data point to the generation of a hyperactive super-enhancer driving *EVI1* overexpression in OC. These findings emphasize the importance of epigenetic control in the regulation of *EVI1* expression, as previously shown in 3q26-rearranged AML. Since OC tumor cell lines are strongly dependent on EVI1, interference with this super-enhancer, leading to loss of *EVI1* expression, could be exploited to inhibit tumor growth. For this purpose, we generated GFP-tagged *EVI1* cell line models (e.g. SKOV3), which will be used to discover small molecules to target the activity of this super-enhancer. In conclusion, we discovered a new mechanism of enhancer-mediated overexpression of the *EVI1* oncogene as a molecular driver in ovarian cancer, with possible implications for therapy.

#3041 The small MAF transcription factor MAFG is a potent driver of melanoma.

O. Vera, M. Martinez, Z. Soto-Vargas, X. Xu, **F. Karreth**;
Moffitt Cancer Center, Tampa, FL

While common mutations in potent proto-oncogenes and tumor suppressors induce melanoma formation, no recurrent mutations associated with the late stages of melanomagenesis have been identified. Instead, non-mutational mechanisms such as the deregulation of transcriptional or epigenetic programs typically promote the malignant progression and metastasis of melanoma. We have previously identified the small MAF transcription factor MAFG as a critical target of the melanoma suppressor miRNA miR-29, prompting an in-depth evaluation of the role of MAFG in melanoma. MAFG expression is elevated in melanoma compared to melanocytes and increases with tumor stage. Ectopic expression of MAFG in human melanocytes and melanoma cells enhances proliferation in vitro and promotes melanoma growth in vivo. Moreover, MAFG overexpression in $Braf^{V600E}$; $Pten^{FL/+}$ mice accelerated melanomagenesis, significantly shortening overall survival. Despite being a critical NRF2 dimerization partner, NRF2 was dispensable for the effects of MAFG. Moreover, MAFG overexpression in melanoma cells had no effect on the activity of NRF2 transcriptional reporters, nor did it induce transcriptional programs associated with NRF2. RNA sequencing and pathway analysis revealed MAFG-mediated effects on melanoma-associated processes such hypoxia, the PI3K/AKT pathway, and pigmentation. Indeed, MAFG induced HIF1a under normoxic conditions, enhanced AKT phosphorylation, and downregulated MITF and its target genes in the pigmentation pathway in melanoma cells. Interestingly, MAFG also potently enhanced AXL expression, suggesting that MAFG may promote melanoma, at least in part, by affecting the MITF/AXL balance that is associated with melanoma phenotype switching. We next analyzed whether MAFG is required for melanoma. Interestingly, silencing MAFG in human melanoma cells robustly inhibited growth in vitro. Moreover, the CRISPR/Cas9-mediated knockout of MAFG in an aggressive $Braf^{V600E}$; $Pten^{FL/FL}$ model potently prevented melanoma formation. Given the mild phenotype of MAFG whole-body knockout mice, our results suggest targeting of MAFG or its downstream pathways as a viable therapeutic approach in melanoma. In conclusion, our study establishes MAFG as a potent driver of melanoma development and nominates it as a therapeutic target.

#3042 Unraveling the mechanism of YAP toxicity in neuroendocrine solid tumors: Insights from Merkel cell carcinoma.

F. Bahar[1], T. C. Frost[2], V. Ananthapadmanabhan[1], J. L. Schnabel[1], M. Thakuria[1], J. A. DeCaprio[1];
[1]DFCI/Harvard Medical School, Boston, MA, [2]AstraZeneca, Boston, MA

The Hippo pathway, a pivotal regulator orchestrating organ size and tissue growth, has emerged as a central player in cancer biology. The downstream transcription factor YAP within this pathway has been implicated in diverse oncogenic processes. YAP activation contributes to drug resistance, metastasis, and poor clinical outcomes in many solid tumors. Conversely, YAP exhibits growth-suppressive effects in neuroendocrine (NE) solid cancers, a paradox that remains poorly understood. Analysis of RNAseq data from the Cancer Cell Line Encyclopedia (CCLE) revealed a distinct classification of tumors into YAP1-expressing (YAP^{on}) and non-expressing (YAP^{off}) subgroups, with hematopoietic malignancies and NE solid tumors featured prominently in the latter. Merkel cell carcinoma (MCC) is a rare, high-grade, NE carcinoma of the skin with two distinct etiologies. Virus-positive MCC contains integrated Merkel cell polyomavirus that expresses the viral T antigens and virus-negative MCC caused by sunlight exposure and extensive UV damage. Bulk RNAseq performed with more than 60 MCC tumors revealed that YAP expression displayed an inverse correlation with an NE gene expression signature. To gain insight into why YAP expression is so low in MCC, we generated MCC cell lines with inducible expression of YAP. Expression of YAP led to growth arrest and cell death. We performed a genome-wide CRISPR-Cas9 screen to identify genes that when lost enable MCC cells to tolerate YAP expression. Functional enrichment analysis of the positively selected genes uncovered a variety of signaling pathways. Intriguingly, the CRISPR screen revealed a positive enrichment of non-canonical BAF complex members, including BRD9 and SMARCD1. To validate this finding, we treated MKL-1 cells with a BRD9 inhibitor, observing a substantial reduction in YAP toxicity. These findings open avenues for the development of targeted therapeutic strategies for high grade NE cancers, addressing a critical gap in our understanding of YAP biology in the context of MCC and beyond.

#3043 MYC activation and PTEN loss synergistically activate proliferation in a mouse model of lethal prostate cancer.

M. Rubenstein[1], T. Jones[1], J. Hicks[1], A. Rege[2], Q. Zheng[1], C. Gomes-Alexandre[1], G. Hubbard[1], S. Yegnasubramanian[1], C. Bieberich[2], A. DeMarzo[1]; [1]Johns Hopkins University School of Medicine, Baltimore, MD, [2]University of Maryland Baltimore County, Baltimore, MD

Prostate cancer kills 30,000 men per year in the U.S. Yet, of all primary prostate cancers, only a relatively small percentage are aggressive and have the potential to become life threatening. In terms of genomic copy number alterations, concurrent amplification of MYC and loss of tumor suppressor PTEN is the strongest predictor of prostate cancer specific mortality. We have previously shown, in a novel mouse model, that combined MYC overexpression and Pten loss results in the development of precursor lesions (PIN) that lead to aggressive metastatic prostatic adenocarcinoma, yet overexpression of MYC alone or Pten loss alone result only in precursor lesion development. Here, we performed genome wide transcriptome analysis using bulk RNA seq to obtain clues regarding the synergy between MYC overexpression and Pten loss. Prostates harboring PIN lesion were dissected from mice engineered to have MYC activation alone, Pten loss alone, and the combination thereof (BMPC mice), as well as invasive primary adenocarcinomas and metastatic lesions from BMPC mice. Principal Components Analysis (PCA) analysis separated the lesions into highly distinct groups. Genes contributing the most to the first principal component were related to inflammation and cell proliferation/cell cycle progression by functional annotation. The proliferation-related genes were increased somewhat by MYC overexpression alone, were not increased Pten loss, and were more consistently increased by combined MYC overexpression and Pten loss in BMPC. Strikingly, mice with combined MYC overexpression and Pten loss showed approximately 2-4 fold higher Ki67 proliferation index than mice with MYC activation alone. PIN lesions driven by MYC overexpression or PTEN loss alone were characterized by Gene Set Enrichment Analysis (GSEA). Among the pathways with the highest negative enrichment scores in PIN samples with PTEN loss were those that generally describe ribosome biogenesis and translation. PIN lesions with Pten loss showed lower hybridization signals for the 45S rRNA, which was increased by MYC alone and somewhat more in BMPC PIN lesions. Our results demonstrate that combined activation of MYC and Pten loss drive increased cell proliferation beyond that seen with either gene alteration alone. These findings suggest that a key part of the molecular mechanisms by which MYC and PTEN alterations may synergize to drive aggressive prostate cancer is related to increased tumor cell proliferation. Surprisingly, we uncovered the novel finding that Pten loss, in the absence of MYC overexpression, is associated with decreased expression of genes coding for proteins that mediate translation, as well as decreased 45S pre-rRNA. Since ribosome biogenesis is a key driver of cell proliferation, it is likely that loss of both copies of PTEN alone, in the absence of MYC overexpression, would be selected against in early lesions in prostate cancer.

#3044 Novel agents with efficacy against germline mutant RUNX1 familial platelet disorder with myeloid malignancy (FPD-MM).

C. P. Mill[1], W. C. Fiskus[1], C. D. DiNardo[1], P. K. Reville[1], J. A. Davis[1], C. E. Birdwell[1], K. Das[1], H. Hou[1], K. Takahashi[1], S. Loghavi[1], J. D. Khoury[2], K. Bhalla[1]; [1]UT MD Anderson Cancer Center, Houston, TX, [2]Univ of Nebraska, Omaha, NE

RUNX1 is a master-transcriptional regulator involved in normal and malignant hematopoiesis. Germline, mono-allelic, missense mutations in RUNX1 cause large deletions or truncations that are mostly loss-of-function mutations. They cause familial platelet disorder (RUNX1-FPD), which evolves into myeloid malignancy (FPD-MM), e.g., MDS or AML. Although curative in some patients, allogeneic stem cell transplantation from matched, un-related donors carries the risk of GVHD and relapse in FPD-MM. Thus, there is a need for novel therapies to revert FPD-MM back to FPD. LINCS1000-CMap analysis, of the RUNX1 knockdown RNA-Seq signature revealed homoharringtonine (HHT or omacetaxine) and the anthelmintic fenbendazole (analog of mebendazole (MB)) as the top expression mimickers. In our current studies, we demonstrate that treatment with HHT or MB induced significantly greater loss of viability in seven patient-derived samples of FPD-MM vs RUNX1-FPD. Analyses conducted on BMA cells harvested longitudinally from the same patient at the RUNX1-FPD versus FPD-MM stage demonstrated greater chromatin accessibility in FPD-MM cells along with increased mRNA expressions of MYB, MECOM and BCL2. Following HHT treatment, scRNA-Seq analysis demonstrated a marked reduction in the HSC population, but concomitant increase in the macrophage population in FPD-MM. This was associated with positive enrichment of apoptosis signaling and TP53 targets gene-sets, while negatively enriching those of c-Myc targets. CyTOF analysis demonstrated that HHT treatment reduced c-Myc, EVI1, MCL1, BFL1 and CDK6 expression in phenotypically characterized FPD-MM stem-progenitor cells. Utilizing an FPD-MM sample harboring Runx1 K194N, also detected in other pedigree members with FPD or FPD-MM, we established the first ever cell line (GMR-AML1) expressing germline mtRUNX1. GMR-AML1 cells exhibited high surface expression of CD117 (c-KIT), CD123 (IL-3R) and CD33. GMR-AML1 cells in which Runx1 was knocked-out by CRISPR-gRNA were outcompeted in vitro and in vivo, by cells that retained Runx1. Treatment with HHT or MB induced loss of viability in GMR-AML1 cells (LD50: 40 or 330 nM, respectively). HHT also caused concordant decline in ATAC-Seq and RNA-Seq peaks in ribosomal genes involved in protein translation. Treatment with MB inhibited cell cycle and protein translation. CyTOF analysis revealed that MB treatment also depleted CDK6, RUNX1, c-Myc and EVI1 in phenotypically defined FPD-MM stem cells. Finally, in the GMR-AML1 cell xenograft, treatment with omacetaxine or MB significantly reduced AML burden and improved overall survival of NSG mice. These preclinical findings highlight the molecular features associated with progression of RUNX1-FPD to FPD-MM and highlight HHT or MB as effective against cellular models of FPD-MM.

#3045 PPAR-α antagonist enhances immunotherapy and anti-angiogenic therapy to inhibit murine renal cancer.

M. Gillespie[1], V. Chen[2], I. Howard[1], K. Smith[1], D. Freund[2], N. Standifer[2], D. Burdette[2], T. W. Dubensky[2], S. Whiting[2], D. Panigrahy[1];
[1]Beth Israel Deaconess Medical Center, Harvard Medical School, Boston, MA, [2]Tempest Therapeutics, Brisbane, CA

Peroxisome proliferator activated receptor alpha (PPARα) is a transcription factor and master regulator of fatty acid oxidation. PPARα ligands modulate the switch between co-activator and co-repressor transcription complexes at PPARα-controlled target genes. In addition, PPARα has been shown to transrepress NF-κB signaling and inhibit angiogenesis. Renal cell carcinoma (RCC) expresses high levels of PPAR-α and is a highly angiogenic cancer. Current frontline treatments for RCC include chemotherapy, anti-angiogenics, and immunotherapy but are limited by the immune suppressive state of the tumor microenvironment. TPST-1120 is a novel PPARα antagonist for the treatment of cancer patients that binds in the ligand binding domain, positioning the AF-2 activation helix in an inactive conformation. The inactive conformation has a lower affinity for co-activator motifs and reduces activation of PPARα regulated genes. In a CHO-based reporter cell line, TPST-1120 potently competed against the PPARα-specific agonist GW7647 (IC_{50} = 36 nM at 20 nM GW7647) and an endogenous PPARα agonist oleoylethanolamide (OEA; IC_{50} = 15 nM at 30 μM OEA). Furthermore, in an enzyme fragment complementation assay, we demonstrated that TPST-1120 inhibited agonist-induced binding of PPARα to MED1 by destabilizing the co-activator complex thereby stabilizing the inactive conformation of PPAR-α. In a murine model of renal cell adenocarcinoma (RENCA), TPST-1120 treatment for 12 days (30 mg/kg qd) reduced tumor growth by 52% as a monotherapy ($p<0.0001$). Consistent with these findings, TPST-1120 inhibited tumor angiogenesis and proliferation as quantified by Ki67 levels. Combination treatment with current frontline therapeutics resulted in synergistic tumor inhibition of 74% with anti-PD1 (200 ug Q3D for 12 days) and 81% with cabozantinib (15 mg/kg QD for 15 days) ($p<.0001$). Flow cytometry-based analysis of tumors demonstrated increased CD8+ T cell infiltration in the TME as well as decreases in M2 and elevations in M1 macrophages. Importantly, we demonstrate that TPST-1120 can reverse an immunosuppressive class of immune cells to promote anti-tumor immunity and anti-angiogenesis in kidney cancer in the absence of overt toxicity. These data support advancement of TPST-1120 into RCC.

#3046 The estrogen signaling pathway reprograms prostate cancer cell metabolism and supports proliferation and disease progression.

C. Lafront, L. Germain, G. H. Campolina-Silva, C. Weidmann, L. Berthiaume, H. Hovington, H. Brisson, C. Jobin, L. Fregeau-Proulx, R. Cotau, K. Gonthier, A. Lacouture, P. Caron, C. Menard, C. Atallah, J. Riopel, E. Latulippe, A. Bergeron, P. Toren, C. Guillemette, M. Pelletier, Y. Fradet, C. Belleannee, F. Pouliot, L. Lacombe, E. Levesque, E. Audet-Walsh;
Universite Laval, Quebec, QC, Canada

Just as the androgen receptor (AR), the estrogen receptor α (ERα) is expressed in the prostate and is thought to influence prostate cancer (PCa) biology. Yet, the incomplete understanding of ERα cellular functions in PCa hinders our ability to fully comprehend its clinical relevance and restricts the repurposing of estrogen-targeted therapies for treatment of this disease. Using two human PCa tissue microarray cohorts, we first demonstrated that nuclear ERα expression was heterogeneous between patients, being only detected in half of tumors. Positive nuclear ERα levels were correlated with disease recurrence, progression to metastatic PCa, and patient survival. Using *in vitro* and *in vivo* models of the normal prostate and PCa, bulk and single cell RNA-seq analyses revealed that estrogens partially mimic the androgen transcriptional response and induce specific biological pathways linked to cellular proliferation and metabolism. Bioenergetic flux assays and metabolomics confirmed regulation of cancer metabolism by estrogens, supporting proliferation. Using cancer cell lines and patient-derived organoids, selective estrogen receptor modulators, a pure anti-estrogen, and genetic approaches impaired cancer cell proliferation and growth in an ERα-dependent manner. Overall, our study revealed that, when expressed, ERα functionally reprograms PCa metabolism, is associated with disease progression, and could be targeted for therapeutic purposes.

#3047 Interrogating TEAD protein interactions in cancer.

A. Guarnaccia, J. Lill, A. Dey;
Genentech, Inc., South San Francisco, CA

The Hippo signaling pathway is a major regulator of cellular growth and is frequently deregulated in cancer. The main effectors of the Hippo pathway are the TEAD transcription factors which function by interacting with other co-effector proteins to modulate transcriptional outputs. Notably YAP and TAZ interact with TEAD to mediate oncogenic transcriptional programs, and blocking interaction of TEAD with YAP and TAZ is a sought-after mechanism for small molecule TEAD inhibitors. However, the interaction network of TEAD extends well beyond YAP and TAZ to a variety of additional cofactors, including chromatin remodelers, epigenetic factors, and other transcriptional regulators. Thus, the impact of inhibiting TEAD could extend to unanticipated protein interactions and cellular functions. The purpose of this study is to investigate, define, and interrogate TEAD interaction networks, providing foundational knowledge for interrogating TEAD biological functions and pharmacological effects. We are employing mass spectrometry-based technologies combined with chemical and genetic tools and biochemistry to interrogate TEAD protein interaction networks. We have performed affinity purification coupled with mass spectrometry for TEAD and have identified dozens of significant interacting proteins. TEAD interactions include expected proteins, such as known Hippo pathway members, as well as unexpected protein interactions, such as DNA damage response proteins. Cellular assays probing these DNA damage protein interactions implicate TEAD as a crucial factor for efficient DNA repair mechanisms and maintaining genomic stability. These results raise questions towards a combinatorial effect for TEAD inhibitors and DNA damaging chemotherapeutic agents. Altogether, these ongoing proteomic studies are providing insights into TEAD interaction networks, leading to a deeper understanding of TEAD biology, and providing foundational knowledge that can inform the development of TEAD inhibitors as effective cancer therapies.

#3049 Similarities between ovarian cancer and endometriosis: The role of STAT3.

A. A. Kloeckner, S. R. Walker;
University of New Hampshire, Durham, NH

Endometriosis is a painful gynecological disease that affects over 190 million women worldwide. This disease is classified by the presence of endometrial-like cells growing in and around the female reproductive system. Instead of lining the uterus, these ectopic cells shed off and cluster together forming lesions that attach to different surfaces of the female reproductive system. In particular, endometriosis cells interact with and form lesions within the mesothelial cells that line the peritoneum. There is currently no cure, and many of the therapies aiming to help with pain management come with unfavorable tradeoffs. Our research on ovarian cancer led us to investigate potential overlapping characteristics with endometriosis. Growing ovarian cancer cells in 3D causes spheroids to form which mimic the physical features of tumors and are also able to better represent cell-cell and cell-environment interactions. Analysis of the endometriosis cell lines 12Z and hEM3 demonstrated that they could also form spheroids. As both ovarian cancer cells and endometriosis cells interact with mesothelial cells, we wanted to determine if endometriosis spheroids were able to clear the mesothelial layer comparable to ovarian cancer spheroids. Evaluation of 12Z and hEM3 cell lines demonstrated that endometriosis spheroids were able to undergo mesothelial clearance. While the exact cause of endometriosis is not known, different proteins have been identified as important factors in the progression of endometriosis. The Signal Transducer and Activator of Transcription 3 (STAT3) is a transcription factor involved in cell differentiation, proliferation, apoptosis resistance, angiogenesis, and metastasis. In endometriosis cell lines, STAT3 is constitutively active, which makes it a promising potential therapeutic target. To verify that STAT3 is important in endometriosis, siRNA was used to reduce the expression of STAT3 in two endometriosis cell lines, 12Z and hEM3. Both cell lines showed a decrease in cell viability. In addition, reducing the expression of STAT3 in the endometriosis cells appeared to decrease mesothelial clearance ability. Our lab previously identified statins as potential STAT3 inhibitors by using the Broad Institute's CLUE tool. After statin treatment, 12Z and hEM3 spheroids showed a decrease in cell viability and clearance ability. Taken together, these data suggest that STAT3 plays a key role in endometriosis and that the repurposing of statins may provide a benefit to patients with endometriosis.

#3050 Evaluating the role of ΔNp63α in driving growth and metastasis of pancreatic ductal adenocarcinoma.

D. H. Ryan, C.-H. Tai, X. Zhang, M. Palestino Dominguez, C. Alewine;
National Cancer Inst. - Bethesda Campus, Bethesda, MD

Pancreatic ductal adenocarcinoma (PDAC) is the third leading cause of cancer-related deaths in the US and is rising in incidence. PDAC tumors may be either classical or basal in transcriptomic subtype, and PDAC patients with basal tumors have worse prognosis and may have increased resistance to chemotherapy. Previous studies have shown that ΔNp63α drives basal program expression. The goal of this project is to investigate whether ΔNp63α expression is sufficient to increase pancreatic cancer cell growth, metastasis and chemoresistance and whether these cells can outcompete ΔNp63α non-expressers in mixed tumors. Non-ΔNp63α expressing human PDAC cell lines AsPC1 and HPAFII were stably transduced to express either ΔNp63α or mCherry (control). For both AsPC1 and HPAFII, ΔNp63α-expressing and control cells had similar proliferation rates and susceptibility to chemotherapy agents oxaliplatin and SN38 when grown in culture. When control or ΔNp63α-expressing AsPC1 cells were implanted orthotopically into the pancreas of athymic nude mice, there was no significant difference in primary tumor mass and pathological analysis of lungs and livers did not reveal any significant difference in metastatic burden. Bulk RNA sequencing of primary tumors confirmed that tumors in mice inoculated with AsPC1-ΔNp63α had significantly upregulated expression of genes associated with the basal subtype. Collectively, these data suggest that while ΔNp63α drives the basal program in PDAC, its expression is insufficient to cause resistance to these chemotherapies or a growth or metastatic advantage in an immunodeficient setting. Further work is needed to elucidate the mechanism by which ΔNp63α contributes to more aggressive PDAC tumors.

#3051 JunAP, a peptide antagonist against the activator protein 1 transcription factor complex, demonstrates cancer cell cytotoxicity and reduced invasion in vitro and tumor regression in vivo in TNBC models.

K. Mendelson, Z. F. Mattes, S. Leong, R. Ramirez, M. Koester, C. Scuoppo, J. Diehl, E. Gallagher, J. Gonzales, F. Abbate, L. Ghamsari, G. Merutka, B. J. Kappel, A. Vainstein-Haras, J. A. Rotolo;
Sapience Therapeutics, Inc., Tarrytown, NY

The activator protein 1 (AP-1) transcription factor is a dimeric complex consisting of proteins from the JUN, FOS, MAF, and ATF families. AP-1 complexes have been identified as novel therapeutic targets in cancer due to their role in tumor growth, invasion, metastasis, angiogenesis and chemoresistance. Dimerization of components of the AP-1 complex via leucine zipper domain interactions is required for DNA binding and subsequent transcriptional activity. We designed a peptide (Jun antagonizing peptide, JunAP) targeting the basic leucine zipper motif of AP-1 to antagonize AP-1 complex formation and prevent associated activity. Fluorescence polarization and DNA ELISA assays demonstrate target binding and selectivity of JunAP towards AP-1 family members, co-immunoprecipitation experiments reveal that JunAP blocks protein-protein interactions between cJun and its key binding partners, and reporter assays confirm inhibition of AP-1 transcriptional activity in vitro. Pathway analysis of RNA sequencing data confirmed by qPCR analysis shows that JunAP disrupts key pathways required for cell survival and migration. Corresponding functional in vitro assays reveal that JunAP exhibits an inhibitory effect on invasion in Boyden chamber assays and demonstrates potent cytotoxicity in Jun-dependent cells. Further, in a BT549 triple negative breast cancer subcutaneous xenograft model, administration of JunAP results in tumor regression, demonstrating the anti-cancer potential of targeting the AP-1 complex. In summary, these data support JunAP as a potent peptide antagonist of the AP-1 transcription factor family that warrants further development as a potential therapeutic option for AP-1 driven tumors.

#3052 Investigating the role of FOXA1/2 & HNF4α in pancreatic ductal adenocarcinoma.

W. A. Orellana, K. Gillis, P. Fang, G. Fort, E. L. Snyder;
Huntsman Cancer Institute, Salt Lake City, UT

PDAC represents a formidable challenge with an alarmingly low 5-year survival rate of less than 12%. Integrated genomic, transcriptomic, and proteomic analyses have identified two distinct PDAC subtypes: classical and basal. The critical difference between these subtypes lies in the expression of endodermal lineage specifiers, with the classical subtype expressing FOXA1, FOXA2 (FOXA1/2), and HNF4α, critical for pancreatic cell-fate determination, while the basal subtype downregulates these genes, leading to the loss of endodermal identity. We reason that the transcription factors (TF), FOXA1/2 and HNF4α, that play critical roles in pancreatic development, are not only biomarkers of the classical subtype but are essential regulators of PDAC subtype differentiation state. Despite their relevance in other cancers, their specific functions in PDAC remain largely unexplored. We aim to define the functional roles of FOXA1/2 and HNF4α in the classical PDAC subtype, exploring their regulation of growth and cellular identity. Previous published work in our lab has shown that exogenous HNF4α restrains growth in a panel of human and murine PDAC cell lines. Furthermore, we have shown that HNF4α regulates the classical subtype program of PDAC. While FOXA1/2 and HNF4α cooperatively enact gene expression changes in normal tissue, the extent to which cooperative interactions between these TFs are required to activate the classical gene expression program of PDAC remains unknown. Overall, we will test the central hypothesis that FOXA1/2 and HNF4α are critical regulators of the transcriptional network governing the cellular identity of classical PDAC. To test this hypothesis, we will be reconstituting and modulating the expression of these factors in human and murine PDAC cell and organoid lines. We will assess gene expression changes through RNA-seq and genomic localization of these TFs through ChIP-seq. We have conducted bulk RNA sequencing on *Foxa1/2*-positive and negative organoids to transcriptionally identify differences brought on by *Foxa1/2* deletion and found over 2,200 differentially expressed genes. *Foxa1/2* deletion led to a significant decline in the classical PDAC signature based on gene ontology. Furthermore, we show that HNF4α can inhibit organoid growth in the absence of FOXA1/2. We discovered that HNF4α targets, such as *Lgals4,* expression levels are unaltered at the RNA level independent of FOXA1/2. By assessing the roles of FOXA1/2 and HNF4α in PDAC, we aim to determine the transcriptional network governed by these factors in the classical subtype of PDAC

#3053 PTEN as a double-edged sword regulates EGFRL858R-induced lung cancer progression.

Jan-Jong Hung

National Cheng Kung University, Tainan, Taiwan

Lung cancer is the major cause of death worldwide. Activation of oncogenes or inhibition of tumor suppressors causes cancer formation. Previous studies have indicated that Pten, as a tumor suppressor, inhibits cancer formation. In this study, we studied the role of Pten in $EGFR^{L858R}$-induced lung cancer *in vivo*. Interestingly, loss of Pten increased bronchial cell hyperplasia but decreased alveolar cell hyperplasia in $EGFR^{L858R}$*$Pten^{-/-}$-induced lung cancer. Syatematic analysis of gene expression by RNA-seq showed that a number of genes related to ciliogenesis were upregulated in $EGFR^{L858R}$*$Pten^{-/-}$-induced lung cancer and subsequently showed that bronchial ciliated cells were hyperplastic. Several critical ciliogenesis-related genes, such as mucin5a, DNAI2 and DNAI3, were found to be regulated by NR2F1. Next, NR2F1 was found to be inhibited by overexpression of Pten, indicating that Pten negatively regulates NR2F1, thereby inhibiting the expression of ciliogenesis-related genes and leading to the inhibition of bronchial cell hyperplasia during $EGFR^{L858R}$-induced lung cancer progression. In addition, we also found that Pten decreased Akt phosphorylation in A549, Kras mutant, and H1299 cells but increased Akt phosphorylation in PC9, $EGFR^{L858R}$, and $H1299^{L858R}$ cells, suggesting that Pten may function as a tumor suppressor and an oncogene in lung cancers with Kras mutation and EGFR mutation, respectively. PTEN acts as a double-edged sword that differentially regulates $EGFR^{L858R}$-induced lung cancer progression in different genomic backgrounds. Understanding the Pten in lung cancer with different genetic backgrounds will be beneficial for therapy in the future.

#3054 Investigating novel players involved in AR cistrome reprogramming.

E. J. Gardner;
University at Buffalo, Buffalo, NY

Advancements in the treatment of aggressive prostate cancer (PCa) have led to the development of second-generation AR-targeted therapeutics for advanced PCa. Unfortunately, many patients who initially respond to these treatments develop resistance and progress. Several mechanisms of resistance are being studied. We have focused on the roles of a reprogrammed AR cistrome from a canonical to a non-canonical cistrome in resistant disease. The premise of this study is based on previous studies by others and studies in our lab that suggest enrichment in non-canonical AR activity and adaptation to enzalutamide in advanced PCa cell lines and patient-derived xenografts. We aim to develop an ecosystem map of canonical and non-canonical AR activity to understand the drivers of therapeutic resistance and their vulnerabilities. We hypothesize that through combined transcriptomic/chromatin accessibility profiling at single-cell resolution and proteomics studies, we can holistically capture non-canonical AR activity. To provide invaluable information, as PCa is highly heterogeneous and not all cancer cells may be contributing to the resistance pathway that is of interest, we use castrate-resistant PCa (CRPC) and enzalutamide-resistant CRPC patient-derived xenograft (PDX) models and patient tissue samples as our disease models on our multi-omic assay platform to capture and study dynamic interplays and novel players driving a non-canonical AR cistrome and treatment resistance. Our preliminary data revealed potential transcriptional factor (TF) candidates that may modulate non-canonical AR cistrome. We verified the enrichment of these TF in PDX models of treatment-resistant PCa at the gene and protein level. Integration of our ongoing global proteomic studies will provide a holistic view of the contributions of the TF to the AR non-canonical switch.

#3055 Characterizing the role of HNF4α isoforms in human PDAC.

P. Fang[1], A. Kabir[2], G. Fort[1], E. L. Snyder[1];
[1]University of Utah, Salt Lake City, UT, [2]Huntsman Cancer Institute, Salt Lake City, UT

Pancreatic ductal adenocarcinoma (PDAC) is a deadly and recalcitrant malignancy with a 5-year survival rate of 12%. Transcriptomic studies have classified PDAC into a classical or basal-like subtype. The classical subtype has a better prognosis, response to chemotherapy, and express higher levels of endodermal lineage specifiers compared to the basal-like subtype. However, the field lacks a comprehensive understanding of the key subtype-specific regulators. Functional analysis of transcription factors associated with each subtype are needed to elucidate their roles in regulation of PDAC subtypes and to identify therapeutically targetable vulnerabilities. Previous work in our lab demonstrated that HNF4α is a key regulator of the classical subtype. Using genetically engineered mouse models, our lab showed that loss of HNF4α leads to an increase in tumor burden, a shift from glandular to poorly differentiated histology, and a decrease in the classical subtype score. However, while murine PDAC only express one set of HNF4α isoforms, human PDAC express both sets of HNF4α isoforms, suggesting murine PDAC may not fully recapitulate human disease. There are 2 subsets of HNF4α isoforms driven by expression from 2 distinct promoters, P1 and P2. P1 and P2 isoforms are differentially expressed within the gastrointestinal (GI) tract and play dichotomous roles in GI malignancies. In HNF4α-positive human PDAC, P2 isoforms are always expressed but there is variable expression of P1 isoforms. Based on the differential role of HNF4α isoforms in both normal tissue and cancer, we hypothesize that P1 isoforms will restrain tumor growth and promote greater classical/GI differentiation compared to P2 isoforms. We utilized CRISPRi to selectively inhibit transcription at the P1 or P2 promoter in HNF4α-positive, human cell lines expressing both isoforms. To test for sufficiency, we exogenously expressed P1 or P2 isoforms in HNF4α-negative, human cell lines. We then performed Incucyte, CRISPRi competition, and anchorage-independent growth assays. We performed RNA-seq and ChIP-seq on both exogenous and endogenous HNF4α isoforms. Functional assays revealed that HNF4α isoforms regulated growth in a context dependent manner. Exogenous P1 isoforms significantly inhibited growth while loss of endogenous P1 isoforms was dispensable for growth. Exogenous P2 isoforms inhibited growth to a lesser degree while loss of endogenous P2 isoforms led to a significant reduction in growth. Despite ChIP-seq analysis revealing very similar binding profiles, RNAseq analysis revealed that P1 isoforms are significantly more transcriptionally active than P2 isoforms and are stronger inducers of GI differentiation. Taken together, our data demonstrates that P2 isoforms are more compatible with growth in PDAC compared to P1 isoforms, which promote a more differentiated cell state. Mechanistically, this may be due to the increased transcriptional activity of P1 isoforms.

#3056 Copper chelation modulates YTHDF2 RNA-binding protein localization and global translation, in neuronal cancers.

J. L. Bell[1], D. K. Abruzzese[2], E. Kasiou[2], V. Vu Pham[1], J. B. Bertoldo[1], F. Michniewicz[2], O. Vittorio[2];
[1]Children's Cancer Institute, Sydney, Australia, [2]University of New South Wales, Sydney, Australia

Cancers are dependent on copper for growth, angiogenesis and metastasis and copper chelators are in clinical trials against breast cancer, however the mechanisms of this emerging cancer treatment are still largely unexplored. We previously demonstrated that copper chelation has efficacy in mouse models of neuroblastoma and glioma. Multiomics analyses in neuronal cancers suggested that RNA-binding proteins were deregulated by copper chelator treatment. We found that the “RNA Binding” gene set was the most significantly ranked molecular function list using differentially expressed RNAs after copper chelation treatment (GO:0003723, p-value 1.02e−32). We subsequently found that the copper chelator drug decreased global protein synthesis, MYC/MYCN expression, as well as the amount a key methylated (m6A) RNA-binding protein called YTHDF2 in glioma cells, by RNA-seq (-log2FC 0.3, p-value 0.005) and western blot. This downregulation was also clear in neuroblastoma and glioblastoma cell lines. Interestingly, copper chelation also shifted YTHDF2 protein location into the nucleus. YTHDF2 knock-out (DepMAP Chronos dependency score, -0.32) and knock-down studies (siRNA pool, 38% decrease in cell confluence) in neuroblastoma cell lines and others, indicated that YTHDF2 depletion is selective against neuronal cancer cell growth. YTHDF2 was found to be a MYCN transcriptional target. Moreover, as YTHDF2 protein also binds MYCN transcripts (the principal oncogene in neuroblastoma), and copper signaling mRNAs, it appears that copper signaling, YTHDF2 and MYCs operates in an oncogenic-axis. Ongoing studies are investigating novel YTHDF2 inhibitors and their neuronal cancer efficacy. Our work represents a significant breakthrough in drugging oncogenic post-transcriptional processes either directly, or indirectly via depleting copper.

#3057 The TARZN complex binds to *de novo* enhancer mutations and promotes oncogenic expression in T-ALL.

N. Zaal Anuar[1], C. Goh[1], B. Chua[1], S. Tan[1], J. R. Costa[2], M. R. Mansour[2], T. Sanda[1], D. Kappei[1];
[1]National University of Singapore, Singapore, Singapore, [2]University College London, London, United Kingdom

TAL1 is overexpressed in 40-60% of T-cell acute lymphoblastic leukaemia (T-ALL) cases and forms an oncogenic core regulatory circuit (CRC) with other transcription factors such as LMO1, LMO2 and GATA3. In 5% of T-ALL cases an insertion of a consensus GT dinucleotide is observed upstream of the *TAL1* gene, termed the “Mutation of TAL1 enhancer” (MuTE), driving *TAL1* overexpression. Using an *in vitro* reconstitution DNA pull-down assay combined with quantitative mass spectrometry, we identified nine candidate proteins that preferentially bound to the MuTE sequence compared to the WT sequence. Among the candidates, we demonstrate by reciprocal immunoprecipitation experiments coupled to quantitative mass spectrometry that the RNA methyltransferase TARBP1 and the zinc finger proteins ZBTB2, ZBTB25 and ZNF639 formed a complex that we term TARZN. Interestingly, the TARZN complex also bound to *de novo* super enhancer sites upstream of the *LMO1* and *LMO2* genes in T-ALL cells, indicating a putative common mechanism between these different non-coding driver mutations. Furthermore, knock-down of all TARZN members resulted in lower TAL1 protein expression in MuTE-positive but not in MuTE-negative T-ALL cells. Overall, these data suggest that the TARZN complex cooperatively promotes oncogenic expression in T-ALL.

MOLECULAR/CELLULAR BIOLOGY AND GENETICS: Signaling Pathways That Regulate Metabolism 1
Poster Session

#3061 A positive feedback loop between GLS1 and c-Myc drives tumor aggressiveness.
J. Yang, F. Chen, F. Yang, **Y. Teng**;
Emory University, Atlanta, GA

Both GLS1 and c-Myc are upregulated in head and neck squamous cell carcinoma (HNSCC) primary tumors and further increased in metastatic tumors. However, the regulation between these two molecules remains largely unknown. GLS1 is a critical enzyme that regulates glutamate, which plays an important role in cancer metabolism that supports cancer growth and survival. Our bioinformatic analysis of the TCGA HNSCC cohort revealed a strong correlation between c-Myc and GLS1 expression. We describe the importance of c-Myc in regulating GLS1 and vice versa. c-Myc protein directly binds to the promoter of the GLS1 gene and upregulates its expression at the transcriptional level. Interestingly, blocking GLS1 signaling in HNSCC cells by lentiviral shRNA knockdown or CB-839 treatment downregulates USP1, one of the best characterized human DUBs, which in turn reduces c-Myc protein stability via the ubiquitin-proteasome pathway. The GLS1-c-Myc axis thus represents a novel positive feedback loop that is critical for driving the aggressiveness of HNSCC. As the treatment of HNSCC remains a major challenge, these novel findings provide the molecular basis for combining GLS1-specific inhibitors with c-Myc-targeted therapy for the treatment of HNSCC patients.

#3062 Unraveling the role of RCC2 in glioblastoma by mutational analysis and a murine model of glioma.

W. L. Ho, P. Or, A. M. Chan;
The Chinese University of Hong Kong, Shatin, Hong Kong

Glioblastoma (GBM) is a brain malignancy characterized by being highly aggressive, lethal, yet treatment modalities remain limited. Recent studies have implicated *R*egulator of *C*hromosome *C*ondensation *2* (RCC2), a guanine nucleotide exchange factor (GEF) for RalA, as a potential regulator in glioblastoma pathogenesis. RCC2 has been shown to play a role in promoting glucose metabolism through BACH1-dependent upregulation of hexokinase II (HK2)(1). In this study, we investigated the functional mechanism of RCC2 in gliomagenesis using two complementary approaches. First, the relevance of RCC2 structural regions on its downstream functions were examined. By superimposing the three-dimensional crystal structure of RCC2 onto RCC1 (Regulator of Chromosome Condensation 1), a related GEF, we identified several unique regions within the RCC1-like domain of RCC2. A panel of point, substitution, and deletion mutants were generated, and pulldown experiments were performed to assess their relative binding affinity with BACH1. Additional assays to assess their relative ability to modulate the expression of HK2 and other cellular parameters will be discussed. The structure-functional characterization of distinct regions within RCC2 may identify unique sequences within RCC2 that could have relevance to glucose metabolism, cell proliferation and cell motility. Additionally, we have established a murine glioma model utilizing a *Pten* heterozygous mice expressing a GFAP-Cre-recombinase transgene (*Gfap-cre;Pten*$^{fl/+}$). Glioma were induced by stereotaxically injected lentiviral constructs expressing either with HRasV12 oncogene alone or together with RCC2. Neurological symptoms were monitored over a period of 7 months, and histopathological analysis was performed to evaluate the morphological and molecular features of the tumors. We showed that co-expression of HRasV12 and RCC2 exhibited earlier emergence of neurological manifests in both male and female groups (Log-rank test, $p<0.05$) when compared to HRasV12 alone. Overall, our study provides insights into both the structural mechanism of RCC2 in gliomagenesis through mutational analysis of RCC2 and the functional relevance through a murine model of glioma.

(1)Liu, T. et. al. Cancer Lett (2022) 549:215914.

Funding: This work is supported by a General Research Fund grant (#14113519) from the University Grants Committee of Hong Kong.

#3063 Defining oncogene-specific metabolic vulnerabilities in a mouse model of hepatocellular carcinoma.

K. Al-Shami[1], M. Snaebjornsson[1], F. Vogel[1], L. Schlicker[1], P. Poller[1], D. Dauch[2], A. Schulze[1];
[1]German Cancer Research Center (DKFZ) and DKFZ-ZMBH Alliance, Heidelberg, Germany, [2]University Hospital, Tubingen, Germany

Despite the continued success of advanced cancer therapies, hepatocellular carcinoma (HCC) represents a substantial challenge to current treatment modalities that are not sufficiently effective for the management of advanced disease. Metabolic reprogramming is a hallmark of cancer and many oncogenic signaling pathways impact on cellular metabolism. Here, we are investigating changes in metabolism in different oncogene-driven mouse models of liver cancer to identify selective metabolic vulnerabilities associated with HCC that could be implicated in tumor initiation and progression to be exploited for cancer therapy. Transposon-based vectors coding for different combinations of oncogenes, either *Myc* and *Akt1*^{Myr} (CaMIA) or *Myc* and *Nras*^{G12V} (CaMIN), were transduced by hydrodynamic tail vein injected into C57BL/6 mice. The resulting liver tumors and control livers were subjected to a comprehensive profiling of polar metabolites (metabolomics) and lipids (lipidomics and total fatty acids) as well as changes in gene expression (transcriptomics). Despite similar overall survival, the two models display marked differences in the presentation of the tumors, with CaMIA showing larger aggressive tumors, while CaMIN livers contain numerous small tumor nodules. Both models also showed evidence for the deregulation of intermediate metabolism, indicating activation of aerobic glycolysis and deregulation of glutamine metabolism. Lipidomic analysis revealed substantial lipidome remodeling in both models. Oncogene-specific alterations included elevated levels of lysophosphatidylcholine (LPC) in CaMIN tumors, while CaMIA tumors displayed high levels of ether phospholipids compared to CaMIN and normal liver. Moreover, the fraction of polyunsaturated fatty acids (PUFAs) was enhanced in lipids from CaMIN tumors, while monounsaturated fatty acids (MUFAs) were enriched in CaMIA tumors. Furthermore, tumors from both genotypes produced higher levels of oxylipins, a class of lipid mediators involved in signaling and inflammation, compared to normal liver. Transcriptome analysis confirmed these metabolic alterations and revealed evidence for enhanced inflammatory signaling in CaMIN. In addition, analysis of tumor microenvironment composition disclosed specific differences in stromal components, indicative of immune evasion through checkpoint activation. Experiments in primary murine liver cancer cell lines confirmed oncogene-specific metabolic rearrangements and suggest elevated sensitivity towards inhibitors of lipid remodeling. Future experiments will investigate the role of altered lipid metabolism in tumor development and immune evasion in liver cancer.

#3064 Unmasking the deadly tango: PKA and lipid genes in prostate cancer's bone invasion.

P. Sanchis[1], N. Anselmino[2], E. Labanca[2], A. Sabater[1], J. Bizzotto[3], G. Pascual[3], R. Seniuk[3], S. Lage-Vickers[3], A. Mitrofanova[4], P. Valacco[3], A. Toro[3], J. Cotignola[3], N. Navone[2], E. Vazquez[3], G. Gueron[3];

[1]1- CONICET - IQUIBICEN. 2- Universidad Argentina de la Empresa (UADE), Instituto de Tecnologia (INTEC)., Buenos Aires, Argentina, [2]Department of Genitourinary Medical Oncology and The David H. Koch Center for Applied Research of Genitourinary Cancers, The University of Texas MD Anderson Cancer Center, Houston, TX, [3]CONICET - IQUIBICEN, Buenos Aires, Argentina, [4]Department of Biomedical and Health Informatics, Rutgers School of Health Professions, Rutgers Cancer Institute of New Jersey, New Brunswick, NJ

About 88% of metastatic prostate cancer (PCa) cases involve bone metastasis. When PCa cells spread to the bone, a metabolic adaptation to the new environment takes place, partly influenced by factors secreted by the homing organ. Thus, we hypothesize that metabolic reprogramming, both in the tumor and bone niche drive PCa bone metastasis. In this work, we carried out an integrative *in vitro*, *in vivo*, and bioinformatics approach to identify key regulators governing the metabolic behavior of PCa cells. We performed an indirect co-culture between PCa (PC3) and bone progenitor (MC3T3 or Raw264.7) cells. PCa cells displayed a strong transcriptional (RNA-seq) activation of lipid metabolism, including PPAR-signaling, fat digestion, and PI3K-Akt pathway. Accordingly, treatment with the conditioned media (CM) of the co-culture promoted lipid accumulation in PC3 cells (Bodipy 493/503 staining). To assess the clinical relevance of the *in vitro* model, we performed an unsupervised clustering analysis using transcriptomics data from human PCa and bone metastatic samples (GSE74685). Results showed that the metabolic genes deregulated in PC3 by the co-culture, could accurately cluster samples in primary tumor or bone metastasis. We next performed a multivariable Cox regression analysis and built a prognostic model, identifying a novel signature of 5 lipid-associated genes, *PPARA, VDR, SLC16A1, PAPSS2* and *GPX1*, associated with a 23-fold higher risk of death in PCa patients (SU2C-PCF dataset). The expression of this signature was validated in a PDX pre-clinical model (MDA PCa PDX series) when comparing MDA-PCa-183 growing intrafemorally vs. subcutaneously. In order to identify the central hubs regulating this transcriptional phenotype, we performed an Ingenuity Pathway Analysis (QIAGEN), showcasing that the lipid-related signature deregulated by the bone niche is indeed modulated by the Protein Kinase A (PKA). Accordingly, the expression of these signature was downregulated by PKA inhibition (H89; PKA inhibitor). Moreover, secretome analyses (ESI MS/MS) revealed that bone secreted type I collagen (Col1a1) and fibronectin (Fn1) regulate PKA activity in PCa cells. Further, we investigated whether PKA could modulate critical mechanisms for bone progression, focusing on osteopontin (*SPP1*), a secreted protein involved in the adhesion and invasion of PCa cells, whose regulatory mechanism in tumor cells is yet to be elucidated. Strikingly, we observed not only that the activation of PKA using Forskolin in PCa cells activated *SPP1* expression, but also that PKA inhibition led to a significant impairment of the *SPP1* induction triggered by bone soluble factors secreted during the PC3/MC3T3 co-culture. Altogether, we showcase PKA as a central hub of PCa energetic metabolism during bone progression and outline a lipid-associated gene signature that can be targeted to halt metastatic PCa.

#3065 Targeting of metabolic reprogramming in lung cancer by utilizing patient-derived organoid tissue for precision medicine.

C. Wu[1], J. D. Nguyen[1], G. Theodore[1], E. Rodriguez[2], S. Spector[3], E. Kim[1], T. Khan[4], P. Puente[5], Y. Wang[1], D. M. Nguyen[2], C.-B. Chen[1], D. Lim[1], L. G. Feun[2], N. Savaraj[1], M. Wangpaichitr[1];

[1]Univ. of Miami/VA Medical Ctr., Miami, FL, [2]Univ. of Miami, Miami, FL, [3]Nova Southeastern Univ./VA Medical Ctr., Miami, FL, [4]University of Southern California, Los Angeles, CA, [5]Univ. of Illinois Chicago, Chicago, IL

In a preliminary pilot study, we reported elevated activity of indoleamine 2,3-dioxygenase 1 (IDO1) in serum from cisplatin-resistant (CR) lung cancer patients compared to cisplatin-sensitive (CS) patients. This heightened IDO1 activity was associated with increased tryptophan (TRP) catabolism, resulting in the upregulation of kynurenine (KYN) production. The detection of KYN can now be readily achieved through immunohistochemistry (IHC). We demonstrated that this upregulation contributed to increased Treg (regulatory T cell) and MDSC (myeloid-derived suppressor cell) populations resulting in an immunosuppressive tumor microenvironment. To investigate this effect, we used dual inhibition of IDO1/TDO2 (tryptophan2,3-dioxygenase 2) in an orthotopic mouse model of CR-Lewis lung carcinoma. This resulted in a significant reduction in tumor volume compared to LLC-CS ($n=7$, $p<0.01$), confirming the role of TRP catabolism in CR tumorigenesis. To determine the relevance of the data derived from this mouse model to clinical settings, we established 50 patient-derived organoid tissues (PDOT) from patients with NSCLC. PDOT is an experimental ex vivo tissue model developed to recapitulate the intricate features of lung architecture, including the lung acinus. Upon optimizing our collection and growth protocols, each PDOT successfully developed into a spherical body within 14 days. Furthermore, through bulk RNA-seq analysis, we showed that PDOT closely mirrors the expression of key molecular markers (PD-L1 and mutations), as observed in the original tumor tissues. PDOT from patients possessing high levels of PD-L1 and KYN were exquisitely sensitive to dual inhibition with 2-3-fold greater sensitivity compared to patients with undetectable KYN expression in growth inhibition assays ($GI50=20\pm5.5\mu M$ vs. $65\pm7.5\mu M$). Increased lipid peroxidation was detected via flow cytometry by accumulation of the C11-BODIPY reporter dye in the dual inhibition treatment group. Moreover, we integrated PDOT with a novel 3D microfluidic culture that can be supplied with patient-matched peripheral blood mononuclear cells (PBMC) to assess immune response. Using CyTOF, we showed that dual inhibitors with Atezolizumab (anti-PD-L1) enhanced immune effector (CD8+, NK) and suppressed immunosuppressive (Treg, MDSC) populations. We believe that our swift progress in PDOT development may bridge the divide between cancer biomarker expression and patient trials by timely complementing conventional drug studies based on cell lines and xenografts to facilitate the design of personalized therapies. As a result, the extensive reporting that we have contributed for KYN expression profiling in CR has the potential to serve as a valuable companion diagnostic tool in the future. This can assist in applying precision oncology by finding the most appropriate patients for immunotherapies.

#3066 Lung cancer cells overcome nutrient stress by upregulating an integrin αvβ3/AMPK/OXPHOS axis.

A. Nam, S. Jain, A. Campos, R. M. Shepard, T. von Schalscha, S. M. Weis, H. I. Wettersten, D. A. Cheresh;
University of California San Diego - UCSD, La Jolla, CA

Tumor cells are exposed to various forms of stress within the tumor microenvironment, and those cells that adapt often gain stem-like properties that facilitate tumor initiation and metastasis. Here, we show that lung cancer cells exposed to nutrient stress adapt and survive by converting their metabolism from glycolytic to oxidative phosphorylation (OXPHOS). This is based on the cell's ability to upregulate expression of integrin αvβ3, a driver of tumor initiation, progression, and drug resistance. Mechanistically, integrin αvβ3 recruits and activates c-Src, promoting sustained AMPK activity leading to activation of PGC-1α, which promotes the expression of mitochondrial OXPHOS complexes. In fact, ectopic expression of integrin β3 was sufficient to drive OXPHOS-dependent metabolism even in the absence of stress. Furthermore, pharmacological targeting of this pathway not only rendered integrin αvβ3+ cells sensitive to nutrient depletion but also prevented their ability to undergo tumor initiation. These findings reveal that targeting integrin αvβ3 or its pathway can prevent cancer cell metabolic flexibility and their capacity to adapt to stress within the tumor microenvironment.

#3067 SLC7A5/LAT1 promotes the Warburg Effect for TNBC progression through Trp/QPRT/NAD+ pathway.

M. Y. W. Fedoroff, L. Zhao, L. Saeednejad Zanjani, J. He;
Thomas Jefferson University, Philadelphia, PA

SLC7A5/LAT1 is a cross-membrane transporter that functions in uptake of large neutral amino acids into cells. Many pathological studies have shown that LAT1 is highly expressed in cancer tissue from various origins such as lung, biliary tract, breast, prostate, bone, and their metastatic legions. High LAT1 expression has been recognized as a significant prognostic marker in various cancers. Our TCGA data analysis showed that the expression level of LAT1 is higher in TNBC tumors compared with normal breast tissues. The higher expression level of LAT1 is linked with poor overall and progression-free survival. Dysregulation of amino acid transporters lead to metabolic reprogramming, which changes intracellular amino acid levels, contributing to the pathogenesis of cancer. However, it remains elusive whether and how LAT1 re-wires the cellular metabolic programs to promote TNBC tumor proliferation. In this study, we showed that inhibition of SLC7A5/LAT1 significantly reduced TNBC cell proliferation, viability, migration capability while promoting apoptosis. Mechanistically, we found significant positive correlations of LAT1 with PKM2 and LDHA in breast cancer tissues, which are key enzymes in mediating glycolysis and lactate fermentation or the Warburg Effect. Knock down LAT1 via siRNA decreased the expression levels of p-PKM2 and p-LDHA in TNBC cells. Tryptophan, a major substrate amino acid transported into cytosol by LAT1, is the precursor for the de novo synthesis of nicotinamide adenine dinucleotide (NAD+). The enzyme quinolinic acid phosphoribosyltransferase (QPRT) catalyzes the conversion from quinolinate, a product of tryptophan degradation, to NAD+. We showed LAT1 inhibition reduced the expression level of QPRT, cytosolic NAD+/NADH ratio as well as lactate production. Addition of L-Tryptophan increased the levels of p-PKM2 and p-LDHA while knockdown of LAT1 reversed tryptophan-mediated increase of PKM2 and LDHA activities, suggesting that LAT1 may regulate PKM2/LDHA through Trp/QPRT/NAD+ pathway for promoting the Warburg Effect. Additionally, we found upregulations of SLC7A5/LAT1, p-PKM2 and p-LDHA in doxorubicin-resistant cells and PDX mouse model compared with their corresponding controls. Collectively, these results provide evidence that overexpression of LAT1 in TNBC drives cancer progression and drug resistance by reinforcing the Warburg Effect, suggesting LAT1 as a promising therapeutic target for addressing TNBC. Our ongoing work will evaluate whether inhibiting LAT1 genetically or pharmacologically reduces xenograft tumor growth and enhances the sensitivities of TNBC resistant cells to chemotherapy in vivo. Our investigation will elucidate the underlying mechanisms involved in these processes.

#3068 CD146mediates intimate crosstalk between adipocytes and triple-negative breast cancer cells and drives tumor metastasis through lipid metabolic reprogramming.

H. Sun[1], K. Huang[1], B. Sun[1], J. Lin[1], R. Yang[1], J. Li[1], S. Wang[1], D. Zeng[2], H. Lin[1], Y. Liang[1];

[1]First Affiliated Hospital of Shantou University Medical College, Shantou, China, [2]Cancer Hospital, Shantou University Medical College, Shantou, China

Background & Aim: In the tumor microenvironment, the adipocytes enhance the invasiveness of breast cancer (BC) by remodeling the lipid metabolism, especially in triple-negative breast cancer (TNBC). The cell adhesion molecule CD146 was highly expressed in TNBC and predicted poor distant metastasis free survival (DMFS) in patients. Meanwhile, CD146 was known to alter the obesity process by regulating the metabolic level of the body. In this study, we aimed to explore the molecular mechanism of CD146 in tumor metastasis mediating by lipid metabolic reprogramming between adipocytes and TNBC cells.
Methods: CD146 knockout (KO) or overexpression cell models were constructed by CRISPR/Cas9 or lentivirus. Cells labeled with luciferase were injected in tail vein of Balb/c-nude mice and monitored lung metastasis by IVIS Kinetic system *in vivo*. Transwell and wound healing assays were analyzed cell aggressiveness *in vitro*. We synthesized anti-CD146 nanobodies, which significantly degraded CD146 protein and inhibitd its function. RNA-seq and Lipidomics in CD146 knockout models were performed to analyze the role of CD146 in TNBC cell metabolism. Immunofluorescence was used to detect the intracellular content of Lipid Droplet (LD) and protein localization. Finally, we used oleic acid (OA) and adipocyte-conditioned medium (CM) to mimic the tumor microenvironment.
Results: CD146 was highly expressed in TNBC and predicted poor DMFS survival. Inhibition of CD146 suppressed tumor aggressiveness and lung metastasis *in vitro* and *in vivo*. According to the bioinformatics and RNA-Seq analysis, we showed that CD146 was intimately involved in the lipid metabolic pathway, particularly fatty acid metabolism, and revealed that inhibiting CD146 in TNBC elevated the intracellular triglyceride level through lipidomic assay. Meanwhile, knockout of CD146 promoted LD accumulation and decreased fatty acid oxidation (FAO) and mitochondrial ATP levels. In molecular mechanism, we found that adipocytes secrete high level of IL6 and fatty acid, which activated JAK/STAT3 signaling and FAO mediating by CD146 in TNBC cells. Blocking CD146 using its nanobody inhibited IL6/JAK/STAT3 activities and ACADM, leading to impairment of FAO and lung metastasis suppression *in vitro* and *in vivo*.
Conclusions: In this study, we demonstrate the crucial role of CD146 in the crosstalk between tumor cells and adipocytes in the tumor microenvironment. CD146 promotes the utilization of fatty acids through fatty acid oxidation and activates the downstream inflammatory pathway response with adipocyte-secreted IL-6, thereby driving BC aggressiveness. Our study has important implications for the development of TNBC therapeutics to block CD146-driven FAO process, inflammatory response and tumor metastasis.

#3069 Targeting lactic acid sensing GPR132 in ccRCC.

D. Wang;
University of Miami Miller School of Medicine, Miami, FL

Clear cell renal cell carcinoma (ccRCC) is the most common and aggressive subtype of kidney cancer, accounting for 70-80% of the cases. Despite the improvements in tumor therapeutics, patients with metastatic clear cell tumors still have a five-year survival rate lower than 10%. Most of the ccRCC tumors harbor loss of VHL tumor suppressor gene on chromosome 3, leading to constitutively stabilized HIF, activation of downstream pathways involved in glycolysis, angiogenesis and metastasis and a highly acidic, vascularized, and immunosuppressive tumor microenvironment (TME). Such molecular alterations lead to the buildup of lactic acid within the tumor microenvironment. Long has been considered as a byproduct of hypoxic tumor metabolism, but recent studies have demonstrated a pro-tumorigenic role of lactic acid. Therefore, elucidating the molecular mechanisms on how tumor cells take advantage of lactic acid can identify potential novel therapeutic options. To understand how ccRCC cells sense extracellular lactic acid, I explored the concept of a lactate sensor. The currently known lactate sensors are GPR81 and GPR132. By querying TCGA data, GPR81 is reduced in ccRCC tumors and does not predict patient outcome while GPR132 is elevated in ccRCC tumors compared to normal kidney and demonstrates a strong negative effect on survival. Therefore, GPR132 stands out as a potential lactate sensor in ccRCC with meaningful impact on patient survival. Previously, GPR132 has been shown to be involved in tumor associated macrophage M1 to M2 transition upon lactic acid exposure. However, GPR132 exerts a striking impact on ccRCC tumors. Depleting GPR132 significantly decreased the HIF2α level in multiple ccRCC cell lines, establishing a molecular connection between lactic acid, GPR132 and HIF2α. Furthermore, due to suppressed HIF2α signaling, GPR132 knockout led to decreased lactic acid uptake through MCT1. Such decreased lactic transporter MCT1 abrogated the elevated aggressive phenotype in ccRCC cells when exposed to lactic acid. Metabolically, GPR132 knockout led to decreased lipid deposition. In addition, such deprivation of lipid droplet is not replenished when cells are exposed to lactic acid. Furthermore, by conducting an isotype-tracing experiment, GPR132 knockout actively decreased lactic acid uptake by the tumors and limit their resources to regenerate TCA cycle intermediates and build up lipid droplets. More importantly, GPR132 knockout led to defective mitochondria activities and activation of apoptosis, both of which led to significantly suppressed ccRCC growth *in vitro* and *in vivo*. This suggested that GPR132 likely affects ccRCC fitness through multiple layers of signaling mechanisms. Overall, our study has revealed that lactate sensing GPR132 is a critical signaling pathway for ccRCC tumor development in a glycolytic feed-forward context. As a membrane bound receptor, GPR132 holds immense potential as a novel therapeutic target in ccRCC.

#3070 CDK12 is a novel therapeutic target in glioblastoma.

Jeong-Yeon Mun[1], Chang Shu[1], Qiuqiang Gao[1], Mike-Andrew Westhoff[2], Georg Karpel-Massler[3], Markus D. Siegelin[1]

[1]Department of Pathology & Cell Biology, Columbia University Medical Center, New York, NY, [2]Department of Pediatrics and Adolescent Medicine, Ulm University Medical Center, Ulm, Germany, [3]Department of Neurological Surgery, Ulm University Medical Center, Ulm, Germany

Glioblastoma (GBM), the most common primary brain tumor in adults carries a highly unfavorable prognosis of only one to two years despite treatment with the standard of care, involving surgery, temozolomide and radiation. Patient-derived xenograft (PDX) GBM cultures were assessed for their susceptibility to loss of CDK12 function, which was either mediated genetically (shRNA) or by the novel inhibitor, SR-4835. GBM metabolism was measured by utilizing extracellular flux analysis as well as LC/MS based carbon tracing analyses. In vivo efficacy was determined by orthotopic GBM models in mice. Based on Clustered Regularly Interspaced Short Palindromic Repeat (CRISPR) and shRNA library screens in multiple GBM cell cultures we identified CDK12 as essential for the growth of GBM. Consistently, loss of function of CDK12 (genetically and pharmacologically) led to a reduction of growth of GBM patient-derived xenograft (PDX) lines *in vitro*. Notably, SR-4835 reduced GBM growth in the low nanomolar range and synergistically enhanced the potency of temozolomide. Extracellular flux analysis and metabolite screening analyses, including carbon tracing (U13C-Glucose, U13C-Glutamine) suggested that loss of function of CDK12 elicited a substantial inhibition of cellular respiration, causing energy deprivation with subsequent cell death with apoptotic features. On the molecular level, loss of function of CDK12 increased ATF4 along with pro-apoptotic Noxa, whereas anti-apoptotic Mcl-1 decreased. In turn, adenoviral mediated ectopic expression of Mcl-1 inhibited cell death mediated by loss of function of CDK12 in GBM cells. In an orthotopic murine PDX model of GBM animals receiving treatment with SR-4835 had a significantly longer overall survival without induction of toxicity as compared to mice treated with vehicle. In summary, these findings suggest that CDK12 is a novel treatment target for GBM and that CDK12 is an important driver of energy metabolism in GBM to partially mediate apoptotic resistance. Moreover, SR-4835 enhanced the potency of temozolomide in GBM models. Therefore, the novel CDK12 inhibitor, SR-4835 should be tested in a clinical trial in patients suffering from GBM.

#3071 Differential susceptibility of breast cancer cells to mitochondrial dysfunction induced by Wnt inhibitors.

Y. Kam, L. Winer, G. W. Rogers, N. Romero;
Agilent Technologies, Inc., Lexington, MA

Advances in research have shown that cancer cells have distinctive bioenergetic alterations to meet their energy requirements. It has been established that certain cancers are significantly reliant on mitochondrial respiration, suggesting that modulation of mitochondrial function may have therapeutic value. The Wnt signaling pathway is a potential therapeutic target of cancer, including breast and colorectal cancers. Recent findings suggest that bi-directional crosstalk between Wnt signaling and mitochondrial function plays a crucial role in tumorigenesis, as well as differentiation and self-renewal of stem cells. In this study, 71 agents known to alter Wnt signaling were screened for effects on mitochondrial function in BT474 and Hs578T breast cancer cell lines, which have highly oxidative and highly glycolytic bioenergetic phenotypes, respectively. This screen was performed using the Agilent Seahorse XF Mito Tox assay, which enables sensitive detection and characterization of mitochondrial modulators via a standardized, quantitative parameter, the Mito Tox Index (MTI). The MTI facilitates the comparison of drug efficacy by detecting modes of mitochondrial toxicity, inhibition, and uncoupling. The MTI-based screening of the Wnt modulators identified one inhibitor and two uncouplers as potent agents inducing mitochondrial dysfunction for both BT474 and Hs578T. Despite their distinctive bioenergetic phenotypes, MTI-based dose-response assays revealed no significant differences in the efficacy of these modulators between BT474 and Hs578T cell types. In contrast, significant differential effects on ATP production rates were detected, showing cellular energy depletion induced by these agents. Using the Agilent Seahorse XF Real-Time ATP Rate assay, BT474 cells showed significant metabolic energy crisis in the presence of all 3 compounds, whereas Hs578T cells maintained stable total ATP production. This differential impact on ATP production rate corresponds directly to differences in cell viability, with BT474 showing higher susceptibility to these compounds. These results suggest that the anti-cancer efficacy of mitochondrial modulators can be different depending on the metabolic phenotype of the target cell and should be considered in therapeutic design.

#3072 BXQ-350: A novel biologic that allosterically activates glucosylcerebrosidase and demonstrates signs of activity in cancer patients.

G. H. Tapolsky, C. Cruze, R. Furnish, M. Gazda, T. Stephens, L. Stamper, N. Wilkins, R. Takigiku;
Bexion Pharmaceuticals, Inc, Covington, KY

Background: Ceramides, glucosylceramides and sphingosine-1-phosphate (S1P) are key bioactive signaling molecules. Ceramides are proapoptotic and mitigate chemoresistance while glucosylceramides and S1P promote cancer cell proliferation, activate multiple oncogenic pathways, promote chemoresistance and stimulate a pro-tumoral microenvironment. Many studies have shown a better prognosis and longer survival for patients with high ceramides levels, while high S1P and glucosylceramides levels are associated with shorter survival and worst prognosis. Levels of ceramides, glucosylceramides and S1P are controlled by enzymes involved in sphingolipid metabolism, including glucosylcerebrosidase (Gcase) and sphingosine kinase (Sphk).
Methods: BXQ-350 is a nanovesicle of Saposin C, an allosteric activator of enzymes involved in sphingolipid metabolism; preclinically, BXQ-350 was investigated in different *in vitro* and *in vivo* models. Clinically, BXQ-350 was investigated in a first-in-human Phase 1 safety dose and escalation study in cancer patients with recurrent advanced solid malignancies (NCT02859857).
Results: Preclinical results demonstrated that BXQ-350 allosterically activates Gcase *in vitro*, in cells and *in vivo* in a significant and dose-dependent manner; as expected, *in vivo*, Gcase activation results in lower levels of glucosylceramides, as much as 2/3 lower for picomolar concentrations of BXQ-350. An increase in ceramides and a decrease in S1P are also observed. By impacting glucosylceramides, ceramides and S1P, BXQ-350 rebalances the S1P/ceramide rheostat in favor of an antitumoral state and homeostasis. By lowering S1P and glucosylceramides, BXQ-350 modulates the innate and adaptive immune response and repolarizes macrophages towards the antitumoral M1 phenotype, inhibits differentiation and activity of immunosuppressor of MDSCs, and promotes the proliferation of CD4+ and CD8+ Tcells as well as their activity. Clinical results showed BXQ-350 was safe and well-tolerated (no DLT, no MTD). Also, 13 patients (~17.8% of evaluable patients) had a clinical benefit up to cycle 6 and beyond (PR, SD). Among patients with PFS > 6 months, there were 4 recurrent CRC patients: 1 patient had a PFS of ~12 months, 2 of ~18 months, and 1 is still on study after 6 years. Furthermore, there were signs that BXQ-350 may alleviate symptoms of CIPN as 4 out of 10 patients with chronic CIPN at time of enrollment experienced an improvement of their symptoms.
Conclusions: Preclinical and clinical results demonstrated that BXQ-350 activates Gcase and modulates sphingolipid metabolism leading to a novel anticancer MOA that had not been clinically tested. Additional studies are ongoing to further elucidate BXQ-350's MOA.

#3073 ACTL6a drives metabolic reprogramming and chemoresistance in head and neck squamous cell carcinoma.

Mehri Monavarian, **Andrey Finegersh**

Stanford University School of Medicine, Palo Alto, CA

Actin like protein 6A (ACTL6a), a subunit of the SWI/SNF chromatin remodeling complex, is amplified in a third of all squamous cell carcinomas including head and neck (HNSCC) cancers. Recent studies implicate ACTL6a as an oncogenic driver that potentiates SWI/SNF-related chromatin remodeling; however, the underlying mechanisms in HNSCC progression yet to be elucidated. Using the HNSCC cell lines FaDu, SCC90, and SCC2, ACTL6a knockdown (siACTL6a) led to a significant reduction in cell proliferation compared to control when measured by sulforhodamine B but not resazurin, suggesting up-regulation of oxidative phosphorylation with siACTL6a. We used RNA-seq datasets of siACTL6a in FaDu cells and found that there was a significant up-regulation of components of complex I and IV of the electron transport chain compared to control. Gene set enrichment analysis also demonstrated a significant up-regulation in glycolysis in ACTL6a amplified tumors within the HNSCC TCGA dataset. Since metabolism is a key driver of chemotherapy resistance, we studied effects of ACTL6a expression on cisplatin-mediated cytotoxicity. Compared to control, siACTL6A of the HNSCC cell lines FaDu and SCC2 had significantly decreased IC50 to cisplatin, indicating ACTL6a mediates toxicity. We also observed significantly decreased migration in a transwell migration assay in siACTL6A FaDu and SCC2 cells compared to control. We are studying the effects of shRNA directed against ACTL6a using a syngenic *in vivo* tumor model with a mouse oral cavity (MOC2) cell line that grows in C57BL/6J mice. Subcutaneous injection of MOC2 cells demonstrated significantly decreased tumor growth in shACTL6a cells compared to control. We are performing additional studies to identify specific mechanisms of ACTL6a mediated metabolic reprogramming in tumor cells. In conclusion, ACTL6A amplification is common in HNSCC and facilitates metabolic reprogramming, which drives tumor proliferation, cell migration, and drug resistance.

#3074 Regulating lactate levels in triple negative breast cancer presents a promising avenue for therapeutic intervention.

C. P. Prasad, S. M. Umar, A. D. J. R., A. Kashyap, M. Rathee;
All India Institute of Medical Sciences (AIIMS) New Delhi, New Delhi, India

Introduction: Among all subtypes of breast cancer, triple-negative breast cancer (TNBC) is associated with the most unfavorable prognosis, emphasizing the critical need to pinpoint therapeutic targets tailored to TNBCs. Lactate, produced as a by-product of aerobic glycolysis, acts as an oncometabolite and plays a substantial role in promoting tumor aggressiveness, particularly in TNBCs. In our ongoing laboratory investigations, we are actively exploring strategies to mitigate the influence of lactate on TNBCs.

Methods: The experiments utilized two triple-negative breast cancer (TNBC) cell lines, i.e., MDA-MB231 and MDA-MB468. The inhibitors employed in this study are FOXY5, XAV939, PFK15, and Quercetin. Protein expression was examined using Western blotting and Immunofluorescence assays. Trans-well and wound healing assays were employed to assess cell migration and invasion. Colony formation assays (CFU) were utilized to investigate stem cell potential and proliferation. In vivo experiments were conducted using 4T1-orthotopic Balb/c mice.

Results: Using triple-negative breast cancer (TNBC) cells, we have demonstrated the pivotal role of the WNT/β-catenin signaling pathway in promoting the generation of extracellular lactate, thus driving the progression and metastasis of TNBCs. Additionally, we have shown that inhibiting lactate production in TNBC cells, and consequently impeding cell migration and invasion, can be achieved by using recombinant WNT5A or its mimicking hexa-peptide FOXY5. Similarly, employing a β-catenin inhibitor such as XAV939 can yield comparable outcomes in relation to TNBC cells. In an alternative approach, we conducted inhibition experiments targeting PFKFB3 (6-phosphofructo-2-kinase/fructose-2,6-bisphosphatase), a key regulator of aerobic glycolysis in cancer cells. Our findings indicate that a combined approach involving siPFKL and iPFKFB3 is more promising in suppressing lactate production in TNBCs when compared to the effects of individual iPFKFB3 treatment.

Conclusions: Our present investigations suggest that employing inhibitors targeting the WNT/β-catenin signaling pathway, PFKP, and PFKEB3 could be a promising therapeutic strategy to effectively reduce lactate levels in TNBCs.

#3075 Different roles of EPAC1 and EPAC2 in ovarian cancer: Implications for precision targeting in cancer therapy.

Z. Gao, W. Yuan, L. T. Lee;
University of Macau, Macau, China

There are two distinct functional isoforms of Exchange proteins directly activated by cAMP (EPACs), EPAC1 and EPAC2, which exhibit fundamental distinctions in structure, expression patterns, signaling specificity, and subcellular localization. This diversity suggests that EPAC1 and EPAC2 can operate independently, synergistically, or antagonistically, contributing to the wide range of reported functions and impacts in different cancers and studies. We compared the function of EPAC1 and EPAC2 in ovarian cancer using *in vitro* and *in vivo* models and further explored the underlying mechanism in the regulation of metabolism reprogramming. Selective inhibition of EPAC1 and EPAC2 markedly reduced proliferation in ovarian cancer cell lines, leading to cell death and cycle arrest. RNA-seq analysis indicated different downstream signaling pathways triggered by EPAC1 and EPAC2, with EPAC2 specifically linked to functions in energy metabolism. Treatment with an antagonist or knockdown of EPAC2 resulted in attenuation of both glycolysis and oxidative phosphorylation (OXPHOS), while EPAC1 did not induce such effects. Furthermore, inhibition of EPAC2 induced mitochondrial dysfunction, manifested by reduced ATP production, decreased mitochondrial membrane potential, and increased burden of reactive oxygen species (ROS). Our data also revealed that EPAC2 governs the MAPK pathway and mediates the mitochondrial unfolded protein response (UPRmt) in ovarian cancer cells. By delineating the distinctions between EPAC1 and EPAC2 within ovarian cancer cells, this project revised the prevailing understanding of EPACs and suggests the potential for precise targeting of EPAC isoforms as a viable strategy in cancer therapy.

#3076 Unveiling the therapeutic potential of β-catenin inhibition in triple negative breast cancers: Targeting the Warburg effect.

S. M. Umar, S. kahol, A. D. JR, A. Kashyap, S. R. Mathur, A. Gogia, S. Deo, C. P. Prasad;
All India Institute of Medical Sciences (AIIMS) New Delhi, New Delhi, India

Introduction: Triple Negative Breast Cancer (TNBC) exhibits increased glycolysis, known as the Warburg effect. Recent research, including our own Nanostring nCounter studies, identify β-catenin as an oncoprotein linked to elevated glycolysis in TNBC tumors. Our current research explores the impact of β-catenin inhibitors on glycolysis in TNBC cell lines and an *in vivo* CDX model.
Method: We employed immunohistochemistry to assess 98 TNBCs for the presence of β-catenin, PFKP, LDH-A, and MCT1 proteins, exploring their correlation with clinicopathological factors. In *in-vitro* experiments using MDA-MB-231, MDA-MB-468, and 4T1 cell lines, we investigated how β-catenin inhibitors (XAV939 & Axitinib) affected aerobic glycolysis components, and TNBC cell characteristics (proliferation, migration, invasion, and stemness). For *in-vivo* validation, 4T1 TNBC xenografts were employed to confirm our findings.
Results: Among the 98 TNBC patients, 63 (64%) displayed cytoplasmic /or nuclear β-catenin staining. Additionally, cytoplasmic accumulation of PFKP was observed in 52/98 (53%), increased cytoplasmic LDH-A expression in 57/98 (58%), and membranous MCT-1 expression in 50/98 (51%) TNBC patients. Notably, significant positive correlations were found between nuclear/cytoplasmic β-catenin and cytoplasmic PFKP ($p = 0.001$) as well as membranous MCT1 ($p = 0.014$). Furthermore, β-catenin, PFKP, LDHA, and MCT1 proteins were overexpressed in all TNBC cell lines thereby supporting their glycolytic nature. Comparative analyses between XAV939 and Axitinib revealed that Axitinib significantly reduced various TNBC cell parameters, including migration, invasion, lactate production, colony-forming ability, and expression of aerobic glycolytic pathway proteins. In the *in-vivo* studies, 30mg/kg Axitinib in a female Balb/c-4T1 xenograft model resulted in a substantial reduction in tumor volume and weight.
Conclusion: Our findings show that increased levels of β-catenin play an important role in regulating aerobic glycolysis in TNBCs. Furthermore, our findings also highlight Axitinib's potential as an effective therapeutic agent for the treatment of β-catenin-positive TNBCs.

#3077 Integrin expression during ovarian cancer progression.

N. Bano, **E. M. Schmelz**;
Virginia Tech, Blacksburg, VA

During peritoneal dissemination, ovarian cancer cells exfoliate from the primary tumor and aggregate in the peritoneal fluid. This elicits survival signals via changes in mitochondrial morphology and function. As spheroids adhere to secondary sites, mitochondrial function is restored in the form of recovery of mitochondrial morphology, increased mitochondrial membrane potential, glucose uptake and increased proliferation. These findings suggested a mitochondrial phenotypic switch from mitophagy in spheroids to upregulation of mitobiogenesis upon spheroids adhesion to secondary sites. Hence, our objective was to identify critical receptors that facilitate the adhesion of spheroids to secondary sites, focusing on integrins that facilitate cell-extracellular matrix (ECM) attachment and activate downstream signaling cascades. To investigate changes in integrin expression, we mimicked three major stages of ovarian cancer progression by developing adherent stage, spheroid stage and adherent spheroid stage using our mouse ovarian surface epithelial (MOSE) cell lines representing benign (MOSE-E) stage as well as slow-developing (MOSE-L) and fast-developing disease (MOSE-L_{TICv}) in biologically relevant conditions. Using RT qPCR and Western blotting, we determined gene and protein expression levels of integrins and adhesion related genes. Confocal microscopy was used to determine protein localization during ovarian cancer progression. RT qPCR result indicated differential up-regulated expression of integrins in both spheroid and adherent spheroid stage, suggesting the role of different integrins during the stages of ovarian cancer progression. Specifically, we observed a decrease (integrin α5, α6) or increase (α2**β**;1) of integrins after aggregation and an upregulation of **β**;1, α2, αV, α3, α5 and immunomodulatory integrins such as αE and αM in adherent spheroids, indicating their role in mediating specific steps during progression of ovarian cancer from tumorigenesis to metastatic implantation. We also observed increased expression levels of extracellular matrix proteins and their modulators, and cell-to-cell adhesion genes during ovarian cancer progression that was more pronounced in the MOSE-L_{TICv} cells which suggests their association with an aggressive cancer phenotype. Overall, this project will aid in the identification of adhesion targets to develop new anti-metastatic treatments that will reduce mortality in women with ovarian cancer.

#3078 Role of HuR in metabolic reprogramming of BRAF mutant melanoma treated with dabrafenib.

A. Loftus[1], M. Zarei[2], H. Graor[2], O. Hajihassani[2], C. Boutros[1], J. M. Winter[1], L. D. Rothermel[1];
[1]UH Cleveland Medical Center, University Heights, OH, [2]Case Western Reserve University, Cleveland, OH

Introduction: Oncogenic BRAF mutations are present in about 50% of melanoma and are clinically targetable by BRAF inhibitors such as dabrafenib. While BRAF inhibitors show high rates of clinical response, that response is transient and resistance inevitably develops. Previously we have demonstrated that BRAF inhibitors induce a metabolic shift towards the mitochondrial oxidative phosphorylation. We have shown that inhibition of wild type isocitrate dehydrogenase 1 (wtIDH1), a vital anaplerotic and anti-ROS enzyme, demonstrates synergy with dabrafenib in vitro and in vivo. IDH1 expression has been found in pancreatic cancer to be posttranscriptionally regulated by the RNA-binding and stress response protein, HuR (ELAVL1) under nutrient and chemotherapy stress. We hypothesize that HuR functions as a survival mechanism in melanoma under BRAF inhibition, regulating metabolic reprogramming including the expression of IDH1.

Methods: The human BRAF V600E mutant melanoma cell line, A375, was used for all experiments. HuR and IDH1 expression was suppressed by siRNA oilgos through lipofectamine transfection, as validated by immunoblot analysis. The bioenergetic assay was conducted using Seahorse XFp mini extracellular analyzer to measure the oxygen consumption rate (OCR) under nutrient stress, both with and without dabrafenib exposure. The impact of HuR on IDH1 expression was further explored using qPCR and Immunoblot. Ivosidenib was used for pharmacologic inhibition of wtIDH as previously described.

Results: Mitochondrial respiration (OCR) increased in parental A375 BRAF mutant melanoma cells following nutrient stress with low glucose conditions akin to the tumor microenvironment. OCR was further increased after dabrafenib exposure. Immunoblot analysis revealed that dabrafenib treated cells at 6-hour and 12-hour time points displayed HuR translocation from nucleus to cytoplasm, as detected in cytoplasmic lysates. Transient HuR silencing blocked the adaptive OCR response to both low glucose and BRAF inhibition. This suggests that HuR is involved in the metabolic response to acute BRAF inhibition in BRAF mutant melanoma. HuR cytoplasmic translocation is associated with increased IDH1 expression 24 hours after dabrafenib exposure. However, there is no increase in IDH1 levels under nutrient or treatment stress in HuR knockdown cells, indicating that IDH1 is regulated by HuR. Transient IDH1 knockdown, as well as pharmacologic IDH1 inhibition, blocks the OCR response of melanoma cells to BRAF inhibition and low glucose. This indicates that IDH1 is important in the HuR metabolic response to targeted therapy.

Conclusion: We find that BRAF mutant melanoma cells adapt to acute dabrafenib exposure via HuR mediated expression of IDH1 to upregulate mitochondrial metabolism. This demonstrates a targeted therapy induced metabolic vulnerability that can be exploited by wtIDH1 inhibition.

#3079 AMPK-HIF-1α signaling enhances glucose-derived *de novo*serine biosynthesis to promote glioblastoma growth.

H. Yun, J.-H. Lee;
Dong-A University, Busan, Korea, Republic of

Cancer cells undergo cellular adaptation through metabolic reprogrammin to sustain survival and rapid growth under various stress conditions. However, it remains unknown how brain tumors modulate their metabolic flexibility in the naturally serine/glycine (S/G)-deficient brain microenvironment. We used a range of primary/stem-like and established glioblastoma (GBM) cell models *in vitro* and *in vivo*. To identify regulatory mechanisms of S/G deprivation induced metabolic flexibility, we employed high throughput RNA-sequencing, transcriptomic analysis, metabolic flux analysis, metabolites analysis, chromatin immunoprecipitation (ChIP), luciferase reporter, nuclear fractionation, cycloheximide-chase, and glucose consumption. The clinical significances were analyzed in the genomic database (GSE4290) and in human GBM specimens. The high throughput RNA-sequencing and transcriptomic analysis demonstrate that the *de novo* serine synthesis pathway (SSP) and glycolysis are highly activated in GBM cells under S/G deprivation conditions. Mechanistically, S/G deprivation rapidly induces reactive oxygen species (ROS)-mediated AMP-activated protein kinase (AMPK) activation and AMPK dependent hypoxia-inducible factor (HIF)-1α stabilization and transactivation. Activated HIF-1α in turn promotes expression of SSP enzymes phosphoglycerate dehydrogenase (PHGDH), phosphoserine aminotransferase 1 (PSAT1), and phosphoserine phosphatase (PSPH). In addition, HIF-1α-induced expression of glycolytic genes (*GLUT1*, *GLUT3*, *HK2*, and *PFKFB2*) promotes glucose uptake, glycolysis, and glycolytic flux to fuel SSP, leading to elevated *de novo* serine and glycine biosynthesis, NADPH/$NADP^+$ ratio, and proliferation and survival of GBM cells. Analyses of human GBM specimens reveal that levels of overexpressed PHGDH, PSAT1, and PSPH are positively correlated with levels of AMPK T172 phosphorylation and HIF-1α expression and poor prognosis of GBM patients. Our findings reveal that metabolic stress-enhanced glucose-derived *de novo* serine biosynthesis is a critical metabolic feature of GBM cells and highlight the potential to target SSP for treating human GBM.

#3080 Activation of mTORC2/Akt is amplified during glutamine starvation and is mediated by GCN2.

Tatiana Hernandez[1], Nikhil Patel*[1], Jedrick Magsino[1], Jay Kavia[1], Aparna Ragupathi[1], Alysta Paneque[1], Tracy G. Anthony[2], Guy Werlen[1], Estela Jacinto[1]

[1]Biochemistry and Molecular Biology, Rutgers Univ.-Robert Wood Johnson Medical School, Piscataway, NJ,[2]Nutritional Sciences, Rutgers, The State University of New Jersey, New Brunswick, NJ

Highly proliferative cells like cancer cells depend on glucose and glutamine to augment flux through metabolic and biosynthetic pathways. The mechanistic target of rapamycin (mTOR) integrates signals from nutrients and other growth signals to maintain metabolic homeostasis. Whereas mTOR complex 1 (mTORC1) is activated by the presence of nutrients to promote anabolic metabolism, mTORC2 is activated by nutrient fluctuations, leading to increased Akt phosphorylation at Ser473. How mTORC2 signaling can be augmented by nutrient starvation remains poorly understood. Here, we found that General Control Nonderepressible kinase 2 (GCN2), an amino acid starvation-sensing kinase, conveys glutamine depletion to mTORC2. mTORC2 enhances Akt phosphorylation and Akt feeds back to mTORC2 to augment its activity during glutamine starvation. Amino acid starvation in vivo also enhances mTORC2/Akt signaling via GCN2. Our findings reveal that manipulating the GCN2/mTORC2/Akt signaling cassette could have therapeutic benefit to more effectively starve cancer cells.

#3081 Targeting lipid kinases to enhance autophagy inhibition for the treatment of pancreatic cancer.

E. G. Schechter, J. M. DeLiberty, C. A. Stalnecker, K. L. Bryant;
University of North Carolina, Chapel Hill, NC

Pancreatic ductal adenocarcinoma (PDAC) is characterized as the most KRAS-addicted cancer type, with KRAS mutations found in >95% of cases. Mutant KRAS relies on dysregulated metabolism to support growth. One dysregulated pathway upregulated in PDAC is autophagy, a lysosome-mediated process that degrades proteins and organelles to supply macromolecules for growth. Our lab and others have shown that inhibition of KRAS or the mitogen activated protein kinase (MAPK) components, MEK or ERK, further increases PDAC dependency on autophagy as a resistance mechanism. Cotreatment with ERK MAPK inhibitors and the autophagy inhibitor chloroquine (CQ) decreased autophagic flux, inhibited proliferation, and induced apoptosis in PDAC cells. CQ is the only FDA-approved autophagy inhibitor, and it demonstrates low potency *in vivo*, motivating our studies to identify strategies to improve autophagy inhibition in PDAC. We utilized a CRISPR-Cas9 loss-of-function screen to identify sensitizers to CQ in PDAC and identified 25 autophagy-related targets.

We hypothesize that targeting the autophagy pathway at multiple nodes will increase the efficacy of CQ treatment in PDAC. To validate hits identified in the CRISPR-Cas9 screen, I designed an siRNA array that contained three distinct oligos for each target. I quantified changes in proliferation in a panel of four PDAC cell lines after siRNA-mediated suppression of the target genes following 3- or 6-day time points.

I hypothesized that targets identified to be non-essential on their own would allow for potential synthetic lethality with CQ. To test this, I performed a 3-day knockdown followed by 3-day exposure to a dose response of CQ. I found that suppression of lipid kinases *PIP4K2A*, *PIP4K2C*, or *PIK3C3* shift the dose response to CQ in a panel of PDAC lines. This indicates that loss of those targets sensitizes PDAC cells to CQ treatment. Furthermore, we found that pharmacological inhibition of VPS34, the lipid kinase encoded by *PIK3C3* by the ATP-competitive inhibitor SAR-405 synergizes with CQ.

My future studies will be focused on validating other targets identified in the loss-of-function CRISPR-Cas9 screen. I will measure changes in autophagic flux and apoptosis due to the loss of validated targets. The long-term goal of this project is to enhance the translatability of autophagy inhibition for patient care through identifying combinational approaches to improve CQ response in PDAC.

#3082 The liver microenvironment promotes glycolysis in metastatic colorectal cancer by activating her3.

M. G. Rathore, K. Curry, C. Boutros, Z. Wang, J. Winter, R. Wang;
Case Western Reserve University School of Medicine, Cleveland, OH

Background: Liver metastasis occurs in ~80% of all metastatic colorectal cancer (mCRC) and the liver has a unique endothelial cell (EC)-rich microenvironment that promotes cancer cell survival. We previously reported that liver ECs secrete soluble factors to promote CRC growth via activating CRC-associated the HER3 signaling pathway. The present study reports that ECs promote mCRC growth by shifting cancer metabolism towards glycolysis and elucidates the involved signaling pathway.

Methods: We performed mass spectrometry to profile the metabolic changes in mCRC treated with/without HER3 inhibition in a syngeneic, orthotopic mCRC model. We also performed Seahorse and lactate ELISA assays to determine the effect of liver EC-secreted factors on CRC metabolism. To further determine the role of HER3 in promoting glycolysis and CRC growth in the liver, we used siRNA silencing of HER3 and pharmacological inhibition of HER3 downstream signaling proteins to identify the key mediator(s) of HER3-induced metabolic shift in CRC.

Results: We determined that HER3 inhibition leads to increased oxidative phosphorylation metabolites (OXPHOS) and decreased glycolysis metabolites in CRC liver metastases. Conditioned medium containing EC-secreted factors decreased oxygen consumption (determined by Seahorse, a readout of OXPHOS) and increased lactate secretion (determined by ELISA, a readout of glycolysis) in CRC. As HER3 inhibition reversed the metabolic shift and increased OXPHOS as an alternative survival strategy, we found that simultaneous inhibition of HER3 and OXPHOS synergistically blocked CRC cell and tumor growth. Lastly, we found that PFK2 is activated by HER3 signaling, determined by phosphorylation, and determined that the HER3-AKT-PFK2 signaling axis is the key mediator of EC-induced metabolic shifts.

Conclusions: We identified that the liver microenvironment activates HER3 and the downstream AKT-PFK2 signaling to promote glycolysis and growth in CRC liver metastases by activating AKT-PFK2-dependent glycolysis. Our findings highlighted the potential of combining HER3 and OXPHOS inhibitions as a potential strategy for treating patients with mCRC.

#3083 Unveiling the role of chemotherapy-resistant, slow-cycling cancer cells in driving cancer cachexia.

J. Cho, H.-Y. Lee;
Seoul National University, Seoul, Korea, Republic of

Cancer cachexia, a systemic disease marked by substantial, involuntary weight loss, predominantly affecting muscle and adipose tissue, manifests in patients with advanced-stage cancer. The emergence of cancer cachexia poses significant challenges to cancer treatment, diminishing the efficacy of anticancer medications, and the resultant muscle loss adversely impacts the daily lives of patients, diminishing the overall quality of life. Notably, cancer cachexia is implicated in 30-40% of cancer-related deaths, underscoring the pivotal need to comprehend its underlying principles and propose apt interventions to enhance both survival rates and the well-being of cancer patients. Based on our previous findings, cancer cells exhibiting a slow cell cycle, resistant to widely employed clinical chemotherapy agents, exhibit the formation of proinflammatory tumor microenvironment. The escalation of systemic inflammatory cytokines has long been suggested as a potential mechanism contributing to cancer cachexia. Building upon these insights, we hypothesized that slow-cycling cancer cells (SCCs) featuring resistance to chemotherapy are pivotal contributors to cancer cachexia. We investigated the impact of drug-resistant SCCs on the loss of differentiated myotubes and lipid droplets *in vitro* and muscle and fat loss in *in vivo* conditions. Interestingly, these cells induced more severe muscle and fat losses. Upon scrutinizing this cell population, we found the overexpression of a particular membrane protein, Protein A. The increase of this Protein A enhanced the release of exosomes from the cell through a novel mechanism distinct from its classical functions, consequently amplifying the release of inflammatory substances originating from cancer cells. In summary, our study elucidates that chemotherapy-resistant cancer cells, characterized by a slow cell cycle, intensify the secretion of inflammatory substances in a manner contingent upon the overexpression of a membrane protein A, which leads to the depletion of muscle and fat located in the distal peripheral regions.

#3084 Aldob regulates fructose metabolism to confer ferroptosis and immune response in colorectal cancer harboring microsatellite instability.

Y.-C. Chang[1], **C.-L. Chen**[2];

[1]Department of Biomedical Imaging and Radiological Sciences, National Yang Ming Chiao Tung University, Taipei, Taiwan, [2]Department of Pathology, Taipei Medical University and Taipei Medical University Hospital, Taipei, Taiwan

Microsatellite instability (MSI) is a genetic alteration that occurs during cancer progression, specifically in colorectal cancer. Objective evidence demonstrates that colorectal cancer patients with MSI have better survival rates than those without MSI. Moreover, patients with both dMMR and MSI respond equally well to immunotherapy. We evaluated the MSI status of colorectal cancer specimens and identified an activation of aldolase B (ALDOB), the primary regulator of fructose metabolism, in the MSI group. Our analysis of the cancer cell panel revealed that the expression level of ALDOB in MSI+ cells (HCT116 and LoVo) was significantly higher than that in the microsatellite stable (MSS) group (SW480 and HT29). We also discovered a significant negative correlation between ALDOB and numerous dMMR-related genes, such as *MLH1* and *MSH2*. We investigated how fructose concentration and pathway activation affected MSI occurrence. Our results demonstrated that abnormal fructose metabolism leaded to SLC7A11-mediated ferroptosis. SLC7A11 functioned as the active subunit and generated glutathione, GPX4, and lipid epoxides in response to transported cystine. This may explain the better clinical outcomes observed in colorectal patients with MSI. On the other hand, we also observed that ALDOB could increase certain immune ratios, such as $CD4^+$ T cells and B cells. This aligns with the implementation of immunotherapy in the MSI community, which has been proven to yield positive effects. Consistent results were still being shown. Our study revealed significant increases in various chemokines and cytokines in media conditioned with fructose. It was interesting to note that fructose resulted in more significant changes than glucose. Based on the gathered evidence, it could be posited that ALDOB plays a crucial role as a promoter of fructose metabolism, leading to the induction of ferroptosis and immune responses in MSI colorectal cancer. The findings shed new light on known consequences and provide new avenues of information.

#3085 Cholesterol sulfotransferase SULT2B1b suppresses prostate tumor growth and regulates cholesterol metabolism in prostate cancer cells.

J. Yang, D. Wusiman, T. L. Ratliff;
Purdue University, West Lafayette, IN

Prostate cancer (PrCa) ranks as the second leading cause of cancer death in males in the United States. The 5-year survival rate drops drastically from 100% in patients with early-stage confined PrCa to 30% in those with advanced metastatic PrCa. Patients with advanced PrCa face limited long-term treatment options, often developing resistance to androgen-deprivation therapy and chemotherapy. Identifying and targeting pivotal molecules or pathways in advanced PrCa can substantially enhance patient survival. Our previous findings unveiled an inverse relationship between cholesterol sulfotransferase SULT2B1b and the severity of human PrCa. The highest levels of SULT2B1b were observed in the epithelium of normal prostates, with a progressive decrease as cancer advanced. The lowest levels were found in the most advanced metastatic samples. This study aims to determine whether SULT2B1b performs any active and critical functions in PrCa progression and assess whether it regulates cholesterol metabolism in PrCa cells. We generated SULT2B1b knockout (KO) clones from mouse PrCa cell line MyC-CaP and established inducible SULT2B1b overexpression lines from androgen receptor (AR)+ LNCaP and AR- PC3 human PrCa cells. These modified mouse and human cells were implanted into syngeneic FVB mice and immunodeficient NRG mice, respectively. MyC-CaP KO cells formed significantly larger tumors compared to parental cells, accompanied by reduced survival rates. In contrast, both LNCaP and PC3 tumors with induced SULT2B1b exhibited smaller sizes compared to control tumors, leading to improved survival rates. To investigate the impact of SULT2B1b on cholesterol metabolism and the underlying mechanisms behind SULT2B1b-regulated tumor growth, we examined genes related to lipoprotein signaling and cholesterol metabolism in MyC-CaP SULT2B1b KO cells using PCR arrays and qRT-PCR. Genes responsible for cholesterol uptake and synthesis (e.g. *Ldlr*, *Cyp51*, *Sorl1, Pcsk9* and *Insig1*) were among the top upregulated genes, while genes controlling cholesterol efflux (e.g. *Abca1*) and esterification (e.g. *Soat1* and *Soat2*) were downregulated in KO cells. Consistent with these gene expression patterns, intracellular cholesterol levels significantly increased in KO cells. Interestingly, although SULT2B1b did not affect cell proliferation under normal conditions, KO cells exhibited faster growth than parental cells when cultured in lipid-depleted or charcoal-stripped media, possibly due to altered intracellular cholesterol levels. In summary, these findings align with the expression pattern of SULT2B1b in human PrCa, demonstrating that SULT2B1b inhibits tumor growth, whereas its removal promotes tumor growth. This suggests SULT2B1b may serve as a critical tumor suppressor in PrCa. Its modulation of tumor growth may occur through the regulation of cholesterol metabolism.

#3086 *NAPRT* silencing in oncometabolite-producing cancers confers therapeutic vulnerabilities to NAD$^+$ depletion.

K. J. Noronha[1], K. N. Lucas[1], **S. J. Zhao**[1], J. Edmonds[1], S. Friedman[1], M. A. Murray[1], S. Liu[1], J. Liang[2], S. Paradkar[1], H. Zeng[2], R. K. Sundaram[1], J. Spurrier[3], M. Raponi[3], D. Sajed[4], B. M. Shuch[5], J. C. Vasquez[1], R. S. Bindra[1];

[1]Yale University, New Haven, CT, [2]Sichuan University, Chengdu, China, [3]Alphina Therapeutics Inc., New Haven, CT, [4]Ronald Reagan UCLA Medical Center, Los Angeles, CA, [5]UCLA, Los Angeles, CA

Cancer associated mutations in citric acid cycle enzymes cause overproduction of 2-hydroxyglutarate (2HG), fumarate, or succinate, commonly referred to as oncometabolites. These oncometabolite-producing mutations are prevalent in 70% of gliomas, >76% of hereditary leiomyomatosis and renal cell carcinoma, and >25% of paraganglioma and pheochromocytomas, respectively and contribute to their progression. These oncometabolite-producing cancers harbor vulnerabilities in multiple cellular pathways because of their competitive inhibition of alpha ketoglutarate dependent dioxygenases, which includes the ten eleven translocation (TET) enzymes. As a result, a DNA hypermethylation phenotype is observed in oncometabolite producing cancers. Our group has found that DNA hypermethylation results in silencing of nicotinate phosphoribosyl transferase (NAPRT). NAPRT is a rate-limiting enzyme in the Preiss-Handler pathway, which is vital for NAD+ biosynthesis. We have shown that the NAPRT gene is hypermethylated in regions surrounding and within a CpG island in the promoter. Hypermethylation of the NAPRT gene also occurs in patient tumor samples. Methylation of the promoter appears to control expression of mRNA and protein. We now show that silencing of NAPRT expression occurs in patient samples of oncometabolite-producing tumors. Furthermore, oncometabolite-producing cancer models that silence NAPRT are extremely sensitive to nicotinamide phosphoribosyl transferase (NAMPT) inhibitors, which further prevents NAD+ biosynthesis via inhibition of the NAM Salvage Pathway. Furthermore, NAD+ is used to synthesize poly-ADP-ribose (PAR) chains by Poly (ADP-ribose) Polymerases (PARPs) to recruit other DNA damage response proteins, suggesting that NAMPTis and PARPis may synergize in oncometabolite-producing cancers. Ongoing studies are investigating the role of histone and DNA demethylating enzymes in NAPRT silencing and the efficacy of NAMPTis in NAPRT silenced models *in vivo*. Overall, our findings indicate that NAPRT-silencing can be therapeutically targeted in oncometabolite-producing cancers and elucidates how oncometabolite induced hypermethylation can impact diverse cellular processes from metabolism to DNA repair.

#3087 The m^{6}A methyltransferase RBM15 drives the growth of triple-negative breast cancer cells through the stimulation of serine and glycine metabolism.

S. Park[1], Y.-Y. Park[2], J.-H. Lee[1];
[1]Dong-A University, Busan, Korea, Republic of, [2]Chung-Ang University, Seoul, Korea, Republic of

N^6-adenosine methylation (m^{6}A) is critical for controlling cancer cell growth and tumorigenesis. However, the function and detailed mechanism of how m^{6}A methyltransferases modulate m^{6}A levels on specific targets remains unknown. In the current study, we identified significantly elevated levels of RBM15, an m^{6}A writer, in basal-like breast cancer (BC) patients compared to non-basal like BC and linked it to worse clinical outcome. Gene expression profiling uncovered correlations between RBM15 and serine and glycine metabolism genes including PHGDH, PSAT1, PSPH, and SHMT2. RBM15 influences overall m^{6}A levels and, specifically, m^{6}A of serine and glycine metabolism genes via direct binding to target RNA. Further RBM15 effects on cell growth were largely dependent on serine and glycine metabolism. Thus, RBM15 coordinates cancer cell growth through altered serine and glycine metabolism suggesting RBM15 as a new therapeutic target in BC.

CHEMISTRY: High-Throughput Screening and New Assay Technology
Poster Session

#3090 Development and performance of the National Cancer Institute's HTS384 NCI60 screen: A modernized platform to support drug discovery and development by the worldwide cancer research community.

N. P. Coussens[1], T. S. Dexheimer[1], E. M. Jones[1], T. Silvers[1], J. R. Britt[1], R. C. Taylor[2], M. W. Kunkel[2], J. H. Doroshow[2], B. A. Teicher[2];
[1]Frederick National Laboratory for Cancer Research, Frederick, MD, [2]National Cancer Institute, Bethesda, MD

The NCI60 screen was established in the 1980s and introduced in the 1990s as a screening service for the worldwide cancer research community. The screen features 60 human tumor cell lines that represent 9 cancer types including non-small cell lung, colon, central nervous system, ovarian, renal, prostate and breast, as well as leukemia and melanoma. On a weekly basis, synthetic molecules, natural products, and biologics are screened against the 60-cell line panel to evaluate their anticancer potential. On average, more than 13,000 compounds are screened annually for investigators throughout the world. Cell growth and cytotoxicity were assessed by the sulforhodamine B (SRB) assay, performed in a 96-well format, that measures cellular protein content with an absorbance readout and enabled unprecedented throughput in the 1980s. Although the SRB assay supported a robust screening platform for three decades, its sensitivity and throughput are limited. Recently the NCI's DCTD introduced the HTS384 NCI60 as a modernized screening platform. While the same 60 cell lines are evaluated, the HTS384 NCI60 is fully automated and performed in a 384-well format to enable a higher throughput. Additionally, the 48-h test agent exposure period of the SRB assay was increased to 72 h, which may result in lower 50% growth inhibition values (GI_{50}) for some agents. A highly sensitive CellTiter-Glo luminescence readout for cell viability, based on cellular ATP content, was selected to enable comparisons of the NCI60 monolayer data to 3D cell culture models where the same assay chemistry can be applied. The HTS384 NCI60 was evaluated by screening a library of 1,003 U.S. Food and Drug Administration-approved and investigational oncology agents at five concentrations. Assay performance of the 60 cell lines was assessed from the controls of 30 - 60 microplates per cell line. The average doubling time of the 60 cell lines during the 72-h exposure period ranged between 19 h for NCI-H460 (17 - 23 h, *n* = 57) to 117 h for MDA-MB-468 (43 - 272 h, *n* = 60). The average signal-to-background ratio of all 60 cell lines was 89 (3,413 microplates) and ranged from 6 for OVCAR-5 (3 - 13, *n* = 54) to 229 for SF-539 (141 - 566, *n* = 60). The average coefficient of variation for microplate vehicle controls (*n* = 14) of all 60 cell lines (*n* = 3,413) was 5.2% and ranged from 3.2% for SK-MEL-28 (1.4 - 7.7%, *n* = 60) to 11.1% for HL-60(TB) (5.2 - 20.2%, *n* = 59). The average Z'-factor value of all 60 cell lines (*n* = 3,413) was 0.82 and ranged between 0.66 for HL-60(TB) (0.39 - 0.84, *n* = 59) to 0.89 for MALME-3M (0.79 - 0.95, *n* = 59), SF-295 (0.49 - 0.97, *n* = 59), SK-MEL-28 (0.74 - 0.95, *n* = 60), and UO-31 (0.8 - 0.94, *n* = 54). The development and performance of the HTS384 NCI60 screen will be described. This project was funded in part with federal funds from the NCI, NIH, under contract no. HHSN261201500003I.

#3091 Discovery of highly selective ligands with unique binding modes for challenging oncology targets using DNA-encoded chemical libraries.

Y. Zhang, A. Keefe, M. A. Clark;
X-Chem, Inc., Waltham, MA

DNA-encoded chemical library (DEL) technology enables the efficient screening of large collections of encoded compounds and has emerged as a powerful tool for hit identification in recent years. The technology allows for the multiplexed interrogation of target-ligand binding interactions and results in DEL hits with unusual binding modes and desirable selectivity. This screening methodology is particularly effective for oncology targets. Examples of discovery of highly selective ligands for challenging oncology targets, including kinases, protein-protein interactions, and receptors, will be presented. We will illustrate how DEL campaign strategies directly aim at novel binding modes, and provide molecular details around the uniqueness of these interactions. Furthermore, we will show how these novel binding modes lead to unique pharmacology with direct benefit to patients. Lastly, we will demonstrate how X-Chem's high-quality encoded libraries enhance the tractability and novelty of chemical equity discovered with the platform.

#3092 MICRO-TAG: A novel fluorescence-based real-time cellular target engagement platform for drug discovery.

I. Babic[1], N. Bryan[1], C. Cunningham[2], A. Sampson[2], D. Starczynowski[2], **E. Nurmemmedov[1];**
[1]Nerd Bio, San Diego, CA, [2]Cincinnati Children's Hospital Medical Center, Cincinnati, OH

Success of drug discovery programs can be amplified by adopting emerging technologies that can interrogate drug targets within their physiological context. Cell target engagement (CTE) presents a combined biological & biophysical method, which provides quantitative evaluation of target-drug interaction within the native environment of the cell. The currently available luminescence-based CTE methods are limited to measurement of end-point signal and poor resolution, thereby limiting their mechanistic and stoichiometric insight. We have developed MICRO-TAG, a novel fluorescence-based CTE platform, which relies on complementation of split-RNAse A. It enables interrogation of target engagement without interfering with folding, localization and function of target proteins - all within the physiological milieu of the cell. Uniquely, this new platform allows for quantitation and monitoring of CTE in real- time in the cell. It enables extraction of important parameters from target-drug interaction: target thermal profile and temperature of aggregation (T_{agg}), time required to reach equilibrium (t_{eq}), apparent association rate (K_{on}) and physiologically relevant drug:target binding affinity (K_D). We provide data demonstrating potential and utility of MICRO-TAG platform on drug targets, such as KRAS, MTH1, EGFR, and UBE2N. The platform demonstrates relevance for discovery of novel drug candidates targeting challenging drug targets such as transcription factors. This highly scalable and quantitative novel method for assessing drug-target interaction within cells can enhance drug discovery programs, and offers potential to rapidly identify clinically relevant hit compounds for challenging drug targets.

#3093 Combining lab automation with data analysis automation to enable high-throughput screening of patient-derived organoids.

A. Lin[1], M. Le Compte[1], T. Gilcrest[2], E. Cardenas De La Hoz[1], G. Roeyen[3], J. Hendriks[4], F. Lardon[1], C. Deben[1];
[1]University of Antwerp, Antwerp, Belgium, [2]Orbits Oncology, San Francisco, CA, [3]University Hospital of Antwerp, Edegem, Belgium, [4]University Hospital Antwerp, Edegem, Belgium

Although patient-derived tumor organoids (PDOs) better-represent patient tumors compared to traditional in vitro cell cultures, limitations of PDO analysis remain a major hurdle for high-throughput screening (HTS) applications. In particular, current PDO analysis fall short in at least 1 of 2 major criteria: 1) accurate recapitulation of patient tumor or 2) scalability. To address this, we have developed an automation-compatible protocol to satisfy these 2 major criteria to facilitate the adoption of PDOs for HTS applications[1]. Our novel protocol leverages live-cell imaging techniques to capture the dynamic interactions and intricate complexities of PDOs, which allowed for more precise and comprehensive analysis. To further enhance the accuracy and efficiency of our approach, we developed a fully automated image and data analysis pipeline (Orbits). Using label-free detection of organoids from brightfield images, Orbits integrates growth-rate-based drug response metrics with drug synergy metrics to significantly improve the identification of synergistic drug interactions. Here, present the results of our HTS protocol on 10 distinct drug combination strategies, specifically focusing on the repurposed drug candidate Auranofin, a Thioredoxin reductase inhibitor. We screened on 10 PDOs sourced from healthy lung, non-small cell lung cancer, and pancreatic ductal adenocarcinoma. Not only were we able to distinguishing cytostatic from cytotoxic drug responses at a single-organoid level, we identified drug candidates that can synergistically enhanced the efficacy of Auranofin in a tumor selective manner. Our study presents a major step forward in the field of PDO-based drug discovery, offering a robust protocol for HTS and automated data analysis. The implementation of our method will accelerate the discovery of effective therapeutic strategies, ultimately translating to improved patient outcomes. [1] Le Compte, M., et al *JoVE* 190 (2022)

#3094 Biophysics in kinase drug discovery programs: Spectral shift technology from fragment screening to mechanism of action.

C. Legros[1], V. Porkolab[2], M. Sigoillot[2], O. Mirguet[1];
[1]Eurofins Discovery, Celle Levescault, France, [2]Eurofins Cerep, Celle Levescault, France

Using Eurofins Discovery's state-of-the art Hit-Finding platform, our experts designed an optimized screening cascade combining cutting-edge High-throughput Screening (HTS) technologies with the latest Biophysics techniques. With advanced technologies, such as the Echo® MS and RapidFire MS for HTS, and SPR, MST, TSA, nanoDSF and ITC for Biophysics, the cascade is effective for primary screening, orthogonal assays and evaluating Mechanism of Action (MoA). There are many biophysical approaches which bring value to drug discovery programs, and it is the target properties which drive the selection of the most suitable technology. In this presentation, we will highlight the novel Spectral Shift technology, one of the techniques employed by the Dianthus (well-known for the MST-TRIC). The goal was to rapidly implement an assay that monitors the ability of PIM3 to bind to ATP, as well as to compounds and fragments in solution. Using the Echo MS' acoustic-droplet ejection, nanoliter dispensing in 394-well plates, robust data by Spectral Shift were quickly generated for the fragment-based screening campaign. Hits were confirmed in Dose-response with µM-range affinity values (K_D), and TSA was used as an orthogonal assay for the identification of stabilizers among the selected PIM3 binders. For a defined set of 826 proprietary fragments, a single dose screening at 600µM using Spectral Shift was run, leading to the identification of 11% of potential binders. The 100 fragments were then confirmed in dose-response titration and 80 binders were confirmed. The top 30 binders were selected for orthogonal characterization using TSA. This led to the selection of the top 6 confirmed fragments, on which a MoA study in MST-TRIC was performed. Following this evaluation, 3 allosteric binders were identified, with K_D from 355 to 550µM (affinity of orthosteric binders from 55 to 333µM). Biophysics plays an important role in drug discovery by qualifying valuable assets and increasing the success rates of future Hit-finding programs. The fragment hits selected in this PIM3 Kinase project, which show ADP-Glo™ activities, are now ready for crystallography studies (NMR & X-ray co-crystallization).

#3095 A high-throughput phenotypic screen to identify small molecule inhibitors of Werner helicase.

C. A. Moomau, Y. Lu, X. Zhang, X. Zhai, L. Gu, Q. Sheng, F. Li, Y. Chen;
Allorion Therapeutics, Natick, MA

Werner helicase (WRN) is a RecQ DNA helicase involved in genome maintenance and DNA damage repair. It has recently been shown to be essential to cancer cells with high microsatellite instability (MSI-H). In MSI-H cancer cells, WRN depletion was shown to induce DNA damage and disrupt mitoses, resulting in a distinct phenotype of enlarged and fragmented nuclei. Here, we present a high-throughput phenotypic screen to identify compounds that selectively induce enlarged nuclei in MSI-H cancer cells. In HCT116, an MSI-H colorectal cancer cell line, approximately 40% of cells exhibited enlarged nuclei when WRN was depleted using siRNA. In contrast, fewer than 10% of control cells displayed this phenotype. In HT29, a microsatellite stable (MSS) cancer cell line, no such difference in nuclear morphology was observed, suggesting that the phenotype is specific to MSI-H cells. We used high content imaging to screen our in-house diversity library of approximately 175,000 compounds in 384-well format. 4,260 compounds induced enlarged nuclei in HCT116 cells, a 2.4% hit rate. After re-screening hits in HCT116 along with two additional MSI-H cancer cell lines, SW48 and SNU-407, and counter-screening in HT29 cells, 144 hits were confirmed to specifically enlarge nuclei in MSI-H but not MSS cells. Using the ADP-Glo Kinase Assay, two of these compounds were confirmed to inhibit WRN ATPase activity, suggesting WRN inhibition as a potential mechanism for their specific effects in MSI-H cells. This screen will also identify compounds which selectively kill MSI-H cells through mechanisms beyond direct inhibition of WRN, including interaction with WRN complex members or other members of DNA damage repair pathways. Validation studies including the assessment of cell viability and DNA damage in a panel of MSI-H and MSS cell lines will be performed. Our study proposes a phenotypic screening strategy for identifying small molecules with the potential to target WRN and uncover additional novel mechanisms for treating MSI-H cancers.

#3096 CETSA Navigate HT: A new paradigm for high-throughput screening.

H. Almqvist, **V. Brehmer**, L. Arnold, T. Friman, S. Lundgren, D. Martinez Molina;
Pelago Bioscience, Stockholm, Sweden

The CEllular Thermal Shift Assay (CETSA) technology is a powerful way to assess target engagement across various matrixes. By the introduction of the high-throughput format (CETSA Navigate HT), this technology offers a reliable high-throughput screening method in natural cellular environments that can successfully be applied in compound screening for hit identification and confirmation already during lead generation. Due to its broad applicability to native, full length protein targets in the live cellular environment, without the need for expensive and time-consuming protein and/or compound labelling efforts, CETSA Navigate HT may be regarded as a new paradigm for high-throughput screening and actives generation. As a case study to demonstrate the applicability of CETSA Navigate HT in hit identification, we have applied the technology for primary screening of a 12000 compound library for CDK4, a protein targeted in several cancers. Hits identified from this screen are privileged from the onset by binding to the target in a physiologically relevant cellular matrix and in a binding-mode agnostic way. This is in contrast to traditional screening methods targeting activity or in vitro interactions where cellular activity is addressed in later stages. Data from follow up studies using functional assays will be presented as well as mass spectrometry based CETSA selectivity profiling and comparison to commercially available de novo CDK4/6 inhibitors.

#3097 CETSA HT: Employing rapid high-throughput target engagement technology in primary screening of P53.

M. Kacal, **T. Friman**, L. Arnold, V. Brehmer, D. Martinez Molina, S. Lundgren;
Pelago Bioscience AB, Solna, Sweden

The confirmation of target engagement for candidate drugs is a fundamental requisite in drug discovery. A significant portion of projects fail to reach the clinic due to lack of efficacy or failure to show lead candidates interacting with the intended target in a more complex environment. The utility of using the CETSA® (CEllular Thermal Shift Assay) technology to measure target engagement in intact cells is increasingly exploited in high throughput screening, where examples demonstrate low false positive rates in screens of up to 500K compounds. The p53 tumor suppressor protein, a crucial guardian against cancer, functions as a transcription factor that mediates cancer suppression by regulating genes involved in a wide range of cellular processes such as DNA repair, cell cycle and apoptosis. Unfortunately, frequent mutations in the TP53 gene hinder p53's tumor suppressor role in human cancers, thus designating it as a promising target for anticancer therapy. However, attempts to restore p53 function for therapeutic purposes have not yet advanced to clinical approval, highlighting the complexities in leveraging p53 for cancer treatment. Its undruggable nature, attributed to the absence of accessible deep pockets, lack of enzymatic activity, and its intracellular location, further complicates targeted interventions with both low and high molecular weight drugs. Here, we demonstrate the analysis of a high-throughput plate based CETSA® HT screen on the challenging target p53, performed using AlphaLISA® SureFire® Ultra™ technology and our newly developed high-throughput screening platform. Hits identified from this screen are privileged from the onset by binding to the target in a physiologically relevant cellular matrix and in a binding-mode agnostic way. This is in contrast to traditional screening methods targeting activity or in vitro interaction where cellular activity is addressed in later stages. This assay cascade highlights a rapid target-to-hit lead generation strategy placing the emphasis on finding chemical matter that interacts with endogenous target in living cells first, followed by analysis of hit material activity. The ‘shortcut’ to chemical matter active in living cells represents significant potential cost savings in comparison to assay development time on recombinantly produced proteins and/or modified cell lines for traditional HTS screening approaches that still rely on target engagement assessment downstream.

#3098 CETSA for navigating your chemistry and exploring the biology of protein degraders .

V. Brehmer, S. Lundgren, T. Friman, D. Amadio, A. Chernobrovkin, D. Martinez Molina;
Pelago Bioscience, Stockholm, Sweden

Protein degradation is a non-classical modality with the potential to tackle therapeutically interesting proteins, previously deemed undruggable. In this area, CETSA is a powerful technology for identifying new binders, assessing target engagement, and investigating the mechanism of action of the degraders in the intact cell environment - without the need to modify your compound, the proteins or the cellular environment. CETSA can provide insights into the binding of the degrader to both the E3 ligase and the protein of interest (POI), as well as follow the downstream cellular and molecular effects. Here we will exemplify how CETSA can be applied in various stages of drug discovery to provide biologically relevant data to guide the design and optimization of new degraders. For example, CETSA can provide valuable information of the cell permeability and the in-cell performance of the degrader, which is important for understanding how the degrader enters cells and reaches its target proteins. By combining data from CETSA with data from degradation readout, in our case quantitative proteomics, it is possible to correlate cellular target engagement potencies with degradation efficiency and importantly, also identify any drug:protein binding that does not result in degradation By using the proteome-wide CETSA Explore format, the selectivity of the degrader and the downstream protein consequences of the elimination of the target protein could be studied.

#3099 A new HTS ELISA for monitoring NRAS activity to expedite drug discovery.

H. Park, J. Weber, M. Carlson, M. Jelinek;
Active Motif, Carlsbad, CA

Oncogenic mutations in the KRAS, HRAS, and NRAS isoforms of the RAS gene family alter GTP binding and hydrolysis leading to errant over activation of the MAPK/ERK pathway. While the total of all such RAS mutations drives some 20-25% of all human cancers, each isoform tends to favor particular mutations that are cancer specific. Many evolving treatment strategies for these cancers target these mutant isoforms to minimize off target effects. NRAS mutations are seen in about one-fifth of cutaneous melanomas and patients with NRAS mutation melanomas have a poorer prognosis due to the high aggressiveness of RAS mutant tumors, a lack of efficient targeted therapies, or rapidly emerging resistance to existing treatments. Furthermore, there is no currently authorized targeted treatment for NRAS-mutated melanoma. As a result, there is a growing need for assays which can quantify activated NRAS. Here we describe the development of a highly specific and sensitive ELISA for determining the active NRAS protein in high throughput compatible (HTS) format.

A NRAS specific recombinant antibody was developed via cloning of immunoglobulin variable regions from antigen positive B cells isolated by FACS from rabbits immunized with a NRAS peptide corresponding to a region of low homology between the RAS isoforms. Immunoblotting and a bead-based multiplex ELISA with all three RAS isoforms were used to confirm antibody specificity with recombinant HRAS, KRAS, and NRAS proteins over a wide concentration range.

The new immunoassay enables in-well lysis of cells cultivated in 96-well plate. Activated NRAS in the lysate is collected on the test plate and detected using the NRAS specific antibody via chemiluminescence. We anticipate that this assay will further the discovery of novel NRAS specific therapeutics. EGF treatment of MCF7 cells demonstrated activation in cells expressing wildtype NRAS in preliminary assay validation. Evaluation of assay performance in mutant NRAS melanoma cell lines will be presented.

#3100 Interactive analysis of drug testing data for functional precision oncology with Breeze 2.0.

Swapnil Potdar[1], Filipp Ianevski[1], Aleksandr Ianevski[1], Ziaurrehman Tanoli[1], Krister Wennerberg[2], Brinton Seashore-Ludlow[3], Olli Kallioniemi[4], Paivi Ostling[4], Tero Aittokallio[1], Jani Saarela[1]

[1]Institute for Molecular Medicine Finland (FIMM), HiLIFE, University of Helsinki, Helsinki, Finland,[2]Biotech Research & Innovation Centre (BRIC), University of Copenhagen, Copanhagen, Denmark,[3]Department of Medical Biochemistry and Biophysics, Chemical Biology Consortium Sweden (CBCS), Science for Life Laboratory, Karolinska Institutet, Stockholm, Sweden,[4]Department of Oncology-Pathology, Science for Life Laboratory, Karolinska Institutet, Stockholm, Sweden

High throughput screening (HTS) is used to screen large numbers of small molecules in cell-based assays to predicting their potential therapeutic response and when applying approved drug libraries using HTS it becomes drug repurposing. The Drug Sensitivity and Resistance Testing (DSRT) platform established at FIMM has been extensively used in testing panels of approved and investigational drugs on cells, both conventional cell lines and primary cell models derived from cancer patient samples. The results help in deepen our understanding of drug efficacy in individual patients and across specific disease to guide future patient stratification.

Breeze 2.0 is an open access, web-based platform for interactive analysis of drug screening data in real time. Breeze accepts raw data in a simple tabular format and generates detailed quality control metrics, plots, dose-response curve fits, drug response quantification in form of IC50/EC50/AUC and Drug Sensitivity Scores (DSS). Besides tabular results, Breeze generates interactive, informative, and intuitive visualizations, such as plate heatmaps, scatterplots, barplots, clustered heatmaps, circular plots, for further analysis. Based on manually-curated published datasets available through Breeze 2.0, users can instantly compare their drug response patterns with the existing DSRT profiles from patient samples, as well as cell lines. Importantly, Breeze 2.0 has integrated curated reference DSRT data tested on bone marrow samples from healthy control individuals, which plays a crucial role in understanding cancer-selective drug response by de-prioritizing generally toxic compounds. The end-users can select multiple healthy controls or relevant patient/cell line samples and choose the drugs of interest to visualize the overlaid dose responses, as well as response quantification metrics. Breeze 2.0 is built in R, PHP, MySQL and is freely accessible at https://breeze.fimm.fi/v2

#3101 Developing a drug repurposing screen for head and neck squamous cell carcinoma using a novel c-Rel bioassay.

K. A. Altwegg[1], K. E. King[2], D. Blivis[1], T. C. Voss[1], N. J. Martinez[1], W. C. Weinberg[2], M. J. Henderson[1];
[1]NIH-NCATS (National Center for Advancing Translational Sciences), Rockville, MD, [2]US Food and Drug Administration, Silver Spring, MD

Head and neck squamous cell carcinoma (HNSCC) is the sixth most common cancer worldwide. Approximately 890,000 new cases are diagnosed each year, while incidence continues to rise and is anticipated to increase by 30% by 2030. HNSCC occurs most often in men in their 50-60s, although the incidence among younger individuals is increasing. Current standard of care practices include surgical resection, followed by adjuvant radiation or chemoradiation. HNSCC tumors exhibit frequent mutation of CDKN2A (22% of tumors) and TP53 (72% of tumors). Additionally, two members of the TP53 gene family, TP63 and TP73, are frequently altered in HNSCC. TP63 encodes two major isoforms, ΔNp63 which lacks the main transcription activation domain and acts as a dominant-negative inhibitor of transactivation (TA), and TAp63 (contains a p53-like TA domain). ΔNp63 is overexpressed in a majority of HNSCC tumors. Our lab has reported ΔNp63α interacts with activated c-Rel (a nuclear factor-KB family member) in HNSCC, thereby promoting uncontrolled proliferation, a key alteration in the pathogenesis of cancers. Consistent with a role in growth regulation, ΔNp63α:c-Rel complexes bind a promoter motif and repress the cyclin-dependent kinase inhibitor p21WAF1 in both human HNSCCs and normal keratinocytes overexpressing ΔNp63α. The direct relationship between ΔNp63α and activated c-Rel is observed by strong nuclear co-localization in the proliferating compartment of primary head and neck SCC. Stimulation of HNSCC cells with TNFα results in the induction of the c-Rel oncoprotein that binds to ΔNp63, displacing and inactivating the tumor suppressor TAp73 from ΔNp63-TAp73 complexes. Using western blot analysis in human HNSCC cell lines, we confirmed that stimulation with TNFα enhances nuclear c-Rel localization. We then set out to design a high throughput screening bioassay for the purpose of evaluating compounds that can inhibit c-Rel accumulation in the nucleus under TNFα stimulation. By preventing activated c-Rel from interacting with ΔNp63α in the nucleus we aim to decrease uncontrolled proliferation and restore the tumor-suppressive functionality of the ΔNp63-TAp73 complex. A 384-well immunocytochemistry assay was developed using a confocal microscopy readout and an automated image analysis algorithm to quantify nuclear translocation. The optimized assay will be used to screen the NCATS collection of approved drugs and investigational oncology agents. Top candidates will undergo further investigation in vitro, ex vivo, and in vivo to explore the possibility of repurposing the small molecules for HNSCC therapeutics.

#3102 A high-throughput screening method for discovering potent P-glycoprotein modulators from the chemical library in Tohoku University.

Norihiko Sugisawa[1], Shinobu Ohnuma[1], Takayuki Doi[2], Michiaki Unno[1]

[1]Tohoku University Graduate School of Medicine, Sendai, Japan,[2]Tohoku University Graduate School of Pharmaceutical Science, Sendai, Japan

Background: Drug development is important for cancer therapy to improve patient outcomes. In most cases, drug development starts in discovering candidate compounds from a chemical library in high-throughput screening (HTS). Tohoku University Graduate School of Pharmaceutical Science owns the original chemical library consisting of thousands of original chemical compounds. P-glycoprotein (P-gp), a major drug efflux transporter mediates multi-drug resistance (MDR) in cancer cells. Therefore, P-gp modulators could revere MDR and increase chemosensitivity. The aim of this study is to reveal an adequate method of HTS for discovering potent P-gp modulators from the chemical library in Tohoku University.
Methods: The chemical library in Tohoku University had 5861 compounds in the present study, and the collection contains over 7 thousand compounds in 2023. P-gp overexpressing KB-V1, human epidermal carcinoma cell lines were obtained, and calcein AM, P-gp substrate was employed for fluorescent substrate efflux assays. A plate reader-based calcein AM efflux assay for HTS was established to select candidate compounds as P-gp modulators. After the primary HTS, structures of the candidate compounds were analyzed, then several analogous compounds were extracted from the chemical library. For the validation of the hit compounds in HTS and the analogs, a flow cytometry-based calcein AM efflux assay was conducted. In addition, reversal effects of P-gp modulators on the cytotoxicity of paclitaxel were measured in a cell proliferation assay.
Results: Of 5861 compounds in the chemical library, 53 compounds showed 2-fold or higher fluorescence intensity, and then 13 compounds showed 3-fold or higher fluorescence intensity in a plate reader-based assay for the HTS. Especially 2 candidate compounds showed over 5-fold fluorescence intensity. In the analysis for structures of the candidate compounds, 20 analogous compounds were extracted from the chemical library. To verify the result of the plate reader-based assay, a flow cytometry-based assay was conducted for 53 hits and 20 analogs. As a result, the 2 candidate compounds that selected in the plate reader-based assay showed 60-fold, the highest fluorescence intensity in a flow cytometry-based assay. The other compounds showed less fluorescence intensity than these 2 candidates. In addition, both candidates enhanced the paclitaxel-induced cytotoxicity in a cell proliferation assay.
Conclusions: A plate reader-based calcein AM efflux assay in HTS was an adequate method for discovering potent P-gp modulators from the chemical library in Tohoku University.

#3103 Alternative cell counting and viability detection using NexGreen/PI fluorescent stain on multiple low- and high-throughput image cytometry platforms.

J. Mukherjee, C. F. Nitta, M. Pierce, S. Hem, D. Browe, D. Kuksin, L. L. Chan;
Revvity Health Sciences, Inc., Lawrence, MA

In the past decade, the increase in cell and gene therapy products such as biologics, antibodies, and CAR-T has significantly increased the need for precise, robust, and consistent cell counting and viability measurements. Simplified and automated workflows benefit from assays that measure sample characteristics independent of their buffer, media, or storage conditions. Reliable and robust results are thus required to maintain quality control of downstream processes. In this work, we demonstrate a novel fluorescence-based dye, NexGreen/PI, capable of live and dead cell detection comparable to AO/PI in multiple cell buffer/media conditions. Jurkat cells of different viabilities (low, intermediate, and high) were stained in parallel with either NexGreen/PI or AO/PI for 1-2 minutes and measured on multiple image cytometer platforms including low-throughput (Cellometer K2, Auto2000, and Spectrum) and high-throughput (Cellaca MX, Cellaca PLX, and Celigo) instruments. Both NexGreen/PI and AO/PI dyes are used as equal volumes added to cell samples (ex: 20 uL cells + 20 uL dye). Additionally, we tested if difficult to analyze cells in “spent” media (typically with a lower pH) or in PBS can be stained using NexGreen/PI compared to AO/PI. Results on the high-throughput platforms show that NexGreen/PI staining can discriminate between live and dead Jurkats, analogous to AO/PI in samples of low (10-25%), intermediate (40-60%), and high (80-95%) viabilities. Measured viability of all samples using NexGreen/PI was within 5% of the paired AO/PI-stained samples. Cell concentration results with either NexGreen/PI or AO/PI also show counts with less than 6% difference. Low-throughput instrument results are similar and show that viabilities of Jurkat cells match within 5% of each other independent of sample (low, intermediate, or high viability), while cell concentrations differ up to 6% when comparing NexGreen/PI and AO/PI. Cells in “spent” media or washed and resuspended in PBS can exhibit low AO signal intensity that can be difficult to detect in a robust fashion. NexGreen/PI-stained cells, however, showed an unaltered fluorescence signal in these “tricky” cell samples. In this work, we demonstrated the capability of NexGreen/PI to measure cell counts and viability using low- and high-throughput instruments, which enables fit-for-purpose for a wide range of samples. Thus, our experiments demonstrate that NexGreen/PI is scalable and can be of significant value for use in automation and high-throughput systems where multiple samples in different mediums can be precisely measured.

#3104 A NanoBRET target engagement assay for querying domain selectivity at full-length polymerase theta in live cells.

S. Edenson[1], M. Slater[2], C. Corona[2], M. Beck[3], J. Vasta[3], K. Teske[3], A. Michaud[3], M. Robers[3];
[1]Promega, San Marcos, CA, [2]Promega, San Louis Obispo, CA, [3]Promega, Madison, WI

In HR-deficient cells, Polymerase Theta (Pol-theta) serves to repair double strand breaks and has emerged as a therapeutic target in HR-deficient cancers. Encoded by the POLQ gene, Pol-theta is a large (290 Kda) protein with two distinct functional domains (polymerase, helicase), separated by an unstructured region. Each domain of Pol-theta has proven vulnerable to small molecule inhibitors, with a number of molecules undergoing clinical evaluation. Unlike the helicase domain, target engagement at the polymerase domain requires cooperativity with DNA fragments. Here we describe a novel NanoBRET Target Engagement assay that enables domain-specific analysis of small molecule occupancy in live cells. To observe the high affinity-state of small molecule inhibitors to the polymerase domain, we have developed a cell-permeable pol domain NanoBRET probe, along with a novel work flow to introduce small DNA fragments into live cells. Together these components form a nucleoprotein complex with full length polymerase theta. This assay method can be used to quantify and rank-order engagement to the polymerase domain in live cells. To enable domain-selectivity analysis, we have developed a second NanoBRET probe directed to the helicase domain. Together these two NanoBRET probes allow for the mechanism of action studies at Pol-theta in living cells.

#3105 Computational integration with phage library to optimize clones of DEFB4A antibodies for cancer diagnostics and therapeutics.

Y. Guo[1], J. Yom[1], A. Han[1], Z. Guo[1], E. Zewdu[1], R. Gonzalez[1], T. Qu[1], B. Gilmore[1], X. Liu[1], W. Fu[1], X. Hu[2];
[1]Origene Technologies Inc, Rockville, MD, [2]OriGene Wuxi Biotechnology Co., Ltd, Wuxi, China

DEFB4A, a human beta-defensin, functions as a potential cancer biomarker, with elevated expression observed in various cancers, making it a candidate for diagnostic and prognostic applications. Additionally, its role in immune modulation suggests that DEFB4A may hold promise as a target for novel cancer treatments, particularly in the context of immunotherapy. This study aimed to develop a stable and high-affinity DEFB4A antibody for clinical and pre-clinical use. To achieve this, a combination of high-diversity phage libraries and computation-assisted analysis was employed to generate single-chain variable fragments (ScFv) clones specifically targeting DEFB4A. This research presents a robust approach for the generation of DEFB4A-targeting single-chain variable fragments (ScFv) from a phage library characterized by a high diversity of 10^9 unique clones and high titer of 10^{13} cfu/mL. Computational optimization was then applied to enhance the affinity, stability, and expression of these candidates through rational design and virtual mutagenesis programs. The binding activity of the optimized mutants was validated using biophysical methods such as surface plasmon resonance (SPR) and thermal stability assays. The process showed a remarkable 100-fold increase in affinity and stability. Additionally, the selected ScFv clone was further employed in immunohistochemistry (IHC) to detect DEFB4A in breast, prostate, and gastric cancers, showing higher expression levels compared to initial clones.

This study highlights the synergy of high-diversity phage libraries and computational methods in crafting DEFB4A antibodies with enhanced affinity, stability, and expression. The findings advance the field of antibody engineering, emphasizing the crucial integration of experimental and computational approaches. This work lays the groundwork for the development of high-performance biologics with diagnostic and prognostic applications across diverse cancer types. Furthermore, it demonstrates the possibility of integrating computational approaches in antibody development, offering the promise of expediting the process in the future.

#3106 Integrated *in vitro* and machine learning approaches for targeted drug screening in gliomas with concurrent NF1 and ATRX loss.

S. Dubey[1], S. Mohapatra[2], M. Yuan[3], C. G. Eberhart[3], F. J. Rodriguez[1];
[1]UCLA - University of California Los Angeles, Los Angeles, CA, [2]Massachusetts Institute of Technology, Cambridge, MA, [3]Johns Hopkins University School of Medicine, Baltimore, MD

Neurofibromatosis type 1 (NF1) frequently precipitates the development of brain and nerve tumors, with subsets of associated solid tumors demonstrating an aggressive phenotype often characterized by alpha thalassaemia mental retardation X-linked (ATRX) loss. In response, we executed an in vitro high-throughput drug screening utilizing a 10,000-compound library in an NF1-associated ATRX mutant glioblastoma cell line (JHH-NF1-GBM1) and in U251 cells with ATRX knockout, mimicking the concurrent loss of ATRX and NF1. The screening protocol aimed to pinpoint compounds selectively targeting vulnerabilities arising from the co-occurrence of ATRX and NF1 loss. To enhance the precision of our results, we employed an unsupervised-supervised machine learning approach. Unsupervised models identified distinctive chemical groups associated with heightened sensitivity in ATRX/NF1-deficient cells. Subsequently, supervised models were trained, and their uncertainty estimates were utilized to further narrow down the selection of hit compounds. We also utilized pre-trained models to predict ADME and toxicity properties, facilitating a further filtration. This multi-step in vitro screening, coupled with in silico analyses, successfully identified promising compounds, subsequently validated through biophysical characterization. The integration of machine learning in our screening pipeline enhances the identification of potential targeted therapies for aggressive tumors (gliomas) characterized by ATRX/NF1 loss, offering a comprehensive and efficient approach to drug discovery in the pursuit of more effective treatments.

#3107 SMASH: Single molecule antibody screening with high-throughput imaging system.

Jihye Jo[1], Changju Chun[2], Byeong-Kwon Sohn[2], Booyoung Yu[1], Jiyu Lee[2]

[1]Proteina Co., Seoul, Korea, Republic of,[2]Seoul National University, Seoul, Korea, Republic of

Larger, more diverse antibody libraries are being screened in recent years. Despite enabling the high-throughput screening of extensive libraries, the process for identification and characterization of antibodies remains laborious and time-intensive. Here we report a platform that not only compiles hit finding and validation processes, but also provides high-resolution binding affinity as well as rank order among the library being screened. We streamlined the library construction and affinity screening via microscale transient expression in HEK293T cells with designed antibody sequence and direct quantification of antibody-antigen binding affinity which reduced the timeline from multiple weeks to a single week. We constructed the single-chain fragment antigen binding (scFab) libraries by replacing the duplex DNA fragment in CDR of interest while preserving the human framework of Fab. We have demonstrated that the SPID technique allows to detect antibody-antigen interactions from just dozens of pg of scFabs in total. This allowed us to bypass the conventional DNA cloning or even PCR amplification to achieve the minimum amount of DNA plasmids for expressing scFabs to be analyzed such as BLI and SPR. Therefore, we assembled the DNA plasmids through in vitro ligation with high efficiency and directly introduced it to HEK293T in 96-well microplate with microscale (200 ul) for transient transfection, which only takes three days for library generation. Next, we utilized SPID to quantify the number of single molecules between free and antigen-bound fractions of scFab, resulting in occupancy at the antibody-antigen binding equilibrium. This technique facilitated the determination of binding affinity (K_D) for 200 antibody-antigen pairs within a 6-hour TAT encompassing both measurement and analysis. In total, we utilized 4,000 times less antibody for characterization while achieving enhanced sensitivity compared to both BLI and SPR methods. As a proof-of-concept, we generated a library consisting of 720 variants of Trastuzumab in scFab format to probe the landscape of CDRs affecting affinities against HER2 showing nM to low uM dynamic range of K_D. Out of 720 analyzed variants, 5% were deleterious, 38% provided substantial changes, 40% showed little/no change, 17% enhanced affinity to HER2. To validate the robustness of the platform, we extensively expanded the library screening, assessing over 2,000 antibody variants for their affinity against more than three different therapeutic targets. To conclude, we demonstrated an efficient approach for monitoring changes in affinity resulting from single mutations in scFab. This rapid screening of site-saturated libraries would lead to a combinational variant library that our platform can screen. Ultimately, our platform aims to identify potential candidates for therapeutic antibody development throughput the phases of antibody discovery, maturation, and engineering.

#3108 Antibody labeling reagents to rapidly screen for the binding and internalization of therapeutic antibodies.

R. W. Holly;
Thermo Fisher Scientific, Eugene, OR

Introduction: There is a growing need in the immunotherapy research field for tools to rapidly screen novel therapeutic antibodies, whether looking for cells expressing IgG, target binding, or tracking internalization. Thermo Fisher Scientific has developed the next generation of Invitrogen™ Zenon™ reagents to enable screening of potential therapeutic antibodies, working across a variety of sample types including primary B cells and hybridomas, while being compatible with a wide range of platforms including flow cytometry, high content imaging, and in-incubator imaging systems.

Methods: The Invitrogen™ Zenon™ Alexa Fluor™ Plus IgG Labeling Reagents to screen for antibody binding provide a fast, versatile, and reliable method to evaluate antibody binding to cell surface antigens. Zenon screening reagents are labeled with Invitrogen Alexa Fluor Plus 488, Alexa Fluor Plus 594, or Alexa Fluor Plus 647 dyes (i.e., labeling reagent). The labeling reagent is directed against the Fc portion of an intact mouse or human IgG primary antibody. The formation of the zenon-antibody complex is rapid and requires no purification steps. The Invitrogen™ Zenon™ pHrodo™ Deep Red Labeling Reagents for screening antibody internalization provides a highly sensitive method for monitoring antibody internalization. Zenon pHrodo Deep Red utilizes the same screening reagent as Zenon Alexa Fluor Plus reagents, replacing Alexa fluor dyes with the pH-sensitive dye, pHrodo Deep Red. The pHrodo Deep Red sensors have minimal fluorescence at neutral pH and only upon entry into the late endosome and lysosome do they brightly fluoresce. Zenon pHrodo Deep Red Labeling Reagents are perfectly suited for screening the endocytosis and degradation of potentially therapeutic antibodies including antibody-drug conjugates.

Results: Live cells stained with Zenon-labeled antibodies show remarkable signal to background in both flow and imaging applications, while retaining their signal following fixation. Therapeutic antibodies such as anti-Her2 labeled with Zenon pHrodo Deep Red show as bright fluorescent puncta upon lysosomal degradation in the Alexa Fluor 647 channel and co-localize with lysosomal markers such as Invitrogen™ LysoTracker Red dye. Both Zenon Alexa Fluor Plus and Zenon phrodo Deep Red are ideal reagents for screening antibody panels of up to 96 different antibodies.

Conclusions: Thermo Fisher Scientific has developed sensitive and rapid Zenon reagents to allow for high throughput therapeutic antibody screening. In addition to Zenon reagents, Thermo Fisher Scientific has developed additional tools that allow for specific monitoring of antibody and protein uptake into the lysosome for degradation. These tools not only greatly improve the workflow from our existing portfolio, but allow for increased sensitivity allowing the field to make decisive decisions when selecting candidate immunotherapies.

Acknowledgments: I would like to thank the whole team that worked to develop these new labeling reagents including: Maria Olson and Chris Langsdorf.

#3109 Development of novel mono and bivalent nanobodies against EGFR for targeted cancer therapy.

D. C. Aguilar Cortes[1], M. O. Heitrich[1], M. M. Fernandez[2], S. Werbajh[1], G. Canziani[1], V. Zylberman[1], E. L. Malchiod[2], O. L. Podhajcer[1], S. E. Vinzon[1];
[1]Fundacion Instituto Leloir (FIL), Buenos Aires, Argentina, [2]UBA-CONICET, Buenos Aires, Argentina

Introduction: The epidermal growth factor receptor (EGFR) plays a central role in the tumorigenesis of various solid tumors, rendering it a noteworthy target for cancer therapy. Nanobodies (Nbs) offer an appealing therapeutic approach due to their low immunogenicity, rapid clearance, and high targeting specificity. The aim of this study is to isolate, design, and characterize Nbs directed against EGFR.
Methods: The Nb library was constructed following llama immunization with cells overexpressing EGFR. After three rounds of panning the phage-display library (both in solid phase and solution), individual clones were screened for EGFR reactivity using ELISA against Virus-Like Particles. Positive clones were sequenced, cloned into an expression vector, and then purified by immobilized metal affinity chromatography (IMAC). The Nbs were characterized through immunofluorescence (IF), flow cytometry (FACS), and surface plasmon resonance (SPR). The most promising candidates were used to design bivalent constructs, which were subsequently characterized by SPR and in a cell proliferation assay.
Results: We successfully constructed an EGFR-targeted Nb library, which allowed the selection of multiple EGFR-specific Nbs following the optimization of the panning strategy. Two of the candidates exhibit strong binding to native EGFR in cells and outperform the gold standard anti-EGFR Nb 7D12. They demonstrate enhanced binding parameters in surface plasmon resonance (SPR) assays, with fast association and slow dissociation rates. The homo/heterodimeric bivalent constructs show improved affinity and the ability to inhibit cancer cell proliferation.
Conclusion: We were able to develop novel mono and bivalent nanobodies with enhanced binding properties which can be used for targeted cancer therapy.

#3110 An enhanced and cost-efficient method for neoantigen immunogenicity screening method: Double Barcode Neoepitope Scan™.

S. Kim, M.-H. Jung, H.-J. Hwang, S. Oh, S.-E. Hong, S. Paik, H.-S. Kim;
Theragen Bio, Sungnam-si, Korea, Republic of

Neoantigens, HLA bound peptides generated by tumor-specific mutations, have emerged as promising targets for cancer immunotherapeutic. However, the significant challenge in neoantigen-based therapies is that the neoantigens are rare and difficult to predict. Therefore, in addition to prediction algorithms, the optimization of validation methods is essential for the reliable selection of highly immunogenic neoepitopes. In this study, we have developed a cost-effective screening method to validate large scale of neoantigen candidates. The DNA library-based methods have been employed for antigen selection and T cell receptor identification. We improved the DNA library-based neoantigen screening method by adding two barcodes to each minigene transcribing multiple neoantigen candidates and pooled synthesis of minigenes. We initially designed the barcodes to allow analysis in a 10 by 10 format for screening of hundreds of neoantigens so that PCR with each barcode result in amplification of ten candidates. The second barcode allowed the deconvolution of immunogenicity results without the need for synthesis of individual peptides. In this method B cell was used as antigen-presenting cell, which were co-transfected with mRNA for a minigene pool, 41BBL, and OX40L after expansion with CD40L/IL4/IL21. The resulting B cells were co-cultured with T cells and T cell responses were evaluated using ELISpot. To validate the method the TESLA consortium reported tetramer positive neoantigens were included in minigene. In results, the neoantigens including each barcode were amplified to form a pool of ten neoantigens as a minigene and confirmed that the neoantigens were equally amplified by nested PCR. The neoantigen pools synthesized as mRNA were transfected for presentation in B cells. The result of the targeting a neoantigen pool containing tetramer-positive neoantigens of the TESLA consortium showed a positive for ELISpot. In conclusion, our optimized screening method, employing the double barcode system, offers a time- and cost-efficient approach for the selection of immunogenic neoantigens without the need for individual peptides. This method will facilitate large-scale screening to identify actual neoantigens with immunogenic potential, contributing to the development of neoantigen-targeted vaccines.

#3111 Preclinical development of a peptide-based immune-surveillance PET tracer for immuno-oncology stratification.

A. W. Sinkjaer[1], D. K. Sell[1], I. M. Dawoodi[1], B. Bakhshinejad[2], C. Stavnsbjerg[1], A. Kjaer[1];

[1]Copenhagen University Hospital - Rigshospitalet & University of Copenhagen, Copenhagen, Denmark, [2]University of Copenhagen, Copenhagen, Denmark

Introduction: Cancer immunotherapies, such as immune checkpoint inhibitors (ICIs), have become an integral part of cancer treatment. However, significant differences in their effectiveness persist among individual patients. This variability partly stems from poorly immunogenic tumors, referred to as "cold" tumors, characterized by low levels of tumor-infiltrating leukocytes (TILs). Studies indicate that lower levels of TILs, specifically CD4+ and CD8+ T-cells, lead to reduced efficacy of certain immunotherapies. Therefore, the imaging of these cell types could be invaluable in screening cancer patients to predict the effectiveness of a prescribed immunotherapeutic agent before and during treatment. CD4+ T-cells, identified by their high expression of CD4 receptors, could serve as a potential molecular imaging target for an immuno-oncology relevant PET tracer. For this purpose a peptide-based PET tracer offer several beneficial characteristics such as relatively low circulation time, cell penetration, and low development costs.

Methods: All peptides were identified through peptide phage display (PPD) and commercially synthesized (>95% purity). These peptides underwent screening for their binding affinity to recombinant human CD4 and a negative control protein using surface plasmon resonance (SPR) on a Biacore X100. Peptides exhibiting specific binding to CD4, as determined by SPR, were further selected for FITC-labeling (>95% purity). FITC-labeled peptides were applied in fluorescence-based cell assays conducted on the SUP-T1 (CRL-1942) cell line and an established SUP-T1 CD4 knockout (KO) cell line. Flow cytometry assays were performed using a Fortessa X-20, while live cell imaging was conducted on either a LSM980 or LSM900 confocal microscopy. Simultaneously, an *in silico* docking method was employed, utilizing ColabFold—an online complex predictor powered by AlphaFold2—for CD4-peptide docking analysis.

Results: Several peptides successfully identified via PPD exhibited binding to recombinant human CD4 as shown by SPR screening. The FITC-labeling and assessment against SUP-T1 and corresponding CD4 KO cell line unveiled specific CD4 binding within a subset of peptides, as observed in both flow cytometry and confocal microscopy. *In vitro* data was compared to CD4-peptide docking results to create a list of peptides for future *in vivo* studies.

Conclusions: Multiple peptides successfully identified via PPD showed robust *in vitro* CD4 binding through SPR screening. Select peptides also demonstrated specific CD4 binding in cell assays, corroborated by docking results. Future prospective for the high performing peptides include *in vivo* PET/CT Ga-68 or Cu-64 imaging in tumors with high and low CD4+ T-cell infiltration.

#3112 Colorectum metabolome map revealed etiological and survival heterogeneity in cancers of different subsites: Challenging the proximal versus distal classification.

Abhishek Jain[1], Caroline Johnson[1], Domenica Berardi[1], Sajid Khan[2], Montana Morris[2]

[1]Yale School of Public Health, new haven, CT,[2]Yale School of Medicine, new haven, CT

Objective: Colorectal cancer (CRC) is usually classified as proximal, distal and rectal cancer. clinicopathological, molecular features and risk factors do not change abruptly and variations exist even among the refined subsites, which may contribute to the failure of mechanism-targeted therapies for CRC and poor accuracy of potential CRC biomarkers. We generated a CRC metabolome map describing etiological and survival heterogeneity in cancers of different subsites of the colorectum.
Design: Utilizing 372 tumor tissues with matched normal mucosa liquid chromatography-mass spectrometry was applied to examine metabolomics profiles along 7 subsites of the colorectum: cecum (n=63), ascending colon (n=44), transverse colon (n=32), descending colon (n=28), sigmoid colon (n=75), rectosigmoid colon (n=38) and rectum (n=92). Linear regression showed distribution of metabolites along the subsites. Survival heterogeneity along subsites were statistically tested by cox regression analysis. Metabolome profiles were obtained from invitro cultures of 310 human microbial species.
Results: 40 and 76 significantly altered metabolites (including bile acids, lysoPCs and LysPEs) among tumors and normal mucosa showed metabolic heterogeneity existed among CRC subsites. Gradual changes in metabolites abundance with significantly linear trend from cecum to rectum: 23 metabolites in tumor, 30 metabolites in normal mucosa and 15 metabolites in both tumor and normal mucosa, revealed concentration gradient depends on the disease status. Exclusively significant alteration of metabolites only in one subsite showed the differences in cancers among the 7 subsites of colorectum. We identified the metabolites associated with survival were different and unique to each subsite. Integration of microbial metabolome with CRC metabolome revealed microbial metabolites contributed to etiological and survival heterogeneity among CRC subsites.
Conclusions: Gradual changes of metabolites from cecum to rectum and the association of different metabolites with CRC risk and survival in each subsite of colorectum, revealed the differences in cancers along the colorectum and challenge the simple classification of CRC in LCC, RCC and rectum. Human microbial metabolites contributed to etiological and survival heterogeneity among CRC subsites.

#3113 Development of HTS enzymatic assays for WRN helicase and exonuclease functions.

H. Pham, M. Ali, A. Ramos Martinez, R. Lowery;
BellBrook Labs, Madison, WI

WRN, a double strand break repair enzyme with ATP-dependent DNA-helicase and 3'- >5' exonuclease activities, is under intense focus as a therapeutic target because of its synthetic lethality in tumors with microsatellite instability. To accelerate discovery of WRN inhibitors, we developed and validated homogenous, fluorescence-based high throughput assays for WRN helicase and exonuclease enzymatic activities using the Transcreener HTS Assay platform, which relies on highly selective antibodies to detect nucleotides in a homogenous (mix-and-read) format with far red fluorescent readouts. We produced the WRN helicase domain (aa 500-946, N-terminal 6xHis) in BaV-infected insect cells and optimized detection of its dsDNA-dependent ATPase activity using the Transcreener ADP^2 Assay in FP, TR-FRET, and FI detection modes. Optimal reaction conditions included 50 µM ATP (approximate K_m) and saturating concentration (100 nM) of a 3' flapped duplex DNA oligomer; these conditions yielded a good signal with 250 pM WRN, a kcat of 300 min^{-1}, and a Z' of 0.85. An IC_{50} of 35 nM was determined for the probe inhibitor NSC-617145, and a 1,280 compound pilot screen (Tocris 2.0 Micro) identified multiple hits that were confirmed in dose response experiments. We produced the WRN 3'-5' exonuclease domain (aa 1-133-6xHis) in E. coli and used the Transcreener dAMP Exonuclease Assay to allow direct, FP-based detection of dAMP monomers released from a 52 bp dsDNA oligomer with a 5' overhang. With saturating DNA present (1 µM), the assay produced a good signal with 1 nM enzyme; the Z' value was 0.89. There are no published inhibitors for the WRN exonuclease, but suramin inhibited with an IC_{50} of approximately 100 nM. These assays allow sensitive, robust, quantitative detection of WRN ATPase and exonuclease activities using an extensively validated HTS platform; they should be valuable tools for screening and optimizing small molecules targeting specific WRN functions.

#3114 Development of HTS enzymatic assays for RNA helicases: DDX3, DDX5, DDX17, RIG-1 and MDA5.

M. Ali, **H. Pham**, A. Ramos Martinez, R. Lowery;
BellBrook Labs, Madison, WI

RNA helicases are a broad class of enzymes that bind and modify RNA in an ATP-dependent manner and play diverse roles in RNA metabolism, regulation of gene expression, and innate immunity. Several RNA helicases, especially in the dead box helicase (DDX) family, have been shown to be dysregulated in cancer, and there have been limited efforts to develop small molecule inhibitors. To accelerate development of selective helicase inhibitors while avoiding off target effects, especially with helicases that promote tumor immunity, we are assembling a panel of high throughput biochemical assays using the Transcreener ADP^2 assay for homogenous detection of RNA-dependent ATPase activity with a far-red fluorescence polarization (FP) readout. Here we describe development of assays for DDX3, DDX17 and DDX5, which have all been implicated in cancer, and the Rig-1-like receptor (RLR) helicases, RIG-1 and MDA5, which trigger expression of type I interferons important for tumor immunity. We produced the recombinant enzymes using BaV-infected insect cells, as full-length polypeptides, or in some cases truncated to remove disordered N-terminal domains. We determined RNA substrate and cofactor requirements and kinetic parameters with the purified enzymes and optimized the assays for initial velocity detection of RNA-dependent ATPase activity with a Z' value greater than 0.7, ensuring a sufficient signal window for inhibitor screening and dose response assays. We validated each of the helicase ATPase assays for HTS by screening a collection of bioactives (Tocris 2.0) and confirming hits in dose response mode with the enzymatic assay and with thermal shift assays to confirm target binding. These assays will enable screening and hit-to-lead/SAR for DDX helicases that drive tumorigenesis as well as selectivity profiling to avoid off target effects with RLR helicases that promote tumor immunity.

#3115 Systematic analysis of gene mutations and therapeutic efficacy via *ex vivo* hematological vitroscreen platform.

F.-J. Chou, S. Cairo, M. Gilardi, A. Andar, K. Abarca-Heidemann, M. Mancini;
Champions Oncology, Inc. (Hackensack, NJ), Hackensack, NJ

Acute myeloid leukemia (AML) is a common hematological malignancy found in adult patients, and FMS-like tyrosine kinase 3 gene (FLT3) mutation occurs in about 30% of patients. In 2019, a phase 3 clinical trial suggested that gilteritinib treatment resulted in significantly longer survival than salvage chemotherapy in relapsed or refractory FLT3-mutated AML patients. Targeting FLT3-mutants in AML has become one of the important therapeutic strategies in this decade. The ex vivo hematological VitroScreen platform provides a powerful tool to evaluate the performance of FLT3 inhibitors and other test articles. With Champions Oncology's primary hematological repository (https://www.championsoncology.com/hematological-vitroscreen) and proprietary LUMIN Bioinformatics platform, we classified models based on patient responses, clinical annotation, NGS data, and cell surface markers. In this Ex vivo study, we tested gilteritinib in 30 AML patients, and 8 of models were identified as FLT-3 mutants' carrier. Fold changes of cell viability after gilteritinib treatment were assessed based on quantitation of the ATP present. FLT3-mutants models showed significantly higher sensitivity to gilteritinib than FLT3-WT models (IC50, 132.56 nM vs. 234.16nM) in a 6-day assay. Only 25% of models in the FLT3-mutants group had higher IC50 than the average of all AML models (n=28, IC50 = 204.05 nM), compared to 53% in the FLT3-WT group. Our preclinical data highly match the observations in previous clinical trials, which suggest that VitroScreen is a reliable high throughput tool for drug development of drug resistant cancers.

#3116 Bioluminescent 3D tumors with immune cell co-culture for high throughput screening (HTS).

F.-J. Chou, S. Kamali, M. Gilardi, B. Walling, A. Andar, K. Abarca-Heidemann, M. Mancini;
Champions Oncology, Inc. (Hackensack, NJ), Hackensack, NJ

In the past decade, cancer immunotherapy has revolutionized the cancer treatment strategy. Immune-oncology (IO) drugs play an important role in treating various malignancies. Immunotherapies work by re-educating and boosting patients' immune systems to recognize and eliminate cancer cells. The immune co-culture assay provides invaluable information to understand the tumor microenvironment (TME) and observe the immune response after IO drug treatment. Recent advancements in the Champions TumorGraft3D (CTG3D) platform provides more consistent and accurate information for preclinical drug evaluation, but also efficiently simulate the tumor-Immune microenvironment (TIME) and interactions between cancer organoids and immunocyte. However, current analytic approaches in organoid-immune co-culture studies are still highly reliant on flow cytometry and high-resolution confocal imaging endpoints to provide the study outcome. There is a need for a fast and cost-effective co-culture platform to help set up experimental conditions. Easily traceable tags (e.g. bioluminescent and fluorescent) can quickly help establish reliable the effector (E) cell to tumor (T) cell conditions, thus enabling the user to test multiple immune-cell activator or engagers concentrations in a cost-effective and rapid manner. At Champions Oncology we provide stable Luc/GFP-tagged CTG3D models. We have built a reliable CTG3D-immune co-culture platform with various indications (including colon, prostate, gastric, non-small cell lung cancer, and leukemia) which can be used in co-culture with autologous TIL, allogenic TIL and NK cells, thus providing users a fast and cost-effective option to optimize the E:T ratio and monitor the drug performance.

EXPERIMENTAL AND MOLECULAR THERAPEUTICS: Antibody-Drug Conjugates
Poster Session

#3121 Therapeutic potential of a HER3 antibody-drug conjugate for the treatment of HER3-expressing cancers .
T. O'Hare, J. Cleveland, V. M. Jansen, D. Dornan;
Elevation Oncology, Inc., Boston, MA

To address the need for targeted therapy in the treatment of HER3-positive solid tumors, the human HER3 mAb, seribantumab, was evaluated in the context of an antibody-drug conjugate (ADC). As a proof-of-concept, seribantumab was conjugated with a cleavable valine-citrulline linker and monomethyl auristatin E (MMAE) payload via the stochastic cysteine conjugation method to yield HER3-ADC1. A drug-antibody ratio of 4 was selected for preclinical assessment in HER3-expressing models. Methods: HER3-ADC1 was evaluated *in vitro* and *in vivo*, with patritumab deruxtecan (patri-DXd) as a comparator. Binding to BT474 breast carcinoma cells (HER3 high; immunohistochemical (IHC) staining intensity 3+) was measured by flow cytometry. Internalization properties were established using seribantumab and patritumab coupled to Fab-AF488 following 4 hours incubation in SK-BR-3 breast adenocarcinoma (HER3 high; IHC 3+) and HCC1569 breast carcinoma (HER3 low; IHC 0-1+) cell lines. *In vitro* cytotoxicity was evaluated for HER3-ADC1, isotype-MMAE and free MMAE payload as well as patri-DXd, isotype-DXd and free deruxtecan payload in BT474 cells, SK-BR-3 cells and NCI-H446 lung carcinoma (HER3 low; IHC 0-1+) cells. *In vivo* anti-tumor activity was assessed for HER3-ADC1, isotype-MMAE, patri-DXd and isotype-DXd in patient derived xenograft (PDX) models of pancreatic (HER3 high; IHC 3+) and breast cancer (HER3 low; IHC 0-1+). Results: HER3-ADC1 binding to cancer cells, endocytosis, MMAE release, and inhibition of proliferation were dependent on HER3 expression. In assays investigating antibody internalization, seribantumab displayed similar internalization capacity as patritumab. For both HER3 mAbs, internalization was greater in a HER3 high than a HER3 low cell line. In cytotoxicity assays, HER3-ADC1 and patri-DXd displayed HER3 expression level-dependent cell killing. HER3-ADC1 outperformed patri-DXd in HER3 high cell lines based on *in vitro* cytotoxicity. HER3-ADC1 and patri-DXd were ineffective against NCI-H466 cells with low HER3 expression. In a PDX model of pancreatic cancer (HER3 high), HER3-ADC1 induced tumor regression, while isotype-MMAE had only a moderate anti-tumor effect. Both patri-DXd and isotype-DXd had moderate anti-tumor effects, indicating a lack of HER3 target dependence. In a PDX model of breast cancer (HER3 low), HER3-ADC1 and isotype-MMAE lacked anti-tumor activity; isotype-DXd had a moderate anti-tumor effect and patri-DXd had a substantial anti-tumor effect. Conclusions: HER3-ADC1 demonstrated target-dependent *in vitro* cytotoxicity and *in vivo* anti-tumor activity in a HER3-expressing pancreatic cancer PDX model. Results from *in vitro* and *in vivo* studies highlight the promising therapeutic potential of a seribantumab-based ADC for patients with HER3-expressing cancers. Additional results on the optimization and characterization of HER3-ADC1 will be presented.

#3122 Preclinical development of a novel camptothecin-based antibody-drug conjugate targeting solid tumors expressing Claudin-6.

N. Tsang[1], N. Veillard[1], E. Horsley[1], K. Havenith[1], N. Janghra[1], K. Zaitseva[1], C. Oblette[1], I. Kirby[1], P. W. Hogg[1], F. Zammarchi[2], L. de Haan[1], P. H. van Berkel[1];

[1]ADC Therapeutics, London, United Kingdom, [2]Myricx Bio, London, United Kingdom

Claudin-6 is a member of the claudin family and consists of four transmembrane helices, two extracellular loops, and an amino- and carboxyl-terminal tail with a PDZ-binding motif in the cytoplasm. It is involved in the formation of tight junctions and is expressed in developing human epithelial structures during early-to-mid gestation while expression in iadult tissues is mostly absent. Claudin-6 expression is upregulated in ovarian cancer, testicular cancer, endometrial cancer, non-small cell lung cancer (NSCLC) and gastric cancer. Here, the generation and preclinical characterization of a novel Claudin-6 specific antibody-drug conjugate (ADC) is described, composed of a humanized IgG1 directed against human Claudin-6 site-specifically conjugated a novel payload containing a valine-alanine cleavable linker and a camptothecin warhead with a drug to antibody ratio of 6. FcγR-mediated effector function of the ADC was abrogated via mutations in the Fc portion of the antibody. The purpose of this study was to evaluate the expression of Claudin-6 in different tumour indications and characterise the *in vitro* and *in vivo* anti-tumour activity in human cancer cell lines and patient-derived xenograft (PDX) models. In addition, the tolerability of the ADC was evaluated in a repeat-dose toxicity study cynomolgus monkeys. Cell binding studies using Fabs showed high affinity binding to Claudin-6, while affinity for Claudin-9 was 16-fold lower with no binding to Claudin-3 and Claudin-4. Cross-reactivity with cynomolgus monkey and mouse Claudin-6 was also demonstrated. Fcgamma receptor binding studies confirmed the strongly reduced binding of the antibody to FcγI, FcγI,IIa, FcγIIb and FcγIIa, consistent with the introduction of mutations in the Fc domain of the antibody. *In vitro*, the Claudin-6 ADC showed potent and specific cytotoxicity against various Claudin-6-expressing solid cancer cell lines, including OVCAR3, PA-1, OV-90, FU-97, BeWo, NTERA-2 and NUGC3 in comparison to a non-binding control ADC conjugated to the same payload, and it also showed potent bystander killing. *In vivo*, a single dose intravenous (IV) of the Claudin-6 ADC demonstrated potent anti-tumour activity in multiple solid tumour xenograft models, including OVCAR3 and PA-1. Furthermore, administration of the Claudin-6 ADC to cynomolgus monkeys was well tolerated up to 40 mg/kg IV when given on Day 1 and 22. Cell membrane expression of Claudin-6 was confirmed by immunohistochemistry (IHC) in ovarian cancer (70%), testicular cancer (98%), endometrial cancer (30%), NSCLC (28%) and gastric cancer (24%), confirming expression of Claudin-6 in indications with high unmet need. In summary, this novel Claudin-6 ADC demonstrated potent, specific anti-tumour activity in Claudin-6 expressing cancer-derived models and was well tolerated in cynomolgus monkey, supporting future clinical development of this ADC.

#3123 Preclinical characterization of AMB302/GQ1011, a first-in-class FGFR3 antibody-drug conjugate (ADC) with topoisomerase 1 inhibitor against diverse FGFR3 overexpression or alteration.

Byeongkwi Min[1], Sunghyun Lee[1], Wonsik Jung[1], Lina Wang[2], Yajun Sun[2], Hyejin Kim[1], Nam-Gu Her[1], Paul H. Song[2], Gang Qin[2], **Do-Hyun Nam**[1]

[1]Aimed Bio Inc., Seoul, Korea, Republic of,[2]GeneQuantum Healthcare Suzhou Co., Ltd., Suzhou, China

Background: Molecular alterations of oncogene FGFR3 in various cancers include FGFR3 gene fusions, activating mutations, and overexpression as a driver mutation. AMB302/GQ1011 is a novel FGFR3-targeting ADC conjugated with an innovative topoisomerase I inhibitor (TopoIx) using intelligent Ligase-Dependent Conjugation (iLDC) technologies developed by GeneQuantum (GQ), providing high homogeneity, excellent druggability, and superior linker stability. Based on preclinical characterization, AMB302/GQ1011 exhibits impressive anti-tumor activities against bladder cancer (BC), head and neck squamous cell carcinoma (HNSCC), and glioblastoma (GBM) with either FGFR3 overexpression or FGFR3 alterations including gene fusions, demonstrating potential as a first-in-class FGFR3 ADC against FGFR3 relevant solid tumor indications.
Methods: For biomarker analysis, patient tissue microarrays and tissue blocks were subjected to IHC staining for FGFR3 to assess its real-world intensity. To characterize AMB302/GQ1011, in vitro assays and ex vivo plasma stability were evaluated to confirm the anti-tumor effect and linker stability. In vivo anti-tumor effects of AMB302/GQ1011 were assessed on various CDX and PDX models with FGFR3 overexpression or alterations. The potential toxicity profile of AMB302/GQ1011 was evaluated in NHP via repeated intravenous infusions.
Results: AMB302/GQ1011 conjugates a novel FGFR3-targeting antibody (Aimedbio Inc.) with TopoIx (GQ) via a cleavable linker through iLDC platform. In IHC analysis, we detected high and widespread FGFR3 expression in various tumors. In in vitro cytotoxicity assay, AMB302/GQ1011 showed excellent antitumor activity against FGFR3-expressing cells. In various CDX and PDX models with FGFR3 expression or alterations, AMB302/GQ1011 demonstrated superior efficacy compared with benchmark ADCs and FGFR pan-inhibitors. AMB302/GQ1011 dramatically prolonged survival in GBM orthotopic PDX models with F3-T3 fusion by >150% in combination with TMZ. Particularly, in combination with an immune checkpoint inhibitor (ICI), AMB302/GQ1011 exhibited an excellent synergistic antitumor effect. In a monkey toxicity study, AMB302/GQ1011 demonstrated a high tolerability up to 60 mg/kg dosing, without severe adverse effects.
Conclusion: AMB302/GQ1011 demonstrated a potent antitumor efficacy in vitro and in vivo models with FGFR3 overexpression and alterations across various solid tumors. Notably, AMB302/GQ1011 suggests the potential for combination with ICI treatment. Moreover, AMB302/GQ1011 exhibited excellent tolerability at high doses in NHP, indicating its safety profile. Our data suggest that AMB302/GQ1011 has potential to become a first-in-class FGFR3-targeting ADC for solid tumors with FGFR3 overexpression or alterations.

#3124 MRG006A, a novel glypican-3-targeting antibody-drug conjugate, demonstrated potent anti-tumor activity and good safety profile in preclinical studies.

Yanchun Wang[1], Hongfeng Li[1], Hao Shen[2], Wenchao Liu[1], Shoujia Liu[1], Kequan Yin[1], Haili Xu[1], Xueyuan Cui[1], Wei Li[1], Wei Liu[1], Xiangyu Wu[1], Liu Yang[2], Tian Ma[1], Zhongrun Zhao[1], Jun Wang[3], Feifei Cui[2], **Lei Fang**[2], Minmin Qin[3], Chaohong Hu[1]

[1]Shanghai Miracogen Inc., Shanghai, China,[2]Concept to Medicine Biotech Co., Ltd., Shanghai, China,[3]Lepu Biopharma Co., Ltd., Shanghai, China

Background: Hepatocellular carcinoma (HCC) is one of the most challenging cancers with high unmet medical need. Glypican-3 (GPC3) is an oncofetal glycoprotein anchored to the cell surface via GPI (glycosylphosphatidylinositol) and frequently over-expressed in HCC with limited expression in normal adult tissues, which makes it an appealing antibody-drug conjugate (ADC) target for HCC. MRG006A is a potentially first-in-class GPC3-targeting ADC composed of a novel humanized IgG1 antibody conjugated to a proprietary linker-payload platform utilizing a potent topoisomerase 1 inhibitor via a peptide-based cleavable linker.

Materials and Methods: As a GPC3-targeting ADC intended for clinical therapy of GPC3-expressing cancers, the mechanism of action and therapeutic potential of MRG006A were investigated in a series of preclinical studies, including (1) MRG006A and its antibody moiety binding to human GPC3 expressed on cells assessed by flow cytometry; (2) binding affinity to human and cynomolgus monkey GPC3 measured by SPR (surface plasmon resonance); (3) internalization in Huh7 cells assessed by pHAb Reactive Dye and confocal microscopy; (4) *in vitro* cytotoxicity against a panel of HCC cell lines (Huh7, HepG2, Hep3B and GPC3-negative SK-HEP-1); (5) anti-tumor activity of MRG006A evaluated in Huh7 and HepG2 cell line-derived xenograft (CDX) as well as a panel of HCC patient-derived xenograft (PDX) mouse models with a different expression level of GPC3; (6) plasma stability of MRG006A evaluated in human, cynomolgus monkey, rat and mouse plasma; and (7) an exploratory pharmacokinetic (PK) and toxicology study of MRG006A in cynomolgus monkey.

Results: The GPC3-targeting ADC, MRG006A, and its antibody moiety exhibited superior binding activity to GPC3-expressing cancer cell lines than a clinical antibody benchmark and similar nanomolar binding affinity to both human and cynomolgus monkey GPC3, which makes cynomolgus monkey suitable for toxicological studies. Rapid internalization of MRG006A antibody was observed in GPC3-expressing Huh7 cells, and MRG006A maintained comparable internalization capability to the naked antibody. More importantly, MRG006A exhibited potent GPC3-dependent cytotoxic activity in a panel of HCC cells expressing varying levels of GPC3. Administrations of MRG006A resulted in a robust and dose-dependent tumor growth inhibition of multiple CDX models and HCC PDX models. Remarkable stability of MRG006A was shown in the plasma of various species tested. MRG006A demonstrated a favorable PK and safety profile with good tolerability in the exploratory toxicology study.

Conclusion: Overall, the preclinical study results suggest that MRG006A is a feasible ADC drug candidate for treating GPC3-expressing cancers in clinical studies. MRG006A was aimed to submit IND in China and the U.S in 2024.

#3125 TCX-101, a novel antibody-drug conjugate targeting a tumor-associated carbohydrate antigen for the treatment of solid tumors.

F. G. Gomes, F. Muraca, G. M. Schmidt Garcia Moreira, K. Rosch, M. Brautigam, P. Sondermann, **M. Ocker**;
TACALYX GmbH, Berlin, Germany

Tumor-associated carbohydrate antigens (TACAs) are short oligosaccharides expressed on the surface of cancer cells and play key roles in cellular communication, immune evasion, apoptosis and metastasis. TACAs are therefore interesting targets for antibody-based therapies in cancer. We have generated an antibody (TCX-101) against a TACA structure with improved binding affinity compared to other monoclonal antibodies (mAbs) against the same target as shown by surface plasmon resonance (~ 10x superior KD), as well as high level of specificity against glycan species related to the target, as accessed by glycan array, flow cytometry, and immunocytochemistry or immunofluorescence. Immunohistochemistry studies on fresh-frozen tissue microarrays showed high expression of the target in various solid tumors (e.g. gastrointestinal, lung, and breast) and only low expression in normal tissues. *In vitro*, TCX-101 has ~ 4x higher maximum binding, ~ 2x faster binding kinetics, ~ 4x faster cellular internalization and induces ~ 2x higher antibody-dependent cellular cytotoxicity than a reference antibody. Monomethyl auristatin E (MMAE) was used in a drug-antibody ratio (DAR) of 4 to generate an antibody-drug conjugate (ADC). This ADC was effective in *in vitro* toxicity assays against murine B16 melanoma cells induced to express the target (measurable effect on WT cells), as well as human breast cancer MCF7 WT cells (~ 25x less activity on target-knockout MCF7 cells, Table 1). When tested *in vivo*, TCX-101 was highly effective in two different xenograft mouse models (B16, MCF7) with more than 95% tumor growth inhibition compared to vehicle, and no signs of toxicity (no weight loss, no histophatological findings). A fully humanized version of TCX-101 with improved binding properties (EC50 6.27 nM vs. 8.13 nM) was generated and will be evaluated in further *in vivo* experiments. In conclusion, TCX-101 is a promising ADC for the treatment of various solid tumors.

Table 1

	IC50 [nM] TCX-101-MMAE 4 DAR
B16 KI	7.64
B16 WT	no killing observed
MCF7 WT	1.97
MCF7 KO	45.97

#3126 A novel pegylated bispecific antibody-drug conjugate (P-BsADC) JY207b targeting cancers co-expressing PD-L1 and CD47.

Y. Wen, Shumin Liu, Weidong Lyu, Yang Lei, Shuangyu Tan, Zibin Wu, Shuqiang Yin, Qiudong Zhuo, Dechun Wu;
Shenzhen Enduring Biotech, Ltd., Shenzhen, China

ADCs have showed improved efficacy and target selectivity comparing to the non-specific small molecule cytotoxicity drugs. However, conventional IgG based ADC has been hindered in solid tumor therapies by the poor tumor penetration, low internalization efficiency, unexpected efflux from tumor cells, and narrow therapeutic window due to the on target/off tumor toxicity, etc. To address these issues, we have developed the pegylated bispecific ADC platform and proved the concept with JY207, which targets PD-L1 and CD47 with a 30k PEG-MMAE linker-payload. JY207 has demonstrated advantages in tumor penetration, internalization efficiency, without efflux post internalization, lacking Fc related toxicity, and better tumor inhibition than DS-8201a in a model positive for Her2, PD-L1 and CD47. In this study, we further improved the compound by site-specific conjugating the fusion protein of two scFvs that target PD-L1 and CD47, with a 40K PEG-MMAE linker-payload. As expected, the new compound JY207b retained all the advantages of JY207. Additionally, JY207b did not bind to human red blood cells at all even though an ultra-sensitive detection method was employed, while CD47 antibodies with reported low affinity bound >90% red blood cells under our ultra-sensitive detection method. Meanwhile, JY207b could still preferentially bind to CD47/PD-L1 double positive tumor cells, thus reducing the possibility of on-target toxicities. In the *in vitro* cytotoxicity assays, the compound JY207b demonstrated strong potencies in CD47/PD-L1 double positive tumor cells, with almost no killing effect to CD47 or PD-L1 single positive tumor cells. In CDX models and a PDX model of transplanted tumor tissues from lung cancer patients, the compound JY207b demonstrated strong tumor inhibition efficacies at low doses. More interestingly, although the elimination half-life (T1/2) of JY207b in mice is 59.17±3.824 hours, the elimination time of JY207b in tumors is beyond 1 week by the IVIS imaging examination, which allows for weekly dosing in PK unfavorable mouse animals for pegylated protein drugs. Moreover, preliminary repeated-dosing toxicological study has found the maximum tolerated dose of JY207 in CD47/PD-L1 double transgenic mice to be 50mg/kg. These studies suggested favorable anti-tumor effect of JY207 both in vitro and in vivo, and its mechanism of action has been well described. These findings provide evidence for the efficacy of JY207 as a clinical treatment for patients with CD47/PD-L1 double positive cancers.

#3127 Development of three-dimensional cancer cell line spheroid models for the *in vitro* functional characterization of cytotoxic antibody-drug conjugates.

Jodi Wong, Andrea Hernandez Rojas, Allysha Bissessur, Lemlem T. Degefie, Araba P. Sagoe-Wagner, Samir Das, Vincent Fung, Kevin Yin, Renee Duan, Sam Lawn, Laurence Madera, Catrina Mi Jung Kim, Alex Wu, Mark E. Petersen, Raffaele Colombo, Jamie R. Rich, Stuart D. Barnscher

Zymeworks Inc., Vancouver, BC, Canada

Background: Antibody-drug conjugates (ADCs) are an effective class of cancer therapeutics which have gained prominence for the treatment of several malignancies. A cytotoxic ADC consists of a linker-payload conjugated to a monoclonal antibody, which targets a distinct tumor-associated antigen (TAA) to enable the delivery of the cytotoxic payload to cancer cells. Presently, there is a need for *in vitro* models that better recapitulate *in vivo* tumor tissue complexity to aid in the screening and evaluation of ADCs during preclinical development. Hence, efforts have been made to develop *in vitro* three-dimensional (3D) models with improved translation to *in vivo* tumor models compared to traditional two-dimensional (2D) cancer cell line monolayer models. We aimed to generate monoculture cancer cell line spheroids in a high-throughput manner. Subsequently, we sought to evaluate the spheroid penetration capability of structurally distinct ADCs and to assess the 3D cytotoxic activity of a variety of microtubule inhibitor (MTI) and topoisomerase 1 inhibitor (TOPO1i)-bearing ADCs targeting multiple TAAs, comparing to activity in 2D models.

Methods: Monoculture cancer cell spheroids were generated by seeding cells from a variety of tumor types, using an automated liquid-handling robot, into microtiter plates treated with ultra-low attachment coating, which allows for scaffold-free self-assembly of cancer cells into a 3D arrangement. Following spheroid formation by incubation for 2-3 days under standard culturing conditions, spheroids were treated with ADCs at a range of concentrations for functional evaluation: the spheroid penetration capability of ADCs of different antibody formats was assessed using high-content confocal imaging of spheroids treated with fluorescently labeled antibodies; the cytotoxic activity of ADCs was characterized using an ATP quantification luminescent reagent, live/dead cell fluorescent stains, and confocal imaging.

Results: Monoculture spheroids of varying morphologies were successfully and reproducibly generated with a large panel of >50 cancer cell lines derived from ≥10 tumor types. Antibodies with different formats demonstrated target-mediated binding and a range of spheroid penetration depths. Additionally, MTI and TOPO1i ADCs evaluated in a panel of cancer cell spheroids demonstrated robust 3D cytotoxicity and differentiated activity when compared to the 2D monolayer assay. In a number of cases, the potency trends across multiple ADCs in 3D cytotoxicity assays were more predictive of *in vivo* efficacy compared to the 2D assay. Taken together, our high-throughput spheroid assays present important and straightforward *in vitro* tools to aid in the screening and selection of therapeutic cytotoxic ADC candidates for the treatment of solid tumors.

#3128 HRA00184-C004, preclinical characterization of a novel tissue factor-targeted antibody-drug conjugate.

H. Ying, L. You, N. He, S. Xu, P. Pu, S. Lin, J. Feng, Z. Zhang, X. Ye, M. Hu, F. He;
Shanghai Hengrui Pharmaceutical Co., Ltd., Shanghai, China

The physiological function of tissue factor (TF) is to initiate coagulation cascade by forming complex with plasma Factor VII after vascular injury. For Tisotumab vedotin (Tivdak), a TF targeting antibody-drug conjugate (ADC) approved for the treatment of cervical cancer, bleeding events were prespecified as adverse effects (AEs) of interest, besides ocular toxicity and peripheral neuropathy (known MMAE payload related AE). In order to mitigate the bleeding risk, a next generation of TF-targeting ADC is developed by Hengrui Pharmaceuticals. HRA00184-C004 is a novel ADC comprising a differentiated TF-targeted antibody (HRP07132) conjugated to a proprietary topoisomerase I inhibitor (Dxh, an exatecan derivative) via a protease-cleavable linker. In contrast to most TF-targeting antibodies, the naked HRP07132 does not interfere the interaction between TF and Factor VII or Factor X, has no impact on coagulation function in prothrombin time and thrombin generation assay, therefore reduced bleeding incidence is expected for HRA00184-C004. Meanwhile, HRA00184-C004 exhibited not only potent growth inhibition against multiple TF-expressing cancer cell lines but also bystander-killing effect *in vitro*. HRA00184-C004 also displayed robust and sustained anti-tumor activities in the PDAC HPAFII (TF high), TNBC MDA-MB-231 (TF moderate) and NSCLC H358 (TF low) TF-expressing xenograft models. Furthermore, in cynomolgus monkey, HRA00184-C004 is well-tolerated over a 6-week period with 12 mg/kg dosing every 3 weeks with acceptable PK profile. Notably, neither coagulation disorder nor skin rash was observed, which are superior to the historical NHP data reported by Tivdak. In conclusion, with the encouraging efficacy in preclinical study and promising safety profiles in NHPs, HRA00184-C004 has demonstrated the best-in-class potential and is scheduled to advance into clinical development.

#3129 BYON4413, an *in vivo* active CD123-targeting antibody-drug conjugate, combines effectively with azacitidine and venetoclax in acute myeloid leukemia cell lines.

M. M. van der Lee[1], T. van Achterberg[1], K. Hersmus[1], A. Brouwers-Vos[2], M. van der Vleuten[1], M. Pruis[2], W. Kappers[1], G. Verheijden[1], G. Huls[2], G. van Wigcheren[1], R. Ubink[1], A. Sesink[1], A. MacInnes[1], J. Schuringa[2], W. Dokter[1];

[1]Byondis B.V., Nijmegen, Netherlands, [2]University Medical Center Groningen, University of Groningen, Groningen, Netherlands

Background: CD123, the alpha chain of the interleukin-3 receptor (IL-3Rα), is overexpressed in multiple hematologic malignancies and found particularly highly expressed on the surface of acute myeloid leukemia (AML) cells. Furthermore, increased CD123 expression on leukemic stem cells relative to non-neoplastic hematopoietic stem cells makes CD123 an attractive tumor-associated target for an antibody-drug conjugate (ADC). BYON4413 is an ADC that consists of a novel humanized IgG1 anti-CD123 antibody site-specifically conjugated with Byondis' proprietary duocarmazine linker-drug technology, ByonZine® and ByonShieLD®. The efficacy of BYON4413 is studied as monotherapy and in combination with azacitidine and venetoclax (AZA/VEN), since the AZA/VEN regimen is the standard of care (SOC) for AML patients who are ineligible for intensive chemotherapy.

Method: A panel of CD123+ and CD123- hematological cell lines and AML patient-derived bone marrow mononuclear cells (BMMCs)/peripheral blood mononuclear cells (PBMCs) were utilized in *in vitro* studies to determine the cytotoxic effects of BYON4413. The induction of apoptosis and cell killing by BYON4413 in a triple combination with AZA/VEN was studied *in vitro* using the CD123+ AML cell lines MOLM-13 and MV4-11. AML patient and cell line-derived xenograft models were used to investigate the *in vivo* efficacy of BYON4413.

Results: *In vitro* studies with human AML cell lines show that BYON4413 is highly effective in eradicating CD123+ cells while having little impact on CD123- cells. These results were confirmed *ex vivo* with AML patient-derived BMMCs/PBMCs. BYON4413 effectively killed AML patient-derived blasts while largely sparing healthy hematopoietic cells. The triple combination of BYON4413 with AZA/VEN enhanced both apoptosis and cell killing of AML cell lines compared to the singular BYON4413 treatment. *In vivo* studies demonstrate that BYON4413 is remarkably efficient at reducing the tumor burden in AML patient- and cell line-derived xenograft models.

Conclusions: Preclinical studies show that BYON4413 has potential to be an effective targeted therapy against CD123+ hematological malignancies such as AML. The enhanced efficacy of BYON4413 together with AZA/VEN suggests that a clinical benefit from the triple combination may be achievable and is worth further exploration. A first-in-human dose-escalation and expansion trial with BYON4413, designed to enroll R/R AML and high-risk MDS patients, is scheduled to start in Q2 2024.

#3130 *In vitro* characterization of a novel TROP2-targeting antibody-drug conjugate OBI-992.

T.-M. Kuo, T.-Y. Chang, J.-Y. Huang, W.-C. Tang, C.-J. Lin, Y.-C. Wu, C.-H. Lu, H.-C. Weng, Y.-J. Chen, Y.-H. Tsao, C.-Y. Wei, L. Shen, W.-F. Li, M.-T. Lai; OBI Pharma, Inc, Taipei, Taiwan

BACKGROUND

TROP2, a transmembrane glycoprotein widely expressed on epithelial cancers, has emerged as an attractive target for antibody-drug conjugate (ADC) development. Sacituzumab govitecan, a TROP2 ADC conjugated to topoisomerase inhibitor (TOP1) SN-38, has been approved for patients with triple-negative breast cancer. This study aims to investigate the characteristics of a novel TROP2 antibody (R4702) and its ADC OBI-992, which is derived from the conjugation of R4702 with a TOP1 inhibitor exatecan.

METHODS

Clinical study: Prognostic roles of TROP2 and TOP1 in patients were accessed through the “Kaplan-Meier plotter” database from more than 1055 colon cancer patients.

In vitro study: An ELISA study was conducted to investigate the binding epitope of R4702. Cell binding assay and Surface Plasmon Resonance were carried out to measure non-specific binding activity and binding affinity, respectively. DNA damage activity, cytotoxicity, and immunogenic cell death (ICD) effects of three TOP1 inhibitors exatecan, deruxtecan (Dxd), and SN-38, were evaluated. Cytotoxicity of OBI-992 along with other ADC was measured in both 2D and 3D spheroids cancer cells (gastric cancer NCI-N87, pancreatic cancer Capan1, and prostate cancer DU145). TROP2 and BCRP expression as well as potential mutations in TOP1 were investigated in TROP2 ADCs-induced resistant colon cancer cells. The synergistic effects of the combination of OBI-992 with PARP inhibitors were evaluated.

RESULTS

Clinical study: Positive correlations between high mRNA expressions of both TROP2 (p=0.0075) and TOP1 (p=0.043) with poor overall survival for colon cancer patients were found.

In vitro: The R4702 antibody displayed different binding epitopes from sacituzumab and datopotamab. In addition, R4702 showed lower non-specific binding and better binding affinity to TROP2 antigen than datopotamab. The payload exatecan demonstrated excellent ICD effects. Relatively higher cytotoxicity was observed by exatecan when compared to that of Dxd and SN-38. OBI-992 exhibited excellent activities on cell growth inhibition in 2D cell cultures and 3D cell spheroids. TROP2 down-regulation and BCRP upregulation were not found in OBI-992-induced resistant cells. A mutation R364H was identified in TOP1 in the resistance study with OBI-992, which is critical for the binding to TOP1 inhibitors camptothecin analogs. Finally, a synergistic effect of OBI-992 and PARP inhibitors (talazoparib, rucaparib, niraparib, and olaparib) on the enhancement of cancer cell killing and DNA damage was observed.

CONCLUSION

High expression of both TROP2 and TOP1 is associated with poor survival in patients with colon cancer. R4702 is a novel TROP2 antibody with a unique binding epitope and low non-specific
binding. Exatecan and exatecan-conjugated ADC OBI-992 showed high cytotoxic activities. Combination of OBI-992 with PARP inhibitors have potential in TROP2-expressing malignancies.

#3131 Novel CDH17-targeting antibody-drug conjugate exhibits anti-tumor efficacy in preclinical models of gastrointestinal cancers.

P. Wong[1], L. He[2], K. Chow[1], K. Wong[1], C. O[1], D. Wong[3], J. M. Luk[3], P.-C. Lo[2], K. Wong[1];
[1]Arbele Limited, Hong Kong, Hong Kong, [2]City University of Hong Kong, Hong Kong, Hong Kong, [3]Arbele Corp, Seattle, WA

Antibody-drug conjugates (ADC) for oncology indications have been developed, however, only few of them are approved for the treatment of gastrointestinal (GI) cancers, which represent as a huge unmet medical need. As such, we developed a novel ADC of which monomethyl auristatin E (MMAE), an antimitotic agent, was conjugated to a cadherin-17 (CDH17)-targeting monoclonal antibody via protease-cleavable peptide valine-citrulline linker. CDH17 is highly restricted to the intestinal adherent junctions which is not accessible in healthy individuals. In contrast, it is overexpressed and becomes reachable in over half of the gastric and pancreatic cancer patients and in more than 95% of patients with colorectal cancer, making it a perfect target for ADC. Our ADC is designed to deliver MMAE specifically to CDH17-expressing tumors to exert the cytotoxic effect of MMAE on cancer cell, mitigating the undesired off-target cytotoxicity. LC/MS analysis revealed that MMAE was conjugated in a drug-to-antibody ratio of 4 with a yield of higher than 75%. ELISA showed that the binding of naked antibody and ADC to CDH17 was comparable (EC_{50}, 0.17 nM & 0.3 nM, respectively), indicating the conjugation process did not affect antigen binding. This ADC also bound to different CDH17-expressing cell lines, including pancreatic AsPC1 and gastric AGS (EC_{50}, 2.1 nM & 1.53 nM, respectively). By labelling the ADC with pH-sensitive fluorescent indicator, we illustrated that ADC internalization only occurred in CDH17+ but not CDH17- cells, suggesting the high specificity of the ADC. Similarly, the ADC showed selective killing on CDH17+ cells (EC_{50}, 0.02-0.5 nM), and the data together proposed a positive correlation between ADC internalization level and its cytotoxicity (R^2 = 0.4307). This supported the specificity and safety of the ADC in killing CDH17+ cancer cells only without affecting normal cells. Furthermore, a preliminary *in-vivo* study on subcutaneous AsPC1 xenograft model demonstrated that the ADC significantly suppressed tumor growth without causing any changes in body weight. Our ADC would potentially be a “First-in-class” ADC for the treatment of GI cancers with minimal adverse systemic toxicity. Further pharmacokinetics, safety, and other IND-enabling studies are underway.

#3132 A novel dual drug antibody-drug conjugate targeting hTrop2 has synergetic anti-tumor activity in solid tumor models.

J. Zhu, X. Zhao, E. Li, H. Xu, L. Nie, G. Chen, H. Wang;
BioRay Pharmaceutical Co., Ltd., San Diego, CA

Antibody-drug conjugates (ADCs) are emerging therapeutic agents for targeted cancer treatment with remarkable clinical success. However, tumor heterogeneity and microenvironment complexity are still the major factors contributing to drug resistance, recurrence, and metastasis, which cannot be resolved with a mono therapy strategy. We've developed a novel dual drug ADC (BiADC), BR113, by conjugating an anti-hTrop2 antibody with a drug linker of a Topoisomerase I inhibitor payload, and another drug linker of an immune stimulator. Our studies show that the homogeneous ADC containing two distinct payloads is a new promising drug class, with two different anti-tumor MOAs, synergistic antigen-specific cell killing potency, desirable pharmacokinetic profiles, and minimal toxicity at therapeutic doses. In the cancer cells and human PBMC co-culture assay, BR113 exerts significantly more potent killing on cancer cells than two individual single-drug ADCs and the combination of two single-drug ADCs, which suggested a synergy on anti-tumor effects of this dual-drug ADC. In the xenograft mouse model studies, BR113 exhibits greater treatment effect and survival benefit than the combo of two single-drug ADCs at various doses. This robust superior anti-tumor activity is further confirmed in a hTrop2-MC38 syngeneic model with a prolonged anti-tumor protection against the tumor re-challenge. Finally, the novel BiADC, BR113, is well tolerated in hTop2 humanized mice after repeated administration. Our findings highlight the therapeutic potential of the BiADC format for treating refractory advanced solid tumors. The outstanding anti-tumor activity across various CDX tumor models and its favorable safety profile in mice support further evaluation of the innovative BiADC, BR113.

#3133 A novel bispecific antibody-drug conjugate targeting HER2 and Trop-2 displays potent antitumor activity in a variety of tumor models with promising preclinical characteristics.

H. Zhong, Y. Xiong, H. Huang, Y. Pan, N. Wang, B. Sun, S. Liu, W. Yuan, D. Liu, J. Fang, **H. Bao**;
BiOneCure Therapeutics, Inc., Germantown, MD

Antibody-drug conjugates (ADCs) have exhibited considerable advancements in cancer therapy, though their efficacy is often confined to specific patient subsets or results in modest clinical responses due to low and heterogenous expression of drug targets in tumors. Targeting more than one tumor-associated antigens (TAAs) represents a new strategy to broaden treatment applicability and minimize on-target toxicity of ADC. Our analysis of co-expression of HER2 and Trop-2, two clinically validated ADC targets, in tumors of various histological malignancies manifests the great potential for an ADC simultaneously targeting these two antigens. We describe here a novel bispecific ADC (BIO-201) designed to co-target HER2 and Trop-2. This compound comprises a bispecific anti-HER2/Trop-2 antibody conjugated with a novel topoisomerase I inhibitor via a cleavable linker. BIO-201 demonstrates increased or comparable cell binding and internalization compared to parental antibodies. In in vitro cytotoxicity assays, BIO-201 effectively kills cancer cells with an IC50 in the sub nM range, irrespective of whether they co-express HER2 and Trop-2 or express only one antigen. Co-culture studies reveal that BIO-201 possesses a good bystander killing effect on drug target-negative tumor cells. In vivo studies further demonstrate the superior anti-tumor activity of BIO-201 in various tumor xenograft models, including those expressing different levels of HER2 and/or Trop-2, as well as models resistant to HER-2-targeting therapies. Moreover, BIO-201 exhibits favorable plasma stability, preclinical pharmacokinetics (PK), and toxicity profiles. In conclusion, these findings suggest that the anti-HER2/Trop-2 bispecific ADC, BIO-201, holds significant promise as an effective therapy for a diverse range of cancers, especially those expressing heterogenous levels of HER2 or Trop-2, and has the potential to benefit a broad patient population.

#3134 SDP03923-000-9106, a novel and optimized LIV-1 ADC with superior anti-tumor efficacy in breast cancer xenograft models.

Yanling Gong, Xing Sun, Changyong Yang, Simeng Chen, Wei Zhang, Cheng Liao

Jiangsu Hengrui Pharmaceuticals Co., Ltd., Shanghai, China

Background: LIV-1, also known as SLC39A6 or ZIP6, is a transmembrane protein belonging to the zinc transporter family. LIV-1 is a promising target for antibody-drug conjugate (ADC) therapy due to its broad expression in tumors and limited normal tissue expression. Ladiratuzumab vedotin, a LIV-1 targeting ADC with payload of MMAE, is now in phase I clinical trial stage and is the only LIV-1 ADC under clinical development worldwide. The preliminary clinical results demonstrated promising efficacy in TNBC (ORR=32%) but no response in HR+/HER2- breast cancer (ORR=0%), and typical MMAE-related adverse events were observed. Herein, we presented a novel LIV-1 directed ADC, SDP03923-000-9106, consisting of a LIV-1 mAb developed in house conjugated to a proprietary topoisomerase I inhibitor via a cleavable linker with an optimized average drug-to-antibody ratio (DAR) of 6.
Method: The *in vitro* binding affinity of SDP03923-000-9106 against LIV-1 protein was measured by Surface Plasmon Resonance (SPR) assays. The expression levels of LIV-1 in different cancer cell lines were detected by flow cytometry and IHC staining. *In vitro* activity against cancer cell lines was analyzed by CellTiter Glo assays following 10 days of treatment. The *in vivo* anti-tumor activities were investigated in both CDX and PDX models of breast cancer.
Results: SDP03923-000-9106 is a novel anti-LIV-1 ADC comprised of a humanized LIV-1 monoclonal antibody conjugated to the potent topoisomerase I inhibitor (a novel exatecan derivative designed by Hengrui with a better liposolubility and cellular permeability) by a cleavable linker. SDP03923-000-9106 had an optimal drug-to-antibody ratio (DAR) of 6 and showed strong binding affinity to LIV-1 and favorable internalization. SDP03923-000-9106 exhibited robust anti-tumor activity in cell lines across breast cancer, esophageal squamous cancer, gastric cancer, prostate cancer and non-small cell lung cancer. In the LIV-1 highly expressed breast cancer cell line of MCF-7, SDP03923-000-9106 demonstrated a strong inhibitory effect with IC_{50} of 5.36 nM. Moreover, in a LIV-1 high-expressing patient-derived xenograft model of breast cancer, SDP03923-000-9106 showed pronounced tumor regression at both doses of 3 and 10 mg/kg and showed stronger anti-tumor activity (TGI: 109%) at the same dose of 3 mg/kg versus BMK-MMAE (TGI: 75%; BMK-MMAE is synthesized by Hengrui using the published structure of Ladiratuzumab vedotin).
Conclusion: In summary, SDP03923-000-9106 is a novel LIV-1 targeted ADC with a highly permeable payload demonstrating great anti-tumor activity across multiple types of tumors in preclinical studies. The promising preclinical data support advancing SDP03923-000-9106 into clinical testing, and Investigational New Drug (IND) application to NMPA has been submitted.

#3135 BSI-730, a bispecific antibody targeting HER2 and PD-L1 for the development of a first-in-class bispecific ADC.

X. Hao[1], H. Li[1], X. F. Liu[2], J. Liu[1], W. Dai[1], Y. Pan[1], H.-H. Hu[1], J. Li[1], S. Xia[1], Q. Lyu[1], **H. M. Davis**[2], M. Chen[1], Z. Peng[1];
[1]Biosion, Inc., Nanjing, China, [2]Biosion USA, Inc., Newark, DE

Background: Antibody-drug conjugates (ADCs) have become a promising therapeutic option for patients with cancer. Bispecific ADCs targeting two tumor-associated antigens have potential differential anti-tumor advantages. HER2 and PD-L1 are co-expressed in some tumor cell types, such as breast cancer, gastric cancer, lung adenocarcinoma and urothelial carcinoma. A bispecific ADC targeting HER2 and PD-L1 should provide therapeutic benefit, particularly for patients with HER2 low cancer. Dual-target mediated cytotoxicity combined with PD-L1 mediated immunotherapy provides an innovative approach for cancer patients.

Experimental procedures: An anti-PD-L1 monoclonal antibody was identified from A/J mice immunized with PD-L1-ECD-Fc and screened by the Biosion proprietary SynTracer® High Throughput Endocytosis Platform. A “knob-in-hole” bispecific antibody, BSI-730, targeting HER2 and PD-L1 was created with trastuzumab and the humanized anti-PD-L1 scFv. Target binding specificity, binding activity, and affinity of BSI-730 were evaluated by protein-based ELISA, cell-based FACS and Biacore-based SPR, and the ligand blocking activity of PD-L1 portion was measured by competitive ELISA and cell-based FACS. The internalization activities on various cancer cell lines with different expression levels of HER2 and PD-L1 were evaluated by using the SynTracer® Platform.

Summary: BSI-730, a HER2/PD-L1 bispecific antibody, showed comparable binding affinity to HER2 as compared to trastuzumab, as well as comparable bioactivity to the parental anti-PD-L1 antibody regarding PD-L1 binding and PD-1/PD-L1 blocking. Based on a cell-based reporter assay, BSI-730 was able to reverse PD-L1 mediated T-cell suppression and exhibited comparable potency to the parental anti-PD-L1 antibody. The internalization of BSI-730 on HER2 low cancer cell lines was stronger than that of trastuzumab whereas the internalization of BSI-730 on HER2 high cancer cell lines was comparable to that of trastuzumab.

Conclusion: BSI-730 is a novel bispecific antibody for the development of a first-in-class bispecific ADC with the potential advantage of increased potency that can be further investigated to treat HER2 and PD-L1 co-expression tumors, particularly HER2 low tumors.

#3136 Towards development of a novel biparatopic trop2-ADC.

Y. Wu, B. Jiang, J. Rivera, F. Wang, J. Zhou, L. Liu, S. Hudson, W. Draper, J. Li, X. Min, H. Chen, **Z. Wang**;
RemeGen Biosciences, Inc., South San Francisco, CA

Background: Trophoblast cell surface antigen 2 (TROP-2) is a member of Tumor-associated Calcium Signal Transducer family (TACSTD2), which is a 35kDa transmembrane protein with 4 N-linked glycosylation sites. The overexpression of TROP2 in various cancers is associated with poor prognosis and increased risk of metastasis. Anti-TROP2 antibody drug conjugates (ADCs) are emerging as an innovative therapeutic intervention for cancer treatment. While these efforts were rewarded by the FDA approval of Trodelvy (Sacituzumab govitecan), a Trop2 targeted ADC, in 2020 for the TNBC patients, tumor heterogeneity could present one of the limitations for the Trop2-targeting therapy, leading to drug resistance. Here, we report our effort in developing a novel biparatopic TROP2 ADC which demonstrate superior cell killing activity compared with the monospecific TROP2 ADC, including certain resistant cell lines for the approved therapy.

Methods: Various biparatopic Abs were engineered using two different mAbs targeting the two non-overlapping epitopes of Trop2. The physical stability and biological activities were characterized. Binding competition assay was utilized for epitope binning using SPR. Cell binding affinity was determined using flow cytometry. Cellular internalization activity was measured using Incucyte system, and tumor cell killing efficacy was evaluated in multiple cancer cell lines. CDX mouse models were utilized to investigate the TROP2-ADC *in vivo* efficacy.

Results: We identified a biparatopic TROP2 mAb using two monospecific TROP2 mAbs with A recognizing the same epitope as Trodelvy, and B binding to a non-overlapping epitope vs Sacituzumab's. mAb-B demonstrates superior ability to recognize a few resistance cell lines to mAb-A. The biparatopic TROP2 mAb-A/B displays a KD of 0.81 nM protein binding compared with 6.42 nM and 0.26 nM, respectively for mAb-A and mAb-B. Importantly, the biparatopic mAb-A/B demonstrates significantly faster cellular internalization activity compared to those of the individual mAbs, signifying the biparatopic scaffold could drive receptor clustering and subsequently enhance the internalization, trafficking to the lysosome and degradation of the target. As expected, the ADC of the biparatopic mAb-A/B conjugated with a TOPi payload shows cancer cell killing efficacy in both *in vitro* and *in vivo* experiments. Furthermore, we tested mAb-A , -B and biparatopic mAb-A/B for their binding affinity to 14 missense mutations in TROP2 ECD expressed in HEK293 cells. Interestingly, mAb-A showed decreased binding in 5 mutant cell lines, while mAb-B and biparatopic mAb-A/B maintains activity.

Conclusion: We have engineered a novel TROP2 biparatopic antibody with unique biological features as well as superior in vitro and in vivo activities. Such a biparatopic ADC presents its potential to be a best-in-class ADC therapy by overcoming the limitation of the monospecific ADC therapy such as drug resistance.

#3137 Development of AT2604, a highly efficacious ADC targeting alkaline phosphatases ALPP and ALPPL2.

B. K. S. Yeung, X. Koh, W. Ling, W. Tan, Y. Wu, X. Zhang, H. Tan, S. Liu, C. Zhong, B. Zou;
Axcynsis Therapeutics, Singapore, Singapore

Placental alkaline phosphatases, ALPP and ALPPL2, are highly homologous, membrane-bound proteins involved in fetal development. Despite having limited expression in normal tissues, they are highly differentiated in tumor cells making them ideal targets for antibody drug conjugate (ADC) development.
AT2604 is an ADC that consists of a humanized IgG1 anti-ALPP/ALPPL2 antibody that displays specificity over other human alkaline phosphatases and is cross reactive to NHP ALPPL2 but not to murine ALPPL2. The anti-ALPP/ALPPL2 antibody shows high target binding affinity and internalization into ALPP and ALPPL2 positive cells. AT2604 utilizes AxcynCYS™ technology for site-specific conjugation to achieve a highly homogeneous (>97%) DAR4 ADC product. The payload is the clinically validated microtubule disrupting agent monomethyl auristatin E (MMAE) conjugated to the antibody via a protease-cleavable peptide linker approved for ADC use.
When evaluated in mouse xenograft models of gastric (NCI-N87) and pancreatic (HPAC) cancer, AT2604 displayed strong tumor growth inhibition (>90%) at 1 mg/kg (QW3x2 dosing) in both models. Furthermore, a pre-tox study in non-human primates concluded AT2604 has a HNSTD of 10 mg/kg (QW3x3 dosing) and did not exhibit any non-reversible adverse effects; implying that AT2604 possesses an improved safety profile over other vedotin-based ADCs. Taken together, the data supports the continued development of AT2604 towards evaluation in human trials.

#3138 Discovery of AT65474, a highly selective anti-CLDN6 ADC with a proprietary payload.

C. Zhong, Y. Wu, X. Zhang, Y. Cheng, Q. Wang, P. Du, S. Liu, B. Zou;
Axcynsis Therapeutics, Singapore, Singapore

CLDN6 is a membrane-bound oncofetal protein and a promising target for cancers such as ovarian and testicular cancer. CLDN6 shares high sequence homology with other CLDN family members which are expressed in normal tissues, making a high degree of selectivity required for CLDN6-targeting therapies. In particular, CLDN6 is closest to CLDN9 in sequence with a difference of only three residues in the extracellular loops, making it challenging to generate a highly selective antibody.

We report the development of a humanized anti-CLDN6 antibody with high affinity and high selectivity for targeted cells which displays > 800-fold higher binding affinity for CLDN6 over CLDN9. The antibody was refined for use as an ADC and incorporates AxcynCYS^{TM} technology for site-specific conjugation which can reproducibly achieve high DAR4 ratios of greater than 97% by HIC analysis. AT65474 is an ADC candidate that incorporates a proprietary payload derived from an FDA approved drug that was optimized in-house for increased potency and improved PK properties to limit systemic exposure. In vitro, the payload displays broad sub-nanomolar activity across a wide range of cancer cell lines including those resistant to paclitaxel, DM1, MMAE and DXd. The payload is conjugated via an enzyme-cleavable linker optimized for solubility, stability, and high drug to antibody ratios.

We provide evidence characterizing AT65474 as a highly potent ADC with high DAR4 homogeneity and strong in vivo activity at low doses. Compared with a benchmark ADC in clinical development, AT65474 shows stronger binding, higher internalization, superior in vitro cytotoxicity, and stronger bystander killing effect. When evaluated in PA-1 and OV90 xenograft models of ovarian cancer, AT65474 displays significantly higher efficacy over the benchmark ADC. Furthermore, we show that AT65474 displays an ADCC effect that contributes to tumor suppression in the OV90 model. AT65474 was shown to be well tolerated in all xenograft mouse models and a pre-tox study in non-human primates. The combined data support further development of AT65474.

#3139 BL-M11D1, a novel CD33-targeting ADC, demonstrates robust anti-tumor efficacy in preclinical evaluation.

W. Wan[1], S. Zhao[1], S. Zhuo[1], Y. Zhang[1], L. Chen[1], R. Li[1], **J. S. Khalili**[2], X. Sa[1], Y. Yan[2], X. Shen[1], Y. Zhu[2];
[1]Sichuan Baili Pharmaceutical Co., Ltd., Chengdu, China, [2]SystImmune Inc., Redmond, WA

CD33, is a transmembrane receptor expressed on cells of myeloid lineage. It is therapeutically targeted in cancer due to overexpression broadly among hematopoietic malignancies including AML. To develop a promising therapeutic anti-tumor agent, we generated BL-M11D1, a CD33-Ed-04 ADC. It is built on gemtuzumab, a specific monoclonal antibody against CD33, having a wt Fc that can mediate ADCC in vitro. BL-M11D1 is composed of gemtuzumab, a cathepsin B cleavable linker, and a novel topoisomerase I inhibitor agent (Ed-04). The novel Ed-04 is a derivative of the alkaloid camptothecin and mediates cell cycle arrest at the S phase and subsequent apoptosis. BL-M11D1 achieves a high drug-to-antibody-ratio (DAR=8) with a highly stable linker and is readily internalized and trafficked to lysosomal cellular compartments. The antitumor efficacy of BL-M11D1 was evaluated in xenograft tumor models. BL-M11D1 exhibited strong tumor inhibition capacity toward the human hematopoietic malignancies engrafted xenograft models. In summary, these studies suggest BL-M11D1, a novel CD33-targeting ADC, is potentially efficacious in the treatment of CD33-expressing disease. The clinical phase I trial is being undertaken to evaluate safety, dosing and observations of preliminary signs of efficacy.

#3140 BL-M05D1, a novel claudin 18.2-targeting ADC, demonstrates specific potent anti-tumor efficacy in preclinical evaluation.

W. Wan[1], K. Dinkel[2], A. Sanford[2], S. Zhao[1], S. Zhuo[1], Y. Zhang[1], L. Chen[1], R. Li[1], **J. S. Khalili**[2], X. Sa[1], Y. Yan[2], X. Shen[1], Y. Zhu[2];
[1]Sichuan Baili Pharmaceutical Co., Ltd., Chengdu, China, [2]SystImmune Inc., Redmond, WA

Claudin 18.2, is a member of the tight junction protein family, and an isoform of claudin18. It is therapeutically targeted in cancer due to its limited expression in normal tissue and prevalent expression in a variety of human carcinomas. To develop a promising therapeutic anti-tumor agent, we generated BL-M05D1, an anti-Claudin 18.2-Ed-04 ADC. It is comprised of a novel, specific monoclonal antibody against Claudin 18.2 (5103F3), having a wt Fc that can mediate ADCC and CDC in vitro. BL-M05D1 is composed of (5103F3), a cathepsin B cleavable linker, and a novel topoisomerase I inhibitor agent (Ed-04). The novel Ed-04 is a derivative of the alkaloid camptothecin and mediates cell cycle arrest at the S phase and subsequent apoptosis. BL-M05D1 achieves a high drug-to-antibody-ratio (DAR=8) with a highly stable linker and is readily internalized and trafficked to lysosomal cellular compartments. The antitumor efficacy of BL-M05D1 was evaluated in xenograft tumor models. BL-M05D1 exhibited strong tumor inhibition capacity toward the human gastric cancer cell MKN-45-Claudin18.2 (#C11D) xenograft model, and human pancreatic cancer cell Patu8988s-Claudin18.2 (#C7G) xenograft model. In summary, these studies suggest BL-M05D1, a novel Claudin 18.2-targeting ADC, is potentially efficacious in the treatment of Claudin 18.2-expressing carcinomas. The clinical phase I is being undertaken to evaluate safety, dosing and observations of preliminary signs of efficacy.

#3141 LCB02A an antibody drug conjugate (ADC) targeting CLDN18.2 expressing solid tumors.

E. Baek, C.-W. Chung, C. Park, T. Jang, Y. Jeong, S.-A. Lee;
LegoChem Biosciences, Yuseong-gu, Korea, Republic of

Claudin18.2 (CLDN18.2) is an isoform of CLDN18 with very limited expression in gastric epithelial cells in normal tissues, and aberrant overexpression in gastric, pancreatic, esophageal, ovarian, lung, and other solid tumors. This expression pattern presents a significant hurdle in developing an ADC targeting CLDN18.2 due to potential on-target toxicity to the gastrointestinal (GI) tract. LCB02A is an antibody-drug conjugate (ADC) that targets CLDN18.2, composed of a topoisomerase 1 inhibitor (TOPO1i) as payload (DAR4) linked to the CLDN18.2 specific binding PR301839 hClaudin18.2 (CLDN18.2) is an isoform of CLDN18 with very limited expression in gastric epithelial cells in normal tissues, and aberrant overexpression in gastric, pancreatic, esophageal, ovarian, lung, and other solid tumors. This expression pattern presents a significant hurdle in developing an ADC targeting CLDN18.2 due to potential on-target toxicity to the gastrointestinal (GI) tract. LCB02A is an antibody-drug conjugate (ADC) that targets CLDN18.2, composed of a topoisomerase 1 inhibitor (TOPO1i) as payload (DAR4) linked to the CLDN18.2 specific binding PR301839 humanized IgG1 antibody utilizing LegoChem Biosciences' *ConjuAll*^{TM} technology. LCB02A showed potent *in vitro* cytotoxicity in CLDN18.2 expressing gastric and pancreatic cancer cell lines. LCB02A also showed excellent anti-tumor efficacy in various gastric and pancreatic cell line-derived xenograft (CDX) models and patient-derived xenograft (PDX) models. Preliminary toxicity assessment in cynomolgus monkeys (CLDN18.2 cross-reactive species) demonstrated that LCB02A was well tolerated, with repeat doses of up to 60 mg/kg. In conclusion, LCB02A is a promising ADC for the treatment of CLDN18.2 expressing solid tumors including gastric cancer (GC) and pancreatic ductal adenocarcinoma (PDAC). umanized IgG1 antibody utilizing LegoChem Biosciences' *ConjuAll*^{TM} technology. LCB02A showed potent *in vitro* cytotoxicity in CLDN18.2 expressing gastric and pancreatic cancer cell lines. LCB02A also showed excellent anti-tumor efficacy in various gastric and pancreatic cell line-derived xenograft (CDX) models and patient-derived xenograft (PDX) models. Preliminary toxicity assessment in cynomolgus monkeys (CLDN18.2 cross-reactive species) demonstrated that LCB02A was well tolerated, with repeat doses of up to 60 mg/kg. In conclusion, LCB02A is a promising ADC for the treatment of CLDN18.2 expressing solid tumors including gastric cancer (GC) and pancreatic ductal adenocarcinoma (PDAC).

#3142 NN3201, a novel c-Kit targeting ADC, exhibits robust preclinical anti-tumor efficacy in SCLC and GIST models.

C. Kim, J. Cho, T. Wi, J. Moon, H.-J. Ko, J. Lee, J. Park, Y. Lee, S. Kim, J.-O. Kim, **J. Song**, S.-H. Lee, S. Park;
Novelty Nobility, Inc., Seongnam-si, Korea, Republic of

c-Kit (CD117) is a type III receptor tyrosine kinase (RTK), which is known to be activated upon binding to its cognate ligand stem cell factor (SCF) to induce critical signaling pathways involved in cell proliferation, survival, and differentiation. Indicative of poor prognosis, overexpression and activating mutations of c-Kit have been implicated in a variety of human cancers including small cell lung cancer (SCLC), gastrointestinal stromal tumors (GIST), and acute myelogenous leukemia (AML). While imatinib, a small molecule c-Kit inhibitor, has been a beneficial treatment for GIST, resistance eventually develops to the drug, moreover, shows limited efficacy in c-Kit overexpressing tumors such as SCLC. Herein, we developed NN3201, a novel c-Kit targeting antibody-drug conjugate (ADC), comprised of fully human 2G4 antibody with a picomolar binding affinity to c-Kit and cytotoxic monomethyl auristatin E (MMAE) as the payload. NN3201 displayed potent *in vitro* cytotoxicity in various wild-type and mutant c-Kit positive SCLC and GIST cell lines with IC_{50} in the nanomolar range. In addition, NN3201 was rapidly internalized and inhibited c-Kit-mediated signaling., NN3201 treatment resulted in the increased proportions of the sub G1 and G2/M in the c-Kit positive cancer cell lines, indicating that release of MMAE induced cell cycle arrest. Moreover, bystander effect was confirmed by co-culturing c-Kit high and negative cell lines. Most importantly, in mouse xenograft models, NN3201 showed a remarkable tumor growth inhibition of several wild type, mutant c-Kit positive, and imatinib resistant SCLC and GIST cell lines. Enhanced anti-tumor activity and delayed tumor growth were observed in an SOC-treated (etoposide and carboplatin) SCLC xenograft model, by NN3201 in comparison to second line SOC (topotecan or irinotecan). In the GLP study, repeated intravenous administration of NN3201 was well tolerated at all doses (0.5, 1, 2 mg/kg Q3Wx3) without unscheduled death. Dose-dependent, yet transient, cytotoxicity of NN3201 was observed in the bone marrow. We confirmed HNSTD (Highest Non-Severely Toxic Dose) of NN3201 to be 2 mg/kg through exploratory and GLP repeat dose toxicity studies as no serious irreversible toxicity was observed. Accumulating data suggest that NN3201 is a promising therapeutic alternative for the treatment of SCLC and GIST regardless of wild-type or activating mutations in c-Kit.

#3143 The ADC payload PNU-159682 is highly active in a wide range of cancer indications by inducing DNA damage and cell death via a distinct mode of action.

M. Kaiser[1], U. Fiedler[1], D. Gerlach[2], N. Kraut[2], L. Bammert[1];

[1]NBE Therapeutics, Basel, Switzerland, [2]Boehringer Ingelheim, Vienna, Austria

During the last decade antibody-drug-conjugates (ADCs) have become an important and validated treatment modality for cancer patients. Here, we introduce a unique next generation ADC platform based on Sortase-mediated antibody conjugation (SMAC-Technology) yielding in very homogenous and stable drug conjugates with limited systemic, but powerful anti-tumor activity. The highly potent payload used is a proprietary derivative of the Anthracycline PNU-159682. Our PNU-159682-based ADCs are known to not only induce DNA damage in the target cell, but importantly also trigger immunogenic cell death and thus, stimulating anti-tumor immunity offering untapped combination potential. ADCs based on the SMAC-Technology platform currently undergo clinical development. In this work, we present functional studies that were performed to further elucidate the mode of action (MoA) of the ADC payload PNU-159682 and to investigate any potential liabilities with respect to sensitivity, which could limit treatment options for cancer patients. Flow cytometry-based readouts verified that PNU-EDA, a derivative of PNU-159682, is a highly potent inducer of DNA damage, cell cycle arrest and cell death. Interestingly, PNU-EDA arrests cells and inhibits DNA synthesis in S-phase in contrast to other Anthracyclines such as Doxorubicin, which leads to a block in the G2/M-phase. High-throughput cell line panel sensitivity screens confirmed that the activity of PNU-EDA is broad and not restricted to specific cancer indications. Notably, a correlation between lower potency and increased ABCB1 (MDR1) expression levels was observed for PNU-EDA, but not for parental PNU-159682. More detailed mechanistic insights were obtained by performing a genome-wide CRISPR-Cas9 KO screen, which revealed a partial dependency of the PNU-EDA potency on the proficiency of the TC-NER DNA damage repair mechanism. This finding further highlights a distinct MoA of PNU-159682 compared to Doxorubicin or other DNA-targeting compounds such as Cisplatin. Overall, our screens and mechanistic studies verified that PNU-159682-based ADCs efficiently kill cancer cells via a particular MoA and thereby, offer highly promising therapeutic options to a diverse and large population of cancer patients.

#3145 HRA00242-C004, a novel anti-PSMA ADC with high DAR reveals potent *in vitro* and *in vivo* anti-tumor efficacy.

G. Lin, H. Zhang, Z. Xu, L. You, Z. Xue, Y. Mao, X. Yang, B. Hu, S. Lin, J. Feng, Z. Zhang, X. Ye, M. Hu, F. He;
Shanghai Hengrui Pharmaceutical Co., Ltd., Shanghai, China

Prostate cancer (PCa) is the second most common cancer, and it is the fifth leading cause of cancer-related death among men. The incidence rates of PCa are 37.5 per 100,000 in developed countries and 11.3 per 100,000 in developing countries, while mortality rates are 8.1 per 100,000 in developed countries and 5.9 per 100,000 in developing countries[1]. As androgen receptor (AR) signaling plays an essential role in PCa initiation and disease progression, androgen deprivation therapy (ADT) has been a backbone of treatment for patients with advanced disease[2]. However, patient responses to ADT vary, and most patients eventually develop castration-resistant prostate cancer (CRPC) which remains large unmet clinical need[3]. Prostate-specific membrane antigen (PSMA), a transmembrane glycoprotein located on the cell membrane, is specifically and highly expressed in PCa with an extremely low expression level in non-prostatic tissues[4], which makes it an ideal target for the treatment of PCa[5].Here, we presented a PSMA-directed ADC, HRA00242-C004, which features a differentiated topoisomerase I inhibitor payload DXh conjugated via a cleavable linker to a humanized anti-PSMA IgG1 antibody (HRP04732). HRP04732 showed good binding affinity in both protein and cell-level assays, and a better cell internalization profile when compared with the reference antibody (AB-PG1-XG1-006, published sequences from US8114965B2). HRA00242-C004 exerted strong inhibition effect on cell lines with different PSMA expression levels. *In vivo* efficacy study, HRA00242-C004 showed potent anti-tumor activity in PSMA medium expression human prostate cancer 22RV1 xenograft model without significant weight loss during the experiments. Moreover, HRA00242-C004 demonstrated satisfactory PK profiles in SD rats and cynomolgus monkeys without any toxicity observed in PK assays. Compared with AB-PG1-XG1-006-DXh (the reference ADC), HRA00242-C004 exhibited a longer elimination half-life as well as higher serum exposure level of both the total antibody and the intact ADC. Meanwhile, as employing the same linker-payload as SHR-A1811, HRA00242-C004 has potential good plasma stability which was consistent with the results of PK study. In summary, with a highly permeable payload, high DAR, potent *in vitro* and *in vivo* anti-tumor efficacy, HRA00242-C004 demonstrated the best-in-class potential.

1.CA Cancer J. Clin. 2021, 71, 209-249.2.Nat. Rev. Urol. 2019, 16, 645-654.3.J. Clin. Oncol. 2015, 33, 1151-1156.4.World J Surg. 2006; 30: 628-36.5.Front Oncol. 2018; 8: 653-63.

#3146 HRA00130-C004, a novel anti-DLL3 ADC with bystander effect, high DAR and favorable safety profiles.

Q. Yao, C. Xue, Z. Xu, L. You, Z. Xue, Y. Mao, S. Lin, J. Feng, Z. Zhang, X. Ye, M. Hu, F. He;
Shanghai Hengrui Pharmaceutical Co., Ltd., Shanghai, China

Small Cell Lung Cancer (SCLC) is a highly aggressive neuroendocrine tumor, accounting for ~15% of all new lung cancer cases[1]. It is estimated that there are 250,000 new SCLC cases and at least 200,000 deaths globally each year[2]. SCLC exhibits high recurrence after first-line treatment, poor response to subsequent therapies, and rare survival[3]. Lacking of recommended treatments for prolonging survival remains a problem over decades[4]. DLL3 is an inhibitory ligand of the Notch receptor. It binds to its Notch receptor through a cis-interaction, thus, mediates inhibition of Notch pathway to facilitate neuroendocrine tumorigenesis[5]. DLL3 is highly upregulated and aberrantly expressed on the cell surface in SCLC and other high-grade neuroendocrine tumors with limited expression in normal tissues[6].Here we presented a DLL3-directed ADC, HRA00130-C004, which features a differentiated topoisomerase I inhibitor payload DXh conjugated via a cleavable linker to a humanized IgG1 antibody. HRA00130-C004 strongly inhibited the proliferation of cell lines with different DLL3 expression. In the bystander killing assays, HRA00130-C004 was able to kill both DMS53 cells (DLL3 over-expressed) and U-2OS (DLL3-negative) cells when they are co-cultured. The *in vivo* treatment of HRA00130-C004 resulted in a dramatic and sustained inhibition of tumor growth in H1184 (DLL3 high) and DMS53 (DLL3 low) xenograft models. No obvious weight loss was observed during the experiment. Furthermore, HRA00130-C004 demonstrated a favorable PK profile and satisfactory molecular integrity in rats with 3mg/kg dosing and cynomolgus monkeys with 10 mg/kg dosing. The exposure of total antibody and intact ADC was consistent. Moreover, HRA00130-C004 was well tolerated in rats and cynomolgus monkeys with no related adverse findings, which indicated its favorable safety profiles. In summary, taking advantage of Hengrui's DXh platform, HRA00130-C004 has demonstrated great potency and good safety profiles. These data support the future clinical development of HRA00130-C004.

1.CA Cancer J. Clin., 2018, 68, 7; 2.J. Natl. Compr. Cancer Netw. 2018, 16, 1171; 3.Mol. Ther. Oncolytics, 2021, 20, 470; 4.Journal of Cancer, 2022, 13, 2945; 5.Cellular Oncology, 2019, 42, 261; 6.Journal of Hematology and Oncology 2019, 12, 61;

#3147 DXC025, a novel anti-MUC1/EGFR bispecific antibody-tubulysin conjugate with a function linker, exhibits potent anti-tumor efficacy.

Xingyan Jiang, Junxiang Jia, Huihui Guo, Xiangfei Kong, Yongfang Xu, Sishi Ye, Yong Du, Zhicang Ye, Qikuang Cen, Lingli Zhang, Yongxiang Chen, Gaituo Chen, Lu Bai, Yunxia Zheng, Wei Zheng, Jun Zheng, Juan Wang, Wenjun Li, Yuanyuan Huang, Linyao Zhao, Yifang Xu, Mengmeng Liu, Binbin Chen, Meng Dai, Miaomiao Chen, Zhixiang Guo, Qingliang Yang, **Robert Y. Zhao**

Hangzhou DAC Biotechnology Co., Ltd., Hangzhou City, China

Antibody-drug conjugates (ADCs) have become a promised drug class in cancer therapy. Armed with three main components-an antibody, a linker molecule, and a cytotoxic agent (“payload”), plus sites of the antibody conjugation and the distribution of tumor-associate antigens, nowadays ADCs have proved the unique ability of the precision of targeted therapy, a great leap forward from traditional chemotherapeutic approaches that cause widespread effects without specificity. Both epidermal growth factor receptor (EGFR) and mucin 1 (MUC1) are tumor-associated antigens (TAA) that are co-expressed in many solid tumors, such as, colon cancer, non-small cell lung cancer (NSCLC), esophageal cancer, epidermal cancer, and pancreatic cancer. In particular, MUC1, a glycoprotein essential for the formation of the epithelial mucous barrier, is hypoglycosylated and dimerizes with EGFR, a potent oncoprotein, in transformed cells. For our anti-Muc1 ADC clinical program, for treatment of colon and pancreatic cancers, it was found out that the highly glycosylated transmembrane Muc1 had much more turning over rates on the luminal surface of epithelial cells. Here, we first designed and generated bispecific Fab/scFv antibodies targeting both MUC1 and EGFR, using the knob-into-hole technology. The addition of the affinity- and internalization-optimized anti-EGFR arm to the other single Muc1 arm was aimed to broaden tumor selectivity and to reduce on-target toxicity, for the treatment of gastrointestinal tumors in comparison to individual full IgG1-ADC, either EGFR or Muc1-ADC. Indeed, many of generated anti- MUC1/EGFR bispecific antibodies (BsAbs) showed strong binding affinity in $MUC1^{modetate}EGFR^{modetate}$ cells, in addition to both MUC1 and EGFR highly expressed cells. Internalization assays demonstrated that the BsAbs were endocytosed in tumor cells co-expressing EGFR and MUC1 more efficiently than monoclonal antibodies targeting MUC1. The selected BsAbs were subsequently conjugated with tubulysin B analogs with varieties of Tubulysin B analog payloads and function peptidyl spacer/linkers to generate bispecific ADC (DXC025) candidates. DXC025 candidates exhibited very potent cytotoxicity in vitro against epidermal cancer, lung adenocarcinoma, and pancreatic cancer cell lines with IC_{50} of single or tens digital pM. In in vivo cell-derived xenograft (CDX) models, DXC025 candidates demonstrated much superior efficacies of tumor growth inhibition in comparison with parental (monoclonal), either Muc1- or EGFR- ADC for the treatment of gastrointestinal tumors. These results indicated that the MUC1/EGFR-ADC (DXC025) would be a promising ADC candidate for targeted treatment of either Muc1- or EGFR-expressing gastrointestinal tumors.

#3148 ABBV-706 is a novel SEZ6-targeted topoisomerase 1 inhibitor ADC for SCLC and other neuroendocrine cancers.

E. J. Faivre[1], M. A. Pysz[2], E. O hAinmhire[1], L. Kreckler[1], K. Doyle[1], A. D'Souza[2], Z. Ding[2], T. Sondkar[2], D. Maji[2], F. Zhao[1], A. Phillips[1];
[1]AbbVie Inc., North Chicago, IL, [2]AbbVie Inc., South San Francisco, IL

Lung cancer has the highest rates of incidence (2.1 million cases/year) and mortality (1.8 million deaths/year) among all cancers worldwide. Approximately 15% of lung cancers are small cell lung cancer (SCLC). SCLC is typically diagnosed at late stages, with approximately 70% of patients having extensive stage disease at time of diagnosis. Unfortunately, these patients have a dismal 5-year survival rate of approximately 3%. In contrast to non-small cell lung cancer (NSCLC), there has been little advancement in the treatment of SCLC, with no biomarker directed therapies available for patients. SEZ6 is overexpressed in most SCLC's and other neuroendocrine tumor types. This overexpression and limited normal tissue expression suggest SEZ6 would be a good target for the development of an antibody drug conjugate (ADC). Validation of SEZ6 as an ADC target was supported by signs of clinical activity for ABBV-011, a SEZ6-targeting calicheamicin ADC. Preclinical and clinical data suggest an increased therapeutic index for Top1i ADCs relative to calicheamicin ADCs. Furthermore, Top1i inhibition is an effective mechanism of action in SCLC with topotecan approved in 2L, although significant toxicity limits broad utility. As such, we hypothesized that a SEZ6-Top1i ADC would enable effective Top1 inhibition in tumor cells and reduce toxicity relative to ABBV-011 or systemic chemotherapy, driving increased therapeutic benefit. ABBV-706 is an ADC comprised of the same SEZ6 targeting antibody as ABBV-011 conjugated to AbbVie's topoisomerase-1 (Top1) inhibitor. ABBV-706 is a potent anti-proliferative agent in SEZ6 positive SCLC cell lines, with sub- to low-nanomolar activity. SEZ6 dependence was demonstrated by the correlation of SEZ6 mRNA expression to ABBV-706 growth inhibition. On-target Top1i activity was confirmed in cells treated with ABBV-706 as measured by dose-dependent induction of γ-H2AX, a marker of DNA damage, and G2/M arrest. ABBV-706 possessed superior anti-tumor activity compared to ABBV-011 in a panel of SCLC cell line-derived xenograft (CDX) and patient-derived xenograft (PDX) models with a range of SEZ6 expression levels. In addition, ABBV-706 had activity in the setting of resistance to cisplatin/etoposide (1L SoC in SCLC), in combination with cisplatin, and in SEZ6-expressing neuroendocrine liver and cervical PDX models. ABBV-706 has favorable pharmacokinetics and is well-tolerated in cynomolgus monkeys with bone marrow and gastrointestinal tract toxicities common to other Top1 inhibitors. ABBV-706 shows promise as an agent for the treatment of SCLC and other difficult to treat SEZ6 expressing neuroendocrine tumors. ABBV-706 has completed dose escalation, and dose expansion is currently ongoing in a Phase 1 FIH clinical study (NCT05599984).

#3149 Development of a novel site-specific ADC glycan platform with potential for improved *in vivo* efficacy and stability of the ADC in animal studies.

T.-Y. Huang, Y.-C. Hsieh, K.-S. Fung, Y.-C. Huang, C.-S. Shia, M.-F. Chiang, N.-H. Wang, W.-F. Li, M.-T. Lai;
OBI Pharma, Inc., Taipei, Taiwan

Antibody-drug conjugates (ADCs) represent a promising modality for delivering cytotoxic drugs to targeted tumor cells while avoiding off-tumor toxicities. Despite successes in the past 20 years, development of effective ADCs with broad therapeutic window remains challenging due to the complexity of conjugation technologies and the instability of the linkers. Most platforms currently in the market as well as under clinical development may face limitations ascribed to the heterogeneity of ADCs with various drug-to-antibody ratio (DAR). This likely resulted from random conjugation and poor overall biophysical characteristics caused by linker hydrophobicity. The limitations may impact the efficacy, safety, bioavailability, and the robustness of manufacturing process of these therapeutic agents. OBI developed a unique glycan ADC platform (GlycOBI) to enable a site-specific conjugation, which is in a 'Plug and Play' format and compatible with any antibodies, linkers, and payloads in various DAR. This is an efficient and scalable process to generate homogenous ADCs. This platform overcomes the limitations of traditional ADCs, resulting in the improvement of efficacy and stability. We developed a non-genetic, engineering-free approach to generate site-specific homogenous ADCs. This was achieved by utilizing OBI proprietary enzymatic technology (EndoSymeOBI), followed by the click chemistry to conjugate the hydrophilic linker-payload via the glycan site that naturally occurs on the antibody's Fc region. The conjugation process avoids disrupting the antibody structure, ensuring the related ADC has similar biophysical characteristics compared to native antibody. Furthermore, OBI linker technology improves the conjugation efficiency of the payload, as well as reduces the aggregation propensity, and expands the half-life of the ADC products. Anti-TROP2 and anti-HER2 ADCs are developed based on OBI glycan ADC platform (GlycOBI) using a topoisomerase I inhibitor, exatecan, as the payload. Both ADCs demonstrated greater chemical stability in serum stability studies compared to competitor ADCs. Additionally, they showed broad activity against different cancer cell lines in vitro as well as in mouse xenograft models. The preclinical data presented here suggest that GlycOBI is an outstanding ADC platform to improve the performance of ADCs. Further investigations, including studies in the clinical settings, are warranted.

EXPERIMENTAL AND MOLECULAR THERAPEUTICS: Cancer Biology and Metastasis
Poster Session

#3153 Regulation of ATF4-mediated stress responses by NUAK2 in ovarian cancer.

Li Chen[1], Oscar GW Wong[1], Claire LY Cheung[1], Esther SY Wong[1], Karen KL Chan[2], Hextan YS Ngan[2], **Yusanne YS Chan**[1], Annie NY Cheung[1]

[1]Department of Pathology, The University of Hong Kong, Hong Kong, China, [2]Department of Obstetrics & Gynaecology, The University of Hong Kong, Hong Kong, China

NUAK family kinase 2 (NUAK2) a member of the AMPK-related serine/threonine kinase family with crucial roles in various cancer cellular processes. The aim of this study was to elucidate the expression and functions of NUAK2 in ovarian cancer while investigating the underlying molecular mechanisms. Analysis of several publicly available databases suggested a significant increase in NUAK2 mRNA levels in ovarian cancer compared to normal tissue. The overexpression of NUAK2 in ovarian cancer was confirmed by immunohistochemistry of NUAK2 in our local collection of ovarian tumor tissues comprised of carcinomas of various histological types (N=88) as well as benign and borderline tumors (N=19). Intense nuclear NUAK2 immunoreactivity was observed in serous and clear-cell carcinomas. Furthermore, nuclear expression of NUAK2 was significantly correlated with higher tumor grade and poorer overall and disease-free survival. Knocking out NUAK2 in SKOV3 cells by CRISPR-Cas9 resulted in suppressed cell growth and migration. Transcriptome by RNA sequencing and pathway enrichment analysis of SKOV3 cells overexpressing NUAK2 revealed activation of activating transcription factor 4 (ATF4) -dependent unfolded protein response (UPR) in the cell. NUAK2 knockout exaggerated the reactive oxygen species level induced by the endoplasmic reticulum (ER) stress inducer tunicamycin treatment. NUAK2 upregulated ATF4 protein expression during ER stress, facilitating its translocation into the nucleus upon exposure to tunicamycin. SKOV3 with NUAK2 knockout grew significantly slower than its parental line in mice as demonstrated by *in vivo* imaging. Collectively, our study highlights NUAK2 as an oncogene in ovarian cancer and underscores its involvement in the UPR pathway.

#3154 The role of nuclear kinases in pancreatic carcinogenesis.

K. LaRue[1], A. Sigafoos[2], L. Flores[1], B. Tader[1], M. Fernandez-Zapico[1];
[1]Mayo Clinic Graduate School of Biomedical Sciences, Rochester, MN, [2]Mayo Clinic Department of Oncology, Rochester, MN

Pancreatic ductal adenocarcinoma (PDAC), the most common histological subtype of pancreatic cancer, is a devastating disease predicted to be the second leading cause of cancer deaths in the next 15 years. Thus, there is an urgent need to develop new treatment approaches based on a better understanding of cellular and molecular mechanisms controlling this dismal progression. PDAC development is marked by nuclear morphological changes likely resulting in changes in chromatin organization and gene expression. Oncogenic KRAS, present in more than 90% of tumors, plays a key role in disease initiation and progression and is sufficient to induce these nuclear morphology changes. Work from our lab has identified the nuclear lamina protein Emerin as a mediator of KRAS-induced nuclear morphology changes. Further, a BioID experiment identified a KRAS-induced interaction of Emerin with a group of nuclear kinases belonging to the ribosomal S6 kinase (RSK) and mitogen- and stress- activated protein kinase (MSK) families. *In silico* analysis identified candidate MSK and RSK phosphorylation sites in Emerin. Thus, we hypothesize that the nuclear kinase families RSK and MSK can act as effectors of the KRAS-Emerin axis to regulate PDAC nuclear morphology. Further studies will be done to confirm if Emerin can be phosphorylated by RSK and MSK, and to validate that this relationship is dependent on oncogenic KRAS signaling and if its nuclear morphological changes are regulated by this GTPase. Overall, this work aims to define a novel signaling axis for RSK and MSK in controlling nuclear dynamics that play a role in disease progression of PDAC, which can lead to the identification of new therapeutic targets.

#3155 Metabolic stress induces an intrinsic inflammatory CAF phenotype that regulates stromal architecture in pancreatic cancer.

Y. Zhang[1], S. Maganti[2], J. Hope[2], L. Lin[2], C. Galapate[2], F. Carrette[2], L. Bradley[1], C. Commisso[2];
[1]Sanford Burnham Prebys Med. Discovery Inst., San Diego, CA, [2]Sanford Burnham Prebys Medical Discovery Institute, San Diego, CA

Macropinocytosis is a critical amino acid supply pathway that fuels the metabolism of tumor cells and cancer-associated fibroblasts (CAFs) in pancreatic ductal adenocarcinoma (PDAC). PDAC tumors are deficient in glutamine, a critical amino acid that tumor cells and CAFs use to sustain their cellular fitness. We have previously shown that both PDAC cells and CAFs stimulate macropinocytosis as an adaptive response to glutamine depletion. How these linked metabolic mechanisms might co-operate to control stromal architecture remains elusive. In this study, we employed glutamine starvation and 5-(N-ethyl-N-isopropyl)-amiloride (EIPA), a selective inhibitor of macropinocytosis, to investigate how metabolic stress impacts the tumor microenvironment. We find that concomitant suppression of glutamine metabolism and macropinocytosis synergizes to drive an intrinsic inflammatory CAF phenotype that requires metabolic stress-induced ERK/MAPK signaling. Utilizing immunocompetent syngeneic mouse models of PDAC, we find that blocking macropinocytosis in these glutamine-depleted tumors diminishes tumor growth and reorganizes the tumor stroma by decreasing collagen deposition, increasing vasculature expansion and enhancing the infiltration of both CD8+ and CD4+ T cells. Alterations in the stromal landscape under these conditions are linked to the enhancement of CAFs that display an inflammatory signature while simultaneously suppressing more myofibroblastic identities within the tumor. Interestingly, we find that these effects on the tumor microenvironment can be harnessed to improve therapeutic responses. We determine that combining macropinocytosis inhibition with immune checkpoint blockade reduces PDAC tumor burden and significantly inhibits metastasis. We also find that macropinocytosis inhibition enhances drug delivery, thereby improving the efficacy of gemcitabine chemotherapy. Our findings demonstrate that intratumoral metabolic stress plays a critical part in preserving and modulating the tumor stroma.

#3156 Unveiling the functional role of HDGFRP3 in pediatric medulloblastoma: Implications for growth, progression, and radioresistance.

S. S. R. Nirzhor, P. Pitta Venkata, S. Abdulsahib, P. Subbarayalu, S. Timilsina, M. K. Rao;
UT Health Science Center at San Antonio, San Antonio, TX

Introduction: Medulloblastoma (MB) is the most common malignant brain cancer in children. Although long-term survival has improved in recent years, only a modest percentage of patients survive high-risk disease. The quality of life for those who survive is substantially reduced due to the high toxicity associated with the radiation and chemotherapy. Therefore, identification of safe and potent therapeutic approaches that can sensitize the therapy response in MB without inducing toxicity will lead to more efficient treatment of MB patients. We recently discovered that targeting HDGFRP3, a protein highly expressed in MB, and can block MB growth and improve the efficacy of radiation therapy. HDGFRP3 is a multifaceted protein that plays important roles in diverse cellular processes. Our investigation sheds light on the functional role of HDGFRP3 in MB, focusing on its involvement in growth, progression, and radioresistance where we report HDGFRP3 as a novel oncogenic driver of these processes.
Methods: Human MB cell lines (DAOY, D556, D425, and HDMB03) were purchased from the American Type Culture Collection and cultured in standard medium. MB cancer cells were transfected with siRNA specific to HDGFRP3. These knockdown cells were analyzed for cell viability, migration, invasion, colony formation, stemness, cell cycle, apoptosis assays for functional role assessment. Real-time qPCR and western blotting were performed to validate the downstream targets of HDGFRP3 in MB models.
Results: Our findings demonstrate that HDGFRP3 functions as an oncogene in MB, as its overexpression promotes cancer growth, while its depletion results in decreased tumor growth in MB models. Furthermore, we provide evidence that HDGFRP3 knockdown results in decreased migratory potential of MB cells as well as a reduction in stemness. Interestingly, HDGFRP3 depletion improved the efficacy of standard of care radiation in multiple MB models. At present, in vivo studies are validate the oncogenic role of HDGFRP3 in preclinical animal models of MB.
Conclusions: In conclusion, our data suggests HDGFRP3 facilitates MB growth, progression, stemness as well as resistance to radiation therapy. Our comprehensive investigation into HDGFRP3's functional role in MB presented here provides valuable insights into its potential as a therapeutic target and opens avenues for further research into novel treatment strategies for the pediatric brain tumors.

#3157 The crosstalk between STAT3 and p53/ERK signaling regulates brain metastasis.

S. L. Zeller, E. Spirollari, J. V. Wainwright, S. J. Hanft, C. D. Gandhi, **M. Jhanwar-Uniyal**;
New York Medical College/WMC, Valhalla, NY

Brain metastasis (BM) affects approximately 10% of cancer patients with metastatic disease, representing a major cause of morbidity and mortality. BM is a complex multi-step process involving various immune checkpoint proteins. Mitogen-activated protein kinase (MAPK), particularly extracellular signal-regulated kinases 1/2 (ERK1/2), and signal transducer and activator of transcription 3 (STAT3) are implicated in tumorigenesis and are critical upstream regulators of Programmed Death Ligand 1 (PD-L1) expression, a common immunotherapy target. Tumor suppressor p53 is shown to regulate STAT3 and ERK1/2 signaling, which are dysregulated in various malignancies. We hypothesize that p53 along with STAT3 and ERK1/2 play a critical role in the initiation and maintenance of BM. Twenty-six BM tumors with various primary sites of origin were used following IRB guidelines. $pSTAT3^{Tyr705}$, $pERK1/2^{Thr202/Tyr204}$, mutant p53 ($p53^{mt}$), and PD-L1 expression was determined by immunohistochemistry. Gene expression analysis of BM was performed on a cDNA microarray. Human brain metastatic breast cancer cells (MDA-MB-231) were treated with STAT3 inhibitor (NSC74859) or MAPK inhibitor (U0126) in regular or astrocytic media to determine cell proliferation and migration by MTT assay and scratch-wound, respectively. ERK1/2 signaling pathway status was determined by Western blotting. Results demonstrated: 1) $pSTAT3^{Tyr705}$ and $pERK1/2^{Thr202/Tyr204}$ were expressed profusely at tumor margins, while $p53^{mt}$ was uniformly expressed throughout. 81% of BM expressed $p53^{mt}$ while 86% and 63% expressed $pERK1/2^{Thr202/Tyr204}$ and $pSTAT3^{Tyr705}$, respectively. Venn analysis displayed significant overlap between expression, with 62% overlap between $p53^{mt}$ and $pERK1/2^{Thr202/Tyr204}$ and a 50% overlap between both $pSTAT3^{Tyr705}$ and $pERK1/2^{Thr202/Tyr204}$ with $p53^{mt}$. Expression of PD-L1 was seen in a majority of BM tumors. 2) Gene expression analysis demonstrated alterations in 32 STAT3- and MAPK-associated genes; these included upregulation of stathmin-1 and stathmin-like 3, which control microtubule dynamics in STAT3-related cell migration, and changes in cytokine-related genes, suggesting altered immune responses. 3) Cell proliferation showed augmented growth in astrocytic media ($p \leq 0.05$) and was significantly decreased following treatment with NSC74850 or U0126 ($p \leq 0.01$). While migration showed a trend towards significance in reduction following NSC74859 ($p=0.08$), migration stagnated following U0126 treatment in astrocytic media ($p \leq 0.01$). 4) $pERK1/2^{Thr202/Tyr204}$ expression was reduced following U0126 or NSC74859 treatment. These findings suggest activation of STAT3 and ERK1/2 promote BM and suppression of these pathways may lead to a reduction in cell viability and motility. Therefore, this provides compelling evidence for the use of STAT3 and ERK1/2 along with p53 as potential targets for immunotherapy in brain metastatic disease.

#3158 TUSC2 suppresses energy metabolism in lung cancer cells with opposite effects in normal bronchial epithelial cells.

J. Tonello[1], M. Berger[2], A. Shanker[1], **A. Ivanova**[1];
[1]Meharry Medical College, Nashville, TN, [2]Geneprex, Inc, Austin, TX

Introduction: TUSC2 (TUmor Suppressor Candidate 2) is a tumor suppressor gene from the human 3p21.3 chromosomal region frequently deleted in lung cancers. Independently of deletion, reduced expression of TUSC2 is observed in ~ 80% of lung cancers, mesothelioma, breast, head-and neck, osteosarcoma, glioblastoma, and other cancers, suggesting a critical anti-tumor role of TUSC2. TUSC2 resides in mitochondria and is involved mitochondrial respiration/energy metabolism, ROS production, Ca^{2+} flux to/from mitochondria, etc. Studies on tumor-bearing mice treated with TUSC2-containing plasmid encapsulated in lipid nanoparticles (quaratusugene ozeplasmid) and Phase I and II clinical trials of quar oze in lung cancer patients provides a strong rationale to further study the tumor-protective mechanisms of TUSC2 protein. Main scientific question. We asked if and how human lung cancer cells, A549 and H358, that have ~80-90% decrease in TUSC2 expression, change their energy metabolism in response to re-introduction of TUSC2 as compared to Beas2B, a normal bronchial epithelial cell line. Cancer cells rely heavily on anaerobic glycolysis, while normal epithelial cells use mitochondrial respiration as a primary way of energy production.
Methods: Transient transfection of TUSC2-expressing plasmid to 3 cell lines; qPCR to confirm TUSC2 delivery; Seahorse analysis of energy production that measures in real time Oxygen Consumption Rate (OCR) and Extracellular Acidification Rate (ECAR) in different conditions.
Results: All three cell lines demonstrated high transfection efficiency. Seahorse analysis revealed that TUSC2 re-introduction to TUSC2-deficient cancer cells consistently suppressed both glycolytic and mitochondrial ATP production, thus leaving cells without sufficient energy to support their vital functions. We found a significant decrease in basal and maximal respiration, spare respiratory capacity, ATP production, glycolysis and glycolytic capacity in cancer cell lines transfected with TUSC2-expressing plasmid. Unlike cancer cells, both glycolytic and mitochondrial metabolism of normal epithelial cells Beas2B were significantly strengthened after the introduction of TUSC2, suggesting a beneficial role of TUSC2 for the metabolic health of normal cells. The experiments were repeated four times; Student T-test was used to calculate statistical significance.
Therapeutic Significance: These experiments suggest that TUSC2 plasmid delivery to cancer patients, and thus quar oze therapeutic use, may target and disrupt the metabolism of cancer cells, triggering either senescence or apoptotic pathways, while on the other hand, supporting the metabolism of normal epithelial cells. These data have high therapeutic significance, suggesting that one of the anti-tumor mechanisms of quar oze action in patients is the suppression of cancer cell metabolism resulting in cancer cell death.

#3159 *VHL1* activation with a CRISPR-based gene activation platform causes increased *MLKL* expression and triggers necroptosis in renal cell carcinoma.

M. S. Meng, R. M. Kemper, T. J. Nelson, N. A. Hathaway, D. J. Crona;
UNC Eshelman School of Pharmacy, Chapel Hill, NC

Background: Kidney cancer is a common and deadly disease. Over 90% of all kidney cancers are classified as renal cell carcinoma (RCC), of which clear-cell RCC (ccRCC) is the most predominant subtype. *VHL* is a tumor suppressor and plays a pivotal role in ccRCC development. While >50% of ccRCC patients present with pathogenic *VHL* mutations, deep deletions and low *VHL* expression are also common. Over the past two decades, therapeutic advances have been made for metastatic ccRCC; however, none directly target *VHL*, and the five-year overall survival for metastatic ccRCC remains ~12%. Here, we used a fusion protein, consisting of a deactivated Cas9 (dCas9) linked to the histone acetyltransferase protein p300, to determine if *VHL* activation initiates programmed cell death in a preclinical model of ccRCC.

Methods: Caki-1 cells are a human ccRCC line, are wild-type *VHL* with low-moderate expression. Caki-1 cells were stably transduced with our dCas9-p300 system via lentivirus, and then transfected with either sgRNAs targeting *VHL* or a non-targeting (NT) sgRNA. Ten targeting sgRNAs were designed, with eight starting within -120 bp from the *VHL1* transcriptional start site (chr3:10141778), and two starting within +50 bp after the TSS. *VHL* gene expression changes from baseline were evaluated by RT-qPCR at 8h, 24h and 48h after sgRNA transfection. At 24-72h, Caki-1 cells were harvested and stained with Annexin V and propidium iodide; apoptosis and necrosis were then assessed by flow cytometry. Last, to determine whether *VHL* reactivation triggered necroptosis, *MLKL* gene expression changes were evaluated by RT-qPCR at 8h, 24h and 48h.

Results: Four targeting sgRNAs met internal thresholds for evaluation within our dCas9-300 system: sgRNA3 bp), sgRNA4, sgRNA9, and sgRNA10. Significant increases in *VHL* expression were observed at 8h for sgRNA3 and sgRNA10 (62.4% and 56.5%, respectively; both $P<0.0001$, n=3), at 24h for all four sgRNAs (range 91.1-236.1%; all $P<0.0001$, n=3), and again at 48h for all four sgRNAs (range 84.4-194.4%; $P<0.0001$, n=3). At 48h and 72h, sgRNA4 (6.78% and 7.35%) and sgRNA9 (6.71% and 6.76%) showed evidence of necroptosis activation. sgRNA4 demonstrated significantly increased *MLKL* expression at 24h and 48h (199.6% and 144.6%; both $P<0.0001$, n=3) as did sgRNA9 (192.7% and 235.6%; both $P<0.0001$, n=3) suggesting necrosome activation.

Conclusions: To our knowledge, this is the first study to associate *VHL* reactivation with increased *MLKL* expression and necroptosis initiation. These data support continued development of an experimental system we have pioneered (PMID: 31712774), which will leverage chemical-induced proximity to reactivate *VHL*.

#3160 PufA promotes proliferation, migration and tumorigenesis through NF-kB pathway in cholangiocarcinoma.

C.-P. Chen[1], C.-N. Yeh[2], Y.-R. Pan[2], Y.-T. Hsiao[2], C.-H. Lo[2], C.-H. Lin[2], C.-E. Wu[1];
[1]Chang Gung University, Taoyuan City, Taiwan, [2]Chang Gung Memorial Hospital-Linkou branch, Taoyuan City, Taiwan

Cholangiocarcinoma (CCA) exhibits a poor prognosis despite the recent advances in targeted therapy and immunotherapy. Therefore, exploring the novel mechanism of CCA tumorigenesis and identifying the effective targeted therapy is critical for advanced CCA to improve future treatment. A novel biogenesis factor of the 90S pre-ribosome named PufA, is higher expressed in tumors than normal tissue based on the TCGA databank implying the role of CCA tumorigenesis. Our results showed that PufA expression was significantly associated with larger tumor size, more lymph node metastasis, more tumor relapse, death, and unfavorable survivals in 205 patients with resectable CCA in Chang Gung Memorial Hospital. We demonstrated the inhibited effect of cell survival, migration ability, and the sphere-formation potential by silencing of PufA in CCA cell lines. Tumor growth is also suppressed in PufA knockdown xenograft mice. Mechanistic investigation showed that PufA was expression associated with nuclear factor kappa B p65 (RELA) activity and facilitated activity of the NF-κB transactivation. RELA, a transcription factor, is the principal regulator of the inflammatory response and is crucial for the homeostasis of the immune system and the expression of the immune checkpoint. Furthermore, decreased PufA levels also downregulated PD-L1 expression in CCA. Together, these findings suggested that the PufA-RELA axis could be a potential target for further application of targeted therapy in combination with immunotherapy.

#3161 PCTK1 driven glutamine metabolic adaptation in brain metastasis.

L. Zhang[1], F. Lowery[2], C. Zhang[1], Y.-W. Huang[1], Y.-J. Jiang[1], Y. Duan[1], D. Yu[1];
[1]UT MD Anderson Cancer Center, Houston, TX, [2]NCI, Washington DC, DC

Brain metastasis (BrM) is the most common malignancy of the central nervous system and the median survival time of patients with BrM is less than 1 year. Although recent impressive advances in targeted therapy and immunotherapy enable more effective control of the systemic diseases, the incidence of BrM upon disease recurrence is steadily increasing. Unfortunately, there is no effective treatments for BrM. To surmount this challenge, we have performed an *in vivo* human kinome screening to uncover novel kinases that promote breast cancer (BC) BrMs in mice and may serve as therapeutic targets. We identified >20 different kinases enriched in BrM lesions of our mouse models and PCTK1 is one of the top “hits”. We transduced PCTK1 expression vector and the control vector into MDA-MB-231 human BC cells to generate 231.PCTK1 and 231.vector cells, respectively. Intra-carotid injection of the 231.PCTK1 cells into mice induced BrM significantly faster with shortened mouse survival than that of the control 231.vector cells, confirming PCTK1 as a BrM-promoting kinase. However, when 231.vector or 231.PCTK1 cells were injected into the mouse’ mammary glands, PCTK1 overexpression did not lead to enhanced primary tumor growth, suggesting that its pro-tumoral functions are BrM-specific. To uncover how PCTK1 promotes BrM but not primary tumor, we examined whether PCTK1 may confer growth advantage in BrM by utilizing the unique metabolic microenvironment of the brain. We analyzed the relationship between PCTK1 gene expression and gene expression of members of the glutamine metabolism pathway in TCGA database. We found that in the brain tumors, such as low-grade glioma, PCTK1 positively correlated with the expression of glutamine metabolizing genes, including glutaminase 1 and 2 (GLS and GLS2). To evaluate whether PCTK1-overexpressing cells can uptake glutamine from the media directly, we cultured 231.PCTK1 and 231.vector cells in low-nutrient BME media plus 5% d.FBS, with addition of different concentrations of glutamine. The PCTK1-overexpressing cells showed a clear growth advantage at glutamine concentrations ranging from 400 µM to 2 mM. Then, we knocked down PCTK1 in MDA-MB-231 cells by shRNAs and found that PCTK1 knocking down reduced the cell proliferation in 5% d.FBS.BME with 500 µM glutamine, a physiological glutamine level in the brain. We measured the expression of GLS, an enzyme that converts glutamine to glutamate, one of the key steps in the glutamine metabolism, and found that knockdown PCTK1 in MDA-MB-231 cells dramatically reduced the GLS expression, which indicates that PCTK1 can modulate glutamine metabolism in cancer cells. In summary, our data suggest that PCTK1 promotes BC BrM, at least partly, through increasing glutamine metabolism. Currently, we are exploring whether targeting PCTK1 or inhibiting glutamine metabolism can deter BrM progression. Our studies may reveal novel therapeutic targets for BrM inhibition.

#3162 Antagonizing beta-2 adrenergic receptor's function triggers death in glioma cells and down-regulates survivin.

O. Algranatti[1], J. Yae Lee[2], J. Angelastro[1];
[1]UC Davis School of Veterinary Medicine, Davis, CA, [2]UC Davis Graduate Studies, Davis, CA

Introduction: Epidemiological studies showed that beta-adrenergic antagonists caused a low incidence of several cancer types. Glioblastoma highly expresses beta-2-adrenergic receptors. GBM accounts for 50% of central nervous system cancers. After standard-of-care therapeutic intervention, there is a survival time of 15 months. Our goal is to develop a translational therapy that will trigger the death of GBM cells while preserving healthy cells
Methodology: Salmeterol xinafoate is a biased agonist that activates the G-protein pathway. Biased agonists activate signaling through the G-protein or the beta-arrestin pathway of G-protein coupled receptors. Dose-response experiments were performed using beta1 and beta2-adrenergic receptor antagonists and biased beta2-adrenergic receptor agonists to determine loss of glioma cell viability in GBM5, GBM12, and LN229 glioma cell lines. Western immunoblotting gauged survivin expression levels in all three lines. Epoxomicin was used to inhibit the proteasome complex. Annexin V and propidium iodide were employed to measure apoptotic or necrotic cell death.
Results: Disrupting beta2-adrenergic receptor signaling by salmeterol xinafoate led to cell death of glioma cells but spared healthy neuron-glia cells using similar doses. Salmeterol xinafoate revealed greater efficacy for killing glioma cells than beta1 and beta2-adrenergic receptor antagonists. To determine the mechanism of glioma cell death, LN229 cells were treated with escalating doses of Salmeterol xinafoate, and at 24 hours, annexin V staining showed early apoptosis, and Annexin V/propidium iodide co-staining also showed late apoptosis. Propidium iodide revealed minor necrosis in LN229 glioma cells. Western immunoblotting showed salmeterol xinafoate downregulated survivin in a dose-dependent manner. However, the epoxomicin's inhibition of the proteasome complex prevented dose-escalated downregulation of survivin for all three glioma cell lines.
Conclusion: The bitopic structure of salmeterol enables this drug to bind to the beta2-adrenergic receptors ligand binding site and an exosite site by its aryloxyalkyl tail that may contribute to the increased efficacy. Salmeterol xinafoate triggers glioma cell death by apoptosis at least in one glioma cell line. Salmeterol Xinafoate down-regulates survivin through protease degradation. Promising results show that the FDA-approved drug salmeterol xinafoate enables a favorable transition to the clinic. Repurposing this drug for GBMs may be combined with the current standard-of-care chemotherapies to enhance more significant loss of tumor volume and increase patient survival.

#3163 (Phospho)proteomic analysis reveals vulnerabilities in refractory metastatic colorectal cancer.

M. Marinucci[1], G. F. Boot[1], L. Zaidi[1], C. Esposito[1], M. Coto Llerena[1], S. Soysal[2], O. Kolmar[2], C. Ng[1], S. Piscuoglio[1];
[1]University of Basel, Basel, Switzerland, [2]St. Clara Hospital and University Hospital Basel, Basel, Switzerland

Proteomic networks are crucial for cellular homeostasis maintenance and, indeed, their aberrant regulation is implicated in cancer development and progression. Understanding alterations underlying these pathways, provides a way to design therapeutic interventions in human cancer. Improvements in mass spectrometry analysis have unlocked our potential to unveil cancer vulnerabilities. Here, we performed (phospho)proteomic analysis and ex-vivo drug testing on a cohort of refractory metastatic colorectal cancer (mCRC) tissues and matched patients-Derived Organoids (PDO) to identify new putative druggable biomarkers. The comparison between the proteome and phosphoproteome of 10 mCRCs tissues with their matched PDOs normalized to a pool of 6 colon mucosa tissues highlighted a strong overall correlation (R= 0.57 and R=0.6, respectively) suggesting a good level of similarity. Applying GSEA on our proteomic dataset, we identified up-regulation in MYC, cell cycle and MTORC1 signaling pathways in mCRC tissues and PDO, while kinase enrichment analysis highlighted an increase in Casein Kinase II (CKII) activity, an important cell cycle regulator. Our ex-vivo experiments showed that silmitasertib-mediated CKII inhibition reduced the cell viability in our PDO models, but with an overall modest effect. Analysis revealed that, even though not statistically significant, high Wnt signaling score correlated with an higher resistance to silmitasertib treatment (R=0.61; p=0.08). Previous works highlighted that MAPK activity is increased after silmitasertib treatment and responsible for resistance mechanisms to CKII inhibition. Strikingly, the combined trametinib-mediated MEK blockade and CKII blockade resulted in a synergistic interaction leading to enhanced antitumor activity, especially in PDO harboring high Wnt (R=0.74; p=0.022) and cell cycle (R=0.69; p=0.04) pathway activity. Moreover, the combined treatment strongly reduced S6 activity and RAPTOR expression, overcoming the significant effect exerted by the single agents. Surprisingly, none of them altered baseline MAPK activity, suggesting that silmitasertib and trametinib synergize their activity via inactivating the MTORC1-S6 axis in an ERK-independent manner. We are currently integrating genomic and transcriptomic data to better characterize the observed drug synergy. Taken together, our findings propose the silmitasertib and trametinib combination as a new therapeutic opportunity for refractory mCRC patients and strengthen the use of PDO as a suitable model for drug screening.

#3164 The *in vivo* Hollow Fiber model is a valuable tool in drug development of selective KRas inhibitors.

P. Metzger, C.-W. Franzke, E. Dikici, G. Sommerkamp, F. Fimm-Todt, J. E. Ehlert, C. Obodozie, **H. Weber**;
Reaction Biology Europe GmbH, Freiburg, Germany

The proto-oncogene KRas is a well-described small GTPase that functions as a molecular switch for major physiological signaling pathways involved in cell proliferation, differentiation and survival. It has been shown that activating mutations in KRas are among the most common oncogenic drivers of tumorigenesis. Missense mutations of KRas result in constitutive activation due to impaired hydrolysis of GTP which enhances tumor-promoting downstream signaling pathways. Most KRas mutations are located in exon 2 or 3 including the most frequently altered glycine 12, which is present in most pancreatic cancers as well as in colorectal cancers and lung adenocarcinomas.

A panel of cancer cell lines harboring different KRas mutations such as G12C, G12V or G12D was selected to test KRas inhibitors in several cellular assays: phosphorylation assays, 2D and 3D proliferation assays. Applying the cellular pERK AlphaLISA assay showed high selectivity of several inhibitors for specific KRas mutants, while RAF and MEK inhibitors did not show significant selectivity in the tested cancer cell lines. The KRas inhibitors were then examined in a cellular 2D and a 3D spheroid proliferation assay to determine the inhibitory effect on cell growth. These cellular assays revealed a high selectivity for a specific KRas mutant, which was even more pronounced in the 3D format than in the 2D setup.

The transferability of the cellular data obtained to in vivo was tested in the Hollow Fiber mouse model. The Hollow Fiber model allows the simultaneous study of multiple cell lines implanted in separated drug-(but not cell-) permeable fibers in a single mouse with a study duration of only 16 days. AMG510 (Sotorasib), a drug approved for tumors with a G12C Kras mutation, and MRTX1133, which is currently in clinical phase and shows activity in tumors with a G12D Kras mutation, were screened for their inhibitory effect on the pancreatic tumor cells MiaPaCa-2 (G12C Kras mutation), AsPC-1 (G12D Kras mutation) and BxPC-3 (wt Kras) in the in vivo Hollow Fiber model in female NMRI nude mice. While the growth of BxPC-3 tumor cells was not affected by either inhibitor, the growth of AsPC-1 tumor cells in particular was selectively and significantly inhibited by MRTX1133.

In summary, the in vivo Hollow Fiber model is a fast and cost-effective model that can play an prominent role in drug development as a link between in vitro and in vivo xenograft studies by providing rapid and transferable evidence for in vivo efficacy.

#3165 Targeting angiogenesis for improved survival in mantle cell lymphoma.

S. Singh[1], A. sircar[1], A. Odier[1], N. Epperla[1], N. Muthusamy[1], S. Parekh[2], L. Sehgal[1];
[1]The Ohio State University Wexner Medical Ctr., Columbus, OH, [2]Icahn School of Medicine at Mount Sinai,, New York, NY

Mantle cell lymphoma (MCL) is a subtype comprising 6% of all NHL cases and is characterized by overexpression of cyclin D1 due to chromosomal translocation t(11;14) in the nodal MCL subtype. One of the best discriminatory genes between these conventional and indolent MCL tumors is SOX11; in addition, SOX11 has been shown to promote angiogenesis in MCL. Further SOX11 protein expression in MCL patients correlated with increased microvascular density and poor outcomes. Bulk transcriptomics analysis was performed on MCL patients (n=24) and CD19-purified B cells from healthy donors (HD,n=3). To understand the role of the angiogenic process in MCL, we queried 141 genes related to angiogenesis (GO:0001525). Our analysis showed that many genes involved in angiogenesis were predominantly overexpressed in MCL compared to HD, including *FLT1* and *KDR* (p-value;0.05; FC>2). SOX11 has been shown to regulate PDGFA in MCL cell lines. Consistent with this observation, we also see upregulated PDGFA levels in MCL patients. However, PDGFA upregulation was not statistically significant in our analysis. Further expression of *VEGFR2* is overexpressed in MCL Patients (n=122) compared to naïve or activated-B cells from HD. We validated that VEGFR2 protein levels were higher in MCL primary patients than in healthy donor PBMC. Further, in two independent cohorts, high *VEGFR2* expression shows significant adverse effects on 5-year overall survival (OS). To explore the potential of targeting VEGFR, we utilized lucitanib, which potently and selectively inhibits VEGFRs. Treatment with lucitanib resulted in a dose-dependent decrease in cell viability and cellular death as determined by Annexin PI staining; further, MCL cells treated with lucitanib showed inhibition of autophosphorylation of VEGFR2 and demonstrated PARP cleavage associated with cytotoxicity *in-vitro*. To assess the role of VEGFR2 inhibitor lucitanib as a single agent in MCL growth *in-vivo*, we utilized two different murine models of MCLs. First, we used cell-line-derived xenograft (CDX) models of MCL where Jeko-1 and HS5 cells were injected together, followed by treatment (lucitanib;15mg/kg QOD; IP) and measured tumor volume until the ERC of any experimental mice was reached. Kaplan-Meier survival graphs were plotted, demonstrating that lucitanib treatment prolongs survival *in-vivo*. Further, to confirm if the lucitanib can provide an overall survival benefit in the systemic PDX MCL model, we injected the PDX cells via the tail vein in NSG mice and followed human-B2M levels for disease progression, and overall survival was the endpoint. Lucitanib treatment significantly prolonged median overall survival significantly in the systemic MCL model. Our data demonstrates that targeting angiogenesis in MCL can provide therapeutic benefits, as demonstrated in preclinical MCL models.

#3166 Lipid nanoparticles as an efficient transfection method for the delivery of elephant TP53 and retrogene9 into osteosarcoma cells.

M. Sanborn, A. Rogers, G. Mitchell, R. Kennington, M. Sharp, J. D. Schiffman, L. M. Abegglen;
University of Utah Huntsman Cancer Institute, Salt Lake City, UT

Lipid nanoparticles (LNPs) continue to be at the forefront of nanotechnology research due to their versatile and effective ability to deliver DNA, RNA, and small molecules through the cell membrane. Since LNPs are formulated with lipids found naturally in cells, they generate a lower risk for immunogenic response and cause significantly less cell death than traditional transfection methods, such as electroporation. Our microfluidics assembled LNPs have shown transfection efficiencies over 80%, substantially higher than observed with other transfection techniques, and continues to increase over the first 72 hours. We previously reported that elephant *TP53* (*EP53*) induces apoptosis in cancer cells at higher rates than human *TP53* (*huTP53*), and elephant *TP53* RETROGENE9 (*EP53-R9*) contributes to apoptosis through transcription independent mechanisms. To further characterize the effectiveness of these genes, osteosarcoma cell lines were transfected with *huTP53, EP53, and EP53-R9* nanoplasmid and mRNA loaded LNPs. Cells treated with *EP53* and *huTP53* nanoplasmid-loaded LNPs had significantly increased caspase activity and cell death compared to those treated with the empty vector control ($P<.0001$), with over 90% of all cells treated with either type of p53 dead after 72 hours. Immunocytochemistry was performed to image cells using confocal microscopy, which showed a 36-fold increase in *TP53* signal in the nucleus of nanoplasmid LNP treated cells after 72 hours as compared to untreated osteosarcoma cells. In contrast, cells treated with the mRNA LNPs had a 7-fold increase in *TP53* signal over 72 hours, though the transfection efficiency was equivalent to the nanoplasmid treated cells. Future studies will assess the efficacy of *EP53* and *EP53-R9* LNPs *in vivo* in osteosarcoma mouse models. These results demonstrate the potential of LNP mediated delivery of *EP53* and *EP53-R9* to be developed as a new treatment approach for cancer patients.

#3167 Impact of gemcitabine modification on redox-driven responses in pancreatic cancer organoids cultured in distinct 3D microenvironments.

B. Han[1], S. Zhao[1], E. Agyare[2], X. Zhu[2], J. Trevino[3], S. Rogers[4], E. Velazquez[1], J. Brant[5], P. Eliahoo[6], J. Barajas[1], B. X. Hoang[1];
[1]Keck School of Medicine of USC, Los Angeles, CA, [2]Florida A&M University, Tallahassee, FL, [3]Virginia Commonwealth University, Richmond, VA, [4]Univeristy of Florida, Gainesville, FL, [5]University of Florida, Gainesville, FL, [6]University of Southern California, Los Angeles, CA

Pancreatic ductal adenocarcinoma (PDAC) poses a formidable challenge in oncology, characterized by its high lethality and limited treatment options. The advanced stage at diagnosis, aggressive metastasis, and the constrained efficacy of conventional therapeutic drugs collectively contribute to the grim prognosis associated with PDAC. Gemcitabine, a nucleoside analog and the longstanding standard chemotherapy for pancreatic cancer, encounters a significant hurdle in its efficacy due to the development of resistance. To establish a cancer-acquired resistance model applicable to Gem-modified drugs, it is crucial to account for the dense extracellular matrix (ECM) composition characteristic of PDAC. In this investigation, we employ three-dimensional (3D) cell culture models, specifically utilizing pancreatic cancer patient-derived organoids (PDOs) within a 3D matrix with tunable density and stiffness by incorporating variations in transglutaminase crosslinking rates. PDAC cells from different patients exhibit diverse adaptations within these altered gel matrix environments, manifesting differences in morphology, doubling time, and responses to drugs. Notably, PDAC cells display pronounced stemness characteristics in the dense matrix, featuring a more rounded and compact appearance and an increase in ABC transporters.Addressing the challenge of gemcitabine resistance, modifications such as gemcitabine conjugates with stearate (Gem-S) have shown promise in preclinical studies. Exploring the effects of both Gem and Gem-S in a viscoelastic-specific ECM model derived from PDAC patient-derived organoids, distinct responses based on matrix stiffness come to light. The physical properties of the matrix exert a significant influence on cellular function, thereby impacting the effectiveness of therapeutic agents. Intriguingly, within a stiffer environment, Gem-S demonstrates higher sensitivity compared to Gem, suggesting the potential application of Gem-S in the dense pathological PDAC environment. Further investigation reveals that Gem-S treatment induces a noteworthy increase in reactive oxygen species (ROS) and HIF-1 expression compared to Gem. Surprisingly, the role of multidrug transporters in Gem-S sensitivity is limited, while the downregulation of NRF (Nrf2) after Gem-S treatment hints at distinct mechanisms underlying the development of drug resistance. This study provides valuable insights into the intricate interplay between gemcitabine resistance and the PDAC microenvironment. Understanding the matrix-specific responses opens avenues for tailored therapeutic interventions, offering the potential for improved outcomes in PDAC patients.

#3168 Amphiphilic dendrimer-mediated siRNA delivery for precision regulation of cAMP pathway in cancer cells.

W. Yuan[1], Z. Gao[1], L. Peng[2], L. T. Lee[1];
[1]University of Macau, Macau, Macao, [2]Aix-Marseille University, Marseille, France

Exchange proteins directly activated by cAMP (EPACs) are involved in multiple cellular processes. The two EPAC isoforms (EPAC1 and EPAC2) have fundamental differences in structure, expression pattern, and signaling specificity, indicating that they may function independently. Therefore, the highly specific regulation of EPAC1 and EPAC2 could be beneficial in targeting cAMP pathway-related therapies. Small RNA molecules could theoretically target genetic components based on Watson-Crick base pairing, offering a unique and promising approach to achieve precision medicine. In this study, we successfully design small interfere (si)RNAs that specifically target EPAC1 and 2, without cross-reactivity with other isoforms. The use of the amphiphilic dendrimer (AD) efficiently delivers siRNAs, resulting in significant down-regulations of EPAC1 and 2 mRNA and protein expressions in multiple cancer cells, including ovarian, breast, colon, and pancreatic cancers. Functional analysis demonstrate that EPAC1 and EPAC2 regulate cancer progression depending on different mechanisms. siEPAC2-AD is more potent compared to siEPAC1-AD in suppressing cell proliferation by altering energy metabolism. Hence, this siEPACs-AD system not only enhances the drug specificity and reduces potential side effects, but also provides a new strategy for precision pharmaceutical control of the cAMP/PKA/EPAC signaling pathway for cancer treatment.

Keywords: EPAC1; EPAC2; siRNA; amphiphilic dendrimer; cAMP signaling; cancer

#3169 The role and mechanism of m6A methylation modification of LncRNA-ATB in regulating the invasion and metastasis of colorectal cancer.

Y. Lang#[1], **J.-L. Lin#**[1], J.-P. Kang[2], L. Yang[3], D. Zhou[4], C.-B. Fang*[5], F. Ye*[1], W.-w. Tang*[1];
[1]The First Affiliated Hospital of Xiamen University, School of Medicine, Xiamen University, The School of Clinical Medicine of Fujian, Medical University, Xiamen, China, [2]Zhangzhou Municipal Hospital, Zhangzhou Municipal Hospital Affiliated of Fujian Medical University, Zhangzhou City, China, [3]Weifang people's Hospital, Weifang Medical University, Weifang, China, Weifang City, China, [4]Application Technique Engineering Center ofNatural Cosmeceuticals, Collegeof Fuijan Province, Xiamen Medical College, Xiamen City, China, [5]Prince of Wales Hospital, The Chinese University of Hong Kong, Hong Kong, Hong Kong

Background: The epigenetic modification of LncRNA N6-methyladenosine (m6A) methylation plays a wide role in the invasion and metastasis of various malignant tumors. However, the role of LncRNA-ATB m6A methylation modification in colorectal cancer (CRC) has not been systematically elucidated.
Methods: Detect the regulatory effect of ALKBH5 on LncRNA-ATB by Luciferin reporter gene. LncRNA-ATB expression was detected by IHC and qPCR in CRC tissues and cells. Transwell and scratch tests were used to detect the effect of ALKBH5 overexpression after LncRNA-ATB knockdown and replacement on the invasion and migration ability of CRC cells. Western blotting was used to detect the expression changes of MMPs proteins.
Results: ALKBH5 could regulate the methylation level of the LncRNA-ATB 3' UTR region ($p<0.05$). ALKBH5 overexpression in CRC cells led to a significant decrease in the expression level of LncRNA-ATB ($p<0.05$). LncRNA-ATB exhibited elevated expression in CRC cells and demonstrated significantly higher levels in CRC tissues compared to paracancerous tissues ($p<0.05$), indicating the potential tumor-promoting effect of LncRNA-ATB in CRC, with the mechanism possibly regulated by ALKBH5-mediated m6A demethylation. ALKBH5 overexpression inhibited the proliferation and migration of CRC cells after LncRNA-ATB knockdown. However, this inhibitory effect was attenuated upon LncRNA-ATB rescue, accompanied by an increase in MMP9 and a decrease in TIMP1.
Conclusion: LncRNA-ATB plays a crucial role in ALKBH5-mediated m6A demethylation, regulating the invasion and metastasis of CRC. The ALKBH5-LncRNA-ATB m6A demethylation-MMPs signaling axis has been identified as a key regulatory pathway promoting CRC migration. m6A modification of lncRNA-ATB modulated by ALKBH5 provides a theoretical basis for novel therapeutic strategies for patients with metastatic CRC.
FUNDING: This study was supported by the National Natural Science Foundation of China (Grant No. 81702414), Natural Science Foundation of Fujian Province of China (Grant No. 2020J05306) and Xiamen Science and Technology Planning Project (Grant No. 3502Z20194003).

#3170 Epigenetic identification and functional characterization of a novel RING finger protein tumor suppressor in nasopharyngeal carcinoma and esophageal carcinoma.

X. Chai, F. Luo, S. Bao, L. Meng, A. T. C. Chan, B. B. Y. MA, Q. Tao, L. Li;
The Chinese University of Hong Kong, Hong Kong, Hong Kong

RING finger proteins play crucial roles in normal physiology and pathophysiology as important regulators of ubiquitin-dependent proteasomal protein degradation. Many RING finger proteins have also been implicated in tumorigenesis either as oncogenes or tumor suppressors. Through cancer CpG methylome studies, we identified RING finger protein 150 (RNF150) as a methylated target gene in nasopharyngeal carcinoma (NPC) and esophageal carcinoma (ESCC). RNF150 was found to be ubiquitously expressed in human normal tissues but frequently downregulated in NPC and ESCC cells due to its promoter methylation. Its downregulation is associated with poor survival in patients with head and neck cancer and esophageal cancer. We also found that RNF150 is a functional tumor suppressor by inhibiting tumor cell growth and inducing cell cycle arrest in NPC and ESCC cells. Furthermore, ectopic expression of RNF150 inhibited NPC and ESCC cell migration/invasion by suppressing epithelial-mesenchymal transition (EMT) through upregulation of epithelial marker E-cadherin and downregulation of mesenchymal markers (vimentin, N-cadherin, Snail, and Slug). RNF150 is located in the cytoplasm and represses several oncogenic signaling pathways including the Wnt/β-catenin and NF-kB signaling pathways. Liquid chromatography-mass spectrometry (LC-MS) was performed to elucidate RNF150 binding proteins. KEGG enrichment analysis showed that glycolysis/gluconeogenesis, pyruvate metabolism, central carbon metabolism in cancer, and AMPK signaling were the top 4 pathways with significant enrichment, suggesting potential targeting of metabolic molecules by RNF150. Thus, our results provide insights into a new ring finger protein member, RNF150, as a functional tumor suppressor for NPC and ESCC. Our study also suggests a potential epigenetic biomarker for the early dection of NPC and ESCC.

#3171 The effect of estrogen and phytoestrogens in Inflammatory breast cancer.

E. A. Peterson-Peguero[1], K. Rodriguez-Martir[1], M. Ganshert[2], D. Negron-Figueroa[1], A. N. Colon-Ortiz[1];
[1]University of Puerto Rico - Rio Piedras, San Juan, PR, [2]Loyola University Chicago, Chicago, IL

Inflammatory breast cancer is an aggressive and lethal type of breast cancer. Frequently, this cancer is diagnosed in an advanced stage with metastasis. IBC diagnosis is associated with a worse survival rate than other types of breast cancer. The presence of dermal and stromal tumor emboli blocking the lymphatic vessels under the skin is considered a hallmark of IBC and assumed to be responsible for the high metastatic behavior and aggressiveness of IBC disease. To this date, there are no effective targeted therapeutics, especially for those patients that account for approximately 20-40% of IBC cases with triple-negative breast cancer (TNBC) classification. Several studies have shown that estrogen can exert non-genomic effects in IBC and non-IBC TNBC, mediated by the expression of alternate estrogen receptors including estrogen receptor alpha-36, and GPR30. In this context, estrogen can activate non-genomic signaling pathways involved in the acquisition of oncogenic phenotypes such as increased motility and invasion in IBC cells. Phytoestrogens, naturally derived structural analogs to 17β-estradiol (E2), were evaluated as an alternative treatment option using *in vitro* IBC cell models (SUM149 and SUM190). Given the estrogenic properties of phytoestrogens, the drugs were hypothesized to interact with targets in pathways similar to E2 in non-genomic signaling. Several phytoestrogens including coumestrol (Cou) can induce a cytotoxic effect in TNBC. We hypothesize (1) that estrogen non-genomic signaling has an active role in the aggressive metastatic phenotype of IBC, and (2) that Cou has anticancer activity by inhibiting estrogen non-genomic signaling in IBC. To test these hypotheses, IBC cells were treated with E2 or Cou to determine their effects on the activation of downstream kinases by western blot and phospho-kinase array assays. In addition, transcriptional effects upon treatment with Cou were identified using RNA-seq. A dose-response curve in 2D and 3D models was generated to determine the half-maximal inhibitory concentration (IC_{50}) of Cou. Finally, treatment using the IC50 of Cou caused a decrease in cell viability in the TNBC cell line. Also, in comparison to E2, Cou decreases migration, proliferation, and tumor emboli formation in IBC cell lines. In addition, IBC cells were treated using monotherapy and combination therapy with phytoestrogens including Cou, genistein (GN), and/or 8-prenylnaringenin (8-PN). Observed reductions of cell viability in IBC cell lines treated with the different phytoestrogens and combinations make them worthy of further characterization as anti-cancer therapies in *in vitro* and *in vivo* models. In summary, IBC cells are responsive to E2 making this signaling pathway attractive for the development of innovative therapeutic strategies with phytoestrogens as potential candidates for treatment.

#3172 Significance of PELP1 signaling in liver cancer progression.

U. Pratap, K. Nassar, X. Yang, A. Baker, R. Gopalam, W. C. Arnold, T. Adeniran, M. Hernandez Fernandez, G. R. Sareddy, S. Viswanadhapalli, L. Sun, R. K. Vadlamudi;
UT Health San Antonio, San Antonio, TX

Background: Hepatocellular carcinoma (HCC) is the fastest-rising cause of cancer-related mortality in the United States. Furthermore, advanced HCC has a very poor prognosis, with a median survival time of only about ten months. Effective new targeted therapies are urgently needed for the treatment of HCC. Proline, glutamic acid-, and leucine-rich protein 1 (PELP1) is a protooncogene. PELP1 signaling has been implicated in the development of several cancers, however, its role in the progression of HCC remains unclear. The goal of this project is to investigate the significance and therapeutic potential of targeting PELP1 in HCC.
Methods: In this investigation, we have used six HCC cell lines (HUH7, HEP3B, SNU398, SNU475, SNU423, and SNU449). Using immunohistochemistry (IHC), the expression of PELP1 in HCC tissue microarrays was examined. PELP1shRNA lentiviral particles were used to create PELP1 knockdown (KD) cells. Using well-established in vitro tests for cell proliferation, colony formation, and apoptosis, the effects of PELP1 KD or PELP1 inhibitor (SMIP34) were investigated. RNA-seq, RT-qPCR, Western blotting, IHC, reporter gene assays, and signaling pathway analysis were used in mechanistic investigations. Preclinical evaluations were conducted using mice xenograft models.
Results: TNM plot analysis showed that HCC samples had increased PELP1 expression relative to normal tissue. Immunohistochemistry analysis of tissue microarray confirmed that HCC specimens overexpressed PELP1 in comparison to normal specimens. PELP1 knockdown with shRNA dramatically decreased HCC cell invasion, clonogenicity, and proliferation. Similarly, PELP1 inhibitor SMIP34 treatment significantly reduced cell viability, invasiveness, colony forming capacity, and induced apoptosis of HCC cells. RNA-seq analyses using PELP1 KD cells confirmed that PELP1 modulates the ribosome and the eukaryotic translation elongation pathways. Mechanistic studies confirmed that SMIP34 treatment contributed to the disruption of the Rix complex, which is crucial for ribosomal biogenesis. Puromycin labelling studies confirmed that PELP1 KD or SMIP34 treatment contributes to the reduction of ribosomal biogenesis and new protein synthesis. Furthermore, PELP1 KD or treatment with SMIP34 dramatically slowed the progression of HCC tumors in xenograft models. IHC analysis revealed reduced levels of the proliferation marker Ki67 in PELP1 KD/SMIP34 treated HCC xenograft tumors compared to controls.
Conclusions: Overall, the results of our study point to PELP1 as a potential therapeutic target for HCC intervention.

#3173 Impact of hypoxia on the integrated stress response activated by imipridones ONC201 and ONC206 in pediatric diffuse midline glioma cells.

T. J. Roady[1], N. Stubbs[2], J. Chen[1], Y. Xia[1], A. S. Uruchurtu[1], X. Tian[1], L. Zhou[1], W. S. El-Deiry[1];
[1]Legorreta Cancer Center at Brown University, Providence, RI, [2]Morehouse School of Medicine, Atlanta, GA

Diffuse midline gliomas (DMGs) are highly aggressive, high-grade gliomas which typically arise in children and young adults. With currently approved treatments the median survival from time of diagnosis for pediatric DMG is 8-10 months with only 10% of children living to 2 years post diagnosis. Despite being only 15% of the cases it makes up 40% of the pediatric brain cancer deaths making it the leading cause of death for all pediatric glioma cases. Two recent clinical studies, NCT03416530 and NCT03134131, have shown the clinical efficacy of Dordaviprone (ONC201/TIC10) for the treatment of DMG; increasing median survival to 22 months in patients following radiation treatment prior to recurrence. Imipridone ONC206, a chemical derivative of ONC201, is under clinical development for treatment of pediatric and adult patients with primary brain tumors (NCT04732065 and NCT04541082). To further improve treatment, we must continue to study how the tumor microenvironment impacts the efficacy of imipridones. One crucial aspect of all brain cancers is hypoxia, so the IC50s of the SU-DIGP-25, SU-DIPG-XIII and SU-DIPGIV pediatric DMG cell lines treated with ONC201 or ONC206 were measured using the CellTiter-Glo assay under conditions of hypoxia and normoxia. Imipridones mediate apoptosis through the upregulation of the TRAIL death receptor DR5 and the activation of the integrated stress response (ISR), so western blots were used to show changes in the ISR protein expression in ONC201 treated DMG cells at multiple different degrees of hypoxia. To understand how hypoxia inducible factors (HIFs) play a role in resistance and susceptibility to ONC201 or ONC206, HIF-1a, HIF-2a, and HIF-3a were knocked down showing altered ISR protein expression after treating with the imipridones under hypoxic and normoxic conditions.

#3174 Crosstalk between protein translation and DNA replication during stress response and cancer therapy.

F. Wang;
Case Western Reserve University, Cleveland, OH

Tumor microenvironment, which includes both various types of cells (tumor cells, stromal cells, immune cells, *etc.*) and an interstitial fluid system, plays a key role in tumorigenesis, therapy response, and disease outcome. While the cell component has been heavily studied in cancer treatment, the interstitial fluid system has not. A key feature of the fluid system is constant oscillation of osmolytes such as salt, glucose, and proteins due to unstable blood supply and tumor metabolism, resulting in cycles of osmotic stress and recovery. Yet, how this osmotic stress - recovery cycle mediates tumorigenesis and cancer therapy remains poorly understood. Our unpublished results reveal sequential activation of molecular events during osmotic stress and recovery. In the stress stage, protein translation, transcription, and DNA replication are inhibited. Following recovery, protein translation resumes, gene transcription is greatly upregulated, but DNA replication is not immediately recovered. It turns out that a DNA replication checkpoint is activated during recovery; as a result, DNA replication is halted. Defects in activating protein translation inhibition during stress fail to activate the replication checkpoint during recovery, indicating a causative link from protein translation inhibition to DNA replication checkpoint activation. Many genes involved in this crosstalk are altered in a wide range of human tumors. Ovarian cancer cells that are resistant to standard of care (for instance, cisplatin) demonstrate defects in this crosstalk; however, they were also more sensitive to a combination of osmotic stress followed by the presence of replication checkpoint inhibitors during recovery than parental cancer cells. These findings highlight a unique role of the interstitial fluid system in tumor development and therapy response. They also suggest a new anticancer strategy by combining osmotic stress with checkpoint inhibitors. Key words: Tumor microenvironment; osmotic stress; protein translation control; DNA replication checkpoint; cancer therapy

#3175 Dear ABBIE, edit that colon cancer.

D. C. Aguilar, A. Gallegos;
SOHM, INC., Chino Hills, CA

Genome editing has exciting potential for gene therapy of cancers. Colorectal cancer is the third most occurring cancer in both men and women. The current treatments for colon cancers include surgery, radiofrequency ablation, chemotherapies and immunotherapies. These either involve removal of intestinal tissue that can alter the quality of life of the patient, or require doses of drugs that generally result in various side effects. ABBIE (A Binding Based Integrase Enzyme) genome editing can insert operational gene sequences into a chosen site in the genomic DNA of cells via its targetability and integrase activity. The ABBIE system offers ease of use, faster time to a readout and decreased time per genome editing experiment. SW480 and Caco-2 colon adenocarcinoma cells were used with the ABBIE system to integrate a GFP donor sequence into a safe harbor locus of the genome. Integration is to be confirmed with fluorescence microscopy and DNA sequencing. The colon cancer cell line will then be edited with the ABBIE genome editing system to include a gene cassette that overexpresses caspase genes into the genomic DNA of these cells. ABBIE-Edited colon cancer cell lines are expected to exhibit increased apoptosis as compared to non-edited controls or controls edited with DNA that do not have the caspase genes. This strategy will help lead to novel and more targetable treatments for colon cancer.

#3176 Otopetrin 3 promotes cell proliferation and regulates glycolysis via interaction with MYC in colorectal cancer.

H.-J. Jang, W. Jee, S.-M. Park, Y.-r. Park, S. Kim, J. Jung;
Kyung Hee Univ. College of Korean Medicine, Seoul, Korea, Republic of

Otopetrin 3 (OTOP3) stands out as a pivotal regulator of intracellular pH through its control over proton transportation into cells, affecting fundamental cellular processes. Previous studies have shown that OTOP3 is associated with the prognosis of colorectal cancer (CRC) patients. However, the mechanism underlying OTOP3 regulation remains unclear in cancer. Our investigation reveals OTOP3 as a potent oncogene in CRC, with higher OTOP3 levels correlating with diminished overall survival rates in CRC patients. Comparative analysis between cancerous and normal colon cells highlights a pronounced overexpression of OTOP3 in cancer cells. Suppression of OTOP3 expression significantly curtailed CRC cell proliferation, colony formation, migration, and invasion, concurrently inducing apoptosis and cell cycle arrest, ultimately leading to cancer cell death. Moreover, through CHX, FBS inactivation, and MG132 treatment experiments, it was confirmed that OTOP3 regulates c-Myc expression and stability through ubiquitination and has a critical impact on CRC cell proliferation and growth. Additionally, OTOP3's modulation of HK2, PKM2, and LDHA, underscores its role in impacting cancer cell behavior via glycolytic pathways. In summary, the overexpression of OTOP3 in CRC cells drives cell proliferation and growth through the regulation of c-Myc, impacting crucial cellular processes. Additionally, it promotes these processes by influencing glycolysis. These findings provide valuable insights into potential therapeutic targets for CRC treatment, possibly involving OTOP3 and its associated pathways.

#3177 Angiopoietin-like 4 suppress clear cell renal cell carcinoma via inhibition lysosomal acid lipase.

Z. Jin[1], U. De[1], T. Tithi[1], J. Kleberg[2], A. Nataraj[3], E. Jolley[4], B. Davies[5], W. Zhang[1], R. Kolb[1];
[1]University of Florida College of Medicine, Gainesville, FL, [2]University of Florida College of Liberal Arts and Sciences, Gainesville, FL, [3]University of Florida College of Public Health and Health Professions, Gainesville, FL, [4]Florida State University Interdisciplinary Medical Sciences Division, Tallahassee, FL, [5]University of Iowa, Iowa city, IA

Renal cell carcinomas(RCC) account for about 76,000 new cancer cases annually in the U.S. and 403,000 cases world wide. Clear cell RCC (ccRCC) is both the most common and aggressive subtype, accounting for 75-85% of cases with a 5-year survival rate of 50-69% for all cases and only 10% for metastatic disease. In our study, we report thatANGPTL4 is highly upregulated in ccRCC compared to other types of cancers and normal kidney tissues. However, we identified a cohort of patients with significantly lower expression of ANGPTL4 which had a worse prognosis compared to rest of the patients with higher expression of ANGPTL4. This subset of patients had a lower frequency of mutated VHL and were enriched for genes related to lipid metabolism. In transplant tumor models using RCC cell lines with wild-type VHL, we found that ANGPTL4 suppresses tumor growth. Moreover, loss of ANGPTL4 in ccRCC cell lines reduces colony formation in a lysosomal acid lipase (LAL) dependent manner, a phenotype that is rescued by expression of nANGPTL4. This data indicates that ANGPTL4 suppresses ccRCC tumors in a cancer cell intrinsic manner via regulation of LAL activity. This cohort of patients with low ANGPTL4 may be more dependent on lipid metabolism and less likely to respond to anti-angiogenic TKI plus immune checkpoint inhibitor therapy.

#3178 Vitamin B1 derivative, fursultiamine, prevents colon cancer growth.

S. Poludasu, C. Pompoco, K. Ramana;
Noorda College of Osteopathic Medicine, LLC, Provo, UT

Colon cancer is the second deadliest type of cancer in the United States, with surgical resection being the primary treatment modality for localized early-stage colon cancer. Still, more treatment and prevention options are needed to help improve the outcomes for colon cancer as they are currently limited to invasive procedures. One promising option is fursultiamine, a disulfide lipid-soluble vitamin B1 derivative, which has anti-oxidative and anti-inflammatory activity that could aid in preventing colon cancer. We hypothesize that supplementation of fursultiamine could be an effective chemopreventive treatment to control the growth and spread of colon carcinogenesis. Human colorectal adenocarcinoma (SW480) cell lines were incubated with complete media (CM) or human recombinant endothelial growth factor (EGF 20 ng/ml) in the absence and presence of fursultiamine. The cell viability was examined by MTT assay in a concentration- (0-150 uM) and time (24 and 48 h) - dependent manner. Our results indicate that fursultiamine prevents SW480 cell death in a dose-dependent manner. Apoptosis was detected by using Annexin-V staining and live and death cell assay. Our results suggest that fursultiamine prevents SW480 cell proliferation by inducing apoptotic cell death. The production of reactive oxygen species (ROS) and activation of caspase-3 were examined by specific assay kits. Treatment with fursultiamine resulted in the decreased production of ROS and activation of caspase-3. The expression of anti-apoptotic, pro-apoptotic, and pro-inflammatory factors was analyzed using antibody arrays. The results demonstrated that treatment with fursultiamine increased the expression of pro-apoptotic factors such as Bad, Bax, cleaved caspase 3, Fas/CD95, and FADD. Further, fursultiamine increased expression of the tumor suppressor genes p53, p27, and p21. We next planned to examine this vitamin B1 derivative's effect in preventing cancer growth in nude mice xenograft models. In conclusion, our in vitro results indicate that fursultiamine, a vitamin B1 derivative, prevents colon cancer growth through increased regulation of pro-apoptotic pathways and tumor suppressor proteins and thus has the potential for further development as a chemopreventative agent.

#3179 Spindle assembly checkpoint as a therapeutic target for *TP53*-mutated myeloid neoplasms.

A. Arsana, H. Huang, A. Al-Kali, M. Shah;
Mayo Clinic, Rochester, MN

Introduction TP53-mutated (*TP53*^{mut}) myeloid neoplasms (MN) are a distinct entity of myeloid neoplasms with no effective therapies and poor survival (Grob et al, Blood 2022). The TP53-deficient state facilitates the downstream dysfunction of the spindle assembly checkpoint (SAC), predisposing to genomic instability. Recently, a SAC protein, threonine tyrosine kinase (TTK), has emerged as an attractive therapeutic target. Upregulation of TTK has been described in various solid tumors. It is stipulated that targeting SAC proteins might result in extreme level of genomic instability that even cancer cells could not tolerate. We hypothesized that inhibition of TTK with a small molecular inhibitor—TTKi may offer a promising therapeutic strategy for *TP53*^{mut} MN.

Method We evaluated relative *TTK* mRNA expression and its association with *TP53*^{mut} and complex karyotypes (CK) in the BEAT AML cohort (Tyner et al., 2018). We used myeloid cell lines, OCI-AML-3, THP-1, and U937 cell lines that harbor-near diploid, moderately aneuploid, and highly aneuploid karyotype, respectively. The efficacy of TTKi CFI-402257 (AbMole) was tested using cell viability, apoptosis, and colony-forming unit (CFU) assays using the standard protocol. Finally, we tested the efficacy of CFI-402257 using the diagnostic bone marrow mononuclear cell (BMMC) cells from *TP53*^{mut} MN patients.

Results Among 591 AML patients in the BEAT AML cohort (41.6% diploid, 35.9% non-CK, 22.7% CK), *TTK* mRNA expression was progressively higher with increasing chromosomal abnormality burden. *TTK* expression was 1.96-fold higher in *TP53*^{mut} AML compared to *TP53*^{wt} AML (P=0.0008). Further stratified by *TP53*^{mut} VAF, there was a trend towards higher expression of *TTK* in *TP53*^{mut} VAF≥50 compared to the cases with VAF<50 (P=0.06). Next, the treatment with TTKi (CFI-402257) led to a dose-dependent reduction in cell viability across all cell lines, with *TP53*^{mut} cells (U937 and THP-1) being more sensitive than *TP53*-wildtype (*TP53*^{wt}) OCI_AML-3 cells. Similarly, TTKi inhibited the CFU potential of THP-1, U937, and OCI-AML-3 cells. Finally, TTKi induced dose-dependent apoptosis in *TP53*^{mut} MN patient BMMC but not in healthy donors, resulting in a significant reduction in colony-forming potential.

Conclusion Overexpression of TTK was strongly associated with *TP53*^{mut} and CK in AML. Inhibition of TTK-induced dose-dependent apoptosis in all myeloid cell lines tested with *TP53*^{mut} highly aneuploid cell line (U937)—traditionally the most chemorefractory phenotype—being the most sensitive. TTKi induced preferential and dose-dependent inhibition of viability and cell proliferation potential in *TP53*^{mut} MN compared to healthy donor cells, implying a therapeutic window. Further pre-clinical and clinical studies are indicated to evaluate SAC inhibition as a therapeutic strategy for *TP53*^{mut} MN.

#3180 Suppression of the CPEB3 ribozyme modulates the progression of glioblastoma.

C. Chen[1], E. Wang[1], L. Tong[1], M. Nikan[2], D. A. Bota[1], C. Benavente[1], A. Luptak[1];
[1]University of California, Irvine, Irvine, CA, [2]Ionis Pharmaceuticals, Carlsbad, CA

Glioblastoma multiforme (GBM) is the most aggressive primary malignant brain tumor in adults, with a poor prognosis that highlights a dire clinical need for innovative therapeutic interventions. Despite significant advances in diagnoses and multimodality therapies, the overall prognosis for patients with GBM remains poor, with a median survival time of 15-18 months. Therefore, there is an unmet medical need to develop alternative treatment strategies to improve clinical outcomes. Dysregulation of post-transcriptional control and translational machinery have been implicated in malignant tumor development. Cytoplasmic polyadenylation element binding proteins (CPEB1-CPEB4) are RNA-binding proteins that regulate poly(A) tail elongation of target mRNAs and subsequently contribute to phenotypic changes in cancer cells. Notably, a self-cleaving ribozyme was identified in the *CPEB3* gene, but its role in cancer is wholly unexplored. Considering the role of CPEB3 as a tumor suppressor gene and the promotion of cancer progression through the downregulation of CPEB3, our hypothesis is that the CPEB3 ribozyme regulates CPEB3 expression, and its activity contributes to the progression of tumors. Using antisense oligonucleotides (ASOs) as an approach, we demonstrated that inhibition of CPEB3 ribozyme resulted in an increase of CPEB3 mRNA and protein expression. Blocking the CPEB3 ribozyme led to a significant reduction in cell proliferation, migration, and invasion in GBM cell lines. Gene set enrichment analysis (GSEA) revealed the downregulation of epithelial-mesenchymal transition (EMT), angiogenesis, and hypoxia gene sets in GBM cells treated with ASO compared to Ctrl-ASO. We further measured VEGFA mRNA and protein expression and found that ASO-treated GBM cells secreted significantly less VEGF in conditioned media. Inhibition of the CPEB3 ribozyme also mitigated the EMT process in GBM cells. Subsequently, ASO strategies were applied to patient-derived glioma stem cells (GSCs), representing a clinically relevant model for pre-clinical therapeutic intervention. We found that treatment of CPEB3 ribozyme ASO up-regulated CPEB3 mRNA and inhibited cell proliferation in GSCs. Furthermore, the combination of ASO and temozolomide chemotherapy exhibited a more pronounced decrease in GSCs proliferation compared to individual treatment alone. Collectively, this study highlights the significance of the CPEB3 ribozyme in GBM and explores therapeutic approaches focused on targeting CPEB3 in cancer.

#3181 Immune modulatory activity of radio-sensitizing gold nanoparticle.

T. Kulkarni[1], S. Dutta[1], H. Parent[1], K. Perry[2], Y. Mackeyev[3], **S. Bhattacharya**[1];
[1]Mayo Clinic Florida, Jacksonville, FL, [2]Elizabeth City State University, Elizabeth City, NC, [3]University of Texas Houston Health Science Center, Houston, TX

Radiation therapy (RT) is frequently used in the neoadjuvant setting in borderline resectable and some resectable pancreatic ductal adenocarcinoma (PDAC) and in the definitive setting in locally advanced PDACs which is third leading cause of cancer associated death. Higher doses of RT improve overall treatment outcomes but increasing the dose significantly above 50Gy in standard 2Gy fractions risks profound gastrointestinal (GI) toxicity. Additionally, genotoxic stress such as RT, can induce CXCL12 secretion by cancer associated fibroblast (CAFs) and overexpression of CXC motif chemokine receptor 4 (CXCR4) in cancer cells. CXCL12-CXCR4 downstream signaling results in immune suppression and consequent enhanced tumor growth and metastasis and poor prognosis in PDAC. To overcome these clinical challenges, we have developed multimodal gold nanoparticle constructs (GNPs) by functionalizing the CXCR4 antagonists to (i) bind to CXCR4 and mediate GNP internalization, (ii) abolish the feedback immune inhibitory signals mediated by CXCR4 overexpression, and (iii) enhance therapeutic benefit of radiation. To achieve these multimodal activities, we have covalently attached the CXCR4 antagonist, AMD070, to thiol-terminated polyethylene glycol (PEG) to synthesize AMD-PEG which was then conjugated with GNPs to produce AMD-PEG-GNP. In our experiment AMD-PEG-GNP has successfully inhibited CXCL12-CXCR4 downstream signalling such as reduction of ERK phosphorylation in PDAC cells. To analyze the radiosensitization role of GNP nanoconjugates, PDAC cells were incubated with AMD-PEG, PEG-GNP and AMD-PEG-GNPs for 4 hours and then treated with increasing doses of radiated, from 1-4Gy. AMD-PEG-GNP demonstrated a systematic enhancement on reactive oxygen species (ROS) production and downregulation of a colony formation. Collectively, the results from in vitro study with PDAC cells confirm that the nanoconjugate with AMD070 enhances radio-cytotoxicity and impair CXCL12-CXCR4 downstream signaling. Hence AMD-PEG-GNP has strong merit to enhance radiation dose locally and simultaneously restrict RT induced immunosuppression in PDAC.

#3182 Role of Frizzled 7 in melanoma development and metastasis.

M. Nihal[1], S. A. Umar[2], A.-B. A. Chang[2], N. Ahmad[3], H. Chang[2];
[1]William S. Middleton Memorial Veterans Hosp., Madison, WI, [2]University of Wisconsin-Madison, School of Medicine and Public Health, Madison, WI, [3]University of Wisconsin-Madison, Madison, WI

The frizzled (Fzd) family of proteins are 7-transmembrane G-protein coupled receptors (GPCRs) that transduce signals mainly for Wnt ligands. There are 10 Fzds identified in mammals, and they are involved in multiple cellular and biological functions via signaling through the canonical Wnt/beta-catenin, planar cell polarity, and calcium signaling pathways. Our previous work revealed a pro-metastasis role of Fzd6 in melanoma. This project focuses on Fzd7, a homolog of Fzd6, in melanoma. We found that *FZD7* is highly expressed in multiple melanoma cell lines. siRNA knockdown of *FZD7* does not affect cell proliferation but significantly reduces cell invasion in A375, Hs294T, and SK-MEL28 cells *in vitro*. To determine the *in vivo* role of Fzd7 in melanoma, we generated Fzd7 knockout YUMM1.7 cell lines for xenograft experiments using CRISPR. All three Fzd7 knockout clones showed a significant reduction in primary tumor growth when xenografted in C57BL/6 mice. To determine the potential mechanism of Fzd7 in melanoma growth and invasion, we performed bulk RNA-Seq on the YUMM1.7 knockout cell lines and identified 215 downregulated and 31 upregulated genes (with a fold change of 2, $p<0.05$). We are in the process of confirming these transcriptional profile changes. Further functional analysis will be performed using gain- and loss-of-function approaches to determine the downstream mechanisms of Fzd7 in melanoma growth and invasion.

EXPERIMENTAL AND MOLECULAR THERAPEUTICS: Cancer Immunotherapy and Drug Delivery
Poster Session

#3184 Development of an innovative bifunctional CPL976-MMAE conjugate based on a bispecific anti-PD-L1/ ant-AXL antibody with a dual mechanism of action.

K. Lacek, **A. Jablonska**, O. Abramczyk, M. Janowska, F. Mitula, A. Sowinska, A. Bojko-Matuszek, T. Kornatowski, D. Kolakowski, M. Bojko, M. Skupinska, W. Pyra, M. Gorka, J. Hucz-Kalitowska, E. Mroz, M. Choros, J. Pieczykoland, M. Wieczorek, D. Popiel;
Celon Pharma SA, Kazun Nowy, Poland

Background: Tumor immunotherapy, especially the combination of PD-1/PD-L1 inhibitors and chemotherapy, has developed rapidly. However, the systemic side effects induced by chemotherapy remain a crucial problem that needs to be addressed. Antibody-drug conjugates (ADCs) are exceptional as a target-specific prodrugs that greatly improve the therapeutic window of chemotherapy drugs. Therefore, we designed the ADC based on a bispecific anti-PD-L1/anti-AXL antibody with toxic MMAE (Monomethyl auristatin E) for precise targeting of cancer cells and reduction of the side effects.
Materials and Methods: The CPL976-MMAE conjugate was prepared with site-specific conjugation technology of Fc-glycan remodeling and click-chemistry. The binding to the extracellular domain of AXL and PD-L1 was confirmed with use of the Surface Plasmon Resonance (SPR). After the conjugation with MMAE, cytotoxicity and selectivity of the ADC were evaluated on the human cancer cell lines with different expression levels of AXL and PD-L1. The ADC's ability to force internalization of targets was shown on a panel of cell lines. The effectiveness of ADC was evaluated based on changes in the cell cycle and of treated cells. The high efficacy of the conjugates was confirmed in a mouse model of MDA-MB-231 xenografts in bi-weekly intravenous injection of 6 doses.
Results: CPL976-MMAE showed improved cellular uptake, selectivity, and anticancer activity, compared to unconjugated MMAE in the cancer cell lines with different expression of the targets AXL/PD-L1. We confirmed ADCs efficacy using cells expressing high levels of AXL and PDL-1 shown as arrest in G2-M phase of the cell cycle and dose-depended apoptosis. The in vivo experiment on a mouse xenograft model confirmed complete tumor reduction (8/8) after ADC treatment, despite the application of an 11 times lower dose in comparison to the free-MMAE control group and was well-tolerated by mice. Importantly, even after the withdrawal of 976-MMAE for 3 weeks, no tumor regrowth was observed.
Conclusions: We presented a new, ADC based on bispecific anti-PD-L1/anti-AXL antibody conjugated with MMAE, that combines the effects of cancer growth inhibition by interaction with AXL and immunotherapy by disruption of the PD-1/PD-L1 axis, with selective delivery of MMAE to cancer cells. The simultaneous action of delivering the toxin and acting on both therapeutic targets provides a potent synergistic anti-tumor effect, that can lead to complete tumor eradication and potentially overcome the primary and secondary resistance to PD-1/PD-L1 targeted therapies.

#3185 Glatiramer acetate enhances tumor retention and mitigates systemic toxicity of toll-like receptor 9 agonists as intratumoral immunotherapy.

H. Gong[1], D. J. Griffin[2], C. E. Groer[1], X. Wu[1], M. M. Abdelaziz[1], S. Wu[1], L. Xu[1], L. M. Forrest[1], C. J. Berkland[1];
[1]University of Kansas, Lawrence, KS, [2]Kinimmune, Inc., St. Louis, MO

Pathogen-associated molecular patterns (PAMP) are conserved molecular structures produced by microorganisms that are recognized as foreign by receptors of the innate immune system. Unmethylated cytosine-guanine oligodeoxynucleotides (CpG ODNs) are a storied drug class from the PAMP family that ligates Toll-like receptor 9 (TLR9). CpG ODNs have shown promising antitumor effects in preclinical studies by inducing potent pro-inflammatory immune responses. However, there are still practical challenges that have hindered clinical success, including inefficient *in vivo* delivery and severe immune-related toxicities caused by systemic exposure to CpG. We previously identified that glatiramer acetate (GA), an FDA-approved, lysine-rich polypeptide, could be applied as a cationic drug delivery vector for CpG delivery proximal to the injection site while mitigating systemic release of pro-inflammatory cytokines. To dive into the mechanism and evaluate pharmacological efficacy in more pathological models that simulate colorectal carcinoma, we validated the biodistribution of GA-CpG complexes (or R4B) and explored their safety and antitumor immunity in multiple mouse colorectal carcinoma models. In the CT26 single tumor model, intratumoral R4B treatment displayed comparable antitumoral efficacy as CpG treatment. Genome-wide transcriptome analysis showed that R4B treatment elicited much more prominent immune system response pathways in both lesions and spleens. The biodistribution study proved that R4B localized and gradually released CpG around the injection site while ‘naked’ CpG diffused away from the injection site quickly. In the CT26 dual tumor-bearing model, intratumoral administration of R4B generated systemic immune efficacy that led to an abscopal effect on distant untreated cancers, comparable to treatment with CpG alone. Notably, R4B treatment accomplished these effects with greatly mitigated systemic pro-inflammatory cytokines compared to CpG alone. These data help further elucidate the noncanonical role of glatiramer acetate to serve as a nucleic acid delivery scaffold that potentiates the safety of CpG adjuvant for cancer immunotherapy.

#3186 An Erythrocyte-αPD-1 conjugate suppresses cancers resistant to checkpoint blockade immunotherapy: A first-in-human study.

L. Yang[1], X. Nie[2], Z. Chen[1], Y. Liu[2], J. Zheng[3], X. Gao[2];
[1]Zhejiang Provincial People's Hospital, Hangzhou, China, [2]Westlake University, Hangzhou, China, [3]Westlake THerapeutics, Hangzhou, China

Background: Immune checkpoint blockade (ICB) therapy has revolutionized cancer treatment, yet resistance to this therapy can lead to immune escape and disease progression. Here, we introduce WTX-212, an erythrocyte-antibody conjugate covalently linking anti-PD-1 antibody to erythrocyte membranes. Unlike conventional antibodies, WTX-212 naturally accumulates in the spleen and remodels the splenic immune landscape in tumor-bearing mice. Pre-clinical studies have demonstrated that T cells activated by WTX-212 reduce the splenic reservoir of immunosuppressive myeloid cells, including those within tumors. This results in a systemic anti-tumor immune response and suppression of tumor growth in xenograft tumor models resistant to anti-PD-1 immunotherapies. A first-in-human (FIH) clinical trial is now investigating its potential in human cancer patients.

Methods: The FIH trial (NCT05707325) is aimed to investigate the safety, pharmacokinetics, mechanisms and preliminary efficacy of WTX-212 in cancer patients with advanced malignancies. All of patients had previously received anti-PDs therapies and developed resistance to these treatments. By November 15th, 2023, 7 patients across two cohorts had received WTX-212 monotherapy (1×10^{11}-2×10^{11} cells, Q3W IV). The tumor lesions were assessed using RECIST v1.1 criteria. Blood and tumor samples were collected for correlative analysis.

Results: 7 patients with various solid tumors, having undergone a median of 3.1 prior lines of therapy (ranging from 1-6), received WTX-212 monotherapy. No dose-limiting toxicities or treatment-related adverse events greater than Grade 3 were reported. WTX-212 was detectable in peripheral blood at the end of cycle in a dose dependent manner. Disease control, including partial remission (PR) and stable disease (SD), was observed in 5/7 patients (DCR, 71%). One patient with esophageal cancer achieved a PR with a significant 44% reduction in target lesion size after two cycles of treatment. Two patients, one with esophageal cancer (3 lines prior therapies) and another with HPV-negative cervical cancer (4 lines prior therapies), maintained disease control for over 30 weeks after WTX-212 treatment. Consistent with preclinical findings, WTX-212 systemically induced anti-tumor responses, leading to a reduction of myeloid-derived suppressor cells (MDSCs) particularly the PMN-MDSC subset in 6/7 patients (reductions ranging from 24%-82% compared to baseline), and a median 1.5-fold increase of T cells in 7/7 patients in the peripheral blood after the 1st cycle of treatment.

Conclusion: The initial promising data support further investigation and exploration of the combination therapy strategies to expand the therapeutic potential of WTX-212 in cancer patients. Erythrocyte-drug conjugation may serve as a unique strategy for targeting the peripheral immune system to treat cancers.

#3187 Enhancing STING activation by cyclic dinucleotide-manganese particles for systemic cancer immunotherapy.

X. Zhou[1], X. Sun[1], W. Gong[1], Z. Wan[1], T. Krieger-Burke[2], V. Yuzbasiyan-Gurkan[2], Y. L. Lei[1], J. Moon[1];
[1]University of Michigan, Ann Arbor, MI, [2]Michigan State University, East Lansing, MI

Background: Activating the innate immune pathway of stimulator of interferon genes (STING) can elicit potent anti-tumor immunity via the production of type-I interferons (IFN-I). However, cyclic-dinucleotide (CDN) STING agonists have undesirable pharmacological properties. Most CDNs in clinical development are administered intratumorally, thus precluding their utility against advanced cancer. Here, we report the development of a new nanoparticle system for the systemic delivery of CDN STING agonists with potent efficacy, favorable pharmaceutical properties, and acceptable safety profiles.
Methods: Various metal ions were screened for synergy with CDNs for IFN-I response from bone marrow-derived dendritic cells. Lipid nanoparticles carrying CDN and manganese ions (termed SNP) were synthesized. Mice bearing syngenetic tumors (including CT26 and B16F10) as well as genetically engineered mouse models were treated by intravenous administration of SNP, followed by tumor monitoring and immune profiling of the tumor microenvironment. White New Zealand rabbits bearing VX2 tumors as well as healthy mongrel dogs were treated with SNP and evaluated. Lastly, human tumor biopsies derived from head and neck squamous cell carcinoma (HNSCC) patients were incubated with SNP or soluble STING agonists and analyzed for immune activation.
Results: We identified that Mn^{2+} achieved strong synergy with CDN STING agonists for inducing IFN-I production. SNP carrying CDN and Mn^{2+} was dosed intravenously in mice, leading to robust IFN-I response, remodeling of the immunosuppressive tumor microenvironment, and expansion of anti-tumor $CD8^{+}$ T cells. Intravenous SNP therapy resulted in robust anti-tumor efficacy in multiple murine tumor models, including CT26, B16F10, and a genetically engineered mouse model of MMTV-PyMT triple-negative breast cancer. We have also observed robust anti-tumor efficacy of SNP against VX2 squamous carcinomas in rabbits and have demonstrated the safety of intravenous SNP therapy in healthy dogs. Mechanistically, the efficacy of SNP therapy was dependent on the host STING expression but independent of the tumor STING expression. In addition, the anti-tumor efficacy of SNP was decreased in mice lacking *Ifnar1* or *Ifngr1* expression in the B16F10 melanoma model, showing the crucial effects of IFN-I and IFN-II responses. Moreover, SNP treatment led to robust IFN-I responses from fresh human tumor biopsies derived from HNSCC patients.
Conclusions: SNP empowers highly effective systemic cancer immunotherapy via nanotechnology. It also underscores the potential of utilizing metal ions for immune-mediated disease treatment.

#3188 Chitosan-glycerol injectable gel for intratumoral retention of immunotherapeutics.

R. L. Kobrin, S. M. Mantooth, D. A. Zaharoff;
North Carolina State University, Raleigh, NC

A novel, injectable chitosan-glycerol hydrogel was developed and characterized. Upon injection with co-formulated therapeutics, the gel vastly improved molecule retention at the injection site, as compared to molecule delivery in less viscous media.

Methods. The hydrogel was formed through a centrifugation process. 70% deacetylated, medium viscosity chitosan was dissolved in 0.1M HCl. Glycerol was then added, followed by vortexing. Next, 1x PBS and 1M NaOH were added to neutralize the mixture, which induced gelation. After hydrogel centrifugation at 10,000 rpm for 5 minutes, a hydrogel was separated from precipitate. Several formulation parameters were tested, including chitosan:glycerol volume ratio, chitosan concentration, chitosan degree of deacetylation, and chitosan molecular weight. The retention of model therapeutics, formulated in hydrogel or saline vehicles, following injection in agar-based tumor phantoms was quantified via absorbance and fluorescence readings. To assess biocompatibility, a non-contact cell viability assay was performed utilizing 3T3 fibroblasts seeded in the bottom of transmembrane wells with hydrogels added to the upper chamber. After 48 hours, cells were collected and counted utilizing trypan blue.

New Data. A hydrogel for intratumoral therapeutic delivery was constructed with several desirable qualities, including biocompatibility and injectability through a 25-gauge needle. Different relative glycerol to chitosan volumes, from 5 to 95 w/v % glycerol, were tested to determine a range of gelation conditions. Glycerol volume most significantly impacted gelation conditions independent of chitosan concentration, with gelation occurring between 70-85% relative volume glycerol. Increasing chitosan solution concentration and chitosan molecular weight increased the range of chitosan:glycerol ratios resulting in gelation. The hydrogel improved load retention at the agar tumor phantom injection site for various sizes of model therapeutics compared to less viscous solutions. Cytotoxicity testing of the hydrogel showed a statistically insignificant difference between the live:dead cell ratios of the experimental and negative control groups.

Conclusion. An injectable, biocompatible hydrogel was created through the neutralization and centrifugation of a chitosan-glycerol solution. The hydrogel displays physiological pH, injectability through a 25-gauge needle, biocompatibility, and vastly improved therapeutic load retention at the injection site compared to less-viscous delivery media. Chitosan-glycerol hydrogels may be useful for intratumoral delivery and retention of immunomodulators within the tumor microenvironment.

#3189 A novel monoclonal antibody targeting TM4SF4 enhances antitumor activity through regulation of cellular levels of immune checkpoint ligands and antibody dependent cellular cytotoxicity.

Yeon-jee Kahm[1], Chang-Kyu Heo[2], Rae Kwon Kim[1], Uhee Jung[1], Byung-Chul Shin[1], Won-Yong Kim[1], Bum-Jin Kim[3], Sung-Chul Kim[3], Chun-jeih Ryu[4], Eun-Wie Cho[2], In-Gyu Kim[1]

[1]Korea Atomic Energy Research Institute, Daejeon, Korea, Republic of,[2]Korea Research Institute of Bioscience and Biotechnology, Daejeon, Korea, Republic of,[3]Algok Bio. Inc., Bellevue, WA,[4]Sejong University, Seoul, Korea, Republic of

Transmembrane 4 super family member 4(TM4SF4) protein has been shown to be involved in EMT-associated stemness through autocrine of insulin-like growth factor 1(IGF1) and osteopontin(OPN) in non-small cell lung cancer(NSCLC) cells. However, its potential as a therapeutic target has not been evaluated. In this study, anti-human TM4SF4 monoclonal antibodies(anti-hTM4SF4 mAbs) were prepared in mouse as part of a strategy for developing anticancer drug using humanized antibody. A synthetic peptide(15 mer, 126-140th AA) derived from the extracellular loop(ECL) 2 of human TM4SF4 exposed on outer cell surface was used as an immunization antigen. Among the selected anti-hTM4SF4 mAbs, ECL-2B7 and ECL-12A8 showed the best affinity for the antigen(Kd), approximately 2.66 nM and 8.34 nM, as determined by surface plasmon resonance analysis. Using mouse xenograft of NSCLC cell line, it was confirmed that ECL-2B7 was superior to ECL-12A8 in producing humanized antibody. ECL-2B7 inhibited EMT-associated stemness of TM4SF4 positive cancer cells by blocking cellular signaling events such as IGF1Rβ and CD44 and their downstream signals, PI3K/AKT/GSK3β/NF-κB and JAK2/STAT3 pathways. ECL-2B7 also enhanced antitumor activity by downregulating cellular and exosomal level of PD-L1 and B7-H4, immune-checkpoint ligands that elicit immunosuppression of T cell, and by mediating antibody-dependent cellular cytotoxicity. Treatment with OPN- and IGF1-neutralizing antibodies suppressed intracellular PD-L1 and B7-H4 level. It means that the regulation of PD-L1 and B7-H4 levels by TM4SF4 is closely related to the autocrine action of OPN and IGF1 induced by TM4SF4. Using patient-derived xenograft model, it was confirmed that the ECL-2B7 has excellent antitumor activity that effectively inhibits tumor progress. These results strongly suggest that it is necessary to construct humanized antibody based on ECL-2B7 to confirm its potential as a novel anticancer drug.

#3190 Twin Fc-immune cell engager (ICE): A novel antibody platform for cancer immunotherapy with enhanced avidity for Fcγ receptors and complement.

E. S. Choi, H. Park, J. Bae, K.-J. Lee, E. Kim, S. Yoon, D. Lee, G.-H. Yang;
Centenaire Biosciences Inc., Seongnam-si, Korea, Republic of

Immunoglobulin G (IgG)-based mAbs have become a dominant class of cancer immunotherapy due to their excellent drug-like properties, long half-life, and generally safe profiles. Typical IgG-based therapeutic mAbs have strong binding to target antigens owing to the valency effect of two antigen-binding fragments (Fabs). However, the single crystallizable fragment (Fc) lacks the valency effect to engage immune effector elements. As Fcγ receptors (FcγR) such as FcγRIIa and FcγRIIIa and C1q complement component have low affinity for Fc, IgG-based mAbs require high antibody opsonization density to exhibit avidity for these low affinity Fcγ receptors and C1q. This may also account for the suboptimal efficacy of IgG-based mAbs against tumors with less abundant antigen. To enhance effector functions of IgG1 by overcoming such limitation, we devised a novel platform, Twin Fc-ICE, in which a single Fab region is attached by two Fc regions which allow for high avidity binding to Fcγ receptors and C1q. The two Fc regions of Twin Fc-ICE are arranged in parallel, not in tandem, to adopt natural topologies of multiple Fc regions presented by IgG1-opsonized targets. Supporting the avidity effect of Twin Fc-ICE for FcγR binding, we showed that CTN001, a Twin Fc-ICE with trastuzumab Fab, have markedly increased binding to FcγRs including FcγRI, FcγRIIa and FcγRIIIa compared with trastuzumab. The avid FcγR binding was further demonstrated by flow cytometry analysis of human blood which revealed significantly increased binding of CTN001 relative to trastuzumab for immune cells expressing activating FcγRs such as natural killer (NK) cells, monocytes, and dendritic cells (DCs). The monovalent antigen binding of Twin Fc-ICE requires Fab with high affinity. However, provided that high affinity is achieved, the monovalent Fab adds to the two Fc regions to maximize the Fc load on cancer cells expressing low levels of antigen. Indeed, flow cytometry analysis revealed that treatment of CTN001 alone results in higher Fc load on HER2-expressing cancer cells than combination of two anti-HER2 IgG1 mAbs, trastuzumab and pertuzumab. In consistent with increased Fc load on target cells and avid FcγR binding, CTN001 induces enhanced effector functions such as CDC, ADCC and ADCP against HER2-expressing cancer cells compared with trastuzumab, which will be presented in a separate poster. CTN001 exhibits comparable thermal stability with trastuzumab and can be readily purified to >95% purity with typical purification platforms. The serum half-life of CTN001 at 10 mg/kg intravenous dose in rats is found non-inferior to that of trastuzumab (~12 days versus ~7 days). Taken together, Twin Fc-ICE provides an optimized platform with drug-like properties, which leverages avidity effects of Fc to potentiate therapeutic efficacy of antibody.

#3191 Chk1/2 inhibition enhances response to lurbinectedin treatment in small cell lung cancer.

A. Sanchez Sevilla Uruchurtu[1], T. Roady[1], A. Anderson[2], W. S. El-Deiry[1];

[1]Brown University, Providence, RI, [2]Metropolitan Regional Career and Technical Center, Providence, RI

Small cell lung cancer (SCLC) remains a significant clinical concern, with only a 7% 5 year survival rate; therefore, there remains an unmet need for efficacious treatments. Lurbinectedin was FDA approved in 2019 to treat platinum-resistant SCLC. Preliminary experiments in SCLC cell lines indicated an increase in intracellular pChk1 when treated with lurbinectedin. Based on these data and our understanding of the role of checkpoint kinases in the DNA damage response (DDR), we hypothesize that the activity of Chk1 is indicative of upregulated DDR activity as a result of double stranded breaks and replicative stress induced by lurbinectedin. In subsequent experiments, we sought to identify the role of Chk1 and Chk2 in the tumor cell response to lurbinectedin by inhibiting their activity using prexasertib (LY2606368, Acrivon Therapeutics). Cell viability experiments indicate decreased tumor cell viability when three SCLC cell lines (H1048, H1105, H1417) are treated with prexasertib as a single agent and in combination with lurbinectedin. Western blot analysis of intracellular proteins from the same SCLC cell lines treated with both drugs demonstrate dose-dependent effects on cell death marker cPARP, DNA damage marker γH2AX, and DDR/cell cycle pathway kinases cdk1 and 2. Ongoing experiments seek to replicate results using alternative Chk1/2 inhibitors, and to explore the effect of lurbinectedin-Chk1/2 inhibitor combination treatment on antitumor immune effector function by in vitro co-culture.

#3192 A novel long acting pegylated T cell engager targeting CD3 and cd19 with effective tumor killing and no potential CRS risk in CD19+ hematologic malignancies.

S. Liu, Y. Wen, W. Lyu, S. Yin, Y. Lei, D. Wu, Z. Wu, Q. Zhuo;
Shenzhen Enduring Biotech, Ltd., Shenzhen, China

The development of bispecific T cell engagers represents a highly effective immunotherapy strategy for the treatment of hematologic malignancies. However, Blinatumomab, a bispecific T cell engager of CD3/CD19, has disadvantages in clinical setting due to the adverse pharmacokinetics (PK), which resulted in less than 2 hours of in vivo elimination half-life, neurotoxicity, and cytokine release syndrome. In this study, a bispecific antibody JY108 was developed to target CD19 and CD3e with much reduced affinities towards both targets (revealed by Biacore assay results). JY108 was prepared by a patented pegylation bispecific linker technology, which could address the limitations of current therapeutic approaches. *In vitro* cytotoxicity assay results demonstrated that the EC50s of the drug specific cytotoxicity of T cells mediated by JY108 are in the concentrations of ng/ml, while blinatumomab mediated cytotoxicity to the same CD19+ cells are in the concentrations of pg/ml. Despite the weaker in vitro cytotoxicity than Blinatumomab, JY108 presents comparable tumor inhibition effects with Blinatumomab in different i*n vivo* studies, which include the PBMC reconstructed models with established MEC-1 or Farage tumors, the delayed drug administration on human PBMCs/tumor co-transplanted model of Raji. In addition, JY108 prolonged the survival of animals with Nalm6 brain metastasis more significantly than Blinatumomab at the same dosage. Furthermore, the PK study revealed that at the different dosages, the circulation $T_{1/2s}$ of JY108 in mice are above 20 hours, which is expected to result in more significant efficacious benefits in clinical setting. Meanwhile, the completed package of GLP-toxicity study did not observe any drug related tox to the model animals (including no cytokine release in vivo, no neurotoxicity, no respiratory toxicity, etc.), and JY108 did not induce significant cytokine release than the blank control to the whole blood or PBMCs from healthy donor in vitro. In the efficacious concentrations of exerting cytotoxicity to CD19+ tumor cells in the presence of PBMC, JY108 did not induce significant cytokine release than the blank control, while blinatumomab always induced significant cytokine release. We postulated that the lower CD3 affinity of JY108 most probably resulted in the decoupling of the signaling for activating the gene expression of cytokines from the secretion of the polarized lytic granules by T cells, which resulted in a much milder T cell activation by JY108. Currently, JY108 is a phase I trial candidate and awaits further evaluations.

#3193 Utilizing a pH sensitive peptide (pHLIP) for antigen-directed T cell therapy.

A. M. Yurkevicz, Y. Liu, P. M. Glazer;
Yale University, New Haven, CT

Many targeted therapies, such as antibody drug conjugates (ADCs) and chimeric antigen receptor (CAR) T cell therapies, rely on the identification of an optimal antigen as the cell marker for targeting cancer cells. However, there is a paucity of antigen candidates that are sufficiently specific to epithelial cancers. Therefore, technologies that can mark tumor cells for immune recognition could prove beneficial in the treatment of these solid cancers. pH low insertion peptides (pHLIPs) act as a unique delivery platform that can specifically target the acidic microenvironment of tumors, sparing healthy tissue in the process. We developed a pHLIP-peptide conjugate (pHLIP-SIINFEKL) to deliver the SIINFEKL peptide, an immunogenic fragment of ovalbumin, to investigate antigen delivery and recognition to tumors *in vivo*. When processed intracellularly, SIINFEKL is presented for immune recognition through the major histocompatibility complex (MHC) class I pathway. We observed selective delivery of pHLIP-SIINFEKL both *in vitro* and *in vivo* using fluorescently labeled constructs. *In vitro*, treatment of melanoma tumor cells with pHLIP-SIINFEKL resulted in recognition by SIINFEKL-specific T cells (OT1), leading to T cell activation and effector function. Mechanistically, we show that this recognition by OT1 cells was abrogated by siRNA knockdown of the β2 microglobulin (β2m) component of MHC class I in the target tumor cells, indicating that an intact antigen processing pathway in the cancer cells is necessary to mediate the effect of pHLIP-directed SIINFEKL delivery. *In vivo*, pHLIP-SIINFEKL treatment of tumor-bearing mice resulted in recruitment of OT1 T cells and suppression of tumor growth in two syngeneic tumor models in immunocompetent mice, with no effect when mutating either the pHLIP or SIINFEKL components of the conjugate. These results suggest that pHLIP-mediated peptide delivery can provide a novel approach to decorate solid tumors with engineered antigens for enhanced immune recognition and anti-tumor efficacy.

#3194 Discovery of T cell receptor mimic antibody against MAGE-A4 with single B-cell cloning platform.

H. Cheng, Y. Wu, T. Shi, Y. Yu, M. Wang, C. Jia, W. Xin, **H. Liu**, T. Yang, D. Yao;
ChemPartner Biologics Co., Ltd, Shanghai, China

Antibody therapeutics has been proven clinically against various cancer types and have achieved great success. Majority of the therapeutic antibodies target cell surface or extracellular proteins. Most of the tumor-specific antigens that control cell growth, proliferation, and death are intracellular, and traditional antibody therapies fail to recognize intracellular antigen targets. Such tumor specific intracellular targets consist of overexpressed self antigens, oncofetal protein, cancer testis antigens, viral protein and neo-antigens of mutant proteins. Recently, an emerging approach to target these neo-epitopes has been developed called T-cell receptor-like/TCR-mimic antibodies as they recognize similar epitopes to those of T cell receptors which target specific peptide-MHC complexes(pMHC). TCR mimic antibodies open a new avenue for targeting intracellular antigens yet there are lots of challenges for generating highly selective and potent TCR mimic antibodies. MAGE-A4, melanoma-associated antigen A4, is a member of the MAGE protein family of cancer-testis antigen (CTA). In healthy adult, MAGE-A4 expression is restricted to immune-privileged sites. But MAGE-A4 is widely expressed on many cancers such as lung cancer, head and neck squamous cell cancer, synovial sarcoma(SS), ovarian cancer, urothelial cancer and melanoma. The decapeptide GVYDGREHTV(amino acids 230-239) derived from MAGE-A4, can be presented by HLA-A*02:01 molecule, elicits specific cytotoxicity T cell response. Afami-cel, a genetically modified autologous T cell therapy against this pMHC complex, showed promising potency for patients with metastatic SS. So MAGE-A4/ HLA-A*02:01 may be a good target for TCR mimic antibodies and cancer immunotherapy. In the present study, we utilized a newly established single cell cloning platform LyTARS to generate TCR mimic antibodies against HLA restricted MAGE-A4 peptide. Recombinant HLA-A*02:01 MAGE-A4 protein was used to immunize mice and plasma B cells from immunized mice were sorted and loaded onto LyTARS system. Clones that showed reactivity to recombinant HLA-A*02:01 MAGE-A4 but not to irrelevant pMHC (WT-1) were exported and sequenced. Purified antibodies were extensively characterized by the specificity, affinity, and potency by ADCC. Results demonstrated that the TCR mimic antibodies identified have sub-nano molar affinity by protein based ELISA, bind to peptide pulsed T2 cells that endogenously expressing HLA with nano-Molar apparent affinity. TCR mimic antibodies also demonstrated antibody dependent cell killing with the potency of sub-nanomolar. In summary, we have generated and extensively characterized a panel of high affinity and selective TCR mimic antibodies against HLA-A*02:01 MAGE-A4 using a newly established single cell cloning platform.

#3195 SHR-4602, next generation of HER2-targeting ADC with potent anti-tumor efficacy overcoming the resistance of HER2 ADC with Topo I inhibitor payload in xenograft models.

Y. Tian, X. Sun, C. Yang, C. Liao;
Jiangsu Hengrui Pharmaceuticals Co., Ltd., Shanghai, China

Background: Current clinical HER2-targeting ADCs (i.e. DS-8201) have shown promising clinical efficacy in HER2 expressing or mutant cancer patients. However, most of them will ultimately experience disease progression due to different mechanisms. Herein, we presented a novel HER2 ADC, SHR-4602, which demonstrated good *in vitro* and *in vivo* anti-tumor activities and could overcome the resistance caused by HER2 ADC including DS-8201 analogue (synthesized using DS-8201 structure) and SHR-A1811 (composed of trastuzumab, a cleavable linker, and a Topo I inhibitor payload, in phase III clinical trials) in xenograft models.

Method: We used a stable enzyme-cleavable linker technology to conjugate the HER2 ADC using the amino acid sequence of pertuzumab and ER300 (eribulin derivative). The *in vitro* biological and anti-tumor activities were assessed by a series of assays. The *in vivo* anti-tumor efficacies were evaluated in the JIMT-1 (HER2 low expressing) as well as the SHR-A1811 and DS-8201 analogue induced JIMT-1 resistance (caused by treating with SHR-A1811 followed by DS-8201 analogue for a long-term) xenograft models in BALB/c nude mice.

Results: Through the SPR assay, SHR-4602 exerted single nanomolar binding affinity to human and rhesus monkey HER2, but no binding activity against rat HER2. It demonstrated varying inhibitory activity on the proliferation of cancer cell lines with various HER2 expression levels, with the IC_{50} at the range of 0.007 nM to 8.21 nM. SHR-4602 showed highly efficient internalization in NCI-N87 HER2 expressing cells and could be translocated to the lysosome followed by releasing ER300. The cytotoxic activity of SHR-4602 was predominantly mediated by released ER300 through microtubule dynamics inhibition, G_2/M arrest and apoptosis induction. Furthermore, SHR-4602 showed a strong *in vitro* bystander effect in the co-culture of HER2 positive/negative cells. SHR-4602 showed significant anti-tumor efficacy in JIMT-1, SHR-A1811 and DS-8201 analogue both-resistant JIMT-1 xenograft models. In SHR-A1811 and DS-8201 analogue both-resistant xenograft models, treatment with 10 mg/kg SHR-A1811 or DS-8201 analogue exerted negligible anti-tumor activity (TGI% < 17%), whereas SHR-4602 at 2.5, 5 and 10 mg/kg significantly inhibited the tumor growth ($p < 0.001$, vs. vehicle), with TGI% of 84.96%, 101.64% and 113.11% on Day 42, respectively, which indicated a superior anti-tumor efficacy against SHR-A1811 and DS-8201 analogue both-resistant xenograft models.

Conclusion: SHR-4602 represents a new generation HER2-targeting ADC to deliver a potent cytotoxin to HER2 expressing tumor cells and may be more efficacious to the tumors in which current anti-HER2 therapies are ineffective. SHR-4602 is now in the phase I clinical development stage for advanced malignant solid tumors (NCT05819684).

#3196 Overcoming lung cancer drug resistance: Enhanced cellular delivery using lipid-extracted nanoliposomes.

M. Alqaryan, R. Allahyani, D. Lee, R. Campbell;
MCPHS University, Worcester, MA

Background: Lung cancer causes substantial cancer deaths in the U.S. Drug resistance remains a major issue. Nanoliposomes demonstrate enhanced drug targeting and resistance-overcoming potential. Incorporating lipid extracts derived from target cells shows improved delivery over conventional nanoliposomes. This study examined the effects of lung cancer cell lipid extract nanoliposomes against target and non-target cell populations from different environments.
Method: Cellular Membrane Lipid-Extracted Nanoliposomes (CLENs) were fabricated with DOPC, DOTAP, ChaGo-K-1 lipid extract, cholesterol, PEG5000, and rhodamine fluorescent label was incorporated for uptake studies. The liposome size was reduced by probe sonication. Particle size and polydispersity index (PDI) were measured by dynamic light scattering. Zeta potential was quantified by laser Doppler micro-electrophoresis. Four cell lines were utilized: ChaGo-K-1 NSCLC target, A549 pulmonary microenvironment control, 4T1 extra-pulmonary control, and normal lung fibroblasts off-target control. All cell lines were cultured in 48-well plates at a seeding density of 10,000 cells/mL and incubated for 24 hours. Freshly prepared CLENs were added to all cell lines and incubated for an additional 24 hours. Cells were washed with PBS, and fluorescence intensity was then quantified and qualified by a microplate reader to measure the cellular uptake of the CLENs.
Results: The mean particle size and PDI of the ChaGo-K-1 CLENs were 117 ± 0.7 nm and 0.216 ±0.009, compared to 126 ± 0.5 nm and 0.195 ± 0.008 for the control, respectively. Both formulations were within the optimal size range for drug delivery and tumor cell penetration. The zeta potential of the ChaGo-K-1 CLENs was -1.75 ± 1.81 mV compared to -1.74 ± 6 mV for the control. Quantification and qualification of cellular uptake using fluorescence intensity measurements revealed a 3.2-fold increase in ChaGo-K-1 CLENs compared to conventional liposomes without ChaGo-K-1 lipid extracts. This demonstrates that the inclusion of the lipid extracts in the CLEN significantly enhanced selectivity and delivery to target cancer cell populations.
Conclusion: Higher uptake occurred with target cells using CLENs with lipid extracts versus standard liposomes. NSCLC-derived CLENs show potential to improve selective delivery and overcome drug resistance. Further, in vivo studies evaluating selective NSCLC tumor accumulation and efficacy enhancement are warranted.

#3197 Addressing drug metabolism and pharmacokinetics (DMPK) challenges of small molecule-drug conjugates (SMDCs).

A.-S. Rebstock[1], H.-G. Lerchen[1], H. Wong[2], B. Stelte-Ludwig[1], M. Wiedmann[1], A. J. Johnson[2], R. Izumi[2], A. Hamdy[2];
[1]Vincerx Pharma, Monheim, Germany, [2]Vincerx Pharma, Palo Alto, CA

Background: SMDCs are gaining momentum with potential advantages over antibody-drug conjugates (ADCs), eg, better tumor penetration and lack of immunogenicity. We have developed a novel platform technology with tailored solutions for ADCs and SMDCs with intracellular and extracellular cleavage options. Key features of the SMDC technology comprise of a small molecule ligand such as an αvβ3 integrin binder showing efficient tumor homing and a linker extracellularly cleaved by neutrophil elastase (NE) in the tumor microenvironment allowing for seamless release of different payload classes.[1] Our lead SMDC VIP236[2] is currently in a Phase 1 clinical trial for the treatment of advanced solid tumors (NCT05712889). SMDCs often have a shorter half-life compared with ADCs, which may result in more frequent dosing schedules. Here we show significant reduction of clearance and drastic prolongation of half-life of SMDCs achieved by adding a second binding moiety.

Methods: Payloads such as kinesin spindle protein inhibitors (KSPi), cyclin-dependent kinase 9 inhibitors (CDK9i), and monomethyl auristatin E (MMAE) have been linked via elastase-cleavable linkers to one or, via a branched linker, to two αvβ3 integrin binding moieties. Cytotoxicity of SMDCs was measured in cell lines with or without NE. Monovalent and bivalent SMDCs were investigated in DMPK studies in rats while monitoring the conjugate and the released payload.

Results: Payloads were coupled to the NE-cleavable peptides via different linkages. MMAE was conjugated via sterically hindered ester bonds, CDK9i was conjugated via sulfoximide bonds, and KSPi payloads were coupled via amide bonds. Each of these SMDCs was highly stable in plasma and buffer. Without NE, in vitro cytotoxicity of SMDCs in each cell line was poor with IC50 in the micromolar range. In contrast, in the presence of NE, potency increased, and cytotoxicity (IC50) was in the low nanomolar to picomolar range depending on the cell line and payload. In each case, the SMDCs reached similar potency as the free payload indicating efficient cleavage of the SMDC by NE. In DMPK studies of SMDCs in rat, none or trace levels of free payload (<0.1% as compared to the respective conjugates) was measured. With each of the SMDCs and independent of the conjugated payloads, a remarkable impact on exposure was observed when attaching a second binding ligand. The SMDCs with two ligands showed a 37- to 81-fold reduced plasma clearance as compared with the respective monovalent SMDCs, which parallels a 12- to 57-fold increase in half-life (eg, 2.1 h and 28 h for mono and bivalent MMAE SMDCs respectively). Initial in vivo studies in a cell line-derived xenograft model showed efficacy of bivalent SMDCs with once weekly dosing.

Conclusion: Our technology platform comprises NE-cleavable SMDCs with promising options to tune the DMPK profile for a longer half-life.

1. Lerchen et al, *AACR* (2023). 2. Lerchen et al, *Cancers* (2023).

#3198 An analysis of breast cancer membrane lipid-modified nanoliposomes for enhanced targeting of triple-negative breast cancer.

C. Ayertey, P. Amid, M. H. S. Almozain, R. B. Campbell;
McPhs University, Worcester, MA

Background: Every breast cancer diagnosis is unique in its own way. Triple-negative breast cancer (TNBC), has a highly aggressive phenotype characterized by a rapid growth rate profile, increased risk of metastasis and recurrence. TNBC is devoid of epidermal growth factor receptor 2, estrogen, and progesterone receptors. All three are commonly present in other forms of breast cancer disease. The aim of this study was to develop a cell membrane lipid-extracted nanoliposomes (CLENs) for selective targeting compared to conventional nanoliposomal varieties. An additional objective was to investigate the role of microenvironment on targeting using cell model of TNBC, and representations of non-target tissue environments for comparison.
Method: Lipid extracts (LE) obtained from 4T1, a murine mammary carcinoma cell line from a BALB/cfC3H mouse was used to formulate the CLENs (cell membrane lipid-extracted nanoliposomes) with different ratios of 1,2-dioleoyl-sn-glycero-3-phosphocholine (DOPC), a phospholipid used in most conventional drug delivery liposomes. Different lipid compositions and ratios were employed to evaluate cellular uptake in target, non-target and off-target cells. The target cell line, 4T1, off-target and non-target cell populations included CRL-2089, normal breast fibroblasts, SKBR3 a (human breast cancer), and A549 a (lung cancer) cell lines. Other studies involved determination of molecular charge and zeta potential of various nanoliposomal preparations and corresponding fluorescence studies in vitro.
Results: The physicochemical properties of CLENs such as particle size and surface charge characteristics were vital when assessing benefit of the lipid-based preparations. The size of the CLENs typically ranged between 130 - 165 nm and zeta potential values were negatively-charged. The inclusion of 70 mol% of LE in preparation of 4T1-CLENs demonstrated increased cellular uptake and binding by the 4T1 target cells compared to the control DOPC (100%). The highest degree of selectivity was observed in early cell binding events, and with studies involving more extended incubation time points under different experimental conditions. Off-target cells demonstrated reduced uptake by comparison. Overall, 4T1-CLENs was most efficient when applied against intended target 4T1 cells, when compared to relevant control cell populations. In conclusion, studies performed to date suggest the notion that lipid extracts derived from TNBC improves targeting.

#3199 Nano gelasomes: Novel lamellar metal-protein suprastructures for nucleic acid delivery.

A. Suresh Babu, **D. Suresh**, Z. Li, A. Upendran, R. Kannan;
University of Missouri, Columbia, MO

There is considerable interest in the development of self-assembled charged nanocarriers that form organized, predictable structures to enhance stable packaging and delivery of nucleic acid materials *in vivo*. However, the synthesis of stably-charged, organized nanostructures is highly challenging, requiring a controlled balance of nanomaterial components, stabilizers, and hydrophobic forces. Herein, we report a significant step forward in the controlled lamellar assembly of a charged complex between ultra-small 2 nm gold nanoparticles and a lipidoid within an organic matrix to form Gelasomes. These spherical suprastructures feature an intricate 3D concentric arrangement with a constant interlayer distance (4nm). The cationic lipidoid within this arrangement aids in the highly efficient packaging of nucleic acid materials in the nanoparticle. To demonstrate the potential biomedical applications of Gelasomes, we have loaded siRNA (AXL or YAP), mRNA (EGFP), or CRISPR components (Cas9 mRNA and guide RNA) and validated their functionality by *in vitro* or *in vivo* studies. Gelasomes with AXL siRNA (~20 bp) demonstrated rapid uptake (<2 hrs), successful endosomal escape, remarkable transfection efficiency (99.87 ± 0.04 %), gene downregulation (97 ± 2.8 %), and disassembly within the cell (<24 hrs). *In vivo* downregulation studies in Lung Cancer PDX (Gelasomes with AXL siRNA) and CDX (Gelasomes with YAP siRNA) models confirm the gene-silencing capability (91% or 38 % respectively) of Gelasomes underscoring their potential in advancing nanomedicine. Similarly, Gelasome loaded with EGFP mRNA (1 kb) showed 47 ± 8.54 % expression efficiency within 48 h of treatment *in vitro*. We also show the packaging of larger nucleic acids such as CRISPR Cas9 mRNA (5 kb) along with the guide RNA (100 bp) *in vitro* for generating knockouts, that achieved an editing efficiency of ~6%. Together, the results from this study pave the way for the development of adaptable, biodegradable, and functionally versatile supraparticles for medical applications.

#3200 Assessing the utility of cell membrane lipid-extracted nanoliposomes (CLENs) as a targeted drug delivery system for pancreatic cancer.

K. Alshammari, S. Verdery, S. George, R. Campbell;
Massachusetts College of Pharmacy and Health Sciences, Worcester, MA

Background: Pancreatic cancer is a challenging type of cancer to treat as evidenced by a 9% 5-year survival and a dismal rate of mortality. Nanoparticles represent a revolutionary treatment method, primarily due to characteristics including cellular absorption, boosting therapeutic effectiveness, and mitigating side effects through localized actions. For nanomedicine, optimizing liposome formulations is crucial for achieving the highest level of specificity in drug targeting. This study aims to evaluate cellular interaction of pancreatic cancer lipid-extract modified nanoliposomes when compared to unmodified varieties *in vitro*.
Method: Cell membrane lipid-extracted nanoliposomes (CLENs) were prepared via the thin film evaporation technique. The composition included various compositions and ratios of DOPC, DOTAP, Cholesterol, DPPE-PEG-$_{5000}$, and lipid extracts derived from MS1-VEGF target cells. MS1-VEGF was the cellular model of pancreatic cancer used for this study. Cellular binding studies were performed using cellular suspension and adherent cell populations. Studies were performed in 48-well plates under different experimental conditions including alterations in time of incubation, and periods of cellular exposure to dual humidified and oscillation environments in the presence of lipid-extracted (LE) nanoliposomal preparations and conventional controls.
Results: The particle size for nanoliposomes employed for this study was approximately 115 ± 0.7 nm for control and 128 ± 2.7 nm for experimental (lipid extract-modified) nanoliposomes. Following cellular exposure to different lipid extract concentrations (typically 0 to 100 nmoles per ml of growth medium), the fluorescence values demonstrated increased cellular uptake with greater LE content for floating and adhered MS1-VEGF cell populations. With the floating cells, LE-modified nanoliposomes demonstrated significantly higher fluorescence intensity values compared to conventional nanoliposomes. Similarly, with MS1-VEGF adherent cells, LE-modified nanoliposomes targeted cells to a greater extent compared to unmodified controls.
Conclusions: The increased cellular uptake of CLENs designed for targeting pancreatic tumor cells (both floating and adherent cells) demonstrated an improvement over the use of conventional nanoliposomes under similar experimental conditions. Further research is needed to fully explore the potential use of CLENs for targeting and treatment of pancreatic cancer.

#3201 Preclinical development of a novel Romidepsin nanoparticle for the treatment of T-Cell lymphoid malignancies.

I. Pal, A. Illendula, A. Joyner, T. M. Deddens, D. P. Damera, T. E. Fox, M. E. Dunlap-Brown, K. D. Jayappa, T. P. Loughran, Jr., D. J. Feith, **O. A. O'Connor**; University of Virginia, Charlottesville, VA

The histone deacetylase inhibitors (HDACi) have long been regarded as an important class of drugs for treating T-cell lymphoid malignancies (TCL). Romidepsin (Romi), a bicyclic peptide, was approved for patients with relapsed or refractory cutaneous (CTCL) and peripheral T-cell lymphomas (PTCL). Unfortunately, the approval of Romi for relapsed/refractory PTCL was withdrawn due to a negative Phase 4 post-marketing requirement. Given its potent activity against Class I HDACs, Romi is considered one of the most effective HDAC inhibitors studied and used in patients with TCL. Herein, we report on a first-in-class nanoparticle of Romi (NanoRomi) with a superior safety and efficacy profile compared to the free drug in preclinical models of PTCL and large granular lymphocyte leukemia (LGLL). We developed a first-in-class NanoRomi using our proprietary amphiphilic di-block copolymer-based nanochemistry platform. NanoRomi was characterized in cell viability, flow cytometry, and western blotting (WB) assays to determine the concentration-effect relationships with regard to the induction of apoptosis and histone acetylation in cell lines representative of TCL and LGLL, as well as primary LGLL patient PBMC samples. In addition, we performed extensive *in vivo* modeling using murine xenografts of CTCL, including repeated dose toxicity, biodistribution, efficacy, and survival studies. Cytotoxicity assays demonstrated superior/comparable activity of NanoRomi (IC50: 1.1-2.3 nM) compared to free Romi (IC50: 4.8-10.6 nM) across all PTCL and LGLL cell lines studied, while in primary LGLL samples, NanoRomi exhibited superior cytotoxicity (2-fold) compared to Romi. WB analysis showed that NanoRomi induced apoptosis and increased acetylation of histone H3 and H4 in a time and concentration-dependent manner in cell lines representing CTCL, ALK+-ALCL, and LGLL. Repeat dose toxicity studies in CTCL xenografts confirmed that the overall tolerability of NanoRomi was substantially better than Romi. Tracking studies with a fluorescent dye (DiO) in the NanoRomi demonstrated preferential localization of NanoRomi in tumors of mice compared to the normal organs after 6 hours of drug administration. NanoRomi exhibited superior efficacy in the murine CTCL xenograft models, including a significant improvement in overall survival compared to Romi. Collectively, these data show that NanoRomi exhibits markedly superior pharmacokinetics, tolerability, and efficacy in models of TCL. We anticipate that the improved activity and tolerability of NanoRomi relate to the altered pharmacologic profile and superior bioavailability of the drug, which optimizes the effects of the drug for its influence on epigenetic biology. This unique platform offers the prospect of improving the tolerability and efficacy of epigenetic treatment strategies in these challenging diseases.

#3202 Investigating the induction of ferroptosis by nano drug delivery system.

E. M. Jacob[1], S. Y. Kim[2], P. Sirohi[3], M.-E. Wang[1], M. L. Davis[1], A. R. Bawcom[1], A. Chilkoti[3], M. R. Wiesner[3], J. Huang[1], M. Chen[1];
[1]Duke University School of Medicine, Durham, NC, [2]Washington and Lee University, Lexington, VA, [3]Duke University, Durham, NC

Prostate cancer is the second leading cause of cancer-related death in U.S. men. Genomic and clinical associations have identified loss of RB function as a dominant mechanism driving prostate cancer lethality. We recently demonstrated that ferroptosis induction *in vivo* by ferroptosis inducers blocks *RB1*-deficient prostate tumor growth and metastasis and leads to improved survival of the mice. As all ferroptosis inducers are newly discovered, there is a great need to improve their therapeutic potential through different avenues, including innovative drug delivery systems. Poly Lactic-co-glycolic acid (PLGA) is an FDA-approved biodegradable polymer. Due to their strong biocompatibility and consistent release, PLGA-based nanotherapeutics are an attractive carrier for small molecule drugs. This study aims to further improve the efficacy of ferroptosis induction against lethal *RB1*-deficient prostate cancer through PLGA-based ferroptosis-induced nanoparticles (NPs). The PLGA NPs encapsulating JKE-1674 were synthesized using the solvent evaporation method. The NPs were characterized using dynamic light scattering (DLS) and scanning electron microscopy (SEM) to assess the physicochemical properties of the NPs. The cell-killing efficacy of free-form or PLGA NP encapsulated JKE-1674 was then evaluated in vitro. Our analyses showed that the particle size and polydispersity index (PDI) of JKE-1674 PLGA NPs were 160.8 nm and 0.049, respectively. SEM images of JKE-1674 PLGA NPs further validated the DLS data. These findings suggest that encapsulation of JKE-1674 within the PLGA NPs results in a stable and biocompatible formation. Critically, JKE-1674 encapsulated by PLGA NPs is as potent as JKE-1674 in its free form to induce ferroptosis and associated lipid peroxidation in various human prostate cancer cell lines. This study presents the first effort to develop and validate PLGA-based ferroptosis-induced nanotherapeutics. Based on our *in vitro* data, we will test the *in vivo* efficacy of JKE-1674 PLGA NPs against lethal *RB1* deficient prostate cancer.

#3203 Extravasation and metastasis dynamics are cytoplasmically controlled by the epitranscriptome.

O. R. Grafinger[1], G. Thillainadesan[1], B. Su[1], Y. Mo[2], X. Xu[2], S. Mar[1], M. Sheng[1], S. Al Islam[1], J. Geddes-McAllister[3], M. G. Coppolino[3], H. H. He[2], G. Zheng[2], K. J. Jerzak[1], H. S. Leong[1];

[1]Sunnybrook Research Institute, Toronto, ON, Canada, [2]University Health Network, Toronto, ON, Canada, [3]University of Guelph, Guelph, ON, Canada

Non-coding RNA (ncRNA) and RNA binding proteins (RBPs) primarily reside in the nucleus to regulate splicing, transcription, and transcript stability. However, their role(s) in the cytoplasm were unclear until now. Evidence now suggests that ncRNAs within the cytoplasm play an important role in cancer invasion. In concert with MT1-MMP, a protease involved in invadopodia formation, long non-coding RNAs (lncRNAs) and RBPs form cytoplasmic complexes with MT1-MMP, which we termed “R-bodies” and are abundant in invasive breast cancer cells. RNA immunoprecipitation sequencing (RIP-seq) of only the cytoplasm identified the RNA at the core of these complexes to be metastasis-associated lung adenocarcinoma transcript 1 (MALAT1), a lncRNA which has been previously described as playing a fundamental role in cancer but only within the nucleus. Further investigation revealed that R-body-associated-MALAT1 was m6A-epigenetically marked. Depletion of any component of R-bodies and inhibition of m6A epigenetic marking of MALAT1 halted R-body formation and subsequent cell invasion. Importantly, we demonstrate that this cytoplasmic complex can be functionally targeted using RNA therapy against m6A-MALAT1 as well as drugs which inhibit the methyltransferase responsible for the m6A methylation of MALAT1. The identification of R-bodies has far-reaching implications and links the roles of cytoplasmic ncRNA and RBPs to the progression of disease.

#3204 Antitumor activity of a coencapsulated liposomal formulation of ceramides and doxorubicin in neuroblastoma models.

V. Bensa[1], M. Biscaia-Caleiras[2], M. Ponzoni[1], J. N. Moreira[3], C. Brignole[1], **F. Pastorino[1]**;
[1]IRCCS Istituto Giannina Gaslini, Genoa, Italy, [2]Bluepharma- Industria Farmaceutica, S.A, Coimbra, Portugal, [3]University of Coimbra, CIBB, Faculty of Pharmacy, Coimbra, Portugal

***Background*:** Neuroblastoma (NB) represents the most frequent and aggressive form of extracranial solid tumor of infants. Targeted therapies are severely limited by the lack of specific receptors, thus chemotherapy and radiotherapy remain the main treatment choices, which expose NB patients to systemic toxicity. Recently, we have demonstrated that cell surface Nucleolin (NCL) represents a novel cellular target for NB therapy.
***Methods*:** The cytotoxic potential of pH-sensitive nanocarriers (NC), decorated with the NCL-recognizing F3 peptide and incorporating a combination of the PI3K/Akt signaling inhibitors, C6-Ceramide (C6-Cer) or C18-ceramide (C18-Cer), and the topoisomerase II inhibitor doxorubicin (DXR) (F3-NC[C6-Cer/DXR] and F3-NC[C18-Cer/DXR], respectively), was tested *in vitro* on a panel of NB cell lines. Cytotoxicity was evaluated in monolayer and in multicellular tumor spheroid models, by MTS proliferation and Cell Titer Glo 3D cell viability assays, respectively. Apoptotic/necrotic cell death was investigated by Real Time-Glo Annexin VApoptosis and Necrosis assay.
***Results*:** F3-NC[C6-Cer/DXR] and F3-NC[C18-Cer/DXR] resulted significantly more effective, in term of reduction of NB cell viability, compared to the corresponding “drugs”-loaded untargeted NC formulations. Both formulations triggered apoptotic cell death, even if in a different kinetic profile. In particular, NB cells treated with F3-NC[C6-Cer/DXR] underwent apoptotic cell death earlier with respect to those treated with F3-NC[C18-Cer/DXR]. Interestingly, F3-NC[C6-Cer/DXR] exerted a significant superior cell killing effect when compared both to F3-NC[C18-Cer/DXR] and to F3-NC encapsulating only DXR, suggesting the importance of the combination treatment to enhance the antitumor effect against NB cells.
***Conclusion*:** Our preliminary findings demonstrate that the co-encapsulation and delivery of C6-Ceramide and DXR by NCL-recognizing nanoparticles exert potent antitumor effects against NB models *in vitro*. Ongoing *in vivo* experiments on clinically relevant mouse NB models (i.e. recapitulating primary tumor growth, metastases, and minimal residual disease) will allow us to define the possible use of F3-NC[C6-Cer/DXR] as an innovative therapeutic strategy for relapsed/refractory NB.
***Funding**:* AIRC IG n. 24397 to PF; CInTech (PRR) C644865576-00000005 to JNM.VB is recipient of AIRC ID 24397 contract. MBC is recipient of PD/BDE/150664/2020 (FCT) fellowship.

#3205 MicroRNA-peptide polyelectrolyte complex nanoparticle-hydrogel composite attenuates mesothelioma growth.

A. Singh[1], A. Caleb[2], J. P. Schneider[2], C. D. Hoang[1];
[1]National Institutes of Health, Bethesda, MD, [2]National Institutes of Health, Frederick, MD

Diffuse pleural mesothelioma (DPM) is a biologically unusual, aggressive asbestos-associated cancer affecting the entire pleura surface. DPM defies current standard multimodal therapies due to intrinsic chemoresistance and inability to achieve negative-margin resection of complex surface anatomy. Hence, current non-specific drug regimens ultimately fail because the biology of this tumor is poorly understood and even if surgically resected, tumor inevitably recurs from residual microscopic tumor foci. These various clinical challenges led us to develop a therapeutic platform delivering microRNA (miRNA), a novel anti-cancer agent therapeutic regimen, with the goal of eradicating residual microscopic tumor foci thereby improving the efficacy of multimodal therapy. We engineered a peptide-based biodegradable hydrogel that can be injected or sprayed directly to coat anatomic surfaces (surface-fill hydrogel; SFH), functioning as a therapeutic depot. Properties of SFH allow us to specify critical composition parameters such as biopersistence time, therapeutic payload, cell-specific targeting etc. In the first step of SFH formulation, miRNA complexed with different amphiphilic cationic peptides varying in length (19-26 amino acids) and amines (9-17), to form stable nanoparticles. Flash nanocomplexation (FNC) were used to produce highly scalable and kinetically controlled assembly of miRNA-peptide polyelectrolyte complex (PEC) nanoparticles (NPs), which utilizes a confined impinging jet (CIJ) mixer to achieve turbulent micromixing of the NPs components, yielding highly uniform and stable NPs. Next, NPs were encapsulated into another peptide hydrogel, formed via self-assembly of amphiphilic cationic peptide HLT2, thus forming a surface-fill hydrogel NPs composite. The SFH-NPs composite was not toxic to DPM cells and demonstrated efficient release of miRNA-peptide NPs from the SFH matrix in-vitro. The uptake of FAM-labeled miRNA-peptide NPs was confirmed by flowcytometry. Biodistribution analysis of NPs in mice bearing luciferase-positive DPM xenografts treated locally with Cy3-miRNA-SFH composite showed that Cy3-miRNA was concentrated in tumor cells but not in other organs. Furthermore, miR-215 exhibiting potent anti-tumor activity in DPM was used to study the therapeutic efficacy of SFH miRNA-nanoparticle composites. Subcutaneous DPM xenografts treated locally with miR-215 SFH composite shrank tumor significantly. Thus, delivery of specific miRNA-peptide PEC nanoparticles via SFH therapeutic platform in preclinical models of DPM displayed potent anti-cancer effects. Together, this new generation microRNA-peptide polyelectrolyte complex nanoparticles-SFH composite is a very promising delivery platform that could be extended for a diverse array of locoregional therapies.

#3206 Tumor-targeted nanoparticles for cancer therapy.

H. Kang[1], B. Upton[2], J. Nagy[2], T. Triche[1];
[1]Children's Hospital Los Angeles, Los Angeles, CA, [2]NanoValent, Bozeman, MT

Introduction: Untargeted cancer therapy is often toxic, limiting the maximum tolerated dose (MTD) and thus potential cure. Targeted therapy with antibody-drug conjugates (ADCs) has demonstrated greater efficacy, as with those directed at HER2 for triple negative breast cancer and other HER2 expressing tumors. However, ADC drug-antibody ratio (DAR) is limited, typically 3 to 1. In contrast, antibody-targeted nanoparticles deliver thousands of drug molecules per nanoparticle, with potentially greater anti-tumor effect.

Experimental Procedures: Antibody targeted nanoparticles (TNP) were created that preferentially deliver cytotoxic molecules to tumor cells. TNPs were created with various antibodies and payloads and evaluated for their efficacy against 12 different adult and pediatric malignancies (see below), using tumor xenografts in NOG-SCID mice. Survival of control, free drug, and TNP treated animals was compared. MED was also determined. Non-tumor bearing animals treated at the same dose and schedule were evaluated for evidence of toxicity. PK/PD metrics were obtained and drug delivery to normal and tumor tissue was evaluated microscopically and by mass spectroscopy.

Data: Plasma TNP drug levels persist for 48 hours, compared to free drug which is undetectable by 2 hours. Microscopically, nanoparticles accumulate in tumor tumor tissue but not normal tissue. Drug levels are typically 15 times higher in tumor tissue than normal tissue by quantitative mass spectroscopy. The minimum effective dose (MED) is reduced 25-fold for Ewing sarcoma, from 50 mg/kg to 2 mg/kg. TNPs also cross the blood-brain barrier (BBB), and were used to treat orthotopic GBM PDX xenografts, prolonging animal survival 3-fold over control or free drug treated animals. Ewing sarcoma, osteosarcoma, triple negative breast cancer, GBM, hepatoma, and adult ALL, bearing animals all showed complete tumor ablation and 100% survival when treated biweekly at 10mg/kg. Pancreatic, prostate, and ovarian Ca showed 100% survival in TNP treated mice after all control animals had died but remained tumor bearing with slow but progressive tumor growth when treated identically. Lung and colorectal Ca and melanoma bearing animals treated similarly with TNPs showed 50-80% survival at the time of control animal death. No animal in any study showed evidence of off-target toxicity.

Conclusions: Tumor antigen targeted, cytotoxic molecule containing nanoparticles have been created that show broad utility in the treatment of at least a dozen different adult and pediatric cancers. Six of 12 types showed complete tumor ablation when treated at 10mg/kg biweekly injections, and the remainder showed enhanced anti-tumor effect and survival compared to free drug treatment. We conclude that use of tumor antigen targeted, small molecule cytotoxic containing nanoparticles results in dramatically enhanced tumor response and in many case, complete tumor ablation where the same free drug fails to do so.

#3207 Chemical fabrication and characterization of a novel nanoparticle of the histone deacetylase (HDACi) romidepsin.

Samir Zuberi[1], Deepthi P. Damera[1], Ipsita Pal[1], Susan Walker[2], Ramesh Katla[1], Colin Haws[3], Akhil Gajjala[1], Andrea Joyner[1], Kallesh D. Jayappa[1], David J. Feith[1], Todd E. Fox[2], Thomas P. Loughran[1], Owen A. O'Connor[1], **Anuradha Illendula**[1]

[1]Department of Medicine, Division of Hematology/Oncology, University of Virginia, Charlottesville, VA,[2]Department of Pharmacology, University of Virginia, Charlottesville, VA,[3]National Resilience, Boston, VA

Introduction: Histone Deacetylase inhibitors (HDACi) are important drugs for the treatment of patients with PTCL (peripheral T-cell lymphoma). Romidepsin (R), a potent Class I HDACi, is given intravenously, weekly for three to four consecutive weeks. R has a half-life of three hours and is extensively protein bound. The indication for R in PTCL was recently withdrawn due to a failed Phase 4 study. Given the need for new drugs in PTCL, and the importance of epigenetically targeted drugs for the disease, we developed a first-in-class nanoparticle of R (NR) deploying a proprietary nanochemistry platform.
Methods: We modified the bulk nanoprecipitation method with FDA approved and Generally Recognized as Safe (GRAS) materials, specifically including PEGylated amphiphilic diblock copolymers, to develop NR combinatorially. By combining a drug and polymer solution with an anti-solvent, we produced core-shell structured NR particles with “stealth” properties. To achieve high R loading, stability, purity, scalability, and reproducibility, we devised a multi-pronged optimization system by modulating parameter sets in tandem. We determined the optimal parameters for the "lockdown" formulation. We purified NR by using centrifugal filters and determined stability by storing at 4°C. We used Cryo-electron microscopy (cryo-EM), Dynamic Light Scattering (DLS), and Liquid Chromatography-Mass Spectrometry (LC-MS) to determine the morphology, size, PDI, and drug concentration of NR. We developed fluorescent-NR with DiO dye to test bioavailability. We tested NR in T-cell lymphoma cell lines for histone acetylation and apoptosis induction. Furthermore, we investigated the *in vivo* pharmacokinetics and toxicity of NR in PTCL xenograft mouse model and quantified the drug by LC-MS.
Results: The physiochemical analysis of NR demonstrated that the particles were spherical, with a hydrodynamic diameter of 46 ±5 nm and PDI of 0.15 - 0.2. NR had a negative zeta potential and an exceptional drug encapsulation efficiency of over 50% (>500 µg/mL). NR exhibited high stability with respect to size, PDI and drug concentration for over two years. Flow cytometry and western blot analyses indicate NR induces apoptosis and histone acetylation in a time and dose-dependent manner, equivalent to or better than that observed for R. NR’s AUC increased 25-fold when administered intravenously. NR had superior tolerability, and DiO-NR confirmed superior biodistribution in tumor in a PTCL xenograft mouse model.
Conclusion: We developed a cutting-edge approach with minimum excipients, which enabled NR scale up with batch-to-batch reproducibility and high quality co-packaging of fluorescent dye and drug. NR improved R’s pharmacokinetic profile and efficacy in pre-clinical xenograft mice models. Our versatile technology enables Chemistry Materials and Controls products, an essential step in clinical product development.

#3208 A nano sized system for the treatment of gastrointestinal cancers.

D. Vaskovich[1], R. Acurcio[2], R. Kleiner[1], B. Carreira[2], A. Matos[2], H. Florindo[2], R. Satchi-Fainaro[1];
[1]Tel Aviv University, Tel Aviv, Israel, [2]University of Lisbon, Lisbon, Portugal

Despite the recent progress in cancer immunotherapies, most patients do not benefit from the currently available immune checkpoint blockers, and many develop severe immune-related adverse events. Therefore, it is urgent to develop alternative, effective immunotherapeutic approaches. An example of non-responsive cancers are gastrointestinal (GI) cancers, which account for 26% of the global cancer incidence and 35% of all cancer-related deaths. In many GI cancers, the failure of immunotherapies to yield clinical response is partially attributed to the inefficient antigen presentation by DC, which results in insufficient T cell stimulation despite their expression of tumor-associated antigens (TAA). To overcome these hurdles, we designed novel polymeric-based nanoparticles (NP) to deliver a combination of GI cancers antigens of CEACAM5 protein and toll-like receptor ligands to DC. We chose to encapsulate CEACAM5 antigens because it is overexpressed in GI cancers, such as gastric cancer, colorectal cancer, and pancreatic cancer. With this approach, we aim to modulate the tumor milieu-immune cell interactions to an anti-cancer phenotype in order to control tumor growth and improve overall survival. Our NP present an average diameter below 200 nm, narrow polydispersity index, slightly negative surface charge, spherical morphology, and high antigens and immune potentiators loading. Cy5-labeled NPs were found to be extensively internalized by DC, which triggered their activation *in vivo*, shown by the increasing expression of DC-related co-stimulatory molecules such as CD80, CD86, and CD40. Furthermore, we assessed the immunotherapeutic effect of our NP on mouse models and on a human 3D multi-cellular spheroid *ex-vivo* model, composing the patient's tumor cells and peripheral blood mononuclear cells (PBMC). We found that the NP successfully induced a potent immune-mediated anti-tumor response against CEACAM5-positive GI tumors, sensitizing the tumor microenvironment to other therapies and decreasing tumor volume, ultimately leading to prolonged survival. Taken together, the developed NP induced a strong antigen-specific immune response and overall sensitized CEACAM5-expressing GI cancers to the clinically relevant treatments *in vivo*, that so far have shown limited clinical outcomes in addition to a specific T cell anti-tumor activity that was shown on our patient-derived *ex vivo* model.

#3209 Antibody mediated targeted drug delivery approach for pancreatic cancer.

N. Dan[1], S. Setua[2], P. Shaji[3], S. Kumari[4], M. M. Yallapu[3], **S. S. Khan**[3], S. Chauhan[3];
[1]University of connecticut, Connecticut, NY, [2]University of Maryland, Baltimore, MD, [3]University of Texas Rio Grande Valley, Edinburg, TX, [4]National Institutes of Health, Bethesda, MD

Pancreatic ductal adenocarcinomas, originating from the epithelial cell lining of ducts, account for approximately 95% of tumors in this category, showcasing a survival rate of less than 5-7%. Unfortunately, little progress has been seen in the outcomes of patients with PDAC as tumor develops high desmoplasia and chemo-resistance to chemotherapeutic drugs, such as gemcitabine (Gem). The therapies are unable to penetrate to the fibrotic tumors leading to insufficient availability of the therapeutic drugs at the tumor site. We and others have shown that MUC13 is aberrantly expressed in pancreatic tumors but not in normal pancreas, which makes MUC13 as an excellent protein for specifically targeting pancreatic tumors. Herein, we demonstrate a unique ability of our in-house generated mouse and humanized monoclonal antibody of MUC13 to penetrate and target pancreatic cancer. These antibodies have been conjugated with our recently developed novel patented superparamagnetic iron oxide nanoparticles (SPIONS) to deliver therapeutics specifically to pancreatic tumors. In this study, we are using curcumin that depletes tumor microenvironment and gemcitabine to investigate the efficacy of the MUC13 conjugated SPION in delivery of therapeutic drugs. Our results demonstrate that enhanced uptake of MUC13-SPION formulation in MUC13 positive (MUC13+) PanCa cells, compared with MUC13 null (MUC13-) cells as demonstrated by immunofluorescence, Prussian blue staining and flow cytometry experiments. Interestingly, the formulation resulted in sustained delivery of curcumin (CUR), enhanced inhibition of cell proliferation, migration and invasion in MUC13+ cells as compared with MUC13- cells, which suggests the targeting efficacy of the formulation. In PanCa orthotopic mice model, MUC13-SPION efficiently targeted pancreatic tumors resulting in significant tumor accumulation. We observed inhibition of tumor volume, metastasis, gem resistance and improved survival in mice treated with the formulation. Additionally, the tumor tissues from treated mice showed extensive downregulation of PCNA and expression of key proteins in SHH pathway, such as SHH, Gli-1, Gli-2, Patched 1, SMO, which has been associated with cancer progression and drug resistance. In conclusion, the results indicate high therapeutic significance of MUC13-SPIONS for achieving pancreatic tumor specific delivery of drugs.

#3210 Raptamer-drug conjugates as molecularly targeted cancer therapeutics.

S. P. Vega[1], N. E. Ward[1], U. Saini[1], L. Castan-Chibas[1], G. Kaushik[2], D. Ciznadija[2], D. Chatterjee[1], M. J. Heffernan[1], A. Varadhachary[1], M. Ritchie[2]; [1]Fannin, Houston, TX, [2]Champions Oncology, Rockville, MD

The use of aptamers as a therapeutic targeting moiety holds the promise of building on the success of antibody-drug conjugates (ADCs). While ADCs are an attractive modality, they face limitations, including limited penetration into solid tumors and a complicated production process for large-scale manufacturing. Aptamers have several potential advantages over antibodies as a targeting moiety including: (i) a smaller size that enables better tumor penetration; (ii) chemical synthesis which allows rapid scale-up and ease of incorporating modifications; (iii) a superior safety profile from lack of immunogenicity and (iv) room temperature stability. Therefore, the use of aptamers in conjunction with drugs (similar to ADCs) holds promise for development of targeted therapeutics. We have identified a novel therapeutic target for certain cancers (COF-01) using proteomics data and immunohistochemistry from patient-derived tumors. Both the COF-01 protein and related mRNA expression was shown to be significantly increased in non-small cell lung cancer, head and neck cancer and pancreatic cancer. Here, we present a new therapeutic approach that targets COF-01-positive cancer cells using next generation aptamer conjugates. We performed a cell- and protein-based selection using our proprietary bead-based combinatorial libraries to generate next-generation base-modified ssDNA aptamers (Raptamers) against COF-01. Binding affinities of the COF-01 Raptamer candidates were determined by concentration curves using biolayer interferometry. The dissociation constants for the COF-01 Raptamers ranged from 80 nM - 200 nM. COF-01-specific Raptamer-drug conjugates (Rap-DCs) were developed by conjugating the Raptamers to monomethyl auristatin E via a cleavable linker. *In vitro* efficacy data showed the COF-01 Rap-DC can selectively induce cytotoxicity in different types of COF-01-positive human cancer cells (A431, CAL 27, BxPC-3). There was a significant decrease in cell viability of COF-01-positive cells when compared to COF-01-negative control cells (IC_{50} values ranged from 5.19 nM - 14.11 nM). *In vivo* efficacy testing in a COF-01-postive cell-derived xenograft mouse model showed a significant decrease in tumor volume in animals treated with the COF-01 Rap-DC when compared to saline- and erlotinib-treated controls. This provides proof-of concept for the use of high-affinity Raptamers against novel molecular targets, such as COF-01. This platform can be used to develop Rap-DCs against emergent neo-antigens on cancer cells that have escaped chemotherapy.

#3211 Development of first in class zip code drug conjugate in pancreatic ductal adenocarcinoma.

M. Cinar[1], P. Ganji[1], A. Pisarev[2], L. Martinez-Medina[3], D. S. R. Bandi[4], P. K. Puvvula[3], S. Chang[5], D. Maneval[3], B. El-Rayes[6], **L. Bernal-Mizrachi[1]**;
[1]Emory University School of Medicine, Atlanta, GA, [2]Kodikaz Therapeutic Solutions,LLC, New York, NY, [3]Kodikaz Therapeutic Solutions, LLC, New York, NY, [4]University of Alabama, Birminghan, AL, [5]Kodikaz Therapeutic Solutions, LLD, New York, NY, [6]University of Alabama, Birmingham, AL

Pancreatic ductal adenocarcinoma (PC) is the fourth most common cancer-related cause of death in Western countries. It is projected that PC will become the second most prevalent cause of cancer-related mortality by the year 2030. Although chemotherapy may offer certain advantages to those who have been diagnosed with pancreatic cancer, its effectiveness is notably constrained by the emergence of chemoresistance and excessive toxicity. In recent studies, it has been established that circulating tumor DNA (ctDNA) serves as a mechanism for cell-specific genetic transfer. We discovered that transposon sequences (known as Zip Codes, ZC) were responsible for ctDNA cell targeting. Therefore, we investigated the possibility of hijacking these ZC to deliver drugs specifically. We began by determining whether PDCA ZC synthesized chemically could target PDCA cells selectively. To achieve this, ZC sequences were labeled with CY5 for high-throughput microscopy. Results show that numerous PDCA-ZC were specific and efficient at targeting PC cell lines while sparing other cancer cell lines. The AluSc8 (PCZC) sequence was chosen for further investigation. The specificity of PCZC for targeting cells was validated using pancreatic islet cells. Based on these findings, we developed a technique for conjugating PCZC with SN38 via a CL2A linker. The results indicated that PCZC-SN38 was a very effective agent at killing PC cells (IC50: 1
µg), but not other cancer cell lines. The therapeutic efficacy of PCZC-N38 was evaluated in vivo using PDX (patient-derived xenografts, Garcia et al Plos One 2013). Maximum tolerated dose testing (MTD) (dosing from 1 to 21 mg of PCZC-SN38/Kg) failed to reach an MTD. Subsequently, we evaluated the efficacy signal of PCZC-SN38 by administering PCZC-SN38 to animals three times per week for three weeks at concentrations of 3 and 30 mg/kg of DNA (equivalent to 0.05 and 0.5 SN38 mg/kg). We used animals treated with vehicle, PCZC alone, and irinotecan (either once per week (50 mg/kg) or three times per week (0.5 mg/Kg) as a comparison. PCZC-SN38 decreased tumor growth by 41% and 70%, respectively, when compared to the vehicle or PCZC alone. The observed efficacy did not result in a change in body weight. In contrast, every animal administered irinotecan at a dosage of 50 mg/kg died within a week. On the contrary, animals that were given irinotecan at a dosage of 0.5 mg/kg demonstrated a growth inhibition of 60% and exhibited remarkable tolerability. Currently, research is being undertaken to determine the therapeutic efficacy of PCZC-SN38 at higher doses. The results outlined in this study illustrate the preliminary application of PC targeted drug delivery using a PC zip code drug conjugate. The results of our study demonstrate an innovative methodology for targeting PC cells specifically with therapeutic cargo material and supports further preclinical development of PCZC-SN38 for PC.

#3212 Development of a Trop2/CD3 bispecific antibody with modulated Trop2 binding affinity as a novel immunotherapy for advanced gastrointestinal cancer treatment.

C. O[1], **P. Wong**[1], K. Chow[1], K. Wong[1], D. Wong[2], J. M. Luk[2], K. Wong[1];
[1]Arbele Limited, Hong Kong, Hong Kong, [2]Arbele Corp, Seattle, WA

Trophoblast cell surface antigen 2 (Trop2) is considered as a potential therapeutic target because its over-expression in tumors is found to be associated with poor prognosis of patients with different cancers. Trop2-directed antibody-drug conjugates have been approved for the treatment of solid tumors, however, the expression of Trop2 in a broad range of epithelial tissues, even in low expression, would limit their clinical benefits. The present work generated a novel Trop2/CD3 bispecific antibody with its binding affinity towards Trop2 being well-modulated to mitigate the chance of on-target off-tumor effect. By linking a humanized anti-Trop2 monoclonal antibody with a CD3-binding scFv, a Trop2/CD3 bispecific antibody was produced. In order to adjust the bispecific antibody's affinity to the tumor target, ProABC-2 was used for in-silico paratope prediction (Ambrosetti F et al., 2020). A complementarity-determining residue (CDR) variant was produced and its binding to Trop2 antigen was analyzed using biolayer interferometry. The binding of both wild type (WT) and variant antibodies to Trop2-positive cancer cells, the activation of T cells upon target engagement and the redirection of T cell-mediated killing on cancer cells expressing high level of Trop2 were examined. The binding affinity of CDR variant to Trop2-expressing tumor cells was significantly reduced, which led to a slower induction of cytokines and T-cell proliferation, less acute T-cell activation, and a milder cytotoxic effect. This allowed the bispecific antibody to have a higher level of safety by restricting the cytotoxicity only to cancer cells that expressed high level of Trop2. Our novel Trop2/CD3 bispecific antibody not only showed potent anti-tumor activity, but also demonstrated a lower risk of on-target off-tumor toxicity. Monkey toxicity and other IND-enabling studies are beginning to further bring the drug candidate into clinical trial.

Table showing EC50 values of Trop2/CD3 bispecific WT and CDR variant antibodies in different assays

		WT	**CDR variant**
Binding affinity (M)	Trop2	4.62E-11	2.14E-10
Cytotoxicity (M)	AsPC1 (low Trop2 level)	1.24E-11	No killing effect
	SW480 (medium Trop2 level)	1.25E-12	2.25E-11
	NCI-H596 (high Trop2 level)	5.65E-12	5.89E-10
Receptor occupancy (%)	Trop2	0.65	2.75
	CD3	0.08	5.83
Cytokine induction (M)	IL-2	4.82E-11	5.42E-11
	IFNγ	6.46E-13	2.59E-11
T cell activation (M)	CD25+ marker	2.02E-12	2.39E-10
	CD69+ marker	3.81E-13	7.40E-11
T cell proliferation (M)	Ki-67 marker	3.54E-12	8.80E-11

#3213 A novel CDH17/PD-1 bispecific antibody for treatment of advanced gastrointestinal cancers.

K. Wong[1], **P. Wong**[1], K. Chow[1], C. O[1], D. Wong[2], J. M. Luk[2], K. Wong[1];
[1]Arbele Limited, Hong Kong, Hong Kong, [2]Arbele Corp, Seattle, WA

Targeting immune checkpoints like programmed death receptor 1 (PD-1) with monoclonal antibodies has achieved durable responses in a range of cancers, however, immune-related adverse events may occur in a subset of patients. As such, we developed a bispecific antibody targeting cadherin-17 (CDH17) and PD-1 with a hope to rejuvenate specifically the exhausted T cells within tumor microenvironment. In healthy individuals, CDH17 is expressed at a restricted level in intestinal epithelial junction that is not accessible to biologics, however, in gastrointestinal cancers, CDH17 is overexpressed and can be targeted by antibodies. Our new CDH17/PD-1 bispecific antibody would reactivate anti-tumor immunity with reduced risk of on-target off-tumor toxicity. Different bispecific antibody formats were designed, cloned, and expressed. Strong binders were first identified using CDH17 and PD-1 ELISA. The binding affinities to CDH17 and PD-1 of the selected candidate were examined using biolayer interferometry. The effect of these bispecific antibodies on blocking PD-1/PD-L1 axis in T cells was demonstrated in a cell-based reporter assay. T-cell mediated killing on CDH17-positive GI cancer cells and induction of T cell activation markers upon antibody treatment were also studied. A total of 7 CDH17/PD-1 bispecific antibodies of different formats were screened. Of these candidates, one, named ARB204, was selected because of its potent binding to both antigens in ELISA (i.e., EC_{50} values: CDH17, 1.6nM; PD-1, 0.4nM) and biolayer interferometry (i.e., K_D values: CDH17, 2.4E-09M; PD-1, 6.02E-11M). ARB204 blocked PD-1/PD-L1 axis in the reporter assay with EC_{50} value 4.4nM. Notably, ARB204 redirected T cells to eradicate CDH17-positive pancreatic AsPC1 cells with an EC_{50} value of 3.5nM. No cytotoxicity against CDH17-negative cancer cells were seen. ARB204 effectively bound CDH17 on GI cancer cells and PD-1 on T cells. This bispecific design allowed selective T-cell mediated killing on cancer cells expressing CDH17, mitigating the risk of off-tumor toxicity. ARB204 warrants further studies on its immune checkpoint inhibition in animal models.

EXPERIMENTAL AND MOLECULAR THERAPEUTICS: Epigenetic Targets
Poster Session

#3217 Discovery of novel inhibitors of the epigenetic regulator Kat6a histone acetyl transferase and characterization of their anti-tumor activity.

L. J. Holsinger[1], R. Rai[1], R. R. Nagawade[2], B. K. Pal[2], S. G. Pawar[2], K. A. Putta[2], S. S.C.[2], M. Jaleel[2], J. Wang[1], A. L. Hannah[1];
[1]ISOSTERIX, INC., San Carlos, CA, [2]Sai Life Sciences Limited, Medchal-Malkajgiri, India

KAT6A and its paralog KAT6B are histone acetyltransferases (HATs) which direct chromatin structural rearrangement and subsequent changes in gene transcription through acetylation of histones, primarily specific lysine residues on histone H3. KAT6A is modified in cancer, including genomic amplification, overexpression, mutation, as well as genetic rearrangement, resulting in the production of fusion proteins. Dysregulation of this MYST family member and its acetyl transferase activity is known to drive gene expression and tumorigenic progression in cancers. An inhibitor of KAT6A and KAT6B entered phase 1 clinical trials (NCT04606446). With continuous daily dosing, durable partial responses were seen in estrogen-receptor positive (ER+) breast cancer patients who had progressed on a prior endocrine therapy and CDK4/6 inhibitor. In that study, evidence of dose dependent pharmacodynamics (H3K23Ac inhibition) was observed in peripheral blood mononuclear cells and paired tumor biopsies (Sommerhalder, ASCO2023). Isosterix has developed a series of structurally diverse small molecule KAT6A-selective inhibitors which engage at the active site in the acetyl CoA substrate binding pocket. Lead compounds are selective for KAT6A and have significant potency and cellular activity in a variety of assays; they inhibit KAT6A-mediated histone acetylation in a biochemical assay as well as pharmacodynamic dose-dependent inhibition of histone acetylation in the breast cancer tumor cell line ZR-75-1. These compounds reduce cell viability of ZR-75-1 in 10 days with continuous compound administration, confirming the dependence of this cell line on KAT6A acetyl transferase activity for proliferation and cell cycle progression. Lead inhibitors are orally bioavailable with excellent pharmacokinetic properties in rodents. They demonstrate dose-dependent anti-tumor efficacy with minimal weight loss with continuous daily dosing in mouse xenograft tumor models. Inhibitors against this novel epigenetic target demonstrate the potential for efficacy in not only ER+ breast cancer but also other tumor indications which exhibit transcriptional induction dependent on KAT6A-directed chromatin remodeling. Selection of a lead candidate is planned for early 2024 with IND enabling studies to follow.

#3218 Combination drug screen identifies novel epigenetic therapies to enhance menin inhibitor efficacy in KMT2A rearranged and NPM1 mutant AML.

T. M. Totiger, S. Chaudhry, S. Montoya, M. Affer, A. K. Sondhi, A. Chirino, C.-H. Volmar, S. Brothers, J. Watts, J. Taylor;
University of Miami, Miami, FL

Background: Acute myeloid leukemia (AML) with KMT2A-rearrangements have a poor prognosis and so there is an urgent need for novel therapies. Menin inhibitors have shown promising anti-leukemic effects in KMT2A-rearranged and NPM1-mutated AML. However, the efficacy of menin inhibitors as single agents may be limited by the development of resistance mutations. Combining menin inhibitors with other epigenetic drugs may present a strategy to enhance their therapeutic potential. In this study, we performed a combination drug screen using an epigenetic drug library in KMT2A-rearranged (MV4;11) and NPM1-mutant (OCI-AML3) AML cell lines to identify synergistic therapies that can be used in conjunction with menin inhibitors.
Methods: During assay optimization, MV4;11 and OCI-AML3 cells were treated with the menin inhibitor DSP-5336, and their viability was assessed. Quality control metrics were applied with Z' values consistently greater than 0.5 for all assay plates and then the cells were subjected to a small molecule compound library screen containing a set of 932 epigenetic drugs. The screening process included a systematic evaluation of each drug's effect on cell viability in combination with the DSP-5336.
Results: The combination drug screen demonstrated robust performance in both MV4;11 and OCI-AML3 cell lines, with reliable quality control metrics. Among the epigenetic drugs tested, five compounds were identified as potential hits that synergistically enhanced the efficacy of DSP-5336 across both cell lines.The five identified compounds exhibited enhanced anti-leukemic effects when combined with the menin inhibitor in either one of the cell lines. The targets of these drugs varied, including histone deacetylases, histone acetyltransferases and BRD4 inhibition, suggesting many alternate mechanisms of action involving epigenetic modulation. Remarkably, one of the 5 hits C301-3161, a KAT2A inhibitor, showed limited activity in either cell line alone but increased cell killing with DSP-5336 in both cell lines, highlighting its potential as a specific therapeutic for combining with DSP-5336 in AML patients.
Conclusions: Our findings suggest combining menin inhibitors with other epigenetic drugs may improve AML treatment outcomes. The combination drug screen successfully identified four novel compounds that synergistically enhance menin inhibitor efficacy in both KMT2A-rearranged and NPM1-mutant AML cell lines. These compounds hold significant promise as potential therapeutic candidates for further investigation. Future studies should focus on elucidating the underlying mechanisms of action for each hit and evaluating their effects in preclinical animal models. Ultimately, this research may pave the way for the development of innovative combination therapeutic strategies for AML patients with KMT2A-rearragned and NPM1-mutant AML.

#3219 STAT3 inhibition synergizes with epigenetic therapy to suppress glutamine metabolism and clonogenic potential in non-small cell lung cancer.

J. An, Y.-Y. Chen, J. Park, S. Baylin, M. Topper;
Johns Hopkins University, Baltimore, MD

Non-small cell lung cancer (NSCLC) remains one of the deadliest cancers with metastatic disease being the primary driver of mortality. Therefore, there is a critical need for therapies that prevent disease dissemination in both early and late-stage disease presentations. Among the recent novel therapeutic combinations that have transformed the treatment landscape of NSCLC is an approach developed in our lab and others utilizing DNA methyltransferase inhibition (DNMTi) paired with histone deacetylase inhibition (HDACi) to sensitize patients to immunotherapy. However, most patients do not benefit durably from epigenetic therapy alone or in combination with other therapies.

In this study, we identified STAT3 as an actionable target in tumor cells that synergizes with epigenetic therapy (DNMTi+HDACi). We and others have previously shown that STAT3 signaling is augmented after epigenetic therapy. To interrogate the importance of this finding, we treated a panel of 12 human NSCLC cell lines with STAT3i+epigenetic therapy and identified five cell lines demonstrating a synergistic reduction of cell viability. These *in vitro* monolayer observations were recapitulated in an intermediate complexity 3D model, thus providing orthogonal validation of response applicability in a more treatment-resistant setting. In addition to phenotypic characterization, we deployed RNA sequencing to define the whole transcriptome consequences of our novel therapeutic paradigm. These transcriptional data showed that STAT3i+epigenetic therapy suppressed cell cycle and activated apoptotic pathways, which were validated by immunoblotting and flow cytometry-based approaches. We further demonstrated a significant and durable reduction in colony formation after treatment with STAT3i+epigenetic therapy. Additionally, we observed significant perturbation of a subset of genes involved in both epithelial-to-mesenchymal transition and suppression of glutamine and fatty acid metabolism.

Reliance on glutamine is considered a hallmark of cancer metabolism. Furthermore, glutamine metabolism has been implicated in the plasticity between epithelial and mesenchymal cancer cell states, which is required for metastatic success. Additionally, survival of metastatic cells requires upregulation of pathways that promote anchorage-independent growth and anoikis resistance, which are suppressed in our phenotypic and transcriptional data, respectively. Taken together, our results suggest **1.** STAT3i+epigenetic therapy diminishes the ability of NSCLC cells to survive and return to a colony-forming state and **2.** This phenotype is associated with metabolic dysfunction. Our studies therefore provide a basis for the development of novel strategies to intercept metastatic recolonization by impairing circulating tumor cells from seeding distant sites.

#3220 Osimertinib-induced epigenetic and transcriptional reprogramming drives a BRD4-POUF-PDGFRB-YAP-EMT axis of resistance in NSCLC.

A.-V. Hartley, C. Weston, S. Baldacci, W. Feng, M. Al-Dulaimi, C. Gentile, M. Booker, M. Tolstorokuv, C. Kadoch, P. Janne;
DFCI/Harvard Medical School, Boston, MA

Acquired resistance to Osimertinib continues to pose a major limitation to achieving durable therapeutic responses in EGFR mutant non-small cell lung cancer (NSCLC). While multiple actionable genetic mutations have been identified as the underlying molecular basis of resistance, a genomic mechanism cannot be identified in >50% of Osimertinib resistant tumors and thus an effective combinatorial treatment strategy cannot be deployed for these patients. Recently, we identified YAP/TEAD activation and ERK1/2 reactivation as two major non-mutational counter-regulatory pathways that diminish the efficacy of Osimertinib, promoting establishment of the drug tolerant persister (DTP) and resistant states. Moreover, it is well known that cancer cells escape tyrosine kinase inhibitor (TKI) therapy by developing dependence on alternate, non-mutated receptor tyrosine kinases (RTKs) through a treatment-induced “RTK switch” phenomenon. The link however between alternate RTK signaling and YAP/TEAD/ERK1/2 has never been explored in the context of Osimertinib resistance. In this study, we systemically uncover transcriptional de-repression of, and critical dependence on PDGFRβ as part of a novel “RTK switch” mechanism deployed by cells to evade Osimertinib-induced death. Genetic or pharmacologic co-inhibition of PDGFRβ renders NSCLC cells more sensitive to Osimertinib during drug naïve, DTP and resistant phases of treatment through suppression of ERK1/2 reactivation, YAP activity/nuclear translocation and YAP-mediated induction of EMT factors, SLUG and Zeb2. Importantly, compared to Osimertinib alone, co-targeting EGFR and PDGFRβ robustly suppresses tumor regrowth following treatment cessation both *in vitro* and *in vivo* which is consistent with a reduction in the DTP cell population. These data auspiciously demonstrate a two-fold utility of concomitant PDGFRβ inhibition: to enhance the initial efficacy of Osimertinib and to eliminate the DTP and resistant cells following chronic Osimertinib treatment. Further mechanistic studies from integration of ATAC-seq, CUT&RUN and RNA-seq reveal that Osimertinib induces the dynamic cooperativity of chromatin modulator BRD4 with pluripotent POU-domain transcription factors Oct-4, Pit-1 and Brn-3 at putative proximal enhancer elements, facilitating upregulation of PDGFRβ. Collectively, we demonstrate a novel treatment-induced BRD4/POUF epigenetic/transcriptional mediated “RTK switch” that involves co-opting PDGFRβ signaling to activate YAP/TEAD and ERK1/2 as a means of driving adaptive resistance to Osimertinib. These data provide compelling rationale for combined anti-EGFR and PDGFRβ targeted therapy to improve patient outcomes.

#3221 Targeting ARID1A-mutated gastric cancer cells with synthetic lethal approaches.

Menghan Fang[1], Youfen Lin[2], Chaorong Xue[2], Kaiqin Sheng[2], Zegeng Guo[2], Yuting Han[2], Hanbin Lin[2], Yuecheng Wu[2], Stephen B. Howell[3], Xu Lin[2], **Xinjian Lin**[2]

[1]Department of Pathology, Fujian Medical University Cancer Hosptial, Fuzhou, China,[2]Key Laboratory of Gastrointestinal Cancer (Fujian Medical University), Ministry of Education, Fujian Medical University, Fuzhou, China,[3]Department of Medicine and the Moores Cancer Center, University of California, San Diego, San Diego, CA

AT-rich interaction domain 1A (ARID1A) functions as a tumor suppressor gene, and its loss or inactivation is a common occurrence in various human malignancies, including around 30% of gastric cancers (GC). This study aimed to identify potential therapeutic targets for GC cells with ARID1A deficiency. After robust screening from a chemical library consisting of 551 diverse protein kinase inhibitors, we identified the AKT inhibitor AZD5363 as being the most potent lead compound in inhibiting viability of ARID1A$^{-/-}$ cells. A synthetic lethality between loss of ARID1A expression and AKT inhibition by AZD5363 was validated in both GC cell model system and xenograft model. Mechanistically, AZD5363 treatment induced pyroptotic cell death in ARID1A-deficient GC cells through activation of the caspase-3/GSDME pathway. Furthermore, ARID1A occupied the AKT gene promoter and regulated its transcription negatively, thus the GC cells deficient in ARID1A showed increased expression and phosphorylation of AKT. Our study demonstrates a novel synthetic lethality interaction and unique mechanism between ARID1A loss and AKT inhibition, which may provide a therapeutic and mechanistic rationale for targeted therapy on patients with ARID1A-defective GC who are most likely to be beneficial to AZD5363 treatment.

#3222 Acute and long-term responses to treatment with the HDAC inhibitor quisinostat in preclinical models of glioblastoma.

K. Orndorff, J. McNamara, M. Stavnichuk, C. Lo Cascio, C. White, E. Luna Melendez, G. Uzunalli, N. Sanai, S. Mehta;
Barrow Neurological Institute, Phoenix, AZ

Introduction: High expression of histone deacetylases (HDACs), particularly HDAC1, is strongly associated with poor prognosis for glioblastoma (GBM) patients. Quisinostat is a second-generation, class I-II selective HDAC inhibitor with high specificity for HDAC1 and potent anti-tumor activity. Here, we evaluated GBM PDX tissues and glioma stem cells (GSCs) for cellular, transcriptomic and phenotypic changes after acute and long-term treatment with quisinostat.

Methods: Multiple GBM PDX models and PDX-derived GSCs were treated with quisinostat, radiation, or a combination of quisinostat and radiation. Tissue and cells were processed for RNA-seq, qRT-PCR, and immunofluorescence assays to examine alterations in neuronal signaling, cell fate, DNA damage, and markers of stemness and differentiation.

Results: Bulk RNA sequencing of tumor tissue revealed that chronic co-treatment with quisinostat and radiation led to increased cellular expression of neuronal signaling and neuronal development pathways compared to the untreated control group. Increase in expression of neuronal signaling genes was also observed upon *in vitro* treatment of GSCs with quisinostat. Immunocytochemistry and immunofluorescence staining confirmed changes in neuronal signaling and neuronal cell fate proteins after quisinostat treatment.

Conclusions: Quisinostat treatment induces a shift in tumor cells towards a neuronal-like cell fate. Considering that GSCs have been shown to establish synaptic junctions with healthy neurons to evoke enhanced excitatory currents within glioma cells and contribute to treatment resistance, further investigation of this shift upon HDAC inhibition is crucial. Ongoing studies are aimed at evaluating the significance of these cellular and molecular changes resulting from quisinostat treatment and whether the quisinostat-induced cell fate changes can be exploited for future combination therapy for GBM.

#3223 Embryonic ectoderm development (EED) inhibitor APG-5918 (EEDi-5273) and MDM2 inhibitor alrizomadlin (APG-115) synergistically inhibit tumor growth in preclinical models of prostate cancer (PCa).

Y. Yin[1], Y. Yang[1], E. Liang[2], B. Li[1], H. Wang[1], D. Yang[1], Y. Zhai[1];

[1]Ascentage Pharma (Suzhou) Co., Ltd., Suzhou, China, [2]Ascentage Pharma Group Inc., Rockville, MD

Advanced PCa, especially castration-resistant PCa, represents an urgent unmet treatment need. Dysregulation of the polycomb repressive complex 2 (PRC2), which mediates trimethylation of histone H3 at lysine 27 (H3K27me3) and leads to gene silencing, is common in PCa and correlates with poor prognosis. EED, a core PRC2 component, is crucial for histone methyltransferase activity. MDM2, a negative regulator of p53, is often amplified or overexpressed in PCa and associated with metastasis and poor clinical outcomes. We evaluated antitumor activity and molecular mechanisms of EED inhibitor APG-5918/EEDi-5273 and MDM2 selective inhibitor alrizomadlin in preclinical PCa models. Human castration-resistant (22Rv1) and androgen-dependent (LNCaP) PCa cell lines were used in antiproliferation assays. Cell viability was determined by CellTiter-Glo luminescent assays. Western blotting was used to explore mechanisms of action. Subcutaneous 22Rv1 and LNCaP cell line-derived xenograft (CDX) models were established to evaluate antitumor effects of APG-5918 and alrizomadlin *in vivo*. Single-agent APG-5918 or alrizomadlin had limited inhibition on PCa cell growth; combined, they demonstrated synergistic antitumor activity. In the 22Rv1 CDX model, single-agent alrizomadlin (100 mg/kg) or APG-5918 (100 mg/kg) administered for 26 days exerted no/limited antitumor activity, with treatment-to-control (T/C) values of 93.39% and 49.89%, respectively. In contrast, the doublet enhanced antitumor activity (T/C value, 33.22%), with a synergistic index of 1.40. In the LNCaP CDX model, APG-5918 (100 mg/kg) administered for 28 days exhibited minimal antitumor effects (T/C value on last day of dosing, 80.32%). Alrizomadlin (100 or 50 mg/kg) showed limited antitumor activity (T/C value, 47.61%). Combined treatment significantly enhanced antitumor activity (T/C value, 15.69%), with a synergistic index of 2.44. Regarding putative mechanisms, western blot analyses showed that APG-5918 downregulated oncogenic drivers and DNA methylation factors (UHRF1, DNMT1) and on-target-related pharmacodynamic markers (H3K27me3, EED, EZH2). Alrizomadlin markedly downregulated UHRF1 and DNMT1, and upregulated p53 and p21 expression. Combined treatment further enhanced downregulation of DNMT1, UHRF1, cell cycle pathway proteins (pRb, CDK6), antiapoptotic protein MCL-1, and synergistically increased cleavage of PARP-1, a marker of apoptosis. In summary, we show that targeting EED and MDM2 synergistically enhances antitumor activity in PCa cell lines and CDX models. Mechanistically, this combination likely modulated pathways related to DNA methylation, cell cycle, and apoptosis. The findings provide a scientific rationale for future clinical development of APG-5918 and alrizomadlin for PCa patients.

#3224 Identifying the molecular mechanisms underlying progesterone receptor downregulation in endometrial cancer.

X. Meng, L. Lamont, S. Yang;
Carver College of Medicine, University of Iowa, Iowa City, IA

Background: Endometrial cancer (EC) is the most common gynecologic cancer. Cancer survival has improved over the past four decades for all the most common cancers except cervical and EC, calling for significant treatment advancements. Progesterone receptor (PR) is a favorable prognostic marker for EC and other solid tumors. However, PR expression has been shown to be reduced or lost in these malignant tumors, which correlates with worse patient survival and limits the effectiveness of progestin therapy. Thus, restoring functional PR expression is vital to sensitizing tumor cells to progestin therapy, enhancing EC clinical interventions, and improving patient outcomes. In this project, we aim to restore functional PR expression.

Methods: To visualize PR expression in real-time, we constructed an innovative endogenous PR reporter gene transfected EC cells. This system facilitated screening potential small molecular PR inducers from the FDA-approved oncology drug library. Sixteen drugs were identified to increase PR expression; topoisomerase II inhibitors (Top IIi), mitoxantrone and idarubicin were the top hits. Drug effect of Top IIi, as well as HDAC inhibitor romidepsin, dual PI3k/HDAC inhibitor CUDC-907, and PHB2 inhibitors, fluorizoline (FLZ) and rocaglamide (RocA), were evaluated as single drug or in combination. Potential PR repressors, including G9a, HDAC2, PHB2, and Top2A, were knocked down using siRNA, shRNA, or CRISPR-Cas9 in EC cells and PR expression was analyzed. A chromatin immunoprecipitation (ChIP) assay was also conducted to validate bona fide PR repressors.

Results: Mitoxantrone and idarubicin were validated to be effective PR inducers. G9a, HDAC2, PHB2, and Top2A were confirmed PR repressors. Single treatment with mitoxantrone, idarubicin, romidepsin , CUDC-907 , FLZ , and RocA achieved effective inhibition of EC cell proliferation and enhanced PR expression except FLZ and RocA. Combined romidepsin with Topi or PHB2i demonstrated additive or synergistic effects. More importantly, dual treatment of CUDC-907 with mitoxantrone enhanced PR expression compared to a single treatment or no treatment control. Our mass spectrometry and ChIP assay by specific antibodies against HDAC2 and PHB2 revealed that potential mechanisms include PHB2 forming a complex with HDAC2 that binds on the PR promoter, thus inhibiting PR transcription.

Conclusion: Co-treatment of CUDC-907 with Top2Ai increased PR expression and enhanced cell death in EC cell lines, indicating a potential treatment strategy. *In vivo* studies utilizing our EC-PDX models will further validate the efficacy of restoring PR expression and suppressing EC tumor growth. Further studies of the molecular mechanisms behind this strategy will be conducted.

#3225 Profiling the DNA regulome to discover direct inhibitors of the brachyury transcription factor.

Alexander Joel Federation, Yang Gao, Brian McEllin, Tonibelle Gatbonton-Schwager, Andrea Gutierrez, Julia Robbins, Bodhi Hueffmeier, Erin Broderick, Daniele Canzani, William Fondrie, Lindsay Pino

Talus Bioscience, Inc., Seattle, WA

Background: The human genome encodes more than 1,600 transcription factors (TFs), along with additional cofactors, chromatin regulators, and structural proteins that collectively execute the regulatory instructions encoded within the nuclear DNA. Dysfunctions of these proteins, collectively known as the Regulome, are known to drive multiple conditions such as cancer, autoimmune conditions, and fibrosis. Despite their importance, many of these proteins are considered undruggable due to challenges in modeling their activity in vitro.
Methods: We have addressed these shortcomings by implementing a live-cell Regulome profiling approach that quantifies the global activity of TFs without the need for cell manipulation or genome engineering, called TF-Scan. The technology coupled rapid, automated purification of the DNA-bound proteome coupled to scalable Data Independent Acquisition (DIA) quantitative mass spectrometry proteomics and machine learning.
Results: We completed a screen of covalent compounds across 8 tissue types to discover hotspot sites on TFs that control their DNA-binding activity. A chordoma cell line was included in this screen. The screen identified compounds capable of binding to and disrupting the activity of several previously undruggable transcription factors, including brachyury. Hit validation and hit-to-lead medicinal chemistry resulted in a covalent chemical probe for brachyury, with activity in cell line models of chordoma.
Conclusion: Phenotypic drug discovery in live, unmodified human cells with systematic regulome profiling enables the discovery of compounds that disrupt previously undruggable targets by multiple mechanisms of action.

#3226 PRMT1 is a critical dependency in clear cell renal cell carcinoma with roles in post- transcriptional regulation and DNA damage response.

J. Walton[1], K. Arevalo[2], A. Ng[2], J. Meens[1], C. Karamboulas[1], P. Prinos[3], B. Raught[1], E. Chen[1], C. Arrowsmith[1], L. Ailles[1];
[1]University Health Network, Toronto, ON, Canada, [2]The University of Toronto, Toronto, ON, Canada, [3]The Structural Genomics Consortium, Toronto, ON, Canada

The majority of sporadic renal cell carcinoma (RCC) cases present as the clear cell subtype (ccRCC) and are associated with the biallelic inactivation of the von Hippel-Lindau (*VHL*) gene, leading to constitutive activation of the cellular hypoxia response and deleterious alterations to gene expression, metabolism, and growth. Despite the near ubiquity of VHL loss, evidence suggests that it alone is insufficient to drive tumor establishment. Additional loss of function (LOF) mutations in epigenetic regulatory proteins including *PBRM1*, *SETD2* and *BAP1* have been identified as tumor drivers. The frequency and penetrance of these mutations in epigenetic regulators implicates a vulnerability in ccRCC that may be exploited to develop new therapies. To explore this vulnerability, the Ailles lab completed a screen of the Structural Genomics Consortium's (SGC) epiprobe library - a panel of inhibitors targeting an array of epigenetic regulators in patient derived ccRCC models. Among the several promising targets identified, a particularly favorable inhibition profile was noted for MS023, an inhibitor of the type I protein arginine methyltransferase family (PRMT1/3/4/6 and 8). PRMTs transfer methyl groups to nuclear histones and cytoplasmic targets, influencing gene expression, mRNA processing and viability. This growth inhibition was corroborated using an additional type I PRMT compound, GSK3368715. CRISPR-mediated deletion of type I PRMT targets indicated that PRMT1 is the main enzyme responsible for growth inhibition in our ccRCC models. Furthermore, genetic depletion of PRMT1 *via* shRNA phenocopied pharmacological inhibition and proliferative growth was restored in the presence of MS023 by overexpressing PRMT1. Finally, MS023 treatment of mice bearing ccRCC cell line and patient derived xenografts led to significant inhibition of tumor growth *in vivo*. Transcriptomic profiling of chemical treatment and PRMT1 genetic depletion demonstrated that PRMT1 inhibition triggers a significant down regulation of genes related to cell cycle progression and DNA damage. ccRCC cells treated with MS023 accumulated significant levels of DNA damage before undergoing cell death, with several DDR-related proteins being down-regulated. Proximity ligation and proteomic analysis (Bio-ID) revealed that PRMT1's interactors skew heavily towards RNA metabolism regulators and widespread alterations in mRNA processing were noted with MS023 treatment. Evidence continues to mount that PRMT1 is implicated in the biology of cancer, but to our knowledge, no thorough investigations have been performed in the context of ccRCC. Our data suggests that inhibition of PRMT1 inhibits processing of mRNA transcripts, compromises DDR mechanisms, leading to an accumulation of double stranded breaks, cytostasis and cell death. Thus PRMT1 represents a viable therapeutic target in ccRCC.

#3227 Developing brain-penetrating MAT2A inhibitors for *MTAP*-deleted brain metastatic cancer and GBM.

S. Ki, J. Kim, J. Na, I. Koh, H. Cho, H. Lee, H. Jung, G. Cho, M. Moon, Y. Shin, S.-K. Park;
SK Biopharmaceuticals Co., Ltd., Seongnam, Korea, Republic of

Background: Homozygous deletion of *MTAP* is one of the most frequent genetic alterations in various solid tumors including glioblastoma (GBM), mesothelioma, pancreatic cancer and lung cancer. While *MTAP*-deleted cancers are associated with a poor prognosis, there are no approved drugs for the treatment of patients with *MTAP* deficiency. MAT2A has emerged as a potential target for selective anticancer effects in *MTAP*-deleted cancers. However, development of brain-penetrating MAT2A inhibitors are yet to be reported in preclinical or clinical stages despite of high *MTAP* deletion fraction in GBM and brain metastatic cancers. Here, we present highly potent and selective MAT2A inhibitors capable of brain penetration for *MTAP* deleted cancer therapy.
Methods: A MAT2A biochemical enzyme assay was performed with phosphonate colorimetric kit. To evaluate *in vitro* and *in vivo* activities of compounds, S-adenosylmethionine (SAM) and symmetrical dimethyl arginine (SDMA) levels were measured using LC-MS/MS and high-content screening systems. Cell growth inhibition assay was evaluated to confirm the selectivity in isogenic pairs of HCT116 WT and *MTAP*-deleted cells. *In vivo* efficacy was conducted using the *MTAP*-deleted HCT116 xenograft.
Results: To develop novel brain penetrating scaffolds, we focused on interaction of hydrogen bond acceptor in the scaffolds with arginine residue Arg313 in MAT2A protein and the improvement of physicochemical properties, including logP and logBB. A series of MAT2A inhibitors significantly inhibited MAT2A enzymatic activity, resulting in the reduction of intracellular SAM level, the direct product of MAT2A. These compounds showed highly potent inhibition of SDMA and cell proliferation in *MTAP*-deleted cells, while displaying minimal effect on *MTAP*-WT cells, showing >100-fold selectivity towards *MTAP*-deletion over *MTAP*-WT. Furthermore, anti-proliferative activity of MAT2A inhibitors were observed in *MTAP*-deleted cancer cells across various cancer types, including GBM, breast cancer, and non-small cell lung cancer. Remarkably, mouse pharmacokinetic study revealed high level of plasma and brain exposure with outstanding brain-to-plasma ratio (> 0.75). Robust tumor growth inhibition as well as reduction in tumor SAM levels were observed as monotherapy in an *MTAP*-deleted HCT116 xenograft model.
Conclusion: We have identified novel brain-penetrating MAT2A inhibitors displaying encouraging *in vitro* and *in vivo* pharmacological profiles, indicating the potential use of these compounds as therapeutic agents for *MTAP* deleted brain metastatic cancer and GBM.

#3229 IACS-16559, a CBP/P300 bromodomain inhibitor for the treatment of specific AML subsets.

Ciro Zanca, Michael Soth, Guang Gao, Jason Gay, Ningping Feng, Christopher Bristow, Kang Le, Quanyun Xu, Phuong Nguyen, Yongying Jiang, Teresa Perry, Faika Mseeh, Paul Leonard, Jason Cross, Virginia Giuliani, Joe Marszalek, Philip Jones, Tim Heffernan

The University of Texas MD Anderson Cancer Center, Houston, TX

Block in differentiation and accumulation of undifferentiated blasts are hallmarks of Acute Myeloid Leukemia (AML) and epigenetic processes have been shown to play a critical role in hematological malignancies. Paralogs CREBBP and EP300, in association with co-factors, are hijacked during leukemogenesis by aberrant transcriptional factors, thus driving blast proliferation and maintaining the undifferentiated phenotype. Here, we introduce IACS-16559, a bromodomain inhibitor targeting CREBBP/EP300. IACS-16559 is highly selective for the bromodomains of CBP and EP300 versus BRD4, showing a dose-dependent inhibition of H3K27 acetylation residue *in vivo* and *in vitro*. In addition, IACS-16559 pharmacokinetic properties show low clearances, high oral exposures and predicted QD dosing in human. We screened AML cell lines *in vitro* for their response to IACS-16559 and identified specific subtypes of AML that exhibit heightened sensitivity to CBP/EP300 inhibition, specifically AML with AML1-ETO and MLL-AF9 rearrangements, and AML featuring mutations in the nucleophosmin (NPM1c) gene. IACS-16559 inhibited proliferation of AML responder cell lines *in vitro*, halted cell cycle progression, with an accumulation of cells in G1 and a decrease of cells in S phase. IACS-16559 did not induce apoptosis across a panel of AML cell lines, indicating that induction of apoptosis is not a major mechanism of action of CBP/EP300 inhibition. To augment the anti-tumor effects of IACS-16559, we prioritized the pharmacological combination of CBP/EP300 and MLL-Menin inhibitors. This combination synergistically impeded cell proliferation and potently triggered apoptosis *in vitro* and *in vivo*, whereas none of the individual agents alone had this effect. The changes in gene and surface marker expression produced by these treatments, as single agents and in combination with synergistic effects, were in line with an induced myeloid differentiation phenotype. Collectively, our findings provide a compelling basis for further exploring the use of a CBP/EP300 bromodomain inhibitor in conjunction with an inhibitor of the MLL-Menin interaction in a subset of AML patients with MLL rearrangements or NPM1 mutations.

#3230 Discovery of selective BRM (SMARCA2) ATPase inhibitors for the treatment of BRG1 (SMARCA4) mutant cancers.

J. Y. Lee[1], N. Brooks[2], B. Antonakos[1], B. Perria[2], C. Langan[2], B. D. Jones[2], R. S. Flack[2], Z. Li[1], D. Terry[1], R. Wallace[3], R. Bondi[3], G. Sis[3], R. Baracani[3], M. McVean[3], G. Kolakowski[3], D. Osimboni[1], K. Wilson[1];

[1]Foghorn Therapeutics, Cambridge, MA, [2]Loxo@Lilly, Indianapolis, IN, [3]Loxo@Lilly, Louisville, CO

BRM (SMARCA2) and BRG1 (SMARCA4) are highly homologous ATPases that are members of the BAF (also known as the mSWI/SNF) chromatin remodeling complex. BRM and BRG1 are mutually exclusive enzymatic subunits of BAF complexes, and functional genomic screens have shown a synthetic lethal relationship between the two genes. BRG1 is frequently mutated in cancer, including in approximately 10% of non-small cell lung carcinomas. Selective inhibition of BRM is a mechanism by which BRG1-mutated cancer cell growth would be affected by losing BRM function, while normal tissues should be spared as they still express functional BRG1. Given that the ATPase domains of BRM and BRG1 are 92% identical, the identification of selective enzymatic inhibitors of BRM has been challenging. Here, we report the discovery of novel, highly potent compounds that selectively inhibit BRM over BRG1 as seen in cell-based transcription and proliferation assays, that also possess excellent oral pharmacokinetics. Our lead compounds inhibit BRM in a cell-based reporter assay with an unbound IC_{50} of 1 nM and are greater than 20-fold selective over BRG1. They are also selective against other helicases and do not show any significant activity in off-target screening panels. Dosing of mice carrying BRG1-mutant xenografts causes target gene modulation that is correlated with compound exposure. Treatment of A549 and RERF-LC-AI xenografts with lead compounds led to tumor growth inhibition of 87% and 96%, respectively, at well-tolerated doses, and significant tumor growth inhibition was also achieved in multiple other BRG1-mutant models. The results suggest that our compounds have first-in-class potential as potent and selective BRM ATPase inhibitors for the treatment of BRG1-mutated cancers, and we are planning to file an IND in 2024.

#3231 Pharmacological inhibition of the m^{6}A RNA reader, YTHDC1, as a novel approach to targeting biomolecular condensates in cancer.

R. C. Centore[1], M. Charles[2], M. Arora[1], Y. Chen[1], M. Watson[2], C. Kelley[1], M. Czekalska[2], M. Rebmann[2], M. Ghandi[1], J. Cattin[2], N. Bharatham[2], P. Radhakrishnan[1], A. Howarth[2], G. Rudlaff[1], W. E. Arter[2], S. Qamar[2], K. Saar[2], D. Williamson[2], A. Seeber[1], T. Knowles[2], **S. Arora[1]**;
[1]Transition Bio, Watertown, MA, [2]Transition Bio, Cambridge, United Kingdom

Epigenetic dysregulation is a hallmark of cancer, and tumors have evolved complex mechanisms to fine-tune oncogenic gene expression. In acute myeloid leukemia (AML), one such regulatory mechanism involves post transcriptional modification of RNAs. The most abundant post transcriptional modification is methylation of adenosine at the N6 position (m^{6}A). This modification is catalyzed by the m^{6}A “writer”, METTL3 and METTL14 complex, and is removed by “erasers” such as FTO and ALKBH5. m^{6}A RNAs can regulate a variety of cellular processes which can impact tumor phenotypes, including RNA stability, splicing, and nuclear export; and METTL3 catalytic inhibitors are currently in clinical development for AML and other cancers (NCT05584111).The m^{6}A “reader”, YTHDC1, has been recognized as a critical contributor to the proliferation and survival of AML cells. As the primary nuclear m^{6}A reader, YTHDC1 localizes with m^{6}A marked RNAs in phase-separated assemblies, termed biomolecular condensates, helping to maintain the stability of oncogenic transcripts such as *MYC*. Here, we have employed our proprietary microfluidics based screening platform (termed PhaseScan^{TM}) to identify modulators of YTHDC1 biomolecular condensates. Evaluation of early screening hits helped identify that disruption of the interaction between YTHDC1 and m^{6}A RNA is a functionally relevant mechanism of action (MoA) that results in dissolution of YTHDC1 condensates. Using computational and knowledge based approaches, we have identified other structurally distinct inhibitors that occupy the RNA binding pocket of YTHDC1 and disrupt its interaction with m^{6}A RNA at nanomolar potencies. These compounds disrupt cellular YTHDC1 condensates, suppress oncogenic gene expression, and result in anti proliferative and pro-differentiation phenotypes in AML cell lines. Compounds are selective for YTHDC1 over other YTH family members and are also selective in dissolving YTHDC1 condensates over other nuclear and cytosolic condensate systems. Our optimized chemical matter has suitable ADME properties to support *in vivo* studies. Thus, targeting YTHDC1 biomolecular condensates represents a novel approach to the treatment of AML.

#3232 LSD1 inhibition transcriptionally reprograms neuroendocrine prostate cancer exposing unique therapeutic vulnerabilities.

S. M. Jasmine[1], A. Mandl[1], S. L. Dalrymple[1], S. Kim[1], J. Dias[2], M. Kleppe[2], C. Celatka[2], A. Tapper[2], I. Coleman[3], P. Nelson[3], H. Rienhoff[2], S. R. Denmeade[1], W. Brennen[1];

[1]Johns Hopkins University, Baltimore, MD, [2]Merck, Boston, MA, [3]Fred Hutchinson Cancer Center, Seattle, WA

Therapeutics have been developed to target castration-resistant prostate cancer (CRPC) classified as adenocarcinoma (CRPC-Adeno). However, an increasing frequency of CRPC-Adeno tumors progress to the highly aggressive and lethal neuroendocrine prostate cancer (NEPC) by acquiring a neuroendocrine (NE) phenotype as a mechanism of therapeutic resistance. This transformation from CRPC-Adeno to NEPC requires distinct epigenetic reprogramming by lysine-specific demethylase 1 (LSD1), which can be exploited for development of novel therapies to target NEPC. LSD1 is upregulated in NEPC and promotes a stem-like transition state through lineage plasticity which enables the cancer cell to undergo NE differentiation. We have shown that LSD1 inhibition reduces the NE program, driving NEPC towards a non-neuroendocrine state through ASCL1 suppression and YAP1 re-expression. This less aggressive non-neuroendocrine state exposes unique vulnerabilities for the development of novel combination therapies to treat this lethal disease.

#3233 EP102: Pharmacological Inhibition of METTL3 causes tumor growth inhibition and prolongs survival in preclinical models of NSCLC, ovarian and squamous cell carcinoma.

G. Fraser, C. Sorlet, N. Parmentier, E. Brunel, C. Coremans, S. Rorive, A.-F. Hartiel, K. Oukoloff, G. Dutheuil;
EPICS Therapeutics, Gosselies, Belgium

METTL3 is the RNA methyltransferase predominantly responsible for the addition of N-6-methyladenosine (m6A), the most abundant epigenetic modification to mRNA. The prevalence of m6A and the activity and expression of METTL3 have been linked to the appearance and progression of numerous hematological and solid tumor cancers. EPICS has discovered and optimized small molecule inhibitors of METTL3 ("M3i"). The aim of the current study is to evaluate the efficacy of M3i in various CDX mouse tumor models. M3i compound potency was evaluated in vitro by measuring enzymatic inhibition of METTL3/14 by scintillation proximity assay (IC_{50} = 2 nM). The anti-proliferative effects of M3i were measured in cell viability assays following a 72h treatment of A549 (NSCLC, IC_{50} = 190 nM), SKOV3 (ovarian, IC_{50} = 9 nM) and FaDu (hypopharyngeal squamous cell carcinoma, IC_{50} = 24 nM) cells. Complementary data in all three cell lines demonstrates a clear concentration-response for a target engagement biomarker (m6A; IC_{50} = 2-8 nM, across cell lines) as well as M3i-induced changes in biomarkers of oncogenic drivers. M3i (30 mg/kg, IP, QD) was tested in vivo in mouse models using FaDu (subcutaneous implant) in addition to A549 and SKOV3 (both orthotopic implants); all animal models were performed by LabCorp (MI, USA). Daily M3i treatment significantly prolonged survival in all three disease models consistent with efficacy on tumor growth inhibition as measured by imaging (A549, SKOV3) or direct measurement of tumor volume in the case of subcutaneous implant (FaDu). M3i has previously been shown to be effective in mouse CDX and PDX models of AML. The current results extend the application of METTL3 inhibitors to include the treatment of various types of solid tumors. The efficacy of M3i as a single-agent on tumor growth inhibition and survival advances the validation of METTL3 as a cancer target and provides additional evidence for the applicability of mRNA epigenetic mechanisms to the treatment of solid tumors.

#3234 A new vulnerability to BET inhibition due to enhanced autophagy in *BRCA2*-deficient pancreatic cancer.

S. Archasappawat[1], E. Lee[1], K. Ji[1], J. Pena[2], V. F. Vega[2], R. Gangaraju[1], N. S. Beesabathuni[1], M. J. Kim[1], Q. Tian[1], P. Shah[1], L. Scampavia[2], T. Spicer[2], C.-I. Hwang[1];

[1]University of California, Davis, Davis, CA, [2]The Herbert Wertheim UF Scripps Institute for Biomedical Innovation & Technology, Jupiter, FL

Pancreatic ductal adenocarcinoma (PDAC) is the third leading cause of cancer-related deaths in the United States, with the lowest five-year survival rate of all cancers. Around 10% of pancreatic cancer diagnoses are thought to be familial pancreatic cancer (FPC). *BRCA2* pathogenic variants have been identified to be closely associated with FPC. Personalized medicine approaches that are tailored to FPC patients based on their mutation profiles could improve patient outcomes and minimize adverse effects. This study aims to identify novel potential drug candidates for *BRCA2*-deficient PDAC and dissect its underlying molecular mechanisms. To discover new vulnerabilities for *BRCA2*-deficient pancreatic cancer, we performed high-throughput drug screening (HTS) using isogenic murine *Brca2* knockout (KO) and control PDAC cells. The HTS assay revealed that JQ1, a small molecule inhibitor of the bromodomain and extra-terminal domain protein (BET) family, selectively induced cytotoxicity in *Brca2* KO cells. JQ1 significantly decreased the cell viability of *Brca2* KO cells in vitro and suppressed the growth of *Brca2* KO tumors in vivo compared to the controls. The transcriptomic analyses showed that JQ1 treatment resulted in upregulation of the gene sets associated with macroautophagy. Multi-orthogonal autophagy assays, including live cell imaging of fluorescence-based autophagy reporter, also supported that *Brca2* KO cells had a constitutively higher basal level of autophagic activities compared to the controls, and JQ1 further induced autophagic flux in *Brca2* KO cells. Moreover, blocking the autophagy process by pharmacological inhibition or knocking down essential autophagy genes rescued JQ1-induced cell death in *Brca2* KO cells, indicating that the increased autophagy is responsible for JQ1-mediated cell death in *Brca2* KO cells. In conclusion, we found that BRCA2 deficiency elevated autophagic flux, and extensive autophagy was further activated by BET inhibition, culminating in autophagy-dependent cell death in *Brca2*-deficient pancreatic cancer cells. Our findings suggest that BET inhibition could be a promising therapeutic strategy for treating *BRCA2*-deficient pancreatic cancer.

#3236 Discovery of hydrazide-based HDAC8 selective PROTACs.

Y. Xiao[1], Y. Liu[1], N. Awasthee[1], C. Meng[1], M. He[2], S. Hale[1], R. Karki[3], Z. Lin[3], R. Kridel[2], D. Liao[1], G. Zheng[1];
[1]University of Florida, Gainesville, FL, [2]Princess Margaret Cancer Centre, University Health Network, Toronto, ON, Canada, [3]Washington University in St. Louis, St. Louis, MO

HDAC8 plays crucial roles in biological processes and is a highly desirable target for therapeutic interventions. However, due to the conserved catalytic domain among HDACs, developing specific inhibitors for these isozymes has proven challenging. HDAC8 also has deacetylase-independent activity which cannot be blocked by an inhibitor. Previously we reported the discoveries of a potent HDAC3 degrader XZ9002 and an HDAC3/8 dual degrader YX968. In this study, we carried out further optimizations based on the warhead of YX968 through rational design, which led to the discovery of YX862 and YL246, novel hydrazide-based HDAC8 selective PROTAC degraders with single-digit nanomolar DC50 and excellent selectivity. We demonstrated that the degradation of HDAC8 affects its non-histone substrates; however, it does not trigger profound histone hyper-acetylation and gene expression alteration, highlighting the unique role of HDAC8. The PROTACs developed in this study are well-characterized HDAC8 degraders without triggering pan-HDAC inhibition which represent valuable tool compounds for exploring the biological and therapeutic potential of HDAC8 in cancers and beyond.

#3237 KDM1A/LSD1 inhibition enhances chemotherapy response in ovarian cancer.

J. D. Johnson[1], Y. Chen[2], S. Jayamohan[1], Y. He[2], D. Jamwal[1], N. Pandey[1], E. Kost[1], R. K. Vadlamudi[1], G. R. Sareddy[1];
[1]UT Health Science Center at San Antonio, San Antonio, TX, [2]Central South University, Changsha, China

Background: Ovarian cancer (OCa) is the deadliest of all gynecological cancers. The standard treatment for OCa is platinum-based chemotherapy, such as carboplatin or cisplatin in combination with paclitaxel. Most patients are initially responsive to these treatments; however, nearly 90% will develop recurrence and inevitably succumb to chemotherapy-resistant disease. Recent studies have revealed that the epigenetic modifier lysine-specific histone demethylase (KDM1A/LSD1) is highly overexpressed in OCa. However, whether KDM1A plays a role in chemoresistance and whether its inhibition enhances chemotherapy response in OCa is unknown. In this study, we explored the hypothesis that KDM1A inhibition will sensitize OCa cells to standard-of-care chemotherapy.
Methods: Transduction of KDM1A-specific shRNA was used to generate KDM1A knockdown (KD) cells. Cell viability, colony formation, and apoptosis assays were used to determine the impact of KDM1A KD on sensitization of SKOV3, OVCAR8, and OVCAR5 OCa cells to cisplatin, carboplatin, and paclitaxel. The combination effect of KDM1A inhibitors (NCD38 and SP2509) and chemotherapy drugs was further determined. Mechanistic studies were conducted using RNA-sequencing, RT-qPCR, and Western blotting. *In vivo* efficacy ofKDM1A knockdown with or without chemotherapy was determined using OCa orthotopic xenograft models.
Results: Analysis of TCGA datasets revealed that KDM1A expression is negatively correlated with OCa survival, and its expression is high in patients who do not respond to chemotherapy. Further, Western blotting results show that treatment with chemotherapy drugs cisplatin, carboplatin, and paclitaxel increased KDM1A expression in OCa cells. KDM1A-KD or KDM1A inhibition sensitized OCa cells to chemotherapy drugs in reducing cell viability, survival, and enhancing apoptosis. Moreover, knockdown of KDM1A sensitized carboplatin-resistantA2780-CP70 cells to carboplatin treatment. RNA-seq studies revealed that KDM1A-KD and cisplatin-regulated genes showed negative correction with epithelial-mesenchymal transition (EMT) and positive correlation with apoptosis-related pathways. Importantly, KDM1A KD in combination with cisplatin significantly reduced the tumor growth in the orthotopic OCa xenograft model.
Conclusion: These results suggest that the combination of KDM1A inhibitors with chemotherapy is a viable therapeutic approach for the treatment of OCa

#3238 Therapeutic targeting of the genome guardian sirtuins in metastatic prostate cancer.

S. Giri;
Medical College of Wisconsin, Wauwatosa, WI

Introduction: The effective treatment paradigm for the lethal form of metastatic prostate cancer (mPCa) remains challenging. Almost all mPCas eventually develops therapy resistance against androgen receptor (AR) inhibitors (e.g., Enzalutamide, Abiraterone) or to poly (adenosine diphosphate-ribose) polymerase (PARP) inhibitors (Olaparib, Niraparib, Talazoparib) (HRRd) when used as monotherapy. Although the patients in the ARSi+PARPi combination produced significantly longer radiologic progression-free survival (rPFS), a substantial number had attained therapy resistance by the end of the study tenure. So, a newer therapy is urgently needed. In recent years, a new targetable therapeutics development domain has been unfolding with an expanding understanding of the role of SIRTuins in prostate cancer cell survival, invasion, and progression to an aggressive metastatic state. Here, we will investigate the therapeutic efficacy of SIRT1/7 inhibitor (SIRT1/7i) and determine synergy with DNA-damaging PARP inhibitor combinations through a battery of cell and molecular assays using various prostate cancer cellular models.

Methods: We have treated the mPCa cell lines 22Rv1, LAPC4, PC3 and LnCAP as well as prostate epithelial cell line RWPE1 with SIRT1 inhibitor SIRT1-IN-2 (MedChemExpress, HY-146689), SIRT7 inhibitor 97491 (MedChemExpress, HY-135899) and AR inhibitor Enzalutamide individually as well as in combination of PARP inhibitor Olaparib. The treatment of the SIRT1 and SIRT7 monotherapy arm was 72 hours long, and combination therapy continued for 7 days. The cell viability was assessed with CellTiter-Glo® 2.0 Cell Viability Assay (Promega). The cell cycle progression and proliferation analysis were done using flow cytometry through Propidium iodide staining and AnnexinV-FITC apoptosis detection chemistry. Cell survival was orthogonally assessed using colony counting assays. We adopt RAD51 foci counting assays and COMET assays for evaluating treatment-induced genome instability.

Results: The preliminary result suggested that the SIRT1i+Olaparib and SIRT7i+Olaparib combination significantly sensitized the mPCa cell lines 22Rv1, PC3, and LnCAP for cell death compared to the prostate epithelial cell RWPE1. Upon the combination treatment, the mPCa cell lines showed elevated apoptotic cell death, reconfirmed through colony counting assay.

Conclusion: Therapeutic combination treatment of SIRT1 and SIRT7 inhibition with Olaparib could be an effective treatment option for aggressive metastatic prostate cancer.

#3239 Targeting the GAS41 YEATS domain in non-small cell lung cancer with novel small molecules.

A. Winkler, D. Listunov, B. Linhares, J. Ray, S. Weaver, S. Zolov, V. Keshamouni, J. Grembecka, T. Cierpicki;
University of Michigan, Ann Arbor, MI

Background: Glioma amplified sequence 41 (GAS41) belongs to the Yaf9, ENL, AF9, Taf14, and Sas5 (YEATS) domain family of epigenetic reader proteins. This domain preferentially recognizes acetylated lysine residues on chromatin to facilitate gene expression by recruiting chromatin remodeling and transcription activating complexes. The *YEATS4* gene encoding for GAS41 protein is frequently amplified in NSCLC patient samples relative to normal lung tissue, and GAS41 protein is overexpressed in NSCLC cells. In knockdown experiments using NSCLC xenograft mouse models, GAS41 has been shown to be essential for NSCLC tumor growth. In mutagenesis studies, the YEATS domain residues responsible for acetylation reader activity were found to be essential for NSCLC cellular proliferation and tumor progression. Thus, the YEATS domain of GAS41 represents an attractive target for the development of small-molecule inhibitors as potential therapeutics for NSCLC.

Results: We developed the first-in-class small-molecule inhibitors for the GAS41 YEATS domain. Using an NMR-based fragment screen, we identified a hit with low millimolar binding affinity. Structure-based drug design followed by extensive medicinal chemistry optimization yielded the potent and selective inhibitor DLG-369 with sub-micromolar inhibition of the GAS41 YEATS domain interaction with acylated histones. Using the NanoBRET platform, we showed that DLG-369 selectively disrupts the association of GAS41 YEATS with chromatin in mammalian cells. Furthermore, DLG-369 inhibits proliferation of NSCLC cell lines without affecting normal lung fibroblasts. In transcriptomic experiments, DLG-369 treatment regulates expression of multiple genes in NSCLC cells, including upregulation of the critical tumor suppressor genes *CDKN1A* and *CYR61* and downregulation of chemokine genes *CXCL5* and *CXCR4* associated with NSCLC progression.

Conclusions: We developed DLG-369, a potent inhibitor of the GAS41 YEATS domain with activity in NSCLC cellular models. DLG-369 potently binds to the YEATS domain acetylation reader pocket and disrupts GAS41 recognition of acetylation in cells. DLG-369 potently reduces proliferation and drives differential expression of key genes associated with NSCLC. DLG-369 can serve as a chemical probe to further interrogate the biological role of the GAS41 YEATS domain in NSCLC and other cancers for potential therapeutic implications.

#3240 Synthetic lethal strategy of an EZH1/2 dual inhibitor, HM97662, for the treatment of ARID1A-mutated solid cancers.

Y.-Y. Kim, S. Jung, S. Han, J. Byun, G. Lee, M. Lee, J. Park, T. Kong, H. Han, S. Lee, Y. Ahn;
Hanmi Pharmaceutical Co., Ltd., Hwaseong-si, Korea, Republic of

Enhancer of zeste homolog 2 (EZH2), an enzymatic subunit of polycomb repressive complex 2 (PRC2), is known to catalyze tri-methylation of histone H3 at lysine 27 (H3K27me3), leading to repression of the transcription of its target genes involved in cell cycle regulation, cell proliferation, cell differentiation, and tumor suppression. It has been proposed that epigenetic regulators could serve as novel drug targets, and EZH2 is one of the targets with considerable therapeutic potential. Meanwhile, synthetic lethality is a phenomenon whereby individual genes in a pair can be knocked-out without affecting cell viability, while disruptions of both genes concurrently cause cell death. It has been shown that loss-of-function (LOF) mutations of component proteins in SWI-SNF chromatin remodeling complex, including PBRM1, ARID1A, SMARCA4, and so on, are synthetic lethal with inhibition of the histone methyltransferase EZH2. Especially, ARID1A-mutated solid tumors are vulnerable to EZH2 inhibition. Given that ARID1A is mutated in approximately 10% of all tumor types, inhibiting EZH2 activity could be a promising therapeutic strategy for cancer patients with this mutation. Although the methyltransferase activity of PRC2 is mainly contributed by EZH2, EZH1 also plays a compensatory role in maintaining tri-methylation of H3K27 and directly binds to chromatin, modulating its condensation. These emphasize that blocking both EZH1 and EZH2 might have greater anti-tumor effect than EZH2 alone. Herein, we introduce a novel EZH1/2 dual inhibitor, HM97662, which concurrently suppressed the methyltransferase activity not only wild-type EZH1, but also wild-type and gain-of-function (GOF) mutant EZH2 at nanomolar concentrations. HM97662 potently repressed tri-methylation of H3K27me3 in TOV-21G (ovarian cancer) and HT-1376 (bladder cancer) cell lines with ARID1A LOF mutation. HM97662 also showed a wide and strong growth inhibitory effect in various solid cancer cell lines harboring ARID1A mutation. HM97662 exhibited potent antitumor activities in xenograft mouse models with various ARID1A-mutated cancer cells including ovarian, bladder, small cell lung cancer, prostate, and gastric cancers (e.g. TOV-21G, HT-1197, NCI-H128, LNCap, and MKN-45, respectively). Once-daily oral dosing of HM97662 greatly inhibited tumor growth in a dose-dependent manner without significant clinical signs compared to known EZH2 selective or EZH1/2 dual inhibitors. HM97662 also exhibited a synergistic effect in combination with second-line standard of care in small cell lung cancer. In conclusion, these preclinical studies demonstrated that HM97662 as an EZH1/2 dual inhibitor, holds promising therapeutic potential for ARID1A-mutated solid cancers. It is crucial to evaluate the effectiveness of HM97662 in subsequent clinical trials.

#3241 Elevated H3K27 trimethylation mediates adaptation to DNA demethylation in BRAF^{V600E}-mutated colorectal cancer.

H. Lee[1], A. Saw[1], V. K. Morris[1], A. K. Singh[1], S. Napolitano[2], A. Sorokin[1], P. Kanikarla Marie[1], O. Coker[1], O. E. Villarreal[1], N. Esmaeili Anvar[1], K. Rai[1], S. Kopetz[1];

[1]University of Texas MD Anderson Cancer Center, Houston, TX, [2]Universita degli Studi della Campania "Luigi Vanvitelli", Napoli, Italy

Background: BRAFV600E in colorectal cancer (CRC) defines a unique subgroup of patients with poor prognosis and scarcely benefit from BRAF inhibitor-based treatment. Interestingly, BRAFV600E tumors demonstrated profound CpG island methylator phenotype (CIMP), suggesting extensive epigenetic dysregulation. Thus, we investigated epigenomic regulations in this subset of tumors with treatment-induced DNA demethylation.

Methods: We treated six cell lines and two patient-derived xenograft (PDX) models of BRAFV600E CRC with vehicle, 5-azacitidine (DNMTi), vemurafenib (BRAFi), and combination treatment. PDX tumors treated with either vehicle or 5-azacitidine were collected on day 21 and sequenced for DNA methylation (Infinium HumanMethylation 450k BeadChip array), histone marks (ChIP-seq), chromatin accessibility (ATAC-seq), and gene expression (RNA-seq). Comprehensive post-translational modifications (PTMs) in histones with DNMTi or BRAFi treatment were assessed by mass spectrometry (MS). The combinational effect of 5-azacitidine with EZH2 or RNF2 inhibitors (Polycomb repressive complex activity (PRC) inhibition) was assessed through cell viability assays and colony formation assays in BRAFV600E CRC cell lines.

Results: Analysis of TCGA COAD/READ tumors demonstrated a higher DNA methylation profile in BRAFV600E tumors than wild-type tumors even among the CIMP population (FDR < 1e-4). The combination of DNMTi with BRAFi showed selective additivity in vitro; however, did not improve efficacies in PDXs. The 5-azacitidine treatment induced profound demethylation in PDXs compared to control samples, predominantly attributed to promoter regions (48%). However, DNA demethylation failed to reactivate classic CIMP markers or tumor suppressor genes in CRC (e.g., CDKN2A, MGMT). Interestingly, demethylated genomic regions gained H3K27 trimethylation, repressive histone mark, in azacitidine-treated samples compared to control (9,431 vs 5,147 peaks respectively). We validated the elevation of H3K27 trimethylation as well as additional histone PTMs following DNMTi in MS-based histone analysis. Finally, combining a demethylating agent with EZH2i or RNF2i, which either deplete H3K27 trimethylation or block the PRC activity respectively, has demonstrated additive growth inhibitory effects in BRAFV600E CRC cell lines ($p < 0.05$).

Conclusions: This study unveiled intriguing aspects of demethylation agent treatment, which led to the compensatory engagement of other epigenomic markers, particularly repressive histone marks, resulting in limited efficacies to azacitidine treatment in preclinical BRAFV600E CRC models. This finding suggests the existence of adaptive interactions between epigenetic modifiers and potential clinical strategies in combinational epigenetic therapeutics.

#3242 TNG917 is a clinical-grade, potent and selective inhibitor of EHMT1/2 for the treatment of immune cold tumors.

A. Lu, B. Haines, J. Lei, W. Zhang, M. Zhang, D. A. Whittington, M. L. D. Ferdinez, Y. Yu, S. R. Meier, A. Choi, A. Bejnood, M. Bandi, K. Lazarides, X. Pan, L. Gu, A. W. Tsai, S. Sudsakorn, C. Liang, J. Come, B. Williams, S. Throner, J. Vacca, J. P. Maxwell, J. N. Anderson, A. Huang, C. Min, **Y. P. Chen**;
Tango Therapeutics, Boston, MA

CRISPR-based functional genomics screening can be designed to identify novel cancer cell intrinsic targets that increase tumor immunogenicity. Using a FACS-based CRISPR sorting screen for PD-L1 expression, we identified Euchromatic histone-lysine-*N*-methyltransferase 1 and 2 (EHMT1/2) as negative modulators of the interferon signaling pathways. EHMT1 and EHMT2 are histone methyltransferases that mono- and di-methylate lysine 9 of histone H3 to repress gene transcription of defined target genes. Gene knockout or pharmacological inhibition of EHMT1/2 in cancer cells resulted in de-repression of gene promoters, upregulation of interferon-stimulated genes (ISGs), and secretion of pro-inflammatory cytokines. Here, we present the preclinical characterization of TNG917 - an oral and highly selective EHMT1/2 inhibitor with low nanomolar cellular potency, and favorable pharmacodynamic and pharmacokinetic properties. In humanized and syngeneic mouse models, treatment with TNG917 in combination with anti-PD1 promoted a T-cell-infiltrated tumor microenvironment, led to significant anti-tumor activity, and resulted in survival benefit. In summary, our in vitro and in vivo studies provide a rationale for the clinical development path of TNG917, in combination with checkpoint inhibition, in patients with immune cold tumors.

#3244 EWS-FLI1-driven upregulation of UGT3A2 unlocks drug sensitivity pathway in Ewing sarcoma.

O. Olaoye[1], C. Harrington[2], K. Ross[1], B. A. Seong[1], L. de Waal[2], J. Qi[1], J. Roth[2], K. Stegmaier[1];
[1]DFCI/Harvard Medical School, Boston, MA, [2]Broad Institute, Cambridge, MA

Ewing sarcoma (ES), an aggressive pediatric bone tumor, presents a clinical challenge, particularly for metastatic or relapsed disease. The hallmark genetic alteration involves the fusion of the FET RNA-binding protein, EWSR1, with an ETS transcription factor, typically FLI1, resulting in the EWS-FLI1 fusion oncoprotein. EWS-FLI1 orchestrates a unique epigenetic program, leading to the aberrant expression of genes crucial for cell-cycle regulation, DNA damage response, and cell migration.

Targeting the EWS-FLI1 fusion oncoprotein is a daunting task, which has prompted us to pursue other strategies in parallel. Here, we present an innovative approach harnessing the power of phenotypic drug screens to uncover amenable pathways for targeted medicines in ES. Leveraging data from the Broad Institute's repurposing dataset encompassing 4,518 drug molecules screened across 578 adherent cancer cell lines using the high-throughput multiplexed screening platform known as PRISM, we identified compounds with selective efficacy against ES.

The top-ranking compound identified for selective ES toxicity in the screen was R112, an ATP-competitive inhibitor of Spleen Tyrosine Kinase (SYK). In low-throughput evaluation, R112 induced selective ES cell death when compared to other sarcomas. However, the reported target of R112, SYK, is a dependency in ES based on the Cancer Dependency Map (DepMap) resource.

Subsequent validation of compounds identified in the PRISM screen as selectively toxic in ES revealed that while majority of them induced selective ES cell death, their reported targets were diverse and not linked to known dependencies in ES. Notably, one of the emerging compounds, luteolin, a natural compound known for its antioxidative properties, stood out and was selected for further studies alongside R112.

Comprehensive genome-wide CRISPR-rescue screens identified *UGT3A2*, encoding a UDP glycosyltransferase, along with its solute carrier, *SLC35B4*, as pivotal genes that when deleted rescued both R112 and luteolin-induced cytotoxicity in ES cells. UGT3A2, a direct target gene of EWS-FLI1, demonstrated hyperexpression in EWS-FLI1-positive ES cells and no expression in most cancer and normal cells. While ES cells do not depend on UGT3A2 for survival, this abnormal elevation of *UGT3A2* expression emerged as a key determinant driving their hypersensitivity to a subset of additional small molecules identified from the PRISM screen. Despite divergent mechanisms and direct targets, these drugs shared a common phenoxy motif, which UGT3A2 glycosylated.

This specific EWS-FLI1-induced UGT3A2 upregulation, thus, unveils a novel biomarker for drug sensitivity,paving the way for precision medicine strategies tailored for Ewing sarcoma.

Beyond Ewing sarcoma, this work holds promise in reshaping therapeutic paradigms and offering new avenues for discovering safe and enhanced treatments across a spectrum of cancers.

#3245 Use of hypomethylating agents to reprogram the epigenome in large granular lymphocyte leukemia.

A. Sabzevari, I. Pal, T. Deddens, T. Fox, A. Ratan, D. J. Feith, T. P. Loughran, Jr.;
University of Virginia, Charlottesville, VA

Large granular lymphocyte (LGL) leukemia is a rare heterogeneous blood cancer that is characterized by the clonal lymphoproliferation of CD8+ T cells (T-LGL leukemia) or, less frequently, natural killer cells (NK-LGL leukemia). These cells evade activation induced cell death, allowing them to accumulate as highly cytotoxic lymphocytes that contribute to autoimmune attacks, neutropenia, and anemia. Frontline treatments are limited to repurposed, nonspecific immunosuppressive agents with limited efficacy and incomplete response rates. As there are no FDA-approved antineoplastic agents for LGL leukemia, our research explores novel therapeutic avenues for this orphan disease. Somatic activating mutations in the transcription factor *STAT3* are the most common molecular alteration found in >50% of patients, and STAT3 signaling is dysregulated in almost all LGL leukemia patients. In the largest molecularly profiled LGL leukemia patient cohort to date, we found that *STAT3* mutations frequently co-occur with mutations in chromatin and epigenetic modifying genes, suggesting crosstalk and cooperativity between STAT3 activation and epigenetic dysregulation. Moreover, *TET2*, which promotes DNA demethylation, is frequently inactivated in LGL leukemia via loss-of-function mutations and promoter hypermethylation. As DNA hypermethylation is an emerging hallmark of LGL leukemia, we evaluated the therapeutic potential of two epigenetic agents, azacitidine (AZA) and cladribine (CLAD), that directly and indirectly inhibit DNA hypermethylation, respectively. We hypothesize that AZA and CLAD will 1) exhibit cell intrinsic efficacy, 2) reprogram the epigenome of LGL leukemia through DNA hypomethylation to normalize aberrant gene expression, and 3) induce cytokine-mediated immune responses. AZA and CLAD cytotoxicity was assessed by the Cell Titer Glo viability assay in human LGL leukemia cell lines. Each exhibited potent anti-leukemic effects with IC50 values in the low micromolar and nanomolar ranges. Western blotting analysis demonstrated the decrease in protein expression of DNA methyltransferases and phosphorylated STAT3 levels with treatment in a time- and dose-dependent manner. We also explored the immunomodulatory effects of these hypomethylating agents since LGL leukemia is a pro-inflammatory malignancy with cytotoxic lymphocytes. Preliminary findings using the Isoplexis platform suggest that AZA and CLAD induce production of anti-inflammatory cytokines in LGL leukemia cells. Ongoing studies will identify differential methylation, chromatin accessibility, and gene expression using RRBS, ATAC-seq, and RNA-seq of AZA or CLAD treated samples to define the mechanisms and consequences of DNA demethylation. Uncovering the reprogramming capabilities of AZA and CLAD could allow for the potential repurposing of these inhibitors for treatment of LGL leukemia patients.

EXPERIMENTAL AND MOLECULAR THERAPEUTICS: Immune Modulators and Antisense Molecules
Poster Session

#3248 Metabolic rewiring shifts engineered TCR T cell bioenergetics to enhance cytotoxicity.

R. Pillai[1], X. Zhang[2], Y. Abassi[2],
[1]Rashmi Pillai (Individual), San Diego, CA, [2]Agilent Technologies, San Diego, CA

Background: Adoptive T cell-based transfer has shown tremendous success in hematological cancers. However, an important obstacle to using cell and gene therapy for solid tumors is the aggressive tumor microenvironment (TME). To significantly improve prognosis of subjects undergoing immunotherapy, it is essential to incorporate unique methods to drive T cell energy production and metabolism towards empowering T cells to dismantle the suppressive TME. This can promote anti-tumor effects and persistence of the transfused engineered T cells. In the present study we present a simple metabolic preconditioning process that improves T cell performance and bioenergetics.
Methods: Using the Agilent xCELLigence RTCA eSight, and Seahorse XF Analyzer we assessed the killing efficiency, and bioenergetics of engineered T-cells after pretreating with Arginine. Briefly, engineered TCR T-cells against MART-1 were generated by transducing $CD3^+$ T-cells (Hemacare, Seattle, WA) with retrovirus SAMEN-DMF5 with a CD34 marker gene, against MART-1. The TCR T cells were pre-conditioned in 6mM Arginine for 7 days, followed by a killing assay using MART-1 expressing melanoma cell line as target cells (624.38) at the E:T ratio of 5:1. Target melanoma cells, 624.38 cells, were engineered to express a red-fluorescent nuclear protein. The comparison was made with transduced T-cells grown in RPMI (no added amino acid supplementation, and non-transduced T cells. The cytotoxicity assay was assessed using real-time impedance and live cell imaging data collected on xCELLigence RTCA eSight. Concurrently, the metabolic profiling of the engineered T-cells was examined by the XF96 Analyzer.
Results: Supplementing the growth medium with 6 mM Arginine significantly increased the potency of MART-1 engineered T cells (up to 6-fold) and bioenergetic studies revealed increased spare respiratory capacity, basal respiration, and ATP production via mitochondrial respiration.
Conclusions: Arginine pre-conditioning improved TCR T cell potency through metabolic rewiring favoring mitochondrial respiration. For Research Use Only. Not for use in diagnostic procedures RA45236.3483333333

#3249 Simple, rapid, and robust bioluminescent cell-based assay for detecting neutralizing antibodies against AAV in serum.

Morten Seirup, Kirsten Wingate, Jeff Nelson, Kara Machleidt, Vanessa Ott, Trish Hoang, Marjeta Urh

Promega Corporation, Madison, WI

Adeno-associated viruses (AAV) are prevalent gene therapy vectors, delivering therapeutic transgenes to treat various diseases including cancer and rare monogenic diseases. Individuals with pre-existing immunity to AAVs are less likely to benefit from AAV-based therapies due to both, a reduction in cellular AAV uptake and activation of a cytotoxic T-cell response to transduced cells, decreasing efficacy or changing the safety profile. Measurement of serum neutralizing antibodies (NAbs) against AAV is essential to determine treatment eligibility and to identify clinical trial candidates. Here we introduce a cell-based assay using NanoLuc® luciferase to detect NAbs in serum samples. The superior brightness of NanoLuc® luciferase in our AAV reporter system results in the need of low concentrations of AAV and a short 24h assay time. The minimal AAV concentration in our assay aids in detecting low NAb titers in serum samples, reducing false negatives and enhancing decision-making accuracy. Testing 60 human serum samples against a range of AAV serotypes, we found that a large fraction of the population had pre-existing NAbs to at least one serotype, and of the pre-exposed individuals a majority displayed NAbs against multiple AAV serotypes. Interestingly, fewer samples were seropositive for AAV-DJ than for either parental serotype (AAV2, AAV8 or AAV9), highlighting the assays utility in the development of engineered capsids. Furthermore, the broad dynamic range of our assay facilitates serum sample categorization into four NAb tiers: negative, low, medium, and high using a single serum dilution. Neutralizing titers (ND_{50}) which was determined by serial dilution of the serum samples strongly agreed with the assigned NAb tiers. Our study with 40 naïve mice further validated the assay's robustness, showing a clear correlation between NAb levels and injected AAV viral loads. Taken together, this rapid, highly sensitive, and reliable assay enabled by NanoLuc® AAV reporter technology precisely measures NAbs against AAVs in both human and animal serum. Further validation of the assay is required for future use in a clinical setting.

#3250 LNA gapmer to gastrin inhibits growth and metastases of human pancreatic cancer in mice.

G. Chekuri[1], W. Chen[1], N. Shivapurkar[1], H. Cao[1], R. N. Kularatne[2], S. Stern[2], J. P. Smith[1];
[1]Georgetown University, Washington, DC, [2]National Cancer Institute, Frederick, MD

Background: Pancreatic cancer has a poor prognosis and novel strategies are needed to improve the survival. Gastrin stimulates growth of pancreatic cancer by an autocrine mechanism and RNAi techniques that decrease gastrin expression have been shown to inhibit growth of this malignancy in vitro. Locked nucleic acid (LNA) Gapmers are antisense oligonucleotides (ASO) that have long half-life and stability in vivo, hence represent a potential method to deliver RNAi for cancer therapeutics. We developed an LNA Gapmer that selectively downregulates gastrin expression in pancreatic cancer cells in culture. The goal of this project was to test this anti-gastrin Gapmer in vivo as a novel therapy for pancreatic cancer.
Methods: The anti-gastrin LNA Gapmer was modified using thiol-click chemistry to conjugate a peptide to the 5' end and render the Gapmer target-specific with the ability to bind selectively to the cholecystokinin-B receptor that is over-expressed in pancreatic cancer. Forty athymic nude mice with established AsPC-1 human pancreatic orthotopic tumors were divided into four groups of equal tumor size. Mice (N=10 per group) were treated with PBS (controls), an untargeted LNA-Gapmer, the CCK-BR targeted Gapmer (60nM), and the CCK-BR targeted Gapmer (120nM) intraperitoneally twice a week for 4 weeks. Growth was monitored by luciferase IVIS imaging. At necropsy, tumors were excised, and metastases counted.
Results: Mean tumor mass was 43% smaller in mice treated with the targeted Gapmer-120nM (P=0.0007). Untargeted and targeted Gapmer 60nM slightly decreased tumor mass but this difference was not significant. Compared to PBS control-treated mice, metastases were significantly less in mice treated with the untargeted Gapmer by -39% (p=0.01); in the targeted Gapmer-60nM by -44% (p=0.003), and with the targeted Gapmer-120nM by -72% (p<0.0001). Gastrin mRNA analysis of the tumors by qRT-PCR confirmed downregulation of gastrin.
Conclusion: Novel LNA Gapmers that downregulate gastrin mRNA expression decrease growth and metastases of pancreatic cancer in a dose-related fashion.

#3251 QTOLIMOD: A specific TLR9 agonist nanomedicine with high anti-solid tumor activity.

F. Su[1], J. Bai[1], C. Li[1], Y. Wu[1], J. Li[1], X. Zhao[2], Y. Yang[2], **R. J. Lee**[2];
[1]Zhejiang Haichang Biotechnology Co., Ltd., Hangzhou, China, [2]The Whiteoak Group, Inc., Rockville, MD

Background Toll-like receptor 9 (TLR9) agonists are extensively studied for cancer treatment, but face challenges in delivery, clearance, and side effects. Our study showed that QTOLIMOD, a 26nt CpG-ODN delivered via QTsome™ lipid nanoparticle, significantly inhibited tumor growth in MC38-bearing mice (TGI%=99.06%, $p<0.001$). Here, we report QTOLIMOD's potential for complete tumor rejection, prevention of recurrence, and advantages in safety and immune-cell induction.

Methods C57BL/6 mice were subcutaneously inoculated with 1×10^6 MC38 cells. To assess drug tissue distribution, Cy5-labeled naked CpG-ODN or QTOLIMOD were intratumorally injected and in vivo imaging was conducted. ELISA was utilized to determine the levels of cytokines in serum and tumor samples. Once the tumor volume reached an average size of 80-100 mm^3, mice were grouped and intratumorally injected with saline, vehicle, or QTOLIMOD. Tumor volume was calculated using the formula: length × $width^2$ × 1/2.

Results Following intratumoral injection of QTOLIMOD or naked CpG-ODN, free CpG-ODN were significantly reduced within 24 hours, while QTOLIMOD exhibited extended duration of action up to 7 days. Anatomical examination revealed that a dose of 5 mg/kg naked CpG-ODN caused liver and spleen enlargement in mice, whereas QTOLIMOD at the same dose did not cause the adverse events. Immunohistochemical assay indicated a significant increase in the infiltration of macrophages, dendritic cells, and CD8+ T cells at the tumor site after dosing. IL-10, IFN-γ, and IL-12 were significantly upregulated in the tumor samples, but not in the serum. In a dose escalation experiment, tumor suppression were observed with intratumoral injection of 0.5, 1, 1.5, or 2 mg/kg (every 3 days, 5 doses), resulting in tumor growth inhibition rates ranging from 92.5% to 98.8%. In the QTOLIMOD treated groups, complete tumor rejection was achieved in 4 out of 6 animals in the 0.5 mg/kg group and in all animals in the 1-2 mg/kg groups within 56 days. To investigate the effect of QTOLIMOD on tumor recurrence, cured mice were re-inoculated with MC38 tumor cells at a distant site. All cured mice rejected newly inoculated tumors without additional injection, resulting in 100% survival for up to 60 days. In a dosing frequency experiment, mice were administered with QTOLIMOD at 1 mg/kg once every 3, 5, 7, or 14 days for a total of 5 doses. The results suggested that fortnightly dosing of QTOLIMOD is more effective than more frequent dosing.

Conclusions QTOLIMOD exhibits a high intratumoral retention rate, resulting in increased safety, while effectively promoting the expansion and infiltration of immune cells associated with tumors. Moreover, QTOLIMOD demonstrates potent efficacy in inhibiting tumor growth, potentially leading to complete eradication. Furthermore, treatment with QTOLIMOD effectively prevents tumor from recurrence, offering promising long-term effect.

#3252 Anti-tumor effect of the combination of a lipid nanoparticle suspension of an AKT-1 antisense oligonucleotide (WGI-0301) with tyrosine kinase inhibitors in an orthotopic murine tumor model.

F. Xie[1], T. Lin[1], C. Wang[2], J. Wei[2], R. J. Lee[2], B. Zhao[1], Y. A. Men[2];

[1]Zhejiang Haichang Biotech Co., Ltd., Hangzhou, China, [2]The WhiteOak Group, Inc., Rockville, MD

Background: Archexin is a fully phosphorothioated 20-mer antisense oligonucleotide, complementary to AKT-1 mRNA, which leads to the inhibition of translation and the downstream pathway activities of AKT-1 mRNA. WGI-0301 is a proprietary lipid nanoparticle formulation (QTsomeTM) of Archexin designed to enhance delivery. A phase I clinical study of WGI-0301 as monotherapy in patients with advanced solid tumors is currently ongoing in the U.S. Given the limited efficacy of TKIs compared to immunotherapy and growing incidence resistance, WGI-0301 combined with TKIs may augment the therapeutic response to TKIs by enhancing angiogenic blockade, inhibiting AKT-1, and overcome resistance. Methods: The anti-tumor effect of combining WGI-0301 with Lenvatinib/Sorafenib/Cabozantinib was assessed using a Hep3B-Luciferase orthotopic mouse tumor model. We divided sixty-four female Balb/c nude mice into groups (8 mice per group), including vehicle control, WGI-0301 (8 mg/kg), Lenvatinib (10 mg/kg), Sorafenib (20 mg/kg), Cabozantinib (20 mg/kg), WGI-0301+Lenvatinib (8+10 mg/kg), WGI-0301+Sorafenib (8+20 mg/kg), and WGI-0301+Cabozantinib (8+20 mg/kg). We administered treatments via tail vein injection (vehicle/WGI-0301, QW4 weeks) or oral administration (Lenvatinib/Sorafenib/Cabozantinib, QD28 days). We monitored body weight twice weekly and measured tumor burden using bioluminescence with an IVIS (Lumina III) imaging system twice weekly as well. Treatment was suspended between Day 29 and Day 70 for survival observation.

Results: The tumor growth inhibition (TGI) rates of the combination of WGI-0301 with Lenvatinib/Sorafenib/Cabozantinib were 66.05%, 86.81%, and 75.89%, respectively. These values were higher than those of the Lenvatinib/Sorafenib/Cabozantinib single drug group with TGI rate of 50.84%, 55.68%, and 47.84%. The tumor bioluminescence signal intensities of the two drugs combination (56.74*108, 22.28*108, and 40.40*108 photon/s) were slightly lower than that of the Lenvatinib/Sorafenib/Cabozantinib single drug group (81.97*108, 73.95*108, and 86.96*108 photon/s). The median survival time was 35.0, 46.0, 55.5, and 51.5 days in the vehicle, WGI-0301+Lenvatinib, WGI-0301+Sorafenib and WGI-0301+Cabozantinib, respectively. The median survival time of Sorafenib, the two-drug combinations were 55.5, 55.5, 58.0, and 53.5 days, which was significantly prolonged compared to the vehicle in the mice bearing the Hep3B-luc orthotopic tumor model. No severe adverse effects were observed in the drug combination groups.

Conclusion: The combination of WGI-0301 with TKIs demonstrated superior anti-tumor efficacy over TKI monotherapy in the absence of substantial increase in toxicity. This finding warrants further robust clinical investigation in patients with advanced HCC.

#3253 Novel gene & protein-carrying vector BC-PIV expressing immunomodulatory molecules potently stimulates anti-tumor immunity against solid tumors in mice.

M. Fukumura[1], J. Ohtsuka[1], T. Ohtsuka[1], H. Nakajima[2], T. Nosaka[3];
[1]BioComo Inc., Mie-Gun, Japan, [2]Yokohama City University Graduate School of Medicine, Yokohama, Japan, [3]Mie University Graduate School of Medicine, Tsu, Japan

Background: Cancer immunotherapy such as immune-checkpoint inhibitors or CAR-T cell therapy has emerged as an effective therapeutic modality for some cancers such as hematological malignancies. However, they still show little efficacy for many solid tumors, because of their immune suppressive microenvironment. BC-PIV is a replication-deficient viral vector derived from human parainfluenza virus type 2, that can convey two ectopic genes simuoltaneously and uniquely display ectopic proteins with intact steric structure on the surface of viral particles. Furthermore, BC-PIV itself can induce maturation of dendritic cells with efficient induction of CD80/86. These unique characteristics of BC-PIV make it an attractive tool for improving anti-tumor responses under immunesuppressive milieu of solid tumors.
Aim and Methods: To develop novel immunotherapy using BC-PIV, we have introduced various immunomodulatory molecules into BC-PIV and tested their anti-tumor efficacy *in vivo*. To activate CD4/8 positive T cells, we introduced genes for OX-40L, 4-1BBL, GITRL, CD30L, OX40L/4-1BBL, OX40L/GITRL, or 4-1BBL/GITRL (collectively, TNFRSF ligands) to BC-PIV. All gene products were effectively presented on BC-PIV envelope. For expansion of T, B, and NK cells, or for promoting migration of immune cells, genes for IL-7, CCL19, IL-7/CCL19, IL-7/CCL21, or IL-12 (P40/P35) were introduced. CT-26 murine colon cancer cells ($5X10^5$) were implanted into syngeneic Balb/c mice at one or both side(s) of their ventral wall. Approximately 10^7 viral particles derived from BC-PIV carrying immunomodulatory molecules were directly injected into tumors that had grown to 5-7mm in diameter, and the anti-tumor efficacy was assessed by monitoring the tumor size.
Results: In the mice treated with BC-PIV carrying TNFRSF ligands, tumor regression was observed at the virus administered site, but also at the non-treated, distant site, possibly due to the Abscopal effect. Moreover, these mice maintained efficient anti-tumor responses and rejected tumors when they were re-challenged with CT-26 cells at 8 months after the initial BC-PIV treatment, showing that BC-PIV/ TNFRSF ligands induced sustained anti-tumor immunity. In the BC-PIV/IL-7/CCL19-treated mice, the tumors began to shrink about six days after the single injection of the virus. This effect was even more enhanced by concurrent administration of anti-PD-1 antibody.
Conclusions: BC-PIV carrying TNFRSF ligands, cytokines or chemokines induced efficient, sustained anti-tumor immunity and eradicated tumors in *in vivo* solid tumor model. Unique characteristics of BC-PIV, being able to deliver two genes simultaneously and to display ectopic proteins with intact steric structure on the viral surface, make this vector an attractive, novel platform for next generation cancer immunotherapy.

#3254 Development of novel luminescent assays for sensitive and specific quantitation of double-stranded RNA in mRNA vaccines.

R. Moravec, J. Wang, J. Hartnett, M. Cong, **J. Grailer**;
Promega, Madison, WI

mRNA-based therapeutics have shown clinical efficacy, evidenced by the success of the mRNA vaccines for SARS-CoV-2. Personalized mRNA vaccines containing patient-derived tumor mutations are now entering the clinic and have shown promise. Delivery of mRNA-encoded therapeutic proteins (e.g., antibodies) is also under development. mRNA drug substance is typically generated by in vitro transcription (IVT). One byproduct and contaminant of IVT is the formation of double-stranded RNA (dsRNA). dsRNA is highly immunogenic, can induce inflammation and cell death, and inhibit protein translation, including the protein encoded by the therapeutic mRNA. As such, dsRNA must be measured for all IVT products to ensure safety and efficacy. However, existing dot bot and ELISA technology to detect dsRNA is neither sensitive nor quantitative. Herein, we describe the development of novel assays for sensitive and specific quantitation of dsRNA in IVT products and following encapsulation of IVT products in lipid nanoparticles (LNPs). First, NanoBiT® split luciferase technology was applied to detect dsRNA in IVT products. dsRNA binding domains were genetically attached to either SmBiT or LgBiT. In the presence of dsRNA, the SmBiT and LgBiT constructs bind via the dsRNA binding domains, resulting in dimerization and the complementation of functional NanoBiT® luciferase. NanoBiT® then generates light which is proportional to the amount of dsRNA in the sample. The assay detects dsRNA greater than or equal to 30 base pairs and is independent of the size and sequence of the dsRNA contaminant. The assay does not cross-react with single-stranded RNA or DNA and is highly sensitive, with a limit of detection less than 100 pg/ml. As a complementary tool to the biochemical assay, we developed a cell-based bioassay to detect dsRNA encapsulated in LNPs. dsRNA/LNPs are taken up by endocytosis where Toll-like receptor 3 (TLR3) detects dsRNA. Activation of TLR3 initiates a signaling pathway that is detected by a TLR3 pathway-specific promoter driving luciferase expression. This pathway likely represents the most physiologically-relevant readout of dsRNA bioactivity. Both assays are developed in “add-mix-read” format with no wash steps or media transfer, and exhibit robust, sensitive, and repeatable performance for specific detection of dsRNA in mixed solutions.

#3255 Targeting CD4+FOXP3+ Tregs to enhance anti-tumor immunity.

T. Akimova[1], L. Wang[2], Z. Bartosh[2], E. Eruslanov[3], S. Albelda[3], S. Singhal[3], V. Aishwarya[4], **W. W. Hancock**[1];
[1]University of Pennsylvania and Children's Hospital of Philadelphia, Philadelphia, PA, [2]Children's Hospital of Philadelphia, Philadelphia, PA, [3]University of Pennsylvania, Philadelphia, PA, [4]AUM LifeTech, Philadelphia, PA

We strive to improve the outcomes of cancer immunotherapy by using a new generation of chemically modified self-delivering antisense oligonucleotides (ASO), termed FANA ASO, to target the key T-regulatory (Treg) cell transcription factor, FOXP3. We tested five murine FANA in 2 murine tumor models (TC1, MC38) and studied 19 human FANA FOXP3 in vitro with human healthy donor PBMC, followed by use of clinical samples from lung cancer patients and patients with mesothelioma, as well as testing in humanized mice (hu-PBMC-NSG). In murine studies, we treated mice on day 7 after tumor inoculation with Scramble control or murine FANA FOXP3, 50 mg/kg for 14 days, i.p. In the TC1 lung tumor model, we found an average 38% decrease of tumor volumes, p = 0.0007, and 22% of tumors were completely resorbed. In the MC38 colon carcinoma model, we found a 49% decrease of tumor volumes, p = 0.0182, and 13.6% of tumors were completely resorbed. In both tumor models, we observed an ~50% decrease of Foxp3 mRNA by qPCR, and decreased numbers of intratumoral Tregs by flow cytometry. This was accompanied by significant decreases ($p<0.05$) of the mRNA and protein intratumoral levels of multiple exhaustion markers: LAG-3, CTLA-4, PD-1, Tim-3, Tigit, CD244, CD160 and VISTA, and increased expression of perforin and granzyme-b by intratumoral T cells. In addition, there were no changes in FOXP3 mRNA expression or in the numbers of Tregs in draining lymph nodes and in spleens of tumor bearing mice, suggesting that intratumoral Treg have enhanced sensitivity to FANA FOXP3 in vivo. We identified the best 5 of 19 human FANA FOXP3 and showed these had no toxic effects on cell viability or division, and downregulated FOXP3 expression over 50% in PBMC from healthy donors ($p<0.05$). Human Treg, pre-incubated with FANA FOXP3 for 3 hours, retained only 60.3% of their suppressive function in vitro. FANA FOXP3 treatment of lung cancer tumor samples and mesothelioma pleural effusion samples resulted in a 56.4% decrease in FOXP3 mRNA expression and a 61.5% decrease in Treg numbers (all $p<0.05$). Moreover, tumor FOXP3+ Treg had 36.7% less FOXP3 protein per cell, and downregulated CD39 expression compared to Scramble control. Targeting of cancer samples with human FANA FOXP3 in vitro was associated with increased division of CD4+ and CD8+ cells, and with downregulation of multiple exhaustion molecules, including CTLA-4, Tim-3, PD-1, LAG-3 and TIGIT. Humanized mice, treated with two human FANA FOXP3 compounds (50 mg/kg, 7days), demonstrated an absence of apparent toxic effects and human FOXP3 mRNA was downregulated by 47.4% in the blood, by 74.2% in lymph nodes and by 51.8% in the spleens (all $p<0.05$). Hence, targeting of intratumoral Tregs using FANA FOXP3 results in enhanced immune responses to solid tumors without inducing autoimmunity, and studies are underway in combination with checkpoint inhibitors and/or CAR-T cell therapy.

#3256 Novel SOX2-targeting bioPROTACs for the treatment of cancers.

J. Choi, S. Lim, X. Bai, H. Song, Y. Oh, Y. Yong, S. Lee;
EPD Biotherapeutics Inc., Seoul, Korea, Republic of

Targeted protein degradation (TPD) technology has been developed showing the therapeutic potential to modulate historically 'undruggable' disease-associated proteins. Currently, proteolysis targeting chimeras (PROTACs) using small-molecule binders represent the TPD field, and PROTAC-induced proximity between target proteins and E3 ligases enables specific degradation of target proteins. However, substantial amounts of clinically relevant cancer targets such as transcription factors lack active sites or allosteric binding pockets for small molecules which challenges the development of classical PROTACs for these targets. SOX2 is one of the pluripotency transcription factors and has been well-known for its crucial role in tumor development through promoting cancer cell survival, metastasis, stemness, and drug resistance. Numerous studies have also reported SOX2 amplification and overexpression in various tumor tissues. Thus, SOX2 has been validated as an attractive anticancer target, but directly targeting SOX2 has been proved to be difficult since SOX2 is an "undruggable" transcription factor. EPD Biotherapeutics develops EPDeg™, a next-generation engineered protein degrader platform in order to overcome the limitations of small molecule-based PROTAC. Here we report a series of SOX2-targeting bioPROTACs, being composed of a nanobody against SOX2 with high affinity and several ubiquitin E3 ligases with deletion of natural substrate binding domain to allow highly selective degradation of SOX2 protein. To evaluate the in vitro efficacy, SOX2 bioPROTACs were generated by mRNA IVT with CleanCap ® and modified uridine. First, robust degradation of SOX2 with a half-maximal degradation concentration (DC_{50}) of the picomolar range was observed with the treatment of SOX2 bioPROTACs in multiple SOX2-overexpressing cancer cell lines. The degradation was ubiquitin- and proteosome-dependent manner, and neither nanobody nor ubiquitin E3 ligase alone affected SOX2 protein level. Then, SOX2 bioPROTACs led to significant cancer cell growth inhibition caused by apoptotic cell death with a half-maximal growth inhibition concentration (GI_{50}) of the picomolar range. Notably, chemo-resistant cancer cell lines expressing SOX2 protein in high levels were sensitized to chemotherapy in combination with our SOX2 bioPROTACs. Furthermore, i.v. injection of one of our lead candidates formulated with LNP significantly inhibited tumor growth in the A549 xenograft model, proving the in vivo anti-tumor efficacy of SOX2 degraders for the first time in the world. Taken together, EPD's SOX2 bioPROTACs show potent in vitro and in vivo anti-tumor efficacy as first-in-class SOX2 degraders and provide new insights for the therapeutic potential of transcription factor-degrading strategies.

#3257 Unleashing immune power: How mRNA-encoded modulators suppress tumor growth.

D. Wang, z. zhang, p. wang, b. duan, x. qiang, q. gu;
WuXi App Tec, Shanghai, China

Subsequent to the emergence of the COVID-19 pandemic, an increased number of nucleic acid-based therapeutics have secured clinical endorsement. Unlike conventional protein-targeted therapies, nucleic acid therapeutics provide the potential for long-lasting effects and can be further categorized into oligonucleotides, single-guide RNA (sgRNA), and messenger RNA (mRNA). In this study, we aim to explore the anti-tumor properties of mRNA-encoded CD3-EpCAM Bispecific Antibody (BsAb) and mRNA-encoded IL-12 protein.

We conducted qPCR, flow cytometry, and ELISA analysis to assess the dynamic concentration of mRNA-encoded CD3-EpCAM BsAb and mRNA-encoded IL-12 protein within tumor cells post-transfection. We then accessed their effects on anti-tumor and immune activation in vitro via flow cytometry and ELISA. Furthermore, using in vivo imaging system (IVIS), we were able to determine the biodistribution of mRNA-encoded BsAb in vivo. Efficacy was evaluated in subcutaneous tumor xenograft models with mRNA content in tumors examined via qPCR. Moreover, we analyzed the activation of tumor-infiltrating immune cells post mRNA-encoded IL-12 treatment. Finally, to ascertain the preliminary safety of mRNA-encoded BsAb and mRNA-encoded IL-12 protein, we conducted serum biochemistry analysis and histopathological examination of various organs.

In this comprehensive preclinical evaluation, we found that both mRNA-encoded BsAb and mRNA-encoded IL-12 promoted the activation and cytotoxicity of human T cells, exhibiting significant inhibitory effects on tumor growth in vivo while maintaining a favorable safety profile. Our findings provide compelling evidence that mRNA therapeutics hold significant research value and exhibit promising potential for clinical applications.

#3258 A potential oncogenic role and immunoregulatory mechanisms of MZB1 in melanoma.

G. Chhabra, C. A. Shirley, J. M. Krien, M. A. Ndiaye, N. Ahmad;
University of Wisconsin-Madison, Madison, WI

While immune checkpoint blockade (ICB) therapies have drastically improved melanoma treatment, a majority of patients fail to achieve a durable response. Thus, there is a critical need to advance our understanding of melanoma immune evasion mechanisms and identify novel targets capable of enhancing ICB responses. MZB1 (Marginal Zone B and B1 Cell Specific Protein), an immune regulator gene, is differentially expressed in metastatic melanoma compared to primary melanoma or normal skin. In a limited number of cancers, MZB1 has been shown to function as either an oncogene or a tumor suppressor. However, its role and significance in melanoma is not known. In this study, we determined the functional significance and immunoregulatory mechanisms of MZB1 in human melanoma cell lines using MZB1 overexpression (OE) (in SK-MEL-2, and SK-MEL-28) and CRISPR knockout (KO) (in A375 and Hs294T) lines. MZB1 OE significantly increased melanoma cell proliferation and expression of the proliferation markers Ki67 and PCNA, while MZB1 KO yielded the opposite effect. To identify immunoregulatory mechanisms associated with MZB1, we performed differential gene expression analysis of 770 immune-related genes using NanoString nCounter technology. nSolver analysis identified 153 differentially expressed genes (DEGs) as a result of MZB1 knockout in Hs294T cells (adjusted $p < 0.05$, 1.5-fold change cutoff). MZB1 KO strongly reduced the expression of the HLA class-II family genes and altered the expression of various cytokines, suggesting an immunoregulatory role of MZB1. Further, MZB1 KO significantly downregulated genes related to cancer progression and metastasis promotion. Additionally, MZB1 KO reduced expression of common “cancer stem cell” genes, such as RXRG, ALDH1A1, AQP1, NFATC2, LPAR1, indicating MZB1 expression in melanoma may promote a dedifferentiated or neural crest-like state. In addition, an Ingenuity Pathway Analysis (IPA) of the DEGs revealed many cancer-related functions altered upon MZB1 KO (p adjusted < 0.05) and displayed a negative enrichment for cancer-promoting pathways including tumor growth, metastasis, and proliferation. IPA regulatory analysis predicted MZB1 KO to decrease the activation of oncogenic signaling components including PI3K, MEK, and ERK1/2. Further, IPA predicted that MZB1 inhibition could positively sensitize melanoma cells towards higher immune responses by activating mechanisms associated with T cell proliferation and activation, leukocyte migration, and macrophage activation. Overall, our study suggests MZB1 promotes oncogenic signaling in melanoma to drive proliferation and dedifferentiation, as well as regulates a wide range of immune-related genes that may be responsible for immune evasion in melanoma cells. Thus, MZB1 merits further investigation to determine if the immune consequences yielded by targeting MZB1 can complement ICB approaches in the management of melanoma.

EXPERIMENTAL AND MOLECULAR THERAPEUTICS: Mechanisms of Drug Resistance 2
Poster Session

#3261 Improving targeted therapy in female patients with lung squamous cell carcinoma.
M. Momcilovic, D. Shackelford;
UCLA - University of California Los Angeles, Los Angeles, CA

Non-small cell lung cancer (NSCLC) will claim the lives of ~60,000 female patients in the US in 2023. Lung squamous cell carcinoma (LUSC) is a subtype of Non-Small Cell Lung Cancer (NSCLC) that comprises ~30% of NSCLC and is characterized by high metabolic activity. Specifically, LUSC typically exhibits elevated rates of both glucose and glutamine metabolism driven by the PI3K-AKT-mTOR and KEAP1/NRF2 pathways. Further, a paucity of identifiable genetic drivers in LUSC has resulted in a lack of effective targeted therapies for patients with this devastating disease. Despite recent advances in therapy, the 5-year survival rate for patients with advanced NSCLC is 6%, underscoring the need for better treatment options. Importantly, no significant sex bias is seen in the newly diagnosed cases of lung cancer (~50%M/~50%F) (American Cancer Society, 2023), yet there are no sex-specific therapeutic approaches in clinical use. We demonstrated that the catalytic mTOR kinase inhibitor TAK228 can be utilized to effectively treat LUSC tumors via inhibition of glycolysis, an approach that is currently being evaluated on two phase I/II clinical trials (NCT02417701, NCT04250545), launched as a direct result of our pre-clinical work. However, our pre-clinical data suggests that despite the potential benefit of TAK228 inhibition in LUSC, a subset of tumors are resistant to TAK228 despite on-target activity of mTOR inhibitor, leading to the rationale of the current hypothesis, namely the possibility that sex-specific differential effects of TAK228 may exist. To evaluate this hypothesis, we have generated preliminary data demonstrating that sex is a determinant of TAK228 response in LUSCs, whereby male mice are significantly more sensitive to mTOR inhibition than females. Follow-on experiments have demonstrated that the anti-estrogen therapy (Letrozole) sensitized previously resistant female mice bearing LUSCs to TAK228, suggesting an estrogen-related link to TAK228 resistance in females. Additionally, RNASeq and biochemical analyses identified pathways that are upregulated in TAK228 resistant female mice with LUSC tumors. These results suggest that the estrogen may play a key role in the observed pattern of female resistance to mTOR inhibition. As such, the goal of the current proposal is to evaluate the catalytic mTOR kinase inhibitor TAK228, in combination with anti-estrogen therapy as a therapeutic strategy to treat LUSC in females.

#3262 Elucidating the mechanism of resistance to tyrosine kinase inhibitors in *ROS1*-and *ALK*-fusion non-small cell lung cancer: The role of CD74.

V. Ho, M. Izumi, M. Lee, D. Shibahara, I. S. Kobayashi, S. S. Kobayashi;
Beth Israel Deaconess Medical Center, Boston, MA

The therapeutic landscape in treating advanced oncogene-mutated non-small cell lung cancer (NSCLC) was revolutionized with the advent of tyrosine kinase inhibitors (TKIs). Despite the efficacious breakthrough and improved patient outcomes, disease progresses once more due to the seemingly inevitable development of drug resistance in tumor cells. This poses a considerable predicament in the clinical management of oncogene-mutated NSCLC and signifies the importance of elucidating the mechanism of resistance in tumor cells that harbor these genomic alterations which give rise to oncogenic drivers. Recent evidence suggests that drug-tolerant persister (DTP) cells, which are tolerant to initial exposure to TKIs give rise to acquired drug-resistant cells. Currently, the mechanism by which tumor cells undergo a drug-tolerant state is not well understood in NSCLCs driven by *ALK* or *ROS1* fusion. Previously, we identified *CD74* as a gene that may play a role in a drug-tolerant state in *EGFR*-mutated lung cancer via single-cell RNA-sequencing (scRNA-seq). Here, we sought to determine whether the CD74 signaling also leads to resistance to TKIs in NSCLCs with *ALK* or *ROS1* fusion. We showed that CD74 expression increased at both the mRNA and protein levels after treatment with respective TKIs in *ALK* and *ROS1* fusion cells lines. Notably, the *ALK* and *ROS1* fusion cell lines also exhibited an increase in mRNA expression levels of upstream and downstream genes of CD74. Additionally, we generated CD74 knock-out and overexpression models in two cells lines, HCC78 (*SLC34A2-ROS1* fusion) and H2228 (*EML4–ALK* fusion), to further examine the role of CD74 expression in DTP cells. We demonstrated that resistance to TKIs were dependent on CD74 expression. Furthermore, it was determined that anti-CD74 antibody-drug conjugates, in combination with TKIs, synergistically induced apoptosis in these cell lines. In conclusion, our data suggest that CD74 can be a therapeutic target in NSCLC with *ALK* or *ROS1* fusion.

#3263 VEGFA mediates traditional EGFR-TKI resistance in non-small cell lung cancer with EGFR exon 20 insertions.

Y. Yang[1], C. Liu[1], G. Yang[2], H. Xu[1], S. Lei[1], Y. Wang[1];

[1]Cancer Hospital, Chinese Academy of Medical Sciences and Peking Union Medical College, Beijing, China, [2]Department of Respiratory Medicine, Shandong Cancer Hospital and Institute, Shandong First Medical University and Shandong Academy of Medical Sciences, Jinan, China

Background: Epidermal growth factor receptor (EGFR) exon 20 insertions (Ex20ins) accounted for 4%-12% of EGFR mutations and showed primary resistance to EGFR tyrosine kinase inhibitors (EGFR-TKIs) which is an urgent issue to be solved. In our previous studies, we found that antiangiogenetic therapy had certain advantages for patients with Ex20ins in the real-world practice. Previous research showed the tumor microenvironment has been associated with resistance to targeted therapy in sensitive mutations. However, the mechanism of resistance of EGFR-TKIs and the advantage of antiangiogenetic therapy in patients with EGFR Ex20ins were still unclear.

Methods: In this study, patients with EGFR exon 19 deletion (19del), exon 21 p.L858R (21L858R), and Ex20ins were collected to identify the efficacy of EGFR-TKIs. Stable cell lines expressing were established and used to compare signaling pathway activation. Matrigel angiogenesis assay was conducted in different cell lines. Next, we evaluated the efficacy of various treatments combined with antiangiogenetic agents or not in mouse models.

Results: We collected 23 patients with EGFR sensitive mutations and Ex20ins, respectively, and found Ex20ins presented primary resistance to TKIs and poor survival outcomes. Based on the RNA sequence of stable cell lines, it was found that Ex20ins had a higher level of VEGFA expression and enriched in MAPK pathway compared to EGFR 19del and 21L858R. Immunohistochemical studies also revealed that a higher level of VEGFA expression was observed in a cohort of NSCLC patients with Ex20ins mutation compared with 19del or L858R. Matrigel angiogenesis assay has shown consistent result that Ex20ins promoted angiogenesis *in vivo*. Further experiments in mouse models identified that in the group of Osimertinib, mobocertinib alone, chemotherapy alone, mobocertinib or chemotherapy combination with bevacizumab, Osimertinib achieved the worst efficacy and additional utility of antiangiogenetic agents had a more favorable efficacy.

Conclusion: Our study highlights the potential of VEGFA as a mechanism of resistance to EGFR-TKIs and induces immunosuppression microenvironment in NSCLC with Ex20ins. Furthermore, the findings suggested that antiangiogenetic therapy could be a promising therapeutic approach.

Keywords: VEGFA, targeted therapy, resistance, EGFR exon 20 insertions, non-small cell lung cancer

#3264 Characterization of EGFR ectodomain mutation in acquired resistance to cetuximab in colorectal cancer.

N. Joshi[1], R. G. Deal[1], G. Bogatcheva[1], J. N. Higginbotham[1], M. Ramirez[1], B. P. Brown[2], Q. Liu[1], J. Meiler[2], B. Singh[1];
[1]Vanderbilt University Medical Center, Nashville, TN, [2]Vanderbilt University, Nashville, TN

Colorectal cancer (CRC) remains the second leading cause of cancer-related deaths in the United States (US). Individuals with surgically unresectable stage four CRC have a five-year overall survival rate of 13%. Targeting of the receptor tyrosine kinase (RTK), EGF receptor (EGFR) with therapeutic monoclonal antibodies (cetuximab, panitumumab) is approved for use in wild-type (WT) KRAS/NRAS/BRAF (RAS/RAF) advanced CRC. However, these antibodies as a single agent have response rates of 12-17% and expected progression-free survivals of only 3-4 months. Accordingly, resistance may be present at the outset (de novo resistance) or develop during treatment (acquired resistance). Here, we report the identification of an EGFR ectodomain missense mutation acquired *in vitro* in response to treatment with anti-epidermal growth factor receptor (EGFR) antibody cetuximab. Using 2D and 3D drug sensitivity assays, our results demonstrate that this EGFR ectodomain mutation in addition to being resistant to cetuximab and panitumumab, also could not be targeted by the oligoclonal antibody cocktail MM-151. To determine whether this EGFR ectodomain mutation is necessary and sufficient to impart cetuximab resistance, we engineered CRC lines to inducibly overexpress mutant EGFR and showed that this was sufficient to induce cetuximab resistance. Further structural, and functional characterization is underway for this ectodomain mutation that confers resistance to cetuximab and will be shared during the meeting. These findings necessitate the need for additional treatment strategies for a subset of subjects with mCRC who do not respond to treatment with cetuximab/panitumumab and MM-151.

#3265 Secretome core fucosylation drives clonal drug resistance expansion and hypoxic control of metastasis.

M. D. Aldonza, K. Son, J.-Y. Cho;
Seoul National University, Seoul, Korea, Republic of

Cancer secretome is a reservoir for aberrant glycosylation. How therapies alter this post- translational cancer hallmark and the consequences thereof remain elusive. Here, we show that an elevated secretome fucosylation is a pan-cancer signature of both response and resistance to multiple targeted therapies. Large-scale pharmacogenomics revealed that fucosylation genes display widespread association with resistance to these therapies. In cancer cell cultures, xenograft mouse models, and patients, targeted kinase inhibitors distinctively induced core fucosylation of secreted proteins less than 60 kDa. Label-free proteomics of N-glycoproteomes identified fucosylation of the antioxidant PON1 as a critical component of the therapy-induced secretome (TIS). N-glycosylation of TIS and target core fucosylation of PON1 are mediated by the fucose salvage-FUT8-SLC35C1 axis with PON3 directly modulating GDP-Fuc transfer on PON1 scaffolds. Core fucosylation in the Golgi impacts PON1 stability and folding prior to secretion, promoting a more degradation-resistant PON1. Global secretome and PON1-specific de-N-glycosylation both limited the expansion of resistant clones in a tumor regression model. We defined the resistance-associated transcription factors (TFs) and genes modulated by the N-glycosylated TIS via a focused and transcriptome-wide analyses. In a spontaneous lung metastasis mouse model, global secretome and PON1-specific core fucosylation functionally drive hypoxia and hypoxic selection of drug-resistant clones. Our findings demonstrate that core fucosylation is a common modification indirectly induced by targeted therapies that paradoxically promotes resistance and metastasis.

#3266 Plk1 promotes Pdcd4 degradation to enhance enzalutamide resistance in prostate cancer.

Q. Wang, Q. Zhang, Y. Zhang, X. Liu, H.-S. Yang;
University of Kentucky, Lexington, KY

The androgen receptor (AR) signaling pathway plays critical role in the development of prostate cancer (PCa), including castration-resistant prostate cancer (CRPC). As a result, androgen signaling inhibitors (ASIs) like abiraterone and enzalutamide (ENZ) have emerged as the first-line treatment for CRPC. Nevertheless, the limited success of ASIs underscores the urgency of developing new approaches for managing CRPC patients who have become unresponsive to ASIs. Programmed cell death 4 (Pdcd4) is a tumor suppressor, which is frequently down-regulated during PCa progression. It has been shown that reduced Pdcd4 expression promotes both AR-dependent and AR-independent growth in PCa. In this study, we found that down-regulation of Pdcd4 led to acquisition of ENZ resistance in PCa. We also observed that down-regulation of Pdcd4 resulted in activation of mTORC2 activity. Additionally, knockdown of Rictor, a component of mTORC2 complex, enhanced sensitivity to ENZ treatment in PCa. These findings suggested that activation of mTORC2 due to Pdcd4 loss contributes to ASI resistance in PCa. To understand how Pdcd4 is down-regulated in the PCa, we identified that polo-like kinase (Plk1) phosphorylated Pdcd4 at Ser239. Phosphorylation of Pdcd4 by Plk1 led to ubiquitin-mediated proteasomal degradation of Pdcd4. Over-expression of the phosphomimic Pdcd4(S239D) in 22Rv1 cells promoted tumor cell growth in cultured cells and mice. Taken together, our data suggest that targeting Plk1/Pdcd4/mTORC2 signaling axis holds promise as a strategy to overcome ENZ resistance in PCa.

#3267 Understanding the role of dNTP pool on double-strand break and resistant to therapy in quiescent hypoxic glioblastoma.

E. R. Usoro, D. Monroe, K. Carver, E. Steinbeck, A. Williams, S. Aycox, W. Daddacha;
Augusta University, Augusta, GA

Glioblastoma (GBM) is the deadliest type of primary brain tumor. After surgical resection of GBM, chemotherapy and radiotherapy (RT) are used as treatment modalities to induce double-strand breaks (DSBs), the most cytotoxic and lethal form of DNA damage. However, an inadequate oxygen supply and the high metabolic demand in rapidly growing solid tumors like GBM result in severe hypoxic regions, contributing to altered cellular metabolism and resistance to these cancer therapies. These subpopulations of resistant and refractory hypoxic cancer cells are clinically significant as they lead to poor prognosis and adverse clinical outcomes in patients. Ionizing radiation (IR) and chemotherapeutics such as temozolomide induce DNA damage, such as base deletions, single-strand breaks (SSBs), and DSBs. Rapidly replicating cells are more sensitive to these therapeutic agents partly due to replication-induced conversion of SSB and other manageable damages to highly lethal DSB. A balanced deoxyribonucleoside triphosphate (dNTP) is crucial for DNA replication, repair, and maintenance of genomic stability. Cellular dNTP is mainly regulated by ribonucleotide reductase (RNR) and the SAM- and HD-domain-containing protein (SAMHD1). RNR boosts the cellular dNTP pool through the *de novo* synthesis, while SAMHD1 depletes the pool by hydrolyzing dNTPs. Also, previous studies have shown that hypoxic cancer cells have low dNTP levels due to oxygen dependency of its rate-limiting RNR enzyme, which could result in reduced DNA replication and cell cycle arrest. Here, we show the direct relationships between dNTP levels, DNA replication, and DSB induction in hypoxic GBM cancer cells, which is currently unknown. To bridge this knowledge gap, we exposed GBM cells to severe hypoxia and utilized cellular dNTP analysis to demonstrate that their dNTP pool can be elevated. Our results show that elevating the cellular dNTP pool relieved hypoxia-induced cell cycle arrest as determined by flow cytometry and increased their DNA replication. A single-cell microscopic analysis also revealed that increasing the dNTP pool significantly enhanced the induction of DSBs following exposure to IR and bleomycin. Furthermore, we detected an increased efficacy of DSB-inducing agents in hypoxic GBM, as demonstrated by apoptosis pathway activation. Our result suggests that increasing the intracellular dNTP pool in hypoxic GBM will stimulate DNA replication, increase genotoxin-induced DSB, and improve DSB-inducing therapeutic efficacy. In conclusion, this study provides a preclinical justification for using cellular dNTP modulation as a novel therapeutic strategy and an adjunct to classical DSB-inducing agents in hypoxic GBM.

#3268 A novel signaling axis of APE1-redox-sensitive SOX9 activation underlying reflux-condition-associated chemoresistance in esophageal adenocarcinoma.

H. Lu[1], L. Chen[1], F. Ballout[1], D. Peng[1], Z. Chen[1], J. Que[2], S. Chen[1], O. G. McDonald[1], A. Zaika[1], W. El-Rifai[1];
[1]University of Miami, Miami, FL, [2]Columbia University, New York, NY

Chronic gastroesophageal reflux disease (GERD), characterized by the reflux of acidic bile salts (ABS) into the esophagus, stands as the primary risk factor for esophageal adenocarcinoma (EAC). EAC, known for its aggressive nature and limited response to therapy, exhibits a disheartening 5-year survival rate of less than 20%. Overcoming drug resistance remains a pressing challenge in achieving optimal therapeutic outcomes for EAC patients. Previous studies from our team have unveiled that exposure to ABS leads to the overexpression of Apurinic/apyrimidinic endonuclease (APE1), which orchestrates various oncogenic pathways in EAC cells. In this study, we delve into the influence of ABS in driving APE1-redox-mediated activation of the SOX9 pathway, thus contributing to the chemoresistance observed in EAC. To identify the enrichment of the SOX9 pathway and the heightened downstream target genes in EAC, we analyzed RNA sequencing data and public databases. Cell models, patient tissue arrays, pL2-IL1β transgenic mice, and de-identified xenografts derived from EAC patients (PDXs) were employed to investigate the signaling axis of APE1-redox-SOX9 in oxaliplatin resistance of EAC. Our analysis of public databases unveiled a significant enrichment of the SOX9 pathway in EAC patients. RNA sequencing data from EAC cells exposed to ABS, with or without APE1-knockdown, suggested APE1's involvement in the GERD-activated SOX9 signaling pathway. Immunohistochemistry staining of human patient tissue arrays, along with immunofluorescent staining of L2-IL1ß transgenic mice, confirmed the co-overexpression of APE1, SOX9, and ALDH1A1 in EAC. Furthermore, APE1 silencing led to the downregulation of SOX9 and exhibited synergistic effects with oxaliplatin in chemo-resistant EAC cells. Mechanistically, we uncovered that APE1's redox function is crucial for AKT-GSK3ß-mediated SOX9 stability. Treatment with the APE1-redox-specific inhibitor, APX2009, sensitized patient-derived xenograft (PDX) tumors to oxaliplatin by repressing SOX9-regulated chemoresistance genes. This study sheds light on a novel signaling axis involving APE1-redox-AKT-GSK3ß-SOX9 in Barrett’s carcinogenesis. The pharmacological inhibition of APE1-redox function presents itself as a promising therapeutic approach to target the previously intractable SOX9 signals, potentially overcoming chemoresistance in EAC.

#3269 APE1/NF-κB/PRDX2 activated by reflux conditions mediates chemoresistance in esophageal adenocarcinoma by suppressing ferroptosis.

L. Chen[1], H. Lu[1], F. Ballout[1], D. Peng[1], Z. Chen[1], J. Que[2], S. Chen[1], O. McDonald[1], A. Zaika[1], W. El-Rifai[1];
[1]University of Miami Miller School of Medicine, Miami, FL, [2]Columbia University, Miami, FL

Background: Esophageal adenocarcinoma (EAC) stands out as one of the most lethal malignancies, characterized by a discouragingly low 5-year survival rate of less than 20%. Accumulating lines of evidence indicate that ferroptosis, a novel type of cell death, can regulate drug resistance. Peroxiredoxin 2 (PRDX2), an antioxidant enzyme, plays an antioxidant protective role in the cells under stress by regulating redox homeostasis. We aimed to elucidate the role of PRDX2 in regulating reactive oxygen species (ROS), ferroptosis, and chemoresistance in EAC.
Methods: In this investigation, we analyzed RNA sequencing data and public databases to uncover the aberrant overexpression and potential chemoresistance function of PRDX2 in EAC. We employed transient acidic bile salts exposure (ABS) and repeated ABS exposure (rABS) to mimic gastroesophageal reflux disease, the main risk factor for EAC, in *in vitro* cell models. EAC cells and 3D organotypic culture (OTC) served as platforms to delve into the anti-ferroptosis function and regulatory mechanisms of PRDX2. The findings were validated using patient-derived xenografts (PDX) and human EAC tissue microarrays (TMA).
Results: Elevated PRDX2 level was observed in both EAC patients and cell lines exhibiting poor responsiveness to chemotherapy. Intrinsic overexpression of PRDX2 emerged as a crucial factor in the recovery from ABS-exposure-induced lipid peroxidation. Silencing PRDX2 heightened the sensitivity of EAC cells to Oxaliplatin by inhibiting ferroptosis in a GPX4-dependent manner. Mechanistically, we found ABS activate the APE1/redox/NF-kB signal axis, leading to the upregulation of PRDX2 transcription. The co-overexpression of APE1 and PRDX2 was identified through both immunofluorescent staining in cells/OTC and immunohistochemistry staining in TMA. Moreover, the APE1-redox-specific inhibitor, APX2009, significantly sensitized EAC cells to Oxaliplatin by repressing PRDX2 and inducing ferroptosis. Remarkably, the combination therapy of Oxaliplatin and APX2009 achieved a synergistic effect in EAC-PDX tumors.
Conclusion: The study unveils a novel signaling axis, APE1/NF-kB/PRDX2, linking disease-associated ROS unbalance and ferroptosis-related chemoresistance. Targeting PRDX2 signaling by APE1-redox-specific inhibition provides a potential novel strategy for combined chemotherapies in refractory EAC.

#3270 SH3GLB1 is involved with hydrogen peroxide/akt signaling in glioblastoma multiforme cells.

C.-H. Chien[1], K.-Y. Chang[2],

[1]School of Medicine, I-Shou University, Kaohsiung City, Taiwan, [2]National Institute of Cancer Research, National Health Research Institutes, Tainan City, Taiwan

Glioblastoma (GBM), a malignant brain tumor, has poor survival outcomes due to recurrence or drug resistance. In our previous studies, it was found that superoxide dismutase 2 (SOD2) was associated with temozolomide (TMZ) resistance. Moreover, SOD2 can convert $O_2^{\bullet-}$ to H_2O_2, and H_2O_2 redox signaling is vital for physiological reactions and promotes tumor progression. We used cell lines, patient primary cells and pharmacological inhibitors/activators to confirm the significance of H_2O_2 signaling. We used the cultured cells to verify roles of H_2O_2 signaling in the plasticity of cell fate and did animal experiments to identify the optimal treatment strategy. In the present study, SOD2 was found to be the upstream mediator, and combining SOD inhibitor and TMZ, the cells showed reduced SH3GLB1 and autophagy levels. We then found that SH3GLB1 was regulated by H_2O_2 through AKT signaling using experiments of regulating redox homeostasis. The change of intracellular H_2O_2 levels in mitochondria following the treatments is similar to that in cytosol, however, the cell fate of parental or resistant cells was quite diverse. Notably, CCCP, a mitochondrial membrane potential disrupter, increased endogenous H_2O_2 production, and TMZ-increased SH3GLB1 levels can be reversed by $HgCl_2$, reflecting the aquaporin function. In animal models, a combination of TMZ and 4-hydroxynonenal reduced growth of the SH3GLB1-knockdown resistant cells, along with suppressed autophagy levels. Our results characterizing the mechanism of H_2O_2-SH3GLB1 axis signaling in acquired TMZ resistance of GBM cells will provide new therapeutic strategies against the disease in the future.

#3271 The casein kinase 2/IKZF1 axis attenuates ceramide accumulation through up-regulation of acid ceramidase: Implications for use of CK2 inhibitors in high-risk pediatric B-cell acute lymphoid leukemia.

J. A. Hengst[1], D. Bastihalli Tukaramrao[1], T. Fox[2], A. Sharma[1], D. Desai[1], S. Dovat[1];
[1]Penn State College of Medicine, Hershey, PA, [2]University of Virgina School of Medicine, Charlottesville, VA

Casein Kinase II (CK2), a growth-promoting non-oncogene, is frequently over-expressed in pediatric high-risk B-cell acute lymphoblastic leukemia (B-ALL) leading to proliferation and survival. CK2 phosphorylates the tumor suppressor IKZF1 (IKAROS) resulting in a loss-of DNA-binding activity. Loss of IKZF1 function is associated with poor prognosis in high-risk B-ALL. As such, inhibition of CK2 using silmitasertib (CX-4945), to restore IKZF1 function, is being therapeutically investigated in high-risk B-ALL. CK2 also phosphorylates/activates the mammalian ceramide synthases to increase production of the pro-apoptotic sphingolipid, ceramide (Cer). Therefore, we hypothesized that inhibition of CK2 with CX-4945 would exert both pro-death (restoration of IKAROS function) and pro-survival (decreased Cer production) effects on B-ALL cells. Moreover, this suggests that targeting the sphingolipid metabolic pathway in tandem with CX-4945 could be a novel strategy for treatment of high-risk B-ALL. To this end, we examined the effects of CX-4945 on sphingolipid levels and the enzymes of the sphingolipid metabolic pathway. Unexpectedly, we determined that CX-4945 dose-dependently increased expression of ceramide synthase 1 (CERS1) and acid ceramidase (AC) proteins, in an IKZF1 dependent manner. Increased CERS1 expression/production of C18:0 Cer has been linked to enhanced mitophagy (i.e., lysosomal clearance of damaged mitochondria) in head and neck squamous cell carcinoma. Induction of mitophagy by CX-4945 was confirmed by western blot analysis of mitofusin-1 and Drp-1 levels. Up-regulation of AC, a lysosomal protein, metabolizes C18:0 Cer to sphingosine for recycling and prevents Cer-induced lysosomal membrane permeabilization. Thus, induction of mitophagy and metabolic breakdown of Cer could potentially reduce the apoptotic efficacy of CX-4945 in B-ALL cell lines. We, therefore, tested whether inhibition of AC would synergize with CX-4945 to enhance B-ALL cell death. Indeed, synergy was observed with the AC inhibitor, SACLAC, in multiple cell lines. Consistent with the observation of synergy between CX-4945 and SACLAC, the combination also enhanced cleavage of PARP indicating an enhancement of cell death. We are currently testing the efficacy of a combination of CX-4945 and AC inhibitors in cell-line derived xenograft models of human B-ALL. Together, these findings indicate that simultaneous targeting of CK2 and AC represents a rationally selected combinatorial therapeutic strategy that overcomes the ability of cancer cells to adapt to single agent targeted therapies by altering pro- and/or anti-apoptotic pathways.

#3272 PJA1 inhibits docetaxel-induced pyroptosis and results in chemoresistance in nasopharyngeal carcinoma.

N. Liu, Y.-Q. Li, S.-Y. Huang;
Sun Yat-sen University Cancer Center (SYSUCC), Guangzhou, China

Background: Nasopharyngeal carcinoma (NPC) is highly prevalent in South China. More than 70% of patients are diagnosed with locoregionally advanced NPC (LA-NPC) at initial presentation, and the addition of induction chemotherapy (IC) to concurrent chemoradiotherapy is recommended for these patients. However, chemoresistance is a main reason for treatment failure in NPC patients, and the exact regulatory mechanism underlying chemoresistance in NPC remains to be elucidated.

Methods: A gene expression dataset and STRING database were used to identify core module and gene that are related to the efficacy of docetaxel-cisplatin-5-fluorouracil (TPF) IC in NPC patients. *In vitro* and *in vivo* functional experiments were used to test the effects of PJA1 on docetaxel chemoresistance of NPC cells. The flow cytometric analysis, western blot, and lactate dehydrogenase (LDH) release assays were performed to determine the effects of PJA1 on GSDME-mediated cell pyroptosis. Co-immunoprecipitation, mass spectrometry, immunofluorescence staining, and ubiquitination assays were performed to explore the regulatory manners between PJA1 and PGAM5-DRP1 axis. Finally, multiplex immunofluorescence and immunohistochemical staining were used to evaluate the clinical significance of PJA1 -PGAM5-DRP1 axis in patients with NPC.

Results: PJA1 was identified as a key E3 ligase of the top-ranked module ubiquitin-proteasome system dysregulation that involved in NPC chemoresistance, which was highly expressed in NPC patients with nonresponse to the TPF IC. PJA1 facilitated the docetaxel resistance of NPC cells through inhibiting the GSDME-mediated pyroptosis. Mechanistically, PJA1 promoted the degradation of the mitochondrial protein PGAM5 by increasing its K48-linked ubiquitination at K88, further increasing the phosphorylation of DRP1 at S637 and reducing the mitochondrial reactive oxygen species (ROS) production, in turn resulting in a suppressive of GSDME-mediated pyroptosis. PGAM5 knockdown fully restored the docetaxel sensitization effect of PJA1 knockdown. Moreover, RTA402, a pharmacological inhibitor of PJA1, enhanced the docetaxel sensitivity of NPC cells. Clinically, high PJA1 expression indicated resistance to TPF IC an inferior survival in NPC patients.

Conclusions: Our study emphasizes the essential role of E3 ligase PJA1 in regulating chemoresistance in NPC and provides new therapeutic strategies for NPC patients based on targeting the ubiquitin-proteasome system.

#3273 Tirapazamine sensitizes homologous recombination-proficient cancers by enhancing DNA damage andferroptosis.

Y. Jiang, H. Estephan, Y. Wang, F. Aljarbou, N. V. Lopera, E. Moon, E. M. Hammond, A. J. Giaccia;
Oxford Institute for Radiation Oncology, Department of Oncology, University of Oxford, Oxford, United Kingdom

Despite its success in HR-deficient tumors, the application of PARP inhibitors (PARPis) in HR-proficient cancers is very limited. Since the majority of cancers are HR-proficient, there is a need for developing strategies to extend the use of PARPis to HR-proficient cancers. We investigated whether the hypoxic cytotoxin, tirapazamine (TPZ) sensitizes HR-proficient cancer cells to PARPis under normoxia and hypoxia (2% O_2), and found that TPZ enhanced PARPi cell killing to a greater extent under hypoxia compared to normoxia. Mechanistically, this enhanced killing was due to the induction of DNA double-strand breaks and free radicals that lead to ferroptotic cell death. To determine the role of hypoxia in the anti-tumor effect of the combination treatment, we examined the efficacy of TPZ and PARPi treatment in hypoxic spheroids and subcutaneous xenograft models derived from a panel of HR-proficient human non-small cell lung cancer (NSCLC) cells. We found that PARPis combined with TPZ significantly inhibited the growth of the hypoxic NSCLC spheroids. In addition, the combination treatment significantly inhibited the growth of A549 and CORL105 xenografts that possess significant hypoxic fractions, but did not significantly inhibit the growth of well-oxygenated Calu3 and H3122 xenografts. Taken together, this study demonstrates that TPZ can sensitize HR-proficient tumor cells to PARPi through the introduction of DNA strand breaks and free radicals, suggesting that TPZ treatment can broaden the usage of PARPi to HR-proficient cancers.

#3274 Trefoil factor 1 suppresses stemness and enhances chemosensitivity of pancreatic cancer.

J. Yamaguchi, T. Kokuryo, Y. Yokoyama, M. Sunagawa, T. Baba, T. Ebata;
Nagoya Univ. Graduate School of Medicine, Nagoya, Aichi, Japan

Background and Aims: Pancreatic cancer is one of the most lethal malignancies, partly due to resistance to conventional chemotherapy. The chemoresistance of malignant tumors is associated with epithelial-mesenchymal transition (EMT) and the stemness of cancer cells. The aim of this study is to investigate the availability and functional mechanisms of trefoil factor family 1 (TFF1), a tumor-suppressive protein in pancreatic carcinogenesis, to treat pancreatic cancer.
Methods: To investigate the role of endogenous TFF1 in human and mice, specimens of human pancreatic cancer and genetically engineered mouse model of pancreatic cancer (KPC/TFF1KO; Pdx1-Cre/ LSL-$KRAS^{G12D}$/ LSL-$p53^{R172H}$/ $TFF1^{-/-}$) were analyzed by immunohistochemistry (IHC). To explore the efficacy of extracellular administration of TFF1, recombinant and chemically synthesized TFF1 were administered to pancreatic cancer cell lines, a xenograft mouse model and a transgenic mouse model.
Results: The deficiency of TFF1 was associated with increased EMT markers of cancer cells (Snail and Zeb1) in mouse models of pancreatic cancer, KPC. Analysis of the survival of patients who underwent chemotherapy for recurrent pancreatic cancer revealed that the expression of TFF1 in cancer cells was associated with better survival. Also, in the mouse model of pancreatic cancer, KPC mice showed improved survival when treated with gemcitabine, the KPC/TFF1KO mice did not. Pancreatic cancer cell lines were administered with gemcitabine and/or chemically synthesized TFF1, revealing that addition of TFF1 downregulated gemcitabine-induced EMT markers (Snail, Slug, ZEB1, and αSMA), Wnt pathway activation (β-catenin, TCF7, and EPHB3). In addition, TFF1 inhibited the expression of cancer stemness markers (CD133 and NANOG3) and the ability to form tumor sphere. Importantly, TFF1 accelerated the apoptosis of cancer cells induced by gemcitabine *in vitro*. *In vivo*, combined treatment of gemcitabine and subcutaneous administration of TFF1 arrested tumor growth in xenograft mouse model. Also, KPC mice with combined treatment showed the better survival rather than gemcitabine-alone treatment, with lower expression of CD133, high expression of ZEB1, and lower nuclear translocation of β-catenin.
Conclusion: These results indicate that TFF1 can contribute to establishing a novel strategy to treat pancreatic cancer patients by enhancing chemosensitivity.

#3275 PHGDH-mediated serine-glycine-one-carbon metabolism drives ferroptosis- and chemotherapy-resistance in colorectal cancer.

G. Liang[1], J. Chen[1], X. Wen[1], Z. Zhang[1], Z. Chen[1], Y. Chen[1], Z. Xian[1], X. He[1], X. Wu[2], P. Lan[1], T. Hu[1];
[1]The Sixth Affiliated Hospital of Sun Yat-sen University, Guangzhou, China, [2]Sun Yat-sen Memorial Hospital of Sun Yat-sen University, Guangzhou, China

Background and Aim: Ferroptosis is an iron-dependent form of programmed cell death characterized by lipid peroxidation, with the potential as a novel cancer therapy. The application of ferroptosis-inducers has been limited to preclinical studies due to toxic side effects and drug-resistance. Our study aims to explore the metabolic mechanism in regulating ferroptosis-resistance, thereby identifying combinational therapeutic target for ferroptosis-inducers.
Methods: The ferroptosis-resistant CRC cell lines were induced by chronic exposure to ferroptosis inducer Erastin and verified by cell viability assay. Metabolomics and transcriptomics were performed to identify the metabolic characteristics in ferroptosis-resistant CRC cells. Quantitative RT-PCR and western blot was applied to confirm the differentially expressed serine-glycine-one-carbon metabolism (SGOC) enzymes. The MTT cell viability assay, colony formation assay, 3D spheroid formation assay and cell derived xenograft (CDX) model were carried out to investigate the therapeutic effect of targeting SGOC key enzyme-phosphoglycerate dehydrogenase (PHGDH) in combination of ferroptosis inducers. Gene set enrichment analysis (GSEA) was performed to identify molecular mechanism for the upregulation of SGOC enzymes based on RNA-seq data from TCGA-COAD cohort.
Results: Metabolomic and transcriptomic data revealed that SGOC metabolism was significantly increased in ferroptosis-resistant CRC cells. Moreover, the mRNA and protein level of SGOC key enzyme-PHGDH were remarkably upregulated in ferroptosis-resistant CRC cells. PHGDH inhibitor NCT-503 or knockdown of PHGDH exhibited a great synergistic effect with ferroptosis inducers for CRC cells in vitro or in vivo. Additionally, targeting PHGDH could dramatically restore the sensitivity of ferroptosis-inducers in ferroptosis-resistant cells. The RNA methyltransferase-like 3 (METTL3) was identified as the upstream regulator responsible for the upregulation of PHGDH in an m^6A-dependent manner. The ferroptosis stress induced deacetylation of METTL3, thereby promoting its nuclear translocation and enzyme activity.
Conclusions: In summary, we have uncovered that CRC cells resisted ferroptosis inducers via METTL3-PHGDH axis. Targeting PHGDH combined with ferroptosis inducers exhibited with synergistic effect for CRC in vitro and in vivo. Our findings identified the metabolic vulnerability in ferroptosis-resistant CRC cells, which could serve as a novel therapeutic target.

#3276 The effects of extracellular ATP signaling on the anticancer activities of macrophages.

J. M. Manouchehri, L. M. Marcho, M. A. Cherian;
The Ohio State University Wexner Medical Ctr., Columbus, OH

Among cancers in women worldwide, breast cancer has the highest incidence and the highest mortality. Patients with triple negative breast cancer (TNBC) have a markedly worse outcome in comparison to patients diagnosed with hormone-dependent and human epidermal growth factor receptor-positive breast cancers due to the aggressive and rapidly progressive nature of the disease and the deficit in specifically targeted therapies available. Therefore, there is a need for new therapeutic approaches. Extracellular ATP has been shown to cause cell death in an autocrine and paracrine manner and is also a known danger signal that causes immune activation. Our published data reveals that at high micromolar concentrations extracellular ATP (eATP) can induce cell death through the eATP-gated ion channels, purinergic P2RX7 and P2RX4 receptors. We also showed that in the context of chemotherapy treatment, eATP modulates TNBC cell death at submicromolar concentrations. A feature of the tumor microenvironment is a pronounced increase in the concentrations of eATP (micromolar) to levels that are closer to the threshold for cytotoxicity than in normal tissues (nanomolar). In addition, we discovered that chemotherapy induces the release of eATP from TNBC cells, further augmenting its concentration. Despite this, eATP is rapidly degraded to adenosine by extracellular ATPases (eATPases). It should be noted that extracellular ATP release and activation of its receptor, P2XR7, are prerequisites for the activation of a complex of proteins known as the NLRP3 inflammasome that is critical for IL-1β and IL-18 secretion and the induction of a highly inflammatory form of programmed cell death known as pyroptosis. The objective of this study was to evaluate if augmenting eATP levels using extracellular ATPase inhibitors will increase the efficacy of chemotherapy against THP-1 and differentiated THP-1 cells to undergo an inflammatory form of cell death known as pyroptosis. We treated THP-1 and differentiated THP-1 cells with increasing concentrations of the chemotherapeutic agent paclitaxel in the presence of eATPase inhibitors POM-1 and PSB 069 with eATP content and cell viability being assessed. Additionally, we examined NLRP3 inflammasome activation by immunoblot analysis. We analyzed the oligomerization of NLRP3 and ASC, the cleavage of caspase 1 and gasdermin and the secretion of IL-1β and IL-18, all components of pyroptosis. These results reveal that eATP modulates the chemotherapeutic response in the monocytic THP-1 and differentiated THP-1 cells, which could be exploited to augment the anticancer effects of macrophages on TNBC cells. These preclinical experiments could be applied to develop effective therapies that increase the depth and length of responses to chemotherapy and immunotherapy in TNBCs by augmenting pyroptosis of tumor associate macrophages through enhanced eATP.

#3277 PAI-1 mediates resistance to MET-targeted therapy in non-small cell lung cancer.

T. Higashihara[1], Y. Thu[1], K. Suzawa[2], K. Date[1], A. Matsuoka[1], D. Mizuno[1], R. Yoshichika[1], N. Hayashi[1], F. Mukohara[1], M. Yoshikawa[1], K. Shien[2], H. Yamamoto[2], S. Toyooka[1];

[1]Okayama University Graduate School of Medicine, Dentistry and Pharmaceutical Sciences, Okayama, Japan, [2]Okayama University Hospital, Okayama, Japan

[Purpose] The mesenchymal epithelial transition factor receptor (MET) is a potential therapeutic target in various cancers, including non-small cell lung cancer (NSCLC). In NSCLC, the activation of MET pathway is thought to occur through diverse mechanisms that influence properties affecting cancer cell survival, growth, and invasiveness. These tumors show oncogene addiction to MET and exhibit remarkable responses to MET-Tyrosine Kinase Inhibitors (TKIs). However, the long-term effectiveness of MET-TKIs is usually limited due to acquired drug resistance. The mechanisms underlying primary and acquired resistance to MET-TKIs in the management of NSCLC remain unclear. In this study, we investigated the mechanisms acquired for crizotinib in *MET*-amplified lung carcinoma cell lines. [Experimental Designs] Two *MET*-amplified lung cancer cell lines, EBC-1 and H1993, were established for acquired resistance to MET-TKI crizotinib and were functionally elucidated. The factors contributing to the resistance mechanism were assessed by genomic and transcriptomic data, and the alterations hypothesized to confer resistance were validated. [Results] Multiple mechanisms underlay acquired resistance to crizotinib in *MET*-amplified lung cancer cell lines. In EBC-1-derived resistant cells, the drug resistance mechanism was mediated by the overexpression of *SERPINE1* , the gene encoding plasminogen activator inhibitor-1 (PAI-1). Crizotinib resistance was overcome by combination therapy with PAI-1 inhibitor and PAI-1 knockdown. Another mechanism of resistance in different subline cells of EBC-1 was evaluated as epithelial to mesenchymal transition (EMT) with the upregulation of antiapoptotic proteins. In the H1993-derived resistant cells, the phosphorylated forms of MEK and ERK were observed to be upregulated and MEK inhibitors could be a potential therapeutic strategy for overcoming the resistance. [Conclusions] In this study, we revealed the different mechanisms of drug resistance to MET-TKI treatment and presented some possible strategies to overcome the resistance.

#3278 Analysis of the mechanism of resistance to selpercatinib in thyroid cancer cells with *RET/PTC1* fusion gene.

M. Amitani, K.-i. Ito;
Shinshu University, Matsumoto, Japan

Purpose: Precision oncology, in which molecularly targeted drugs are selected based on genetic mutations, has begun in thyroid cancer, and drugs targeting *BRAF*, *RET*, and *NTRK* are already in clinical use. However, as with previous therapeutic agents for malignant tumors, there have been cases of resistance to these drugs either initially or during treatment, and the mechanisms of drug resistance need to be elucidated. So far, little is known about the mechanisms of resistance to molecularly targeted drugs in thyroid cancer. To overcome resistance to the RET inhibitor, selpercatinib (SEL), and to consider next therapeutic strategies, we aimed to elucidate the mechanisms of resistance to SEL.
Method: We used papillary carcinoma cell lines TPC-1 and CUTC48, which harbor the *RET/PTC1* fusion gene. We established an SEL-resistant subline (TPC-1/SELR) in TPC-1 by long-term exposure to SEL. The growth inhibitory effect of drugs was analyzed using the WST assay. The alteration of intracellular signal transduction was analyzed by western blotting.
Result: The 50% inhibitory concentration (IC_{50}) for SEL in the parental TPC-1 was 3 nM, while growth inhibition in TPC-1/SELR did not reach 50% even at more than 100 nM of SEL. On the other hand, growth inhibition by SEL in CUTC48 did not reach 50% even at more than 100 nM of SEL. The sensitivity to SEL in CUTC48 was comparable to that in TPC-1/SELR, and CUTC48 showed an intrinsic resistance to SEL. TPC-1/SELR showed increased phosphorylation of EGFR, Erk, Akt, and mTOR compared to TPC-1. In CUTC48, phosphorylation of EGFR and Erk was not increased compared to that of TPC-1, while phosphorylation of Akt and mTOR was increased. We investigated the growth inhibitory effect of an mTOR inhibitor everolimus and found that TPC-1 (IC_{50}: 1.3 nM), TPC-1/SELR (5 nM) , and CUTC48 (9.4 nM) were all highly sensitive to everolimus.
Discussion: Our results showed that Akt and mTOR phosphorylation were elevated in the SEL-resistant TPC-1/SELR and the SEL-intrinsic resistant CUTC48 in common, suggesting the involvement of activation of the Akt-mTOR pathway in SEL resistance in thyroid cancer. The inhibition of the Akt-mTOR pathway in parallel with RET may have therapeutic potential to overcome SEL resistance in thyroid cancer.

#3279 MUC1 is necessary for the inflammatory memory response to osimertinib resistance in NSCLC cells.

N. Haratake[1], A. Bhattacharya[1], A. Nakashoji[1], H. Ozawa[1], M. Shimokawa[2], D. Kufe[1];
[1]Dana-Farber Cancer Institute, Boston, MA, [2]Yamaguchi University, Yamaguchi, Japan

Emergence of resistance is an invariable outcome in cancer progression that may involve memory of cancer cells to treatment. The oncogenic MUC1-C protein confers pleotropic resistance of cancer cells to diverse cytotoxic and targeted agents by unclear mechanisms. We demonstrate that MUC1-C regulates the interferon (IFN) type I/II pathways in H1975 non-small cell lung cancer (NSCLC) cells selected for osimertinib resistance (H1975-OR). Targeting MUC1-C in H1975-OR cells suppressed STAT1 and inflammatory IFN signaling in association with reversing the osimertinib-resistant phenotype. Studies of H1975-OR cells selected for growth in the absence of osimertinib demonstrate that revertant H1975-RT cells retain MUC1-C-dependent memory necessary for recalling osimertinib resistance. Mechanistically, osimertinib treatment of H1975-RT cells activates the *MUC1* gene at a (i) promoter-like signature (PLS) by MUC1-C and STAT1, and (ii) proximal enhancer-like signature (pELS) by PBAF and JUN/AP-1. Targeting MUC1-C in osimertinib-treated H1975-RT and MGH170 NSCLC MET-amplified cells isolated from a patient refractory to osimertinib treatment suppressed induction of STAT1 and downstream IFN-stimulated genes (ISGs) encoding MX1, OAS1 and ISG15. Targeting MUC1-C, STAT1, PBRM1/PBAF and JUN/AP-1 further confirmed their dependencies for reemergence of osimertinib resistance in H1975-RT and MGH170 cells. In support of these results, high MUC1-C protein expression analyzed by IHC is associated with shorter progression free survival for patients treated with osimertinib. These findings and the demonstration that MUC1-C is upregulated in NSCLC cells from patients refractory to osimertinib indicate that MUC1-C drives osimertinib resistance in NSCLC cells by promoting an inflammatory memory response.

#3280 ASCL2$^{\pm}$ tumor cells modulate the response of colorectal cancer to MAPK targeting therapy.

O. E. Villarreal, H. M. Lee, H. Tran, A. Machado, J. Alshenaifi, C. W. Wong, O. Coker, R. Minelli, M. Peoples, A. Hernandez Martinez, N. Fowlkes, P. Kanikarla, K. Lin, C. Bristow, A. Viale, J. R. Marszalek, J. P. Shen, S. Kopetz;
The University of Texas MD Anderson Cancer Center, Houston, TX

Colorectal cancer (CRC) is commonly treated with MAPK pathway inhibitors (MAPKi) including EGFRi, BRAFi, and most recently KRAS G12C inhibitors. However, clinical trials repeatedly demonstrate that durability of benefit is short-lived in many patients. While genomic mechanisms of acquired resistance have been described, this explains a small minority of patients and further research is needed to determine the underlying biology limiting MAPKi therapy durability in CRC.

Potential responsible mechanisms were explored using transcriptomic data from patients treated with MAPKi combination therapy, showing upregulation of stem-related signatures in nonresponders (FDR<0.001), therefore CRC stem markers with the greatest expression increase were identified. The top markers (ASCL2, LGR5, LRIG1) were evaluated using a metacohort of single cell RNAseq (scRNAseq) data from patients with CRC (n=72), and ASCL2 was selected for further study due to its high marker coexpression and tumor cell specificity (OR=8.27, p<0.0001). Additionally, ASCL2 expression increased in multiple patient-derived organoid and xenograft (PDX) models that were treated with a spectrum of MAPKi therapies (BRAFi, EGFRi, G12Ci, MEKi, SOSi). As such, we postulated that ASCL2$^{\pm}$ tumor cells play an important role in the limited response durability of MAPKi therapy in CRC.

To investigate, ASCL2 reporter models were treated with MAPKi therapy, resulting in the significant enrichment of ASCL2$^{\pm}$ tumor cells, independent of driver mutation or treatment regimen used. Using Single Cell BarcodeSeq, by combining molecular barcoded PDXs with single cell transcriptomics, we found that MAPKi therapy engaged intrinsic cellular plasticity resulting in cells transitioning into the ASCL2$^{\pm}$ phenotype. Additional patient-level data confirmed enrichment of the ASCL2$^{\pm}$ transcriptomic signature at progression while on MAPKi therapy. Characterization of ASCL2$^{\pm}$ cells showed higher stem cell frequency ($p=9.7x10^{-62}$), clonogenic capacity (p<0.0001), expression of stem-related genes, and retention of phenotypic plasticity, indicating ASCL2$^{\pm}$ tumor cells feature stem-like abilities, as previously described, which include therapy resistance. Lastly, depletion of ASCL2$^{\pm}$ tumor cells resulted in improved initial response to MAPKi therapy (p<0.0001) and, more importantly, prolonged cell growth inhibition.

Overall, we observe that MAPKi therapy enriches stemness programs in CRC and demonstrate MAPKi drives cells into a transient ASCL2$^{\pm}$ stem-like state with limited sensitivity to MAPK inhibitors. Further studies are underway to identify vulnerabilities that will enable targeting of ASCL2$^{\pm}$ tumor cells. Ultimately these findings will help guide future optimization of MAPKi regimens to prolong response durability and improve outcomes for patients with CRC.

#3281 Silencing of necroptosis related genes in endocrine-resistant breast cancer cells causes PFKFB3 induced arrest of necroptosis and contributes to resistance.

B. C. Jones[1], T. Onal[2], S. Sengupta[2], C. M. Sevigny[3], L. Jin[2], P. R. Pohlmann[4], A. Shajahan-Haq[5], **R. Clarke**[2];
[1]Lombardi Comprehensive Cancer Center, Georgetown University Medical Center, Washington DC, Washington, DC, [2]The Hormel Institute, University of Minnesota, Austin, MN, [3]The Jackson Laboratory, Bar Harbor, ME, [4]MedStar Georgetown University Hospital, Washington, DC, [5]Lombardi Comprehensive Cancer Center, Georgetown University Medical Center, Washington, DC

Approximately 70% of newly diagnosed breast cancer patients are estrogen receptor positive. Patients treated with approved treatment strategies may develop resistance to these therapies. Because of this problem in treatment, new treatment regimens need to emerge. Altered reprogramming of metabolism and an intense dependence on glycolysis are hallmarks of cancer, which is necessary to support the high energy demand of rapidly proliferating cancer cells. Rapidly dividing cancer cells are known to have increased energy requirements and altered reprogramming of glucose metabolism, leading to an increased reliance on glycolysis. The conversion of fructose-6-phosphate to fructose-1,6-bisphosphate, a critical rate-limiting step in the glycolysis pathway, is greatly influenced by an allosteric activator produced by the enzyme PFKFB3 (6-phosphofructo-2-kinase/fructose-2,6-bisphosphatase 3), thus making PFKFB3 an important regulator of glycolytic flux. Furthermore, PFKFB3 has been shown to be overexpressed in many human cancers, including breast cancer, and upregulated by estrogen. In our previous studies, we have shown that endocrine-resistant BC cells growth is strongly reduced by PFKFB3 targeting using PFKFB3 inhibitors, glucose uptake is reduced, triggered to necroptosis by RIPK1 and MLKL phosphorylation, and PFKFB3 inhibition reduces tumor size in mouse xenografts. In this study, we showed that silencing of RIPK1 and MLKL, genes involved in necroptosis, by siRNAs followed by inhibition of PFKFB3 by PFK158 did not induce necroptosis in endocrine-resistant BC cells. Furthermore, we further confirmed that phosphorylation of MLKL and RIPK occurs with PFKFB3 inhibition. In summary, this study reveals that necroptosis induced by PFKFB3 inhibition contributes to resistance by arresting necroptosis in endocrine-resistant BC cells after silencing of necroptosis-related genes.

#3282 Endocrine resistance genes driving cross-resistance to current combination therapies in HR-positive breast cancer.

Z. Huang, N. Wortelboer, C. Beaufort, S. N. Ortak, D.-w. Chan, H. H. Dag, J. Helmijr, J. Martens, M. Jansen;
Erasmus MC Cancer Institute, Rotterdam, Netherlands

Introduction: Treatment failure to multiple treatment lines in hormone receptor positive (HR+) patients brings cross-resistance into the stage. The study aimed to determine if tamoxifen resistance genes cause cross-resistance to commonly employed metastatic breast cancer (combination) treatments.
Materials & Methods: Parental and tamoxifen resistant MCF7A models (BCAR3, BCAR4, EGFR, AKT1 and AKT2) were cultured for 10 days with different concentrations of tamoxifen and fulvestrant (endocrine therapy), ribo-, abema-, and palbociclib (CDK4/6 inhibitors) and alpelisib (PIK3CA inhibitor). Compounds were tested as mono- and combination therapy in replicate experiments estimating cell growth using the Sulforhodamine B assay and half maximal inhibitory concentration (IC50) was calculated by Graphpad PRISM v5 software. Resistance was declared when IC50 was significantly different from parental ($p<0.05$, Mann-Whitney U test).
Results: The BCAR3, BCAR4 and EGFR models were not only resistant to tamoxifen but also to fulvestrant monotherapy (see table). In the two AKTs models the initial results could not be reproduced and were excluded from the study. The BCAR4 model was also resistant to all CDK4/6- and PIK3CA-inhibitors monotherapy. Analysis of the combination regimens demonstrated cross-resistance in the BCAR4 model for all compound combinations tested, in the EGFR model for all combinations except fulvestrant combined with alpelisib, and in the BCAR3 model only for tamoxifen combined with alpelisib.
Discussion/Conclusion: Tamoxifen resistance genes BCAR3, BCAR4 and EGFR show various degrees of cross-resistance to other breast cancer treatments. It might be worthwhile to evaluate these genes or their associated biological pathways as predictive biomarkers for cross-resistance in HR+ breast cancer patients treated with the mentioned (combination) therapies.

Summary of median IC50 (IQR) for different conditions

	parental	BCAR3	BCAR4	EGFR	AKT1	AKT2
Monotherapy						
Tamoxifen	**9.8 (7.0)**	**47.3 (121) ****	**2210 (1280) ****	**515 (495) ****	**8.0 (21.3)**	**3.8 (21.8)**
Fulvestrant	**0.1 (0.35)**	**0.8 (0.8) ****	**309 (407) ****	**11.4 (37.7) ****		
Ribociclib	**479 (285)**	**423 (1102)**	**3099 (1212)****	**719 (669)**		
Abemaciclib	**94.9 (82.5)**	**28.9 (52.6)**	**206 (197) ***	**189 (172)**		
Palbociclib	**138 (163)**	**91.1 (107)**	**608 (347) ****	**158 (128)**		
Alpelisib	**14.1 (676)**	**322 (94.0)**	**1424 (372) ****	**375 (356)**		
Combination therapy Tamoxifen with						
Ribociclib	**1.7 (1.0)**	**17.2 (29.0)**	**111 (159) ***	**54.4 (35.8) ***		
Abemaciclib	**2.5 (1.9)**	**6.0 (10.7)**	**19.5 (15.0) ****	**40.0 (53.6) ***		
Palbociclib	**1.6 (2.0)**	**5.4 (4.6)**	**74.9 (80.9) ***	**29.2 (3.1) ***		
Alpelisib	**2.1 (0.3)**	**9.6 (12.4)***	**157 (69.9) ***	**17.8 (9.9) ***		
Combination therapy Fulvestrant with						
Ribociclib	**0.07 (0.02)**	**0.1 (0.3)**	**14.4 (8.8) ***	**6.9(16.8) ***		
Abemaciclib	**0.07 (0.02)**	**0.1 (0.1)**	**4.6 (2.6) ****	**2.6 (6.5) ***		
Palbociclib	**0.2 (0.1)**	**0.2 (1.6)**	**5.6 (0.9) ***	**1.3 (1.5) ***		
Alpelisib	**0.05 (0.05)**	**1.6 (20.6)**	**13.3 (8.1) ***	**2.1 (0.9)**		
***:p<0.05, **:p<0.01 compared to parental cell line.**						

#3283 Role of HA, HAS3, UGT1A9 in metastatic renal cell carcinoma and sorafenib resistance.

A. K. Sharma, K. Aguilar, C. S. Panda, V. B. Lokeshwar;
Augusta University, Augusta, GA

Introduction: Despite numerous available treatments, metastatic renal cell carcinoma (mRCC) remains highly lethal, with over 90% of patients succumbing within 5 years. Sorafenib (SF), a second-line treatment for mRCC, exhibits modest efficacy, and the underlying molecular basis for its failure is elusive. Hyaluronic acid (HA), implicated in promoting cell proliferation, invasion, and motility through CD44 and RHAMM receptors, represents a potential player in SF resistance. Hymecromone (HC), a non-toxic dietary supplement, is known to inhibit HA synthesis and downregulate CD44 and RHAMM mRNA levels. This study investigates the elusive mechanisms of SF resistance and evaluates the effectiveness of the HC+SF combination as a targeted therapy for advanced RCC, providing insights into a novel and potentially impactful treatment approach.

Methods: HA levels were measured in normal and tumor kidney specimens using ELISA-like assay and IHC. Similarly, HAS3 and UGT1A9 (A9) levels and SF glucuronidation were measured by qPCR and a glucuronidation assay using tumor microsomes. Response to SF+HC combination was examined in A9 and HAS3 knockdown and overexpression cell lines (transfectants) and primary RCC spheroids by proliferation, apoptosis, motility, and invasion assays. Target analysis was performed by immunoblot. Treatment efficacy was evaluated in subcutaneous and orthotopic xenograft mouse models, with bioluminescence imaging.

Results: SF failure in mRCC was linked due to its glucuronidation and inactivation by A9. Tumor microsomes from patients who developed mRCC glucuronidated SF 5-fold higher than from non-mRCC patients. A9 levels were elevated (8-10 folds) in mRCC patients' tumor along with HA and HAS3 (5-10 folds) as compared to non-mRCC patients and normal kidney tissues. HC treatment downregulated A9 promoter activity and inhibited SF-glucuronidation in RCC cells. SF (5uM) and HC (20, 40ug/ml) combination inhibited RCC cell and primary tumor spheroid proliferation (>90%), motility/invasion (>80%), and induced apoptosis (5-fold) and downregulated HAS3 expression (>80%), and HA synthesis in RCC cells. While A9 and HAS3 transfectants both were resistant to SF+HC treatment, A9 and HAS3 - KO transfectants were sensitive to SF. Endothelial cells co-cultured with either A9 or HAS3 transfectants were resistant to SF+HC treatment. SF+HC upregulated apoptosis effectors, but downregulated CD44, RHAMM, and phospho-Met levels in EV but not in A9 or HAS3 transfectants. HC (100 or 200mg/kg) and SF (30mg/kg) oral combination abrogated Caki-1 tumor growth (>80%), without serum/tissue toxicity. HC+SF treatment decreased A9, HA and HAS3 levels, Ki67 index and microvessel density. Both A9 and HAS3 overexpressing tumors were resistant to treatment.

Conclusion: This study demonstrates the mechanism of SF failure in mRCC and proposes a safe, oral adjunct combination for effective treatment.

#3284 Transcription factor YBX1 elevating the sorafenib IC50 in hepatocellular carcinoma cell lines.

D. Kwabiah[1], A. AyalaPazzi[2], K. Doxtater[1], S. Leslie[1], M. K. Tripathi[1];
[1]University of Texas Rio Grande Valley, McAllen, TX, [2]UT SouthWestern Medical Center, Dallas, TX

Hepatocellular carcinoma (HCC) is the most common form of liver cancer which accounts for more than 90% of occurrences of liver cancer cases. Surgical therapies such as liver transplantation and hepatectomy may help cure hepatocellular carcinoma diagnosed in its early stages. Advanced stages of the disease have a poor prognosis and a high refractoriness because of drug resistance. Sorafenib is a tyrosine kinase inhibitor that has been approved for the systemic treatment of patients with advanced HCC. However, the efficacy of this medication has shown a limited prolongation of the overall survival in patients with advanced HCC. The mechanism of resistance to sorafenib in advanced HCC is poorly understood. The TCGA analysis of the HCC patient cohort shows an elevated expression of YBX1 in tumors as compared to normal. The expression is also correlated with progression, metastasis, and poor survival of HCC patients. Transcription factor YBX1 is involved in the regulation of drug resistance in different cancers, especially breast and colorectal cancers. Our lab is interested in understanding if YBX1 is involved in sorafenib resistance in HCC. Different HCC cell lines procured from ATCC SK-Hep1, Huh-7luc, and C3A, were analyzed for their IC50 values for sorafenib using MTT assays, at different time points. SK-Hep1 showed 8.780µM and 8.174µM, HepG2luc 4.659µM and 3.596µM at 48 and 72 hrs respectively. Overexpression of YBX1 in the SK-Hep1 cell line increased the cell survival and IC50 value of sorafenib at 48 and 72 hrs at 13.19µM and 10.64µM respectively. This supports the hypothesis which demonstrates the role of YBX1 in mediating resistance to sorafenib in advanced HCC. YBX1 could be a major therapeutic target and by inhibiting its action could improve the sensitivity of advanced HCC to sorafenib. We have developed YBX1 overexpressing and knockdown (GFP expressing) cell lines, FACS sorted and Puromycin selected for further mechanistic studies. We are also further developing the sorafenib-resistant HCC cell lines to understand the mechanism underlying sorafenib resistance in HCC. Protein and RNA analyses revealed a relative increase in YBX1 overexpression in sorafenib-resistant cell lines as compared to its parental cell lines. Understanding the mechanism of YBX1-induced drug resistance to sorafenib and its associated signaling pathways could help improve the sensitivity of advanced hepatocellular carcinoma to treatment by sorafenib and thus improve the livelihood of its patients.

#3285 Elevated expression of breast cancer stem cell marker alpha6-integrin is associated with reduced anti-estrogen efficacy in breast cancer.

G. Viteri[1], S. Angeloni[2], U. Soto[2], E. J. Brantley[2];
[1]Loma Linda Univ. School of Pharmacy, Loma Linda, CA, [2]Loma Linda Univ. School of Medicine, Loma Linda, CA

Most women diagnosed with breast cancer have tumors expressing the estrogen receptor and are prescribed agents such as aromatase inhibitors or the anti-estrogens tamoxifen or fulvestrant. However, up to 40% of these patients will experience relapse due to endocrine therapy resistance even when these agents are used in combination with cyclin dependent kinase inhibitors. A small population of cells within tumors known as breast cancer stem cells are generally resistant to endocrine therapy and are believed to promote patient relapse. We previously found that breast cancer stem cell marker α6-integrin is expressed at elevated levels in cells that are resistant to the anti-estrogen tamoxifen. We thus hypothesized that elevated levels of α6-integrin confer resistance to anti-estrogens. Quantitative PCR analyses revealed that tamoxifen-resistant and fulvestrant-resistant mammospheres (breast cancer spheroids) exhibit increased α6-integrin expression as compared to antiestrogen-sensitive mammospheres. Cells with enforced α6-integrin expression were less responsive to tamoxifen and fulvestrant than control cells. Further, pharmacological or genetic inhibition of α6-integrin enhanced anti-estrogen efficacy. Our data suggest that targeting α6-integrin represents a viable strategy to overcome endocrine therapy resistance.

#3286 Synergistic impact of long non-coding RNA TUG1 depletion in overcoming temozolomide chemoresistance in glioblastoma.

Hidekazu Kito, Yuji Kibe, Miho Suzuki, Keiko Shinjo, Yutaka Kondo

Nagoya University, Nagoya, Japan

Glioblastoma (GBM) stands out as the most prevalent and aggressive primary brain tumor in adults, marked by a high mortality rate. Standard therapy involves temozolomide (TMZ) chemotherapy, an alkylating agent. However, most cases develop resistance to TMZ, necessitating the development of new treatment options to overcome TMZ-resistant GBM. Long non-coding RNAs (lncRNAs) constitute a class of RNA molecules that, despite not encoding proteins, play pivotal roles in regulating diverse cellular processes. Overexpression of specific lncRNAs in cancer is linked to crucial aspects of cancer progression, such as cell proliferation, apoptosis, and metastasis. Taurine upregulated gene 1 (TUG1) is a highly expressed lncRNA in GBM, playing a crucial role in preventing excessive DNA replication stress and associated DNA damage (Nat Commun 2023).This study aimed to investigate the combined effects of TUG1 depletion and TMZ in TMZ-resistant GBM. First, we established a TMZ-resistant U251MG cell line, U251MG-R, characterized by a low DNA methylation level of the O6-methylguanine-DNA methyltransferase (MGMT) promoter. We observed that TMZ increased DNA replication stress in the U251MG-R. Depleting TUG1 by using antisense oligonucleotide (TUG1-ASO) sensitized U251MG-R cells to TMZ. Treatment with TMZ or TUG1-ASO alone inhibited cell proliferation, with the most significant inhibition observed when both were combined. Next, we employed a xenograft mouse model to evaluate the efficacy of intravenous TUG1-ASO treatment coupled with a tumor-specific drug delivery system (antiTUG1-DDS). The combination of antiTUG1-DDS with TMZ displayed the most effective suppression of tumor growth compared to either TMZ or antiTUG1-DDS alone. Targeted therapy aimed at TUG1 may be a promising approach for overcoming TMZ resistance in GBM.

#3287 Learning to target CDK4/6 inhibitor resistance via a breast cancer-specific atlas of cellular mechanisms.

A. Yaari[1], E. Farias[1], F. Guedes[1], O. Priebe[1], L. McDaniel[1], T. Earnest[1], T. Ideker[2], **M. A. Sherman**[1];
[1]Serinus Biosciences Inc., New York, NY, [2]University of California, San Diego, San Diego, CA

Development of resistance to targeted, chemotherapeutic, and immune-oncology treatments alike is a major barrier to long-term remission in advanced cancer patients. We developed an integrated computational-experimental platform to mitigate treatment resistance by identifying therapeutics that selectively target clinical resistance mechanisms. The key innovation is the computational framework that comprehensively maps tumor-specific mechanisms of response and resistance to a treatment based on clinicogenomic and/or preclinical pharmacogenomic data. It then screens for drugs or targets that are synthetically lethal with these resistance mechanisms. Here we present the identification of therapeutic options that mitigate resistance to CDK4/6 inhibitors as a case study. Leveraging a breast cancer-specific atlas of cellular architecture, our framework learned genetic mechanisms of CDK4/6 inhibitor resistance from a high-throughput phenotypic screen of ~700 cell lines treated with the clinical CDK4/6 inhibitor palbociclib. The learned mechanisms formed a parsimonious set of hierarchically linked protein complexes that coordinate G1-to-S transition ($P=5.6\times10^{-12}$). The mechanisms unified distinct resistant populations such as samples resistant due to CDK4/6-Rb checkpoint bypass and those resistant due to growth factor receptor activation. Applied to 70 ER+ metastatic breast cancer patients in a real-world dataset, the learned resistance mechanisms accurately predicted patient response to palbociclib ($P=3\times10^{-4}$, log-rank test). Computationally screening 20K clinical-grade small molecules and gene targets for therapeutic options synthetically lethal with the learned resistance mechanisms identified the known CDK4/6 resistance targets CDK2, CCNE1, and E2F. It also identified a target that, to our knowledge, has not previously been rigorously evaluated for its potential to mitigate CDK4/6 inhibitor resistance. In-vitro, monotherapy inhibition of the target by siRNA selectively decreased growth of breast cancer cell lines resistant to CDK4/6 inhibitors by 52% compared to CDK4/6i sensitive cell lines (P=0.023, Mann-Whitney U-test). As a combination therapy, inhibition of the target by siRNA selectively increased the sensitivity to palbociclib by nearly an order of magnitude in an otherwise resistant breast cancer cell line (expected vs observed IC_{50}: 9.7 uM vs. 1.3 uM) while not having a substantial effect in a palbociclib-sensitive cell line (expected vs observed IC_{50}: 0.57 uM vs. 0.56 uM). Finally, while monotherapy inhibition of the target and CDK4/6 induced cell cycle arrest, the combination strongly induced apoptosis in cell lines resistant to CDK4/6 inhibitors. These results highlight how computational deconvolution of tumor resistance mechanisms enable algorithmic identification of therapeutic options to target treatment-resistant cell populations.

#3288 Identification of Annexin A1 as a novel driver of lenvatinib resistance in hepatocellular carcinoma.

C. GU, C. LEUNG, T. LEE;
Hong Kong Polytechnic University, Hong Kong, Hong Kong

Hepatocellular carcinoma (HCC) is the third leading cause of cancer-related deaths worldwide. Lenvatinib has recently been approved by the FDA for front-line treatment of HCC patients at advanced stages. However, the survival benefit of lenvatinib is modest due to the development of acquired drug resistance. In this study, we aimed to investigate the mechanisms underlying lenvatinib resistance in HCC and to identify potential therapeutic targets to combat lenvatinib resistance. For this purpose, we established a lenvatinib-resistant (LenR) HCC patient-derived tumor xenograft (PDTX) by administering four rounds of lenvatinib treatment, and their genetic profiles were analyzed using single-cell RNA sequencing (scRNA-seq). Based on single-cell regulatory network inference and clustering (SCENIC) analysis, Annexin A1 (ANXA1), the top gene that was enriched in the HCC cell-like cluster of LenR tumors, was identified and was consistently observed in LenR HCC cell lines and LenR tumors derived from *Tp53*^{KO}/*C-Myc*^{OE} and RIL175 HCC mouse models. Using an *in vitro* differentiation model, limiting dilution assay, apoptosis assay and correlation analysis, we demonstrated the role of ANXA1 in the regulation of cancer stemness-driven lenvatinib resistance. Mechanistically, ANXA1 regulates cancer stemness and drug resistance by driving the STAT3/S100A6 signaling cascade, and ANXA1 expression is regulated by SOX2 via promoter activation, as demonstrated by a chromatin immunoprecipitation (ChIP) assay. Using the same set of scRNA-seq data, we showed that LenR HCC tumors reshaped the tumor microenvironment (TME) by inducing M2 macrophage polarization, as evidenced by a higher M2/M1 ratio of tumor-associated macrophages (TAM) in LenR HCC tumors than in their mock counterparts. Based on this observation, we further demonstrated the *in vitro* role of secretory ANXA1 in LenR HCC cells in inducing macrophage polarization towards the M2 phenotype. In conclusion, ANXA1 may regulate lenvatinib resistance intrinsically via the promotion of cancer stemness and extrinsically via the induction of an immunosuppressive TME.

#3289 APOBEC3A drives tumor evolution through activation of ERVs in non small cell lung cancer.

H. Isozaki, R. Sakhtemani, N. Nikpour, S. Monroe, M. Lawrence, A. Hata;
Massachusetts General Hospital, Charlestown, MA

Acquired drug resistance to even the most effective anti-cancer targeted therapies remains an unsolved clinical problem. Although many drivers of acquired drug resistance have been identified, the underlying molecular mechanisms shaping tumor evolution during treatment are incompletely understood. We recently demonstrated that lung cancer targeted therapies commonly used in the clinic induce the expression of cytidine deaminase APOBEC3A (A3A), leading to sustained mutagenesis in drug-tolerant cancer cells persisting during therapy. Preventing therapy-induced A3A mutagenesis by gene deletion decreased the chromosomal aberration events and delayed the emergence of drug resistance. Thus, inhibition of A3A may represent a potential therapeutic strategy to prevent acquired resistance. Understanding the regulatory mechanisms of A3A may provide alternative approaches to inhibit A3A mutagenesis. Using a panel drug screen, we found that DNA methyltransferase (DNMT) inhibitor remarkably induces A3A in non-small cell lung cancer cells. RNA-seq profiling revealed that targeted therapy as well as DNMT inhibitor treatment activate expression of distinct classes non-coding repetitive RNA elements, including endogenous retrovirus (ERVs), in drug-tolerant persister cells. Activation of intracellular viral sensing pathways by introduction of exogenous nucleic acids mimicking viral elements induced A3A expression. While the transcription factor NFkB was acutely activated by targeted therapy, TBK1-IRF3 signaling was activated at later time points. These findings suggest that reactivation of ERVs may underlie A3A mutagenic activity and tumor evolution during targeted therapy.

#3290 FTO mediates tumor growth and resistance to erlotinib in NSCLC.

A. Rastogi, R. Qiu, **N. Puri**;
University of Illinois College of Medicine (Rockford), Rockford, IL

Lung cancer, among the most common cancer types, ranks first in cancer associated deaths. Nearly 85% of the lung cancer cases are non-small cell lung cancer (NSCLC). Epidermal growth factor receptor (EGFR), an established marker for NSCLC, is frequently overexpressed on the cell surface. Amplifying mutations often render these receptors activated in a ligand independent manner, therefore, therapies such as erlotinib, an EGFR tyrosine kinase inhibitor (EGFR-TKI), target these activating mutations and inhibit tumor growth. Nevertheless, patients acquire resistance to EGFR TKI within 9-14 months of treatment. Recent studies show that fat mass and obesity- associated (FTO) gene, initially identified to increase the body mass index, plays a major role in cancer development and acquired therapy resistance in several cancer types. FTO demethylates m6A mRNA and modulates tumorigenesis, and drug resistance. In this study, we explored the functions of FTO in EGFR TKI resistance in NSCLC. To study the expression of FTO in erlotinib resistant cells, we used wildtype-EGFR NSCLC cell lines (H2170, H358) and mutant EGFR NSCLC cell lines (H1975, PC9) that were rendered resistant to erlotinib. Our RT-qPCR results demonstrated that FTO was upregulated by 1.7-3.0 fold in erlotinib resistant H2170, H358, PC9 and H1975 cells. FTO protein was upregulated by 1.3-1.6 fold as seen by western blotting, and by 1.7 to 2.6 fold in the nucleus of erlotinib resistant H1975, H2170 and PC9 cell lines by immunofluorescence. Furthermore, we investigated FTO inhibition with Dac51 (FTOi) on cell viability and cell migration properties. MTT cell viability assay showed a 9-17% decrease in cell viability when treated with a combination of Dac51 and erlotinib compared to Dac51 alone in erlotinib resistant H2170 and PC9 cells, respectively. The combinatory treatment showed an additive effect compared to the Dac51 and erlotinib treatments alone. Wound healing assay revealed an 18% open wound area after 48-hour treatment with both Dac51 and erlotinib compared to 0.1% after treatment with erlotinib alone in erlotinib resistant H2170 cells. To evaluate the effect of siRNA mediated FTO (siFTO) knockdown on cell viability and energy metabolism, MTT and luciferase assays were performed. MTT assay showed a 21-28% decrease in viability in erlotinib resistant H1975, H2170, PC9 cells, demonstrating increase in the erlotinib efficacy, as compared to the mock siRNA treatment. Luciferase assay showed an inverse relationship between the FTO and ATP, where the latter was upregulated by 1.3 to 3.4 folds in erlotinib resistant H1975, H2170 and PC9 cells, when treated with siFTO, suggesting its involvement in the energy requirements of the NSCLC cells. In conclusion, our study suggests FTO was upregulated in erlotinib resistant NSCLC cells on both the gene and protein levels. FTO could mediate resistance to EGFR TKI possibly through cell proliferation and migration and help with prognosis of NSCLC patients.

EXPERIMENTAL AND MOLECULAR THERAPEUTICS: Molecular Glues
Poster Session

#3294 The GSPT1 molecular glue degrader MRT-2359 is active against prostate cancer.

R. Tiedt[1], M. Schillo[1], A. Osmont[1], D. Bonenfant[1], R. Narayan[2], O. Wallace[2], M. Warmuth[2];
[1]Monte Rosa Therapeutics, Basel, Switzerland, [2]Monte Rosa Therapeutics, Boston, MA

We have previously described our GSPT1 molecular glue degrader MRT-2359, which was optimized to achieve preferential antiproliferative activity in non-small cell lung cancer (NSCLC) and small cell lung cancer (SCLC) expressing high N-MYC or L-MYC mRNA. A clinical trial with this new drug candidate is ongoing (NCT05546268). Here, we present pre-clinical profiling of MRT-2359 across hundreds of cancer cell lines representing multiple cancer types, aiming at identifying other cancers where preferential sensitivity is associated with high expression of a MYC family member. These studies showed that prostate cancer cell lines clearly segregate into groups that are either sensitive or insensitive. Sensitive prostate cancer cell lines could be further divided into two subgroups: (1) androgen receptor positive cell lines displaying higher c-MYC mRNA expression levels than the other prostate cancer cell lines, (2) neuroendocrine prostate cancer cell lines with or without high N-MYC. The latter is in line with our previous observation that the neuroendocrine phenotype is generally associated with heightened sensitivity to MRT-2359 independently of MYC status. The insensitive cell lines were androgen receptor and neuroendocrine negative and displayed lower c-MYC mRNA levels. GSPT1 degradation in androgen receptor-positive cell lines led to rapid and deep loss of c-MYC protein as well as reduction of androgen receptor, including the splice variant AR-V7 that is associated with resistance to agents targeting androgen signaling. In androgen receptor-negative cell lines, the levels of c-MYC protein decreased only modestly upon GSPT1 degradation. Finally, in immunocompromised mice, xenografts of the AR-V7-positive cell line 22RV1 and the neuroendocrine prostate cell line NCI-H660, both of which are sensitive to MRT-2359 in vitro, were treated with several MRT-2359 dose regimens including continuous as well as intermittent (5 days on / 9 days off) dosing. Most regimens led to marked tumor regression. Tumors of both models fully regressed after a 4-week course of 10 mg/kg MRT-2359 once daily, and no tumor regrowth could be detected after cessation of treatment. No significant in vivo response was observed for xenografts of the insensitive cell line PC-3. These data support the clinical investigation of MRT-2359 in prostate cancer.

#3295 Pharmacological characterization of CYRS1542: A potent and orally available GSPT1 molecular glue degrader for the treatment of neuroendocrine solid cancer with a favorable safety profile.

Min Sung Joo[1], JaeYung Lee[1], Joonhyung Lee[1], Eun-Jung Kim[1], Seogbeom Song[1], Jeonghyeon Lee[1], Joonwoo Nam[1], Heuijoon Park[1], Jaewoo Park[2], Keon Wook Kang[2], Wooseok Han[1]

[1]Cyrus Therapeutics, Seoul, Korea, Republic of,[2]College of Pharmacy, Seoul National University, Seoul, Korea, Republic of

Neuroendocrine cancers (NECs) are relatively rare compared to other malignancies, but their clinical behavior can be exceptionally aggressive. Two particularly challenging subtypes of NECs, Small Cell Lung Cancer (SCLC) and Neuroendocrine Prostate Cancer (NEPC), are worthy of attention due to their rapid progression, limited treatment options, and high mortality rates. At the molecular level, SCLC and NEPCs necessitate the presence of TP53 and RB1 mutations (Beltran et al., 2016; George et al., 2015). The frequency of TP53 mutations in SCLC is particularly noteworthy, with studies consistently reporting a high incidence (89~92%) (Chen et al., 2022; Sivakumar et al., 2023). A recent study has unveiled intriguing parallels between NECs and hematological malignancies, shedding light on their shared genetic features and analogous patterns of therapeutic susceptibility (Balanis et al., 2019). GSPT1, a translation termination factor, plays a key role in releasing the complete polypeptide from the ribosome. As cancer cells are dependent on translation processes to express elevated levels of oncoproteins, GSPT1 degradation would have lethal consequences. Specific CRBN modulators possess the capability to induce GSPT1 degradation via the ubiquitin-proteasome pathway. GSPT1 degradation leads to a halt in translation termination, activating the Integrated Stress Response (ISR) and subsequently triggering TP53-independent apoptosis. Despite GSPT1 degradation in cancer cells is appealing due to its potential to disrupt the production of critical proteins necessary for cancer cell survival and growth, the challenge lies in doing so without causing excessive harm to normal cells, as GSPT1 is also indispensable for their vital cellular functions. Remarkably, the ongoing development of GSPT1-targeted agents in clinical trials has raised intriguing questions about the mechanisms by which a therapeutic index can be established. Recently, we have identified CYRS1542 as an orally bioavailable GSPT1 molecular glue degrader (MGD) (Joo et al., 2023). Here, we present a pharmacological characterization of CYRS1542 as a potent and orally bioavailable GSPT1 MGD with the ability to effectively treat aggressive neuroendocrine cancers. In various NEC in vivo models, including an orthotopic model, CYRS1542 demonstrated dose-dependent and excellent anti-tumor efficacy comparable to the clinical stage GSPT1 MGD. Furthermore, it demonstrates improved safety profiles in a broad spectrum of normal cells, resulting in a higher therapeutic index compared to the clinical GSPT1 MGD.

#3296 IK-595, a best-in-class MEK-RAF molecular glue, drives broad and potent anti-tumor activity across RAS-MAPK pathway-altered cancers as a monotherapy and in combination.

E. Haines, R. Catterall, V. De Jesus, D. Hidalgo, J. Cavanaugh, M. Sanchez-Martin, J. D. Manna, M. Burke, B. Li, S. R. Wessel, A. Yang, S. Santillana, J. Ecsedy, X. Zhang, S. K. Ruppel;
Ikena Oncology, Boston, MA

Alterations in the RAS/RAF/MEK/ERK pathway are the most common drivers of oncogenesis. Although MEK is a clinically validated cancer target and several MEK inhibitors have been approved by the FDA, their clinical utility has been limited to BRAF V600 mutant cancers and NF1 mutant neurofibromas. We developed the molecular glue, IK-595, a potent inhibitor of the MEK-RAF complex, to overcome the limitations of available MEK inhibitors. IK-595 traps MEK in an inactive complex with all RAF isoforms, as well as mutant forms of BRAF (Class I, II, and III), and blocks RAF-dependent MEK phosphorylation, thereby alleviating CRAF-mediated MEK reactivation that limits the efficacy of approved MEK inhibitors in RAS/RAF-driven tumors. We demonstrate that IK-595 leads to potent and prolonged inhibition of MEK and ERK1/2 phosphorylation in RAS-mutant cancer models. Importantly, IK-595 has a much slower off-rate binding to MEK and retains CRAF longer in an inactive complex with MEK than other MEK/RAF inhibitors, allowing for prolonged target engagement and durable pathway inhibition in RAS/RAF mutant cancer cells. IK-595 exhibits potent single agent activity across a wide range of cancer model indications harboring various RAS/MAPK pathway alterations, including KRAS, NRAS, BRAF and NF1 mutations, and BRAF and CRAF fusions. The benefits of combining IK-595 with inhibitors targeting key resistance mechanisms both within the RAS/MAPK pathway and across parallel survival pathways has also been observed in multiple models. Additionally, IK-595 improved the response of KRAS-driven tumor models to standard of care chemotherapeutic agents, expanding the potential clinical opportunity for IK-595. Key to the design of IK-595 is its PK profile that enables transient high plasma drug exposure and flexible dosing schedules. Intermittent dosing of IK-595 every other day (QOD) or every three days (Q3D) in KRAS-mutant mouse tumor models shows similar efficacy and improved tolerability compared to daily dosing (QD), affording a larger therapeutic window. Preclinical pharmacology studies provide clear guidance to the clinical development plan of IK-595, where flexible dosing schedules, multiple expansion cohorts in RAS/RAF altered patient populations, and combination therapies with mediators of resistance will be explored. IK-595 is a novel MEK-RAF molecular glue that prolongs pathway inhibition, minimizing the potential for resistance, while providing an optimal therapeutic window for patients with RAS/RAF-driven cancer.

#3297 Discovery and evaluation of GT19870, a GSPT1/Myc molecular glue drug (MGD) with oral bioavailability for targeting c-Myc and n-Myc-addictive blood cancer and solid tumors.

L. Ma, Y. Tong, Z. Yang, Q. Zhou, H. Yan, R. Xu, D. Chen;
Kintor Pharmaceutical Limited, Suzhou, China

c-Myc and n-Myc are oncogenic transcriptional factors driving tumor initiation, progression and poor prognosis in a variety of blood cancers and solid tumors, such as acute myeloid leukemia (AML), B-cell malignancies, castration resistance prostate cancer (mCRPC), small cell lung cancer and (SCLC) and neuroblastoma. Both c-Myc and n-Myc dysregulations have been directly linked to the poor clinical outcome in some of these cancers which are addictive to deregulated Myc proteins. Therefore, it is highly warranted to discover and develop novel therapeutical agents for targeting Myc-addictive cancers. GT19870 was discovered through a SAR effort for Myc degradation with improved bioavailability (F % 92.52) from GT19630, a GSPT1/Myc degrader series [1-4]by using phenotypic screenings with c-Myc-addictive HL-60 AML cells and growth factor-dependent hematopoiesis progenitor TF-1 cells, followed by c-Myc ELISA and Western blot assays. GT19870 selectively inhibited the proliferation of HL60 cells with an IC_{50} of 2.6 nM as compared to an IC_{50} of 70.03 nM (26.5-fold selectivity) and effectively degraded c-Myc protein with an IC_{50} of 2.54 nM and IC_{90} <10 nM in HL-60 cells, as compared to an IC_{90}>30 nM in CD3/CD28-stimulated PBMC assays. GT19870, as a MGD, was confirmed to selectively degrade GSPT1, a neo-substrate, by proteomic and Western Blot assays. Further, GT19870 was tested in SCLC, triple negative breast cancer (TNBC) and brain cancer cell panels, in which GT1987 was revealed potent anti-proliferation activities with an IC_{50}<50 nM in 9 of 19 SCLC, 8 of 13 TNBC, and 7 of 24 brain cancer cell lines tested. Importantly GT19870 was also shown potent antitumor activities with IC50 of ≦5.4 nM in 8 of 8 SCLC patient derived organoids. Furthermore, GT19870 (salt form-GT19884) was demonstrated to induce target-engaged (c-Myc and n-Myc) tumor regression in AML, SCLC, mCRPC and neuroblastoma xenograft and PDX models with in a dose ranges of 3-12 mpk/qd/po. In brief, GT19870 is an oral MGD degrading GSPT1/c-Myc/n-Myc. This novel MGD has been demonstrated target-engaged antitumor activities in vitro and in vivo with selectivity of c-Myc degradation in c-Myc-addictive cancer cells as compared to growth factor-stimulated TF-1 cells and CD3/CD28 activated PBMC. GT19870 has been progressing IND enabling stage. References 1. Ma L et al, ASH, 2021 2. Ma L et al, AACR, 2022 3. Nishida Y et al, ASH, 2022 Nishida Y et al, ASH, 2023

#3298 Unlocking the potential of OPM-383: A novel LRRK2 inhibitor in cancer therapy.

M. Riveiro, P. Blom, K. Shoji, J. Hoflack;
ONCODESIGN PRECISION MEDICINE (OPM), Dijon, France

Background: Leucine-rich repeat kinase 2 (LRRK2) plays a pivotal role in regulating various cellular processes, such as cell proliferation, survival, and inflammation. LRRK2 exhibits dual functionality as a serine-threonine kinase and as a GTPase. It is involved in the modulation of multiple signaling pathways, including WNT, MAPK, NF-kB and mTOR. Germline mutations in LRRK2 are associated with an increased risk of cancer, particularly hormone-related and colorectal cancers. LRRK2 also promotes tumor cell growth and survival in papillary renal and thyroid carcinomas, DLBCL and cholangiocarcinoma cells. OPM has designed and developed a novel oral LRRK2 inhibitor, OPM383, using its proprietary Nanocyclix® technology. In this study, we have evaluated the pharmacokinetic (PK) properties, efficacy and tolerability of OPM383 in a colon carcinoma model and a panel of patient-derived organoids.
Materials and Methods: In vitro potency of our Type I inhibitor, OPM383, against full-length wild-type LRRK2 and the G2019S pathogenic LRRK2 mutant was assessed in in a Lanthascreen cell assay. For PK studies, we analyzed OPM383 plasma levels using UPLVC/MS-MS. Evaluation of inhibition of LRRK2 phosphorylation (Ser935) was assessed by western blot. MC-38 cells were inoculated into C57BL/6 mice. When tumor masses reached 75 mm^3, mice were randomized to receive OPM383 (50 mg/kg, orally, daily), anti-PD1 antibody (10 mg/kg, ip, twice weekly), or their combination. OPM383 was also evaluated in patient-derived organoids using the SEngine-Paris® platform.
Results: OPM-383 inhibited wild-type LRRK2 and LRRK2[G2019S] with an IC_{50} of 42 nM and 33 nM, respectively. OPM383 is highly selective among a panel of >400 protein kinases (only 6.7% cross-reactivity at 100 nM). The compound is permeable, metabolically stable and possesses drug-like properties. OPM-383 exhibited a favorable pharmacokinetic profile in mice (AUC of 11858 h*ng/mL and T max of 3 hours at a dose of 30 mg/kg via oral administration). Preliminary e-ADME results indicated moderate inhibition of CYP3A4BFC but no significant inhibition of CYPs 1A2, 2D6, 3A4BQ, 2C19, and 2C9 by OPM-383. After 90 minutes of oral administration in CD1 mice, we observed the inhibition of LRRK2 phosphorylation (Ser935) in the brain, kidney, and PBMCs. In assessing its potential antitumor effects, OPM383 was tested on a panel of patient-derived organoids. Notably, OPM383 inhibited the proliferation of 7 out of 29 patient-derived organoids after 6 days of exposure at various concentrations (<10 µM). In mice bearing subcutaneous MC38 tumors, OPM383 significantly inhibited tumor growth compared to the vehicle-treated group.
Conclusion: This study characterizes a potent first-in-class LRRK2 inhibitor in cancer models. The findings suggest that OPM383 could serve as an attractive lead scaffold for designing and synthesizing a new class of kinase inhibitors for potential applications in cancer therapy.

#3299 Harnessing PIKfyve as a therapeutic vulnerability in neuroendocrine prostate cancer.

Y. Zheng[1], K. G. Rogers[1], A. G. Kamat[1], S. N. Yee[1], R. Mannan[1], X. Jiang[1], R. Kannaiyan[1], X. Cao[1], Y. Wang[2], Y. Qiao[1], A. M. Chinnaiyan[1];
[1]University of Michigan, Ann Arbor, MI, [2]University of British Columbia, Vancouver, BC, Canada

Neuroendocrine prostate cancer (NEPC) represents an aggressive subtype characterized by the independence on androgen receptor (AR) signaling and the acquisition of neuroendocrine features. Despite its rarity among prostate cancer cases, NEPC carries a particularly poor prognosis with limited treatment options. Our prior investigation demonstrated the heightened efficacy of targeting PIKfyve with ESK981 in AR- prostate cancer models, prompting further exploration. In this study, we expanded our investigation to assess the efficacy of ESK981 monotherapy across five NEPC models, encompassing one cell line xenograft and four patient-derived xenografts (PDXs). Our findings revealed consistent tumor inhibition and notable regression in select models. Comparative analysis highlighted the superior effectiveness of ESK981 in NEPC compared to AR+ prostate cancer, as evident through percent tumor growth inhibition (%TGI) assessments. Early evaluations post five days of treatment (PD5) unveiled that PIKfyve inhibition induced apoptotic cell death specifically in NEPC models, confirmed through immunoblotting and TUNEL staining in a time-dependent manner. Intriguingly, PD5 TUNEL positivity correlated with endpoint %TGI, suggesting its potential as a predictor for long-term efficacy. To further delineate the role of PIKfyve in NEPC, we successfully established two novel ex vivo NEPC cell lines from these PDXs, overcoming the constraint of limited publicly accessible NEPC cell lines, and confirmed their NEPC characteristics. Employing a doxycycline-inducible PIKfyve knockdown system in these cells demonstrated significant tumor inhibition in xenograft models, albeit with a lower %TGI compared to ESK981 monotherapy. In conclusion, our results illuminate the preferential cytotoxicity of PIKfyve inhibition in NEPC tumors compared to AR+ prostate cancer, advocating PIKfyve as a compelling therapeutic target. This study provides a strong rationale for advancing ESK981 into clinical trials for NEPC patients, underscoring its potential in addressing this challenging malignancy.

#3301 Translational research of CDK12/13 inhibitor, CTX-439, informing clinical trial strategy.

H. Yamakawa[1], S. Ebara[1], A. Mizutani[1], M. Yoshida[1], M. Sugiyama[1], K. Yamamoto[2], D. Komura[3], M. Kakiuchi[3], S. Ishikawa[3], K. Yusa[4], **D. Morishita**[1]; [1]Chordia Therapeutics Inc., Fujisawa, Japan, [2]MetCoding, Ibaraki, Japan, [3]The University of Tokyo, Tokyo, Japan, [4]Kyoto University, Kyoto, Japan

Gene dysregulation is a hallmark of cancer, arising from genetic alterations that invariably lead to dysregulated transcriptional programs. This dysregulation renders cancer cells highly dependent on certain gene expression regulators, leading to a potential for novel therapeutic strategies. Consequently, ongoing research aims to develop small molecules targeting RNA transcriptional processes. Cyclin-dependent kinase 12/13 (CDK12/13) is a member of the cyclin-dependent kinase family of serine/threonine protein kinases. CDK12/13 regulates the RNA transcription elongation by phosphorylating RNA polymerase II and promotes the elongation of transcripts, specifically those involved in DNA damage responses, such as BRCA1/2. The inhibition of CDK12/13 is expected to exert a synergistic effect when combined with PARP inhibitors and chemotherapeutic reagents. Therefore, we developed a novel small molecule inhibitor, CTX-439 (former name: CRD-1835439). Additionally, we demonstrated that CTX-439 exhibits a preclinical efficacy *in vitro* and *in vivo* [*Cancer Res*. (2022) 82 (12_Supplement): 5485]. To identify potential strategies for a clinical trial of CTX-439, in the current study, we conducted translational research to elucidate (1) pharmacodynamics (PD) markers to monitor the suppression of CDK12/13 in humans, (2) patient selection biomarkers to determine sensitivity to CTX-439, and (3) combination strategies with other key medications. Firstly, to identify PD markers of CTX-439, we performed a comprehensive analysis employing RNA-seq, Pol II-ChIP-seq, and Poly(A)-seq. We confirmed that CTX-439 induced the usage of intronic polyadenylation sites by inhibiting CDK12, resulting in the production of shortened mRNA. Of these transcripts, PCF11 emerged as a potential PD marker for clinical trials, which was confirmed using qPCR analysis of human blood. Secondly, to clarify the indication of CTX-439, we performed an *in vitro* survey involving 400 cell lines and 100 PDX-derived organoids (PDXOs) to identify biomarkers displaying sensitivity and insensitivity to CTX-439. Furthermore, a significant anti-tumor effect of CTX-439 was revealed in PDX models that showed sensitivity in the survey. CTX-439 exhibited a synergistic effect in combination with PARP inhibitors both *in vitro* and *in vivo*, highlighting its potential for use in combination strategies. Additionally, CTX-439 showed an anti-tumor effect when combined with other chemotherapy and molecular-targeted drugs. Collectively, the results from these translational research studies provide a foundation for developing a clinical trial by clearly defining PD monitoring, patient stratification biomarkers, and combination strategies. These findings highlight the therapeutic potential of CTX-439 as a single-agent and in combination with inhibitors, such as PARP, for the treatment of cancers characterized by transcriptional addiction.

#3303 Paralogue selective p300 degraders induce synthetic lethality in pre-clinical models of CBP-deficient and p300-dependent malignancies.

S. Thiyagarajan, C. Abbineni, K. Chaitanya T, A. Apte, I. Iqbal, N. Kumar R, A. A B, A. Kumar, D. Madhu Babu, S. Shwetha, A. Manna, M. Mandal, R. Panigrahi, S. Marappan, S. Gore, M. Fairus, L. Jin, S. Mukherjee, G. Daginakatte, S. Chelur, K. Nellore, M. Ramachandra, **S. Samajdar**;
Aurigene Oncology Limited, Bangalore, India

EP300 (or p300) acts as histone acetyltransferase (HAT) and transcriptional adapter or co-activator regulating transcription via chromatin remodeling. Both histone and non-histone proteins are acetylated by p300. In addition to HAT function, p300 has crotonyl-transferase activities, and that p300-catalyzed histone crotonylation directly stimulates transcription to a greater degree. p300 functions by scaffolding or as co-activator and enhancer of different transcription factors like HIF1a, BRCA-1, p53, NFκB, c-Myc, estrogen receptor (ER) and androgen receptor (AR) and other proteins such as PD-L1 and FOXP3. Selective targeting of p300 is expected to lead to therapeutic efficacy in CBP-mutant and p300-dependent malignancies with high degree of tolerability because of sparing of the other paralog CBP in normal cells. CBP mutant cancers comprise of several solid and hematological malignancies including 10% to 15% of non-small cell and small cell lung cancers harboring loss-of-function (LOF) aberrations. p300-dependent malignancies include prostate cancer, in which p300 plays a major role for androgen-dependent and -independent transactivation of the AR, MYCN-amplified neuroblastoma and ER+ breast cancers. Since the conventional CBP/p300 inhibitors do not discriminate between CBP and p300 proteins due to high sequence homology, we adopted a degrader approach, which has the potential to lead to paralog selectivity due to differentiated ternary complex formation. Herein we report best-in-class novel, potent and paralog selective p300 degraders with excellent selectivity over CBP and and other bromodomain containing proteins such as BRD4 by implementing molecular modeling, iterative medicinal chemistry and SAR based approaches. Synthetic lethality has been demonstrated while selectively degrading p300 in the cell lines having LOF mutation of another paralogue, CBP. Identified selective p300 degraders displayed excellent selectivity towards p300 degradation across tested cell lines and are orally bioavailable. Selective antiproliferative activity was observed in a panel of cell lines with CBP mutations or p300 dependency including AR+ / ER+ cell lines along with the downregulation of target genes. In summary, we have identified highly selective degraders of p300 with desirable profile. Efforts are underway to advance them further towards nominating a development candidate.

#3304 Modulation of enhancer accessibility by SMARCA2 PROTACs synergize with TEAD inhibitors to suppress growth of SMARCA4 mutant lung cancers.

S. Kotagiri, N. Blazanin, M. Qudrattulah, Y. Xi, J. Wang, **Y. Lissanu**;
UT MD Anderson Cancer Center, Houston, TX

The SWI/SNF chromatin remodeling complex is frequently mutated in non-small cell lung cancer with a frequency of 33% in advanced stage disease, making it the most commonly altered complex in lung cancer. Among the various subunits of the SWI/SNF complex, *SMARCA4* and *ARID1A* are by far the most frequently mutated. Importantly, multiple clinical reports have shown that *SMARCA4* mutant lung cancers have one of the worst prognosis among genetically defined lung cancer subtypes and lack response to both immunotherapy and KRAS G12C inhibitors. Recent reports, and our own data, have identified the paralogue *SMARCA2* to be synthetic lethal to *SMARCA4* suggesting SMARCA2 could be a high value therapeutic target. Unfortunately, the discovery of selective inhibitors of SMARCA2 has so far been challenging. To overcome this hurdle, we have recently developed novel, potent and selective SMARCA2 degrading small molecules based on proteolysis targeting chimera (PROTAC) technology. We demonstrated that YD23, our lead SMARCA2 PROTAC, potently and selectively induced degradation of SMARCA2. Importantly, we showed that YD23 selectively inhibits growth of *SMARCA4* mutant lung cancer cells. Mechanistically, we demonstrated that YD23 decreased chromatin accessibility only in *SMARCA4* deficient cells. In particular, SMARCA2 degradation profoundly decreased chromatin accessibility at enhancers of a number of genes with cell cycle and cell growth regulatory roles. Gene expression profiling and pathway analysis indicated that cell cycle genes were downregulated by YD23 consistent with the reduced chromatin accessibility at their *cis*-regulatory regions. We further showed that YD23 robustly inhibited growth of *SMARCA4*-mutant xenograft tumors. While this is promising, SMARCA2 degradation by itself does not induce regression of tumors highlighting the need for identification of efficacious combination strategies. Using integrative gene expression, ATAC-Seq and CUT&RUN assays, we uncover a critical role for YAP/TEAD transcription factor signaling axis in mediating pro-growth phenotypes in *SMARCA4* mutant tumors. Finally, we show that the combination of TEAD inhibitors synergizes with YD23 to induce profound tumor growth inhibition. In conclusion, our study provides a mechanistic basis for the anti-tumor action of SMARCA2 degraders and introduces a novel combination strategy for future clinical development against a genetically defined subtype of lung cancer with dismal prognosis.

#3305 Golcadomide (CC-99282) is a novel CELMoD® agent with antiproliferative activity and combinatorial potential in disease models of chronic lymphocytic leukemia.

A. Lopez-Girona[1], M. Jimenez-Nunez[2], D. Sobradillo[2], S. Carrancio[1], P. Janardhanan[1], G. Deb[1], L. Groocock[1], D. Pierce[1], N. Bence[1], M. Rolfe[1]; [1]Bristol Myers Squibb Company, San Diego, CA, [2]Bristol Myers Squibb Company, Seville, Spain

Chronic Lymphocytic Leukemia (CLL) is an adult leukemia characterized by the accumulation of incompetent B lymphocytes expressing CD19, CD20, CD23, and CD5. Current therapies include chemotherapy and combination with targeted therapies such as ibrutinib (Bruton's tyrosine kinase inhibitor), venetoclax (BCL2 inhibitor), and obinutuzumab (anti-CD20). The tumor microenvironment promotes CLL development and drug resistance. Golcadomide (GOLCA, CC-99282) is an oral cereblon E3 ligase modulator (CELMoD®) agent with immunomodulatory and tumor cell-autonomous activities under clinical investigation for R/R non-Hodgkin lymphomas and CLL/SLL. Here we investigated the effect of GOLCA on inhibiting proliferation and inducing apoptosis of CLL preclinical models by degrading Ikaros and Aiolos. We also studied its combination with other anti-CLL agents. A panel of 10 CLL cell lines and 15 primary CLL patient samples were used to assess efficacy of GOLCA alone or in combination with ibrutinib (Ibru), venetoclax (Ven), and obinutuzumab (Obi). Primary CLL cells were grown ex vivo in a co-culture system with CD40L expressing fibroblasts designed to mimic the CLL lymph node microenvironment. Substrate degradation, viability, cell cycle and immunophenotyping were assessed by flow cytometry. GOLCA showed potent in vitro antiproliferative activity on 6 out of 10 CLL cell lines, including those with high-risk features, with IC_{50} of 1-20 nM. It also inhibited CLL stimulated cell proliferation and induced apoptosis in all evaluated patient samples in the co-culture system, with low to sub-nanomolar IC_{50}, independent of IGHV mutation status and other chromosomal characteristics. Cell-cycle analysis confirmed inhibition of proliferation in the 5 patient samples evaluated after 3 days of treatment with GOLCA, with a dose-dependent decrease in the fraction of cells in the S phase. GOLCA also demonstrated degradation of the proximal substrates Ikaros and Aiolos in tumor and T cells from CLL patient samples. In combination with Obi, Ven, and Ibru, GOLCA led to synergistic or additive tumor cell toxicity in most patient samples evaluated, suggesting potential clinical benefit of these targeted agent combinations. Additive tumor toxicity was observed in two out of four patient samples when GOLCA was combined with Ibru. We have previously demonstrated that GOLCA induces immune activation in T cells from healthy donor PBMCs. In co-cultures of CLL PBMCs and CD40L-expressing fibroblasts, GOLCA increased T cell numbers and activation characteristics. Ven inhibited this immune activation, while Obi or Ibru maintained the immune activation. Collectively, these findings suggest that GOLCA, alone or in combination with targeted agents, may produce clinical benefit in CLL patients.

#3306 RGT-M001, a first-in-class small molecule mRNA degrader of the oncogenic transcription factor c-Myb, demonstrated remarkable single agent anti-tumor efficacy in cancer patient-derived xenograft model.

N. Lu[1], **P. Soulard**[1], K. Li[1], H. Sadlish[1], C. Yates[1], X. Gu[1], I. Kays[1], J. Lee[1], S. Hasson[1], Z. Weng[2], S. Xi[1], T. Wager[1];
[1]Rgenta Therapeutics, Inc., Woburn, MA, [2]University of Massachusetts Medical School, Worcester, MA

Dysregulated transcription factors (TFs) represent a unique class of drug targets that drive aberrant gene expression programs involved in the major hallmarks of cancers. However, developing drug-like small molecules targeting TF proteins for clinical purposes has proven to be extremely challenging. Here, we present a novel and innovative approach to degrade the RNA transcript of the master oncogenic transcription factor C-MYB, thereby preventing its undesirable expression, using potent and orally available small molecules.

C-MYB is a transcription factor that regulates differentiation and proliferation programs in normal cells, including hematopoietic, stem and epithelial cells. In numerous cancer types, such as adenoid cystic carcinoma (ACC), leukemia, colorectal cancer, and breast cancer, C-MYB is a well-established oncogenic transcription factor, overactivated via different mechanisms, including chromosomal translocations and gene amplification.

Here, we leveraged our integrative RNA-targeting platform to identify and validate actionable cryptic exon target sites in the human *C-MYB* gene. We identified RGT-M001, a potent small molecule that can selectively induce the inclusion of the cryptic exon into the final *C-MYB* transcripts, resulting in a robust decrease of *C-MYB* canonical transcripts and C-MYB protein in cells. In a functional assay, we demonstrated that RGT-M001 has potent cell-killing activity against a large panel of cancer cell lines overexpressing *C-MYB* (EC50 ~ 20 - 300nM), while sparing normal cells. To confirm RGT-M001's on-target effect, we demonstrated a robust correlation between RGT-M001 cell-killing activity and the knockdown of C-MYB RNA and protein.

We further investigated the anti-tumor activity of RGT-M001 in an ACC patient-derived xenograft (PDx) mouse model harboring *C-MYB-NFBI* fusion. Recurrent or metastatic ACC is a malignant neoplasm of predominantly salivary gland origin for which effective approved therapies are lacking; the best reported ORR being 15.6% for lenvatinib. As a single agent, RGT-M001 reduced in vivo *C-MYB* transcript levels by >80% at peak drug exposure and induced a remarkable tumor growth inhibition response (~70% TGI) in the ACCX11 PDx mouse model, surpassing the therapeutic benchmark Lenvatinib (40% TGI). Importantly, the RGT-M001 regimen was well tolerated. Finally, we showed that the combination of RGT-M001 with the Notch Inhibitor AL-101 resulted in complete inhibition of tumor growth.

In conclusion, these data demonstrate that small molecules targeting RNA are a safe and effective approach to address previously undruggable protein targets. Down-regulation of *C-MYB* by our RNA-targeting small molecules is an attractive therapeutic strategy to treat ACC and other cancers driven by *C-MYB* dysregulations.

#3307 c-Met targeting chaperone-mediated protein degrader for therapeutic intervention in NSCLC.

H. Chae[1], J. Kim[2], S. Lee[1], H. Yoo[1], H.-K. Kim[2], Y.-J. Yu[2];
[1]Oncozen Co.,Ltd., Seoul, Korea, Republic of, [2]Jeonbuk National University, Jeonju, Korea, Republic of

The interaction between E3 ligases and chaperones is crucial for proteostasis, regulating more than 10% of total proteasomes and over 30% of human E3 ligases (Kevei, 2017). Chaperones also can recognize their substrates and direct them to degradation by the ubiquitin-proteasome system (UPS). Developing a targeted protein degradation (TPD) technology that utilizes these advantageous attributes of chaperones, termed chaperone-mediated protein degradation (CMPD) technology, would broaden the range of disease-causing target proteins and would efficiently degrade them by recruiting various intracellular E3 ligases through interaction with chaperones, compare to other TPD approaches. The c-mesenchymal-epithelial transition (c-MET) is recognized as primary cause of drug-resistance to EGFR inhibitors in non-small cell lung cancer (NSCLC). Herein, to degrade the c-MET, we synthesized bifunctional small molecule compound inducing c-MET and chaperones in proximity, termed CMPD-MET degrader, and evaluate it in MET-mutant NSCLC cell lines and mouse xenograft models.
The efficacy and potency of CMPD-MET degrader were assessed using H596 and H1437 cells *in vitro*. Cell proliferation was measured using MTT assay and c-Met degradation assay was conducted, along with the examination of proteasome-dependent degradation via western blot. An *in vivo* H596 xenograft model gauged impact of CMPD-MET degrader via I.P. administration.
In NSCLC with MET Exon 14 skipping mutation cell line H596 and H1437, treatment a OZD-MET degrader resulted inhibition of cell proliferation with IC_{50}< 5 μM and subsequent proteasome-dependent c-MET degradation with DC_{50} ranging from 4-6 μM for 24h. The degradation of c-MET levels significantly induced by OZD-MET degrader, especially, the c-Met was degraded by 70.4% and 51.7% at 5 μM for 24h in H596 and H1437 cells, respectively. Also, OZ-MET degrader effectively suppressed c-MET mediated signaling and showed cleavage of PARP-1 in a dose-dependent manner. OZD-MET degrader induced selective degradation of c-MET showing at least more than about 5-fold selectivity over other chaperones-regulated client proteins.In the H596 xenograft model, OZD-MET degrader was administered in 5 dosage groups (minimum dose is 2.5 mg/kg) resulted in dramatic reduction in tumor size compared to the vehicle-treated group. Remarkably, administration of OZD-MET degrader revealed more than 90% degradation of c-Met in tumor tissues compared to the vehicle groups via western blots and fluorescence image. In contrast, c-MET inhibitor treated group showed no effect on degradation of c-MET in tumor tissues.
In summary, we developed a novel c-Met targeting chaperone-mediated protein degrader, showed highly potent and selective proteasome-dependent c-MET degradation and notable inhibition of tumor size in xenograft models. These results provide a strong foundation for further evaluation in clinical trials.

#3308 A selective FGFR1/2 degrader overcomes endocrine resistance in ER+/*FGFR1-amplified* and*FGFR1/2*-mutant breast cancer.

Y. Uemoto[1], C.-C. Lin[1], B. Wang[2], D. Ye[1], E. Bikorimana[1], A. Servetto[3], L. Formisano[3], F. Napolitano[1], R. Chica Parrado[1], S. Mendiratta[1], C. Chen[2], A. B. Hanker[1], C. L. Arteaga[1];

[1]Harold C. Simmons Comprehensive Cancer Center, Dallas, TX, [2]UT Southwestern Medical Center, Dallas, TX, [3]University of Naples "Federico II", Naples, Italy

FGFR1 amplification and *FGFR1/2* activating mutations are associated with resistance to antiestrogens in the estrogen receptor-positive (ER+) breast cancer. In this study, we investigated selective degradation of FGFR1/2 using the proteolysis-targeted chimera (PROTAC) DGY-09-192 as a novel therapeutic strategy to overcome resistance to antiestrogens in ER+ breast cancers harboring *FGFR1*-amplification or *FGFR1/2* activating mutations.

Treatment of ER+/*FGFR1*-amplified CAMA1 and MDA-MB-134 breast cancer cells with DGY-09-192 degraded FGFR1 and suppressed phosphorylation of FGFR1 and its downstream targets FRS2, AKT, and ERK1/2. DGY-09-192-mediated FGFR1 degradation were rescued by a proteasome inhibitor, MG132, suggesting that the antitumor activity of DGY-09-192 depends on proteasome-mediated degradation. Growth of CAMA1 and MDA-MB-134 cells were modestly inhibited by single-agent DGY-09-192 or the ER degrader fulvestrant, but the combination completely arrested cell proliferation. Treatment of female NSG mice bearing established ER+/*FGFR1*-amplified patient-derived xenografts (PDXs) with single-agent DGY-09-192 (40 mg/kg/day, i.p.) or fulvestrant (5 mg/week, s.c.) delayed tumor growth, respectively. However, treatment with DGY-09-192 + fulvestrant induced tumor regression in all mice (n=7), suggesting that a FGFR1 degrader plus an antiestrogen can serve as an effective therapeutic combination for ER+/*FGFR1*-amplified breast cancer.

Next, we examined whether ER+ breast cancer cells harboring *FGFR1/2* hotspot mutations are sensitive to DGY-09-192. Ectopic expression of $FGFR1^{N546K}$, the most common *FGFR1* mutation in breast cancer, activated FGFR1 signaling and induced resistance to fulvestrant compared to MCF7 cells transduced with wild-type *FGFR1*. EFM-19 cells harboring $FGFR2^{K659E}$ exhibited resistance to fulvestrant *in vitro.* Treatment of both cell lines with DGY-09-192 degraded the mutant $FGFR1^{N546K}$ and $FGFR2^{K659E}$, respectively, blocked phosphorylation of the FGFR downstream targets, and markedly inhibited cell proliferation. These results suggest that PROTAC-mediated degradation of FGFR1/2 effectively blocks the growth of ER+, F*GFR1/2*-mutant breast cancers resistant to antiestrogens.

Conclusions: DGY-09-192 induced FGFR1/2 degradation and blocks FGFR downstream signaling in ER+/*FGFR1*-amplified and *FGFR1/2*-mutant breast cancer cells. The combination of DGY-09-192 and fulvestrant exhibited superior antitumor effects relative to each monotherapy alone *in vitro* and/or *in vivo*. Therefore, PROTAC-mediated FGFR1/2 degradation represents a promising therapeutic strategy for ER+ breast cancers harboring *FGFR1*-amplification or *FGFR1/2* activating mutations.

#3309 Discovery of potent and selective bivalent CDK2 degraders that demonstrate activity in CCNE1^{amp} driven tumors.

A. Gerson-Gurwitz, P. Yang, **S. Fish**, G. Blanco, H. Gao, K. Hayashi, M. Hocker, A. Jamborcic, A. Richters, M. E. Spalding, J. Toth, D. Tran, L. Yang, S. You, A. Burritt, A. Campos, G. Parker, K. Freeman-Cook, P. A. Thompson, S. Bailey;
Plexium, San Diego, CA

Introduction: The Cyclin-Dependent Kinases (CDKs) with their cyclin binding partners, are associated with cell cycle progression and transcriptional regulation. Targeting CDKs is a key oncology therapeutic strategy with CDK4/6 inhibitors demonstrating significant clinical benefit in HR^{+}/HER2^{-} metastatic breast cancer, the most prevalent subtype. However, 30% of patients develop acquired resistance in the clinic with cyclin E1 (CCNE1) amplification/overexpression and CDK2 activation implicated as a major resistance mechanism to CDK4/6i breast cancer therapy. Additionally, CCNE1/CDK2 activation has also been associated with poor prognosis in ovarian and endometrial cancers. Selective targeting of CDK2 using small molecule inhibitor-based approaches have recently advanced into the clinic. Targeted protein degradation of CDK2 provides an alternative strategy that has the potential to eliminate the activity of the CCNE1/CDK2 complex, as well as CDK2 complexed with other cyclins, including cyclin A, and provide improved clinical benefit.

Results: Discovery efforts at Plexium have identified CDK2 bivalent degraders that consist of a CDK2-binding moiety, a linker and a high affinity cereblon-binding ligand. Cereblon binding potency was found to correlate with potent and deep degradation of CDK2. Degradation was blocked in the presence of a proteasome inhibitor as well as in a cereblon knock-out cell line, confirming that CDK2 degradation is mediated by the ubiquitin proteasome system and through engaging cereblon. Proteome-wide analysis demonstrated that CDK2 was selectively depleted without significantly modulating other CDKs or known cereblon neo-substrates. Selective degradation was achieved despite lack of selectivity for binding/inhibition of other CDKs and was confirmed to be dependent on the formation of a CRBN-CDK2 ternary complex. Dose dependent CDK2 degradation resulted in dose dependent inhibition of Rb phosphorylation, cell cycle arrest, senescence-associated phenotypes and antiproliferative activity in CCNE1 amplified cancer cell lines. The *in vitro* data was used to evaluate the PK/PD drug exposure-response relationship *in vivo* and deep CDK2 degradation was demonstrated both *in vitro* and *in vivo*.

Conclusions: These data provide validation for CDK2 degradation as a therapeutic approach. Potent and selective CDK2 bivalent degraders were exploited as tools for studying the sensitivity of CCNE1 amplified tumor models to CDK2 degradation and dependence on E3 ligase. This proof-of concept study supports Plexium's current approach of discovering novel CDK2 molecular glue degraders for the treatment of CDK4/6 inhibitor-naïve and -resistant HR^{+}/HER2^{-} breast cancer, and CCNE1 amplified ovarian and endometrial cancers.

EXPERIMENTAL AND MOLECULAR THERAPEUTICS: Novel Antitumor Agents 3
Poster Session

#3313 Discovery of a potent, selective, and orally available small molecule for disruption of the SOS1-RAS interaction.

D. Ki[1], H. Yu[2], D. Kim[2], Y. Jeon[2], S. Jo[2], J. Nam[1], E.-J. Kim[1], S. Kim[1], H. Choi[1], J. Kim[1], J. Yu[1], S. Choi[2], W. Han[1];
[1]Cyrus Therapeutics, Seoul, Korea, Republic of, [2]Kanaph Therapeutics, Seoul, Korea, Republic of

KRAS mutations represent one of the most common genetic alterations in many cancers including non-small cell lung cancer (NSCLC), pancreatic ductal adenocarcinoma (PDAC), and colorectal cancer (CRC). While Sotorasib and Adagrasib, KRAS G12C inhibitors, have received approval, they exhibit limited responsiveness in clinical trials and are not applicable to various other KRAS mutation types. SOS1 (Son of Sevenless 1) functions as a guanine nucleotide exchange factor (GEF) on RAS, facilitating the transition of inactive GDP-bound RAS to its active GTP-bound state. In addition, SOS1 plays a pivotal role in negative feedback by actively contributing to the reactivation of ERK during treatment with inhibitors targeting the RTK/RAS/MAPK pathway. Inhibiting SOS1, which impedes the reactivation of ERK, has the potential to enhance the effectiveness of inhibitors targeting the RTK/RAS/MAPK signaling cascade and prevent the emergence of resistance mechanisms via H-RAS and N-RAS bypass pathways. Therefore, combining the inhibition of SOS1 with inhibitors targeting the RTK/RAS/MAPK pathway may enhance outcomes and mitigate relapse associated with observed resistances. Here, we present the discovery of a potent, selective, and orally bioavailable small molecule SOS1 inhibitor that effectively disrupts the interaction between SOS1 and RAS. It has demonstrated remarkable synergy effects with RTK/RAS/MAPK pathway inhibitors, significantly impeding the growth of tumors carrying KRAS or EGFR mutations *in vivo*. Overall, our development candidate has demonstrated significant therapeutic potential in combination with inhibitors targeting the RTK/RAS/MAPK pathway for cancers bearing activating mutations in this pathway.

#3314 Molecular profiling of covalent menin inhibitor, BMF-219, in KRAS-mutated solid tumors.

A. A. Momin, T. Rughwani, N. Tanataweethum, K. Mordec, R. Lin, M. Chin, D. Lu, P. Somanath, M. Balakrishnan, T. Butler;
Biomea Fusion, Inc., Redwood City, CA

Menin is an epigenetic protein that drives oncogenic function through transcriptional control directed by its various cofactors such as MLL1 (KMT2A) and MYC. BMF-219 is a covalent menin inhibitor currently under investigation in a dose-finding study evaluating safety and tolerability in adults with KRAS-driven Non-Small Cell Lung Cancer (NSCLC), Pancreatic Adenocarcinoma (PDAC), or Colorectal Cancer (CRC) (NCT NCT05631574). We previously showed that BMF-219 induces effective killing of solid tumor cells irrespective of their KRAS mutation subtype (AACR 2022, abstract 2665) and perturbs genomic binding of MYC and its binding partner MAX, in acute leukemia cells (ASH Abstract 2021). To probe into the underlying mechanism and the potential pathways engaged, BMF-219-induced effects were evaluated in CRC, PDAC and NSCLC cell lines. Cells treated with relevant concentrations of BMF-219 versus vehicle were assessed for menin and MYC protein levels, along with treatment effects on cell cycle and induction of apoptosis. In addition, bulk RNA-seq analysis was performed on the cell lines treated with BMF-219 in a time course study. BMF-219 induces a dose-dependent decrease in menin protein levels in the solid tumor cell lines tested following 24 hours treatment, with the least impact observed in a KRAS WT cell line. The effect of BMF-219 on c-MYC protein levels were variable and highly cell-type dependent, with the CRC metastatic tumor cell line SW620 exhibiting the highest reduction. Differential expression (DE) analysis of bulk RNA-seq data comparing BMF-219 treated versus vehicle treated cells, identified significant alterations in transcript abundance at 6- and 24-hours post treatment. The magnitude of change in the transcript abundance showed a dose-dependent response without significant alteration of a panel of housekeeping genes. GSEA analysis identified pathways associated with cell cycle, cell division and MYC-regulated were significantly differentially expressed across multiple cell lines. These data suggest similar molecular pathways are altered by BMF-219 across KRAS-mutated solid tumor cells. Additional insights into key pathways and modulators will be reported. Collectively, these data suggest that the functional pathway alterations induced by BMF-219 in solid tumor cells are likely pan-KRAS and are similar across different solid tumor indications. This provides further support for advancing the clinical investigation of BMF-219 in KRAS-driven solid tumors.

#3315 Preclinical studies of TSN1611, a potent, selective, and orally bioavailable KRAS^{G12D} inhibitor.

E. Shang, B. Zhong, T. Zhang, C. Dong, S. Ma, A. Yang, Z. Jia, R. Zheng, J. Li, H. Fu, L. Lai;
Tyligand Bioscience (Shanghai), Ltd., Shanghai, China

Background: KRAS mutations are the most frequently encountered driver oncogene, involved in ~25% of all human cancers [1,2]. KRAS^{G12D} is the predominant KRAS mutation isoform, detected in approximately 35% of pancreatic cancer, 13% of colorectal cancer, and 5% of NSCLC [3]. Compared to KRAS^{G12C}, targeting KRAS^{G12D} has proven to be more challenging since the target protein lacks a reactive amino acid residue for irreversible inhibitory modification by a ligand. Herein, we disclose TSN1611, a potent and selective KRAS^{G12D} inhibitor, which possesses favorable oral PK profiles and demonstrates significant *in vitro* and *in vivo* anti-tumor activity in various KRAS^{G12D}-mutant models.

Method: Biochemical HTRF assay was used to measure the inhibition of TSN1611 to both GDP-bound and GTP-bound state of KRAS^{G12D}. Biophysical SPR method was used to directly measure the binding of TSN1611 to GDP-bound KRAS^{G12D} and KRAS^{WT}. Cell based activities were evaluated in a series of *in vitro* cell proliferation assay utilizing Ba/F3 cells engineered with KRAS^{G12D} or non-KRAS^{G12D} mutations and tumor cell lines harboring KRAS^{G12D} mutation. Human cancer cell-derived xenograft models of HPAC (pancreatic) and GP2D (colorectal) were used to evaluate its *in vivo* antitumor effect. *in vitro* and *in vivo* PK studies were performed in mouse, rat, and dog. Systematic nonclinical safety evaluations, including safety panel screen testing, safety pharmacology studies, and repeat-dose toxicity studies were carried out to assess its preliminary toxicity profile.

Results: TSN1611 inhibited both active (GTP-bound) and inactive (GDP-bound) forms of KRAS^{G12D} protein at IC_{50} 1.23 and 1.49 nM, respectively; the K_D value of its direct binding to KRAS^{G12D} protein is 1.93 pM in SPR assay. TSN1611 demonstrated potent anti-proliferation activity against several tumor cell lines harboring KRAS^{G12D} mutation, and excellent selectivity over cells of NRAS, HRAS, and other KRAS isoforms. It also showed dose-dependent anti-tumor efficacy in GP2D and HPAC models. Mechanism of action studies concluded that the antitumor effect of TSN1611 is resulted from its effective inhibition of KRAS signaling pathway. Oral bioavailability and safety profile across multiple species supported its further development.

Conclusion: TSN1611 is a selective KRAS^{G12D} inhibitor. It exhibited excellent selectivity and activity both *in vitro* and *in vivo*; it demonstrated favorable physicochemical properties, oral PK profiles, and brain penetration potential; it also showed acceptable margins of safety. The preclinical data supports further development. Pending regulatory submission and review, the phase I/II study is planned to start in H1 of 2024.

References: [1] Cox, A.D. *et al. Nat. Rev. Drug. Discov.* 2014, *13*, 828. [2] Indini, A. *et al. Pharmaceutics* 2021, *13*, 653. [3] Moore, A. R. ***et al.*** *Nat. Rev. Drug. Discov.* 2020, *19*, 533.

#3316 LY3962673, an oral, highly potent, mutant-selective, and non-covalent KRAS G12D inhibitor demonstrates robust anti-tumor activity in KRAS G12D models.

X. Gong[1], H. Gao[1], M. H. Bender[1], W. Ming[1], Y. Zhang[1], T. R. Stewart[1], C. Yu[2], W. Xu[2], A. X. You[2], W. Bian[2], B. Li[1], T. Wang[1], H. Bian[1], M. Tandon[1], A. Capen[1], R. N. Cavitt[3], B. D. Anderson[3], W. Bocchinfuso[3], A. Klippel[4], C. Iyer[1],
[1]Loxo@Lilly, Indianapolis, IN, [2]Loxo@Lilly, Shanghai, China, [3]Eli Lilly and Company, Indianapolis, IN, [4]Loxo@Lilly, New York, NY

KRAS G12D mutations are activating oncogenic events that occur in approximately 35%, 13%, and 4% of pancreatic, colorectal, and non-small cell lung cancers, respectively, and less commonly in other cancers. We previously demonstrated that LY3962673 is a highly potent inhibitor of KRAS G12D and is selective against wild-type (WT) KRAS in mutant -cell lines and -*in vivo* models. Here, we describe the mechanism by which LY3962673 inhibits KRAS G12D and report a more comprehensive evaluation of LY3962673 activity across a panel of genetically and histologically diverse cancer cell lines, as well as in multiple patient-derived xenograft (PDX) models.

LY3962673 is a non-covalent KRAS G12D inhibitor with high affinity binding to KRAS G12D-GDP (Kd 0.071 nM) compared to KRAS G12D-GTPγS (Kd 26.7 nM). In a panel of cancer cell lines with KRAS G12D mutations, non-G12D mutations or KRAS WT, LY3962673 selectively suppressed MAPK signaling and inhibited the growth of KRAS G12D mutant cancer cells while sparing KRAS WT and non-G12D mutant cells. Sensitivity to LY3962673 varied among the KRAS G12D-mutant cells tested, suggesting that not all cell lines share the same dependence on KRAS G12D for their growth and survival. Furthermore, in multiple KRAS G12D-mutant PDX models representing diverse tumor types, LY3962673 demonstrated anti-tumor activities, ranging from tumor growth inhibition to robust tumor regression. LY3962673 also showed enhanced efficacy when combined with other anti-cancer agents.

Taken together, the findings underscore the potential of LY3962673 as a monotherapy or in combination with other anti-cancer agents, as a promising oral therapeutic option for a range of cancer types with KRAS G12D mutations.

#3317 KRAS^{multi} inhibitor BI 3706674 shows efficacy in KRAS-driven preclinical models of cancer that supports clinical testing in patients with tumors harbouring KRAS^{G12V} mutations and KRAS wild-type amplifications.

A. Tedeschi[1], D. H. Peng[2], F. Schischlik[1], L. Herdeis[1], O. Schaaf[1], V. Santoro[1], D. Gerlach[1], F. Savarese[1], J. Lipp[1], C. Haslinger[1], F. Rocchetti[1], J. Popow[1], H. J. Huber[1], B. Wilding[1], M. Treu[1], J. Fuchs[1], J. Broeker[1], T. Wunber[1], M. Gmachl[1], K. Rumpel[1], M. Rees[3], M. Ron[3], J. Roth[3], M. Williams[2], C. Deckard[2], V. Ramamoorthy[2], J. R. Daniele[2], J. A. Ajani[2], F. Meric-Bernstam[2], S. Kopetz[2], M. Kim[2], D. L. Gibbons[2], C. P. Vellano[2], J. R. Marszalek[2], T. P. Heffernan[2], D. McConnell[1], M. Pearson[1], N. Kraut[1], D. Rudolph[1];

[1]Boehringer Ingelheim RCV GmbH & Co KG, Vienna, Austria, [2]The University of Texas MD Anderson Cancer Center, Huston, TX, [3]Broad Institute of MIT and Harvard, Cambridge, MA

Alterations in KRAS are a main cancer driver. Amplifications of the KRAS wild-type (wt) allele account for ~7% of all KRAS-driven cancers and are frequent in gastric (~5%), esophageal (~13%) and gastroesophageal junction cancers (~12%). KRAS^{G12V} mutations account for ~28% of pancreatic cancers, 9% of colorectal cancers and 6% of lung adenocarcinoma. There is an urgent medical need to identify targeted therapies for these frequent KRAS alterations. Herein, we describe BI 3706674, a novel, potent and orally bioavailable small molecule inhibitor of the KRAS oncogene for clinical testing in patients with tumors harboring KRAS^{G12V} mutations and KRAS wild-type amplifications. BI 3706674 binds non-covalently to multiple KRAS mutant alleles, including the KRAS wt allele, in the GDP-bound state and thereby disrupts oncogenic signaling. Importantly, BI 3706674 is highly selective for KRAS vs HRAS or NRAS, and it is therefore expected to be well-tolerated in normal tissues. In two large cancer cell line panels (PRISM and Horizon), BI 3706674 shows sensitivity across a wide range of KRAS alleles (KRAS wt amplifications and KRAS mutations e.g., G12A/C/D/V, G13D and Q61H). The strongest sensitivity was observed for cell lines with KRAS wt amplifications (relative copy number (CN) of > 10) followed by cell lines with KRAS^{G12V} mutations along with significant pharmacodynamic (PD) biomarker modulation (e.g., down-regulation of DUSP6 mRNA). *In vivo*, BI 3706674 was well-tolerated and showed dose-dependent efficacy in cell line-derived and patient-derived xenograft models of human gastric cancer with KRAS wt CN > 10 and diverse tumor types with KRAS^{G12V} mutations. A twice daily oral dose of 30 mg/kg induced significant tumor regression and PD biomarker modulation. Combination of BI 3706674 with standard of care therapies and novel agents are being tested in preclinical models to guide clinical development. Results of the ongoing pre-clinical analysis will be shared. A Phase I clinical trial is in preparation in patients with advanced solid cancers harboring KRAS^{G12V} mutations and KRAS wt amplifications to evaluate safety, tolerability, pharmacokinetic and pharmacodynamic properties, and efficacy of BI 3706674.

#3318 GFH375 (VS-7375): An oral, selective KRAS G12D (ON/OFF) inhibitor with potent anti-tumor efficacy.

Feng Yan[1], Tao Jiang[1], Tao Liang[1], Lijian Cai[1], Leitao Zhang[1], Xiaoming Xu[1], Yanhui Zhao[1], Xiaoling Lan[1], Xiaohui Zhang[1], Meng Liu[1], Qiang Liu[1], Jinting Gao[1], Fubo Xie[1], Xueyan Gao[1], Li Wang[1], Jingyang Zhang[1], Hongcan Ren[1], Dong Liu[1], Siyuan Le[1], Lili Tang[1], Silvia Coma[2], Yaofeng Cheng[2], Nathan Sanburn[2], Jonathan A. Pachter[2], **Fusheng Zhou**[1], Jiong Lan[1], Qiang Lu[1]

[1]Genfleet Therapeutics, Shanghai, China, [2]Verastem Oncology, Needham, MA

Background: KRAS is the best-known oncogene but had long been considered ‘undruggable’ until the approval of the first KRAS G12C inhibitor sotorasib in 2021. However, most current clinical-stage KRAS inhibitors target the KRAS G12C mutation. Inhibitors of other KRAS mutants such as KRAS G12D, the most frequent KRAS mutation in human cancer, are needed for patients. We have developed GFH375 (VS-7375), an oral, selective KRAS G12D inhibitor targeting both “ON” (GTP-bound) and “OFF” (GDP-bound) states of KRAS proteins. The in vitro potency, selectivity, and in vivo efficacy of monotherapy and combination therapy with avutometinib, a unique RAF/MEK clamp, were evaluated in preclinical studies.

Methods: Biochemical and cellular assays were used to investigate inhibition to KRAS cycling and signaling. CellTiter-Glo assay was performed to determine the effects on proliferation of tumor cell lines. Several KRAS G12D CDX tumor models were employed to study the in vivo pharmacodynamic and anti-tumor effects.

Results: GFH375 inhibited both nucleotide exchange on GDP-bound KRAS G12D and interaction between GMPPNP-bound KRAS G12D with RAF1 with single-digit nanomolar IC_{50} values. GFH375 suppressed phosho-ERK1/2 (p-ERK) level with sub-nanomolar IC_{50} values and potently inhibited cell proliferation across a panel of KRAS G12D tumor cell lines. GFH375 showed high selectivity for KRAS G12D relative to non-G12D KRAS variants, KRAS wild type cells, and NRAS, HRAS, or BRAF mutated cells. Following a single oral dose, GFH375 produced deep and durable inhibition of p-ERK in KRAS G12D CDX tumors. GFH375 demonstrated dose-dependent anti-tumor activity with tumor regressions at 10 or 30 mg/kg given orally twice daily in multiple KRAS G12D PDAC and CRC CDX tumor models. GFH375 also showed strong anti-tumor efficacy in an intracranial KRAS G12D tumor model starting as low as 10 mg/kg orally twice daily. Strong synergy between GFH375 and avutometinib was observed in vitro and was validated in vivo as anti-tumor activity of GFH375 was further enhanced by avutometinib.

Conclusions: GFH375 is a highly potent and selective orally active inhibitor of KRAS G12D (ON/OFF) and demonstrated promising anti-tumor activity in multiple KRAS G12D tumor models. GFH375 was also effective in an intracranial tumor model. GFH375 showed strong synergy with avutometinib in vitro and in vivo. GFH375 is currently in IND-enabling development in preparation for clinical studies of monotherapy and potentially in combination with other agents for patients with KRAS G12D mutant tumors.

#3319 The MTA-cooperative PRMT5 inhibitor, MRTX1719, demonstrates increased anti-tumor activity in combination with KRAS mutant-selective inhibitors in *MTAP* del,*KRAS*-mutant cancers.

L. Waters, R. Aranda, X. Helu, L. Vegar, K. Moya, A. Calinisan, A. Hebbert, J. Hallin, D. Vanderpool, D. M. Briere, J. G. Christensen, **P. A. Olson**, L. D. Engstrom;
Mirati Therapeutics, San Diego, CA

MRTX1719 is an MTA-cooperative PRMT5 inhibitor that leverages the increased concentration of the metabolite MTA in cancer cells harboring a homozygous deletion of the *MTAP* gene (*MTAP* del) under investigation in clincial trials. MRTX1719 preferentially binds to the PRMT5•MTA complex to selectively inhibit PRMT5, an essential gene for all cells, in *MTAP* del cancer cells while sparing PRMT5 activity in normal *MTAP*-wildtype cells. *MTAP* del occurs in ~10% of all cancers, and these patients exhibit remarkably poor survival. Among pancreatic cancer, *MTAP* del occurs in ~ 25% of patients and of these ~30% have co-occurring *KRAS* G12D mutations. In addition, ~15% of lung adenocarcinoma patients harbor *MTAP* del and of these ~13% harbor *KRAS* G12C. While recently approved KRAS G12C mutant selective inhibitors demonstrate anti-tumor activity, strategies to address drug resistance and maximize clinical benefit are warranted. Combination of MRTX1719 with adagrasib or the KRAS G12D inhibitor MRTX1133 in CDX models harboring both a *KRAS* mutation (G12C or G12D) and homozygous *MTAP* deletion resulted in increased anti-tumor activity compared to either single agent. This includes the pancreatic KP4 model in which initial tumor regression in response to single agent MRTX1133 was observed, followed by adaptative resistance and tumor progression with monotherapy while co-administration with MRTX1719 continued to result in marked tumor regression. Mechanistically, combination treated animals demonstrated strong inhibition of both PRMT5 and RAS pathway signaling and combinatorial targeting of these pathways converged on enhanced inhibition of RB-1 phosphorylation. We also characterized this combination treatment in the context of resistance to KRAS selective inhibitors or MRTX1719 to evaluate the benefit of combination over sequential treatment. Finally, an *NF1* mutant, *MTAP* del malignant peripheral nerve sheath tumor (MPNST) PDX model was treated with MRTX1719, the SOS1 inhibitor MRTX0902, or the combination, and a similar increase in anti-tumor activity was observed in the combination treatment compared to either monotherapy alone. These results suggest that the combination of an MTA-cooperative PRMT5 inhibitor with a KRAS mutant selective or KRAS pathway inhibitor may lead to deeper and more durable responses in *MTAP* del cancer patients with co-alterations in the KRAS pathway.

#3320 *In vivo* and *in vitro* experience with novel direct Pan-RAS inhibitors.

Tariq Arshad[1], Howard Donninger[2], Goeff Clarke[3], Joe Burlison[3], Rob Monsen[3], Mike Sabo[3]

[1]Qualigen Therapeutics, Carlsbad, CA,[2]Dept. Pharmacology and Toxicology University of Louisville,, University of Louisville, Louisville, KY,[3]University of Louisville, Louisville, KY

RAS oncogenes are frequently activated by mutations in human cancer, where they act as driving elements of the disease. Mutation rates can range from ~25% of Non Small Cell Lung cancers to over 90% of pancreatic cancers. RAS proteins can also be hyper-activated to drive cancer at a significant frequency in the absence of RAS gene mutations when their protein regulatory systems are damaged. Thus, RAS may be the most frequently activated oncoprotein in cancer. We have developed a series of novel, direct, RAS inhibitors with a unique binding site on RAS. The binding of the agents alters the structure of the RAS effector loop and blocks the association with RAS downstream effectors. We used in silico library screening followed by Medicinal Chemistry optimization to develop the compounds. We have validated the agents using Microscale Thermophoresis and NMR to quantify binding to recombinant RAS protein. We have used mutant and wild type RAS driven tumor cell lines in 3D growth and protein-based RAS signaling assays to quantify and characterize the action of the family of inhibitors. We have used xenograft assays to demonstrate compound anti-tumor activity in RAS driven cell lines and pdx systems. We have identified compounds that can bind mutant and wild type K, H, N and M-RAS. We can suppress the association of mutant and wild type RAS protein with its effector RAF-1 in treated cells. The compounds can suppress 3D growth of mutant or wild type RAS driven tumor cell lines and repress tumor development in vivo. The compound family bind to a different site than either clinical agent AMG-510 (K-RAS G12C specific) or MRTX-1133 (K-RAS G12D specific). They exhibit distinct RAS signal inhibition patterns compared to these agents. They can also co-operate with the clinical agents and reduce drug resistance effects.

#3321 KRAS^{multi} inhibitor BI 3706674, an orally bioavailable, direct inhibitor of diverse oncogenic KRAS variants drives tumor regression in KRAS^{G12V}-driven preclinical models.

David Hwa Peng[1], Antonio Tedeschi[2], Lorenz Herdeis[2], Otmar Schaaf[2], Fabio Savarese[2], Francesca Rocchetti[2], Johannes Popow[2], Heinrich J. Huber[2], Birgit Wilding[2], Matthias Treu[2], Julian Fuchs[2], Joachim Broeker[2], Tobias Wunberg[2], Firoella Schischlik[2], Jesse Lipp[2], Mariah Williams[1], Vaness Chandler[1], Charles E. Deckard[1], Vandhana Ramamoorthy[1], Joseph R. Daniele[1], Scott Kopetz[1], Michael Kim[1], Don L. Gibbons[1], Christopher P. Vellano[1], Joseph R. Marszalek[1], TImothy P. Heffernan[1], Darryl McConnell[2], Mark Pearson[2], Norbert Kraut[2], Dorothea Rudolph[2]

[1]TRACTION, UT MD Anderson Cancer Center, Houston, TX, [2]Boehringer Ingelheim, Vienna, Austria

Alterations of KRAS are observed in approximately one in seven of all human tumors, making KRAS one of the most prevalent oncogenic drivers. Gain-of-function missense mutations in KRAS, leading to its aberrant activation, are found in ~90% of pancreatic cancer, ~40% of colorectal cancer and ~30% of lung adenocarcinoma, with KRAS^{G12V} mutations accounting for ~28%, 9% and 6% of the cases, respectively. The poor outcome associated with these tumor types as well as the lack of targeted inhibitors for the KRAS^{G12V}-mutant allele calls for the urgent need to identify therapies able to effectively address this allele. BI 3706674 is a novel, potent and orally available small molecule inhibitor of the KRAS oncogene. BI 3706674 binds non-covalently to multiple KRAS mutant alleles, including KRAS^{G12V}, in the GDP-bound state, and blocks downstream oncogenic signalling. Here, we show that BI 3706674 has a strong anti-proliferative activity in a panel of KRAS^{G12V}-mutant cancer cell lines *in vitro*, along with significant pharmacodynamic (PD) biomarker modulation (including inhibition of ERK1/2 phosphorylation and down-regulation of DUSP6 mRNA). *In vivo,* a twice daily oral dose of 30 mg/kg was well tolerated, while inducing tumour regression in several mutant KRAS^{G12V} patient-derived xenograft (PDX) models across multiple different tumor types. Feedback activation of upstream signalling pathways including receptor tyrosine kinases, such as the EGFR, has been suggested to limit the efficacy of GDP-KRAS-targeting compounds in preclinical studies. Clinical combination trials involving KRAS^{G12C} inhibitors such as adagrasib and sotorasib and anti-EGFR modalities are further supporting these findings. Here we show that a combination with anti-EGFR antibodies (e.g., Cetuximab) potently enhances the response observed for BI 3706674 in models of KRAS^{G12V}-mutant colorectal cancer. The deeper response observed upon combination of BI 3706674 with Cetuximab across multiple xenograft models provides a strong rationale for the clinical investigation of this combination therapy. Moreover, based on our *in vitro* mechanistic studies and *ex vivo* organoid platform we have identified prospective mechanisms of resistance and opportunity for novel drug combinations with BI 3706674 that can potentially translate into clinical trials.

#3322 Sigma-2-Erastin inhibits PC tumor growth through lipid ROS-DUSP6-MAPK signaling.

K. S. Bishnupuri[1], K. F. Newcomer[1], Q. Gong[1], L. Ye[1], S. Vangveravong[1], R. Takchi[1], B. T. Keller[2], D. M. Spitzer[1], W. G. Hawkins[1];
[1]Washington University School of Medicine in St. Louis, St. Louis, MO, [2]Accuronix Therapeutics, Inc., St. Louis, MO

Introduction: Pancreatic cancer (PC) is a malignancy with poor prognosis and high mortality with a very low 5-year survival rate. Currently, apoptosis and autophagy are the central mechanisms of programmed cell death (PCD) that maintain cellular homeostasis and regulate cell fate. With the recent emergence of 'ferroptosis' as a new type of PCD and its close association with the pathophysiological processes of many diseases including tumors, it is viewed as a potential mechanism to improve systemic treatment of PC. Considering the opportunity to regulate both apoptosis and ferroptosis by a single agent, our group has developed a cancer-targeted small molecule consisting of a sigma-2 ligand (a known apoptotic inducer) delivery moiety linked to an inhibitor of the cystine importer xCT (dm-Erastin, a known ferroptotic inducer) and named it as Sigma-2-Erastin (S2E) or ACXT-3102. The study presented here is aimed at determining the efficacy of ACXT-3102 in PC and defining its underlying mechanism of action.
Methods: Using *in vitro* and *in vivo* tumor xenograft models of human PC, we determined the effects of ACXT-3102 treatments in regulating PCD of PC cells and defined the signaling pathway involved in mediating the effects.
Results: As assessed by TitreGlo assays, we observed dose-dependent inhibition of PC cell (BxPC-3, AsPC-1 & PANC-1) viability. Following the WES-analysis of signaling proteins, we observed that ACXT-3102 induces PC cell death by combinatorial regulation of apoptotic and ferroptotic PCD via lipid ROS-DUSP6-MAPK/ERK-mediated signaling pathway. Interestingly, the results of this study demonstrated a hyperactivation of MAPK/ERK signaling by increased phosphorylation instead of inhibition involved in inducting apoptotic cell death as represented by significant increases in expression of cleaved Capase-3/7 and PARP. In addition, ACXT-3102 treatments deceased GPX4 expression along with an increase in lipid ROS production as key markers of inducing ferroptotic cell death. Results from the murine model of human tumor xenografts using AsPC-1 cells further demonstrated significant decreases in tumor volume and increases in survival proportions in ACXT-3102-treated mice.
Conclusions: ACXT-3102, an orally administered conjugate of sigma-2 ligand and Erastin induces PCD of human PC by uniquely regulating apoptosis and ferroptosis together. Therefore, ACXT-3102 offers a novel and improved therapeutic strategy for treating patients of fatal human carcinomas, especially those, which are difficult to diagnose at an early stage.

#3323 Novel Pan-RAS inhibitor ADT-007: A unique mechanism of antitumor selectivity in pancreatic and colorectal carcinoma models.

J. Wang[1], A. B. Keeton[1], S. Ramesh[1], P. Johnson[1], Y. Y. Maxuitenko[1], J. B. Foote[2], C.-H. Huang[1], K. L. Berry[1], K. Fadlalla[1], B. D. S. Reddy[2], G. P. Nagaraju[2], E. Nurmemmedov[3], I. Babic[3], V. Gaponenko[4], X. Chen[1], B. F. El-Rayes[2], D. J. Buchsbaum[2], G. A. Piazza[1];

[1]Auburn University Harrison College of Pharmacy, Auburn, AL, [2]University of Alabama at Birmingham, Birmingham, AL, [3]Nerd Bio, San Diego, CA, [4]University of Illinois Chicago, Chicago, IL

Multiple types of RAS mutations activate RAS isoforms, HRAS, NRAS, or KRAS, that drive oncogenic signaling leading to uncontrolled cell proliferation and tumor development. RAS mutations occur de novo in approximately one-third of all human cancers, and are especially prevalent in pancreatic, colorectal, and lung tumors. Where RAS mutations are less frequent in other cancers, such as breast cancer, RAS can be pathologically activated by growth factor receptors that engage numerous downstream effectors.

The currently FDA-approved KRAS-targeted drugs are designed to covalently inactivate only G12C KRAS mutants, however, this mutation is only prevalent in lung cancer. The most common mutations in pancreatic ductal adenocarcinoma (PDAC) are KRAS-G12D, KRAS-G12V, and KRAS-G12R. Our novel class of pan-RAS inhibitors, exemplified by ADT-007, addresses the urgent need for pan-RAS inhibitors with antitumor activity in cancers harboring these common mutations. These pan-RAS inhibitors have unique pharmacological properties that allow for selective killing of cancer cells harboring RAS mutations. ADT-007 inhibited growth of an array of carcinoma tumor cell lines in vitro with single digit nM IC50 values regardless of RAS mutant allele, and inhibited RAS activation and MAPK/AKT signaling. Because it is a pan-RAS inhibitor, ADT-007 may not be susceptible to commonly reported mechanisms of resistance to covalent KRAS inhibitors, such as activation of wild type (WT) alleles or secondary RAS mutations. Differentiated normal epithelial or hepatic cells, and tumor cells with WT RAS were insensitive to ADT-007 due to enzymatic detoxification of ADT-007 via glucuronidation, representing a novel mechanism of tumor selectivity. An orally bioavailable prodrug of ADT-007 (ADT-1004) is well tolerated in vivo, and produced sustained concentrations of ADT-007 well above IC50 values in plasma and even higher levels in tumors. Daily oral administration of ADT-1004 significantly inhibited RAS signaling and tumor growth in orthotopic and PDX mouse models of pancreatic cancer.

#3324 Discovery of a novel SOS1 inhibitor, AIG01012, targeting pan-KRAS mutant cancers.

J. Kim, S. Park, S. Kim, S. Lee, K. Yoo, H.-J. Lee, J. Kang, K.-O. Lee;
AIGEN Sciences, Seoul, Korea, Republic of

Targeting the SOS1-KRAS interaction represents a pivotal strategy in mitigating aberrant KRAS signaling, which is implicated in numerous malignancies. At AIGEN Sciences, Inc., we have harnessed an advanced human-in-the-loop (HITL) AI-based drug discovery platform (AIGEN ChemTailor). This innovative platform allows online learning through expert feedback, optimizing our drug development endeavors. We designed a potent SOS1 inhibitor, AIG01012 using AIGEN ChemTailor in combination with fragment-based drug discovery (FBDD) and molecular modeling techniques. We conceived numerous compounds and shortlisted the leading candidates for extensive testing after meticulous computer simulations. AIG01012 manifested substantial inhibitory effects against several KRAS mutant interactions with SOS1, specifically SOS1-KRAS WT, SOS1-KRAS G12C, SOS1-KRAS G12D, SOS1-KRAS G12V, and SOS1-KRAS G13D. However, its inhibitory capacity did not extend to the SOS2-KRAS G12C interaction. AIG01012 demonstrated remarkable inhibitory effects in 3D cell proliferation assays across various cell lines, including H358, MIA-PaCa2, SW837, AsPC-1, A427, SW620, Capan-2, A549, DLD-1, MKN-1, and H1666. Moreover, AIG01012 showed synergistic antiproliferative effects when combined with approved drugs such as sotorasib (for lung cancer with KRAS mutations), trametinib (a MEK inhibitor), and Osimertinib (targets specific EGFR mutations) in either H358 or PC-9 cell lines. Mouse studies further confirmed its favorable pharmacological properties, and its efficacy was evaluated in subsequent mouse tumor model. In summary, utilizing our human-in-the-loop (HITL) AI platform, AIGEN ChemTailor, we have efficiently derived AIG01012 as a potent SOS1 inhibitor that targets a wide range of KRAS interactions. With its notable in vitro and in vivo outcomes, AIG01012 is set for further exploration and prospective clinical trials as a significant contender in KRAS-targeted cancer treatments.

#3325 HBW-012-D and HBW-012-E are novel, potent, selective, safe, and bioavailable KRAS G12D inhibitors with superior anti-tumor efficacy in mice.

N. Lee, Y. Li, G. Liu, J. Li, J. Ren;
Chengdu Hyperway Pharmaceuticals, Chengdu, China

Purpose: This study is to characterize newly identified KRAS G12D small molecule inhibitors HBW-012-D and HBW-012-E, both showing improved oral bioavailability than MRTX1133, the known clinical compound with poor bioavailability. Method: Through our medicinal chemistry efforts, we have aimed to design novel small-molecule KRAS G12D inhibitors that are orally bioavailable. The compounds were screened via pERK and cell viability (CTG) assays in multiple cell types. The optimized compounds were further evaluated based on their pharmacokinetic (PK) properties and toxicity. The anti-tumor efficacy of the leads was confirmed in the GP2D (colorectal carcinoma with KRAS G12D mutation) mouse xenograft tumor model. Result: As shown in the table, HBW-012-D and HBW-012-E have significantly better potency and PK characteristics than MRTX1133. In the mouse GP2D model, comparing head-to-head with the same vehicle and protocol (50 mg/kg, twice daily, orally), MRTX1133 hardly inhibited tumor growth, whereas HBW-012-D inhibited tumor growth well (58 % tumor growth inhibition), and HBW-012-E not only completely inhibited tumor growth but also further regressed tumor size by around 40%. Preliminary toxicity tests showed that HBW-012-D and HBW-012-E are safe: weak inhibition of CYP450 enzymes, negative mini-Ames test, excellent kinase selectivity, and no obvious abnormalities in the 14-day rat or mouse toxicity test. Conclusion: New KRAS G12D inhibitors, HBW-012-D and HBW-012-E, were identified. Their preclinical profile, including potency, efficacy, and PK data, are all superior to MRTX1133, and their safety meets the criteria of clinical development. They show potential as a preferred oral treatment option for patients with tumors mediated by the KRAS G12D mutation, such as pancreatic cancer that still lacks effective treatments.

in vitro data

IC 50 (nM)	**MRTX1133**	**HBW-012-D**	**HBW-012-E**
AGS (G12D, stomach, pERK)	1	0.8	0.46
AsPC-1 (G12D, pancreas, 3D CTG)	10.88	3.09	
GP2D (G12D, colon, 3D CTG)	1.38	0.67	0.69
MKN-1 (WT, stomach, 3D CTG)		>3000	
Rat PK @ 100 mg/kg oral			
Cmax (ng/mL)	9	82	1444
AUC0~t (mg.h/mL)	20	258	5724

#3326 PMR-116, a second generation RNA Polymerase I inhibitor.

L. Furic[1], N. Hein[2], R. Ferreira[3], K. Panov[4], A. Huglo[1], R. Rebello[1], E. Kusnadi[1], D. Drygin[5], M. Haddach[5], R. Hannan[2],
[1]Peter MacCallum Cancer Centre, Melbourne, Australia, [2]ANU, Canberra, Australia, [3]ANU, Melbourne, Australia, [4]Queen's University Belfast, Belfast, United Kingdom, [5]Pimera Inc, San Diego, CA

Introduction: Inhibition of RNA Polymerase I, the enzyme responsible for the synthesis of ribosomal RNAs, the nucleic scaffold of ribosomes, has been proven as a novel therapeutic target as most cancer cells are "addicted" to ribosome biogenesis.
Methods: In collaboration with Pimera Inc, we developed and tested the efficacy of a second generation RNA polymerase I inhibitor, PMR-116, in various pre-clinical cancer models. On-target activity of PMR-116 was confirmed in peripheral blood cells isolated from patients with solid tumors enrolled in a phase I trial of PMR-116.
Results: PMR-116 potently inhibits Pol I transcription with ~200 fold higher selectivity towards Pol I compared to Pol II transcription. PMR-116 inhibits rRNA synthesis by stalling the Pol I complex at the rDNA promoter preventing promoter escape and consequently elongation. PMR-116 anti-cancer activity was evaluated against a panel of over 100 cancer cell lines representative of 20 major types of solid and haematological malignancies. This new Pol I inhibitor exhibited broad anti-proliferative and cytotoxic activity with an IC50 ranging from 32-4500nM and a median IC50 of 300nM. In contrast, cells derived from normal tissues were significantly less sensitive (IC50 ranging from 6-33µM).
In vivo, PMR-116 significantly improved survival and reduce tumor burden in several preclinical models such as Vk*MYC transgenic model of indolent multiple myeloma, CT26 xenograft model of colorectal cancer, MMTV-PyMT transgenic model of metastatic breast cancer, mixed-lineage leukemia (MLL)-eleven nineteen leukemia (ENL)+Nras acute myeloid leukemia (+/-p53 mutation) and patient-derived xenografts of prostate cancer and AML.
In a phase I trial of PMR-116, on-target activity of PMR-116 was observed in cells derived from the peripheral blood.
Conclusion: PMR-116 significantly reduced cancer growth in a wide range of tumor models, including GEMM, syngeneic and PDX models. PMR-116 is undergoing clinical testing in phase I in solid tumors with the objective to determine maximum tolerated dose and identify a phase II dose.

#3327 L-pampo™, a TLR2/3 agonist, enhances anti-tumor immune responses and synergistically improves the anti-tumor efficacy of immune checkpoint inhibitors in cold tumors.

Guentae Kim[1], Yoonki Heo[1], Hye Jung Kim[1], Sejung Park[1], Byung Cheol Ahn[1], Won Suk Lee[2], Chan Kim[2], Hong Jae Chon[2], Eunyoung Chun[1], Jung Sun Yum[1]

[1]CHA Vaccine Institute, Seongnam-si, Korea, Republic of,[2]CHA Bundang Medical Center, CHA University School of Medicine, Seongnam-si, Korea, Republic of

Introduction: Immunotherapy is a promising therapeutic approach for a wide range of cancers. However, some tumors called "cold tumors" lack infiltrating T-cells and are not responsive to immune checkpoint inhibitors (ICIs), leading to worse clinical outcomes. This study demonstrates that L-pampo, a novel TLR2/3 agonist, promotes an anti-tumor immune response in cold tumors. Also, combining L-pampo with ICIs can improve the anti-tumor efficacy more safely than standard-of-care (SoC) chemotherapies.

Method: We utilized syngeneic tumor models using CT26 colon cancer and 4T1 triple-negative breast cancer (TNBC). L-pampo was administered alone or in combination with ICIs such as anti-PD-1 (aPD-1) and anti-CTLA-4 (aCTLA-4) antibodies to tumor-bearing mice (n=8/group). Tumor size was measured every three days, and the survival rate was monitored until day 60. On day 21 or 27 after transplantation, we analyzed the tumor weight and tumor-infiltrating immune cells. Furthermore, we assessed the respective anti-tumor efficacies and safety of L-pampo and SoC chemotherapies (FOLFOX and paclitaxel).

Result: In the CT26 colon cancer model, L-pampo effectively reduced the tumor size compared to the vehicle group (83.7%). The combination of L-pampo and ICI reduced tumor size by 86.1% (with aCTLA4) and 90.5% (with aPD-1), while the ICI alone did not effectively inhibit tumor growth (aPD-1; 17.3%, aCTLA-4; 23.6%). Notably, the triple concurrent treatment with L-pampo, aPD-1 and aCTLA-4 reduced tumor size by 96.6% and induced completed tumor regression in 1 out of 8. In the 4T1 TNBC model, L-pampo reduced tumor size by 64.2% compared to the vehicle treatment, and combined treatment with L-pampo and a-PD-1 suppressed tumor growth compared to aPD-1 alone (9.6% vs. 61.5%). Additionally, L-pampo improved median overall survival in each tumor model (CT26; 25.5 vs. 35.5, 4T1; 29.5 vs. 53.5 days). To compare the anti-tumor efficacy of L-pampo and conventional cytotoxic chemotherapy, we treated tumor-bearing mice with FOLFOX or paclitaxel as SoC regimen, respectively. Compared with each chemotherapy, L-pampo revealed comparable antitumor efficacies (Tumor growth inhibition CT26; 75.6% vs. 70.6%, 4T1; 65.5% vs. 58.8%). Interestingly, L-pampo inhibited tumor growth without significant adverse effects. In contrast, conventional chemotherapies induced acute hematological side effects such as leukopenia/neutropenia/thrombocytopenia and rapid weight loss. Furthermore, L-pampo increased the active cytotoxic T-cells infiltration through antigen-presenting cells stimulation within the tumors.

Conclusion: This study suggests that L-pampo, a novel TLR2/3 agonist, can be a potent anti-tumor agent, improving the anti-tumor efficacy of ICIs in cold tumors with enhanced anti-tumor immunity and minimal toxicities than conventional chemotherapies.

#3328 Oridonin derivative compounds target STATs to inhibit triple-negative breast cancer.

G. Vontz[1], J. Li[2], Z. Liang[1], R. Ma[3], P. Wang[2], H. Chen[2], J. Zhou[2], Q. Shen[1];
[1]LSU Health New Orleans, New Orleans, LA, [2]University of Texas Medical Branch, Galveston, TX, [3]University of Georgia, Athens, GA

Breast cancer remains the second leading cause of cancer related deaths in women. Despite the development of targeted treatments and immunotherapies, triple-negative breast cancer (TNBC) continues to evade effective treatment. TNBC lacks sufficient expression of druggable markers, ER, PR, and Her2, and exhibits especially aggressive characteristics including later diagnosis, lower survival rate, and higher rates of metastasis and reoccurrence. Currently, cytotoxic chemotherapy and radiation remain the standard of care for TNBC. Our work utilizes compounds from nature to develop therapies for TNBC with improved efficacy and safety. Oridonin, a natural kaurene-type diterpenoid enriched in the medicinal herb *Rabdosia rubescens*, is a promising anticancer agent, but exhibits limited bioavailability and potency. Our team successfully developed oridonin derivative CYD0618 compound that exhibits significantly improved solubility and anticancer activity. This study aims to characterize the mechanism of action of CYD0618 on TNBC cells. We found that CYD0618 reduces the proliferation of TNBC cells *in vitro* with IC_{50}s at the nanomolar level. We also found CYD0618 has high potency against TNBC *in vivo*. Within a xenograft mouse model, CYD0618 suppresses the growth of TNBC tumors and extends animal survival. Using Western blot to probe for putative targets, we found CYD0618 reduces activation of STAT3, a transcription factor critically involved in proliferation, survival, and transformation of epithelial cells. Because STAT3 is constitutively active in ~70% of human cancers, there has been a tremendous effort to develop STAT3 targeting therapies; however, none has achieved FDA approval. In addition to STAT3, we show CYD0618 also suppresses other STAT transcription factors. Compared to selective STAT3 degradation by PROTAC treatment, poly-STAT targeting by CYD0618 exhibits superior activity against TNBC cells. Our study identifies CYD0618 as a novel poly-STAT inhibitor with promising activity against TNBC.

#3329 Development of HM-001 as a therapeutic drug for non-muscle invasive bladder cancer.

Shinji Mima[1], Monta Sakaki[1], Noriaki Kiya[1], Atsunari Kawashima[2], Norio Nonomura[2], **Chihaya Kakinuma**[1]

[1]HOIST Co., Ltd., Osaka, Japan,[2]Department of Urology Graduate School of Medicine, Osaka University, Osaka, Japan

HM-001 is a drug containing sodium chlorite as the active ingredient that is being developed as a drug for non-muscle invasive bladder cancer (NMIBC), and is currently undergoing physician-led clinical trials. It has been discovered that sodium chlorite generates radicals in an acidic environment, and phosphatidylserine on the surface of tumor cells acts as a Lewis acid to generate radicals. HM-001, like other anticancer drugs and BCG, is intended to be injected into the bladder, retained, and then excreted. GLP studies using the same administration method has been completed, and no toxic changes have been observed in human trial doses. The efficacy of HM-001 against NMIBC was evaluated using an orthotopic transplantation model of UM-UC-3, a bladder cancer cell line. In the model, cells were transplanted into the bladder of SCID mouse after epithelial removal with trypsin, 600, 800, 1,600, and 3,200 ppm of HM-001 were administered once a week, and the weight of the excised bladder was calculated. After 4 weeks, the tumor weight was calculated and the tumor weight suppression rate in the control group was evaluated. As a result, the medicinal efficacy was confirmed at concentrations of 800ppm or higher. On the other hand, the UM-UC-3 model is a commonly used model, but it mimics CIS (carcinoma in situ) and can only partially mimic NMIBC. That is, other models are needed to evaluate efficacy for low- and high-grade NMIBC other than CIS. Therefore, we established high-grade and low-grade PDX and evaluated the effectiveness of HM-001 against low- and high-grade PDX through ex vivo testing. First, patient-derived tissue was transplanted into SCID mice, allowed to grow, and then removed. After extraction, they were cut into 2 mm3 pieces, exposed to HM-001 at 800, 1600, and 3200 ppm for 2 hours, and then transplanted into SCID mice. As a result of comparing the tumor size after transplantation with the control group, a dose-dependent tumor regression effect was confirmed in high-grade and low-grade PDX. NMIBC is divided into low-, medium-, and high-risk categories, with different treatment methods and drugs used for each. In particular, low-grade forms are restricted to low- and intermediate-risk groups. The results of this study show that HM-001 is effective not only for high-risk (including CIS) NMIBC but also for low- and intermediate-risk (low-grade) NMIBC.

#3330 BPP, a dual functional inhibitor, targets MLL-rearranged acute myeloid leukemia: Unraveling mechanisms and expanding therapeutic horizons.

T.-L. Chen[1], T.-L. Su[2], T.-C. Lee[2];

[1]National Chung Hsing University, Taichung, Taiwan, [2]Academia Sinica, Taipei, Taiwan

Refractory/recurrent acute myeloid leukemia (AML) poses a formidable clinical challenge, with MLL translocations implicated in approximately 10% of AML cases and a staggering 75% in infant leukemia, bearing an unfavorable prognosis. Our investigation focuses on BPP, a dual-functional inhibitor capable of inducing DNA cross-linking and suppressing angiogenesis. In a diverse panel of solid tumor and leukemic cells, BPP exhibited exceptional sensitivity against MLL-rearranged AML cell types. In MOLM13 and MV4-11 xenograft models, BPP showcased outstanding tumor suppression, with some tumors even achieving complete remission. In-house acute toxicity testing, BPP treated group showed excellent safety margin in both blood chemistry and pathological examination. Remarkably, BPP demonstrated significant cytotoxicity not only in FLT3-WT AML but also in FLT3-ITD AML. Delving into the mechanism, BPP was found to induce FLT3-ITD and MLL degradation by triggering DNA damage and ER stress. Comet assays revealed a dose-dependent accumulation of DNA fragments in MLL cells upon BPP exposure.The involvement of the KMT2A gene in chromosomal translocation in THP1 cells was highlighted, with BPP treatment resulting in a significant increase in Heat-shock protein. Notably, the combination of ganetespib, an FDA-approved HSP90 inhibitor, with BPP exhibited synergistic effects in both in vitro and in vivo models, inducing synthetic lethality and inhibiting HR repair. Furthermore, BPP not only reduced leukemic stem cells in colony formation assays but also demonstrated sensitivity in relapsed/refractory (R/R) and multiple drug-resistant patient samples. These findings collectively position BPP as a promising candidate for the treatment of MLL-rearranged AML, offering multifaceted therapeutic potential.

#3331 Preclinical combination of ONC206 with radiotherapy and temozolomide in a GBM mouse orthotopic model.

L. Zhou, L. Zhang, J. Zhang, S. Zhang, W. S. El-Deiry;
Brown University, Providence, RI

Glioblastoma multiforme (GBM) is the most common form of primary malignant brain tumor in adults. It is also the most aggressive and lethal. Standard of care therapy comprises maximal safe surgical resection followed by adjuvant alkylating agent temozolomide (TMZ) and radiotherapy (RT). There have only been five drugs and one device ever approved by the FDA for the treatment of GBM. The five-year survival rate for GBM patients has shown no notable improvement in the last three decades. We previously reported that the first-in-class imipridone small-molecule Dordaviprone (ONC201) decreases protein chaperone ClpX to unleash mitochondrial protease ClpP activity, integrated stress response and cell death. Preclinical combination of ONC201 (100 mg/kg weekly) with radiotherapy and Temozolomide in a GBM mouse orthotopic model results in reduced tumor burden and prolonged survival. The second generation imipridone ONC206 also activates integrated stress response and decreases ClpX in GBM cells but ONC206 is approximately 20 times more potent than its parent imipridone ONC201. ONC206 0.08 uM in combination with 12.5 uM TMZ and 2 Gy RT reduced the cell viability of GBM cells significantly compared to all single treatments and double treatments. During a short-term treatment of a GBM mouse orthotopic model, ONC206 (50 mg/kg weekly, half of ONC201 doses) synergizes with TMZ and RT to induce more tumor cell apoptosis and inhibits more tumor cell proliferation compared to other groups with single or double treatments. There are two ongoing clinical trials with ONC206: single weekly or multiple-day weekly dose regimens of single-agent, oral ONC206 in patients with recurrent, primary central nervous system (CNS) neoplasms (NCT04541082) and ONC206 alone or in combination with radiation therapy in treating patients with diffuse midline gliomas that is newly diagnosed or has come back (recurrent) or other recurrent primary malignant CNS tumors (NCT04732065). Future studies evaluating the role of immune function, mitochondrial metabolism, dopamine receptors, the ISR and TRAIL pathway in the synergistic effect would support further development of the triple combination regimen of ONC206, TMZ and radiation therapy for GBM clinical trial.

#3332 Kalkitoxin thiol amide suppresses the breast cancer metastasis to bone and brain.

Y. Soh, S. Shrestha, S. Kim;
Graduate School_Jeonbuk National University, Jeonju, Korea, Republic of

Introduction: Breast cancer is the primary frequently diagnosed cancer worldwide, with a high fatality rate. Metastasis resulting from advanced breast cancer increases mortality in patients. MDA-MB-231 is triple-negative breast cancer that does not have any of the receptors that are commonly found in breast cancer. The lipopeptide toxin kalkitoxin thiol amide (KTA), generated from the marine cyanobacterium Moorena producens (formerly Lyngbya majuscule), has a wide range of biological and pharmacological effects. Its promise as a therapeutic agent for treating bone metastases from breast cancer is still uncertain. This study aimed to determine whether KTA could prevent breast cancer from metastasis to mice's bones and to elucidate any potential mechanisms causing this inhibition.
Experimental Procedures: MDA-MB-231 cells were transfected with pGL4.50 (Luc2/CMV/Hygro) vector using LipofectamineTM 2000. Positive clones of MDA-MB-231 cells were selected after treatment with 300 µg/ml hygromycin for one week. After cancer implantation to the heart, bioluminescent imaging of femurs was measured upto 5 weeks and signal intensity of KTA-treated groups was compared with the vehicle group.
Summary: KTA decreased breast cancer cell proliferation, migration, and invasion. KTA prevented MDA-MB-231 cells from breast cancer metastasizing to the bone and brain via inhibiting MAPK and STAT signaling. The epithelial-mesenchymal transition markers, which are responsible for distant metastasis, are highly opposed by KTA. Compared to mice in the control group, mice receiving KTA displayed considerably less bone and brain metastasis, a lower tumor burden, and less bone destruction in the murine breast cancer bone metastasis model.
Conclusion: KTA has new inhibitory effects on cancer cell invasion and migration both *in vitro* and *in vivo*. From these findings, KTA may have therapeutic promise for treating breast cancer patients with distant metastases.

#3333 Targeting the MDM2-p53 interaction: Time- and concentration-dependent studies in tumor and normal human bone marrow cells reveal strategies for an enhanced therapeutic index.

Elaine Willmore[1], Maria Ahn[2], Suzanne Kyle[1], Yan Zhao[1], Huw Thomas[1], Kenneth S. Rankin[1], Luke Bevan[2], Lynsey Fazal[2], Keisha Hearn[2], Nicola Wilsher[2], Justyna Kucia-Tran[2], Nicola Ferrari[2], Nicola Wallis[2], Neil Thompson[2], John Lyons[2], Duncan Miller[1], Celine Cano[1], Martin E. M. Noble[1], Ian R. Hardcastle[1], Steven Howard[2], Gianni Chessari[2], John Lunec[1], David R. Newell[1], **Steve R. Wedge**[1]

[1]Newcastle University, Newcastle upon Tyne, United Kingdom,[2]Astex Pharmaceuticals, Cambridge, United Kingdom

Aim We aimed to design an MDM2-p53 antagonist with a differentiated tolerability profile that could be used to treat patients with wild-type *TP53* malignancies. As part of an alliance between Newcastle University, Astex Pharmaceuticals, and Cancer Research Horizons, we discovered ASTX295, a potent inhibitor of the MDM2-p53 interaction that is currently under clinical investigation in patients with solid tumors (NCT03975387). We selected ASTX295 as a compound with a predicted short plasma half-life, which we hypothesised would help to mitigate the dose-limiting neutropenia and thrombocytopenia observed with earlier MDM2-p53 antagonists in clinical studies. To examine this hypothesis *in vitro*, we determined time- and concentration-dependent responses to ASTX295 treatment in healthy volunteer-derived human bone marrow cells, megakaryocytes, and in a panel of human tumor cell lines.

Methods Samples containing bone marrow cells from healthy patients undergoing hip surgery were obtained under the ethical approval of the Newcastle Biobank (REC 12/NE/0395). Following Lymphoprep™ separation, cells were treated *ex vivo* with ASTX295 and seeded for Granulocyte-macrophage (GM) colony-forming assays in methylcellulose. Megakaryocytes were obtained from *in vitro* differentiation of CD34+ stem/progenitor cells. Human tumor cell lines (including *MDM2*-amplified SJSA-1) were treated with ASTX295 *in vitro* and seeded at low density for colony-forming assays. Exposures of 6, 12, or 24h were examined, and the data plotted to calculate LC_{50} values.

Results The clonogenic survival of tumor cells was time-dependent, with LC_{50} values (mean ± SEM) in SJSA1 cells being 238 ± 46nM and 75 ± 7nM respectively (n = 3-4), following a 12h or 24h exposure to ASTX295. Time-dependent effects were also evident in five human bone marrow samples but with LC_{50} values of 1.9, >3, >10, >10, and >10uM being achieved at 12h, and 860 ± 268nM at 24h. Megakaryocytes showed similar time-dependent sensitivities in which daily treatment of 2 or 6h over three days did not induce apoptosis while significant cell death was observed when the treatment time was extended to 16-24h daily. In contrast, short, daily pulse treatment of 2-6h in cell lines (MV4-11, MOLM-13, SJSA-1) over three days was sufficient to induce cell death.

Conclusions ASTX295 is a potent antagonist of the MDM2-p53 interaction. Collectively, our *in vitro* data suggest that a shorter exposure to ASTX295 (up to 12h), may help to spare healthy bone marrow cells whilst killing tumor cells. Hence, intermittent exposure to an MDM2-p53 antagonist could favourably modulate its therapeutic index. The predicted short plasma half-life of ASTX295 should provide flexibility in controlling the duration of exposure *in vivo*, potentially enabling a more bone-marrow sparing approach to MDM2-p53 antagonism to be utilised.

#3334 Combined treatment with PG3 and Nelfinavir induced synergistic apoptosis though sustained activation of integrated stress response.

X. Tian, W. S. El-Deiry;
Brown University, Providence, RI

Integrated stress response (ISR) activation has been linked to many human diseases, including cancer and neurological diseases. The ISR controls protein synthesis and proteostasis. ISR main effector ATF4 transcriptional factor regulates the balance between survival and cell death. Under acute ISR, ATF4 promotes cell adaptation and survival. Sustained ISR leads to ATF4-mediated apoptosis. In many cancers, mutations or overexpression of oncogenes, results in enhanced cell proliferation and increased protein synthesis, which activate the ISR. Therefore, protein translation is reduced to maintain proteostasis. In other words, many cancers are primed by the ISR. Therefore, additional push by small molecule ISR-inducers will disrupt the balance and force cancer cells to enter apoptosis. Nelfinavir activates ATF4 through inhibition of eIF2α specific phosphatases CReP and GADD34. PG3 upregulates ATF4 through the HRI/eIF2α/ATF4 pathway. We hypothesize that combined treatment of PG3 and Nelfinavir will sustain upregulation of ATF4, and lead to ATF4-mediated cell apoptosis. Cell viability assays indicated that the combined treatment potently and synergistically inhibited cell viability in colorectal cancer cell lines HT29, SW480 and HCT116 $p53^{-/-}$, osteosarcoma cell line U2OS and breast cancer cell lines MCF7 and T47D. The combined treatment sustained the induction of ATF4 and enhanced the expression of its proapoptotic target genes, CHOP and PUMA, and cell apoptosis. We confirmed that the enhanced induction of ATF4, CHOP and PUMA is through the ISR because ISRIB (ISR inhibitor) blocked the combined treatment-induced upregulation of ATF4, CHOP and PUMA.

#3335 A novel and potent IRE1α RNase inhibitor, HM100168 as a promising therapeutic strategy in solid cancers.

J. Kim, S. Jung, M. Kim, W. Park, J. Byun, S. Park, M. Lee, Y.-Y. Kim, J. Park, S. Hong, M. Kim, Y. Ahn;
Hanmi Pharmaceutical Co., Ltd., Hwaseong-si, Korea, Republic of

Protein folding homeostasis in the endoplasmic reticulum (ER) is regulated by a signaling network called the unfolded protein response (UPR). Inositol-requiring enzyme 1α (IRE1α) is an ER membrane-resident kinase/RNase that mediates signal transmission in the most evolutionarily conserved way of the UPR. The IRE1α-XBP1 pathway, one of the most essential branches of the UPR, is activated in various types of cancer. When IRE1α is activated, the spliced form of XBP1 (XBP1s) is generated to activate the transcription of many pro-survival genes to prevent cellular death and relieve cellular stress. IRE1α plays an instrumental pro-tumoral role in various cancers, such as glioblastoma, myeloma, lung adenocarcinoma, and breast cancers, as well as high IRE1α activity is associated with poor prognoses. Moreover, IRE1-XBP1 plays an essential role in the UPR and ER stress responses, which have been implicated in the development of drug resistance. Thereby, blockade of the IRE1α-XBP1 pathway is crucial as it is considered as a potential anti-cancer strategy. Here, we developed a potent and selective IRE1α RNase inhibitor, which have a hydroxy-aryl-aldehydes (HAA) moiety that binds to IRE1α within the RNase catalytic site. Our lead compound, HM100168, potently inhibited the RNase activity of human IRE1α at nanomolar concentrations without affecting its kinase activity. Experiments were performed on MCF7 breast cancer cells to confirm the inhibitory effect in the mRNA and protein levels of XBP1s, which was increased by tunicamycin (TM), a ER stress inducer. HM100168 strongly inhibited XBP1s levels in a dose-dependent manner, displaying the potent IC_{50} values. We tested cell growth inhibition activity in 3D as well as 2D cell culture condition of various cancer cell lines. Interestingly, HM100168 effectively inhibited cell proliferation of diverse cancer cell lines in both 2D and 3D culture condition. In addition, we explored the promising anti-cancer effects of HM100168 and its synergistic potential when combined with anti-tumorigenic agents. As a result, HM100168 in combination with anti-tumorigenic agents significantly enhanced suppression of tumor growth in human cancer cell transplanted mice. In conclusion, we have identified a novel compound with unique properties that specifically blocked the endonuclease activity of IRE1α. HM100168 inhibited IRE1α endonuclease activity, without affecting its kinase activity after endoplasmic reticulum stress *in vitro*. The identification of this novel IRE1α inhibitor supports the hypothesis that the IRE1α-XBP1 axis is a promising target for anticancer therapy. Also, co-targeting of IRE1α-XBP1 in combination with anti-tumorigenic agents can be considered a novel approach to overcome cancer resistance. Further preclinical studies will be performed and reported soon after the establishment of a preclinical candidate.

#3336 Regulation of liver X receptor protein stability by novel ligands in pancreatic cancer cells.

A. Bagchi, K. T. Gamage, S. R. Gilbertson, C.-Y. Lin;
University of Houston, Houston, TX

Liver X Receptors (LXRs) are nuclear receptors that act as ligand-modulated transcription factors. LXRs are overexpressed in various cancers, including pancreatic cancer, and targeting LXR with small molecule ligands has emerged as a promising therapeutic strategy in cancer. Current small molecule LXR ligands were originally developed for the treatment of atherosclerosis and other metabolic diseases. To identify ligands specifically targeting cancer cells, we screened a focused library of drug-like molecules predicted to bind to LXR using molecular docking. In the screen, novel LXR ligand GAC0001E5 (1E5) exhibited significant anti-proliferative effects in human pancreatic ductal adenocarcinoma (PDAC) cell lines. Functionally, 1E5 is an LXR inverse agonist which decreases LXR target gene expression and a “degrader” of LXR proteins following prolonged treatment. We posit that this novel ligand inhibits PDAC cells by downregulating the expression of LXR target genes. To test this hypothesis, we treated cancer cells with the previously described LXR inverse agonist SR9238 and examined its effect on cancer cell proliferation. Interestingly, treatments with SR9238 had no effect on pancreatic cancer cell proliferation as compared to the novel ligand 1E5 and the 1E5 derivative KD-95, suggesting that LXR inverse agonism was insufficient to inhibit cell proliferation. To determine whether SR9238 has similar effects on LXR protein levels as novel ligands, we performed western analysis of protein expression following ligand treatment. In contrast to the novel ligands 1E5 and KD-95, treatments with SR9238 increased LXR protein levels. Furthermore, time-course studies in cycloheximide treated cells indicated that novel ligands decreased protein stability whereas SR9238 had the opposite effect. Inhibition of proteasomal degradation and autophagy abolished the effects of 1E5 and KD-95 in a cell line-dependent manner. Related to these observations, previously published data revealed that knockdown of LXR expression greatly diminished PDAC cell proliferation. Taken together, these findings indicate that LXR expression is essential in pancreatic cancer cells and suggest that the novel ligands may disrupt its involvement in protein-protein interactions and non-genomic mechanisms.

#3337 Inhibition of KIF18A leads to mitotic arrest and robust anti-tumor activity in chromosomally instable tumors.

M. S. Lynes, S. Khan, T. Hotz, B. A. Sparling, M.-M. Zablocki, D. Gotur, P. Boriack-Sjodin, K. W. Duncan, S. J. Blakemore, S. J. Silver, R. A. Copeland; Accent Therapeutics, Lexington, MA

KIF18A is a plus-end directed kinesin known to play a role in mitosis by facilitating chromosome alignment and spindle microtubule dynamics. Knockdown or knockout of KIF18A has been shown to inhibit proliferation in cells with whole genome doubling or aneuploidy, cellular states characterized by chromosomal rearrangements. These alterations render cells particularly vulnerable to disrupted mitosis upon KIF18A loss. As such, KIF18A is a compelling target in a subset of tumors with chromosomal instability (CIN), which have ongoing chromosomal segregation defects. We have identified potent and selective small molecule inhibitors of KIF18A. A proprietary tool compound, ATX020, inhibits KIF18A ATPase activity with an IC_{50} of 14.5 nM; KIF18A is selectively inhibited over other kinesins including CENPE (IC_{50} > 10 µM) and EG5 (IC_{50} 5.87 µM). ATX020 exhibits robust cellular activity, with anti-proliferative activity observed in chromosomally instable ovarian cancer cell lines such as OVCAR-3 (IC_{50} 53.3 nM) and OVCAR-8 (IC_{50} 0.54 µM). Upon treatment with ATX020, Annexin V is robustly induced in sensitive cell lines, demonstrating that KIF18A-dependent cell lines undergo apoptosis upon KIF18A inhibition. In KIF18Ai sensitive cells, a dose-dependent upregulation of phospho-Histone H3 and gamma-H2AX is observed upon ATX020 treatment in OVCAR-3 and OVCAR-8 cells, consistent with the induction of mitotic arrest and DNA damage. In contrast, CIN negative Ovarian cancer cells that are insensitive to KIF18A loss, such as A2780 and OVK18, proliferate normally upon ATX020 treatment, and Annexin V, phospho-Histone H3, and gamma-H2AX are not induced. In sensitive cell lines, ATX020 induces a dose-dependent cell cycle arrest in G2/M, consistent with the role of KIF18A in facilitating mitosis. OVCAR-3 cells treated with ATX020 exhibit fragmented nuclei and malformed mitotic spindles, in contrast to A2780 cells where cell division is unaffected, suggesting that KIF18A is dispensable in CIN negative cells. This selective dependency is also observed *in vivo*, where administration of ATX020 leads to dose-dependent tumor growth inhibition in an OVCAR-3 cancer cell line-derived xenograft model, with significant tumor regression observed at 100 mpk/day. In contrast, OVK18 tumors are unaffected by ATX020 administration, as expected based on the lack of cell cycle and proliferation effects in that cell line. Together, these data demonstrate a critical role for KIF18A in facilitating mitosis in a subset of chromosomally instable cells. These effects are selective, with KIF18A-independent cell lines proceeding through the cell cycle normally in the presence of inhibitors. Small molecule inhibition of KIF18A is therefore expected to have robust efficacy in solid tumors with high levels of chromosomal instability such as Ovarian cancer.

#3338 Development of a CK2α inhibitor for treatment of wnt-driven colorectal cancer.

D. Cawkill;
Apollo Therapeutics Ltd, Cambridge, United Kingdom

A novel, potent and highly selective orally bioavailable small molecule inhibitor of Casein Kinase 2α (CK2α) has been developed and validated in pre-clinical models of wnt-driven colorectal carcinoma; and is poised to enter clinical development.CK2α is considered as a positive regulator of wnt signaling and tumorigenesis. The wnt pathway is known to be sensitive to and amplified by CK2α activity at multiple nodes and can be inhibited by loss of CK2α function. The human genetics of colorectal cancer (CRC) have been well characterized and approximately 80% tumors are identified as being wnt pathway mutation driven. CRC tumors can be further stratified into consensus molecular subtypes (CMS), with iCMS2 representing 37% of CRC patients, being characterized by ongoing wnt pathway upregulation. Development of CK2α inhibitors as a targeted therapy for CRC is therefore mechanistically well aligned to the wnt signaling drive and may serve as a promising therapeutic strategy for this cancer. A novel small molecule binding site on CK2α has been exploited to design and develop an inhibitor with K_i of 95 pM and exquisite selectivity over the kinome. This inhibitor has been comprehensively characterized using *in vitro*, *ex vivo* and *in vivo* pharmacology studies. Cellular mechanism of action studies in CRC cell lines have quantified the potency of target engagement, inhibition of known CK2α phospho-sites, inhibition of tumorigenic wnt pathway activity, and induction of apoptosis. This CK2α inhibitor was also profiled in a high content screen of CRC patient-derived organoids established from various driver mutation backgrounds. Use of these *ex vivo* models has validated the potent cytotoxic activity of CK2α inhibition in tumor samples with wnt-driven characteristics and highlights the potential therapeutic efficacy of CK2α inhibition in this setting. *In vivo* CRC xenograft studies have confirmed anti-tumor efficacy and developed the understanding of pharmacokinetic pharmacodynamic relationship between free plasma concentration of drug and inhibition of CK2α-specific biomarker in the tumor. The preclinical data presented establishes the strong rationale for clinical development of a novel CK2α inhibitor for the treatment of locally advanced or metastatic solid tumors, with an emphasis on wnt-driven CRC.

#3340 RMC-5127, a first-in-class, orally bioavailable mutant-selective RASG12V(ON) inhibitor is central nervous system (CNS)-penetrant and demonstrates anti-tumor activity in a preclinical intracranial xenograft model.

Z. Chen, A. Eriksson, B. Lee, J. Dinglasan, N. Montazer, J. Cregg, A. Edwards, K. Sanders, J. A. M. Smith, D. Wildes, M. Singh, Z. Wang, J. Jiang; Revolution Medicines, Inc., Redwood City, CA

Patients with advanced cancers harboring activating mutations in RAS, particularly those with non-small cell lung cancer, often develop brain metastases leading to increased morbidity and mortality. $KRAS^{G12V}$ is the second most frequent RAS mutation in RAS-addicted cancers, including pancreatic cancer (34 %), colorectal cancer (21 %), and non-small cell lung cancer (19%). RMC-5127 is an orally bioavailable, mutant-selective tri-complex inhibitor of the GTP-bound (ON) form of RAS^{G12V}. RMC-5127 non-covalently binds to an abundant intracellular chaperone protein cyclophilin A (CypA), resulting in a binary complex that engages RAS^{G12V}(ON) to form a high-affinity tri-complex that sterically inhibits RAS binding to effectors. RMC-5127 drove deep suppression of RAS pathway activity, inhibited cell proliferation, and induced apoptosis in a panel of $KRAS^{G12V}$ mutant human cancer cells *in vitro* but only caused submaximal inhibition in the panel of K/N/HRAS wildtype cancer cells, indicative of selectivity for $KRAS^{G12V}$ over K/N/HRAS wildtype. Repeated oral dosing of RMC-5127 resulted in profound and durable anti-tumor activity in subcutaneous CDX and PDX models of $KRAS^{G12V}$ mutant NSCLC, PDAC, and CRC *in vivo*. Dose-dependent exposure of RMC-5127 was observed in the whole brain of naïve mice, indicating the compound is brain penetrant. An intracranial xenograft model of $KRAS^{G12V}$ tumors was established in immunodeficient mice to assess the CNS anti-tumor activity of RMC-5127. The intracranial tumor exposure of RMC-5127 was comparable with that observed in the whole brains of naïve mice and was sufficient to drive robust pharmacodynamic responses in the brain tumor. Moreover, RMC-5127 exhibited profound and durable anti-tumor activity in the intracranial model, with tumor regressions at well-tolerated doses. The anti-tumor activity of RMC-5127 in intracranial tumors was consistent with that in subcutaneous tumors at equivalent tumor exposures. In conclusion, these preclinical data demonstrate that RMC-5127 is a CNS-penetrant RAS^{G12V}(ON) inhibitor and support further study to determine the potential to benefit patients with advanced RAS^{G12V}-mutated cancers, including those that have developed or are at risk of developing brain metastases.

#3341 Targeting CXCR4 via the small molecule inhibitor NMX1 as a therapeutic strategy to treat high-risk malignancies.

Patrick Sipila[1], Son Tran[1], Chunfen Zhang[1], Laura G. Corral[2], Kyle W. H. Chan[2], Cathy A. Swindlehurst[2], Aru Narendran[1]

[1]Department of Oncology, University of Calgary, Calgary, AB, Canada,[2]NovoMedix, San Diego, CA

Introduction: Cytokines are secreted by various cells of the immune system, endothelium, and stroma that play a critical role in cell survival. The activation of C-X-C chemokine receptor type 4 (CXCR4) by its ligand SDF-1 leads to signaling by the AKT and mTOR pathways. CXCR4 is highly expressed in several types of cancer and contributes to tumor growth, metastasis, and resistance to therapy. Interleukin 11 (IL-11) is a cytokine that often drives disease progression, as well as contributing to tumor immune evasion. NMX1 (NovoMedix) is a novel oral small molecule that inhibits mTOR signaling, CXCR4 expression, IL-11 secretion, and activates AMPK. In animal models of breast cancer, NMX1 effectively prevented tumor growth and metastasis, while also protecting from doxorubicin-induced cardiotoxicity. In this study, we investigated the anticancer activity of NMX1 in preclinical models of high-risk pediatric and adult malignancies.
Methods: Cell viability assays using alamar blue were performed in a panel of pediatric and adult cancer cells, including leukemia, brain, breast, lung, neuroblastoma, and sarcoma. Cells were treated with increasing concentrations of NMX1 ranging from 250 nM to 16 µM for 96 hours, followed by determination of half maximal inhibitory concentrations (IC_{50}). To validate target modulation, the level of IL-11 and CXCR4 was determined by ELISA and immunoblot, respectively. Protein kinase activity was assessed by phosphorylation levels. Induction of apoptosis was confirmed by caspase-mediated PARP cleavage. To identify effective drug combinations, NMX1-treated cells were screened with a comprehensive drug library. Synergy was evaluated in the top candidates by dose-response matrices and SynergyFinder. Safety and tolerability was tested in animal models.
Results: NMX1 treatment induced cytotoxicity at micromolar concentrations in diverse types of cancer, with IC_{50} values ranging from 0.2-8.7 µM and 0.4-4.4 µM for leukemia and solid tumor cells, respectively. NMX1 induced cancer cell death by PARP cleavage and apoptosis. Mechanistically, CXCR4 expression, mTOR signaling, and IL-11 secretion were decreased upon treatment with NMX1, validating effective target modulation. The drug combination screen identified several candidates in a tumor type-dependent manner. Synergistic effects were observed using NMX1 combined with clinically relevant concentrations of rucaparib, linsitinib, and crizotinib, which target PARP, IGFR, and c-MET, respectively.
Conclusions: Our study shows antitumor activity by NMX1 through inhibition of CXCR4, IL-11, and mTOR signaling, providing an effective therapeutic strategy for high-risk and refractory malignancies. Preclinical data on feasible drug combinations and biological correlates of activity support development of early phase clinical studies involving NMX1.

#7277 Discovery of INV-9956, an orally available and highly selective Cyp11A1 inhibitor for the treatment of castration-resistant prostate cancer with drug resistant AR mutations.

C. Bai, D. Chen, Z. Xia, S. Huang, L. Lin, Z. Zeng, J. Su, Y. Sun;
IONOVA Life Science Co., Ltd., Shenzhen, China

Androgen Receptor (AR) signaling plays a profound role in prostate cancer and development. Efforts in harnessing androgen and AR axis for castration-resistant prostate cancer treatment have led to discovery of several therapeutics, including AR antagonists and Cyp17 inhibitors. However, resistance to these approved therapeutics has emerged, and remained a significant unmet medical need. Among the prominent resistance mechanisms of action are restored androgen signaling via AR amplification and overexpression, and gain-of-function mutations occurring at AR ligand binding domain that can be agonized by existing AR antagonists and/or non-androgenic steroids such as glucocorticoids. Targeting Cyp11A1 that catalyzes the formation of pregnenolone is effective to ablate biosynthesis of androgens and all steroids and thus holds promise to deliver coverage of a significant percentage of drug resistant AR mutations and benefit CRPC patients post treatment with AR antagonists or Cyp17 inhibitors. Here we present discovery and characterization of INV-9956, an orally available, selective, and potent Cyp11A1 inhibitor with well-acceptable pharmacokinetic properties. INV-9956 potently inhibits biosynthesis of pregnenolone and other androgens in H295R cells with IC50 at single-digit nanomolar, suppresses proliferation of prostate cancer cell lines harboring major clinically acquired drug resistant AR LBD mutations, such as AR L702H using coculture assays. Orally administered INV-9956 showed consistent dose dependent PK/PD correlations across animal species. Particularly, INV-9956 displayed pronounced tumor inhibition superior to known competitors in a CRPC VCaP xenograft model and in a “humanized” animal model. Furthermore, INV-9956 displayed a good tox profile in 14-day repeated dosing rat and dog studies, supported by a high selectivity to Cyp11A1 over other Cyp family members, clean hERG and mini-Ames, and no significant off-target activity in a safety panel screen. The promising preclinical profiles of INV-9956 lend strong support to its potentials in addressing unmet needs in CRPC treatments and warrant clinical development.

EXPERIMENTAL AND MOLECULAR THERAPEUTICS: Novel Therapeutics
Poster Session

#3344 Widespread *BRCA1/2*-independent homologous recombination defects are caused by alterations in RNA binding proteins.

B. Kaundal[1], D. J. McGrail[2], Y. Li[1], R. S. Smith[3], B. Feng[4], H. Dai[1], L. Hu[1], B. Dennehey[1], S. Awasthi[1], M. L. Mendillo[3], A. K. Sood[1], G. B. Mills[5], S.-Y. Lin[1], S. Yi[6], N. Sahni[1];

[1]UT MD Anderson Cancer Center, Houston, TX, [2]Center for Immunotherapy and Precision Immuno-Oncology, Cleveland Clinic, Cleveland, OH, [3]Northwestern University Feinberg School of Medicine, Chicago, IL, [4]GSK Oncology Experimental Medicine Unit, Waltham, MA, [5]Knight Cancer Institute, Oregon Health and Sciences University, Portland, OR, [6]Livestrong Cancer Institutes, Department of Oncology, Dell Medical School, The University of Texas at Austin, Austin, TX

Summary: Defects in homologous recombination DNA repair (HRD) both predispose to cancer development and produce therapeutic vulnerabilities, making it critical to define the spectrum of genetic events that cause HRD. However, we found that mutations in *BRCA1/2* and other canonical HR genes only identified 10-20% of tumors that display genomic evidence of HRD. Using a networks-based approach, we discovered that over half of putative genes causing HRD originated outside of canonical DNA damage response genes, with a particular enrichment for RNA binding protein (RBP)-encoding genes. These putative drivers of HRD were experimentally validated, cross-validated in an independent cohort, and enriched in cancer-associated GWAS loci. Mechanistic studies indicate that some RBPs are recruited to sites of DNA damage to facilitate repair, whereas others control the expression of canonical HR genes. Overall, this study greatly expands the repertoire of known drivers of HRD, with implications for basic biology, genetic screening, and therapy stratification.

#3345 PP1 phosphatase complex at the hub of the integrated stress response: A potential therapeutic target in multiple myeloma.

S. Xiong[1], J. Zhou[2], T. Tan[2], S.-M. Toh[2], T.-H. Chung[2], T. Sanda[2], W. Chng[3],

[1]Department of Medicine, Yong Loo Lin School of Medicine, National University of Singapore, Singapore, Singapore, [2]Cancer Science Institute of Singapore, National University of Singapore, Singapore, Singapore, [3]Department of Hematology-Oncology, National University Cancer Institute of Singapore, National University Health System, Singapore, Singapore

Protein phosphatase-1 (PP1) is a class of eukaryotic enzyme that catalyzes more than half of the phosphoserine/threonine dephosphorylation reactions, and plays essential roles in cell division, glycogen metabolism and protein synthesis. The substrate specificity of PP1 holoenzyme complex is mediated by PP1-interacting proteins and its catalytic subunits. Of note, PPP1R15B/CReP and PPP1R15A/GADD34 are regulatory subunits of PP1 complex that regulates global protein synthesis and mRNA translation through eIF2α dephosphorylation. Notably, PPP1R15B is constitutively expressed, whereas the expression of PPP1R15A is stress-inducible. Previous studies showed that multiple myeloma (MM), a hematological malignancy arising from immunoglobulin-secreting plasma cells, is characterized by continual ER stress and high dependency on the unfolded protein response (UPR). The integrated stress response (ISR) activated by eIF2α phosphorylation is the fastest reaction pathway of the UPR; however, its functional role and therapeutic potential in MM remains largely unknown.

In this study, we performed gene expression analysis and super-enhancer (SE) profiling in MM cell lines, primary patient samples, normal CD138+ plasma cells and memory B cells. we found that PPP1R15B is highly expressed in MM cells as compared to healthy controls, but did not observe significant upregulation of PPP1R15A in MM cells. In addition, higher expression of PPP1R15B predicted poor overall survival of MM patients, suggesting its clinical relevance in MM pathogenesis. Depletion of PPP1R15B significantly reduced cell viability, proliferation and induced G2/M phase cell cycle arrest. Gene Ontology analysis of downregulated genes in response to PPP1R15B knockdown indicates significant association with the UPR pathway. Immunoblot analysis showed activation of ER stress pro-apoptotic executors PUMA, NOXA, and cleavage of caspase-12 in PPP1R15B knockdown cells.

Furthermore, we examined the therapeutic effects of eIF2α dephosphorylation inhibitors, Salubrinal and Raphin1, on MM cells. Raphin1 is a selective inhibitor of PPP1R15B that binds strongly to the PPP1R15B-PP1c complex, whereas Salubrinal inhibits both PPP1R15A-PP1c and PPP1R15B-PP1c complex. Our data showed that both Salubrinal and Raphin1 inhibited MM cell proliferation in a dose-dependent manner, while sparing normal plasma cells. MM cell lines with elevated PPP1R15B expression level were more sensitive to Salubrinal or Raphin1 than those with lower PPP1R15B level. Similar changes in the expression patterns of ISR-related genes were observed in response to eIF2α dephosphorylation inhibitors. Taken together, our study suggests that targeting PPP1R15B-PP1c complex or maintaining eIF2α hyperphosphorylation may serve as a new therapeutic approach in MM, which warrants further investigation.

#3346 JMJD6 as a novel tumorigenic factor and therapeutic target in group 3 (MYC-driven) medulloblastoma.

M. Kling[1], D. Kumar[2], S. Ray[2], S. Joshi[2], D. Coulter[2], **N. K. Chaturvedi**[2];
[1]Creighton University, Omaha, NE, [2]University of Nebraska Medical Center, Omaha, NE

Medulloblastoma (MB) is the most common type of childhood brain cancer worldwide. Although current treatment with surgery and extensive chemoradiation has led to increased survival rates, many MB patients still die from the disease. Moreover, surviving patients suffer severe long-term side effects as a consequence of treatment. It is therefore crucial to develop more effective and less toxic therapies. The most aggressive subtype of MB tumors often exhibits amplification or overexpression of the MYC oncogene. Patients with MYC-amplified MB exhibit a high frequency of cerebrospinal tumor dissemination, often experience treatment resistance and have extremely poor prognoses. While the MYC oncogene is established as the oncogenic driver in Group 3 MB, it has remained undruggable. Thus, targeting regulatory components of MYC and the signaling pathways regulated by it is of great potential therapeutic value. Studies have revealed that MB has very few germline mutations in cancer predisposition genes, suggesting that dysregulated epigenetic pathways might be critical in MB pathogenesis. Particularly, dysregulation of epigenetic modifiers, including histone methyltransferases and histone demethylases, is very common in Group 3 MB, compared to other MB subgroups. Therefore, it is important to identify such epigenetic modifiers that may have controls on MYC and its tumorigenic activities and explore these as the epigenetic drug-candidate targets in Group 3 (MYC-driven) MB. In this regard, we found that protein arginine demethylase Jumonji C domain-containing protein 6 (JMJD6), an emerging key epigenetic enzyme in cancers, is a novel regulator of MYC expression in MYC-driven MB. We observed high levels of JMJD6 that not only mirror MYC expression in the most aggressive MB but also correlate with poor outcomes in these patients. Knockdown of JMJD6 decreased MYC expression, cellular proliferation/survival and stemness in MYC-amplified MB cells. Mechanistically, our results revealed that JMJD6 forms complexes with proteins involved in maintaining and regulating the promoter-pause at super-enhancers, suggesting that JMJD6 can regulate MYC at the transcription level. Moreover, our in vivo analyses of JMJD6 inhibition, either with inducible gene knockdown or a pharmacologic small molecule inhibitor, demonstrated anti-MB potential with suppressed MYC expression. Based on this background and preliminary observations, we hypothesize that JMJD6 plays crucial roles in the most aggressive MB by regulating MYC expression and hence MYC-driven tumorigenesis. Accordingly, we hypothesize that targeting the JMJD6-MYC axis by JMJD6 inhibition can serve as a powerful therapeutic strategy for MYC-driven MB.

#3347 KIFC1 inhibition elicits antineoplastic activity in small cell lung cancer by inducing anaphase catastrophe.

N. Nakagawa[1], M. Tokunaga[1], M. Ka[1], Y. Sugiura[1], T. Iida[1], T. Ando[1], K. Watanabe[1], X. Liu[2], E. Dmitrovsky[2], H. Kage[1], M. Kawakami[1];
[1]University of Tokyo, Tokyo, Japan, [2]Frederick National Laboratory for Cancer Research, Frederick, MD

Cancer cells often have more than two centrosomes (supernumerary centrosomes) and this is one of the hallmarks of cancer. We previously demonstrated that CDK2 antagonism inhibits clustering of supernumerary centrosomes at mitosis leading to multipolar cell division and apoptotic death in non-small cell lung cancer. This antineoplastic process was designated anaphase catastrophe. Anaphase catastrophe can preferentially affect cancer cells sparing normal cells with two centrosomes. On the other hand, as CDK2 functions in normal cell cycle progression, its inhibition can also affect normal and malignant cells. Identification of a novel drug target that would preferentially cause anaphase catastrophe is needed. The motor protein KIFC1 affects centrosome clustering. Small cell lung cancer (SCLC), known for its poor prognosis with limited therapeutic options, displays disruptions in the cell cycle checkpoint mechanism due to inactivation of p53 and RB. We hypothesized SCLC was susceptible to mitotic abnormalities, including anaphase catastrophe. In this study, we explored the possibility of KIFC1 as a novel therapeutic target that triggers anaphase catastrophe in SCLC. In-silico GEO database analysis revealed elevated levels of KIFC1 and PLK4 in SCLCs compared with other cancers and normal tissues. PLK4 plays a key role in centrosome amplification. Our in-silico analysis results imply that centrosome amplification and their clustering frequently occur in SCLC. We performed in-vitro functional analysis of KIFC1 inhibition in SCLC cell lines (NCI-H146, SHP77, NCI-H209, and NCI-H524 cells), using siRNAs and CRISPR-Cas9 system for genetic inhibition and AZ82, a specific KIFC1 inhibitor, for pharmacologic inhibition of KIFC1. Cell proliferation was measured by the CellTiter-Glo Luminescent Assay and apoptosis was scored by annexin V and PI staining followed by flow cytometry analysis. Cell growth was reduced and apoptosis was statistically significantly increased after genetic inhibition of KIFC1 by siRNAs and by use of the CRISPR-Cas9 system in SCLC cell lines. These antineoplastic effects also occurred after AZ82 treatments, in a dose-dependent manner in these SCLC cell lines. To examine the mitotic status of SCLC cells after KIFC1 inhibition, SCLC cells were stained with α-tubulin antibody and DAPI before analysis with a fluorescence microscope. Besides normal bipolar mitotic cells, multipolar mitotic cells were observed, and their population was increased after KIFC1 knockdown with siRNAs. This indicated that clustering of supernumerary centrosomes was inhibited by targeting KIFC1 in SCLC cells. Taken together, KIFC1 is a potential therapeutic target to induce anaphase catastrophe in cancer cells. Targeting KIFC1 is a novel therapeutic strategy to consider for SCLC that currently has limited treatment options.

#3348 Identification of circSPINT2 as a tumor suppressive circular RNA sensitizing lung cancer to 3rd generation EGFR-TKI treatment.

M.-L. Wang[1], S.-H. Shiou[1], Y.-C. Chen[1], M.-L. Tsai[1], N. Verusingam[1], A.-K. Ong[2];
[1]Taipei Veterans General Hospital, Taipei, Taiwan, [2]Universiti Tunku Abdul Rahman, Selango, Malaysia

Introduction: Lung cancer remains a high incidence and mortality globally. Adenocarcinoma is the most common type of lung cancer with around 50% of patients in Asia expressing mutated EGFR, which makes EGFR an effective therapeutic target to treat lung adenocarcinoma (LAC). Unfortunately, resistance to EGFR-TKI often occurs in patients through either dynamic EGFR mutation, driver oncogenic pathway shift, or transdifferentiating to evade EGFR-TKI treatment. circRNAs are a type of RNA molecule with a circular shape. Their importance in several biological processes and disease progression was intensively studied recently, and have emerged as promising diagnostic, prognostic, and monitoring biomarkers for diseases like cancer. CircRNAs' unique circular structure and resistance to degradation make them robust candidates for non-invasive diagnostics of cancers.

Aims: This study aimed to identify and investigate the involvement of a novel circular RNA (circSPINT2) in acquired resistance against the 3rd generation EGFR-TKI Osimertinib.

Materials & Methods: Comparative circRNA sequencing (circRNA-Seq), qRT-PCR, sanger sequencing, and RNase R treatment were applied to identify and verify the identity of Osimertinib-resistance-related circRNA. Biotinylated circRNA pull-down assay, miRNA-seq, and in-silico analysis were employed to delineate the downstream miRNA-mRNA regulatory axis. Osimertinib-resistant mouse xenograft model was established to explore the molecular mechanisms associated with both circSPINT2 and Osimertinib resistance.

Results: We identified circSPINT2 as particularly downregulated in Osimertinib-resistant cell lines (OR) using circRNA-Seq. Overexpression of circSPINT2 in resistant cells increased cellular sensitivity to Osimertinib, whereas knockdown of circSPINT2 conferred Osimertinib resistance in parental cells. The circSPINT2-dependent regulation of Osimertinib sensitivity is mediated through modulating apoptosis. *In-vitro* analysis indicated high circSPINT2 increased tumor suppressor RBP1 expression by sequestering oncogenic hsa-miR-1296 further improving Osimertinib sensitivity. Molecular and histologic analysis of subcutaneous xenograft tumors corroborated our *in-vitro* results.

Conclusion: Our study demonstrated circSPINT2 functions as a tumor suppressor, improving Osimertinib sensitivity via the hsa-miR-1296/RBP1 axis. circSPINT2 may serve as a prognostic and cancer biomarker to monitor Osimertinib resistance in LAC patients.

#3349 Identification of new potential vulnerabilities for differentiation-based therapeutic strategies against osteosarcoma.

C. Cascini[1], D. Lecis[1], V. Cancila[2], K. Scotlandi[3], C. Tripodo[2], M. P. Colombo[1], **C. Chiodoni**[1];
[1]Fondazione IRCCS Istituto Nazionale dei Tumori, Milan, Italy, [2]University of Palermo School of Medicine, Palermo, Italy, [3]IRCCS Istituto Ortopedico Rizzoli, Bologna, Italy

Osteosarcoma (OS), a mesenchymal bone tumor affecting mainly children and adolescents is characterized by a particularly aggressive behavior, with 20% of patients showing lung metastasis already at diagnosis. Current OS treatment strategies rely on multi-drug chemotherapy, and the prognosis for metastatic cases remains grim, underscoring the pressing need for novel therapeutic approaches. OS is considered a differentiation-related disorder, stemming from the inability of mesenchymal stem cells or osteoblastic progenitors to progress towards terminal differentiation. In our study we explored the impact of targeting ZEB1, a transcription factor known to play a pivotal role in maintaining mesenchymal and stemness characteristics in cancer, on OS cells. We employed CRISPR-Cas9 and shRNA interference techniques to inhibit ZEB1 expression in mouse immune competent OS models. In vitro, ZEB1 deficiency significantly diminished the stemness potential of OS cells, as assessed by spheroid formation assays, while promoting osteogenic differentiation. In vivo, ZEB1 deletion in OS cells led to a significant reduction in primary tumor growth. Tumors originating from ZEB1 KO cells exhibited a more differentiated morphology and higher extracellular matrix deposition compared to controls. Intriguingly, the absence of ZEB1 in tumor cells also influenced the immune infiltrate, with ZEB1-deficient tumors showing significantly fewer pro-tumoral CD206+ M2-like macrophages. This observation is in line with the significant down-modulation of CCL2 expression we detected in ZEB1 KO cells. When injected intravenously, ZEB1-deficient cells produced fewer and smaller lung metastases than control cells. Transcriptional changes induced by ZEB1 deletion were investigated by gene expression profile (GEP) and identified 849 down-regulated and 1093 up-regulated genes in ZEB1 knockout (KO) clones versus ZEB1-competent controls. Gene set enrichment analysis showed a down-modulation of pathways related to cellular proliferation and survival, such as MTORC1 signaling, MYC targets, GM2 checkpoint, E2F targets and oxidative phosphorylation in the absence of ZEB1. Single gene analysis identified among the most up-regulated genes in ZEB1-deficient cells Sfrp1, a negative regulator of the WNT/b-CAT pathway, which in turn regulates MYC, whose pathway is indeed repressed in ZEB1 KO cells. We hypothesize that a high expression of SFRP1 could vicariate the effects of ZEB1 inhibition on OS cell stemness, differentiation state, and in vivo aggressiveness, and therefore could act as a tumor suppressor, which could be potentially exploited for therapeutic strategies.

#3350 The pan-quadruplex drug QN-302 targets up-regulated genes in pancreatic cancer and in other cancer types and correlate with poor patient prognosis.

S. Neidle[1], A. A. Ahmed[1], T. Arshad[2];

[1]University College London (UCL), London, United Kingdom, [2]Qualigen Therapeutics Inc, Carlsbad, CA

We have previously disclosed (Ahmed et al, ACS Med Chem Lett, 2020) a novel small molecule G-quadruplex binding compound, QN-302, that is highly potent in pancreatic ductal adenocarcinoma (PDAC) cells and in several in vivo models for this disease. QN-302 was invented at University College London UK and has been subsequently developed by Qualigen Therapeutics Inc. It was cleared by the FDA in August 2023 for clinical evaluation and is currently in a Phase 1 clinical trial at select oncology centers in the USA. Genes that are significantly down-regulated by QN-302 are mostly up-regulated genes in human PDAC. We report here that some of these genes are also up regulated in other cancer types, whose expression frequently correlates with poor patient prognosis. We have used human cancer data from https://www.proteinatlas.org which contains pathology information based on mRNA and protein expression data from 17 different forms of human cancer, together with millions of in-house generated immunohistochemically stained tissue sections, images and Kaplan-Meier plots showing the correlation between mRNA expression of each human protein gene and cancer patient survival. We have revisited the RNA-seq data for QN-302 in PDAC MIA-PACA2 cells exposed to QN-302 for 24 hrs. (GSE151741 at https://www.ncbi.nlm.nih.gov/geo/) in detail and now identify a small group of eleven down-regulated genes, all with >3-fold expression changes. Interestingly all these genes and their gene products have been previously identified as playing a role in human PDAC (they also have varying roles in other cancer types). Some have been validated as anticancer targets. 10/11 of these genes (https://www.proteinatlas.org/) have been previously reported as being over-expressed in significant fractions of large (>150) groups of human cancer patients from The Cancer Genome Atlas (TCGA) project. Members of the PDAC susceptible gene panel are mostly disfavored in prostate, lung and breast cancer. However, the patient data does not discriminate between cancer sub-types nor does it show resistant data. They are especially favored in colorectal, liver and renal cancers, suggesting that QN-302 may have anticancer effects in these cancers as well as in PDAC. We also do not exclude the strong possibility that each cancer type also has its own group of G-quadruplex containing genes that are sensitive to QN-302.

#3351 Identifying novel therapies from unbiased screens in AML with MECOM re-arrangement.

C. E. Birdwell[1], W. C. Fiskus[1], C. P. Mill[1], T. M. Kadia[1], N. Daver[1], C. D. DiNardo[1], K. Sasaki[1], J. A. Davis[1], K. Das[1], H. Hou[1], M. Cerebelli[2], K. N. Bhalla[1]; [1]UT MD Anderson Cancer Center, Houston, TX, [2]NCATS, NIH, Bethesda, MD

EVI1 is a transcriptional regulator encoded from the MECOM locus (3q26.2). Aberrant EVI1 expression is observed in ~10% of *de novo* AML, of which about half are due to inv3(q21;q26.2) or t(3;3)(q21;q26.2) chromosomal rearrangements [3q26.2-r]. 3q26.2-r AMLs generally have a stem-like phenotype, are refractory to current therapy options and exhibit poor overall survival. Therefore, there is an unmet need to develop novel targeted therapies with improved efficacy in repressing EVI1 and its targets, thereby improving outcomes in AML with EVI1 overexpression. We conducted an unbiased high-throughput drug screen, utilizing a library of mechanistically annotated drugs (NCATS Mechanism Interrogation Plates [MIPE 5.0]), against seven AML cell lines (3q26.2-r: UCSD-AML1, HNT-34, AML191, AML194; non-3q26.2-r AML: SET-2, MV4-11, OCI-AML3). This exploited the mechanistic redundancy in the library to identify druggable, target-level dependencies in 3q26.2-r AML, exhibiting absolute potency and relative activity as compared to other AML subtypes. BRD4 was identified as an absolute dependency in 3q26.2-r AMLs. An unbiased epigenetic modifier CRISPR screen in UCSD-AML further confirmed BRD4 as a dependency, confirming previous reports of BET inhibition (BETi) efficacy in 3q26.2-r AML. Comparison of 3q26.2-r versus other AML cell lines also identified XIAP, mTOR, PIK3CA and Bcl-xL as druggable vulnerabilities in 3q26.2-r AML. In follow-up experiments, IAP family inhibitors/SMAC mimetics induced significantly more dose-dependent apoptosis in 3q26.2-r versus the other AML cell lines, which was associated with reduction of IAP proteins, p-ERK, MCL1 and Bcl-xL, but increase in levels of cleaved caspase-3 and PARP. BETi (mivebresib) also induced dose-dependent apoptosis, and reduced EVI1, c-Myc, c-Myb, IAP proteins, and CDK4/6, while increasing levels of HEXIM1 and cleaved PARP. Consistent with this, co-treatment of mivebresib with SMAC mimetic birinapant or IAP inhibitor LCL161 was synergistically lethal against 3q26.2-r cells. Co-targeting the other identified druggable vulnerabilities from the drug screen with BETi (mTOR/PI3K with BGT-226 and dactolisib, Bcl-xL with navitoclax and A1155463, as well as CBP/p300 (with GNE781, identified through the CRISPR screen), exerted synergistic lethality in 3q26.2-r AML cells. Finally, in a xenograft model of 3q26.2-r AML in immune-depleted mice, while monotherapy with LCL161 or dactolisib significantly reduced the AML burden with minimal toxicity, co-treatment with mivebresib and LCL161 or dactolisib was superior in reducing AML burden in the xenograft model. These findings demonstrate promising preclinical activity of BETi and IAP protein or mTOR/PI3K antagonists in the cellular models of AML with EVI1 overexpression. This supports the rationale to determine *in vivo* efficacy of these BETi-based combinations against this therapy-resistant AML sub-type.

#3352 A CRISPR-enabled function genomics profiling platform in acute leukemia: Updates from a pilot study of Function (Fx) Heme utilizing fresh patient samples.

K. C. Dykes[1], T. R. Tan[1], K. Hodel[2], K. Tran[2], M. Meyers[2], L. Hagmann[2], M. Baltay[2], P. Kilfeather[2], Y. Li[2], C. Schmedt[2], S. Sampath[2], S. Sampath[2], T. N. Tanaka[1], S. Corbel[2];

[1]UC San Diego Moores Cancer Center, San Diego, CA, [2]Function Oncology, San Diego, CA

Introduction: In this study we utilized a novel primary cell CRISPR/Cas9 profiling approach to identify gene dependencies in fresh acute myeloid leukemia (AML) and acute lymphoid leukemia (ALL) patient samples. The primary aim of this prospective study was to demonstrate the feasibility of the CRISPR-based personalized functional genomic testing with fresh patient samples in the clinical setting.

Methods: AML and ALL patient peripheral blood samples (10-16 mL) were obtained at time of initial diagnosis and/or at relapse, and if feasible post-treatment. Primary cells were transduced with lentivirus harboring Cas9 enzyme and a 'drug targets' sgRNA panel. Transduced cells were harvested at early (input) and Day 8 timepoints, and sgRNA distribution was assessed by amplicon sequencing of DNA barcodes. Changes in barcode abundance were quantitated and aggregated to calculate gene-level phenotype scores, enabling identification of gene dependencies.

Results: 37 patients were included in the study, 23 with AML, 9 with Philadelphia (Ph) (+) ALL, 5 with Ph (-) ALL. The majority of patients had adverse or poor risk disease. The average age of patients was 52.6, range 18-84. 23 were male, 14 female; 20 identified as white, 17 as other. 20 patients were sampled at initial diagnosis, 12 were sampled at time of relapse and 5 at time of refractory disease. Serial samples were collected from 9 patients. 34 patients received treatment following sample collection. The majority of patients received intensive chemotherapy or a hypomethylating agent with venetoclax, however 15 patients received some form of targeted therapy. At the time of the abstract submission, Fx Heme results were available for 23 patients and among these, we identified potential treatment targets in 10 samples (43%). Importantly, 60% of the positive samples have a dependency on a gene clinically targetable by an approved leukemia drug. In addition, our profiling platform enabled the discovery of novel druggable dependencies in 100% of the positive samples.

Conclusions: With this pilot study we demonstrated that utilizing small volume fresh patient samples to assess CRISPR-defined gene dependencies on targeted therapies in AML and ALL is feasible, timely, and results in clear Fx Heme dependency gene output. Our data indicates that CRISPR-based comprehensive functional profiling has the potential to add valuable information beyond traditional NGS methods to determine the optimal therapy for patients with AML and ALL. Future directions include translating further into the clinical setting and correlating Fx Heme dependence with response to targeted treatment in acute leukemia patients.

#3353 The emerging role of extracellular HSP90 in prostate cancer progression to a metastatic phenotype.

K. O'Neill, J. Zigmond, R. Bergan;
University of Nebraska Medical Center, Omaha, NE

Background: Metastasis is the central cause of lethal prostate cancer (PCa). Mechanisms regulating metastasis represent high-potential therapeutic targets for preventing development of lethal PCa. Inhibitors of extracellular heat shock protein 90 (eHSP90) have been shown to inhibit prostate cell motility. In contrast to the intracellular HSP90 (iHSP90), whose biology has been extensively studied, and whose therapeutic targeting is associated with systemic toxicity, the biology of extracellular HSP90 is not well understood. We undertook a series of investigations to better understand eHSP90 biology in PCa.
Methods: Human PCa cells were subjected to cellular stress by heat shock combined with serum starvation. Resultant conditioned media was probed for matrix metalloproteinase 2 (MMP-2) by zymography and subject to scratch-wound and Boyden chamber invasion assays. Expression of HSP90 and CDC37 was measured by Western blot. Plasma from patients with PCa and healthy controls was probed for eHSP90 by ELISA.
Results: We have examined expression of iHSP90 and eHSP90 after cellular stress, induced by heat shock and serum starvation, in human PC3, LNCaP, C4-2B, 1532NPTX and 1532CPTX PCa cell lines. Cell stress induces increased eHSP90 in all PCa cell lines examined. This is associated with a decrease in MMP-2 activity in conditioned media. Conditioned media from stressed cells was also shown to decrease invasion of PC3 cells, consistent with changes in MMP-2. Of high interest, the addition of protease inhibitors to conditioned media led to a complete reversal of the MMP-2 response: its activity increased with cellular stress. When measuring HSP90α in plasma from healthy controls (N = 20) and patients with PCa (N = 40, 20 localized and 20 metastatic), we demonstrated a significant (p=.001) >2 fold increase in PCa compared to control. Further, a significant increase in HSP90α was observed when low versus high T stage lesions were compared. There was no statistically significant difference in HSP90α for those with metastasis to regional lymph nodes, non-regional lymph nodes, bone, or liver.
Conclusion: We demonstrate that increased eHSP90 due to cellular stress is a response observed across all PCa cell lines examined and should be considered typical. Its association with extracellular MMP-2 activity is dependent on the presence of other proteases and indicates a complex regulatory mechanism. Examination of eHSP90 in humans supports its association with aggressive disease. These factors support further investigation of underlying biology and therapeutic opportunities.

#3354 Capturing tumor heterogeneity to personalize therapy in young patients with hormone receptor positive breast cancer.

I. Segatto[1], M. Mattevi[1], A. Dall'Acqua[1], L. Musco[1], F. Ruggiero[1], G. Di Giustino[1], A. Favero[1], G. Rampioni Vinciguerra[2], N. Crestan[1], L. Pellizzari[1], R. Spizzo[1], R. Bomben[1], F. Vit[1], A. Vecchione[2], L. Gerratana[1], F. Puglisi[1], S. Massarut[1], T. Perin[1], G. Baldassarre[1], **B. Belletti**[1];

[1]Centro di Riferimento Oncologico (CRO) di Aviano, IRCCS, Aviano, Italy, [2]Universita degli Studi di Roma La Sapienza, Roma, Italy

Background: Breast cancer (BC) in young women (Y) is a distinct entity in terms of prognosis. Although triple negative and HER2 positive subtypes are enriched in Y patients, the hormone receptor (HR) positive subtype (luminal, LBC) remains the most common. A thorough understanding of LBC biology in Y women has not been reached yet, also hampered by lack of appropriate models that faithfully recapitulate these tumors in molecular and preclinical studies.
Methods: To investigate molecular determinants of progression and therapeutic resistance, we collected a large panel of fresh specimens (N=226) from Y (< 40 years) and nY (>55 years) LBC patients, characterized by targeted sequencing and used to generate Patient-Derived Organoids (PDO) and Xenografts (PDX). A selected panel of Y and nY LBC patients (N=96), sharing similar clinical-pathological features, was used for whole exome sequencing (WES) and transcriptomic analyses.
Results: We generated stable LBC PDO (N=32, 13 from Y patients), with a success rate of 50% and stable LBC PDX (N=15, 11 from Y patients), with a success rate 17%. Our targeted panel of NGS, covering most mutated genes in LBC at high coverage (1000x), revealed a significantly higher number of Y patients displaying mutations in PIK3CA and in PIK3CA+TP53. However, these data were not observable in WES analyses (200x), likely because many of those mutations displayed a VAF < 5% (20% of PIK3CA and 30% of TP53). The transcriptomic analysis showed an enrichment in signatures of aggressiveness in the Y LBC subgroup. The EGF family member AREG (Amphiregulin) was the most enriched gene in tumors from pre- versus post-menopausal patients. Following validation in a larger panel of LBC, both at RNA and protein level, we tested the impact of AREG in LBC cell lines. AREG expression was timely induced by growth factor and hormonal stimulation. Furthermore, stimulation using amphiregulin induced the activation of EGFR and its downstream pathway, creating a positive feedback loop. Relevant to the Y LBC phenotype, a consistent and time dependent induction of AREG transcription was induced following estrogen and progesterone stimulation, indicating that, in LBC, AREG might act as a transcriptional target of ESR1. Finally, high levels of amphiregulin reduced response to tamoxifen and CDK4/6 inhibitors in LBC cells and PDOs.
Conclusions and Perspectives: Our study provides valuable molecular and biological insights into LBC in Y women. We identified distinct genetic and transcriptomic profiles, including PIK3CA and TP53 mutations and AREG overexpression, which may be exploited to plan more targeted and efficient treatments. The establishment of a living biobank of PDO and PDX from LBC patients of Y age will enable preclinical trials, facilitating discovery of biomarkers and therapeutic strategies tailored to the unique biology of Y LBC.

#3355 Unraveling the molecular mechanisms of glioma migration: Exploring the role of cell intrinsic and stromal ephrin receptor-ligand signaling.

J. Moon[1], X. Gao[1], P. Ding[1], F. Bilal[1], S. Rindhe[1], N. Gao[1], D. P. Dave[2], M. Henkemeyer[1], E. A. Maher[1], R. M. Bachoo[1];
[1]UT Southwestern Medical Center, Dallas, TX, [2]University of Texas at Arlington, Arlington, TX

Diffuse invasion, a hallmark of malignant gliomas, makes these tumors surgically incurable and is the ultimate cause of death. While glioma cells can migrate along blood vessels and in neuron-rich regions, their preferred route of migration is along white matter (WM) tracts, which allows tumor cells to spread to the contralateral hemisphere with devastating neurocognitive consequences. The underlying mechanisms of in vivo glioma cell migration are poorly understood. There is emerging evidence that glioblastoma multiforme (GBM) cells may hijack migration mechanisms used during brain development. Accordingly, we used a neonatal plasmid electroporation GBM model (CRISPR-Cas9, -Cre,gRNAs targeting NF1, p53, PTEN, and piggyBac-glast) to generate a highly penetrant diffusely invasive glioma models with preference for migration along myelinated fiber tracts including the corpus callosum (CC). To test the in vivo role of integrin-mediated migration, tumors were generated using conditional integrin β1f/f (ITGB1) or focal adhesion kinase (FAKf/f) mice. Both ITGB1 and FAK null GBM cells (confirmed by western blot analysis) showed diffuse infiltration similar to WT mice, suggesting that integrin signaling is not essential for in vivo GBM cell migration. Next, we tested the role ephrin-signaling using a series of transgenic neonatal mice, including EPH-B1-/-, -B2-/-, -B1/2-/-, -kinase-dead (KD) and a gain-of-function mutant). EPH1/2-/- GBM, but not the other genetic models, consistently formed tumors which showed no diffuse single-cell infiltration, but rather grew as a solid expanding mass. An extensive panel of in vitro studies comparing WT and EPHB1/2-/- GBM patterns of growth and migration, including time-lapse random walk, neurosphere radial migration, migration along patterned surfaces, and laminin-coated confined 3D channels, showed similar patterns of migration, despite the marked differences in vivo. These contrasting in vivo and in vitro results raise the possibility that EPH-B1/2 receptors may require their cognate ephrin ligands to facilitate migration through the WM tracts. To test this hypothesis, we are using Ephrin-B1f/f, B2f/f mice for in vivo cell-type specific deletion in WM tract stroma cells and primary astrocytes derived from these mice for ex vivo co-culture studies. Our preliminary data suggest that EPH/EPHRIN interactions may regulate GBM cell migration.

#3356 Inhibiting phospholipase D1 reduces pancreatic carcinogenesis in mice.

H. A. Addassi[1], K. Matsukuma[2], G. G. Mackenzie[1];
[1]UC Davis, Davis, CA, [2]UC Davis, Sacramento, CA

New therapeutic targets are needed for pancreatic ductal adenocarcinoma (PDAC), a leading cause of cancer-related death worldwide. Phospholipase D (PLD) is a lipid-signaling enzyme that appears to play a critical role in cell proliferation, survival/apoptosis, and downstream oncogenic transformation. Elevated PLD1 or PLD2 (the two classical mammalian isoforms) activity has been shown to promote tumor progression in various cancer types, however, the role and mechanisms of PLD in pancreatic cancer are not yet understood. Thus, the objective is to determine the role of PLD1 regulation in pancreatic carcinogenesis through genetic and pharmacological inhibition. To evaluate the role of PLD1 in tumor growth, we subcutaneously transplanted human MIA PaCa-2 pancreatic cancer cells expressing endogenous PLD1 levels (Ctr KD cells), or MIA PaCa-2 cells in which PLD1 was knocked down (Pld1 KD cells), into immunodeficient nude mice. After 18 days post implantation, tumors that arose from Pld1-KD cells presented a significantly smaller tumor size ($p<0.05$) and had reduced levels of Bcl-xL and Bcl-2, compared to controls (Ctr KD). Then, to assess the role of PLD1 in the tumor microenvironment, we implanted KPC pancreatic cancer cells into C57BL/6 wild-type (WT) or C57BL/6 PLD1 knockout (*Pld1*$^{-/-}$) mice with and without treatment with gemcitabine. Fourteen days after tumor implantation, the growth of KPC tumors was attenuated in *Pld1*$^{-/-}$ mice by 49% ($p<0.05$). Treatment with gemcitabine reduced tumor growth by 51.6% ($p<0.05$) in WT mice and by 79.5% ($p<0.03$) in *Pld1*$^{-/-}$ mice. Moreover, we evaluated the effects of PLD1 genetic ablation by crossing *LSL-Kras*$^{G12D/+}$*; Ptf1Cre/+* (*KC*) mice into PLD1 knockout (*Pld1*$^{-/-}$) mice to generate *KC; Pld1*$^{-/-}$ mice. At 8 months of age, *KC; Pld1*$^{-/-}$ mice had significantly smaller pancreases ($p<0.05$) compared to *KC* mice. Interestingly, PLD1 ablation increased phosphorylation of ERK and c-Jun in *KC; Pld1*$^{-/-}$ mice compared to *KC* mice. Finally, to assess whether pharmacological inhibition of PLD can inhibit pancreatic carcinogenesis, *KC* mice received daily intraperitoneal injections of a small molecule inhibitor of PLD1 and PLD2 (FIPI) at a dosage of 3 mg/kg of body weight for a duration of 5 weeks. Treatment with FIPI reduced acinar-to-ductal metaplasia ($p<0.05$) and reduced cell proliferation ($p<0.01$), when compared to vehicle-treated KC controls. Additionally, FIPI treatment was safe demonstrating no significant differences in body weight between the groups and no significant alteration in the serum levels of liver enzymes, including aspartate aminotransferase, alanine aminotransferase and alkaline phosphatase. In conclusion, these findings reveal PLD1 plays a critical role in pancreatic carcinogenesis and might represent a novel therapeutic target.

#3357 Identifying mechanisms of acquired resistance to lorlatinib utilizing a genome-wide CRISPR-Cas9 screen.

Joshua Renn Kalna[1], Smita Matkar[1], Emily O'Drisoll[2], Skye Balyasny[1], Matteo Calafatti[1], Mark Gerelus[3], Dave Groff[1], Tina Acholla[1], Colleen E. Casey[1], Paul Kamitsuka[3], Grant Li[1], Steven J. Pastor[4], Gabriela Witek[1], Kateryna Krytska[1], Jarrett Lindsay[3], Ophir Shalem[5], Yael P. Mosse[6]

[1]Oncology Research, Children's Hospital of Philadelphia, Philadelphia, PA,[2]Genetics and Epigenetics, Perelman School of Medicine, University of Pennsylvania, Philadelphia, PA,[3]Pharmacology, Perelman School of Medicine, University of Pennsylvania, Philadelphia, PA,[4]Bioinformatics, Children's Hospital of Philadelphia, Philadelphia, PA,[5]Pathology and Laboratory Medicine, Children's Hospital of Philadelphia, Philadelphia, PA,[6]Oncology, Children's Hospital of Philadelphia, Philadelphia, PA

Survival rates for neuroblastoma (NB), a predominantly pediatric solid tumor arising from the sympathoadrenal neural crest, have improved incrementally from 25% to 50% over three decades with dramatic escalation in therapy intensity. Gain-of-function mutations in anaplastic lymphoma kinase (*ALK*), of which 85% occur at residues F1174, F1245, and R1275, confer inferior survival compared to patients with wild-type *ALK*. Lorlatinib, a third generation ALK inhibitor, has completed Phase 1 testing in the NANT Consortium and has moved to frontline therapy in the Children's Oncology Group. The robust and sustained activity observed with minimal toxicity is transient in relapse patients harboring *MYCN* amplification and ALK activation. We aim to elucidate and target mechanisms of acquired resistance that emerge from lorlatinib treatment. We utilized the Brunello library, a genome-wide CRISPR-CAS9 loss of function screen targeting 19,114 genes (4 sgRNA per gene), which allows for a high confidence of detection of hits. We screened four clinically representative cell lines: Kelly (ALK^{F1174L}, *MYCN*-amplified, $p53^{P117T}$), SMS-SAN (ALK^{F1174L}, *MYCN*-amplified), LAN5 (ALK^{R1275Q}, *MYCN*-amplified), and SY5Y (ALK^{F1174L}, *MYCN*-nonamplified). sgRNAs were ranked according to the degree of depletion or enrichment. We validated top depleted targets through cell-based assays and immunoblotting. We identified several actionable targets across multiple NB cell lines that, when depleted, increase the efficacy of lorlatinib, including *FGFR2*, *BCL2L1*, *SOX11*, *SMARCA2*, and *SMARCD2*. Genetic knockout of *FGFR2* led to a 40% reduction ($p<0.05$) in KO cells upon lorlatinib treatment compared to control. PROTAC degradation of the anti-apoptotic BCL-xL (*BCL2L1*) revealed the combination of lorlatinib and the PROTAC led to a decrease in IC50 *in vitro*. Additionally, we identified conserved core components of the SWI/SNF complex, a subfamily of ATP-dependent chromatin remodelers, as well as SOX11, a regulator of the SWI/SNF complex and transcription factor of the core regulatory circuitry in adrenergic high-risk NB. In conclusion, we identified actionable targets across four NB cell lines that, when depleted, increase the efficacy of lorlatinib. Depletion of FGFR2 led to increased sensitivity to lorlatinib, however enzymatic inhibition showed minimal effect. Future investigation into dual targeting of ALK and FGFR2 through novel alternative methods is warranted. Furthermore, we observed a synergistic relationship between lorlatinib and a BCL-xL PROTAC *in vitro*. Ongoing *in vivo* studies will test the combinatorial efficacy in lorlatinib-naïve and resistant models. Finally, we are investigating epigenetic remodeling by the SWI/SNF complex and its regulators in NB cells during lorlatinib treatment through targeted genetic manipulation of *SOX11* to understand its role as a master transcriptional regulator of *MYCN* and *FGFR2*.

#3358 Tribbles 1 (TRIB1) pseudokinase forms a complex with and activates Akt in GBM cells.

K. Singh, C. Han, H. Manring, S. J. Haque, A. Chakravarti;
The Ohio State University, Columbus, OH

Glioblastoma (GBM; WHO grade 4) is the most aggressive form of glioma with a dismal 5-year survival rate. The current therapies are largely ineffective and therapy resistance is commonly encountered. We have recently shown that TRIB1, a Ser/Thr pseudokinase contributes to therapeutic resistance in GBM cells by activating both ERK and Akt pathways. Here we show that, increased expression of TRIB1 contributed to RT/TMZ resistance by activating pro-survival Akt signaling resulting in increased viability of GBM cells. High level of Akt phosphorylation/activation is correlated with poor prognosis of GBM patients. Many pan Akt inhibitors have been developed which are currently in various phases of clinical trials. The three Akt isoforms (1, 2 and 3) are known to play a role in cancer during proliferation, transformation and metastasis. A previous report has shown that TRIB1 interacts with Akt1 in *Drosophila* and blocks its activation. In this study we show that Akt binds and forms a complex with TRIB1 in GBM cells and this interaction could be isoform and cell line specific.

We utilized patient derived xenograft (PDX) GBM cell lines and established GBM cell lines in this study. Stable TRIB1 overexpressing cell lines were generated by antibiotic selection. Co-immunoprecipitation (Co-IP) was performed utilizing Anti-FLAG or anti-c-Myc magnetic agarose beads to evaluate protein-protein interactions. Western blotting was done to detect protein levels. The FLAG tagged TRIB1 deletion mutants were a generous gift from Dr. Takuro Nakamura (Division of Carcinogenesis, The Cancer Institute, Tokyo, Japan). Cells were transfected using Lipofectamine 2000 reagent.

Co-IP studies showed that TRIB1 formed a complex with Akt in PDX GBM cell lines. We then transiently transfected respective TRIB1 deletion mutants lacking either N and C terminal residues in HEK 293 cells and performed Co-IP with Anti-FLAG magnetic agarose beads. We observed that all TRIB1 deletion mutants except TRIB1-ΔN2 (lacking first 160 amino acids) were able to pull down Akt. The western blot results showed that each Akt isoform had a variable protein expression across different cell lines. Co-IP studies in the PDX cell lines showed that TRIB1 interacted with all three Akt isoforms in T08-387 cells whereas TRIB1 consistently interacted with only Akt3 but not Akt1/2 in GBM30 cells that lack wild-type p53 expression.

Our data suggest that TRIB1 forms a complex with Akt in PDX GBM cell lines. The potential Akt binding site on TRIB1 lies between 90-160 amino acids. TRIB1 can interact with different Akt isoforms in a cell type dependent manner thereby playing a role in their activation and consequent tumorigenic processes. Therefore, targeting TRIB1 mediated Akt activation could be considered a better therapeutic option over targeting Akt directly, which may decrease Akt's oncogenic activities without risking the toxicity associated with available Akt- specific inhibitors.

#3359 *HEY1::NCOA2 fusion* disturbs the transcriptional program of chondrogenic differentiation and activates oncogenes in mesenchymal chondrosarcoma tumorigenesis.

W. Qi, W. Rosikiewicz, B. Xu, **L. Wang**;
St. Jude Children's Research Hospital, Memphis, TN

Mesenchymal chondrosarcoma (MCS) is a rare high-grade mesenchymal neoplasm occurring in bone and soft tissue. It accounts for 2%~10% of all chondrosarcomas and affects mainly adolescents and young adults. Genetically, this tumor is characterized by the recurrent HEY1::NCOA2 fusion. To functionally characterize the fusion in MCS tumorigenesis, we generated stably transduced iPSC-derived mesenchymal stem cells (iPSC-MSC) with inducible expression of HEY1::NCOA2. We previously demonstrated that the expression of HEY1::NCOA2 significantly enhanced cell proliferation, upregulated PDGFB/PI3K/AKT signaling, and induced genes that are involved in chondrocyte differentiation. In this study, we evaluated the impact on chondrogenic lineage differentiation and dysregulated pathways resulting from HEY1::NCOA2 expression and further elaborated oncogenic pathways in MCS tumorigenesis. We first successfully established the differentiation culture of inducing iPSC-MSC on chondrogenic lineage differentiation, showing an increase in glycosaminoglycans and the expression of differentiation markers (COL1A1, COL2A1, ACAN, COMP, SOX9 and COL10A1) at 7-, 14-, and 21-days post treatment with differentiation medium. The iPSC-MSC-HEY1::NCOA2 cells and control cells were cultured for chondrogenic lineage differentiation. During differentiation culture, we collected cells from each condition at multiple time points to (1) monitor the expression of differentiation markers and (2) perform transcriptomic profiling. Principal component analysis showed that cells with the expression of *HEY1::NCOA2* possessed a distinct feature from parental cells and control cells, however, *HEY1::NCOA2* did not simply suppress chondrogenic differentiation. The differential gene expression indicated that HEY1::NCOA2 fusion disrupted genes related to fine tuning of chondrogenic differentiation (*SOX9*, *COMP*, and *IGF1*) and activated oncogenes (*PDGFB, BCL2, CCND1, IGF2*, etc.). Notably, we demonstrated that both *BCL2 (*an anti-apoptotic protein) and *COMP (*possess antiapoptotic function that protects chondrocytes against death and blocks activation of caspase 3) were directly targeted and consistently upregulated by *HEY1::NCOA2* fusion. In addition, the functional classification of genes (n=86) consistently increased with HEY1:: NCOA2 expression through differentiation of the chondrogenic lineage demonstrated that the PI3K / AKT pathway was the most significantly enriched, which further supports targeting the PDGFB/PI3K/AKT axis in MCS therapy. Together, this study sheds light on how *HEY1::NCOA2* fusion shapes key mechanisms of chondrogenic differentiation and exerts oncogenic activation. Our findings provide the rationale for anti-apoptosis along with anti-PDGFB/PI3K/AKT signaling in the treatment of mesenchymal chondrosarcoma.

#3360 Myristoylated alanine-rich C-kinase substrate (MARCKS) as a target for pathological tunneling nanotubes in glioblastoma.

Lauren C. Nassour-Caswell[1], Nicholas J. Eustace[2], Shane T. Rich-New[3], Taylor L. Schanel[1], Hasan Alrefai[1], Andee M. Beierle[1], Manoj Kumar[1], Patricia H. Hicks[1], Johsua C. Anderson[1], Christopher D. Willey[1]

[1]Radiation Oncology, University of Alabama at Birmingham, Birmingham, AL,[2]City of Hope, Pasadena, CA,[3]Biochemistry and Molecular Genetics, University of Alabama at Birmingham, Birmingham, AL

Background: Glioblastoma (GBM) is a lethal brain malignancy with a median survival of <2 years due to relapse in 100% of cases. Tunneling nanotubes (TNTs) facilitate the development of treatment resistance by establishing tumor-promoting networks between GBM and surrounding cells. Only having emerged in 2004, many key players remain to be identified which is why we propose that MARCKS regulates TNT directionality through phosphorylation of its effector domain (ED).

Methods: We quantified TNT sinuosity, numbers, branching points, and average length in (3) PTEN-null doxycycline-inducible U87-MARCKS-mutant models in serum-free conditions. Mutants overexpress MARCKS as wild-type (U87-WT), non-phosphorylated (U87-NP), or pseudo-phosphorylated (U87-PP). TNTs were characterized using immunofluorescence, confocal imaging, ICY manual TNT plugin, and negative staining. We also investigated a cytotoxic peptide derived from MARCKS-ED, termed MED2, on PTEN-null brain tumor-initiating cell (BTIC) TNTs. Statistical analysis was conducted with one or two-way ANOVA and multiple comparisons.

Results: The most striking difference between all mutants is the loss of rigidity and directionality in U87-NP TNTs. Negative staining revealed U87-NP TNTs have deformed bodies with clubbed tips compared to ordered filaments in U87-WT and U87-PP. 4h MED2 treatment in non-mutated BTICs results in cytotoxicity as well as truncated TNTs that phenotypically resemble U87-NP.

Conclusions: This is the first report supporting MARCKS to be a novel regulator of TNTs through ED phosphorylation. Future directions will investigate the functionality of TNTs in U87 mutants to determine if the lack of MARCKS phosphorylation renders TNTs nonfunctional. Defining MARCKS' role in GBM TNTs not only advances the field of cellular communication but also offers a new perspective on GBM treatment.

Quantitative TNT Characterization

	Sinuosity	TNT Number	Branch Points	Average Length	MARCKS/F-actin Correlation
U87-WT	1.00 +/- 0.00	29.0 +/- 2.94	17.0 +/- 2.94	9.80 +/- 1.74	R^2=0.9245
U87-NP	1.21 +/- 0.10	11.5 +/- 1.29	9.00 +/- 0.82	9.90 +/- 1.79	R^2=0.5497
U87-PP	1.03 +/- 0.02	34.3 +/- 11.2	8.50 +/- 3.41	7.90 +/- 1.05	R^2=0.7249
P-value	WT vs. NP: P=0.0026 WT vs. PP: P=0.7804 NP vs. PP: P=0.0070	WT vs. NP: P=0.0126 WT vs. PP: P=0.5344 NP vs. PP: P=0.0025	WT vs. NP: P=0.0053 WT vs. PP: P=0.0036 NP vs. PP: P=0.9616	WT vs. NP: P=0.9975 WT vs. PP: P=0.0363 NP vs. PP: P=0.0312	U87-WT: P<0.0001 U87-NP: P<0.0001 U87-PP: P<0.0001
BTIC + No treatment	1.00 +/- 0.00	13.5 +/- 1.29	8.00 +/- 1.83	23.2 +/- 10.3	Not determined
BTIC + 3μM MED2	1.48 +/- 0.33	13.3 +/- 3.5	7.50 +/- 1.92	15.0 +/- 11.7	Not determined
P-value	NT vs. MED2: P=0.0198	NT vs. MED2: P>0.9999	NT vs. MED2: P>0.9999	NT vs. MED2 P=0.2003	Not determined

#3361 Surfaceome and cancer testis antigen profiling of lung adenocarcinoma by large-scale transcriptomic analysis.

S. Andrew[1], A. Elliott[2], G. W. Sledge, Jr.[2], S. V. Liu[3], B. Halmos[4], V. K. Lam[5], T. K. Owonikoko[1];
[1]UPMC Hillman Cancer Center, Pittsburgh, PA, [2]Caris Life Sciences, Phoenix, AZ, [3]Lombardi Comprehensive Cancer Center, Washington, DC, [4]Montefiore Medical Center, Bronx, NY, [5]Johns Hopkins University School of Medicine, Baltimore, MD

Background: The emergence of improved modalities to target tumor specific and tumor associated antigens in solid tumors (e.g. antibody-drug conjugates, bi-specific antibodies, and adoptive cell therapy) underscores the need to efficiently identify and validate new therapeutic targets.
Methods: We examined differential expression of surfaceome genes (Fonseca et al., 2016) and cancer testis (CT) antigen genes (Almeida et al., 2009) among major lung adenocarcinoma genomic subtypes; conducting comprehensive surfaceome/CT antigen profiling of 9002 NSCLC adenocarcinoma samples using data generated by RNA sequencing (whole transcriptome) at Caris Life Sciences (Phoenix, AZ). NSCLC tumors were stratified into 5 subgroups based on the presence of specific driver mutations: *ALK* fusion (N=325), *EGFR* mutant (N=1739), *KRAS* mutant (no *STK11* or *KEAP1* mutation; N=2561), *KRAS* + *STK* or *KEAP1* mutation (N=1264), and Pan-WT (no mutation in *ALK*, *EGFR*, *KRAS*, *STK11*, or *KEAP1* detected; N=3113). Fold-change in expression was calculated by dividing the median value for a specific subgroup by the median of all other groups combined. Significance was tested by Mann-Whitney U test, with p-values adjust for multiple hypothesis testing (Benjamini-Hochberg).
Results: Surfaceome genes with the highest median expression overall included *CD74*, *TMBIM6*, and *CD44*, while the highest median expression among CT antigens was observed for *SPAG9*, *KIAA0100*, and *RQCD1*, yet the expression of these genes across the 5 driver mutation-based subgroups was similar (fold-changes ranged 0.93-1.06). To identify driver-associated candidate genes with relatively high expression, genes with subgroup-specific median expression >75th-percentile and with significant differences when compared to all other groups were ranked by fold-change. While several candidate surfaceome genes were associated with a specific subgroup, *CLDN10* was identified among the top 3 candidates for both *ALK* fusion and *KRAS* + *STK11*/*KEAP1* mutant subgroups: *ALK* fusion (*GRIN2A*, 3.03-fold; *CLDN10*, 2.53-fold; *SLITRK6*, 1.86-fold), *EGFR* mutant (*SFTPC*, 3.82-fold; *MUC21*, 1.99-fold; *ATP13A4*, 1.60-fold), *KRAS* mutant (*VSIG1*, 1.86-fold; *AREG*, 1.47-fold; *C15orf48*, 1.25-fold), and *KRAS* + *STK11*/*KEAP1* mutant (*ABCC2*, 4.03-fold; *MUC13*, 3.21-fold; *CLDN10*, 3.00-fold). The top driver-associated CT antigen candidates included *LEMD1* (1.42-fold) in *ALK* fusion, *TMEM108* (1.27-fold) in *EGFR* mutant, *XAGE1D* (1.7-fold) in *KRAS* mutant, and *CABYR* (1.52-fold) in *KRAS* + *STK11*/*KEAP1* mutant subgroups.
Conclusion: Our analysis revealed several surfaceome and CT antigen candidate genes with relatively high expression across lung adenocarcinoma, as well as differential expression of candidate genes within specific genomic subtypes. These findings can help prioritize the validation and development of novel therapeutic targets in lung adenocarcinoma.

#3362 Describing the molecular landscape of cervical cancer metastases: Implications for future therapeutic targets.

M. J. Hadfield[1], S. Wu[2], A. Farrell[2], M. Oberly[2], G. Sun[1], P. Thaker[3], J. Wellcome[4], M. Anderson[4], D. Dizon[1];
[1]Brown University/Legorreta Cancer Center, Providence, RI, [2]Caris Life Science, Phoenix, AZ, [3]Washington University/Siteman Cancer Center, St. Louis, MO, [4]University of South Florida, Tampa, FL

Introduction: Cervical Cancer (CC) is a heterogenous disease with multiple histological sub-types. Early screening has led to a reduction in disease related mortality, but a significant number of patients present with or progress to advanced disease. Studies between the molecular and immune alterations in CC primaries (CCP) and CC metastases (CCM) are needed to explore potential therapeutic strategies.
Methods: Relationships of CCM and alterations detected by NGS (592, NextSeq; WES, NovaSeq) were investigated in 2,668 (1,393 primary Cervix samples, 383 local metastatic GYN samples, and 892 distant metastatic samples) CC samples (Caris Life Sciences, Phx, AZ). PD-L1+ was tested by IHC (22c3, >1%). Tumor mutational burden (TMB) was measured by summing somatic mutations per tumor (H: >10 mt/MB). Immune infiltrates estimated by deconvolution of WTS data (NovaSeq) using Quantiseq. Statistical significance determined by chi-square and Mann-Whitney U and adjusted for multiple comparisons ($q<0.05$).
Results: Hierarchical clustering of CCM sites by alterations (mutations, amplifications and fusions) frequency revealed CCM to Liver (n=77) and Lymph Nodes (n=265) as the most distinct from CCP while Vagina/Vulva (V/V) (n=196) and Lung (n=115) CCM were most similar. Lymph Nodes had decreased *TP53*-mt (6.6% vs 14.7%) and *ARID1A*-mt (4.53% vs 8.27%) but higher *BRCA1*-mt (3.03% vs 0.87%) compared to CCP ($p<0.05$). Liver had higher *BRCA1*-mt (6.67% vs 0.87%), *ASXL1*-mt (8.47% vs 2.96%) and *APC*-mt (4% vs 0.65%) compared to CCP ($p<0.05$). CCM to Lymph Nodes had higher median TMB (median [range]: 6 [0-101] vs 5 [0-460], $q<0.05$) and HPV16/18+ rate compared to CCP (81.2% vs 66.8%, $p<0.05$). CCM to Liver had lower expression of *CTLA4* compared to CCP (1.67-fold decrease), similarly, Ovary/FT had significantly lower expression of immune checkpoint (IC) gene expression (*CD80*, *CD86*, *CD274*, *PDCD1*, *PDCD1LG2*, *CTLA4*, *HAVCR2*, *IDO1*, *LAG3*, *IFNG*: 2.23-4.66-fold decrease) ($q<0.05$). While Lymph Nodes had higher expression of the IC genes compared to CCP (1.30-1.49-fold, $q<0.05$). CCM to Liver and Ovary/FT had lower median infiltration of immune cells while Lymph Nodes had higher compared to CCP of Macrophage M1 (2.7% vs 1.03% vs 3.35% vs 3.1%), B cells (3.7% vs 3.5% vs 5.6% vs 4.3%), CD8 T cells (0% vs 0% vs 1.01% vs 0.75%), and Tregs (1.6% vs 0.74% vs 2.86% vs 2.5%) ($q<0.05$). CCM to Liver and Ovary/FT had lower median IFN score while Lymph Nodes had higher median IFN score ($q<0.05$) compared to CCP, similarly, Ovary/FT had a lower % of T-cell inflamed tumors with Lymph Nodes having higher T-cell inflamed tumors compared to CCP (7.89% vs 47.4% vs 29.3%, $q<0.05$).
Discussion: CCM to Lymph Nodes and Liver had the most distinct molecular and immune landscape compared to CCP while Ovary/FT had a similar molecular profile but a distinctively cold immune profile compared to CCP. Additional studies to evaluate the potential therapeutic targets are warranted.

#3363 LIG1 inactivation selectively inhibits growth of BRCA1 mutant cells in vitro and in vivo.

L. Martires, L. G. Ahronian, C. Pratt, N. Das, X. Zhang, D. A. Whittington, H. Zhang, B. Shen, J. Come, P. McCarren, M.-S. Liu, C. Min, T. Feng, H. Jahic, E. Brophy, D. Aird, J. N. Andersen, A. Huang, F. Li, W. D. Mallender, **H. E. Nicholson**;
Tango Therapeutics, Boston, MA

Women harboring a mutation in the *BRCA1* gene have a >7X increased risk of developing breast cancer and >35X increased risk of developing ovarian cancer in their lifetime compared to women lacking such mutations. While PARP1/2 inhibitors are efficacious in the *BRCA* mutant setting, this efficacy is limited and resistance develops readily. Additional therapeutic targets beyond PARP1/2 are needed to treat cancer patients with *BRCA* mutations. We performed CRISPR screens in 11 *BRCA1/2* wild-type and 2 *BRCA1* mutant cancer cell lines to identify targets that are synthetic lethal with *BRCA1* mutations. In addition to USP1, PARP1 and POLQ, we identified the DNA ligase gene *LIG1* as a novel target that when knocked out kills *BRCA1* mutant cells selectively. Internal analysis of *BRCA* mutations in breast and ovarian cancer cell lines in the Project Achilles database further validated the hyperdependence of *BRCA1* mutant cells on *LIG1*. Single-gene perturbation of *LIG1* using CRISPRn, CRISPRi, and RNAi confirm the lethal effect of *LIG1* inactivation in *BRCA1* mutant cell lines, but not *BRCA1/2* wild-type cell lines. This loss of viability could be rescued by complementing with an exogenous wild-type *LIG1* cDNA, demonstrating the on-target nature of the genetic tools. Using a degradable DNA Ligase I fusion protein, we demonstrate a strong correlation between DNA Ligase I protein level and viability in *BRCA1* mutant cells. Enzymatically inactive DNA Ligase I mutant protein (LIG1^{K568A}) was unable to rescue the loss of viability caused by endogenous *LIG1* depletion supporting the tractability of this target from a small molecule inhibitor perspective. These data were reproduced *in vivo* using *BRCA1* mutant MDA-MB-436 derived tumors, in which tumor growth was inhibited >80% upon loss of *LIG1*.Mechanistically, DNA ligase I plays a critical role in DNA replication and damage repair by sealing nicks in the phosphodiester backbone of DNA. When these nicks are not repaired, they are marked by the addition of PAR chains. Consistent with this mechanism, we demonstrated that inactivation of *LIG1* leads to increased PARylation. The induction of PARylation was proportional to the level of inactivation of LIG1 protein, supporting a correlation between LIG1 activity and DNA nick repair. Together, these data support DNA ligase I as a synthetic lethal target in the context of *BRCA1* mutations.

#3364 PELO is a synthetic lethal target in chromosome 9p21-deleted or MSI cancers.

E. M. Chan[1], P. Borck[2], N. Bick[2], K. Jankovic[1], I. Boyle[2], L. Parker-Burns[1], K. Foster[2], A. Lau[2], A. Borah[2], J. Dempster[2], F. Vazquez[2];
[1]Columbia University Irving Medical Center, New York, NY, [2]Broad Institute, Cambridge, MA

Homozygous deletion of chromosomal region 9p21.3 is one of the most frequently observed somatic copy number alterations in cancers, occurring in approximately 15% of all cancers. Many of the 9p21.3-deleted cancers are further characterized by poor clinical outcomes including subsets of glioblastoma, pancreatic, esophageal, and urothelial cancers. Large deletions of chromosomal regions may also provide unique therapeutic opportunities. Specifically, cancer-specific therapeutic opportunities can arise from co-deletions of passenger genes neighboring tumor suppressors. As such, we sought to identify novel therapeutic targets associated with Ch9p21.3 loss in cancers and identified the pelota mRNA surveillance and ribosome rescue factor (PELO) as the top preferential dependency in 9p21.3-deleted cancers. Intriguingly in another analysis, we identified PELO to be amongst the top preferential dependencies in cancers with microsatellite instability (MSI), which accounts for subsets of colorectal, endometrial, gastric, and ovarian cancers. Given the strength of PELO as a candidate synthetic lethal target in two distinct cancer subsets, we performed focused validation with CRISPR interference across multiple cell lines. Knockdown of PELO preferentially impaired the viability of MSI or 9p21-deleted as compared to control (9p21-proficient and microsatellite stable) cells. Further validation with patient-derived organoid and in vivo xenograft models confirmed these findings. We next sought to refine the predictive biomarkers for PELO dependency and identified loss of FOCAD (a 9p21.3 gene and an interactor of the SKI mRNA surveillance pathway) as necessary and sufficient for PELO dependency in the 9p21.3-deleted context. Our findings implicate splicing alterations involving TTC37, a key protein in the SKI mRNA surveillance complex, as the underlying cause of PELO dependency in MSI cancers. Together, we found that loss of large deletions of 9p21.3 and MSI independently impair the SKI complex, uncovering a dependency upon PELO and highlighting a novel functional interaction between PELO and the SKI complex. Furthermore, the strength of this synthetic lethal interaction in a broad range of cancers with poor outcomes underscores the potential of PELO as a promising drug target for patients with 9p21.3-deleted or MSI cancers.

#3365 Reliable detection of potentially therapeutically actionable ecDNA using clinical-grade NGS in a large pan-cancer cohort.

Matteo Repetto[1], Klaus Wagner[2], Shalabh Suman[3], Peter Krein[2], Pavitra Rao[3], Maria Arcila[3], Christian Hassig[2], Mark Donoghue[4], Alexander Drilon[1], Michael Berger[3]

[1]Early Drug Development Service, Memorial Sloan Kettering Cancer Center, New York, NY,[2]Boundless Bio, Inc., San Diego, CA,[3]Pathology and Laboratory Medicine, Memorial Sloan Kettering Cancer Center, New York, NY,[4]Memorial Sloan Kettering Cancer Center, New York, NY

Background Focal high-level oncogene amplifications (FH-amp) (e.g., *MYC, EGFR*) frequently occur on extrachromosomal DNA (ecDNA), highly transcribed units of circular non-chromosomal DNA. FH-amp on ecDNA promote intra-tumoral heterogeneity, resistance to therapies, and poor prognosis. Recently, a Phase 1 clinical trial exploring ecDNA-directed treatments has begun. However, to date, bioinformatic detection of ecDNA has relied on whole-genome sequencing data, and no standard method exists to detect ecDNA on targeted NGS. We thus sought to explore the feasibility of detecting ecDNA in a large cohort of patients with solid tumors sequenced with the targeted NGS panel, MSK-IMPACT, and describe the pan-cancer prevalence of oncogenes amplified on ecDNA.
Methods We utilized a novel bioinformatic ecDNA-diagnostic algorithm, ECHO, to determine the presence of oncogene FH-amp on ecDNA (including HSR) vs. chromosomal in clinical-grade NGS data. 72,651 tumor samples profiled by MSK-IMPACT were queried for high level oncogene FH-amp (*AR, CCNE1, CDK4/6, EGFR, FGFR1-4, KRAS, MDM2, MDM4, MET, MYC, MYCL*, and *MYCN*) above a fold-change of three, and subsequently annotated with ECHO. Patients with concomitant oncogenic driver mutations or fusions (e.g., *EGFR L858R, EML4-ALK*) were excluded based on the hypothesis that they might be mutually exclusive with oncogene FH-amp.
Results FH-amp of any above listed oncogene were found in 3065 (4.2%) samples. Cancer types with frequent FH-amp without concomitant driver alterations were liposarcoma (LPS) (61% FH-amp; 43% were ecDNA+), glioblastoma (GBM) (22%; 72%), gastroesophageal adenocarcinoma (GE AD) (10%; 57%) squamous cell lung cancer (7%; 18%), and breast cancer (BRCA) (7%; 23%). Among tumors with oncogene FH-amp, GBM and GE AD had high frequencies of ecDNA+ FH-amp of *EGFR* (39% and 15% of all EGFR ecDNA+). LPS had the highest frequency of ecDNA+ FH-amp of *CDK4* (64%), followed by GBM (15%). The majority of ecDNA+ *FGFR1* and *FGFR2* FH-amp were in BRCA (75% and 47%). *EGFR* in GBM and EGFR or *FGFR2* in GE AD were ecDNA+ in more than 90% of patients, while *CDK4* in LPS and *FGFR1* in BRCA were ecDNA+ in 45% and 39% respectively.Evaluation the relationship between ecDNA+ by ECHO and amp FC range showed higher ecDNA+ in samples with higher level amp (FC > 5; 58% ecDNA+) compared to lower level amp (FC 4~5; 12%, FC 3~4; 6% ecDNA+).
Conclusions A novel ecDNA clinical diagnostic tool, ECHO, was successfully applied to a large clinical cohort of patients enriched for actionable oncogene amplifications sequenced with MSK-IMPACT. The results demonstrate that detection of ecDNA using clinical-grade NGS assays is feasible and that key oncogene FH-amp on ecDNA (e.g., *EGFR, FGFR2*) are common in select tumor types. ECHO may be developed as a clinical trial device to prospectively identify patients with oncogene ecDNA+ FH-amp for clinical testing of ecDNA-directed therapies.

#3366 FoRx-06-428 is a novel PARG inhibitor with potent anti-tumor efficacy in preclinical cancer models.

O. Querolle[1], U. Lucking[1], L. Iacovino[1], A. Freudenmann[1], G. Rossetti[1], M. Gysin[1], S. Bologna[1], V. Dionellis[1], M. Malattia[1], A. Potenza[1], N. Bocquet[1], I. Konstantinova[1], A. Goutopoulos[1], S. Sotiriou[1], T. Halazonetis[2], T. Bashir[1], F. Zenke[1];

[1]FoRx Therapeutics AG, Basel, Switzerland, [2]University of Geneva, Geneva, Switzerland

The formation of poly(ADP-ribose) (PAR) chains from NAD+ precursors by PARP enzymes is a characteristic posttranslational modification during DNA damage repair. PAR chains function as docking platforms for DNA repair proteins that are required to resolve DNA lesions. Equally important is the subsequent removal of PAR chains from protein substrates to conclude the repair process and restore genomic integrity. Poly(ADP-ribose) glycohydrolase (PARG) is the key enzyme in this process and has recently garnered significant attention as a novel cancer target. FoRx-06-428 is a novel, orally bioavailable and highly potent, low molecular weight PARG inhibitor. It binds to the catalytic domain of human PARG with high affinity, as evidenced by surface plasmon resonance (SPR), and displays potent inhibition of enzymatic activity. FoRx-06-428 shows selective reduction of viability in a panel of cancer cell lines highlighting therapeutic potential in multiple cancer indications. Pharmacological inhibition of PARG leads to accumulation of PAR chains and is indicative of target engagement, accompanied by modulation of DNA damage response markers, such as phosphorylation of replication protein A (pRPA) and phosphorylation of H2AX (γH2AX). Compelling anti-tumor efficacy as single agent was observed in several xenograft models (breast and gastric cancer) with excellent tolerability. Dose-dependent accumulation of PAR chains was demonstrated *in vivo* and constitutes a tractable target engagement biomarker for clinical exploration. Sensitivity to PARG inhibition is partly driven by distinct genomic instabilities, such as defects in homologous recombination (HR) repair, however the activity of PARG inhibitors is also influenced by aberrations in other cancer-relevant pathways. This report represents the first disclosure of the pharmacological characterization of FoRx-06-428 and highlights the value of PARG inhibition as a novel targeted approach to treat DNA repair-deficient cancers.

#3367 R-loop type determines the orientation of transcription-replication conflicts attenuated by transcription factor IIS.

R. C. Duardo[1], J. Marinello[1], M. Russo[1], S. Morelli[1], S. Pepe[1], F. Guerra[1], B. Gomez-Gonzalez[2], A. Aguilera[2], **G. Capranico**[1];
[1]University of Bologna, Bologna, Italy, [2]Centro Andaluz de Biologia Molecular y Medicina Regenerativa-CABIMER, Seville, Spain

During human Topoisomerase I (Top1) catalytic activity, a transient Top1-DNA cleavage complex (Top1cc) forms to allow DNA relaxation. Top1ccs can be stabilized by antitumor Top1 poisons, such as clinically-effective camptothecin analogs. Camptothecin-stabilized Top1ccs can lead to R-loop-dependent transcription-replication conflicts (TRCs), single-end DNA double-strand breaks (seDSBs) and genome instability in cancer cells. To define the genomic location of TRCs and the underlying mechanisms, we integrated genomic maps of Top1cc-induced DNA cleavage by END-seq and DNA:RNA hybrids by DRIP, determined the cell-cycle specificity of micronuclei formation and the effects of elongation transcription factor IIS (TFIIS). We have defined the genomic sites of both seDSBs and increased R-loop levels (gains) induced by Top1ccs. seDSBs are highly enriched at regions with R-loop gains at highly-transcribed genes in early replicating zones. Kinetics analyses of R-loops and genomic ChIP data of RNA polymerase II (RNAPII) revealed that R-loop gains can either be upstream or downstream of RNAPII. TFIIS effects showed that downstream R-loop gains can follow RNAPII backtracking and arrest. seDSB strandness showed that co-directional TRCs occur mainly at downstream hybrid-associated RNAPII, whereas head-on TRCs occur mainly at upstream hybrid-associated RNAPII. Therefore, Top1ccs can increase two structurally-different R-loops and R-loop-associated backtracked RNAPII causes co-directional TRCs at higher rate than head-on collisions. Moreover, Top1ccs trigger micronuclei formation at G1/early S, but not late S/G2, which are attenuated by TFIIS. Thus, our findings establish a role of RNAPII backtracking at highly-transcribed genes in Top1cc-induced co-directional TRCs and micronuclei formation. The findings can accelerate the development of new effective strategies to treat cancer patients. (Supported by Associazione Italiana per la Ricerca sul Cancro, Milan, Italy - IG 2019 - ID. 23032 to C.G. and by the European Union - NextGenerationEU through the Italian Ministry of University and Research under PNRR - M4C2-I1.3 Project PE_00000019 "HEAL ITALIA" to G.C., CUP J33C22002920006).

#3368 Combination of a chk1/2 dual inhibitor (prexasertib) and gemcitabine reveals a novel intrinsic synergy mechanism in head and neck squamous cell carcinoma.

V. C. Palve, H. L. Walker-Mimms, R. Chaudhary, V. Izumi, N. Chaudhary, B. Fang, J. Koomen, J. A. Guevara, P. C. Rodriguez, C. H. Chung, D. R. Duckett; Moffitt Cancer Center, Tampa, FL

Head and neck squamous cell carcinoma (HNSCC) presents a challenging clinical scenario due to its recurrence propensity despite existing treatments. Altered intrinsic signaling pathways significantly contribute to therapeutic resistance, demanding exploration of novel strategies to induce tumor cell demise. Dysregulated cell cycle and DNA damage repair constitute pivotal events driving HNSCC progression, offering potential therapeutic targets.CHK1 and CHK2, pivotal regulators of the DNA replication checkpoint, are promising targets in HNSCC. The convergence of DNA-damaging agents with DNA checkpoint inhibitors represents a burgeoning paradigm in cancer management. Our study delves into elucidating the intrinsic signaling mechanisms triggered by the synergistic action of the CHK1/2 dual inhibitor (Prexasertib) and the nucleoside analog (Gemcitabine) in HNSCC.Our study unveiled a robust synergistic effect between Prexasertib and Gemcitabine, inducing substantial cell death in multiple HNSCC cell lines and mouse model. Remarkably, the combination rapidly induced DNA damage and reduced tumor growth in vivo. To unravel the underlying intrinsic signaling mechanism provoked by the Prexasertib/Gemcitabine combination, we conducted comprehensive molecular analyses.Proteomic profiling uncovered distinct alterations in key signaling pathways upon combination treatment. We identified unique overexpression of an embryonic stem cell-specific transcription factor pivotal in genomic stability regulation, solely induced by single-agent Prexasertib. Specifically, the combination therapy showcased unique modulation of critical genes involved in DNA repair, replication, and cell cycle regulation. These alterations included overexpression or suppression of key genes associated with DNA stability and cell proliferation pathways, accompanied by evidence of CHK1/2 inhibition-mediated DNA damage response accompanied by cleavage of CHK-2 and caspase-3 proteins, validated through Western blots.Additionally, functional assays including the colony formation assays demonstrated markedly reduced survival rates with the combination treatment compared to single-agent therapy. Cell cycle analysis revealed a replication catastrophe and increased pH2AX across multiple HNSCC cell lines following combination treatment.Our findings highlight the significance of CHK1/2 inhibition coupled with nucleoside analog-induced DNA damage in unveiling novel intrinsic signaling mechanisms in HNSCC. These insights offer a promising avenue for targeted therapeutic strategies to enhance treatment efficacy and outcomes in HNSCC.This work has been supported by the MGC, FC, P&MC, and BBSR at the H. Lee Moffitt Cancer Center & Research Institute, a comprehensive cancer center designated by the National Cancer Institute (P30-CA076292).

#3369 Dual inhibition of ATR and PI3K pathways promotes cell death in platinum-resistant endometrial cancer cells by increasing DNA damage.

K. R. Ibanez[1], T.-T. Huang[1], S. Sotiriou[2], Y. G. Lin[3], J.-M. Lee[1];

[1]Center for Cancer Research, National Cancer Institute, National Institutes of Health, Bethesda, MD, [2]Roche Pharma Research and Early Development (pRED), Roche Innovation Center Basel, F. Hoffmann-La Roche Ltd., Basel, Switzerland, [3]Genentech, Inc., South San Francisco, CA

Background: Endometrial cancer (EC) is the most common gynecologic malignancy with increasing incidence and mortality in the U.S. Among the four subtypes characterized by the Cancer Genome Atlas, the serous-like copy number high (CNH) subtype which occurs in 15-25% of EC is associated with poor prognosis and platinum resistance, requiring alternative treatment options. ~85% CNH EC cases have impaired G1/S checkpoint regulation, making cells rely on ATR-mediated G2/M cell cycle checkpoints for optimal DNA replication and repair. Additionally, over 80% of ECs exhibit PI3K pathway activation (e.g., *PIK3CA* mutations), linked to enhanced DNA repair and drug resistance. Therefore, we hypothesized that dual ATR and PI3Kα inhibition would enhance DNA damage, increasing cell death in EC.

Methods: CNH EC cell lines included platinum-resistant (KLE, MFE280, HEC1A, ARK2) as well as platinum-sensitive (ARK1) lines used to evaluate the activity of ATR inhibitor (ATRi) camonsertib and PI3Kα inhibitor (PI3Kαi) inavolisib. Cell growth was assessed by 3-day XTT and 9-12-day colony-forming assays. The degree of combination synergy, additivity, or antagonism was calculated using SynergyFinder with a reference highest single agent (HSA) model. An HSA synergy score > 10 indicates synergy, -10 to 10 suggests additivity and < -10 represents antagonism. DNA damage endpoints were measured by alkaline comet assay and immunoblotting for γ-H2AX. Data were repeated in triplicate, analyzed using one-way ANOVA test, and shown as mean ± SD. $P < 0.05$ was statistically significant.

Results: All tested EC cell lines showed sensitivity to clinically attainable doses of ATRi monotherapy (IC_{50} 0.09 - 0.98 μM), but varying sensitivity to PI3Kαi monotherapy (IC_{50} 0.03 - 67.01 μM) unrelated to their *PIK3CA* mutation status. Combination treatment using clinically attainable concentrations (camonsertib < 6 μM; inavolisib < 10 μM) yielded additivity in all cell lines independent of platinum sensitivity (HSA synergy scores -0.8-10.0). Notably, increased cytotoxic effects were observed in both *PIK3CA* wild-type (KLE) and *PIK3CA*-mutant (MFE280 and HEC1A) platinum-resistant lines by colony-forming assays (4.8- to 15.4-fold decrease in colony-forming ability relative to ATRi; 1.5- to 3.5-fold decrease relative to PI3Kαi). ATRi and PI3Kαi combination induced greater DNA damage, evidenced by elevated mean comet tail moment relative to ATRi (increased 2.5- to 6.7-fold; $P < 0.01$) or PI3Kαi (increased 2.1- to 5.6-fold; $P < 0.01$) regardless of *PIK3CA* mutation status. Increased γ-H2AX levels were found in HEC1A cells with combination treatment (3.2-fold increase relative to ATRi; 16-fold increase relative to PI3Kαi).

Conclusion: Our results suggest that dual inhibition of ATR and PI3K pathways induces greater cell death by increasing DNA damage in platinum-resistant EC cells independent of *PIK3CA* mutation status.

#3370 Anti-tumor activity of Debio 0123 in combination with sacituzumab govitecan in preclinical models of breast cancer.

L. Piggott, E. Rodrigo Imedio, F. Staehli;
Debiopharm International S.A., Lausanne, Switzerland

Background: Debio 0123 is a WEE1 inhibitor that has previously shown significant preclinical efficacy in combination with DNA damaging agents and is currently being investigated in phase 1 clinical studies either as a monotherapy or in combination with different standard therapies. Sacituzumab govitecan (SG) is a TROP2 directed antibody-drug-conjugate (ADC) carrying an SN38 payload that has recently gained approval in TNBC and ER+ve breast cancer after demonstrating improvements in survival versus standard therapies. Despite these promising data some patients still do not respond to SG treatment, develop resistance or experience toxic side effects. Herein we present preclinical data that demonstrates Debio 0123 improves tumor response to SG in breast cancer models and provides sustained complete responses and anti-metastatic activity.

Methods: Synergy between Debio 0123 and SG was evaluated in breast cancer cell lines, with varying levels of TROP2 expression, *in vitro* using standard cytotoxicity assay in a matrix combination format. Efficacy of Debio 0123 and SG as monotherapies or in combination was further assessed *in vivo*, in both $TROP2_{high}$ and $TROP2_{low}$ subcutaneous breast cancer xenograft models at different doses.

Results: *In vitro*, Debio 0123 in combination with SG demonstrated synergistic tumor cell killing in all 4 breast cancer cell lines tested, at all concentrations. *In vivo*, $TROP2_{high}$ MDA-MB-468 breast cancer xenograft tumors treated with Debio 0123 at 30mg/kg QD resulted in minimal anti-tumor activity as a monotherapy but completely regressed 100% of the tumors in combination with SG. Furthermore, 40% of these complete regressions were sustained for up to 100 days post-treatment initiation. These data were then further replicated at a reduced dose of SG. In the $TROP2_{low}$ MDA-MB-231luc model, Debio 0123 significantly improved response to SG resulting in a 2-fold improvement in tumor growth inhibition. Additionally, combination treatment significantly inhibited metastasis of these tumors to the lung and lymph nodes as monitored by bioluminescence. Collectively, these results lead to a significant improvement in animal survival as a combination compared to either treatment as a monotherapy.

Conclusion: These results demonstrate that Debio 0123 synergizes with, and significantly improves breast cancer tumor cell response to, SG regardless of TROP2 expression levels (both *in vitro* and *in vivo*), leading to complete regressions and inhibition of metastasis. Collectively these data support Debio 0123 in combination with SG could be a potential therapeutic approach for improving responses in patients with breast cancer.

#3371 PRMT blockade induces defective DNA replication stress response via ATR suppression and synergizes with PARP inhibition.

D. Bisht[1], Y. Li[1], L. E. Dobrolecki[2], C. Sallas[2], X. Zhang[1], T. D. Kerr[3], Y. Wang[1], S. Awasthi[1], B. Kaundal[1], S. Wu[1], W. Peng[4], M. L. Mendillo[5], Y. Lu[1], C. R. Jeter[1], G. Peng[1], J. Liu[1], S. N. Westin[1], A. K. Sood[1], M. T. Lewis[2], J. Das[6], S. Yi[7], M. T. Bedford[1], D. J. McGrail[8], N. Sahni[1];

[1]The University of Texas MD Anderson Cancer Center, Houston, TX, [2]Baylor College of Medicine, Houston, TX, [3]Center for Immunotherapy and Precision Immuno-Oncology Cleveland Clinic, Cleveland, OH, [4]University of Houston, Houston, TX, [5]Northwestern University Feinberg School of Medicine, Chicago, IL, [6]University of Pittsburgh School of Medicine, Pittsburgh, PA, [7]The University of Texas at Austin, Austin, TX, [8]Center for Immunotherapy and Precision Immuno-Oncology, Cleveland Clinic, Cleveland, OH

Aberrant protein arginine methylation has been observed in multiple cancer types, making it an attractive drug target. Proteins can undergo asymmetric arginine methylation by type I protein arginine methyltransferases (PRMTs), predominately by PRMT1 and to a lesser extent PRMT4, or symmetric arginine methylation by type II PRMTs, predominately PRMT5. Here, we performed targeted proteomics following inhibition of PRMT1, PRMT4, and PRMT5 across cancer cell lines. We found that inhibition of both type I and type II PRMTs suppressed levels of total and phosphorylated ATR protein in cancer cell lines, and down-regulated expression of the ATR gene. Loss of ATR from PRMT inhibition resulted in defective DNA replication stress response activation in following exogenous replication stress. Since PARP inhibitors are known to induce replication stress, we next combined PRMT inhibition with PARP inhibition and found inhibition of PRMT1 or PRMT5 greatly exacerbated PARP inhibitor induced DNA damage. Based on this observation, we assessed the combination of PARP and PRMT inhibition in a panel of cell lines. While inhibition of both type I and type II PRMTs were synergistic with PARP inhibition in both cells with intact and deficient homologous recombination, type I PRMT inhibition resulted in higher toxicity in non-malignant cells. Therefore, we validated the synergy of combined PARP/PRMT5 inhibition in primary patient-derived organoids. Finally, we demonstrate that the combination of PARP and PRMT5 inhibition improves overall survival in both BRCA-mutant and wild-type patient-derived xenograft models without any detectable hematological toxicities typically associated with PARPi combination therapies. Taken together, these results demonstrate that PRMT5 inhibition may be a well-tolerated approach to improve tumor sensitivity to PARP inhibition.

#3372 Clinical genetic testing results in metastatic prostate cancer patients.

T. Crawford[1], E. Barrett[1], T. Al-Saleem[2], M. Tayeb[1], H. Symecko[1], C. Orr[1], V. Narayan[1], S. Takvorian[1], R. Parikh[1], Y.-N. Wong[1], K. Robinson[1], L. Aiello[2], C. Wolfe[1], D. Mann[1], K. Spielman[1], S. Domchek[1], K. Maxwell[1];

[1]University of Pennsylvania, Philadelphia, PA, [2]Corporal Michael Crescenz Veterans Affairs Medical Center, Philadelphia, PA

Background: A proportion of prostate cancers (PCa) are hereditary, driven by likely pathogenic/pathogenic germline variants (PGVs) in DNA repair genes. PGVs in *BRCA2* contribute to aggressive prostate cancer biology and overall poorer survival. Genetic testing and targeted sequencing panels help identify PGV carriers who are susceptible to aggressive PCa and may be candidates for targeted therapy with PARP inhibitors. Prior research suggested a high rate of 10-20% of metastatic PCa (mPCa) patients have PGVs in DNA repair genes; however, many of these studies reported highly selected research cohorts. The real-world rate of DNA repair PGVs and whether any genotype-phenotype correlations exist in broader, more racially diverse clinical populations are not well understood.

Patients and Methods: We studied two prospective cohorts of males with PCa who presented for genetic testing due to meeting NCCN personal history genetic testing criteria for prostate cancer (metastatic or high risk/very high risk localized). We report PGV frequencies of mPCa patients who underwent genetic testing in a point of care model at the Basser Center within Penn Medicine (Penn-POC, n=596), and a cancer genetics practice at the Corporal Michael Crescenz VA Medical Center in Philadelphia (VA-GT, n = 171). PGVs were identified in *ATM, BRCA1, BRCA2, CHEK2, EPCAM, HOXB13, MLH1, MSH2, MSH6*, *NBN, PMS2, TP53*.

Results: The Penn-POC and VA-GT cohort included 437 (73.3%) and 59 (34.5%) self-identified white patients, respectively, and 121 (20.3%) and 107 (62.6%) self-identified black patients, respectively. In the Penn-POC and VA-GT cohorts, 7.2% and 7.6% patients were found to carry a PGV, respectively, and 11.9% and 18.1% of patients had variants of uncertain significance (VUS), respectively. The most common PGVs in the Penn-POC cohort were in *BRCA2* (2.2%), *ATM* (1.9%), and *BRCA1* (1.3%). The most common PGVs in the VA-GT cohort were in *BRCA2* (2.9%), *ATM* (1.1%), and *CHEK2* (1.2%). PGV rates were not statistically different between self-identified white and black patients in either cohort (Penn-POC p= 0.4036; VA-GT p=0. 0.4061). Overall PGV frequencies between the Penn-POC and VA-GT cohorts are not statistically different. There is a correlation between carrier status and age at diagnosis with a significant difference between carriers and non-carriers (p=0.0433) as well as with family history of first degree relatives with PCa (p=0.0184). However, there was not a significant correlation between carrier status and clinical stage at diagnosis, Gleason grade group, or other clinical variables.

Conclusions: We report a lower rate of DNA repair PGVs in two prospectively ascertained, racially diverse cohorts of mPCa patients, approximately 7%, compared to the previously reported rates of 10-20%. Our results suggest age and family history, but not other pathological variables are clinical predictors for carrying a PGV in mPCa patients.

#3373 Protein kinase D1 alleviate etoposide induced DNA damage through up regulation of alpha-catenin.

S. Shukla, S. Serrano, M. Al-Toubat, T. Osumi, K. Balaji;
University of Florida, Jacksonville, FL

Interaction between E-cadherin and β-catenin at cell-cell adherens junctions is pivotal in cell adhesion, and dysregulation of these genes is associated with disease progression in various solid tumors, notably in prostate cancer. α-catenin acts as a physical linker between the cadherin/β-catenin complex and actin cytoskeleton, through its mechanosensory properties has potential to modify interactions between cadherins and cytoskeleton and results in sensitivity of cells to DNA damage and toxicity. Membranous β-catenin interacts with the cellular cytoskeleton through threonine 120 (T120) phosphorylation and its association with α-catenin. We want to investigate the role of protein Kinase D1 (PrKD1) in DNA damage response, using various prostate cancer cell lines; PrKD1-silenced cells (LNCaP sh-PrKD1) and overexpression of PrKD1 (C4-2 PrKD1). PrKD1 silence and overexpress cells were treated with PrKD1 inhibitor and Etoposide to observe the effect of DNA damage repair altering various genes in prostate cancer cells. Silencing α-Catenin increased p-γH2AX (ser-139) expression in C4-2 PrKD1 cells. Conversely silenced PrKD1 (LNCaP sh-PrKD1) cells represented decreased α-Catenin expression, and increased p-γH2AX (ser-139). Overexpression of PrKD1 in prostate cancer cells increased α-catenin levels and conferred resistance to etoposide-induced DNA damage. Silencing PrKD1 compromised DNA damage protective effect. Furthermore, we elucidate the role of Protein kinase D1 (PrKD1), a unique serine-threonine kinase that phosphorylates β-catenin at T120, in this interaction. We treated C4-2 and C4-2 PrKD1 cells with PrKD1 inhibitor and immuno-precipitated β-Catenin complex represented decrease in β-Catenin (T-120) and α-Catenin than untreated C4-2 PrKD1 cells. We observed crosstalk between α-catenin and PrKD1 in DNA damage repair. In-silico analysis affirmed that the loss of T120 phosphorylation disrupts β- and α-catenin interaction. PrKD1 inhibitor decreased cell viability in dose response fashion, and also decrease the p-γH2AX (ser-139) in C4-2 PrKD1 cells than C4-2 cells. In vitro findings were corroborated in a mouse prostate cancer PDX xenograft model by inhibiting PrKD1 kinase activity, resulting in reduced β-catenin T120 phosphorylation and α-catenin levels. In vivo experiments with PrKD1 inhibitor represented tolerability in mice and its efficacy in modulating α-catenin and PrKD1 expression to inhibit tumor progression. Study for the first time provides a mechanistic basis of the protective role of PrKD1 against DNA damage.

PREVENTION / EARLY DETECTION / INTERCEPTION: Animal and Cellular Models of Cancer Prevention and the Study of Biological/Biochemical Mechanisms
Poster Session

#3377 Exploring the role of obesity-induced exosome secretion and associated proteins in endometrial cancer pathogenesis: A roadmap for prevention through exosome inhibition.

T. Sakaue[1], **K. Dorayappan**[2], R. Zingarelli[2], W. Khadraoui[2], M. Anbalagan[3], J. Wallbillich[4], M. Wascovich[2], P. Paramita[2], A. Suarez[2], C. Cosgrove[2], L. G. Maxwell[5], H. Koga[1], D. O'Malley[2], D. Cohn[2], S. Karuppaiyah[2];
[1]Kurume University School of Medicine, Kurume, Japan, [2]The Ohio State University, Columbus, OH, [3]Tulane University School of Medicine, New Orleans, LA, [4]Wayne State University, Detroit, MI, [5]Inova Fairfax hospital, Virginia, VA

Introduction: Endometrial cancer (EC) is the leading gynecologic malignancy in the U.S., with obesity implicated in 57% of cases. This study explores the molecular workings of oncogenic protein expression (TMEM205, STAT5, and FAS) and their role in regulating exosome secretion. Understanding these mechanisms is crucial for unraveling pathways involved in obesity-related EC, informing the development of innovative strategies for prevention and treatment.
Methods: The isolated exosomes were quantified using nanoparticle tracking analyzer (NTA) and their size measured by Transmission electron microscopy (TEM). TMEM205, STAT5, FAS and PIAS3 expression was confirmed by IHC, ELISA and RT-PCR in patient and high fat diet treated mouse tissue. Endometrial hyperplasia was developed in immunocompetent mice using high fat diet (HFD; 45 kcal% fat diet) for 16 weeks.
Results: Our study investigates exosome secretion and the regulation of oncogenic proteins in adipose and uterine tissues from obese EC patients compared to non-obese EC samples. Analyzing the effects of a 45% kcal high-fat diet (HFD) on mice over 24 weeks, we observed higher body weight and increased adipose tissue in the HFD group, along with enlarged uterine horns and heightened inflammation. This correlated with elevated exosome secretion and increased expression of TMEM205, FAS and STAT5, while the tumor suppressor gene PIAS3 was downregulated. The identified small molecule inhibitor, DAP-5, selectively targeting TMEM205 and exosome secretion, demonstrated a significant reduction in body weight and adipose tissue accumulation when administered to HFD mice. Additionally, DAP-5 treatment restored normal uterine morphology and reduced the expression of exosome-related proteins.
Conclusion: This study offers central insights into the mechanisms underlying obesity-mediated TMEM205 expression and exosome secretion, shedding light on their role in the pathogenesis of EC. Additionally, it provides pre-clinical evidence supporting the initiation of the first in-human studies for exosome-targeted therapies aimed at preventing obesity-mediated EC.

#3378 Acinar cell susceptibility for tumor development in the pancreas: Targeting the critical regulators for therapy.

Z. Pan[1], J.-L. Van den Bossche[1], E. Rodriguez-Aznar[1], P. Janssen[1], O. Lara[1], G. Ates[1], A. Massie[1], D. Luc De Paep[2], I. Houbracken[1], M. Mambretti[1], I. Rooman[1];

[1]Vrije Universiteit Brussel (VUB), Jette, Belgium, [2]Universitair Ziekenhuis Brussel, Jette, Belgium

Acinar to ductal metaplasia (ADM) or acinar cell dedifferentiation is one of the most notable features of chronic pancreatitis. It is also considered the initial step of pancreatic cancer development when oncogenic mutations accumulate. However, its precise mechanism and regulatory pathways remain unclear. This study profiled the transcriptome of dedifferentiated acinar cells from both humans and mice. Differential expression analysis integrated with a systematic literature search revealed several potential regulators (e.g., GDF15, GFRA1, MXRA5, CXCL17), of which the expression pattern over time was validated by qRT-PCR. We also focused on multiple conserved pathways of cell survival, among which SLC7A11 (xCT) is transiently upregulated in both species. The xCT subunit, integral to the cystine/glutamate antiporter system xc-, plays a critical role in cell survival across various cell types. To elucidate its role in acinar dedifferentiation, we employed gene silencing, pharmacological inhibition, and a knock-out mouse model. Acinar cells with diminished xCT function exhibit increased ferroptosis linked to lipid peroxidation. Antioxidants such as N-acetylcysteine and ferroptosis inhibitors like Ferrostatin-1 can mitigate lower glutathione levels and lipid ROS accumulation. Similarly, in mouse acute pancreatitis, xCT prevents lipid peroxidation. Our findings indicate that xCT fuels the glutathione pool and maintains ROS balance during ADM, thereby preventing pancreatic acinar cells from ferroptosis, a form of cell death rarely reported in relation to ADM. Next to xCT, a future and similar comprehensive study of the aforementioned genes could provide valuable insights into the dynamic changes that occur during acinar cell dedifferentiation and pave the way to the discovery of new intervention targets to suppress tumorigenesis in chronic pancreatitis.

#3379 Single-cell profiling reveals dynamic epithelial and immune cell interactions in the progression of lung adenocarcinoma.

H. Chen[1], B. Zhu[1], J. Fujimoto[1], Y. Tian[1], J.-R. Li[2], C. Li[1], P. Chen[1], A. Reuben[1], M. Nilsson[1], X. Le[1], A. Poteete[1], S. M. Hubert[1], D. L. Gibbons[1], I. I. Wistuba[1], J. Wu[1], C. Cheng[2], J. V. Heymach[1], J. Zhang[1];

[1]The University of Texas MD Anderson Cancer Center, Houston, TX, [2]Baylor College of Medicine, Houston, TX

Background: Lung adenocarcinoma (LUAD) is a leading cause of cancer-related deaths. Our understanding of LUAD initiation and progression is limited, impeding early diagnosis and effective treatment. A comprehensive single-cell transcriptomic analysis, unraveling the malignant transformation from normal lung to LUAD, will provide key insights into the initiation and development of this challenging disease. However, human tissues are not amendable for such analysis.

Methods: We generated two mouse models, a genetically engineered mouse model with $Kras^{G12D}$ activating mutation (GEMM) and a carcinogen urethane-induced mouse tumor model (CITM) in the same 129S4 background. Single-cell transcriptome sequencing was conducted on lung tissues collected at five time points after induction for each model. The LUAD and its precursors were defined by experienced lung cancer pathologists as normal lung, hyperplasia, adenoma and adenocarcinoma. This analysis aimed to characterize the dynamic interaction between epithelial and immune cells, providing insights into the initiation and progression of LUAD.

Results: A comprehensive analysis identified a total of 12 major cell types, revealing a gradual increase in the proportion of epithelial cells during LUAD progression. EpiC 1, 2, 5 and 8 were consistently found in normal lung epithelium and various stages of abnormal epithelia, indicating their role as background components in lung tissues. In contrast, EpiC 4 emerged from hyperplasia and EpiC 0 and 3 emerged from early adenoma, while EpiC 6 and 7 were predominantly present in adenocarcinoma. Further investigation into the developmental trajectory of AT2 cells indicated a clear separation between normal (EpiC 1, 2, 5 and 8) and tumor cells (EpiC 0, 3, 4, 6 and 7). Cancer hallmark analysis revealed that tumor clusters exhibited higher scores in KRAS_SIGNALING_UP, HYPOXIA, APOPTOSIS, and P53_PATHWAY compared to normal epithelial clusters, suggesting the potential activation of these pathways in the tumorigenesis. Furthermore, the proportion of Macro_C1qc increased over time, accompanied by Macro_C1qc exhibiting the highest M2 signature score. This indicates a unique enrichment of M2-like macrophages in LUAD tissues. Remarkably, a notable increase in ligand-receptor pairs contributed significantly to the signaling from macrophages to tumor cells during progression. The dynamic regulatory interplay between Macro_C1qc and tumor cells was notably mediated by Thbs-Sdc1, App-Cd74, Spp1-Cd44 and other L-R pairs across various time points.

Conclusion: We constructed a single-cell LUAD developmental atlas of dynamic tumor-immune cell interactions, which sheds light on the initiation and progression of LUAD. Notably, our findings underscore a potential crucial role of macrophages, particularly M2 in lung tumorigenesis.

#3380 HER2 overexpression induces breast tumorigenesis in a non cell autonomous manner by inducing oxidative stress in the tissue microenvironment.

S. B. Gurler, O. Wagstaff, L. Dimitrova, F. Chen, R. Pedley, W. Weston, I. Donaldson, B. A. Telfer, D. Novo, K. Pavlou, G. Taylor, Y. Ou, K. Williams, A. Gilmore, K. Brennan, A. Ucar;
University of Manchester, Manchester, United Kingdom

Breast cancer is the most common cancer type in the world. Approximately 70% of pre-malignant breast tumours, known as ductal carcinoma *in situ* (DCIS), and 20% of invasive breast tumours overexpress HER2. Although molecular mechanisms of HER2 function in breast tumour cells have been extensively studied, our knowledge on how HER2 drives breast tumourigenesis at its pre-malignant stage is quite limited. Here, we investigate the HER2-overexpression driven cellular events at the earliest stages of breast tumourigenesis using *in vitro*, *in vivo and ex vivo* models. Using mouse models of HER2+ breast cancer and clinical samples of patients with DCIS, we showed that breast cancer stem cells (BCSCs) reside in HER2-negative population of tumour cells and arise from a HER2-negative cell-of-origin. Proteomics and metabolomics analyses of mammary ducts isolated from the MMTV-Neu mice at the pre-cancerous stage showed that *HER2/Neu* overexpression alters the energy metabolism in mammary epithelial cells *in vivo*. Furthermore, we have observed an accumulation of reactive oxygen species levels in pre-cancerous mammary ducts, which consequently causes oxidative stress induction and DNA damage in both HER2-positive and HER2-negative epithelial cells. Collectively, our findings indicate that HER2 overexpression in normal mammary epithelia may lead to a genotoxic tissue microenvironment that may consequently result in the accumulation of further somatic mutations in HER2-negative cell populations, which contain BCSCs and their cell-of-origin. Our findings therefore illustrate a novel mechanism explaining the HER2-driven breast tumour initiation and thus provide new avenues of research for developing novel preventive approaches against breast cancer.

#3381 Diversifying the breast cancer cell line repository with ACRJ-BC24, ACRJ-BC24α, and ACRJ-BC24β: Novel TNBC cell lines derived from an Afro-Caribbean patient.

I. Allen[1], S. Clarke[1], J. Ravix[2], A. P. Sanchez Covarrubias[3], A. Omotoso[2], D. Cornwall[1], S. N. Chin[1], S. Harrison[4], C.-H. Claude-Henry Volmar[2], S. Saigh[2], B. B. Cortes[1], E. Smith[2], R. Thompson[1], C. Ragin[4], S. George[2], **S. A. Badal[1]**;

[1]Univ. of the West Indies - Mona Campus, Kingston 7, Jamaica, [2]University of Miami, Miami, FL, [3]University of Miami, Kingston 7, FL, [4]Fox Chase Cancer Center, Philadelphia, PA

Breast cancer is a leading global health burden; however, women of African ancestry are disproportionately affected and have an increased risk of developing more aggressive breast cancer, triple-negative breast cancer (TNBC), and consequently suffering poorer outcomes. One factor contributing to this cancer disparity is the lack of diverse representation in preclinical models and clinical trials. Cell lines are widely used preclinical models, though of the breast cancer cell lines commercially available, only 8% are derived from women of African ancestry, compared to 90% from women of European ancestry. Thus, diversifying cancer cell lines would better represent the population as a whole and strengthen the translatability of results. The aim of this study was to develop and characterize three novel breast cancer cell lines derived from a woman of African-Caribbean ancestry, ACRJ BC24 parent, ACRJ BC24α, and ACRJ BC24β. Characterization assays included cell line authentication, growth curve analysis, western blots, immunohistochemistry staining, flow cytometry, whole-genome sequencing (WGS), RNA-sequencing (RNA-seq), xenografts, and karyotyping. Short tandem repeat profiling confirmed the novelty and human origin of the cell line. WGS confirmed the cell lines to be of 100% African ancestry. The ACRJ-BC24 parent, α, and β lines have been passaged over 70 times in vitro with a doubling time of 70 hours, 133 hours, and 70 hours, respectively. All cell lines were confirmed triple-negative, CD49f+ and EpCAM-, as well as CD44+ and CD24-, suggesting a basal-like subtype. Additionally, all the ACRJ BC24 cell lines expressed vimentin but not E-Cadherin, suggesting a mesenchymal phenotype. Expression of N-cadherin is demonstrated in the parent and α line, but not in the β line, showing varying levels of epithelial-mesenchymal transition amongst the lines. Additionally, varying intensity of expression of CD49f was observed between the three ACRJ BC24 lines, further confirming a biological distinction. Cytotoxicity of 10 chemotherapy drugs was assessed against the 3 novel cell lines and established lines (MCF7, T47D, HCC70, and HCC1806). Differential viability was observed among the cell lines as gemcitabine and docetaxel were most potent against ACRJ BC24α with IC_{50}s of 4.6 nM and 10 nM respectively compared to all other cell lines. Our findings confirm the need for increased representation of Black breast cancer cell lines among the preclinical panel for drug screens. The inclusion of these three novel Afro-Caribbean breast cancer cell lines in preclinical models will provide further insight into the current disparities among Black and White breast cancer cell lines.

#3383 Growth suppression and selective disruption of actin by alpha-santalol in human melanoma SK-MEL2 cells.

A. Bommareddy, **R. Chandrasekaran**, M. Lu, D. Penate;
Florida Atlantic University, Boca Raton, FL

Alpha-santalol, a major component of sandalwood oil has been shown to have chemopreventive and anti-tumor effects in different pre-clinical cancer models. The present study was undertaken to determine the *in vitro* efficacy of alpha-santalol on SK-MEL2 human melanoma cells and an immortalized human keratinocyte cell line (HACaT). In this study, we employed MTT assay, Trypan blue assay, wound healing assay, and confocal microscopy for imaging phalloidin/DAPI stained cells to investigate the cytotoxicity, cell viability, migratory potential respectively of the cells treated with different concentrations of alpha-santalol and DMSO for given time periods. Results showed that alpha-santalol treatment significantly decreased SK-MEL2 cell viability, wound healing, while only affecting HACaT cells at higher concentrations. Alpha-santalol treatment also disrupted actin cytoskeleton in SK-MEL2 cells, whereas HACaT cells were more resistant to this effect. In conclusion, the present study reveals selective growth inhibitory and anti-migratory effects of alpha-santalol in human melanoma cells and warrants future studies to systemically explore the mechanistic details involved in its growth inhibitory and antimigratory effects.

#3384 Rapid and automated tumor cell phenotyping based on annexin-mediated enforce blebbing response.

W. Huang[1], Z. Wang[1], D. W. Au[2], B. Tang[1], B. Qi[1], **W. C. Cho**[2], Y. Lin[1];
[1]The University of Hong Kong, Hong Kong SAR, China, [2]Queen Elizabeth Hospital, Hong Kong SAR, China

Introduction: Accumulating evidence supports the tight correlation between the physical characteristics of cells (including morphology, mechanical, and electrical properties) with the progression of cancer. Cellular blebbing, a distinctive feature observed during apoptosis and cell migration, has gained significant recognition. However, existing tools such as atomic force microscopy and optical tweezers have limitations in terms of throughput and complexity. Microfluidics has emerged as a promising technology to overcome these limitations.
Methods: In this study, we developed a novel microfluidic device with a double-layer compression mechanism to induce controlled blebbing of cells. We implemented a convolution-based tracing program to enhance the accuracy and efficiency of cell area measurement. The device was used to examine the enforced blebbing response of two human breast cancer cell lines (MDA-MB-231 and MCF-7) and investigate the potential of blebbing as a marker for drug resistance using a human lung cancer cell line (HCC4006). Additionally, we elucidated the role of annexin-6 (A6) in enforced blebbing and its underlying mechanism.
Results: Our microfluidic device successfully implemented a double-layered design that induced cell deformation through compression from the second pressurized polydimethylsiloxane layer. The findings revealed that highly invasive cell lines, such as MDA-MB-231 and osimertinib-resistant HCC4006, required significantly higher critical compression levels compared to their non-invasive counterparts (MCF-7 cell line) or osimertinib-sensitive cells. Moreover, the drug-resistant groups exhibited a greater compression strain requirement for blebbing compared to the control group, indicating their enhanced resilience against disruptive forces and superior survivability. Prior studies have demonstrated that A6 protein is recruited to the site of membrane injury and facilitates the formation of blebs, thereby contributing to cellular repair processes. Our further investigation into the role of A6 protein demonstrated its involvement in cell blebbing. Knockdown of A6 resulted in a notable 27% reduction in cellular volume, reflecting reduced intracellular pressure, and a corresponding 1.7-fold increase in the critical compressive strain necessary for inducing blebbing.
Conclusion: Our microfluidic device allows for rapid and simultaneous testing and automated analysis of hundreds of cells, making it suitable for applications such as cell sorting, highly invasive and drug-resistant cancer cell detection, without the need for labeling. Furthermore, it serves as a powerful tool for fundamental studies of membrane and cytoskeleton dynamics. The label-free nature of the device, coupled with its high throughput capabilities, highlights its potential in future applications, including cancer monitoring and drug-resistance screening.

#3385 Modeling evolutionary fitness in resistant cancers based on a common adaptability trait.

B. Singh, V. N. Sarli, A. Lucci;
UT MD Anderson Cancer Center, Houston, TX

Cancer is composed of a major subpopulation of proliferative cells and a minor subpopulation of highly adaptable cells. Although it is evident that cancer is an evolution like process driven by rare adaptable cancer cells that persist under various selection pressures, most of our knowledge about cancer comes from studying proliferative cancer cells. To overcome the hurdle in modeling adaptable cancer cell state that defeats all currently offered therapies, we are exploiting a linkage that exists between different adaptability substates such as metabolic, regulatory, and structural substates. Our studies, thus far carried out with aggressive triple-negative breast cancer and melanoma cell lines, suggest that it is feasible to apply severe metabolic challenges as realistic selection pressures/bottlenecks for modeling highly abnormal and highly adaptable cancer cells that drive cancer evolution and therapy resistance. The most significant aspect of our approach is an ability to model rare resistant cells (approximately 0.01% of cells) that survive in reversible quiescence under selection pressures. Monitoring of cells under microscope for several weeks under a severe and prolonged metabolic challenge, for example, a lack of glutamine in culture medium, revealed perhaps most interesting and cancer-relevant cells that survive in quiescence for weeks and then advance to generate therapy-resistant cells. Such microscopic monitoring revealed a significant heterogeneity among surviving cells. As examples, 1) surviving cells differ in the depth of quiescence, some cells trying to proliferate sooner than others; 2) as cells progress from quiescence to proliferation, their fate is far from certain: cells may progress to yield few cells, tiny colony, or large colony and then stop proliferating and in most instances die (abortive attempts at evolution). Of significance, the cell lines derived inflammatory breast cancer (IBC), an aggressive subtype of breast cancer, possessed a higher evolutionary fitness than non-IBC cell lines. This approach also eliminates 99.99% of cells that proliferate in cell culture but would not survive selection pressures in the body. The adaptable cells that survived the bottleneck and then proliferated indefinitely were highly resistant and metastatic. Molecular analyses of adaptable cells, including gene expression microarrays, CGH microarrays, and whole genome sequencing revealed mechanisms for their plasticity (exemplified by markers of high EMT), and for generating cellular diversity by altering epigenome (exemplified by low TET2) and by structural modifications in transcriptome (exemplified by high FTO). We conclude that the phenotype-based approach described here is good at modeling deep intrinsic resistance and may be useful in developing strategies for improving outcomes in resistant cancers. Supported by a State of Texas Grant for Rare and Aggressive Cancers.

#3386 Changes in extracellular vesicle miRNAs from three-dimensional ovarian cancer cell models reflect physiological changes and cancer survival.

N. Godbole[1], A. Ravichandran[2], D. Guanzon[1], A. Lai[1], F. Carrion[3], P. Kalita de Croft[1], L. Perrin[4], J. Hooper[4], L. Bray[2], C. Salomon[1];
[1]University of Queensland, Brisbane City, Australia, [2]Queensland University of Technology, Brisbane City, Australia, [3]Universidad del Alba, Santiago, Chile, [4]Mater Research Institute, Brisbane City, Australia

Ovarian Cancer (OC) is the most common gynaecological malignancy and the eighth most diagnosed cancer in females worldwide. Currently, it is the fifth leading cause of cancer-related mortality among patients globally, largely due to delayed diagnosis, chemotherapy resistance, high metastasis rates, and subtype heterogeneity. Recent OC research highlights extracellular vesicles (EVs) as pivotal contributors to intercellular communication and disease progression, elucidating the intricacies of OC pathology. EVs, diverse membrane-derived vesicles released by most cells, carry molecular cargoes containing proteins and nucleic acids. Studies indicate that the biogenesis, packaging, and release of EVs are highly dependent and sensitive to the cellular microenvironment and depend on the in-vitro and in-vivo modelling systems. Labs use varied model systems—2D monolayers, animal models, and innovative 3D models—to investigate EVs' ovarian cancer roles. Therefore, in this study we aimed to compare the miRNA profiles associated with EVs in 3D ovarian cancer cell models, and to identify the pathophysiological relevance of the EVs isolated from these models to the patient derived EVs.In this study, two OC epithelial cell lines, SKOV-3 and OVCAR-, were initially cultured as 2D monolayers and embedded within Gelatin Methacryloyl hydrogels. Over nine days, multiple assays observed spheroid formation within the cell-laden hydrogels. EVs isolated from the cell-conditioned media were characterized per MISEV 2018 guidelines. Small RNA sequencing identified statistically significant miRNAs, subject to gene ontology and gene rank analyses. EVs from a cohort of 60 OC patients were used to identify survival-associated miRNA profiles.Our findings in the cell-laden hydrogels demonstrated OC cell growth, proliferation, and aggregation into spheroidal structures, establishing an ideal 3D model. The isolated EVs were characterized for size, concentration, morphology, and surface markers. Small RNA sequencing revealed 18 significantly different EV-associated miRNA species across 3D vs 2D models, influencing apoptosis, angiogenesis, migration, and proliferation in ovarian cancer. Notably, 3D model-derived EV-associated miRNAs mirrored patient-derived EV-associated miRNA profiles, indicating their pathophysiological relevance.This study establishes a robust 3D OC model in hydrogels, showcasing growth, proliferation, and aggregation capabilities. Differential miRNA profiles between 3D and 2D model EVs highlight the critical roles of these miRNAs in essential ovarian cancer processes. Moreover, similarities between 3D model and patient-derived EV-associated miRNA profiles emphasize the clinical relevance of our model.

#3387 Spatial analysis revealed distinct molecular and immune landscape in genetic versus carcinogen-induced lung adenocarcinoma precancer mouse models.

B. Zhu[1], P. Chen[1], J.-R. Li[2], M. Aminu[1], C. Li[1], H. Chen[1], Y. Tian[1], F. R. Rojas[1], P. Edwin Roger[1], O. Shi[1], M. B. Nilsson[1], A. Poteete[1], S. M. Hubert[1], K. B. Khan[1], W. Lu[1], X. Song[1], J. Zhang[1], D. L. Gibbons[1], L. M. Solis Soto[1], I. I. Wistuba[1], J. V. Heymach[1], C. Cheng[2], J. Wu[1], J. Zhang[1];
[1]UT MD Anderson Cancer Center, Houston, TX, [2]Baylor College of Medicine, Houston, TX

Introduction: Our understanding of early carcinogenesis of lung adenocarcinoma (LUAD) is still rudimentary. Single-cell technologies have unveiled the intricate interaction between tumor cells and tumor microenvironment (TME) with unprecedented precision. However, the spatial context of single-cell phenotypes within TME during LUAD early carcinogenesis remain poorly understood. Here, we sought to characterize human-relevant murine LUAD precancer models to elucidate the molecular and immune changes in the spatial context during early LUAD carcinogenesis to inform lung cancer interception strategies.
Methods: We have developed genetically engineered mouse models (GEMMs) (129S4 KrasG12D) and carcinogen-induced LUAD precancer model (CITM) (129S4 Urethane). Lung tissues were collected at various time points after induction and analyzed using whole exome sequencing (WES), imaging mass cytometry (IMC), and spatial transcriptomics (10x Visium).
Results: Pathological image analysis demonstrated a significantly higher tumor burden ($p<0.01$) in the 129S4 KrasG12D model compared to the 129S4 Urethane model across different time points. WES revealed a progressive increase in tumor mutation burden (TMB) from precancers to invasive LUADs in both models, with the CITM model having significantly higher TMB ($p<0.05$) at matched timepoints than GEMM model. IMC assessed 39 biomarkers in 284 regions of interest (ROIs) and identified 1.4 million individual cells with 17 major cell types. Macrophages were the most prevalent immune cell type in TME, representing 9.00% of total cells in GEMM and 8.29% in CITM. The percent immune cells of the total cells progressively decreased from early-stage hyperplasia to late-stage adenocarcinoma in both models. The CITM exhibited a significantly ($p<0.05$) higher immune proportion than the GEMM model at hyperplasia and adenoma stages, with no significant difference at the invasive adenocarcinoma tumor cores between these 2 models. On the other hand, CITM had a significantly higher overall immune proportion ($p<0.05$) and the CD8 T cell and B cell proportions than GEMM tumor adjacent lung tissues at the adenocarcinoma stage leading to a significantly higher immune cell gradient between tumor adjacent lung tissues and tumor cores in CITM models. Spatial transcriptomics (ST) data demonstrated an increased presence of immune response signaling at the tumor adjacent lung tissues compared to the tumor core in the latest stage.
Conclusion: Spatial analysis revealed different molecular and immune landscapes in the genetic and carcinogen-induced LUAD precancer models, leading to distinct cellular spatial arrangements within the tumor microenvironment in each model. Overall, innate immunity, particularly macrophage, probably plays critical roles during early carcinogenesis of LUAD regardless of carcinogen exposure.

#3388 Targeting liver specific βII-Spectrin to prevent the development of metabolic dysfunction associated steatohepatitis (MASH) through CEACAM1 axis.

K. Bhowmick[1], K. Ohshiro[1], X. Xiang[1], S. John[1], X. Yang[1], N. Beauchemin[2], M. I. Hassan[3], T. Mohammad[3], **L. Mishra**[1];
[1]Feinstein Institute for Medical Research, New York, NY, [2]The Rosalind and Morris Goodman Cancer Institute, Montreal, QC, Canada, [3]Jamia Millia Islamia, New Delhi, India

Background: Obesity and pro-inflammatory alteration of the gut microbiome are risk factors for gastrointestinal (GI) cancers, including liver cancer (HCC). Dysregulated TGF-β signaling and loss of CEACAM1 activity are implicated in fatty liver disease. Clinically, 40% of human liver and GI cancers have genetic alterations in the TGF-β pathway members. CEACAM1 expression is significantly decreased in the liver of patients with Metabolic dysfunction-associated steatohepatitis (MASH). In contrast, in hepatocellular carcinoma (HCC), high CEACAM1 is associated with invasion, metastasis and poor prognosis. We hypothesized that TGF-β signaling and βII-Spectrin modulate MASH and HCC through CEACAM1.
Methods: Wild type and the liver-specific βII-Spectrin (*Sptbn1*) knockout (LSKO) mice fed a high-fat diet (HFD) or Western diet (WD) and analyzed for *Ceacam1* expression, changes in immune cell population, liver inflammation, and cancer. We used Alphafold and molecular modeling to identify the CEACAM1 and SPTBN1 interaction sites.
Results: Single cell sequencing analysis of MASH mice liver revealed that Ceacam1 expression is significantly decreased in hepatocytes. Interestingly, we found that CEACAM1 levels are restored to normal in tissues from liver-specific βII-Spectrin knockout (LSKO) mice. Transcriptomic and multiplex imaging analysis suggest that proinflammatory TGF-β signaling is activated and infiltration of CD11b+ cells is increased in MASH liver. These phenotypes are blocked in LSKO mice. Furthermore, siRNA-knockdown of βII-Spectrin blocks diet-induced obesity, fibrosis, lipid accumulation, tissue damage, and cancer susceptibility. We have also found that CEACAM1 interacts with the Smad3 adaptor, βII-Spectrin. Furthermore, structural analysis of CECAM1 and βII-Spectrin revealed critical residues involved in the interaction.
Conclusion: These data suggest that βII-Spectrin regulates CEACAM1 expression in the liver and is a potential target for therapeutic intervention to treat MASH and prevent progression to HCC.

#3389 Intraductal ablative procedure for local preventive intervention in rat models of breast cancer.

E. Zaluzec[1], M. Ashry[1], E. G. Phelps[1], **K. Kempinska**[1], E. Kenyon[1], L. Kenny[1], M. Volk[1], K. Powell[1], J. M. Hix[1], C. Mallett[1], M. Kiupel[2], E. M. Shapiro[1], L. F. Sempere[1];

[1]Michigan State University, East Lansing, MI, [2]Michigan State University, Lansing, MI

There are limited options for primary prevention of breast carcinoma (BC). Prophylactic mastectomy and systemic hormonal therapy are only recommended for high-risk individuals. Prophylactic mastectomy is a drastic surgery that removes the entire breast, including the epithelial cell-lined ductal trees where BC arises but also uninvolved stroma. Even with a 90% risk reduction, many women are deterred from prophylactic mastectomy due to its associated risk of infection, lymphedema, painful recovery time, and mental health toll. Hormonal therapies, tamoxifen and raloxifene, reduce BC risk by upwards of 50% but also increase the risk of uterine cancer and stroke. Thus, new interventions to reduce the risk of BC and minimize deterrents are necessary. Intraductal (ID) injection is a minimally invasive procedure that avoids systemic toxicity by cannulating a needle directly into the ductal tree opening to directly administer a solution to the epithelial cells. We previously reported that ID infusion of 70% ethanol (EtOH) as a cell-killing solution prevents tumor formation in an aggressive genetically engineered mouse model of BC with minimum collateral tissue damage. Here, we investigated the therapeutic efficacy of EtOH-based ablative solutions in a Methyl-N-Nitrosourea (MNU) chemically induced rat model of BC to assess scalability of this procedure towards clinical trials. Two weeks after tumor induction, rats received ID infusions of a solution containing 70% EtOH to ablate epithelial cells, ethyl cellulose (EC) to minimize collateral tissue damage, and/or Tantalum Oxide (TaO_x) to visualize infused ductal trees via micro-CT imaging. EtOH-infused glands had the longest tumor latency (273 days vs 97 days in control group, $p < 0.0001$). No statistically significant differences were noted in epithelial ablation or collateral tissue damage between treatment groups receiving ID injections of 70% EtOH with varying concentrations of EC, but there was a trend to lower collateral damage with EC-containing solutions. Local clearance of TaO_x in infused mammary glands enabled post-procedure MR imaging surveillance after 15 d of ID procedure. This preclinical study demonstrates that ID injection of a refined solution containing 70% EtOH and TaO_x is an efficacious and scalable procedure for primary prevention of BC.

#3390 Development of hypoxia responsive targeted polymersomes drug therapy validated using patient derived xenograft of triple negative breast cancer.

Y. S Ramakrishnan[1], S. Ambhore[1], C. Edvall[1], J. Mohammed[1], S. Mallik[1], D. M Tuvin[2], V. Sathish[1];
[1]North Dakota State University, Fargo, ND, [2]Sanford Broadway Clinic, Fargo, ND

Introduction: Eliminating triple-negative breast cancer (TNBC) resistance to neoadjuvant chemotherapy is a critical unmet clinical need. TNBC accounts for 20% of breast cancer and is more aggressive due to increased metastasis, high recurrence rate, and significant resistance to chemotherapy (e.g., Doxorubicin, DOX). Napabucasin (NAPA, a small organic molecule) is recognized to kill cancer stem cells by targeting the transcription factor STAT3 pathway and is currently in clinical trials. Our previous *in vitro* results showed significant effects with hypoxia-responsive targeted polymersomes compared to control in MDA-MB-231 and Patient-Derived Xenograft (PDX) TNBC cells. Further, we observed increased NRP-1 expression in TNBC patient-derived xenograft (PDX) cells under hypoxic (0.2% oxygen) conditions compared to normoxia (21% oxygen). Hence, we hypothesize that targeted hypoxia-responsive polymersome drug therapy would reduce the tumor growth of the PDX mouse model of triple-negative breast cancer *in vivo*.

Methods: We have established the TNBC PDX mouse model with two major phases, initial propagation (F1-F3) and final study phase (F3-F6), for *in vivo* study (TNBC tumor samples received from Sanford Broadway Clinic, Fargo, IRB approved). We utilized 3-6 months old female adult NSG mice (Jackson Lab) weighing 18-25 g. PDX tumor-bearing female NSG mice were administered polymersome-encapsulated drug (doxorubicin and other groups) by intravenous injection twice a week for 4 weeks and then observed the animals for an additional week. The percentage of tumor volume growth was calculated on these treatment groups and compared to vehicle. The tumors from all the groups were excised and dissected after the treatment and fixed in 10% formalin for histological evaluation. Tumors from all the groups after treatment were stained using hematoxylin and eosin to analyze the tumor core necrosis, and the average area of necrosis was compared among all the groups.

Results: The TNBC PDX mouse model treated with DOX alone and a combination of encapsulated DOX with NAPA showed significant weight loss compared to the control (over 4 weeks). DOX-alone treated mice have shown reduced tumor growth and exhibited a significant difference compared to the control group. Notably, the targeted DOX-encapsulated polymersome demonstrated a much lower tumor volume and displayed a marked difference compared to non-targeted vehicles, free-DOX, and saline. In the initial analysis, we observed a higher necrosis in the tumor of the targeted DOX-encapsulated polymersome compared to the control.

Summary and Conclusion: Overall, the hypoxia-responsive targeted polymersomes showed potent antitumor activity in the novel TNBC PDX animal model. With further developments, the targeted polymersomes might have translational potential as drug carriers for treating TNBC.

#3391 Effects of repeated psychological stress on NNK-induced lung cancer development in young female mice.

F. Jenkins[1], L. P. Stabile[1], J. R. Nedrow[1], K. Day[1], J. D. Latoche, Jr.[1], P. M. Tarwater[2], J. Manculich[1], **D. H. Bovbjerg**[1];
[1]UPMC Hillman Cancer Center, PIttsburgh, PA, [2]Texas A&M University, College Station, TX

Lung cancer is the second most common cancer in both men and women in the US and the leading cause of cancer death. Among younger US women, lung cancer incidence rates have in recent years become higher than rates seen in men, despite comparable histories of tobacco use. The possible contribution of stress to higher lung cancer risk in young women has received little research attention despite preclinical evidence that exposure to stress-related neuroendocrine responses can cause DNA damage. The present study used a well-established lung cancer model in young female mice (*in vivo* exposure to NNK) along with a mouse stress model to explore their independent and combined effects on lung cancer development. In addition, we explored one possible biological pathway by chronic administration of a beta-adrenergic receptor blocker (propranolol). We also tested the use of *in vivo* imaging for repeated monitoring of tumor development over time. Cohort 1 (n=60) had 4 groups: Home cage control, NNK treatment alone, repeated stress (RS) alone and NNK+RS. Cohort 2 (n=60) had the same 4 groups with the addition of administration of propranolol in drinking water. Cohort 3 (n=48, imaging cohort) had 3 groups: Home cage control, NNK alone and NNK+RS. FVB/N (4-6 wk) were purchased from a commercial supplier and acclimated with gentle handling for two weeks. The repeated stress protocol began week-3 and continued for the duration of the study. It combined two well-established rodent models: social disruption stress via changes in cage mates at the time of cage cleaning (2x/week) and a 90-minute restraint stress immediately prior to cage change (1x/week). NNK or saline treatment began on week-4 (IP; 2x/week; 3 mg/injection) and continued for 4 weeks. 21 weeks after stress initiation, the mice in cohorts 1 and 2 were sacrificed, lungs removed, inflated and tumors counted and sized. Mice in cohort 3 were imaged by Hounsfield-calibrated micro-CT (μCT) at baseline, 14, 19 and 23 weeks. The entire lung space, excluding the heart, was defined as a volumetric region of interests (VOIs). The VOIs were subjected to thresholding to segment the lungs into air space and tissue space compartments. The volume of tissue space of each animal was ratioed against its own baseline tissue space volume. Results from Cohort 1 revealed significantly greater numbers and overall size of lung tumors in stressed mice that received NNK. No significant effects were seen in the absence of NNK. Results from Cohort 2 revealed no significant differences between stressed and unstressed groups treated with propranolol. Cohort 3 revealed a pattern of results with stressed mice generally showing the highest lung tumor volume levels (Hounsfield Units), which reached significance at 19 weeks in preliminary analyses.
Conclusion: In this study, we found that repeated stress increased lung tumor burden in female mice treated with NNK, and that a beta-adrenergic pathway may be involved.

#3392 Generation and characterization of transgenic oncopig model for lung cancer.

Kirtan Joshi[1], Nagabhishek Sirpu[2], Amanda Schmelzle[3], Ravikanth Poonooru[3], Benjamin Nelson[3], Pradeep Subramanyam[3], Colleen Garrett[4], Mariana Sponchiado[3], Sarah Schlink[4], Samantha Gerb[4], Jesse Porter[5], Dae Kim[6], Jeffrey Kunin[5], Jeffrey Bryan[7], Timothy Hoffman[8], Bhanu Telugu[3], Jussuf Kaifi[9], Satyanarayana Rachagani[10]

[1]Department of Medicine and Surgery, University of Missouri - Columbia, Columbia, MO,[2]Roy Blunt NextGen Precision Health Institute, University of Missouri - Columbia, Columbia, MO,[3]National Swine Resource and Research Center, University of Missouri - Columbia, Columbia, MO,[4]Veterinary Medicine And Surgery, University of Missouri - Columbia, Columbia, MO,[5]Department of Radiology, University of Missouri - Columbia, Columbia, MO,[6]Department of Veterinary Pathobiology, University of Missouri - Columbia, Columbia, MO,[7]Department of Veterinary Medicine and Surgery, University of Missouri - Columbia, Columbia, MO,[8]Department of Medicine-Division of Hematology and Oncology, University of Missouri - Columbia, Columbia, MO,[9]Department of Surgery-Section for Thoracic Surgery, University of Missouri - Columbia, Columbia, MO,[10]Department of Veterinary Medicine And Surgery, University of Missouri - Columbia, Columbia, MO

Lung cancer (LC) is the leading cause of cancer-associated death in the United States. Preclinical findings in small animal models do not translate into human clinics. There is an urgent need to develop relevant preclinical large animal models for LC. We describe a novel method to induce LC in transgenic pigs carrying Cre-inducible $Kras^{G12D}$ and $TrP53^{R167H}$ mutations (Oncopigs).

The Oncopigs (n=12; 9 females, and 3 males) at 9 weeks of age were anesthetized and adenovirus ($1x10^{11}$ PFU) carrying Cre recombinase gene (Ad-Cre) ± polybrene (1:100) ± IL-8 (5 ng/ml) was injected via flexible bronchoscopy with two techniques: (1) Bronchial lavage (n=6) and (2) Transbronchial needle injection (n=6) into different lung lobes. As controls, a combination of polybrene ± IL-8 was injected without AdCre into the contralateral lobes in the same pigs (n=8). Oncopigs were monitored via clinical monitoring, blood counts, basic metabolic panel, and contrast-enhanced computed tomography (CT) imaging for LC progression and metastasis at 3-, 4-, 7-, 10-, 16-, and 26 weeks post-intervention.

All animals tolerated the injections with expected weight gains. Blood counts and metabolic panels remained normal during LC progression. At the site of injection/lavage, lung masses were detected on CT imaging at 3 weeks post-injections. However, a decrease in masses was observed on CT at 7 weeks post-intervention. The decrease in size of the lung masses coincided with increasing attenuation. No distant metastases were observed on CT imaging. Lavage-based lesions appeared to be more heterogeneous with surrounding inflammatory changes. Transbronchial-injection-based lesions appeared more consolidated and coin-shaped without surrounding inflammatory changes. Control injection sites did not show any mass growth on CT imaging.

Immunohistochemistry analysis on lung tumors revealed increased pancytokeratin, trichrome, E-cad, Ki-67, IBA, and CD3 expression. Further, immunofluorescence revealed decreased E-Cad, CK-19, and Zo-1 expression, whereas increased expression of N-Cad, FN1, snail, CD44, α-SMA, and γ-catenin, was observed in the LC and metastatic tissue compared to normal.

We successfully generated and characterized a novel transgenic Oncopig LC model. There is robust tumor production status post AdCre delivery. One of four Oncopigs had carcinomatous metastatic skin growth. The remaining 7 Oncopigs are monitored longitudinally for tumor growth and development of metastasis.

#3393 Deciphering colorectal cancer: A model to study sex-based differences and role of estrogen amidst obesity.

P. Wele, H. Shi, X. Wu;
Miami University, Oxford, OH

Worldwide statistics indicate that obesity is increasing globally, mostly due to the consumption of Western diet. The literature points out that obesity is a potent risk factor for the development of colorectal cancer (CRC). Interestingly, CRC incidence is higher in men compared to women, and the sex hormone estrogen protects reproductive-age females from CRC despite obesity. In this project, we aim to understand the sex-based differences and protective role of estrogen in obesity-influenced CRC. An improved mouse model was devised where the effects of obesity and estrogen in CRC could be meticulously studied. We deployed 4-5-week-old male and female FVB/NJ mice and performed either sham surgery (males and females) or bilateral ovariectomy (OVX) (females). Post one week of recovery, all mice were randomly sub-grouped into either low-fat diet (LFD, 10% fat) or high-fat diet (HFD, 60% fat) groups, weekly injected with a colon-specific carcinogen azoxymethane (AOM; 5 mg/kg for week 1, 10 mg/kg for weeks 2-6), and cyclically every 4-5 days injected 17-beta-estradiol (E2; 4 µg/mouse) to a group of OVX mice for the study period of 22 weeks. The body weight of all mice was tracked every week. A whole-body composition analysis after 22 weeks showed that males and OVX females are more obese compared to females with sham surgery and OVX females with E2 injection (OVX+E2), respectively. Additionally, mice on HFD had a higher body weight compared to those on LFD; however, the absence of estrogen in OVX females led them to have higher body weight compared to sham and OVX+E2 females. Moreover, a significant difference was observed in the tumor size between males and females, females and OVX females, and OVX and OVX+E2 females. Study models have rarely incorporated both sex-dependent differences and diet-induced obesity in understanding CRC. With the current study model, it is anticipated to learn more about these differences at molecular, cellular, and metabolic levels.
Acknowledgments: 1) NIH/NCI R15 [To HS, XW]; 2) Miami University CFR Faculty Research Grants [To HS, XW, JZ]; 3) Miami University's College of Education, Health, and Society Interdisciplinary Research Seed Grant [To HS, XW, JZ]; 4) Sigma Xi Grants in Aid Research [To PW]; and 5) We thank Jazzminn Hembree (Director of Laboratory Animal Resources, Miami University) and Laboratory Animal Resources, Dr. Jiangjiang Zhu (Department of Human Sciences, Ohio State University), Dr. Jing Zhang (Department of Statistics), and Dr. Ramiro Malgor (Director of Histology Core Facility, Ohio University)

#3394 Participation of molecular iodine and PPARG in prostate cancer progression and neuroendocrine differentiation.

C. Montes de Oca, L. Alvarez, C. Aceves, B. Anguiano;
Universidad Nacional Autonoma de Mexico (UNAM), Queretaro, Mexico

Introduction: Advanced prostate cancer (PCa) therapy is based on androgen deprivation; however, cancerous cells develop resistance, and can develop a highly aggressive neuroendocrine (NE) phenotype. Molecular iodine (I_2) has antitumoral effects in breast cancer models, in which PPARG receptors represent the main mechanism of action described. In PCa though, PPARG is considered pro-tumoral and I_2 effects have not been fully studied. Hence, the aim of this study was to analyze I_2 individual and combined effects with androgen deprivation by using both androgen dependent (AD) and independent (AI), *in vitro* and *in vivo* PCa models.

Methods: *In vitro.* I_2 effects in cell viability and invasion were analyzed in AD (LNCaP) and AI (DU145, PC3) PCa cells. LNCaP cells were also treated with androgen receptor (AR) antagonists. PPARG participation in I_2 effects was assessed with GW9962 (antagonist) and rosiglitazone (agonist). NE phenotype was induced in LNCaP by prolonged culture under androgen-depleted conditions and was assessed by measuring the growth and length of neurite-like projections. RT-qPCR was employed to assess the expression of NE markers (*SYP, ENO2*), and lipogenic genes (*FASN, SREBF1*). *In vivo.* Eighteen weeks-old TRAMP mice were subjected to sham surgery or castration, and were provided or not with I_2 (0.025%, drinking water) for four weeks. Prostates were subjected to histopathological analysis (H&E and Masson's trichrome) and IHC (AR, SYP, PPARG). Scoring systems were used to grade the severity of high proliferative intraepithelial lesions (HPIN), and desmoplasia.

Results: I_2 decreased the cell viability and invasion capacity of all PCa cells tested, and when supplied with AR antagonists further enhanced their antiproliferative effects in LNCaP cells. I_2 failed to induce the expression of PPARG target genes, and GW9662 did not prevent I_2-induced decrease in cell viability. Like androgen deprivation, I_2 also caused NE-like morphology in LNCaP cells, but unlike androgen deprived LNCaP cells, I_2 treated cells had decreased expression of NE markers. In TRAMP mice, I_2 increased the presence of HPIN, reduced nuclear AR protein detection, and had no effect on PPARG. As expected, castration reduced HPIN, caused epithelial atrophy and desmoplasia; decreased total AR levels and PPARG nuclear levels. However, the number of NE (SYP-positive) cells did not change. The addition of I_2 to castration did not modify the score of epithelial lesions but increased the desmoplasia and the presence of NE cells.

Conclusions: I_2 exhibited *in vitro* antineoplastic effects over epithelial cells, however, these effects did not translate into the *in vivo* model. PPARG did not seem to mediate I_2 effects. Overall, our data suggest that tumoral microenvironment may interfere with I_2 epithelial-specific antitumoral effects.

Funding: PAPIIT-UNAM (IN217223, IN202322) and CONAHCYT (774791).

#3395 Polyisoprenylated cysteinyl amide inhibitors: Effects on RAS signaling pathway intermediates and viability of mutant *KRAS* African American lung cancer cell line.

Justin K. Mensah-Mamfo[1], Kweku Ofosu-Asante[1], Jassy Mary S. Lazarte[1], Amarender Goud Burra[1], Sofia A. Lugo[2], Yong Huang[3], Ite A. Offringa[2], Nazarius S. Lamango[1]

[1]Florida A&M University, Tallahassee, FL,[2]University of Southern Carlifornia, Los Angeles, CA,[3]University of Florida, Gainesville, FL

Mutated *KRAS* is the most common cancer driver gene in lung adenocarcinomas in all racial and ethnic groups, including Blacks/African Americans (B/AAs). Drugs developed to combat KRAS-driven cancers become less effective due to intrinsic changes in the cells resulting in resistance and relapse. Due to the enormous challenges encountered in developing direct KRAS inhibitors, agents targeting alternative downstream RAS mediator kinase enzymes of the MAPK and PI3K/AKT signaling pathways have been developed. However, other avenues that directly target KRAS and similar cancer drivers must be explored to obtain alternative effective therapies. PCAIs constitute a group of potential anticancer agents that we developed to specifically disrupt and suppress signaling by hyperactive G-proteins such as mutated KRAS. In previous studies, PCAIs stimulated MEK1/2, ERK1/2, p90RSK and AKT phosphorylation resulting in cell death. The present study aims to determine whether specific inhibitors of the kinases can reverse PCAIs-stimulated phosphorylation and cell death. PCAIs were thus tested against the KRAS mutant NCI- cell line H23 (from a B/AA patient) and compared to $KRAS^{G12C}$ inhibitor Sotorasib and other kinase inhibitors drugs. The EC_{50} values for the PCAIs NSL-YHJ-2-27 and NSL-AB-45 were 4.1 ± 0.3 and 5.5 ± 0.1 µM, respectively, compared to Gefitinib (EGFR), Sotorasib ($KRAS^{G12C}$), Dabrafenib (BRAF), Selumetinib (MEK1/2), Ulixertinib (ERK1/2) and Ipatasertib (AKT) whose EC_{50} values were 83 ± 12.9 µM, 38 ± 5.5 µM, 33 ± 1.2 µM, 71 ± 5.3 µM, 11 ± 0.2 µM, 12 ± 1.0 µM, respectively. The results indicate that the PCAIs are more effective against NCI-H23 than the other kinase inhibitor drugs. Future work will determine the effects of co-treating cells with the PCAIs and the respective kinase inhibitors on cell viability and PCAIs-induced phosphorylation of the kinases. Supported by grants U54CA233396, U54CA233444, and U54CA233465 from the National Institutes of Health (NIH)/National Cancer Institute (NCI) and the Norris Comprehensive Cancer Center core grant, award number P30CA014089 from the NIH/NCI

PREVENTION / EARLY DETECTION / INTERCEPTION: Cancer Control and Survivorship
Poster Session

#3399 Prediction of cardiac adverse events (AE) in trastuzumab treated breast cancer patients (pts) via a comprehensive genomic and DNA methylation blood based assay.

S. Gordon, C. Barbacioru, D. Gaile, D. Tolkunov, N. Zhang, C. Espenschied, J. Wang, T. Dinman, K. Banks, A. Das, H.-Y. Chuang, H. Eltoukhy; Guardant Health, Redwood City, CA

Background: *ERBB2* (HER2) targeted therapy is an important therapeutic class used to treat HER2-positive breast cancer (BC) but has been associated with a risk of cardiotoxicity. Identifying pts likely to experience this AE could allow for early intervention and/or a change in treatment plan. Previous studies have demonstrated the ability to detect changes in methylation patterns of pts who had cardiotoxicity from anti-HER2 therapy. Here, we report a retrospective study assessing the feasibility of using the Guardant Infinity platform (genomic and epigenomic NGS analysis) to predict severe cardiac AE in pts treated with trastuzumab.

Methods: Samples (n=46) from female pts with BC undergoing treatment with trastuzumab without prior record of heart failure and with a blood sampling <300 days prior to a documented heart failure event defined a positive case cohort. 70 blood samples were matched to the positive case cohort in all above attributes but without record of patient heart failure to comprise a negative cohort. The >20K differentially methylated regions on Guardant Infinity platform may be useful for detection of specific disease attributes such as treatment-associated AE. To explore this, mixture models were first trained using 880 BC samples unrelated to heart failure to distinguish methylation signals coming from tumor versus non-tumor cfDNA. The resulting normalized methylation signals represent the posterior probabilities of the region molecules to be derived from tumor cells. A subset of methylation regions were selected based on significance of association between heart failure status and normalized methylation signals in the positive and negative AE cohorts. A penalized logistic regression model was then trained on the normalized signals of the selected methylation regions to predict whether a patient would have future cardiac AE.

Results: A 10-fold cross validation of the penalized logistic regression models trained on normalized methylation signals produced an area under the curve of 0.78 for predicting heart failure status, suggesting feasibility of using blood-based methylation signals to predict cardiac AE on this platform. The differentially methylated regions selected as model predictors show a clear separation in hypermethylation status between positive versus negative cohorts.

Conclusion: Our results show the prediction of cardiac AE in BC pts undergoing trastuzumab treatment in advance of documented heart failure using a blood-based assay designed for simultaneous comprehensive genomic and epigenomic profiling. Given the relatively small sample size within this study, further refinement and validation of the classification models is warranted and ongoing.

#3400 Single-cell proteogenomics analysis of AML samples treated with decitabine and venetoclax reveals divergent treatment escape mechanisms.

Y. Kim, Z. Li, A. Maiti, T. Tanaka, H. Uryu, K. Furudate, K. Hayes, N. Daver, N. Pemmaraju, T. M. Kadia, F. Ravandi, N. J. Short, M. Ohanian, G. Borthakur, N. Jain, G. C. Issa, L. Masarova, S. M. Kornblau, W. G. Wierda, S. Loghavi, S. A. Wang, G. Garcia-Manero, H. Kantarjian, C. D. DiNardo, M. Y. Konopleva, K. Takahashi;

The University of Texas MD Anderson Cancer Center, Houston, TX

The combination therapy of hypomethylating agents and venetoclax (HMA+Ven) has emerged as a standard of care for acute myeloid leukemia (AML) patients unfit for intensive chemotherapy. Nonetheless, significant clinical challenges persist including relapse and treatment resistance, to which our understanding remains incomplete. Previous studies have revealed genetic (RAS/RTK pathway mutations and *TP53* mutations) and phenotypic (monocytic differentiation) resistance mechanisms. In this context, we hypothesized that integrative assessment of both genetic and phenotypic factors could further unveil the contributors of HMA+Ven resistance. To determine the predictors of treatment response, we first analyzed the baseline characteristics of 208 newly diagnosed, secondary, and relapse/refractory AML patients treated with Decitabine and Venetoclax (Dec+Ven). While complex cytogenetics, KRAS and TP53 mutations were significantly associated with treatment resistance, phenotypic factors such as bone marrow cell compositions or French-American-British (FAB) classifications were not. To identify the factors of resistance at the cellular level, we performed a single-cell targeted DNA-antibody sequencing (DAb-seq) on a subset of 33 patients. In total, 60 multi-timepoint bone marrow samples were analyzed, which included five patients with paired baseline-relapse timepoints. From all five patients, we identified that stem-like cells were largely eradicated and replaced by more differentiated cells such as monocyte-like or erythroid-like cells. At relapse, we identified three patterns of phenotypic shifts: monocytic shift, erythroid shift, and mixed monocytic/erythroid shift. The phenotypic shifts were not always associated with the expansion of new genetic mutations, except for in two cases: one patient had monocytic shift accompanied by the expansion of *KRAS* mutation, and another patient had erythroid shift accompanied by the expansion of *NRAS* mutation. To examine the mechanisms behind the phenotypic shifts, we performed a single-cell RNA sequencing on three of the relapsed patients. As a result, we confirmed the upregulation of BCL2L1 in the patient with erythroid shift (N=1), and MCL1 in the patients with monocytic shifts (N=2), but not BCL2 in both. These findings are consistent with known dependency of these cells on non-BCL-2 anti-apoptotic proteins such as MCL-1 and BCL-xL. To summarize, we conclude both genetic and phenotypic factors play a role in Dec+Ven resistance. Most importantly, we report that divergent phenotypic transitions, from stem-like toward more differentiated phenotypes (monocytic or erythroid), were frequently observed in AML relapse following Dec+Ven therapy. Close monitoring of phenotypic alterations during HMA+Ven treatment may facilitate the precise identification of AML patients predisposed to relapse.

#3401 Uncovering virus induced dysregulated processes in cancer and their impact on outcomes.

M. Soleimanpour moghadam, A. Khosh, D. Ebrahimi;
Texas Biomedical Research Institute, San Antonio, TX

The National Cancer Institute has designated several viruses such as EBV, HBV, HCV, HIV, HPV, and HTLV as agents that either cause cancer or increase the risk of developing cancer. However, extensive analyses of tumor genome and transcriptome datasets have identified numerous additional virus types, the functional implications of which remain largely unknown. Viral infection often dysregulates unique molecular processes within tumor cells and alters the composition of immune cells in the tumor microenvironment. For instance, HPV-positive tumors have been shown to exhibit a significantly elevated expression of the DNA editing enzyme APOBEC3B compared to HPV-negative tumors. Furthermore, HPV positive tumors display and increased number of C-to-T mutations induced by this protein. The genome and transcriptome of tumor tissue biopsies contain a wealth of information about these virus-associated signatures. However, advanced signal processing approaches are needed to extract these viral signatures from complex tumor datasets, and elucidate their specific roles in cancer. Here, we developed a quantitative approach to investigate the link between viral infection and dysregulation of a seven-membered A3 enzyme family (A3A/B/C/D/F/G/H). The primary role of these enzymes is to restrict viral infections by inducing C-to-U mutations in viral genomes. However, at least three members of this enzyme family (A3A/B/H) can also induce mutations in cellular DNA, and drive tumor formation and evolution. We used NMF (Nonnegative Matrix Factorization) to deconvolute the expression profiles of A3 enzymes in >10,000 bulk RNAseq datasets from diverse TCGA tumors. This analysis revealed the expression profiles of A3 enzymes within tumor and tumor microenvironment cells including various immune cells. Next, we conducted an association analysis to identify the link between the presence of viral infection and the proportion of each of these tumor and tumor microenvironment expression profiles. As expected, our analyses revealed strong associations between tumor-specific A3 expression profiles and infections by oncolytic viruses such as HPV. Notably, and somewhat unexpectedly, our analyses also revealed associations with viruses about which little is known in the field of cancer. For example, in certain tumors, we identified a robust association between bacteriophages and a tumor-specific A3 expression profile characterized by A3B upregulation. Taken together, our analyses provide evidence for the link between A3 dysregulation and infection by viruses including bacteriophages.

#3402 Integration of microRNAs and transcriptome signatures identifies the persistent infection of hepatitis C virus-induced hepatocellular carcinoma.

W.-H. Su, C. S. Shabangu, S.-C. Wang;
Kaohsiung Medical University, Kaohsiung, Taiwan

MicroRNAs (miRNAs) are short non-coding RNAs (ncRNAs) of ~22 nucleotides that mediate gene expression through various functions, including gene silencing, which can lead to translation repression and degradation of target mRNAs. Dysregulation of miRNA function has been associated with numerous diseases, particularly cancer, including hepatocellular carcinoma (HCC). During the progression of HCV-HCC, the function of miRNAs may be altered thereby altering gene expression to favor HCC. Therefore, the involved miRNA-mRNA interaction needs to be further studied. In addition, there are many clinical studies have shown that HCV patients who do not adequately control their diet which are prone to fatty liver accumulation (steatosis), it may increase the possibility of liver cirrhosis. In the current study, we aim to investigate the function and effects of persistent HCV-induced miRNAs expression in liver hepatocellular carcinoma progression and gene expression and to explore the mechanisms and regulatory genes of liver steatosis caused by HCV patients in a high-fat environment. We used the Huh751 cell line and the infected with the HCV JFH1 replicon of low-viral load S2 cells. We used an HCV miRNA array for initial identification of potential candidates. These miRNAs were analyzed for KEGG pathways via DIANA. Next, we identified miRNA-mRNA targets in 3 databases (miRDB; miRPathDB; TargetScan) and analyzed the targets for KEGG pathways using ShinyGO. The target miRNA-mRNA candidate genes were then compared with long-term JFH1 replicon infectious cell (L-HCV) NGS mRNA data to integrate miRNA-mRNA. The identified genes were analyzed in The Cancer Genome Atlas (TCGA) for survival, biological process, and expression in LIHC Big Data. Hsa-miR-215, hsa-mir-10b, and hsa-let-7a of L-HCV miRNAs group showed high significance for LIHC overall survival with a hazard ratio >1.0. Moreover, miRNAs associated with L-HCV survival were LIHC-specific but not in other cancers. Through systematic integration of these findings, we identified HMOX1 and BMF genes as being specifically associated with HCC and regulated by hsa-miR-215-5p, hsa-miR-10b-5p, and hsa-miR-7a-5p. In addition, we also found that the expression of the adipogenesis genes, FABP4 and adipogenesis gene, SREBP1, as well as the viral non-structural protein, NS3, was significantly increased in the HCV-high-fat group; and the expression of the gene IRS1, which is involved in hyperinsulinemia, showed a decreasing trend. The main cause of HCC is that HCV inhibits the expression of hsa-miR-215-5p, hsa-miR-10b-5p, and hsa-miR-7a-5p, leading to alter the expression of target genes, these have a significant effect on survival, suggesting that an essential role in virus-related liver cancer. In the future, we will further explore the regulatory mechanisms between these genes and HCV in a high-fat environment.

#3403 Disentangling the obesity paradox in high-grade serous epithelial ovarian cancer.

Evan W. Davis[1], Nancy Barone[1], Charles Roche[2], Gyorgy Paragh[3], Andre Klein[4], **Rikki Cannioto**[1]

[1]Cancer Prevention and Control, Roswell Park Comprehensive Cancer Center, Buffalo, NY,[2]Diagnostic Radiology, Roswell Park Comprehensive Cancer Center, Buffalo, NY,[3]Dermatology; Cell Stress Biology, Roswell Park Comprehensive Cancer Center, Buffalo, NY,[4]Information Technology, Roswell Park Comprehensive Cancer Center, Buffalo, NY

Background: Previously published evidence suggests an 'obesity paradox' in epithelial ovarian cancer, where excess adiposity is linked to better survival. However, prior studies did not jointly consider skeletal muscle, a key prognostic factor in cancer. Addressing this gap, our study examines the combined effects of adiposity and muscle phenotypes on mortality in high-grade serous epithelial ovarian cancer (HGSOC), offering novel insights into the role of body composition in patient outcomes.

Methods: 343 HGSOC patients from the Body Composition and Epithelial Ovarian Cancer (BComES) Cohort at Roswell Park were included in this analysis. Body composition was derived from sliceOmatic software using computed tomography images obtained prior to chemotherapy. Body composition was quantified as surface area (cm^2) at L3 for intermuscular adipose tissue (IMAT), visceral adipose tissue (VAT), subcutaneous adipose tissue (SAT), total adipose tissue (TAT), and skeletal muscle index (SMI). SMI<38.5 cm^2/m^2 was defined as low SMI, a proxy for sarcopenia. For each adipose depot, phenotypes were categorized as: 1) low adiposity/high SMI (optimal/referent); 2) high adiposity/high SMI; 3) high adiposity/low SMI (e.g., sarcopenic obesity); and 4) low adiposity/low SMI (e.g., cancer cachexia). Multivariable Cox models adjusted for age, tumor stage, and surgical debulking status were used to estimate Hazard Ratios (HR) and 95% Confidence Intervals (CI) representing associations of each body composition phenotype with mortality.

Results: High IMAT and VAT were associated with increased mortality in patients with high SMI (HR=1.80, 95% CI: 1.18-2.74 and HR=1.96, 95% CI: 1.27-3.04, respectively) and low SMI (HR=1.65, 95% CI: 1.05-2.61 and HR=1.70, 95% CI: 1.04-2.80). High SAT and TAT were also associated with increased mortality in patients with high SMI (HR=1.74, 95% CI: 1.14-2.67 and HR=2.04, 95% CI: 1.31-3.18), but associations were shy of significance for patients with low SMI (HR=1.37, 95% CI: 0.85-2.23 and HR=1.58, 95% CI: 0.95-2.61). Lastly, low SMI and low adiposity was associated with increased mortality for VAT (HR= 1.65, 95% CI: 1.01-2.70), SAT (HR=1.88, 95% CI: 1.14-3.10), TAT (HR=1.97, 95% CI:1.19-3.26) and IMAT (HR=1.46, 95% CI: 0.85-2.53).

Conclusions: In this study, we observed no support for an obesity paradox. Rather, we observed compelling evidence linking high adiposity phenotypes with striking increases in HGSOC mortality, regardless of SMI. Notably, as the cachectic phenotype was also linked to substantial increases in mortality, unwittingly assigning patients with low adiposity and low muscle to a reference group in adiposity research could falsely induce an ‘obesity paradox’. Importantly, as body composition can be modified through diet and exercise, our data establishes it as a potential therapeutic target alongside chemotherapy to improve outcomes in this deadly disease.

#3404 Body weight trajectory among patients with non-small-cell lung cancer receiving immune checkpoint inhibitors.

T.-Y. D. Cheng, B. Kinder, R. T. Akasheh, C. M. Mahenge, C. J. Presley, P. G. Shields, X. Nguyen, A. Shendre, Z. Li, L. Li;
The Ohio State University, Columbus, OH

Objectives: Body weight is an important prognostic factor in patients with lung cancer. As immunotherapy involves toxicities, body weight may be affected during the treatment course. The objective of this study is to examine the trajectory of weight changes at 180 and 365 days after the initiation of immune checkpoint inhibitors (ICIs) among patients with NSCLC.

Methods: Retrospective chart review and data extraction were performed among patients receiving ICIs at the Ohio State University Comprehensive Cancer Center between 2015 and 2021. Patients with NSCLC were included in this study if their initial treatment entailed a PD-1/PD-L1 ICI), either alone or in combination with chemotherapy/targeted cancer drugs, and if they also had their body weights recorded on ICI initiation and 180 days after (± 30 days) treatment initiation. A subset of these patients who had body weight data on day 365 of ICI initiation were included in additional analysis. Percentages of change in body weight relative to pre-ICI were calculated ([weight at 180 or 360 days minus pre-ICI weight] divided by pre-ICI weight x 100%) and examined by treatment regimen and pre-ICI body mass index (BMI) using t-tests. A sensitivity analysis was performed by excluding 11 patients with cachexia defined by the presence of ICD-9 (799.4) or 10 (R64) codes in their medical records.

Results: A total of 554 patients with NSCLC received any ICI; 139 patients met the inclusion criteria, of which 96 had body weight data on day 365. The mean age of diagnosis was 63.8 (SD=10.1); 80% were White and 18.7% were Black. The median time on ICI was 195 days (inter-quartile range, 55-392 days) among patients with ICI only and 255 days (inter-quartile range, 126-479 days) among patients with ICI combined with chemotherapy or targeted cancer drugs. Among patients receiving ICI only, body weight increased among those with normal weight (BMI <25.0; mean change = +7.57%, P=0.013) but decreased among those classified as overweight (BMI = 25.0 to 29.9; −5.2%, P=0.037) or obese (BMI ≥30; −6.5%, P=0.025). Decreases in weight were also observed for patients with obesity and receiving a combined treatment (−9.65%, P=0.043). After one year of treatment, weight changes among patients receiving ICI only remained significant in the normal weight group (+15.6%, P=0.007), but not among patients with other BMIs and treatment regimens. These associations remained similar after excluding the patients with cachexia.

Conclusions: Body weight change during ICI therapy may vary by treatment regimen and pre-ICI BMI among patients with NSCLC. Whether the weight changes are related to toxicities and survival warrants further research to shed light on weight management, ICI efficacy, and prevention of treatment-related adverse events. Funding: The study was in part funded by NIH/NCI R37CA248371, OSUCCC CCSG P30CA016058, and Pelotonia Institute for Immuno-Oncology (PIIO) at OSUCCC.

#3405 CT-assessed body composition and tumor immunologic characteristics in patients with non-small-cell lung cancer.

T.-Y. D. Cheng, **C. M. Mahenge**, R. T. Akasheh, A. S. Yilmaz, B. Kinder, X. Nguyen, M. Pietrzak, C. J. Presley, P. G. Shields;
The Ohio State University, Columbus, OH

Objectives: Obesity is associated with higher immunotherapy efficacy, but body mass index is a convoluted marker of adipose and muscle tissue. We conducted a discovery scale study to assess the association of skeletal muscle and adipose tissue areas annotated on computed tomography (CT) scan images with selected tumor immunologic characteristics among patients with non-small-cell lung cancer (NSCLC).

Methods: We analyzed publicly available data from 102 patients (mean age = 67.2, 47.1% female, and 70.6% stage I-II) who had diagnostic CT images in The Cancer Image Archive. All patients had the 12th thoracic vertebra (T12) image, and a subset (62 patients) had the 3rd lumber vertebra (L3) image. Paravertebral muscle areas on T12 and skeletal muscle and adipose tissue areas on L3 were annotated using Slice-O-Matic. RNA-seq data were provided by The Cancer Genome Atlas and Clinical Proteomic Tumor Analysis Consortium; percentages of CD8, regulatory T cells, and activated NK cells were identified using the CIBERSORT. ESTIMATE algorithm was used to derive the stromal score and the immune score. Differences in the immune markers were examined using ANOVA adjusting for stage, histology, and study.

Results and Conclusion: Patients with higher paravertebral muscle area (3rd tertile) had the lowest stromal scores, compared to the 2nd and 1st tertile ($P<0.05$). Patients in the 2nd tertile of paravertebral muscle areas had the highest immune score and *CD274* (*PD-L1*) gene expression. Among the body composition types classified using L3 images, low muscle/high adiposity was associated with lower stromal scores, and low muscle was associated with lower immune scores, compared to high adiposity and high muscle/low adiposity types. Other immunological markers did not differ across the body composition types.

Significance: These findings suggest associations between deconvoluted skeletal and adipose tissue components and tumor markers relevant to immune checkpoint inhibitor efficacies in NSCLC. Further validation using immune phenotyping in a large patient sample is warranted. Funding: The study is in part supported by NIH/NCI R37CA248371 and OSU Comprehensive Cancer Center - James.

#3406 Transcriptomic analysis reveals differentially expressed pathways in colon tumors of cancer patients with vs without obesity: Results from the ColoCare Study.

V. M. Bandera[1], T. Lin[1], C. Himbert[2], E. M. Glenny[3], A. Tan[4], J. Ose[1], C. Warby[1], O. Aksonova[1], A. Carpanese[5], C. Stubben[1], D. Nix[1], K. Boucher[4], P. Schirmacher[6], I. Strehli[1], J. Jedrzkiewicz[1], L. C. Huang[4], J. N. Cohan[4], A. Brobeil[6], M. A. Schneider[6], C. Kahlert[6], E. M. Siegel[7], A. T. Toriola[8], D. Shibata[9], C. I. Li[10], J. C. Figueiredo[11], B. Gigic[6], J. Roper[5], S. Hursting[3], C. M. Ulrich[1];

[1]University of Utah Huntsman Cancer Institute, Salt Lake City, UT, [2]Massachusetts General Hospital, Boston, MA, [3]University of North Carolina at Chapel Hill, Chapel Hill, NC, [4]University of Utah, Salt Lake City, UT, [5]Duke University, Durham, NC, [6]Heidelberg University Hospital, Heidelberg, Germany, [7]Moffitt Cancer Center, Tampa, FL, [8]Washington University School of Medicine, St. Louis, MO, [9]University of Tennessee Health Science Center, Memphis, TN, [10]Fred Hutchinson Cancer Center, Seattle, WA, [11]Cedars Sinai Medical Center, Los Angeles, CA

Despite the rise of global obesity rates and obesity's implication in increased colon cancer risk, the understanding of mechanisms underlying these associations and opportunities for interception are limited. This work leveraged transcriptomic data from colon tumors to identify pathways and biologically relevant functions that characterize the tumors among obese vs nonobese individuals. Fresh-frozen colon tumor samples were collected from 155 patients who underwent surgery without neoadjuvant treatment as part of the ColoCare Study at Huntsman Cancer Institute, Utah, and Heidelberg University Hospital, Germany. RNA was sequenced using the NovaSeq X. The DESeq2 R package identified differentially expressed genes stratified by body mass index (BMI) at diagnosis (>30 kg/m^2 vs <30 kg/m^2) adjusting for age, sex, study site, and tumor stage. Genes with *padj* < 0.2 were entered into Ingenuity Pathway Analysis (IPA) software for pathway and expression analyses. Significant pathways were identified using Fischer's Exact Test as the probability of molecules' association with canonical pathways due to chance. The analysis was also repeated testing a median BMI categorization of >27.7 kg/m^2 vs <27.7 kg/m^2 using *padj* < 0.1 for IPA entry. Patients were 49% female, 63±14 years old, 47% stage III with a mean baseline BMI of 28.8±6.0 kg/m^2. In colon tumors of those with >BMI 30 kg/m^2, 213 genes were differentially expressed compared to BMI <30 kg/m^2. IPA identified five upregulated pathways (neurovascular coupling signaling, adrenergic receptor signaling, activation of N-methyl-D-aspartate receptors and postsynaptic events, response to elevated platelet cytosolic Ca^{2+}, docosahexaenoic acid signaling) and one downregulated pathway (WNT/B-catenin signaling) in patients with vs without obesity (p <0.05). The top predicted functional pathways, based on activation z-scores, identified in expression analysis included significant activation in chromosomal instability and aberration, size of body, phosphorylation of L-tyrosine, protein kinase cascade, and cell death and survival categories among colon tumors in obese patients. Using a median BMI categorization, 458 genes and 35 pathways were differentially expressed in those with BMI > 27.7 kg/m^2 vs < 27.7 kg/m^2. Both BMI models had good agreement with 5 pathways consistently significantly (z-score > |2|) up- or down-regulated, including predicted downregulation of organismal death and increased body size and phosphorylation of L-tyrosine in the higher BMI group. Colon tumors from patients with a higher BMI had pathways associated with more aggressive tumors, such as increased chromosomal instability and decreased cell death. Our ongoing work investigates the role of the adipose-tissue tumor microenvironment among patients, and the potential for interception using parallel mouse models.

#3407 Physical activity and post-menopausal breast cancer in the Multiethnic Cohort Study.

J. K. Gill[1], G. Maskarinec[2], S.-Y. Park[2], L. Wilkens[2], L. Le Marchand[2];
[1]California State University, Fullerton, Fullerton, CA, [2]University of Hawai'i Cancer Center- University of Hawaii at Manoa, Honolulu, HI

Much research has been conducted on the relationship between physical activity and breast cancer, with meta-analyses showing 10 – 21% reduction in breast cancer risk for postmenopausal women with high compared to low level of physical activity. However, few studies have explored this relationship in non-Caucasian women. We analyzed data from 74,177 post-menopausal African American, Caucasian, Japanese American, Latina, and Native Hawaiian women in the Multiethnic Cohort in Hawaii and California. Data on physical activity (hours and metabolic equivalents (METs)) was based on a self-administered questionnaire at baseline (1993–1996). Multivariate Cox proportional hazards models provided estimates of hazard ratios (HRs) and 95% confidence intervals (CIs) adjusted for risk factors. We observed no associations between breast cancer risk and hours of moderate/vigorous activity per week (HR=1.01, 95% CI: 0.91-1.10, Ptrend=0.71), MET-hours of moderate/vigorous activity per week (HR=1.03, 95% CI: 0.94-1.13, Ptrend=0.92), and total METs-measured as average MET level per day multiplied by 7 (HR=0.94, 95% CI: 0.86-1.03, Ptrend=0.37) when comparing the highest quartile to the lowest. When examining the data across race/ethnicity, we observed a reduction in risk of breast cancer for total METs (HR=0.75, 95% CI: 0.61-0.94, Ptrend=0.05) among Latina women. Analysis across strata of BMI showed no differences across subgroups. In this study, we did not observe any consistent protective association between physical activity and breast cancer risk.

#3408 'Survivor mentality': The meaning of survivorship among Black cancer survivors.

Nathaniel Woodard, Jingle Xu, Deirdre F. Lea, John L. Milner, Paulette Duggins, Karia Coleman, Ashley L. Bryant, Carmina G. Valle, Stephanie B. Wheeler, Jessica Carda-Auten, Tammy A. Triglianos, Rachel Hirschey

University of North Carolina at Chapel Hill, Chapel Hill, NC

Purpose: To explore how Black adults who have been diagnosed with cancer perceive and interpret the term 'cancer survivor'.
Procedures: This study is a secondary analysis of qualitative data from a project identifying physical activity determinants among Black U.S. residents living past a cancer diagnosis. Semi-structured telephone interviews began with an inquiry into perceptions of the term 'cancer survivor.' Eligible participants were age 18 or older, self-identified as Black, and were living beyond a cancer diagnosis. Interviews were audio recorded and transcribed verbatim. Applying directed content analysis, 5 researchers independently applied a codebook generated from the interview guide to a subset of transcripts. The codebook was refined through iterative discussions to address coding discrepancies and achieve replicability. Remaining transcripts were then coded and a report of grouped narrative summaries was generated. Themes and subthemes were organized to present the meaning and significance of 'cancer survivorship' among the sample. The partnering community advisory board aided in and reviewed the interpretation of study findings.
Results: Participants were 19 survivors of nine different types of cancer. Most participants were women (89.5%), 68.4% held a bachelor's degree or greater, and the mean age was 56 (SD=12). Emergent themes describing perceptions of 'cancer survivorship' included 1) cancer 'survivor' terminology preferences, 2) outset of cancer 'survivorship,' 3) 'survivor mentality' and mental fortitude, and 4) advocacy for those affected by cancer. Many participants identified as 'cancer survivors' and preferred this to 'in remission,' but some preferred different terms or identities (e.g., warrior or thriver). Many believed survivorship began once an individual completed cancer treatment, but some felt survivorship began at cancer diagnosis. Survivor mentality was raised as a mindset providing some individuals the mental fortitude to complete cancer treatment, especially among those embracing a survivor identity during treatment. Some participants raised advocacy, providing support to others diagnosed with cancer, and sharing cancer information and their experience as part of what it means to be a survivor.
Conclusions: Acceptance of the term "cancer survivor" and what it means to be a "survivor" vary among Black individuals living past a cancer diagnosis. The identities held by those diagnosed with cancer may have implications for their cancer experiences and outcomes. Many Black cancer survivors may perceive working to improve the lives of others with cancer as part of what it means to be a survivor. Partnering with Black cancer survivors in cancer prevention and control efforts may be mutually appealing and beneficial to improve the lives of individuals living past a cancer diagnosis.

#3409 AGEing and lifestyle after a cancer diagnosis: A balanced equilibrium for survivorship?.

D. P. Turner[1], B. A. Krisanits[1], M. E. Ford[2], L. L. Peterson[3], S. E. Steck[4], P. D. Bos[1], V. J. Findlay[1];
[1]Virginia Commonwealth University, Massey Cancer Center, Richmond, VA, [2]Medical University of South Carolina, Charleston, SC, [3]Washington University, St Louis, MO, [4]University of South Carolina, Columbia, SC

In the US, over 18 million people are living with a cancer diagnosis and that number may double by 2050. There is a need to unite research across the cancer continuum to address the needs of cancer survivors to ensure optimal quality of life and improve mortality outcomes. Health constructs that influence cancer survivorship are multifactorial, highly dynamic, and vary across the lifespan. This makes assigning their impact on the well-being and future outcomes of cancer survivors challenging. As a pathophysiological process that lies at the intersection between societal, environmental, and biological constructs, it is proposed that the irreversible accumulation of metabolites called advanced glycation end products (AGEs) can inform on quality of life and mortality outcomes for cancer survivors. It is proposed that AGE accumulation as a result of societal, environmental, and biological constructs overwhelm the fragile equilibrium that maintains AGE homoeostasis to impact tumor biology and cancer outcomes. The relationships between health constructs and AGE exposure are epitomized by nutritional behavior. The consumption of cheaper unhealthier often ultra-processed foods are inherently AGE laden and the excessive consumption of foods high in fats and sugars that promote obesity and increase cancer risk readily provide reactive intermediates that fuel AGE formation in cells and tissues. Our collaborative epidemiological studies assign high levels of AGE consumption with increased breast cancer risk, aggressiveness, and mortality, which is supported by translational studies showing that circulating AGE levels in breast cancer patients correlate with worse disease-free survival and other poor prognosis indicators. Critically, this group has also shown that chronic AGE consumption by mice increases prostate tumor growth ($p<0.001$), and causes a rapid progression through prostate intra-epithelial neoplasia ($p=0.049$), adenocarcinoma ($p=0.042$) and metastasis ($p=0.001$). Consumption of the high AGE diet caused a regulatory program of stromal activation conducive for tumor growth. As a bio-social determinant of health AGE accumulation and its pathogenic effects serve as informative and/or functional markers indicative of the current health status and well-being of cancer survivors and may inform of potential future outcomes. Our studies show that physical activity and dietary intervention (cardiac rehabilitation) reduced systemic AGE levels in breast cancer survivors. Therefore, prevention and control interventions aimed at reducing AGE exposure represent viable strategies for improving quality of life and disease recurrence for cancer survivors.
This research was made possible in part by Grant Numbers R01-CA259415, R01-CA245143, R21-CA194469, and U54-CA210962 from NIH-NCI. Its contents are solely the responsibility of the authors and do not necessarily represent the official views of NIH.

#3410 Financial toxicity among patients with advanced prostate cancer in the United States.

I. Singh[1], B. Vaselkiv[1], E. Rencsok[1], K. Autio[2], D. Enting[3], A. Morgans[4], J. Nowak[5], K. Kensler[6], D. Nanus[6], R. Dreicer[7], B. Lewis[8], O. Sartor[9], E. Heath[10], P. Kantoff[11], D. Kaye[12], D. George[12], L. Mucci[1];

[1]Harvard School of Public Health, Boston, MA, [2]Memorial Sloan Kettering Cancer Center, New York, NY, [3]Guy's and St Thomas' NHS Foundation Trust, London, United Kingdom, [4]Dana Farber Cancer Institute, Boston, MA, [5]Cancer ABCs, Brooklyn, NY, [6]Weill Cornell Medical College, New York, NY, [7]University of Virginia School of Medicine, Charlottesville, VA, [8]Tulane University School of Medicine, New Orleans, LA, [9]Mayo Clinic, Rochester, MN, [10]Karmanos Cancer Institute, Detroit, MI, [11]Convergent Therapeutics, Cambridge, MA, [12]Duke University School of Medicine, Durham, NC

Background: Advanced prostate cancer is defined as metastatic hormone-sensitive prostate cancer (mHSPC) or castration-resistant prostate cancer (CRPC). Newer and aggressive treatments are leading to increasing lifespans in this population. As such, studying quality of life could have a large impact on the survivorship experience. An important component of quality of life is financial toxicity, defined as the financial burden and distress that can arise for patients and their families because of cancer treatment.

Objectives: To understand the prevalence and predictors of financial toxicity in advanced prostate cancer.

Methods: IRONMAN (International Registry of Men with Advanced Prostate Cancer) is a prospective cohort of patients with newly diagnosed mHSPC or CRPC enrolling in 15 countries. Financial toxicity was collected using the EORTC QLQ-C30 (“has your physical condition or medical treatment caused you financial difficulties?”) at enrollment and every three months thereafter. For this analysis, we studied 997 patients cared for at 37 US sites enrolled from 7/2017 to 7/2023. We examined baseline and longitudinal reports of financial toxicity across clinical and demographic factors: age at enrollment, race and ethnicity, disease state, marital status, education, employment, military status, and type of health center. We conducted adjusted risk difference analysis and multivariable regression modeling to identify predictors of financial toxicity using a generalized estimating equations approach to calculate odds ratios (OR and 95% confidence intervals, CI).

Results: At enrollment, 125 (13%) patients reported experiencing “quite a bit” or “very much” financial toxicity. 21% of Black patients experienced toxicity compared to 10% of White patients. Even after incorporating all other predictors, Black patients experienced 5% (95% CI: 0, 11) greater toxicity than White patients. Independently of other predictors, patients >75 experienced 11% (CI: -17, -4) lower toxicity compared to those <65 years (while patients in the 65-74 group experienced 6% less, CI: -12, 1). Toxicity was 6% greater in patients with mHSPC (CI: 2, 10) than in patients with CRPC, and disabled or unemployed patients were at substantially higher risk. In the multivariable longitudinal analyses, older age (> 75) remained associated with significantly lower odds for financial toxicity (OR: 0.30, 0.15-0.61) while mHSPC (OR: 1.91, 1.14-3.20) and being unemployed (OR: 2.69, 1.03-6.99) or disabled (OR: 5.14, 2.29-11.6) were associated with higher odds.

Conclusions: Financial toxicity is prevalent in advanced prostate cancer, especially in patients who are Black, younger than 75, diagnosed with mHSPC, or unemployed/disabled. These results may inform identification of patients at high risk for financial toxicity to support delivery of patient-situation-informed care by clinicians and targeted aid for patients at highest risk.

#3411 Health-related quality of life trajectories in older breast cancer survivors and noncancerous controls over ten years: SEER-MHOS analysis.

E. Lee[1], M. Azevedo Daruge[1], K. Ferdowsi[1], J. Zhu[2];
[1]University of Central Florida, Orlando, FL, [2]Advent Health, Orlando, FL

Background: The adverse effects of cancer treatment on health-related quality of life (HRQOL) are the primary concern of older women diagnosed with breast cancer. The interplay of transient and progressive functional impairments caused by cancer therapies alongside the accelerated physical declines associated with the normal aging process are all negatively correlated to HRQL, yet it remains unclear whether this is an effect of cancer or solely aging; therefore, this study examined HRQL trajectory over ten years after diagnosis between cancer cases and controls.
Methods: The cancer group included 1467 women (age ≥ 65) diagnosed with primary breast cancer in 1998 - 2012, registered in the Surveillance, Epidemiology, End Results (SEER) cancer registry, and completed Medical Health Outcomes (MHO) surveys before and after cancer diagnosis. Propensity score-matched controls were randomly selected with a 1:1 ratio. Participants reported their HRQOL using SF-36/VR-12. It was summarized into two summary scores (Physical Component Summary [PCS] and mental component summary [MCS]) and eight domain scores (physical functioning [PF], role limitation due to physical health [RP], bodily pain [BP], general health [GH], vitality [VT], social functioning [SF], mental health [MH], and role limitation due to emotional problem [RE]). Hierarchical linear modeling was utilized to assess the main effects of time and group and the interaction effect between time and group on HRQOL trajectory.
Results: At diagnosis, cases fared worse than controls for all HRQOL domains and summary scores. Over the ten years, PCS, PF, GH, RP, SF, and VT worsened over time (all *P* for time < 0.05), while MCS, MH, and RE remained relatively constant over time (all *P* for time ≥ 0.05). Older women with breast cancer had lower HRQL over time than controls in PCS, GH, and RP domains, while they showed higher HRQOL than controls post 4 - 7 years in PF, SF, RE, and VT domains (all *P* for group < 0.05). However, only RE showed a statistically significant interaction effect (*P* =0.035), improving over time in cases but worsening in controls.
Conclusions: This research shows both older women with breast cancer and propensity-matched controls experiencing deterioration of HRQOL, particularly physical health domains, over ten years after baseline, with cases' HRQOL kept lower than controls over time. Needs assessment and more efficient interventions to improve physical health HRQOL among older women are warranted.

#3412 Benralizumab for treatment of eosinophil-related cutaneous adverse events associated with checkpoint inhibitors and anticancer targeted therapies: Phase 2 study.

Mario E. Lacouture[1], **Tara Maier**[1], Alexander Pan[1], Anna Chen[1], George Dranitsaris[2], Neil J. Shah[3], Sarat Chandarlapaty[4], Chau Dang[4], Devika Gajria[4], Allison Gordon[1], Neil Iyengar[4], Pedram Razavi[4], Mark Robson[4], Ezra Rosen[4], Serena Wong[4], Ucalene Harris[1], Kwami Ketosugbo[1], Cindy Bravo[1], Manu Jain[1], Alina Markova[1]

[1]Dermatology Service, Department of Medicine, Memorial Sloan Kettering Cancer Center, New York, NY,[2]Department of Public Health, Falk College, Syracuse University, New York, NY,[3]Sidney Kimmel Center for Prostate and Urologic Cancers, Memorial Sloan Kettering Cancer Center, New York, NY,[4]Evelyn H. Lauder Breast Center, Memorial Sloan Kettering Cancer Center, New York, NY

Background: Eosinophil-related cutaneous adverse events (ercAEs) are common toxicities of PI3K inhibitors, antibody drug conjugates (ADCs), checkpoint inhibitors (CPIs), and targeted cancer therapies. While systemic corticosteroids are effective, their use is limited by additional toxicities and high recurrence. Benralizumab is an anti-IL-5Rα monoclonal antibody that induces eosinophil depletion via antibody-dependent cellular cytotoxicity, and is FDA-approved for severe eosinophilic asthma but has not been studied for ercAEs.

Methods: We conducted a single-center, single-arm, Phase 2 trial (NCT04552288) of benralizumab in cancer patients with Grade 2/3 ercAEs from PI3K inhibitors, ADCs, CPIs or targeted therapies. Patients received benralizumab 30 mg subcutaneously every 4 weeks for 3 doses, then every 8 weeks for 3 doses. The primary endpoint was clinical response, defined as reduction in ercAE Grade to 0/1 at Week 4. Secondary endpoints included changes in quality of life, rash body surface area (BSA), cytokines and eosinophil biomarkers, as well as adverse events (AEs).

Results: Forty-seven patients were enrolled, predominantly with breast (55.3%), bladder (10.6%), melanoma (10.6%), or kidney (6.4%) cancer. Baseline ercAEs were Grade 2 (48.9%) and Grade 3 (51.1%), most often from PI3K inhibitors (46.8%), CPIs (21.3%), tyrosine kinase inhibitors (8.5%) or ADCs (8.5%). Overall, 32 of 42 evaluable patients (76.2%) had clinical response by Week 4, with decreased ercAE grade (mean 2.4 to 0.9, $p<0.0001$), improved quality of life, reduced rash BSA, decreased peripheral and skin eosinophils (all $p<0.0001$), and cytokine changes. Clinical response by Week 4 was seen in all patients with ercAEs from alpelisib (PI3K inhibitor; n=18) or enfortumab vedotin (ADC; n=4); p-value for both: $p<0.05$. Mild-to-moderate mucositis, diarrhea, and xerosis were the most common AEs, all unrelated to benralizumab.

Conclusions: Benralizumab demonstrated favorable safety and efficacy for Grade 2/3 ercAEs from cancer therapies, especially alpelisib and enfortumab vedotin. Larger placebo-controlled trials are warranted to confirm these preliminary findings.

#3413 Physical activity and sedentary behavior of cancer survivors compared to individuals without cancer in NHANES.

A. Pavy, S. E. Steck;
University of South Carolina, Columbia, SC

INTRODUCTION: Physical activity may improve quality of life and reduce mortality among cancer survivors. As cancer death rates continue to decrease, the population of cancer survivors is expected to grow, therefore making it important to study their health behaviors. Research has been conducted on prevalence of physical activity and sedentary behaviors of survivors of certain cancers, however, little research has been conducted comparing cancer survivors to individuals without cancer. The purpose of this study was to update previously published results from earlier National Health and Nutrition Examination Survey (NHANES) cycles (2007-2010) with more recent data comparing physical activity and sedentary behavior among cancer survivors and individuals without cancer.
METHODS: Using the NHANES 2011-2018, we identified 1320 cancer survivors and 19,109 participants without cancer who provided data on recreational, work-related, and transportation-related physical activity and sedentary behavior. The included participants were over 20 years of age, not pregnant at the time of the survey, and were more than three years from their cancer diagnosis, if applicable. Comparisons between cancer survivors and individuals without cancer were conducted for duration of total physical activity (min/day) and sedentary time per day. To account for the complex sampling design, weighted multivariable analysis was used to calculate odds ratios (ORs) and 95% confidence intervals (CIs).
RESULTS: Compared to individuals without cancer, cancer survivors reported less average ± standard error physical activity minutes per day (190.06 ± 5.24 and 147.29 ± 13.14, respectively), and slightly more sedentary hours per day (6.95 ± 0.09 and 7.56 ± 0.36, respectively). However, after adjusting for age, race and ethnicity, sex, educational status, body mass index, and smoking status, there was no association between physical activity duration or sedentary time and cancer survivor status. The OR (95%CI) for more than 60 minutes per day of physical activity was 1.00 (0.83, 1.20) compared to no physical activity, and for more than 8 hours of sedentary time per day was 1.00 (0.82, 1.21) compared to less than 5 hours per day.
DISCUSSION: In a previous publication of earlier cycles of NHANES (2007-2010), cancer survivors reported higher physical activity but also higher sedentary time per day compared to individuals without cancer. However, these results were not supported in this updated analysis using more recent NHANES cycles (2011-2018). After adjustment for important covariates, we did not find differences between cancer survivors and individuals without cancer in reported physical activity or sedentary time. Further research in other populations is needed to corroborate these findings and document whether they reflect a growing awareness of the negative impact of sedentary behavior in cancer survivorship.

POPULATION SCIENCES: Biomarkers of Endogenous or Exogenous Exposures, Early Detection, Biologic Effects, and Prognosis
Poster Session

#3417 Dissecting tumor microenvironment to predict clinical outcome in prostate cancer.

Aritri Bhattacharjee[1], Manjusha Biswas[1], **Amjad Husain**[1], Asim Kr Das[2], Sourav Karmakar Karmakar[2], Tapan Mondal[2], Pinaki Roy[2], Manas Kr Mondal[2], Badal Kumar Sahu[2], Nabendu Murmu[3], Partho Nath[3], Chandra C. Ghosh[1], Pradip Kumar Majumder[1]

[1]CanFinis Therapeutic Private Limited, Kolkata, India,[2]Nilratan Sircar Medical College and Hospital, Kolkata, India,[3]Chittaranjan National Cancer Institute, Kolkata, India

Prostate cancer is one of the major causes of cancer death in males, and its prevalence is particularly high in developed countries such as the United States and Western Europe. However, death rates in developing and underdeveloped countries are greater, presumably, due to a lack of routine clinical check-ups, poor health awareness, inadequate screening resources, and clinical intervention. Much progress has already been made using cutting-edge technologies like whole genome sequencing, RNAseq, phosphoproteomics, and targeted transcriptomic Nanostring profiling, etc. However, understanding of the prostate tumor microenvironment as a whole in clinical samples remains very limited. Here we use the latest genomic, proteomics, and metabolomic tools not only to understand the biology of prostate cancers but also their correlation with patient demography and clinical outcome. We recruited 80 patients from both tertiary research hospitals and clinical centers in the eastern region of India. All of their demographic information is collected along with their clinical outcome. Pathological evaluation revealed only 50 patients with positive Prostate Carcinoma. We performed a detailed analysis using experimental data (from genomic, and proteomic) in a cohort of patients' routine biomarkers (PSA and PSMA), histopathology, and clinical outcome. Our data demonstrate no linear correlation of any of the individual markers or parameters like AR status, PSA, Prostate Specific Acid Phosphatase, Prostate-Specific Membrane Antigen (PSMA), Alpha-methylacyl-CoA racemase (AMACR), Mesothelin, PD-L1, and other potential genomic and proteomic alterations or any histopathological readouts. However, a clear understanding of the relationship between these multiparameter data, disease pathology, and clinical outcomes in a group of patients has been established. The heterogeneity of these individual data for tumor microenvironments will lead us to identify novel biomarkers for the clinical response of targeted drugs, accelerating personalized treatment strategies.

#3418 Preoperative nutritional status and overall survival among non-metastatic colorectal cancer patients: The ColoCare Study.

B. Gigic[1], V. Damerell[1], T. Lin[2], J. Ose[2], C. Kahlert[1], J. C. Figueiredo[3], C. I. Li[4], M. Schneider[1], D. Shibata[5], E. M. Siegel[6], A. T. Toriola[7], C. M. Ulrich[2]; [1]Heidelberg University Hospital (UKHD), Heidelberg, Germany, [2]University of Utah and Huntsman Cancer Institute, Salt Lake City, UT, [3]Samuel Oschin Comprehensive Cancer Institute, Cedars-Sinai Medical Center, Los Angeles, CA, [4]Fred Hutchinson Cancer Research Center, Seattle, WA, [5]University of Tennessee Health Science Center, Memphis, TN, [6]H. Lee Moffitt Cancer Center and Research Institute, Tampa, FL, [7]Washington University St. Louis, St. Louis, MO

Introduction: Preoperative malnutrition in colorectal cancer (CRC) patients undergoing major abdominal surgery is a common and serious issue that affects postoperative recovery and clinical outcomes. The aim of this study was to evaluate the associations between preoperative nutritional status and overall survival (OS) of prospectively followed, non-metastatic CRC patients.

Methods: The target cohort consisted of 415 patients with newly-diagnosed stage I-III CRC who underwent curative surgery at the Heidelberg University Hospital in Germany. Nutritional status was evaluated using predefined accessible laboratory parameters (haemoglobin, albumin, total protein, and thrombocytes), and the Geriatric Nutritional Risk Index (GNRI), a screening tool to identify patients with malnutrition: *(GNRI) = 14.89×serum albumin concentration (g/dl) + 41.7×present weight/ideal weight*. Ideal weight was calculated as follows: *height(cm)-100-[(height(cm)-150)/4]* for men and *height(cm)-100-[(height(cm)-150)/2.5]* for women. Patients were categorized into normal *vs.* out of normal range for laboratory parameters and into four grades of nutrition-related risk: major risk (GNRI: <82), moderate risk (GNRI: 82 to <92), low risk (GNRI: 92 to ≤98), and no risk (GNRI: >98). Vital status has been obtained through study-specific follow-ups or the tumor registry. OS was calculated as the interval between the date of surgery and the date of death from any cause or the last follow-up examination. Using Cox proportional hazards regression, we examined associations of the nutritional status with OS. Models were adjusted for potential confounders.

Results: After a median follow-up of 2.24 years for OS, 13% (54) of the 415 patients died. Of all patients, 35.1%, 3.4%, 12.5%, and 10,8% had values out of the normal range for haemoglobin, albumin, total protein, and thrombocytes, respectively. Further, 6.4%, 33.8%, 29.7%, and 30.2% of the patients had major, moderate, low, and no nutrition-related risk, respectively. Patients with out of normal range haemoglobin and thrombocyte values had a significantly increased risk of death (HR_{Hb}: 2.8; 95% CI, 1.6-4.9, p<0.001 and HR_{Thr}: 3.0; 95% CI, 1.5-6.1, p=0.003). The major nutrition-related risk group had a significantly increased risk of death compared to the no nutrition-related risk group (HR_{GNRI}: 7.2; 95% CI, 2.7-19.3, p<0.001). We did not observe significant associations between preoperative albumin and total protein values and OS among CRC patients.

Conclusion: Patients with out of normal range levels of preoperative haemoglobin and thrombocytes had a significantly worse OS. Further, the GNRI may have a close relationship with the prognosis in non-metastatic CRC patients. Findings from this study yield important clinical information that could help to strategically combat malnutrition prior to surgery in order to improve clinical outcomes.

#3419 Demographic, health history, and lifestyle factors in association with biomarkers of colorectal cancer prognosis: A pilot study.

U. Zanif[1], I. Tai[1], S. Yip[2], S. Babinszky[3], K. Milne[3], P. Watson[3], R. Murphy[1], P. Bhatti[1];
[1]BC Cancer Research Centre, Vancouver, BC, Canada, [2]BC Cancer Agency, Vancouver, BC, Canada, [3]BC Cancer Research - Deeley Research Centre, Victoria, BC, Canada

Background/Objectives: Multiple demographic, health history, and lifestyle factors have been associated with prognosis of colorectal cancer (CRC), but the mechanisms underlying these associations remain poorly understood. Knowledge of these mechanisms could reveal new strategies to improve outcomes among CRC patients. The primary objective of this project was to explore the association of these factors, which were assessed pre-diagnostically, with expression of two biomarkers in CRC tumors, SPARC and PD-L1, for which lower and higher levels of expression, respectively, have been previously associated with poorer CRC prognosis.
Methods: Participants were drawn from the British Columbia Generations Project (BCGP). At the time of recruitment, they completed a detailed questionnaire that ascertained demographic factors (e.g., biological sex and household income), health history (e.g., personal history of CRC screening), and lifestyle factors (daily fruit and vegetable consumption and alcohol consumption). Formalin-fixed paraffin-embedded blocks (FFPE) with adequate volumes of tumor were obtained for 49 incident CRC cases diagnosed within the BCGP. Cores were extracted from the blocks to create tumor tissue microarrays (TMAs). Slides created from thin sections of the TMAs were stained with SPARC and PD-L1 antibodies and then imaged and analyzed to calculate H-scores as measures of expression in both epithelial and non-epithelial tissues. Linear regression analyses were conducted to evaluate associations between the various factors and ln-transformed H-scores.
Results: Compared to non-smokers, smokers, on average, had 47% lower SPARC H-scores (p=0.05) in the epithelial tissues of their CRC tumors. Individuals with incomes higher than $74,999/year had 33% higher SPARC H-scores (p=0.04) in their CRC tumor non-epithelial tissues than those who earned less than $74 999/year. Females had 2.8-fold greater PD-L1 H-scores (p=0.005) in their CRC tumor epithelial tissues than males. Compared to those without a history of CRC screening, those with a history of CRC screening had 2.2 and 2.0-fold greater PD-L1 H-scores in their epithelial and non-epithelial CRC tumor tissues, respectively.
Conclusion: Larger-scale studies with prognostic data are needed to confirm our findings, but our results suggest that differences in the expression of SPARC and PDL-1 may contribute to the previously observed impacts of some demographic, healthy history, and lifestyle factors on CRC prognosis.

#3420 Androgen receptor $(CAG)_n$ polymorphism: A genomic marker for prostate cancer prognosis independent of histopathological parameters.

G. M. Pascual[1], A. Sabater[2], J. Bizzotto[1], R. Seniuk[1], P. Sanchis[1], C. M. Roggero[3], C. Scorticati[4], O. Mazza[4], E. Vazquez[1], A. Toro[1], G. Gueron[1], J. Cotignola[1];

[1]CONICET - IQUIBICEN, Ciudad Autonoma de Buenos Aires (CABA), Argentina, [2]1-CONICET - IQUIBICEN. 2-Universidad Argentina de la Empresa (UADE), Instituto de Tecnologia (INTEC), Ciudad Autonoma de Buenos Aires (CABA), Argentina, [3]CONICET-IHEM, Ciudad de Mendoza, Argentina, [4]Universidad de Buenos Aires, Hospital de Clinicas Jose de San Martin, Departamento de Urologia, Ciudad Autonoma de Buenos Aires (CABA), Argentina

The androgen receptor (AR) serves as a pivotal transcription factor in prostate cancer (PCa) development. Its transcriptional activity is linked to the number of glutamines in the N-terminal domain. While current screening for PCa and prognostic biomarkers include serum prostate-specific antigen (PSA) levels and histopathological characteristics (specifically, ISUP grade and margin involvement), the heterogeneity of these tumors underscores the need for additional markers to enhance clinical management.

Thus, this study aimed at characterizing an Argentinian PCa patient cohort based on the CAG polymorphism $(CAG)_n$ in *AR* and establish associations between genotypes and clinical-pathological characteristics to refine disease prognosis.

We designed a hospital-based case-case study for PCa patients to determine the association between *AR* polymorphisms and PCa biochemical relapse after radical prostatectomy (RP). We retrospectively recruited 112 patients histologically diagnosed with PCa at the Hospital de Clínicas José de San Martín, Buenos Aires, Argentina. All patients underwent RP as their primary therapeutic strategy. All patients were, by definition, Hispanics, predominantly of Caucasian ancestry and, at a lesser extent, Amerindian or African. Written informed consent and institutional review board approval were acquired.

Blood samples were collected post-RP for genomic DNA extraction using the CTAB method. $(CAG)_n$ in *AR* was genotyped by fluorescent PCR followed by capillary electrophoresis, and correlations between genotypes and clinical-pathological variables were analyzed using R.

Results categorized patients into three subgroups based on the length of the CAG tandem repeat in *AR*: long (>23 repeats, n=29), medium (20-23 repeats, n=44), and short (<20 repeats, n=38). No associations were found between the length of the polymorphism and age of diagnosis, pre-RP PSA serum values, ISUP grade, and margin involvement. However, patients with family cancer history had a higher frequency of the intermediate-length allele (p=0.02). Moreover, among patients with pre-RP PSA <10 ng/ml and intermediate-length allele had 2.72-fold risk of biochemical recurrence (BCR) (HR=2.72, 95%CI=1.05-7.03, p=0.039). Furthermore, multivariable BCR analysis including the ISUP grade and margin involvement as co-variates showed that the $(CAG)_n$ in *AR* was independent of these histopathological parameters (HR_{adj}=3.37, 95%IC=1.24-9.10, p_{adj}=0.017).

Altogether, the *AR* polymorphism is associated with family history of cancer. Consequently, determining the number of CAG repetitions in *AR* through a blood sample could serve as an independent prognostic marker in patients with PSA <10 ng/ml prior to PR, independent of the histopathological features.

#3421 Associations of circulating levels of tryptophan-kynurenine metabolites and inflammation biomarker neopterin with overall survival among patients with stage I-III colorectal cancer.

V. Damerell[1], E. H. van Roekel[2], S. Brezina[3], D. E. Kok[4], T. Lin[5], D. D. B. Holthuijsen[2], J. Ose[5], C. Himbert[5], S. J. M. Eussen[6], A. Ulvik[7], F. J. B. van Duijnhoven[4], J. C. Figueiredo[8], C. I. Li[9], E. M. Siegel[10], M. Schneider[1], D. Shibata[11], A. A. Toriola[12], A. B. Ulrich[1], P. M. Ueland[7], M. P. Weijenberg[2], A. Gsur[3], E. Kampman[4], C. M. Ulrich[5], B. Gigic[1];

[1]Heidelberg University Hospital (UKHD), Heidelberg, Germany, [2]GROW School for Oncology and Reproduction, Maastricht University, Maastricht, Netherlands, [3]Center for Cancer Research, Medical University of Vienna, Vienna, Austria, [4]Wageningen University & Research, Wageningen, Netherlands, [5]University of Utah and Huntsman Cancer Institute, Salt Lake City, UT, [6]School for Cardiovascular Diseases (CARIM), Maastricht University, Maastricht, Netherlands, [7]BEVITAL, Bergen, Norway, [8]Samuel Oschin Comprehensive Cancer Institute, Cedars-Sinai Medical Center, Los Angeles, CA, [9]Fred Hutchinson Cancer Research Center, Seattle, WA, [10]H. Lee Moffitt Cancer Center and Research Institute, Tampa, FL, [11]University of Tennessee Health Science Center, Memphis, TN, [12]Washington University St. Louis, St. Louis, MO

Introduction: Dysregulation of the kynurenine pathway of tryptophan metabolism has been linked to the development of inflammation-related chronic diseases, such as colorectal cancer (CRC). Circulating concentrations of certain kynurenine metabolites, the kynurenine/tryptophan ratio (KTR), and the pro-inflammatory marker neopterin increase during inflammation, particularly in response to interferon-gamma. However, comprehensive data on the associations between inflammation markers and kynurenine metabolites and clinical outcomes in CRC patients are lacking. To address this gap in knowledge, we investigated associations of circulating kynurenine metabolites and neopterin with overall survival (OS) in prospectively followed non-metastatic CRC patients.

Methods: Pre-surgery blood samples from 2,101 stage I-III CRC patients participating in the international FOCUS consortium were used to measure circulating levels of nine tryptophan-kynurenine pathway metabolites and neopterin using liquid chromatography-tandem mass spectrometry. Multivariable linear regression models and Spearman partial correlation analyses were conducted to quantify associations between kynurenine metabolites and neopterin. Based on the results from correlation analyses, a subset of patients (n=984) was categorized into different groups (‘kynurenine metabolite/neopterin‘; i.e. ‘low/high‘, ‘high/high‘) using the median biomarker concentration as cut-off. Associations of biomarkers with OS were assessed using Cox proportional hazards regression models. All models were adjusted for age at diagnosis, sex, tumor stage, tumor site, circulating creatine levels and cohort.

Results: Tryptophan was inversely correlated with neopterin ($r=-0.21$, $\beta=-0.48$, $P_{linear}<0.001$). Neopterin was positively correlated with kynurenine (kyn) ($r=0.25$, $\beta=0.57$, $P_{linear}<0.001$), the KTR ($r=0.42$, $\beta=0.87$, $P_{linear}<0.001$), 3-hydroxykynurenine ($r=0.26$, $\beta=0.32$, $P_{linear}<0.001$), anthranilic acid ($r=0.29$, $\beta=0.36$, $P_{linear}<0.001$), and quinolinic acid (QA) ($r=0.41$, $\beta=0.56$, $P_{linear}<0.001$). After a median follow-up of 3.2 years for OS, 14% (141) patients deceased. While patients with ‘high neopterin’ levels had a 43% increased risk of death (HR, 1.43, 95%CI 0.95-2.16), the ‘high kyn/high neopterin‘ patient group had a 52% increased risk of death (HR, 1.52, 95%CI 1.04-2.22). Similarly, the ‘high QA/high neopterin‘ and ‘high KTR/high neopterin‘ patient groups had a 85% and 89% increased risk of death, respectively ($HR_{QA/Neopt}$, 1.85, 95%CI 1.24-2.75, $HR_{KTR/Neopt}$, 1.89, 95%CI 1.27-2.80).

Conclusion: Tryptophan-kynurenine pathway activation correlates with inflammation marker neopterin in CRC. Combined associations of kynurenine metabolites and neopterin may be a promising predictor for OS among stage I-III CRC patients.

#3423 Spatial-resolved single-cell analysis of the tumor microenvironment in Alaska Native colorectal cancer patients.

H. Yin[1], D. Redwood[2], K. Smythe[3], D. Jones[3], M. Houghton[3], K. C. Barry[3], A. L. Koehne[3], E. Donato[3], C. Yeung[3], M. Lin[3], J. J. Tiesinga[4], T. A. Harrison[1], S. S. Thomas[3], L. Hsu[3], J. C. Figueiredo[5], L. Li[6], T. K. Thomas[2], C. Li[3], U. Peters[3], J. R. Huyghe[3];

[1]University of Washington, Seattle, WA, [2]Alaska Native Tribal Health Consortium, Anchorage, AK, [3]Fred Hutchinson Cancer Center, Seattle, WA, [4]Alaska Native Medical Center, Anchorage, AK, [5]Cedars-Sinai Medical Center, Los Angeles, CA, [6]Ochsner Health Foundation, New Orleans, LA

Tribal Health Organizations recognize the high rates of colorectal cancer (CRC) among Alaska Native peoples and are undertaking initiatives to address it. The tumor microenvironment (TME) is a complex ecosystem including tumor, stromal, and immune cells. Understanding the cell composition and spatial organization of the TME among Alaska Native patients with CRC will provide new insights into disease progression. We performed spatial profiling on 3 tissue microarrays (TMA) from 37 patients using the Akoya Biosciences' s PhenoCycler system. Patients with CRC were selected from a nested case-control study which includes 16 patients who died of CRC and 21 patients who lived as long as patients with lethal CRC and matched on age at diagnosis, sex, tumor site and tumor stage. We designed a 40-antibody panel that captured tumor, epithelium, stromal, vascular, and immune cells, as well as cell functional states (e.g., PD1). Initial images were processed using QuPath for image stitching, artifact removal, background subtraction, cell segmentation, and measurement of average intensity of each marker per cell. Cell quality control (QC) was performed to filter out low quality cells based on cell size and log10-transformed sum of intensity. After quantile normalization and arcsinh transformation, cells that passed QC were clustered using the R package 'Seurat' and manually annotated based on the cell type and function marker intensities for each cluster. We identified 1.17 million cells and 15 cell types. Those cell types included 3 stromal and vascular cells, 1 epithelium, 1 mixed immune cluster, and 10 different immune cells. We quantified each cell type as a fraction of total cells on a per-patient basis. Among the subset of immune cells, the proportions of macrophages, CD4+T cells, and CD8+T cells were high (21%, 11.2%, and 14.5%, respectively), and the proportion of B cells was low (5.1%). We also identified regulatory T cells, cytotoxic CD8+T cells, and monocytes at 1-3%. We observed differences in the composition of cell clusters by CRC-specific death. The frequency of epithelium was higher among patients with lethal CRC, and the frequency of CD4+T cells and CD8+T cells were higher among patients without lethal CRC. In summary, the overall composition of tumor and immune cells varies between patients with and without CRC-specific death, indicating TME heterogeneity. Further investigation of spatial domains and relationships with clinical molecular features may facilitate discovery of novel predictors of CRC-specific death among Alaska Native peoples. We are clustering cell types into different cellular neighborhoods using spatial information and conducting statistical analysis integrating RNA sequencing data from the same patients. Further, we are generating spatial profiling data for an additional 5 TMAs comprising 60 additional patients and will present results of the combined data analyses.

#3424 Assessing a DNA methylation-based telomere length estimator in individuals with a heavy smoking history.

L. Grieshober[1], S. Graw[2], M. J. Barnett[3], G. E. Goodman[3], C. Chen[3], D. C. Koestler[4], C. J. Marsit[5], J. A. Doherty[1];
[1]Huntsman Cancer Institute, University of Utah, Salt Lake City, UT, [2]Everest Clinical Research Corporation, Markham, ON, Canada, [3]Fred Hutchinson Cancer Center, Seattle, WA, [4]University of Kansas Medical Center, Kansas City, KS, [5]Rollins School of Public Health, Emory University, Atlanta, GA

Telomere length (TL) and DNA methylation are associated with age and smoking exposure, as well as aging-related outcomes including lung cancer and mortality. A DNA methylation-based TL score (DNAmTL) was developed to estimate TL using DNA methylation array data, both in blood. DNAmTL effectively estimates telomere-related aging using 140 CpGs that are moderately enriched in sub-telomeric regions and not included in existing epigenetic clocks. We examined DNAmTL in individuals with a heavy smoking history (mean 56 pack years, range 11-185) in a nested lung cancer case-control study of 350 cases and 350 controls from the β-Carotene and Retinol Efficacy Trial identified through 2005. Twenty-two controls became cases with additional follow-up through 2013, so 328 controls and 372 cases were considered for these analyses. Leukocyte TL was measured using quantitative polymerase chain reaction (T/S ratio, log2-transformed), and DNA methylation was assayed on the Illumina EPIC array, in blood samples obtained on average 4.9 years prior to diagnosis in cases. We observed weak positive Pearson correlations between DNAmTL and TL in cases (r=0.19, p=0.0003) and controls (r=0.14, p=0.009) that persisted after age-adjustment: r=0.16, p=0.002 and r=0.14, p=0.014, respectively. Age-adjusted DNAmTL, but not TL, was longer for female compared to male cases (T=3.6, p=0.0004) and controls (T=2.2, p=0.03), and for those in the placebo compared to the intervention arm in cases (T=2.1, p=0.03) and controls (T=2.3, p=0.02). Linear regression models of TL and DNAmTL adjusted for age, sex, and race and ethnicity were not statistically significant for smoking variables at blood draw (pack years, current vs former smoking status, cigarettes smoked per day during smoking history, years smoked, years since quit), nor asbestos exposure in either cases or controls. Longer age-adjusted DNAmTL was associated with a lower hazard ratio (HR) for time to lung cancer death (0.60, 95% Confidence Interval (CI): 0.37-0.97) among cases (n=313 lung cancer-specific mortality events) in Cox proportional hazards models adjusted for age, sex, race and ethnicity, and time from blood draw to diagnosis with stage as a stratification variable (early I/II, advanced III/IV, unknown). Analogous age-adjusted TL model showed a similar direction but did not reach statistical significance (HR 0.86, CI: 0.71-1.05). Further adjustment of these models by DNA methylation-estimated leukocyte proportions of granulocytes, monocytes, natural killer, CD8+T, and CD4+T (excluding B cells) yielded similar results for age-adjusted DNAmTL (HR 0.54, CI: 0.31-0.92) and age-adjusted TL (HR 0.87, CI: 0.71-1.05). Our results illustrate that while DNAmTL may not be closely associated with smoking exposure among heavily exposed individuals, shorter DNAmTL may be more strongly associated with lung cancer mortality than TL in individuals with a heavy smoking history.

#3425 Genetic predisposition to obesity and survival in women with breast cancer.

C. Bodelon, A. Lori, M. Landry, J. Hodge, P. P. Choudhury, Y. Wang, L. E. McCullough, A. V. Patel, L. R. Teras;
American Cancer Society, Atlanta, GA

Background. Higher body mass index (BMI) is associated with poor survival after breast cancer diagnosis. BMI is a heritable trait. A polygenic risk score (PRS) for BMI has been associated with cardiometabolic traits and found to modify weight loss interventions. Whether BMI genetic scores affect survival in women with breast cancer is unknown.

Methods. This analysis was conducted in the Cancer Prevention Study II Nutrition cohort. Women diagnosed with non-metastatic breast cancer between 1992 and 2017 were included in the analysis if they had genotype data. Analyses were restricted to unrelated, postmenopausal women at the time of diagnosis who were of European ancestry (N=3,566). Deaths through 2020 were identified through linkage with the National Death Index. Primary cause of death was based on the International Classification of Disease codes. Pre-diagnosis BMI was self-reported (median 1.3 years from BMI measurement to diagnosis, interquartile range (IQR): 0.6, 1.9). We constructed a PRS using findings from a published meta-analysis of BMI genome wide association studies (GWAS) that included ~700,000 individuals and the PRSice tool.Hazard ratios (HR) and 95% confidence intervals (CI) between the PRS and all-cause mortality were estimated using Cox proportional hazards regression and Fine and Gray models for cause-specific mortality to account for competing risks. Models were adjusted for age and GWAS-specific statistically significant (P<0.05) principal components for population stratification. Mediation was estimated using the mediation R package.

Results. The median age at diagnosis was 71.5 years (IQR: 66.3, 76.8). Most women were overweight (33.5%) or obese (18.4%) and were diagnosed with localized stage (63%) and estrogen receptor positive (65%) breast cancer. During a median follow-up of 14.5 years (IQR: 9.7-19.8), there were 1,825 (51.2%) deaths, including 301 breast cancer and 337 cardiovascular disease (CVD) specific deaths. In multivariable models, a 5 Kg/m^2 increase in BMI was associated with increased risks of all-cause mortality (HR=1.09, 95% CI: 1.04, 1.15), breast cancer-specific mortality (HR=1.27, 95% CI: 1.13, 1.42), and CVD-specific mortality (HR=1.25, 95% CI: 1.11, 1.41). The PRS was highly predictive of pre-diagnostic BMI (P<0.001). A 1-standard deviation increase in the PRS was associated with statistically increased risk of all-cause mortality (HR=1.06, 95% CI: 1.02, 1.11). Risks of breast cancer (HR=1.07, 95% CI: 0.96, 1.19) or CVD (HR=1.01, 95% CI: 0.90, 1.12) specific mortality did not reach statistical significance. We estimated that 27% of the PRS and all-cause mortality association was mediated by BMI (95% CI: 12%, 91%; P=0.004).

Conclusions. Women with breast cancer predisposed to higher BMI were at increased risk of all-cause mortality. A BMI-related PRS may be a useful tool to identify women with breast cancer in need of additional interventions and/or surveillance.

#3426 Real-world biomarker testing rates and trends among patients with advanced non-small cell lung cancer in the US.

Y. Chen, A. Carlson;
University of Minnesota, College of Pharmacy, Minneapolis, MN

Background: Broad biomarker profiling before treatment initiation for non-small cell lung cancer (NSCLC) is recommended. Patients may not receive or receive inadequate biomarker testing before treatment initiation. This study assesses rates and trends of biomarker testing in community and academic oncology practices in the US.
Methods: A descriptive cohort study was conducted using electronic health records from an NSCLC registry. Patients who initiated NSCLC treatment following diagnosis of advanced NSCLC (stage IIIB/IIIC/IV) from 01/01/2015-12/31/2021 were identified. Patient demographics (age, gender, race, region) along with histology type (squamous/non-squamous) and hospital type (academic/community) were included. The percentage of patients receiving tests for any of the nine biomarkers before and during therapy was calculated and compared.
Results: 8,769 patients were identified with advanced NSCLC; 65.9% having non-squamous cell carcinoma; 22.4% having squamous cell carcinoma; 11.7% unknown. 13.4% of patients were from academic centers, 78.7% from community hospitals, 8.0% unknown. The majority (59%) were 65+ years; 47.3% were female. Overall, 83.2% had biomarker testing at some point in treatment; only 66.3% before treatment initiation. Over time, biomarker testing rates prior to treatment initiation increased (46.9% in 2015 to 73.8% in 2021). The use of biomarker testing in non-squamous cell carcinoma was greater than in squamous cell carcinoma. The most frequent biomarker testing before treatment initiation were PD-L1 (52.2%), EGFR (51.6%), and ALK (50.7%), followed by ROS1 (46.9%), BRAF (39.5%), and KRAS (34.1%). Testing rates for the newest biomarkers NTRK, MET, and RET were 20.4%, 28.4%, and 28.0%, respectively. Testing rates were similar between academic centers and community-based hospitals, except for the newest biomarkers, where use in academic settings was greater. Biomarker testing rates were higher among female patients (χ^2 P-value<0.001); rates by race were similar (χ^2 P-value=0.83).
Conclusion: While the use of biomarker testing in advanced NSCLC is growing, 26% of patients remained untested before treatment initiation. Biomarker testing in non-squamous cell carcinoma is higher than in squamous cell carcinoma, in keeping with the guideline emphasis on biomarker testing for that histology type. Results suggest that further dissemination of guideline recommendations to obtain biomarker test results prior to treatment initiation is important to optimize treatment decisions in the NSCLC landscape.

#3427 Serum metabolites and pancreatic ductal adenocarcinoma in two prospective cohorts.

T. Zhang, S. C. Moore, S. Fu, K. Wang, D. Albanes, S. J. Weinstein, K. Yu, R. Z. Stolzenberg-Solomon;
National Cancer Institute, Rockville, MD

Objective: Metabolomics may provide insight to understand the etiology and potential mechanisms for pancreatic ductal adenocarcinoma (PDAC) development beyond established risk factors of smoking, diabetes, and adiposity. We extended our previous metabolomic study by including additional participants from the Prostate, Lung, Colorectal, and Ovarian Cancer Screening Trial (PLCO) with the aim to examine prospective associations between serum metabolites and incident PDAC.

Method: We measured 1483 known metabolites in pre-diagnostic serum (up to 24 years) in two PDAC nested case-control studies within the PLCO (360 cases-control pairs) of mostly non-smoker men and women and Alpha-Tocopherol, Beta-Carotene Cancer Prevention Study (ATBC, 372 cases-control pairs) male smokers using liquid chromatography, high resolution/accurate mass spectrometry. Controls were incidence-density sampled and matched to cases by age, blood draw date, sex, race/ethnicity, and cohort. We used conditional logistic regression to calculate odds ratios and 95% confidence intervals for PDAC per standard deviation increase in $\log_{10}$-metabolite levels in each cohort and combined using fixed-effect meta-analyses and stratified by follow-up time. We also performed ElasticNet regression in each cohort to identify metabolites. We assessed associations of 72 predefined metabolic pathways with PDAC by comparing Fisher's statistic of metabolite p-values per pathway with a null distribution based on 500,000 permutations.

Results: Sixty-six metabolites were associated with PDAC at a false discovery rate (FDR)<0.05 with 26 below the Bonferroni threshold ($P<3.4\times10^{-5}$). Among the 66 metabolites, 14 and 15 were selected in ElasticNet regressions in ATBC and PLCO, respectively, with two in both cohorts. Notable findings include: fibrinopeptide B(1-9); seven modified, di- or poly-peptides; eight xenobiotics related to tobacco smoke; amino acids, carbohydrates, and TCA cycle metabolites known to be regulated by mutant KRAS (aspartate, glutamate, lactate, pyruvate, and α-ketoglutarate); four secondary bile acids and three aromatic amino acids (tryptophan, phenylalanine, and tyrosine) that were positively, while four fibrinogen cleavage peptides were inversely associated with PDAC. Among the top identified metabolites, aspartate, α-glutamyltyrosine, pyroglutamylglutamine, and Glu-Gly-Asn-Val showed time-varying associations overall ($P\leq0.05$) with greater magnitudes within the first 5 years after blood draw. Thirteen metabolic pathways were associated with PDAC (Bonferroni $P\leq0.05$).

Conclusion: Our study suggests pre-diagnostic circulating metabolites, particularly those potentially related to subclinical disease, microbiome, and tobacco metabolism are associated with PDAC. The identified metabolites along with other known risk factors might be useful in algorithms to model disease risk and progression.

#3428 Association of adipokines and inflammation biomarkers with cancer risk in men.

D. DeMoulin, H. Cai, Q. Cai, W. Zheng, X.-O. Shu;
Vanderbilt University Medical Center, Nashville, TN

Using pre-diagnosis fasting plasma samples from 4,040 participants of the Shanghai Men's Health Study which enrolled 61,464 men ages 40-70 during 2001-2006, we prospectively evaluated the associations of adipokines and inflammation biomarkers with cancer risk. Levels of leptin, resistin, adiponectin, plasminogen activator inhibitor type-1 (PAI-1), interleukin-6 (IL-6), interleukin-8 (IL-8), tumor necrosis factor-alpha (TNFa), monocyte chemoattractant protein-1 (MCP-1), and insulin were measured by Luminex assays, and C-reactive protein (CRP), measured by ACE Clinical Chemistry System. Biomarker levels were categorized by tertile distribution. The Cox regression model was applied to derive hazard ratios (HR) and 95% confidence intervals (CI) for cancer risk in association with biomarkers with adjustment for potential confounders. Principle component analysis (PCA) was performed to assess associations with multiple biomarkers, and tertile scores for each component were used in analyses. During 15-years of follow-up, 318 cancer cases were identified, including 85 lung, 49 gastric, 17 liver, and 61 colorectal cancer (CRC) cases. Analyses adjusted for age, education and income showed that 3rd vs 1st tertile of TNFa (HR=1.7, 95%CI=1.0-3.0) and adiponectin (HR=4.0, 95%CI=1.1-14.4) was associated with lung and liver cancer risk, respectively. High levels of leptin, insulin, and CRP were each associated with CRC risk: respective HRs were 2.3 (95%CI=1.1-4.7), 2.1 (95%CI=1.0-4.2), and 2.0 (95%CI=1.1-3.9). After further adjustment for known cancer risk factors, TNFa-lung cancer (HR=1.8, 95%CI=1.1-3.1); leptin-CRC (HR= 3.2, 95%CI=1.3-7.7); insulin-CRC (HR=2.1, 95%CI=1.0-4.5); and CRP-CRC (HR=2.0, 95%CI=1.0-4.0) associations remained statistically significant. The adiponectin-lung cancer association lost significance. PCA identified 4 principal components (PC). High PC1 score (main loadings: TNFa, leptin, and insulin) was associated with CRC risk (HR=2.3, 95%CI=1.1-5.0 for 3rd vs 1st tertile p_{trend}=0.02). High PC2 score (main loadings: adiponectin, IL-8, MCP-1) and PC3 (main loadings: resistin and PAI-1) were associated with liver cancer risk: HR=5.2 (95%CI=1.1-24.3) for the 3rd vs 1st tertile, p_{trend}=0.03 and HR=4.7 (95%CI=1.0-21.7), for the 3rd vs 1st tertile, p_{trend}=0.03, respectively. High PC4 score (main loadings: IL-6 and CRP) was associated with lung cancer risk (HR=1.7, 95%CI=1.0-3.0, for the 3rd vs 1st tertile, p_{trend}=0.04). These associations, except the PC1-CRC association, lost significance after further adjustment of known cancer risk factors. Our study found that high plasma levels of insulin, CRP, and their combination were associated with CRC risk, high resistin and adiponectin levels with liver cancer risk, and high TNFa levels with lung cancer risk. Some biomarker-cancer associations may be explained by their correlations with known cancer risk factors, especially smoking.

#3429 Using metabolomics to identify biomarkers mediating the associations of adiposity in childhood and early adulthood with mammographic breast density in premenopausal women.

Kayla R. Getz[1], Myung Sik Jeon[1], Lili Liu[2], Lei Liu[2], Chongliang Luo[1], Jingqin Luo[1], Adetunji T. Toriola[1]

[1]Public Health Sciences, Washington University School of Medicine in St. Louis, St. Louis, MO,[2]Biostatistics, Washington University School of Medicine in St. Louis, St. Louis, MO

Introduction: Mammographic breast density (MBD), a strong predictor of breast cancer risk, is highly influenced by body mass index (BMI) in childhood and early adulthood, but the mechanisms elucidating this relationship are undetermined. To our knowledge, no study has explored the mediating role of biomarkers on the relationship between early-life adiposity and MBD. The goal of this study is to discover metabolites that mediate the relationship between BMI at ages 10 and 18 with MBD in premenopausal women.

Methods: This study includes premenopausal women who had their screening mammogram at Washington University in St. Louis, MO, and provided a fasting blood sample. Metabolon performed untargeted metabolomic profiling, detecting 1,074 metabolites. Metabolites missing >300 observations were excluded, leaving 828 metabolites; the other missing values were imputed using the nearest neighbor method. To mitigate batch effect, we normalized the metabolite peak area data using ComBat. Volumetric percent density (VPD) was calculated in 700 women using Volpara software. BMI at age 10 was estimated using the Stunkard pictogram, and BMI at age 18 was calculated from self-reported weight at 18 and height at study initiation. To assess the mediating role of the 828 metabolites, we performed high dimensional mediation analysis using the *hima* R package adjusting for potential confounders. Missing values in the covariates and BMI measures included in the mediation analysis were imputed using multivariate imputation by chain equations. Associations were considered significant if FDR p-value <0.1.

Results: Four metabolites (glutamate, beta-cryptoxanthin, phytanate, and cortolone glucuronide (1)) mediated the relationship between BMI at age 10 and VPD; and 2 metabolites (glutamate, beta-cryptoxanthin) mediated the relationship between BMI at age 18 and VPD. Glutamate and beta-cryptoxanthin significantly mediated the relationship between both BMI measures and VPD, but glutamate was the strongest mediator across both time points. Glutamate mediated 6.7% (FDR p-value=0.06) and 9.3% (FDR p-value=0.008) of the total effect between BMI at age 10 and 18, respectively, on VPD. Beta-cryptoxanthin mediated 4.1% (FDR p-value=0.06) and 6.3% (FDR p-value=0.04), of the total effect between BMI at age 10 and 18, respectively, on VPD. Additionally, phytanate mediated 2.6% (FDR p-value=0.06) and cortolone glucuronide (1) mediated 2.0% (FDR p-value=0.07) of the total effect between BMI at age 10 and VPD.

Conclusion: Amino acid, lipid, cofactor/vitamin, and xenobiotic metabolites mediated the associations of BMI in early-life and VPD in premenopausal women. This innovative study offers insight into the biological mechanisms underlying the link between early-life adiposity and MBD, which can support future research into breast cancer prevention.

#3430 Mosaic loss of the Y chromosome is associated with prostate cancer risk.

R. L. Kelly, W. Zhou, K. M. Barnao, C. D. Young, A. K. Hubbard, S. M. Khan, W.-Y. Huang, S. J. Chanock, M. J. Machiela;
National Cancer Institute, Rockville, MD

Mosaic loss of the Y chromosome (mLOY), a type of clonal hematopoiesis, is the most frequent chromosomal alteration observed in leukocytes of aging men. mLOY is a putative biomarker of genomic instability with evidence of associations with risk of some solid tumors, but more studies are needed to refine associations and identify potential mechanisms for cancer risk. Prostate cancer (PCa), the most common non-cutaneous cancer in males, is also associated with aging. To further investigate potential relationships between mLOY and PCa, we examined DNA derived from leukocytes of male participants in two large biobanks: the UK Biobank (UKBB; N = 210,103) and the Prostate, Lung, Colorectal, and Ovarian Cancer Screening Trial (PLCO, N = 26,795). Of the 236,898 male participants without previous cancer diagnosis, 14,253 (6.0%) were diagnosed with incident PCa after DNA collection. High-density genotyping array data collected during the studies were used to create virtual karyotypes for detecting mLOY in whole blood samples utilizing a phase-based detection method in MoChA software. Analyses were restricted to men without cancer at genotyping and multivariable regression models were adjusted for age, smoking status, and genetic similarity. Men with detectable mLOY were older (mean = 62 vs 56 years) and more likely to be smokers (14.8% vs 9.7%) than men without mLOY. A total of 3,848 (27.0%) men with PCa and 42,835 (19.2%) men free of PCa had detectable mLOY. mLOY clonal fraction ranged from 0.01% to 72.1% of total leukocytes. 18.7% of PCa cases and 13.6% of men free of PCa had high clonal fraction mLOY, defined as greater than 10% of leukocytes with mLOY. Fixed effect meta-analysis of multivariable models from UKBB and PLCO produced evidence for a positive association between mLOY in leukocytes and incident PCa; (Odds Ratio (OR) = 1.062, 95% Confidence Interval (CI) [1.020, 1.107], P-Value (p) = 0.004). The effect estimate was the same in men with low clonal fraction of mLOY (OR = 1.062, 95% CI [1.012, 1.113], p = 0.014) and men with high clonal fraction of mLOY (OR = 1.065, 95% CI [0.998, 1.137], p = 0.057). Age at PCa diagnosis was not associated with mLOY or the clonal fraction of mLOY. A sub-analysis of separate participants from PLCO with mLOY detected in buccal cells (n = 18,011) also showed a small positive effect between mLOY and PCa risk, but the relationship did not reach statistical significance (OR = 1.036, 95% CI [0.877, 1.224], p = 0.673)). Our investigation of the relationship between mLOY and PCa in two large prospective studies provides additional evidence for an association between mLOY detected in the blood and increased PCa risk, meriting additional studies of potential biologic mechanisms underlying the relationship.

#3431 Genetically determined circulating lactase/phlorizin hydrolase concentrations and risk of colorectal cancer: A two-sample mendelian randomization study.

S. Han[1], J. Yao[1], H. Yamazaki[2], S. Streicher[3], J. Rao[4], R. Nianogo[1], Z.-F. Zhang[1], B. Huang[5];
[1]UCLA Fielding School of Public Health, Los Angeles, CA, [2]Graduate School of Medicine, Kyoto University, Kyoto, Japan, [3]University of Hawaii Cancer Center, University of Hawaii at Manoa, Honolulu, HI, [4]UCLA David Geffen School of Medicine, Los Angeles, CA, [5]Keck School of Medicine of USC, Los Angeles, CA

Background: Colorectal cancer (CRC) ranks as the third most common cancer worldwide. Despite its established connection with genetic, dietary, and lifestyle factors, gaps remain in the understanding of its etiology. Lactase-phlorizin hydrolase (LPH) plays a critical role in milk digestion and influences crucial nutrient absorption and gut microbiota composition. A direct relationship of CRC risk with LPH level remains unexplored. Our study aims to elucidate the potential causal link between genetically determined LPH levels and CRC risk.
Methods: We applied a two-sample Mendelian Randomization (MR) strategy to investigate the causal link between elevated LPH levels and CRC risks. Genetic instruments for LPH (one *cis*-variant and three *trans*-variants) were derived from the Fenland Study, and CRC-associated summary statistics for these instruments were extracted from the FinnGen Study, PLCO Atlas Project, and Pan-UK Biobank. Primary MR analyses focused on a *cis*-variant (rs4988235) for LPH levels, with results integrated via meta-analysis. MR analyses using all variants were also undertaken. This analytical approach was further extended to assess CRC subtypes, specifically colon and rectal cancer.
Results: Meta-analysis across the three datasets illustrated an inverse association between genetically predicted LPH level and CRC risk (OR: 0.92 [95% CI, 0.89-0.95]). Subtype analyses revealed associations of genetically predicted elevated LPH levels with reduced risks for both colon cancer (OR: 0.92 [95% CI, 0.89-0.96]) and rectal cancer (OR: 0.92 [95% CI, 0.87, 0.98]). Consistency was observed across varied analytical methods and different datasets.
Conclusions: Our study suggests an inverse relationship between genetically determined LPH level and CRC risk. Further exploration is warranted to unveil the underlying mechanisms and validate LPH's potential role in CRC prevention.

#3432 Blood metabolomic profile of glioma risk: A pooled, multi-cohort analysis in COMETS.

J. Huang[1], B. Zhao[1], S. J. Weinstein[2], M. L. Neuhouser[3], S. C. Moore[2], H. Eliassen[4], D. J. Cote[5], L. Le Marchand[6], L. Mucci[4], Y. Yang[7], V. Stevens[7], W. Zheng[8], X.-O. Shu[8], **D. Albanes**[2];

[1]National Clinical Research Center for Metabolic Diseases, Changsha, Hunan, China, [2]National Cancer Institute, Bethesda, MD, [3]Fred Hutchinson Cancer Center, Seattle, WA, [4]Harvard TH Chan School of Public Health, Boston, MA, [5]Keck School of Medicine of the University of Southern California, Los Angeles, CA, [6]University of Hawaii Cancer Center, Honolulu, HI, [7]American Cancer Society, Atlanta, GA, [8]Vanderbilt University Medical Center, Nashville, TN

Although gliomas are relatively rare, they are among the most lethal malignancies. Yet, with the exception of ionizing radiation and family history, their etiologic factors remain largely unknown. We conducted an untargeted metabolomics investigation pooling nested case-control studies from 9 prospective cohorts (median age 63 years, 59% women) in the Consortium of Metabolomics Studies (COMETS). One cancer-free control was individually matched to each of the 803 glioma cases based on age, sex, self-identified race/ethnicity, and blood collection date. Using an ultrahigh-performance LC-MS/MS platform (Metabolon, Inc.), we identified 874 known metabolites in pre-diagnostic serum or plasma, and logistic regression models conditioned on the matching factors) estimated odds ratios (ORs) and 95% confidence intervals for the associations between 1-SD increases in circulating metabolites and glioma risk (Bonferroni corrected significance threshold $P=5.7\times10^{-5}$). A total of 58 metabolites were associated with glioma ($P<0.05$), with the top three being 3-methylglutarylcarnitine (OR=1.19; P=0.001), cholate (OR=0.85; P=0.001) and a sphingomyelin (SM) (d18:2/21:0, d16:2/23:0, OR=1.19; P=0.002). Analysis restricted to cases diagnosed >5 years after blood collection showed 51 metabolites associated with risk ($P<0.05$), including SM d18:2/23:1 (OR=1.32; $P=5.2\times10^{-5}$), and two other SMs (d18:2/21:0, d16:2/23:0 and d17:1/24:1(15Z)) (ORs=1.27 and 1.26, respectively; $P<5.6\times10^{-4}$). Our findings were not materially altered with further adjustment for smoking, BMI, height and diabetes. Analysis restricted to high-grade glioma cases (n=595) showed similar associations, whereas low-grade glioma (n=207) showed fewer metabolites related to risk (top signals of sphingosine, sphinganine and *L*-glutamic acid, each inversely associated). We did, however, observe that the 2-hydroxyglutarate/alpha-ketoglutarate ratio was significantly associated with low-grade disease (OR=2.9; P=0.0008), which was most pronounced among cases diagnosed >10 years following blood collection (OR=9.99; P=0.003). Glioblastoma (n=485) showed similar positive risk estimates including for 3-methylglutarylcarnitine which achieved Bonferroni significance (OR=1.35; $P=3\times10^{-5}$) and several SMs. In contrast, the top metabolite for astrocytoma risk (n=88) was tyrosine (OR=0.55; P=0.002). Gene-set and principal components analyses confirmed that the sub-pathways of SM, dihydro-SM, fatty acid, and dihydroceramide metabolism were significantly associated with overall glioma risk, and dihydro-SM, dihydroceramide, SM, lactosylceramide, glutathione, and purine metabolism were associated with high-grade glioma (all P values <0.05). These novel findings regarding altered metabolic pathways/dysregulation occurring years before glioma diagnoses may be related to etiologic factors or subclinical disease.

#3433 Characterization of co-occurring clonal hematopoiesis to identify high risk clones associated with hematologic cancer risk.

K. M. Barnao[1], A. K. Hubbard[1], W. Zhou[1], I. Chan[2], D. Tran[2], Y. Cao[2], S. J. Chanock[1], K. L. Bolton[2], M. J. Machiela[1];
[1]National Cancer Institute, Bethesda, MD, [2]Washington University School of Medicine, St. Louis, MO

Clonal hematopoiesis (CH) is the age-related clonal expansion of hematopoietic cells as a result of acquired mutations in driver genes, commonly referred to as clonal hematopoiesis of indeterminate potential (CHIP), or due to large-scale mosaic chromosomal alterations (mCAs). While the type and genomic location of CH exhibits varying associations with hematological parameters as well as lymphoid and myeloid malignancy risk, few studies have examined the co-occurrence of CH types. We characterized the frequency of co-occurring CH and examined the association of co-occurring CH with various cancer-related phenotypes to identify potential high-risk clones associated with hematologic cancer risk.

We analyzed sequencing and genotyping array data from 453,807 participants in the UK Biobank to detect CHIP and mCAs. In total, 83,240 (18.3%) individuals had at least one detectable type of CH, with increasing age strongly associated with increasing frequency of CH ($P < 2\times10^{-16}$). The most common type of CH was mCAs (N= 67,081 (14.7%)), with mosaic loss of the Y (mLOY) and X (mLOX) chromosomes being most frequently observed in males and females, respectively. We noted inverse associations between mLOY or mLOX with autosomal mCAs, but positive associations between some autosomal mCAs (e.g., chr3 and chr18 mCAs). CHIP was detected in 20,354 (4.5%) individuals, with mutations in *DNMT3A*, *TET2*, and *ASXL1* most common. Similar to mCAs, some forms of CHIP were inversely associated (e.g., *DNMT3A* CHIP with most other CHIP mutations) while others displayed positive associations (e.g., *JAK2* CHIP with *NFE2* CHIP), suggesting both instances of mutual exclusivity as well as cooperation. We likewise noted several instances of CHIP and mCAs co-occurring (e.g., *MYD88* and chr18 mCAs) and overlapping (e.g., *JAK2* and 9p24 mCAs) more frequently than expected.

Compared to those with no CH, participants with CH had notable alterations in blood cell counts, leukocyte telomere length (LTL), and elevated hematologic cancer risk even after adjusting for age, sex, smoking, and genetic ancestry. Furthermore, co-occurring CH had more pronounced associations, with the greatest alterations and hematologic cancer risk generally noted in participants with overlapping CHIP and mCAs (e.g., *MYD88* and 3p22 mCAs). These findings highlight substantial enrichment in CH co-occurrences, particularly in the positional overlap of CHIP and mCAs, and indicate an increased risk of hematological malignancies when CH types overlap (HR = 29.5, 95% CI [24.0, 36.3], $P < 2\times10^{-16}$). Overall, this study details the landscape of co-occurring CH and nominates high risk co-occurrences with strong implications for future hematological malignancy risk.

#3434 Effect modification by levels of sex hormones in the association between adiposity and cancer incidence in the UK Biobank.

L. Lucas, Y. Lu, E. L. Giovannucci, M. Song;
Harvard T.H. Chan School of Public Health, Boston, MA

Introduction: The association between adiposity and cancer risk differs between sexes for some cancer types.
Methods: We prospectively examined adiposity in relation to cancer incidence according to sex hormones in the UK Biobank. Adiposity was assessed by body mass index (BMI) and visceral adipose tissue (VAT), the latter predicted using determinants of age, height, weight, hip circumference, waist circumference, and race. Serum sex hormone binding globulin (SHBG), testosterone, and estradiol were measured using a biochemistry assay and were classified as high or low based on median levels. Cancer incidence was ascertained using ICD-10 codes through cancer registry linkage. For cancer types showing a sex difference in the association between adiposity and cancer incidence, we assessed multiplicative and additive interaction with sex hormones in men and women separately and corrected for multiple testing using false discovery rate. We used Cox regression to calculate the multivariable hazard ratio (HR) of cancer per increase between the 90^{th} to 10^{th} percentile of adiposity (BMI or predicted VAT).
Results: During a median follow-up of 13.1 years, we documented 23,964 and 21,045 incident cancer cases among 217,460 men and 256,163 women, respectively. Adiposity showed a much stronger association with higher risk of colorectal, esophageal, and liver cancers in men than women. In men, BMI was more strongly associated with higher risk of colorectal cancer in low vs. high levels of SHBG (HR (95%CI) of 1.47 (1.31-1.64) vs. 1.12 (0.94-1.33) (adjusted $P_{interaction}$ = 0.027). In contrast, BMI showed a stronger association in high vs. low levels of SHBG with esophageal (HR = 2.39 vs. 1.62) and liver cancers (HR = 3.24 vs 1.96) in men (adjusted $P_{interaction}$ = 0.038 and 0.027, respectively). Among women, BMI was associated with a higher risk of esophageal cancer in those with low SHBG (HR=1.68) but not in those with high SHBG (HR=0.64) (adjusted $P_{interaction}$ = 0.025). Similar patterns were observed for predicted VAT. Men with high SHBG levels and high adiposity (BMI and predicted VAT) had 7.63 (5.08-11.46) and 8.92 (5.72 to 13.90), respectively, times higher risk of liver cancer compared to men with low SHBG levels and low adiposity. No effect modification by estradiol or testosterone was detected for any of the cancers studied.
Conclusions: The association between adiposity and colorectal, esophageal, and liver cancer differed by sex. SHBG may be an important factor underlying these differences.

#3435 History of breastfeeding in relation to circulating inflammatory biomarkers.

N. Lin[1], J. M. Mongiovi[2], L. V. Farland[3], T. Huang[1], H. Eliassen[2], M. K. Townsend[2], S. S. Tworoger[2], K. L. Terry[1], N. Sasamoto[1];
[1]Brigham and Women's Hospital, Boston, MA, [2]Harvard T.H. Chan School of Public Health, Boston, MA, [3]University of Arizona, Tucson, AZ

Background: History of breastfeeding has been associated with reduced risk of various chronic diseases in which chronic inflammation is involved in disease etiology, including cardiovascular disease, type II diabetes, breast cancer, and ovarian cancer. However, few studies have investigated the long-term impact of breastfeeding on systemic inflammation. Thus, we aimed to examine the associations between breastfeeding history and circulating inflammatory biomarkers at midlife.
Methods: We conducted a cross-sectional analysis including 3,448 parous women with plasma inflammatory biomarkers in the Nurses' Health Study and Nurses' Health Study II. We examined self-reported history of ever breastfeeding (ever vs. never) and lifetime total duration of breastfeeding (never, < 6 months, 7-11 months, 12+ months) prior to the time of blood draw. We calculated the geometric means of eight inflammatory biomarkers [i.e., high sensitivity C-reactive protein (hsCRP), interleukin-6 (IL6), sIL6Rα, IL8, IL10, sIL2-receptor-α(Rα), soluble tumor necrosis factor α receptor 2 (sTNFR2), B-cell activating factor (BAFF), C-X-C motif chemokine ligand 13 (CXCL13)] by self-reported history of breastfeeding status adjusted for age, body mass index (BMI), smoking status, duration of oral contraceptive use, parity, proinflammatory diet, analgesic use, menopausal status, and cohort. Tests for trend were calculated using the median value of each lifetime breastfeeding duration category and modeling as a continuous variable. We also conducted stratified analyses by menopausal status and BMI (< 25kg/m^2 vs. ≥ 25kg/m^2) at blood draw.
Results: Overall, we did not observe statistically significant differences in circulating inflammatory biomarker levels by history of breastfeeding among parous women. When stratifying by menopausal status at blood draw, total breastfeeding duration was inversely associated with sTNFR2 levels among premenopausal women (P-trend = 0.03) but not among postmenopausal women. Plasma IL8 levels were suggestively inversely associated with breastfeeding duration among postmenopausal women (P-trend = 0.07) but not among premenopausal women. Among women with BMI ≥ 25 kg/m^2, plasma BAFF levels were lower in parous women who ever breastfed compared to those who never breastfed [1382.5 (95%CI = 1242.0 - 1539.0) pg/ml vs. 1611.9 (95%CI = 1424.9 - 1823.4) pg/ml; p = 0.03], and suggestively inversely associated with total breastfeeding duration (p-trend = 0.07) but no statistically significant association was observed in women with BMI < 25kg/m^2. IL10 was inversely associated with total breastfeeding duration among women with BMI ≥25 kg/m^2 (P-trend = 0.007), but not in women with BMI < 25kg/m^2.
Conclusion: Overall, history of breastfeeding was not associated with inflammatory biomarkers at mid-life, however the association may vary by menopausal status and BMI.

#3436 Circadian rhythm dysregulation with risk of gastrointestinal cancers: A large-scale prospective analysis.

Y. Kang, S. Mok, X. Zong, Y. Cao;
Washington University in St. Louis, St Louis, MO

Introduction: The incidence of multiple gastrointestinal (GI) cancers has been rising among younger adults with unknown etiology. Circadian rhythm dysregulation due to increasing exposures to artificial lighting, irregular work hours, and frequent travel, has been recently linked with multiple diseases. Disruption of the circadian clock drives *Apc* LOH to hyperactivate Wnt signaling and enhances MYC-dependent glycolytic metabolism to accelerate colorectal cancer progression. However, the association between circadian rhythm dysregulation, quantified by relative amplitude (RA)--a parameter derived from rest-activity patterns, and risk of colorectal and other GI cancers has not been evaluated in epidemiologic studies.

Methods: We prospectively examined the associations between RA and risk of incident GI cancers among 87,653 UK Biobank participants who wore an Axivity AX3 triaxial accelerometer over 7 days (2013-15) with follow-up to 2021. RA was derived and averaged across all valid days, using the difference between the mean activity levels during the most active 10-hour period and the least active 5-hour period. Cox models were used to estimate relative risks (RRs) and 95% confidence intervals (CIs).

Results: During 512,074 person-years, 1,079 incident GI cancer cases occurred. After multivariable adjustment, lower RA was associated with an increased risk of overall GI cancer (RR per SD [standard deviation] = 1.12, 95% CI 1.04-1.21, P for trend = 0.01). Compared to individuals in the highest tertile (T1), those with RA in the lowest tertile (T3) had a 25% increased risk of overall GI cancer (RR = 1.25, 95% CI 1.05-1.50). The positive associations with GI cancers were mainly driven by gastric cancer (RR per SD = 1.33, 95% CI 1.02-1.74, P for trend= 0.04) and colon cancer (RR per SD = 1.13, 95% CI 1.00-1.28, P for trend = 0.03).

Conclusion: In this large-scale, prospective analysis of accelerometer data, circadian rhythm dysregulation was associated with subsequent risk of GI cancers, primarily gastric and colon cancer. To our knowledge, this is among the first population-based studies reporting the positive link between circadian rhythm dysregulation with cancer risk.

#3437 Stromal tumor-infiltrating lymphocytes in association with body size and composition among Black and White women with breast cancer.

Rand T. Akasheh[1], Thaer Khoury[2], Song Yao[2], Angela Omilian[2], Chi-Chen Hong[3], Elisa V. Bandera[4], Bonnie Qin[4], Nur Zeinomar[4], Christine Ambrosone[2], Ting-Yuan David Cheng[1]

[1]Internal Medicine, The Ohio State University Wexner Medical Center, Columbus, OH,[2]Roswell Park Comprehensive Cancer Center, Buffalo, NY,[3]Roswell Park Comprehensive Cancer Center, Bufalo, NY,[4]Rutgers Cancer Institute of New Jersey, New Brunswick, NJ

Background: Obesity is a major risk factor for breast cancer and negatively affects disease prognosis. Tumor-infiltrating lymphocytes (TILs) in the stroma of breast tissue play a major role in eliminating cancer cells and modulating immunotherapy efficacy. We aim to study the association between body size and composition with stromal TILs in breast tumor tissue by race.
Methods: The study included 920 Black and 395 White women with newly diagnosed invasive breast cancer who have stromal TIL scores from the Women's Circle of Health Study (WCHS). Body mass index (BMI), waist circumference (WC), and waist-to-hip ratio (WHR) were measured during the home interview. Pre-treatment H&E-stained tumor tissue sections were reviewed by our study pathologist and stromal TILs were scored on a scale of 0-100% at 10% increment according to the recommendations of the International TILs Working Group. Linear regressions adjusting for age at diagnosis, tumor grade, stage, and molecular subtype were used to test the differences in TILs across the categories of body size and composition indicators separately for Black and White women.
Results: A higher stromal TILs score was associated with more aggressive breast cancer features, including higher grade, larger tumor size, more advanced stage, hormone receptor (HR) negativity, and human epidermal growth factor receptor 2 (HER2) positivity in both Black and White women (all $P<0.05$). Among Black women, WHR >0.90 vs ≤0.85 was associated with lower TILs overall ($\beta = -3.5\%$, $P = 0.045$) and in triple-negative tumors ($\beta = -12.3\%$, $P = 0.003$). Among White women, BMI 25.0 - 29.9 vs <25 was associated with higher TILs in HR-/HER2+ tumors ($\beta = 28.1\%$, $P = 0.031$). A pattern suggested that BMI ≥30 vs <25 was associated with lower TILs in both HR-/HER2+ ($\beta = -10.2$, $P=0.52$) and triple-negative ($\beta = -12.8$, $P=0.14$) tumors, although the associations were not significant. No association was observed between TILs and any of the body composition parameters in women with HR+ tumors.
Conclusions and Relevance: Body size and composition correlate with stromal TILs mainly in patients with HR- tumors, and this relation may be race-dependent. These findings suggest that body size and composition potentially modulate breast cancer treatment outcomes at least in part through TILs-dependent mechanisms. Funding: This work was in part supported by grants from the US National Institutes of Health (P01CA151135, R01CA100598, R01CA185623, P30CA016056, P30CA072720, K07CA201334, and R37CA248371), US Army Medical Research and Material Command (DAMD-17-01-1-0334), the Breast Cancer Research Foundation (CBA), and the Philip L. Hubbell family.

#3438 Associations between estimated endotoxin exposure and circulating immunological markers among male farmers.

S. C. Ezennia, L. E. Beane-Freeman, V. C. Chang, S. Xie, G. Andreotti, M. C. Friesen, J. N. Hofmann;
NIH-NCI, Bethesda, MD

Occupational exposure to endotoxin has been associated with reduced lung cancer risk. Farmers who perform certain tasks (e.g., raising hogs) can be highly exposed to endotoxin. The mechanisms through which endotoxin could confer a lower risk of lung cancer, while likely to be immune mediated, are not clear. To address this gap, we evaluated associations between estimated endotoxin exposure and circulating immunologic markers among male farmers in the Biomarkers of Exposure and Effect in Agriculture (BEEA) study. Our investigation included 122 non-smoking farmers from Iowa, oversampling those raising hogs (n=61). We evaluated 58 serologic markers, including some linked to lung cancer, that were measured using multiplex bead-based assays. Based on an algorithm linking personal air measurements in BEEA and published data to reported farming tasks, we estimated cumulative endotoxin exposure in the last 30 days and 12 months before sample collection. We used multivariable linear regression to estimate geometric mean ratios of immune markers across exposure quartiles, overall and by season of sample collection. Higher endotoxin exposure in the last 30 days was associated with increased levels of FGF-2, MIP-3A/CCL20, and sIL-4R ($P_{trend} \leq 0.02$), and with decreased levels of MDC/CCL22 ($P_{trend} = 0.02$). In analyses stratified by season, the positive associations with FGF-2 and MIP-3A/CCL20 were most apparent in the winter ($P_{trend} = 0.002$ and 0.03, respectively); we also observed an inverse association with sCD27 levels in the summer ($P_{trend} = 0.03$). Similar patterns were observed for endotoxin exposure in the last 12 months. This study is the first to use novel algorithm-based endotoxin exposure estimates to evaluate associations with intermediate lung cancer-related markers. Several markers were associated with endotoxin levels in an exposure-response manner. Our findings suggest possible biological mechanisms through which endotoxin may reduce risk of lung cancer.

Table 1. Associations between estimated endotoxin exposure in the last 30 days and selected serum im

#3439 Factors affecting the performance of existing epigenetic clocks to predict chronological age in colorectal tumor and normal tissues.

C. L. Benson II[1], F. Moratalla-Navarro[2], A. Diez-Villanueva[2], M. A. Devall[3], V. Moreno[2], S. L. Schmit[4], F. R. Schumacher[1];
[1]Case Western Reserve University, Cleveland, OH, [2]Catalan Institute of Oncology (ICO), Barcelona, Spain, [3]University of Virginia, Charlottesville, VA, [4]Cleveland Clinic, Cleveland, OH

Epigenetic age (EA) may serve as a risk stratification biomarker for early-onset colorectal cancer (EOCRC, <50 years old), which has been rising substantially in recent decades. We utilized publicly available data in a descriptive analysis to compare epigenetic clocks in colorectal tissue and to investigate differences between chronological age (CA) and biological age, as measured by EA, in relation to demographic and clinical features. We analyzed DNA methylation (DNAm) array data on 144 participants (96 CRC cases, 48 healthy controls) from the Colonomics Study (CLX; Barcelona, Spain) and 331 CRC cases (51 EOCRC, 316 average-onset (≥50) colorectal cancer (AOCRC)) from The Cancer Genome Atlas (TCGA) as well as corresponding demographic and clinical variables. Among CLX participants, the 96 CRC cases provided colon tumor and paired normal mucosa samples, while the 48 controls provided healthy colon mucosa samples. TCGA included primary tumor samples from 331 cases with colon or rectal adenocarcinoma (TCGA-COADREAD). The 2013 Horvath clock estimated EA based on CA, while epiTOC, estimated the relative stem cell division rate from tissue biospecimens. We examined the correlations between CA and EA stratified by case/control status, sample type, sex, and age of onset (TCGA only). Tissue from CLX controls demonstrated a strong, positive correlation ($r>0.9$) between CA and EA for both the 2013 Horvath and epiTOC clocks. Using the Horvath clock, CA and EA correlations in normal mucosa and tumor tissue samples from CLX varied, with $r = 0.74$ and $r = 0.41$, respectively, and were weaker using the epiTOC clock, with $r = 0.26$ (normal) and $r = 0.10$ (tumor). When CLX cases were stratified by sex, the CA and EA (Horvath) correlations among female cases were $r = 0.80$ (normal) and $r = -0.12$ (tumor), while the correlations for males were stronger at $r = 0.58$ (normal) and $r = 0.31$ (tumor). This is in comparison to the epiTOC clock with females showing correlations of $r = -0.02$ (normal) and $r = 0.41$ (tumor), while males had $r = 0.06$ (normal) and $r = 0.11$ (tumor). In TCGA, correlations for EOCRC were $r = -0.20$ (Horvath) and $r = -0.08$ (epiTOC) and for AOCRC were $r = 0.29$ and 0.20, respectively. By sex, correlations for females with EOCRC for Horvath and epiTOC were $r = -0.09$ and $r = -0.07$, respectively, while correlations for males with EOCRC were $r = -0.02$ and $r = -0.08$, respectively. For TCGA cases with AOCRC, the correlations between CA and EA were $r = 0.35$ and $r = 0.22$ for females, and $r = 0.26$ and $r = 0.20$ for males, respectively for Horvath and epiTOC. This study revealed substantial variability in the ability of existing epigenetic clocks to accurately predict chronological age, with tissue type and sex strongly influencing the resulting correlations. Our findings highlight the importance of considering these factors when choosing an epigenetic clock.

#3440 Etiology of prostate cancer with the *TMPRSS2:ERG* fusion: A systematic review of risk factors.

Colleen B. McGrath[1], Alaina H. Shreves[2], Megan R. Shanahan[1], Hannah E. Guard[1], Manelisi V. Nhliziyo[1], Kathryn L. Penney[1], Tamara L. Lotan[3], Michelangelo Fiorentino[1], Konrad H. Stopsack[1], Lorelei A. Mucci[1]

[1]Harvard T.H. Chan School of Public Health, Boston, MA,[2]Division of Cancer Epidemiology and Genetics, National Cancer Institute, Bethesda, MD,[3]Johns Hopkins University School of Medicine, Baltimore, MD

Background: The *TMPRSS2:ERG* gene fusion is the most common somatic alteration in primary prostate cancer and an early event in carcinogenesis. There are emerging data highlighting etiologic differences in prostate cancer by *TMPRSS2:ERG* status. This systematic review synthesized evidence from epidemiologic studies on prostate cancer risk factors for tumors with and without the *TMPRSS2:ERG* fusion.

Methods: A systematic literature search was performed in Ovid MEDLINE, EMBASE, and Web of Science without language restriction for studies published by September 27, 2022. Studies that assessed associations between epidemiologic and genetic factors and prostate cancer risk by tumor *TMPRSS2:ERG* (ERG) fusion status in human populations were included.

Results: Of 3,071 records identified, 20 publications comprising prospective cohort and case-control studies from five study populations (published 2009-2022) were included. Risk factors included germline genetic variants, circulating hormones, diet, lifestyle factors, and medications. The included studies suggested that taller height and higher total and free circulating testosterone levels tended to be associated with higher risk of ERG-positive, but not ERG-negative prostate cancer. CAG repeat length in the androgen receptor (*AR*) gene, related inversely to transcriptional activity, appeared to be associated with a lower risk of ERG-positive, but not ERG-negative prostate cancer. There was statistical evidence for etiologic differences for several germline single nucleotide polymorphisms (SNPs) by ERG status. Excess body weight, greater vigorous physical activity, greater lycopene intake, and calcium channel blocker use appeared to specifically be associated with a lower risk of ERG-positive tumors. Associations of other potential etiologic factors, including diabetes mellitus, baldness, aspirin use, circulating antioxidant levels, and sex hormones other than testosterone, with ERG-positive prostate cancer were null or inconclusive. Most associations had low precision, and the results were based on few distinct study populations, highlighting a need for replication.

Conclusions: Prostate cancer with the *TMPRSS2:ERG* fusion may be an etiologically distinct subtype impacted by certain modifiable and hormonally-acting risk factors that align with the established mechanistic role of this gene fusion in androgen, insulin, and growth factor pathways. The findings suggest a potentially distinct genetic predisposition to prostate cancer with or without the *TMPRSS2:ERG* fusion. More broadly, these findings suggest that considering molecular subtypes of prostate cancer, beyond *TMPRSS2:ERG*, may strengthen etiologic understanding of prostate cancer and evidence for prevention.

#3441 Application of a maternal comorbidity index to predict childhood cancer risk: A population-based case-control study in Denmark.

T. Adenekan[1], J. E. Heck[1], C. Yin[1], J. Hansen[2];
[1]University of North Texas, Denton, TX, [2]Danish Cancer Institute, Copenhagen, Denmark

Background: Maternal health has been found to be an indicator of children's health and has also been found to affect the risk of childhood diseases. Children are especially susceptible to in-utero exposures. A mother's health conditions before and during pregnancy could have important consequences for her child's health, including cancer development, as was observed in some prior studies.
Objectives: This study aimed to identify the impact of varying maternal comorbidities on the development of childhood cancers. This study applied an Obstetric Comorbidity Index (Bateman et al, 2013) to examine maternal comorbid conditions in childhood cancer risk.
Methods: Using maternal and birth records, and cancer records from the Danish Cancer Registry, we conducted a population-based case-control study with two population groups- the first population included cases (n=2578) and controls (n=64450) with ICD-10 diagnoses from 1994-2013, and the second population included cases (n=8339) and controls (n=208475) with ICD-8 and 10 diagnoses from 1977-2013. Maternal comorbidities were ascertained from the National Patient Register using the Obstetric Comorbidity Index. We estimated the risk of childhood cancer using conditional logistic regression.
Results: Multiple gestation pregnancy (OR=1.17, 95% CI 1.05, 1.30), maternal pre-existing diabetes (OR=1.68, 95% CI 1.14, 2.48), congenital heart disease (OR=2.62, 95% CI 1.13, 6.09) and previous cesarean delivery (OR=1.35, 95% CI 1.03, 1.75) showed an increased risk of childhood cancers (all types combined). Children born to mothers between the ages of 35 and 39 also had a higher risk of cancer as compared to those born before. In the 1977-2013 population, there was an increased risk of acute lymphocytic leukemia (ALL; OR=1.08, 95% CI 1.04, 1.13) and rhabdomyosarcoma (OR=1.13, 95% CI 1.01, 1.27) for each unit of increase on the Obstetric Comorbidity Index. There was also an increased risk of retinoblastoma (OR=1.16, 95% CI 1.01, 1.32) for each unit of increase on the maternal comorbidities index in the 1994-2013 population. Examining mothers that had a score of one or more in the Obstetric Comorbidity Index, there was a higher risk of ALL (OR=1.43, 95% CI 1.26, 1.62), non-Hodgkin lymphoma (OR=1.50, 95% CI 1.17, 1.91), Burkitt lymphoma (OR=1.71, 95% CI 1.12, 2.61), and rhabdomyosarcoma (OR=1.58, 95% CI 1.10, 2.26) for children whose mothers with at least one maternal comorbidity. A similar trend was observed in the 1994-2013 population for ALL, non-Hodgkin lymphoma, and Burkitt lymphoma.
Conclusion: The results of the study show varying effects of exposure to one or more maternal comorbidities on individual pediatric cancer types, and an overall increased risk of most cancers development in children with exposure of mothers to 1 or more maternal comorbidities.

#3442 Factors modifying the association between hormonal contraception and risk of early-onset breast cancer.

L. R. Teras[1], E. L. Deubler[1], M. E. Sherman[2], C. Bodelon[1], L. E. McCullough[1], J. M. Hodge[1], S. Chantaprasopsuk[1], A. V. Patel[1];
[1]American Cancer Society, Atlanta, GA, [2]Mayo Clinic College of Medicine and Science, Jacksonville, FL

Breast cancer rates among women younger than 50 years-old have been steadily increasing since the mid-1990s. There is consistent evidence that use of combination estrogen and progesterone oral contraceptives (OCs)—including contemporary formulations with lower estrogen—increases breast cancer risk. It is unclear, however, if this risk varies by factors such as progestin type in the OC formulation, timing of OC use, histopathologic characteristics of the breast cancer, or individual patient characteristics. This study included premenopausal women aged <50 years and cancer-free when they enrolled in the U.S.-based American Cancer Society Cancer Prevention Study-3 cohort between 2006 and 2013 (n=101,838 women). At enrollment participants responded to a detailed life history questionnaire including questions about type, brand, duration, and recency of OC use. Incident breast cancers diagnosed between 2006-2018 were identified through cancer registry linkages (n=759). Participants were followed until the first of 1) breast cancer diagnosis, 2) age >50 years, or 3) December 31, 2018. Multivariable hazard ratios (HRs) and 95% confidence intervals (CIs) were used to estimate associations between OC use and breast cancer risk. On average, participants were 39.3 years at baseline and were followed for 5.7 years (up to 12.3 years). Current versus never use of OCs for 10+ years was associated with a higher risk of breast cancer (10-<20 years: HR=1.46, 95% CI: 1.03-2.07; 20-<30 years: HR=1.66, 95% CI: 1.14-2.41; 30+ years HR= 2.51, 95% CI: 0.77-8.16). Cessation of OC use progressively attenuated the association down to the null 15 years after discontinuation of use (HR=1.04, 95% CI: 0.73-1.49). Associations with current OC use varied by generation of progestin in the formulation (first generation: HR=1.37, 95% CI: 0.93-2.02; second: HR=1.79, 95% CI: 1.20-2.67; third: HR=1.65, 95% CI: 1.13-2.42; fourth: HR= 0.91, 95% CI: 0.49-1.67). The strongest associations were observed for use of formulations with norgestrel: HR=2.82, 95% CI: 1.54-5.19; norgestimate: HR=1.80, 95% CI: 1.19-2.72; and levonorgestrel: HR=1.56, 95% CI: 1.00-2.43. The OC-breast cancer associations were primarily limited to localized, grade 1 or 2, and ER+ disease. Race, income, body mass index, physical activity, alcohol use, cigarette smoking, parity, and breastfeeding did not appear to modify the associations. There were also no clear differences in the associations based on age at first or last OC use or timing relative to pregnancy. Current, long-term OC use was associated with increased risk of early-onset breast cancer. These data suggest that risks may vary with progestin content, and future studies are needed to define formulations that minimize breast cancer risk while still maximizing protection against other female cancers.

POPULATION SCIENCES: Risk Prediction Modeling, Screening, Early Detection, and Preneoplastic and Tumor Markers
Poster Session

#3446 Associations of non-steroidal anti-inflammatory drug use and circulating inflammatory proteins with gallbladder dysplasia.

L. Rosa[1], P. Cook[2], R. M. Pfeiffer[3], T. J. Kemp[4], A. Hildesheim[3], B. Pehlivanoglu[5], V. Adsay[6], E. Bellolio[7], J. Araya[8], L. Pinto[4], C. Ferreccio[1], G. Aguayo[9], E. Vinuela[10], J. Koshiol[3];

[1]Advanced Center for Chronic Diseases (ACCDiS), Pontificia Universidad Catolica de Chile, Santiago de Chile, Chile, [2]University of North Carolina, Chapel Hill, NC, [3]National Cancer Institute, Rockville, MD, [4]National Cancer Institute, Frederick, MD, [5]Dokuz Eylul University, Izmir, Turkey, [6]University School of Medicine and Koc, University Research Center for Translational Medicine, Istanbul, Turkey, [7]Universidad de La Frontera, Temuco, Chile, [8]Universidad de La Frontera & Hospital Dr. Hernan Henriquez Aravena, Temuco, Chile, [9]Pontificia Universidad Catolica de Chile & Hospital Sotero del Rio, Santiago de Chile, Chile, [10]Pontificia Universidad Catolica de Chile & UDA Hospital Sotero del Rio, Santiago de Chile, Chile

Background: Most gallbladder cancer (GBC) cases arise from the metaplasia-dysplasia-GBC sequence, and chronic inflammation has been associated with its development. The use of non-steroidal anti-inflammatory drugs (NSAIDs) has been associated with reduced risk of GBC; however, little is known about these associations with preneoplastic lesions. We thus aimed to study the associations of the use of NSAIDs and inflammatory proteins with gallbladder dysplasia, a precursor to GBC.

Methods: Associations of NSAIDs and gallbladder dysplasia were evaluated in 1,925 Chilean cholecystectomy patients, 82 with dysplasia and 1,843 with gallstones but not dysplasia. In addition, we measured 33 circulating inflammatory proteins in a subsample of 68 dysplasia cases diagnosed at the time of sample selection and 136 gallstone controls. Age- and sex-adjusted odds ratios (ORs) and 95% confidence intervals (95% CIs) were calculated, and associations of inflammatory proteins and gallbladder dysplasia were analyzed.

Results: NSAID use was inversely associated with gallbladder dysplasia (OR: 0.48, 95% CI: 0.26-0.83). Comparing the highest versus lowest category of each immune-related protein, eight proteins were inversely associated with dysplasia with ORs ranging from 0.30 (95%CI: 0.12-0.77) for IL-33 to 0.76 (95%CI: 0.59-0.99) for MIP-1B. Of those, GRO remained associated with dysplasia (OR: 0.64, 95%CI: 0.45-0.91) and BCA-1 was borderline-associated (OR: 0.74, 95%CI: 0.54-1.01) in the multivariable logistic regression model additionally adjusted for sex, age and NSAID use.

Conclusion: NSAID users were less likely to have gallbladder dysplasia, suggesting that NSAIDs might be beneficial for gallstones patients. Prospective studies are needed to understand the inverse association of immune-related markers and dysplasia, and to evaluate the biological effect of NSAIDs in GBC.

Research supported by general funds from the Intramural Research Program of the US National Institutes of Health, National Cancer Institute, Division of Cancer Epidemiology and Genetics, and the Office of Research on Women's Health, National Institutes of Health.

#3447 Potential for reduction in invasive cancer incidence by interception of preneoplastic lesions.

P. Pradhan[1], I. Ghobrial[2], C. Marinac[2], B. O'Donnell[2], S. Syngal[2], T. Rebbeck[1];
[1]Harvard T.H. Chan School of Public Health, Boston, MA, [2]Dana-Farber Cancer Institute, Boston, MA

Background: Preneoplastic lesions (PNL) are morphologically identifiable lesions lack the ability to invade surrounding tissue but can progress to invasive cancer. Thus, PNL present an opportunity to identify individuals at elevated cancer risk and identify opportunities for early detection and interception of cancer.
Objective: We used published data sources to estimate the impact of intercepting progression of PNL to invasive cancer across multiple anatomic sites. We estimated the hypothetical number of cancers that could be avoided in the United States population if interception was successful in preventing a percentage of individuals with PNL from progressing to invasive cancer.
Methods: Estimates of prevalence, latency, and probability of percent progression of PNL to invasive cancer were obtained from literature. We considered PNL associated with invasive tumors of the breast, bladder, cervix, colorectum, esophagus, liver, lung, oropharynx, pancreas, prostate, skin (melanocytes), skin (squamous cells), and stomach as well as precursors to leukemia and myeloma. We modeled a cohort of 100,000 individuals from which we estimated the number of cases that could be avoided if interception of a PNL before it progressed to an invasive cancer case was successful. Results were stratified for race and sex; positive- and negative-predictive values were calculated.
Results: For PNL with a higher prevalence and percent progression per year, there were more invasive cancers that could be avoided if interception was successful. Detection of PNL associated with pancreas, stomach, oral, and prostate cancers had the greatest potential to avoid invasive cancers in the US population. For example, if 95% of pancreatic intraepithelial neoplasia lesions were detected, 15% progressed to pancreas cancer, and assuming a 43% prevalence over a 5-year latency period, 1,226 potential invasive pancreatic cancer cases could be avoided per year. Similarly, 998 potential invasive stomach cancer cases could be avoided earlier if 95% of gastric intestinal metaplasia lesions were detected assuming 42% progressed to invasive cancer with a 19% prevalence and a 4-year latency period. Additionally, if we could intercept 5% to 95% of all PNL from becoming invasive cancer, we would avoid between 176 to 8,515 number of invasive cases being diagnosed. When stratified by race, symptomatic multiple myeloma can be avoided in individuals with monoclonal gammopathies of undetermined significance if this condition is detected earlier among Black individuals.
Conclusion: By detecting PNL and preventing them from advancing to invasive cancer, we can avoid substantial mortality as well as the costs and morbidities associated with treating more advanced cancers.

#3448 A novel liquid biopsy lung cancer detection method using a coverage and fragment end motif machine learning analysis.

B. Leatham, M. Salmans, M. Smith, M. Wang, A. Carson, K. Fathe, B. Lee;
Genece Health, Inc., San Diego, CA

Lung cancer remains the leading cause of cancer death in the United States. One reason for this high mortality is that >40% of cases are diagnosed at a late stage, where the 5-year survival rate is low. Liquid biopsy molecular testing has transformed lung cancer care through the identification of driver mutations when tissue is inaccessible. It also has promise as a tool in early detection and diagnosis, thereby reducing mortality. The existing paradigm for lung cancer screening and diagnosis includes low dose CT (LDCT) scans and tissue biopsy. LDCT scans yield a visualization of lung abnormalities. However, many of these abnormalities are difficult to characterize and next steps are often unclear to physicians. One option is to continue to monitor the patient, which may risk a delay in cancer treatment. Up to 15% of all individuals who are put on a monitoring regime will ultimately be diagnosed with lung cancer. A second option is to biopsy the nodule, which risks unnecessary invasive procedures and expenses to patients. 42-62% of indeterminate nodules detected by LDCT are found to be benign after biopsy. Furthermore, 15% of transthoracic needle biopsies result in complications. Genece Health aims to decrease uncertainty in cancer diagnosis and improve patient outcomes through a minimally invasive liquid biopsy assay that detects the presence of lung cancer. The technology utilizes a proprietary algorithm that leverages machine learning models to detect lung cancer signals in low-pass whole genome sequencing (LP-WGS) of patient cfDNA isolated from plasma. To establish assay performance, 50 clinical lung cancer samples from a commercial biobank, and 100 presumed normal samples were collected in Streck cfDNA BCT Devices. Following cfDNA extraction from plasma, LP-WGS was performed. Sequencing data was then processed to generate fragment end-motif and size (FEMS) and fragment coverage data that was input into Genece Health's proprietary machine learning classifier to generate a final cancer prediction score. In addition, a limit of detection was determined using three late-stage lung cancer samples, with tumor fractions estimated using whole exome sequencing and ichorCNA scores. Our results show >80% specificity, >90% sensitivity, and a limit of detection of <1% tumor fraction. Through this testing, we demonstrate the assay's ability to detect lung cancer across various lung cancer stages, including early stage disease, and histologies. Genece has developed a highly sensitive and specific lung cancer detection liquid biopsy assay. We present this assay as a cost-effective approach to discriminate between benign and malignant nodules identified by LDCT. In addition, this assay has the potential to be applied across the cancer care continuum. For example, future work will involve characterizing the assay's ability to be applied in early cancer screening.

#3449 Is AI-enhanced breast ultrasound ready for breast cancer screening in low-resource environments? A systematic review.

A. Bunnell[1], D. Valdez[1], F. Strand[2], Y. Glaser[3], P. Sadowski[3], J. A. Shepherd[1];
[1]University of Hawai'i Cancer Center, Honolulu, HI, [2]Karolinska University Hospital, Solna, Sweden, [3]University of Hawai'i at Manoa, Honolulu, HI

Purpose. Screening mammography is unavailable in many low-resource areas. We ask if the state-of-the-art in artificial intelligence (AI)-enhanced breast ultrasound (BUS) is sufficiently accurate to be used for primary breast cancer screening in low-resource regions.
Background. Since the 1980s, high-income countries have implemented mammographic screening programs, leading to breast cancer mortality reduction in screened women.[1] Mammography is unavailable in many low-resource regions, such as the USAPI. Furthermore, travel difficulties and lack of radiologists hinder implementation. AI combined with portable BUS may address limitations of the high-income paradigm. In this systematic review, we ask if AI-enhanced BUS can detect/segment lesions (Objective 1) and classify lesions as cancerous (Objective 2).
Methods. Two reviewers independently assessed articles from 1/1/2016 to 8/6/2023 from PubMed, Google Scholar, and citation searching. Studies which report on AI development and report performance on a patient-wise, held-out test set met the inclusion criteria. Studies were characterized by AI task and clinical application time. Dataset composition and performance were examined via narrative data synthesis. QUADAS-2 bias assessment was performed using criteria for each AI task. Success in (2) is defined by meeting minimum screening performance guidelines.[2,3]
Results. PubMed yielded 281 studies, Google Scholar yielded 225 studies, and a manual citation search yielded 41 studies. From 382 unique full texts evaluated, 52 articles met all inclusion criteria: 3 frame selection, 2 real-time detection, 2 combination, 14 segmentation-only, and 31 classification-only. Lesion segmentation-only models achieved a 90th percentile Dice similarity coefficient of 0.913 on generally small datasets. The best evidence for lesion cancer classification reported 0.976 area under the curve. All studies faced elevated bias and applicability concerns under QUADAS-2.
Conclusion. Reported performance for (1) is insufficient to introduce AI-enhanced BUS for breast cancer screening. Evidence supporting AI-enhanced BUS for (2) is dependent on few studies relying on internal datasets, limiting generalizability. Geographically diverse clinical trials are needed to confirm and improve robustness of performance of AI-enhanced BUS for (1) and (2).
References. 1. Marmot MG, et al. The benefits and harms of breast cancer screening: an independent review. *British journal of cancer*. 2013;108(11):2205-2240. 2. Lehman CD, et al. National Performance Benchmarks for Modern Screening Digital Mammography: Update from the Breast Cancer Surveillance Consortium. *Radiology*. 2017-04-01 2017;283(1):49-58. doi:10.1148/radiol.2016161174 3. Rosenberg RD, et al. Performance Benchmarks for Screening Mammography. *Radiology*. 2006-10-01 2006;241(1):55-66. doi:10.1148/radiol.2411051504

#3451 Association of multi-level factors with cervical cancer screening in healthcare settings.

R. Rathod[1], E. Hu[1], S. Pruitt[1], J. A. Tiro[2], J. Chubak[3], J. Haas[4], S. J. Atlas[4], G. Kruse[5], A. E. Hughes[1];
[1]UT Southwestern Medical Center, Dallas, TX, [2]The University of Chicago, Chicago, IL, [3]Kaiser Permanente Washington, Seattle, WA, [4]Massachusetts General Hospital, Boston, MA, [5]University of Colorado School of Medicine, Aurora, CO

Background- Few studies have examined the independent contribution of patient, clinician and system factors associated with completing cervical cancer screening.

Methods- Using a large retrospective cohort created from electronic health record data, we examined the association of patient- and provider-level characteristics with cervical cancer screening among unknown- and average-risk, screen eligible women who entered the cohort at a primary care visit in 1 of 3 U.S. healthcare systems (Kaiser Permanente Washington, Parkland Health, Mass General Brigham) between 2010-2019. The outcome was time, in days, from cohort entry to screening. We fit piecewise exponential (PWE) survival models, nesting patients hierarchically within provider seen and the facility at the time of their analytic cohort entry visit. We excluded patients whose visit was with providers at their non-principal facility (principal defined as the facility that they saw most patients in 2010). The analysis was stratified by healthcare setting.

Results- Median time from cohort entry until screening varied across settings (202-1063 days) and across providers and clinics (between cluster variance= 0.11-0.77, 0.06-1.18, respectively). Many patient-level characteristics (age, cohort entry year, race/ethnicity, number of comorbidities, smoking status, primary care visit within 12 months before cohort entry, and insurance), some of the provider-level characteristics (provider specialty and sex) and social determinants of health measures (Local Isolation Score Hispanic) were associated with time to screening. In the adjusted PWE models, for all three settings: a) Younger patients (21-49 years old) (vs older patients (50-65 years)); b) Hispanic and Non-Hispanic Asian/Pacific Islander (vs Non-Hispanic White); and c) patients seeing ob-gyn providers (vs family medicine providers) had shorter time to screening. Patients with a) higher (vs lower) comorbidity burden, and b) Medicare insurance (vs Commercial) were less likely to receive screened.

Conclusion- By identifying characteristics at multiple levels that are associated with the outcome, our results help us identify targets for interventions to improve and increase timely cervical cancer screening in healthcare settings.

#3452 Senescence-associated secretory phenotype (SASP) aging index is associated with cancer risk in the Atherosclerosis Risk in Communities (ARIC) Study.

S. Wang[1], Z. Rao[1], A. H. Blaes[1], J. Coresh[2], C. E. Joshu[2], J. S. Pankow[1], B. Thyagarajan[1], P. Ganz[3], E. A. Platz[2], W. Guan[1], A. Prizment[1];
[1]University of Minnesota, Minneapolis, MN, [2]Johns Hopkins University, Baltimore, MD, [3]University of California, San Francisco, San Francisco, CA

Background: The accumulation of senescent cells, which release SASP proteins damaging neighboring cells, contributes to aging and age-related diseases, such as cancer. Therefore, SASP proteins could be used as biomarkers for individuals' aging process, but no studies have tested if SASP protein-based aging index is associated with cancer risk. We created a SASP-aging index based on the 72 SASP proteins reported in Tanaka et al. [2018] and examined its association with cancer risk in the ARIC study.
Methods: ARIC is an ongoing cohort of White and Black females and males initiated in 1987, followed for cancer until 2015 (median follow-up=17.3 yrs). At Visit 2 (1990-92), 5000 plasma proteins were measured using SomaScan -- an aptamer-based assay in 10,834 participants (aged 46-70 yrs, 55% female, 76% White): 3,347 participants developed cancer during follow-up and 7,487 participants stayed cancer-free. In the training set of 67% randomly selected cancer-free participants, we constructed the SASP-aging index by applying Ridge regression to train the 72 SASP proteins against chronological age. The SASP-aging index was validated in the remaining 33% of cancer-free participants (test set). We calculated age acceleration as residuals after regressing the SASP-aging index on age in participants after excluding the training set. We used Cox proportional hazards regression to estimate hazard ratio (HR) and 95% confidence intervals (CI) for the risk of any type of cancer per 5 years increase in age acceleration, employing Barlow's method [1994] to account for the exclusion of the training set. HR was adjusted for age, sex, race, center, education, BMI, smoking status, alcohol intake, aspirin use, diabetes, and eGFR. We also estimated HRs for obesity-related, smoking-related, and the most common cancers (breast, prostate, colorectal, and lung).
Results: In the test set, Pearson correlation coefficient between the SASP-aging index and age was 0.50. Age acceleration was significantly associated with the risk of any type of cancer [HR (95% CI) per 5 years=1.21 (1.08-1.36)]. There was a suggestion of a higher HR for any type of cancer in females [1.26 (1.07-1.48)] than males [1.18 (1.00-1.39)] [p-interaction=0.08], but HRs were similar across race and smoking status [p-interaction>0.50]. Age acceleration was significantly associated with the risk of obesity-related cancers [1.36 (1.20-1.54)]. A significant association was also found with smoking-related cancers [1.43 (1.24-1.65)] and this association remained significant even among never smokers [1.39 (1.07- 1.82)]. Age acceleration was also significantly associated with colorectal [1.34 (1.03-1.75)] and lung cancer risk [1.63 (1.31-2.02)] but not with breast or prostate cancer risk.
Conclusion: SASP protein-based aging index shows promise as a potential biomarker for cancer risk.
Funding: NHLBI, NCI, NPCR

#3453 U.S. Geographic and socio-demographic characteristics of Voyage Study participants.

A. M. Berry, J. A. Grimm, C. R. Kirt, E. J. Kirsch, R. E. Dixon, W. Z. Fan, K. A. Bohn, J. St. Sauver, K. J. Yost, L. J. Finney Rutten, J. E. Olson;
Mayo Clinic, Rochester, MN

The Voyage Study is a large-scale, prospective cohort study of long-term health outcomes among participants with a valid multi-target stool DNA (mt-sDNA) test order. Recently, the Voyage Study achieved its enrollment target of 150,000 participants. The intent of this descriptive analysis is to provide baseline geographic and socio-demographic characteristics of Voyage Study participants to set the stage for future comparisons to the broader mt-sDNA user population.
Participants were randomly selected from all persons in the U.S. or Puerto Rico who had a valid order for mt-sDNA screening during the enrollment period (10/18/2019 - 10/17/2023). Enrolled participants completed a baseline questionnaire that collected socio-demographic and health information. Participant characteristics and baseline survey answers were compared between regions using chi-square tests where appropriate. Regional geographic data was aggregated for the broader mt-sDNA user population during the enrollment period, though no formal comparisons were made between the broader population and the Voyage population at this time.
Analyses were limited to 139,369 participants with available baseline questionnaire data. Voyage participants were more likely to reside in the Midwest, Northeast, or Southeast (29.9%, 22.5%, 22.6% respectively) and less likely to reside in the Southwest and West (11.6%, 13.4%). During the enrollment period, differential participation was also observed in the mt-sDNA user population, with the Midwest, Northeast, and Southeast having the greatest proportion (25.4%, 22.2%, 26.7%) and the Southwest and West having the lowest proportion of mt-sDNA users (13.8%, 11.9%). In the Voyage cohort, Midwest participants reported the lowest education attainment as characterized by years of school completed (14.1% high school or below, 59.2% college or greater), while participants in the West reported the highest education attainment (7.9% high school or below, 67.3% college or greater). The West also had the highest percentage of participants reporting an income of $100,000 or greater (51.6%), with the Southeast being the lowest (42.2%), as compared to the other regions.
We report here early results of geographic and socio-demographic characteristics from a new research resource that will enable future analyses of health outcomes and behaviors in a population of mt-sDNA users. We observed that the greatest percentage of Voyage participants resided in the Midwest, Northeast, or Southeast, and that there was differential socio-demographic participant characteristics based on region. Future analyses will compare long-term healthcare outcomes and differences in colorectal cancer incidence and mortality between the broader mt-sDNA user population and the Voyage cohort.

#3454 Cell-free DNA methylation and fragmentomic signatures identify tissue damage and predict cancer risk.

N. Cheng[1], K. Skead[2], T. Oullette[1], S. Bratman[3], D. De Carvalho[3], D. Soave[4], P. Awadalla[1];
[1]Ontario Institute for Cancer Research, Toronto, ON, Canada, [2]Regeneron Genetics Center, New York City, NY, [3]Princess Margaret Cancer Centre, Toronto, ON, Canada, [4]Wilfrid Laurier University, Toronto, ON, Canada

Cell-free DNA (cfDNA) epigenetic and fragmentomic profiling has emerged as prominent non-invasive approaches for early cancer detection and subtyping. However, owing to difficulties in observing the early development of human malignancies, most cancer biomarker and evolution studies to date have primarily examined biologics following a diagnosis. Utilizing cfDNA as a screening tool for early disease detection requires assessment of blood plasma samples collected from asymptomatic individuals prior to the diagnosis of cancers. Here, we leverage the Ontario Health Study (OHS), a prospective longitudinal population cohort, to assess cfDNA profiles in blood plasma collected from participants that developed breast (n=476), prostate (n=342) and pancreatic (n=32) cancers throughout the study follow up time between 2009 and 2019. We performed cell-free methylated DNA immunoprecipitation and high-throughput sequencing (cfMeDIP-seq) on baseline plasma samples from incident cancer cases up to eight years prior to diagnosis, in addition to matched controls (n=404) with no history of cancer through follow-up. Genome-wide plasma cfDNA differential methylation analysis revealed significantly hypermethylated regions, particularly among CpG island and shore regions, were predictive of early breast cancers, and overlapped hypermethylated regions in solid cancer tissues relative to adjacent normal tissues and peripheral blood leukocytes. Using a repeated cross-validation strategy we found that as few as 200 hypermethylated regions can identify individuals with breast cancer in blood up to seven years prior to diagnosis among discovery set samples (AUC=0.725) and are highly generalizable to samples processed in separate batches (AUC = 0.650). Remarkably, integrating biomarker hypermethylated regions with fragmentomic features including fragment length and 5' tetranucleotide motif proportions further increased accuracy for detecting individuals with early prostate cancers (AUC=0.804). In addition, we observed shared genome-wide cfDNA methylome changes associated with aging and heavy alcohol consumption in cfDNA. We identified increased shedding of tissue-specific methylation markers from liver and pancreatic tissue among individuals consuming more than three drinks a week relative to non-drinkers, reflective of potential signatures of tissue damage.

#3455 Prevalence of monoclonal gammopathy of undetermined significance (MGUS) in a Western Nigerian population.

C. M. Vachon[1], C. Allmer[1], D. Moonen[1], A. Norman[1], J. Cook[1], S. Slager[1], O. A. Rotimi[2], O. C. De Campos[2], T. M. Dokumu[2], D. Murray[1], S. Kumar[1], E. Brown[3], L. B. Baughn[1], **S. Rotimi**[2];

[1]Mayo Clinic, Rochester, MN, [2]Covenant University, Ota, Nigeria, [3]University of Alabama, Tuscaloosa, AL

Monoclonal gammopathy of undetermined significance (MGUS) is a premalignant condition characterized by plasma cell production of monoclonal (M) protein and is a requisite precursor to multiple myeloma (MM). African American (AA) individuals have a two-fold higher incidence of MGUS and MM compared to White individuals. However, data are limited on individuals from Africa, especially using sensitive MGUS detection methods. We examined the prevalence of MGUS in a sample of the general population in Nigeria. Individuals aged 40 and over (n=343) were recruited through health promotion events in Ado-Odo Ota Local Government Area of Ogun State, Nigeria, and provided informed consent, a blood sample, and a short questionnaire. Serum was screened at Mayo Clinic for heavy chain (HC)-MGUS using the matrix-assisted laser desorption/ionization-time of flight (Mass-Fix) assay, which has high sensitivity for detection of M-proteins; serum free light chains (FLC) were also measured. FLC was abnormal if the kappa (>0.26 mg/dL) or lambda (>0.33 mg/dL) light chain (LC) was elevated and FLC ratio (kappa/lambda) was outside the reference range (0.26-3.10). LC-MGUS was defined as an abnormal FLC in the absence of a HC. Age- and sex-adjusted prevalence rates were directly standardized to 2010 United States (US) population for comparison to published studies. Logistic regression was used to examine the association of age, sex, and BMI with HC-MGUS. The mean age of participants was 55 years (SD=10.9), and 74.6% were female. Of these, 216 (63%) had both parents from the Yoruba tribe, 89 (26%) from the Igbo tribe and 38 (11%) from other tribes. Overall, 33 participants (9.6%) had HC-MGUS, with 8 (2.3%) having an M-protein above 0.2 g/dL; 6 (1.7%) had LC-MGUS. HC-MGUS was predominantly IgG isotype (48.5%), followed by IgA (27.3%), biclonal (15.2%) and IgM (9.0%). Prevalence of HC-MGUS was 8.3% for ages 40-49, 7.7% ages 50-69 and 22% ages 70 and above. Standardized to the US population, age and sex adjusted MGUS prevalence ages 50 and older was 17.3% (95% CI: 9.8%-24.9%) and HC-MGUS was 14.7% (95% CI: 7.7%-21.8%), similar to previously published rates of HC-MGUS using Mass-Fix screening of AA individuals (16.5%, 95% CI: 12.2%-20.8%) (PMID: 35316833). In models that included age, sex and BMI, older age was positively associated with HC-MGUS (OR=3.1, 95% CI: 1.1-8.7 for ages 70+ compared to <50), while female sex (OR=0.53, 95% CI: 0.24-1.2) and overweight/obesity (OR=0.34, 95% CI: 0.16-0.75 for BMI > 25 vs. <25) were inversely associated with HC-MGUS. We observed similar prevalence of HC-MGUS at ages 50 and above among Western Nigerian and AA populations when screened using mass-spectrometry. Older age was positively associated with HC-MGUS while overweight and obesity were inversely associated. Studies of MGUS in indigenous African populations may provide insight to unique cancer risk factors compared to other populations.

#3456 The role of particulate matter exposure in racial differences in colorectal cancer mortality in metropolitan Detroit.

Natalie Gail Snider[1], R. Blake Buchalter[2], Theresa Hastert[1], Gregory Dyson[1], Carina Gronlund[3], Elena M. Stoffel[4], Ed Peters[5], Laura Rozek[6], Ann Schwartz[1], Kristen Purrington[1]

[1]Oncology, Wayne State University School of Medicine, Detroit, MI,[2]Case Comprehensive Cancer Center, Cleveland, OH,[3]Epidemiology, University of Michigan, Ann Arbor, MI,[4]Internal Medicine, University of Michigan Health System, Ann Arbor, MI,[5]Epidemiology, University of Nebraska Medical Center, Omaha, NE,[6]Oncology, Georgetown University School of Medicine, Washington, DC

Colorectal cancer (CRC) is the third most diagnosed cancer in the United States and the third leading cause of cancer-related deaths. Non-Hispanic Black (NHB) individuals have the highest rates of CRC incidence and mortality in the United States. These disparities are highly influenced by social determinants of health (SDOH). Neighborhood quality, a well-established SDOH, has been shown to influence cancer outcomes, oftentimes more heavily in minorities. Additionally, neighborhood quality is known to influence an individual's risk of exposure to harmful environmental contaminants including ambient air pollution as a result of systemic racism such as segregation and historic redlining, leading to environmental injustices. Fine particulate matter (PM2.5) exposure has been shown to increase the risk of CRC mortality, however, its effects by race have not yet been examined. We sought to understand whether higher rates of exposure to PM2.5 played a role in racial differences in CRC survival in metropolitan Detroit. Patient data including census tract at diagnosis, demographics, and clinical features were obtained from the metropolitan Detroit cancer surveillance system registry. Ambient PM2.5 concentration data at the census tract were obtained from the Environmental Protection Agency (EPA) Remote Sensing Information Gateway (RSIG) and converted to annual averages to use in an interval-censored Cox proportional hazards regression model. We found that PM2.5 exposure partly attenuated the effect of race on overall mortality in all patients (NHB vs NHW: Hazard Ratio (HR) = 1.24, 95% Confidence Interval (CI) 1.20 - 1.27, $p < 0.0001$, NHB vs NHW after accounting for PM2.5: HR = 1.19, 95% CI = 1.16 - 1.23 $p < 0.0001$) and the effect was stronger among patients under 50 than over 50, though still significant in both models. Additionally, the effect of PM2.5 on mortality was much stronger among NHB patients than NHW patients (NHB HR = 1.30, 95% CI = 1.17 - 1.45, $p < 0.0001$; NHW HR = 1.06, 95% CI = 1.02 - 1.11 $p = 0.008$) and especially strong among NHB patients under 50 (HR = 2.51, 95% CI = 2.38 - 3.38, $p < 0.0001$) compared to any other group. We conclude that ambient air pollution, particularly PM2.5, disproportionately affects mortality risk in NHB CRC patients. These results highlight the importance of environmental justice research in biomedical research, and the need for a better understanding of environmental impact on tumor biology to prevent tumor progression and mortality among all patients.

#3457 Distinct signatures of tumor-associated macrophage subpopulations predict survival in renal cell carcinoma.

Youngsoo Han[1], Aidan Shen[2], Zhaohui Wang[2], Aliesha Garrett[2], **Chongming Jiang**[2]

[1]Bioengineering Department, University of California, Los Angeles, Los Angeles, CA, [2]Terasaki Institute for Biomedical Innovation, Los Angeles, CA

Background: Comprising 90% of renal cancer cases in adults, renal cell carcinoma (RCC) is marked by significant heterogeneity in its tumor microenvironment. This study aims to test the hypothesis that tumor-associated macrophages (TAMs) play a role in modulating RCC progression and patient response to treatment. We explored the prognostic implications of TAM signatures on RCC survival, leveraging immunomics to decipher TAM-related alterations in the tumor microenvironment.

Methods: Utilizing independent single-cell RNA-seq data from human RCC samples, we crafted 8 distinct RCC TAM signatures reflective of TAM presence. A LASSO Cox regression model was developed to prognosticate survival, tested against the TCGA dataset and independently validated across multiple RCC cohorts. Model performance was corroborated through Kaplan-Meier survival plots, receiver operating characteristic (ROC) curves, principal component analysis, and t-SNE analyses.

Results: We identified two TAM signatures that correlate positively with patient survival, indicative of the abundance of specific subsets of TAMs in RCC. These signatures showed a strong association of specific TAM markers and macrophage infiltration. Survival analysis demonstrated that specific TAM signature gene expressions are significant prognostic markers. Forest plots underscored their prognostic relevance. A 32-gene risk score model was established, successfully stratifying patients into distinct risk categories, with low-risk patients exhibiting markedly improved overall survival.

Conclusions: The study underscores the positive association between abundance of specific TAM subsets of and RCC patient survival. The precision of our LASSO Cox regression model, informed by novel abundance markers of specific TAM subsets, advances our understanding of TAM roles in TIME and RCC progression. These TAM signatures could potentially provide additional insights and targets to enhance the efficacy of RCC treatments.

Keywords: Tumor associated macrophage, renal cell carcinoma, prognosis, tumor microenvironment, immunomics.

#3458 DNA methylation-predicted blood protein levels and breast cancer risk.

J. K. Kresovich[1], **B. Reid**[1], D. A. Byrd[1], K. M. O'Brien[2], Z. Xu[2], C. R. Weinberg[2], D. P. Sandler[2], J. A. Taylor[2];
[1]H. Lee Moffitt Cancer Center, Tampa, FL, [2]National Institute of Environmental Health Sciences, Durham, NC

Background: Blood DNA methylation (DNAm) profiles can be used to predict a variety of human physiologic traits that are associated with breast cancer incidence and plasma concentrations of over 100 proteins, including those involved in inflammation, coagulation, metabolism, and growth. DNAm predictions of circulating proteins, here referred to as "DNAm proteins," may be useful in providing molecular insights into breast cancer etiology and could be a valuable resource for personalizing breast cancer risk prediction.
Methods: The Sister Study is a nationwide, prospective cohort of 50,884 women with a family history of breast cancer designed to identify novel environmental and biological risk factors for breast cancer. Epigenome-wide DNAm data were previously generated using the HumanMethylation450 or MethylationEPIC arrays on baseline blood samples collected from two case-cohort samples, for a combined sample of 4,479 women. This sample included 2,151 (48%) women who were selected because they were diagnosed with breast cancer (1,673 invasive cancer and 478 ductal carcinomas *in situ*) in the 15 years (mean: 7.9 years) following blood draw. Blood levels of 109 DNAm proteins were estimated from DNAm profiles using the method developed by Gadd et al. (eLife, 2022). Weighted Cox regression models were used to estimate associations between these DNAm proteins and incident breast cancer; associations were considered statistically significant at a False Discovery Rate (q) ≤ 0.10.
Results: In age and platform adjusted models, higher breast cancer rates were associated with higher DNAm-predicted blood concentrations of RARRES2, IGFBP4, and CCL21 and lower predicted concentrations of F7, SELL, CXCL9, CD48, and IL19. The strongest associations were observed for RARRES2 (per 1-SD increase, HR: 1.24, 95% CI: 1.10, 1.40, P= 6×10^{-4}, q= 0.03) and F7 (per 1-SD increase, HR: 0.82, 95% CI: 0.74, 0.91, P= 3×10^{-4}, q= 0.03). Estimates were similar after adjustment for known breast cancer risk factors and excluding those diagnosed within two years of their blood draw. Associations appeared stronger for invasive breast cancer.
Conclusions: Using novel DNAm-based estimates of blood proteins, we identified associations between circulating proteins and breast cancer incidence. IGFBP4 and RARRES2 have previously been reported to be higher in newly-diagnosed breast cancer patients. We also identify new potential protein biomarkers related to immune response (CCL21, SELL, CXCL9, CD48, and IL19).

#3460 Predicting cessation of immune checkpoint inhibitor therapy due to severe adverse events with an integrated autoimmune disease polygenic risk score.

P. Middha[1], R. Thummalapalli[2], Z. Quandt[1], Princess Margaret Lung Group, M. A. Gubens[1], C. M. Lovly[3], G. Liu[4], M. C. Aldrich[5], A. J. Schoenfeld[2], E. Ziv[6]; [1]University of California San Francisco, San Francisco, CA, [2]Memorial Sloan Kettering Cancer Center, New York, NY, [3]Vanderbilt University Medical Center and Vanderbilt Ingram Cancer Center, Nashville, TN, [4]Princess Margaret Cancer Centre, Temerty School of Medicine, Dalla Lana School of Public Health, University of Toronto, Toronto, ON, Canada, [5]Vanderbilt University Medical Center, Nashville, TN, [6]Helen Diller Family Comprehensive Cancer Center, Institute for Human Genetics, University of California San Francisco, San Francisco, CA

Background: Immune checkpoint inhibitors (ICIs), including anti-PD1/PD-L1 and anti-CTLA4 agents, have changed the landscape of cancer therapy. However, 6-30% of patients treated with ICIs can develop severe immune-related adverse events (irAEs) depending on the type of therapy used, often leading to cessation of treatment. Hundreds of genetic variants have been associated with autoimmune disorders, and recent genetic studies have developed polygenic risk scores (PRS) for composite risk of autoimmune disease (PRS_{AID}). We used data from an ongoing observational study of patients with non-small cell lung cancer (NSCLC) treated with ICIs to evaluate the association between PRS_{AID} and cessation of ICI therapy due to severe irAEs.

Methods: Our cohort comprises 1,316 advanced NSCLC patients who received ICI therapy from four institutions between 2009 and 2022. Genotyping was performed using the Affymetrix Precision Medicine Array, and imputation was performed using 1000 Genomes Reference. To evaluate cessation of therapy due to severe irAEs, we conducted a thorough review of electronic health records. We identified permanent discontinuation of ICIs due to irAEs as cessation for at least 6 months without any disease progression. We tested the association of a previously published PRS_{AID} (PMID: 35393596) with cessation of ICI due to any severe irAE. PRS_{AID} was converted to a standard normal distribution. We conducted an unconditional logistic regression model to evaluate the association between a standardized PRS_{AID} and discontinuation of ICI therapy due to severe irAEs. All models were adjusted for age at diagnosis, sex, type of ICI therapy, recruitment site, and 5 ancestry-informative principal components.

Results: Of the 1,316 participants with genotype and outcome data, 171 (13.5%) of patients stopped ICI therapy due to severe irAEs. The most common irAEs leading to discontinuation were colitis, hepatitis, and pneumonitis. The PRS_{AID} predicts the cessation of therapy due to severe irAEs with an odds ratio (OR) per standard deviation (SD) of 1.20 (95% confidence intervals [CI]=1.02-1.41, p=0.03). The association was stronger in individuals with high genetic risk (top 25th percentile compared to bottom 75th percentile of the PRS_{AID}) (OR=1.60, 95% CI = 1.11-2.28, p=0.01). When we stratified the analysis by therapy type, we found an OR of 1.17 (95% CI-0.98-1.39, p = 0.08) for the anti-PD1/PD-L1 monotherapy groups and an OR of 1.48 (95% CI=0.94-2.40,p=0.09) for the dual anti-PD1/PD-L1 and anti-CTLA4 therapy group.

Conclusions: An integrated PRS for autoimmunity can predict the cessation of ICI therapy due to severe irAEs in patients with advanced cancer. These findings suggest that PRS may help determine which patients may benefit from careful monitoring or even preventative measures for irAEs during ICI therapy.

#3461 Shorter leukocyte telomere length and higher risk of primary liver cancer in a prospective cohort study.

S. Karnam[1], K. Demanelis[1], K. B. Beckman[2], R. Wang[3], J. Adams-Haduch[3], W.-P. Koh[4], J.-M. Yuan[1];
[1]University of Pittsburgh, Pittsburgh, PA, [2]University of Minnesota, Minneapolis, MN, [3]University of Pittsburgh Medical Center, Pittsburgh, PA, [4]National University of Singapore Yong Loo Lin School of Medicine, Queenstown, Singapore

Background: Telomeres are conserved tandem repeats at chromosome ends that are vital to maintaining chromosomal stability and preventing degradation. Shorter telomere lengths (TL) are typically associated with older biological age or poor health status and can activate programmed cell death, whereas longer telomere lengths can be indicative of younger age or abnormal replication processes with oncogenic mutations. Previous research has identified a link between telomere length and carcinogenesis, but relatively few studies have investigated TL and primary liver cancer (PLC) risk despite it being one of the leading causes of cancer worldwide. The goal of this analysis was to study this association in a large prospective cohort.
Methods: Data was extracted from the Singapore Chinese Cohort Health Study, a cohort of 63,257 men and women aged 45-74 years at enrollment during 1993-1998. Telomere length was measured in peripheral leukocytes of 26,540 participants who provided baseline blood samples, using a validated quantitative polymerase chain reaction (qPCR) method. PLC incidence and death among cohort participants was annually surveilled using the nationwide Singapore Cancer Registry and the National Birth and Death Registry from study enrollment to 2015. For statistical analysis, a *t* test was performed to examine the differences in TL between participants who developed incident PLC and those who remained free of PLC. Cox proportional hazard method was used to estimate the hazard ratios (HRs) and their 95% confidence interval (CI) of PLC incidence according to TL quartiles.
Results: Over a 12-year follow-up, 199 participants developed incident PLC. The relative TL was significantly lower in participants with incident PLC than those without (-6.7%, $p < 0.001$). Multivariate Cox regression model showed an inverse association between TL quartile and risk of PLC (p for trend = 0.009). Compared with the lowest quartile, HRs (95% CIs) of PLC for the 2nd, 3rd, and highest quartile of TL were 0.78 (0.54-1.12), 0.75 (0.51-1.11), and 0.57 (0.37-0.88), respectively, after adjustment for age, sex, alcohol use, body mass index, and smoking status.
Conclusion: The present analysis demonstrated a statistically significant association between shorter telomere length and increased risk of PLC in a large prospective cohort of Singaporean Chinese. This inverse association for PLC is different from those for other cancer types in the same cohort. These results warrant further studies such as using Mendelian randomization to quantify genetic variation in TL with PLC development.

#3462 Mendelian randomization analysis of 27 cardiometabolic trait related polygenic scores identifies genetic risk for cardiometabolic and cardiovascular events in a large prospective study of breast cancer survivors.

P. N. Fiorica[1], H. Sheng[1], C. A. Laurent[2], J. M. Roh[2], V. S. Lee[2], A. Zimbalist[2], I. J. Ergas[2], Q. Zhu[1], R. K. Cheng[3], E. Rillamas-Sun[4], C. Iribarren[2], J. S. Rana[2], M. Nguyen-Huynh[2], D. L. Hershman[5], L. H. Kushi[2], C. B. Ambrosone[1], M. L. Kwan[2], H. Greenlee[4], S. Yao[1];
[1]Roswell Park Comprehensive Cancer Center, Buffalo, NY, [2]Kaiser Permanente Northern California, Oakland, CA, [3]University of Washington School of Medicine, Seattle, WA, [4]Fred Hutchinson Cancer Center, Seattle, WA, [5]Herbert Irving Comprehensive Cancer Center, New York, NY

Background: CVD is the most common cause of non-cancer death in breast cancer patients. Due to cancer treatment-related cardiotoxicities, breast cancer survivors are at increased risk of cardiometabolic disease (CMD) and cardiovascular disease (CVD). In addition to treatment-related factors, behavioral risk factors such as diet, smoking, and obesity are shared between CVD and breast cancer. While clinical factors influencing the risk of CVD in breast cancer patients are well studied, the effects of genetic factors are less known.

Methods: To investigate genetic factors contributing to risk of CMD and CVD in women with a history of breast cancer, we performed a Mendelian randomization analysis to explore the relationships between 27 polygenic scores (PGS) for CMD and CVD phenotypes selected from the PGS Catalog and literature and 13 incident CMD and CVD events in a large prospective cohort of 3,699 breast cancer survivors in the Pathways Study. Fine-Gray sub-distribution hazard ratios (HRs) and 95% confidence intervals (CIs) associated with one standard deviation of PGS were derived with adjustment for epidemiologic, clinical, and treatment factors. The time scale was defined as time since date of breast cancer diagnosis to first of incident event, health plan disenrollment, death, or end of study (12/31/2019). The proportional hazards assumption was tested using Schoenfeld residuals, and no violation was found.

Results: We identified 19 PGS-CMD/CVD associations that met Bonferroni significance ($P<1.17\times10^{-4}$). Five PGS were associated with increased risk of dyslipidemia: apolipoprotein B (HR=1.52, 95% CI,1.38-1.65), LDL cholesterol (1.49, 1.36-1.63), total cholesterol (1.43, 1.31-1.56), triglyceride levels (1.24, 1.14-1.34), and coronary artery disease (1.22, 1.13-1.33). Four PGS were associated with increased risk of hypertension: systolic blood pressure (1.36, 1.25-1.48), diastolic blood pressure (1.21, 1.11-1.32), fasting glucose adjusted for BMI (1.19, 1.09-1.30), and hypertension (1.41, 1.29-1.54). PGS for atrial fibrillation was associated with increased risk of arrhythmia (1.40, 1.25-1.57) and any cardiovascular disease (1.22, 1.12-1.32). PGS for coronary artery disease and myocardial infarction were both associated with increased risk of ischemic heart disease (1.43, 1.21-1.70 and 1.38, 1.17-1.62, respectively).

Conclusion: Our study provides strong evidence for the potential use of PGS to predict the risk of CVD and CMD in women with a history of breast cancer. Future studies may explore the use of PGS to identify women with breast cancer at high risk of CVD-related outcomes and strategies to mitigate this risk.

#3463 Beyond staging systems in cutaneous squamous cell carcinoma: Validation of two thresholds for a model-estimated metastatic risk.

O. F. Steijlen[1], L. Pozza[2], B. Rentroia-Pacheco[1], C. J. Eggermont[1], D. Bellomo[2], S. Alex[2], J. Dwarkasing[2], A. L. Mooyaart[1], L. M. Hollestein[1], M. Wakkee[1]; [1]Erasmus Medical Centre, Rotterdam, Rotterdam, Netherlands, [2]SkylineDx, Rotterdam, Netherlands

Background: Cutaneous squamous cell carcinoma (cSCC) is the second most common skin cancer, therefore causing a death toll comparable to that of melanoma, despite its low propensity to metastasize (2-5%). We recently developed a clinicopathological (CP) model that predicts absolute metastatic risk in cSCC patients. We have recently shown that, in a nationwide Dutch cohort, the model enhances the risk stratification provided by the American Joint Committee on Cancer, eighth edition (AJCC) and the Brigham and Women's Hospital (BWH) staging systems. The current study aims to evaluate the refined risk stratification and designed risk thresholds in an independent, nationwide UK cohort.

Methods: In the Dutch cohort, we defined patients at increased risk within the low-risk group (AJCC: T1-T2, BWH: T1-T2a) as those with an estimated risk above 1%; and in the high-risk group (AJCC: T3-T4, BWH: T2b-T3), as those with a risk above 3.5%. Both risk thresholds were evaluated in the nested case-control (NCC) cohort (n=696), sampled from the nationwide UK cohort (n=31981). The CP model was applied to the NCC cohort and results were binarized as CP Low-Risk or CP High-Risk. Weighted metrics were computed to adjust for the difference in proportion of cases and controls between NCC and nationwide cohorts.

Results: In the low-risk group as per AJCC (T1-T2) and BWH (T1-T2a), the metastatic risk is respectively 0.93% and 1.07%. Within this group, CP High-Risk patients represent respectively 1.69% and 6.11% of the AJCC and BWH groups and have increased metastatic risk of 7.54% in AJCC and 5.36% in BWH. In the high-risk group as per AJCC (T3-T4) and BWH (T2b-T3), the metastatic risk is respectively 7.79% and 13.80%. Within this group, CP High-Risk patients represent respectively 7.42% and 24.40% of the AJCC and BWH groups. They have an increased metastatic risk of 27.92% in AJCC and 24.07% in BWH.

Conclusions: This study validates the designed risk thresholds in an independent nationwide cohort. Differences in performance compared to the Dutch cohort can be explained by the exclusion of patients with multiple missing variables and worse annotation of pathological features in the UK cohort. Additionally, this study confirms that our risk model can enhance cSCC staging systems by a refined risk stratification in both low-risk and high-risk groups. Specifically, the CP High-Risk subgroup within the staging systems' low-risk group might benefit from heightened surveillance and diagnostic screening, such as lymph node ultrasonography. Similarly, the CP High-Risk subgroup within the staging systems' high-risk group could be considered for intensified surveillance and (adjuvant) treatment. In conclusion, adding the CP model to current cSCC staging systems would enable more personalized decisions about follow-up and treatment, while also facilitating the management of healthcare resources.

#3464 Development and prospective validation of an estrogen receptor positive breast cancer risk model to identify women who could benefit for risk-reducing therapies.

T. U. Ahearn[1], S. Mukhopadhyay[1], J. Balasubramanian[1], N. Chatterjee[2], M. Garcia-Closas[3], P. Pal Choudhury[4];
[1]National Cancer Inst. Div. of Cancer Epidemiology & Genetics, Rockville, MD, [2]Johns Hopkins Bloomberg School of Public Health, Baltimore, MD, [3]Institute of Cancer Research, London, United Kingdom, [4]American Cancer Society, Atlanta, GA

Background: Breast cancer risk-reducing therapies such as tamoxifen and aromatase inhibitors are effective for ER-positive (ER+) but not for ER-negative disease. As these therapies have side effects it is important to identify women at risk of ER+ disease. We developed and validated ER-specific risk prediction models in a prospective cohort and evaluated the expected gains of predicting ER+ vs overall disease.
Methods: The iCARE-Lit model integrates established questionnaire-based risk factors and a 313 variant polygenic risk score. We reparametrized the iCARE-Lit model to estimate risk of ER+ and ER- disease separately by obtaining relative risks from published literature for ages at menarche, menopause, first childbirth, and parity to account for their heterogeneous associations with risk of ER-defined subtypes. We estimated 5-year (yr) absolute risk (AR) for ER+ disease using an overall and ER+ model. We evaluated model performance in the Prostate, Lung, Colorectal and Ovarian (PLCO) Cancer Screening Trial prospective cohort. This included evaluation of calibration (expected-to-observed (E/O) ratio) and discrimination (area under the receiver operating characteristic curve (AUC)), among 46,571 self-reported non-Hispanic White women aged 50-75 yrs (1,052 ER+ cases with 5 yrs of follow-up from enrollment). We compared projected risk stratification of the overall and ER+ models among eligible US women in terms of proportions of women and future ER+ cases identified above the 3% 5-yr AR threshold recommended for risk-reducing interventions in the US.
Results: In predicting ER+ disease in PLCO, on average the overall and ER+ AR were well calibrated; however, models overpredicted risk at the ≥3% 5-yr AR threshold, (E/O = 1.31 (1.20, 1. 42) and 1.23 (1.13, 1.34), respectively. Risk discrimination was similar from the overall and ER+ models (AUC=0.65 (0.64-0.67) and 0.66 (0.64-0.67), respectively. The overall model projected that 16% of women in the US could be eligible for risk-reducing therapies, compared to 11% when using ER+ model, resulting in ~1.4 million less women crossing the risk threshold when using the ER+ score. However, the percentage of ER+ cases in the US population projected to occur within 5-yrs among eligible women was larger for the overall (38%) than ER+ (32%) risk score.
Conclusion: Findings suggest that ER-specific risk scores might not offer a substantial advantage compared to overall risk scores to identify women eligible for risk-reducing therapies. Further risk-benefit analyses are needed to quantify the potential gains of predicting ER+ vs overall breast cancer.

#3465 Association with total reproductive year and the risk of biliary tract cancer in women.

C. Maeng[1], K. Han[2], J.-H. Park[3], J. Hong[4];

[1]Kyung Hee University, Seoul, Korea, Republic of, [2]Soongsil University, Seoul, Korea, Republic of, [3]Korea University, Ansan, Korea, Republic of, [4]Sungkyunkwan University, Seoul, Korea, Republic of

Background: Many studies have reported that female reproductive factors, such as parity, age at menarche or menopause, breastfeeding, or age at first birth, were associated with or not associated with the development of biliary tract cancer (BTC). Our study was planned to determine whether a long-term rather than transient exposure was associated with the risk of BTC, including total reproductive year, which was defined as the time from menarche to menopause throughout the life cycle.

Methods: This nationwide cohort study included 1,059,533 women with natural menopausal women aged 40-69 years who underwent the periodic health check-up provided by the Korean National Health Insurance System in 2009. The median follow-up period was 9.3 years. Cox proportional hazard regression analysis was performed to estimate the risk of BTC based on the female reproductive factors.

Results: During the 9,867,152 person-years of follow-up, 4,198 patients (0.4%) were newly diagnosed with BTC. The incidence of BTC was significantly increased in subjects younger than 40 years at menopause compared with those aged 40 years or older (HR 1.341, 95% CI, 1.095-1.642). This trend was consistent even when menopause age was subdivided into 5-year intervals (<40 vs. 40−44, 45−49, 50-54, and ≥ 55 years) for those aged 40 years or older. When compared by categorization into four quartiles, the incidence of BTC tended to be numerically lower than that of the bottom 25% with the lowest age of menopause (designated as Q1 reference group). Compared to those with total reproductive year of 30 years or more, the incidence of BTC increased significantly in the group with less than 30 years of total reproductive year (HR 1.106, 95% CI, 1.014-1.206). This tendency was significantly reproduced in comparison by categorizing the entire group into quartiles. Compared to the lower 25% group (designated as Q1 reference group), the risk of BTC showed a significant linear inverse correlation with the longer total reproductive year. Q1 group has significantly higher incidence of BTC compared to the other groups ($p < 0.001$). This trend was repeated in various subgroup analysis.

Conclusions: In conclusion, this study demonstrated that women under the age of 40 at menopause had an increased risk of BTC compared to those over 40 years of age. Similarly, a longer period of total reproductive year was associated with a lower risk of BTC, suggesting a protective female hormonal effect on BTC. Total reproductive year may be more reliable indicator in that it reflects the actual lifetime exposure to female hormones.

#3466 Prognostic implications of lymph node micrometastasis in patients with gastric cancer.

A. Yamamoto, H. Okamoto;
Tsuru Municipal General Hospital, Tsuru, Japan

Purpose: The clinical significance of lymph node micrometastasis (LNMM) remains controversial in gastric cancer (GC). In this study, we investigated the prognostic impact of patients with LNMM GC.Methods: A total of 624 patients with pathologically lymph node metastasis negative (pN0) and N1 status (pN1) who underwent gastrectomy between 2004 and 2018 were enrolled in this retrospective study. The diameter of tumor cell clusters in metastatic lymph nodes was measured in 120 patients with pN1 GC. Results: Patients with lymph node tumors of diameter < 1500 μm (LNMM) had significantly better prognosis than those with tumors of diameter ≥ 1500 μm ($p = 0.012$; log-rank test). Cox's proportional hazards model revealed that LNMM ($p = 0.016$), several dissected lymph nodes ($p = 0.049$), and the provision of adjuvant chemotherapy ($p = 0.002$) were independent prognostic factors for overall survival of patients with pN1 GC. There was no significant difference in overall survival between patients with LNMM who received chemotherapy and those who did not ($p = 0.332$). Conclusions: LNMM is associated with favorable prognosis and could be an independent prognostic marker in patients with pN1 GC. LNMM in GC may be considered as one of the factors preventing adjuvant chemotherapy.

#3467 Tumor immune and microbial characteristics of colorectal cancer according to age at diagnosis and detailed anatomical location.

T. Ugai[1], Y. Takashima[1], Y. Zhong[1], J. P. Vayrynen[2], D. Buchanan[3], J. Huyghe[4], L. Hsu[4], C. Qu[4], S. Thomas[4], C. Thomas[4], S. Gallinger[5], R. Grant[6], U. Peters[4], A. I. Phipps[7], J. Nowak[1], S. Ogino[1];

[1]Brigham and Women's Hospital, Boston, MA, [2]University of Oulu, Oulu, Finland, [3]University of Melbourne, Melbourne, Australia, [4]Fred Hutchinson Cancer Center, Seatle, WA, [5]University of Toronto, Toronto, ON, Canada, [6]Ontario Institute for Cancer Research, Toronto, ON, Canada, [7]Fred Hutchinson Cancer Center,, Seatle, WA

Background: Colorectal cancer is a heterogeneous disease, exhibiting spectra of tumor characteristics that vary across age at diagnosis and anatomical location. We hypothesized that tumor immune and microbial characteristics of colorectal cancer might change with age at diagnosis and detailed anatomical location.

Methods: We utilized a pooled dataset of colorectal cancer cases (N= 958 to1413 depending on variables) with available immune cell density or microbial data in the Nurses' Health Study, Health Professionals Follow-up Study, and Ontario Familial Colon Cancer Registry. We examined whether there were statistically significant trends in tumor immune and microbial according to age at diagnosis and detailed primary tumor location (cecum, ascending, hepatic flexure, transverse, splenic flexure, descending, sigmoid, rectosigmoid, rectum) using Spearman's correlation test. The densities of immune cells were determined by using multiplex immunofluorescence, including T cells (CD3, CD4, CD8, CD45RA, CD45RO, FOXP3) and macrophages (CD68, M1-like, and M2-like) in tumor intraepithelial and stromal regions. We conducted stratified analyses by microsatellite instability (MSI) status.

Results: The density of memory (both $CD4^{\pm}$ and $CD8^{\pm}$) T cells in tumor epithelial areas continuously increased as age at diagnosis increased (P for trend <0.005). Compared to later-onset colorectal cancer, early-onset colorectal cancer had a lower density of memory T-cells. With respect to tumor site, $CD3^{\pm}CD4^{\pm}$ and $CD3^{\pm}CD8^{\pm}$ T densities in tumor epithelial areas were highest in the cecum compared to other subsites, and there was a statistically significant decreasing trend from the cecum to rectum (P for trend <0.005). We also observed significant decreasing trends for CD68+, M1-like, and M2-like macrophage densities in combined tumor (intraepithelial and stromal) regions from the cecum to rectum (P for trend <0.005). The proportion of *F. nucleatum*-positive colorectal cancers gradually decreased from the cecum to rectum (P for trend <0.005). Similar trends were observed in separate analyses in non-MSI-high cases.

Conclusions: This study suggests that certain tumor immune and microbial characteristics in the tumor microenvironment, specifically T cell and macrophage densities and *Fusobacterium nucleatum* positivity, change gradually according to age at diagnosis and/or detailed anatomical location. Age and anatomical location spectra in tumor immune and microbial characteristics will shed light on the etiology of colorectal cancer (including early-onset colorectal cancer), leading to better-personalized cancer prevention and treatment.

#3468 Emerging lessons from patient-reported hospital discharge experiences among hospitalized cancer patients with frequent emergency department use.

S. Kurteva, R. Tamblyn;
McGill University, Montreal, QC, Canada

Background: While teamwork is essential to providing high-quality patient-centered care, challenges in interprofessional collaboration and decision-making in the hospital settings are common, especially for cancer patients. The purpose of this study was to identify emerging themes related to hospital discharge experiences among patients hospitalized for cancer who became frequent emergency department (ED) users following their hospital discharge.
Design & Methods: A cohort of cancer patients discharged from an academic health center in Montreal (Canada) between October 2014 and November 2016 was assembled. Frequent ED (FED) users were identified as patients who had a > 4 ED visits in the year following hospital discharge using health administrative claims from the provincial universal health care program. Qualitative analysis of telephone interviews conducted with patients 30 days' post-discharge were used for in-depth exploratory analyses to characterize hospital discharge experiences and transition process from the hospital to the community.
Results: A cohort of 1253 cancer patients was formed. The mean age was 70.9 (SD=11.8) and the most frequent cancers included 488 (38.9%) respiratory and 309 (24.6%) upper digestive cancer. Overall, 14.5% (n=182) of patients became FED users. Content analyses revealed the most common emerging themes from the FED patients interviews on hospital discharge experiences. These included:1. Early hospital discharge putting patients at high risk of being re-admitted and going back to the ER shortly after that. Some patients mentioned post-discharge complications and emerging of new health issues that could have been avoided if patient was kept in the hospital for longer.2. Lack of communication between different specialists at the hospital. Some patients mentioned the help of a nurse as crucial during inpatient stays in maintaining communication between doctors. 3. Lack of communication of medications prescribed. Some patients mentioned the lack of communication of what doses was modified, what medications were stopped and which ones were newly prescribed.4. The need to schedule follow-up appointments at the time of hospital discharge. This becomes especially important for vulnerable patients who have been on pain medication during the hospital stay, affecting their cognitive abilities and making post-discharge planning more difficult.
Conclusions: This study using integrated data from administrative claims and patient interviews provided insights into the challenges related to hospital discharge experiences and transition into community among hospitalized cancer patients with frequent emergency department use. Application of our findings could assist in hospital discharge preparation and improvement in healthcare delivery and health outcomes.

#3469 Exploring the impact of a giant inflatable colon on the level of awareness, knowledge, and intent for colorectal cancer screening among men attending two state fairs in the Midwest.

A. E. Sedani[1], K. K. Rifelj[1], M. S. Bevel[2], C. L. McCall[1], M. Rogalla[1], L. Laliberte[3], K. Ellis[4], R. J. Pratt[5], C. R. Rogers[1];
[1]Medical College of Wisconsin, Milwaukee, WI, [2]Medical College of Georgia, Augusta, GA, [3]MNGI Digestive Health, Minneapolis, MN, [4]Masonic Cancer Center, Minneapolis, MN, [5]University of Minnesota, Minneapolis, MN

Purpose: This study aimed to evaluate the influence of an interactive inflatable colon as an effective educational tool to increase colorectal cancer (CRC) awareness, knowledge, and screening intention among men attending the Wisconsin (WI) and Minnesota (MN) state fairs.
Methods: Eligible study participants were self-identified men aged 18-75 who spoke English, were residents of WI or MN, and able to read in English. The study was employed during the final operating weekend of both the 2023 WI State Fair (August 11-13) and the MN State Fair (September 1-3). Eligible participants completed: (1) a pre-survey, (2) an unguided tour of the inflatable “Super Colon”, and then (3) a post-survey. The primary outcomes of interest were change in awareness (two items), knowledge (four items), and behavioral intent to obtain CRC screening (one item) from pre- to post-survey. Chi-square tests were used to examine study site differences and to explore the association between demographics and behaviors (awareness, knowledge, intentions) before entry to the Super Colon. McNemar’s test were employed to test if there were significant differences in the distributions from pre- to post-survey.
Results: A total of 940 eligible participants were included in the study sample. The men self-identified their race/ethnicity as Non-Hispanic (NH) White (72%), followed by NH other (12%), NH Black (9%), and Hispanic (8%). Race and ethnicity significantly varied by study site (<.0001) with participants from WI more likely being members of racial/ethnic groups that are often medically underserved (33% vs. 24% in MN). Only 13% of participants had walked through an inflatable colon before. Of those who were screening-age appropriate (age 45 or older), 89% had been screened for CRC previously. With the exception of one question, baseline CRC knowledge was relatively high among our study sample. Interestingly, having higher confidence of their awareness level was inversely associated with higher knowledge. As a result of touring the Super Colon, a significant improvement in confidence in individuals’ knowledge of CRC (<.0001), knowledge regarding a colon polyp (<.0001), and intentions to be screened in the future (<.0001) were observed. Most participants (95%) agreed that the Super Colon is an effective educational tool to teach people about CRC.
Conclusion: Since both encouraging CRC screening uptake and increasing research study participation among men can be a difficult task, these findings emphasize the crucial role of community-based educational initiatives in achieving these goals. Our findings affirm how the three-dimensional interior of the Super Colon is as an effective educational tool for promoting CRC early detection screening behaviors among men and increasing their awareness.

#3470 Evaluation of the association between sickle cell disease and breast cancer using the *All of Us* Research Program dataset.

I. T. Jubilee II, L. K. Evans, K. P. Lemieux;
Xavier University of Louisiana, New Orleans, LA

Background: The *All of Us* Research Program (AoURP) dataset was used to evaluate pharmacological treatment modalities in patients with both breast cancer (BC) and sickle cell disease (SCD). This study aims to identify treatment strategies for sickle cell patients with BC that may inform improved treatment options for patients living with either or both conditions, as there is an imminent need in this patient population.
Methods: We investigated the relationship between SCD and BC using the AoURP dataset. Criteria were female patients with a confirmed diagnosis of concomitant SCD and BC were selected. Hematologic, antineoplastics, and immunomodulating agents prescribed to patients were identified. Analysis was conducted in a Jupyter Notebook environment by way of R. Using FDA-approved and off-label indications, medication use patterns were used to reverse-engineer patient information and identify trends between SCD and BC.
Results: Nine female patients had concomitant diagnoses of SCD and BC, which aligned with the inclusion criteria. African Americans were significantly represented in this cohort, making up sixty-seven of patients. Twenty-two percent of patients did not indicate race, while eleven percent of patients identified as Caucasian. All patients included in the study were prescribed anemic therapy. Eleven percent of patients were prescribed an FDA-approved medication for SCD. Seventy-eight percent of patients were prescribed hormone-targeted BC medications. Thirty-three percent of patients were prescribed the immunotherapy regimen, Dinutuximab with adjunctive interferon-alpha. Eleven percent of patients were prescribed cytotoxic therapy.
Conclusion: Further investigation is warranted for dinutuximab use in BC treatment, specifically the triple negative subtype, as currently no targeted therapeutic options exist, and prognosis is poor. The data suggests dinutuximab with adjunctive interferon-alpha may be promising for triple-negative BC patients with SCD.

#3471 Predictors of cancer related distress among patients with colorectal cancer.

C. N. Zivanov[1], R. Kalbfell[1], J. Zarate Rodriguez[1], S. Sathe[1], J. Vetter[1], M. Jeon[1], D. Chao[1], K. A. Ohman[1], J. Ose[2], B. Gigic[3], E. M. Siegel[4], D. Shibata[5], C. I. Li[6], J. C. Figueiredo[7], C. M. Ulrich[2], A. T. Toriola[1];

[1]Washington University in St. Louis, St. Louis, MO, [2]Huntsman Cancer Institute, Salt Lake City, UT, [3]Heidelberg University Hospital, Heidelberg, Germany, [4]Moffitt Cancer Center, Tampa, FL, [5]University of Tennessee Health Science Center, Memphis, TN, [6]Fred Hutchinson Cancer Center, Seattle, WA, [7]Samuel Oschin Comprehensive Cancer Institute at Cedars-Sinai Medical Center, Los Angeles, CA

Background: Colorectal cancer (CRC) incidence among patients under age 50 has increased drastically over the past few decades. Given that increased cancer-related distress is associated with worse oncologic outcomes, studies are needed to assess the psychosocial wellbeing of CRC survivors across the shifting demographic and socioeconomic landscape.

Methods: The ColoCare Study is a prospective cohort study of newly-diagnosed CRC patients enrolled across six US and European sites. We analyzed ColoCare data from the Washington University site, which has high accrual of Non-Hispanic Black (NHB) patients. Cancer-related distress was measured using a validated Cancer and Treatment Distress (CTXD) tool with 4-point Likert scales ranging from 0-3 with higher scores indicating greater distress. Covariate-adjusted linear regression analyses were used to evaluate sociodemographic, lifestyle, and clinical factors as predictors of cancer-related distress 12 months following CRC diagnosis.

Results: This analysis included 156 participants enrolled from April 2017 to September 2022 who completed a 12-month CTXD questionnaire: 51.4% male; mean age 55.3 (SD 13.1) years; 64.8% Non-Hispanic White; 33.1% NHB; mean 12-month CTXD score 0.75 (SD 0.70). In covariate-adjusted models, predictors of increased distress at 12 months (Table 1) included recurrence or new metastasis (regression coefficient (β)=0.63, 95% confidence interval (CI)=0.35-0.91), stage II ((β=0.49, 95% CI=0.15-0.84) or stage III (β=0.37, 95% CI=0.02-0.72) disease, current smoking (β=0.33, 95% CI=0.10-0.56), female gender (β=0.22, 95% CI=0.00-0.44) and age (β= -0.01, 95% CI -0.02-0.00). Race and social vulnerability index were not predictors of distress in this analysis.

Conclusion: Among CRC survivors, those with younger age, female gender, active smoking, advanced stage, and disease progression may benefit from targeted cancer-related distress assessment and interventions.

Multiple Linear Regression Analysis Estimating 12-Month CTXD Scores

Variable	Regression Coefficients	95% Lower CI	95% Upper CI	P-value
Age	-0.01	-0.02	0.00	***0.015**
Gender: Female vs. Male	0.22	0.00	0.44	***0.050**
Race: Black vs. White	0.01	-0.26	0.29	0.933
Race: Other vs. White	-0.17	-0.91	0.57	0.650
Social Vulnerability Index	0.15	-0.26	0.56	0.463
BMI	0.00	-0.02	0.02	0.908
Smoking Status: Current vs. Former/Never	0.33	0.10	0.56	***0.006**
Stage II vs. Stage I	0.49	0.15	0.84	***0.006**
Stage III vs. Stage I	0.37	0.02	0.72	***0.040**
Stage IV vs. Stage I	0.41	-0.08	0.91	0.100
Neoadjuvant Treatment: Yes vs. No	0.09	-0.19	0.38	0.510
Adjuvant Treatment: Yes vs. No	-0.23	-0.53	0.07	0.133
Stoma at 6 months: Yes vs. No	-0.21	-0.68	0.25	0.364
Recurrence or New Metastasis: Yes vs. No	0.63	0.35	0.91	***<0.001**

#3472 Tailored cancer outreach efforts of a community outreach core working with Native Hawaiian and Pacific Islanders in Hawai‘i.

Mark Lee Willingham Jr.[1], **Kevin D. Cassel**[1], Angela Sy[2], Munirih Taafaki[2], Tressa P. Diaz[3], Antoinette Kleiner[3], Angelina G. Mummert[4]

[1]University of Hawai'i Cancer Center, Honolulu, HI,[2]John A. Burns School of Medicine, University of Hawai‘i at Mānoa, Honolulu, HI,[3]University of Guam, Margaret Perez Hattori-Uchima School of Health, Mangilao, Guam,[4]Cancer Research Center, Mangilao, Guam

Background The Community Outreach Core (COC) of the Pacific Island Partnership for Cancer Health Equity (PIPCHE) aims to improve health equity for historically underserved populations including Native Hawaiians and other Pacific Islanders (NHOPIs), and Filipinos. PIPCHE is a partnership between the University of Hawai'i Cancer Center and the University of Guam whose efforts are focused in Hawai'i, Guam and the U.S. Affiliated Pacific Islands (USAPI). The COC directly addresses the disproportionately high rates of health disparities and cancer incidence and mortality found within NHOPIs often due to multiple complex historical, social, cultural, and environmental factors. Cancer is the second leading cause of death in Hawai'i between 2014-2018, as well as the second most common cause of death in nearly all USAPI jurisdictions. The COC uses research-tested, community-engaged approaches to modify determinants of cancer in these groups.

Methods Outreach efforts have addressed NHOPI cancer inequities by raising awareness of high cancer burdens experienced by these underserved communities. Efforts include resource sharing and data collection at various venues in Hawai‘i such as health/wellness fairs, public housing, and Pacific Islander churches. Outreach Advisory Council meetings were held biannually with community health leaders to discuss ongoing and future initiatives/resource sharing. The COC provided health providers and students with cultural competency training on more efficient strategies to work with these unique NHOPI groups. The COC provided presentations and short talks across the U.S, including a Health Providers Symposium on lung cancer across the Pacific. Outreach efforts have included tailored NCI-based Screen to Save (S2S) colorectal cancer education to NHOPIs.

Results Forty-seven major outreach events were conducted from 2021 to November 2023. These include: 1 Health Providers' Cancer Symposium, 5 Outreach Advisory Council meetings, 5 Cultural Competency trainings and class lectures, 11 conference/community and short talk presentations, and 25 community outreach events. There were 1,900 attendees reached during these regional and national outreach activities. The COC works with professional audiences at the national level to inform these groups about cancer and the health burdens of NHOPIs. A total of 97 Pacific Islanders received the S2S education and completed a pre-posttest with positive increases in means found for all 14 questions.

Conclusion The PIPCHE COC has been able to reach NHOPIs though community partnerships to deliver culturally tailored cancer prevention education and efforts within Hawai‘i, as well as shed light nationally of the cancer burdens these populations face. The S2S education has been able to raise awareness of cancer screenings and holds promise as a potential strategy to address cancer burdens of NHOPI communities.

#3473 Bringing cancer information and resources to our diverse vulnerable populations: Cancer Wellness Hubs pop-up model.

Elena Nieves[1], Rosa Barahona[1], Marya Shegog[2], Dana Dornsife[2], **Lourdes A. Baezconde-Garbanati**[1]

[1]Keck School of Medicine of USC, Los Angeles, CA,[2]Lazarex Cancer Foundation, Danville, CA

Background: To achieve cancer health equity, we must provide a safe space where we recognize the cultural and cancer challenges among the communities that we serve. The Lazarex Cancer Foundation, in collaboration with USC NCCC, has established the Cancer Wellness Hubs pop-up model to provide information in a culturally sensitive and language specific way. This leads to making educated, accurate and timely decisions in the cancer journey. The actions we take allow us to help reduce the cancer burden. We bring education and connection to cancer support services into the neighborhoods of our most vulnerable populations.

Methods: During the period of 08/2021 - 07/2023 we teamed up with several YMCAs across LA County including East LA, Koreatown, and South LA, as well as with other community-based organizations to bring cancer information to the community. The hubs have supported culturally specific community events such as Chinese New Year, Dia de los Muertos, and Celebration of Life. A speaker series was developed to provide education, guidance, consultation, comfort, and support to enhance the community members' trust and reduce their fear regarding cancer, cancer screening, treatment, clinical trials, and survivor skills. Our cancer experts responded to frequently asked questions on cancer to manage a variety of topics including the importance of clinical trial participation. Holistic wellness workshops were provided to engage the community members in mind-body, health practices.

Results: We provided cancer information to 5,000+ individuals between 08/2021-07/2023. The majority identified as females (79%), including survivors, family members, and caregivers. Over 1,200 have attended our speaker series, and 3,773 have received information. We have supported organizations such as Celebrate Life Cancer Ministry and the Men's Cancer Network, Inc. and their support groups reaching 260 individuals. From Jan-July 2023, 112 community members received individualized follow-up to support increase knowledge and access services such as establishing a medical home, cancer screening, genomic testing, clinical trials & navigation, financial planning and mental, social, or emotional support.

Conclusion: By creating a safe space and inviting environment for our community members, our diverse communities in LA County are becoming better informed about cancer. Considerable education has been provided to help equip our vulnerable diverse communities with the knowledge needed throughout a cancer journey. Information provided includes screening guidelines, the importance of participation diversity in clinical trials, self/ patient advocacy, and accessing trustworthy, reliable sources. This pop-up model is reaching communities in their own *backyard* enhancing our ongoing effort to reduce cancer disparities and create health equity.

#3474 Racial disparities in receipt of surveillance mammography after breast cancer diagnosis.

J. G. Wilkerson[1], F. Wang[2], Y. Raveendran[1], T. Akinyemiju[3];

[1]Duke Cancer Institute, Durham, NC, [2]Duke University Cancer Institute, Durham, NC, [3]Duke University School of Medicine, Durham, NC

Background: The 5-year survival rate for breast cancer (BC) stands at an estimated 91%, with approximately 3.8 million BC survivors in the U.S. This large population of breast cancer survivors remains at risk of loco-regional recurrence, with variations noted across racial groups. White survivors face a locoregional breast cancer recurrence rate of 1.8%, whereas Black, Asian, and Hispanic survivors experience higher rates of 3.9%, 3.6%, and 3.1%, respectively. Notably, Black BC survivors with recurrent breast cancer exhibit a median survival time of 1.8 years compared with 3.6 years observed for White BC survivors. Current recommendations from the U.S. Preventative Services Task Force and the American College of Radiology advocate for surveillance through annual mammography and routine clinical visits following breast-conserving surgery and lumpectomies. However, there are gaps in the data available regarding disparities in the utilization of surveillance mammography by race/ethnicity. Thus, the goal of this study is to estimate race/ethnic disparities in surveillance mammography utilization and its impact on survival among breast cancer survivors at a large comprehensive cancer center.

Methods: A retrospective cohort study of female breast cancer survivors ≥19 years diagnosed and/or treated at the Duke Cancer Institute (DCI) between 2014 and 2022 was conducted. Data was abstracted on patient socio-demographics, cancer type (invasive ductal and ductal in situ carcinomas) and utilization of surveillance mammography within 2-5 years post initial breast cancer diagnosis. Chi-squared testing will be used to analyze rates of mammography surveillance receipt among different races presenting with BC at DCI. Kaplan-Meier estimates will be used for analysis on survival.

Results: A total of 10,904 women with a mean age of 43.7 years were included in the study. The study cohort is comprised of 69% non-Hispanic (NH) White, 24% NH Black, 2.2% Hispanic, 0.5% NH Native American, 1% NH other, and 3.2% NH Asian women. There were 1,791 cases of ductal in situ carcinomas and 9,113 invasive ductal carcinoma cases. NH Black women had the lowest 5-year relative survival rate (81.5%) of all represented racial groups: NH White 89.1%, Hispanic 95.3%, NH Native 87.8%, Asian 97.9%, and NH Other 88.0%. Ongoing analysis will be completed to estimate disparities in the use of post-treatment surveillance mammography amongst breast cancer survivors.

Conclusions: This study will inform efforts to increase post-treatment surveillance and improve adherence to survivorship guidelines with the ultimate goal of reducing mortality disparities among breast cancer survivors.

#3475 Prediction of nausea or vomiting, and fatigue or malaise in cancer care.

R. Vienne, Q. Filori, V. Susplugas, H. Crochet, L. Verlingue;
UNICANCER Centre Leon Berard, Lyon, France

Introduction : Natural language processing has recently achieved unprecedented performances for several medical tasks, but requires additional improvements in oncology. Moreover, very few projects have assessed the potential of language models to help prevent the most frequent serious or severe medical events in medical oncology. We aim at predicting nausea or vomiting (ICD10 code R11), and fatigue or malaise (ICD10 code R53) from patients' medical reports.
Material and methods: The study included all the patients of Centre Léon Bérard between 2000 and 2023 that have not refused to share their data for this analysis. We have retrieved all the clinical notes and manual coding of hospitalization stays in ICD10, in French. We have pretrained a BERT language model with a masking strategy on this data and then fine-tuned it and compared it to several medical pretrained open source models (DrBert and K-memBERT). The labels were medical events leading to or associated with a hospitalization in the 90 days after every patients' notes. For OncoBERT, we included sequential reports from the patients' history, along with a time-encoding layer, and integrated it in a final transformer layer.
Results: We analyzed 140,523 patients, representing 2,515,957 pseudo-anonymized text reports and 6.6M hospitalizations codes in total. The medical texts were consultations reports (56%), end-of-stay reports (17%) and hospitalization summaries (9%). The most frequent types of oncology treatments received by the patients at each time point were 18.8% for chemotherapy, 10.8% for targeted therapies and 1.3% for immunotherapies. The most frequent medical events were nausea or vomiting (20% of patients with 1 or more events), and fatigue or malaise (18% of patients with 1 or more events). In the final dataset, nausea and vomiting (R11) accounted for 16% of the labels while malaise and fatigue (R53) accounted for 24.7% of the labels. We performed random undersampling of reports without any event to balance the label dataset. The fine-tuning on R11 and R53 achieved the performances of 0.58 macro-aucpr (OncoBERT) and 0.50 macro-aucpr (best open-source model) on the validation set.
Conclusion: The language models achieved high performance on the prediction of the most frequent serious medical events in our hospital dedicated to cancer care. We plan to validate the external performances of these models on collaborating hospitals and prospectively and improve the interpretations that we will present at the congress.

BIOINFORMATICS / COMPUTATIONAL BIOLOGY / SYSTEMS BIOLOGY / CONVERGENT SCIENCE: Application of Bioinformatics to Cancer Biology 3 Poster Session

#3479 Evaluation of subclonal deconvolution pipelines using reference cell-lines and patient plasma samples.

X. Dong, Y. Huang, T. Zhang, S. Jia, P. Du;
Predicine Inc., Hayward, CA

Background: Intratumor heterogeneity plays a pivotal role in treatment resistance, emphasizing the need for a comprehensive understanding of tumor clonal architecture. While various methods exist for extracting this information from bulk tumor sequencing data, few studies have evaluated the entire workflow, from sample processing to subclone calls.
Methods: To address this gap, we utilized cell lines with known copy number changes and somatic mutations, constructing 12 ground truth sample sets with varying cellular proportions and tumor purities. These cell lines underwent NGS pipeline using PredicineWES+ with increased sequencing depth across ~600 cancer-related genes. Subclonal analysis workflows, including FACETS, PyClone, and ECLIPSE, were implemented to to assess variant assignment and cellular fractions. The subclone analysis was extended to 91 plasma samples from cancer patients.
Results: Our findings indicate that subclonal decomposition effectively segregates mutations from distinct cell lines. Notably, analyzing multiple samples with different proportions of the same subclones outperformed deconvolution from single mixture samples. In plasma samples from cancer patients, nearly one-third exhibited subclonal clinically actionable variants.
Conclusions: The established subclonal deconvolution pipeline enhances biomarker analysis from assays utilizing WES with boosted sequencing depth for selected genes.

#3480 Alterations in the tumor microenvironment and key signaling pathways in naturally-occurring canine gliomas mirror those seen in human patients.

N. A. Lanman[1], S. Utturkar[1], H. Kothandaraman[1], D. Dhawan[1], D. Liu[1], M. Zhang[2], M. Beyers[3], D. W. Knapp[1], R. T. Bentley[4];
[1]Purdue University, West Lafayette, IN, [2]University of California, Irvine, Irvine, CA, [3]Leidos Biomedical Research, Inc., Frederick National Laboratory for Cancer Research, Frederick, MD, [4]University of Liverpool, Liverpool, United Kingdom

Background: Malignant gliomas are the most common type of primary brain tumors, with patient outcomes that are generally dismal. Recently, pet dogs have been assessed as a valuable model in which to study gliomas. Gliomas in pet dogs occur at similar rates to those seen in humans, and a recent study comparing canine and human gliomas identified high similarity in terms of mutational rates, aneuploidy, the timing of mutations, and methylation patterns. Here, we further compare naturally-occurring canine and human gliomas, focusing on the tumor microenvironment (TME) and key pathways dysregulated in human gliomas.

Methods: Spontaneously occurring gliomas from adult and pediatric human, and canine patients were utilized for this study. RNA, whole genome/whole exome, and bisulfite sequencing data from adult and canine samples were downloaded from the Genomic Data Commons and the National Cancer Institute's Integrated Canine Data Commons, respectively. Pediatric tumor RNA-seq and genomic data were obtained from the Gabriella Miller Kids First database. Normal adult human and canine brain tissue served as control tissue. Only tumors with a clear diagnosis of astrocytoma, oligodendroglioma, or oligoastrocytoma were included in this study.

Results: Overall, we found that key canonical pathways that are altered in human gliomas are also altered in canine gliomas. A comparison of high-grade gliomas in pet dogs to normal canine brain tissues showed significant abnormal gene expression in 3 canonical oncogenic pathways of human GBM: the TP53, RB1, and RTK/RAS/PI3K pathways. Similarities between species included increased expression of PDGF, and receptors PDGFRA and PDGFRB. Frequent copy number alterations and mutations were also observed in PDGFRA and EGFR. Differences between species include the mutation rate of TP53, which we found to be mutated frequently in adults but not in pediatric or canine gliomas, however, expression of TP53 as assessed by RNA-seq was significantly increased in both adult and canine gliomas. IDH1, which drives methylation, was significantly overexpressed in adults but underexpressed in canine. Correspondingly, each of the promotor regions of TERT, PD1 and MGMT was hypermethylated in adults, but hypomethylated in canine. Although an analysis of the TME from RNA-seq data revealed an influx of immune cells in adult, pediatric and canine gliomas, there was a concurrent influx of immunosuppressive cells. Gene expression profiles of astrocytomas and oligodendrogliomas show differences in alterations of immune-related and TME-specific pathways.

Conclusion: We found that similar TME and pathway alterations were observed between human and canine gliomas, and that TME alterations were different between canine astrocytomas and oligodendrogliomas. The canine TME, like that in humans, appears to be immunosuppressive.

#3481 Comparative spatial transcriptomic analysis of monoclonal antibodies targeting the same molecule: A comparison between cetuximab and panitumumab.

J. Choi[1], J. Park[1], M. Lim[1], D. Lee[1], J. Lee[1], H. Choi[2], H.-J. Im[3];

[1]Portrai, Inc., Seoul, Korea, Republic of, [2]Portrai, Inc. / Seoul National University Hospital, Seoul, Korea, Republic of, [3]Portrai, Inc. / Graduate School of Convergence Science and Technology, Seoul National University, Seoul, Korea, Republic of

Background: In recent years, multiple therapeutic monoclonal antibodies have been developed that target the same molecules. Examples include trastuzumab and pertuzumab for HER2, cetuximab (CTX) and panitumumab (PNT) for EGFR, as well as pembrolizumab and nivolumab for PD-1. Currently, comparative studies between different monoclonal antibodies with same target primarily focus on comparing their efficacy, which makes it challenging to discern the factors contributing to their varied effectiveness. In this study, we conducted a comparative analysis of CTX and PNT using integrated data of fluorescence imaging and spatial transcriptomics (ST) to explore their distribution, as well as the associated cell types and genes in tumor tissues.

Method: A FaDu cancer cell line, which has high EGFR expression, was used to establish tumor model in BALB/C nude mice. In the tumor model, fluorescence dye-conjugated CTX or PNT was intravenously administered. In vivo fluorescence imaging was conducted at 0, 2, and 40 hours. Tumor tissues at 2 and 40 hours were dissected for drug distribution images and 10X Visium ST. SPADE algorithm [1], CellDART [2], and Stopover analysis [3] were employed for integrative analysis, cell type deconvolution, and topological association of interesting genes.

Results: In vivo imaging demonstrated that both antibodies exhibited high tumor uptake at 2 hrs, with further increase observed at 40 hrs post-injection. Initially, CellDART analysis confirmed that in the 2 hrs sample, both CTX and PNT exhibited a distribution similar to cancer cells among the various cell types. However, in the 40 hrs sample, the distribution pattern resembled that of cancer cells and inflammatory macrophages for both antibodies. A stopover analysis revealed a higher concordance between CTX distribution and EGFR expression in both the 2 and 40 hrs samples compared to that of PNT. Lastly, the top 100 up-regulated differentially expressed genes which are highly associated with drug distribution were identified through SPADE analysis. Notably, when we checked the intersection between CTX and PNT administered samples for these genes, there was 83% discordance in the associated genes in the 2 hrs sample and 93% in the 40 hrs sample.

Conclusion: In the examination of the distribution patterns of two distinct therapeutic antibodies targeting EGFR within cancer tissues, a notable observation was made: while the cell types exhibited similarity, the associated genes demonstrated divergence, with different degrees of alignment with the intended target. This analytical approach, scrutinizing the distribution of different antibodies within tissue sharing a common target, holds promise as a widely applicable method for elucidating divergent therapeutic effects.

References: 1. Nucleic Acids Res, 2021 Jun 49;10:e552. Nucleic Acids Res 2022 Jun 10;50:e57.3. bioRxiv 2022.11.16.516708

#3482 Single-cell transcriptome analysis reveals that PLK4 signature genes are highly associated with cancer proliferation and hotspot mutations in non-small cell lung cancer (NSCLC).

Y. Kim[1], J. Hwang[1], Y. Park[2], D. Kim[3], K. Na[1], S. Lee[3], S. Baek[1], S.-s. Kang[4], S. Yang[1], M. Kim[1], H. Han[1], C. Lee[1], Y. Han[1], M. Hong[5], J. Lee[5], S. Lim[5], K.-H. Pyo[2], B. Cho[5];

[1]Department of Research Support, Yonsei Biomedical Research Institute, Yonsei University College of Medicine, Seoul, Korea, Republic of, [2]Yonsei New Il Han Institute for Integrative Lung Cancer Research, Yonsei University College of Medicine, Seoul, Korea, Republic of, [3]Brain Korea 21 PLUS Project for Medical Science, Yonsei University College of Medicine, Seoul, Korea, Republic of, [4]JEUK Institute for Cancer Research, JEUK Co., Ltd, Gumi, Korea, Republic of, [5]Division of Medical Oncology, Yonsei Cancer Center, Yonsei University College of Medicine, Seoul, Korea, Republic of

Background: Polo-like kinase 4 (PLK4) is a member of the polo-like kinase family known for its precise regulation during the cell cycle and its key role in centriole duplication, which is essential for proper cell division. Dysregulation of PLK4 is associated with abnormal centriole number, genomic instability and cancer development. In our previous study, we proposed PLK4 as a potential therapeutic target and biomarker for LUAD patients with *TP53* mutations by bulk RNA-seq analysis and confirmed its association with drug resistance. In this study, we analyzed the expression of *PLK4* and its association with cell cycle at the cellular level by scRNA-seq in NSCLC data.

Methods: In a previous study, we analyzed NSCLC data from The Cancer Genome Atlas (TCGA) database using the UCSC Xena data portal. In this study, we analyzed E-MTAB-6653 dataset from the single cell expression atlas(https://www.ebi.ac.uk/gxa/sc/home).

Results: In the previous study, we demonstrated that *PLK4* expression is higher in primary tumors compared to normal tissues in NSCLC. Higher *PLK4* expression in patients is associated with an unfavorable prognosis. Using genes highly correlated with *PLK4*, we confirmed a significant association between *PLK4* and *TP53* mutation by statistical analysis. Using the Drug Gene Interaction database, we observed an association between the drug resistance-related genes *PBK* and *BIRC5* with *PLK4*, and these genes were also correlated with *TP53* mutation. In this study, we investigated the association between *PLK4* and the cell cycle using single cell RNA-seq. First, we performed data pre-processing to selectively isolate NSCLC cells. Using a set of 87 PLK4 signature genes obtained from previous research, we stratified the samples into *PLK4* high and low groups based on the expression of these genes. We then analyzed cell cycle related genes in both groups and observed a higher expression of G2/M phase related genes in the *PLK4* high group compared to the *PLK4* low group. We also examined the expression of *PLK4* signature genes based on pathological differences and found higher expression in tumor tissue compared to normal tissue. There was also an increasing expression gradient from the tumor margin to the tumor core. Finally, using Gene Ontology analysis of both groups, we confirmed the upregulation of genes associated with transcription and translation, as indicated by the GO terms obtained.

Conclusion: In a previous study, the association between *PLK4* expression, *TP53* mutation and drug resistance was identified by bulk RNA-seq. In the current study, we used single cell RNA-seq to verify the correlation between *PLK4* and cell cycle in NSCLC. In addition, we observed that the expression of *PLK4* signature genes increased towards the tumor core based on pathological differences.

#3483 SIRT7 as a potential therapeutic target for drug resistance in lung adenocarcinoma: Insights from histone modification-related genes.

K.-H. Pyo[1], Y. Park[1], G.-T. Lee[2], J. Ahn[3], S.-J. Choi[2], Q. Kejia[2], T. Lee[2], Y. Kim[2], J. Hwang[2], B. Cho[4];

[1]Yonsei New Il Han Institute for Integrative Lung Cancer Research, Yonsei University College of Medicine, Seoul, Korea, Republic of, [2]Department of Research Support, Yonsei Biomedical Research Institute, Yonsei University College of Medicine, Seoul, Korea, Republic of, [3]Severance Biomedical Science Institute, Yonsei University College of Medicine, Seoul, Korea, Republic of, [4]Division of Medical Oncology, Department of Internal Medicine and Yonsei Cancer Center, Severance Hospital, Yonsei University College of Medicine, Seoul, Korea, Republic of

Background: Lung cancer is one of the leading causes of cancer-related deaths worldwide. Understanding the molecular mechanisms underlying its development and progression is crucial for the development of targeted therapies. In recent years, histone modification has emerged as a key player in the epigenetic regulation of gene expression, and its involvement in lung cancer has gained significant attention. Histone modifications, including methylation, acetylation, phosphorylation, and ubiquitination, influence chromatin structure and, consequently, gene transcription. Aberrant histone modifications can lead to dysregulated gene expression patterns, contributing to the initiation and progression of lung cancer. In this study, we investigated the expression patterns of 55 histone modification-related genes and identified an epigenetic tumor regulator as a potential therapeutic target.

Methods: We obtained 55 histone modification-related genes from dbHiMo (http://hme.riceblast.snu.ac.kr/). Transcriptomic (n= 576), clinical data (n=706) and survival data (n=641) of lung adenocarcinoma (LUAD) were downloaded from XenaTCGA database (https://xenabrowser.net/). The transcriptomic and IC50 values with 87 lung cancer cell lines and 310 drugs were downloaded from DepMap portal (https://depmap.org/portal/). RNA-seq data of GSE197555 was downloaded from GEO database (https://www.ncbi.nlm.nih.gov/geo/). All statistical analysis was performed using R.

Results: Among a total of 55 genes related to histone modifications, 6 genes including *KAT2A*, *SIRT7*, *CARM1*, *KDM5B*, *HDAC1* and *PRMT3* were significantly overexpressed in tumor tissues in LUAD transcriptome data from TCGA. Out of these 6 genes, 3 (*KAT2A*, *SIRT7* and *CARM1*) showed significant differences in survival analysis with disease-free interval in the adjuvant therapy-received TCGA LUAD dataset. All three demonstrated that as their expression levels increased, the prognosis became worse. The expression levels of *SIRT7* and *KAT2A* were highly positively correlated with the IC50 value of trametinib, which is MEK inhibitor. Among these two genes, the expression level of *SIRT7* was up-regulated in trametinib-treated group in resistance to MEK inhibitor in the H460 cell line. However, sensitive to MEK inhibitor in A549, the *SIRT7* expression level was down-regulated in the trametinib-treated group.

Conclusion: The histone modification-related gene *SIRT7* was found to be associated with resistance to trametinib. In this study, these findings suggest that SIRT7 may serve as a potential therapeutic target related to drug resistance in combination therapy with dabrafenib and trametinib.

#3484 Mechanism of BRAF V600E resistance revealed by cell panel screening and bioinformatics.

K. Hu, Q. Yang, P. Pan, F. He;
Pharmaron, Inc., Beijing, China

The BRAF V600E mutation is pivotal target in the treatment of melanoma. Dabrafenib, one of the most potent inhibitors approved by the FDA, exhibits differential sensitivity across different cancer types. To explore the underlying mechanisms responsible for the resistance of certain cancers to Dabrafenib, we tested a panel of 20 BRAF V600E positive cancer cell lines. Our results showed that 15 of these cell lines demonstrated sensitivity to Dabrafenib, whereas the remaining 5 exhibited resistance. We then investigated the correlation between Dabrafenib potency and gene expression patterns based on public high throughput sequencing data via bioinformatics methods. The results uncovered that the cell lines resistant to Dabrafenib showed low expression of MAP3K1, alongside with elevated expression of G0S2 and PIK3CG. These alterations are known to promote tumor cell proliferation, migration, and invasion, thereby contributing to a reduced sensitivity to BRAF inhibitors. Subsequent in vitro experiments validated the findings derived from our analysis. This unbiased, bioinformatics-driven approach provides valuable insight into the reasons behind treatment resistance and aids in the development of next-generation treatment approaches for inhibitor-resistant cancers.

#3485 Global DNA methylation level is associated with the sensitivity of cytotoxic and senotherapeutic drugs in gastrointestinal tumors.

K. Lin, X. Wang, Y. Luo, **H. Yu**;
The Sixth Affiliated Hospital of Sun Yat-sen University, Guangzhou, China

Background: Gastrointestinal cancer has become a severe burden around the world. Marker-guided treatment and clinical trials with sensitive anti-tumor drugs are critical for improving cancer survival. The decreasing DNA methylation levels of repetitive elements, such as LINE-1 and ALU, have been identified as the common biomarkers in cancer and aging. However, it remains unclear whether the methylation levels of repetitive elements can imply the drug sensitivity in gastrointestinal cancer. We investigated the association of LINE-1 and ALU methylations with the sensitivity of cytotoxic and senotherapeutic drugs in gastric cancer (GC) and colorectal cancer (CRC).

Methods: The profiles of DNA methylation and gene expression were obtained from GC and CRC patients from the TCGA cohorts. Then, we calculated the averaging methylation level of two repetitive elements (LINE-1 and ALU) to quantify the global methylation levels by using the probes targeting the repetitive elements in 450K methylation array. The sensitivity of anti-tumor drugs, including the cytotoxic (oxaliplatin and fluorouracil) and five senotherapeutic agents (Dasatinib, Nutlin-3a, Navitoclax, Rapamycin, ABT737), were inferred with Oncopredict R package based on the gene expression profile. The Pearson analysis was conducted to test the correlation between DNA methylation and drug sensitivity.

Results: The ALU methylation was associated with the sensitivities of cytotoxic (oxaliplatin: r = 0.171, P = 0.001; fluorouracil: r = 0.158, P = 0.002) and senotherapeutic agents (Dasatinib: r = 0.162, P = 0.002, Nutlin-3a: r = 0.109, P = 0.037, Navitoclax: r = 0.007, P = 0.931, Rapamycin: r = 0.144, P = 0.006, ABT737: r = 0.054, P = 0.523) in GC, while the association of LINE-1 methylation with drug sensitivities was observed in less drugs with weak correlation, including the cytotoxic (oxaliplatin: r = 0.132, P = 0.013; fluorouracil: r = 0.122, P = 0.019) and senotherapeutic agents (Dasatinib: r = 0.129, P = 0.014, Nutlin-3a: r = 0.109, P = 0.037, Rapamycin: r = 0.110, P = 0.034). In CRC, there was no correlation between DNA methylation levels of repetitive elements and drug sensitivity except Dasatinib (ALU: r = -0.107, P = 0.043).

Conclusion: DNA methylation of repetitive elements could serve as a biomarker for cytotoxic and senotherapeutic drugs in GC. In addition, our findings suggested the promising value of ALU and LINE-1 methylation-guided chemotherapy with senotherapeutics in GC.

Keywords: global DNA methylation, repetitive elements, gastrointestinal cancer, drug sensitivity, senotherapeutics

#3486 Triple hormone receptor signatures as novel prognostic markers in breast cancer.

Mohamed Omar[1], J. Chuck Harrell[2], Rulla M. Tamimi[3], Luigi Marchionni[1], Tan Ince[1]

[1]Pathology and Laboratory Medicine, Weill Cornell Medicine, New York, NY,[2]Virginia Commonwealth University, Richmond, VA,[3]Department of Population Health Sciences, Weill Cornell Medicine, New York, NY

Background: Tumor phenotype across various cancers, including breast cancer, is predominantly shaped by a synergy between genomic alterations and the cell-of-origin from which the tumor originates. These elements collectively influence crucial aspects like tumor aggressiveness, treatment response, and patient prognosis. While existing research highlights that the role of cell-of-origin in shaping the molecular architecture of breast cancer, leveraging this information for actionable clinical insights has proven challenging. Here, we introduce two robust models leveraging cellular ancestry signatures of breast luminal cells to improve patient stratification and outcome prediction.

Methods: In this study, we developed a unique gene signature anchored in the expression levels of triple hormone receptors (THR)—namely androgen (AR), estrogen (ER), and vitamin D (VDR)—in breast cancer cells. Building on this, we formulated two distinct mRNA markers, THR-50 and THR-70, aimed at categorizing breast tumors based on their THR expression profiles. These markers were rigorously validated across 65 independent breast cancer studies, involving a total of 6,679 patients, utilizing Kaplan-Meier survival curves, Cox proportional hazards models, and unsupervised clustering analyses.

Results: Our findings indicate that both THR-50 and THR-70 are robustly associated with overall survival and recurrence-free survival in breast cancer patients across all datasets evaluated. Importantly, these THR signatures demonstrate broad applicability across various breast cancer subtypes, grades, and treatment phases—unlike existing prognostic markers that tend to be subtype-specific. Additionally, the THR signatures have revealed four unique patient clusters with divergent survival outcomes, three of which are ER-positive and one is ER-negative. Additionally, we developed an immune-based signature (i20) which can further categorize patients within the ER-negative cluster into two subgroups: one with a highly favorable prognosis, comparable to the ER-positive subtypes, and another that is characterized by exceedingly poor survival outcomes.

Conclusion: The THR-based cellular ancestry signatures open a new avenue in understanding the intricacies of breast cancer biology. These signatures offer a robust and stable framework for developing other prognostic markers, thus providing an enhanced stratification of existing breast cancer categories as well as creating new classifications with more distinct survival estimates.

#3487 Molecular dynamic simulations of RAS family protein interactions: Mutant KRAS binding with wildtype HRAS and NRAS.

I. Silverman[1], M. S. Gerber[2], A. Shaykevich[1], Y. F. Stein[1], A. Siegman[1], S. Goel[3], R. Maitra[1];
[1]Yeshiva University, New York, NY, [2]Albert Einstein College of Medicine, Bronx, NY, [3]Rutgers Cancer Institute of New Jersey, New Brunswick, NJ

Introduction: Mutations in the *KRAS*, *HRAS*, and *NRAS* genes are frequently associated with worse patient outcomes. Previous analyses of the structure and function of the associated proteins have been explored but not conclusively. The actual binding conformations of the three isoforms, especially when mutated are essential in designing inhibitory drugs. Recent studies have identified important interactions between the three isoforms that affect the oncogenic strength of the others when they are mutated. We use a bioinformatics approach to examine the modifications of the structural properties, mechanisms, and kinetic energies of eight KRAS mutants interacting with wildtype HRAS, and again with wildtype NRAS.
Methodology: AlphaFold AI predicted models of KRAS, HRAS, and NRAS were downloaded from Uniprot and relevant mutations were induced using PyMOL. Pairs of KRAS mutants and either HRAS or NRAS were submitted to ClusPro for docking. PyMOL was used to separate proteins by chain identities before being repaired in GROMACS. Molecular dynamics simulations (MDS) were performed between proteins using GROMACS, a Linux based MDS software that renders a topology regulated by Newton's Laws. XmGrace was used to analyze structure, *MMPBSA.py* was used to derive energy calculations, and VMD was used to visualize the interaction mechanisms.
Results: RMSF data indicated C-terminus residues in KRAS mutants and WT-HRAS and WT-NRAS are the most mobile in their interactions. Notably, when WT-HRAS interacts with G12R, G12S, G12V, and Q61H, its C-terminus decreases fluctuation. G13D had the greatest binding strength and strength fluctuation with WT-HRAS. G12V had the greatest binding strength with WT-NRAS. All other mutants had weaker binding with WT-NRAS than WT-KRAS. WT-HRAS had stronger binding at residue Val187 with WT-KRAS than all mutants did. WT-HRAS residues Cys184, Lys185, and Cys186 each had weaker binding energies with WT-KRAS than most mutants did. WT-KRAS residues Gln25 and Lys117 both exhibited stronger binding energy in interactions with WT-HRAS than most mutants did. WT-NRAS had stronger binding at residues Met182 and Met189 with WT-KRAS than all mutants did. Residue Pro185 in WT-NRAS did not have significant interaction with WT-KRAS, but had a strong interaction with all mutants. WT-NRAS residue Val187 had weaker binding energy with WT-KRAS than most mutants. WT-KRAS residues Tyr32 and Asp38 both exhibited weaker binding energy in interactions with WT-NRAS than most mutants did.
Conclusion: MDS between KRAS mutants and WT-HRAS and WT-NRAS present notable structural modification and binding kinetics. In each KRAS mutation, different segments of the protein complexes are involved in the interaction, indicating unique inhibitory methods are required to approach each mutant.

#3488 Decoding splicing isoforms and adaptive evolution in melanoma brain metastases through single cell long-read RNA sequencing.

L. Lu[1], C.-K. Shiau[1], K. Fukumura[2], H. Lin[1], Y. He[1], T. Pan[1], L. Norberg[2], J. Ritchie[2], J. T. Huse[2], R. Gao[1];
[1]Northwestern Univ. Feinberg School of Medicine, chicago, IL, [2]The University of Texas MD Anderson Cancer Center, houston, TX

Melanoma brain metastasis (MBM) is the third most common origin of metastasis to the brain, with a median overall survival of 8.9 months. Alternative splicing plays a critical role in cancer pathogenesis through altered protein coding complexity in tumor cells, which however has been poorly studied in MBM due to technical limitations. Long-read single cell RNA sequencing has the unique strength of measuring transcript isoforms and mutations simultaneously in individual cells due to its capacity of measuring full-length transcripts. In this study, we employed high throughout single cell long-read RNA sequencing (scNanoRNAseq) onto patient-matched MBM and extracranial metastasis (ECM) tumor pairs to evaluate the extent to which splicing isoforms impact adaptive clonal evolution in MBM. Our results showed that MBM tumors had distinct genetic alterations and ecological cellular compositions compared to matched ECM tumors, indicating that tumor clones were adaptively expanded in brain microenvironment. Comparative isoform analysis revealed that hundreds of genes expressed different combinations of isoforms (DCIs) involved in glucose and lipid metabolic pathways. Interestingly, our data demonstrated that ~10% of splicing related genes themselves were alternatively spliced including both spliceosome members and splicing activators. Furthermore, we calculated temporal changes of isoform usages along with tumor cell evolutionary lineages to quantify their impact on adaptive clonal expansion in MBM. Taken together, our work improves the understanding of transcriptional and splicing dynamics inherent in the adaptive evolution of MBM, providing evidence for developing new therapeutics targeting tumor cell-specific and MBM-specific splicing isoforms.

#3489 MetFlow: Automated nextflow pipeline for Ion AmpliSeq methylation assay designs.

R. Bedre, D. Kaul, A. Sharma, A. Hatch, L. Pickle, N. Li, F. Hyland;
Thermo Fisher Scientific, Carlsbad, CA

Introduction: DNA methylation plays a crucial role in development and progression of cancer. Identification of DNA methylation profiles in cancer is indispensable for early detection. To address this research need, Ion AmpliSeq™ offers targeted next-generation sequencing (NGS) methylation community amplicon panels for DNA methylation profiling in cancer-associated genes. However, the process of designing custom methylation amplicon panels using the Ion AmpliSeq primer design pipeline is intricate, labor-intensive, and time-consuming. Here, we developed a one-step, fully automated, faster, and reproducible nextflow-based primer design pipeline (MetFlow) for development of custom Ion AmpliSeq™ methylation panels. MetFlow streamlines the development of custom methylation panels for cancer-related genes, and thus significantly reduces the time and effort traditionally required for amplicon design.

Methods: The fully automated MetFlow pipeline is implemented using Nextflow. MetFlow necessitate an input configuration file for the execution of methylation Ion AmpliSeq™ designs. The configuration file specifies the essential parameters, including target CpG input, reference genome, pool number, and amplicon lengths, which are required for designing the amplicons. The MetFlow pipeline designs candidate amplicons for CpG targets on both Watson and Crick strands, facilitating the subsequent creation of files required for the generation of a methylation panel.

Results: The fully automated MetFlow pipeline has been used for designing the customized Ion AmpliSeq™ methylation amplicon panel(s) for cancer and age-related genes. The amplicons lengths in these AmpliSeq™ methylation panels were ranged from 125 bp to 175 bp for formalin-fixed, paraffin-embedded (FFPE) research samples. These customized methylation panels were run on the Ion GeneStudio™ S5 sequencer followed by performance analysis using Ion Torrent™ Suite. The published data for these custom amplicon panels suggest that the Ion AmpliSeq™ has sufficient read depth and mapping efficiency, higher sensitivity and accuracy for methylation measurement, and strong correlation (r=0.993) for methylation profiling among sample replicates.

Conclusion: We present MetFlow, an advanced automated primer design pipeline for designing the custom Ion AmpliSeq™ methylation amplicon panels tailored to targeted NGS applications in cancer research. The custom designed Ion AmpliSeq™ methylation panels exhibited sufficient read depth, higher sensitivity and accuracy, and reproducibility.

For Research Use Only. Not for use in diagnostic procedures.

#3490 Unveiling sex differences in lung adenocarcinoma through multi-omics integrative protein signaling networks.

C. Chen[1], E. Saha[1], D. L. DeMeo[2], J. Quackenbush[1], C. M. Lopes-Ramos[1];
[1]Harvard T.H. Chan School of Public Health, Boston, MA, [2]Harvard Medical School, Boston, MA

Sex differences in lung adenocarcinoma (LUAD) are evident in incidence rates, prognostic outcomes, and therapy responses, yet the underlying molecular mechanisms driving these disparities remain underexplored. In this study, we conducted a comprehensive proteogenomic analysis encompassing 38 females and 73 males with LUAD from the Clinical Proteomic Tumor Analysis Consortium (CPTAC) dataset. Employing Transcription Inference using Gene Expression and Regulatory data (TIGER), we inferred sex-differentially activated transcription factors (TFs) from The Cancer Genome Atlas (TCGA) LUAD gene expression data and identified sex-differentially activated kinases using CPTAC protein phosphorylation data. We further constructed a comprehensive kinase-TF signaling network by integrating these sex-differentially activated kinases with TFs, identifying all paths shorter than 3 in the protein interaction networks to highlight druggable pathways. Our analyses revealed that many proteins exhibit not only sex-biased abundance but also sex-biased phosphorylation and acetylation. Furthermore, these sex-biased proteins were associated with critical biological pathways including cell proliferation, immune response, and metabolism. Using kinase-TF signaling networks, we found substantial sex bias in the activities of clinically actionable TFs and kinases, including the glucocorticoid receptor (*NR3C1*), *AR*, *AURKA*, *CDK6*, and *MAPK14*. Leveraging the PRISM cancer cell line screening database, we identified several small-molecule drugs, such as glucocorticoid receptor agonists and aurora kinase inhibitors, potentially exhibiting sex-specific efficacy as LUAD therapeutics. Our findings showed that the activity of some clinically relevant TFs and kinases differ by sex in LUAD, underscoring the need to consider sex as a biological variable and the utility of multi-omics integrative protein signaling networks in advancing our understanding of cancer biology and the development of sex-aware therapeutics.

#3491 Tumor subtype classification of HPV-associated head and neck cancers is central to key clinically relevant variables.

B. F. Garb[1], S. Li[1], T. Qin[1], E. Lopez[1], S. Soppe[1], S. Patil[1], L. Rozek[2], N. D'Silva[1], M. Sartor[1];
[1]University of Michigan, Ann Arbor, MI, [2]Georgetown University, District of Columbia, DC

Cancer types are typically categorized according to the cell of origin, but within these groupings there exists vast heterogeneity. Thus, subtypes based on molecular features are often defined that have clinical utility as prognostic biomarkers, aid in selection of therapeutic strategies, or are associated with treatment response. Head and neck cancer (HNC) is the seventh most common cancer globally and projected to have 54,540 new cases in the U.S. in 2023. Within the US, HPV(+) HNC is now more prevalent than HPV(+) cervical cancer, and it is expected to continue to rise. Although there is wide morphologic and epigenetic diversity within HPV(+) HNC, tumor subtyping is not yet widely used for this cancer population, largely because of HPV(+) HNC's unique tumorigenesis process. Unlike other cancers that are driven by specific genetic signatures, HNC is driven by viral gene mechanisms. Given the large degree of heterogeneity among HPV(+) HNC cases and the lack of key mutations to define subtypes, the classification of HPV(+) HNSC subtypes requires a more sophisticated approach.
In this study, we introduce a robust, ensemble machine learning (ML) classifier for subtyping HPV(+) HNC that was trained on multiple cohorts and gene feature sets from RNA-seq data, and rigorously tested to ensure high reproducibility. The results classify HPV(+) HNC into the two main recognized subtypes: IMU (immune strong) and KRT(highly keratinized). Using a cohort of 227 patients, we show that the IMU/KRT classification is highly correlated with key clinically relevant variables in HNC. Of 41 molecular, clinical, and epidemiologic variables tested, 24 significantly associated with subtype. The IMU subtype was significantly associated with CD8 T-cells (p-value = 4.21×10^{-9}), Dendritic cells (p-value = 1.65×10^{-8}), B-cells (p-value = $2.20E^{-8}$), and epithelial to mesenchymal transition (p-value = 0.00013146). The KRT subtype is significantly associated with keratinization (p-value = 7.11×10^{-9}), HPV integration (p-value = 3.14×10^{-6}), radiation resistance (p-value = 0.00307), female sex (p-value = 0.00641), and high T stage (p-value = 0.0324). Genetic, epigenetic, and HPV gene-related variables were also among those significantly associated with subtype.
HPV(+) HNC subtypes have been shown to be associated with survival, with KRT-like patients having worse clinical outcomes than IMU. Given the different carcinogenic processes underlying IMU and KRT tumors, our ensemble ML subtype classifier web tool will help inform future studies of HPV(+) HNC. Future work to assess how HPV(+) subtypes can be incorporated into precision treatment strategies is well-motivated by our findings.

#3492 Comprehensive analysis of hematological malignancies with optical genome mapping and Bionano VIA™Software.

J. Wisotsky, A. Raski, W. Sherman, M. Roytman, S. Al-Saffar, J. Hauenstein, A. Wing Chun Pang, V. Wasnikar, N. Miller;
Bionano Genomics, San Diego, CA

The current standard for analysis of samples with suspected hematological cancer is karyotyping, fluorescence in situ hybridization (FISH), and/or chromosomal microarray (CMA). However, these methods have several limitations for the detection of structural variants (SVs) or copy number variants (CNV) that are smaller than 5 Mbp (karyotyping). Additionally, they are limited in their ability to detect low allele fraction (LAF) events and cannot detect the absence of heterozygosity (AOH) or the loss of heterozygosity (AOH/LOH - FISH and karyotyping).

Optical genome mapping (OGM) from Bionano can enable accurate detection of SV and CNV events of sizes down to 5 kbp, with high sensitivity to detect LAF events down to 5% variant allele fraction. Bionano's VIA™ software provides visualization and analysis support for OGM SV events including an improved Circos plot and ideogram for whole genome review. VIA incorporates CNV calling from OGM data using the SNP-FASST3 algorithm which also allows for accurate copy number calling at allele fractions as low as 10%. CNV detection performance was evaluated using 280 CNV events ranging in size from 175 kbp to 8 Mbp on the 22 autosomal chromosomes. Sensitivity and PPV were calculated for each size range separately.

Using SNP-FASST3, VIA also adds the ability to detect AOH/LOH events from OGM data. By analyzing locations where known SNPs disrupt the specific nucleotide sequence motif used by the DLE-1 labeling enzyme, a B-allele frequency can be calculated and enable AOH/LOH detection at low allelic fractions. AOH/LOH performance using SNP-FASST3 was evaluated using a cohort of constitutional and cancer samples analyzed with orthogonal methods as well as with simulated events. Sensitivity for 20-25 Mbp AOH events was 92% with PPV greater than 90% at 25% aberrant cell fraction.

The VIA 7.0 release also includes the ability to create a customizable decision tree using supplied reference annotation files for CNV, AOH and SV event pre-classification. VIA resources include a panel of target variants derived from various medical societies for clinical analysis guidelines specific to Acute Myeloid Leukemia (AML), Myelodysplastic Syndrome (MDS) and an aggregation of all hematological malignancy guidelines (pan-heme). These methods, combined with tools for expert review and reclassification of variants, allow users to conduct whole genome interpretation and report results.

These new features in VIA provide a streamlined workflow for analyzing heterogeneous hematological cancer samples and demonstrate the analytical performance of updated approaches for detection of CNV and AOH/LOH regions at low allele fractions using optical genome mapping alone.

#3493 Read-level methylation pattern extraction for high-multiplex large-scale targeted NGS assay.

M. Jin[1], M. Kaneko[2], S. Cen[2], H. Li[2], W. Guo[1], X. Zhou[2], A. Fujihara[2], T. Iwata[2], L. Storino Ramacciotti[2], D. Paralkar[2], G. Cacciamani[2], M. Aron[2], O. Ukimura[2], I. Gill[2], G. Liang[2], A. L. Abreu[2], J. Bhasin[1], **X. Yang**[1], X.-Y. Jia[1];

[1]Zymo Research Corp., Irvine, CA, [2]University of Southern California, Los Angeles, CA

The abnormal changes in DNA methylation are linked to the early stages of carcinogenesis. Identifying these epigenetic changes in circulating tumor DNA (ctDNA) can reveal potential biomarkers for the early diagnosis of various cancers. However, analyzing such data poses bioinformatics challenges due to the lack of sensitivity in detecting the low abundance ctDNA signals in biopsy samples, which are often overwhelmed by the complexity of libraries containing hundreds of targeted regions. Read-level methylation analysis holds the promise of more in-depth DNA methylation detection due to the wide coverage and high sensitivity of rare signals. However, this approach is hindered by the absence of a standardized workflow capable of generating interpretable reports suitable for both bench scientists and professional bioinformaticians. Here, we present a bioinformatics workflow that examines next-generation sequencing (NGS) data and characterizes the read-level methylation patterns of amplicons. Compared to other currently available tools, our method is designed to work with high-multiplex, large-scale targeted assays. It effectively eliminates the undesired noise derived from sequencing byproducts such as false CpG calls, dimers, and off-target alignments. Additionally, to accommodate the substantial volume of data generated by state-of-the-art NGS platforms, the workflow enables parallel processing of samples compatible with both cloud-based and on-premises computing resources. This workflow provides a comprehensive per-sample visualization of DNA methylation patterns and reports read-level methylation results in a “pattern-as-a-feature” table. In this table, the occurrence of an amplicon epiallelic haplotype (pattern) for every sample is represented as a “feature column” and is aggregated with all patterns discovered in the experiment. These read-level patterns, along with other information, can be used to develop machine learning algorithms to reiteratively harvest true predictive features and penalize confounding signals in predicting cancer diagnosis.

#3494 KINOMO: A non-negative matrix factorization framework for recovering intra- and inter-tumoral heterogeneity from single-cell RNA-seq data.

S. Tagore, Y. Wang, J. Biermann, E. K. D'Souza, K. D. Luthria, R. Rabadan, E. Azizi, B. Izar;
Columbia University, New York, NY

Single-cell RNA-sequencing (scRNA-seq) is a powerful technology to uncover cellular heterogeneity in tumor ecosystems. Due to differences in underlying gene load, direct comparison between patient samples is challenging, and this is further complicated by the sparsity of data matrices in scRNA-seq. Here, we present a factorization method called KINOMO (Kernel dIfferentiability correlation-based NOn- negative Matrix factorization algorithm using Kullback-Leibler divergence loss Optimization). This tool uses quadratic approximation approach for error correction and an iterative multiplicative approach, which improves the quality assessment of NMF-identified factorization, while mitigating biases introduced by inter-patient genomic variability. We benchmarked this new approach against nine different methods across 150 scRNA-seq experiments and find that KINOMO outperforms prior methods when evaluated with an adjusted Rand index (ARI), ranging 0.82-0.91 compared to 0.68-0.77. Thus, KINOMO provides an improved approach for determining coherent transcriptional programs (and meta-programs) from scRNA- seq data of cancer tissues, enabling comparison of patients with variable genomic backgrounds.

#3495 Multi-omic landscape of squamous cell lung cancer.

I. Y. Narvaez-Bandera, A. Lui, E. Welsh, D. Ercan, V. Rubio, H. Ackerman, G. Li, L. Darville, M. Liu, B. Fang, S. Eschrich, B. Fridley, J. Koomen, E. Haura, G. M. DeNicola, E. Flores, P. Stewart;
Moffitt Cancer Center, Tampa, FL

Patients with lung squamous cell carcinoma (LSCC) require new drug targets and improved biomarkers due to a lack of targetable genomic drivers and low response rates to immune checkpoint blockade. In a previous study, we analyzed a cohort of 108 LSCC patients by integrating DNA copy number variation, somatic mutations, RNA-sequencing, and expression proteomics. The principal discovery was the identification of three proteomic subtypes, with the majority (87%) of tumors comprising two of these subtypes. The "Inflamed" subtype showed enrichment for B-cell-rich tertiary lymphoid structures, while the "Redox" subtype exhibited enrichment for redox pathways and NFE2L2/KEAP1 alterations but had notably lower immune infiltration. We hypothesized that these subtypes would result in distinct metabolic signatures. Using ultra-high-performance liquid chromatographic separation on a HILIC column, followed by analysis on a Q Exactive HF high resolution mass spectrometer, we performed untargeted metabolomics on 87 tumors from the same LSCC proteogenomics cohort. A total of 7,392 features were obtained from this analysis, leading to the identification of 446 metabolites through m/z and retention time matching against an internal reference library. To understand if metabolomics could recapitulate our proteomic subtypes, we applied consensus clustering and non-negative matrix factorization (NMF) and assessed the resulting clusters using a Random Forest (RF) supervised classifier. Area Under the Curve (AUC) values for consensus clustering (5 clusters, AUC = 0.72), NMF (4 clusters, AUC = 0.73), and proteomics subtypes (Stewart et al. Nature communications. 2019:10:3578) (3 clusters, AUC = 0.74) suggest that metabolite abundances do indeed recapitulate the proteomic subtypes. Differential expression between Redox and Inflamed yielded 29 differentially expressed metabolites (p-value < 0.05 and 1.5 fold change). Glutathione, a key redox metabolite, was modestly elevated in the Redox proteomic subtype (0.58 log2 ratio, p = 1.14E-05). Notably, we identified glutathione metabolism (p = 1.29-5) and arginine biosynthesis (p = 5.22-4) as among the most significant pathways among differentially expressed metabolites. Glutathione, a key redox metabolite, was modestly elevated in the Redox proteomic subtype (0.58 log2 ratio, p = 1.14E-05). In conclusion, metabolomics recapitulates the proteomic subtypes, and there are distinct differences between these subtypes at the metabolite level. Ongoing work is developing a novel, network-based analysis framework to integrate these data quantitatively.

#3496 EpigenPlot: A tool for the gene-level methylation analysis of colorectal tumors.

D. Muller, B. Gyorffy;
Semmelweis University, Budapest, Hungary

Introduction. Aberrant DNA methylation patterns are frequent in colorectal adenocarcinoma (CRC) tissues. The investigation of this layer of epigenetic regulation holds the promise of a better understanding of tumour progression and the identification of novel biomarker candidates.
Purpose. Our goal was to collect and analyse publicly available DNA methylation data of colorectal samples and create a user-friendly tool for exploring and visualizing the CRC methylome.
Methods. We used Illumina Infinium Methylation Arrays, which is a popular platform for genome-wide methylation analysis of large cohorts. Gene Expression Omnibus database (GEO) and TCGA-COAD (The Cancer Genome Atlas Colon Adenocarcinoma) datasets including normal colorectal mucosa, adenoma, and adenocarcinoma samples were systematically collected and filtered. Differentially methylated regions were identified using the Kruskal-Wallis test. Genes with significant methylation changes were further analysed using ROC (Receiver Operator Characteristic) analysis. Finally, we established a web application using the shiny R package.
Results. We assembled a database including methylation data of 2,586 samples. Adenoma and adenocarcinoma samples were globally hypomethylated. Hypermethylation ($p < 0.05$, $\Delta\beta >= 0.2$) in adenocarcinoma samples was predominantly present in regions near proximal promoters. Out of the 74 previously proposed biomarkers examined, 50 had a cross-validated AUC of over 0.8. FDA-approved biomarkers BMP3, NDRG4, and SEPT9 have shown the highest performance in the TSS200 region (cvAUC = 0.8, 0.83, and 0.76, respectively). Genes with the highest performance were ITGA4 (5'UTR, first exon: cvAUC = 0.9), MDFI (5'UTR: cvAUC = 0.9), CNRIP1 (5'UTR, first exon: cvAUC = 0.89). The established web application can visualize methylation at CpG sites and gene regions, and KEGG pathway genes. The platform is available at https://epigenplot.com.
Conclusion. We collected and analysed a sizeable database of colorectal tissue data. Gene regions with the best performance include previously proposed and novel diagnostic biomarker candidates. The web platform provides an tool for the efficient exploration of the assembled data.

#3497 Glioma Immune Microenvironment Composition Calculator (GIMiCC): A method of estimating the proportions of eighteen key cell types from human brain tissue assayed using Illumina DNA methylation microarray technology.

S. C. Pike[1], J. K. Wiencke[2], Z. Zhang[1], A. M. Molinaro[2], D. C. Koestler[3], B. C. Christensen[4], K. T. Kelsey[5], L. A. Salas[4];
[1]Dartmouth College, Hanover, NH, [2]University of California San Francisco, San Francisco, CA, [3]University of Kansas Medical Center, Kansas City, KS, [4]Dartmouth-Hitchcock Medical Center, Lebanon, NH, [5]Brown University, Providence, RI

Precise detection of both tumor subclass and immune composition is critical in the pursuit of personalized immunotherapeutic treatment strategies for glioma. DNA methylation (DNAm) biomarkers are promising on both fronts. DNAm-based biomarkers for molecular classification have been developed and integrated into World Health Organization (WHO) diagnostic criteria. However, prediction of the tumor microenvironment is not as well defined. To fill this gap, we present GIMiCC, an approach for cellular deconvolution of DNAm microarray data for four WHO 2021 tumor subclasses: glioblastoma, oligodendroglioma, grade 2/3 astrocytoma and grade 4 astrocytoma. Using data from 17 isolated cell types, we describe the derivation of the deconvolution libraries and test the method on independent datasets from the Cancer Genome Atlas (TCGA) and the DKFZ molecular neuropathology classifier (PMID: 29539639). We utilize GIMiCC to illustrate that DNAm-based glioma classification is unlikely to be biased by compositional variation. In addition, we utilize GIMiCC to identify composition independent DNAm alterations that are associated with high immune infiltration. Our future work aims to optimize GIMiCC and advance the clinical evaluation of glioma with this new tool.

#3498 A novel combination of tissue-informed, comprehensive genomic profiling (CGP) and non-bespoke blood-based profiling for quantifying circulating tumor DNA (ctDNA).

T. Driessen, C. Lo, W. Zhu, R. Tell, J. Freaney, H. Nimeiri, K. Sasser;
Tempus, Chicago, IL

Background: Estimating quantitative circulating tumor fraction in liquid biopsy samples is a promising area of clinical development for monitoring therapeutic molecular response and correlates with patient outcomes. Here we introduce a sensitive measure of estimating ctDNA tumor fraction (ctDNA TF) using a novel combination of tissue-informed CGP with a non-bespoke, blood-based liquid biopsy panel.
Methods: Advanced pan-solid tumor samples were sequenced with both the Tempus xF/xF+ (105/523 gene, liquid biopsy) and Tempus xT (648 genes, solid-tumor with matched buffy coat) NGS assays (samples collected within 90 days). A normal distribution was fit against the somatic variants detected in solid-tissue and variants with variant allele fractions (VAF) within two standard deviations were used as selected biomarkers in the corresponding liquid biopsy to calculate a tumor-informed ctDNA TF for each sample.
Results: In the initial validation set (n=79 samples also sequenced with low-pass whole genome sequencing), the linearity of tumor-informed ctDNA TF was compared to mean VAF (R^2=0.26, slope=0.55), ichorCNA (R^2=0.84, slope=0.84), and tumor-naive ctDNA TF (R^2=0.71, slope=0.90). In a larger validation set (n=12,080), 37.5% samples had no variants detected in both xF and/or xT. Of the remaining samples, the linearity of tumor-informed ctDNA TF was compared to mean VAF (R^2=0.21, slope=0.55) and tumor-naive ctDNA TF (R^2=0.65, slope=0.81). In a follow-up analysis, we required 5 or more variants be detected in both xF and xT (n=1,659 samples) and compared the linearity of tumor-informed ctDNA TF to mean VAF (R^2=0.37, slope=0.64) and tumor-naive ctDNA TF (R^2=0.68, slope=0.98). In samples that received xF+ profiling (n=567), 24.3% had no variants detected in both xF+ and xT. The linearity of tumor-informed ctDNA TF of the remaining samples was compared to mean VAF (R^2=0.01, slope=0.26) and tumor-naive ctDNA TF (R^2=0.63, slope=1.02). Increasing the required number of variants to 5 or more had marginal improvement in linearity of tumor-informed ctDNA TF to mean VAF (R^2=0.12, slope=0.47) and tumor-naive ctDNA TF (R^2=0.67, slope=1.13).The limit-of-blank of the tumor-informed ctDNA TF approach was established to be 0% in both xF and xF+, and the limit-of-detection was ≤0.1% demonstrating that tumor informed ctDNA TF is a sensitive measure in detecting tumor fraction at low concentration levels.
Conclusion: Here we introduce a novel sensitive and specific tumor-informed, non-bespoke approach for estimating ctDNA TF. Linearity improves with increased panel size and increased variant number. These results suggest that a tumor-informed ctDNA TF can be utilized to improve the sensitivity of existing methods for estimating tumor fraction to help in treatment decisions using Tempus' tissue and liquid comprehensive NGS genomic profiling platform.

#3499 Non-small cell lung cancer (NSCLC) histology classification using DNA methylation data captured from liquid biopsies.

L. Tung[1], D. Tolkunov[1], C. Barbacioru[1], D. Kale[1], S. Shell[1], J. Tsai[1], L. Drusbosky[1], K. Parikh[2], H.-Y. Chuang[1];
[1]Guardant Health, Redwood City, CA, [2]Mayo Clinic, Rochester, MN

Background: Non-small cell lung cancer (NSCLC) makes up ~85% of lung cancers, and its major subtypes are adenocarcinoma (AD) and squamous cell carcinoma (SC). The histology classification of NSCLC has significant therapeutic and prognostic implications. As liquid biopsies are rapid and non-invasive, computational methods to classify NSCLC subtypes using cell-free DNA (cfDNA) are desired.
Methods: Using The Cancer Genome Atlas (TCGA) NSCLC methylation data, we developed a method to classify AD and SC subtypes from cfDNA samples. We mapped TCGA methylation data to Guardant Infinity's promoter regions and transformed them to allow for the transfer of the TCGA trained model to Infinity cfDNA epigenomic data. An advantage of this approach is that TCGA training data originates from the primary tumor, while cfDNA samples have low tumor fraction (TF) and may also contain signals from metastatic tumors. We trained a penalized Logistic Regression model with LASSO. To better fit the model to Infinity cfDNA data, we performed region filtering.
Results: Our model effectively classified AD and SC subtypes from TCGA samples (AUC 0.97) (10-fold cross validation; Table 1). When evaluating on cfDNA samples with epigenomic TF ≥ 1%, the final model shows reasonable performance (AUC 0.94) (Table 1); the performance decreases when reduced to TF > 0.05% (AUC 0.89) as expected (Table 1). When evaluating cfDNA from uncategorized lung samples, the predicted AD probabilities have significant association with *KRAS* mutations (p-value = 0.027).

Table 1: Model evaluation on tissue TCGA samples and cfDNA Infinity samples (different TF cutoffs)

Sample type	N samples	AUC	Accuracy	Sensitivity	Specificity	Precision	F1 score
tissue TCGA	907	0.97	0.93	0.94 +/- 0.02	0.93 +/- 0.02	0.94 +/- 0.02	0.94 +/- 0.01
cfDNA Infinity	17 (TF ≥ 1%)	0.94	0.88	0.83 +/- 0.3	0.91 +/- 0.17	0.83 +/- 0.3	0.83 +/- 0.21
cfDNA Infinity	29 (TF > 0.05%)	0.89	0.83	0.88 +/- 0.23	0.81 +/- 0.17	0.64 +/- 0.28	0.74 +/- 0.2

Conclusion: Our results show that the penalized Logistic Regression model trained with tissue TCGA methylation data through mapping, transformation, and region selection can classify NSCLC subtypes from cfDNA samples. This method may offer a fast, non-invasive tool to inform subtype-based clinical decisions, especially in the setting of poorly-differentiated carcinomas, and to identify subtype switches upon resistance to targeted therapies.

#3500 Refining diagnosis of renal cell carcinoma subtypes through single-cell resolution transcriptomic signatures.

M. Kim, A. Madrigal, Z. Mehrjoo, K. I. Glennon, M. Arseneault, M. Park, F. Brimo, S. Tanguay, H. S. Najafabadi, Y. Riazalhosseini;
McGill University, Montreal, QC, Canada

A remaining challenge in the field of renal cell carcinoma (RCC) is diagnosis of rare or mixed subtypes, which hampers the delivery of the most effective healthcare to patients. While a new classification scheme, integrating molecular characteristics of tumors, is emerging, it requires a deep understanding of the tumor heterogeneity and etiopathogenesis of each subtype. We have generated and analyzed single-cell transcriptome profiles of 38 human RCCs and normal kidneys 16 RCCs with diverse histological subtypes and established gene signatures specific to each cell type. We have applied these gene signatures to bulk RNA-sequencing data of 1000 RCC tumors with different histological subtypes and normal kidneys from The Cancer Genome Atlas (TCGA) to characterize different cancer types and cellular origins. Unsupervised clustering analysis of TCGA data shows diagnostic discrepancies for 9.3% cases and subclassifies each major subtype (clear cell, papillary and chromophobe) into clusters with differential clinical outcomes.[KM1] . The pathological marker expression in misdiagnosed tumors is consistent with clustering-based classification, not their original diagnosis. Notably, using unique and subtype-specific gene signature patterns, we identified clear cell papillary renal cell tumor (ccpRCT), which is a newly classified benign entity and the main tumor type representing the mis-diagnosed tumors. These observations have further been confirmed by reviewing histological images of the tumors by an experienced genitourinary pathologist. Interestingly, our gene signatures reveal that ccpRCT does not originate from proximal tubule cells unlike clear cell and papillary RCCs. Taken together, our approach suggests a potential new classification method connected to clinical behaviors and drug responses based on overall transcriptomic differences.

#3501 Concurrent amplification of TBXT and highly activated enhancers in extrachromosomal DNA (ecDNA) drives chordoma tumorigenesis.

B. Zhao[1], M. Ines[1], L. Ye[1], X. Wu[1], A. Soragni[2], A. Futreal[1], K. Akdemir[1];
[1]UT MD Anderson Cancer Center, Houston, TX, [2]UCLA, Los Angeles, CA

Chordoma, a rare bone cancer characterized by limited actionable clinical targets, exhibits a pivotal hallmark in the activation of the developmental transcription factor gene TBXT (Brachyury) through its association with highly active enhancers. TBXT amplification emerges as a major causative factor in familial chordomas, yet the amplification mechanism and its consequential impact on genomic instability remain inadequately elucidated. In this study, we conducted a comprehensive analysis of multiple genomic and epigenomic sequencing datasets, including WGS-seq, H3K27ac ChIP-seq, and ATAC-seq in six chordoma cell lines, and HiC data in two of them, to unravel the mechanisms of structural variations and their biological implications. Notably, our focus extends to JHC7 cells, which exhibit extrachromosomal amplification of a 2.4M region encompassing TBXT and the associated enhancers. The existence of such extrachromosomal DNA (ecDNA) in JHC7 was further validated through DNA FISH and Sanger sequencing. Comparing JHC7 with CH22, a chordoma cell line lacking TBXT amplification, revealed heightened chromatin relaxation and increased DNA rearrangements in JHC7. Interestingly, FISH results showed significant genomic ploidy heterogeneity within JHC7 cells, a finding demonstrated by nucleus FACS sorting. Single-cell multiomic analysis, combining snRNA-seq and snATAC-seq, demonstrated heterogeneous gene expression and distinct copy number variations among JHC7 cells. However, the amplification of the TBXT locus was observed in nearly all cells examined, indicating the rapid genomic evolution in the cultured JHC7 cells. These results collectively show that TBXT is extensively amplified through the formation of ecDNA, providing a fitness advantage to chordoma cells and concurrently exacerbating genomic instability. The findings in this study provide an insight for understanding the pathogenesis of chordoma and may inform the development of targeted therapeutic strategies.

#3502 Multi-omics approach to cholangiocarcinoma-related biology and development of precision medicine.

W. Kwon, I. Kang, S. Lee;
Laboratory of Integrative Precision Oncology, Seongnam-si, Korea, Republic of

Introduction: Cholangiocarcinoma is a diverse tumor entity characterized by distinct tumor biology and clinical phenotypes, which are influenced by the unique tumor microenvironment (TME) and anatomical location—whether intrahepatic, peri-hilar, or distal extrahepatic. Consequently, there is a clear need for a precision strategy that relies on cancer-specific, multi-omic features, moving away from traditional molecular subtypes derived from bulk RNA sequencing.
Methods: We conducted thorough multi-omic analyses utilizing data from the Cancer Dependency Map (DepMap) project. This encompassed cancer-specific molecular characterization through various omics data, genome-wide loss-of-function screening employing the CRISPR-Cas9 system, and drug sensitivity assessments via compound screening. These efforts aimed to reveal cancer-specific molecular subtypes with clinical relevance. The identified cancer-specific molecular signatures were subsequently validated in independent translational cohorts.
Results: Through integrative profiling of the transcriptome in bile duct cancer cell lines (n=39) obtained from the Cancer Cell Line Encyclopedia (CCLE), we unveiled cancer-specific molecular subtypes exhibiting distinct tumor biology across all omics layers, coupled with clinical relevance and prognostic significance. The major molecular features of each subtype demonstrated reproducibility in validation cohorts. Additionally, subtype-specific molecular biomarkers, encompassing mutational signatures and metabolites, were identified. Finally, we analyzed target drugs with subtype-specific genetic dependencies to formulate a precision strategy tailored to the distinct molecular characterizations of each subtype.
Conclusions: A thorough analysis utilizing a multi-omics dataset uncovered precision strategies founded on cancer-specific molecular subtypes of cholangiocarcinoma, both in terms of tumor classification and discriminative therapeutic opportunities. It is imperative to conduct prospective translational studies in conjunction with clinical trials, all centered around the cancer-specific molecular subtypes, to establish a precision strategy for effectively managing cholangiocarcinoma.

#3503 New generation drug development from *in-silico* identification to preclinical evaluation in glioblastoma.

Mahesh Arunachalam, Shreyas Gaikwad, Sharavan Ramachandran, Sanjay K. Srivastava

Immunotherapeutics and Biotechnology, Texas Tech University Health Sciences Center, Abilene, TX

Glioblastoma(GBM) is the most common malignancy of the central nervous system in adults. Despite medical advancements, stagnant survival rate improvements (<13%) and failure of conventional treatments such as temozolomide, have warranted the need for novel drug discovery methodologies. Considering the enormous potential of drug repurposing, we developed a method to identify a safe, active, and effective treatment for GBM. This method comprises two key stages, drug-target prediction and preclinical functional evaluation. Stage 1 fabricated a novel five phase in-silico pipeline for drug-target prediction against Ephrin-Type-A Receptor 2, chosen through preliminary literature and genomic analysis. Around 1562 FDA approved drugs were screened against the developed criterion and analyzed for bond type, location, repulsion, Gibbs free energy, stability, interactions over time, blood brain barrier permeability, and possible false positives (PAINS). Our results provided five plausible hits: Empagliflozin, Mycophenolate mofetil, Canagliflozin, Rivaroxaban, and Carvedilol. We subsequently evaluated the anti-proliferative effects of these hits using Sulforhodamine-B cytotoxicity assay on glioblastoma cell lines U251 and SF295. Our results demonstrated that Canaglifozin and Empagliflozin reduced the proliferation of GBM cell lines with IC50 value ranging from 30-40 µM. On the other hand, Mycophenolate mofetil (IC50: 5µM) and Carvedilol (IC50:16µM) also exhibited significant cytotoxic effects. Effects of Mycophenolate mofetil and Carvedilol were further evaluated in pancreatic cell line SUIT-2 where results exhibited cytotoxic responses similar to those observed in GBM. Furthermore, Annexin V/FITC analysis showed apoptosis in SUIT-2 cells by Carvedilol. Taken together, our results show the anti-cancer repurposing candidates extracted from our in-silico pipeline show significant cytotoxic effects of compounds identified through in-silico screening. Further studies are currently underway in our laboratory to delineate the anti-cancer mechanism, toxicity and off-target effects of these compounds.

#3504 ARS2 and paraspeckle interactions: A nexus for lncRNA mediated drug resistance and cancer progression in hepatocellular carcinoma.

G. Thillainadesan, H. S. Leong, O. Alawamry;
Sunnybrook Research Institute, Toronto, ON, Canada

Paraspeckles, elaborate sub-nuclear assemblies composed of the lncRNA *NEAT1-2* and a cohort of RNA-binding proteins, have a noted association with cancer progression and drug resistance. The specific mechanisms, however, have remained obscure. Our investigation into Hepatocellular Carcinoma (HCC) reveals a critical interaction: the sequestration of ARS2—an RNA-binding protein vital for the suppression of mRNA transcripts and the maturation of miRNAs—within paraspeckles. This sequestration leads to increased levels of *NEAT1-2*, derails miRNA processing, and diminishes the gene-silencing function of ARS2, thereby enhancing the expression of oncogenic genes. This discovery positions the ARS2-paraspeckle axis as a pivotal factor in cancer biology and a promising target for future treatments.

#3505 Classification of cancer subtypes by cfDNA fragmentomics analysis.

L. Zhu[1], C. Dai[1], S. Gan[2], S. Jia[1], P. Du[1];
[1]Predicine, San Francisco, CA, [2]Predicine Huidu (Shanghai) Medical Sciences, Shanghai, China

Introduction Fragmentation patterns of cell-free DNA (cfDNA) from whole genome sequencing offer insights into nucleosome occupancy, providing a tool to infer epigenomic and transcriptomic information. The nucleosome complex, the primary protector of cfDNA, is reflected in the size distribution of cfDNA fragments, with a mode fragment size of 167 bp corresponding to the wrapping of DNA around a single nucleosome. Nucleosome occupancy patterns at transcription factor binding sites (TFBS) exhibit differences between circulating tumor DNA in cancer patients and normal plasma controls, as well as among different tumor subtypes. Therefore, cfDNA fragmentomics can be employed for cancer subtyping analysis.
Methods We utilized the Griffin framework to classify tumor subtypes based on nucleosome profiling of cancer-specific TFBS and tumor subtype-specific chromatin accessibility regions from low-pass whole genome sequencing data of cfDNA. For prostate cancer subtyping, AR and ASCL1 binding sites were used to distinguish between androgen receptor-dependent prostate cancer (ARPC) and neuroendocrine prostate cancer (NEPC). ER and ERBB2 were employed for breast cancer subtyping to differentiate between ER-positive and ER-negative tumor subtypes.
Results Nucleosome profiling patterns at AR binding sites (ARBS) were compared among over 500 prostate cancer plasma samples and 42 normal plasma backgrounds. The ARBS nucleosome profiling abnormality score (ARBS score) was quantified by comparing its GC-corrected fragment central coverage with the normal background using a standard Z-score.Majority of prostate cancer samples with a high ARBS score could be classified as ARPC. For 12 samples with high tumor fraction but low ARBS score and no AR copy number amplification, we found that 8 had a high ASCL1 nucleosome profiling abnormality score. All these samples also exhibited RB1 copy number loss, suggesting that these 8 samples likely belong to NEPC. Nucleosome profiling of 171 breast cancer plasma samples at breast cancer-specific ER binding sites revealed that majority of samples had a high ERBS abnormality score, indicating likely ER-positive breast cancer.
Conclusion Our results demonstrate that nucleosome profiling of tumor cfDNA exhibits distinct patterns across different tumor types. Integrating nucleosome profiling at cancer-specific transcription factor binding sites can facilitate cancer subtyping, highlighting its potential clinical utility for patient stratification.

BIOINFORMATICS / COMPUTATIONAL BIOLOGY / SYSTEMS BIOLOGY / CONVERGENT SCIENCE: Artificial Intelligence and Machine/Deep Learning 2
Poster Session

#3509 Using generative AI for filtering and comprehension of drug target discovery screen results.

A. Rech[1], **Y. Goltsev**[2], N. Samusik[2], A. Kaznadzey[2];
[1]University of Pennsylvania, Philadelphia, PA, [2]Cellformatica, Inc., Menlo Park, CA

Recent advancements in generative AI, including models such as GPT-4 and LLAMA2, have been rapidly integrated into cancer research. Cellformatica, Inc. has developed a pipeline designed to enhance the accuracy of functional and genomic drug target discovery screens by reducing the incidence of false positives and refining the interpretation process. This pipeline is capable of conducting comprehensive investigations, including genome-wide analyses, and is accessible via web and API interfaces. At the core of the pipeline is the use of the extensive global corpus of scientific literature to assess the relevance of each gene within the context defined by the experimental design of the screen. To address the issue of AI-generated inaccuracies, often referred to as 'hallucinations,' the pipeline incorporates a custom-tuned language model (LLM) component within the generative AI framework. This fine-tuning process is specifically tailored to the gene set under investigation. The pipeline's multi-agent architecture is a distinctive feature. It scores candidates based on three orthogonally-tuned criteria: effectiveness, confidence, and novelty. In benchmarking tests, this multi-agent scoring system has outperformed GPT-4 and has proven particularly adept at identifying candidate targets that may have been overlooked in previous research. These candidates are recognized for their significant therapeutic potential and are corroborated by existing scientific findings. The versatility of the Cellformatica pipeline is demonstrated through its application in three distinct areas of cancer research. First, it has been employed to optimize chimeric antigen receptor (CAR) T-cell therapies, a form of immunotherapy for cancer treatment. Second, the pipeline has been used to elucidate the network of chemotactic molecules that orchestrate immune cell infiltration and tissue remodeling in the lungs of patients with COVID-19. Third, it has been used to spatially define signaling pathways in humanized xenograft murine tumor experiments, for which existing cross-species database knowledge is limited. These applications underscore the pipeline's potential to contribute to the understanding and treatment of complex diseases.

#3510 A radiogenomic approach for triple-negative breast cancer risk stratification.

H. Noor[1], Y. Zheng[1], A. Mantz[1], R. Zhou[1], A. Kozlov[2], W. B. DeMartini[1], S.-t. Chen[3], S. Okamoto[4], D. Ikeda[1], S. Mattonen[5], S. Napel[1], M. L. Telli[1], G. Sledge[1], A. Kurian[1], M. Satoyoshi[1], O. Gevaert[1], H. Itakura[1];

[1]Stanford University School of Medicine, Stanford, CA, [2]University of Utah, Utah, UT, [3]Department of Diagnostic Radiology, Chang Gung Memorial Hospital, Taiwan, Taiwan, [4]St. Marianna University School of Medicine, Kawasaki, Japan, [5]Western University, London, ON, Canada

Background: Triple-negative breast cancer (TNBC) is an aggressive disease that accounts for 15-20% of all breast cancers. Expressions of ER, PR and HER2 receptors are lacking in this disease, and thus targeted therapies are not effective. TNBC has a shorter relapse-free survival, higher metastasis rate and decreased overall survival compared with other breast cancers. However, when undergoing standard treatment, some patients respond well, while others have poor outcome, suggesting TNBC heterogeneity. Early stratification of patients with long versus short survival could identify the subgroup of patients who would not benefit from exposure to toxicity of chemotherapy treatment. Here, we developed a non-invasive radiogenomic approach for TNBC risk stratification.
Methods: A transcriptomic-based prognostic gene signature was previously developed using the TCGA-BRCA cohort (n=860). Briefly, LASSO Cox regression model analysis with the 'glmnet' R package was used to identify the transcriptomic signature gene-set consisting of 50 genes. We tested this signature to prognosticate overall survival in a Stanford cohort (n=63) and a previously published SCANB cohort (n=604). The patients were stratified into high- and low-risk groups based on the median risk-score. Next, we developed a machine learning model that identified a radiomic feature set to predict the prognostic transcriptomic risk-groups. Radiomic features were extracted from pre-treatment breast MRI. Radiomics features were extracted using PyRadiomics. The model utilized Decision Tree Classifier and LeaveOneOut method was used for cross-validation.
Results: The transcriptomic signature low-risk group was significantly associated with improved overall survival in the two TNBC cohorts, with hazard ratios of 0.11 [95% CI: 0.01-0.88] for the Stanford cohort and 0.71 [95% CI: 0.52-0.97] for the SCANB cohort (log-rank p-values p=0.012 and p=0.032, respectively). Including this transcriptomic signature in a multivariate analysis, which adjusted for clinical features (patient age, grade, stage and Ki67%), the transcriptomic prognostic signature remained a significant prognostic factor ($p<0.05$). The radiomic feature set (consisting of 20 features) predicted the high- and low-risk transcriptomic groups with a mean accuracy of 72.2% and a mean AUROC of 71%. The precision, F1 and recall scores were 67%, 74% and 82%, respectively. In an independent dataset consisting of 116 Stanford TNBC patients, we used this model to predict risk groups based on the MRI radiomics features, and evaluated the prognostic effects of predicted risk groups. The overall survival of the predicted high-risk group was significantly poorer than the predicted low-risk group (p=0.013).
Conclusions: We present a prognostic model that can non-invasively stratify TNBC patients for low versus high mortality risk using radiomic features derived from pre-treatment patient MRI data.

#3511 iQC: machine-learning-driven prediction of surgery reveals systematic confounds in cancer whole slide images from hospitals by protocol.

A. J. Schaumberg[1], M. S. Lewis[2], R. Nazarian[2], A. Wadhwa[2], N. Kane[2], G. Turner[1], P. Karnam[1], P. Devineni[1], N. Wolfe[1], R. Kintner[1], M. B. Rettig[2], B. S. Knudsen[3], I. P. Garraway[2], S. Pyarajan[1];

[1]VA Boston Healthcare System, Boston, MA, [2]VA Greater Los Angeles Medical Center, Los Angeles, CA, [3]University of Utah, Salt Lake City, UT

Problem: This 21st century has produced an eruption of research using AI for the detection and diagnosis of cancer. Yet, an often-unspoken core premise in this field of computational pathology is that a glass slide suitably represents the patient's disease. Here, we report systematic confounds may dominate slides from a medical center, such that slides are unsuitable for diagnosis.

Methods: We mathematically define high quality data as a whole slide image set where the patient's surgery may be accurately predicted by an automated system. Our system "iQC" accurately distinguished biopsies (i.e. thin strands of tissue) from nonbiopsies, e.g. transurethral resections (TURPs) or prostatectomies, only when the data appeared high quality, e.g. bright histopathology stains and few artifacts. Thus, when the data are of high quality, iQC (i) accurately classifies pixels as tissue, (ii) accurately generates stats that describe the distribution of tissue, and (iii) accurately predicts surgical procedure from those stats. We compare iQC against the published HistoQC tool.

Results: iQC holds all data to the same objective quality standard. We validate this standard in five Veterans Affairs Medical Centers (VAMCs) and the public Automated Gleason Grading Challenge (AGGC) dataset. For the surgery prediction task, we report an AUROC of 0.9966-1.000 at VAMCs that produced high quality data and AUROC=0.9824 for AGGC. In contrast, we report AUROC=0.7115 at the VAMC that produced poor quality data. A pathologist found poor quality may be explained by faded histopathology stains and VAMC protocol differences. Supporting this, iQC's novel stain strength statistic finds this VAMC had weaker stains ($p < 2.2e-16$, two-tailed Wilcoxon rank-sum test; Cohen's $d=1.208$) than the VAMC that contributed most of the slides. Additionally, iQC recommended only 2 of 3736 (0.005%) VAMC slides for review due to inadequate tissue. In contrast, HistoQC in its default configuration excluded 89.9% of VAMC slides because tissue was not detected, but we reduced this to 16.7% with our custom HistoQC configuration.

Conclusion: Our surgery prediction AUROC may be a quantitative indicator positively associated with data quality for a dataset. Unless data are poor quality, iQC accurately locates tissue in slides and excludes few slides. iQC is, to our knowledge, the first automated system in computational pathology that validates quality against objective evidence, e.g. surgical procedure data available in the EHR/LIMS, which requires no efforts or annotations from anatomic pathologists.

#3512 Joint probabilistic modeling of multimodal metabolic data with UnitedMet.

A. X. Xie, C. Bradshaw, C. Tosh, W. Tansey, E. Reznik;
Memorial Sloan Kettering Cancer Center, New York, NY

Metabolites play a crucial role in the functioning of biological systems. Measurements of metabolite abundances by metabolomics and metabolic pathway activity by isotope-tracing are powerful approaches to study metabolic phenotypes. However, large-scale measurements of metabolite levels and pathway activity remain extremely scarce due to the technical challenges. Motivated by the strength of RNA-metabolite covariation, we present UnitedMet, a Bayesian probabilistic method for end-to-end joint modeling of RNA-sequencing and metabolic datasets that is capable of dimensionality reduction, data integration and metabolic modality prediction. UnitedMet demonstrates high accuracy predicting metabolite levels and isotopologue distributions from gene expression data in human tumor samples. To evaluate UnitedMet's efficacy in clinical applications, we inferred metabolomic profiles and isotope labeling patterns from the RNA sequencing data of clear cell renal cell carcinoma (ccRCC) patients enrolled in TCGA and clinical trials. Correlation analysis between genetic mutations and predicted metabolic phenotypes revealed that BAP1 mutations were associated with increased contribution of glucose to TCA cycle in ccRCC. Increased TCA cycle activity was found to be associated with disease progression and poorer clinical outcome. UnitedMet, therefore, provides a solution that could be broadly applicable to enhance multimodal metabolomic datasets and facilitates comprehensive study of interplays between metabolic profiles, molecular alterations and human phenotypes.

#3513 A CNN-based approach with efficient transfer learning improves microRNA-mRNA prediction.

Chen-Hao Peng[1], Hui-Yu Chen[1], Da-Chuan Cheng[1], Eric Y. Chuang[2], Chien-Yueh Lee[3]

[1]Department of Biomedical Imaging and Radiological Science, China Medical University, Taichung City, Taiwan, [2]Graduate Institute of Biomedical Electronics and Bioinformatics, National Taiwan University, Taipei, Taiwan, [3]Innovation Frontier Institute of Research for Science and Technology, National Taipei University of Technology, Taipei City, Taiwan

MicroRNAs play a crucial role in post-transcriptional regulation, influencing over 60% of human protein-coding genes by targeting specific mRNA sites to suppress protein translation. Various predictive algorithms aim to discern potential microRNA-mRNA pairs. Current approaches primarily employ sequence alignment, machine learning, and deep learning, yet encounter challenges such as complex data pre-processing, time-consuming model generation, and limited binding site precision. Additionally, some methods rely on inefficient RNN-based models, resulting in sluggish predictions. To address these issues, we proposed a CNN-based algorithm combined with transfer learning for direct and precise prediction of microRNA-mRNA binding sites, eliminating the need for extensive preprocessing. We introduced two models in this study: the per-based model and the miRNA-target binding decision model. The former screens potential target sites on 3'-UTR sequences, while the latter guides the decision-making process for miRNA-target pairs. The per-based model utilized a public database, extracting 786,447 human microRNA-mRNA pairs verified by CLIP-seq. It employed sequence alignment approaches to determine putative binding sites and per-base binding states. MicroRNA sequences and seed regions served as the initial convolutional kernels in the deep learning model, combined with encoded full-length 3'-UTR sequences of mRNAs as inputs for the fine-tuned U-Net architecture. For the miRNA-target binding decision model, we excluded the per-based model's decoder and initialized a new classification layer for target-site prediction. Leveraging experimental validation datasets from public databases, we extracted 2,846 binding and 1,058 non-binding human microRNA-mRNA pairs. The pre-trained model was fine-tuned on these 3,904 pairs. Both models underwent training with cycle learning rate, focal loss, gradient clipping, and weighted decay to address dataset imbalances. The dataset was split into 80% training and 20% testing data, with balanced accuracy as the evaluation metric. The per-based model achieved a robust 82.14% balanced accuracy on the test data, excelling in handling imbalanced datasets in per-based tasks. It swiftly and accurately identified nucleotide binding states. The miRNA-target binding decision model outperformed existing methods with a balanced accuracy of 80.39% on the test data. In contrast to many deep learning methods requiring additional preprocessing, our algorithm directly predicts per-base binding states from full-length sequences. It seamlessly transfers knowledge from the per-based to the miRNA-target model. Importantly, our approach relies solely on seed regions, eliminating the need for prior knowledge and enhancing microRNA target prediction reliability. This advancement holds promise for biomedical and clinical researchers, offering valuable insights.

#3514 A deep learning model for detection and characterization of tertiary lymphoid structures in H&E-stained images from pancreatic ductal adenocarcinoma.

C. Zhao[1], J. Jia[2], M. Lv[2], J. Feng[1], Y. Wang[1], Y. Liu[1];

[1]Renji Hospital affiliated with Shanghai Jiao Tong University School of Medicine, Shanghai, China, [2]Shanghai Jiao Tong University, Shanghai, China

Tertiary lymphoid structures (TLSs) are ectopic aggregates of a number of immune cells in nonlymphoid tissues under chronically inflamed environments and cancer. Emergence evidence suggested that TLSs were found in diverse cancers and TLSs have been referred as an independently predictive biomarker for immunotherapy response, especially immune checkpoint inhibitors. Moreover, the density and mature status of TLSs often positively associated with the favorable outcomes in cancers. Pancreatic ductal adenocarcinoma (PDAC) is one of the leading causes of cancer-related mortality with low survival rate in the whole world. Here, we developed a multi-resolution machine learning model for detection of TLSs from hema-toxylin and eosin (H&E) stained digital pathology slides as a potential clinical biomarker in PDAC. We selected 120 H&E slides (patients) with a total of 1,896 TLSs manually annotated as immature or mature TLSs by two pathologists. We also used immunohistochemistry (IHC) for CD20 and CD23 markers as a reference standard for H&E-based manual annotations. Our model mainly included detection and segmentation of individual TLSs. First, we used a transformer convolutional neural network to build a classification task to detect the presence of immature or mature TLSs. Then the instance segmentation model was applied to quantify the number of lymphocytes per unit square to validate the presence and maturation of TLSs. F1-score, calculated by the harmonic mean of precision (positive predictive value) and recall (sensitivity), was finally used to quantitatively evaluate the performance of model for each H&E slide. In validation dataset with 250 H&E slides (patients), we selected 50 slides to calculate F1-score, suggesting that our machine learning model achieved high F1-scores for detection and classification of immature TLSs (mean = 0.87, range from 0.79 to 0.95), and mature TLSs (mean = 0.92, range from 0.86 to 0.97). We further stratified 370 PDAC patients into three groups with mature TLSs (23%), immature TLSs (16%), and no TLSs (61%), respectively. Combined the clinical information, survival analysis revealed that patients with mature TLS had better survival outcomes than those without TLS (HR = 0.63; 95% CI, 0.44 - 0.90; P = 0.010). We developed a machine learning model that can accurately detect and classify TLSs in PDAC, and also demonstrated the prognosis value of predictive TLSs in H&E slides by automatedly machine learning model. These data highlight the promise of machine learning model for automated identification and quantification of the TLS on H&E slides in PDAC pathology.

#3515 SynAI: An AI-driven cancer drug synergism prediction platform.

K. Yan[1], R. Jia[2], S. Guo[2];

[1]Crown Bioscience, Inc., Leiden, Netherlands, [2]Crown Bioscience, Inc., Suzhou, China

Introduction: The SynAI solution is an adaptive AI-driven *in silico* drug synergism screening solution aiming to discover the potential therapeutic value of compounds at an early development stage. Given one of both compound inputs in SMILE sequences, SynAI can predict the potential Bliss score of compounds in any given cell line without the need for compound synthesis or structural analysis.The evaluation version of SynAI is accessible at https://synai.crownbio.com
Methods: The AI core of SynAI was constructed using the MLP (multi-layer perceptron) network under the PyTorch machine learning framework. The AI core of SynAI was trained against NCI-Almanac and DrugCombDB datasets. In total, these datasets consist of over 12 million *in vitro* synergism tests across 150 cancer cell lines of different origins. On average, each cell line is tested against over 6000 two-compound combinations of FDA-approved cancer drugs. One MLP network was trained for each cell line. Essentially, these networks predict the Bliss score for any combination of SMILE-based feature sets known as molecular fingerprints. The networks were trained against the NCI Almanac set and verified against NCI and DrugCombDB using n-fold cross-validation to avoid model overfitting. During the training, a hyperparameter tuning (HT) study was performed for SynAI and other popular algorithms; allowing an objective comparison of SynAI performances.
Results: Compared to existing synergism prediction platforms, SynAI yields similar performance in all categories (cf. Table 1) but provides more flexibility for data input using SMILE sequences directly. In addition, the AI core of SynAI can be constantly updated with new inputs from different cell lines and drug combinations. Table 1. Pearson cross correlation (PCC) between measured and predicted Bliss scores of NCI test set

PCC Score	**Cell Lines**		
Algorithm	**MCF7**	**OVCAR-8**	**SK-MEL-5**
SynAI	**0.68 ± 0.02**	**0.56 ± 0.07**	**0.86 ± 0.02**
RF	0.64 ± 0.02	0.55 ± 0.03	0.89 ± 0.02
GBX	0.66 ± 0.02	0.48 ± 0.05	0.88 ± 0.02
RNN	0.54 ± 0.12	0.43 ± 0.06	0.83 ± 0.08

Conclusions: Its adaptive and dynamic nature allows SynAI to learn from new data feeds from future studies and has significant potential in reducing the time and cost of synergism screening.

#3516 AI-derived features of 3D glandular networks are associated with likelihood of biochemical recurrence post radical prostatectomy.

J. Salguero[1], H. Abdeltawab[1], K. Hammouda[1], G. Corredor[1], S. Hawley[2], P. Mutha[1], R. Dhamdhere[1], S. Medina[1], T. Pathak[1], K. Bishop[3], R. Serafin[3], T. Mirtti[4], P. Lal[5], L. True[3], J. Liu[3], A. Madabhushi[6];

[1]Emory University, Atlanta, GA, [2]Canary Foundation, Palo Alto, CA, [3]University of Washington, Seattle, WA, [4]University of Helsinki & Helsinki University Hospital, Helsinki, Finland, [5]University of Pennsylvania, Philadelphia, PA, [6]Emory University and Georgia Institute of Technology, Atlanta, GA

Introduction: Prostate cancer is the most common cancer in American men and is mainly diagnosed from two-dimensional histology sections. Recently, three-dimensional (3D) prostate histopathology has emerged as a valuable strategy to enhance the understanding of the disease by increasing microscopic sampling of specimens. This strategy enhances the microscopic examination of specimens by facilitating the analysis of the volumetric shape of cells and glands, as well as the pathway structures through entire biopsies and other morphological features. These aspects hold the potential to be linked with biochemical recurrence (BCR) outcomes. This study highlights the potential of features derived from the 3D structure of glands in samples of patients with prostate cancer for identifying patients who are at higher risk of BCR.

Methods: Radical prostatectomy specimens were collected from 50 patients along with 5-year postoperative BCR follow-up from the University of Washington. A total of 118 *ex vivo* whole-biopsy 3D pathology images were obtained from RP by an open-top light-sheet microscopy platform. Images were converted into a synthetic CK8 immunofluorescence dataset using an image-sequence translation model. From these 3D images, a glandular structure mask was generated by a computer-vision algorithm. The 3D structure of prostate glands was modeled through a Tree-structure Extraction Algorithm for Accurate and Robust Skeletons (TEASER), which provides a simplification of the length of the gland, its shape, and its pathway. 91 features were then extracted from the glandular skeleton architecture. A 3-fold cross-validation approach was used in which patients were divided into training (D_1) and test (D_2) sets of 33 and 17 patients, respectively. Fisher's score, used to select features based on their correlation to the outcome, was applied to D1 to identify the top 5 features most correlated with BCR. We then utilized these features to train a K-Nearest Neighbors classifier on D_1, aimed at predicting whether a patient would experience BCR. The model's performance was evaluated on D_2 and averaged across all folds.

Results: The classifier was able to accurately differentiate between BCR+ and BCR- patients, achieving an average ROCAUC of 0.73 (±0.04) in D_2. Significant differences in 3D skeletal features were observed between BCR+ and BCR- groups ($p<0.05$). Among the five selected features, three were related to the length and diameter of the gland, with the longest glands observed in BCR- patients. The remaining two features pertained to gland curvature and tortuosity, revealing more twisted glands in BCR+ patients.

Conclusion: Features derived from a skeleton model of the 3D glandular structure of biopsies showed promise in identifying patients with prostate cancer who are at a higher risk of BCR. Additional, multi-site independent validation of these findings is warranted.

#3517 A deep learning-based virtual staining system with multimodal-attention for precision medicine.

Z. Zhou[1], Y. Jiang[2], R. Li[1], L. Xing[1];
[1]Stanford University, Stanford, CA, [2]Wake Forest University School of Medicine, Winston Salem, NC

Purpose: This study introduces a novel multimodal-attention-based virtual mIF staining (MAS) system designed for efficient, reliable virtual mIF staining from label-free fluorescence images. Our goal was to overcome the performance bottleneck and time-cost limitations associated with traditional mIF techniques and thereby enhance their clinical utility.
Method and Materials: Our approach involved developing a cutting-edge MAS model. This model is built upon a sophisticated end-to-end generative convolutional neural network (CNN) architecture. It ingeniously leverages autofluorescence and 4',6-diamidino-2-phenylindole (DAPI) slides as inputs to generate mIF images. To achieve this, we equipped the model with feature extractors enhanced by pretrained masked auto-encoders (MAEs) and a self-attention combination strategy. These components worked harmoniously to extract antigen-label-related features and precisely locate specific cells within the images.
Results: In our comprehensive study, we engaged 94 gastric cancer patients, utilizing the MAS system for automated virtual mIF staining of seven biomarkers, namely CD3, CD20, FOXP3, PD1, CD8, CD163, and PDL1, in both cancerous and non-cancerous tissues. Importantly, the MAS-produced virtual mIF stains matched the quality of traditional manual stains. Furthermore, we validated the prognostic accuracy for gastric cancer using these virtual mIF images, demonstrating their ability to provide clinical information that is as reliable and valuable as that obtained from manually stained mIF images.
Conclusions: Our study identifies the MAS system as an important advancement in mIF staining, enhancing personalized medicine with its efficiency and quality. This tool holds significant potential to enable personalized medicine efficiently and cost-effectively, streamlining the process of diagnosing diseases, making prognoses, and developing treatment plans.

Quantitative Comparison of Ablation Experiments for MAS system in predicting multiple biomarkers

Biomarkers	Index	U-Net (Avg±Std)	ReU-Net (Avg±Std)	Att-ReU-Net (Avg±Std)	MAS (Avg±Std)
CD3	PSNR	27.053±4.10	27.419±4.15	28.073±4.00	**28.546**±4.40
CD3	SSIM	0.733±0.07	0.724±0.07	0.728±0.05	**0.742**±0.07
CD20	PSNR	28.835±4.66	**29.244**±4.76	28.672±4.52	29.243±4.99
CD20	SSIM	0.921±0.058	0.921±0.057	0.915±0.051	**0.923**±0.051
FOXP3	PSNR	31.769±3.29	31.838±3.10	31.098±3.20	**31.862**±3.11
FOXP3	SSIM	0.613±0.11	**0.618**±0.11	0.617±0.112	0.617±0.12
PD1	PSNR	27.908±4.47	27.950±4.43	30.283±4.37	**31.717**±4.17
PD1	SSIM	0.654±0.13	0.659±0.13	0.694±0.12	**0.726**±0.11

#3518 Next generation H&E cell modeling: Using same-slide multiplex immunofluorescence (mIF) data to train H&E.

B. Arbiv, A. Bart, T. Dankovich, R. Elran, S. Bookstein, A. Laniado, T. Dicker, S. Dagan, O. Puig, K. Bloom, E. Markovits;
Nucleai, Chicago, IL

Haematoxylin & Eosin (H&E)-based deep learning algorithms require a large number of human-based cell annotations for model training, and are limited by what a human eye can see. Multiplex immunofluorescence (mIF) offers a more comprehensive and accurate method for classifying cells because annotations are based on cell status, i.e. whether a cell expresses certain markers or not. In this study, we leverage mIF-based cell type predictions[1] to enhance H&E model performance.We used a publicly available CODEX/PhenoCycler dataset[2] consisting of 140 tissue cores obtained from 35 patients with colorectal cancer, which were stained with 56 protein markers and subsequently with H&E. mIF data was used to create over 60,000 prediction-based annotations on the corresponding H&E-stained images that were used to train deep learning H&E classifiers.

The final model performance reached AUC of 0.91 when evaluated on the H&E test annotations and 0.90 on the mIF predictions. Notably, the mIF annotations-based H&E model surpassed the manual annotations-based H&E model in effectively identifying challenging cell types, demonstrating its superior performance. These findings highlight the potential of leveraging mIF cell type predictions to train accurate and automated H&E models.

[1]Markovits et al, BioRxiv, https://doi.org/10.1101/2022.11.09.515776[2]Schürch et al, Cell. 2020,182(5): 1341-1359.PMID: 32763154

#3519 Reconstructing a latent representation of gene expression from genomic alterations to improve clinical utility of real-world clinicogenomics data.

M. Baron, S. Kumar, F. Kuperwaser, D. Tracy, E. Vucic, J. Sherman;
Zephyr AI, McLean, VA

Background: Molecularly and clinically well-annotated patient datasets are ideal for studying tumor biology and developing robust machine learning (ML) models for predicting outcome and treatment response. These data however rarely exist in real-world settings or in sufficient quantities within research contexts. Large publicly available datasets like The Cancer Genome Atlas (TCGA) which provid multi-omic profiles for diverse cancer types, have profoundly advanced cancer research and facilitated development of novel therapies and personalized medicines. However, the absence of patient outcome data tied to treatment limits the applicability of these data for understanding and modeling treatment response. Real-world clinicogenomics cohorts, such as the AACR Project GENIE, on the other hand are typically very rich in clinical annotations, including treatment regimens and outcomes measures. These data are however sparsely annotated for patient tumor molecular profiles, rarely exceeding ~100's of genes profiled. We hypothesized that it would be possible to reconstruct latent tumor mRNA representations from limited genomic and clinical data available in real-world clinicogenomic cohorts, and that these reconstructed expression profiles would be useful for a variety of clinically meaningful downstream applications.

Methods: We developed an ML model, called Mut2Ex, to reconstruct tumor gene expression profiles using genetic information available on commercial next generation sequencing panels using a Principle Label Space Transformation (PLST) we adapted to regression problem, along with embeddings from clinical information (OncoTree code, sex and stage) generated by a language model. Mut2Ex was trained on ~1200 cell lines from DepMap representing 26 cancer types, to generate ~2000 reconstructed mRNA gene profiles that were applied to a variety of clinical tasks. We used Mut2Ex to reconstruct mRNA profiles for ~10,000 tumors from TCGA and ~180,000 tumors from AACR Project GENIE.

Results: Reconstructed mRNA expression by Mut2Ex was highly correlated with true expression in cell lines (rho = 0.926, [0.924-0.928 95% CI, N = 1184]). Compared to true expression, reconstructed profiles recapitulate sub-clusters within cancer types, PAM50 subtyping in breast tumors, survival signatures in colorectal tumors and multiple oncogenic signatures in a pan-cancer manner. Analysis of reconstructed expression for AACR Project GENIE tumors revealed expected enrichment of known driver genes within expression subtypes and enrichment of oncogenic signatures associated with distinct clinical outcomes in a cancer type specific manner.

Conclusions: Our flexible analytic framework for reconstructing gene expression profiles from clinicogenomics data substantially augments the clinical utility and value of data acquired in real-world settings.

#3520 A scalable single cell RNA-seq pipeline leveraging machine learning and high-quality references for cell-type prediction.

A. Dasgupta[1], G. Duclos[2], R. Miragaia[3], B. Manry[1], E. Jacob[2], N. Markuzon[2], A. Rotem[2];
[1]AstraZeneca US, Gaithersburg, MD, [2]AstraZeneca US, Waltham, MA, [3]AstraZeneca UK, Cambridge, United Kingdom

Single cell RNA-seq (scRNA-seq) technology transformed our understanding of biology at the cell level. Inferring cell types provide insights into the relative abundance of, and genomic differences between, different cell types. Current methods leverage known cell type markers and genomic similarity measures to attribute cell types to groups of cells.

We present a scalable machine learning-based pipeline that can leverage high quality reference annotation data to infer cell types quickly for multiple scRNA-seq experimental samples. This pipeline leverages two machine learning technologies: variational autoencoders (VAE) to create a low-dimensional representation of the reference transcriptome; and, supervised learning methods that use this representation to learn cell types from the reference data. This pipeline can quickly score new experimental data using GPU-enabled computing platforms and provide probabilities of a cell being each cell type present in the reference data.

This novel pipeline is evaluated using 5 public reference data sets. We evaluate whether VAE-based representations benefit supervised learning, compared to PCA and t-SNE. We next evaluate different supervised learning methods for predictive performance. Finally, we compare the pipeline's performance with commonly-used cell type prediction algorithms (Seurat, scANVI). We find that using a VAE is generally better than both PCA and t-SNE for feature generation to predict cell type. Using the VAE representation, there is no significant difference in accuracy between logistic regression and other supervised learning algorithms. Finally, using logistic regression as the learning machine, this pipeline is as accurate as Seurat and better than scANVI, while running about 2-5x faster than Seurat.

Algorithm	PBMC (10X)	HLCA	Eraslan snRNA	Blueprint Breast	Blueprint Lung
Our pipeline	92 (87-95)	92 (88-93)	93 (90-97)	89 (80-96)	97 (95-99)
Seurat	96 (95-97)	90 (94-98)	94 (93-97)	96 (87-98)	98 (94-99)
scANVI	91 (84-95)	72 (78-86)	92 (88-96)	94 (80-97)	88 (86-100)

Table 1 Balanced accuracy (%) from leave-one-subject-out cross-validation across 5 public data sets. Intervals are the range of the metric across the cross-validation folds.

#3521 Robust inference of PTEN deletion in prostate cancer from routine histopathology whole slide images using attention-based deep learning.

F. Scarfo[1], M. Omar[2], L. Marchionni[2];

[1]IRCCS Ospedale San Raffaele, Milan, Italy, [2]Weill Cornell Medicine, New York City, NY

The diagnostic workup of prostate cancer (PCa) requires a thorough manual histopathological inspection of prostate tissue specimens stained with hematoxylin and eosin (H&E). While immunohistochemistry and advanced molecular tests like FISH could uncover key genetic alterations, they are not cost-effective and often require special training, necessitating the development of more effective tools that can accurately infer the status of such alterations directly from the tissue morphology depicted in routine H&E-stained glass slides. PTEN deletion, which is present in 15-20% of PCa, is significantly associated with tumor aggressiveness and negative prognostic impact. Deep learning (DL) models can be trained to predict the presence of PTEN deletion on routine whole slide images (WSIs) and select patients that could benefit from further treatment. In this study, we trained and tested the performance of a weakly supervised, multiple-instance learning network on a cohort of 449 WSIs radical prostatectomy specimens stained with hematoxylin & eosin. Our model demonstrated robust performance in predicting PTEN loss based on tumor morphology alone. Through the model, we also generated attention heatmaps of the most informative tiles of each slide, allowing us to quantify the different cellular components, thus inferring the morphological features associated with PTEN loss. This study shows that DL is a potential tool that can assist the pathologist in accurately inferring the molecular status of key genetic alterations using the tissue morphology depicted in histopathology slides. Moreover, the morphological information that can be obtained by attention-based models can be leveraged to close the gap between the pathologist's morphological analysis and the interpretability of artificial intelligence models.

#3522 Application of large language models to nucleotide sequences for profiling signaling pathway disruptions in ovarian cancer patients.

D. K. Chebanov, N. S. Tatevosova;
BioAlg Corp., Covina, CA

Ovarian cancer is a challenging disease, often exhibiting recurrence after initial treatment. The complexity arises from simultaneous disruptions in multiple signaling pathways within tumor cells, rendering targeted inhibitors ineffective in providing sustained therapeutic impact. While targeted sequencing panels can identify specific therapeutically relevant events, they often fail to capture the complete picture of targetable tumor driving aberrations, and provide biomarkers relevant to disease resistance and/or recurrence. A potential solution lies in comprehensively defining the landscape of signaling pathway alterations by identifying molecular triggers underlying their dysregulation. While individual DNA mutations sometimes may not lead to carcinogenesis or changes in tumor cell behavior, combination of deactivating mutations in suppressor genes, can influence tumor development and prognosis, warranting a comprehensive delineation of their effect on the broad signaling network level. To this end, we propose the Large Language Models (LLMs), which have been successful in natural language processing, particularly in understanding context. Such tools are essential for discerning the effect of mutation combinations, their physical proximity to other mutations, and functional gene regions. We obtained mutation annotation files for 177 ovarian cancer patients from the TCGA database, reconstructing consensus nucleotide sequences using a reference genome. To input this data into LLMs, we generated embeddings for these sequences using the Nucleotide Transformer algorithm, pre-trained on 500 million variants of the reference genome. Additionally, we extracted data on detected disruptions in 10 signaling pathways (Cell Cycle, HIPPO, MYC, NOTCH, NRF2, PI3K, RTK RAS, TP53, TGF-Beta, WNT) for these patients from TCGA. Each pathway was associated with the percentage of its alteration. We trained a deep learning algorithm on these data to predict a combination of 10 numerical values, each corresponding to the percentage of disruption for a given signaling pathway. Our findings revealed that nearly half of the patients exhibited disruptions in 5 or more signaling pathways. The algorithm developed enables the determination of the extent of disruption in each pathway based on whole exome sequencing results. This approach facilitates more informed treatment strategy planning and enhances the efficient development of new drugs for ovarian cancer treatment.

#3523 Self-supervised foundation model captures high-dimensional morphology data from single cell brightfield images.

K. Saini, S. Zhang, R. Carelli, K. B. Jacobs, A. Wong-Thai, C. Luengo, V. Lu, A. Mavropoulos, A. Jovic, J. Mei, T. Vollbrecht, S. C. Boutet, M. Salek, M. Masaeli; Deepcell Inc., Menlo Park, CA

Our knowledge of cancer biology has advanced with the characterization of distinct cell types and cell states within heterogeneous tumor environments. Many methods for imaging and sorting tumor cells require biomarker labels that alter cell characteristics and create a selection bias. The use of label-free single-cell methods should further improve cancer studies involving viable, unperturbed cells for downstream assays such as RNA-Seq, cell culture expansion, and functional assays. To eliminate biomarkers and enable broader assessment of cells, we developed REM-I, a platform that characterizes and sorts unlabeled single cells based on high-dimensional morphology. Cells are captured with brightfield imaging and processed in real-time by self-supervised deep learning models to generate quantitative AI embeddings representative of cell morphology. A significant technical challenge in building REM-I was developing an AI model based on extracted features from cell images without prior knowledge of cell types, cell preparation, or other application-specific knowledge. Accordingly, we developed the Human Foundation Model (HFM), a hybrid architecture that combines self-supervised learning (SSL) and morphometrics (computer vision) to extract 115 dimensional embeddings representing cell morphology from high-resolution REM-I cell images. SSL produces a foundation model with high generalization capacity that enables hypothesis-free sample exploration and efficient generation of application-specific models. Meanwhile, computer vision extracts features that represent measurable and interpretable concepts (e.g., cell size, shape, texture, intensity). The training process for the HFM self-supervised backbone model utilizes the discriminatory power of supervised tasks. Using synthetic cells and three cancer cell lines, we trained and then validated the reproducibility and generalization capabilities of the resulting model. Results show combining deep learning and morphometrics improve interpretability of data and enable rapid characterization and classification of tumor cells with high accuracy. We also report on the Deepcell® Axon data suite, a tool to analyze data and customize reusable workflows. This includes the ability to store and manage data, visualize high dimensional data as low-dimensional projections, and train classifiers to identify and sort cell populations. To enable compatibility with user-preferred downstream analysis pipelines, Axon provides data export options for images, plots, and embeddings. Our approach allows users of all skill levels to access and interpret AI-enabled morphological profiling. Applications of REM-I include hypothesis-free evaluation of heterogeneous tumor samples, label-free cancer cell enrichment, characterization of distinct cell states, and multi-omic integration.

#3524 Leveraging ChatGPT for literature-based inference of drug-gene relationships in cancer.

Y. Shin, **M. Ning**, L.-J. Wang, Y. Huang, Y.-C. Chiu;
UPMC Hillman Cancer Center, Pittsburgh, PA

Approximately 5,000 new articles are indexed by PubMed daily, many providing critical insights into novel gene-drug relationships. However, searching and distilling the wealth of biomedical literature to infer specific pharmacogenomic relationships between a gene and a drug poses a significant burden for researchers. Recent advances in large language models, such as ChatGPT, offer a promising solution to tackle this challenge. This study aims to prototype a literature-based inference for drug-gene relationships in the context of cancer using ChatGPT, marking an exploratory effort in this emerging domain. Our approach involves developing an automated pipeline that integrates the Application Programming Interfaces (APIs) of PubMed and ChatGPT, specifically GPT-3.5. Given a gene, a drug, and a disease, the pipeline searches PubMed for relevant articles and extracts their abstracts. Leveraging prompt engineering techniques, we formulated a prompt that facilitates accurate summarization of these abstracts. The output of our pipeline includes three key components: 1) a concise, one-sentence summary elucidating the relationship between the drug-gene pair; 2) a step-by-step explanation of the inference process; and 3) the confidence level associated with the generated summary. Our approach was able to confirm well-known gene-drug relationships in cancer, such as palbociclib and *CDK4*. We further examined a challenging case of CX-5461, an inhibitor of ribosomal RNA synthesis currently under clinical investigation for various cancers. Until recent evidence emerged in 2021, this drug was mischaracterized as an RNA-Pol I inhibitor, whereas it primarily targets topoisomerase II beta (*TOP2B*). Notably, our pipeline correctly identified *TOP2B* as the primary target of CX-5461, despite an extensive body of literature prior to 2021 supporting the RNA-Pol I relationship. To evaluate the sensitivity of our pipeline, we conducted a systematic assessment using a mixture of relevant and irrelevant abstracts. Utilizing bevacizumab, VEGF, and hepatocellular carcinoma as a demonstrating example, we showed that ChatGPT achieved nearly 95% accuracy even when only 30% of the abstracts were relevant to the case. In summary, this pilot research serves as a foundational step towards the utilization of large language models in the field of drug discovery and development. Our ongoing efforts involve the rigorous evaluation of our approach across a diverse spectrum of drug targets and cancer types, as well as the optimization of prompts through state-of-the-art prompt engineering techniques.

#3525 Towards the efficient design of shared neoantigen peptide cancer vaccines using artificial intelligence.

G. Zhang[1], J. Du[1], X. Gao[1], T. Wang[1], Z. Wang[1], Q. Zhang[1], T. Liu[1], D. Chen[1], R. Zhu[1], Y. Zhao[1], C. Li[2], M. Toh[2], **L. Lai**[1];
[1]Xtalpi, Beijing, China, [2]CK Life Sciences Development Limited, Hong Kong, Hong Kong

Background: The advent of immune checkpoint inhibitors has improved morbidity and mortality for some cancers, and recent breakthroughs in gene & cell therapy have shed light on curing some types of blood cancers. However, many cancers remain intractable and the development of novel, effective and safe therapies continue to be a priority. Cancer vaccines as a cancer immunotherapy approach has seen a resurgence in recent years, due to the success of mRNA vaccines for the COVID-19. However, the accurate prediction of immunogenicity of cancer vaccines remains elusive.
Methods: Our models predict the probability of a given peptide derived from the protein of interest to be presented by MHC-I or MHC-II. For MHC-I antigen presentation model development, over 17 million entries in the dataset were collected from published literature and available databases, e.g., IEDB, with peptide lengths ranging from 8 to 11. The peptides were restricted to 150 unique MHC-I alleles. Similarly, ~4 million entries with peptide lengths ranging from 13 to 21 were collected for MHC-II antigen presentation model development, and the peptides were restricted to 19 unique MHC-II alleles. To develop advanced antigen presentation models, a language model was chosen as the backbone network and contrast learning was used to better discriminate the peptide-MHC match versus mismatch. Overall, both MHC-I and MHC-II presentation models were constructed with about 30 million parameters. To validate the model prediction accuracy, automated peptide synthesis and surface plasmon resonance (SPR) technologies were applied.
Results: Using open-sourced data, our developed AI models surpassed the performance of state-of-the-art prediction algorithms, the latest versions of NetMHCpan and MixMHCpred, for both MHC-I and MHC-II antigen presentation. Furthermore, to validate the algorithm accuracy and the peptide immunogenicity, 28 predicted patentable peptides derived from mutated TP53 protein were synthesized and their binding to respective common HLA alleles were validated using SPR. We found that greater than 80% of the peptides display binding affinities that are stronger than the positive control, suggesting that AI significantly improves neoantigen peptide vaccine design.
Conclusions: We developed advanced AI algorithms to rapidly design shared neoantigen T cell epitopes with predicted strong binding affinity to MHC-I and MHC-II. We envision that the epitopes predicted and designed by our AI algorithms possess great potential in advancing the field of off-the-shelf cancer vaccine development and hold the promise of significantly benefiting patients, once translated into the clinic.

#3526 GAIN-BRCA: A graphical explainable AI-net framework for breast cancer subtype classification using multiomics data.

J. Patel, S. K. Shakyawar, S. Sethi, C. Guda;
University of Nebraska Medical Center, Omaha, NE

Higher standards for precise distinction and classification among the four breast cancer subtypes, i.e., Luminal A, Luminal B, HER-2-enriched, and Basal, are essential to delivering customized treatment in precision oncology. The effective integration of readily accessible multi-omics datasets from the same patient may improve the accuracy of subtype prediction algorithms and help decipher reliable molecular features for the prediction and prognosis of breast cancer. Previous models for predicting breast cancer subtypes relied mostly on concatenation and autoencoder methods but rarely utilized graph-based integration to leverage the biological associations among omics datatypes. To overcome these limitations, we developed a graph-based multi-omics integration method using features from mRNA, DNA methylation, and miRNA data and synthesized features from their interactions. GAIN-BRCA computes weightage scores from miRNA-mRNA and DNA methylation-mRNA interactions to derive a new transformed feature vector without compromising biological information. The neural network architecture was designed and trained on the transformed features to classify breast cancer subtypes. Neural network prediction accuracies were compared using concatenated, autoencoder, and GAIN-BRCA-based integrated datasets. GAIN-BRCA outperforms the existing similar models MOGONET (Acc: 0.72) and moBRCA-net (Acc: 0.86) with an accuracy of 0.91. These transformed features were then processed using SHAP, and the top 357 features were selected for functional characterization and pathway analysis. We identified specific pathways and genes related to each breast cancer subtype separately. The most enriched pathways found in each subtype are ribonucleotide reductase signaling and glucocorticoid signaling pathways in luminal A, PFKB4 signaling pathway in luminal B, adipogenesis and DNA methylation and transcriptional signaling in HER2+, and the role of OCT4 in mammalian embryonic stem cell pluripotency in basal. Similarly, the most discriminated gene features are BRAF, ESR1, KRAS, MAPK1, SMARCE1, PPP3CA, and TGFBR2 in luminal A, TGFB3 and NCOA3 in luminal B, HNF4A, SIN3A, and SOX9 in HER2+, and POU5F1 and FOXA2 in basal subtypes. The GAIN-BRCA framework, combined with SHAP, weighs independent omics as cross-disciplinary rather than multidisciplinary and presents a distinctive picture for each subtype. As a result, the framework presents the importance of features about the corresponding subtype, which might lead to a greater understanding of the molecular basis of breast cancer subtypes.

#3527 Application of a deep learning based drug sensitivity prediction model on a novel anticancer drug.

N. M. Chand, V. Vishnudas, M. A. Kiebish, A. Thakurta, N. R. Narain, S. Gesta, G. M. Miller;
BPGbio Inc., Framingham, MA

Discovery of a candidate drug molecule through the preclinical stages is an iterative multiparametric process until a candidate is selected for investigational new drug submission enabling studies. This iterative approach takes up significant time and effort to design, synthesize, and test new compounds. A specific testing step is evaluation of half maximal inhibitory concentration (IC50) of compounds on cell line (CL) models. To augment CL testing, computational approaches predicting the IC50 of a drug can be used to guide choice of optimization as the molecule goes through hit to lead optimization onto candidate selection. DeepDSC [1] is a deep learning (DL) model developed to predict the IC50 in a specific CL of a given drug by integrating public data from large-scale drug screens and high-throughput RNAseq profiling. The Cancer Cell Line Encyclopedia (CCLE) [2] and Genomics of Drug Sensitivity (GDSC) [3] projects compiled pharmacological profiles of 23 and 139 drugs across 491 and 655 cancer CLs, respectively. A 10-fold cross validation (CV) approach was employed to train DeepDSC on the datasets independently and reported the average root mean squared error (RMSE) and the coefficient of determination (R^2) on the held-out sets across the folds. However, the model's generalizability to novel compounds not in the dataset, specifically compounds that are structurally dissimilar, is yet to be tested. In this regard, the DeepDSC model was retrained, with modifications, on a subset of the GDSC dataset - GDSC2 - to access the generalizability of DL models on BRG399, a proprietary microtubule targeting agent (MTA) developed by BPGbio Inc. GDSC2 was used since data generated for BRG399 and GDSC2 share the same potency assay (CellTiter-Glo [6]). The GDSC2 set was split into training and held-out sets using a 80-20 random split. Further, we chose to optimize the learning rate for both the autoencoder and feed forward networks (FFN), and the L2 regularization factor for the FFN only. Hyperparameters were optimized using 5-fold CV on the training set. Finally, we evaluated the predictive performance of the model on BRG399, which was not present in the training set. We encoded each compound in GDSC2 (n=234) using Circular Fingerprints [4] and observed an average Jaccard (or Tanimoto) distance (JD) [5] of 0.892 across 27261 drug pairs. BRG399 showed an average JD of 0.873 across 234 drug pairs, with the most similar compound JD of 0.785. Our retrained DeepDSC model had RMSE 1.15 and R^2 0.82 on the training set and RMSE 1.19 and R^2 0.86 on the held-out set. However, on BRG399 tested CLs (n=101) model had RMSE 1.84 and $R^2 < 0$, which indicated that predictions were on average worse compared to a mean-predictor model for BRG399. These results suggest that DL models that can generalize predictions to a held-out set for compounds that were present in the training set may not accurately predict IC50 of novel compounds not in the training set.

#3528 Constructing knowledge graph of N^6-methyladnosion regulations in cancer from literature using ChatGPT-4.

S. Jo[1], X. Wu[1], Y. Zeng[2], A. Das[2], T.-H. Zhang[2], D. A. Spellman[2], A. Ferris[2], S.-J. Gao[2], J. Zhang[3], Y.-C. Chiu[2], Y. Huang[2];
[1]University of Pittsburgh, Pittsburgh, PA, [2]University of Pittsburgh School of Medicine, Pittsburgh, PA, [3]The University of Texas at San Antonio, San Antonio, TX

N^6-methyladenosine (m^6A) is the most abundant mRNA modification with a crucial role in cellular processes. Its involvement in cancers is well-established. Dysregulation of m^6A is linked to cancer initiation, progression, and therapy resistance, impacting the tumor microenvironment (TME) and promoting metastasis. Understanding m^6A's regulatory role in cancer is essential for identifying new therapeutic targets. We considered the construction of a knowledge graph (KG) representing molecular regulatory mechanisms (MRMs) of m^6A in healthy conditions and different cancers from PubMed papers. Such a KG consists of interconnected triplets of (head node, regulatory relationship, tail node), each denoting regulation between genes or a gene and a phenotype/process. Advances in natural language processing (NLP) have provided tools such as SemRep and GNBR to automate the extraction of these triplets from the literature. However, these methods don't extract contextual information, such as the type of cancers or cells in which these MRMs occur, leading to contradictory regulations in the constructed KG. In addition, existing approaches were designed to extract generic regulatory relations and therefore struggled in properly capturing unique concepts associated with m^6A regulatory mechanisms. To tackle this challenge, we designed a novel ChatGPT-4 prompt to extract relational graphs from papers tailored for m^6A regulatory mechanisms. An annotated dataset of 400 titles on m^6A-related MRMs were created to evaluate the performance. We then applied the prompt to 1023 papers to create a m^6A Molecular Regulatory Mechanism Knowledge Graph (m6A-MRM-KG). This graph illuminates m^6A's roles in gene expression regulation, especially in cancer and immunity. Anticipated to enhance our understanding of cancer development, it provides insights into potential therapeutic strategies. The m6A-MRM-KG not only organizes information but also empowers researchers to uncover novel insights in the dynamic relationships of m^6A modifications in diverse biological contexts.

#3529 Leveraging deep learning for fully automated analysis of pre-clinical mouse positron emission tomography.

H.-Y. Lee, M. Goryawala, T. Sproul, M. Louie, D. Suhy;
Earli Inc., Redwood City, CA

Turning early-cancer diagnosis into actionable treatment often relies on highly accurate and sensitive imaging techniques to guide surgical intervention or to monitor therapeutic efficacy. Earli is developing a highly sensitive, orthogonal approach that uses genetic constructs to usurp dysregulated cancer pathways to force the tumor to produce a PET reporter gene, enabling the use of radiotracers amenable to positron emission tomography/computed tomography (PET/CT) to guide precision imaging. However, analysis of PET/CT images using standard manual and semi-automated methods is challenging resulting in reduced experimental throughput and user variability, highlighting the need for a fully automated PET/CT analysis pipeline using Deep Learning (DL). To increase pre-clinical throughput and reduce inter-user variability, we developed an automated DL processing pipeline in Python to perform three major tasks: separation of multi-mouse bed data for PET uptake quantification by mouse, segmentation of tumors and background organs, and quantification of PET signal for PK/PD analysis. Preclinical PET/CT data was acquired using a 4 animal, multi-mouse bed and separated into individual mice by co-registering the reconstructed CT image against a multi-mouse bed reference mask using a rigid 3D Euler transformation algorithm and cropping at fixed indices. Following mouse separation, a 3D nnUNet architecture is used to perform semantic segmentation of regions of interest (ROI) on CT for bi-hemispheric subcutaneous tumors, lungs, liver, kidneys, spleen, and the bladder. nnUNet was trained on PET/CT of 311 mice consisting of a mixture of naïve and tumor-bearing animals subcutaneously implanted with H1299 cells using a five-fold cross-validation strategy with 1000 epochs per fold. Model performance was evaluated by comparing the network prediction to the reference manually annotated masks using the Dice coefficient. PET uptake is reported as percent injected dose per milliliter (%ID/mL) or standardized uptake value (SUV). Segmentation performance results for the hold-out set identified mean Dice scores greater than 0.80 for all ROIs, reflecting the similarity between model predictions and human annotations. The automated pipeline reduced the analysis time from 5.5-6 hours per mouse when using traditional manual/semi-automatic approaches to approximately 15 minutes. In summary, we developed a fully automated DL-based PET/CT quantification pipeline for pre-clinical mouse studies that provides accurate ROI segmentation and PET uptake quantification, significantly increasing experimental throughput and reducing inter-user variability. Further improvements to model inference include loss functions weighted for poor performing ROIs and addition of lung nodule segmentation for eventual translation to humans as an accompaniment to Earli's theranostic programs.

#3531 PRESS*NET*: Patient stratification and biomarker discovery using multi-modal knowledge graph framework.

K. C. Bulusu[1], J. Cohen-Setton[1], I. Kagiampakis[2], M. Goncalves[1], G. Edwards[1], S. Jayabalan[3], S. Shikare[1], K. Tsang[1], B. Sidders[1], E. Jacob[3];
[1]AstraZeneca UK, Cambridge, United Kingdom, [2]AstraZeneca US, San Francisco, CA, [3]AstraZeneca US, Waltham, MA

Background: Multiomics data is critical to obtain a near comprehensive picture of disease progression and drug response. In addition, the generation of response and survival biomarkers, and the segmentation of patients into subtypes with distinct, actionable 'omic signatures and survival trajectories, is vital for personalised medicine research and successful trial design. However, as the volume and diversity of data increases, so too does the challenge of effective multiomic data integration. Knowledge graphs (KGs) can capture heterogeneous data and relationships between entities in a flexible and scalable data structure, making them suitable for this domain. We have developed PRESS*net*, a framework for building Patient KGs and analysing clinical data for novel patient stratification hypotheses and clinical biomarker discovery.

Methods: PRESS*net* is an end-to-end framework that turns raw patient data into graph-derived insights. Firstly, the user chooses which modality files to include, what assumptions to make about data processing, and which graph algorithms to use. PRESS*net* then automatedly creates a patient KG of the input data, where nodes represent patients and their associated features. In addition, biomedical prior knowledge, for example in the form of gene-pathway or gene-gene relationship data, is also integrated with the graphs. Insights are generated from the KG via community detection, graph embedding generation, and graph neural networks; these generate hypotheses for novel patient subtypes or biomarkers for clinical outcomes. As graph algorithms capture interrelationships between nodes, PRESS*net* offers biomarkers that are composite, i.e. that can contain features from multiple 'omics and clinical features.

Results: We applied PRESS*net* to the MSK 2022[1] cohort of IO-treated LUAD patients, and it uncovered prognostic composite biomarkers that stratified biomarker-positive patients from the whole cohort with a p value < 0.001 (95% CI) for OS, including known markers of poor prognosis such as STK11, RBM10, KRAS and KEAP1 mutations, and high neutrophil/lymphocyte ratio. We also generated embeddings of patients in the cohort and predicted survived/deceased status with an AUC of 0.82, outperforming published state-of-the-art.

Conclusions: We have successfully developed a generalisable framework for generating insights from patient data using state-of-the art knowledge graph data science. PRESS*net* can generate novel stratification and biomarker hypotheses that can potentially inform the next generation of IO targets and clinical biomarkers.

Footnotes[1] Vanguri et al., "Multimodal integration of radiology, pathology and genomics for prediction of response to PD-(L)1 blockade in patients with non-small cell lung cancer", Nat Cancer. 2022

#3532 Transforming genomic data into images for enhanced deep learning in precision oncology.

M. Islam, L. Xing;
Stanford University School of Medicine, Palo Alto, CA

Purpose: In the realm of cancer treatment and research, the analysis of genomic data stands as a cornerstone for diagnosis and therapy. Recognizing this, our study embarks on an ambitious journey to revolutionize how we interpret such data. By converting complex genomic data into a two-dimensional (2D) image format leveraging feature correlations, we pave the way for more profound insights and applications in clinical decision-making. This innovative approach utilizes 2D convolutional neural networks (CNNs) to analyze these structured images, promising a leap forward in the accuracy and utility of such data.

Methodology: The core of our method involves a novel transformation of tabular genomic data into an image format. We start with m patient samples, each characterized by n genes, and calculate a pairwise correlation matrix to capture the intricate relationships between these genes. Concurrently, we generate an Euclidean distance matrix that represents the distances between n points in a 2D grid. The next step involves the optimization of the Gromov-Wasserstein discrepancy to align these two matrices, resulting in a transformation matrix, T. When applied to the tabular data, T transforms it into m distinct, informative images. These images are then processed using a 10-layer CNN, comprising a convolutional layer (3x3 kernel), three dense layers, two relu layers, and a dropout layer.

Data Sources: We created images, termed 'genomaps', from genomic data collected from three diverse patient groups: 130 individuals (cancerous and normal) from Stanford Hospital, 230 breast cancer patients from The Cancer Genome Atlas (TCGA), and a larger group of 1572 patients from the Memorial Sloan Kettering (MSK) Cancer Center. The created genomaps are visually interpretable, offering clear differentiation between cancerous and non-cancerous samples, which is pivotal for accurate analysis.

Outcomes: Our method demonstrates a remarkable 8% improvement in survival prediction accuracy in comparison to the existing methods. The employment of DeepSHAP in our analysis has allowed us to identify critical genes with greater precision than conventional methods. The p53 gene family, notably TP53 and TP63, was identified as significantly mutated in over 50% of all cancer types analyzed. Another critical discovery was the ERBB gene family, encompassing EGFR, ERBB2, ERBB3, ERBB4, which plays a dual role in tumor proliferation and influencing the immune response against tumors, a factor critical for immunotherapy strategies.

Conclusion: This research introduces a transformative approach to represent genomic data, utilizing 2D CNNs for in-depth analysis. It sets a new benchmark in classification and regression accuracy, offering a more interpretable pathway for biomarker discovery, significantly contributing to the field of personalized medicine and cancer research.

#3533 Spatially Resolved Laser-Activated Cell Sorting (SLACS) and AI integration for enhanced pathological analysis and biomarker discovery.

H. Jang[1], A. C. Lee[2], S. Lee[2], S. Kwon[1];

[1]Seoul National University, Seoul, Korea, Republic of, [2]Meteor Biotech, Seoul, Korea, Republic of

This study focuses on the integration of Artificial Intelligence (AI) with Spatially Resolved Laser-Activated Cell Sorting (SLACS) for enhanced pathological analysis and biomarker discovery. The primary approach involves using AI to automatically analyze slide images, identifying critical areas associated with diseases such as cancer or cells emitting specific signals. AI algorithms efficiently segment these significant regions or cellular groups, facilitating targeted analysis.

Following the AI-driven segmentation, SLACS comes into play, isolating the identified cells from the slide for further examination. This precise sorting allows for the focused study of cells relevant to disease processes, enhancing the efficiency and accuracy of pathological analysis.

The separated samples obtained through SLACS are then subjected to detailed analysis. This step is crucial for understanding the cellular mechanisms at play in disease states and for the identification of potential biomarkers. These biomarkers are vital for developing targeted therapeutic strategies and advancing personalized medicine.

By combining AI's advanced image processing and pattern recognition capabilities with the precision of SLACS, this integrated approach significantly improves the identification and analysis of disease-related cellular characteristics. It streamlines the process of isolating and studying specific cell populations, contributing to a deeper understanding of disease mechanisms and progression.

In conclusion, the synergistic application of AI and SLACS represents a significant advancement in pathological research and biomarker discovery. This methodology not only enhances the accuracy of disease marker identification but also opens new avenues for research and clinical application.

#3534 GeneLLM: Unveiling gene functions through literature-driven transformer embeddings.

A. Jararweh, K. Virupakshappa, O. S. Macaulay, A. Segura, O. M. Oyebamiji, Y. Hu, A. D. Sahu;
University of New Mexico, Albuquerque, NM

INTRODUCTION: Our understanding of gene properties has advanced through representation learning such as Alpha fold. Representation learning involves encoding the relationships between genes by embedding them into a numerical space. These embeddings, which capture complex genetic interactions and characteristics, can then be leveraged by machine learning models to predict various gene properties. Current embeddings derive from transcriptome or sequence data. Over the past 150 years, numerous experimental assays have uncovered gene functions and interactions- comprehensive knowledge documented in the literature but not always evident in transcriptome or sequence data. It has been posited that leveraging this knowledge to create gene embeddings; however, could result in machine learning models biased towards well-studied genes.

METHODS AND RESULTS: We tested this hypothesis by developing a novel knowledge-embedding framework, GeneLLM. During training, GeneLLM learns to comprehend summaries of every gene- a compressed form of published knowledge- using Large Language Models (LLMs), fine-tuned for downstream tasks mapping cellular properties and biochemical processes. Despite the expected bias towards well-known genes, GeneLLM surprisingly showed high predictive power for an array of gene properties. Compared to baseline models, GeneLLM boosted an increase in performance of 20.3% correlation in gene conservation across species, 8.6% and 57.2% prediction accuracy in subcellular localization and gene ontology respectively. GeneLLM also showed competitive results on solubility prediction with 0.91 accuracy and a correlation of 0.71 for tissue-specific expression levels for 1001 cell lines. We also showed that the bias toward well-known genes could be mitigated by combining GeneLLM representation with transcriptome or sequence-based embedding. The combined embeddings exhibited superior performance to their individual components which suggests that GeneLLM extracts views complementary to existing embedding methods.

CONCLUSION: The GeneLLM framework demonstrates the ability of LLMs to extract information from the rich knowledge available about the nexus of genes and their cellular traits. It also illustrates how bias in knowledge representation is complementary to other transcriptome and sequence-based information. This ability of GeneLLM to advance our understanding of genes, their roles in cellular processes, and their impact on oncogenesis, as well as in response and resistance mechanisms, highlights its potential in cancer research.

#3535 Seeking novel therapeutic targets in oncology using machine learning.

M. Quazi[1], S. Sirimulla[1], C. G. Bologa[2], A. Pushechnikov[1], N. Savchuk[1], **T. I. Oprea**[1];
[1]Expert Systems, Inc., San Diego, CA, [2]University of New Mexico School of Medicine, Albuquerque, NM

We developed 42 machine learning models using Knowledge Graphs (KGML), informed by data from Pharos (1), based on major resources like DepMap (2), Reactome (3), and STRING (4). Focused on 41 blood cancers, we utilized cancer-specific positive genes and 440 shared negative genes, using metapath and XGBoost (5).

Analysis of the top 500 genes from each model revealed 3,842 genes strongly linked to cancers, with 519 classified as “Tchem,”i.e., small molecule modulators are known (6). We focused on Tchem proteins given the notion that small molecules perturbing these proteins are already known, which accelerates drug discovery. A separate, 1SVM (one-class support vector machine) model was built using mode-of-action drug targets (6) (Tclin, N = 704) as input. This 42nd model evaluates the likelihood that a gene shares the characteristics of Tclin targets (“Tclin-like”). Of the 519 Tchem genes, 132 have “Tclin-like” probability above 50%. The top five “Tclin-like” genes are GAPDH, AKT1, HRAS, TLR4 and TP53, respectively; their role in cancer is well studied.

Our focus shifted to 19 genes that have limited or no known cancer associations, as evaluated by the DISEASES platform (7) - see Table 1. Three genes (LPAR5, GPR18 and FCER2) are associated with primary bone diffuse large B cell lymphoma, and 2 (ADCY1 and PLD1) with B cell prolymphocytic leukemia. Additional studies may elucidate their role in these malignancies. Five genes (IRAK3, EPHB1, ITPKB, ACVR2B and CAMK2D) are predicted to be relevant in 10 or more blood cancers. Machine learning may uncover overlooked, but potentially promising drug targets for leukemias, lymphomas and myelomas.

References 1. Kelleher KJ, et al. *Nucl Acids Res.* 2023; 51:D1405-16.2. Tsherniak A, et al. *Cell.* 2017; 170:564-76.e16.3. Gillespie M, et al. *Nucl Acids Res.* 2022; 50:D687-92.4. Szklarczyk D, et al. *Nucl Acids Res.* 2023; 51:D638-46.5. Binder J, et al. *Commun Biol.* 2022; 5:125.6. Oprea TI, et al. *Nat Rev Drug Discov.* 2018; 17:317-32.7. Grissa D, et al. *Database.* 2022; 2022:baac019.

Table 1: “Tclin-like” targets lacking known cancer associations.

Gene	**41 Cancer counts**	**Disease names**
LPAR5	1	primary bone diffuse large B cell lymphoma
ADCY1	1	B cell prolymphocytic leukaemia
ITPKB	15	
PLD1	1	B cell prolymphocytic leukaemia
PRKCE	2	hepatosplenic T cell lymphoma; acute leukaemia of ambiguous lineage
EPHB1	17	
GPR18	1	primary bone diffuse large B cell lymphoma
FRK	3	chronic myeloid leukaemia; acute myeloid leukaemia therapy related; NK cell leukaemia
CAMK2D	13	
IRAK3	20	
TRPV4	1	primary central nervous system lymphoma
ACVR2B	14	
TRPC6	1	Hodgkin lymphoma
FCER2	1	primary bone diffuse large B cell lymphoma
GRM8	1	acute myeloid leukaemia therapy related
CAMK2A	1	hepatosplenic T cell lymphoma
BLK	4	
ADORA3	1	acute leukaemic transformation of myeloproliferative neoplasm
PIM1	8	

#3536 Paracell: A high throughput, deep learning-based pipeline for single-cell phenotypic profiling.

D. L. Nguyen[1], J. T. Chao[2];
[1]Queen's University, Kingston, ON, Canada, [2]Sunnybrook Research Institute, Toronto, ON, Canada

Variants of uncertain significance constitute the vast majority of missense variants, hampering the utility of genetic testing, despite its remarkable impacts on clinical diagnosis and decision-making. Although the sequencing and interpretation of genetic variants have been drastically improved in recent years, only about 2% of novel missense variants are currently clinically actionable. Therefore, a robust and scalable pipeline is desperately needed to provide functional evidence critical for variant interpretation. In this work, we demonstrate Paracell, a deep learning-based phenotypic profiling pipeline that leverages subcellular segmentation, high-dimensional single-cell phenotyping, and machine learning to classify the functional impact of variants. Paracell captures heterogeneity in cellular phenotypes and protein colocalization between variants and their signaling partners, as well as subcellular markers, and enables analysis at a single-cell resolution. Using a classification model trained on single-cell features extracted by Paracell, we were able to accurately classify cells from loss-of-function (LoF) variants based on their impact. After aggregating cellular profiles on a variant level, our pipeline was able to distinguish LoF variants from functional ones with high sensitivity and specificity. Our work demonstrates that Paracell is a robust and scalable method that can sensitively detect differences in single-cell phenotypic profiles. The systematic application of this pipeline will provide valuable functional evidence for variant interpretation, enhancing their clinical utility and accelerating personalized cancer care.

#3537 Assessing machine learning models of drug response predictions using orthotopic patient-derived xenograft.

Y.-H. Chien, R. Pippa, W. Andrews, J. Rodriguez, K. Buck, D. Gorospe, E. Valencia, B. Carapia, E. Eastwood, J. Sperry, J. Nakashima, L. Do;
Certis Oncology Solutions, San Diego, CA

Accurate prediction of drug response using machine learning (ML) remains a significant challenge in drug development as well as in personalized cancer therapy. Furthermore, there is a scarcity of rigorous external validation studies for evaluating drug response prediction models. Even when available, such validations are often confined to in-vitro studies. Orthotopic patient-derived xenograft (O-PDX) mice serve as essential preclinical models that closely replicate the human tumor microenvironment and assess the therapeutic response to cancer treatments. We present CertisAI^{TM}, a novel ensemble of machine learning models that have been trained on a vast array of experimental high-throughput screenings of both monotherapies and combination therapies, incorporating over 4500 investigational and FDA-approved drugs across 10 major cancer indications. The results of our ML drug response prediction models show an average R^2 of 0.75 and RMSE of 0.62 (across internal 5-fold cross-validation) for all 10 cancer prediction models. Our evaluation of CertisAI's drug response predictions within O-PDX pharmacology studies has shown a notable overall correlation between actual observed tumor growth inhibition (TGI) and predicted TGI, with an r value of 0.45 across seven indications. The most accurate prediction model achieved an r value of 0.7 for colorectal cancer, encompassing 37 treatments in 6 O-PDX studies. Altogether, these results highlight CertisAI’s potential in enhancing pre-clinical model selection as well as personalized treatment strategies in oncology.

BIOINFORMATICS / COMPUTATIONAL BIOLOGY / SYSTEMS BIOLOGY / CONVERGENT SCIENCE: Database Resources, Statistical Methods, and Other Tools
Poster Session

#3541 Systematic assessment of the mechanism of action landscape of glue compounds.
L. Hu, C. Karan, A. Califano;
Columbia University Irving Medical Center, New York, NY

We have recently completed a large-scale project to elucidate the Mechanism of Action (MoA) of clinically relevant compounds in over twenty tumor specific contexts. Many novel, translationally relevant findings have arisen from this work, including (a) the identification of context-specific inhibitors of many proteins considered to be poor pharmacologic targets—including transcription (co-)factors and undruggable signaling proteins; (b) graph theory-based elucidation of drug polypharmacology; and (c) identification of MoA overlap between previously unrelated drugs. However, a limitation of the study is it relies on the existing repertoire of small-molecular inhibitors that is heavily biased towards specific target classes. Compounds that inhibit master regulators (MR) of tumor state are missing or under-represented. In this new project, we explore an extra molecular space of “molecular glues”, as they might be more effective modulators of MRs. Similar to our prior oncology drug study, we will leverage the automated PLATE-Seq technology and the VIPER algorithm to characterize compound MoA in a proteome-wide fashion. Specifically, we will first generate genome-wide RNA-Seq profiles of patient-matched cell lines using a panel of ~150 glue compounds, including a subset of them named PROteolysis TArgeting Chimeras (PROTACs) that were designed to degrade therapeutic targets by recruiting them to E3 ligases. We will analyze the PLATE-seq perturbational profiles with a set of complementary algorithms including the VIPER, which, akin to a multiplexed, tissue-specific gene reporter assay, can accurately measure the differential activity of over 6,000 regulatory/signaling proteins, by assessing the enrichment of their transcriptional targets in differentially expressed genes. Current effort of this project is focused on six PDA cell lines including three MAPK-pathway dependent (M+) and three MAPK-pathway independent (M-) contexts, each one representing the gastrointestinal lineage state (GLS), morphogenic state (MOS), and acinar to ductal metaplasia-like state (ALS). Using this data, we explore similarity-based connections between PLATE-seq perturbational profiles and the Connectivity Map (CMAP) that contains transcriptional consequences of chemical and genetic perturbations. We will also compare PLATE-seq perturbational profiles to tissue-specific differential expression signatures that distinguish cell lines sensitive to compounds in the Cancer Therapeutics Response Portal (CTRP) and Broad Repurposing Hub, each of which houses results from exposing hundreds of compounds exposed to dozens to hundreds of cell lines. Taken together, the data and analyses will help understand MoAs and polypharmacologies/off-targets of molecular glues, which also serve to enable interpretation and prioritization of new candidate MoA for molecular glues by comparing them to compounds with known targets and MoAs.

#3542 The Chemical Probes Portal: An essential resource providing expert advice on chemical tools for cancer research.

Domenico Sanfelice[1], Albert Antolin[2], Alisa Crisp[1], Yi Chen[1], Paul Brennan[3], Susanne Muller[4], Bissan Al-Lazikani[5], Aled Edwards[6], Paul Workman[1]

[1]The Institute of Cancer Research, Sutton, United Kingdom,[2]ProCURE, Catalan Institute of Oncology, Oncobell, Bellvitge Institute for Biomedical Research (IDIBELL), Barcelona, Spain,[3]University of Oxford, Oxford, United Kingdom,[4]Institute of Pharmaceutical Chemistry, Johann Wolfgang Goethe University; Structural Genomics Consortium (SGC), Buchmann Institute for Life Sciences, Johann Wolfgang Goethe University., Frankfurt, Germany,[5]Department of Genomics Medicine and the Institute of Data Science in Oncology, MD Anderson Cancer Center, Houston, TX,[6]Structural Genomics Consortium, University of Toronto, Toronto, ON, Canada

Background: The Chemical Probes Portal (Portal) serves as a vital resource in the realm of cancer research and biomedical science generally - offering expert guidance on high-quality chemical tools, usually protein inhibitors, crucial for studying physiological and pathological processes and validating therapeutic targets. Researchers often grapple with selecting suitable chemical probes, inadvertently utilizing tools ill-suited for their purpose, and not following best practice, thereby contaminating the scientific literature and wasting valuable time and resources. To address this challenge, the Portal (https://www.chemicalprobes.org) was established as a non-profit, independent online platform, meticulously curating, annotating, and scoring the quality of chemical probes and providing associated information and advice.

Results: The Portal stands apart as the sole expert-curated public resource evaluating the quality and utility of small-molecule chemical tool compounds for use in cancer research and wider biomedical research. More than 250 experts, comprising scientific leaders in chemical biology, medicinal chemistry, pharmacology, and related fields, contribute their experience and insights to assess featured chemical probes. Since 2021, a progressively updated and enhanced version of the Portal has been operational, housing over 1000 compounds targeting 500+ proteins across diverse families, now including PROTACs and molecular glues. We also flag 254 ‘Unsuitables’, which are compounds that should not be used to interrogate a specific protein target. Additionally, the Portal now offers informative pages, providing advice delineating guidelines for selecting well-validated compounds, including those suitable for rodent studies, necessitating specific pharmacokinetic and pharmacodynamic properties. Best practice use requires employing high-quality chemical probes from more than one distinct chemical class that target the same protein, incorporating an inactive control compound, and following the recommended concentration range - all aimed at mitigating off-target risks.

Conclusion: The enhanced Chemical Probes Portal provides a vital platform for researchers to navigate and evaluate chemical probes, easily and effectively. It employs a rigorous expert review to ensure the quality of the probes listed. The resource not only aids high-quality probe selection but also provides advice through an Information Centre, offering guidelines, FAQs, and additional information on probe criteria and use. The continuous expansion and outreach efforts aim to make the Portal an indispensable tool for cancer researchers and the broader biomedical research community. Researchers are encouraged to participate in the Portal's development and contribute to the robustness of chemical probe use in scientific endeavors.

#3543 TWNeoDB: A web-based database for tumor neoantigens in the Taiwanese population.

Y.-H. Tseng[1], C.-H. Wu[1], C.-Y. Sung[1], H. K. Yang[2], M.-H. Tsai[1], L.-C. Lai[1], T.-P. Lu[1], K. C. Chao[2], E. Y. Chuang[1], C.-Y. Lee[3];
[1]National Taiwan University, Taipei, Taiwan, [2]China Medical University, Taichung, Taiwan, [3]National Taipei University of Technology, Taipei, Taiwan

Tumor neoantigens are highly immunogenic. Two types of neoantigens have been reported for their ability to be shared among patients. One is a mutated tumor-specific antigen (mTSA) derived from somatic mutations in tumor cells. The other is an aberrantly expressed TSA (aeTSA), influenced by epigenetic changes or abnormal RNA splicing. Tumor neoantigens can bind with the major histocompatibility complex (MHC) and be recognized by the T cell receptor (TCR). Consequently, they can trigger the immune system to attack cancer cells. Until now, some neoantigen databases have been available, they mostly focus on the Western population and primarily contain peptides derived from mTSAs. In contrast, our database provides peptides not only from mTSA but also from aeTSA with a strong emphasis on the Taiwanese population.

Initially, we obtained public sequencing raw data from the NCBI database and employed a neoantigen pipeline for analysis, identifying potential neoantigens. The data collection criteria included samples from Taiwanese individuals, with paired DNA-seq or RNA-seq from both normal and tumor tissues of the same patients. RNA sequencing datasets were utilized to identify aeTSAs and mTSAs, whereas DNA sequencing datasets served for mTSA identification. Additionally, human leukocyte antigen (HLA) genotyping was performed for every sample. The identified peptides were further compared to previously validated data available on IEDB. This data was used to develop a web-based database with several functionalities. Users can search for specific peptides and download relevant data from the website. The website also included data cross-referenced and validated with IEDB. In addition, we incorporated clinically validated peptides capable of stimulating T cells to release cytotoxins or interferons. A machine-learning-based LightGBM model was trained to predict immunogenicity for these peptides through a series of cross-validations based on random data splitting. Users can access comprehensive information on tumor-specific peptides in the online database.

We collected sequencing data from 243 patients, spanning five different types of cancer. The predominant HLA genotype is HLA-A*11:01, a common allele in the Taiwanese population. Peptide characteristics, such as hydrophobicity, binding affinity, and binding stability, have been calculated and stored in the database. Notably, the LightGBM model excelled in predicting immunogenicity, achieving an AUC of 0.95 on the training dataset and 0.8 on the testing dataset. Implemented in the online database, this model allows users to forecast their own candidates. The state-of-the-art database serves as a comprehensive platform for gathering Taiwanese-specific neoantigens, contributing to the advancement of personalized cancer vaccines and immunotherapies.

#3544 OncoKB™, MSK's precision oncology knowledge base: 2023 updates.

S. P. Suehnholz, **M. Nissan**, H. Zhang, R. Kundra, C. Lu, A. Dhaneshwar, N. Fernandez, B. Preiser, M. E. Arcila, M. Ladanyi, M. F. Berger, A. Syed, A. Brannon, R. Levine, A. Dogan, A. Drilon, D. B. Solit, N. Schultz, D. Chakravarty;
Memorial Sloan Kettering Cancer Center, New York, NY

OncoKB™ is Memorial Sloan Kettering Cancer Center's (MSK) FDA-recognized precision oncology knowledge base that contains detailed, evidence-based information about the oncogenic effect and therapeutic implications of individual somatic mutations and structural alterations present in patient tumors. Since its public release in 2016, OncoKB™ has expanded to include annotation for >7,500 alterations in ~820 cancer-associated genes. OncoKB supports variant interpretation by the cBioPortal for Cancer Genomics, is used to annotate >15,000 MSK patient sequencing reports annually and its data is publicly available through the website (www.oncokb.org). Programmatic access to OncoKB™ data via its web-based API is freely available to users in an academic setting while users from commercial and hospital settings require a fee-based license.

OncoKB™ utilizes its Therapeutic Levels of Evidence system to classify variants based on their tumor type-specific sensitivity or resistance to matched standard care or investigational targeted therapies. To date, OncoKB includes 49 Level 1 genes as well as MSI-H and TMB-H (included in the FDA drug label), 24 Level 2 genes (included in professional guidelines), 35 Level 3A genes (predictive of drug response in well-powered clinical studies), 27 Level 4 genes (predictive of drug response based on compelling biological evidence), and 11 R1/R2 resistance genes. In 2023, OncoKB™ captured the following notable changes in precision oncology drug development: Level 1 annotation of *ESR1* ligand-binding domain mutations in breast cancer and promotion from Level 2 to Level 1 of *ERBB2* amplification in colorectal cancer following the FDA drug approvals of elacestrant and tucatinib + trastuzumab, respectively. Additionally, KRAS G12C became a Level 2 biomarker in pancreatic and colon cancers with the listing of adagrasib and sotorasib as systemic therapy options for *KRAS G12C*-mutant disease in the NCCN pancreatic and colon cancer guidelines. *IDH1/2* mutations in low grade glioma were annotated as Level 3A based on compelling clinical evidence demonstrating response to the *IDH*-specific inhibitor vorasidenib. Lastly, noting emerging data with the *KRAS* G12X-specific inhibitor, RMC-6236, OncoKB™ included all alleles at *KRAS* position G12 as Level 4.

In sum, six novel clinically actionable biomarkers (all Level 1) and 14 follow-on precision oncology therapies for existing leveled biomarkers were added to OncoKB™ in the past year. OncoKB™'s current focus includes coverage of additional cancer-associated genes, annotation of germline alterations and incorporation of OncoKB™ data into an electronic health record system.

#3545 Atlas of therapeutic targets: Evolution of druggable proteome.

I. Babic, **E. Nurmemmedov**;
Nerd Bio, San Diego, CA

Selection of therapeutic targets and modalities is of fundamental importance in drug discovery, as it can have a direct impact on the economics of drug discovery as well as its success rate. With the advancement of chem-bio and proteomics methods together with advent of artificial intelligence, the scope of the druggable proteome is expanding. The choice of drug targets gains further importance as we link it to potential clinical efficacy and safety, genetic variation and patient populations. Drug targets are often selected based on inadequate understanding of target biology, tractability by existing toolbox of therapeutic modalities and insufficient insight into possible clinical outcome. We have developed an “Atlas of Therapeutic Targets”, an interactive resource that provides classification of drug target families with linked information on clinical and investigational drugs. The atlas also provides key insights and score for tractability of targets with various therapeutic modalities. Particularly, our scoring system grades the targets on dimensions such as ligandability, involvement in protein-protein complexes, structural disorder, hotspot analysis and cross-referencing with known targets, thus yielding a total tractability score of 1-10. Dissection of targets based on such dimensions, enables critical evaluation therapeutic modalities as well tools and methodologies needed for their conversion into successful drug discovery programs. We curate 900+ human drug targets, analysis of which indicates the continued dominance of privileged target families across disease areas, but also the growth of novel first-in-class mechanisms. This atlas will be available as a resource for the wide drug discovery community.

#3546 Putting genes in context by linking gene signatures to established cancer hallmarks.

O. Menyhart, W. Kothalawala, B. Győrffy;
Semmelweis University, Budapest, Hungary

The concept of the "Hallmarks of Cancer" provides a valuable framework for understanding fundamental organizing principles common to various types of cancers. However, the absence of a consensus gene set for cancer hallmarks poses data comparison and integration challenges, resulting in diverse biological interpretations across studies.

Here, we first established a consensus cancer hallmark-gene set by merging data from available mapping resources. We searched the scientific literature for relevant publications from which a list of hallmark genes could be reconstructed. By consolidating data from seven publications, we identified 6,763 candidate cancer hallmark genes associated with ten cancer hallmarks. Of these, 1574 genes were part of at least two resources, forming a "core" hallmark gene set.

Then, we compared the enrichment of cancer hallmarks by analyzing the prognostic genes associated with overall survival across twelve solid tumor types. Notably, the hallmark "tissue invasion and metastasis" was most prominent in the stomach (p=1.2E-11), pancreatic (p=1.5E-09), bladder (p=1.8E-08), and ovarian cancers (p=0.0002), aligning with their heightened potential to spread. "Sustained angiogenesis" predominated in lung squamous carcinomas (p=4.5E-08), while "genome instability" showed strong enrichment in lung adenocarcinomas (p=1.3E-09), liver (p=1.4E-10), pancreatic (p=1E-5) and kidney cancers (p=0.0025). Compelling evidence links lifestyle choices like alcohol consumption and smoking to genomic instability across tumors, suggesting a potential common underlying mechanism of tumorigenesis.

Pancreatic cancers displayed the highest enrichment of hallmarks (8 out of 10), emphasizing the disease's complexity, while in melanomas, liver, and kidney cancer, a single hallmark („genomic instability") was enriched among the prognostic markers of survival. These findings underscore the utility of the hallmark concept as an effective organizational tool, particularly when establishing a clear connection between genes and biological functions.

Finally, we integrated the data into a publicly accessible and user-friendly online tool (available at www.cancerhallmarks.com) that allows users to identify the most relevant cancer-associated "candidate hallmark genes" in their datasets.

In summary, we have established a consensus list of genes associated with cancer hallmarks. The analysis of survival-associated genes revealed a unique pattern of hallmark enrichment for each tumor type.

#3547 The ISB Cancer Gateway in the Cloud (ISB-CGC): Access, explore and analyze large-scale cancer data through the Google Cloud.

F. Seidl[1], L. Hagen[2], J. Wilson[1], B. Aguilar[2], D. Bleich[1], L. Wolfe[2], P. Gundluru[1], P. Venkatesan[1], M. Tian[2], S. Paquette[2], E. Lee[2], D. Huffman[1], D. Pot[1], W. Longabaugh[2];

[1]ISB-CGC, Rockville, MD, [2]ISB-CGC, Seattle, WA

Rapid growth of cancer data in recent decades has made data discovery and wrangling difficult for the average cancer research lab. Our mission at the ISB Cancer Gateway in the Cloud (ISB-CGC), part of the NCI's Cancer Research Data Commons ecosystem, is to democratize access to large cancer datasets. Funded by the NCI, we have performed ETL processes on data from GDC and PDC projects such as TCGA, TARGET, and CPTAC. We generated hundreds of BigQuery tables containing data such as mutations, gene expression, and protein abundance, which enable data analysis in the cloud via SQL. BigQuery analyses are inexpensive and rapid even when scaled to petabyte sized inputs, for example we ran 6.6 billion correlations in 2.5 hours with a total cost of about one dollar. These data can also be accessed affordably from Google Cloud VMs where researchers can develop analysis pipelines in Python, R, and workflow languages such as CWL. We present two recent collaborations: In one BigQuery was used to develop machine learning algorithms that calculated genetic risk scores from TCGA glioblastoma and ovarian cancer copy number variation. In another example researchers combined SQL queries of our BQ tables with data from the ISPY2 Trial initiative and generated an R shiny app that can dynamically create data visualizations for genes of interest in different TCGA cohorts.

#3548 OKAIN: A comprehensive oncology knowledgebase for the interpretation of clinically actionable alterations.

Z. Yang, M. Wang, H. Qin, Y. Yu, Y. Zheng, Z. Li, X. Meng, X. Dong, L. Wang, K. Wang, A. Wang;
OrigiMed Co., Ltd, Shanghai, China

Background: The increased use of Next-Generation Sequencing (NGS) in clinical genetic testing has resulted in the identification of several genetic variations with possible therapeutic implications. Several knowledgebases, such as OncoKB, have been curated to better understand the clinical implications of somatic mutations in cancer. While thorough annotation of gene variations of Chinese pharmaceuticals is not recorded in the majority of those databases. As a result, we developed OKAIN (https://szcube.origimed.com), an algorithm tool that assesses clinically actionable mutations using a precision oncology knowledge database.
Methods: OKAIN employs a weighted evidence analysis system to deliver final clinical annotation outcomes for intricate variations. This process commences with a weighted analysis of all therapeutic efficacy evidence for a specific genomic variant related to a particular drug, to determine the highest degree of efficacy for that drug. The top efficacy level is then assessed against numerous variants of the gene, resulting in efficacy data for all variants of the gene in relation to the medication.
Results: To date, OKAIN has collected 15,654 pieces of evidence on 471 genes associated with cancer. This comprises 2,600 pieces of Level A evidence (included in FDA/NMPA labeling or clinical professional guidelines) on 66 genes, 180 Level B evidence (included in extensive retrospective studies or prospective investigations) on 31 genes, 676 Level C evidence (included in small-scale retrospective studies or early-stage prospective studies) on 81 genes, and 5,562 Level D evidence (included in case reports and preclinical studies) on 188 genes. For Level A evidence, 864 pieces of evidence were derived from either the NMPA label or CSCO guidelines. As an illustration, Befotertinib was approved by NMPA as a first-line treatment for locally advanced or metastatic non-small cell lung cancer (NSCLC) in adult patients with either *EGFR* exon 19 deletion or L858R mutation. This indicates that adult Chinese patients with locally advanced or metastatic NSCLC who have *EGFR* exon 19 deletion or L858R mutation can potentially experience benefits from administering Befotertinib.
Conclusion: OKAIN acts as a precision oncology knowledgebase for the assessment of clinically actionable alterations, integrating exhaustive data related to cancer-associated genomic variants and therapeutic efficacy. It is a beneficial tool for medical professionals and patients, providing an enhanced means of understanding and approaching precision oncology.

#3549 PMed-TRIAL PDX database: Integrated multidimensional information to facilitate new drug development.

X. Chen, Y. Guo, L. Van, J. Caggiula, X. Gu, **D. Wen**;
Shanghai LIDE Biotech Co., Ltd., Shanghai, China

PDX models play a crucial role in pre-clinical research for new drugs. In recent years, research based on PDX models has entered the 'Big Data Era.' On the one hand, there are numerous factors influencing drug responses, such as cancer types, genetic backgrounds, clinical treatment histories, and more. Therefore, selecting the appropriate PDX models for drug efficacy testing based on relevant information has become increasingly important. On the other hand, conducting in-depth genomics and transcriptomics analyses on PDX models allows us to gain a deeper understanding of the mechanisms of drug efficacy and drug sensitivity. After years of effort, LIDE have successfully built and maintained over 1800 PDX models from 40 different cancer types. And in this year (2023), we launched LIDE's PMed-TRIAL PDX database website. As a comprehensive database of PDX models, it includes fundamental PDX clinical information, medication history, growth curves, and standard of care (SOC) data. It also contains whole exome sequencing data and RNA-seq data. Cancer is a complex and heterogeneous disease characterized by tumor heterogeneity, encompassing both inter-tumor diversity (between patients) and intra-tumor variability (within a single patient), thereby complicating drug responsiveness. PDX models preserve heterogeneity of individual patients, and a robust PDX cohort is essential for accurately representing inter-tumor heterogeneity. LIDE's PDX cohorts effectively capture representative molecular subtypes across various major cancer types, highlighting their potential as a valuable resource for pre-clinical trials. LIDE's PMed-TRIAL PDX database comes with a concise and efficient web user interface. Users can search and filter models using keywords, such as drug names, gene symbols, and other information. The website can now be accessed via the following URL (https://pmed.lidebiotech.com:8000/).

#3550 PerturbDB: A resource for revealing gene functions and cancer-associated phenotypes.

B. Yang, M. Zhang, Y. Shi, Y.-M. Dong, X. Ma, J. Zhang, D. Lu, J.-Y. Liao, **D. Yin**;
Sun Yat-Sen University, Guangzhou, China

Perturb-seq is a high-throughput technique that combines clustered regularly interspaced short palindromic repeats (CRISPR)-based screens with single-cell RNA sequencing (scRNA-seq) readouts for high-content phenotypic screens to comprehensively map the transcriptional effects of genetic perturbations, showing great advantages in revealing disease-associated gene functions and mechanisms in high volumes. Despite the rapid accumulation of Perturb-seq datasets, no dedicated database exists for reusing these valuable information. In this study, we developed a platform called PerturbDB (http://research.gzsys.org.cn/perturbdb) to facilitate users to unveil genotype-phenotype relations, especially gene functions and regulatory networks involved in several classical cancer associated phenotypes using 37 Perturb-seq datasets from 15 studies. By reanalyzing 3,429,829 single-cell transcriptomes from the knockdown of 3214 genes across 10 different cell lines, we identified 749 classical cancer phenotype-related genes and 373 functional gene clusters annotating potential novel functions. Utilizing Marker genes scoring and the InferCNV algorithm, we identified genes involved in 9 malignant phenotypes, which consists of sustaining proliferative signaling (362 genes), resisting cell death (120 genes), inducing angiogenesis (145 genes), tissue invasion and metastasis (321 genes), enabling replicative immortality (160 genes), deregulating cellular metabolism (247 genes), avoiding immune destruction (95 genes), unlocking phenotypic plasticity (231 genes), and chromosome instability (231 genes). Additionally, functional clusters were calculated utilizing Principal Component Analysis (PCAs) and the HDBSCAN package to introduce unknown gene functions related to the cancer associated phenotypes. Perturbation clusters (PCs) were identified by comparing similarities in the transcriptomes of perturbed cells, suggesting individual genes in the same functional cluster perform similar gene functions, and therefore novel functions of 735 genes can be inferred from the known functions of neighboring genes. The PGSEA tool was developed to facilitate functional analysis of genes not yet included, which helps users to predict gene functions through a combination of PerturbDB datasets and personalized RNA-seq datasets. This study will greatly expand our understanding of genes involved in emblematic cancer associated phenotypes and their coordinated functions and regulatory networks.

#3551 Continued analysis of extensive data towards Genome in a Bottle benchmarks for a new tumor normal pair.

J. Wagner[1], J. McDaniel[1], G. L. Rosen[2], N. D. Olson[1], V. Patel[1], C. Xiao[3], A. Liss[4], J. Zook[1];
[1]National Institute of Standards and Technology (NIST), Gaithersburg, MD, [2]Drexel University, Philadelphia, PA, [3]NIH/NLM/NCBI, Bethesda, MD, [4]Massachusetts General Hospital, Boston, MA

Here, we detail in-progress genome-scale measurements from a variety of technologies of the first tumor normal benchmark from the Genome in a Bottle (GIAB) consortium. We created the first broadly-consented tumor cell line from a pancreatic ductal adenocarcinoma with matched normal pancreatic and duodenal tissue. Data is being collected from a large homogeneous batch of the tumor cell line and paired normal tissues. As we receive data we make it publicly available on the NCBI hosted GIAB FTP site, https://ftp.ncbi.nlm.nih.gov/ReferenceSamples/giab/data_somatic/. When complete, this dataset will include WGS measurements from Illumina, ONT, Hi-C, Bionano, single cell WGS, PacBio HiFi and Onso, and Element. Analysis and development of a variant calling benchmark using this data is ongoing in collaboration with an open working group of the GIAB consortium.

Initial Hi-C and optical mapping data from the tumor cell line indicates substantial aneuploidy from translocations that cause large deletions. We found roughly 17 large inversions and translocations and 16 chromosomes with extensive loss of heterozygosity due to missing >30% of one copy, in addition to a few smaller duplications. Low coverage single cell sequencing that provides ploidy estimates across chromosomes showed that most of the large deletions appear in all or nearly all cells with some variation in a few cells. These observations are consistent with bulk WGS analyses from two batches of cells. Additionally, many of the observed large deletions correspond to deletions seen in the population of TCGA chromosomal Loss of Heterogeneity samples. Examining somatic SNVs in non-repetitive regions, we find that close to 60% occur in almost all cells in diploid regions, 30% occur in almost all cells in haploid regions, and 5% in only some cells in diploid and haploid regions, respectively. We take these results to indicate the cell line is relatively homogeneous and stable with most CNVs being deletions. As such, we plan to explore using long reads, ultralong reads, and Hi-C data to generate a near-complete genome assembly of the dominant tumor clone as well as a complete diploid assembly of the normal. With this personalized genome assembly, we will explore aligning tumor and normal reads to each haplotype of the normal to characterize somatic variants, including variants in minor clones. Building on the methods GIAB and T2T have developed to polish diploid assemblies of GIAB's normal genomes and mosaic variant characterization, we will develop benchmarks for somatic variants against the normal assembly as well as standard references.

#3553 OralDB, A integrative data portal for oral and oropharyngeal cancer omics and clinical research.

J. Wang, P. Lam,, Y. Su, J. Wang;
The University of Hong Kong, Pokfulam, Hong Kong

Oral and oropharyngeal cancer is one of the more common cancers worldwide, with a poor prognosis in advanced stages and a higher incidence in Asian populations than in other regions. Its affected Affected areas include the lips, gums, tongue, the inside of the cheeks, the roof of the mouth, the floor of the mouth, the tonsils, and the oropharynx. Currently, the distribution of RNA expression data and clinical data in oral and oropharyngeal cancer is fragmented, impeding effective data mining for the discovery of novel biological markers and testing of new hypotheses. We constructed an oral and oropharyngeal cancer-specific database with expression dataRNA expression and clinical data from more than 4,356 patients in 41 studies. The RNA Expression data from 23 genome-wide platforms are carefully processed and quality-controlled, while clinical data is standardized and tightly managed. With the support of this oral and oropharyngeal cancer-specific database oral cancer-specific database, we have created an open-access web resource, the Oral and Oropharyngeal Cancer Browser, to facilitate researchers interested in oral and Oropharyngeal cancer to quickly access and analyze all currently published RNAoral cancer expression data and clinical data. Users can perform a meta-analysis of Oral and oropharyngeal oropharyngeal cancer to quickly understand the results of tumor versus non-malignant tissue (normal), differential gene expression, and expression-survival associations. Flexible options for survival analysis, comparative analysis, and correlation analysis based on a single dataset are also available. At the same time, the database also accepts the user's own input data and allows the user to do theircarry out their own analysis by combining the input data with the existing data in the database.

#3554 Using All of Us cancer data on the Researcher Workbench to advance career development.

Karriem S. Watson[1], Rubin Baskir[1], Division of Engagement and Outreach, All of Us Research Program, Karen Hubbard[2], **Hannah L. Park**[3], Lin Zhu[4]

[1]All of Us Research Program, National Institutes of Health, Bethesda, MD,[2]City College of New York, New York City, NY,[3]University of California, Irvine, Irvine, CA,[4]Temple University, Philadelphia, PA

This session will provide an overview of the All of Us Research Program (All of Us) dataset, discuss a mechanism to build the capacity of research institutions using the All of Us dataset, and outline the career benefits researchers experienced from using the dataset. All of Us is building a national health dataset to accelerate medical breakthroughs. It is used by cancer researchers to advance health research and career development. This dataset is large and diverse, both in the data types available as well as the demographics of participants: as of April 2023, health data from 413,450+ participants is available to researchers, from a variety of distinct data types, including survey responses, physical measurements, electronic health records, whole genome sequencing, wearable data, and genotyping arrays, with 75% of participants self-identifying as underrepresented in biomedical research and about 45% of participants self-identifying as racial and ethnic minorities. Researchers already leverage this dataset, with All of Us data used in more than 210 publications across peer-reviewed journals. In addition, this dataset is useful for cancer researchers - All of Us EHR data indicates over 60,700 participants are diagnosed with at least one type of cancer, and more than 10% of research projects underway (725/6,945 as of September 2023) using the All of Us dataset are cancer-related, making it the top condition studied by researchers. To help build capacity at research institutions, All of Us collaborated with the NCI Center to Reduce Cancer Health Disparities (CRCHD) Partnerships to Advance Cancer Health Equity (PACHE) to develop a Notice of Special Interest (NOSI) titled Administrative Supplements to Support "All of Us" and Health Disparities-Related Pilot Research Projects at NCI CRCHD-Funded PACHE Partnerships. The focus of this NOSI was on P20 and U54 awards associated with research projects led by PACHE researchers interested in exploring the connections between social determinants of health outcomes and populations experiencing cancer health disparities. NIH awarded investigators at the following institutions: City College of New York, University of California, Irvine, and Temple University.

Principal investigators of these awards will provide an overview of their work, describe how they analyze the All of Us dataset, and discuss how their use of the dataset has helped advance their career as cancer researchers:

Karen Hubbard (City College of New York)

Project Title: Relative and Intersectional Analysis of social determinants of Lung Cancer Risk among Black and Hispanic All of Us respondents

Hannah Lui Park (University of California, Irvine)

Project Title: Improving breast cancer risk assessment and prevention in Asian American women

Lin Zhu (Temple University)

Project Title: Elucidating the Roles of Metabolic Syndrome and Non-Alcoholic Fatty Liver Disease among Asian American Patients with Chronic Hepatitis B

#3555 COSMIC: two decades of curating somatic variants in cancer.

Zbyslaw Sondka, Madiha Ahmed, Joanna Argasinska, David Beare, Nidhi Bindal Dhir, Denise Carvalho-Silva, Manpreet Singh Chawla, Stephen Duke, Ilaria Fasanella, Muhammed Fouzan, Avirup Guha Neogi, Susan Haller, Bhavana Harsha, Balazs Hetenyi, Leonie Hodges, Alex Holmes, Steven Jupe, Rachel Lyne, Madhumita Madhumita, Thomas Maurel, Karen McLaren, Sumodh Nair, Helder Pedro, Amaia Sangrador-Vegas, Helen Schuilenburg, Zoe Sheard, Michael Starkey, Rebecca Steele, Sari Ward, Jennifer Wilding, Siew Yit Yong, Jon Teague

COSMIC, Wellcome Sanger Institute, Cambridge, United Kingdom

In 2004, COSMIC was one of the first initiatives to integrate global data on somatic mutations in cancer. At the time it was explicit that the fragmentation of genetic datasets was a major obstacle to understand the processes driving cancer. A team of expert curators and bioinformaticians was tasked with identifying and cataloguing data related to somatic variants, as well as relevant demographic, clinical, and patient information from published studies and making these data easily accessible to the research community. Over the last two decades we have witnessed the incredible progress in cancer genomics enabling whole genome studies, resulting in the exponential growth of data generated by cancer research. During its first year, COSMIC integrated data from 1672 scientific papers, cataloguing 1755 unique mutations across 21 genes. At present, twenty years later it is common for a single publication to describe tens of thousands of genome-wide mutations and now COSMIC includes 24 million genomic variants collected from more than 1.5 million patient samples acquired from over 29,000 scientific publications. Today, an important part of COSMIC's mission is to help translate this information for improving cancer treatment and patient care. To achieve this, the main catalogue of somatic mutations is supported by 6 accompanying resources that focus on different aspects of molecular oncology. The Cancer Gene Census and Cancer Mutation Census describe the roles of genes and mutations in oncogenesis, based on literature curation and analysis of the core mutation catalogue. COSMIC 3-D visualises mutation frequency in the context of the protein structure, and Mutational Signatures catalogues the mutagenic processes behind the nature of mutations at the genome level. To help target molecular alterations in clinical practice, Actionability and the catalogue of mutations causing drug resistance inform the availability of therapeutic options for cancer and how their efficacy is influenced by the genetic profile of the cancer. The ongoing development of sequencing techniques and new diagnostic methods as well as computational approaches, including deep learning and use of generative AI, give us hope that the next 20 years will be equally revolutionary for data-driven oncology. However, the abundance of new sources of diverse datasets makes data fragmentation an evolving challenge for the whole research community. Developing and adopting common standards for data formats, management and usage will be critical to assure inclusive, efficient, and effective translation of genomic research into a clinical practice.

#3556 A pan-cancer *ex vivo* drug screen database for next-generation pharmacogenomics and functional precision oncology.

A. Markus[1], K. Pichotta[1], J. Quinn[1], J. White[1], C. Tosh[1], J. Liu[2], E. Coyne[1], W. Tansey[1];

[1]Memorial Sloan Kettering Cancer Center, New York City, NY, [2]Weill Cornell Medicine, New York City, NY

Large-scale drug screens across thousands of drugs and biological models enable pan-cancer analyses that can reveal novel insights into therapeutic response and resistance. Existing databases, such as the Cancer Dependency Map only screen established 2D cell lines, which are known to poorly translate to patients. Ex vivo models such as patient-derived cells, spheroids, and organoids, have consistently demonstrated superior translatability from drug screening responses as they better replicate the original tumor. However, the cost, complexity, and difficulty of developing and screening ex vivo models has thus far prevented the establishment of any large-scale database comparable to existing cell line databases. We present the pan-preclinical (PPC) project, a large pan-cancer database of ex vivo drug responses comprising 2.1M raw dose-response measurements with curve-level summary statistics and metadata. The PPC database is assembled from over 30 previously published ex vivo studies and contains 2,880 ex vivo models spanning 106 cancer subtypes tested against subsets of 3,023 drugs. Compounds are harmonized across studies and paired with detailed chemoinformatics derived from PubChem. Each ex vivo sample is matched to an underlying patient and paired, where available, with genomics, transcriptomics, and clinical information such as sex, treatment history, and overall survival. Two thirds of the underlying studies did not originally make the underlying drug screening data available at publication time, making the PPC database a novel resource beyond data integration. Results: To investigate the power of the PPC database, we developed a preliminary computational modeling and statistical analysis pipeline. A hierarchical Bayesian factor model was developed to estimate dose-response curves, remove batch effects across studies, and impute missing drugs. Low-dimensional projections of ex vivo drug responses show biologically meaningful clustering. Statistical analyses of both observed and imputed drug responses recapitulate standard of care drugs as significantly effective across several cancer types. Overall, we envision the PPC project laying the foundation for the next generation of large-scale pharmacogenomic analyses and aiding in the coming era of functional precision oncology.

#3557 A pancancer gamma delta T cell repertoire atlas.

X. Yu[1], S. Li[2], L. Cen[1], X. Wang[1];
[1]Moffitt Cancer Center, Tampa, FL, [2]Dartmouth College, Lebanon, NH

While representing only a small portion of T cell population, Gamma delta (γδ) T cells have unique contributions to both innate and adaptive immunity. Compared to αβ T, γδ T cells have a more diverse TCR repertoire, allowing them to recognize a broader range of tumor antigens. Recent breakthrough discoveries indicate that the antitumor efficacy of γδ T cells can be potentiated or rescued through targeted therapeutic approaches. Despite their functional and translational significance, a comprehensive understanding of the γδ T cell repertoire within tumor tissues has yet to be fully achieved.In this work, we generated a pan-cancer γδ T cell repertoire Atlas through reanalyzing RNA-seq data from more than 11,000 tumors in TCGA utilizing TRUST4, an advanced computational method for reconstruction of TCR repertoires. This allowed us to offer the most accurate and comprehensive examination of the γδ TCR landscape spanning 33 cancer types, marking it the largest collection of γδ clones on human cancer to date. We processed 660 billion RNAseq reads, identified ~3 million CDR3 reads, applied a series of stringent filtering criteria to remove biologically implausible, ambiguous sequences, and out-of-frame TCRs, which resulted in 22,205 unique γδ TCR clones from 6,751 tumors. TCR gene enrichment scores were calculated to represent overall expression of γδ in each tumor. The γδ enrichment is highly variable between and within cancer types. As expected, tumors traditionally classified as immune-cold (UVM and GBM) show the lowest scores. Cancers intrinsically related to lymphatic system (LAML, THYM and DLBC), exhibit the highest scores. Beyond THYM, the top five solid-tumor cancers carrying the highest enrichment are PRAD, KIRC, TGCT, LUAD and KICH. We further profiled the clone counts, spectrum of clone sizes, CDR3 length, V-J pair usage, and clonality in 33 cancers. Overall, a dominant presence of large clone segment is not observed in most cancers. The most prevalent V-J pairs are TRGV10/9/2-TRGJ1 for γ, and TRDV1-TRDJ1 for δ chain. Cancers including LAML, KIRC, LUAD, SKCM, CESC, LUSC, STAD, display a relatively higher proportion of intermediate to larger clones. THYM exists the highest γδ diversity, with the lowest clonality and most diverse V-J pairs. In addition, we evaluated the prognostics value of γδ genes by multivariate Cox regression, adjusting for age, sex, stage, and tumor purity, and identified 38 γδ genes associated with patient survival with $p<0.05$ in 25 cancer types. Finally, within HNSC, we observed higher γδ gene enrichment ($p=1.6e-9$) and clone diversity ($p=0.014$) in HPV+ vs. HPV- tumors. The γδ gene enrichment is also found associated with patients' survival ($p=0.002$) in HPV+, but not in HPV- HNSC. Similarly, COAD tumors with high Microsatellite Instability (MSI) shows higher γδ gene enrichment and clone diversity compared to MSI low COAD. Collectively, our findings serve as a foundational resource for γδ T cell research in oncology.

.

#3558 An integrated data platform to support the international alliance for cancer early detection.

B. Walsh[1], L. Beckman[1], J. Burchett[1], M. Peterkort[1], J. Lee[1], M. Fitzsimons[2], P. Vassilatos[2], B. Bajracharya[2], C. Barnes[2], J. Qureshi[2], R. Grossman[2], C. Yakura[1], Y. Lu[3], S. Burge[4], D. Kelberman[3], E. Watson[1], **K. Ellrott**[1];

[1]OHSU, Portland, OR, [2]University of Chicago, Chicago, IL, [3]University College London, London, United Kingdom, [4]Cambridge, Cambridge, United Kingdom

Cancer early detection is one of the most critical areas of cancer research, as it offers the greatest potential for improving patient outcomes. The International Alliance for Cancer Early Detection (ACED) is a global partnership of world-leading cancer research institutions in the UK and US, established in 2019 to accelerate and revolutionize research in this field. ACED brings together the expertise of the Canary Center at Stanford University, the University of Cambridge, the Knight Cancer Institute at Oregon Health and Sciences University, University College London, and the University of Manchester, together with Cancer Research UK, with the goal of catalyzing new collaborations and research in the field of early detection. One of the major challenges to enabling international collaborations across different institutions is the ability to collect, share and discover datasets between researchers and institutions. To enable collaboration on innovative data science, fundamental functions include, 1) controlled data sharing mechanisms; 2) structured metadata to enable data exploration and data discovery; and 3) enabling easy computational access to that data. To advance researchers' collaboration, ACED began development of an Integrated Data Platform (IDP). The ACED-IDP is based on the Gen3 software platform developed by the University of Chicago's Center for Translational Data Science. Based on software systems originally developed for the NCI's Genomic Data Commons, Gen3 has been used in several other data projects including The Blood Profiling Atlas in Cancer (BloodPAC), Australian BioCommons and numerous other research data platforms. The unique nature of ACED required unique innovations to be made for the development of the IDP. Each of the member institutions within the alliance has different existing computer infrastructures, separate authentication platforms and heterogeneous data types forming the basis of their research. The IDP sought a cloud-ready strategy, while still being cognizant of the extreme costs associated with cloud egress fees that hamper researchers' ability to download data. Additions were made to the Gen3 platform to allow for hybrid cloud support, allowing on-premises as well as cloud object storage systems to be linked to the platform. This innovation permits each institution to share files using the mechanisms that they see fit. To unify the various datasets, the standard Gen3 schema was replaced with one derived from the Fast Healthcare Interoperability Resources (FHIR) standard. To support import from clinical data sets, tooling to enable import and export Observational Medical Outcomes Partnership (OMOP) data has been integrated. With this platform in place, we hope to advance international collaborations and accelerate early cancer detection research.

#3559 A validated bioinformatics tool-set for predicting TCR specificity.

A. Wilm, F. Schmidt, M. Wirawan, M. Cooray, K. Wu, K. Fink, D. MacLeod;
ImmunoScape, Singapore, Singapore

Background: The T-cell receptor (TCR) is a transmembrane receptor on T cells, which is responsible for recognizing any foreign antigen derived peptide, presented on infected or abnormal cells by the MHC-I complex. Predicting TCR specificity computationally is a long-standing problem. Many methods leverage large libraries of TCR sequences and cognate epitopes as input for machine learning and predict specificity from sequence alone. Most methods generally do not perform very well, especially in the case of unseen peptides, i.e. for cases where peptides were not part of the input library.
Methods: Here we describe three independent but interacting in-silico modules for TCR discovery. 1) The first module predicts specificity from deep phenotypic T cell profiles. We produce these profiles using a high-throughput pipeline, which combines multiplexed CyTOF with subsequent VDJ CITE-Seq. The generated multiomics data is aggregated into a database called TCAPS, which is the basis for machine learning models. These models can predict T cell specificity from the deep phenotype alone, i.e. without TCR sequence information. The resolution however is limited to the target class and hence the actual epitope has to be determined through subsequent deorphanization. This deorphanization step is augmented by the other two modules also described here. 2) The second module enables ultrafast sequence similarity search, which is used to find similar TCRs with known epitope specificity 3) The third module ranks TCR candidates for prioritisation for in-vitro validation. This is achieved by running the Alphafold-based structure prediction program TCRDock.
Results: 1) We demonstrate how TCR specificity can be correctly predicted from multiomics deep T-cell profiles and specifically highlight two in-vitro validated predictions, for which the corresponding epitope/antigen were not part of the input panel. 2) Using a recently published TCR clustering benchmark TCRScapes, we demonstrate the superior performance of our ultrafast sequence similarity search. 3) We furthermore showcase TCRdock-directed experiments on TCRs specific for SF3B1mut-induced splice variants. TCRdock correctly ranked TCR candidates, including artificial combinations, whose functionality we prove through in-vitro validation.
Conclusions: We describe three modules for TCR discovery and demonstrate their utility by benchmarking and in-vitro validation of multiple predictions, including two examples against unseen epitopes/antigens.

#3560 Quantified kinematics and wearable sensors to predict serious adverse events in patients undergoing cancer therapy trials.

E. Tran[1], L. Nocera[2], A. Kolatkar[2], A. El-Khoueiry[2], J. Thomas[2], P. Kuhn[2], A. Zeng[2], M. Kai[3], M. Karuturi[3], J. Nieva[2],
[1]UCSD School of Medicine, San Diego, CA, [2]USC Norris Comprehensive Cancer Center, Los Angeles, CA, [3]MD Anderson, Houston, TX

Background: Serious adverse events (SAEs) are a critical determinant of drug toxicity in clinical trials. However the drivers of toxicity may be related to patient factors as much or more than drug related factors. Prior studies have shown that time in non-sedentary activity predicted toxicity in cancer patients receiving highly emetogenic chemotherapy. SAEs are a critical determinant of drug toxicity in clinical trials. However, predicting SAEs using conventional PS scales measurements, such as ECOG is challenging because measurements can vary among observers. Prior studies have used activity trackers to measure physical activity and showed that time spent in non-sedentary activity predicted toxicity in cancer patients receiving highly emetogenic chemotherapy. Here, we sought to extend these findings to early phase clinical trial participants by examining data collected in two single-arm, observational, prospective studies at USC Keck and MD Anderson centers. We explored the use of out-of-clinic wearable sensors as an objective metric of frailty so as to identify patients at risk for therapy complications.

Methods: Adult patients diagnosed with cancer and enrolled in early stage clinical trials across USC Keck and MD Anderson centers were included in parallel single-arm, observational, prospective studies. Patients used a consumer grade wearable activity tracker (Fitbit) and the study examined associations between the number of severe adverse events to activity levels measured by metabolic equivalents (METs) and get-up-go times across the first 30 days. Trends were assessed using t-tests.

Results: 36 eligible patients were included in METs activity analysis. There was a total of 16 recorded incidences of SAEs within the first 30 study days, with 10 patients experiencing at least one SAE. The median non-sedentary time for patients with no SAEs was 27.5 hours above 1.5 METs per week, compared to 21.5 hours for those with at least one SAE occurrence (p-value=0.0146, r^2=0.1629). The median get-up-go times for those without SAEs was 10.0 seconds (n=26) and with SAEs was 9.8 seconds (n=10), (p-value=0.828, r^2=0.0014).

Conclusions: Non-sedentary time, as an objective measure of activity, can be used to identify those patients who are at greatest risk for SAEs in clinical trials. Widely available and inexpensive consumer grade sensors can be used as a stratification tool. Findings should be confirmed in larger patient cohorts across a wider variety of trial settings.

Figure 1: Weekly non-sedentary hours vs. presence of SAE in first 30 days of trial enrollment

#3562 Comparison of spatial co-localization measures for studying the tumor immune microenvironment with application to ovarian cancer.

B. L. Fridley[1], A. Soupir[2], J. Wrobel[3], C. Colin-Leitzinger[2], M. K. Townsend[2], A. B. Lawson[4], K. L. Terry[5], J. M. Schildkraut[3], S. S. Tworoger[2], L. C. Peres[2]; [1]Children's Mercy Hospital, Kansas City, MO, [2]Moffitt Cancer Center, Tampa, FL, [3]Emory University, Atlanta, GA, [4]Medical University of South Carolina, Charleston, SC, [5]Brigham And Women's Hospital, Boston, MA

Introduction: The spatial contexture of the tumor immune microenvironment (TIME) has been associated with survival among cancer patients, including women with high-grade serous ovarian cancer (HGSOC). However, an assessment of statistical approaches to quantify the spatial characteristics of the TIME has not been conducted. Moreover, it is unknown which statistical approach is most sensitive in identifying spatial co-localization of two cell types in the TIME.
Methods: Using the R package scSpatialSIM that simulates spatial single-cell protein data (i.e., multiplex immunofluorescence data), we completed a simulation study to compare four methods for assessing co-localization of cell types in the TIME (Ripley's K, Nearest Neighbor G, Dixon's segregation statistic, and a spatial interaction variable). The simulation study varied the cell abundance (e.g., low vs high), the co-localization (e.g., co-localization, random, segregation), and the variation in the marked point process. In addition to the simulated data, we assessed the four methods in large epidemiological studies (Nurses' Health Study [NHSI/NHSII], New England Case Control Study [NECC], African American Cancer Epidemiology Study [AACES], and North Carolina Ovarian Cancer Study [NCOCS]) including 756 women with HGSOC. Multiplex immunofluorescence was conducted using AKOYA Biosciences OPAL™ platform to measure cytotoxic T cells (CTLS) and regulatory T cells (Tregs). Cox proportional hazards regression models were fit to estimate the association of spatial co-localization of CTLS and Tregs with overall survival.
Results: In the simulation study, we found that Ripley's K was the most powerful approach for assessing co-localization for a variety of simulation scenarios. Surprisingly, the other approaches (Nearest Neighbor G, Dixon's Segregation statistic, and spatial interaction statistic) were unable to detect the simulated co-localization of two cell types in most simulation scenarios. In the analysis of women with HGSOC in the epidemiological cohorts, we were able to detect significant co-localization of CTLS and Tregs in 40.2%, 12.2%, 21.2%, and 17.0% of samples using Ripley's K, Nearest Neighbor G, Dixon's statistic, and the interaction variable methods, respectively. However, the level of co-localization was not associated with survival.
Conclusions: We found that Ripley's K was the most powerful at detecting simulated co-localization of two cell types in the TIME. Similarly, Ripley's K identified the highest level of significant spatial co-localization of CTLS and Tregs in the application to HGSOC. However, we did not observe an association of co-localization of CTLS and Tregs with overall survival. Future work is needed to develop powerful approaches for quantifying the spatial contexture of the TIME, along with assessment of the statistical properties of these methods.

#3563 Multi-modal mutational signatures elucidate the comprehensive consequences of mutational processes.

C. D. Steele, L. Alexandrov, A. Khandekar;
University of California San Diego - UCSD, San Diego, CA

The development of mutational signatures defined individually in the contexts of single/double base substitutions, insertions and deletions, structural variants and copy number variation have led to improved understanding of cancer mutagenesis and potential for improved patient stratification. We hypothesized that combining these contexts into a multi-modal mutational signature framework may improve the accuracy of assigning mutational processes to samples, and provide a holistic view of the full repertoire of mutations conferred from such processes. In order to develop multi-modal signatures, bespoke feature engineering was required for each mutational modality to enhance signal, in addition to individual modality matrix normalization so that the data could be harmonized and analyzed as a whole. These methods, and subsequent signature extraction were developed on 2,438 whole genome sequenced cancers from 21 distinct cancer types from the PCAWG consortium for which all modalities of data were available, incorporating a 348 channel signature definition. Deployment of these methods identified multi-modal signatures that encompass multiple mutation types known to associate with specific processes, for example SBS, indel and rearrangement channels defining a signature of homologous recombination deficiency. In contrast, some signatures remain defined by a single mutational modality, highlighting the distinction between broadly mutational processes, and more focused mutation processes. Multi-modal signatures show promise in increasing accuracy for difficult to assign signatures, such as those for homologous recombination deficiency, and therefore in improving patient stratification for life-saving treatment.

#3564 Survival-based grouping of genetic variants: A novel statistical framework with an application to *TP53* mutations.

X. Liu[1], H. Shi[2], E. Montellier[3], P. Hainaut[3], W. Wang[1];
[1]UT MD Anderson Cancer Center, Houston, TX, [2]Rice University, Houston, TX, [3]Univ. Grenoble Alpes, Grenoble, France

Advancements in genotyping and sequencing techniques, coupled with the growing magnitude of genome databases, have led to comprehensive investigations into the impact of genetic variants on human diseases, including cancers. It is commonly acknowledged that genetic variants have homogeneous effects on clinical outcomes, i.e., variants exhibit similar effects within a certain group but are distinct from those in other groups. However, such grouping information is typically unknown, and identification of the underlying genetic variation groups is crucial for understanding their functional consequences, facilitating patient management, and improving risk prediction. To resolve this challenge, we introduce a novel statistical framework called Survival-based Clustering of Predictors (SCP) in Cox regression to group genetic variants based on patient survival outcomes. Built upon a penalized Cox regression model, SCP considers different genetic variants, as well as additional patient-specific features if needed, as survival predictors and then searches for homogeneity among the coefficients for individual variants to recover the underlying grouping structure. Focusing on *TP53*, the most frequently mutated gene in cancer that has resulted in a wide range of functions and clinical outcomes, we apply SCP to group *TP53* germline mutations with the age of cancer diagnosis as the time-to-event. Using datasets from four Li-Fraumeni syndrome (LFS) cohorts at MD Anderson, NCI, and DFCI, we obtained 75 recurring *TP53* germline mutations from 513 patients and clustered these mutations into high-, medium-, and low-risk groups. Hotspot mutations such as R175H, R248Q, G245S, and R273C are in the high-risk group as supported in many *TP53* studies, while several non-hotspot mutations such as R290H, V218G, and G244D also exhibit strong positive effects and are grouped together with hotspot mutations. Overall, mutations in all three risk groups, obtained through applying SCP, are highly consistent with a yeast functional assay-based approach for grouping *TP53* mutations, supporting the utility of SCP for survival-based grouping of genetic variants. The contribution of our study is three-fold. Statistically, our method fills a critical gap in the survival analysis literature, offering a novel statistical framework for clustering predictors in Cox regression based on survival outcomes. Clinically, we provide a timely solution to the patient outcome-based grouping of *TP53* mutations, facilitating clinical management of *TP53* mutation carriers. Biologically, we bring fresh insights into knowledge for the most frequently observed genetic variants in cancer, providing new hypotheses to *TP53*-related biological research.

#3565 The Cox proportional hazards mixed model enables accurate estimation of the total effect somatic SNVs have on treatment outcomes.

K. Taraszka, A. Gusev;
Dana-Farber Cancer Institute, Boston, MA

Heritability is the variation in disease susceptibility attributed to genetic variation and is a fundamental parameter for interpreting disease architecture and making predictions. In the context of germline genetics, variance component models are commonly used to estimate heritability for continuous or case-control phenotypes (under the liability threshold model, LTM). However, models for time-to-event (TTE) outcomes have been largely unstudied. This has limited the characterization of age-of-onset and treatment response phenotypes, the latter particularly relevant for clinical studies. Here, we propose and evaluate a Cox proportional hazard Mixed Model (COXMM) to enable accurate estimation for TTE phenotypes with censoring. We apply these methods to Real World data from the Profile cohort from Dana-Farber Cancer Institute, a large prospectively collected tumor sequencing cohort with detailed clinical annotation. We implemented an efficient COXMM with a random effect modeled by the genetic relatedness across individuals, and benchmarked its performance in extensive simulations. We simulated phenotypes according to generative models reflecting either LTM or TTE models. For TTE phenotypes, data followed various Weibull distributions with independent censoring. Across TTE simulations, COXMM produced unbiased estimates while the classic case-control heritability estimator showed significant downward bias. Likewise, restricting only to cases and estimating the heritability of age-of-onset as a normalized continuous phenotype produced biased estimates, due to the artificial exclusion of controls. For example, for an age-of-onset with heritability of 0.8 and 40% of individuals in the study being cases, COXMM correctly inferred the heritability to be 0.80 +/- 0.007, compared to 0.32 +/- 0.004 for a conventional case-control model, and 0.09 +/- 0.02 for a conventional case-only age-of-onset model. In the Profile cohort, we analyzed the impact of somatic SNVs on progression free survival (PFS) and overall survival (OS) in patients with non-small cell lung cancer (N=954 and N=1796, respectively). We restricted to somatic SNVs present in at least 5% of patients. For OS, we observed that the COXMM heritability estimate was significantly larger than those computed by case-control status and using a normalized case-only age/duration (COXMM: 0.19 +/- 0.003; Case-Control: 0.07 +/- 0.2; Duration: 0.04 +/- 0.01). We observed a similar phenomenon for PFS as well (COXMM: 0.11 +/- 0.01; Case-Control: 0.03 +/- 0.4; Duration: 0.03 +/- 0.02). These results demonstrate that somatic features are most strongly associated with TTE and can be accurately estimated with COXMM. COXMM enables the efficient quantification of TTE heritability for diverse clinical phenotypes and outperforms existing methods.

#3566 Mohs surgery trends in 104 cases of pediatric melanoma.

Z. G. Brandt, X. Wu, J. Kennard, J. Griffin, P. Silberstein;
Creighton University School of Medicine, Omaha, NE

Background: Cutaneous melanoma is rare in children with a global incidence of two to five cases per million people per year, accounting for roughly 1% of all pediatric malignancies.[5] However, the incidence of pediatric melanoma in the United States is increasing.[1] Mohs Micrographic Surgery (MMS) is a standard treatment for adult skin cancer due to its low recurrence rates and tissue preservation. However, it is less commonly used to treat melanoma in children because the required infrastructure is not widely accessible and many pediatric surgeons are not familiar with MMS.[4] With more limited treatment options for pediatric melanoma, it is important to question the role of socioeconomic factors that may contribute to MMS treatment of pediatric patients with melanoma.[2]
Purpose: The purpose of the study is to investigate pediatric patients with melanoma and assess their tumor characteristics by comparing various skin cancer treatments (Mohs, other treatments [local excision], or no treatment).Methods: This is a retrospective cohort study of pediatric patients (age < 21 years) diagnosed with cutaneous Melanoma who received MMS between 2004 and 2020 in the National Cancer Database (NCDB). Descriptive statistics were collected on the following variables: the year of diagnosis, sex, race, tumor stage, tumor behavior, primary site, and surgical procedure. Overall survival was determined via the Kaplan-Meier test.
Results: 104 cases of pediatric melanoma treated with MMS were identified. Per statistical analysis, it does not appear that surgical frequency has varied yearly from 2004 to 2020 ($r^2 = 0$). The median age of patients analyzed was 18 years old. Most patients were female (64.4%, N = 67), White (100%, N=104), non-Hispanic (100%, N=104), and had private insurance (87.3%, N = 90). 70.2% (N=73) of cases were defined as early-stage (stage 0 or I). 72.1% (N=75) of cases were identified as invasive. 45.2% (N=47) of MMS were performed with a margin of 1 cm or less, 19.2% (N=20) were performed with a margin of 1 cm or more, and the remaining had unspecified margins. The most common primary site for MMS was skin of the trunk (33.7%, N=35), followed by the upper limb and shoulder (16.3%, N=17), and the lower limb and hip (15.4%, N=16). All patients were alive at the last contact, with a median overall survival of 182 months (15.2 years).
Discussion: MMS is used commonly in adults to treat a variety of skin tumors that can have aggressive traits such as melanoma. Although it offers low recurrence rates and tissue-sparing treatment in adult populations, MMS frequency has not changed within the pediatric population. MMS is mainly seen in privately insured, White patients with an early stage of melanoma; this is likely due to lower rates and delayed diagnosis in patients with darker skin that would otherwise present with metastatic disease. Given its clinical advantages and low rate of use, further research should address barriers that affect the availability of MMS in the pediatric population.

#3568 Managing large-scale cancer research data programs.

J. Klenk[1], D. Mikdadi[1], C. Owens[1], A. Maggio[1], B. Singh[1], E. Barner[1], T. Davidsen[2], E. Kim[2];
[1]Deloitte, Arlington, VA, [2]National Cancer Institute, Rockville, MD

Purpose: The National Cancer Institute's (NCI's) Cancer Research Data Commons (CRDC) is a data ecosystem for the cancer research community that provides cloud-based, secure storage and analytic tools for many cancer data types, including genomic, proteomic, imaging, and clinical data. CRDC requires a carefully designed, federated data governance framework to enable CRDC's goals to sustain a collaborative data environment where researchers can access timely, accurate, and relevant cancer data.
Methods: In 2023, CRDC chartered a Data Governance Framework of Committees and Working Groups across all CRDC components to: Enable diverse data type sharing; provide secure data access; optimize common infrastructure components and functions; and adhere to FAIR data principles (Findable, Accessible, Interoperable, and Reusable). We considered many designs for the CRDC Data Governance Framework, including fully centralizing or decentralizing decision-making bodies. Implementing a fully centralized data governance framework for a diverse data ecosystem like CRDC would risk top-down decisions that do not meet the unique needs of the CRDC and cancer research community. A fully decentralized data governance framework risks inconsistencies and compliance challenges. Additional governance design considerations included a federated approach that emphasizes clear roles and responsibilities; prioritizing cross-component policies to ensure consistency and promote operational efficiency; defining measurable performance standards; and keeping data owners, stewards, and users informed, trained, and supported.
Results: We have determined that long term sustainment of CRDC requires a federated governance approach with broad stakeholder participation through Committees and Working Groups. Currently established CRDC governance committees include the Enterprise Architecture Review Team (EART), Submission Review Team, Data Standards Working Group, and Data Advisory Board consisting of cancer research domain experts, researchers, and skilled cloud engineers and developers. In 2023, the CRDC EART defined data lifecycle stages and identified technical optimization opportunities for submission coordination and indexing. The established governance groups are working to identify optimization opportunities for data quality checks, submission review workflows, study acceptance criteria, data submission reviews, and cross-CRDC emerging data standards requirements.
Conclusions: Sustaining large, complex, cancer research data requires a federated governance approach with participation from all relevant stakeholder groups and cannot simply be top-down imposition of policies, standards, and procedures. The newly established CRDC federated governance framework will contribute to improving the long-term sustainability of the CRDC infrastructure and ensuring CRDC data drive meaningful research outcomes.

#3569 Using AI to automatically process data from unstructured health records of patients with lung cancer.

M. Aldea[1], P. Rolland[2], S. Simon[1], A. Poplu[2], M. Wartelle[1], B. Vignal[2], J.-C. Louis[2], F. Lion[1], A. Borie[2], D. Planchard[1], C. Robert[1], S. Michiels[1], F. Andre[1], F. Barlesi[1], F. Le Quay[2], B. Besse[1];

[1]Gustave Roussy, Villejuif, France, [2]Lifen, Paris, France

Introduction: Structured databases created from electronic health records (EHR) are crucial for cancer research. Manual data entry into databases is both labor-intensive and error-prone. We aimed to develop an artificial intelligence (AI)-driven approach for automatically inputting patient information from EHRs.
Methods: A REDCap database for 53 patients with advanced lung cancer treated with first line immuno+/-chemotherapy at Gustave Roussy between 02/2021-06/2023 was manually populated by physicians with demographics, risk factors, cancer history, and treatment data, with 137 variables/patient. Given unstructured medical letters and a schematic description of each variable, generative AI was used to find, quote and process variables into a structured form. We directed large language model actions with prompt engineering and tailored few-shot examples. Mortality data were auto-extracted from the French public registry, INSEE. We assessed consistency between manual (MDE) and automated data entry (ADE), with a secondary manual review for mismatches performed by a senior physician.
Results: In total, 7,261 data points were assessed. ADE averaged 10 minutes per patient inclusive of quality checks vs 1 h for MDA. The concordance rate between ADE and MDE was 90.2% (6,550/7,261) with a discordance of 6.8% (496/7,261). Data was missing in 0.8% (59/7,261) of cases for both methods, 1% (73/7,261) for ADE and 1.1% (83/7,261) for MDA. After checking discordances, ADE correctness was 95.3% (6,922/7,261) (Table), MDE was 93.8% (6,809/7,261). Errors in ADE (207/7,261) were due to algorithm refinement needs (70%) and missing EHR information (30%).
Conclusion: Generative AI has a strong potential for identifying and structuring data from EHRs, yielding consistency superior to manual entry by physicians and 85% reduced amount of time. This may enhance the efficiency, accuracy, and scalability of EHR-to-database conversions. ADE for >1000 patients will be presented at the meeting.

ADE correctness

100%	95-99%	90-94%	80-89%
Sex; Age; Life status; Last follow-up; Metastatic from diagnosis	Molecular alterations; Metastatic sites; Progression sites; Treatment type	Tobacco & cannabis consumption; Histology; PDL1 score; Progression event	Pack years; Date of diagnosis & first metastasis; Stage; Date of start treatment

ENDOCRINOLOGY: Molecular, Preclinical, and Clinical Endocrinology 1
Poster Session

#3572 Role of the gut microbiome in androgen production and prostate cancer treatment resistance.

A. I. Cruz Lebron[1], P. A. Balbuena-Almodovar[1], L. Mummert[1], S. Ernst[1], M. Markowski[1], M. Rudek[1], J. Ridlon[2], K. S. Sfanos[1];
[1]Johns Hopkins University School of Medicine, Baltimore, MD, [2]University of Illinois at Urbana-Champaign, Urbana, IL

Metastatic prostate cancer is often treated via a combination of androgen deprivation therapy (ADT) and the androgen receptor axis-targeted therapies abiraterone acetate + prednisone (AA/P) or enzalutamide. Unfortunately, most individuals undergoing these treatments develop resistance, termed “castration resistance”, through an unknown mechanism. Previous studies demonstrate a potential link between the gut microbiota and the treatment efficacy of endocrine therapy in metastatic castration resistant prostate cancer (mCRPC). This may be due in part to gut bacterial communities with the machinery to synthesize androgens using mechanisms distinct from human cells. For example, the bacterial *desAB* genes (e.g., “desmolase”) that were first described in the gut commensal bacterial species *Clostridium scindens* convert cortisol and prednisone to the androgenic metabolites 11β-hydroxyandrost-4-ene-3,17-dione (11OHAD) and Δ1-adrenosterone (Δ1-AT), respectively. We hypothesize that androgen synthesis by the gut microbiota promotes treatment resistance to AA/P in advanced prostate cancer. This study aims to determine if androgen-converting gut bacterial species as well as circulating and fecal androgen levels correlate with AA/P treatment response in individuals with mCRPC using a combination of metagenomics and metabolomics. We further aim to demonstrate the relationship between gut bacterial androgen production and prostate cancer treatment response using an *in vivo* mouse model. Metagenomic sequencing showed an imbalance in microbial communities and identified the presence of androgen-synthesizing bacteria such as *C. scindens* in fecal samples of individuals undergoing treatment with AA/P. We also demonstrate that the relative abundance of *C. scindens*, as well as other species reported to generate androgens, are significantly enriched during metastatic disease progression on AA/P. Furthermore, targeted quantitative PCR of the bacterial desmolase (*desA*) gene demonstrated that absolute levels of desmolase are significantly higher in AA/P non-responders relative to AA/P responders, and trended higher in individuals with rising prostate-specific antigen (PSA) versus stable PSA while on AA/P. Targeted LC/MS/MS analyses of fecal samples demonstrated the presence of testosterone, dihydrotestosterone, 11OHAD, Δ1-AT, and other androgen metabolites in association with rising PSA levels in the AA/P cohort. Furthermore, we demonstrate that *C. scindens* converts hydrocortisone and prednisone into 11OHAD and Δ1-AT, respectively, *in vitro* at 48- and 72h post-treatment, which recapitulates prior published studies. Finally, we have established a prostate cancer mouse model using a VCaP xenograft in which tumor growth was significantly inhibited by abiraterone acetate in comparison to treatment with ADT alone. Additional studies will use this mouse model to study the effects of androgen metabolism by gut bacteria on AA/P efficacy. Overall, this study ascertains the ability of the human gut microbiota to harbor androgen-synthesizing bacteria, which in turn can be an alternative source of androgens that could impact the efficacy of the anti-androgen therapies used to treat metastatic prostate cancer.

#3574 Cancer testis antigen expression correlates with stromal natural killer cell activation and longer overall survival in small bowel neuroendocrine tumors.

R. I. Ayabe, Y. D. Seo, B. Melendez, R. Lazcano, B. C. Fields, K. Wani, S. Johnson, M. Chelvanambi, C. Hudgens, S. D. Hernandez, N. J. Ajami, J. A. Wargo, A. J. Lazar, D. M. Halperin, J. S. Estrella, J. E. Maxwell;
The University of Texas MD Anderson Cancer Center, Houston, TX

Background: Patients with small bowel neuroendocrine tumors (SBNET) frequently present with metastatic disease and the efficacy of available therapies, including immune checkpoint blockade (ICB), is limited. Toward developing novel immunomodulatory strategies, we interrogated the tumor immune microenvironment of SBNETs using bulk transcriptional and digital spatial profiling (DSP).
Methods: Patients with SBNET who underwent resection at MD Anderson Cancer Center from 2003-2016 were retrospectively analyzed. Overall survival (OS) was assessed using the Kaplan-Meier method and the Cox proportional hazards model was used for multivariate analysis (MVA). Bulk transcriptional profiling was performed using the Nanostring PanCancer-Immune Panel. DSP with whole human transcriptome was performed using PanCK to segment tumor and adjacent stroma; 88 distinct regions were analyzed using differential gene expression and Reactome pathway enrichment pipelines.
Results: Resected SBNET from 42 patients were selected for transcriptional analysis. Unsupervised clustering of gene expression demonstrated dichotomization into high and low cancer testis antigen (CTA) expression. CTA-high patients (n=12) demonstrated elevated expression of type-I interferons (IFN), and CTAs such as PRAME, GAGE1 and MAGEA3 and had significantly longer OS compared to CTA-low patients (n=30; median OS not reached vs 1975 days, p=0.008). MVA controlling for age, sex, stage, and Ki-67% confirmed CTA-high status as an independent predictor of longer OS (hazard ratio [HR] 0.2, 95% confidence interval [CI] 0.05-0.83, p=0.014). A pilot DSP experiment on 4 CTA-high and 4 CTA-low tumors confirmed differential gene expression in the PanCK+ tumor compartment of these samples (R2=0.09, p=0.001). In particular, epigenetic modification genes (e.g., H2BC8, H4C8, H3C1, p<0.001) and epigenetic pathways (e.g., DNA methylation, histone acetylation) were enriched in CTA-high tumors. CTA-high tumors exhibited increased M2 macrophage presence (p=0.025) and increased NK cell activation within the PanCK- stromal compartment (p=0.001).
Conclusions: High CTA and type-I IFN expression in resected SBNET identifies patients with longer survival, agnostic of stage or grade. While CTA expression has been implicated in tumor immunogenicity, this is the first work to identify a clinically relevant signal in SBNET. Increased IFN in CTA-high tumors, corroborated by increased stromal NK cell activation, suggests that enhanced immunogenicity may drive this survival difference. Spatial transcriptomic analysis reveals epigenetic differences in CTA-high tumors and highlights the potential for combination epigenetic modifiers and immunotherapy in future trials.

#3575 The estrogenic endocrine disrupting compounds bisphenol-a (BPA) and alpha-zeranol (aZAL) induce early mammary hyperplasia in female ACI rats.

C. Winz, B. Liu, C. Xie, S. Rohatagi, E. Li, P. Furmanski, N. Suh;
Rutgers University - New Brunswick, New Brunswick, NJ

Endocrine disrupting compounds (EDCs) found in food-grade plastics, drinking water, and foodstuffs, pose a threat to human health. Estrogenic EDCs are capable of binding and activating the estrogen receptor (ER). Since breast tissue relies on estrogen signaling for growth and renewal, excessive estrogen stimulation is associated with breast cancer development. Breast cancer is a leading cause of cancer-related death in women. Only 5-10% of all breast cancer cases can be attributed to genetic causes, and the proportion of breast cancers of the luminal subtype are increasing in the United States for reasons unknown. Estrogenic EDCs may be able to initiate breast cancers through their estrogenic activities. The present study assessed two EDCs: the plasticizer bisphenol-A (BPA) and the mycotoxin alpha-zeranol (aZAL). To assess the estrogenic effects of these EDCs in an *in vivo* model, we utilized the ACI rat strain due to its sensitivity to estrogen-induced mammary carcinogenesis. The hypothesis of this work was that BPA and aZAL will induce mammary gland proliferation and estrogen signaling at early timepoints post-exposure. Estrogen, BPA, or aZAL were implanted into the backs of female ACI rats in silastic tubes at either a 9 gram doses. At a timepoint of 5 days post implantation, we saw no overt toxicity of our treatment. Both BPA and aZAL resulted in increased glandular proliferation and hyperplasia in a comparable manner to estrogen. Immunohistochemistry and qPCR revealed that the estrogen signaling marker progesterone receptor (PGR) was significantly upregulated in the estrogen, BPA, and aZAL treatment groups compared to control. The percent positivity of PGR staining in the mammary glands were 21.5% +/- 4.2%, 25.7% +/- 1.7%, 27.9% +/- 3.8%, and 8.18% +/- 2.5% respectively. Additionally, PCNA, a marker of cell proliferation, was significantly upregulated in the estrogen and aZAL treatment groups. The percent positivity of PCNA staining in the mammary glands were 7.67% +/- 2.56%, 49.6% +/- 5.2%, and 41.0% +/- 11.5% respectively. Additionally, the weight of the pituitary gland, an estrogen-sensitive endocrine organ, significantly increased in both the estrogen and aZAL treatment groups. Overall, this study demonstrated that the estrogenic EDCs BPA and aZAL induced mammary gland proliferation and hyperplasia in a comparable manner to estrogen. This is concerning due to the routine detection of these two compounds in human biosamples. More information is needed to assess the risk of exposure to these compounds as it pertains to breast cancer and other hormonal cancers.

#3576 CRISPR Cas9 mediated MADD deletion can induce autophagy via downregulation of MAPK and PI3K/AKT/mTOR signaling in anaplastic thyroid cancer.

V. Bakthavachalam, M. Madhayan, M. Sanborn, J. Rehman, P. Bellur;
University of Illinois at Chicago, Chicago, IL

Thyroid cancer is a highly prevalent endocrine malignancy with one of the fastest growing incidences of all cancers in the United States. Anaplastic thyroid cancer (ATC) has an incidence of about 1.7% of all thyroid cancers, but it causes over 40% of thyroid cancer-related deaths with a median survival period of less than one year. This is why agents that inhibit the aberrant signaling pathways which drive ATC aggressiveness are of significant interest. MAPK-activating Death Domain-activating protein (MADD) plays a key role in cancer cell survival and proliferation. MADD is constitutively expressed at higher levels in most tumor tissues and cancer cells relative to normal tissues. Studies using shRNA suggest that MADD prevents apoptosis in ATC cells. For a more definitive and mechanistic analysis of MADD in ATC, we used conditional CRISPR-Cas9 gene editing to target MADD. We observed that MADD deletion in ATC cells induced spontaneous apoptosis and also activated the autophagy pathway in human ATC cells through downregulation of ERK and mTOR signals involving the MAPK and PI3K/Akt/mTOR signaling pathways. Transcriptomic analysis of publicly available TCGA data showed several PI3K/AKT/mTOR pathway genes were positively correlated with MADD levels. RNA sequencing data of ATC lines demonstrated that enhanced activity of the PI3K/AKT/mTOR signaling pathway was correlated with a worse prognosis in ATC. Targeted MADD deletion in ATC cells combined with treatment using ERK/PI3K/Akt/mTOR/autophagy inhibitors resulted in enhanced cell death compared with MADD deletion alone. Further, MADD deleted 8505C-ATC cells showed significantly delayed tumor formation in an orthotopic nude mouse model. These findings suggest that combining MADD deletion with inhibitors of PI3K/Akt/mTOR pathway could provide an attractive new therapeutic option for ATC.

#3577 The role of PLXND1 in lineage plasticity and progression to neuroendocrine prostate cancer.

B. Chen, P. Xu, J. C. Yang, S. Ning, L. Wang, C. Nip, A. C. Gao, C. Liu;
UC Davis, Sacramento, CA

Background: Neuroendocrine prostate cancer (NEPC) is a lethal subtype of prostate cancer and is commonly associated with therapy resistance and poor prognosis. Treatment-induced NEPC (t-NEPC) predominantly develops by lineage plasticity from adenocarcinoma in response to androgen receptor signaling inhibitors, such as enzalutamide. However, the mechanisms underlying the lineage plasticity and progression to NEPC are unclear. PLXND1 (PlexinD1) is a cellular receptor of the semaphorin family and has important functions in modulating the cytoskeleton and cell adhesion. However, the role of PLXND1 in lineage plasticity to NEPC development and progression is not well established.
Methods: We performed transcriptomic analysis on NEPC patients' cohorts and the enzalutamide-resistant prostate cancer cell lines. Correlation of PLXND1 with neuroendocrine feature genes and AR-targeting genes was determined. Kaplan-Meier method and the Cox proportional hazards model was used to estimate the correlation between PLXND1 expression level and patients' survival. Immunohistochemistry was used to analyze PLXND1 expression in prostate adenocarcinoma and NEPC. Cell viability was determined in C4-2B MDVR, CWR22Rv1, and H660 cells after knocking down PLXND1 using siRNA or knocking out PLXND1 using CRISPR/CAS9. Organoids viability of patient-derived xenografts was measured after knocking down or knocking out PLXND1.
Results: Our analysis on different patient cohorts suggests that PLXND1 is highly expressed in NEPC patients, and the expression of PLXND1 is positively correlated with neuroendocrine feature genes (CHGA, ENO2, SYP, and NCAM1). Kaplan-Meier survival analysis shows that high expression of PLXND1 is significantly associated with the poor prognosis of prostate cancer patients. PLXND1 is overexpressed and negatively regulated by androgen receptor signaling in enzalutamide-resistant cells and prostate cancer patients' cohorts. Furthermore, downregulation of PLXND1 expression suppressed proliferation of the NEPC cells and viability of the PDX tumor organoids.
Conclusions: PLXND1 expression is elevated in NEPC and correlated with the poor survival of prostate cancer patients, suggesting it is a potential molecular indicator and therapy target for NEPC.

#3578 A systematic NEN spheroid drug screen reveals a novel drug resistance mechanism in small bowel NETs.

C. G. Tran[1], L. C. Borbon[1], D. H. Tow[1], J. Shilyansky[1], G. Li[1], J. Egan[1], S. K. Sherman[1], E. Abusada[1], J. Tang[2], R. govindan[3], R. C. Fields[3], T. A. Braun[1], C. H. Chan[1], C. Chandrasekharan[1], D. Spitz[1], D. E. Quelle[1], A. M. Bellizzi[1], J. R. Howe V[1], **P. Ear**[1];

[1]University of Iowa, Iowa City, IA, [2]University of Helsinki, Helsinki, Finland, [3]Washington University, St. Louis, MO

Neuroendocrine neoplasms (NENs) are rare cancers that arise from neuroendocrine cells. NENs are classified as well-differentiated neuroendocrine tumors (NETs) and poorly differentiated neuroendocrine carcinomas (NECs). Small bowel NETs (SBNETs) and pancreatic NETs (PNETs) are generally slow growing but they commonly metastasize to the liver and can become aggressive cancers. NECs are rapidly growing, and patients have poor prognosis. Little is known about the drug sensitivity profile of SBNETs, PNETs and NECs due to a paucity of cellular and animal models of these malignancies. We have successfully cultured NEN cells from clinical samples as patient-derived spheroids (PDS) and showed that they express appropriate tumor markers. We systematically screened 20 NEN (12 SBNET, 5 PNET, and 3 NEC) spheroid cultures against a library of 175 compounds (147 FDA-approved anti-cancer drugs, 8 lab selected compounds, and 20 structurally diverse molecules) and compared their drug sensitivity profiles to identify the most effective drug classes and to better understand the biology of each NEN subtype. Top drug hits were validated for their anti-tumor properties in NEN PDS and patient-derived xenograft (PDX) mouse models. Our NEN PDS cultures identified common and unique drug sensitivity profiles for each type of NEN. SBNET spheroids were more resistant to many classes of anti-cancer drugs, which was due to overexpression of cytochrome P450 genes. Consistent with clinical findings, PNET spheroids showed increased sensitivity to tyrosine kinase and mTOR/PI3K inhibitors compared to SBNET & NEC spheroids. NEC spheroids showed the broadest sensitivity to many anti-neoplastic compounds. The top candidate drug identified from our screen was romidepsin, a histone deacetylase inhibitor. Romidepsin displayed anti-tumor properties *in vitro* and *in vivo* for all 3 NEN models and was highly synergistic with rapamycin, an mTOR inhibitor similar to the SBNET approved drug everolimus. Excitingly, low-dose romidepsin effectively inhibited tumor growth when combined with low-dose rapamycin in an SBNET PDX mouse model. These NEN PDS drug screens enabled direct drug testing in primary tumor cultures to identify promising drugs that could be used alone or in combination with currently approved-NEN therapies. Histone deacetylase inhibitors, such as romidepsin, may be effective against SBNETs. NEN PDS models also serve as a valuable resource for understanding the unique biology and mechanisms of drug resistance for specific NEN subtypes.

#3580 Understanding and overcoming innate and acquired resistance to type I and II RAF inhibitors in anaplastic thyroid cancer using translational functional genomics.

P. Zeng[1], J. Meens[2], J. Barrett[1], M. J. Cecchini[1], S. B. Ryan[1], N. Pan[1], A. Karimi[1], L. Jarycki[1], A. E. Dawson[1], M. Shaikh[1], D. Palma[1], E. Winquist[1], P. C. Boutros[3], L. Ailles[2], A. C. Nichols[1];

[1]Western University, London, ON, Canada, [2]University of Toronto, Toronto, ON, Canada, [3]University of California, Los Angeles, Los Angeles, CA

Anaplastic thyroid cancer (ATC) is one of the most lethal human cancers, with some patients succumbing to the disease within weeks of diagnosis. Despite a subset of *BRAF*^{V600E} mutant ATC patients responding to monomeric type I RAF inhibitor (RAFi) dabrafenib in combination with MEK inhibitor (MEKi) trametinib, almost all patients rapidly develop adaptive or acquired resistance. These patients, along with those who do not harbor the *BRAF*^{V600E} alteration, have limited treatment options. To understand the mechanism of resistance to dabrafenib and trametinib, we utilized multi-region whole genome sequencing and single nuclei profiling of ATC patient tumors to unravel genomic, transcriptomic, and microenvironmental evolution during type I RAFi and MEKi therapy. Single-cell nuclei sequencing of matched primary and resistant ATC patient tumors identified transcriptomic reactivation of MAPK-pathway, along with immunosuppressive macrophage proliferation, underlie the development of acquired resistance. Our translation genomics led us to hypothesize that deeper inhibition of the MAPK-pathway can be efficacious in overcoming treatment resistance. Screening of a panel of type II RAFis revealed that ATC cell lines are exquisitely sensitive to the type II RAFi naporafenib. We further demonstrate that naporafenib in combination with MEKi trametinib can durably and robustly overcome both innate and acquired treatment resistance to dabrafenib and trametinib using ATC cell lines and patient-derived xenograft models, including in a PDX model from an ATC patient who developed acquired resistance to dabrafenib and trametinib. Finally, we describe a novel mechanism of acquired resistance to type II RAF inhibitor and MEK inhibitor through compensatory mutations in *MAST1*. Taken together, our work using translational and functional genomics have unraveled the differential mechanisms of treatment resistance to type I and type II RAFi in combination with trametinib, and rationalizes the clinical investigation of type II RAFi in the setting of thyroid cancer.

#3581 IGFR1 and MEK inhibition synergize to mediate anti-tumor activity in adrenocortical carcinoma.

S. Kumar, N.-Y. Sun, Y. Arakawa, D. Varghese, C. D. Hoang, J. M. Hernandez, Y. Pommier, C. Thomas, J. Del Rivero, N. Roper;
National Cancer Institute Center for Cancer Research, Bethesda, MD

Adrenocortical carcinoma (ACC) is an aggressive and rare endocrine malignancy with limited treatment options and poor prognosis. IGF2, the ligand for IGFR1, is highly expressed in ACC. However, linsitinib, an IGFR1 inhibitor, failed to improve overall survival over placebo in a randomized, phase 3 clinical trial of metastatic ACC. We hypothesized that combination therapy with IGFR1 inhibition may have greater anti-tumor efficacy in ACC than IGFR1 inhibition alone. To test this hypothesis, we performed high-throughput cell toxicity screening of 2803 clinical-stage compounds with linsitinib in an ACC cell line. MAPK inhibitors were among the top screening hits. MEK inhibitors were chosen for further evaluation given the safety, tolerability, and broad clinical activity of these FDA-approved agents. IGFR1 and MEK inhibitors were strongly synergistic in cytotoxicity across ACC cell lines, ACC organoid short-term cultures derived from surgical tissue resections (PDOs), and PDX-derived organoids (PDXOs). Genetic depletion of IGF2 significantly inhibited growth with cobimetinib and genetic depletion of MEK1 inhibited growth with linsitinib in ACC cell lines. Combination IGFR1 and MEK inhibition downregulated ERK phosphorylation and increased apoptosis compared to either IGFR1 or MEK inhibition alone. Linsitinib combined with cobimetinib significantly reduced tumor growth compared to either linsitinib or cobimetinib alone in an ACC xenograft model. Our study provides preclinical support for testing the combination of IGFR1 and MEK inhibition in patients with ACC.

#3582 PPAR gamma acetylation governs mammary adenocarcinoma tumor growth via acetylated residues that determine DNA sequence-specific binding.

L. Tian[1], X. Jiao[2], C. Wang[1], A. Ertel[1], R. Soccio[3], E. R. Chen[3], B. Győrffy[4], G. Di Sante[2], Z. Zhong[1], S. Addya[1], P. A. McCue[1], A. V. Kossenkov[5], J. Achinger-Kawecka[6], S. Clark[6], **R. G. Pestell**[2];

[1]Thomas Jefferson University, Philadelphia, PA, [2]Baruch S. Blumberg Institute, Wynnewood, PA, [3]Perelman School of Medicine at the University of Pennsylvania, Philadelphia, PA, [4]Semmelweis University, and RCNS Cancer Biomarker Research Group, Budapest, Hungary, [5]The Wistar Institute, Philadelphia, PA, [6]Garvan Institute of Medical Research, Darlinghurst, Australia

Background: HER2/neu overexpression in breast cancer confers a lipogenic phenotype. Although the introduction of anti-Her2 therapies has led to dramatic improvements in survival, nearly all patients with metastatic Her2-positive breast cancer will progress on treatment suggesting the importance of developing coextinction approaches targeting multiple pathways. Peroxisome proliferator-activated receptor γ (PPARγ), which is expressed in a variety of malignancies, governs biological functions through transcriptional programs. PPARγ binds additional DNA cis elements associated with other transcription factors, including C/EBPs, NFκB and AP-1 proteins, to promote non-canonical signaling. Defining the mechanisms governing the selection of canonical versus non-canonical PPARγ binding sequences may provide the opportunity to design regulators with distinct functions and side effects. PPARγ1 acetylation at K268/293 participates in the regulation of adipose tissue differentiation (1), and the conserved lysine residues (K154/155) govern lipogenesis in breast cancer cells (2). Although Cre based *Ppary1* gene deletion in mammary tumor oncomice showed *Ppary1* participates in the onset and progression of ErbB2-induced mammary tumorigenesis (3), the molecular mechanisms and the post-translational modifications of PPARγ governing *Ppary1* tumorigenic function remained to be determined.

Methods: Herein, we defined the role of PPARγ1 acetylation in breast cancer growth in immune-deficient mice using distinct breast cancer cell lines (MCF10-Ras, MCF10A-NeuT). Furthermore, using ChIP and ChIP-Seq we show that the acetylated residues of *Ppary1* altered preference of *cis*-element binding in chromatin to augment *Ppary* non-canonical binding.

Results: Herein, the PPARγ1 acetylated residues K154/155 were shown to be essential for the induction of transcriptional modules governing growth factor signaling, cellular apoptosis, and autophagy in mice. The K154/155 residues determined the selection of genome-wide DNA binding sites, altering the selection from canonical to non-canonical (C/EBP) DNA sequence-specific binding. The gene signature reflecting the acetylation-dependent genomic occupancy provided predictive value in patient survival outcomes.

Conclusions: Endogenous *Ppary1* promotes mammary tumor onset and progression. PPARγ1 breast tumor induction involves K154/155, which governs transcriptional programs (growth, apoptosis, and autophagy) via transcriptional complex binding to canonical *vs.* non-canonical regulatory elements. *Ppary1* acetylation participates in ErbB2-induced breast cancer tumor growth and inflammation and may represent a relevant target for therapeutic coextinction.

References: (1) Qiang L, *et al.* Cell 2012;150:620-322. (2) Tian L, *et al.* Oncotarget 2014;5:7303-153. (3) Jiao X, *et al.* Cancers (Basel) 2021;13.

#3583 Enzalutamide and flutamide induce cytotoxicity in desmoplastic small round cell tumor independent of the androgen receptor.

J. W. Magrath[1], I. N. Goldberg[1], D. D. Truong[2], A. B. Hartono[1], S. Sampath[1], C. E. Jackson[1], A. Ghosh[1], D. L. Cardin[1], H. Zhang[1], J. A. Ludwig[2], S. B. Lee[1]; [1]Tulane University School of Medicine, New Orleans, LA, [2]The University of Texas MD Anderson Cancer Center, Houston, TX

Desmoplastic Small Round Cell Tumor (DSRCT) is a rare, pediatric cancer caused by the EWSR1::WT1 fusion protein. DSRCT predominantly occurs in males, which comprise 80-90% of the patient population. While the reason for the male prevalence remains unknown, one hypothesis is that the androgen receptor (AR), when stimulated by testosterone in males, plays a critical role in DSRCT tumor growth. As a rare pediatric cancer, DSRCT model systems including cell lines and patient-derived xenografts are scarce. Further, DSRCT cell lines have been thought to seed xenograft tumors poorly, with studies commonly using 5-10 million cells for one xenograft. Using a recently established DSRCT cancer stem cell (CSC) model, we sought to establish DSRCT xenografts from fewer cells to enable large-scale xenograft feasibility and reliability. To our surprise, we were able to consistently seed tumors with as few as 100 cells, not only from CSC spheres but also from standard adherent cells. We hypothesized that mouse sex may explain our ability to seed xenografts with so few cells, as many previous studies have utilized female mice. This observation led us to comprehensively investigate the role of the AR in DSRCT. Here, we demonstrate that AR is highly expressed in DSRCT relative to other fusion-driven sarcomas and that the AR antagonists - enzalutamide and flutamide - reduce DSRCT growth. We further elucidate a novel interaction between AR and EWSR1::WT1, which may explain their co-occupancy in a subset of regulatory genomic regions. However, despite these findings, which suggest an essential role for AR in DSRCT, we find that DSRCT cell lines can form xenografts in female mice at the same rate as male mice and AR depletion does not significantly alter DSRCT growth *in vitro*. Further, we demonstrate that AR antagonists remain effective in DSRCT cells depleted of AR, establishing an AR-independent mechanism of action. Intriguingly, high-dose enzalutamide treatment reduces EWSR1::WT1 oncoprotein expression and could explain its toxicity. DSRCT cells express high levels of NR3 nuclear receptors, including the glucocorticoid receptor (GR). Enzalutamide was shown to act on GR in AR-negative prostate cancer cell lines, which could possibly explain its effect on DSRCT independent of AR. Further examination of this mechanism may provide promising therapeutic implications for DSRCT and other fusion proteins driven by the EWSR1 promoter.

#3584 Context matters: Genomic profiling of PR isoform-specific actions in breast cancer stem cells reveals novel therapeutic insights for ER+ breast cancer.

N. E. Gillis[1], T. H. Truong[1], J. Finlay-Schultz[2], C. A. Sartorius[2], C. A. Lange[1];
[1]University of Minnesota, Minneapolis, MN, [2]University of Colorado Anschutz Medical Campus, Aurora, CO

Exposure to progesterone is a recognized risk factor for breast cancer, and *PGR* polymorphisms are associated with various malignancies. The two progesterone receptor (PR) isoforms, full length PR-B and truncated PR-A, are expressed from the *PGR* gene in breast tissue and play crucial roles in normal physiology. An imbalance in the expression ratio of these isoforms, favoring increased levels of PR-A, is common in breast cancer and is associated with resistance to tamoxifen in Luminal A-type tumors. Notably, PRs have recently been implicated in promoting endocrine resistance and driving the expansion of cancer stem-like cell (CSC) populations implicated in early dissemination and maintenance of metastatic populations. Because prior gene expression studies were primarily conducted in 2D culture conditions, the isoform-specific molecular and epigenetic mechanisms underlying PR actions in advanced ER+ breast cancer remain elusive. Our goal was to define progesterone-driven gene expression in CSC cells by employing transcriptomic profiling of T47D cells cultivated in spheroid-culture conditions (3D) expressing exclusively PR-A or PR-B. Utilizing CUT&RUN, we have mapped the genomic binding sites unique to each PR isoform and identified shared sites. This genomic data has been integrated with phenotypic studies in cells expressing a single PR isoform. Our findings indicate that PR-A acts as a regulator of the cell cycle and senescence, while PR-B plays a pivotal role in cell metabolism and intracellular signaling. We find little overlap between PR-regulated gene sets derived from the same hormone-treated cells harvested from 2D relative to 3D conditions. Our genomic profiling of PRs in this 3D model system has unveiled novel strategies to combat CSC outgrowth and late recurrence in luminal breast cancer patients. This work has shifted our prior understanding of the role of PRs in gene regulation within the CSC population, and offers potential insights for therapeutic interventions in ER+ breast cancer.

#3585 DNA-PK inhibition to enhance radiation sensitivity in metastatic pancreatic neuroendocrine cancer.

P. G. Rychahou[1], A. Chauhan[2], Z. Chow[1], T. Izumi[1], Q. Chen[1], E. Y. Lee[1], D. Napier[1], L. Anthony[1], M. J. Cavnar[1], C. M. Townsend, Jr.[3], B. Evers[1]; [1]University of Kentucky, Lexington, KY, [2]University of Miami, Miami, FL, [3]University of Texas Medical Branch, Galveston, TX

Gastroenteropancreatic (GEP) neuroendocrine tumors (NETs) are neoplasms originating from the gastrointestinal track and pancreas. Unfortunately, most patients at the time of diagnosis have extensive metastatic disease and are not candidates for curative surgical resection of metastatic tumors. In such cases, targeted radiation therapy (RT) can slow the progression of metastatic disease, but eventually tumors develop resistance to radiation therapy. In this study, we examined whether DNA-PK inhibition could sensitize pancreatic NETs to radiation therapy and enhance the radiation therapy effect in a preclinical model of pNET metastasis.

Methods. We used 96-well clonogenic assays to evaluate the efficacy of the DNA-PK inhibitor peposertib in combination with RT *in vitro* in QGP-1 and BON pancreatic NET cell lines. Double-strand break-induced DNA repair was visualized with confocal laser scanning microscopy using γ-H2AX immunofluorescence after peposertib treatment alone or in combination with RT. Western blot analysis was used to confirm inhibition of DNA-PKcs (pDNA-PKcs S2056) combination RT. The efficacy of peposertib in combination with RT was evaluated in QGP-1 and BON human xenograft models in athymic nude mice and a BON preclinical lung metastasis model.

Results. Clonogenic assays demonstrated absence of cytotoxicity from peposertib alone at doses below 1000 nM and a strong radiosensitizing effect at 200 nM in both QGP-1 and BON cell lines. Pretreatment with peposertib or treatment within 2 h after RT suppressed colony formation; treatment at later timepoints did not enhance radiotherapy. Immunofluorescence analysis revealed high numbers of γH2AX foci with peposertib therapy alone at 96 h or when given 2 h after RT. Western blot analysis confirmed inhibition of DNA-PK Ser2056 after RT in combination with peposertib. DNA-PK inhibition in combination with RT led to remarkable repression of pNET growth both in subcutaneous xenografts (>90%) and in the preclinical lung metastasis model (>90%).

Conclusions. Our results showed several advantages of targeting DNA-PK to enhance radiation sensitivity in high-grade pNETs: (1) DNA-PK inhibition alone disrupts DNA damage response in pNETs as demonstrated by strong H2AX phosphorylation. (2) DNA-PK inhibition is most effective at enhancing radiotherapy either right before or after radiation therapy administration. This demonstrates that extended DNA-PK inhibition is not necessary to achieve marked responses during pNET radiotherapy. (3) DNA-PK inhibition 30 min before radiation therapy is sufficient to greatly reduce pNET tumor growth or metastasis progression in pNET preclinical models. In summary, selective DNA-PK inhibition provides a potent therapeutic strategy for disruption of non-homologous end joining DNA double-strand break repair and may offer a novel therapeutic approach in advanced NET radiotherapy.

#3586 A Hedgehog-dependent signaling axis drives neural plasticity and oncogenic reprogramming in gastroenteropancreatic neuroendocrine tumors.

S. Duan[1], R. A. Sontz[1], M. Deymier[2], J. L. Merchant[1];

[1]University of Arizona College of Medicine, Tucson, AZ, [2]Arizona Genetics Core, Tucson, AZ

Background: Neuroendocrine tumors (NETs) represent heterogenous malignancies whose origins and etiology remain poorly understood. *Men1*-driven reprogramming of neural crest-derived glial cells was recently implicated in NET development. In these studies, aberrant Sonic hedgehog (SHH) pathway activation known to pattern neural cell fate coincided with the neuroendocrine phenotype in mice. Here, we investigated the hypothesis that loss of menin encoded by the *MEN1* gene drives SHH-dependent oncogenic reprogramming of NETs by modulating the neural crest cell fate.

Methods: Glial cell specific *Men1* deletion was accomplished by expressing *Cre* recombinase downstream of the human glial fibrillary acidic protein promoter (*GFAP*$^{\Delta Men1}$). Hedgehog (HH) activation of *Men1*-deficient glial cells was blocked by deleting the gene encoding primary ciliary protein *Kif3a* required for transducing SHH signaling. The resulting *GFAP*$^{\Delta Men1}$ mice were evaluated for NET development and dysregulated hormone profiles. To identify aberrant SHH activation leading to neuroendocrine reprogramming, we performed single cell RNA- and Assay for Transposase Accessible Chromatin sequencing on *GFAP*$^{\Delta Men1}$ NETs and primary glial cultures. Hyperactivation of SHH in human gastroenteropancreatic (GEP)-NETs was confirmed by immunofluorescent staining and western blot. Lastly, primary mouse and human NET organoids were treated with an agonist and inhibitors of HH signaling and evaluated for ERK/AKT activation, proliferation, and transcript fluctuations indicative of neural crest cell reprogramming.

Results: *GFAP*$^{\Delta Men1}$ mice developed NETs in the pancreas, pituitary, and small intestine. Astonishingly, impaired SHH activation in GFAP^{+}/*Men1*$^{-/-}$ cells abolished the development of NETs and restored hormone levels to that of wild type mice. *GFAP*$^{\Delta Men1}$ NETs and glial cultures showed increased SHH signaling and chromatin accessibility of HH pathway genes, whereas additive *Kif3a* deletion blocked HH activation. Moreover, menin negative glial cells demonstrated a phenotypic shift in neuroglial lineages that suggested SHH-mediated reprogramming of neural crest-derived cells following the loss of menin. Consistent with hyperactive SHH activation in the *GFAP*$^{\Delta Men1}$ mice, human GEP-NETs overexpressed SHH and downstream signaling targets. Functionally, SHH induced ERK/AKT activation, cell proliferation, and neuroendocrine transcript expression in human and mouse NET organoids, whereas pharmacological inhibition of HH signaling reversed these effects.

Conclusions: Our observations implicate neural crest-derived glial cells as potential neuroendocrine cell precursors that are susceptible to transformation through increased HH signaling. These studies warrant future investigation into the delivery of Hedgehog inhibitors in the adjuvant setting for NET treatment.

#3587 Evidence that membrane progesterone receptors (mPR) play a key role in cancer metastases in most cases of metastatic cancer.

J. H. Check[1], D. Check[2], B. Neumann[3], C. Wilson[2],

[1]Cooper Medical School of Rowan University (CMSRU), Melrose Park, PA, [2]Cooper Institute for Reproductive Hormonal Disorders, Mt. Laurel, NJ, [3]Inspira Health Network, Vineland, NJ

An immunomodulatory protein called the progesterone induced blocking factor (PIBF) is essential for the fetal semi-allograft to escape immune surveillance. Many cancer cell lines make both mPRs for PIBF and the protein itself. The progesterone receptor (PR) antagonist mifepristone added to cancer cell line cultures down-regulated mRNA for PIBF and the PIBF protein. This IRB approved study (that required a compassionate use IND from the FDA) evaluated oral mifepristone 200mg per day (majority) or 300mg in patients with very advanced cancers with no more treatment options available. Patients would remain under the care of their primary oncologists (FDA requirement). Because the nuclear (n) PR may be protective against cancer spread, only patients with cancers negative for the nPR were treated. Patients with the following types of cancers received mifepristone: non-small cell lung cancer (NSCLC) (n=9), small cell lung cancer (SCLC) (n=2), colon (n=3), pancreatic (n=2), thymic epithelial cell (n=1), transitional cell carcinoma of the renal pelvis (n=1), malignant fibrous histiocytoma (n=1), glioblastoma multiforme stage IV (n=1), leiomyosarcoma (n=1). All 21 patients showed significant palliative benefits, especially but not limited to, marked reduction in pain and marked improvement in energy, decreased dyspnea on exertion, and return of mental clarity. For those who had repeat CT evaluation no one failed to show shrinkage and decrease in malignant lesions and 2 (leiomyosarcoma and SCLC) showed complete remission after a few months on mifepristone. Five patients (3 females, 2 males) with SCLC (1), NSCL (n=3) and fibrous osteosarcoma (n=1) survived at least 5 years with 2 dying from cancer unrelated causes (SCLC and NSCLC). Two are still alive (NSCLC with EGFR mutation and brain metastases). The male with fibrous osteosarcoma died after stopping mifepristone in favor of a new drug recommended by his oncologist. Two patients lived over 2 years. Most would have lived longer had they not stopped mifepristone. Other observations: significant palliative benefits are seen within 3 weeks of taking mifepristone before any evidence of significant tumor regression. After a period of time, some lesions (especially in the primary location) may start growing slowly, but this is not a sign of loss of drug efficacy and long good quality life is still probable if one remains on the drug. The cancer spreads rapidly if one stops the mifepristone. The usual reason for stopping the drug was intervention by the primary oncologist suggesting a new clinical trial because there has not been complete remission of the cancer or some tumor growth (usually slow) or finances. Not one patient had a side effect. Hopefully this study will generate interest in treating patients with advanced cancer with mifepristone, especially those devoid of the nPR. These data support the role of mPRs in cancer proliferation.

#3588 Androgen synthesis disruption, ferroptosis induction and prostate cancer inhibition by androgen and vitamin D combination.

B. Park, J. Vaquiz, O. Igbekoyi, **B. Chatterjee**;
UT Health Science Center at San Antonio, San Antonio, TX

Background: Metastatic castration-resistant prostate cancer (CRPC) is a fatal condition that progresses to end-of-life within two years, and it is the fifth leading cause of cancer death in men globally. New avenues for preventing or delaying lethal CRPC progression are a critical unmet need. Hormonal vitamin D_3 (calcitriol) inhibits prostate cancer - both castration sensitive and castration resistant - in preclinical models, as documented widely. However, vitamin D as an anti-cancer therapeutic is clinically untenable since prostate tumor suppression in patients requires hormone dosing at a supraphysiologic level which induces hypercalcemia and other toxicities.

Results: Herein we provide the first evidence that a subnanomolar, non-calcemic calcitriol dose can inhibit CRPC cell proliferation, G1 to S phase transition, clonal growth, migration, and invasion *in vitro*, and xenograft growth *in vivo*, only upon concurrent dosing with 5α-DHT at a physiologic or subphysiologic level. Calcitriol as a single treatment is non-inhibitory at a subnanomolar dose. HSD3β1, a hydroxysteroid dehydrogenase, was markedly induced by calcitriol, while DHT cotreatment reduced the induction. HSD3β1 catalyzes conversion of dehydroepiandrosterone, an adrenal androgen, to androstenedione (AED) - a rate-limiting step in the androgen biosynthesis pathway. AKR1C3, an aldo-keto reductase which promotes androgen biosynthesis, was also reduced by calcitriol/DHT cotreatment. In contrast, AKR1D1, an androgen-inactivating 5β-reductase, was robustly induced by a non-calcemic calcitriol dose in the presence of DHT, not by calcitriol singly. AKR1D1 converts AED and testosterone to 5β-diols. HSD3β1 and AKR1C3 are elevated in CRPC. Disruption of androgen biosynthesis and net reduction of the intratumor androgen pool are expected outcomes of reduced HSD3β1 and AKR1C3, and elevated AKR1D1. The hormone pair led to LC3B induction, ferritin degradation, and induction of *ALOX-5* and *NCoA4* - the genes which regulate ferroptosis, indicating autophagy mediated ferroptosis (ferritinophagy). Apoptosis and necroptosis were absent. We conclude that vulnerabilities created by combined androgen and non-calcemic vitamin D dosing can lead to cell death by ferroptosis, and this hormone pairing may be a new avenue for arresting CRPC clinical progression.

Significance: The translational potential of our results is bolstered by the precedent that supraphysiologic testosterone improved serum PSA scores and other clinical parameters for a subset of therapy-inert CRPC patients who received repeated cycles of once-a-month single testosterone dosing- a protocol known as bipolar androgen therapy (BAT)[1]. Our findings may offer a strategic framework for enhancing the efficacy of BAT by including oral dosing of a non-calcemic level of vitamin D_3. W81XWH-21-1-0307 (DoD); IK6 BX004207 (VA). Ref 1: Nat Rev Urol 2023; PMID 36543976

#3589 Understanding the role of Pax5 in development of taxane-resistant NE-like prostate cancer.

S. Bhattacharya, R. Islam, S. Bodas, J. Mishra, D. Das, K. Datta, S. Dutta;
University of Nebraska Medical Center, Omaha, NE

Background: Resistance to the existing Androgen Receptor Signaling Inhibitor (ARSI) therapies led to higher incidences of aggressive therapy-induced neuroendocrine-like prostate cancer (t-NEPC) with predominant small cell-like characteristics, dismal overall survival, and an ultimate resistance to taxane chemotherapies. t-NEPCs are mostly treated with platinum-based drugs with etoposide and/or taxane but have less selectivity and high systemic toxicity, which often limits their clinical and therapeutic potential. During t-NEPC transformation, upon chromatin reprogramming associated with epigenetic alterations and altered transcriptional activity, adenocarcinoma loses its luminal features to adopt neurobasal characteristics. The following study aims to unravel the mechanism of developing t-NEPC taxane resistance upon acquiring such adaptive neuronal characteristics.
Objective: The primary objective is to delineate how chromatin modifications along with epigenetic regulation facilitates the adaptive neuronal characteristics and dictates the development of t-NEPC taxane resistance.
Methods: We generated various t-NEPC cell lines either by genetic modification (DKD) or therapeutic pressure (C4-2BER). We performed RNA-Seq, ATAC-Seq and acetylated Histone (H3K18 and H3K27) ChIP-Seq in our developed t-NEPC models and compared with adenocarcinoma. We next compared ATAC Seq and Acetylated histone ChIP Seq with RNA Seq in C4-2B and C4-2BER and performed functional assays.
Results: Our ATAC Seq and acetylated histone footprints (Ac H3K18 and Ac H3K27 ChIP Seq) analyses revealed an enhanced chromatin accessibility during t-NEPC transformation. Overlapping RNA seq suggested newly transcribed neuronal genes with higher extent of promoter accessibility. Transcription Factor mapping among newly accessible gene promoters revealed preferential Pax5 binding, whose expression occurs selectively in t-NEPC unlike adenocarcinoma. Pathway analysis of differentially expressed neuronal genes in t-NEPC suggested an involvement of Pax5 in axonal guidance, neurotransmitter regulation, and neuronal adhesion, which are essential for strong cellular communication. Furthermore, Pax5 depletion disrupts cellular interaction in t-NEPC, thereby, sensitizing them to taxane therapies.
Conclusions: Our study concludes that continuous AR ablation with ARSIs, leads to chromatin alterations with epigenetic changes, thereby allowing Pax5 transcriptional activation in t-NEPC. This altered transcriptional activity promotes gene expression necessary to govern taxane-resistant t-NEPC development.

#3590 Tumor intrinsic production of glucocorticoids in ovarian carcinoma.

P. Hanjra[1], E. Stur[1], S. Cole[2], S. Lutgendorf[3], A. Sood[1];
[1]UT MD Anderson Cancer Center, Houston, TX, [2]University of California, Los Angeles, Los Angeles, CA, [3]University of Iowa, Iowa City, IA

Background: Cortisol is a glucocorticoid (GC) known to be produced by the hypothalamic-pituitary-adrenal (HPA) axis. Dysregulation of the HPA axis is prevalent in patients with ovarian cancer. These patients have elevated nighttime levels of cortisol and increased tumoral expression of the glucocorticoid receptor (GR); both of which correlate with shortened overall survival (OS). We hypothesize that outside the HPA axis, ovarian cancer may have tumor-intrinsic production of GC. In this study, we examined whether 11 beta-hydroxysteroid dehydrogenase 1 (11β-HSD1; enzyme which activates cortisone to cortisol) has steroidogenic activity in the ovarian cancer tumor microenvironment (TME).
Methods: We used the Genotype-Tissue Expression (GTex) Portal and the Cancer Cell Line Encyclopedia (CCLE) to determine expression of steroidogenic enzymes in the ovary and ovarian cancer cell lines. We further performed UMAP analysis of a single-cell RNA-seq dataset of tumor samples from patients with ovarian carcinoma to cluster for cell type. ELISAs were performed to quantify cortisol production and secretion by cells stimulated with metabolite, cortisone. Subcellular fractionation and Western blotting were performed to measure protein expression of 11β-HSD1, GR, and phospho-Ser 211 GR.
Results: HSD11B1 mRNA (which encodes 11β-HSD1) is detectable in bulk ovarian tissue at a median expression of 78.19 transcripts per million (TPM) as measured in the GTex data. *In vitro*, primary human ovarian fibroblasts express functional 11β-HSD1 and produce and secrete cortisol upon cortisone stimulation in a time-dependent manner, with a mean total secretion of 17.91 ± 0.21 ng/ml at 12 hours. Analysis of scRNA-seq data identifies that cancer-associated fibroblasts (CAFs) may be a source of HSD11B1 in the ovarian TME, with roughly 9% of CAFs expressing HSD11B1. In HeyA8 ovarian cancer cells (positive for 11β-HSD1), cortisone stimulation *in vitro* results in cortisol production with a mean total secretion of 22.04 ± 5.46 ng/ml at 12 hours. Moreover, this cortisol results in GR activation in an 11β-HSD1-dependent manner.
Discussion: We identify 11β-HSD1 as a potential mechanism of GC production within ovarian cancer, with CAFs being a putative source. We further show that 11β-HSD1 activity can lead to activation of the GR within cancer cells.

#3591 Upregulation of CXCL8 is an early step in the oncogenic transition of human thyroid cells by *BRAF*^{V600E}.

R. Sarkar, P. Bolel, J. Klubo-Gwiezdzinska, M. C. Gershengorn;
NIH National Institute of Diabetes and Digestive and Kidney Diseases (NIDDK), Bethesda, MD

Introduction: BRAF^{V600E} is one of the most common oncogenic mutations in human thyroid cancers, especially in papillary thyroid carcinoma (PTC). However, the early molecular changes caused by this mutation have not been studied previously in human thyrocytes *in vitro*.

Methods: Primary cultures of cells derived from noncancerous thyroid tissue of patients (at least n=3) were infected with *BRAF*^{V600E} adenovirus to mimic the mutated condition. Changes induced by the infection were measured at early times (<24h). Transcriptome analysis was performed on infected thyrocytes (n=6) to determine the highest differentially expressed genes between the control and infected groups, which were then verified at the gene and protein levels. RNAi downregulation experiments were performed to determine the cross-regulatory function of the genes.

Results: The induction of *BRAF*^{V600E} mutation, confirmed at the protein level, increased proliferation of the cells, and morphological changes were observed at approximately 24h post-infection. The decreased expression of thyroid-specific genes, viz. TSHR, TG, and TPO were observed after >72h post-introduction of *BRAF*^{V600E} mutation. Transcriptome and protein expression analysis of *BRAF*^{V600E}-positive thyrocytes showed the overexpression of chemokines *CXCL8* and *CXCL12*, and upregulation of endothelial cell-specific molecule 1 (ESM1). These molecules are known to be associated with increased neoangiogenesis and proliferation. Functional studies showed that siRNA knockdown of *CXCL8* decreased the expressions of *CXCL12* and *ESM1*, whereas knockdown of either *CXCL12* or *ESM1* did not decrease the expression of *CXCL8*.

Conclusion: Increased proliferation, de-differentiation, upregulation of chemokines, and endothelial-specific factor are effects associated with *BRAF*^{V600E}-driven thyroid carcinogenesis. CXCL8 appears to play an important early regulatory role in this process.

CLINICAL RESEARCH: Adoptive Cellular Therapy 1
Poster Session

#3595 A retrospective analysis of the clinical characteristics of metastastic solid cancer patients with cytokine-induced killer cells combined immune checkpoint inhibitor immunotherapy.

J. Choi[1], J. Kim[1], D. Yang[2], G. Nam[3];

[1]Konyang Univ. Hospital, Daejeon, Korea, Republic of, [2]Konyang Univ. College of Medicine, Daejeon, Korea, Republic of, [3]GC Cell Corp., Yongin City, Korea, Republic of

Background: Cytokine-induced killer cells (CIKs), obtained through ex vivo expasion from peripheral blood mononuclear cells, are phenotypically and functionally shared with both T and NK cells. Within the T cell group, it can be classified into a group that simultaneously expresses CD3 and CD56 molecules (range: 30% to 70%) and a group representing CD3+ CD56- phenotype (range: 20% to 60%). It also contains a small population (< 30%) of CD3 CD56+ NK cells. They can exhibit potent MHC-unrestricted cytotoxicity for both hematologic and solid tumors, but they are not harmful in hematopoietic precursors and normal tissues. Anti-programmed death-1 (PD-1) antibodies reinvigorate T cell-mediated antitumor immunity. PD-1 blockade antibody might significantly increase the cytotoxic potency of CIK cells via increasing proliferative capacity and IFN-r secretion. This retrospective study is the first to combine CIK cells with PD-1/PD-L1/CTLA-4 blockade(Immune checkpoint inhibitors, ICIs) in patients with metastatic solid cancers.
Methods: We analyzed 225 heavily treated metastastic solid cancer patients receiving CIK cell (Immunecell-LC, GC cell inc provide.) and with ICIs. Blood Sampling for CIK cells production was performed after 3 days after ICIs administration. Patients received a single intravenous infusion of activated autologous CIK cells every 2 weeks. ICIs was administered according to the protocol of each drug regardless of the CIK cells administration date. The primary end points were safety and adverse event (AE) profiles. Objective responses, overall survival (OS), progression-free survival (PFS), and diseae control rate were secondary end points.
Results: Treatment-related AEs occurred in 154/225 patients. Grade 3 or 4 toxicities, including fever and chills, were observed in 28 patients. All treatment-related AEs were tolerable and no death due to autoimmune disease. When administration ICIs, CIK cells exhibited excellent antitumor properties and increased IFN-γ secretion. Objective responses (complete or partial responses) were observed in 67 of the 225 patients. One patients with hepatocellular carcionma had complete response. In most patients who showed an objective response, the effectiveness was maintained for more than 6 months. The overall disease control rate in the patients was 58.9%. At the time of this report, the median OS and PFS were 18.6 and 7.1 months in hepatocellular carcinoma patients and were 13.1 and 6.5 months in triple negative breast cancer patients, respectively.
Conclusion: Treatment with activated autologous CIK cells and ICIs was safe and exerted encouraging antitumor activity in metastastic solid cancers. Phase 2 clinical studies for each tumor type will be conducted.
Keywords: Cytokine-induced killer cells, Immune check inhibitors, Safety, Objective response

#3596 Metabolic reprogramming of the tumor microenvironment to enhance the functionality of TCR-edited T cell in colorectal cancer and liver metastases.

A. Potenza, C. Balestrieri, M. Spiga, L. Albarello, F. Pedica, A. Ferrari, O. A. Botrugno, B. Camisa, E. Tiziano, C. Sirini, M. Casucci, C. Iozzi, D. Abbati, U. Elmore, G. Di Lullo, G. Casorati, C. Doglioni, G. Tonon, P. Dellabona, R. Rosati, L. Aldrighetti, P. Monti, E. Ruggiero, C. Bonini;
IRCCS San Raffaele Scientific Institute, Milan, Italy

In solid malignancies, T cells functionality is intertwined with metabolic reprogramming within the tumor microenvironment (TME), which supports the increased energy request of cancer cells and suppresses the effector function and cytokines production of the immune infiltrate. In primary colorectal cancer (CRCs) and related liver metastases, we revealed extensive transcriptional remodeling across tumors, being metabolic pathways among the major drivers of this variance. Accordingly, extracellular adenosine, accumulating in the TME for the hydrolysis of ATP by CD39 and CD73, has been recognized as a novel inhibitory mediator, which binds preferentially to the A2A receptor (A2Ar) to exert its immunosuppressive activity. By high dimensional flow cytometry, we revealed that CD39 is a major driver of T-cell exhaustion in primary and metastatic CRCs. Therefore, we sought to disrupt CD39 in TCR-edited T cells (TCR_{ED}). By CRISPR/Cas9, we disrupted both the α and β chains of the endogenous TCR together with *ENTPD1*, the gene encoding for CD39, and redirected T cell specificity against the HER2 antigen. $TCR_{ED}CD39_{KO}$ T cells outperformed their competent counterpart in eliminating patient-derived organoids (PDOs) from primary and metastatic tumors both *in vitro* and *in vivo*. Given the role of CD39 in starting the biochemical cascade leading to adenosine production, we aimed at investigating the direct role of adenosine on the functional advantage observed with $TCR_{ED}CD39_{KO}$ T cells. We challenged our cellular products with target cells in the presence or absence of adenosine and observed that $TCR_{ED}CD39_{KO}$ T cells are superior to their competent counterpart in the ability to release cytokines, while the effect is completely abolished when adenosine is present. Also, when $TCR_{ED}CD39_{KO}$ T cells were challenged with PDOs, the exogenously added adenosine nullifies the functional killing advantage given by the $CD39_{KO}$. To gain more insights into the pathway, we also generated $TCR_{ED}A2Ar_{KO}$ T cells. In line with the different roles of CD39 and A2AR on the ATP/adenosine pathway, the disruption of the adenosine receptor resulted in a significant advantage in PDO killing in the presence of adenosine only. We then evaluated the influence of $CD39_{KO}$ in the metabolic capacity of T cells and revealed that $TCR_{ED}CD39_{KO}$ T cells have a greater potential to rely on the mitochondrial other than glycolytic functions, which explains higher functionality and persistence. Further evaluation on the metabolic effect of $CD39_{KO}$ are currently ongoing. Overall, we showed that the ATP/adenosine cascade is relevant for T cells functionality and metabolic status and can be harnessed in adoptive cell therapy strategies to counteract the immunosuppressive TME.

#3597 Multimodal γδ T cell cytotoxicity overcomes cellular therapy reprogramming.

C. B. Nattress[1], D. Fowler[2], P. Vlckova[1], C. Hutton[3], M. Ramos Zapatero[1], J. Sufi[1], F. Cardoso Rodriguez[1], A. Campbell[1], A. Kanouta[2], M. Buschhaus[1], K. Chester[1], J. Anderson[2], V. Li[3], M. Barisa[2], J. Fisher[2], C. Tape[1];

[1]University College London (UCL) Cancer Institute, London, United Kingdom, [2]University College London-Great Ormond Street Hospital (UCL-GOSH) Institute of Child Health, London, United Kingdom, [3]The Francis Crick Institute, London, United Kingdom

Colorectal cancer (CRC) is a devastating disease that kills ~700,000 people worldwide annually. Current immunotherapies struggle against both microsatellite stable (MSS) disease and the immunosuppressive CRC tumor microenvironment (TME). Despite these challenges, tumor infiltrating γδ T cells confer a prognostic benefit to CRC patients and can kill cancer via antibody independent cytotoxicity (AIC) and antibody-dependent cellular cytotoxicity (ADCC). We hypothesized that γδ T cells can be exploited as an 'off-the-shelf' anti-CRC biotherapeutic but their complex interactions within the CRC TME need to be elucidated. To explore the patient-, donor-, and mechanism-specific interactions of γδ T cells with CRC, we performed single-cell profiling of >1,000 CRC patient-derived organoid (PDO) and human Vγ9Vδ2 T cell cultures. γδ T cells from multiple donors were used either unmodified or engineered to secrete a modified IL-15 cytokine (stIL15-γδs). The addition of anti-tumour IgG further allowed us to study anti-PDO ADCC, with antigen specificity assessed with antigenKO PDO models. Using 126-plex Thiol Organoid Barcoding in situ (TOB*is*) mass cytometry (MC) (Qin et al., Nature Methods, 2020) (Sufi and Qin et al., Nature Protocols, 2021), we measured cell-type specific signaling across multiple γδ donors and CRC PDOs, including post-translational modifications (PTMs), cell-state, and immunological phenotype. We found that stIL15-γδs exhibit superior proliferation, purity and viability both *in vitro* and *in vivo*. stIL15-γδs demonstrated significant cytotoxicity against all CRC PDOs tested, commonly outperforming standard-of-care chemotherapies even when challenged against our previously-defined chemorefractory MSS patients (Zapatero et al., Cell, 2023). The susceptibility of PDOs to ADCC differs substantially and is not associated with antigen density and %positivity or PDO tumor mutational burden. Minimal differences in ADCC capability were seen between stIL15-γδs donors which were not associated with γδ phenotype or pre- and post-experiment FcγR CD16 expression. Crucially, we found that stIL15-γδ signaling is reciprocally regulated in a PDO-specific manner, with significant regulation of stIL15-γδ cell-state, PTM signaling and immunological phenotype observed. Increased dysregulation of stIL15-γδs during AIC negatively correlates with PDO cytotoxicity — indicating PDOs negatively reprogram γδ T cellular therapies. However, when γδ T cells engage in ADCC (via anti-tumour IgG), stIL15-γδ signaling recovers, leading to substantial anti-PDO cytotoxicity. Furthermore, stIL15-γδs could perform significant cytotoxicity against all chemoresistant MSS PDOs tested, representing the patient population with greatest unmet clinical need. These results demonstrate that multimodal γδ T cell cytotoxicity can overcome tumor-specific cellular therapy reprogramming.

#3598 A new strategy for T cell therapy: T cells secreting TCR anti-CD3 bispecific T-cell engager.

Hanli Sun, Jiao Huang, Kai Zhan, Wanli Wu, Xianqing Tang, Min Liu, Shanshan Guo, Hongjun Zheng, Yingjie Huang, **Shi Zhong**

XLifeSc Ltd., Guangzhou, China

TCR-engineered T (TCR-T) cells and TCR-anti-CD3 bispecific T-cell engagers (TCEs) are potent TCR-based therapeutic agents with distinct advantages and limitations in tumor treatment. TCR-T cells offer durable persistence within patients but necessitate personalized manufacturing and lack the capacity to harness bystander T cells. Conversely, TCEs are readily available as "off-the-shelf" products and can recruit bystander T cells, yet they exhibit a shorter lifespan. In our study, we sought to merge the merits of both approaches by engineering T cells to secrete a TCR-anti-CD3 TCE specific for alpha fetoprotein (AFP), a tumor-associated antigen abundantly expressed in hepatocellular carcinoma (HCC). We initially identified a TCR with specificity for the $AFP_{158-166}$ peptide bound to HLA-A*02:01 and enhanced its affinity to picomolar via phage display. To facilitate efficient secretion by T cells, we adapted the high-affinity TCR to a single-chain format (scTCR) and fused it with a CD3-specific single-chain antibody fragment (scAFP-TCE). Our findings demonstrated that scAFP-TCE effectively redirected bystander T cells to engage in the lysis of HCC cells. Moreover, scAFP-TCE could be secreted by T cells transduced with lentiviral particles encoding the TCE gene. These transduced T cells exhibited potent antitumor activity both independently and by enlisting bystander T cells. This innovative T cell strategy, combining the bystander-recruiting ability of fusion proteins with the durable persistence seen in T cell therapy after a single infusion, presents a promising alternative to conventional TCR-based therapeutic agents. We anticipate that this novel approach may hold substantial potential for enhancing HCC treatment and expanding the scope of TCR-based immunotherapies.

#3599 Recombinant chimeric antibody-based gamma-delta TCR targeting GPC3 induces potent antitumor response against hepatocellular carcinoma.

D. Li[1], T. Liang[1], Z. Duan[1], H. Zhang[2], C. Liu[2], M. Ho[1];
[1]National Institutes of Health (NIH), Bethesda, MD, [2]Eureka Therapeutics, Inc., Emeryville, CA

Background and Significance: Hepatocellular carcinoma (HCC), a major type of primary liver cancer, is the third leading cause of cancer-related death worldwide. While Glypican-3 (GPC3) is highly upregulated in HCC, it is minimally expressed in normal tissues. The research in our laboratory has been focused on the development of GPC3 as an immunotherapeutic target for liver cancer. Despite many clinical trials, there has not been any approved therapy targeting GPC3 largely due to the combination of antigen heterogeneity, poor tumor penetration, and the inability to induce a durable, potent immune response in the tumor microenvironment (TME). Here, we made a recombinant chimeric antibody-based T cell receptors (named AbTCR) targeting GPC3 and explored its anti-tumor efficacy in xenograft mouse models.
Methods: The AbTCR constructs were built by fusing an antigen recognition domain (hYP7 scFv or HN3 VH) specific for GPC3 to the gamma-delta TCR constant region along with a secondary T cell signaling activation motif. The NFAT-tdTomato reporter cell line was established and used to measure the AbTCR-triggered T cell signaling upon stimulation with tumor cells. Anti-tumor efficacy of AbTCR-T cells was determined via luciferase-based cell killing assay as well as multiple HCC xenograft mouse models.
Results: The hYP7 GPC3 AbTCR-T cell not only enhances antigen-binding capacity and T cell activity, but also induces infiltration and expansion of T cells in the TME, thereby causing robust liver tumor regression in mice.
Conclusion: Our data show that new hYP7-directed GPC3 AbTCR is a promising strategy for treating liver cancer. This work provides a rationale for the use of hYP7 GPC3 AbTCR in clinical studies for treating HCC and other GPC3-positive solid tumors.

#3600 Reversal of iNKT cell dysfunction in cholangiocarcinoma.

K. Htwe, K. Soontrapa, S. Jirawatnotai, S. Prasopporn, P. More-Krong, S. Sampattavanich, A. Wongkajornsilp;
Mahidol University, Bangkok, Thailand

Invariant natural killer T (iNKT) cells are CD1d-restricted unconventional T cells possessing innate and adaptive immunity with high anti-tumor activities. Yet, the effectiveness of iNKT cell therapy in clinical trials is limited due to iNKT cell dysfunction after exposure to the tumor microenvironment. Aggressive cholangiocarcinoma (CCA) cell lines were used to study iNKT cell reactivity. These CCA cell lines lacked CD1d molecules and responded poorly to iNKT cells. The iNKT cells became dysfunctional after the exposure to CCA by 48 h. In this study, we overcame iNKT cell dysfunction by searching for a small molecule to prevent or reverse the gene sets regulating iNKT cell dysfunction, thus prolonging anti-tumor activity. It was found that P53 and estrogen early response pathway gene sets were enriched in dysfunctional iNKT cells which were reversed by vorinostat, an HDAC inhibitor. Anti-CCA activity of iNKT cells was regained with a subtherapeutic dose of vorinostat as protection. Interestingly, vorinostat could not totally recover the anti-tumor effect of iNKT cells that have already developed into the dysfunctional stage. Significant tumor size reduction was seen in the humanized mouse model after iNKT cell adoptive therapy was given in combination with vorinostat compared to monotherapy with either iNKT cell or vorinostat alone. This study demonstrated that inhibiting the gene sets regulating iNKT cell dysfunction by vorinostat could prevent iNKT cell dysfunction, and prolong its anti-tumor activities. This combination could be a novel treatment option for CD1d-negative CCA patients resistant to standard chemotherapy.

#3601 Improving killing of renal cell carcinoma through the combined effects of TCR engineered CD4+ and CD8+ T cells.

Muna Igboko[1], Long Chen[1], Stefan Barisic[2], Elena Cherkasova[1], David Allan[1], Mala Chakraborty[1], Joseph Clara[1], Angie Parrizzi[1], Kyra Carney[1], Rosa Nadal Rios[1], Robert Reger[1], Richard Childs[1]

[1]NIH National Heart, Lung & Blood Institute, Bethesda, MD,[2]Oregon Health & Science University, Portland, OR

Patients with late-stage kidney cancer have poor long-term survival rates. Our lab isolated a low affinity CD8 dependent TCR named BZ-4 from CTLs of a patient who had immune-mediated regression of renal cell carcinoma (RCC) following an allogeneic stem cell transplant and found this TCR recognized a human endogenous retrovirus type E (HERV-E) derived 10-mer peptide, CT-RCC-1. The BZ-4 clone belongs to the Vβ7.1 family and binds to CT-RCC-1 in an HLA-A11 dependent manner. Adoptive infusion of CD8+ BZ-4 transduced T cells is currently being explored in an NIH phase I trial (NCT03354390). Because CD4+ T cells have been shown to augment the anti-tumor effects of TCR-modified CD8+ T cells, we hypothesized that CD4+ T cells genetically engineered to co-express BZ-4 and CD8 would recognize and kill RCC tumors expressing the CT-RCC-1 and would improve the in vivo proliferation and tumor cytotoxicity of CD8+ BZ-4 T cells. CD4+ T cells isolated from healthy donor PBMCs were transfected via Sleeping Beauty electroporation with the control MART-1 reactive TCR (DMF5), BZ-4, or BZ-4 alongside the CD8 co-receptor (BZ-4-8). CD8+ T cells were similarly transfected with DMF5 or BZ-4. Following magnetic bead enrichment, 66% to 84% (mean 77%) of transfected T cells stained positive for Vβ7.1. TCR engineered T cells were subsequently tested for their ability to lyse a) luciferase transduced HLA A-11 expressing RCC tumors and b) a T2 cell line modified to express both HLA A-11 and luciferase that was peptide-pulsed with decreasing concentrations (5×10^{-1}, 5×10^{-2}, 5×10^{-3} & 5×10^{-4} ug/mL) of CT-RCC-1. CD4+ T cells expressing BZ-4 or BZ-4-8 as well as CD8+ T cells expressing BZ-4 or DMF5 were used either alone or in combination in cytotoxicity assays. For combined T cell groups, the total effector/target ratio was maintained at the same ratio as individual T cell groups. For T-2 targets, CD4+ BZ-4 T cells exhibited no cytolytic activity in contrast to both CD8+ BZ-4 T cells and CD4+ BZ-4-8 T cells, which were highly cytolytic to target cells. For RCC tumor targets, CD4+ BZ-4 T cells exhibited no cytolytic activity at 48, 72 and 96 hours in contrast to both CD8+ BZ-4 T cells and CD4+ BZ-4-8 T cells, which exhibited high levels of tumor killing at these timepoints. Remarkably, CD4+ BZ-4-8 T cells alone or in combination with CD8+ BZ-4 T cells demonstrated tumor cytotoxicity that was comparable to that observed with CD8+ BZ-4 T cells alone. In conclusion, these data show that CD4+ BZ-4 T cells transfected with the CD8 co-receptor acquire the ability to lyse RCC tumors at levels comparable to that observed in CD8+ BZ-4 T cells. Additional experiments are planned to evaluate whether mixtures of CD8+ BZ-4 T cells with CD4+ BZ-4-8 T cells will augment the ability of TCR modified T cells to proliferate in vivo and kill human RCC tumors compared to CD8+ BZ-4 T cells alone in tumor bearing NSG mice.

#3602 TRAIL-NK-92 MI as a novel adoptive therapy for castration-resistant prostate cancer (CRPC): Preliminary *in vitro* results.

M. Schwermann[1], P. Srinivasan[1], W. MacDonald[1], V. Tajiknia[1], A. Schmidt[1], S. Zhang[1], L. Carlsen[1], A. George[2], C. Purcell[1], S. Lu[3], M. Hadfield[3], A. Mega[3], B. Carneiro[3], W. El-Deiry[3];

[1]Legorreta Cancer Center at Brown University, Providence, RI, [2]Yale School of Medicine, New Haven, CT, [3]Legorreta Cancer Center and Lifespan Cancer Institute at Brown University, Providence, RI

Introduction: Natural killer (NK) cell tumor infiltration and higher expression of activating receptors NKp30 and NKp46 are associated with improved clinical outcomes in prostate cancer (PC). Activation of NK cells by androgen receptor inhibitors enhanced the killing of PC cell lines (Schwermann 2023). These findings support the therapeutic potential of strategies inducing NK cell activation to treat CRPC. NK cells induce apoptosis of cancer cells via TNF-related apoptosis-inducing ligand) (TRAIL) binding of death receptor 5 (DR5), which is overexpressed in PC cells. This is the first report of adoptive therapy utilizing high expression of TRAIL as a novel therapeutic strategy.

Methods: We transduced NK-92-MI and CD4+ (Jurkat) cell lines with human TRAIL (pLVX-EF1alpha-TRAIL-IRES-eGFP).Transduced cells were pre-treated with simvastatin or atorvastatin (4uM) for 36h, followed by stimulation (IL-2 100 IU/ml and IL-12 100 ng/ml) for 2h. The eGFP-expressing cells were then sorted by FACS. PC (PC3, DU145, LNCaP, and 22Rv1), fibroblast (IMR-90), and brain endothelial (hCMEC/D3) cell lines were used in co-culture experiments with non-transduced and transduced NK cells and CD4+ cells. These experiments were quantified using the ImageXpress Confocal HT instrument. Viability assays were performed using Annexin-PI and flow cytometry staining for caspases 3/7.

Results: Transduced NK-92 MI cells with TRAIL displayed increased surface expression of TRAIL (control[C]: 4.38%±1; TRAIL-overexpression[NK-TRAIL]: 78.54%±3.76; p<0.001). Co-culture of PC cell lines with TRAIL-NK-92 MI cells resulted in significant tumor-induced apoptosis compared to co-culture with non-transduced NK cells after 48 hours (LNCaP + NK [C]: 16.52%±5, LNCaP + NK-TRAIL: 73.19%±6; PC [C]: 14.4%±3, PC3 + NK-TRAIL: 79%±8; 22Rv1 [C]: 16.78%±1.7, 22Rv1 + NK-TRAIL: 76%±8; DU145 [C]: 13%±4, DU145 + NK-TRAIL: 59.1%±10; p<0.001). This enhanced cytotoxic function was also observed in CD4+ cells expressing high levels of TRAIL. Annexin-PI staining as well as Caspase 3 and 7 showed increased apoptosis in PC co-cultured with NK-TRAIL. Co-culture of NK-TRAIL cells did not affect the viability of the non-malignant cells (IMR-90 and hCMEC/D3) over 48h (IMR-90 + NK: 4.6%±1, IMR-90 + NK-TRAIL: 4.47±2, p=0.9; hCMEC/D3 + NK: 2.7%±0.8, hCMEC/D3 + NK-TRAIL: 2.2±0.5, p>0.99). These results align with the lower expression of DR5 on non-malignant cells compared to PC cell lines (IMR-90: 1.46%±0.5, hCMEC/D3: 1.9%±0.8, LNCaP: 92.3%±4.5).

Conclusion: Transduced NK-92 MI cells with human TRAIL-induced higher levels of apoptosis of PC cell lines compared with non-transduced NK cells in co-culture experiments. The results highlight the potential of TRAIL-expressing adoptive cell therapy for CRPC. Engaging adoptive therapies with specific targets (anti-PSMA CAR) might increase the therapeutic potential of this strategy.

#3603 NKX101, an allogeneic off-the-shelf CAR NK cell therapy targeting NKG2D-Ls, has potent anti-leukemic activity alone or in combination with Ara-C.

C. Cho, N. Kimura, J. Sood, D. Juat, M. Zhang, C. Chan, T. Geng, K. Hansen, J. Trager;
Nkarta Inc., South San Francisco, CA

Introduction: NKG2D-Ligands (NKG2D-Ls) are a family of immunomodulatory proteins that are upregulated on damaged or transformed cells but have limited expression on normal tissues. Natural killer (NK) cells target and eliminate NKG2D-L^{+} cells through NKG2D receptor binding and subsequent activation. NKX101 is an allogeneic, off-the-shelf healthy donor-derived chimeric antigen receptor (CAR) NK cell therapy candidate engineered to express an NKG2D-L targeting CAR and membrane-bound IL-15 for extended persistence. In a clinical trial, NKX101 treatment combined with modified lymphodepletion incorporating cytarabine (Ara-C) has shown promise for the treatment of relapsed/refractory (r/r) AML, including generating complete responses (CR) with MRD negativity (MRD^{-}). To support the rationale of NKX101 combined with modified lymphodepletion, we developed assays to (i) investigate the cytotoxic activity of NKX101 against individual NKG2D-Ls, (ii) determine the effect of Ara-C pre-treatment on NKG2D-L expression on AML cell lines, and (iii) evaluate the combined anti-leukemic activity of NKX101 and Ara-C.

Methods: NKX101 cells were generated from peripheral blood leukopaks from healthy donors. CHO-K1 cells were engineered to stably express individual NKG2D-Ls or transduced with empty vector controls and were combined with NKX101 cells for cytotoxicity experiments. AML cell lines were treated with increasing levels of Ara-C and evaluated for NKG2D-L expression by flow cytometry. To measure NKX101 cytotoxicity against AML cell lines, NucRed™-labeled target cells were pre-treated with Ara-C using IC_{50} and IC_{90} concentrations and co-cultured with NKX101. Specific cell killing of target cells was measured using an Incucyte® instrument for five days. Assessment of the contribution of each agent was determined using a dose-response matrix of increasing concentrations of NKX101 and Ara-C to generate specific cytotoxicity values. Combination effects were analyzed using the SynergyFinder Plus web application.

Results: Expression of a single NKG2D-L was sufficient to trigger NKX101 cytotoxicity against target cell lines, further validating NKG2D-Ls as therapeutic targets. Flow cytometry analysis revealed that pre-treatment with Ara-C upregulated NKG2D-Ls on AML cell lines in a dose-dependent manner. NKX101 showed enhanced anti-leukemic activity against AML cells pre-treated with Ara-C compared to untreated controls, demonstrating that the combination can enhance NKX101 potency. Assessment of the combination of NKX101 and Ara-C using a dose-response matrix revealed that the two modalities combine to potently kill AML cells in a synergistic manner, supporting continued investigation of NKX101 CAR NK cell therapy after lymphodepletion incorporating Ara-C for the treatment of r/r AML.

#3604 NKX101, an allogeneic off-the-shelf NKG2D CAR-NK cell therapy, has potent in vitro cytotoxicity against patient-derived AML leukemic stem cells and non-leukemic stem cell blasts.

K. Hansen, C. Cho, N. Kothari, D. Shook, J. Trager;
Nkarta Inc., South San Francisco, CA

Introduction: Acute myeloid leukemia (AML) is a malignancy of immature myeloid cells characterized by rapid proliferation of abnormal myeloblasts. Treatment options for patients with AML are limited, especially for relapsed/refractory (r/r) disease. Leukemic cells with stem cell features, known as leukemic stem cells (LSCs), have been implicated as the origin of relapse in minimal residual disease positive (MRD^{+}) AML (Khaldoyanidi et al. 2022, Kamel et al. 2022). NKX101 is an allogeneic, off-the-shelf, healthy donor-derived chimeric antigen receptor (CAR) NK cell therapy candidate engineered to express an NKG2D CAR and membrane bound IL-15. In a clinical trial, NKX101 has shown promise for the treatment of r/r AML, including generating complete responses (CR) with MRD negativity (MRD^{-}). In this study, we utilize a flow cytometry-based approach to (i) evaluate the cell surface expression of NKG2D-Ls on normal cells vs. primary AML blasts, (ii) assess the expression pattern of NKG2D-Ls on AML blast subsets, and (iii) determine NKX101 cytotoxic killing of LSC and non-LSC AML blasts.
Methods: NKX101 cells were generated from peripheral blood leukopaks from healthy donors. Cryopreserved bone marrow mononuclear cells (BMMCs) were obtained from AML patients (n=20) and healthy donors (n=10) in accordance with approved IRB protocols. AML somatic mutation status was determined using an Illumina TruSight® Myeloid Sequencing Panel. NKX101 cytotoxicity against patient-derived AML blasts was assessed using a flow cytometry-based assay that measured specific cytotoxicity and AML blast/LSC markers. NKG2D-L expression was determined using flow cytometry with antibodies specific to individual NKG2D-Ls.
Results: Utilizing patient-derived primary samples, we demonstrate that NKG2D-Ls are expressed on AML blast cells and expressed at higher levels on AML blast cells compared to healthy normal hematopoietic cells ($p = 0.002$). Furthermore, we show that NKG2D-Ls are expressed at similar levels on LSCs compared to non-LSC AML blast populations. Target cell specific flow cytometry-based cytotoxicity assays revealed that NKX101 potently kills patient-derived AML blasts in a dose-dependent manner. Moreover, NKX101 had similar cytotoxic potency against both LSC and non-LSC AML blasts.
Conclusions: In summary, we show that NKG2D-Ls are expressed on the surface of both LSC and non-LSC AML blasts and at levels above those observed in normal hematopoietic cells. Additionally, the ability of NKX101 to potently kill AML LSC blasts suggests that NKG2D-L targeting may be a viable mechanism for eliminating LSCs in the blood and bone marrow of patients with r/r AML. Taken together, these data support NKG2D-Ls as promising therapeutic targets for AML and support further investigation of NKX101 CAR-NK therapy for the treatment of r/r AML.

#3605 Phase II study of pembrolizumab in conjunction with lymphodepletion, TIL ACT, and high- or low-dose IL-2 in patients with metastatic melanoma.

M. Hasanov[1], **S. Kiany**[2], M.-A. Forget[2], R. L. Bassett[2], M. A. Davies[2], A. Diab[2], J. E. Gershenwald[2], I. C. Glitza[2], J. E. Lee[2], A. Lucci[2], J. L. McQuade[2], S. P. Patel[2], M. I. Ross[2], H. A. Tawbi[2], J. Wargo[2], M. K. Wong[2], C. Bernatchez[2], P. Hwu[3], C. Haymaker[2], R. N. Amaria[2];

[1]The Ohio State University Comprehensive Cancer Center, Columbus, OH, [2]UT MD Anderson Cancer Center, Houston, TX, [3]Moffitt Cancer Center, Tampa, FL

Background: In metastatic melanoma (MM) patients (pts), adoptive cell transfer (ACT) using tumor-infiltrating lymphocytes (TIL) can yield lasting responses. However, TIL ACT with high-dose IL-2 has notable toxicities. Anti-PD1 (pembrolizumab) is FDA approved for MM treatment. Our study aimed to merge TIL infusion with anti-PD1 in two arms, comparing high (HD, arm 1) and low (LD, arm 2) IL-2 doses.

Methods: After tumor harvest and TIL expansion, pts were lymphodepleted with cyclophosphamide and fludarabine, followed by infusion with their ex-vivo expanded TIL combined with IL-2 (arm 1: 720,000 IU/kg IV q 8 hrs up to 15 doses; arm 2: 2 million IU SC for 14 days). Pts were given 200 mg of IV anti-PD1 starting 21 days post-TIL infusion, followed by doses every 3 weeks for up to 2 years. Blood was taken before lymphodepletion and before the first two anti-PD1 doses for flow cytometry and cytokine analysis The primary endpoint of the study was determination of overall response rate by RECISTS 1.1 criteria. Enrollment aimed for 18 pts per arm, monitoring the primary ORR endpoint using a Bayesian rule. Enrollment would halt in any arm if the ORR dropped below 40%.

Results: The median age was 50 years (n=14: 6 F and 8 M). Of these 14 pts, 8, 2, 2, and 2 had cutaneous, uveal, mucosal, or unknown primary melanoma. Pts had a median of 3 lines of prior therapies (range 1-6), including anti-PD-1 (n=13). In arm 1, one pt had a partial response (PR) for 10 months, 2 had stable disease (SD), 3 had progressive disease (PD), and 1 was not evaluable (NE). In arm 2, one pt had an ongoing PR for over 76 months, 1 had SD, and 5 had PD. Due to ORR <40% in each arm, enrollment was stopped after treatment of 14 pts. There was no significant different in progression-free survival or overall survival between the two arms (p=0.99 and p=0.71, respectively). In general, toxicity levels were comparable in both arms; however, pts in arm 2 had slightly lower grade 3 febrile neutropenia (57% vs. 71%) and shorter hospitalization (median 16 days vs. 18 days) than pts in Arm 1. While no correlation was observed between the phenotype of the TIL product and clinical response, both PR pts received high numbers of TIL (38.6x10^9 and 93.7x10^9; mean: 32.6x10^9 cells), with a high CD8+/CD4+ T cell ratio (284.7 and 2.7; median: 2.7). IL-2 dose did not affect circulating Treg frequency, phenotype, or proliferation by flow cytometry 3 weeks post TIL infusion. IL-2 dose was not associated with CD4+ non-Treg and CD8+ T cell phenotype or proliferation. Addition of anti-PD1 reduced expression of checkpoints but did not boost T cell proliferation.

Conclusion: Our treatment strategy did not yield any distinct difference between low and high dose IL-2, suggesting the potential of low-dose IL-2 as an alternative. Anti-PD1 did not have any appreciable effect on immune states potentially due to the cohorts being comprised of a heavily pre-treated heterogenous pt population.

#3606 Tumor-specific CD8$^{\pm}$ Tc9 cells activate host CD4$^{\pm}$ T cells to control antigen-lost tumors.

L. Xiao, Q. Yi;
Houston Methodist Research Institute, Houston, TX

Cancer immunotherapies relying on targeted destruction of cancer cells by potent antitumor T cells have achieved unprecedented success in recent years. As a main form of cancer immunotherapies, adoptive T cell therapy (ACT) has shown a durable response in certain cancer patients. However, this response is often short-lived and tumor relapse occurs due to the outgrowth of antigen-lost-variant (ALV) tumors and poor antitumor immune response. Here, We reported that adoptively transfer of murine tumor-specific CD8$^{\pm}$ Tc9 but not Tc1/CTL cells achieved long-term control of tumor growth in vivo. Here, we demonstrated that murine tumor-specific Tc9 cells not only killed antigen-expressing primary tumors but also controlled the outgrowth of antigen-lost relapsed tumors by recruiting and activating host effector CD4$^{\pm}$ T cells that recognized relapsed tumors. Tc9 cells secreted IL-24 and recruited CCR7-expressing conventional type-2 dendritic cells (cDC2) into tumor-draining lymph nodes to prime host CD4$^{\pm}$ T cell response against relapsed tumors. Depleting host CD4$^{\pm}$ T cells or deficiency in CCR7 expression impaired Tc9 cell ability to control the outgrowth of relapsed tumor. We also observed that intratumoral *IL24* expression was positively correlated with gene signatures of cDC2 and CD4$^{\pm}$ T cells in human cancers and expression of *IL24* and cDC2 and CD4$^{\pm}$ T cell gene signatures were associated with patient's overall survival. Thus, this study uncovers a novel mechanism underlying activation of tumor-specific CD4$^{\pm}$ T cells in vivo.

#3607 Case study: Efficacy and persistence of autologous T cell therapy targeting SLC45A2 in uveal melanoma.

S. Singh[1], E. Ryu[1], K. M. Campbell[2], **A. Smith**[3], S. Phillips[1], L. Soto[1], I. Lai[4], G. Lizee[1], B. Vincent[5], M. Thompson[3], W. Hoos[3], S. Patel[1], C. Yee[1];
[1]MD Anderson Cancer Center, Houston, TX, [2]University of California, Los Angeles, Los Angeles, CA, [3]H37 Institute, Durham, NC, [4]CTMC, Houston, TX, [5]University of North Carolina at Chapel Hill, Lineberger Comprehensive Cancer Center, Chapel Hill, NC

Background: Metastatic uveal melanoma (UM) is an aggressive cancer, with a 1-year overall survival of < 50%. While the bispecific T-cell engager tabentafusp is approved for HLA-A2+ patients with gp100+ UM, there are limited treatment options for patients who do not express HLA-A2. We present a strategy and proof-of-concept for designing and manufacturing a tumor-selective endogenous T-cell therapy (ETC) for a patient with metastatic UM.
Methods: PBMC were collected by apheresis in 2013 upon first diagnosis with uveal melanoma; 8 years later, following progression, cryopreserved PBMC were used to generate autologous antigen-specific T cells for adoptive therapy. The validated tumor antigen SLC45A2 was found to be overexpressed in the patient's metastatic tumor based on RNA expression profiling. Peripheral blood derived SLC45A2-specific HLA-A2402-restricted central memory CD8+ T cells were generated via a process of in vitro priming, IL-21 treatment, tetramer-guided sorting and cell expansion. Clinical response was assessed via longitudinal CT imaging and ctDNA-based MRD monitoring. Persistence of transferred T cells was measured via serial flow cytometry and RNA-sequencing of PBMCs, along with TCR and RNA sequencing of tumor tissue collected post infusion.
Results: A 39 year old male received SLC45A2-specific ETC therapy and checkpoint inhibitor treatment for advanced metastatic UM (GNAQ (Q209P), BAP1 (E398*, LOF). Bulk RNAseq data from baseline biopsies were queried for known tumor-associated antigens, and *SLC45A2* was expressed at high levels. The patient experienced widespread disease stabilization with minimal toxicity. SLC45A2-specific CD8+ T cells persisted in circulation up to 181 days after the first infusion and 43 days after the second infusion, ranging from 6.7% - 1.5% of total circulating CD3 T cells. T cell clones from the infusion product included the dominating TCR subclone in tumor tissue collected 6 weeks post infusion, comprising 33% of the TCRá and 26% of TCRâ population. SLC45A2-specific T cells were identified in the tumor infiltrating lymphocytes in a separate lesion collected 10 months after the first infusion. A duodenum lesion progressed during treatment, and RNAseq demonstrated reduced expression of genes associated with HLA presentation and *SLC45A2* and reduced TIL infiltration, suggesting tissue-specific immune editing of the tumor cell population.
Conclusions: 1. Tumor-reactive antigen-specific T cells can be isolated and expanded for adoptive therapy using PBMCs cryopreserved for > 8 years. 2. Following infusion, peripheral blood and tumor profiling support the persistence of transferred T cells in a patient with metastatic uveal melanoma. 3. Disease stabilization in aggressive metastatic UM was achieved with minimal toxicity. Overall, our study provides evidence and rationale for utilizing autologous antigen-specific T cells for treating rare cancers.

#3608 Nonpathogenic *E. coli* engineered to surface display human cytokines for enhanced immunotherapy.

Shaobo Yang[1], Michal Sheffer[1], Isabel Kaplan[1], Zongqi Wang[2], Mubin Tarannum[1], Roman Shapiro[1], Yasmin Abdulhamid[1], Rebecca Porter[1], David Barbie[1], Robert Soiffer[1], Jessica Little[1], Jerome Ritz[1], Mengdi Yang[3], Valeria Marquez-Pellegrin[3], Jiahe Li[2], Rizwan Romee[1]

[1]Medical Oncology, DFCI/Harvard Medical School, Boston, MA,[2]Biomedical Engineering, University of Michigan, Ann Arbor, Ann Arbor, MI,[3]Bioengineering, Northeastern University, Boston, MA

Background: Poor trafficking, exhaustion and low persistence of adoptively transferred T and NK cell-based therapies in solid tumors remain major barriers in the field. Leveraging safety, tumor tropism and ease of genetic manipulation in bacteria present potentially a novel approach to overcome these barriers. Prior approaches to bacteria-based biologics delivery encounter issues of low concentration and fast clearance. In this study, we hypothesized that displaying immune-activating cytokines on outer membrane of *Escherichia coli (E. coli)* could modulate immunosuppressive tumor microenvironment (TME) enhancing migration, activation, and tumor control mediated by T and natural killer (NK) cells.

Methods: To investigate our hypothesis, we expressed human and murine cytokines: IL-15, decoy resistant IL-18 (DR-18), and IL-21 on outer membrane of a non-pathogenic facultative bacteria *E. coli* K-12. We first evaluated their ability to activate human mesothelin (MSLN) NK cell CARs *in vitro* and performed gene expression analysis. For the *in vivo* experiments we used C57BL/6 mouse model with syngeneic tumor cell lines MC38 and B16F10. We also assessed the ability of human cytokine-displaying bacteria with human MSLN-CAR NK cells in NSG mice carrying human mesothelioma H226.

Results: OmpA displaying murine DR-18 on bacterial surface was most effective in tumor control. After optimization, intra-tumoral injection of the bacteria resulted in 50% of cured mice bearing MC38 and 30% of cured mice bearing B16F10. Rechallenging these mice with respective cells showed no tumor growth, indicating induction of tumor-specific immune memory. Tumor tissue analysis showed upregulation of CD8 T and NK cells and depletion experiments demonstrated the contribution of these cells to tumor control. When systemically injected, the bacteria inhibited tumor growth with no side effects. Bio-distribution analysis demonstrated bacterial enrichment in TME. Through the utilization of *in vitro* killing assays by NK cells, YiaT232 scaffold with human DR-18 emerged as the optimal candidate. RNA-sequencing demonstrated that bacteria with DR-18 were capable of upregulating IL-12 and oxidative phosphorylation pathway in NK cells. Furthermore, administration of bacteria displaying DR-18 and systemic (IV) MSLN-CAR-NK cells led to better tumor control (vs soluble DR-18 or bacteria alone) in NSG mice carrying mesothelin-high H226.

Conclusions: Here we develop a novel platform for immunotherapy involving surface display of cytokines in non-pathogenic *E. coli*. The bacteria were safe and demonstrated tumor tropism and CD8 T and NK cells were identified as the major effector cells mediating tumor control in immune-competent mice. Subsequently, we could display human DR-18 on these bacteria which resulted in superior tumor control in NSG mice when combined with MSLN-CAR-NK cells, paving the way for clinical translation in the near future.

#3609 Chimeric cytokine receptors increase memory phenotypes and improve expansion and efficacy of CAR-T cell therapies.

J. R. Newcomb[1], J. Ren[1], S. Syed[1], Z. Caruolo[1], L. Webb[1], C. McKay[1], S. Kwei[1], C. Novina[2], F. Mermelstein[1];
[1]Dynamic Cell Therapies, Watertown, MA, [2]Dana Farber Cancer Institute, Boston, MA

Cytokine activation of T cells can promote T cell proliferation, memory and improve T cell function in driving tumor cell killing. However, systemic administration of cytokines at therapeutic doses is also associated with unacceptable toxicities. To overcome this limitation, we have engineered a system of private cytokine signaling to affect T cell homeostasis, identity, and function. Specifically, we have engineered chimeric cytokine receptors (CCRs) composed of single-chain variable fragments (scFvs) that bind specifically to small molecules such as fluorescein or DOTA. These scFvs are fused to transmembrane and intracellular domains of all members of the common gamma-chain (γ-chain) family of cytokine receptors. CCRs that permit private cytokine signaling were introduced into known CAR-T cell therapies and their impact on CAR-T cell phenotype, function, and anti-tumor activity was tested. First, CCR-containing T cells were tested for activation-induced changes in phenotype and expansion following stimulation with small molecule conjugates *in vitro*. The most promising results were obtained using either the IL-7Rα- or IL-2Rβ/γ-containing CCR's. CCR-containing constructs were then transduced into one of two different anti-BCMA CAR-T constructs, ide-cel or cilta-cel, using a lentiviral transduction system. CAR-T cells containing each CCR were then compared with CAR-T cells lacking CCRs for phenotype and function *in vitro*. Results indicated that engineering the IL-7Rα CCR with both of these CAR-T's led to increased expansion, cytokine secretion and improved tumor cell killing. Next, CAR-T cells expressing the IL-7Rα CCR were compared to CAR-T cells lacking CCR for efficacy and durability in a mouse model of human multiple myeloma. IL-7Rα CCR-expressing CAR-T cells demonstrated improved long-term tumor control compared to ide-cel and cilta-cel alone. In addition, IL-7Rα CCR-expression increased T cell numbers in blood, spleen and bone marrow of tumor-bearing mice. These increases were particularly evident in the $CD8^{+}$population of CAR-T cells *in vivo*. These results demostrate that private cytokine signaling using small-molecule activatable CCRs can improve efficacy and durability of CAR-T cells. We are testing these CCRs in mouse models of human solid tumors to assess their ability to overcome the immunosuppressive microenvironment.

#3610 Utilizing fructose metabolism to fuel anti-tumor immunity.

T. Schild[1], R. Chirayil[2], L. Haughton[1], P. Wallisch[1], M. Berishaj[1], D. A. Scheinberg[1], K. R. Keshari[1];
[1]Memorial Sloan Kettering Cancer Center, New York City, NY, [2]Columbia University Medical Center, New York City, NY

Consumption of fructose in the form of high fructose corn syrup is elevated in the western diet, but it is not fully understood how fructose metabolism influences anti-tumor immunity. Fructose is canonically metabolized in the intestine and the liver and can shunt into glycolysis. In certain tumor types, fructose metabolism becomes deregulated, allowing tumor cells to metabolize fructose to power their biosynthetic processes. Similarly, reprogramming immune cells to be able to efficiently metabolize fructose may help us power immunotherapy to work in difficult to treat cancers, especially in individuals who have high fructose in their blood or in the tumor microenvironment (TME). Imparting effector T cells with the ability to use fructose for fuel can overcome one of the major metabolic limitations of the TME: limited nutrient supply. As T cells become activated, they alter their metabolism to support growth and proliferation. Activated CD8+ T cells upregulate their glycolysis which results in increased biosynthetic processes, such as synthesis of macromolecules and effector cytokines. However, tumor cells also consume substantial amounts of glucose, resulting in a glucose-depleted microenvironment, which could be one of the major barriers to immunotherapy working in solid tumors. Therefore, we engineered T cells to overexpress a fructose transporter, GLUT5, which is normally not expressed in the immune compartment at high levels. We hypothesized that increased fructose uptake by CD8+ T cells will ameliorate exhaustion caused by the glucose-low tumor microenvironment. Indeed, we determined that GLUT5 T cells are more efficient in killing in low glucose supplemented with fructose. We also observed that GLUT5 expression restores T cell glycolytic capacity under fructose to that of unexhausted T cells under glucose replete conditions. Similarly, GLUT5-expressing T cells proliferate faster *in vitro* and exhibit an improved ability to control B16 tumor growth *in vivo*. Additionally, combining GLUT5 cell infusion with checkpoint inhibition resulted in durable tumor control and prolonged mouse survival. Further, engineered CD19-targeted CAR T cells with expression of GLUT5 were more metabolically active and cytotoxic in low glucose conditions, mimicking the TME. In conclusion, GLUT5 expression in effector CD8+ and CAR T cells may allow immunotherapy to function in solid tumors under low glucose conditions.

#3611 A patient-derived organoid platform to assess the effectiveness of γδTCR cell therapy in solid tumors.

Andrea Bisso[1], Rene Overmeer[2], Sjoerd Baardman[1], Chris Coomans[1], Cesar Oyarce[2], **Sylvia F. Boj**[2]

[1]Gadeta B.V., Utrecht, Netherlands,[2]HUB Organoids B.V., Utrecht, Netherlands

Recent advances in cancer immunotherapy have positively impacted the life expectancy of patients for an extensive range of clinical indications. With new treatment strategies and druggable targets being identified at an increasing pace, the number of patients eligible for cancer immunotherapy is expected to expand steadily. However, promising therapeutic developments face hurdles in translating preclinical findings into therapy since conventional 2D cancer models hold low clinical predictive value. HUB developed an innovative alternative, building on the discovery that adult stem cells proliferate and organise into three-dimensional organotypic structures when embedded into the extracellular matrix. Patient-derived organoids are generated from healthy and malignant tissues, and they recapitulate complex characteristics of the original parental tissue, including molecular heterogeneity and morphological and functional traits. Cell therapies have achieved positive results in treating haematological cancers. Recently, the unique tumour-targeting properties of γδ T cell receptors have been leveraged to develop safer and more effective strategies. HUB and Gadeta joined efforts to explore the therapeutic potential of GDT002 - i.e. αβ T cells engineered with a Gadeta proprietary new γδTCR - to target solid cancers. A preclinical basket trial was performed using patient-derived organoids from several tumour types (colorectal, breast, head and neck, ovarian cancers) cocultured with GDT002. The results showed broad reactivity of GDT002 against solid tumor PDOs. Interestingly, GDT002 was particularly efficient at killing ovarian cancer-derived PDOs, allowing Gadeta to move GDT002 to clinical trials for this indication confidently. This study reveals that our tumor organoid co-culture with engineered T cells platform holds significant value for the preclinical development of cellular therapies.

#3612 Preclinical & clinical activity of autologous mRNA engineered chimeric antigen receptor monocytes for targeted cancer immunotherapy.

Yuxiao Wang[1], Michele Gerber[1], Michael Gorgievski[1], Josephine D'Alessandro[1], Neha Diwanji[1], Ronald Vale[2], Siddhartha Mukherjee[3], Daniel Getts[1]

[1]Myeloid Therapeutics, Cambridge, MA,[2]HHMI, Cambridge, MA,[3]Columbia Univerisity, Cambridge, MA

Introduction: The tumor microenvironment (TME) is a dynamic and multifaceted system that comprises largely myeloid lineage immune cells including neutrophils, macrophages, dendritic cells and monocytes. When activated, these cells are can effectively infiltrate TME and orchestrate anti-tumor immune response. Reprogramming myeloid cells by arming them with a tumor specific chimeric antigen receptor (CAR) presents an attractive strategy to overcome current limitations in solid tumor treatment. In this study, we present the isolation and mRNA-based engineering of monocytes with chimeric antigen receptors (CARs), followed by their in vivo application for cancer treatment in rodent models and in human T cell lymphoma patients.

Results: Engineered monocytes demonstrated the abilities to infiltrate the TME, undergo activation, and differentiate into macrophages and dendritic cells. Upon CAR activation, these reprogrammed myeloid cells utilized both direct and indirect mechanisms to eliminate tumor cells. This included direct tumor cell killing through phagocytosis and TNF-associated mechanisms. Furthermore, engineered monocytes exhibited the capacity to recruit natural killer (NK) cells and T cells to the TME. In the case of T cells, these engineered myeloid cells facilitated the presentation of neoantigens to T cells and stimulate an adaptive immune response. In patients with T cell lymphoma, treatment with engineered monocytes expressing a CAR targeting CD5 exhibited a favorable safety profile and was associated with TME remodeling, expansion of novel T cell clones, and promising survival outcomes.

Conclusions: These findings underscore the potential of reprogrammed myeloid cells as a novel avenue for cancer immunotherapy, offering hope for improved treatments and outcomes in the fight against cancer.

#3613 Screening iPSC lines for optimal characteristics of differentiation into immune effector cells for clinical programs.

B. A. Morse, Jr., A. Cogburn, A. Chialastri, M. S. Hall, O. Manor, A. Lebid, D. Kim, L. Cocka, D. J. Perry, C. Budd, A. Kolluri, L. Campion, T. Nishimura, M. Naso, H. Levitsky;
Century Therapeutics, Philadelphia, PA

Engineered Induced Pluripotent Stem Cells (iPSCs) are the core foundational technology for Century Therapeutics. In our constant effort to identify iPSC lines with diverse functional activity, we have derived a large panel of clinical-grade peripheral blood mononuclear cell (PBMC)-derived and gamma-delta T cell-derived IPSC lines (PiPSCs and TiPSCs, respectively) from multiple donors. These lines have been screened by multiple criteria to select the top lines for clinical development in our iPSC-derived NK (iNK) and T cell (iT) programs. Initial screening included in-depth genomic and transcriptomic analysis of PiPSC and TiPSC lines to eliminate those with any unwanted genetic abnormalities, as well as to build multi-omics datasets for correlating gene polymorphisms and transcript variation to function. Next, all lines were differentiated to iNK or iT effector cells, and phenotypically characterized throughout the differentiation process. In those studies, 86.5% of PiPSCs and 69.2% of TiPSCs lines were compatible with our protocols and able to be successfully differentiated and acquire NK cell and gamma delta T cell phenotypes respectively. Yield and lineage commitment (%CD56+ for NK cells and %CD3+ for T cells) variability was found to be higher across clones than donors in this initial analysis. Finally, we evaluated in vitro cytotoxicity, cytokine secretion, and persistence for all clones that met differentiation thresholds (>90% lineage commitment). As part of that evaluation, 39 PiPSCs lines were differentiated to iNK cells. Cytotoxicity against tumor lines was observed to be consistently between 85-100% at an effector to target ratio of 1:1. Although no trends in functionality were found to be associated with the PBMC donor, iPSC lines derived from CD34+ enriched PBMCs exhibited higher levels of innate killing as compared to those derived from bulk PBMCs. For this presentation, we will present genetic, transcriptomic , and phenotypic correlations with favorable differentiation and functional efficacy and illustrate how our screening process enables efficient selection of founder lines with the highest therapeutic potential for allogeneic cell therapies.

#3614 T cell receptor-engineered T cell therapy using TCR gene derived from an HLA-A2 hepatoblastoma patient who was completely cured by administration of glypican-3 peptide vaccine.

T. Terada[1], K. Ohnuki[1], M. Shimomura[1], T. Suzuki[1], Y. Amaishi[2], K. Takeichi[2], S. Okamoto[2], N. Fujinami[1], K. Takenouchi[1], N. Tsukamoto[1], K. Shoda[1], T. Yoshikawa[1], T. Nakatsura[1];

[1]National Cancer Center, Kashiwa, Japan, [2]Takara Bio Inc., Kusatsu, Japan

Glypican-3 (GPC3) is highly expressed in many of hepatocellular carcinoma, hepatoblastoma, ovarian clear cell carcinoma, and squamous cell lung carcinoma, but not expressed in almost all normal tissues, making it an excellent target for cancer immunotherapy. We identified each HLA-A24 and -A2-restricted GPC3-derived peptide and had conducted various clinical trials administering these peptides. All five cases of refractory hepatoblastoma, who had repeated relapses and remissions, are surviving for more than 9 years without recurrence by the only administering these peptide vaccines. We established many kinds of peptide-specific CTL clones with high avidity from PBMC of one of the female HLA-A*02:01-positive refractory hepatoblastoma patient treated with GPC3-derived peptide. Through collaborating research with Takara Bio Inc., which has siTCR technology and extensive experience in developing TCR-T cell therapies including NY-ESO-1 TCR-T, we identified most effective two kinds of TCR by creating a viral vector, preparing TCR-expressing T cells, and evaluating them in various in vitro/in vivo experiments. These TCR-gene engineered T cell can kill cancer cells presenting glypican-3-derived peptides, so this TCR-T therapy has proven to be a promising treatment for patients with cancers that are HLA-A2 positive and express GPC3. The development of TCR-T has been overshadowed by the overwhelming increase in the number of CAR-Ts developed in recent years, but while CAR-Ts have struggled in solid cancers, there have been some reports of successful cases in TCR-Ts and remains a promising treatment. Although GPC3 is a membrane protein, it is not necessarily expressed on the cell membrane and is often expressed within the cell, so we believe that TCR-T is more effective than CAR-T, which targets GPC3. TCR-T cell therapy targeting GPC3 has not yet been implemented anywhere in the world, and we hope this TCR-T therapy as an effective treatment for hepatocellular carcinoma, an intractable cancer with a 10-year survival rate of only 15%, refractory childhood hepatoblastoma, ovarian clear cell carcinoma and lung squamous cell carcinoma that are difficult to respond to anticancer drugs. This development was based on an unmet medical need, and HLA-A2 is found not only in 40% of Japanese, but also in many Caucasians, making it versatile and possible for international expansion.

#3615 Targeting high-risk neuroblastoma by TGFβ imprinted natural killer cells.

J. A. Ayala-Cuesta[1], Y. Chu[1], K. Foley[1], M. Tian[1], K. Klose[1], A. S. Mendelowitz[1], T. P. Cripe[2], D. A. Lee[2], M. S. Cairo[1];
[1]New York Medical College, Valhalla, NY, [2]Nationwide Children's Hospital, The Ohio State University, Columbus, OH

Background: Neuroblastoma (NB) is a common malignant extracranial solid tumor in children, responsible for 11% of cancer deaths in pediatric patients under 15 (Smith et al, Cancer, 2014). High-risk neuroblastoma is a metastatic disease in children aged 18 months or older with L2, M, or MS disease with amplification of the MYCN oncogene (Chuang Pediatr Blood Cancer 2021). Recent analyses by COG show that HR Neuroblastoma still has a 5-year event free survival of 51% despite an extensive treatment regimen (Steven et al, ASCO, 2022). To address improved tumor targeting and overcome antigen escape, chimeric antigen receptor (CAR) technology to Natural Killer (NK) cell therapy has been adapted (Chu/Cairo, et al, Frontiers in Oncology, 2019). TGFβ is a potent mechanism of the NK cell anti-tumor resistance and is present at elevated levels in the NB tumor microenvironment (TME) (Foltz, Cancers, 2018). Studies demonstrated that blockade of TGF-β signaling in NK cells caused the accumulation of NK cells that produce IFN-γ and neutralization of TGF-β prevented NKG2D downregulation and also restored NK cell anti-tumor reactivity (Nayyar/Chu/Cairo, et al Frontierls in Oncology, 2018). ROR1, a transmembrane protein is highly expressed on the majority of NB (Rebagay/Yan *Front Oncol*, 2012). Our group has successfully expanded functional and active peripheral blood NK cells (exPBNK) with irradiated feeder cells and electroporated CAR mRNA to exPBNK (Chu/Cairo, et al Cancer Immunol Res, 2015).
Objective: To determine in vitro cytotoxicity against neuroblastoma cells by ex vivo expanded TGFβ imprinting (TGFβi) NK cells.
Methods: TGFβi NK cells are generated by culturing expanded NK cells with irradiated K562-41BBL-mbIL21 in 50 IU/mL IL-2 plus 10 ng/mL TGFβ every 2-3 days for two weeks. NK and TGFβi NK cells specific in-vitro cytotoxicity were compared via luciferase reporter assay against ROR1^{+} NB cell lines as we previously described (Chu/Cairo, et al, JITC, 2022). Cytokine/chemokine levels secreted by NK and TGFβi NK cells were compared using ELISA assays (Chu/Cairo, et al, JITC, 2022).
Results: We have successfully expanded TGFβi NK cells. These TGFβi NK cells showed significantly enhanced in vitro cytotoxicity against NB cells compared to NK cells under TGFβ environment (20±2.4% vs 0%; $p<0.001$) at E:T=3:1 and consistently, TGFβ-imprinting NK secreted significantly high level of TNF-alpha (393.7pg/ml±16.77pg/ml) against NB cells ($p<0.001$) compared to NK cells (79.7pg/ml±14.7pg/ml) under TGFβ environment.
Conclusion: Our data indicate TGFβi NK cells may be a promising novel therapy to overcome the immunosuppression of TGFβ in the tumor microenvironment for pediatric NB tumors. We will further engineer these TGFβi NK cells to express anti-ROR1 CAR to enhance the targeting specificity against NB tumors and investigate the anti-tumor effects of anti-ROR1 CAR TGFβi NK cells against NB tumors *in-vitro* and *in-vivo* (Funded by U54 CA232561).

#3616 *In vivo* expansion patterns of anti-BCMA CAR T-cell in relapsed/refractory multiple myeloma: Comparative immunomonitoring of idecabtagene vicleucel and ciltacabtagene autoleucel.

M. Kocoglu, A. P. Rapoport, E. Gebru, D. Omili, D. Yamoah, R. Mulatu, J. Yared, N. M. Hardy, M. Kallen, A. Z. Badros, **D. Atanackovic**;
University of Maryland Greenebaum Comprehensive Cancer Center, Baltimore, MD

Introduction: Chimeric antigen receptor (CAR) T cell (CAR-T) treatments have revolutionized the treatment of multiple myeloma (MM). Two CAR-T cell products targeting B cell maturation antigen (BCMA) have received approval for the treatment of MM: idecabtagene vicleucel (idecel) and ciltacabtagene autoleucel (ciltacel). A comparative analysis of in vivo CAR-T responses in patients receiving these novel cellular therapies has not been performed, especially not in the real-world setting.
Methods: We prospectively enrolled 23 MM patients treated with idecel or ciltacel in our study GCCC2043. Blood samples were obtained at apheresis, pre-lymphodepleting (LD) chemotherapy, on days 0, +7, +14, +21, +28 and at +3 months post CAR-T. Samples were stained using BCMA or control CAR detection reagents, monoclonal antibodies against T cell surface antigens, and analyzed using flow cytometry.
Results: Baseline clinical characteristics, pre-apheresis and pre-LD absolute lymphocyte counts were comparable between groups. There were no G3 cytokine release syndrome (CRS) events whereas G1/2 CRS and all-grade Immune Effector Cell-Associated Neurotoxicity Syndrome (ICANS) events were not significantly different between cohorts. The global overall response rate (ORR) was 78.3% (n=18) and 60.9% (n=14) at days 30 and 90, respectively. At +1 month, 72.7% (8/11) of idecel and 83.3% (10/12) of ciltacel cohort had an objective response (p=0.625). There was no statistical ORR difference between idecel and ciltacel cohorts at 3, 6, and 9 months. Two-way ANOVA of CAR-T expansion studies revealed a trend towards an effect of treatment type (p=0.0595). Time to peak CAR-T numbers was significantly shorter for idecel (p=0.0127), however, ciltacel showed a significantly more pronounced CAR-T expansion (p=0.043) and longer persistence. Peak CAR-T expansion was associated with clinical responses across cohorts at +1 (p=0.034) and +3 months (p=0.050). Day +30 responses were indicative of Day +90 and Day +180 responses (p<0.001, p=0.011). There was no difference in CD8+ CAR T cell peak levels, however, CD4+ CAR T cell peak levels were much higher (p=0.019) for ciltacel vs. idecel. Similarly, there were significantly higher (p=0.002) CD4+/CD8+ double-positive CAR-T peak levels in ciltacel vs. idecel patients. There was no significant difference in the distribution of T cell memory subtypes at peak level.
Conclusions: We demonstrate here for the first time significant differences in CAR T cell expansion and persistence patterns following infusion of either idacel or ciltacel. Studies are underway at our institution investigating anti-BCMA CAR T cell responses in more detail and larger numbers of patients. Such studies have the potential to identify predictive/prognostic biomarkers and/or lead to further optimization of myeloma-targeting CAR-T.

#3617 Expansion and persistence of anti-BCMA CAR T cells correlates with durability of responses in multiple myeloma patients.

K. Wu, K. Law, G. Ledergor, C. Liu, Z. Fan, V. Gurunathan, A. Lea, M. Clark, S. Kwek, A. Cheung, J. Wolf, A. Chari, A. Kumar, J. Eyquem, T. Martin, L. Fong; UCSF - University of California San Francisco, San Francisco, CA

Background: Chimeric antigen receptor (CAR) T cells targeting B-cell maturation antigen (BCMA) can induce >70% response rates in patients with relapsed/refractory multiple myeloma (RRMM). However, most patients ultimately relapse. There are two FDA-approved CAR T products: ciltacabtagene autoleucel (cilta-cel) and idecabtagene vicleucel (ide-cel), the former having much more durable responses. The mechanisms that mediate more durable responses with these CAR T cells is unknown. Previous studies have shown that specific cell states in the apheresis and infusion products are associated with long-term efficacy of anti-BCMA CAR therapy in MM and the relationship between durability of response and CAR T cell persistence remains unclear.
Methods: We analyzed serial bone marrow and PBMC samples from 20 MM patients who received BCMA CAR T therapy, including cilta-cel, ide-cel, and JCARH125. Flow cytometry and single-cell RNAseq were used to evaluate the features of CAR T cells that are associated with durable clinical responses.
Results: While CAR T cells were detectable but variable among patients at 1-month post infusion, the frequency of CAR T cells in bone marrow at 1-month post-infusion is positively correlated with progression free survival (PFS) in all MM patients (p=0.009). This association was also evident in patients just treated with cilta-cel (p= 0.008). By 6 months, CAR T cells could still be detected by high-throughput flowcytometry in the cilta-cel-treated patients, but CAR T cells were not detectable in most of the patients receiving the other 2 products. Cilta-cel CAR T cells predominantly possessed an effector-like surface phenotype at 1-moth post infusion in both CD8+ and CD4+ compartments in bone marrow. These CAR T cells shifted to effector memory and central memory T cell states by 6 months, respectively. For ide-cel and JCARH125, patients with more durable responses (>6mos) there was a significantly higher proportion of CAR T cells with CD8+ effector memory-like state at 1-month post infusion.
Conclusions: Our data demonstrate that distinct anti-BCMA CAR T cell treatments lead to very different cellular outcomes: Cilta-cel CAR T cell treatment leads to greater expansion and persistence compared to other anti-BCMA CAR T cells. Cilta-cel CAR T cells also shift from the initial effector state to a memory phenotype. These results provide insights into features of more efficacious anti-BCMA CAR T cells that can help guide the future development of more durable treatments for MM.

#3618 High-avidity BCMA CAR and high-affinity, non-cleavable CD16 Fc receptor incorporated in off-the-shelf CAR T cells promote multi-antigen targeting and durable anti-tumor cytotoxicity in the treatment of multiple myeloma.

J. Reiser[1], A. O'Connor[1], B. Hancock[1], S. Markov[1], B. Groff[1], A. Gutierrez[1], M. Meza[1], M. Jelcik[1], Y. Pan[1], A. Garcia[1], B. Goulding[1], M. Denholtz[1], T. Lee[1], R. Abujarour[1], R. Bjordahl[1], A. Rehm[2], R. Clarke[1], J. Goodridge[1], B. Valamehr[1];

[1]Fate Therapeutics, San Diego, CA, [2]Max Delbruck Center, Berlin, Germany

Immune cell therapy has proven highly effective for the treatment of multiple myeloma (MM). However, key challenges remain that include disease relapse, limited patient access, and inability to effectively combine with existing standard-of-care therapies. Rapid progress in the development of off-the-shelf, multiplexed-engineered, induced pluripotent stem cell (iPSC)-derived cell therapies enables large-scale manufacture of immune cells incorporating multiple novel synthetic controls of cell function to improve cell fitness, enhance cell function, and enable synergistic combination with existing effective therapies such as CD38-targeted antibody (mAb) therapy. We have developed an iPSC-derived chimeric antigen receptor T (CAR-iT) cell therapy that uniquely leverages elements of both adaptive and innate immunity by incorporating a BCMA-targeted CAR (BCMA-CAR) derived from a scFv domain exhibiting high-binding affinity in the low nanomolar range, and a high-affinity, non-cleavable CD16 (hnCD16) Fc receptor to enable antibody-dependent cellular cytotoxicity with mAb therapy. The genetic deletion of CD38 gene was also incorporated to eliminate the possibility for CD38-mediated fratricide, and genetic deletion of TRAC gene was introduced to remove the potential risk of graft-versus-host disease in an allogeneic setting. These CAR iT cells, which were generated from a clonally-derived iPSC line, demonstrated homogenous expression of each genetic edit (>95% BCMA-CAR and hnCD16; <1% CD38 and TCR surface expression). Using a stringent, disseminated xenograft mouse model of multiple myeloma, MM.1S, which was allowed to achieve complete systemic engraftment during the initial 4 days, treatment with BCMA-CAR iT cells demonstrated comparable tumor cell clearance ($p=0.0024$ vs. vehicle at Day 17) to primary BCMA-CAR T cells ($p=0.002$ vs. vehicle). In combination with a CD38-targeted mAb to exploit hnCD16 and biallelic CD38 KO, BCMA-CAR iT cells are capable of dual-antigen targeting to address antigen escape and promote durable tumor control. To this end, a single dose of BCMA-CAR iT cells combined with daratumumab exhibited near complete TGI for the duration of the study ($p<0.0001$ vs. vehicle at Day 37). Together, these studies demonstrate CAR iT cells incorporating a high-avidity BCMA CAR and high-affinity, non-cleavable CD16 Fc receptor can uniquely leverage elements of both adaptive and innate immunity and can be combined with CD38-targeted mAb to potentially outcompete primary BCMA CAR T cells. As these CAR iT cells can be administered off-the-shelf, key challenges associated with current immune cell therapy, such as patient access and inability to synergize with standard-of-care therapies, can be addressed for the treatment of relapsed / refractory MM.

#3619 Post CAR-T lymphocytosis as a surrogate of BCMA CAR-T expansion, response, and prognosis in multiple myeloma.

M. Mejia Saldarriaga[1], D. Pan[2], C. Unkenholz[3], T. Mouhieddine[2], J. Fein[1], J. Monge[1], C. Rosenbaum[1], R. Pearse[1], D. Jayabalan[1], C. Gordillo[4], H. Chan[4], M. Mapara[4], G. Inghirami[1], S. Lentzsch[4], R. Reshef[4], A. Rossi[2], S. Parekh[2], S. Jagannath[2], S. Richards[2], R. Niesvizky[1], M. Bustoros[1];

[1]Weill Cornell Medicine, New York, NY, [2]Mount Sinai, New York, NY, [3]Weill Cornell Medicine School of Medicine, New York, NY, [4]Columbia University Irving Medical Center, New York, NY

Introduction: Expansion of chimeric receptor antibody (CAR)-T cells after infusion has been described as important marker in multiple myeloma (MM); however, the phenomenon of overt lymphocytosis has not been reported. We describe the kinetics of absolute lymphocyte count (ALC) after BCMA CAR-T in MM as a marker of depth of response and progression-free survival (PFS).

Methods: 158 patients (pts) were included (93 pts ciltacabtagene autoleucel (cilta-cel) and 65 pts idecabtagene vicleucel (ide-cel) from three institutions. Baseline characteristics, cytokine release syndrome (CRS), immune effector cell-associated neurotoxicity syndrome (ICANS), ALC on day -5 through 14, and outcomes were collected. A cohort of 84 pts who received CD19 CAR-T for non-Hodgkin lymphoma (NHL) as comparator. Peripheral blood (PB) flow cytometry was performed on days 7, 14 and 21 in 4 patients.

Results: Early ALC increase after BCMA CAR-T was frequent, with a median max ALC 1.3 $x10^3$/uL (IQR 1-4.4) from a median baseline of 0. However, when compared to ide-cel, cilta-cel had a higher median Max ALC (2 $x10^3$/uL (1 - 4.4) vs 0.8 (0.7 - 2.8), p < 0.001), longer time-to-max ALC (11 vs 12 days, p = 0.003), and higher absolute ALC increase (2.1 $x10^3$/uL vs 0.7 $x10^3$/uL, p <0.001), while there were no differences in ALC before lymphodepleting conditioning or day 0. Higher max ALC was associated with CRS (OR 4.8, CI 1.3-17.2, p 0.01). Max ALC and absolute increase in ALC were significantly associated with deeper response (VGPR vs PR or less), improved PFS and duration of response (DoR) in univariable analysis. Max ALC >1 $x10^3$/uL (HR 0.4, 0.2-0.7, p <0.001) and non-paraskeletal EMD (HR 2.1, 1.2-.4, p <0.01) remained associated with PFS/DoR in multivariable model after adjusting for CAR-T Product, high-risk cytogenetics, and number of previous lines. PB flow cytometry in 3 responder patients (max ALC range 2-14 $x10^3$) showed expansion of CD3+ BCMA CAR-T from day 7 (BCMA CAR-T <0.2% of CD3+ cells) to day 14 (BCMA CAR-T range 54-88.6%), while a non-responder (max ALC 0.4 $x10^3$) patient had no expansion despite presence of CD3+ BCMA CAR-T at day 7, 14 and 21. BCMA CAR-T had higher max ALC when compared to CD19 CAR-T (median 1.3 $x10^3$ vs 0.4 $x10^3$ (0.2-0.7), p < 0.001), while there were no differences in baseline ALC between BCMA and CD19 CAR-T. Median max ALC did not differ between response status after CD19 CAR-T (0.4 $x10^3$ (0.2-0.7) vs 0.6 (0.3-0.7), p = 0.3).

Discussion: Post-CAR-T lymphocytosis is common after BCMA CAR-T therapy for MM and is associated with response, PFS, and DoR after adjusting for other prognostic variables. A cut-off of max ALC > 1 $x10^3$ identified patients with superior PFS, while max ALC <0.5 $x10^3$ represents high-rates of poor response and early progression. ALC expansion correlated with BCMA CAR-T expansion as assessed by flowcytometry, supporting ALC assessment as an accessible surrogate that is clinically applicable and accessible.

CLINICAL RESEARCH: Biomarkers in Clinical Trials
Poster Session

#3623 Quantifying pharmacodynamic markers of radioligand therapies in tumor by multiplex immunofluorescence and automated quantitative analysis (AQUA) algorithms.

J. Santos[1], V. Nyanchama[1], V. Romanet[2], E. Dammassa[2], L. Kattenhorn[3], Y. Huang[3], J. Lim[3], X. Li[1], J. Deeds[3], L. Iaconis[3], E. Pacia[1], M. McLaughlin[3], N. Dakappagari[1], **J. Bordeaux**[1];

[1]Navigate BioPharma Services, Inc., a Novartis subsidiary, Carlsbad, CA, [2]Novartis Biomedical Research, Basel, Switzerland, [3]Novartis Biomedical Research, Cambridge, MA

Purpose: Due to profound clinical successes observed with radioligand therapies (RLT) across multiple cancers coupled with advances in drug handling and delivery logistics recently, clinical trials investigating RLTs are on the rise. Ionizing radiation produced by radioisotopes linked to antibodies causes double-stranded breaks either directly or via generation of reactive oxygen species. This type of DNA damage is associated with an increase in proteins mediating cell cycle arrest (e.g., p21/CIP1) and repairing damaged DNA (e.g., CHK2 and γH2Ax). Additionally, proliferating cells (identifiable by Ki67) are most susceptible to ionizing radiation as DNA is exposed during the mitotic phase of the cell cycle. We incorporated these biologically verified markers into a multiplexed fluorescence immunohistochemistry (mFIHC) assay for robust quantitation of the pharmacodynamic activity of RLTs and gain insights into the DNA damage response in on-treatment tumor core biopsies.
Study Design: We designed a novel mFIHC assay incorporating antibodies to p21, pCHK2, γH2Ax, Ki67, CK to quantitatively characterize DNA damage across five tumor indications of commercially available ovarian cancer, colorectal cancer, gastric cancer, endometrial (uterine) cancer, and breast cancer formalin-fixed paraffin-embedded (FFPE) tissue blocks. We successfully validated this mFIHC assay using automated staining (Bond RX), imaging (PhenoImager HT), and combined with hypothesis-driven spatial profiling algorithms (e.g., AQUA Technology).
Results: Sensitivity and specificity were confirmed on known positive and negative controls. Reproducibility and precision were observed across instruments, operators, and independent experiments for all markers The frequency of p21 ranged from 5% - 8%, pCHK2 from 3% - 36%, pH2Ax from 0% - 8%, Ki67 from 4% - 61%, and CK cells ranged from 25% to 87%. Over 56 unique parameters were evaluated. The prevalence of p21, pCHK2, and γH2Ax ranged from 0% to >30% across five tumor indications tested and were highly concordant.
Conclusion: The validated mFIHC assay examines the expression of proteins mediating cell cycle arrest and DNA damage in tumor and stromal cells. This panel may be used to further understand the complexity of DNA damage response pathways in tumor and non-tumor areas in the context of RLT clinical trials.

#3624 A low-cost kit for gentle, effective and timely extracellular vesicle (GET EVs) isolation: Accelerating development of RNA-based liquid biopsies for neuroendocrine neoplasms.

B. Su[1], M. Jeyhani[2], X. Yang[3], J. Nanayakkara[3], R. Wunsche[4], N. Renwich[3], S. Tsai[2], H. Leong[1];

[1]Department of Medical Biophysics, University of Toronto, Biological Sciences Platform, Sunnybrook Research Institute, Toronto, ON, Canada, [2]Department of Mechanical and Industrial Engineering, Toronto Metropolitan University, Keenan Research Centre for Biomedical Science, St. Michael's Hospital, Institute for Biomedical Engineering, Science and Technology (iBEST), Toronto, ON, Canada, [3]Laboratory of Translational RNA Biology, Department of Pathology and Molecular Medicine, Queen's University, Kingston, ON, Canada, [4]Department of Mechanical and Industrial Engineering, Toronto Metropolitan University, Toronto, ON, Canada

Extracellular vesicles (EVs) are cell fragments released by all cells, making them promising platforms for cancer biomarker development. Effective isolation of ultra-pure EVs for downstream analyses is key for EV-based liquid biopsy development. However, current EV isolation methods such as ultracentrifugation (UC) and other commercialized EV isolation kits are lackluster because of damage to EVs, length of time required, and low EV recovery rates. In response, we developed an “GET EV” kit which is based on the principles of lipid energy states, also known as the aqueous two-phase system (ATPS) to isolate EVs from any media. Nanoscale flow cytometry (nFC) analysis revealed that ATPS has greater EV enrichment capability (21.4× vs. 10.9× times fold enrichment) and higher EV recovery efficiency (97.6% vs. 69.3% recovery) than UC. Other EV isolation kits were tested and were inferior to ATPS in terms of EV recovery and EV-RNA recovery. EV subpopulations as determined by EV biomarkers (CD9, CD63, CD81, etc.) were confirmed by nFC. “Omics” studies (small RNA sequencing and proteomics) also confirmed the presence of expected EV markers. We developed an RNA-based liquid biopsy for Neuroendocrine Neoplasms (NENs) by quantitating the presence of EVs containing miR-375, an established biomarker for NENs. Using the GET EVs kit, we isolated EVs from healthy volunteer and patient plasma samples of NEN patients. RT-qPCR demonstrated enriched expression of miR-375 in EVs isolated from Lung and GI NEN patient plasma samples. Our study establishes the use of GET EV kits to efficiently, rapidly, and gently isolate EVs from small plasma samples (250 uL). This is a low-cost innovation that will finally enable the development of other RNA-based Liquid Biopsies for other disease sites with significant diagnostic and prognostic implications.

#3625 Metabolic phenotypes of doxorubicin-induced cardiotoxicity in breast cancer patients.

S.-R. Jun[1], K. Wallis[1], R. D. Landes[1], V. K. Todorova[1], L. Su[2], S. Makhoul[3], **P.-C. Hsu**[1];
[1]University of Arkansas for Medical Sciences, Little Rock, AR, [2]UT Southwestern Medical Center, Dallas, TX, [3]CARTI Cancer Center, Little Rock, AR

Background. Doxorubicin (DOX) is a highly effective chemotherapy agent that is commonly used in combination with other chemotherapy regimens to treat a wide range of cancers, including 32% of breast cancer (BC) cases. Although DOX has greatly increased the number of long-term cancer survivors, some DOX recipients have experienced DOX-induced cardiotoxicity (DIC). Currently, there are no validated markers that can predict the early development of DIC. Cardiac troponin released by cardiomyocytes has been used in non-clinical studies as a marker of myocardial injury; however, the false positive rates are high, and the predictive value on cardiotoxicity is limited. Therefore, novel biomarkers of DIC are urgently needed to identify patients who are at an increased risk, allowing early detection of the cardiotoxicity before it causes permanent cardiac damage.

Methods. Untargeted metabolomics profiling was performed for plasma samples from a cohort of 28 breast cancer patients who developed abnormal cardiac function (ABN) and those who maintained normal cardiac function (NML). Blood samples were collected before, during, and after DOX-containing chemotherapy. Using both baseline observations and pre-post changes, machine-learning techniques were used to identify metabolite markers that can be used as early indicators of DIC in BC patients. Area under the receiver operating characteristic curve was reported to evaluate the performance of significant metabolites, and metabolite set enrichment analysis (MSEA) and network analysis were used to extrapolate known associations between metabolites and diseases.

Results. Significant separation of plasma metabolomics profiles between ABN and NML patients at baseline was observed. From 1,124 metabolites, abundance of 59 metabolites were found to differ between ABN and NML patients at baseline. Across all patients, levels of 78 metabolites changed between baseline and after the 1st chemotherapy cycle. Of the 6 metabolites identified in both baseline and pre-post data, ABN patients had higher levels of dicarboxylic acids suberate and sebacate derived from ω-oxidation of fatty acids at baseline than NML patients. Enrichment analysis on the metabolites from the pre-post analysis suggested myocardio injury and carnitine palmitoyltransferase deficiency. Network analysis of metabolite-disease interactions further suggests potential impact on neurological health after chemotherapy.

Conclusion. The metabolomics phenotype identified is indicative of impaired beta-oxidation at baseline for ABN patients. In addition, our findings suggest neurotoxic effect from DOX, implicating the potential brain-heart axis involved behind the cardiotoxicity phenotype.

#3626 Day 21 early bone marrow response does not offer high concordance with response bone marrow in the induction chemotherapy setting of *FLT3* mutant acute myeloid leukemia.

V. Lok[1], S. Hahn[1], N. N. Shah[2], D. A. Kerr[2], I. M. Borrello[2], E. M. Sotomayor[2], D. M. Swoboda[2];
[1]USF Health Morsani College of Medicine, Tampa, FL, [2]Tampa General Hospital Cancer Institute, Tampa, FL

Purpose: Day 14 early bone marrow biopsies are routinely initiated to determine need for reinduction chemotherapy, but poorly predict true response and risk overtreatment. Day 21 (D21) bone marrow biopsies have been performed in the context of trials utilizing *FLT3*-targeted therapies in combination with induction chemotherapy (Stone et al. NEJM 2017). However, the utility of D21 bone marrow responses is not well defined.
Methods: We retrospectively identified 26 newly diagnosed *FLT3* mutant AML patients who underwent induction chemotherapy with midostaurin and Next Generation Sequencing (NGS) of bone marrow aspirate within a week of diagnosis.
Results: 19/26 (73%) of patients had both D21 and response bone marrow biopsy. Of the remaining 7 patients, 4 patients did not have D21 bone marrow, 2 died of unrelated complications prior to response bone marrow, and 1 did not have recovery marrow available for assessment. Our cohort included 13 (50%) men with a median age of 57 years (range, 21 - 73 years). All patients had ECOG of 0 - 1. 96% of cases were de novo AML and 81% had normal cytogenetics. FLT3 ITD mutations were detected in 17 (65%) patients with a median FLT3 ITD ratio of 0.305 (range, 0.03 - 1) and median FLT3 VAF of 23.8% (range, 3.2 - 80.6%). 7 patients (26.9%) underwent additional allogeneic stem cell transplant.
In the 19 patients evaluable for analysis, 13/13 (100%) patients with blast % ≤ 5 at D21 achieved a complete response (CR) based on recovery marrow. 4/6 (67%) patients with blast % > 5 at D21 which were considered to have residual disease based on pathology review (median blast % 11 (range, 6 - 17%) ultimately achieved a CR. The 2 patients that did not achieve a CR has a blast % of 29% and 9% on D21 marrow. Thus, the positive predictive value of D21 early bone marrow response corresponding with the response bone marrow was only 33% in our patient cohort. Of the 4 patients that did not have D21 marrow but had recovery marrows available for review, the CR rate was 100%.
No other significant differences in initial disease characteristics were seen. There were no differences proportion of co-mutations in *NPM1, DNMT3A, TP53, IDH2*, and *IDH1*, and higher FLT3 ITD ratio nor FLT3 VAF corresponded with ability to clear D21 bone marrow. Additionally, there were no differences in minimal residual disease (MRD) and overall survival (OS) between the groups.
Conclusions: Our study suggests early bone marrow response in the context of *FLT3*-mutant disease is not dependent on inherent disease characteristics and does not correspond to overall response to targeted induction chemotherapy. The utility of these marrows in is this population needs to be studied further in a larger cohort to better understand the clinical necessity to avoid unnecessary cost/procedures to patients and even more importantly unnecessary reinductions.

#3627 Volrustomig a novel PD-1/CTLA-4 bispecific antibody leads to robust increase in peripheral and intra-tumoral pharmacodynamic biomarkers in solid tumors from FTiH study.

I. Achour[1], M. Kuziora[1], F. Song[1], S. Eck[1], L. Meinecke[1], J. Blando[1], J. Pearson[1], M. Saraiya[1], C. Eisen[1], F. Segerer[1], M. Schick[1], N. Triltsch[1], M. Surace[1], G. Silva Boos[1], H. Hessel[1], M. Bui[1], K. Pratsch[1], A. Andoni[1], S. D. Gainer[1], D. Freeman[1], D. Subramaniam[1], B. Tran[2];
[1]AstraZeneca US, Gaithersburg, MD, [2]Peter MacCallum Cancer Centre,, Melbourne, Australia

Background: Volrustomig (MEDI5752) is designed to fully inhibit PD-1 while preferentially inhibiting CTLA-4 on activated PD-1+ T cells. In a FTiH trial, volrustomig demonstrated meaningful clinical activity in patients with solid tumors (including 1L RCC and NSCLC), acceptable safety profile, sustained PD-1 receptor occupancy, and T cell proliferation at levels greater than seen with clinically tolerable doses of CTLA-4 inhibitors with co-administration of anti-PD(L)-1. We sought to further characterize volrustomig pharmacodynamic effect in the periphery and tumor to demonstrate its biological activity and inform dose optimization.

Methods: Pre- and on-treatment blood samples from 86 patients enrolled in dose exploration were collected. Peripheral T cell profiling was assayed by flow cytometry, RNAseq, TCRSeq and serum proteomics. Paired tumor biopsies (N=17), pre- and at week 6 on-treatment, were analyzed for T cell infiltration and function using RNAseq and computational image analysis of immune cell marker density detected by histochemistry and multiplex immune fluorescence assays.

Results: Volrustomig achieved dose-dependent peripheral pharmacodynamic changes of biomarkers specific to CTLA-4 blockade at ≥ 225mg. At C1D8 with doses ≥ 500mg, increases in CD4 T cell proliferation (ki67), activation (ICOS), and memory T cells (1516%, 321% and 88%, respectively) were seen, each greater than observed with historical controls of patients treated with tremelimumab 3mg/kg (T3) in combination with durvalumab. Similarly, CD8 proliferation and activation were also higher than T3 at C1D8 with 300% and 161% increase respectively. Additional CD4 and CD8 T cell proliferation and activation was observed at C2D8 supporting the benefit of repeat dosing. Higher peripheral T cell clonal expansion at doses ≥ 500mg was seen and associated with PFS and OS benefit. In patients with paired biopsies, volrustomig achieved robust T cell mediated anti-tumor activity including increases in T cell infiltration (CD8+, 2.3 fold, p=0.04), proliferation (CD8+ Ki67+, 2.1 fold, p=0.04) and, T cell cytotoxicity and activation (GrB+, 2.2 fold, p=0.01; T cell effector and IFNg gene signatures, > 2-fold, p< 0.01). Additionally, volrustomig increased CD8 proliferation in tumor compared to historical control durvalumab alone (>2-fold increase in 70% vs 50% patients).

Conclusion: Voltrustomig demonstrated robust peripheral and intra-tumoral T cell activation and proliferation, broadening the pool of antigen experienced T cells, at levels greater than seen with dual checkpoint blockade currently used in the clinic.

#3628 Combined mek and jak inhibition *in vitro* is an effective strategy in overcoming jak inhibitor resistance in primary myelofibrosis (PMF).

S. B. Reynolds, S. Matono, M. Kandarpa, K. Pettit, M. Ribick, M. Talpaz, Q. Li;
University of Michigan, Ann Arbor, MI

Introduction Primary myelofibrosis (PMF) is a myeloproliferative neoplasm arising from various mutations in myeloid-committed hematopoietic progenitor cells. Treatment of PMF is challenging as Jak inhibitor resistance is common, making the expansion of molecular characterization and novel therapeutic target identification in PMF essential. The main goals of this study are to determine both the presence of Ras activity in PMF and the impact on Ras/MAP Kinase pathway targeting in the disease.

Methods Integrated genomic-transcriptomic sequencing analyses were performed on peripheral blood mononuclear cells (PBMCs) purified from 27 patients with PMF at a single institution; protein was then obtained from whole cell lysates. Ras activity was then assessed by applying Ras binding domain (RBD) to sample in an ELISA and was compared between patients with PMF, essential thrombocythemia (ET), polycythemia vera (PV) and healthy donors. Statistical analyses were conducted using two-way unpaired t-tests. The next set of *in vitro* studies aimed to evaluate the effects of MEK inhibition in PMF. Cell viability studies were first performed on human erythroleukemia (HEL) cells to identify IC50 values. Colony forming assays in methylcellulose-enriched media formulated for the growth of CD34+ cells were then performed in 4 conditions: Ruxolitinib and Cobimetinib monotherapy, combined therapies and untreated sample.

Results As previously reported in our initial study, Ras activity in 21 patients with MF was 1.74 fold higher than healthy donors (13 volunteers, p=0.0304) and 1.64 fold higher than in PV/ET (12 patients, p=0.0462). We also reported previously on Ras activity from differential enrichment of myeloid and lymphoid cells from PBMC samples, where a key observation was that myeloid contribution to Ras activity in PMF patients with *RAS*/MAP Kinase pathway mutations was 3.8 times higher in Ras/MAP Kinase WT patients (p=0.0012), potentially suggesting that *RAS* pathway mutations have a predominance in myeloid cells. In HEL cell viability assays, cobimetinib and ruxolitinib, when utilized in tandem, resulted in more cell growth inhibition than either agent individually. This same finding was recapitulated in colony forming assays in 4 different patients with varying levels of sensitivity to Jak inhibitors, in all of whom ruxolitinib and cobimetinib lead to a greater reduction in colony formation than ruxolitinib monotherapy.

Discussion Data from colony forming assays of bone marrow from patients with PMF identifies at least an additive effect of combined Jak and Ras/MAP Kinase (specifically Mek) inhibition on CD34+ colony formation. The specific observation that Ras pathway inhibition may be utilized as a means of overcoming Jak inhibitor resistance in PMF is a novel finding in this field and may be a valuable avenue for future early-phase clinical trials.

#3629 Prevalence of claudin18.2 expression in gastric/gastroesophageal junction adenocarcinoma among patients in TranStar101 and TranStar102 clinical trials.

Li Shen[1], Carol Mao[1], Alan Lin[1], Ying Gu[2], Jenny Milata[2], Lijuan Zhang[1], Chuan Qi[1], Jenny Yao[2], Steven Yu[1], Changjun Yue[3], Lin Shen[4], Yelena Janjigian[5], Xueming Qian[1], Wen-I Chang[2], Caroline Germa[2]

[1]Suzhou Transcenta Therapeutics Co., Ltd, Suzhou, China,[2]Transcenta Therapeutics, Princeton, NJ,[3]LabCorp Central Lab, Torrance, CA,[4]Beijing Cancer Hospital, Beijing, China,[5]Memorial Sloan Kettering Cancer Center, New York, NY

Background: Claudin18.2 (CLDN18.2) is a tight junction protein highly specific to gastric mucosa, and a validated target for gastric cancer (GC) treatment. Immune checkpoint therapy targeting PD-1 combined with chemotherapy has been approved as the first line therapy of GC. Understanding the expression profiles of CLDN18.2 and PD-L1 could guide the development of combination therapies to maximize the benefits of these two agents. This study investigated the prevalence of CLDN18.2 expression in gastric/gastroesophageal junction adenocarcinoma (G/GEJC) screening samples from studies Transtar101 (NCT04396821 in US) and TranStar102 (NCT04495296 in China), and its correlation with various clinical characteristics and PD-L1 expression.
Methods: CLDN18.2 expression in formalin-fixed, paraffin-embedded (FFPE) G/GEJC tissue samples was prospectively detected by an immunohistochemistry-based LDT using an in-house anti-CLDN18.2 antibody (Clone14G11) on the Leica Bond III stainer. CLDN18.2 expression was assessed by scoring the staining intensity (0, 1+, 2+, 3+) and the percentage of positive tumor cells. Positive CLDN18.2 expression is defined as the cutoff at ≥10% of tumor cell with ≥1+ staining intensity for this evaluation. PD-L1 expression was assessed by combined positive score (CPS) using Agilent's PD-L1 IHC 28-8 pharmDx. Both assays were conducted in CAP/CLIA certified LabCorp central lab.
Results: 547 G/GEJC patient samples had CLDN18.2 results as part of the screening procedures for the clinical trials. Of these patients (454 GC/93 GEJC), 439 (80%) were Asian, 29 (5%) were Caucasian, 2 (0.4%) were other ethnic group, and 77 (14%) were not recorded; 434 (79%) were primary tumors and 113 (21%) were metastasis; 201 (37%) were core needle biopsies (CNB), 108 (20%) were surgical resections (SR) and 238 (44%) had no information. 311 (57%) samples had positive CLDN18.2 expressions (≥10%/≥1+). No significant difference in CLDN18.2 positive rates were found between TranStar101 and TranStar102 studies (p=0.801), Asian and Caucasian (p=0.612), GC and GEJC (p=0.373), primary and metastatic specimens (p=0.055) or CNBs and SRs (p=0.715). Out of 83 TranStar102 specimens that had both CLDN18.2 and PD-L1 results, 15 (18%) had PD-L1 CPS≥5, 59 (71%) had positive CLDN18.2, and 10 (15%) had both positive CLDN18.2 and PD-L1 CPS≥5. No correlation (p=0.393) was observed between PD-L1 scores (CPS<5 or CPS≥5) and CLDN18.2 expression (≥10%/≥1+ or <10%/≥1+).
Conclusions: Data suggested CLDN18.2 expression levels were independent of PD-L1 status, and support the use of Transcenta 14G11 antibody for CLDN18.2 detection regardless of sample collection methods, location, and patient demographics. An anti-CLDN18.2 companion diagnostic device based on 14G11 is being developed (CLDN18.2 IHC 14G11 pharmDx, Agilent Technologies, Inc.).

#3630 Measuring EGFr on extracellular vesicles in human plasma samples.

D. A. Olsen, T. F. Hansen, I. Brandslund, J. S. Madsen;
Lillebaelt Hospital, University Hospital of Southern Denmark, Vejle, Denmark

Introduction: Extracellular vesicles (EVs), secreted extracellularly by almost all types of cells, play a pivotal role in intercellular communication and have emerged as valuable indicators in disease progression. Their potential for cancer diagnostics and monitoring is particularly noteworthy. Epidermal growth factor receptor (EGFr) is a major driver of several cancers and serve as an important target or co-target in cancer treatment. The purpose of this study was to develop an assay for measuring EGFr on EVs directly in plasma samples. Additionally three assays were developed to measure the total concentration of plasma EVs.
Methods: Recognizing the expected low concentrations of EGFr on EVs, the immunoassays were developed using Single molecule array (Simoa) technology, which has shown up to a 1000-fold improvement in sensitivity as compared to conventional immunoassay approaches. Commercial available calibrator material and antibodies against surface markers (EGFr, CD9, CD63 and CD81) were used to develop four assays: CD81-EGFr, CD81-CD9, CD81-CD63, and CD9-CD63. Plasma samples from healthy individuals (n=13) and small cohorts of various cancer patients (n=30, lung, colorectal, ovarian) were used for development, validation and testing.
Results: Each assay was tested for dilution linearity, limit of detection, analytical variation and pre-analytical stability of EVs. EGFr on EVs was lower in cancer patients (median: 489 $x10^6$ EVegfr/mL) compared with healthy individuals (median: 663 $x10^6$ EVegfr/mL). Conversely, total EV concentrations were markedly higher in plasma from cancer patients compared with healthy individuals (CD81-CD9: 9157 vs 4088, CD81-CD63: 3634 vs 1582, CD9-CD63: 9538 vs 1210, median values $x10^6$ EV/mL). Positive correlations were observed among the total EV assays ($r=0.6$, $p<0.0001$).
Conclusion: The developed assays allow measurement of EGFr on EVs and total EVs in human plasma samples. Notable, total EV concentrations were highly increased in cancer as compared with healthy individuals. The assays are now ready for a comprehensive validation using large cohorts of cancer samples.

#3631 Preclinical and clinical pharmacodynamic characterization of BBI-355, a novel, orally bioavailable, and selective CHK1 inhibitor being evaluated in the first-in-human Phase 1/2 POTENTIATE clinical trial of patients with cancer harboring oncogene amplifications.

D. Liao, R. Hansen, S. Chowdhry, E. Holmes, J. Wiese, A. Steffy, A. Pferdekamper, E. Tse, S. Garcia, R. Reynolds, S. Weymer, K. Wagner, C. Hassig, S. Kasibhatla;
Boundless Bio, San Diego, CA

Pharmacodynamic (PD) biomarkers play an integral role in the rational development of novel therapeutic agents. Critically, PD biomarkers enable the measurement and confirmation of a drug's intended effect in early clinical trials. Integration of PD biomarker assessments in early therapeutic development can inform the relationship between drug dose and regimen, target modulation, and biological tumor response, which are fundamental to determining the efficacy and safety of novel therapeutic agents. Boundless Bio is evaluating a novel, orally available, and selective Checkpoint Kinase 1 (CHK1) inhibitor, BBI-355, in the Phase 1/2 clinical trial, POTENTIATE (NCT05827614), in patients with solid tumors harboring oncogene amplification including those on extrachromosomal DNA (ecDNA). ecDNA-enabled oncogene amplification endows cancers with significant genomic plasticity, which can facilitate resistance to targeted therapy (Nathanson et al., 2014), and which is also associated with significantly shorter survival (Kim et al., 2020). While ecDNA provides a fitness advantage to cancer cells, its unique features also confer certain liabilities, including elevated DNA replication stress (RS). Elevated RS results in DNA damage and makes ecDNA+ cancers hyper-reliant on the master regulator of RS, CHK1, which manages DNA replication and repair to maintain cell viability (Chowdhry, 2022). Due to their elevated RS and hyper-reliance on CHK1, ecDNA+ cancer cells are rendered more susceptible to CHK1 inhibition than cancer cells that lack ecDNA. Prior clinical CHK1 inhibitor programs have lacked effective clinical PD biomarker assays. Here, we present preclinical data supporting the use of phosphorylated-CHK1 Ser345 (pCHK1-S345), a proximal marker of RS, as a PD biomarker for CHK1 inhibition by BBI-355. In preclinical studies, BBI-355 treatment induced pCHK1-S345 protein expression by immunoblotting in tumor cell lines in vitro and in xenograft tumors in vivo, which corresponded with tumor cell cytotoxicity. We went on to demonstrate in rats the utility of skin as a tumor surrogate tissue to detect CHK1 inhibitor PD effect through induction of pCHK1-S345 expression by immunohistochemistry. Finally, and for the first time, PD activity of a CHK1 inhibitor in humans was demonstrated by increased pCHK1-S345 expression by immunohistochemistry in skin biopsies from patients enrolled on the POTENTIATE study and treated with BBI-355. In conclusion, pCHK1-S345 is a useful PD biomarker for confirming clinical on-target activity of BBI-355 and may be useful to inform the pharmacologically active range of BBI-355 to support clinical development.

#3632 Cytokine profiles associated with ICI myocarditis using machine learning approaches identifies novel cytokines and implicated pathways.

R. Jaber Chehayeb, D. Hong, N. W. Chen, C. Matute Martinez, R. Jayakrishnan, A. Ferrigno Guajardo, D. Lin, Y. Im, S. Halene, J. VanOudenhove, J. Hwa, A. Jha, J. M. Kwan;
Yale University School of Medicine, New Haven, CT

IntroductionImmune checkpoint inhibitors (ICIs) are effective for a growing number of cancer indications. ICI-mediated T cell activation can lead to immune related adverse effects, including ICI myocarditis, which has up to a 50% mortality. To date, only a few cytokines have been reported to be associated with ICI myocarditis. We evaluated an expansive repertoire of cytokines associated with ICI myocarditis and the pathways they regulate.
MethodsA total of 173 cardio-oncology patients were enrolled in the biomarker study, including 55 who were on ICI. Blood samples of patients who were on ICI for cytokine profiling were sampled when patients presented with symptoms concerning for ICI myocarditis. 71 different cytokines were evaluated and analyzed using Point Biserial correlation analyses and machine learning (XGboost) and explainable artificial intelligence (SHAP) to identify cytokines associated with ICI myocarditis. Analyses were performed to identify pathways associated with ICI myocarditis.
Results28 cytokines were associated with ICI myocarditis and machine learning revealed top features associated with ICI myocarditis in the entire cohort with IL33 being the top feature, Accuracy of 0.895, AUC of 0.902, F1 score of 0.73. SHAP was also used to identify features associated with ICI myocarditis and found IL10, CXCL9, CXCL13, CCL3, were positively associated with ICI myocarditis while CCL22, IL33, TNFSF10, CCL8, and CCL24 were negatively associated with ICI myocarditis. 90% of cytokines identified in the correlation model were also identified in SHAP and XG Boost. Top KEGG and GO pathways associated with ICI myocarditis identified by XGBoost and SHAP features include the cytosolic DNA sensing pathway, response to influenza A, IL17, PI3K-Akt, JAK-STAT and lipid/atherosclerosis pathways
ConclusionsIdentifying pathways associated with ICI myocarditis could provide insights into optimization of immunosuppression strategies

Table of cytokines associated with ICI myocarditis identified by SHAP

Cytokine	Direction
IL10	Upregulated
CXCL9	Upregulated
CXCL13	Upregulated
IL7	Upregulated
CCL3	Upregulated
IFNL2	Upregulated
KITLG	Upregulated
IL27	Upregulated
FLT3LG	Upregulated
CCL22	Downregulated
IL12	Downregulated
CCL2	Downregulated
IL33	Downregulated
TNFSF10	Downregulated
CCL8	Downregulated
CCL21	Downregulated
FGF2	Downregulated
CCL24	Downregulated
CX3CL1	Downregulated

#3633 Multi-parametric characterization of extracellular vesicles in the aqueous humor of uveal melanoma eyes undergoing brachytherapy.

S. Sirivolu[1], C.-C. Peng[2], P. Neviani[2], J. L. Berry[1], L. Xu[1];
[1]Keck School of Medicine, University of Southern California, Los Angeles, CA, [2]Children's Hospital Los Angeles, Los Angeles, CA

Introduction: Aqueous humor (AH), fluid in the anterior chamber of the eye, is a liquid biopsy source of tumor information in uveal melanoma (UM). Extracellular vesicles (EVs) have recently been characterized in the AH of retinoblastoma eyes, however, have not been investigated in UM. EVs are small membrane-enclosed particles secreted by virtually every cell type with a role in intercellular communications. We hypothesize that tumor-derived EVs are detectable in the AH of UM eyes and that understanding the type of vesicles present may help us better understand their function, particularly for cancer. Small extracellular vesicles (sEVs) have been shown to promote tumorigenesis, treatment resistance, and metastasis, leading to the discovery of clinically-relevant biomarkers for multiple cancer types. As the diversity and role of sEVs in the AH of UM patients has never previously been reported, this project is a first step towards investigating new biomarkers of clinical utility. Our aim is to use single particle analysis to characterize sEV subpopulations in the AH of UM patients by quantifying their size, concentration, and phenotypes based on cell surface markers, specifically tetraspanin co-expression patterns.
Methods: sEVs were analyzed from paired pre- and post-brachytherapy AH samples collected from 19 UM patients. AH samples from 5 glaucoma patients served as the control cohort. Unprocessed AH underwent Nanoparticle Tracking Analysis for size quantification and Single Particle-Interferometric Reflectance Imaging Sensor analysis for fluorescent particle count and tetraspanin immunophenotyping; counts were subsequently converted to percentages for analysis. Statistics were performed using Mann-Whitney U, ANOVA, and Tukey's tests.
Results: AH derived from UM eyes (pre-brachytherapy) displayed a broader sEV size distribution than glaucoma eyes, with more diverse sEV subpopulations. Both tumor and nontumor AH samples demonstrated a dominant CD63+ sEV subpopulation. A significantly higher percentage of CD63/81+ sEVs (P= 0.0217) and CD9/63/81+ sEVs (P= 0.0146) were found in post-brachytherapy samples compared to pre-brachytherapy.
Conclusions: sEV subpopulations in UM eyes demonstrate increased heterogeneity in comparison to nontumor eyes. Our results are consistent with prior studies reporting that the CD63+ sEV subtype is an AH-specific biomarker enriched across multiple ocular diseases. The increase in CD63/81+ sEVs and CD9/63/81+ sEVs after brachytherapy is presumably a result of radiation-induced release of these vesicles, suggesting a tumor-derived origin of these subpopulations. CD63/81+ sEV subpopulation was previously reported to also be a tumor-derived subpopulation in AH of retinoblastoma eyes. Further study of the cargo carried by these sEV subpopulations may uncover molecular mechanisms pivotal to UM and other ocular cancers.

#3634 Copy number alterations in chromosome 19 genes associate with reduced immune infiltrate and adverse outcomes in lung cancer.

B. S. Henick, Y. Georgis, B. O. Herzberg, C. P. Concepcion-Crisol, A. M. Taylor;
Columbia University, New York, NY

Deleterious mutations in *STK11/LKB1*, *KEAP1,* and *SMARCA4* have been shown to be associated with adverse response to immunotherapy in several lung cancer cohorts. However, the biological and clinical implications of deletions of these genes, which all reside on chromosome 19p (chr19p), has not been extensively described. We sought to first characterize the association between immune infiltration and these copy number changes in chr19p. To do this, we analyzed mutation, copy number, and gene expression data from non-small cell lung cancer cohorts in the Cancer Genome Atlas (TCGA). Chr19p is frequently deleted across cancers in the TCGA dataset, with higher rates in lung adenocarcinoma. In both lung adenocarcinoma and squamous cell carcinoma, nearly half of TCGA tumors have deletion of chr19p including *STK11*, *KEAP1,* and *SMARCA4*, and these tumors are enriched for *STK11* mutation. Immune infiltrate (estimated by methylation patterns) was not significantly associated with *STK11* mutation but was significantly reduced in tumors with chr19 deletion when controlling for tumor type and overall copy number load. In addition, low-level deletion of any of these genes correlated with decreased expression of immune signaling pathways.

Based on these findings, we next wanted to characterize the association between chr19p copy number and immunotherapy response. We previously reported that low-level deletion of STK11 correlated with an immunosuppressive, treatment-refractory phenotype in samples collected from non-small cell lung cancer (NSCLC) patients with resectable disease in a phase II study of neoadjuvant atezolizumab + chemotherapy. To confirm these findings in a larger cohort, we examined the AACR GENIE NSCLC biopharma collective (BPC) dataset. A subset of this cohort included patients treated with immunotherapy (atezolizumab, nivolumab, and/or pembrolizumab) and with copy number data available or GISTIC analysis of individual genes (n = 204). Here, deletion of any of these three genes correlated with worse overall survival, and this was statistically significant for STK11 deletion. Overall, our data suggests that a broader set of patients, defined by copy number changes in these genes, may experience this adverse immunobiology. Further study to elucidate the mechanistic implications of this association is warranted.

#3635 Insulin-like growth factor receptor predicts poor prognosis in early-stage non-small cell lung cancer.

H. nagamine, M. Yashiro, M. Mizutani, A. Sugimoto, Y. Matsumoto, Y. Tani, K. Sawa, K. Yamada, H. Kaneda, T. Watanabe, K. Asai, S. Suzuki, T. Kawaguchi; Osaka Metropolitan University, Osaka, Japan

Introduction: Insulin like growth factor receptor (IGF1R) is involved in the proliferation and metastasis of various cancers. However, the clinical significance of IGF1R in non-small cell lung cancer (NSCLC) remains to be unclear. In this study, we retrospectively evaluated the correlation between IGF1R expression and clinicopathological features of NSCLC.

Method: A total of 782 specimens of NSCLC patients who underwent surgical resection of primary lung cancer between 2010 and 2019 at Osaka Metropolitan University Hospital was enrolled in this study. Immunohistochemical staining of IGF1R were performed, and the correlation between IGF1R expression and clinicopathological features of NSCLC, especially in recurrence free survival (RFS) and overall survival (OS), was evaluated. We also evaluated an association between IGF1R and programmed death ligand 1 (PD-L1) expression.

Results: IGF1R expression was positive in 279 (35.8%) patients. IGF1R-positive group had significantly longer smoking histories (median smoking index, 1,000 vs 600, p <0.01) and a higher proportion of squamous cell carcinomas (35.1% vs 14.1 %, p <0.01). IGF1R-positive group also significantly expressed PD-L1 (24.4% vs 6.4%, p<0.01). IGF1R-positive group had significantly worse RFS (10-year recurrence-free rate; 42.7% vs 53.7%, p <0.01) and OS (10-year survival rate; 54.4% vs 67.3%, p <0.01). RFS and OS were significantly worse in the IGF1R-positive NSCLC patients at stage 0 and stage I (10-year recurrence-free rate; 49.0% vs 62.9%, p <0.01, 10-year survival rate; 57.4% vs 74.2%, p<0.01), but not in stage II (10-year recurrence-free rate; 52.0% vs 43.8%, p=0.68, 10-year survival rate; 63.4% vs 47.5%, p=0.95) and III (10-year recurrence-free rate; 20.7% vs 20.8%, p=0.77, 10-year survival rate; 38.3% vs 54.6%, p=0.18). IGF1R expression was associated with poorer RFS and OS in early-stage NSCLC.

Conclusion: IGF1R is a predictor of poor prognosis in resected early-stage NSCLC.

#3636 Myeloid cell rebound associated with GD2-CAR-T cell therapy in solid tumor patients.

Michael P. Brown[1], Tessa Gargett[2], Nga T. H. Truong[2], Orazio Vittorio[3], David S. Ziegler[4]

[1]Cancer Clinical Trials Unit, Royal Adelaide Hospital, Adelaide, Australia,[2]Translational Oncology Laboratory, Centre for Cancer Biology, Adelaide, Australia,[3]School of Biomedical Sciences, University of NSW, Sydney, Australia,[4]Kids Cancer Centre, Sydney Children's Hospital, Sydney, Australia

GD2 is a validated cancer immunotherapy target with highly restricted normal tissue expression. Promising activity of GD2-CAR-T cell therapy in diffuse midline glioma and neuroblastoma has promoted interest in this therapy. We initiated three phase 1 clinical trials of escalating doses of intravenously administered autologous GD2-CAR-T cells in patients with advanced GD2-positive solid tumors.

Emerging evidence suggests that CAR-T cells may increase circulating myeloid derived suppressor cells (MDSCs) and that this event may be mediated and/or triggered by CAR-T cell-derived cytokines and chemokines. These findings may help to explain the limited persistence of CAR-T cell therapy in solid tumor patients. Hence, we sought evidence of MDSC generation and secretion of relevant cytokines and chemokines in our clinical trial patients.

The CARPETS trial (www.anzctr.org.au: ACTRN12620000622909) recently closed to recruitment after enrolling 12 patients (7 melanoma, 4 colorectal cancer, and 1 sarcoma). No significant adverse events were attributable to CAR-T cell therapy. We opened two other GD2-CAR-T cell therapy trials in 2023: LEVI'S-CATCH (ACTRN12622000675729) in patients with diffuse midline glioma at Sydney Children's Hospital and KARPOS (ACTRN12622001514796) in adult patients with recurrent glioblastoma at Royal Adelaide Hospital. To date, 3 patients have enrolled to LEVI'S-CATCH with the first patient clearing the dose limiting (DLT) evaluation period. Three patients completed enrolment to the first dose cohort of KARPOS without DLTs.

In all CARPETS patients, CAR-T cell expansion, which was measured by by DNA quantitative PCR and flow cytometry, peaked during the 6-week post-CAR-T infusion DLT evaluation period. In 6 CARPETS patients for whom peripheral blood samples were available, we found by flow cytometry, newly formed or increased size of pre-existing subpopulations of non-classical monocytes and/or MDSCs of mononuclear and/or polymorphonuclear class, which peaked at or after the time of peak CAR-T cell expansion. Typically, serum levels of inflammatory cytokines and chemokines such as TNF, IL-6, IL-8, CCL2, GM-CSF, and CXCL10, were detected only after the CAR-T cell infusion with variable patterns of the timing and concentration of analyte observed among the 12 patients.

At the time of writing, blood samples from the first KARPOS patient showed CAR-T cell expansion and the subsequent increases in circulating myeloid derived suppressor cells and inflammatory cytokines. We expect that full data sets for these parameters will be presented for current and future enrolled patients to both studies.

To improve CAR-T cell persistence in solid tumor patients, these data indicate the need for new therapeutic strategies to mitigate effects of CAR-T cell induced myeloid cells with antitumor activity.

#3637 Ultrasensitive assays for combined detection of CEA$^{\pm}$ extracellular vesicles and soluble CEA.

L. Hebert[1], M. Al-Ameen[1], T. Spriggs[1], C. Nelson[1], E. A. Gizzie[1], J. L. Franklin[2], R. J. Coffey[2], **D. A. Routenberg**[1], J. N. Wohlstadter[1];
[1]Meso Scale Diagnostics, LLC, Rockville, MD, [2]Vanderbilt University, Nashville, TN

Colorectal cancer (CRC) is the third most common cancer worldwide and is the second leading cause of cancer death in the United States. Carcinoembryonic antigen (CEA) is a biomarker commonly used in the management of CRC. It is typically present at low levels in the blood of healthy adults but is elevated in CRC samples and some other cancers. CEA is most commonly used to monitor treatment efficacy and as a critical part of post-treatment surveillance for residual disease, recurrence, and/or progression/metastasis. The CRC recurrence rate averages >25%, and liver metastasis occurs in 25-30% of cases. Improved CEA assays could enable earlier determination of treatment failure, detection of lower levels of minimal residual disease (MRD) after treatment, or earlier detection of recurrence. CEA is a GPI-linked membrane protein secreted from CRC cells mainly by enzymatic cleavage of its GPI anchor. However, we have identified alternative secretion of CEA in association with extracellular vesicles (EVs). We hypothesized that the soluble CEA produced by canonical shedding and the alternatively secreted CEA may provide distinct information about the tumor or its microenvironment and serve as independent but complementary biomarkers of CRC. We developed ultrasensitive, multi-marker electrochemiluminescence (ECL) immunoassays for measuring intact EVs presenting CEA, CD73, or both in human plasma. We observed that plasma levels of CEA$^{\pm}$EVs and CD73$^{\pm}$EVs were elevated in some late-stage CRC samples compared to controls. CEA and CD73 double-positive EV (CEA$^{\pm}$CD73$^{\pm}$EVs) levels were also elevated in the same samples, exhibiting a 3-fold improved separation of these samples with CRC from controls, compared to detection of CEA$^{\pm}$EVs. Additionally, approximately 25% of stage IV CRC samples had elevated CEA$^{\pm}$EV and CEA$^{\pm}$CD73$^{\pm}$EV levels while exhibiting low soluble CEA. We confirmed this result in an independent sample set that included samples across all CRC stages, and also identified a few earlier-stage samples that exhibited high CEA$^{\pm}$EVs and CEA$^{\pm}$CD73$^{\pm}$EVs without elevated soluble CEA. Since CEA$^{\pm}$CD73$^{\pm}$EVs and soluble CEA assays identified different subsets of samples, we combined the two assays into a single classifier for late stage CRC and controls, yielding improved receiver operator characteristic (ROC) with area under the curve (AUC) of 0.975 versus 0.927 for the standard soluble CEA assay or 0.788 for CEA$^{\pm}$CD73$^{\pm}$EVs alone. These results suggest that assaying EVs presenting multiple surface markers can increase specificity for the detection of tumor-derived EVs relative to a single marker and that assaying both soluble and EV-associated forms of CEA in plasma may improve the value of CEA measurement in CRC.

#3638 Pathologic endpoints as surrogates for survival endpoints in neoadjuvant immunotherapy clinical trials for non-small cell lung cancer.

R. B. Cameron[1], J. B. Hines[1], A. Esposito[1], C. Bestvina[1], M. C. Garassino[1], V. Torri[2], R. Thawani[1];
[1]UChicago Medicine, Chicago, IL, [2]Institute Mario Negri, Milan, Italy

Background: The use of neoadjuvant immunotherapy alone or in combination has rapidly evolved in the last 5 years. There is significant debate as to whether pathologic complete response (pCR) or major pathologic response (MPR) can be considered a surrogate endpoint for survival. We therefore performed a systematic review and meta-analysis to evaluate the surrogacy of pCR and MPR for event free survival (EFS) in neoadjuvant clinical trials for early-stage NSCLC.

Methods: We performed a systematic literature search on PubMed and reviewed abstracts of the most relevant international conferences until June 2023. Relevant information relative to response rates, Odds Ratios (ORs) of response, 2-years EFS rates and Hazard ratios (HRs) were retrieved from all eligible clinical trials and the association were analyzed. To evaluate patients level surrogacy the association between response rate and 2-year EFS was evaluated. In trials presenting EFS rates by achievement of pCR and MPR a forest plot with random effect model was also produced. For trial level surrogacy, ORs for pCR and MPR and HRs for EFS were retrieved and analyzed using a linear regression model weighted by sample size. R^2 and linear regression slope were used respectively to estimate the proportion of variation in EFS effect explained by pCR effect and the magnitude of change in EFS effect as a function of the magnitude of change in pCR effect. The R^2 with 95% CI were calculated by bootstrapping approach.

Results: Seven RCTs were identified for a total of 2940 patients. At patient level, the R^2 of pCR and MPR with 2-years EFS were 0.82 (0.66-0.94) and 0.81 (0.63-0.93), respectively, with slopes of 0.96 (0.68-1.19) and 0.64 (0.45-0.85), respectively. At trial level, R^2 for association of OR for response and HR for EFS was 0.58 (0.00-0.97) and 0.61 (0.00-0.97) for pCR and MPR, respectively.

Conclusions: While we were able to show a strong correlation between pCR and EFS, trial level surrogacy was not proven. The lack of surrogacy can be related to the high heterogeneity among clinical trials and the still scarce number of data available. More research to reduce the heterogeneity (e.g., pathological evaluation, surgery, and staging harmonization) must be done to introduce pCR as a primary measure to predict EFS.

#3639 *ARID1* mutations may serve as a predictor of MSI and TMB levels in gastric cancer.

C. Xu[1], B. Lian[1], Y. Dai[1], W. Duan[2], F. Zhao[2], **M. Li**[1];
[1]Department of Gastrointestinal Surgery, Xijing Hospital, Air Force Medical University, Xi'an, China, [2]3D Medicines Inc., Shanghai, China, Xi'an, China

Background: *ARID1A* is a gene that produces a protein called BAF250a, which is a component of the chromatin remodeling complex. This complex plays a critical role in regulating gene expression by altering the structure of chromatin. *ARID1A* mutations and MSI-H are mutually exclusive in endometrial cancer, but not in ovarian cancer. *ARID1A* mutations are associated with high TMB in certain types of cancer, such as endometrial and gastric cancer. The relationship between *ARID1B* mutations and MSI-H/TMB is complex, and this study aims to clarify it in gastric cancer.
Methods: The formalin-fixed paraffin-embedded (FFPE) tissues 337 patients with gastric cancer who have underwent next-generation sequencing (NGS) include 733 genes from Nov, 2019 to Mar, 2023 in 3DMed Clinical Laboratory Inc. were investigated in this study. These patients are still being followed up.
Result: In this study, 337 patients with gastric cancer were analyzed for *ARID1A* and *ARID1B* mutations, MSI-H status, and TMB levels. The results showed that 17.8% of the patients had *ARID1A* mutations, 8.9% had *ARID1B* mutations, and 3.6% had both mutations. Additionally, 7.7% of the all patients had MSI-H. The study found that patients with *ARID1* mutations had significantly higher rates of MSI-H compared to unselected patients. Specifically, 35% of patients with *ARID1A* mutations, 30% with *ARID1B* mutations, and 75% with both mutations had MSI-H, compared to 7.7% in unselected patients. Furthermore, TMB levels were higher in patients with *ARID1A* or *ARID1B* mutations compared to wild-type and unselected patients ($p<0.0001$). There was no significant difference observed between patients with *ARID1A* and *ARID1B* mutation subgroups in terms of TMB levels ($p = 0.3515$). However, TMB levels were lower in patients with *ARID1A* or *ARID1B* mutations compared to patients with both mutations ($p = 0.0036$, $p = 0.0104$). These findings suggest that *ARID1* mutations may cause genomic and chromosomal instability in gastric cancer, leading to higher rates of MSI-H and TMB.
Conclusion: The study highlights the potential clinical significance of *ARID1* mutations as a biomarker for predicting MSI-H and TMB levels in gastric cancer, which could help guide personalized treatment strategies for patients with this disease. However, further research is needed to confirm these findings and to determine the clinical implications of *ARID1* mutations in gastric cancer.

#3640 RAB26 accelerates endometrial cancer cell progression by regulating the Hedgehog signaling pathway.

C. Gao[1], Y. Liu[1], Y. Han[2], F. Xue[1], Y. Wang[1];

[1]Tianjin Medical Univeristy General Hospital, Tianjin, China, [2]First Teaching Hospital of Tianjin University of Traditional Chinese Medicine, Tianjin, China

As one of the most common gynecological malignant tumors, endometrial cancer (EC) is continuously being studied since its etiology is still not clear. RAB26, a member of the RAB family, has been shown to influence cell proliferation, metastasis and other malignant phenotypes in several cancers. However, whether and how RAB26 plays roles in EC remain unknown. Our previous study showed that RAB26 was related to the cell cycle-associated protein IK, which has been shown to contribute to carcinogenesis. Herein, we further explored the clinical significance and biological function of RAB26 in EC. Immunohistochemical staining of 615 endometrial tissue samples was conducted to explore whether RAB26 expression was related to the clinicopathological characteristics of EC. In vitro and in vivo experiments were used to evaluate the role of RAB26 in EC and investigate the underlying mechanism. RAB26 expression was higher in EC than in normal endometrium (NE), hyperplastic endometrium (HE) and atypical hyperplastic endometrium (AHE). High RAB26 expression was positively correlated with tumor histological grade (P=0.010), FIGO stage (P=0.042) and tumor size (P=0.003) in EC. RAB26 attenuation inhibited cell proliferation and metastasis but promoted cell apoptosis and caused G0/G1 arrest. After RAB26 attenuation, RNA sequencing data showed that the Hedgehog signaling (SHH) pathway was enriched. Further western blot results confirmed that the levels of SHH pathway proteins (SHH, PTCH1, smo and Gli1) decreased as RAB26 expression was attenuated. Moreover, an agonist of the SHH pathway, purmorphamine, blocked the inhibitory effect of RAB26 attenuation on EC progression. The results of an in vivo study also showed that RAB26 attenuation exerted a significant antitumor effect. Accordingly, RAB26 may act as an oncogenic protein to promote EC progression through the SHH pathway. RAB26 may be a potential target for the treatment of EC patients.

#3641 Pharmacodynamic and predictive biomarker results from the phase I dose escalation study of NGM707, an ILT2/ILT4 dual antagonist antibody, in patients with advanced solid tumors.

L. K. Blum, H.-I. H. Chen, A. De Costa, A. Iyer, G. W. Stone, N. D. Galicia, J. Chan, B. Dampier, K. Wu, U. Jeffry, K. Zhou, J. Sloan-Lancaster, D. Abhayankar, V. Hanes, H. D. Lieu, D. D. Kaplan, J. M. Roda;
NGM Biopharmaceuticals, Inc., South San Francisco, CA

Background: NGM707 is a dual antagonist antibody that binds a shared epitope of the immune inhibitory receptors ILT2 (LILRB1) and ILT4 (LILRB2). In preclinical studies, NGM707 reprogrammed suppressive myeloid cells via blockade of ILT2/ILT4 and enhanced NK and CD8+ T cell activity via blockade of ILT2; furthermore, NGM707 and pembrolizumab acted additively in vitro to enhance CD4+ T cell activation in mixed lymphocyte reactions. NGM707-IO-101 (NCT04913337) is a first-in-human Phase 1/2 clinical trial of NGM707 monotherapy and combination with pembrolizumab. Here we report pharmacodynamic and predictive biomarker data from NGM707-IO-101 monotherapy and combination dose escalation cohorts.
Methods: Eligible patients with advanced or metastatic solid tumors were enrolled into escalating dose cohorts from 6 to 1800 mg NGM707, alone or in combination with 200 mg pembrolizumab, administered Q3W iv. Biomarker assessments of tumors comprised RNA-sequencing and immunohistochemistry (including ILT2, ILT4, CD163) of archival/baseline (N= 41 IHC, 47 RNA) and paired on-treatment tumor biopsies (N=13 IHC, 21 RNA). Peripheral blood biomarker samples were collected on days 1, 4, 8, and 15 of cycle 1 and prior to dosing at each subsequent cycle. Blood biomarker assessments included circulating cytokines/chemokines, PBMC RNA-sequencing, and flow cytometry immunophenotyping. Baseline biomarkers were associated with anti-tumor activity per RECIST v1.1.
Results: Pre-treatment biopsies from patients with disease control (DC) showed higher expression of genes in the 18-gene tumor inflammation signature (TIS) than patients with progressive disease (PD). A composite gene signature incorporating gene sets related to TIS, NK cell activity, and tumor cell proliferation had a statistically stronger association with DC than TIS genes alone. Baseline ILT2/ILT4 target expression (≥1% of tumor area) was observed in 31 (75.6%) patients, with similar levels observed in patients with DC and PD. Pharmacodynamic changes were observed in tumor samples following treatment, including increased expression of gene signatures that reflect myeloid cell activation and a proinflammatory tumor microenvironment. Decreased protein expression of the immunosuppressive myeloid marker CD163 was observed following treatment in both blood and tumor for a subset of patients. Proinflammatory chemokines including CXCL9 increased in serum following treatment.
Conclusion: Baseline gene expression signatures have shown an encouraging association with clinical benefit from NGM707 and merit further investigation as promising predictive biomarkers. Protein and gene expression changes reflecting the expected modes of action of NGM707 and pembrolizumab were observed in both peripheral blood and tumor biopsies following treatment.

#3642 Phenotypic biomarkers of aqueous humor extracellular vesicles from retinoblastoma eyes.

A. Amacker[1], C.-C. Peng[2], B. J. Reiser[2], J. L. Berry[2], L. Xu[2];
[1]Keck School of Medicine of USC, Los Angeles, CA, [2]Children's Hospital Los Angeles, Los Angeles, CA

Purpose: Retinoblastoma (RB) is the most common pediatric intraocular cancer, yet tumor biopsies are contraindicated. This challenge emphasizes the need for investigation of non-tissue biomarkers. Extracellular vesicles (EVs), which are secretory vesicles containing bioactive molecules, have emerged as promising biomarker candidates due to their ability to be phenotyped using known tetraspanin markers. Aqueous humor (AH) provides an exciting liquid biopsy source for intraocular tumor information, with EVs having recently been identified in AH. Our laboratory has previously proposed that CD63/81+EVs are associated with retinoblastoma, but specific tumor-derived markers have not been linked to AH EVs using traditional tetraspanin assays. In this study, we employed MACSPlex, a high-dimensional magnetic bead-based immunoassay, to further explore RB-EV.
Methods: 7 AH samples consisting of two congenital glaucoma (GLC) samples and five RB samples taken at the time of primary enucleation were analyzed. We utilized Macsplex, a multiplex bead-based flow cytometry assay, to analyze the expression profiles of surface markers found on EVs. With 39 capture beads coated with monoclonal antibodies for 37 different EV surface antigens and two negative controls, the mean fluorescence intensity (MFI) of APC conjugated antibody cocktail from three tetrapanins (CD9, CD63 and CD81) on EVs captured by each surface antigen could be measured by flow cytometry. Enrichment ratios were then calculated by normalizing the fluorescence of each signal to the mean fluorescence of CD9, CD63, and C81.
Results: Macsplex analysis of the 2 GLC AH samples demonstrated a strong CD63 dominance compared with RB AH. The mean CD63 enrichment ratio for GLC samples was 2.6 (S.D. = 0.34), and 1.3 (S.D. = 0.27) in RB samples, with a p-value of 0.069. In comparison to the GLC patients, the analysis of EVs in the AH of the 5 RB samples exhibited a greater co-dominance of CD63/CD81 positivity consistent with past research on RB EVs. The mean CD81 enrichment ratio for the 5 RB samples was 1.5 (S.D. = 0.26), in contrast to 0.3 (S.D. = 0.24) in GLC AH, with a p-value of 0.03. Interestingly, 4 out of the 5 RB AH samples demonstrated very strong CD133 signals, which is a known cancer marker. Deeper investigation into one RB AH sample utilizing single tetraspanin detection revealed higher coexpression of CD63 and CD81 with CD133 than seen with CD9. The CD133 enrichment ratio for the CD81, CD63, and CD9 single channel experiments were 6.6, 3.4, and 1.5 respectively.
Conclusions: Comparison between this study and previous work done by our group demonstrate a high concordance between results utilizing Macsplex and Exoview**.** However, this is the first study identifying the expression of CD133, a cancer stem cell marker, on retinoblastoma-derived EVs in AH. Macsplex technology illustrates an incredible clinical potential of AH EVs for characterizing retinoblastoma phenotype *in vivo.*

#3643 Molecular pathogenesis of lung cancer associated with interstitial pneumonia.

D. Mizuno[1], K. Shien[2], A. Matsuoka[1], M. Ohki[1], S. Tomida[3], R. Yoshichika[1], T. Higashihara[1], F. Mukohara[1], N. Hayashi[1], T. Habu[1], M. Yoshikawa[1], K. Suzawa[2], H. Yamamoto[2], D. Ennishi[3], S. Toyooka[1];

[1]Okayama University Graduate School of Medicine, Dentistry and Pharmaceutical Sciences, Okayama, Japan, [2]Okayama University Hospital, Okayama, Japan, [3]Okayama University Hospital, Center for Comprehensive Genomic Medicine, Okayama, Japan

Background: Interstitial pneumonia (IP) is known to be associated with a high risk of developing lung cancer. While common mechanisms have been reported to be involved in the pathogenesis of IP and lung cancer, including genetic and epigenomic alterations or specific signaling pathway activations, many of the molecular mechanisms of lung cancer development in IP lesions remain unknown.

Methods: To clarify the detailed mechanisms of the pathogenesis of lung cancer associated with IP, we performed spatially resolved transcriptomics on lung cancer specimens obtained from usual interstitial pneumonia (UIP) associated lung cancer patients. In a total of 10 patients, including five lung cancers that developed inside the UIP and five lung cancers that originated outside the UIP, regions of interest (ROIs) were selected in the tumoral tissues and their adjacent non-tumor tissues. Then, gene expression profiles were comprehensively analyzed by using GeoMx digital spatial profiler in each ROI.

Results: In the UIP lesions adjacent to lung cancer, increased gene expressions associated with pulmonary fibrosis, such as COL1A1, COL3A1, and APOE, were observed, and gene set enrichment analysis (GSEA) revealed that they were associated with autoimmunity-related pathways. When we compared the tumor lesions developed inside the UIP with outside the UIP, increased gene expressions related to IP mortality were observed in the tumor cells developed inside the UIP. Interestingly, GSEA revealed that the gene set for neutrophil extracellular trap (NETs) formation was found to be upregulated in the tumor cells developed inside the UIP, suggesting that NETs plays an important role in the pathogenesis of lung cancer developed in IP lesion.

Conclusions: In our study, spatially resolved transcriptomics revealed a novel pathway related to the pathogenesis of lung cancer associated with IP.

#3644 Uncover spatial signatures of tumor microenvironment and oncogenic pathways using 6,000-plex single-cell spatial molecular imaging on FFPE skin squamous cell carcinoma.

M. Patrick, **S. He**, S. Ilcisin, D. Kroeppler, P. Danaher, J. Reeves, M. Gregory, H. Zhai, M. Rhodes, J. Beechem;
Nanostring Technologies, Seattle, WA

Background: Tumor progression and therapeutic response are regulated by the tumor microenvironment. Understanding the spatial association and architecture of molecular characteristics and composition of tumor immune microenvironment at single-cell and subcellular resolution encourages improvements in clinical prognosis and immunotherapy benefits. Single-cell Spatial profiling technologies permit the study of transcriptional activity at the spatial, single-cell level and provide abundant, high-resolution information required for the identification of clinical-related features in immuno-oncology.
Methods: We performed an ultra-high-plex RNA assay to detect 6,000 targets simultaneously *in situ* on FFPE human skin squamous cell carcinoma using the CosMx™ Spatial Molecular Imager (SMI). For the selection of regions of interest, four protein markers and DAPI were co-detected on the same tissue slide. Tertiary analysis algorithms were developed for cell typing, co-localization of genes and ligands, cell-cell interaction, and pathway analysis.
Results: Thousands of transcripts were simultaneously detected with high sensitivity and specificity on the FFPE skin squamous cell carcinoma tissue section at single-cell subcellular resolution. We investigated the tumor microenvironment including cell types, their spatial distribution and proportion of diversified immune cells in the tumor compartment. The cell typing results revealed many cancerous subpopulations, which resolved spatially from cells that lacked any defining marker genes. We also assessed distances between immune cells and their nearest functional-related neighbors. Moreover, we revealed the ligands co-localization, as well as spatial patterns of direct cell-cell interactions and signaling pathways. We found that some genes have elevated expression in macrophages which are near cancer compared to those are far from cancer cells, empowering the molecular investigation of novel signaling between immune and cancer cells in tumor immune microenvironment.
Conclusions: Single-cell spatial measurements of 6,000 RNA and four proteins on the same tissue section, along with a large viewing area on archival FFPE tissue, provide a novel tool to reveal the spatial signature of tumor microenvironment and oncogenic pathways, facilitating the next level of cancer and therapeutic research. FOR RESEARCH USE ONLY. Not for use in diagnostic procedures. FOR RESEARCH USE ONLY. Not for use in diagnostic procedures.

#3645 Unraveling spatial complexity of the tumor microenvironment: A whole transcriptomic perspective with Visium HD.

Y. Yin, J. Sapida, D. Sukovich, D. Patterson, A. Tentori;
10x Genomics, Pleasanton, CA

In recent years, advances in spatial transcriptomics have revolutionized our understanding of the tumor microenvironment, providing crucial insights into the complex interplay of different cell types within cancer tissues. In this study, we employed the new, high definition Visium spatial transcriptomics assay (Visium HD) to investigate the intricate molecular landscape of prostate cancer at single-cell scale resolution and across the whole transcriptome. Our research focused on deciphering the spatial heterogeneity of gene expression patterns within the tumor microenvironment, shedding light on the interactions between cancer cells, stromal cells, and vasculature.

The Visium HD assay enables an unbiased exploration of the transcriptome on FFPE tissue sections mounted on standard glass slides. Combining gene expression data with H&E images from the same section, it allows precise characterization of local molecular features and disease states at single-cell scale. We analyzed a set of human prostate adenocarcinoma samples with the Visium HD assay, and identified spatially regulated gene signatures associated with specific cell types and functional pathways. Our findings have recapitulated previously identified molecular markers, including VEGFA and MYC which have been implicated in tumor progression and angiogenesis. The spatial gene expression patterns had good correlation with histological annotations of cancerous and normal tissue within the H&E image. However, Visium HD allowed us to further observe molecular processes and pathways specific to this adenocarcinoma sample. This integrative approach offers valuable implications for personalized cancer therapy and the development of targeted interventions tailored to the spatial context of individual tumors.

Our study underscores the significance of understanding the spatial organization of the whole transcriptome in cancer tissues, and highlights the potential of the Visium HD platform as a powerful tool for unraveling the complexities of the tumor microenvironment. These insights pave the way for the development of innovative therapeutic strategies and precision medicine approaches, ultimately contributing to improved outcomes for cancer patients.

#3646 A spatially resolved single cell proteomic atlas of small bowel adenocarcinoma.

Z. Dereli, B. Bozorgui, H. Wang, J. Weinstein, M. Overman, **A. Korkut**;
UT MD Anderson Cancer Center, Houston, TX

Small bowel adenocarcinoma (SBA) is a rare malignancy associated with poor prognosis. The cellular and proteomic heterogeneity within the tumor immune microenvironment (TIME) of SBA is a likely driver of prognosis, disease progression and response to therapy. There is, however, a major gap in our knowledge of tumor and immune interactions in SBA. Cyclic Immunofluorescence (CycIF), an antibody-based, highly multiplexed imaging technology for spatially resolved single cell level proteomic profiling, is well suited to map the proteomic heterogeneity and organization of TIME in SBA. Here, using CycIF, we have generated a spatially resolved single-cell proteomic atlas of TIME for 136 tumor and normal samples from clinically and genomically annotated SBA patients (N=37). The SBA TIME Atlas covers information on expression levels, spatial position, and cell morphology for > 40 proteomic markers of tumor-intrinsic processes and states, diverse immune cell types, immune checkpoints, and tumor vascularization. In total, we collected proteomics data from > 600,000 cells. Using a hierarchical decision tree of cell type markers, we have generated the cell identity annotations for > 350,000 cells, with positional information. A comprehensive computational analysis of the SBA atlas revealed various spatial and heterogeneity features that may impact the TIME organization in fine detail. Using those features, we have compared the proteomic heterogeneity in tumor vs. normal cell populations, identifying spatial and single-cell correlates of key clinical variables (e.g., patient survival, age, sex, disease stage, metastatic status). We have also performed differential analyses of spatial features involving protein markers and cell types with respect to genomic alteration states and have mapped the spatial enrichment of likely actionable immune check proteins to immune and tumor cells. Such mapping may guide future therapeutic decisions. Overall, we expect that the SBA TIME Atlas will provide a useful resource and inform future translational studies, as well as basic research for better mechanistic understanding and treatment of this disease.

#3647 Digital spatial transcriptomic reveals different epithelial and immune cells signatures across endometriosis-related diseases: From simple ovarian endometriosis to ovarian cancer.

V. Iacobelli, C. Nero, S. Alivernini, G. Scaglione, F. Camarda, F. Sillano, R. Trozzi, A. Piermattei, B. Tolusso, G. Mantini, L. Giaco, G. Anderson, G. Zannoni, E. Gremese, A. Fagotti, G. Scambia;
A. Gemelli University Hospital, University of the Sacred Heart, Rome, Italy

Endometriosis represents a pressing medical concern, imposing a relevant burden on patients including potential malignant transformation into endometriosis-associated ovarian cancer (EAOC). Despite the process of cancer development remains unclear, immune cells abnormalities arose as putative biomarkers in the neoplastic progression. One-third of ovarian endometriosis cases exhibit PD-1/PD-L1 expression levels comparable to those observed in cancer. To substantiate the biological basis of these findings, this study aimed to elucidate the spatial transcriptomic profile of epithelial and immune components from different endometriosis-related conditions, along with their genetic interplay. Formalin-fixed paraffine embedded (FFPE) specimens from 4 ovarian endometriosis (OE) cases, two of which displayed elevated levels of PD-1/PD-L1 expression and were referred to as cancer-like endometriosis (CLE), 1 Clear Cell Ovarian Cancer (CCOC) and 1 Endometrioid Ovarian Cancer (EOC) were cut in 5um section for spatial transcriptomic analysis using GeoMX Human Whole Transcriptome Atlas (WTA) probe-set (>18000 genes). For all sections, the regions of interest (ROIs) were identified using a set of morphology markers: anti-human CD3, CD68 and PanCK antibodies. Spatial transcriptomic analysis revealed condition-specific gene enrichment of epithelial and immune cells across the different conditions. In spite of similar H&E findings, $PanCK^{pos}$ epithelial cells from CLE showed an increased expression of genes involved in stress response and defense regulation pathways (e.g. CXCL6, S100A9, and PECAM-1), when compared to OE, in which $PanCK^{pos}$ cells were enriched in DUSP1/2 and VIM. Interestingly, in CCOC, location-specific gene-enrichment was found in $PanCK^{pos}$ cells, with a significant up regulation of tumor suppressor genes (e.g. EGR-1, NR4A1) in normal-looking peri-tumoral epithelium compared to cancerous intra-tumoral $PanCK^{pos}$ cells. Similarly, in the immune compartment, spatial transcriptomic analysis revealed that $CD3^{pos}$ cells from CLE displayed an up-regulation of genes involved in IL-17 signaling, response to oxydative stress and complement activation (e.g. CXCL6, HMOX1, S100A9, and PECAM-1), when compared to OE. Moreover, in CCOC, $CD68^{pos}$ cells of the tumoral mass showed over-expression of tumor growth and progression markers (e.g. SPP1) compared to their counterpart in the outer area of the tumoral mass. In this first comprehensive spatial transcriptomic study of endometriosis-related diseases with GeoMx WTA, our findings uncovered remarkable differences in epithelial and immune cells among different stages and tissue locations. Importantly, CLE emerged as a transitional entity with a unique immune profile. Ongoing analysis of six additional samples will further refine our results.

#3648 The spatial organization of cells expressing MYC and BCL2 affects immune microenvironment composition and prognosis in DLBCL.

S. Shridar[1], M. M. Hoppe[1], P. Jaynes[1], G. Kumar[2], S. Jasoria[3], Z. Meng[1], V. Rajan[1], K. Kannan[2], C. Tripodo[4], **A. D. Jeyasekharan**[1];
[1]National University of Singapore (NUS), Singapore, Singapore, [2]The University of Texas MD Anderson Cancer Center, Houston, TX, [3]Birla Institute of Technology & Science, Pilani, Pilani, India, [4]University of Palermo, Palermo, Italy

Point process analyses are widely used in ecology and geography to understand the impact and relevance of spatial distribution of points in a complex system. To date, only few studies have explored point process analyses in the context of tumor heterogeneity. Malignancies often show variable patterns of cellular distribution, and the relationship of these topographic variables with underlying biological processes and clinical outcomes is not well understood. Here, we performed spatial point process analyses in diffuse large B-cell lymphoma (DLBCL), leveraging advances in multiplexed immunohistochemistry and cellular phenotyping, with downstream multi-omic and clinicopathological analyses.

We have demonstrated that survival in DLBCL is strongly associated with the fraction of malignant cells showing co-expression of the oncogenes MYC and BCL2 in the absence of BCL6 (M+2+6-). These cells display non-random spatial organization within tumor infiltrates, deviating from a poisson distribution. We therefore modeled the spatial organization of M+2+6- cells within DLBCL, using x-y coordinate information from multiplexed fluorescent immunohistochemistry (mfIHC) in four independent cohorts (N=449 patients). We derived spatial point patterns, upon which Geyers point process models were applied. We observed that patients could be divided into two groups based on these: one group showed “clustered” spatial organization, while the other displayed a “dispersed” M+2+6- cell distribution. Cases with predominantly “dispersed” M+2+6- cells showed shorter overall survival in all analyzed cohorts ($P < 0.05$ in 4/4 cohorts).

We performed multi-omic analyses to identify potential biological explanations for this association between topography and clinical outcome. Using digital spatial profiling of the transcriptome from CD20, CD3 and CD68 compartments in 47 DLBCL samples, we observed that lymphomas with an M+2+6- ‘dispersed’ phenotype had an immunologically cold microenvironment enriched in Tregs and exhausted CD4+ and CD8+ T cells. Through an integration with single-cell transcriptomic analyses (N=22 samples) we observed that malignant B-cells from cases with M+2+6- ‘dispersed’ phenotype expressed genes implicated in cell migration and adhesion, but also in potentially targetable immune checkpoints such as LAG3.

In summary, by integrating multiplexed immunophenotyping and point process analysis with molecular profiling in the setting of DLBCL, we show that a dispersed pattern of distribution of the M+2+6- subclonal fraction uniquely confers poor prognosis, and associates with a potentially reversible immune cold microenvironment composition. This represents the first demonstration that the spatial distribution of malignant cell subpopulations in lymphoma can embody biological and clinical significance.

#3649 A novel spatial multi-omic approach for biological discoveries in colonic diseased tissues using a comprehensive Immuno-Oncology Proteome Atlas and Whole Transcriptome Atlas.

A. Rosenbloom[1], S. Bonnett[1], M. Conner[1], C. Kang[1], E. Piazza[1], B. Filanoski[1], R. Meredith[1], H. Yi[1], L. Hamanishi[1], E. Ignacio[1], N. Nelson[2], M. Prater[2], V. Devgan[1], R. Van Eijsden[1], M. Moon[1], L. Isgur[1], T. Theisen[1], M. Hoang[1], G. Geiss[1], J. M. Beechem[1];

[1]NanoString Technologies, Inc., Seattle, WA, [2]Abcam plc, Cambridge, United Kingdom

The advancement of spatially resolved, multiplex proteomic and transcriptomic technologies has revolutionized and redefined the approaches to complex biological questions pertaining to tissue heterogeneity, tumor microenvironments, cellular interactions, cellular diversity, and therapeutic response. While spatial transcriptomics has traditionally led the way in plex, multiple studies have demonstrated a poor correlation between RNA expression and protein abundance, owing to transcriptional and translational regulation, target turnover, and most critically, post-translational protein modifications. Therefore, a more holistic, ultra-high-plex, and high-throughput proteomic atlas approach becomes critical for the next phase of discovery biology. Here, we present a barrier-breaking, spatial proteomics panel that was designed to accelerate scientific discoveries. A Digital Spatial Profiler platform is uniquely suited to support high-plex proteomics, allowing for the simultaneous analyses of proteins from discrete regions of interest (ROIs) in FFPE tissue sections while preserving spatial context. The assay relies upon abcam antibodies coupled to photocleavable DNA barcodes readout with NGS sequencing, allowing for theoretically unlimited plex. Here we introduce the Human Immuno-Oncology Proteome Atlas (IPA), a 570+ antibody-based proteomic discovery panel, compatible with immunohistochemistry on FFPE tissues with NGS readout. IPA is the highest-plex, most comprehensive, antibody-based multi-omic panel to date focusing on key areas of immuno-oncology, oncology, immunology, epigenetics, metabolism, cell death, and signaling pathway regulation. Here we demonstrate the performance of IPA on various cell lines and tissue. Additionally, we show the power of IPA, using the spatial multi-omic assay along with the GeoMx® Whole Transcriptome Atlas (> 18,000 transcripts), a 40-plex custom antibody panel and microbiome-curated RNA custom spike-in (~220 transcripts) to evaluate 70 different colon disease samples across 5 pathologies including adenocarcinoma, hyperplasia, and chronic inflammation. This is the highest-plex multi-omic (~610-plex proteins and >18,220 genes) study ever implemented for spatial biology. When we compared the diseased tissue to normal tissue, we observed an upregulation of specific pathways associated with tumorigenesis and inflammation. Furthermore, we observed distinct differences in proteomic and transcriptomic landscape between pathologies. The cutting-edge, data-driven, expert-curated IPA panel is at the forefront of spatial proteomics, empowering the researcher for the acceleration of biological discoveries. FOR RESEARCH USE ONLY. Not for use in diagnostic procedures.

#3650 Deep learning-based image cytometry and co-localization index in tumor immune microenvironment.

Tomoki Abe[1], Kimihiro Yamashita[1], Toru Nagasaka[2], Tomosuke Mukoyama[1], Souichirou Miyake[3], Yasuhiro Ueda[3], Masayuki Ando[1], Yuki Okazoe[3], Takao Tsuneki[1], Yukari Adachi[1], Ryunosuke Konaka[3], Ryuichiro Sawada[1], Hironobu Goto[1], Hiroshi Hasegawa[1], Shingo Kanaji[1], Takeru Matsuda[1], Takumi Fukumoto[3], Yoshihiro Kakeji[1]

[1]Division of Gastrointestinal Surgery, Kobe University Graduate School of Medicine, Kobe, Japan,[2]Association of Medical Artificial Intelligence Curation, Nagoya, Japan,[3]Division of Hepato-Biliary and Pancreatic Surgery, Kobe University Graduate School of Medicine, Kobe, Japan

Background: In pathology, digitizing tissue slides has prompted a remarkable development in image analysis using deep learning. This technological advancement is anticipated to aid in pathological diagnosis and to enhance patient management. Deep learning-based image cytometry (DL-IC) enables accurate cell identification and counting and the acquisition of vast amounts of location information from tissue slides. DL-IC can capture information about the diverse and complex tumor immune microenvironment(TIME) and its constituent cells and help identify biomarkers to predict patient treatment efficacy and prognosis. This study will introduce a spatial interaction map and co-localization index (CLI) for the analysis of TIME using DL-IC.

Materials and Methods: Cu-Cyto, a deep learning-based image analysis technology, was used in this study; bit-pattern kernel filtering technology, which can accurately count cells while avoiding the determination of multiple cell counts, was used by Cu-Cyto (Abe T, et al. Anticancer Res. 43:3755, 2023). First, the accuracy of cell counting using Cu-Cyto was evaluated. Second, tumor tissue slides with immunohistochemical (IHC) and hematoxylin-eosin (H&E) staining were prepared from surgical specimens of patients with rectal cancer who had undergone neoadjuvant chemoradiotherapy (NACRT), and the relationship between the co-localization index (CLI) of cancer cells and $CD8^{\pm}$T cells and prognosis was investigated. CLI was defined to predict cell- cell interactions on the basis of the relative distances between different cell types (Nagasaka T. PCT/JP 2021/021455).

Results: The performances of three versions of Cu-Cyto were evaluated according to their learning stages. In the early stage of learning, the F1 score for immunostained $CD8^{\pm}$ T cells (0.343) was higher than that for non-immunostained cells (adenocarcinoma cells [0.040] and lymphocytes [0.002]). In the latest stage of learning, the F1 scores for adenocarcinoma cells, lymphocytes, and $CD8^{\pm}$ T cells were 0.589, 0.889, and 0.911, respectively. Next, we examined the correlation of CLI between cancer cells and $CD8^{\pm}$ T cells with prognosis: patients with a higher CLI significantly prolonged five-year disease-free survival (P=0.038), while there was no substantial difference in five-year overall survival (P=0.57).

Conclusion]: Cu-Cyto performed well in cell determination. In particular, IHC was able to increase the learning efficiencies in the early stages of learning. The CLI calculated using Cu-Cyto ts an objective, reproducible, and innovative quantitative approach for assessing cell-cell interactions, which has been shown to be associated with recurrence-free survival in patients with rectal cancer after NACRT. Its performance is expected to improve even further with continuous learning, and the DL-IC can contribute to the implementation of precision oncology.

#3651 Mutational analysis and spatial phenotyping to decipher racial disparities in pancreatic adenocarcinoma.

D. J. Salas-Escabillas[1], N. Ma[2], B. B. Cheikh[2], A. Pratapa[2], T. Pichardo[3], K. Langley[3], J. Clark[3], N. Steele[3], N. Jhaveri[2], D. Kwon[4], H. C. Crawford[3];
[1]University of Michigan, Ann Arbor, MI, [2]Akoya Biosciences, Inc., Marlborough, MA, [3]Henry Ford Pancreatic Cancer Center, Detroit, MI, [4]Henry Ford Health, Detroit, MI

Background: Pancreatic cancer has a 5-year survival of only 12%. This is due to the lack of effective treatments and virtually no early detection methods. To compound this already poor prognosis, African Americans face a 20% higher incidence and worse mortality compared to non-African American patients. With a substantial portion of the data and tools employed for studying pancreatic cancer failing to adequately represent this demographic we aim to gain more insight into the differences associated with worse outcomes for African Americans with pancreatic cancer. To achieve this, we conducted an in-depth analysis of tumor mutational burden using whole exome sequencing and the cutting-edge PhenoCycler®-Fusion 2.0 spatial biology platform, to uncover disparities in spatial immune and metabolic phenotypes.

Methods: Using an ultrahigh-plex discovery panel of markers encompassing cell lineage, immune checkpoints, tissue architecture, activation, metabolism, proliferation, and stress, we sought to analyze the differences in spatial phenotypes, cellular neighborhoods and functional pathways across the two groups. Additionally, we performed laser capture microdissection on a cohort of patients containing equal numbers of African American and non-African American pancreatic cancer samples. Tumor, stroma, and adjacent normal areas were identified by a board-certified pathologist. These annotations were used to laser capture on 10-micron sections with 7 sections for each patient. We performed whole exome sequencing on these sections and different areas and compared between groups.

Results: Through our investigation using these two technologies, we can find differences in the tumor microenvironment between African Americans and non-African Americans. We can see potential associations in the increased mortality and incidence of this group while also building a foundation of racially diverse data to be used for future studies. Whole exome sequencing has revealed distinct mutational patterns among African American patients, involving common genes that exhibit unique mutation profiles when compared to those previously observed in non-African American patients. Moreover, whole-slide spatial phenotyping reveals the differential tumor-immune landscapes and the key cellular and molecular niches that contribute to tumor progression and prognosis. These findings underscore the imperative need for a more systems biology exploration of the variations within these groups, with the aim of developing more effective and personalized treatment approaches.

#3652 Spatial transcriptomic study of the tumor microenvironment in HNSCC.

C. Schroyer, S. Zhou;
Labcorp, Morrisville, NC

Background: The complex and dynamic nature of the tumor-immune microenvironment (TME) presents challenges for identification of robust and predictive biomarkers in immuno-oncology (IO). Standard multiplex immunohistochemistry (mIHC) or multiplex immuno-fluorescent assays (mIF) allow for the phenotyping on the cellular level but are limited by the number of markers available and the detection systems. Gene expression or next generation sequencing (NGS) platforms provide high-plex bulk data sets about the TME, but the spatial context of the tumor and immune cell interactions is lost. The NanoString GeoMx® Digital Spatial Profiler (DSP) combines spatial context, utilizing fluorescent morphological markers, with molecular profiling capabilities. This combination allows for the quantitative analysis of high-plex analyte abundance which can be traced back to a region of interest within a sample, providing biological inference in the region of interest.

Methods: Formalin-fixed paraffin-embedded (FFPE) specimens from HNSCC patients were cut in 5µm sections for all analyses. Whole section tissue analysis was previously performed utilizing the NanoString nCounter® PanCancer IO 360™ Panel. Tumor inflammation signatures (TIS), an 18-gene signature measuring the adaptive immune response within tumors, was generated for each specimen and categorized each as immune-hot or immune-cold based on predefined parameters. Four specimens were selected based on their TIS score and two sets of cut sections were processed by either Labcorp lab in Morrisville, NC or Nanostring lab in Seattle, WA for precision evaluation, using the GeoMx Human Whole Transcriptome Atlas (WTA) panel (18,000 genes) with the NanoString GeoMx digital spatial profiling technology. The TME regions of interest (ROI) were identified using a set of morphology markers consisting of panCK, CD45 and Syto13; 12 ROIs were selected from each sectioned tumor material. The same ROIs were selected at the two testing sites with matching tissue location and morphology characters.

Results: GeoMx WTA panel provided an unbiased view of 18,000 protein-coding genes at specific TME regions. These counts were successfully mapped to the 12 ROIs on the tissue. A pseudo-TIS score was generated using the same 18 gene signature from the WTA panel for each ROI. The pseudo-TIS scores from ROIs from the four specimens showed consistency with the specimen-wise TIS score, yet variations were observed across different TME/ROI within each specimen. Whole transcriptome expression results showed high correlation between the two testing sites, providing confidence in the reproducibility of the technology. High resolution fluorescent staining images were able to be fed to downstream quantitative digital analysis to generate complementary spatial data.

CLINICAL RESEARCH: Circulating Nucleic Acids 3
Poster Session

#3656 Target enrichment of methylated circulating tumor DNA for colorectal cancer detection.
H.-Y. Huang, R. Vijaya Satya, W.-C. Chan, E. Atolia, J. Babiarz, B. Zimmermann, T. Kawli;
Natera, Inc., Austin, TX

Aberrant DNA methylation changes are one of the earliest signatures of cancer development. Methylation profiling of circulating tumor DNA (ctDNA) from plasma has emerged as a promising approach for early cancer detection (ECD). However, the set of methylation targets that can successfully distinguish cancer through liquid biopsy will vary depending on cancer type and subtype. Here, we explored a methylation target enrichment workflow and developed a methylation-based classification model to distinguish between patients with colorectal cancer (CRC) and healthy individuals. First, CRC-specific CpG targets were identified by comparing the methylation landscape of CRC and normal samples (tissue and blood) available in The Cancer Genome Atlas (TCGA) database and Gene Expression Omnibus (GEO) datasets. This analysis resulted in >800 CRC-specific CpG targets for initial evaluation. To develop and test the classification model, CRC patients and healthy individuals with plasma samples were included. A machine learning model was used to evaluate the highest performing CpG targets that effectively discriminated between CRC patients with detected ctDNA ("CRC ctDNA-positive") and healthy individuals. Correlation between methylation levels of the high performing CpG targets and the variant allele frequency (VAF) among CRC ctDNA-positive patients was calculated. In total, 86 patients were included in this proof of concept study (mean age, 62 ±12 years; male, 55%). 50 CRC ctDNA-positive patients (24% stage I, 40% stage II, 24% stage III, and 12% stage IV) and 36 healthy normals were included in the analysis. We investigated this cohort to identify the highest performing CpG targets among the >800 potential CpG targets that provided effective discrimination between CRC patients and healthy individuals. Using the highest performing CpG targets, observed methylation level was correlated with VAF of single nucleotide variants detected by ctDNA testing (R^2: 0.8). In summary, we developed a cost-effective methylation target enrichment workflow and utilized machine-learning algorithms to demonstrate the potential use of ctDNA methylation markers in early detection. Additional studies are needed to confirm that these and other markers can accurately distinguish between patients with CRC and healthy individuals.

#3657 Customized liquid biopsy assay for monitoring EWSR1 fusions in sarcomas.

A. Li[1], J. C. Thierauf[1], B. Gonda[1], R. Purohit[1], S. T. Kaluziak[1], E. Codd[1], S. N. Dybel[1], E. Choy[2], G. M. Cote[2], J. K. Lennerz[1], A. Iafrate[1];
[1]Massachusetts General Hospital, Harvard Medical School, Boston, MA, [2]Mass General Cancer Center, Massachusetts General Hospital, Boston, MA

Background: Gene fusions involving EWSR1 are involved in certain rare sarcomas and sarcoma-like tumors such as, for example, Ewing sarcoma, clear cell sarcoma, hyalinizing clear cell carcinoma, and clear cell odontogenic carcinoma. EWSR1-FLI1 fusions are found in Ewing sarcoma, while EWSR1-ATF1 and EWSR1-CREB are characteristic of clear cell sarcoma among others. Liquid biopsies involve obtaining tumor-derived materials through minimally invasive methods such as blood or other body fluid collection. Analysis of cell-free DNA (cfDNA) is an attractive method to identify gene fusions and monitor tumor recurrence and minimal residual disease (MRD). However, the structural complexity of oncogenic rearrangements poses challenges for the detection using plasma assays. We present a novel assay to monitor fusion positive tumor DNA in a busy oncology clinic.

Methods and Patients: Patients with EWSR1 fusion positive sarcomas are identified through clinical RNA-based sequencing. Tumor DNA isolated from biopsy or surgical samples is sequenced to map the intronic breakpoint and customized primers spanning the breakpoint are designed for each patient. The breakpoint is subsequently confirmed through PCR. The product length of ~100bp accounts for the small shedding size of tumor cfDNA. A quantitative TaqMan assay is designed to confirm EWSR1 fusions. The limit of detection is determined by a dilution series of tumor DNA. cfDNA is extracted from blood samples of the patients at multiple timepoints, the tumor burden is quantified by TaqMan Assay and subsequently correlated with clinical findings from imaging studies such as tumor progression or remission.

Results: We consented 10 patients with EWSR1 fusion positive tumors to participate in this study. Plasma samples were collected for 8, resulting in 26 total timepoints. Breakpoints were identified in 9 patients and confirmed with PCR on original tumor DNA. TaqMan assays were designed for 5 patients and showed correlation between the tumor burden detected in EWSR1-ATF1 copies in cfDNA extracted from patient blood and the therapeutic response to treatment found through imaging studies. One patient was followed over the period of 9 months, and a total of 5 plasma timepoints were collected. The patient started with a low number of EWSR1-ATF1 copies of <1ng/ul, while on a lurbinectedin/irinotecan therapy and showed a mixed response in the CT scan. After withdrawing from that therapy and starting other therapy regimens, the EWSR1-ATF1 copies increase to 8ng/ul, correlating with tumor progression observed in CT scans.

Conclusion: Our results suggest that ESWR1 fusions in sarcomas can serve as biomarkers to measure tumor burden. Our approach using an individually tailored cfDNA TaqMan assay could provide a valuable monitoring tool to inform clinicians about tumor progression or MRD. With these proof-of-principle findings we can now determine clinical validity and utility.

#3658 Longitudinal tumor-informed ctDNA monitoring with the originally developed OTS-Assay system.

S. S. Nishizuka[1], H. Hiraki[1], A. Yashima-Abo[1], T. Iwaya[2];

[1]Iwate Medical University Institute for Biomedical Sciences, Yahaba, Japan, [2]Iwate Medical University School of Medicine, Yahaba, Japan

Background: Cancer Genome Profiling (CGP) tests are now widely available in daily practice. However, only a very small fraction of patients have the opportunity for genome-guided therapies. Somatic mutations from cancer specimens are unique to individual patients and hold utility as individual tumor markers in blood. We have developed an original circulating tumor DNA (ctDNA) monitoring system, called OTS (Off-The-Shelf)-Assay, at Iwate Medical University Hospital, Yahaba, Japan.

Patients and Methods: Between April 2022 and October 2023, 79 patients who received the OTS-Assay were enrolled in the present analysis. The OTS-Assay includes three steps: (a) OTS-Scan (somatic mutation identification by either tissue or blood), (b) OTS-Select (somatic mutation selection), and (c) OTS-Monitor (periodical somatic mutation quantification as ctDNA). For the OTS-Select, we established an originally developed >90 stepwise selection algorithm. One of the determinants is the availability of appropriate digital PCR (dPCR) probes for individual patients. Here, we search the probes for individual patients from the dPCR probe library, OTS-1000ex, which consists of >1000 probes against frequently reported human somatic mutations (Quantdetect, Tokyo, Japan).

Results: All 79 patients were subject to the analysis. The cancer stage of all the patients was advanced. More than 10 tumor types were enrolled, including esophagus (n=42), colorectal (n=12), breast (n=7), lung (n=4), pancreas (n=3), hematological (n=3), and others (n=8). Fifty patients received OTS-Scan, and 29 patients had received a CGP test before the OTS-Assay (i.e., OTS-Scan was not needed). Seventy-five patients received OTS-Select, meaning that four patients had somatic mutations that were designated for ctDNA monitoring. All 79 patients received at least one OTS-monitor. The number of OTS-Monitors received ranged from 1 to 11 during the 19-month period, and the average interval was 3.0 months. The average pretreatment variant allele frequency (VAF) was 4.96% and the majority of the follow-up VAF was less than 1%. More than 90% of the patients had at least one clinical validity defined by: (a) early relapse prediction, (b) treatment efficacy evaluation, or (c) no relapse corroboration.

Conclusion: The OTS-Assay system provides stable longitudinal ctDNA monitoring at the range of less than 1% of VAF using the originally developed dPCR probe library. The sensitivity and affordability of the OTS-Assay system allows frequent monitoring, which leads to obtaining important clinical information in the context of advanced cancer therapy.

#3659 Development of customized circulating tumor DNA panel for minimal residual disease detection in biliary tract cancer.

Y. Shinohara[1], S.-K. Low[2], T. Nakamura[1], Y. Kimura[3], T. Murakami[3], K. Kiyotani[2], S. Hirano[1];
[1]Hokkaido University Faculty of Medicine, Sapporo, Japan, [2]Japanese Foundation for Cancer Research, Tokyo, Japan, [3]Sapporo Medical University, Sapporo, Japan

Biliary tract cancer (BTC) is a rare type of abdominal cancer and is more frequent in Asian countries than in Western. The 5-year survival rate for BTC is very low 7 to 20% and only 20% of BTC patients could undergo curative-intent surgery. BTC diagnosis based on biopsy and cytology are low in sensitivity that prompted the necessity to identify alternative biopsy. Liquid biopsy, specifically circulating tumor DNA (ctDNA) is known for the accessibility and low invasiveness received great interest for their potential uses in various clinical applications for patients with insufficient tumor tissue, including mutation profiling, treatment monitoring, and cancer detection. However, the panel available in the market up-to-date focused mainly targeted, actionable alterations and thus not suitable for minimal residual disease (MRD) monitoring. In this study, we aimed to develop a customized ctDNA panel for MRD monitoring in BTC. In this study, 124 BTC patients undergone curative resections were enrolled at Hokkaido University and Sapporo Medical University from May 2019 to April 22. All enrolled patients have BTC diagnosis confirmed by pathological diagnosis after surgery, and without other malignant tumors. Genomic profiles of FFPE tissue were conducted using Ampliseq CCP. 13 patients were excluded for high fragmentation. Referring to the genomic profiles of 111 patients in our study and 1924 patients in TCGA established a customized panel using Ion Ampliseq HD technology. The Ampliseq HD panel claims to detect variants at 0.1% LOD for ctDNA detection. It also integrates molecular barcodes to reduce NGS-related errors. The designed panel was 258 Amplicons and 20 genes including eleven therapeutically targetable genes. Clinical characteristics of ctDNA detection were also assessed. Results:The panel validation: concordance of the mutation allele frequency (MAF) between the NGS standard control and Ampliseq HD panel showed a coefficient of determination (R2) of 0.96. Also, concordance of MAF Ampliseq CCP and Ampliseq HD panel on FFPE tumor profiling showed R2 of 0.78. When assessing 70% of BTC patients were covered to have at least one tumor-derived Ampliseq HD panel. When assessing using plasma cell-free DNA, 55% of BTC patients were detected to have at least one tumor-derived ctDNA. Distribution of detected altered top4 genes using Ampliseq HD panels shows TP53 35%, KRAS 10%, SMAD4 5%, ARID1A 2.5%. Clinical characteristics may affected the concordance of plasma and FFPE tumor tissue; stage (P=0.035), size of tumors (P=0.0088), subtype (P=0.013), LN metastasis (P=0.11). Conclusions: A highly sensitive ctDNA customized panel for BTC was established. We also found that clinical characteristics of the BTC affects the detection of ctDNA from blood liquid biopsy. Future study: MRD evaluation using this customized panel.

#3660 Plasma cell free DNA hydroxymethylation profiling reveals anti-PD1 treatment response and resistance biology in non-small cell lung cancer.

G. D. Guler[1], Y. Ning[1], C. Coruh[2], T. Phillips[2], M. Nabiyouni[2], K. Hazen[1], A. Scott[1], W. Volkmuth[1], S. Levy[2];

[1]ClearNote Health, San Mateo, CA, [2]ClearNote Health, San Diego, CA

Background: Treatment with immune checkpoint inhibitors (ICIs) targeting programmed death-1 (PD-1) can yield durable anti-tumor responses, yet not all patients respond to ICIs. Current approaches to select patients who may benefit from anti-PD-1 treatment are insufficient. 5-hydroxymethylation (5hmC) analysis of plasma-derived cell free DNA (cfDNA) presents a novel non-invasive approach for identification of therapy response biomarkers which can tackle challenges associated with tumor biopsies such as tumor heterogeneity and serial sample collection.

Methods: 151 blood samples were collected from 31 non-small cell lung cancer (NSCLC) patients before therapy start and at multiple timepoints whilst on therapy. Blood samples were processed to obtain plasma-derived cfDNA, followed by enrichment of 5hmC-containing cfDNA fragments through biotinylation via a two-step chemistry and binding to streptavidin coated beads. 5hmC-enriched cfDNA and whole genome libraries were prepared in parallel and sequenced to obtain whole hydroxymethylome and whole genome plasma profiles, respectively.

Results: Comparison of on-treatment timepoint to matched pre-treatment samples from same patients revealed that anti-PD-1 treatment induced distinct changes in plasma cfDNA 5hmC profiles of responders, as judged by RECIST, relative to non-responders. In responders, 5hmC accumulated over genes involved in immune activation such as IFNγ and IFNα response, inflammatory response, and TNFα signaling, whereas in non-responders 5hmC increased over epithelial to mesenchymal transition genes. The Molecular Response to anti-PD-1 treatment, as measured by 5hmC changes in plasma cfDNA profiles were observed early, starting with the first cycle of treatment. Comparison of pre-treatment plasma samples revealed that anti-PD-1 treatment response- and resistance-associated genes can be captured by 5hmC profiling of plasma-derived cfDNA.

Conclusions: These results demonstrate that 5hmC profiling can identify response and resistance associated biological pathways in plasma samples, offering a novel method for non-invasive prediction and monitoring of immunotherapy response in NSCLC.

#3661 Non-coding RNAs as biomarkers for early detection of lung cancer.

G. S. Casagrande[1], A. P. Filho[1], A. P. Siqueira[1], R. S. Chiarantano[1], F. d. Vazquez[1], M. A. Molina[2], C. Pedraz-Valdunciel[2], A. Gimenez-Capitan[2], R. M. V. Reis[1], L. F. Leal[1];

[1]Barretos Cancer Hospital, Barretos, Brazil, [2]Hospital Universitari Dexeus, Barcelona, Spain

Introduction: Screening programs proven to reduce lung cancer deaths in high-income countries. Biomarkers detection in body fluids may guide more precise selection of high-risk subjects but this approach has not been currently employed for lung cancer screening. **Aims:** To identify ncRNA-based signatures for early detection of lung cancer in liquid biopsies. **Methods:** This is a case-control prospective study, conducted at the Barretos Cancer Hospital Screening Program. We analyzed miRNAs in plasma and sputum samples from high-risk subjects (n=51), and patients (n=44) diagnosed with non-small cell lung cancer (NSCLC), no metastatic, at Barretos Cancer Hospital (Brazil). We analyzed circRNAs in plasma samples from high-risk subjects (n=100), and patients (n=86) with NSCLC at Hospital Universitari Quiron Dexeus (Spain). Samples were subjected to RNA isolation followed expression analysis, for miRNA expression was used *nCounter Human V3 microRNA* painel, and for circRNA expression was use a nCounter customized painel (NanoString). Counts were normalized by housekeeping, and differentially expressed miRNAs were filtered out according to fold-change (≥|1.5|), p-value (≤0.05). **Results:** All cancer patients were diagnosed with adenocarcinoma (n=68), squamous cell carcinoma (n=41) and others/no information (n=36). No differences were observed related to age, sex, and tobacco exposure between high-risk and cancer groups (p>0.05). For Brazilian group, we observed six differentially expressed miRNAs in plasma able to distinguish cancer from non-cancer samples - three miRNAs upregulated, and three miRNAs downregulated -, and three of them presented with high accuracy (AUC = 0.70). For sputum, we observed four differentially expressed miRNAs able to distinguish cancer from non-cancer samples, and the 4-miRNA signature present with high accuracy (AUC = 0.73). None of miRNAs were shared between plasma and sputum. In both sample types we have miRNAs associated with zinc finger (*ZNF99* and *ZNF268*), that predicted to be involved in regulation of transcription by RNA polymerase II. In Spanish cohort, we observed 4-circRNA signature with high accuracy (AUC = 0.745). These four circRNAs are associated with insulin resistance and proto-oncogenes. **Conclusion:** We identified ncRNA-based biomarkers in biofluids potentially to be employed in lung cancer screening programs to better guide selection of high-risk subjects for early detection of lung cancer.

#3662 Cell-free DNA dynamics following neuroblastoma resection.

Joshua N. Honeyman[1], Andrew Chi[1], Shakeel Modak[2], Fiorella Iglesias Cardenas[2], Michael P. La Quaglia[1], Neerav N. Shukla[2], J. Ted Gerstle[1]

[1]Department of Surgery, Memorial Sloan Kettering Cancer Center, New York, NY,[2]Department of Pediatrics, Memorial Sloan Kettering Cancer Center, New York, NY

Introduction: Prior studies have demonstrated the utility of circulating tumor DNA (ctDNA) as a biomarker in the postoperative period for oncologic risk stratification. However, its utility may be limited in the early postoperative period by surgical trauma causing an increase in total cell-free DNA (cfDNA) due to tissue destruction, inflammation, and wound healing. No studies have identified the optimal timing of postoperative sample collection in pediatric patients undergoing resection of high-risk neuroblastoma. The purpose of this study is to assess the postoperative dynamics of cfDNA following neuroblastoma resection to determine optimal timing for ctDNA investigations.

Methods: An institutional database of banked cell-free DNA samples was retrospectively queried for patients with a diagnosis of neuroblastoma who had blood samples collected prior to resection and postoperative samples collected within 2 months of the operation. Plasma was collected from whole blood samples. cfDNA was extracted from plasma samples using the QIAGEN QIAsymphony SP system, and samples were quantified using the Advanced Analytical Fragment Analyzer Automated CE System with the High Sensitivity Genomic DNA Analysis Kit.

Results: Seventeen patients were identified undergoing 18 total operations and 37 total blood draws yielding cfDNA. There were 12 male and 5 female patients. Median age at operation was 5.5 years (range 1.4y to 20.5y). Two patients were INRG stage L2, and 15 patients were stage M. Operative indications were primary tumor resection in 10 patients and resection of recurrence/progression in 8 patients. Three postoperative samples were drawn within 10 days of the operation, and 16 samples were collected between postoperative weeks 4 and 6. There was a statistically significant difference (p=0.029) in cfDNA yield between each timepoint sampled: preoperative (median 6ng/mL, range 2-30ng/mL), 0-10 days postop (median 34ng/mL, range 15 - 85 ng/mL), and 4-6 weeks postop (median 6ng/mL, range 2 - 17ng/mL). Pairing the pre- and post-operative samples for each patient, those drawn within 10 days had a median increased yield of 180% (range +67% to +652%) while the samples collected at 4-6 weeks had a median decreased yield of 23% (range -55% to +491%; p = 0.047). Of note, there were three outliers in the 4-6 week group who had increases in cfDNA yield of >200%. On further review of these charts, each patient was being treated for obstructive uropathy at the time the postoperative sample was collected.

Conclusion: Plasma cfDNA yield increases in the early postoperative period before dropping by postoperative week 6. Tumor resection may be associated with an overall decrease in total cfDNA. Postoperative renal pathology may cause a persistent elevation in cfDNA. Further studies are necessary to clarify the role of ctDNA in the management of patients with neuroblastoma.

#3663 Extending and analytical validation of a hematological cancer panel for simultaneous detection of driver mutations, copy number variations and translocations in tissue and blood samples.

Y. Huang, T. Zhang, F. Xie, J. Dong, X. Wang, Z. Zhao, S. Luo, K. Zhou, S. Jia, P. Du;
Predicine Inc, Hayward, CA

Background Hematological cancers represent approximately 9.4% of all new cancer cases in the US, with varying prevalence among different age groups. For instance, Acute Lymphocytic Leukemia (ALL) is more prevalent in children (less than 15 years), while Multiple Myeloma and Non-Hodgkin Lymphoma are commonly identified in older population (65 or older). Each hematological cancer subtype has distinct mutation and expression profiles, necessitating the coverage of various variant types, including point mutations, gene copy number variations (CNVs), and translocations. In this study, we extend the PredicineHEME panel to encompass long-range translocation and CNV detections.

Methods The extension of the original PredicineHEME panel involves three key modifications. First, a genome-wide SNP backbone was incorporated to enhance the sensitive detection of both gene and chromosomal-level CNVs and Loss of Heterozygosity (LOH). Second, additional coverage of translocation breakpoint regions was added, considering the panel's application in liquid biopsy samples. Coverage included the most frequently found translocations in major hematological cancers. Third, the driver gene list was supplemented to include genes and mutations treated as active therapeutic targets in clinical studies. Analytical validation was conducted using contrived reference materials, cell lines with known biomarker status, and healthy and clinical samples with known mutations or translocation status.

Results The expanded panel underwent balanced testing with healthy normal saliva gDNA samples to ensure even capture of targeted genomic regions. Assay testing followed CLIA/CAP guidelines on analytical validation materials. The Limit of Detection for SNV/INDEL and known translocation breakpoint reached as low as 0.3%. Our assay detected over 90% of covered and reported translocation breakpoints in the validation materials. Chromosome arm level CNVs reported in the validation materials were detected with 100% sensitivity and specificity.

Conclusions The expansion of the PredicineHEME panel underwent analytical validation, meeting design expectations. With this extension, the assay can effectively detect driver mutations (SNVs/INDELs), CNVs at gene and chromosomal levels, and targeted large translocations in major hematological cancers.

#3664 Evaluation of on-treatment tumor molecular dynamics using plasma whole genome sequencing (pWGS) and whole exome sequencing (pWES) of circulating tumor DNA (ctDNA) in patients (pts) with metastatic non-small cell lung cancer (NSCLC): An exploratory analysis of KEYNOTE-598.

Minita Shah, EJ Dettman, Andrew Albright, Cai Chen, Julie Kobie, Vinay Varadan, Ayman Samkari, Carol Pena, Razvan Cristescu, Z Alexander Cao

Merck & Co., Inc., Rahway, NJ

Background: ctDNA-based pWES is a promising tool to examine tumor genomics using a non-invasive liquid biopsy to serially monitor changes during tumor evolution and treatment. Here, we evaluate on-treatment tumor molecular dynamics using ctDNA-based pWGS and pWES in pts with metastatic NSCLC that responded to pembrolizumab (pembro) monotherapy and later experienced PD in KEYNOTE-598 (NCT03302234).

Methods: In KEYNOTE-598, pts had metastatic NSCLC (PD-L1 tumor proportion score ≥50%) and received first-line pembro ± ipilimumab for ≤35 cycles. Cell-free DNA (cfDNA) was isolated and sequenced from plasma samples at baseline (BL), during on-treatment response (cycle 5 [C5]), and at PD (discontinuation [D]) from pts with objective response to pembro monotherapy and subsequent PD. ctDNA burden (tumor fraction [TF]) was estimated using low-pass pWGS by quantifying tumor content in cfDNA as a function of aneuploidy. All samples with TF >1.5% underwent high-depth pWES. ctDNA burden was estimated from pWES data using maximum somatic allele frequency (MSAF). Correlation between TF and MSAF was evaluated using the Spearman coefficient (r). Variant allele frequency (VAF) and normalized VAF (nVAF) were used to determine variant clonality.

Results: In total, 23 pts with initial response to pembro and subsequent PD had plasma samples available from BL, C5, and D. Samples from 22 pts had TF >1.5% by pWGS and underwent pWES. MSAF by pWES was correlated with TF by pWGS at BL (r = 0.68), C5 (0.80), and D (0.59). ctDNA TFs at BL and D (mean = 8.1% and 4.9%, respectively) were higher than C5 (2.0%). In a pooled variant-level analysis (nVAF >0.25) of samples from pts with high TF (≥2.5%) at both BL and D (n = 10), 786 (46%) of variants were present at BL and D, 391 (23%) were present at BL only, and 540 (32%) were present at D only. Variants shared between BL and D had higher clonality (mean nVAF = 0.46) than BL-only (0.38) or D-only variants (0.4). In general, shared variants had similar nVAFs at BL and D but in some pts nVAFs increased at D, suggesting evolution of tumor subclones during treatment. *TP53* was mutated in 9 of 10 pts with high TF and was shared at BL and D in 6 pts (mean nVAF = 0.49), present at BL only in 1 pt (0.11) and at D only in 2 pts (0.43). *KRAS G12V* and *Q61H* hotspot mutations were observed in 2 pts at D-only and may be related to immune editing.

Conclusions: Comprehensive pWES is feasible with sufficient ctDNA burden (TF ≥2.5%). ctDNA dynamics demonstrated molecular profiles characteristic of recurrence with high TF at BL and D and were consistent with radiographic determination of response/progression. Tumor variants at BL and D generally had a common clonal trunk with clones disappearing or appearing de novo.

#3665 Stratifying prostate cancer patients through circulating genes related to prostate cell subtypes, drug targets, and therapeutic resistance.

Seta Derderian[1], Edouard Jarry[2], Arynne Santos[1], Mohanachary Amaravadi[1], Quentin Vesval[3], Lucie Hamel[1], Raphael Sanchez-Salas[4], Alexis Rompre-Brodeur[4], Wassim Kassouf[4], Raghu Rajan[5], Marie Duclos[6], Fadi Brimo[7], Armen Aprikian[4], Simone Chevalier[8]

[1]Uro-oncology Research Group, Cancer Research Program, McGill University Health Centre Research Institute, Montreal, QC, Canada,[2]Urology, Centre Hospitalier Regional et Universitaire de Lille, Lille, France,[3]Urology, Centre Hospitalier Regional et Universitaire de Rennes, Rennes, France,[4]Deparments of Oncology and Surgery, McGill University, Montreal, QC, Canada,[5]Deparment of Oncology, McGill University, Montreal, QC, Canada,[6]Deparment of Radiation Oncology, McGill University, Montreal, QC, Canada,[7]Deparment of Pathology, McGill University, Montreal, QC, Canada,[8]Deparments of Oncology, Surgery, and Medicine, McGill University, Montreal, QC, Canada

Stratification remains an obstacle for the optimal treatment of prostate cancer (PCa) patients throughout the treatment trajectory. Targeting the androgen receptor (AR) kills the majority of luminal-like cells, which are AR-positive and express Prostate Specific Antigen (PSA). However, a subset of surviving AR-positive cells develop resistance to treatments while AR-negative cells of the neuroendocrine (NE) or stem-like phenotypes emerge through selection. We reported on the clinical relevance of cell-subtype genes in whole blood RNA of advanced PCa patients. Here, we studied an expanded panel of genes to include drug targets and therapeutic resistance as predictive biomarkers to stratify patients at diagnosis and at the advanced stage of disease.Genes were chosen based on literature review, results of clinical trials in PCa, and PCa transcriptomic data. Technical validation of TaqMan RT-qPCR assays was carried out for each gene, including rigorous testing of reproducibility. Whole blood RNA was extracted from 26 healthy controls with no prostatic disease, 16 patients prior to prostatectomy, and 43 blood samples from 28 metastatic cases. Gene overexpression was defined as the 99.5% confidence interval of expression in controls. Clinical data were retrieved from patients' charts.A panel of 64 genes was built, showing overexpression in advanced PCa but low or no expression in normal blood (including whole blood, white and red blood cell populations and platelets). Testing in control blood showed no correlation with age. The proportions of patients' white blood cells did not correlate with gene expression in their blood. Overall, up to 44/64 genes were overexpressed in at least one patient sample. Patients with prostatic intraductal carcinoma at prostatectomy showed more circulating genes, including more NE and stemness genes, and more PCa cell subtypes represented. Intermediate and high-risk patients showed more circulating NE genes. In metastatic patients, signatures of luminal, NE, stemness, and resistance to AR inhibitors or taxanes were associated with progression. PCa-specific luminal genes were associated with shorter overall survival. Treatment resistance genes correlated with lines of treatment and current taxanes. Two targetable NE genes were overexpressed in distinct categories of patients, suggesting that they may benefit from more specific treatments.In conclusion, phenotypic and functional differences in circulating gene patterns of PCa patients correlate with pathological features, treatments, progression. They may be clinically meaningful to stratify patients and predict therapeutic response. Circulating genes encoding drug targets may justify clinical trials to offer personalized treatments and impact on lethal PCa.

#3666 Multi-cancer early detection using metrics of DNA methylation based epigenetic instability.

S.-J. Thursby, Z. Jin, S. B. Baylin, M. Brock, T. Pisanic II, H. Easwaran;
Johns Hopkins University, Baltimore, MD

Cancers present significant changes in DNA methylation, which has proven to be highly useful in cell-free DNA (cfDNA) based cancer detection. Cancer epigenomes are marked by a high degree of intra- and inter-tumor epigenetic variation, indicative of the high level of epigenetic instability. However, the nature of the regions with high epigenetic instability and its utility as biomarker has not been explored. Here we developed a novel methodology and metric to measure the degree of epigenetic perturbation, termed the Epigenetic Instability Index (EII), for multiple cancer screening through cfDNA. Our novel methodology provides a sample specific score of epigenetic perturbation in relation to the expected normal state as opposed to only looking at CpG sites that change between samples. Through machine learning, we have elucidated 269 CpG-island regions which sufficiently capture the epigenetic instability in cancers. We have built classifier models using the EII metrics of these 269 regions and demonstrate that they can efficiently identify breast and lung cancer cases from cfDNA methylation data. Particularly, the models can differentiate even Stage IA of NSCLC with ~75% sensitivity at 95% specificity and early-stage breast cancer at ~68% sensitivity and 95% specificity. The EII metrics perform significantly better than metrics that measure absolute DNA methylation levels. Our studies highlight the potential of measuring epigenetic instability from cfDNA in any given sample in addition to traditional methods of methylation measurement for non-invasive screenings via liquid biopsies.

#3667 Nucleic acid quantification in uveal melanoma aqueous humor.

C. Chang[1], S. Pike[2], M. Reid[3], C.-C. Peng[3], B. Xu[2], J. Berry[3], L. Xu[3];

[1]Univeristy of Southern California, Los Angeles, CA, [2]Keck School of Medicine of the University of Southern California, Los Angeles, CA, [3]Children's Hospital Los Angeles, Los Angeles, CA

Introduction: Uveal melanoma (UM) is the most common primary adult intraocular cancer. Though radiation brachytherapy is often employed for UM treatment, half of UM patients develop systemic metastases. In large tumors with macular involvement, the disease and its treatment can lead to blindness. Clinically, UM prognosis is estimated by tumor size, location, American Joint Cancer Commission (AJCC) staging, and histologic findings. Prognostic UM biomarkers have been established but lesions <2 mm in height, particularly near the fovea, are difficult to biopsy, and thus physicians often do not perform biopsies on such tumors. Therefore, the use of aqueous humor (AH) as a liquid biopsy is a promising methodology. The purpose of the study was to quantify analytes in AH samples collected at diagnosis and post-brachytherapy from UM eyes with varying tumor sizes and AJCC Stages to analyze correlations between analyte (dsDNA, microDNA, and protein) concentrations and tumor features.

Methods: This case series study included 119 UM AH samples from 66 UM eyes and 16 control AH samples collected from age-matched non-UM glaucoma (GLC) eyes analyzed for unprocessed analytes using Qubit fluorescence assays.

Results: Most UM AH samples contained quantifiable analyte concentrations (dsDNA: 94.1%, miRNA: 88.0%, protein: 95.2%) and at higher concentrations than GLC controls (dsDNA, P=0.008; miRNA, P<0.0001; protein, P=0.007). In samples taken at diagnosis, concentrations were higher at more advanced AJCC stages; comparing most advanced Stage III (n=8) to least advanced Stage I (n=24), median dsDNA was 4 times greater (P<0.0001), protein was 3 times greater (P<0.0001), and miRNA was 2 times greater (P=0.001). Analytes were quantifiable in >70% of pre-brachytherapy samples from eyes with tumors <2 mm tall (n=17). Height was positively associated with analyte concentrations at diagnosis (dsDNA: R=0.43, P=0.0007; miRNA: R=0.35, P=0.01; protein: R=0.39, P=0.005). In paired samples (n=53), all analyte concentrations were significantly higher post-therapy compared to diagnosis pre-therapy (Ps<0.01).

Conclusions: Although AH analytes were also quantifiable in smaller, less advanced tumors, AH samples from eyes with larger, more advanced tumors had higher analyte concentrations. The detection of prognostic biomarkers in AH may allow for early UM recognition and guide personalized treatment.

#3668 Plasma cell-free DNA profiling for deciphering cellular origins and immune competence in cancer patients.

L. Andersen, A. Frydendahl, T. V. Henriksen, C. Demuth, M. H. Rasmussen, I. Nordentoft, K. Birkenkamp-Demtroder, J. S. Pedersen, S. Besenbacher, L. Dyrskjot, C. L. Andersen, N. J. Birkbak;
Aarhus University Hospital, Aarhus N, Denmark

Plasma cell-free DNA (cfDNA) originates from apoptotic cells in the blood, providing a real-time insight into the biology of various cell types. The fragment coverage pattern of cfDNA across the genome is known to reflect the distinct chromatin status of originating cells. While extensive research has focused on fragments derived from cancer, known as circulating tumor DNA (ctDNA), for inference about cancer biology, cfDNA fragments from healthy cells have received little attention. Our study explores the potential of cfDNA to decipher the relative abundance of distinct blood cell types, particularly immune system cell types.
We collected a cohort of 273 bladder (BC) and colorectal cancer (CRC) patients and 45 healthy controls for plasma whole genome sequencing and assessed the fragment coverage profile at transcription start sites (TSS) of protein coding genes. A significant negative correlation was observed between TSS coverage and whole blood gene expression (Spearman's rho = -0.65). Furthermore, TSS coverage revealed a bimodal distribution, characterized by modes corresponding to high and low gene expression levels in blood cells. This may suggest the cfDNA coverage profile as a binary expression status classifier to distinguish between expressed and unexpressed genes in blood cells. We further evaluated TSS with differential coverage between age groups of healthy individuals and relapse status of cancer patients. Notably, out of the TSS that significantly differentiated middle-aged (aged 40-65) from older individuals (aged 65+), 31 were also able to distinguish relapse from non-relapse patients. Among these TSS were CD36, SLAMF7, TABBP and PDCD1, known to be involved in immune related pathways. Finally, we evaluated coverage at cell-type specific TSS and found dendritic cells (P-value: CRC = 8e-06, BC = 5.1e-3), monocytes (CRC = 1.6e-04, BC = 2.5e-3), and NK cells (CRC = 8.5e-04, BC = 0.026) to exhibit a significant increase in coverage in the cancer cohorts compared to healthy controls. Conversely, T-cells showed a decrease in coverage (CRC = 0.041, BC = 0.062).
In conclusion, cfDNA coverage profile may identify TSS with differential coverage between patient groups and characterize a shift in blood cell type composition as a response to cancer. Future work may show if fragment coverage quantifies the relative contribution of cfDNA from distinct immune cell types. We anticipate our analysis to illuminate the utility of plasma cfDNA as a biomarker for cancer patient's immune competency, enabling improved patient stratification for treatment, leveraging their distinct immune capabilities.

#3669 Clinical application of urinary DNA methylation biomarkers for identifying patients with non-muscle invasive bladder cancer.

G. Bonora[1], Z. Zhu[1], B. Gould[1], B. Xiang[1], K. Zhou[1], S. Jia[1], R. Li[2], P. Du[1];
[1]Predicine, Inc., Hayward, CA, [2]Moffitt Cancer Center, Tampa, FL

Introduction

Differences in DNA methylation along cell-free DNA (cfDNA) fragments are known to exist between cancer patients and healthy individuals. Profiling these aberrant methylation patterns in urinary cfDNA (ucfNDA) holds great promise for the non-invasive detection and monitoring of bladder tumors, including non-muscle invasive bladder cancer (NMIBC). Here, we analyzed fragment-level DNA methylation patterns in urine samples obtained prior to repeat transurethral resection of a bladder tumor (reTURBT) from a cohort of NMIBC patients. The results were compared to traditional clinical disease assessment and mutation-based tumor fractions. We found a strong concordance between DNA methylation abnormality and clinical diagnosis, as well as tumor fractions, highlighting the potential of epigenetic alterations as a non-invasive indicator of bladder cancer status.

Methods

Patients with high-risk NMIBC (n = 30) were prospectively enrolled prior to reTURBT. The PredicineEPIC™ genome-wide methylation analysis and PredicineBEACON™ MRD profiling was performed on pre-repeat TURBT urine samples. Abnormally methylated genomic fragments were detected against a background model built from a panel of plasma samples from healthy donors.

Results

DNA methylation abnormality was significantly higher ($p = 4.8 \times 10^{-6}$) in samples classified as NIMBC positive by a clinical pathologist (n = 19) compared to negative samples (n = 11), as well as compared to hold-out healthy donor samples (n=24; $p = 7.0 \times 10^{-9}$). Classifying the samples based on a DNA methylation score cut-off derived from healthy donor samples, 24 / 30 samples showed concordant disease status. Furthermore, DNA methylation abnormality scores correlated positively with mutation-based tumor fractions (r = 0.62), with higher grade samples showing a stronger correlation (r = 0.81; n = 13) than lower grade samples (r = 0.54; n = 17).

Conclusion

We demonstrate the utility of methylation patterns extracted ucfDNA samples obtained prior to reTURBT to detect and monitor NMIBC. Urinary DNA methylation patterns were highly concordant with clinical pathology status and as well as tumor fractions determined from mutation analysis.

#3670 Reducing the patient burden for ctDNA biomarkers: Advancing small volume home-based collection technologies.

B. R. Evans[1], R. J. Foley[2], S. M. Townson[1], E. J. Welch[3], C. E. Frame[1], D. D. Donovan[1], J. M. Fahey[1], K. P. Bateman[1];
[1]Merck & Co., Inc., Rahway, NJ, [2]Guardant Healthcare, Palo Alto, CA, [3]Tasso, Inc., Seattle, WA

There is broad consensus from regulatory agencies, clinicians and patients for the need to move to decentralized trials while focusing on patient-centric approaches with the COVID-19 pandemic being the catalyst. This requires the development of new sample collection capabilities and workflows to ensure that the necessary biomarkers can be measured. Circulating tumor DNA (ctDNA) has become an increasingly important biomarker for cancer detection and genetics, and monitoring patients during treatment. Typical measurements of ctDNA involve venous draws of >10mls of whole blood that require patients to be in clinic. Here, we test the feasibility of using a new collection device, Tasso+, to collect capillary blood for ctDNA analysis using the Guardant360 panel. A pilot of whole blood microsamples (< 1 mL) with a cfDNA yield of 0.7-1.4 ng/ml spiked to 0.5% MAF with Seraseq ctDNA reference material. This resulted in detection of ~20% of the total expected variants across variant classes showing the feasibility of using the G360 panel to detect low volume/low MAF samples. Initial testing of Tasso+ collected samples revealed a 5-10x increase in high MW gDNA compared to traditional venipuncture. SPRI bead-based size selection was used in the extraction protocol to remove >95% of the high MW DNA, resulting in a 35% loss of target cfDNA fraction. Traditional venipuncture samples and Tasso+ samples were collected from 5 cancer patients and run using the G360 platform. Microsamples detected 75% of the variants across all variant classes found in venipuncture samples. Tasso+ lost sensitivity of variants when the MAF was <0.5%. To expand usage of Tasso+ to at-home collection of blood for ctDNA analysis, we sought to determine if lyophilization of the Streck DNA BCT RUO tube reagent could still provide stability to samples and a potential framework for at-home collections. Venipuncture and Tasso+ samples were collected from control patients, pooled and spiked with Seraseq cfDNA reference material. Samples were aliquoted into standard liquid Streck tubes or tubes with lyophilized reagent at the concentration per manufacturer's directions and evaluated for stability over time. The Tasso+ samples with a target MAF between 0.5%-2.0% detected ~26% of all variants compared to the standard samples with a similar MAF. Lyophilization of the Streck reagent had minimal effect (<20% reduction in variants detected) on the reagent's performance as there were approximately an equal number of total variants detected when comparing liquid and lyophilized samples for both the standard tubes and Tasso+ samples. Overall, these results provide support and a framework for using a home-based patient-centric sampling approach for monitoring ctDNA from cancer patients in clinical development.

#3671 Analytical performance of the Oncomine™ Dx Express Test, a CE-IVD NGS liquid biopsy assay for identification of clinically relevant variants.

M. Jasti, S. Raut, D. Hassell, N. Ezzedine, D. Garcia, S. Wunsch, N. Siepert, E. Martinez, E. Ostrowska, J. Schagemann, J. Gu, T. Jayaweera, L. He, A. Cheng; Thermo Fisher Scientific, AUSTIN, TX

For in vitro Diagnostic use only. Not available in all regions including the United States.

Introduction

Minimally invasive blood-based liquid biopsy using cell-free total nucleic acid (cfTNA) and next generation sequencing (NGS) has substantially evolved in the field of clinical diagnostics for oncology, for detection of molecular therapeutic targets in non-small cell lung cancer (NSCLC). Here we describe analytical validation results for cfTNA using the CE-IVD Oncomine™ Dx Express Test (ODxET) assay, a qualitative in vitro diagnostic test that uses targeted NGS technology, the Ion Torrent Genexus™ Dx Integrated Sequencer to detect SNV, indel and copy number gain present in 42 genes and fusions in 7 genes from cfTNA isolated from NSCLC plasma samples.

Methods

Plasma samples from NSCLC patients were screened for variants of interest on several important gene loci. Screening involved isolation of cfTNA from K2-EDTA-derived plasma using the Genexus™ Cell-Free Total Nucleic Acid Purification kit on an automated purification system and sequencing was performed on the Genexus™ Dx integrated sequencer using the ODxET assay. Plasma samples having clinically relevant variants from the set of screened plasma samples were used to perform the validation studies.

Results

Analytical sensitivity and specificity of NSCLC plasma samples were characterized through determination of limit of detection (LOD) and limit of blank (LOB), respectively. The LOD level tested for DNA SNVs, and indels at 5 ng (minimum) input level ranged from 0.62% to 1.82% allelic frequency (AF), while 30 ng (maximum) input shows the LOD level ranging from 0.23% to 0.42% AF. The LOD for the tested RNA fusions ranged from 4.2 to 19.6 molecular counts for 5ng input and 4.9 to 8.0 molecular counts for 30ng input. Furthermore, LOB for the ODxET assay was determined by testing wild type (WT) cfTNA extracted from 30 healthy donor blood plasma samples, which were confirmed to be negative at all variant locations. The analytical accuracy study shows the false positive rate at 0.20% for SNVs, 0% for indel locations and fusion targets. In addition, the analytical reproducibility study shows 99.64% intra-run repeatability call rate for DNA variants and 98.75% for RNA variants.

Conclusion

In conclusion, we establish that the ODxET assay on Ion Torrent Genexus Dx Integrated Sequencer, is fast and efficient while demonstrating high sensitivity, specificity, and reproducibility for testing NSCLC liquid biopsy samples.

#3672 Development of liquid biopsy HPV (Human Papilloma Virus) cell free DNA (cfDNA) based approach for prognosis of cervical cancer.

G. Dagar[1], A. Gupta[1], R. Chauhan[1], A. Shankar[1], D. N. Sharma[1], M. A. Macha[2], A. A. Bhat[3], R. Goyal[4], V. Suri[1], M. Singh[1];
[1]All India Institute of Medical Sciences (AIIMS), New Delhi, India, [2]Islamic University of Science and Technology, Pulwama, Jammu and Kashmir, India, [3]Obesity and Cancer Program, Sidra Medicine, Doha, Qatar, [4]Lady Hardinge Medical College, New Delhi, India

Introduction: Recent progress in the analysis of blood samples for circulating tumor cells or cell-free circulating tumor DNA (ctDNA) has shown that liquid biopsies may have potential applications in the detection and monitoring of cancer. Human papillomavirus (HPV) circulating cell-free (ccf) DNA may act as a unique marker for the prognosis of high-risk HPV-related cancers. However, detection of circulating markers for cervical cancer (CC) requires extremely sensitive techniques that can measure circulating human papillomavirus DNA. Here, we used the sensitive droplet digital PCR (dd PCR) based approach for the detection and quantification of circulating human papillomavirus DNA in plasma from patients diagnosed with cervical cancer at baseline and subsequent follow up with intention of validating its utility as a prognostic marker in CC.

Method: Blood sera form 34 Patients diagnosed with cervical cancer (Stage 1-1V) at AIIMS Delhi was collected at baseline and after 3 months of the treatment. 10 healthy controls were also recruited in the study after due approval from AIIMS IEC. Plasma samples were stored at -80°C. ccf DNA was isolated from 1 ml of plasma and further processed to detect the presence of circulating high risk Human papilloma virus (HPV) i.e., HPV-16 and HPV18 cf DNA using dd PCR.

Result: The median cf DNA concentration was 9.3 ng/uL (range 3-26.6) for all patients while median cf DNA concentration was 7.2 ng/uL (Range 3-57.3) for healthy controls (n=10). Furthermore, the levels of cfDNA decreases post 3 months of treatment with average concentration of 8.07 ng/uL (Range 4.6-19.3). We further processed our samples for dd PCR based screening to detect low copy no HPV cf DNA and ddPCR detection yielded a positive rate of 51% (18/35) for circulating HPV18 DNA while a positivity of 88.5% (31/35) was seen for the circulating HPV16 DNA in the sera of CC patients. By comparing HPV16 and HPV18 genotypes, we observed detection of circulating HPV 16 DNA more frequently than circulating HPV18 DNA in CC patients coming at our center. Furthermore, we found that copies of circulating viral DNA (HPV18 and HPV16) decreased post induction therapy in CC patients indicating progression ability of thid marker.

Conclusion: In the current studies we provide evidence that cell free DNA concentration in CC patient can predict tumor burden and detection of low copy no of circulating HPV DNA could be a promising indicator for prognosis in cervical cancer patients and can predict recurrence of the disease.

#3673 Monitoring treatment response in patients with metastatic colorectal cancer using cfDNA fragmentomics testing: The DOLPHIN trial.

D. E. van Steijn[1], R. J. A. Fijneman[1], G. R. Vink[2], J. M. L. Roodhart[3], M. Koopman[3], M. J. Lahaye[1], M. N. J. Braat[4], V. M. H. Coupe[5], D. A. van den Broek[1], G. A. Meijer[1], H. Wang[5], M. J. E. Greuter[6], B. I. Lissenberg-Witte[6], L. Rinaldi[7], E. Peters[8], A. Konicki[8], N. C. Dracopoli[8], N. F. M. Kok[1], V. E. Velculescu[8];
[1]Netherlands Cancer Institute, Amsterdam, Netherlands, [2]University Medical Center Utrecht, Utrecht University. Netherlands Comprehensive Cancer Organisation (IKNL)., Utrecht, Netherlands, [3]University Medical Center Utrecht, Utrecht, Netherlands, [4]University Medical Center Utrecht, Amsterdam, Netherlands, [5]Amsterdam University Medical Center, Amsterdam, Netherlands, [6]Amsterdam University Medical Centers, Amsterdam, Netherlands, [7]Delfi Diagnostics, Balitmore, MD, [8]DELFI Diagnostics, Baltimore, MD

Background: Accurate monitoring of treatment response in patients with metastatic colorectal cancer (mCRC) is important to decide when to adjust treatment regimen or to proceed to local therapy of metastases. At present, clinical response is determined by computed tomography (CT) imaging-based assessment of changes in tumor size. However, this monitoring approach is constrained by limited sensitivity in detecting lymph node and peritoneal metastases, as well as inter-reader variability. Detection of circulating tumor DNA (ctDNA) is indicative of the amount of neoplastic cells and may have added clinical value to CT imaging for assessment of treatment response and guidance in treatment decision making in mCRC patients. We recently developed a tumor mutation-independent ctDNA test that utilizes low-coverage whole genome sequencing to analyze the plasma cell-free DNA (cfDNA) fragmentome to measure the ctDNA tumor fraction: the DELFI-tumor fraction (DELFI-TF) score.
Aim: The DOLPHIN study aims to investigate whether the DELFI-TF ctDNA assay can provide a sensitive, affordable and broadly applicable ctDNA test to monitor treatment response of mCRC patients.
Methods: The prospective, observational, multi-center DOLPHIN study is a substudy of the Prospective Dutch ColoRectal Cancer cohort (PLCRC). Clinical data, images and blood samples from 400 patients receiving systemic therapy in 8-10 Dutch hospitals will be collected. Blood samples will be drawn longitudinally in conjunction with regularly scheduled CT imaging. Plasma cfDNA will be analyzed for tumor-specific fragmentation patterns using the DELFI-TF score. Droplet digital PCR ctDNA-testing of RAS/RAF hotspot mutations will be performed as reference, when feasible. Primary endpoint is the association between ctDNA changes and clinical response. Secondary endpoints are the association between ctDNA changes and radiological response according to RECIST and to serum carcinoembryonic antigen (CEA) at various time points during systemic treatment, lead time of ctDNA-testing compared to CT imaging to detect progressive disease, and the prognostic value of longitudinal ctDNA-testing.
Results: Since the inclusion of the first patient in March 2023, 117 patients have been included in the DOLPHIN study (November 2023). Seven hospitals throughout the Netherlands are currently open for patient inclusion and more sites have been approached to participate.
Discussion: The DOLPHIN study will assess the added clinical value of longitudinal ctDNA-testing in treatment response monitoring of mCRC patients and whether imaging can be complemented and/or partly replaced by ctDNA-testing. The results of this study may lead to novel strategies for monitoring treatment response and to ctDNA-guided treatment decision making in mCRC patients.

#3674 Blood-based differentiation of malignant and benign pancreatic lesions using analysis of fragmentation patterns in cell-free DNA.

C. T. Marcinak[1], M. D. Stephens[1], B. R. McDonald[1], N. Merali[2], S. M. McGregor[1], S. M. Weber[1], A. E. Frampton[2], S. Sivakumar[3], R. M. Minter[1], M. Murtaza[1]; [1]University of Wisconsin - Madison, Madison, WI, [2]University of Surrey, Guildford, United Kingdom, [3]University of Birmingham, Birmingham, United Kingdom

Pancreatic ductal adenocarcinoma (PDAC) remains lethal, with a five-year survival rate of less than 10%. For patients with pancreatic cystic lesions (PCL), analysis of DNA from cyst fluid has shown promise in determining the risk of malignant transformation. However, obtaining cyst fluid requires an invasive procedure. We recently developed an approach for blood-based cancer detection by analyzing fragmentation characteristics in plasma cell-free DNA (cfDNA). In this study, we evaluate the performance of this method in differentiating between patients with malignant and benign pancreatic lesions. We collected plasma samples from 81 patients at the time of endoscopic evaluation or surgical resection of a PCL. We simultaneously obtained plasma samples from 209 PDAC patients and 56 healthy individuals. Using plasma cfDNA whole genome sequencing data from patients with PDAC and healthy individuals, we trained and cross-validated an ensemble machine learning model based on 10 genomic features capturing plasma cfDNA fragmentation patterns. This model was applied to sequencing data from patients with PCL for independent evaluation of diagnostic performance. In training and cross-validation, the model demonstrated an area under the receiver operating characteristic curve (AUROC) of 0.90 for differentiating PDAC samples from healthy individuals. Of the 81 PCL patients, ten patients (12.3%) were found to have a malignant PCL, with either high-grade dysplasia or invasive carcinoma. The trained model showed an AUROC of 0.78 for differentiating malignant from benign lesions, achieving 50% sensitivity and 62.5% positive predictive value at 95% specificity. Our results are a novel demonstration that a peripheral blood test based on plasma cfDNA analysis can enable differentiation between malignant and benign pancreatic lesions. This approach may improve risk-stratification and clinical decision-making regarding the necessity for surgical resection. Larger studies and clinical trials to validate these results and evaluate their impact on outcomes are warranted.

#3675 Design of high-performance tumor-informed minimal residual disease (MRD) panels from low FFPE tumor input.

M. LaBella[1], A. Acevedo[1], R. Patel[1], K. Haug[1], S. Ganesh[1], E. Buser[1], N. Xu[1], S. Carlson[1], K. Trettin[1], S. Ratzel[1], K. Hara[2], P. Msaouel[3], K. Sircar[3], C. Tang[3], D. Muzzey[1], G. Gould[1];

[1]Myriad Genetics, Inc., Salt Lake City, UT, [2]The University of Texas MD Anderson Cancer Center, Houstin, TX, [3]The University of Texas MD Anderson Cancer Center, Houston, TX

Background: Minimal residual disease (MRD) testing can detect cancer recurrence months to years earlier than the current standard of care, enabling earlier treatment of recurrence and improved patient outcomes. Tumor-informed MRD assays typically utilize formalin-fixed paraffin-embedded (FFPE) tumor tissue, which is available in limited quantities for some patients, for example, following core needle biopsy (CNB), after neoadjuvant treatment or when patients need multiple tests from the same tumor sample. To determine the lower limit of tissue input, we evaluated our MRD assay performance across a range of extracted tumor volumes.

Methods: Resected tumors and CNBs were sectioned, H&E stained, and macro-dissected. Tumor gDNA was extracted, quantified, prepared into libraries and sequenced. Sequenced libraries were aligned and evaluated for depth of coverage, variation of coverage, and duplication rate. Somatic calling was performed on matched tumor and normal samples. Up to 1000 target sites were selected for high-depth targeted sequencing of the tumor and normal gDNA for confirmation of somatic variant calls. The positive predictive value (PPV) was computed as the percent of putative somatic variant sites that were present in the tumor capture library and absent in the normal capture library.

Results: Extracted tumor volumes varied by almost two orders of magnitude, from 0.06mm^3 (equivalent to needle core or fine needle aspirate biopsies) to 5mm^3 (achievable with resected tumor). gDNA amount varied linearly (3.6ng to 1549ng) with tumor tissue input, indicating the low tissue to paraffin ratio did not have an adverse effect on yield. Tumor gDNA inputs into library prep ranged from 2.5ng to 100ng. DNA amounts above 100ng into library prep had no discernable benefit. Below 10 ng, depth of coverage and the coefficient of variation in coverage indicated poor-quality libraries. Samples with ~10 ng of gDNA input into library prep showed depth of coverage comparable to higher inputs and saturated the achievable library complexity. Additionally, PPV of somatic calling was consistent across the range of gDNA inputs from 10-100 ng, demonstrating equivalent assay performance.

Conclusion: Tumor-informed MRD assays have immense potential for increasingly sensitive treatment response and recurrence monitoring that can inform better treatment decisions. FFPE tumor tissue is a critical input into MRD assays but is a limited resource. This study supports a minimum DNA input of 10 nanograms for a single attempt at extraction, corresponding to a tissue volume of 0.2mm^3 or a single 10µm slide with a 20mm^2 area, representing one of the lowest tissue input requirements for an MRD assay. Low FFPE tissue requirements expand the patient population that benefit from MRD testing by utilizing samples that have low tumor content, are post-neoadjuvant therapy or do not meet the tumor volume requirements of competing MRD offerings.

#3676 A circulating tumor fraction DNA biomarker response stratified by *ESR1* mutation status correlates with overall survival in patients with HR+ HER2- metastatic breast cancer.

M. M. Stein[1], **K. Kaneva**[1], S. Hyun[1], C. Sangli[1], M. Ting-Lin[1], R. Ben-Shachar[1], J. Freaney[1], K. Sasser[1], J. Guinney[1], H. Nimeiri[1], M. Cristofanilli[2]; [1]Tempus Labs, Chicago, IL, [2]Weill Cornell Medicine, New York City, NY

Background: *ESR1* mutations (*ESR1m*) are acquired resistance mutations that evolve during treatment with aromatase inhibitor (AI) therapy in approximately 40% of ER+ HER2- metastatic breast cancer (mBC) patients and are indicative of poor outcomes. Patients with *ESR1m* acquired on AI may retain treatment response if switched to selective estrogen receptor degraders (SERDs) like fulvestrant. Circulating tumor DNA (ctDNA) analysis can detect the emergence of *ESR1* mutations and simultaneously determine molecular response to therapy through changes in quantitative ctDNA tumor fraction (ctDNA TF). We used real-world data (RWD) to study the combined effect of acquired *ESR1* mutation status and ctDNA TF dynamics on overall survival in ER+ HER2- mBC.

Methods: Tempus xF Monitor is a ctDNA assay that measures quantitative molecular changes in ctDNA TF by utilizing diverse genomic events, dynamically weighting somatic variant allele frequencies and copy number variants, while using germline information to inform these estimates and providing single nucleotide variant (SNV) results on 105 genes including *ESR1*. Non-responders (NR) were characterized as < 50% reduction in ctDNA TF while responders (MR) experienced ≥ 50% reduction in ctDNA TF. We selected a cohort from the deidentified Tempus multimodal database of 101 HR+ HER- mBC patients with a baseline xF test up to one year prior to or 3 months post AI therapy start. Real-world overall survival (rwOS) was defined as the interval from AI start to death, censored on the last known physician follow-up. Kaplan Meier analysis and Cox proportional hazards models were fitted to evaluate the relationship between *ESR1m* and MR/NR status with rwOS.

Results: In our evaluable cohort, (n=101), median age 59, *ESR1m* was detected in 29.7% (n=30) patients. *ESR1m* patients had shorter rwOS compared to *ESR1* WT patients (median *ESR1m* rwOS 63.8 months, median rwOS not reached for *ESR1* WT; p=0.013, HR=3.45 [1.9-9.2]). Across the cohort, regardless of *ESR1* status, 23.8% (24/101) of patients were characterized as ΔctDNA TF MR, 60.4% (61/101) as NR and 15.8% (16/101) of patients with ctDNA TF values below the limit of blank (b-LOB). Within the NR group, 35.5% (22/61) were also *ESR1m*, while only 20.8% (5/24) and 18.8% (3/16) *ESR1m* patients were in the MR and b-LOB group, respectively. Patients with combined *ESR1m* + NR ΔctDNA TF (n=22) experienced shorter rwOS (p=0.015) compared to MR ΔctDNA TF patients with WT *ESR1* (p=0.024, HR=6.61 [1.3-34.2]).

Conclusions: xF Monitor is a ctDNA assay that tracks changes in quantitative ctDNA TF and simultaneously monitors for the emergence of *ESR1m*, providing a diagnostic that identifies resistance to AI therapy and enables early switch to therapies that could improve outcomes in a patient population with poor prognosis. A larger prospective clinical study is needed to validate these findings.

#3677 Hybrid capture based sequencing from urinary cell free DNA from colorectal cancer patients.

A. Eberhard, T. Moser, L. Ziegler, G. Vlachos, I. Lazzeri, M. Loibner, A. Gerger, E. Heitzer;
Medical University of Graz, Graz, Austria

Background: The study of body fluids other than blood is gaining increasing attention in the field of liquid biopsy. Since urine offers a truly non-invasive sampling method, it is a particularly interesting specimen. Evidence suggests that urine cell-free DNA (ucfDNA) harbors information about renal and bladder cancer. However, not much is known about ucfDNA in colorectal cancer (CRC) patients. Therefore, we aimed to test the feasibility of a hybrid capture based NGS approach with and without preanalytical stabilization of urine samples.
Methods: Urine samples were collected from 20 patients with metastatic CRC (mCRC), aliquoted and stored unstabilized or stabilized (urine collection/stabilization solution under development at PreAnalytiX (QIAGEN/BD company) and Streck urine Preserve) at room temperature. Urine cfDNA was isolated at the day of donation and after 3 days. Matched blood samples were additionally collected in PAXgene Blood ccfDNA Tubes (PreAnalytiX). cfDNA from blood and urine was isolated using the QIAsymphony platform (QIAGEN). cfDNA samples were analyzed using the AVENIO ctDNA Analysis Kit (Roche), a hybrid-capture based approach enriching for 17 clinically relevant genes.
Results: While all stabilized ucfDNA yielded high quality libraries, library preparation failed in 66.7% of unstabilized urine samples, demonstrating that without stabilization ucfDNA rapidly degrades after urine donation. In native samples, in which sequencing data could be obtained, sequencing depth was significantly decreased compared to stabilized samples. For stabilized samples, sequence analysis revealed full concordance between urine and plasma for putative germline variants. However, when using less than 50ng of input material of ucfDNA, a low signal-to-noise ratio with a high number of false positive low level variants was observed. We therefore adjusted the limit of detection for ucfDNA to 0.5%, at which CRC-related mutations were detected in ucfDNA in one patient. Although these variants, were not observed in plasma cfDNA, they could be detected in all stabilized urine samples, which hints to true variants.
Conclusion: Our data demonstrate that a hybrid-capture based analysis approach is feasible for ucfDNA form CRC patients and that urine may provide complementary information about a patient's tumor that may be missed in plasma. Yet, due to degradation and lower concentrations, immediate stabilization of urine after donation is required. Moreover, the limit of detection needs to be adjusted if low amounts of input DNA is available only.

#3678 Beyond detection: AI-based classification of breast cancer invasiveness using cell-free orphan non-coding RNAs.

Mehran Karimzadeh[1], Taylor B. Cavazos[1], Nae-Chyun Chen[1], Noura K. Tbeileh[1], David Siegel[1], Amir Momen-Roknabadi[1], Jennifer Yen[1], Jeremy Ku[1], Selina Chen[1], Diana Corti[1], Alice Huang[1], Dang Nguyen[1], Rose Hanna[1], Ti Lam[1], Seda Kilinc[1], Philip Murzynowski[1], Jieyang Wang[1], Xuan Zhao[1], Andy Pohl[1], Babak Behsaz[1], Helen Li[1], Lisa Fish[1], Kim H. Chau[1], Laura J. Van't Veer[2], Laura J. Esserman[2], Patrick A. Arensdorf[1], Hani Goodarzi[2], Fereydoun Hormozdiari[3], Babak Alipanahi[3]

[1]Exai Bio Inc., Palo Alto, CA,[2]UCSF, San Francisco, CA,[3]Exai Bio Inc., San Francisco, CA

Background: Approximately 1 in 8 women will be impacted by breast cancer in their lifetimes. Earlier detection of breast cancer through screening has improved survival. Liquid biopsies have the potential to complement existing screening methods by enabling earlier detection and differentiating invasive cancer (IBC) from ductal carcinoma in-situ (DCIS). We previously demonstrated high sensitivity and specificity for early detection of IBC by using a blood-based liquid biopsy platform to analyze a novel category of cancer-associated small RNAs, termed orphan RNAs (oncRNAs). Here, we developed a test that could not only detect the presence of cancer, but also classify the invasiveness of breast cancer.

Methods: We utilized The Cancer Genome Atlas (TCGA) small RNA profiles to discover a library of 20,538 oncRNAs that were significantly enriched among 1,103 breast tumors compared to 349 controls from normal tissues spanning multiple tissue sites, limited to female samples. The diagnostic performance of these oncRNAs was assessed in an independent cohort of serum samples from 708 women, including 380 breast cancer patients (221 IBC and 159 DCIS; mean age: 58.0 ± 13.4 years) and 328 age-matched controls (mean age: 58.4 ± 13.7 years). We sequenced the small RNA content from 1 ml of serum from these patients at an average depth of 21.6 million 50-bp single-end reads. We detected 19,736 (96%) of the breast cancer-specific oncRNA library within at least one sample in this cohort. We then trained a multi-class generative AI model using 5-fold cross-validation to predict IBC, DCIS, and absence of breast cancer (IBC or DCIS).

Results: Our oncRNA-based generative AI model achieved an overall AUC of 0.95 (95% CI: 0.94-0.97) for prediction of breast cancer versus cancer-free controls. At 90% specificity, overall model sensitivity is 90.0% (86.5%-92.8%). For DCIS and stage I IBC, the model has a sensitivity of 88.1% (82.0%-92.7%) and 90.4% (81.9%-95.8%) respectively, both at 90% specificity. In the second step, restricting to samples flagged as cancer, we observed an overall AUC of 0.9 (0.87-0.93) and sensitivity of 62.4% (55.3%-69.1%) at 90% specificity for discriminating against invasive breast cancer.

Conclusions: We have demonstrated the potential utility of oncRNAs as the foundation for a liquid biopsy platform for sensitive and accurate early detection of breast cancer. Our liquid biopsy assay has the potential to complement standard of care by not only detecting breast cancer but also differentiating IBC from DCIS.

#3679 Development and validation of prognostic signatures comprising neutrophil-specific long non-coding RNAs (LncRNAs) for predicting survival in urothelial carcinoma.

H. Y. Su, C.-T. Lin, S.-Y. Huang, Y.-H. Chen, C.-W. Kuo;
Kaohsiung Chang Gung Memorial Hospital, Kaohsiung, Taiwan

Background: Tumor-associated neutrophils profoundly influence the tumor immune microenvironment (TME), impacting urothelial carcinoma (UC) progression, metastasis, and survival. Long non-coding RNAs (lncRNAs) have emerged as critical players in cancer biology. Recognizing neutrophils as influential contributors to tumor biology, our study aimed to explore neutrophil-specific lncRNAs and evaluate their prognostic significance in UC.
Methods: In the GSE24890 dataset, 46 lncRNAs were identified with elevated expression in neutrophils compared to other immune cells, thus designating them as neutrophil-specific lncRNAs. To establish a tailored prognostic model, the TCGA BLCA dataset served as the internal training set. Candidate lncRNAs underwent filtration and selection through univariate Cox regression analysis, followed by the construction of a risk score employing LASSO and multivariate Cox regression algorithms. We used IMVigor210 dataset as external validation for this lncRNA model.
Results: Ten lncRNAs exhibiting correlation with overall survival (OS) were initially identified through univariate Cox regression. Following LASSO regression and subsequent multivariate Cox regression analysis, a refined set of 9 lncRNAs was selected to construct the risk model, represented by the formula: Risk score = (-0.096 × FAM13A-AS1 expression level) + (0.157 × FAM27C expression level) + (-0.294 × HCG27 expression level) + (-0.037 × HOTAIRM1 expression level) + (-0.137 × LINC-PINT expression level) + (-0.279 × LINC00612 expression level) + (-0.058 × LINC00967 expression level) + (0.187 × LINC01018 expression level) + (-0.288 × LINC01138 expression level). Kaplan-Meier survival analysis of the BLCA cohort revealed that patients in the high-risk group experienced significantly worse OS compared to those in the low-risk group ($p < 0.001$). The area under the curve (AUC) values at 1, 3, and 5 years were 0.66, 0.67, and 0.66, respectively. In the multivariate Cox regression model, the risk score remained an independent prognostic factor ($p < 0.001$; HR 2.5; 95% CI 1.91-3.30). The validity of the risk score was further confirmed in the IMVigor210 dataset, demonstrating discriminative predictive ability for OS between high- and low-risk groups ($p = 0.027$).
Conclusions: This study underscores the interplay between neutrophils and lncRNAs in UC. Neutrophil-related lncRNAs identified may serve as promising therapeutic targets and prognostic markers for UC.

#3680 Prognostic value of serum biomarkers in pancreatic adenocarcinoma: Results from a Swiss single center cohort analysis.

E. D. Chiru[1], M. Knufike[2], M. Sonderegger-Stalder[1], R. Mosimann[1], A. Sgries[1], R. Rosenberg[1], E. Burri[1], S. Mitrovic[1], M. Voegeli[1], K. Mertz[1], A. Angelini[1], M. Vetter[1];

[1]Cantonal Hospital Baselland, Basel, Switzerland, [2]Eidgenossische Technische Hochschule Zurich, Zurich, Switzerland

Introduction: Inflammatory and nutritional biomarkers, such as neutrophil to lymphocyte ratio (NLR), C-Reactive Protein (CRP), lactate dehydrogenase (LDH) and albumin, are valuable prognostic indicators, refining stratification strategies in oncological patients. This study aims to delineate the impact of these markers on overall survival in patients with pancreatic adenocarcinoma, in order to aid in clinical risk stratification.

Methods: We conducted a retrospective analysis on patients with adenocarcinoma of the pancreas, treated at the Cantonal Hospital Baselland (January 2018 - February 2022). Clinical data, including diagnosis, treatment, and blood markers, were extracted from electronic records. The analysis incorporated the computation of median values for each blood marker, followed by survival analysis and determination of Cox proportional hazard ratios with a 95% confidence interval.

Results: Our cohort included 43 patients, 53% women, 44% men, median age 73 years (IQR 14.75) with adenocarcinoma of the pancreas. Most patients (56%) had advanced distant disease and 25% of these did not receive any oncological therapy. At least one cycle of chemotherapy was administered in 85% of patients. NLR<4 was reported in 63% of cases, normal albumin levels in 72%, normal LDH levels in 79%, and normal CRP levels in 47%. In the multivariate Cox regression analysis, there was a significant higher risk for death with metastatic disease (HR 6.216 CI 2.00-19.28, p=0.002), age ≥75 (HR 4.88, CI 1.65-14.39, p=0.004) and CRP>10 (HR 3.38, CI 1.18-9.66, p=0.023) and lower risk with addition of chemotherapy (HR 0.076, CI 0.02-0.29, p<0.001). NLR, LDH and albumin levels did not significantly correlate with higher HR for death. At a median follow-up period of 8.5 months (IQR 14), the median overall survival was 9 months (IQR 14.5) with a worsening prognostic for increased CRP (p=0.00027), NLR>4 (p=0.051), albumin <35g/l (p=0.0024), LDH >250 U/l (p=0.037). Better survival rates were seen in patients receiving chemotherapy 75% vs 20 for those without chemotherapy (p<0.0001) and in those with local disease 80% vs 60% for metastatic disease p=0.034). Age ≥75 years carried a significant poorer prognostic (p=0.0017), while gender was not relevant. However, due to small sample size, age adjusted survival was not carried out and age was considered not relevant for the survival analysis.

Conclusion: Beyond the expected factors like stage of disease and therapy, an increased CRP appears to carry significant correlation with hazard ratio for death among patients with adenocarcinoma of the pancreas. In our cohort, abnormal CRP, NLR, albumin and LDH levels demonstrated significant association with shorter survival period, underscoring the potential utility of these biomarkers in prognostic stratification and their incorporation into routine oncological assessments.

#3681 Transcribed ultraconserved regions are associated with survival in multiple tumor types.

Ana Carolina Rodrigues[1], Douglas Adamoski[2], Daniela F. Gradia[1], **Jaqueline Carvalho de Oliveira**[1]

[1]Genetics, Federal University of Parana (UFPR), Curitiba, Brazil,[2]Brazilian Biosciences National Laboratory (LNBio), Brazilian Center for Research in Energy and Materials (CNPEM), Campinas, Brazil

Ultraconserved regions (UCRs), encompassing 481 genomic segments identical across humans, mice, and rats, and conserved in other species, are distributed across all human chromosomes except 21 and Y. Over 90% of these regions, termed transcribed ultraconserved regions (T-UCRs) are expressed in at least one human tissue. Although extensively studied in the context of cancer since their discovery, the prognostic significance of T-UCRs in a pan-cancer context has not been explored. For this, TCGA data extracted from the TANRIC platform was utilized, differential expression and survival analysis was performed on different tumor types. Our analysis revealed that approximately 300 UCRs were expressed in the majority of the 20 tumor tissues. Additionally, it was noted that all examined tumor tissues expressed a higher number of UCRs compared to their non-tumor counterparts. Through t-distributed stochastic neighbor embedding (t-SNE) analysis, UCR expression patterns could distinguish primary tumor origins and types. Regarding the prognostic value, we identified 100 (20,8%) T-UCRs associated with disease-specific survival (DSS) and 102 (21.2%) T-UCRs associated with progression-free interval (PFI). Those T-UCRs are particularly important in the survival outcomes of kidney renal clear cell carcinoma (KIRC) and low-grade gliomas (LGC). In addition, we verified that uc.44, uc.48, uc.135, uc.144, uc.153, uc.217, uc.255, uc.256, uc.344, uc.357, uc.390, uc.427 and uc.436 were associated with survival of more than one tumor. Particularly, uc.135 high expression was associated with poor prognosis in Kidney Renal Papillary Cell Carcinoma (KIRP) and LGC, and good prognosis in KIRC. Uc.135 are mapped on MECOM gene, coding an oncoprotein acting as transcriptional regulator and involved in apoptosis, proliferation, and cell differentiation. Our findings suggest that analysis of T-UCRs expression have the potential to be used as predictive biomarkers and can help in studying the mechanisms and specific roles of the highlighted T-UCRs in cancer.

#3682 Pre-surgical blood metabolites associated with ovarian cancer prognosis.

N. Lin[1], O. A. Zeleznik[1], J. Avila-Pacheco[2], C. B. Clish[2], A. F. Vitonis[1], D. W. Cramer[1], K. L. Terry[1], N. Sasamoto[1];
[1]Brigham and Women's Hospital, Boston, MA, [2]Broad Institute of MIT and Harvard, Boston, MA

Background: Ovarian cancer has a poor prognosis with a 5-year survival less than 50%, resulting > 14,000 deaths in the US annually and > 150,000 globally. Identifying prognostic biomarkers at time of diagnosis and elucidating the biological dysregulation among those who are more likely to progress after first-line treatment could inform personalized treatment strategies. Thus, we evaluated metabolites and metabolomic profiles in pretreatment blood associated with survival in women with high-grade serous ovarian cancer, the most common and most deadly histologic subtype.
Method: We examined plasma metabolites in blood samples collected prior to ovarian cancer treatment in 80 high-grade serous ovarian cancer patients who participated in the PreOperative Pelvic Mass Study, a clinic-based study enrolling women undergoing surgery for a pelvic mass. Liquid chromatography tandem mass spectrometry was used to measure 524 known metabolites. We excluded metabolites with coefficient of variation ≥ 25% (n = 104), then removed metabolites with missing in > 20% of the samples (n = 3). Metabolites missing in < 20% of the samples were imputed to be half the minimum value for that metabolite, resulting in 417 unduplicated metabolites. All metabolite values were transformed to probit scores to achieve normality. Cox proportional hazard models were used to calculate the hazard ratios (HRs) and 95% confidence intervals (CIs) adjusting for age at diagnosis, body mass index (BMI), and stage. False discovery rate (FDR) was used for multiple testing correction. Metabolite set enrichment analysis (MSEA) was used to identify metabolite classes associated with prognosis.
Results: Overall, none of the individual metabolites were significantly associated with survival after multiple testing correction (FDR > 0.05). However, 32 metabolites were associated with survival with p< 0.05, with 12 metabolites being associated with worse survival (HR range: 1.38 - 1.98) and 20 metabolites being associated with better survival (HR range: 0.54 - 0.73). MSEA revealed triglycerides (normalized enrichment score (NES) = 3.14), cholesteryl esters (NES = 2.43), and phosphatidylcholines (NES = 2.30) were positively associated with risk of death (FDR < 0.001). Steroids and steroid derivatives (NES = -1.93), sphingomyelins (NES = -2.45), and carnitines (NES = -2.27) were negatively associated with risk of death (FDR < 0.001). Diglycerides (NES = 1.96), lysophosphatidylethanolamines (NES = 1.72), and phosphatidylcholine plasmalogens (NES = 1.58) were positively associated and phosphatidylethanolamines (NES = -1.93) was negatively associated with risk of death with FDR < 0.05.
Discussion: In this study, we explored plasma metabolites associated with mortality in high-grade serous ovarian cancer patients and observed multiple classes of lipid-related metabolites being associated with worse prognosis.

#3683 Prognostic value and biological correlates of LINE1 hypomethylation in oropharyngeal cancer.

M. Casarotto[1], R. Guerrieri[1], P. Boscolo-Rizzo[2], M. Schiappacassi[1], S. D'Andrea[1], V. Lupato[3], S. Chiocca[4], M. Tagliabue[4], R. De Berardinis[4], A. Menegaldo[5], A. Piccinato[6], P. Stritoni[6], M. Ansarin[4], D. Politi[6], G. Fanetti[1], G. Giurato[7], J. Polesel[1], **E. Fratta**[1];

[1]Centro di Riferimento Oncologico di Aviano (CRO), IRCCS, Aviano, Italy, [2]University of Trieste, Trieste, Italy, [3]Santa Maria Degli Angeli General Hospital, Pordenone, Italy, [4]European Institute of Oncology (IEO) IRCCS, Milano, Italy, [5]AULSS 2 Marca Trevigiana, Treviso, Italy, [6]AULSS 3 Serenissima, Mestre, Italy, [7]University of Salerno, Salerno, Italy

Background. We have recently demonstrated that LINE-1 hypomethylation is a negative prognostic factor in oropharyngeal squamous cell carcinoma (OPSCC). HPV-positive patients with LINE-1 methylation <55% showed an almost 5-fold higher risk of death than hypermethylated once, with an overall survival as poor as HPV-negative patients. Somatic *TP53* mutations are a common feature in HPV-negative OPSCC, whereas their presence has been reported in only a small subset of HPV-related OPSCC. At present, little is known about the correlation between LINE-1 methylation and p53 expression status and/or *TP53* mutation in OPSCC. **Methods**. Since 2019, an ongoing prospective study has been enrolling patients with OPSCC in nine cancer centers in Northern Italy. HPV16 E6 DNA was quantified using real-time quantitative PCR (qPCR). LINE-1 methylation was evaluated by methylation-specific qPCR. p53 expression was detected by immunohistochemical staining. *TP53* exon mutations were analyzed by Next Generation Sequencing. **Results**. Up to date, 134 OPSCC patients have been enrolled, including cancer of the tonsil (n=74; 55.2%), base of tongue (n=47; 35.1%), and other subsites (n=13; 9.7%). HPV16 DNA was found in 54.3% of cases: 65.7% in base of tongue, 57.1% in tonsil, and 16.7% in other subsites (p<0.001). LINE-1 methylation was higher in HPV16-positive patients (median: 55.8%, interquartile rage [IQR]: 42.5-68.5) than HPV16-negative ones (median: 40.7; IQR: 23.9-59.1; p=0.003). Nevertheless, the median LINE-1 methylation was lower (50.7%) among HPV-16 OPSCC patients who relapsed than those who did not (56.0%), thus confirming the findings previously reported. However, data from the present investigation are presently not mature to purse the study aims (median follow-up: 12.3 months). The correlation between LINE-1 hypomethylation and p53 expression has also been evaluated in OPSCC patients. p53 expression was categorized into three groups (0%, 1-49%, and ≥50%) based on the overall intensity of nuclear staining of the tumor cells. p53 was considered null, overexpressed, or wild type when its nuclear staining was 0 %, ≥50%, or ranged between 1% and 49%, respectively. Of note, the highest level of LINE-1 methylation was observed in OPSCC tissues with nuclear p53 staining between 1% and 49% (57.8%), whereas OPSCC patients with p53 expression ≥50% showed a decline of LINE-1 methylation levels (40.6; p=0.026). Interestingly, LINE-1 methylation was lower in OPSCC patients harboring *TP53* mutations in both HPV16-negative (24.8%) and HPV16-positive (24.0%) OPSCC patients, even if statistical significance was reached only in the HPV-negative group (p=0.015). **Conclusion**. Preliminary results confirm the potential of LINE-1 methylation to identify HPV16-positive patients with poor prognosis. In addition, this study suggest that *TP53* mutations might influence LINE-1 methylation, irrespective of HPV status.

#3684 Comprehensive error suppressing approach allowing enhanced minimal residual disease detection in lung cancer patients.

H. Bao[1], F. Meng[2], Z. Xia[2], Q. Sun[2], S. Wang[2], W. Tang[1], N. Li[1], M. Wu[1], J. Zhang[1], B. Zhu[1], D. Zhu[1], X. Wu[1], R. Yin[2], Y. Shao[1];
[1]Nanjing Geneseeq Technology Inc., Nanjing, China, [2]Department of Thoracic Surgery, Jiangsu Key Laboratory of Molecular and Translational Cancer Research, Jiangsu Cancer Hospital & Nanjing Medical University Affiliated Cancer Hospital & Jiangsu Institute of Cancer Research, Nanjing, China

Objective: Identifying minimal residual disease (MRD) in postoperative lung cancer patients is crucial for timely cancer intervention. However, current fixed panel methods suffer from low sensitivity, whereas personalized panels face challenges as long yield time and require patient tissue samples. Our objective was to develop an accurate and efficient method for detecting circulating-tumor DNA (ctDNA) in post-surgery lung cancer patients.
Methods: The study retrospectively enrolled 39 lung cancer patients (14 relapse, 25 non-relapse) with 63 post-surgical plasma samples. The mutational profiles of cell-free DNA (cfDNA) were obtained using SHIELDINGTM ULTRA Panel by Geneseeq, covering hotspots in 2365 cancer-associated genes. A comprehensive error suppressing algorithm, which combines intra-run sampling adaptive noise control, cfDNA fragment profiling, normal pool, and white blood cell background, was utilized to eliminate the background artifacts. The plasma ctDNA status were identified under both tumor-informed and tumor-naïve scenarios.
Results: Our method yielded results on par with personalized panels, achieving a sensitivity of 85.7% at the specificity of 92.0%, with a negative predictive value (NPV) of 92.0% in longitudinal analysis. The ctDNA positive patients had a 21-fold increased risk (Hazard Ratio [HR] = 20.7, p = 9.2 ×10^(-5)) compared to the ctDNA negative patients. Remarkably, the landmark analysis using 39 samples (<= 7 days post-surgical) showed a 57.1% sensitivity at 100.0% specificity. Patients with a landmark (<= 7 days post-surgical) ctDNA positive status showed an increased risk of 16.2 times (HR = 16.2, p = 3.5 ×10^(-6)). Furthermore, we found that our approach could maintain its level of performance under tumor-naïve scenario, showing HRs of 12.7 (p = 1.3 ×10^(-4)) for longitudinal ctDNA positive patients and 12.3 (p = 3.7 ×10^(-5)) for landmark ctDNA positive patients. The ctDNA status determined by the tumor-informed and tumor-naïve approaches showed a substantial agreement, yielding a concordance of 90.5% (Cohen's Kappa = 0.738).
Conclusion: Herein, we report a comprehensive error suppressing approach for removing background artifacts by fixed MRD panel, allowing an enhanced MRD detection in post-surgical lung cancer patients. Our approach, which accurately identified ctDNA status at a cost-effective rate, outperformed other fixed panels while showing comparable performance with personalized panels. Furthermore, our method can be utilized under tumor naïve scenarios when personalized panels are unfeasible in the absence of tumor information. Finally, the faster turnout time of fixed panel makes our approach more suitable for clinical landmark MRD detection than a personalized panel.

#3685 Improved detection of minimal residual disease in colorectal cancer patients using adaptive noise cancellation algorithm.

H. Bao, W. Tang, N. Li, M. Wu, J. Zhang, B. Zhu, X. Wu, Y. Shao;
Nanjing Geneseeq Technology Inc., Nanjing, China

Objective: Existing methods for detecting circulating-tumor DNA (ctDNA) through fixed panels exhibit constrained sensitivity, while customized panels are time-consuming and rely on prerequisite tumor mutation profiles. Here, we aimed to introduce an adaptive noise cancellation approach for efficient Minimal Residuals Disease (MRD) detection in colorectal cancer patients employing a fixed panel under both tumor-informed and tumor-naïve situations.
Methods: 108 plasma samples were collected from 52 colorectal cancer patients (11 relapse, 41 non-relapse) at various post-surgical timepoints. Comprehensive mutational profiling of plasma samples was conducted using a fixed MRD panel (SHIELDINGTM ULTRA) that encompasses hotspots in 2365 cancer-related genes. Background errors were removed by an adaptive noise cancellation algorithm relying on DNA fragment profiling, normal pool, and white blood cell background and intra-run plasma sampling. Variants were called both with (tumor-informed) and without (tumor-naïve) the present of tumor tissue.
Results: Our longitudinal analysis of 108 plasma samples yielded 90.9% sensitivity, 97.6% specificity and 97.6% negative predictive value in the tumor-informed scenario. The ctDNA positive patients exhibited significantly higher risk than those with negative ctDNA status (Hazard Ratio = 87.2, p = 3.5×10^(-5)). For landmark analysis, 33 plasma samples (≤7 days post-operation) were assessed, yielding a remarkable performance of 66.7% sensitivity and 100% specificity. Our approach showed robustness under tumor-naïve scenario, illustrating 90.9% sensitivity, 92.7% specificity and 97.4% NPV for the longitudinal analysis. This corresponded to an increased risk of 49 times in the ctDNA positive patients (HR = 49.0, p = 2.2×10^(-4)). Notably, the results of tumor-naïve samples closely aligned with those of tumor-informed samples, showing a concordance of 92.6% and substantial agreement (Cohen's Kappa = 0.691).
Conclusion: Our method stands as an ultra-sensitive tool for identifying colorectal patients at high risk of recurrence. By employing an adaptive noise cancellation algorithm, our fixed panel approach demonstrates superiority over existing fixed panels in accuracy and proves to be a cost-effective alternative to personalized panels. Significantly, it extends potential clinical utilization towards tumor-naïve patients, which is not feasible for personalized panels.

CLINICAL RESEARCH: Circulating Tumor Cells 1
Poster Session

#3689 Optimizing CTC isolation techniques for molecular characterization of circulating tumor cells in clear cell renal cell carcinoma: A comparative study of EpCAM-based and density-based methods.

Joanna Bialek, Anne Muthe, Stefan Yankulov, Felix Kawan, Georgios Gakis, **Gerit Theil**

University Clinic and Outpatient Clinic for Urology, Medical Faculty of Martin Luther University Halle-Wittenberg, Halle (Saale), Germany

Introduction: Renal cell carcinoma (RCC) belongs to the most invasive cancers with the high molecular intrapatient heterogeneity. Circulating tumor cells (CTCs) are cells that detach from the tumor, reflecting the activity of the metastatic procedure. The most popular CTCs isolation methods are based on EpCAM signal detection on epithelial tumor cells. The clear cell RCC (ccRCC) originate from epithelial entity, since that is the EpCAM-based method suitable to isolate CTCs in this cancer. However, the prone of CTCs to EMT is known, which may in consequence downregulate the EpCAM expression and change the cell profile (hybrid phenotype). This is one of the points challenging the CTCs isolation by RCC disease. In our study, we compare the effectivity of antibody-based and density-based isolations technics in ccRCC patients to detect potential markers in CTCs.
Purpose: Our aim was to find a precise and costs effective method to isolate and characterize CTCs from ccRCC patients.
Materials and Methods: Prospective blood samples (3mL) from pulmonary and/or osseous metastatic ccRCC patients were collected during the immunotherapy and from the healthy donors. CTCs were isolated using EpCAM beads (RCC n=13; healthy n=15) or density-based (RCC n=13; healthy n=15) method. Expression of potential RCC biomarkers (mucin-1 (Muc1), androgen receptor (AR)) was identified using qPCR (Real-Time PCR) followed by dPCR (digital PCR), the results status received from both methods was evaluated.
Summary: Based on our prior results, we first isolated CTCs based on EpCAM beads. Using qPCR we analyzed expression of genes, which we previously associated to the RCC (Muc1, PD-L1, AR). The results revealed differences in Muc1 (40% of tested patients positive but none of the healthy donors), when PD-L1 did not differed and AR was not detected. Applying more precise dPCR did neither show any expression. We continued our investigations with isolation of CTCs using density-based method. We confirmed more frequent expression of Muc1 by RCC Patients than by donors, as in our EpCAM cohort. PD-L1 was similar in both groups. Results of AR obtained using qPCR were confusing, showing deviations within same patients. The use of dPCR displayed significant differences in expression between RCC patients (77%; median [range] 0.28 [0.00 - 0.62] and donors (60%; 0.04 [0.00 - 0.51] confirming dPCR as optimal tool for molecular CTC characterization.
Conclusions: Based on our results we demonstrate higher expression of Muc1 and AR in CTCs of metastatic ccRCC patients. The isolation technic should be adapted to the disease status and treatment choice. Further investigations confirming Muc1 and AR as ccRCC biomarkers are required.

#3690 Monitoring prostate specific membrane antigen or androgen receptor expression on circulating stromal cells in advanced prostate cancer patients and their correlation with patient response.

D. M. Kasabwala[1], R. C. Bergan[2], R. Alpaugh[3], D. C. Danila[4], T. L. Chuang[4], B. Y. Hurtado[4], D. L. Adams[5];
[1]Rutgers, The State University of New Jersey, New Brunswick, NJ, [2]University of Nebraska Medical Center, Omaha, NE, [3]Fox Chase Cancer Center, Philadelphia, PA, [4]Memorial Sloan Kettering Cancer Center, New York, NY, [5]Creatv MicroTech, Inc., Monmouth Junction, NJ

Background: Metastatic Prostate cancer (mPCa) mortality rates are high despite numerous treatment options against various mechanisms of action, including targeted therapies, i.e. prostate specific membrane antigen (PSMA)-targeted therapy (Pluvicto) or anti-androgen receptor (AR) (Enzulamide, Biculamide). Further, tumor biomarkers (i.e. PSMA and AR) can change over time and with resistance mechanisms that develop after treatments. This suggests that primary biopsies may not represent later PCa tumors necessitating a way to identify patients that may respond to later line therapies. Blood based biopsies can be used to monitor PCa treatment, which can include circulating tumor cells (CTCs) and the newly discovered cancer associated macrophage like cells (CAMLs), a cancer specific circulating phagocytic stromal cells. Interestingly, while PSMA & AR have been identified in CTCs, they have not been evaluated in CAMLs, nor have PSMA & AR expressions in CTCs & CAMLs been evaluated in anti-AR therapy settings. We measured CAMLs & CTCs in mPCa to evaluate their PSMA & AR expression, including in patients treated with anti-AR therapy.
Methods: We evaluated CAMLs & CTCs in a multi-institutional prospective pilot study using n=30 mPCa patients with progressive disease, prior to starting a new line of therapy (T0). Whole peripheral blood (7.5mL) was filtered for CAMLs & CTCs and stained for PSMA (n=15) & AR (n=15). In addition, 15 patients were treated with anti-AR therapy as standard of care and responses by PET/CT were compared against AR expression. When possible, follow up samples (T1) were also procured.
Results: CTCs were identified in 16% (n=5/30) of patients and CAMLs were identified in 96% (n=29/30), with 53% of patients having hyperengorged CAMLs ≥50 µm (n=16/30). CTCs in patients were not statistically significant for worse outcomes PFS HR= 0.1748, p=0.546 nor OS (HR= 1.303, p=0.865), nor were CAMLs prognostic for PFS or OS. However, patients with ≥50 µm CAMLs did have significantly worse PFS (HR= 5.9, CI95% 2.2-16.3, p=0.001) and worse OS (HR= 3.1, CI95% 1.3-7.1, p=0.016). Further, PSMA CAML/CTC expression was high in 60% (n=9/15) of patients and AR CAML/CTC expression was high in 53% (n=8/15). Of the n=15 patients who received anti-AR therapy after T0, high AR expressing CAMLs/CTCs (n=8/15) had a ~250% better mPFS of 10.3 months (mons) (progressing at 2.2-32.6 mons) vs low AR CAMLs/CTCs mPFS of 4 mons (progressing at 0.2-7.2 mons). Additional mOS analysis from T1 samples and 2-year survival is ongoing.
Conclusion: We utilized liquid biopsies to monitor the expression of two common cell surface receptors (PSMA & AR) in CAMLs and CTCs in mPCa. Further, in a small subset of patients treated with AR therapy, high AR CTC/CAML expression appeared to correlate with better response rates, though larger prospective studies are needed.

#3691 Molecular profiling using next generation sequencing with high purity enrichment of circulating tumor cells.

S. Park, J. Choi, **A. Jeong**, H. Kim, J. Oh, I. Jang, H. Kang, J. Lee, S. Pak, M.-J. Song, J. Kim, H.-C. Lee;
Cytogen Inc., Seoul, Korea, Republic of

Purpose: In the area of liquid biopsy, coupled with next generation sequencing (NGS), circulating tumor cells (CTCs) and circulating tumor DNA (ctDNA) can serve as an alternative substrate to tumor tissue for mutation detection and companion diagnostic purpose. Emerging evidence shows that complementary sequential CTCs and ctDNA profiling provide promising benefit for prognosis and treatment. In contrast to well-established ctDNA extraction methods, the process of isolating intact CTCs for NGS analysis is yet to be fully elucidated. Here, we show that the isolation and harvest of viable CTCs by CytoGen's Smart Biopsy™ System enable the attainment of sufficiently high purity for NGS analysis in metastatic breast cancer.

Methods: Targeted panel sequencing for CTC was developed to detect representative mutated genes, using the Oncomine™ Comprehensive Assay Plus (501 genes) and the Oncomine™ Pan-Cancer Cell-Free Assay (52 genes). Analytical validation was performed with breast cancer cells MDA-MB-231 (50 to 5 cells) which were spiked into 5 mL healthy blood, to mimic CTC. The CytoGen's Smart Biopsy™ system was applied to isolate the CTC. Then, CD45 depletion and whole genome amplification were performed. Sequencing was carried out on Ion S5™ XL systems using an Ion 550™ Chip Kit. Subsequently, sequencing data was analyzed using Ion Torrent software with default configurations.

Results: As a result of targeted panel sequencing using Oncomine™ Comprehensive Assay Plus, representative mutated genes (*BRAF*, *KRAS*, *TP53*, *NF2 and NOTCH3*) in breast cancer were detected in at least 20 MDA-MB-231 cells. In the results using Oncomine™ Pan-Cancer Cell-Free Assay, mutated genes (*BRAF*, *KRAS* and *TP53*) were successfully detected even with only 5 MDA-MB-231 cells. These results suggest that clinical sample of breast cancer could be applied with promising sensitivity and specificity for detection of representative mutated genes.

Conclusion: Molecular analysis of CTCs is a challenge since CTCs are very rare in the blood and there are technical limitations in isolating CTCs with sufficient purity. In this study, we developed the process for NGS analysis on very low number of CTCs with high purity, isolated using CytoGen's Smart Biopsy™ system. Overall, these process could provide information for diagnosis and appropriate treatment of metastatic breast cancer along with the results of our ongoing clinical trials.

#3692 Genomic profiling with the novel single-cell IMPACT assay reveals evidence of genetic heterogeneity among CTCs in late-stage breast cancer patients.

Zbigniew T. Czyż[1], Clara Chaiban[1], Adithi Ravikumar Varadarajan[2], Cacilia Kostler[1], Vadim Dechand[2], Jonas Grote[3], Thomas Ragg[3], Bernhard Polzer[2], Jens Warfsmann[2], Christoph A. Klein[1]

[1]Experimental Medicine and Therapy Research, University of Regensburg, Regensburg, Germany,[2]Division of Personalized Tumor Therapy, Fraunhofer Institute for Toxicology and Experimental Medicine, Regensburg, Germany,[3]quantiom bioinformatics GmbH & Co. KG, Weingarten, Germany

Introduction: Liquid biopsy enables minimally invasive molecular profiling of systemic cancer for diagnosis, therapy selection and longitudinal monitoring of minimal residual disease. Cell-based liquid biopsy methods are particularly well suited to examine the extent of genetic heterogeneity and clonal diversity among metastatic cancer cells, which are believed to be the major determinants of therapeutic failure. However, isolation and molecular profiling of circulating tumor cells (CTCs) from body fluids is challenging due to methodological constrains.

Methods: To overcome these challenges, we have developed a workflow for detection, isolation, and mutational profiling of CTCs. The workflow utilizes the FDA-approved CellSearch System® and a novel method for single-cell Integrated Mutation Profiling of Actionable Cancer Targets (scIMPACT). Our workflow was optimized for reliable detection of copy number variations (CNVs) and single nucleotide variations (SNVs) in single CTCs. The method was then applied to 31 CTCs alongside with 15 matched germline samples.

Results: After implementation of a customized Bayesian neural network based algorithm, accounting for biases introduced during amplification of single-cell DNA and prioritizing the detected mutations, we achieved a sensitivity of 91% and a specificity of 96%, AUC = 0.98. The CTC analysis revealed presence of CNVs affecting known oncogenes and tumor suppressor genes (including *MYC*, *CCND1*, *FGF4*, *TP53* and *RB1*) as well as SNVs classified as pathogenic (e.g., ARID1A Q775*). Notably, in the examined specimens most of the chromosomal aberrations (51-82%) were clonal across all cells of a given patient. In contrast, most of the detected somatic SNVs (67-96%) were sub-clonal and thus present only in a subset of CTCs.

Conclusion: In summary, the novel scIMPACT workflow enabled reliable and accurate genomic profiling of patient-derived CTCs in late-stage breast cancer patients. Our proof-of-concept study revealed evidence of genetic diversity of SNVs among the examined CTCs, which might have been acquired late in progression but relevant for therapy escape in the studied cases. Further analyses are still needed for assessing the generalizability of our finding as well as for deeper understanding of the molecular basis orchestrating the establishment and maintenance of heterogeneous genotypes of CTCs in breast cancer.

#3693 Molecular and functional characterization of circulating CK+/CD45+ cells in breast cancer.

C. Reduzzi[1], E. Nicolo`[1], L. L. Ozimski[2], M. Silvestri[3], L. Gerratana[4], M. S. Serafini[1], E. Molteni[4], N. Bayou[1], A. K. Strickland[1], H. Liu[5], V. Cappelletti[3], N. Aceto[2], M. Cristofanilli[1];

[1]Weill Cornell Medicine, New York, NY, [2]ETH Zurich, Zurich, Switzerland, [3]Fondazione IRCCS Istituto Nazionale Tumori, Milano, Italy, [4]Universita` degli Studi di Udine, Udine, Italy, [5]Northwestern University, Chicago, IL

Background: Circulating tumor cells (CTCs) are considered a key element in metastatic progression and represent a validated prognostic biomarker in breast cancer (BC). CTCs in BC are normally defined as epithelial cells (positive for EPCAM or cytokeratin, CK) lacking the expression of the leukocyte marker CD45. Circulating cells expressing both EPCAM/CK and CD45 (dual positive, DPcells) have however been reported in BC but not investigated. It is believed that DPcells derive from the heterotypic cell fusion of tumor and immune cells, but this hypothesis has not been demonstrated yet. We recently reported, for the first time, the association of DPcells with worse survival in a cohort of 341 BC patients (pts) [Reduzzi et al. ASCO 2022] supporting their tumor origin. Here, we further investigated their malignancy and metastatic potential by molecular profiling and functional experiments.

Methods: The study consisted of 2 components: A) Single CTCs and DPcells were enriched from the blood of BC patients with the CellSearch platform, and isolated with the DEPArray system. Single cells underwent whole genome amplification and lowpass whole genome sequencing for single cell copy number alteration (CNA) profiling; B) DPcells and CTCs were investigated in the blood of immunodeficient (NSG) and immunocompetent (FVB) mouse models using various cell lines (LM2, 4T1, MVT1). To test their metastatic potential, DPcells from the primary tumor of FVB donor mice were transplanted into recipient NSG mice, and the metastatic burden in the lungs and liver quantified, in comparison with control CD45- tumor cells.

Results: We analyzed 73 DPcells and 18 CTCs collected from 16 BC pts: Aberrant genomes were observed in 28% and 93% of evaluable cells, respectively. When collected from the same pt, CTCs showed clonal CNA profiles, while DPcells were highly heterogeneous. *In vivo*, DPcells could only be detected in the blood of FVB mice but not in NSG mice. They were very rare, comprising of only about 3% of the total CTC count. When DPcells and control tumor cells were isolated from the primary tumor of 10 donor mice and transplanted into the tail vein of 10 recipient mice, we observed no significant differences in the metastatic colonization of the lungs and liver by the two population, indicating that DPcells do in fact possess metastatic ability, and to a similar extent as control cancer cells.

Conclusions: DPcells can have an aberrant genome, supporting their malignancy. Contrary to CTCs, DPcells' CNA profiles are not clonal and, i*n vivo*, they can only be observed in immunocompetent models; both observations support the tumor/immune fusion hypothesis. Finally, DPcells show metastatic potential in mice, in line with the association with worse survival we previously observed in BC pts. Overall DPcells seem a new CTC subpopulation that should not be neglected anymore. More studies are needed to better understand their origin and phenotypic/molecular features.

#3694 Genomic profiling of single cancer cells using the novel single-cell integrated mutational profiling of actionable cancer targets (scIMPACT) assay.

C. Chaiban[1], A. Ravikumar Varadarajan[2], J. Grote[3], T. Ragg[3], I. Blochberger[1], V. Dechand[2], J. Warfsmann[2], C. A. Klein[1], Z. T. Czyż[1];
[1]University of Regensburg, Regensburg, Germany, [2]Fraunhofer ITEM-R, Regensburg, Germany, [3]Quantiom Bioinformatics GmbH & Co. KG, Weingarten, Germany

Liquid biopsy provides opportunities to guide therapy decisions using biomarkers such as circulating tumor cells (CTCs) even years after the primary tumor resection. For this, novel methods permitting the genomic profiling of CTCs are needed to characterize systemic cancer spread and identify clinically targetable genomic alterations. Hence, we developed an assay based on the FDA-approved MSK-IMPACT® assay to analyze the genomes of single-cells. We present a series of benchmarking experiments using well-characterized cell lines to demonstrate the performance of our new Single-Cell Integrated Mutation Profiling of Actionable Cancer Targets (scIMPACT) assay.The scIMPACT assay was developed using Ampli1® WGA products of single-cell and pool samples. The workflow consists of an optimized library preparation protocol followed by targeted sequencing with the scIMPACT panel. A bioinformatics mutation calling workflow facilitates the detection of single nucleotide variations (SNVs), indels, and copy number variations (CNVs). To account for WGA associated bias, we developed an in-house proprietary machine learning based classifier algorithm. Two sample collectives were prepared and used for training and validating the workflow. The first collective, including genomic libraries of MDA-MB-453, BT474, BT549 and ZR-75.1 samples, was used for training of the mutation detection workflow. The second collective, consisting of HCC1395/HCC1395BL cell lines representing matched tumor and normal cells, was used to validate the performance of the assay. The scIMPACT assay identified somatic mutations in all WGA products as predicted from bulk gDNA samples and published literature. Notably, evidence of genetic heterogeneity was reported at the single cell level. Pertaining to the SNV detection, the training collective displayed 91% sensitivity and 96% specificity (AUC=0.98) while the validation collective demonstrated similar performance with 84% sensitivity and 96% specificity (AUC=0.90) proving the applicability of our workflow across different datasets. Furthermore, CNV analysis showed high concordance between matching gDNA and WGA samples. Our workflow enables mutational profiling with high specificity and sensitivity and accurate CNV detection in single cells. The scIMPACT assay has been successfully adapted to analyze samples at the single-cell level. Therefore, our method can be applied for the genomic profiling of patient-derived CTCs.

#3695 Monitoring response to immunotherapy using cell free DNA fragmentomes.

B. Alipanahi[1], L. Sivapalan[2], J. Medina[1], Z. L. Skidmore[1], P. Ghanem[2], E. Peters[1], G. Pereira[2], N. Rao[2], K. Velliangiri[2], A. Konicki[1], S. Cristiano[1], L. Millberg[1], J. Carey[1], K. Lumbard[1], N. Niknafs[2], B. Chesnick[1], J. Tom[1], A. Leal[3], B. Levy[2], P. Forde[2], P. Bach[1], N. C. Dracopoli[1], R. B. Scharpf[2], V. Velculescu[2], L. Rinaldi[1], V. Anagnostou[2];

[1]Delfi Diagnostics Inc., Baltimore, MD, [2]The Sidney Kimmel Comprehensive Cancer Center, Johns Hopkins University School of Medicine, Baltimore, MD, [3]NYU Grossman School of Medicine, New York, NY

BACKGROUND: The rapid detection of disease progression in patients receiving immune checkpoint inhibitors (ICIs) is challenging since there are no reliable biomarkers of clinical response. Liquid biopsy assays may address this unmet need by using cell-free DNA (cfDNA) to monitor treatment responses. Current targeted next-generation sequencing cfDNA assays are costly and have limited assay sensitivity for detection of cancer-specific mutations at low mutant allele frequency (MAF). Here, we demonstrate the utility of DELFI Tumor Fraction (DELFI-TF), a tumor- and mutation-independent cfDNA fragmentome approach to monitor treatment response in patients with metastatic non-small cell lung cancer (mNSCLC).

METHODS: Overall, 422 longitudinal blood samples were collected from 141 mNSCLC patients of which 109 were treated with immunotherapy and 32 with targeted therapy (TT). Plasma-derived cfDNA was processed with whole genome sequencing at low coverage (~4x). Circulating tumor burden was quantified as the maximum MAF (maxMAF) of tumor-derived variants detected using a 500+gene panel. Matched white blood cells were used to filter out germline and clonal hematopoietic variants. A random forest regression model was trained with maxMAF as the response using fragmentation-derived features. The accuracy of DELFI-TF was assessed using leave one patient out cross-validation in the ICI cohort and holdout validation in the cohort of patients receiving TT. For survival analyses, we used the median baseline scores to define low/high DELFI-TF and maxMAF.

RESULTS: In the ICI cohort, DELFI-TF scores were strongly correlated with the maxMAF ($r=0.94$, $p<0.001$, Pearson). At baseline, DELFI-TF and maxMAF both differentiate responding from non-responding tumors ($p = 0.01$ and $p = 0.001$ for DELFI-TF and maxMAF respectively; Wilcoxon). Patients with high DELFI-TF or maxMAF had significantly shorter progression-free survival (PFS) compared to low DELFI-TF or maxMAF (17.0 vs 4.7 months, $p < 0.001$; 17.0 vs 4.6 months, $p < 0.001$; Log-Rank respectively) and similar overall survival (OS) (DELFI-TF high 11.4 vs low 34.1 months, $p<0.001$; maxMAF high 10.9 vs low 34.1 months, $p < 0.001$, Log-Rank). Changes in DELFI-TF and maxMAF at the earliest timepoint were highly correlated ($n=109$; $r=0.90$; Pearson). In the validation cohort of TT patients, DELFI-TF at baseline outperformed maxMAF in distinguishing patients with PFS and OS benefits (DELFI-TF PFS 36.4 vs 11.5 months, $p = 0.03$; maxMAF PFS 21.9 vs 15.9 months, $p=0.6$; Log-Rank) (DELFI-TF OS high 37 months vs low not reached (NR), $p < 0.05$; Max MAF OS high 37 vs NR, $p = 0.1$, Log-Rank). The majority of TT patients (81%) had consistent changes with DELFI-TF and maxMAF from baseline to the earliest timepoint.

CONCLUSIONS: DELFI-TF is a tumor and mutation independent approach that is cost-efficient with high performance comparable to current ctDNA assays for estimating tumor burden and monitoring response in cancer patients.

#3696 Liquid biopsy biomarker analysis during treatment with ^{177}Lu-PSMA-617 in castrate resistant prostate cancer.

J. M. Sperger, M. N. Sharifi, L. Nunamaker, V. Carreno, A. H. Chang, S. R. Reese, C. Linebarger, A. K. Taylor, G. C. Bliitzer, J. Floberg, S. G. Zhao, J. M. Lang; University of Wisconsin-Madison, Madison, WI

Background: Prostate-Specific Membrane Antigen (PSMA) is a highly expressed prostate cancer (PCa) cell surface protein regulated by androgen receptor signaling and the target of the recently approved radioligand therapy ^{177}Lu-PSMA-617. While some patients have dramatic responses to this therapy, rates of upfront or acquired resistance are high even in patients with PSMA-PET-avid disease, and better biomarkers of ^{177}Lu PSMA-617 response and resistance are needed to select patients more effectively for this therapy. To address this need, we evaluated the relationship between longitudinal circulating tumor cell (CTC) androgen signaling and PSMA expression to ^{177}Lu-PSMA-617 response or resistance in patients with metastatic prostate cancer. We leveraged a CTC androgen signaling signature that we have previously shown is prognostic for patients with metastatic prostate cancer treated with AR signaling inhibitors.
Methods: Longitudinal blood samples were collected from 20 patients for circulating tumor cell (CTC) analysis at C1D1, C2D1, C4D1, and C6D1. CTCs were isolated with antibodies to EpCAM followed by parallel enumeration, analysis of cell surface expression of PSMA and RNA extraction for AR or neuroendocrine marker transcriptional profiling.
Results: CTC samples were assessed for PSMA cell surface protein expression prior to treatment and on treatment. *FOLH1* (PSMA) gene expression was detected from CTCs at baseline that persisted through treatment. Gene expression representative of AR pathway activation was present in 70% of the cohort at baseline and 50% of patients at C2D1. Concordant with these observations, no significant decrease in CTC number or PSMA protein expression was seen from baseline to C2D1. However, increased CTC AR pathway activation at C2D1 was associated with increased mean serum PSA (155 vs 21.93 ng/ml) and was associated with decreased duration of response.
Conclusions: Improved tools to predict who will respond to ^{177}Lu-PSMA-617 and detect early treatment resistance and disease progression are needed. Here, we show that persistent CTC burden, CTC AR signaling, and CTC PSMA expression are common early in treatment with ^{177}Lu-PSMA-617 and may be associated with lower likelihood of clinical response. Further ongoing studies are needed to elucidate the relationship between these liquid biopsy results and clinical outcomes.

#3697 Proof-of-concept study to enumerate large oncosomes using the RareCyte CTC platform.

E. Papp[1], J. Vandesompele[2], P. B. Vermeulen[3], L. Y. Dirix[3], M. Kockx[2];

[1]CellCarta, Montreal, QC, Canada, [2]CellCarta, Antwerp, Belgium, [3]GZA Hospital Sint-Augustinus & University of Antwerp, Edegem, Belgium

Introduction: Large oncosomes (LO) are produced by tumor cells and can be detected in blood from cancer patients. The clinical utility of enumerating and characterizing LOs along with CTCs has been demonstrated, especially in settings where CTC counts are low. The RareCyte CTC platform has the potential to capture LOs along with CTCs. We performed a pilot study to evaluate the RareCyte CTC platform's potential to analyze LOs using established preanalytical procedures.

Methods: Metastatic breast cancer patients' (N=10) blood smears labelled with RarePlex® Enumeration panel kit were re-evaluated to identify objects with LO-like characteristics at 10x magnification, along with negative control slides (N=5). LO-like objects were annotated and re-scanned at 40x magnification using the CyteFinder® imaging instrument. After establishing the criteria for LO identification, LO enumeration was performed on a cohort of MBC patients (N=6). Sets of five blood smear slides stained with the RarePlex® Enumeration panel kit were reviewed and LO counted. Total LO counts were established by extrapolating LO counts to 7.5 mL plasma. Pearson correlation was used to determine the level of correlation between LO counts and previously obtained CTC counts.

Results: The established identification criteria enabled the consistent enumeration of LOs at 10X magnification. Total LO count was 9.6 on the negative control slides. In MBC patients the mean total LO count was 306.2 (range 3.2 - 792). There was a significant positive correlation between LO and CTC count (r=0.855, p=0.3). In samples with CTC>0 (N=3), the average total LOs count was 588, about six times higher than CTC count. In CTC=0 patient samples (N=3) the mean total LO count was 24.3 (range 3.2-36).

Conclusions: We report a novel protocol to quantify large oncosomes using the RareCyte CTC platform using established preanalytical workflows. The strong CK/EpCam staining in LOs and the strong correlation of LO count with CTC count indicates their tumoral origin. Due to their higher abundance, LOs combined with CTCs offer a more sensitive tool for treatment response monitoring. Due to its broad range, LO counts in patients with CTC=0 may reveal therapy response dynamics undetectable with CTC enumeration alone. Ongoing work focuses on the parallel detection and integrated evaluation of HER2 by immunofluorescent staining of CTCs and LOs, along with digital PCR based HER2 quantification using cfDNA from matched blood plasma samples.

#3698 Characterization of circulating rare events in non-small cell lung cancer.

J. Seo, S. N. Shishido, J. Mason, C. R. Velasco, J. Mullin, R. Prabakar, J. Hicks, P. Kuhn;
USC - University of Southern California, Los Angeles, CA

Non-small cell lung cancer (NSCLC) is the most frequent type of lung cancer, accounting for about 80 - 85% of all diagnoses. Unfortunately, 75% of NSCLC diagnoses are made when cancer has already spread and the prognosis is poor. Therefore, biomarker investigation that might allow for early detection of NSCLC is critical to improving patient outcomes. The purpose of this study is to demonstrate the feasibility of liquid biopsy to detect and identify circulating rare events, such as circulating tumor cells (CTCs), associated with NSCLC. Here we apply our non-enrichment-based High Definition Single Cell Assay (HDSCA) workflow which utilizes an immunofluorescence staining technique and an unsupervised rare event detection algorithm to identify the circulating rare cells and acellular events in samples collected from 206 NSCLC patients and 60 healthy individuals. We detected a heterogeneous population of circulating rare events in NSCLC, including epithelial, mesenchymal, and endothelial cells, as well as acellular events such as oncosomes. Cancer-associated circulating rare events with statistically significant prevalence in NSCLC compared to healthy individuals were observed. Molecular characterization using multiplexed targeted proteomics based on imaging mass cytometry and genomic analysis by single-cell copy number profiling confirmed the phenotypic heterogeneity and genomic profiles of the detected circulating rare events. In this study, our results demonstrate the use of the extended capabilities of liquid biopsy to identify a comprehensive overview of circulating rare events that can provide clinically valuable biomarkers in NSCLC.

#3699 Identifying novel resistance biomarkers in circulating tumor cell-expressed transcriptomes of metastatic castration-resistant prostate cancer patients treated with androgen receptor signaling inhibitors.

H. Cho[1], J. Cha[1], K.-H. Han[1], J.-S. Chung[2];

[1]Inje University, Gimhae, Korea, Republic of, [2]Haeundae Paik Hospital, Busan, Korea, Republic of

Introduction: For individuals with metastatic castration-resistant prostate cancer (mCRPC), therapeutic options include androgen receptor signaling inhibitors (ARSIs) like abiraterone or enzalutamide, as well as taxane-based chemotherapy. Despite this, establishing the best treatment approach is still debated, with varied responses to treatments observed. Notably, around 30%-40% of mCRPC patients either do not benefit from ARSI therapy or quickly become resistant. PSMA PET/CT demonstrates prognostic significance in forecasting responses to ARSI treatments, underscoring its utility in managing mCRPC. Nevertheless, the effectiveness of blood test-measured PSMA expression levels in diagnosing and treating prostate cancer remains uncertain. Consequently, there is a crucial demand for predictive biomarkers, particularly those indicating therapeutic resistance, to customize treatments according to the unique tumor biology of individual patients.

Materials and Methods: We recruited 21 healthy donors and 60 ARSI-treated metastatic castration-resistive prostate cancer patients. We isolate the circulating tumor cells (CTCs) using lateral magnetophoretic microfluidic technology. The EpCAM-labeled CTCs were specifically isolated by microfluidic technology and analyzed for cell enumeration and transcriptomic analysis. Prostate cancer and epithelial-related six genes (PSMA, PSA, AR, AR-V7, EpCAM, and KRT19) were detected by droplet digital PCR (ddPCR) method.

Results: In ARSI-treated groups, the connection between transcript expression and CTC count is differentiated by the presence or absence of a PSA response. Specifically, 41.7% (25/60) of the ARSI group exhibited a PSA non-response, defined as less than a 50% reduction from the baseline level. These patients demonstrated elevated PSA, PSMA, and AR-V7 mRNA expression levels. Kaplan-Meier survival analysis indicated that patients with high PSMA, PSA, and AR-V7 expressions and a higher CTC count experienced poorer PSA-PFS, radiological-PFS, and overall survival (OS) than those with lower expression levels. This trend was echoed in the findings of the proportional hazards model. Notably, patients with higher PSMA mRNA expression faced significantly lower PSA-PFS (HR: 2.28, 95% CI: 1.20-4.33, $p = 0.012$), radiological-PFS (HR: 4.75, 95% CI: 2.27-9.93, $p < 0.001$), and OS (HR: 6.99, 95% CI: 2.93-16.73, $p < 0.001$) than those with lower expression. The Cox model presented analogous results for CTC count and PSA mRNA levels. However, other transcripts, such as AR, KRT19, and EpCAM, did not correlate significantly with the response to ARSI treatment.

Conclusions: The study's conclusion revealed that PSMA, PSA, and AR-V7 are biomarkers resistant to ARSI treatment among the CTC-derived transcriptomic genes.

#3700 Genomic alterations on first-line panitumumab plus FOLFIRI in metastatic colorectal cancer.

A. Avallone[1], F. Giuliani[2], G. Nasti[1], V. Montesarchio[3], G. Santabarbara[4], S. Leo[5], U. Malapelle[6], G. Rosati[7], C. Lotesoriere[8], E. Tamburini[9], A. Colombo[10], F. Pepe[6], C. Cardone[1], A. Leone[1], C. Vitagliano[1], G. Russo[6], G. Troncone[6], D. Giannarelli[11], A. De Stefano[1], A. Budillon[1];

[1]Inst. Nazionale Tumori IRCCS - Found. Pascale, Napoli, Italy, [2]National Cancer Research Centre Istituto Tumori Giovanni Paolo II, Bari, Italy, [3]AORN dei Colli, Napoli, Italy, [4]AORN S.G.Moscati, Avellino, Italy, [5]Ospedale Vito Fazzi, Lecce, Italy, [6]University of Naples Federico II, Napoli, Italy, [7]Ospedale San Carlo, Potenza, Italy, [8]IRCCS Saverio de Bellis, Castellana Grotte, Italy, [9]Tricase City Hospital, Tricase, Italy, [10]Casa di Cura Macchiarella, Palermo, Italy, [11]Fondazione Policlinico Universitario A. Gemelli, Roma, Italy

Background: IMPROVE is a randomized, non-comparative multicenter, phase 2 study evaluating continuous or intermittent FOLFIRI/PANI, in first-line in patients (pts) with unresectable RAS/BRAF wild-type metastatic colorectal cancer (mCRC). In this trial intermittent FOLFIRI/PANI strategy produced a longer progression-free survival (PFS) on treatment, 17.6 months (mts) vs 11.3 mts, a reduced skin severe toxicity, 18% vs 30%, without any detrimental effect on overall survival (OS), 36.2 mts vs 36.2 mts. The trial also included a prospective genomic alterations (GAs) analysis on circulating tumor DNA with the aim to explore emergence of GAs under the selective pressure of FOLFIRI/PANI.

Methods: We analyzed paired plasma samples (basal and PD) by a commercially available NGS panel enabled to simultaneously analyze KRAS, NRAS, BRAF and PIK3CA hotspot mutations from blood samples. Among them, inspecting default calling parameters on proprietary analysis software (Ion Reporter software 5.2.0), only variants with ⩾5X allele coverage and a quality score ⩾20, within an amplicon that covered at least 1000X alleles was considered. As clonality, the threshold of 0.5% of variant allele frequency (VAF) was established to classify mutations as clonal (VAF⩾0.5%) or subclonal (VAF<0.5%).

Results: Of the 137 pts enrolled in the trial, GAs basal analyses were available for 84 pts. Among these, in 55 (65.5%) no GAs were detected (ND). In the remaining cases, the analysis relieved the presence of mutations for PIK3CA (N=14), KRAS (N=12), NRAS (N=2) and BRAF (N=1). According to the clonality threshold, these GAs were classified as subclonal (SC) in 12 cases (14.3%) and clonal (CL) in 17 (20.2%) cases. Survival analysis according to basal GAs clonality showed a median PFS of 16.6 mts (95% IC 13.0-20.2), 12 mts (95% IC 9.1-14.9) and 25.8 mts (95% IC 17.2-34.5) for ND, CL and SC group, respectively. Median OS was 47.7 mts for ND group (95% IC 34.9-60.5), 26.8 mts for CL (95% IC 25.8-27.8) and not reached for SC group. Moreover, we performed GAs analysis on 61 cases of which basal and PD samples were available. Forty-two cases (68.9%) resulted ND, 7 (11.5%) with SC and 12 (19.7%) with CL GAs.At PD, among 42 ND basal cases, 29 remained ND (69%), 8 (19%) and 5 cases (11.9%) developed SC and CL GAs, respectively. In the SC group, 1 kept SC (14.3%), 4 (57.1%) and 2 (28.6%) cases became ND and CL GAs, respectively. In the CL group, 10 (83.3%) kept CL GAs, 1 (8.3%) case became ND and 1 (8.3%) CL.

Conclusions: These findings suggest that classical GAs associated with anti-EGFR resistance are infrequent with up-front use of anti-EGFR/chemotherapy. Moreover, our data show that basal SC GAs rarely evolve to CL GAs at progression disease and do not affect survival of pts with anti-EGFR/chemotherapy treatment. An update will be provided at the congress. NCT04425239

#3701 Urine-based liquid biopsy test for the detection of residual bladder cancer in radical cystectomy patients.

R. Arya, H. Valentine, U. Satyal, R. Chelluri, M. Li, P. Abbosh;
Fox Chase Cancer Center, Philadelphia, PA

The gold standard therapy for muscle-invasive bladder cancer (MIBC) is neoadjuvant chemotherapy followed by radical cystectomy (RC) and urinary diversion. Some patients may have their disease completely eradicated by chemotherapy as ~35% of patients achieve a pathologic complete response (pCR) when evaluated from RC specimens. RC with urinary diversion is a life-altering operation with high complication rates and therefore determining who are complete responders would improve quality of life and could decrease costs and still achieve a high cure rate via RC avoidance. Unfortunately, current methods cannot accurately identify complete responders. Our lab has developed a urine-based liquid biopsy test in which DNA isolated from urine and germline is isolated and subjected to panel exome sequencing for enumeration of somatic variants. This occurs under the premise that tumor DNA identified (as mutant alleles) is a marker of residual disease while the absence of tumor DNA (meaning the absence of mutant alleles) can indicate a pCR.

A 55 gene panel was designed to be used for exonic sequencing of urinary DNA (uDNA) to identify mutations indicative of bladder cancer or therapeutic targets. We have shown that most mutations in tumor tissue are detectable as mutations in urine (Mu). We also showed that the presence or absence of residual Mu after completion of chemotherapy strongly associates with residual disease or pCR at the time of RC, respectively. Therefore, this test could be used after neoadjuvant therapy to better identify patients for RC avoidance.

To optimize this test, we are currently evaluating pre-analytical factors affecting the yield, purity, and integrity of uDNA and the quality of sequencing data using prospectively collected samples from patients with MIBC. We are also testing commercial and novel preservatives to identify one that maintains cell-free DNA integrity, yield, and mutation detection accuracy to enable temporary ambient temperature storage without compromising mutation detection, permitting shipping/centralized testing. Lastly, we are comparing two library preparation approaches: classical hybrid capture-based (Agilent SureSelect XT^{HS}) and amplicon+hybrid capture-based (Agilent HaloPlex^{HS}) to determine which performs the best for identifying the variants in a sample. Our results showed that both sequencing depth and the quality bases mapped was higher when utilizing the SureSelect XT^{HS} kit as compared to HaloPlex^{HS} using approximately the same number of reads. This improvement may also increase the power to detect rare alleles.

Studies described herein will enable liquid biopsy tests to accurately identify patients with pCR after neoadjuvant therapy and might safely avoid radical cystectomy.

#3702 Dissecting circulating tumor cells phenotype in a cohort of locally advanced non-small cell lung cancer patients undergoing neoadjuvant chemotherapy.

R. Leporati, T. Beninato, S. Iadecola, C. Andreon, F. Murianni, M. Balsamo, A. Martinetti, B. Lombardi Stocchetti, L. Mazzeo, S. Manglaviti, M. Occhipinti, M. Brambilla, A. Prelaj, C. Proto, R. Miceli, L. Roz, G. Sozzi, F. De Braud, G. Lo Russo, G. Bertolini;
Fondazione IRCCS Istituto Nazionale dei Tumori, Milan, Italy

Background: Platinum-based neoadjuvant chemotherapy (pb-NACT) is the primary treatment approach for locally advanced non-small cell lung cancer (LA-NSCLC), despite offering only a limited overall survival (OS) gain. Cisplatin-induced cell damage has been shown to activate the SDF-1/CXCR4 axis in preclinical models of NSCLC, resulting in the recruitment of a cell subset co-expressing the stemness marker CD133 and CXCR4 (SDF-1 receptor) at distant sites. These cells, known as metastasis-initiating cells (MIC), exhibit prometastatic activity. By longitudinally monitoring circulating tumor cells (CTC) in the blood of LA-NSCLC patients (pts) undergoing pb-NACT, our objective is to assess the potential prognostic significance of CTC number and phenotype.
Methods: Between February 2019 and August 2023, a total of 61 pts with LA-NSCLC undergoing pb-NACT, were included in the study. Blood samples were obtained at baseline (T1), post-pb-NACT (T2), and post-surgery (T3) for the characterization of CTC, including total CTC, CXCR4+CTCs, and CXCR4+CD133+ MIC. This characterization utilized a validated marker-independent strategy combining Parsortix and DEPArray™ technologies. Logistic regression models were employed to examine the association between CTC subsets and the response to pb-NACT (Disease Control Rate [DCR], Overall Response Rate [ORR]), while Cox-regression models were used to assess their association with survival endpoints (event-free survival [EFS], OS, disease-free survival [DFS]).
Results: Out of the 61 enrolled patients, 34 had available CTC data for analysis. In this population, DCR was 64.7%, and the ORR 29.4%. Surgery was performed in 14 pts (41.2%). At baseline (T1), elevated levels of CXCR4+CTCs were linked to a lower DCR (10 vs 3/mL, odds ratio [OR]=0.02, 95% confidence interval [CI]: 0-0.40, p=0.008), as well as shorter EFS (10 vs 3/mL, HR=4.20, 95% CI: 1.84-9.58, p=0.002) and OS (10 vs 3/mL, HR=3.14, 95% CI: 1.25-7.88, p=0.004). At the post- CT time point (T2), higher levels of MIC were associated with shorter EFS (3 vs 0/mL, HR=1.41, 95% CI: 1.00-1.99, p=0.047) and OS (3 vs 0/mL, HR=1.55, 95% CI: 1.03-2.34, p=0.035). Although the sample size was limited, a higher number of MIC at the post-surgery time point (T3) showed a trend toward reduced DFS.
Discussion: CTC could serve as a novel biomarker for assessing the effectiveness of pb-NACT in LA-NSCLC. Elevated levels of CXCR4+CTC both at baseline and after pb-NACT, along with increased MIC post-pb-NACT and post-surgery, indicate unfavorable prognostic factors for survival. Specifically, a higher baseline of CXCR4+CTCs may be linked to a suboptimal response to treatment, suggesting the potential need for treatment intensification in patients exhibiting elevated CXCR4+CTC baseline levels.

#3703 Utility of circulating tumor DNA (ctDNA) from cerebrospinal fluid (CSF) for prognosis of patients with recurrent high grade glioma.

B. M. Holle[1], S. Nandakumar[1], C. Kreitzer[1], T. Song[1], M. Tartaro[1], C. J. Hertz[2], J. Rafailov[3], C. Campos[1], A. S. Reiner[1], R. Young[1], A. Meng[1], L. Pasquini[1], A. R. Brannon[1], N. D. Socci[1], M. E. Arcila[1], D. B. Solit[1], M. F. Berger[1], N. Schultz[1], I. K. Mellinghoff[1], A. M. Miller[1];

[1]Memorial Sloan Kettering Cancer Center, New York, NY, [2]Weill Cornell Medicine, New York, NY, [3]NYU Grossman School of Medicine, New York, NY

High-Grade Gliomas (HGGs) are the most aggressive primary brain tumors in adults and molecular characterization is crucial for diagnosis and optimal disease treatment. Due to the eloquent location of many HGGs, upfront or repeat tumor sampling may be sub-optimal. Hence, there is an urgent need to develop alternative, minimally-invasive means to obtain diagnostic information and determine the expected clinical behavior. Here we report that circulating tumor DNA (ctDNA) from cerebrospinal fluid (CSF) can be used to identify disease defining genomic alterations and to track clonal evolution. Additionally, we demonstrate that detection of CSF ctDNA is positively correlated with leptomeningeal disease and overall survival suggesting that CSF ctDNA should be integrated into clinical decision making in the clinic.

Our study includes 315 samples from 254 patients with recurrent glioma treated at Memorial Sloan Kettering Cancer Center who underwent CSF collection for routine clinical care and were sequenced using the MSK-IMPACT targeted clinical sequencing assay (468 and 505 genes). Alterations were classified as oncogenic based on OncoKB. 23% of genomic alterations detected were identified using a secondary bioinformatics analysis, following an informed approach with less stringent mutation calling criteria and Gaussian Mixture Model to call copy number events. CSF ctDNA positivity was determined by the presence of at least one oncogenic disease defining alteration or any shared alteration with the tumor.

Within this cohort, we found 198 CSF ctDNA positive (63%) and 117 CSF negative (37%) samples. Of note, CSF ctDNA positivity was the highest amongst histone mutant tumors with 94% CSF ctDNA positivity compared to 56% CSF ctDNA positivity for IDH-WT tumors. We noticed considerable evolution of the cancer genome in patients with sequential biopsies with only 35% of alterations shared between the tumor and the CSF, in particular within the growth signaling pathways (e.g. PDGFRA). The majority of the shared alterations were clonal, and we noticed the emergence of new clonal events in the CSF.

Our cohort demonstrated that patients with positive CSF ctDNA had a significantly shorter overall survival compared to those who were CSF ctDNA negative (4.83 months vs 11.83 months, HR 2.1, $p < 0.001$). In tandem with secondary clinical analysis, radiographic findings also correlated with CSF ctDNA positivity. Specifically, the presence of enhancing disease and contact of the tumor with the ventricular space were positively associated with detection of CSF ctDNA. Additionally, CSF ctDNA was associated with positive cytology in 21/21 cases (100%).

With our improved bioinformatics pipeline we hypothesize ctDNA from CSF may be used as a prognostic biomarker for survival, but confirmation requires further validation in a prospective study.

#3704 Whole genome and targeted proteome analysis of single cancer cells.

A. Alyasin[1], K. Weidele[2], C. Botteron[2], C. A. Klein[1], Z. T. Czyż[1];
[1]University of Regensburg, Regensburg, Germany, [2]Fraunhofer ITEM-R, Regensburg, Germany

The simultaneous genome and proteome analysis of very rare single cells would enable addressing important biological and diagnostic questions particularly in cancer. Here, we introduce a novel genome and proteome (G&P) analytic workflow, a method allowing comprehensive analysis of single-cell DNA and targeted profiling of protein expression in single cells. As a proof of concept, we demonstrate the capability of the method by quantifying copy number of the *ERBB2* gene alongside with protein expression levels of HER2 and phospho-HER2 in single cells. The G&P workflow utilizes antibodies conjugated with DNA oligonucleotides designed to enable their amplification alongside the single-cell genome facilitating parallel genome and proteome profiling by either quantitative PCR (qPCR) or sequencing. We utilized antibodies targeting cytokeratin 8/18/19, HER2 and phospho-HER (Tyr1248). Performance of each DNA-conjugated antibody was assessed by immunofluorescence staining in a variety of breast cancer cell lines (MDA-MB231, MDA-MB453, BT474 and MCF7) and sample types. Stained cells were isolated by manual micromanipulation and subjected to whole genome amplification (WGA). Protein expression levels, derived from quantification of the amplified DNA tags, were measured by qPCR. Shallow whole genome sequencing was employed to facilitate genome-wide profiling of copy number variations (CNVs), including the *ERBB2* locus. We successfully developed and tested a G&P workflow allowing parallel genome-wide CNV profiling and quantification of three target proteins. G&P measurement yielded concordant results to immunofluorescence quantification for all tested markers. Furthermore, the workflow allowed direct correlation of copy numbers of the *ERBB2* gene with HER2 expression in single cancer cells. Notably, the method enabled measurements of cellular and molecular responses at the single-cell level to lapatinib treatment, i.e. monitoring of the HER2 pathway activation level. Our novel multiplex G&P technique is capable of generating multiparametric measurements linking DNA copy numbers and expression levels of selected genes of interest. The method is optimized for analysis of single cells from rare cell populations and is readily translatable to study circulating tumor cells (CTCs) and disseminated cancer cells (DCCs), enabling for the first time pathway analysis via phosphoprotein analyses of these cells.

#3705 Development and analytical validation of a novel assay for HER2 assessment on circulating tumor cells using Parsortix® isolation and BioView imaging technologies.

M. Ciccioli[1], A. Young[1], L. Vlietinck[1], C. Johnson[2], A.-S. Pailhes-Jimenez[1];
[1]ANGLE Europe Limited, Guildford, United Kingdom, [2]BioView, Billerica, MA

Background. HER2 testing in tissue biopsies is extensively performed in breast cancer (BC) patients. However, tissue biopsy is invasive and repeated examination is impractical. Additionally, lack of concordance between primary tumor and metastatic sites are often observed. Liquid biopsy, on the other hand, enables less invasive and recurrent sample collection for ongoing monitoring. In this study, we developed an end-to-end Research Use Only assay for concomitant evaluation of HER2 gene amplification and protein overexpression in circulating tumor cells (CTCs).
Methods. Blood was drawn from healthy volunteers into Streck Cell-Free DNA tubes, spiked with SKBR3 (HER2+) and Hs 578T (HER2-) breast cancer cells and processed on ANGLE's Parsortix® PC1 System, a microfluidic device that captures CTCs from metastatic breast cancer patients' blood based on their size and deformability, without relying on specific markers. Captured cells were harvested and spun onto positively charged slides and stained with the Portrait HER2 immunofluorescence (IF) panel, consisting of a nuclear dye, epithelial and mesenchymal markers, leukocytes' markers, and an antibody targeting HER2. Slides were then de-stained and subjected to HER2 FISH using a commercially available kit. All slides were imaged twice using BioView Allegro Plus, a platform equipped with artificial intelligence for automated imaging, CTC candidate identification and reporting. First, an automated scan after IF was performed to identify CTCs based on marker expression and morphology profiles. Second, an automated relocation of the CTCs based on IF results and reimaging using higher magnification to ensure precise analysis of the FISH signals in single cells. The workflow is being implemented in a cohort of BC patients.
Results. Following IF, HER2 protein expression in SKBR3 cells was significantly higher (p<0.0001) than that of HER2-negative cells, with 100% analytical specificity and sensitivity. Following FISH, 100% of the cells were de-stained and presented sharp HER2/CEP17 foci, with 96% of the SKBR3 cells and only 4% of the Hs 578T cells displaying HER2 amplification. Additionally, in a small cohort of metastatic BC patients', 100% of the identified CTCs are retained and evaluable from IF to FISH.
Conclusions. An assay integrating HER2 identification by IF and FISH to characterize CTCs in metastatic BC patients was successfully developed. The assay enables the identification of both HER2 protein and gene copy information from each target cell with minimal cell loss, with the potential for minimally invasive patient monitoring during treatment and better classification of patients who may qualify and benefit from HER2-targeted therapies. An added value of the assay is the practicality of utilizing preserved blood samples, allowing streamline batch shipping of clinical samples.

#3706 Single cell and cell-free nucleic acid analyses of liquid biopsy specimens from a blood collection tube using a new droplet digital PCR system.

L. Jackson, C. Cochran, C. Gould, S. Kreston, J. Bello, B. D'Alessio, J. Riley, A. Tubbs, G. A. Pestano;
Biodesix, Inc., Boulder, CO

Introduction: Liquid biopsy-based testing has increasingly been adopted by oncologists for biomarker-driven diagnostics, therapy selection, and patient monitoring. Unlike tissue-based approaches, the target analytes in blood specimens are often rare events that must be discriminated from a background of non-tumor derived material. Droplet digital PCR (ddPCR) is an ideal platform for detection of rare nucleic acid markers in the clinic, because it is highly sensitive and specific, robust, and quantitative. Additionally, the workflow is simple to adopt and execute. The QX600 System is a new ddPCR instrument designed for advanced multiplexing which enables simultaneous detection of up to 6 unique fluorophores in a single well. This capability can decrease the sub-sampling needed for detection of multiple analytes. The objective of our study was to develop multiplexed ddPCR assays for detection of cell-based and cell-free circulating biomarkers from a single tube of whole blood.
Methods: Tumor cells were enriched from the buffy coat fraction of whole blood collected in fixative-containing cfDNA BCT based on size and morphology using a microfluidics-based system. Enriched tumor cells were enumerated by immunofluorescence (DAPI+/Pan-CK+/CD45-), and gene expression was measured using the QX600 for a panel of cytokeratins (CK) and PD-L1 in CTC negative, NSCLC donor specimens (n=8). Results were compared to CTC positive, contrived specimens (whole blood spiked with breast tumor cell line MCF7 cells; n=5). For ctDNA analysis of the plasma fraction, a multiplexed ddPCR assay was designed to test for five actionable mutations prevalent in NSCLC, including EGFR del19, L858R, T790M, KRAS G12C, BRAF V600E, and wildtype EGFR. To evaluate performance of the multiplexed assay, concordance evaluation was conducted using cfDNA from 8 mutation-positive NSCLC donors on the QX600 and compared to single assays run on the QX200 system.
Results: CK8 and CK19 were differentially expressed in the cells enriched from the CTC negative NSCLC cohort as compared to the contrived positives ($p=0.0058$, and $p=0.0049$, respectively). All the NSCLC cfDNA samples were positive for the reference variant, and linear regression analysis of the minor variant frequency for ctDNA biomarkers showed good concordance between QX systems ($R^2=0.8847$).
Conclusions: These studies demonstrate proof of concept for single cell and cell-free analysis from a single blood draw into a cfDNA BCT using the QX600 system. Liquid biopsy analysis of CTCs and ctDNA can enable minimally invasive, comprehensive decision making in the diagnostic workup of patients. Future studies will focus on further optimizing the cell enrichment methodology from cfDNA BCT and development of additional multiplexed ddPCR assays for NSCLC-relevant biomarkers on the QX600.

#3707 Characterization of estrogen receptor expression on CTCs during CDK4/6i treatment in HR+/HER2- metastatic breast cancer: Results from the PACE phase II study.

Mara Serena Serafini[1], Carolina Reduzzi[1], Lorenzo Gerratana[2], Rinath Jeselsohn[3], Reshma L. Mahtani[4], Cynthia X. Ma[5], Angela DeMichele[6], Jane Lowe Meisel[7], Kathy D. Miller[8], Yara Abdou[9], Elizabeth C. Riley[10], Rubina Qamar[11], Priyanka Sharma[12], Sonya Reid[13], Harold J. Burstein[14], Sara M. Tolaney[15], Michelle K. DeMeo[15], Yuan Liu[16], Eric Gauthier[17], Yue Ren[18], Meredith M. Regan[19], Huiping Liu[20], Erica L. Mayer[15], Massimo Cristofanilli[1]

[1]Weill Cornell Medicine, New York, NY,[2]CRO Aviano, National Cancer Institute, IRCCS, Aviano, Italy,[3]Dana-Farber Cancer Institute, Boston, MA,[4]Miami Cancer Institute, Plantation, FL,[5]Division of Oncology, Department of Medicine, Washington University School of Medicine, St. Louis, MO,[6]Department of Medicine, Division of Hematology & Oncology, Perelman School of Medicine at the University of Pennsylvania, Philadelphia, PA,[7]Department of Hematology and Medical Oncology, Glenn Family Breast Center, Winship Cancer Institute, Emory University, Atlanta, GA,[8]Indiana University Melvin and Bren Simon Comprehensive Cancer Center, Indianapolis, IN,[9]Lineberger Comprehensive Cancer Center, University of North Carolina, Chapel Hill, NC,[10]Department of Medicine, Division of Medical Oncology, University of Louisville School of Medicine, Louisville, KY,[11]Advocate Aurora Health, Milwaukee, WI,[12]Department of Internal Medicine, University of Kansas Medical Center, Westwood, KS,[13]Vanderbilt University Medical Center, Nashville, TN,[14]Dana-Farber Cancer Institute, Brigham & Women's Hospital, Harvard Medical School, Boston, MA,[15]Department of Medical Oncology, Dana-Farber Cancer Institute, Boston, MA,[16]Pfizer, La Jolla, CA,[17]Global Medical Affairs, Pfizer Inc, San Francisco, CA,[18]Department of Data Sciences, Dana-Farber Cancer Institute, Harvard T.H. Chan School of Public Health, Harvard University, Boston, MA,[19]IBCSG Statistical Center, Division of Biostatistics, Dana-Farber Cancer Institute, Harvard Medical School, Boston, MA,[20]Northwestern University, Chicago, IL

Background Circulating tumor cells (CTCs) are associated with worse survival in metastatic breast cancer (MBC). The PACE study (NCT03147287) enrolled patients (pts) with hormone receptor-positive (HR+)/ human epidermal growth factor receptor 2-negative (HER2-) MBC after progression on CDK4/6 inhibitor (CDK4/6i) and endocrine therapy, and randomized pts to fulvestrant (ful) alone; ful with palbociclib; or ful, palbociclib, and avelumab [Mayer et al., SABCS 2022]. Pts with ≥5 CTCs appear to derive benefit from treatment combinations vs ful alone. In this feasibility analysis, we evaluated estrogen receptor (ER) expression on CTCs to further investigate their monitoring/predictive potential.**Methods** Blood samples were collected from pts enrolled in the PACE study at: baseline (T1), first tumor assessment (T2) and progression (T3). CTCs were enumerated using the CellSearch platform and samples were classified as CTC^{high} or CTC^{low} (cutoff ≥5 CTCs). CTC^{high} samples underwent ER expression quantification with the ACCEPT software [Zeune et al. 2017]. ER expression intensity (ERint) was measured through the *Marker Characterization* function for each CTC; the average was calculated for each sample. **Results** From the 220 enrolled pts, a total of 409 samples (166, 153 and 90 collected at T1, T2, and T3, respectively) were analyzed for ER. Overall, 236 samples were CTC^{low} (T1 = 91, T2 = 97, T3 = 48) and 173 were CTC^{high} (T1 =75, T2 =56, T3 =42). ER was quantified on 3928, 1853, and 2209 CTCs collected at T1, T2, and T3, respectively. Overall, 32.2% of CTCs were ER negative (ER-).The samples' median ERint showed a numerical decrease from T1 to T3 (T1 = 7.27, T2 = 4.58, T3 = 1.31). Similarly, the % of ER positive (ER+) CTCs per sample decreased from baseline to progression: 26.3%, 14.0%, 5.5% at T1, T2, T3, respectively.CTC^{high} samples were then classified as ER+ or ER- (ER+ = mean ER_int >0). At T1, 91 (54.8%) samples were CTC^{low}, 67 (40.4%) were CTC^{high}/ER+, and 8 (4.8%) were CTC^{high}/ER-. At progression, 48 (53.3%) samples were CTC^{low}, 26 (28.9%) were CTC^{high}/ER+, and 16 (17.8%) samples were CTC^{high}/ER-. A numerical increase in the proportion of CTC^{high}/ER- samples was thus observed from baseline to progression (4.8 to 17.8%).**Conclusions** Herein we demonstrated the feasibility of evaluating and quantify ER expression on CTCs with a software-assisted approach to reduce inter-operator variability. In the PACE study, ER expression on CTCs was decreased at progression compared to baseline, possibly suggesting a mechanism associated with treatment resistance. Future analyses are needed to investigate the correlation between ER expression levels on CTCs with survival and treatment response. This, together with information about the mutational status of *ESR1* by ctDNA sequencing, might provide a new perspective on the development of resistance to ful and CDK4/6i in HR+/HER2- MBC.

#3708 Characterization of EpCAM-positive cells for specific detection of disseminated cancer cells in bone marrow of early breast cancer patients.

J. Roth[1], E. Raya[1], S. Hucker[2], H. Koerkel-Qu[1], S. Seitz[1], C. Klein[1];
[1]University of Regensburg, Regensburg, Germany, [2]Fraunhofer ITEM Regensburg, Regensburg, Germany

Obviously, breast cancer cells that disseminated from the primary tumor before surgical resection are responsible for metastasis. However, detection of disseminated cancer cells (DCC) in breast cancer patients during minimal residual disease is still difficult, impeding the study of early systemic cancer and the extraction of clinically relevant diagnostic or therapeutic information. Others and we have shown previously that EpCAM is a suitable DCC detection marker, however not entirely specific in bone marrow. To improve DCC detection, we here compared different methods to enrich DCC exploiting information from our ongoing single cell RNA-seq study. Based on our ongoing scRNA-seq study (see poster of Elia Raya), we generated a qPCR assay to classify candidate DCC based on an expression signature of four genes. This assay categorizes plasma cell-like EpCAM+ cells from healthy donors and candidate DCC from breast cancer patients with high fidelity. With this assay at hand, we compared two enrichment strategies: depletion of CD11b, CD319 and Glycophorin A positive cells from density gradient enriched mononuclear cells (MNC) vs. positive selection of EpCAM+ cells and subsequent addition of markers that separate out DCC among EpCAM+ cells. For this we applied 10x genomics profiling of EpCAM+ cells from bone marrow. We depleted and screened the bone marrow of 221 patients suffering from non-metastatic early breast cancer for EpCAM-positive cells. From 87 patient samples we could isolate EpCAM-positive cells. We performed single cell RNA-sequencing on 64 EpCAM-positive cells from 54 patients of which 84% were classified as cancer cells and 16% of bone marrow origin. Applying the selected gene signature, 76% of isolated cells were classified as DCC, 16% were undefined and 8% as non-cancer bone marrow cell (NCC). Upon positive selection of EpCAM+ cells implementing additional markers, we isolated 53 cells from 14 patients. Of these, 68% showed a DCC or DCC-like-signature, 15 % a NCC and 17% an undefined profile. To get a better understanding of these EpCAM-positive confounder populations we currently perform a scRNA-seq profiling using 10X on the enriched EpCAM+ cells. Our data shows that EpCAM is a promising marker to identify DCCs in the bone marrow of early cancer patients, but it also indicates that we find several groups of confounder cells. To differentiate between these cell types during staining and in our qPCR assay we are currently testing additional markers.

#3709 Single cell analysis from CSF of patients with suspected leptomeningeal metastasis.

C. Koestler[1], G. Feliciello[1], F. Lueke[1], K. Weidele[1], S. Zoubaa[2], P. Hau[2], T. Pukrop[2], M. J. Riemenschneider[2], C. A. Klein[3], **B. Polzer**[1];
[1]Fraunhofer Institute for Toxicology and Experimental Medicine ITEM, Regensburg, Germany, [2]University Hospital Regensburg, Regensburg, Germany, [3]University of Regensburg, Regensburg, Germany

Introduction: Leptomeningeal metastases (LM) are diagnosed in up to 10% of metastatic cancer patients, the most frequent cancers being carcinomas of breast and lung or melanoma. Due to a dismal prognosis and an overall median survival of only four months new approaches for molecular analysis could help to identify individual treatment options. Material and Methods: In this study, we collected 28 cerebrospinal fluid (CSF) samples from patients with different primary tumors but suspected LM. CSF was divided in two parts for standard neuropathologic cytomorphology and detection of circulating tumor cells (CTCs) by using the CellSearch® CTC Kit, respectively. Subsequently, single Cytokeratin-positive CTCs were isolated for whole genome amplification by *Ampli*1™ and molecular analysis. Additionally, we were able to isolate cell-free DNA (cfDNA) from CSF in a subset of patients which we amplified by an adapted *Ampli*1™ library protocol. In a small subset of patients, we collected slices of formalin-fixed paraffin embedded (FFPE) primary tumors and systemic metastases for dissociation and isolation of pure subpopulations by DEPArray™ technology. Isolated CTCs, cfDNA and subpopulations of tumor and stromal cells were analyzed for copy number variations (CNV) applying the *Ampli*1™ LowPass protocol on the Illumina MiSeq™ platform. Results: By comparing results from classical cytomorphology and CellSearch® workflow, we could find high concordance (24/28 samples) with a slightly higher tumor cell detection rate by CellSearch® (11 positive cases vs. 9 by cytomorphology). Importantly, we could confirm the malignant origin of isolated cells by CNV analysis in all patients positive in CellSearch® assay. Moreover, by comparing single cell data with cfDNA analysis of a subset of 20 samples, we could also detect a higher sensitivity for tumor detection in CTC-based analysis (8/20 cases positive) in comparison to cfDNA-based analysis (5/20 cases positive). In a comprehensive analysis of multiple samples of an individual patient, including CTCs and cfDNA from CSF at different time points, CTCs from blood and biopsies from multiple visceral metastasis, we could identify divergent genomic evolution between tumor cells from the central nervous syste Conclusion: In this proof-of-concept study we show that a liquid biopsy-based approach for single cell analysis from CSF holds potential for innovative diagnostic assays for patients with suspected LM. Combining CTC quantification with molecular single cell analysis could enable us to define predictive tests to select novel treatment options for patients with LM in the future.

#3710 Determining the efficacy of blood filtration in patients diagnosed with pancreatic cancer through the liquid biopsy.

D. D. Suresh[1], G. Courcoubetis[1], E. Lin[1], J. Mason[1], N. Nissen[2], S. Gaddam[2], S. Lo[2], S. Pandol[2], P. Kuhn[1], S. Shishido[1];
[1]USC - University of Southern California, Los Angeles, CA, [2]Cedars-Sinai Medical Center, Los Angeles, CA

Cancer becomes lethal as it spreads from the primary site to the rest of the body. Circulating tumor cells (CTCs) are considered a marker of disease progression and have been associated with decreased overall survival. Blood filtration is one such method of removing cancer cells from circulation to improve patient prognosis. This study utilizes the liquid biopsy to assess the efficacy of a proprietary filtration device on the blood of patients with pancreatic ductal adenocarcinoma (PDAC) using the third generation high-definition single cell assay (HDSCA3.0) workflow. Blood samples were collected and analyzed to characterize the CTCs and other rare cells present before and after filtration. Examination of 6 paired portal (PoVB) samples demonstrated a statistically significant decrease in total rare cells, total CK+ cells, and epi.CTCs across all patients due to filtration of the blood. Furthermore, analysis of 2 paired peripheral blood (PB) samples showed a decrease in total rare cells, total CK+ cells, and specific phenotypes of rare cells upon filtration. These preliminary results demonstrate initial proof of concept that this filtration device can remove CTCs from the circulation, which may be used as a potential therapeutic device for PDAC patient care.

#3711 Procedure establishment of EGFR mutation test with circulating tumor cells of lung cancer by in vitro assay.

J. Lee, **H. Kang**, M. Kim, J. Lee, H. Kim, S. Kim, H. Lee, H.-C. Lee, J. Kim;
Cytogen, Inc., Seoul, Korea, Republic of

Introduction: Non-small cell lung cancer (NSCLC) is the most common subtype, accounting for approximately 80% of lung cancer. The treatment for NSCLC has significantly improved since the introduction of targeted therapies. Epidermal growth factor receptor (EGFR) mutations are the most frequently found genetic alterations in NSCLC, and deletion of exon 19 is a representative example. Searching for this mutation may provide important clues to the use of EGFR tyrosine kinase inhibitors in NSCLC. So, the detection of EGFR mutation is important step in cancer diagnosis and determining the drug treatment strategy, but the detection of mutation with tissues has limitations such as clinical challenge to poorly accessible tumor tissues before and after treatment. The aim of this study was to explore the feasibility and utility of implementation of EGFR molecular testing from circulating tumor cells (CTC) in NSCLC. Here, we developed and optimized the procedure of mutated EGFR detection in CTC after isolation with CytoGen's Smart Biopsy™ CTC isolator by cobas® EGFR Mutation Test. This EGFR mutation test in CTC showed the potential to overcome the limitations of tissue biopsy with high sensitivity and specificity in an in vitro assay.
Method: PC-9 cells were used the positive control of EGFR mutation (EGFR exon 19 deletion). Limit of detection (LOD) was performed with PC-9 cells (200 cells to 5 cells, 6 points) spiked into blood sample (5mL, healthy donor) to mimic CTC in the blood of lung cancer patient. CTC were isolated from spiked samples using CytoGen's Smart Biopsy™ CTC isolator, subsequently cobas® EGFR Mutation Test was carried out to detect of EGFR mutation.
Results: In in vitro experiments of recovery test using cell lines spiked into blood from healthy donor, the recovery rate of CytoGen's Smart Biopsy™ CTC isolator showed over 80%. As a result of LOD test, EGFR exon19 deletion mutation of PC-9 cells was clearly detected even in the smallest number of cells were spiked into blood (5 cells in 5mL blood) and was not detected at all in the negative controls. The result suggested that CytoGen's Smart Biopsy™ CTC isolator can isolate CTC with high recovery rate and apply the test of oncogenic mutations including EGFR mutation in CTC.
Conclusions: Confirmation of EGFR mutation is important step in the diagnosis and selection of optimal drug for cancer patients. However, tissue biopsy has several limitations such as difficulties to get tissue samples and inaccurate information due to invasive method and tumor heterogeneity. Detection of EGFR mutation in CTC might overcome and make up for limitations of tissue biopsy. In this study, we optimized the EGFR mutation detection procedure of intact live CTC isolated by CytoGen's Smart Biopsy™ CTC isolator.

CLINICAL RESEARCH: Combination Immunotherapies
Poster Session

#3716 Enhancing anti-tumor responses in triple-negative breast cancer by combining SIRPα inhibition with immunogenic chemotherapy or antibody-drug conjugates.

X. Ma, L.-C. Tsao, T. Wang, C.-X. Liu, M. Gajda, X. Yang, G. Lei, J. Wei, Z. Hartman;
Duke University, Durham, NC

Background: Triple-negative breast cancer (TNBC) is a subtype of breast cancer defined by the absence of hormone receptors and HER2 receptor on tumor cells. Because of a lack of targetable receptors and poor response to PD1/PDL1 immunotherapy, TNBC has limited systemic treatment options. In previous work using a genomic screen (Shuptrine et al., 2017), we identified CD47 as one of the leading factors that contributes to TNBC immune evasion. The CD47-SIRPα axis is an innate immune checkpoint that primarily regulates myeloid cells. In the context of cancer, tumor cells upregulate CD47 to engage SIRPα inhibitory signaling to block phagocytosis. While CD47 or SIRPα blockade alone show limited antitumor effect, therapies that combine blockade of this axis with other treatment agents, such as tumor-antigen specific antibodies, show superior tumor inhibition. Thus, we hypothesize that the addition of SIRPα inhibition to existing TNBC treatments (chemotherapy and Trop2-antibody drug conjugates (ADC)) will improve their treatment efficacy.
Methods: To ascertain the impact of SIRPα inhibition combined with chemotherapy and Trop2-ADC, we utilized and validated a novel SIRPα KO mouse, along with SIRPα mAbs, in our previously utilized models of Triple-Negative Breast Cancer (TNBC) (Crosby et al., 2018). Using both in vitro and in vivo tumor models, we tested the therapeutic impact of SIRPα inhibition/blockade combined with different immunogenic chemotherapies (doxorubicin/cyclophosphamide) and Sacituzumab govitecan (SG) in TNBC.
Results: After validating the loss of SIRPα in KO mice, we found that E0771 TNBC cells had comparable growth rates in WT and SIRPα KO mice. Similarly, we did not observe different anti-tumor responses to Doxorubicin between WT and SIRPα-KO mice. However, we observed more profound suppression of E0771 tumors after cyclophosphamide treatment in SIRPα KO mice than in WT mice. To evaluate the efficacy of SG in inducing antibody-dependent cellular phagocytosis (ADCP), we co-cultured SIRPα KO and WT mouse macrophages with a syngeneic mouse TNBC model (MM3MG-Trop2-WT). We found that SG promotes ADCP in WT macrophages, and SIRPα loss further increased this ADCP, suggesting the potential importance of antibody-mediated phagocytosis as a mechanism of action for SG. *In vivo*, we implanted human TNBC cells (MDA-MB-468) in mice and treated them with SG with and without SIRPα antibody blockade. These studies demonstrated an anti-tumor effect from SG that was potentially enhanced by SIRPα blockade, suggesting the clinical potential of this combination in TNBC.
Conclusion: Our study demonstrates that the addition of SIRPα inhibition to chemotherapy or SG may promote tumor phagocytosis and stimulate stronger antitumor immunity in TNBC. These results support further investigation of SIRPα-targeting combination therapies for TNBC.

#3717 Sudocetaxel Zendusortide (TH1902) triggers the cGAS/STING pathway and potentiates anti-PD-L1 immune-mediated tumor cell killing.

M. Demeule[1], J.-C. Currie[1], C. Charfi[1], A. Zgheib[2], I. Cousineau[2], V. Lullier[2], R. Beliveau[2], C. Marsolais[1], B. Annabi[2];
[1]Theratechnologies, Montreal, QC, Canada, [2]Universite du Quebec a Montreal, Montreal, QC, Canada

The potential impact of the immune tumor microenvironment (iTME) was assessed with respect to the anticancer efficacy of sudocetaxel zendusortide (TH1902), a peptide-drug conjugate internalized through a sortilin (SORT1)-mediated endocytic pathway. In the triple-negative breast cancer (TNBC)-derived MDA-MB-231 immunocompromised xenograft tumor model, TH1902 induced complete tumor regression for more than 40 days after the last treatment. Surprisingly, immunohistochemistry analysis revealed higher staining of CD45 leukocytes and of STING, a master regulator in the cancer-immunity cycle, in comparison to docetaxel. Additionally, in a murine B16-F10 melanoma syngeneic tumor model, weekly administration of TH1902 as a single agent also demonstrated superior tumor growth inhibition than did docetaxel. Although B16-F10 is considered a non-immunogenic “cold” tumor model, we observed a net increase in CD45 leukocyte infiltration within TH1902-treated tumors, especially for tumor-infiltrating lymphocytes and tumor-associated macrophages. Moreover, in TH1902-treated tumors, increased staining of perforin, granzyme B, and caspase-3 was suggestive of elevated cytotoxic T and natural killer cell activities. Combined TH1902/anti-PD-L1 treatment led to increased tumor growth inhibition and median animal survival. Accordingly, TH1902 inhibited cell proliferation and triggered apoptosis and senescence in B16-F10 cells *in vitro*, while inducing several downstream effectors of the cGAS/STING pathway and the cell surface expression of MHC-I and PD-L1. This is the first evidence that TH1902 exerts its antitumor activity, in part, through modulation of the iTME and that the combination of TH1902 with checkpoint inhibitors (anti-PD-L1) could lead to improved clinical outcomes.

#3718 Deciphering the role of TREM2+ tumor-associated macrophages as mediators of immunoresistance in micro-satellite stable colorectal metastases.

M. Mirza[1], M. Cottam[1], M. Raoof[2], K. Idrees[1];

[1]Vanderbilt University School of Medicine, Nashville, TN, [2]City of Hope, Irvine, CA

Introduction: Most Colorectal Cancer (CRC)-related deaths are caused by metastatic disease, and more than 95% of CRC metastases (mCRC) are microsatellite stable (MSS) which respond poorly to Immune checkpoint inhibitors (ICI). Tumor-associated macrophages (TAMs) have been recognized as major drivers of immunoresistance in primary CRC; however, their role in mCRC remains poorly understood. We analyzed primary CRC and major metastatic sites (Liver, Peritoneum, Lungs) using single-cell RNA-sequencing (scRNAseq) to elucidate the TAM driven mechanisms of immunoresistance in the mCRC tumor microenvironment (TME) and used a novel TAM directed targeting strategy to improve responses to ICI in a preclinical orthotopic model of MSS-mCRC.

Methods: Using scRNA-seq, we analyzed 22 samples from 14 patients with mCRC. Target antigens identified were validated using flow cytometry and immunofluorescence (IF). The antitumor activity of anti-TREM2 and anti-PD1 mABs was evaluated in-vivo using CT26 CRC cell line in BALB-C mice, assessing tumor immune response via flow cytometry.

Results: We characterized the TME in MSS-mCRC and identified 17 clusters of malignant epithelial, immune, and stromal cells. Our sub-clustering analysis revealed 6 unique sub-populations of TAMs which were differentially distributed across liver, lung, and peritoneal metastases (PM).Two subsets of TAMs, 5 and 6, were enriched in PM and malignant ascites. TAMs 5/6 expressed canonical lipid-associated genes; TREM2, APOE, and PLTP. TREM2+ TAMs were also enriched in immunosuppressive and pro-angiogenic pathways, and expressed genes known to drive EMT and ECM remodeling in the TME. Thus, TREM2 was identified as a potential therapeutic target. We validated our transcriptomic findings using flow cytometry and IF analysis of MSS-mCRC showing an abundance of TREM2+ TAMs in PM. TREM2+ TAMs co-expressed CD163, known marker for M2-TAMs and stained positive for BODIPY. In an aggressive PM mouse model, treatment with anti-PD1, anti-TREM2, or combination anti-PD1/anti-TREM2 was insufficient to reduce tumor burden. However, a trend towards a reduction in total intratumoral F4/80+CD11b+ TAMs was observed in the combination treatment compared to other groups. All three treatments trended towards increased CD8+ intratumoral T-cell infiltration compared to control mice.

Conclusion: Our study provides new insights into the TME of MSS-CRC metastases at a single-cell level. Our findings indicate that TREM2+ TAMs contribute to the immunosuppressive milieu of MSS-CRC metastases. Targeting TREM2 in combination with anti-PD1 resulted in a modulation of TME via reduction of TAMs paralleled by an increased infiltration of CD8+ T cells. This reprogramming of TME suggests that inhibiting TREM2 might augment response to ICI in MSS-CRC metastases, traditionally resistant to ICI.

#3719 Fasting-mimicking diet plus 2-DG drives antitumor immunity by targeting EDEM3-induced PD-L1 glycosylation.

X. Liu, S. Peng, X. Wang, H. Yu, Y. Luo;
Sun Yat-sen University, Guangzhou, China

The PD-1/PD-L1 axis plays an essential role in immune escape and immunotherapy. Importantly, translated N-linked glycosylation of PD-L1 stabilizes protein, enters the cell membrane binding to PD-1, renders T cells anergic and leads to T-cell exhaustion and dysfunction. Targeting PD-L1 glycosylation as an attractive target by a rational combination of cancer immunotherapies. Cancer-associated fibroblasts (CAFs), a predominant cell component of the tumor microenvironment, exert crucial functions in promoting immune escape and immunotherapy resistance by increasing the tumor PD-L1 expression. However, whether and how CAFs upregulate the glycosylation of PD-L1 has never been reported. This study shows that CAFs can upregulate PD-L1 glycosylation and enhance PD-L1 cell surface expression via glycosyltransferase EDEM3, thus cancer immune evasion. Then, the study delves into the relationship between EDEM3 expression, prognosis and immunogenicity. We demonstrate that EDEM3 plays a role in tumor immunity during tumor progression, as evidenced by EDEM3 expression is only significantly correlated with poor prognosis in the $CD8^+$ T cell-enriched population. In subcutaneous tumor models, we observed high cell-surface PD-L1 expression accompanied by decreased $CD8^+$ T cell infiltration and increased M2 macrophage in immunocompetent mice transplanted with EDEM3 over-expressed CRC cells that promote resistance to PD-1/PD-L1 blockade cancer immunotherapy. By performing bioinformatic analysis, we found that the hexosamine biosynthesis pathway (HBP) is highly affected in EDEM3-upregulated CRC cancer. Subsequently, the production of the UDP-GlcNAc (the end product of HBP metabolic flow), a donor substrate for N-linked glycosylation, is significantly increased in EDEM3 over-expressed CRC cells by LC/MS. Meanwhile, glucose is confirmed to be the primary effector of PD-L1 glycosylation in CRC cells, and the glucose restriction attenuates EDEM3-modified PD-L1 glycosylation by reducing UDP-GlcNAc biosynthesis. Finally, we demonstrate that modulation of glucose metabolism through a fasting-mimicking diet (FMD) in combination with 2-deoxy glucose (2-DG) treatment enhances antitumor immunity, especially in tumors with high-EDEM3 expression that exhibit resistance to immunotherapy. We propose potential therapeutic targets for CRC that inhibit PD-L1 glycosylation through FMD+2-DG and could augment the efficacy of immune checkpoint blockers.

#3720 Utility of oncolytic virus as an immunostimulants and potential for combination therapy with ICIs.

D. Kadowaki[1], S. Kuroda[1], M. Hashimoto[1], N. Kanaya[1], Y. Kakiuchi[1], S. Kikuchi[1], K. Noma[1], H. Tazawa[1], S. Kagawa[1], Y. Urata[2], T. Fujiwara[1];
[1]Okayama Univ. Graduate School of Med., Dentistry & Pharm. Sci., Okayama city, Japan, [2]Oncolys BioPharma Inc., Toranomon, Minato-ku, Tokyo, Japan

Background: Anti-PD-1 antibodies have been approved for a variety of carcinomas, but their efficacy in gastrointestinal cancers is limited. CD8-positive T cells (CD8) of tumor-infiltrating lymphocytes (TILs) and resident memory T cells (TRMs) with long-term anti-tumor immune function have been reported to be associated with the therapeutic efficacy of anti-PD-1 antibodies. Among our oncolytic adenoviruses (OVs), OBP-301, in which the human telomerase reverse transcriptase (hTERT) promoter element drives the expression of the viral E1A and E1B genes, is currently undergoing clinical trials. In the present study, we investigated the usefulness of OVs as immunostimulants and their potential efficacy in combination with anti-PD-1 antibodies.
Methods: The cell lines used were the mouse colon cancer cell line CT26 and the mouse pancreatic cancer cell line PAN02. In vitro, the cytotoxic activity of the OVs and extracellular ATP in the culture supernatant were determined. OBP-502, an OBP-301 variant with the gene cassette of the RGD peptide, and anti-PD-1 antibody were used to examine the antitumor effect on subcutaneous tumors. OBP-702, another OBP-301 variant with the gene cassette of the wild-type p53 tumor suppressor gene, was used to examine the effect of long-term anti-tumor immunity. The effects on memory T-precursor cells (MPEC), CD8 and TRM were immunologically assessed in a rechallenge study.
Results: OBP-502 and OBP-702 showed cytotoxic activity against CT26 and PAN02 cells in vitro, and significantly increased ATP in the culture supernatant. In vivo, the anti-PD-1 antibody/OBP-502 combination therapy significantly increased intratumor CD8 in CT26 and PAN02 subcutaneous tumors compared to each monotherapy. Complete response was achieved in 4 out of 12 mice by the combination therapy against CT26 tumors. When CT26 cells was re-seeded into tumor-free mice cured by the combination therapy, 2 out of 4 mice remained tumor-free. In the CT26 and PAN02 subcutaneous tumor model, OBP-702 increased CD44-positive CD62L-negative MPECs that differentiated into TRMs in the spleen, and this effect was blocked by ATP receptor inhibition. In CT26 and PAN02 bilateral subcutaneous tumor models, OBP-702 had a significant antitumor effect on both OBP-702-treated and -non-treated sides, and TIL analysis showed a significant increase in CD8 and TRM. In a rechallenge study, OBP-702-pretreatment showed significant growth inhibition of re-inoculated tumors.
Conclusion: The OVs showed potent and long-term immune activation by inducing CD8 and TRM in tumors as well as direct anti-tumor effects, and synergistic effects with ICI.

#3721 EZH2 inhibition enhances PD-L1 protein stability through USP22-mediated deubiquitination in colorectal cancer.

J. Yang, J. Huang, Q. Yin, L. Xue;
Peking University Third Hospital, Beijing, China

The regulation of PD-L1 is the key question which largely determines the outcome of the immune checkpoint inhibitors (ICIs) based therapy. The epigenetic mechanism is involved in transcriptional regulation towards PD-L1. However, besides the transcription level, the protein stability of PD-L1 is closely correlated to its function and has drawn more and more attention. In this study, EZH2 inhibition could enhance PD-L1 expression and protein stability, and the deubiquitinase ubiquitin-specific peptidase 22 (USP22) is identified as a key mediator in this process. EZH2 inhibition upregulates the expression of USP22 via canonical mechanism, and upregulated USP22 further stabilize PD-L1. Importantly, a combination of EZH2 inhibitors with anti-PD-1 immune checkpoint blockade therapy could improve the tumor microenvironment, promotes immune cell infiltration, enhances sensitivity to immunotherapy and exerts synergistic anti-cancer effects. In addition, knocking down USP22 could potentially enhance the therapeutic efficacy of EZH2 inhibitor on colon cancer. These findings unveil the novel role of EZH2 inhibitors (EZH2i) in tumor immune evasion by upregulating PD-L1. Although it may be one reason of EZH2i inefficacy due to the fact that it elicits the immune suppressive effect, appropriately utilizing this drawback to arouse PD-L1 expression may convert the tumor into more responsive upon ICI cancer therapy. In addition, the EZH2-USP22-PD-L1 regulatory axis could further facilitating to identify populations sensitive to immunotherapy or provide novel strategy for combined treatment. Therefore, these findings provide valuable insights into the intricate interplay between EZH2 and PD-L1, shedding light on the optimization of combining both immune checkpoint blockade and EZH2 inhibitor based epigenetic therapies to achieve more efficacies and accuracy in cancer treatment.

#3722 Immunotherapy efficacy in advanced hepatocellular carcinoma in a diverse and underserved population in the United States.

F. Bteich[1], L. Bioh[1], K. Desai[1], C. Zhang[2], A. Kaur[3], R. A. Levy[1], A. Wang[1], S. Sultana[1], A. Kaubisch[1], M. M. Kinkhabwala[4], S. Bellemare[4], S. A. Fidvi[2], D. Kanmaniraja[2], R. G. Berkenblit[2], J.-Y. Moon[2], A. A. Adedimeji[2], C. Y. Tow[4], Y. M. Saenger[1];

[1]Montefiore Einstein Comprehensive Cancer Center, Bronx, NY, [2]Albert Einstein College of Medicine, Bronx, NY, [3]Jacobi Medical Center, Bronx, NY, [4]Montefiore Medical Center, Bronx, NY

The incidence of hepatocellular cancer (HCC) in the Bronx is 61% higher than the rest of New York State. Underserved populations are not well represented in clinical trials of immune checkpoint inhibitors. The purpose of this study is to analyze the efficacy of immunotherapy treatment in a diverse and underserved patient population in the Bronx. Study demographics include 194 patients treated with ICI at the Montefiore Einstein Comprehensive Cancer Center (MECCC) between 2017 and 2022. A retrospective electronic medical record (EMR) review was conducted of all adult patients and this sample size was identified as having advanced HCC treated with immunotherapy. Outcome parameters such as overall survival and disease control rate assessed by radiologists using the Modified Response Evaluation Criteria in Solid Tumors (mRECIST 1.1) were reported. Survival was evaluated using parameters such as baseline serum alpha-fetaprotein(AFP) level, its evolution at the 3-month re-evaluation mark, the Child-Pugh(CP) class and MELD-Na score at the time of diagnosis. Categorical variables were analyzed by Chi-squared test and survival was analyzed using Kaplan-Meier (KM) curves. MECCC patients were 40.7% Hispanic and 20.6% Black, compared with 3% and 2% respectively in the landmark IMbrave 150 study. Median overall survival (mOS) on ICI was 9.0 months, 25.0 months for the 100 (51.5%) favorable-prognosis Child Pugh A (CPA) patients included in HCC clinical trials. Disease control rate (DCR) was 58.5% among 123 evaluable patients per mRECIST 1.1. Baseline liver function, as defined by CP and Model for End Stage Liver Disease-Sodium (MELD-Na), correlated with survival ($p<0.001$). Hepatitis C Virus (HCV) and alcoholism were over-represented relative to National Cancer Institute (NCI) data (56.2% vs 4.7% and 38.7% vs 8.2%, respectively). HCV treatment correlated with prolonged survival in infected patients ($p=0.0017$). AFP decline correlated with response ($p=0.001$). Hispanic patients lived longer when clinical variables were controlled for (mOS 52 vs 23 months; $p=0.011$). In summary, our patient population differed significantly in racial composition and etiology of liver disease from clinical trial populations on which ICI was tested. In an underserved HCC population, ICI yielded a DCR of 58.5% and low rates of severe toxicity. This work highlights ICI efficacy in minority groups, a need for earlier HCC diagnosis and for studies of genetics and environmental factors in Hispanics with HCC.

#3724 Targeting the LIFR-LCN2 pathway to sensitize liver cancer to immunotherapy.

Y. Deng, L. Ma;
UT MD Anderson Cancer Center, Houston, TX

Liver cancer, primarily hepatocellular carcinoma (HCC), is highly lethal with limited treatment options and no biomarker to predict therapy response. The current frontline therapies for liver cancer, including sorafenib and the combination of atezolizumab (anti-PD-L1) and bevacizumab (anti-VEGF), have limited therapeutic benefits, which could be attributed, at least in part, to the highly immunosuppressive tumor microenvironment in liver cancer. Leukemia inhibitory factor receptor (LIFR) is frequently downregulated in HCC. My recent studies revealed that in oncogene-induced liver tumors, overexpression of LIFR increased, while knockout of Lifr decreased $CD8^+$ T cell infiltration, which may be mediated by LCN2-dependent inhibition of T cell viability, proliferation, and effector function. In ongoing and future work, I will investigate whether LIFR or therapeutic LCN2 neutralization can sensitize HCC to immunotherapy. If successful, this project will illuminate how to improve liver cancer immunotherapy by targeting the LIFR-LCN2 pathway. Low LIFR expression and high LCN2 expression may be used to select HCC patients who will likely benefit from the combination therapy with the LCN2-neutralizing antibody plus immune checkpoint inhibitors.

#3725 Exosomal Galactin-3 promotes pre-metastatic niche formation that accelerates peritoneal metastases of gastric adenocarcinoma.

Y. Fan, S. Song, M. Pool Pizzi, K. Yoshimura, J. Vykoukal, S. Hanash, J. Ajani;
UT MD Anderson Cancer Center, Houston, TX

Peritoneal carcinomatosis (PC) in gastric adenocarcinoma (GAC) lead to a short median survival (≤6 months). Pre-metastatic niche (PMN) formation, in a distant organ to prepare for tumor seeding and colonization, has long been recognized. However, the precise molecular and mechanistic contributions of exosomes in PMN formation of PC remain unclear. We identify that exosomes promote PMN formation in the peritoneal cavity by patient-derived orthotopic mouse model. Using an in-depth proteomic profiling of paired ascites cells and ascites-derived exosomes from PC patients, we discover that Galectin-3 as the exosomal payload is responsible for PC by promoting PMN formation in both patient-derived orthotopic model and syngeneic mouse model. Inhibition of exosomal Galectin-3 reverses PC. Furthermore, exosomal Galectin-3 activates cancer-associated fibroblasts (CAFs), which further activate the CXCL12/CXCR4 axis to orchestrate the immunosuppressive PMN. Simultaneous inhibition of exosomal Galectin-3, CXCR4, and PD-1 leads to tumor regression and durable anti-tumor responses. Thus, this study provides a rationale for the novel clinical strategy for GAC patients with PC.

#3726 Absence of synergistic effects for PARPi and immunotherapy combinations in ex vivo 3D micro tumor assay for ovarian cancer patients.

L. J. Ceton[1], E. Koedoot[1], T. J. P. Sijsenaar[1], D. J. van der Meer[1], M. Montero Garcia[1], J. van der Valk[1], K. Maad[2], C. de Kroon[3], A. van Altena[4], **W. Vader**[1], J. Kroep[3], N. Ottevanger[4];

[1]VitroScan B.V., Leiden, Netherlands, [2]Oncodia, Uppsala, Sweden, [3]LUMC, Leiden, Netherlands, [4]Radboud University Medical Center, Nijmegen, Netherlands

Introduction: 50% of ovarian cancers are homologous recombination deficient (HRD), with 15% of the patients carrying a BRCA mutation. PARP inhibitors (PARPi) are designed to improve survival in HRD patients, but clinical responses to PARPi often do not match HRD status. In this study, a 3D ex vivo tumor testing platform was applied to quantify patient-specific drug responses to (combinations of) PARPi, chemo- and immunotherapies.

Material and Methods: 81 patients with ovarian cancer eligible for chemotherapy were included in the trial between 2019 and 2022 in the Netherlands (IRB P18.032). Tumor clusters were isolated from ascites and solid tissue, seeded and exposed to three PARPi, standard-of-care chemotherapies and immunotherapies, both single agent and in combination. Ex vivo drug sensitivity was quantified using high-throughput 3D imaging and extraction of morphological features. Bliss scores were calculated for synergy analysis.

Results: Results were generated in two weeks after sample collection. Ex vivo patient-specific response profiles were observed for all drug classes, with a small percentage of patients (7%) showing strong PARPi sensitivity reflected by strong tumor cluster shrinkage upon treatment. Significant correlation of drug sensitivity profiles was observed comparing the different PARPi between themselves, but also comparing PARPi and platinum responses. Interestingly, ex vivo sensitivity to olaparib and immunotherapy combinations demonstrated additive, but no synergistic effects (21 patients, 79 tests). In addition, olaparib responses were shown to be independent of immune responses (SEA).

Conclusion: This study applied a predictive ex vivo 3D micro tumor testing platform to classify patient-specific sensitivity to (a combination of) PARPi, chemo- and immunotherapies in over 80 patients. The current dataset demonstrates the potential of ex vivo testing to identify patients that are responsive to PARPi. No synergistic effects were observed for these drugs in combination with immunotherapies.

Discussion: Evaluation of PARPi responses in a functional 3D micro tumor assay could support identification of responsive patients prior to treatment. Distinct responses were observed for PARPi and immunotherapies. No synergistic but additive effects were measured, suggesting that ovarian cancer patients could benefit from PARPi and immunotherapies. Correlation of clinical and ex vivo drug responses to PARPi in combination with available HRD tests will further validate the platform for predicting patient clinical outcome.

#3727 Synergistic effect of CD47 blockade and EPHA3 treatment on recurrent head and neck cancers.

S. Kim[1], M. Han[1], J. Kim[2], S. Kim[3];
[1]University of Ulsan College of Medicine, Ulsan, Korea, Republic of, [2]Inha University College of Medicine, Incheon, Korea, Republic of, [3]University of Ulsan College of Medicine, Seoul, Korea, Republic of

CD47 acts as a “don’t eat me “signal and suppresses it through its interaction with signal regulatory protein (SIRP-a) on the macrophage. CD47 is expressed in many human cancer cells, including head and neck cancer. Additionally, we reported in a previous study that EphA3 is overexpressed in radioresistant head and neck cancer and may play an important role in the development of radioresistance in head and neck cancer. In our present study, we demonstrated that the blockade of EPHA3 and CD47 attenuates the function of M2-like macrophages and may contribute to macrophage polarization toward the M1 phenotype. Here, we combined a therapeutic strategy of an anti-EPHA3 and an anti-CD47 antibody. Using mRNA sequencing and fluorescence imaging, we showed that the combination treatment could significantly enhance the effectiveness of anti-EPHA3 and anti-CD47 antibodies, in reactivating macrophages and reversing macrophage polarization. In addition to using flow cytometry in vivo, combination treatments can alter the proportion of tumor-associated macrophages (TAMs). Collectively, our findings suggested that the combination treatment of anti-EphA3 and the anti-CD47 antibodies could significantly improve tumor suppression, increase the proportion of M1 macrophages, and decrease the proportion of M2 macrophages.

#3728 Treating pancreatic cancer with "armed" oncolytic adenoviruses and adoptive T-cell therapy.

B. L. Roach, M. Yamamoto;
University of Minnesota, Minneapolis, MN

Introduction: Pancreatic ductal adenocarcinoma (PDAC) is the third leading cause of cancer-related mortalities and is projected to become second by 2030. Although major advancements in cancer treatments have improved outcomes for many cancers, the survival rate for PDAC has not improved in nearly four decades. Two primary features make PDAC refractory. First, the highly immunosuppressive tumor microenvironment (TME) plays a crucial role in impeding the innate and effector arms of the immune system to prevent anti-tumor responses. Second, desmoplasia causes formation of fibrotic tissue within and around tumor tissue, which creates a physical barrier for infiltration of anti-tumor immune cells and therapeutics. The goal of this project is to develop viro-immunotherapies against PDAC that target the immunosuppressive TME and desmoplasia by utilizing “armed” oncolytic adenoviruses (OAds) and adoptive T-cell therapy (CAR T-cells). Three transgenes were selected to “arm” the OAd constructs: i.) TGF-beta blocker, ii.) interleukin-7 (IL-7), and iii.) interferon gamma (IFN-gamma).

Methods: “Armed” replication-deficient adenovirus (Ad) constructs were first generated to isolate transgene function from oncolytic activity. Each transgene was individually cloned into the E1 region of Ad-5 (WT). Viral particles were amplified in 293 cells and purified via ultracentrifugation using a CsCl gradient. Anti-tumor effects were measured using a syngeneic mouse model. C57BL/6 mice were subcutaneously injected with KPC cells (mouse PDAC cell line), and tumors were treated with Ad constructs via intratumoral injection. Tumors were harvested at various time points and stained for immune cell infiltration and fibrosis. Mesothelin-directed CAR T-cells (meso-CARTs) were injected (tail vein) into NSG mice bearing subcutaneous Panc1 tumors after intratumoral injection of Ad constructs.

Results: Tumor growth was significantly inhibited in syngeneic mouse models in the presence of each “armed” Ad construct. Furthermore, significant tumor infiltration of anti-tumor immune cells was induced upon treatment as well as a decrease in fibrosis. Abscopal effects were observed on contralateral tumors after injection of ipsilateral tumors as well as an increase in tumor infiltration of anti-tumor immune cells. Finally, combining meso-CARTs with IFN-gamma-expressing Ad induced the greatest anti-tumor responses.

Conclusions: PDAC is very resistant to conventional therapeutics, so utilizing combination strategies seems essential. The findings in this study have broad implications in the field of pancreatic cancer by shedding light on how the TME can be manipulated to enhance anti-tumor effects to aid in the development of more efficient therapeutics against PDAC. Moreover, therapeutics inducing abscopal effects should be highly valued because most PDAC patients die from metastasis.

#3729 Association between clinical characteristics and treatment outcome of immune checkpoint inhibitor with or without chemotherapy in elderly non-small cell lung cancer patients with high PD-L1 expression.

H. Kawachi[1], S. Takei[1], T. Yamada[1], M. Tamiya[2], Y. Negi[3], Y. Goto[4], A. Nakao[5], S. Shiotsu[6], T. Takeda[7], A. Okada[8], T. Harada[9], K. Date[10], Y. Chihara[11], I. Hasegawa[12], N. Tamiya[13], T. Kijima[3], K. Takayama[1];

[1]Kyoto Prefectural University of Medicine, Kyoto, Japan, [2]Osaka International Cancer Institute, Osaka, Japan, [3]Hyogo Medical University, Nishinomiya, Japan, [4]Fujita Health University School of Medicine, Toyoake, Japan, [5]Fukuoka University Hospital, Nanakuma, Japan, [6]Japanese Red Cross Kyoto Daiichi Hospital, Kyoto, Japan, [7]Japanese Red Cross Kyoto Daini Hospital, Kyoto, Japan, [8]Saiseikai Suita Hospital, Suita, Japan, [9]Fukuchiyama City Hospital, Fukuchiyama, Japan, [10]Kyoto Chubu Medical Center, Nantan, Japan, [11]Uji-Tokushukai Medical Center, Uji, Japan, [12]Saiseikai Shigaken Hospital, Rittou, Japan, [13]Rakuwakai Otowa Hospital, Kyoto, Japan

Background and Aim: The proportion of elderly patients diagnosed with advanced stage lung cancer has been increasing owing to the aging of the population. Thus, formulating a treatment strategy for elderly non-small cell lung cancer (NSCLC) patients is essential. For NSCLC with programmed cell death ligand-1 (PD-L1) tumor proportion score (TPS) ≧ 50%, both immune checkpoint inhibitor monotherapy (ICI mono) and combination therapy of ICI and chemotherapy (ICI/Chemo) have been established as standard treatment options. However, evidence based on the clinical trials specifically for elderly patients is limited, and it is not clear whether ICI mono or ICI/Chemo should be used in elderly NSCLC patients with PD-L1 TPS ≧ 50%. This study aimed to clarify which clinical population will benefit from ICI/Chemo in elderly NSCLC patients with PD-L1 TPS ≧ 50%.

Method: We retrospectively analyzed 199 NSCLC patients aged ≧ 70 years of Eastern Cooperative Oncology Group performance status (ECOG PS) 0-1 with PD-L1 TPS ≧ 50% who were treated with ICI mono or ICI/Chemo. We analyzed the association between treatment outcome and baseline patient characteristics in each group. Comparing the treatment outcome, propensity score matching was used to reduce bias.

Results: Of the 199 patients, 131 received ICI mono, and 68 received ICI/Chemo. The median overall survival (OS; 25.0 vs. 42.2 months, P = 0.116) and median progression-free survival (PFS; 10.9 vs. 11.8 months, P = 0.231) did not significantly differ between the ICI mono and ICI/Chemo groups. Multivariate analysis revealed the factors independently associated with OS: smoking history in the ICI mono group (smoking history/non-smoking history, hazard ratio [HR] 0.36, 95% confidence interval [CI] 0.16-0.78, P = 0.048), and ECOG PS (ECOG PS 1/PS 0, HR 3.84, 95% CI 1.44-10.20, P = 0.007) and histology type in the ICI/Chemo group (Non-squamous cell carcinoma/squamous cell carcinoma, HR 0.17, 95% CI 0.06-0.44, P < 0.001). For patients with ECOG PS 0 (OS: 26.1 months vs. not reached, P = 0.0031, PFS: 6.5 vs. 21.7 months, P = 0.0436) or non-squamous cell carcinoma (OS: 23.8 months vs. not reached, P = 0.0038, PFS: 10.9 vs. 17.3 months, P = 0.0383) in the ICI/Chemo group, PFS and OS were significantly longer than in the ICI mono group.

Discussion and Conclusion: In elderly NSCLC patients with high PD-L1 expression, this study suggested that ECOG PS and histological type may be predictive clinical factor when choosing ICI mono or ICI/Chemo treatment.

#3730 Impact of proton pump inhibitor on ICI with or without chemotherapy for NSCLC with high PD-L1 TPS.

R. Sawada[1], H. Kawachi[1], T. Yamada[1], M. Tamiya[2], Y. Negi[3], Y. Goto[4], A. Nakao[5], S. Shiotsu[6], T. Takeda[7], A. Okada[8], T. Harada[9], K. Date[10], Y. Chihara[11], I. Hasegawa[12], T. Kijima[3], K. Takayama[1];

[1]Kyoto Prefectural University of Medicine, Kyoto, Japan, [2]Osaka International Cancer Institute, Osaka, Japan, [3]School of Medicine, Hyogo Medical University, Nishinomiya, Hyogo, Japan, [4]Fujita Health University School of Medicine, Toyoake, Aichi, Japan, [5]Fukuoka University Hospital, Nanakuma, Fukuoka, Japan, [6]Japanese Red Cross Kyoto Daiichi Hospital, Kyoto, Japan, [7]Japanese Red Cross Kyoto Daini Hospital, Kyoto, Japan, [8]Saiseikai Suita Hospital, Suita, Osaka, Japan, [9]Fukuchiyama City Hospital, Fukuchiyama, Kyoto, Japan, [10]Kyoto Chubu Medical Center, Nantan, Kyoto, Japan, [11]Uji-Tokushukai Medical Center, Uji, Kyoto, Japan, [12]Saiseikai Shigaken Hospital, Rittou, Shiga, Japan

Background and Aim: Immune checkpoint inhibitors (ICIs) have been widely used for the initial treatment of non-small cell lung cancer (NSCLC). Although both ICI monotherapy and the combination of ICI plus chemotherapy (chemo-ICI) are promising therapeutic options for patients with a programmed cell death ligand-1 tumor proportion score of 50% or higher (high PD-L1), the patient's clinical background and biomarkers differentiating the two options are still not well-defined. In our prior research, we found that a history of proton pump inhibitor (PPI) use independently have negative impact with significantly shorter overall survival (OS) and progression-free survival (PFS) in NSCLC patients harboring high PD-L1 with pembrolizumab monotherapy, but not with chemo-ICI. However, this OS data remain immature. Therefore, in our current study, we extended the follow-up period and conduct additional analysis including OS data to confirm this trend.
Method: Advanced NSCLC patients with high PD-L1 who had received pembrolizumab or chemo-ICI as the first-line treatment between March 2017 and December 2020 at 13 hospitals in Japan were analyzed. Survival outcomes were estimated using the Kaplan- Meier method and were compared using the log-rank test.
Results: A total of 425 patients with NSCLC were included in the study, with 271 patients (median [range] age, 72 [43-90] years; 215 [79%] men) receiving pembrolizumab monotherapy as their first-line treatment and 154 patients (median [range] age, 69 [36-86] years; 121 [79%] men) receiving chemo-ICI as their first-line treatment. The median follow-up duration was 22.8 months. Among patients with a history of PPI use, both median PFS (19.3 months vs. 6.8 months; HR, 0.53; 95% CI, 0.35-0.78; P = .003) and the median OS(not reached vs. 20.4 months; HR, 0.53; 95% CI, 0.34-0.85; P = .04) were significantly longer in the chemo-ICI group compared to the pembrolizumab monotherapy group. For patients without a history of PPI use, both median PFS (11.4 months vs. 10.8 months; HR, 0.99; 95% CI, 0.76-1.3; P = .36) and the median overall survival (42.2 months vs. 29.9 months, HR, 0.84; 95% CI, 0.62-1.16; P = .33) showed no significant differences between the groups.
Discussion and Conclusion: This retrospective study showed that a concomitant treatment with PPI is poor prognostic factor in patients harboring high PD-L1 and treated with ICI monotherapy compared with chemo-ICI in Japanese cohort and this tendency is durable in long-term follow-up. These results indicate that when deciding on an ICI treatment, with or without chemotherapy, it is essential to take into account a concomitant treatment with PPI.

#3731 Spliceosome: A gatekeeper for necroptosis.

X. Jiang, X. Ma, S. Balachandran, I. Canadas;
Fox Chase Cancer Center, Philadelphia, PA

Small cell lung cancer (SCLC) is the most aggressive type of lung cancer with a 5-year overall survival of approximately 5%. SCLC has high prevalence of somatic mutations, yet express low to zero neoantigen. Despite promising advances in immunotherapy, highly metastatic SCLC remains a devastating disease and only a small fraction of SCLC patients respond to immunotherapy. These poor survival and lack of therapy options stresses the unmet need to identify novel and effective targeted therapies for metastatic SCLC. Here, we demonstrate that targeting the splicing core component, SF3B1, in SCLC, is a molecular trigger for tumor killing and viral mimicry.SF3B1 inhibition through the small molecule Pladienolide B (PlaB) induces the accumulation of immunogenic double-stranded RNAs (dsRNAs), including right-handed dsRNA conformation (A-RNA), provoking a tumor-intrinsic innate immune response and tumor cell death in SCLC preclinical models. Strikingly, we discovered that PlaB treatment also induces the formation of Z-form nucleic acids (Z-NAs), which are unique, left-handed nucleic acids and necroptosis-activating ligands for the host sensor ZBP1.These endogenous A-RNAs and Z-NAs initiate tumor-intrinsic antiviral interferon (IFN) signaling in SCLC cells leading to tumor-intrinsic immunogenicity and apoptosis. Notably, we also found that Z-NAs derived from spliceosome inhibition trigger the activation of ZBP1, inducing RIPK3-mediated MLKL activation and eventual necroptosis, a highly immunogenic cell-death pathway, in ‘necroptosis competent’ cells, including mouse embryonic fibroblasts (MEFs). This opens unexplored strategies for spliceosome inhibitors to activate anti-tumor immune pathways not only in tumor cells themselves, but also in cells of the Tumor Microenvironment (TME), which too can break tolerance and enhance anti-tumor T cell responses which is crucial to enhance cancer immunotherapy responses. These findings demonstrate a unique and novel spliceosome-targeted mechanism to remodel the immunosuppressive TME of SCLCs. Also, our study suggests that SF3B1 inhibitors and potentially other spliceosome inhibitors might be used not only to selectively kill tumor cells, but also as compounds to generate Z-NAs in tumor cells and cells of the TME and trigger on-demand necroptosis without need for an active virus infection.

#3732 Peripheral pharmacodynamic activity of epcoritamab as monotherapy and in combination with rituximab + lenalidomide in patients with follicular lymphoma.

H. Si[1], J. Zhang[1], M. Wielgos-Bonvallet[1], L. Falchi[2], K. Linton[3], W. Jurczak[4], D. Belada[5], I. Altıntaş[6], M. Sacchi[1], E. Favaro[7], A. Rana[1], D. Hoehn[1], D. Soong[1], C. W. Chiu[1], M. Jure-Kunkel[1];

[1]Genmab, Plainsboro, NJ, [2]Memorial Sloan Kettering Cancer Center, New York, NY, [3]The Christie NHS Foundation Trust and Manchester Cancer Research Centre, Manchester, United Kingdom, [4]MSC National Research Institute of Oncology, Krakow, Poland, [5]University Hospital and Faculty of Medicine, Hradec Kralove, Czech Republic, [6]Genmab, Utrecht, Netherlands, [7]Genmab, Copenhagen, Denmark

Introduction: Epcoritamab (DuoBody®-CD3xCD20) is a subcutaneous IgG1 bispecific antibody that simultaneously binds to CD3 on T cells and CD20 on malignant B cells, inducing activation and cytotoxic activity of T cells to mediate killing of target lymphoma cells. Epcoritamab is approved in the US for the treatment of adults with relapsed/refractory (R/R) diffuse and high-grade large B-cell lymphoma after ≥2 lines of systemic therapy (also approved in Europe, the UK, Japan, and Canada). Here we present the pharmacodynamic effects of epcoritamab as monotherapy (EPCORE NHL-1: NCT03625037) or in combination with rituximab + lenalidomide (R^2) (EPCORE NHL-2: NCT04663347) in peripheral blood of patients with follicular lymphoma (FL), a heterogeneous disease for which many patients have an unmet medical need for efficacious, well-tolerated, off-the-shelf therapies.

Methods: In EPCORE NHL-1 expansion phase, adults with R/R FL received epcoritamab monotherapy; in EPCORE NHL-2, adults with R/R (arm 2) or newly diagnosed (ND) (arm 6) FL received epcoritamab combined with R^2. B-cell markers and T-cell proliferation and activation markers in whole blood were assessed using validated flow cytometry assays. Cytokines in plasma were measured using a validated multiplex immunoassay.

Results: Epcoritamab as monotherapy and in combination with R^2 induced rapid depletion of circulating peripheral B cells ($CD19^{\pm}$) in patients with detectable peripheral B cells at baseline. Additionally, within the first 2 cycles, epcoritamab monotherapy induced a transient elevation of peripheral $CD8^{\pm}$ and $CD4^{\pm}$ T cells expressing proliferation ($Ki67^{\pm}$%) and activation ($HLA\text{-}DR^{\pm}$% and $PD\text{-}1^{\pm}$%) markers. R/R and ND patient groups treated with epcoritamab + R^2 showed a trend for greater induction of proliferating and activated peripheral T cells. Likewise, elevation in T-cell absolute counts was observed from cycle 2 onward, with a trend of higher levels with epcoritamab + R^2 vs epcoritamab monotherapy. In addition, a moderate but transient elevation of circulating cytokines including IFNγ, IL-6, and IL-10 during cycle 1 was observed with epcoritamab monotherapy and epcoritamab + R^2. Importantly, IL-6 and IL-10 returned to approximate baseline levels prior to the subsequent dose. Compared with epcoritamab monotherapy, patients treated with epcoritamab + R^2 showed a trend for lower median levels of IL-6 peaks 24 hours after the first full dose.

Conclusion: The pharmacodynamic activity of epcoritamab combined with R^2 in R/R and ND FL was consistent with epcoritamab's mechanism of action as monotherapy. Epcoritamab + R^2 showed a favorable pharmacodynamic profile with a trend toward increased T-cell activation and T-cell elevation, and lower IL-6 levels. These data support the ongoing phase 3 trial of epcoritamab + R^2 compared with R^2 alone in patients with R/R FL (EPCORE FL-1: NCT05409066).

#3733 Gut microbiota-dependent bile acidtaurodeoxycholic acid, TDCAfacilitates anti-tumor immune responses by modulating cytotoxic CD8 T cell immunity.

W. Li, H. Wang, L. Coughlin, N. Poulides, P. Valle, J. Lichterman, X. Zhan, C. Liao, S. Palmer, X. Li, A. Koh;
UT Southwestern Medical Center, Dallas, TX

Gut microbiota are critical for effective immune checkpoint blockade therapy (ICT) for cancer. However, the underlying mechanisms by which gut microbiota and/or microbiota-derived metabolites augment antitumor response are largely unknown. Here, we utilized a preclinical melanoma (B16-F10) model and treated groups of mice (Jackson, C57BL/6J, female, 6-8 wks, n=14-26 per group) with seven distinct antibiotic treatments to induce unique gut microbiomes and metabolomes. Mice were then treated with ICT (anti-PD-1 and anti-CTLA-4), resulting in markedly heterogeneous tumor phenotypes (tumor volume and weight) as dictated by the specific antibiotic treatment. Using machine learning (e.g. random forest classifier), we identified metabolite candidates most strongly associated with ICT response (i.e. tumor volume and weight).One metabolite candidate, the bile acid taurodeoxycholic acid, TDCA, had previously been identified by my group as associated with anti-PD-1/anti-CTLA-4 response in human melanoma patients (PMID 28923537). Administration of TDCA alone is sufficient to overcome antibiotic-induced ICT hyporesponsiveness in mice. Utilizing both *in vitro*/*ex vivo* immune cell assays and *in vivo* preclinical models, we have validated that TDCA treatment directly boosted the antitumor cytotoxic CD8+ T cell responses (i.e. IFN-gamma production, anti-tumor cytotoxicity, tumor growth, etc.) without affecting innate immune responses. Bulk RNAseq of CD8 T cell analysis indicated that TDCA modulate CD8 T cell function through IFN pathway. Together, our findings suggest that the gut microbial metabolite TDCA could promote immunotherapy efficacy through regulation of CD8+ T cell immunity and has the potential to be utilized as a novel therapeutic agent to enhance ICT efficacy.

#3734 Tumoral and systemic immune modulation with neoadjuvant (NeoAd) intratumoral (IT) TAVO-EP (plasmid IL-12 electro gene transfer) and nivolumab (NIVO) in patients (pts) with operable locoregionally advanced melanoma.

A. A. Tarhini[1], Z. Eroglu[1], J. S. Zager[1], R. J. Gonzalez[1], A. A. Sarnaik[1], C. Cruse[1], D. B. De Aquino[1], E. Abraham[1], D. M. Acevedo[1], A. Richards[1], M. J. Schell[1], D. Kalos[1], P.-L. Chen[1], J. L. Messina[1], D. A. Canton[2], V. K. Sondak[1];

[1]H. Lee Moffitt Cancer Center, Tampa, FL, [2]OncoSec, San Diego, CA

Introduction: IT TAVO-EP (tavokinogene telseplasmid delivered by electroporation) results in localized expression of IL12 in the tumor microenvironment (TME). This study (NCT04526730) evaluated NeoAd TAVO-EP and NIVO. All patients provided a written informed consent (Advarra IRB Pro00041794). Biomarkers of tumoral and systemic immune responses were conducted and correlated with clinical outcomes.

Methods: NeoAd phase comprised up to 3 x4-week cycles of IT TAVO-EP and iv NIVO followed by surgery. Endpoints included pathologic complete response (pCR), near pCR, major response (pMR; pCR + near pCR) and nonresponse (pNR). Biospecimens were collected at screening, C1D8, C2D1 (~30 days from treatment start), pre-surgery (~90 days). Slides cut from FFPE tissue were analyzed by chromogenic immunohistochemistry (IHC) for $CD8^{\pm}$ tumor infiltrating lymphocytes (TIL) and PD-L1 (22C3 CDx assay). RNA extracted from FFPE tissue was subjected to NanoString's IO360 transcriptomic analysis, including Tumor Inflammation Signature (TIS). PBMCs were stained and analyzed via flow cytometry on an LSR Fortessa X-20. Serum samples were analyzed for cytokine levels using Luminex® MAGPIX® platform (15-plex).

Results: 16 pts were treated; 1 with PR declined surgery, 1 with early distant PD did not have surgery, 14 had surgery: 2 pNR, 3 near pCR, 9 pCR; pMR rate 12/15 (80%). In tumor, at baseline, 9/11 pts tested had <20% $CD8^{\pm}$ TIL, 7/11 <10% PD-L1 tumor proportion score (TPS) and 6/10 TIS of ≤0, predicting non-response to anti-PD-1. In 5 pts with evaluable matched tissue at baseline and C2D1: 5/5 had increased peritumoral CD8+ T cells, 4/5 increased CD8+ TIL, 2/5 increased PD-L1, 4/5 increased TIS at C2D1 compared to baseline. Tumoral transcriptome profile revealed significant upregulation of genes involved in innate and adaptive immune responses (IFN-gamma, APM, granzymes, CD8, PD-L1, JAK1, chemokines, others) at C2D1. In blood, proliferating Ki-$67^{\pm}$/$PD\text{-}1^{\pm}$/$CD8^{\pm}$ T cells expanded at C2D1 while total $PD1^{\pm}$/$CD8^{\pm}$ cells decreased. Decrease of $PD1^{\pm}CD8^{\pm}$ cells and other subtypes in blood at C2D1 coincided with TME infiltration by $CD8^{\pm}$ cells. Serum effector cytokines including IL12, IFN-gamma and IL2, showed no biologically meaningful changes following treatment or differences between responders and non-responders.

Conclusions: At baseline, most patients exhibited low CD8+ TIL, PD-L1 and TIS, with enhanced immune activation following treatment in the TME and blood including increased immune-related gene expression, CD8+ TIL, peritumoral CD8+ T cells and TIS. Four of 5 pts with negative predictive baseline biomarkers $[CD8^{\pm}TIL/PD\text{-}L1/TIS]^{low}$ experienced pCRs supporting activity of IL12/anti-PD1 based regimens in this setting.

#3735 Combinatorial targeting of tumor-microenvironment together with antigen vaccination using innovative nano-immuno-gel for enhanced cancer-immunotherapy.

A. K. Sunilkumar[1], M. Salvi[2], S. N. Mohammed[1], Z. T. Zakkariya[1], A. G. Cadena[2], S. Chappan[1], S. P. Radhakrishnan[1], M. Manohar[1], P. Keechilat[3], S. Nair[1], P. Romero[2], C. Jandus[2], **M. Koyakutty**[1];

[1]Amrita Vishwavidyapeetham University, Kochi, India, [2]Ludwig Institute for Cancer Research, Lausanne, Switzerland, [3]Amrita Institute of Medical Sciences (AIMS), Kochi, India

Successful cancer-immunotherapy need to address three critical factors: a) Relieving the immuno-suppressive tumor microenvironment (TME) b) expanding antigen specific, functionally avid effector T cells, c) triggering systemic immunity with a balanced innate-adaptive response for continued effector cell-feeder supply-chain and memory generation. Combinatorial engagement of such multi-elemental components demands smart, engineered immunotherapy systems compared to conventional vaccines. Here, we report an injectable Nano-Immuno-Gel (NIG) that can neutralize immunosuppressive components (e.g., myeloid derived suppressor cells (MDSCs), M2 macrophages (Mϕ) in TME, together with generating strong effector T cells by nano-vaccination, and sustained release of cytokines to enhance systemic immunity against tumor. In a proof-of-concept study, we show that sustained-release of myeloid-suppressive drug from NIG depot efficiently inhibited MDSCs and M2 Mϕ, not only in TME, but also in the circulation and in peripheral systems, thus creating a conducive, hot TME infiltrated with CD8 effector cells. Follow-up antigen vaccination with novel nano-adjuvant enhanced DC-T cell engagement and sustained IL15 release from NIG provided systemic NK/T cell activation, rendering significant control of the tumor growth. Our data demonstrate the potential of rationally engineered multi-functional nano-immuno-gels (NIG) to combine sequential neutralization of the suppressive TME, antigen vaccination, and concurrent systemic immune activation for highly effective combinatorial cancer immunotherapy.

#3736 Bridging the gaps: A cross-species approach to PD-1 and OX40 combination immunotherapy.

M. Sandey[1], D. Ruiz[1], J. Marable[1], D. Bedi[2], P. Agarwal[1];
[1]Auburn University, Auburn, AL, [2]Tuskegee University, Tuskegee, AL

Monoclonal antibodies (mAbs) targeting immune checkpoints, such as PD-1, PD-L1, and CTLA4, have provided unprecedented clinical benefits to human cancer patients. Novel strategies such as combination therapy with OX40 or 4-1BB agonists are currently under investigation in various pre-clinical studies to enhance the therapeutic benefits of immune checkpoint inhibitors. While syngeneic mouse tumor xenograft models offer valuable insights in pre-clinical testing, they fall short in capturing the nuanced heterogeneity within and between tumors and the dynamic tumor-immune interface. In contrast, canine patients with spontaneous neoplasms possess a closely analogous and intact immune system. These canine patients, who receive sophisticated and advanced medical therapy like their human counterparts, can serve as a vital intermediate pre-clinical model system between rodent studies and human clinical trials, potentially reducing clinical trial failures. In this study, we have developed a novel bispecific fusion protein, denoted BsOXPD, that combines OX40 agonism and PD-1 blockade into a single therapeutic. Our bispecific fusion protein employs an anti-PD-1 nanobody (Nb) to bind and block the PD1 pathway and the extracellular domain (ECD) of the OX40 ligand to stimulate the OX40 receptor. We have developed murinized, caninized, and humanized versions of this protein. All versions of the bispecific fusion protein retain their biochemical and functional properties following the murinization, caninization, and humanization processes. Importantly, all versions effectively disrupt the PD-1/PD-L1 axis in murine, canine, and human systems while concurrently acting as potent OX40 agonists. To further improve the humanized version of the BsOXPD, we partially humanized the anti-PD1 Nb by introducing amino acid substitutions in various framework regions. The humanized anti-PD1 Nb still completely inhibited the binding of human PD-L1 to the PD-1 receptor. The caninized version of BsOXPD exhibits no toxicities or immune-related adverse events (irAEs) following intravenous injection at doses of 1 mg/kg or 3 mg/kg body weight in healthy beagle dogs. In summary, we have designed a cross-species Nb-based fusion protein for PD1 blockade and OX40 agonism. Our next goal is to evaluate the therapeutic efficacy of caninized BsOXPD in pet dogs with oral melanoma in neoadjuvant settings. Therefore, our cross-species approach will offer comprehensive insights into the safety, pharmacokinetic (PK) profile, and clinical benefits associated with the concurrent application of PD1 blockade and OX40 agonism.

#3737 Molecular and early clinical characterization of the anti-CD73 antibody S095024 (Sym024).

A. Spreafico[1], J. R. Ahnert[2], D. Sommerhalder[3], M. Almena-Carrasco[4], N. Harouki Crochemore[4], **X. Ianopulos**[5], J. S. Jakobsen[6], E. Armbruster[7], A. Delmas[4], A. des Georges[7], C. Frohlich[6], J. Geronimi[4], M. M. Grandal[6], R. W. Hansen[6], J. Lantto[6], J. Legrand[4], F. Levasseur[4], M. Riva[6], C. Rodrigues[4], V. Seif[4], V. Askoxylakis[5], N. Lakhani[8];

[1]Princess Margaret Canada, Toronto, ON, Canada, [2]MD Anderson Cancer Center, Houston, TX, [3]Texas Oncology-San Antonio Babcock Next Oncology, San Antonio, TX, [4]Servier, Gif-sur-Yvette, France, [5]Servier, Boston, MA, [6]Servier, Ballerup, Denmark, [7]The City University of New York (CUNY), New York, NY, [8]START Midwest, Grand Rapids, MI

Background: Adenosine signaling is a central immunosuppressive mechanism affecting a broad set of immune cell types. Adenosine is generated from extracellular ATP by a group of ectonucleotidases including CD39 and CD73. Suppressing the adenosine pathway via CD73 blockade may enhance the potential of checkpoint inhibitor therapies.S095024 (Sym024) is a fully human, effector-function attenuated antibody that binds to human and cynomolgus CD73 with sub-nM affinity.

Methods: Preclinically, the stoichiometry and conformational structure of the binding interaction between CD73 and S095024 was assessed by SEC-MALS and cryo-EM and the ability of S095024 to inhibit CD73 activity was done *in vitro* covering 3-, 6- and 24-hour incubation periods. The clinical safety, tolerability, pharmacokinetics, and pharmacodynamics of S095024 alone or in combination with Sym021, an anti-PD1 antibody, was investigated in a first-in-human study (NCT04672434) in patients with selected types of advanced solid tumors. Following assessment of single agent S095024 (100 to 1500 mg IV Q2W) in part I, the safety and tolerability of S095024 (300 to 1500 mg IV Q2W) was assessed in combination with Sym021 (200 mg IV Q2W) in part II. A part IIa was added: patients received 3000 mg IV Q2W of S095024 in Cycle 1, followed by 3000 mg S095024 + 200 mg Sym021 from Cycle 2 onwards.

Results: Structural data indicate that S095024 binds to CD73 in a unique configuration by bridging the two monomers of the molecule, interacting in a 1:1 stoichiometry and effectively preventing the conformational state cycling required for catalysis. Functional data using a 20x cell line panel harboring a broad range of CD73 expression levels demonstrates that this interaction modus results in deep enzymatic inhibition. As of 12 Oct 2023, 43 patients have been treated with, S095024 in the FIH study. S095024, as a single agent (N=18) and in combination with PD-1 blockade (N=25) was well tolerated across all dose levels. The most frequent treatment emergent adverse events (≥15% patients) were fatigue, nausea, diarrhea, dyspnea, and vomiting. A dose proportional increase in drug exposure, both in monotherapy and combination, was observed starting at 900 mg. Target engagement assessed both peripherally (free soluble CD73) and intra-tumorally (enzymatic activity), showed a sustained decrease in free soluble CD73 in blood at dose levels ≥1500 mg and dose-dependent CD73 modulation, with >80% inhibition reached at ≥1500 mg in tumor biopsies.

Conclusions: These findings reveal the potential of S095024 (Sym024) to prevent adenosine-mediated tumor evasion and support further clinical investigation.

#3739 Different combination regimens for OX40 agonists and PD-1 inhibitors exert different antitumor effects in OX40 humanized mice.

Y. Li, Y. Zhang, X. Qiu, D. Feng, R. Sun, **D. X. He**;
Shanghai Model Organisms Center, Inc., Shanghai, China

OX40, also known as CD134 or TNFRSF4, is a member of the tumor necrosis factor receptor (TNFR) superfamily which mainly expressed on the surface of activated T cells including Treg cells. Engagement of OX40 with its ligand, TNFSF4, leads to effector T cell expansion and cytokine release, inhibits activation-induced cell death (AICD) and promotes the survival of antigen-specific memory T cells. In contrast to the massive hit of immune checkpoint inhibitors like PD-1 and PD-L1, the benefit of agonistic antibodies in clinical trials has not been completely demonstrated to date. On one hand, higher doses could leads to T cell exhaustion or AICD, paradoxically, with no efficacy improvement. Another hand, the limited understanding of the biology of immune checkpoints underlying “accelerator and brake” should account for the slow clinical progress of OX40-targeted biologics. It seems that the dosing sequence or timing of anti-OX40 and anti-PD-1 is an important consideration in combination therapies. Given this, we firstly evaluated the antitumor effects of two different anti-human OX40 agonists in syngeneic MC38 and Pan02 tumor models, respectively, in hOX40 knockin mice. We observed tumor regressions upon treatment of OX40 agonistic Ab1 in a dose-dependence way in the homozygous hOX40 knockin mice engrafted with MC38 tumors. The anti-hOX40 Ab1 at high-dose (10 mg/kg) led to ~60% TGI, but no response at very low dose (0.1 mg/kg). Furthermore, the homozygous hOX40 knockin mice inoculated with Pan02 pancreatic tumors were treated with a novel strong anti-hOX40 agonist (Ab2) and surrogate anti-mPD-1. Notably, Anit-hOX40 (Ab2) alone at low dose (1 mg/kg, Q3D*9 doses) exerted strong anti-tumor potency (TGI=59.3%, p< 0.005) and no statistical significant antitumor difference was observed between high-dose group (at 5mg/kg) and low-dose group (at 1 mpk) as monotherapy, though anti-hOX40 (Ab2) at 5mg/kg showed the best therapeutic response (TGI=72%, p=0.0002) among all treatment groups. In contrast, the second therapeutic response was observed in the combo group treated with first dosing of 5mg/kg anti-hOX40 (Ab2) combining delayed dosing of 10mg/kg anti-mPD-1 (TGI=64%, p< 0.005) and the concurrent dosing group of Ab2 (5 mg/kg, Q3D×9 doses) plus anti-mPD-1 (2 mg/kg, Q3D×9 doses) (TGI=62.3%, p= 0.001). In conclusion, different human-specific OX40 agonists displayed different anti-tumor activity as monotherapy, and different dose led to different antitumor potency for the same agonist. In terms of different combination regimens, although no advanced benefit was observed for the combination of anti-mPD-1/anti-OX40 (Ab2) in comparison to strong anti-OX40 agonist (Ab2) alone, it demonstrated that the dosing timing and sequence of either anti-PD-1 or anti-hOX40 did has impact on the therapeutic outcome.

#3740 Tusamitamab ravtansine induces immunogenic cell death and synergizes with anti-PD-1 or anti-PD-L1 antibody combination in solid tumor.

C. Nicolazzi, A.-M. Lefebvre, N. Moindrot, C. Larois, M. Classe, **S. Sidhu**;
Sanofi, Vitry-Sur-Seine, France

Tusamitamab ravtansine (SAR408701) is an antibody-drug conjugate (ADC) targeted to carcino-embryonic antigen-related cell adhesion molecule 5 (CEACAM5) and delivering DM4, a maytansinoid cytotoxic. CEACAM5 is highly expressed in several tumor types, including non-squamous non-small cell lung cancer (NSQ NSCLC). It is currently being evaluated in patients with advanced CEACAM5-positive NSQ NSCLC, in a phase II study in combination with pembrolizumab, and a phase III trial as single agent in comparison with docetaxel. Preclinical investigations were performed to determine whether SAR408701 could be beneficially combined with immune checkpoint inhibitors. We, first, demonstrated that the tusamitamab ravtansine payload, DM4, is able to induce robust immunogenic cell death (ICD) using an in vivo vaccination assay. In this assay, immunocompetent mice were “vaccinated” by DM4-treated CT26 cells and then later rechallenged with CT26 tumor cells. Tumor rejection was observed in more than 50% of “vaccinated” mice. The ICD was characterized by the expression or release of danger-associated molecular patterns (DAMPs), and we observed DAMP modulation such as calreticulin (CRT) exposure at the cell surface of dying tumor cells, and the release of the High-Mobility Group Box 1 (HMGB1) in the extracellular space by CT26 cells in response to DM4 treatment. We also showed that DM4-treated CT26 tumor cells implanted into mice or SAR408701 treatment of MC38 tumor-bearing mice induced an elevation of plasmatic level of murine IL-6 and INFγ, revealing potential antitumor immunity modulation by the ADC and its payload. Immunohistochemistry analysis of MC38 tumors also revealed that tusamitamab ravtansine treatment induced a dose-dependent increase of CD8 T-cell infiltration in tumors correlating to dose-dependent efficacy. Finally, tusamitamab ravtansine was combined with immune checkpoint inhibitors (ICIs) in immunocompetent mice bearing MC38 tumor model. In this model, the combination of tusamitamab ravtansine with anti-PD-1 or anti-PD-L1 antibody led to complete response and, even, tumor-free survivors at 120 days post tumor implantation while single agents were inactive or transiently active. In summary, these preclinical data show that tusamitamab ravtansine could be beneficially combined with immune checkpoint and strongly support their evaluation in clinical development.

#3741 Helper/killer hybrid epitope long peptide (H/K-HELP) cancer vaccine augments Th1-dependent CTL induction at tumor-draining lymph node to eradicate solid tumor: its application to develop an innovative combination cancer immunotherapy(iCCI).

T. Iwasaki[1], Y. Yazaki[1], T. Masuko[2], T. Nishimura[3];

[1]Precision Clinic Tokyo, Tokyo, Japan, [2]School of Pharmacy, Kindai University, Osaka, Japan, [3]Cancer Medical Research Center, Fujita Health University, Aichi, Japan

We have initially demonstrated the pivotal role of IFN-γ-producing tumor-antigen-specific Th1 cells for the complete eradication of established tumor mass by CTL. The accumulated evidence has clearly demonstrated that induction of Th1-dependent full activation of CTL at tumor-draining lymph nodes (TDLN) are crucial for inducing complete rejection of solid tumor by CTL. To induce Th1 immunity efficiently at TDLN in tumor-bearing host, we developed an artificially synthesized helper/killer-hybrid epitope long peptide (H/K-HELP), which conjugated killer and helper epitope peptides of cancer antigen by a glycine-linker. In mouse model, OVA-H/K-HELP was selectively presented in vivo by professional DC in vaccinated TDLN and sustained antigen presentation capability of DC to stimulate both CTL and Th1 cells. Thus, in contrast to short peptide, vaccination of OVA-expressing EG7-bearing mice with OVA-H/K-HELP caused a complete eradication of EG7 tumor mass. To apply these basic findings to clinical treatment of cancer patients, we then developed Survivin-H/K-HELP. Treatment of a patient with a triple-negative breast cancer patient with Survivin-H/K-HELP induced a complete response in a triple-negative breast cancer patient concomitantly with the induction of Th1-dependent cellular and humoral immune responses. In this clinical study, the patients showed Th1-dependent C'-fixing IgG antibody production and exhibited IFN-γ-producing Th1 cellular responses. Finally, we also applied H/K-HELP-pulsing DC-vaccine to develop an innovative combination cancer immunotherapy (iCCI). The iCCI consisting of radiation, low dose of immune check point inhibitors (ICIs:Nibolumab, Ipilimumab) and H/K-HELP-pulsed DC, all of which have been shown to initially modulate antitumor immunity at TDLN. Here, we described a successful outcome of a case of the stage IVA inoperable advanced hypopharyngeal squamous cell cancer patient with lymph node-metastasis. The iCCI treatment of the patient caused a complete disappearance of all cancers and the patient has been cancer free for over 15 months so far. Although the destruction mechanism of cancer is not determined, we image this iCCI might improve patient's antitumor immune capability in immune microenvironment around tumor (IMAT) including TDLN and TME. Our developed iCCI will become a promising strategy to overcome inoperable advanced cancers in future.

CLINICAL RESEARCH: Diagnostic Biomarkers 2
Poster Session

#3745 Metabolomic profiling of lipid and metabolite in cirrhosis patients with and without hepatocellular carcinoma.
H. Powell, E. Ruiz, S. L. Grimm, O. Najjar, L. Olivares, M. Scheurer, H. B. El Serag, C. Coarfa, S. Kaochar;
Baylor College of Medicine, Houston, TX

Early detection of hepatocellular carcinoma (HCC) is crucial for improving patient outcomes, as curative treatments are most effective at the early stages of the disease. The lack of robust biomarkers, particularly a non-invasive diagnostic tool, precludes significant improvement of clinical outcomes for HCC patients. Serum metabolites are one of the best non-invasive means for determining patient prognosis. Established biomarkers for HCC including alpha-fetoprotein (AFP), have shown suboptimal performance in early disease stages. This study aimed to develop a combined metabolite and lipid panel to differentiate early-stage HCC from cirrhosis. Unbiased metabolomic and lipidomic analyses of serum samples were performed for 28 and 30 patients with early HCC and cirrhosis, respectively. We developed an unbiased high-resolution liquid chromatography mass spectrometry (LC-MS) based metabolic profiling platform and evaluated differences in the serum global metabolome and lipidome. This method enabled the detection of over 1200 metabolites and up to 800 lipid molecules in this select cohort. We identified 124 metabolites and 246 lipids that were upregulated and 208 metabolites and 73 lipids that were downregulated in HCC compared to cirrhosis. Using multiomic integrative analysis, we identified the overlap between differentially expressed metabolites and lipid and previously published transcriptomic signatures and illustrate that the overlapping signature associates with clinical disease progression. Lastly, we leveraged machine learning models to identify a minimal panel of lipids and metabolites that accurately distinguish between cirrhosis patients with HCC and without HCC. The best performing classifier was derived using Support Vector Machines, achieving a median AUC of 0.98 over 100 cross-validation iterations, and we showed that we need as little as 12 metabolite and lipids for effective discrimination between cirrhosis and early HCC.

#3746 Identification of cancer specific extracellular vesical biomarkers to aid in diagnosis of cancer.

T. A. Hembrough[1], Z. Opheim[1], C. Bandoski[1], I. Isaac[2], M. Mehnert[2], A. Ezrin[1],
[1]Nexosome Oncology, Durham, NC, [2]Biognosys, Schlieren, Switzerland

The limitations of serial tumor biopsies are well known, thus liquid biopsies which allow for repeated plasma-based biomarker analysis are urgently needed. Extracellular vesicles (EVs) represent an extremely stable and emerging proteomic substrate which allows for deep enrichment of biologically relevant signals from plasma, and broad analysis of tumor associated and host response proteins. To identify novel biomarkers, we performed proteomics analysis on EVs purified using size exclusion chromatography and a proprietary buffer system which increases EV and corona protein recovery. Initial DIA mass spectrometry (MS) analysis was performed on EVs from 125 patients (25 each from CRC, breast, NSCLC, ovarian, and normal patients). A subset of 25 normal and 25 ovarian was subjected to a second deeper analysis on a much more powerful DIA platform. Initial analysis identified 204 unique proteins differentially expressed in ovarian cancer patients (>2-fold change; $p<0.05$). Repeat analysis of the ovarian vs normal cohorts on the Biognosys TrueDiscovery™ platform identified 645 differentially expressed, a significant increase in depth of analysis. These cancer exosome associated proteins represent a broad range of host response signals. Taking ~20 of the top proteins, we extended our analysis using ELISAs to determine if the results by MS were reproducible in a simpler format. The ELISA analysis recapitulated the MS results. This confirms that the TrueDiscovery™ platform can easily be translated into a simple, quick and distributable ELISA platform. Extending these results, a blinded cohort of ovarian and normal EVs was analyzed using a predefined cutoff for a host immune response biomarker. This blinded analysis demonstrated sensitivity of 1.0 and specificity of 0.9, exceptionally high values for a single analyte assay, underscoring the potential value of analyzing the host/immune response proteins in the context of the EV microenvironmentKey biomarkers from cancer patient EVs suggests it is possible to track host immunosuppressive environment via antigen presenting cell and check point antagonist biomarkers. In both cases, highly significant differences are seen comparing EVs from normal patient plasma versus cancer patient plasma. Interestingly, when these biomarkers are evaluated in pre-EV enriched plasma, no significant differences are seen. This underscores the unique nature of the EV microenvironment, and suggests that host immune response and tumor microenvironment may be recapitulated in the EV/host response proteome using our unique methods. These data confirm that the EV microenvironment represents a unique oncological ecosystem with highly specific and sensitive disease biomarkers which are not dysregulated in complete plasma. This novel approach to assessing cancer proteomics has great promise for real time, longitudinal analysis of cancer patient tumor/host immune biology.

#3747 Bronchial washing fluid sequencing is useful in the diagnosis of lung cancer with necrotic tumor.

J. Lim[1], H.-T. Shin[1], S. Park[2], W. Ryu[1], L. Kim[1], K.-H. Lee[1], S. Ko[2], S. Lee[3], J. Kim[1], J.-S. Ryu[1];

[1]Inha University College of Medicine, Incheon, Korea, Republic of, [2]Yonsei University Wonju College of Medicine, Wonju, Korea, Republic of, [3]DNA Link, Inc., Seoul, Korea, Republic of

Lung cancers identified with low-dose CT are typically early stage without endobronchial lesions, and most require a pathological diagnosis using invasive procedures. We conducted a study analyzing bronchial washing (BW) fluid using targeted panel sequencing to evaluate its diagnostic performance. And we aimed to elucidate the characteristics of patients group in which this method could be effectively applied. We prospectively enrolled patients with an incidental lung lesion suspected of early-stage lung cancer on chest CT and no visible endobronchial lesion on bronchoscopy from June 2017 to March 2018 at two independent hospitals. Lung cancer was histologically diagnosed using a diagnostic work-up including surgical lung biopsy, percutaneous needle biopsy, endobronchial ultrasound, and other biopsies. BW was performed on each patient in the subsegmental bronchus where the lung lesion was suspected to be located. Among shared genes between the panels for each cohort, we selected 8 genes that are frequently mutated known oncogenes/tumor suppressor genes in lung cancer not to consider passenger mutations for diagnosis. In addition, several filtering criteria were considered to differentiate cancer. Since criterion d considered definitive somatic mutations [known hotspot mutations or loss of function mutations with variant allele fraction (VAF) ≥ 2%] with criterion c (≥ 2 COSMIC11 variants with VAF ≥ 1%), the sensitivity was increased without loss of precision and the sensitivity of sequencing was higher than BW cytology. In total, 164 subjects (114 with lung cancer and 50 with benign) were enrolled. Of lung cancer patients, necrosis was observed on chest CT in 44 (38.6%) patients and malignant cells were identified upon BW cytological examination in 33 (28.9%) patients. Of total, 33 (20.1%) patients had complications related to invasive diagnostic test. By the panel with the criterion d, 42 patients (25.6%) were classified as cancer. The panel showed 100% of specificity, 100% of positive predictive value for diagnosing cancer whereas it had relatively low sensitivity. Twenty patients who were classified as cancer by sequencing despite of negative cytology. In the group with necrosis, the proportion of patients with positive for sequencing only was significantly higher than that of patients with positive for cytology only. In addition, the sensitivity of BW sequencing reached 75% in patients with necrotic tumors. The prevalence of necrotic tumors was significantly higher in SQC than in ADC. The significant proportion (66.7%) of primary tumors with positive for sequencing only and located in outer area had necrosis. This study demonstrated that BW sequencing could be applied for diagnosis in patients with necrotic lung lesion suspected of early-stage lung cancer in chest CT. It would be possible to reduce the frequency of unnecessary invasive procedures and subsequent complications.

#3748 Evaluation of immune cells from patient-derived tumor tissue and peritoneal washing cytology in correlation with immunohistochemical markers in endometrial cancer.

C. Shin, S. Lee, H. Chung, J. Kim, E. Ha, J. Seo, S. Shin;
School of Medicine, Keimyung University, Daegu, Korea, Republic of

Background This study aims to evaluate the characteristics and clinical correlations of tumor-infiltrating lymphocytes (TILs) in endometrial cancer, derived from fresh tumor tissue and peritoneal washing cytology. Furthermore, it seeks to explore the correlation between TILs and immunohistochemical markers in endometrial cancer.

Methods In this study, we investigated the nature of TILs extracted from endometrial tissue and peritoneal washing cytology, along with their correlation with immunohistochemical markers. Samples collected from endometrial cancer patients during surgery, with informed consent, were analyzed for immune cell composition using flow cytometry. We examined the association between pathological findings, a range of immunohistochemical markers (including LVSI, PD-L1, ER, P53, HER2, MLH1, MSH2, MSH6, PMS2, MSI), and the status of tumor-infiltrating immune cells (such as CD3-CD19+ B Cells, CD3-CD16+CD56+ NK Cells, CD4+CD25+ regulatory T cells (Treg), and CD3+CD8+ cytotoxic T cells).

Results Our analysis encompassed 25 endometrial cancer-derived samples. Notable observations include an increase in CD3-CD19+ B cells in the LVSI-positive group and a decrease in the ER-positive group ($p<0.05$, respectively). CD3-CD16+CD56+ NK Cells decreased in the ER-positive group, while CD3+CD8+ cytotoxic T cells were decreased in the HER2-positive group ($p<0.001$, $p<0.05$, respectively). Other immunohistochemical markers showed no significant differences.

Conclusion The study suggests that tumor-infiltrating immune cells from patient-derived tissue and peritoneal washing cytology may reflect the molecular and clinical characteristics of endometrial cancer. However, further research with an expanded sample size and correlation with oncologic outcomes is warranted to validate these findings.

#3749 The evaluation of expression level of Cxcl12 gene in peripheral blood samples of breast cancer patients.

A. Adamnejad Ghafour, S. Tuncer;
Istanbul University, Istanbul, Turkey

Breast cancer, like many other cancer types, is linked to the activation and overexpression of CXCR4. The overexpression of CXCR4 is associated with factors such as tumor growth, angiogenesis, increased metastasis, and therapeutic resistance. Similarly, CXCL12, a specific ligand for CXCR4, plays a significant role in tumorigenesis processes, including survival, migration, and microenvironmental interactions. The CXCL12/CXCR4 signaling pathway has been found to impact the development and progression of breast cancer, regulating proliferation, motility, and metastasis. Hence, molecules within the CXCL12/CXCR4 signaling pathway hold promise for determining breast cancer prognosis, treatment monitoring, and serving as therapeutic agents. The study, conducted at the Istanbul University Institute of Oncology, obtained ethical approval from the Istanbul Faculty of Medicine Ethics Committee. Genetic materials from 300 breast cancer patients and 150 control subjects underwent standard testing, matched based on crucial parameters. Real-time PCR with the MIC qPCR Cycler was statistically analyzed using GraphPad Prism ($p < 0.05$). Descriptive statistics were presented for categorical and quantitative variables, while the Kolmogorov-Smirnov test assessed the normal distribution of quantitative variables. Statistical comparisons between groups were performed using the Mann-Whitney U test and the Kruskal-Wallis test, was used for calculations. Notably, among the three genes—LASP1, CXCL12, and CXCR4—LASP1 exhibited the highest mean expression level at 11.64 with a considerable standard deviation of 11.80. In contrast, CXCL12 had a much lower mean expression level at 2.96 and a tighter distribution, and CXCR4 displayed the lowest mean expression level at 0.37 with a standard deviation of 0.74. The analysis of diagnostic groups indicated no significant differences in mean LASP1 and CXCL12 levels, but a significant variance in mean CXCR4 levels ($p<0.001$). Specifically, CXCR4 expression in group Breast and ovarian cancer was notably lower compared to Breast cancer, Bilateral Breast cancer, and Breast and Other cancer, while group Breast cancer exhibited significantly lower CXCR4 expression compared to groups Bilateral Breast cancer and Breast and Other cancer. However, there was no significant difference in CXCR4 expression between groups of Bilateral Breast cancer and Breast and Other cancer. These findings reveal distinct expression patterns of CXCR4 across diagnostic groups, suggesting potential implications for diagnostic categorization and underlying molecular pathways in breast cancer. Understanding these expression disparities could be crucial in deciphering the molecular intricacies influencing disease progression and treatment responses.

#3750 Dual isolation and profiling of circulating tumor cells and circulating tumor DNA from a single liquid sample using the Genesis Cell Isolation System and Droplet Digital PCR.

Y.-T. Kang[1], A. Bodunrin[2], E. Pusod[1], K. Simonyi[3], A. Corner[4], D. Coe[3], M. Racey[5], E. J. Dreskin[3];
[1]Bio-Rad Laboratories, Ann Arbor, MI, [2]Bio-Rad Laboratories, Pleasanton, CA, [3]Bio-Rad Laboratories, Hercules, CA, [4]Bio-Rad Laboratories, Watford, United Kingdom, [5]Bio-Rad Laboratories, Boulder, CO

Introduction: Recent advances in technology support the use of liquid biopsy as a noninvasive method for cancer monitoring and diagnosis. Circulating tumor cells (CTCs) and circulating tumor DNA (ctDNA) are both regarded as key liquid biopsy biomarkers, offering significant disease-related molecular insights. Despite their potential, dual isolation and profiling have been challenged in a clinical setting by the lack of established platforms and optimized protocols that support this approach. The Genesis System with Celselect Slides™ captures CTCs based on size and deformability, then the enriched cells can be recovered for subsequent downstream analysis. Concurrently, Droplet Digital PCR (ddPCR™) can be utilized to interrogate cell-free DNA (cfDNA) to determine the presence of a range of DNA aberrations present in ctDNA. This study, using a model lung CTC-ctDNA sample, illustrates the feasibility of this dual-biomarker approach to detect cancer-associated nucleic acid mutations simultaneously with CTC enumeration, using commercially available kits and instruments.
Methods: To model lung cancer samples, blood samples were prepared by spiking in two model circulating markers, cultured cancer cells (model CTCs, human lung cancer cell line A549) and fragmented genomic DNA containing *EGFR* mutations (model ctDNA, multiplexed 23 ctDNA [~145 bp band > 95%]), into whole blood from a healthy donor prior to enrichment/extraction. Plasma isolation from the whole blood model samples was performed using either two-step centrifugation or Ficoll-Paque PLUS solution for plasma/buffy coat separation. The extracted plasma layer was used for ctDNA separation, while the remaining cell layer was used for CTC isolation on the Genesis System with a modified protocol.
Results: The Genesis System isolated 78-79% of spiked cancer cells in whole blood at a concentration of 40 cells/ml. Despite additional plasma separation steps and liquid handling, the system isolated CTCs spiked in with minimal cell loss (<6%). With an optimized ctDNA extraction, more than 70% of spiked ctDNA in blood samples in the size range of 120-220 bp was extracted. Using the Bio-Rad QX200 ddPCR System and ddPCR *EGFR T790M* Mutation Detection Assay, blood samples with the model ctDNA spiked in showed positive droplets (17 copies) for *EGFR T790M* while control blood samples without model ctDNA spiked in showed no positive droplets.
Discussion and Conclusions: This work illustrates an optimized protocol for the dual isolation and profiling of CTCs and ctDNA from a single blood sample by using an automated CTC isolation platform and high-sensitivity ddPCR based ctDNA mutation detection. This protocol enables comprehensive liquid biopsy studies using a single blood sample from cancer patients with readily available instruments and kits, which can be applied to many other cancers.

#3751 Diagnostic assessment of Filamin A (FLNA) as a serum biomarker for identification of benign prostatic hyperplasia vs aggressive prostate cancer in a prospective Mexican cohort.

A. Rodriguez[1], A. Mendoza[2], M. Rosenburg[3], J. Castaneda[4], A. A. Melgar[5], B. Ciseros[6], A. G. Gangemi[2], N. M. Chand[7], P. Tekumalla[7], G. Miller[7], A. Thakurta[7], D. Banuelos[8], J. J. Real[9], D. A. Joya[1], A. Romero[10], J. D. Farias[11], E. Cabeza[1], H. H. Remess[12], J. J. R. Delgado[13], H. M. Sanchez[14], I. Barragan[15], M. Rodriguez[16], B. Garcia[17], D. A. S. Sanchez[18], J. Izquierdo[19], E. M. S. Lopez[20], J. Hanao[7], J. G. Frusch[20], N. R. Narain[7], M. A. Kiebish[7]; [1]Hospital General de Occidente, Zapopan, Mexico, [2]Hospital Medica Sur, Mexico City, Mexico, [3]Mid-Michigan Health Centers, Jackson, MI, [4]Hospital Angeles Clinica Londres, Cuauhtemoc, Mexico, [5]Hospital Angeles Pedregal, Mexico City, Mexico, [6]Hospital ABC Santa Fe, Mexico City, Mexico, [7]BPGbio Inc., Framingham, MA, [8]Banuelos Radiologos por Doctores Banuelos, Guadalajara, Mexico, [9]Dr. Juan Jose Real Urologo/Oncologo, Guadalajara, Mexico, [10]Hospital Versalles, Guadalajara, Mexico, [11]Hospital Real San Jose, Zapopan, Mexico, [12]MOLEET Medical Unit/ Clinica Zepeda/ Unidad Medica Especializada Pulido, Zapopan, Mexico, [13]Hospital Star Medica Chihuahua, Chihuahua, Mexico, [14]Hospital La Luz, Mexico City, Mexico, [15]Uromin, Instituto Urologico de Invasion Minima Sc, Guadalajara, Mexico, [16]Laboratorio de Analisis de Moleculas y Medicamentos Biotecnologicos, Instituto de Biotecnologia., Cuernavaca, Mexico, [17]Centro Estatal de la Transfusion Sanguinea del Estado de Jalisco, Zapopan, Mexico, [18]Laboratorio de Analisis Geneticos Especializados Mexico, Mexico City, Mexico, [19]Laboratorio Diagnostico Especializado de Imagen, Zapopan, Mexico, [20]Grupo Terralpe, Mexico City, Mexico

Prostate cancer (PCa) exhibits a significant health risk to aging men, in which effective diagnosis of high gleason (Gleason >7) cancers is of critical need. Currently, the main screening tool utilized for detection of prostate cancer is prostate specific antigen (PSA), however, PSA exhibits limited utility in men with benign prostatic hyperplasia (BPH) due to inherent elevated PSA as the result of an enlarged prostate, resulting in increasing unnecessary biopsies. In Mexico, there is currently a higher incidence of aggressive PCa due to the risk within the overall population as well as the need for increased screening tools. Since, there is a critical unmet need to evaluate novel PCa diagnostic test that could serve as a reflex test within the screening paradigm, we evaluated the recently developed test, pSTATEdx, which measures the cleaved portion of Filamin A (FLNA) via IP-MRM mass spectrometry in conjunction with the patients age, to determine the overall risk of aggressive prostate cancer. In the current study, we analyzed a prospective cohort from Mexico City and Guadalajara evaluating 34 BPH and 44 PCa in men exhibiting symptoms with PSA levels between 4-10 ng/mL, who were all referred for 12 core prostate biopsies due to suspicion of prostate cancer. Additionally, we assessed 41 non-diseased men as controls who had PSA below 1.5 ng/mL, who were not assessed further. Comparison of non-diseased controls with BPH/PCa men exhibited an AUC of 0.99, PPV 0.96, NPV 0.89, OR 118, and P value 2 e-20, thus demonstrating that pSTATEdx had significant utility in assessing prostate health independent of PSA. In comparison with previously published data, FLNA mean levels were 24 ng/mL in previously published American study cohort and 55 ng/mL in the Mexican BPH/PCa cohort with a P value of <0.001. Assessment of patient populations revealed that there was superior diagnostic performance of FLNA for patients between PSA 4-7, which represents an increased unmet need for biopsy decision support. Analysis of BPH compared to all PCa exhibited a sensitivity of 0.94 and specificity of 0.53, PPV 0.64, NPV of 0.91, and OR of 16.4. Diagnostic analysis of BPH compared to high gleason PCa exhibited a sensitivity of 1, specificity of 0.21, PPV 0.38, NPV of 1, and OR of inf in this pilot study. This assessment revealed promising insight that aggressive PCa was not missed using pSTATEdx. pSTATEdx demonstrated diagnostic utility in prevention of unnecessary biopsies in the Mexican population as a reflex test to those patients with PSA levels between 4-7 as well as demonstrated that aggressive prostate cancers were not missed with the risk score. Additional studies are planned in the future to expand the utility of pSTATEdx in Latin America.

#3753 Co-expression proteomic analysis of antibody drug conjugate receptor and payload biomarkers in breast cancer.

N. Ghafourian[1], **S. P. Thyparambil**[1], R. Mortensen[1], J. Chou[1], R. Heaton[1], X. B. Ling[2];
[1]mProbe, Rockville, MD, [2]Stanford University, Palo Alto, CA

The use of antibody drug conjugates (ADC) targeting HER2, and Trop 2 has made a great difference in the treatment of breast cancer. Such agents consist of an antibody targeting the receptor which is conjugated to a payload chemotherapy agent. Chemotherapy involves the use of anti-tubulin agents (e.g. docetaxel), topoisomerase inhibitors etc. We examined 507 breast cancer samples using targeted proteomics to quantitate biomarkers for ADC targets such as HER2, HER3, EGFR and Trop2 in our clinical proteomics (CLIA) laboratory. We also measured biomarkers that are associated with response and biomarkers that are associated with resistance to chemotherapeutic agents. Resistance markers include TUBB3 (taxanes), and response markers include TOPO1 (irinotecan, topotecan). Methods: Formalin fixed, paraffin embedded (FFPE) tissues blocks of breast cancer were sectioned, marked for tumor, laser capture microdissected, digested and analyzed by LC-selected reaction monitoring mass spectrometry. Seventy-two proteins were quantitated. Discussion:In our previous work, we have determined that >740 amol/µg HER2 corresponds to IHC 3+/2+ and FISH +. Based on the HER2 quantitation for each sample, the samples were segregated into three groups. Negative (Group A, <150 amol/µg), High expressors (Group C, >740 amol/µg), and Detected (Group B, 151-739 amol/µg). Groups A, B, and C were 39%, 46%, and 43% of the cases respectively. In Group A (HER2 negative), HER3 was detected in 14% of cases with a 3x range (181-602 amol/µg). EGFR was detected in 53% of samples with 139x range (108-14986 amol/µg). Trop2 was detected in 59% of cases ranging from 256 to 11900 amol/µg. Topo1 was detected in 86% of cases with a 12x range (402-4870 amol/µg) and TUBB3 was detected in 63% of cases at levels ranging from 755 to 11750 amol/µg. In Group B (HER2 detected), HER3 was detected in 38% with a 3x range (178-565 amol/µg). EGFR was detected in 34% at levels ranging from 104-7040 amol/µg. Trop2 was detected in 63% ranging from 157 to 12808 amol/µg. Topo1 was detected in 94% with a 12x range (413-5100 amol/µg). and TUBB3 was detected in 51% of cases at levels ranging from 757 to 9311 amol/µg.In Group 3 (HER2 highly expressed), HER3 was detected in 43% with a 5x range (189- 890 amol/µg). EGFR was detected in 30% at levels ranging from 101 to 565 amol/µg. Trop2 was detected in 68% ranging from 310 to14650 amol/µg. Topo1 was detected in 95% with a 6x range (487- 2885 amol/µg), and TUBB3 was detected in 64% of samples at levels ranging from 829 to 2300 amol/µg. Conclusion:The capacity to multiplex 72 protein biomarkers from 2-3 FFPE sections will help in design of ADCs bispecific antibodies and/or bispecific ADCs.

#3754 High staining reproducibility and scoring precision demonstrated in endometrial cancer stained with PD-L1 IHC 22C3 pharmDx used in conjunction with combined positive score.

J. Hand, A. Morones, D. Moquin, K. Martyniuk, M. Kalpakoff, S. Tabuena-Frolli, J. Milo, S. Hund;
Dako North America - Agilent Technologies, Carpinteria, CA

Background: PD-L1 IHC 22C3 pharmDx (SK006) is a qualitative immunohistochemical (IHC) assay using anti-PD-L1 clone 22C3 to detect PD-L1 in formalin-fixed, paraffin-embedded (FFPE) human endometrial cancer (ENDO) tissues. PD-L1 expression is determined using the Combined Positive Score (CPS) algorithm, which is the number of PD-L1 staining cells (tumor cells, lymphocytes, macrophages) divided by the total number of viable tumor cells, multiplied by 100. Validation testing evaluated the sensitivity and analytical performance of SK006 PD-L1 expression in FFPE ENDO specimens based on two PD-L1 expression cutoffs for all applicable studies: CPS ≥ 1 and CPS ≥ 10. Analytical performance studies included precision (combined precision, intra-run and intra-inter observer) and robustness (time, temperature, pH and re-use) testing.
Methods: FFPE ENDO specimens were stained with SK006 and scored using CPS. Negative percent agreement (NPA), positive percent agreement (PPA), and overall agreement (OA) with two-sided 95% bootstrap confidence intervals (CIs) were used for data analysis, based on PD-L1 binary status (positive/negative) at the evaluated cutoffs. Acceptance Criteria (AC): the lower bound of the two-sided 95% CI computed on percent agreement (NPA, PPA, and OA) must meet or exceed 85%. Sensitivity determined if SK006 could detect a range of CPS expression levels in ENDO specimens. Combined precision measured inter-instrument, -operator, and -day variation nested within the same study. Intra-run measured repeatability within the same run and Inter/Intra-Observer measured scoring reproducibility by 3 pathologists over 3 non-consecutive days. Robustness evaluated the staining performance of SK006 under varying Target Retrieval Solution (TRS) laboratory conditions: time (18-22min), temperature (95-99°C), pH (5.9-6.3) and re-use (up to 3 uses).
Results: The sensitivity data showed that SK006 could detect a range of CPS expression levels in ENDO specimens. Analyses for each analytical validation study, subject to AC, showed NPA, PPA, OA point estimates (PE) of ≥ 95.5% and CI lower bounds (CILB) of ≥ 87.1%.
Conclusion: PD-L1 IHC 22C3 pharmDx (SK006) used in conjunction with CPS provides high staining reproducibility and scoring precision for ENDO specimens at the CPS ≥ 1 and CPS ≥ 10 cutoffs, under standard day-to-day laboratory testing and scoring conditions.

#3755 Impact of antigen retrieval and other parameters on detection of FGFR2b in various solid tumors on a BenchMark ULTRA automated staining platform: Development of a new IHC assay for FGFR2b.

A. S. Watson, C. Le, A. M. Wertheimer, S. Escobedo, L. So, B. Bagevalu Siddegowda, J. D. Palting, S. Marion, **S. P. Stratton**, B. Aggeler;
Roche Tissue Diagnostics, Tucson, AZ

Background: Fibroblast growth factor receptor 2b (FGFR2b) is part of the FGFR transmembrane tyrosine kinase receptor family. This protein has gained more attention in recent years as a tumor progression biomarker in numerous solid tumors. The detection of FGFR2b by immunohistochemistry (IHC) has been used recently in immunotherapy clinical trials with multiple tumor types. During IHC assay development on formalin-fixed paraffin embedded tissue, a thorough study of antigen retrieval through cell conditioning or enzyme incubation, primary antibody incubation, and detection parameters is critical to evaluate staining performance.
Design: A study of an investigational anti-FGFR2b (FPR2-D) assay developed on a BenchMark ULTRA automated staining platform explored the effect of antigen retrieval and detection parameters on staining performance. VENTANA System Software was used to modify steps in the IHC staining protocol resulting in 42 permutations. Ten different solid tumors were stained with these modifications to the assay and subsequently evaluated for FGFR2b expression.
Result:s The results demonstrate that the staining clarity, intensity, and dynamic range within tissue cases of FGFR2b staining can vary widely between different solid tumor types. While most permutations of the initial assay parameters had minimal impact on the staining performance and readability by a pathologist, the order of the enzyme treatment and the cell conditioning steps (in addition to increased incubation time of primary antibody) had a significant impact when comparing across different solid tumors. Detection of FGFR2b seemed to have a greater susceptibility by tumor type to the antigen retrieval process than has traditionally been observed in other biomarkers.
Conclusion: The overall results of this investigation show the importance of an extensive parameter screening approach when evaluating new antibody targets and indication combinations in IHC to ensure optimal staining performance. This is critical to downstream testing and the potential use of new assays in the context of in vitro diagnostics.

#3757 The development of MAGMAS as a potential therapeutic target in temozolomide-resistant glioma.

J. D. Tran[1], J. J. Lepe[2], M. C. Kenney[2], B. C. Das[3], D. A. Bota[2];
[1]California State University, San Bernardino, CA, [2]University of California, Irvine, CA, [3]Long Island University, Brookville, NY

Glioblastoma (GBM) is one of the most aggressive types of brain cancer and remains a significant challenge for drug development in oncology today. Temozolomide (TMZ) is the standard of care for GBM, and resistance to this drug is modulated partly by the DNA repair enzyme O6-methylguanine-DNA methyltransferase (MGMT). Clinical studies demonstrated that low MGMT expression in GBM enhances sensitivity to TMZ and prolongs survival for patients. However, recent clinical studies indicate MGMT is a discordant biomarker since the predictive value of MGMT methylation is relatively low and there is a lack of modalities to inhibit MGMT expression. Furthermore, glioma stem cells (GSC) are another contributing factor for resistance due to tumor heterogeneity, self-renewal capacity and activation of DNA repair responses to overcome the effect of radiation and TMZ treatment. These resistance mechanisms contribute to tumor recurrence and present major impediments for the development of effective treatments.

MAGMAS, 13.8 kDa mitochondria protein, is a translocase of the inner mitochondrial membrane and regulates oxidative phosphorylation. Specifically, MAGMAS regulates the ATP stimulatory activity of DNAJC19 on mtHSP70 that drives the movement of peptides through the TIM23 complex into the mitochondrial matrix. Recent evidence suggests that MAGMAS can regulate oxidative phosphorylation via interactions with the respiratory complexes present in the inner mitochondrial membrane. Previously, our lab has shown MAGMAS overexpression in malignant glioma tissues of patients and murine intracranial xenografts. Additionally, pharmacological inhibition of MAGMAS with the small molecule BT9 promoted cytotoxicity and impaired respiratory functions in malignant glioma cells demonstrating that MAGMAS is a promising potential target for GBM patients. However, further studies are needed to investigate the role of MAGMAS across the spectrum from initial tumorigenesis to disease progression and to further determine how MAGMAS is implicated during the development of treatment resistance.

This study is designed to investigate the role of MAGMAS in GSCs and their contribution to TMZ resistance. We observed temozolomide-resistant (TR) U251-TR and D54 MG-TR GBM cell lines expressed significantly higher levels of MAGMAS and several stem cell markers than their drug-sensitive (S) parental cell lines. Therefore, we hypothesized that silencing MAGMAS re-sensitizes TR GBM cell lines to TMZ. We found that MAGMAS knockdown in D54-MG and U251 S/TR cells in the presence of escalating TMZ concentrations, caused enhanced sensitivity to TMZ. Consistent with these results, inhibition of MAGMAS with the novel BT9 inhibitor enhances the TMZ sensitivity in the TMZ-resistant cell lines. Additional studies of patient-derived cell lines are being utilized further to validate MAGMAS as it is an attractive target in TMZ-resistant GBM patients.

#3758 Evaluation of breast cancer-derived extracellular vesicles as diagnostic indicator for HER2 status.

Sol Moon, Min Woo Kim, Young Kim, Suji Lee, Hyojung Lee, Joon Ye Kim, Seung Il Kim, Jee Ye Kim

Department of Surgery, Yonsei University College of Medicine, Seoul, Korea, Republic of

HER2-low is a new distinct type of breast cancer that is characterized by low levels of the HER2 protein. As treatment paradigms for HER2-low breast cancer are rapidly evolving with the approval of antibody-drug conjugates, identification of HER2-low breast cancer with more sensitive and reproducible HER2 assays is needed. We aimed to investigate the utility of liquid biopsy in isolating tumor-derived extracellular vesicles (TDEs) for diagnosis of HER2 status. We adopted an affinity-based approach to isolate TDEs and performed CNV analysis of the ERBB2/neu genes using the tumor DNA present in TDEs (etDNA). HER2 status of etDNA had been determined by droplet digital PCR using HER2/EIF2C ratio, a highly accurate method to quantify DNA copy number. In our study, we utilized a variety of breast cancer cell lines categorized as HER2-low (MDA-MB-231, MCF7, ZR-75-1) and HER2-high (MDA-MB-453, BT-474, SK-BR-3) to confirm HER2 expression in extracellular vesicles (EVs) by flow cytometry. This analysis successfully demonstrated that EVs effectively reflect the HER2 status of the tumor cells, evidenced by a strong Pearson correlation coefficient ($r=0.987$, $p<0.001$). Further clinical validation was conducted with plasma samples from 22 breast cancer patients. In the clinical study, we observed a significant correlation between the CNV of tumor DNA present in TDEs and the HER2 status of primary tumors ($p<0.01$). Additionally, the Receiver Operating Characteristic (ROC) analysis yielded an impressive area under the curve (AUC) value of 0.838 ($p<0.01$), demonstrating a high level of accuracy in differentiating between high and low HER2 groups, with a sensitivity of 55.6% and a specificity of 100%. In summary, we show potential diagnostic tools for real-time, less invasive determination of HER2 status in primary tumors, providing continuous monitoring methods for HER2 status. Although further validation in larger cohorts and prospective studies is needed, our study indicates that TDE analysis could contribute to the assays for identification of the HER2 status in breast cancer patients.

#3759 First clinical evidence of the tissue nanomechanical signature as a novel diagnostic and prognostic tool in patients with non-small-cell lung cancer.

J. Alcaraz[1], H. Sanz-Fraile[1], **E. Marin**[2], P. Gausa Busquets[3], K. Neal[1], M. Arshakyan[1], M. Rico[1], M. Boada[3], D. Sanchez[3], R. Oropesa Nunez[4], G. Srivastava[4], A. Jizawi[4], S. Nizzero[4], T. Appenzeller[4], M. Gachechiladze[4], M. Loparic[4], M. Plodinec[4], N. Reguart[3],
[1]University Of Barcelona, Barcelona, Spain, [2]August Pi i Sunyer Biomedical Research Institute (IDIBAPS), Barcelona, Spain, [3]Hospital Clinic Barcelona, Barcelona, Spain, [4]ARTIDIS AG, Basel, Switzerland

Introduction: Complex structural remodelling of cells and extracellular matrix during cancer initiation and progression elicit substantial biomechanical alterations, which can be measured by Atomic Force Microscopy (AFM) at the nanoscale level. Clinical and translational evidence indicates that tissue nanomechanical signature (NS) can be a useful tool for rapid cancer diagnosis, and assessment of cancer aggressiveness. We demonstrated that the AFM-based Automated and Reliable Tissue Diagnostics (ARTIDIS) platform represents a valid method for rapid diagnosis, prognosis, and treatment response assessment in patients with breast cancer. Here we aimed to use this platform to examine tumour biopsies from non-small cell lung cancer (NSCLC) patients for the first time.
Methods: This is an ongoing, single center study at the Hospital Clinic of Barcelona and University of Barcelona (UHB) Spain, aiming to enroll 75 patients by January 2024 in the first phase, followed by 200 patients in the expansion phase. To date, 54 matching tumor and non-tumor fresh tissue biopsies were taken by experienced pathologists from fresh surgical resection specimens from 27 patients with previously diagnosed NSCLC. Tissue biopsies were measured with the ARTIDIS device in a blinded manner, without knowing the malignancy status of the biopsy. Routine clinico-pathologic parameters have been collected. The multiparametric nanomechanical signature has been analyzed in an automated manner using the proprietary AI-based ARTIDISNET software platform together with available clinico-pathologic parameters.
Results: In total, the NSCLC tissue samples included 16 squamous cell carcinoma (SCC), 6 Adenocarcinoma (ADC), 1 large cell carcinoma (LCC) and 4 other histological subtypes. Non-tumor tissues exhibited significantly varied composition, including normal lung parenchyma, bronchial tissues, fibrosis and inflammatory changes. Among the 27 patients, 5 patients developed distant progression within 12 months after ARTIDIS measurements. Results analysis showed that the ARTIDIS NS can reliably differentiate malignant NSCLC lesions from non-tumor lung tissue, with a sensitivity of 0.84, specificity of 0.81, positive predictive value (PPV) of 0.79, negative predictive value (NPV) of 0.86 and accuracy of 0.82. In addition, the ARTIDIS NS can differentiate patients with and without distant progression with a sensitivity of 0.62, specificity of 0.81, PPV of 0.42, NPV of 0.90 and accuracy of 0.77.
Conclusions: Here we demonstrated first clinical evidence of the ARTIDIS tissue NS as a novel diagnostic and prognostic tool in patients with NSCLC. This study aims to establish the diagnostic, prognostic, and predictive NS in patients NSCLC. In addition to local expansion at the UHB, study results will be further validated in ARTIDIS clinical program at MD Anderson Cancer Centre, USA.

#3760 The importance of optimizing DNA extraction conditions for formalin fixed paraffin embedded tissues.

M. G. Butler, B. Forson, M. Cowen, J. Ramprakash, D. Ruminski Lowe, **Y. Konigshofer**;
LGC Clinical Diagnostics, Inc., Gaithersburg, MD

The pre-analytic extraction of Formalin Fixed Paraffin Embedded Tissues (FFPETs) appears to have a profound effect on the ability to obtain meaningful data from the DNA therein. FFPETs represent important materials in Pathology that are used to diagnose and analyze cancer. As part of preparing FFPETs, the formalin fixation step preserves the structure of tissues through covalent modifications but can also damage nucleic acids through that same process. Over the last decade, the emergence of Molecular Pathology, which benefits from gentler fixation compared to Histopathology and especially Immunohistopathology, has led to changes in how FFPETs are prepared. However, the remnant FFPETs from over a decade ago may be far from representative of what is now prepared for Molecular Pathology by many laboratories. Here we discuss our optimization of FFPET extraction for gently fixed samples. When we prepared our Seraseq FFPE Homologous Recombination Deficiency (HRD) reference standards using fixation conditions that are recommended for Molecular Pathology and extracted the resulting FFPETs using generic conditions, our initial coverage data from Whole Genome Shotgun (WGS) sequencing was difficult to analyze for changes in copy number across the genome. A major contributor to nonuniform coverage was identified as the formalin reversal step, where deparaffinized proteinase K-digested tissue is heated in water to near boiling to attempt to detach formaldehyde from nucleic acids through hydrolysis. Given the gentler fixation conditions, this step was found to be mostly unnecessary, and omitting it improved the resulting data substantially. A reason for this appears to be that the gentler fixation conditions that are now in use may not protect the DNA from the effects of near-boiling water, where the lack of salt lowers the melting temperature of double stranded DNA fragments and causes them to denature unless they have a higher GC content. Different kits used for the extraction of nucleic acids from FFPETs may benefit from different optimizations to obtain improved sequencing data from today's Molecular pathology samples, and reference standards that represent such samples provide a useful tool for such optimizations.

#3761 A modified SELEX enables the efficient identification of DNA aptamers with potential for specific cancer targeting.

Yang Lin[1], Cho-Yi Chen[2], Zhi-Qian Lin[3], Bing-Hong Chen[3], Yi-Chen Sun[1], Kai-Feng Hung[3]

[1]Department of Opthalmology, Taipei Tzu-Chi Hospital, the Buddhist Tzu-Chi Medical Fiundation, New Taipei City, Taiwan, [2]National Yang Ming Chiao Tung University-Yangming Campus, Taipei, Taiwan, [3]Department of Medical Research, Taipei Veterans General Hospital, Taipei, Taiwan

Background: Aptamers have sparked significant interest in cell recognition due to their superior binding specificity and biocompatibility. Cell recognition can be mediated by targeting the major histocompatibility complex (MHC) that presents short peptides derived from intracellular antigens. Although numerous antibodies have demonstrated a specific affinity for the peptide-MHC complex, the number of aptamers that exhibit comparable characteristics is limited. However, the success rate of aptamer identification is low. This is possibly due to the presence of complementary sequences or sequences rich in quinine and cytosine that are less accessible for primers. Here, we use ovalbumin model antigen to explore whether aptamers with specificity for binding to a defined peptide-MHC complex can be identified. We developed DNA aptamers with modified SELEX by employing systemic consecutive selections with minimal PCR amplification. Furthermore, the other tumour antigen, claudin-6, was also used as a target to determine whether our modification for SELEX can be used with any selection technology.

Methods: To determine whether our modified SELEX has potential for selecting aptamer capable of cancer-specific targeting, we used ovalbumin presented by H-2Kb (to represent the specific antigen presented by MHC) and claudin-6 (a cancer-associated adhesion molecule) as a target for the selection of aptamers. This modified SELEX consisted of consecutive positive and negative selections with minimal PCR amplification. Meanwhile, the selection of candidate aptamers is based on their appearance in multiple rounds rather than enrichment, and is facilitated by several computational tools. The specificity and affinity of the candidate aptamer are validated by flow cytometry, immunohistochemistry, and immunofluorescence analysis with cells with or without these molecules.

Results: After high-throughput sequencing, a total of 211 candidate aptamers were selected for further analysis. The quadruplex forming G-rich sequences (QGRS) mapper, mFold modeling, and NUPACK web servers were used to predict the potential of G-quadruplex formation, resulting in only four potential aptamers. Using MTCQ1-OVA cells with FITC-conjugated aptamers, two aptamers showed selective binding to MTCQ1-OVA cells and had no binding specificity to MTCQ1-WT cells. The binding specificity was further validated by immunohistochemistry in tumour derived from mice inoculated with MTCQ1-WT or MTCQ1-OVA cells. In the pull-down assay, the binding affinity of these two candidate aptamers was 136.2 nM and 155.1 nM affinity.

Conclusions: This preliminary study demonstrated that our modification for SELEX is effective in the selection of aptamers with promising potential for specific cancer targeting. The identification of aptamers may facilitate further application in diverse biomedical fields.

#3762 11,000-plex aptamer based proteomics of bladder cancer urine for the discovery of novel disease biomarkers.

C. Mohan[1], K. Vanarsa[1], J. Castillo[1], L. Wang[2], Y. Lotan[3];
[1]University of Houston, Houston, TX, [2]Central South University, Changsha, China, [3]University of Texas Southwestern Medical Center, Dallas, TX

In search of more accurate, non-invasive biomarkers of bladder cancer (BC), a comprehensive aptamer-based screen of urine proteins was conducted using urine samples from a BC cohort, followed by systems biology analyses. Following an initial 1317-plex screen, an extended 11,000 plex aptamer-based proteomic screen is in progress. Based on the initial screen, 30 urine proteins were next ELISA validated in an independent cohort of 68 subjects, and the results are shown in Table 1. Of 21 urine proteins that discriminated BC from urology clinic controls (UC), urine D-dimer displayed the highest ROC AUC value (0.96) and sensitivity (95%) (Table 1). Furthermore, 9 urine proteins significantly discriminated more advanced BC (T1-T4) from earlier stages (Ta-Tis), with IL-8 and MMP-12 being the best performers. Urine MMP12 exhibited the highest specificity of 80% at fixed sensitivity for identifying advanced BC. Systems biology analysis implicated molecular functions related to extracellular matrix, collagen, integrin, heparin and transmembrane tyrosine kinase signaling in BC susceptibility, with HNF4A and NFKB1 emerging as key molecular regulators. STEM analysis of the dysregulated pathways implicated a functional role for the immune system, complement and interleukins in BC disease progression. Urine C2, D-dimer, and Elastase were additionally ELISA validated in a second BC cohort of Chinese ethnicity. Thus, comprehensive proteomics and independent ELISA validation have uncovered novel urine biomarkers for initial BC diagnosis and subsequent disease progression, that warrant further head to head comparison with current diagnostic tests.

#3763 Comparative spatial analyses of the tumor immune landscape in different mouse models of glioblastoma.

D. Klymyshyn[1], N. Jhaveri[1], A. Pratapa[1], N. Nikulina[1], T. H. Tam[1], N. Nelson[2], R. Dolcetti[3], D. Moi[3], R. Mazzieri[3], T. Mantamadiotis[4];
[1]Akoya Biosciences, Menlo Park, CA, [2]Abcam, Cambridge, United Kingdom, [3]Peter MacCallum Cancer Centre, Melbourne, Australia, [4]Department of Microbiology & Immunology, The University of Melbourne, Parkville, Australia

Background: Despite advances in treatment, glioblastoma (GBM) remains one of the most difficult types of cancer to treat, and the prognosis is poor. The current median survival time for patients with GBM is about 12-15 months, and the five-year survival rate is less than 10%. There is an unmet need for better GBM treatment options, leveraged from relevant experimental models. To develop new therapies, preclinical animal models are important for analyzing the biology of GBM and evaluating the efficacy of novel therapeutic strategies. While a variety of experimental models are used to study GBM, most preclinical investigations involve mice. In this study we utilize a spatial phenotyping application that permits comprehensive characterization and comparison of key proteins in the brain tumor immune microenvironment (TiME), and detailed comparison the TiME between different immune-competent GBM mouse models.
Methods: The Phenocycler-Fusion is a fast spatial biology solution that affords ultrahigh-plex single-cell spatial readouts. We used this solution for the whole slide imaging of mouse FFPE tissues and deep immune phenotyping of >40 proteins, comprising immune cell lineages, activation states and checkpoints, as well as biomarkers for tumor, vascular and neural landscapes of various GBM mouse models.
Results: Via single cell spatial phenotyping, we isolated spatial signatures within the mouse GBM tissue immune microenvironment. We focused on multiple immune biomarkers, including microglia/myeloid cells that were identified via the combinatorial expression of the key markers CD68, Iba-1, F4/80, Tmem119 and CD11b. The macrophages and their biomarker expression profiles exhibited significant inter- and intra-tumoral heterogeneity within different mouse GBM models, indicative of the heterogeneous and complex biology of GBM.
Conclusions: Our work encompasses the development of a custom antibody panel, an imaging workflow, as well as a novel bioinformatic analysis method. Deployment of this workflow on different mouse GBM models allowed us to study cell populations, according to biomarker profiles and spatial distribution. This study provides a deeper characterization of the diverse mouse GBM models to determine the optimal model that most accurately recapitulates the complex TiME of human GBM, including key features such as invasive tumor margins, high vascularity, blood-brain barrier, etc. We anticipate that this approach has enormous potential for a broad range of applications for which biomolecules' spatial information is important and will deepen our understanding of the GBM TiME.

#3764 Spatially resolved immune landscape revealed sex-biased T-cell infiltration in glioblastoma.

Y. Hao[1], G. Reid[1], A. Baker[1], K. L. Fink[2], G. J. Snipes[2], B. E. Mickey[2], A. E. Sloan[3], J. S. Barnholtz-Sloan[4], M. Berens[1];
[1]Translational Genomics Research Institute, Phoenix, AZ, [2]Baylor University Medical Center, Dallas, TX, [3]Piedmont Healthcare System, Atlanta, GA, [4]National Cancer Institute, Bethesda, MD

Glioblastoma (GBM) multiforme is the most aggressive type of brain cancer. These lethal brain tumors are characterized by the inter- and intra-tumor molecular heterogeneity and demonstrated cell plasticity. A male:female distribution of 1.6:1; survival outcome from treatment (debulking, radiation, and temozolomide) benefits females nearly twice that for males. Through spatial transcriptomics, we interrogated the immune landscape of GBM, seeking to tease out whether distinct biological and therapeutic niches in GBM were evident, and to understand how the tumor microenvironments contributed to the heterogeneity of GBM. We designed a set of RNA hybridization probes specifically for portraying the cell identities and cell functional states within GBM tumor. The probe set was used to profile six human GBM samples from male and female cohorts on the Vizgen MERSCOPE platform. An integrated analysis of 505,614 cells from the six samples yielded a rich and varied spatial cell atlas of glioblastoma. Our preliminary findings depict distinct spatial niches of different tumor cell subpopulations that are associated with local environmental factors such as hypoxia. We identified a small cluster of cells that are in neuronal-like state, which could potentially drive invasion. We found spatial proximity of CD4+ cells and cells that express HIF1A, suggesting the dynamic interactions between tumor cells, regulatory T cells and tumor microenvironment. We also observed significant difference in the degree of CD8+ T-cell infiltration in female samples versus male samples. The average CD4+/CD8+ T-cell ratio in males is twice as high as that of females, suggesting intrinsic sex-based differences in immune response to tumor. Expansion of these studies in additional specimens will further illuminate microenvironmental influences on glioma progression and may instruct specific interventions leading to more effective and predictable immune-oncology of this disease.

#3765 Single cell spatial proteomics analysis and computational evaluation pipeline.

Behnaz Bozorgui[1], Zeynep Dereli[1], Guillaume Thibault[2], John N. Weinstein[1], Anil Korkut[1]

[1]UT MD Anderson Cancer Center, Houston, TX, [2]OHSU, Portland, OR

Resolving tissue and proteomic heterogeneity is critical to decoding the structure and function of tumor-immune microenvironment (TIME). Such understanding requires profiling of tumor and immune cell proteomic features with spatial resolution at the single-cell level. Although such spatially resolved methods and data sets are becoming increasingly available, analytical and computational methods that can extract the highly complex features and interactions within TIME are lacking. To address that problem, we have developed a computational pipeline we call the Spatial Proteomics Analysis and Computational Evaluation Pipeline (SPACE). The SPACE pipeline is composed of many analysis modules for processing and mining highly multiplexed imaging-based data types to explore TIME composition, organization, and heterogeneity. The pipeline generates and interprets biomarker expression and positional information from multiplexed images using algorithms for image indexing, image registration, quality control, segmentation, identification and removal of non-specific signals, data normalization, automatic identification of missing data, and adjustment for left-over signals. The accurate intensity measurements at single cell level are then used to calculate the proposed spatial features that represent cellular interactions in TIME. A hierarchical decision tree of cell markers is used to annotate types and identities for individual cells. The SPACE enables statistical and differential analyses of complex spatial features as well as cell types/identities with respect to clinical annotations and genomic alterations. The visualization of spatial and imaging data is made possible through an open-source OMERO image repository and spatial maps that integrate diverse markers in a single representation. Here, we demonstrate the applications of our pipeline in diverse gastrointestinal tumor types (e.g., small bowel adenocarcinoma) and validate the importance of integrating tissue heterogeneity at spatial and single-cell level. The framework is applicable to nearly all highly multiplexed imaging data platforms, including but not limited to, CycIF, CODEX, and imaging mass cytometry.

#3766 Utilizing whole-transcriptome digital spatial profiling for glioblastoma clinical biomarker discovery.

A. Luo, K. Casella, S. Sharma, E. Baraban, C.-H. Lucas, E. Shenderov;
Johns Hopkins University School of Medicine, Baltimore, MD

Objective: *IDH*-wildtype glioblastoma (GBM) is the most aggressive brain tumor in adults. Notable for substantial inter- and intra-tumoral heterogeneity, GBM is highly resistant to standard-of-care treatment. Emerging spatial omics technologies, such as GeoMx Digital Spatial Profiling (DSP), offer novel approaches to interrogate the molecular features of regionally defined cellular ecosystems in cancer. Here, we leverage DSP to study whole-transcriptome gene expression signatures in a spatially defined manner across five *IDH*-wildtype GBMs. Methods: Formalin-fixed paraffin-embedded tumors were assessed histologically and three spatially distinct areas from each tumor were used to construct a custom “spatial” tissue microarray. From each set of three areas, we identified nine spatially distinct regions of interest (ROIs) for bulk transcriptomic analysis according to two histopathological features: distribution (cellular tumor core or tumor periphery) and vascular proximity (near or far). We evaluated normalized target expression data statistically using linear mixed modeling (LMM) with Benjamini-Hochberg correction. Results: 44 profiled ROIs and 8531 transcriptomic targets were analyzed following quality control trimming. 3D principal component analysis and unsupervised hierarchical clustering analysis showed clustering according to tumor specimen as well as distribution (core versus periphery), thereby substantiating the presence of inter- and intra-tumoral transcriptional heterogeneity. LMM-based differential gene expression analysis identified distinct molecular signatures when comparing core and periphery. Specifically, we observed elevated log2-transformed expression of migration and proliferation markers including *LAMC1* (p=0.00297) and *FABP7* (p=0.00434) in core ROIs and neurodevelopmental markers including *NTRK2* (p=0.00734) and *DAAM2* (p=0.00263) in periphery ROIs. Additionally, reactome analysis demonstrated considerable enrichment for the aberrant programmed cell death pathway (R-HSA-9645723, coverage=71.84%) in core ROIs and the MHC class II antigen presentation pathway (R-HSA-2132295, coverage=69.11%) in periphery ROIs. Interestingly, differential gene expression analysis did not reveal any biologically significant targets when subsetting for vascular proximity within cellular tumor core ROIs. However, reactome analysis of this regional subset demonstrated upregulation of various cellular proliferation pathways (G2/M transition, APC/C activity, DNA synthesis, etc.) within vessel-near ROIs when compared with vessel-far ROIs. Conclusions: We preliminarily characterize the molecular heterogeneity of GBM using a spatially guided approach. Ongoing analyses are focused on dataset validation, mixed cell deconvolution, further regional genotyping, and potential biomarkers.

#3767 A novel method to minimize HIER-induced alterations on H&E staining in an integrated mIF-H&E workflow.

K. Hwang, G. Vezeau, E. Olejnik, D. Wood, R. Cardenes, L. Duro, G. Chatterjee, J. H. Lee;
Ultivue, Inc., Cambridge, MA

Background: Hematoxylin and eosin staining (H&E) is widely used as an anatomical assay for clinical diagnosis. Researchers and clinicians also rely on molecular *in situ* techniques, such as multiplexed immunofluorescence (mIF), to gain deeper insights on cellular phenotypes and tissue microenvironment. As a result, there has been significant interest in combining anatomical stains with molecular imaging techniques, most commonly by using a terminal H&E stain after mIF staining. This allows a combination of the two assays but has been observed to show alterations in the H&E staining pattern. In this work we identify heat-induced epitope retrieval (HIER) as the root cause of alterations of the terminal H&E stain after mIF. We further demonstrate a new workflow combining an initial H&E stain with subsequent InSituPlex assay, to avoid these alterations and thus enable co-registration of highly sensitive multiplexed immunofluorescence with an unaltered H&E stain.

Methods: FFPE tissue slides were stained using a standard HIER protocol or a full mIF assay, followed by a standard H&E stain. Slides were imaged using a Zeiss Axioscan.Z1 scanner. Additional H&E-stained slides were prepared, and the H&E stain removed using a destaining protocol before carrying out InSituPlex® mIF staining for multiple markers. Fluorescence and brightfield images of the same slide were overlaid using UltiStacker® to assess qualitative differences between pre- and post-mIF H&E, and UltiAnalyzer.AI® was used to quantify cell densities and signal intensities between mIF image pre- and post-H&E.

Results: Alterations in H&E staining were observed between slides directly stained with H&E and slides stained with a terminal H&E after HIER alone or a full mIF assay. Calculated cell counts and tissue area were consistent throughout, but some tissue microstructures could be difficult to resolve after either HIER or full mIF. Our destaining protocol was successful in removing hematoxylin and eosin from directly-stained H&E slides and allowing subsequent mIF staining. For most biomarkers, qualitative and quantitative differences in InSituPlex mIF staining were minimal. Brightfield and fluorescent images were co-registered with sub-micron accuracy using UltiStacker, enabling molecularly defined cellular phenotyping within a traditional H&E image.

Conclusions: While the mIF to H&E workflow is widely used and is capable of allowing combined anatomical and cellular phenotyping, alterations in the H&E stain exist due to the use of HIER in most mIF protocols. An alternative method is possible in which H&E-stained slides are destained and then restained for mIF or other spatial assays, providing the same valuable combination of assay information but without the HIER-induced alterations in H&E staining pattern.

#3768 Optimization of digital pathology through laser capture microdissection with a 405 nm laser.

Thomas Philipson[1], Marissa Howard[1], Kevin Johnson[2], Amanda Still[1], Furkat Yunusov[1], Emanuel Petricoin[1], Virginia Espina[1], Noel Gonzalez[2], Alan Carpino[2], Lance Liotta[1]

[1]George Mason University, Fairfax, VA,[2]Targeted Bioscience, Jupiter, FL

Tumor cellular heterogeneity is a complex problem in cancer molecular diagnostics and personalized therapy. The tumor is a product of the different types and interactions of host and immune cells. Investigators have created a variety of methods to procure separate subpopulations of the tumor microenvironment for individual analysis. One of the most successful methods of this is laser capture microdissection (LCM). This method captures specific subpopulations of cells under direct microscopic visualization. This LCM technology has successfully been used for over 20 years, revealing a variety of insights into cancer pathogenesis and mechanisms of therapeutic response employed in numerous clinical trials. Nevertheless, there are two drawbacks to the current systems. For UV cutting (365 nm), the tissue is significantly damaged by the UV light energy. Infrared (808 nm) laser systems do not damage the tissue however, this method has low power and poor resolution. Our first hypothesis to be tested is that a new class of near UV 405 nm laser will have small capture areas approaching single cells while simultaneously preventing cellular damage. The second weakness of LCM is the requirement for an open-faced tissue section without a coverslip. Moreover, when visualizing the tissue of interest, the identification of regions of interest is obscured due to the refractive index mismatch between the laser microdissection cap and the tissue surface. We hypothesize that using a volatile organic compound with a refractive index similar to glass would elucidate the tissue region of interest to allow proper visualization. We successfully developed and tested a near 405 nm wavelength LCM system that utilizes a “liquid” coverslip to visualize the sample of interest with higher clarity, resolution, and contrast for immunohistochemistry, immuno-fluorescence, blood smear slides, and conventional hematoxylin-eosin tissue staining. Overall, these critical improvements LCM technology now allow for single-cell tissue capture, system automation, tissue visualization, and opens the door for artificial intelligence-assisted spatial profiling.

#3769 Spatial biology *in situ* hybridization and multiplexed immunohistochemistry detection compatibility using a modified protocol.

S. T. Clarke, M. Voeun, L. Montoya, C. Vonnegut, B. Mandavilli;
Thermo Fisher Scientific, Eugene, OR

In the field of spatial-omics imaging, combining mRNA *in situ* hybridization (ISH) detection with multiplexed protein immunohistochemistry detection (IHC) is desirable. We present a simplified workflow in FFPE tissue sections where ISH is detected using branched ssDNA signal amplification visible by brightfield imaging combined with multiplexed IHC using directly labeled antibodies detected by fluorescence. In multiple studies mRNA expression of PCNA (Proliferating Cell Nuclear Antigen) shows moderate to high nuclear positivity observed in most cancer cells, with gliomas and lymphomas being the few negative exceptions. In contrast, expression of PCNA in adult non-cancerous tissue has low to no expression, with tonsil and bone marrow being the exceptions. We first show the relationship between proliferation as measured by EdU detection, PCNA antibody and PCNA mRNA expression in the embryonic mouse model where PCNA expression is prevalent in developing tissue. Then we demonstrate a simplified working protocol for combining ISH and IHC in FFPE human cancer tissue sections for the co-detection of PCNA mRNA together with IHC using a panel of six protein markers relevant to the tumor microenvironment. For IHC, we directly labeled validated unconjugated antibodies with fluorophores using amine-reactive chemistry and select the degree of labeling (DOL) and titer for optimal signal/background most useful for multiplexing on FFPE tissue. We found important protocol steps to consider for compatibility between IHC and ISH detection method. Loss of IHC protein epitope due to ISH protocol use of proteases and loss of ISH signal due to presence of RNase commonly present in IHC antibody relevant reagents can prevent combining IHC with ISH. Stabilizing IHC through refixation prior to ISH workflow is also required. Modifying the protocols to avoid these incompatible treatments and using directly labeled antibodies provides useful strategies for multiplexing IHC with ISH.

#3770 Comparative analysis of single cell expression and digital spatial profiling in FFPE tumor tissues.

A. Moore, A. O'Hara, P. Vishwanath, L. Turner, H. Latif, C. Mozdzierz, G. Zhou;
GENEWIZ from Azenta Life Sciences, South Plainfield, NJ

Formalin Fixed Paraffin Embedded (FFPE) tissues are a staple in clinical diagnostics associated with solid tumor. Next Generation Sequencing (NGS) approaches characterize genomes, epigenomes, transcriptomes, and proteomes from a single sample source. FFPE blocks from several different tumor tissue types were serially sliced into FFPE slides. Individual slides were then utilized to explore the genome, epigenome, single cell RNA-Seq (scRNA-Seq), and Digital Spatial Profiling (DSP). Here we present a comparative analysis of two transcriptomic modalities within one FFPE tissue sample: fixed-cell scRNA-Seq of the transcriptome and digital spatial profiling of the whole transcriptome. Independent analysis of scRNA-Seq and DSP identified common trends as well as distinct differences within the same sample. Comparative analysis within sample between modalities identified statistically significant differences, driven by local tumor microenvironment, but also highlighted commonalities between methods. Cross sample comparisons showed striking differences, as indicated by tumor type. These studies highlight the strengths of each assay individually, as well as the power of a dual-assay approach for comprehensive analysis of the tumor and its microenvironment. Conclusions from this standalone analysis were further aggregated into downstream multiomics analyses, including proteomics analysis, illustrating the expanding landscape of information that can be extracted from FFPE derived tissue and the potential for novel discovery and diagnostic power integrating these complex data types holds.

#3771 3D correlated multi-scale cellular and molecular architecture of solid tumors.

S.-Y. Lee[1], Y.-C. Wu[1], J. Zheng[1], E. Khalil[1], S. Wang[2], A. Lippert[3], J. Plank[3];
[1]University of Illinois at Chicago, Chicago, IL, [2]University of Chicago, Chicago, IL, [3]Southern Methodist University, Dallas, TX

A solid tumor presents heterogeneous 3D structures at tissue, cell, and molecule levels. To develop advanced cancer diagnostics and therapies, it is important to understand in-depth cellular and molecular architecture of a tumor at multiple scales. Here we introduce novel optical microscopy methodologies for in-depth 3D spatial analysis of tumor tissues: 1) LED photobleaching-mediated 3D multiplex immunofluorescence (IF) microscopy, 2) Correlated 3D multi-resolution optical microscopy, and 3) 3D tissue region-based cell type-selective multi-omics. We built a high-power LED light irradiator with a broad emission spectrum (490-700 nm) that bleaches a broad wavelength of fluorescence signals simultaneously throughout an optically cleared, 400 µm-thick tumor tissue. Cyclic workflow involving IF staining, optical tissue clearing, 3D confocal microscopy, and LED photobleaching enables visualization of multiple cell types in the same whole 400 µm-thick tumor tissue after computational 3D image registration. The constructed multiplex image offers comprehensive 3D cellular landscape of a tumor. We also developed a method for tracking regions of interest (ROIs) in the middle of a large tumor tissue using a UV-activated visible dye in light sheet microscopy. Light sheet microscopy allows imaging an optically cleared large-sized tumor tissue at a low spatial, tissue resolution. To mark the ROI positions on a tumor, the dye is infused into agarose gel surrounding the tumor tissue and be activated and present purple-colored lines where are exposed to UV light sheets in light sheet microscopy. The tumor tissue was physically sectioned at the marked ROI positions using a vibratome after reversing tissue clearing process. Sequential IF staining and high-resolution confocal microscopy permit for visualizing detailed cellular compositions of the ROIs in the tumor. The tissue and cellular-resolution 3D images from light sheet and confocal microscopy are correlatively integrated to display ‘Google Earth’-like multi-scale view of a tumor tissue. To further analyze the ROIs of a tumor at molecular level, we have developed optical microscope-mediated fluorescence lithography methods that allow fluorescently labeling of a selected cell type in ROIs of an optically cleared 3D tumor tissue. After wash free from clearing solution and dissociation of the tumor into cells, fluorescence-marked, intact cells from the ROIs are collected through flow cell sorting. Proteins and mRNAs are extracted from the collected cells and sent to LC-MS/MS analysis and RNA sequencing. The spatial multi-omics method provides in-depth molecular information of selected cells in the ROIs of a tumor. We believe all these 3D microscopy methods will provide powerful spatial analysis tools for better understanding cellular and molecular architecture of solid tumors.

#3772 Tissue-niche-based and cell-type-selective in-depth proteomics.

Y.-C. Wu[1], E. Abi Khalil[1], S. Weng[2], S. Lee[1];
[1]University of Illinois at Chicago, Chicago, IL, [2]University of Chicago, Chicago, IL

Introduction: The development, physiology function, and pathogenesis of the tissues are intricately orchestrated by the spatial organization of diverse cell populations. Proteins are the fundamental components within individual cells that control every function. Therefore, by integrating both information on cellular location and molecular profiling, spatial proteomics has emerged as an indispensable field for understanding mechanisms governing tissue homeostasis, disease progression, and therapeutic responses. Here, I introduce a spatial proteomics method designed to target selective cell phenotypes within definite tissue niches for in-depth spatial biology analysis.
Method: In this approach, we developed a sequential pipeline highlighted with immunofluorescence staining, microscopic photobleaching, fluorescence cell sorting, and liquid chromatography-mass spectrometry (LC-MS) analysis. The process begins with staining 400-µm-thick tissue macrosections with fluorescence-conjugated antibodies to visualize specific cell types of interest. We employed two different fluorescence-conjugated antibodies of the same clone (e.g., Alexa488-anti-CD11c and Alexa647-anti-CD11c antibodies) for the staining on every targeted cell (e.g., CD11c+ immune cells). We then introduced “photobleaching barcodes” using a confocal microscope to photobleach/exhaust either one of the fluorescence signals stained on cells by exposing it to the matched laser. This allows us to create differentiable fluorescence barcodes that label cells at distinct regions, incorporating cell spatial information into our fluorescence detection. After tissue dissociation, barcoded cells were sorted into different groups which were also classified by their original locations in the macrosection. Finally, protein extraction and LC-MS analysis were conducted on the collected cells to enable comprehensive spatial proteomic analysis.
Results: The initial application in investigating dendritic cell (DC) subsets in mouse spleen during lipopolysaccharide (LPS)-induced inflammation reveals significant proteome differences among three splenic DC subsets, categorized by their locations in or outside spleen T-cell zones as well as control DCs. Our result aligns with previously published proteome data in splenic DCs, underscoring the feasibility and reliability of our technology. Currently, we are in the process of evaluating breast cancer cell heterogeneity in human biopsy specimens using our approach to profile the tumor-immune microenvironment.
Conclusion: Spatial proteomic findings from both applications are poised to discover potential drug targets that benefit treatment efficacy for inflammatory diseases and breast cancer. This technology features deep protein profiling for cell-type-specific spatial proteomics and is designed for broad applications across diverse tissue specimens in various diseases.

#3773 Bladder cancer risk stratification with the Oncuria 10 plex bead-based urinalysis assay using three different Luminex xMAP instrumentation platforms.

S. Tanaka[1], T. Sakatani[1], K. Murakami[1], R. T. Waldron[1], W. Morales[1], W. Hogrefe[2], C. J. Rosser[2], H. Furuya[1];
[1]Cedars-Sinai Medical Center, Los Angeles, CA, [2]Nonagen Bioscience Corp, Los Angeles, CA

Introduction and Objectives: Oncuria® is a bead-based multiplex fluorescence immunoassay that coordinately measures 10 protein biomarkers in urine samples. The current study compared assay performance and output when urine samples were evaluated with the Oncuria assay using three different fluorescence-analyzing instruments commonly used in diagnostic laboratories worldwide.
Methods: We compared the performance of the clinically validated Oncuria bladder cancer (BC) multiplex immunoassay when data output was generated on three different analyzer systems. Voided urine samples from 36 subjects (18 with BC and 18 Controls) were reacted with Oncuria test reagents in three 96 well microtiter plates, and consecutively evaluated on the LED/image based MagPix, and laser/flow based Luminex 200 and FlexMap 3D (all xMAP instruments from Luminex Corp., Austin, TX). The BC assay uses magnetic bead based fluorescence technology (xMAP, Multi-analyte profiling; Luminex) to simultaneously quantify 10 protein analytes in urine specimens [i.e., angiogenin (ANG), apolipoprotein E (ApoE), carbonic anhydrase IX (CA9), CXCL8/interleukin-8 (IL-8), matrix metalloproteinase-9 (MMP-9), matrix metalloproteinase-10 (MMP-10), serpin A1/alpha-1 anti-trypsin (A1AT), serpin E1/plasminogen activator inhibitor-1 (PAI-1), CD138/syndecan-1 (SDC1), and vascular endothelial growth factor-A (VEGF-A)].
Results: All three platforms categorized all 10 analytes in identical samples at nearly identical concentrations, with variance across systems typically <5%. While the most contemporary instrument, the FlexMap 3D, output higher raw fluorescence values than the two comparator systems, standard curve slopes and analyte concentrations determined in urine samples were concordant across all three units. Forty-four percent of BC samples registered ≥1 analyte above the highest standard concentration, i.e., A1AT (n=7/18), IL-8 (n=5), and/or ANG (n=2). In Controls, A1AT was higher in one sample.
Conclusions: In conclusion, the Oncuria BC assay performed similarly well across three different flow analysis platforms for all 10 analytes simultaneously evaluated in urine samples. This agreement across instruments indicates that the test is amenable to standardized performance in laboratories using existing xMAP, without requiring costly outlays for new equipment.

#3774 Evaluation of FibraChek™ for non-invasive detection of hepatic fibrosis and hepatocellular carcinoma.

S. Tanaka[1], G. Xie[2], H. Furuya[1], W. Jia[3], C. J. Rosser[4];
[1]Cedars-Sinai Medical Center, Los Angeles, CA, [2]Human Metabolomics Institute Inc, Shenzhen, China, [3]Hong Kong Baptist University, Kowloon, Hong Kong, [4]Nonagen Bioscience Corp, Los Angeles, CA

Introduction and Objectives: The incidence of hepatocellular carcinoma (HCC) has almost tripled since the early 1980s in the United States where it is the fastest rising cause of cancer-related deaths. Advanced liver fibrosis and cirrhosis are ones of major risk factors for HCC. The recent evidence demonstrates that successfully treating the cause of early to moderate hepatic fibrosis may reverse most. For this reason, detecting hepatic fibrosis in an early stage is crucial. Liver biopsy is currently the gold standard for the assessment of hepatic fibrosis in clinical practice. Thus, there is an urgent clinical need for the development of non-invasive blood-based tests because of its ease of obtaining biological material. Previously, we developed FibraChek™, non-invasive blood-based tests. In this study, we tested the performance of FibraChek™ on detecting hepatic fibrosis and HCC in the US.
Methods: The performance of FibraChek™ was evaluated in a single-institutional cohort of 14 prospectively collected subjects presenting for chronic liver disease (NAFLD/NASH) patients with hepatic fibrosis, 19 prospectively collected subjects diagnosed with HCC, and 12 prospectively collected controls from the US. The algorithm uses weighted value of the 5 biomarkers: AST, ALT, Platelet, Taurocholic Acid (TCA) & Tyrosine plus age to derive a risk score. The ability of the test to identify patients harboring hepatic fibrosis or HCC was assessed. Hepatic fibrosis status was confirmed by tissue biopsy or definitive surgery. Diagnostic performance was assessed using AUC.
Results: FibraChek™ provided an AUC of 0.923 with an overall sensitivity of 93.9%, specificity of 81.8%, NPV 91.2% and PPV 81.8%. Interestingly, risk scores in HCC cohort indicated higher than those in patients with hepatic fibrosis. Thus, FibraChek™ may be also able to use for HCC detection.
Conclusions: Serum levels of a biomarker panel enabled the accurate discrimination of hepatic fibrosis and controls. The FibraChek™ test can achieve the easy, efficient, and accurate detection of hepatic fibrosis and HCC in a non-invasive patient setting.

CLINICAL RESEARCH: Metastasis Biomarkers
Poster Session

#3778 Comprehensive analysis of single disseminated cancer cells identifies a stem-like phenotype with strong prognostic impact.

T. Mederer[1], D. Spitzl[1], F. Elsner[1], B. Polzer[2], M. Ried[3], R. Neu[3], T. Robold[3], H.-S. Hofmann[3], C. A. Klein[1];
[1]University of Regensburg, Regensburg, Germany, [2]Fraunhofer-Institute for Toxicology and Experimental Medicine, Regensburg, Germany, [3]University Hospital of Regensburg, Regensburg, Germany

Introduction: Recent studies on disseminated cancer cells (DCCs) in Non-Small-Cell Lung Cancer (NSCLC) patients demonstrated their clinical relevance even in early tumor stages. However, their molecular and phylogenetic link to the primary tumor is currently unclear. Certain genetic alterations, such as TP53 or KRAS mutations, have been proposed to be clonal events and drivers of dissemination and metastasis. In this study, we analyzed the genome and transcriptome of single DCCs to identify the characteristics of early DCCs and their translational clinical value.
Materials and methods: From 2011 to 2019 we prospectively collected and analyzed bone marrow aspirates and lymph node samples from 296 newly diagnosed NSCLC patients undergoing tumor resection with curative intention. Presence of DCC was examined by i) immunocytology (IC) for Cytokeratin (clone A45-B/B3, bone marrow, BM-DCCs) or EpCAM (clone BerEp4, lymph node, LN-DCCs) and ii) immunofluorescent (IF) staining for EpCAM in a live cell suspension (clone HEA-125) from BM or LN. Single cells were isolated using micromanipulation and subjected to Whole Genome Amplification or combined Whole Genome/Transcriptome Amplification for IC and IF, respectively. Sanger sequencing for known hotspot mutations in TP53 and KRAS was performed on single DCCs. Gene expression profiles of DCCs were analyzed by single cell RNA sequencing and the results were compared with clinical data with a mean follow-up of 2.93 years (range 0.03-7.22).
Results: LN-DCCs were found in 44.8% and 59.6% by IC and IF, respectively. CK_{IC}^{pos} BM-DCCs were found in 45.2%, while $EpCAM_{IF}^{pos}$ BM-DCCs were present in 52.8%. LN-DCCs correlated with
reduced tumor-specific survival (TSS, p=0.009) and progression-free survival (PFS, p=0.025). $EpCAM_{IF}^{pos}$, but not CK_{IC}^{pos} BM-DCCs correlated with reduced TSS (p=0.003) and PFS (p=0.083). Genetic analysis of single DCCs revealed that TP53 or KRAS mutations could be found in 3.6% and 2.8% of analyzed BM-DCCs and 5.0% and 29.3% of LN-DCCs for IF and IC, respectively. Single cell RNA-seq showed distinct transcriptomic profiles for LN- and BM-DCCs, and identified a DCC phenotype with high stemness score in the bone marrow. Further analysis of potential transcriptome-based biomarkers identified a novel candidate marker for activated $EpCAM^{pos}$ BM-DCCs that strongly correlates with PFS and TSS (p<0.001).
Conclusions: DCCs in early-stage NSCLC have high prognostic value and predict reduced PFS and TSS. While genetic alterations in the TP53 and KRAS gene were not detected in the majority of analyzed DCCs, transcriptomic phenotypes provided relevant information and identified a subset of activated DCCs that correlate strongly with relapse and poor outcome.

#3779 Genomic and clinical characterization of metastatic patterns using real-word data from a large cohort of colorectal cancer patients.

P. Manca, A. V. Kris, H. Walch, C. Fong, J. Jee, K. Pichotta, N. Schultz, W. K. Chatila, R. Yaeger, F. Sanchez-Vega;
Memorial Sloan Kettering Cancer Center, New York, NY

Background: Colorectal cancers (CRCs) can exhibit disparate metastatic patterns that affect outcomes. We investigated associations between genomic features and organ-specific metastatic tropism and we compared the frequency of actionable alterations detected in patients undergoing longitudinal clinical sequencing.
Methods: We analyzed data for 6574 tumors from 6153 CRC patients, including 4510 primary and 2064 metastatic specimens. All patients had microsatellite stable (MSS) disease and were treated at Memorial Sloan Kettering. Paired primary and metastatic samples were available for 203 patients. Tumors were sequenced with MSK-IMPACT, a targeted DNA sequencing assay that identifies genomic alterations in 341-505 genes. Clinical annotations included sex, stage at diagnosis (Dx), and primary tumor location. History of metastatic disease was automatically retrieved from radiology reports using validated natural language processing methods; time to specific-site metastasis was modeled with Cox regression. False discovery rate (FDR) was used to correct for multiple hypothesis testing. The OncoKB knowledge base was used to identify clinically actionable alterations.
Results: Liver (n=1068, 51.7%) , peritoneal (n=269, 13.0%) and lung metastases (n=263, 12.7%) accounted for the majority of non-primary sequenced specimens. The frequency of actionable alterations (OncoKB Level≥3A) did not vary between unmatched metastatic and primary samples (12.3% vs 11.4%, p=0.302). In primary tumor samples from patients with localized disease at the time of diagnosis, TGFB pathway alterations were associated with increased risk of metastasis to the brain (HR=2.41, p=0.028), bone (HR=2.10, p<0.001), peritoneum (HR=1.82, p=0.001) and liver (HR=1.42, p=0.049). Alterations in the RAS pathway were associated with increased risk of lung (HR=1.47, p=0.009), peritoneum (HR=1.54, p=0.021) and liver (HR=1.44, p=0.026) metastases. By contrast, WNT pathway alterations were associated with a lower risk of developing lung (HR=0.69, p=0.033) and peritoneal metastasis (HR=0.68, p=0.081). Among patients with paired primary and metastatic samples, no significant difference was observed between the frequency of clinically actionable alterations in primary vs. metastatic specimens (16.7% vs. 18.2%, p=0.794). Presence of metastases-private or primary-private alterations did not correlate with site-specific metastasis risk.
Conclusions: The risk of developing metastatic disease and organ-specific dissemination might be linked to genomic abnormalities detectable at the localized stage. No significant difference in the frequency of actionable alterations was observed between primary and metastatic CRC samples.

#3780 From diagnostic labs to rapid near-patient testing: Bridging across RT-qPCR platforms of a clinicopathological and gene expression model for cutaneous melanoma patients.

L. Pozza[1], S. Zumrutcu[1], L. Bosman[1], A. van der Spek[1], M. Moreau[2], D. Tempel[1], J. Dwarkasing[1], **D. Bellomo**[1];
[1]SkylineDx, Rotterdam, Netherlands, [2]Biocartis, Mechelen, Belgium

Background: Gene expression signatures are becoming increasingly common in clinical settings, for diagnosis, risk stratification, and treatment response prediction. However, deployment in clinical practice often entails a molecular platform different from the one used for development. Transporting molecular signatures across platforms ("bridging") cannot be achieved directly, due to differences in scales and distributions in gene expression and requires bespoke methods. Here, we focused on the bridging of a clinicopathological and gene expression model (CP-GEP) across two reverse transcription-quantitative polymerase chain reaction (RT-qPCR) platforms: a single-plex SYBR Green qPCR, and a multiplex TaqMan probe-based qPCR (Idylla TM platform). CP-GEP is a regression model, combining eight genes (plus two housekeeping genes) and two clinicopathologic variables (age and Breslow thickness), able to stratify patients with melanoma into two groups based on their risk of sentinel lymph node metastasis.
Methods: For the bridging, we selected 150 samples of primary melanoma patients who underwent a sentinel lymph node biopsy from a cohort of stage I-III melanoma patients. We measured the expression of the eight genes on both qPCR platforms and quantified them as ΔCt. Within a bootstrapping scheme (500 repeats), for each gene, we learned a mapping ("bridging function") between ΔCt spaces, using all eight genes as regressors. Exploiting the linearity of per-gene bridging functions, we reparametrized the CP-GEP model so that we could directly use it in the target platform. We assessed the performance of the bridging, in terms of Percent Agreement (PA), defined as the percentage of the concordant binary outputs between the original and the bridged models; both in the bootstrapped samples and in 15 samples from an independent cohort.
Results: In the bootstrapped samples, we obtained a PA of 100%, in the intervals for which we had pre-defined acceptance criteria, based on the distance from the cut point; and we had a mean PA of 89.2% [95% CI, 85.23%, 94.6%] when we considered all samples. In the external validation, we achieved a PA of 100%; all performance metrics were identical. The continuous scores of the original and bridged models were in excellent agreement, with an R^2 equal to 0.95 both in the bridging and external validation cohorts.
Conclusions: We showed that a model, combining gene expression and clinicopathologic variables, originally developed on a single-plex SYBR Green RT-qPCR, often used in diagnostic labs, could be robustly reparametrized to be compatible with a multiplex TaqMan probe-based qPCR (Idylla TM platform), more suitable for point-of-care-diagnostics. The ability to transfer models across different molecular platforms can greatly accelerate the translation of fundamental research to clinical practice.

#3781 Tracking triple negative breast cancer (TNBC) evolution in the molecular residual disease (MRD) setting in the c-TRAK TN clinical trial.

M. Coakley[1], R. J. Cutts[1], P. Sritharan[2], S. Hrebien[1], C. Swift[1], K. Dunne[1], L. Kilburn[2], K. Goddard[2], G. Villacampa[2], P. Rojas[3], W. Emmett[3], C. Pipinikas[3], P. Hall[4], C. Harper-Wynne[5], T. Hickish[6], I. Macpherson[7], A. Okines[8], A. Wardley[9], D. Wheatley[10], S. Waters[11], J. M. Bliss[2], I. Garcia-Murillas[1], N. C. Turner[12]; [1]The Institute of Cancer Research, London, United Kingdom, [2]The Institute of Cancer Research, Sutton, United Kingdom, [3]Neogenomics/Inivata, Cambridge, United Kingdom, [4]University of Edinburgh,, Edinburgh, United Kingdom, [5]Maidstone and Tunbridge Wells NHS Trust, Maidstone, United Kingdom, [6]University Hospitals Dorset NHS Foundation Trust, Bournemouth, United Kingdom, [7]The Beatson West of Scotland Cancer Centre, Glasgow, United Kingdom, [8]Breast Unit, The Royal Marsden Hospital, London, United Kingdom, [9]Outreach Research & Innovation Group Ltd, Manchester, United Kingdom, [10]Royal Cornwall Hospitals NHS Trust, Truro, United Kingdom, [11]Velindre University NHS Trust, Cardiff, United Kingdom, [12]The Institute of Cancer Research & The Royal Marsden Hospital, London, United Kingdom

Background: Circulating tumor DNA (ctDNA) to track early tumor clones and to identify the point of origin of clones in relapsed disease, could provide novel insights into the impact of heterogeneity on the development of MRD and relapse in TNBC.

Methods: c-TRAK TN recruited 161 patients (pts) with early TNBC into prospective ctDNA surveillance after curative therapy. Two distinct early tissue samples were provided, and a subset provided a relapse biopsy. Tissue was whole exome sequenced (WES) and relapse plasma DNA underwent error-corrected WES. Clonal evolution analysis was performed for pts who developed MRD with a minimum of 2 samples with WES (n=44), and non-relapse pts with samples before and after neoadjuvant chemotherapy (NAC) (n=16). Clonal structures were inferred with Pyclone; the founding clone as the cluster with highest cellular prevalence (CP). Clones were validated and tracked using the RaDaR ctDNA assay, supplemented with a median of 9 (range 6-45) variants specific to each clone. Cluster hierarchy and phylogenetic tree structure was derived using ClonEvol.

Results: A median of 3 (range 1-5) clones per pt validated. Non-validated clones (12.9%) and pts with only 1 clone validated were removed, resulting in 56 pts for analysis. To assess the impact of spatial heterogeneity, contemporaneous paired early tissue was available from 17 pts who developed MRD. Primary tumor subclones were detected in the MRD or relapse in 88.9% (8/9) pts with a subclone detected in all regions, versus 37.5% (3/8) pts with a subclone unique to 1 region ($p = 0.049$). To assess the impact of NAC, paired tissue before and after NAC, was available in 32 pts. Distinct sub-clonal evolutionary patterns were identified. Subclones increased in CP or were first detected after NAC in 75% (24/32) pts. Subclones present prior to NAC were reduced or lost in 62% (20/32) pts. Sub-clonal persistence was observed in 46.8% (15/32) pts. Subclones first detected following NAC were detected in the MRD in 60% (6/10) pts. Following NAC, subclones reduced or lost re-emerged in the MRD in 30% (3/10) pts, versus subclones that persisted which were detected in the MRD in 100% (9/9) pts ($p=0.003$). In 21 pts, relapse samples were available. Relapse-unique subclones were identified in 57% (12/21) pts, with 2 new subclones in 1 pt. Relapse-unique subclones were not detected in MRD in 41.6% (5/12) pts, and were detected in the MRD in 66.7% (8/12) of pts.

Conclusion: Polyclonal metastasis is a common mode of metastasis in TNBC, with frequent detection of primary tumor subclones in the metastasis. NAC provides an evolutionary bottleneck, with subclones detected post NAC being the most likely to persist into the MRD and subsequent relapse. Relapsed cancer frequently had subclones not detected in the primary cancer, with approximately half of these potentially late arising, and half detectable in MRD suggesting early establishment of diversity.

#3782 IASLC grading system predict distant metastases for resected lung adenocarcinoma.

Y. Wang[1], M. R. Smith[1], Y. Liu[1], M. E. Green[2], O. A. Hassan[3], A. M. Balmaceda[4], T. Sexton[4], W. Li[4], F. Xing[1];
[1]Wake Forest University School of Medicine, Winston-Salem, NC, [2]Eastern Connecticut Pathology Consultants, Manchester, CT, [3]Atrium Health Cabarrus Medical Center, Concord, NC, [4]Atrium Health Wake Forest Baptist Medical Center, Winston-Salem, NC

The International Association for the Study of Lung Cancer (IASLC) proposed a new histological grading system for invasive lung adenocarcinoma (LUAD). However, whether this new grading system is able to predict distant metastases in LUAD patients has not been evaluated. This study investigated the feasibility of using this grading system to predict the occurrence of brain and bone metastases in patients with resectable LUAD which identifies patients who have a high probability of developing distant metastases after surgery. We collected clinical information and pathological reports of 179 early stage LUAD patients who underwent resection during 2008 to 2015 from Wake Forest Comprehensive Cancer Center. All patients were followed up for 5 years and both bone and brain metastasis-free survival were calculated. Tumor grading of all samples was evaluated by both IASLC grading and predominant pattern-based grading systems. The ability of predicting distant metastases using IASLC grading and tumor stage were examined by receiver operating characteristic curves (ROC). 28 out of 179 patients developed distant metastases in five years with a median overall survival of 60 months for metastasis-free patients and 38.9 for patients with distant metastasis. Compared to predominant pattern-based grading system, IASLC grading system showed a stronger correlation with distant metastasis incidence. Complex gland pattern is enriched in patients who developed bone and brain metastases compared to metastasis-free patients. IASLC grading system also showed a superior prediction power of distant metastasis compared to tumor stage with area under curve (AUC) of 0.69 for brain metastasis and 0.71 for bone metastasis. IASLC grading system is capable of predicting the incidence of distant metastasis among early-stage invasive LUAD patients.

#3783 Oral squamous carcinoma, LN metastasis.

H. Kawai, H. S. Eain, T. Ohara, M. W. Oo, Y. So, H. Nagatsuka;
Okayama Univ. Graduate School of Med., Dentistry & Pharm. Sci., Okayama, Japan

Due to genetically unstable nature of cancer cells, they give rise to genetically different variant subclones inside a single tumor. To enable the development of more efficacious therapies, it is crucial to understand cancer heterogeneity and subclone characteristics. Oral squamous cell carcinoma (OSCC) has high heterogeneity and plasticity. C-X3-C motif ligand 1 (CX3CL1) is the chemokine with anti- and pro-tumor functions. Our study reported CX3CL1 functions on cancer subclones with different phenotypes, both in vivo and in vitro. We found that Mouse OSCC (MOC) 1 and MOC2 cells responded in similar manners to CX3CL1 in vitro. However, in vivo, CX3CL1 increases cellular differentiation in indolent cancer (MOC1) while increasing metastasis in aggressive cancer (MOC2). These phenomena are influenced by different phenotypic tumor microenvironments created by indolent and aggressive cancer. From there, we established that when aggressive cancer cells gain CX3CL1 expression, they stimulate protumor immune system, promoting cancer metastasis via lymphatic vessels. A similar phenomenon was observed in metastatic OSCC patient samples, where CX3CL1 expression became intense in metastasis regions, consistent with aggressive subclone (MOC2) character; we correctly predicted patient outcomes by using CX3CL1 as prognostic indicator for long-term follow-up in metastatic OSCC patients. In conclusion, CX3CL1 is the key factor for stimulating aggressive cancer subclones to create new lymphatic networks for lymph node metastasis.

#3784 Methylated DNA markers for detection of peritoneal metastasis in pancreatic cancer.

K. Maheshwari, C. K. Berger, W. R. Taylor, D. W. Mahoney, K. N. Burger, A. M. Delgado, K. A. Doering, H. M. Streich, P. H. Foote, S. P. Cleary, T. E. Grotz, M. L. Kendrick, R. L. Smoot, P. P. Starlinger, C. A. Thiels, M. J. Truty, S. G. Warner, J. B. Kisiel, S. Majumder;
Mayo Clinic, Rochester, MN

Introduction: Laparoscopy with peritoneal lavage enhances staging accuracy in patients with pancreatic ductal adenocarcinoma (PDAC). Occult intra-abdominal metastases are identified by staging laparoscopy in approximately 20% of patients with radiologically localized PDAC. Peritoneal fluid cytology has limited sensitivity in detecting occult intra-abdominal metastasis. Methylated DNA markers (MDMs) can accurately detect PDAC from tumor tissue, blood, and pancreatic secretions. This study aims to assess the feasibility of assaying MDMs in peritoneal lavage fluid obtained at the time of staging laparoscopy for patients with PDAC.

Methods: Peritoneal lavage fluid (25-60 mL) obtained from patients with PDAC at the time of staging laparoscopy was centrifuged for 10 minutes at 1200×g. The pellet was resuspended and aliquoted into 200µL tubes and frozen at -80°C. DNA extracted from one aliquot was assayed for mutant *KRAS (G12A and G13D)* and then bisulfite converted to measure 13 MDMs (*GRIN2D, CD1D, ZNF781, FER1L4, RYR2, CLEC11A, AK055957, LRRC4, MAX.CHR5.4295, HOXA1, PRKCB, SHISA9, NTRK3)* and a normalizing reference gene (*B3GALT6*) using quantitative methylation specific PCR. The association of *KRAS* and the average signal from the 13 MDMs (MDMscore) with intra-abdominal metastasis (Y/N) was assessed with the area under the receiver operator characteristic curve (AUC).

Results: Among 48 PDAC patients, staging laparoscopy revealed intra-abdominal metastasis in 15 (31%). Of the 15 intra-abdominal metastases, 6 were found to have biopsy-confirmed intra-abdominal metastasis and positive peritoneal cytology, 4 were positive on peritoneal cytology alone, and 5 had biopsy-confirmed intra-abdominal metastasis alone. The sensitivity of the MDMscore for intra-abdominal metastasis was 87% (CI: 60-98%) at 90% (CI: 76-98%) specificity whereas the sensitivity for *KRAS* was 40% (CI: 16-68%) at 85% (CI: 68-95) specificity. The AUC for the MDMscore was 0.98 (CI: 0.94-1.00) compared to 0.62 (CI: 0.48-0.77) for that of *KRAS* ($p<0.0001$).

Conclusion: MDMs assayed from peritoneal lavage fluid collected during staging laparoscopy is a novel tool for accurate molecular staging of PDAC. These early results warrant further study in a larger cohort to assess impact on peritoneal staging and its clinical utility in the neoadjuvant treatment paradigm of PDAC.

#3785 Clinical and genomic characterization of melanoma brain metastases.

M. Padilla Mazzeo, H. S. Walch, R. Kumar, J. Eichholz, C. Cooper, N. Nandakumar, J. Shen, I. Khatri, L. Del Balzo, A. Skakodub, E. Miao, D. W. Kelly, K. Kwok Hei Yu, J. Wilcox, B. S. Imber, Y. Yu, Y. Yamada, H. Vasudevan, A. Ilica, N. Schultz, L. R. G. Pike;
Memorial Sloan Kettering Cancer Center, New York City, NY

Introduction: Melanoma has a high propensity for brain metastasis (BM). Although advancements in brain-penetrant treatments have resulted in improved central nervous system (CNS) disease control, BMs remain a significant cause of morbidity and mortality. The molecular features of melanoma BM are poorly defined, and there is an unmet need to identify biomarkers associated with CNS-specific outcomes.
Methods: We retrospectively identified 109 patients with melanoma BM who underwent craniotomy at Memorial Sloan Kettering Cancer Center (MSK) between 01/2014 and 04/2023. BM specimens were sequenced using MSK-IMPACT, an FDA-approved next-generation sequencing assay covering 341-505 genes with 700X coverage. Clinical characteristics and CNS-specific outcomes were available from 107 patients; CNS-specific radiographic endpoints were verified through direct inspection of contrast-enhanced MRI imaging by a board-certified neuroradiologist. Clinical data included baseline characteristics, prior systemic or radiotherapy (RT), and CNS-directed follow up including recording local progression of disease (POD), regional POD, and development of leptomeningeal disease (LMD).
Results: Majority (68%,73/107) patients were male with a median age at the time of primary diagnosis of 56 (range 3-88). Forty-eight patients (45%) had advanced disease (stages III and IV) at the time of initial diagnosis. At the time of BM development, half of the patients had 2-5 intracranial tumors present (50%) with a median diameter of largest BM of 33.4mm (range .9mm-64mm). The median KPS was 80 at the time of BM diagnosis, and 79% had neurologic symptoms prior to resection. 81 patients (76%) were treatment naïve at the time of resection and 56 patients (53%) developed CNS recurrence with the majority of those having local POD (29%,16/56) followed closely by regional POD of 1 lesion (25%,14/56). The most frequent genomic alterations in the cohort were *TERT* (87%), *CDKN2A* (50%), *BRAF* (43%), *NRAS* (28%), and *PTEN* (25%). The median fraction genome altered was 0.3047 and the median tumor mutational burden was 13.2 muts/Mb. We compared the genomic profiles of BM tumors of patients that had no progression, local POD, regional POD, and LMD. Compared to patients with no progression, patients with local POD were more likely to have *RB1* alterations (18.1% vs 2.1%, p = 0.04, q = 0.83) and patients with LMD were less likely to have *TERT* alterations (62.5% vs 93.8%, p = 0.03, q = 0.75).
Conclusions: Our analysis between genomic markers and clinical outcomes in melanoma BM reveals genomic features which may improve prediction and treatment strategies.

#3786 Genomic and transcriptomic characterization of peritoneal, lung and liver metastases of colorectal carcinoma reveals site-specific differences.

N. Crnovrsanin[1], S. Lakbir[2], R. d. Wit[2], S. L. C. Ketelaars[1], N. F. M. Kok[1], P. Snaebjornsson[1], G. A. Meijer[1], S. Abeln[2], R. J. A. Fijneman[1];
[1]Netherlands Cancer Institute, Amsterdam, Netherlands, [2]Vrije Universiteit, Amsterdam, Netherlands

Background: Metastasis in colorectal cancer (CRC) is a critical factor in patient outcomes, with 20% of patients affected at the time of diagnosis and up to 50% developing metachronous metastatic disease later on. Despite the growing importance of metastatic sites as independent predictors of overall survival (OS) and the ongoing development of new treatments, there has been limited effort to personalize systemic treatment based on specific metastatic locations. Aim: This study aims to compare the genomic landscape of different metastatic sites in CRC to detect novel diagnostic and therapeutic targets.
Methods: DNA whole-genome-sequencing and RNA gene expression data from metastatic CRC samples were retrieved from the Hartwig Medical Foundation (HMF). Single nucleotide variants (SNVs), somatic copy number aberrations (SCNAs) and structural variants (SVs) were reported by HMF with their pipelines. In addition, focal amplifications and deletions were identified using GISTIC2 (v6.15.30). We included 464 microsatellite stable samples derived from liver metastases (n=369), peritoneal metastases (n=58) and lung metastases (n=37). We compared DNA mutation frequencies between tumors from different metastatic sites (two-sided Mann-Whitney tests) and performed differential gene expression and pathway enrichment analysis.
Results: Liver metastases had the highest number of focal SCNAs per sample (median 33 vs 17 in peritoneum ($p < 0.001$); vs 18 in lung ($p < 0.001$)). Furthermore, we observed 39 site-specific SCNAs in liver, 9 in peritoneal and 15 in lung metastases. Of these, the most significant focal SCNAs were an amplification within 20q13.12 (79%) and deletion within 1p35.3 (64%) in peritoneal metastases and a deletion within 18q21.1 (84%) in lung metastases. Furthermore, peritoneal metastases displayed less genomic instability, featuring lower ploidy (median 2.65 vs 2.94 in liver ($p=0.025$); vs 3.15 in lung ($p=0.025$)) and lower aneuploidy scores (median 19 vs 26 in liver ($p=0.016$); vs 30 in lung ($p=0.016$)) while having no significant differences in tumor mutational burden or individual SNVs. Analysis of SVs revealed that peritoneal metastases exhibited fewer deletions (≥10kb; 1.3x fold change increase in liver and lung) and fewer duplications (≥1kb; 1.4x fold change increase in liver). Differential gene expression analysis uncovered higher expression of gene sets involved in the apical junction and the TGF-beta-signaling pathway in peritoneal metastases.
Conclusion: Specific focal SCNA and differences in genomic instability exhibit an association with preferential organotropism in CRC metastasis and could offer potential targets for the development of new diagnostic and therapeutic approaches.

#3787 Important role of GPX1 and NF-kb signaling pathway in human gastric cancer including cell proliferation and invasion.

B. Jang, J. Jung, Jr., S. Koh, Sr., K. Lee, Sr.;
Yeungnam University Medical Center, Daegu, Korea, Republic of

Background: Glutathione peroxidases(GPXs) are member of an antioxidant enzyme family. Their role is to eliminate the reactive oxygen species(ROS). Many available studies confirm that over expression of GPXs can promote cancer cell proliferation and invasion. Among the 8 GPXs, Glutathione peroxidase-1 (GPX1) is the most plentiful. Overexpression of GPX1 has been noted to promote invasion, migration, cisplatin resistance and proliferation in breast, colorectal and lung cancer. NF-kB is a ubiquitous nuclear transcription factor in the human body. that key role in cell proliferation, apoptosis and tumor progression. In reliable studies, inhibition of NF-kB expression has been shown to reduce the malignancy of Esophageal squamous cell carcinoma. Accordingly, the purpose of this study is to identify the GPX1 and NF-kB signaling pathway and their correlation with cancer cell proliferation and invasion in vitro using gastric cancer cell.
Methods: In our study, we used cell culture, Northern blotting, cDNA microarray analysis, western blotting, RT-PCR, Zymography, 3-(4,5-dimethylthiazol-2-yl)-2,5-diphenyltetrazolium bromide(MTT) assay, GPX1 knock-down with short hairpin RNS(shRNA), Standard two-chamber invasion assay, Chromatin immunoprecipitation assay.
Results: First, we confirmed that the expression level of GPX1 was up-regulated by HGF(hepatocyte growth factor) in gastric cancer cells. The cells were treated with NF-kB inhibitor, Pyrrolidine dithiocarbamate(PDTC), and analyzed by Western blotting to identify the associated pathway of HGF-induced GPX1 with NF-kB. The HGF-induced GPX1 protein level was down regulated by PDTC. The role of GPX1 associated with NF-kB was determined by knock down GPX1 expression using GPX1-sh RNA. The GPX1-sh RNA treated cells showedvdown regulation of NF-kB and urokinase Plasminogen activator(uPA) also. To fine the upper regulator of GPX1 signaling pathway, we treated AKT inhibitor(LY294002) ant then analyzed by Western blotting to identify associated pathway of HGF-induced GPX1 with AKT. When AKT pathway was inhibited, GPX1 and NF-kB were down-regulated in gastric cancer cell. HGF-mediated cell proliferation and invasion *in vitro* was decreased in GPX1 knock down cell. We identified the putative binding site of GPX1 promotor containing NF-kB binding site and confirmed the function by CHIP assay.
Conclusions: This study aimed to investigate relationship between GPX1 and NF-kB in gastric cancer cells. Results showed that HGF induced GPX1 expression through the NF-kB and AKT pathway and GPX1 may play a significant role in cell proliferation and invasion in gastric cancer. Therefore, GPX1 can be a potential therapeutic target of gastric cancer for the treatment.

#3788 EpCAM+ DCCs isolated from the bone marrow of breast cancer patients display high stemness and potency scores.

E. Raya[1], H. Koerkel-Qu[1], L. Rudhart[1], L.-M. Kohler[1], A. Damboeck[1], C. Irlbeck[2], C. Botteron[2], M. Werner-Klein[1], S. Seitz[3], C. Klein[1];
[1]University of Regensburg, Regensburg, Germany, [2]Fraunhofer-Institut fur Toxikologie und Experimentelle Medizin ITEM, Regensburg, Germany, [3]University Hospital Regensburg St. Josef, Regensburg, Germany

Metastatic dissemination of cancer cells from primary to distant sites often occurs early and it has been shown that their detection is linked to poor outcomes. Eradication of disseminated cancer cells (DCC) has therefore become the primary goal of adjuvant therapies. Since the phenotype of DCC is largely unknown, we set out to search, isolate, and molecularly characterize these candidate metastasis founder cells from bone marrow of breast cancer patients, years before manifestation of metastasis.

We screened more than 200 bone marrow samples of breast cancer patients with no evident metastasis (UICC stage M0) for EpCAM-positive cells. EpCAM positive cells in the bone marrow of healthy donors were used as a negative control. In addition, we isolated DCC from breast cancer patients with manifest metastasis (UICC stage M1). We then performed single cell RNA sequencing after whole transcriptome amplification of the collected DCC and the healthy donor (HD) control cells. To confirm the malignant origin of picked DCCs, we projected the transcriptome data into the bone marrow atlas, inferred copy number alterations, and searched for mutations shared with the matched primary tumor. EpCAM-positive cells from control patients mostly comprised plasma cells. In contrast, DCCs derived from M0-stage breast cancer patient formed a unique, non-overlapping cluster in the bone marrow atlas. UMAP-clustering placed M1-stage DCC clearly separate from M0 stage DCC. Among the collected M0-stage DCCs, we identified at least three separate subclusters. Strikingly, M0-stage DCC displayed much higher stemness and potency scores than M1-stage DCCs, reminiscent of embryonic cells. DCCs, identified by EpCAM, display very high transcriptional stemness scores when isolated before metastatic manifestation. Upon expansion and proliferation, stemness scores are reduced indicating epithelial re-differentiation. The embryonic phenotype of M0-stage DCCs may reflect an early adaptive mechanism that enables DCC to survive in an ectopic environment and may impact on the metastatic potential of the DCC.

#3789 Discovery of liquid biopsy-based novel protein biomarkers for early detection of breast cancer metastasis.

C. Jinno[1], S. Tanaka[1], T. Fujii[2], H. Furuya[1];

[1]Cedars-Sinai Medical Center, Los Angeles, CA, [2]National Cancer Institute, Bethesda, MD

Introduction and Objectives: Despite recent advances in screening and therapeutic technology, breast cancer is still the first leading cause of cancer death among females. When detected early (i.e., SEER Stage Localized), the 5-yr survival rate is 99%. The 5-yr survival rate is still 86% when cancer cells have spread beyond the breast, but this spread is limited to nearby lymph nodes (SEER Stage Regional). However, when the disease is noted to be SEER Stage Distant or metastasis, the 5-yr survival rate is significantly reduced to 31%. The evidence suggests that breast cancer is manageable if distant metastasis could be prevented. Thus, the prevailing idea is that early detection of breast cancer metastasis in surveillance will likely be the best modality to address advanced breast cancer's dismal outcomes. Thus, liquid biopsy may be suitable for "early detection" of pre- and/or micro-metastasis because of its ease of obtaining biological material. In this pilot study, we explored the potential biomarkers for the early detection of breast cancer metastasis using publicly available datasets.
Methods: We obtained 2 publicly available datasets from GEO (GSE102484 and GSE234114) containing primary tumor samples taken from subjects with and without metastatic disease. Both datasets were generated by mRNA microarray (Affymetrix Human Genome U133 Plus 2.0 Array). With these datasets, we performed the differentially expressed gene (DEG) analysis using GEO2R based on GEOquery and *limma* (Linear Models for Microarray Analysis) with a threshold criterion of Log 2 fold change >0 and p-value <0.05 as the cut-off point. The significantly upregulated genes were further screened using VerSeDa (Vertebrate Secretome Database) to select secreted proteins.
Results: In the GSE102484 (N = 683, 582 non-metastasis and 101 metastasis), DEG identified 1798 upregulated and 1472 downregulated genes. Venn diagram analysis between the upregulated genes and VerSeDa identified 337 upregulated genes coding secreted proteins. In the GSE234114 (N = 120, 60 non-metastasis and 60 metastasis), DEG identified 2873 upregulated and 931 downregulated genes. Venn diagram analysis between the upregulated genes and VerSeDa identified 563 upregulated genes coding secreted proteins. By integrating the genes from GSE102484 and GSE234114, 82 commonly upregulated genes that code secreted proteins were identified.
Conclusions: In this study, we identified 82 candidate mRNA biomarkers that are upregulated in breast tumor with metastasis. The panel of biomarkers will be validated in blood-based liquid biopsy samples in the next study.

#3790 HtrA3 promotes malignant progression of colorectal cancer via PI3K-AKT-FOXO1 signaling pathway.

J. Zheng, X. Huang, X.-e. Peng, **Y. Wu**;
Fujian Medical University, Fu Zhou, China

High-temperature requirement protease A3 (HtrA3) is known to contribute to the progression of various carcinomas through tissue-specific actions, yet its precise role in colorectal cancer (CRC) remains unclear. Our study revealed that HtrA3 is significantly upregulated in CRC at both mRNA and protein levels. TCGA database analysis showed that higher HtrA3 expression in colon adenocarcinoma is linked to poorer patient survival. Moreover, increased HtrA3 expression in HCT116 cells boosted their proliferation, migration, and invasion, while decreasing HtrA3 in SW480 cells had the reverse effect. In HCT116 cells with high HtrA3 levels, there was an increase in p-PI3K, p-AKT, and p-FOXO1, which reduced upon treatment with the PI3K inhibitor LY294002. Conversely, in SW480 cells with lowered HtrA3, these molecular levels decreased and rose again after treatment with the PI3K activator 740Y-P. HtrA3 also promoted cell proliferation, migration, and invasion in the presence of LY294002 and 740Y-P. In vivo experiments demonstrated that HtrA3 overexpression accelerated xenograft tumor growth. This study confirms that HtrA3's overexpression in CRC cells promotes their proliferation, migration, and invasion by activating the PI3K-AKT-FOXO1 signaling pathway. Therefore, HtrA3 could be a significant factor in the advancement of CRC and may serve as a potential prognostic marker for guiding targeted CRC therapies.

#3791 A prognostic signature based on inherited genetic polymorphisms for patients with uveal melanoma.

T. Verrier[1], A. Le Ven[1], A. Houy[1], A. Garcia[1], P. Gaelle[1], N. Cassoux[1], M. Rodrigues[1], J. Noirel[2], M.-H. Stern[1];
[1]Institut Curie, Paris, France, [2]Conservatoire National des Arts et Metiers, Paris, France

Introduction: Uveal melanoma (UM) is the most frequent eye malignancy in adults. Two UM subtypes exist, defined by Gene Expression Profiling or by genomic status: GEP class 1/disomy 3 [D3] and GEP class 2/monosomy 3 [M3] defining low-risk or high-risk of developing metastasis, respectively. However, these prognostic signatures require tumor samples, which may be difficult to obtain. We previously identified by a genome-wide association study (GWAS) frequent single nucleotide polymorphisms (SNP) in *IRF4* and *HERC2* associated with risk for D3 or M3 UM, respectively (1). Here, we aim to design a prognostic signature for the D3 and M3 UM subtypes based on these constitutive polymorphisms, available from blood samples.
Experimental Procedures: We used the GWAS cohort of 1476 UM patients genotyped on GSA or Omni5. Risk SNPs coupled with clinical variables were used on a cohort of 497 UM patients (191 D3, 306 M3) in a statistical machine learning process to define a predictive signature of UM subtype. A cohort of 852 UM patients was used for validation.
Results: We retained two SNPs, rs12203592 (in *IRF4*) and rs12913832 (in *HERC2*), tumor diameter and thickness, age at diagnosis and gender. We validated the predictive model in the validation cohort. The predicted high-risk group showed a decrease in time to relapse (TR) (HR: 3.72 [2.57 - 5.41], logrank p-value = 1.35E-15), overall survival (OS) (HR: 3.85 [2.58 - 5.73], logrank p-value = 1.24E-14) and progression-free-survival (PFS) (HR: 3.61 [2.32 - 5.61], logrank p-value = 6.55E-11), compared with the predicted low-risk group.
Conclusion: Common germline polymorphisms contribute to the prediction of metastatic risk in patients with localized uveal melanoma. This information could be especially useful when access to the tumor is problematic.
1. Mobuchon et al, J Natl Cancer Inst, 114, 2, (2022)

#3793 Mutational and gene expression profiles of the primary tumor and matched brain metastasis of epithelial ovarian cancer reveal differences in LAMC3 and MYC target genes.

Rita Trozzi[1], Camilla Nero[1], Marianna Buttarelli[1], Marcello Salvi[2], Luciano Giaco[1], Angelo Minucci[1], Claudia Marchetti[1], Carolina Sassu[1], Federica Persiani[1], Lorenzo De Marco[1], Simona Duranti[1], Camarda Floriana[1], Valentina Iacobelli[1], Ilenia Marino[1], Luca Mastrantoni[1], Flavia Giacomini[1], Alessia Piermattei[1], Mariagrazia Valentini[1], Tina Pasciuto[1], De Bonis Maria[1], Giuseppina Raspaglio[1], Diana Giannarelli[1], Anna Fagotti[1], Davide Cacchiarelli[2], Giovanni Scambia[1]

[1]Fondazione Policlinico Universitario A. Gemelli IRCCS, Rome, Italy,[2]Telethon Institute of Genetics and Medicine (TIGEM), Armenise/Harvard Laboratory of Integrative Genomics, Pozzuoli, Italy

Introduction: Brain metastases (BM) from Epithelial ovarian cancer (EOC) are a rare and late-stage disease manifestation, very poorly biologically characterized. We performed a multi-omics characterisation of primary EOC samples (PT) and the matched BM, to assess differences in mutational and gene expression profiles.

Material and Methods: We retrospectively collected data from EOC patients treated at Fondazione Policlinico Gemelli IRCCS who underwent surgical removal of BM between 2011 and 2022. We collected the formalin-fixed, paraffin-embedded (FFPE) tissue of the PT and the matched BM. An evaluation of single nucleotide variants (SNVs), insertions/deletions (indels) and copy number variations (CNVs) in 523 genes as well as known and unknown fusions and splicing variants in 55 genes was performed (Illumina TruSight Oncology 500 high throughput). Moreover, a bulk RNAseq analysis was conducted utilizing the NEGEDIA Digital mRNA-seq clinical-grade sequencing service. We acknowledged as differentially expressed genes if they exhibited a $-1 \leq \log2(\text{Fold Change}) \geq 1$ and $pAdj \leq 0.05$. To ensure specificity in identifying differential gene expressions pertinent to our tumoral tissues, genes associated with brain-related functionalities were systematically excluded from downstream analyses and identified through meticulous screening via the Human Protein Atlas. Clonal evolution was evaluated with two distinct algorithms: Pyclone VI and Sciclone.

Results: Matched PT/BM FFPE samples were collected from 10 different patients. We identified 21 SNVs: most of them were shared between the PT and the matched BM and TP53, CCND1, IRS2, and FGFR4 mutations emerged as the most frequently detected (shared in 70%, 50%, 50%, and 40% of the cases, respectively). Among 56 CNV detected, most of them were exclusive of the BM samples. Specifically, MYC family genes (MYC, MYCL, MYCN) were the most frequently amplified. At the clonal analysis, each patient showed at least two clusters. The majority of clusters turned out to be consistent among PT and BM demonstrating monoclonal evolution. Gene set variation analysis discovered 50 different gene sets between the PT and the BM ($p < 0.05$). Among them, the E2F targets, G2M checkpoint, MYC targets V1 and MYC targets v2 hallmarks showed higher expression in the BM. We identified 110 significant differentially expressed genes between PT and BM samples, including 27 upregulated and 83 downregulated genes. The gene LAMC3 emerged as notably upregulated in metastatic contexts.

Conclusion: This is the largest cohort present in the Literature of EOC PT and matched BM characterized with a multi-omics analysis. The intersection of LAMC3 and MYC target genes within the MET signalling network, a pathway recognized for bolstering cell motility, introduces a compelling avenue for future research.

#3794 Clinical impact of high-quality liquid biopsy for peritoneal lavage cytology in resectable pancreatic cancer.

M. Tanemura[1], K. Furukawa[2], T. Asaoka[2], D. Marukawa[1], H. Yasuoka[2], Y. Urata[3], D. Yamada[4], S. Kobayashi[4], H. Eguchi[4];
[1]Rinku General Medical Center, Izumisano, Osaka, Japan, [2]Osaka Police Hospital, Osaka, Japan, [3]Oncolys BioPharma Inc., Tokyo, Japan, [4]Osaka University Graduate School of Medicine, Suita, Osaka, Japan

Despite the general trends towards increased cancer survival, pancreatic ductal adenocarcinoma (PDAC) still has a dismal prognosis. Peritoneal recurrence is a major recurrence pattern after pancreatectomy. Peritoneal lavage cytology (CY) is employed widely in the diagnosis and staging of PDAC to rule out patients with occult peritoneal metastasis. However, the importance of CY status both as a sign of irresectability and as a prognostic factor for PDAC remains controversial. The purposes of this study were to determine whether CY+ status precludes radical resection and to propose novel liquid biopsy using peritoneal lavage fluid to detect viable peritoneal tumor cells (v-PTCs). We conducted this study to evaluate use of a new genetically modified telomerase-specific replication-selective adenovirus, expressing GFP (TelomeScan F35) in rapid detection of v-PTC dissemination (Telo-CY). We assessed the clinical utility of high-quality testing of Telo-CY in PDAC patients in comparison with the findings of conventional CY (Conv-CY). This study was approved by the IRB in our Hospital. Patients with resectable cytologically or histologically proven PDAC were enrolled. 100 ml of saline as peritoneal lavage fluid was harvested just after a laparotomy. Half of the fluid was examined by conv-CY, based on Papanicolaou staining and MOC-31 immunostaining, and the remaining half was analyzed to detect v-PTCs by Telo-CY. To distinguish between leucocyte and cells with epithelial origin, cells were stained with anti-CD45 mAb. To further distinguish cells with primary tumor origin, cells were labeled with anti-CEA, anti-CA19-9 and Ep-CAM mAbs. GFP(+) and CD45(-), and either CEA-, CA19-9- or Ep-CAM-(+) cells were counted as v-PTCs. Patients were followed to evaluate its clinical significance. Among 53 patients aged 53-87 years (30 males, 23 females), 5 were conv-CY(+), other 12 were Telo-CY(+). All 53 patients underwent surgical resection (PD/DP/TP=32/14/7). 2 patients were double-CY-(+) [conv-CY(+) and Telo-CY(+)], and peritoneal recurrence occurred at 7-9 months after surgery, despite adjuvant chemotherapy. 3 were conv-CY(+) alone, but Telo-CY(-), and no peritoneal recurrences were observed (0%). Conversely, 10 were Telo-CY(+) alone, but conv-CY(-), and 6 out of 10 patients were relapsed with peritoneal dissemination (60%). Remaining 38 patients were double-CY-negative (conv-CY- and Telo-CY-, conv-CY±), peritoneal recurrence was observed in 3 patients (8.3%). Although CY-positive status predicts poor prognosis and a higher risk of peritoneal dissemination after resection, it is not sufficient to preclude pancreatectomy by conv-CY alone. Combined CY examination with conv-CY and Telo-CY may open the window of opportunity for leading true results, accurately predicting peritoneal recurrence in PDAC patients. The CY status should be confirmed by staging laparoscopy prior to resection.

#3795 Possible role of miR-375-3p in cervical lymph node metastasis of oral squamous cell carcinoma.

M. Saika, K.-i. Nakashiro, N. Tokuzen, H. Shirai, D. Uchida;
Ehime University Graduate School of Medicine, Toon, Ehime, Japan

Latent cervical lymph node metastasis (LNM) is the most important prognostic factor in early oral squamous cell carcinoma (OSCC). However, no clinically useful predictors of LNM in early OSCC are available. In this study, we focused on the microRNAs (miRNAs) involved in the expression of numerous genes and explored those associated with latent cervical LNM in OSCC. Microarray analysis of miRNA expression showed that the expression levels of miR-375-3p were significantly reduced in primary OSCC tissues with latent cervical LNM. Subsequently, we quantified the expression of miR-375-3p by RT-qPCR and digital PCR. Similar to the results of miRNA microarray analysis, miR-375-3p was significantly downregulated in primary OSCC tissues with latent cervical LNM. The results of digital PCR showed a more significant difference than those of RT-qPCR. When the reference value for predicting latent cervical LNM was set to less than 57.85 copies based on the receiver operating characteristic curve, the sensitivity, specificity, accuracy, and area under the curve were 80%, 100%, 90%, and 0.942, respectively. Next, we examined the effects of miR-375-3p mimics on the growth and migration of four human OSCC cell lines (SAS-L1, HSC2, HSC3, and Ca9-22) that do not express miR-375-3p. When an miR-375-3p mimic was introduced into these cells, cell proliferation and migration were significantly suppressed. Total RNA was extracted from these cells reverse-transfected with miR-375-3p mimic for 48 hours. Microarray analysis and Ingenuity Pathway Analysis (IPA) miRNA target filter showed that miR-375-3p overexpression reduced the expression of 266 genes, of which 37 genes had the target sequences of miR-375-3p in their 3'-untranslated region. Among these target genes, CEPT1 and TIMM8A knockdown significantly inhibited the migration of all human OSCC cells, similar to miR-375-3p mimics. Furthermore, IPA core analysis revealed a decrease in expression of genes involved in the activation of PI3K-AKT pathways by miR-375-3p overexpression. These results indicated that downregulating miR-375-3p expression could promote cervical LNM by enhancing cell proliferation and migration in OSCC. We also found that CEPT1 and TIMM8A as novel target genes of miR-375-3p regulated the migration of human OSCC cells. The expression levels of miR-375-3p in primary OSCC tissues appear to be a useful biomarker for predicting latent cervical LNM.

#3796 Investigating unbiased whole transcriptome high-resolution spatial interactions within tumor masses.

M. M. Lee, J. Wilhelmy, T. Ong, W. Wang, B. Yeung, **C. Chang**, C. Fan;
Curio Bioscience, Inc., Palo Alto, CA

Tumor masses contain a diverse array of cell types, including both normal and tumor cells from different lineages, endothelial cells, and immune cells. Interactions among these cellular constituents and their spatial arrangements play a pivotal role in tumor development, progression, and metastasis. While single-cell analysis has provided valuable insights regarding the dissociated cellular composition of tumors, it falls short in elucidating the complex interplay of cell-cell interactions and spatial relationships that may drive tumor cellular behavior and gene expression.

We used the Curio Seeker Spatial Mapping Kits to uncover those spatial relationships in human tumor samples. The method captured whole transcriptomes and preserved the spatial locations of tumor cells, infiltrating immune cells, and normal cells by self segregating gene expression signatures and unbiased clustering. Amongst other findings by using Curio Seeker, we identified areas of immune cell infiltrates that were devoid of tumor cells, signifying zones of potential anti-tumor response.

The high spatial resolution, continuous gene expression maps from the Curio Seeker Spatial Mapping Kits reveal spatial interactions between different cellular populations that enable researchers to better understand how the interplay between tumor cell types and their cellular neighborhoods affect gene expression and tumor cell behavior.

#3797 Unveiling the spatial dynamics of the tumor microenvironment: Integrated RNA and protein profiling on the same slide through automated spatial multiomics analysis.

P. Juricic[1], **A. Manoukian**[1], A. Comberlato[1], P. Bordignon[1], A. Failletaz[1], A. Dikshit[2], E. Doolittle[2], R. Delvillar[2], S. Zhou[2], C.-w. Chang[2], L.-c. Wang[2], S. Brajkovic[1], M. Srinivasan[2], D. Dupouy[1];
[1]Lunaphore, Lausanne, Switzerland, [2]Advanced Cell Diagnostics, Newark, NJ

Spatial biology techniques have revolutionized our approach towards the study of the tumor microenvironment (TME) and its complex cellular interplay. On the one hand, multiplex immunofluorescence (mIF) methods have enabled a precise profiling of immune cells and other key cellular players of the TME while uncovering their spatial distribution and interactions. On the other hand, in situ hybridization (ISH) technologies have shown to provide complementary information to protein profiling such as the mapping of cytokine- and chemokine-expressing cells, essential for comprehending signaling networks and immune activation statuses.

Here, we made use of a novel multiomics approach that combines these two biological inputs by integrating RNAscope™ and sequential immunofluorescence (seqIF™) protocols to achieve same-slide co-detection of RNA and protein targets. The combined workflow is automated on COMET™, an advanced tissue staining and imaging platform. Through precise control over temperature and reagent distribution, the instrument ensures maximum efficiency and reproducibility of the assays. The integrated multiomics protocol allows for up to three RNAscope™ detection cycles combined with twelve seqIF™ cycles, for a final 12-plex RNA + 24-plex protein panel.

We first showed the capacity of COMET™ platform to fully automate the RNAscope™ protocol and demonstrated its sensitivity and specificity with the analysis of positive and negative control genes on HeLa cell pellets, highlighting the flexibility of sample selection. To illustrate the potential multiomics in unravelling the complexity of the TME, we designed a panel of 12-RNA-targeting probes for key biomarkers of tumor-infiltrating lymphocytes and their activation status, including multiple secreted molecules (e.g., cytokines and proteases). This was combined with a 24-antibody panel for the detection of protein biomarkers, selected to enable the single-cell profiling of different players within the TME. We applied this panel to characterize different human FFPE tumor tissues and showed that the co-detection of RNA and protein biomarkers on the same slide allows a better characterization of key cellular components involved in tumor progression and immune response.

Our results highlight the potential of spatial multiomics technologies in enhancing the efficiency of investigations of immune cell behavior and generally the understanding of cellular interplay in the TME. Their full automation on a platform like COMET™ will accelerate analysis and increase robustness by minimizing user intervention, and ultimately helping in the development of prognostic and predictive biomarkers, in the refinement of cancer diagnoses, and in the selection of new personalized therapies.

#3798 Advancements in multiplexed spatial phenotyping.

L. Montoya, S. Clarke, A. Harvey, J. Serafin, M. Voeun;
Leticia Montoya (Individual), Eugene, OR

Spatial omics is an expanding research area focused on integrating spatial knowledge of tissue with transcriptomics (RNA) and proteomics (protein). Understanding the complexity of the biological structure(s) is an important biological process in cancer immunotherapy research which requires accurate target classification. Translational profiling of 4+ targets on a single sample at one time can be difficult in many ways, such as, panel design, staining protocols, and data analysis. Furthermore, to design a reliable multi-target biomarker panel, there are many parts to overcome, such as protein abundance and localization, fluorophore compatibility, varying tissue types, and data characterization, to name a few. To address the needs of high target multiplex ability, labeling methods have advanced in cyclic detection enabling iterative labeling and detection using automated fluidics, however these approaches suffer from low simultaneous target throughput. Thermo Fisher Scientific can now provide a streamline process for tissue labelling; a process that enables sufficient labelling of high multiplexed panels completed within a couple of hours. We show successful detection of a wide range of various protein markers across numerous tissue organs used in various biological research applications with our uniform technique of labelling.

#3799 Spatial biomarker prediction in papillary renal cell carcinoma using artificial intelligence-based immunofluorescent inference.

J. Brewer[1], J. Vento[2], S. Haake[2], **A. Reddy**[1];
[1]Vindhya Data Science, Morrisville, NC, [2]Vanderbilt University Medical Center, Nashville, TN

Papillary renal cell carcinoma (pRCC) accounts for ~15-20% of the global burden for kidney cancers but still lacks effective mechanisms to predict patient responses to therapeutic intervention. Existing therapies targeting kidney cancers (anti-angiogenesis and immunotherapy) intimately involve the tumor microenvironment in their mechanism of action. However, the role of the physical organization of the tumor in determining therapeutic efficacy remains unknown. Previous efforts have utilized transcriptional profiling to stratify patients into treatment categories but here we propose to leverage artificial neural networks ("AI") to infer the expression of marker genes for particular cell types of interest based on ubiquitously expressed immunofluorescence channels, unstained brightfield images, and hematoxylin and eosin (H&E) stained images. We have developed AI models that are capable of the prediction of a range of relevant cell types based on the expression profile of DAPI, type IV collagen, and integrin beta-1, including endothelial cells, T cells, macrophages and other cell types. This work applies an AI model class known as generative adversarial networks (GANs) to produce photo-realistic simulated immunofluorescence images based on the input channels. This approach may allow us to accurately predict complex multiplex immunofluorescence (mIF) images from simpler, more routine histological methods, greatly reducing the cost burden required to profile histopathology images for cell types of interest. Our previous work identified a number of interesting cell-cell association clusters correlated with patient prognosis and this extension of that previous work aims to allow for the prediction of these interactions while obviating the need to perform the original, costly multiplex immunofluorescence assay or even a more reduced immunofluorescence staining panel which may still be out of reach for many clinical pathology labs and the interpretation of which may be challenging. By simplifying and increasing the availability of predictive AI models for digital pathology, we hope to further develop and apply predictive biomarkers for patient prognosis and treatment response in papillary renal cell carcinoma.

#3800 Next generation of spatial biology: High-throughput multiplexed Imaging Mass Cytometry™ with whole slide modes.

Q. Raza, **T. D. Pfister**, J. Chwee, L. Lim, D. Howell, N. Parsotam, D. King, C. Loh;
Standard BioTools Inc, Markham, ON, Canada

Gaining spatial insights into the cellular composition of tumor tissue has tremendous potential to inform clinical and translational researchers about mechanisms behind spatial predictors of immunotherapy success, disease etiology and progression. Imaging Mass Cytometry™ (IMC™) is a high-plex spatial biology imaging technique that enables deep characterization of the diversity and complexity of the tumor microenvironment (TME). IMC supports detailed assessment of cell phenotype and function using 40-plus metal-tagged antibodies simultaneously on a single slide without issues associated with fluorescence-based spectral overlap, tissue autofluorescence or implementation of multiple washing and acquisition cycles.

Currently, IMC enables user-defined regions of interest (ROI) in tissues to evaluate cellular and structural composition. To enhance the IMC user experience, we developed two new whole slide imaging (WSI) modes which enable streamlined workflows using ultrafast preview mode (PM) and high-throughput tissue mode (TM). PM samples the entire tissue at predefined spacing to rapidly capture a low-resolution image of all expressed markers in the antibody panel. PM generates an image in minutes to enable informed ROI placements while leaving the stained tissue intact for higher-resolution imaging. PM and TM are designed so acquisitions can easily occur on the same slide without additional processing steps. TM rapidly acquires images of the whole tissue at lower resolution (7 µm pixel size) at a quality that can be used for quantitative analysis of the tissue spatial biology. Specifically designed for high-throughput applications, TM in combination with a newly available 40-slide loader for the Hyperion XTi™ Imaging System permits automated and continuous imaging of more than 40 large tissue samples (400 mm^2 per tissue) per week.

We showcase the application of WSI modes using the newly developed Maxpar® Human Immuno-Oncology IMC Panel Kit. The 31-marker panel was combined with catalog antibodies to create a 40-plus-marker panel that expands the ability to conduct comprehensive high-plex tumor and immune cell profiling. Tumor tissue microarrays (TMA) and whole tumor tissue sections were stained with the expanded panel. Single-cell analysis of selected ROIs, on whole tumor sections and TMAs, guided by PM data successfully provided quantitative analyses of spatial biology at single-cell resolution. In parallel, TM on whole tumor sections followed by pixel-based analysis provided a spatially resolved quantitative assessment of specific tumor and immune components of the TME.

This work demonstrates the expanded capabilities of IMC and establishes it as a reliable high-plex spatial biology imaging platform with high-throughput imaging capabilities ideally suited for translational and clinical applications.

For Research Use Only. Not for use in diagnostic procedures.

#3801 Spatially resolved laser-activated cell sorting (SLACS) for high throughput spatial cell sorting in tumor research.

S. Lee, A. C. Lee;
Meteor Biotech Co., Ltd., Seoul, Korea, Republic of

Understanding of tumor heterogeneity and the microenvironment is a cornerstone in advancing cancer research and therapy. The Spatially resolved Laser-Activated Cell Sorter (SLACS) represents a novel approach in cancer research, allowing for high-throughput, precise cell isolation while preserving spatial information, which is crucial for studying tumor heterogeneity and the tumor microenvironment. The SLACS instrument utilizes laser-activated technology for selective isolation of cells from heterogeneous tissue samples, optimized for accuracy, speed, and minimal cell damage. This instrument has demonstrated effective isolation of specific cell types from complex tissue matrices, maintaining cell integrity and spatial information. Its high-throughput capacity significantly reduces sample processing time. This groundbreaking tool offers detailed exploration of tumor heterogeneity and the tumor microenvironment, providing valuable insights into cancer biology and potential therapeutic targets.

#3802 Integrating multiplex-staining and multiplex-DIA: Profiling the tumor microenvironment spatial proteome for precision cancer research.

X. Zheng, A. Mund, M. Mann;
University of Copenhagen, Copenhagen, Denmark

Our innovative dual-dimensional multiplexing approach ushers in a new era of spatial proteomic exploration. Multiplex-staining deepens understanding of tumor-stroma interactions. Our robust dimethyl labeling-based multiplex-DIA workflow enhances throughput and proteome depth in the Deep Visual Proteomics (DVP) technology. Now, our audacious integration of multiplex-staining with multiplex-DIA holds the promise of pushing the boundaries of spatial proteome profiling. This innovation combines the power of mass spectrometry (MS) with clinical viability in 1) requiring just one FFPE section for spatial proteome analysis at the resolution of individual cell types; 2) ingeniously transmuting MS revelations into a clinically feasible staining strategy. A force in personalized oncology, our innovation unravels the intricate dynamics of the cancer ecosystem while ensuring direct clinical relevance.

We conducted multiplex immunofluorescent staining on human cancers using the MACSima platform, followed by cellular phenotyping and automated single-cell laser microdissection. Subsequently, we loaded dimethyl-labelled 3-plex tryptic peptides onto Evotips and performed LC-MS analysis using the Evosep One coupled to timsTOF SCP.

Pre- and post-22-plex staining proteome analysis confirmed no significant protein loss, validating microdissection compatibility and excellent recovery. The key findings include: 1) profiling of 21 distinct cell types/subtypes in human tonsil cancer tissues, resulting in the identification of 4941 protein groups from a cellular volume of 110,859 μm^3, equivalent to approximately 55 cells; 2) observation of a loss of CD45RA/RO expression in tumor-infiltrating cytotoxic T cells, contributing to a reduction in MET and PDGF signaling activity within tumor cells; 3) the presence of abundant cytotoxic T cells, B cells, and plasma cells, coupled with a reduction in tumor cell proliferation, indicative of a hot tumor microenvironment. Proteome analysis revealed enhanced immune cell mobility and interactions with tumor cells. Moreover, our workflow facilitated the identification of potential diagnostic markers for mycosis fungoides, a marker-lacking skin lymphoma, where we achieved the identification of 2964 significant proteins out of a total of 6009. In addition, a rare lymphoma case study not only guided ABVD chemotherapy and suggested IL4 inhibition to address chemoresistance but also identified CDK, MCM, and PSMA/B/C/D/E inhibitors as promising candidates for targeted therapy. The integration of multiplex-staining and multiplex-DIA represents a significant stride in advancing personalized diagnostics and therapeutic strategies.

#3803 Spatial architecture of tumor and immune cell lineages in syngeneic mouse tumor tissues.

A. BOSE[1], L. Arvidson[2], E. Alonzo[2], M. J. Smith[1], K. O. White[1], R. A. Heil-Chapdelaine[1], G. Spang[2], M. Norton[2], S. Jensen[2], V. Agrawal[1];
[1]Leica Microsystems, Waltham, MA, [2]Cell Signaling Technology, Danvers, MA

Immune checkpoint blockade (ICB) therapies have demonstrated great clinical benefit in a variety of malignancies, but there are many patients that do not respond. Despite many preclinical and clinical studies, the mechanism of ICB is not completely understood. Development of novel therapies targeting other immunosuppressive mechanisms or combining ICB with conventional chemo or radio therapies have the potential to increase the number of patients that achieve durable responses. However, the optimal therapy or combination of therapies for a patient is likely influenced by which immunosuppressive mechanisms exist within the tumor microenvironment (TME) and the phenotype and function of tumor-infiltrating immune cells. To delineate the mechanisms of immunosuppression we selected FFPE tissue sections from three syngeneic murine cancer models and performed tumor-immune profiling to spatially understand the contributions of both immune cells and cancer cells. Mouse reactive antibodies targeting specific cellular populations will help identify the location of immune cells within the tumor site and can be used for proof-of-concept studies. This approach can lead to novel insights to synergize anti-tumor activity of ICB therapies and will help to identify differences between responders and non-responders. The Cell DIVE Multiplex Imaging Solution allows probing and imaging of dozens of biomarkers on a whole single tissue section with an iterative staining and dye inactivation workflow. At its core, Cell DIVE is a precise and adaptable open multiplexing solution that enables flexibility in antibody selection of biomarker panels used in a multiplexed imaging study. Cell Signaling Technology (CST®) has a broad portfolio of IHC-validated antibodies to detect key proteins in the TME, enabling immune cell detection and phenotyping in tissue. CST offers off the shelf (OTS), ready-to-ship antibody conjugates that have been verified to work on Cell DIVE and offers custom conjugation of IHC-validated antibodies to fluorophores and other detection reagents. CST employs a rigorous approach to IHC validation, followed by verification on the Cell DIVE platform to ensure successful detection of proteins. Here, we demonstrate multiplexed Cell DIVE imaging using a novel panel of dozens of CST biomarker antibodies across multiple mouse syngeneic tumor types. In summary, multiplexed whole slide imaging using validated antibodies and Aivia AI-based image processing software enables spatially resolved tissue analysis of the tumor microenvironment, including new insights into spatial biology.

#3804 Multiparameter cell-cycle measurement enables a better assessment of cancer aggressiveness than Ki67 LI alone.

Jan H. Mueller[1], Julia Ebner[1], Zhihao Huang[1], Maximilian Lennartz[1], Claudia Hube-Magg[1], Frank Jacobsen[1], Stefan Steurer[1], Christian Bernreuther[1], Till S. Clauditz[1], Andreas H. Marx[2], Till Krech[1], Eike Burandt[1], Guido Sauter[1], Ronald Simon[1], Sarah Minner[1], **Elena Bady**[1]

[1]University Medical Center Hamburg-Eppendorf, Hamburg, Germany,[2]Klinikum Fuerth, Fuerth, Germany

Background: Ki67 is expressed in the G1, S, G2 and M phase of the cell cycle. Immunohistochemical determination of the Ki67 labeling index (LI) is a clinically well-established tool for assessing the proliferative activity of tumors and critical clinical decisions are based on this parameter. Other cell cycle associated proteins have been evaluated for clinical utility much less intensively. This for example includes minichromosome maintenance-3 (MCM3) which is expressed earlier in the cell cycle than Ki67.

Design: To evaluate the difference and potential synergy between of Ki67 and MCM3 based proliferation indices, both proteins were analyzed by multiplex fluorescent immunohistochemistry in more than 1,580 colorectal carcinomas that were available in a tissue microarray format and results were compared with clinico-pathological parameters (pT, pN, grade, MSI, p53 status). A deep learning-based framework comprising a deep-learning based algorithm for automated cell and marker detection was used for image analysis.

Results: In our 1,583 evaluable colorectal cancers, the average Ki67 LI was 69% and the average MCM3-LI was 67%. There was a significant overlap between Ki67 and MCM3 staining: Of all panCK positive tumor cells, 56% were positive for both Ki67 and MCM3, 11% were only positive for Ki67, 8% showed positivity only for MCM3, and 25% were negative for both markers. According to the expression of Ki67 and MCM3, the following compartments of proliferating cells were defined: early ($MCM3^{+}/Ki67^{-}$), intermediate ($MCM3^{+}/Ki67^{+}$), and late phase of the cell cycle ($MCM3^{-}/Ki67^{+}$) as well as full proliferation ($MCM3^{+}$ or $Ki67^{+}$). Comparison with clinico-pathological parameters revealed the best p-values for the MCM3 LI in the comparison with pT ($p=2.7e^{-8}$), nodal metastasis (p=0.0002), and p53 alterations ($p=6e^{-11}$) while the “full proliferation” LI was most tightly linked to microsatellite instability ($p=1e^{-10}$). The Ki67 LI was best correlated to the grade (p=0.01).

Conclusion: The combined analysis of MCM3 and Ki67 enables the distinction of cells in early, intermediate, and late phase of the cell cycle. At least in colorectal cancer - a highly proliferative neoplasm - MCM3 quantification alone or in combination with Ki67 often resulted in stronger relationships with clinicopathological parameters than the Ki67 LI alone. These results suggest that a more subtle analysis of cell cycle proteins might enable a better evaluation of cancer aggressiveness than Ki67 measurement alone.

#3805 Intestinal microbiome with chemotherapy response and RAS mutation in patients with advanced or metastatic colorectal cancer: a pilot, exploratory study.

Jwa Hoon Kim[1], Boyeon Kim[2], Soohyeon Lee[1]

[1]Medical oncology, Korea University College of Medicine, Korea University Anam Hospital, Seoul, Korea, Republic of,[2]Cancer research institute, Korea University, Seoul, Korea, Republic of

Intestinal microbiomes interact with the tumor microenvironment, participating in inflammation and immune regulation, and are associated with the response to anticancer therapy. However, there has been limited research exploring the relationship between changes in the microbiome and treatment response in patients with metastatic colorectal cancer (mCRC) during chemotherapy and radiation therapy.This study included all 15 patients with mCRC treated with first-line systemic therapy between October 2021 and February 2023. We conducted 16S rRNA sequencing on baseline stool samples and investigated the association of intestinal microbiome with chemotherapy response and RAS mutation. The QIIME2 and R packages were used for analysis. As a results, Median age was 61 years (range, 35-73), and there were 8 patients with RAS-mutated mCRC. All patients were treated with first-line systemic therapy; FOLFOX (5-fluorouracil and oxaliplatin)-based (n=13) and FOLFIRI (5-fluorouracil and irinotecan)-based chemotherapy (n=2). Of them, 2 patients received short-course radiotherapy (ScRTx) to primary tumor before systemic chemotherapy, where pre- and post-ScRTx stool samples were collected. Among 15 patients, 9 patients (60%) achieved responses. Non-responders tend to exhibit higher alpha diversity (Chao1, Observed ASV) compared to responders. Firmicutes, Lactobacillus, Faecalibacterium, and the [Luminococcus]_gauvreauii_group were more prevalent in responders, whereas Bacteroidota, Prevotella, DTU089, Alistipes, Christensenellaceae_R-7_group, and Porphyromonas in non-responders. Despite no statistical significance, alpha diversity decreased in post-ScRTx compared to pre-ScRTx samples. Akkermansia, Prevotella, and Peptostreptococcus were more prevalent in the post-ScRTx compared to pre-ScRTx samples. Regarding the association of intestinal microbiome with RAS mutation, Bray curtis and weighted unifrac analyses revealed significant differences in beta diversity; higher incidence of Faecalibacterium, Lactobacillus, Prevotella, Anaerofilum, and UCG-005 in the RAS-wild type mCRC, while Bacteroides, Collinsella, Holdemanella, and Anaerostipes in RAS-mutated mCRC.This pilot study suggests the prognostic value of gut microbiomes and its association with RAS mutation in patients with mCRC treated with first line systemic therapy. A microbial functional study with immune cytokine change is planned to confirm these findings in future.

#3806 Impact of tumor-infiltrating lymphocytes, tertiary lymphoid structures, and neutrophil-to-lymphocyte ratio on the prognosis of patients with lung metastases from uterine leiomyosarcoma.

F. Mukohara[1], N. Matsuda[1], H. Yamamoto[2], T. Habu[1], D. Mizuno[1], R. Yoshichika[1], A. Matsuoka[1], T. Higashihara[1], N. Hayashi[1], M. Yoshikawa[1], M. Ohki[1], K. Shien[2], K. Suzawa[2], K. Takahashi[3], S. Toyooka[1];

[1]Okayama University Graduate School of Medicine, Dentistry and Pharmaceutical Sciences, Okayama, Japan, [2]Okayama University Hospital, Okayama, Japan, [3]Kameda Medical Center, Kamogawa, Chiba, Japan

In the tumor microenvironment, tumor-infiltrating lymphocytes (TILs) and tertiary lymphoid structures (TLSs) are known to play a major role in terms of antitumor immunity. It has been reported that the presence of TILs and TLSs is related to the prognosis of various cancers. In addition, neutrophil-to-lymphocyte ratio (NLR) has also been associated with the prognosis in them. We investigated the significance of TILs, TLSs and NLR as a prognosis indicator for lung metastases from uterine leiomyosarcoma. We retrospectively recruited 102 patients undergoing metastasetomy for lung metastases from uterine leiomyosarcoma at Okayama University Hospital from January 2006 to December 2019. TILs were evaluated by immunohistochemical staining of surgically resected specimens of lung metastases using anti-CD3/CD8/CD103/Foxp3 antibodies. TLSs were also evaluated using anti-CD20 antibodies. We counted the number of CD3/CD8/CD103/Foxp3-positive cells and classified TILs into high and low groups. We measured the density of CD20-positive cells and classified TLSs into high- and low-density groups. NLR was calculated from the blood examination immediately before the most recent pulmonary metastasectomy. We determined the cut-off value for NLR using a time-dependent receiver operating characteristic (ROC) curve analysis and classified the patients into NLR-high and NLR-low groups according to the cut-off value. In terms of TILs, both CD3 and CD8 were correlated with the prognosis. The overall survival (OS) was significantly better in patients with CD3-high group ($p = 0.018$), CD8-high group ($p = 0.017$), TLSs-high group ($p = 0.041$) and NLR-low group ($p = 0.018$), respectively. The status of CD103 and Foxp3 did not affect the prognosis. We assessed the impact of the combination of CD8-positive TILs or TLSs and NLR on the prognosis. Regarding CD8-positive TILs and NLR, the OS of CD8-high/NLR-low group was significantly better than that of CD8-low/NLR-high group ($p = 0.0078$). In terms of TLSs and NLR, the OS of TLSs-high/NLR low group was significantly better than that of TLSs-low/NLR-high group ($p = 0.010$). In conclusion, CD3-positive TILs, CD8-positive TILs, TLSs, and NLR are correlated with the prognosis, respectively. The combination of CD8-positive TILs or TLSs and NLR may be indicators to predict the prognosis of the patients with lung metastases from uterine leiomyosarcoma.

#3807 CXCL9:SPP1 macrophage polarity as a prognostic biomarker for localized colorectal cancer after surgical resection.

Y. Bang, J. Choi, H. Kim, K. Park, D. Pyo, Y. Cho, W.-Y. Park;
Samsung Medical Center, Seoul, Korea, Republic of

Background: There is an unmet need for additive predictive biomarkers for the recurrence of stage II/III colorectal cancer (CRC) after surgery. As recent studies showing the potential prognostic role of macrophage polarity defined by CXCL9 and SPP1, instead of conventional M1 and M2, we tried to evaluate the prognostic role of this biomarker in real-world practice setting, delineating biologic mechanisms.
Method: The RNA sequencing data of 273 tumors derived from patietns with stage II/III colorectal cancer who underwent surgical resection in 5 Korean cancer-centers were available for analysis. We initially divided two subgroups based on the ratio of expression level of CXCL9 per SPP1 expressions (CS ratio) and evaluated prognostic outcomes and compared immune cell proportions by deconvolutional method between subgroups.
Result: The CS ratio was higher in consensus molecular subtype (CMS)2 or CMS3 than others, and no significant differences were observed according to sidedness, stage, microsatellite instability status and medical centers. Total 69 (25.3%) patients were classified as low level of CS ratio group, and there were no significant differences in baseline characteristics, including age, sex, CMS, sidedness, stage, microsatellite instability status and medical centers. With a median follow-up of 58.2 months, the low CS ratio group showed poor 5-year recurrence-free survival (50.6 vs. 71.1%, HR=2.27, P = 0.002) and 5-year overall survival (69.7% vs. 85.9%, HR=1.75, P = 0.033). These trends were consistent across the subgroups. In the multivariate analyses including the potential prognostic factors (P < 0.1 in the univariate analyses), low CS ratio was significantly associated with poorer for RFS (adjusted HR = 1.96, P = 0.011) and OS (adjusted HR = 1.81, P = 0.002). These trends were consistent in the TCGA dataset (5 years OS: 69.7% vs. 85.9%, HR=1.98, P = 0.011). The low CS ratio group showed upregulated WNT signaling, and extracellular matrix organization pathway. Immune cell deconvolutional method exhibited the low CS ratio group showed more proportion of neutrophils, monocytes, whereas CD8+T cells, activated memory CD4+T cells were decreased, compared to high CS ratio group.
Conclusions: These results suggest that CS ratio could be an applicable prognostic biomarker in locally advanced colorectal cancer after surgical resection. Based on this classification, more advanced treatment strategy may be required for low CS ratio group to improve surgical outcomes.

CLINICAL RESEARCH: Outcome Investigation with Real World Data
Poster Session

#3811 Impact of antiviral treatment status on risk of extrahepatic cancers in patients with chronic hepatitis C.

M. Tao[1], J. Li[1], T. Wu[1], S. C. Gordon[1], L. B. Rupp[1], S. Trudeau[1], S. D. Holmberg[2], A. C. Moorman[2], P. R. Spradling[2], E. H. Teshale[2], M. A. Schmidt[3], Y. G. Daida[4], M. Lu[1];

[1]Henry Ford Health System, Detroit, MI, [2]Centers for Disease Control and Prevention, Atlanta, GA, [3]Kaiser Permanente-Northwest, Portland, OR, [4]Kaiser Permanente-Hawaii, Honolulu, HI

Background: Eradiation of hepatitis C virus (HCV) infection has been shown to reduce risk of liver cancer among HCV patients; however, there has been spare data on the effect of antiviral treatment on the risk of extrahepatic cancers. Using data from the Chronic Hepatitis Cohort Study (CHeCS), we investigated whether antiviral therapy impacts the risk of extrahepatic cancers among patients with HCV.
Methods: 17,485 HCV patients were included in the study, and they were followed until incidence of cancer including lung cancer, non-Hodgkin lymphoma (NHL), breast cancer or prostate cancer, death, or last follow-up. An extended landmark modeling approach was considered, which included time-varying covariates and propensity score justification for treatment selection bias and used generalized estimating equations (GEE) with a link function as multinominal distribution for a discrete time-to-event data. Death was considered a competing risk.
Results: Compared to untreated patients, patients with HCV treatment had significantly lower risk of lung cancer for direct-acting antiviral (DAA) treatment (hazard ratio (HR) = 0.47, 95% CI, 0.30-0.72) and for interferon-based treatment (IFN) (HR = 0.33, 95% CI, 0.20-0.50). The risk of NHL was only reduced among patients receiving DAA treatment. There were no significant associations between HCV treatment and risks of breast and prostate cancer.
Conclusion: Both DAA and IFN antiviral treatment independently reduce the risk of lung cancer, while the protective association with NHL was limited among HCV patients with DAA treatment. Our findings support the importance of timely initiation antiviral therapy in chronic HCV-infected patients.

#3812 Treatment guideline concordance for patients with metastatic hormone-sensitive prostate cancer (mHSPC) in the United States in IRONMAN, the International Registry for Men with Advanced Prostate Cancer.

H. D. McManus[1], L. Howard[1], K.-A. Crowell[1], T. Hyslop[2], J. Vinson[3], D. E. Rathkopf[4], P. Kantoff[5], L. A. Mucci[6], D. George[1], K. Stopsack[6];
[1]Duke Cancer Institute, Duke University School of Medicine, Durham, NC, [2]Thomas Jefferson University, Philadelphia, PA, [3]Prostate Cancer Clinical Trials Consortium, LLC, New York, NY, [4]Memorial Sloan Kettering Cancer Center, New York, NY, [5]Convergent Therapeutics, Newton Center, MA, [6]Harvard T.H. Chan School of Public Health, Boston, MA

Background: Treatment intensification strategies with an androgen receptor pathway inhibitor (ARPI) and/or docetaxel chemotherapy in addition to androgen deprivation therapy (ADT) are guideline recommended treatment options for patients with metastatic hormone-sensitive prostate cancer (mHSPC). Prevalence of guideline concordant care for mHSPC patients in the US and its changes over time are not well characterized.
Methods: The International Registry for Men with Advanced Prostate Cancer (IRONMAN) is a prospective cohort study of patients with newly diagnosed mHSPC and castration-resistant prostate cancer (CRPC). Therapies are captured by site personnel and by directly capturing data from treating physicians via physician questionnaires (PQ). We included all US patients with mHSPC enrolled from 2018 to January 1, 2023 with a completed PQ at enrollment. We examined patient characteristics, first-line treatments for mHSPC, and guideline concordance of first-line treatments. Guideline concordance was defined as a treatment regimen listed in the first National Comprehensive Cancer Network guidelines version for the year prior to treatment. Patients enrolled in clinical trials were excluded from analysis of treatment guideline concordance.
Results: Among the 636 US participants with mHSPC, physicians completed PQs for 458 participants (72%). Participants had a median age of 68 years (interquartile range 62 - 75). Three hundred eight (78%) were White, 72 (18%) were Black, 13 (3%) were other races/ethnicities: 65 did not report race. First-line treatment for mHSPC based on the PQ was most commonly ADT + ARPI (59%) followed by ADT + docetaxel (17%), ADT monotherapy (14%), ADT + first-generation antiandrogen (3%), ADT + ARPI + docetaxel (3%), and other treatments (5%). Overall, 384 (86%) participants received first-line treatment that was guideline concordant at the time of treatment. Treatment guideline concordance was highest in 2018 (99%) when ADT monotherapy was considered as guideline concordant but then decreased to 80% in 2019 and remained largely stable from 2019 to 2022 (85%). Overall, rates of guideline concordance were similar when stratified by race (88% for White patients vs 85% for Black patients), age (90% for patients <65 years old vs 85% for patients ≥65 years old), and treatment at a Comprehensive Cancer Center (CCC) (87% at CCC vs 86% at non-CCC).
Conclusion: Among patients with mHSPC treated in the US at 38 cancer centers, proportions of guideline concordant first-line treatment were high and remained stable over time, despite changes in approved therapies. Future efforts to understand reasons for treatment decisions will be important to better understand the relatively uncommon situations in which guidelines and actually received treatments differ for patients with mHSPC.

#3813 Relationship between race/ethnicity and oncologic outcomes in patients with biochemical recurrence after primary treatment for prostate cancer.

N. Khan[1], V. Quintero[1], C. Beck[2], M. Dimova-Dobreva[3], B. Patel[1];

[1]Bayer Healthcare Pharmaceuticals, Whippany, NJ, [2]Bayer AG, Wuppertal, Germany, [3]Bayer Consumer Care AG, Basel, Switzerland

Background: Prostate cancer (PC) is the most common form of cancer in men and accounts for ~35% and 24% of all new cancer diagnoses in Black and Hispanic men, respectively. Incidence rates of PC are higher and cancer is diagnosed at a younger age in Black compared to White men. The most frequently utilized primary treatment options are radical prostatectomy (with or without adjuvant radiotherapy) or radiotherapy. Despite the success of primary treatments for localized PC, many patients (pts) will eventually develop biochemical recurrence (BCR), defined as rising prostate-specific antigen (PSA) levels. Pts with BCR are at a higher risk of developing distant metastases and ultimately dying from PC. This targeted literature review aimed to assess the real-world (RW) relationship between race/ethnicity and BCR, and further identify any differences in oncologic outcomes (risk of metastases, PC-specific mortality, and overall survival).

Methods: A targeted literature search was performed using Embase, PubMed, and the past 2 years of American Society of Clinical Oncology conference proceedings. Selected studies were limited to English-language articles focusing on BCR and race or ethnicity among US populations, published between 1/2010 and 7/2023.

Results: Ten studies were selected after title and abstract review. Most studies had a White pt majority (83%-92%). Six studies reported no differences in BCR or oncologic outcomes when pts were stratified by race/ethnicity. Four studies reported a higher BCR risk for Black pts with low-risk PC after radical prostatectomy, but not for pts with high-risk PC. PSA and PSA doubling time (PSADT) were found to be strong predictors of oncologic outcomes.

Conclusions: The FDA draft guidance on diversity plans recommends that clinical trials enroll an adequate number of participants from underrepresented racial and ethnic populations. This requires an understanding of the diversity of the population that will eventually use the treatment and of which race/ethnicity differences in outcomes should be expected and investigated. Based on this targeted review among pts with localized PC, most RW studies had a White pt majority, and the race distribution in these studies aligned with published census and epidemiology data. In addition, findings suggest that race/ethnicity differences were not pronounced among high-risk PC pts in the US when given equal access to care or treatment, and that oncologic outcomes and BCR risk were similar across Black, White, and Hispanic pt populations. Conversely, PSA and PSADT may be stronger prognostic markers for BCR and oncologic outcomes. Future clinical trials are needed to support these RW findings and should aim to actively enroll racial/ethnic minorities to identify potential differences in efficacy and safety, and to help advance the evidence base for pt PC management.

#3814 Molecular background conditioning by temozolomide in neuroendocrine tumors.

E. Trevisani[1], A. Reni[1], I. Torresan[1], A. Rossi[1], M. Borghesani[1], S. Nicolini[1], C. Luchini[2], L. Landoni[3], D. Melisi[1], A. Scarpa[2], M. Milella[1], **A. Mafficini**[2], S. Cingarlini[1];

[1]University and Hospital Trust of Verona, Verona, Italy, [2]ARC-Net Centre for Applied Research on Cancer and University and Hospital Trust of Verona, Verona, Italy, [3]Pancreas Institute of University and Hospital Trust of Verona, Verona, Italy

Temozolomide (TMZ)-based regimens represent a valid therapeutic option in well-differentiated neuroendocrine tumors (NETs G2 and G3). As an alkylating agent, it increases DNA alteration by altering guanine residues, which either triggers cell death or results in novel missense mutations especially in *MGMT* deficient cells. Here, we describe an exploratory case series of TMZ-treated NETs cases that underwent NGS analysis at the University Hospital of Verona. Methods. We included 32 patients (16 G2 and 16 G3). NGS was performed before TMZ treatment for 22 cases (54%), after for 19 (46%) and in both for 4 cases (13%). We performed NGS on tissue samples for 73% of assays and *via* liquid biopsy for the remaining 27%. For tissue NGS, in 77% of samples we used an in-house panel encompassing 174 genes and in 23% commercial test interrogating at least 500 genes. Only ACMG/AMP class IV-V molecular alterations were considered for further analysis. Main Results From 2021 we performed NGS analysis on 32 NETs (G2 and G3) treated with TMZ-based regimes. Most cases (28 pf 32, 84.4%) were pancreatic NETs. Mean Ki-67 at baseline was 24.5% (range 3-60). The mean number treatments prior to TMZ were 1.4 and 0.5 between CAPTEM and subsequent NGS. The top five altered genes at baseline were *MEN1* (32%), *TP53* (14%), *DAXX* (14%), *PTEN* (9%) and *SMAD4* (9%). None of the patients showed a high TMB (>15Mut/Mb) at baseline, while 26% of post-TMZ samples displayed that feature. Mean TMB at baseline and after treatment was 6.51 (range 1-10.6) and 22.9 mut/Mb (range 1-216) respectively. Alterations in DDR systems genes, including *ATM, ATR, CHEK2, BRCA1, BRCA2, MLH1, MLH2, PMS2 MLH6* and *MUTYH,* were found in 8 patients (47%) after TMZ exposure; only one DDR-specific alteration (*MUTYH*) was found at baseline. DDR defects were enriched in patients exposed to higher numbers of treatments. The increase in mean TMB and enrichment in mutations in the DDR system is also confirmed when analysing the 6 cases having both pre- and post-TMZ treatment samples. Among other pathways, cell cycle deregulating genes (*CDKN1A, CDKN2B, CDKN1B, CDK12, CDK6, RB1*) were altered in 2 (11%) and 5 (29%) pre- and post-TMZ NGS samples respectively, the mTOR pathway (*MTOR, NF1, PIK3CA, AKT, TSC1, TSC2, PTEN*) in 2 (11%) and 8 (47%), and the MAPK pathway (*KRAS* and *BRAF*) in 1 (5%) and 2 (12%). Conclusions. The wide and effective use of temozolomide in neuroendocrine tumors, together with the potential therapeutic implications of DDR defects make this topic of great interest. The DDR pathway was one of the most affected by alterations in post-TMZ samples, although the genotoxic agent caused a general increase in the rate of somatic mutation. The status of DDR systems, either germinal or somatic, may represent an important selection and/or stratification parameter for future immunotherapy clinical studies also in neuroendocrine tumours provided that the analysis is carried out in a systematic, comprehensive and longitudinal way.

#3815 Clinical efficacy and safety of HER2 targeted therapy in patients with metastatic colorectal cancer: A systematic review and meta-analysis.

O. E. Villarreal, L. Xiao, J. Allam, A. Sorokin, Y. Yuan, S. Kopetz, K. P. S. Raghav;
The University of Texas MD Anderson Cancer Center, Houston, TX

Background: Therapies targeting HER2 have shown clear benefit in patients with breast or gastric cancer,; and their use in metastatic colorectal cancer (mCRC) has been increasingly explored in recent years. HER2 overexpressed or amplified (HER2-positive) mCRC is seen in 2-8% of all mCRC cases and is enriched in RAS wild-type (WT) tumors, representing a patient population that may benefit from anti-HER2 therapies. Although, several single-arm and some non-comparative randomized clinical trials have now tested the use of diverse dual anti-HER2 therapies in mCRC, no summative analysis have been performed. We conducted a systematic review and meta-analysis to evaluate the overall clinical benefit (efficacy and safety) of dual-HER2 inhibition in patients with RAS-WT HER2-positive mCRC.

Methods: A systematic review of available literature was performed for clinical trials involving patients with mCRC treated with HER2 targeting therapy. Two independent reviewers selected studies and extracted data from PubMed and abstracts published at major international oncology meetings during the past 5 years. Case reports and other studies not meeting inclusion criteria were excluded, therefore a total of 13 studies were used for analysis. Patients with RAS-mutant tumors within each trial were excluded due to known limited benefit of dual HER2 inhibition in this subset. Inverse variance method with random-effects model was used for meta-analysis to determine the overall effect of the therapy on overall response rate (ORR), disease control rate (DCR), progression free survival (PFS) and treatment-related adverse events (TRAE).

Results: Systematic review identified 9 study cohorts which were utilized in the meta-analysis, encompassing a total of 279 patients with mCRC who received Trastuzumab (T) in combination with either Pertuzumab (P), Tucatinib (Tu), Pyrotinib (Py), or Lapatinib (L). Collectively, dual HER2 inhibition showed an ORR of 35.1% (95% CI: 29.4-41.0%), a DCR of 68.3% (95% CI: 62.5-73.9%), and a PFS of 5.2 months (95% CI: 4.4-6.0 months). Pooled TRAE of grade ≥ 3 across studies was 29.9% (95% CI: 18.8-42.4%) but displayed high inter-study heterogeneity ($p<0.0001$, $I^2 = 79\%$), mainly driven by one trial (Pyro-HER2; TRAE = 75.0%, 95% CI: 50.9-91.3%).

Conclusions: Overall, this comprehensive meta-analysis confirms that dual HER2 targeting therapies yield meaningful clinical efficacy, with favorable safety profiles, and improve outcomes in patients with RAS-WT HER2-positive mCRC.

#3817 Real-world clinical outcomes in patients with advanced ROS1+non-small cell lung cancer in the US.

R. Villacorta[1], S. Ray[1], Y. Yuan[1], S. Vijapur[2], S. Kim[2], H. Sun[2], S. Myers[2], V. Lam[3];
[1]Bristol Myers Squibb, Lawrenceville, NJ, [2]Genesis Research Group, Hoboken, NJ, [3]Johns Hopkins University, Baltimore, MD

Introduction: ROS1 rearrangements define a rare molecular subtype of non-small cell lung cancer (NSCLC), occurring in 1-2% of patients (pts) with advanced NSCLC (aNSCLC). Crizotinib and entrectinib received US approval for ROS1+ aNSCLC in March 2016 and August 2019, respectively. Few studies have addressed temporal trends in first-line (1L) utilization since these drugs' approval. This study describes treatment patterns and clinical outcomes in pts with ROS1+ aNSCLC in the US.

Methods: This retrospective study used the nationwide Flatiron Health (FH) electronic health record-derived de-identified database and included adult pts with ROS1+ aNSCLC who received 1L (index) therapy between March 2015 and December 2022. Pts were followed until March 31, 2023, and had ≥ 3 months of follow-up post-index date. Treatment-related (sequence, time to treatment discontinuation [TTD], time to next treatment [TTNT]) and clinical (real-world progression-free survival [rwPFS], overall survival [OS]) outcomes of 1L therapy were assessed using descriptive statistics and Kaplan-Meier methods.

Results: In the FH database, 87,784 pts had aNSCLC, and 242 were ROS1+. The median age was 65 years; most were female (64%), White (67%), non-squamous (91%) and had a history of smoking (52%), with most pts having ECOG performance status 0 (31%) or 1 (35%). 19% had brain metastases prior to or up to 30 days post-index. Median follow-up time was 14.2 months. In 1L treatment, only 59% received ROS1-sensitive TKI monotherapy (i.e. crizotinib, entrectinib, ceritinib), with 97 (40%) and 40 (17%) treated with crizotinib and entrectinib monotherapy, respectively. Median TTD and TTNT for 1L was 6.4 (95% CI: 5.0, 7.6) and 7.6 (95% CI: 6.5, 9.4) months, respectively. Among 1L crizotinib pts, 51% had 2L treatments and 57% of those initiated another ROS1-sensitive TKI (16% entrectinib). Among 1L entrectinib pts, 43% had 2L therapy; of these, 82% initiated another ROS1-sensitive TKI. Median rwPFS was 7.5 (95% CI: 6.2, 9.3) months (1L crizotinib, 8.6 [95% CI: 5.3, 13.0] months; 1L entrectinib, 8.0 [95% CI: 5.3, 13.6] months). Median OS was 29.0 (95% CI: 19.4, 35.9) months (1L crizotinib, 31 [95% CI: 19.4, not estimable [NE]] months; 1L entrectinib, NE). Patients initiated ROS1-sensitive TKIs (crizotinib, entrectinib or ceritinib) in 1L across each year of the study (2015: 67%, 2016: 58%, 2017: 51%, 2018: 47%, 2019: 63%, 2020: 81%, 2021: 52%, 2022: 68%). Overall, 5% received checkpoint-inhibitor (CPI) only, 17% chemotherapy alone, and 7% a chemotherapy/CPI combination.

Conclusion: Compared to relevant clinical trials, ROS1+ aNSCLC pts in this real-world study were older, had greater smoking exposure, and worse overall survival. Only 59% of pts initiated 1L ROS1-sensitive TKI monotherapy. These results highlight potential disparities in the diagnosis and treatment of ROS1+ NSCLC and opportunities for improving clinical outcomes.

#3818 Sociodemographic, access to care and survival outcomes for patients with mantle cell lymphoma: A national cancer database analysis with focus on Hispanics.

E. Toro Velez[1], C. Velez-Mejia[1], D. Rosas[2], Q. Liu[1], J. Michalek[1], A. Diaz Duque[3];

[1]UT Health Science Center at San Antonio, San Antonio, TX, [2]Memorial Healthcare System, Pembroke Pines, FL, [3]Mays Cancer Center, San Antonio, TX

Background: Mantle cell lymphoma (MCL), represents 3% of new cases of non-Hodgkin's lymphomas.(PMID 29348844) MCL affects mainly males; factors like ethnicity, age at presentation can have prognostic implications. Currently, it isn't clear if Hispanics (HI) have a survival difference compared to Non-Hispanics (NH).(PMID 31029647, PMID 25315847). This National Cancer Database (NCDB) analysis aims to clarify how sociodemographic factors affect presentation and survival in HI vs NH patients with MCL.

Methods: Data were analyzed on MCL patients in the United States reported to the NCDB 2004-2019. Demographic and treatment characteristics were compared between ethnic groups. Kaplan-Meier and Cox regression analyses were used to compare overall survival (OS). Multivariate analysis and propensity score matching was performed.

Results: Of 32515 of MCL patients, 1729 were HI, and 29309 NH. Male gender and identification as white predominated for both. HI were diagnosed at a younger median age of 65 years (y) vs 68 y for NH, p<0.001. Most patients were diagnosed between years 2016-2019. Stage IV predominated for HI and NH, p<0.001. As to Charlson-Deyo Score ≥2, HI had 6% vs NH 8%. Government sponsored was the most prevalent primary payer, HI (54%) and NH (60%). HI had a higher percentage of unknown/uninsured, 13% vs 4% for NH, p<0.001. In relation to census median income (2008-2012), the most prevalent bracket for HI and for NH was >$63,000, 29% and 37% respectively. When analyzing median income of less than $38,000, HI were 22% vs 13% for NH, p<0.001. For median distance in miles (mi) between the patient's residence and the hospital that reported the case (Great circle distance), HI lived at a median of 8.2mi, vs NH at median of 11.3mi. Most patients were treated at Academic/Research programs, 50% for HI and 39% for NH, p<0.001. On survival analysis, the survival probability at 2, 5 and 10 for HI was 74%, 57%, 44%, vs for NH was 72%, 54%, 36%, respectively. The median survival (MS) was 7.0 years for HI, vs 5.8 years for NH, with a statically significant difference in OS favoring HI, p=0.00015. On multivariate analysis, not insured status was independently associated with worse OS (HR 1.29, CI 1.08-1.55, p=0,01). The propensity matched analysis showed significant MS difference between HI vs NH (5.8 y vs. 5.6 y).

Conclusion: In this analysis, MCL is a malignancy that presents at advanced stages, affecting mainly the elderly white males. HI compared to NH have a statically significant benefit in OS, which might be driven by a younger population with less comorbidities. Despite HI having limited access to insurance and lower income; sociodemographic differences don't seem to be barriers for HI to access care at academic centers. Newer studies should focus on understanding what genetic and intrinsic disease factors cause HI to have an earlier presentation and a survival advantage over NH.

#3819 Real-world long-term survival outcomes of first-line immunotherapy-based regimens in advanced non-small cell lung cancer.

D. Waterhouse[1], S. Ray[2], K. A. Betts[3], S. Gao[3], Y. Yuan[2], M. Sundar[3], S. Rui[3], D. Stenehjem[4];

[1]Oncology Hematology Care (OHC)/ An affiliate of the US Oncology/SCRI Network, Cincinnati, OH, [2]Bristol-Myers Squibb, Lawrenceville, NJ, [3]Analysis Group, Los Angeles, CA, [4]Department of Pharmacy Practice and Pharmaceutical Sciences, University of Minnesota, Minneapolis, MN

Background: The real-world survival outcomes of first-line (1L) immunotherapy (IO)-based regimens for the treatment of advanced non-small cell lung cancer (aNSCLC) were assessed utilizing the Flatiron Health database from January 2011 to June 2023.

Methods: Adult patients (pts) with aNSCLC receiving 1L IO monotherapy or single-agent IO + chemotherapy on or after January 1, 2016, were identified. Pts were excluded if they had *EGFR/ALK* mutations or unknown histological type. Overall survival (OS) and real-world progression-free survival (rwPFS) of 1L IO monotherapy and IO + chemotherapy were described using Kaplan-Meier analyses.

Results: A total of 14,320 pts were included (5,166 pts receiving IO monotherapy; 9,154 pts receiving IO + chemotherapy). Among pts receiving IO monotherapy, the 1-, 2-, 3-, and 4-year OS rates were 52.3%, 36.5%, 27.4%, and 21.9%, respectively. The corresponding rwPFS rates were 29.2%, 17.5%, 12.7%, and 9.2%. Among pts receiving IO + chemotherapy, the 1-, 2-, 3-, and 4-year OS rates were 50.7%, 32.6%, 23.9%, and 19.2%. The corresponding rwPFS rates were 27.0%, 15.1%, 10.3%, and 7.8%. Table 1 presents the 4-year OS and rwPFS rates stratified by histological type, tumor programmed death ligand 1 (PD-L1) expression level, and Eastern Cooperative Oncology Group (ECOG) performance status. Patients with lower PD-L1 expression level (<1%), worse ECOG performance status (≥2), and squamous cell carcinoma had worse survival outcomes, regardless of the type of 1L treatment received.

Conclusions: The real-world survival rates for patients with aNSCLC who were treated with 1L IO-based regimens were lower than those observed in pivotal trials, which indicates an unmet need for the management of newly-diagnosed aNSCLC. However, on average approximately 1 in 11 pts receiving IO monotherapy and 1 in 13 pts receiving IO + chemotherapy remained progression-free at the four year landmark and achieved an extended period of survival.

Table: 4-year OS and rwPFS rates

	1L IO monotherapy			**1L IO + chemotherapy**		
	PD-L1 <1%	**PD-L1 ≥1-49%**	**PD-L1 ≥50%**	**PD-L1 <1%**	**PD-L1 ≥1-49%**	**PD-L1 ≥50%**
OS by histological type (sample size; 4-year rate, %)						
Squamous	122; 12.7	329; 14.0	814; 15.1	585; 11.7	647; 15.1	295; 23.3
Non-squamous	231; 16.7	516; 20.0	2563; 26.3	2263; 14.9	2058; 20.8	1313; 28.9
OS by ECOG performance status (sample size; 4-year rate, %)						
0-1	193; 17.0	439; 20.8	1880; 27.6	1852; 16.8	1802; 21.9	1065; 28.0
≥2	89; 6.7	261; 14.5	840; 12.7	478; 5.6	452; 11.1	241; 22.8
rwPFS by histological type (sample size; 4-year rate, %)						
Squamous	122; 7.6	329; 4.4	814; 6.8	585; 5.2	647; 8.3	295; 9.2
Non-squamous	231; 5.1	516; 10.0	2563; 11.2	2263; 4.3	2058; 6.3	1313; 14.7
rwPFS by ECOG performance status (sample size; 4-year rate, %)						
0-1	193; 6.9	439; 10.4	1880; 11.9	1852; 5.4	1802; 6.8	1065; 14.5
≥2	89; NA	261; 3.7	840; 5.0	478; 2.2	452; 3.9	241; 8.2

#3820 Impact of primary site in early-stage follicular lymphoma on patient outcomes: Analysis of a large national database.

O. Davis[1], R. Kasht[2], A. Cohoon[3], S. Day[4], S. Ibrahimi[4], A. Asch[4], T. Al-Juhaishi[4];
[1]University of Oklahoma College of Medicine, Oklahoma City, OK, [2]OU Health, Oklahoma City, OK, [3]University of Oklahoma College of Public Health, Oklahoma City, OK, [4]OU Health - Stephenson Cancer Center, Oklahoma City, OK

Introduction: Follicular lymphoma (FL) is the most common indolent Non-Hodgkin lymphoma and is associated with better outcomes compared to other types of lymphoma. Despite this, cure is usually elusive and most patients experience multiple relapses within their lifetime. Previous studies have identified risk factors associated with worse outcomes, but little is known about the role of primary disease site in FL. We sought to investigate the outcomes of patients with extranodal early-stage FL compared to nodal disease using a large national cancer database.
Methods: The Surveillance, Epidemiology, and End Results (SEER) public database was used to identify and extract data for patients with FL. Early-stage disease was defined as stage I or II by the Ann Arbor staging system. Most patients in the database were diagnosed after 2000 so this was used as the diagnosis year cutoff and also to reflect the impact of recent management strategies on outcomes. Patients were divided into two groups based on their primary disease site. These two groups were nodal (includes spleen) and extranodal. Treatment effect (surgery, radiation, or chemotherapy) was analyzed when available. Survival was estimated using the Kaplan-Meier method and compared using log-rank tests. Cox proportional hazards models were used for adjusted survival analyses.
Results: A total of 13,400 patients with FL of all histologic grades diagnosed between 2000 and 2015 were identified in the SEER database. The median age at diagnosis was 65 years (2-100). A majority of patients were Caucasian (81%), had stage I disease (62%), and belonged to the nodal FL group (79%). Median overall survival (OS) for patients with nodal FL was 181 months [95% CI (175-187)]. Median OS for extranodal FL was 189 months [95% CI (179-195)]. Extranodal FL was associated with better OS compared to the nodal group [HR=0.89, 95% CI (0.84-0.96); p-value =0.00012] even after adjusting for age and race [HR=0.84 , 95% CI (0.79-0.90); p-value <0.0001].
Conclusions: In this analysis of a large national cancer database, early-stage FL presenting as extranodal disease can be seen in about 20% of patients and is associated with slightly better outcomes.

#3821 Real world outcomes among patients with newly diagnosed acute myeloid leukemia.

E. D. Pulte[1], L. L. Fernandes[2], J. Wynne[1], E. Hansen[2], A. J. Belli[2], A. Barcellos[2], C. M. Zettler[2], R. Bystrom[1], J. Vallejo[1], W. Gu[1], C. Lerro[1], K. Norsworthy[1], A. DeClaro[1], M. R. Theoret[1], D. Rivera[1], C.-K. Wang[2];

[1]Food & Drug Administration, Silver Spring, MD, [2]COTA Healthcare, New York, NY

Introduction: Treatment options for patients with acute myeloid leukemia (AML) have expanded in recent years. Although new treatments have demonstrated efficacy in clinical trials, less is known about their effect on outcomes in routine clinical practice. We examined outcomes for patients with newly-diagnosed AML (ND-AML) using real world data (RWD).

Methods: This retrospective observational study was conducted using the COTA real-world (rw) database, a de-identified source of longitudinal electronic health record data pertaining to the diagnosis, management, and outcomes of patients with cancer. Adult patients with ND-AML, diagnosed January 1, 2013 to March 20, 2023 were included. First-line treatment regimens were grouped into therapeutic categories and outcomes were summarized. The index date was defined as date of initiation of first-line therapy.

Results: Among 2516 patients with ND-AML included (Table), the most common regimens used were intensive chemotherapy with cytarabine (IC w/ara-C), hypomethylating agents with venetoclax (HMA+ven), and HMA alone. Complete response rate was highest in patients treated with IC w/ara-C or investigational regimen(s). Median overall survival (OS) was 16 mo overall, with highest median OS seen in patients treated with IC w/ara-C and investigational regimen(s). Median OS for patients treated with HMA+ven was 13.5 mo. Thirty-day mortality was lowest in patients treated with IC w/ara-C, CPX-351 (liposomal daunorubicin + cytarabine), and HMA+ven.

Conclusions: Results suggest that IC w/ara-C remains the standard of care for most patients with ND-AML and this regimen has a higher CR rate and median OS. Variation of patient demographics and clinical characteristics across treatment groups did not permit cross-treatment comparisons, though future analyses evaluating these subgroups may provide further insight into effectiveness and safety of AML regimens in routine care for populations underrepresented in clinical trials.

		rwCR rate	Median rwOS	30-day mortality
	N	% (95% CI)	Months (95% CI)	% (95% CI)
Overall	2516	45.3 (43.2, 47.3)	16.0 (14.9, 17.3)	5.9 (5.0, 6.8)
IC w/ara-C	1171	60.6 (57.8, 63.4)	36.4 (31.0, 46.0)	1.6 (0.9, 2.3)
HMA+ ven	300	33.7 (28.3, 39.3)	13.5 (11.4, 15.5)	3 (1.1, 4.9)
Decitabine	242	12.8 (8.9, 17.7)	8.4 (6.7, 9.9)	10.4 (6.5, 14.2)
Azacitidine	206	7.8 (4.5, 12.3)	7.2 (5.3, 9.6)	10.7 (6.4, 14.8)
Investigational	206	61.6 (54.6, 68.3)	21.3 (15.2, 27.8)	3.4 (0.9, 5.9)
Lower dose cytarabine	62	12.9 (5.7, 23.9)	8.7 (5.4, 16.1)	14.9 (5.4, 23.4)
CPX-351 based	61	55.7 (42.4, 68.5)	9.3 (7.3, 15.1)	0.0
No treatment	188	NA	1.9 (1.5, 2.8)	30 (22.7, 36.6)

#3822 Oncotype DX testing and differences in use of chemotherapy by age in an integrated system.

A. Aller[1], L. Lyon[2], L. Habel[2], A. Shirazi[1], R. Liu[1];

[1]Kaiser Permanente - Northern California, San Francisco, CA, [2]Kaiser Permanente - Northern California, Oakland, CA

Introduction: Oncotype DX (ODX) identifies breast cancer patients who are less likely to benefit from chemotherapy. We investigated patient factors associated with clinical application of ODX testing and chemotherapy use.

Methods: We identified a cohort of adult breast cancer patients with stage I-IIA, estrogen receptor positive, human epidermal growth factor receptor 2 negative, lymph node negative disease diagnosed within Kaiser Permanente Northern California between 2015 - 2021 eligible for ODX testing. Chi-square tests were used for bivariate analysis of categorical variables. Multivariable logistic regression was used to identify independent predictors of chemotherapy use in female patients with high risk ODX scores (>25).

Results: 8017 patients were eligible for ODX testing; of which 5,136 received testing (64%) and 576 patients (7%) had high risk ODX. ODX testing increased over the years (45% of eligible patients in 2015; 79% of eligible patients in 2021). Testing was frequent in larger lesions (74%), poorly differentiated tumors (73%), and younger patients (83% in patients <40 years at diagnosis; 12% in patients > 80 years). Chemotherapy was frequently administered in younger patient, and for larger, poorly differentiated tumors. For patients who possessed a high risk ODX score, chemotherapy administration differed by age. In comparison with the 90% of high risk patients <45 years who received chemotherapy, 58% of patients 60+ years at diagnosis with high risk ODX received chemotherapy. Comorbidity index and chemotherapy administration was not statistically significant (Table 1).

Conclusion: Oncologists frequently use ODX testing to guide chemotherapy management. Despite high risk ODX scores, older patients received less chemotherapy compared to their younger counterparts. Further investigation is needed to determine how age impacts clinician decision making and clinical outcomes following ODX testing.

Table 1. Multivariable Logistic Regression Analysis of Factors Associated with Chemotherapy

Women > 60 years with high risk oncotype DX scores (N=467)	Adjusted Odds Ratio (95% Confidence Interval)	P-values (Calculated using the Wald $\chi 2$ Statistic)
Age at Cancer Diagnosis (Reference: 60 - 69 years old)		
70-79	0.62 (0.40-0.96)	0.03
>79	0.11 (0.02-0.55)	0.01
Charlson Comorbidity Index (Reference = 0)		
1	0.76 (0.48-1.22)	0.26
2	0.62 (0.30-1.29)	0.20
3	0.65 (0.26-1.60)	0.35
4	0.54 (0.20-1.44)	0.22
5+	0.37 (0.10-1.35)	0.13

#3823 Clinical outcomes of uveal melanoma patients in the emergency department.

A. A. Beneke[1], **K. Taneja**[2], L. Ladehoff[3], K. Root[1], E. Toloza[4];
[1]University of Florida, Gainesville, FL, [2]Stony Brook University, Stony Brook, NY, [3]University of South Florida, Tampa, FL, [4]Moffit Cancer Center, Tampa, FL

Purpose: Uveal melanoma is a rare ocular malignancy that has not been well characterized at a large scale. Specifically, uveal melanoma diagnosis and outcomes in the emergency department (ED) has not been characterized.
Methods: The Nationwide Emergency Department Sample was queried from the last quarter of 2015 to 2019 to identify patients with a primary diagnosis of uveal melanoma. Multivariable logistic regression, with patient- and hospital-level characteristics as covariates, was used to identify factors associated with increased risk of inpatient admission.
Results: From the last quarter of 2015 to 2019, there were 1,274 ED encounters with a primary diagnosis of uveal melanoma. Most patients were less than 11 years old (43.4%), male (51.1%), or a Medicaid beneficiary (37.8%), and most belonged to a family in the lowest income quartile (32.0%). The median age of these patients was 35 years (IQR: 2-64). Most patients presented to hospitals in the South (53.9%), with a Trauma Level I designation (51.4%), and most to a metropolitan teaching hospital (89.1%). The most common ED outcomes were same-day discharge (61.6%) and admission to the inpatient setting (31.2%). Patients presenting to Trauma Level I hospitals were most likely to be admitted (odds ratio [OR]=2.21; p=0.031). The factors that were most significantly associated with decreased odds of inpatient admission were: patients who were not charged for services (often due to charity) (OR=0.13; p=0.040), Medicaid beneficiaries (OR=0.27; p=0.031), and private insurance beneficiaries (OR=0.34; p=0.047). Among the admitted patients, patients can be discharged to home with self-care (76.2%) or with home-health care (14.9%) or can be transferred to an intermediate-care facility (8.1%). The mean hospital length of stay was 5.7±0.6 days. In-hospital mortality rate for admitted patients was very low (0.8%).
Conclusion: Uveal melanoma patient outcomes are closely related to insurance status, indicating socioeconomic factors as a modulator of patient outcomes.

#3824 Efficacy of trastuzumab in combination with capecitabine and cisplatin vs 5-FU and cisplatin therapy for Korean patients with HER2-positive advanced gastric cancer Health Insurance Review and Assessment service (HIRA) data retrospective analysis.

h. Lee, J.-H. Kim, S. Kang, T. Park, Y. Choi;
Ajou University School of Medicine, Suwon, Korea, Republic of

The combinations of oral fluoropyrimidines and cisplatin such as capecitabine and cisplatin (XP) or 5-FU and cisplatin (FP) are regarded as a standard therapy against HER-2 positive advanced gastric cancer (AGC). Trastuzumab-XP(HXP) and trastuzumab-FP(HFP) is the most common regimen against AGC in Korea. The aim of the present study is to evaluate the effectiveness of trastuzumab-XP vs trastuzumab-FP.

Patients with HER2-positive AGC were assigned to the trastuzumabXP or trastuzumabFP group. We then retrospectively compared the efficacy and safety between both groups. As a first-line chemotherapy, trastuzumab in combination with XP or FP was administered to 2,399 patients: 1,913 with HXP and 486 with HFP. In the HXP group vs HFP group, median progression-free survival (mPFS), and median overall survival (mOS) were 8.02 vs 6.08 months (p <0.0001) and 13.27 vs 9.89 months (p <0.0001). In HFP group, mPFS and mOS were 10.15 vs 5.36 months (p <0.0001) and 15.15 vs 8.90 months (p <0.0001) in comparison HFP-H maintenance to HFP group. In HXP group, mPFS and mOS were 10.64 vs 13.44 vs 5.03 months (p <0.0001) and 20.14 vs 22.18 vs 9.10 months (p <0.0001) in comparison HXP-H maintenance, HXP-HX maintenance, and HXP group.

Trastuzumab in combination with XP and HX maintenance is a potential first-line therapeutic option for patients with HER2-positive AGC.

#3826 Predictive and prognostic factors in NUT carcinoma: A systematic review and individual patient data meta-analysis.

S. K. Abdulwali[1], A. M. El-Sibai[1], S. S. Ali[1], A. M. Alaklabi[1], H. M. Abdalla[1], A. N. Sabbah[1], A. Shafqat[1], N. A. Fawzy[1], B. N. Sabbah[1], A. Badran[2], **T. Z. Arabi**[1]; [1]Alfaisal University, Riyadh, Saudi Arabia, [2]King Faisal Specialist Hospital and Research Centre, Riyadh, Saudi Arabia

Background: NUT carcinoma (NC) is a rare cancer affecting midline structures and involving the lung, bones, and lymph nodes. Data on NC are limited mostly to case reports and case series.
Methods: PubMed, Web of Science, and Scopus were systematically searched for original articles describing confirmed NC patients. A quantitative individual patient data meta-analysis (IPD-MA) analyzing overall survival and risk factors for progression was performed for all NC patients with a clear age at diagnosis. Relevant patient characteristics and clinical parameters were compared in a multivariate Cox regression model.
Findings: Out of 4,701 studies screened, 175 studies met the inclusion criteria for the systematic review. 117 (66.9%) were case reports. 284 patients were included in the IPD-MA. 139 (48.9%) patients were male, 145 (51.1%) underwent surgery, 156 (54.9%) received radiotherapy, and 173 (60.9%) developed metastasis. The mean age at diagnosis was 35.82±18.33 and the median OS was 9 months. 77 (27.1%) patients received platinum-based agents, 39 (13.7%) received taxanes, and 15 (5.3%) received BET inhibitors as part of their first-line regiment. Age at diagnosis, gender, and the aforementioned drugs did not significantly influence OS. Presence of metastasis was an independent predictor of poor survival, while radiotherapy and surgery were significantly associated with better survival (table 1).
Interpretation: NC is associated with poor survival. Surgery and radiotherapy appear to be more effective treatment strategies, while medical modalities may not play a major role in the treatment of NC.

Predictors of overall survival in NUT carcinoma patients.

Parameter	Hazard ratio	95% confidence interval	P-value
Age at diagnosis	0.99	0.99-1	0.35
BET inhibitors	0.61	0.28-1.15	0.16
Platinum-based agents	0.73	0.47-1.13	0.16
Taxanes	1.29	0.78-2.1	0.31
Surgery	0.41	0.29-0.58	<0.0001
Female gender	1.12	0.83-1.51	0.45
Metastasis	1.76	1.26-2.49	0.0011
Radiotherapy	0.48	0.36-0.67	<0.0001

#3827 Optimizing the treatment schedule of radiotherapy combined with VEGFR-TKIs and PD-(L) 1 inhibitors in metastatic colorectal cancer.

Z. Lin, M. Zhai, T. Zhang;
Cancer Center, Union Hospital Tongji Medical College Huazhong University of Science and Technology, Wuhan, China

Background: The oral vascular endothelial growth factor receptor (VEGFR) inhibitor fruquintinib, an innovative Chinese drug, has recently been approved by the U.S. Food and Drug Administration (FDA) for third-line treatment of metastatic colorectal cancer (mCRC) in adults. This study aims to investigate the efficacy and safety of radiotherapy (RT) combined with VEGFR-TKIs (such as fruquintinib) and PD-(L) 1 inhibitors in mCRC, and explore optimal sequence of RT with the systemic regimen.

Methods: This retrospective study enrolled eligible patients with MSS/pMMR mCRC who had received RT in combination with anti-angiogenic drugs (Fruquintinib or Regorafenib) and immunotherapy (IT) between April 2018 and September 2023. Data on treatment response, progression-free survival (PFS), overall survival (OS), and adverse events were collected.

Results: A total of 42 pts were analyzed. For Fru + IT + RT (n = 33) and Reg + IT + RT (n = 9), ORR were 21.2% (7/33) and 11.1% (1/9); DCR were 81.8% (27/33) and 88.9% (8/9), respectively. Median PFS were 6.4 mo and 5.0 mo (P=0.856) while median OS were 17.2 mo and 7.2 mo (P=0.578), respectively. In-depth analysis of Fru + IT + RT treated population, the PFS and OS of 3rd-line treatment were superior to later (≥ 4th) -line treatment (median: 6.7 vs 4.2 mo, P=0.02) and (median: 17.5 vs 8.9 mo, P=0.27), seemingly. Additionally, RT before initiation of Fru + IT demonstrated superior PFS compared to simultaneous/sequential RT with Fru + IT (median 7.1 vs 6.1 vs. 3.2 mo, p<0.001). Simultaneously, pts with interval time ≤1 month, received numerically benefit compared to interval time >1 month between RT and FRU+IT (mPFS: 6.2 vs. 3.8 mo, P=0.16; mOS: not reached vs. 7.65 mo, P=0.08). Further subgroup analysis revealed that men, age ≤56 years, ECOG PS score of 1, primary focal resection, recurrent metastatic disease, liver/pulmonary metastases, and metastatic involvement of organs ≥2, were more favorably treated with Fru for prolonged OS. Intriguingly, the 3rd-line treatment of Fru exhibited a tendency to prolong OS compared to Reg. Cox multivariate regression analysis suggested that the cycle of Fru/Reg combined with PD-1 inhibitor treatment was a common independent influencing factor for PFS and OS. Safety was consistent with previous reports, and the incidence of AE appeared to be lower in Fru + IT + RT than in Reg + IT + RT.

Conclusion: In pts receiving RT of localized lesions, the addition of Fru combined with PD-1 inhibitor could prolong the pts' OS more than Reg plus PD-1 inhibitor. And radiotherapy sequential Fru + IT (interval time ≤1 mo) treatment is expected to be the optimal strategy for MSS/pMMR mCRC.

#3829 Identifying the genetic basis for resistance to aromatase inhibitors (AIs) in metastatic breast cancer (mBC) patients.

N. Singh, S. Agrawal;
ConcertAI, Bengaluru, India

Background: AIs, such as letrozole, anastrozole, and exemestane, are used to treat hormonal receptor positive (HR^{+}) breast cancer (BC) patients. Many patients either respond poorly or relapse on AIs. A comprehensive view of the underlying genomic landscape of such patients may aid in a better understanding of the resistance mechanisms and the development of new targeted therapies. This study leveraged a real-world clinico-genomic dataset of BC patients to identify key biomarkers and the corresponding high frequency mutations in this relapse/refractory patient population.

Methods: This retrospective study used ConcertAI's Genome360^{TM} BC dataset (N=3223). A cohort of HR^{+}/$HER2^{-}$ mBC patients who were either refractory to or relapsed on AIs (N=863) were included. To identify key resistance genes/pathways, only genomic data (from NGS tests) from a biopsy performed after tumor progression on AIs was considered. Prevalence analysis was done only based on known pathogenic/likely pathogenic variants. Pathway analysis of identified biomarkers with the mechanism of action of AIs was performed to identify and validate key resistance pathways. Further, signatures of unique protein alteration were identified within the biomarkers of interest.

Results: The median age of patients at the time of diagnosis was 54 years. Adenocarcinoma and Lobular/Ductal carcinoma were the two most prevalent histologies. 51% of patients in this cohort were treated with AIs in the first line. Table 1 lists the 20 most frequently altered genes observed in this cohort. Genes with a potential role in AI resistance based on pathway analysis are indicated. The most common mutations in selected biomarkers are also provided. These biomarkers were observed at a much lower frequency in patients who responded well to AIs.

Conclusion: This study provides insights into the genetic basis of resistance to AIs in mBC patients, opening up possibilities for development of new treatments to overcome resistance.

Table1: Top 20 biomarkers and their variants found in AI relapse/refractory mBC Patients.

Biomarker	**Prevalence (%)**	**Potential Role in AI Resistance**	**Key Variants**
ESR1	37.81	Yes	D538G, Y537, Y537N, E380Q, Y537C
PIK3CA	37.04	Yes	H1047R, E545K, E542K, H1047L, E726K, N345K
TP53	35.56		
GATA3	14.25	Yes	Frameshift Mutation (Mainly)
CDH1	11.64	Yes	Frameshift Mutation (Mainly)
MAP3K1	9.35		
KMT2C	9.02		
PTEN	8.38	Yes	Frameshift Mutation (Mainly)
ARID1A	8.17		
RB1	7.38	Yes	Frameshift Mutation (Mainly)
DNMT3A	5.31		
ATM	5.30		
TBX3	5.10		
SPEN	4.90		
NF1	4.82	Yes	Frameshift Mutation (Mainly)
AKT1	4.74	Yes	E17K
ERBB2	3.21	Yes	L755S, V777L, D769Y
KRAS	2.74	Yes	G12V, G12D, G12A
BRCA1/2	2.69		
CDKN2A	1.78		

#3830 Comparison of individual patient data from real-world experience with the ADAURA study for resected stage IB-IIIA EGFR-mutated non-small cell lung cancer.

H. Jung, J. Lee, B. Park, S. Park, J.-M. Sun, S.-H. Lee, J. Ahn, M.-J. Ahn;
Samsung Medical Center, seoul, Korea, Republic of

Introduction: In recent data of ADAURA study, adjuvant osimertinib demonstrated clinically significant improvement in overall survival in completely resected stage IB-IIIA with epidermal growth factor receptor (EGFR)-mutated NSCLC. Among 205 patients who experienced recurrence in the placebo arm, 89.8% of patients received subsequential treatment and 79.0% of patients in the placebo arm received EGFR-TKI after recurrence.
Methods: This study included patients with completely resected EGFR-mutated NSCLC who confirmed to pathologic stage II-IIIA between November 2015 and February 2019 at Samsung Medical Center (SMC data). They did not receive adjuvant EGFR-TKI. To compare overall survival between the SMC data and the ADAURA study, the individual patient data (IPD) approach was applied. We assessed the overall survival of individual patient data from real-world experience in comparison to the ADAURA study.
Results: A total of 547 patients were included in this study, with 51.0% at stage IB, 23.8% at stage II, and 25.2% at stage IIIA. The median follow-up duration was 71.4 months (range 1-92). At the time of data lock, 241 patients experienced recurrence in the SMC data. Among them, 230 patients (95.4%) received subsequent treatment, and 214 patients (88.8%) received EGFR-TKI after recurrence. In the stage IB and II, there was no difference of overall survival between the SMC data (reference) and the osimertinib arm of the ADAURA study (HR=0.83, 95% CI, 0.36-1.90, p=0.66 in stage IB; HR=1.08, 95% CI, 0.58-2.03, p=0.81 in stage II). However, in the stage IIIA, the 5-year survival rate was 68% in the SMC data and 85% in the osimertinib arm of the ADAURA study (HR=0.42, 95% CI, 0.24-0.73, p<0.01). In the stage IB-IIIA, the 5-year survival rate was 85% in the SMC data (reference), 78% (HR=1.68, 95% CI, 1.25-2.25, p<0.01) in the placebo arm of the ADAURA study, and 88% (HR=0.81, 95% CI, 0.56-1.16, p=0.24) in the osimertinib arm of the ADAURA study. In the stage II-IIIA, the 5-year survival rate was 77% in the SMC data (reference), 73% (HR=1.29, 95% CI, 0.92-1.82, p=0.14) in the placebo arm of the ADAURA study, and 85% (HR=0.62, 95% CI, 0.41-0.93, p= 0.02) in the osimertinib arm of the ADAURA study.
Conclusions: In this study, the majority of patients received EGFR-TKIs after recurrence. The 5-year overall survival in the real-world data demonstrated superiority over the placebo arm of the ADAURA study. In stage IB and II disease, there was no significant difference between the SMC data and the osimertinib arm of the ADAURA study. Consequently, patients with pathologic stage IIIA are considered strong candidates for adjuvant osimertinib.

#3831 Clinicopathologic determinants of survival in double/triple hit lymphoma: Analysis of a pooled database.

P. A. Haddad[1], S. Gupta[2], A. Gupta[3], C. Graham[2];
[1]LSUHSC-S Feist-Weiller Cancer Ctr./Overton Brooks VAMC, Shreveport, LA, [2]LSUHSC-S Feist-Weiller Cancer Ctr., Shreveport, LA, [3]Overton Brooks VAMC, Shreveport, LA

Background B-cell lymphoma with MYC, BCL2, and/or BCL6 rearrangements are classified as double/triple- hit lymphoma (DTHL). They usually, but not always, tend to be high-grade aggressive B-cell lymphoma with worse prognosis. Despite this classification, DTHL remains a heterogeneous group with varied molecular profiles, biological behavior, and prognosis. Therefore, we conducted this pooled database analysis to identify the prognostic factors, clinicopathological characteristics, and therapeutic strategies influencing survival in this rare disease.
Methods To study the demographic characteristics, molecular and immunohistochemical signatures, therapeutic interventions, survival, and prognostic factors, we compiled a pooled database of 161 cases that fit the diagnostic criteria for DTHL. Kaplan-Meier survival curves were constructed. Cox proportional hazards model and Log-rank tests were used to assess the influence of demographic and clinicopathologic factors on overall survival (OS) and disease-free survival (DFS).
Results A compiled a dataset of 161 patients with confirmed DTHL. The median age was 62 with F:M of 1.08. The median duration of symptoms before diagnosis was 2 months. DTHL involved the lymph nodes (41%), bone marrow (31%), bone (14%), CNS (5%), skin (4%), liver (3%), and spleen (2%). Constitutional symptoms were reported in 20%. The cohort consisted of primary (50%), secondary/transformed (16%), and follicular DTHL. The median OS and DFS of the cohort were 69 and 27 months, respectively. Bone marrow and extra-lymphatic organ involvement were associated with worse DFS and non-significant numerically worse OS. LDH>500 (p=0.006), PAX5-negative (p=0.01), CD79a-negative (p=0.02), and Ki67>80% (p<0.0001) were associated with worse OS. Similarly, CD5+, CD10+, and MUM1+ had worse OS, but did not reach statistical significance. Follicular DTHL was associated with the best median OS and DFS followed by primary then secondary/transformed in decreasing order. Advanced stage and high IPI were also associated with worse non-significant numerical OS. Age and sex did not impact OS. Compared to no treatment, chemotherapy and stem cell transplant had incrementally superior median OS (3 vs. 55 vs. NR months, p=0.008). Frontline intensive chemotherapy yielded similar DFS and OS to CHOP-like regimens. Patients who attained CR as their best response also had a superior median OS (p<0.0001).
Conclusion This study presents clinicopathologic data from a cohort of patients with primary, secondary, and follicular DTHL. It identifies the type of DTHL, IHC profile, LDH levels, type of therapy, and quality of response to treatment as critical determinants of OS.

#3832 Fluid-overload associated large B-cell lymphoma and determinants of outcomes: Analysis of a pooled database.

P. A. Haddad[1], S. Gupta[2], C. Graham[2];
[1]LSUHSC-S Feist-Weiller Cancer Ctr./Overton Brooks VAMC, Shreveport, LA, [2]LSUHSC-S Feist-Weiller Cancer Ctr., Shreveport, LA

Background: Fluid overload-associated large B-cell lymphoma (FOLBCL) is a new WHO lymphoma entity previously known as PEL-like lymphoma or HHV8-unrelated PEL-like lymphoma. It is a rare lymphoma that arises within fluid-filled body cavities without a solid component. FOLBCL occurs in the absence of immunodeficiency and is commonly associated with conditions associated with fluid overload. It expresses mature B-cell phenotype and occasional EBV infection markers. We conducted this study to delineate key clinicopathological characteristics, prognostic indicators, and treatment modalities that affect outcomes in this rare and newly defined lymphoma subtype.
Materials & Methods: To study the demographic characteristics, molecular and immunohistochemical signatures, therapeutic interventions, survival, and prognostic factors, we compiled a pooled database of 115 cases that fit the diagnostic criteria for FOLBCL. Kaplan-Meier survival curves were constructed. Cox proportional hazards model and Log-rank tests were used to assess the influence of demographic and clinicopathologic factors on overall survival (OS).
Results: A total of 115 patients with confirmed FOLBCL were identified. The median age was 74, with a peak incidence between 72 and 82 years. There was a male preponderance with M:F of 2. The pleural, pericardial, and peritoneal cavities were involved in 75%, 34, and 27%. The median duration of symptoms before diagnosis was 1 month. Patients presented with constitutional symptoms and hepatosplenomegaly in 13% and 1%, respectively—no patients presented with lymph node and bone marrow involvement. The median OS of the whole group was 16 months. Patients younger than 70 had better median OS than 70 and older (24 vs. 10 months, p=0.008). The presence of any malignant peritoneal effusion was associated with worse OS when compared to effusion limited to the thoracic cavity (7 vs. 24 months, p=0.005). LDH>500 was also associated with worse OS (p=0.02). Sex, the presence of fluid overload-causing conditions, and serum IL2R levels did not seem to impact OS. MYC re-arrangement had numerically worse OS when present but did not reach statistical significance. Chemotherapy demonstrated superior OS compared to no treatment (24 vs. 7 months, p=0.009). Patients who attained CR as their best response had a superior median OS (p<0.0001).
Conclusion: This study presents updated clinicopathologic data from a pooled cohort of patients with FOLBCL. It identifies the age, the primary location of cavitary disease, LDH, active therapy, and quality of response to treatment as key determinants of OS.

#3833 Primary cutaneous diffuse large B-cell lymphoma-leg type and clinicopathologic determinants of survival: Analysis of a pooled database.

P. A. Haddad[1], M. Amankwah[2];
[1]LSUHSC-S Feist-Weiller Cancer Ctr./Overton Brooks VAMC, Shreveport, LA, [2]LSUHSC-S Feist-Weiller Cancer Ctr., Shreveport, LA

Background: Primary Cutaneous Diffuse Large B-cell Lymphoma-Leg Type (PCDLBCL-LT) is a rare but non-indolent subtype of B-cell lymphoma. While most PCDLBCL-LT starts over the lower extremities, some cases may present at other cutaneous sites. The determinants of survival outcomes in this disease are not very well defined. Therefore, we conducted this pooled database analysis to identify the prognostic factors, clinicopathological characteristics, and therapeutic strategies that influence survival in this disease.
Methods: To study the demographic characteristics, molecular and immunohistochemical signatures, therapeutic interventions, survival, and prognostic factors, we compiled a pooled database of 122 cases that fit the diagnostic criteria for PCDLBCL-LT. Kaplan-Meier survival curves were constructed. Cox proportional hazards model and Log-rank tests were used to assess the influence of demographic and clinicopathologic factors on overall survival (OS) and disease-free survival (DFS).
Results: A total of 122 patients with confirmed PCDLBCL-LT were identified. The median age was 76. There was a male preponderance with M:F of 2.4. Seventy-three percent involved the extremities. The median duration of symptoms before diagnosis was 3.5 months. Involvement of lymph nodes, bone marrow, bone, and CNS occurred in 11%, 3%, 4%, and 3%, respectively. Constitutional symptoms were reported in 5%. The median OS and DFS of the whole group were 39 and 32 months, respectively. Patients younger than 70 had better median DFS (NR vs. 24 months, p=0.02) with a non-significant better median OS. Lymphadenopathy (45 vs. 18 months, p=0.006) and stage T3 compared to T1/T2 (16 vs 41 months, p=0.006) were associated with worse OS. Sex, constitutional symptoms, IHC phenotype, extra-lymphatic/extra-cutaneous organ involvement, and histologic cutaneous patterns did not impact OS. Compared to no treatment, chemotherapy, XRT+/-surgery, and stem cell transplant had numerically better OS without reaching statistical significance (5 vs. 39 vs. 41 vs. NR months, p=0.15). Patients who attained CR as their best response also had a superior median OS compared to responses less than CR and none (61 vs. 23 vs. 11 months, p<0.0001).
Conclusion: This study presents updated clinicopathologic data from a large, pooled cohort of patients with PCDLBCL-LT. It identifies age, lymph node involvement, T stage, type of therapy, and quality of response to treatment as critical determinants of OS.

#3834 Plasmablastic lymphoma provisional prognostic score.

P. A. Haddad[1], J. Lerner[2];
[1]LSUHSC-S Feist-Weiller Cancer Ctr./Overton Brooks VAMC, Shreveport, LA, [2]LSUHSC-S Feist-Weiller Cancer Ctr., Shreveport, LA

Background Plasmablastic Lymphoma (PBL) is a rare and aggressive subtype of non-Hodgkin's lymphoma. It tends to be associated with immunosuppressive clinical contexts, such as HIV infection and immunosuppressive therapies for autoimmune disorders and organ transplants. However, due to the rarity of the disease, which needs to be better understood, varied treatment approaches have been implemented, and no optimal data or guidelines for managing PBL are available. Therefore, we conducted this study to develop a provisional PBL prognostic score (PBLPS) for this rare disease.
Methods We used our constructed PBL database, which contains retrospective data on 300 cases. Such data included demographics such as sex, age, and race. It also included disease presentation symptoms, duration of symptoms before diagnosis, site(s) of the disease, blood counts, coexisting comorbidities, disease immunohistochemical and molecular phenotype, types of treatment, and survival outcomes. Of the 300 cases, 291 had complete survival and outcomes data, the sample chosen for this study. Cox proportional-hazards model and Log-rank tests were used to assess the influence of clinicopathologic factors on overall survival (OS). We included factors that statistically impacted OS and scored them by the impact of their hazard ratios.
Results The median OS of the cohort was 25 months. The following dichotomous variables were identified as impactful prognostic factors in this cohort: LDH>500 (p=0.04), CD4<100 (p=0.006), bone marrow (BM) involvement (p<0.0001), EBER-negative (p=0.01), HHV8+ (p=0.02), and involvement of liver (p=0.003), lungs/pleura (p<0.0001), and upper GI tract (p=0.001). A prognostic model was devised using these variables to identify different levels of risk. Involvement of BM and involvement of any of the worse prognosis organs (liver, lung/pleura, and/or upper GI tract) were each assigned a score of 2 when present. CD4<100, EBER-negative, and LDH>500 were assigned 1 point each as they had the lowest hazard ratios of all the other variables. In this exploratory cohort, we assigned low risk a score of 0, intermediate risk a score of 1-2, and high risk a score of 3-7. This prognostic score system led to our cohort's most optimal risk discriminatory model, where low, intermediate, and high risk had a median OS of NR, 15, and 4 months, respectively (p<0.0001).
Conclusion This PBLPS is a promising new tool for risk-stratifying patients with PBL. However, it still requires prospective validation.

#3835 Clinicopathologic determinants of survival in malignant histiocytic neoplasms: Analysis of a pooled database.

P. A. Haddad[1], D. Keerty[2];

[1]LSUHSC-S Feist-Weiller Cancer Ctr./Overton Brooks VAMC, Shreveport, LA, [2]LSUHSC-S Feist-Weiller Cancer Ctr., Shreveport, LA

Background: Malignant histiocytosis, also known as the M-group per the Histiocyte Society classification, represents a rare, aggressive malignant group of histiocytic neoplasms. It includes histiocytic neoplasms that occur de novo (pMHN) and those that develop in association with other malignant diseases (aMHN). However, little is known about factors that impact MHN clinical outcomes. We conducted this pooled database analysis to delineate key clinicopathological characteristics, prognostic indicators, and treatment modalities that affect survival in these rare diseases.

Methods: To study the demographic characteristics, molecular and immunohistochemical signatures, therapeutic interventions, survival, and prognostic factors, we compiled a pooled database of 281 cases of MHN. Kaplan-Meier survival curves were constructed. Cox proportional hazards model and Log-rank tests were used to assess the influence of demographic and clinicopathologic factors on overall survival (OS).

Results: A total of 281 patients with confirmed MHN were identified, with 77% pMHN and 23% aMHN. The median age was 45, with bimodal peaks between 0-13 and 52-65. There was a male preponderance with M:F of 1.6. Primary sites of involvement were liver (15%), CNS and spleen (13% each), thoracic, GI, and soft tissues (12% each), bones (11%), skin (10%), H&N (8%), and breast, heart, gonads, pancreas, and kidney (1% each). Lymphadenopathy and bone marrow (BM) were involved in 28% and 18%, respectively. Constitutional symptoms occurred in 12% and hemophagocytic syndrome (HPS) in 6%. The median OS of the whole group was 12 months. BM involvement had a worse median OS (5 vs. 60 months, p=0.0002). Stage 1 disease had better median OS than higher stages (p=0.0008). Furthermore, unifocal had better median OS than multifocal/multicentric disease (60 vs. 7 months, p=0.0001). The presence of inflammatory background positively impacted OS (p=0.01). The occurrence of HPS adversely affected OS (p<0.0001). Compared to no treatment, localized therapies such as surgery (S) and/or radiation therapy (RT) and systemic combination chemotherapy (CT) were statistically superior, with a median OS of 3, 24, and 16 months, respectively (p=0.009). Among systemic therapies, SCT and BRAF/MEK inhibitors were superior to conventional chemotherapy (p=0.02). Having CNS or splenic-lymphatic primary involvement tended to have a numerical but non-significant worse median OS than soft tissue or visceral disease. While female sex, size<10cm, and pMHN seemed to have numerically better OS, they did not reach statistical significance. There was no difference in median OS for age.

Conclusion: This study presents updated clinicopathologic data from a pooled cohort of patients with MHN. It identifies BM involvement, stage, extent of the disease, the inflammatory background status, occurrence of HPS, and treatment approach as critical determinants of OS.

#3836 Mast cell leukemia provisional prognostic score.

P. A. Haddad[1], S. Chennapragada[2];

[1]LSUHSC-S Feist-Weiller Cancer Ctr./Overton Brooks VAMC, Shreveport, LA, [2]LSUHSC-S Feist-Weiller Cancer Ctr., Shreveport, LA

Background Mast cell leukemia (MstCL) is a rare but aggressive variant of systemic mastocytosis (SM), defined by the presence of >20% atypical mast cells in the bone marrow. It is further classified into leukemic and aleukemic variants based on the presence or absence of >10% atypical mast cells in the peripheral blood, respectively. There is a wide variation in treatment regimens used to treat MstCL. Despite this, prognosis remains poor. While MstCL often follows an aggressive course, its outcomes vary considerably. We conducted this study to develop a provisional MstCL prognostic score (MCLPS) for this rare disease.
Methods We used our constructed MstCL database, which contains retrospective data on 144 cases. Such data included demographics such as sex, age, and race. It also included disease presentation symptoms, duration of symptoms before diagnosis, site(s) of the disease, blood counts, coexisting comorbidities, disease immunohistochemical and molecular phenotype, types of treatment, and survival outcomes. Of the 144 cases, only 104 had complete survival and outcomes data, the sample chosen for this study. Cox proportional-hazards model and Log-rank tests were used to assess the influence of clinicopathologic factors on overall survival (OS). We included factors that statistically impacted OS and scored them by the impact of their hazard ratios.
Results The median OS of the cohort was 9 months. The following dichotomous variables were identified as impactful prognostic factors in this cohort: Age<55 (6 vs. 15 months), Hgb<10g/dl (3 vs. 29 months), Plt<100K (3 vs. 23 months), leukemic phase (7 vs. 18 months), and complex cytogenetics (2.3 vs. 23 months). A prognostic model was devised using these variables to identify different levels of risk. Each variable was assigned a score of 1 when present for a maximum possible score of 5. In this exploratory cohort, low risk was assigned a score of 0, intermediate risk a score of 1-2, and high risk a score of 3-5. This prognostic score system led to our cohort's most optimal risk discriminatory model, where low, intermediate, and high risk had a median OS of 29, 8, and 2.4 months, respectively (p=0.0006).
Conclusion This MCLPS is a promising new tool for risk-stratifying patients with MstCL. However, it still requires prospective validation.

CLINICAL RESEARCH: Tumor Immune Response 2
Poster Session

#3840 Can serum exosomal content predict response to immunotherapy in hepatocellular carcinoma?.

Niramol Savaraj[1], Pablo Puente[2], Ying-Ying Li[1], Chunjing Wu[1], Jonathan D. Nguyen[1], Medhi Wangpaichitr[1], Peter J. Hosein[3], Lynn G. Feun[3]

[1]Univ. of Miami/VA Medical Ctr., Miami, FL,[2]University of Illinoid, Chicago, IL,[3]Medicine, Univ. of Miami, Miami, FL

While atezolizumab and bevacizumab combination has received FDA approval for the treatment of unresectable hepatocellular carcinoma (HCC), and recently durvalumab + tremelimumab also showed activity over sorafenib, there is no biomarker which can guild which patients can benefit from these regimens. The traditional PD-L1 positivity in the tumor by immunohistochemical staining which can predict possible response to immune checkpoint inhibitor in other solid tumors, such as melanoma and NSCLC, does not appear to apply to HCC. Thus, we attempt to explore whether exosomal content can be useful to predict response. HCC tumors exist in a complex microenvironment and serum exosomes can be generated from either tumor cells, macrophages, or other immune cells. Exosome act as new mediators for cell-cell communication transporting molecules such as lipids, proteins, and RNAs in vivo. Exosomal PD1 and PD-L1 have been implicated for possible biomarkers for immune checkpoint sensitivity. We isolated exosome from serum of unresectable HCC patients who underwent treatment with atezolizumab and bevacizumab. Blood sample was obtained prior to treatment, and then on cycle 3 and at the time of disease progression. Exosomes were isolated using the kit from System BioScience. Twenty patients were entered into the study. Five patients were not treated (received SBRT or other regional treatment), one was lost to follow up and one had atezolizumab only. In terms of antitumor response, eight patients had stable disease, three patients had partial response and two patients had progressive disease. Serum exosomal content data was available in 16 patients. Both PD1 and PDL1 are lowest in the three patients who had response followed by the group who had stable disease. In the two patients who had progressive disease, both exosomal PD-L1 and PD1 appeared to be the highest and did not change during treatment. Unlike in melanoma patients we have studied, other proteins in the antiapoptotic family such as Bcl-2 do not show any differences. While the number of patients are small and accrual is still ongoing, it appears that exosomal PD-L1/PD1 may have clinical value in predicting response to atezolizumab + bevacizumab therapy. Supported by Sylvester Comprehensive Cancer Center grant.

#3841 Tumor-derived microRNA125a induces CART cell apoptosis and failure in B cell malignancies.

O. Sirpilla, R. Sakemura, I. Can, T. N. Huynh, J. H. GIrsch, C. Manriquez Roman, C. M. Stewart, K. Yun, E. J. Ogbodo, L. Mai, O. Gutierrez Ruiz, M. Rodriguez, B. Kimball, H. Xia, J. C. Villasboas, S. Ansell, N. Bennani, P. B. Johnston, J. Paludo, J. Castro, M. Kharfandabaja, S. Parikh, N. Kay, Y. Lin, E. Siegler, S. Kenderian;
Mayo Clinic, Rochester, MN

Despite the remarkable efficacy of chimeric antigen receptor T -cell therapy (CART) for the treatment of B-cell malignancies, durable remission remains limited often due to tumor relapse. We have previously demonstrated that tumor-derived extracellular vesicles (EVs) induced CART cell failure in preclinical models. To characterize the impact of tumor EV induced CART cell dysfunction, we assessed microRNA (miRNA) profiles contained within tumor EVs from two independent patient cohorts and studied how they contributed to CART dysfunction. Our first cohort included patients with chronic lymphocytic leukemia (n=50). We previously showed that CLL patient derived EVs induce a state of CART cell dysfunction. To understand this dysfunction, we interrogated the miRNA cargo significantly enriched in CLL EVs and how their coculture impacts CART signaling by RNAseq. Here, we found a significant enrichment in miR-125a within CLL EVs as compared to healthy donor controls (*p=.0001*). CART cocultured with CLL EVs showed alterations in T cell activation pathways, where miR-125a targets TNFAIP3 and NFkB pathways were activated. These findings implicate miR-125a from CLL EVs in CART dysfunction. Next, we aimed to validate the impact of miRNA on CART cell outcomes in the clinic. We interrogated miRNA profiles from patients with diffuse large B cell lymphoma (DLBCL) treated with CART cell therapy (CART19-28ζ, axicabtagene ciloleucel). EV miRNA cargo was compared between responders (complete remission at 6 months, n=10) and non-responders (no response 1 month post CART19, n=10) to identify differentially enriched miRNAs across groups. miR-125a was again significantly upregulated in EVs of non-responders as compared to responders to CART19 treatment (*fold change=3.28, padj=.018*). To study the direct effect of miR-125a on CART cell functions, we generated and studied the effector functions of CART19-28z following transfection with miR-125a or negative miR control. CART19 cells transfected with miR-125a showed a dose dependent decrease in killing of lymphoma cells as compared to miR-control (*p=.0001*). miR-125a also significantly increased the rate of apoptosis in CART19 cells (*fold change=1.95, p=.024*) and decreased the level of CART proliferation (*fold change=.71, p=.013*) as compared to controls. Notably, miR-125a did not impact tumor cell growth, further verifying a direct CART effect. In summary, our studies demonstrate the impact of tumor derived miRNAs on CART cell outcomes. They identify that miR-125a is 1) associated with CLL EV induced CART dysfunction, 2) significantly elevated in non-responders to CART therapy in the clinic, and 3) able to decrease CART19 efficacy through reduced CART killing/proliferation and increased apoptosis. These results highlight a novel mechanism of CART19 failure induced through miRNA cargo delivery by tumor-derived EVs and the role of miR-125a in inducing CART19 dysfunction.

#3842 Neuroendocrine differentiation and treatment of human SCLC: NRF2 has a role..

S. Hamad[1], H. Joshi[2], Y. Li[3], H. Toma[2], N. Bendjilali[4], S. Jefferys[5], D. Corcoran[5], W. Elbezanti[2], B. Major[6], W. Bernard[7], F. Spitz[1];
[1]Cooper Medical School of Rowan University (CMSRU), Camden, NJ, [2]Cooper University Hospital, Camden, NJ, [3]Cooper University Health Care, Camden, NJ, [4]Rowan University, Glassboro, NJ, [5]University of North Carolina, Chapel Hill, NC, [6]Washington University School of Medicine in St. Louis, St. Louis, MO, [7]University of North Carolina, Chapel Hill, NJ

SCLC is a lethal form of lung cancer and highly metastatic disease with limited therapeutic options. Four main neuro and non-neuroendocrine SCLC molecular subtypes have been identified which further complicate the efforts of finding targeted therapies. NRF2 is a transcription factor that is known to protect cells from oxidative damage by regulating more than 500 cytoprotective genes. NRF2 is frequently mutated in non-small cell lung cancer (NSCLC), however, whether alterations occur in small cell lung cancer (SCLC) is not clear due to limited sequencing data. Recently, our group has discovered a previously unrecognized role of NRF2 signaling pathway in the development of SCLC using a novel genetically engineered mouse model (GEMM). In this study, we have investigated the role of NRF2 in the progression and regression of human SCLC. Human SCLC cell lines were generated with $NRF2^{E79Q/+}$ mutation (one of the most common mutations found in human tumors) to allow the constitutive activation of NRF2 in these cells. Results from hSCLC cell lines showed that NRF2 activation in NRF2-negative SCLCs can significantly inhibit their growth. Further, human SCLC gene expression data showed reduced levels of a NRF2 signature as hSCLC neuroendocrine SCLC transforms to non-neuroendocrine subtypes. As an anti-inflammatory pathway, NRF2 is known to inhibit immune cell gene signature. Our in vivo and invitro studies showed that NRF2 inhibits immune cell infiltration in SCLC; and increases PDL1 protein expression. Currently, we are investigating the effect of NRF2 activation in hSCLC growth, neuroendocrine differentiation and immune gene activation in vitro and in vivo. We are also using immune checkpoint inhibitors to determine the best therapeutic options for each SCLC subtype.

#3843 Role of CD4/CD8 double positive T cells in modulating response to anti-PD-1 treatment in renal cell carcinoma.

S. Sankaran, K. Jaganathan, B. Das, S. V, C. Bhowal, M. M, D. M, M. Nath, R. M, O. M, R. Malhotra, G. K, M. Malhotra, N. Pal Basak;
Farcast Biosciences, Bangalore, India

Presence of CD4+CD8+ Double Positive T (DPT) cells in the tumor microenvironment has been correlated with good prognosis[1]. Renal cell carcinoma (RCC) is reported to have relatively much higher DPT cell sub-populations as compared to other cancer types[1,2]. DPT cells in RCC were reported to express high programmed cell death protein-1(PD-1) and therefore is considered a potential target for checkpoint based immunotherapy[2]. However, the clinical relevance of these DPT cells in determining response to anti-PD-1 has not yet been studied. Using the near native Farcast™ TruTumor RCC histoculture platform, we attempted to elucidate the role of DPT in anti-PD1 response modulation. Fresh surgically resected RCC samples (n=18) along with matched blood were collected from consented patients. Explants were generated and distributed into arms. These arms were treated in culture with nivolumab (anti-PD1:132µg/ml) for 72 hours. The response was evaluated using histopathology and flow cytometry read-outs. DPT cells were gated and expressed as percentage of CD3 using flowcytometry. We observed a significantly higher proportion of DPT cells in RCC (Mean±SEM: 8.2±2.8) compared to head and neck squamous cell carcinoma (Mean±SEM: 1.2±0.4) and ovarian cancer (Mean±SEM: 0.7±0.1). DPT cell population was found to be well preserved on the TruTumor RCC platform post-culture. We stratified samples as high and low DPT cell sub cohorts based on 5% cut-off. Out of 18, 6 samples (33%) showed high DPT cells (with a range of 7-41%). Eighty-three percent (5 out of 6) of high DPT samples elicited a tumor cytotoxicity on treatment with Nivolumab treatment as compared to only 50% (6 out of 12) in low DPT samples. A significant decrease ($p<0.05$) in DPT cells was observed in the high DPT sub cohort upon Nivolumab treatment, with a concomitant increase in activated (Granzyme B+) DPT and cytotoxic T cells (CD8+) sub-populations was observed upon nivolumab treatment. However, total CD8+ proportions remained unchanged. In addition, an increase in effector (CD4+ FoxP3-) and decrease in Treg (CD4+FoxP3+) population was also observed. Only one out of six high DPT samples exhibited no cytotoxicity in response to nivolumab treatment. Interestingly in this non-responder sample there was a 3.1-fold increase in M2-like (CD68+CD206+) macrophages, as compared to a M1-like macrophage polarization observed in the remaining high DPT samples. In summary, our data suggests that presence of high percentage of DPT cells could favour better response to anti-PD1 therapy in RCC patients. The Farcast™ TruTumor platform thus provides powerful insights into the role of various immune cell sub-populations in modulating response to treatment with immune-oncology therapies.

References

1. Nishida, K., et al., Int Immunol. 2020;32:347-357.
2. Menard, LC., et al., Front Immunol. 2018;9:2728.

#3844 Clinical implications of mixed response on prognosis of non-small cell lung cancer (NSCLC) patients treated with Immunotherapy.

S. Lee[1], T. Um[2], J. Lee[1], P. Kim[3], M. Yadav[2], M. J. A. Chuchuca[2], L.-Y. Chung[2], Y. Chae[2];

[1]Kyungpook National University, Daegu, Korea, Republic of, [2]Feinberg School Of Medicine, Northwestern University, Chicago, IL, [3]The University of Texas at Austin, Austin, TX

Background: Current methods for assessing the response of lung cancer patients to therapy (e.g. RECIST criteria) lack consideration for mixed response (MR) where some lesions increase while others decrease simultaneously. MR poses a challenge in deciding the continuation of therapy. Understanding the clinical implications of MR on patient prognosis within radiographic response categories is crucial for establishing effective treatment strategies for NSCLC.
Methods: This study analyzed 177 NSCLC patients with ≥2 lesions receiving first-line systemic treatment with immunotherapy. Clinical response was evaluated by RECIST v1.1 and immune-related RECIST (irRECIST). MR was defined as the simultaneous presence of ≥1 lesion increase and ≥1 lesion decrease during therapy. Two different definitions of MR were utilized. Definition-A (MR-A): the simultaneous presence of one or more lesions increasing ≥5mm and one or more lesions decreasing ≥5mm during therapy (Δ [baseline - first follow-up] ≥ 5 mm); and Definition-B (MR-B): the simultaneous presence of one or more lesions increasing >1mm and one or more lesions decreasing >1mm during therapy (any Δ [baseline - first follow-up]). Subgroup analysis was conducted using 94 patients with only intrathoracic lesions.
Results: Among the 177 patients, tumor responses based on RECIST were 3 CR (1.7%),42 PR (23.7%), 87 SD (49.2%), and 45 PD (25.4%). Based on irRECIST, responses were 3 CR (1.7%), 46 PR (26.0%), 89 SD (50.3%), and 39 PD (22.0%). MR-A and MR-B occurred in 19.8% (n=35) and 45.2% (n=80) of cases, respectively. In the irRECIST PD group, MR-A demonstrated significantly different median progression-free survival (mPFS) and median overall survival (mOS) compared to non-MR-A ($p<0.020$, $p<0.005$, respectively). The mPFS for MR-A group was 1.4 months (range 0.5-52.9) and non-MR-A group was 5.5 months (range 0.2-97.2) with the hazard ratio being 2.91 (95% CI 1.13-7.51). The mOS for MR-A and non-MR-A groups were 4.8 months (range 0.7-61.5) and 11.8 months (range 0.2-97.2), respectively, hazard ratio 4.87 (95% CI 1.43-16.56). No other significant results were found for other RECIST and irRECIST categories. Subgroup analysis of only intrathoracic lesion patients revealed no statistically significant results.
Conclusion: Contrary to our hypothesis, MR did not modify prognosis within the RECIST or irRECIST category. MR-A or MR-B in the RECIST or irRECIST PD group did not show a better prognosis, indicating the complexity of mixed responses in NSCLC patients treated with immunotherapy. Further research with larger cohorts are warranted.

#3846 The obesity paradox in immune checkpoint blockade: A pan-tumor analysis.

S. L. Alden[1], S. Charmsaz[2], M. Brancati[2], H. L. Li[1], A. Warner[1], K. Munjal[2], K. Howe[2], S. Mitchell[2], E. Griffin[2], M. Nakazawa[2], H.-L. Tsai[1], L. Danilova[1], C. Thoburn[1], J. Gizzi[1], A. Hernandez[2], N. E. Gross[1], E. M. Coyne[2], S. M. Shin[2], J. Durham[2], M. F. Konig[1], B. J. Christmas[2], E. J. Lipson[2], J. Naidoo[2], L. C. Cappelli[1], A. Pabani[2], Y. Ged[2], M. Baretti[2], J. R. Brahmer[2], J. Hoffman-Censits[2], T. Y. Seiwert[2], S. Bansal[3], L. Tang[3], E. Jaffee[2], G. Chandler[4], R. Mohindra[5], W. Ho[2], M. Yarchoan[2], C. Kao[2];

[1]Johns Hopkins University School of Medicine, Baltimore, MD, [2]Sidney Kimmel Comprehensive Cancer Center, Johns Hopkins University, Baltimore, MD, [3]Genentech Inc, San Francisco, CA, [4]F. Hoffmann-La Roche Ltd., Basel, Switzerland, [5]F. Hoffmann-La Roche Ltd, Basel, Switzerland

Background: Chronic systemic inflammation mediated by pro-inflammatory cytokines serves as a major mechanism by which obesity contributes to cancer development. Paradoxically, elevated body mass (BMI) has been associated with improved outcomes after treatment with immune checkpoint inhibitors (ICIs) in many tumor types. The interplay between cytokine response and obesity after ICIs is poorly understood. To characterize underlying mechanisms, we investigated cytokine profiles in relation to obesity and clinical outcomes in patients treated with ICIs.

Methods: From June 2021 to October 2022, we enrolled and collected blood samples from patients with advanced or metastatic solid tumors who received ICIs as standard of care at Johns Hopkins. We calculated BMI using height and weight at treatment initiation, with BMI ≥30 obese and BMI <30 non-obese. Underweight patients (BMI <18.5) were excluded. The Bioplex 200 platform (Biorad, Hercules CA) was used to determine the plasma concentration of 37 cytokines at baseline and on-treatment, with the median cytokine value used to differentiate between high and low concentration.

Results: Among 94 patients, 29 (31%) were obese and 65 (69%) were non-obese, with a significant difference in sex (Fisher's exact test, p = 0.02), but no observed difference in age, race, cancer type, autoimmune disease, or presence of immune-related adverse events (irAE) based on BMI category; all the following hazard ratios (HR) are therefore adjusted for sex. Obese patients had improved progression free survival (PFS) (HR 0.41 [95% CI: 0.21-0.80], p=0.01) and overall survival (OS) (HR 0.16 [95% CI: 0.04-0.69], p=0.01). Eighty-six patients had cytokine data at baseline (range: eight days prior to day of initiation). Baseline IL-15 was significantly lower in obese patients (1.71 vs. 2.08, p=0.04), however, there was no difference in PFS (HR 1.49 [95% CI: 0.87-2.56], p=0.15) or OS (HR 1.22 [95% CI: 0.51-2.97], p=0.65) comparing low vs. high baseline IL-15. Eighty-two patients had cytokine data on-treatment (range: 21-349 days after initiation), with significantly lower levels of IL-6 (2.49 vs. 3.45, p=0.04), IL-8 (2.01 vs. 2.92, p=0.01), and IL-15 (1.70 vs. 1.81, p=0.01) in obese vs. non-obese patients, respectively. Low on-treatment IL-8 was associated with improved PFS (HR 0.52 [95% CI: 0.29-0.92], p=0.02) and OS (HR 0.17 [95% CI: 0.05-0.58], p<0.01), and low on-treatment IL-6 was associated with improved OS (0.25 [95% CI: 0.08-0.76], p=0.01).

Conclusions: In a diverse, pan-tumor ICI cohort, we observed a positive relationship between obesity and clinical outcomes with ICIs, with no correlation between obesity and irAEs. We also observed lower on-treatment levels of IL-6 and IL-8 in patients with obesity and that low on-treatment levels of IL-6 and IL-8 correlated with improved survival, suggesting that IL-6 and IL-8 may serve as mediating factors for improved outcomes in obese patients treated with ICIs.

#3847 Dual targeting of EGFL6 and VEGF-A to overcome immune suppression in ovarian cancer.

S. Umamaheswaran[1], L. S. Mangala[1], R. Joseph[1], N. B. Jennings[1], M. S. Kim[1], Y. Wen[1], E. Bayraktar[1], N. Zhang[2], Z. An[2], A. K. Sood[1];
[1]University of Texas MD Anderson Cancer Center, Houston, TX, [2]University of Texas Health Science Center at Houston, Houston, TX

Background: Ovarian carcinomas are known to have a high degree of immune suppression, which may be related, in part, to high levels of vascular endothelial growth factor-A (VEGF-A). Bevacizumab (anti-VEGF antibody) has been shown to increase infiltration of T-cells in the tumor microenvironment (TME). We have also identified EGFL6 as an important angiogenic protein. Here, we examined the biological effects of blocking EGFL6 and VEGF-A in ovarian cancer models.
Methods: We studied the *in vitro* (endothelial tube formation and migration assays) and *in vivo* (ID8$^{KO\text{-}Trp53;Brca2}$ and SKOV3-ip1 models) biological effects of EGFL6 and VEGF-A blockade. Tumor-infiltrating immune cells were studied by flow cytometry and immunohistochemistry staining.
Results: Blocking EGFL6 and VEGF-A simultaneously with monoclonal antibodies in RF24 endothelial cells decreased tube formation and migration significantly, in comparison to VEGF-A blockade alone ($p<0.001$). EGFL6 monotherapy in ID8$^{KO\text{-}Trp53;Brca2}$ tumor bearing syngeneic mice decreased tumor burden (~2.5 fold, $p<0.0001$) and increased the infiltration of IFNγ^{+} (~2.75 fold, $p<0.0001$) and GzmB^{+} (~1.75 fold, $p<0.01$) CD8^{+} T-cells and IFNγ^{+} (~2 fold, $p<0.0001$) and GzmB^{+} (~2 fold, $p<0.01$) CD4^{+} T-cells while decreasing PD-L1^{+} cells (~1.8 fold, $p=0.01$). Dual blockade of EGFL6 and VEGF-A in SKOV3-ip1 tumor bearing nude mice significantly decreased tumor burden (~3.72 fold, $p<0.01$) and angiogenesis (~2.36 fold, $p<0.05$) compared to controls and single-agent blockade. Similar blockade in ID8$^{KO\text{-}Trp53;Brca2}$ tumor bearing mice significantly decreased tumor burden (~4.2 fold, $p=0.0004$), improved CD8^{+} (~3.32 fold, $p=0.0004$) and CD4^{+} (~2.81 fold, $p<0.0001$) T-cell infiltration, NK cell infiltration (~2.3 fold, $p=0.0005$) and decreased myeloid-derived suppressor cells (MDSCs) (~1.92 fold,
$p=0.0278$) compared to EGFL6 and VEGF-A blockade alone.
Conclusions: Our results demonstrate that simultaneously targeting the angiogenesis drivers EGFL6 and VEGF-A in ovarian cancer significantly decreased tumor burden *in vivo* and increased the infiltration of T lymphocytes compared to single-agent blockade.
AACR Category: Tumor Microenvironment and Immune Oncology
Key words: ovarian cancer, immune suppression, angiogenesis, VEGF-A, EGFL6

#3848 Comprehensive protein analysis to identify the proteins responsible for sarcopenia and their impact on antitumor immunotherapy in non-small cell lung cancer.

T. Masuda[1], S. Watanabe[1], T. Wakabayashi[1], S. Tanaka[1], K. Shono[1], R. Suzuki[2], T. Sekiya[1], N. Yanagimura[1], M. Arita[1], A. Ohtsubo[1], T. Tanaka[1], K. Nozaki[1], Y. Saida[1], S. Hokari[1], R. Kondo[1], K. Shima[1], Y. Kimura[1], N. Aoki[1], Y. Ohshima[1], T. Koya[1], K. Sakai[3], K. Nishio[3], M. Yamazaki[1], H. Ishikawa[1], T. Kikuchi[1];
[1]Niigata University Graduate School of Medical and Dental Sciences, Niigata, Japan, [2]Sado General Hospital, Sado, Japan, [3]Kindai University Faculty of Medicine, Osaka, Japan

Background: Previous retrospective studies have shown that sarcopenia (Sar) is associated with poor outcome in cancer patients (pts) receiving immune checkpoint inhibitors (ICIs). We conducted a prospective study to determine whether Sar-related proteins induce Sar and reduce the efficacy of ICI.
Method: Non-small cell lung cancer (NSCLC) pts receiving ICI as first-line treatment at Niigata University Medical and Dental Hospital were eligible. Sar was diagnosed with physical performance and skeletal muscle mass. Comprehensive protein analysis of pre-treatment blood samples was performed to identify factors that correlate with muscle loss and ICI effects.
Result: 41 patients were enrolled from October 2019 through August 2022. PFS for Sar was 4.6 months, 6.7 months for Pre-Sar, and 16.7 months for Non-Sar (P=0.0028). OS for Sar was not reached, 15.7 months for Pre-Sar, and not reached for Non-Sar (P=0.0014). Leptin, IL-1β, IL-12, and Pentraxin 3 were significantly correlated with loss of muscle mass. In contrast, leptin, insulin, IGF-1, GDF-8, Activin A, IL-2Ra, IL-8, MMP-3, osteopontin, and Pentraxin-3 were significantly associated with poor OS. Pentraxin 3 and leptin were associated with both the effectiveness of immunotherapy and sarcopenia. A multivariate analysis that considered factors commonly associated with the effectiveness of immunotherapy, including age, PD-L1 expression rate, and neutrophil-lymphocyte ratio, Pentraxin 3 was determined to be an independent prognostic factor.
Conclusion: This study indicated that Sar-related proteins and inflammatory cytokines are involved in the development of Sar and ICI efficacy.

#3849 Frontline ibrutinib-based therapy enhances CART cell functions in patients with CLL: Analysis of the phase 3 randomized clinical trial ECOG-ACRIN E1912.

T. N. Huynh[1], V. Wang[2], T. Shanafelt[3], E. L. Siegler[1], C. M. Stewart[1], K. Yun[1], L. K. Mai[1], O. Sirpilla[1], J. H. Girsch[1], C. Manriquez-Roman[1], J. M. Feigin[1], M. Rodriguez[1], B. L. Kimball[1], H. Xia[1], R. L. Sakemura[1], I. Can[1], O. L. Gutierrez-Ruiz[1], E. J. Ogbodo[1], E. E. Tapper[1], L. A. J. Fonkoua[1], M. T. Hefazi[1], M. W. Ruff[1], S. Parikh[1], N. E. Kay[1], S. J. Kenderian[1];

[1]Mayo Clinic, Rochester, MN, [2]Dana-Farber Cancer Institute, Rochester, MN, [3]Stanford University School of Medicine, Stanford, CA

Introduction: Despite the remarkable activity of CD19-directed chimeric antigen receptor T cell therapy (CART19), durable remissions remain low, especially in chronic lymphocytic leukemia (CLL). Ibrutinib is an oral irreversible inhibitor of Bruton's tyrosine kinase and is a first line therapy for CLL. Preclinical and early clinical data indicate that ibrutinib plus CART19 may be synergistic through inhibition of IL2-inducible T cell kinase. To systematically study the effects of prior ibrutinib treatment on subsequent CART functions, we utilized blood samples from the pivotal clinical trial E1912 (NCT02048813). E1912 was a phase 3 randomized trial comparing treatment with ibrutinib/rituximab (IR) to fludarabine/cyclophosphamide/rituximab (FCR) in previously untreated patients with CLL, which led to the FDA approval of ibrutinib as a first-line therapy in CLL.

Methods: We evaluated the ex vivo expansion and effector functions of T cells and CART19 generated from patients (n=12) with CLL progression following treatment with IR or FCR. We generated CART19 from longitudinal samples obtained at baseline (pretreatment), 6 months post-treatment, 12 months post-treatment, and disease progression. Isolated T cells were lentivirally transduced to express CD28- or 41BB-costimulated CAR19. To assess antigen specific killing and proliferation, untransduced T cells or CART19 were co-cultured at a 1:1 ratio with the CD19+ cell line, JeKo-1, as a surrogate for CLL cells.

Results: Ex vivo T cell expansion increased from an average of 1.5-fold at baseline to 6.7-fold at 6 months, 11.6-fold at 12 months, and 16.9-fold at progression, following ibrutinib-based therapy ($p = 0.02$, 0.04, and 0.04, respectively). Improved T cell expansion was independent of disease burden ($p = 0.89$, 0.73, and 0.54 for expansion vs B cell count at 6 months, 12 months, and progression). T cell expansion significantly worsened following treatment with FCR-based therapy compared to ibrutinib-based therapy (0.6- vs 11.6-fold at 12 months and 0.9- vs 16.9-fold at progression; $p = 0.031$ and 0.039, respectively). Starting at 6 months post-IR, CART19 demonstrated improved antitumor activity and antigen-specific proliferation against JeKo-1. There was no significant difference in the expansion of 41BB- vs CD28-costimulated CART19 following ibrutinib treatment. However, 41BB-CART19 showed enhanced antigen-specific proliferation upon stimulation with JeKo-1 ($p = 0.008$, 0.02, and 0.02 at 6 months, 12 months, and progression).

Conclusion: Our results indicate significant improvement in T cell expansion and CART19 cell functions in patients with CLL following frontline ibrutinib-based therapy, and worsening T cell functions after FCR treatment. Improvement in T cell functions is independent of malignant B cell eradication and is more significant in 41BB-costimulated CART19.

#3850 Modeling individual variability in CD19 CAR-T therapy: An *in vivo* study with PBMC-humanized mice.

W. Lee, D. Rose, J. G. Keck, J. Yang;
The Jackson Laboratory-West, Sacramento, CA

Chimeric antigen receptor T-cell (CAR-T) therapy targeting CD19 has emerged as a transformative treatment for hematological malignancies. Despite its efficacy, significant inter-patient variability in response and associated toxicities pose challenges for its broader application. Understanding these variations is critical to optimize therapy and predict outcomes. This study aims to capture the individual variability observed in CD19 CAR-T cell therapy responses using PBMC-humanized mouse model, with a focus on efficacy, expansion, and cytokine induction profiles. Three human PBMCs (Donors A, B, C) used throughout the studies were pre-screened for in vivo cytokine induction and humanization levels. Autologous CD19 CAR-Ts with a CD28 costimulatory domain and CD3z chain were generated with varying transduction rates: 92%, 52%, and 95% for Donors A, B, and C, respectively. In the first experiment, irradiated female NSG™-MHC I/II double knock-out (DKO) mice were reconstituted with human PBMCs. Six days post humanization, the mice were treated with equal total number of autologous CAR-Ts. All three CAR-Ts showed efficacy, eradicating CD19 cells in peripheral blood. We observed a moderate but significant body weight loss only in mice treated with Donor B autologous CAR-Ts. Notably, CAR-T expansion varied across three donors and did not correspond with the purity (% transduction) of CAR-Ts. Donor B CAR-Ts with the lowest purity showed the highest CAR-T expansion. Donor B PBMCs resulted in the highest humanization level of CD19+ cells and we hypothesize that more CD19 targets led to higher CAR-T expansion. By measuring 33 cytokines from sera collected 2 days post treatment, we explored if human cytokine induction corresponded to the CAR-T expansion. Contrary to initial expectations, cytokines typically associated with robust CAR-T expansion, such as IL-2, IL-6, IL-10, IFNγ, and TNFα, did not peak in the Donor B cohort. To see if individual variability in efficacy and CAR-T cell expansion shows similar variation with increased targets of CD19 CAR-Ts, we engrafted DKO mice with B cell lymphoma (Raji-luc). Seven days after tumor engraftment, we humanized mice with Donor A, B, or C PBMCs and subsequently treated mice with autologous CAR-Ts. Donor A showed the fastest clearance of Raji-luc measured by IVIS bioluminescence imaging. In parallel with the previous experiment, we observed that Donor B CAR-Ts showed the highest expansion level among the three CAR-Ts. The study illustrates how a PBMC-humanized mouse model can reflect the variability in patient responses to CD19 CAR-T therapy. This model serves as a valuable tool for further investigation into the complex dynamics of CAR-T efficacy and toxicity, potentially guiding more tailored approaches in treatment design.

#3851 Beta-lapachone promotes tumor associated neutrophils (TANs) polarized towards anti-tumor (N1) phenotype.

X. Huang[1], S. Tumbath[1], L. Jiang[1], Y.-X. Fu[2];

[1]Indiana University School of Medicine, Indianapolis, IN, [2]University of Texas SouthwesternMedical Center, Dallas, TX

NAD(P)H:quinone oxidoreductase1 (NQO1) is overexpressed in most solid cancers, emerging as a promising target for tumor selective killing. β-lapachone (β-lap), an NQO1bioactivatable drug, exhibits significant antitumor effects on NQO1^{+} human solid cancer cell lines. It also induces immunogenic cell death in the tumor microenvironment (TME)and synergizes with anti-PD-L1 immunotherapy. However, the interaction between β-lap-mediated anti-tumor immune response and neutrophils, a novel antigen presenting cells(APCs), remains unknown. This study found β-lap treatment increased intracellular ROS formation and DNA damage to kill NQO1^{+} murine tumor cell lines and dicoumarol spared the lethality. Furthermore, flow cytometric analysis of immune cells in TME of subcutaneous tumor models indicated that there is a significant infiltration of neutrophils(CD11b^{+} Gr1^{high} cells) or Tumor Associated Neutrophils (TANs) following β-lap treatment. Depletion of neutrophils by co-addition of anti-Ly6G antibody abolished β-lap-induced anti-tumor efficacy in immune competent mice. Neutrophil mediated tumor cell killing determined *ex vivo* using bone marrow derived neutrophils and it was observed that in the presence of β-lap induced antigen, neutrophils were killing murine tumor cells. Moreover, exposure of these neutrophils to β-lap induced antigen medium induce antitumor N1-like properties, include increase in certain surface markers such as CD95(Fas) and CD54 (ICAM-1) as well as increase in intracellular cytokine IFN-β and decrease in TGF-β revealed by flow cytometric analysis. Corroborating to this, there is a significant increase of CD95 and IFN-β and a decrease in TGF-β were observed with TANs infiltrated into β-lap treated TME compared to vehicle treated tumors. Additionally, TLR/MyD88signaling deficiency decreased β-lap induced neutrophil tumor infiltration. BlockingHMGB1, depleting neutrophils, or TLR4/MyD88 deficiency lessened the antigen-specific T cell response. This study highlights that β-lap kills NQO1^{+} murine tumor cells through ROS production and DNA damage, and neutrophils play a pivotal role in its antitumor effects.

#3852 Comprehensive genomic profiling of recurrent or metastatic head and neck cancer presenting with combined positive score 90 or more.

Y. Saito, K. Hidenori, K. Kobayashi, O. Fukuoka, K. Yamamura, A. Shinozaki-Ushiku, K. Oda, K. Kondo;
University of Tokyo, Tokyo, Japan

Background. Biomarkers that predict response to immune checkpoint inhibitor (ICI) in recurrent metastatic squamous cell carcinoma of the head and neck (RMHNSCC) are not well known. Previously, we have found that Combined positive score (CPS) ≥90 and albumin >3.5 respond well to ICI treatment in patients with RMHNSCC treated with ICI irrespective of addition of chemotherapy. In the present study, we investigated whether RMHNSCC with CPS ≥90 has a characteristic genomic mutational profile.

Methods. CPS measurements were performed on a single tumor specimen at the time of diagnosis of RMHNSCC, as approved by Japanese health insurance. Tumor specimens were obtained from the primary tumor as much as possible, and sections that best reflected anti-tumor immunity were decided by a pathologist. We retrospectively reviewed the results obtained from comprehensive genomic profiling (CGP) testing of RMHNSCC cases with CPS ≥90 who were treated by ICI experienced at our institution.

Results. There were 117 eligible RMHNSCC cases. The number of primary lesions were oral cavity in 28 cases (23.9%), nasopharynx in 10 cases (8.5%), oropharynx in 21 cases (17.9%), hypopharynx in 33 cases (28.2%), and others in 18 cases (15.4%). Of 117 patients, 28 patients (23.9%) had a CPS ≥90. Of the 28 cases, the number of primary lesions were oral cavity in 12 cases (42.9%), nasopharynx in 4 cases (14.3%), oropharynx in 0 cases (0%), hypopharynx in 8 cases (28.6%), and others in 3 cases (10.7%). When ICI was administered, CPS ≥90 had a statistically significantly better prognosis than CPS <90 for OS and PFS. Of the 28 cases with CPS ≥90, CGP test was performed in 6 cases. The primary lesions in the 6 cases consisted of 3 oral cavity, 2 nasopharynx, 1 hypopharynx, and 1 maxillary sinus. All three oral primary cases had co-mutations in the *TERT* promoter and *HRAS*. Two of the nasopharyngeal primary cases had mutations in JAK3 and STAT, respectively. One of the hypopharyngeal primary cases had mutations in FGFR3.

Conclusion. RMHNSCC with CPS ≥90 had unique mutations that could account the enhanced PD-L1 expression, such as *TERT/HRAS* co-mutation, JAK-STAT pathway mutation, and *FGFR* pathway mutation. The above findings may be useful for predicting the efficacy of ICI for RMHNSCC.

#3853 T cell ferroptosis attenuates antitumor immune responses in sickle cell disease.

Z. Zhao[1], B. Hu[2], Y. Deng[1], M. Soeung[1], G. Genovese[1], W. Li[2], P. Msaouel[1], L. Yang[1], C. Lin[1];
[1]UT MD Anderson Cancer Center, Houston, TX, [2]University of Texas Health Science Center, Houston, TX

Background: Sickle cell disease (SCD) is the most common inherited blood disorder and arises from homozygosity for the HbS mutation (GAG>GTG: βGlu6Val) leading to the production of abnormal hemoglobin that cause sickle shaped red blood cells (RBCs). Individuals with SCD are at higher risk than the general population for developing hematologic malignancies or solid tumors such as renal medullary carcinoma (RMC). Although relatively rare, RMC is one of the most aggressive kidney cancers and is the third most common kidney cancer among children and young adults who harbor sickle hemoglobinopathies such as SCD or sickle cell trait (SCT) which occurs due to heterozygosity for the HbS mutation. Molecular profiling studies have shown that most cases involve biallelic inactivation of the *SMARCB1* gene, either through simultaneous hemizygous loss and translocation or by homozygous loss. The loss of *SMARCB1* and subsequent dysregulation of chromatin remodeling are key factors contributing to the development and progression of renal medullary carcinoma. Despite manifesting an inflamed tumor immune microenvironment, RMC consistently demonstrates resistance to conventional immune checkpoint inhibitors (ICI). Ameliorating the efficacy of immunotherapy of RMC is vital for research and potential therapeutic interventions by targeting $CD8^+$ T cells.

Methods: CyTOF was performed by using the spleen of WT mice and SCD mouse model. mRNA was isolated from $CD8^+$ T cells of Peripheral Blood Mononuclear Cell (PBMC) collected from healthy donors and SCD patients followed by bulk RNA sequencing. Hi-C was conducted using $CD8^+$ T cells isolated from PBMC of healthy donors and SCD patients. We employed DNA FISH (Fluorescence in Situ Hybridization) to examine alterations in gene architecture within $CD8^+$ T cells under varying conditions.

Results: RMC tumors exhibit accelerated tumor growth and reduced numbers of tumor resident $CD8^+$ T cells in SCD mice model compared with WT control. $CD8^+$ T cells in the SCD associated tumor microenvironment (TME) are subjected to ferroptosis by downregulation of *SLC7A11*; however, *SMARCB1* loss promotes the resistance of RMC tumor cells to ferroptosis. Genomic architecture of $CD8^+$ T cells is altered under SCD conditions, potentially contributing to immune dysfunction.

Conclusions: Our research has identified significant alterations in the 3D genome architecture of $CD8^+$ T cells in individuals with SCD. These alterations lead to transcriptional inhibition of *SLC7A11*, resulting in $CD8^+$ T cell ferroptosis and a hindered anti-tumor immune response in RMC. These findings elucidate the mechanistic relationship of SCD with ICI resistance in cancers such as RMC and provide novel avenues for therapeutically sensitizing tumors to immunotherapies in individuals with SCD.

Keywords: Sickle Cell Disease, Renal Medullary Carcinoma, SMARCB1, Ferroptosis, Genomic Architecture Alteration, Hi-C, SLC7A11

#3854 Revealing mismatch repair deficiency in Egyptian colorectal cancer patients using next generation sequencing a predictive biomarker for immunotherapy efficacy.

A. S. Youssef[1], M. Ragab[1], H. A. Ateya[1], M. Elberry[1], N. Fathy[1], A. Elleithy[2], A. Zekri[1], **O. S. Ahmed**[1], A. Nassar[1];
[1]National Cancer Institute, Cairo, Egypt, [2]Must University, Cairo, Egypt

Background: The mismatch repair (MMR) deficiency is a potential predictive biomarker for immunotherapy efficacy, particularly in colorectal cancer (CRC), where alterations in various DNA polymerases and MMR genes are prevalent. The accumulation of these genetic aberrations may cause a subsequent neoantigen formation. study aimed to identify the mutational profile of DNA polymerases and MMR genes in Egyptian CRC patients', providing insights into colorectal carcinogenesis and potential implications for immunotherapy.
Material and Methods: Thirty-nine blood samples from Egyptian patients with CRC and twenty-four blood samples from healthy controls were collected. The libraries were prepared by Qiaseq UMI-based targeted panel and sequenced via an Ion proton sequencer. The detected genetic variants with an average coverage of 500x were annotated against Cosmic, dbSNP, and ClinVar databases using Ingenuity Variant analysis (IVA).
Results: Our results revealed that the POLD1andPOLE genes (DNA polymerases) in the CRC patients, when compared with healthy controls, harbored 10 and 13 pathogenic variants (PVs), respectively. These PVs cause a loss of their functionality. The most frequently detected PVs and likely to be novel in the POLD1gene werec.44delC(31%)andc.3008delG(31%), while c.3510delA(18%)andc.2793delT(15%) were detected in the POLE gene. As per MMR genes, our study showed that the MLH1, MLH3, MSH2, MSH3, MSH6, PMS1,and PMS2 harbored 8, 13, 23, 19, 22, 23, and 7 PVs, respectively. The highly frequent PV in the MLH1wasc.469delT (26%), while the novel most frequently detected PV in the MLH3 wasc.1467delA (23%). Moreover, the PVs found highly frequent are c.2647delA (36%) in MSH2,c.1148delA (41%)in the MSH3, and c.2079delA (44%) in the MSH6. RegardingPMS1/2, the most frequently detected PV and likely to be novel was c.1647delA (44%) in PMS1, while c.869delT (13%) was the most prevalent PV in PMS2.
Conclusion: Our results revealed the MMR mechanism deficiency in Egyptian CRC patients offering crucial insights into colorectal carcinogenesis and neoantigen formation. These insights are pivotal for developing ethnic-based personalized immunotherapy strategies in Egyptian CRC patients, shedding light on their role in CRC. Interestingly, we have identified novel variants in the DNA repair enzymes. However, further investigations and validations are required to corroborate these findings and explore their clinical significance in the personalized medicine.

#3855 Kinetics of neoantigen-specific T cells in post-transplant relapse.

B. Neupane, J.-E. Lee, K. Ventura, K. Parr, K. Quann, **S. Ito**;
University of Pittsburgh School of Medicine, Pittsburgh, PA

Introduction: Graft-versus-leukemia effect (GVL) underpins the curative mechanism of allogeneic stem cell transplantation (alloSCT) for acute leukemias. Donor-derived T cells can recognize various antigens, including human leukocyte antigen (HLA), minor-histocompatibility antigens (miHA), over-expressed antigens, or neoantigens derived from somatic mutations of leukemia. However, the role of neoantigens has not been fully investigated in GVL. Here, we aimed to predict neoantigens and identify neoantigen-reactive T cells using samples after alloSCT. Materials: Leukemia blasts were purified from relapsed samples. Recipient saliva or T cells from pre-transplant peripheral blood (PB) were used as a recipient germline control, while donor monocyte or CD34 cells were used as donor controls. DNA/RNA isolated from these specimens were analyzed for whole exome sequencing (WES) paired with RNAseq. Somatic mutations were called using blasts and recipient germline controls by mutect and mpileup and annotation with SnpEff. Somatic mutations with variant allele frequency >20% were screened for neoantigen prediction bound to recipient HLA (IC50 < 500nM) by pVAC-seq. We also genotyped 73 SNPs associated with publicly known miHAs. Serial PB were stained for HLA-A*02:01 tetramers loaded with neoantigens or CMVpp65. T cells were stimulated with neoantigens for 10 days and tested for cytokine production in responses to target or control peptides. Results: We screened neoantigens in 8 patients relapsing after alloSCT (7 acute myeloid leukemia and 1 acute lymphoblastic leukemia) and their donors (4 matched siblings, 1 matched unrelated, 3 haploidentical). In 7 subjects, WES/RNAseq showed an average of 273 somatic mutations per patient (range 108- 609). In one subject, targeted next-generation sequencing was used to detect 2 somatic mutations. Among these mutations, seven out of eight subjects (87.5%) had potential neoantigen candidates, with a median number of 9 antigens per subject. In contrast, only 2 subjects (25%) had potential miHA. UPN8, a responder to donor lymphocyte infusion (DLI), showed dominant CMVpp65-specific T cells at the time of relapse and emergence of TP53- (neoantigen) or HA-2- (miHA) specific T cells after relapse. HA-2-specific T cells upregulated PD-1 expression at the time of graft-versus-host disease (GVHD), indicating activation of these miHA-specific T cells during GVHD. In two subjects (UPN3 and UPN8) who achieved long-term remission after DLI, CD8 T cells specific to neoantigens were detectable by IFN-γ/CD107a production in reaction to mutant peptides (*SDE2*.pK123X or *TP53*.pR248W) from post-relapse samples. Discussion: Our study showed the feasibility of in-silico neoantigens prediction and neoantigen-specific T-cell detection from a subject who developed relapse after alloSCT. Further investigation is needed to test if neoepitope burden and miHA disparity could correlate with transplant outcomes.

#3856 Nodal metastasis as an immune indicator in cancer (ca) therapy.

B. Fugere, J. Chen, T. C. Fugere, F. Mazahreh, N. Thalambadu, A. Safar;
University of Arkansas for Medical Sciences, Little Rock, AR

Introduction: Nodal Metastasis as an Immune Indicator in Cancer (Ca) Therapy Staging (sg) is widely used to identify appropriate treatment options & implement therapy. Tumor-Node-Metastasis (TNM) is the most utilized sg system. In it, nodal involvement is viewed simply as an adverse metric without biologic connotation, and gross metastasis (M1) eclipses other variables and denotes the least favorable sg. Ca's ability to thrive within the lymph node itself was intriguing to us in the immune-oncology (IO) era. Failure to overcome an immunogenic ca (e.g., dysfunctional apoptosis) leads to T-cell exhaustion (TCE) typified by PD-1 expression. Immune Checkpoint Inhibitors (ICI) address TCE by intercepting the PD-1:PDL-1 synapse. We reasoned that immune actions are distinct in tumor beds vs nodes & hypothesized that immunogenic N(+), implies ca's ability to defend itself (e.g., PDL-1 expression); N(0), reflects immune susceptibility and effective clearance outside the tumor bed. In the latter scenario, TCE is nonexistent; ICIs are less beneficial. Tumor beds (T, M) are sanctuaries exempt from immune action due to factors such as hypoxia, acidity, and poor tumor vasculature which lead to poor T-cell trafficking, to name a few. M1 develop from circulating ca stem cells, an immune-exempt entity.

Methods: We examined the interaction between ICIs & nodal involvement dichotomizing surveillance, epidemiology and end results SEER cases into N(0) or N(+) within M1 melanoma & lung cancer. 2005, 2015-17 denote pre-, and post ICI, respectively to provide mature survival data.

Results: Table 1 depicts the 4- or 5-year overall survival in the specified subsets.

	Expectations		SEER results: % Overall Survival at 5-y (melanoma) or 4-y (Lung ca)			
				Pre-ICI	Post ICI	Metric
Melanoma		Mechanism		2005	2015	Increment in 5yr OS
	N(0) favorable prognosis	Immunogenic tumor	N(0): 302 cases	20	29	8 (20 -12)
	N+ Predicts benefit to ICI	T-cell exhaustion in N(+) only	N(+): 210 cases	12	37	N(+): +25 > N(0): +9
				2005	2017	Increment in 4yr OS
Lung Cancer	N(0) similar to N(+)	Less immunogenic tumor	N(0) 9,583 cases	18	18	4 (18 -14)
	N+ Predicts benefit to ICI	T-cell exhaustion in N(+) only	N(+): 17,887 cases	14	20	+6

Conclusions: ICI benefit is more prominent in N(+) ca, where TCE is likely. N(0) ca represents immune-prone ca with less TCE & need to be viewed as a biologically distinct subset. Agents influencing T-cell access (angiogenic)/functionality should be considered in these cases. Finally, we suggest that PDL-1 testing should specify testing sites as nodal vs tumor bed expression.

#3857 Tumor-extrinsic BIRC3 promote sensitivity to checkpoint inhibition immunotherapy in breast cancer.

D. Yang, **J. Sun**, G. Ren, H. Li;
The First Affiliated Hospital of Chongqing Medical University, Chongqing, China

Baculoviral IAP repeat containing 3 (BIRC3) protein play a critical role in breast cancer. Blocking BIRC3 cause apoptosis in tumor cells, but its correlation with tumor immunity remains elusive. TCGA databases were employed to examine the expression of BIRC3 in breast cancer. The correlation between BIRC3 expression and T cell infiltration and function was employed in breast cancer tissues (n=92) by immunohistochemistry. Birinapant, a selective BIRC3 inhibitor, was then used to investigate the effect of BIRC3 blockade on tumor immune microenvironment (TIME) landscape of breast cancer syngeneic mouse models by flow cytometry. Survival analysis suggested that the low expression of BIRC3 was associated with poor overall survival (OS). Additionally, we uncovered the close association between BIRC3 expression and the profiles of immune cells in breast cancer microenvironment based on the TCGA dataset. Interestingly, we found that BIRC3 expression was positively correlated with cytotoxic T lymphocyte infiltration and T-cell effector function by immunohistochemistry. The in vivo experiments suggested that blocking BIRC3 might convert ‘hot’ tumor into ‘cold’ tumor, which was characterized by a decreased of $CD8^+$ T cell infiltration and inhibition of $CD8^+$T cell function. Furthermore, we observed that BIRC3 blocking combined with immune checkpoint blockade therapy (ICT) greatly restrains immunotherapy efficacy of breast cancer model. Our study revealed a positively association between BIRC3 and anti-tumor immune landscape in breast cancer. Notably, we established a validated prognosis model based on BIRC3 and BIRC3 associated immunomodulators in breast cancer.

#3858 Peripheral CD38+ effector memory (EM) T cells are dynamic biomarkers of response to neoadjuvant immune checkpoint blockade (NeoICB) in patients (pts) with resectable dedifferentiated liposarcoma (DDLPS) and undifferentiated pleomorphic sarcoma (UPS).

E. F. Nassif, H. Lu, M. Stanford, K. Millerchip, D. Romero, J. Malke, B. Matejka, J. E. Gershenwald, S. Kumari, D. H. Mak, A. J. Lin, J. K. Burks, W.-L. Wang, A. J. Lazar, N. Somaiah, C. Haymaker, C. L. Roland, **E. Z. Keung**;
UT MD Anderson Cancer Center, Houston, TX

Introduction: NeoICB is a promising approach for pts with DDLPS and UPS. However, biomarkers to identify which pts benefit from this treatment and understanding the mechanisms of response and resistance to ICB remains a challenge. **Methods:** We conducted a randomized phase 2 trial of neoICB (anti-PD1 +/- CTLA4) in pts with resectable DDLPS (n=17) and UPS (n=10). Pts with UPS received concurrent neoICB and radiation. The primary endpoint of the trial was pathological response; 3 DDLPS and 9 UPS pts were responders (R) and 14 DDLPS and 1 UPS pts were non-responders (NR). Peripheral blood mononuclear cells (PBMCs) were collected at baseline, prior to cycle 2 of neoICB (C2D1), and at the time of surgery (SURG). We performed mass cytometry (CyTOF) to identify immune cells associated with response and their dynamic changes with neoICB. We designed a custom 41-parameter panel using CD45 live cell barcoding with 31 markers for immune profiling, of which 23 were selected to detect key cell lineage and 8 to detect signaling markers. Batch correction and high dimensional data analyses were performed using CyCombine and CyTOF workflow R packages. Longitudinal comparisons between immune cell populations were conducted using Mann-Whitney U Test. **Results:** Of 79 available PBMC samples from 27 pts, 63 passed quality control after thawing (≥30% viability) and data clean-up (at least 10,000 events). Data was down-sampled to 5000 events for analysis. Of 19 immune cell types identified, monocytes were the most common followed by CD4+ and CD8+ T cells. There was an early increase in CD38+ effector/effector memory (EM) T cells at C2D1 in pts with DDLPS (CD8+ $p=0.005$, CD4+ $p<0.001$) and a similar increase observed in pts with UPS (CD8+ C2D1 p=NS, SURG $p=0.034$; CD4+ C2D1 $p=0.024$, SURG $p=0.06$) and these cells had higher Ki67 expression than CD38- T cells ($p<0.005$). At baseline, R pts with DDLPS had higher fractions of CD38+ EM CD8+ T cells than NR pts ($p=0.044$). Analysis in the UPS cohort was limited by the low number of NR pts. Higher expression of TIGIT was observed on CD38+ EM CD8+ T cells compared to CD38- counterparts at all time points. **Conclusion:** Peripheral CD38+ EM CD8+ T cells are associated with response to neoICB in pts with DDLPS. Longitudinal peripheral immune profiling reveals an increase in CD38+ EM CD8+ and CD4+ T cells with neoICB in pts with DDLPS and UPS. These cells are proliferative and express higher levels of TIGIT, which could be a future target for therapeutic exploration. Importantly, changes in the peripheral immune populations may precede changes in the tumor microenvironment (TME) as preliminary analyses of the TME did not identify early (C2D1) changes. TME imaging mass cytometry analyses are currently underway to associate peripheral and intratumor changes in immune populations.

#3859 HSP90 blockade activates antitumor immunity by suppressing tumor glycolytic flux in head and neck squamous cell carcinoma.

F. Chen, C. Tang, F. Yang, A. Ekpenyong, R. Qin, N. F. Saba, **Y. Teng**;
Emory University, Atlanta, GA

Accumulating evidence suggests that failure of antitumor immunity may be due to dysregulation of energy metabolism. Head and neck squamous cell carcinoma (HNSCC) exhibits increased activity of two key enzymes, pyruvate kinase M2 (PKM2) and platelet phosphofructokinase (PFKP), which are central to the glycolytic pathway responsible for the conversion of glucose to ATP energy. HSP90 is a molecular chaperone that plays a critical role in the folding, stabilization, and regulation of a wide range of client proteins involved in various cellular processes, including metabolism. However, whether HSP90 signaling contributes to tumor metabolism rewiring and antitumor immune response remains unknown. Using ganetespib as a drug model for HSP90 inhibition and combining results from clinical trials and animal treatment, our study demonstrated that HSP90 inhibition causes an obstruction of glycolytic flux in HNSCC cells by simultaneously suppressing both PKM2 and PFKP at the transcriptional and post-translational levels. In addition, ganetespib enhances T cell-driven antitumor immune responses by promoting CD8+ T cell infiltration into the tumor. Mechanistically, ganetespib downregulates IL8 signaling by inhibiting PKM2 and PFKP-mediated glycolysis in HNSCC cells, which in turn contributes to ganetespib-mediated T cell tumor infiltration. These findings provide a novel molecular basis for the use of effective HSP90 inhibitors to improve the outcome of HNSCC patients.

#3860 Characterizing peripheral immune correlates of tumor response in breast cancer patients immunized with the P10s-PADRE vaccine.

F. Jousheghany[1], J. P. Lee[1], B. Nounamo[1], V. Raj[2], J. L. Faulkner[1], E. Siegel[1], I. Makhoul[3], T. Kieber-Emmons[1], **B. Monzavi-Karbassi[1]**;
[1]University of Arkansas for Medical Sciences, Little Rock, AR, [2]University of Arkansas at Pine Bluff, Pine Bluff, AR, [3]Central Arkansas Radiation Therapy Institute, Inc, Little Rock, AR

Introduction: We demonstrated that vaccination of HR+/HER2− breast cancer subjects with P10s-PADRE cancer vaccine in combination with standard-of-care chemotherapy led to generation of antibodies (Ab), activation of Natural Killer (NK) and T cells, increases in IFNγ and TNFα, and increases in TILs and stromal CD3+ T cells. The current study was conducted to assess the vaccine's efficacy, particularly focusing on tumor shrinkage and pathologic Complete Response (pCR). Additionally, it aims to explore the association of specific peripheral-blood immune responses, such as antibody levels and NK and T-cell activation, with pCR and objective reduction in primary tumor size.
Methods: Blood samples collected at baseline and after treatment of at least 25 subjects were used in characterization of immune responses. Serum and plasma samples were used in ELISA, cytokine, and glycan-array assays to measure anti-peptide and anti-glycan antibodies and blood-cytokine levels. Peripheral blood mononuclear cells (PBMCs) were interrogated by RNA-seq, flow cytometry, and ELISpot assays.
Results: We observed that high levels of anti-peptide and anti-GD2 antibody responses correlated with pCR. Ab response was positively correlated with differential expression of CD56, GZMA, IFNγ, NKp46, and CD8b, among which GZMA and NKp46 showed a statistically significant association. Vaccine-induced functional cellular immune responses (measured by differential expression of IFNγ, GZMA, CD8, CD69, NKp46, CD56, and PRF1) correlated with reduction of primary tumor size. We also observed substantial differences among immune responders vs non-responders in immune gene expression and in cytokine production in post-immune PBMCs after specific and polyclonal stimulation.
Conclusions: The data suggest that immunization of HR+/HER2− breast cancer patients with P10s-PADRE in combination with chemotherapy leads to both humoral and cellular immune responses. While induction of a robust antibody response is a good marker for potential clinical efficacy, vaccine-associated increases of the ratio of CD8+ cells and the expression of CD69, CD8b, GZMA, IFNγ, NKp46, and PRF1 seem to serve as additional efficacy indicators. Future studies are underway to validate these findings and establish reliable prognostic biomarkers.

#3861 Associations of intragenic rearrangement burden with immune cell infiltration and response to immune checkpoint blockade in cancer.

H. Zhang, S. Lee, R. Muthakana, B. Lu, D. Boone, D. Lee, **X. Wang**;
University of Pittsburgh School of Medicine, Pittsburgh, PA

While immune checkpoint blockade (ICB) induces durable cancer remission, only a small subset of patients can receive benefits, whereas a substantial portion of patients encounter severe immune-related adverse events. Further, about 4-29% of patients experience dramatic acceleration of disease progression after ICB treatment. Predictive biomarkers of ICB responses are in high demand to ensure patient benefits and avoid tragic clinical outcomes. In addition to PD-L1 tests, several genetic biomarkers are associated with ICB effectiveness, such as tumor mutation burden (TMB), somatic copy number aberrations, indels, and microsatellite instability. However, none of these neoantigen markers are sufficient to discriminate ICB responders in diverse cancer entities of distinct genetic profiles. In particular, TMB fails to predict in the cancer types with low simple mutation rates, such as triple-negative breast cancer (TNBC), ovarian cancer, and esophageal cancers. In TNBC, high TMB only accounts for 5-10% of patients, whereas a much larger proportion of tumors are inflamed (26-50%), which suggests a possible uncharacterized major source of neoantigens. Similarly, TMB is not predictive of ICB response in ovarian cancers according to the IMagyn050 trial. In esophageal cancer, TMB is not associated with T cell infiltration and does not predict ICB response. Our analyses of Pan-cancer whole genomes revealed that intragenic rearrangement (IGR) burden is a pivotal contributor to immune infiltration in breast, ovarian, esophageal, and endometrial cancers, which correlates with increased Macrophage M1 and CD8+ T cell signatures. IGRs result in exon duplications or deletions through rearrangements of a genomic distance of tens of kilobases. Multivariate regression against spatially counted tumor infiltrated lymphocytes in breast, endometrial, and ovarian cancers suggest that IGR burden is a more influential covariate than other genetic aberrations in these cancers. In the MEDI4736 trial evaluating durvalumab in esophageal adenocarcinoma, IGR burden correlates with patient benefits. In the IMVigor210 trial evaluating atezolizumab in urothelial carcinoma, IGR burden increases with platinum exposure and predicts patient benefits for TMB-low, platinum-exposed tumors. Altogether, we demonstrate that IGR burden contributes to T-cell inflammation and predicts ICB benefits in TMB-low, IGR-dominant tumors, or in platinum-exposed tumors. IGRs as a cryptic class of structural variants have been heretofore overlooked in cancer genomics studies. The association of IGRs with ICB response has not been previously reported in cancer in general. The development of IGR burden-based predictive marker could increase effectiveness of ICB therapy, reduce severe side-effects and unnecessary costs.

#3862 Identification, profiling and clonotypic tracking of tumor-reactive T cells derived from bronchoalveolar lavage in lung cancer patients.

H. Ryu, W. Sun, M. A. Wurscher, V. S. Nair, **E. W. Newell**;
Fred Hutchinson Cancer Center, Seattle, WA

Immunotherapeutic strategies for disinhibiting T cell responses have revolutionized lung cancer treatment. However, the identification of tumor-reactive T cells and the acquisition of adequate tissue for molecular and immune profiling remains a challenge that hinders our ability to adequately characterize the mechanisms of immunotherapy response versus resistance. To address this gap, we are investigating the use of bronchoalveolar lavage (BAL) as an alternative to blood or tumor biopsy samples to identify tumor reactive T cells.

We collected cells from a prospective bronchoscopic biorepository of patients undergoing lung cancer evaluation that were subjected to bilateral BAL, phlebotomy, and tissue sampling. We then employed flow cytometry and single-cell multi-omic analyses to identify, characterize and clonotypically track tumor-reactive T cells obtained from BAL, blood and tumor samples from lung cancer patients. Analysis of BAL samples revealed a significant enrichment of terminally exhausted $CD8^{+}CD39^{+}CD103^{+}$ T cells in BAL from tumor-bearing lungs compared to non-tumor bearing lung BAL and blood PBMCs in 14 patients. We then used single-cell sequencing-based multi-omics to deeply profile bilateral BAL cells, blood PBMCs and tumor tissues from 5 of these patients.

By tracking T cell receptor (TCR) sequences across patient-matched samples, we found BAL derived T cell clonotypes that expressed markers of terminal exhaustion, such as CD39 and CXCL13 in the tumor, which strongly implicates them as being tumor reactive and relatively abundant in BAL. Further validation through functional assays is being used to confirm the tumor reactivity of these clones.

These data demonstrate the feasibility of capturing tumor-specific T cells during bronchoscopy, providing promising opportunities for patient outcome characterization and exploration of novel therapies. This relatively non-invasive and practical test during routine bronchoscopy offers a cost-effective and safe alternative to identifying tumor-reactive T cells from surgical specimens or biopsies.

#3863 Flow cytometry using stabilized whole blood to assess innate and adaptive immune cells (Monocytes, NK, T, and B cells) in immunotherapies.

J. Benko, S. Splitt, **A. Bisconte**, L. Lozza, R. Owen, D. Phippard;
Precision for Medicine, Frederick, MD

Flow cytometry assays using fresh whole blood which are interrogating either an extremely rare cell subset or a depleting immunotherapy, may require samples to be processed from global clinical sites over a wide geographical area, which can pose a major challenge for clinical operations. Precision for Medicine (PfM) has addressed these operational challenges using commercial stabilizers which are added to the blood allowing samples to be frozen at -80°C and subsequently batch processed for sample testing. We have performed a fit for purpose assay qualification of a multiparameter flow cytometry panel allowing the immunophenotypic analysis of monocyte, T cell, B cell and NK immune populations using Cytodelics™ fixed/stabilized healthy donor whole blood. Additionally, the assay was verified in whole blood samples from multiple solid tumor disease states including melanoma, colorectal cancer, head & neck, non-small cell lung cancer to demonstrate clinical application. In these oncology samples, we were able to assess both immune cell frequencies and their activation status in both fresh whole blood as well as fixed whole blood over a short-term sample stability study, where the samples had been stored at -80°C for several months. This data provides a representative example of the use of commercial stabilizing fixatives for clinical studies to extend the stability window of whole blood for subsequent assessment by flow cytometry. Fixed whole blood can be stored at -80°C, shipped on dry ice allowing multiple timepoints in a cohort to be assessed together, thus minimizing assay variability as compared to fresh whole blood analysis, and mitigating the impact of shipping delays and temperature excursions on the samples. With sufficient time for assay development there are several commercial stabilizers that can be tested to determine if the markers in the flow assay are compatible with these reagents, providing a valuable option to assess the impact of immunotherapies on the immune cells of interest and reducing operational challenges in global studies.

#3864 Role of NK/TAM cross-talk on T-CD8+ recruitment and efficacy of chemoimmunotherapy and MEKi combination in "cold" tumors.

L. Nuttin[1], C. Latour[1], S. Revy[1], R. Aucagne[2], G. Lalle[1], F. Ghiringhelli[3], **E. Limagne**[3];
[1]Center Georges-Francois Leclerc, Dijon, France, [2]University Hospital Francois Mitterrand, Dijon, France, [3]Center Georges-Francois Leclerc - INSERM U1231 - Universite Bourgogne, Dijon, France

In patients with non-small cell lung cancer (NSCLC), double platinum-based chemotherapy (cisplatin or carboplatin and pemetrexed) combined with the anti-PD-1 antibody has shown significant clinical benefit and has become the standard of care. In the context of so-called "cold" tumors, the immunogenic capacities of chemotherapies increase danger signals (type I IFNs, CXCL9/10) and favor both infiltration of NK/T-CD8+ cells and response to anti-PD-1. Despite the therapeutic progress represented by this new combination, some patients have limited benefit from chemo-immunotherapy, suggesting that in these patients, the immunogenic capacities of chemotherapy are limited. Recently, we were able to show that KRAS oncogene signaling restricts the ability of the cisplatin/pemetrexed doublet to induce the chemokine CXCL10, lymphocyte recruitment and sensitize to PD-L1 blockade. Thus, the addition of a MEK inhibitor (MEKi) to the chemo-immunotherapy combination restores an immunogenic signal through CXCL10, enabling T-CD8+ to infiltrate the tumor more extensively, making it more sensitive to immunotherapy. Here, we unravel the essential role of NK cells in the immunological and antitumoral effect of chemo-immunotherapy plus MEKi combination in the LLC1 preclinical lung cancer model. We showed that chemo/MEKi combination favors NK cell recruitment and activation in tumor bed through both CXCL10 and NKG2D-ligand (Rae1, Mult1). Then, IFNγ-producing NK cells trigger tumor associated macrophage switch from M2 toward M1 phenotype and amplify T-CD8+ cells recruitment through CXCL9 production by macrophages. Thus, NK cell depletion, CXCR3, CXCL9 or NKG2D-neutralization restrained chemo/MEKi therapeutic efficacy. However, IFNγ also triggers NKG2A-ligand expression (Qa-1b, HLA-E in human) which restrained NK cell activation and CD8+ T cell recruitment. Thus reducing the NKG2A pathway, by using Qa-1b-/- LLC1 cells, enhances chemo-immunotherapy/MEKi anti-tumor efficacy. Similar results were obtained in preclinical “cold” CT26 colon cancer model treated by chemo-immunotherapy. Our results underline a new role for NK cell activation to trigger TAM2/TAM1 switch, CXCL9 expression and amplify CD8 T cell recruitment in “cold” tumor. In a context of resistance to chemo-immunotherapy, MEKi or ICI targeting NK cells could be an interesting way to amplify the anti-tumor immune response by modulating both TAMs biology and the recruitment of CD8+ T cells.

#3866 Azvudine : An emerging immunomodulator in the treatment of cancer and viral infections.

P. Li, L. Jia, Z. Wang, J. Du;
Genuine Biotech, Henan, China

Azvudine (FNC) is a nucleoside analog that has secured approval from the CDE in China for the treatment of both AIDS and COVID-19. In these contexts, it has showed remarkable efficacy and safety when taken orally. Typically, nucleoside analog drugs function by integrating into DNA and impeding DNA synthesis, evident in drugs like 5-FU, Capecitabine, Ara-C, and Gemcitabine. Furthermore, FNC has been reported to exhibit robust anti-tumor properties, curbing cell proliferation, initiating G1 and S phase arrests, and advancing apoptosis across various human cancer cell lines. Grounded in this mode of action, we have ascertained that the anti-tumor effects of FNC intricately align with the expression of deoxycytidine kinase (dCK) both in vitro and *in vivo*. Remarkably, our studies delved into the effects and underlying mechanisms of FNC in enhancing the tumor microenvironment within solid tumors. Our findings, stemming from cell-based assays and *in vivo* animal experiments, elucidate the following: 1. FNC can trigger immunogenic cell death (ICD) in tumor cells. This is evidenced by the surface presentation and liberation of damage-associated molecular patterns (DAMPs) such as Calreticulin, HSP70, HSP90, Annexin A1, and HMGB1, which in turn stimulate both innate and adaptive immune responses. 2. FNC substantially reduces the population of monocytic-myeloid derived suppressor cells (M-MDSC) and Polymorphonuclear-myeloid derived suppressor cells (PMN-MDSC) in the tumor microenvironment. Concurrently, it boosts the infiltration and proliferation of CD8+T, CD4+T and NK cells. This instigates the transformation of the tumor microenvironment from a 'cold' state to a 'hot' one, enhancing the synergistic effects of PD-1 when used in tandem with FNC. This mechanism was substantiated through a high proportion of MDSCs observed in H22 and CT-26 syngeneic models, and contrastingly, a low proportion in MC38 and LL/2 in vivo syngeneic models. Notably, every animal subjected to combined FNC and PD-1 treatment in the H22 and CT-26 *in vivo* models witnessed complete tumor regression. Given these revelations, there's a compelling argument that FNC monotherapy possesses immense potential as an anti-tumor agent. The potent anticancer effects of FNC *in vitro* and *in vivo* warrants further investigation of its anticancer potential as immunomodulator.

#3867 Identification of novel biomarkers of immune toxicity from CAR T-cell therapy using ultrasensitive NULISA™ proteome technology.

Riley Kirkpatrick[1], Joanne Beer[2], Manishkumar S. Patel[1], Akansha Jalota[1], Agrima Mian[3], Ishara S. Ariyapala[2], Qinyu Hao[2], Wei Feng[2], Xiao-Jun Ma[2], Yuling Luo[2], Brian T. Hill[3], **Neetu Gupta**[1]

[1]Inflammation and Immunity, Cleveland Clinic, Cleveland, OH,[2]Alamar Biosciences, Fremont, CA,[3]Hematology and Medical Oncology, Cleveland Clinic, Cleveland, OH

Introduction: The efficacy of anti-CD19 chimeric antigen receptor (CAR) T-cell therapy in patients with relapsed/refractory large B-cell lymphoma (LBCL) is limited by acute toxic events, most notably cytokine release syndrome (CRS) and immune effector cell-associated neurotoxicity syndrome (ICANS). Identification of biomarkers of toxicities can allow for selection of high-risk patients and elucidate targetable mechanisms for mitigation. Previous biomarker studies have been constrained by relatively narrow panels of potential mediators and limited time points. Here, we employed NULISA, a novel ultrasensitive assay capable of simultaneously quantifying 204 inflammatory proteins from a single sample, to identify temporal proteome associations with acute toxicities in anti-CD19 CAR T-cell treated patients.

Methods: Baseline and post-treatment peripheral blood samples from 80 patients with LBCL who underwent anti-CD19 CAR-T cell therapy were collected within specific time intervals. Plasma samples (n=480) were analyzed with NULISA. CRS and ICANS were graded according to ASTCT consensus criteria. Patients were grouped according to their maximum CRS and ICANS scores. Differential protein abundance across the toxicity groups was assessed using linear mixed effects models fit for each protein, including a time by toxicity group interaction. Proteins showing significant associations were subjected to pathway enrichment and network analysis.

Results: Severe CRS and ICANS patient groups showed proteome upregulation beginning on day 1-2 and peaking at day 6-9, followed by extensive downregulation on day 11-16. The strongest upregulated pathway associations of severe CRS and ICANS were inflammatory response, IL-17 signaling, non-genomic action of vitamin D3, regulation of leukocyte proliferation, and cellular extravasation. Downregulated pathways included anti-microbial humoral response and TNFs binding to receptors. In addition to the previously identified inflammatory proteins IL-6, IFNγ, sIL-2Rα, CXCL8, CCL2, our analysis revealed significant association of several novel immune regulators and mediators. These included upregulated Th2 cytokines, IL-17A, IL-22, GZMB, CTLA4, IFNA1;IFNA13, and downregulated S100A12, IL-12B, CCL22, BDNF and TNFSFs, revealing exquisite temporal orchestration of lymphoid and myeloid activities during CRS and ICANS development.

Conclusions: This study represents the most comprehensive characterization of immune response to CAR T-cell therapy to date. Using the novel NULISA technology, we identified new proteins and functional pathways associated with CAR T-cell-induced toxicity, implicating them as potential biomarkers. These previously unidentified factors also provide a platform to further investigate the causative immune mechanisms of acute toxicities in CAR-T cell therapy.

BIOINFORMATICS / COMPUTATIONAL BIOLOGY / SYSTEMS BIOLOGY / CONVERGENT SCIENCE: Multi-omic Analysis and Translational Research Minisymposium

#3872 Multi-ancestral origins of colorectal lesionsMulti-ancestral origins of colorectal lesions.

R. O. Schenck, A. Khan, A. Horning, E. D. Esplin, D. Van Egeren, HTAN-FAP Consortium, W. Greenleaf, J. M. Ford, M. P. Snyder, C. Curtis;
Stanford University, Palo Alto, CA

The widely accepted paradigm that cancer initiation is a monoclonal event has not been definitively resolved. In sporadic cancers this is due to the requirement for longitudinal sampling to study this occult process, which occurs over years to decades. Individuals with familial adenomatous polyposis (FAP) possess a germline APC mutation, leading to hundreds of colonic polyps in adolescence and a 100% lifetime risk of colorectal cancer. Resected colons from FAP patients contain normal mucosa, benign and dysplastic polyps that embed the natural history of colorectal tumorigenesis at different points of malignant progression. Through genome sequencing of 127 independent polyps or mucosa samples from six FAP patients, we characterized the genomic landscape, relative timing of somatic alterations, and clonal dynamics in normal, dysplastic, and invasive colon tissue. Comparison with multi-region sequencing data from FAP patients and sporadic colorectal adenomas and carcinomas indicates similar molecular profiles, with canonical cancer driver genes present across benign and dysplastic premalignant lesions and shared mutational orders. Pairwise sample comparisons and phylogenetic reconstructions revealed extensive heterogeneity and subclonal sharing within a patient's benign and dysplastic lesions, irrespective of location in the colon. These data imply that polyps were initiated from multiple cells from distinct lineages whose most recent common ancestor arose during development. We corroborate these findings using a mechanistic mathematical model, which infers polyclonality in 100% of benign and 83% of dysplastic samples. Based on these findings, we propose a conceptual model of the multi-ancestral origin of intestinal malignancies.

#3873 Understanding spatial organization of cellular plasticity in pancreatic ductal adenocarcinoma.

I. Zamora[1], M. Parikh[1], B. K. Patel[2], L. Bi[1], D. Haviv[3], J. Cao[4], C. Shiau[2], M. Hemberg[5], W. L. Hwang[2], N. Hacohen[2], D. T. Ting[2], A. Mehta[2];
[1]Broad Institute of MIT and Harvard, Cambridge, MA, [2]Massachusetts General Hospital, Boston, MA, [3]Memorial Sloan Kettering Cancer Center, New York, NY, [4]Beth Israel Deaconess Medical Center, Boston, MA, [5]Brigham and Women's Hospital, Boston, MA

Pancreatic ductal adenocarcinoma (PDAC) is notorious for poor survival rates, underscoring the urgency of understanding factors that drive tumor progression. A key player in this process is epithelial-mesenchymal transition (EMT), known for its role in enhancing cancer cell adaptability, resistance to treatment, and metastasis. Our study focuses on EMT within PDAC, using single-cell spatial transcriptomics to explore how the tumor microenvironment influences changes in cellular states. We introduce a novel method involving Gaussian mixture models (GMM) to categorize EMT stages in single-cell data and utilize deep learning for label transfer of these tumor cell states, including intermediate cell states, onto spatial transcriptomic data with limited gene panels and sparse count profiles. We find strong spatial autocorrelation of classical cells and a dispersion of basal cells alongside other cells at intermediate stages of the EMT spectrum. By leveraging the spatial proximity of clonally related cells, we confirm that cells transition along the EMT spectrum in a gradient and infer transition rates. We next leverage density gradients of tumor cells in different states to identify distinct neighborhoods with varying EMT subtype composition. We observe significant variations in cell density among different EMT states. A focus on cancer-associated fibroblasts (CAFs) and macrophages reveals differences in these cells across density contours. We also examine differential ligand-receptor interactions across cell state gradients to better understand the cellular interactions that drive EMT transitions and alter the tumor environment. By leveraging spatial transcriptomics, this research aims to provide new biological insights into PDAC intratumoral heterogeneity, potentially leading to the identification of novel therapeutic targets to disrupt treatment resistance.

#3874 Adaptive heterogeneity enables the survival of residual malignant PDAC cells in response to RAS-GTP inhibition.

L. Tomassoni, U. N. Wasko, A. C. Garcia, T. C. Dalton, P. Laise, S. A. Sastra, C. F. Palermo, A. Califano, K. P. Olive;
Columbia University Irving Medical Center, New York, NY

More than 90% of human pancreatic ductal adenocarcinoma (PDAC) cases are driven by activating mutations in KRAS. RMC-7977 is a potent inhibitor of GTP-bound RAS proteins (RAS(ON)), including both wild type and mutant variants of KRAS, NRAS, and HRAS. The related investigational agent, RMC-6236, is a first-in-class, potent, orally bioavailable, RAS^{MULTI}(ON) inhibitor currently in Phase 1/1b clinical trials (NCT05379985). We performed preclinical studies in a range of models of PDAC, including the highly chemoresistant $K\text{-}ras^{LSL.G12D/+}$, $p53^{LSL.R172H/+}$, $Pdx1Cre^{tg/+}$ (KPC) genetically engineered mouse. RMC-7977 exhibited broad anti-tumor activity at tolerable doses, provoking radiographic responses in KPC pancreatic tumors and extending overall survival by 3-fold, the largest response observed yet in this model. RMC-7977 dosing produced a metronomic effect on RAS signaling in tumor and normal tissues, with full pathway inhibition at 4 hours post treatment that was restored by 24 hours. This pattern yielded tumor-selective effects on apoptosis and proliferation, consistent with RAS oncogene addition in PDAC. To understand the dynamic response of malignant cells following RAS-GTP inhibition, we did single cell RNA sequencing on KPC pancreatic tumors treated with RMC-7977 or vehicle at multiple timepoints. Using the ARACNe and VIPER algorithms [Maroling., et al. 2006; Alvarez., et al. 2016], we performed regulatory network analysis on the expression profiles of >210,000 cells to calculate the activities of >5000 transcriptional regulatory proteins per cell. Additionally, we assessed the impact of treatment on malignant cell subtypes as previously identified by our team based on their sets of hyperactivated developmental transcription factors [Laise., et al. 2022].

As expected, RAS pathway transcription factors, such as FOS and JUN, were repressed relative to controls in malignant cells by 4 hours after treatment with RMC-7977. However, at 24 hours, responses varied by cellular subtype: well-differentiated Gastrointestinal Lineage State (GLS) cells had restored MAPK activity, while poorly differentiated Morphogenic State (MOS) cells were still inactivated. Strikingly, we found that after one week of treatment (in actively regressing tumors, representing a state of residual disease), nearly all malignant cells had assumed the GLS state. Acquisition of resistance after weeks or months of treatment was associated with a restored diversity of malignant cell states, suggesting that the GLS state serves as a regulatory “safe harbor” in which residual malignant cells can undergo evolution and adaptation. Mechanistically, we found that RAS pathway signaling directly activates transcriptional regulators that drive the MOS state, elucidating an early adaptive response to RAS-GTP inhibition that enables residual cells to survive treatment prior to development of acquired resistance.

#3875 Glioblastoma mutational profiles drive cancer cell signaling and immune evasion.

M. Pourmaleki[1], B. D. Greenstein[1], C. J. Jones[1], S. Nandakumar[1], D. A. Navarrete[1], S. Mehta[1], C. Campos[1], T. J. Hollmann[2], N. D. Socci[1], T. Bale[1], S. P. Shah[1], I. K. Mellinghoff[1];

[1]Memorial Sloan Kettering Cancer Center, New York, NY, [2]Bristol Myers Squibb, Princeton, NJ

Glioblastoma multiforme (GBM) is the most common malignant brain tumor in adults with a median survival below two years. Characterization of GBM through gene expression profiling and DNA sequencing has identified disease subgroups and commonly altered genes and pathways, including alterations in the genes encoding neurofibromin-1 (*NF1*) and the epidermal growth factor receptor (*EGFR*). *NF1* and *EGFR* are involved in receptor tyrosine kinase (RTK), RAS/MEK/ERK, and PI3K signaling, and together, are genetically altered in over 60% of adult GBMs. Interestingly, *NF1* and *EGFR* alterations in GBM are almost always mutually exclusive. Here, we designed a multimodal approach integrating spatial proteomics, transcriptomics, and genomics to measure cell composition, immune cell function, cancer cell signaling, cellular spatial organization, gene expression, transcriptional subtypes, and genome alterations in 80 *NF1* and *EGFR* altered human GBMs with extensively curated treatment and survival data. We quantified the spatial expression of 42 proteins in over 31 million single cells measuring RTK/RAS/PI3K and Rb signaling and features of the TME, including 23 cell types covering tumor cells, immune cells, and brain resident cells. In addition to tumor genotype labels, we classified each GBM tumor by its transcriptional subtype (i.e., mesenchymal, classical, or proneural). We identified genotype-phenotype associations in GBM including hyperactive RAS signaling cellular niches, a macrophage-rich TME, and an epithelial-mesenchymal signature in *NF1* altered tumors and hyperactive RTK signaling and an immune desert TME in *EGFR* amplified tumors. Furthermore, we observed spatial heterogeneity in cancer cell signaling patterns suggestive of the presence of different tumor cell clones within different regions of each GBM tumor. Together, we identify several genotype-associated features of GBMs, reinforcing the value of integrating spatial multi-omic data for generation of genotype-driven therapeutic hypotheses, with implications for GBM genotype-based therapeutic stratification.

#3876 A spatial transcriptomic study of a triple-negative breast cancer (TNBC) patient-derived xenograft (PDX) model of residual disease refractory to conventional chemotherapy.

B. Strope, K. Pendleton, W. Bowie, G. Echeverria, **Q. Zhu**;
Baylor College of Medicine, Houston, TX

Combating chemotherapy resistance in TNBC is critical to improving quality of care and reducing fatality. To understand chemoresistance, it has been proposed that the spatial interactions between cell types in the tumor microenvironment (TME) could offer insights into the differential response to therapy and metastatic potential. Thus, this study utilizes spatially resolved transcriptomics (SRT) to profile the spatial interactions in TNBC TME. With the goal of understanding chemoresistance and providing a proof-of-concept for new technology, we launched a longitudinal SRT study of a TNBC PDX of residual disease before, during, and after adriamycin and cyclophosphamide (AC) treatment (Tx). SRT by 10X Visium was performed on Veh, AC-residual tumor (21 d post-Tx), and AC-regrown tumor (50 d post-Tx when tumors regrew). This study is divided into two parts. 1. Due to the lack of specialized tools for processing xenograft reads from SRT, we developed the Xenomake pipeline, which combines xenograft sorting and spatial barcode demultiplexing to assign reads into the host and graft organisms per spatial spot. It permits clustering the spots into stroma-rich (mouse), and epithelial-rich (human) regions. We show that it can find differential cytokines in the stroma (S) and epithelium (E), and finding SS, EE, and SE interactions. 2. Although using PDX necessitates immune-compromised mice, several types of stromal populations are present and analyzable. Thus, using Xenomake, we inferred the localization of stromal cell types in Visium spots including cancer associated fibroblasts (CAF), macrophages (MP), endothelial (ENDO), monocytes, and perivascular cells. We compared the spatial localization profiles (SLP) of stromal cell types across samples. With human reads, we computed the spatial pathway activity map (SPAM) for HALLMARK pathways. We correlated SPAM with stroma cell type SLP to survey stroma-epithelial interactions. Stroma cells are distributed in the tumor periphery in vehicle and AC50, while in AC21 there is a notable increase in stroma abundance and stroma infiltration within tumor mass. SLP of MP (Cd68+ and Csf1r+) is correlated with ENDO (Pecam1+), and CAF (Acta2+ and Pdgfrb+). Additionally, all 3 cell types are correlated with Vim and Cd44 expression. Although all samples show enrichment of MP, ENDO, and CAF, they interact differently with pathway activities of adjacent epithelial cells. In vehicle and AC50, the 3 cell types are colocalized with OXPHOS, MYC targets, E2F pathway, while in AC21, a switch to colocalization with EMT is observed. Further, hypoxia response and glycolysis display anti-correlation with stroma cell types, meaning that these pathway activities are further away from stroma and occupy distinct territories. The results suggest stroma-tumor metabolic crosstalk and ways of targeting residual disease.

#3877 Multi-modal analysis of paracrine signaling in group 3/4 medulloblastoma.

B. Yu, J. Jung, A. Diaz;
University of California, San Francisco (UCSF), San Francisco, CA

Medulloblastoma (MB) is the most common primary brain malignancy in kids, with the group 3 and 4 subtypes (G3/4) being the most aggressive. Recent single-cell genomics studies have identified the G3/4 MB cell of origin and point to disrupted stem-cell differentiation as a key factor in MB pathogenesis. However, surprisingly little is known about the contribution of tumor-supportive paracrine signaling to the ontogeny of this disease. The spatial organization of MB cellular hierarchies is not completely understood. We profiled N=24 G3/4 MBs from UCSF patients via single-nucleus RNA sequencing (snRNA-seq). Of these cases, N=10 were profiled via single-cell assay for transposase-accessible chromatin by sequencing (scATAC-seq). To capture the spatial context, we profiled an additional 20 samples via spatial transcriptomics using the Visium and Xenium platforms. We found that the standard Xenium brain capture set was inadequate, and we developed a highly specific capture set for G3/4 MBs. In particular, our panel resolves cell-type differences in the stage of MB lineage commitment, from rhombic-lip progenitors to more differentiated unipolar brush-like cells. Altogether, over 110,000 nuclear-sequencing libraries and over 1,898,000 spatially-resolved single-cell libraries were generated. We inferred cell-cell communication signals from our snRNA-seq data by identifying co-expressed receptors and their cognate ligands. We then performed an integrated analysis of our snRNA-seq and scATAC-seq data to infer the cis-regulatory enhancers of those signaling genes, as well as the transcription factors that bind them. We employed our spatial transcriptomics data to confirm paracrine signaling networks inferred from nuclear-sequencing data. We found that distinct MB cell types corresponding to different stages of differentiation occupied specific spatial domains. The results of our ongoing analysis of this spatially-resolved single-cell atlas will be presented. This study paves the way for innovative therapeutic strategies targeting paracrine signaling in G3/4 MB.

#3878 Therapy-associated remodeling of pancreatic cancer revealed by single-cell spatial transcriptomics and optimal transport analysis.

J. CAO[1], C. Shiau[2], D. Gong[2], M. T. Gregory[3], X. Yin[2], J.-W. Cho[1], P. L. Wang[2], J. Su[2], J. W. Reeves[3], J. A. Guo[2], N. A. Lester[2], J. Bae[2], R. Zhao[2], M. Hemberg[1], W. L. Hwang[2];

[1]Gene Lay Institute of Immunology and Inflammation, Brigham and Women's Hospital and Harvard Medical School, Boston, MA, [2]Center for Systems Biology, Department of Radiation Oncology, and Center for Cancer Research, Harvard Medical School and Massachusetts General Hospital, Boston, MA, [3]NanoString Technologies, Seattle, WA

The aggressive nature of pancreatic ductal adenocarcinoma (PDAC) is driven by cell-intrinsic features and cell-extrinsic interactions between tumor cells and the desmoplastic stroma, which is infiltrated with heterogeneous populations of cancer-associated-fibroblasts (CAFs) and immune cells. These features are able to drive emergent properties such as chemoresistance through diverse and not yet fully elucidated mechanisms. Through single-nucleus RNA-seq and whole-transcriptome digital spatial profiling of PDAC patient tumors, we previously reported marked heterogeneity in the malignant cells and CAF composition of PDAC. In this project, we performed high-plex single-cell spatial molecular imaging (990-plex SMI, Nanostring) to dissect the therapy-remodeled multicellular neighborhoods and malignant-stroma cell interactions in primary resected human pancreatic cancer with (n = 6) or without (n = 7) neoadjuvant chemotherapy and radiotherapy. SMI of the PDAC samples yielded ~753,000 high-confidence single cells and captured the heterogeneity of malignant cells and CAFs. We identified three malignant subtypes: classical (CLS), basal-like (BSL), and the recently characterized neural-like progenitor (NRP) malignant subtype that exhibits stem-like and neurodevelopmental features. To leverage the single-cell spatial resolution of SMI to further dissect treatment-associated changes in cell-cell interactions, we developed Spatially Constrained Optimal Transport Interaction Analysis (SCOTIA), an optimal transport model with a cost function that includes both spatial distance and ligand-receptor gene expression. Our results uncovered a marked enrichment in ligand-receptor interactions between CAFs and malignant cells in response to treatment. In combination with several complementary methods, including examination of downstream target gene expression and *ex vivo* 3D co-culture of CAF and PDAC cells, we found that IL-6 family signaling was the most consistently enriched interaction between CAFs and malignant cells after treatment. This led us to hypothesize that IL-6 signaling between CAFs and malignant cells may induce chemoresistance in cancer cells. To test this hypothesis, we treated three human cancer cell lines (AsPC1, Panc1, Panc0203) with 5FU with or without IL-6 and discovered that IL-6 induced chemoresistance for two of the lines (Panc1, Panc0203). Taken together, we have integrated novel experimental and computational approaches to enable high-resolution, spatially-guided discovery of treatment-associated remodeling in the pancreatic cancer microenvironment. Further studies will be conducted to dissect additional mechanisms by which candidate cell-cell interactions promote disease progression and/or resistance to cytotoxic therapy, with the ultimate goal of guiding novel therapeutic development.

CHEMISTRY: Identification, Optimization, and Characterization of Protein Degraders and Inhibitors Minisymposium

#3879 Development of potent, highly selective and efficacious SMARCA2 degraders.

L. Yang, W. Tu, L. Huang, L. Leng, W. Jiang, M. Wang, B. Wen, D. Sun, J. Stuckey, S. Wang;
University of Michigan, Ann Arbor, MI

In human lung, melanoma and other types of human cancers, the mammalian SWItch/Sucrose Non-Fermentable (SWI/SNF) helicase SMARCA4 is frequently mutated, which leads to inactivation of its functions. SMARCA2, a close homologous protein of SMARCA4, is an attractive synthetic lethality target for human cancers with SMARCA4 deficiency. Herein, we report the discovery and biological evaluation of potent, highly selective and efficacious SMARCA2 PROTAC degraders exemplified by UM-SMD-3236. UM-SMD-3236 has a DC_{50} value of <1 nM in inducing degradation of SMARCA2 in cells and demonstrates >400-fold selectivity over SMARCA4 protein. Of significance, while UM-SMD-3236 achieves a D_{max} of >95% against SMARCA2, it shows a D_{max} of 50% against SMARCA4 in cells. *In vivo*, a single intravenous dose of UM-SMD-3236 attains 85-93% of SMARCA2 depletion in tumor tissues for 7 days, while showing no reduction of the SMARCA4 protein. Weekly intravenous administration of UM-SMD-3236 is highly effective in inhibition of tumor growth in SMARCA4 deficient xenograft models of human cancer. Importantly, UM-SMD-3236 shows no signs of toxicity in mice at highly efficacious doses. UM-SMD-3236 represents a highly promising SMARCA2 degrader for extensive evaluation as a potential new therapy for the treatment of SMARCA4-deficient human cancers.

References 1. Oike, T.; Ogiwara, H.; Tominaga, Y.; Ito, K.; Ando, O.; Tsuta, K.; Mizukami, T.; Shimada, Y.; Isomura, H.; Komachi, M.; Furuta, K.; Watanabe, S.-I.; Nakano, T.; Yokota, J.; Kohno, T. A Synthetic Lethality-Based Strategy to Treat Cancers Harboring a Genetic Deficiency in the Chromatin Remodeling Factor BRG1. *Cancer Res.* 2013, *73*, 5508-5518. 2. Yang, L.; Tu, W.; Huang, L.; Miao, B.; Kaneshige, A.; Jiang, W.; Leng, L.; Wang, M.; Wen, B.; Sun, D.; Wang, S. Discovery of SMD-3040 as a Potent and Selective SMARCA2 PROTAC Degrader with Strong in vivo Antitumor Activity. *J. Med. Chem.* 2023, *66*, 10761-10781.

#3880 LYTAC targeting galectin-1 to enhance radioimmunotherapy of cancers in the upper aerodigestive tract.

Yuyan Jiang[1], Green Ahn[2], Mobeen Rahman[3], Hongbin Cao[1], Carolyn Bertozzi[2], Qunh Le[1]

[1]Radiation Oncology, Stanford University School of Medicine, Stanford, CA,[2]Chemistry, Stanford University, Stanford, CA,[3]Pathology, Stanford University School of Medicine, Stanford, CA

Non-small cell lung cancer (NSCLC) and head and neck cancer (HNC), ranking respectively as a leading cause of cancer-related death and the sixth most common cancer worldwide. Despite treatment advancements, there's a pressing need for more effective strategies to improve survival and quality of life for NSCLC and HNC patients. Carolyn Bertozzi group recently reported in Nature the groundbreaking protein degraders named lysosome-targeted chimeras (LYTACs), which have bispecific binding affinity that drives cell-surface endocytic receptors to drag membrane or extracellular oncogenic proteins to lysosomes for degradation. They have successfully targeted critical oncoproteins such as epidermal growth factor receptor (EGFR) and more. However, current degradation demonstration was limited to in vitro cancer cells, LYTACs' impact on immune cell modulation and their therapeutic potentials in preclinical animal models remain unknown and require extensive evaluation before venturing to clinical trials.Our group and others have identified galectin-1 (Gal-1) as a multifaceted immunosuppressive biomarker overexpressed in NSCLC and HNC. By interacting with glycosylated receptors (e.g. CD45) on immune cells, it results in apoptosis of cytotoxic T cells, expansion of regulatory T cells, and intratumoral recruitment of myeloid-derived suppressor cells. Despite promising as an immune checkpoint target, effective anti-Gal-1 therapies are currently absent in clinical trials.Through histopathological analyses, we have confirmed substantial LYTAC receptor (cation-independent mannose-6-phosphate receptor, CI-M6PR) expression in ~200 HNC and ~400 NSCLC patient samples. Collaborating with Bertozzi group, we have developed the first Gal-1 targeting LYTAC named G-M6Pn which triggers significant target protein degradation in various human HNC and NSCLC cell lines. Such efficient Gal-1 degradation leads to significant immunosuppression reversal by stimulating CD8+ T cell and natural killer (NK) cell activation while dampening regulatory T cell (Treg) activity in both cell experiments and humanized mouse tumor models, resulting in excellent tumor/metastases control and survival improvement on both NSCLC and HNC models. When synergized with stereotactic ablative radiotherapy, the antitumor immune responses are further amplified and G-M6Pn also mediates ‘abscopal effect’ inhibiting non-irradiated tumors. This study thus contributes to expediting clinical translation of LYTACs as novel immune checkpoint degraders to improve personalized radio-immunotherapy of cancer.

#3881 Discovery of highly potent, selective and efficacious STAT3 PROTAC degraders capable of achieving long-lasting tumor regression.

H. Zhou, D. Wu, L. Bai, R. K. Acharyya, H. Metwally, D. McEachern, B. Wen, D. Sun, S. Wang;
University of Michigan, Ann Arbor, MI

STAT3 (signal transducer and activator of transcription 3) is a transcription factor and a promising therapeutic targets for cancer and other human diseases. We have previously reported the discovery of SD-36 and SD-91 as potent, selective and highly efficacious STAT3 degraders. In the present study, we report the discovery and extensive evaluation of new, highly potent, selective and efficacious new STAT3 degraders. In direct comparison, these compounds are >50-times more potent than SD-36 in inducing STAT3 degradation in cells and demonstrates >500-fold degradation selectivity over other STAT members. Proteomic analysis showed that our best lead compound (UM-STAT3-1218) only reduces the levels of STAT3 protein in cells over other >6,700 proteins. (UM-STAT3-1218) achieves low nanomolar IC_{50} values in leukemia and lymphoma cancer cell lines with activated STAT3. A single intravenous dose of (UM-STAT3-1218) at 3 mg/kg reduces the STAT3 protein for >4 days in xenograft tumor and native tissues, without reducing another other STAT members. Impressively, a single dose of (UM-STAT3-1218) at 3 mg/kg achieves complete and long-lasting tumor regression in multiple xenograft tumor models without any signs of toxicity. Taken together, (UM-STAT3-1218) is a highly promising STAT3 degrader for the treatment of the treatment of human cancers and other human diseases in which STAT3 plays a key role.

#3882 Targeted degradation of undruggable proteins using a novel heterobifunctional proteomimetic platform.

M. Wang[1], M. Truica[2], B. Gattis[1], X. Zhang[1], S. Abdulkadir[2], N. Gianneschi[1];
[1]Northwestern University, Evanston, IL, [2]Northwestern University, Chicago, IL

Of the ~20,000 unique proteins in the human genome, only a subset can be modulated via traditional pharmacological approaches. “Undruggable” targets currently include proteins with pivotal roles in cancer pathogenesis. Our work aims to introduce a new paradigm for engaging these clinically relevant proteins using a modular platform we term the HYbrid DegRAding Copolymers (HYDRACs). HYDRACs multiplex targeting warheads with degradation inducers and have long circulation times plus high cell uptake. Preliminary studies on MYC and RAS, targets of immense pharmaceutical interest, highlight the potential of this platform to revolutionize drug design.

Methods: HYDRACs containing MYC- or RAS- targeting peptides randomly copolymerized with degrons were synthesized using ROMP. Fluorescent and biotin-tags were incorporated for use in uptake and pull-down assays. Viability following treatment with MYC-HYDRACs was performed in multiple cell lines with both cellular (MYC-independent lines) and polymer composition controls. Target engagement was assessed via immunoprecipitation and circular dichroism with protein degradation monitored by WB. Unbiased whole proteome analysis and RNAseq were done to confirm observed effects were selectively on-target. *In vivo* efficacy and biodistribution was assessed in tumor-bearing mice.

Results: HYDRACs show high levels of cell uptake and antiproliferative effects at sub-micromolar concentrations in a formulation- and target-dependent manner. Cells treated with MYC-HYDRACs displayed reduced MYC protein levels, which were rescued by proteasome or neddylation inhibition. Swapping out the degron for various validated E3 ligase recruiters maintained MYC degradation, highlighting the “plug-and-play” nature of this approach. On-target activity was confirmed via RNAseq. Biophysical analysis showed strong HYDRAC-protein interactions, orthogonally supported by the presence of target protein following pull-down of biotin-terminated HYDRACs. Target protein degradation only occurred following treatment with an intact HYDRAC compound. Mice bearing MYC-CaP tumors showed delayed tumor growth following treatment with MYC-HYDRACs, with compound accumulation in the tumor for up to 72 h following a single injection. Generalizability was demonstrated against RAS, with RAS-HYDRACs capable of degrading KRAS across multiple different alleles, acting as a pan-KRAS degrader.

Conclusions: We present a novel platform technology that addresses the challenges inherent to peptide delivery approaches. HYDRACs have the potential to dramatically alter the drug discovery landscape, allowing for the development of cancer-relevant target modulators for which there are no current viable therapies. We envision the HYDRAC platform as a generalizable approach to designing degraders of proteins of interest, greatly expanding the therapeutic armamentarium for TPD.

#3883 Cryo-EM-guided enhancement of target selectivity of a novel p97 inhibitor for treating multiple myeloma and acute myeloid leukemia.

J. Crawford[1], R. Munuganti[1], C. Leung[1], K. Singh[1], E. Gates[1], X. Zhu[1], M. Bally[2], N. Dos Santos[2], M. Sharifiaghdam[2], Z. Nosrati[2], P. Axerio-Cilies[3], A. Berezuk[3], S. Cholak[3], S. Subramaniam[4];

[1]Gandeeva Therapeutics, Burnaby, BC, Canada, [2]BC Cancer Research Centre, Vancouver, BC, Canada, [3]University of British Columbia, Vancouver, BC, Canada, [4]University of British Columbia; Gandeeva Therapeutics, Vancouver, BC, Canada

The AAA ATPase p97, also known as valosin-containing protein (VCP), serves to regulate protein homeostasis by facilitating the translocation of ubiquitinated proteins from membranes or chromatin to the proteasome for degradation. Certain cancers, including multiple myeloma (MM) and acute myeloid leukemia (AML) are known for the intracellular overexpression of proteins, and are thus susceptible to the inhibition of p97 and resulting proteotoxic stress. A known p97 inhibitor, CB-5083 entered human phase 1 clinical trials in 2015, but trials were terminated due to side effects that were later traced to strong interaction of the compound with the phosphodiesterase PDE6. To address this problem, we devised a subtractive approach that leveraged high resolution structures of CB-5083 bound to PDE6 and p97. Using this information, we designed a p97 inhibitor that no longer displayed significant off-target binding but retained strong on-target binding. The optimization process started when we identified the 7-azaindole core from an *in silico* screen as a suitable hit pharmacophore and confirmed the binding mode of several variants of this scaffold in p97 by cryo-EM. Through a structure-guided medicinal chemistry program, we identified GND-135, a potent, on-target binder through the synthesis of less than 100 compounds. The design was supported with about 50 cryo-EM structures throughout the optimization process. Compared to CB-5083, our compound GND-135 displays greatly reduced PDE6 activity (< 1% inhibition at 10 µM versus 89% inhibition for CB-5083) and more potent p97 ATPase inhibition (3 nM IC_{50} versus 12 nM for CB-5083). We also evaluated the pharmacokinetic profile of GND-135 in mice; the half-life and clearance of 6.6 h and 15.9 mL/min/kg respectively were deemed suitable for daily administration. Based on the initial profiling, we carried out an efficacy study in a cell derived xenograft mouse model of AML using a U937 cell line with subcutaneous implantation. In this model, where GND-135 was administered IP (40 mg/kg QD) and CB-5083 was administered orally (40 mg/kg QD) the compounds showed statistically comparable efficacy, which was differentiated from untreated control. Thus, GND-135 is a novel p97 inhibitor lead compound with on-target selectivity powered by cryo-EM driven rational drug design.

#3884 Artificial intelligence (AI)-enabled discovery of GLX1546, a novel and potent inhibitor of ULK1/2 kinases and autophagy.

G. Cui[1], X. Sun[2], W. Zhu[1], Q. Wang[1], J. Li[1], Z. Pan[2], **C. Li**[1];
[1]Galixir, Beijing, China, [2]Galixir, Shanghai, China

Background: Autophagy is an evolutionarily conserved process, critical for the recycling of damaged or excess cellular components, which promotes cell survival and growth under stress conditions. Cancer cells, especially those with RAS mutations, can activate the ULK1/2 (UNC-51-like kinase 1/2)-initiated autophagy pathway for survival and diminish RAS pathway inhibitors' efficacy. The combination of RAS pathway and ULK1/2 kinase inhibitors may provide synergistic or additive effects for RAS mutated solid tumors. We have identified a structurally small molecule, GLX1546, which shows strong inhibition against ULK1/2, as well as autophagy induced by RAS pathway inhibitors in cells.
Methods: Multiple dual-target activity predictive models were constructed and trained using extensive protein-ligand interaction data. These models, in conjunction with in-house built physicochemical property predictive models, were integrated into an AI-driven computational pipeline to perform the *in silico* screening on both ULK1/2 inhibitory activities and drug-like properties. ULK1/2 *in vitro* activities were assessed by enzymatic assays and cellular assays based on the phosphorylation of ULK substrate. The *in vivo* anti-tumor efficacy of GLX1546 was evaluated in A549 CDX mouse model both as monotherapy and in combination with trametinib.
Results: An AI-driven high-throughput virtual screening strategy using deep learning models was implemented for the discovery of novel and potent ULK1/2 small-molecule inhibitors. GLX1546 was developed as a potent ULK1/2 inhibitor with IC_{50} values of 1.13 nM for ULK1 and 4.75 nM for ULK2. Moreover, to address trametinib-induced activation of ULK1/2 in KRAS and BRAF mutated solid tumors, GLX1546 provided IC_{50} values of 54 nM in A549, 21 nM in HCT 116, 67 nM in MIA PaCa-2, and 76 nM in A375 cells against both basal and trametinib-induced pATG13. Furthermore, GLX1546 exhibited good exposure, sound safety, and high oral bioavailability (~100%) in mice. The combination of trametinib (PO, QD) with GLX1546 (PO, BID) in 21-day cycles also led to inhibition of ATG13 phosphorylation and greater tumor growth inhibition than trametinib alone in A549 CDX mouse model.
Conclusions: These results indicate that GLX1546 can inhibit ULK-mediated autophagy induced by trametinib. The combination of GLX1546 with RAS pathway inhibitors may offer a novel cancer therapy for RAS mutated cancers, highlighting AI as an effective tool for drug discovery.
Keywords: AI-driven drug discovery, autophagy, small-molecule inhibitors, ULK

#3885 A ubiquitin-specific proximity labeling method to study drug-induced ubiquitylation.

H.-T. Huang[1], R. J. Lumpkin[2], R. W. Tsai[1], K. A. Donovan[2], S. Su[1], X. Zhao[1], J. Chen[1], E. S. Fischer[2], W. R. Sellers[1];
[1]Broad Institute, Cambridge, MA, [2]Dana Farber Cancer Institute, Boston, MA

Targeted protein degradation is a promising therapeutic paradigm that offers new ways to disrupt protein functions. Currently, most studies that characterize the pharmacological effects of protein degraders utilize target-specific assays and global proteomics. However, information on the direct molecular consequence of protein degraders, i.e., induced protein ubiquitylation, is often lacking. Here we report the development of E-STUB (E3-substrate tagging by ubiquitin biotinylation), a ubiquitin-specific proximity labeling method that identifies ubiquitylated substrates in proximity to an E3 ligase of interest. We demonstrated that E-STUB can accurately identify the ubiquitylated targets induced by protein degraders in both CRBN and VHL systems—two of the most utilized E3 ligases by heterobifunctional degraders—and is likely generalizable to other E3 ligases. While we observed a high level of consistency between ubiquitylation and degradation for the induced substrates, E-STUB also detected ubiquitylation of non-degraded targets, providing novel and complementary insights to global proteomics. We also envision that E-STUB could be specifically used for the development of chemical inducers of proximity that catalyze non-degradative ubiquitylation events. In summary, we expect that the E-STUB approach can be widely useful for studying the principles of chemically induced ubiquitylation and the advancement of targeted protein degradation.

CLINICAL RESEARCH: Application of Real-World Evidence to Cancer Care
Minisymposium

#3886 Analysis of clonal heterogeneity within paired primary and metastatic tumor samples of patients with solid tumors and implications for neoantigen-based personalized cancer vaccines.

A. Obermayer[1], T. Shaw[1], D. Chang[1], J. Davis[1], J. K. Teer[1], X. Yu[1], X. Wang[1], D. Hedges[2], A. Tan[3], R. Rounbehler[2], A. Naqash[4], M. Gatti-Mays[1], A. Ratan[5], M. McCarter[6], H. Colman[7], I. Puzanov[8], S. Arnold[9], M. Churchman[2], P. Hwu[1], W. Dalton[2], G. Weiner[10], J. Conejo-Garcia[11], P. C. Rodriguez[1], B. Salhia[12], A. A. Tarhini[1];

[1]H. Lee Moffitt Cancer Center & Research Institute, Tampa, FL, [2]Aster Insights, Tampa, FL, [3]Huntsman Cancer Institute, University of Utah,, Salt Lake City, UT, [4]Stephenson Cancer Center Oklahoma University, Okalahoma City, OK, [5]University of Virginia, Charlottesville, VA, [6]University of Colorado School of Medicine, Aurora, CO, [7]Huntsman Cancer Institute, University of Utah, Salt Lake City, UT, [8]Roswell Park Comprehensive Cancer Center, Buffalo, NY, [9]Markey Cancer Center, Lexington, KY, [10]University of Iowa, Iowa City, IA, [11]Duke University, Durham, NC, [12]USC Norris Comprehensive Cancer Center, Los Angeles, CA

Background: Neoantigen-based personalized cancer vaccines carry significant promise in treating solid malignancies. However, there are uncertainties regarding the choice between the primary or the metastatic tumor for neoantigen prediction in individual patients. Here, we conducted a thorough examination of somatic variations in 676 patients who had paired primary and metastatic solid tumors.

Methods: Patients were enrolled in the Total Cancer Care protocol (NCT03977402) to which patients provided an IRB-approved written informed consent within the Oncology Research Information Exchange Network (ORIEN). Whole-exome sequencing of 756 primary and metastatic tumor pairs was performed (N = 676 patients). These included Genitourinary (n=83), Gynecological (n=97), Gastrointestinal (n=213), Thoracic (n=33), Cutaneous (n=24), Breast (n=108), Endometrial (n=49), Sarcoma (n=35), Head-and-Neck (n=106) and others (n=8). The data was analyzed through the ORIEN AVATAR Molecular Analysis Pipeline for somatic mutation variant detection and variant annotation. In this analysis, we focused on somatic events that result in an in-frame alteration (such as missense, in-frame deletion and in-frame insertion) and out-of-frame protein-altering mutations (such as frameshifts, de novo start, out-of-frame, and nonstop gain). Clonal population structure was determined based on pyclone-vi.

Results: For in-frame events, bladder cancer, melanoma, and gynecological cancers shared close to 75% of the mutations between paired primary and metastatic cases. In contrast, sarcoma and thyroid cancer had a low overlap (~ 25%) of variants. For out-of-frame events, these events tend to have a lower proportion of shared somatic variants between primary and metastasis than in-frame variants. Oncogenic drivers (e.g., BRAF V600E, KRAS G12A, and TP53 loss-of-function) were highly likely to be present in both paired primary and metastatic tumors. Next, we performed additional analysis on evolutionary selection of protein-coding variants via dN/dS calculation. We found no significant global shift in dN/dS ratio between paired primary and metastatic tumors across malignancies. However, we found increased selection of protein-coding variants in brain and liver metastatic sites, which correlated with increased homologous recombination deficiency within these sites.

Conclusions: Our analysis demonstrates genetic variations that exist when comparing paired primary and metastatic tumors that appear to vary by histology. Variants are potentially undergoing negative selection supported by the preferential loss of out-of-frame events in metastatic tumors and positive selection in specific metastatic sites. Overall, understanding the clonal structure will be key to neoantigen prediction for effective neoantigen-based vaccines.

#3887 The origins and clinical impact of extrachromosomal DNA across 39 cancers.

C. Bailey[1], O. Pich[1], K. Thol[2], J. Luebeck[3], G. Stavrou[2], T. B. K. Watkins[1], N. E. Weiser[4], W.-T. Lu[1], J. Kittel[2], R. Bentham[2], N. Sharma[2], R. Salgado[5], D. Moore[6], M. Litovchenko[2], K. L. Hung[7], A. J. Cornish[8], B. Dameracharla[3], S. Nik-Zainal[9], V. Bafna[3], H. Chang[7], N. McGranahan[2], N. Kanu[2], Genomics England Consortium, P. S. Mischel[7], M. Jamal-Hanjani[2], C. Swanton[1];

[1]Francis Crick Institute, London, United Kingdom, [2]University College London, London, United Kingdom, [3]University of California at San Diego, La Jolla, CA, [4]Stanford University School of Medicine, Stanford, CA, [5]ZAS Hospitals, Antwerp, Belgium, [6]University College London Hospitals, London, United Kingdom, [7]Stanford University, Stanford, CA, [8]The Institute of Cancer Research, London, United Kingdom, [9]University of Cambridge, Cambridge, United Kingdom

Extrachromosomal DNA (ecDNA) is emerging as a major contributor to cancer drug resistance and poor outcome in many cancer types. To understand the underlying genetic and mutational processes associated with ecDNA formation and presence, we conducted an analysis of whole-genome sequencing data from 14,778 cancer patients representing 39 tumor types from the Genomics England cohort. Our findings revealed focal amplifications driven by ecDNA in 17.1% of tumor samples, exhibiting varying frequencies across tissues. Notably, liposarcomas (55.4%) and HER2+ breast cancers (46.4%) displayed higher rates compared to lower rates found in pancreatic adenocarcinomas (2%). In addition to oncogenic amplifications such as HER2 derived from ecDNA during cancer evolution, ecDNAs that did not contain oncogenes were enriched for immunomodulatory genes (e.g., CXCL6, LRRC32, and HLA-G). Immunomodulatory ecDNAs exhibited reduced T cell infiltration.

In the context of intrinsic and environmental mutational processes, deamination clock-like, tobacco smoking, and APOBEC cytidine deaminase signatures positively correlated with ecDNA presence. Conversely, mismatch repair deficiency (MMRd) and POLD1/POLE deficiency signatures exhibited a negative correlation. Mutational processes associated with tobacco exposure, UV light, and spontaneous deamination primarily occurred before ecDNA formation, while signatures of homologous recombination repair deficiency tended to manifest post-ecDNA formation.Notably, ecDNA was enriched at metastatic sites and significantly associated with shorter overall survival in multivariable analysis (HR 1.31, 95% CI 1.17-1.47), underscoring its clinical relevance. This study enhances our understanding of the mutational processes and tissue contexts that shape the ecDNA landscape in human cancer and highlights its implications for clinical outcomes.

#3888 *TOP1* mutations mediate cross resistance to ADCs in metastatic breast cancer.

R. O. Abelman[1], H. Barnes[1], A. J. Medford[1], A. Putur[1], B. Wu[1], C. Weipert[2], G. Fell[3], L. M. Spring[1], S. A. Wander[1], B. Moy[1], A. Varkaris[1], D. Juric[1], L. Ellisen[1], R. Corcoran[1], A. Bardia[1];

[1]Harvard Medical School/Massachusetts General Hospital, Boston, MA, [2]Guardant Health, Boston, MA, [3]Harvard Medical School/Dana Farber Cancer Institute, Boston, MA

Background: Antibody-drug conjugates (ADCs) have improved survival for patients with metastatic breast cancer (MBC). In patients with HER2 negative MBC, two ADCs have FDA approval: sacituzumab govitecan (SG) and trastuzumab deruxtecan (T-DXd), both with topoisomerase-I (topo-I) inhibitor payloads. Given the many other ADCs in development, there is great interest in using ADC after ADC to maximize treatment benefit for patients. However, there is limited understanding regarding resistance mechanisms to ADCs and impact on ADC sequencing. We conducted a translational study to address this, and here we report the incidence of *TOP1* mutations and clinical impact on ADC sequencing.

Methods: All patients with MBC treated with ADCs at a large academic medical institution (Massachusetts General Hospital) who had comprehensive plasma-based genotyping (500 gene GuardantOMNI panel) were included. Since both SG and T-DXd have topo-I inhibitor-based payloads, we particularly focused on *TOP1* mutations, variant allele frequency (VAF), and germline/somatic characterization. Incidence of *TOP1* mutations in the ADC cohort was compared to The Cancer Genome Atlas (TCGA). Clinical “cross-resistance” was defined as progressive disease (PD) as best response to second ADC (ADC2) or treatment time on ADC2 of less than 60 days.

Results: Based on comprehensive plasma-based genotyping we identified 4 distinct *TOP1* mutations: S57C, R364H, W401C, G359E, at a frequency of 6.0% (4/67) at the time of disease progression on ADC compared to a frequency of 0.5% described in primary breast cancer in TCGA. Two of the amino acids found to be mutated are known to form direct interactions with the DNA backbone (G359) or the topoisomerase inhibitor itself (R364). For clinical resistance, one patient was briefly on ADC2 but stopped after 1 dose for toxicity; among the other 3 patients, two had cross-resistance to ADC after ADC, with both ADCs containing topo-I inhibitor payloads. Median duration on first ADC was 455 days compared to a median of 52 days for ADC2. Finally, one patient treated sequentially with 3 ADCs (all with topo-I inhibitor payloads) was found to have rising TOP1 VAF with progressive ADC treatments.

Conclusion: This is the first report describing emergence of *TOP1* mutations under selective pressure from ADCs and the impact on mediating cross-resistance to ADC after ADC with topo-I inhibitor payloads. Novel ADCs with alternative payloads may potentially be more effective when used sequentially after an ADC with a topo-I inhibitor. Further biomarker research is needed to optimize ADC sequencing for patients with *TOP1* mutant MBC.

#3889 Genomic landscape of gynecologic cancers with poor prognosis in Japan, an analysis of the national database of comprehensive genomic profiling tests.

Q. Xi[1], H. Kage[1], M. Ogawa[1], A. Matsunaga[2], A. Nishijima[1], K. Sone[1], K. Kawana[2], K. Oda[1];
[1]The University of Tokyo, Tokyo, Japan, [2]Nihon University School of Medicine, Tokyo, Japan

Objective: Comprehensive genomic profiling (CGP) tests were approved in Japan in June 2019 under universal health insurance coverage for cancer patients who have finished (or almost finished) standardized treatment. All the data are collected to the "Center for Cancer Genomics and Advanced Therapeutics (C-CAT)" under written informed consent. Up to date, over 60,000 CGP data have been deposited with a 99.7% consent rate. This study aims to analyze mutational landscape of gynecologic cancers, especially with poor prognosis, by using this database.
Methods: We analyzed CGP datasets from 3,006 gynecologic cancer patients using FoundationOne® CDx (F1CDx), the most commonly tested in Japan. This study was ethically approved by our institutional ethics committee (#2021341G) and the Information Utilization Review Board of C-CAT (#CDU2022-026N).
Results: Endometrial cancers (n=561) showed high rates of tumor mutational burden-high (TMB-H) (13.9%) and MSI-high (MSI-H) (10.8%), especially in endometrioid carcinomas. *POLE* exonuclease mutations were less frequent (1.4%) compared to TCGA data (7%), while *TP53* mutations were more common (54.4% vs. 29% in TCGA), suggesting the impact of prognosis of the molecular subtypes. Other frequently mutated genes included *PIK3CA* (41%), *PTEN* (35%), *ARID1A* (31%) and *KRAS* (26%). In 839 cervical cancers, TMB-H prevalence was 14.2%, with low MSI-H at 1.5%. TMB-H was significantly higher in squamous cell carcinomas (20.6%) than adenocarcinomas (8.3%). Frequent mutations included *PIK3CA* (32%), *STK11* (20%), *TP53* (20%), *KRAS* (14%), and *CDKN2A* (11%). *TP53* mutations were significantly higher than TCGA data (<5%), particularly in mucinous carcinomas (60%), indicating a prevalence of HPV-independent tumors with poorer prognosis. Actionable mutations were generally more frequent in adenocarcinomas than in squamous cell carcinomas, including *KRAS* (32.2%), *TP53* (29.4%), *CDKN2A* (18.3%), and *ERBB2* (16.7%). In 1,606 ovarian cancers, the ratio of TMB-H was 5.0%, and MSI-H was 1.2%. TMB-H rates varied between 3.3-6.5% across histological types, while the ratio of MSI-H was significantly lower in serous carcinomas (0.3%) than non-serous carcinomas. Pathogenic mutations in the *POLE* exonuclease domain were rare in cervical (0.0%) and ovarian (0.2%) cancers.
Conclusion: The C-CAT database offers insights into the mutational landscape of various cancers and histological subtypes, especially those with poor prognosis, highlighting the unmet needs for drug development in these gynecologic cancers.

#3890 Comprehensive molecular and immunological characterization of early-onset esophagogastric cancer.

L. W. Wu[1], S. K. Deshmukh[2], S. Wu[2], J. Xiu[2], A. Farrell[2], V. Lam[3], E. Lou[4], S. Goel[5], C. Nabhan[2], R. H. Moy[1];
[1]Columbia University Irving Medical Center, New York, NY, [2]Caris Life Sciences, Phoenix, AZ, [3]Johns Hopkins Sidney Kimmel Comprehensive Cancer Center, Baltimore, MD, [4]University of Minnesota, Minneapolis, MN, [5]Rutgers Cancer Institute of New Jersey, New Brunswick, NJ

Background: The incidence of early-onset esophagogastric cancer (EOEGC), defined as age of diagnosis <50, has increased in recent decades. Compared to average-onset esophagogastric cancer (AOEGC), EOEGC are more likely to be genomically stable, have diffuse histology, and present with more advanced disease. Here, we utilized a large real-world data cohort to characterize EOEGC with molecular and immune signatures.
Methods: 5,175 esophagogastric cancer (EGC) samples (<50 yrs, n=530; ≥50 yrs, n=4645) were tested by next generation sequencing (NGS) (592, NextSeq; WES, NovaSeq) and whole transcriptome sequencing (WTS) (NovaSeq) (Caris Life Sciences, Phoenix, AZ). EGC patients with age <50 and ≥50 were classified as EOEGC and AOEGC, respectively. Deficient mismatch repair (dMMR)/microsatellite-instability (MSI) was tested by IHC and NGS. Tumor mutational burden (TMB) totaled somatic mutations per tumor (high>10 mt/MB). Pathway enrichment determined by Gene Set Enrichment Analysis (Broad Institute, Cambridge, MA). Immune cell fractions were calculated by deconvolution of WTS: Quantiseq. Statistical significance was determined using chi-square and Mann-Whitney U test with p-values adjusted for multiple comparisons (q < 0.05).
Results: EOEGC had higher frequency of *CDH1* (18.9% vs 6.5%) but lower frequency of *TP53* (65.9% vs 74.4%) mutations compared to AOEGC (all q<0.05). EOEGC had higher frequency of *CCNE1* (6.8% vs 4.4%), *MYC* (6.1% vs 4.1%) and *FGFR2* (3.45% vs 1.87%) copy number alterations and *ARHGAP26* (5.67% vs 2.2%) fusion. EOEGC had lower frequency of TMB high (3.8 vs 10.1%) and dMMR/MSI-H (1.3% vs 5.7%) (all p<0.05). EOEGC had pathway enrichment of epithelial mesenchymal transition (EMT) (NES: 1.8, FDR: 0.0) and angiogenesis (NES: 1.3, FDR: 0.24). EOEGC had lower median MAPK pathway activity score (MPAS) (-0.16 vs 0.13, p<0.05). Analysis of inferred immune cell infiltrates showed that EOEGC had increased infiltration of B cells (4.7% vs 3.9%) and M2 macrophages (3.6% vs 3%) but decreased infiltration of M1 macrophages (3.7% vs 4%) (all q<0.05). EOEGC had increased T cell inflamed signature (31.3% vs 26.1%, p<0.05) and increased expression of *HAVCR2* (*TIM3*) but decreased expression of *FOXP3* and *CD274* (PD-L1) (FC: 0.84-1.09, all p<0.05). There was no difference in *LAG3*, *CTLA4*, and *IDO1* gene expression.
Conclusion: EOEGC has several unique molecular and tumor immune microenvironment features. In this real world cohort, EOEGC has increased frequency of *CDH1* mutations, *ARHGAP26* fusions, enrichment of EMT and angiogenesis pathways, decreased MAPK pathway activity, decreased frequency of TMB high and dMMR/MSI-H, and a unique immune cell infiltrate with decreased M1 macrophages and increased M2 macrophages. These unique differential characteristics present therapeutic opportunities but also demonstrate the limitations of currently approved therapies in this subset of patients.

#3891 Early real-world experience with repeat multi-cancer early detection (MCED) testing.

R. Abrams[1], R. Shaknovich[2], J. Lipton[3], M. McMillin[4], A. Schneider[5], M. Margolis[2], X. Hou[2], Y. Oh[2], V. Le[2], E. Hubbell[2], R. Jiang[2], J. M. Venstrom[2], **O. K. Gordon**[6];

[1]Colorado Preventive Medicine, Denver, CO, [2]GRAIL, LLC, Menlo Park, CA, [3]Signature Healthcare, Charlotte, NC, [4]University of Illinois College of Medicine at Peoria, Peoria, IL, [5]MD2, Austin, TX, [6]Colorado Preventive Medicine, Los Angeles, CA

Background: An MCED test (Galleri®, GRAIL, LLC, Menlo Park, CA) has been in clinical use since April 2021. We previously reported the results of screening the first ~53,000 individuals in the US with this test from real-world (RW) practice. Here, we report the RW experience with repeated MCED testing in ~5800 individuals.

Methods: This MCED test analyzes targeted methylation in cell-free DNA and uses machine learning to detect a Cancer Signal (CS) and determine its Cancer Signal Origin (CSO). We analyzed results returned through August 2023 for those with a “No Cancer Signal Detected” (NCSD) result in Year 1 and an additional consecutive test. We excluded tests from clinical studies and sites that limited data sharing. Systematic collection of outcomes was attempted for all cases with a “CS detected” (CSD) result and continues via a quality assurance (QA) program.

Results: In this RW cohort, a second test was ordered in 5794 individuals (58% male, average age=61.3 y, range: 24.0-89.0 and 42% female, average age=60.5 y, range: 23.0-89.0). Median interval between blood draws was 12.9 months, and 81% (4693/5794) were tested 10-18 months after the initial test. Among the 5794, 26 received a CSD result in the second test, of which 20 were within 10-18 months, corresponding to a CSD rate (CSDR) of 0.45% (95% CI 0.31%-0.66%; 26/5794). The CSDR was slightly higher in males (0.50% [0.32%-0.81%; 17/3367]) vs females (0.37% [0.2-0.7%; 9/2427]) and was lower than the Year 1 CSDR of 0.95% (95% CI 0.87-1.0; 510/53,744). The top CSOs reported during second tests were: Lymphoid, Head & Neck, Bladder and Urothelial, Colon & Rectum, Anus. Among the 26 CSD cases, the QA program confirmed 12 clinical outcomes (8 with a cancer diagnosis, 4 with no cancer diagnosis), and 14 cases are still under investigation or without outcomes at this time. Among 8 cases with a confirmed cancer diagnosis, accuracy of the 1st CSO prediction was 100%, and diagnoses reflected invasive cancers across multiple cancer types including anus, colon, head & neck, urothelial tract, ovary, and lymphomas. Staging information was available in 5 cases, including 4 stage I cancers (4/5, 80%; anus, head & neck, lymphoma, bladder) and one stage IV cancer (ovary).

Conclusions: A subset of individuals who returned for MCED testing had cancers detected, including cancers without recommended screening, underscoring the potential value of annual screening with this MCED test. There may be systematic differences in this limited population of individuals who returned for repeat screening, reducing the signal detection rate through potential early adopter bias. Clinical data return was incomplete, and confirmed 8 cancers, including 4 stage I cancers. All cancers were found at the predicted CSO, demonstrating the clinical utility of this unique test feature that directs diagnostic work up.

#3892 Systematic generation of a clinicogenomic harmonized oncologic real-world dataset (MSK-CHORD).

Christopher J. Fong, Karl Pichotta, Thinh Tran, Michele Waters, Tom Fu, Mono Pirun, Mirella Altoe, Brooke Mastrogiacomo, Anisha Luthra, Mehnaj Ahmed, Arfath Pasha, Armaan Kohli, Raymond Lim, Tom Pollard, Darin Moore, Benjamin Gross, Avery Wang, Calla Chennault, Ritika Kundra, Ramyasree Madupuri, Ino de Bruijn, Aaron Lisman, Walid K. Chatila, Subhiksha Nandakumar, Anika Begum, Doori Rose, Kenneth L. Kehl, Deborah Schrag, Michael Berger, Jian Carrot-Zhang, Pedram Razavi, Bob Li, Peter Stetson, Nikolaus Schultz, Justin Jee

Memorial Sloan Kettering Cancer Center, New York, NY

Clinical data storage in unstructured notes and siloed datasets present a major challenge for large-scale cancer informatics. Whether natural language processing (NLP) combined with multimodal integration across datasets can produce a mineable resource and improve discovery of relationships between tumor genomics and clinical phenotypes is unknown.

We hypothesized that NLP could automatically annotate a pan-cancer corpus of 82,464 patients with tumor genomic sequencing. To develop algorithms to annotate free-text reports, we leveraged the AACR Project GENIE Biopharma Collaborative (BPC), a structured curation of EMR from five cancer types (non-small cell lung (NSCLC), breast, colorectal, prostate, and pancreatic cancer), to train and validate several Transformer and rule based-based NLP models. After automating the generation of NLP annotations alongside medication, demographic, tumor registry, survival, and tumor genomic sequencing data, we tested whether clinicogenomic relationships not apparent in the smaller BPC cohort might be discoverable in the larger cohort.

In 5-fold cross-validation, NLP Transformers accurately annotated the presence of cancer (AUC=0.99), cancer progression (AUC=0.97), and sites of disease (AUC=0.99) from radiology reports, and presence of prior outside treatment (AUC=0.98) and hormone receptor (HR) and HER2 receptor status (AUC=0.98, 0.98) from clinician notes. In addition, rule-based models, trained on non-BPC data and validated on the whole BPC cohort, annotated smoking status from clinician notes (ACC=0.95), and Gleason score (ACC=1.0), PD-L1 status (ACC=0.98), and mismatch repair deficiency (ACC=0.98) from histopathology reports. NLP annotations were merged with genomic and other structured clinical data to create a Clinicogenomic, Harmonized Oncologic Real-world Dataset (MSK-CHORD). Finally, we tested if associations not apparent in the BPC might be discoverable in MSK-CHORD. We found positive associations between Gleason score and gene-level alterations in prostate cancer including TP53, PTEN and BRCA2 ($q<0.1$), none of which were adequately powered for detection in the BPC. We found PD-L1 status was associated with better survival following immunotherapy treatment in NSCLC, but only in the larger MSK-CHORD was this association statistically significant. In breast cancer, NF1 mutations were associated with prior therapy in both cohorts, but this association was only significant in MSK-CHORD.

The infrastructure generating MSK-CHORD uses a combination of on-premise and cloud computing resources and open-source development operation applications to automate processes. Once annotations are created, data is imported into a local instance of cBioPortal, where researchers can visualize data and perform analyses. The system generating MSK-CHORD demonstrates how large-scale data delivery and integration can fuel cancer research.

CLINICAL RESEARCH: Early Detection and Progression Biomarkers
Minisymposium

#3893 A multimodal spatial-omics atlas of lung precancer and progression to adenocarcinoma.

A. Sinjab[1], F. Peng[1], Y. Liu[1], S. Yang[1], T. Zhou[1], A. G. Serrano[1], J. Feng[1], L. Gomez Bolanos[1], G. Han[1], D. G. Rosen[1], S. G. Swisher[1], A. Spira[2], S. M. D. Dubinett[3], L. M. Solis Soto[1], M. Li[4], J. Fujimoto[5], J. Burks[1], I. I. Wistuba[1], L. Wang[1], H. Kadara[1];
[1]UT MD Anderson Cancer Ctr., Houston, TX, [2]Boston University, Boston, MA, [3]The University of California Los Angeles, Los Angeles, CA, [4]University of Pennsylvania, Philadelphia, PA, [5]Hiroshima University Hospital, Hiroshima, Japan

Understanding the earliest changes during lung adenocarcinoma (LUAD) development can set the stage for discovery of fertile targets for disease interception, thereby mitigating the dire public health burden of LUAD. We previously identified bulk-level molecular and immunological changes that are enriched in normal-appearing tissue (NAT) in the local niche of human LUAD, as well as those that commence in adenomatous premalignant lesions (aPMLs, LUAD precursors) and that are further enriched in LUADs. Yet, in-depth understanding of the identities, states, and properties of specific cell subsets in NAT and precancer that trigger LUAD remain largely elusive due to inherent roadblocks to sampling and characterizing aPMLs that are at the center of this trajectory. Here, we aimed to map molecular profiles, states, and interactions of cell subsets that underlie initiation in lesion-adjacent NAT, and to determine how features of these cells evolve along the aPML-LUAD spectrum. We analyzed an expanding cohort of archived matching NATs, aPMLs and LUADs, including challenging small samples, from up to 17 patients. Samples were analyzed using combined high-resolution, multi-modal Visium spatial transcriptomics (ST, n=17) and proteomics (n=12), as well as single-cell RNA-sequencing of fixed cells (scFFPE-seq) from consecutive sections of the same tissues from 15 patients. We also studied a subset of samples by high-plex spatial proteomics (COMET) or subcellular spatial gene expression analysis (Xenium). In total, we sequenced more than half a million single cells comprising diverse epithelial, immune, and stromal subsets, which were concordant with lineage clusters identified by ST analysis of the same samples. Loss of alveolar differentiation was a hallmark of tumor cell-enriched areas in aPMLs and LUADs, with a more pronounced effect in the LUADs. Alveolar intermediate cells (AICs), which we have previously shown to be involved in LUAD initiation, were found in lesion-adjacent NAT, and their signature was enriched in matching aPMLs and further in LUADs. In line with these findings, trajectory analysis showed that AICs are derived from normal alveolar type 2 cells and likely progress towards tumor cells. Spatial neighborhood analysis pointed towards strong crosstalk between AICs and macrophages. We also noted heterogeneity in immune infiltration including patterns indicative of progressive features along the NAT-aPML-LUAD continuum. For example, B cell lineages were not only increased in abundance in LUADs relative to aPMLs, but they also mobilized into relatively more mature tertiary lymphoid aggregates/structures. While T regulatory cells aggregated close to LUADs, they were rather scattered in matching aPMLs. Our multimodal and spatial atlas of NAT, nearby aPML and LUAD elucidates the earliest cellular events underlying transition of NAT to LUAD and that could inform of targets for interception of this trajectory.

#3894 The temporal influence of the tumor microenvironment in response to checkpoint blockade.

N. F. Greenwald[1], I. Nederlof[2], H. Horlings[2], M. Kok[2], C. Curtis[1], M. Angelo[1];
[1]Stanford University School of Medicine, Palo Alto, CA, [2]Netherlands Cancer Institute, Amsterdam, Netherlands

Immune checkpoint inhibition (ICI) has produced a paradigm shift in treatment across a range of cancer subtypes. However, our understanding of why only certain patients respond, as well as our ability to predict this response, is still quite limited. This is exacerbated by the complexity of the tumor microenvironment (TME), which contains cancer cells, immune cells, and stromal cells. These differing cell types can have context-dependent roles in either promoting or inhibiting anti-tumor immune responses, making it challenging to identify features which reliably correlate with patient outcome. In addition, the roles of these diverse cell types are often influenced by their location within the TME, meaning that assays without spatial information cannot fully resolve this complexity. To address these gaps, we mapped the spatial distribution and phenotype of 21 cell populations across 117 patients with metastatic triple negative breast cancer that received nivolumab (anti-PD1) through the TONIC clinical trial (NCT02499367). We collected metastatic samples prior to and during treatment to understand how anti-PD1 reshaped the TME. We also collected archival material from the original primary tumor for each patient. We generated multiplexed imaging data from these samples, identified the location and phenotype of each cell, and then quantified the spatial distribution, diversity, and functional marker status of all cell populations in the TME. We detected numerous features indicative of a productive immune response that correlated positively with clinical benefit, whereas features indicative of a suppressive microenvironment correlated negatively with clinical benefit. We observed significant temporal effects, where many pre-treatment predictive features were not predictive on-treatment; similarly, many on-treatment predictive features had no predictive power prior to treatment. Intriguingly, we found features in the original primary tumors which predicted subsequent (metastatic) response to immunotherapy. We observed substantial differences in predictive accuracy of multivariate models based on timepoint, with on-treatment samples exhibiting the best performance and primary tumor samples exhibiting the worst. Of note, we observed substantially worse predictive performance when using bulk DNA sequencing data to predict outcome from the same patients, highlighting the importance of spatial information. Taken together, we show that the features associated with a productive anti-tumor immune response are temporally structured, and differ based on what phase of response is profiled. Furthermore, using the primary tumor to assess whether metastatic TNBC patients are good candidates for ICI may miss important predictive signals. These findings shed new light on the determinants of ICI outcome, and may shape the design of subsequent trials to better understand the temporal aspects of ICI.

#3895 Prognostic significance of blood-based multi-cancer detection in cell-free DNA: 4-year outcomes analysis.

C. Swanton[1], M. Margolis[2], E. Hubbell[2], K. N. Kurtzman[2], S. Shih[2], O. Venn[2], M. Seiden[3];

[1]Cancer Evolution and Genome Instability Laboratory, The Francis Crick Institute, London, United Kingdom, [2]GRAIL, LLC, Menlo Park, CA, [3]Gladius Therapeutics, Inc, Philadelphia, PA

Background: The third substudy of the case-control Circulating Cell-free Genome Atlas (CCGA; NCT02889978) study reported an observed 99.5% specificity and 89% cancer signal origin prediction accuracy in true positives using a refined version of a blood-based multi-cancer early detection (MCED) test. A shared cancer signal has been detected across >50 cancer types. Most cancer types do not have recommended screening and are diagnosed once symptoms present. Previous analysis of participant outcomes evaluated the prognostic significance of cancer signal detection by an earlier version of the MCED test with 3-year longitudinal follow-up data. We present a longer follow-up time with an updated statistical model to robustly account for variation in cancer type and stage (ie, a cancer spectrum) when estimating survival hazards.

Methods: The MCED test utilizes targeted methylation sequencing of plasma cell-free DNA (cfDNA) and machine learning classifiers to estimate a cancer signal from tumor-derived cfDNA. We compared observed overall survival of participants with known cancer who had 4-year longitudinal follow-up data to expected survival from Surveillance, Epidemiology, and End Results (SEER) data matched for age, sex, cancer type, and stage to account for changes in the cancer spectrum between “Cancer Signal Detected” (CSD) and “No Cancer Signal Detected” (NCSD) groups using a refined MCED test version. Hazard ratios (HR) and Kaplan-Meier curves were calculated for these groups. A one sample test was used to estimate the HR and confidence interval against a reference survival distribution. A methylation-based estimate of ctDNA abundance was used to quantify the cfDNA tumor methylated fraction (TMeF).

Results: Follow-up data were available for 2471/2513 (98%) evaluable participants with known cancer (median 46.9 mos [IQR: 22.7 - 56.0]). Among 782 (31%) participants with known cancer that died during follow-up, the MCED test detected a cancer signal in 668 (85%). Accounting for the effect of cancer type and stage, the NCSD group had better survival than the CSD group (HR 0.585 [CI: 0.474-0.712]). Both the NCSD group and the CSD group had better survival than expected SEER-based survival ($p<0.05$, HR 0.432 [0.356-0.521] and $p<0.05$, HR 0.737 [0.684-0.791], respectively). TMeF increased with clinical stage ($p<0.05$) and was lower for NCSD cancers relative to CSD cancers for all stages ($p<0.05$).

Conclusions: In the third substudy of CCGA, extended follow-up confirmed the prognostic value of CSD compared to NCSD by the refined MCED test for participants with cancer.

#3896 Time to diagnosis analysis using miRNA-based ovarian cancer prediction models.

J. Webber[1], L. Wollborn[1], S. Mishra[1], S. Alimena[1], B. Testino[1], A. Vitonis[1], D. Cramer[1], D. Chowdhury[2], K. Elias[1];
[1]Brigham and Women's Hospital, Boston, MA, [2]Harvard Medical School, Boston, MA

Background: The recent literature proposes several diagnostic Machine Learning (ML) models for ovarian cancer based on miRNA expression profiling. These ML models are trained and validated on subjects whose miRNA sample was drawn proximate to cancer diagnosis (e.g., within one month). Whether these models remain useful remote from the time of diagnosis, when early detection or prevention would be most relevant, is unclear. Therefore, we examine the effect of time between blood draw and cancer diagnosis on miRNA-based ML model accuracy and the relevance of a cancer probability score, P_C, for estimating long-term cancer risk.

Methods: The study is based on the miRNA expression profiles of 2983 total subjects, which is comprised of 1829 subjects collected as part of the Biobank at Mass General Brigham (MGB), 110 samples from the Pelvic Mass Protocol at Brigham and Women's Hospital (Cramer), and 1044 samples which were obtained from the Prostate, Lung, Colorectal, and Ovarian (PLCO) cancer screening trial. miRNA expression was measured using a pre-specified panel of 179 miRNAs optimized for serum detection using the Fireplex® circulating miRNA assay. We trained ML models using 1865 controls and 74 ovarian cancer subjects (1829 Biobank + 55 Cramer + 55 PLCO). The training cancer samples were drawn between 1 day and 14 years from diagnosis, most within 30 days. The models were then validated on 769 control and 275 ovarian cancer subjects (989 PLCO + 55 Cramer) whose time to cancer diagnosis ranges between 1 and 1814 days (up to 5 years) after blood draw. Performance was reported as Area Under the receiver operator characteristic Curve (AUC).

Results: Among the validation set cases, we observe a decreasing trend in predicted cancer probability (P_C) with increasing log time ($R = -0.34$, $p < 0.0001$), and we see a similar trend in AUC score with time. On samples drawn within 21 days of cancer diagnosis, the ML model offers an AUC = 0.88, which decreases to AUC = 0.72 on samples drawn between 21 days and one year from diagnosis, and later plateaus at AUC ~ 0.72 up to five years from diagnosis.

Out of 2928 total subjects considered in the study, 286 had multiple blood draws taken over a 5-year time period. Using this data, we analyze the change in P_C over time per subject. The results show that P_C, for the average case subject, increased by 7% per year ($p = 0.02$). In contrast, when we applied the same analysis to control subjects, P_C increased by only 1% per year on average ($p = 0.62$). Thus, monitoring changes in P_C at regular intervals could be an informative cancer diagnostic.

In terms of relative risk, subjects with $P_C < 0.5$ had a relative 5-year cancer risk of 0.74, whereas subjects with $P_C > 0.5$ had relative risk 7.4 (i.e., an order of magnitude higher).

Conclusion: The results indicate that miRNA-based ML models can be used to identify individuals at increased long-term risk of ovarian cancer and provide a tool for profiling at regular intervals to allow earlier diagnosis of disease.

#3897 Isolation and molecular characterization of exosomes from glioblastoma patients using a microfluidic device after ultrasound-based opening of the blood-brain barrier.

Abha Kumari[1], Mark Youngblood[2], Andrew Gould[2], Yoon-Tae Kang[1], Li Chen[2], Karl Habashy[2], Chris Amidei[2], Rachel Ward[2], Cristal Gomez[2], Guillaume Bouchoux[2], Michael Canney[2], Roger Stupp[2], Adam M. Sonabend[2], Sunitha Nagrath[1]

[1]University of Michigan, Ann Arbor, MI,[2]Northwestern University, Chicago, IL

Glioblastoma (GBM) is a highly aggressive tumor of the brain. Current techniques of detection like magnetic resonance imaging and tissue biopsy are inaccurate or highly invasive, requiring alternatives like liquid biopsy. Exosomes are nanosized vesicles that contain cargo, reflective of their cellular origin and have been used for early diagnosis of cancer. However, in GBM, the blood-brain barrier (BBB) leads to a paucity of pathological information in blood. This study investigates the effect of opening the BBB on circulating exosomes and their potential for early detection of GBM using a microfluidic platform (^{Glio}ExoChip). In 20 patients enrolled in a clinical trial NCT03744026, a pulsed ultrasound emitter- Sonocloud-9 was implanted into their brains to open the BBB. We show that ^{Glio}ExoChip isolates GBM-specific exosomes with a high capture efficiency using phosphatidylserine and Annexin-V chemistry. Further, the amount of circulating EVs increases twofold after opening the BBB. Finally, the correlation between tumor growth rate and the exosome concentrations is evaluated longitudinally.

Methods: ^{Glio}ExoChip is a microfluidic platform with a polydimethylsiloxane top and a glass bottom, functionalized with neutravidin-biotinylated annexin-V. Experiments are performed with GBM cell-line derived exosomes, followed by patient plasma. Isolated exosomes are characterized using Nanoparticle tracking analysis (NTA), scanning electron microscopy, Bicinchoninic acid (BCA) assay and western blot. Statistical analyses are performed using Student's t-test and Pearson correlation.

Results: The microfluidic device ^{Glio}ExoChip has a high capture efficiency of exosomes derived from GBM cell lines, *i.e.,* 93.03±3.31% and 96.77±0.72% for GBM6 and U87, respectively. NTA and BCA showed that 15 times more exosomes were captured from patient plasma when compared with healthy. Further, western blot proved the presence of a glial protein and Flotillin-1 in exosomes isolated from patients. Exosome concentrations varied with different time points after sonication and had an average twofold increase from the BBB opening. In our longitudinal study with 8 patients, an association between the volumetric enhancement of the tumor and exosome concentrations after sonication shows that the average Pearson correlation among short progression-free survival (PFS) patients was 0.73 (avg. p=0.39), while no correlation was seen among long PFS patients (avg. r value=0.10; avg. p-value=0.54).

Conclusions: A microfluidic approach was used to investigate the role of circulating exosomes using phosphatidylserine-annexin V chemistry in GBM. BBB opening via sonication leads to an increase in the average GBM-specific exosome concentrations in plasma. Thus, exosomes are promising biomarkers for early detection in GBM.

#3898 SJPedPanel: A pan-cancer gene panel for childhood malignancies.

P. Kolekar, V. Balagopal, L. Dong, Y. Liu, S. Foy, Q. Tran, H. Mulder, A. Huskey, E. Plyler, Z. Liang, J. Ma, J. Nakitandwe, J. Gu, J. Maciaszek, D. Payne-Turner, S. Mallampati, L. Wang, J. Easton, J. Klco, X. Ma;
St. Jude Children's Research Hospital, Memphis, TN

Background: Extensive efforts in the past decade have revolutionized our understanding of the genetic underpinnings of childhood malignancies and identified numerous driver alterations that can provide potential targets for novel therapy and are excellent biomarkers for disease monitoring. For these purposes, a whole genome or exome sequencing approach can be resource prohibitive. Numerous gene panels are developed for adult cancers to address these challenges. Due to the dramatic differences in driver gene landscapes between pediatric and adult cancers, a gene panel for childhood cancers is needed.
Results: Here, we have developed a gene panel dedicated to childhood cancers. This panel (2.8 Mbp) covers 5275 coding exons of 357 driver genes, 297 introns frequently involved in rearrangements that generate fusion oncoproteins, commonly deleted regions, such as CDKN2A and PAX5 (for B-/T-ALL) and SMARCB1 (for ATRT), and 7,590 polymorphism sites to detect copy number alterations for interrogating tumors with aneuploidy, such as hyperdiploid and hypodiploid B-ALL or 17q gain neuroblastoma. We used driver alterations reported from an established real-time clinical genomics cohort (n=253) to investigate the effectiveness of this gene panel. Among the 485 pathogenic variants reported, our panel covered 417 variants (86%). For 90 rearrangements responsible for oncogenic fusions, our panel covered 74 events (82%). We re-sequenced 113 previously characterized clinical specimens at an average depth of 2,500X using SJPedPanel and recovered 355 (90%) of the 396 reported pathogenic variants. Among the 30 unique genes of the 41 missed alterations, 29 genes are mutated in pediatric cancers with a low frequency (<0.21%) and hence not covered in the panel. We then investigated the power of this panel in detecting mutations from specimens with low tumor content (as low as 0.1%) using cell line-based dilution experiments and discovered that this gene panel enabled us to detect ~80% variants with allele fraction of 0.2%, while the detection rate decreases to ~50% when the allele fraction is 0.1%. We finally demonstrate its utility in disease monitoring on clinical specimens collected from AML patients in morphologic remission.
Conclusion: Overall, our gene panel enables the detection of clinically relevant genetic alterations including rearrangements responsible for subtype-defining fusions for childhood cancers by targeted sequencing of ~0.15% of human genome. Our panel will significantly enhance the analysis of specimens with low tumor burdens for cancer monitoring and early detection.

EXPERIMENTAL AND MOLECULAR THERAPEUTICS: Drug Discovery 1: New Targets and Approaches Minisymposium

#3900 A high-throughput platform identifies novel drug combinations towards acute myeloid leukemia therapy.

A. R. Soltis[1], B. Zhelyazkova[1], P. Drane[1], E. Eleftheriadis[1], A. Ventresco[1], D. A. Weitz[2], A. Lee[1], A. J. Iafrate[3];
[1]Hunter Biodiscovery, Inc., Boston, MA, [2]Harvard University, Cambridge, MA, [3]Massachusetts General Hospital, Boston, MA

Molecularly targeted therapies have reshaped oncology in recent decades, though not all patients are eligible for such treatments and resistance mechanisms limit clinical benefit. In response, combination therapies, which can induce potent synthetic lethalities, bypass drug resistance, and expand treatment options, are increasingly being developed. A major hurdle limiting novel combination therapy discovery is the sheer combinatorics associated with broadly testing two or more agents. Thus, there is a practical need for methodologies that prioritize test compounds and technologies for rapid and efficient screening. Towards these ends, we have developed a novel combination drug screening workflow that integrates machine learning-based drug synergy predictions with a high throughput droplet microfluidics-based screening platform. Our physical system, or FlowMatrix, consists of 9,216 nano wells arrayed in a 96 x 96 grid in which cells are incubated and drug compounds delivered via emulsified droplets along both its rows and columns to facilitate combination screening. Following multi-day incubation, live cells are imaged with fluorescence microscopy and drug combination synergies are calculated from cellular viabilities. In our current setup, which includes four dose drug treatments with replicates and controls, we capture complete data (control, single agent, and 4x4 drug-drug combination viability measurements) for up to 100 unique drug combinations within the 9,216 dual droplet loaded wells of one FlowMatrix. Our to-date screening efforts have focused on acute myeloid leukemia (AML) specifically, where we have profiled 12,700 AML cell line-drug combinations in our system. This encompasses >3,700 unique drug combinations profiled in 7 distinct AML cell lines with 183 total matrix runs. Among the strongest hits observed in our screens and confirmed with validation studies (~65% confirmation rate) are combinations currently being tested in clinical trials for other cancers and established therapies paired with non-cancer indicated drugs. In particular, we are interrogating combinations involving CDK12 inhibitors, which affect the transcription of DNA repair proteins, splicing, and cancer cell progression, including unexpected partner drugs that potentiate the effects of CDK12 blockade in AML cell lines. We have uncovered additional unexpected synergistic combinations with KIT inhibitors in *RUNX1-RUNX1T1* altered AML lines, ATR inhibitors (including an established combination with Gemcitabine), and the BCL-2 inhibitor Venetoclax, including known partnerships with chemotherapies (e.g. Decitabine and Daunorubicin) and other targeted inhibitors. Deeper studies are underway to further validate and characterize these candidates towards expanding treatment options for AML. Ultimately, our platform may radically enhance drug combination screening potential.

#3901 Therapeutic targeting of LGR5-positive cancer stem cells.

M. Mulero, C. Rice, S. A. Jahdav, W. Pi, A. Lin, M. Nguyen, O. Tai, **S. B. Howell**;
UCSD Moores Cancer Center, La Jolla, CA

Introduction: Destruction of cancer stem cells (CSC) is a major therapeutic goal. LGR5 marks active stem cells in many types of solid cancers. It has been very difficult to isolate good antibodies to native LGR5 and attempts to develop ADCs targeting LGR5 have not advanced. We took the alternative approach of using a natural LGR5 ligand to target monomethylauristatin (MMAE) to LGR5-expressing CSC. An Fc domain was fused to the LGR binding domains of RSPO1 and the sortase reaction was used to conjugate a Gly_3-val/cit-PAB-MMAE linker at the C-terminal end to create FcF2-MMAE. We previously reported its efficacy in ovarian models here document its activity in other aggressive cancer models.

Methods: FcF2-MMAE was produced by transient transfection in HEK293E cells and purified by a sequential Ni-NTA and ion exchange chromatography. OVCAR8 ovarian cancer cells were molecularly engineered to stably express an empty vector (OVCAR8/EV) or LGR5 (OVCAR8/LGR5.6) at a 10-fold higher level. The sortase A enzyme was produced *in E. coli*. Flow cytometry was used to quantify cell surface LGR5 in live cells using an anti-LGR5 antibody.

Results: DEPMAP tools were used to identify cell types with high levels of WNT signaling that drives expression of LGR5. FCM confirmed LGR5 expression in colon LoVo, gastric AGS and neuroblastoma SKNAS cells. All three lines were very sensitive to FcF2-MMAE; GI_{50} values in 2D cultures were: LoVo 4.5, AGS 0.7 and SKNAS 8.6 nM. IC_{50} values for stem cell-derived spheroids grown from these lines were: 11.0, 3.0 and 1.70 nM, respectively. The MTD of FcF2-MMAE was found to be >1.5 nmol/g in mice. The plasma half-life was 29.7 h. A q7dx4 IP dose schedule was found to be more effective than a q4dx4 IP schedule. FcF2-MMAE inhibited *in vivo* SC growth in all 3 models at a dose of 1 nmol/g q7dx4, producing cures in a fraction of AGS tumors and delaying SKNAS growth >2-fold in the absence adverse events. In addition to MMAE, we showed that FcF2-His could be conjugated to the either deruxtecan or PNU159682; FcF2-His loaded with either one of these cytotoxins had low nM or sub nM cytotoxicity and retained the same high selectivity of FcF2-MMAE when tested in isogenic OVCAR8/EV and OVCAR8/LGR5 cells.

Conclusions: FcF2-MMAE has activity in xenograft models of very aggressive tumors driven by high levels of WNT signaling (LoVo, AGS, and SKNAS) and LGR5 expression. Efficacy was obtained at doses well below its MTD indicating a wide therapeutic window. The FcF2 core accommodates multiple types of warheads without loss of targeting selectivity. The ability to switch out one cytotoxin for another provides versatility in targeting different diseases. FcF2-MMAE has advantages over ASCs. Its small size relative to antibodies favors better tumor penetration. The binding domains of RSPO1 also target stem cells expressing LGR4 and LGR6 as well as LGR5, something that cannot be achieved with an ADC. These features support the further development of FcF2-MMAE as a stem cell-targeted therapeutic.

#3902 The Nanoprimer: A significant opportunity to boost the efficacy of cancer therapies.

J. Devalliere, L. Poul, M. Bergere, F. Mpambani, A. Darmon, O. Jibault, M. Germain;
Curadigm, Paris, France

Nanomedicines are among the most promising novel delivery systems and are highly promising as therapeutic agents in oncology. However, their use is still limited by nanoparticle hepatic clearance which is responsible for low delivery to the target site. Moreover, the unintended liver distribution could cause harmful side effects. Curadigm's innovative Nanoprimer technology aims to shift the balance of therapeutics bioavailability and toxicity. The platform is designed to decrease nanomedicines' liver trapping and increase their systemic bioavailability for optimal accumulation in target tissues. This technology can redefine the benefit/risk ratio of therapeutics, improving their clinical outcomes and treatment value. The Nanoprimer is an engineered, biocompatible liposome that transiently and specifically occupies the cells of the mononuclear phagocytic system responsible for sub-optimal therapeutics bioavailability. The Nanoprimer is administered just before the therapeutic, temporarily reducing drug clearance and elimination. Proofs-of-concept were realized by combining the Nanoprimer with different therapeutic agents such as irinotecan-loaded liposomes and nucleic acid-loaded lipid nanoparticles (LNP). One example is a study conducted in collaboration with the Langer Lab at MIT that shows that the Nanoprimer increases mRNA- and siRNA-based therapeutics efficiency by 32% and 49% respectively. Efficacy studies in a triple-negative breast cancer mouse model reveal that the Nanoprimer increases by 2-fold the anti-tumor efficacy of siRNA LNP therapy. Data demonstrate the safety of the Nanoprimer, along with its ability to maximize the inhibition of primary tumor growth and pulmonary metastasis by systemic siRNA LNP treatment. In a collaborative study with the NCL*, the Nanoprimer was shown to stimulate the immune response in a systemic vaccine model using ovalbumin-coated gold nanoparticles (GNP-OVA). Administration of the Nanoprimer before immunization of mice by intravenous injection of GNP-OVA, results in a dramatic increase in anti-OVA antibody levels with IgGs detected as early as 7 days. Furthermore, IgG and IgM antibodies remain elevated at day 28 showing a robust and sustainable immune response. Nanoprimer ability to enhance immune response shows its great potential in immunotherapy, especially for cancer vaccines. Altogether, these data demonstrate that the ubiquitous nature of the Nanoprimer mode of action allows its application to a broad spectrum of therapeutics, from nucleic acid-loaded LNP to immunotherapy. Efficacy studies conducted in mouse models highlight the potential for the Nanoprimer to empower nanotechnology for oncology treatments. *We acknowledge NCL, Frederick National Laboratory for Cancer Research sponsored by the NCI for the help with conducting these experiments.

#3903 Discovery of ULBP6 as a novel immuno-oncology target using pleiotropic signals from 23andMe's genetic and health survey database.

S. Tilk[1], P. Fontanillas[1], W.-J. Chung[2], C. Hom[1], S. Shi[1], A. Diep[1], **K. Gerrick**[1], M. Poggio[1], P. Sood[1];
[1]23andme, Inc., South San Francisco, CA, [2]Loxo@Lilly, Stamford, CT

23andMe has assembled one of the largest platforms for human genetics research that combines genotypes from 14 million individuals, 80% of which are consented to participate in research, with billions of phenotypic data points collected from health survey data. Using these large scale genetic and phenotypic datasets, we have developed a unique target discovery platform that has identified hundreds of pleiotropic genetic variants with opposing directionality of effects in cancer and immune diseases. These immune-oncology (I/O) genetic associations point to already clinically validated immune checkpoint receptors (e.g., CTLA4) and those currently in clinical trials (e.g., CD200R1). This suggests that these I/O genetic associations could be linked to genes that are broadly utilized by tumor cells to evade the immune system and could be used to identify novel therapeutic targets involved in regulating anti-tumor immune response. Here, we utilized expression quantitative trait loci (eQTLs) and annotation of coding single nucleotide polymorphisms (SNPs) to link one of these signals to a causal gene, and identified ULBP6, a stress-induced ligand for the activating immunoreceptor NKG2D found on NK and T cells. ULBP6 is known to be shed from the cell surface of tumor cells to block its interaction with NKG2D to evade immune surveillance. Expression profiling of ULBP ligands in various tumor types using MSD, IHC, bulk and single-cell RNA-seq revealed tumor-intrinsic up-regulation of ULBP6 in squamous cancer subtypes. Collectively, these data suggest that ULBP6 is a promising therapeutic target, and that can potentially enhance anti-tumor immunity.

#3904 Multiplexed flow cytometry based immunophenotyping paired with functional *ex vivo* (MFLEX) drug profiling informs potential efficacy of therapeutic agents in acute myeloid leukemia.

R. Shah, H. Wander, M. Hsueh, M. Floren, W. Liu, P. Cheung, C. Andersen, M. White, N. Kingston, P. M. Gutierrez, L. Drew, G. Fabbri, E. Bibikova, D. Auclair; AstraZeneca US, South San Francisco, CA

Introduction: Acute Myeloid Leukemia (AML) is a heterogenous hematological malignancy with a complex clonal architecture that requires in-depth immunophenotyping for disease characterization. Conventional AML e*x vivo* models for preclinical drug screening lack functional readouts that provide single cell level data to identify drug activity in defined AML subsets with unique immune signatures. Here, we present a novel platform that links Multiparameter Flow cytometry with high-throughput *EX vivo* drug screening (MFLEX) in AML patient-derived cell models to simultaneously detect phenotypic changes and predict cell-subset specific drug responses in AML.

Method: We developed a 21-color high-dimensional immune profiling panel that captures AML heterogeneity by delineating primitive and mature AML blasts along with normal hematopoietic lineages. The panel also includes markers for functional measurement of apoptosis, proliferation, differentiation, and expression of BCL2 family proteins in lymphoid and myeloid cell subsets. *Ex vivo* culture conditions were optimized using physiologically relevant stroma-free cytokine-rich media that supports primary AML cells with minimal phenotypic shift, allowing for high throughput functional drug sensitivity testing. Timepoints and dosing conditions for AML standard of care (SoC) agents were optimized to support combination screens. Multi-parameter datasets were analysed for functional differences and visualized using dimension reduction methods.

Results: We tested MFLEX on clinically annotated AML samples to understand sensitivity profiles to venetoclax and combination partners: 5-azacytidine, cytarabine, fludarabine and gilteritinib. We identified distinct drug sensitivity profiles for venetoclax in AML patients with varying leukemic differentiation states where M0/M1 subtypes were more sensitive to therapy than M4/M5. We also observed cell lineage specific sensitivities, with myeloid blast being more sensitive to venetoclax compared to autologous CD4+ and CD8+ T-cells and this observed difference was correlated with higher expression of BCL2. Our platform demonstrated that patients who previously failed venetoclax therapy could benefit from a combination with 5-azacytidine or fludarabine and this was patient-specific. We further evaluated MFLEX's predictive value for patient clinical response by systematically comparing venetoclax sensitivity in patient-derived xenograft models *in vivo* vs *ex vivo* and found a high correlation between drug responses.

Conclusion: We have established a unique, immune drug screening platform, MFLEX, that has high translational value and can be implemented in clinical trials to identify drug response patterns, novel combinations, and potential biomarkers of response for patient stratification in AML.

#3905 Targeting RNA demethylase ALKBH5 blocks growth and improves therapy response in osteosarcoma.

D. Medina, S. Timilsina, P. Subbarayalu, P. P. Venkata, D. Singh, T. Do, S. Zhou, Y. K. Gupta, D. Zhou, M. K. Rao;
UT Health Science Center at San Antonio, San Antonio, TX

Background: Osteosarcoma (OS) arises primarily in children and adolescents, with a second peak in incidence in those over the age of 50. Unfortunately, outcomes of patients with metastatic or relapsed osteosarcoma have remained abysmal. Moreover, patients who survive have a highly compromised quality of life due to debilitating side effects associated with chemotherapy drugs. Virtually no new drug has been approved for treating OS in the last three decades. Recently our group showed that ALKBH5 is critical for promoting OS growth and metastasis and may thus serve as a unique driver of OS. We therefore hypothesized that epigenetic changes, specifically mRNA demethylation mediated by the RNA demethylase ALKBH5, play a pivotal role in OS growth and metastasis, and hence approaches aimed at inhibiting ALKBH5 activity could prove clinical utility for patients with OS.
Methods: shRNA and CRISPR-Cas9-based knockout were used to study the effect of depleting ALKBH5 in osteosarcoma and the effect it has on growth and metastasis. Fluorescence-based high-throughput screening (HTS) assay was used to identify targets of ALKBH5. FDA-approved and LOPAC compound libraries were used. SPR analysis was used to determine the Mefloquine-ALKBH5 interaction. *In vitro* and *In vivo* intratibial orthotopic models were used to test the efficacy of Mefloquine for blocking OS growth. Experiments are currently underway to test the effect of combining Mefloquine and doxorubicin in inhibiting OS growth and metastasis.
Results: We showed that upregulation of the ALKBH5 attenuates histone H2A monoubiquitination to result in the induction of key pro-tumorigenic genes and consequently unchecked cell cycle progression, incessant DNA replication, and upregulation of DSB repair. Unbiased high throughput screening using a LOPAC library identified mefloquine as a potential ALKBH5 inhibitor. SPR analysis showed the interaction of Mefloquine with ALKBH5 catalytic domain. M^6A dot blot confirmed that mefloquine inhibits the catalytic activity of ALKBH5. Cell-based assays showed reduced short-term and long-term growth with the treatment of mefloquine. *In vivo* models showed a reduction in tumor volume upon mefloquine oral treatment.
Conclusion: Our results establish RNA demethylase ALKBH5 as a novel driver of OS. This project has a direct translational relevance as an FDA-approved drug can be repurposed for treating OS patients as a monotherapy or in combination with doxorubicin and be formally tested in the clinic without much delay.

#3906 *Ex vivo* breast tumors for understanding the patient specific tumor microenvironment remodeling and drug responses.

E. Martin[1], M. Benz[2], K. Hebert[2], E. Byrne[3], F. Lau[1];
[1]Keliomics, Portland, OR, [2]Tulane University, New Orleans, LA, [3]Louisiana State University, Baton Rouge, LA

Breast cancer is a heterogeneous disease driven by cell-intrinsic and cell-extrinsic signaling cues. Many of these cues derive from the tumor microenvironment (TME), which is composed of adipocytes, vasculature, stem cells, immune cells, and the extracellular matrix (ECM). Through these diverse components, the TME modulates cellular proliferation, survival, and ultimately response to therapy. Despite this high-level understanding of tumor-TME crosstalk, no existing pre-clinical models accurately capture the TME *in vitro*. We overcame that hurdle by developing a method to maintain healthy human breast tissue (HBT) alive *ex vivo* for at least 8 weeks. By culturing breast cancer cells in that HBT, we created ex vivo breast tumors (EVBTs) that retained patient-specific features relevant to breast cancer including menopause status, obesity status, and response to therapy. Using these EVBTs, we demonstrate breast cancer subtype-specific alterations in lipid accumulation, ECM remodeling, and cytokine profiles. RNA sequencing showed that breast cancer cell line signatures were retained in the EVBTs system at 1 week and 2 weeks *in vitro*. We demonstrated donor-specific transcriptional changes to the core matrisome gene set. Finally, we demonstrate that our EVBTs retained patient-specific heterogeneity in response to standard of care endocrine therapy and neoadjuvant chemotherapies. Our novel tumor model allows for 1) real-time examination of breast cancer interactions with HBT and the TME and 2) the isolation of breast cancer-specific factors vs. patient-specific factors in the development and progression of breast cancer.

EXPERIMENTAL AND MOLECULAR THERAPEUTICS: Novel Molecular Targets and Biomarkers Minisymposium

#3907 Novel public and tumor-wide neoantigens arising from clonal aberrant splicing events drive tumor-specific T-cell responses across diverse cancer types.

Darwin Kwok[1], Nicholas O. Stevers[1], Takahide Nejo[1], Lee H. Chen[1], Inaki Etxeberria[2], Jangham Jung[1], Kaori Okada[1], Maggie Colton Cove[1], Senthilnath Lakshmanachetty[1], Marco Gallus[1], Abhilash Barpanda[1], Chibo Hong[1], Gary KL Chan[1], Samuel H. Wu[1], Emilio Ramos[1], Akane Yamamichi[1], Jerry YZ Liu[1], Payal Watchmaker[1], Hirokazu Ogino[1], Atsuro Saijo[1], Aidan Du[1], Nadia Grishanina[1], James Woo[1], Aaron Diaz[1], Susan M. Chang[1], Joanna J. Phillips[1], Arun P. Wiita[1], Christopher A. Klebanoff[2], Joseph F. Costello[1], Hideho Okada[1]

[1]UCSF - University of California San Francisco, San Francisco, CA,[2]Memorial Sloan Kettering Cancer Center, New York City, NY

BACKGROUND: Immunotherapy in gliomas is limited by intratumor heterogeneity (ITH) and low mutational burden. We developed a novel comprehensive *in silico* pipeline for detecting tumor-specific splicing events (neojunctions), and across multiple cancer types, we successfully identified a new class of tumor-wide, public, alternatively spliced neoantigens (ASNs) that elicit CD8+ T-cell-mediated immune responses.

METHODS: Our pipeline identified recurring public neojunctions expressed in TCGA RNA-seq (positive sample rate (PSR) > 10%) and not in GTEx normal tissue RNA-seq data (PSR < 1%) across ten cancer types. To characterize tumor-wide neojunctions, we utilized available multi-site RNA sequencing across diverse cancer types. With gliomas, our in-house dataset comprised of 56 patients with approximately 10 maximally-distanced intratumoral biopsy sites per patient (*n*=535). Tumor-wide public neojunction expression was subsequently validated in RNA-sequencing and mass spectrometry (MS) data from patient-derived cell lines (*n*=68) and samples (*n*=447). Two independent algorithms then predicted peptide processing likelihood and HLA-binding affinity of ASN candidates. TCRs identified by *in vitro* sensitization (IVS) of donor-derived CD8+ T-cells followed by 10x VDJ scRNA-seq, were transduced into CD8+ T-cells and co-cultured with tumor cells to evaluate TCR functionality and cytotoxicity.

RESULTS: Pan-cancer analysis identified large subsets of neojunctions that were interpatiently and intratumorally conserved. Our glioma-specific analysis identified 789 public neojunctions, and 8 ASNs were validated in transcriptomic and proteomic glioma data and predicted to be presented by HLA-A*02:01 with high confidence. IVS and subsequent 10x VDJ scRNA-seq on expanded PBMC-derived CD8+ populations cultured against ASN-pulsed dendritic cells identified TCR clonotypes reactive against neojunctions in *RPL22* (*n*=7) and *GNAS* (*n*=1), the latter being highly intratumorally-conserved (detected in > 90% of spatially-mapped biopsies in 17/56 patients (26.78%)). TCR-transduced T-cells demonstrated recognition and immunogenic activation against endogenously processed and presented neoantigens in both pan-cancer cell lines and transfected COS7 cells and cytotoxicity against glioma cell lines. Pan-cancer analysis revealed the detection of both neojunctions in various tumor types beyond gliomas, with the GNAS neojunction notably found tumor-wide in mesothelioma, prostate cancer, and liver hepatocellular carcinoma spatial data.

CONCLUSION: Our unique integrative pipeline identified a novel class public tumor-wide splice-derived neoantigen candidates and ASN-specific TCRs, offering a promising off-the-shelf immunotherapy approach for diverse cancer types and tackling the critical challenge of ITH in immunotherapy resistance.

#3908 DHX9 inhibition as a novel therapeutic for cancer with loss-of-function mutations in DNA damage repair genes BRCA1 and BRCA2.

J. B. Castro, M. H. Daniels, S. Nayak, M. Laidlaw, D. Brennan, B. T. Johnston, J. Wu, A. Raman, C. Lu, S. J. Blakemore, S. J. Silver, P. Boriack-Sjodin, K. W. Duncan, J. A. Sager, R. A. Copeland;
Accent Therapeutics, Lexington, MA

DHX9 is a DEAH-box RNA helicase which can unwind regions of double-stranded DNA and RNA but has a greater propensity for secondary structures such as DNA/RNA hybrids (R-loops), circular RNA and DNA/RNA G-quadruplexes. Given the delicate balance of R-loop formation and resolution in maintaining efficient transcription and replication, the ability of DHX9 to unwind R-loops is important in helping to maintain genomic stability. In addition, DHX9 can interact and regulate a large variety of proteins, including key proteins in DNA damage repair pathways such as BRCA1, ATR, Ku86, and WRN. Previously we demonstrated that DHX9 inhibition was efficacious in microsatellite high (MSI-H) CRC xenograft tumor models. Efficacy attributed to DHX9 loss in MSI-H correlates with defective DNA repair pathways such as mismatch repair (MMR). Here we report results of preclinical studies in ovarian and breast cancer models that indicate patients with Loss-of-Function (LOF) mutations in the DNA damage repair genes BRCA1 and/or BRCA2, may also benefit from DHX9 inhibitor treatment. DHX9 small molecule inhibitor ATX968 was tested for anti-proliferative activity in a large cell panel of 300 cell lines, and bioinformatic analyses was performed to identify molecular variants that co-associate with sensitivity or resistance cell proliferation outcomes. Notably, selective dependency on DHX9 was observed in both ovarian and breast cancer cell lines that exhibit BRCA LOF, as defined by somatic mutations including single-nucleotide variants and/or copy number loss in BRCA1 and/or BRCA2. DHX9 inhibition leads to increased RNA/DNA secondary structures such as R-loops and G-quadruplexes, resulting in subsequent DNA damage and increased replication stress. Cell lines that exhibit BRCA LOF appear unable to resolve this replication stress and show S-G2 phase cell cycle arrest prior to onset of apoptosis. Furthermore, a potent and selective DHX9 inhibitor tool compound was dosed orally *in vivo* to assess DHX9 dependency within multiple human xenografts representing triple negative breast cancer and high-grade serous ovarian cancer with BRCA LOF. In all models, the tool DHX9 inhibitor was dosed orally at 100 mg/kg BID and it was well tolerated for a period of up to 28 days. Robust and significant tumor growth inhibition and regression was observed in multiple BRCA LOF models with minimal tumor growth inhibition observed in BRCA1 and BRCA2 wild type xenograft models. These results extend the opportunity for DHX9 inhibition to provide therapeutic benefit for patients with solid tumors beyond what was previously reported for MSI-H CRC. Together, this preclinical data package validates DHX9 as a tractable new target with potential utility as a novel treatment for patients with defective DNA repair, such as MMR and BRCA1 and/or BRCA2 LOF, across multiple tumor types including colorectal, breast and ovarian cancer.

#3909 PARG inhibitor sensitivity is correlated with accumulation of single strand DNA gaps in preclinical models of ovarian cancer.

R. Ravindranathan, O. Somuncu, Y. Jiao, A. da Costa, B. Lamarre, D. Martignetti, G. Zambrano, S. Mukkavalli, J. Liu, B. Kochupurakkal, J.-B. Lazaro, K. Parmar, G. Shapiro, A. D'Andrea;
Dana Farber Cancer Institute, Boston, MA

Poly (ADP-ribose) glycohydrolase (PARG) is a dePARylating enzyme which promotes DNA repair in conjunction with PARP1 by removal of poly (ADP-ribose) (PAR). Loss or inhibition of PARG results in replication stress and sensitizes cancer cells to DNA damaging agents, suggesting it is a potential therapeutic target for cancer therapy. Indeed, PARG inhibitors are now undergoing clinical development for patients having tumors with homologous recombination deficiency (HRD), such as ovarian and breast cancer patients with *BRCA1/2*-mutation. In this study, we investigated PARG inhibitor (PARGi)-PDD00017273 activity in preclinical models of ovarian cancer cell lines and primary patient-derived organoids. PARGi exhibited sensitivity in a subset of ovarian cancer cell lines that was distinct from PARP inhibitor sensitivity. Initially, we evaluated a PARGi-sensitive cell line, RMUGS. By gradually increasing the concentration of PARGi, we generated drug resistant cells. PARGi treatment resulted in increased S phase specific PAR, DNA-PARylation, DNA damage, and replication stress in the sensitive cells but not in cells with *de novo* or acquired resistance. In the sensitive cells, PARGi exposure also increased accumulation of PAR at the replication fork resulting from unligated Okazaki fragment processing. More importantly, PARGi treatment or PARG loss caused accumulation of single strand DNA (ssDNA) gaps in sensitive cells, as detected by the DNA fiber assays combined with S1 nuclease treatment. Regardless of the *BRCA*-status, the induction of ssDNA gaps in ovarian cancer cells correlated with PARGi sensitivity. Consistent with an increase in ssDNA gaps, PARGi exposure increased p-RPA, a ssDNA surrogate, at the replication fork in sensitive cells. p-RPA sites also colocalized with PAR suggesting that accumulation of PAR occurs at the ssDNA sites, perhaps, leading to the ssDNA gaps. Collectively, these results suggested that toxic accumulation of PAR at the replication fork leads to accumulation of ssDNA gaps due to Okazaki fragment processing defects and ovarian cancer cell killing after PARG inhibition. We further assessed PARG inhibition in patient-derived organoids (PDOs) and patient-derived xenograft (PDX)-derived organoids (PDXOs) as model systems of ovarian cancer. PARGi exhibited monotherapy activity in specific HR-deficient PDOs and PDXOs with *BRCA1* or *RAD51C* mutation and in a HR-proficient PDXO model. Importantly, PARGi exposure resulted in accumulation of ssDNA gaps in organoids of ovarian cancer and this phenotype directly correlated with drug sensitivity. PDOs can therefore be a useful model system for testing PARGi sensitivity. The detection of ssDNA gaps in PDOs may provide a functional biomarker to predict the response to PARG inhibitors in clinical trials.

#3910 The Atlas of Blood Cancer Genomes: A resource for therapeutic and biomarker development.

J. Shingleton[1], R. Pillai[2], S. Ondrejka[3], G. Bhagat[4], A. Chadburn[5], M. McKinney[1], J. Koff[6], D. Soliman[7], M. Czader[8], A. Louissaint[9], S. Li[10], C. Ong[11], A. Behdad[12], A. Evens[13], Y. Natkunam[14], M. Pedersen[15], S. Leppa[16], E. Tse[17], J. Chapman[18], C. Amador-Ortiz[18], Y. Fedoriw[19], A. Evans[20], J. Yan[21], M. Xu[22], K. Naresh[23], C. Parker[24], D. Hsu[1], S. Dave[1],

[1]Duke University, Durham, NC, [2]City of Hope Comprehensive Cancer Center, Duarte, CA, [3]Cleveland Clinic Taussig Cancer Institute, Cleveland, OH, [4]Columbia University Irving Medical Center, New York, NY, [5]Weill Cornell Medicine, New York, NY, [6]Emory University School of Medicine, Atlanta, GA, [7]Hamad Medical Corporation, Doha, Qatar, [8]Indiana University School of Medicine, Indianapolis, IN, [9]Massachusetts General Hospital, Boston, MA, [10]MD Anderson Cancer Center, Houston, TX, [11]National Cancer Centre Singapore, Singapore, Singapore, [12]Cleveland Clinic Florida, Weston, FL, [13]Rutgers Cancer Institute of New Jersey, New Brunswick, NJ, [14]Stanford University School of Medicine, Stanford, CA, [15]University of Copenhagen, Copenhagen, Denmark, [16]University of Helsinki, Helsinki, Finland, [17]University of Hong Kong, Queen Mary Hospital, Hong Kong, Hong Kong, [18]University of Miami Health Systems, Miami, FL, [19]University of North Carolina, Chapel Hill, NC, [20]University of Rochester Medical Center, Rochester, NY, [21]University of Toronto, Toronto, ON, Canada, [22]Yale School of Medicine, New Haven, CT, [23]Fred Hutchinson Cancer Research Center, Seattle, WA, [24]Data Driven Bioscience Inc., Durham, NC

Developing a novel cancer therapy is an expensive, time-consuming, high-risk endeavor that involves identifying a molecular target as well as target indications. This process could be accelerated by a comprehensive interrogation of driver variants and gene expression profiles across cancer types. The Atlas of Blood Cancer Genomes (ABCG) project was initiated to elucidate the molecular basis of all leukemias and lymphomas, building on advances in genomic technologies, our capabilities for data analysis, and economies of scale.

The ABCG project includes collaborators from 25 institutions worldwide who contributed samples from 10,512 patients comprising every type of blood cancer in the World Health Organization classifications. All cases were de-identified and their associated pathology and clinical information entered into a purpose-built web-based system. All cases underwent pathology and clinical data review by experienced hematopathologists and oncologists. Samples were subjected to whole exome DNA and RNA sequencing.

We examined three classes of therapeutic targets with selected examples of application: 1. Surface markers: Surface markers are targets of many approved and experimental therapies in blood cancers (CAR-T cells, monoclonal and bispecific antibodies). We found that CD22, which has been evaluated as a target in diffuse large B-cell lymphoma (DLBCL), is also highly expressed in follicular lymphoma, adult ALL, mantle cell lymphoma, and high-grade B cell lymphoma, all areas of clinical need. We can evaluate the expression of virtually any marker or combination of markers across all blood cancers while noting areas of greatest clinical need within and across diseases, providing the basis to reclassify diseases by therapeutic target. 2. Genetic targets: Our work assesses the entire spectrum of genetic alterations including mutations and fusions. We found targetable alterations including BCR-ABL1 fusions, EZH2 Y641, IDH2 R140Q and BRAF V600E mutations in multiple cancers, albeit at low frequency, pointing to potential new indications for existing drugs in subsets of rare diseases. 3. Complex targets (immune or expression signatures or combinations of gene variants): Past work defined DLBCL immune and other signatures associated with response to avadomide, a novel cereblon inhibitor. We found that these signatures are also highly expressed in large subsets of peripheral T-cell lymphomas and acute myeloid leukemia, both areas of major unmet clinical need. Thus, we can interrogate immune and other signatures across the spectrum of cancers to uncover potential biomarkers of response.

The ABCG project will enable the comprehensive study of genomic and clinicopathological features of all blood cancers. We anticipate that our data, approaches and results will provide a lasting resource for molecular classification and therapeutic development in all leukemias and lymphomas.

#3911 A FGFR-p53 developmental signaling axis drives progression of salivary cancer.

Julia M. R. Billington[1], Adele M. Musicant[2], Jessica L. Cote[3], Jennifer Modliszewski[4], Yi-Hsuan Tsai[4], Luane J. B. Landuau[5], John Powers[1], Renee Betancourt[6], Radhika Sekhri[7], Ricardo J. Padilla[8], Juan C. Hernandez-Prera[9], David N. Hayes[7], Trevor G. Hackman[10], Omer Gokcumen[5], Sarah M. Knox[11], Jimena Guidice[12], Antonio L. Amelio[13]

[1]Department of Tumor Microenvironment & Metastasis, H. Lee Moffitt Cancer Center, Tampa, FL,[2]Graduate Curriculum in Genetics and Molecular Biology, Biological and Biomedical Sciences Program, University of North Carolina at Chapel Hill, Chapel Hill, NC,[3]Department of Cell Biology and Physiology, University of North Carolina at Chapel Hill, Chapel Hill, NC,[4]Bioinformatics Core, University of North Carolina at Chapel Hill, Chapel Hill, NC,[5]Department of Biological Sciences, University at Buffalo, Buffalo, NY,[6]Department of Pathology and Laboratory Medicine, University of North Carolina at Chapel Hill, Chapel Hill, NC,[7]Department of Medical Oncology, University of Tennessee Health Sciences West Cancer Center, Memphis, TN,[8]Division of Diagnostic Sciences, University of North Carolina at Chapel Hill, Chapel Hill, NC,[9]Department of Pathology, H. Lee Moffitt Cancer Center, Tampa, FL,[10]Department of Otolaryngology/Head and Neck Surgery, University of North Carolina at Chapel Hill, Chapel Hill, NC,[11]Department of Cell and Tissue Biology; Program in Craniofacial Biology, University of California San Francisco, San Francisco, CA,[12]Department of Cell Biology and Physiology; McAllister Heart Institute, UNC School of Medicine, University of North Carolina at Chapel Hill, Chapel Hill, NC,[13]Department of Tumor Microenvironment & Metastasis; Head and Neck Oncology Program, H. Lee Moffitt Cancer Center, Tampa, FL

Mucoepidermoid carcinoma (MEC) is the most frequently occurring salivary gland (SG) malignancy. Treatments for high grade (HG) MEC are lacking due to a limited understanding of its diverse histological and clinical features. Consequently, patients with non-resectable HG MEC are often treated with adjuvant radiotherapy and suffer from increased rates of recurrence and metastasis with poor 5-year survival rates (30-50%) as compared to low grade (LG) MEC (76-95%). We previously demonstrated a role for IGF-1 signaling, an important mediator for SG development and branching morphogenesis, in MEC pathogenesis (Musicant et al, 2021). Here, we analyzed transcriptome profiles shared between fetal and adult normal parotid (PAR) tissues with MEC tumors to investigate programs involved in MEC progression. Using this information, we developed the first genetically engineered mouse model (GEMM) of advanced HG MEC via targeted oncogene expression in SG ductal cells. MEC samples from 21 PAR tumors (8 LG/13 HG), 8 age-matched normal, and 3 fetal PAR glands aged between 22-24 weeks of gestation (Saitou et al, 2020) were retrospectively collected from UCSF or UNC Surgical Pathology. RNAseq was performed on FFPE samples using Illumina HiSeq. Differential gene expression, gene set enrichment analyses (GSEA), and alternative splicing analyses were compared between fetal/normal/MEC according to tumor grade and CRTC1 (CREB-regulated transcription coactivator 1)/MAML2 (Mastermind-like 2) (C1/M2) status. Based on these analyses, we developed a GEMM combining C1/M2 expression with TP53 loss. GEMM tumors were subjected to RNAseq and reviewed by two independent pathologists for diagnostic confirmation of HG MEC.GSEA revealed significant overlap between MEC tumors and fetal SG for genes governing proliferation and developmental pathways associated with branching morphogenesis. Interestingly, upregulation of the negatively regulated p53 target FOXM1 along with a mutant-p53 gene signature (Troester et al, 2006) revealed that p53 dysregulation in HG tumors phenocopies that seen in fetal SG. Cre-inducible expression of C1/M2 alone was insufficient to induce MEC-like lesions when targeted to distinct salivary cell types (ductal Krt14-CreER, acinar Mist1-CreER, serous demilune Dcpp1-CreER). However, p53 alteration ($Tp53^{KO}$) with ductal C1/M2 expression drove MEC formation with histological and molecular features of human HG-MEC. Notably, transcriptome profiles implicate an FGFR-p53 developmental signaling axis in MEC progression. Our autochthonous GEMM recapitulates advanced HG-MEC *in vivo* providing the field with a powerful platform for identifying pathways for developing targeted therapies. Taken together, the integrated bioinformatics and mouse modeling of this study provide a critical step toward elucidating salivary MEC progression and suggest a role for FGFR targeted therapies in the treatment of non-resectable HG MEC.

#3912 ATM and PARP combined inhibition demonstrate synergistic antitumor efficacy in osteosarcoma models.

S. N. Kocinsky[1], J. J. Morsby[1], W. C. Wright[1], M. Wierdl[1], C. S. Wechsler[2], G. Alexe[2], P. Geeleher[1], K. Stegmaier[2], L. M. Guenther[1];
[1]St. Jude Children's Research Hospital, Memphis, TN, [2]Dana-Farber Cancer Institute, Boston, MA

Signatures of BRCAness are found in many osteosarcoma (OS) tumors, driving an interest in PARP inhibition (PARPi) for OS treatment. Although PARPi have shown limited efficacy as OS monotherapy, rational combination strategies have not yet been explored for this disease. We performed a genome-scale loss-of-function CRISPR-Cas9 screen in two OS cell lines in the presence and absence of olaparib, a small molecule PARPi. *ATM* knockout (KO) scored highly as a potent synergizer of PARPi across both cell lines. Here we report this screen finding as well as *in vitro* validation of PARPi and ATM inhibition (ATMi) synergy in OS models.

OS cell lines SAOS2 and CAL72 were infected with the Avana genome-scale lentiviral CRISPR library, targeting 20,000 genes with 4 uniquely barcoded guides (sgRNAs) per gene. After infection and antibiotic selection, cells were grown in an IC_{40} dose of olaparib or matched control for 18 days. Following DNA sequencing of barcodes and rigorous quality control, sgRNA dropout hits were calculated against the control arm. *ATM* KO sensitizing to PARPi was first validated utilizing a CRISPR-based genetic approach. *ATM* KO in CAL72 and SAOS2 was performed via lentiviral infection. After KO confirmation by western immunoblotting (WB), *ATM* KO and control KO cells were treated with PARPi in a dose range of 19.5 nM-10 µM. ATP-based and Incucyte assays were used to quantify differential cell viability. Secondly, the combination of a small molecule ATMi and a PARPi was studied in a panel of OS cell lines. Synergistic cytotoxicity was quantified using the Zero Interaction Potency (ZIP) model. DNA damage levels after PARPi and ATMi (by chemical inhibition and genetic KO) were assessed by WB for γH_2AX, a marker of DNA double-stranded breaks (DSBs).

In our genome-scale CRISPR screens, ATM arose as a top druggable hit across both lines. Reassuringly, *PARP1* KO scored as a top resistance mediator to PARPi, confirming biologic relevance of the screen and supporting the known PARP-trapping mechanism of these drugs in OS. At low-throughput, *ATM* KO lines trended toward increased sensitivity to PARPi in short-term viability assays. Combined chemical inhibition yielded highly synergistic ZIP scores across OS cell lines; synergy was achieved with both drugs in the low nanomolar range. γH_2AX levels were substantially increased in the setting of combined PARPi and ATMi (via chemical inhibition or genetic KO) as compared to inactivation of either PARP or ATM alone, indicating increased presence of DNA DSBs.

In conclusion, these data demonstrate synergy of ATM and PARP inhibition, providing promise for their potential combined use in the treatment of OS. Accumulation of DNA DSBs in response to PARP and ATM inactivation suggests a shared role in DNA damage repair as the molecular basis of synergism. Ongoing studies are investigating anti-tumor potential in *in vivo* OS models and exploring the mechanistic impact of the combination in OS tumors.

#3913 Molecular mechanism of action and targets of glucocorticoids in lymphoma therapy.

J. Choi[1], M. Ceribelli[1], J. D. Phelan[1], B. Haupl[2], D. Huang[1], G. W. Wright[1], T. Hsiao[1], V. Morris[1], F. Ciccarese[3], B. Wang[1], S. Corcoran[1], S. Scheich[1], X. Yu[1], W. Xu[1], Y. Yang[1], H. Zhao[1], J. Zhou[1], G. Zhang[1], J. Muppidi[1], G. G. Inghirami[4], T. Oellerich[2], C. J. Thomas[1], W. H. Wilson[1], L. M. Staudt[1];

[1]National Institutes of Health, Bethesda, MD, [2]Goethe University, Frankfurt, Germany, [3]Veneto Institute of Oncology IOV-IRCCS, Padova, Italy, [4]Weill Cornell Medicine, New York, NY

Prednisone is an anti-inflammatory glucocorticoid (GC) that is cytotoxic for normal and malignant B cells and, on this basis, has long been included in combination chemotherapies to treat aggressive B-cell lymphomas. However, the mechanisms by which GCs kill malignant lymphoma cells still largely remains elusive due to the pleiotropic consequences of GC binding to the glucocorticoid receptor (GR; *NR3C1*), a ligand-induced transcription factor. This prompted us to search for critical direct targets of GC action with the hypothesis that GCs may inhibit key survival pathways in lymphomas. To determine effector genes that increase glucocorticoid toxicity, we performed genome-wide CRISPR-Cas9 screens in the presence and absence of prednisolone. Screens in cell line models of Burkitt lymphoma (BL) and diffuse large B cell lymphoma (DLBCL) revealed strong synergy between GC treatment and inactivation of genes encoding components of the B cell receptor (BCR) signaling pathway (≥2 SD). To identify direct transcriptional GR targets and binding sites genome-wide, we performed the cleavage under targets and release using nuclease (CUT&RUN) assay and integrated this dataset with RNA-seq upon GC treatment. The pairwise comparison analysis ($p<0.05$) for GR-bound genes across BL and DLBCL cell lines revealed a significant enrichment of negative regulators of BCR/PI3K signaling and BCR-related tumor suppressors (*LAPTM5, KLHL14, ARID5B, DDIT4, DAPP1, INPP5D*, and *CSK*). Interestingly, expression of CSK, an inhibitor of all Src-family kinases (SFKs), was repressed while that of other BCR negative regulators were directly activated by binding of GR. Combinatorial deletion of activated genes counteracted the toxicity of GC up to 83.9%. In contrast, depletion of CSK paradoxically increased the cytotoxic effects of GC in BCR-dependent aggressive lymphoma with decreased proximal BCR signaling. To gain further insights on CSK function in aggressive lymphomas, we performed phospho-proteome and ubiquitinome profiling by treating lymphoma models with a small molecule inhibitor of CSK kinase activity (CSKi). The CSKi treatment initially increased constitutive BCR signaling, as expected, but then triggered exuberant ubiquitination of the LYN, HCK and BLK, leading to their proteasomal degradation. Consequently, the CSKi blocked BCR-dependent NF-κB activation in ABC DLBCL models and BCR-dependent PI3 kinase activation in models of GCB DLBCL and BL. In summary, inhibition of oncogenic BCR signaling is a major mode of action for GCs. Furthermore, small molecule inhibition of CSK kinase activity potentiated the effect of GCs on oncogenic BCR signaling and strongly synergized with GCs in killing ABC and GCB DLBCL models in vitro and preventing the growth of ABC and GCB DLBCL and patient-derived xenografts, warranting the development of clinical-grade CSK inhibitors for the treatment of these aggressive cancers.

IMMUNOLOGY: Immune Targets and Therapies
Minisymposium

#3914 IGSF8 is a novel innate immune checkpoint and cancer immunotherapy target.

X. Liu[1], Y. Li[2], X. Wu[2], H. Liu[2], H. Liu[2], C. Sheng[1], Q. Ding[2], Y. Tang[2], C. Liu[2], B. Xie[2], X. Xiao[2], Q. Yu[2], R. Zheng[2], X. Hu[1], T. Xiao[2];
[1]Gv20 Therapeutics LLC, Cambridge, MA, [2]Shanghai Xunbaihui Biotechnology Co., Ltd, Shanghai, China

Background: Loss of MHC-I antigen presentation is often associated with T-cell excluded tumors, and represents a common mechanism of both primary and acquired resistance to immune checkpoint blockade (ICB) treatment. MHC-I normally acts as a marker of “self” and cells that lack MHC-I are recognized and killed by innate immunity. In this study, we investigated the mechanism of innate immune evasion in tumors with MHC-I antigen presentation defects.
Methods: Integrating functional genomics, big data, and artificial intelligence, we discovered that IGSF8 expressed on cancer cells is an evolutionarily conserved innate immune checkpoint. IGSF8 is normally expressed in neuronal tissues and is not essential *in vitro* or *in vivo*. However, knockout of IGSF8 in B16-F10 melanoma cell line decreased tumor growth *in vivo*. For clinical relevance of IGSF8 in tumor immunity, we analyzed genomics, transcriptomics, and clinical data from The Cancer Genome Atlas (TCGA). We developed an antibody (GV20-0251) against IGSF8 and tested its function to induce immune cell killing of cancer cells *in vitro* and inhibit tumor growth *in vivo*.
Results: IGSF8 has receptors on both natural killer (NK) cells and dendritic cells (DC) to strongly suppress NK cytotoxicity and antigen presentation. In the TCGA tumor profiles, IGSF8 has highest mRNA expression in melanoma and is significantly overexpressed in many cancer types. IGSF8 also shows frequent copy number amplifications. In addition, IGSF8 expression is associated with low antigen presentation, low immune infiltration, and worse overall survival in patients with low MHC class I expression. Immunohistochemistry staining of various cancers showed that IGSF8 expression was primarily observed in malignant cells with low MHC-I. We developed a cross-species reactive antibody against IGSF8 (GV20-0251) which blocks IGSF8 interaction with NK and DC. Flow cytometry of the tumor infiltrating CD45+ cells revealed that IGSF8 inhibition significantly increased NK and dendritic cell infiltration. GV20-0251 enhances NK killing of cancer cells *in vitro* and increases antigen presentation, NK-mediated cytotoxicity, and T cell signaling *in vivo*. In multiple syngeneic tumor models (B16-F10, CT26, LLC, 4T1 and EMT6), anti-IGSF8 shows single-agent efficacy and is synergistic with anti-PD1 in controlling tumor growth.
Conclusions: IGSF8 is a novel innate immune checkpoint and cancer immunotherapy target. A phase 1 study is ongoing to explore the IGSF8 inhibitor GV20-0251 in patients with advanced or metastatic solid tumors (NCT05669430).

#3915 BMS-986442 (AGEN1777), a novel TIGIT/CD96 bispecific antibody, demonstrates superior monotherapy and combination activity versus conventional anti-TIGIT antibodies in preclinical models.

R. Ward[1], N. Ramsay[1], S. Campbell[1], H. Patel[1], M. Bushell[1], B. M. Morin[1], B. Wensley[1], D. A. Savitsky[1], P. Garcia-Broncano[1], B. Joshi[1], E. Briend[1], O. Ignatovich[1], Z. Jawad[1], N.-P. Rudqvist[1], N. Wilson[2], **D. Chand**[1];

[1]Agenus Inc, Lexington, MA, [2]Bristol Myers Squibb, Redwood City, CA

TIGIT immune checkpoint blockade can enhance anti-tumor immunity, however conventional anti-TIGIT antibodies have shown suboptimal activity in the clinic. Here, we present the first preclinical disclosure of BMS-986442 (AGEN1777), a novel and fully human Fc-enhanced bispecific antibody against TIGIT and CD96 co-receptor, that demonstrates superior pharmacological activity compared to conventional TIGIT monospecific antibodies (mAbs).

Gene expression of TIGIT, CD96, and the co-stimulatory counter-receptor CD226 in tumor samples from patients with cancer was identified using bulk and single cell RNA-sequencing. To target this interaction, Fc-engineered knob-in-hole bispecific antibodies against TIGIT and CD96 were developed and affinity optimized to achieve potent and complete blockade of TIGIT and CD96 ligand interactions. BMS-986442 and corresponding monospecific anti-TIGIT and anti-CD96 monoclonal antibodies were evaluated with or without anti-PD-1 in a variety of human T and NK cell stimulation assays. Mouse surrogate TIGIT/CD96 bispecific antibodies were developed and evaluated as monotherapy or together with anti-PD-1 in colorectal CT26 and breast orthotopic 4T1 tumor bearing mice.

In CT26 and 4T1 tumor-bearing mouse models, the Fc-enhanced TIGIT/CD96 bispecific antibody demonstrated superior tumor control compared to either anti-TIGIT, anti-CD96, or the combination of anti-TIGIT and anti-CD96 mAbs. Tumor control was dependent on co-engaging activating Fcγ receptors, as an Fc-silent bispecific antibody lacked anti-tumor activity. In the tumor microenvironment, efficacy was associated with increased frequency of CD226+ effector and TCF-1+ GrzB- memory precursor CD8 T cells, increased frequency and activation of cytotoxic NK cells, and increased activation of professional APCs, including B cells, MHC Class II monocytes, and dendritic cells as determined by expression of CD40, CD83, and CD86. In primary human *in vitro* assays, BMS-986442 potently enhanced T cell responsiveness and activation compared with conventional anti-TIGIT mAbs alone and in combination with anti-PD-1 (nivolumab). Lastly, BMS-986442 promoted superior NK cell activation in tumor co-culture assays.

In conclusion, BMS-986442 demonstrated a differentiated FcγR-dependent mechanism-of-action to enhance innate and adaptive immune responses compared with anti-TIGIT or anti-CD96 mAbs. BMS-986442 is currently advancing in phase I clinical studies in patients with advanced solid cancers (NCT05543629).

#3916 TNG260, a small molecule CoREST inhibitor, sensitizes STK11-mutant NSCLC to anti-PD1 immunotherapy.

A. Patel[1], S. Sahu[1], K. Geng[1], S. Punekar[1], J. Stephens[1], J. Deng[1], T. Chen[1], L. Ahronian[2], M. Zhang[2], J. Andersen[2], B. Haines[2], K.-K. Wong[1];
[1]NYU Langone Health, New York, NY, [2]Tango Therapeutics, Cambridge, MA

Loss of function (LOF) of the serine-threonine kinase STK11/LKB1, which has been reported in ~15% of non-small cell lung cancer (NSCLC), drives resistance to immune checkpoint therapies such as PD1. *In vivo* CRISPR screens in tumor-bearing immune competent mice identified the Corepressor of Repressor Element 1 Silencing Transcription (CoREST) complex as a synthetic lethal immune evasion target for *STK11*- mutant tumors. Here, we demonstrate that TNG260, a small molecule drug specifically targeting the CoREST complex, can sensitize STK11 mutant lung cancers to anti-PD1 immunotherapy. Combination treatment with TNG260 and anti-PD1 arrested *KRAS*/*STK11* mutant NSCLC tumor growth with no major toxicity observed, as confirmed in both allograft and genetically engineered mouse models (GEMMs) of STK11 mutant NSCLC. Further transcriptional analysis via bulk RNA-seq revealed that treatment of KRAS/STK11 mutant lung tumors with TNG260 promotes genes related to inflammatory responses and suppresses genes related to cell cycle and mitotic checkpoint(s). This phenotype was not observed in STK11 wildtype *KRAS*/*P53* mutant lung tumors. Furthermore, combinational treatment of TNG260 with PD1 antibody showed increased macrophages, neutrophils and dendritic cells signatures *in vivo*. Our data suggests that epigenetic reprogramming via TNG260 sensitizes STK11 mutant NSCLC tumors to anti- PD1 treatment via targeting of the CoREST complex. This work identifies new vulnerabilities in STK11 LOF cancers that can be exploited therapeutically. TNG260 is currently being investigated in combination with pembrolizumab for the treatment of STK11-mutant cancer (NCT05887492), including NSCLC.

#3917 A CXCR4 partial agonist TFF2-MSA improves anti-PD-1 immunotherapy in advanced gastric cancer by selectively targeting PMN-MDSC.

Jin Qian[1], Chenkai Ma[2], Quin T. Waterbury[1], Christine S. Moon[1], Xiaofei Zhi[1], Feijing Wu[1], Ruhong Tu[1], Biyun Zheng[1], Hiroki Kobayashi[1], Leah B. Zamechek[1], Ryan H. Moy[1], Arnold Han[1], Bruce Daugherty[3], Seth Lederman[3], Timothy C. Wang[1]

[1]Irving Cancer Research Center, Columbia University Irving Medical Center, New York, NY,[2]Integrated Diagnostic, Human Health, Health and Biosecurity, CSIRO, Westmead, Australia,[3]Tonix Pharmaceuticals, Inc., Chatham, NJ

Introduction: Advanced gastric cancer poses a challenge for PD-1 immunotherapy due in part to the prevalence of polymorphonuclear myeloid-derived suppressor cells (PMN-MDSCs). PMN-MDSCs are mostly immature granulocytes but coexist with mature neutrophils, complicating their precise targeting. While PMN-MDSCs highly express CXCR4, recent clinical trials suggest that CXCR4 antagonists may provide limited additive efficacy to PD-1 blockade. This study explored the efficacy of a secreted CXCR4 partial agonist, trefoil factor family 2 (TFF2), in the context of anti-PD-1 refractory gastric cancer.

Methods: We fused mouse TFF2 with murine serum albumin to generate a novel TFF2-MSA peptide with extended half-life, and evaluated its therapeutic effects with or without anti-PD-1 antibody. As histidine decarboxylase (HDC) is expressed in immature neutrophils, we used the HDC-GFP transgene to track PMN-MDSC *in vivo*. The HDC-GFP mice received subcutaneous or orthotopic implantation of murine syngeneic gastric cancer cells and subsequent treatments. Additionally, human blood was assessed for both serum TFF2 and immune profiles.

Results: The combination of TFF2-MSA plus anti-PD-1 antibody displayed remarkable synergy, boosting intratumoral cytotoxic CD8 T cells by 50-fold, leading to tumor regression or eradication, 80% reduction of distant metastasis and 2-fold extension of mouse survival. The immunosuppressive HDC-GFP^{+} PMN-MDSCs expressed the highest level of CXCR4 among immune cells, and TFF2-MSA treatment systematically reduced HDC-GFP^{+} PMN-MDSCs in the tumor, blood, spleen and their myeloid progenitors in the bone marrow. In contrast, CXCR4 antagonist AMD3100 in combination with anti-PD-1 failed to restrict tumor growth or PMN-MDSCs. Further single-cell RNA-seq and functional assays revealed that combination of TFF2-MSA plus anti-PD-1 induced a skewing of remaining tumor HDC-GFP^{+}PMN-MDSC compositions from highly immature CD300ld^{+} subsets to less immature subsets expressing interferon-stimulated genes, accompanied by reduced immunosuppression and increased antigen presentation functions. Rather than local reprogramming, this compositional shift stemmed from an IRF1-driven interferon response in splenic HDC-GFP^{+} PMN-MDSCs. In human, PMN-MDSCs marked by LOX1 significantly expanded in the blood of gastric cancer patients compared to healthy donors. Human LOX1^{+} PMN-MDSCs showed an inverse correlation with T cell number, activation, proliferation and the serum TFF2 level.

Conclusions: TFF2-MSA synergizes with PD-1 blockade by selectively targeting CXCR4^{high} PMN-MDSCs. This study provides a rational for a novel combination therapy of the CXCR4 partial agonist, TFF2-MSA, rather than CXCR4 antagonists, plus PD-1 blockade for treatment of advanced gastric cancer.

#3918 Targeting MARCO in combination with anti-CTLA4 leads to enhanced melanoma regression and immune cell infiltration via macrophage reprogramming.

H. Takahashi, P. Perez-Villarroel, R. Falahat, J. J. Mule;
Moffitt Cancer Center, Tampa, FL

Tumor-associated macrophages (TAM) are known to suppress responses to conventional therapeutics and the presence of TAM is generally related to poor prognosis in various cancers. Therefore, depletion of TAM has been one of the main strategies to break the ceiling of efficacy in cancer treatment. However, to date, TAM depletion strategies have not been successful in clinical trials[1]. Here, we introduce an approach to target TAM by employing Macrophage Receptor with Collagenous Structure (MARCO), a class A scavenger receptor, as a novel immune checkpoint. Previously, we showed MARCO to be the most upregulated mRNA in murine and human dendritic cells following their uptake of dead tumor cells (TP-DC)[2]. We also showed ex vivo treatment of TP-DC with anti-MARCO mAb (ED31) led to enhanced anti-tumor responses in vivo[3,4]. The aim of this current study was to explore whether targeting MARCO using ED31 could improve the efficacy of an immune checkpoint inhibitor in murine models of melanoma. In C57BL/6 mice with B16F10 tumors, adding ED31 to anti-CTLA4 mAb (αCTLA4) resulted in enhanced tumor regression and longer survival ($p=0.001$, $p<0.05$ vs αCTLA4 monotherapy; $p<0.05$, $p<0.01$ vs ED31 monotherapy, respectively). To explore the immune mechanism of ED31 with αCTLA4, we focused on the tumor microenvironment (TME) by flow cytometry. TME immune-profiling consistently revealed that one time treatment with this combination resulted in a rapid increase in the number of tumor infiltrating lymphocytes (TIL) including $CD8^{\pm}$T (2.8-fold) and $CD4^{\pm}$T cells (2.9-fold), NK cells (2.5-fold), activated $CD11c^{\pm}$DC (2.2-fold) and $F4/80^{\pm}$Mφ (2.5-fold), compared to αCTLA4 monotherapy (all with $p<0.0001$; vs αCTLA4 monotherapy, vs ED31 monotherapy, vs control, respectively). As measured by chemokine production using murine bone marrow-derived, in vitro M-CSF induced Mφ phenotypes (M1: polarized by IFNγ and LPS, M2: polarized by IL4, TAM-like Mφ: polarized by a supernatant from B16F10 cell line culture), ED31 exposure switched the pattern of chemokine productions from M2 and TAM-like Mφ into an M1 pattern. In vivo depletion of each immune cell type had a diminishing effect on the treatment efficacy ($p<0.001$ for CD8 depletion, $p=0.01$ for CD4-depletion, $p<0.01$ for NK1.1 depletion). However, Mφ depletion had a more profound impact by completely abrogating the anti-tumor efficacy and the associated survival benefit, in addition to completely reversing the increase in TIL infiltration and canceling the increase of M1 chemokines in vivo (all with $p<0.05$ vs Mφ depletion). These preclinical data support the proof-of-concept that a combination strategy of targeting MARCO along with αCTLA4 can lead to enhanced anti-tumor responses through utilizing TAMs rather than their depletion.

[1] Immunity 2023;56:2188. [2] J Immunol 2003;171:2879. [3] Cancer Immunol Immunother 2010;59:875. [4] PLoS One 2013;8:e67795.

#3920 BND-35, a novel anti-ILT3 antibody for remodulation of the tumor microenvironment.

T. Peretz, Y. Pizem, L. Iancovici, E. Peled, M. Hakim, S. Hashmueli, I. Mandel, Y. Sapir, T. Ben Moshe;
Biond Biologics, Misgav Industrial Park, Israel

Background: ILT3 (LILRB4) is expressed in various suppressive myeloid cells including tumor associated macrophages (TAM), myeloid derived suppressor cells (MDSCs) and tolerogenic dendritic cells (DCtol). The binding of ILT3 to its ligands induces an immunosuppressive phenotype in myeloid cells, mediates the inhibition of T cells activity and generates an immunosuppressive tumor microenvironment (TME) which supports tumor growth. The inhibition of ILT3 can restore the anti-tumor activity of myeloid cells and T cells, and thus remodulate the TME from immunosuppressive to pro-inflammatory. Here we describe preclinical characterization of BND-35, a humanized IgG4, ILT3 antagonist antibody developed for the treatment of solid tumors.
Methods: BND-35 binding to ILT3 was evaluated by flow cytometry, ELISA and surface plasmon resonance. We investigated the ability of BND-35 to block ILT3 interactions with APOE and fibronectin, to enhance the pro inflammatory activity of various myeloid cells and reverse ILT3-mediated immune suppression of T cells by different suppressive myeloid cells using ELISA and in vitro and ex vivo cell-based assays. The anti-tumor activity of BND-35 was also evaluated in vivo in hILT3 transgenic mouse tumor models as well as in tumoroid systems generated from cancer patients.
Results: BND-35 binds ILT3, but not other ILT-family receptors, with low nanomolar affinity and blocks its interaction with APOE and fibronectin in a concentration-dependent manner. ILT3 blockade with BND-35 restored the pro-inflammatory activity of FcR-stimulated DCs and THP1 cells inhibited by fibronectin. BND-35 was also shown to restore an M1 phenotype in cancer patients' derived monocytes differentiated in the presence of autologous tumor cells. In addition, BND-35 restored T cell activity (both, CD4 and CD8 T cells) inhibited by either DCtol, MDSCs or M2 cells as a single agent and in combination with anti PD-1. BND-35 enhanced immune activity in a unique system of patient-derived tumoroids as evidenced by the secretion of pro-inflammatory cytokines. In vivo, blocking ILT3 activity with BND-35 resulted in decreased tumor growth and induced a pro-inflammatory phenotype in tumor resident T cells and myeloid cells populations as a single agent and in combination with anti PD-1.
Conclusions: BND-35 is an anti-ILT3 antagonist antibody that was shown to induce potent pro inflammatory activity of myeloid cells and enhance T cells activity inhibited by ILT3 expressing myeloid suppressive cells in multiple in vitro, ex vivo and in vivo models. By doing so, BND-35 can lead to TME remodelling from immunosuppressive to proinflammatory. Safety, tolerability, and anti-tumor activity of BND-35 will be explored in a first-in-human clinical trial in cancer patients with solid tumors.

IMMUNOLOGY: Understanding and Targeting Pathogenic Inflammation in Solid Tumors Minisymposium

#3921 The aged tumor microenvironment limits CD8^{+} T cell control of cancer.

A. Chen[1], S. Jaiswal[1], D. Martinez[1], C. Yerinde[1], K. Ji[1], V. Miranda[1], M. E. Fung[2], S. A. Weiss[2], M. Zschummel[1], K. Taguchi[1], C. S. Garris[1], T. R. Mempel[1], D. R. Sen[1];

[1]MGH/Harvard Medical School, Boston, MA, [2]Harvard Medical School, Boston, MA

Aging is associated with progressive loss of immune function, which parallels the rise in cancer incidence. The etiology and impact of age-related CD8^{+} T cell dysfunction in cancer remain poorly understood. Here, we demonstrate that increased tumor growth in aged hosts is associated with reduced CD8^{+} T cell infiltration and function. The transfer of young antigen-specific CD8^{+} T cells fails to restore tumor control in aged hosts due to the rapid induction of CD8^{+} T cell dysfunction. The aged tumor microenvironment drives a novel age-associated dysfunctional state (T_{ADys}) that is functionally, transcriptionally, and epigenetically distinct from canonical CD8^{+} T cell exhaustion. Overall, this study focuses on understanding the cell-intrinsic and -extrinsic effects on CD8^{+} T cell immunity in aging and explores a proper strategy to improve CD8^{+} T cell control of cancer.

#3922 Quaking modulates anti-tumor immunity by regulating antigen processing and presentation in dendritic cells.

Y. Li, J. Hu, C. Yee;
UT MD Anderson Cancer Center, Houston, TX

Dendritic cells are essential players in anti-tumor immunity. One of their critical roles is to process and present tumor associated antigens to T cells, thereby inducing antigen-specific T cell response. However, cellular factors and molecular pathways regulating antigen processing and presentation by DCs are not fully understood.Here, we revealed a potential regulatory role of a transcriptional co-activator, Quaking (QKI), and its binding partner, PPARδ in antigen processing and presentation by DCs. Consistent with our previous studies in neural stem cells and microglia, we found QKI and PPARδ enhance phagocytosis in DCs by upregulating genes involved in the formation of phagosome and endosomes. QKI- or PPARδ-deficient DCs showed reduced $CD8^+$ T cell priming capacity *in vitro. In vivo* tumor models suggested DC-specific knocking out of QKI or PPARδ promoted the tumor growth. Furthermore, ablation of QKI or PPARδ in DCs limited the effectiveness of immune checkpoint blockade in multiple tumor models.Together, these revealed a transcriptional regulation of antigen processing and presentation by DCs through QKI and PPARδ. Our data also suggested that perturbing this important function of DC would subvert their anti-tumor activity, highlighting the pivotal role of DCs in an effective anti-tumor immune response.

#3923 Targeting immunosuppressive TREM2^{+}tumor associated macrophages in prostate cancer.

A. J. Lee, K. Adusei, M. Praharaj, F. Shen, X. Wang, K. Bhatia, T. Nirschl, J. C. Zarif;
Johns Hopkins University School of Medicine, Baltimore, MD

With over 250,000 new cases annually, prostate cancer (PCa) is amongst the most diagnosed cancers in the United States. Despite a near-perfect 5-year survival rate in patients with localized disease with androgen deprivation therapy (ADT), about 10-20% of patients on ADT eventually develop castration-resistant prostate cancer (CRPC). Immunotherapies are typically ineffective in treating these treatment-resistant patients due to the abundance of immunosuppressive tumor-associated macrophages (TAMs) and lack of infiltrating lymphocytes. We propose to target these immunosuppressive macrophages through the triggering receptor expressed on myeloid cells 2 (TREM2), which has been identified as a major mediator of suppressive macrophage function but has not been studied in the context of PCa and CRPC. For this study, we analyzed publicly available RNA-seq datasets to query for TREM2 expression amongst patients with a range of prostate cancer disease states and cell types, measured tumor growth kinetics in two subcutaneous models of prostate cancer, and compared tumor immune infiltrates by flow cytometry. Our analysis of the TCGA prostate adenocarcinoma (PRAD) and the Stand Up to Cancer/Prostate Cancer Foundation (SU2C/PCF) datasets implicate *TREM2* expression with prostate cancer progression, by Gleason score and progression-free status, and with worse overall survival of patients with metastatic CRPC (mCRPC). Manual curation and analysis of 10 single-cell RNA-seq datasets with a total of 84 patients, encompassing primary PCa, CRPC, and mCRPC indicate that *TREM2* is highly and specifically expressed on TAMs in prostate cancer, with macrophages from patient-matched tumor samples expressing higher *TREM2* compared to normal adjacent tissue. B6CaP tumors, with a luminal cytokeratin profile, high AR expression, and high Myc expression, show slower tumor growth in *Trem2*$^{-/-}$ mice compared to tumors in *Trem2*^{wt} mice. On the other hand, RM1 tumors show no difference in growth kinetics on *Trem2*$^{-/-}$ mice. A major difference between the B6CaP and RM1 tumor microenvironments is the level of macrophage infiltration, where only 2-5% of immune cells in RM1 tumors are macrophages, compared to the 40-50% in B6CaP tumors. RM1 cells co-implanted with *Trem2*$^{-/-}$ macrophages show slower tumor growth, compared to tumor cells co-implanted with *Trem2*^{wt} macrophages, confirming the role of *Trem2*-expressing macrophages in mediating tumor growth. Consistent with previous reports of suppressive Trem2 signaling, we also observed higher levels of inflammatory cytokine production in *ex vivo* stimulated *Trem2*$^{-/-}$ TAMs. By targeting TREM2 in prostate cancer, we find that TAMs are less suppressive, more inflammatory, and permit cytotoxic lymphocyte infiltration to enhance anti-tumor responses by synergizing with chemo and immune checkpoint therapy.

#3924 Dual COX-2/sEH inhibition enhances immunotherapy and chemotherapy to induce bladder cancer regression.

K. L. Vazquez[1], E. Rothenberger[2], W. Wang[3], S. Hwang[4], D. R. Bielenberg[5], B. D. Hammock[4], D. Panigrahy[1];
[1]Beth Israel Deaconess Medical Center/Harvard Medical School, Boston, MA, [2]Harvard University, Boston, MA, [3]Purdue University, West Lafayette, IN, [4]University of California, Davis, Davis, CA, [5]Boston's Children Hospital, Boston, MA

Unresolved inflammation plays a critical role in bladder cancer initiation and progression. Chemotherapy (e.g. gemcitabine and cisplatin), the standard of care for advanced bladder cancer, disrupts inflammation resolution and is only partially effective in preventing tumor recurrence after treatment. Immunotherapy has emerged as a potential treatment option for bladder cancer patients, however it is ineffective in 80% of patients and can induce a pro-inflammatory cytokine storm. Therefore, there is a critical unmet medical need to improve chemotherapy and immunotherapy in bladder cancer. To address this, we have developed dual COX-2/sEH inhibitors (e.g. PTUPB). This lead compound is representative of a newly patented class of “dual acting” molecules that target two important enzymes in the arachidonic acid cascade with nanomolar binding affinity: cyclooxygenase-2 (COX-2) and soluble epoxide hydrolase (sEH). Oral dosing of PTUPB is well-tolerated in animal models. Since chemotherapy and immunotherapy both induce tumor-promoting inflammation via an eicosanoid/cytokine storm, we hypothesized that dual COX-2/sEH inhibition would enhance immunotherapy in experimental bladder cancer via anti-inflammatory mechanisms. When syngeneic (MB49) bladder tumors reached ~200 mm3 in immunocompetent mice, treatment was initiated with PTUPB, anti-CTLA-4, anti-PD1, gemcitabine & cisplatin, or various combinations thereof. Here we demonstrate that chemotherapy and/or immunotherapy stimulated sEH and COX-2 expression in tumor tissue which was counter-regulated by PTUPB. While monotherapy treatment with PTUPB, gemcitabine & cisplatin, anti-PD1 or anti-CTLA-4 suppressed tumor growth compared to control, the tumors escaped single treatments by the end of the study. Remarkably, dual COX-2/sEH inhibition in combination with chemotherapy (gemcitabine and cisplatin) and/or immune checkpoint blockade (anti-CTLA-4 or anti-PD1) induced sustained tumor regression via synergistic anti-tumor activities. Chemotherapy and/or immunotherapy induced the expression of ER stress response genes (e.g. BiP and CHOP) and angiogenic factors (e.g. EGF and VEGF-C) in bladder cancer tissue, which were repressed by PTUPB. PTUPB also prevented chemotherapy-induced toxicity and prolonged survival in an orthotopic MB49 tumor model. Taken together, our results demonstrate dual COX-2/sEH inhibition as a novel therapeutic approach to enhance immunotherapy in bladder cancer without overt toxicity.

#3925 Cancer-associated fibroblast-derived Dickkopf-1 impairs anti-tumor immunity in breast cancer by suppressing NK cell-mediated cytotoxicity.

S. Lee, B. Ricci, R. Faccio;
Washington University School of Medicine in St. Louis, St. Louis, MO

Despite early diagnosis, 10-20% of breast cancer patients experience metastatic disease within 5-10 years. While it is established that breast cancer cells have the capacity to evade immune responses, the mechanisms driving this evasion remain elusive. Therefore, finding ways to enhance anti-tumor immunity is crucial to improve patient outcomes. Dickkopf-1 (DKK1) is a Wnt inhibitor whose levels correlate with poor prognosis and decreased immune infiltration in various cancers. In this study, we used mice orthotopically injected with the PyMT, EO771, and 4T1 breast cancer lines. In all models, we found elevated DKK1 serum levels, and its neutralization with an αDKK1 Ab resulted in a significant reduction in primary tumor growth but also in metastatic dissemination. To identify the source of DKK1, we examined its expression in the tumor. DKK1 was detected in stromal cells with a fibroblast-like morphology but not in cancer cells or immune infiltrates. Co-staining confirmed colocalization between DKK1 and the CAF marker αSMA. To address the role of CAF-derived DKK1, we specifically deleted DKK1 in CAFs by generating FSP1CreDkk1fl/fl and αSMACreERT2Dkk1fl/fl mice. Both models showed a significant reduction in primary tumor growth while maintaining comparable serum DKK1 levels, indicating locally produced DKK1 supports tumor growth. To understand how DKK1 promotes tumor progression, we conducted bulk RNAseq of tumor cells isolated from IgG or αDKK1 treated mice. While no changes related to cell viability or cell cycle were observed, immune response-related genes were upregulated in αDKK1-treated cells. In support of this, αDKK1 did not reduce tumor growth in NSG immune-compromised mice. To pinpoint the immune cell targeted by DKK1, we depleted T, NK cells, or macrophages in WT tumor-bearing mice treated with αDKK1. Remarkably, only NK cell depletion negated αDKK1 anti-tumor effects. In vitro assays further demonstrated that rDKK1 or the presence of CAFs reduced NK cell cytotoxicity against tumor cells while αDKK1 restored it. To assess whether DKK1 levels correlated with tumor progression and immune suppression in breast cancer patients, we analyzed DKK1 serum levels and circulating NK cells at the diagnosis of metastatic bone disease and 15-18 months after standard care. DKK1 levels were significantly elevated in patients with progressive bone disease compared to those with stable disease. Importantly, NK cells from the progressive disease cohort had reduced perforin and granzyme B expression at the follow-up visit compared to baseline, indicating reduced cytotoxicity. Furthermore, rDKK1 reduced perforin in NK cells from healthy donors. In sum, our data show DKK1 is an important regulator of breast cancer progression, and we report for the first time DKK1 directly impairs NK cell cytotoxicity, creating an immune suppressive environment resistant to treatment.

#3926 ARF6-dependent endocytic trafficking of the interferon-gamma receptor drives adaptive immune resistance and response to immune checkpoint blockade.

Y. Wee[1], J. Wang[1], E. C. Wilson[1], C. P. Rich[1], A. Rogers[1], Z. Tong[2], E. DeGroot[3], Y. Gopal[3], M. Davies[3], H. A. Ekiz[1], J. K. Tay[1], C. Stubben[1], K. M. Boucher[1], J. M. Oviedo[2], K. C. Fairfax[2], M. A. Williams[1], S. L. Holmen[1], R. K. Wolff[1], **A. H. Grossmann**[1];
[1]University of Utah Huntsman Cancer Institute, Salt Lake City, UT, [2]University of Utah, Salt Lake City, UT, [3]MD Anderson Cancer Center, Houston, TX

Interferon-gamma (IFNγ)-driven adaptive immune resistance (AIR) in cancer begins at the plasma membrane where cytokine signaling is initiated. Cytotoxic CD8+ T cells secrete IFNγ, eliciting tumor-intrinsic IFNγ signaling and expression of immunosuppressive genes, which are critical for effective therapeutic response to anti-PD-1 and anti-CTLA-4 immune checkpoint blockade (ICB). Although the IFNγ receptor (IFNγR) is expressed in all cell types, its surface density can determine a cell's responsiveness to ligand. Mechanistic control over this process remains a mystery. Herein we report that the endocytic trafficking protein ADP-Ribosylation Factor 6 (ARF6) is critical for IFNγ-driven AIR during primary tumor progression and in the setting of ICB therapy. The IFNγR1 subunit of the receptor is constitutively internalized in a ligand-independent manner. ARF6 is necessary for endocytic recycling of IFNγR1 and determines the steady-state surface density of the receptor. Loss of ARF6 results in lysosomal degradation of the receptor and controls IFNγR1 protein levels in melanoma, non-small cell lung cancer, colorectal cancer, and triple-negative breast cancer. IFNγ activates ARF6 in parallel with JAK1-STAT1 signaling, suggesting a positive feedback loop that allows tumor cells to dynamically respond to immune attack. Silencing ARF6 reduces tumor intrinsic IFNγ signaling and downstream expression of immunosuppressive genes. In murine melanoma, loss of ARF6 causes resistance to systemic ICB therapy. Likewise, low expression of ARF6 in patient tumors correlates with inferior outcomes with ICB. Our data provide new mechanistic insights into tumor immune escape, defined by ARF6-dependent adaptive immunity, and support that ARF6-dependent endomembrane trafficking of the IFNγ receptor shapes clinical outcomes of ICB therapy.

Private Information

#3927 Metabolic inhibition of BATF2 dampens type-I interferon-mediated immune sensing of cancer.

W. Gong[1], H. Taner[1], Y. Wu[2], Z. Li[1], W. Cheng[1], C. Donnelly[3], F. Nor[1], Y. He[1], Z. Fitzsimonds[1], J. Li[1], H. Wen[4], S. Chinn[1], Y. Xie[2], J. Moon[1], Y. L. Lei[1]; [1]University of Michigan School of Dentistry, Ann Arbor, MI, [2]Michigan State University, East Lansing, MI, [3]Duke University Medical Center, Durham, NC, [4]Ohio State University, Columbus, OH

Background: The type-I interferon (IFN-I) system appeared before adaptive immunity during evolution as the primary defense system for metazoans. Initiating cancers frequently disable this first line of defense before establishing T-cell exhaustion programs. However, the molecules linking IFN-I, danger signals, and unique metabolic conditions in the tumor microenvironment (TME) remain to be discovered.

Methods: We performed centered log-ratio transformation on the cluster composition data using the R-package ALDEx2 to compare the clusters in single-cell data sets. IFN-I signatures were quantified using qPCR and ELISA. ChIP was performed to examine the H3K27me3 epigenetic marker on the promoters of BATF2 and IFN-I genes in bone marrow-derived macrophage (BMDM). For the cigarette smoke carcinogen-induced head and neck squamous cell carcinoma (HNSCC) model, experimental mice were fed with water containing 50 μg/mL of 4-NQO for 16 weeks and then switched to regular feeding water. We started monitoring 10 weeks post-treatment for the number, location, and diameter of the lesions. TME analysis was performed using single-cell RNA-Seq and multispectral imaging.

Results: We analyzed three large independent cohorts of patients and found that BATF2 strongly correlated with the immunogenicity of HNSCC, with a stronger correlation coefficient than *STING*. We generated *Batf2*$^{-/-}$ BMDM and found that *Batf2* deficiency rendered cells insensitive to STING agonists. However, the dsRNA-induced IFN-I activation was not affected by *Batf2* deletion. BATF2 interacted with STING, promoting its phosphorylation and oligomerization. Glutamine is enriched in the TME. We found that glutamine inhibited the BATF2-STING pathway by increasing a repressive epigenetic marker, H3K27me3, on the promoters of *BATF2* and *IFNB1*. The expression of BATF2 in cancer cells resulted in IFN-I- and γδ T-cell-dependent tumor rejection. Single-cell immune profiling showed that Batf2-expressing tumors contained significantly expanded Cxcl10^{+} myeloid cells and γδ T-cells. Utilizing the 4-NQO-induced HNSCC model, we found that BATF2 limited suppressive myeloid cells and expanded effector cells in the TME, serving as a potent tumor suppressor.

Conclusion: BATF2 is a glutamine-responsive tumor suppressor that limits tumor initiation by engaging the STING-γδ T-cell pathway.

Acknowledgments: This work was supported by NIH grants R01 DE026728, U01 DE029255, R01 DE031951, and U01 DE033330

MOLECULAR/CELLULAR BIOLOGY AND GENETICS: Advances in Cancer Genomics: Carcinogenesis, Tumor Evolution, and Heterogeneity Minisymposium

#3928 Genomic landscape and estimation of immune infiltration of soft tissue sarcoma histology subtypes from the ORIEN network.

A. C. Soupir[1], O. E. Ospina[1], D. Hedges[2], J. K. Teer[1], M. D. Radmacher[2], D. M. McKean[2], N. Seligson[3], M. McCarter[4], B. Wilkey[5], G. Riedlinger[6], J. Groundland[7], B. J. Miller[8], B. Schneider[9], R. Patel[10], A. Rafeh-Naqash[11], S. Edge[12], B. Salhia[13], C. Moskaluk[14], M. Johns[15], M. L. Churchman[2], O. Hampton[2], D. Liebner[16], B. L. Fridley[1], A. S. Brohl[1];

[1]H. Lee Moffitt Cancer Center, Tampa, FL, [2]Aster Insights, Hudson, FL, [3]University of Florida, Gainesville, FL, [4]Univerity of Colorado Denver, Denver, CO, [5]University of Colorado Anschutz, Denver, CO, [6]Rutgers Cancer Institute of New Jersey, New Brunswick, NJ, [7]Huntsman Cancer Institute, Salt Lake City, UT, [8]Holden Comprehensive Cancer Center, Iowa City, IA, [9]IU Health Simon Cancer Center, Indianapolis, IN, [10]UK Markey Cancer Center, Lexington, KY, [11]University of Oklahoma Health Sciences Center, Oklahoma City, OK, [12]Roswell Park Comprehensive Cancer Center, Buffalo, NY, [13]University of Southern California, Los Angeles, CA, [14]University of Virginia, Charlottesville, VA, [15]Emory, Atlanta, GA, [16]Ohio State University, Columbus, OH

Sarcomas encompass a group of malignant diseases arising from mesenchymal origins. Given their rarity and diversity, a fundamental understanding of the genomic underpinnings for many sarcoma subtypes is still lacking. Studies are often limited to one or several of the more common subtypes or a narrow evaluation of a broader sampling. We therefore report on one of the largest comprehensive omics evaluation in sarcomas to date, including whole exome sequencing (WES; n = 1170) and RNA-sequencing (n = 983) of tissues from 29 different sarcoma histologic subtypes collected at 13 institutions in the US as part of the Oncology Research Information Exchange Network (ORIEN). We identified recurrent somatic mutations previously identified in sarcomas (e.g. *TP53*, *KIT*) as well as other cancer types (e.g. *BRCA1*). The burden of putatively pathogenic driver point mutations was higher in metastatic samples (median = 3) as compared to primary tumor samples (median = 2; $p < 0.001$). We observed frequent copy number alterations including whole genome doubling more commonly in metastatic compared to primary tumors (23.4% vs. 16.9%; $p = 0.0.25$). Inspection of gene expression dimensionality reduction (UMAP) showed separation of gastrointestinal stromal tumors (GISTs), leiomyosarcomas, myxoid liposarcomas, and well/de-differentiated liposarcomas from the other histologies. Differential expression analysis for these four histologies with gene set enrichment analysis highlights the diversity of disease-specific pathways and need for sarcoma subtype-specific translational focus. Estimation of immune cell abundances based on RNA-seq followed by hierarchical clustering identified five immune subtypes. The subtypes ranged from low (clusters A, B) to high (clusters D, E) immune infiltration with higher abundance of T, B, Natural Killer (NK), and myeloid cells (FDR < 0.01). Intermediate immune group C was predominantly composed by GISTs and marked by an enrichment for NK cells (FDR < 0.01) compared to all groups except the immune “hot” group E; however, this immune group exhibited modest infiltration by other immune cell types. Notably, we observed significant differences in the overall survival of patients with sarcomas in immune enriched (C, D, E) compared to immune depleted clusters (A, B; $p = 0.002$). In summary, we report the genomic and expressional landscape of over 1000 sarcomas, representing one of the largest comprehensive profiling efforts in this disease. We identify the mutational and copy number variation landscape and observe differences between primary and metastatic samples. We highlight expression pathways that are enriched in histologic subtypes that cluster most distinctly from others, providing a subtype-specific roadmap for further translational efforts. Finally, we define immune enriched or depleted sarcoma subgroupings that carry a prognostic impact.

#3929 Comparative genomics of breast cancer in indigenous African and western populations first results from the E-Predict study.

S. S. Lueong[1], P. D. Derliche Tonouo[2], A. A. Z. Tiofack[2], R. N. Kenfack[2], J. R. Kuiate[3], E. D. B. Mbassi[4], S. N. Ananga[4], E. O. Atenguena[5], G. Simo[6], A. J. Njouendou[7], W. Ndaka[8], Z. Sando[5], E. Mayemi[9], R. Tayou[10], G. G. G. Aghoagni[11], A. Sango[12], B. Pokam[8], A. T. Bambara[13], J. T. Siveke[1];

[1]German Cancer Consortium (DKTK), partner site Essen/Dusseldorf, a partnership between DKFZ and University Hospital Essen, Essen, Germany, [2]The Cameroon Consortium for translational Cancer Research, Dschang, Cameroon, [3]Research Unit of Microbiology and Antimicrobial Substances (RUMAS), Department of Biochemistry, Faculty of Science, University of Dschang, Dschang, Cameroon, [4]Faculty of Medicine and Pharmaceutical Sciences, University of Douala, Douala, Cameroon, [5]Faculte de Medecine et des Sciences Biomedicales, Universite de Yaounde I, Yaounde, Cameroon, [6]Molecular Parasitology and Entomology Unit (MPEU), Department of Biochemistry, Faculty of Science, University of Dschang, Dschang, Cameroon, [7]6Department of Biomedical Sciences, Faculty of health Sciences, University of Buea, Buea, Cameroon, [8]Department of Biomedical Sciences, Faculty of health Sciences, University of Buea, Buea, Cameroon, [9]Department of pathology, Yaounde general hospital, Yaounde, Cameroon, [10]Department of medical oncology, Douala Bonasama District Hospital, Douala, Cameroon, [11]Douala Gynaeco-Obstetric and Pediatric Hospital, Douala, Cameroon, [12]Douala Gynaeco-Obstetric and Pediatric Hospital, Douala, Douala, Germany, [13]Departement de Chirurgie, Service de Chirurgie Viscerale et Digestive, Centre Hospitalier Universitaire Yalgado Ouedraogo, Ouagadougou, Ouagadougou, Burkina Faso

Breast cancer (BC) stands as the foremost female malignancy globally and is the most prevalent cancer in numerous developing countries, particularly in sub-Saharan Africa (SSA). Over the past decade, significant strides in comprehending the pathobiology of the disease and tumour dynamics have greatly enhanced treatment options, particularly in industrialized nations. Regrettably, SSA countries have witnessed only marginal, if any, improvements, with mortality rates surpassing incidence rates. Unfavourable outcome, early onset and high-grade tumours are predominant in SSA. Despite these challenging clinical phenotypes, there is currently a limited understanding of the primary molecular drivers, primarily due to a dearth of reliable data. Furthermore, there is a paucity of research conducted in, and pertinent to, the challenges of the disease in low-income countries (LICs), despite a rising incidence and higher mortality-to-incidence ratios. We thus established an international translational cancer research consortium in five distinct African countries. This initiative has contributed to the creation of a high-quality repository of biomaterials. Additionally, we have conducted whole exome sequencing on the initial 100 cases of breast cancer, comparing the molecular architecture of these tumors with data from The Cancer Genome Atlas (TCGA). We examining and compared the clinical disease phenotypes between indigenous African women and Western patients. A higher proportion of grade III tumors was observed in African patients aged between 30 to 59 years as compared to other patients within the same age group. In comparative molecular analyses, we found a significantly elevated tumor mutational burden in African patients (median of >15/MB) in contrast to other populations within the TCGA (median ~ 0.7/MB). Gene sets featuring co-occurring mutations, predicted to be associated with survival using the TCGA dataset, showed high mutation rates in the African cohort. Notably, co-occurring mutations between *PIK3CA* and genes linked to genomic instability, such as *BIRC6* (HR: 11.7, p = 2.7e-05), *KMT2C* (HR: 4.7, p = 4.01e-04), *NEB* (HR: 3.84, p = 0.48), and *PCLO* (HR: 4.9, p = 0.016), among others, strongly correlated with poor overall survival and were highly mutated within the African cohort. Interestingly, within the TCGA, patients with early breast cancer onset exhibit twice as many mutations in *KMT2C*, a gene known for its association with DNA damage repair, genomic instability, and showed an improved response to immune checkpoint inhibition. These initial findings suggest that breast cancer genomics in indigenous African populations may exhibit substantial differences, potentially warranting consideration for distinct therapeutic modalities for these patients.

#3930 The therapeutic implications of consensus genomic subtypes of gastric adenocarcinoma.

Yun Seong Jeong[1], Young-Gyu Eun[2], Sung Hwan Lee[3], Sang-Hee Kang[4], Sun Young Yim[5], Eui Hyun Kim[6], Joo Kyung Noh[2], Bo Hwa Sohn[1], Ju-Seog Lee[1]

[1]UT MD Anderson Cancer Center, Houston, TX, [2]Kyung Hee University, Seoul, Korea, Republic of, [3]CHA Bundang Medical Center, Seongnam, Korea, Republic of, [4]Korea University Guro Hospital, Seoul, Korea, Republic of, [5]Korea University College of Medicine, Seoul, Korea, Republic of, [6]Yonsei University College of Medicine, Seoul, Korea, Republic of

Background: Gastric adenocarcinoma (GAC) is heterogeneous lethal disease in genomic and clinical level. Although the clinical relevance of genomic and molecular subtypes of GAC has been demonstrated, differences in classification methods have made it difficult to use these findings in clinical applications. We aim to examine a consensus of genomic subtypes and correlate them with clinical outcomes.

Method: We collected genomic data from 2527 GAC tumors and divided the data into discovery (n = 1427) and validation sets (n = 1100). A cluster of clusters approach (COCA) was used to find consensus subtypes of gastric tumors. We constructed the GAC predictor of the integrated consensus subtype with 120 genes (GPICS120) and applied it to the validation data set in order to validate the clinical significance of the new subtypes. By analyzing genomic and proteomic data we evaluated each subtype's potential response rate to standard and experimental treatments such radiation therapy, targeted therapy, and immunotherapy and further validated their functional significance in cell line models.

Results: We identified 6 clinically and molecularly distinct genomic consensus subtypes (CGSs) by integrating 8 previously established genomic subtypes. CGS1 is characterized by worst prognosis, remarkably high stem cell characteristics, high IGF1 expression, and low genomic alterations. CGS2 showed canonical epithelial gene expression patterns. CGS3 and CGS4 are characterized by high copy number alterations and low immune activity. CGS5 has highest mutation burden and moderately elevated immune activity that is characteristics of MSI-high tumors. The majority of CGS6 tumors have extremely high methylation, high immune activity, and are EBV-positive. The most intriguing finding is that CGS1 is the most responsive to immunotherapy whereas CGS3 is significantly associated with benefit of chemoradiation therapy due to high basal level of ferroptosis. Furthermore, we showed that ferroptosis inducer statin sensitized radiation-resistant GAC cells to ionizing radiation, suggesting that statin can be used to enhance the efficacy of chemoradiation in GAC and it would warrant further investigation in preclinical models.

Conclusion: Consensus subtype is robust classification system and can serve as the basis for future clinical trials as well as pre-clinical research into targeted subtype-based therapies.

#3931 Breast cancer genomic architecture contributes to immune escape across metastasis.

Lise Mangiante, Kathleen Houlahan, Cristina Sotomayor Vivas, Alvina Adimoelja, Seongyeol Park, Aziz Khan, Sophie Pribus, Zhicheng Ma, Jennifer Caswell-Jin, Christina Curtis

Stanford University School of Medicine, Stanford, CA

Clinically, breast tumors are stratified based on the expression of three receptors - estrogen receptor (ER), progesterone receptor (PR) and human epidermal growth factor receptor-2 (HER2). Breast cancer is a highly heterogeneous disease, and a more detailed understanding of its genomic drivers, mechanisms of immune evasion, and evolution may inform more effective and personalized treatment. Previously, we established a genome-driven breast cancer classification scheme that defines 11 integrative subgroups (ICs) of disease with distinct copy number aberrations (CNAs), transcriptional profiles, and clinical outcomes. Specifically, we identify four subgroups of ER+ disease (IC1, IC2, IC6, IC9) with a persistent risk of lethal distant relapse up to two decades after diagnosis, each with focal copy number drivers and two distinct subgroups of triple-negative disease (Curtis et al. Nature 2012; Rueda et al. Nature 2019). These findings nominate new therapeutic strategies, however, it is not known how mutational processes and genomic architecture differ across the ICs to sculpt the development and evolution of disease, nor how their microenvironments differ. To interrogate the genomic and immune landscape of breast cancer throughout the disease continuum, we established a meta-cohort of 2,873 breast tumors spanning pre-invasive (ductal carcinoma in situ), primary invasive, and metastatic breast cancer, including 1,865 with whole-genome sequencing, 1,738 with whole-transcriptome sequencing, and 730 with both modalities. We developed a fully containerized bioinformatic workflow to interrogate copy number alterations, complex classes of structural variation, and neoantigens. Analysis of this large clinically curated compendium identifies highly concordant mutational signatures and higher order genomic features in high-risk ER+ (IC1,2,6,9) and HER2+ (IC5) tumors, including distinct patterns of structural variation. In contrast, triple-negative tumors (predominantly IC10) were characterized by global genomic instability and tandem duplications, whilst a third group is largely genomically stable. These distinct genomic architectures were associated with specific tumor microenvironments. As expected, triple-negative tumors were immune-enriched. In contrast high-risk ER+ and HER2+ tumors demonstrated immune-depleted profiles, as compared to typical risk ER+ tumors. These microenvironment classifications were maintained from primary tumors to metastatic lesions, except triple-negative tumors that exhibited increased immune depletion during metastasis. Taken together, our data demonstrate that complex structural alterations established early in breast cancer contribute to immune evasion, and persist throughout the life history of the tumor through metastasis.

#3932 Multi-omics characterization of molecular features and global-local genomic ancestry analysis of colorectal cancer in Hispanic-Latinos.

E. I. Velazquez Villarreal[1], S. Rajpara[1], Y. Jin[2], M. Postel[1], B. Waldrup[1], F. Wu[1], D. Loza[1], H.-J. Lenz[3], D. W. Craig[2], J. D. Carpten[2];
[1]Keck School of Medicine of USC, Los Angeles, CA, [2]Beckman Research Institute of the City of Hope, Los Angeles, CA, [3]Norris Comprehensive Cancer Center KSOM, Los Angeles, CA

Introduction: Clinical factors and molecular characteristics play pivotal roles in shaping therapeutic strategies and prognoses in colorectal cancer (CRC), the second leading cause of cancer-related mortality in the United States. Despite an overall decline in mortality, the Hispanic/Latino (H/L) population in the Los Angeles area exhibits mortality rates up to 20% higher than their Caucasian American counterparts, often with diagnoses at a younger age and advanced disease stages. Few studies have utilized substantial H/L sample sizes and integrated comprehensive clinical and multi-omics data to conduct integrative translational analysis of reported genomic alterations and their implications for colorectal tumorigenesis.
Methods: We collected clinical, DNA, and RNA sequencing data from 36 primary CRC Tumor/Normal (T/N) samples and 82 primary CRC T/N samples within the H/L population in the Los Angeles area through the Participant Engagement and Cancer Genome Sequencing (PE-CGS) Network and the Oncology Research Information Exchange Network (ORIEN), respectively. Additionally, we retrieved two CRC samples with spatial transcriptomic (ST) data from the 10xGenomics database. This data underwent Whole Exome and RNA sequencing analysis. Furthermore, we conducted global and local genomic ancestry analyses to establish correlations between self-ancestral identification and the five main superpopulations. ST data was analyzed using recently released bioinformatics tools. Clinical and genomic data were integrated.
Results: In these studies, distinct age-of-onset, Amerindian (AMR), and survival patterns were observed, with significant mutations identified in key genes, including APC, TP53, KRAS, and PIK3CA. Cancer heterogeneity was evident, influenced by mutation type, microsatellite instability, subsite, and ethnicity. Ancestry analysis indicated genetic diversity, with a predominant AMR heritage and cases showcasing substantial European genetic proportions alongside AMR ancestry. Additionally, RNA sequencing has been conducted, with ongoing transcriptomic analysis in both studies, and the results are set for presentation at the annual meeting. The ST analysis generated initial maps, delineating diverse cellular populations and revealing the samples' distinct immunological and inflammatory signals.
Conclusion: Our study has delved into the molecular profiling of CRC tumors among H/L patients, contributing essential insights into the DNA and RNA level characterization of CRC tumors and the multifaceted clinical and genomic heterogeneity within our aimed population. It also provides crucial insights into CRC tumor heterogeneity and the tumor microenvironment. These findings serve as the cornerstone for forthcoming sample analyses within our PE-CGS project to potentially lead to the development of personalized treatments.

#3933 Comprehensive molecular characterization of mitochondrial mutational landscape across the evolution of lung adenocarcinoma.

A. Singh[1], S. Dasgupta[2], A. L. Koppayi[3], L. Rooper[4], V. Mishra[1], D. Sidransky[5], N. Agrawal[1], K. Suresh[5], E. Izumchenko[1];
[1]University of Chicago, Chicago, IL, [2]University of South Alabama, Alabama, AL, [3]Northwestern University, Chicago, IL, [4]John Hopkins University, Baltimore, MD, [5]Johns Hopkins University School of Medicine, Baltimore, MD

The human mitochondrial genome is prone to genetic alterations, which lead to somatic mutations, changes in mtDNA copy number and altered expression of respiratory chain subunits. This is in part due to the fact that mtDNA has a limited ability to repair itself when it is damaged. Although a buildup of somatic mutations in mtDNA has been associated with increased cancer risk, the role of mtDNA alterations in malignant transformation of lung adenocarcinoma has not been addressed. Therefore, a clear understanding of changes in mtDNA along the pathway of lung tumorigenesis is critical for identifying molecular biomarkers related to carcinogenesis and tumor progression. Like all solid tumors, lung adenocarcinoma is thought to be initiated and to progress through a series of genetic alterations, including changes in mtDNA. Lungs resected for primary adenocarcinomas often harbor minute discrete foci of cytologically atypical pneumocyte proliferations designated as atypical adenomatous hyperplasia (AAH). Evidence suggests that AAH represents an initial step in the progression to adenocarcinoma in situ (AIS), minimally invasive adenocarcinoma (MIA) and ultimately fully invasive adenocarcinoma (ADA). In this study we used a unique cohort of 52 patients with matched specimens (n=133) representing different steps of disease progression (AAH, AIS, and MIA) coupled with novel ultra-deep mitochondrial sequencing (mtDNA-Seq) method to assess the mtDNA mutational landscape throughout the continuum of lung adenocarcinoma development. Utilizing a custom bioinformatics workflow, somatic mutations were detected in a subset of the premalignant non-invasive lesions, with overall higher mutational load observed in MIA and ACA specimens. Additionally, large degree of inter-patient heterogeneity were observed for mtDNA copy numbers in conjunction with the clonal histological evolution of pulmonary neoplasia. Moreover, an appreciable number of coding and non-coding mutations from regulatory regions of the mtDNA were detectable in the precursor AAH lesions and the continuum of LUAD progression. Majority of shared mutations showed heteroplasmic transition with increase in fractional abundance in ADA, compared to the AHH lesions, thereby indicating spatial clonal expansion as they progressed histologically. Here we report the first comprehensive characterization of mitochondrial mutational landscape in dynamic evolution of lung adenocarcinoma, and provide insight into the heterogeneity of clonal events associated with the progression from noninvasive to malignant disease.

#3934 Smoking's influence on divergent paths to lung cancer.

E. J. Evans, Jr.[1], F. Marongiu[2], E. Lim[3], O. Pich[3], Y. Zhuang[1], D. Gao[1], W. Hill[3], C. Murphy[3], R. Turner[3], M. Ghosh[1], Y. Miller[1], M. Jamal-Hanjani[4], C. Swanton[3], J. DeGregori[1];

[1]University of Colorado Anschutz Medical Campus, Aurora, CO, [2]Unversity of Cagliari, Cagliari, Italy, [3]The Francis Crick Institute, London, United Kingdom, [4]University College London, London, United Kingdom

Lung cancer is the leading cause of cancer mortality in the world. Many studies have highlighted how mutagens from cigarette smoke promote specific mutations such as G12 mutations in *KRAS*, contributing to clonal evolution that leads to lung cancer. Despite the indisputable correlation between smoking and lung cancer, people who have never smoked account for the 7th leading cause of cancer mortality. Given the differences in predominant exposures, we hypothesize that the clonal evolution between people with and without smoking histories are markedly different. Therefore, we analyzed lung samples from people with different cigarette smoking exposure to elucidate smoking's effect on the somatic mutational landscape in the progression to lung cancer. To observe somatic mutations subjected to different exposures of smoking, we used a rare-mutation detection technique called DuplexSeq to analyze somatic variants from 200+ lung samples. We acquired DNA from cells from bronchoscopy brushings and lung punches of histologically normal tissue from people with and without lung cancer and who currently, formerly, or never smoked cigarettes. Through collaborations, we characterized mutations using bioinformatic pipelines, various databases, and statistical methods. In samples from people who smoke, we observe an enhancement of mutations with higher variant allele frequencies and pervasive positive selection acting on mutations in many cancer-associated genes. From our bronchoscopy brushings, *NOTCH1* mutations show the most definitive increase of protein-altering variants, while *NF1* and *KRAS* show a predominance of driver mutation in lung punches. Unexpectedly, people without lung cancer who never smoked had a notable presence of pathogenic mutations in *PTEN* and *PIK3CA*. Furthermore, multiple punches from the same individual highlight how expansions of mutations have stronger similarity within an individual than across individuals regardless of smoking status. This association points to the importance of the inherent lung microenvironment in influencing the mutational landscapes in lung cancer progression. Altogether, these results show how smoking increases the oncogenicity of observable mutations in the lung but does not preclude the presence of oncogenic clones, emphasizing the value of precision diagnoses and prevention. Ongoing research will be centered around functional assays to determine the impact of observed mutations on tissue function and longitudinal studies using mutational landscapes as a proxy for lung cancer risk.

MOLECULAR/CELLULAR BIOLOGY AND GENETICS: Novel Mechanisms of Oncogenesis and New Therapeutic Targets Minisymposium

#3935 Involvement of nanoscale physical communication in obesity-associated breast cancer severity.

T. Saha, B. B. Srinivasan, S. Sengupta;
Harvard Medical School, Brigham and Women's Hoapital, Cambridge, MA

Obesity is a risk factor for several cancers, including breast cancer, and contributes up to 20% of cancer-related deaths. Growing evidence from both clinical and preclinical studies indicates that increased obesity is associated with increases in cancer incidence, progression, metastasis, and therapeutic resistance. According to the Centers for Disease Control and Prevention (CDC), more than 70% and 40% of American adults can be classified as overweight and obese, respectively. However, treatment strategies for dealing with cancer in obese patients have not advanced apart from lifestyle interventions. However, several signaling mechanisms have been proposed related to the inflammatory and metabolic impact of obese adipocytes in promoting cancer progression. However, a lack of mechanistic understanding led to no specific treatment strategies have been proposed which can specifically downregulate the key regulator by which obese adipocytes promote cancer progression. Thus, translational research initiatives are immediately needed to provide mechanistic justifications for these striking statistics in order to better serve this growing segment of the population.

Here, we have shown the role of nanoscale physical communication between breast cancer cells and adipose tissue in promoting cancer progression. Using high-resolution optical and electron microscopy, we have found that breast cancer cells form nanoscale tubular communications with obese adipocytes. Moreover, the cancer cells hijack mitochondria from obese adipocytes. However, coculturing cancer cells and obese adipocytes in the Boyden chamber, allowing exosomal and paracrine communication but blocking direct physical communication, revealed negligible mitochondria transfer. This observation indicates an active transfer of mitochondria via nanotube. A significantly higher rate of mitochondria transfer from obese adipocytes to cancer cells has been observed than non-differentiated pre-adipocytes. The transfer of mitochondria results in an increase in the metabolism of the cancer cells. The mechanistic investigation of the nanotube formation revealed actin's presence as the major component in the nanotube. The exocyst-GTPase protein complex has a prime contribution in actin remodeling and nanotube formation. Inhibition of exocyst-GTPase using a pharmacological inhibitor results in a significant reduction in nanotube-mediated mitochondria transfer.

Conclusion: Our goal is to (i) investigate the direct physical connection between adipocytes and cancer cells and the effect on cancer progression and (ii) eliminate mortality related to obesity-associated breast cancer severity by introducing a new therapeutic strategy. Here, we have shown how cancer cells communicate with obese adipocytes and receive additional metabolic power for proliferation. The *in vivo* investigation of the same is under progress.

#3936 Altered endosomal pH regulation: molecular mechanisms of oncogenesis and therapeutic dependencies.

H. Dopeso[1], Y. Zhu[1], L. Gusain[1], T. Basili[1], D. Brown[1], F. Derakhshan[1], E. da Silva[1], R. Koche[1], P.-J. Hamard[1], X. Guo[2], E. Toska[3], E. DeStanchina[1], H. Zhang[1], J. Reis-Filho[1], B. Weigelt[1], F. Pareja[1];

[1]Memorial Sloan Kettering Cancer Center, New York, NY, [2]Johns Hopkins Bloomberg School of Public Health, Baltimore, MD, [3]Johns Hopkins University, Baltimore, MD

ATP6AP1 and *ATP6AP2,* which we previously identified to be recurrently altered in granular cell tumors (GCTs), encode for accessory proteins of the vacuolar (V)-ATPase, which controls endosomal acidification. The mechanistic basis of how *ATP6AP1/AP2* loss of function (LOF) leads to oncogenesis remains to be elucidated. Here, we sought to unravel the molecular mechanisms downstream of *ATP6AP1/AP2* inactivation resulting in oncogenesis and identify associated therapeutic dependencies. Using CRISPR/Cas9 technologies, we generated *ATP6AP1*-knock out (KO), *ATP6AP2*-KO and non-target (NT) control immortalized Schwann cells, the likeliest cell of origin of GCTs. Compared to NT controls, *ATP6AP1/AP2*-KOs displayed increased cellular proliferation, migration, and anchorage independent growth. *ATP6AP1/AP2*-KOs, but not NT controls, demonstrated *in vivo* tumorigenesis upon subcutaneous implantation in NSG mice. In addition, *ATP6AP1/AP2*-KOs, compared to NT controls, displayed abnormal bulk endocytic function, evidenced by reduced endocytic cargo delivery to lysosomes in a DQ-Red BSA assay, and increased LC3BII/LC3BI ratio and expression of the autophagy marker GABARAP, indicating altered autophagic flux. ATAC-seq analysis of our cell modes revealed changes in chromatin accessibility upon *ATP6AP1/AP2* inactivation, affecting transcription factors (TFs) associated to the Wnt pathway, including LEF/TCF (canonical Wnt) and NFAT (non-canonical Wnt), and TFs associated to autophagy pathways, among others. RNA-sequencing analysis revealed expression changes in key Wnt pathway components upon *ATP6AP1/AP2* LOF, such as biphasic modulators (*DKK1*, *DKK2* and *SFRP1*), secreted ligands (*WNT2*, *WNT9a* and *WNT7B*), transcriptional regulators (*TLE1*, *TLE2*, *TLE3* and *TLE4*) and receptors (*LGR5*, *FZD7* and *FZD1*). Consistent with these findings, *ATP6AP1/AP2*-KOs displayed upregulation of downstream canonical (MYC, Cyclin D1) and non-canonical (NFATC1, CALM1) Wnt targets at the mRNA and protein levels, and increased sensitivity to pharmacologic inhibition of the Wnt pathway, with significantly lower IC50s to IWR-1, compared to NT controls. Lastly, *ATP6AP1/AP2*-KOs displayed increased sensitivity to pharmacologic inhibition or induction of autophagy and/or endocytic processes, with lower IC50s to Chloroquine, N-Ethylmaleimide, Torin-1 and Bafilomycin-A1 compared to NT controls. Taken together, we demonstrate that *ATP6AP1*/*AP2* inactivation leads to the acquisition of oncogenic properties *in vitro* and in *vivo*, altered endocytosis and autophagy. Furthermore, our findings suggest that *ATP6AP1/AP2* LOF results in chromatin accessibility changes leading to activation of an oncogenic transcriptional program with increased signaling via the Wnt pathway. Notably, inactivation of these genes results in unique and previously unknown vulnerabilities, offering potential avenues for therapeutic exploration.

#3937 Investigating the role of fibulin 3 in pancreatic tumorigenesis.

H. Song[1], J. Hsu[1], X. Lin[1], S. Ogawa[2], V. Pantazopoulou[2], K. Peck[2], C. Bottomley[2], S. Okhovat[2], M. Stamp[2], K. Curtis[2], J. D. Esko[1], D. D. Engle[2];
[1]University of California, San Diego, La Jolla, CA, [2]Salk Institute for Biological Studies, La Jolla, CA

Pancreatic ductal adenocarcinoma (PDA) is a highly lethal malignancy with a five-year survival rate of less than 11%, making it one of the deadliest cancers. Notably, 95% of PDA cases exhibit *KRAS* mutations, contributing to highly dysregulated cell signaling networks. Despite extensive research into the interplay of various oncogenic pathways in pancreatic tumorigenesis, targeted therapies against these signaling networks have displayed modest efficacy, with most patients rapidly developing therapeutic resistance. Recent studies highlight the significance of the carbohydrate antigen 19-9 (CA19-9) as a functional biomarker linked to disease progression and resistance. However, understanding the detailed functions of CA19-9-modified proteins in PDA has been limited due to the lack of adequate models for synthesizing CA19-9. To address this challenge, we have developed unique mouse and 3D organoid culture models capable of producing CA19-9. CA19-9 elevation in mice with *KRAS*-mutations results in an aggressive PDA phenotype through increased tumor proliferation and microenvironment (TME) remodeling. Furthermore, our research has identified Fibulin 3 (FBLN3), an extracellular matrix glycoprotein, as a secreted, CA19-9-modified protein that stimulates tumorigenesis. In this study, we found that FBLN3 not only facilitates tumor proliferation but also drives epithelial-mesenchymal transition (EMT) and promotes STAT3 pathways activation in the CA19-9^{pos}, *KRAS*-mutant PDA organoids. Additionally, in both CA19-9^{pos}, *KRAS*-mutant PDA mouse models and human PDA, FBLN3 is expressed by cancer-associated fibroblasts (CAFs), suggesting its role in TME remodeling. These findings have significant implications for providing novel insights into PDA biology and paracrine signaling mechanisms, identifying FBLN3 as a potential therapeutic target for the improved treatment of this devastating disease.

#3938 A novel mouse model reveals potential therapeutic strategies for RIT1-driven lung adenocarcinomas.

A. Mozzarelli[1], A. Cuevas-Navarro[2], A. Urisman[3], P. Castel[1],
[1]NYU Grossman School of Medicine, New York, NY, [2]Memorial Sloan Kettering Cancer Center, New York, NY, [3]University of California San Francisco, San Francisco, CA

Gain-of-function oncogenic mutations in *RIT1* have been identified in lung adenocarcinoma and are mutually exclusive with other reported driver mutations, highlighting the role of RIT1 as a cancer driver. RIT1 is a poorly-studied non-classical RAS GTPase and, to date, there are no reported genetically-engineered mouse models of RIT1-driven lung adenocarcinoma. Here, we have generated a conditional knock-in allele within the endogenous mouse *Rit1* locus, introducing the most frequent mutation observed in lung adenocarcinomas ($RIT1^{M90I}$). Upon intranasal administration of adenovirus encoding the Cre recombinase to induce somatic recombination in the mouse lungs, we observed the formation of discrete adenomas. Although $Rit1^{M90I}$ mutation can promote lung tumor initiation in mice, we found that this phenotype is less penetrant than the common $Kras^{G12D}$ mutation. Immunohistochemistry analysis of $Rit1^{M90I}$ and $Kras^{G12D}$ tumors showed expression of typical histological markers associated with lung adenocarcinoma (i.e., TTF1 and SPC), as well as increased levels of Ki67 and pERK expression. Next, to develop potential pharmacological strategies for RIT1-driven lung tumors, we first explored drugs that inhibit the RAS/MAPK pathway and are either FDA-approved or under clinical development. *In vitro* experiments with cell lines carrying the $RIT1^{M90I}$ mutation demonstrated high sensitivity to SHP2, MEK, RAF, and RAS inhibitors. *In vivo*, SHP2 and RAS, but not MEK, inhibitors slowed down tumor progression in both cell line and patient-derived xenografts. Our results indicate that, although RAS signaling might be needed for RIT1-dependent growth, these tumors are not sensitive to MAPK inhibition as a monotherapy and, hence, other pathways could contribute to tumor growth. Therefore, we decided to explore whether targeting RIT1 directly, could be a more beneficial strategy for these tumors. In order to inhibit oncogenic RIT1 directly, we have undertaken two complementary approaches. First, because RIT1 mutations were shown to impair its proteolysis, we explored whether restoring RIT1 proteasomal degradation could be a promising strategy. Recently, the development of Proteolysis Targeting Chimeras (PROTAC) has demonstrated that targeted degradation can be used as a pharmacological approach for the treatment of cancer. Therefore, we have tested successfully several proof-of-concept PROTAC approaches that caused degradation of oncogenic RIT1 in different cellular models. Second, we used a chemical biology approach to assess whether covalent inhibitors directed against the closely-related GTPase KRAS could cross-react and bind to oncogenic RIT1. We have identified a molecule that binds RIT1 and we are currently characterizing it in our preclinical models. Overall, our work provides comprehensive insights into the oncogenic role of RIT1 in lung cancer emphasizing its potential as a therapeutic target.

#3939 Ror2, a novel key regulator driving cell fate decisions throughout pancreatic tumor progression.

S. Benitz[1], A. Steep[2], M. Nasser[1], J. Preall[3], U. Mahajan[4], I. Loveless[1], H. McQuithey[1], E. Davis[1], H.-J. Wen[1], D. Long[1], T. Metzler[5], S. Zwernik[1], D. Salas-Escabillas[1], L. Huang[1], N. Steele[1], I. Regel[4], F. Bednar[6], H. Crawford[1];

[1]Henry Ford Health System, Detroit, MI, [2]Center of Translational Data Science, Chicago, IL, [3]Cold Spring Harbor Laboratory, Cold Spring Harbor, NY, [4]Ludwig Maximilian University of Munich, Munich, Germany, [5]Technical University of Munich, Munich, Germany, [6]University of Michigan, Ann Arbor, MI

Introduction: Reprogramming of pancreas cell fate drives development of pancreatic ductal adenocarcinoma (PDAC). Acinar cells, the most probable origin of pancreatic cancer, undergo a rapid cell identity switch towards a duct-like phenotype upon $Kras^{G12D}$ expression and when combined with pancreatitis or the loss of acinar differentiation factors. Metaplastic and dysplastic duct-like cells are heterogeneous with a proportion acquiring features reminiscent of gastric lineages. While some gastric signatures are maintained in the classical PDAC subtype, they are eroded in the more aggressive, basal-like PDAC. Since subtype identity has a major impact on prognosis and therapeutic targetability, druggable targets that regulate cellular reprogramming in pancreatic cancer can be exploited to increase sensitivity to therapy.

Methods: To elucidate mechanisms responsible for early reprogramming, pancreatic tissue of mice with conditional $Kras^{G12D}$ expression and loss of Pdx1 was analyzed by single-nucleus ATAC-seq. Expression of identified target genes was studied in precancerous lesions and PDAC by using multiplex RNAscope and IHC staining. Computational analyses of publicly available sequencing data were used to establish correlation to PDAC subtype identity. Genes were functionally studied in PDAC cell lines.

Results: By performing snATAC-seq and RNA-seq of early transformed pancreatic tissue, we discovered that acinar cells with the combined expression of $Kras^{G12D}$ and loss of Pdx1 activate expression of a gastric metaplastic gene signature accompanied by elevated levels of the receptor kinase Ror2. Ror2 is also highly expressed in distinct subpopulations of metaplastic and dysplastic cells, associated with a gastric neck cell phenotype and enhanced proliferative capacity. In contrast, $Ror2^{Low}$ lesions are characterized by a gastric pit cell-like and a senescent phenotype. Genetic ablation of Ror2 resulted in a shift in lesion identity, enriching those with a pit cell and senescent identity. In PDAC, we found that Ror2 anti-correlates with a similar gastric pit cell phenotype that is maintained in the classical subtype PDAC but is strongly associated with the more aggressive basal-like subtype. Overexpression of ROR2 in human PDAC cell lines with a classical differentiation induced loss of the classical gene signature as well as epithelial-to-mesenchymal transition. Moreover, ROR2 enforces a strong dependency on AKT signaling, causing increased vulnerability of ROR2-expressing cells to AKT inhibition, but increased resistance to the KRAS inhibitor MRTX1133.

Conclusions: We discovered Ror2 as a critical determinant of precancerous lesion as well as PDAC subtype identity. Its role in driving an aggressive PDAC phenotype that is inherently resistant to Kras inhibition suggests that inhibiting this receptor tyrosine kinase will enhance sensitivity to the new generation of targeted therapies.

#3940 Nuclear translocation of HER3 promotes breast cancer progression and dissemination recruiting immune cells via CXCL1 and CXCL8.

T. Cheytan, R. Wurth, N. Hahnen, E. Donato, C. Klein, R. Weber, D. Colombo, J. Krijgsveld, M. Sprick, A. Trumpp;
German Cancer Research Center, Heidelberg, Germany

Breast cancer is a highly complex multifactorial disease, which can be driven by the aberrant regulation of different signaling pathways including receptor tyrosine kinase (RTK) signaling. Notably, while RTKs have been classically described as transmembrane receptors, they can also translocate to the nucleus, even though the functional importance of this process remains largely unexplored for most RTKs. Here, we report a novel role for the nuclear form of the RTK human epidermal growth factor receptor 3 (HER3) in driving primary breast cancer growth and metastasis. Firstly, using different patient-derived organoids (PDOs) established from metastatic breast cancer patients, we demonstrated the robust translocation of the activated phosphorylated HER3 receptor (pHER3) from the plasma membrane to the nucleus in response to its ligand Neuregulin 1 (NRG1). Interestingly, the nuclear translocation was observed not only in the HER2-positive breast cancer subtype but also in luminal and triple-negative breast cancer-derived cells. In order to decipher the functional role of nuclear HER3 (nHER3), we identified and mutated its nuclear localization signal, resulting in decreased nuclear translocation of the receptor while its membrane form remained intact. This reduction in nHER3 remarkably impeded primary tumor growth and metastatic spread in different patient-derived xenograft (PDX) models. Conversely, selective overexpression of HER3 in the nucleus led to increased primary tumor growth and metastatic burden in vivo. In order to decipher the mechanism of action of nHER3, we performed co-immunoprecipitation followed by global mass spectrometric analysis to identify the protein binding partners of the receptor in the nucleus. Specifically, nHER3 was found to interact with different transcription factors such as the AP-2 family of transcription factors and with major chromatin remodeling complexes like the nucleosome remodeling and deacetylase (NuRD) complex, implicating its role in transcriptional regulation. Furthermore, gene expression analysis of PDOs expressing the wild-type or the mutated form of HER3 revealed the modulation of several key growth regulators such as early growth response 3 (EGR3) by nHER3. The nHER3-EGR3 axis further controlled downstream effectors like the immune chemoattractants CXCL1 and CXCL8. Accordingly, PDX from breast cancer cells overexpressing nHER3 showed significantly increased immune infiltration, suggesting a possible role of nHER3 in regulating the tumor microenvironment. Altogether, we report here a novel non-canonical role of the nuclear form of HER3 receptor in driving breast tumorigenesis, with key implications for our understanding and targeting of RTK signaling in breast cancer.

#3941 Wild-type KRAS dosage in mutant KRAS lung cancer: Implications for tumorigenesis and therapeutic response.

T. Ivanisevic[1], G. Vande Velde[2], P. Zhao[1], W. Magits[1], R. N. Sewduth[1], A. A. Sablina[1];
[1]VIB-KU Leuven Center for Cancer Biology, Leuven, Belgium, [2]Nuclear Medicine and Molecular Imaging, Leuven, Belgium

Lung adenocarcinomas (LUAD) are frequently driven by activating mutations in the Kirsten rat sarcoma viral oncogene homolog (KRAS). Previous studies have suggested that wild-type (wt)-RAS signaling may modulate cancer progression and drug resistance in these tumors. However, the interplay between oncogenic KRAS and wt-RAS-like GTPases in lung cancer biology and treatment remains debated. Here, we investigated the impact of increased wt-KRAS dosage in LUAD harboring mutant KRAS on lung cancer phenotypes and response to anti-KRAS therapies. Increased wt-KRAS dosage occurs in LUAD due to the loss of LZTR1, a proteostatic regulator of RAS-like GTPases. *LZTR1* mutations, deletions, or downregulation co-occur with oncogenic KRAS mutations in more than 40% of LUAD patients. Using a global protein stability screen, we identified LZTR1 as the main regulator of the stability of wt-KRAS, but not of the oncogenic KRAS mutants. Proteomic analysis of LUAD cells confirmed that LZTR1 loss leads to elevated expression of wt-KRAS, but not of KRAS-G12D, indicating that *LZTR1* loss affects wt-RAS rather than mutant KRAS signaling. *LZTR1* loss in LUAD patients is associated with poor prognosis and hypoxic expression signatures. In a mouse model of *Kras*-mutated LUAD, *Lztr1* haploinsufficiency promoted tumor initiation and progression. Moreover, *Lztr1* loss results in hypoxic tumors with inflamed, tortuous, insufficiently perfused, and leaky vessels. Integrative proteomic and phosphoproteomic analysis revealed increased RAL/TBK1 pathway activity in *LZTR1*-depleted lung cancer cells and *Lztr1*-deleted tumors. This leads to enhanced secretion of proangiogenic and proinflammatory factors, such as VEGF and TNFα, by *LZTR1*-deficient cells and an increased number of neutrophils in *Lztr1*-deleted tumors. TNF-activated neutrophils present at vascular branching points can modulate vascular remodeling by influencing the formation and function of blood vessels. Pharmacological inhibition of RAL/TBK1 signaling with amlexanox, an anti-NF-κB/TBK1 drug, reduces TNFα secretion, decreases the number of neutrophils, and normalizes the tumor-associated vasculature. We demonstrated that increased wt-KRAS dosage, but not other small GTPases, mimicked the effects of LZTR1 loss on RAL/TBK1 signaling and VEGF secretion, suggesting that LZTR1 loss alters the heterogeneity of KRAS-mutated lung cancer by modulating wt-KRAS levels. Furthermore, MRTX1133 a selective inhibitor of KRAS-G12D, showed limited effect in the *Kras-G12D*, *Lztr1*-loss LUAD model, whereas the combination of MRTX1133 and amlexanox suppress tumor growth, likely due to the restoration of the tumor vasculature by RAL/TBK1 inhibition. Our study reveals novel insights into the role of wt-KRAS dosage in mutant KRAS lung cancer and identifies potential therapeutic strategies to target patients with dysregulated KRAS proteostasis due to LZTR1 loss.

POPULATION SCIENCES: Cancer Disparities Research
Minisymposium

#3942 Mailed at-home self-sampling for HPV testing increases screening participation among under-screened patients in a U.S. safety net health system: Results of the PRESTIS trial.

Jane R. Montealegre[1], Elizabeth Y. Chiao[2], Matthew L. Anderson[3], Susan G. Hilsenbeck[4], Shaun Bulsara[4], Susan L. Parker[1], Maria Daheri[5], **Trisha L. Amboree**[1], Kathleen M. Schmeler[6], Maria L. Jibaja-Weiss[7], Mohammad Zare[8], Ashish A. Deshmukh[9], Michael E. Scheurer[10]

[1]Behavioral Science, UT MD Anderson Cancer Center, Houston, TX,[2]Epidemiology, UT MD Anderson Cancer Center, Houston, TX,[3]Obstetrics and Gynecology, University of South Florida Morsani School of Medicine, Tampa, FL,[4]Medicine, Baylor College of Medicine, Houston, TX,[5]Harris Health System, Houston, TX,[6]Gynecologic Oncology, UT MD Anderson Cancer Center, Houston, TX,[7]School of Health Professions, Baylor College of Medicine, Houston, TX,[8]Family and Community Medicine, University of Texas Health Science Center-Houston, Houston, TX,[9]Medical University of South Carolina, Charleston, SC,[10]Pediatrics, Baylor College of Medicine, Houston, TX

Background: In global settings, self-sampling for human papillomavirus (HPV) testing is associated with a pooled 2-fold increase in cervical cancer screening participation over usual care among underscreened persons. The Prospective Evaluation of Self-Testing to Increase Screening (PRESTIS) Trial is the first pragmatic randomized controlled trial (RCT) in the U.S. to evaluate the effectiveness of mailed at-home self-sampling for HPV testing in a safety net health system setting. Safety net systems provide care to medically underserved individuals at elevated cervical cancer risk. We hypothesized that patients who were mailed a self-sampling kit would have greater screening participation compared with those receiving usual care; and that patient navigation, a patient-centered intervention to address barriers to care, would further increase participation.
Methods: PRESTIS is a three-arm pragmatic RCT of n=2,270 patients in a U.S. safety net health system who are under-screened for cervical cancer (i.e., no Pap in 3.5 years or Pap/HPV co-test in 5.5 years). Eligible participants were identified through the electronic health record (EHR) and randomized to arms: 1) telephone recall to provider-performed screening (usual care); 2) telephone recall + mailed self-sampling kit for HPV testing; or 3) telephone recall + mailed self-sampling kit + telephone-based patient navigation. Self-sampled swabs were tested for high-risk (HR)-HPV. HR-HPV+ patients were navigated to clinical follow-up. The primary outcome, incidence of screening participation, was ascertained by EHR review at 6 months post-randomization and defined as return of a completed kit or attendance for provider-performed screening.
Results: Participants were enrolled 02/2020-08/2023. Primary outcomes have been ascertained for n=2,115 participants. Participants were predominantly Hispanic/Latina (68.6%); 53.4% indicated Spanish as primary language; and 60.3% were uninsured. Mean age was 47.9 years (SD: 10.4 years); median time since last screening test was 9.5 years (range: 1.6-21.7 years). In intent-to-treat analyses, screening participation was 15.3% (95% CI 13.0% - 17.9%) in Arm 1; 44.0% (40.4% - 47.6%) in Arm 2; and 51.4% (47.7% - 55.0%) in Arm 3. Relative incidence of screening in Arms 2 and 3 versus Arm 1 was 2.90 (2.42 - 3.47) and 3.36 (2.82 - 4.01), respectively. Relative incidence of screening in Arm 3 versus Arm 2 was 1.16 (1.04 - 1.29).
Conclusion: Compared with usual care, mailed at-home self-sampling increased screening participation among an under-screened population by almost three-fold when used alone and over 3.3-fold when combined with telephone-based patient navigation. After FDA approval, self-sampling for HR-HPV testing has the potential to dramatically increase participation in cervical cancer screening in underserved populations.

#3943 Refined race and ethnicity categories for an EHR-based cohort to study disparities in liver cancer risk.

M. C. DeRouen[1], C. A. Thompson[2], A. J. Canchola[1], A. Cortella[1], P. Inamdar[1], J. Chu[1], S. Nie[3], M. Vu[4], M. Somsouk[1], M. M. Tana[1], A. D. Rubinsky[1], I. Cheng[1], M.-O. Klm[1], M. Segal[1], C. Ho[5], Y. G. Daida[3], S.-Y. Liang[4], H. B. El-Serag[6], S. L. Gomez[1], S. Shriff-Marco[1];

[1]UCSF - University of California San Francisco, San Francisco, CA, [2]UNC - University of North Caroline Chapel Hill, Chapel Hill, NC, [3]The Center for Integrated Healthcare Research-Kaiser Permanente Hawai'i, Honolulu, HI, [4]Palo Alto Medical Foundation Research Institute, Palo Alto, CA, [5]California Pacific Medical Center, Sutter Health, San Francisco, CA, [6]Baylor College of Medicine, Houston, TX

Purpose: To develop a schema for harmonized, detailed characterization of race and ethnicity data for an electronic health record (EHR)-based cohort linked to cancer registry data to assess disparities in hepatocellular carcinoma (HCC) risk.

Methods: We assembled an cohort of adults with 1+ encounter in 2000-2017 by pooling EHR data from three healthcare systems (Kaiser Permanente Hawai'i, Sutter Health, San Francisco Health Network). EHR data to define sociodemographic and clinical factors were linked to population-based state cancer registries for data on incident HCC (ICD-03 site/histology C22.0/8170-8175) through 2017. We extracted, harmonized and developed schemas to characterize multiple response race and ethnicity data across systems. We used Cox proportional hazards regression to examine disparities in HCC risk across racial and ethnic groups, comparing observations across categorization schema.

Results: The cohort included 4,248,553 adults; 2,916 had incident HCC. A race and ethnicity schema that prioritized small populations and disaggregation of heterogenous groups defined 16 categories and was used to analyze pooled data from Kaiser Permanente Hawai'i and Sutter Health. With this schema, we observed variation in HCC risk across ethnic groups that are typically aggregated into larger ethno-racial categories (e.g., Asian American). Compared to non-Hispanic (NH) White males, Vietnamese American males had greater risk of HCC (hazard ratio (HR): 7.42; 95% CI: 4.25, 12.96) as did American Indian/Alaska Native, Black, Chinese American, Hispanic, Native Hawaiian, and Pacific Islander males; Asian Indian, Filipino, Japanese, and Korean American males did not. Among females, every group except American Indian/Alaska Native, Asian Indian American, and Pacific Islander females had greater risk of HCC than the NH White group. Due to less granular data from San Francisco Health Network during our study period, we developed a second, grouped schema aggregating categories from the detailed schema; it resulted in seven race and ethnicity categories and was used to analyze pooled data from all three healthcare systems. Compared to the categorization of race and ethnicity used by the US Census, which also has seven categories, we observed different patterns in HCC risk disparities for the smallest groups (i.e., American Indian/Alaska Native and Native Hawaiian).

Conclusions: Analysis of a large EHR-based cohort linked to cancer registry data using a race and ethnicity characterization schema that prioritizes small populations yields valuable knowledge on disparities in HCC risk. Thus, to advance research on health disparities using EHR data, researchers must critically assess racial and ethnic categories typically available from healthcare system data repositories. We offer recommendations to operationalize EHR data on race and ethnicity to facilitate its meaningful use in research.

#3944 Addressing stomach cancer disparities by assessing *Helicobacter pylori* infections among American Indian adults from the Navajo Nation.

D. Pete[1], N. R. Salama[1], J. W. Lampe[1], M. C. Wu[1], A. I. Phipps[2];
[1]Fred Hutchinson Cancer Center, Seattle, WA, [2]University of Washington, Seattle, WA

Background. The Navajo Nation, the largest tribe in the United States (US), is experiencing a high burden of stomach cancer, possibly due to a high prevalence of *Helicobacter pylori (Hp)* infection. *Hp* is a major risk factor for stomach cancer and *Hp* strains that carry the *cagA*-gene are linked to greater gastrointestinal disease severity. Yet little research has investigated the prevalence and correlates of *Hp* and *cagA* infection in Navajo people. We assessed the prevalence and correlates of *Hp* infection and *cagA*-gene carriage in adult tribal members residing in the Navajo Nation.
Methods and Material. We conducted a community-based cross-sectional study in the Navajo Nation in 2021 during the COVID-19 pandemic. Participants were recruited using online and offline platforms, including social media, a study website, newspaper advertisements, flyers, word of mouth, and community outreach. Stool samples collected from participants were analyzed with droplet digital PCR for *Hp* 16S and *cagA* virulence genes. Demographic characteristics, health, and dietary factors were collected from self-administered health and food questionnaires sent via mail.
Results. Of 99 participants, half (49.5%) were 18-44 years old and 73.7% were female. About sixty percent (57.7%, 95% CI: 47.6-67.3) of participants were infected with *Hp*, twice the US population prevalence (27%). Among *Hp*-infected participants, 76.7% (95% CI: 64.0-86.6) were *cagA*-gene positive, four times the *cagA* gene prevalence in White people (19%). Controlling for age and sex, monthly use of Navajo herbal medicines was positively associated with *Hp* infection (OR=3.73, 95% CI: 1.05-17.87). No significant associations with *Hp* and *cagA*-gene were observed with other risk factors such as older age, males, lower education, and high sodium intake.
Conclusion. A substantial proportion of Navajo adults in our study had *Hp* and *cagA*-positive infections. Given studies showing the antibacterial activity of Indigenous herbal medicines, monthly use of Navajo herbal medicines was an unexpected risk factor for *Hp* infection. This observation may be due to reverse causality, where participants with gastrointestinal conditions used Navajo herbal medicines for gastrointestinal symptom relief, particularly when participants had limited access to healthcare services due to the COVID-19 pandemic. Possible environmental transmission of *Hp* in the preparation of herbal medicines (i.e., water source, utensils) could be another source of exposure. Given the high burden of *Hp* and *cagA*-positive infections, culturally tailored health education strategies and interventions addressing these infections present an opportunity for research and cancer prevention among Navajo adults.

#3945 The development of a culturally adapted tobacco prevention curriculum for LGBTQ+ youth across California: Formative research.

M. Fine[1], Z. Surani[1], L. J. Finster[1], J. T. Greene[2], C. L. N. Kajiwara[2], R. Zaldivar[3], **B. Halpern-Felsher**[2], R. W. Haile[1];
[1]Cedars-Sinai Medical Center, Los Angeles, CA, [2]Stanford University School of Medicine, Palo Alto, CA, [3]The Wall Las Memorias, Los Angeles, CA

Purpose: LGBTQ+ youth exhibit some of the highest rates of tobacco use and tobacco-related morbidity and mortality, making access to cancer prevention at an early age particularly critical. The purpose of this study is to develop an LGBTQ+ culturally tailored tobacco prevention curriculum within the Stanford Tobacco Prevention Toolkit, to help prevent LGBTQ+ students from starting or escalating the use of any tobacco product.
Methods: A community-based participatory research (CBPR) was established between the Cedars-Sinai Cancer Research Center for Health Equity, facilitated by Community Outreach and Engagement, in collaboration with The Wall Las Memorias and the Stanford REACH Lab to conduct basic formative focus groups in the LGBTQ+ community. Seventy-six participants were recruited, and 9 focus groups were conducted (33 participants among LGBTQ+ youth; 19 community advocates and educators; and 24 parents/caregivers/guardians). A thematic analysis was conducted to identify lesson topics and subject matter content to be included in the curriculum and the best strategies to deliver the lesson to LGBTQ+ youth.
Results: Several themes emerged from the focus groups, including an overall theme noting a desire for more safe spaces and peer support to discuss tobacco, vaping, and marijuana use among LGBTQ+ youth. LGBTQ+ youth noted tobacco, vaping, and marijuana were very accessible through friends and social groups in the school setting. They also expressed that tobacco, vaping, and marijuana use were associated with pressures to fit in, an increasing ‘normalization’ of marijuana use, and social media channels that glorify vaping and tobacco use. LGBTQ+ youth also expressed that they do not see tobacco prevention messaging relevant to themselves or their peers nor through their preferred information channels. Parents, educators, and community advocates expressed that they would like to be offered opportunities for education and direct involvement in LGBTQ+ research. With this information, the REACH Lab is developing the LGBTQ+ curriculum.
Conclusions This CBPR approach builds upon the existing validated set of curricula contained in the Stanford Tobacco Prevention Toolkit, which is theory-driven and has reached over 3 million middle and high school students. Once completed, the LGBTQ+ Focused Tobacco Prevention Curriculum will be added to the Tobacco Prevention Toolkit and will be the first informed/validated tobacco prevention program for LGBTQ+ youth.

#3946 Weaving equity into the fabric of health: A deep dive into race, social determinants of health and facility type in pancreatic adenocarcinoma care.

C. Wu, Z. Song, R. Akhund, C. McLeod, L. Wood, H. Chen, J. Rose, S. Bhatia, A. Gillis;
University Of Alabama At Birmingham, Birmingham, AL

Introduction: Pancreatic adenocarcinoma (PDAC) remains one of the deadliest malignancies, with significant differences in survival rates observed among various racial and ethnic groups. Despite advancements in care, ongoing racial disparities stress the need to uncover underlying causes. This study seeks to evaluate the interplay of race, social determinants of health, and treatment facility on overall survival (OS) of PDAC patients.
Methods: In this retrospective cohort study, we identified PDAC patients from January 1, 2004, to December 31, 2019, using National Cancer Database (NCDB) data. Patients not receiving treatment (surgery, chemotherapy, or radiation) or who were missing race were excluded. We performed a multivariable cox proportional hazards regression to explore the race and all-cause mortality relationship, stratified by facility type and income status. Patients were divided into income quartiles (SES) with the lowest SES represented by median zip code level income ≤$40,227, while highest SES indicated income levels ≥$63,333. Treating facility type included community or academic hospital. A two-sided P-value <0.05 was considered significant.
Results: The total cohort included 210,520 patients. The average age of the cohort was 66.4 (SD:10.7) years and most patients were white (80%, N=168,467), male (52.2%, N=109,844), treated at academic facility type (65.5%, N=136,623), and the highest SES was the largest (38.4%, N=71,205). In unadjusted analysis, Black patients had lower OS than Whites (HR: 1.05 (95% CI: 1.04-1.07, p<0.001)). As SES increases there was a corresponding decrease in hazards (p<0.001). In the multivariable subgroup analysis, survival were not significant for Black and White patients in highest SES at academic facilities (p=0.8). Of note, highest SES Black patients in community hospitals had worse survival than highest SES White patients (HR: 1.08 (95% CI:1.01-1.16, p=0.03)). However, lowest SES Blacks treated at academic facilities had superior survival compared to lowest SES Whites (HR: 0.93 (95% CI: 0.89-0.96, p<0.001)).
Conclusion: Survival differences among Black individuals were linked to SES and facility type. Highest SES was not protective for Black patients treated at community hospitals compared to their White counterparts, indicating additional factors driving outcomes. These findings highlight the intricate influence of race, SES, and perhaps biology on survival outcomes. Addressing these complexities through targeted research and intervention is crucial for reducing health disparities and fostering a more equitable healthcare landscape.

#3947 Non-BRCA variants in hereditary breast and ovarian cancer patients in the Northern Mexico population.

C. H. Burciaga-Flores, Sr.[1], D. C. Perez-Ibave[1], M. L. Garza-Rodriguez[1], O. Vidal-Gutierrez[1], C. M. Villarreal-Garza[2], D. Aguilar y Mendez[2];
[1]Universidad Autonoma de Nuevo Leon, Monterrey, Mexico, [2]Hospital Zambrano Helion Tec Salud, Monterrey, Mexico

Background: Hereditary cancer syndromes explain 5-10% of all cancer cases. Germline pathogenic variants in BRCA1 and BRCA2 genes (BRCA) are present in 2-3% of all breast cancer (BC), and 15% of all ovarian cancer (OC) cases. BRCA1 and BRCA2 pathogenic variants (PV) represent 25-28% of BC and 40% of OC patients with a positive familial history. BRCAs are the most studied genes for the prevalence, family history, preventive surgeries, and target treatment options in both BC and OC. There are other genes, important in the diagnosis, pathogenesis, and treatment options of the patients: TP53, PALB2, CHEK2, among others. This study aims to identify the prevalence of non- BRCA genes related to the development of hereditary breast and ovarian cancer syndrome in patients of Northeast Mexico.
Methods: This is a multicenter study that recruited patients from two reference oncology centers in Nuevo Leon, Mexico: the CECIL (The CUCC Early Cancer Detection Clinic) Hereditary Cancer Registry and Hereditary Cancer Program from Tec Salud. From March of 2016 to March of 2023, a total of 872 patients meeting NCCN criteria were evaluated by Medical Geneticists from both centers and were tested with NGS multigene cancer panels.
Results: A total of 665 (76.26%) patients with a clinical diagnosis of HBOC (Hereditary Breast Hereditary Cancer Syndrome) were included. We found 310 (46.6%) patients had at least one variant, 180 (58%) with at least one pathogenic variant, and 130 (41%) with a VUS (a variant of uncertain significance). BRCA1 was found in 79 (43.8%) and BRCA2 in 32 (17.7%) of all PV. Non-BRCA PV were found in 69 (38.3%) patients: 4 ATM, 2 BLM, 3 BRIP1, 22 CHEK2, 4 CDKN2A, 5 MUTYH, 10 PALB2, 4 RAD51C, 2 SDHA, 2 TP53, 2 WRN, CDH1, CDK4, DICER, MSH3, NBN, PTEN, RAD50, USH2A one of each. Is remarkable that 19 of the 22 patients with CHEK2 and 5 of the 10 patients with PALB2 had the recurrent PV c.707T>C and c.2167_2168del, respectively.
Conclusions: Non-BRCA PV in Northern Mexico corresponds to one-third of the BC and OC cases, including HRD (homologous recombination deficiency) genes. HDR patient carriers are potential targets of iPARP therapies. This project reinforces the fact that multigene panels should be employed to ensure a complete diagnosis in hereditary cancer patients.

#3948 HPV45 and HPV52 prevalence, within-type variants, and precancer/cancer risks differ by race/ethnicity.

Aimee J. Koestler[1], Chase W. Nelson[1], Meredith Yeager[2], Zigui Chen[3], Laurie Burdett[2], Sambit K. Mishra[2], Michael Dean[2], Elizabeth Suh-Burgmann[4], Thomas Lorey[5], Phillip E. Castle[1], Mark Schiffman[1], Lisa Mirabello[1]

[1]Division of Cancer Epidemiology and Genetics, National Cancer Institute, National Institutes of Health, Rockville, MD, [2]Cancer Genomics Research Laboratory, Leidos Biomedical Research, Inc., Frederick, MD, [3]Department of Microbiology, The Chinese University of Hong Kong, Hong Kong, China, [4]Division of Research, Kaiser Permanente Northern California, Oakland, CA, [5]Regional Laboratory and Women's Health Research Institute, Division of Research, Kaiser Permanente Northern California, Oakland, CA

Introduction: Persistent infection with a high-risk HPV (HR-HPV) type causes cervical cancer and many other cancers in both men and women. Our published data have shown that the distribution of specific HPV16/35 sublineages and genetic variants differ around the world and confer greater risk of cervical precancer/cancer in the populations where the virus is thought to have originated and coevolved. More studies are needed to evaluate the relationship between race/ethnicity, HR-HPV genetic variation, and precancer/cancer risk.

Objective: To evaluate HPV45 and HPV52 genetic variation, and how it relates to a woman's race/ethnicity and cervical precancer/cancer risk, using HPV whole-genome sequencing of 774 HPV45+ and 719 HPV52+ women in the NCI-Kaiser Permanente Northern California (KPNC) HPV Persistence and Progression cohort; and compared to HPV16/35.

Methods: We viral genome sequenced 557 HPV45+ and 345 HPV52+ controls (women with benign infections [≤CIN1]), and 94 HPV45+ and 227 HPV52+ precancer/cancer cases (CIN3+). We evaluated HPV45 and HPV52 prevalence for each type by a woman's self-reported race/ethnicity, and compared them to HPV16 and HPV35 using existing comparable NCI-KPNC data. To assess associations between HPV45 and HPV52 genetic variation (viral sublineages and SNPs) and infection outcome, we used Fisher's Exact Tests and logistic regression to estimate the OR and 95% CI.

Results: For HPV45, we determined that sublineages have varying histology-specific precancer/cancer risk (ORs ranged from 2-14), and that the sublineage distribution significantly varied by race/ethnicity ($p < 0.001$). By race, the HPV45 A2 sublineage was most prevalent in Asian/PI women and was associated with the highest risk of CIN3+ in these women compared to other races/ethnicities (OR=5.7, 95% CI=1.5-29.4), while the B2 sublineage was associated with increased risk of CIN3+ in Black women only (OR=6.1, 95% CI=1.2-33.6). The prevalence of each HR-HPV type (HPV16/35/45/52) significantly varied by race/ethnicity ($p < 0.001$). For each type, White was the most reported race/ethnicity; however, Black women were a greater proportion of the HPV35+ cases compared to other types (15% vs 8-10%), and Asian/PIs were a greater proportion of HPV52+ cases (26% vs 10-13%). HPV52 genome analyses are still underway; we will present the complete study results (i.e., sublineage risk by race) at AACR.

Conclusions: We conducted the largest studies of HPV45 and HPV52 genome variation to date. We demonstrate that specific HPV45 sublineages vary by race and are associated with an increased risk of precancer/cancer for specific races/ethnicities, and that HPV52 infection has a greater prevalence in Asian/PI women compared to other racial groups. Our data suggest that certain HR-HPV types and specific sublineages of these types are more common in specific racial/ethnic groups and potentially linked to differing risks by race.

TUMOR BIOLOGY: Genetic Drivers and Therapeutic Achilles' Heels of Childhood Cancers
Minisymposium

#3949 SMARCAL1 is a novel synthetic lethal target in ALT+ osteosarcoma and neuroblastoma.

M. Wierdl[1], J. L. Catlett II[2], N. Ocasio-Martinez[2], J. D. Johnson, Jr.[1], A. Herman[3], N. V. Dharia[2], G. Alexe[2], E. A. Sweet-Cordero[4], E. Bernstein[5], K. Stegmaier[2], **L. M. Guenther**[1];

[1]St. Jude Children's Research Hospital, Memphis, TN, [2]Dana-Farber Cancer Institute, Boston, MA, [3]Broad Institute of MIT and Harvard, Cambridge, MA, [4]UCSF School of Medicine, San Francisco, CA, [5]Icahn School of Medicine at Mount Sinai, New York, NY

Osteosarcoma (OS) is an aggressive pediatric solid tumor that is difficult to treat with established therapies. We performed CRISPR/Cas9 screening in 13 OS cell lines as part of the Dependency Map project. Mining this data to identify genes whose knockout (KO) leads to selective anti-viability in OS, we observed the helicase *SMARCAL1* as a selective dependency in OS ($p<0.0001$; effect size = -0.275). Given the genomic instability of OS and SMARCAL1's related, established role in replication stress, we first validated our screens by CRISPR KO in OS lines in vitro. This demonstrated selective antiviability of *SMARCAL1* KO in dependent OS lines. To orthogonally validate *SMARCAL1* dependency, we deployed a dTAG system, utilizing a hetero-bifunctional small molecule targeting the tagged protein for degradation by an E3 ubiquitin ligase. We observed antiviability of dependent lines after SMARCAL1 degradation. In parallel, in order to ascertain importance of this gene in vivo, we performed a barcoded CRISPR pooled screen against pre-selected OS dependencies in an OS cell line xenograft in NSG mice. After sequencing of tumor gDNA, we identified *SMARCAL1* as a top hit, suggesting relevance *in vivo*.We next investigated biomarkers of *SMARCAL1* dependency. A role for SMARCAL1 has been described in alternative lengthening of telomeres (ALT). We asked whether ALT+ OS cell lines are enriched for *SMARCAL1* dependency. We found a correlation between ALT+ OS and *SMARCAL1* dependence in our CRISPR screens. We then asked if this extends to other ALT+ tumors. Neuroblastoma (NB), the most common extracranial pediatric solid tumor, is enriched for ALT. When we looked specifically at NB models, we observed that *SMARCAL1* was the most enriched dependency in ALT+ NB compared with other NB lines ($p<0.0001$; effect size = -0.785). We then performed *SMARCAL1* KO in 2 ALT+ ATRX-altered NB lines and one ALT+ ATRX-WT NB line. We found that *SMARCAL1* KO led to antiviability in the ATRX-altered ALT+ cell lines, while the ALT+ ATRX-WT cell line was unaffected. This suggests that dependency on *SMARCAL1* is specific to ATRX alteration, rather than ALT alone.In order to confirm synthetic lethality between ATRX and SMARCAL1, we next utilized a human OS line not included in the DepMap screen, which has biallelic inactivation of *SMARCAL1*. We infected this line with our SMARCAL1 dTAG, leading to constitutive overexpression of SMARCAL1, and then performed ATRX KO. We observed that SMARCAL1 overexpression rescued the antiviability effect of ATRX KO. This could be reversed by degradation of exogenous SMARCAL1, suggesting that ATRX and SMARCAL1 can compensate for one another. Taken together, these findings demonstrate that *SMARCAL1* is a selective dependency engendered by the loss of WT ATRX in OS and NB and that SMARCAL1 is playing a critical role in mediating ALT. Studies are ongoing to determine the mechanism of SMARCAL1's activity and potential for targeting this enzyme for therapeutic benefit.

#3950 Dedifferentiation unveils origin of Ewing sarcoma.

U. Kapoor[1], C. Hafemeister[1], L. Shaw[2], K. Muelbacher[1], J. Moldaschl[3], D. Egger[4], S. Toegel[2], C. Kasper[3], M. Farlik[2], F. Halbritter[1], H. Kovar[1];
[1]St. Anna Children's Cancer Research Institute, Vienna, Austria, [2]Medical University of Vienna, Vienna, Austria, [3]University of Natural Resources and Life Sciences (BOKU), Vienna, Austria, [4]Leibniz University Hannover, Hannover, Germany

Ewing sarcoma (ES) is an aggressive pediatric bone tumor in adolescents primarily driven by the expression of the fusion oncogene EWS::FLI1. Although the etiology of ES remains controversial, human mesenchymal stem cells (hMSCs) are considered to be the likely cell of origin. This is not only due to their ability to tolerate ectopic EWS::FLI1 expression, but also because the transcriptome of EWS::FLI1 expressing hMSCs is highly similar to that of primary Ewing tumors. However, to date a cellular differentiation-based model of ES does not exist. With the intent to understand ES histogenesis, this study aims to establish the first comprehensive single-cell differentiation atlas (both transcriptome and epigenome) of juvenile bone marrow-derived hMSCs with and without EWS::FLI1 expression. We sought to study the consequences of inducing the EWS::FLI1 oncogene expression at various time points of hMSC differentiation into adipo-, chondro-, osteo- and neuro-genic lineages. Our workflow utilizes physiology-mimicking conditions including serum-free differentiation, hypoxia, and growth/differentiation as spheroids. We pooled bone marrow-derived hMSCs isolated from eleven healthy juvenile donors, engineered them to conditionally express EWS::FLI1, and carried out multi-lineage differentiation for 10 days where EWS::FLI1 was induced daily for 24h or 72h. This temporally resolved atlas of 105 samples representing normal and perturbed differentiation allowed us to map ES patient tumor data to multiple lineages and time-points across stages of lineage commitment. Single-cell RNA-seq analysis of ~271,000 transcriptomes revealed an apparent and dynamic dedifferentiation in the presence of EWS::FLI1 across all four lineages. Preliminary analysis of genes detected in the EWS::FLI1 high cluster uncovers a specific lineage preference and time window that shares the transcriptomic signature with tumor cells, indicating the potential cell/stage of tumor-origin. Our results provide new insight into the enigmatic cell of origin of Ewing sarcoma, laying the foundation for the development of much-needed pre-clinical models for tailoring therapies. This study is supported by a generous grant (#20) of the Alex’s Lemonade Stand Foundation (ALSF) Crazy8 Program.

#3951 Timing the development of chemoresistance in relapsed pediatric cancer.

S. Blay[1], M. Layeghifard[1], S. Davidson[1], D. Chen[1], A. Schwertschkow[1], V. Ramaswamy[1], M. Taylor[1], E. Papaemmanuil[2], A. Villani[1], D. Malkin[1], L. Alexandrov[3], M. Cowley[4], A. Shlien[1];

[1]SickKids, Toronto, ON, Canada, [2]Memorial Sloan Kettering Cancer Center, New York City, NY, [3]University of California, San Diego, CA, [4]Children's Cancer Institute, New South Wales, Australia

Survivors of pediatric cancer face lifelong battles with severe morbidities, which includes a significant risk of recurrence. Pre-existing genetic variation within primary tumors may offer certain cell populations an evolutionary advantage, increasing the likelihood that some will be resistant to treatment. But the inherent complexity of the tumor means finding these markers of resistance has yet to be fully explored across childhood cancer. To address this, we developed a pipeline that combines clonal evolution reconstruction with mutational signature extraction at the subclonal level to elucidate changes in mutational processes. Using this pipeline to analyze 1,743 pediatric tumor genomes we found a common pattern of parallel evolution in most pediatric cancers, irrespective of their tissue of origin. Further, we detected therapy-associated mutational signatures linked to specific treatments such as temozolomide, platinum, fluorouracil, and thiopurine in post-treatment tumor subpopulations. Of 235 samples with known treatment exposure, 37.9% displayed one or more treatment-associated signatures. In the context of the phylogenetic tree, we identified specific subpopulations with therapy signatures. In multi-sample cases, resistant subpopulations had ancestors present in primary tumors at the time of diagnosis, suggesting certain subpopulations possessed the ability to withstand chemotherapy-induced pressures from an early stage and then expanded following treatment. Finally, we observed differences in the timing of mutational signatures between antimetabolite and alkylating agent treatments, reflecting the mechanisms of these drugs. Antimetabolite agents showed subclonal mutational signatures occurring in later branches, likely due to dependence on cell cycling. In contrast, alkylating agents displayed signatures in both early and late subpopulations, as they are unaffected by cell cycle state. Thus, investigating mutational signatures at the subclonal level unveils new insights into the clonal dynamics of pediatric cancers and the development of chemoresistance. This research offers valuable insights for identifying pediatric cancer patients at greater risk of recurrence, enabling the development of more effective treatment plans to enhance their quality of life and overall survival rates.

#3952 Multiomic single-cell tumor evolution models of minimal residual disease in pediatric B-cell acute lymphoblastic leukemia.

S. M. Foltz[1], A. Loren[2], C. Chen[1], R. Mehta[2], E. Li[3], J. Xu[2], F. Alikarami[1], K. M. Bernt[1], K. Tan[1];
[1]Children's Hospital of Philadelphia, Philadelphia, PA, [2]University of Pennsylvania, Philadelphia, PA, [3]Stanford University School of Medicine, Palo Alto, CA

Detection of minimal residual disease (MRD) after initial diagnosis (IDX) and therapy is a strong prognostic marker for relapse in pediatric B-cell acute lymphoblastic leukemia (B-ALL). Previous studies have explored clonal genetic and gene expression changes between initial diagnosis and relapse. However, studying tumor cells present at MRD is challenging due to their low abundance. Examining the genomic profiles of leukemia cells that resist induction chemotherapy and understanding their evolutionary relationship to cells present at diagnosis may lead to a better understanding of the cells that eventually seed relapse. We analyzed somatic point mutations, indels, and copy number variants from 41 pediatric B-ALL patients with high-risk B-ALL. We specifically focused on patients from the following four common high-risk subtypes: KMT2A-rearranged, Ph+, Ph-like, and iAMP21, who had detectable disease at the end of induction. Leukemic burden at end-induction (day 29) ranged from 0.03% to 66.00%. Data were generated in partnership with the National Cancer Institute's Human Tumor Atlas Network and the Children's Oncology Group.

Our data set of 41 patients includes 39 with paired initial diagnostic and end-induction samples that we used to create tumor evolution models based on single cells across disease stages. We produced single-cell multiome gene expression (scRNA) and chromatin accessibility (scATAC) profiles (10x Genomics) with a median of 7428 leukemic blast cells at IDX (range: 2490-14219) and 1907 at MRD (range: 240-10167) after filtering. We called somatic mutations from scRNA and scATAC using SComatic and Monopogen, and we detected copy number changes using Numbat and EpiAneufinder. We also designed a targeted DNA sequencing panel including 335 variants based on B-ALL literature and database searches to produce scDNA (Mission Bio) for 24 patients (16 IDX-MRD pairs) with a median of 2346 cells profiled at IDX (range: 340-8849) and 1828 at MRD (range: 596-5133). We built tumor phylogenies based on somatic SNVs and CNVs with COMPASS. Using multiple tools and complementary single-cell omics data types to detect somatic changes improved our confidence in the events used for tumor evolution tree construction.

Our approach allowed us to define recurrent genomic events and patterns across pediatric B-ALL subtypes and to describe the clonal evolution of cells measured at initial diagnostic and end-induction disease stages. We were also able to link cell-specific mutation events to their transcriptional and epigenomic signatures, including mapping mutation events along the B-cell development trajectory and within differentially expressed gene pathways. Some cases showed dramatic shifts in subclonal structure between IDX and MRD that may be related to therapy-induced clonal selection, such as a loss of *NRAS* hotspot mutation.

#3953 BET inhibitor increases DNA damage, modulates Wnt signaling, and suppresses osteosarcoma growth in naïve and metastatic disease models.

N. Riyahi[1], P. H. Pandya[1], B. J. Bailey[2], E. A. Dobrota[2], C. Young[2], H. E. Shannon[2], F. Barghi[1], R. Malko[1], K. Bijangi-Vishehsaraei[1], M. A. Trowbridge[3], K. Coy[3], F. M. Kennedy[3], A. L. Sinn[3], S. Angus[1], M. J. Ferguson[1], M. Saadatzadeh[1], K. E. Pollok[1],
[1]Indiana University School of Medicine, Indianapolis, IN, [2]Herman B Wells Center for Pediatric Research, Indianapolis, IN, [3]Preclinical Modeling and Therapeutics Core, Indiana University Melvin and Bren Simon Comprehensive Cancer Center, Indianapolis, IN

Osteosarcoma (OS) is an aggressive bone cancer in pediatric adolescent and young adult patients. Survival rate for metastatic and relapsed OS patients remains dismal at <30%. Additionally, no effective standardized salvage therapy currently exists for these patients, in part, due to genomic complexities arising from moderate levels of replication stress (RS). Bromodomain and extra-terminal domain protein inhibitors (BETi) are an underexplored option to target RS for BETi creates an imbalance between transcription-replication kinetics resulting exacerbation of oncogenic RS and cell death. BET proteins are epigenetic readers that play a role in regulating gene expression networks as well as DNA replication and repair. We tested the hypothesis that BET inhibition leads to decreased OS cell growth and potentiates the efficacy of salvage therapy via gene dysregulation and increased DNA damage and RS. Combination index and Bliss independence analyses of bivalent BET inhibitor (BETi) AZD5153 or PROTAC ARV825 in combination with salvage agents demonstrated additive-to-synergistic cell growth inhibition in OS lines. Increased apoptotic-mediated cell death was observed following AZD5153+topotecan. In addition, γ-H2AX levels and comet assays demonstrated that BETi+topotecan induces its effect, in part through increased RS *in-vitro*. AZD5153 monotherapy significantly suppressed OS tumor growth in patient-derived xenografts (PDXs) derived from both naïve (PDX96) and metastatic (TT2) OS compared to vehicle ($p<0.05$). Moreover, AZD5153 reduced lung metastatic lesions and increased survival in the 143B OS lung colonization model. *In-vivo* mechanisms of drug-induced tumor response were evaluated. Anti-tumor effect correlated with increased γ-H2AX following AZD5153 exposure in PDX96, indicative of increased RS. RNA-seq analysis and protein validation from vehicle versus BETi-treated PDX96 highlighted dysregulation of several key genes involved in DNA damage response including elevated TXNIP, a tumor suppressor which can induce DNA damage and apoptosis. Downregulation of TCF7, a downstream effector of the Wnt pathway, was also observed following BETi. Global kinome profiling and validation experiments revealed increased activity and expression of EphA2 and EphA4 receptors both implicated in development of drug resistance. Furthermore, in BETi-treated PDX96 tumors, Wnt/β-catenin pathway activation emerged as tumors rebounded once BETi treatment was stopped. TT2 PDX was resistant to commonly used salvage agents ifosfamide and irinotecan; however, combination BETi+ topotecan increased the probability of survival compared to each agent alone ($p<0.05$) and was well tolerated. These data collectively suggest that BET inhibition alone or in combination with low-dose salvage therapy holds promise as novel treatment strategies in aggressive OS.

#3954 Increased mosaic chromosomal alterations among survivors of childhood acute myeloid leukemia.

X. Zhang[1], N. Qin[2], Q. Dong[1], C. Chen[1], J. Easton[1], H. Mulder[1], X. Chen[1], K. Shelton[1], C. Im[3], Y. Yasui[1], G. Armstrong[1], K. K. Ness[1], M. M. Hudson[1], P. Auer[4], J. Zhang[1], Z. Wang[1];

[1]St. Jude Children's Research Hospital, Memphis, TN, [2]Nanjing Medical University, Nanjing, China, [3]University of Minnesota, Twin City, MN, [4]Medical College of Wisconsin, Milwaukee, WI

Background: We previously characterized point mutations of clonal hematopoiesis (CH) including single nucleotide variants or small insertion/deletions residing in a set of cancer-related genes (e.g., *DNMT3A* and *TET2*), and found that CH point mutations occurred at a much higher prevalence in childhood cancer survivors (CCS) than in age-sex-race matched community controls. However, mosaic chromosomal alterations (mCAs), another form of CH with megabase-scale structural alterations (copy gain, copy loss and copy-neutral loss of heterozygosity), have not been examined.
Methods: Detection of mCAs was performed on whole-genome sequencing (WGS, 30X) data from 5-year CCS with the Mosaic Chromosomal Alterations (MoChA) caller which utilizes phased genotypes, coverage, and B allele frequency (BAF) at heterozygous sites (HETS). We implemented the pipeline established by the TOPMed consortium to detect low mutant cell fractions (CF >1%). Variant filtration criteria: minor allele frequency <1%, the read depth of either allele <5, and only one variant retained in each 1Kb window. Called mCA filtration criteria: <100 HETS; lod score <5; relative coverage >2.9 or BAF deviation >0.16 and relative coverage >2.5. Autosomal mCAs (CF ≥1%, HETS >100 and length >1Mb) retained. Multivariable Cox models evaluated the association between mCAs and specific late-effects including all-cause mortality, obesity, myocardial infarction (MI) or cardiomyopathy (CMP); multivariable logistic models evaluated the association between mCAs and childhood cancer diagnoses. All models were adjusted for age, sex and therapeutic exposures.
Results: In our evaluation of 4,330 CCS (median age at blood draw: 26.8 years) and 433 controls (33.6 years) with WGS data from the St. Jude Lifetime Cohort, the prevalence of mCAs was slightly higher among CCS than community controls (4.83% vs. 4.16%). Among CCS, mCAs were associated with therapeutic exposures (alkylating agents: odds ratio [OR]=1.48, 95% CI=1.09-2.00; antimetabolites: 1.53, 1.02-2.31; corticosteroids: 0.60, 0.40-0.91). In contrast to recent mCA studies in the general population, we observed no co-occurrence with CH point mutations, and no associations with late-effects including all-cause mortality, obesity, MI or CMP. Interestingly, mCAs were significantly associated with the primary diagnosis of acute myeloid leukemia (AML, OR=2.86, 95% CI=1.63-5.01). Furthermore, this finding was replicated in 2898 5-year survivors from the Childhood Cancer Survivor Study (OR=3.77, 95% CI=1.94-7.33).
Conclusion: mCAs were not associated with age-related morbidities and mortality among CCS. However, we identified a striking association between mCAs and previous diagnoses of AML independent of treatment exposures. If validated among AML patients at the time of diagnosis, mCAs, which reflect the underlying genome instability, may serve as a diagnostic biomarker for AML.

#3955 A proteogenomic study of high-grade glioma among adolescents and young adults.

N. Tignor[1], M. P. Koptyra[2], S. Chowdhury[1], W. Ma[1], J. Rokita[2], M. Gritsenko[3], X. Song[1], G. B. Marino[1], E. Z. Deng[1], F. Petralia[1], A. Krek[1], D. Rykunov[1], F. da Veiga Leprevost[4], N. Hosseini[4], K. S. Rathi[2], Y. Hu[5], S. Migliozzi[6], T. Yaron[7], W. Fu[1], B. Zhang[2], Y. Zhu[2], M. A. Brown[2], J. R. Whiteaker[8], Clinical Proteomics Tumor Analysis Consortium (CPTAC), Children's Brain Tumor Network (CBTN), M. Mesri[9], A. I. Robles[9], K. Rodland[10], L. C. Cantley[11], A. Iavarone[6], K. Aldape[9], M. Cieślik[4], A. I. Nesvizhskii[4], J. E. Ippolito[12], J. B. Rubin[12], A. G. Paulovich[8], H. Zhang[5], A. Ma'ayan[1], T. Liu[3], P. B. Storm[2], A. C. Resnick[2], B. R. Rood[13], P. Wang[1];

[1]Icahn School of Medicine at Mount Sinai, New York, NY, [2]Children's Hospital of Philadelphia, Philadelphia, PA, [3]Pacific Northwest National Laboratory, Richland, WA, [4]University of Michigan, Ann Arbor, MI, [5]Johns Hopkins University, Baltimore, MD, [6]University of Miami Miller School of Medicine, Miami, FL, [7]Columbia University Vagelos College of Physicians and Surgeons, New York, NY, [8]Fred Hutchinson Cancer Center, Seattle, WA, [9]National Cancer Institute, Rockville, MD, [10]Oregon Health & Science University, Portland, OR, [11]Dana-Farber Cancer Institute, Harvard Medical School, Boston, MA, [12]Washington University School of Medicine in Saint Louis, Saint Louis, MO, [13]Children's National Hospital, Washington, DC

To unravel the molecular mechanisms underlying high-grade glioma (HGG) in adolescent and young adult (AYA) patients, we conducted a comprehensive proteogenomic analysis for 34 AYA (age 15-40) and 59 pediatric (age 0-15) HGG cases. Our approach involved whole genome sequencing, methylation profiling, RNA sequencing, and a suite of mass spectrometry-based proteomic experiments, including global proteomic, phosphoproteomic, and glycoproteomic profiling. The proteomics study successfully identified and quantified approximately 11,000 proteins, 33,000 phosphosites, and 3000 glycopeptides with a 50% missing filtering threshold. To identify the unique characteristics of AYA HGG in contrast to both pediatric and adult HGG, we further integrated a proteogenomic dataset of 99 adult GBM tumors previously published by CPTAC and collaborators (PMID: 33577785).

Our study unveiled a collection of mutations, copy number variations, epigenetic modifications and gene fusions that exhibited different frequencies across tumors from pediatric, AYA, and adult patients. Moreover, the influence of these genetic variations on RNA/protein activities also varied across different age groups. Clustering analysis using age-dependent molecular profiles revealed striking differences in RNA/protein/phosphosite activities between patients aged 15-26 and 26-40. Additionally, significantly better overall survival (OS) was observed in the 26-40 age group compared to all other age groups, highlighting distinct biological characteristics within the AYA category that differentiate adolescents from young adults.By leveraging proteogenomic datasets from normal brain tissues (PMID: 30518843), we identified genes, proteins, and pathways with differential age-dependent molecular profiles between tumor and normal brain tissues. Notably, this analysis highlighted significant alterations in proteins from the oxidative phosphorylation, tricarboxylic acid (TCA) cycle, and myelin sheath pathways in tumors compared to normal tissues, some of which were found to be sex-specific.To search for prognostic markers, we introduced a novel approach called Trans-Population Survival Analysis through Interpolation of Age-Dependent Tumor Molecular Profiles. Applying this method on the kinase activity scores derived from the phosphoproteomic data, we identified 150 kinases whose activities were significantly associated with OS among AYA patients. Additionally, employing a causal network analysis tool, we pinpointed six kinases causally linked to OS, suggesting their potential as treatment targets. This study not only characterizes the molecular landscape of AYA HGG but also explores the disease trajectory across the lifespan. Our findings shed light on the intricate interplay of various factors influencing glioma etiology and patient outcomes, paving the way for a deeper understanding of HGG in the AYA population.

Tuesday, April 9, 2024

IMMUNOLOGY: Adaptive Immunity in Tumors
Poster Session

#3959 Unraveling the anti-tumor partnership of CD169$^{\pm}$ macrophages and CD8$^{\pm}$ T cells in a preclinical breast cancer model.
N. Couturier, M. Boutet, K. Nishitani, W. Guo, G. Lauvau;
Albert Einstein College of Medicine, Bronx, NY

In this study, we describe both the individual and the cooperative mechanisms by which CD169$^{\pm}$ macrophages (MP) and CD8$^{\pm}$ T cells support an anti-tumor immune response against breast cancer tumors. Breast cancer is the second leading cause of death in women of all ages each year, thus a deeper understanding of the molecular determinants that promote tumor development and suppress the anti-tumor immune response is still greatly needed. Here we use high dimensional flow cytometry, functional assays, and new mouse models to investigate the MP - T cell anti-tumor partnership. With our collaborators, we developed a preclinical mouse model of breast cancer by genetically engineering mammary stem cells to harbor three cancer driver mutations that are frequently associated in human patients: functional loss of the tumor suppressor genes p53 and mixed-lineage leukemia protein 3, and constitutive activation of the PI3 kinase. To characterize the immune cells in this tumor model, we developed a powerful 30-color high dimensional spectral flow cytometry panel to track and phenotype most known immune cell subsets. We found that CD169$^{\pm}$ MP rapidly infiltrated and outnumbered all other populations during tumor growth, suggesting that they play an important role in shaping the tumor microenvironment. Surprisingly, although current literature describes breast cancer MP to be highly immunosuppressive, our phenotypic analysis showed only low expression of the pro-tumor MP markers TREM2 and CD206, but extremely high expression of the anti-tumor markers FOLR2 and CD64. To further investigate if these MP promoted or prevented tumor growth, we selectively depleted CD169$^{\pm}$ MP in tumor-bearing mice and observed significantly accelerated tumor growth compared to the non-depleted control group, suggesting that these MP promoted anti-tumor responses. MP depletion also affected tumor-infiltrating CD8$^{\pm}$ T cells, which produced lower effector functions (e.g., secretion of IFNγ, CCL3, TNF), indicating that MP may also boost anti-tumor CD8$^{\pm}$ T cell responses. To further test if CD8$^{\pm}$ T cells control tumor growth, we depleted either CD8$^{\pm}$ or CD4$^{\pm}$ T cells in tumor-bearing mice and observed that only CD8$^{\pm}$ but not CD4$^{\pm}$ T cell depletion accelerated tumor growth compared to the control group. MP have been documented to provide type I IFN signals to CD8$^{\pm}$ T cells via the triggering of the STING pathway. To explore this mechanism in our model, we created a CD169^{cre}STING$^{flox/KO}$ mouse in which MP lack functional STING. Tumors in these mice grew much faster compared to those in the control group, consistent with the hypothesis that STING sensing occurs in tumor MP and promotes anti-tumor effector CD8$^{\pm}$ T cell responses. Overall, our data provide evidence for an unexpected anti-tumor role for CD169$^{\pm}$ MP in breast tumors, presumably through enhancing anti-tumor effector CD8$^{\pm}$ T cell responses.

#3960 Establishment of humanized mouse models engrafted with luciferase-expressing acute myeloid leukemia cell lines.

E. Bayon, A. Mersni, A. Wetzel, J. Ville, **K. Ho Wang Yin**;
Transcure Bioservices, Archamps, France

Introduction: Because acute myeloid leukemia (AML) is a very aggressive and quickly developing cancer, for which actual treatments are either inefficient, poorly tolerated, or leading to resistance, there is a strong need for an effective platform to evaluate novel therapies. Our aim is to provide a relevant humanized mouse model as a precious tool to evaluate innovated treatments to cure AML.
Methods: Mice were humanized with CD34+ hematopoietic stem cells to reconstitute a complete human immune system. Three AML cell lines, namely OCI-AML2, OCI-AML3 and MOLM-14, all expressing mCherry and luciferase, were intravenously engrafted at different doses in non-humanized and CD34-humanized mice. Tumor proliferation was monitored by bioluminescence imaging (BLI) thanks to luciferase expression on tumor cells. Their expression of mCherry was also exploited to determine the presence of tumor cells in blood and tissues using flow cytometry.
Results: All AML cell lines engrafted in mice, but we observed different growth kinetics and homogeneity depending on the humanization of mice and the dose injected. Indeed, tumor grew more slowly and heterogeneously in humanized mice, which underlines the role of human immune cells reconstituted in mice. This was improved by increasing the number of tumor cells injected. Tumor cells were found in femurs, spleen, kidneys, ovary, lungs, and uterus depending on the cell line. Mice survival was also highly affected by the tumor cell line engrafted. We observed that MOLM14 was the most aggressive model, while OCI-AML3 reached a steady state and were tolerated by mice over a long period.
Conclusion: We established 3 different AML cell lines in a model of humanized mice which nicely recapitulates the growth of tumor cells in target organs. These 3 models behave differently in terms of growth kinetic, tolerability by mice, and organs infiltrated, which gives plenty of opportunities to evaluate novel therapies designed to cure AML.

#3961 Impact of CD8 resident memory T cells on antitumor immunity and response to cancer immunotherapy.

S. Corgnac, Jr., I. DAMEI, Jr., **F. Mami-Chouaib, Sr.**;
Gustave Roussy, Villejuif, France

$CD8^{\pm}$ resident memory T (T_{RM}) cells expressing the CD103 integrin accumulate in human lung tumors and are associated with a favorable prognosis. We have previously demonstrated that a high density of $CD103^{\pm}CD8^{\pm}$ T cells in human lung tumors is a biomarker of response to immune checkpoint blockade (ICB) immunotherapy. However, a large fraction of human tumors is only weakly infiltrated by $CD8^{\pm}$ T_{RM} cells, and the reason of this T_{RM} desert is not explained. Therefore, defining the molecular signals that give rise and maintain T_{RM} cells within the tumor microenvironment (TME) and the mechanisms that potentiate antitumor T_{RM} functions are important challenges. Data obtained in pre-clinical mouse colorectal cancer and melanoma models demonstrate that knocking-out CD103 impairs antitumor T-cell immunity and response to ICB and therapeutic peptide vaccine. Moreover, immunization of melanoma-bearing mice with the cancer vaccine results in a dramatic decrease in the percentage of $CD103^{\pm}$ T_{RM} cells among $CD8^{\pm}$ tumor-infiltrating T lymphocytes (TIL). Algorithm analyses applied to spectral cytometry data of TIL support the conclusion that upon activation with the peptide vaccine a T_{RM} subset gives rise to tumor-specific effector T cells. The mechanisms associated with the decrease in CD103 expression on $CD8^{\pm}$ T cells and lead to a T_{RM} differentiation shift will be presented as well as the key role of TGF-b in $CD8^{\pm}CD103^{\pm}$ T_{RM} formation and persistence in the TME. Our data demonstrate that tumor $CD8^{\pm}CD103^{\pm}$ T_{RM} are capable of mounting a potent antitumor immunity and suggest that a fine balance between diverse signals in the tumor ecosystem is required to induce their differentiation and thereby optimize response to cancer immunotherapy.

#3962 A CCR6$^{\pm}$Th1-like CD4$^{\pm}$T-cell cluster involved in HEV formation predicted lung cancer patients requiring anti-CTLA-4 therapy.

H. Kagamu, S. Yamasaki, A. Mouri, O. Yamaguchi, A. Shiono, F. Nishihara, Y. Miura, K. Hashimoto, H. Imai, K. Kaira, K. Koabayashi, K. Horimoto;
Saitama Medical University International Medical Center, Hidaka city, Japan

Background: CD4$^{\pm}$ T cells are known to help in cytotoxic T-cell priming, clonal proliferation, migratory and infiltrative capacity, and target cell killing function by licensing dendritic cells. Although CXCR3$^{\pm}$ CCR6^{-} classical Th1 CD4$^{\pm}$ T cells are thought to be essential for acute cellular immunity, such as antiviral responses, the details of Th1-type CD4$^{\pm}$ T cells required for anti-tumor immunity as a long-term chronic T cell immune responses over years remain unclear. We reported the Th7R, a CCR6 expressing Th1-like CD4$^{\pm}$ T cell cluster predicted anti-PD-1 antibody therapy efficacy and postoperative recurrence-free survival.
Objective: In this study, we focus on two Th1-like CD4$^{\pm}$ T cell clusters, Th1 and Th7R, to determine their functions and roles in long-lasting anti-tumor immune phenomena.
Methods: We studied patients with advanced stage lung cancer treated with immune checkpoint inhibitors (Pembrolizumab monotherapy n=63, Ipilimumab + Nivolumab n=148) and stage I-II lung cancer patients undergoing surgery (n=54). Mass cytometry, single cell RNA sequencing, and immunohistochemical staining were performed using peripheral blood, tumor-infiltrating lymphocytes and lymph node T cells. These studies were approved by the IRB of Saitama Medical University International Medical Center, and all patients gave written consent.
Results: Unlike classical Th1, which highly expresses *PRF1*, *GZMB*, *GNLY*, and *NKG7*, Th7R expressed *LTβ*, *CXCR6*, *CTLA-4*, *CD28*, and *CXCL13*. Analysis of HEV index (MECA79$^{\pm}$ /CD31$^{\pm}$ vessels) by MECA79 and CD31 staining of tumor tissues showed that Th7R in peripheral blood correlated with tumor tissue HEV index, suggesting that LTβ and CXCL13 expressed by Th7R are involved in HEV formation.Th1 mainly expressed PD-1 and did not express CTLA-4, whereas Th7R expressed both PD-1 and CTLA-4. When pre-treatment peripheral Th7R quartile was used to analyze OS after Ipilimumab + Nivolumab treatment, both the top 25% and intermediate 50% patients showed favorable prognosis, but the lower 25% had significantly poor OS. In contrast, only the top 25% Th7R patients but not the intermediate 50% and lower 25% patients who were treated with Pembrolizumab had favorable OS. Thus, it is likely that the Th7R intermediate 50% patients required anti-CTLA-4 therapy to achieve antitumor immune responses. These results may be useful for stratification of patients requiring anti-CTLA-4 antibody therapy as well as for predicting the therapeutic response of Ipilimumab + Nivolumab.
Conclusion: Th7R exhibits LTβ and CXCL13 expression, which is absent in classical Th1, and may help maintain sustained T-cell immunity through HEV/TLS formation. Th7R may be a biomarker to select the patients who benefit from anti-CTLA-4 treatment.

#3963 Indoleamine 2,3-dioxygenase 1 (IDO1) regulates immune evasion in lymphoma.

J. Park[1], S.-J. Yoo[1], Q. Hu[2], C. M. Fielder[2], H. Yoon[2], J. Hong[3], B.-S. Kim[4], Y. Koh[3], T. Kim[2], S.-S. Yoon[3], C. Yan[2];
[1]Seoul National University, Seoul, Korea, Republic of, [2]Vanderbilt University Medical Center, Nashville, TN, [3]Seoul National University Hospital, Seoul, Korea, Republic of, [4]Eunpyeong St. Mary Hospital, Seoul, Korea, Republic of

Recently, anti-programmed death (anti-PD) therapy has been at the forefront of cancer therapy. However, the clinical efficacy of anti-PD therapy in DLBCL remains obscure. The marginal response to anti-PD therapy in DLBCL indicates that different mechanisms of immune evasion other than the PD-1/PD-L1 pathway may be present. To investigate the mechanisms of resistance to anti-PD therapy in DLBCL, we assessed gene expression in patients with DLBCL in public database. Accordingly, we found indoleamine 2,3-dioxygenase 1 (IDO1), a key enzyme responsible for tryptophan catabolism, is highly expressed in DLBCL. IDO1 expression is upregulated by IFN-gamma produced by T cells in tumor microenvironments (TMEs) of various cancer types. Upregulated IDO1 leads to the production of kynurenine, which creates an immunosuppressive TMEs. However, it remains unknown whether IDO1 induces immune evasion in DLBCL and if so, which subsets of IDO1 expressing cells are responsible for immune evasion in DLBCL. To address these questions, we first determined the intrinsic role of IDO1 in lymphoma cells. We knocked down IDO1 expression (IDO1 KD) in a human DLBCL RC-K8 cell line using short hairpin RNA. We observed decreased cell proliferation in IDO KD lymphoma cells compared with control cells. We also found increased susceptibility to apoptosis in IDO1 KD RC-K8 cells compared with IDO1 WT control, when these were co-cultured with THP-1-derived macrophages or activated Jurkat T lymphocytes. These data suggest that lymphoma IDO1 has an intrinsic role of lymphoma progression and makes lymphoma sensitive to cytotoxic immune cells. To validate the anti-tumor effect of IDO1 deficiency in immune cells, we assessed EL4 lymphoma growth and immune TME of lymphoma in syngeneic wild type (WT) and *Ido1* knock-out (KO) mice. The growth of EL4 lymphoma tumor was significantly suppressed in *Ido1* KO mice compared to WT mice (*Ido1* KO: 621.9mm^3 vs WT: 1228mm^3, N=22, P<0.001). Immune TME assessment revealed a decreased frequency of regulatory T cells, yet, the increased proportions of B cells, MHC II+ antigen-presenting cells, monocytes, and NK cells in *Ido1* KO tumors compared with WT control. In summary, IDO1 is highly expressed in DLBCL. IDO1 up-regulation may drive lymphoma progression both intrinsically and extrinsically (immune evasion). This data suggests that IDO1 overexpression may be one of the mechanisms of resistance to anti-PD therapy. We will extend our studies to determine a combination effect of IDO1 inhibitors with immune checkpoint inhibitors including anti-PD therapy in DLBCL.

#3964 A cancer survival program against activated T cell attack.

M. X. Wang, B. E. Mauch, A. F. Williams, T. Barazande-Pour, F. Araujo Hoffmann, S. H. Harris, C. P. Lathrop, C. E. Turkal, M. H. Paw, D. A. G. Gervasio, T. Tran, T. Guo, G. A. Daniels, S. J. Park, M. J. Hangauer;
University of California San Diego - UCSD, La Jolla, CA

The immune-cancer interactions downstream of immune checkpoint inhibition present the next targetable interface of cancer immunity. Despite evidence for cytotoxic T lymphocyte (CTL) infiltration and cytolytic activity within immunotherapy-responsive tumors, partial responses and acquired resistance are common, indicating additional barriers for complete tumor elimination. We report a survival program engaged within residual cancer cells exposed to weeks of activated CTLs. Contrary to immune-evasion mechanisms, we observe a residual antigenic cancer cell subpopulation which activates CTLs, survives within IFNγ-high environments, and withstands CTL-induced apoptosis. This cancer survival program, termed immune-induced persistence, is reversibly-driven (non-genetic) and prevents the complete CTL-mediated elimination of cancer cell populations by supporting the survival of quiescent cancer 'persister' cells against activated CTL attack. Persister cells display sublethal caspase activity and caspase-dependent DNA damage, consistent with CTL-induced genomic instability, and depend on the inhibitors of apoptosis proteins for survival. Notably, immune-induced persistence presents a markedly distinct survival program than drug-induced persistence, including distinctive apoptotic profiles, stress response pathways, and vulnerabilities. Thus, cancer cell populations can transiently adopt non-redundant survival programs in response to various cytotoxic environments. Features of immune-induced persistence are observed within CTL-treated human cancer cell lines, immune-treated human tumor slice cultures, and intratumor transcriptional heterogeneity programs. Under continued CTL exposure, persistent cancer populations give rise to genetically distinct cancer clones, including stably resistant immune escape variants, modeling acquired resistance to cancer immunotherapies. We propose sublethal interactions between effector immune cells and cancer persister cells as a critical and targetable variable at the interface between activated immunity and cancer.

#3965 A cytolytic effector CD8+ T cell response is associated with remission in adult T-cell leukemia/lymphoma.

E. Guillen[1], E. Liu[1], Y. Wang[1], A. Shastri[1], A. Sica[1], A. Verma[1], X. Zhang[1], J. Ramos[2], H. Ye[1], G. Lauvau[1];
[1]Albert Einstein College of Medicine, Bronx, NY, [2]University of Miami, Miller School of Medicine, Miami, FL

Introduction: Adult T-cell leukemia/lymphoma (ATLL) is a rare blood cancer that develops in 3-5% of human T-lymphotropic virus-1 (HTLV1) carriers when the combination of viral oncoproteins and somatic mutations lead to malignant transformation of HTLV1 infected CD4+ T cells. ATLL has the worst overall survival among peripheral T cell lymphomas and remains a fatal disease despite efforts to improve outcomes over the last 35 years. First-line combination chemotherapy rarely achieves a durable response and two immune-modulating treatments (α-CCR4 and α-PD-1 monoclonal antibodies) failed in clinical trials. These findings highlight an urgent need to improve our understanding of the functional state of host immunity in ATLL patients. A host immune response against HTLV1 is pivotal in preventing ATLL development. Malignant ATLL cells can escape immune surveillance by preventing antigen presentation and engaging immune checkpoints. The prospect of an ATLL clone inducing systemic suppression was suggested in the literature but has not been directly examined. Furthermore, HTLV1-specific CD8+ cytotoxic T lymphocytes (CTLs) play an important role during viral latency, yet it remains unknown if they play a clinically relevant role during ATLL treatment.

Methodology: In this work, we hypothesized that malignant ATLL cells will exhibit a suppressive immune phenotype and that effective therapeutic interventions will augment anti-ATLL CTLs to promote durable remission. We implemented an immune profiling approach to analyze PBMC samples from ATLL patients. Specifically, we developed a powerful 30-marker spectral flow panel to discriminate malignant ATLL cells from non-transformed lymphocytes (T, B, and NK cells) and monitor the expression of key transcription factors and markers associated with proliferation, cytolysis, and exhaustion. We analyzed diagnostic samples from the Montefiore-Einstein ATLL Biobank and samples collected during a phase 2 clinical trial aimed to assess the efficacy of a promising Belinostat/Zidovudine/Interferon-α combination therapy against ATLL (NCT02737046).

Results: Our findings reveal that malignant ATLL cells exhibit an immune phenotype associated with robust immunosuppression and yet distinct from other suppressive immune cells (i.e., regulatory T cells). Additionally, we discovered that ATLL patient samples contained a unique population of phenotypically exhausted CD8+ T cells, the proportion of which was drastically reduced in patients under remission. Remarkably, a decrease in this exhausted subset correlated with the expansion of highly cytolytic CD8+ CTLs.

Conclusion: Altogether, our findings suggest that ATLL cells may drive CD8+ CTLs into exhaustion to achieve immune evasion and that a robust anti-ATLL CTL response actively contributes to a remission state.

#3966 NK receptors enable TCR-mediated CTL recognition and killing of cancer cells expressing non-mutated tumor-associated antigens.

B. Dong[1], N. Obermajer[2], T. Tsuji[1], J. Matsuzaki[1], C. Bonura[1], H. Withers[1], M. Long[1], C. Chavel[1], S. H. Olejniczak[1], H. Minderman[1], R. P. Edwards[2], W. J. Storkus[2], P. Romero[3], P. Kalinski[1];

[1]Roswell Park Comprehensive Cancer Center, Buffalo, NY, [2]University of Pittsburgh School of Medicine, Pittsburgh, PA, [3]University of Lausanne and Ludwig Institute for Cancer Research, Lausanne, Switzerland

Background: Responsiveness or ignorance of antigens presented to naïve T cells by dendritic cells (DC) involves the CD28-driven “signal 2”, but it is unclear how activated CTLs respond to the same non-mutated tumor-associated antigens (TAAs) presented by cancer versus healthy cells to avoid autoimmunity. Since $CD8^{\pm}$ T cells express activating NK receptors (NKRs) and NKR ligands are commonly expressed by cancer cells but not healthy tissues, we evaluated the crosstalk between NKRs and TCR during recognition of cancer cells by DC-primed TAA-specific CTLs.

Methods: Associations between DNAM-1, NKG2D, CTL markers, and patients’ survival was analyzed using TCGA. *In vitro* sensitization was used to induce human TAA-specific CTLs by TAA-loaded DCs. The roles of DNAM-1 and NKG2D in CTL recognition and killing were tested using IFN-γ ELISpot, conjugate formation, degranulation, and cytotoxicity assays. The mechanisms and molecular effects of NKR-mediated costimulation were analyzed using IsoPlexis, calcium flux, western blot, and RNA sequencing. Double-transduction of T cells with TCR and NKR constructs or pre-treatment of cancer cells by chemotherapy was used to manipulate the levels of NKRs on T cells or their ligands on cancer cells.

Results: TCGA analysis revealed that DNAM-1 and NKG2D are strongly associated with intratumoral $CD8^{\pm}$ T cells rather than NK cells, being critical for the long-term survival of melanoma patients. Human DC-primed CTLs significantly upregulated DNAM-1 and NKG2D compared to naïve $CD8^{\pm}$ T cells, but retained strict dependence on TCR in cancer cell recognition. Unexpectedly, blockade of DNAM-1 and NKG2D prevented the TCR-mediated CTL recognition and killing of cancer cells expressing low-TAA levels, but were redundant in the recognition of high-TAA-expressing cancer cells. DNAM-1, and to a lesser extent NKG2D, lowered TCR activation threshold and enhanced proximal TCR signaling and CTL polyfunctionality. NKR overexpression in TCR-transgenic T cells or chemotherapy-driven elevation of NKR ligands on cancer cells allowed effective recognition and killing of weakly immunogenic cancer cells.

Conclusions: Reduced TCR activation threshold in the presence of NKR costimulation enables CTL activation by low levels of cognate MHC I-peptide complexes on cancer cells. Our data helps explain the ability of non-mutated “self” antigens to mediate tumor rejection in the absence of autoimmunity, and provides new tools to enhance the effectiveness of cancer therapies.

#3967 ISM9182A, a novel HPK1 inhibitor, exhibits immune modulatory activity and robust monotherapy anti-tumor effects in preclinical studies.

C. X. Chen[1], C. Pu[1], J. Peng[1], X. Ding[1], H. Lu[1], X. Ding[1], M. Zhang[1], S. Bavadekar[2], **S. Rao**[2], F. Ren[1], A. Zhavoronkov[2];
[1]Insilico Medicine, Shanghai, China, [2]Insilico Medicine, New York, NY

The hematopoietic progenitor kinase 1 (HPK1 or MAP4K1) is a member of the Ste20 serine/threonine kinase super family that negatively regulates immune cells, including T cells, B cells and dendritic cells (DCs). Thus HPK1 is an attractive immuno-oncology target in many tumor types. Here, we report ISM9182A as a novel, potent, and selective inhibitor of HPK1.ISM9182A demonstrated nanomolar enzymatic potency against HPK1 with >100-fold selectivity against other MAP4K family kinases. ISM9182A inhibited the phosphorylation of SLP-76 at Ser376 dose-dependently with an IC50 of 30nM in human peripheral blood mononuclear cells. Moreover, ISM9182A enhanced IL-2 and IFNγ secretion upon CD3/CD28 co-stimulation in a dose-dependent manner without affecting T cell proliferation. Treatment of human pan T cells with ISM9182A also significantly reversed PGE2-mediated immunosuppression of human pan T cell activation and further boosted IL-2 and IFNγ secretion compared to CD3/CD28 co-stimulation. In monocyte-derived DCs stimulated with TNF-α/IL-1β/PGE-2, ISM9182A significantly upregulated CD80, CD86, and CD83 expression, demonstrating its potency to promote DC maturation. ISM9182A showed no obvious toxicity towards human T cell, B cells, and monocytes without CD3/CD28 co-stimulation. *In vivo* PK data revealed favorable ADME properties and good oral bioavailability of ISM9182A across different species. In a CT-26 murine syngeneic mouse model, oral administration of ISM9182A exhibited potent antitumor effects with p-SLP76 inhibition in both murine spleen and tumor, without body weight loss. In summary, ISM9182A is a potent and selective HPK1 inhibitor and a promising immuno-oncology agent.

#3968 Class I HLA-independent lysis of cancer cells by tumor-infiltrating CD8 T cells.

H. Xie, A. Jiang, J. Perera, A. Dey, N. Smith, M. Sade-Feldman, R. T. Manguso, N. Hacohen, R. W. Jenkins;
Massachusetts General Hospital, Harvard Medical School, Boston, MA

T cell-based therapies have transformed cancer treatment, although intrinsic or acquired resistance develops in nearly half of the patients. Tumor-infiltrating CD8+ T lymphocytes (TILs) are key determinants of anti-tumor immunity by secretion of cytotoxic granules, such as granzymes and perforin, and effector cytokines, such as TNFa and IFNg. A deep understanding of how CD8+ TILs eliminate cancer cells will help identify resistance mechanisms and develop new therapeutic strategies. Here, we demonstrate that TILs eliminated matched melanoma cells in a time and dose-dependent manner but in a class I HLA-independent fashion. Specifically, blocking class I HLA-TCR interaction either by the deletion of B2M (resulting in loss of class I HLA surface expression) or TCR genes did not alter the activity of these TILs. We further confirmed that TIL-mediated killing is contact-dependent. After excluding the potential roles of CD1d and MR1-restrictive T cells, gamma delta T cells, and NKG2D in TIL-mediated killing, a whole-genome CRISPR/Cas9 screen was performed in cancer cells. We identified that genes involved in JAK-STAT and cell-extrinsic apoptosis pathways are necessary for TIL-mediated killing. Together, these findings demonstrate that expanded CD8 TILs from melanoma patients are capable of eliminating melanoma cells via a novel, class I MHC-independent mechanism by coactivation of both JAK-STAT and cell-extrinsic apoptosis pathways.

#3969 Alzheimer's disease-associated amyloid precursor protein improves anti-tumor immunity by inhibiting ceramide-mediated lethal mitophagy and restoring mitochondrial fumarate metabolism in aging T-cells.

M. Kassir, H. G. Lee, N. Oleinik, W. Wofford, C. Walton, F. Atilgan, P. Chakraborty, K. Calisir, O. Sahin, S. Mehrotra, B. Ogretmen;
The Medical University of South Carolina (MUSC), Charleston, SC

The association between Alzheimer's disease (AD) and lower cancer incidence has been observed in several epidemiological studies without much mechanistic insight. We aimed to understand this cancer resistance mechanism linked to AD and exploit it for broader cancer therapies. A hallmark of AD is the accumulation of amyloid precursor protein (APP) in neuronal mitochondria, inhibiting mitophagy, abrogating the clearance of dysfunctional mitochondria, and contributing to AD pathology. In addition to neurons, mitophagy plays an important role in T-cells, where excessive ceramide-dependent mitophagy in aging T-cells inhibits their energy metabolism and limits their anti-tumor functions. Thus, attenuation of ceramide-dependent mitophagy plays a favorable role in enhancing aging T-cell anti-tumor function. Given that APP is also processed in T-cells, we hypothesized that APP accumulates aberrantly in aging Alzheimer's T-cells, inhibiting mitophagy and enhancing T-cell anti-tumor activity. Employing techniques of lipidomics, metabolomics, imaging, molecular biology, and genetic models, we show that AD T-cells from a mouse model and human patients are protected against aging-associated ceramide-dependent mitophagy, which enhanced their secretion of inflammatory anti-tumor cytokines. The excessive localization of APP to the T-cell mitochondria, where it inhibits the accumulation of ceramide synthase 6 (CerS6) and C14/C16-ceramides, attenuated the levels of mitophagy and protected the Alzheimer's T-cells from metabolic defects observed in aging, namely protecting against the exhaustion of fumarate pools. Both in vitro and in vivo re-supplementation of fumarate to aging WT mouse T-cells effectively rescued their viability, cytokine production, and tumor killing capacity both *in vitro* and in adoptive T-cell transfers to mice with melanoma, functionally mimicking the AD phenotype. The fumarate supplementation also led to a decrease in ceramide-dependent mitophagy in the WT aging T-cells, indicating an interplay between ceramide-dependent mitophagy and fumarate metabolism which contributes to the protection of the anti-tumor function in aging AD T-cells. Moreover, we show that Alzheimer's mice that express APP in the brain and T-cells, but not AD mice that express APP only in the brain, are protected against the growth of both carcinogen-induced and allografted tumors. Finally, transfer of mitochondria from AD T-cells to aging WT T-cells improved their metabolic fitness and anti-cancer functions. In summary, we show that AD-associated APP improves anti-tumor immunity of aging T-cells by inhibiting ceramide-mediated lethal mitophagy and restoring mitochondrial fumarate metabolism. These data provide a novel mechanism to explain reduced cancer incidences in AD patients.

#3970 Impairment of tumor reactive CD8 T cells in liver cancer.

R. S. Trehan[1], M. Soliman[1], X. Wang[2], P. Huang[1], N. Kedei[1], X. Zhu[1], M. Seifert[1], M.-R. Benmebarek[1], A. Nur[1], F. Korangy[1], C. Ma[1], T. F. Greten[1]; [1]National Cancer Institute, Bethesda, MD, [2]Albert Einstein College of Medicine, Bronx, NY

Tumor reactive (TR) CD8 T cells in the liver have been studied in the setting of both immunotherapy and cellular therapy with the predominant dogma that these cells have equivalent functionality in the liver as compared to other organ sites. Herein, we detail that TR+ CD8 T cells are functionally impaired in the liver immune microenvironment in mice with liver tumors.TR+ CD8 T cells were studied in BALB/c and C57BL/6 mice injected intrahepatic, intravenous, and subcutaneously with either a colon (CT26) or a melanoma (B16F10) cancer cell line to create intrahepatic, pulmonary and subcutaneous tumors, respectively. Additionally, an αCD8 antibody with IgG control was used to conduct functional studies. Samples were analyzed using flow cytometry and liver weights were measured. A high frequency of TR+ CD8 T cells were found in the liver in mice with intrahepatic tumors. Despite ~70% of CD8 T cells being tumor reactive in intrahepatic tumors, liver tumor growth kinetics were faster than subcutaneous tumors. Higher proportion of the TR+ CD8 T cells were found to be exhausted in the liver tumor by flow cytometry. Functional depletion of the CD8 T cells caused a fivefold higher tumor growth in the subcutaneous model but in contrast had no effect on intrahepatic tumors. In conclusion, despite the high frequency of “killer” tumor reactive T cells in the liver, the growth kinetics of the liver tumors, flow cytometry as well as functional studies demonstrate the impairment of TR+ CD8 T cells in the liver. We aim to dissect the mechanisms mediating intrahepatic TR CD8+ T cell exhaustion in primary liver tumors as well as metastatic models. Additionally, we aim to determine significant costimulatory molecules specific to intrahepatic exhaustion which could lead to better therapeutic models.

#3971 Progesterone impacts regulatory T cell activity to promote immunosuppression in the mammary gland.

E. I. Chowanec, L. R. Werner, C. R. Hagan;
University of Kansas Medical Center, Kansas City, KS

Estrogen and progesterone signaling together drive hormone-receptor positive breast cancer growth and progression. However, there have been limited studies on the independent role that progesterone and its receptor, the progesterone receptor (PR), play in the development of breast cancer. Studies in the Hagan lab have shown that progesterone signaling promotes mammary tumor growth and changes the immune landscape of the mammary gland towards immunosuppression. Regulatory T-cells (Tregs) are immune cells known to promote immunosuppression in the tumor microenvironment. The data from our lab shows that among hormone receptor positive breast cancers, higher levels of PR expression correlates to higher levels of Tregs in the tumor microenvironment. To determine if progesterone signaling increases the number of Tregs in the tumor-bearing mammary gland, we used a syngeneic orthotopic murine tumor model, E0771 cells, engineered to express mouse PR or control empty vector. Mice were treated with progesterone or placebo for 7 days before implantation of the modified E0771 cells. The results of this study show that progesterone promoted tumor growth, and flow cytometry analysis at tumor endpoint showed that PR-positive tumors treated with progesterone harbored more Tregs than mice treated with placebo. Additionally, initial studies using flow cytometry and RNA-seq indicate increased Treg activity following progesterone treatment in PR+ tumor-bearing mice. As progesterone treatment promoted tumor growth and Treg recruitment in progesterone receptor-positive tumors, these data imply that progesterone treatment may promote the release of secreted factors impacting the immune cells in the mammary microenvironment. To determine if progesterone treatment results in cytokine or chemokine changes that may affect Treg recruitment, cytokine arrays and enzyme-linked immunosorbent assays (ELISAs) were performed using cell culture supernatant from murine mammary tumor cells expressing progesterone receptor (E0771-PR) treated with progesterone (0-72 hours). E0771-PR cells treated with progesterone showed higher levels of cytokines and chemokines that have been linked to Treg recruitment and differentiation, such as MCSF. Our findings demonstrate that progesterone signaling promotes an immune suppressed microenvironment in the mammary gland through an increase in Tregs. This evidence provides rationale to investigate the use of anti-progestins as a mechanism to overcome the immune-cold tumor microenvironment seen in progesterone receptor positive breast tumors.

#3972 Personalized immune-organoid co-culture system for modeling the anti-tumor immune response in breast cancer patients.

C.-H. Hong[1], W.-J. Ryu[1], S. Park[2], T. Kim[1], Y. Hwang[1], H. Han[1], S. Jo[2], T. Kweon[2], G. Kim[1], M. Kim[1], H. Park[1], J. Sohn[1];

[1]Yonsei Cancer Center, Yonsei University College of Medicine, Seoul, Korea, Republic of, [2]Yonsei University College of Medicine, Seoul, Korea, Republic of

Recent studies have reported the effectiveness of immune checkpoint blockade (ICB) therapy in breast cancer patients. However, only a subset of patients benefits from ICB therapy due to various immunosuppressive mechanisms. The development of personalized predictive models for the anti-tumor immune response is essential to broaden the indication of ICB therapy. Here, we suggest a novel model platform using a co-culture system with patient tumor-derived organoids and matched immune cells to predict the immune response of individual patients. We successfully established fifty-nine cases of patient-derived breast cancer organoids with matched peripheral blood mononuclear cells (PBMCs) (subtype: Luminal A, 18.6%; Luminal B, 28.8%; Triple-negative breast cancer, 35.6%; HER2-positive, 17.0%). Three rapidly proliferating organoids (one Luminal B and two TNBC organoids) were selected to develop an immune-organoid co-culture (IOC) system. To mimic the anti-tumor immune response, cytotoxic immune cells were expanded from PBMCs by modified cytokine-induced killer (CIK) cell expansion protocol utilizing IL-2/IL-15. The CIK cells were co-cultured with patient-derived tumor organoids for killing assay to enable the prediction of ICB responsiveness *in vitro*. The CIK cells were expanded in the IOC system by stimulation of PBMC with IL-2/IL-15 in the presence of matched tumor organoids for 11 to 14 days. The CIK cells exhibited tumor organoid-specific killing (measured by Caspase-3, 15.22% ± 8.58, mean ± SEM) on organoid co-culture and showed induction of CD107a and CD137 expression in CD8+ T cells and NK cells with the PD-1 blocking antibody. The CIK-mediated tumor organoid deaths and immune cell activation were reduced by HLA class I blocking antibody (W6/32) treatment, confirming HLA-TCR mediated immune response and killing of tumor organoids in the IOC system (-14.85% in organoid-specific lysis and -7.46% in CD107a expression). In the live cell imaging of the IOC system, the interaction between T cells and tumor organoid cells and subsequent induction of Caspase 3 was noted. Our IOC system could directly measure the immunogenic tumor organoid killing by immune cells on ICB treatment in individual breast cancer patients. Moreover, the analysis of immune receptor profiles may reveal immune modulating mechanisms in each patient. We expect the IOC system to serve as a useful platform for personalized immunotherapy and exploration of combinatory therapy to enhance the anti-tumor efficacy of ICB in breast cancer patients.

#3973 Cancer B cell blueprint reveals dysfunctional extra-follicular dominance with therapeutic opportunity.

J. Ma[1], Y. Wu[1], L. Ma[2], X. Yang[1], T. Zhang[1], G. Guo[2], J. Fan[1], X. Zhang[3], Q. Gao[1];

[1]Zhongshan Hospital Fudan University, Shanghai, China, [2]Zhejiang University, ZheJiang, China, [3]Shanghai Institute of Immunity and Infection, Shanghai, China

B cells are essential components of humoral immunity but harbor multifaceted functions across cancers. To decode tumor-infiltrating B cells, we generated the B cell blueprint encompassing single-cell transcriptome, BCR repertoire, and chromatin accessibility data across 20 cancer types (483 samples, 266 patients). Strikingly, B cells harbored extraordinary heterogeneity and composed of 15 subsets, which were grouped into two independent developmental paths (extra-follicular [EF] versus germinal-center [GC]) exhibiting organ preference. Of note, colon adenocarcinoma and hepatocellular carcinoma are the two representative types of cancer enriched for GC and EF pathways, respectively. We affirm that EF-dominant cancers correlate with dysregulated immune responses and worse clinical outcomes. We then identify the dynamic metabolic-epigenetic-signaling networks in fine-tuning tumor-infiltrating B cell differentiation and managing the balance between the EF and GC pathways. Atypical memory (AtM) B cells, the primary progenitors of EF-derived ASCs, exhibit an exhausted and bystander phenotype and develop independently of the GC pathway. We find that the AtM B cells reside in the center of immature TLSs and spatially relocate to the periphery during TLS maturation. Finally, we mechanistically link these findings to specific transcription factors and epigenomic regulations. We demonstrate that the glutamine-derived metabolite α-ketoglutarate (αKG) could increase the expression of AtM B cell associated transcription factors Tbet and BATF and promote their differentiation, accompanied by the activation of mammalian target of rapamycin complex 1 (mTORC1) signaling. Consequently, AtM B cells acquire an immunoregulatory function that dampens anti-tumor T cell responses and fosters an immunosuppressive microenvironment.

#3974 Macronutrient composition dictates MASH-associated HCC immunosurveillance through microbiota alteration and metabolic adaptation.

N. T. Ryujin[1], J. Huang[1], A. Nguyen[1], J. Edwards[1], Y. Cheng[2], J. Wen[1], A. Damania[1], N. Ajami[1], S. Rosario[3], M. Long[3], L. Alexandrov[2], **S. Shalapour**[1];
[1]UT MD Anderson Cancer Center, Houston, TX, [2]University of California San Diego, La Jolla, CA, [3]Rosewell Park Comprehensive Cancer Center, Buffalo, NY

Hepatocellular carcinoma (HCC) is the most common form of liver cancer, with an estimated incidence of over one million cases by 2025. The advances in vaccines against HBV and HCV have led to a decrease in the number of virus-related cases; however, the obesity epidemic has contributed to a drastic increase in metabolic dysfunction-associated steatohepatitis (MASH) related HCC cases (e.g., obesity and type 2 diabetes induced HCC). Considering this trend, we aim to understand how lifestyle choices, like food composition, in combination with alcohol consumption at a “social drinking level” impacts host metabolism, and subsequently the development of MASH-induced HCC. We hypothesize that the impact of dietary composition on dysbiosis and immune cells, particularly adaptive immune cell metabolic status, will drive the phenotype. We have developed a MASH-induced HCC murine model, with long-term dietary intervention including seven different customized diets: normal chow (NC), ketogenic, solid high fat diet (sHFD), or isocaloric liquid Lieber DeCarli Diets (LDC): high fat/low carb (HF), high fat/low carb with ethanol (HF-EtOH), low fat/high carb (LF), and low fat/high carb with ethanol (LF-EtOH). Mice began special diet in late adolescences and disease progression was monitored over the course of a year, where mice developed HCC. Our model allowed for a comprehensive understanding of MASH-induced HCC where disease initiation could be studied beyond known contributors like obesity or body mass index (BMI). The animal model was analyzed comprehensively with high-parameter flow cytometry (FC), 16S sequencing, bulk RNA-seq, scRNA/ATAC-seq, and WGS. Long-term diet intervention led to macronutrient specific microbiota dysregulation, alterations in systemic metabolism and suppression of adaptive immune response, consequently impacting the progression of HCC. Customized dietary interventions showed a specific phenotype regarding HCC development and progression with distinct mutational genotype and particular response to immunotherapy. T and B cell subpopulation deficiency had a significant impact on MASH-induced HCC development in a macronutrient composition dependent manner. In summary, each dietary intervention showed a distinct pattern and effect on dysbiosis, systemic metabolic reprograming, cellular transcriptomic and epigenetic alteration, and particularly immune cell effector function. Additionally, some compositions supported the immuno-escape mechanism of malignant cells through regulation of their MHC machinery. Collectively, these accumulated data construct an atlas for understanding the underlying molecular mechanisms contributing to lifestyle-induced HCC providing the knowledge needed to advance effective strategies for treatment and prevention.

#3975 A therapeutic screening platform for assessing antigen-specific T cell-mediated tumor killing *in vitro*.

E. Klaver, H. Leonard, E. Lieverse, O. Brand, O. Reelfs, C. Kirkham, L. Schewitz-Bowers, **L. Brackenbury**;
Charles River Laboratories, Bristol, United Kingdom

Many cancers remain resistant to conventional therapies, consequently there has been an exponential rise in the number of therapeutics harnessing the power of the immune system in an oncology setting, with several remarkable examples of success. High frequencies of infiltrating tumor-specific T cells have been linked to improved patient outcomes, which highlights the importance of uncovering how therapeutics can enhance their function. To explore this functionality in a preclinical setting it is critical to have physiologically relevant models. Here, we demonstrate that common issues, such as low precursor frequencies and restricted HLA-types can be overcome via access to HLA-typed samples and use of expansion platforms which attain high numbers of antigen-specific T cells. Furthermore, we show how these systems enable vaccine immunogenicity screening and assessment of therapeutic efficacy. Healthy blood donations were screened for HLA type and antigen-specific T cells were expanded by either co-culture with peptide-pulsed dendritic cells or polyclonal stimulation following multimer enrichment and FACS sorting. Following expansion, the large number of antigen-specific T cells generated enabled the T cells to be assessed via phenotyping, cytokine secretion, or functional killing assays in a 2D or 3D tumor setting. Tumor targets with either 1) endogenous antigen expression, 2) antigen introduced via lentiviral overexpression or 3) peptide loading of MHC class I were utilized. Validated readouts for measuring antigen-specific killing included flow cytometry and time-lapse imaging (IncuCyte), alongside quantification of antigen-specific IFNγ responses by ELISpot. These pre-clinical platforms represent a suite of physiologically relevant T cell assays which can be used to perform candidate selection in tumor associated antigen/neoantigen vaccine drug development programs, pharmacological inhibition of checkpoint pathways, or co-stimulatory agonist discovery. In combinatorial approaches with radio- or chemotherapy, the development of novel immunotherapies offers hope to many patients with treatment-resistant cancers.

#3976 Single-cell TCRα/β and TCRγ/δ immune receptor profiling and immunophenotyping using a 96-well plate sorted-cell approach.

A. Chenchik, T. Liu, M. Makhanov, D. Hu, L. Kobzik, K. Ghias, P. Diehl;
Cellecta, Inc., Mountain View, CA

Single-cell immune receptor profiling is a revolutionary approach that allows investigators to combine clonotype repertoire identification with paired-chain information and the phenotype of cells (e.g., cell subtype). Single-cell immune receptor profiling can be performed using a medium-throughput approach (1,000-5,000 cells) using microwell arrays or droplet microfluidics technologies. However, these assays are more complicated to run and require expensive reagents and limited sequencing throughput when compared to bulk immune receptor profiling methods.

Here, we describe a low-throughput, single-cell immune profiling strategy using sorted cells in 96-well plates. The plate is pre-aliquoted with either T-cell receptor (TCR) α/β or TCR γ/δ primers along with 30 crucial T-cell markers. We perform multiplex RT-PCR amplification and sequencing of the CDR3 regions. The resulting data provides the abundant clonotype counts along with the chain pairing information for these α/β and γ/δ chains, together with the T-cell subtype information using gene-expression profiles. By analyzing the TCR gene rearrangement at the single-cell level, researchers can better understand T cell development, proliferation, and clonality, which are crucial for studying diseases such as cancer, immunodeficiency, and autoimmunity. Furthermore, single-cell TCR sequencing when combined with RNA sequencing datasets, facilitates the identification of γδ T cells. This method provides a standardized tool for identifying potential γδ T cell-based cancer immunotherapies. The technology's cost-effectiveness and ability to analyze clonotypes and immunophenotypes of cells in a single assay make it a valuable tool for unraveling the immune dynamics in various diseases.

#3977 Neoadjuvant chemotherapy and radiation shape the local and regional adaptive antitumor immune response in lung squamous cell carcinomas..

R. Krupar[1], J. Nieder[2], J. Braegelmann[3], M. Haarmann[3], T. Goldmann[4], S. Ruane[1], T. Milbich[1], C. Boehm[1], L. Ruff[1], J. Ribbat-Idel[1], C. Watermann[2], S. Perner[5], C. Kuempers[2];

[1]Aignostics GmbH, Berlin, Germany, [2]University Hospital Schleswig-Holstein, Campus Luebeck, Luebeck, Germany, [3]Faculty of Medicine and University Hospital Cologne, Cologne, Germany, [4]Research Center Borstel, Leibniz Lung Center, Borstel, Germany, [5]Institute of Haematopathology, Hamburg, Germany

Chemotherapy (CT) and radiotherapy (RT) are known for their stimulating as well as inhibiting effects on the anti-tumor immune response. This study aimed to understand how CT and RT change the local immune microenvironment of the tumor and the regional immune response in draining lymph nodes. Evaluations were performed on lung squamous cell carcinomas (LUSC) with a special focus on tertiary lymphoid structures (TLS) and lymph follicles.

A cohort of 21 untreated LUSC (naiveLUSC) and 21 matched neoadjuvantly treated LUSC (neoLUSC) was compiled. Digitized H&E whole slide images of the tumor and of two representative probes of a proximal and distal lymph node were assessed. A pathologist blinded to the groups assigned tumors to one of three immunophenotypes (inflamed, excluded, desert) by visual analysis. Tertiary lymphoid structures (TLS) in the tumor area and lymph follicles in the regional lymph nodes were counted and characterized according to their maturation status (with/without germinal center). RNAseq analyses were performed for a subset of tumors.

NeoLUSC tended to more frequently have a desert immune phenotype (6/21 versus 1/21, p=0.0931). The mean number of TLS was significantly reduced in neoLUSC compared to naiveLUSC (4 versus 9, p=0.0179). Additionally, neoLUSC had a significantly lower likelihood for the presence of mature TLS with germinal centers (3/21 versus 9/21, p=0.0327). While the mean number of lymph follicles in regional lymph nodes was comparable between neoLUSC and naiveLUSC, neoLUSC had a significantly reduced number of mature lymph follicles (20% versus 41% of lymph follicles, p=0.0376) in distant lymph nodes and showed a similar, but less pronounced trend in proximal lymph nodes. In general, the amount of TLS correlated with the amount of lymph follicles in naiveLUSC patients (p=0.0154), but not in neoLUSC patients. Across the complete cohort, long-term survivors (>2 years) tended to have higher numbers of lymph follicles in lymph nodes than short term survivors (1.6 versus 1.1 lymph follicles/mm2, p=0.0805). RNAseq analysis revealed a significant upregulation of inflammatory gene sets and downregulation of cell cycle associated gene sets in neoLUSC as compared to naiveLUSC.

This study demonstrates that CT and RT are potent, but multimodal influencers of the local tumor immune microenvironment as well as the regional immune response of the draining lymph nodes. While gene expression results underline the inflammation promoting effect of CT and RT, histological evaluations suggest that CT and RT negatively affect the adaptive anti-tumor immune response by reducing the development and maturation of TLS and lymph follicles in the lymph nodes. Next steps include an artificial intelligence based cell characterization and spatial evaluation of the tumor immune microenvironment to further unveil functional changes induced by CT and RT.

#3978 B-cell activating factor (BAFF) enhances antitumor immunity.

K. Aziz, K. Munjal, K. Howe, M. Yarchoan;
Johns Hopkins University School of Medicine, Baltimore, MD

Immunotherapies that modulate T cell function have been firmly established in cancer immunotherapy, whereas the potential for B cells in the antitumor immune response is not as well understood. B cell-activating factor (BAFF) is a cytokine belonging to the TNF ligand family that activates B cells and is linked to autoimmunity. Our preliminary research has identified BAFF as a target for enhancing antitumor immunity through enhancing presentation of tumor neoantigens and inducing tertiary lymphoid structures which can orchestrate tumor-specific T cell immune responses and correlate with improved clinical response. Since broad activation of B cell response could be detrimental and possibly induce autoimmune side effects, identification of specific B cell receptors that coordinate anti-tumor immunity is prudent. BAFF has three known receptors (BAFF-R, TACI and BCMA), and the effects of these specific BAFF ligand-receptor interactions on antitumor immunity are not known. Here we first generated BAFF-overexpressing cell lines using genomic editing [KPC-BAFF (pancreas), B16F10-BAFF (melanoma), and PancO2-BAFF (pancreas)] and examined their tumor growth in syngeneic immunocompetent host. Secondly, we investigated the effects of BAFF-overexpression on tumor response when individual receptors are knocked out using BAFF-R-KO, TACI-KO and BCMA-KO mice. Our results show significantly hindered tumor growth when the BAFF expressing stable cell lines are introduced to immunocompetent host, compared to parental cell lines. Tumor response experiments in receptor knockout mice is currently in progress. Successful identification of the BAFF receptor candidate that drives anti-tumor response is an exciting prospect for clinical translation. Development of agonists for the specific receptor may allow selective modulation of this particular B cell function in context of cancer therapy without perturbation of broad systemic humoral immunity.

#3979 PD-1 signals regulate NKG7 that is required for CD8+ T cells to sustain cytotoxicity and durable antitumor memory responses.

Zhiming Mao[1], Joanina Gicobi[1], Jacob Hirdler[2], Xin Liu[2], Michelle Hsu[1], Emilia Dellacecca[1], Wenjing Zhang[3], Fabrice Lucien-Matteoni[1], Haidong Dong[1]

[1]Immunology, Mayo Clinic College of Medicine and Science, Rochester, MN,[2]Urology, Mayo Clinic College of Medicine and Science, Rochester, MN,[3]Virology and Gene Therapy, Mayo Clinic College of Medicine and Science, Rochester, MN

Cytotoxic CD8+ T cells play a key role in response to anti-PD-1/PD-L1 immune checkpoint inhibitors (ICI) therapy. However, the exact effector molecules that are regulated by PD-1 signals in cytotoxic CD8+ T cells have not been completely defined. Lack of this knowledge is a crucial problem in addressing how to overcome the low clinical response rate to ICI therapy. When exploring why certain patients not responding to ICI therapy, we found non-responders did not have an elevated NKG7 expression in CD8+ T cells as responders to ICI therapy. The difference in NKG7 expression in CD8+ T cells between non-responders and responders to anti-PD-1 therapy prompted us to investigate the potential role of PD-1 signaling in regulating NKG7 expression. To that end, we generated a CD8+ T cell-specific *Pdcd1* conditional knockout mice (CD8 E8ICre-*Pdcd1*$^{fl/fl}$, also known as CD8-PD-1 cKO) where *Pdcd1* is deleted after thymic selection of single positive CD8+ T cells. We observed a delayed tumor growth and prolonged survival in CD8-PD-1 cKO mice compared to control mice after B16-OVA melanoma tumor challenge. On Day 12, when the CD8-PD-1 cKO mice demonstrated their ability to control tumor growth, we conducted single cell RNA sequencing on isolated tumor infiltrating CD8+ T cells, revealing a significant increase of *Nkg7* expression in effector CD8+ T cells in the *Pdcd1* deficient CD8+ T cells compared to the control wild type T cells. *Pdcd1*-deficient effector CD8+ T cells also had increased expression of genes linked to NFAT/Calcineurin signaling pathway including *Nfatc1*, *S100a4*, *Tbet* and *Tox,* suggesting *Nkg7* could be regulated by *Pdcd1* via the NFAT pathway. To determine the impact of increased NKG7 expression in CD8+ T cells, we used OVA protein as a surrogate tumor antigen in vaccination. We found a complete B16-OVA tumor rejection in CD8-PD-1 cKO mice compared to control mice when tumor cells were injected on day 7 after vaccination with OVA protein and poly (I:C) (as an adjuvant), but only a partial rejection on day 21. The CD8-PD-1 cKO mice that were tumor-free for 30-40 days rejected 2nd tumor challenge with B16-OVA tumors. This long-term protection is tumor antigen (OVA) specific because these mice did not reject B16F10 tumor cells that do not express OVA antigen. We also found effector memory CD8+ T cells with high cytotoxicity increased in the spleen of CD8-PD-1 cKO mice after OVA antigen immunization compared to control. In conclusion, we found NKG7 is one of the effector molecules in *cytotoxic* CD8+ T cells, which can be regulated by PD-1 signals through NFAT signaling. Targeting the PD-1-NFAT pathway may be a new option to overcome low responses of T cells to ICI therapy in treatment of refractory cancer.

#3980 Investigating the role of host obesity in promoting immunotherapy resistance.

H. N. Ogbonna, Z. Roberts, H. Kvarnberg, F. Dempsey, P. N. Song, A. G. Sorace, L. Norian;
University of Alabama at Birmingham, Birmingham, AL

Obesity is linked to an increased risk of various cancers, including renal cell carcinoma (RCC). Many RCC patients have obesity at diagnosis and treatment initiation, and our lab has found that this significantly impairs immunotherapy outcomes. Both preclinical and clinical reports, from our lab and others, have demonstrated that obesity reduces the efficacy of CD8+ T cell-dependent immunotherapy by increasing pro-tumorigenic IL-1β. Combining anti-PD-1 based therapy with anti-IL-1β triggers the recruitment of CD8+ T cells and improves the efficacy of anti-PD-1 based immunotherapy. However, the mechanistic links between obesity and increased IL-1β production remains unknown. Our objective is to identify mechanisms promoting IL-1 β-driven immunosuppression within renal tumors of obese mice. In our *in vivo* studies, we utilized a BALB/c mouse model of diet-induced obesity (DIO) and lean controls in combination with the Renca-Luc RCC cell line. Using flow cytometry and western blot, we respectively assessed leukocyte populations producing IL-1β and tumor energetics. Flow cytometry revealed that intra-tumoral IL-1β is produced primarily by tumor associated macrophages (TAMS). Immunoblotting demonstrated that increased IL-1β production is linked to altered mitochondrial function and ATP production. These early findings support the hypothesis that obesity driven IL-1β expression is mediated by tumor-associated macrophages and that mitochondrial dysfunction drives immune suppression. Understanding these molecular and immune-related mechanisms may pave the way for novel strategies to reduce immunosuppression in obese RCC patients, thus improving immunotherapeutic efficacy and overall clinical outcomes.

#3981 Immune targeting progesterone receptor in hormone receptor positive breast cancer.

A. E. Wilson[1], J. Wei[1], G. Lei[1], X.-Y. Yang[1], C.-X. Liu[1], M. Gajda[1], T. Wang[1], C. Hagan[2], Z. C. Hartman[1];
[1]Duke University School of Medicine, Durham, NC, [2]University of Kansas Medical Center, Kansas City, KS

Background: Hormone receptor positive (HR^+) breast cancer (BC) is a subtype of BC that is characterized by expression of estrogen receptor (ER) and progesterone receptor (PR). A cornerstone treatment for this subtype of BC is endocrine inhibition therapy (EIT), in which estrogen and ER are suppressed using antagonists to suppress tumor growth. However, patients eventually obtain resistance to EIT. Metastatic HR^+BC is the deadliest form of BC, with no cure. Current therapies currently only utilize the ER-axis, with no PR-targeted therapies. Little is known about the role of PR in these BCs, but we have found evidence for an immunosuppressive role for PR in HR^+BC. Yet, it is unclear how PR mediates immunosuppression and if this axis can be therapeutically targeted. We hypothesized that PR confers local immunosuppression through the stimulation of immunosuppressive transcriptional activity and that we can immunologically target this axis using a PR vaccine.

Experimental methods: To assess the immune impact of PR, we expressed the isoforms of PR (A, B and A+B) in mouse mammary cancer cells and assessed their capacity to elicit PR signaling. We assessed the impact of PR expression on T cell activity in targeting PR^+ mammary tumors that express GFP, along with using GFP-specific JEDI $CD8^+$ T cells. We explored the ability of PR to protect against GFP xenoantigen immune responses by engrafting PR^+ mammary cells into immune competent and deficient mice. Lastly, we engineered 1st generation adenoviral vectors encoding mouse and human PR and utilized two antiprogestins (Mifepristone and Onapristone) in vivo. Using our vectors, we vaccinated BALB/c in the footpad and assessed PR-specific immunity using IFNγ ELISPOT.

Results: Using PR signaling reporters, we found canonical PR signaling activity in the absence of progesterone (P4) by PR-A and in the presence of P4 by PR-B, but the most profound activation of PR signaling was seen through combined expression of PR-A and B. While expression of these genes did not confer striking cytotoxic T cell resistance in vitro, combination of PR-A+PR-B in 67NR cells permitted successful tumor engraftment in immune competent mice, despite xenoantigen expression. GFP expression did not alter tumor growth in immunodeficient mice, suggesting a key role in modulating local anti-tumor immunity. The use of either Mifepristone or Onapristone significantly suppressed tumor engraftment in immune competent mice in vivo. We found that an Ad-PR vaccine could elicit T cell responses against human PR-specific epitopes, a potential step towards immune targeting these BCs.

Conclusions: We found that murine PR-A and PR-B can confer robust P4 signaling that is linked to an immunosuppressive phenotype in vivo. We developed a PR vaccine that elicited PR-specific T cell responses in vivo. We are currently examining the mechanisms that underlie PR-mediated immunosuppression and exploring the potential of PR vaccines in HR^+BC.

#3982 Evaluating the effects of obesity on immune responses in renal tumors.

F. Dempsey, L. Norian;
University of Alabama at Birmingham, Birmingham, AL

Understanding the effects of obesity on cancer progression and treatment is a critically important area of research. Obesity is reaching epidemic proportions in our country and is known to increase the risk for many cancers, including renal cell carcinoma, which is among the ten most common cancers in both men and women. Our lab has shown that obesity leads to worse outcomes in advanced renal cancer patients treated with immunotherapy as compared to lean patients, but the cause for this difference is unknown. To investigate this further, we utilized a murine model with diet-induced obese mice and lean mice that were challenged with orthotopic renal tumors. The tumors grew out over three weeks and were harvested for flow cytometry staining. We stained for markers associated with immune function to better characterize what might be causing patients with obesity to be less responsive to immunotherapy. Our preliminary findings show that DIO mice had a greater tumor burden than lean controls over time. We also found that there compositional differences in multiple subsets of T cells in DIO versus lean mice. In the future, we will expand our murine studies to evaluate the phenotype and function of both tumor cells and immune cells. Additionally, we will continue these studies in human samples to further examine associations between obesity and immunotherapy outcomes.

#3983 Antigen-presenting cancer-associated fibroblasts provide an alternate mechanism for CD4 T cell activation in murine pancreatic ductal adenocarcinoma.

S. Maru, L. Andaloori, K. Howe, K. Munjal, J. Leatherman, E. J. Pearce, E. M. Jaffee;
Johns Hopkins University, Baltimore, MD

Despite the advent of immune checkpoint inhibitors (ICI) that have markedly changed the treatment landscape for select tumors, pancreatic ductal adenocarcinoma (PDAC) remains unresponsive to such an approach. Features of the PDAC tumor microenvironment that contribute to treatment resistance, including the influence of cancer-associated fibroblasts (CAF) on immune and tumor cells, remain poorly understood. Antigen-presenting CAFs (apCAFs) express MHC-II and activate CD4 T cells in genetically engineered PDAC mouse models, but are rarely found in human PDAC. In a human PDAC atlas consisting of six published single-cell RNA-sequencing datasets, we identified 370 apCAFs out of 8736 total CAFs, the majority of which were from one dataset. Understanding apCAF regulation can reveal how to promote their differentiation and enhance T cell activating capacity in PDAC.
Methods: Two KPC clones that differ in sensitivity to ICIs, sKPC (sensitive) and rKPC (resistant), derived from the autochthonous KPC murine model of PDAC, were implanted orthotopically into the pancreas or subcutaneously into the flank of syngeneic C57BL/6 mice. Tumors were harvested at 14-28 days post implantation for quantification of T cells, dendritic cells, and CAFs. To evaluate function, apCAFs were sorted and $CD11c^{\pm}$ and $CD4^{\pm}$ T cells were isolated from tumors. Naïve $CD4^{\pm}$ T cells were also isolated from OT-II mice. apCAFs and $CD11c^{\pm}$ cells were pulsed with OVA and co-cultured with OT-II $CD4^{\pm}$ T cells, or co-cultured with sKPC tumor infiltrating $CD4^{\pm}$ T cells in the presence of endogenous peptides.
Results: Total CAFs are equivalent between tumors, but apCAFs are significantly more abundant in sKPC tumors. Furthermore, the apCAF to dendritic cell ratio within these tumors ranged from 5:1 to 50:1. $CD11c^{\pm}$ dendritic cells sorted from sKPC tumors and pulsed with OVA peptide robustly activate naïve OT-II $CD4^{\pm}$ T cells, as expected from professional APCs; sorted apCAFs also activate naïve OT-II $CD4^{\pm}$ T cells, although to a lesser degree. When apCAFs or $CD11c^{\pm}$ dendritic cells are cultured with tumor-infiltrating $CD4^{\pm}$ T cells, however, they upregulate CD4 activation markers to a similar extent.
Conclusions: apCAFs are more abundant in tumors derived from ICI-sensitive KPC clones and greatly outnumber dendritic cells. Functionally, apCAFs from sKPC tumors stimulate tumor-derived CD4 T cells to the same degree as $CD11c^{\pm}$ dendritic cells, implicating a role in activation of the immune response in ICI-sensitive tumors. Although a small proportion of the tumor microenvironment, the apCAF subset may be enhanced in number and function by CAF-targeted modulators to affect the antitumor response; transcriptomics analyses are currently underway to identify regulators of apCAFs. Such a strategy could provide a solution to the currently unmet need for new and more effective treatments for PDAC patients.

#3984 Full-length TCR and BCR repertoire analysis, integrated with mRNA and surface proteins characterization, in a tumor mouse model.

A. Rezvan[1], X. Shi[1], M. Sen[1], S. Widmann[2], **A. Tyznik**[2];
[1]BD Biosciences, San Jose, CA, [2]BD Biosciences, San Diego, CA

Full-length TCR and BCR analysis with single-cell multiomic assays provides an understanding of immune responses, offering insights into the complete receptor structure and functionality that is crucial for accurately assessing the diversity and specificity of immune repertoires. Studying mouse immune cell heterogeneity can be achieved by simultaneous mRNA and surface protein profiling. However, when coupled with full-length TCR and BCR analysis, this integrated approach provides a more comprehensive understanding of immune responses and cellular function in healthy and diseased conditions. In this study, we used the MC38 colon carcinoma model to study T and B cell heterogeneity and clonotype diversity. We stained single-cell suspensions prepared from bone marrow, thymus, spleen and tumor tissues with 20 AbSeq (CITE-Seq) antibody oligos and sample-multiplexing tags. We then loaded 50,000 isolated T and B cells into two lanes of an 8-lane microwell cartridge for single-cell capture by a single-cell analysis system. To aid in the simultaneous analysis of clonality and gene expression, we carried out library preparation using a full-length TCR/BCR multiomic assay and a mouse immune response panel. The combination of mRNA and protein expression confirmed the elevated expression of exhaustion and activation markers in tumor-infiltrating lymphocytes (TILs). We identified high-frequency clonotypes within TILs and tracked their frequency across other tissues. Tumor-burdened mice splenic T cells showed shared TCR combinations with TILs, which were absent in healthy tissue. The results show the ability to successfully profile T and B cell receptors using a full-length TCR/BCR multiomic assay in a mouse tumor model and the use of transcriptome, protein and TCR/BCR clonal information to investigate immune cell characteristics across multiple samples.

#3985 Immune-competent “NoGlow” transgenic mice overcome restrictive tolerance to multiple xenoantigens and simultaneously permit identification, tracking, and temporal gene expression in tumor cells.

T. N. Trotter, A. Wilson, J. McBane, C. Dagotto, X. Yang, J. Wei, G. Lei, H. Thrash, H. K. Lyerly, Z. Hartman;
Duke University, Durham, NC

The ability to temporally regulate gene expression and track labeled cells make animal models powerful biomedical tools. However, sudden exposure to xenobiotic genes (e.g. GFP, luciferase (luc), or rtTA3) triggers inadvertent immune responses that can significantly suppress foreign gene expression or result in complete rejection of transplanted cells. Although germline expression of foreign genes somewhat addresses these challenges, native fluorescence and bioluminescence abrogates their utility as cellular reporters and spatiotemporally restricted expression can lead to suboptimal xenoantigen tolerance. Even in endogenous cancer models, we find that the means of tissue-directed expression of the same foreign gene yield significant differences in overall tolerance. Thus, the degree of tolerance to foreign genes strongly impacts the utility of different genetic modification and can strongly influence experimental outcomes and interpretations. To overcome these unwanted immune responses and enable reliable cell tracking/gene regulation, we developed a novel mouse model that selectively expresses antigen-intact but non-functional forms of GFP, luc, and rtTA3. These "NoGlow" mice possess no detectable background fluorescence or luminescence and mount limited adaptive immune responses against transgenic xenoantigens even after vaccination. Furthermore, we demonstrate that NoGlow mice allow tracking and tetracycline inducible gene regulation of triple-transgenic cells expressing GFP/luc/rtTA3, in contrast to transgene-negative immune competent mice which completely eliminate these cells. Notably, this model enables de novo metastasis from orthotopically implanted, triple-transgenic tumor cells, despite high xenoantigen expression. Finally, we observed model and sex-based differences in immune tolerance to the encoded xenoantigens after activation by different tissue-specific CREs, illustrating the obstacles of tolerizing animals to foreign genes and validating the utility of NoGlow mice to dissect the mechanisms of central and peripheral tolerance. Altogether, the NoGlow model provides a critical resource for in vivo studies across multiple disciplines, including oncology, developmental biology, infectious disease, autoimmunity, and transplantation.

#3986 Exploring nonsense-mediated decay inhibition as a novel approach to improve immunogenicity in small cell lung cancer.

L. A. Torres Fernandez[1], V. Bohm[2], L. Maas[1], A. Schollhorn[3], J. Kaufmann[4], J. D'Rozario[1], L. Kaiser[1], N. Gehring[2], M. Peifer[4], C. Gouttefangeas[3], R. K. Thomas[1], J. George[1];

[1]Department of Translational Genomics, Medical Faculty, University of Cologne, Cologne, Germany, [2]Institute of Genetics, department of RNA biology, University of Cologne, Cologne, Germany, [3]Institute for Immunology, University of Tubingen, Tubingen, Germany, [4]Center for Molecular Medicine Cologne (CMMC), University of Cologne, Cologne, Germany

Cancer immunotherapy has revolutionized the field of oncology and is one of the most promising treatments for lung cancer. Small cell lung cancer (SCLC) is highly aggressive and patients often relapse due to chemotherapy resistance. In the recent years, chemotherapy has been combined with immune checkpoint inhibition (ICI) for SCLC treatment, leading to improved responses in some patients, but also leaving a high number of non-responders to address. Paradoxically, SCLC has one of the highest tumor mutational burden, including remarkably abundant frameshifts (FS) which could create highly immunogenic neoantigens (NeoAg). However, FS-harbouring transcripts are often degraded via Nonsense-Mediated Decay (NMD). We therefore aimed to inhibit the NMD pathway to increase the immunogenicity of SCLC.

Our lab has so far profiled the mutational landscape of more than 400 SCLC patients and generated over 100 patient-derived xenotransplant models. We analyzed genome and transcriptome sequencing data of multiple tumors to interrogate the NMD target repertoire in SCLC. We determined tumor-specific mutations and predicted NeoAg based on the HLA-I-binding ability of mutant peptides. Upon NMD inhibiton, we validated the expression and presentation of NeoAg via transcriptomics, proteomics and HLA-I-immunopeptidomics. NMD-sensitive mutated transcripts included a wide range of somatic alterations beyond FS-mutations, suggesting an overall increase of potential tumor-specific NeoAg. We furthermore evaluated immunogenicity after NMD perturbation employing *in vitro* co-cultures as well as immunocompetent *in vivo* mouse models. Inhibition of NMD in tumor cells resulted in an HLA-I-dependent enhancement of T cell-mediated tumor killing *in vitro*, and *in vivo* experiments showed reduced tumor growth accompanied by increased immune infiltration upon controlled induction of NMD inhibition.

Altogether, NMD inhibition in SCLC led to an upregulation of NeoAg expression in tumor cells accompanied by enhanced T cell responses *in vitro* and *in vivo*. Our strategy provides a novel approach for the treatment of low immunogenic tumors which could be combined with ICI to enhance the efficacy of immunotherapy.

#3987 PD-L1 antigen stability using PD-L1 IHC pharmDx on human cancer tissues.

M. Kalpakoff, E. Olander, K. Jones, S. Hund, T. Evans, J. Barreto, D. Moquin, G. Toland, S. Tabuena-Frolli, K. Kersch, K. Kulangara, J. Musser; Agilent Technologies, Inc., Carpinteria, CA

Diagnostic evaluation and selection of potential pembrolizumab-responsive patients is achieved by determining the programmed cell death ligand-1 (PD-L1) expression using the companion diagnostic PD-L1 IHC 22C3 pharmDx assay, for several indications. PD-L1 expression is evaluated by immunohistochemistry (IHC) and is currently the most widely used selective biomarker for response to pembrolizumab anti-PD-1 therapy. Antigen stability on cut tissue sections, also referred to as cut section stability (CSS), and its impact on IHC results is of interest when determining PD-L1 positive or negative status for clinical trials and diagnostic purposes. Since the stability of cut sections from formalin-fixed paraffin-embedded (FFPE) tissue relies on retention of PD-L1 antigenicity following tissue sectioning, the aim of these studies was to measure CSS across multiple tumor indications using combined positive score (CPS). The impact of aged cut sections was evaluated for PD-L1 expression based on pathologist CPS scores of blinded and randomized stained sections. To assess CSS, fresh unstained 4µm cut tissue sections were stored in the dark at 2-8 °C. Staining was performed according to the instructions for use at predefined timepoints. Studies included neoplastic specimens from biliary tract adenocarcinoma (BTAC), cervical cancer (CC), colorectal (CRC) and gastric (GC) carcinoma, esophageal cancer (EC), head and neck squamous cell carcinoma (HNSCC), nasopharyngeal (NPC), ovarian (OC), renal cell (RCC), and triple negative breast (TNBC) carcinoma. Data for each indication and timepoint were used to evaluate average drift in CPS scores over time, starting with scores from a set of respective slides stained at timepoint zero, prior to aging of unstained cut slides. CSS for each specimen within each indication was based on the intersection point of the two-sided 95% confidence interval for the regression line on CPS drift with allowable drift limits. Overall CSS for each indication was defined based on the specimen that exhibited the shortest shelf-life. Linear regression analysis was performed to evaluate average CPS drift over time and define the CSS per indication. This analysis identified the following CSS (in days) for each tumor type when stored at 2-8 °C: 105 (CC), 113 (OC), 115 (BTAC), 135 (EC), 163 (GC), 180 (RCC), 197 (HNSCC), 231 (TNBC), 240 (NPC), and 300 (CRC). The minimal shelf life for unstained cut sections stored at 2-8 °C across the 10 indications in these studies was 105 days, indicating a possible minimum threshold for indications tested when sectioned specimens are stored at 2-8 °C. These data provide high confidence in determining PD-L1 expression on properly stored aged cut sections. Commercial claims may be shorter based on region, as specified in the local instructions for use.

#3988 Deep spatial immunophenotyping of lymphoid aggregates in pancreatic cancer using multi-omic integration of ultra high-plex proteomics and transcriptomics.

D. Gong[1], J. Cao[2], P. Wang[3], N. Jhaveri[4], Y. Hou[4], B. B. Cheikh[5], H. Ji[5], M. Gregory[6], J. Reeves[6], M. Patrick[6], C. Shiau[3], J. Su[3], J. A. Guo[1], J. M. Beechem[6], M. Hemberg[2], W. L. Hwang[3], R. Park[7],

[1]Massachusetts Institute of Technology (MIT), Cambridge, MA, [2]Brigham and Women's Hospital, Boston, MA, [3]Massachusetts General Hospital, Boston, MA, [4]Akoya Biosciences, Menlo Park, CA, [5]Massachusetts Institute of Technology (MIT), Menlo Park, CA, [6]NanoString Technologies, Seattle, WA, [7]MD Anderson Cancer Center, Houston, TX

The most well-described mechanism of immune evasion in PDAC is exclusion of immune cells by a desmoplastic stroma, but such immune exclusion is not uniform. Through single-nucleus RNA-seq and whole-transcriptome digital spatial profiling of patient tumors, we previously reported marked heterogeneity in the immune composition of PDAC. Here, we developed a novel multi-omics workflow integrating single cell spatial proteomics (96-plex, Akoya Phenocycler®-Fusion) and transcriptomics (990-plex, Nanostring CosMx) in primary patient PDAC tumors to systematically study spatial relationships and functional states of malignant, stromal, and immune cells. Consecutive sections from four independent tumors enabled whole slide proteomic assessment of >3.5M cells, and transcriptomic assessment of >200K cells. Strikingly, we observed an abundance of immune cell aggregates in all tissue sections, up to 57 within a 1 cm2 tumor section. Aggregates were diverse in composition with representation of myeloid cells, CD8+ T cells, and stromal cells, including fibroblasts and nerves. B/T lymphoid aggregates were well vascularized with co-localized CD31+CD34+ endothelial cells and appeared at various phases of maturation towards putative tertiary lymphoid structures (TLSs) containing CD38+ B cells, CD4+ T cells, and CD21+ follicular DCs. These tissues were enriched for interferon stimulated genes in T cells and type 1 interferon response signatures in malignant cells and cancer associated fibroblasts (CAFs) forming inflammatory multicellular hubs that have been associated with improved response to immune checkpoint blockade. Surprisingly, B cells, in addition to macrophages and CD8+ T cells, were major producers of interferon gamma (B cells: 13.7%, macrophages: 36.6%, CD8+ T cells: 12.1% of IFNG+ cells). Finally, to gain insight into the necessary factors for TLS formation in PDAC, we quantified the expression of chemokines and adhesion molecules associated with TLS initiation. Activated dendritic cells expressed CCL19 and CCL21, endothelial cells expressed CCL21, and in concert with inflammatory CAFs (iCAFs), CXCL12. Malignant cells expressed CXCL13 and CCL20 and displayed high levels of cell adhesion molecules ICAM1, VCAM1, and ICAM2. Together, our data suggests that the functions of lymphoid tissue organizer cells can be substituted by endothelial cells, dendritic cells, iCAFs, and, surprisingly, malignant cells. Our spatial immunophenotyping study of pancreatic cancer thus highlights the marked immune heterogeneity of the disease and suggests a central role for malignant and stromal cells in mediating diverse mechanisms of immune evasion and engagement. Functional studies will be conducted to investigate these mechanisms of tumor-immune crosstalk and identify novel immunotherapeutic vulnerabilities for this deadly disease.

IMMUNOLOGY: Adoptive Cell Therapies 3: CAR-T Cells
Poster Session

#3992 Tandem CAR-T cells against mesothelin and MUC16^{ecto}to overcome tumor-antigen heterogenicity.

D. Salas-Benito, F. Birocchi, A. Armstrong, A. A. Bouffard, T. Kienka, F. Korell, M. B. Leick, T. Berger, M. V. Maus;
Mass General Cancer Center, Charlestown Navy Yard, MA

Introduction: Antigen heterogeneity is a challenge for CAR-T cell therapy in solid tumors due to antigen escape when targeting a single antigen. In ovarian cancer (OC), mesothelin (meso) and Mucin16 (MUC16) are two of the most overexpressed antigens. Moreover, CA125, which is part of MUC16, is lost in some OC patients, but the ectodomain remains on the cell surface. Targeting both antigens (Meso and MUC16^{ecto}) with a tandem-CAR configuration could overcome antigen heterogeneity to improve CAR-T cell efficacy in OC.

Material and Methods: We designed a library of different CARs with tandem Meso and MUC16^{ecto} scFv combinations with varying G4S linker lengths, fused to a CD8 hinge/transmembrane domain and 41BBz intracellular domain. A series of constructs was then tested in an NFAT-GFP reporter system in Jurkat cells to determine which configuration induced maximal T cell activation and antigen-binding capacity via flow cytometry. We identified the top 2 activators and binders, produced primary human tandem CAR-T (TanCAR) cells by LV transduction, and tested their cytotoxicity *in vitro*against dual antigen-expressing or single antigen-expressing tumor cells using luciferase killing assays and Incucyte. We measured the cytokine production with a Luminex® Multiplex Assay and used a z-Movi® Cell Avidity Analyzer to test the tandem scFv avidity towards the antigens. Also, we examined TanCAR activity against a mixed tumor model in NSG mice. Their *in vitro* and *in vivo* activity were compared to CAR T cells targeting either single antigen (SS1-anti-Meso or 4H11-anti-MUC16^{ecto}).

Results: We found that TanCAR1 and TanCAR3 as the configurations with the best activation and binding capacity in response to cognate antigen. TanCAR1 and TanCAR3 had superior *in vitro* cytotoxic capacities compared to SS1 or 4H11 in tumor models expressing both antigens and in mixed cultures of tumor cells expressing one, both, or neither target antigen. From this mixed culture, we analyzed the remaining tumor cell populations by flow cytometry and observed an overgrowth of the population not targeted by CAR. In response to tumor cells, tandem CARs also produced INFg, IL6, IL-18, IL-13, and GM-CSF regardless of whether one or two antigens were expressed. For further experiments, we pursued TanCAR1 due to its slightly better functionality compared to TanCAR3. TanCAR1 had the same avidity for cells expressing the single antigens as SS1 or 4H11 CARs, but an intermediate avidity for the double Ag-expressing cell line compared to the single CARs. Finally, we tested TanCAR1-T cells in an *in vivo* mixed tumor model, showing that they better controlled and reduced tumor growth compared to either SS1 or 4H11.

Conclusion: Targeting Meso and MUC16^{ecto} through a tandem CAR design allows for a better anti-tumor response compared to CAR T cells targeting a single antigen. This approach may combat antigen heterogeneity by preventing antigen escape.

#3993 A tunable safety switch for solid tumor CAR T-cell therapy.

K. Misawa, M. Taleb, S. Banerjee, W.-R. Vista, N. K. Chintala, P. S. Adusumilli;
Memorial Sloan Kettering Cancer Center, New York, NY

On-target off-tumor toxicity, cytokine release syndrome (CRS), and immune effector cell-associated neurotoxicity syndrome (ICANS) are severe immune-related adverse events (irAEs) that are frequently associated with Chimeric Antigen Receptor (CAR) T-cell therapy. Current efforts to manage such therapy-related toxicities involve incorporation of an inducible suicide agent within CAR constructs, such as iCaspase-9 or herpes simplex virus type 1 thymidine kinase that can be selectively activated to produce toxic effects within CAR T cells and attenuate their activity. However, while activation of these agents helps to mitigate or overcome such unwarranted toxicities, the therapeutic benefit of CAR T cells anti-tumor activity is also compromised. Therefore, to continue maintenance of CAR T cells' therapeutic function while minimizing irAEs, an ideal safety switch should 1) rapidly inhibit the activation and proliferation of CAR T cells exposed to the target antigen, 2) reversibly inhibit activity without inducing CAR T cell elimination and 3) be clinically translatable for safe application in patients. Our laboratory investigated one such safety switch to inhibit CAR T-cell activity while maintaining their therapeutic function. We showed that incorporating a mutant variant of c-KIT D816V (KITv) in the intracellular domain of mesothelin-targeting second-generation CAR T cells (M28z-KITv) improved efficacy in solid tumors with low antigen, or an immunosuppressive environment. Herein, we evaluate the use of Dasatinib, a clinically available multitarget (BCR, SRC, c-KIT) tyrosine kinase inhibitor (TKI), as a tunable safety switch to reversibly inhibit M28z-KITv CAR T-cell functional activity. In cohorts of mice established with lung adenocarcinoma, daily administration of Dasatinib starting on day 1 or day 3 after CAR T-cell administration stabilized tumor growth, which otherwise continued to regress in untreated mice, indicating inhibition of CAR T-cell functional activity. Upon discontinuation of Dasatinib, tumors regressed, indicating reversal of CAR T-cell functional activity. In an experiment conducted to investigate functional persistence of CAR T cells upon long-term exposure to Dasatinib (1 month), we noted uninhibited activity of CAR T cells to rechallenged tumors. Dasatinib, thus may act as a tunable safety switch to regulate M28z-KITv CAR T-cell activity without compromising its therapeutic function.

#3994 N glycosylation inhibition hinders immunosuppressive tumor microenvironment cells improving CAR T cell efficacy.

C. Sirini, B. Greco, C. Balestrieri, B. Camisa, L. Falcone, R. El Khoury, O. Botrugno, G. Giovannoni, G. Tonon, E. Brunetto, M. Cangi, F. Pedica, A. Bergamini, F. Ciceri, C. Bonini, M. Casucci;
IRCCS San Raffaele Scientific Institute, Milano, Italy

Adoptive transfer of CAR T cells demonstrated impressive results against B-cell malignancies, but still limited efficacy against solid tumors. In this context, multiple challenges need to be overcome, including poor tumor recognition and strong immunosuppression within the tumor microenvironment (TME). Our Unit has recently reported that pharmacological inhibition of N-glycan synthesis in cancer cells increases CAR T cell efficacy by improving tumor recognition and preventing T cell exhaustion. In this project, we investigated the role of N-glycosylation blockade on TME cells in the context of colorectal cancer (CRC) and pancreatic adenocarcinoma (PDAC)-derived liver metastases, exploiting CEA-specific CAR T cell therapy. To understand the effect of N-glycosylation blockade on TME cells (both M2-like macrophages, M2-M and Hepatic stellate cells, HepSCs), we analyzed the phenotypic and transcriptional profile and we performed in vitro functional assays, such as tripartite co-cultures, suppressive assays and released-cytokines analysis. *In vitro* studies revealed that N-glycosylation inhibition abolishes the ability of both TME cells to restrain T cell proliferation and increases the elimination of cancer cell lines and patient-derived tumor organoids (PDOs from CRC-liver metastases). Interestingly, these effects were associated with profound phenotypic and transcriptional changes in M2-M and HepSCs. In particular, the treatment was able to inhibit M2-polarization in terms of surface markers expression, IL-10 secretion and gene expression profile, and was shown to hinder the activation of HepSCs. Moreover, to evaluate the effect of N-glycosylation inhibition on TME cells *in vivo*, we exploited immunodeficient mice reconstituted with a human immune system (huSGM3), engrafted intra-liver with tumor cells and treated with CEA CAR T cells. Interestingly, in this *in vivo* model, the presence of human immune cells supports CAR T cell responses and helps recreate an immune TME more representative of the human disease. Importantly, using these mice we observed that N-glycosylation inhibition improves CEA CAR T cells fitness, enhancing their antitumor activity in terms of survival. This effect is associated with a modulation of human immune TME populations and in particular with the downregulation of immunosuppressive genes in tumor-infiltrating human immune cells (from scRNAseq and Nanostring analysis). Overall, these data suggest that blocking N-glycosylation can help overcome multiple barriers that currently limit CAR T cell efficacy in solid tumors, acting not only on tumor cells, but also on immunosuppressive tumor microenvironment cells.

#3995 A novel chimeric Fas signal redirect receptor enhances the durability of anti-tumor activity and serial killing potential of CAR T cells.

C. Ecker, **E. Peralta**, H.-Y. Chu, L. Loter, M. Tsuda, E. Avramis, M. Denholtz, A. Witty, T. Lee, B. Valamehr;
Fate Therapeutics, San Diego, CA

Chimeric antigen receptor (CAR) T-cell therapies have demonstrated remarkable success in hematological malignancies but only modest efficacy in solid tumors. Apoptosis induced by Fas receptor signaling can be a substantial barrier to CAR T-cell antitumor activity, as many solid tumors express high levels of Fas ligand (FasL). Here we describe a novel synthetic construct where the ectodomain of Fas receptor is fused to the signaling endodomain of a stimulatory receptor, creating a Fas signal redirect receptor (Fas-SRR). This unique design not only prevents Fas-dependent cell death, but also augments the long-term killing potential of induced pluripotent stem cell (iPSC)-derived CAR-T (CAR-iT) cells. Fas-SRR constructs with unique T-cell activation signaling endodomains were designed and compared to two control arms: a dominant negative receptor (Fas-DNR), which blocks Fas signal but does not promote activation; and a Fas-41BB fusion receptor, where the 41BB endodomain is fused to FasR ectodomain to direct activation upon FasL:Fas engagement. Fas-SRR designs were validated in Jurkat reporter cells treated with Fas agonist to measure signal redirection via Fas-SRR. To conduct a head-to-head comparison, CAR-iT cells were engineered to express a CAR under the regulation of the TRAC locus and to express either a Fas-DNR, a Fas-41BB, or FAS-SRR constructs at high purity (>90% transgene expression). No major differences were seen in maturation phenotype (>95% TRAC-CAR expression) of these cells, indicating compatibility of the FAS-SRR constructs with CAR-iT cell generation. Functional testing of the Fas-SRR$^{\pm}$ CAR-iT cells was performed in a long-term restimulation assay where effector cells were repeatedly exposed to target cells over multiple rounds of co-culture. Complete loss of target cell lysis was observed by round six in the co-cultures with FAS-DNR cells, where loss of CAR-iT cell persistence led to accumulation of target cells. After eight rounds of co-culture, the Fas-41BB cells and the majority of Fas-SSR cell constructs also began to exhibit minimal activity toward target cells. However, the top Fas-SRR cell constructs continued to show durable antitumor activity (>97% cytolysis) through the end of the 9-round rechallenge assay. Of note, GSEA analysis identified significant upregulation of NFkB and RELA target genes in cells having the top FAS-SRR construct versus the less durable designs. These results reinforce the advantage of attenuating Fas-FasL interactions to prevent apoptosis and, more importantly, demonstrate the unique therapeutic value in redirecting Fas signaling to improve T-cell potency over an extended duration. Additional studies are underway to further investigate the implications of Fas signal redirection in CAR T and CAR-iT cells and to further understand the module of genes involved in supporting serial stimulation performance.

#3996 Secreted cytokine-αPDL1 fusion proteins improve solid tumor chimeric antigen receptor (CAR) T-cell therapy.

L. Christian[1], J. P. Murad[1], L. Lopez[1], A. Park[1], J. Yang[2], E. Lee[3], C. Trac[1], S. Forman[1], S. J. Priceman[1];

[1]Beckman Research Institute of The City of Hope, Duarte, CA, [2]Ohio State University, Columbus, OH, [3]Georgia Institute of Technology, Atlanta, CA

Background: Success of Chimeric Antigen Receptor (CAR) T cells therapy for solid tumors are limited by the suppressive solid tumor microenvironment (TME), T cell exhaustion, lack of persistence, and poor trafficking to tumors. Strategies to improve this include therapeutic combinations, such as checkpoint inhibition (CPI) or cytokine support. However, CPI therapy has largely failed because of refractory and resistant tumors and cytokine administration can lead to lethal toxicities. To this end, we propose that enabling CAR T cells to secrete bi-functional fusion proteins consisting of cytokine modifiers (ie: IL12, IL15, or TGFβ-trap) combined with checkpoint inhibition (αPDL1 scFv) can provide tumor PDL1 sequestered cytokine activity and local tumor-immune modulation to boost solid tumor CAR T cell efficacy, enhance CPI impacts, and safely improve durable outcomes. **Methods:** Mouse T cells dual transduced to express surface CAR targeting prostate or ovarian solid tumors in addition to secretable cytokine fused to an αPDL1 scFv were generated. *In vitro*, the PDL1 blockade capacity and tumor-surface cytokine presentation of supernatants from dual transduced CAR T cells was assessed on PDL1 induced tumor cells. Further, secreted fusion protein transduced CAR T cells were assessed for function, phenotype, and cytokine release in a repetitive tumor rechallenge assay. *In vivo*, mouse CAR T cells dual transduced with fusion proteins and appropriate controls were assessed for anti-tumor efficacy, survival kinetics, and toxicity in immunocompetent solid tumor mouse models of prostate cancer and intraperitoneal disseminated ovarian cancer. **Results:** CAR T cells were shown to be successfully dual transduced, and secreted αPDL1-cytokine fusion proteins exhibiting functional PDL1 binding characteristics *in vitro*. CAR T cells engineered with αPDL1-IL12 fusion protein had greater anti-tumor activity and CAR specific expansion compared to other tested fusion proteins in *in vitro* co-culture assays. In a syngeneic prostate tumor model, mice receiving CAR T cells with αPDL1-IL12 fusion T cells out competed other cytokine fusion combinations. In a syngeneic ovarian tumor model we safely achieved 100% curative response rate with CAR secreting αPDL1-IL12 fusion in contrast to CAR with αPDL1^{mut}IL12 control along with tumor regional PDL1 blockade on myeloid subsets within the TME. **Conclusions:** Our findings suggest that CAR T cells engineered to secrete αPD-L1-IL12 fusion protein show improved tumor control, less systemic toxicity, and enhanced expansion which promotes eradication of disease in two independent *in vivo* tumor models with two unique solid tumor CAR targets. We believe this strategy has the potential to improve solid tumor CAR T-cell efficacy and enhance durable innate immune responses.

#3997 PARP inhibitors plus anlotinib as bridging therapy for TGFβ-insensitive CAR-T cell therapy targeting MSLN and CD19 in advanced ovarian cancer.

Huayi Li[1], Minghua Xiang[1], Jiahao Liu[1], Wei Mu[2], Li Zhu[2], Xuejiao Zhao[1], Gordon B. Mills[3], Qinglei Gao[1], **Yong Fang**[1]

[1]Department of Gynecological Oncology, Cancer Biology Research Center, Tongji Hospital, Tongji Medical College, Huazhong University of Science and Technology, Wuhan, China,[2]Department of Hematology, Tongji Hospital, Tongji Medical College, Huazhong University of Science and Technology, Wuhan, China,[3]Department of Cell, Development and Cancer Biology, Oregon Health and Sciences University; Knight Cancer Institute, Portland, OR

Background: The efficacy of chimeric antigen receptor (CAR) T cell therapy remains modest for the treatment of solid tumors due to restricted T cell infiltration and immunosuppressive tumor microenvironment (TME). Leveraging the window of opportunity between leukapheresis and infusion using bridging therapy might improve TME and potentiate CAR-T cell therapy. Here, we assessed the potential of poly (ADP-ribose) polymerase (PARP) inhibitors plus anlotinib as bridging therapy for CAR-T cells with resistance to TGFβ and capability of rapid expansion by bait-and-switch strategy of dual-targeting mesothelin (MSLN) and CD19 in preclinical models of advanced ovarian cancer.

Methods: Immunocompetent mice bearing ID8 tumors were treated with niraparib (21 days) plus anlotinib (14 days) and euthanized at different timepoints (0, 7, or 14 days since discontinuation) to quantify tumor-infiltrating T cells and profile T cell functions. CAR-T cells transfected with dominant-negative TGFβRII dual-targeting MSLN and CD19 were produced by IASO Biotherapeutics. NSG mice bearing MSLN-positive cell- or patient-derived xenografts (CDX or PDX) of ovarian cancer received CAR-T cells alone or after bridging therapy (niraparib plus anlotinib followed by a wash-out period of 7 days). Tumor volume was balanced before CAR-T cell infusion. Replication-deficient NALM6 cells pre-treated with mitomycin C were injected to provide CD19 antigen. A PET scan that visualized granzyme B release was used to track CAR-T cells and assess immune-mediated tumor killing.

Results: Niraparib combined with anlotinib increased tumor-infiltrating T cells without impairing T cell functionality. The effects of promoting T cell infiltration remained significant at 14 days after discontinuation, which might associate with lasting activation of cGAS-STING pathway and secretion of downstream chemokines (CXCL10 and CCL5), and normalized tumor vasculature featured by better perfusion and reduced leakage. The engineered CAR-T cells could resist TGFβ and displayed improved proliferation, cytotoxicity, cytokine release, and in vivo antitumor activities upon CD19 stimulation. Importantly, bridging therapy significantly increased CAR-T cell infiltration, curbed tumor growth, and prolonged survival in mice bearing SKOV3 CDX, HRD-negative PDX, and another multidrug-resistant PDX. PET imaging showed that bridging therapy increased tumor-infiltrating CAR-T cells and boosted tumor-killing capability.

Conclusions: PARP inhibitors plus anlotinib as bridging therapy facilitated CAR-T cell infiltration and enhanced antitumor activities in multiple preclinical models of advanced ovarian cancer, and an early phase I trial (NCT05141253) is ongoing to evaluate PARP inhibitors plus anlotinib as bridging therapy for CAR-T cell therapy in patients with refractory MSLN-positive ovarian cancer.

#3998 Preclinical efficacy of a synthetic Notch-based combinatorial immunotherapy against colorectal cancer with HER2 amplification.

M. Cortese[1], E. Torchiaro[1], A. D'Andrea[2], C. Petti[1], F. Invrea[1], L. Franco[1], C. Donini[2], V. Leuci[2], S. M. Leto[1], V. Vurchio[1], F. Cottino[1], C. Isella[2], S. Arena[2], F. Vigna[2], A. Bertotti[2], L. Trusolino[2], D. Sangiolo[2], E. Medico[2];

[1]Candiolo Cancer Institute - IRCCS, Candiolo, Italy, [2]University of Turin, Turin, Italy

HER2 amplification occurs in about 5% of colorectal cancers (CRC) and is only partially associated with clinical response to combined HER2/EGFR targeted treatment. An alternative approach, based on Adoptive Cell Therapy (ACT) using T cells engineered with anti-HER2 Chimeric Antigen Receptor (CAR), proved toxic due to "on-target off-tumor" activity. Therefore, we developed a combinatorial ACT strategy to safely target HER2 amplification in CRC using a synNotch-based artificial regulatory network. A synthetic Notch receptor was employed in which the extracellular domain is an anti-HER2 scFv and the intracellular domain contains the GAL4VP64 artificial transcription factor. Engagement of the HER2-synNotch by overexpressed HER2 on the surface of target cells induces GAL4VP64 cleavage and translocation to the nucleus, where it drives expression of a CAR under a GAL4-responsive promoter. In this way, only cells co-expressing both HER2 and the CAR target are killed. Carcinoembryonic antigen (CEA) was selected as a colon-specific CAR target: CEA expression is indeed restricted to the digestive tract and is increased in CRC. The natural killer cell line NK-92 was chosen as effector to be engineered. NK-92 cells transduced with HER2-synNotch and inducible CEA-CAR lentiviral vectors were subsequently sorted in the OFF and ON state to select those with the higher CAR induction after synNotch engagement. Subsequently, cloning of sorted cells led to identification of an optimally responsive clone (clone 5F), in terms of specificity and amplitude of CAR induction. The 5F clone demonstrated significant activity *in vitro* and *in vivo* specifically against HER2amp CRC models, with no effects on cells with physiological HER2 levels. *In vitro*, the 5F clone displayed selective cytotoxicity against HER2amp/CEA+ CRC cells, with minimal killing activity against HER2amp/CEA- cells, or HER2norm/CEA+ cells. Additional assays on 3D organoids highlighted better recruitment and infiltration by the 5F clone respect to NK-92 WT cells, only in HER2amp models. *In vivo*, NK-92.5F significantly impaired tumor growth in two different HER2amp CRC models, with no effect on HER2norm CRC cells. To further improve survival, tumor penetration and *in vivo* efficacy of the NK-92.5F clone, a more complex system was built, in which HER2 synNotch engagement drives expression of both the CEA-CAR and IL2. 5F-IL2 cells displayed further increased cytotoxicity *in vitro*. *In vivo*, 5F-IL2 cells drastically increased survival of mice carrying HER2amp CRC xenografts with respect to the parental 5F clone. The observed selective therapeutic efficacy both *in vitro* and *in vivo* of this innovative HER2 synNotch/CEA-CAR system, and its future evolutions, opens perspectives for possible clinical applications in cases of HER2amp CRC resistant or partially responsive to HER2/EGFR blockade.

#3999 Augmentation of antitumor effects by CAR-T cells secreting anti-PD-1 single-chain antibody fused with IL-21.

Y. Li[1], J. Zhao[1], X. Cheng[2], H. Li[2], R. Tian[1], Q. He[1], S. Wang[1];

[1]Institute of Biophysics, Chinese Academy of Sciences, Beijing, China, [2]CD(Suzhou)Biopharma Co.,Ltd., Suzhou, China

Background: Chimeric antigen receptor (CAR) T cell therapy has shown remarkable responses in hematologic malignancies. However, many patients suffer from limited response and tumor relapse due to lack of persisting CAR-T cells and immune escape. Delivery of immunomodulatory cytokines is one of the strategies to improve immune function; however, the systemic effect of cytokines can be detrimental.

Methods: To prevent the toxic effects of cytokines, we proposed the concept of targeting cytokines to tumor-specific T cells in vivo. To this end, we developed CAR-T cells secreting a fusion protein (PD-1Ab21) composed of anti-PD-1 single chain antibody and IL-21, which target IL-21 to CAR-T cells to promote their proliferation and differentiation into memory cells while blocking the PD-1 signal of CAR-T cells. The secretion and functions of PD-1Ab21 were identified. The proliferation and differentiation of CAR-T cells secreting PD-1Ab21 (PD-1Ab21-CAR-T) were compared in vitro with that of the conventional CAR-T cells. The therapeutic effects of CAR-T cells secreting PD-1Ab21 were studied in immunodeficient mice engrafted with human Burkitt lymphoma Daudi, multiple myeloma cell U266 and Her2/neu+ breast cancer cell BT474.

Results: The results showed that the culture supernatant of PD-1Ab21-CAR-T cells, like anti-PD-1 antibody, blocked the binding of PD-1 to PD-L1 and stimulated STAT3 phosphorylation in human T lymphocytic leukemia cell Hut78 with the same activity as IL-21. In the conventional culture milieu with high dose of IL-2, the proliferation of the PD-1Ab21-CAR-T cells was not different from that of conventional CAR-T cells. While cultured with low dose of IL-2 that could not support the proliferation of conventional CAR-T cells, the PD-1Ab21-CAR-T cells still showed significant proliferation. A major fraction of the PD-1Ab21-CAR-T products was shown to co-express CCR7, CD62L and CD45RA, and express high level of TCF-1, indicating a memory stem-like phenotype. While the most of conventional CAR-T cells showed effector phenotype defined as CD45RA+CCR7-. Furthermore, adoptive transfer of PD-1Ab21-CAR-T cells exhibited significantly improved CAR-T cell expansion and resulted in superior tumor eradication in the xenograft models of human B-cell malignancy, multiple myeloma and Her2/neu+ breast cancer. The enhanced cellular function by secreting PD-1Ab21 was mediated through an autocrine and/or paracrine manners.

Conclusion: We developed an enhanced CAR-T cells. Our data provide preclinical evidence to support the translation of this design for an improved CAR-T cell-mediated anti-tumor response.

#4001 Monocyte transcriptome profiles associated with clinical response in patients with B-cell non-Hodgkin's lymphoma receiving CD19-directed CAR-T therapy.

A. de Menezes Silva Corraes, P. Wang, R. Bansal, H. Zhang, Z. Shao, K. Regan, E. Moreno Cortes, A. Khurana, N. Bennani, Y. Wang, P. Hampel, J. Paludo, P. Johnston, H. Murthy, M. Iqbal, S. Ansell, J. Munoz, A. Rosenthal, M. Kharfan-Dabaja, J. Castro, S. Kenderian, H. Dong, Y. Li, Y. Lin;
Mayo Clinic, Rochester, MN

Background Although CAR T-cell therapy has achieved remarkable response in patients (pts) with B-cell non-Hodgkin's lymphoma (NHL), 20-30% of pts still have primary refractory disease (PD1), and another 30-40% relapse (PD2). We and others have shown that monocytes can modulate T-cell functions and impact clinical response to chemoimmunotherapy in NHL. Given that monocytes nadir and recovery kinetics differ from lymphocytes post lymphodepletion chemotherapy, we hypothesize that monocyte phenotype at peak CAR-T expansion and in the early month post CAR-T can modulate immune responses.
Methods scRNAseq were performed on peripheral blood mononuclear cells of NHL pts prior to lymphodepletion chemotherapy (pre), at peak CAR-T expansion (peak), and one month following CAR-T (M1). Seurat v4.3.0 was used for unsupervised hierarchical clustering analysis. Lugano criteria was used to determine clinical responses which were categorized as CR (complete remission), PD1, or PD2.
Results We analyzed 129,981 monocytes from 77 samples of 32 pts (16 CR, 4 PD1, 12 PD2) and 5 healthy controls. Unsupervised hierarchical clustering analysis identified 13 monocyte clusters: 4 classical monocyte (CM) clusters with transcriptome profiles for enriched signaling in IL-6, TGFβ, EMT, and p53; 2 intermediate monocyte (IM) clusters enriched for IL-1 or CD38 signaling; 2 non-classical monocytes (NM), one with increased CD36 expression; 3 monocytic MDSC clusters with enrichment of TGFβ, SIRPα, and HIF1α signaling; and 2 lymphoma-associated monocytes, expressing CD163 or CD169. At Pre and Peak, the distribution of the monocyte clusters was similar in pts with CR, PD2, or PD1, with only a slight decrease in the percent of NM in the PD2 group at Pre and slight increase of CD36 NM in PD1 at Peak. Compared to Pre, all pts had increased percent of CD36 NM and IL-1 IM at Peak. Interestingly, while the distribution of monocyte clusters was similar at Pre and Peak across clinical responses, GSEA showed that monocytes in CR pts, compared to PD1 and PD2, had gene expression enrichment of MYC target V2 pathway at Pre and TGFβ pathway at Peak. At M1, pts in PD1 had increased percent of p53 and TGFβ CM and decreased percent of NM. In contrast, pts with CR had decreased percent of IL-6 CM, p53 CM, TGFβ CM, IL-1 IM and increased percent of NM. Notably, as pts with CR and PD2 may appear similar clinically at M1, pts with PD2, compared to CR, have increased IL-6 CM, IL-1 IM, and decreased NM. In addition, GSEA showed that PD2 pts had increased IFNα response. Our results demonstrate that monocyte phenotype differences at Pre and Peak could be associated with CAR-T clinical response, and that persistent inflammatory monocyte signaling at M1 in pts with clinical response is associated with relapse. These data suggest a role for development of monocyte biomarkers to predict response and therapeutic targeting.

#4002 Investigating CAR-T cell efficacy and activation in the disseminated NALM6-luc human B-cell acute lymphoblastic leukemia model.

P. Pandey, **D. Draper**, S. Barnes, Y. Xing, D. Germain, L. Kucharczyk, R. Stacey;
Labcorp Early Development, Ann Arbor, MI, MI

Introduction: Chimeric Antigen Receptor T (CAR-T) cell therapy has emerged as a promising approach for treating hematological malignancies, particularly B-cell acute lymphoblastic leukemia (B-ALL). This study aimed to delve into the activation dynamics and therapeutic efficacy of CD19 CAR-T cells in a disseminated NALM6-luc human B-ALL murine model.
Experimental design: NALM6-Luc-mCh-Puro cells were implanted intravenously in female NSG (NOD.Cg-Prkdcscid Il2rgtm1Wjl/SzJ) mice. Animals were treated with CD19 CAR-T cells alone and in combination with ibrutinib. The anti-tumor activity was assessed, and the persistence and activation of CAR-T cells in the blood were evaluated using flow cytometry. Additionally, ddPCR analysis was employed to quantify CAR copy numbers, providing insights into the T-cell persistence over time.
Results: Treatment with CD19 CAR-T cells exhibited notable anti-cancer activity and that activity was enhanced in combination with ibrutinib, in line with other reports. The increased time to progression was noted as 69.2% for the CAR-T group and 138.4% for the combination of CAR-T and ibrutinib compared to control. Flow cytometry analysis showed that CAR-T cells persisted in the blood throughout the study. The mean CAR-T absolute cell count for both CAR-T and CAR-T plus ibrutinib treated groups increased from 2 cell/µL blood on Day 0 to 11 and 51 cells/µL of blood, respectively, by Day 39. The progressive increase of PD-1+ and LAG-3+ percentage cells correlates positively with tumor burden, indicating a dynamic link between biomarker upregulation and the presence of tumor cells in mice. ddPCR analysis revealed an initial CAR copy decrease in all groups, followed by gradual increase in tumor-bearing mice treated with CD19 CAR-T cells, with a dramatic increase observed by Day 39. Results from CAR-T treated and CAR-T plus ibrutinib treated groups were comparable, showing mean copy numbers per ng of DNA increasing from less than 1 on day 4 to 17.9 and 23.3, respectively, on day 39. Importantly, no changes were noted in non-tumor implanted mice, emphasizing the tumor dependency for CAR-T cell expansion.
Conclusion: This study emphasizes the marked anti-cancer activity of CD19 CAR-T cells in the NALM6-Luc-mCh-Puro B-ALL murine model. Comprehensive analysis of CAR-T cell persistence and activation, including insights from ddPCR, provides a robust understanding of therapeutic response dynamics. The observed in vivo anti-cancer efficacy aligns with the persistence of CAR-T cells revealed by flow cytometry and the dynamic expansion captured through ddPCR analysis. Our results indicate ddPCR and flow cytometry as complementary and independent methods for assessing the systemic CAR-T cell persistence, contributing to optimizing therapy for B-cell acute lymphoblastic leukemia.

#4003 TBK1 inhibition enhances CAR-T cell efficacy against patient-derived organotypic tumor spheroids.

L. Maggs[1], Y. Sun[1], G. Cattaneo[1], M. Ventin[1], F. Chen[1], M. Q. Rasmussen[1], X. Wang[1], C. R. Ferrone[2], S. Ferrone[1], R. W. Jenkins[1];
[1]Massachusetts General Hospital, Boston, MA, [2]Cedars-Sinai, Los Angeles, CA

Novel therapeutic strategies are needed to improve the efficacy of chimeric antigen receptor (CAR)-T cells in the treatment of solid tumors. Here, we set out to evaluate novel therapeutic strategies to improve the efficacy of B7-H3 (*CD276*) directed (B7-H3.CAR-T) using 3D microfluidic cultures of patient-derived organotypic tumor spheroids (PDOTS). PDOTS are generated from fresh patient tumor tissue and contain tumor cells, autologous immune cells and stromal cells, therefore recapitulating key features of the tumor microenvironment (TME), enabling the study of tumor-immune dynamics. We confirmed activity of B7-H3.CAR-T in PDOTS, although a strong correlation between B7-H3 expression and CAR-T efficacy was not observed. Mechanistic studies subsequently demonstrated dynamic upregulation of co-inhibitory receptors on CAR-T cells following target cell encounter leading to CAR-T cell dysfunction and limiting CAR-T efficacy in B7-H3 expressing tumors. PD-1 blockade restored CAR-T activity in monotypic and organotypic tumor spheroids with improved tumor control and upregulation of effector cytokines. Given the emerging role of TANK-binding kinase 1 (TBK1) as an immune evasion gene, we examined the effect of TBK1 inhibition on CAR-T efficacy. Similar to PD-1 blockade, TBK1 inhibition restored CAR-T activity in monotypic and organotypic tumor spheroids, prevented CAR-T cell dysfunction, and enhanced T cell proliferation. Inhibition or deletion of TBK1 also enhanced sensitivity of cancer cells to immune-mediated killing. Taken together, our results demonstrate the feasibility and utility of *ex vivo* profiling of CAR-T cells using PDOTS, and suggest that targeting TBK1 is a novel strategy to enhance CAR-T efficacy by overcoming tumor-intrinsic and -extrinsic resistance mechanisms.

#4004 Fine-tuning affinity/avidity of anti-CAIX CAR T cells to mitigate on-target off-tumor toxicity in clear cell renal cell carcinoma.

S.-C. Yuan[1], Y. Wang[1], R. Abbas[1], P. Mathenge[1], C. Chien[1], C. D. Coherd[1], B. Bajoua[1], M. R. Chang[1], N. Murugan[1], G. M. Kastrunes[1], G. Wang[2], S.-M. Hoang[3], W. A. Marasco[1];

[1]Dana-Farber Cancer Institute, Boston, MA, [2]Yale University, New Haven, CT, [3]Lumicks, Waltham, MA

On-target off-tumor toxicity (OTOT) is one of the major hurdles preventing tumor-associated antigen (TAA) targeted therapy from effectively treating patients with solid tumors due to the shared presence of the same TAA on normal tissues. We have previously demonstrated high expression of carbonic anhydrase IX (CAIX) in ccRCC patient samples and low-density expression on healthy bile duct epithelium. In 2006, a clinical trial was stopped due to OTOT bile duct toxicity observed in patients infused with anti-CAIX CAR T cell therapy. To address the issue of OTOT in the bile duct, we performed affinity/avidity fine-tuning of the anti-CAIX CAR G36 to specifically target ccRCC tumor cells with high CAIX expression while sparing cholangiocytes with low CAIX expression. We generated a complementarity-determining region (CDR) single variant mutagenesis library of G36 and displayed the library on yeast for screening. Using flow cytometry, we were able to identify six populations based on antigen-binding affinity: high, med-high, med, med-low, low, and loss of binding. These libraries were sequenced via PacBio, a next generation sequencing (NGS) platform that excels in long-read sequencing, providing a powerful tool to detect single mutations in the scFv. The results were analyzed to identify enriched mutations compared to the wild-type G36, and inspected using *in silico* modeling and docking. Furthermore, enriched mutants from med-low and low populations were tested in CAR-T format for their cytotoxic capacity on tumor cells and bile duct cholangiocytes, as well as their avidity. We demonstrate that mutations in CDR2 and CDR3 of the heavy chain successfully mitigate OTOT toxicity on cholangiocytes with physiological levels of CAIX expression while maintaining tumor-killing capacity, shedding light on CDR mutagenesis as a useful tool to mitigate OTOT toxicity.

#4005 HER2 TKIs enhance the anti-tumor activity of HER2-targeting CAR-T and CAR-NK cells against NSCLC.

Y. Yang, M. B. Nilsson, A. Poteete, J. He, Q. Huang, J. V. Heymach;
UT MD Anderson Cancer Center, Houston, TX

Approximately 3% of non-small cell lung cancer (NSCLC) cases harbor *ERBB2*/HER2 mutations. Notably, the majority of actionable HER2 mutations in NSCLC are in-frame insertions in exon 20. Current HER2-targeting approaches, including antibody-drug conjugates (ADCs) such as trastuzumab deruxtecan, have shown promising response rates. To explore novel strategies for targeting HER2-positive NSCLC, we investigated chimeric antigen receptor (CAR)-based therapies to enhance the anti-tumor activity of immune effector cells. We engineered a series of HER2 CAR constructs utilizing scFvs derived from trastuzumab, pertuzumab, and FRP5, recognizing distinct domains of HER2. These scFvs were integrated into second-generation BB3z (with 4-1BB and CD3z intracellular domains) and third-generation 28BB3z (with CD28, 4-1BB, and CD3z intracellular domains) CAR backbones, which were subsequently transduced into activated T and natural killer (NK) cells to generate CAR-T and CAR-NK cells, respectively. High transduction efficiencies were achieved, with over 80% in CAR-T cells and over 50% in CAR-NK cells. We next evaluated their activity against a panel of NSCLC cell lines expressing varying levels of HER2 *in vitro* using firefly luciferase assays. All HER2 CAR-T cells demonstrated more than 90% killing against H2170 (HER2 high) and H322 (HER2 medium) at an effector:target (E:T) ratio of 10:1, whereas HER2 CAR-T cells yielded a killing effect of 35% against A549 (HER2 low) cells. HER2-targeting CAR-NK cells also displayed potent cytotoxicity against HER2-expressing NSCLC cells. Moreover, we observed that treatment of HER2 mutant and HER2 amplified NSCLC cells with low doses of HER2 tyrosine kinase inhibitors (TKIs) such as poziotinib enhanced the expression of HER2 on the cell surface. This upregulation resulted in enhanced activation of HER2 CAR-T and CAR-NK cells in coculture experiments as measured by CD107a expression on effector cells. Additionally, treatment with the HER2 TKI poziotinib potentiated the killing activity mediated by HER2 CAR-T and CAR-NK cells. Using a HER2 YVMA duplication patient-derived xenograft (PDX) NSCLC model, we observed that the *in vivo* combination of poziotinib with HER2 CAR-NK cells exhibited superior anti-tumor activity as compared to poziotinib treatment alone. In conclusion, HER2 CAR-T and CAR-NK cells effectively target HER2-mutant and HER2-positive NSCLC, and their combination with HER2 TKIs enhances vulnerability to HER2-targeting strategies.

#4006 IL12-secreting CAR-T cells eliminate the requirement for lymphodepletion and promote epitope spreading via local antigen presenting cells.

Aditya Mohan, Steven Shen, Kelly Hotchkiss, Sarah Quackenbush, John Sampson, Peter Fecci, Anoop Patel

Duke University Medical Center, Durham, NC

Introduction: EGFRvIII is a commonly studied tumor-specific antigen in glioblastoma (GBM) and poses an enticing target for immunotherapy. Its varied expression, however, complicates its effectiveness as a Chimeric Antigen Receptor (CAR) T cell target. Given the increasing prominence of Interleukin-12 (IL12) in treating solid tumors, its synergy with EGFRvIII specific CARs in treating preclinical models of GBM is explored.
Methods: To simulate tumor heterogeneity, mice were implanted with equal ratios of CT2A and CT2A EGFRvIII+ cells. We developed EGFRvIII-specific third-generation CAR T cells, both with and without IL12 using a MSGV retrovirus backbone and transduced them into murine T cells. Their antitumor effectiveness was gauged by evaluating survival rates, and their capability to enhance and modify the tumor environment was determined using single-cell sequencing.
Results: Standalone EGFRvIII CARs were unsuccessful in curing mice with heterogeneous tumors. However, 60% of mice treated with EGFRvIII CARs combined with IL12 were long term survivors. IL12 secreting CARs exhibited prolonged persistence in vivo, and there was no need for prior lymphodepletion before ALT introduction. Our studies reveal that EGFRvIII CARs secreting IL12 can eliminate EGFRvIII negative tumor cells by drawing on the inherent CD8 T cell compartment. Moreover, IL12 prominently impacted microglia among all Antigen Presenting Cells in the tumor environment, amplifying antigen presentation processes and broadening epitope exposure.
Conclusion: By leveraging IL12, EGFRvIII CARs can counteract antigen heterogeneity in tumors by recruiting endogenous CD8 T cells and polarizing microglia. These IL12-secreting CARs outlast their traditional counterparts without requiring lymphodepletion. Harnessing CAR-T cells that secrete IL12 represents a novel strategy for overcoming tumor heterogeneity and treating GBM in a clinical context.

#4007 AIC100 CAR-T cells targeting ICAM-1 are efficacious against solid tumors in xenograft mouse models of non-small cell lung cancer (NSCLC) and cervical cancer (CC).

A. Birt, S. Josiah, K. L. Joyce, S. Alla, M. P. Gallagher, J. Puc, H. Nguyen, E. Walsh Martin, S. Gupta;
AffyImmune Therapeutics Inc., Natick, MA

Purpose: Establish preclinical proof of concept efficacy with CAR T cells (AIC100) in xenograft models of solid tumors (NSCLC and CC) expressing high levels of surface ICAM-1.

Experimental: AIC100 is a third generation CAR T cell with micromolar affinity to ICAM-1, tuned lower than most CARs used to date in pre-/clinical studies. Affinity tuned AIC100 drug product is expected to selectively bind and kill tumor cells while safely sparing healthy cells. AIC100 also co-expresses somatostatin receptor 2 (SSTR2), which enables *in vivo* monitoring of AIC100 distribution and expansion by DOTATATE PET/CT imaging. To test preclinical efficacy of AIC100 in NSCLC and CC, four xenograft mouse models were generated using tumor cell lines known to have ICAM-1 expression (verified by flow cytometry) to test efficacy of AIC100. Reporter cell lines transfected with Luciferase were H226 NSCLC adenocarcinoma, H441 NSCLC squamous cell carcinoma, HeLa CC adenocarcinoma and SW756 CC squamous cell carcinoma. AIC100 efficacy was established by in vitro cytotoxicity prior to in vivo studies. NSG mice (n=10 per cell line) were inoculated via tail vein injection ($1.0x10^6$ cells) in cell growth media. Mice were imaged to ensure solid tumor formation which occurred in all mice within 3-5 days in the lung. At D0, mice were randomized into 2 groups (n=5 per group) of vehicle (PBS) and AIC100. At D1, mice were injected with AIC100 ($1.0x10^7$ live T cells) or vehicle. Mice were followed by weight and clinical observations 2x weekly and imaging by IVIS weekly. The study continued until vehicle group was euthanized due to tumor related co-morbidities at which time the study concluded.

Results: AIC100 showed clear treatment benefit in both models of NSCLC and CC. In CC HeLa model, in mice treated with AIC100, primary tumors were significantly reduced by D8 and eliminated in 5/5 mice by D22. In CC SW756 model, in mice treated with AIC100, tumor growth was reduced in size by D22. In NSCLC H441 model, in mice treated with AIC100, primary tumors were largely eliminated in 5/5 mice by D15. In NSCLC H226 model, in mice treated with AIC100, tumors were significantly reduced by D8 and largely eliminated by D57 (4/5 mice). A clear survival benefit was observed in AIC100 treated mice in NSCLC H226 xenograft model. These results show treatment benefit by AIC100 in 2 tumor models per indication and establish proof of concept for the potential development of AIC100 as a treatment for ICAM-1 expressing NSCLC and CC cancers.

Conclusions: AIC100 has significant treatment benefit in NSCLC and CC tumors with ICAM-1 expression in *in vivo* preclinical studies.

#4008 DASH CAR-T: accelerating CD276-targeted immunotherapy for pancreatic cancer.

Haiying Wang, Tian Deng, Hao Li, Yue Yao, Yuan Tian, Hongwei Wang, **Pengfei Jiang**

Shanghai Hrain Biotechnology Co., Ltd., Shanghai, China

B7 homolog 3 protein (B7-H3), recognized as CD276, is a pivotal immune checkpoint molecule extensively expressed in cancer cells, presenting a limited presence in normal tissues. Immunohistochemical analysis of 150 pancreatic cancer patients revealed positive CD276 staining in 66% of cases, with elevated expression correlating to diminished disease-free survival. Additional findings from an independent study on 59 patients highlighted significantly elevated CD276 levels, particularly in lymph node metastasis and advanced pathology. This study introduces an innovative Chimeric Antigen Receptor T (CAR-T) therapy targeting CD276, leveraging our DASH CAR-T manufacturing platform. Significantly, our approach reduces the ex vivo cell expansion time from 10 days to 1-2 days. T cells were enriched, activated, and transduced with a CD276 CAR-encoding retroviral vector, achieving the final product in 2-3 days. In preclinical models, our shorten-time CAR-T against CD276 exhibited superior expansion and heightened tumor-killing efficacy. Remarkably, DASH CAR-T demonstrated superior tumor control compared to conventional CAR-T, requiring only one-tenth of the dosage. This research advances our understanding of CD276 in pancreatic cancer and presents a transformative approach in CAR-T therapy manufacturing. The shortened production timeline and enhanced therapeutic outcomes underscore the potential clinical impact of our novel CAR-T strategy, offering a more efficient and potent treatment option for pancreatic cancer.

#4009 Discovery of inhibitory CAR target DSG1 for damping NECTIN4 on-target off-tumor toxicity in iPSC-derived CAR-T cell therapy.

Matthew S. Hall, Christopher M. Dower, Michael Miller, John Wheeler, Jill Carton, Ohad Manor, Hyam Levitsky

Century Therapeutics LLC, Philadelphia, PA

Century Therapeutics is developing NECTIN4 targeted induced Pluripotent Stem Cell (iPSC) derived Chimeric Antigen Receptor (CAR) T cell therapy. NECTIN4 targeted antibody drug conjugate enfortumab vedotin, while generally well tolerated, causes severe skin adverse events in some patients, thought to be driven by on-target off-tumor toxicity against NECTIN4 displaying skin keratinocytes. We include a safety switch in our first clinical-stage iPSC-derived CAR-NK cell therapy, CNTY-101, which provides an antibody target for elimination of the engineered cells should that be necessary. An additional method for reducing the incidence and severity of this type of adverse event is through the incorporation of an inhibitory CAR, also known as a NOT-gate, directed against antigen expressed on normal skin keratinocytes, but the optimal surface protein to target with such an inhibitory CAR for a NECTIN4 targeted therapy is unknown. Here, we identify DSG1 (Desmoglein-1) as a top inhibitory CAR target for NECTIN4 targeted CAR-T cell therapy by conducting a multi-omics analysis of public single-cell RNAseq, bulk RNAseq, and protein microarray immunohistochemistry datasets. We find that DSG1 is constitutively and uniformly displayed on the surface of skin keratinocytes in the layers of epidermis where they display NECTIN4, and DSG1 gene expression in normal skin is uniformly high across individuals. Conversely, DSG1 mRNA and protein are rarely expressed in NECTIN4 expressing cancer indications including bladder, breast, non-small cell lung, ovarian, and pancreatic. Further, autoimmune antibodies specific to DSG1 have been described, suggesting that DSG1 is targetable by a CAR in situ. Finally, DSG1 is not expressed by our iPSC-derived CAR-T cells. While NECTIN4 expression is greatest in skin keratinocytes, epithelial cells in other tissues express NECTIN4 at lower levels. In this study, we compare the expression levels of NECTIN4 to targets associated with tissue and cell-type specific on-target off-tumor toxicity in primary CAR-T cell clinical trials. Our findings support the strategy of DSG1-directed inhibitory CAR incorporation into NECTIN4 specific CAR-T cell therapeutic candidates.

#4010 Assessing impacts of tumor burden and CAR-T cell dosage on the toxicity and efficacy profile of CD19 CAR-T therapy in a PBMC-humanized mouse model.

W. Lee, D. Rose, J. G. Keck, J. Yang;
The Jackson Laboratory, Sacramento, CA

Chimeric antigen receptor T-cell (CAR-T) therapy is a significant advancement in treating hematological malignancies, yet it faces challenges due to its variable therapeutic responses and the risk of severe toxicities. This study delves into the effects of tumor burden and CAR-T cell doses on the toxicity profile of the therapy, employing a PBMC-humanized mouse model engrafted with luciferase-labeled Raji B cell lymphoma (Raji-luc). By exploring high vs. low tumor burden and high vs. low CAR-T dose scenarios, we aim to gain insights into the dynamic relationship between these factors and CAR-T-induced toxicity and efficacy. In the first experiment, we established PBMC humanized mouse models with a high tumor burden and a low tumor burden. 10 days (high burden) or 7 days (low burden) after the Raji-luc inoculation, mice were engrafted with 10M human PBMCs and dosed with CD19 autologous CAR-Ts. In mice with low tumor burden, CAR-T treatment demonstrated significant efficacy, as evidenced by IVIS imaging, while the high tumor burden model exhibited reduced efficacy. CAR-T treatment in Raji-bearing mice did not induce weight loss in either high or low burden models. CD19 CAR-T cells effectively reduced the target cell population in peripheral blood, with greater expansion observed in the higher tumor burden model. We also evaluated human cytokine levels post-CAR-T treatment, revealing higher cytokine induction in the high tumor burden model, peaking at 2 days post-treatment. Secondly, in a CAR-T dose-response study, we treated PBMC-humanized Raji-bearing mice with 10M, 15M, and 20M CAR-T cells. Higher CAR-T cell doses (15M and 20M) resulted in observable toxicity measured by body weight loss, while the 10M dose did not. All CAR-T doses effectively slowed tumor growth and induced significant CAR-T cell expansion. Selected human cytokines, such as IL-5 and RANTES, demonstrated a dose-response correlation with CAR-T treatment. Additionally, IL-6 and IL-10 were significantly correlated with tumor burden rather than CAR-T doses. The differential cytokine responses observed in our study provide valuable insights into the utility of the PBMC-humanized mouse model for investigating the biological responses associated with CD19 CAR-T therapy. Our findings underscore the utility of the PBMC-humanized mouse model in assessing variability in toxicity and cytokine responses to CAR-T therapy. This model offers valuable insights into the factors influencing CAR-T treatment outcomes and provides a platform for planning more precise treatment and enhancing the safety and efficacy of CAR-T therapy.

#4011 Locoregional GPC3 chimeric antigen receptor (CAR)-T cell therapy is associated with improved tumor control in hepatocellular carcinoma by enhancing CAR-T cell trafficking and functionality.

J. Wang, K. Tsang, J. Qiu, B. Feng;
The Chinese University of Hong Kong, Hong Kong, Hong Kong

Despite the rapid development of anti-cancer immunotherapy, the prognosis of hepatocellular carcinoma (HCC) patients is far from satisfactory. Glypican-3 (GPC3) CAR-T cell therapy has shown varied patient response. One of the potential reasons of low response rates may be due to the limited CAR-T cell infiltration. Therefore, locoregional GPC3 CAR-T therapy has been a promising option, with a hope of enhancing CAR-T cell tumor penetration. In this study, the therapeutic efficacy and underlying mechanisms of locoregional GPC3 CAR-T cell delivery were explored using HCC mouse xenografts. Orthotopic NOD-scid IL2Rg^{null} (NSG) HCC models were established by tumor fragment implantation into the liver. CAR-T cell injections were performed via the tail vein and portal vein to simulate systemic and locoregional administrations, respectively. Compared to the systemic treatment, locoregional therapy could better control the tumor growth, and was associated with improved liver function. In addition, the locoregional therapy group demonstrated a higher percentage of tumor-infiltrating CAR-T cells which showed an increased expression level of the cytotoxicity marker *GZMB* and a reduced level of the exhaustion marker *LAG3*. Moreover, significantly higher IFN-gamma level was found in the blood of the locoregional therapy group, indicating a better CAR-T cell functionality. In conclusion, we have demonstrated that locoregional administration of CAR-T cells is associated with increased CAR-T cell infiltration and better therapeutic efficacy. Additionally, CAR-T cells being injected locoregionally are correlated with enhanced functionality and reduced exhaustion phenotype. These findings highlight the potential of locoregional GPC3 CAR-T therapy as a promising treatment strategy for HCC patients.

#4012 SOT302: Dual expression of exogenous glutamine oxaloacetate transaminase (GOT2) and TP53-induced glycolysis and apoptosis regulator (TIGAR) enhance CAR T cell activity in preclinical solid tumor models.

Emily Kuiper, Samyabrata Bhaduri, Daniel Garafola, Kshitij Sharma, Jennifer Coccia, Kathleen Whiteman, **Amy Jensen-Smith**

SOTIO Biotech, Inc., Boston, MA

Background: Despite success in hematological malignancies, CAR T therapy has had limited efficacy against solid tumors. The suppressive tumor microenvironment limits CAR T activity through various mechanisms including competition for available nutrients and chronic stimulation resulting in reduced effector functions or T cell exhaustion. CAR T cells with enhanced metabolic fitness or more durable memory phenotype could potentially improve the clinical outcome in solid tumors. GOT2 plays an important role in mitochondrial function and maintenance of redox homeostasis. We have previously demonstrated enhancement of CAR T cells overexpressing GOT2. TIGAR is an enzyme known to promote antioxidative activites and reduce reactive oxygen species and has a role in protecting against apoptosis. Here we tested SOT302 CAR T cells expressing both GOT2 and TIGAR in preclinical solid tumor models.
Results: Expression of GOT2 and TIGAR transgenes were confirmed by qRT-PCR and western blot. Activity of GOT2 and TIGAR were confirmed by measuring aminotransferase activity (AST) and glutathione production, respectively. Compared to control CAR T cells, SOT302 is enriched for CD8+ Tscm cells and has a higher percentage functional, non-senescent (CD28+CD57-) cells. SOT302 has similar cytokine expression and cytotoxicity in standard co-culture assays compared to controls. SOT302 cells were chronically stimulated with plate-bound antigen every 3-4 days for 4 rounds. SOT302 had greater expansion of cells and were less exhausted and had better cytolytic capacity compared to controls. SOT302 cells were then evaluated in tumor xenograft mouse models. Consistent with our previous findings, CAR T cells expressing the single GOT2 transgene were more efficacious compared to CAR T cells alone. Expression of the single TIGAR transgene had no apparent benefit over CAR alone, however SOT302 cells expressing both GOT2 and TIGAR had superior anti-tumor activity compared to CAR alone and CAR+GOT2. No overt toxicity or significant body weight loss was observed. Ex vivo analyses to measure peripheral expansion, tumor infiltration and exhaustion were also performed. Preliminary findings indicate that SOT302 has better peripheral expansion compared to CAR alone and similar expansion compared to CAR+GOT2 controls. SOT302 cells had better tumor infiltration compared to both the CAR alone and CAR+GOT2 cells. Tumor infiltrating SOT302 cells also exhibited lower levels of exhaustion compared to CAR alone or CAR+GOT2 controls.
Summary: SOT302 cells express exogenous GOT2 and TIGAR transgenes and have superior anti-tumor activity in preclinical solid tumor models. These data suggest that SOT302 may be a promising candidate for patients with solid tumor cancers.

#4013 Increasing mitochondrial respiration by silencing MCJ/DnaJC15 enhances CD8 CAR-T cell therapy efficacy.

M.-H. Wu[1], E. L. Giddings[2], F. Valenca-Pereira[1], C. Pham-Danis[1], F. Cendali[1], M. C. Yarnell[1], A. J. Novak[1], J. Henao-Mejia[3], R. A. Flavell[4], A. D'Alessandro[1], M. E. Kohler[1], M. Rincon[1];

[1]University of Colorado Anschutz Medical Campus, Aurora, CO, [2]University of Vermont, Burlington, VT, [3]University of Pennsylvania, Philadelphia, PA, [4]Yale University, New Haven, CT

Chimeric antigen receptor (CAR)-T cell therapy is a promising treatment against leukemia and lymphoma. However, poor initial treatment response and post-therapy relapse have found to be common and remained to be resolved. Modulating T cell immunometabolism is considered a novel therapeutic approach to enhance CAR-T cell therapy. We have identified MCJ (*DnaJC15*) as an endogenous negative regulator of Complex I of the electron transport chain in mitochondria. MCJ is abundantly expressed in mouse CD8 cells relative to other immune cells. We propose that MCJ can be a therapeutic target to enhance mitochondrial respiration in CD8 CAR-T cells. We will show that loss of MCJ in mouse CD8 cells leads to superior anti-tumor response against melanoma. In addition, we will show that MCJ-deficient murine CD8 CAR-T cells have enhanced killing activity against leukemia both *in vitro* and *in vivo*. We have recently revealed that MCJ is also expressed in human CD8 cells and the levels of MCJ are heterogenous among human population. Similar to murine CD8 cells, MCJ knockdown in human CD8 cells enhances mitochondrial membrane potential and effector functions. We have designed a new CAR construct to silence MCJ in human CD8 CAR-T cells. MCJ-deficient human CD8 cells show superior cytotoxicity against leukemia with increased mitochondrial metabolism. Together, these data demonstrate that MCJ is a promising target to improve CAR-T cell therapy through modulating the T cell metabolism. We are currently investigating the effect of MCJ-deficient CD8 CAR-T cells against solid malignancy.

#4014 Humanized mouse model to assess PBMC donor derived autologous CD19 CAR Ts for efficacy against Raji tumors and related cytokine release.

S. Ramalingam, D. Cai, L. Shopland, J. G. Keck;
The Jackson Laboratory, Sacramento, CA

Immuno-oncology cell therapies engage the immune system to treat cancer. In recent years, adoptive T-cell therapy with CD19-specific chimeric antigen receptors (CARs) has shown promise for treatment of various malignancies, including acute lymphoblastic leukemia. However, CAR-T-cell therapies have been hampered by various adverse events, including cytokine release syndrome (CRS). To predict and minimize CRS effects from CAR-T therapies, a human immune preclinical murine model that combines efficacy and toxicity readouts is essential. Here, we describe the development of PBMC humanized mouse model based on the NSG-MHC I/II-DKO strain to study autologous CD19 CAR-T treatment related tumor growth inhibition and CRS *in vivo*. Three different PBMC donors were used to generate CAR-T (CD28-Cd3z) directed against a CD19 epitome. Our preliminary data demonstrate that CD19 CAR-T treatment stimulated dynamic and PBMC donor dependent cytokine release with IFN-g, IL-10, IL-4, IL-2, IL-6 and TNF. Our model showed elevation of shared proinflammatory cytokines (IFN-g, IL-10, IL-2 and TNF) observed in humans after CD19 CAR-T treatment. Currently, we are evaluating our PBMC based cytokine release model in CD19 CAR-T cells tumor control study. Our results to date indicate that PBMC-engrafted NSG-MHC I/II-DKO mouse models are vital platforms to screen adoptive T-cell therapy for potential CRS.

#4015 Improvement of CAR T cell potency against low-density targets like L1CAM and FGFR4 in rhabdomyosarcoma.

C. Piccand[1], A. Timpanaro[2], S. Anton-Joseph[1], M. Bernasconi[1], J. K. Rossler[3];

[1]University of Bern/Inselspital, Bern, Switzerland, [2]Seattle Children's Hospital, Seattle, WA, [3]Novartis, Basel, Switzerland

Rhabdomyosarcoma (RMS) is the most common pediatric soft tissue sarcoma. Overall survival rates are low for metastatic RMS, emphasizing the urgent need of improved therapies. Chimeric Antigen Receptor (CAR) Ts have shown remarkable results against hematological malignancies, but CAR T cell therapy remains challenging in solid tumors, mainly due to a lack of ideal tumor specific targets, and of the immunosuppressive tumor microenvironment (TME). To maximize antitumoral activity against RMS and to address optimal CAR T persistence *in vivo*, novel CAR constructs were investigated against upregulated RMS targets. By surfaceome profiling, we recently identified L1CAM as promising candidate for RMS CAR T cell therapy, and confirmed CD276 and FGFR4 expression. CD276- (CD276.CD28HD.28TM.28CSD.3z) and Dual-CAR Ts targeting both CD276 and FGFR4 (F8-FR4.CD28HD.28TM.28CSD.3z) showed tumor eradication in an orthotopic RMS model, whereas FGFR4-CAR Ts exhibited only a partial response *in vivo.* Moreover, CD276-CAR Ts showed a limited activity against RMS tumors expressing lower amounts of CD276, eradicating the tumor in 1/5 mice, underlying the need of improved CAR T cell potency against low-density target-expressing tumors. First, to improve FGFR4-CAR Ts activity, we optimized the recognition of FGFR4 epitope by modifying the CAR moiety “hinge”. We replaced the CD28-derived hinge with various hinges of different length: no hinge, IgG4 (12aa), IgG4CH3 (119aa), and IgG4CH2CH3 (229aa). Luciferase assays showed effective *in vitro* killing capacity of FGFR4-CAR Ts expressing an IgG4-derived hinge, with a tumor cell survival less than 10% at Effector to Target (E:T) ratio of 5:1. They also released the double amount of IFN-γ (50pg/ml) compared to the other constructs, when co-incubated with Rh4 cells. Next, to verify the potential of L1CAM as CAR T target for RMS, we generated a panel of L1CAM-CARs expressing either a long (IgG4CH2CH3, 229aa) or a short (CD28, 35aa) Hinge, and a CD28- or 41BB-derived costimulatory domain (CSD). L1CAM.IgG4CH2CH3Hinge.28TM.28CSD.3z CAR Ts outperformed the other constructs, killing ~60% of Rh30 at the E:T ratio of 1:1 and more than 90% at the E:T ratio of 5:1. They also exhibited a 3-fold higher IFN-γ release (120 pg/ml) compared to the other constructs. However, although our examination of patient-derived TMA revealed a strong immunoreactivity for L1CAM, more expressed in aggressive RMS subtypes, the selected L1CAM-CAR Ts against Rh30 cells, exhibiting ~10’000 L1CAM copies, showed limited activity in an *in vivo* pilot study. Based on these results and on the RMS TME investigation, which revealed consistent collagen (COL4A1, COL4A2 and COL18A1) deposition in RMS-derived mice tumor xenografts, we hypothesize that co-expressing a collagenase, able to partially degrade the dense extracellular matrix surrounding tumors, will lead to an improved CAR T cell infiltration and activity *in vivo*.

#4016 mRNA encoding a CAR specific stimulating protein (CSSP) mediates tumor metabolism regulated (TMR) CAR signaling for CAR-T expansion beyond the tumor microenvironment.

Frederic Vigant, Anirban Kundu, Michael Betts, Sid P. Kerkar, Gregory I. Frost

Exuma Biotech Corp., West Palm Beach, FL

Background: Unlike hematologic targets, TMR Chimeric Antigen Receptors with binding restricted to antigen in the tumor microenvironment lack CAR dependent stimulatory signals for proliferation outside the tumor. Increased exposure to CAR-T is associated with improved clinical outcomes and therefore tools to safely and selectively increase proliferation represent potential adjunctive CAR-T therapeutics. Therefore, we developed a surrogate CAR Specific Stimulating Protein (CSSP) approach encoded by synthetic mRNA for expression in antigen presenting cells to boost CAR-T proliferation *in vitro* and *in vivo*.
Methods: NFAT-Luc reporter lymphocytes were transduced with lentivectors encoding TMR CARs with or without epitopes reactive to CSSP's in the CAR. Subsequently, PBMCs were transfected with LNPs containing synthetic mRNAs for either GFP or candidate membrane bound CSSPs. Transfection efficiency was confirmed by microscopy and flow cytometry. The activity of CSSP's expressed in monocytes cultured with T cells expressing CAR variants with NFAT-luc reporter was measured by luciferase expression and compared to CD3 stimulation. Additionally, the kinetics of CAR stimulation with monocytes expressing CSSPs were determined by serial luciferase measurements. Finally, the proliferation of PBMCs transduced with a TMR-HER2 CAR co-cultured with CSSP treated purified monocytes were evaluated.
Results: Following exposure of PBMCs expressing CSSPs to TMR-CAR-expressing NFAT T cells, CAR specific luciferase signaling was readily detectable compared to non-specific CD3 stimulation, indicating that the CSSPs were capable of CAR specific stimulation through the CD3ζ chain of the CAR. Two of the CSSP variants demonstrated stimulation in a CAR specific fashion at levels similar to or greater than non-specific CD3 stimulation. In kinetic experiments, stimulation of NFAT could be detected over a period of 8 days, indicating persistence of the CSSP similar to GFP in antigen presenting cell controls. Finally, co-culture of CSSP mRNA expressed in purified monocytes were capable of TMR-HER2-CAR T cells stimulation, which do not proliferate when cultured with HER2 antigen expressing cells under physiologic conditions.
Conclusion: TMR-CAR-T cells can achieve proliferative capacity outside the tumor microenvironment using synthetic mRNA encoding CAR Specific Stimulatory Proteins. This novel mRNA approach may provide additional tools to promote the proliferation and/or persistence of solid tumor targeted CAR-T cells outside the tumor environment.

#4017 CAR T cell-mediated cytotoxicity and cytokine release in response to varying levels of antigen expression on target cells.

S. Barnes[1], D. Sullivan[1], D. Lazar[2], K. Haupt[3], D. Califano[1], S. Chvatal[1], D. Millard[1];
[1]Axion BioSystems, Atlanta, GA, [2]Axion BioSystems, Madison, WI, [3]Promega Corporation, Madison, WI

The development of immunotherapies relies on the use of in vitro potency assays, which are crucial for understanding the complex interactions between immune cells (effectors) and cancer cells (targets). Chimeric antigen receptor (CAR) T-cell therapy is an immunotherapeutic approach that exhibits promise; however, varying levels of antigen expression on the surface of tumor cells can influence the efficacy of CAR T cell-mediated killing. To fully understand the impact of target antigen density on CAR T cell activity, we utilized a matrix approach to assess both target cell death, using an impedance-based in vitro potency assay to quantify CAR T cell-mediated cytotoxicity, as well as cytokine release with homogeneous Lumit™ immunoassays. SKOV3 (high HER2 expression), A549 (low HER2 expression), or MDA-MB-231 (no HER2 expression) target cells were seeded into a 96-well microplate with embedded electrodes in the substrate that detect the attachment and proliferation of target cells. HER2 CAR T cells were added after 24 hours at effector-to-target (E:T) ratios of 1:5 or 1:1 and target cell cytolysis was recorded continuously by the Maestro Z for 72 hours. Cytolysis of the target cells was calculated by comparing the treated wells to no treatment control wells and full lysis wells (1% TritonX). At 72 hours post CAR T cell addition, complete killing was observed in SKOV3 cells at the 1:1 ratio, while A549 cells exhibited only 80% cytolysis. MDA-MB-231 cells showed 20% cytolysis, likely due to nonspecific killing by non-engineered T cells, as approximately only 78% of the CAR T cell population was CAR positive. Because the cytolysis assay was label-free, cytokine analysis was able to be multiplexed with the same plates. To assess release of pro-inflammatory cytokines, TNF-α and IFN-γ, we collected supernatant post-antigen exposure at 24, 48, and 72 h. At the 1:1 E:T ratio, CAR T cells co-cultured with target cells expressing low (A549) or high (SKOV3) levels of HER2 had the highest TNF-α production at 24 hours, with CAR T cells co-cultured with SKOV3 cells releasing 30.6% more TNF-α when compared to A549 cells. The highest levels of IFN-γ were detected in both A549 and SKOV3 groups at the 1:1 E:T ratio, with the highest levels observed from CAR T cells co-cultured with SKOV3 cells at 72 hours, releasing approximately 1459.6 +/- 357.3 pg/mL of IFN-γ, compared to 1093.8 +/- 387.5 pg/mL IFN-γ released by CAR T cells co-cultured with A549 cells. As expected, CAR T cells co-cultured with MDA-MB-231 cells did not release any detectable TNF-α or IFN-γ at either E:T ratios during the duration of the experiment. Future work will continue to explore multiplexed potency assays for the evaluation of CAR T cell therapies.

#4018 An innovative *in vivo* model for CAR-T cell therapy development: Tolerability and efficacy evaluation of CD19-targeting CAR-T cells on human lymphoma using the chicken CAM assay.

Yan Wang[1], Xavier Rousset[1], Chloe Prunier[1], Emilien Dosda[1], Alejandra Gutierrez-Guerrero[2], Pauline Abrial[2], Inna Menkova[2], **Jean Viallet**[1]

[1]Inovotion, La Tronche, France,[2]Allogenica, Villeurbanne, France

BACKGROUND Chimeric antigen receptor (CAR) T cell therapy is a revolutionary approach in cellular immunotherapy, where a patient's T cells are genetically engineered to recognize and attack cancer cells. In the last decade, several CAR-T cell therapies have been approved by the FDA. However, this encouraging outcome was obtained only with certain blood cancers, like B cell leukemias, lymphomas, etc. Many research / clinical trials are now underway worldwide to extend the CAR T-cell therapy benefits to a large spectrum of cancers, using rodents. This model presents several drawbacks, such as the immunodeficiency of humanized models, ethical constraints, time, and cost. An alternative, pertinent, 3Rs-compliant *in vivo* model for developing CAR-T therapy is urgently needed. Xenografts on the chicken embryo's ChorioAllantoic Membrane (CAM) have proven extremely valuable for *in vivo* cancerology studies. In this work, we evaluated *in vivo* the anti-tumor efficacy of CD19-targeting CAR-T cells on human lymphoma using Inovotion's CAM assay.

METHODS Human lymphoma Raji cells (ATCC) were grafted on the CAM on embryonic development day (EDD) 9. A 2nd generation of CD19-targeting CAR-T cells (CAR-T-(CD3/4-1BB)) developed by Allogenica (France) were co-injected at EDD9 at E/T (effector CAR-T cell *vs* target Raji cell) ratio 1:1. One group was injected with CAR-T (CD3/4-1BB) only once at EDD9 and a second group received a first injection of CAR-T (CD3/4-1BB) at EDD9 and a second injection at EDD13. Embryonic viability was checked daily. On EDD18. The efficacy of CAR-T therapy was evaluated basing on tumor weight, metastatic invasion in the lower CAM and CAR-T infiltration in tumors detected by qPCR. Activation of the chicken embryo immune system was detected as well.

RESULTS The treatment with CAR-T-(CD3/4-1BB) cells was well tolerated *in ovo*, no significant embryo mortality/abnormality was observed. CAR-T-(CD3/4-1BB) cells prevented tumor formation (tumor weight was 88.67% to 90.62% lower than control, $p < 0.001$); and prevented metastasis formation in the lower CAM (86.88% to 81.43% lower than control, $p < 0.001$).

CONCLUSION Different to *in vitro* models and immunodeficient murine models, chicken embryo possesses a progressively mature immune system. Our results show that CAR-T-(CD3/4-1BB) cells can prevent tumor formation and metastatic invasion when co-injected with tumor cells. Inovotion's CAM assay is a viable alternative *in vivo* model for developing CAR-T cell therapy on a large spectrum of cancers. It is fully 3Rs-compliant.

#4019 Development of mRNA chimeric antigen receptor T cells targeting MET in aggressive B-cell lymphomas.

P.-H. Chen[1], R. Raghunandan[2], M. Muschen[1], S. G. Katz[1];
[1]Yale School of Medicine, New Haven, CT, [2]Yale University, New Haven, CT

Multiple versions of CAR T cells targeting the cell surface protein CD19 are approved by the FDA to treat refractory B-cell malignancies. However, durable remissions range from 60% in B-cell leukemias to 40% in B-cell lymphomas. Major reasons for resistance to CD19-CAR treatment relate to heterogeneous or loss of CD19 expression. In addition, CD19-CAR leads to B-cell depletion which increases the risk for infection. These limiting factors necessitate research into alternative targets for CAR therapy against B-cell lymphomas.Using a large data set from clinical trials, we found that approximately 30-70% of diffuse large B-cell lymphomas (DLBCL) express MET. We hypothesize that these MET-positive B-cell lymphomas can potentially be targeted with chimeric antigen receptor (CAR) T-cells against MET receptor. We constructed a second-generation anti-MET-CAR by fusing the scFv fragment of an anti-MET monoclonal antibody with the human CD28 hinge/transmembrane/cytoplasmic domain and CD3ζ cytoplasmic domain. Stable MET-CAR Jurkat cells showed increased CD69 expression upon stimulation by MET-positive lymphoma cell lines such as Karpas-422 and OCI-LY3. Using primary human T cells, we further demonstrated that the mRNA MET-CAR T-cells mediated cytotoxicity against DLBCL cell lines. Of note, while CD19-CAR T-cells showed only low level of cytotoxicity against the CD19-/MET+ OCI-LY3 cell line, MET-CAR T cell was able to mediate substantial tumor cell lysis.In summary, the preliminary data demonstrate that MET-CAR is capable of mediating cytotoxicity against MET-positive DLBCL. Some cell lines such as OCI-LY3 are negative for CD19 but positive for MET expression, and MET-CAR is capable of mediating cell lysis while CD19-CAR is ineffective. These results suggest that some large B-cell lymphomas negative for CD19, either intrinsic or secondary to loss of CD19 as a result of resistance mechanism, may show MET expression and will likely benefit from MET-targeted immunotherapy.

#4020 Donor-dependent anti-tumoral efficacy of human CD19 CAR T cells in a leukemic xenograft mouse model.

P. Metzger[1], C. N. Castro[1], J. F. Hummel[1], M. Roman Azcona[2], D. Antony[2], C. Mussolino[2], D. Zurr[3], S. Adamsky[3], H. Weber[1];
[1]Reaction Biology Europe GmbH, Freiburg, Germany, [2]Medical Center - University of Freiburg, Freiburg, Germany, [3]Lepton Pharmaceuticals Ltd, Zichron Yakkov, Israel

The recent advances in cellular immunotherapies have revolutionized the treatment options for hematological malignancies. Among others, genetically engineered T cells to express chimeric antigen receptors targeting CD19 have shown clinical success in patients with B cell malignancies. However, depending on the study design only one to two thirds of the patients experience a complete response upon CD19 CAR T cells treatment. Antigen escape, immune suppressive microenvironment, CAR T cell dysfunction as well as lack of CAR T cell persistence have been discussed to be reasons for the lack of sustained therapy response. Well established models for the preclinical evaluation of cellular therapies are needed for the evaluation of next generation CAR T cells as well as novel combination therapies.

Here, we describe a xenograft animal model of human acute lymphoblastic leukemia (NALM-6 cells) with a suboptimal treatment response to human CD19 CAR T cells from three different donors. First, the activation status and memory phenotype of the CAR T cells from the different donors was characterized by flow cytometry and the anti-tumoral efficacy of the CD19 CAR T cells was evaluated in an in vitro co-culture killing assay using luciferase expressing NALM-6 cells. Next, CD19 CAR T cells from three donors were injected in NALM-6_luc tumor bearing animals. The tumor growth was monitored by bioluminescence imaging and the phenotype of the transferred CAR T cells was checked by flow cytometry.

The frequency of memory T cells differed between the donors whereas the T cells from all donors exhibited all low expression of activation markers. In vitro, all three donors showed high and comparable anti-tumoral killing efficacy independent of their memory status. In vivo, CD19 CAR T cells from all three donors delayed the tumor growth significantly although none of the animals had a complete remission. In line with the individual memory status of the CAR T cells prior to infusion, there were slight differences in the kinetics of the anti-tumoral response. The flow cytometric analysis revealed that the transferred CAR T cells were almost absent in the peripheral blood and spleen whereas for individual animals tumor cells and highly activated CAR T cells were detectable in the bone marrow of the animals.

In summary, the NALM-6_luc xenograft model is a value tool for evaluating next generation cellular therapies and novel combination strategies to overcome the current limitations of cellular therapies.

#4021 The development of CAR T cell therapeutics targeting tumor specific CD146.

E. Uzuner[1], H. Mole[1], C. W. Wong[1], M. L. Fernandez Carro[1], R. Leshem[1], K. Sefton[1], H. Tovey[2], A. Picken[2], M. Blot-Chabaud[3], A. F. L. Hurlstone[1];
[1]University of Manchester, Manchester, United Kingdom, [2]FUJIFILM Diosynth Biotechnologies, Billingham, United Kingdom, [3]Aix-Marseille University, Marseille, France

Chimeric antigen receptor (CAR) T cells represent a promising class of "living drugs" for cancer treatment. These primary T cells are genetically engineered to express a synthetic antigen receptor, incorporating various domains to enhance their effector functions. While CAR T cells have shown success against liquid cancers, their application to solid cancers is hindered by significant "on-target/off-tumor" toxicities due to the absence of specific target proteins. In this study, we aim to enhance the tumor specificity of CAR T cells by targeting a tumor-specific version of CD146. CD146 is a glycoprotein widely expressed in several solid tumors, particularly melanoma and ovarian cancer. However, it is also expressed on benign cells, such as endothelial cells, pericytes, and smooth muscle cells. Nevertheless, a CD146 isoform exists that is enriched in cancer cells.
We assessed CAR activity using flow cytometry to measure surface CD69 expression (an early activation marker) on CAR-expressing Jurkat cells co-cultured with various CD146-positive and CD146-negative human melanoma and ovarian cancer cell lines. The killing ability of primary CAR-T cells was evaluated by measuring the relative luciferase activity of target cells, and their effector functions were further analyzed by ELISA for the secretion of IFN-g and TNF-a.
Through multiple rounds of protein engineering, we have developed a CAR construct capable of reprogramming T cells to respond to a tumour-enriched CD146 isoform. Our CAR demonstrated antigen-dependent activation of Jurkat cells when co-cultured with CD146-positive human melanoma and ovarian cancer cell lines, comparable to a CAR targeting pan-CD146. Moreover, primary CAR T cells exhibited proportional killing activity and other effector functions.
We have successfully engineered a CAR with specificity for a tumour-enriched isoform of CD146. Our future work will involve rigorously evaluating the tumor selectivity of our CAR, as well as assessing the ability of primary CAR T cells expressing this CAR to control tumor growth in vivo.

IMMUNOLOGY: Combination Approaches
Poster Session

#4025 A phase II trial of neoadjuvant gemcitabine, cisplatin plus tislelizumab followed by concurrent chemoradiotherapy in locoregionally advanced nasopharyngeal carcinoma: Clinical efficacy, safety and the biomarker analysis.

X.-Y. Li, S.-Y. Xie, Q.-Y. Chen, H.-Q. Mai, L.-Q. Tang;
Sun Yat-sen University Cancer Center (SYSUCC), Guangzhou, China

Immune checkpoint inhibitors (ICIs) have been widely used in recurrent or metastatic nasopharyngeal carcinoma (NPC), but the addition of ICIs to chemoradiotherapy in locoregionally advanced (LA) NPC requires further investigation. We conducted a phase II, single-arm trial to evaluate the efficacy and safety of neoadjuvant gemcitabine, cisplatin (GP) plus tislelizumab followed by concurrent chemoradiotherapy (CCRT) in LA-NPC. All participants received 3 cycles of GP chemotherapy plus tislelizumab (200 mg) followed by 3 cycles of cisplatin-based CCRT. The primary endpoint was the clinical complete response rate (CR) after neoadjuvant chemoimmunotherapy (NAT). The secondary endpoints include pathological CR rate, progression-free survival (PFS), overall survival (OS), locoregional relapse-free survival (LRRFS), distant metastasis-free survival (DMFS), etc. Pretreatment blood samples and paired (pre-/post-NAT) tissue biopsies were collected to perform full-spectrum peripheral T-cell profiling, PD-L1 and tertiary lymphoid structures (TLS) staining. Among all 63 participants, the CR rate after NAT reached 41.3% (95% CI, 28.8%-53.8%), far exceeding our hypothesized CR rate of 22%. The objective response rate (ORR) and pCR rate after NAT were 88.9% (95% CI, 80.9% to 96.9%) and 74.6% (95% CI, 62.1% to 84.7%), respectively. As of July 15th, 2023, after the median follow-up of 25 months, the 2-year PFS and OS were 98.4% and 100%. The incidence of grade 3-4 immunotherapy-related adverse events was 1.6%. The compliance of CCRT was not compromised. Patients who achieved CR had significantly more circulating CD4+ and CD8+ effector memory T cells (Tem), regulatory T cells (Treg) and follicular helper T cells (Tfh). The peripheral abundance of LAG3+ Tem and Tfh were independently predictive of NAT response. The number and maturation of TLS significantly increased after NAT in the CR group, but not in the Non-CR group. GP chemotherapy plus tislelizumab followed by CCRT was highly therapeutic and safe in treating LA-NPC, further randomized phase III studies are awaited.

#4026 The combination of DLL4/VEGF-a blockade and immunomodulation can eliminate MHC class I negative tumors in mice.

Diana I. Albu, Rachael Duffy, Amy Daniel Ulumben, Jason Kong, Jessica Zolotarevsky, Melissa Brundin, Mei Su, Ruturaj Jadhav, Kris F. Sachsenmeier, Bing Gong, Thomas J. Schuetz, Alberto Visintin

Compass Therapeutics, Boston, MA

CTX-009 is a bispecific antibody targeting VEGF-A and DLL4 which is undergoing clinical investigation in patients with multiple tumor types, including biliary tract and colon cancers. In biliary tract cancers, checkpoint inhibitor therapy has been shown to improve outcomes when combined with chemotherapy. In an effort to increase the breadth and duration of response of CTX-009, we set out to investigate the combined anti-tumor efficacy of this bispecific antibody and immunotherapy in preclinical models. Here we report the evaluation of the combination of the mouse surrogates of CTX-009 and CTX-471, an agonistic anti-mouse CD137 antibody, or monoclonal antibodies that disrupt the PD-1/PD-L1 signaling axis. Coupling VEGF-A/DLL4 targeting with either CD137 agonism or PD-1/PD-L1 blockade markedly increased the anti-tumor efficacy of the individual treatments alone in multiple syngeneic mouse tumor models. Tumor growth inhibition was accompanied by pharmacodynamic evidence consistent with enhancement of anti-tumor immunity. Notably, the combination of CTX-009 and CTX-471 retained potent anti-tumor activity even in a tumor line (MC38) which was made MHC I deficient through the deletion of the beta 2 microglobulin gene. This system may model the clinically relevant unmet need characterized by tumor escape through the loss of antigen presentation machinery such as HLA LOH. Interestingly, the model cell lines CT26 and MC38 failed to thrive in the B2M-deficient setting and depletion of NK cells markedly increased their ability to grow. This implies that NK cells might be involved in controlling tumor growth in this setting, and that the combined action of CTX-471 and CTX-009 in the tumor stroma enhances NK cell activity. The findings presented here suggest that CTX-009 may provide enhanced clinical benefit when combined with immunomodulatory agents, such as agonistic anti-CD137 antibodies or PD-1/PD-L1 blockers in tumors where immune checkpoint inhibitors have failed.

#4027 From tumor progression to therapeutic control: Combinatorial targeting of immune vulnerabilities in TNBC.

A. Poissonnier[1], E. V. Egeland[2], W. Horton[1], S. Sivagnanam[1], O. Stapleton[3], R. Erbe[3], N. Kirchberger[1], K. Betre[1], A. Skaist[3], L. Danilova[3], A. Fields[1], P. Ordentlich[4], A. C. Adey[1], E. J. Fertig[3], L. M. Coussens[1];

[1]OHSU Knight Cancer Institute, Portland, OR, [2]2Dept. of Tumor Biology, Institute for Cancer Research,, Oslo, Norway, Norway, [3]Johns Hopkins Univ., Sidney Kimmel Comprehensive Cancer Center, Baltimore, MD, [4]Syndax Pharmaceuticals, Inc, Waltham, MA

Triple-negative breast cancer (TNBC) is an aggressive form of breast cancer, associated with limited treatment options and high mortality rates. Although immune checkpoint inhibitors (ICIs) show promise, early clinical results indicate benefits in only a specific subset of patients with TNBC. Preclinical evidence indicates that infiltrating macrophages contribute to breast tumor progression by restricting $CD8^{\pm}$ T cell infiltration, activation, and cytotoxicity within tumor microenvironments. Preliminary data has revealed that immune-competent mammary tumor-bearing MMTV-PyMT transgenic mice have slowed tumor progression following sequential combination of a microtubule poison (paclitaxel; PTX) to enhance tumor immunogenicity, plus a macrophage-depleting/reprogramming agent such as a colony-stimulating factor 1 receptor blocking antibody (αCSF1R), and undergo primary tumor regression in 60% of transgenic mice when an ICI targeting PD-1 is applied (3x therapy) by a $CD8^{\pm}$ T cell-dependent mechanism. Response to 3x therapy is associated with localized $CD8^{\pm}$ T effector and resident memory cell expansion, and increased antigen-specific clonal expansion at primary tumor sites. We hypothesized that epigenetic plasticity was limiting T cell memory and thus impeding long-term tumor control. Using a class 1 benzamide histone deacetylase (HDAC) inhibitor (e.g., entinostat) sequentially added to PTX/αCSF1R/αPD-1 therapy (4x) resulted in primary tumor stasis in 100% of mice, and significantly enhanced overall survival, in two transgenic mouse models of breast cancer (MMTV-PyMT and C3-(1)-TAg). Cohorts were analyzed at distinct time points for primary and metastatic tumor burden, in addition to immunophenotyping (flow cytometry), transcriptional (bulk and scRNA-Seq), epigenetic (sciATAC-Seq), and T cell receptor (TCR) changes correlating with 4x responses. Improved outcome and tumor stasis was associated with increased presence of long-lived central and stem-like memory $CD8^{\pm}$ T cell infiltration, intra-tumoral B memory cell, and $CD4^{\pm}$ T follicular helper cell infiltration. Tumor stasis was achieved by B and T cell-dependent mechanisms where B cell depletion led to decreased T cell cytotoxicity. Adoptive serum transfer (AST) from 4x-treated MMTV-PyMT mice into either 3x-treated or untreated MMTV-PyMT mice elicited tumor stasis and control. These preclinical studies indicate the complexity of myeloid, B cell and T cell interactions that are co-opted by tumors, and identify novel paths to therapeutic tumor control by targeting vulnerable immune communication programs.

#4028 Inhibition of IL25 IL17RA improves immune related adverse events of checkpoint inhibitors and reveals antitumor activity.

X. Hu, S. Bukhari, C. Tymm, K. Adam, S. Lerrer, B. Henick, R. Winchester, **A. Mor**;
Columbia University Irving Medical Center, New York, NY

Immune checkpoint inhibitors (ICI) have improved outcomes and extended patient survival in several tumor types. However, ICI often induces immune-related adverse events (irAEs) that warrant therapy cessation, thereby limiting the overall effectiveness of this class of therapeutic agents. Currently, available therapies used to treat irAEs might also blunt the antitumor activity of the ICI themselves. Therefore, there is an urgent need to identify treatments that have the potential to be administered alongside ICI to optimize their use. Using a translationally relevant murine model of anti-PD-1 and anti-CTLA-4 antibodies-induced irAEs, we compared the safety and efficacy of prednisolone, anti-IL-6, anti-TNFα, anti-IL-25 (IL-17E), and anti-IL-17RA (the receptor for IL-25) administration to prevent irAEs and to reduce tumor size. While all interventions were adequate to inhibit the onset of irAEs pneumonitis and hepatitis, treatment with anti-IL-25 or anti-IL-17RA antibodies also exerted significant additional antitumor activity. Mechanistically, IL-25/IL-17RA blockade reduced the number of organ-infiltrating lymphocytes. These findings suggest that IL-25/IL-17RA may serve as an additional target when treating ICI-responsive tumors, allowing for better tumor control while suppressing immune-related toxicities.

#4029 HPK1 inhibitor reinvigorates exhausted tumor-infiltrating CD8 T cells and synergizes with anti-PD-1 blockade in gynecologic malignancies.

J. Park[1], Y. Lee[1], S. Kim[1], **S. Lim**[2], A. Park[2], J. Kim[2], J. Lee[2], S. Kim[1], S.-H. Park[3], J.-Y. Lee[1];

[1]Yonsei University College of Medicine, Seoul, Korea, Republic of, [2]1ST Biotherapeutics, Inc., Yongin-si, Korea, Republic of, [3]Korea Advanced Institute of Science and Technology, Daejeon, Korea, Republic of

HPK1 (Hematopoietic Progenitor Kinase 1) is a negative intracellular immune checkpoint that interferes with the priming and activation of T cells. In recent years, several HPK1 inhibitors have been discovered as novel immune-oncology drugs with promising potential to improve anti-tumor immune responses. However, there has been no study showing the effects and potential application of HPK1 in gynecologic malignancies. Therefore, we investigated the expression and role of HPK1 in tumor-infiltrating CD8 T cells (CD8 TILs) and how the selective small molecule kinase inhibitor, FB849, affected the reinvigoration of exhausted CD8 TILs in gynecologic cancers. We isolated TILs from patients with newly diagnosed endometrial (*n*=53) and ovarian cancer (*n*=46). The immunological properties and HPK1 signaling pathway of CD8 TILs were explored using flow cytometry. TILs were *in vitro* stimulated with anti-CD3 in the presence of FB849 and/or anti-PD-1, and their proliferation was assessed. We observed that HPK1 marked severely exhausted PD-1$^{\pm}$CD8 TILs, and high HPK1 expressers had more exhausted PD-1$^{\pm}$CD8 TILs compared to low HPK1 expressers. In addition, FB849 could successfully restore the effector function of exhausted CD8 TILs. In particular, the reinvigorating capacity of FB849 was negatively correlated with phosphorylated SLP76$^{\pm}$PD-1$^{\pm}$CD8 TILs in endometrial cancer. In addition, FB849 further enhanced anti-PD-1-mediated reinvigoration of CD8 TILs in endometrial cancer. However, there was no synergistic effect of FB849 + anti-PD-1 in terms of proliferative capacity in ovarian cancer. Overall, the results of our present study provide a rationale for clinical trials investigating the anti-tumor efficacy of FB849 ± anti-PD-1 tailored to the respective properties of gynecologic malignancies.

#4031 P-selectin as an emerging target for the treatment of primary and secondary brain tumors.

E. Yeini[1], R. Frommer-Shapira[2], A. Talianski[2], P. Ofek[1], S. Pozzi[1], N. Albeck[1], D. Ben-Shushan[1], G. Tiram[1], S. Golan[1], R. Kleiner[1], R. Sheinin[1], S. Reich-Zeliger[3], R. Grossman[4], Z. Ram[1], H. Brem[5], T. Hyde[5], P. Magod[1], D. Friedmann-Morvinski[1], A. Madi[1], R. Satchi-Fainaro[1];

[1]Tel Aviv University, Tel Aviv, Israel, [2]Sheba Medical Center, Ramat Gan, Israel, [3]Weizmann Institute of Science, Rehovot, Israel, [4]Rambam Health Care Campus, Haifa, Israel, [5]John Hopkins Hospital, Baltimore, MD

Glioblastoma (GB) is an aggressive type of brain cancer with a high mortality rate. It is a highly angiogenic tumor exhibiting an extremely invasive nature. As such, its brain microenvironment plays a crucial role in its progression. Microglia are the brain resident immune cells that have been shown to facilitate GB cell invasion and immune suppression. The mechanism by which GB cells alter microglia behavior is yet to be fully understood. One proposed mechanism involves adhesion molecules such as the Selectins family of proteins which are expressed on the surface of endothelial and immune cells and are involved in immune modulation and cancer immunity. We have previously shown that one member of the Selectin family, P-Selectin (SELP), is expressed by GB cells. Here, we investigated the functional role of SELP in GB-microglia interactions. First, we found that microglia cells facilitate the expression and secretion of SELP by GB cells, and that GB cells facilitate the expression of P-Selectin ligand-1 (PSGL-1) by Glioma-associated microglia/macrophages (GAMs). We then showed that SELP mediates GAMs-enhanced GB invasion and proliferation in our unique 3D-bioprinted *ex vitro* models and has a role in GAMs activation state. These findings were validated *in vivo*, showing that inhibition or downregulation of SELP leads to reduced tumor growth, increased overall survival, and improved immune response. Single-cell RNA-seq analysis of the tumors revealed an increase in pro-inflammatory GAMs signature, reduction in cancer cell tumorigenesis potential, and improved T cell activation. Thus, combining SELP inhibition with other immune checkpoint inhibitors, such as anti-PD-1, may have a synergistic effect by harnessing both the innate and the adaptive immune systems against the tumor. Furthermore, we found SELP/PSGL-1 axis to be involved in the progression of brain metastasis originating from melanoma, and breast, and lung cancer. Thus, we have begun an investigator-initiated clinical trial, testing the efficacy of the anti-SELP antibody, Crizanlizumab, alone or in combination with anti-PD-1 antibody, Nivolumab, for GB and melanoma brain metastasis patients (NCT05909618). Crizanlizumab, approved by the FDA and EMA for sickle cell pain crisis (VOC, Vaso-Occlusive Crisis) of sickle-cell anemia patients, was proven to be safe for human use, and efficient in inhibiting SELP function. As such, it has the potential to reduce tumor burden and improve patient outcomes. This work can improve our understanding of GAMs function, which may pave the way for new and effective treatments for primary and secondary brain tumors.

#4032 ATRA induces an interferon response to reprogram the immunosuppressive tumor microenvironment and overcomes resistance to immune checkpoint inhibition in murine models of LKB1-deficient non-small cell lung cancer.

W. P. Crosson, R. Li, R. Salehi-Rad, R. J. Lim, J. Abascal, B. P. Kahangi, E. Perez Reyes, M. Oh, C. Dumitras, N. Edgar, R. Chew, R. Jocobo, A. Tfayli, Z. Jing, K. Krysan, L. Tran, S. M. Dubinett, B. Liu;
UCLA - University of California Los Angeles, Los Angeles, CA

Lung cancer remains the deadliest form of cancer, claiming 1.8 million lives worldwide in 2020. While treatment options have improved with the advent of immune checkpoint inhibitors (ICI), many patients do not respond to immunotherapy or develop resistance following initial response. A significant subset of non-small cell lung cancer (NSCLC) patients harbors somatic co-mutations in *Kirsten rat sarcoma virus (KRAS)* and *Liver kinase 1 [LKB1,* also known as *serine/threonine kinase 11 (STK11)]* genes, whose tumors are characterized by an immunosuppressive tumor microenvironment (TME) that are resistant to ICI. Our studies revealed that *all-trans* retinoic acid (ATRA), a metabolite derived from vitamin A, sensitized a murine model of NSCLC with increased tumor mutational burden (*Kras* ^{G12D} *P53*$^{-/-}$*Lkb1*$^{-/-}$; KPL-3M) to PD-1 blockade. The ATRA and anti-PD-1 combination therapy improved local and systemic T cell activation and generated systemic tumor-specific immunity. To understand ATRA-mediated anti-tumor effects, we performed single cell RNA sequencing (scRNA-seq) of KPL-3M murine tumors with or without 6 daily ATRA treatments. scRNA-seq analysis revealed a reduction of neutrophils as well as an enrichment in T cell and natural killer (NK) cell populations in the TME. Furthermore, scRNA-seq analysis revealed elevated expression of interferon (IFN) downstream genes in multiple immune subpopulations in the TME. Preliminary *ex vivo* studies indicated that ATRA increases NOX2 levels, intracellular reactive oxygen species (ROS), and IFN signaling in the neutrophils in KPL-3M tumors. Our findings suggest that ATRA may reshape the TME by activating IFN signaling in multiple cell subtypes to sensitize resistant tumors to ICI immunotherapy.

#4033 Leukocyte-based biomimetic nanoparticles for combined targeted and immunotherapy in osteosarcoma.

G. Romano[1], B. Ha[1], J. T. Yustein[2], F. Taraballi[3];
[1]Drexel University College of Medicine, Philadelphia, PA, [2]Emory University School of Medicine, Atlanta, GA, [3]Houston Methodist Hospital, Houston, TX

Osteosarcoma is the most diffuse bone cancer in the pediatric population, with most patients showing resistance to therapy. All patients are administered systemic high-dose cytotoxic chemotherapy regimens. Many targeted and immune therapy approaches are currently in clinical trials for treating osteosarcoma, but single treatments are not showing promise. While combined targeted and immunotherapy appears to be a possible avenue, developing solutions for patients who show intolerable toxicity or lack of synergy is critical. Nanoparticles (NPs) have successfully been used to prolong the half-life of drugs, favor extended release, reduce systemic toxicity, and reach beyond biological barriers. Biomimetic NPs represent an emerging class of NPs as a system to mimic naturally occurring processes. One class of biomimetic NPs is leukosomes, leukocyte-based biomimetic NPs that target inflamed tissues. Leukosomes are synthesized by integrating proteins isolated from the membranes of circulating leukocytes in the NPs' wall. Leukosomes' biomolecular profile helps them adhere to tumor-inflamed vasculature and promotes their self-tolerance and ability to evade immune clearance from the mononuclear phagocyte system (MPS). We have demonstrated the feasibility of a "one-two punch" approach for leukosome-mediated bone cancer treatment. Specifically, the first "punch" (a multi tyrosine kinase inhibitor, mTKI) induces an immunogenic response, which is subsequently targeted by leukosomes delivering a second class of compounds (immunomodulating nucleic acids, second "punch"). Indeed, even a single mTKI administration increases the amount of leukosomes localized to tumors, which is amplified by a second dosage in a dose-dependent manner. Importantly, leukosome infiltration was paralleled by an increase in immune infiltration, especially in Cd8+ T-cell abundance and macrophages. After several iterations and protocol adjustments, leukosome compositions and microfluidic parameters have been optimized to load either siRNA or mRNA. Current experiments are optimizing the "second punch" targeting immune checkpoint inhibitors (siRNAs vs. PD1/PDL-1). Interestingly, we showed the leukosomes produced using the membranes of human or mouse macrophages pre-treated with LPS show increased surface concentration of adhesion molecules (e.g., Siglec-1) that further enhance their localization at the inflamed site while decreasing filtration by the MPS. In addition to increased delivery to the tumor site, this strategy reduces the therapeutic strain because it is sequential ("one-two punch") and uses nucleic acids instead of antibodies to target immune checkpoints. Overall, our work describes a novel rationale-based sequential approach that can be *paradigm-shifting* in the field as it harnesses treatment-induced inflammation to boost intratumoral drug delivery.

#4034 Lag3 blockade enhances the anti-tumor effect of dual GITR agonism and PD-1 blockade in a preclinical melanoma model.

R. R. Maniyar[1], Y. Elhanati[2], L. Mangarin[1], Y. Marouf[1], A. Ahmed[1], B. Greenbaum[2], J. Wolchok[1], T. Merghoub[1];
[1]Weill Cornell Medicine, New York, NY, [2]Memorial Sloan Kettering, New York, NY

Immune checkpoint blockade (ICB) therapies, specifically anti PD-1 and anti CTLA-4, have resulted in tremendous success in the clinic. However, a substantial number of patients still relapse due to either inherent or acquired resistance to ICB therapies. In this scenario, activation of T cell co-stimulation pathways along with ICB emerges as a promising strategy to improve anti-tumor responses. Engagement of Glucocorticoid induced TNFR Related protein (GITR) costimulatory molecule, leads to enhanced activation of cytotoxic T cells while destabilizing suppressive T regulatory cells in the tumor microenvironment. Additionally, combining GITR agonism with PD-1 blockade improves the anti-tumor response in a murine model of advanced melanoma resistant to ICB, positioning GITR as an attractive immunotherapeutic target. In this study, we evaluated the therapeutic efficacy of combining blockade of the immune checkpoint LAG3 with GITR agonism for treating ICB-resistant advanced melanoma, using the B16 model. The combination of LAG3 blockade with GITR agonism was well tolerated, leading to better tumor control and improved survival. Our data revealed increased B cell infiltration and activation within tumors and draining lymph nodes (LNs) of treated mice. B cell depletion diminished the anti-tumor effect of the combination therapy, suggesting that B cells play an active role in controlling tumor growth. Spleens from treated mice exhibited increased lymphocytic hyperplasia, along with more and larger germinal centers. B cell receptor sequencing revealed an increased clonality and reduced entropy. Treating B cells with GITR agonism and LAG3 blockade *in vitro* led to increased activation and proliferation, suggesting a direct effect of these therapies on B cells. Furthermore, adding LAG3 blockade to the dual combination of GITR agonism and PD-1 blockade resulted in superior tumor control and increased B cell activity in the draining LNs. Collectively, our findings suggest that the humoral response significantly contributes to the anti-tumor responses elicited by ICB when combined with GITR agonism. This triple combination therapy (LAG3 blockade + PD1 blockade + GITR agonism) holds promise as a safe and potent therapeutic strategy to overcome ICB resistance. Further investigation into the mechanism of action by which GITR agonism leads to enhanced B cell responses when combined with ICB is warranted in order to design more effective therapies for cancer treatment.

#4035 Lipid-based nanoparticle combination immunotherapy with sitravatinib for the systemic treatment of high-risk neuroblastoma.

Miranda Diaz-Infante[1], Griffin Kane[1], Christina Lusi[1], Meghan Brassil[1], Kim Wigglesworth[2], Christian Alarcon[3], Jason Shohet[2], Prabhani Atukorale[1]

[1]Biomedical Engineering, University of Massachusetts Amherst, Amherst, MA,[2]UMass Chan Medical School, Worcester, MA,[3]Kansas City University, Kanas City, KS

We seek to develop a systemic, innate immunomodulatory nanoparticle therapy that combines synergistically with sitravatinib for the treatment of high-risk neuroblastoma, where metastasis is the largest hurdle for current treatment modalities. Here, we utilize a unique lipid-based nanoparticle (LNP) system comprised of co-encapsulated agonists of the Stimulator of Interferon Genes (STING) and Toll-like Receptor 4 (TLR4) pathways (immuno-NPs) that can be safely administered in the systemic blood circulation for delivery to the tumor microenvironment (TME) and uptake by perivascular innate antigen-presenting cells (APCs). STING/TLR4 agonists together promote the synergistic production of Type I interferon β (IFNβ), a key activator of anti-tumor immunity from the TME itself. Here, we also focus on sitravatinib, an investigational drug shown to inhibit receptor tyrosine kinases such as discoidin domain receptor 2 (DDR2), which can inhibit the sustained remodeling of collagen around primary tumors. The inhibition of such is vital to treatment as sustained collagen remodeling can facilitate the metastasis of cancer cells via epithelial-mesenchymal transition (EMT). We hypothesize that the downstream effects of sitravatinib treatment will augment tumor clearance and increase the therapeutic efficacy of immuno-NPs with respect to recruiting APCs. Our early pilot studies in humanized mice bearing orthotopic SH-5YSY tumors show that immuno-NPs are effective at tumor clearance. We found that mice inoculated subcutaneously with syngeneic 9464D-GD2 tumors showed decreased tumor growth when treated with our novel combination therapy in comparison to monotherapy controls. In both humanized and syngeneic tumor models, our ongoing mechanistic studies involve quantification of EMT in primary tumors, systemic nanoparticle deposition at metastatic sites, and the mechanistic impact of combination therapy on IFNβ-promoted elimination of metastasis. Here, we have proposed and tested an immunotherapy with great promise for treating neuroblastoma. However, the impact of nanoparticle-based immunotherapy reaches far beyond neuroblastoma: it has the potential to be a platform for the development of immunotherapies specific to other highly metastatic cancer types.

#4036 Integrating dendrimers and peptide-based biologics to co-target immune checkpoints and oncogenic pathways for HNSCC treatment.

D. Kim, P. Rawding, M. Iida, K. Kostecki, B. Mehall, D. Wheeler, S. Hong;
University of Wisconsin-Madison, Madison, WI

The utilization of peptides as cancer therapeutics has tremendous potential given their nature of mimicking protein functionalities while maintaining a high degree of modularity in their molecular design. However, their translation into the clinic remains a challenge due to their inferior binding kinetics, poor bioavailability, and short plasma half-life. To address these, we employed multivalent dendrimers that improve the binding and stability of the peptide-based biologis. We herein present a translatable, modular nanoparticle platform, utilizing generation 7 (G7) poly(amidoamine) (PAMAM) dendrimers conjugated with engineered peptides (dendrimer-peptide conjugates, DPCs). This approach capitalizes on the multivalent binding effect mediated by dendrimers. We found that DPCs functionalized with peptides targeting programmed death-ligand 1 (PD-L1, $DPC^{PD\text{-}L1}$), a crucial immune checkpoint protein in HNSCC, exhibit significantly lower K_D at 163 nM, which was three orders of magnitude stronger than free peptides. Furthermore, $DPC^{PD\text{-}L1}$ prolonged the serum half-life to 10.8 hours, approximately 14 times longer than that observed with PD-L1-binding peptide alone. The enhanced binding kinetics and plasma stability of $DPC^{PD\text{-}L1}$ were translated into the *in vivo* efficacy, as evidenced by a significant 40% reduction in tumor volume after four injections of $DPC^{PD\text{-}L1}$ at a dosage of 50 mg/kg in mice bearing oral carcinoma (MOC1) tumors. The transcriptomic analysis of $DPC^{PD\text{-}L1}$-treated tumor tissues revealed an increased population of CD4- and CD8-positive lymphocytes while decreasing the regulatory T cells and tumor cell proliferation, which is likely related to the observed efficacy. Expanding on this study, we have employed peptides designed to bind to the epidermal growth factor receptor (EGFR), a key player in the oncogenic pathways of HNSCC. These peptides were conjugated to G7 PAMAM dendrimer, forming DPC^{EGFR}. Similar to $DPC^{PD\text{-}L1}$, DPC^{EGFR} displayed improved binding affinity as proven by biophysical measurements and a series of *in vitro* assays. All these results highlight the versatility of our DPC platform, suggesting its potential applicability not only for targeting immune checkpoint proteins but also for intervening oncogenic pathways. With its simplicity, modularity, and versatility, this platform indicates the possibility of broadening its scope to incorporate multiple targeting and therapeutic factors, paving the way for its clinical translation, and providing new avenues in HNSCC treatment.

#4037 Optimizing the efficacy of anti-VEGF/cytotoxics/anti-PD-1 scheduling in a lung cancer mice model through B and T cells monitoring.

G. Sicard[1], D. Protzenko[1], S. Giacometti[1], R. Fanciullino[1], F. Barlesi[2], **J. Ciccolini**[1];
[1]Aix-Marseille University, Marseille, France, [2]Paris Saclay University, Paris, France

The exact modalities of combinatorial regimens associating Immune Checkpoint Inhibitors (ICI) with other treatments are yet to be defined. Understanding how and when cytotoxics best reshape tumor immunity could help optimizing the scheduling of ICI's. *In vivo* studies were performed on C57BL/6 mice grafted with LL/2lung cancer cells. A longitudinal immunomonitoring study on tumor, spleen and blood after multiple treatments including Cisplatin, Pemetrexed and anti-VEGF as single agents and in combination was performed for up to 21 days to determine the best time-window during which immune checkpoint inhibitors should be added. Finally, an efficacy study was conducted comparing the antiproliferative performance of various schedules of anti-VEGF, Pemetrexed-Cisplatin doublet, plus anti-PD-1 (i.e., immunomonitoring-guided scheduling, concurrent dosing or a random sequence). Immunomonitoring showed marked differences between treatments, organs and time-points. However, harnessing tumor immunity (i.e., promoting CD8 lymphocytes or increasing the CD8/Treg ratio) started on D7 and peaked on D14 with the anti-VEGF followed by cytotoxics combination. Therefore, a two-week delay between anti-VEGF/cytotoxic and anti-PD1 administration was considered the best sequence to test. Efficacy studies then confirmed that this sequence achieved higher anti-proliferative efficacy compared to other treatment modalities (i.e. -71% in tumor volume compared to control at the end of the study). Anti-VEGF and cytotoxic agents show time-dependent immunomodulatory effects, suggesting that sequencing is a critical feature when combining these agents with immune checkpoint inhibitors. Our efficacy study confirmed that sequencing treatments further enhances anti-proliferative effects in lung cancer models compared to concurrent dosing.

#4038 TU2218 (TGFβRI/VEGFR2 dual inhibitor) maximizes the benefit of cancer immunotherapies.

Jihyun Lee, Nam-Hoon Kim, Jeong Su Park, Jihyun Noh, Sowon Bae, Hun-Taek Kim

TiumBio Co., Ltd., Seongnam-si, Korea, Republic of

Approved anti-PD-1 antibodies play a pivotal role in driving innovative clinical outcomes through combination with cytotoxic agents, targeted therapies, or other immune checkpoint inhibitors in various cancers. Anti-PD-1 antibody-based combination therapies have led to a paradigm shift in cancer treatment from cytotoxic agents or targeted therapy to immunotherapy. Considering this change in the regimen, the clinical development of TU2218 aims to accelerate approval and clinical application by improving the efficacy and safety of clinically proven combination therapies. TU2218 is characterized by the following four mechanisms of action: 1) improvement of T lymphocyte activity, 2) suppression of Treg, 3) improvement of costimulatory signal defects, and 4) overcoming endothelial cell anergy. Based on the mechanisms of action, TU2218 is expected to show significant clinical effects when combined with immune checkpoint inhibitors by lowering the intensity of immune evasion and changing more favorably to immune checkpoint inhibitors. To test the feasibility of various combination options based on TU2218, in vivo efficacy studies were conducted in 4T1, MC38, and CT26 syngeneic tumor models. In the 4T1 of TNBC type, a level of tumor reduction was significant to $p<0.001$ on TU2218 and anti-PD-1 antibody combination group compared to vehicle, whereas anti-PD-1 antibody alone or anti-PD-1 antibody and paclitaxel combination group was not significant. Combination therapy with anti-CTLA4 antibody and anti-PD-1 antibody has been approved for some cancers but has therapeutic limitations due to safety issues such as immune-related toxicity and needs improvement. In the MC38, the effectiveness of a dose-sparing strategy of anti-CTLA4 antibody was evaluated by adding TU2218 to the anti-CTLA4 antibody and anti-PD-1 antibody combination regimen to improve safety concerns. In the anti-CTLA4 antibody sparing group, co-administration of TU2218 maintained the anti-tumor activity despite reducing 90% or 60% of the original anti-CTLA4 antibody dose. In effect, the difference in anti-tumor activity between the group with a reduced dose of anti-CTLA4 antibody and the group without was not statistically significant. In CT26, the efficacy of Lenvatinib and anti-PD-1 antibody combination therapy was compared with the combination of Lenvatinib, anti-PD-1 antibody, and TU2218. The efficacy of the Lenvatinib anti-PD-1 antibody, and TU2218 combination group was superior to that of TGI 99% and CR 67% than the Lenvatinib and anti-PD-1 antibody combination group of TGI 76% and CR 17%. Moreover, a statistical difference in anti-tumor activity between the two groups was significant at $p<0.001$. Collectively, the combination therapies using TU2218 not only improved efficacy but also showed high safety profiles without weight loss or any toxicity signs, supporting the feasibility of the combination strategy of TU2218.

#4039 Enhanced anti-cancer efficacy of the AhR Inhibitor DA-4505 in combination with anti-PD-1 treatment: Attenuation of lung metastasis and elimination of tumor.

D. Kim[1], S. Baek[2], S. Yang[2], Y. Kim[2], J. Hwang[2], S. Lee[1], S.-s. Kang[3], M. Kim[4], H. Han[4], K. Na[4], C. Lee[4], Y. Han[4], T. Han[5], H. Doh[5], J. Cho[5], D. Kim[5], D. Cha[5], J. Kim[4], Y. Byeon[4], Y. Kim[4], M. Yun[6], J. Lee[7], M. Hong[7], S. Lim[7], K.-H. Pyo[6], B. Cho[7];

[1]Brain Korea 21 PLUS Project for Medical Science, Yonsei University College of Medicine, Seoul, Korea, Republic of, [2]Yonsei University College of Medicine, Seoul, Korea, Republic of, [3]JEUK Institute for Cancer Research, JEUK Co., Ltd.,, Gumi, Korea, Republic of, [4]Severance Biomedical Science Institute, Yonsei University College of Medicine, Seoul, Korea, Republic of, [5]Dong-A ST Research Institute, Yongin, Korea, Republic of, [6]Yonsei New Il Han Institute for Integrative Lung Cancer Research, Yonsei University College of Medicine, Seoul, Korea, Republic of, [7]Division of Medical Oncology, Department of Internal Medicine and Yonsei Cancer Center, Severance Hospital, Yonsei University College of Medicine, Seoul, Korea, Republic of

Background: The Aryl hydrocarbon receptor (AhR) is one of the most predominant regulators of cancer metabolism. AhR plays a crucial role in inhibiting the activation of immune cells and promoting the growth of tumor cells. Here, we propose that a best-in-class AhR inhibitor, DA-4505, improves anti-tumor efficacy in combination with anti-PD-1.

Methods: To explore the anti-tumor effects, DA-4505 was administered at a daily dose of 10 mg/kg either alone or in combination with anti-PD-1 (10 mg/kg) in a syngeneic mouse model. Tumor volume, survival rates, and metastasis were measured, and immune profiles were evaluated using mIHC, flow cytometry, and scRNAseq.

Results: The synergistic anti-tumor effects of the DA-4505 and aPD-1 combination therapy were observed across four mouse tumor models (CT26, 4T1, LLC, TC1). The combination group demonstrated a significant improvement in anti-tumor efficacy compared to the monotherapy groups. Despite the moderate response of aPD-1 in the CT26 colon tumor model, the combination group displayed heightened anti-tumor effects through increase in CD8 T cell activity (P<0.05). In the LLC and TC1 lung cancer models, the combination therapy demonstrated improved anti-tumor effects and survival rates (P<0.001). Notably, the LLC model exhibited a significant increase in M1-type macrophages, while the TC1 model showed a significant augmentation in functional markers of $CD3^{\pm}$ T cells within the combination group (P<0.05). In both models, there was a significant reduction in the ratio of immunosuppressive M-MDSC and PMN-MDSC in the combination group. Immune depletion assays elucidated that DA-4505 mediated anti-tumor effects by increase in $CD8^{\pm}$ T cells, NK cells, and macrophages in the CT26 model. In contrast, the LLC model exhibited the contribution of macrophages and $CD4^{\pm}$ T cells to anti-tumor effects in the combination group (P<0.05). To assess the impact on metastasis inhibition, an orthotopic model of 4T1 mouse tumor was established, revealing a significantly increased anti-tumor effects and survival rate in the combination group, accompanied by a reduced lung metastasis ratio. H&E staining confirmed diminished migration of tumor tissue to adjacent areas. scRNAseq analysis of CT26 tumor samples indicated consistent changes at the gene expression level, reflecting a decrease in metastasis-related MMP and VEGF genes in the combination group and an increasing trend in cytotoxicity-related genes following DA-4505 treatment.

Conclusion: The AhR inhibitor, DA-4505, has demonstrated enhanced anti-tumor efficacy when administered in combination with anti-PD-1. Furthermore, it not only promoted tumor elimination but also demonstrated significant efficacy in inhibiting metastasis. This study highlights the potential of combining AhR inhibitors with immunotherapies for clinical treatment.

#4040 Hypoxia-induced HIF-1α/USP3 pathway promoting immune escape in lung squamous cell carcinoma.

X. Zhang[1], H. Huang[1], C. Ding[1], C. Chen[2], Y. Li[2], H. Liu[2], **C. Jun**[3];
[1]Department of Lung Cancer Surgery, Tianjin Medical University General Hospital, Tianjin, People's Republic of China, Tianjin, China, [2]Tianjin Lung Cancer Institute, Tianjin Key Laboratory of Lung Cancer Metastasis and Tumor Microenvironment, Tianjin Medical University General Hospital, Tianjin, People's Republic of China, Tianjin, China, [3]Tianjin Medical University, Tianjin, China

Background: Immune escape poses a significant mechanism for tumor progress as well as enormous challenge for the treatment of lung squamous cell carcinoma (LUSC). The close association between hypoxic environments and tumor immune escape, with PD-L1 serving as a key marker, has garnered considerable attention. This study aims to delve into the molecular mechanisms underlying the regulation of PD-L1 deubiquitination by the hypoxia-induced HIF-1α/USP3 pathway, shedding light on the immune escape mechanisms in LUSC.
Methods: NSCLC cells were cultured under hypoxia condition and the expression of USP3, HIF-1α and PD-L1 were measured by Western blot. Chromatin Immunoprecipitation (ChIP) and Co-immunoprecipitation (CO-IP) were employed to elucidate the direct regulatory mechanisms of the HIF-1α/USP3 pathway in PD-L1 deubiquitination. In vitro T cell-mediated killing assays was used to investigate the functional roles of USP3 in antitumor immunity in NSCLC.
Results: We demonstrated that hypoxia score was increased in LUSC and negatively correlated with CD8+ T cell infiltration. Hypoxia as a major factor triggering LUSC cell immunosuppression and against T cell surveillance via stabilization of PD-L1. Mechanistically, USP3, induced by HIF-1α, is required for hypoxia-mediated PD-L1 stabilization in LUSC cells. USP3 inhibits the ubiquitination and degradation of PD-L1. The combination of USP3 inhibitors with PD-1/PD-L1 monoclonal antibodies significantly enhances the anti-LUSC effect, possibly through promoting the infiltration of CD8+ T and NK cells.
Conclusion: This research unveils a novel mechanism by which hypoxia, through the HIF-1α/USP3 pathway, regulates PD-L1 deubiquitination, thereby promoting immune escape in LUSC. Furthermore, our study provides a new strategy involving USP3 inhibitors in combination with PD-1/PD-L1 monoclonal antibodies, offering novel insights for molecular targeted therapy and reversal of drug resistance in LUSC.

#4041 Translational assessment of triple combination with Tislelizumab (anti-PD-1), LBL-007 (anti-LAG-3) and Surzebiclimab (anti-TIM-3) highlights its strong anti-tumor activity and clinical potential in solid tumors such as HNSCC.

Hengrui Zhu, Jinhui Zhang, Han Yan, Xiao Ding, Juan Yang, Yu Jiang, Minjuan Deng, Haoxuan Song, Fangfang Ping, Fuyun Sun, Xiaoyu Li, Lijie Zhang, Bin Jiang, Weiwei Song, Zhirong Shen, Wei Jin, Jiyuan Zhang, Yun Zhang

BeiGene (Beijing) Co., Ltd, Beijing, China

Background: Therapeutics targeting PD-(L)1 have demonstrated impressive clinical activity in several type of cancers. However, only a small proportion of patients develop long-term response and resistance frequently occurs. LAG-3 and TIM-3 are inhibitory immune checkpoints frequently upregulated and co-expressed with PD-1 on tumor-infiltrating T cells, contributing to T cell dysfunction. Thus, we hypothesized that simultaneously targeting PD-1/LAG-3/TIM-3 would further restore T cell response and the triple combination of Tislelizumab (Tisle, anti-PD-1), LBL-007 (anti-LAG-3) and Surzebiclimab (Surze, anti-TIM-3) would provide greater clinical benefit.**Methods:** To evaluate the rationale and the anti-tumor activity of triple combination, LAG-3 and TIM-3 expression were analyzed in *in vitro* T cells, syngeneic mouse models and cancer patients with anti-PD-(L)1 therapy. The effects of dual blockade of PD-1/LAG-3, PD-1/TIM-3 and the triple blockade of PD-1/LAG-3/TIM-3 on T cell function were evaluated in *in vitro* activated PBMCs and the anti-tumor efficacy were evaluated in syngeneic mouse models. Relevant gene expression and immune signatures were ranked across 31 solid tumor types in TCGA.**Results:** Both LAG-3 and TIM-3 expression on T cells were upregulated by anti-PD-1 treatment in syngeneic mouse tumors, similar trend was observed in cancer patients with anti-PD-(L)1 therapy. Dual combination of Tisle/LBL-007 or Tisle/Surze enhanced IFNγ production in *in vitro* activated human T cells. The dual blockade of PD-1/LAG-3 or PD-1/TIM-3 significantly enhanced tumor growth inhibition compared with anti-PD-1 monotherapy in syngeneic mouse models. The triple combination of Tisle/LBL-007/Surze further enhanced IFNγ production in *in vitro* activated T cells. In a mouse MC38 colon carcinoma model, the triple blockade of PD-1/LAG-3/TIM-3 demonstrated enhanced anti-tumor activity compared with either dual combination, evidenced by trend of increased tumor growth inhibition and higher tumor-free incidence rate. Finally, the responsiveness of PD-1/LAG-3/TIM-3 triple combination was predicted using 5 signatures, including early effector T cell signature, inflamed signature, LAG-3, TIM-3 and PD-L1 expression. The *in silico* analyses indicated strong potential in clinical utility such as squamous cell carcinoma of the head and neck (HNSCC).**Conclusions:** The concurrent blockade of PD-1/LAG-3/TIM-3 represents a promising strategy to enhance T cell function and anti-tumor activity. The results demonstrated the therapeutic potential of the triple combination. A Ph2 study evaluating Tisle in combination with LBL-007 and/or Surze in first-line treatment of recurrent or metastatic HNSCC (NCT05909904) is recruiting.

#4042 Cbl inhibition increases the response of cytotoxic T cells to sub-optimal stimulation and drives enhanced anti-tumor responses alone or in combination with PD-1 blockade.

L. Yamashiro, S. Marubayashi, R. Rayaji, A. Battsooj, K. Mrouj, H. Singh, Y. Lee, A. Chen, L. Shen, A. Mailyan, K. Yu, M. Podunavac, J. Yu, D. Liu, C. Hardman, J. Yin, S. Gangam, K. Lawson, M. Leleti, M. Walters, D. DiRenzo;
Arcus Biosciences Inc., Hayward, CA

INTRODUCTION: Herein, we describe a series of experiments to define the unique biology of dual Cbl-b/c-Cbl (Cbl) inhibition in amplifying T cell activation and anti-tumor responses. Through their E3 ubiquitin ligase activity, Cbl-b and c-Cbl have been shown to negatively regulate multiple signaling proteins downstream of the T cell receptor (TCR), suggesting that inhibition may yield enhanced anti-tumor T cell activity. Indeed, using a dual Cbl-b/c-Cbl small molecule inhibitor, we demonstrate that Cbl blockade enhances T cell activity under standard and sub-optimal stimulation conditions. Moreover, Cbl inhibition increases mouse syngeneic tumor control alone or in combination with α-PD-1, as described below.

METHODS: Human $CD8^+$ T cells were isolated from healthy human blood and activated using α-CD3 or α-CD3/CD28 stimulation. Mouse OT-I splenocytes were stimulated with SIINFEKL or lower affinity ovalbumin peptides and cytokine production was assessed. For tumor studies, mice were inoculated with syngeneic cancer cells and were treated with Cbl inhibitor (30 mg/kg, QD) +/- α-PD-1 (10 mg/kg, Q5D) starting at a tumor volume of 75 mm^3.

RESULTS: Human $CD8^+$ T cells, stimulated in the presence of a Cbl inhibitor, demonstrated a concentration-dependent increase in activation hallmarks including cytokine secretion (IL-2, IFN-γ and granzyme B), proliferation, and the presence of highly polyfunctional cells. Furthermore, using serially stimulated $CD8^+$ T cells with reduced overall activity, Cbl inhibition showed a marked enhancement of IFN-γ production and cytotoxicity compared to controls upon re-stimulation. We then used an antigen-specific T cell assay where OT-I splenocytes were stimulated by peptides with optimal or reduced TCR affinities, Cbl inhibition produced significantly higher IFN-γ levels with all peptides relative to controls demonstrating that Cbl inhibition can increase the response of T cells to sub-optimal stimulation. Using mouse CT26 and MC38 tumor models, Cbl inhibition was able to significantly enhance tumor control in combination with α-PD-1 and as a monotherapy in CT26 tumors. Notably, a greater number of tumor antigen-specific cytotoxic T cells were found in Cbl inhibitor-treated tumors. Higher expression levels of the co-stimulatory molecule CD226 and the TCR in these anti-tumor cells were also observed, demonstrating the unique biology of Cbl inhibition in enhancing anti-tumor responses. Finally, Cbl inhibition had no effect on the growth or survival of cancer cells *in vitro* consistent with the notion that enhanced tumor control was driven by immune activity.

CONCLUSIONS: Altogether, these data demonstrate that pharmacologic Cbl inhibition robustly enhances T cell activity *in vitro* and *in vivo* and provide a mechanistic rationale for targeting Cbl-b/c-Cbl to amplify anti-tumor immune responses.

#4043 Nanoparticle-mediated combination therapy to synergistically harness Type I interferons and senescence in the pancreatic tumor microenvironment.

P. Atukorale[1], M. Ruscetti[2], L. Chibaya[2], C. Lusi[1], K. DeMarco[2], G. Kane[1], M. Brassil[1], C. Parikh[2], K. Murphy[2];
[1]University of Massachusetts - Amherst, Amherst, MA, [2]University of Massachusetts Chan Medical School, Worcester, MA

We seek to combine a unique innate immunomodulatory nanoparticle (NP) system with RAS inhibitors for a multi-faceted therapy that mitigates the formidable drug delivery challenges in pancreatic ductal adenocarcinoma (PDAC). PDAC has quickly risen to the third most deadly cancer largely due to its fibrotic, desmoplastic, and immunosuppressive tumor microenvironment (TME) that limits delivery and efficacy of chemo- and immunotherapeutics. We have engineered unique lipid-based NPs that co-encapsulate agonists of the Stimulator of Interferon Genes (STING) and Toll-like Receptor 4 (TLR4) pathways. NPs can be safely delivered in the systemic blood circulation to achieve TME deposition, uptake by innate antigen-presenting cells (APCs), and robust, synergistic production of Type I interferons by dual STING/TLR4 activation. Here, we hypothesize that combination therapy of proinflammatory NPs with tumor senescence-inducing RAS inhibitors, tremetinib and palbociclib, will not only augment $CD8^{\pm}$ T cell recruitment to the TME but enhance their sustained activation by mitigating local immunosuppression. In mice bearing orthotopic transplant *KPC* tumors or *KPC* GEMMs, combination NP/inhibitor treatment promoted significant NP delivery to tumors, APC and natural killer (NK) cell activation, and $CD8^{\pm}$ T cell-mediated clearance, compared to monotherapies and untreated controls. Unexpectedly and strikingly, these studies also showed that, besides innate immune cells, combination therapy also promoted Type I interferon and other proinflammatory cytokine production by PDAC tumor cells, which are otherwise notoriously unresponsive to current state-of-the-art treatments. Further, in *KPC* GEMMs, 25% of mice exhibited apparent complete responses following combination treatment, which, to our knowledge, is challenging to achieve in this model. Current studies include the mechanistic elucidation of immune- and tumor-intrinsic factors that govern efficacy of our combination therapy. In conclusion, these findings strongly corroborate the use of this NP-based system as a platform therapy for similar drugs and across other aggressive cancers. They also strongly make the case for the rational design of combination therapies to achieve synergistic therapeutic outcomes with minimal systemic toxicities.

#4044 Potentiated antitumor activity of poly-γ-glutamic acid combined with anti PD-L1 blockade on murine models of colorectal cancer.

Jae-Pyung Jang, Chan-Hee Yoo, Kyung-Soo Hahm, Do Young Lee, Young-Chul Park, **Jae Chul Choi**

BL Corporation, Yongin, Gyeonggi-do, Korea, Republic of

Objective: Immune checkpoint inhibitors(ICIs) have been shown to be key role in cancer therapy. Especially, antibodies targeting programmed cell death ligand1(PD-L1) promoted T cells to activate immune response against cancer cells. However, the current ICIs still have insignificant to motivate effective antitumor immunity by blocking PD-1/PD-L1 pathway and the regulatory network of PD-L1 by cytokines in the tumor microenvironment remains to be uncovered. Previously, we have reported the anti-cancer effects of combination treatment with a natural product, poly-γ-glutamic acid(γ-PGA), and PD-1 blockade. Now, we show that combination therapy with anti PD-L1 and γ-PGA can overcome the limits of ICIs and enhance anticancer effect in murine colorectal cancer.
Design: *In vivo* efficacy studies were performed by intraperitoneal injection of antibody targeting PD-L1 and oral administration of γ-PGA in C57BL/6 model transplanted with mouse tumor cell lines. Systemic changes in immunophenotype was measured by tumor volume size and body weight. The splenocyte was isolated from mice and the populations of myeloid-driven suppressor cells(MDSCs) and CD4/CD8 T cells were analyzed by FACS. Also, the significant cytokines activated by T- cell, IFN-γ and IL-2, were measured by ELISA.
Results and Conclusions: In murine model of colorectal cancer, γ-PGA and anti PD-L1 blockade combination therapy significantly improved anti-tumor activity compared with single agents. In addition, tumoral infiltration of $CD8^{\pm}$ T cells and IFN-γ productions were increased by γ-PGA, and its antitumoral activity was attenuated by antibody-mediated depletion of these cells, indicating that g-PGA suppressed tumor growth in a CD8 T cell-dependent manner. Therefore, our results suggest that γ-PGA promote ICI-mediated antitumor responses by the transformation of "cold tumors" into “hot tumors”

#4045 Dependence of human immune cell type, and impact of IL-7R or TLR1/2 agonism, upon trastuzumab-mediated ADCC.

M. Bryant, G. Tut, N. Harrison, E. Welsh, I. Morano, A. Kaur, A. Pegg, H. Chan, Z. Li, J. Cowley, C. Brady, J. Gordon, N. Barnes, O. Qureshi;
Celentyx Ltd, Birmingham, United Kingdom

Targeting of tumors over-expressing HER2 using trastuzumab provides clinical benefit for patients by inhibiting HER2 signalling and enhancing immune responses against the tumor by antibody-dependent cell-mediated cytotoxicity (ADCC). Cytokines such as IL-7 augment cytotoxic anti-viral responses through up-regulation of FasL, whereas TLR1/2 agonists enhance T cell cytotoxic responses but may also promote tumor cell survival. We therefore investigated the ability of IL-7R or TLR1/2 agonism to enhance trastuzumab-mediated ADCC.

We first determined the contribution of various human immune cell subsets (e.g. monocytes, T cells, NK cells) to deliver ADCC of human tumor cells using a live high-content imaging assay in both 2D and 3D formats. Our results demonstrate that trastuzumab evoked immune cell dependent, concentration-dependent killing of tumor cells that exhibited some differential sensitivity dependent upon the cell culture format. We then tested trastuzumab-mediated killing in the absence or presence of IL-7R or TLR1/2 agonism, and noted evident donor and immune cell dependent modulation of the cytotoxic response. Modulation of this cytotoxic response was associated with differential immune cell marker expression when analysed by flow cytometry.

Our findings provide mechanistic insight into trastuzumab-mediated ADCC and highlight how cytokine receptor and TLR pathways may modulate this response.

#4046 Orally active PD-L1 inhibitor MAX-10181 in combination with temozolomide effectively prolonged survival in GBM animal model study.

Y. Wang[1], Z. Feng[1], Q. Zhao[1], W. Zhang[2], Y. Jiang[2], Y. Huang[2], C. Qi[2], C. Zhang[2];
[1]Maxinovel Pharmaceutical, Inc., Shanghai, China, [2]Wenzhou Medical University, Wenzhou, China

Treatment of glioblastoma (GBM) with PD-1/PD-L1 immuno therapy is highly challenging due to the limited brain blood barrier (BBB) penetration of the marketed antibody drugs. During the past several years, we have successfully developed orally active, BBB penetrating, small molecule PD-L1 inhibitor MAX-10181 which is in the phase II clinical development. To demonstrate the utility of PD-1/L1 immuno therapy for the treatment of GBM, we completed the study of MAX-10181 in combination with Temozolomide (TMZ) in GL-261 animal model study. In this study, the combination of MAX-10181 with TMZ effectively prolonged the survival by 50% in comparison with TMZ single therapy. Details of this study will be reported in this meeting.

#4047 Unraveling synergistic therapeutic strategies involving FAK inhibition and immunotherapy using anti-PD1 antibody in KRAS and LKB1-driven lung cancer.

J. Koo, C. Tucker-Burden, M. Roy, C. Huang, W. Zhou, M. Gilbert-Ross, H. Fu, S. S. Ramalingam, A. I. Marcus;
Emory University, Atlanta, GA

Lung cancer presents a global health challenge demanding innovative preclinical models forresearch and therapeutic advancement. Genetically engineered mouse models (GEMMs) have seenremarkable growth in complexity and application over the past two decades. Our work leveragesthese models and is specifically designed to address the pressing need for effectiveimmunochemotherapies in the context of KRAS and LKB1 (KL) mutant lung adenocarcinoma,which shows resistance to most immunotherapies. Our study centers around a preclinicalsyngeneic orthotopic mouse model we developed using mouse lung and metastatic tumor cell linesderived from KL-GEMM. This model, optimized to mimic human lung cancer closely, providesan ideal platform for exploring the intricate interplay between the immune system and tumorprogression. Furthermore, we have previously shown the LKB1 mutant cell lines and tumormodels are uniquely sensitive to FAK inhibitors, and therefore we wanted to test whether thecombination of a FAK inhibitor with anti-PD1 therapy can improve sensitivity. The combinatoryadministration of FAK inhibitor (VS-6063) with anti-PD1 mAb synergistically increased anti-tumor response and survival outcome compared with single-agent therapy in the KL-mediatedsyngeneic orthotopic lung cancer model. By using GEMM-derived syngeneic cell lines, we haveevaluated the potential for creating innovative immunochemotherapies, customized for KL co-mutant lung adenocarcinomas with promising clinical potential. Furthermore, using this modelenables a deeper understanding of the KL mutant disease's pathogenesis, the impact of sex-biasedcancer development, and the assessment of novel immunochemotherapy treatment strategies in theKL genetic sub-type of lung adenocarcinoma.

#4048 Comparative effects of SOS1 inhibitor with IL-6 blockade and their combination on Kras mutant lung cancer.

Katherine E. Larsen, Maria J. Arredondo Sancristobal, Melody Zarghooni, Avantika Krishna, Maria T. Grimaldo, Nastaran Karimi, Arnav Gaitonde, Michael J. Clowers, Seyed Javad Moghaddam

UT MD Anderson Cancer Center, Houston, TX

Despite recent advances in treatment, lung adenocarcinoma (LUAD), particularly harboring *Kras* mutations, is still the leading cause of cancer mortality. We and others have previously shown that Kras mutant LUAD development and progression is associated with intrinsic inflammatory characteristics driven by epithelial NF-κB activation, increased levels of IL-6 (which is transcriptionally regulated by NF-κB), and activation of the IL-6-responsive transcription factor STAT3. We further demonstrated that IL-6 blockade suppresses lung tumorigenesis by reducing tumor-associated immunosuppressive myeloid populations and induction of a T cell-mediated anti-tumor response. The recent discovery of a novel SOS1-targeting compound (BI-3406) that selectively inhibits the KRAS-SOS1 interaction and leads to anti-proliferative activity has opened up the possibility to more efficiently inhibit Kras mutant lung cancer. Accordingly, in this study we used a mouse model of KRAS mutant LUAD (CC-LR) to compare the therapeutic effects of BI-3406, IL-6 blockade, and MEK inhibitor (trametinib). We also tested whether inhibiting IL-6 driven pro-tumor immune response would provide a synergistic/additive response and increase the tumor inhibitory effect of either BI-3406 or Trametinib. Eight cohorts of 14-week-old female mice were treated with either anti-IL-6 antibody, trametinib, or BI-3406, or their combinations for 4 weeks, and their tumor burden was compared at the end of study. We observed a significant reduction in tumor multiplicity and tumor area in response to all monotherapies, with the highest effect in the trametinib treated cohort. Neither combination therapy led to decreased tumor burden over either of the monotherapy regimens in our model. However, we observed an increase in T helper 1 and CD8 T expressing IFNγ cell populations in the cohort treated with Trametinib and anti-IL-6 Ab combination. In addition, using qPCR analysis of RNA extracted from the whole lung we found a higher expression of IFNγ along with a reduced expression of IL-10 in the cohort treated with BI-3406 and anti-IL-6 Ab combination. This suggests that these combinations may have the potential to improve the anti-tumor immune responses. Hence, we conclude that further adjustment of the treatment regimen (doses, interval, duration) may allow to obtain improved anti-tumor efficacy with these combinations. Overall, this study provides a new research perspective for the improvement of currently available treatment modalities for patients with Kras mutant lung cancer that could be further explored preclinically.

#4049 The beta-carboline Harmine sensitives microsatellite stable colorectal cancer mouse model to anti-PD-1 through upregulating MHC-I dependent antigen presentation machinery and improving the infiltration of CD8 T cells into the tumor microenvironment.

Ruize Gao[1], Kris Van Moer[1], Coralie Pulido[2], Anais Oudin[2], Diane Murera[1], Teresa L. Ramos[1], Margaux Poussard[1], Andreas Schlapfer[3], Annette Ives[3], Christian Auclair[3], **Bassam Janji**[1]

[1]Department of Cancer Research - Tumor Immunotherapy and Microenvironment (TIME) Group, Luxembourg Institute of Health, Luxembourg City, Luxembourg,[2]Department of Cancer Research - Animal Experimental Core facility, Luxembourg Institute of Health, Esch-sur-Alzette, Luxembourg,[3]AC Bioscience SA, Epalinges, Switzerland

Colorectal cancer (CRC) is the most common gastrointestinal cancer and the third leading cause of cancer-related death in both sexes. Mismatch repair deficient/microsatellite instability-high (MSI) colorectal cancer patients benefit from immune checkpoint blockades (ICBs)-based immunotherapy; however, this benefit has not been translated into microsatellite stable (MSS) colorectal cancer. It has been proposed that the loss of major histocompatibility complex class I (MHC-I) in tumor cells limits the use of ICB in colorectal cancer. Harmine displays a number of biological and pharmacological properties affecting the immune response and tumor phenotype. Here, we assessed the impact of combining harmine, also referred to as ACB1801 molecule, on improving the responsiveness of ICB in the mouse MSS CRC model. Our results showed that combining ACB1801 significantly improves the therapeutic benefit of anti-PD-1 in the CT26 CRC mouse model by decreasing tumor growth and improving the survival of tumor-bearing mice. The improvement of anti-PD-1-based therapy by combining ACB-1801 was associated with a modification of the immune landscape of tumors as evidenced by an increase in the CD8+ T cells and a decrease in the Treg infiltrations into the tumor microenvironment. By profiling the cytokine/chemokine network, we showed that ACB1801 induced the expression and the release of the proinflammatory chemokine CXCL10 by CRC tumor cells *in vitro*, which could be responsible for driving CD8+ T cells to the tumor microenvironment. Mechanistically, we showed that ACB1801 increased the expression of MHC-I genes, including TAP1 and TAPASIN, and improved the antigen loading on MHC-I in CRC cells *in vitro*. Overall, our study highlights the value of combining ACB1801 and anti-PD-1 as a therapeutic opportunity to convert MSS colorectal cancer into an “immune hot” cancer, which may define the future treatment paradigm of colorectal cancer for which there is a great unmet need.

#4051 Optimizing breast cancer therapy by modulating oxygen consumption.

A. Assouvie[1], S. Budhu[1], M. Mane[2], M. Bah[1], J. Zurita[2], I. Serganova[1], S. Min[2], J. Koutcher[2], V. Ponomarev[2], J. Wolchok[1], T. Merghoub[1];
[1]Weill Cornell Medicine, New York City, NY, [2]Memorial Sloan Kettering Cancer Center, New York City, NY

Immune checkpoint blockade (ICB) has achieved great clinical responses in multiple cancers. However, only a subset of patients with triple negative breast cancer (TNBC), a highly hypoxic tumor, respond to ICB. In TNBC, the immune checkpoints PD-1/PD-L1 and adenosine receptor (A2aR) are often activated to escape anti-tumor responses. These two immune checkpoints are sensitive to hypoxia. We propose that blocking tumor oxygen consumption using deferiprone (DFP), phenformin (Phen) and metformin (Met) will improve the efficacy of PD-1/PD-L1 and A2aR blockade. We generated two mouse breast cancer cell lines (4T1 and E0771) expressing green fluorescent protein (GFP) fused to Firefly luciferase under the control of the hypoxia reporter element (HRE). This construct, which we called HRE/TGL, serves as a hypoxia reporter, with GFP expression and luciferase activity increasing in hypoxic conditions. To induce hypoxia *in vitro*, we used two approaches: 1) we incubated cells in a hypoxia chamber (3% oxygen), and 2) treated cells with cobalt chloride, which chemically mimics hypoxia by inducing the expression of the hypoxia master regulator HIF1α. Both 4T1-HRE/TGL and E0771-HRE/TGL cells exhibited increased GFP expression and luciferase activity within hypoxia conditions. We orthotopically implanted these cells into mice. We measured luciferase activity *in vivo* using the IVIS spectrum imaging system overtime after tumor implantation. We observed high luciferase activity in 4T1-HRE/TGL tumors. Next, we examined the effects of DFP, Phen and Met on cell hypoxic responses by performing immunoblotting against HIF1α and phosphorylated AMPK (p-AMPK) on 4T1 and E0771 cells. We observed that, unlike Phen or Met, DFP increased HIF1α and p-AMPK expression. Binding of HIF1 proteins to HREs is known to activate the expression of the HRE promoter. To confirm our results, we treated 4T1-HRE/TGL and E0771-HRE/TGL cells with low (10μM) or high (100μM) doses of the drugs *in vitro*. We observed that, while DFP increased GFP expression and luciferase activity, Phen had no consistent measurable effect. We observed similar results *in vivo*. Finally, we examined the effect of DFP, Phen and Met either alone or in combination with anti-PD-1 on tumor progression and survival in mice bearing 4T1 or E0771 tumors. Contrary to what expected, we did not observe better tumor control and survival after treatment with these drugs. In addition, DFP, Phen and Met failed to improve the anti-tumor effect of anti-PD-1 treatment in both TNBC models. Future experiments will focus on charactering the adenosine pathway *in vivo* in 4T1 and E0771 tumors and examine how drugs targeting A2aR and oxygen consumption (DFP, Phen and Met) influence the activation of immune cells within the tumor microenvironment and potentially combinate these two strategies to improve their anti-tumor efficacy.

#4052 Neutrophil recruitment and activation promotes cutaneous adverse effects with T cell immunotherapies.

D. Hirschhorn[1], L. Kraehenbuehl[1], S. Budhu[1], V. Estrada Navarro[1], L. B Mangarin[1], Y. Marouf[1], J. Ricca[1], B. Gasmi[1], O. De Henau[1], Y. Li[1], C. Cortez[1], H. Linda[1], I. Schulze[1], C. Liu[1], K. Panageas[2], M. Lacuoture[3], G. A. Rizzuto[1], M. Egeblad[4], J. D. Wolchok[1], T. Merghoub[1];

[1]Weill Cornell Medicine, New York, NY, [2]Memorial Sloan Kettering, New York, NY, [3]Memorial Sloan Kettering Cancer Center, New York, NY, [4]Johns Hopkins University, Baltimore, MD

Immune-based therapies that induce tumor regression are often accompanied by immune-related adverse events (irAEs) which can occasionally present with severe and lethal symptoms. Currently, there are no well-defined preventative approaches to uncouple anti-tumor immunity from irAEs. Currently approved immunotherapies include agents that activate T cell responses, such as antibodies blocking immune checkpoints and infusion of tumor-derived, T cell receptor-transgenic or chimeric antigen receptor-modified T cells. While the beneficial and toxic effects of T cell-based therapies in the clinic are being extensively explored, the precise mechanisms underlying their activity remain the subject of investigation. In this study, we treated preclinical models of established melanomas with tumor-specific adoptive CD4+ T cell transfer in combination with T cell co-stimulation via OX40 agonism or CTLA-4 blockade. We found that, despite adequate T cell stimulation, acute local inflammation plays an important role in tumor elimination and the manifestation of irAEs. While stimulated T cells are necessary for initiating a therapeutic response, activation of endogenous neutrophils constitutes an important and necessary effector mechanism for both tumor destruction and the development of irAEs. Extensive neutrophil extracellular traps (NETs) were associated with irAEs. Furthermore, melanoma patients treated with immune checkpoint blockade with skin rashes equivalent to irAEs found in mice showed increased survival and NETs in biopsies from both rashes and tumors. Our results bring forward a novel paradigm where T cells prime an anti-tumor immune response that is followed by an inflammatory effector mechanism provided by the innate immune system, resulting in both curative and undesirable side effects in mice and patients.

#4053 Targeting oxygen consumption with metformin and phenformin have differential effects on immune cells in the tumor microenvironment.

S. Budhu[1], A. Assouvie[1], M. Bah[1], S. Verma[1], I. Serganova[2], M. Mane[3], J. Zurita[3], J. Koutcher[3], V. Ponomarev[3], J. D. Wolchok[1], T. Merghoub[1]; [1]Weill Cornell Medicine/Sandra and Edward Meyer Cancer Center, New York, NY, [2]Weill Cornell Medicine, New York, NY, [3]Memorial Sloan Kettering Cancer Center, New York, NY

T cell immune checkpoint blockade (ICB) has shown remarkable promise in melanoma and other cancers. However, most patients do not show clinical benefit. This is because tumors can activate multiple checkpoints and immunosuppressive pathways to evade anti-tumor immune responses. Inhibition of these immune suppressive mechanisms and immune checkpoints or repolarizing the tumor microenvironment (TME) to become more accessible to the immune system may be necessary for maximal therapeutic efficacy of immunotherapies. There is increasing evidence that tumor hypoxia can attenuate the antitumor immune response by promoting immune suppression and inhibiting direct killing by cytotoxic immune cells. We propose that blocking tumor oxygen consumption using drugs that target the mitochondrial complex I (phenformin and metformin) will enhance the efficacy of immunotherapies such as ICB in preclinical models such as B16 melanoma. In this study, we examined how low oxygen levels (hypoxia) influence T cell effector function such as cytotoxic activity and cytokine production in vitro. We co-cultured B16 melanoma cells in the presence of tumor specific T cells (Pmels) and incubated at 37ºC in either normoxia (~21% O2) or hypoxia (3% O_2) and assessed killing and intracellular cytokine production 24 - 48 hours later. We show that the ability of tumor antigen-specific T cells to kill tumor cells or make effector cytokine such as IFNγ and TNFα is significantly reduced in hypoxia settings. We also examined the effects of hypoxia targeting drugs (metformin and phenformin) on T cell priming and activation. When T cells were activated in the presence of each drug in vitro, there was enhanced expression of T cell activation markers (CD25, Granzyme B) as well as an increase in their differentiation into central memory T cells. We next determined whether these drugs could alter the TME in vivo by treating C56BL/6J mice bearing established B16 tumors with phenformin and metformin and then examine the effects on the immune system in the tumor, tumor draining lymph nodes and spleen by flow cytometry. We found that these three drugs have differential effects on both the innate and adaptive the immune system in the tumors and periphery. Finally, we tested whether these drugs could delay B16 melanoma growth in vivo as a monotherapy or in combination with anti-PD1. We found that while both drugs can significantly delay tumor growth as monotherapies, only metformin showed improved anti-tumor efficacy when combined with anti-PD-1 in vivo. These studies show that while both drugs target tumor oxygen consumption (via inhibition of complex I), and can delay B16 tumor growth in vivo, they have differential effects on the TME and will need further considerations when combining with immune based therapies such as ICBs.

IMMUNOLOGY: Immune Modulation with Cytokines
Poster Session

#4057 Beyond IL-2: The promise of anti PD-1-attenuated IL-2 fusion protein in cancer immunotherapy.

S. Amar[1], Y. Liubomirski[1], E. Yeini[1], M. Monsonego[1], T. Weiss[1], G. Tiram[1], A. Katyal[1], O. Avramoff[1], A. Krinsky[1], K. Reshef[1], S. Dulberg[1], A. Kaminitz[1], D. Bar On[2], I. Ben Eliezer[2], O. Iancu[2], T. Taura[2], D. Wilson[2], P. Ayton[2], R. Satchi-Fainaro[1], **A. Madi**[1];
[1]Tel Aviv University, Tel Aviv, Israel, [2]Teva Pharmaceutical Industries Ltd., Tel Aviv, Israel

PD1$^{\pm}$ CD8$^{\pm}$ tumor-infiltrating T-cells have been at the forefront of cancer immunotherapies due to their antigen-specificity, cytotoxicity, proliferative capacity, and stem-like/memory properties. IL-2 is essential for T cell growth and proliferation, however, its systemic administration at a high dose was associated with intolerable toxicities, while low-dose treatment contradicted the intended therapeutic effect by activating regulatory T cells.To overcome the limitations of IL-2, we fused modified IL-2 sequences with reduced affinity for the murine IL-2 receptor to a PD1 antibody designed to target the PD1$^{\pm}$ T cells found in tumors. The resulting murine PD1 antibody-attenuated-IL-2 (mAnti-PD1-IL2Att) demonstrated similar IL-2 potency on PD1$^{\pm}$ cells as native IL-2, but diminished potency by orders of magnitude on PD1^{-} cells. The agent was furthermore designed to bind PD1 non-competitively with known PD1-blocking antibodies, so that it could be used in combination with them to achieve effective anti-tumor response. We demonstrated that mAnti-PD1-IL2Att exhibits potent anti-tumor activity, resulting in complete tumor regression in a syngeneic MC38 colorectal cancer model, and significant anti-tumor activity in other models of different tumor types. The mechanism was evaluated by immunophenotyping and single-cell RNAseq. Shortly after the first administration of mAnti-PD1-IL2Att, CD8$^{\pm}$ T cells, rather than Tregs, emerged as the primary responding cells; these CD8$^{\pm}$ T cells exhibited increased proliferation and activation with reduced expression of exhaustion markers (PD1$^{\pm}$Tim3$^{\pm}$). Following subsequent doses, there was a notable increase in the number of effector cells, followed by a prolonged generation of effector and memory cells at a later stage. Myeloid cells exhibited increased transcriptional programs related to chemotaxis, co-stimulation, and co-inhibition, including the upregulation of the PD1-PDL1 pathway. By contrast, blockade of PD1 with a naked PD1 antibody led to distinct cellular responses and less pronounced anti-tumor activity, and a combination of the blocking antibody with PD1-attIL-2 was superior to either agent alone. Together, our findings suggest that mAnti-PD1-IL2Att potent anti-tumor activity was driven by its direct targeting of PD1$^{\pm}$ on tumor-infiltrating CD8$^{\pm}$ T-cells, shedding light on the specific changes in their dynamic differentiation trajectory and their impact on the tumor microenvironment.

#4058 Nanoparticle delivery of interleukin-2 induces anti-tumor immune response and therapeutic efficacy in mouse tumor models.

R. Wang[1], A. Wallstrum[2], N. White[2], P. Kumar[1], T. Watcharawittayakul[2], N. A. Crumrine[2], C. Baker[2], J. Saito[2], M. Reda[2], W. Ngamcherdtrakul[2], W. Yantasee[1]; [1]Oregon Health & Science University, Portland, OR, [2]PDX Pharmaceuticals, Inc., Portland, OR

Immune checkpoint inhibitors (ICIs) have demonstrated robust responses in some solid tumor types. However, the low response rate, which is associated with lack of pre-existing tumor-infiltrating lymphocytes (TILs), remains a significant challenge. Interleukin-2 (IL-2) can effectively expand TILs and has been FDA-approved for metastatic renal cancer and melanoma. However, IL-2 has several drawbacks—including short circulation half-life, dose-limiting toxicities, and counterproductive activation of regulatory T cells (Tregs)—resulting in less than 10% complete response rate. Numerous efforts have been made to enhance IL-2 formulations, but none have yet received FDA approval.

In this study, we utilized our proprietary nanoparticle platform (Pdx-NP™) to improve IL-2 formulation. Pdx-NP™ can load IL-2 with near-complete binding, resulting in a 160-nm nanoconstruct (IL2-NP), suitable for both local and intravenous administrations. To evaluate the efficacy, we utilized bilateral melanoma (B16F10) and colon (MC38) tumor models, in which the local tumor was treated intratumorally for 3 doses and the distal tumor was left untreated to assess the systemic anti-tumor immune response. In the B16F10 model, IL2-NP treatment demonstrated favorable immune profiles in local and distal tumors and the draining lymph nodes, such as increased CD8+ T cell proliferation, CD8+ T cells/Treg ratio, and recruitment of dendritic cells and macrophages, compared to saline or free IL-2 counterparts. These positive immune responses translated into significant growth reduction of IL2-NP treated tumors and improvement in survival of the mice compared to free IL-2. In the MC38 tumor model, the IL2-NP treatment resulted in complete regression of both local and distal tumors in 43% of the mice. When combined with ICIs (αPD-1 and αCTLA-4), the treatment achieved a cure rate of 100%, whereas ICIs alone yielded only a 29% cure rate.

In conclusion, IL2-NP induces robust proliferation and activation of TILs and is efficacious both as a monotherapy and in combination with ICIs. This is due to the ability of Pdx-NP™ to protect and retain therapeutics within tumors, with an 8-fold increase in tumor accumulation over the free drug counterpart. Our ongoing efforts are focused on the targeted delivery of IL-2 to tumors upon systemic administration, using αPD-L1 antibody-conjugated Pdx-NP™. This antibody-conjugated nanoparticle has an elimination half-life ($t_{1/2}$) of about 25 hrs in non-human primates. Paired with αPD-L1 for tumor homing, this nanoconstruct is hypothesized to enhance IL-2 accumulation in tumors compared to free IL-2, which has $t_{1/2}$ of only 1.5 hrs in human. The current clinical landscape of cancer immunotherapy focuses on combinational approaches, and our versatile Pdx-NP™ platform, which is capable of co-delivering different classes of therapeutics, is well suited for this endeavor.

#4059 Vitokine-2: A TIL-targeting tumor activable engineered IL-2 for cancer treatment.

S. V. Challa, Y.-T. Hsieh, K. Gelinas, A. Umana, W.-c. Weng, T. Berisha, C. Stephens, Y. Li, J. Xu;
Cugene, Waltham, MA

Background: Interleukin-2 is the first approved immune-oncology (IO) drug to treat multiple metastatic cancers with durable and curative antitumor effects. Yet, its application is restricted due to severe toxicity, short half-life, and a small fraction of response rate. To reduce toxicity and improve efficacy, we developed Vitokine-2, a tumor infiltrating lymphocyte (TIL)-targeting, tumor activable, and precision engineered IL-2 that remains inert systemically but activated in the tumor microenvironment (TME).

Methods: Through protein and structure-guided precision engineering, the biological activity of IL-2 was optimized, concealed, guided to exhausted TILs, and activated at TME. The biological activity was determined by measuring proliferation (Ki67) of CD8+ T and NK cells using human peripheral blood mononuclear cells (PBMCs). Pharmacokinetics (PK), pharmacodynamics (PD), and anti-tumor efficacy were evaluated in mice, encompassing healthy and multiple syngeneic tumor mouse models.

Results: Vitokine-2 was inactive in stimulating CD8+T and NK cell proliferation in vitro. Yet, its biological activity was fully restored following the cleavage and release of the concealing domain. Vitokine-2 displayed a significantly prolonged in vivo pharmacokinetic profile due to half-life extension, concealing and reduction of target sink. Administration of Vitokine-2 in mice resulted in minimal or no detectable activation, proliferation, and expansion of cytotoxic CD8+T and NK cells in the systemic circulation. However, marked CD8+ T cell proliferation and expansion with enhanced expression of granzyme B, a cytotoxic functional biomarker, was observed within the TME. The effect was specific to cytotoxic lymphocytes but not regulatory T cells. Corroborating with the expansion and enhanced functionality of CD8+ T cells in TME, robust antitumor efficacy was observed with Vitokine-2 but not with the non-activable IL-2 counterpart. Furthermore, dose-dependent tumor killing efficacy and complete eradication of tumors were demonstrated in multiple syngeneic tumor models. Vitokine-2 was found to be safe and well tolerated with minimal interferon gamma release and body weight loss even at much higher doses.

Conclusion: Vitokine-2 is a TIL-targeting, tumor activable and precision engineered IL-2. It demonstrated robust anti-tumor efficacy with minimal systemic toxicity. It is safe, well tolerated, and permits high dose administration, yielding a widened therapeutic window. Vitokine-2 presents a paradigm-shifting, potentially a first-in-class, highly safe and efficacious IO therapy with an immense potential to address both IO-responsive and unresponsive patient population.

#4060 Characterization of MDNA113, a tumor-targeting anti-PD1-IL-2^{SK} immunocytokine with conditional activation to increase tolerability and maximize efficacy.

A. Sharma, M. D. To, Q. Liu, F. Merchant;
Medicenna Therapeutics, Toronto, ON, Canada

Background-MDNA113 consists of an IL-13 decoy receptor-binding domain (MDNA213) fused to anti-PD1-IL-2^{SK} (MDNA223) immunocytokine using a matrix metalloprotease (MMP) sensitive linker (PSL). MDNA213 is an IL-13 superkine with high selectivity towards IL-13Rα2, a tumor associated antigen overexpressed in numerous aggressive solid tumors with limited expression in normal tissues. IL-13Rα2 overexpression is associated with MMPs abundancy in tumor microenvironment (TME) and poor clinical outcomes. MDNA223, a fusion of 'not-alpha, beta enhanced' IL-2 superkine with anti-PD1 is designed to facilitate cis-binding to PD1 and IL-2Rβγ on CD8^{+} T cells. MDNA223 is superior to co-administration of anti-PD1 and IL-2 agonist at inhibiting both immunologically 'hot' and 'cold' tumors in mice. MDNA113 is designed to target and accumulate in tumors via the MDNA213 domain, which also attenuates immune stimulation by hindering IL-2R activation to reduce peripheral activity. The dual targeting/masking MDNA213 domain is released within tumor microenvironment following MMP cleavage of PSL to fully restore IL-2R agonism while maintaining PD1/PDL-1 blockade.

Methods-*In vitro* signaling studies were performed in reporter cell assays and human PBMCs. Tolerability and pharmacodynamic studies were conducted in mice. Tumor growth inhibition was assessed in syngeneic mouse tumor models in monotherapy and combination settings.

Results-MDNA113 showed reduced IL-2R agonism (~38-fold) while maintaining PD1/PD-L1 blockade compared to MDNA223 (non-masked) in cell-based reporter assays. Capacity to stimulate human PBMC proliferation was reduced while potency in CD8+ T cell p-STAT5 signaling also decreased. MMP cleavage of MDNA113 to release MDNA213 domain fully restored IL-2R signaling. Systemic delivery of MDNA113 to mice showed reduction, but not complete blockade, of lymphocyte expansion compared to equimolar dose of MDNA223. A 3x increase in MDNA113 restored lymphocyte expansion to a similar level achieved with MDNA223, indicating a 'partial masking' effect of MDNA213 domain. Accordingly, MDNA113 was better tolerated than MDNA223 in viability studies in mice. In syngeneic tumor models, equimolar treatment with MDNA113 and MDNA223 (non-mask version) resulted in similar extent of tumor growth inhibition. In contrast, in vivo activity was partially compromised when mice were treated with a non-cleavable version of MDNA113, consistent with a role for MMP-cleavage to restore full anti-tumor effect within TME.

Conclusion-MDNA113 is a tumor-targeting and conditional-activatable anti-PD1/IL-2^{SK} fusion characterized with potent PD1/PDL1 blockade and 'not-alpha, beta enhanced' IL-2R agonism. MDNA113 is better tolerated than the non-mask version while achieving similar effect on tumor control, therefore offering a much broader therapeutic index.

#4061 Preclinical characterization of MBS309, a conditionally active PD-1-dependent IL-2 mutation with significantly superior anti-tumor efficacy with safety.

J. Li, **G. Lin**, L. Zhang, F. Li;
Beijing Mabworks Biotech Co Ltd, Beijing, China

Although PD-1/PD-L1 therapies have shown significant benefit among a range of tumor types, the majority of malignancy patients do not respond or develop resistance after initial tumor regression. Development of new modality to overcome primary and acquired resistance to anti-PD-1/PD-L1 therapy is a huge unmet medical need, and IL-2 is believed a potentially powerful approach for that. However, the current clinical application of IL-2 in cancer immunotherapy has been limited by its severe toxicity. Herein, we developed MBS309 (PD1/IL2m), a novel PD-1-targeted IL-2 mutation with significantly enhanced therapeutic window. MBS309 has the similar high affinity and blockade efficacy with monoclonal antibody to PD-1, and its IL-2 mutation has reduced binding to IL-2Rβγ and abolished binding to IL-2Rα. Our *in vitro* assays, including HEK-blue assay and $CD3^{+}$ T cell assay, both indicated that the IL-2 receptor agonist activity of MBS309 was conditionally induced only the antibody cis-binding to both PD-1 and IL-2 Rβγ. And the maximal agonist activities of MBS309 in HEK-blue assay and $CD3^{+}$ T cell assay were much lower than wild-type IL-2 and RG6279 analog enabling its high tolerated drug doses *in vivo*. In our *in vivo* tumor murine models, 1mg/kg MBS309 showed much better suppression effect in MC38/hPD-L1 tumor than 1mg/kg RG6279 analog and Pembrolizumab (1mg/kg) combination with wild type IL-2 (0.1mg/kg) ; And MBS309 at the dosage of 5mg/kg can significantly inhibit tumor growth in PD-1 resistant Pan-02 xenograft models without any side-effects observed, while RG6279 analog at the dosage of 5mg/kg induced severe body reduction of the mice and resulted in 80% (4/5) mice death after two dosages. MBS309 showed similar PK profile with anti-PD-1 monoclonal antibody and much better than RG6279 analog in mouse model. 20mg/kg of MBS309 was well tolerated in mouse, while 10mg/kg of RG6279 analog or PF-07209960 analog show severe toxicity and resulted in death of all the mice. Pharmacodynamic studies in murine models showed that MBS309 prioritized active tumor infiltrated $PD\text{-}1^{+}$ CD8 T cells rather than other organs. Taken together, MBS309 effectively expands tumor infiltrated T-cells, and avoids system immune cytokine side effects compared to other PD-1-targeted 2nd generation IL-2Rβγ agonist modalities currently in clinical development. And it shows much higher anti-tumor effect compared to anti-PD-1/-L1 antibodies alone in both PD-1 sensitive and resistant tumor models. MBS309 has demonstrated a favorable safety profile and highly anti-tumor activities *in vivo*, which has the potential to supporting its clinical development for the treatment of cancer.

#4062 A novel method for generating regulated cytokine therapeutics: Safety and activity of a conditionally active cLAG3-IL2 capable of delivering IL2 to LAG3+ cells while remaining inert on LAG3- cells.

J. Killebrew, S. Okada, L. Amon, D. Bienvenue, L. Carlucci, D. Colby, W. Curtis, K. Daniels, A. Etheridge, Z. Kraft, J. Nguyen, S. Notonier, J. Pham, M. Sprague, K. Thomas, D. Hollenbaugh, J. Mulligan;
Bonum Therapeutics, Inc., Seattle, WA

IL-2 is a powerful cytokine central to the generation of an effective immune response. However, its use in cancer immunotherapy has been limited by toxicities arising from its broad activity as well as the narrow patient population in which efficacy is seen. To address these limitations, many strategies have been pursued including IL-2 attenuation and targeting of IL-2 activity. These approaches, however, retain unacceptable toxicity and/or are not targeted to the appropriate cell populations. Using a novel approach that takes advantage of the ability of an antibody to bind specifically and competitively to two distinct antigens, we have generated a conditionally active cLAG3-IL2 therapeutic that targets IL-2 to $LAG3^{\pm}$ cells while remaining inert on IL-2Rβγ+ cells lacking LAG3 expression, even at high treatment doses. As a marker of antigen-activated and tumor-specific T cells, LAG3 is an ideal target toward which to direct IL-2 activity. In vitro, using both reporter cell lines and receptor binding assays, the regulated cLAG3-IL2 demonstrates >100 fold difference in activity in the presence or absence of LAG3. In primary immune cells, regulated cLAG3-IL2 preferentially induces IL-2 cis-signaling in activated human $LAG3^{\pm}$ CD8 T cells compared to $LAG3^{-}$ T cells. In mouse syngeneic tumor models, cLAG3-IL2 inhibits tumor growth while avoiding clinical signs of IL-2-mediated toxicity at doses well above the level where the non-regulated IL2 is toxic. Additionally, cLAG3-IL2 does not induce expansion of circulating $LAG3^{-}$ IL-2Rβγ+ cell populations, including NK cells and $LAG3^{-}$ T cells. In the TME, cLAG3-IL2 drives the expansion and activation of tumor-specific CD8+ T cells. Furthermore, cLAG3-IL2 demonstrates robust combinatorial activity with anti-PD1. These results demonstrate the strength of the Bonum platform, currently applied to multiple target/effector pairs including PD1, PDL1, ATP, LRRC15 and effectors IFNα, IL12 and TGFβ inhibition, and support the clinical development of our conditionally active cLAG3-IL2.

#4063 SAR445877, an anti-PD-1 antibody-IL-15 mutein fusion protein restores function to exhausted T cells.

I. Pratumchai[1], M. Bernardo[2], K. L. Marquardt[1], C. Zhu[2], F. Menas[3], R. Carrio[4], T. Byers[4], D. Shaffer[2], X. Li[2], J. R. Teijaro[1];
[1]The Scripps Research Institute, San Diego, CA, [2]Sanofi, Boston, MA, [3]Sanofi, Madrid, Spain, [4]Sanofi, Orlando, FL

During persistent viral infections and cancer, antigen-specific T cells become exhausted, express elevated levels of inhibitory receptors and gradually lose their functional potential. Immune checkpoint blockade can restore function of exhausted T cells to result in tumor clearance, however, only a minority of cancer patients see durable tumor control. Immune-stimulatory cytokines can augment the antitumor efficacy of checkpoint blockade, but their clinical use is marred by substantial toxicity. SAR445877 (SAR'877, formerly KD050), is a novel antibody-cytokine fusion protein consisting of Fc silenced human anti-PD-1 IgG1 fused to a mutated interleukin-15 (IL-15)/IL-15 receptor alpha sushi domain fusion, which can cis-activate direct cytokine stimulation to effector T cells and alleviate off target binding and the resultant toxicity. Here, we leveraged existing models of chronic antigen exposure to characterize the potential of SAR'877 to restore activity of exhausted T cells.C57BL/6 mice exposed to lymphocytic choriomeningitis virus (LCMV) Clone 13 develop persistent viral infection that results in development of dysfunctional, exhausted T cells. We tested the SAR'877 murine surrogate molecule (mKD050) using the LCMV Clone-13 (CL13) infection model for its ability to promote T cell function *in vitro*, *in vivo,* and to control viral infection. Treatment of exhausted T cells with mKD050 *in vitro* was able to increase expansion and cytokine production of antigen-specific CD8 T cells which was superior to anti-PD-1 antibody or non-targeting antibody-IL15/IL-15Ra fusion protein (mntKD050). Moreover, *in vivo* treatment of CL13 infected mice with mKD050 increased the numbers and functional output of antigen-specific CD4 and CD8 T cells compared to anti-PD-1 or mntKD050 treatments. Further, mKD050 increased the frequency of antigen-specific $TCF1^{+}TIM\text{-}3^{-}$ stem-like CD8 T cells, which are critical to maintaining the T cell pool during chronic viral infection and cancer. The enhanced T cell function observed following treatment with mKD050 translated to hastened clearance of CL13. Finally, the hastened CL13 clearance observed following mKD050 treatment required an intact CD4 T cell compartment. Given the robust activity of mKD050 in reinvigorating dysfunctional T cells in a mouse model of chronic viral infection, we utilized the MIMIC CD8 T cell exhaustion model to explore whether SAR'877 could rescue the function of exhausted human T cells. SAR'877 stimulated proliferation and functional activity of exhausted human CD8 T cells *in vitro*. SAR'877 more potently induced proliferation and IFNγ and granzyme B production compared to anti-PD-1 and non-targeted IL15 mutein alone. Together, these results demonstrate that the PD-1 targeted IL15 mutein SAR'877 rescues the functional activity of chronically stimulated, exhausted T cells.

#4064 hetIL-15 and Fenofibrate combination alters the metabolic fitness of tumor-infiltrating CD8$^{\pm}$T cells leading to TNBC tumor eradication in mice.

D. Stellas[1], S. Karaliota[2], V. Stravokefalou[1], K. C. Goldfarbmuren[3], B. Myers[2], G. N. Pavlakis[1], B. K. Felber[1];
[1]National Cancer Institute at Frederick, Frederick, MD, [2]Frederick National Laboratory for Cancer Research, Leidos Biomedical Research, Inc., Frederick, MD, [3]Advanced Biomedical Computational Science, Frederick National Laboratory for Cancer Research, Leidos Biomedical Research, Inc., Frederick, MD

Introduction: Tumor-infiltrating cytotoxic CD8$^{\pm}$T cells frequently undergo an altered state of differentiation referred to as "exhaustion" and, as a result, they fail to control tumor growth. IL-15 is a cytokine which stimulates the generation, proliferation and cytotoxic function of tumor CD8$^{\pm}$T and NK cells. We have produced the native heterodimeric form of IL-15 (hetIL-15) which has advanced in clinical trials. The aim of this study was to overcome the exhaustion of the tumor-infiltrating CD8$^{\pm}$T cells and to increase their cytotoxicity, using Fenofibrate (FF), a PPAR-α agonist, in combination with hetIL-15.
Experimental Procedures: We have evaluated the therapeutic efficacy of hetIL-15 immunotherapy as a monotherapy and in combination with FF in the murine EO771 orthotopic breast cancer model. The effects of hetIL-15 and/or FF on immune cells and on tumor microenvironment were analyzed by flow cytometry, transcriptomics, metabolomics and proteomics. The metabolic profile of tumor-infiltrating T cells was performed with Seahorse analysis.
Results and Conclusions: hetIL-15 monotherapy resulted in tumor eradication in 40% of treated mice and increased survival. Seahorse analysis of tumor-infiltrating CD8$^{\pm}$T cells confirmed a rise in oxygen consumption rate (OCR) with substantial increase of spare respiratory capacity. Upon hetIL-15 treatment, tumor-infiltrating CD8$^{\pm}$T cells showed elevated extracellular acidification rate (ECAR), resulting in a pronounced shift in the OCR/ECAR ratio in comparison to control, confirming their increased proliferating status. These tumor-infiltrating CD8$^{\pm}$T cells also showed increased mitochondrial potential and/or mass and fatty acid (FA) uptake, as evidenced by increased MitoTracker and Bodipy staining, respectively. Transcriptomic analysis revealed increased expression of genes involved in several metabolic pathways such as oxidative phosphorylation, FA oxidation and glycolysis. Monotherapy with FF had no effect on tumor growth delay, whereas the FF- hetIL-15 combination resulted in complete eradication of the tumors in 85%. Combination therapy reshaped the tumor microenvironment, resulting in higher IFN-γ and in differentially expressed metabolites as shown by tumor proteomics and metabolomics, respectively. The combination treatment increased the mitochondrial function, FA uptake and OCR, revealing a more metabolically active phenotype. We conclude that hetIL-15 supports a favorable metabolic profile of intratumoral effector lymphocytes, important for their function. Our data suggest that metabolic reprogramming of tumor specific CD8$^{\pm}$T cells using FF is a promising strategy to overcome T cell exhaustion and to promote survival in a metabolically hostile tumor microenvironment.

#4065 Entinostat synergizes with the IL-15 superagonist N-803 and anti-PD-1 to engage cDC1 and stem-like TCF-1^{+} CD8^{+} T and NK cells to overcome colorectal tumors refractory to anti-PD-1 therapy.

C. M. Minnar, M. Miyamoto, A. S. Khelifa, G. Lui, K. L. Lothstein, P. L. Chariou, T. J. Meyer, A. Lobanov, M. Cam, J. Schlom, S. R. Gameiro;
National Cancer Institute, Bethesda, MD

Background: Immune checkpoint blockade (ICB) has limited efficacy in colorectal carcinoma (CRC), where ~85% of patients harbor microsatellite stability (MSS). A minor subset of CRC patients (~15%) harbor microsatellite instability (MSI) and demonstrate improved responses to ICB ranging from 30-50%. Combination therapy has the potential to increase the response rate. Entinostat, a class I HDAC inhibitor, has demonstrated potential to enhance ICB efficacy, such as αPD-1 and immunostimulatory cytokines. N-803, a heterodimeric IL-15 superagonist that enhances proliferation and activation of CD8^{+} and NK cells has demonstrated to enhance the clinical benefit of Nivolumab in non-small cell lung cancer patients that were relapsed or refractory to αPD-1 monotherapy. Here, we investigated the antitumor efficacy and mode of action of combination therapy comprising αPD1, Entinostat, and N-803 in αPD1-refractory CT26 and Jak1-deleted MC38 CRC tumor models.

Methods: Entinostat, N-803, and αPD1 alone or in combination were administered to mice bearing established CT26 or Jak1-deleted MC38 tumors. Antitumor efficacy, survival, and protective memory upon tumor rechallenge were monitored. Comprehensive flow cytometric profiling of the tumor microenvironment (TME), tumor-draining lymph node (tdLN), and spleen cell populations was conducted. CT26 tumor and tdLN immunomes were examined by single-cell transcriptomics. Cytokines and chemokines were examined in the TME and sera. Antigen-specific IFNg T cell responses were evaluated by ELISpot.

Results: We demonstrated that combination therapy with Entinostat, N-803 and αPD1 elicits potent suppression of CT26 and Jak1-deleted MC38 tumors, with median overall survival increasing 33% to not reached. These effects were associated with increased activation, infiltration, cytokine production, and cytolytic function of tumor CD8^{+} T and NK cells, and increased sera IFNg and TNFα. Tumor resolution and protective memory were associated with development of p15e-specific T cell responses. Increased migration of CD8^{+} T cells and cross-presenting dendritic cells (cDC1) to the tdLN, as well as significant enrichment of cross-presentation genes in tumor cDC1s was observed. Transcriptomic and phenotypic analyses demonstrated increased stem-like TCF-1^{+} CD8^{+} T cell accumulation in the tdLNs and TME of mice treated with triple combination.

Conclusions: Combination therapy with Entinostat plus N-803 and αPD1 synergized to promote a sustained antitumor response and prolonged survival. We hypothesize the antitumor effects were due to collaborative efforts of CD8^{+} T and NK cells, and cDC1 cells in tdLN and TME. These results provide a rationale for the clinical testing of αPD1, Entinostat and N-803 combination for patients with CRC, including those with acquired resistance to ICB.

#4066 Generation of tumor targeted self-assembling split IL-12 subunits for the treatment of cancer.

J. Heiber, P. Gurel, R. G. Newman, K. Dreaden, Y. Zhao, C. Wang, S.-P. Pearson, J. Chamoun;
Mural Oncology, Waltham, MA

A major milestone in immuno-oncology was the development of immune checkpoint inhibitors, resulting in significant benefits for numerous patients. However, many patients are not responsive, become refractory, or cannot tolerate the treatment due to toxicity or side effects, demonstrating the need for additional immunotherapies. Cytokines are a class of promising immunomodulatory proteins being explored as therapeutics, but their success has been limited due to their rapid clearance or pleiotropic properties. Classically known as 'signal 3' of an endogenous immune response, IL-12p70 is a heterodimeric cytokine comprising p35 and p40 subunits. When administered exogenously, IL-12 is a potent stimulator of the immune system and can have profound anti-tumor activity; however, the clinical use of IL-12 has been limited due to poor systemic tolerability. Therefore, developing an immunotherapy that can be systemically administered and improve the therapeutic index could capitalize on the potential clinical benefit of IL-12. Mural Oncology has developed an innovative approach to mitigate the toxicity of IL-12 by splitting the heterodimer into inactive p35 and p40 monomers. The individual subunits are separately fused to two non-competitive antibody fragments targeting a highly expressed tumor-associated antigen. The goal of this approach is to conditionally activate IL-12 preferentially in the tumor microenvironment (TME). This is achieved by sequential administration of the targeted subunits, which will drive assembly and activity of the IL-12 heterodimer primarily at the tumor site, reducing systemic exposure and thereby potentially reducing associated toxicities. To engineer the split IL-12 subunits, a structure-based rational design approach was used to remove the natural intra-molecular disulfide bond and generate variants that maintained affinity between the p35 and p40 monomers. The engineered subunits were characterized using analytical methods and screened for the pair with the strongest affinity. Additionally, the candidate pair was assessed for receptor binding and functional activity on human T cells through phosphorylation of STAT4 and secretion of IFN-γ. Pharmacokinetics and pharmacodynamics were evaluated in mouse models with and without tumors demonstrating that dual targeting led to an increase in tumor retention, rapid clearance from circulation, and dose dependent release of IFN-γ. The results thus far demonstrate that the innovative approach of tumor targeted self-assembling split IL-12 has the potential to enhance the overall therapeutic potential of this cytokine. A development candidate will be identified and moved into clinical testing in cancer patients to enable us to fully understand if this design approach holds true in the clinical setting.

#4067 Development of tumor-restricted IL-12 with antigen-dependent expression and localized IL-12 activity.

S.-H. Huang[1], T. M. Davenport[2], H. F. Moffett[2], B. D. Weitzner[2], L. Cassereau[1], L. E. Baker[2], B. Hammerson[2], S. Zhuang[1], C. Saechao[1], L. Song[2], J. Mimms[2], D. Chian[1], C. Sims[1], H. Hiraragi[1], M. J. Lajoie[2], S. E. Boyken[2], **B. Boldajipour**[1];

[1]Lyell Immunopharma, South San Francisco, CA, [2]Outpace Bio, Seattle, WA

IL-12 is an immune-stimulatory cytokine that can modulate the tumor microenvironmnent (TME) to enhance the cytotoxic activity of T and NK cells; however, IL-12 expression by T cells caused severe toxicity in a previous clinical trial. Using Outpace's OutSmart™ technology, we designed a tumor-restricted IL-12 (trIL-12) that is under control of an activation-inducible promoter and auto-inactivates within minutes after secretion.

T cells were engineered via lentiviral vectors (LVV) to express wild-type single-chain IL-12 (WT scIL-12) or trIL-12 under the control of an activation-inducible promoter; a second LVV introduces an NY-ESO-1 TCR. Kinetics of IL-12 expression was measured by qPCR and MSD technology; kinetics of IL-12p70 heterodimer half-life was measured using Octet bio-layer interferometry (BLI). T-cell cytotoxicity and cytokine production was evaluated in vitro after repeated stimulation with NY-ESO-1 expressing target cells using Incucyte and MSD. IL-12 activity in bystander cells was measured by detection of IFN-γ using flow cytometry. In vivo T-cell function of trIL-12-engineered NY-ESO-1 TCR T cells was measured in NSG MHCI/II KO mice bearing A375 xenografts. trIL-12 activity in a fully immune-competent mouse model was measured in B6 mice implanted with B16F10 tumor cells engineered to express murine surrogates of trIL-12.

Expression of WT scIL-12 under the control of an activation-inducible promoter peaks within 6 hours after activation and produces sufficient IL-12 to improve T-cell function in vitro and in vivo. trIL-12 was created by inclusion of a cleavable linker and elimination of the covalent disulfide bond between the p35 and p40 subunits of IL-12p70, resulting in dissociation of the functional cytokine within 10 minutes post-cleavage. Additional mutations further reduce the IL-12p70 half-life. trIL-12 activates the IL-12-producing T cells, as well as proximal bystander T-cells in direct co-culture, but it does not have the ability to activate distal bystander T-cells separated by Transwell membranes. In xenograft mouse models, trIL-12-expressing T cells have improved proliferation upon antigen recognition and display potent anti-tumor activity and cytokine production without showing systemic IL-12 accumulation. Furthermore, in fully immune competent mice, expression of a murine trIL-12 surrogate by tumor cells led to generation of potent anti-tumor responses without systemic trIL-12 accumulation and reduced systemic IFN-γ.

trIL-12-engineered T cells generate potent anti-tumor activity in vitro and in vivo. Unlike WT scIL-12, trIL-12 activity is localized to the region around the producing T cell and systemic IL-12 exposure is not observed in vivo. Collectively, these preclinical data suggest that trIL-12 may enable the development of potent T-cell therapeutics while maintaining an acceptable safety profile.

#4068 *In vitro* masked effect, *in vivo* anti-tumor activity and toxicology study of KGX101, an interleukin-12 prodrug, in monotherapy or in combination with anti-PD-L1 antibody.

Shumin Yang, Nuo Li, Jing Wang, Li Ma, Yi Zhao, Hui Chen, Haixiang Wu, **Weidong Jiang**

Shanghai KangaBio Co., Limited, Shanghai, China

Interleukin-12 (IL-12) has long been limited in its clinical use due to its short half-life ($t_{1/2}$) and dose-related toxicity, despite its remarkable ability to activate effector functions in T cells and natural killer (NK) cells. To address these challenges, we engineered an IL-12 prodrug called KGX101. In KGX101, the C-terminus of IL-12 is fused with ADCC-impaired IgG1 Fc to extend its half-life. Meanwhile, the N-terminus is concealed with its corresponding receptor soluble domains, IL-12Rβ1 and IL-12Rβ2, using tumor-specific protease cleavable linkers. This innovative design prevents systemic immune system overactivation. Once the linker is cleaved by tumor microenvironment (TME)-specific proteases, KGX101 functions like IL-12, effectively stimulating T cells and NK cells, reshaping the TME, and displaying significant potential in cancer therapy. To confirm KGX101's masking effect, we conducted IFNγ induction efficacy tests using peripheral blood mononuclear cells (PBMCs) from three donors. KGX101 demonstrated a 300 to 2500-fold reduction in activity compared to unmasked IL-12-Fc. Importantly, the masking effect of KGX101 was nearly abolished after protease digestion, affirming its mechanism of action. To further establish KGX101's effectiveness, we conducted *in vivo* antitumor studies in hPBMC xenograft mouse models using human colorectal cancer HCT116 and PD-L1-overexpressed human malignant melanoma A375. Mice were subcutaneously implanted with a specific mixture of cancer cells and hPBMCs, and then intravenously injected with PBS or KGX101 at various dose levels twice a week for 4-5 cycles. Compared to the PBS control group, KGX101 demonstrated up to a 42% tumor growth inhibition (TGI) in the HCT116 model at 0.18 mg/kg and a 76% TGI in the hPD-L1-A375 model at 0.06 mg/kg. Analysis of tumor-infiltrating lymphocytes (TILs) revealed that KGX101 increased the percentage of T cells in the tumor environment in a dose-dependent manner. We also evaluated the combination of KGX101 with an anti-PD-L1 antibody in an HCT116/hPBMC xenograft mouse model, which showed limited response to anti-PD-L1 monotherapy. The TGI% for KGX101 at 0.06 mg/kg, anti-PD-L1 antibody at 1 mg/kg, and their combination were 36.56%, 6.93%, and 66.22%, respectively, demonstrating a promising antitumor synergy. In terms of pharmacokinetics, a single dose of KGX101 at 0.06 mg/kg and 0.18 mg/kg in the HCT116/hPBMC xenograft mouse model resulted in a serum half-life ranging from 52.75 to 64.87 hours, while the $t_{1/2}$ in *Cynomolgus* monkeys was approximately 3 days. In a 4-week repeat dose toxicity study in *Cynomolgus* monkeys, the highest non-severely toxic dose (HNSTD) of KGX101 was determined to be 0.1 mg/kg. The results from nonclinical toxicology studies support the potential of KGX101 as a well-tolerated therapy for the First-in-Human (FIH) clinical trial.

#4069 IL12-expressing genetically engineered myeloid cells remodel the stromal dense and T cell poor tumor microenvironment and premetastatic niche of F42010 murine osteosarcoma.

K. Jackett, A. Browne, S. Kaczanowska, M. Clements, R. Kaplan, K. Wessel, B. Ball, J. Cronk;
National Institutes of Health (NIH), Bethesda, MD

Treatment options for patients with metastatic and recurrent osteosarcoma are poor. The development of immunotherapies for osteosarcoma has been hindered by the lack of immunocompetent preclinical models that recapitulate the stromal dense, myeloid-rich, T cell poor, and overall immunosuppressive microenvironment of human osteosarcoma. We hypothesized that the syngeneic murine osteosarcoma model F42010 may serve as a useful immunocompetent preclinical model of osteosarcoma suitable for developing novel immunotherapies for osteosarcoma. To test this, we used flow cytommetry, bulk RNA sequencing, and immunohistochemistry to characterize the stromal and immune compartments of this model. We found that the F42010 osteosarcoma model recapitulates the ECM-rich and immunosuppressive nature of human osteosarcoma primary tumor and pre-metastatic microenvironments, characterized by increased myeloid infiltrate expressing suppressive markers and lymphocyte exhaustion. Finally, we used this model to test the utility of a myeloid immunotherapy for osteosarcoma, IL-12 secreting genetically engineered myeloid cells (IL12-GEMys) that can reverse immune suppression in the pre-metastatic niche and tumor microenvironment. IL12-GEMy treatment augmented immune activation and significantly extended survival by delaying tumor growth. Our findings highlight that the F42010 osteosarcoma model effectively replicates key features of the osteosarcoma tumor microenvironment and is a valuable model for developing novel tumor microenvironment and pre-metastatic niche modulating immunotherapies for osteosarcoma.

#4070 CIS-demasking cytokine linker technology allows a selective cytokine delivery to activated immune cells while sparing others and peripheral toxicity.

A. Morello, C. Mary, v. Thepenier, M. Seite, J. Durand, C. Batty, K. Biteau, J. Taurelle, G. Teppaz, A. Georges, N. Poirier;
OSE Immunotherapeutics, Nantes, France

Immunocytokines are promising new therapeutic approaches to enhance T-cell response by delivering interleukins into the tumoral site. Fusion of wild-type or attenuated interleukins to anti-PD-1 antibody has shown some efficacy to preferentially cis-activate PD1-expressing T-cells but on-target/off-tumor activity on PD-1-negative cells is still observed due to the high affinity of the cytokine to its receptor leading a broad systemic effect, toxicity, high clearance and low tumor biodistribution limiting the potential of some immunocytokines (e.g. anti-PD-1/IL-2/IL-15/IL-21). Various strategies have emerged to achieve localized cytokine activation using conditional strategies (*e.g.* allosteric modulators, MMP-cleavable linkers or pH-dependent binding) that remain challenging due to high dependency to specific TME composition (MMP, acidosis...). We developed the OSE-Cytomask® Platform, a universal and innovative linker technology allowing exclusive cytokine CIS-demasking upon binding of the fused antibody to its target without TRANS-activation associated with undesired effects (*e.g.* Toxicity). A series of different linkers were screened for optimal cis-activation of cytokine on PD1-expressing vs PD1-negative T-cells using different cytokines fused to a high-affinity anti-PD1. OSE-Cytomask® linker technology decreases IL-2 or IL-15 cytokine activity (pSTAT5 signaling) on PD1-negative cells while maintaining high activation of PD1-transduced T-cells even in co-culture. We confirmed activity of OSE-Cytomask® Immunocytokine on (PD1+) human T-cells while very low activation has been observed in naïve T-cells. Importantly, Cytomask® linker technology does not induce TRANS-activation on PD1-negative T-cells illustrating an innovative and strict CIS-demasking mechanism of action. *In vivo*, Anti-PD-1/IL-15 and/or anti-PD1/IL-2 OSE-Cytomask® molecules illustrated reduced toxicity after single or multiple injections (2mg/kg). High T-cell proliferation has been observed in tumor-micro-environment where PD1-expressing T cells are located. Low T-cell proliferation in periphery was seen, illustrating the potential of CIS-demasking technology to target the right T-cells at the right place. Altogether, OSE-Cytomask® linker technology illustrates specific intrinsic property to mask cytokine on naïve peripheral immune cells not expressing the target of the antibody while allowing selective CIS-demasking of the cytokine and CIS-activation of activated immune cells expressing (*e.g.* PD-1). This linker technology could be used with a broad range of cytokine to abrogate OFF-tumor cytokine activity associated with toxicity while selectively CIS-activating activated immune cells in the TME.

#4071 The first-in-class PD1-IL18 conjugate BPT567 induces potent anti-tumor immunity by preferentially activating PD1$^{\pm}$IL18R$^{\pm}$ intratumoral effector T cells in *cis*.

K. Martin[1], T. Luu[2], J.-P. Carralot[1], L. Gremlich[1], P. Herzig[2], C. Herr[1], R. Meoded[1], P. Moosmann[1], A. Goepfert[1], A. Zippelius[3], V. Pattabiraman[1], B. Kreft[1]; [1]Brightpeak Therapeutics AG, Basel, Switzerland, [2]Department of Biomedicine, Cancer Immunology, University of Basel and University Hospital Basel, Basel, Switzerland, [3]Department of Biomedicine, Cancer Immunology & Medical Oncology, University Hospital Basel, University Hospital Basel, Basel, Switzerland

Antibody-cytokine conjugates leverage orthogonal mechanisms of action (MoA) in one molecule to induce potent antitumor immune responses. PD-1-targeting conjugates are of particular interest since they preferentially target antigen-experienced PD-1$^{\pm}$ CD8$^{\pm}$ T cells enriched in the tumor microenvironment (TME) while simultaneously blocking the PD-(L)1 pathway and inducing potent cytokine receptor stimulation in the same CD8$^{\pm}$ T cell *in cis (cis*-signaling*)*. Interleukin 18 (IL-18) is a proinflammatory cytokine able to integrate both innate and adaptive immunity resulting in profound anti-tumor immune responses mediated by T effector and NK cells. BPT567 has been generated via chemical conjugation of the anti-PD-1 Ab Lipustobart^{TM} to an enhanced human IL-18 variant of increased potency and reduced sensitivity to IL-18 binding protein (IL-18BP). BPT567 is designed to specifically target and activate a subset of tumor-infiltrating PD-1$^{\pm}$ IL18R$^{\pm}$ CD8$^{\pm}$ T effector cells recently described to exhibit superior cytotoxic and proliferative activity (Codarri Deak et al., Nature 2022). Due to its ability to signal *in cis*, BPT567 shows enhanced potency as well as increased resistance to IL-18BP when analyzing IFNγ release *in vitro* in PD-1$^{\pm}$ cells. Subsequent PD-1 receptor occupancy analyses showed that it is fully sufficient for BPT567 to engage a low number of PD-1 receptors to induce maximum IFNγ release in NK92 cells expressing human PD-1. Strikingly, despite addressing overlapping epitopes in PD-1, even a 200-fold excess of pembrolizumab has no impact on the *in vitro* potency of BPT567. *In vivo*, BPT567 exhibits strong anti-tumor efficacy at significantly lower IL-18 doses compared to the combination of an untargeted antibody-IL-18 conjugate and an anti-PD1 Ab further corroborating the importance of *cis*-signaling as a unique MoA of this PD1-IL18 conjugate. Detailed analyses of tumor-infiltrating immune leukocytes (TIL) revealed that BPT567 triggers a preferential expansion of CD8$^{\pm}$ T effector memory cells within the TME. In line with this finding, activity in the MC38 tumor model is dependent on the presence of CD8$^{\pm}$ T cells while depletion of other immune cell subsets (e.g. NK cells, CD4$^{\pm}$ T cells, macrophages) had no impact on efficacy. Although not required for anti-tumor efficacy, CD4$^{\pm}$ T cells are essential for proficient formation of an immunological memory. In an effort to confirm findings generated in murine models in relevant human *ex vivo* systems, we analyzed the release of cytokines and chemokines in dissociated cells isolated from primary human tumor explants. Also in this human model, BPT567 is able to induce significantly stronger IFNγ release compared to either single agents or the combination of untargeted IL-18 and an anti-PD1 Ab, thus confirming the unique MoA of the PD1-IL18 conjugate triggering superior TIL activation in *cis*.

#4072 Unleashing natural IL-18 activity using an anti-IL-18BP blocker antibody induces potent immune stimulation and anti-tumor effects.

A. Menachem[1], Z. Alteber[1], G. Cojocaru[1], T. Kfir[1], D. Blat[1], O. Leiderman[1], M. Galperin[1], L. Sever[1], N. Cohen[1], K. Cohen[1], R. Granit[1], S. Vols[1], M. Frenkel[1], L. Faigenbloom[1], L. Soffer[1], K. Meyer[1], K. Menachem[1], H. Tilleman[1], D. Morein[1], I. Borukhov[1], A. Toporik[1], M. Perpinial Shahor[1], E. Tatirovsky[1], P. Ferre[2], **E. Ophir**[1];

[1]Compugen Ltd., Holon, Israel, [2]Compugen Ltd., Toulouse, France

IL-18 is an inflammasome induced proinflammatory cytokine that augments T and NK cell activity and stimulates IFNγ production. The activity of IL-18 is naturally blocked by a high affinity endogenous binding protein (IL-18BP). IL-18BP is induced in the tumor microenvironment (TME) in response to IFNγ upregulation in a negative feedback mechanism. By evaluating 88 human tumor specimens and serum samples we were able to show that IL-18 is upregulated in the TME (median 11.2ng/gr) compared to serum samples (median 0.3ng/ml). Moreover, we showed that most of the IL-18 is bound by IL-18BP. IL-18BP-bound IL-18 levels were largely above the amount required for T cell activation *in vitro* (1.2ng/gr), implying that blocking IL-18BP has the potential to release IL-18 in tumors above the minimum range required for immune system stimulation. Next, to assess whether tumor endogenous IL-18 levels released by IL-18BP blockade are sufficient to provoke anti-tumor responses, COM503, a high affinity (<1pM) anti-IL-18BP Ab, was generated and examined in T and NK cell-based assays. In a co-culture assay of tumor cells with ex-vivo stimulated human tumor infiltrating $CD8^{\pm}$ lymphocytes, COM503 was able to displace IL-18 from a pre-formed complex and enhance IFNγ (197%, p<0.01) and TNFα (84% p<0.01) secretion. Additionally, COM503 induced human NK cell activation as reflected by increased IFNγ secretion (26-fold, p<0.001). Finally, in human ex vivo dissociated tumor cells assay, COM503 mediated an increase in Granzyme B (25%), IFNγ (38%), TNFα (58%) and IL-12 (50%) production. *In vivo*, administration of an anti-mouse IL-18BP Ab resulted in potent anti-tumor responses and increased survival across multiple mouse tumor models. In orthotopic E0771 tumor model, anti-IL-18BP Ab induced significant tumor growth inhibition (91% TGI, p<0.0001), as well as pronounced TME-localized immune modulation. This modulation included an increase in $CD8^{\pm}$ T cells expansion (108.5%, p=0.015) and activation, specifically in polyfunctional effector $IFN\gamma^{\pm}GrB^{\pm}CD8^{\pm}$ T cells (259%, p=0.02) and $IFN\gamma^{\pm}TNF\alpha^{\pm}$NK cells (77%, p=0.001). Similarly, anti-tumor effects were shown in $MC38OVA^{dim}$ model (58% TGI, p<0.001), accompanied by a robust TME-localized immune modulation including increased $CD8^{\pm}$ T cells expansion (85%, p=0.009) and IFNγ secretion (76%, p=0.052). In contrast to immune modulation in the TME, no increase in inflammatory cytokines and lymphocyte numbers or activation state was observed in serum and spleen. Taken together, our data suggest that IL-18 is upregulated in the TME, mostly bound by IL-18BP, and could be exploited to induce pronounced TME-localized immune modulation. Anti-IL-18BP Ab approach has a leading edge in inhibiting tumor growth while avoiding peripheral toxicity associated with administration of a cytokine. COM503 is currently undergoing IND-enabling studies.

#4073 Decoy-resistant IL-18 enhances checkpoint inhibitor combinations beyond anti-PD-1 *in vitro* and *in vivo*.

J. N. Lindquist[1], K. Qin[2], A. M. Ring[2], H. Uppal[1];

[1]Simcha Therapeutics, Inc., San Francisco, CA, [2]Fred Hutchinson Cancer Center, Seattle, WA

Background: Interleukin-18 (IL18) is a proinflammatory cytokine that modulates both innate and adaptive immune responses. Historically, wild-type recombinant IL-18 has shown limited anti-tumor efficacy in preclinical models and clinical trials, likely due to upregulation of IL-18 binding protein (IL-18BP), a negative regulator of the IL-18 signaling axis. Accordingly, an engineered IL-18 cytokine capable of interacting with the IL-18 receptor, but resistant to IL-18BP interactions (i.e., “Decoy-Resistant IL-18”, DR-18), has demonstrated enhanced therapeutic potential in mouse tumor models, both as a single agent and in combination with anti-PD-1 [1, 2]. Here we evaluated murine DR-18 in combination with additional checkpoint inhibitors beyond anti-PD-1 in a set of mouse tumor models, and tested human DR-18 activity *in vitro*/*ex vivo* for activation of human immune cells and anti-tumor activity.

Results: Treatment with mDR-18 elicited strong efficacy as a single agent and combination activity with immune checkpoint inhibitors (ICIs) across diverse syngeneic mouse models of solid tumors. As a single agent, mDR-18 demonstrated robust single agent activity in tumor growth inhibition for MC38 (>80%), CT26 (>60%) and B16-F10 (>55%). Combination treatment of mDR-18 with anti-PD-1, anti-CTLA-4, or anti-LAG-3 increased the efficacy for the MC38 (>85-95%), CT26 models (>80-85%), while the B16-F10 (>60%) showed smaller efficacy enhancement with the combinations. *In vitro* assays revealed human DR-18 (ST-067) activated immune cells and enhanced A549 tumor cell killing over 72hrs. Furthermore, *ex vivo* studies of 3D patient-derived tumor spheroids demonstrated that ST-067 impaired growth and increased immune cell infiltration, highlighting the potential of hDR-18 to enhance immune activity within the human tumor microenvironment.

Conclusion: These studies expand the breadth of IL-18/checkpoint synergism beyond anti-PD-1 and confirm enhanced human immune response *in vitro* with the clinical candidate ST-067. Taken together, these findings strengthen the rationale for clinical combination of ST-067 with ICI agents in patients with solid tumors.

1.Zhou T, Damsky W, Weizman OE, et al. IL-18BP is a secreted immune checkpoint and barrier to IL-18 immunotherapy. *Nature*. 2020;583(7817):609-614. doi:10.1038/s41586-020-2422-62.Minnie SA, Waltner OG, Ensbey KS, et al. Depletion of exhausted alloreactive T cells enables targeting of stem-like memory T cells to generate tumor-specific immunity. *Sci Immunol*. 2022;7(76):eabo3420. doi:10.1126/sciimmunol.abo3420

#4074 Discovery of WTX-518, an IL-18 pro-drug that is conditionally activated within the tumor microenvironment and induces regressions in mouse tumor models.

K. R. Morris, H. Brodkin, K. Economides, D. J. Hicklin, J. LePrevost, C. Nagy-Domonkos, C. Nirschl, A. Salmeron, C. Seidel-Dugan, C. Spencer, Z. Steuert, W. M. Winston;
Werewolf Therapeutics, Watertown, MA

Systemic administration of proinflammatory cytokines is a promising approach to treat cancer. IL-18 has been shown to promote activation of both innate and adaptive anti-tumor responses in pre-clinical models. Specifically, IL-18 has been shown to impact macrophage suppressive function as well as drive CD4+ T cells towards a TH1 phenotype. However, IL-18 therapies have been hampered by a lack of efficacy due to the suppressive activity of IL-18 binding protein (IL-18BP), which binds to IL-18 and prevents its interaction with its receptor. Several groups have taken the approach of modifying IL-18 to render it resistant to IL-18BP as a potential strategy to enhance anti-tumor activity. To explore the therapeutic benefit of delivering a conditionally-activated IL-18 to the tumor microenvironment, we have developed inducible polypeptides (INDUKINE™ molecules) consisting of mouse IL-18 or IL-18BP resistant IL-18 (BPR IL-18) tethered via protease-sensitive linkers to a high affinity antibody blockade domain, and a half-life extension (HLE) domain which improves exposure in the tumor. IL-18 INDUKINE™ molecules are inactive until reaching the tumor microenvironment, where the linkers are cleaved by intra-tumoral proteases, releasing active IL-18. Intraperitoneal (i.p.) administration of an IL-18BP resistant IL-18 (BPR IL-18) INDUKINE™ molecule led to complete tumor regression in the MC38 tumor model. In contrast, equimolar doses of wild-type IL-18 INDUKINE™ protein were not as efficacious. Moreover, BPR IL-18 INDUKINE treatment led to increased activation and frequencies of NK cells and tumor specific CD8 T cells in MC38 tumors. WTX-518 is a novel INDUKINE™ molecule that is designed to selectively deliver active human BPR IL-18 to the tumor microenvironment. WTX-518 is inducible in vitro, either when tested using a reporter assay or primary immune cells. Importantly, the active BPR IL-18 payload is resistant to IL-18BP in reporter or primary immune cell assays. WTX-518 is also selectively inducible, as incubation *ex vivo* with various primary human tumors led to the release of active BPR IL-18, while WTX-518 was stable in human serum and after exposure to primary cells from healthy tissues. Pharmacological and efficacy data support continued preclinical development of this innovative and differentiated engineered IL-18 therapy.

#4075 Targeting attenuated IL-18 to PD-1: A next generation checkpoint inhibitor with enhanced anti-tumor activity.

X. Zhou, J. Takimoto, S. Yoon, N. Khanna, **B. Rabinovich**;
Fuse Biotherapeutics Inc., Boston, MA

PD-1 antagonists have shown strong clinical proof of concept, but the development of next-generation versions that can target tumors that weakly respond and/or acquire drug resistance is a critical medical need. Lymphocytes, including T cells and NK cells, upregulate PD-1 and other immunoregulatory receptors in response to neoantigens. Such immunoregulation is important for maintaining the persistence of immune responses in a controllable manner so that immune pathology does not overwhelm the host. In addition to microbial proteins, neoantigens are often expressed by tumor cells. These 'tumor antigens' are derived from mutated genes or proteins not presented during T cell education. As such, many established tumors contain areas of chronic inflammation, including a subset of PD-1+ T cells that can be 'de-immuno-regulated' by anti-PD-1 antagonist antibodies, thus enhancing anti-tumor activity. IL-18 is a cytokine that delivers a 'danger' signal to NK cells and T cell subsets that express the IL-18 receptor complex (RC) and increases their capacity to kill, induces proliferation, diminishes terminal exhaustion, and sustains survival. Importantly, IL-18RC is expressed on progenitor exhausted T cells, the population of T cells in solid tumors that is most active and responds to anti-PD-1, but not terminal exhausted T cells. The latter have been shown to be non-responsive to PD-1 antagonism. Thus, we engineered an anti-PD-1-IL-18 antibody to enhance anti-tumor immune responses. Such a therapeutic requires two key characteristics: resistance to inhibition by IL-18BP, IL-18's natural antagonist, and PD-1-dependent cis-restricted binding to the IL18RC on PD-1+ cells to reduce trans-based systemic toxicity. We have engineered an IL-18BP-resistant mutant of IL-18 and generated variants with different degrees of attenuation for PD-1-dependent cis targeting. Attenuation was achieved by sterically hindering the capacity of IL-18 to bind the IL-18RC while maintaining cis activity without a requirement for proteolytic activation. We identified a variant of IL-18 that is 10,000-fold attenuated and, when fused to an anti-PD-1 antibody, mediated (1) PD-1-dependent cis activity in vitro equivalent to ~5x that of anti-PD-1 alone and (2) tumor shrinkage in mouse tumor models, including an ~80% frequency of complete responses. Due to the high degree of IL-18 attenuation, we were able to dose mice without toxicity to levels at which full PD-1 antagonism is maintained. To our knowledge, this anti-PD-1-IL-18 variant is the first PD-1 targeted cytokine capable of activating PD-1+ T cells via the cytokine's receptor and fully antagonizing PD-1 as a single agent. Thus, targeting a highly attenuated variant of IL-18 that retains strong cis activity to PD-1 holds promise as a clinical candidate for the treatment of cancer indications that respond weakly to anti-PD-1 and/or are associated with acquired resistance.

#4076 Interleukin-18 engineered for resistance to IL-18 binding protein (IL-18BP) and half-life extension to enhance its therapeutic potential.

J. Chamoun, C. DiLea, K. Dreaden, P. Gurel, J. Heiber, R. G. Newman, S.-P. Pearson, C. Wang, Y. Zhao, **M. Whitmore**;
Mural Oncology, Waltham, MA

Interleukin-18 (IL-18) possesses a unique combination of innate and acquired immune functions with high potential to be transformative in cancer immunotherapy of solid tumors. In clinical studies, recombinant wild-type IL-18 was limited by rapid upregulation of IL-18 binding protein (IL-18BP), which serves as a negative feedback checkpoint of the IL-18 pathway. As its name implies, IL-18BP tightly binds to IL-18, thereby blocking its ability to activate the IL-18 receptor. We have focused our protein engineering efforts to obtain variants of IL-18 that are resistant to IL-18BP suppression while retaining IL-18 biological activity. To further capitalize on the immunological effects of IL-18, the IL-18BP resistant variants were fused to half-life extension protein scaffolds for enhanced in vivo exposure. Rational protein design and combinatorial approaches were used to generate a pool of IL-18 variants that were screened for potency and resistance to IL-18BP. Several IL-18 variants showed undetectable binding to IL-18BP (up to 1 mM IL-18BP) and displayed a spectrum of potencies relative to recombinant wild-type IL-18. Importantly, these variants retained their full biological activity in the presence of super-physiological levels of IL-18BP, as tested with in vitro cell-based IFN-γ release assays. In vivo pharmacokinetic studies in mice compared several IL-18BP resistant variants fused to a half-life extension scaffold with a non-half-life enhanced IL-18BP resistant variant. The half-lives for the fusion proteins ranged from 15 - 30h, while the non-fused variant showed a half-live of 0.6h. Furthermore, the IL-18 variants displayed a more durable, Th1 immune response compared to a non-half-life enhanced variant. Thus, IL-18 variants with strong resistance to IL-18BP that are fused to a half-life extension protein scaffold displayed enhanced pharmacokinetic and pharmacodynamic properties in preclinical mouse models. These protein engineering modifications will enable us to select an appropriate development candidate with enhanced pharmaceutical properties to achieve the full therapeutic potential of IL-18 to assess in patients with cancer.

#4077 T cell targeting with PD-1-selective immune cell engagers based on GlycoConnect™ (GC™-ICEs) show excellent efficacy and tolerability.

R. van Geel, M. Verhagen, E. Post, W. Vugs, S. Popal, S. van Berkel, F. van Delft;
Synaffix - A Lonza Company, Oss, Netherlands

Engagement of T cell cells to harness a patient's immune system is a promising approach in immuno-oncology. An immunocytokine, *i.e.* a tumor-targeting antibody (fragment) genetically fused to an immunostimulatory cytokine, is specifically designed for this purpose. Fusion antibody-immunocytokines, based on molecular architectures generated by a variant of DNA recombinant technologies, have recently entered the clinic. Earlier we have demonstrated how GlycoConnect™, a site-specific conjugation technology anchoring on the native antibody glycan[1], can be applied for attachment of various cytokines, including RLI or IL-15, without prior antibody engineering. The immunostimulatory activity of these GlycoConnect™ immune cell engagers (GC™-ICEs) can be modulated by tailoring linker design and payload stoichiometry. In this presentation, we demonstrate the GC™-ICE with either IL-15 or RLI can be applied to selective targeting of T cells, based on PD-1-selective binding and activation, using either protease-sensitive or non-cleavable linkers. We will show how such T cell targeting can be achieved leading to significant tumor volume reductions in syngeneic mouse models. Moreover, we have found that the GC-ICE™ can be applied without inducing systemic immune activation, thereby displaying a promising therapeutic index. In vitro and in vivo studies will be presented to showcase the biological activity of these GC™-ICEs in comparison to conventional immunocytokines obtained via genetic engineering.

[1]Wijdeven et al., Enzymatic glycan remodeling-metal free click (GlycoConnect™) provides homogenous antibody-drug conjugates with improved stability and therapeutic index without sequence engineering. *mAbs* 2022, 14, DOI: 10.1080/19420862.2022.2078466.

#4078 WTX-712, a conditionally active IL-21 INDUKINE™ molecule, induces a strong anti-tumor phenotype through a differentiated mechanism.

J. M. Sullivan, P. A. Aderhold, H. R. Brodkin, C. Nagy-Domonkos, K. Economides, D. J. Hicklin, N. Ismail, Y. Lewis, C. Seidel-Dugan, W. M. Winston, A. Salmeron;
Werewolf Therapeutics, Watertown, MA

Despite great strides seen recently in the development of immunotherapies such as immune checkpoint inhibitors (ICI), many patients do not respond or acquire resistance, highlighting a need for alternative immunotherapies. As potent immunomodulators, cytokines have been explored as treatments for cancer, but their use has been limited due to toxicity and poor pharmacokinetics (PK). One of these key cytokines, interleukin 21 (IL-21), is a pluripotent cytokine that activates anti-tumor T cell responses, induces B cell activation, and promotes generation and maintenance of germinal centers and tertiary lymphoid structures. IL-21 acts on a broader range of cells and does not induce vascular leak syndrome compared to IL-2, another common-gamma chain family member. Half-life extended IL-21 (IL-21-HLE) drives robust anti-tumor activity in several syngeneic tumor mouse models. Of particular interest, IL-21-HLE showed superior anti-tumor activity compared to IL-2-HLE in the EMT-6 and Renca models, both of which are highly resistant to anti-PD-1/PD-L1 treatment. Although IL-21-HLE and IL-2-HLE induced a similar frequency of tumor infiltrating CD8+ T cells, IL-21-HLE treatment led to higher polyfunctionality in CD8+ T cells than IL-2-HLE treatment. Of note, IL-21-HLE induced greater amounts of effector cytokines, Granzyme B and perforin, than IL-2-HLE. Transcriptomic analysis revealed that IL-21 drives upregulation of a type I IFN signature in the tumor promoting an anti-tumorigenic microenvironment. Clinical activity of IL-21 has been hampered by poor PK and adverse events at dose levels associated with signs of efficacy. To overcome these limitations Werewolf Therapeutics has developed WTX-712, an IL-21 INDUKINE™ molecule, which contains wild-type human IL-21, an inactivation domain, and a half-life extension domain tethered together by protease sensitive linkers. In preclinical studies with mouse syngeneic tumor models, WTX-712 is inactive in the periphery, and wild-type IL-21 is selectively released within the tumor, resulting in anti-tumor efficacy with an expanded therapeutic window compared to IL-21-HLE. Anti-tumor efficacy was linked to expansion and activation of tumor infiltrating CD8 T cells with increased polyfunctionality. We will show additional mechanistic data evaluating the effect of WTX-712 dosing on immune populations, including tumor spatial profiling using different models.

#4079 EGL-001 is a novel immunocytokine designed to specifically target and disarm T regulatory cells in the tumor microenvironment.

F. Kotsias[1], C. Janot-Sardet[1], P. Pamela Caudana[1], E. Russo[1], M. Dubois[1], A. Zucchetti[1], M. Tkach[1], S. Lemoine[1], I. Z. Mamedov[1], A. Lladser[1], J. Denizeau[2], A. Meola[3], C. Sedlik[2], E. Borcoman[2], F. Rey[3], P. Guardado-Calvo[3], B. Vanhove[1], **M. Gostissa**[1], E. Piaggio[2];

[1]Egle Therapeutics, Paris, France, [2]Institut Curie, Paris, France, [3]Institut Pasteur, Paris, France

Introduction Immune checkpoint blockade (ICB) therapies targeting PD-1/PD-L1 or CTLA-4 have greatly improved clinical outcome in many cancers. However, multiple mechanisms of resistance to ICB severely limit the number of patients experiencing long-term survival benefits. Overcoming resistance to ICB represents a significant challenge for drug development. Regulatory T cells (Tregs) in the tumor microenvironment (TME) prevent effector T cells (Teffs) from mounting a productive immune response and have been implicated in ICB resistance. Novel therapeutic strategies aimed at disarming Tregs in the TME could restore anti-tumor responses and sensitize patients to ICB therapy. Treg survival is dependent on interleukin-2 (IL-2), which signals in Tregs via the high affinity IL-2 receptor (IL-2R). Tumor-associated Tregs differentiate from tumor-associated Teffs and from peripheral Tregs by higher expression of CD25, the IL-2R alpha chain. Tregs in the TME also express higher surface levels of CTLA-4 as compared to peripheral Tregs. Thus, CD25 and CTLA-4 overexpression could allow preferential targeting of tumor-associated Tregs.

Methods and Results We used single-cell RNA sequencing data from cancer patients and flow cytometry analysis of human tumor samples to verify that CD25 and CTLA-4 are selectively overexpressed in tumor-associated Tregs as compared with peripheral Tregs or other T cells. Based on these findings, we developed EGL-001, a novel immunocytokine (ICK) comprising a humanized IgG1 directed against CTLA-4 fused to a Treg-specific IL-2R antagonist IL-2 mutein, to selectively target tumor infiltrating Tregs. EGL-001 IgG1 moiety binds membrane CTLA-4, as demonstrated by flow cytometry, and competes with CTLA-4-CD80/86 interaction, as evaluated by ELISA. EGL-001 IL-2 mutein moiety binds to CD25, as demonstrated by bio-layer interferometry, and specifically blocks high-affinity IL-2R signaling in Tregs. Signaling blockade is further potentiated by a CTLA-4 dependent CD25 downmodulation process evidenced by confocal microscopy and flow cytometry. We demonstrate that EGL-001 unique tumor-associated Treg-targeted dual mechanism of action results in increased Treg apoptosis and decreased Treg frequencies in multiple in vitro, ex vivo and in vivo systems. Importantly, EGL-001 only minimally affects IL-2 signaling and survival of Teffs, which are then expected to be unleashed from Treg cell-mediated suppression. Accordingly, EGL-001 induces anti-tumor responses in mice in combination with anti-PD1 therapy.

Conclusions EGL-001 is an ICK with a novel and unique mechanism of action combining ICB and Treg selective IL-2 starvation, designed to specifically disarm and deplete tumor-associated Tregs. Based on our preclinical data, EGL-001 is being developed as a cancer immunotherapeutic to improve patients' response to ICB and counteract ICB resistance.

#4080 IBB0979, A novel B7H3/IL-10 immunocytokine of monovalent anti-B7H3 antibody fused with IL-10 homodimer.

X. Jiang, C. Wu, Z. Chen, **L. Yin**;
SUNHO (China) BioPharmaceutical Co.,Ltd., Nanjing, China

Background: This study demonstrates the preclinical evaluation of a novel B7H3/IL-10 immunocytokine IBB0979. IBB0979 was designed to solve the problems of immune cell exhaustion and drug resistance in current immunotherapy. As the tumors progress, the domination of progenitor exhausted T cells (which are the major target cells of current PD-1/L1 based immunotherapy) will be replaced by terminally exhausted T cells (which are the major target cells of IL-10) causing resistance of current PD-1/L1 based therapies. Thus, IL-10 is a potent activator of antigen-specific CD8+ T cells in the tumor microenvironment and can restore the tumor-killing activity of tumor-infiltrating lymphocytes by restoring the oxidative phosphorylation metabolism of terminally exhausted T cells. B7H3 is highly expressed on various tumors but expressed at lower levels in normal tissues and blood vessels, which makes it an ideal target for developing cancer treatment. Also, B7H3 antibody extended the half-life and performed tumor-targeted delivery of IL-10, which improves the safety and efficacy of IL-10.
Methods: We designed several structures of B7H3 antibody and IL-10 bifunctional fusion protein. Binding activity to B7H3 and IL-10 receptor was evaluated by both ELISA and FACS. C57BL/6J mice bearing MC38-hB7H3 cell line were used to evaluate the anti-tumor efficacy of IBB0979. Preclinical PK and toxicity study was also performed in cynomolgus monkeys to describe the safety profile of IBB0979.
Results: Preclinical study showed that IBB0979 has high affinity to both targets and exhibited potent TGI in C57BL/6J mice bearing MC38-hB7H3 cell line, with TGI of 100% at 0.3mg/kg, 1mg/kg and 3mg/kg. An *in vivo* study in cynomolgus monkeys showed that after intravenously administered with 1 mg/kg, 2 mg/kg and 6 mg/kg of IBB0979 once a week for 29 days (5 times in total, given on days 1, 8, 15, 22 and 29), MTD was not reached up to 6 mg/kg which is significantly higher than the 10-20 μg/kg tolerated by IL-10 cytokines alone.
Conclusion: IBB0979 is the world's first B7H3/IL-10 immunocytokine receiving IND approvals from both the FDA and the NMPA, showing excellent preclinical efficacy and safety profile. The Phase I clinical trial is currently on-going, with the first patient dosed in July 2023 and achieved SD at first efficacy evaluation after 2 cycles of administration. Since B7H3 is overexpressed in a wide range of cancers including lung, prostate, glioma, thyroid, head and neck, rectal, breast, skin, renal cell, and ovarian cancers, IBB0979 has the potential to become a next-generation therapy for resolving T cell exhaustion in cancer patients.

#4081 rhIL-7-hyFc (efineptakin-alfa, NT-I7) increases tumor-specific CD8+ T cells despite FOLFOX cytotoxicity effect.

Soung-Min Lee[1], Miyoung Kim[1], **Taekyung Yu**[2], Sara Ferrando-Martinez[3], Sun-Kyoung Im[1], Mankyu Ji[1], Donghoon Choi[1]

[1]NeoImmuneTech, Inc., Gyeongsangbuk-do, Korea, Republic of,[2]Research Institute of NeoImmuneTech, Co., Ltd., Pohang, Korea, Republic of,[3]NeoImmuneTech, Inc., Rockville, MD

rhIL-7-hyFc (efineptakin-alfa; NT-I7) is a potent T cell amplifier, comprised of two molecules of interleukin-7 (IL-7) fused to the hybrid Fc domain of IgD/IgG4 immunoglobulin. NT-I7 safely, significantly, and persistently increases the absolute lymphocyte counts (ALC) in humans in a dose-proportional manner. Importantly, this increase is primarily due to an increase in T cells (1). Previous studies have shown that NT-I7 not only significantly increases the number of CD8+ T cells in peripheral blood but also dramatically boosts the presence of tumor-infiltrating CD8+ T cells, including both tumor-specific (p15E+PD-1+) and tumor non-specific (PD-1-) CD8+ T cells in mice (2). FOLFOX is a chemotherapy regimen composed of 5-fluorouracil, leucovorin, and oxaliplatin that inhibits DNA duplication and eradicates rapidly dividing cells (3). Although the mechanism of FOLFOX results in direct tumor killing, it also has the potential to kill newly dividing lymphocytes during NT-I7 treatment (4-6). Therefore, in this study, we aimed to evaluate the feasibility of combining FOLFOX with NT-I7 in a syngeneic MC38 mouse tumor model. Our results show that NT-I7 improves the efficacy of FOLFOX, irrespective of the timing of NT-I7 administration: simultaneous administration or delayed 3 hours, or 2 days after FOLFOX administration. This improvement persists despite a significant decrease in ALC for the first 6 days, which was significantly lower than the ALC observed with FOLFOX alone. FOLFOX decreases the absolute numbers of tumor non-specific CD8+ T cells. However, adding FOLFOX does not affect the NT-I7-driven increase of tumor-specific CD8+ T cells within the tumor. Taken together, our data demonstrate that FOLFOX does not compromise NT-I7's ability to increase tumor-specific T cells within the tumor and the combination enhances the anti-tumor response irrespective of the timing of NT-I7 administration.

#4082 Anchored IL-12 synergizes with an epigenetic modulator to promote immune remodeling and overcome anti-PD1-refractory murine tumors.

A. S. Khelifa[1], K. L. Lothstein[1], M. Miyamoto[1], R. Tighe[2], S. Battula[2], H. L. Kaufman[2], J. Schlom[1], S. R. Gameiro[1];
[1]National Cancer Institute, Bethesda, MD, [2]Ankyra Therapeutics, Cambridge, MA

Background Most patients with solid malignancies harbor innate or acquired resistance to immune checkpoint blockade (ICB), prompting the need for novel therapeutic strategies. Interleukin-12 (IL-12) is a promising cytokine for cancer therapy due to its ability to bridge innate and adaptive immunity. However, a narrow therapeutic index limits the use of systemic IL-12 therapy. Here, we investigated the tumor-suppressive effects and mode of action of intra-tumorally delivered murine Interleukin-12 anchored to aluminum hydroxide (referred as mANK-101) in combination with the class I HDAC inhibitor entinostat, in various ICB-refractory murine tumor models, including CT26 (colorectal) and MOC-1 ($HPV16^{neg}$). We hypothesized that combining Entinostat with an anchored form of IL-12 could overcome systemic toxicity while maintaining anti-tumor activity.
Methods Entinostat and intra-tumoral mANK-101 were administered to mice bearing well-established αPD-1-refractory CT26 (colorectal) and MOC-1 ($HPV16^{neg}$) tumors. Antitumor activity, survival, and protective memory upon tumor rechallenge were evaluated. Comprehensive proteomic and immune cell analysis was performed in MOC-1 tumors, tumor-draining lymph node (tdLN), and periphery. Tumor-specific T cell responses were examined.
Results We demonstrate that intra-tumoral mANK-101 synergizes with entinostat to suppress multiple αPD1-refractory tumors, resulting in significant tumor eradication (62-88%), survival benefit ($P < 0.0001$), and protective memory, including CT26 (colon, Kras $G12D^{mut}$) and MOC-1 (oral, $HPV16^{neg}$). Analysis of MOC-1 tumor-bearing mice demonstrated these effects to be associated with peripheric activation of $CD8^{\pm}$ and NK lymphocytes, augmented polyfunctional $IFNγ^{\pm}/TNFα^{\pm}$-producing $CD8^{\pm}$ T cells, $CD8^{\pm}$ T cell effector memory, and tumor-specific T cell responses. Significant decrease in $CD4^{\pm}$ Tregs and increased CD8/Treg ratio were also observed. Ongoing functional studies, proteomic and immune cell analysis at the tumor site, tdLN, and periphery, including single cell transcriptomics and epigenetic studies, will allow for a deeper understanding of the synergistic effect of mANK-101 with the epigenetic modulator Entinostat.
Conclusions Collectively, these findings form a rationale for the clinical combination of intralesional delivery of ANK-101 with entinostat for patients with ICB-refractory malignancies, including colorectal and $HPV16^{neg}$ head and neck cancers.

#4083 Pre-clinical development of IAMA-005, a long-acting cytokine fusion of modified IL-2 and IFN-α.

L. Liu, Z. Han, Y. Fan, Q. Pan;
Nanjing JSIAMA Biopharmaceuticals, Ltd., Nanjing, China

In 1990s, both IL-2 and IFN-α were approved as the first two immunotherapies for metastatic melanoma and renal cell carcinoma; IFN-α was also approved for hairy cell leukemia. Although the response rates are relatively low, along ~25%, those who responded have long term survival benefits. However, the severe toxicity especially in high dose prohibited their broad use in oncology. Recently, there have been tremendous interests in modifying these two cytokines in the efforts to reduce the toxicity and enhance the activity. One such effort is to enhance the binding of IL-2 to the intermediate affinity β/γ receptors, which are expressed and function on CD8 T cells and NK cells. Another effort is to reduce the binding of IL-2 to high affinity α/β/γ receptors which mostly expressed on Treg and stimulate the growth of Treg cells, which suppress immune responses. Recently, whether it's better to target intermediate affinity or high affinity for cancer therapy has become controversial with some studies showing that high affinity receptor engagements are required for robust anti-tumor activity while others favoring intermediate affinity receptor engagement for better efficacy; However, the clinical comparison is still lacking to be sure which approach is better. Here we have developed a long-acting novel IL-2-Fc-IFN-α fusion molecule termed IAMA-005 that has mutations to reduce the toxicity effects of IL-2 and IFN-α. We have characterized this molecule preclinically both *in vitro* and *in vivo*. IAMA-005 has demonstrated a potent tumor cell killing activities in numerous cancer cell lines including BT-474, SK-OV-3, NCI-N87, OE19, HCC-1954, MDA-MB-231, MDA-MB-468. When combined with IAMA-004 (a Her2-CD47-CD16 tri-specific antibody) *in vitro*, the tumor cell killing activities were dramatically increased. In addition, IAMA-005 was also tested in patient-derived *Ex-Vivo* fluids (one malignant pleural effusion and one malignant asities) and demonstrated excellent tumor cell killing efficacies. In addition, the killing activities of IAMA-005 could be attributed to the specific part of the fusion molecule because of the TME immune cell compositions. The *in vivo* assays to demonstrate efficacy and safety are ongoing and will be presented in the poster. These results suggest that this fusion cytokine molecule may be used in monotherapy in certain indications and an excellent complementary therapeutic to antibody targeted therapies or immunotherapies when used in combination.

#4084 Potent anti-tumor activity of ABN202 (anti-EGFR antibody-interferon-beta mutein) through direct cytotoxicity and indirect immune activation against non-small cell lung cancer, regardless of EGFR mutation status.

H. Park[1], S. Cho[1], H. Park[1], M. Jo[1], J. Park[2], M. Seo[2], J. Kim[2], S. Hong[3], K. Song[4], C. Lee[5], H. Jeong[5], S. Lee[1], N. Kim[1], J. Choi[1], Y. Shin[2];
[1]ABION Inc., Seoul, Korea, Republic of, [2]Department of Molecular Medicine and Biopharmaceutical Sciences, Seoul National University, Seoul, Korea, Republic of, [3]Research Institute of Pharmaceutical Sciences, Seoul National University, Seoul, Korea, Republic of, [4]College of Pharmacy, Duksung Women's University, Seoul, Korea, Republic of, [5]Genopharm Inc., Seoul, Korea, Republic of

Epidermal growth factor receptor (EGFR) is overexpressed or mutated in many patients with non-small cell lung cancer (NSCLC). Targeting EGFR mutation by tyrosine kinase inhibitors (TKIs) has significantly improved overall survival (OS) in patients with EGFR mutations. However, many patients experience tumor recurrence due to various resistance mechanisms. Therefore, there is an unmet medical need for new treatment strategies for patients with EGFR-positive NSCLC, regardless of EGFR mutation status. ABN202 is an antibody-cytokine fusion protein (ACFP) that serves as a platform technology compromising the IFN-β mutein (ABN102) fused to various antibodies for specific tumor targeting. In a previous study, we designed ABN202 (αEGFR) to comprise an EGFR targeting antibody (Cetuximab) and IFN-β mutein (ABN102) and we confirmed anti-cancer activities of ABN202 against EGFR-positive NSCLC. In this study, the direct cytotoxicity of ABN202 (αEGFR) was evaluated in human NSCLC cell lines with various driving mutations and EGFR expression levels. The indirect immune activation was tested in human peripheral blood mononuclear cells (PBMCs) and human IFNAR1/2 knock-in (KI) mice. The *in vivo* efficacy was evaluated in human NSCLC xenograft mouse models and human IFNAR1/2 KI mouse models. ABN202 (αEGFR) demonstrates potent anti-tumor activity through direct cytotoxicity and indirect immune activation in NSCLC, regardless of EGFR mutation status. Taken together, we suggest that ABN202 (αEGFR) is a promising drug candidate against NSCLC, regardless of EGFR mutation status.

#4085 The anti-VISTA x MSLN bispecific antibody-interferon beta mutein fusion protein: A trispecific immunocytokine with potent therapeutic efficacy against malignant pleural mesothelioma.

H. Park[1], H. Kim[2], M. Seo[2], J. Park[2], T. Kim[2], J. Choi[2], J. Park[2], K. Song[3], C. Lee[4], H. Jeong[4], J. Choi[1], Y. Jeon[5], Y. Choi[6], S. Hong[7], Y. Shin[2];
[1]ABION Inc., Seoul, Korea, Republic of, [2]Department of Molecular Medicine and Biopharmaceutical Sciences, Seoul National University, Seoul, Korea, Republic of, [3]College of Pharmacy, Duksung Women's University, Seoul, Korea, Republic of, [4]Genopharm Inc., Seoul, Korea, Republic of, [5]Department of Thoracic and Cardiovascular Surgery, Samsung Medical Center, Sungkyunkwan University School of Medicine, Seoul, Korea, Republic of, [6]Department of Pathology and Translational Genomics, Samsung Medical Center, Sungkyunkwan University School of Medicine, Seoul, Korea, Republic of, [7]BitD Inc., Siheung, Korea, Republic of

Background Malignant pleural mesothelioma (MPM) is a rare and highly fatal cancer primarily induced by asbestos exposure. The 5-year overall survival rate for MPM patients is less than 20%. Before the FDA approval of the combination of immune checkpoint inhibitors (Nivolumab + Ipilimumab, CHECKMATE-743), chemotherapy was the only systemic therapy for MPM. However, the predominant histological type of MPM, epithelioid MPM, comprising approximately 70% of cases, showed limited clinical benefits from immune checkpoint inhibitors when compared to non-epithelioid histology. Consequently, there is an unmet medical need to develop a new anti-cancer drug specifically for the treatment of epithelioid MPM. In this study, we discovered that V-domain Ig suppressor of T cell activation (VISTA), an immune checkpoint protein, and Mesothelin (MSLN), a tumor differentiation antigen, are co-expressed in epithelioid MPM. Subsequently, we developed a biomarker-based anti-VISTA x MSLN bispecific antibody (BsAb) and anti-VISTA x MSLN BsAb-IFN-β mutein fusion protein (trispecific immunocytokine) for the treatment of epithelioid MPM.

Method We designed and screened various structures of the anti-VISTA x MSLN BsAb. To produce the trispecific immunocytokine, we fused IFN-β mutein (R27T/C17S), which exhibits improved stability, productivity, and pharmacokinetic properties compare to recombinant IFN-β. The *in vitro* efficacy of the trispecific immunocytokine was tested in human MPM cell lines, and its *in vivo* efficacy was evaluated in a human MPM xenograft mouse model and a human IFNAR1/2 Knock-in (KI) mouse model.

Results We demonstrated a strong positive correlation between the expression levels of VISTA and MSLN in epithelioid MPM. The Anti-VISTA x MSLN BsAb showed improved binding affinity and antibody-dependent cell cytotoxicity (ADCC) activity. The trispecific immunocytokine displays analogous biological activities to both Anti-VISTA x MSLN BsAb and IFN-β mutein. The trispecific immunocytokine exhibited potent *in vivo* and *in vitro* anti-cancer activities against epithelioid MPM preclinical models, operating through both direct cytotoxicity and indirect activation of immune cells.

Conclusion The trispecific immunocytokine demonstrated robust *in vitro* and *in vivo* anti-cancer efficacy in the epithelioid MPM model. Our findings suggest that the trispecific immunocytoine is a promising drug candidate for epithelioid MPM.

#4086 ABN202 (anti-Trop-2-interferon-beta mutein): A potent antibody-cytokine fusion protein for the treatment of Trop-2 positive solid tumors.

H. Park[1], H. Lee[1], M. Seo[2], D. Kim[2], S. Bang[2], J. Lee[2], S. Hong[3], K. Song[4], C. Lee[5], H. Jeong[5], S. Lee[1], N. Kim[1], J. Choi[1], Y. Shin[2];
[1]ABION Inc., Seoul, Korea, Republic of, [2]Department of Molecular Medicine and Biopharmaceutical Sciences, Seoul National University, Seoul, Republic of Korea., Seoul, Korea, Republic of, [3]Research Institute of Pharmaceutical Sciences, Seoul National University, Seoul, Republic of Korea., Seoul, Korea, Republic of, [4]College of Pharmacy, Duksung Women's University, Seoul, Republic of Korea., Seoul, Korea, Republic of, [5]Genopharm Inc., Seoul, Republic of Korea., Seoul, Korea, Republic of

Trop-2, trophoblast cell-surface antigen 2, is a type 1 transmembrane glycoprotein overexpressed in many solid cancers, including breast, lung, pancreatic, bile duct and bladder cancer. Overexpression of Trop-2 in cancer patients is associated with disease progression and poor prognosis. The antibody-drug conjugate (ADC) targeting Trop-2, Sacituzumab-govitecan (Trodelvy®), is approved for patients with triple-negative breast cancer (TNBC) and bladder cancer. However, Trop-2 targeting ADCs exhibit a high frequency of grade 3/4 adverse events and a short duration of response. Therefore, there is an unmet medical need for new treatment strategies beyond ADCs. In a previous study, we designed ABN202 (αTrop-2) to comprise a Trop-2 targeting antibody (Sacituzumab) and IFN-β mutein (ABN102) for the Trop2-positive tumor-specific delivery of ABN102. We confirmed anti-cancer activities of ABN202 against Trop-2 positive bladder cancer. In this study, we evaluated *in vitro* and *in vivo* anti-cancer efficacy of ABN202 (αTrop-2) in Trop-2 positive TNBC, bile duct cancer and bladder cancer cell lines. To identify response biomarkers for ABN202 (αTrop-2), we analyzed cell lines exhibiting both response and non-response to ABN202 (αTrop-2). In conclusion, ABN202 (αTrop-2) demonstrated potent anti-cancer efficacy compared to Trodelvy®. Our results support ABN202 (αTrop-2) as a promising drug candidate against Trop2-positive solid tumors.

IMMUNOLOGY: Vaccines, Antigens, and Antigen Presentation 1
Poster Session

#4090 Gut microbiota mimics as a source of cross-reactive tumor rejection antigens.

V. Panneton[1], M. Gigoux[1], A. Zebboudj[2], N. Sadek[1], H. Choi[1], L. M. Mangarin[1], M. M. George[1], G. Kulakowski[3], J. G. Magalhaes[3], J.-M. Carpier[3], T. Dugat[3], C. Gaal[3], F. Strozzi[3], L. Tibaldi[3], L. Chene[3], J. D. Wolchok[4], V. P. Balachandran[2], T. Merghoub[4];

[1]Swim Across America and Ludwig Collaborative Laboratory - Department of Pharmacology - Weill Cornell Medicine, Parker Institute for Cancer Immunotherapy and Sandra and Edward Meyer Cancer Center - Weill Cornell Medicine, New York, NY, [2]Memorial Sloan Kettering Cancer Center, New York, NY, [3]Enterome, Paris, France, [4]Swim Across America and Ludwig Collaborative Laboratory - Department of Pharmacology - Weill Cornell Medicine, Parker Institute for Cancer Immunotherapy and Sandra and Edward Meyer Cancer Center, Department of Medicine - Weill Cornell Medicine, New York, NY

The crosstalk between gut microbiome and anti-tumor immunity has recently gained attention in clinical settings. The administration of antibiotics during immune checkpoint blockade (ICB) therapies has been correlated with poorer outcomes in cancer patients, suggesting that microbiome alterations affect overall responses to ICB. The establishment of microbiota-specific T cell clones with tumor cross-reactivity potential was proposed as one of the mechanisms linking the microbiome to anti-tumor responses. Vaccine-based strategies aimed at reactivating these dormant pools of T cells to help eliminate tumors have been proposed as an alternate approach, but the parameters required for successful responses remain poorly understood. Here, we performed in silico selection of bacterial peptides derived from healthy mice based on their mimicry of either tumor-associated antigens (TAAs) or neoantigens expressed by murine melanoma cells and not healthy tissue. We show that in silico predicted peptide binding affinity to MHC I correlates with experimental MHC I binding, a key factor associated with strong immune responses. Moreover, we confirmed that a significant proportion of selected peptide candidates can provoke an immune reaction in a vaccination setting. From this group of peptides, we selected candidates which triggered cross-reactive immune responses against TAAs or neoantigens. Data from preliminary tumor challenge experiments with prophylactic peptide vaccination and ICB allowed us to define key parameters such as target gene expression levels which can predict the cross-reactive potential of bacterial peptides that mimic tumor antigens. These findings provide novel insights into the design of gut microbiome peptide-based tumor vaccines and pave the way for establishing combinatorial therapies with immunomodulatory drugs.

#4091 A novel cancer vaccine based on hyaluronic acid nanogel combined with adoptive T cell therapy induces complete regression of established tumors and long-lasting memory CD8$^{\pm}$ T cells.

F. Momose[1], T. Nakai[2], K. Yabuuchi[2], M. Yamane[1], T. Hayashi[1], L. Wang[1], Y. Nakagawa[2], S. Aso[2], T. Katsumata[2], T. Shimoboji[2], Y. Miyahara[1];
[1]Mie University Graduate School of Medicine, Mie, Japan, [2]Asahi Kasei Corporation, Tokyo, Japan

Background: We have developed nanosized hydrogel particles (nanogels) to create new nanomaterials for biomedical applications. In particular, Hyaluronic Acid, partially hydrophobized by chemical modification with cholesteryl groups, has a distinguished characteristic to form physically cross-linked NanoGel particles. HANG efficiently forms a stable complex with an antigenic polypeptide (HANG-Vaccine) through hydrophobic interactions. In this study, we investigated the efficacy of HANG-V against tumors resistant to immune checkpoint inhibitors (ICIs) and adoptive TCR-T therapy.
Methods: C57BL/6-derived B16F10 melanoma and BALB/c-derived CMS5a sarcoma are both known to be resistant to ICIs and adoptive TCR-T therapy. The efficacy of HANG-V was tested by using each tumor-bearing mice treatment model. HANG-V was prepared by mixing gp100 or CMS5a neoantigen (Ag) with HANG, respectively.
Results: HANG-V was subcutaneously injected into B16F10-bearing C57BL/6 on days 7, 11, and 15, and CD8$^{\pm}$ T cells from Pmel-1 mice were intravenously administered on days 8 and 12. Surprisingly, complete regression of established B16F10 tumors with more than 100 mm^2 were observed. Vaccinated mice survived with changing hair color of mice into white, while non-vaccinated mice were all dead by day 25. Moreover, gp100-specific CTLs was observed abundantly in systemic including tumor site. Even two months after the treatment, transferred T cells with memory phenotype were persistently detected in peripheral bloods. Furthermore, booster vaccination elicited robust expansion of these memory T cells persisting for more than one year. In similar experimental settings, we treated CMS5a tumor-bearing mice by HANG-V combined with adoptive transfer of CD8$^{\pm}$ T cells from DUC18 mice, whose T cells are specific for mutated ERK2 neoAg. All mice survived as well with complete reduction of established CMS5a tumors, rejected a rechallenge with CMS5a and induced an Ag-specific CTL responses on more than 2 years. Notably, by using neoantigen-knockout CMS5a, we obtained results suggesting that HANG-V with TCR-T therapy potently induced the so-called “antigen spreading”. Furthermore, induction of Ag-specific CTLs was associated with CD44 hyaluronic acid receptor which expressed in APCs crucial for cross-presentation to CD8$^{\pm}$ T cells.
Conclusions: HANG-V strongly enhanced the efficacy of adoptive TCR-T cell therapy against ICI refractory tumors leading to total tumor suppression. Furthermore, HANG-V induced potent and persistent Ag-specific CTLs systemically through interaction with CD44 hyaluronic receptor, allowing long-term protection of tumor recurrence with memory CD8$^{\pm}$ T cells. Our studies may propose crucial insights for clinical application of HANG vaccine with adoptive T cell therapy in patient with ICI-resistant tumors with poor prognosis.

#4092 Characterizing the endogenous retroviral envelope protein ERVMER34-1 as a target for a therapeutic cancer vaccine.

M. Maldonado, M. Iida, M. Gracia Hernandez, L. Le, R. N. Donahue, C. Palena, J. Schlom, D. H. Hamilton;
NIH-NCI, Bethesda, MD

Endogenous retroviruses (ERVs) are remnants of retroviral germline infections which occurred over the course of evolution and constitute between 5-8% of the human genome. Although ERV protein expression is typically silenced epigenetically in normal adult human tissues, previous studies have shown that some ERVSs, can be aberrantly expressed in multiple cancer types. This atypical expression of ERVs in tumors may represent a class of immunologically relevant tumor-associated antigens that can potentially be targeted clinically using therapeutic cancer vaccines. For the first time, this study evaluates the ERV envelope protein ERVMER34-1 as a potential target for a therapeutic cancer vaccine. We first assessed the expression of ERVMER34-1 in multiple tissues and found that ERVMER34-1 protein is absent in most healthy adult tissues and over expressed in multiple types of human carcinomas. ERVMER34-1 specific T-cells were detected in PBMCs of cancer patients but not healthy donors following an overnight stimulation. However, reactive T-cells are readily expanded from both healthy donor and cancer patient PBMCs following a 7-day in-vitro stimulation. Importantly, reactive CD8+ T cells selectively killed human carcinoma cells expressing the target antigen. Based on these findings, we rationally designed a ERVMER34-1 therapeutic cancer vaccine and assessed its immunogenicity and anti-tumor efficacy in established syngeneic murine tumors expressing the full-length ERVMER34-1 protein. Our rationally designed ERVMER34-1 cancer vaccine significantly mediated tumor regression and extended survival as a monotherapy and in combination with checkpoint blockade. Altogether, our work supports the clinical development of a therapeutic cancer vaccine targeting the retroviral envelope protein ERVMER34-1 as a potential first-in-class immunotherapeutic target for the therapy of several carcinoma types.

#4093 Modeling tumor immunoediting under immune selective pressure to inform neoantigen landscape dynamics for effective cancer vaccines.

M. M. George[1], J. Lihm[2], H. Choi[1], Y. Elhanati[2], S. Martis[2], M. Luksza[3], B. Greenbaum[2], J. D. Wolchok[1], T. Merghoub[1];
[1]Weill Cornell Medicine/Sandra and Edward Meyer Cancer Center, New York, NY, [2]Memorial Sloan Kettering Cancer Center, New York, NY, [3]Mount Sinai School of Medicine, New York, NY

Tumor specific neoantigens, encoded by somatic mutations, are recognized by T cells, inducing anti-tumor immune responses. This renders neoantigens viable targets for personalized cancer vaccines. However, the identification of immunogenic neoantigens remains suboptimal. Understanding how immune selective pressure-mediated tumor evolution and neoantigen editing contribute to emergence of immunogenic neoantigens may improve prediction accuracy. In this study, we aimed to model tumor evolution and heterogeneity under immune pressure using three preclinical models of lung cancer with common driver mutations, Kras G12D/+ and p53 -/-, namely KPA, KPC, and HKP1, subcutaneously implanted in immunocompetent C57BL/6 (B6) and immune-deficient Rag1-/- mice. Our data suggest that despite shared driver mutations identified by whole exome and RNA-seq, tumor growth in vivo varied between tumor models. KPA tumors were immunogenic, as they were controlled in B6 mice but rapidly progressed in Rag1-/- mice, suggesting immunoediting of KPA-specific neoantigens. In contrast, HKP1 was non-immunogenic, with tumors progressing regardless of immune competency. KPC showed moderate tumor control in B6 mice, which was lost in Rag1-/- mice. We then estimated the cancer cell fraction on every mutation based on phylogenetic reconstruction. Immunogenic KPA tumors had significantly lower mutation burden in B6 than in Rag1-/- mice and the fraction of cell line mutations edited in vivo was significantly higher, suggesting active immunoediting in the former. Non-immunogenic HKP1 tumors did not show significant differences in mutation burden nor fraction of mutations edited between B6 and Rag1-/- mice. The immunogenicity was reflected in the immune infiltrate levels within tumors, with KPA being highly infiltrated by activated CD4 and CD8 T cells compared to KPC. HKP1 tumors showed increased infiltration of suppressive regulatory T cells. T cell receptor (TCR) sequencing on lung tumors showed that clonal expansion is strongly associated with immunogenicity. KPA tumors showed significantly higher TCR clustering with less diversity compared to KPC and more than HKP1. Following a simple approach to study the immunogenicity of shared neoantigens to elicit cross-protective anti-tumor responses, mice were immunized with whole irradiated (IR) tumor cell lines and implanted with live tumor cells (matched and unmatched). While immunization with IR-KPA protected against corresponding tumor implant and moderately against KPC, it did not protect against HKP1, indicating lack of immunogenicity of mutations shared between KPA and HKP1. Further studies testing the anti-tumor responses and characteristics of neoantigens shared between these three related tumor cell lines will inform the conditions under which tumors may escape or regress and help improve neoantigen identifying algorithms.

#4094 Immune modulatory cancer vaccines against IDO1 and PD-L1 trigger distinct pathways and cooperatively reduce tumor growth in preclinical models.

M. Chapellier[1], E. Martinenaite[1], P. Patel[1], L. Svendsen[1], S. Munir Ahmad[2], H. Jorinde Glockner[2], M. Carretta[1], E. Sutanto-Ward[3], J. DuHadaway[3], S. Dey[3], S.-C. Shen[3], D. Ghaban[3], M. Iglesias[1], M. Biller[1], I. Lecoq[1], A. J. Muller[3], M. Hald Andersen[2], A. Wakatsuki Pedersen[1];
[1]IO Biotech, Copenhagen, Denmark, [2]Center for Cancer Immune Therapy, Copenhagen, Denmark, [3]Lankenau Institute for Medical Research, Wynnewood, PA

While immune checkpoint inhibitors have shown clinical efficacy in many cancers, drug and immune resistance remain challenging. Indoleamine 2,3-dehydrogenase (IDO1) and Programmed Death Ligand 1 (PD-L1) both contribute to immunosuppression, leading to immune escape and cancer progression. In this context, vaccination to promote T-cell immunity against IDO1^{+} and PD-L1^{+} cells is an attractive strategy that demonstrated encouraging clinical results in melanoma (Kjeldsen et al. Nat Med 2021). Our study aims to further evaluate the efficacy and mode of action of combined IDO1 and PD-L1 peptide vaccines.
Mice injected with tumor cells and treated with IDO1 or PD-L1 peptides were monitored for tumor growth. Vaccine activity was determined by IFNγ Elispot assay. Gene expression analysis was performed on tumors using Nanostring nCounter PanCancer IO360 Panel. IDO1 and PD-L1 expression were also examined via multiplex immunofluorescence in a human tumor tissue microarray (TMA) panel. Human IDO1 and PD-L1 specific CD4^{+} T cell clones were isolated and expanded from melanoma patients treated with IDO1/IO102 or PD-L1/IO103 peptide vaccines in combination with aPD1 therapy.
Immunofluorescence analysis of murine tumor sections showed expression of IDO1 and PD-L1 by different cell populations. Vaccination against each target led to expansion of specific T cells in splenocytes and reduced tumor growth in MC38 and CT26 models. Combining IDO1 and PD-L1 treatments further enhanced the anti-tumor response. Gene expression analysis of tumors revealed distinct signatures following monotherapy and combination treatments. While PD-L1 vaccination predominantly enhanced the cytotoxic effector T cell function in the tumor microenvironment (TME) and concomitantly increased gene signatures associated with enhanced activation of T effector cells, IDO1 vaccine primarily exerted its effect via reduction in the immune suppression loop. TMA analysis of IDO1^{+} and PD-L1^{+} cells in human tumors also revealed that they represent largely distinct cell populations. Lastly, IDO1 and PDL1-specific CD4^{+} T cell clones from melanoma patients treated with IO102-IO103 vaccine could selectively target cells differentially expressing IDO1 or PDL1.
Our data collectively show that cells expressing IDO1 and PD-L1 represent distinct populations in the TME thus targetable by the IDO1-PD-L1 vaccination approach. The vaccines targeting IDO1 and PD-L1 cooperatively reduce tumor outgrowth, and each contributes to the anti-tumor effect through distinct molecular programs regulating immunosuppression in the TME and T cell activation respectively. These data are supported by ex vivo functional assays using target specific T cells from vaccinated patients. Altogether, our data support the use of a dual antigen approach to reduce the immunosuppression and enhance anti-tumor effect.

#4095 Targeting alternative classes of tumor antigens to improve immunotherapy for microsatellite stable, mismatch repair-proficient colorectal cancer.

R. Dolcetti[1], B. Zeng[1], J. Ye[2], T. Shamekhi[2], M. Harpur[1], D. Moi[1], S. Roth[1], R. Ramsay[1], D. Duscharla[2], A. W. Purcell[2], P. Faridi[2], R. Mazzieri[1];
[1]University of Melbourne, Melbourne, Australia, [2]Monash University, Clayton, Australia

Background: The clinical outcomes of immunotherapy for microsatellite stable (MSS) colorectal cancer (CRC) remains unsatisfactory. The development of more effective immunotherapies is hampered by limited knowledge of the appropriate target antigens, also considering the low burden of mutations generating neoantigens of these tumors. Alternative classes of MSS CRC antigens may provide actionable epitopes.
Methods: We have characterized the immunopeptidome of 2 MSS CRC cell lines derived from the primary tumor (SW480) and a metastatic lymph node (SW620) of the same patient. Given the low mutational burden of MSS, we focused on peptides belonging to alternative sources of HLA-A*02 epitopes, such as proteasomal cis-spliced peptides derived from cancer testis antigens and linear epitopes derived from Human Endogenous Retroviruses (HERVs), which are frequently reactivated in CRC. Peptide immunogenicity was functionally validated based on their ability to expand HLA-A*02$^{\pm}$ donor T cells (>3) specifically killing targets cells presenting the relevant peptides or HLA-matched CRC cell lines. *In vivo* epitope immunogenicity was verified by analyzing polyfunctional responses of human CD8$^{\pm}$ T cells obtained from NSG-A2 mice humanized with A*02$^{\pm}$ donor PBMCs and immunized with epitope-loaded nano-emulsions selectively targeting human Clec9A$^{\pm}$ dendritic cells. Therapeutic exploitation of the novel epitopes was investigated by adoptive transfer of epitope-specific T cells in NSG-A2 mice injected with SW620 cells. Epitope-specific T cell responses were investigated in PBMCs from 10 MSS CRC patients and 7 donors.
Results: Among >50,000 HLA-bound peptides identified by in depth immunopeptidomics analysis, 11 cis-spliced peptides and 5 HERV peptides were functionally validated as immunogenic. Epitope-specific T cells showed specific cytotoxic activity against SW480 and SW620 CRC cells. Globally, cis-spliced peptides were more immunogenic *in vitro* than HERV-derived peptides. The immunogenicity of both groups of peptides was confirmed *in vivo* in humanized mice. Adoptively transferred HERV or cis-spliced epitope specific T cells significantly inhibited the growth of SW620 cells *in vivo*, with cis-spliced epitope-specific T cells being more effective. Therapeutic efficacy of Clec9A-targeting vaccines exploiting these epitopes is currently under investigation. T cell responses specific for cis-spliced and HERV epitopes were detected in PBMCs from 3/4 MSS CRC HLA-A*02$^{\pm}$ patients but in none of 4 HLA-A*02^{-} MSS CRC patients or 7 healthy donors (4 HLA-A*02$^{\pm}$ and 3 HLA-A*02^{-}).
Conclusions: We have identified and validated a new class of immunogenic HLA-A*02 epitopes derived from alternative classes of MSS CRC antigens. We also provide the proof of principle supporting their therapeutic exploitation to improve the management of these poorly immunogenic tumors.

#4096 Comparative molecular profiling of sporadic and Lynch syndrome MSI tumors: Unraveling insights for vaccine design.

Hagay Ladany[1], Mark Grossman[2], Julian Hess[3], Nicole Lu[3], Derin Keskin[4], Catherine J. Wu[4], Nir Hacohen[5], Erika Hissong[2], Richard Gallon[6], John Burn[6], Wendy Frankel[7], Rachel Pearlman[7], Heather Hampel[8], Zsofia Stadler[9], Gad Getz[3], Yosef E. Maruvka[1], Steven Lipkin[2]

[1]Technion, Haifa, Israel,[2]Weill Cornell Medical College, New York, NY,[3]Broad Institute, Cambridge, MA,[4]Dana-Farber Cancer Institute, Boston, MA,[5]Massachetest General hospital, Boston, MA,[6]Newcastle University, Newcastle, United Kingdom,[7]The Ohio State University Wexner Medical Center, Comprehensive Cancer Center, Columbus, OH,[8]Ohio State University, Columbus, OH,[9]Memorial Sloan Kettering Cancer Center, New York, NY

Lynch Syndrome (LS) is a hereditary syndrome that predisposes carriers to colorectal cancer (CRC). The hallmark of LS is microsatellite instability (MSI), resulting from a defective DNA mismatch repair (MMR) system. MSI cases have hyper-elevated frameshift mutation rates including “shared” hotspot mutations recurrently across patients. Frameshift mutations can generate neopeptides that activate the immune system. These open the door for preventive vaccines. However, preventive vaccines work best with neopeptides that happen early during tumorigenesis.Here we present 83 newly sequenced adenomas and carcinomas from Lynch syndrome carriers and combine them with previously published 68 Lynch cases and 133 Sporadic cases, thus generating the largest currently available colorectal neoplasiaMSI cohort. We leveraged this large cohort to analyze the molecular landscape of adenomas vs carcinoma tumors and Lynch vs sporadic tumors. Employing our recently developed MSIDetect tool on our WGS samples, we identified microsatellite instability in 75% of adenomas, which is higher than previously reported. We found that about 30% of normal adjacent tissues showed MSI, suggesting early mismatch repair defects. This early MSI occurrence supports the potential effectiveness of preventive vaccines.We observed comparable levels of SNVs, microsatellite Indels, and single base signature activity among Lynch adenomas and carcinomas, as well as sporadic carcinomas while adjusting for variations in coverage across different datasets. Moreover, using RNA sequencing data and PCA analysis we found that adenoma and carcinoma cluster together. This large cohort enabled us to identify (as fast as we know for the first time) MS-indels that tend to have a second MS-indel in the same locus. The high similarities observed between Lynch and sporadic tumors allow for their combination in one vaccine.Using the combined MSI cohort we generated a set of about 300 neopeptides that emerged from frequent mutations (>5% in our cohort) with a strong binding affinity for at least one HLA type. We evaluated that a set of about 60 neopeptides per person from that list is predicted likely to initiate an immune response in ~99.5% of the carriers.These findings hold promise for the development of a preventive vaccine capable of targeting early tumorigenic stages. This work is approved under Weill Cornell IRB exemption 1810019672

#4097 LNP-mRNA neoantigen vaccines to intercept progression of pre-invasive to invasive lung adenocarcinoma.

Y. He[1], S. Zhong[2], B. Bhinder[1], G. Markowitz[1], A. Singh[1], E. Gardner[1], M. Ko[1], N. K. Altorki[1], S. Jiang[2], V. Mittal[1];
[1]Weill Cornell Medicine, New York, NY, [2]Cornell University, Ithaca, NY

The widespread use of chest computed tomography in lung cancer screening has led to the detection of ground-glass opacity (GGO) nodules, which typically harbor pre-invasive or minimally invasive adenocarcinoma and 20-40% of GGO nodules progress to invasive lung adenocarcinoma within 4 years. Lack of approved treatments to intercept disease progression has imposed challenges in the clinical management of patients with GGOs. Previous studies showed that GGO nodules have substantially lower rates of HLA deletions than invasive/metastatic lung cancer, suggesting that GGO nodules constitute a critical window of vulnerability for immune interception. We therefore sought to identify the most immunogenic and cytotoxic neoantigens in patients with GGO nodules and to develop LNP-mRNA cancer vaccines to intercept the disease progression from pre-invasive to invasive adenocarcinoma. Whole exome and RNA sequencing of a large cohort (>300) patients identified potential neoantigen candidates, with KRAS-G12C, KRAS-G12D and EGFR-L858R as the most frequently predicted shared neoantigens consistent with >40% GGO patient population harboring either mutant KRAS or EGFR driver oncogenes. LNP-mRNA vaccines targeting KRAS-G12C and EGFR-L858R showed marked immunogenicity as determined by ELISPOT assays. Moreover, KRAS-G12C vaccination induced CD4+ T cell responses whereas EGFR-L858R vaccination triggered CD8+ T cell responses. Both these vaccines are being tested in GGO immunoprevention studies. Our data suggest the potential of KRAS and EGFR vaccines in the treatment of early disease, particularly in EGFR mutant patients who fail to respond to immunotherapy.

#4098 A citrullinated-ENO1 peptide vaccine delayed tumor growth and markedly improved overall survival in a mouse model of triple-negative breast cancer.

R. A. Leon Letelier, H. Katayama, Y. Chen, Y. Cai, F. Hsiao, B. Arun, S. Hanash;
The University of Texas MD Anderson Cancer Center, Houston, TX

Purpose: To evaluate the impact of a novel citrullinated-enolase 1 (cit-ENO1) peptide-based vaccine on the immune response, tumor growth and overall survival in a mouse model of triple-negative breast cancer (TNBC).
Background: Cancer vaccines have consisted primarily of mutated or overexpressed proteins in cancer. We have uncovered dysregulated protein citrullination by peptidyl arginine deiminases (PADI) as a feature of triple negative breast cancer inducing immunogenicity to citrullinated proteins. On the basis of these findings, we investigated a novel vaccine based on cancer-selective cit-ENO1 peptides that we identified from mass spectrometry analysis of the surfaceome and immunopeptidome in TNBC. We assessed the extent to which the vaccine elicited an immune response and delayed tumor growth and improved overall survival in a syngeneic mouse model of TNBC.
Experimental Design: We immunized female B6129SF1/J mice with cit-ENO1 peptides or corresponding unmodified ENO1 (unm-ENO1) peptides as antigens, together with the TLR3 agonist poly I:C as an adjuvant, once a week, for three weeks. PBS or poly I:C alone were used as controls. One week post the last round of immunization, draining lymph nodes (LN) and immunized skin were harvested, and T cell phenotypes evaluated using flow cytometry. To assess anti-cancer efficacy, mice were immunized with cit-ENO1 or unm-ENO1 peptides, followed by orthotopic implantation with murine BRCA1$^{co/co}$; MMTV-Cre; p53$^{+/-}$ TNBC cells. Tumor growth and overall survival were assessed.
Results: Cit-ENO1 peptide vaccination induced a statistically significantly greater percentage of activated CD8+ PD-1+ effector T cells as well as CD8+ CD44+ CD62L- effector memory T cells in the LNs compared with either the control groups or the unm-ENO1 peptide. CD8+ PD-1+ T-cells were also significantly elevated in immunized skin of cit-ENO1 vaccinated mice. Both cit-ENO1 and unm-ENO1 vaccine increased CD4+ PD-1+ T cells from the LNs and immunized skin. Remarkably, the cit-ENO1 vaccine but not the um-ENO1 vaccine significantly delayed tumor growth and markedly improved overall survival compared to respective controls.
Conclusion: Cancer-selective cit-ENO1 peptides induced a potent anti-cancer immune response and significantly delayed tumor initiation and progression in a preclinical, immune competent mouse model of TNBC.

#4099 AMP-peptide vaccination against multiple p53 mutant epitopes promotes lymph node delivery to generate potent, functional T cell immunity.

M. P. Steinbuck, X. Cabana-Puig, E. Palmer, M. M. Jung, T. Williams, K. Osaer, J. Zhang, C. M. Haqq, P. C. DeMuth;
Elicio Therapeutics, Boston, MA

Background p53 is the most commonly mutated gene in human cancer, prevalent in nearly all tumor types. Despite its significant medical relevance and the knowledge that human T cells recognize these mutations[1,2], immunotherapies designed to promote responses against mutated p53 (mp53) have not had the hoped-for clinical impact[3]. The Amphiphile (AMP) platform improves the potency of vaccine immunotherapy by programming the delivery of vaccine components to the lymph nodes where efficient uptake by immune cells initiates tumor-targeted immune responses. AMP-modification of vaccine components (peptide antigens, molecular adjuvants) results in covalent conjugation to albumin-binding lipids. Upon injection, AMP-vaccines associate with tissue-resident albumin which efficiently distributes to draining lymph nodes. This approach was shown to promote activation of polyfunctional, cytotoxic T cells with promising safety and improved clinical outcomes in a Phase 1 trial of ELI-002, an mKRAS AMP therapeutic vaccine (AMPLIFY-201 NCT05726864). Application of this strategy to p53 mutations with ELI-008 offers the potential for improved immunotherapeutic activity in a setting of significant unmet need.

Methods Following immunization of C57BL/6J mice with AMP-modified or soluble comparator vaccines consisting of mp53 peptides and CpG adjuvant, analyses were performed 7 days after the third bi-weekly dose. To assess antigen-specific T cell responses, ELISpot (IFNγ, GzmB), multiplexed proteomic, and flowcytometric analysis of effector cytokines (IFNγ, TNFα, IL-2) were performed following antigenic stimulation. Responses were determined in secondary lymphoid tissues and lung. Cytolytic capabilities of antigen-specific T cells were evaluated by monitoring specific killing of IV-transferred antigen-pulsed target cells.

Results AMP-immunization generated robust immune responses yielding strong T cell activation against common p53 hot spot mutations (R248W, R248Q, R175H, G245S, R273H, Y220C, C135Y, R158H, H214R). Responses to AMP-vaccination were characterized by the generation of increased frequency of polyfunctional T cells (IFNγ, TNFα, IL2) specific to mp53 epitopes. Induced T cells demonstrated significant levels of cytolytic activity including GzmB production and elimination of target cells *in vivo*. Non-lymph targeted vaccines using soluble comparators were inactive.

Conclusions AMP-conjugation permits efficient delivery directly to the lymph nodes and thus improves the immunogenicity of peptide vaccination. These substantially improved immune responses induced by ELI-008 represent a promising therapeutic opportunity for targeting cancer in a large fraction of human tumors. The AMP-platform technology is simple, rapid and scalable, promising broad clinical, off-the-shelf application for treating p53 mutated tumors.

#4100 AMP-peptide vaccination against mutant BRAF epitopes promotes lymph node delivery to generate potent, functional T cell immunity.

M. P. Steinbuck, X. Cabana-Puig, E. Palmer, M. M. Jung, T. Williams, K. Osaer, J. Zhang, C. M. Haqq, P. C. DeMuth;
Elicio Therapeutics, Boston, MA

Background Mutations in BRAF cause ~8% of human cancers[1]. Nonetheless, therapies designed to promote immune responses against mutated BRAF (mBRAF) have led to limited clinical success[2], despite evidence confirming T cell recognition of these mutations[3,4]. The Amphiphile (AMP) platform improves the potency of vaccine immunotherapy by programming the delivery of vaccine components to the lymph nodes where efficient uptake by resident immune cells initiates tumor-targeted immune responses. AMP-modification of vaccine components including peptide antigens and molecular adjuvants results in covalent conjugation to albumin-binding lipids. Upon injection, AMP-vaccines associate with tissue resident albumin which efficiently distributes to draining lymph nodes. This approach was shown to promote activation of polyfunctional, cytotoxic T cells with promising safety, and improved clinical outcomes in a Phase 1 trial of ELI-002, an mKRAS AMP therapeutic vaccine (AMPLIFY-201 NCT04853017). Application of this strategy to prevalent BRAF mutations with ELI-007 offers the potential for improved therapeutic activity in a setting of significant unmet need, as BRAF inhibitors benefit only a fraction of patients, with near universal progression.

Methods Following multi-dose immunization of C57BL/6J mice with AMP-modified or soluble comparator vaccines consisting of mBRAF V600E/K peptides and CpG adjuvant, immunological readouts were performed 7 days after dosing. Antigen-specific T cell responses were assessed after *ex vivo* re-stimulation of cells with mBRAF overlapping peptides. Assays included analysis of antigen-specific T cell frequencies, multiplexed proteomics determining polyfunctionality, and effector function and cytotoxic potential evaluation. Responses were determined in secondary lymphoid tissues (spleen), as well as lung, to which many BRAF driven cancers metastasize.

Results AMP-immunization generated robust *in vivo* immune responses yielding strong T cell activation against mBRAF epitopes. Non-lymph node targeted vaccination using soluble comparators were inactive with no response above mock treated mice. Responses to AMP-vaccination were characterized by the generation of significantly increased frequency of Th1-skewed, polyfunctional T cells (IFNγ, TNFα, IL2) specific to mBRAF V600E and V600K. Induced T cells further exhibited mBRAF-specific cytotoxic function.

Conclusions AMP-conjugation enhances efficient delivery directly to the lymph nodes and thus improves the immunogenicity of peptide vaccination. These enhanced immune responses provide an encouraging therapeutic opportunity to treat >90% of BRAF-mutated cancers[5] with the AMP-mBRAF vaccine, ELI-007. Moreover, the AMP-platform technology is simple, rapidly executable, and scalable, promising broad clinical off-the-shelf application for BRAF.

#4101 Immune inhibition of murine colorectal cancer by a p53 peptide mucosal vaccine.

S. Wang, Z. Cao, K. W. Janczak, Y. Feng, M. Green, E. R. Fearon, J. R. Baker Jr.;
University of Michigan, Ann Arbor, MI

Colorectal cancer (CRC) is among the most common cancers with high morbidity and mortality for patients despite multi-modality treatment options. Immune checkpoint inhibitors often have impact in the 15% of CRC patients with microsatellite instability-high status CRCs but have limited utility in the remaining 85% of CRC patients. Given the presence of p53 mutations in CRC, we pursued a vaccine approach against tumor cells expressing murine CRC Trp53 codon 270 missense alleles (codon 273 mutation in human cancer) using a combination of R270H p53 peptide, wild type p53 recombinant protein and used a mucosal adjuvant (MA) to drive epithelial immune responses. The vaccine (p53/MA) was studied in a CDX2-CreERT2 (tamoxifen-induced Cre-Lox) transgenic mouse CRC model where tumors arise in the cecum and proximal colon epithelium following combined $Apc^{\Delta 580}$, $Kras^{G12D}$, and $Trp53^{R270H}$ mutations (AKP model). The p53/MA vaccine treatment was administered intranasally to the mice at defined time points after tamoxifen tumor induction. p53/MA vaccinated animals had increased anti-p53 IgG ($p<0.01$), IgG2a ($p<0.01$), and IgG2b ($p<0.001$) in sera compared to control mice. The treatment enhanced antigen-specific Th1 and Th17 cellular immune responses, as shown by increasing of IFN-γ ($p<0.05$), IL-17a ($p<0.01$) and IL-2 ($p<0.01$) both in splenocytes and draining lymph nodes measured by Luminex assay. Vaccinated mice also showed significant more cells producing IFN-γ ($p<0.001$) and IL-17a ($p<0.001$) as analyzed by ELISpot. Importantly, the immunized animals had decreased tumor size/volume ($p<0.001$) and prolonged survival ($p<0.05$) compared to control animals that received only saline or MA respectively. Tumors from vaccinated mice also showed more mononuclear cell infiltrates than tumors from the control animals. In conclusion, novel p53/MA vaccinations can induce significant p53-specific immune responses and anti-tumor effects in the mouse AKP CRC model.

#4102 Treatment with androgen receptor targeting vaccines provides an overall survival benefit in AR-V7 expressing tumor models.

R. D. Marek, J. Wei, T. Wang, X.-Y. Yang, G. Lei, Z. C. Hartman;
Duke University, Durham, NC

Background: Androgen receptor (AR) signaling inhibition is part of the mechanism behind many effective prostate cancer therapies, including androgen deprivation and next generation anti-androgens. However in castration resistant prostate cancer up to 50% of treatment resistance has been linked to AR amplification or expression of the constitutively active RNA splice variant, AR-V7. Although the use of immune checkpoint blockade has failed to demonstrate clinical success, immunotherapeutic interventions remain attractive as prostate cancer's relatively slow progression provides time for anti-tumor immune responses to develop. Cancer specific vaccines have the potential to enable and enhance tumor specific immune responses by stimulating and directing T cell immunity to important oncologic targets. We hypothesized that a cancer vaccine designed to induce a T cell response against cells expressing high levels of AR would result in an anti-tumor effect and potentially prevent or delay the development of therapeutic resistance.

Methods: Adenoviral vaccines against AR (Ad-AR) or AR splice variant 7 (Ad-AR-V7) were used to evaluate the potential of AR targeting vaccination in mouse models. We evaluated AR and AR variant specific adaptive responses produced by our vaccines with naïve and tumor-bearing mice by ex vivo peptide restimulation. We challenged vaccinated mice with multiple syngeneic subcutaneous tumor models that we engineered to express AR-V7, including a $PTEN^{-/-}$ $p53^{-/-}$ prostate tumor cell line. Finally we tested our vaccines in a therapeutic regimen, vaccinating mice after implanting our subcutaneous AR-V7 expressing models.

Results: Across multiple strains of mice, AR or AR-V7 targeting adenoviral vaccination induced robust adaptive immune responses against the N-terminal domain of AR. Vaccination with either Ad-AR or Ad-AR-V7 resulted in significant anti-tumor responses, providing a significant overall survival benefit and complete tumor rejection by the majority of mice vaccinated against AR or AR-V7. Similarly tumor bearing mice treated with Ad-AR or Ad-AR-V7 vaccination displayed tumor growth inhibition or complete tumor regression resulting in an overall survival benefit. Additionally, we found that vaccine responses were unaffected by the use of the approved antiandrogen drug enzalutamide, suggesting that vaccinations could be deployed in tandem with standard-of-care therapies.

Conclusions: Vaccination against AR and AR splice variants can induce AR specific adaptive immune responses capable of inhibiting the growth of AR-V7 expressing tumor models, illustrating the potential of AR and its splice variants as immunologic targets in prostate cancer.

#4103 Novel mRNA-encoded HPV vaccine with APC maturation signal and endolysosomal trafficking domain demonstrates superior T cell-mediated immunogenicity and efficacious tumor clearance *in vivo*.

Liang Du, Hongya Han, Jingshu Ma, Zhenxing Yang, Jinjuan Mao, **Jijun Yuan**, Bo Ying

Abogen Bioscience, Suzhou, China

Human Papillomavirus (HPV), particularly HPV16, is a known causative agent of cancers in various anatomical sites, notably the anogenital and oropharyngeal regions. Despite the availability of prophylactic HPV vaccines for almost two decades, vaccination rates among young females, who are at a heightened risk for cervical intraepithelial neoplasia (CIN) and subsequent invasive cancer, remain suboptimal. The current standard of care for cervical cancer, involving invasive surgery and chemotherapy-based treatments, underscores the pressing need for safer and more effective therapeutics to enhance patient survival and quality of life.

In this context, while several HPV16-E6/E7 targeted therapeutic vaccines are in development and clinical trials, their clinical efficacy has been limited due to inadequate antigen presentation and suboptimal immunogenicity. Addressing this, our team has developed a novel, highly immunogenic mRNA therapeutic cancer vaccine, engineered to activate a robust T cell-mediated adaptive immune response and exhibit strong anti-tumor potential.

Our innovative approach includes the design of an HPV16-E6/E7 mRNA vaccine (ABO2101) that incorporates a unique antigen-expressing cassette. This cassette features endolysosomal trafficking domains and antigen presenting cell (APC) activation stimulators, enhancing both Class I and Class II antigen presentation and APC maturation, thereby amplifying antigen-specific T cell responses.

In both murine and human-derived experimental models, ABO2101 has demonstrated a significantly more potent adaptive T cell response against HPV16 antigens compared to other HPV16 mRNA therapeutic vaccines.

In antitumor efficacy evaluations using TC-1 tumor-bearing mice, ABO2101 single-dose administration successfully eradicated both early-stage (50 mm^3) and advanced (500 mm^3) tumors. This was accompanied by a marked increase in HPV16-specific CD8+ cytotoxic T lymphocytes within the tumor microenvironment.

Moreover, in prophylactic and adjuvant therapy models, ABO2101 prevented tumor growth across various dosages, indicating its robust preventative capabilities.

Further, the combination of ABO2101 with immune checkpoint inhibitors, including PD-1 and CTLA-4 antibodies, displayed a synergistic effect in both immune-oncology sensitive and resistant animal models, suggesting a potential for combinational clinical therapy.

In conclusion, our development of ABO2101, a mRNA-based HPV16-E6/E7 therapeutic cancer vaccine inclusive of APC maturation signals, represents a groundbreaking advancement in HPV-associated cancer treatment, as supported by our compelling preclinical data.

#4104 Randomized phase II trial of imiquimod with or without 9vHPV vs observation in patients with CIN 2 and 3.

S. S. Sheth[1], J. Oh[2], S. Bellone[1], E. R. Siegel[3], N. Buza[1], A. Iwasaki[1], **A. D. Santin**[1],

[1]Yale University, New Haven, CT, [2]Korea Advanced Institute of Science and Technology, Daejeon, Korea, Republic of, [3]University of Arkansas for Medical Sciences, Little Rock, AR

Introduction: We report the results of a randomized phase II trial of imiquimod, a topical immune-response modulator, vs imiquimod plus a 9-valent human papillomavirus vaccine (9vHPV) vs surveillance in cervical intraepithelial neoplasia (CIN) 2 and 3 patients.

Methods: We randomly allocated 133 patients with untreated CIN 2/3 in equal proportions to a 4-month treatment with self-applied vaginal suppositories containing imiquimod (arm B) or imiquimod plus 9vHPV (arm C) vs clinical surveillance (arm A). The main outcome was efficacy, defined as histologic regression to CIN 1 or less. Secondary outcomes were HPV clearance and treatment tolerability. Exploratory objectives included the comparison of cervical CD4/CD8 T-cell infiltration at baseline, mid-study, and post-treatment by flow-cytometry.

Results: Of the 114 evaluable patients 77% and 23% had CIN2 and CIN3, respectively. Histologic regression to CIN1 or less was observed in 95% of patients in the Arm B: imiquimod group and 84% in the Arm C: imiquimod+9vHPV compared with 79% in Arm A: surveillance ($p=0.043$ and 0.384, respectively). The difference between either treatment arm compared with control did not reach the prespecified $\alpha=0.025$. No significant differences were noted in HPV clearance. The number of tissue-resident memory CD4/CD8 T-cells in cytobrush samples demonstrated a >5-fold increase in Arm-B: imiquimod when compared to Arm-A: surveillance ($p<0.01$). Imiquimod treatment was well tolerated. In contrast, there was no significant difference in T-cell responses among participants in Arm-C compared to Arm-A. Imiquimod treatment was well-tolerated.

Conclusions: Although imiquimod induced a higher percentage of regression to CIN1 or less and significant increases in CD4/CD8 T-cells infiltrating the cervix, it did not meet its prespecified statistical outcome for efficacy. A higher regression rate than expected was observed in the surveillance arm of this prospective trial. Future clinical trial with imiquimod targeting CIN3 patients are warranted.

#4105 Immune-modulating vaccines targeting CD73.

Y. Luo, T. Shi, H. Wang, B. Liu, J. Wei;
Department of Oncology, Nanjing Drum Tower Hospital, Affiliated Hospital of Medical School, Nanjing University, Nanjing, China

Background: To realize the generalizable regulation of the tumor microenvironment (TME), immune-modulating vaccines are developed to target shared antigens expressed by immunosuppressive cells and cancer cells. CD73, also known as ecto-5'-nucleotidase, is a pivotal enzyme in the adenosine metabolic pathway and is expressed on the surface of multiple cancer cells and immunosuppressive cells in the TME. In this study, we aim to develop a CD73-targeting immune modulatory peptide vaccine by predicting antigen sequences, screening immunogenic antigen peptides, and assessing their anti-tumor efficacy and capacity to improve the TME.

Methods: The expression level of CD73 on various cancer cell lines were evaluated by flow cytometry. Several online software were used to predict CD73-derived peptides that bind to the mouse MHC-I (major histocompatibility complex class I) molecules. Cells from the draining lymph nodes of healthy mice and peptide-immunized mice were harvested and stimulated by the synthetic peptides *in vitro*. T cell activation level, IFN-γrelease degree and their cytolytic capability towards cancer cells was measured. CD73-derived peptides were mixed with CpG to treat 4T1 tumor-bearing mice and the changes in the TME were investigated by flow cytometry. The online website (www.camoip.net) was used to analyze the correlation between CD73 expression and patient survival in the TCGA Breast invasive carcinoma (BRCA) cohort.Results: 4T1 exhibited a strikingly elevated surface expression of CD73 compared to other mouse cancer cell lines. Three CD73-derived peptides (EP1, EP2, EP3) consisting of 8-10 amino acids were synthesized. *In vitro* stimulation experiments indicated that EP1 and EP3 significantly elicited T-cell responses in draining lymph nodes. After stimulation, the proportions of $CD25^{+}$, $CD69^{+}$, $CD107a^{+}$, and $CD137^{+}$ cells markedly increased in $CD8^{+}$ T cell populations. These cells also displayed enhanced cytotoxicity against 4T1 tumor cells. *In vivo* experiments demonstrated that EP3 induced a pronounced anti-tumor response in an established 4T1 tumor model without evident toxicity. Moreover, subcutaneous injection of EP3 improves the TME by promoting antigen-specific $CD8^{+}$ T-cell responses, reducing M2 macrophages, and inducing neutrophil maturation. High tumor CD73 expression was also found to be associated with poor outcomes among BRCA patients, which further indicated clinical relevance.

Conclusions: In this study, we successfully identified an immunogenic vaccine targeting CD73. It expressed dual functionality by effectively triggering cytotoxic T-cell responses that directly killing CD73-highexpressing tumor cells and regulating the tumor microenvironment through eliminating immunosuppressive cells with elevated CD73 expression. These findings hold promise for a novel immune-modulating vaccine and suggest a potential therapeutic avenue for the treatment of breast cancer and other types of cancer.

#4106 A novel synthetic long peptide vaccine composition targeting multiple PD-L1 T-cell epitopes exhibits anti-tumor efficacy in a syngeneic mouse colorectal cancer model.

K. Lin, M. Toh;
CK Life Sciences Development Limited, Hong Kong, Hong Kong

Background Cancer immunotherapy targeting immune checkpoints has shown promising clinical anti-tumor efficacy over the past decades. Monoclonal antibodies against PD-1 or PD-L1 have demonstrated clinical efficacy in a wide spectrum of cancer types. Despite the clinical success of therapies using immune checkpoint inhibitors (ICI), only a subset of patients shows long-lasting tumor remission, while resistance and toxicities to these agents remain to be addressed. This supports the need to explore alternative immunotherapeutic approaches or additional therapies for synergistic combinations to augment the anti-tumor efficacy for cancer patients receiving ICI therapies.
Methods As an active immunotherapy approach, we developed a blend of four novel synthetic peptide vaccines each containing one PD-L1 T-cell epitope with individual covalent conjugation of the carrier protein, keyhole limpet haemocyanin (KLH), which is to break immune tolerance towards self-molecules. The four PD-L1 epitopes range from 30 to 40 amino acids in length, which target different domains of mouse PD-L1 protein. The PD-L1 peptides were synthesized using the technique of solid-phase peptide synthesis and purified by high performance liquid chromatography. All naked peptides were conjugated to KLH protein by thiol-maleimide reaction, followed by dialysis for purification. The peptide vaccines were formulated with a Toll-like receptor 9 agonist CpG ODN 1826 and aluminum hydroxide gel for animal immunization.
Results These synthetic long PD-L1 peptide vaccines are highly immunogenic in a syngeneic BALB/c mouse model for a cell-mediated immune response when admixed and formulated with adjuvants. The vaccine composition is well tolerated by the mice with no evidence of toxicity and autoimmunity. *In vivo* administration of the vaccine formulation can elicit a positive PD-L1-specific T cell response in splenocytes with an IFN-γ ELISPOT assay. Moreover, *in vivo* vaccination of these PD-L1 peptide vaccines in a CT26 syngeneic mouse preventive colorectal cancer model exhibits a potent anti-tumor activity, with a 54% tumor growth inhibition ($p<0.001$) in tumor volume compared to that of the adjuvant-control group at the end of the study.
Conclusions Taken together, our data demonstrate a proof-of-concept that T cell-based PD-L1 peptide vaccines are a promising therapeutic strategy for inducing anti-tumor immunity to combat cancers.

#4107 Evaluating the efficacy of personalized neoantigen cancer vaccine in preclinical model: A promising step towards precision immunotherapy.

T. Ghosh Halder[1], K. Gutowsky[1], S. Ng[1], T. Thode[1], A. Weston[1], E. Kelley[1], J. Soria-Bustos[2], J. A. Giron[2], T. Bargenquast[3], M. Kaadige[1], S. Tripuraneni[1], B. Durbin[1], S. Rheinschmidt[1], S. Adamson[1], M. Gordon[3], J. Moser[3], J. Altin[2], R. Soldi[1], S. Sharma[1];

[1]TGen (The Translational Genomics Research Institute), Phoenix, AZ, [2]TGen (The Translational Genomics Research Institute), Flagstaff, AZ, [3]HonorHealth Research Institute, Scottsdale, AZ

Background: In the past decade, immunotherapy has transformed cancer treatment, with the development of immune-checkpoint inhibitors and adoptive cell therapies. A novel frontier is personalized vaccines targeting neoantigens unique to tumor cells. Vaccines based on neoantigens have several advantages. First, neoantigens are exclusively expressed by tumor cells and can, therefore, elicit truly tumor-specific T cell responses, thereby preventing 'off-target' damage to nonmalignant tissues. Second, neoantigens are de novo epitopes derived from somatic mutations, which presents the possibility to circumvent T cell central tolerance of self-epitopes and thus induce immune responses to tumors. One of the major challenges is the optimal neoantigen discovery/selection. Our study combines in silico HLA binding models with the 'MHC-PepSeq' platform to enhance neoantigen prediction, creating a personalized neoantigen peptide vaccine. We aim to demonstrate its efficacy in a mouse CT26 colon cancer model.

Methods: Our method involved whole exome sequencing of tumor and normal DNA to identify neoantigens expressed in CT26 tumors, generating a peptide library. The peptides were further filtered using an in-silico prediction algorithm and our proprietary peptide-MHC binding assay (PepSeq assay), to determine those exhibiting the highest binding affinity with mice HLAs. Vaccines were prepared by dissolving these peptides in sterile PBS. Mice (BALB/C) were subcutaneously implanted with CT26 tumors, then immunized with the vaccine via IV injection in combination with a TLR7/8 agonist. Mice received a second vaccine dose on Day 14, and some groups were treated with an anti-PD-1 agent. Tumors and spleens from the mice were collected, processed into single-cell suspensions, and analyzed by single-cell sequencing, TCR analysis, IHC, and flow cytometry assays. Peripheral blood mononuclear cells (PBMCs) were collected and utilized in MHC tetramer assays.

Results: Preliminary in vivo studies demonstrated significant tumor growth restrictions (TGI around 70%) and prolonged tumor-free survival in some mice. Our data showed the generation of neoantigen-specific T cells in vaccinated mice. Remarkably, vaccinated, tumor-free mice, when re-challenged with the same tumor cells, maintained their tumor-free status, suggesting the vaccine induced post-treatment immunological memory. Combining the vaccine with checkpoint inhibition resulted in better tumor growth restriction in mice (TGI around 93%).

Conclusion: Overall, our data suggests that our personalized neoantigen vaccine platform has the potential to evoke robust and durable immune responses and, when paired with suitable complementary therapies and immune adjuvants, may serve as an effective cancer treatment.

#4108 Safety and feasibility of personalized neoantigen DC vaccines in postoperative esophagus squamous cell carcinoma: A Phase 1b trial.

Yueyun Chen, Hua-Shan Shi, Yang Hu, Yong Yuan, Yu-Shang Yang, Heng Xu, Li Yang, Zhen-Yu Ding

West China Hospital, Sichuan University, Chengdu, China

Background: Immunotherapy, currently stands at the forefront of esophagus squamous cell carcinoma (ESCC) research. Yet, the landscape of post-surgical adjuvant therapy, particularly for patients resistant or unresponsive to initial immunotherapy, remains unexplored. Addressing this, our prospective study evaluates the efficacy of a personalized neoantigen-loaded dendritic cell vaccine (Neo-DCVac) as a novel adjuvant in ESCC patients after neoadjuvant immunochemotherapy (nICT).
Methods: Neo-DCVac, designed for 12 ESCC patients post-radical mastectomy following nICT. The vaccine regimen included five doses at weeks 1, 2, 4, 6, and 8, followed by bi-monthly boosts for a year. The primary endpoints were safety and immune response post-vaccination, with 1- and 2-year overall survival (OS) and progression-free survival as secondary endpoints. The T-cell response to neoantigen peptides was evaluated using ELISPOT, flow cytometry, ELISA, and single-cell sequencing to investigate the vaccine's mechanism of action.
Results: From April 2021 to October 2023, a total of 12 ESCC patients were enrolled. The occurrence of all-grade AEs was 38.5% (5/12), all of grade 1-2, with no dose-limiting toxicities. No treatment interruptions or treatment-related deaths were observed. Till October 27 2023, the median follow-up was 31.2 months. Survival analysis revealed 1-year and 2-year disease-free survival (DFS) and overall survival(OS) rates of 88.3%, 66.7%, and 100.0%, 91.7%, respectively. Patients with diver genes had a longer median DFS (not reached) compared with patients without diver genes (10.8 months, P = 0.001). Post-vaccine immunization, all patients showed a marked increase in peripheral blood T cell subtypes (CD3, CD4, CD8), with significant neoantigen peptide response in 75% (9/12) as evidenced by ELISPOT and ELISA tests. Single-cell sequencing coupled with CoNGA analysis revealed a distinct MAIT cell population, displaying 65 clonotypes and 146 cells with consistent GEX profiles and TCR sequences. GLIPH2 analysis on Neo-Vac immunotherapy patients identified shared peptide-MHC specificities, notably in patient ES0-01, and similar patterns in patients ES0-04 and ES0-07, suggesting T cell expansion and neoantigen-specific responses post-vaccination.
Conclusions: The neoantigen DC vaccine demonstrated favorable safety and exhibited notable efficacy in ESCC.
Clinical trial information: NCT05023928. Research Sponsor: No.

#4109 Discovery of a novel cancer-specific antigen for therapeutic targeting using the Oncotope platform.

J. S. Manavalan[1], D. Mor[2], J. Davis[1], S. Saini[2], I. Pal[3], D. Feith[3], Y. Hikichi[4], E. Davis[1];
[1]Cancer Antibodies Inc, Longwood, FL, [2]Augusta University, Augusta, GA, [3]University of Virginia, Charlottesville, VA, [4]Tuning Fork Bio, Cambridge, MA

Identification of druggable cancer-specific surface antigens is hindered by the complexity of cancer's molecular diversity and the risk of normal cell cross-reactivity. We developed the Oncotope Platform that rapidly identifies multiple cancer-specific cell surface targets not expressed on normal cells (JCO 2022). In this study, we generated polyclonal antibodies to human Triple Negative Breast Cancer (TNBC; Hs578T, ATCC). Following this, we used the Oncotope Platform to filter the anti-TNBC antibody-enriched serum, to yield cancer specific polyclonal antibodies. Using a Protein Microarray, we assessed the binding affinity of both the Total Anti-TNBC Serum (before filtration) and the Oncotope Filtered Anti-TNBC Serum towards approximately 25,000 human proteins. Our results identified antigens that exhibited significantly higher affinity binding to the Oncotope Filtered Anti-TNBC Serum than the Total Anti-TNBC Serum. One of these antigens ZIP7, a zinc transporter situated in the ER and Golgi, has been shown to activate cell proliferation related signaling pathways in TNBC. Our findings revealed the aberrant cell surface expression of ZIP7 on TNBC cells and its potential as a therapeutic target. Flow cytometry analysis using rabbit polyclonal antibodies against ZIP7 revealed substantial binding to TNBC cells, while no significant binding was observed with normal breast epithelial (NBE) cells from the same patient (Hs578BsT, ATCC). Additionally, cytotoxicity assays, employing the same antibodies and a secondary anti-rabbit ADC, showed the preferential killing of TNBC cells over NBE cells (Table 1). In summary, our study marks a breakthrough in identifying cancer-specific antigens with therapeutic potential. The Oncotope Platform, in combination with protein microarrays, enables rapid identification of unique cancer-specific antigens absent in normal cells. Specifically targeting ZIP7 on TNBC cell surfaces highlights its promise for precision cancer therapy.

Table 1

Cell Line	Incubated with:	%Binding Flow Cytometry (1:400 Ab dilution)	%Cytotoxicity (4ug/ml Ab conc.)
TNBC (Hs578T)	Total Anti-TNBC Serum	96.65	94.5 +/- 2.5
	Oncotope Filtered Anti-TNBC Serum	97.46	79.2 +/- 2.1
	ZIP7 Polyclonal antibody ((Proteintech 11200-1-AP)	46.2	73.2 +/- 0.5
Normal Breast Epithelial cells (Hs578Bst)	Total Anti-TNBC Serum	92.95	92.3 +/- 3.0
	Oncotope Filtered Anti-TNBC Serum	20.39	17.9 +/- 4.5
	ZIP7 Polyclonal antibody ((Proteintech 11200-1-AP)	6.37	14.1 +/- 1.6

#4110 Identification of tumor peptides for therapeutic mRNA vaccination in a mouse multiple myeloma model.

A. Van der Vreken[1], F. Thery[2], S. Meulewaeter[3], K. Vanderkerken[1], E. De Bruyne[1], K. De Veirman[1], L. Franceschini[1], R. Verbeke[3], F. Impens[2], J. Lentacker[3], K. Breckpot[1], E. Menu[1];

[1]Vrije Universiteit Brussel, Brussels, Belgium, [2]VIB, Ghent, Belgium, [3]Ghent University, Ghent, Belgium

Background: Multiple myeloma (MM) is a plasma cell cancer for which immunotherapy holds the promise of durable control. To date, cancer vaccines mainly focused on tumor-associated antigens with survivin eliciting protective T-cell responses in both preclinical and clinical studies. Given the success of mRNA vaccines in medicine, we developed Galsomes, lipid nanoparticles containing mRNA and α-galactosyl ceramide to activate both $CD8^+$ T cells and invariant natural killer (iNK) T cells, both potential anti-MM effectors.

Materials and Methods: Mouse 5T33MM cells were studied by PCR and flow cytometry (FCM) for expression of survivin and CD1d, respectively. Intravenous (IV) prime-boost Galsome vaccination was performed with a 7-day interval in C57BL6/KalwRij mice that received an IV injection of 5^x10^6 5T33MM cells 3 days earlier. As a control, mice were injected with saline. After 2 weeks, MM burden was studied by serum electrophoresis and FCM, incl. expression of CD1d and PD-L1 on MM cells. Activation of iNKT cells and survivin-specific T cells was studied by measuring IFN-γ secretion in ELISA and dextramer staining. Immunopeptidomics was used to identify new vaccine candidates for which Galsome vaccination is ongoing.

Result: The 5T33MM cells showed expression of survivin and CD1d, making it a suitable model for Galsome vaccination. Two weeks following prime-boost vaccination, the serum M-protein was reduced, though not significantly. In contrast, MM cells were significantly reduced in bone marrow and spleen. Expression of CD1d and PD-L1 on MM cells was high but unchanged by Galsome vaccination. Activation of iNKT cells and survivin-specific T cells following prime vaccination was shown. However, following boost vaccination these cell populations reduced significantly compared to control. We repeated prime-boost vaccination in healthy mice, observing a similar outcome. This suggests that the negative effect of the boost Galsome vaccination was not related to immune dysfunctionality due to MM progression. So, we studied the impact of survivin mRNA in the vaccine, as survivin is also expressed in activated T cells, making them a potential target. We observed that iNKT cells and ovalbumin-specific T cells were more reduced when ovalbumin mRNA was paired with survivin mRNA in the Galsomes. To identify other vaccine candidates, we studied peptides eluted from MHC-I/peptide complexes on 5T33MM cells. We selected 4 vaccine candidates including the MM idiotype based on immunogenicity, pathway classification and abundance. mRNA and Galsomes were prepared, and the efficacy of these Galsomes in 5T33MM mice is currently under evaluation.

Conclusion: These data show that Galsome vaccination has the potential to reduce MM cell levels. To reach higher efficacy, careful selection of the vaccine antigen is required. Moreover, combination with other immunotherapies might be needed to reach durable disease control.

#4111 Multi-peptide cancer vaccines targeting KRAS induce significant anti-tumor efficacy.

C. Li, M. Toh;
CK Life Sciences Development Limited, Hong Kong, Hong Kong

Background and objective: *Kirsten rat sarcoma viral oncogene homologue (*KRAS) is frequently mutated in human cancers. KRAS mutants offer the potential for the development of cancer-specific immunotherapy, as epitopes harbouring mutations are strong neoantigens to which the immune system generates cancer-specific anti-tumor effects. However, previous clinical trials of KRAS-targeted vaccines failed to generate satisfactory anti-cancer efficacy. Evidence suggested that CD4 T cell activity plays a critical role in augmenting the cytotoxic effect of CD8 T cells. Here, we design long peptides based on the MHC II hotspots on the entire KRAS protein that activate both CD4 and CD8 T cells to kill KRAS-driven cancer cells. Long peptides also cover a wider range of HLA alleles to increase their utility in a broader spectrum of patients. Our objective is to create a multi-peptide vaccine simultaneously targeting the mutant and wild-type (WT) regions of human KRAS protein.

Methods: By selecting MHC II hotspots via multiple epitope prediction algorithms, we designed and synthesized 8 long peptides with lengths between 25 to 30mers. One of them harboured a G12D mutation, while the others covered the WT regions of KRAS. In addition, the corresponding *keyhole limpet hemocyanin (*KLH) conjugated peptides were also generated. We first demonstrated their immunogenicity in mouse *in vivo* models. Different combinations of peptides adjuvanted with either CpG oligodeoxynucleotide + aluminum (CpG+alum) or complete/incomplete Freud's adjuvant (CFA/IFA) were immunized into Balb/c mice before determining the immune response by mouse interferon γ (mIFNγ) ELISPOT assay. Subsequently, an *in vivo* prophylactic anti-tumor study was conducted by immunizing this multi-peptide vaccine in Balb/c mice and observing the growth inhibition of the CT26-derived tumors.

Results: T cell responses were observed in two peptide mixes with or without G12D mutation, suggesting that both mutant-harbouring peptide and WT peptides were immunogenic. We showed that KLH-conjugated peptides and CpG+alum elicited stronger immune responses than the naked peptides and CFA/IFA respectively. Furthermore, peptide mapping showed that the G12D mutant-harbouring peptide and two other WT peptides may contribute to the overall T cell response in the Balb/c mouse. In the prophylactic anti-tumor study (n = 10), immunization of KRAS naked peptide and KLH-conjugated peptide vaccines significantly inhibited tumor growth by 51.2% (****$p < 0.0001$) and 44.7% (***$p < 0.001$) respectively, compared to control. Subsequent mIFNγ ELISPOT assay showed that the tumor inhibitory effect was attributed to the activation of antigen-specific T cell response of the vaccines.

Conclusion: Our multi-peptide vaccines targeting both the mutant and WT regions of KRAS could generate KRAS-specific T cell responses and elicit significant anti-tumor effect in mouse models.

#4112 Identification of Th1-specific epitopes from non-mutated KRAS lesions for off-the-shelf cancer vaccines.

Y. Choi, J. Lim, H.-H. Park, J. Kang, H. Jung;
Aston Sci., Seoul, Korea, Republic of

Background KRAS is crucial for cell growth, differentiation, and signaling. Mutations in the KRAS gene (i.e., codon 12 or 13) are frequently associated with the development and progression of cancer, particularly lung, colorectal, and pancreatic cancers. Recently, it has been captured that KRAS targeting cancer vaccine research and clinical trials have been conducted in certain tumor types and vaccine approaches are encouraged to move forward. It has been well known that the tumor-eradicating efficacy of cancer vaccines arises from Th1 epitope selection. While tumor growth may persist after immunization with non-selected epitopes (including full-length), immunization with a highly selected Th1-specific epitope vaccine can lead to tumor regression by suppressing the activation of immune inhibitory cells. The Th-Vac® discovery platform uses a combination of in-silico, in-vitro, and in-vivo studies to precisely identify Th1-specific epitopes. It consists of two modules: module 1 (in-silico) and module 2 (in-vitro and efficacy evaluation). The aim is to identify MHC class II epitopes that are specific to antigens for CD4+ T cells, displaying the most favorable binding affinity across diverse alleles. Th1-specific epitope vaccines aim to boost and sustain T cell immunity against tumor antigens, overcoming the lack of a precise T cell response or pre-existing tolerance in the immunosuppressive TME. This study aimed to explore Th1-specific epitopes for KRAS vaccine to be potentially effective in numerous KRAS mutation-driven cancers.

Methods Peptide sequence candidates that have highly potential of MHC class II binding affinity were comprehensively predicted via a module 1 (ASEP program). All of peptides selected in ASEP were synthesized as 15 mers. Each peptide was evaluated for immunogenicity using ELISpot and/or FACS analysis in module 2 (2a for in vitro and 2b for in vivo immunologic evaluation) of the Th-Vac® discovery platform. Specifically, in Module 2b, immunogenicity was evaluated using a 38-mer peptide formed by combining five overlapping peptides selected in 2a. These kinds of immunogenicity evaluations were conducted using type 1 and/or type 2 cytokine(s) produced by CD4+ T cells.

Results In ASEP prediction, twelve peptides were selected as potential candidates demonstrating a high affinity to MHC class II, which were in different lesions of common mutation of KRAS. In module 2 using ELISpot and FACS analysis, two epitopes (non-mutated sequences) were finally selected as Th1-specific epitopes based on the type 1 T cell response.

Conclusion Unlike previous vaccines using mutant lesions, in this study, two non-mutated Th1-specific epitopes are under the in-vivo efficacy studies as mono and combining regimen(s) in certain tumor types. Additionally, the Th-Vac® platform was fully validated in terms of the performance and its application would be expanded beyond a cancer vaccine.

#4113 AST-301,a pDNA-based cancer vaccine encoding HER2-ICD, enhances anti-tumor effect of HER2-ADC in a HER2-expressed gastric cancer xenograft model.

J. Kang[1], H.-H. Park[1], J. Choi[1], J. Lim[1], S.-Y. Jang[2], M.-A. Kim[2], M.-K. Park[2], Y.-H. Park[3], S. Lim[3], C.-W. Chung[3], J. Choi[4], E. Joung[1], A. Y. Kim[5], H. Jung[1]; [1]Aston sci., Seoul, Korea, Republic of, [2]Korea testing & Research institute, Hwasun, Korea, Republic of, [3]LegoChem Biosciences, Inc., Daejeon, Korea, Republic of, [4]Jeonbuk National University Medical School, Jeonju, Korea, Republic of, [5]Aston sci. USA, Inc., Seoul, Korea, Republic of

Background: In gastric cancer, the HER2 overexpression (6% to 29.5% of gastric cancers) is considered to increase proliferation activity and suppress apoptosis of the cancer cells. However, HER2-targeting therapy in gastric cancer has not been fully evaluated. Currently, new approaches with HER2-tageted antibody-drug conjugates (ADCs) have led to promising results in HER2-related solid tumors. ADCs may have immune-modulating properties and that the payloads delivered by ADCs may induce immunogenic cell death. Based on this rationale, ADC and cancer vaccine combination would be potentially synergistic to improve clinical outcomes. This study was conducted to evaluate an synergistic effect and immune response of the combination of AST-301 and HER2-ADC in HER2-expressed gastric cancer xenograft model. AST-301 phase 1 study (PN109) was completed and phase 2 randomized-control trials (CornerStone-001, CornerStone-003) have been conducted in breast cancer and gastric cancer.

Methods: NCI-N87 cells were mixed with the same amount of matrigel at $1x10^7$ cells to formation tumors in the flanks of athymic BALB/c nude mice. After the tumor size of mice reached 100-200 mm^3, all of them were randomly classified into four groups (n=7/group) and drug administration was initiated. AST-301 (100 μg/animal, intradermal injection, mixed with rhuGM-CSF as an immune adjuvant) was administered once a week to a total of fourth. LCB01 (1 mg/kg, intravenous injection) was administered to once. Enhertu (1 or 3 mg/kg, intravenous injection) was administered to twice for four weeks. The relative tumor size and TGI rate at day 25 were key endpoints of efficacy. To evaluate the mechanism underlying the enhanced anti-tumor effect due to the combined administration of AST-301 and HER2-ADCs, immune-cell profiling was also conducted using FACS analysis.

Results: Our previous study has shown that AST-301 has anti-tumor effects in human gastric cancer xenograft athymic BALB/c nude mouse model. It was showed that adding AST-301 to LCB01 or Enhertu inhibited tumor growth based on a TGI rate at days 25; AST-301 combining with LCB01 vs LCB01 mono (52 % vs 43 %), AST-301 combining with Enhertu vs Enhertu mono (42 % vs 24 %).As an explorative endpoint, it was observed that myeloid-derived suppressor cells (MDSCs) elevation was modestly inhibited in tumor site in AST-301 mono or certain combination regimen adding AST-301. It was remarkable (or observed or captured) that MDSCs elevation was inhibited in tumor site in the combination groups of all ADCs with AST-301 compared to normal saline groups.

Conclusion: With combining AST-301 and HER2 ADCs, it was demonstrated that anti-tumor effect was likely synergistic in the athymic mouse model. Phase 2 study of AST-301 in HER2-expressed gastric cancer has been on going (CornerStone-003, NCT 05771584).

#4114 AST-201 (pUMVC3-hIGFBP2 N-terminus) demonstrates anti-tumor effect in an ovarian cancer mouse model.

J. Lim[1], **J. Kang**[1], H.-H. Park[1], J. Choi[2], J. Choi[1], S.-Y. Jang[3], M.-A. Kim[3], M.-K. Park[3], M. Disis[4], E. Joung[1], A. Y. Kim[5], H. Jung[1];
[1]Aston Sci., Seoul, Korea, Republic of, [2]Jeonbuk National University Medical School, Jeonju, Korea, Republic of, [3]Korea testing & research institute, Hwasun, Korea, Republic of, [4]Center for Translational Medicine in Women's Health University of Washington, Seattle, WA, [5]Aston Sci. USA, Inc., Seattle, WA

Background: IGFBP2, known to enhance the invasion capacity of ovarian cancer cells, has been suggested that its inhibition could be potentially a treatment strategy of ovarian cancer. AST-201 (pUMVC3-hIGFBP2) is a therapeutic cancer vaccine using a plasmid DNA encoding IGFBP2 N-terminus. In a phase 1 study (NCT01322802) completed, 100 μg AST-201 (intradermal immunization, id) showed not only a significant efficacy by inducing the Th1-cell immunity against IGFBP2 but also safety and tolerability profiles in ovarian cancer patients. The primary objective of this study is to evaluate whether the administration of AST-201 alone and the combination with pembrolizumab could show anti-tumor efficacy and/or synergic effect in the ID8-Luc2 ovarian cancer mouse model. Also, immunological responses were observed as explorative endpoint.

Methods: AST-201 (100 μg/animal, id, mixed with mGM-CSF as an immune adjuvant) was immunized to mice (C57BL/6) once a week for a total of 4 times on different days, either alongside pembrolizumab (10 mg/kg, intraperitoneal injection) twice a week for a total of 3 times on different days. Also, AST-201 was immunized was a mono treatment. The efficacy was evaluated by a tumor growth inhibition (TGI) rate at the last day, and immune cell profiling via FACS analysis was conducted with splenocytes and tumor tissues collected at 8 weeks after the first injection.

Results: As a primary endpoint, a TGI rate at Day 55 of AST-201 mono treatment was 67%, comparing to a control group ($p<0.05$). The anti-tumor effect of AST-201 combining with pembrolizumab was better than standard dose pembrolizumab, based on a TGI rate at Day 55 (78% vs 66%, not significant). Immune profiling showed that AST-201 and pembrolizumab combination regimen could inhibit a tumor growth by transforming TME into inflamed-type (‘hot’) form the low immunoreactivity, which was supported by increased $CD4^{+}T_{EM,}$ and $CD8^{+}T_{EM}$ and T helper cells in splenocyte and TIL analysis.

Conclusion: A study demonstrated that AST-201 (IGFBP2 cancer vaccine) showed an anti-tumor effect as mono treatment and would be potentially leading to a synergistic effect with a combination regimen of pembrolizumab. Phase 2 randomized-controlled study of AST-201 in ovarian cancer will be initiated under the MRCT strategy (CornerStone-004 study, NCT05794659).

#4115 Unleashing the power of MHC associated peptide proteomics: Immunogenicity assessment of oncology drugs.

S. Pattyn;
ImmunXperts, a Q2 Solutions Company, Gosselies, Belgium

Bispecifics targeting multiple antigens or epitopes have been showing great promise for treatment of cancer. However, managing unwanted immunogenicity has become a challenge in the development cycle of these promising therapeutics as there is a trend towards higher unwanted immune responses compared with classical monoclonal antibodies. A thorough assessment of their immunogenic potential leads to safe biotherapeutics with high treatment efficacy. MAPPS assays (MHC associated peptide proteomics) enable the precise identification of all the regions of a protein that may evoke an immune response. This information is key for correct risk assessment and for modulating biotherapeutics. High-sensitive MAPPS workflow leads to higher numbers of identified peptides (self + non-self peptides) and gives the deepness of analysis required for confident immunogenicity derisking and modulation. We show the importance of peptides presented by HLA-DP and HLA-DQ (next to the standard HLA-DR presented peptides). Next, we also show the first ever comparison of presented peptides in true immune cells: dendritic cells (as compared to monocyte derived dendritic cells) and B cells.

TUMOR BIOLOGY: Detection, Treatment, and Prevention of Metastasis
Poster Session

#4119 CXCR4/CB2 heterodimer antagonizes CXCR4-mediated metastasis and tumor growth *in vivo*.

N. M. Pennant[1], A. B. Hartono[2], S. Liu[2], C. Massey[2], C. Lee[2], T. Stoyanova[2], C. V. Hinton[1];
[1]Clark Atlanta University, Atlanta, GA, [2]University of California, Los Angeles, Los Angeles, CA

The G-protein-coupled chemokine receptor (GPCR), CXCR4, is ubiquitously expressed in malignant tumor tissues, and controls migration and other tumor survival mechanisms upon interaction with its chemokine agonist, stromal cell-derived 1α (SDF1α). The CXCR4/SDF1α axis is relevant to shaping the tumor microenvironment mainly the metastatic spread of primary tumors to distal organs and immune response; thus, expression of CXCR4 in tumors is vital to tumor aggressiveness, survival probability, and metastasis-associated mortality. CXCR4 signals through a homodimer, but also forms heterodimers with other chemokine and non-chemokine GPCRs. We've demonstrated that CXCR4 forms a heterodimer with the GPCR, cannabinoid receptor 2 (CB2), in human breast and prostate cell lines *in vitro*. The cannabinoid system has earned interest as anticancer therapeutic targets by modulating growth, migration, angiogenesis, *etc*. In our model, CXCR4-mediated, pro-tumor signaling was reduced by the physical heterodimer, and the dimer was induced by simultaneous treatment with agonists (*SDF1α and AM1241*) for respective receptors. The resultant heterodimer negatively interfered with migration, cytoskeletal rearrangement, motility associated proteins, and signaling that coordinates movement. Given that cannabinoids have been shown to reduce metastasis and profession of clinical tumors, **we hypothesize that a heterodimer of CXCR4 and CB2 disrupts CXCR4-mediated metastasis, and ultimately, decrease tumor progression *in vivo***.Herein, we tested our hypothesis in an *in vivo* model of spontaneous metastasis NSG male mice. Luciferase-containing human prostate cancer cells (DU145 RFP/Luc) were implanted subcutaneously. Once tumors reached 40mm^3, mice were randomized by volume, weight and age, and divided into 4 treatments: vehicle, SDF1α, AM124, and SDF1α/AM124(combo) for daily intraperitoneal injections. Tumors reaching 400mm^3 were excised, and treatments continued for 3 weeks. Spontaneous metastasis was monitored via IVIS imaging at 2- and 3-weeks post-tumor removal. We observed reduced tumor growth, and decreased incidence rates of metastasis to the lung in the combination treatment group, which, based on our *in vitro* data, is representative of a CXCR4/CB2 heterodimer. This novel definition of heterodimerization could reveal and exploit new mechanisms for CXCR4 regulation in tumor metastasis. The CXCR4/CB2 heterodimer may attenuate responses triggered individually by CXCR4 without toxicity and side effects experienced with current CXCR4 antagonists.

#4120 Adherent-to suspension transition by hematopoietic factors in metastatic dissemination of circulating tumor cells.

H. Park;
Yonsei University, Seoul, Korea, Republic of

Although metastasis is the foremost cause of cancer-related death, a specialized mechanism that reprograms anchorage dependency of solid tumor cells into circulating tumor cells (CTCs) during the metastatic cascade remains elusive. We discovered a biological phenomenon referred to as Adherent-to-Suspension Transition (AST) that reprograms adherent cells into suspension cells via aberrant induction of hematopoietic transcriptional regulators, which are hijacked by solid tumor cells to disseminate into CTCs. During dissemination, tumor microenvironment triggers epigenetic alteration of AST factors in the invasive front of solid tumors to evoke spontaneous cell-matrix dissociation, acquire anoikis resistance, and bypass immune surveillance of CTCs, however, in the absence of lineage differentiation and EMT. Using mouse models and de novo metastatic patient specimens, we uncovered how Adherent-Suspension Plasticity (ASP) dictates anchorage plasticity during the dissemination and colonization process within the metastatic cascade. Finally, we demonstrate therapeutic strategies that target AST factors to specifically abrogate CTC formation and suppress distant metastases. Together, these findings underscore an important early mechanism of how cancer cells spread and highlight novel targets for the development of anti-metastatic therapy. Furthermore, AST opens unexplored scenarios how reprogramming anchorage dependency orchestrates physiological events such as development, organ morphogenesis and immune cell activation.

#4121 Unveiling discordant views of a novel drug's influence on cell motility from proteomics and immunofluorescence perspectives.

W. Chen[1], N. Woods[1], H. Law[1], F. Qiao[1], S. Jagadesan[2], C. Guda[2], R. Bergan[1];
[1]UNMC Eppley Institute, Fred & Pamela Buffett Cancer Center, Omaha, NE, [2]University of Nebraska Medical Center, Omaha, NE

Introduction: Metastasis is a leading cause of death in patients with solid tumors. Our group has discovered KBU2046, a selective inhibitor of cell motility (Nature Communications 2018). We conducted a time-course immunofluorescent staining to investigate the impact of KBU2046 on the cell adhesion and motility components of human prostate cancer cells. Our objective was to compare our findings with our proteomic analysis results in order to gain insights into the novel molecular mechanisms of KBU2046 in modulating cell motility.
Experimental Procedures: Proteomics analysis. We treated PC3 cells with KBU2046 or vehicle (N=3/group) and quantified protein expression using Liquid Chromatography/Tandem Mass Spectrometry (LC-MS/MS). In separate experiments (N=4), we performed LC-MS/MS after Tandem Mass Tag (TMT) labeling on isolated membrane fractions. We used bioinformatics tools, including Gene Set Enrichment Analysis (GSEA), Gene Ontology (GO), Kyoto Encyclopedia of Genes and Genomes (KEGG), Ingenuity Pathway Analysis (IPA), and protein-protein interaction (PPI) network analysis, to characterize significantly differentially expressed proteins upon KBU2046 treatment and tried to verify by Western blots. Immunofluorescence (IF) staining. Following treatment of PC3, 1532CPTX, and 1532NPTX cells with KBU2046 or vehicle at various intervals, cells were stained for β1, β5 integrin, actin, and DAPI. Images were acquired by a Zeiss LSM 800 Confocal Laser Scanning Microscope.
Results: The proteomics analysis demonstrated that KBU2046 was having a major impact on cell motility processes, consistent with our prior functional studies. Despite conducting Western blot analysis, we could not confirm the candidate proteins linked to cell adhesion. Using IF, we examined changes in cell adhesion proteins over time in response to KBU2046 treatment. The time-course IF investigation revealed that KBU2046 affects adhesion proteins kinetically by altering their subcellular localization over time rather than altering their total expression level. This finding corroborates KBU2046's known effects on cell motility, demonstrating that a kinetic-based analysis yields important new information not directly represented in a single time point screen, although functionally related.
Conclusions: Our study underscores the importance of integrating proteomic and imaging methodologies to procure a holistic comprehension of the molecular mechanisms that govern cell behavior, especially those that relate to highly dynamic processes. Through these methodologies, we have obtained a more profound understanding of how cells regulate motility and how that process can be therapeutically modulated.

#4122 Integrin avb3 and HSPG targeting agents prevent extracellular vesicles uptake and breast cancer metastasis.

E. Muro-Blanc[1], R. Bayona-Ramon y Cajal[2], M. Cano-Galietero[3], S. Garcia-Ortega[1], C. Falciani[4], L. Bracci[4], A. J. Schuhmacher[2], S. Hummer[1], S. Ramon y Cajal[1];

[1]Vall d'Hebron Research Institute (VHIR), Barcelona, Spain, [2]Aragon Health Research Institute (IIS Aragon), Zaragoza, Spain, [3]Spanish Biomedical Research Network in Oncology (CIBERONC), Madrid, Spain, [4]University of Siena, Siena, Italy

INTRODUCTION: Metastasis is the major cause of cancer-related deaths (90%). Intercellular communication between cancer cells and with cells in their environment plays a significant function in tumor progression. In fact, secreted factors like cytokines and extracellular vesicles (EVs) can either halt or stimulate tumorigenesis as well as metastasis. We have previously reported, that the integrin B3 (ITGB3) is required for metastasis of breast cancer cells in vivo (Sese et al. Oncotarget, 2017). We furthermore demonstrated, that EVs mediated colony growth is dependent on ITGB3 and that endocytosis mediated uptake of EVs relies on the interaction of ITGB3 with integrin av (ITGav) and heparan sulphated glycoproteins (HSPGs) (Fuentes et al. Nat. Commun., 2021).
OBJECTIVE: The objective of this work is focused on identifying inhibitors targeting the ITGav/B3/HSPGs complex to prevent extracellular vesicle uptake in cancer cells and to test their ability to prevent metastasis.
METHODOLOGY. Inhibitors targeting ITGB3/ITGAV or HSPGs were either commercially available or obtained through collaborations and single chain antibodies (scFv) were produced in house. Inhibition of fluorescent labeled EVs was determined by FACS analysis or Incucyte based measurements and the efficacy of inhibitors was determined in a dose dependent manner. Toxicity of inhibitors was studied by crystal violet-based assay in normal and tumor cell lines. Tail vein injection of luciferase labeled MDA-MB-231 cells into nude mice was used as model to study metastatic diseases under treatment with the identified inhibitors. Metastasis formation was monitored by bioluminescence imaging and lungs were examined pathologically at end point. Overall survival was determined.
RESULTS: Among the tested Integrin and HSPGs targeting compounds, we identified an integrin-binding antibody, an integrin binding scFv, an RGD-mimetic compound and an HSPGs-binding peptide as inhibitors of EV uptake. Inhibition was validated in a dose dependent manner and toxicity studies did not show adverse effects. Three of those inhibitors, targeting either ITGB3/ITGAV or HSPGs were tested in mice models in vivo and all inhibitors could significantly reduce the formation of metastasis and strongly increase the overall survival.
CONCLUSION: We have identified four drug candidates that target the ITGav/B3/HSPGs complex and are able to prevent EV uptake, demonstrating that EV uptake is a druggable process. Even more, the inhibitors tested in vivo could strongly reduce metastasis formation and increase overall survival. This data supports our hypothesis, that targeting EV mediated intercellular communication is a valuable approach to combat cancer metastasis.

#4123 Attenuating breast cancer metastasis with BCL-X_L-targeting PROTACs.

M. E. Carelock[1], P. Zhang[2], M. Jiao[1], U. De[1], Z. Jin[1], R. M. Stump[3], S. G. Williams[3], G. Zheng[2], W. Zhang[1];
[1]University of Florida College of Medicine, Gainesville, FL, [2]University of Florida College of Pharmacy, Gainesville, FL, [3]University of Florida College of Agriculture and Life Science, Gainesville, FL

B-cell lymphoma X-large (BCL-X_L) emerges as a significant player in cancer progression. In our recent findings, we unveil the efficacy of proteolysis-targeting chimeras (PROTACs) directed against BCL-X_L, demonstrating their capacity to not only eliminate cancer cells but also target tumor-induced regulatory T cells (TI-Tregs). Notably, BCL-X_L's role in promoting breast cancer metastasis extends beyond its anti-apoptotic function. We posit that BCL-X_L-targeting PROTACs (BCL-X_L-Ps) hold promise for treating metastatic breast cancer. Their potential lies in directly eliminating circulating tumor cells during vulnerable stages and/or triggering anti-cancer immunity through Treg cell depletion. Our experiments underscore the potency of IAP-based PROTACs in facilitating BCL-X_L degradation via the ubiquitin-proteasome system (UPS) while mitigating on-target platelet toxicity. Treatment of breast cancer-bearing mice with these compounds demonstrates a tangible reduction in breast cancer metastasis to the lungs. Additionally, our studies reveal a significant depletion of tumor-infiltrating Tregs in mice treated with BCL-X_L-Ps. While affirming BCL-X_L as a viable therapeutic target for breast cancer metastasis, further exploration into the mechanisms behind BCL-X_L-P targeting is imperative. Our future endeavors will be devoted to unraveling whether our BCL-X_L-Ps effectively target both tumor-intrinsic BCL-X_L, potentially inducing tumor cell death, and tumor-infiltrating Tregs, thereby fostering an adaptive immune response against the tumor cells.

#4124 Patient-derived ex vivo models to test drug responses of disseminated cancer cells in various metastatic niches.

L. Wohrl[1], C. Botteron[1], K. Weidele[1], S. Treitschke[1], D. Das[1], M. Werner-Klein[2], M. Hoffmann[1], N. Stojanović Guzvić[1], S. Materna-Reichelt[1], F. Weber[2], S. Engelmann[3], R. Mayr[3], M. Guzvić[3], S. Haferkamp[4], S. Seitz[3], C. A. Klein[2], C. Werno[1];

[1]Fraunhofer Institute for Toxicology and Experimental Medicine ITEM, Regensburg, Germany, [2]University of Regensburg, Regensburg, Germany, [3]Caritas St. Josef, Regensburg, Germany, [4]University Medical Center, Regensburg, Germany

Metastases arise from disseminated cancer cells (DCCs) that often lodge to distant organs long before diagnosis of the primary tumor. Unfortunately, the efficacy of (neo-)adjuvant therapies against DCCs remains uncertain. Here, we harnessed novel patient-derived ex vivo models to identify promising candidate therapies targeting DCCs and explored the impact of the unique microenvironment of metastatic target organs on the phenotypes and drug responses of DCCs. We screened disaggregated lymph node (LN) or bone marrow (BM) samples from melanoma, breast, and bladder cancer patients without distant metastasis for the presence of DCCs. Then, we expanded DCCs in patient-derived xenografts, adherent cell culture, or three-dimensional culture. LN and BM suspensions were spiked with allogeneic and autologous tumor cells to unravel the impact of different metastatic niches on DCCs. Automated high-throughput microscopy of disaggregated patient LNs was used to evaluate drug effects on DCCs in the autologous microenvironment. We established 13 cell lines from melanoma DCCs, three organoid models from breast cancer DCCs, and two organoid models from bladder cancer DCCs. The origin of each model was confirmed by assessment of histomorphology, marker expression, and genetic profiles. We screened a comprehensive panel of chemotherapeutics, targeted drugs, and antibody-drug conjugates across these in vitro models, and thereby identified compounds with the potential to eradicate DCCs. We further found that the LN and BM microenvironments differentially affected phenotypes and drug responses of cancer cells particularly when immune modulating drugs were used. Of note, ex vivo drug testing, performed directly on LN suspensions containing DCCs, revealed candidate therapeutics within a time frame acceptable for personalized treatment decisions. In conclusion, we report that the microenvironment of the specific metastatic niche impacts DCC drug responsiveness. Employing DCC-derived in vitro models in drug response assays that include specific niches may help to develop (neo)-adjuvant, personalized therapies and to discover novel therapeutics against metastasis.

#4125 Exploring the efficacy of alpelisib and combined PI3Kα-S6K inhibition in LIN28B-mediated colorectal cancer metastasis.

A. E. Shin[1], K. Sugiura[1], S. W. Kariuki[1], D. A. Cohen[1], C. J. Lengner[2], P. A. Sims[1], J. T. Gabre[1], A. K. Rustgi[1];

[1]Vagelos College of Physicians and Surgeons, Columbia University Irving Medical Center, New York, NY, [2]University of Pennsylvania, Philadelphia, PA

Introduction: Colorectal cancer (CRC) is the third most diagnosed cancer worldwide. LIN28B, an RNA-binding protein that regulates mRNA translation, has garnered significant interest in recent cancer research. Our lab has established that LIN28B is an oncogene and promotes CRC metastasis. However, the exact mechanisms through which LIN28B exerts these effects remain elusive.

The phosphatidylinositol 3-kinase (PI3K)/AKT signaling pathway is altered in 50-70% of CRCs and is characterized by *PIK3CA* gene mutations in 20-30% of CRC cases. *PIK3CA* encodes the catalytic subunit p110α of the PI3Kα enzyme, which is critical for PI3K/AKT signaling. Activation of this pathway is associated with worse CRC prognosis. Among the components of this signaling cascade, the ribosomal protein S6 kinase (S6K) is a crucial downstream effector, playing a pivotal role in protein synthesis and cell growth. Despite the frequent occurrence of *PIK3CA* mutations in CRC, targeted therapies for *PIK3CA*-mutant CRC are lacking. Alpelisib, a PI3Kα-specific inhibitor approved by the FDA for a subset of *PIK3CA*-mutant breast cancers, remains largely unassessed in CRC. *We hypothesize that LIN28B-mediated CRC metastasis is facilitated by the activation of the PI3K/AKT pathway, representing a potential target for Alpelisib or other related inhibitors.*

Results: Our data indicate that LIN28B expression in CRC cells promotes liver metastasis in mouse models of metastatic CRC (mCRC). Furthermore, LIN28B expression activates the PI3K/AKT pathway, as measured by an AKT phosphorylation array. Treatment of CRC cells with SC79, a pan-AKT activator, enhanced cell migration and invasiveness. Similarly, *Villin*^{Cre}*;R26*^{Pik3ca} transgenic mice, expressing a constantly active mutant form of PI3Kα in the intestinal epithelium, demonstrated crypt hyperplasia and an amplified propensity for tumorigenesis, mirroring the effects of LIN28B expression in CRC. Importantly, Alpelisib effectively hinders LIN28B-driven CRC progression in cell lines, transgenic mice-derived organoids, and mCRC mouse models, as well as the growth rate of CRC patient-derived organoids (PDOs). The effects observed with Alpelisib treatment were replicated with inhibition of S6K using either LY25284702 or PF4708671. Moreover, a combination of low-dose Alpelisib with low-dose LY25284702 or PF4708671 synergistically restricted the growth of PDOs.

Conclusion: Our data provide compelling evidence that the PI3K/AKT pathway regulates LIN28B-mediated CRC metastasis, and its inhibition by Alpelisib is feasible. This underscores the potential for precision medicine in CRC, offering targeted therapies to *PIK3CA*-mutant CRC patients who lack specific treatment options. Furthermore, our study highlights the clinical advantages of combined inhibition strategies for improved anti-metastatic outcomes, a field in dire need of interventions in mCRC.

#4126 The inhibitory effect of statins on distant metastasis and recurrence of endometrial cancer.

K. Kim[1], J. Yoo[2], R. Broaddus[3], E. Jeong[1], M. Hunter[1], T. Kim[1], J.-W. Jeong[1];

[1]University of Missouri, Columbia, MO, [2]Yonsei University MIRAE Campus, Wonju, Korea, Republic of, [3]University of North Carolina, Chapel Hill, NC

Endometrial cancer (EC) is the most common gynecologic malignancy. The most common histological type is endometrioid endometrial cancer (EEC). While the majority of patients present with early-stage and low-grade EEC and have an excellent prognosis, a subset develops distant recurrence derived from EEC after initial treatment of the primary. However, the exact mechanism of distant metastasis and recurrence from EEC is still unclear. In addition, the lack of suitable pre-clinical models is a significant barrier to research for distant metastasis and recurrent cancer derived from EEC. Our preclinical EEC model, the ablation of both *Mig-6* and *Pten* in the uterus (*Pgr*$^{cre/+}$*Mig-6*$^{f/f}$*Pten*$^{f/f}$; *Mig-6*$^{d/d}$*Pten*$^{d/d}$), dramatically accelerates the development of EEC compared to single ablation of either gene. The ablation of both *Mig-6* and *Pten* in the uterus (*Pgr*$^{cre/+}$*Mig-6*$^{f/f}$ *Pten*$^{f/f}$; *Mig-6*$^{d/d}$*Pten*$^{d/d}$ mice) displayed distant metastases into the ovary, diaphragmatic skeletal muscle, lymph node, and lung. However, the *Pten*$^{d/d}$ mice exhibited endometrial cancer without distant metastases. After hysterectomy of EEC confined to uterus, *Mig-6*$^{d/d}$*Pten*$^{d/d}$ mice exhibited recurrent EEC in abdomen and lung. To identify prognostic factors for distant metastatic and recurrent EEC, we performed transcriptomic analysis in endometrial hyperplasia, a precancerous condition, from *Pten*$^{d/d}$ and *Mig-6*$^{d/d}$*Pten*$^{d/d}$ mice. Our transcriptomic analysis identified that cholesterol biosynthesis was the most significantly activated pathway in *Mig-6*$^{d/d}$*Pten*$^{d/d}$ mice compared to *Pten*$^{d/d}$ mice. Statins, also known as HMG-CoA reductase inhibitors, are the most common cholesterol-lowering drugs. We evaluated the effect of atorvastatin on tumorigenesis and recurrence of EEC. *Mig-6*$^{d/d}$*Pten*$^{d/d}$ mice treated with atorvastatin displayed significant reduction of tumor size compared to vehicle treated group. For vehicle-treated group, our pathological analysis revealed EEC outside the uterus, therefore EEC had disseminated to involve the ovary, diaphragmatic skeletal muscle, lymph node, and lung. However, EEC was confined to the uterus in the atorvastatin treated group. Furthermore, atorvastatin treatment reduced the rate of recurrent EEC development. This data demonstrated that atorvastatin has a remarkable inhibitory effect on metastasis and recurrence of EEC in *Mig-6*$^{d/d}$ *Pten*$^{d/d}$ mice. Our results suggest that statins suppress development of distant metastasis and recurrence in mouse models of EEC with *Pten* and *Mig-6* deficiency by inhibiting cholesterol biosynthesis.

#4127 Combined inhibition of RAF, MEK, and FAK attenuates melanoma brain metastases and prolongs survival in preclinical models.

Karly A. Stanley[1], Jared D. Almazan[1], Tursun Turapov[1], David A. Kircher[1], Gennie L. Parkman[2], MiKaela N. Field[1], Katie M. Culver[1], Christopher M. Stehn[1], Silvia Coma[3], Jonathan A. Pachter[3], Howard Colman[1], Sheri L. Holmen[1]

[1]Huntsman Cancer Institute, Salt Lake City, UT,[2]Weber State University, Ogden, UT,[3]Verastem Oncology, Needham, MA

Despite promising results from recent FDA-approved therapies, many advanced melanoma patients develop resistance to both immunotherapy and targeted therapy. A common resistance mechanism to targeted therapy is upregulation of the PI3K/AKT signaling pathway, which has also been shown to promote the development of melanoma brain metastases. Historically, AKT inhibitors have failed in the clinic due to their limited efficacy or intolerable toxicity. Proteomic analysis comparing non-metastatic vs brain metastatic primary tumors in mice revealed focal adhesion kinase (FAK) as an AKT1 specific effector and a potential alternative therapeutic target. FAK is a non-receptor tyrosine kinase that localizes primarily to focal adhesions to regulate cell migration. To determine whether targeting FAK alone or in combination with the RAF/MEK inhibitor avutometinib reduces brain metastases and prolongs survival, we utilized both autochthonous and syngeneic melanoma mouse models. Mice with either subcutaneous tumors or established brain metastases were treated with FAK inhibitor, RAF/MEK inhibitor, or the combination of FAK and RAF/MEK inhibitors. Each cohort was assessed for tumor onset, growth, metastasis, and survival. Our results show that combined RAF/MEK/FAK inhibition significantly delays tumor onset, causes regression of established tumors, prevents the development of brain metastases, promotes the regression of established brain metastases, and prolongs survival. In addition, patient-derived BRAF V600E melanoma xenograft mouse models resistant to the BRAF inhibitor dabrafenib and the MEK inhibitor trametinib, were sensitive to combined RAF/MEK/FAK blockade. The addition of the BRAF inhibitor encorafenib to these models further enhanced the effect on tumor growth. These results support the initiation of a clinical trial evaluating the efficacy of the RAF/MEK inhibitor avutometinib in combination with the FAK inhibitor defactinib in patients with brain metastases from cutaneous melanoma. Additionally, we are assessing non-canonical roles of FAK in modulating the tumor microenvironment to determine whether avutometinib and defactinib also enhance the efficacy of immune checkpoint inhibition in this disease.

#4128 Biofield therapy suppressed invasion and metastases of human pancreatic cancer.

P. Yang, S. Chakraborty, P. Nguyen, D. Deng, A. Cusimano, D. Wei, L. Cohen;
The University of Texas MD Anderson Cancer Center, Houston, TX

The NIH categorizes Biofield Therapy (BT) as therapeutic approaches within energy medicine that involve using the body's energy field (biofield) for therapeutic benefit. Although controversial, in some cases devices have been developed that mimic the electromagnetic fields (EMF) that are emitted from people when delivering BTs. We previously reported that BT significantly inhibited the growth of pancreatic cancer cells and liver metastasis in their relevant animal models mediated in part through modification of the cell cycle, reductions in cell voltage potentials, and down regulation of PI3K/Akt pathways. We expanded this research to examine the potential role of BT in anti-invasiveness in human pancreatic ductal adenocarcinoma (PDAC) cells and animal models. We found that PANC-1 cells treated with BT (15 min) displayed 55% less invading cells than that of untreated incubator control and sham control cells ($P < 0.001$). Similar results were observed in human PDAC L3.7 cells and mouse pancreatic cancer KPCY cells. These experiments were replicated 8 times for Panc-1 cells and 4 times for L3.7 cells. Additionally, migration capacity was tested using the transwell migration and scratch assays. Consistent with the result of cell invasion assays, BT treatment also led to significant reduction of migration of PANC-1 and L3.7 cells by 34% and 41%, respectively, compared to sham controls. Two additional therapists independently replicated the anti-invasiveness and anti-migratory effects of BT on these PDAC cells. This suggests the replicability of these findings across studies and therapists. In a repeated PANC-1 mouse orthotopic model, we found that only a third of BT treated mice had visible liver nodules whereas liver metastasis was observed in more than half of mice in the untreated colony control and sham control groups. Furthermore, BT treatment significantly reduced liver tumor burden by 73% compared to that of the sham control group ($p < 0.05$), which was similar to that observed in the previous study. Similar to the prior PANC-1 mouse model, in the current study BT treatment had only a moderate impact on the growth of primary pancreatic tumor. We assessed certain markers indicative of cell status as well as pathways associated with migration and invasion and these will be presented at the meeting. Our findings suggest that exposure to BT reduced cellular invasion and migration processes and profoundly reduced metastasis of pancreatic tumor in an animal model. This study is in part supported by Emerald Gate Charitable Trust.

#4129 Mitochondria-targeted antioxidant MitoQ inhibits human breast cancer metastasis in mice.

T. Capeloa, **P. Sonveaux**;
Universite catholique de Louvain (UCLouvain), Brussels, Belgium

In oncology, the occurrence of distant metastases often marks the transition from curative to palliative care. Such outcome is highly predictable for triple-negative and HER2-positive breast cancer patients, even if tumors are detected early, and there is no treatment to prevent metastasis. Here, considering that mitochondria are bioenergetic sensors of the tumor microenvironment, we report in preclinical mouse models that human breast cancer relapse is not a fatality: local recurrence and metastatic dissemination can be prevented by MitoQ, a mitochondria-targeted antioxidant that already underwent Phase I safety and Phase II efficacy trials in humans for pathologies other than cancer. Metastatic prevention was confirmed in the MMTV-PyMT model of spontaneously metastatic mouse breast cancer. After oral delivery, MitoQ was effective at nanomolar concentrations at which nonmalignant cells were spared. In anticipation of future clinical trials, a robust signature of the response to MitoQ was defined, applicable to bulk primary tumor biopsies.

#4130 Targeting epigenetically-driven inflammation for PDAC metastasis prevention in high-risk individuals.

J. Handler, R. Kalhor;
Johns Hopkins University, Baltimore, MD

Background: Pancreatic ductal adenocarcinoma (PDAC) is a lethal cancer with a dire prognosis, in large part due to the late stage at which it is diagnosed in most patients. High-risk individuals (HRIs) identified through family history or germline genetic testing are candidates for imaging-based screening, yet even with intensive surveillance, metastasis often occurs between scans. Our study aims to address this critical clinical challenge by investigating the epigenetic determinants of PDAC metastasis and developing novel strategies for metastasis prevention in HRIs.
Methods: Innovative transplantation models of PDAC liver and peritoneal metastasis incorporating DNA barcodes for subclonal tracking were developed to facilitate the identification of subclones with high or low metastatic potential. An in-depth epigenomic characterization and comparison of these subclones was performed utilizing assay for transposase-accessible chromatin with sequencing (ATAC-seq) and RNA-seq.
Results: Metastasis-high subclones demonstrate widespread chromatin accessibility differences relative to their metastasis-low peers. These differences are linked to expression changes for genes involved in motility, differentiation, survival, and particularly inflammation. Top epigenetically activated genes in metastasis-high subclones include the pro-inflammatory cytokines IL-1α and IL-23α and the pro-inflammatory cytokine receptor IL-18R1.
Discussion: These findings highlight the role of epigenetic changes in PDAC metastasis, especially activation of inflammatory pathways resulting from altered chromatin accessibility. These insights provide a foundation for exploring anti-inflammatory agents for PDAC metastasis prevention. Targeting inflammation, alongside imaging-based screening, could significantly improve outcomes for HRIs.

#4131 Combination therapeutic strategy to fight against triple-negative breast cancer.

Laura Svajda[1], Ivan Ranđelović[1], Sara Eszter Surguta[1], Marcell Baranyi[2], Istvan Kenessey[1], Mihaly Cserepes[1], Jozsef Tovari[1]

[1]National Institute of Oncology and National Tumor Biology Laboratory, Budapest, Hungary, [2]Semmelweis University, Budapest, Hungary

Triple-negative breast cancers (TNBCs) lack estrogen-and progesteron receptors and human epidermal growth factor receptor-2 (HER2) which limits the therapeutic approaches. The high metastasizing capability of TNBCs is in correlation with the poor oxygenation of the cancerous breast tissue. This leads to the activation of the hypoxia-inducible-factor 1 (HIF-1), which induces multiple target genes that are involved in tumor progression and metastasis formation. This makes HIF-1 an attractive drug target, however, HIF-1 inhibitors failed if applied in monotherapy. Therefore, our aim is to investigate the combined therapeutic effect of HIF-1 inhibitor acriflavine and paclitaxel, a commonly used taxane in TNBC treatment. The synergy assessment of the two drugs was carried out by utilizing Sulforhodamine B assay on TNBC cell lines. The *in vivo* toxicity and efficacy of the drug combination was tested on NOD SCID mice with orthotopically inoculated MDA-MB-231 cell line. Quantitative and qualitative analysis of multiple genes involved in tumor progression was performed by mRNA and protein expression level assessment with qPCR, western blot and immunohistochemistry methods. HIF-1 stimulation was achieved by either incubating the cells at 1% oxygen level or through CoCl2 treatment. The *in vitro* mRNA expression studies demonstrated that acriflavin possesses a hypoxic-effect-mitigating property on the expression of metastasis-involved- and HIF-1 target genes. Acriflavine alleviated the epithelial-mesenchymal transition of TNBC cells by increasing the expression of the epithelial marker, E-cadherin. At protein level, we detected decrease in HIF-1alpha and Phospho-Protein kinase B (Akt) and increase in p53 tumor suppressor gene expression in response to acriflavine treatment. We further established MDA-MB-231 xenograft model in mice for investigating *in vivo* toxicity and efficacy. The drug combination efficiently reduced the tumor size and the macrometastasis formation compared to the control groups. The protein analysis of frozen tumor tissue samples indicated that the combination therapy decreased the HIF-1alpha expression and the amount of Phospho-Akt and Phospho-Mitogen-activated protein kinases (pMAPK/pERK) in CoCl2treated mice. Additionally, expression of epithelial markers increased and that of mesenchymal markers decreased. The combination therapy led to a decrease in the platelet-derived growth factor receptor beta (PDGFRB) as well. To conclude, we identified a novel drug combination which can efficiently combat TNBC by inhibiting HIF-1 signaling, mitigating cell migration and metastasis formation and suppressing the activation of the Phosphoinositide 3-kinase (PI3K) and MAPK pathways. This work was supported by the Hungarian Thematic Excellence Program (TKP2021-EGA-44) and the National Laboratories Program - National Laboratory for Tumor Biology (NLP-17).

#4132 Low-dose carbon monoxide therapies suppress cancer metastasis.

T. Zhang[1], C. Zhang[1], X. Chen[1], X. Yang[2], Q. Mao[2], G. Zhang[1], Z. Chen[1], A. Tan[1], J. Xiang[1], E. Hissong[1], Y.-T. Chen[1], B. Wang[2], **N. Du**[1];
[1]Weill Cornell Medicine, New York, NY, [2]Georgia State University, Atlanta, GA

Metastasis is the primary cause of cancer-related deaths. Novel systemic therapies for metastatic cancer are urgently needed. Carbon monoxide (CO) is an endogenously produced signaling molecule in the human body with demonstrated pharmacological activities, including organ protection and anti-inflammation. We determined the therapeutic effect of low-dose CO and CO prodrugs on cancer progression in this study. We found that low-dose CO inhibits the migration of cancer cell lines including breast, pancreatic, colon, prostate, liver, and lung cancer. We showed that low-dose CO inhibits lung metastasis of breast cancer and liver metastasis of pancreatic cancer in preclinical mouse models. Further, to provide safer and more reliable CO delivery, we developed metal-free, organic CO prodrugs and showed that CO prodrugs inhibit tumor growth and metastasis. We demonstrated that low-dose CO blocks the transcription of heme importers, leading to diminished intracellular heme levels. Altogether, our work lays a strong foundation for the development of CO-based systemic cancer therapies.

#4133 Hyaluronidase inhibitor delphinidin inhibits cancer metastasis.

J. J. McGuire[1], T. Taguchi[2], G. Tombline[1], V. Paige[1], M. Janelsins[1], N. Gilmore[1], A. Seluanov[1], V. Gorbunova[1];
[1]University of Rochester, Rochester, NY, [2]Salk Institute for Biological Sciences, Rochester, CA

Cancer remains a formidable global health challenge, with metastasis being a key contributor to its lethality. Abundant high molecular weight hyaluronic acid, a major non-protein component of extracellular matrix, protects naked mole rats from cancer and reduces cancer incidence in mice. Hyaluronidase plays a critical role in degrading hyaluronic acid and is frequently overexpressed in metastatic cancer. We investigated the potential of targeting hyaluronidases to reduce metastasis. High throughput screening identified delphinidin, a natural plant compound found in fruits and vegetables, as a potent hyaluronidase inhibitor. Delphinidin-mediated inhibition of hyaluronidase activity led to an increase in high molecular weight hyaluronic acid in cell culture and in mouse tissues, and significantly reduced proliferation, migration and invasion of breast (EO771), prostate (RM1), and melanoma (B16-F10) metastatic cell lines. Addition of exogenous hyaluronidase partially reversed all of these effects. Moreover, delphinidin treatment suppressed melanoma (B16-F10) metastasis in a spontaneous mouse model of metastasis. These results provide a proof of principle that inhibition of hyaluronidase activity suppresses cancer cell migration, invasion and metastasis. These results combined with the lack of adverse effect make delphinidin an attractive potential therapeutic option for inhibition of metastasis. We believe further investigation is warranted to fully elucidate the mechanisms and optimize the use of delphinidin in cancer therapy.

#4134 The abscopal effect of combination IRE with αPD-1 treatment against PDACs.

Q. Cao[1], N. A. Egan[2], W. Peng[2], C. Li[1];

[1]UT MD Anderson Cancer Center, Houston, TX, [2]University of Houston, Houston, TX

Pancreatic ductal adenocarcinoma (PDAC) is associated with a high capacity of metastatic dissemination, which results in a dismal 5-year relative survival rate. Irreversible electroporation (IRE) represents an innovative intervention utilizing short high-voltage electric pulses to induce cell death through either permanent membrane lysis or disruption of cellular homeostasis. Previous studies from our lab have demonstrated that the combination of IRE and immune checkpoint blockade using anti-PD-1 antibody (αPD-1) enhances the infiltration of CD8+ cytotoxic T cells, significantly prolonging survival in an orthotopic murine PDAC model. However, the impact of IRE/αPD-1 on metastatic PDAC tumors, known as the abscopal effect, remains unclear. In this investigation, we bilaterally implanted C57BL/6J mice with subcutaneous KRAS* PDAC tumors, treating the right flank tumors with or without IRE, in conjunction with or without αPD-1 administered intraperitoneally. Tumor growth in both the treated (with or without IRE) and untreated (abscopal) left flank tumors was closely monitored until humane euthanasia or long-term survival. In a separate study, mice serum and tumor tissues were collection on the 5th day post-IRE/αPD-1 treatment. Luminex cytokine assays were conducted on the collected serum, and immunostaining was performed on tumor tissue. Results demonstrated significantly enhanced antitumor activity in both IRE-treated and untreated tumors on mice treated with combined IRE and αPD-1, leading to a marked extension of overall survival. Luminex cytokine assays revealed a substantial increase in crucial cytokines, including IL-2, IFN-gamma, IL-18, IL-19, and IL-3, known for their pivotal roles in fostering cytotoxic T lymphocyte development, promoting T cell differentiation into effector T cells, and facilitating the recruitment of effector CD8+ T cells to the tumor microenvironment. Moreover, immunofluorescence staining of tumor tissue illustrated a notable accumulation of CD169+ macrophages in IRE-treated tumors compared to untreated tumors. Tumors from the combined IRE with αPD-1 group exhibited increased CD8+ T cell accumulation compared to other groups. These data suggest IRE combined with PD-1 blockade promotes robust antitumor immune, leading to systemic antitumor activity and robust abscopal effect.

#4135 First demonstration of magnetic particle imaging for sentinel lymph node identification.

O. C. Sehl[1], A. R. Mohtasebzadeh[1], K. Guo[1], P. Kim[1], B. Fellows[1], M. Weyhmiller[1], P. J. Foster[2], P. W. Goodwill[1], J. M. Greve[1];
[1]Magnetic Insight, Inc., Alameda, CA, [2]Robarts Research Institute, Western University, London, ON, Canada

Sentinel Lymph Node (LN) biopsy involves the identification and surgical removal of the first LN(s) that drain from a primary tumor to evaluate for metastasis by histopathology [1]. For several tumor types, the standard of care is to manage the regional LN basin separately from the primary tumor. For head and neck cancer, melanoma, and complex breast cancer cases, pre-surgical imaging is required to determine the number and location of LN(s) to remove. Most sentinel LN biopsies are performed with nuclear imaging, which relies on short-lived radiotracers and can have poor image quality, making it challenging to identify sentinel LNs in complex anatomies. An alternative and non-inferior workflow uses a non-radioactive iron oxide magnetic tracer (ferucarbotran) with a magnetic probe [2], however this tool can only be used intraoperatively. In this abstract we introduce magnetic particle imaging (MPI) as a pre-surgical imaging technology that detects iron oxides with high sensitivity at mm-scale resolution [3]. **Our objective is to demonstrate that MPI provides sensitive and quantitative tracking of ferucarbotran pharmacokinetics from four anatomical sites to primary draining LNs in mice. Methods:** Ferucarbotran was administered intradermally to C57BL/6 mice at a standard clinical dose of 0.675 mg Fe/kg to the forepaw, hindpaw, or base of tail, or tongue (n = 4). Full-body 2D and 3D imaging was performed after 20 mins, 24 h, and 48 h, and 144 h using MOMENTUM imager (Magnetic Insight Inc.). MPI signal was quantified at the injection site and draining LNs. LNs of interest were extracted to verify MPI signals ex vivo then were processed for Perl's Prussian iron staining. **Results:** After 20 minutes, MPI signal was seen at the injection site and primary LNs. The pharmacokinetics of ferucarbotran to LNs varied based on administration site. For hindpaw, signal was present in the popliteal LN (1.4% of tracer). For forepaw, ferucarbotran accumulated in the primary axillary LN (9%). For base of the tail, signal was observed in inguinal LN (2%). For tongue, MPI signal was detected in cervical LNs (14%). In all mice, MPI signal at the injection site decreased over time and signal in primary LNs persisted for at least 6 days. **Conclusions**: We demonstrated MPI is a quantitative, hotspot imaging technique for identifying primary LNs. As iron oxide tracer pharmacokinetics varies with injection site, this imaging technique could provide fundamental information required for surgical planning. Unlike nuclear imaging, persistence of MPI signal for several days provides tremendous flexibility in clinical workflow and introduces the potential for an image-guide delayed SLN biopsy [4] . This preclinical LN imaging is timely as our team is actively building and testing the world's first large-bore, clinical-scale MPI scanner.[1] Leong SP, *Clin Exp Metastasis* (2022). [2] Alvarado MD, et al. Ann Surg Oncol (2019). [3] Sarnitas EU, et al. J Magn Reson (2014). [4] Karakatsanis A, et al. Ann Surg Oncol (2023).

#4136 Tracking metastatic dissemination and tumor growth using longitudinal imaging and ctDNA.

W. Liu[1], B. Ding[2], H. Sonya[1], C. Martinez-Ruiz[1], C. Naceur-Lombardelli[1], C. Richard[1], H. Lee[2], C. Veiga[2], K. Patel[1], A. Huebner[1], A. Hackshaw[3], C. Abbosh[4], A. M. Frankell[5], G. Royle[2], C. Swanton[5], M. Jamal-Hanjani[1];

[1]University College London Cancer Institute, London, United Kingdom, [2]University College London, London, United Kingdom, [3]Cancer Research UK and UCL Cancer Trials Centre, London, United Kingdom, [4]Cancer Research UK Lung Cancer Centre of Excellence, London, United Kingdom, [5]Francis Crick Institute, London, United Kingdom

Metastatic lung cancer is a heterogeneous disease, characterized by different patterns of clinical progression and therapy response. The scale of this heterogeneity on a lesion specific level has yet to be quantified but is of clinical importance because it may provide an indication of molecular mechanisms underpinning metastasis growth. Currently, whether metastasis growth patterns can be predicted by the primary tumor or governed by metastasis specific characteristics is not known. Furthermore, circulating tumor DNA (ctDNA) has proven useful to predict disease relapse, but how closely it reflects metastatic growth post relapse is unclear. In 104 patients enrolled in the TRACERx study with disease relapse post-surgical resection of the primary tumor, lesion volumetric dynamics were tracked in 460 metastases. Total volume growth rate (TVGR) was calculated using CT imaging performed between disease relapse and death. All patients had whole exome sequencing (WES) of the primary tumor. For 19 patients enrolled in the PEACE autopsy study WES and RNAseq from 60 metastases visible on imaging prior to death and subsequently sampled at autopsy were analyses. In 29 patients, ctDNA was used to track 200 tumor-specific mutations to assess tumor burden and detect metastatic subclones. High TVGR correlated with poor survival (hazard ratio for death 1st vs 2nd tertile was 0.21, p<0.001; 2nd vs 3rd tertile was 0.51, p=0.04). Primary tumor subclonal whole genome doubling was predictive of high TVGR. There was considerable heterogeneity in the growth rate of metastases within patients. The anatomical location of metastases contributed to this, extrathoracic soft tissue and pleura had the highest growth rates, whilst lymph node and adrenal the lowest (p<0.001). Molecular attributes differed between metastases, with fast growing metastases being enriched for proliferation pathway gene expression. It was observed that the most prevalent population of cells, or clone, in the fastest growing metastasis within a patient was exclusive to that metastasis, suggesting that genomic features that characterize the clone might support rapid growth. ctDNA tracked with tumor burden post relapse and patients with extrathoracic relapse had higher levels of ctDNA. In 9 patients, metastasis specific mutations identified at autopsy and in ctDNA, were used to determine the proportion of ctDNA shed by different metastatic sites. ctDNA subclonal fraction was found to track with changes in lesion volumes during disease progression. This work highlights significant heterogeneity in metastatic growth rates which can potentially be attributed to the presence of distinct genomic features which may dictate tumor growth rate. ctDNA accurately reproduces patterns of radiological disease progression and when combined with longitudinal imaging and tumor DNA sequencing, can accurately reconstruct the natural history of cancer evolution.

#4137 Feasibility of a novel image guided injection tool for non-surgical implantation of orthotopic tumors.

T. M. Kierski[1], J. D. Rojas[1], N. Beaumont[1], T. Charity[2], R. D. Marek[2], K. H. Young[2], G. M. Palmer[2], R. C. Gessner[1], **T. J. Czernuszewicz**[1];
[1]Revvity, Durham, NC, [2]Duke University, Durham, NC

The purpose of this study was to evaluate a novel device for non-surgical implantation of tumor cells using ultrasonic (US) image guidance. There are a variety of mouse model cancer types (e.g. sub-cu, orthotopic, genetically engineered). Orthotopic tumors are increasingly prevalent but usually require surgery, which reduces throughput and injures the surrounding anatomy. Injections are an alternative to surgery, but usually require image guidance or extensive training. US guided injection systems exist, but are suboptimal because they require significant training, as the US beam is not necessarily coplanar with needle location or trajectory, reducing accuracy and throughput. We tested a new approach to image guided injection which ensures that the US beam is coplanar with the needle. To test the efficacy of the image guided injection device across a variety of common orthotopic tumors, we delivered luc-tagged cells to the prostate (2.5e5 cells in 40 µL, PC3, N=8), liver (2e6 cells in 100 µL, Hep G2, N=5), and brain (1.75e5 cells in 100 µL, U87-MG, N=3). The brain tumor model was introduced via intracardiac injection to simulate metastases. Between 3 and 8 mice were injected for each tumor model. For injection, animals were anesthetized and positioned on motion stage. A 1 mL syringe was mounted to the adjustable injection gantry with the needle co-planar with the US beam, and the target organ was visualized with US. Cells were delivered to the targets using the US live stream as a guide. Between 1 to 3 weeks after the injections, tumors were confirmed via BLI with an IVIS (Revvity, Waltham, MA, USA). For each of the three tumor cell lines, animal preparation and injections could be performed in 10 mins by recently-trained novice users. All three cell lines could be effectively delivered to the orthotopic host tissues, and this was confirmed by using BLI of the cells. This study represents the first time a co-planar US beam and needle delivery mechanism was used for the purpose of non-surgical implantation of orthotopic tumors. Future developments of this platform could include improvements to automation of needle placement and trajectory to ensure successful payload delivery by novice users.

#4138 Evaluation of breast triple-negative 4T1-derived tumor metastatic development in gender-different mouse.

C. Shao, M. He, L.-H. Tsai;
HD Biosciences Co., Ltd., San Diego, CA

Background and Objective: Breast cancer in men is a rare and less-studied case, with therapeutic strategies predominantly relying on clinical treatment protocols established for women. To support the clinical treatment concept, Dr. Martin-Martinez's lab observed no differences in the time of orthotopic breast mammary fat pad tumor development, necrosis, or color change of tumor tissue between male and female mice. However, the clinical treatment readout, especially tumor metastasis, is different in men and women, and current models for breast cancer are inadequate due to the absence of metastases. It is necessary to evaluate the development of breast cancer 4T1-derived tumor metastasis in male and female mice.
Method and Result: 4T1-Luc breast cancer cells were implanted in male and female Balb/c mice via various routes, including inguinal fat pad injection, tail vein injection, caudal artery injection, portal vein injection, and Intratibial Injection. Illuminance images showed no significant differences in tumor metastatic development between genders for inguinal fat pad, tail vein, and intratibial injections. However, following caudal artery injection, early-stage metastasis differed; male mice developed femoral head metastasis, while female mice developed lung metastasis. In the late stage, male mice displayed lung and femoral bone metastasis, while female mice primarily showed lung metastasis with barely bone metastasis.
Conclusion: While both male and female mice showed similar primary breast tumor development, mouse gender affected tumor metastasis differently, particularly when tumor cells went through the caudal artery. Male mice presented earlier femoral head metastasis and less lung metastasis than female mice. Based on this work, sex hormones would affect both hormone-related and nonhormone-related tumor metastasis. To elucidate whether this phenomenon is caused by estrogen or androgen or to test if a drug has any beneficial effects, HD Biosciences provides established tumor metastatic cell-delivering platforms and over 1000 cancer cell lines for target validation and drug efficacy study.

#4139 Prolyl 4-hydroxylase subunit alpha 1 acts as a novel target for lung adenocarcinoma brain metastasis.

Y. He[1], Z. Luo[2], Y. Dong[3], **R. Wan**[4], X. zhang[1], h. Bai[1], J. Wang[1];

[1]CAMS Key Laboratory of Translational Research on Lung Cancer, State Key Laboratory of Molecular Oncology, Department of Medical Oncology, National Cancer Center/National Clinical Research Center for Cancer/Cancer Hospital, Chinese Academy of Medical , beijing, China, [2]Department of Clinical Medicine, Southwest Medical University, Luzhou, China, Luzhou, China, [3]Chinese Academy of Medical Sciences and Peking Union Medical College, beijing, China, [4]Cancer Hospital, Chinese Academy of Medical Sciences and Peking Union Medical College, Beijing, China

Lung cancer is the most lethal cancer worldwide, with a high incidence of distant metastasis. Many lung adenocarcinoma (LUAD) patients experience brain metastasis during the disease process with unfavorable prognosis. Our previous study has discovered that P4HA1 was exclusively upregulated in brain metastatic cells. Through the analysis of single-cell RNA sequencing of LUAD samples, we found that the expression of P4HA1 in brain metastatic tumor cells is higher than that in primary tumor cells. This finding was further confirmed by immunohistochemical staining. Significantly, a strong presence of P4HA1 in primary tumors is associated with a reduced duration of disease-free survival in individuals with LUAD. Overexpression of P4HA1 in A549 and PC9 cell lines significantly increased the incidence of brain metastasis in BALB/c nude mice, whereas knockdown of P4HA1 in high brain metastatic cells significantly decreased the incidence of brain metastasis and reduced the tumor foci in brain with improved survival. Utilization of DHB, a P4HA1 inhibitor, exerts both therapeutic and preventive effects in relieving brain metastases in nude mice. Furthermore, remarkable inhibition of tumor growth by DHB was observed in patient derived xenograft (PDX) models. RNA sequencing analysis demonstrated that the reduction of P4HA1 expression had a substantial impact on cell adhesion and extracellular matrix (ECM)-receptors interactions. Western blotting analysis verified that the decrease in P4HA1 expression led to a drop in the expression of adhesion molecules ICAM1, VCAM1, NCAM1, as well as integrin molecules ITGA2 and ITGA3. Furthermore, when endothelial cells were co-cultured with conditioned medium from tumor cells, it was observed that the expression of the tight junction molecule ZO1 was reduced after co-culturing with conditioned medium from P4HA1 knockdown A549 cells. The results from the in vitro blood-brain barrier (BBB) model and in vivo biofluorescence imaging indicate that P4HA1 promoted brain metastasis of LUAD via modulating the ability of tumor cells to cross the blood-brain barrier. In conclusion, our study reveals that overexpression of P4HA1 promotes metastatic spread to the brain, and targeting P4HA1 could be a promising therapeutic strategy for the treatment of lung adenocarcinoma brain metastasis.

#4140 Enhanced microglial phagocytosis of metastatic brain tumor cells with *Cd24a/Cd47* depletion.

T. Tsuji[1], H. Hirose[1], M. Shindo[1], R. Hartantyo[1], Y. Saito[1], K. Hosoya[2], H. Yoshida[2], D. Kato[1], A. Yoshizawa[2], Y. Arakawa[1], H. Ozasa[2], T. Hirai[2], H. Wake[1]; [1]Nagoya University Graduate School of Medicine, Nagoya, Japan, [2]Kyoto University Graduate School of Medicine, Kyoto, Japan

Despite the robust homeostasis of the brain, its high prevalence of tumor metastasis is intriguing and the underlying mechanism may contribute to the development of novel therapies. Microglia have emerged as promising therapeutic targets due to their role in brain parenchymal homeostasis. However, with evidence for both pro- and anti-tumorigenic functions, their role in brain metastasis (BrM) remains unclear. Here, we show that the microglial response to tumor cells within a single host is heterogeneous and can alter tumor fate. Single-cell RNA sequencing was performed on five surgically resected metastatic brain tumors, and the transcriptome of tumor-associated microglia was extracted by single-cell variational inference (scVI). Evidence for the coexistence of cytokine-secreting and angiogenesis-supporting subsets, as well as subsets associated with phagocytosis and antigen presentation, within each tumor sample was determined. To demonstrate the intra-tumoral functional heterogeneity of tumor-associated microglia, we established a metastatic brain tumor model that allows us to visualize the metastatic process and the dynamic microglial response in vivo by injecting mCherry-tagged allogeneic cancer cells into the internal carotid artery of *CX3CR1-EGFP* mice. Metastasis formation was suppressed in microglia-depleted mice, identifying a dominant microglial response that promotes tumor growth. However, continuous in vivo imaging of the BrM model revealed tumor-eradicating anti-tumor microglia coexisting with pro-tumor microglia in the same host. The transcriptome of anti-tumor microglia supported that they are enriched for phagocytosis, antigen processing and antigen presentation genes. The subset was identified in microglia extracted from human samples. We then examined the immune checkpoint of microglial phagocytosis in the tumor transcriptome and identified *Cd24a* and *Cd47*. Simultaneous deletion of both genes in cancer cells enhanced microglial phagocytosis, reduced tumor volume and improved survival, and rescue of both genes reversed these anti-tumor effects. The microglial dependency was addressed by microglial depletion experiments, and the anti-tumor effects were reproducible in nude mice lacking mature T cells. These results suggest that there are distinct immune cell subtypes that respond to lung tumor metastases in the brain and either promote tumor growth or inhibit metastasis through phagocytosis. Furthermore, anti-tumor activity in mouse models can be enhanced by genetic deletion of *Cd24a* and *Cd47* in tumor cells, which regulate phagocytosis by microglia.

#4141 Quantitative measurement of 3D tumor spheroid invasion using live cell time-lapse imaging.

G. Yang, T. Wang, P. Ye, **X. Zhang**;
Agilent Technologies, Inc., San Diego, CA

90% of the death of cancer individuals is related to cancer metastasis[1]. The invasion and migration of cancer cells into surrounding tissues and chambers is the first step of metastasis[2]. To have a better and more in-depth understanding of the pathophysiological activities involved in metastatic cancer, accurate and reliable methods for evaluating cell invasion are urgently needed. Compared to the 2D cell model, the 3D system mimics the natural physiological properties and conditions, such as structure, physiology, biological signals of living tissues, cell-matrix interactions[4]. In this study, we followed the commonly used protocol for 3D tumor invasion assay[3] to generate spheroids in Ultra-Low-attachment (ULA) round bottom 96-well plate and subsequently embedded them in Matrigel® (5 mg/mL). After polymerization, the Matrigel that contains tumor spheroid was submerged in 100 µL cell culture media. The invasion of the 3D spheroid in the presence or absence of drug treatment was monitored and quantified using the brightfield and fluorescence live cell time-lapse image acquisition and image analysis functions of the Agilent xCELLigence RTCA eSight. The progress of spheroid invasion and the drug-inhibitory effects on tumor invasion were quantified by tracking and calculating the area of invasive protrusion from the spheroid. Our data show that 1) different types of cancer cells had different metastatic potentials demonstrated by the level of invadopodium extending into the Matrigel at desired time points; 2) the invasion of 3D HT1080 spheroid was inhibited by cytochalasin D (Cyto D), an inhibitor of actin polymerization, and GM6001, a potent broad-spectrum inhibitor of matrix metalloproteinases (MMP), in a dose-dependent manner; 3) Cyto D exhibited higher efficacy of inhibiting tumor invasion than GM6001. In summary, our approach by combining the 3D tumor spheroid invasion model with the RTCA eSight's capability of live cell imaging and automatic quantification of the area of invasive protrusion can facilitate and enhance the development of new treatments at the preclinical stage in the future.

#4142 Obesity contributes to CD8+ T cell dysfunction before and after lung metastasis in a mouse model of ER+ breast cancer.

A. E. Williams, L. M. Arendt;
University of Wisconsin-Madison, Madison, WI

Obesity is known to worsen the overall prognosis of breast cancer patients. Breast cancer patients with a body mass index (BMI) of ≥30 kg/m^2 have an increased risk for metastatic disease compared to patients with a BMI in the normal range. Although immune cells like neutrophils and myeloid derived suppressor cells have been studied in breast cancer metastasis of the lung, little is known how T cell populations change before and after metastasis. To investigate these gaps, we fed 3-week-old female FVB/N mice either a low-fat diet (LFD) or high-fat diet (HFD) for 16 weeks to induce obesity. One group was set as a tumor-naïve control and the other was injected estrogen receptor positive (ER+) TC2 cells into the mammary fat pad. Tumors grew to 0.5 cm in diameter then were surgically removed. Lung tissue was collected 8 weeks after tumor removal to examine progression of metastatic disease, and T cell populations were quantified in tumor-naïve and metastatic lung tissue from obese and lean mice using flow cytometry. Lungs from naïve obese mice showed a significant increase of total CD45+ immune cells. CD8+ T cells from naive obese mice expressed higher levels of programmed cell death protein-1 (PD1), a marker of T cell dysfunction or T cell activation. Metastatic lungs also showed increases in CD45+ immune cells and PD-1+ expression on CD3+ cells and CD8+ cells. Overall, metastatic lungs showed higher levels of PD-1 expression than naïve lungs on more cell types, evidence of more immune dysfunction or activation. To further investigate how obesity alters the function of T cells, CD45+ cells were sorted from lungs from lean and obese mice with and without metastasis, and gene expression was examined using the NanoString nCounter Immune Exhaustion panel. Immune cells from the lungs of obese non-tumor-bearing mice showed increased expression of markers for increased TCR signaling. This may indicate more T cell activation which leads to exhaustion in obese naïve mice. In metastatic lungs from obese mice, immune cells showed impaired interferon and tumor necrosis factor signaling. In addition, immune cells from metastatic lungs of obese mice also had upregulated expression of genes associated with senescence which may indicate a combination of both exhaustion and senescent phenotypes are present. This was not seen in immune cells from naïve samples, indicating that obesity leads to more chronic T cell dysfunction in metastatic lungs. Overall, even without pathogenic interference, obesity contributes to more T cell signaling and impaired CD8+ T cell activation that leads to higher T cell dysfunction once metastasis is present.

TUMOR BIOLOGY: In Vivo Imaging and Anatomical and Molecular Pathology
Poster Session

#4146 Brain permeable bioluminescent substrates for NanoLuc based reporters.

C. Gao[1], Y. Su[2], Y. Wu[2], C. Fitzgerald[1], T. H. Uyeda[1], H. Wang[1], T. A. Kirkland[3], M. Z. Lin[2], W. Zhou[1];
[1]Promega Corporation, San Luis Obispo, CA, [2]Stanford University, Stanford, CA, [3]Promega Corporation, Madison, WI

Non-invasive imaging methods for tracking gene expression, cell growth and migration and other biological events in vivo are indispensable tools for biomedical studies. Bioluminescence imaging (BLI) can achieve sensitive detection with low background *in vivo*, which is desirable for body imaging of small animals. Yet, BLI in the central nervous system (CNS) is challenging because many luciferase substrates show limited permeability of the blood-brain-barrier (BBB). To address this issue, we developed a family of new brain-permeant NanoLuc (NLuc) substrates, cephalofurimazine (CFz). CFz family paired with Antares, a fusion of CyOFP and NLuc that emits orange light instead of blue, produces an order of magnitude more signal from the brain than the standard combination of D-luciferin with firefly luciferase and matches the peak output of AkaLumine with AkaLuc but without the need of ATP. One of the substrates in the family, CFz-9, not only produces outstanding signal as other CFz substrates when paired with Antares, but also is able to be formulated into lyophilized cake that can be reconstituted in aqueous buffers for i.p. injections. Toxicity studies demonstrate that CFz-9 and its reconstituted solutions are non-toxic to mice and thus multiple injections are allowed.

#4147 Chitosan luminescent rare-earth doped nanoparticles as cancer cell tracking for imaging tumors and their immune response.

R. Osorio-Arciniega[1], E. Lucero-Meza[1], B. Can-Uc[2], I. Rocha-Mendoza[1], P. G. Fournier[1], G. Hirata[2], **P. Juarez**[1];
[1]Center for Scientific Research and Higher Education of Ensenada (CICESE), Ensenada, Mexico, [2]CNYN: Centro de Nanociencias y Nanotecnologia, Ensenada, Mexico

Background: Cancer is a group of diseases characterized by the unregulated growth of cells, which can be hard to diagnose due to the high false negatives or positives derived from technical and human mistakes.The detection of solid tumors during resection surgery is also a common issue, so contrast agents are used for both cancer diagnosis and tumor visualization during surgery, facilitating the tumor resection procedure. Nevertheless, they cause long-term problems because they accumulate in specific tissues, low penetration, and rapid clearance from the circulation. It is necessary to study new contrast agents that improve tumor detection to address these issues.Here, we synthesized two different kinds of luminescent nanoparticles (LNPs) conjugated with chitosan (Ch) and functionalized with folic acid (FA) for breast cancer detection. We compared *in vitro* its physicochemical characteristics and effects on the proliferation of cancer cells. Evaluated its impact on the immune system *in vivo* and implemented a differential imaging process to resemble a refined 3D visualization of cluster cells using Light Sheet Microscopy.
Results: Luminescent nanoparticles (LNPs) synthesized by sol-gel method and functionalized with FA using EDC-NHS coupling revealed high-intensity yellow emission at 540 nm wavelength with a quantum yield of ~ 36%. *In vitro* viability assay at different times with 293T epithelial cells, MDA-MB-231, and T-47D cancer cells demonstrated biocompatibility and high improvement of cellular uptake by LNP functionalized with FA for cancer cells versus normal cells. Light-sheet microscopy analysis of cell-LNP interactions to visualize tagged MDA-MB-231 clusters with LNP/Ch-FA showed positive interactions due to higher stability and adherence. Biodistribution and effects on the immune system by LNP/Ch-FA nanoparticles inoculated in mice were evaluated by flow cytometer analysis. LNP/Ch-FA were well tolerated *in vivo.* No adverse effects were observed macroscopically. Peripheral blood analysis from animals injected with LNP/Ch-FA after 2 or 6 days of the treatment showed that a single injection of the different NPs did not have any effects on the amount of circulating neutrophils or monocytes in peripheral blood when assessed 2 or 6 days after the injection. With T cells, the core NP induced a significant decrease in circulating T cells (-31%, p=0.045) that seemed specific to the CD4+ T cells (-33%, p=0.0479). However, conjugation of the NP to chitosan prevented this effect.
Conclusions: Our work presented significant evidence that could allow a better understanding of LNPs conjugated with Ch and functionalized with FA for possible upcoming clinical applications that could work singly or in synergy with the present detection techniques to boost accuracy and precision for cancer detection without compromise the inmunosystem.

#4148 Extracellular matrix biophysical properties change during nevus to melanoma progression.

A. Kavuturu, M. A. Constantino, A. Sassano, G. Merlino;
National Institutes of Health, Bethesda, MD

Cutaneous malignant melanoma is one of the most aggressive forms of skin cancer and its major etiological risk factor is ultraviolet (UV) solar radiation. The extracellular matrix (ECM) has been shown to influence many of the hallmark characteristics of tumor development, survival, and progression across several types of cancer, including melanoma. Interactions between the tumor and the ECM often results in rearrangement, cross-linking, and deposit of specific ECM proteins, which can contribute to stiffening of the tissue and tumorigenesis. To simulate tumorigenesis, we have previously used a hepatocyte growth factor (HGF) transgenic mouse model, which develops melanoma nevii when exposed to UVB radiation. This model is highly representative of human melanoma lesions in terms of biological, genetic, and etiologic criteria. In general, microrheology involves injecting beads into a medium, tracking movement of the beads using two-photon microscopy, and using the movement to calculate the viscosity and elasticity of the medium. The physical properties of the ECM during tumorigenesis have not been well studied at the cellular level, and microrheology has rarely been used *in vivo.* In our *in vivo* microrheology study, we injected fluorescent beads into the skin of these transgenic mice. Then, we used intra-vital microscopy with particle tracking to image the beads and measure changes in ECM elasticity as nevii grow into melanoma tumors. These results, combined with transcriptomic analysis of ECM regulation and proteomic analysis of ECM signaling, could provide unique insights into components of the extracellular matrix that are involved in melanoma tumor development and offer opportunities for therapeutics to target oncogenesis. <!--EndFragment-->

#4149 Real-time intravital trafficking of tumor infiltrating lymphocytes in breast cancer models.

S. Ahn[1], K. Akyildiz[1], H. Kim[1], P. Kim[2];

[1]IVIM Technology, Seoul, Korea, Republic of, [2]KAIST (Korea Advanced Institute of Science and Technology), Daejeon, Korea, Republic of

Cancer immunotherapy utilizing the immunoreactive efficiency of immune cells via adoptive cell therapy (ACT) has been a novel method of cancer treatment. In tumor microenvironment, immune cell reactivity of tumor-infiltrating lymphocytes (TILs) can facilitate cancer cell attack, which finally derives efficient suppression of tumor growth. However, the conventional evaluation for cancer immunotherapy has been generally performed by *ex vivo* methods, providing restricted information on lymphocyte motility and immune cell dynamics within the tumor microenvironment. *In vivo* data with the dynamic behavior of TILs in breast cancer can provide new insight to investigate novel targets of immune checkpoint inhibitors. In this research, longitudinal intravital imaging of motility trafficking of TILs in breast cancer animal models has been performed by utilizing intravital microscopy to unveil the immunoreactive dynamics of T cell activity in early stage. In vivo analysis of TIL motility within different breast cell lines, including 4T1 (mouse breast cancer cell), MDA-MB-231 (human triple-negative breast cancer cell), and MCF7 (human breast cancer cell), respectively, has been investigated for immune responses to cancer. We've monitored spatiotemporal dynamics of TIL over 11 days in breast cancer xenograft mouse model generated by tumor implantation into the dorsal skinfold imaging chamber and adoptive T cell transfer by blood circulation. In the results, the adoptive immunoreactivity of TIL has been differentiated by the timepoint of adoptive T cell transfer, distance proximity of T cells in tumors, and breast cancer types. Furthermore, anti-cancer effect coordinated with dendritic cells behaviors showed induced immune responses with accumulated dendritic cells with increased TIL count over time in breast cancer model treated with various cancer therapy such as immunotherapy, radiation therapy and anti-cancer drug (anti-PD-L1), which implied a relationship between programmed death-ligand 1 expression levels and TIL/ dendritic cell motility. The result demonstrates that intravital TIL motility trafficking analysis in cancer model can be an invaluable assessment method to explain the detailed cellular/molecular mechanism of immune response to cancer involved with T lymphocytes, dendritic cells, and immune checkpoint inhibitors to accelerate the efficiency of cancer immunotherapy.

#4150 Development of a three-dimensional spatialomics map of lethal prostate cancer driven by clinical imaging.

J. E. Ippolito[1], D. H. Ballard[1], K. Bergeron[1], R. Chidambaram[2], A. Elumalai[1], T. J. Fraum[1], H. Jing[1], P. Kamelin[2], E. H. Kim[1], C. Kita[3], A. Klim[1], A. Knesis[2], M. Lim[3], J. Luna[1], H. Nakhoul[1], T. Ragan[2], K. J. Rothschild[3], S.-K. Song[1], K. Utt[1], C. Weimholt[1], G. Yagnik[3], E. Yew[2], P. M. Angel[4], R. R. Drake[4]; [1]Washington University School of Medicine in St. Louis, Saint Louis, MO, [2]TissueVision, Inc., Newton, MA, [3]AmberGen, Inc., Billerica, MA, [4]Medical University of South Carolina, Charleston, SC

Prostate adenocarcinoma (PCa) is the most common malignancy and the second leading cause of cancer-related mortality in United States men. Following treatment for localized PCa, up to 50% of these men can experience disease recurrence, with subsequent metastasis and death. This indicates that there is suboptimal identification of lethal PCa at the time of diagnosis, despite advancements in imaging, genomics, and biomarkers. To improve the noninvasive diagnosis of lethal PCa at initial diagnosis, we have developed a novel magnetic resonance imaging (MRI) method, diffusion basis spectrum imaging (DBSI), that noninvasively measures cancer, stromal, and immune cell contributions to the prostate tumor microenvironment (TME). To validate DBSI for PCa, we have applied novel technologies to matched prostatectomy specimens that include (i) fully automated tissue section processing with serial 2-photon tomographic (STP) imaging of the sections to generate 3D volumetric structural maps of the tumor tissue and (ii) multiplex MALDI mass spectrometry imaging of untargeted glycans and extracellular matrix (ECM) peptides and of proteins targeted with novel photocleavable-mass-tagged antibodies (MALDI-IHC) to spatially resolve hundreds of biomolecules from the TME. To establish the feasibility of this approach, we recruited a patient with an unusually aggressive prostate cancer consisting of Gleason 5+4 acinar adenocarcinoma histology with intraductal growth that was locally invasive and lymph node positive at prostatectomy (stage T3bN1). This patient also had the unusual finding of low activity on prostate specific membrane antigen positron emission tomography (PSMA-PET). Following gross sectioning of the prostate with MRI-guided 3D printed molds to co-register clinical DBSI with histology, a 5-mm thick tissue cross-section containing tumor and normal prostate was imaged with high resolution ex vivo DBSI followed by 3D structural mapping with STP imaging. Selected slides in the 3D stack were subject to multiplexed MALDI imaging to identify relationships between cellular and molecular heterogeneity with tumor structure identified with DBSI and STP imaging. We discovered unique structural differences in the prostate tumor compared with the surrounding stroma based upon collagen and glycan modifications to the ECM that were recapitulated with second harmonic maps of collagen from STP imaging as well as stromal maps generated from DBSI imaging. Additional novel protein and glycan ECM components were expressed in this tumor known to be associated with poor patient outcomes. Together, these data represent the first evidence successfully linking noninvasive in vivo clinical imaging and de novo spatialomics technologies with potential to improve PCa diagnostics. This advanced imaging workflow can be applied to any tissue type, underscoring its relevance to translational cancer research.

#4151 Development of a cancer-activated biologic imaging platform for early lung cancer diagnosis.

M. Goryawala[1], H.-Y. Lee[1], L. Tong[2], T. Patil[1], A. Harwig[1], C. Xia[1], S. Ramachandran[1], D. Wodziak[1], D. Felsher[2], T. Sproul[1], D. Suhy[1];
[1]Earli Inc., Redwood City, CA, [2]Stanford University, Palo Alto, CA

Current modalities, such as LDCT and fluorodeoxyglucose positron emission tomography (FDG PET), for early lung cancer imaging, rely upon proxies resulting in poor specificity and/or sensitivity. They are also unreliable for discriminating benign versus malignant lesions resulting in the requirement of longitudinal analyses euphemistically called “watchful waiting”. Lung biopsies are marred by significant false negative rates and pose complications of collapsed lungs or bleeding in up to 22% of procedures and death rates up to 1%. To overcome these obstacles, Earli is developing a non-invasive, highly specific cancer-activated imaging platform that usurps dysregulated gene expression within malignancies to force only cancer cells to produce a synthetic biomarker that can be localized using PET imaging. EARLI-204 is a lipid nanoparticle that contains a DNA nanoplasmid comprised of a cancer-activated promoter driving selective expression of a functionally inactivated somatostatin receptor 2 ($SSTR2_{fi}$) gene. Abrogation of internalization and signal transduction allows the safe use of $SSTR2_{fi}$ as an ectopically expressed PET reporter gene (PRG). Following administration, EARLI-204 transfects tumor and normal cells but transcriptional activation only within cancer cells results in selective cell-surface expression of $SSTR2_{fi}$ that can be imaged with FDA-approved SSTR2 PET tracers. H1299 human lung cancer cells engineered to express SSTR2 (H1299-SSTR2) revealed a discernable PET signal with as little as 31,000 engineered cells. Mixed cell titration studies using subcutaneous (SQ) tumors with H1299-SSTR2 and non-expressing H1299-wt cells suggest tumors with between 0.1% and 1% H1299-SSTR2 cells had a significant PET signal, compared to tumors with 100% H1299-wt. This result sets a benchmark transfection of ~1% to achieve a PET signal. Intratumoral (IT) dose titration of EARLI-204 revealed that 5 ug of EARLI-204 generates a significant PET signal. Consistent with the H1299-SSTR2 studies, IHC shows ~1% of tumor cells express the PRG at a 5 ug IT dose level. Furthermore, we measured 70 copies of EARLI-204 DNA per cell resulting in 22,629 SSTR2 mRNA copies/25 ng at a 5 ug IT dose level. IV dosing of EARLI-204 in SQ and intralung tumor models results in cancer-activated expression of $SSTR2_{fi}$ in both SQ and small (<4 mm) lung tumors with significantly increased ($p < 0.05$) PET signal. For lung tumors, analyses showed 1 copy of EARLI-204 DNA/ cell resulting in 780 SSTR2 mRNA copies/25 ng. The results demonstrate an effective molecular imaging platform for drug discovery ranging from in vivo screening to building PK-PD-efficacy relationships and enabling human dose projection for the Earli PET localization drug. The benchmarks and findings established with this preclinical imaging pipeline are currently being evaluated in large animals such as dogs and pigs, and will be translated to humans in planned clinical trials.

#4153 PET/CT imaging of pancreatic ductal adenocarcinoma with a claudin-4 binding peptide in preclinical mouse model.

J. Seo, J. Wang, A. J. Kare, S. K. Tumbale, B. Wu, M. N. Raie, M. Pandrala, K. W. Ferrara;
Stanford University, Palo Alto, CA

There is a critical need to develop new imaging and therapeutic strategies for pancreatic cancer. Current positron emission tomography (PET) imaging assessments of pancreatic ductal adenocarcinoma (PDAC) rely on ^{18}F-FDG as a radiopharmaceutical. To increase the sensitivity of PDAC detection, we identified Claudin-4 (CLDN4), a tight junction transmembrane protein, as a PDAC biomarker through spatial transcriptomic and proteomic analyses. CLDN4 expression has previously been reported to be enhanced in 99% of primary and 100% of metastatic pancreatic cancer tissue samples and in 10 of 11 precancerous pancreatic intraepithelial neoplasia (PanIN) specimens. A small fragment of naturally occurring Clostridium perfringens enterotoxin (CPE) was previously reported to bind to the extracellular loop domain of CLDN4 protein (PDB:7kp4) with nanomolar (nM) affinity (K_d). A CLDN4 binding peptide (C4BP) was developed as a radioligand by modifying the n-terminus of C4BP which does not impact receptor binding. Here, we designed and synthesized a DOTA-PEG_1-C4BP ligand on a rink amide resin using a microwave-assisted peptide synthesizer. Radiolabeling of DOTA-PEG_1-C4BP (2 nmol) with $^{64}CuCl_2$ (70 MBq) conferred ^{64}Cu-C4BP (28 MBq/nmol) with 80% non-decay corrected yield and >99% radiochemical purity. PET/CT imaging of ^{64}Cu-C4BP (~0.1 µg/mouse) performed in an inducible PDAC (*Kras*$^{LSL\text{-}G12D/+}$;*Rosa26*$^{LSL\text{-}tdTomato/LSL\text{-}tdTomato}$(*KT*);*Ptf1a*^{CreER};*Trp53*$^{fl/fl}$) model at 84 day after tamoxifen injection resulted in ~25% injected activity per cubic centimeter (IA/cc) accumulation in metastases and at ~18% IA/cc retention in pancreatic tumors within 30 minutes of tail vein injection with minimal background accumulation. *Ex vivo* PET imaging confirmed the localized accumulation of ^{64}Cu-C4BP in transgenic mice within the colon, pancreas, and liver. Blocking of ^{64}Cu-C4BP accumulation with the cold compound in a xenograft model (NOD/SCID) bearing Capan-1 PDAC tumors demonstrated the specificity of ^{64}Cu-C4BP binding. Here we report that CLDN4 is a promising target and ^{64}Cu-C4BP is a promising ligand for the detection of pancreatic cancer.

#4154 PET imaging to characterize the tumor microenvironment in a breast cancer model of obesity.

S. E. Lynch, C. Crawford, A. Hunt, L. Sligh, B. M. Larimer, S. E. Lapi, A. G. Sorace;
The University of Alabama At Birmingham, Birmingham, AL

Introduction: Obesity is known to reduce efficacy for cancer treatment patients and is thought to modulate the tumor microenvironment and glucose metabolism. In this study, we aim to quantify obesity-induced differences in the breast cancer tumor microenvironment with positron emission tomography (PET) imaging of hypoxia, glucose metabolism, and granzyme B. These experiments are testing the hypothesis that tumors in obese mice have increased glucose metabolism and hypoxia, measured by [^{18}F]F-fluorodeoxyglucose (FDG) and [^{18}F]F-fluoromisonidazole (FMISO) uptake. We also hypothesize that immunotherapy (IMT) increases immune activation, as measured by [^{68}Ga]Ga-Granzyme B peptide (GZP), and that obese mice will respond less to immunotherapy than lean mice.
Methods: C57/Bl6 mice were placed on a high-fat diet (HFD) with 60% kcal fat (n=18) or low-fat diet (LFD) composed of 10% kcal fat (n=18) to induce obesity. Blood serum was collected for analysis of cholesterol levels prior to tumor implantation. Body weight and food intake were measured weekly. 14 weeks after initiating each diet, $5x10^5$ E0771 cells were implanted into the 3rd mammary fat pad and allowed to grow to 50-150mm^3. Tumor-bearing mice were imaged with [^{18}F]F-FDG and [^{18}F]F-FMISO PET to measure glucose metabolism and hypoxia, respectively prior to treatment. Following imaging, mice began treatment with either saline (n=6/diet) or checkpoint blockade IMT with 200 ug anti-PD-1 and 100 ug anti-CTLA-4 (n=12/diet). After 3 doses of IMT, mice were imaged with [^{68}Ga]Ga-GZP PET to measure immune activation. Tumor volume measurements and treatment administration occurred every 3 days. Metrics of standardized uptake value (SUV) including mean, max, and peak were quantified from imaging data. A one-way independent ANOVA or independent t-test was used to compare differences between groups.
Results: HFD-fed mice had significantly increased body weight ($p<0.0001$) and serum cholesterol ($p=0.005$) compared to LFD-fed mice. SUVmean for tumor hypoxia ($p=0.003$) and glucose metabolism ($p=0.02$) were significantly increased at baseline in HFD-fed mice compared to LFD-fed mice. IMT increases immune activation for both LFD-fed ($p=0.009$) and HFD-fed mice ($p=0.05$). IMT treatment significantly reduces tumor burden for LFD mice ($p<0.0001$), but not HFD mice ($p=0.096$).
Conclusions: Obesity plays a role in the reduction of the effectiveness of immunotherapy. At baseline, tumors of obese mice have increased tumor glucose metabolism and hypoxia. Although immunotherapy increases immune activation, this is not sufficient to reduce tumor burden or improve overall survival. Understanding obesity-induced differences in tumor biology may provide imaging-directed treatment decision making.

#4156 Monitoring early chemotherapy response in murine pancreatic ductal adenocarcinoma using non-invasive hyperpolarized magnetic resonance spectroscopic imaging with ^{13}C-pyruvate.

Irina Heid, Anna-Maria Schmidmuller, Simon Baller, Jason G. Skinner, Geoffrey J. Topping, Wolfgang Gottwald, Hussein Trabulssi, Rupert Ollinger, Katja Steiger, Roland Rad, Franz Schilling, Rickmer F. Braren

TUM School of Medicine and Health, Klinikum rechts der Isar, Technical University of Munich, Munich, Germany

Background: Pancreatic ductal adenocarcinoma (PDAC) is a rarely operable cancer with a very poor prognosis. Nearly 100% of affected patients receive one of two alternative first-line chemotherapies during the course of their disease: 1.) Gemcitabine-Abraxane (G/A) or 2.) FOLFIRINOX. Treatment success varies widely between the patients due to individual molecular, structural tumor and metabolic heterogeneity. In this project, we use hyperpolarized 13C-pyruvate magnetic resonance spectroscopic imaging (HP-MRSI) to non-invasively characterize early metabolic changes in murine endogenous PDAC in response to the mentioned chemotherapies.

Methods: 18 KPC (*Ptf1a*$^{wt/cre}$(C)*Kras*$^{wt/G12D}$(K)*Trp53*$^{fl/fl}$(P)) mice with 74 distinct tumour nodules, visually identified based on T2-weighted anatomical imaging, were used in this study. The conversion of pyruvate to lactate was detected by HP-MRSI, performed on 7 T preclinical system using modified 3D balanced steady-state free precession (bSSFP) sequence on day 0 pre-therapy and on day 3 post-therapy. 100µg/g G (intraperitoneally) and 30µg/g A (intravenously) were applied twice on day 0 post-scan and day 2 (n=6). FOLFIRINOX (60µg/g 5-Fluoruracil, 27µg/g Irinotecan, 12.8µg/g Oxaliplatin, 60µg/g Leucovorin) was injected intravenously once on day 0 post-scan (n=6). Vehicle mice (n=6) were left untreated. Area under the curves (AUC) of lactate to pyruvate time-courses (AUC_l/AUC_p) were calculated. Primary murine PDAC cell lines were established from biopsies of 58 imaging region, sequenced using 3'RNA-Seq (Poly-ASeq) method and analysed using Dseq2 R package.

Results: G/A and FOLFIRINOX-treated tumors exhibited heterogeneous metabolic responses in distinct nodules, while non-treated group tumors remained stable. A significant difference in metabolic changes (p = 0.01, ANOVA) from day 0 to day 3 was observed between FOLFIRINOX, G/A, and non-treated groups. Low glycolytic tumors showed a positive trend, more pronounced with FOLFIRINOX than G/A treatment. Metabolically active nodules with high AUCl/AUCp on day 0 reduced lactate turnover under therapy. These findings suggest that metabolic HP-MRSI can detect treatment-induced changes in tumor composition and subtype-specific epithelial/mesenchymal plasticity, correlating with the metabolic phenotype. Further investigation will include histology, subtype-specific biomarkers, transcriptional signatures, and regional transcriptome analysis to explain molecular changes in metabolism.

Conclusions: We have applied a non-invasive approach for detection of metabolic changes under chemotherapy in murine PDAC. These findings will contribute in the long term to the establishment of predictive imaging biomarkers for PDAC.

#4157 Combining hyperpolarized magnetic resonance and positron emission tomography to interrogate prostate cancer metabolism.

M. Wang[1], J. S. Enriquez[1], P. Dutta[1], J. Han[1], P. Shepherd[1], D. Frigo[1], F. Pisaneschi[2], P. K. Bhattacharya[1];
[1]UT MD Anderson Cancer Center, Houston, TX, [2]UT Health Houston, Houston, TX

Background: There is an unmet clinical need for imaging biomarkers to distinguish indolent from aggressive prostate cancer (PCa). Many advanced and aggressive PCa patients receiving anti-androgens (enzalutamide) develop resistance. It is hypothesized that dysregulated cell metabolism is a key driver for PCa progression and therapy resistance. Two pathways commonly involved in PCa are glycolysis and fatty acid metabolism. Therefore, metabolic imaging and metabolomics were performed on enzalutamide sensitive/resistant, Androgen Receptor dependent (AR+) and AR independent (AR-) patient derived xenograft (PDX) tumors. To interrogate both pathways, [1-^{13}C]-pyruvate hyperpolarized magnetic resonance spectroscopy (HP-MRS) and [^{18}F]-fluorodeoxyglucose positron emission tomography (^{18}F-FDG) for glycolysis, and [^{18}F]-fluoro-pivalic acid positron emission tomography (^{18}F-FPIA) for fatty acid metabolism were employed. ^{1}H Nuclear Magnetic Resonance (NMR) spectroscopy and liquid chromatography with tandem mass spectrometry (LC-MS-MS) were employed for validation purposes.

Methods: [1-^{13}C]-labeled pyruvic acid was hyperpolarized using a DNP HyperSense polarizer following standard protocol. Anatomical MRI and ^{13}C-MRS were obtained on different PCa PDX mouse models at two different time points using a Bruker 7T scanner. The PDX models included AR+ enzalutamide sensitive (183-A, 180-30), AR+ enzalutamide resistant (274-4), and AR- (144-4, 114-B). The time points imaged were before and after 7 days of treatment with enzalutamide. ^{1}H-NMR spectroscopy was performed on extracted tissue. Simultaneously, ^{18}F-FPIA-PET imaging were acquired on the same models on an Albira trimodal PET station.

Results: The dynamic metabolic flux ratio, lactate-to-pyruvate (Lac/Pyr) was determined *in vivo* and used as a treatment response marker. The Lac/Pyr ratios were significantly higher in resistant tumors compared to sensitive tumors ($p<0.01$). The enzalutamide sensitive group had a lower Lac/Pyr ratio after treatment, while the enzalutamide resistant group had a higher Lac/Pyr ratio. After treatment, there was also a decrease in [^{18}F]-FDG uptake, corresponding to the HP-MRS data. This was expected as both Pyruvate and [^{18}F]-FDG interrogate the glycolytic pathway. As for the fatty acid metabolic imaging, PET imaging also revealed that [^{18}F]-FPIA is transported into the tumors, and we are currently exploring how its uptake varies between AR (+/-) PCa-PDX tumors and enzalutamide resistant/sensitive models. *Ex vivo* NMR and mass spectrometry-based metabolomics validated the *in vivo* HP-MRS data with higher lactate levels in drug resistant tumors.

Conclusion: Combining HP-MRS and PET presents an exciting opportunity to realize imaging-based personalized medicine in different AR (+/-) PCa-PDX preclinical models by interrogating glycolysis and fatty acid oxidation pathways.

#4158 Non-invasive mapping of acidosis and extracellular lactosis for assessing tumor invasion *in vivo*.

Anais Choffart[1], Remy Chiaffarelli[1], Max Zimmermann[1], Laura Kuebler[2], Andre F. Martins[3]

[1]Werner Siemens Imaging Center, Department of Preclinical Imaging, Universitatsklinikum Tubingen, Tubingen, Germany,[2]Cluster of Excellence iFIT (EXC 2180) "Image-Guided and Functionally Instructed Tumor Therapies", Universitatsklinikum Tubingen, Tubingen, Germany,[3]German Cancer Research Center (DKFZ), German Cancer Consortium (DKTK), partner site Tubingen, Heidelberg, Germany

Tumor cells typically display a hyperglycolytic metabolic phenotype characterized by increased lactate production, known as the Warburg effect. This drift in oxidative metabolism often results in a more acidic microenvironment. This adverse microenvironment represents a unique metabolic signature in cancer cells with more invasive phenotypes. However, to date, there are no effective methods available to evaluate cancer progression and metastatic potential *in vivo*. To bridge this gap, we have developed a molecular imaging technique (CEST-MRI) that can track extracellular pH (pH_e; acidoCEST) and extracellular lactate levels (shiftCEST) simultaneously to discern different cancer phenotypes.

In this study we have generated and selected *in vivo* two PyMT derived murine breast cancer cell lines, a parental and a G6 metastatic. We first characterized the cell's metabolism by analyzing key biomarkers with qPCR, Western Blot and microscopy, and confirmed their distinct metabolic profiles with Seahorse and RNA Sequencing. Notably, the metastatic PyMT exhibited a more active metabolism, aligning with the invasive phenotype observed by spheroid invasion assay. Herein, we combined the injection of iopamidol and shift reagent (SR) to perform quasi-simultaneous acidoCEST and shiftCEST. First, we assessed the approach *in vitro* by introducing iopamidol and SR into phantoms containing the individual contrast agents, and the combination in pure water and cells supernatants at different pH_e and lactate levels. We performed LDH assays to cross-validate the extracellular concentrations and monitored the pH with a micro pH meter (Mettler-Toledo). *In vivo*, the cells were injected orthotopically in the 4th mammary fat pad of C57BL/6N mice. Hybrid shift/acidoCEST sequences were optimized and acquired following the injection of the iopamidol+SR solution. Preclinical shift/acidoCEST enabled the simultaneous and accurate determination of extracellular acidosis and lactosis, revealing increased acidification in the metastatic models despite lower lactate secretion. Metastatic tumors exhibited a negative correlation between tumor volume and pH_e, indicating the significance of acidity in mutagenesis and invasion. In contrast, no correlation was observed for the parental non-metastatic tumor. Additionally, the metastatic tumors had lower levels of lactate than the parental tumors, which could be attributed to their higher mitochondrial activity, reflecting a diverted metabolic fitness.

In summary, our study highlights the efficacy of shift/acidoCEST as a reliable method for non-invasive metabolic imaging, enabling the simultaneous detection of extracellular acidity and lactate production by MRI. This research introduces a unique platform for assessing the metabolic aggressiveness of cancer, emphasizing the significance of acidity and lactate production as crucial biomarkers in cancer invasion.

#4159 Noninvasive measurement of murine glioblastoma *in vivo* with a benchtop ultrasound instrument.

T. M. Kierski[1], J. D. Rojas[1], M. Thang[2], S. D. Hingtgen[2], P. G. Durham[2], P. A. Dayton[2], **T. J. Czernuszewicz**[1], R. C. Gessner[1];
[1]Revvity, Durham, NC, [2]UNC Chapel Hill, Chapel Hill, NC

The purpose of this study was to evaluate a new *in vivo* approach for rapidly measuring tumor volumes in rodent models for glioblastoma (GBM). GBM is the most common primary brain tumor with <5% of patients surviving >5 years post diagnosis. These poor outcomes underscore the importance of researching new treatment options, and murine models play a vital role in this. Noninvasive measurements of murine GBM tumors are commonly performed using CT and MRI but these tools are costly and time-consuming to use. BLI can quickly detect the presence of GBM cells *in vivo*, but image data can be challenging to correlate to tumor volume. In this study we demonstrate the feasibility of imaging GBM *in vivo* through the intact mouse skull using a benchtop robotic ultrasound scanner. This approach could offer researchers a means to quickly size tumors in the murine brain noninvasively. To test feasibility of this approach, a female athymic nude mouse aged 16 weeks was implanted with 2e5 U87 GBM cells in the brain. The tumor was given 25 days to develop prior to ultrasound imaging. After imaging, the brain was harvested for *ex vivo* validation of tumor presence and volume. Imaging was performed using a Vega ultrasound system (Revvity, Waltham, MA, USA) with the mouse in supine position and fur removed from head with depilatory cream. *In vivo* imaging consisted of a contrast-enhanced acoustic angiography (AA) scan to assess tumor perfusion. An *ex vivo* B-mode scan of the brain was collected after sacrificing the animal to validate the location and size of the tumor without interference from the skull. The tumor volumes were measured in each image and compared. 3D segmentations in the *ex vivo* and *in vivo* images yielded volumes of 43.1 mm^3 and 44.6 mm^3, respectively, a 3.5% variance. In the *in vivo* AA image, the borders of the tumor were adequately well-defined for volume estimation, despite some shadowing from the sagittal suture of the skull. In the B-mode image of the excised brain, the tumor appeared hyperechoic compared to the contralateral hemisphere. Images were acquired in < 2 min. This pilot study demonstrates a potential alternative to CT and MRI for monitoring of GBM volumes *in vivo*.

#4160 V7 targeted liposomes detect pancreatic adenocarcinoma via multispectral optoacoustic tomography.

H. Agarwal[1], P. Chuong[2], W. E. Grizzle[3], B. H. Edil[1], A. Jain[1], L. R. McNally[1];

[1]OU Health Stephenson Cancer Center, Oklahoma City, OK, [2]University of Louisville, Louisville, KY, [3]University of Alabama at Birmingham, Birmingham, AL

Purpose: Pancreatic ductal adenocarcinoma (PDA) remains one of the most aggressive malignancies with a 5-year survival rate of 9-10%. Insufficient early detection coupled with limitations in operating surgery renders PDA as one of the most challenging tumors to treat. Accurate localization of tumor margins can tremendously improve surgical treatment outcomes in patients. Recently, nanotechnology has emerged as a promising platform for theranostic applications in the field of drug discovery, although the clinical success is limited by their tumor-specific uptake. Hypoxia due to aberrant vascularization is a hallmark of PDA and can be exploited for active targeting. pH-low insertion peptide variant 7 (V7) is used as hypoxia and acidosis-dependent biomarker for selective targeting of pancreatic cancer tissue. This work is focused on using IR 780 contrast agent loaded, V7 peptide conjugated liposomes for the active targeting of PDA towards enhanced surgical outcomes.

Methods: Liposomes encapsulating IR780 dye were prepared using thin film hydration technique. V7 peptide was conjugated to liposomes using an SMCC linker and liposomes were characterized for their size, polydispersity and surface potential. In-vitro uptake of IR780-V7-liposome by S2VP10 at pH 7.4, 6.8, and 6.6 was evaluated through NIR fluorescence imaging using an Odyssey Infrared System. Athymic mice were orthotopically implanted with S2VP10 cells. After tumors were 3 mm, V7-liposomes and untargeted liposomes (0.01 OD) were intravenously injected and biodistribution and tumor specific uptake was accessed using multispectral optoacoustic imaging (MSOT).

Results: Dynamic light scattering (DLS) revealed the size of liposomes to be 109 nm with a polydispersity index of 0.198 and zeta potential of +35.8 mV. Surface conjugation of V7 peptide was confirmed using the zeta potential measurement. NIR fluorescence imaging in S2VP10 cells established enhanced tumor specific uptake of V7 conjugated liposomes than passively targeted liposomes ($p<0.05$). Biodistribution of V7-liposomes demonstrated tumor specific accumulation (PDAC tumor 23.7 a.u, liver 3.6 a.u., and kidney 1.1 a.u.) while untargeted liposomes had the greatest uptake in liver (PDAC tumor 2.1 a.u., liver 6.3 a.u., and kidney 0.7 a.u.) $p<0.05$.

Conclusion: pH-specific actively targeted liposomes can be used to specifically target PDA with minimal off-target binding effects. V7-IR780-liposome formulation can be used to efficiently deliver contrast agent for imaging tumor margins and to expand the potential of MSOT towards clinical applications.

#4161 Identification of pancreatic adenocarcinoma using urokinase plasminogen activator probe detected using optoacoustic imaging.

V. Kim[1], P. Chuong[2], R. Bynum[1], W. Grizzle[3], L. R. McNally[1];
[1]OU Health Stephenson Cancer Center, Oklahoma City, OK, [2]University of Louisville, Louisville, KY, [3]University of Alabama at Birmingham, Birmingham, AL

Purpose: Diagnosing and treating pancreatic cancer remains a challenge. The hypovascularized nature of pancreatic cancer renders modern chemotherapeutics and cancer detection contrast agents ineffective. A promising approach to the challenges is the adoption of a novel imaging technique known as Multispectral Tomography (MSOT). We hypothesize that a urokinase plasminogen activator (UPA) probe will enhance the detection of orthotopic pancreatic cancer xenografts.
Methods: Pancreatic tumor cell lines (Panc1, MiaPaca-2, S2VP10, and S2C9) were assessed for UPA-receptor expression using western blot analysis. UPA peptide was synthesized and to the HiLyte-750 NIR dye. Flow cytometry and immunofluorescence were utilized to examine the specificity and activity of this UPA-750. The UPA-750 binding efficiency was assessed through a competitive inhibition assay with a UPAR-blocking antibody using fluorescence microscopy. Then SCID mice (5 mice/group) received orthotopic implantation of S2C9 (1.5 x 105) or MiaPaCa2 (2.0 × 106) pancreatic tumor cells. UPA-750 or 750 dye alone was IV injected into mice after the tumors reached 3mm. Biodistribution and accumulation of UPA-750 were observed through MSOT images taken at 2-hour intervals over 8 hours and at 24 hours. UPA-750 in the tumor, liver, and kidney was confirmed through ex vivo fluorescent imaging.
Results: UPAR expression was observed in every pancreatic cancer cell line, with the greatest relative abundance in S2P9 cells (3.0X), followed by S2VP10 (2.5X), Panc1 (1.77X), and MiaPaca-2 (1.3X). Application of the UPAR blocking antibody on S2CP9, S2VP10, MiaPaCa2, and SKOV3p1 (positive control) cell lines resulted in the inhibition of cellular binding of the UPA-750, as evidenced by fluorescence microscopy. UPA-probe was successfully observed in pancreas tumor slices with peak intensity at 4-hrs of imaging by MSOT. Ex vivo NIR fluorescence imaging confirmed UPA-750 signal in pancreatic tumors but not in liver or kidney.
Conclusion: UPA-probe exhibits potential as a marker for pancreatic cancer.

#4162 Peptide-targeted probe identifies pancreatic cancer using optoacoustic imaging.

E. Sanderson[1], T. Husarova[2], L. McNally[3],

[1]University of Oklahoma, Norman, OK, [2]Military University Hospital Prague, Prague, Czech Republic, [3]University of Oklahoma, Oklahoma City, OK

Introduction: Advanced pancreatic ductal adenocarcinoma (PDAC) suffers from inadequate early detection, inoperability, and poor outcomes. While tumor identication in an intraoperative setting largely utilize ultrasound, ultrasound suffers from insufficient resolution and lacks the ability to identify molecular features to differentiate tumor from non-tumor. To overcome these limitations, we utilized optoacoustic imaging combined with a pH-sensitive peptide-based probe, V3, to identify pancreatic cancer in orthotopic mouse models.

Methods: The V3 peptide was synthesized using microwave chemistry which resulted in a peptide of >90% purity. The V3 peptide was conjugated to a fluorescent dye and dialyzed to make the V3-750 probe. S2VP10 cancer cell line was plated in a 6-well plate and acclimated to 7.4, 6.8, and 6.6 pH media to mimic a healthy microenvironment and the acidic tumor microenvironment found in pancreas cancer. Cells were treated with 1 micromolar of V3-750 probe for 1 hour, then imaged on the near-infrared fluorescence imager. Treated cells were loaded into tissue mimicking phantoms and imaged using multispectral optoacoustic tomography. Athymic mice were orthotopically implanted with S2VP10 cells and tumor grew to 3 mm. V3-750 was intraveneously injected and mice were imaged 3h after injection with MSOT.

Results: Signal values for the samples displayed a trend that the V3-750 probe has higher signal values in the 6.8 and 6.6 pH as compared to the 7.4 pH. MSOT data supported this trend, with the signal values from the 6.8 and 6.6 pH being greater than the 7.4 pH by 10-fold ($p<0.05$). Biodistribution demonstrates peak tumor-specific uptake at 3h post injection (3.1 a.u., 0.003 a.u. liver, 0.002 a.u. kidney).

Conclusion: The heightened signal values for the acidic pH's from the fluorescence imaging and the MSOT suggest that the V3-750 probe can contrast acidic cancer cells from healthy cells because it targets the acidic cancer microenvironment.

#4163 Improving the dynamic range of pH low insertion peptides for targeted imaging of pancreatic tumors.

R. Bynum, E. Sanderson, B. H. Edil, A. Jain, L. R. McNally;
OU Health Stephenson Cancer Center, Oklahoma City, OK

Objective: Current intraoperative imaging modalities such as near-infrared fluorescent imaging (NIR) or ultrasound are limited due to operator experience and depth, and targeted imaging of pancreatic tumors would be beneficial. However, specific pancreatic tumor biomarkers available for targeting in a novel imaging protocol are lacking. As such, we focus on developing a novel targeted imaging paradigm utilizing multispectral optoacoustic imaging (MSOT) to target the acidic microenvironment of pancreatic tumors. Peptides know as pH low insertion peptides (pHLIPs) when bound to dye allow for contrasted imaging selectively based on pH using MSOT. We have identified the need for a pHLIP with improved dynamic range to improve imaging accuracy. Here, we synthesize the novel pHLIP V7FS for comparison to V3 with aims of improving the dynamic range of imaging with MSOT in pancreatic cancer.
Methods: Using microwave chemistry, V7FS and V3 were synthesized with >90% purity. Peptides were conjugated to HiLyte 750 dye, and peptide-dye conjugation confirmed via spectroscopy. Intraoperative measurements of human pancreatic tumor and surrounding uninvolved tissue were obtained using a microsensor. Near-infrared fluorescent imaging was used to measure probe uptake in S2VP10 and S2013 pancreatic cancer cells lines grown in pH specific media (7.4, 6.8, 6.6) in replicates. MSOT was then used to image probes in phantoms mimicking tissue and then in mice with pancreatic tumors from orthotopically implanted S2VP10. Statistical analysis was performed using ANOVA.
Results: Compared to surrounding uninvolved pancreatic tissue, human pancreatic tumor was more acidic with pH 6.2-6.7 vs 7.2-7.3 ($p<0.01$). Signal at pH 7.4, 6.8 and 6.6 was higher for V7FS-750 compared to V3-750 ($p=0.0105$). Signal for V7FS-750 was centered around pH 6.6 and signal for V3-750 centered around pH 6.8. Interaction between probe and pH did not reach significance ($p=0.745$). Peak uptake in orthotopic murine models was observed at 3 hours following intravenous injection.
Conclusions: V7FS-750 was shown to have higher signal accumulation compared to V3-750 favoring a more acidic environment (pH 6.6 vs pH 6.8). This novel pHLIP was demonstrated to be viable for use in an imaging paradigm utilizing MSOT in an orthotopic murine model. Continued improvement in the dynamic range of these probes is promising for the use of pHLIPS in imaging of pancreatic cancer with MSOT.

#4164 Hybrid photoacoustic imaging and fast ultrasound localization microscopy to probe the tumor microenvironment.

S. Zhao, S. Basu, R. H. Campbell, Y. Zhao, Y.-S. Chen;
University of Illinois Urbana Champaign, Urbana, IL

Photoacoustic (PA) imaging can map the physiological conditions of tissues and track the biodistribution of contrast agents. Ultrasound localization microscopy (ULM) with microbubbles provides deep-tissue super-resolution blood vessel images and blood velocity maps. The integration of these techniques offers a potential tool for oncological applications, such as visualizing tumor hypoxia and vasculature. Additionally, because PA imaging and ULM can share the same ultrasound detector and data-acquisition system, PA images can seamlessly fuse with ULM images without requiring post co-registration processing. However, the acquisition time of ULM is considerably longer (several minutes per frame) compared to PA imaging (10 milliseconds to 100 milliseconds per frame), limiting the simultaneous acquisition of the two imaging modalities. To address this issue, we developed a deep learning model based on U-Net to accelerate the frame rate of ULM using information from sparse microbubble locations and power Doppler images. By enabling fast ULM acquisition, we developed an interleaved PA/fast ULM imaging technique to simultaneously capture photoacoustic and ULM images. Our experiments demonstrated up to a 16 times improvement in acquisition speed with U-Net, utilizing in vivo mouse brain and skin tumor data. The hybrid imaging sequence achieved super-resolution vascular and tissue oxygenation imaging with less than 2 seconds of acquisition time per frame in vivo. The implementation of this rapid dual imaging scheme enables the longitudinal monitoring of 3D tumor microvasculature and hypoxia conditions using a common linear ultrasound transducer. We monitored tumor growth of epidermoid carcinoma (A431) in a mouse model from Day 7 to Day 17 of tumor implantation, and the results reveal a significant decrease in tumor vasculature density and oxygen saturation as the tumor grew larger over time. The results indicate a positive relationship between oxygen saturation and vessel density. Our findings showcase the potential of this innovative technique for advancing deep tissue, high-resolution, multi-biological parameters imaging in oncological research.

#4165 Influence of halogens in squaraine dye on optoacoustic signal.

K. Belligund[1], W. MacCuaig[1], C. Wickizer[2], Y. Shao[2], L. R. McNally[1];
[1]OU Health Stephenson Cancer Center, Oklahoma City, OK, [2]University of Oklahoma, Norman, OK

Optoacoustic imaging has grown in clinical relevance due to inherent advantages in sensitivity, resolution, and contrast, compared to standard modalities, such as fluorescence. However, guiding principles for development of small molecule contrast agents specific for optoacoustic imaging is lacking. This study assesses the influence of specific structural features of small molecule dyes, specifically squaraine dyes, that result in optoacoustic activity. Through computational models, *in vitro* testing, and *in vivo* experimentation this study assesses the effects of halogens on small molecule squaraine dyes to increase optoacoustic signal. By using the aid of our computational model, we decorated the squaraine scaffold with heavy halogenation of squaraines increased optoacoustic activity (2.12 a.u. vs. 0.21 a.u., $p<0.001$). Density functional theory models suggest the origin of increased optoacoustic signal is due to increases in transition dipole moment which manifested experimentally as increased absorbance in the NIR wavelength range and decreased fluorescence quantum yield, respectively. This study provides an insight into the structure-function relationships that lead to guiding principles for designing optoacoustic-specific contrast agents. Further developments of squaraines and other types of optoacoustic agents will further increase relevance of optoacoustic imaging in a clinical setting.

#4166 TSPO-targeted near-infrared optical probe for early identification and localization of high-risk premalignant pancreatic lesions.

S. Sharma, D. Hernandez, X. Wen, J. Wang, C.-D. Pham, B. Huang, H. C. Manning;
The University of Texas MD Anderson Cancer Center, Houston, TX

Background: Pancreatic cancer is the third most prevalent cause of cancer death in the U.S. with a ~10% survival rate. Surgery represents one of the best opportunities for extending survival and potential cures. Fluorescence-guided surgery (FGS) employing near-infrared (NIR) fluorescence-based targeting agents improves resection margins, allowing removal of small lesions not visible under white light. We previously reported a targeted NIR tracer (V-1520) of translocator protein (TSPO) expression that demonstrated proof-of-principle utility in high-grade pancreatic lesions arising in *Ptf1a-Cre; LSL-Kras$^{G12D/+}$; Smad4$^{flox/flox}$ (KCS)* of pancreatic cancer. The purpose of the present study is to evaluate the utility of V-1520 to identify low-grade, premalignant yet high risk lesions in *KCS* mice; in this scenario we attempted to model use of V-1520 to remove lesions likely to manifest as future recurrence. We compared the uptake of the tracer in these mice from weaning to adulthood to systematically evaluate the efficacy of FGS as a function of lesion grade.

Experimental: The tracer, V-1520, was synthesized and *KCS* mice were generated as reported.[1] Mice were injected with 30µg of V-1520 intravenously 24 hours before imaging. Images were acquired using the 800nm channel. *KCS* and WT mice were imaged as a function of from 4 to 11 weeks age. After imaging, tumor tissues and major organs were harvested for *ex-vivo* imaging, histopathology and Cryo-Fluorescent Tomography (CFT).

Summary: We found, V-1520 prominently localized in low-grade, premalignant PanIN cystic lesions with malignancy potential, as well as pancreatic tumors with and without local invasion. In contrast, V-1520 did not accumulate in healthy pancreata of KCS or WT mice. Mice as young as 4 weeks exhibited localized accumulation of the tracer with low grade PanIN and early dysplasia. The fluorescence intensity was further enhanced in mice with higher grade disease, whereby the pathology was characterized by high-grade cyst formation, increased nuclear/cytoplasm ratio, acinar to ductal metaplasia and invasion. Low and high-grade neoplasia was characterized by high TSPO immunoreactivity, consistent with *in-vivo* imaging. Confocal microscopy was used to colocalize V-1520 accumulation and TSPO immunoreactivity; V-1520 was found to prominently localized to premalignant epithelia pancreatic cancer cells. CFT illustrated that the primary localization of V-1520 included the liver, kidneys, and pancreatic diseases.

Conclusion**:** These studies suggest the utility of V-1520 to identify high-risk pancreatic lesions that could be removed with surgery. Encouragingly, the V-1520 was capable of differentiating tumors from surrounding non-tumor tissue at an early stage, which could lead to better resections and delay and/or prevent recurrence in the future. 1. *Clinical Cancer Research* 26(22), 15 Nov. 2020 5914-5925

#4167 Selective imaging of cancer-associated fibroblasts in the breast cancer microenvironment with near-infrared fluorescent probes.

M. S. Michie[1], J. Du[1], J. Ye[1], K. Duncan[1], M. Y. Berezin[1], S. Achilefu[2];
[1]Washington University School of Medicine in St. Louis, St. Louis, MO, [2]UT Southwestern Medical Center, Dallas, TX

Tumors consist of a complex mixture of resident and infiltrating cells that can support their survival and evasion of treatment. Selective detection of genetically stable cells in the tumor microenvironment (TME) offers insight into tumor biology beyond the malignant cells, which are the focus of most molecular imaging approaches to cancer detection. Motivated by the goal of non-invasively understanding the primary breast TME, we have developed fluorescent molecular probes that target cancer-associated fibroblasts (CAFs), a major component of the stromal compartment of many tumors, and emit light in the near-infrared (NIR) spectral window, providing access to deeper tissues than visible probes. We synthesized and characterized a series of CAF-targeted antibody- and small molecule-based fluorescent imaging agents utilizing a highly hydrophilic NIR dye and ligands that target Fibroblast Activation Protein (FAP). FAP is a key cell-surface marker of breast cancer CAFs with an S1 phenotype, which are modulators of immunosuppression, metastatic spread, and are associated with worse outcomes, especially in HER2+ and triple-negative breast cancer. Modifications to the chemical structure of the linker and targeting ligands allowed us to alter the specificity and brightness of the CAF-probes *in cellulo*. Imaging of a co-implanted tumor model of SKBR3 human breast cancer cells and FAP expressing fibroblasts after administering our lead small-molecule CAF imaging agent revealed selective tumor targeting of CAF-rich tumors compared to cancer cell predominant tumors with favorable pharmacokinetics and tumor-to-background ratio (TBR) greater than 2. Similar imaging studies with MMTV-PyMT transgenic mice, an established murine model of breast cancer, showed analogous enhanced uptake in mammary tumors (TBR > 2) and clearance over 24 hours. NIR fluorescence also correlated with CAFs isolated from PyMT tumor tissue via flow cytometry, consistent with our hypothesis that this agent can specifically detect endogenous CAFs. This study identified a novel, bright, and water-soluble FAP-specific NIR agent for *in vivo* imaging, setting the stage for simultaneous optical imaging of malignant cells and activated fibroblasts in the TME to elucidate cancer-host interactions.

#4168 Pre-clinical demonstration of Raman spectroscopy-assisted photothermal therapy for prostate cancer.

S. Lee[1], G. Beaudoin[2], J. Yeoh[2], F. Leblond[2], M. Trifiro[1], M. Paliouras[3];
[1]McGill University, Montreal, QC, Canada, [2]Polytechnique Montreal, Montreal, QC, Canada, [3]Guzzo Nano Research, Terrebonne, QC, Canada

Prostate cancer (PCa) ranks among the most prevalent malignancies in men. The combination of ultrasound and fine-needle aspiration biopsy has greatly facilitated early diagnosis and expanded the range of treatment options. Traditional treatments primarily involve anti-androgens and androgen deprivation therapy; however, a recurrence occurs in approximately 30% of cases following these interventions. Our current focus is on the exploration of photothermal therapies using nanoparticles for precise tumor ablation. Among these nanoparticles, multiwalled carbon nanotubes (MWCNTs) exhibit unique structural, optical, and thermal properties that make them exceptionally appealing for biomedical applications, especially as a foundation for photothermal therapy. Our platform employs the copper (I)-catalyzed azide alkyne cycloaddition of prostate-specific membrane antigen (PSMA)-targeting peptidomimetic (Glu-urea-Lys) ligand to the MWCNTs. We used confocal microscopy to observe a significantly enhanced binding of the targeted Glu-urea-Lys-MWCNTs to the surfaces of PSMA-expressing LNCaP cells compared to IgG-MWCNTs and to PSMA-null PC3 cells. Raman microscopy further confirmed the increased presence of Glu-urea-Lys-MWCNTs on LNCaP spheroids compared to non-targeting MWCNTs. We also confirmed enhanced photothermal cell ablation *in vitro* using the targeted MWCNTs. Based on *in vitro* evidence, we established LNCaP and PC3 xenografts in *nu/nu* mice and evaluated the therapeutic efficacy. Using fluorescence-based imaging, we observed the enhanced localization of Glu-urea-Lys-MWCNTs within the tumors. Furthermore, we collected the tumors and conducted *ex vivo* analysis using Raman microscopy for a label-free detection of the targeted MWCNTs, which complemented the fluorescence imaging and laying the foundation for real-time Raman imaging *in vivo*. Subsequently, we applied photothermal ablation of the tumor xenografts based on a pre-optimized treatment protocol established from COMSOL simulations and prior experiments. This treatment led to complete tumor ablation with minimal recurrence and minimal non-specific damage. In conclusion, we have assessed the effectiveness of our targeted nano-photothermal platform in a pre-clinical model of PCa. Further studies will aid in the transition of photothermal therapy to clinical trials. Moreover, we aim to investigate the role of photothermal therapy in the PCa tumor microenvironment and whether such an approach can trigger post-therapeutic activation of immune responses against the tumor. Ultimately, we anticipate that our nanotherapeutic platform will contribute to a focused therapeutic approach where targeted MWCNT-laser treatment exploits overexpressed tumor markers in conjunction with various irradiation strategies to enhance ablation while minimizing damage to surrounding tissue.

#4169 A deep learning approach to guide acquisition region selection for imaging mass cytometry.

F. Schneider[1], S. Kala[2], S. Lim[2], C. Hupple[2], N. Lane[2], **J. R. Mansfield**[1];
[1]Visiopharm, Horsholm, Denmark, [2]Standard BioTools, South San Francisco, CA

The growth in cancer immunotherapy agents requires an understanding of the immune contexture of the tumor microenvironment. This can be aided by high-plex imaging and analysis to obtain phenotypes of specific cells and study their biodistribution and interactions. Imaging Mass Cytometry™ (IMC) is the method of choice for single-step staining and high-plex imaging of tissues, avoiding the complications of autofluorescence and cyclic imaging.
IMC has expanded its capabilities with three distinct imaging modes: Preview, Cell, and Tissue. The Preview Mode is a rapid scanning system that captures a comprehensive overview of the stained tissue, mapping out the distribution of over 40 markers and revealing tissue heterogeneity. This enables researchers to make informed decisions about which areas warrant closer examination on the same. Building on this, Cell Mode offers high-resolution imaging for detailed analysis of the Regions of Interest (ROI) identified during Preview, all using the same slide. Tissue Mode complements these by providing a fast acquisition of the entire tissue at a lower resolution, which is optimal for quantitative pixel-based analysis of tissue biology. These modes support automated, continuous imaging of more than 40 large tissue samples (400 mm2) weekly. Following Preview Mode, the selection of ROIs for high-resolution imaging is a critical step, enhanced by automated AI algorithms to ensure it is informed by biomarker expression.
Tissue sections of colon adenocarcinoma were stained with a 30-marker IMC panel of structural, tumor, stroma, immune cell, and immune activation markers. Images were acquired on Hyperion XTi™ (Standard BioTools), first in Preview Mode, then in Cell Mode with automatic selection of ROIs using Phenoplex™ (Visiopharm). ROIs were automatically selected based on two criteria: 1) actively proliferating and non-proliferating tumor regions; 2) cold and hot tumor regions as identified by hotspots of lymphoid and myeloid immune markers within stromal or epithelial tumor regions.
Single cell analysis of the high-resolution images obtained in Cell Mode, was performed as a multi-step workflow using Phenoplex. Tissue segmentation was used to divide the tissue into epithelial tumor (E-Cadherin/panCK), stromal, and tumor margin regions; cell segmentation was based on Iridium DNA channels; and phenotyping was performed using the guided highplex workflow. These data were used to compare the immune contexture through a series of t-SNE plots partitioned by spatial region and clinical variables.
This work demonstrates that the multi-modal features of Hyperion XTi can greatly accelerate the ability of IMC users to gain useful insights from complex biological samples. Phenoplex enables a comprehensive workflow for the analysis of this complex data, providing automated ROI selection, and phenotyping and spatial analyses of high-resolution IMC images for biological assessment.

#4170 Artificial intelligence (AI)-based multi-modal approach using H&E and CT image for predicting treatment response of immune checkpoint inhibitor (ICI) in non-small cell lung cancer (NSCLC).

D. Jeong[1], J. Park[2], H. Song[2], J. Moon[2], T. Lee[2], C. Ahn[2], S. Park[1], S.-H. Lee[1], C.-Y. Ock[2], H. Lee[1];
[1]Samsung Medical Center, Seoul, Korea, Republic of, [2]Lunit, Seoul, Korea, Republic of

Background: Previously, AI-powered spatial tumor-infiltrating lymphocyte analysis in H&E whole-slide image (WSI) showed promising performance in predicting ICI outcomes. However, there were several innate limitations of tissue analysis, including the time lag between tissue biopsy and actual ICI administration, during which tumor microenvironment (TME) has changed, and analyzing a part of a single tumor tissue would not fully assess immunogenicity of multiple metastatic tumors. To overcome the challenges, we developed multiple-instance learning (MIL)-based models and applied them to predict the treatment response of ICI in a real-world dataset.

Method: MIL-based models were trained under the cross-validation scheme for CT scans (N=456) separately, based on CT image analyzers. Lunit SCOPE IO (Lunit, South Korea), an AI-based H&E WSI analyzer, identifies various classes of cells within TME and segments tumor regions from WSI (AI-HE-TIL). An AI-based CT image analyzer detects nodules on the CT image (AI-CT). The final ensemble score per patient is computed by the average of all model predictions from CT and pathology image inputs. Single and ensemble performances for predicting responder and non-responder patients to ICI are measured in an independent cohort of 208 NSCLC patients.

Results: In the overall cohort, the AUROC values for AI-HE-TIL, AI-CT, and the ensemble were 0.6372, 0.6759, and 0.7307, respectively. The high ensemble score group (≥ median) has prolonged progression-free survival (PFS) of ICI (median PFS 5.0 months vs 2.1 months, hazard ratio [HR] 0.54, P < 0.0001). It correlates with PD-L1 expression, as tumor proportion score (TPS) ≥ 50% subgroup had higher ensemble score (median 0.312 vs 0.257, P = 0.0295). Interestingly, among TPS ≥ 50% subgroup, the high ensemble score shows significantly favorable PFS of ICI (median PFS 6.7 months vs 2.9 months, HR 0.46, P = 0.0002). In subgroup analysis according to tissue harvest site (primary tumor vs lymph node or distant metastasis), the AUROC values of AI-HE-TIL and AI-CT for the subgroup harvested from the primary tumor (N=111) were 0.6568 and 0.6658, respectively, and those for the subgroup harvested from the metastatic lesion (N=97) were 0.6162 and 0.6973, respectively, implying AI-CT is relatively not affected by tissue harvest site.

Conclusion: AI-powered multi-modal approach of using H&E image and CT image shows complimentary, and synergistic effect to predict ICI clinical outcomes in advanced NSCLC, even in the subgroup of PD-L1 high population.

#4171 Utilizing biopsy-free virtual histology for improved clinical efficiency in the dermatologic surgical setting.

Rachel Wahhab[1], Nelly Kokikian[1], Jingxi Li[2], Jason Garfinkel[3], Stephanie Martin[3], David Beynet[3], Aydogan Ozcan[2], Philip Scumpia[1]

[1]Division of Dermatology, University of California, Los Angeles, Los Angeles, CA,[2]Department of Electrical Engineering and Bioengineering, University of California, Los Angeles, Los Angeles, CA,[3]Dermatology, Veterans Affairs Greater Los Angeles Healthcare System, Los Angeles, CA

The ability to accurately define tumor margins may enhance tissue sparing and increase efficiency in the dermatologic surgery process, but no device exists that serves this role. Reflectance Confocal Microscopy (RCM) provides non-invasive cellular resolution of the skin. The only clinically-approved RCM device is bulky, non-portable, and requires a tissue cap which makes mapping of the underlying tissue impossible. We recently combined “virtual histology”, a machine learning algorithm with RCM images from this standard RCM device to generate biopsy-free histology to overcome these limitations. Whether virtual histology can be used with a portable, handheld RCM device to scan for residual tumor and tumor margins is currently unknown. We hypothesize that combining a handheld RCM device with virtual histology could provide accurate tumor margin assessment. We determined whether our established virtual histology algorithm could be applied to images from a portable RCM device and whether these pseudo-stained virtual histology images correlated with histology from skin specimens. The study was conducted as a prospective, consecutive non-randomized trial at a Veterans Affairs Medical Center dermatologic surgery clinic. All patients greater than 18 years of age with previously biopsied BCC, SCC, or SCCis were included. Successive confocal images from the epidermis to the dermis were obtained 1.5 microns apart from the handheld RCM device to detect residual skin cancer. The handheld, in-vivo RCM images were processed through a conditional generative adversarial network-based machine learning algorithm to digitally convert the images into H&E pseudo-stained virtual histology images. Virtual histology of in-vivo RCM images from unbiopsied skin captured with the portable RCM device were similar to those obtained with the standard RCM device and virtual histology applied to portable RCM images correctly correlated with frozen section histology. Residual tumors detected with virtual histology generated from the portable RCM images accurately corresponded with residual tumors shown in the frozen surgical tissue specimen. Residual tumor was also not detected when excised tissue was clear of tumor following surgical procedure. Thus, the combination of virtual histology with portable RCM may provide accurate histology-quality data for evaluation of residual skin cancer prior to surgery. Combining machine learning-based virtual histology with handheld RCM images demonstrates promise in providing insights into tumor characteristics and has the potential to assist the surgeon and better guide practice decisions to more efficiently serve patients, leading to decreased layers and appointment times. Future work is needed to provide real time virtual histology, convert horizontal/confocal sections into vertical or 3D sections, and to perform clinical studies to map tumors in tissue.

#4172 Pathology supervised approaches for ROI placement and segmentation to overcome caveats and pitfalls in high-plex spatial profiling.

S. Hernandez[1], C. J. Arrechedera[1], P. Rocha[2], L. Kostousov[1], S. Barnes[1], K. Khaja[1], L. M. Solis-Soto[1];
[1]UT MD Anderson Cancer Center, Houston, TX, [2]Hospital del Mar, Barcelona, Spain

Background: Tissue-based high-plex platforms evaluate numerous biomarkers in limited tissue sections. Certain tissue features and assay technical limitations may jeopardize the accuracy of this analysis. In this study, we aim to determine tissue specific features that influence image-based region of interest (ROI) selection and segmentation for spatial profiling of carcinomas, and to develop pathology approaches to overcome them.
Methodology**:** A total of 317 samples from different carcinoma types processed with the GeoMx Digital spatial profiling protein assay protocol were assessed to identify deviations from original strategies for ROI placement and segmentation (Table 1). ROI were selected by a pathologist. The initial strategy for all cases was to place rectangles ROIs of 660*785 µm in tumor area and to segment based on morphology biomarkers as indicated in Table 1. Strategies to overcome technical and tissue specific features were recorded and quantified.
Results: A total of 2068 ROIs and 4422 AOIs were evaluated. In all the cases, tissue displayed specific features that limited planned ROI placement and segmentation. Table 1 describes these features by tissue type and profiling strategies. A total of 970 ROIs were solved using different annotation type or changes in segmentation strategy, 584 bypassed the limitations by changing the processing protocol; and 322 were not solved due to non-compliance with assay requirements.
Conclusions: We identified tissue features that limit the planned ROI selection and segmentation in spatial high-plex profiling, mainly due to tissue processing, distinct histology, type of sample, and presence of adjacent non-neoplastic tissue. A deep understanding of tumor architecture, biology and platform related technical limitations is needed to select areas of analysis for spatial profiling.

Table 1: ROI and segmentation strategy methodology and tissue specific features with pathology appro

		Histological type (Profiling segments)						
		Anal Carcinoma (Tu/TME)	**Lung NSCLC (Tu/TME)**	**Lung NSCLC TMA (Tu/Tcells/ Mϕ)**	**Lung NSCLC TMA (Tu/TME)**	**CRC MT Tu/Immune**	**Breast Ca Tu/Immune/else**	**Pathology Approach (ROIs)**
Methodology	**Samples**	48	33	80	80	6	70	
	Biopsy type	Incisional (Core/other), Whole tissue	Incisional (Core/other)Whole tissue	TMA	TMA	Whole tissue	Core	
	Morphology markers/mIF Channels	Syto13: FITC/525 PanCK: Cy3/568 CD45: Texas red/615 CD68: Cy5/666	Syto13: FITC/525PanCK: Cy3/568CD20: Texas red/615CD3: Cy5/666	Syto13: FITC/525 PanCK: Cy3/568 CD68: Texas red/615 CD3: Cy5/666	Syto13: FITC/525 PanCK: Cy3/568 CD68: Texas red/615 CD3: Cy5/666	Syto13: FITC/525 PanCK: CD45: Texas red/615	Syto13: FITC/525 PanCK: Cy3/568 CD45: Texas red/615	
	Strategy for segmentation	Tumor (PanCK+) TME (PanCK-)	Tumor (PanCK+)TME (PanCK-)	Tumor (PanCK+) T cell (CD3+) Mϕ (CD68+)	Tumor (PanCK+) TME (PanCK-)	Tumor (PanCK+) Immune (CD45+)	Tumor (PanCK+) Immune (CD45+) Else (PanCK-CD45-)	
	Total ROIs/AOIs	224/435	144/252	80/218	82/162	944/1573	594/1782	
Tissue specific features (ROI number/percentage)	**Folds (ROIs)**	10	1	0	0	9	5	Draw Polygons (25)
	Adjacent* Non-Tumoral tissue	22	7	9	7	388	40	Draw Polygons (473)
	Tissue Derived Autofluorescence	3	105	0	1	0	45	Draw Polygons (13). New segment to exclude autofluorescence (141)
	Sample Size	26	19	1	2	5	138	Polygons (191)
	Necrosis	13	0	1	1	217	6	Polygons (238)
	Biological absence of morphology marker	10	0	0	0	0	5	Polygons non segmented for Tu and TME (15)
	Solid tumors with scant TME	0	21	0	0	0	9	Polygons non segmented for Tu and TME (30)
	Eosin autofluorescence	0	0	0	0	0	584	Stained new section with Validated PanCK in Cy5/666 channel (584)
	Failure to reach the minimum number of cell requirements	13	36	22	2	249	43	Excluded segments (322) New scan to select more areas (43)

TUMOR BIOLOGY: In Vivo Imaging and Humanized Models
Poster Session

#4177 High-throughput *in vivo* monitoring of splenomegaly and tumor burden in a murine breast cancer model.
C. McMannus, **T. J. Czernuszewicz**, R. C. Gessner, J. D. Peterson;
Revvity, Durham, NC

Splenomegaly is a valuable parameter in mouse model cancer studies, as it can reflect the magnitude of cancer burden, hematopoietic activity, immune status, and can provide an indirect measure of cancer treatment efficacy. In liquid cancer models specifically (leukemia/lymphoma), spleen sizing is important as it is usually the only measure of *in vivo* tumor burden that can be assessed noninvasively without genetic labeling of tumor cells. Magnetic resonance imaging (MRI) and contrast-enhanced computed tomography (CT) are highly effective at evaluating spleen size in small animals. However, these techniques can impose limitations on large-cohort study designs due to high cost, long scan time, and ionizing radiation. Ultrasound is an alternative method with lower cost, high frame rate, and no ionization, but can suffer from poor inter-user variability, limited 2D field-of-view, and low throughput due to manual operation. In this work, we evaluated a novel 3D automated ultrasound scanner (Vega, Revvity, Inc.) for rapid assessment of splenomegaly in a murine cancer model. Female BALB/c mice (n=10) were implanted with 5e5 4T1 (ATCC) cells on the right flank. Mice were imaged at five timepoints over 25 days to track longitudinal progression of both spleen and tumor enlargement. Images were segmented manually in 3D using the “Slice Draw” and “Fill Between Slices” effects in SonoEQ v2.0.1 (Revvity, Inc.) to quantify tissue volume. After the final timepoint, mice were euthanized, and spleen weight was measured *ex vivo*. An additional cohort of age-matched mice without tumors (n=7) were imaged at the final timepoint to serve as controls. Imaging revealed a substantial enlargement of the spleen over time, from 30 ± 3 mm^3 to 545 ± 105 mm^3, representing an 18-fold increase. In the same time span, tumor volume grew to 1966 ± 87 mm^3. Correlation analysis demonstrated good agreement between ultrasound volumes and *ex vivo* spleen weights ($R^2 = 0.90$). The results in this study demonstrate that noninvasive, nonlabelled quantification of murine spleen size with automated ultrasound is feasible, robust, and fast. The average time to acquire the spleen image for each mouse was less than 30 seconds. Future studies will apply this workflow in liquid cancer models, as well as explore using machine learning approaches to automatically segment spleen borders for faster data analysis.

#4178 Non-invasive shortwave infrared imaging of cytotoxic T lymphocyte infiltration for monitoring responses to combination immunotherapy and chemotherapy.

Jay V. Shah[1], Jake N. Siebert[1], Xinyu Zhao[2], Shuqing He[2], Richard E. Riman[3], Mei Chee Tan[2], Mark C. Pierce[1], Edmund C. Lattime[4], Vidya Ganapathy[1], Prabhas V. Moghe[1]

[1]Biomedical Engineering, Rutgers University, Piscataway, NJ,[2]Engineering Product Development, Singapore University of Technology and Design, Tampines, Singapore,[3]Materials Science and Engineering, Rutgers University, Piscataway, NJ,[4]Rutgers Cancer Institute of New Jersey, New Brunswick, NJ

Although triple-negative breast cancer (TNBC) can be treated with anti-PD-1 checkpoint immunotherapy in combination with chemotherapy, there remains a challenge in effectively monitoring therapeutic responses. Current non-invasive clinical imaging tools to evaluate response to treatment are reliant upon measurements of tumor volume and may fail to distinguish true progression from increased immune cell infiltration. Invasive biopsy sampling and immunohistochemistry (IHC) can elucidate changes in the immune landscape of treated tumors, but these methods are not conducive to providing real-time information. This study presents shortwave infrared (SWIR) imaging as a potential tool to detect treatment-induced cytotoxic T lymphocyte (CTL) infiltration non-invasively and in real time using rare earth metal-doped nanoparticles encapsulated in human serum albumin nanocomposites (ReANCs). ReANCs were chemically conjugated with anti-CD8α antibodies as targeting ligands to facilitate binding of the nanoprobes to CTLs with high specificity in a syngeneic mouse model of breast cancer. After treating the mice with combination anti-PD-1 and doxorubicin, volumetric analysis of the mammary fat pad tumors did not show any significant impact of treatment compared to single treatment and untreated control mice. However, increased CTL infiltration in the tumors of mice that received combination treatment was detected by *in vivo* SWIR imaging. CTL infiltration was validated with *ex vivo* IHC staining, and a monotonic relationship was observed between SWIR fluorescence and CD8 positivity. IHC staining of other immune markers, including CD45, CD3, CD4, and PD-L1, showed that combination treatment may influence in the expression of these markers, presenting additional targets that could be imaged with ReANCs in the future. In conclusion, the increase in SWIR signal from CD8-targeted ReANCs in tumors treated with combination immunotherapy and chemotherapy and the relationship with IHC staining highlight the ability to use SWIR imaging for non-invasive assessment of changes in immune dynamics following treatment.

#4179 Magnetic resonance imaging and bioluminescence imaging for evaluating tumor burden in orthotopic glioblastoma.

Mingrui Guo[1], Ruisong Su[1], Jeff W H Chor[1], Zheyan Zhang[1], Mandy Tan[1], Xing Qi Teo[2], Haosheng Feng[2], Kuan J. Lee[2], Li Hua[1], Longyun Zhang[1], Jie Cai[1], Guanping Mao[1], Jingjing Wang[1], Keefe Chng[1], Weiping Han[2], Colin Guo[1]

[1]Crown Bioscience, San Diego, CA,[2]Institute of Molecular and Cell Biology, Agency for Science, Technology and Research (A*STAR), Singapore, Singapore

Accurate monitoring of orthotopic tumors in oncological research is critical. While conventional surgical exposure method or imaging methods such as bioluminescence imaging (BLI), ultrasound imaging (US) and computed tomography (CT) have different advantages and limitations. Magnetic Resonance Imaging (MRI) offers a non-invasive modality with high sensitivity. This study compares BLI and MRI in tracking tumor progression, focusing on the human glioblastoma multiforme (GBM) orthotopic xenograft mouse model. To establish the GBM model, human glioblastoma cells U87 MG-luc, expressing firefly luciferase, were intracranially implanted in female BALB/c nude mice. In-life tumor growth was assessed longitudinally every 3-4 days using BLI (IVIS Lumina S5, PerkinElmer, US) and MRI (Bruker BioSpec 117/16, 11.7T ultra-high field scanner, Germany) with a T2-weighted sequence. Mice were randomized into two groups (n=8) based on the MRI-derived tumor volume and BLI signal on the 3rd day post inoculation. One day after grouping, each cohort received specific treatments: one with the standard vehicle control and the other with Temozolomide (TMZ) (10mg/kg, 5 days/week, oral gavage). This treatment lasted until day 21, after which whole brains were removed and tumors excised from surrounding normal tissue and weighed. The results from both BLI and MRI showed that the control group exhibited consistent tumor growth, while TMZ treatment significantly inhibited tumor growth by day 21. However, some differences were observed, particularly for small tumor size, with more accurate measurement with MRI compared to BLI. By day 7 (3 days post treatment), MRI indicated a Tumor Growth Inhibition (TGI) of 32.63%, whereas BLI indicated a 5.04% increase in the TMZ-treated group compared to the control group. From day 11 onwards, both methods demonstrated a TGI exceeding 70% with TMZ treatment. Moreover, there was a pronounced difference in tumor weight correlations: MRI assessments showed a strong correlation (R^2=0.9967) with extracted tumor weights, whereas in contrast to BLI showed a weaker correlation (R^2=0.5371). The lower correlation for BLI, could be explained by the hypoxia and necrosis commonly observed in larger tumors or after treatment leading to decrease of ATP and reduction of bioluminescence. BLI offers rapid 2D imaging but lacks precision in determining location and depth of GBM tumor. Moreover, it requires luciferase engineered cell lines. In contrast, MRI provides high-resolution 3D imaging without genetic modifications, providing precise anatomical evaluations. Our study highlights the advantages of MRI over BLI for longitudinal monitoring of orthotopic GBM models. MRI imaging modality opens the possibility to use more clinically relevant patient derived xenograft (PDX) models of GBM in an orthotopic manner, improving the clinical transability to evaluate new GBM treatment modalities.

#4180 Evaluation of CD38 pharmacodynamics in multiple myeloma using PET with a Ga-68 labelled peptide.

A. Sharma, K. Gupta, A. Mishra, G. Lofland, I. Marsh, D. Kumar, G. Ghiaur, P. Imus, S. P. Rowe, R. F. Hobbs, C. B. Gocke, S. Nimmagadda;
Johns Hopkins University, Baltimore, MD

Introduction: Multiple myeloma (MM) is a disease of plasma cells that primarily arises in the bone marrow. CD38 is a receptor expressed uniformly and with high density in MM. Several CD38 targeted therapeutics are in clinic for MM. However, how those therapeutics engage or modulate CD38 is poorly understood particularly in lesions that cannot be assessed with routine blood testing. CD38 specific radiotracers for positron emission tomography (PET) could be helpful for detection of MM and for assessing therapy response early by measuring CD38 pharmacodynamics non-invasively. Here, we report the development of a first-in-class peptide-based PET radiotracer, [^{68}Ga]AJ206, evaluation of its pharmacokinetics (PK), specificity for non-invasive CD38 detection, and its potential to evaluate therapy induced CD38 pharmacodynamics in mouse models of MM.

Methods: A bicyclic peptide, AJ206, was synthesized and its binding affinity for CD38 was determined by surface plasmon resonance. AJ206 was labelled with Gallium-68 in high radiochemical yields and purity. In vitro uptake of [^{68}Ga]AJ206 was carried out in four MM cell lines with variable CD38 expression (MOLP8, MM1S, RPMI8226, and U266). PK and biodistribution of [^{68}Ga]AJ206 were evaluated by PET in cell line derived xenografts, in patient derived xenografts (PDXs) and in a disseminated disease model. PET data was corroborated by ex vivo biodistribution studies. [^{68}Ga]AJ206 in vivo specificity for CD38 was confirmed by co-injection of non-radioactive AJ206 (1 mg/kg) and cross-correlative immunohistochemistry (IHC) of matched xenografts. Furthermore, ability of [^{68}Ga]AJ206 to quantify CD38 pharmacodynamics was established by treating PDX models with all-trans retinoic acid (ATRA) and cross validating PET imaging observations with IHC.

Results: AJ206 exhibits high affinity (K_D,19 nM) for human CD38. In vitro binding assays showed variable [^{68}Ga]AJ206 uptake in MM cells that correlated with receptor density measured by flow cytometry. Dynamic PET-MR imaging revealed high and specific uptake of [^{68}Ga]AJ206 in MOLP8 tumor within 5 min that retained for at least 90 min. In contrast, [^{68}Ga]AJ206 exhibited rapid clearance from normal tissues providing high contrast images at 60 minutes and a high tumor-to-muscle ratio of 27.1±2.7. Tumor uptake was reduced by > 80 % in mice receiving blocking dose, confirming the specificity of the radiotracer. Also, [^{68}Ga]AJ206 could detect CD38 expression in different MM xenografts, PDXs and disseminated disease models which was corroborated by flow cytometry and IHC findings. Moreover, [^{68}Ga]AJ206 successfully quantified the increased CD38 expression in PDXs following ATRA treatment.

Conclusion: [^{68}Ga]AJ206 is a CD38 specific high affinity peptide-based PET imaging agent that can be used to non-invasively quantify CD38 pharmacodynamics in MM, with potential applications in other diseases with CD38 involvement.

#4181 AXL-specific single domain antibodies show diagnostic potential and anti-tumor activity in acute myeloid leukemia.

N. Vandewalle[1], H. Satilmis[1], E. M. Verheye[1], R. Fan[1], Y. Wang[1], T. W. M. De Groof[1], T. Kerre[2], N. De Beule[3], A. De Becker[3], E. De Bruyne[1], E. Menu[1], K. Vanderkerken[1], K. Breckpot[1], N. Devoogdt[1], K. De Veirman[1];

[1]Vrije Universiteit Brussel, Jette, Brussels, Belgium, [2]Ghent University Hospital, Ghent, Belgium, [3]Universitair Ziekenhuis Brussel, Jette, Brussels, Belgium

Rationale: AXL expression has been identified as a prognostic factor in acute myeloid leukemia (AML) and is detectable in approximately 50% of AML patients. In this study, we developed AXL-specific single domain antibodies (sdAbs), cross-reactive for both mouse and human AXL protein, to non-invasively image and treat AXL-expressing cancer cells.

Methods: AXL-specific sdAbs were induced by immunizing an alpaca with mouse and human AXL proteins. SdAbs were characterized using ELISA, flow cytometry, surface plasmon resonance and the AlphaFold prediction software. A lead compound was selected and labeled with ^{99m}Tc for evaluation as a diagnostic tool in mouse models of human (THP-1 cells) or mouse (C1498 cells) AML using SPECT/CT imaging. For therapeutic purposes, the lead compound was fused to a mouse IgG2a-Fc tail and *in vitro* functionality tests were performed including viability, apoptosis and proliferation assays in human AML cell lines and primary patient samples. Using these *in vitro* models, its anti-tumor effect was evaluated as a single agent, and in combination with standard of care agents venetoclax or cytarabine.

Results: Based on its cell binding potential, cross-reactivity, nanomolar affinity and GAS6/AXL blocking capacity, we selected sdAb20 for further evaluation. Using SPECT/CT imaging, we observed tumor uptake of ^{99m}Tc-sdAb20 in mice with AXL-positive THP-1 or C1498 tumors. In THP-1 xenografts, an optimized protocol using pre-injection of cold sdAb20-Fc was required to maximize the tumor-to-background signal. Besides its diagnostic value, we observed a significant reduction in tumor cell proliferation and viability using sdAb20-Fc *in vitro*. Moreover, combining sdAb20-Fc and cytarabine synergistically induced apoptosis in human AML cell lines, while these effects were less clear when combined with venetoclax.

Conclusions: Because of their diagnostic potential, sdAbs could be used to screen patients eligible for AXL-targeted therapy and to follow-up AXL expression during treatment and disease progression. When fused to an Fc-domain, sdAbs acquire additional therapeutic properties that can lead to a multidrug approach for the treatment of AXL-positive cancer patients.

#4182 Development and evaluation of orthotopically and subcutaneously implanted luciferase-labeled prostate cancer xenograft models for therapeutic assessment.

K. Draheim, E. Rainbolt, B. John, C. Clouse, A. Wong, B. Wolff, J. Avery, C. Hall, P. Fadden, **A. Avrutskaya**;
Charles River Laboratories, Inc., Wilmington, MA

Introduction: Prostate cancer is the most common male-specific cancer in many western countries including the US and the second most prevalent cause of cancer deaths in American males after lung cancer. The establishment of clinically relevant prostate cancer models is crucial for advancing our understanding of the disease and evaluating potential therapeutic interventions. In this *in vivo* project we characterize the tumor growth and response to therapy of two luciferase (luc) tagged human prostate cancer xenograft models of metastatic PC3M and non-metastatic DU145 cell lines. These models aim to replicate the variable clinical behavior of prostate cancer to provide valuable pre-clinical platforms to test existing and novel therapies. As a first step, these studies evaluate the effect of standard of care cytotoxic agents paclitaxel and carboplatin and the newer AXL kinase inhibitor bemcentinib alone and in combination on tumor growth kinetics and agent tolerability.
Methods: PC3M-luc and DU145-luc cells were implanted subcutaneously on right flank or orthotopically into the prostate of NCG triple immunodeficient mice (Charles River). Subcutaneous tumor progression and treatment responses were monitored using calipers and bioluminescent imaging (BLI), with the capacity to detect developing metastases prior to necropsy. Orthotopic implants were monitored exclusively using BLI.
Results: Orthotopic and subcutaneous implants of PC3M-luc demonstrated spontaneous metastasis to lungs and bones, replicating the established behavior of this cell line and effectively modeling metastases observed in prostate cancer patients. In contrast, orthotopic and subcutaneous implants of DU145-luc model did not metastasize. Both PC3M-luc and DU145-luc models independent of the tumor implant placement responded to paclitaxel treatment, with enhanced effects observed when combined with carboplatin. Notably, bemcentinib exhibited no activity as a single agent but showed promise when used in combination with cytotoxic agents.
Conclusion: The development of orthotopic and subcutaneous PC3M-luc and DU145-luc prostate cancer models provides a valuable platform for assessing the effectiveness of established and novel therapies. These models mimic various clinical presentations of prostate cancer and promise to offer insights into disease progression and therapeutic strategies. Future studies will focus on durable responses and the assessment of other combination therapies for improved treatment outcomes.

#4183 Utility of the highly immunodeficient SRG rat for combined drug efficacy, pharmacokinetics, and toxicology studies in tumor-bearing animals.

D. Begemann[1], C. Dunn[1], D. Robertson[1], L. Keach[1], E. Baldwin[1], R. Walton[1], A. Van Engelenburg[2], J. Durrant[2], L. Healy[2], K. Aw Yong[3], M. J. Schlosser[1], **F. K. Noto**[1];

[1]Hera BioLabs, Lexington, KY, [2]Dallas Tissue Research, Dallas, TX, [3]Charles River Laboratories, Wilmington, MA

Immunodeficient rodents are vital pre-clinical disease models. Historically, immunodeficient mice have been standard for hosting human cell and tissue xenografts, enabling cancer drug efficacy and tolerability testing. However, an immunodeficient rat that supports a variety of human cancer types provides a larger model for easier surgical manipulation and serial blood and tumor tissue sampling, allowing for efficacy, pharmacokinetics, and toxicology testing in the same animal. We created a Sprague Dawley *Rag2 -/-, Il2rg -/-* rat (*SRG Rat®; SRG)* that is highly supportive of human cell and tissue engraftment. The SRG rat lacks B, T, and NK cells and is more immunodeficient than the Nude rat.

Here we show comparative pathology between the SRG rat and its parental strain, the CRL Sprague Dawley (CD). We also present data from an efficacy study in tumor bearing SRG rats, demonstrating that serial blood draws and tumor biopsies can be performed in tumor bearing animals to assess drug pharmacokinetics and pharmacodynamics within a single study. First, we assessed 10 SRG (5/sex) and 10 CD (5/sex) at 8-10 weeks of age. Body weight, hematology, and clinical chemistry parameters were measured. Microscopic examinations were performed on routine H&E slide preparations.

Male and female SRG displayed lower mean body weight when compared to sex- and age-matched CD. Compared to CD, SRG had reduced lymphoid tissue and circulating monocytes, and highly reduced circulating lymphocytes, neutrophils, eosinophils, and basophils; expected phenotypes for this severely immunodeficient rat. Thymus was not present in SRG rats, spleens were grossly smaller, and bone marrow cellularity was decreased compared to CD. Microscopically, mandibular lymph nodes and lymphoid tissue in spleen, lung, and intestine were not observed in SRG rats, consistent with the 92% decrease in circulating lymphocytes.

To demonstrate the utility of the SRG for tumor inhibition, pharmacokinetics, and pharmacodynamics, we inoculated rats with human VCaP prostate cancer cell-derived tumors, then treated these animals and collected serial blood samples and tumor biopsies to assess tumor biomarkers. Treatment led to decreased PSA and AR, two key proteins expressed in prostate cancer, correlating to decreased tumor growth.

These data demonstrate that the SRG rat is suitable for toxicology studies and has comparable pathology to the CD rat, except for reduced lymphoid tissue and WBCs, which are expected phenotypes. In addition, the SRG rat supports the growth of human cancer tissue for treatment studies. The large size of the SRG rat and comparative pathology to the CD rat support its value as an immunodeficient model for assessing toxicity during efficacy testing for de-risking safety concerns in the presence of the human target tissue.

#4184 Change of oncological features on tumor and immune cells after anti-PD-1 antibody to pancreatic cancer orthotopic model in CD34+ HSC based humanized mice.

Sujin Park[1], Eun-young Koh[2], Inha Yoo[1], Ji Hye Jeong[2], Eunsung Jun[3]

[1]Department of Medical Science, AMIST, Asan Medical Center, University of Ulsan College of Medicine, Seoul, Korea, Republic of,[2]Department of Biochemistry and Molecular Biology, Asan Medical Center, University of Ulsan College of Medicine, Seoul, Korea, Republic of,[3]Division of Hepatobiliary and Pancreatic Surgery, Department of Surgery, Asan Medical Center, AMIST, University of Ulsan College of Medicine, Seoul, Korea, Republic of

(a) To investigate novel therapeutic agents in pancreatic cancer, animal models that recapitulate the features of the human immune system are necessary. We aim to analyze an orthotopic model in CD34+HSC-based humanized mice and to prove that is an indispensable model for immune-oncology therapy research.
(b) We established an orthotopic tumor model using luciferase-expressing BxPC3 cells in humanized NSG mice. After inoculation of tumor cells, anti-PD-1 Ab was administered to mice 5 times a week by I.P. injection. Tumor formation and progression were monitored using IVIS. To compare the subsets and immune-check point receptors of human immune cells in blood and tumor tissue, Flow cytometry and immunohistopathology were used. Additionally, we compared the distribution of various cells included in the tumor and the mRNA expression level of each cell through a single cell RNA sequence. We also establish primary cell lines and organoids with the humanized mouse tumor for further evaluation.
(c) After inoculation of BxPC3_Luc cell line into mice pancreas, we monitored tumor growth using a noninvasive imaging method of IVIS. When we compared the tumor growth between the anti-PD-1 treatment and control, there was no significant difference. Using FACS, we analyzed the various markers of human immune cells in mouse blood and tumor tissue. In blood, PD-1 expression of CD8+ T cells decreased, and Tim-3 expression increased in anti-PD-1 group. And, PD-1 expression of CD4+ T cells decreased in anti-PD-1 group. In tumor tissue, we also verified the decrease of PD-1 expression on tissue infiltrating CD8+ T cells and CD4+ T cells in the anti-PD-1 group. Especially in the more responsive mouse among anti-PD-1 group, activation markers in cytotoxic T cells (CD8+), helper T cells (CD4+), and regulatory T cells (CD4+FOXP3+CD25+) increased, and also, M1 macrophage (CD86+) expression was increased. Furthermore, we compared the mRNA expression levels of various cells in the tumor microenvironment according to anti-PD-1 Ab treatment through single cell RNA seq analysis. It was confirmed that the expression of genes related to proliferation and growing decreased, while the expression of genes related to apoptosis increased in cancer cells. Finally, we constructed primary cancer cells and organoids from tumor tissue and confirmed that the immune-oncological characters of these models are maintained after passaging.
(d) We successfully established a pancreatic orthotopic model in a humanized mouse and analyzed the changes in immune cells and tumor cells after anti-PD-1 treatment. In addition, by obtaining tumor tissue-based preclinical models, we laid the foundation for future immune-oncologic experiments. We hope that these attempts and results will help in the development and drug verification of new immunotherapy agents for refractory solid tumors such as pancreatic cancer.

#4185 Neutralizing human IFN-β combined with anti-human PD-L1 and anti-human CTLA-4 treatment increased control of endometrial tumor growth in a novel HLA-A matched BLT humanized mice.

Zhe Yuan[1], Guorui Zu[1], Xiao Sun[1], Emmanouil Papasavvas[1], Lily Lu[1], Joel Cassel[1], Peter L. Lutes[2], Mark Cadungog[2], Joseph Salvino[1], Luis J. Montaner[1]

[1]The Wistar Institute, Philadelphia, PA,[2]Christiana care, Newark, DE

High concentrations of type I interferon can induce growth arrest and apoptosis in cancer cells upon acute exposure, while low concentrations of the same can provide significant pro-survival benefits upon chronic exposure. In vitro data show the dependence of cancer cells on self-generated IFN-I leads to their demise if the IFN-β gene is disrupted, but they manage to persist when provided with IFN-β from an external source. Importantly, murine models show that inhibition of myeloid-associated INF-β can limit tumor growth. As blockage of type I interferon can also restore the CD8+ T cell function after chronic viral infection, we sought to determine the effects of neutralizing anti-human IFN-β antibody 7859 (N-anti-IFN-β) when added to T-cell directed immunotherapy in BLT humanized mice implanted with HLA-A matched human endometrial cancer PDX specimens. Specifically, we tested the combination of immunotherapy with N-anti-IFN-β combined with anti-human PD-L1 and anti-human CTLA-4. N-anti-IFN-β was first characterized for neutralizing activity to confirm specific neutralization of IFNβ and not human IFN-β. HLA-A matched genotyped CD34 stem cells and thymus (BLT humanized mice) and clinical endometrial tumors (PDX) were joined in BLT humanized mice before infusions with N-anti-IFN-β with or without anti-human PD-L1 and anti-human CTLA-4, anti-human PD-L1 and anti-human CTLA-4 alone, and IgG control antibodies intraperitoneally twice per week over three weeks. Tumor sizes were measured weekly and weighted at the end of the study. Human leukocytes infiltrating PDX were assessed by IHC and flow cytometry. Leukocyte subset activation, exhaustion, and tumor-specific T-cell function were measured. Anti-human PD-L1 and anti-human CTLA-4 reduced tumor growth by 82.9% ($p<0.0001$), but quickly increased the T cell exhaustion markers PD-1 and LAG3. The addition of N-anti-IFN-β to immunotherapy significantly decreased the tumor growth rate by 96.2% ($p<0.0001$) also significantly different from immunotherapy alone ($p=0.0009$) N-anti-IFN-β monotherapy reduced tumor growth rate by 42.4% ($p=0.0032$). While there was an increase in infiltrating CD4 and CD8 T-cells in combination therapy, reductions in expression of PD-1 and LAG3 were observed when compared to immunotherapy or N-IFN-β groups alone Analysis was done with Prism software. The use of a novel HLA-A matched BLT humanized mice with human tumor PDX model shows that neutralization of IFN-β can increase the T-cell anti-tumor activity and tumor repression of immunotherapy with anti-human PD-L1 and anti-human CTLA-4 treatment.

#4186 Development of an orthotopic A549 lung carcinoma model in CD34^{+} humanized NCG mice and response to treatment with paclitaxel and pembrolizumab.

A. Avrutskaya[1], E. Rainbolt[1], B. John[1], C. Clouse[1], M. Stackhouse[1], C. Currie[1], S. Scatigno[1], S. Bronson[2], J. Rowe[2], C. Hall[1], **D. P. Harris**[1];
[1]Charles River Laboratories, Inc., Durham, NC, [2]Charles River Laboratories, Inc., Wilmington, MA

Translational in vivo models are needed to expedite the discovery of new treatments for lung cancer. One such approach is the use of humanized mouse models that enable immunotherapies targeting human immune cells to be evaluated for efficacy and tolerability. We developed an orthotopic lung carcinoma model in humanized mice (HuCD34 NCG), utilizing serial bioluminescence imaging to evaluate the activity of paclitaxel and pembrolizumab as single and combination agents. Paclitaxel, which disrupts microtuble function, and pembrolizumab, a PD-1-targeting immunotherapy, are both approved for the treatment of certain types of lung cancer. Paclitaxel kills cancer cells directly, and may also promote anti-tumor responses through enhanced presentation of tumor antigens and activation of T cells. Immunodeficient NCG mice were humanized with cord blood-derived hCD34^{+} stem cells from 3 donors. High levels of human cell engraftment, with expected frequencies of hCD45^{+} cells and other immune subsets, was observed by 14 weeks post-injection. Luciferase expressing A549 cells were implanted orthotopically into the pulmonary space of the left lobe of the lung, and animals were subsequently flux sorted into treatment groups. Tumor burden, measured by luciferase expression, increased progressively in untreated animals, and moribundity was often associated with clinical indications of respiratory distress. Treatment with paclitaxel significantly decreased the tumor burden and extended survival. In contrast, pembrolizumab did not control tumor growth or extend survival. There was no synergistic effect with the combination therapy, in fact, the addition of pembrolizumab was associated with a modest increase in tumor burden and disease progression. Comparative analysis of immune cell composition, function and persistence in lung and other tissues provided insights into the distinct pharmacodynamic responses associated with the different treatment regimens. This model establishes a robust in vivo platform to identify novel therapies for the treatment of lung cancer.

#4187 Transcriptome profiling and characterization of peritoneal metastasis ovarian cancer xenografts in humanized mice.

Sung Wan Kang[1], Ji-young Lee[1], Ok-Ju Kang[1], Yong-Man Kim[1], Eun Kyung Choi[2], Shin-Wha Lee[1]

[1]Obstetrics and Gynecology, Asan Medical Center, University of Ulsan College of Medicine, Seoul, Korea, Republic of,[2]Radiation Oncology, Asan Medical Center, University of Ulsan College of Medicine, Seoul, Korea, Republic of

Background: Although immunotherapy has not yet been as successful in ovarian cancer (OC), it remains a potential therapeutic strategy. Preclinical models of OC are necessary to evaluate the efficacy of immuno-oncology (IO) drugs targeting human cancer and immune components but have been underutilized. Developing mouse models with a humanized (Hu) immune system can help understand the human immune response to IO drugs, including immune checkpoint inhibitors (ICIs), which have demonstrated limited effectiveness in OC patients.

Methods: We established OC xenograft Hu-mouse models by intraperitoneally injecting luciferase-expressing SKOV-3 Luc and OVCAR-3 Luc OC cells into $CD34^{\pm}$ Hu-mice. Tumor growth was monitored through bioluminescence imaging (BLI). We assessed the efficacy of PD-1 blockade with pembrolizumab in the SKOV-3 Luc Hu-mouse model. The immune profiles of the tumors were characterized using colorimetric immunostaining and flow cytometry. Additionally, we analyzed RNA-seq data to investigate the gene expression signature of pembrolizumab refractory tumors.

Results: We confirmed tumor development in both OC cell lines within $CD34^{\pm}$ Hu-mice. In these models, human lymphocyte and myeloid cell subsets were present in the tumors, draining lymph nodes, blood, and spleens. The SKOV-3 Luc tumor-bearing Hu-mice did not respond to pembrolizumab monotherapy. These tumors exhibited a high presence of tumor-infiltrating macrophages. Tumors in Hu-mice unresponsive to pembrolizumab showed a lower abundance of $CD8^{\pm}$ T-cells, memory B cells, plasma cells, and a higher proportion of naïve M0 macrophages and mast cells compared to the PBS control. Furthermore, we identified 43 significantly enriched gene sets in these tumors. The differentially expressed genes (DEGs) were predominantly enriched in HDAC class I, RB1, KLF1/3, TCF21, MYD88, SMARCE1 target genes, and genes associated with epithelial-mesenchymal transition (EMT) and fibroblasts.

Conclusion: Our xenograft Hu-mouse model of OC provides a valuable tool for investigating the efficacy of IO drugs. The insights gained from this model offer potential avenues to explore mechanisms of resistance to PD-1/PD-L1 blockade in OC.

#4188 Kyinno PBMC humanized mouse platform: Pioneering service in biomedical research.

T. Liu, G. Wu, F. He, L. Luo, Z. Guo, S. Li, J. Ning, **F. Hao**;
Kyinno Biotechnology Co., Ltd, Beijing, China

Tumor immunotherapy is the use of the human immune system to kill tumors. Compared with traditional chemotherapy and radiotherapy, immunotherapy has significant advantages such as significant efficacy, long-lasting effects, and low toxicity. Wild-type mice are widely used as preclinical models for immunotherapy due to their normal immune system, but they have many shortcomings, such as only being able to inoculate mouse tumor cells, differences between mouse and human immune systems, etc., which cannot accurately simulate the interaction between drugs and tumor cells in the human body. Humanized mouse models include PBMCs humanized mouse models, HSC humanized mouse models, and human embryonic bone, liver, and thymus tissue (BLT) transplantation models. Among them, the PBMCs humanized mouse model is widely used due to its simple preparation, short cycle, and high levels of hCD3+ T cells in the peripheral blood of mice. To assist in the development of immunotherapy, KYINNO has established a PBMC humanized mouse platform that can perform in vivo drug efficacy verification of various immunotherapeutic drugs such as CD3 bispecific antibodies or multi-specific antibodies, immune checkpoint inhibitors, etc. We screen many PBMC donors and select PBMC donors with light GvHD and good hCD3+ T cell reconstruction effects. The drug administration window of the PBMC humanized model has been extended to 6 weeks. Platform verification has been performed on subcutaneous and intravenous injection models of various tumors. Overall, we successfully established the PBMC humanized mouse platform, which is a powerful tool for immunotherapy.

#4189 BALB/c-hIL12RB1/hIL12RB2: A robust model for preclinical research in human IL-12 therapy.

Y. Fang, H. Wang, J. Xing, L. Yang, J. Zhao, X. Gao, C. Ju;
Gempharmatech Co., Ltd., Nanjing, China

Interleukin-12 (IL-12) is a multifaceted cytokine primarily produced by antigen-activated dendritic cells, macrophages, and neutrophils. Its receptor is a composite of IL12RB1 and IL12RB2, and the union of these two subunits forms a high-affinity receptor complex proficient in mediating IL-12 signaling. As a pivotal regulator of innate and adaptive immunity, IL-12 plays a crucial role in steering the differentiation of naïve T cells into Th1 cells. It is renowned as a T cell stimulatory factor, fostering T cell proliferation. Furthermore, IL-12 has the capacity to augment the activation of cytotoxic lymphocytes and natural killer cells (NK), thereby enhancing interferon (IFN-γ) production. Empirical evidence consistently demonstrates that IL-12 synergistically exerts anti-tumor effects in conjunction with various immune cells, such as T cells and NK cells. Its effectiveness in preclinical studies has solidified IL-12 as an appealing drug target, leading to the development of activating antibodies, therapeutic IL-12 proteins, and tumor vaccines as potential treatments.

To delve deeper into the functionality and therapeutic potential of IL-12, we have engineered a humanized mouse model, known as BALB/c-hIL12RB1/hIL12RB2. Notably, this model fully preserves the intracellular domains of mouse IL12RB1 and IL12RB2 proteins, ensuring the normal propagation of intracellular signaling. It also effectively expresses human IL12RB1 and IL12RB2. In vitro functional validation experiments have verified that BALB/c-hIL12RB1/hIL12RB2 mice can proficiently generate IFN-γ when induced by human IL-12.

Furthermore, in vivo efficacy experiments have yielded compelling results. Intratumoral administration of human IL-12 mRNA in BALB/c-hIL12RB1/hIL12RB2 mice led to a significant suppression in the growth of CT26 tumors, culminating in complete tumor regression. Subsequent rechallenge experiments conducted after the discontinuation of treatment revealed no tumor recurrence, signifying the enduring inhibitory effect of hIL12 mRNA on mouse tumors.

In conclusion, the development of BALB/c-hIL12RB1/hIL12RB2 mice stands as a robust model for advancing preclinical research in the realm of human IL-12 therapy.

#4190 Patient-derived xenograft (PDX) models with differential HER2 expression for preclinical evaluation of HER2-targeted therapies.

X. Yang, S. Guo, H. Wang, X. Su, J. Zhao, X. Gao, C. Ju;
Gempharmatech Co., Ltd., Nanjing, China

Human epidermal growth factor receptor 2 (HER2) is a critical therapeutic target in gastric cancer. However, the varying expression levels of HER2 in patients present a significant challenge in selecting the appropriate HER2-targeted therapies. Patient-derived xenograft (PDX) models offer a valuable tool to address this clinical concern.

We established a panel of PDX models derived from gastric cancer patients, each representing a distinct range of HER2 expression levels. These models were subsequently treated with HER2-targeted drugs, including Trastuzumab (Herceptin), Margetuximab, and Enhertu.

Our results demonstrated differential drug responses corresponding to the varying HER2 expression levels in the PDX samples. Trastuzumab, Margetuximab, and Enhertu exhibited distinct efficacies across the HER2 expression spectrum. This underscores the significance of selecting the right therapeutic approach based on the HER2 status of individual patient.

Our collection of PDX models with differential HER2 expression levels provides a robust platform for preclinical evaluation of HER2-targeted therapies. This approach not only addresses the clinical challenge of HER2 heterogeneity but also facilitates a more personalized and effective treatment strategy for gastric cancer patients.

#4191 Delayed onset of GvHD in PBMC humanized NCG-B2m KO mice provides an enhanced model for oncology studies.

S. Bronson, D. Harris, A. Avrutskaya, C. Eberle, J. Rowe;
Charles River Laboratories, Inc., Wilmington, MA

Humanized mice are specialized animal models incorporating components of the human immune system. These models are valuable tools for assessing the efficacy of human immunotherapies on tumors. Humanized mice are created by injecting human $CD34^{+}$ hematopoietic stem cells (HSCs) or human peripheral blood mononuclear cells (PBMCs) into an immunodeficient mouse. PBMC humanized (HuPBMC) mice engraft within a few weeks and can recapitulate a robust human T cell population. One challenge when using HuPBMC mice is the onset of graft versus host disease (GvHD), limiting their lifespan compared to $hCD34^{+}$ HSC humanized mice. The onset of GvHD varies in the HuPBMC model depending on the donor cells. The development of xenogeneic GvHD is dependent on the expression of major histocompatibility complex (MHC) on host cells and lowering MHC expression can delay the onset of GvHD.NCG-B2m KO mice lack beta-2 microglobulin, a component of MHC I, and have lower cell surface expression of MHC I molecules. This leads to a decrease in recognition of host cells by human immune cells. Here we compared the onset of GvHD between HuPBMC NCG-B2m KO mice and HuPBMC NCG mice. PBMC donor variability was also compared between the two PBMC humanized models by evaluating multiple donors and assessing additional collections from the same donor. After the PBMC engraftment was characterized, HuPBMC NCG mice and HuPBMC NCG-B2m KO mice were enrolled in tumor studies comparing outcomes and tumor growth kinetics in mice treated with human immune checkpoint blockade therapy.NCG and NCG-B2m KO mice were injected with $1x10^{7}$ PBMCs from individual donors. Animals were weighed three times a week to monitor for changes in body weight and general health status. Peripheral blood was collected at day 10, 20, 30, 40, 60 and 90 post injection for flow cytometry screening of human immune cell engraftment ($hCD45^{+}$, $hCD3^{+}$, $hCD4^{+}$ and $hCD8^{+}$). Human PBMCs isolated from additional collections from the same donors were also injected into both NCG-B2m KO mice and NCG mice and flow cytometry was performed. HuPBMC NCG-B2m KO mice survived longer than HuPBMC NCG mice allowing for the potential use in longer term tumor studies before the results are confounded by GvHD. PBMC humanized mice are an important model for translational research using immunotherapies and the PBMC humanized NCG-B2m KO model provides an expanded study window ideal for oncology studies.

#4192 In-depth evaluation of chemotherapy-induced mucositis in intestinal organoids using holotomography.

Mahn Jae Lee[1], Jaehyeok Lee[2], Weisun Park[3], Geon Kim[3], Hye-Jin Kim[2], YongKeun Park[3]

[1]Graduate School of Medical Science and Engineering, Korea Advanced Institute of Science and Technology, Daejeon, Korea, Republic of,[2]Bioscience, Tomocube Inc., Daejeon, Korea, Republic of,[3]Physics, Korea Advanced Institute of Science and Technology, Daejeon, Korea, Republic of

Intestinal mucositis is a prevalent adverse event associated with antineoplastic therapies, such as chemotherapy, which still lacks a targeted and effective treatment regimen. The difficulty in preclinical prediction and prevention of drug-induced intestinal mucositis is attributed to the intricate underlying mechanisms of its onset and the broad spectrum of patient-specific responses to chemotherapeutic agents. Advancements in regenerative medicine have enabled the generation of intestinal organoids from adult stem cells, serving as a personalized model to emulate disease pathology and simulate individual drug responses. Various imaging techniques are employed to evaluate the responses of the organoids to pharmacological agents, but the inherent complexity of their three-dimensional (3D) architecture poses significant challenges in organoid imaging. These challenges are exacerbated by the standard preparation processes for imaging, including fixation and staining, which do not allow for the observation of dynamic, real-time effects of drugs on living organoids. In this study, we focused on meticulously examining the histopathological alterations in small intestinal organoids subjected to chemotherapeutic agents that induce mucositis, specifically 5-fluorouracil and irinotecan. Employing holotomography, a label-free real-time 3D imaging technology, we were able to visualize the destructive processes affecting the intestinal organoids, including the breakdown of the epithelial lining, the exfoliation of dead cells, and the alteration of the villus/crypt structure. Furthermore, we propose a novel methodology for quantifying the viability of intestinal organoids. This quantification is essential for assessing the extent of damage caused by the chemotherapeutic agents and for determining the maximum drug concentrations that can be deemed safe for use, thereby minimizing the risk of inducing mucositis while maintaining therapeutic efficacy. These results provide new insights into the toxic mechanisms of chemotherapeutic drugs and highlight the importance of using organoid models in drug safety evaluation throughout the development phase.

#4193 Digital PCR as a novel way to assess chimerism of humanized immune system mice.

N. Smith[1], S. Hansen[2], R. S. Livingston[2], S. Smith[2], P. Roesch[1], M. M. MacBride[1];
[1]Taconic Biosciences, Inc., Rensselaer, NY, [2]IDEXX BioAnalytics, Columbia, MO

Humanized immune system (HIS) mice contain human and murine immune cells. Analysis of chimerism in HIS mice is typically accomplished via flow cytometry, but this requires collecting a 75 µl blood sample and access to a flow cytometer. Repeated bleeding can negatively affect the health of HIS mice, limiting serial analysis. Digital PCR offers a novel method for chimerism analysis, which uses much smaller blood volumes and can be performed on clotted or frozen samples, sample types unsuitable for flow cytometry. A digital PCR assay directly comparing the presence of three human genes and one murine gene was developed. This assay was validated in the huNOG-EXL HIS mouse engrafted with CD34+ hematopoetic stem cells from 3 unique donors via blind comparison with chimerism data from flow cytometry. At 10 weeks post engraftment, the digital PCR assay showed excellent correlation for all three human genes against chimerism as measured by flow cytometry of the peripheral blood. This assay represents a new, user-friendly, rapid tool for the analysis of HIS mice and may permit serial chimerism measurement using 10 µL whole blood. This assay may be useful to investigate other mouse-human chimera models, including mice harboring functional human hepatocytes, tumors, and other cells.

#4194 An in-silico approach to identify genes required for polyamine transport.

V. Millington, L. von Kalm;
University of Central Florida, Orlando, FL

The purpose of this study was to use an in-silico approach to identify genes required for polyamine transport. Polyamines are small positively charged molecules that control vital cellular processes including cell proliferation and growth. Cells obtain polyamines by biosynthesis or transport from the extracellular environment. Cancer cells require high levels of polyamines to sustain rapid growth, and therapies aimed at polyamine depletion are considered promising. The FDA approved drug difluoromethylorthinine (DFMO) blocks polyamine biosynthesis, however, in most cases malignant cells evade the biosynthetic block by increasing transport. Thus, a dual therapy that simultaneously targets polyamine biosynthesis and transport is needed. The mechanism of polyamine transport is poorly understood in multicellular eukaryotes and identification of genes involved in polyamine transport has largely relied on an inefficient hit-or-miss 'educated guess' approach. To increase the probability of identifying genes involved in polyamine transport, we adopted an in-silico approach comparing protein-protein interactions with the protein product of the human ATP13A3 gene across multiple databases. We used ATP13A3 because our work, and the work of others, has shown that ATP13A3 and its Drosophila ortholog 'anne' are required for polyamine transport. We searched for high confidence protein interactors with ATP13A3 in four databases, BioGRID, STRING, NextProt, and GPS-Prot, prioritizing hits that occurred in more than one database. We next asked if any of the high priority hits had orthologs in Drosophila. We chose to study the candidate genes in Drosophila because we have utilized the sophisticated genetic resources available in this organism to develop novel assays to identify positive and negative regulators of polyamine transport. Using the criteria described, we identified four candidates that occurred in three databases, and one that occurred in two databases. In addition, a very high confidence match to the human gene SLC15A was observed in one database and included in the group of candidate genes. To determine the validity of our candidate gene enrichment approach we are currently testing each gene for roles in polyamine transport.

#4195 Activity of IMM-1-104 alone or in combination with chemotherapy in RAS-altered pancreatic cancer models.

P. King[1], J. Funt[1], S. Kolitz[2], P. Nair[1], J. d. Jong[1], A. Yamamura[1], M. Johnson[1], J. Zhang[3], K. Fowler[1], A. Travesa[1], A. Axel[1], C. Walker[1], B. J. Zeskind[3], B. M. Hall[1];

[1]Immuneering Corporation, San Diego, CA, [2]Immuneering Corporation, Cambridge, MA, [3]Immuneering Corporation, New York, NY

Introduction: Addiction to the MAPK pathway drives a large proportion of cancers, and pancreatic tumors almost universally display RAS mutations. IMM-1-104, a once-daily oral treatment being evaluated in a Phase 1/2a trial for RAS-mutant solid tumors [NCT05585320], offers a novel deep cyclic inhibition (DCI) approach in targeting the MAPK pathway at MEK. Traditionally, MAPK-targeted drugs inhibit the pathway chronically causing serious class-effect toxicities and limited durability due to resistance. In contrast, IMM-1-104's unique pharmacokinetic (PK) profile was designed to drive pulsatile MEK inhibition, with the goal of improving tolerability and providing more durable activity across a broad range of MAPK-driven tumors. Phase 1 dose escalation of IMM-1-104 revealed no dose-limiting toxicities, high oral bioavailability, plasma half-life of approximately 2-hours, and pharmacodynamic (PD) data supporting DCI of the MAPK pathway.

Experimental Procedures: IMM-1-104 responses in humanized 3D tumor growth assays (3D-TGA) were combined with NGS data using machine learning (ML) to refine a pharmacogenomic response model. Evaluation of databases such as AACR Project GENIE enabled prediction of patient alignment of preclinical models based on genomic profile, identification of patient populations displaying MAPK pathway addiction and projected sensitivity to IMM-1-104 mono- or combination therapy. To test combinations with approved chemotherapy agents, IMM-1-104, gemcitabine (GEM) and nab-paclitaxel (PAC) and 5-fluorouracil (5FU) were evaluated in tumor xenograft models with drugs alone or across multiple combinations.

Summary of New Data: IMM-1-104 showed promising combination effects when treated with GEM or PAC in 3D-TGA pancreatic cancer models. In a MIA PaCa-2 tumor xenograft model, IMM-1-104 alone showed greater tumor growth inhibition (TGI) than any single or combination chemotherapy tested. Further, combinations of IMM-1-104 plus chemotherapy resulted in near complete responses in a majority of animals. At day 39, antitumor activity (TGI%) was 103% for IMM-1-104 at 125 mg/kg BID PO, 25.2% for GEM at 60 mg/kg IP Q4D, 62.2% for PAC at 10 mg/kg IV Q4D and 36.6% for 5FU at 50 mg/kg IP Q4D. Based on these results and additional 3D-TGA pharmacogenomics data, ML modeling was advanced to query the GENIE database and identify biomarkers of response and resistance with the goal of further informing mono and combination treatment options with IMM-1-104 in pancreatic cancer.

Conclusions: The Phase 2a portion of the ongoing IMM-1-104 clinical study includes five arms, three of which focus on patients with pancreatic cancer, where IMM-1-104 will be evaluated as both monotherapy and in select combinations with approved chemotherapeutic agents. The new *in vitro*, *in vivo* and ML modeling data presented here further support an advancing translational roadmap for IMM-1-104 in pancreatic cancer.

TUMOR BIOLOGY: Models to Study Immune Cells in the Tumor Microenvironment
Poster Session

#4199 Comprehensive 3D liver cancer model to study the tumor microenvironment for therapy development.
F. Bonanini, R. Dinkelberg, V. van Duinen, J. Heijmans, D. Gouber, T. Hagens, N. Kortekaas, M. Caro Torregrosa, D. Kurek, P. Vulto, **K. Bircsak**; MIMETAS, Oegstgeest, Netherlands

Liver cancer, or hepatocellular carcinoma (HCC), is a formidable malignancy characterized by the uncontrolled growth of cells within the liver tissue. It represents a global health concern, with risk factors including chronic viral infections (such as hepatitis B and C), excessive alcohol consumption, fatty liver disease, and certain genetic conditions. The silent progression of HCC complicates early detection, emphasizing the need for a deeper understanding of the liver tumor microenvironment, which plays a crucial role in disease development. The liver model presented here incorporates a wide array of relevant liver cell types, including hepatocytes, endothelial cells, stellate cells, and resident immune cells. This is complemented by a complete vascularization system, allowing for fluid flow across a micro vascular network that faithfully models the dimensions of liver sinusoids. All these elements are seamlessly integrated into an automated and high throughput platform known as the OrganoPlate®. To model the liver tumor microenvironment, hepatocellular carcinoma cells were integrated into healthy liver tissue model. The resulting model allowed for the observation of integrated cancer colonies, providing a more realistic platform for therapy development compared to monocultures. Simultaneously, the liver's particle clearance mechanisms were investigated using fluorescent imaging. Endothelial cell phagocytosis of E. coli particles and resident macrophages' internalization of dextran molecules were studied to explore hepatic delivery of macromolecules and nanoparticles via the systemic circulation. The integration of hepatocellular carcinoma cells within healthy liver tissue revealed the formation of integrated cancer colonies, offering insights into the complex interactions within the liver tumor microenvironment. Fluorescent imaging showcased endothelial cell phagocytosis of E. coli particles and resident macrophages' internalization of fluorescent molecules. These findings elucidate the liver's particle clearance mechanisms, providing a foundation for understanding immunological processes and designing efficient drug delivery systems. Understanding the liver tumor microenvironment is critical for developing effective therapies for HCC. The integration of hepatocellular carcinoma cells within healthy liver tissue offers a more realistic platform for therapy development compared to traditional monocultures. We believe this system holds the potential for a groundbreaking progress in liver modelling which, besides including functional hepatic cells, also reflects the cellular organization and interactions found within the liver lobule. In conjunction with its high throughput capability, this has the potential to revolutionize drug discovery and develop therapies for complex liver diseases.

#4200 A novel 3D culture platform, *E-slice*, retains intact tumor microenvironment and tumor infiltrating immune cells.

Viridiana Leyva-Aranda[1], Thomas Gallup[1], Jose Maldonado[2], Corina Margain[1], Sang Yun[1], David Gallup[1], Min Kim[3], Kyuson Yun[2]

[1]EMPIRI, Inc., Houston, TX,[2]Department of Neurology, Houston Methodist Research Institute/Weill-Cornell Medical College, Houston, TX,[3]Department of Surgery, Houston Methodist Research Institute/Weill-Cornell Medical College, Houston, TX

Human cancer tissue is a complex ecosystem with heterogeneous cell types that communicate with each other dynamically to promote tumor progression and immune evasion. Hence, experimental systems that destroy or select for cancer cells in culture have often failed to accurately predict clinical responses of new drugs. Therefore, a technology that can retain the intact tumor microenvironment (TME) and accurately predict cancer patient's response to anti-cancer treatments, including immunotherapies, will greatly benefit patients and dramatically reduce the cost of new drug development.

E-slice is a proprietary 3D human tumor culture platform that maintains individual patient tumor's unique ecosystem and the TME *ex vivo* for up to 30 days. It is generated by making thin sections of intact, fresh tumor tissues and culturing them in serum-free, defined media. As such, immune components and the TME in *E-slices* faithfully recapitulate human tumors *ex vivo*. We demonstrate that *E-slices* can be used to: 1) measure viability changes upon anti-cancer agent treatment longitudinally; 2) retain the native TME and tissue architecture since *E-slices* are never dissociated or artificially reconstituted; 3) culture any solid tumor types from patient needle biopsy cores or surgical samples, PDX, or mouse models; 4) perform high content drug screening on human tissues; 5) discover secreted biomarkers and to 6) discover or validate molecular mechanisms of action or therapy resistance; and 7) measure immunotherapy responses *ex vivo* from human tissues.

Importantly, it has been shown to accurately predict individual patient treatment responses to chemotherapies and targeted therapies in 4-8 days, paving the way for evidence-based personalized treatment selections in a clinically actionable time frame. Furthermore, single cell RNA-sequencing analysis demonstrates that *E-slices* can retain the viability and molecular phenotypes of tumor infiltrating immune cells for up to 8 days *ex vivo*, providing a unique platform to study human tumor-immune interactions and evaluate efficacy of immune modulators on human tumor tissues *ex vivo*.

#4202 A novel 3D model investigating the pathophysiology of prostate cancer bone marrow metastasis.

Jianhui Yang[1], Hani Awad[2], Hiroshi Miyamoto[3], Omar Aljitawi[4], Peter Van Veldhuizen[5]

[1]Department of Medicine, University of Rochester Wilmot Cancer Institute, Rochester, NY,[2]Center for Musculoskeletal Research, University of Rochester, Rochester, NY,[3]Department of Pathology & Laboratory Medicine, University of Rochester Medical Center, Rochester, NY,[4]Hematology/Oncology Division, University of Rochester Medical Center, Rochester, NY,[5]Department of Internal Medicine, University of Rochester Medical Center, Rochester, NY

Our study is aimed to apply a 3-dimensional (3-D) *in vitro* model emulating the extracellular matrix (ECM) of the bone marrow microenvironment (BMM) to explore the interaction of disseminated Prostate Cancer (PC) cells and ECM. Wharton's Jelly (WJ), which histologically and biochemically resembles the ECM part of the hematopoietic stem cell (HSC) niche, was decellularized as a novel 3-D culture platform, named as decellularized WJ matrix (DWJM). CD133, a critical marker of PC stem cells (PCSC), was chosen to initially evaluate the PCSC phenotype of DU-145 cells cultured using DWJM by flow cytometry and Image-Stream. DWJM was used to culture PC Cell line DU-145 cells. Enriched CD133(+) cells by Fluorescence-Activated Cell Sorting (FACS) were further analyzed for functional phenotypes of PCSC, and the mechanism of reactivated expression of CD133 was also investigated. A small percentage (about 2-5%) of CD133(+) DU-145 cells were detected after DU-145 cell culturing using DWJM for 3-7 days. Sorted CD133+ cells formed more colonies *in vitro* and manifested some characteristics of Epithelial-to-Mesenchymal Transition (EMT), including increased nuclear to cytoplasmic ratio and spindle-cell morphology. The undetectable expression of CD133 mRNA and protein in parental DU-145 cells was at least partly caused by promotor methylation, while culturing using DWJM reactivated the expression of CD133 by demethylating the CD133 DNA promotor. Taken together, our *in vitro* findings provide preliminary findings to support the possible conversion of disseminated PC cells to PCSC by epigenetic modulation in the BMM, and these early findings warrant further validation using an *in vivo* mouse model.

#4204 Subcutaneous vs. orthotopic tumor models: A comparative assessment.

K.-A. Bright, S. Barnes, D. Germain, L. Kucharczyk;
Laboratory Corporation of America, Ann Arbor, MI

The failure of murine tumor models to adequately simulate the native biological milieu and tissue architecture of human malignancies, has fomented much discourse surrounding the discord that exists between experimental outcomes and clinical settings. Orthotopic (OT) models, which are generated by the engraftment of tumor cells or fragments into recipient organs of the same histotype from which they were derived, has the advantage of recapitulating the appropriate vasculature, as well as cellular and stromal components as the site of origin. In the context of immunotherapy, there is increasing evidence that subcutaneous (SC) tumors bear a vastly different immunological profile compared to OT implants, a phenomenon dictated by tissue-specific recruitment of various immune subsets, and subsequently, impacts overall response. Therefore, establishing cancer models that better represent the natural tumor environment is imperative for addressing some of the foibles inherent to preclinical mouse models. To demonstrate the significance of the anatomical site of the tumor, we present a comparative assessment of the MC38 murine colon carcinoma model, in the context of SC and OT settings. In the SC model of MC38, administration of either 5mg/kg anti-mPD1, anti-mPDL1, or anti-mCTLA-4, failed to elicit any notable anti-tumor activity, as evidenced by 0% incidences of complete regressions (CR) and tumor free survivors (TFS) for all three therapeutic agents, and incidences of 11%, 5% and -22% increase in time to progression (ITP), respectively. However, mice bearing OT tumors, exhibited meaningful response to 5mg/kg anti-mPD1 and anti-mPDL1, both evoking incidences of 25% CR, 25% TFS and 108% ITP. Though the anti-mCTLA-4 treated cohort did not produce any CRs or TFS, there was, nonetheless, a 50% incidence of ITP. Taken together, the data clearly illustrates the distinct disparities in response between SC and OT tumors, with respect to immunomodulatory agents. Characterization of immune phenotype within both settings, and interrogation of additional mouse models are ongoing. The exigencies and profound limitations associated with bench to bedside translation have long encumbered the drug development process. Despite staggering financial investment in oncology research, effective treatments for a myriad of cancers remain elusive, and only 3.4% of cancer drug candidates are conferred with clinical approval. Employing modalities that adequately reproduce the molecular and structural frameworks of human tumors, is crucial to better elucidating the natural trajectory of cancer progression, thus facilitating more accurate evaluation of drug activity and therapeutic response in preclinical settings. OT models therefore represent a more disease-relevant preclinical approach compared to their subcutaneous counterparts, as they more reliably preserve the intrinsic infrastructure and complexities of patient tumors *in situ*.

#4205 Investigating micro-environmental changes in a syngeneic radio-recurrent prostate cancer model.

S. D. White[1], X. Huang[2], I. Mills[3], S. K. Liu[4];
[1]University of Toronto, Toronto, ON, Canada, [2]Sunnybrook Research Institute, Toronto, ON, Canada, [3]University of Oxford, Oxford, United Kingdom, [4]Sunnybrook Health Sciences Centre, Toronto, ON, Canada

Approximately 1 in 8 men in Canada will be diagnosed with prostate cancer (PCa) in their lifetime, with ~20% presenting with high-risk disease. A standard treatment is radiotherapy (RT) and while many patients respond well to RT, up to 40% of men with high-risk disease can recur, often within the prostate. It can be challenging to salvage prostate relapses due to the morbidity of re-irradiation and the high rate of subsequent progression. The tumor micro-environment (TME) is altered after radiotherapy with increased immune-suppressor and immune-stimulatory effects occurring concurrently. Therapies capitalizing on these changes in the TME might provide an advantage to tackling radiation-recurrent cancer. Identifying TME changes in radio-recurrent PCa is the first step; however, existing PCa animal models do not accurately model the TME. Our collaborator's lab has created the DVL3 mouse model with a clinically relevant TME. It forms tumors with distinct glandular morphology and displays micro-environmental responses to RT like what is seen in high-risk PCa patients, making this model an innovative tool for investigating radio-recurrence. The objective of this study is to create a radio-recurrent DVL3 PCa cell line to explore changes in the TME both *in vitro* and *in vivo* via orthotopic injection. To generate the radio-recurrent model, the DVL3 Parental cells (DVL3-Par) underwent a conventionally fractionated RT schedule (78Gy/39fx), herein referred to as DVL3-CF cells. The first part of the project involves *in vitro* characterization. Radiation resistance was evaluated via clonogenic assay which demonstrated a significant increase in clonogenic survival in the DVL3-CF cells relative to DVL3-Par. Characterization of DVL3-CF cells demonstrates that they are more proliferative at baseline, they recover quicker following G2/M blocks, they have decreased senescence following high dose radiation, and they are more invasive *in vitro*. The second part of the project evaluates the radio-recurrent model *in vivo* using an orthotopic mouse model as this best emulates the TME and clinical tumor progression. Parental and CF cells will be injected orthotopically into the prostate of C57/BL-6 mice and monitored for growth by MRI which will provide information on tumor volume as well as vasculature. At the time of sacrifice, the prostate and draining lymph nodes will be cryo-preserved and formalin fixed for downstream histological analysis. Transcriptional analyses, MRI data, and histological analysis of the tumors and draining lymph nodes will be compared across the radio-recurrent model and its parental cell line to evaluate environmental changes and potentially implicated mechanisms. This study will elucidate some of the complex interactions that are occurring within the TME of radio-recurrent PCa, increasing our understanding of mechanisms of radio-recurrence.

#4206 Regional transcriptomic profiling of the head and neck squamous cell carcinoma tumor microenvironment paired with murine models identify extracellular matrix components that mediate tumor progression and immune suppression.

John D. Aleman[1], Khoa A. Nguyen[1], Erica Wong[1], Yao Ke[2], Hanne T. Lind[2], Clifford G. Tepper[3], Andrew C. Birkeland[4], Christian D. Young[1], Sana D. Karam[5], Xiao-Jing Wang[2]

[1]Pathology, University of Colorado Anschutz Medical Campus, Aurora, CO,[2]Department of Pathology & Laboratory Medicine, University of California Davis, Sacramento, CA,[3]Department of Biochemistry and Molecular Medicine, University of California Davis, Sacramento, CA,[4]Department of Otolaryngology-Head and Neck Surgery, University of California Davis, Sacramento, CA,[5]Department of Radiation Oncology, University of Colorado Anschutz Medical Campus, Aurora, CO

Purpose: A substantial contribution to the poor prognosis for head and neck squamous cell carcinoma (HNSCC) patients is the progression to distant metastasis. This occurs in 30% of patients over the course of their disease, and radically reduces the 5-year survival rate to under 50%. Investigations in recent years have begun to unveil the intricate interplay of the extracellular matrix (ECM) in both tumor-intrinsic signaling and immunoregulation. However, studies conducted in the context of metastatic have been limited. Here, we employ spatial transcriptomics on HNSCC patient biopsies to identify ECM components that may contribute to cancer progression and immune suppression.
Experimental design: Comprehensive transcriptome profiling of HNSCC patient biopsies was conducted using the GeoMx Digital Spatial Profiler (DSP). This approach allowed us to characterize regions of the tumor microenvironment (TME) by immunofluorescent staining for subsequent bioinformatic analysis. To investigate the biological consequences of associations observed in our dataset, we performed *in vivo* murine studies. We have produced a series of SCC C57BL/6 murine cell lines derived from $Smad4^{-/-}Kras^{G12D}$ Keratin15+ stem cells, which faithfully mimic the clinical progression of HNSCC tumors, including metastasis. Using these murine models, we applied relevant pharmacologic inhibitors and genetic knockdown of targets identified with our GeoMx DSP analysis. *In vitro* immune-based and functional assays were conducted to elucidate the underlying mechanisms contributing to SCC progression.
Results: GeoMx DSP analysis revealed that laminins were enriched in stage IV HNSCC patient stroma, relative to lower stage patients. This coincided with TGFβ enrichment and inversely associated with signatures of anti-tumor immune infiltration. Analysis of The Cancer Genome Atlas data revealed similar inverse correlations in SCCs, distinct from breast cancer and lung adenocarcinoma. Our metastatic SCC murine lines likewise exhibited elevated levels of these laminin proteins, accompanied by high levels of laminin-binding integrins and TGFβ-Smad signaling. Independent of impacting cell proliferation, shRNA knockdown of laminin decreased tumor volume in an immune-competent setting. Targeting laminin-integrin signaling with the small molecule inhibitors Galunisertnib and Buparlisib also reduced the metastatic capacity of these cells in C57BL/6 mice.
Conclusions: Spatial transcriptomic profiling of the HNSCC TME uncovers intricate associations and promising targets not readily discernible in bulk RNAseq analyses. Validation through genetic and pharmacological approaches in immune-competent models underscores their potential as strategies to reduce HNSCC burden.

#4207 Zoledronic acid reduces quiescent bone-disseminated human ER+ breast cancer tumor cell burden and estrogen-responsiveness in a pre-clinical model.

J. N. Cheng, J. B. Frye, S. A. Whitman, **J. L. Funk**;
University of Arizona, Tucson, AZ

Unique to early-stage ER+ breast cancer, ER+ tumor cells already bone disseminated at time of diagnosis can remain dormant at this site until an initiating event (e.g., activating ESR1 mutation acquisition) allows for osteolytic bone metastases (BMET) progression even decades later. Adjuvant use of anti-resorptive bisphosphonates, but not denosumab, reduces BMET risk in post-menopausal women with early stage breast cancer, suggesting protective effects may be unrelated to changes in bone turnover. Pre-clinical modeling of dormant, bone-disseminated ER+ breast cancer cells may enhance our understanding and thus our ability to better target these inherently treatment-resistant cells. In studies reported here, a model of bone-disseminated ER+ dormancy was characterized and used to query effects of zoledronic acid (ZA) on dormant cells. When female nude mice were inoculated (intracardiac) with human ER+ MCF-7 cells labelled with DiD, a membrane dye that dissipates with each cell division, DiD-positive tumor cell number in harvested tibial bone marrow remained unchanged from 24 hours to 28 days post-tumor cell inoculation. When 17ß-estradiol (E2) treatment (0.72 mg 60-day pellets) was initiated on D28 following tumor cell inoculation, detectable DiD+ tumor cell number in harvested tibial bone marrow increased 1.8-fold within one week (D35 vs. D28, $p < 0.0001$), consistent with initiation of E_2-stimulated proliferation, and osteolytic, histology-confirmed BMET appeared subsequently with 60% incidence by 6-weeks post-start of E2 treatment. When mice were instead zoledronic acid-treated during the 28d dormancy period (70 ug/kg subcutaneously on D7 and on D21 post-inoculation), DiD-positive cell number in marrow harvested on D28 was reduced by more than half vs. vehicle-treated controls ($p< 0.05$). Moreover, DiD-positive cell numbers on D35, one week after start of E2-treatment, remained unchanged in tibial marrow of ZA-treated mice and were thus substantially (3.8-fold) lower than controls ($p< 0.001$). When followed for 6-weeks after initiation of E2 treatment, no osteolytic BMET were detected in ZA-treated mice. In toto, these results recapitulate clinical findings, thus validating the methodologic approach, and suggest that in addition to reducing dormant ER+ tumor cell burden in bone, bisphosphonates may also alter their estrogen responsiveness. Acknowledgements: Special thanks to undergraduates Alyssa Magee and Geethika Ameneni for assistance with data acquisition, and the METAvivor Foundation and NIH-NCI (NCI R03 CA181893, R01 CA174926, P30 CA023074, T32 CA009213) for financial support.

#4208 In-vitro modeling of Sonic Hedgehog signaling identifies the extracellular matrix as a regulator of tumor invasion outcomes.

E. A. Carrasquillo-Dones[1], H. M. Rosado-Galindo[1], A. M. Reyes-Ramos[1], W. Torres-Garcia[1], S. Cifuentes[1], J. P. Rios-Grant[1], G. Ortiz-Soto[2], N. A. Ramos-Acevedo[1], M. Acevedo-Esquilin[1], M. Colon-Vargas[1], I. Almodovar-Rivera[1], C. Mora[1], M. M. Martinez-Montemayor[2], M. Domenech[1];
[1]University of Puerto Rico - Mayaguez, Mayaguez, Puerto Rico, [2]School of Medicine Universidad Central del Caribe, Bayamon, Puerto Rico

Preclinical models of Sonic Hedgehog (SHH)-driven tumors support the therapeutic benefit of pharmacological inhibitors, yet clinical outcomes are conflicted due to biphasic tumor responses that include complete remission or faster disease progression. In such studies, the activity of the SHH pathway in the tumor-adjacent stroma supported or restrained tumor progression. Our prior studies show that altered SHH ligand levels can lead to faster tumor growth during pharmacological inhibition suggesting a role for the SHH pathway strength in the biphasic tumor responses of a triple-negative breast cancer (TNBC) model. In this study, the role of SHH pathway strength altered by tumor-fibroblast proximity was examined on the tumor growth, invasion, and transcriptional activity using in vitro and in vivo models. Tumor spheroid models composed of TNBC cell lines and fibroblasts were used to monitor SHH signal strength as a function of the culture modality and SHH ligand levels. In vitro, SHH signal strength was altered by tumor-fibroblast proximity and ligand concentration. Mixed cultures exhibited significantly higher SHH activity and reduced invasion than adjacent cultures. This effect was reversed by pharmacological inhibition of SMO, confirming the involvement of an SHH-dependent mechanism. In a tumor xenograft model, tumor metastasis outcomes were suppressed by pharmacological inhibition of the SHH pathway, but opposite results were observed in tumor xenografts composed of co-injected with fibroblasts indicating that the biphasic tumor response can be driven by the fibroblasts. Spatial transcriptional analysis identified extracellular matrix (ECM) activities in fibroblasts as the top altered bioprocesses in both *in vitro and in vivo*. This finding was confirmed in cultures, where fibroblast-derived decellularized matrix stimulated tumor invasion of single TNBC spheroids at levels observed in co-cultures. Further analysis of differentially expressed genes (DEGs) identified a small leucine-rich repeat proteoglycan (SLRP) as the primary ECM target altered by variations in SHH signal strength in fibroblasts. Furthermore, we confirmed the role of SLRP cues in governing tumor invasion potency within spheroid cultures embedded in a collagen hydrogel matrix. While high levels of SLRP in the matrix inhibited spheroid invasion, low SLRP matrix promoted spheroid invasion and increased secondary invasion sites. These findings agreed with the Vimentin expression levels observed in TNBC cells and confirmed the potency of SLRP in regulating tumor invasion outcomes. In summary, our study underscores the significance of ECM remodeling activities in fibroblasts and the role of SLRPs in governing tumor invasion, with implications for understanding the impact of altering SHH signaling activity in TNBC.

#4209 Unraveling the effects of the microenvironment on glioblastoma multiforme invasiveness using a xeno-free 3D hydrogel platform.

A. I. Ferrer Diaz, J. Huang;
TheWell Bioscience, North Brunswick, NJ

Glioblastoma multiforme (GBM) is a grade IV astrocytoma and the most common type of adult brain malignancy. The overall survival of patients diagnosed with GBM is less than 5 years. Therefore, it is imperative to understand the mechanisms contributing to GBM progression, invasiveness, and survival. This study aimed to evaluate the effect of the extracellular matrix (ECM) on GBM cell invasion by performing the traditional invasion assay as well as novel *in vitro* invasion assay strategies. A significant challenge with *in vitro* cell invasion assays is the use of animal-based ECM: the components of animal-based ECM are not characterized; the batch-to-batch variability of animal-based ECM can influence experimental findings and affect potential clinical applications; and the temperature-sensitive operation protocols make the use of animal-based ECM time-consuming and difficult for automated high-throughput assays. These challenges can be circumvented using VitroGel®, a synthetic xeno-free, bio-functional hydrogel resembling the physiological ECM with tunable biophysical and biochemical properties. In this study, we harnessed the properties of the synthetic xeno-free hydrogel system to examine how different mechanical strengths and functional ligands as well as cytokines and serum within the hydrogel matrices or in the outer well, affect GBM cell invasion. The results indicated that adjusting the mechanical strength of the ECM system affects GBM cell invasion. We further showed that the bio-functional ligands within the hydrogel matrix, such as matrix metalloproteinases, RGD peptide, and others, stimulated cell invasion. This finding exemplifies the importance of using a well-characterized ECM system given that it is difficult to evaluate how specific ECM components contribute to cell invasion using the undefined animal-based ECM. Since the composition of the hydrogel system is chemically defined, we could further control the cytokine milieu within the matrix to understand how the ECM composition affects cell migration. To demonstrate this, we added the cytokine TGF-β1 to the hydrogel and examined GBM cell invasion. Indeed, we showed that adding TGF-β1 to the synthetic VitroGel enhanced GBM cell invasion, thus illustrating that incorporating factors inside the matrix is a powerful method to evaluate chemotaxis. Altogether, this study demonstrates the potency and flexibility of using a xeno-free hydrogel for a myriad of invasion assay applications.

#4210 Stromal remodeling danger signals regulate “second-touch” antigenic encounters and promote CD8+ T cell effector differentiation in the TME.

A. Papadas, D. Hong, A. Cicala, A. Gibbons, D. J. Lagal, Y. Huang, Y. Dou, F. Asimakopoulos;
UC San Diego, La Jolla, CA

Tumor immune infiltration (“hot” tumor microenvironment, TME) constitutes a powerful predictor of outcomes and immunotherapy efficacy, however underlying mechanisms remain elusive. Recent evidence shows that TME-repriming of incoming CD8+ T cells is required for full effector functionality. Reminiscent of the “second-touch” hypothesis proposed by Klaus Ley for CD4+ differentiation, tumor-draining lymph node (TDLN) priming (“first-touch”) generates antigen-specific stem-like TCF1+CD8+ T cells. These stem-like CD8+ T cells then migrate to the tumor periphery where “second-touch” antigenic encounters with non-migratory $CCR7^{neg}$ dendritic cells (DC) (importantly, the cross-presenting cDC1 subset) leads to effector CD8+ T cell differentiation and tumor entry. These second-touch encounters occur within specialized stromal niches that are rich in antigen-presenting cells (APC). We have hypothesized that productive APC:CD8+ interactions require stroma-derived signals that emulate provisional matrix remodeling in embryonic development and/or adult wound healing. Thus, stroma remodeling by the expanding tumor translates into a conserved “danger signal” that licenses APC to activate CD8+ T cell responses. We have focused on a prototypical pathway of provisional matrix remodeling, the regulated proteolysis of the matrix proteoglycan versican (VCAN) to generate a bioactive fragment endowed with immunostimulatory activities, versikine. Stromal VCAN proteolysis at the site releasing versikine is associated with T-cell infiltration across human solid and liquid tumors. To investigate the mechanisms by which versikine regulates first- and second-touch antigenic encounters, we dissected the immune microenvironment of versikine-replete tumors of immunocompetent models at single-cell resolution. Non-migratory $Ccr7^{neg}$ cDC1 in versikine-replete tumors overexpress MHC-I and MHC-II antigen presentation machinery (Tap1, Ciita), maturation (Irf7, ISGs, Tlr3) and co-stimulation markers (Cd86, 4-1BBL), while $Ccr7^{pos}$ DC (mregDC) markedly overexpress Cd40 compared to control mregDC. In parallel, Cd4+ Tfh-like cells (overexpressing Cd40lg, Icos and Maf) accumulate in versikine-replete tumors, mirroring the accumulation of CD4+ T-cells in the stroma of human tumors displaying intense VCAN proteolysis. Consequently, versikine-replete tumors demonstrate expansion of late effector CD8+ T cells (Gzmb+Prf1+). Versikine reverses anti-PD-1 refractoriness in the “cold” model, Lewis Lung Carcinoma (LLC). In “warm” tumor models, versikine with anti-PD-L1 suffices to eradicate tumors and establish immune memory with resistance to tumor rechallenge. Our presentation will focus on the mechanistic dissection of stromal signals regulating antigen presentation across models as well as approaches for translation into novel vaccine platforms.

#4212 Mimicking HCC complex biology and diverse treatment response in a patient-derived microfluidic model.

O. Mocellin[1], A. Robinson[1], A. Olczyk[1], S. Treillard[1], T. Olivier[1], C. P. Ng[1], J. Heijmans[1], A. Stok[1], G. van Tienderen[2], M. Verstegen[2], S. Trietsch[1], H. Lanz[1], P. Vulto[1], J. Joore[1], **K. Queiroz**[1];

[1]MIMETAS, Oegstgeest, Netherlands, [2]Erasmus MC-University Medical Center Rotterdam, Rotterdam, Netherlands

Hepatocellular carcinoma (HCC) is the most common primary liver malignancy and is closely associated with progressive stages of liver diseases. Its transformation, survival, progression and metastasis have been associated with regulation mechanisms orchestrated by the tumor stroma. Patient differences in tumor composition and cellular signaling are reflected in the diversity of therapy response. Hence, comprehensive in vitro models that capture patient-specific tumor and stromal components are necessary to elucidate and evaluate anticancer therapy. Patient-derived dissociated HCC cells from eight different patients were combined with tumor-derived fibroblasts and endothelial cells within a microfluidic setup comprising 64 parallel chips in a microtiter plate format. Cultures were challenged with an individual or combinatorial treatment from a panel of tool compounds for 72 hours in an automated setup. We used immunofluorescence and high content confocal imaging to assess the structural and biological interaction between cancer cells and the associated stroma. Viability assessment, artificial intelligence-based vascular morphology characterization and multiplexed chemokine/cytokine release measurements were used to elucidate patient and drug-dependent effects of single or combinatorial treatments. Cellular interaction within the microfluidic platform led to a vascularized tumor construct, with hepatocellular carcinoma aggregates being enveloped and traversed by a lumenized and interconnected vascular plexus, in association with tumor-derived fibroblasts. Compound treatment led to profound differences across the tested parameters, indicating different anticancer effects in conjunction with the biological diversity of the patient material. Finally, morphological assessment revealed distinct compound-induced effects on the tumor's vascular organization. We present a vascularized patient-derived HCC model that includes relevant cellular players of the tumor microenvironment found in vivo. These co-cultures are highly suitable for studying specific cell types as well as patient-specific responses. We envision that this system has the potential to provide a platform for understanding the interplay between different cell types present in hepatocellular carcinomas, with sufficient scalability ease of use for industrial and clinical implementation.

#4213 Multiplex digital spatial profiling of proteins and RNA in MC38 mouse colorectal cancer syngeneic model.

M. Chen, H. Liu, X. Tu, S. Guo, **X. Chen**;
Crown Bioscience, Inc., Suzhou, China

Introduction Characterization of the tumor microenvironment (TME) has become an essential step for the understanding of the complexity of cell interactions and the discovery of biomarkers for prediction and prognosis of immunotherapy response[1]. The NanoString GeoMx® Digital Spatial Profiler (DSP) technology includes the ability to quantitatively assess RNA and protein levels as well as sample multiple user-defined regions of interest, specifically focused on defining heterogeneity and TME interactions[2]. This technology has been widely used to identify biomarkers in clinical surgical specimens, but its applications in preclinical models are still needed. MC38 colorectal cancer syngeneic model is one of the most utilized models for assessing anti-cancer immunotherapies. In this study, we present the spatial profiling of proteins and RNA on MC38 model treated with anti-PD-1 through GeoMx® DSP technology.

Methods GeoMx protein panel was used to detect the target protein expression differential in tumor-rich region and immune-rich region within MC38 subcutaneous tumor sections treated. Mice were treated with vehicle or anti-PD-1 (10mg/kg, BIW x 4 doses, ip). Whole Transcriptome Atlas (WTA) was employed, and then a comprehensive assessment of the data and comparison was performed.

Results Two morphology markers, CD45 and PanCK, were used to separate tumor-rich region and immune-rich region. The GeoMx® protein data showed that the abundance of VISTA in tumor-rich region differed significantly (log2(fold-change) = 0.67, $p < 0.01$) in anti-PD-1 group compared to vehicle group. While in immuno-rich region, GITR was significantly altered (log2(fold-change) = 0.79, $p < 0.05$) in anti-PD-1 group (TGI value = 50.39%). From WTA data, we observed the upregulation of 839 genes, while 1048 genes were downregulated in immuno-rich region in anti-PD-1 group compared with vehicle group ($p < 0.05$). For tumor-rich regions, 550 genes were upregulated while 782 genes were downregulated in anti-PD-1 group versus vehicle group ($p < 0.05$). From the gene set enrichment analysis, we found that interferon alpha and interferon gamma, which are related to tumor immunity and immunotherapy response, were upregulated in anti-PD-1 group.

Conclusion Both the differential expressing genes and proteins in TME of MC38 syngeneic models treated with anti-PD-1 could be well detected by GeoMx® DSP, which has the potential to provide insightful data for use in biomarker discovery in preclinical cancer models.

References

1. Charmsaz S, Collins DM, Perry AS, Prencipe M. Novel Strategies for Cancer Treatment: Highlights From the 55th IACR Annual Conference. Cancers (Basel) 2019; 11(8).
2. Toki MI, et al. High-plex predictive marker discovery for melanoma immunotherapy-treated patients using digital spatial profiling. Clin. Cancer Res. 2019;25:5503-5512.

#4214 Tissue-engineered 3D model for elucidating the role of the bone niche in osteosarcoma therapy response.

A. D. Peasah[1], C. Monette[1], J. Lee[1], M. Tai[1], E. Sweet-Cordero[2], F. Yang[1];
[1]Stanford University, Stanford, CA, [2]University of California San Francisco, San Francisco, CA

Introduction. Osteosarcoma (OS) is an aggressive pediatric bone cancer whose 5-year survival rate has remained stagnant for nearly 40 years, and often exhibits high therapy resistance. Experimental models that can elucidate how the OS bone niche modulates OS signaling and drug response could accelerate discovery of new targeted therapies. Our group has recently reported a biomaterials-based 3D *in vitro* model of OS with bone matrix mimicking cues: a gelatin microribbon scaffold coated with hydroxyapatite particles (GelHA μRBs). We demonstrated this 3D OS model can better mimic *in vivo* signaling and drug responses than standard 2D culture. However, the potential of this 3D model for probing OS-bone niche crosstalk has not yet been investigated. We hypothesize that OS-bone crosstalk will modulate OS drug response and signaling. To test this hypothesis, here we aim to establish a 3D model to assess the effect of tissue engineered (TE) bone on OS drug response and signaling.

Methods. Gel μRBs were fabricated by wet spinning as previously described. To generate tissue engineered bone, human mesenchymal stem cells (hMSCs) were encapsulated (15 M/mL) in GelHA μRBs and cultured in osteogenic medium for 28 days. A PDX-derived OS line (OS052) was used. Three groups were studied: OS monoculture, separate coculture (paracrine only), and OS cells seeded directly on TE bone (paracrine plus direct contact). For all groups, 96K OS cells were seeded per sample. OS cells were labeled with firefly luciferase to allow tracking of OS cell viability and proliferation using bioluminescence. Gemcitabine, a standard chemotherapy drug for OS, was used as the model drug (0.001 to 1 uM). Outcome analyses include cell viability, proliferation, gene expression, and immunostaining.

Results. TE bone enhances OS resistance to gemcitabine in both separate coculture and direct seeding on bone, as shown by bioluminescence. At 1 uM, OS cell death in monoculture, separate coculture, and seeding on bone was on average 98.19%, 82.05%, and 64.44%. These results indicate that both paracrine signaling from osteoblasts and direct contact with bone ECM contribute to OS drug resistance. TE bone did not significantly impact OS proliferation over 7 days as shown by bioluminescence. Ongoing studies will assess the effect of TE bone on OS expression of key proteins in the bone niche (RANK/RANKL/OPG) and OS response to cabozantinib, a cMET inhibitor whose antiproliferative effect may be osteoblast-mediated.

Conclusions. Here we report a tissue engineered 3D model to study the crosstalk between OS cells and bone niche. The results support our hypothesis that bone niche contributes to OS drug resistance, which is mediated through both paracrine signals and ECM. This model can be used to further elucidate the mechanisms through which the bone niche influences OS progression and drug resistance, and for screening potential drug candidates that target such crosstalk.

#4215 Single-cell proteomic characterization of the tumor microenvironment in humanized NOG-EXL patient-derived xenograft (PDX) models.

D. Stueckmann[1], J. Meens[2], S. Zhang[2], S. Hui[2], S. Sivapatham[3], S. Chevrier[3], J. Pfeil[1], L. Martin[2], M. Komisarenko[2], P. Dube[4], S. Prendeville[5], H. Jackson[1], A. Finelli[2], G. Bader[1], B. Bodenmiller[3], K. A. Lawson[2], L. Ailles[2];

[1]University of Toronto, Toronto, ON, Canada, [2]Princess Margaret Cancer Centre, University Health Network, Toronto, ON, Canada, [3]University of Zurich, Zurich, Switzerland, [4]Taconic Biosciences, Inc., Rensselaer, NY, [5]University Health Network, Toronto, ON, Canada

Introduction:

$CD34^{+}$ hematopoietic stem cell (HSC) derived humanized mice engineered to express human cytokine transgenes are promising models for the evaluation of novel immunotherapeutic treatments. While flow cytometry-based analyses have confirmed the presence of many human immune cell populations within humanized mice bearing patient-derived tumor xenografts (PDX), comprehensive high-dimensional immunophenotyping of the tumor microenvironment (TME) of these models remains limited. Beyond this, the relative influence of PDX vs. donor CD34+ HSC populations on TME composition is poorly understood. Here, we characterize the quantity and diversity of immune cell subpopulations in the TME, bone marrow, and spleen of humanized NOG-EXL (huNOG-EXL) mice using Cytometry by Time-Of-Flight (CyTOF) data with > 60 features.

Methods:

We performed CyTOF analysis on 250 dissociated samples from primary tumors (n = 15; n = 6 head and neck cancer, n = 6 ovarian cancer, n = 3 renal cell carcinoma), as well as xenograft (n = 59), spleen (n = 88), and bone marrow (n = 88) samples from huNOG-EXL mice (Taconic). Each sample was profiled with two partially overlapping antibody panels; an innate immunity-focused panel (40 features), and an adaptive immunity-focused panel (40 features).

Results:

CyTOF data were collected from over 10 million live immune cells for each of the adaptive and innate antibody panels. Unbiased clustering of single-cell marker expression revealed clusters corresponding to all major lymphoid and myeloid cell types. Therapeutically relevant cell states were identified including exhausted CD8+ T cells marked by PD-1 and Tim-3 expression, and PD-L1+ macrophages. Hierarchical clustering of bone marrow and spleen samples suggested that systemically, immune composition was not driven by tumor-intrinsic factors alone with many samples clustering on the basis of CD34+ stem cell donor ID. Conversely, clustering PDX samples revealed strong consistency in xenografts originating from the same primary tumor sample regardless of the chosen stem cell donor. The immune composition of primary tumor samples showed greater similarity with matched PDX samples versus unmatched PDX samples, further supporting that tumor-intrinsic factors drive immune composition in xenografts.

Conclusions:

We provide a high-resolution characterization of the immune phenotypes present in huNOG-EXL PDX models across three cancer types. These data captured substantial heterogeneity in the immune composition of humanized xenograft samples, and we demonstrate that immune composition in humanized xenografts is strongly driven by tumor-intrinsic features. Overall, this resource data supports the use of these models for immuno-oncology studies with future work focused on functionally validating specific immune cell populations of interest.

#4216 Indication agnostic evaluation of CAR T cell function using patient-derived immunocompetent tumoroid modelling platform.

D. O. Ochola[1], H. Dell mundo[1], P. Samuel[1], N. Korkorina[2], **B. Dave**[1];
[1]Spanios, Houston, TX, [2]SNAP Biolabs, Houston, TX

Introduction: Engineered T cells redirected towards tumor-specific cytotoxicity is a promising immunotherapeutic modality that has been well characterized for efficacy against B cell malignancies and evaluated in multiple tumor types. However, the development and optimization of CAR T cell therapies requires a rigorous preclinical model for the evaluation of CAR T cell function, tumor killing, cytokine production, and memory responses.
Experimental Procedure: We are evaluating our model platform Custom Organoid Modelling Platform for Accurate and Speedy SolutionS (COMPASS 2) as a comprehensive platform for testing developmental and functional stages of CAR T cells including activation, memory, and exhaustion. We are performing qualitative and quantitative analyses of surface markers to recapitulate the complexity of human cancer. Additionally, since CAR T cells mediate crosstalk with other immune components in the TME, we also evaluate and monitor the presence of B cells, NK cells, macrophages, and endogenous T cells. Triple Negative Breast Cancer (TNBC); Immunophenotyping (IP); Immunofluorescence (IF); Fluorescence Activated Cell Sorting (FACS); T regulatory (Treg).
Summary of Results: Our evaluation of COMPASS 2 for functional testing of CAR T cells demonstrates the feasibility of the platform in preclinical CAR T cell evaluation. We showed T cell infiltration and analyzed cytokine production that may alter tumor cells and TME. Crosstalk with other immune cells will be evaluated. We are currently evaluating the tumor volume changes using an EGFRvIII-targeted CART cell therapy on TNBC model systems, followed by apoptosis and EGFR analysis using FACS.
Conclusion: Our COMPASS 2 model platform enables studies that require recapitulating hurdles to CAR therapy, including antigen escape, T cell dysfunction and trafficking; to reveal an essential role of the endogenous immune response mediating the antitumor effect following CAR therapy.

#4217 An engineered breast tumor microenvironment model, with single-cell spatial resolution, to assess spatial dynamics of tumor evolution.

H. R. Helms, K. A. Oyama, A. E. Davies, E. M. Langer, L. E. Bertassoni;
Knight Cancer Institute, Oregon Health & Science University, Portland, OR

Cellular heterogeneity is a prominent feature of the tumor microenvironment, and the organization of these cells has been linked to clinical outcomes such as disease progression and drug resistance. While retrospective analysis of patient tumors has produced a myriad of insights, samples are limited and highly complex making it challenging to validate causality. Here we present an engineered breast tumor microenvironment model, with single cell spatial resolution, to systematically identify which cell phenotypes and their spatial arrangements may be driving ductal carcinoma in situ disease progression. A microfluidic dispenser (Biopixlar, Fluicell) was optimized to enable the spatial patterning of single cells to replicate native histology. To demonstrate the high spatial precision of our method, we first replicated an annotated 2D section of a breast tumor biopsy region of interest (ROI) using MCF10A, MDA-MB-231, primary mammary fibroblasts, THP-1 derived macrophages, and primary mesenchymal stem cells. The XY coordinate of each cell was identified to create a print map matching the original biopsy. Deposited cells adhered to their intended target with an average print fidelity of 2.4 µm. Next, the stromal compartment of the ROI was altered to include phenotypes associated with tumor promoting microenvironments (i.e. cancer associated fibroblasts, M2 macrophages) and the core of the MCF10A ring filled with MDA-MB-231. Each deposited cell contained a fluorescent tag corresponding with its cell type to facilitate real time spatial tracking and annotation. The tumor microenvironments were live cell imaged for 24 hours at 5 minute intervals. MCF10A cells spread to form their junctions and create a cohesive ring, MDA-MB-231 cells proliferated and rapidly moved around within the confined space, and the cells of the stromal compartment spread to create a dense tissue like structure. The microenvironments were cultured for an additional 2-6 days, fixed, and stained for markers of proliferation, phenotype shifts, cell-cell junctions, and morphology. Unlocking the relative contributions of the specific cell types in ductal carcinoma in situ tumor microenvironment to the overall evolution of invasive breast cancer may hold the answer for many questions in early detection, treatment, and cancer avatar models.

#4219 Establishing CAF-like and TAM-like transformation induced by TNBC culture supernatant in 3D in-vitro culture as a model for targeted drug testing.

B. Sapkota[1], N. Chintalaramulu[1], A. Pandit[1], S. Thota[1], R. Begum[1], A. Mansouri[2], J. Adamec[2], J. Francis[1];
[1]Louisiana State University, Baton Rouge, LA, [2]Louisiana State University Health Sciences Center, New Orleans, LA

Several previous studies have highlighted the significance of cell-to-cell communication, or crosstalk, between tumor cells and non-tumorigenic cells in the context of cancer progression and metastasis. Within the tumor microenvironment (TME), these interactions have the potential to alter the phenotypes and behaviors of normal cells. The use of 2D in-vitro cultures has been limited due to their inability to accurately replicate the intricate in-vivo TME. Conditioned medium (CM) derived from cultured cancer cells contains secreted factors that may influence the phenotype and functionality of normal cells. In our investigation, the exposure of normal murine fibroblast NIH3T3 and macrophage RAW 264.7 cells to conditioned medium (CM) obtained from malignant mammary epithelial 4T1 cells (4T1CM) resulted in a modified phenotype with enhanced cell viability. Treatment with 4T1CM led to the upregulation of genes, including α-smooth muscle actin (αSMA), IL-10, CD206, and vascular endothelial growth factor (VEGF), in NIH3T3 and RAW 264.7 cells compared to their respective control cells. Additionally, NIH3T3 cells treated with 4T1CM exhibited an epithelial-mesenchymal transition (EMT) phenotype, as indicated by the regulation of EMT markers such as E-cadherin, β-catenin, N-cadherin, and Vimentin. Notably, RAW 264.7 cells treated with 4T1CM showed an upregulation of cyclooxygenase-2 (COX-2) and programmed death-ligand 1 (PDL-1), suggesting a propensity for an inhibitory immune response. Moreover, NIH3T3 cells conditioned with 4T1CM demonstrated an upregulation of stemness markers, including sex determining region Y-box 2 and Aldehyde dehydrogenase. In summary, our study highlights the potential role of 4T1CM in transforming normal NIH3T3 and RAW 264.7 cells into cancer-associated fibroblasts (CAFs) and tumor-associated macrophages (TAMs). Ongoing proteomics analysis aims to map differentially expressed proteins potentially regulating the 4T1CM-induced transformation. To further investigate, a series of experiments using mono- and co-cultures of these cells are underway, specifically targeting the transformed macrophages and fibroblasts with the aim of either re-educating or eliminating them. This treatment involves drug combinations that specifically target the identified signaling pathway intermediates, offering novel therapeutic intervention strategies.

#4220 Combined light sheet and multispectral imaging facilitates the detection of tumor-associated tertiary lymphoid structures in the KP NSCLC model.

N. O'Brien[1], B. Appelt[2], M.-L. Moerbitz[2], J. P. J. Mueller[1], F. Herting[1], P. Umana[2], C. Murgia[2], S. Colombetti[2], T. Poschinger[1];
[1]Roche Diagnostics GmbH, Penzberg, Germany, [2]Roche Glycart AG, Schlieren, Switzerland

Tertiary lymphoid structures (TLS) have recently emerged as a predictive biomarker in cancer immunotherapy. Their consideration in preclinical drug development is impeded by rare and transient appearance and random distribution, making them difficult to analyze with conventional sampling methods. We applied whole-organ tissue clearing and 3D staining of B and T cell clusters to comprehensively identify TLS in a KP GEMM of NSCLC using 3D Light Sheet Fluorescence Microscopy (3D LSFM). To further investigate cellular composition of TLS we performed 3D LSFM-educated sectioning of relevant ROIs and cyclic immunofluorescence of the same samples. 3D LSFM facilitated correlation of tumor features and location with T cell infiltration as well as the analysis of number, size and location of TLS. The majority of TLS were located in proximity to bronchi instead of intratumorally. LSFM-guided multiplex immunofluorescence revealed further details on cellular composition and maturation status of TLS. This combination of 3D and 2D imaging modalities offers a holistic approach for the identification of TLS in whole murine tumors or organs. The technology could help studying effects of immunotherapy on de novo formation or maturation of TLS.

#4221 Characterization and comparison of hypoxia inducing factors on tumor growth and metastasis in 2D and 3D tumor models.

J. McDonald[1], L. L. Chan[1], S. Kessel[1], B. Lin[1], P. Weingarten[2],

[1]Revvity Health Sciences, Inc., Lawrence, MA, [2]ImmunityBio, Culver City, CA

The monocarboxylic acid transporter 4 (Mct-4), a downstream biomarker of hypoxia inducing factor (HIF)-1α, is involved in the cellular response to hypoxia, as indicated by the hypoxic response element in its promoter region. Using a tumorsphere assay as an in vitro 3-dimensional (3D) model generated using 384-well ultra-low attachment (ULA) plates for cell proliferation analysis using a plate-based image cytometer, we identify a hypoxic response in the tumorsphere model that is distinct from that of cells grown under 2-dimensional (2D) normoxic conditions and demonstrate a key role for Mct-4 in enabling 3D growth. The tumorsphere model yields evidence of an essential role for Mct-4 in multiple cell lines which were genetically modified to underexpress and overexpress Mct-4, evidence not apparent in a standard 2D model of growth in the same cell lines. In addition, we identify the effects of overexpressing Mct-4 in cancer cell migration using a transwell chamber assay. We also show that the response to hypoxia may be circumvented by transfection with a CMV promoter driven Mct-4, which confers constitutive 3D growth, wherein tumorsphere growth inhibition by small molecule HIF-1α inhibitors is mitigated. Finally, we demonstrate quantifiable gene/protein expression differences between 2D and 3D cancer models based on the normoxic and hypoxic conditions. Therefore, the tumorsphere 3D model generated using 384-well ULA plates in combination with high-throughput image cytometer is demonstrated to provide a convenient, robust, and reproducible tool and method for the elucidation of mechanisms of action underlying tumor growth and migration in the hypoxic tumor microenvironment.

#4223 The dual immunestimulatory and immunesuppressive role of MRC5 fibroblast cells in 3D coculture with T cells and tumor cells.

I. Arnkil, C. Hekim, E. Narvi, E.-L. Ihantola, E. Elbasani, A. Thotakura;
Immuno-Oncology, Oncology R&D, Orion Corporation, Turku, Finland

Introduction: Cancer-associated fibroblasts (CAFs) alter anti-tumor immune responses and modulate resistance to immune checkpoint inhibitors. The mechanisms of crosstalk between tumor cells, CAFs, and T cells remain not fully understood, and studying these multicellular interactions requires adoption of novel tools in preclinical research. Here, we established a spheroid co-culture model comprising of tumor cell lines, a fibroblast cell line, and primary human T cells, for studying the immunomodulatory effects of fibroblasts on T cell responses *in vitro,* in the context of immunotherapies.
Methods: For setting up the 3D co-culture, A375 or OV-90 tumor cells were seeded alone or with MRC-5 fibroblasts in 96-well ultra-low attachment round bottom plates in complete growth medium supplemented with 1% Geltrex matrix. The cells were centrifuged, and spheroids were allowed to form for 24 hours. After spheroid initiation, activated T cells and treatments with anti-PD1 antibody or an immune stimulatory drug were added. Spheroid co-cultures were live imaged by Incucyte SX5 for 72 hours taking images every 4 hours, after which treatment responses were evaluated by flow cytometry and measuring IFN-γ accumulation with ELISA.
Results: To mimic fibroblast and T cell interactions in tumor microenvironment we built and optimized an *in vitro* 3D co-culture assay using various tumor cell lines. With this assay we found that depending on the tumor cell interaction, fibroblasts MRC-5 cell line have either immune-suppressive or immune-promoting properties. IFN-γ secretion of T cells in the assay indicated that MRC-5 cells suppressed T cells when co-cultured with A375 cells, while with OV-90 cells T cells activation was enhanced. In addition to the IFN- γ secretion, T cells in MRC-5 OV-90 interaction significantly upregulated 4-1BB expression on both CD4 & CD8 T cells. Interestingly we noticed that MRC-5 fibroblasts could modulate T cell responses to anti-PD-1 treatment in the co-culture depending on the tumor cell used.
Conclusion: Here, we established a spheroid co-culture model, which will allow studies of the immunomodulatory crosstalk occurring in tumor microenvironment. Our model revealed a bifunctional role of MRC-5 fibroblasts in altering T cell phenotype. This finding is in line with literature highlighting the ability of fibroblasts to act as either tumor promoters or tumor suppressors depending on tumor microenvironment. We believe that this model, would aid in elucidating mechanisms of interaction between CAFs and T cells, potentially leading to discoveries of novel targets for immuno-oncology drug development. Additional studies, such as gene expression analysis using single cell RNA sequencing, are warranted to further validated the model and to better understand the kinetics of these interaction occurring in the co-culture with various tumor cell lines.

#4224 The application of sophisticated image analysis to a T cell killing assay in 3D deciphers the dynamics of the different components of the tumor microenvironment.

R. Kerwin[1], I. Rohleff[2], M. Blanchard[1], K. Lashuk[2], B. Walker[1], **J. B. Schueler**[2];
[1]Animantis, San Diego, CA, [2]Charles River Laboratories, Inc., Freiburg, Germany

We developed an in vitro protocol to generate tumor-specific cytotoxic lymphocytes (CTL) by priming T cells from healthy donors on HER2+ breast cancer cell line SKBR-3. Subsequently, these primed CTLs were tested in a 3D immune cell killing assays in a life cell imaging device. An image analysis workflow was applied to understand the T cell movement in spatial relation to the tumor and the kinetic of tumor cell killing. The activity of the CTLs was compared with non-activated CD8+T cells, staurosporin and CD8+ T cells, unspecifically activated by αCD2/αCD3/αCD28 beads. The tumor cells were expressing mKate whereas the T cells were label-free. By analyzing a combination of different masks, we could computationally measure tumor spheroid characteristics and dynamic attributes such as changes in shape, percent of cells expressing red fluorescentce, and relative average distance of T cells from the spheroid in each timelapse assay. This process was applied at each frame to determine the average T cell distance from its corresponding spheroid center and subsequently calculate the average T cell flux over the course of each assay by linking data between image frames. Additional measurements allowed for the quantification of tumor debris accumulation over time both relative to the primary tumor mass and in absolute terms. Our analyses revealed that bead-activated T cells approached the tumor spheroid with the highest speed and infiltrated the spheroid homogeneously. In contrast the CTLs approached the spheroid slower and started tumor cell killing from the rim of the spheroid towards the center. The reduction of spheroid area over time displayed a very similar kinetic when co-cultured with CTL or bead-activated T cells. At the end of the experiment the CTLs induced a more pronounced shrinkage of spheroid size. Interestingly the size of the spheroid and the red fluorescence intensity were not necessarily aligned. The positive control Staurosporin induced a fast reduction of the mKate signal, whereas the spheroid area did not change over time. In summary, the bead-activated T cell approached the spheroid fast, infiltrated the complete area and induced tumor cell killing homogenously across the tumor area. The CTL approached the spheroids slower but started killing earlier from the outside towards the center of the spheroid. The observed differences in infiltration and killing characteristics of the investigated T cell types lead to a better understanding of T cell biology in the context of the tumor biology, which can be translated into applications during dug development. Taken together, with the applied image analysis algorithm we were able to deconvolute the biological processes in the assay in much more detail. The additional read-outs increase the translational value of the assay tremendously in the context of drug development as well as precision medicine.

#4225 Analysis of the landscape of cancer-associated neurons (CANs) in diverse cancers through retrograde tracing and single cell molecular profiling.

V. Thiel, S. Renders, J. Panten, Daniel Azorin, Nicolas Dross, Albrecht Stenzinger,Sebastian Scholch, Frank Winkler, M. Sprick, A. Trumpp;
German Cancer Research Center, Heidelberg, Germany

Hyperinnervation emerges as a common hallmark in the tumor microenvironment (TME) of most cancers, with clinical studies establishing a direct link between increased innervation and poor prognosis. Despite the acknowledged pivotal role of the TME, previous molecular profiling excluded tumor-infiltrating neurons due to the unique anatomical characteristics of peripheral neurons. While their axons extend into tumor masses, their DNA- and mRNA-containing cell bodies reside in adjacent ganglia, rendering them absent from virtually all large data sets analyzing tumor material. To fill this critical gap of the role of neurons for cancer growth, therapy resistance and metastasis, we developed a multi-layered approach to unravel the molecular basis of the neural influence in a.o. pancreatic (PDAC), colon cancer and melanoma including their metastasis. First, we unveiled a complex neural network within tumors and metastases through tissue clearing and 3D imaging of patient-derived xenografts, GEMMs, and human samples. This approach was complemented by the introduction of 'Trace-n-Seq,' a novel methodology integrating retrograde axonal tracing, FACS analysis, and single-cell RNA sequencing of neurons innervating both healthy organs and tumors. Expanding this technique unveiled the molecular profiles of over 3000 individual sympathetic, parasympathetic, and sensory neurons infiltrating various tumors, metastases, and pancreatitis, which were compared to neurons innervating healthy organs. Thereby we identified novel neuronal subtypes and observed tumor-induced neuronal reprogramming. Our single-cell data, when integrated with scRNA sequencing of PDAC, unveiled comprehensive neuronal interactions. An interactome analysis identified key genes in tumor/stroma-nerve signaling. To address the functional consequence of hyperinnervation of PDAC tumors, we show data demonstrating that surgical or pharmacological denervation of tumors caused a reduction in tumor size, concomitant with diminished stromal and increased immune compartments. Our data also suggest that the anti-cancer activity of paclitaxel -not oxaliplatin- was partially dependent on its ability to directly target CANs. In fact, in a neoadjuvant setting, PDAC patients treated with Gemcitabine/nab-paclitaxel, but not FOLFIRINOX, displayed a reduction in neuronal structures, underscoring the clinical significance of these observations. In summary, our comprehensive approach has elucidated the role of neurons in PDAC, melanoma, pancreatitis, and metastasis, leveraging innovative tools for studying the molecular programs of CANs at the single-cell level. These insights not only unveil novel mechanisms orchestrated by neuronal activity but also pave the way for imminent clinical trials, aiming to combat PDAC by targeting cancer-associated neurons.

#4226 Human-derived hydrogels for 3D models of bone and osteosarcoma organoids and adipose tissue interactions.

C. G. Sanchez[1], A. Raz[2], H. Lassiter[1], T. Frazier[1];
[1]Obatala Sciences, Inc., New Orleans, LA, [2]Tulane Medical School, New Orleans, LA

The goal of the study was to determine the metabolic and morphological changes, via high Content Imaging, in 3D models of osteosarcoma cancer cells using human derived hydrogels with different protein composition, Obagel and Obagel ECM. Furthermore, we evaluated the relevance of the adipose tissue microenvironment in Adipose Derived Stem Cells (ADSC) linage and Tumoroids development.
Methods: Adipose derived Stem cells were cultured in a modified 3D human and fat and bone linage differentiation as studied via histology and Immunofluorescence. Osteosarcoma spheroids were cultured in Obatala Sciences' human-derived hydrogels ObaGel and ObaGelECM and control media. Organoid structure and phenotypic changes were analyzed via live cell imaging on the Incucyte S3 and Nikon high content imaging device. Then, adipocyte-cancer cell crosstalk was evaluated using pooled adipocytes co-cultured with KHOS spheroids. Adipose derived Stem cells were cultured in a modified 3D human derived hydrogel dictates that promotes the differentiation potential toward fat and adipose tissue simultaneously in microenvironments within the organoid. Furthermore, the results demonstrated that ObaGel and ObaGel-ECM 3D cultures can support the growth and proliferation of KHOS tumor spheres during an extended culture period. Metabolic changes and phenotypic changes associated to ObaGel and ObaGel-ECM differentially facilitated tumoroids growth and migratory behavior.
Conclusions: Human derived hydrogels are developed to support 3D culture of Bone and Osteosarcoma cells to recapitulate the phenotypic changes associated with their metastatic potential. The use of human derived 3D culture systems can accelerate the understanding of the role of the microenvironment in bone development and the pathogenesis and progression of Cancers like Osteosarcoma as well as screening for drug development.

#4227 Human-derived hydrogels to support phenotypic changes in ER+ breast cancer cell line.

C. G. Sanchez[1], K. Hamel[1], E. Rogers[1], J. Robinson[1], H. Lassiter[1], T. Frazier[1], C. Williams[2];
[1]Obatala Sciences, Inc., New Orleans, LA, [2]Xavier University, New Orleans, LA

Adipose tissue plays a critical role in breast cancer incidence, progression, and response to therapy. The development of human derived 3D culture systems can accelerate the understanding of the role of environmental factors in the progression of Breast cancer as well as a model for preclinical studies during drug development. MCF-7 spheroids were cultured in Obatala Sciences' Obavate and human-derived hydrogels ObaGel® and ObaGel®-ECM and control media. Organoid structure and phenotypic changes were analyzed via live cell imaging on the Incucyte S3. Migration studies were performed and gene expression analysis of EMT markers. Finally, adipocyte-breast cancer cell crosstalk was evaluated using pooled adipocytes co-cultured with MCF-7 spheroids. The results demonstrated that ObaGel® and ObaGel®-ECM 3D cultures support the growth and proliferation of MCF-7 tumorspheres during an extended culture period. In addition, MCF-7 cells exhibit the characteristic morphology of tumorsphere-forming cells when cultured in Obavate, with morphological changes in the ObaGel® and ObaGel®-ECM 3D. ObaGel® and ObaGel®-ECM differentially supports MCF-7 migratory behavior and phenotypic changes characteristic of EMT. Conclusions: Human derived hydrogels are developed to support 3D culture of breast cancer cells and to recapitulate the phenotypic changes associated with their metastatic potential. Furthermore, the use of a human derived 3D coculture system provides a platform for the understanding of adipose tissue-breast cancer cell interactions as it relates to breast cancer initiation, progression, and treatment response. Defining these interactions will support the development of a tool for future use in patient stratification and precision medicine in identifying underlying causes of breast cancer progression and response to treatments.

TUMOR BIOLOGY: Organoid Models of Cancer 2
Poster Session

#4230 Patient-derived tumoroid platforms with progressing tumor microenvironment representability reveals efficacy and resistance patterns in pre-clinical HSP90i regimen testing for improved clinical insights.

H. Del Mundo, D. O. Ochola, **B. Dave**, P. Samuel;
Spanios, Houston, TX

Introduction: Drug candidates advance to phase I clinical trial after rigorous optimization at preclinical stage and yet nine out of ten drug candidates fail during clinical trials and approval stage. Lack of clinical efficacy is a major contributor (~ 50%) towards this 90% of the failure at clinical trials. Tremendous efforts are being taken to demonstrate drug efficacy in preclinical studies by mitigating the biological discrepancy of molecular target between human disease and the model used for the validation. Herein this study, we aim to showcase therapeutic responses of heat-shock protein 90 (HSP90) inhibitor regimens (HSP90i only and HSP90i + Doxorubicin combination) against three-dimensional (3D), patient-derived tumoroid (PDT) model platforms with progressing tumor microenvironment (TME) representability by incorporating supplementary TME structure, immunity, and oxygenation. Revelations on efficacy and resistance patterns of such drug treatments on increasingly complex models is aimed at providing unique insights to tumor and drug-drug interplay.
Methods: Human Uterine Adenosarcoma PDT models were prepared across three COMPASS (Custom Organoid Modeling Platform for Accurate SolutionS) platforms: 1) COMPASS 1a - Non-scaffold 2) COMPASS 3b - Scaffold + Immune cells and 3) COMPASS 3d - Scaffold + Immune cells + Oxygenation. The various platforms were tested against two regimens A) HSP90i only [50 nM and 100 nM] and B) HSP90i [50 nM and 100 nM] + Doxorubicin [50 nM]. Tumor size and volume assessment were carried out on Days 3 and 7 post-treatment -with statistical done via one-way ANOVA, followed by student's t test for significance ($p<0.05$, n=3).
Results: While a simpler platform COMPASS 1a showcased the therapeutic efficacy of monotherapeutic HSP90i [at 100 nM] ($p<0.05$), progressively complex models (COMPASS 3b and COMPASS 3d) have otherwise indicated the lack of significant tumor volume changes. On the other hand, current findings on combination therapies of HSP90i and Doxorubicin have revealed persistent therapeutic resistance (even suggestive of patterns of increasing tumor growth) on COMPASS 1a, necessitating further comparisons on the more complex models.
Conclusion: Our results demonstrate the need to test drugs in context of TME and oxygenation to help stratify patients to develop better clinical trials based on patient tumor characteristics of vascularization and immunogenicity. We plan to test several different drug modalities and cancer types for these parameters to demonstrate the need and effectiveness of testing prior to taking the drugs to the clinic.

#4231 A biobank of bladder cancer organoids as a platform for screening new therapeutic approaches.

Emilie Decaup[1], Claire Beraud[1], Anne Sophie Bajeot[2], Xavier Game[2], Nicolas Monjotin[1], Pascal Rischmann[2], Philippe Lluel[1], Mathieu Roumiguie[2]

[1]Urosphere SAS, Toulouse, France,[2]CHU Toulouse, Toulouse, France

In patients with bladder cancer (BC) immune therapies have recently demonstrated an improvement for overall survival rates compared to chemotherapy alone. However, several challenges persist and it remains an unmet need to develop novel therapeutic strategies. Organoids have emerged as a promising animal-free tool revealing patients' heterogeneity and allowing large preclinical therapeutic screening. Urosphere developed a BC organoids biobank with phenotypic, pharmacological and molecular characterization. The aim of this study was to demonstrate the relevance of our organoids models and their use for validation of therapeutic approaches such as targeted or CAR-T cell therapies using EGFR as target. Molecular characterization of the organoids was performed by exome and whole transcriptome sequencing. Cell architecture and differentiation were assessed by labeling cytokeratins (CK) 5, 17 and 20, and uroplakin 3 (UPK3). Proliferation and tumor status were validated with Ki67 and GATA3, respectively. To evaluate targeted-therapy, organoids were treated with erlotinib for 5 days and cell viability was measured with CellTiter-Glo3D® (CTG) assay. To validate CAR-T cell approach, organoids were co-cultured with anti-EGFR or control anti-CD19 CAR-T cells at 4 effector:target ratios. Cell viability was measured with CTG and Caspase-Glo® 3/7 3D assays. Pro-inflammatory and granzyme B release were analyzed by Luminex® assay. Phenotypically, organoids showed proliferating structures whose tumor status was confirmed by GATA3 expression. Cellular heterogeneity present in original tumors was also found, with differential expression of CKs showing the presence of basal (CK5/CD17) and/or differentiated superficial (CK20/UPK3) cells. Organoids from 2 models with high transcriptomic EGFR expression were selected and protein expression was confirmed by immunofluorescence. For targeted therapy, erlotinib presented significant efficacy in both models with a better activity in the model presenting the highest EGFR expression. After 48h of co-culture with anti-EGFR CAR-T cells, a decrease of cell viability associated with an increase of apoptosis was observed. After 72h of co-culture, an increase in the secretion of pro-inflammatory cytokines (IFN-γ and TNF-α) and granzyme B by anti-EGFR CAR-T cells was also observed. In co-cultures with organoids higher expressing EGFR, CAR-T cells activation appeared higher compared to those co-cultured with organoids lower expressing EGFR. Organoids reproduce characteristics of the tumor from which they are derived, making them a predictive preclinical model. In an EGFR targeting approach, the use of organoids to evaluate both targeted- and CAR-T cell therapies was validated with concordant results. This robust translational model is fully transposable to other therapeutic approaches, whether in a traditional culture model or in a co-culture system.

#4232 Exploring chemotherapy resistance in pancreatic cancer: Insights from a 3D organoid model.

H. Lee;
Yonsei University College of Medicine, Seoul, Korea, Republic of

Pancreatic cancer is marked by a dismal prognosis, with a 5-year survival rate at approximately 10%. A key contributor to its lethality is the development of chemotherapy resistance, followed by early metastasis. However, studies elucidating the mechanisms behind chemotherapy resistance in pancreatic cancer are limited. Previous research has relied on 2D cell line models, which present limitations, such as uniform cell types that fail to capture tumor heterogeneity and an inaccurate representation of clinical realities, wherein resistance often develops gradually rather than through continuous exposure to high drug concentrations. In this study, we developed a more sophisticated organoid model of chemotherapy resistance. Six organoids from three patients were matched to study chemotherapy resistance in a personalized context. Comprehensive whole-exome sequencing and transcriptomic analyses were performed, along with an examination of chemotherapy resistance protein expression and EMT-related markers. Notably, differential expression levels of CK19 and Vimentin were observed between samples. Our analysis also focused on the expression of the ATP-Binding Cassette Subfamily G Member 2 (ABCG2) gene in chemoresistant organoids. Western blot analysis indicated a significant increase in ABCG2 expression in these organoids compared to controls. According to the Moffitt RNA signature, the primary and corresponding chemoresistant organoids retained their molecular subtype classifications both before and after developing chemoresistance. Gene set enrichment analysis uncovered significant upregulation of pathways related to DNA repair and cell cycle regulation, particularly the G2M checkpoint, in chemoresistant organoids. Furthermore, gene ontology functional analysis suggested a notable overrepresentation of activities related to amino acid transmembrane transport and extracellular matrix constituents, underscoring their potential role in the chemoresistance phenotype.

#4233 Rapid and robust generation of ex vivo tumoroid samples from fresh patient samples in a serum-free, conditioned medium-free system.

C. Paul, A. Bullock, A. Chatman, B. Balhouse, C. Yankaskas, P. Shahi Thakuri, M. Dallas, D. Kuninger;
Thermo Fisher Scientific, Frederick, MD

Functional precision oncology describes a method in which an individual patient's cancer cells are tested for response to various treatments ex vivo to aid in therapy selection. In many cases, these cultures take the form of tumoroids, which are 3D, patient-derived "mini tumors" that retain phenotypic and genotypic characteristics of the patient cancer. While interest in functional precision oncology is increasing due to strong correlation between patient responses and those experimentally observed using matched tumoroid models in the literature, a lack of standardization has precluded its widespread translation to clinical settings. To study the ability to generate short-term tumoroid cultures using a commercially available, serum-free, and conditioned medium-free system, we processed fresh tumor resection samples and performed culture in Gibco™ OncoPro™ Tumoroid Culture Medium. Tumor resection samples spanning a variety of indications were stored in supplemented Hibernate™-A Medium (including antibiotics) and shipped overnight on gel packs to a central tissue processing site. Samples were minced, enzymatically dissociated, and counted. Average yields of ~2000-12,000 cells per mg of tumor resection tissue were observed, with lower yields in lung, head and neck, and breast cancer samples and higher yields in endometrial and colorectal cancer samples. Donor-to-donor variability generated a wide range of yields within a given indication. Similarly, cell viability following dissociation ranged widely, reaching as low as 20% for some samples and exceeding 90% for others. Though yields and initial viability varied, dissociated cells that were plated in OncoPro Tumoroid Culture Medium formed tumoroids in >85% of samples within 7 days of tissue receipt. Both mutational profiles and gene expression patterns were highly conserved (>90%) between initial tumor samples and cells cultured in OncoPro for 7 days. Computational approaches designed to identify cell-type specific signatures from bulk RNA sequencing data indicated that immune cell population signatures were present after one week in OncoPro medium. Additionally, we have developed methods to analyze tumoroid response to compounds and candidate cell therapies by both plate reader- and imaging-based analyses using ~1.2e6 initial tumor cells per 96-well plate. Due to the high success rate of tumoroid formation from fresh tumor samples and retention of donor-specific characteristics in OncoPro Tumoroid Culture Medium, we believe that it will be a valuable tool for functional precision oncology of solid tumor samples.

#4234 Personalized therapeutic screening in patient derived organoids for gastroenteropancreatic neuroendocrine tumors.

Steven D. Forsythe[1], Srujana V. Yellapragada[1], Stephen G. Andrews[1], Jaydira del Rivero[2], Jonathan M. Hernandez[3], Naris Nilubol[1], James P. Madigan[1], Samira M. Sadowski[1]

[1]Neuroendocrine Cancer Therapy Section, National Cancer Institute, Bethesda, MD,[2]Developmental Therapeutics Branch, National Cancer Institute, Bethesda, MD,[3]Surgical Oncology Program, National Cancer Institute, Bethesda, MD

Introduction Gastroenteropancreatic Neuroendocrine Neoplasms (GEP-NENs) are a rare subset of cancers which nevertheless are a rising health burden. Development of new therapies suffers from several bottlenecks, including low patient accrual and poor understanding of tumor characteristics. Patient tumor organoids (PTOs) are a novel model capable of improving screening of patient tissue in an accurate, standardized, and high-throughput capacity. In this study, we utilized patient tumors for creation of high-fidelity PTOs from a variety of GEP-NEN primary origins to evaluate therapy responses.

Methods Tumors from patients undergoing clinically guided surgeries were processed within two hours of resection and dissociated into single-cell suspension. Cells were encapsulated into Matrigel and cultured into two groups. The first group was grown for 10 days to assess viability then treated with a panel of clinically approved therapies and novel treatments recommended by high throughput NEN cell line screening for treatment sensitivity using the MIPE 5.0 library. The second group was grown for long-term expansion and biobanking, followed by characterization using immunohistochemistry and genetic profiling to ensure tumor cell maintenance.

Results From March 2023-November 2023, 14 patients provided 30 tumors for PTO development. These included small intestine (n=5), pancreatic (n=8), and gastric (n=1) neuroendocrine tumors. Long-term culture (>3 passages) was successful for 23/30 (77%) specimens, with passage timing related to tumor grade. PTOs maintained immunohistochemical characteristics of the parent tumor types and demonstrated similar genetic profiles, including neuroendocrine tumor cell markers synaptophysin, chromogranin A, and matched grade-based Ki67 proliferative index. The early-stage therapeutic screening was performed for 12/14 (86%) patients, demonstrating tumor grade dependent treatment efficacy and showing clinically dose relevant sensitivity towards approved small molecule inhibitor therapies including cabozantinib and sunitinib in a patient and tumor origin-dependent manner. Testing of effective therapy classes recommended by cell line treatment panels suggested high level treatment efficacy for proteosome inhibitors, MEK inhibitors, and topoisomerase inhibitors.

Conclusion Development of GEP-NEN PTOs is feasible for long term culture and standard of care therapy testing. Further study demonstrated the successful application of novel therapeutic options in PTOs for patients with GEP-NENs.

#4235 PD3D® models as jacks-of-all-trades for cancer research and therapy response prediction.

Lena Wedeken[1], Samantha Forbrig[1], Katja Herrera-Glomm[1], Juergen Loskutov[1], Ulrike Pfohl[1], Irina Piven[1], Michael Poehle[1], Manuela J. Regenbrecht[1], Barbara Seller[1], Cynthia Yapto[1], Sabine Finkler[2], Larissa Ruhe[2], Quirin Graf Adelmann[2], Christoph Reinhard[1], Marie Flechner[3], Katja Uhlig[3], David Kaul[4], Siyer Roohani[4], Maya Niethard[5], Rica Sauer[6], Christian R. A. Regenbrecht[1]

[1]CELLphenomics GmbH, Berlin, Germany,[2]ASC Oncology GmbH, Berlin, Germany,[3]Branch Bioanalytics and Bioprocesses IZI-BB, Fraunhofer Institute for Cell Therapy and Immunology, Potsdam, Germany,[4]Department of Radiation Oncology, Charite - Universitatsmedizin Berlin, Berlin, Germany,[5]Department of Orthopedic Oncology, Sarcoma Center, Helios Klinikum Berlin-Buch, Berlin, Germany,[6]Institute of Pathology, MVZ am Helios Klinikum Emil von Behring GmbH, Berlin, Germany

Physiologically relevant *in vitro* tumor models are crucial in any research setting from preclinical drug development to functional precision oncology. Patient-derived 3D cell culture models (PD3D®) are validated cancer models which recapitulate the biology of the original tumor tissue. PD3D® can be used to model intratumoral heterogeneity in medium and high throughput screens. Using a reverse clinical engineering approach, PD3D® models are already applied in personalized oncology to identify treatment for an individual patient. We successfully established a living biobank of more than 500 PD3D® models, spanning from common cancers like colorectal, breast (incl. TNBC), non-small cell lung and pancreatic carcinoma, to orphan indications including various subtypes of sarcomas. Not surprisingly, PD3D® model morphology and culture requirements differ between tumor entities. Treating PD3D® models with standard of care drugs in a semi-automated high-throughput assay, we observed heterogeneity in drug sensitivity between models of the same cancer type, recapitulating clinical response of patients. Combining drug sensitivity profiles with genomic and proteomic data of the same PD3D® models, we successfully identified a biomarker for predicting chemosensitivity towards MEK-targeting drugs. For application of PD3D® in truly personalized oncology, we developed a protocol that allows us to generate a PD3D® culture and perform a drug sensitivity assay for an individual patient within a therapy-relevant timeframe. Within 38 days we identified a systemic therapy for a young patient with a relapsed metastasized synovial sarcoma. After surgery and initiation of recommended chemotherapy, the patient is now under remission. To further expand the scope of PD3D® for therapy response prediction, we established a method for irradiation of PD3D® cultures with different dosages of photon and proton radiation. We observed significant, model specific differences in radiosensitivity between PD3D® sarcoma models which also reflect clinically heterogenous responses. Additionally, PD3D® models can be employed for a tumor organoid-on-chip platform (TumOC), delivering real-time information on physiological parameters like drug response-mediated oxygen consumption in a microfluidic system. In conclusion, PD3D® models act as jacks-of-all-trades in current and future cancer research, delivering robust and reliable data that not only is of academic value, but speeds up the drug development process, and are ready for prime time in functional precision oncology.

#4236 PDX-derived organoids (PDXO) are valuable tools to unveil the shortcomings of new anti-cancer drug candidates.

Y. Wang, L. Feng, H. Liu, J. Zhang, K. Hu, P. Pan, F. He;
Pharmaron, Inc., Beijing, China

Introduction: Tumor organoids are increasingly being used as predictive preclinical cancer models, as they reflect the original tumor features and patient drug responses. However, systematic comparisons between organoids and traditional 2D cell lines or 3D spheroids are lacking.
Method: We established over 30 PDX-derived organoid (PDXO) models with KRAS mutations and tested three inhibitors targeting the KRAS pathway: VS-6766(RAF/MEK inhibitor), Trametinib (MEK inhibitor), and MRTX1133 (a Phase II drug targeting KRASG12D) against these models.
Results: IC50 results indicated that most models responded to treatment. For some cell lines we detected differential drug responses in 2D vs. 3D testing with 3Dspheroids being more sensitive to inhibitors than 2D cell lines (on average ~10 fold). PDXO models exhibited greater individual differences in drug response, with a subset of models demonstrating no sensitivity to MRTX1133. This is consistent with published results showing that some KRASG12D-mutant PDX models were less sensitive to MRTX11331. Similarly, the clinical trial data for the KRASG12C inhibitor Adagrasib revealed distinctions in the response of patients2. Further analysis with WES (whole exome sequencing) and RNA-sequencing identified potential genotypic mutations and differential expressions of signaling pathways related to drug resistance. Subsequent drug combination testing showed that targeting these pathways could enhance the MRTX1133 efficacy in the resistant PDXO models.
Summary: Our research confirms that drug testing on organoids predicts responses in mouse models and clinical trials. In combination with multi-omics and bioinformatics analysis, the platform can be used for evaluating drug resistances, identifying new targets, developing new drug combination therapies, and ultimately improving the creation of new cancer therapeutics.

#4238 Modeling*RET*-rearranged non-small cell lung cancer (NSCLC): Generation of lung cell progenitors from patient-derived induced pluripotent stem cells (iPSCs).

P. Marcoux, J. Hwang, C. Desterke, J. Imeri, A. Bennaceur Griscelli, **A. Turhan**;
Universite Paris Saclay, Villejuif, France

Rearranged during Transfection (RET) oncogenic rearrangements can occur in 1-2% of lung adenocarcinomas. While RET-driven NSCLC models have been developed using various approaches, no model based on patient-derived induced pluripotent stem cells (iPSCs) has been described yet. Patient-derived iPSCs hold great promise for disease modeling. However, generating iPSCs with specific oncogenic drivers, like *RET* rearrangements, presents challenges due to reprogramming efficiency and genotypic variability within tumors. To address this issue, we aimed to generate lung progenitor cells (LPCs) from patient-derived iPSCs carrying the somatic mutation RET^{C634Y} which is commonly associated with hereditary medullary thyroid carcinoma. Additionally, we have established a RET^{C634Y} knock-in iPSC model to validate the effect of this oncogenic mutation during LPC differentiation. We successfully generated LPCs from RET^{C634Y} iPSCs using a 16-days protocol and showed an overexpression of cancer-associated markers as compared to control iPSCs. Transcriptomic analysis revealed a distinct signature of NSCLC tumor repression, suggesting a lung multilineage lung dedifferentiation, along with an upregulated signature associated with RET^{C634Y} mutation potentially linked to poor NSCLC prognosis. These findings were validated using the RET^{C634Y} knock-in iPSC model, highlighting key cancerous targets such as *PROM2* and *C1QTNF6*, known to be associated with poor prognostic outcomes. Furthermore, the LPCs derived from RET^{C634Y} iPSCs exhibited a positive response to the RET inhibitor Pralsetinib, evidenced by the downregulation of the cancer markers. This study provides a novel off-the-shelf iPSC model of RET-driven NSCLC, paving the way for exploring the molecular mechanisms involved in RET-driven NSCLC to study disease progression and to uncover potential therapeutic targets.

#4239 Pancreatic cancer organoids from the Human Cancer Models Initiative biobank reflect disease genotypes, capture patient heterogeneity, and are amenable to therapeutic screening.

S. Friend, R. Demerath, M. Graziano, **J. Clinton**;
ATCC, Gaithersburg, MD

Pancreatic cancer is the fourth leading cause of cancer-related death in the United States (~3% of all cancer cases) and has one of the lowest 5-year relative survival rates. There is a lack of clinically representative, easily available, validated, in vitro pancreatic cancer models that reflect the genomic and phenotypic diversity of the disease. The Human Cancer Models Initiative (HCMI) is an international collaborative project devoted to the development and distribution of approximately 1,000 novel human primary tissue-derived tumor models supported with clinical and molecular annotation. These models were manufactured, characterized, and validated at a not-for-profit biobank and made available for academic and commercial use in basic research, compound screening, and drug development. Available pancreatic cancer organoids (PCOs) from the HCMI biobank (n=46 unique models, n=41 unique donors) were acquired and subjected to a targeted next-generation sequencing hybridization capture, pan-cancer panel of 663 genes. Data were compared to publicly available clinical and genotyping results from the patient's tumor (n=42) that the model was derived from as well as cancer datasets such as The Cancer Genome Atlas (TCGA). A subset of models was cultured following standard procedures and tested for response to chemotherapeutics (cisplatin, nab-paclitaxel), KRAS-targeting inhibitors (MRTX1133, KR-pep-2D), or PARP inhibitors (PJ34, olaparib) at three time points. A luminescent ATP viability assay was used to assess response. PCOs from the HCMI were predominantly derived from primary tumors (75%), had an adenocarcinoma ductal histological type, and were from female patients (56%) with an average age of 65 years at diagnosis. Models had mutations in key disease-relevant driver genes including KRAS, TP53, SMAD4, and/or CDKN2A at frequencies similar to the TGCA cohort. Sequencing revealed mutations in genes less commonly associated with pancreatic cancer, including BRCA, APC, BRAF, TGFBR2, and ARID1A, albeit at lower frequencies. Most models had mutations in KRAS including G12D, G12V, G12C, and G12R variants. Significant but not complete concordance was seen in comparison with the mutation status of the patient's respective tumor, indicating potential genotypic drift had occurred. Response to acute treatment varied by model, genotype, timepoint, and drug. Chemotherapeutics like Cisplatin were broadly cytotoxic while MRTX1133 exhibited greater toxicity in models with KRAS G12D variants as compared with KRAS wild type. Patient-derived cancer organoids from the HCMI recapitulate genotypes seen in patient populations and respond to therapeutic treatment in vitro.

#4240 A comprehensive i*n vitro* tumor model: One-stop simultaneous isolation and culture of tumoroids, CAFs and TILs for advancing immuno-oncology research.

Y. KO[1], S. Kim[1], H. Park[1], S. Jang[2];

[1]AMIST, Asan Medical Center, University of Ulsan College of Medicine, Seoul, Korea, Republic of, [2]Asan Medical Center, University of Ulsan College of Medicine, Seoul, Korea, Republic of

The tumor microenvironment (TME), composed of a diverse array of cells, jointly participates in tumor formation and has attracted attention as a direct or indirect therapeutic target. Among the tumor-forming cells, cancer cells, cancer-associated fibroblast (CAF), and tumor-infiltrating lymphocytes (TILs) comprise major proportion and players in tumor biology. Therefore, an in vitro tumor model composed of at least above three major cellular players better mimics a patient's tumor. Here, we developed a patient-derived tumor model containing tumoroids, CAFs and TILs isolated from the patient's tumor tissue by using one-stop isolation culture system. Our one-stop culture system utilizes a Transwell-based method that concurrently segregates cancer cells, CAFs, and TILs based on distinct characteristics such as cell size, migration speed, and growth. Lung tumoroids, fibroblasts, and TILs segregated in Matrigel-coated upper Transwell chamber, Transwell pores and in the lower chamber, respectively. Lung tumoroids maintain the patient's lung cancer tissue characteristics and genetic features during extended *in vitro* cultivation. Fibroblasts extracted from the Transwell pores exhibit significant similarity to CAFs found in patient tissue. TILs in the lower part of the Transwell chamber closely resemble those found in the original cancer tissue analyzed by FACS. We have also refined the functionality of TILs through a two-week expansion process. Patients' tumor composed of 0.15 to 95.3 % of EpCAM positive tumor cells, 0.14 to 19.4 % of CD90 positive fibroblasts and 3.98 to 91.2 % of immune cells in FACS analysis. By reassembling three main cellular components of the tumor in a proper proportion, we developed a co-culture platform for a patient-derived tumor model reproducing patient-specific TME conditions. The co-culture platform showed a potential not only for an experimental model but also to use a predictive test of personalized immunotherapy responses for lung cancer patients.

#4241 Development of stroma cells-rich oral cancer organoid for functional analysis of tumor microenvironment.

A. Shimoda, S. Shiiya, H. Yoshii, K. Mitsudo, M. Kioi;
Yokohama City Univ. School of Medicine, Yokohama, Japan

Background: Tumor microenvironment (TME), composed of cancer cells, endothelial cells, fibroblast, immune cells, and etc, plays crucial roles in tumor progression and treatment resistance. Thus, it is extremely important to find its role involved in the interaction of TME. However, it is more difficult to examine the biological activities of those cells in vitro assay. The purpose of this study is to develop stroma cells-incorporating preclinical model, termed stroma cells-rich oral cancer organoid, for functional analysis of TME.
Materials and Methods: We have first developed the stroma cells-rich oral cancer organoid by selecting the types of stroma cells such as endothelial cells, fibroblast, ratio of those cells, culture method, 3-D methods, culture media, and supplement of growth factors. Then, growth rate, morphology, radiosensitivity, and drug response were analyzed to investigate the effect of TME. Finally, the function of tumor-associated macrophage was determined using this organoid model. The growth rate of cancer cells and drug response were investigated using the organoid treated with supernatant of M1 and M2 macrophages polarized from THP-1 monocyte.
Results: Oral cancer cells were co-cultured with endothelial cells (ECs) and mesenchymal stem cells (MSCs) in a particular ratio in 3D-culture, and the formed organoid became sphere. The vascular formation in the organoid was confirmed by immunofluorescent analysis. The organoid also showed higher tumorigenicity in nude mice when inoculated, compared to cancer cells alone or mixed cells with ECs and MSCs. Cell viability of luciferase-expressing tongue cancer cells (OSC-19-luc) in the organoid was assessed after treatment with cisplatin using the IVIS system showing that OSC-19-luc organoid was resistance to cisplatin compared to 3D-cultured OSC-19-luc alone or OSC-19-luc co-cultured with ECs/MSCs. The supernatant of M1 or M2 macrophage had no effect on cancer cell growth in the organoid. However, when the organoid was treated with cisplatin in the presence of M2 macrophage supernatant, the drug sensitivity was low compared to those of M1 suggesting that secretory factor from M2 macrophage may lead to drug resistance of oral cancer cells in the presence of TME.
Conclusions: We have successfully established stroma cells-incorporating preclinical model that recreates the tumor microenvironment by co-culturing stromal cells. This will serve as a platform that can recapitulate the tumor biology and drug response profiles of cancer cells derived from individual oral cancer patients. This will also enable us to elucidate the role of other factors in TME and to identify novel targets for the treatment of chemo-resistant oral cancer.

#4242 Preserving lung cancer patient mutations in 3D organoid models: Advancing cancer research through innovative culture systems.

J.-y. Park, S. Gu, J. Lee, N.-G. Lee, D. Choi, S. Park, J. Kim, J. Rheey;
Gradiant Bioconvergence, Seoul, Korea, Republic of

Lung cancer is one of the most prevalent cancers worldwide. There are currently many anticancer drugs available, but they have numerous issues in terms of treatment, such as drug resistance and recurrence. Culturing systems that can replace a patient's cancer tissue are crucial, and the existing 2D culturing systems have many limitations. Patient-derived cancer organoid culture is the most advanced culture system for understanding mechanism of cancers. Using a 3D organoid culture system, we have successfully established a culture system for lung cancer using biopsy/surgical specimens and malignant effusions, including a long-term culture system. There are two critical indicators to determine the success of 3D organoid culture. One is whether the organoids retain their cancer-specific mutations from patient's lung cancer tissue, and the second is whether the organoids grow well and can be maintained in long-term culture for more than 20-30 passages. We typically assess gene mutations in EGFR, ALK, ROS, and P53 when evaluating lung cancer organoids. We confirm these mutations when we establish organoids, and currently we have established a total of 127 patient-derived lung cancer organoids. Among the 127 organoids, we completed NGS analysis on 108 of them and validated that 86.5% exhibit similarity when compared to lung cancer tissues. Additionally, we achieved a 100% retention of mutations in the long-term culturing of these organoids. Our studies indicate that patient-derived lung cancer organoids represent a meaningful organoid system for cancer tissue replacement and treatment response in the context of precision cancer medicine.

#4243 Revolutionizing cancer research, new drug screening approach with vascularized cancer organoid platform mimicking patient tumor microenvironment.

M. Lee, Y.-J. Yoon, **Y.-S. Lee**, J. Rheey;
Gradiant Bioconvergence, Seoul, Korea, Republic of

Patient-derived organoids (PDOs) are improving our understanding of cancer heterogeneity and personalized medicine. In particular, patients' intrinsic and acquired treatment resistance is being evaluated with PDOs, which has become an essential factor in developing new anticancer drugs and designing successful clinical trials. However, there are obstacles to cancer heterogeneity and patient-specific cancer therapy due to lack of understanding of tumoral diversity resulting from the tumor microenvironment (TME). Complex direct and indirect interactions between various types of TME cells and the resulting tumoral diversity are challenges that must be addressed for customized cancer therapy. Standard cancer therapy targets tumor cells without considering possible damage on the tumor microenvironment that could impair therapy response. Therefore, the construction and analysis of a platform for co-culturing cancer organoids with other cell types that make up the TME over a long period of time is necessary. We generated and performed characterization of blood vessel organoid (BVO). The BVO expressed endothelial marker CD31 and pericyte marker PDGFRβ. We attempted to co-culture with patient-derived lung cancer organoid (LCO) on Matrigel by dissociating the constructed BVO, and it was confirmed that BVO and LCO were interconnected after 10 days. This new platform was treated with Gefitinib and Poziotinib, and after 5 days of drug treatment, the IC50 value increased compared to LCO-only culture. Additionally, flow cytometry analysis confirmed that co-culturing with BVO during drug treatment resulted in a lower percentage of dead LCO cells compared to LCO-only culture. Image-based analysis also verified that co-culturing with blood vessels enhances the viability of LCOs when treated with drugs. Taken together, the co-culture of cancer organoids and BVOs present a platform that closely mimics the in vivo TME compared to the existing cancer organoid culture method. This innovative platform demonstrates higher drug resistance than existing approaches, offering a novel method for drug screening.

#4244 Clinical response assessment of immune checkpoint inhibitors in mismatch repair-deficient endometrial cancer using a T cell organoid coculture system.

Ju Hee Oh, Eun Hye Choi, Ji Eun Lee, Eun Ji Nam

Yonsei University College of Medicine, Seoul, Korea, Republic of

Endometrial cancers with the mismatch repair deficiency (MMR-D) phenotype exhibit characteristics such as an increased burden of tumor mutations and the presence of tumor-infiltrating lymphocytes (TILs) involved in tumor invasion. While monotherapy using immune checkpoint inhibitors (ICIs) has shown clinical improvement in MMR-D endometrial cancer (EC), observed response rates ranging from 30% to 50% suggest the existence of inherent resistance mechanisms. One notable feature of MMR-D tumors is the high proportion of tumor-infiltrating lymphocytes (TILs) encompassing various lymphocytes with diverse effects on immune interactions. Therefore, we aim to assess the feasibility of a self T-cell-tumor organoid co-culture platform for individual MMR-D endometrial cancer patients. We provide evidence that co-culturing self-tumor organoids with peripheral blood lymphocytes can be utilized to evaluate ICI responsiveness in MMR-D endometrial cancer patients. The application of a specific T-cell organoid co-culture platform to a cohort of patient resistant to monotherapy ICIs offers a means to anticipate the timing for minimal immunotherapeutic intervention and the appropriate timing for combination therapy.

#4245 Selection of AAV capsids by evaluating transgene delivery using human organoid models.

Y. Fu[1], Z. Qi[2], Z. Zuo[2], S. Chiang[2], **A. Ouyang**[3], G. Gao[2], S. Guan[2], J.-Q. Chen[3], R. Zhang[2], C. Wang[1];
[1]Innovec Biotherapeutics, Beijing, China, [2]ACROBiosystems, Beijing, China, [3]ACROBiosystems, Newark, DE

Recombinant adeno-associated viruses (AAVs) play a pivotal role in gene therapy, a promising approach aimed at treating various genetic disorders by introducing modified genetic material into cells or tissues. These AAV capsids are utilized as a vector in transferring genetic material into host cells. In discovery research, many AAV serotypes are developed in parallel to identify the optimal subtype for subsequent preclinical and clinical use. However, gene therapies have found limited success in clinical translation, in part, due to variable transgene delivery efficacy between traditional in vitro and in vivo models and human models. This study presents an organoid-based approach that mimics human physiology, as well as organ-specific features and cell diversity within an organ. Organoids are 3D structures derived from stem cells that resemble the cellular architecture and functionality of a specific organ. Compared to conventional 2D cell cultures, organoids provide a more comprehensive modeling of complex cell signaling, cell-cell and cell-extracellular matrix interactions, simulating the complex interplay between various cell types and functions. Within this study, several human-based organoid models were built, cerebral and cardiac, and verified by identifying the expression level of known marker genes through RNA sequencing. Five different AAV serotypes were utilized to evaluate transgene efficacy using each type of organoid model. Expression of delivered GFP transgene within each organoid was then compared to evaluate transduction and select the optimal AAV serotype in comparison to commercial wild-type AAVs. We outline the use of human organoid as an improved preclinical model for selecting AAV serotypes and evaluating transgene delivery efficacy to help provide better guidance for gene therapy development when moving into clinical research.

#4247 Miniaturizing patient-derived organoid screening assays for predictive drug testing.

Y. Abouleila[1], R. Verkerk[1], M. Doorn[1], T. Voskuilen[1], G. Harada[2], M. Watanabe[2], L. Smabers[3], H. Kyan[2], T. Kumagai[2], Y. Hikichi[2], R. Overmeer[1], J. Roodhart[3], K. Matsuno[2], C. Verissimo[1], S. Boj[1];

[1]HUB Organoids, Utrecht, Netherlands, [2]Yamaha Motor, Shizuoka, Japan, [3]Utrecht Medical Center, Utrecht, Netherlands

Colorectal cancer (CRC) ranks as the third leading cause of both cancer incidence and cancer-related mortality. A significant portion of CRC patients diagnosed with de novo metastatic disease face limited benefits from conventional treatment options, often accompanied by substantial side effects. This underscores the pressing need for more effective preclinical models to predict patient responses in clinical settings. Patient-derived organoids (PDOs or HUB Organoids®) represent a pivotal breakthrough in preclinical modeling. These organoids are directly derived from patient tissue, faithfully mirroring the patient's disease. While HUB Organoid Technology is currently applicable for preclinical drug screening, it is essential to expedite the transition from patient diagnosis to the delivery of PDO-based results to directly benefit patients. In a collaborative effort with Yamaha Motor, we have optimized the Yamaha CELL HANDLER™ for the automated transfer of organoids, offering enhanced precision and efficiency in handling a significantly reduced number of organoids per screening plate, compared to conventional methods. Moreover, we have developed an image-based readout system that enables precise quantification of organoid numbers, ensuring high assay quality. Utilizing this developed automated platform, we conducted a proof-of-concept investigation into PDO responses to chemotherapy in comparison to corresponding patient responses. The correlation between PDO and patient responses demonstrated a strong connection, highlighting the potential of the developed automated platform for predictive drug testing. In summary, this work signifies the development of an automated workflow that synergizes patient-representative HUB Organoids® with cutting-edge robotics from Yamaha Motor. The described workflow reduces the number of organoids needed per screening well, streamlining patient response prediction, potentially leading to faster diagnoses, and ultimately optimizing patient outcomes.

#4248 Patient-derived MTAP-deleted bladder cancer organoid model: A unique platform for drug development.

M. Schwermann[1], B. Carneiro[2], S. Lu[2], A. De Souza[2], M. Hadfield[2], A. Mega[2], G. Lagos[2], S. Khaleel[2], D. Golijanin[2], S. Holder[2], P. Srinivasan[1], W. MacDonald[1], A. George[3], L. Zhou[1], L. Zhang[1], W. El-Deiry[2];

[1]Legorreta Cancer Center at Brown University, Providence, RI, [2]Legorreta Cancer Center and Lifespan Cancer Institute at Brown University, Providence, RI, [3]Yale School of Medicine, Providence, RI

Introduction: Approximately 30% of advanced bladder cancer (BCa) tumors exhibit MTAP gene deletion, which has been associated with luminal subtype BCa, poor response to chemotherapy, and shorter progression to metastatic disease (De Souza 2023). MTAP deletion has been proposed as a potential biomarker for response to pemetrexed and an emerging class of PRMT5 and MAT2A inhibitors in development for MTAP-deleted tumors. Here, we describe the first patient-derived 3D model of BCa with MTAP deletion and its translational potential as a drug sensitivity platform.

Methods: A patient (pt) with metastatic BCa harboring MTAP deletion underwent a pelvic lymph node biopsy. A fresh tumor sample was processed under collagenase/dispase solution for 30 minutes and filtered through a 70-um cell strainer. Cells were cultures in low attachment plates with MammoCult™ Basal Medium (Stem Cell Technologies). After 5 passages and 3D spheroid formation, immunostaining for cytokeratin (CK) 5 and 6, GATA3, CK20, and Ki67 staining were performed to confirm the urothelial origin. The MTAP-del was confirmed by a western blot of the organoid specimen and compared to other BLCa cell lines (UMUC, RT4, J82, and 5637). The viability assays were performed using the CellTiter-Glo® 3D Cell kit. Next-generation sequencing (NGS) of primary BCa tumor revealed deletion of MTAP, CDKN2A, CDKN2B, and mutations in p53, TERT, and KDM6A.

Results: The patient organoid sample was positive for the luminal CK5/6 markers and negative for GATA3. Ki67 and CK20 were primarily expressed in the nucleus of the same sample. The organoid retained morphologic and immunohistochemical features of the patient's primary bladder tumor, showing the same squamous differentiation and similar Ki-67 proliferative index. The organoid displayed no evidence of the MTAP protein by western blot (similar findings with the MTAP-del cell lines UMUC and RT4). The organoid showed sensitivity to pemetrexed [pemetrexed IC50=0.12 uM (other MTAP-del BLCa IC50: 0.1-0.23 uM)] and resistance to gemcitabine and cisplatin [Gem IC50=55 nM (other BLCa IC50: 1-29 nM), Cis IC50=90.5 uM (other BLCa IC50: 2-17 uM).

Conclusions: We describe the first patient-derived MTAP-deleted BCa organoid recapitulating the features of the primary tumor. The organoid displayed sensitivity to pemetrexed as described with MTAP-deleted BCa. The organoid represents a unique platform for testing novel therapeutic strategies for MTAP-deleted BCa.

#4249 Establishment and analysis of patient-derived high-grade serous ovarian cancer organoids for disease modeling and drug testing.

T. Kallunki[1], A. R. Lauridsen[1], A. Skorda[1], A. Lahtinen[2], M. L. Bay[1], B. Rasmussen[1], K. Huhtinen[2], T. Muranen[2], J. Oikkonen[2], J. Hynninen[3], S. Hautaniemi[2]; [1]Danish Cancer Institute, Copenhagen, Denmark, [2]University of Helsinki, Helsinki, Finland, [3]University of Turku and Turku University Hospital, Turku, Finland

Purpose: Ovarian cancer is the most lethal gynecologic cancer. Majority of ovarian cancers belong to the subgroup of high-grade serous ovarian cancer (HGSC). Its standard treatment is surgery and chemotherapy with platinum and taxane-based compounds, for which almost all patients become resistant. We have established a panel of patient derived 3-dimensional (3D) HGSC long-term tumor organoid cultures for personalized disease modeling, drug screening and evaluation of the efficiency of potential new treatments to be used in preclinical research.

Methods: Tumor tissues or ascites from > 30 HGSC tumors were set up as long-term 3D organoid cultures (PDOs). RNA and whole genome sequencing was performed from the original tumors and from PDOs. Pluripotency and proliferation were assessed via high-throughput immunofluorescent detection of PAX8 and Ki67. Resistance towards standard treatment and response to additional selected drugs and drug combinations were evaluated in cell death and proliferation assays. Imaging and image-based quantifications were performed under 3D setup. PDOs were set up for *in vivo* drug testing in immunodeficient NOD/Shi-scid/IL-2Rgnull (NOG) mice.

Summary: A set of HGSC PDOs of different longitudinal, prospective, and multiregional samples has been established representing the three evolutionary states of HGSC: evolving, maintaining and adaptive state. They are ready to be used as rational and effective models for studying drug interventions. Supportively, results of preclinical studies with PI3K inhibitor Alpelisib matched the published patient responses. Tumor evolutionary analysis based on data of longitudinal, prospective, and multiregional collected samples suggest further targetable pathways that can mediate chemotherapy resistance and pinpoint potential targets for drug intervention.

Conclusion: Inhibition of these pathways with simultaneous targeting of other cellular functions, such as lysosomal-mediated cell death, may be highly effective alternative treatment option. 3D imaging and efficient image analysis are necessary tools to understand tumor organoid biology and drug responses to assist development and pre-clinical evaluation of new treatments. This study is a part of the DECIDER project (https://www.deciderproject.eu/, NCT04846933).

#4250 Adherent and spheroid cell models of patient-derived xenograft for drug development and translational research.

Lars Winkler, Joshua Alcaniz, Maria Stecklum, Wolfgang Walther, Jens Hoffmann

Experimental Pharmacology and Oncology Berlin-Buch GmbH, Berlin, Germany

Introduction: The development of new drugs in cancer therapy comprises toxicity and efficacy tests with increasing complexity. First and foremost, in vitro experiments are performed with well-established cancer cell lines, which are subsequently validated in animal experiments as prerequisite for clinical trials. Until a few years ago, there were gaps in the complexity chain between in vitro and in vivo experiments. Ethical considerations have led to use of systems like organ on a chip or mini-organ 3D in vitro models. In cancer research, cell cultures or organoids are generated from patient tumor material. However, these cultures only reflect the tumor of one patient, which is why panels of patient tumors should be used to evaluate the effectiveness of drugs on different patients. In vivo panel screens of patient derived xenografts (PDX) mouse models need high numbers of animals and takes several months. A pre-screen with in vitro models generated from in vivo PDX tissues allows large scale and faster pre-screens complementing in vivo systems for more focused in vivo analyses.
Methods: Currently we have a pool of more than 600 established PDX models of 21 tumor entities. From this pool, cancer tissues of glioblastoma, mesothelioma, gastric, head/neck, lung and breast cancer were processed in single cell suspensions and cultured under defined conditions to obtain adherent cells or spheroids. The generated PDX in vitro cultures were analyzed for cellular impurities, cancer stem cell content and perpetuation of *in vivo* PDX characteristics. FACS analyses for tumor specific markers, chemo sensitivity assays and growth characteristics of the PDX derived cell lines (especially for glioblastoma) were analyzed.
Results: From PDX tissues used, 90% grew as adherent and/or spheroid PDX derived in vitro cultures, in which mouse cells were entirely depleted. A high percentage of these cultures showed enriched cancer stem cell features and stem cell marker expression. Tumor marker expression and standard drug sensitivity data correlate to the in vivo PDX and derived in vitro cell culture models. RNAseq data were used to predict drug sensitivities in silico for untested drugs and drug combinations on our newly established PDX derived glioblastoma cell lines. Initial screens with predicted candidates were performed. Promising conditions were successfully repeated in corresponding animal PDX models.
Conclusion: The newly developed technology for establishment if in vitro cell cultures from PDX efficiently generates stably growing cell lines possessing all key features of the original PDX. These cell lines can be used for initial pre-screens to optimize and improve selection of pharmacologically active drugs or drug combinations before initiating in vivo PDX studies.

#4251 Establishment of hormone-dependent endometrial tumoroids in a conditioned-medium free, serum-free medium.

C. Yankaskas, B. Balhouse, C. Paul, P. Shahi Thakuri, S. Salen, M. Kennedy, M. Dallas, D. Kuninger;
Thermo Fisher Scientific, Frederick, MD

Tumoroids, also known as cancer organoids, are self-assembled three-dimensional cultures of patient-derived tumor cells. Compared to traditional 2D cancer cell lines, tumoroids better maintain key characteristics of the original tumor including the genotype and transcriptome, which lead to better *in vitro* modeling of clinically relevant functional responses such as drug sensitivity. An under-studied aspect of tumoroid cultures has been their ability to recapitulate dependence on hormone signaling *in vitro*, with some reports indicating hormone dependence is lost over time in culture. To investigate this, we utilized Gibco™ OncoPro™ Tumoroid Culture Medium and defined tissue-specific supplements, FGF10 and beta-estradiol, that when added to the medium enabled the derivation of endometrial tumoroids from tumor resections. Derivation of tumoroid lines compatible with long-term growth depended on a variety of factors, including tissue quality and time from resection to culture initiation. Each of the 15 samples processed formed tumoroids when initially seeded into culture. 11/15 samples reformed tumoroids through multiple passages (typically 1-2 weeks per passage) over 1-3 months in culture. 7/15 samples met our high criteria for stable tumoroid line growth of >5 passages and reaching >5 cumulative population doublings (from initial number of cells seeded post-resection) in culture. Next-generation sequencing of the established tumoroids and the uncultured tumor material demonstrated a high degree of correlation (pearson's r>0.9) of genomic mutations in a targeted panel; few differentially expressed genes were detected beyond down-regulation of immune-related genes, presumably because the medium is optimized for outgrowth of cancer epithelial cells, and immune cells do not persist during long-term culture. Endometrial tumoroids were capable of growing embedded in basement membrane extract (BME) or in suspension with dilute BME added and could be cryopreserved and recovered. Endometrial tumoroids retained gene expression levels (both presence and absence) of estrogen receptor and progesterone receptor for up to the 20 passages tested *in vitro*. A subset of the models was tested and showed increased growth rates in response to increased concentrations of beta-estradiol. Of those tested, 2/3 tumoroid cultures stopped growing within 1-2 weeks after removal of beta-estradiol from the medium, demonstrating dependence on this hormone for growth. Maintenance of hormone receptor expression and dependency should enable *in vitro* studies to understand the signaling mechanisms and potential ways to modulate them in the context of cancer. Overall, this method provides a toolset for studying endometrial cancer, particularly hormone dependency, and may be more broadly applicable to other gynecological or hormone dependent cancers.

#4252 Evaluation of NXI-101 in non-small cell lung cancer (NSCLC) using patient-derived organotypic tumor spheroids (PDOTS): Targeting a novel tumorigenic pathway.

J. Vail[1], H. Maeng[2], J. Jang[2], K. Boo[2], J.-I. Youn[2], A. Martin[1], A. Goldman[3], K. Yoon[2], **M. A. Perricone**[1];
[1]Xsphera Biosciences, Inc., Boston, MA, [2]NEX-I, Seoul, Korea, Republic of, [3]Harvard Medical School, Boston, MA

ONCOKINE-1 (OK-1), a soluble protein that is released by tumor cells, is implicated in the resistance of immunotherapy. Here we evaluated the efficacy of NXI-101, a monoclonal antibody that binds and neutralizes OK-1, in a model of patient-derived organotypic tumor spheroids (PDOTS) derived from non-small cell lung carcinoma (NSCLC) patients. NSCLC PDOTS were treated with NXI-101 and the effects of the drug were evaluated on day 3 post-treatment. Cytotoxicity was measured by Hoechst/Propidium Iodide staining and quantified by measuring the area-weighted percentage of cell death. Significant cytotoxicity was observed in 2 out of 10 patient tumors (20%) as a monotherapy and 4 out of 10 (40%) when used in combination with atezolizumab. The therapeutic response for both treatments was positively correlated ($p<0.05$) with the level of OK-1 expression, determined by immunohistochemistry using tissue sections taken on the day of tumor specimen collection. NXI-101 alone and in combination with atezolizumab had immunomodulatory effects that were associated with cytotoxic response. For example, transcriptomic analysis, Nanostring IO 360 Panel, indicated that the drug treatments resulted in the inhibition of TGF-β pathways and stimulated a number of immune pathways in 3 of the 4 responsive PDOTS. These pathways include interferon-α, JAK-STAT, and dendritic cell activation markers. We also observed evidence of activation of these same pathways in 2 of the 6 non-responsive PDOTS. These data support the prospects of NXI-101 as a first-in-class therapeutic for the treatment of NSCLC when used alone or in combination with an immune checkpoint inhibitor. Moreover, the findings highlight the PDOTS platform's substantial value in capturing patient-specific tumor response variability and providing robust support for the mechanistic evaluation of cancer therapeutics.

#4253 High expression of specific gene profiles in organoids from African American pancreatic cancer tumors.

B. D. Lyn-Cook[1], F. Nouri Emamzaden[2], B. Word[2], G. Hammons[2];
[1]FDA-NCTR (National Center for Toxicological Research), Jefferson, AR, [2]National Center for Toxicological Research, Jefferson, AR

Pancreatic cancer remains one of the leading causes of cancer-related deaths in the United States with limited therapies for advanced stages of this disease. African Americans have the highest morbidity and mortality rates of pancreatic cancer compared to other racial groups. Many factors are known to contribute to this disparity such as, socioeconomic and lifestyle factors. One of the major factors contributing to this disparity is the lack of African Americans with pancreatic cancer in clinical trials or genomic databases. In order to gain insight into the biology or genetic differences that may exist in signals driving the aggressiveness of this cancer in this population more studies are needed. Innovative *in vitro* models are needed to investigate possible differences in molecular changes that may exist in African Americans. Studies have shown that organoids developed from metastatic and primary tumors can give sights into genetic and epigenetic changes detected in several type of cancers. Using a Human Pancreatic Adenocarcinoma TagMan Array 96 (Applied Biosystems), which contained 76 genes known to be expressed in pancreatic cancer, pancreatic organoids from African American metastatic tumors revealed high expression levels of specific genes. Usually K-ras is highly expressed in pancreatic tumors but it was not significantly expressed in the organoids from African Americans metastatic tumors. However, preliminary results from organoids, compared to pancreatic cancer cell line spheroids, showed significantly increased gene expression of HSP90AA1 (13-fold), MMP1(36-fold), BRACA2 (20-fold), MDM2 (19-fold), RB1 (14-fold), Rel (12-fold), STAT1 (15-fold), STAT5B (5-fold), and TGFBR1 (1- fold). High expression of HSP90AA1 is related to poor prognosis, constitutively expression of STAT5B confers gemcitabine chemoresistance and promote invasiveness, and mutations in BRCA2 can increase pancreatic cancer risk. Further studies are being done to validate these findings in African American pancreatic tumors and to ascertain their relevance to the metastatic progression phenotype.

#4254 Genetically engineered human lung organoid models for lung cancer evolution study.

S. Moon, R. Kim, D. Lee, K. Park, W. Lee, S. Lee, Y. Park, J. Kim;
Genomic Medicine Institute, Medical Research Center, Seoul National University, Seoul, Korea, Republic of

Initial cellular events in a transitional period from normal to cancer cells, such as transcriptomic or epigenetic dynamics, are poorly understood. Observing these is more challenging than in cancer progression, especially for humans. Mapping this phenomenon in early cancer evolution is crucial, as we can identify targetable molecules to inhibit cancer development at the precancerous stage. Immortalized human cancer cell lines hardly capture these appropriately as they have lost usual cellular characteristics. Normal organoids harbor stem cells and their differentiated cells, reflecting the epithelial physiology of tissues, and are more suitable models for cancer evolution studies. To establish a human cancer development model in vitro, we genetically engineered normal human airway organoids derived from adult stem cells into small cell lung cancer (SCLC). We used CRISPR-Cas9 systems to induce non-homologous end-joining in both *TP53* and *RB1*, the most frequently mutated genes of SCLC. First, we knocked out *TP53* of the airway organoids, selected by Nutlin-3a, an MDM2 antagonist, for 3-4 weeks, demonstrating 88-89% editing efficiencies calculated from Sanger sequencing results. Most mutations were one base pair deletion or insertion, which induced frameshift mutation in *TP53*. They did not show a significant difference from wild-type organoids morphologically at bright-field microscopy. Subsequently, we targeted *RB*1 on *TP53*$^{-/-}$ airway organoids to induce SCLC. We used Palbociclib, a CDK4/6 inhibitor, to enrich the mutated cells. They had 67.1% efficiency, and 20.4% had a 7-base pair deletion mutation. In the initial period, they seemed to have similar shapes to *TP53*$^{-/-}$ organoids. Unexpectedly and interestingly, however, we noticed more rapidly proliferating and disorganized organoids disrupting their original round shapes appeared in 4-5 weeks. The cells were indiscriminately piled up on the airway organoids' apical and basolateral surfaces, indicating their malignant traits. Their chaotic proliferation represented the rapidly progressing clinical feature of SCLC with a median survival of 7-16 months with treatment. This is the first work constructing the SCLC development model from the normal human airway organoid. By sequentially single-cell sequencing this organoid model changing to tumorous condition, we can capture the multi-omics landscape during the initial evolution of SCLC.

#4255 A systematic framework for efficient generation of expandable patient-derived 3D sarcoma models.

C. Dagostino[1], W. Hussain[1], J. Paluncic[1], M. Zoccoler[2], J. Pablik[3], D. Richter[1], L. Knol[1], A. Banito[4], J. Wagner[5], I. Mateska[6], D. E. Stange[3], I. Oehme[7], S. Richter[8], S. M. Pfister[4], S. Frohling[9], C. Scholl[10], J. Weitz[11], K.-D. Schaser[12], C. Heining[1], H. Glimm[1], C. R. Ball[1];

[1]National Center for Tumor Diseases Dresden (NCT/UCC), a partnership between DKFZ and Faculty of Medicine and University Hospital Carl Gustav Carus, TUD Dresden University of Technology; Helmholtz-Zentrum Dresden - Rossendorf (HZDR), Dresden, Germany, [2]Technical University of Dresden, Dresden, Germany, [3]University Hospital Carl Gustav Carus Dresden, Dresden, Germany, [4]Hopp Children's Cancer Center Heidelberg (KiTZ), Heidelberg, Germany, [5]German Cancer Research Center (DKFZ) and National Center for Tumor Diseases (NCT), Heidelberg, Germany, [6]National Center for Tumor Diseases (NCT/UCC), Dresden, Germany, [7]Hopp Children's Cancer Center Heidelberg (KiTZ); Clinical Cooperation Unit Pediatric Oncology (B310), German Cancer Research Center (DKFZ) and German Cancer Consortium (DKTK); National Center for Tumor Diseases, Heidelberg, Germany, [8]University Hospital Carl Gustav Carus, Technical University Dresden, Dresden, Germany, [9]National Center for Tumor Diseases (NCT), Heidelberg, Germany, [10]German Cancer Research Center (DKFZ), Heidelberg, Germany, [11]University Hospital and Faculty of Medicine Carl Gustav Carus, Technische Universitat Dresden, Dresden, Germany, [12]University Hospital Carl Gustav Carus at TU Dresden, Dresden, Germany

Introduction: Sarcomas are rare connective tissue tumors with over 100 described subtypes. High heterogeneity within and among sarcoma sub-entities and low incidence contribute to poor therapeutic success. Patient-derived 3D models (PDMs), i.e. organoids and spheroids, closely recapitulate features of the original tumor, e.g. cell-to-cell interaction, differentiation potential and heterogeneity. However, PDMs are rarely available or even lacking for most sarcoma sub-entities, constituting a major hurdle for sarcoma precision oncology and research. Here, we present a highly efficient and systematic framework to generate long-term 3D models for distinct sarcoma subtypes, which we developed within the HEROES-AYA consortium.

Methods: Tumors were received directly after surgery and processed within 24 hours. After enzymatic dissociation, cell clumps were seeded in 384-well plates with and without Matrigel. Each tumor was cultivated on an array of 140 distinct culture conditions, differing in contribution and concentration of pathway inhibitors and activators. Organoid and spheroid growth was assessed over time via imaging and AI-based algorithms to identify best-growing conditions.

Results: Initially, we combined Ewing sarcoma (EwS) secreted factors and potentially relevant cytokines to generate a matrix of 140 diverse media, named Media Test Plate (MTP). The MTP was tested on five EwS tumors, allowing the identification of optimal culture conditions with 100% efficiency. When transplanted in NSG mice, the established PDMs showed tumorigenicity potential and Ewing sarcoma-specific CD99 marker expression. The MTP was then tested on four synovial sarcomas (SyS) and five myxoid liposarcomas with a 75% and 50% success rate, respectively. The optimal media, as identified by MTP, allowed the cultivation of one EwS and one SyS out of two, respectively, even with limited cell count. Additional PDMs generated include one undifferentiated, one alveolar soft tissue and one spindle cell sarcoma. Established cultures were characterized by Ki67 positivity, ranging from 40% to 70%, and expression of sarcoma subtype-specific markers. EwS models resulted 100% CD99 positive, while TLE1 positivity in SyS models was ≈90%. DNA and RNA sequencing of PDMs will show whether they resemble the genetic and transcriptional features of the original tumors. Conclusions: We here present a novel systematic protocol to generate organoids and spheroids from different sarcoma subtypes. To date, no such systematic protocol is available for sarcoma models generation. Our success rate is comparable to the one of intestinal and pancreatic organoids and exceeds those of 2D and PDX sarcoma cultures, which is ≈20%. Current work aims to adapt the MTP to a broad range of sarcoma subtypes, including rare entities. The efficient generation of expandable PDMs from a wide range of sarcomas will further fuel basic and translational research.

#4256 Autologous organoids and T cell co-cultures as a powerful personalized platform for immunotherapy development.

C. Beaurivage[1], B. Sridharan[2], S. Mucuk[1], K. Nadwodny[2], D. Poore[2], A. Schepers[1], F. Pourfarzad[1], **S. F. Boj**[1];
[1]HUB Organoids B.V., Utrecht, Netherlands, [2]GlaxoSmithKline, Collegeville, PA

Recent advances in cancer immunotherapy have had a positive impact on the life expectancy of patients for an extensive range of clinical indications. With new treatment strategies and druggable targets being identified at an increasing pace, the number of patients eligible for cancer immunotherapy is expected to expand steadily. However, promising therapeutic developments face hurdles in translating preclinical findings into therapy since conventional 2D cancer models hold low clinical predictive value. We developed an innovative alternative, building on the discovery that adult stem cells proliferate and organize into three-dimensional organotypic structures when they are embedded into extracellular matrix. Patient-derived organoids are generated from normal and malignant tissues and stored as high-quality biobanks that yield highly reproducible results. HUB Organoids® recapitulate complex characteristics of the parental tissue, including molecular heterogeneity, as well as morphological and functional traits. Since cancer progression and response to immunotherapy are governed by immune cell interactions in the tumor microenvironment, we developed an assay in which colorectal (CRC) and non-small cell lung cancer (NSCLC) tumor organoids are co-cultured with paired tumor infiltrating lymphocytes (TIL) that are simultaneously expanded as a source of tumor reactive cells. Paired resources allow for the screening of immune-modulatory therapies under physiologic conditions, not depending on peptide-pulsing and alloreactivity. We quantify tumor organoid killing and TILs reactivity by combining imaging-based analysis of apoptotic cells with flow cytometry to measure cytokine release by cytotoxic TILs. Here, we show that our system is robust and reproducible with an establishment rate of 75%, allowing for expansion of TILs that preserve T cell receptor repertoires. First line expansion of both PDO and TIL components can be used to effectively build coculture models and probe the tumor and immune components, respectively. Our system offers a powerful tool for the development and validation of cancer immunotherapy and can help to stratify cancer patients for susceptibility to various types of immunotherapies. We certify that the research use of each of the HBS marked above was conducted according to the expectations of each institution.

#4257 A novel 3D co-culture platform for patient-specific immune-oncology treatment.

T. Light, **S. Kamali**, M. Gilardi, A. Andar, K. Abarca-Heidemann, M. Mancini;
Champions Oncology, Inc. (Hackensack, NJ), Hackensack, NJ

Lung cancer is the leading cause of global cancer-related mortality resulting in ~1.8 million deaths. annually. Over the past decade, the contribution of tumor microenvironment (TME) in lung cancer progression has been highly appreciated and provided significant improvements of survival outcomes for patients. That includes the complexity of the tumor immune microenvironment (TIME) playing a critical role in cancer progression. However, drug resistance usually arises and there is an urgent need for novel immune cell-based therapies. 3D tumor cell structures that recapitulate the architecture and functionality of the original tumor have revolutionized the understanding of disease mechanisms and testing potential therapeutics. However, there are certain drawbacks that need to be overcome. For example, these models mainly consist of only the epithelial compartment and lack signals from the microenvironment. Recent advances with engineering co-culture systems with immune cells at Champions Oncology help to emulate cell-cell and immune cell infiltration. We have successfully established a biobank of TumorGraft3D (CTG3Ds) derived from non-small cell lung cancer (NSCLC) patient-derived xenografts as well as their autologous and allogeneic immune cells (TILs, PBMCs) to establish a proprietary co-culture platform to investigate disease mechanisms and test potential therapeutics. In brief, surgical resections from patients were used to generate patient-derived xenografts organoids, and matched immune cells were expanded using standard rapid expansion protocol. The combination of a comprehensive staining system and high-content imaging as an endpoint allowed for 3D confocal analysis and deep evaluation of cancer-immune cellular interaction at the single cell level. Our pipeline of image analysis not only differentiates cancer-immune cell spatial distribution and cellular death but also allows for the evaluation of tumor infiltration and drug cytotoxicity. The characterization of the platform showed proliferation of the cancer cells and functional immune profiling by flow cytometry. The molecular profile of the organoids composing the platform showed a tight overlap with the original tumor highlighting the clinical relevance of the model. In addition, this novel co-culture platform has been tested with several NSCLC models to test the efficacy of various therapeutics such as immune-checkpoint inhibitors (ICIs) in reproducible, cost-effective, and patient-specific manner. In summary, Champion's novel co-culture platform allows screening of novel immune targeting agents to determine impacts tumor cytotoxicity. Furthermore, our lung cancer tumorGraft3D platform serves as a powerful tool to facilitate the practice of precision medicine by investigating a variety of therapeutic modalities, alone or in combination, to identify patient-specific treatment strategies.

#4258 An innovative PDX and patient-derived 3D platform for improved translatability of new medical entities.

S. Kamali, S. Cairo, F.-J. Chou, T. Light, M. Gilardi, B. Walling, C. Baer, H.-W. Tsai, A. Andar, K. Abarca-Heidemann, M. Mancini;
Champions Oncology, Inc. (Hackensack, NJ), Hackensack, NJ

The preclinical platform landscape in oncology has radically changed in the last 15 years, mainly due to an increased ability to generate patient-derived models. Multiple 3D tumor cell cultures methods, either from established cell lines or from primary cultures, have been developed to assess the activity of therapeutic agents in vitro. These methods are strongly influenced by the experimental conditions, such as cell culture conditions, the presence of 3D supports like Matrigel, and the experimental design of the assay, such as the choice of the dose and the duration of the assay. The ability of these methods to predict drug efficacy in the patient relies not only in the optimization of the experimental settings, but also on the representativeness of the patient population, and on the prevention of model drifts due to clonal selection and/or tumor cell adaptation to culture conditions with passages. In this project, we aimed to develop an innovative 3D cell model platform that addresses all these experimental challenges. To do so, we took advantage of our low passage Tumorgraft platform, a bank of more than 1500 patient-derived xenografts (PDXs) well characterized at molecular and pharmacological level and highly representative of the patient population, to generate the Tumorgraft3D platform. We derived TumorGraft3D models from low passage PDXs, by using proprietary, indication-specific culture conditions. By keeping these models at low passage, we were able to avoid clonal drifts. Moreover, the use of indication specific media allowed the preservation of patient's and PDX's tumor histology, molecular traits at genetic, gene expression and proteomic level, and displayed proliferation rates that recapitulate those observed in the parental PDXs. So far, we have successfully developed over 100 models from breast, ovarian, prostate, NSCLC, colorectal and gastric indications, with success rates up to 90%. Ex-vivo testing of standard of care highlighted different response profiles in accordance with the molecular feature of these models. The tumor dissociation process and culture conditions optimized with PDXs were also used for the development of 3D cultures derived from patients' samples. These data demonstrated that our 3D platform can integrate the complementarity of our PDX and patient-derived 3D platform, which lies in the possibility of evaluating test agent activity in the repeatable and reproducible setting provided by the patient-derived 3D models, as well as in models directly derived from patients with more heterogeneous and indication-specific establishment success rate, and throughput dependent on the amount of primary tumor material.

#4259 A novel human model of lung squamous cell carcinoma to deconvolve the cell-intrinsic effects of key dysregulated pathways.

J. Ogden[1], R. Sellers[1], A. Oojageer[1], S. Sahoo[1], A. Chaturvedi[2], **C. Lopez-Garcia**[1];
[1]Cancer Research UK Manchester Institute (Alderley Park), Manchester, United Kingdom, [2]The Christie NHS Foundation Trust, Manchester, United Kingdom

Tractable, patient relevant models are needed to investigate the essential components of normal cell transformation. We developed a unique in vitro model of early lung squamous cell carcinoma (LUSC) genetic alterations and driver pathway dysregulation using genetically modified primary human bronchial basal cells (hBCs) from three independent donors. The co-operation of ubiquitous and early LUSC alterations (TP53 and CDKN2A loss) and commonly deregulated pathways including squamous differentiation (SOX2), PI3K signaling (PTEN) and the oxidative stress response (KEAP1) was investigated using a combinatorial approach, culminating in eight unique hBC mutants harboring cumulative pathway alterations in a $TP53^{-/-}$/$CDKN2A^{-/-}$ background. Phenotypes indicative of mutant hBC transformation were investigated using proliferation assays, organotypic cultures and anchorage independent growth assays. Organotypic cultures revealed LUSC pathway alterations to drive dramatic changes in airway histology, ranging from a normal epithelium to severe dysplasia. Furthermore, these analyses confirmed the role of SOX2-overexpression in initiating transformation by inducing squamous cell commitment and anchorage independent growth. We also identified a co-operation of SOX2-overexpression with the oxidative stress response and PI3K pathways to drive more advanced lesions in-vivo and in-vitro. Importantly, we were able to map changes in the expression of immunomodulatory factors with the pathway dysregulation. We demonstrated that this strategy constitute an alternative and patient-relevant system to model LUSC and identify genotype-phenotype correlations of clinical relevance.

TUMOR BIOLOGY: The Extracellular Matrix in Cancer
Poster Session

#4262 AI-driven analysis of collagen characteristics in the tumor immune microenvironment predicts immune checkpoint inhibitors treatment responsiveness in gastric cancer.

M. Kim[1], E. Redekop[2], Y. Choi[1], S. Lee[3], J.-H. Cheong[4], Y. Aoki[5], K. Shitara[5], T. Hwang[1];
[1]Mayo Clinic, Jacksonville, FL, [2]University of California, Los Angeles, CA, [3]The Catholic University of Korea, Seoul, Korea, Republic of, [4]Yonsei University College of Medicine, Seoul, Korea, Republic of, [5]National Cancer Center Hospital East, Kashiwa, Japan

Background: Recent studies indicate a correlation between increased stromal composition in tumors and resistance to immune checkpoint inhibitors (ICIs) across various cancer types. Specifically, the extracellular matrix (ECM) within the stromal compartment significantly influence the tumor microenvironment, affecting cancer cell proliferation and immune cell recruitment. However, identifying and quantifying the ECM at the collagen fiber level in whole slide images (WSIs) is challenging due to its inherent heterogeneity and complexity. In this work, we utilized statistical analysis and a deep learning (DL)-based approach to identify and assess collagen in the ECM, examining its characteristics in relation to the ICIs treatment response in gastric cancer.
Methods: We analyzed 116 WSIs of hematoxylin and eosin (H&E) stained slides before ICIs treatment from three institutions. Responders were defined as those with a complete response or partial response (N=18); those with stable disease (SD) (N=34) or progressive disease (PD) (N=64) were considered non-responders (N=98). For non-responders, post-treatment H&E slides were available for 21 patients; SD (N=5) and PD (N=16). We applied a DL-based second harmonic generation (SHG) synthesis algorithm to tumor regions identified by a tumor detection model. We then calculated various collagen properties, including volume, fiber orientation and alignment, waviness, straightness, and fiber thickness, based on collagen fiber centerlines extracted from the generated SHG images. An attention-based multiple instance learning (ABMIL) model was trained to automatically predict the treatment response solely based on collagen features. The dataset of 116 pre-treatment slides was divided into training and validation subsets using stratified 3-fold cross-validation. The area under the curve (AUC) was used to assess the performance of the trained models.
Results: Collagen fiber features were significantly associated with ICIs response. Notably, ICIs responders have a decrease in collagen waviness and fiber orientation variation (p-value<0.05, by Mann-Whitney U test). Among non-responders, the PD group showed a statistical decrease in waviness after treatment (p-value<0.05, by Mann-Whitney U test). The ABMIL model achieved a mean AUC score of 0.823, with a standard deviation of 0.023.
Conclusion: This study provides a comprehensive analysis of collagen in the ECM, and its properties in relation to gastric cancer ICIs response within Tumor Immune Microenvironment. We also developed a model using collagen features and demonstrated high accuracy in predicting treatment response.

#4263 Prostate cancer cell-derived small extracellular vesicles regulate monocyte migration via STEAP4 and promote a monocyte transitional state.

N. M. Naranjo[1], A. Testa[1], S. K. Yadav[1], U. P. Naik[1], L. Yu[1], W. K. Kelly[1], Q. Liu[2], J. Ding[2], H. Yang[1], H. Tang[2], C. E. Verrillo[1], C. D. Hooper[1], L. R. Languino[1]; [1]Thomas Jefferson University, Philadelphia, PA, [2]The Wistar Institute, Philadelphia, PA

Our group has previously shown that prostate cancer (PrCa)-derived small extracellular vesicles (sEVs) are powerful cell communication mediators as they carry an array of proteins that have the ability to change recipient cell functions. Here, we describe a novel pathway of cancer cell-monocyte communication mediated by sEVs. Since sEVs carry cargoes that alter recipient cell phenotypes, we analyzed via proteomic analysis sEVs released from PC3 PrCa cells. Using CRISPR Cas9 methods, we downregulated IFIT3 (Interferon-induced proteins with tetratricopeptide repeats-3, member of the interferon-stimulated gene family) in PC3 PrCa cell (IFIT3KO). We then isolated sEVs from PC3 or IFIT3KO cells by using differential ultracentrifugation followed by iodixanol density gradient. Our proteomic analysis of IFIT3KO sEVs compared to PC3 sEVs shows that IFIT3 downregulation results in a significant upregulation of a metalloreductase, STEAP4 (six-transmembrane-epithelial antigen of the prostate 4), which is increased in PrCa cells and promotes PrCa cell proliferation and survival. STEAP4 is also known to promote an anti-inflammatory response in monocytes and macrophages. We then, investigated whether PrCa sEVs enriched in STEAP4 have a causal effect on monocyte functions and phenotype by using adhesion and migration assays as well as flow cytometry. Our results show that while all PrCa sEVs stimulate the adhesion of healthy donor or non-metastatic PrCa patient monocytes, only PrCa sEVs expressing STEAP4 increase their migration. In parallel, we provide evidence that all PrCa sEVs affect some of the M2 (CD163 or CD204) and M1 (CD80 or HLA DR) polarization markers analyzed in healthy donor monocytes. We show that there is a transitional state induced by PrCa sEVs in healthy donor monocytes, which occurs in a STEAP4-independent manner. This state mimics the non-metastatic PrCa patient monocyte phenotype. In conclusion, we describe a unique pathway whereby PrCa cell sEVs expressing STEAP4 promote monocyte migration with partial changes to their polarization.

Funding: This study was supported by NCI P01-CA140043, R01-CA224769, Pennsylvania DOH - Cure award to L.R.L

#4264 The TWEAK-Fn14-NF-kB signaling axis enhances expression of integrin AVB3 in a post-chemotherapy tumor microenvironment.

O. Lujano Olazaba, M. Robinson, C. Gallo, M. Shammas, K. Shelby, L. Cruz, S. F. Gilbert, C. D. House;
San Diego State University, San Diego, CA

High grade serous ovarian cancer (HGSOC) patients initially respond to chemotherapy but a majority relapse with chemoresistant disease. Research supports the notion that tumor-initiating cells (TICs), a subpopulation of drug resistant stem-like tumor cells, are responsible for facilitating relapse and therapies targeting these fecund cells may prolong remission. The tumor microenvironment (TME) plays a crucial role in therapy resistance, and tumor relapse. Cytotoxic chemotherapies have been shown to modify the stroma of the TME which may favor the survival of TICs displaying specific adhesion proteins. We and others have shown that NF-kB transcription factors RelA and RelB respond to signals from the ovarian TME to promote proliferation, chemoresistance, and survival. Our results further show that RelA and RelB regulate expression of specific integrins. Recently we found that TNF-like inducer of apoptosis (TWEAK), a cytokine involved in tissue repair, and its only known receptor Fn14, are enriched following chemotherapy, leading to enhanced chemoresistance and survival of TICs. TWEAK also induces expression of specific integrins in ovarian TICs. Therefore, we hypothesize that NF-kB mediated integrin expression enables adhesion and survival of TICs to a chemotherapy modified extracellular matrix (ECM) to facilitate tumor repopulation and relapse. Using magnetic activated cell sorting (MACS) for CD117+ TICs, we found that a significant majority are enriched for integrin AVB3. Supporting a role for TWEAK-Fn14-NF-kB in mediating integrin expression we further show that integrin AVB3, but not AVB5 or A5B1, was significantly increased in CD117+ TICs in the presence of TWEAK and was dependent on Fn14 as demonstrated through knockdown experiments. RNA-sequencing analysis of tumor cells grown in spheroid conditions with RelA or RelB shRNA knockdown relative to control, show ITGAV is dependent on RelA while ITGB3 expression is dependent on RelB. Taken together, our findings suggest CD117+ TICs have enhanced expression of AVB3 and is further induced by TWEAK mediated NF-kB activity for adaptation to a stressful post-chemotherapy environment. Ongoing in vitro and in vivo studies are investigating the therapeutic benefit of targeting AVB3 or TWEAK in CD117+ TICs for prevention of adhesion and tumor repopulation following chemotherapy. These studies will uncover interactions between TICs and ECM through their unique expression of integrins and clarifies the role of NF-kB transcription factors RelA and RelB in regulating TIC survival in the post-chemotherapy TME.

#4265 ZEB1-regulated hyaluronan network in the lung tumor microenvironment.

S. Lee[1], J. Park[1], E. Kim[1], S. Cho[1], S. Park[2], J. Kurie[3], Y.-H. Ahn[1];
[1]Ewha Womans University, Seoul, Korea, Republic of, [2]Deargen, Inc., Daejeon, Korea, Republic of, [3]University of Texas MD Anderson Cancer Center, Houston, TX

In the tumor microenvironment, hyaluronan surrounds neighboring cells as one of the major components of the extracellular matrix and stimulates the epithelial-mesenchymal transition (EMT) of various epithelial cancer cells. However, the mechanism of how the hyaluronic network is formed by cancer cells and regulates cancer progression and metastasis has not been known in detail. Therefore, we investigated the role of the hyaluronan network built-up by cancer cells in regulating cancer progression and metastasis in the tumor microenvironment. Our study demonstrated that ZEB1, an EMT-inducing transcription factor, reconstructs the hyaluronan network to induce the expression of ITIH2, a hyaluronan-binding protein, and hyaluronic acid synthase-2 (HAS2). ZEB1 was also shown to control the isoform switching of CD44, a hyaluronan receptor. ITIH2 knockdown and HAS inhibition reduced the formation of hyaluronan cables and inhibited cancer cell migration and invasion. In addition, the treatment of a specific ITIH2 inhibitor identified through deep learning-based screening suppressed the formation of hyaluronan cables, cell migration, and metastasis. These findings suggest that targeting the hyaluronan network could be a novel strategy for suppressing lung cancer progression and metastasis in the tumor microenvironment.

#4266 Evaluation of integrin alpha v beta 5 as a novel target for non-small cell lung cancer via tumor intrinsic and host immune regulation.

B. P. Kahangi[1], W. P. Crosson[1], J.-A. Lee[1], C. Dumitras[1], T. Zhang[1], R. Salehi-Rad[2], L. M. Tran[2], M. Palazzolo[1], D. Conklin[2], S. M. Dubinett[2], B. Liu[2];
[1]UCLA - University of California Los Angeles, Los Angeles, CA, [2]David Geffen School of Medicine at University of California Los Angeles, Los Angeles, CA

Lung cancer is the leading cause of cancer related deaths worldwide, with the most prevalent subtype being non-small cell lung cancer (NSCLC). As only a subset of patients exhibits durable clinical responses to current treatments, including targeted therapy and immunotherapy, new treatment options are needed. Integrins (ITGs) are a diverse class of heterodimeric, transmembrane receptors that bind extracellularly to the extracellular matrix (ECM) and intracellularly to the cytoskeleton to integrate signals bi-directionally between the extracellular environment and cell interior. One of 18 α subunits is paired with one of 6 β subunits to create the 24 known αβ ITGs in mammals. ITGs are expressed at low levels in normal tissue and can be upregulated in cancer cells in response to stress signals in the tumor microenvironment (TME). Altered expression of ITGs is associated with enhanced cell proliferation, metastasis, and immune evasion. Targeting of the diverse ITG family members by inhibitors not specific to individual isoforms has obscured understanding of potentially distinct functions of each heterodimer. Through data mining of a genome wide CRISPR screening publicly available at the DepMap portal, we have identified a novel cancer dependency to ITG αvβ5 in approximately 40% of NSCLC cell lines. Using small molecule ITG αv inhibitors, we have mirrored sensitivity of NSCLC cell lines to their ITG αvβ5 CRISPR scores, suggesting that these inhibitors function specifically through ITG αvβ5 in cell lines. RNA sequencing analysis following αvβ5 inhibition in human NSCLC cell lines revealed downregulation of YAP and E2F1 target genes with alterations in gene ontologies associated with cell cycling and cell death in sensitive, but not resistant, lines. This is consistent with the known function of YAP driving gene transcription promoting cell proliferation and survival, and of E2F1 being implicated in regulating the proliferation and self-renewal of cancer stem cell (CSC). Additional changes to immune processes, specifically perturbations to interferon (IFN) pathways, were identified in response to ITG αvβ5 inhibition, suggesting that ITG αvβ5 may play a role in host anti-tumor immune responses. Pharmacological inhibition of ITG αvβ5 also led to a reduction of tumor growth in NSCLC murine models accompanied with increased CD8 T cell activation. These findings support ITG αvβ5 as a unique target of cancer dependency in NSCLC whose inhibition promotes anti-tumor responses through both tumor intrinsic and host immune regulatory mechanisms.

#4267 Inflammation mediated expression of integrin αvβ3 potentiates KRAS driven PDAC oncogenesis.

R. M. Shepard, A. D. Campos, Z. M. Ortega, H. I. Wettersten, T. Von Schalscha, S. M. Weis, D. A. Cheresh;
University of California San Diego - UCSD, San Diego, CA

Understanding how pancreatic epithelial cells respond to inflammation and why some become tumorigenic and aggressive could identify new methods of early detection and novel therapeutic targets to control disease progression. Here, we leveraged an in vivo model in which mice with pancreas-specific expression of mutant Kras progress from pre-malignant intraepithelial neoplasias (PanINs) to pancreatic ductal adenocarcinoma (PDAC) following caerulein-induced chronic pancreatitis. During the transition from PanINs to PDAC, we observe two classes of neoplastic lesions: classically-described PanIN tubular structures that are highly organized and previously uncharacterized atypical highly disorganized lesions that are marked by robust integrin αvβ3 expression, observations which are consistent with human pancreatitis and PDAC. In vitro, we report that immune-, stroma-, and tumor cell-derived inflammatory cytokines induce β3 expression in a STAT3-dependent manner leading to increased integrin αvβ3. Considering that we previously established αvβ3 as a driver of cancer cell stress tolerance, drug resistance, and a stem-like phenotype, the acquisition of αvβ3 during chronic inflammation may promote tumorigenesis. Indeed, using the spontaneous tumor mouse model and xenograft models of human PDAC, we find that cells with an inability to upregulate β3 during tumor initiation fail to form tumors. These findings implicate integrin αvβ3 as a critical driver of inflammation-mediated pancreatic tumorigenesis.

#4268 Engineered hydrogel elucidates contributions of matrix mechanics to pathobiology of adenocarcinoma and identify matrix-activated therapeutic targets.

R. Cruz-Acuna[1], S. W. Kariuki[1], K. Sugiura[1], S. Karaiskos[1], E. M. Plaster[2], C. Loebel[2], G. Efe[1], T. Karakasheva[3], J. T. Gabre[1], J. Hu[1], J. A. Burdick[4], A. K. Rustgi[1];

[1]Columbia University Irving Medical Center, New York, NY, [2]University of Michigan, Ann Arbor, MI, [3]Children's Hospital of Philadelphia, Philadelphia, PA, [4]University of Colorado, Boulder, CO

Dysregulation of the extracellular matrix (ECM) properties disturbs tissue homeostasis and contributes to pathological conditions, such as cancer. Recent studies have demonstrated that ECM stiffening is associated with metaplasia-dysplasia-adenocarcinoma sequence in the esophagus. This underscores a compelling need to develop a physiologically-relevant 3D culture model to enable the study of the independent contribution of matrix stiffness to the initiation and progression of esophageal adenocarcinoma (EAC). Such a model will then serve as a platform for pre-clinical drug screening in the context of matrix properties. In this context, we have engineered a hyaluronic acid-based 3D hydrogel platform that supports the growth and differentiation of patient-derived Barrett's esophagus (BE) organoids, a precursor to EAC, as well as patient-derived EAC organoids. The engineered biomaterial 3D platform allows control over matrix stiffness to better recapitulate the mechanically dynamic esophageal cancer microenvironment and help identify therapeutic targets in EAC.Our data demonstrates that BE and EAC organoid density, growth and proliferation can be controlled by matrix stiffness. RNA sequencing data show that increased matrix stiffness promotes changes in the transcriptional profiles of BE and EAC organoids, revealing enrichment of pathways associated with tumorigenesis and disease progression. Furthermore, we demonstrate through molecular and functional assays that increased matrix stiffness endows stem-like properties to the EAC organoids via Yap-Sox9 mechano-activation. Finally, targeted therapy studies in our in vitro and in vivo engineered environments revealed that Yap inhibition regressed the effects of increased matrix stiffness in EAC organoids. In summary, our data suggest that matrix mechanics have a significant role in activation of EAC-associated signaling pathways in patient-derived BE and EAC organoids. We also demonstrate that the engineered hydrogel serves as a platform to identify potential therapeutic targets to disrupt the contribution of pro-tumorigenic matrix mechanics in EAC. Together, these studies establish an engineered patient-derived organoid culture platform that can be used to elucidate underlying matrix-mediated mechanisms of the metaplasia-dysplasia-adenocarcinoma sequence and inform the development of novel therapeutics that target ECM stiffness in EAC. FUNDING SOURCES: NCI P01CA098101, U54 CA163004 and NIDDK K01 DK133620.

#4269 Effect of PAX3-FOXO1 fusion gene on cell-extracellular matrix interaction of Rhabdomyosarcoma.

Chandra Kaladhar Vemula, Ivan Chavez, Anthony Chronopoulos, Jinseok Park

Hematology and Oncology, Children's Hospital of Los Angeles Foundation, Los Angeles, CA

Background Rhabdomyosarcoma (RMS) is the most common childhood soft tissue sarcoma, categorized by two subtypes, fusion protein-positive (FPRMS) and negative (FNRMS), based on the existence of PAX3-FOXO1 fusion gene (P3F). Different features between the two subtypes could guide the use of distinct treatment approaches. We discovered that FNRMS exhibited enrichment of gene sets related to cell-extracellular matrix (ECM) interaction than FPRMS. ECM, providing physical support as a scaffold, regulates cancer development. We hypothesize that a distinct molecular feature, P3F, may cause the difference in cell-ECM interaction between FPRMS and FNRMS.

Methods To confirm the higher cell-ECM interaction of FNRMS vs. FPRMS, we used confocal reflection microscopy (CRM), enabling us to monitor the fibrous structures of ECM. We generated the spheroids with FNRMS and FPRMS cell lines by hanging drop method and embedded them into collagen type I. Then, we assessed orientation and dynamic changes in the structure of collagen fibers surrounding spheroids. Also, we analyze the transcriptome of FPRMS cells with P3F knockdown to confirm if P3F regulates cell-ECM interaction negatively via RNA seq. Additionally, we examined ECM surrounding spheroids of P3F knockdown FPRMS cells if P3F modulates fibrous structures of ECM, indicating cell-ECM interaction.

Results We showed that collagen fibers are oriented more perpendicular to the FNRMS spheroid surface, indicating the strong pulling and pushing effect of cells. However, fibers surrounding FPRMS spheroids showed parallel alignment to their surfaces, reflecting passively pushed by the spheroids. Additionally, fibers near FNRMS spheroids showed greater displacement than those near FNRMS spheroids, which suggests stronger cell-ECM interaction in FNRMS than in FPRMS. Furthermore, P3F knockdown FPRMS cells exhibited significant enrichment of gene sets related to cell-ECM interaction. Their CRM results showed that collagen fiber orientation was significantly perpendicular to the surfaces of spheroids of P3F knockdown FPRMS cells than those of control cells. P3F knockdown cell spheroids also displayed enhanced displacement of ECM fibers than control cells. These results suggest that P3F suppresses cell-ECM interaction, consistent with higher cell-ECM interaction of FNRMS than FPRMS.

Conclusions The PAX3-FOXO1 gene may regulate cell-ECM interaction negatively, causing distinct features between FPRMS and FNRMS, which is crucial for various cellular functions and suggest different treatment between the two RMS subtypes.

#4270 Differential expression of the αVβ3 integrin affects small extracellular vesicle cargo and promotes small extracellular vesicle pro-tumorigenic activity *in vivo* via its downstream effector, NgR2.

C. E. Verrillo, F. Quaglia, N. Naranjo, A. Testa, L. R. Languino;
Thomas Jefferson University, Philadelphia, PA

It is known that small extracellular vesicles (sEVs) are released from cancer cells and contribute to cancer progression via crosstalk with recipient cells. These sEVs are being investigated as powerful biomarkers and possible therapeutic agents for prostate cancer (PrCa), which remains the leading cause of cancer death among men in the United States. We have previously reported that sEVs expressing the αVβ3 integrin, a protein upregulated in aggressive neuroendocrine prostate cancer (NEPrCa), contribute to neuroendocrine differentiation (NED) in recipient cells. sEVs used in this study were isolated by iodixanol density gradient and characterized by nanoparticle tracking analysis, immunoblotting, and single vesicle analysis. Our proteomic profile of sEVs containing αVβ3, when compared to control sEVs, shows a downregulation of typical effectors involved in apoptosis and necrosis, and an upregulation of tumor cell survival factors. This subset also contains an αVβ3 downstream effector, NgR2, a member of the Nogo receptor family and a novel marker for NEPrCa. We have previously shown that NgR2 promotes NED and cell motility, and upregulates RhoA, a protein associated with aggressive phenotypes of PrCa. In this study, we show that the expression of NgR2 increases tumor growth *in vivo*. We also show that the downregulation of NgR2 inhibits tumor growth and NED. Furthermore, we report that sEVs containing αVβ3 are loaded with higher amounts of NgR2 as compared to sEVs that do not express αVβ3. Mechanistically, we demonstrate that sEVs containing NgR2 do not affect the sEV marker profile, but, when injected *in vivo* intratumorally, they promote tumor growth and induce NED. We confirm that the transfer of NgR2 into recipient cells is sufficient to promote tumor growth and show that NgR2 mimics the effect of sEVs containing αVβ3 since it displays increased growth of NgR2 transfectants *in vivo,* as compared to control cells. Overall, our results describe a new mechanism mediated by sEVs containing αVβ3 and NgR2 that promotes cancer progression.

Acknowledgements: NIH R01-CA224769; DoD W81XWH2210826

#4271 The ITGA2 (CD49b) collagen receptor excludes the $CD8^+$ T cell infiltration in pancreatic ductal adenocarcinoma.

Ibrahim Ragab Eissa, Eric D. Abston, Darshini Kuruppu, Yongtao Wang, Guoliang Qiao, Motaz Qadan, Michael Lanuti, Kenneth K. Tanabe

Massachusetts General Hospital /Harvard Medical School, Boston, MA

BACKGROUND: Pancreatic ductal adenocarcinoma cancer (PDAC) is characterized by an enriched extracellular matrix and limited T cell infiltration, which poses challenges for immunotherapy. The significant accumulation of collagen type I (COL1) in PDAC tumor microenvironment raises questions about its functional role in PDAC progression and its interactions with the cellular compartments. **OBJECTIVE**: The objective of this study was to investigate whether the collagen receptors expressed by cancer cells modulate the anti-tumor activity of $CD8^+$ tumor-infiltrated lymphocytes ($CD8^+$ TILs).**METHODS**: Collagen receptor expression patterns in PDAC were examined using flow cytometry, western blot, multiplex immunofluorescence, RNA seq, and scRNA seq databases in KPC and treatment-naïve PDAC that were resected from patients. The KPC cell line, known as Hy15549, was established from KPC mouse model (Ptf1-Cre; LSL-KRAS-G12D; Trp53 Lox/+). Using CRISPR-Cas9, we conducted targeted deletions for either ITGA2(CD49b) or ITGB1(CD29), as well as generating double knockouts for both CD49b and CD29. Growth of these cell lines implanted into the flanks of immunocompetent, immunodeficient mice was measured, as well as after $CD8^+$ T cell depletion in immunocompetent mice. We analyzed TILs using FACs. We used multiplex immunofluorescence to analyze tumors microenvironment including collagen fiber alignment. Downstream signaling pathways were assessed using RNA seq and western blot. **RESULTS:** CD49b is highly expressed specifically in PDAC cancer cells, as assessed in both KPC cell flank tumors and resected human PDAC. Using adhesion assay, we found that CD49b specifically binds to Col1 rather than ColIV. $KPC^{CD29b\ KO}$ exhibited a complete loss of adhesion to both Col1 and ColIV. Tumor growth of the $KPC^{CD49b\ KO}$, $KPC^{CD29\ KO}$, $KPC^{CD49b\ CD29\ KO}$ was observed to be significantly slower than KPC^{WT} despite identical in vitro growth kinetics. Knockout of CD49b in tumors promoted intratumoral infiltration of $CD8^+$ T cells and significantly impeded tumor growth. Tumor growth by $KPC^{CD49bKO}$ was rescued by depletion of $CD8^+$ T cells. In contrast to observations in immune-competent mice, $KPC^{CD49bKO}$ tumor growth was similar to KPC^{wt} in immunodeficient nude mice. Analysis of downstream signaling in $KPC^{CD49bKO}$ tumors revealed a decrease of FAK as well as pFAk expression pathway. The proteomic profiling of $KPC^{CD49bKO}$ revealed an increase of CXCL10 chemokine. Moreover, In the absence of CD49b, the orientation of collagen fiber alignment appeared more scattered, with thinner fibers. This altered alignment could potentially contribute to immune cell infiltration.**Conclusion:**These findings reveal a previously unreported function of CD49b in PDAC cancer progression and the immune response within the TME. Together, our study reveals a mechanism underlying immune exclusion and suggests a novel immunotherapeutic target in PDAC.

#4272 Disruption of hyaluronan metabolism alters glioma cell proliferation by ligand dependent and independent mechanisms.

E. R. Neves, J. Mueller, A. Anand, K. Selting, H. Xu, R. Remy, B. Harley, **S. Pedron-Haba**;
University of Illinois Urbana-Champaign, Urbana, IL

Hyaluronan (HA) is the main constituent of the brain extracellular matrix and is an essential component of the glioblastoma (GBM) tumor microenvironment. The biosynthesis and catabolism of hyaluronan has multiple roles in tissue architecture and cell signaling. Dysregulation of these mechanisms is crucial in pathological processes such as cancer, inflammation or tissue remodeling. The role of HA is believed to be strongly dependent on its size (molecular weight), location, and cell receptor density and activity. HA is produced intracellularly by HA synthases (HAS1-3) and can also be catabolized endogenously by hyaluronidases (HYAL1-3).The fabrication of controlled microenvironments provided by three dimensional (3D) models helps to elucidate the role of HA signaling in GBM tumors. We exploit here the advantages of these models to understand the role of hyaluronan in the local behavior of GBM after radiation therapy and selected targeted inhibitors. We have established engineered brain tumor biomaterials based on functionalized hydrogels to monitor the response of patient-derived xenograft cell populations with different molecular signatures in combination with microfluidic devices. We have analyzed shifts in metabolism, hyaluronan secretion, as well as hyaluronan synthetic enzymes (HAS) and hyaluronidases (HYAL) activity in an array of patient derived GBM cells. We reveal that endogenous HA plays a role in mitochondrial respiration and cell proliferation in a tumor subtype dependent manner. We also show that HA fragments can enhance tumor metabolism and growth through ligand dependent and independent mechanisms. We provide bioengineered platforms and strategies to predict and stratify tumors in order to achieve more efficient combinatorial treatments targeting endogenous hyaluronan production. This work emphasizes the potential of these preclinical models to predict and accelerate cancer treatments, more relevant in malignancies with limited treatment options.

#4273 Genetically engineered mesenchymal stromal cells degrade hyaluronic acid to disrupt the ECM and enhance cancer therapy outcomes.

A. T. Browne, M. Clements, W. Ju, R. Kaplan;
National Institutes of Health (NIH), Bethesda, MD

The extracellular matrix (ECM) is a vital component of cancer pathophysiology. However, little is known about how to modulate the ECM for therapeutic benefit effectively. Hyaluronic acid (HA) is a polysaccharide component of the ECM with increased deposition during tissue injury or inflammation. HA in the tumor microenvironment (TME) has been linked to aggressive cancer progression. We have found enhanced ECM remodeling behavior linked to pre-metastatic niche formation and metastatic progression. To remodel this ECM-enriched microenvironment, we developed HA-targeting genetically engineered mesenchymal stromal cells (GEMesys) expressing hyaluronidase (Hyal), the enzyme responsible for HA degradation. We examined the impact of Hyal-GEMesys in osteosarcoma (F42010), rhabdomyosarcoma (M-3-9M), and pancreatic cancer (Panc02) syngeneic murine models. Hyal-GEMesys delivered to tumor-bearing mice homed to primary tumor sites and successfully degraded HA in the TME. The degradation of HA also resulted in a significant remodeling of collagen. T cells in Hyal-GEMesy treated tumors display an activated CD4+CD44+ phenotype with a reduction of LAG3+PD1+ exhaustion markers. Additionally, Hyal-GEMesy treatment results in a significant decrease in hypoxic regions within tumors and reorganization of the tumor vasculature to a more normalized phenotype, marked by diminished CD31 expression. Hyal-GEMesy treatment reduces tumor volumes in osteosarcoma, rhabdomyosarcoma, and pancreatic cancer models and enhances chemotherapeutic efficacy. These findings suggest that reorganizing the tumor ECM with Hyal-GEMesys holds the potential to dismantle the protective stroma of the tumor, which often shields malignant cells from therapeutic reach, and combining anti-cancer and anti-stroma agents can enhance anti-tumor efficacy and patient outcomes.

#4274 Unraveling collagen signatures in cancer-associated fibroblasts: A biomarker-driven approach.

A. Hettich, N. I. Nissen, M. A. Karsdal, **N. Willumsen**;
Nordic Bioscience, Herlev, Denmark

Background: The tumor microenvironment (TME) plays a crucial role in driving tumor development. Among the constituents of the tumor stroma, cancer-associated fibroblasts (CAFs) are a significant component. CAFs are actively involved in tumor progression by modulating the architecture of the TME through increased deposition of various collagens resulting in tumor fibrosis. Several studies have shown that CAFs have heterogeneity within, and between, individual tissues. TGF-β is thought to be the main driver of tumor fibrosis, however, the field lacks a characterization of the specific collagen deposition of CAFs from different tissues. In this study, we investigated the fibrotic activity of CAFs from various tissues by measuring the production of three specific collagen peptides in vitro by use of non-invasive clinically validated biomarkers.
Methods: Primary human CAFs from pancreas (pCAF), colon (cCAF), breast (bCAF) and lung (lCAF) were cultured over a 12-day period in ficoll-based media under both unstimulated conditions and TGF-β stimulation. Additionally, cells were subjected to treatment with the ALK5/TGF-β1 receptor kinase inhibitor (ALK5i). The assessment of collagen I (PRO-C1), collagen III (PRO-C3), and collagen VI (PRO-C6) formation was conducted in the cell supernatant at day 3, day 6, day 9, and day 12 using competitive enzyme-linked immunosorbent assay (ELISA).
Results: For lCAFs, cCAFs, and pCAFs, the addition of TGF-β led to a notable elevation in the levels of PRO-C1, PRO-C3, and PRO-C6 within the supernatant. Conversely, in the case of bCAFs, stimulation with TGF-β did not elicit remarkable alterations in the levels of PRO-C1 and PRO-C3 compared to unstimulated cells. Notably, bCAFs exhibit elevated intrinsic activity (high PRO-C3) even in the absence of TGF-β stimulation whereas lCAFs and cCAFs exhibited relatively low level of PRO-C3. Additionally, across all different CAFs, the introduction of ALK5 inhibitor (ALK5i) to the culture medium resulted in a considerable reduction in PRO-C1, PRO-C3, and PRO-C6 levels, returning them to the baseline of the unstimulated control or even lower. Distinct collagen formation patterns were observed among the various CAFs. CAFs derived from breast cancer exhibited the highest release of PRO-C1 and PRO-C3, while CAFs isolated from colon cancer displayed the highest levels of PRO-C6.
Conclusion: These findings underscore the heterogeneity in collagen production among different CAFs, providing valuable insights into the extracellular matrix dynamics within distinct tumor microenvironments. Moreover, non-invasive biomarkers demonstrate the capability to differentiate between different CAF subtypes. Lastly, our model proves to be a valuable tool for anti-fibrotic drug screening, as evidenced by the consistent suppression of TGF-β1 signaling and reduced levels of PRO-C1, PRO-C3, and PRO-C6 upon treatment with ALK5i across all cases.

#4275 Targeting tumor extracellular matrix to improve response to therapy.

O. M. T. Pearce;
Queen Mary University of London, London, United Kingdom

Introduction. Building on our previous findings that tumor extracellular matrix (ECM) composition associates with immune cell phenotype (Pearce et al, Cancer Disco, 2018), and ECM can directly educate tumor-associated immune phenotypes (Puttock et al, Nat Commun, 2023), we present here the identification of specific ECM components that associate with tumor immune phenotype, and discuss our approach to target these components as a way to improve anti-tumor immunity and immunotherapy response.

Methods. We use a combination of transcriptomics, proteomics, glycomics, and spatial tissue analysis to identify correlations between ECM composition and the immune landscape in breast and ovarian cancers. Correlations are tested within a decellularized tumor model made from patient samples which allow immune cell movement, interaction with ECM, and tumor killing to be measured in real-time.

Results. Through our analysis pipeline we have identified a specific ECM molecule that appears to regulate the spatial location of tumor infiltrating CD8 T-cell populations via post-translational modifications that are present on the molecule. Deletion of this molecule in injectable orthotopic murine models dramatically alters the immune landscape within the tumor. Within an in vitro decellularized tumor tissue model the *in situ* deletion of the ECM molecule drives tumors into an inflamed phenotype which is more responsive to cell-based cancer therapy.

Conclusions. Tumor ECM can direct immunity in two ways. These are educating or stimulating immune cells to develop specific phenotypes that tend to be immunosuppressive, and secondly directing the movement of cells within the tissue. These immunosupressive effects can be overcome through small modifications to ECM structure, indicating therapeutics that make subtle changes to ECM composition may be used in combination with current cell-based therapies to improve tumor response.

#4277 CREB-ROCK driven extracellular matrix remodeling exasperates pancreatic cancer progression.

S. Jinka, S. Mehra, V. Krishnamoorthy, A. Bianchi, K. Rajkumar, A. Adams, H. Amirian, S. Singh, E. W. Box III, E. Dickey, N. L. Alberto, B. Yuguang, J. Datta, N. Merchant, N. Nagathihalli;
University of Miami, Miami, FL

Background: Pancreatic Ductal Adenocarcinoma (PDAC) is characterized by a heightened oncogenic mutational burden, an immunosuppressive tumor microenvironment, and a dense desmoplastic stroma. During the tumor progression from *in situ* carcinoma to intraductal neoplasia, cancer cells manage to evade the stromal compartment and infiltrate into the ducts. This invasive tumor progression is often associated with the overexpression of extracellular matrix (ECM) modulating genes. Despite this correlation, there are currently no effective and specific inhibitors of ECM-altering pathways. By understanding the signaling mechanism, the ECM remodeling pathways may be intercepted to prevent invasive tumor progression. This study aims to elucidate the role of cAMP-response element binding protein 1 (CREB1) and its downstream effectors in regulating PDAC ECM remodeling.
Methods: The Cancer Genome Atlas (TCGA) was quired for *CREB1* expression and other ECM modulators in PDAC patients. *In vitro*, CRISPR/CAS9-based genomic editing was utilized to knockout CREB1 in the murine KPC cell line, on which RNA-seq analysis was performed. To investigate the effects of CREB in PDAC progression, a novel conditional CREB1 knockout ($CREB^{fl/fl}$) was created in LSL-$Kras^{G12D/+}$; $Trp53^{R172H/+}$; $Pdx1^{Cre/+}$ (KPC) mice ($KPCC^{-/-}$). Tumors were extracted and histologically evaluated. Immunoblotting and staining were conducted on both *in vitro and in vivo* samples. Chromatin immunoprecipitation sequencing (ChIP-seq) and qPCR were performed on the KPC $CREB^{KO}$. Eukaryotic Promoter Database (EPD) and ENCODE databases were explored to evaluate the transcriptional role of CREB in regulating ECM genes.
Results: Patient PDAC samples data from TCGA revealed elevated levels of *CREB1, ROCK1,* and *ROCK2* compared to normal pancreatic tissues. When comparing high *CREB* expression to low *CREB* expression, upregulation of several ECM genes was noted, including *ROCK1* and *ROCK2* in patients with high *CREB* expression. In $CREB^{KO}$, RNA-seq analysis revealed the downregulation of key ECM genes, including *Mmp3, Mmp10, Lama3,* and *Fn1* compared to CREB wildtype. In our novel murine conditional knockout model, a substantial reduction in fibrosis was observed. In both *in vitro* and *in vivo*, immunoblot and staining demonstrated a marked reduction in the expression of ECM remodeling proteins upon CREB deletion. Through ChIP-seq, the direct involvement of CREB1 in the transcriptional regulation of *Rock1* and *Rock2* was established. EPD and ENCODE were utilized to confirm and validate our CREB regulation experimental findings.
Conclusion: These findings demonstrate the role of CREB in PDAC progression, which may provide a potential target to intercept ECM remodeling via inhibition of the CREB-ROCK axis to suppress PDAC tumor progression and invasion.

#4278 Role of WNK1 in extracellular matrix modification in breast cancer.

P. Suman, S. Kakkat, S. S. Patil, V. Ramirez, E. A. Turbat-Herrera, S. Singh, C. Sarkar, D. Chakroborty;
University of South Alabama, Mobile, AL

Introduction: Breast cancer (BCa) is the most common cancer and the second leading cause of cancer related deaths in women in the United States. Metastatic dissemination of cancer cells remains the leading cause of mortality in BCa. Therefore, determination of the mechanisms that promote metastasis is important for development of new therapeutic strategies. The extracellular matrix (ECM), which is the main non-cellular component of the tumor microenvironment (TME), plays an important role in BCa progression and metastasis. The cancer-associated fibroblasts (CAFs) are the principal cell types that together with BCa cells drive the modification of ECM during cancer development. Lysine deficient receptor protein kinase 1 (WNK1), a widely expressed serine threonine kinase that regulates blood pressure and electrolyte balance in the body, and is highly overexpressed in BCa microenvironment. The aim of the present study was to investigate the role of WNK1 in modification of ECM in BCa.

Methods: The clinical relevance of WNK1 overexpression in BCa was determined by immunohistochemically staining human BCa sections, analyzing data from publicly available databases and creating orthotopic mouse models of BCa using 4T1 mouse BCa cells followed by treatment of the tumor bearing mice with WNK1 inhibitors, WNK-IN-11 and WNK463 (10 mg/kg , oral for 10 days). *In vitro* assays were conducted using 4T1 cells and mouse embryonic fibroblasts (MEFs) to determine the regulatory role of WNK1 on cancer cells and fibroblasts.

Results and Conclusion: Our results indicated that WNK1 is strongly expressed in BCa cells and fibroblasts, the two most abundant cell types in the BCa microenvironment. Furthermore, WNK1 expression strongly correlated with expressions of matrix regulatory and cross-linking genes. Our results demonstrated that WNK1 inhibitors significantly reduced orthotopic 4T1 growth and metastasis. WNK1 inhibition also significantly inhibited collagen deposition in tumor tissues, which is a negative prognostic indicator in BCa. *In vitro* proliferation and migration assays using 4T1 cells and MEFs identified that WNK1 inhibitors (1-100nM) can significantly inhibit the proliferation and migration of 4T1 cells and MEFs. Results from co-culture studies with 4T1 cells and MEFs further indicated that WNK1 inhibition in MEFs could significantly reduce the invasive properties of 4T1 cells. Taken together, our results suggest that blocking the actions of WNK1 in BCa may be a promising therapeutic approach.

#4280 Regulatory T cells contribute to tumor cell dissemination by extracellular matrix remodeling.

A. Garcia-Santillan, J. Y. Lichtenberg, H. Shen, M. G. Dozmorov, A. L. Olex, P. Y. Hwang, **P. D. Bos**;
Virginia Commonwealth University, Richmond, VA

Regulatory T (Treg) cells function to enforce peripheral tolerance and are potent suppressors of tumor immunity. In breast cancer, we have shown that Treg cells promote tumor growth by favoring alternative activation of macrophages via suppression of IFN-γ. The tumor-associated extracellular matrix (ECM) is a key regulator of metastatic dissemination and is emerging as a critical regulator of tumor immunity. However, the reciprocal effects of the immune system on the ECM remain elusive. Using murine *in vivo*, *ex vivo* and bioengineering models we describe Treg cell-dependent changes in the tumor ECM that facilitate tumor cell movement and metastatic dissemination. Further, Treg cell-dependent matrisome signatures correlate with survival in human breast cancer samples. This work underscores a previously unrecognized role of Treg cells on the ECM that facilitates metastasis and is consistent with tissue Treg cell emergent function as critical regulators of tissue repair and cancer.

#4281 BMP signaling impaired telocytes-Foxl1+disrupt the extracellular matrix network enabling the development of colitis-associated cancer.

V. Reyes Nicolas, A. B. Alfonso, J. Raisch, F. M. Boisvert, M.-A. Lauzon, N. Perreault;
Universite de Sherbrooke, Sherbrooke, QC, Canada

The relationship between colon stem cells (SCs), its surrounding niche microenvironment like the extracellular matrix (ECM) and the mesenchymal niche cells is complex and dynamic. ECM proteins are not only a scaffolding system for SCs, but their biophysical properties also contribute to localizing signals and creating gradients leading to the SCs homeostasis. Foxl1+-Telocytes (TC^{FoxL1+}) are mesenchymal niche cells implicated in cell-cell communication and the production of BMP ligands. Upon chronic inflammation, mice lacking BMP signaling in TC^{FoxL1+} (*BmpR1a*$^{\Delta FoxL1+}$), developed colonic tumors with microenvironment exhibiting abnormal TC^{FoxL1+} structure, increased BMP expression and myofibroblastic-like cancer-associated fibroblasts (myCAF) subpopulation. Yet, how the TC^{FoxL1+} influences SCs niche ECM proteins during tumorigenesis is less understood. We aimed to investigate how the loss of BMP signaling in TC^{FoxL1+} affects ECM network impacting the niche microenvironment promoting the development of CAC. DSS-based chronic inflammatory challenge in mutant and control mice, quantitative-MS-based strategy was performed to determine the proteome of the transformed regions solely in epithelial-mesenchymal tissue following colon deconstruction. Expression of the proteins of interest were validated by Western Blots or immunostainings. Quantitative analysis of collagen network was assessed using phyton pipeline U-net in Sirius red-stained colon analyzed under polarized light. Differential significant expression of 798 proteins, with 342 upregulated and 456 downregulated, were found in the tumors of mutant mice compared to controls. Mfap5 involved in CAF activation was the highest upregulated protein. We found upregulated, laminin subunits α4 and β2, decorin, lumican as well as transgelin (myCAF marker), which are proteins known for contributing to the stiffening of the ECM during colorectal cancer. Adamdec1 which prevents aberrant ECM accumulation and thrombospodin-1, an ECM glycoprotein whose low levels have been related to tumor growth, were both found to be downregulated. Data extracted from Python's U-Net pipeline demonstrated that tumors, in mutant mice, exhibited higher frequencies of straighter collagen fibers compared to wavier fibers in controls. Collagen fiber distribution was shown to present an even angle distribution in controls whereas *BmpR1a*$^{\Delta FoxL1+}$ mice presented a preferential orientation. These results suggest that defective TC^{FoxL1+} commits the surrounding niche microenvironment, especially its ECM, toward the development and progression of CAC.

#4282 Crosstalk between the immune system and the extracellular matrix in the context of melanoma and aging.

E. I. Harper, Y. Chhabra, A. Carey, M. Ramos Rocha, L. Huser, V. Wang, A. Dixit, A. Weeraratna;
Johns Hopkins University, Baltimore, MD

Aging is an independent prognostic factor for the diagnosis of melanoma. The extracellular matrix of the skin has well-documented changes with age, such as the loss of HAPLN1, which can lead to differential metastasis in aged individuals. The aged microenvironment can contribute to the phenotype switch, where aged individuals have smaller primary tumors but more metastases, i.e., going instead of growing. The extracellular matrix (ECM) has been shown to modulate the immune response either through direct binding of ECM proteins or through mechanotransduction, but it is unclear how aging affects this crosstalk. Our hypothesis is that the ECM can modulate immune response to melanoma and affect response to immune checkpoint blockade (ICB) therapy. Melanoma cells cultured on cell derived matrices (CDMs) from young and aged human fibroblasts show differential levels of expression of PD-L1, a ligand that binds to PD-1 on T cells to induce T cell exhaustion. Antibodies targeting PD-1/PD-L1 are one of the main ICB treatments available to melanoma. We are also investigating T cell motility on young and aged CDMs, as well as correlating T cell infiltration in murine tumors with ECM signatures as identified by second harmonic generation microscopy. Therefore, we have compiled evidence that aging affects the crosstalk between the extracellular matrix and the immune system, providing a new horizon for therapeutic improvement of response in older patients.

#4283 NAMPT-enriched small extracellular vesicle promotes liver cancer via activation of SLC27A4-mediated glycolysis.

L. Yeung, T. Ng, J. Yam;
University of Hong Kong, The - Li Ka Shing Faculty of Medicine, Pok Fu Lam, China

Introduction: Tumor-derived small extracellular vesicles (sEV) act as a major mediator of the tumor microenvironment (TME) and are reported to regulate various metabolic pathways.
Methods: Small extracellular vesicles (sEV) were collected from normal human hepatocyte and metastatic HCC cell lines using differential ultracentrifugation. Mass Spectrometry proteomic analysis was employed to identify NAMPT to be enriched in metastatic HCC-sEV. The glycolytic effect of NAMPT-sEV was analyzed by seahorse glycolytic assay.
Result: Mass spectrometry protein analysis revealed nicotinamide phosphoribosyl transferase (NAMPT) to be upregulated in metastatic HCC-sEV. NAMPT is a rate-limiting enzyme essential for maintaining cellular level of nicotinamide dinucleotide (NAD+). However, the underlying pathway of sEV-NAMPT-induced metabolic consequence in HCC remains largely unknown. This study elucidated sEV-NAMPT's carcinogenic role by establishing NAMPT-knockdown (NAMPT-KD) stable clone in metastatic HCC cell lines, which significantly hampered the promoting effect of HCC-sEV in glycolysis. sEV-mediated *in vitro* and *in vivo* tumor growth was also inhibited. Through sEV treatment, we found that sEV-NAMPT significantly elevate SLC27A4 in both transcription and protein level of recipient cells. Mechanistically, it is demonstrated that SLC27A4 expression was enhanced by NF-κB transcription factor, which is activated upon binding of sEV-NAMPT to toll-like receptor 4 (TLR4). SLC27A4 mainly function as a long-chain fatty acid transporter or acyl-CoA synthetase. Lipidomic and metabolomic analysis unveiled SLC27A4 to be positively correlated with intracellular triacylglycerol (TG) and dihydroxyacetone phosphate (DHAP) level. Elevation of TG aggravates lipolysis by hepatic lipase and promotes conversion of glycerol-3-P to DHAP, which is an intermediate metabolite that transit between lipid metabolism and glycolysis. This study uncovers a regulatory axis of sEV-NAMPT-mediated SLC27A4 in glycolysis, apart from conventional fatty acid-related metabolisms. Clinically, we explored the therapeutic potential of targeting sEV-NAMPT by inhibitor FK866. Treatment of NAMPT-inhibitor significantly hampered tumor growth in various HCC *in vivo* models, which suggested an alternative therapeutic strategy for HCC.
Conclusion: NAMPT is enriched in metastatic HCC sEV. sEV-NAMPT regulates the promoting effect of HCC-sEV in glycolysis and oncogenesis. SLC27A4 function as the downstream target that promotes HCC progression via glycolysis. NAMPT inhibitor FK866 are proven to reduce *in vitro* and *in vivo* tumorigenic ability of metastatic HCC-sEV, which may serve as potential HCC treatment option.

#4284 Macrophage reprogramming and immune suppression through extracellular vesicles loaded eIF4A1in ovarian cancer.

S. Mittal, I. Pulikkal Kadamberi, S. Kumar, J. George, M. singh, A. Geethadevi, P. Chaluvally-Raghavan, S. Pradeep;
Medical College of Wisconsin, Wauwatosa, WI

Background- In ovarian carcinoma (OvCa), macrophages are reprogrammed toward pro-tumorigenic phenotypes, including releasing anti-inflammatory cytokines and expressing immunosuppressive molecules. However, how these macrophages acquire their phenotype remains largely unexplored. To understand the mechanism driving pro-tumorigenic phenotype in macrophages, we studied the role of tumor cell-derived extracellular vesicles (EVs) in the cross-talk with macrophages in OvCa. We found that EVs from ovarian cancer cells contain eukaryotic translation initiation factor 4A1 (eIF4A1). eIF4A1 containing EVs from ovarian cells enhanced macrophage translational activity and PD-L1 expression. However, the detailed mechanism that explains how eIF4A1-packaged EVs induce immunosuppressive phenotype in macrophages is necessary to develop novel immunotherapy strategies for advanced OvCa treatment.

Methods- We performed SUnSET assay (surface sensing of translation) to determine whether eIF4E-EVs affect global translation in macrophages. SILAC (Stable isotope labeling by amino acids) based mass spectrometry was used to identify the downstream targets of eIF4A1 in macrophages. We isolated murine peritoneal macrophages from naïve C57BL/6 female mice and co-cultured the macrophages with EVs derived from ovarian cancer cell lines. The expression of PD-L1, CD206, interleukin-6 (IL-6), and other inflammatory cytokines on EVs treated macrophages was evaluated using flow cytometry and a cytokine array kit. Further, we created a Rab27aKO ovarian cancer in vivo model to study the effect of eIF4A1 packaged EVs on the immune suppressive ability of macrophages and tumor progression.

Results- Our study shows that tumor cells employ EVs to deliver eIF4A1 to the tumor microenvironment, facilitating the release of cytokines such as IL-6 and the expression of PD-L1 on macrophages and supporting tumor growth. In addition, our data shows that eIF4A1-EVs enhance protein synthesis in macrophages. Our data show that in the Rab27aKO ovarian cancer in vivo mouse model, intravenous injection of eIF4A1-packaged EVs increased the tumor burden, metastasis, and ascites accumulation as compared to PBS control. eIF4A1-EVs treatment increased the infiltration of tumor-associated macrophages (TAM) in ascites. We also found increased expression of PD-L1 and CD206 on TAM isolated from ascites

#4285 Tumor-on-chip co-culture system: A comprehensive tool in personalized medicine to study cancer progression.

S. Kamali, M. Gilardi, B. Walling, A. Andar, K. Abarca-Heidemann, M. Mancini;
Champions Oncology, Inc. (Hackensack, NJ), Hackensack, NJ

As a part of the rapidly advancing organ-on-chip field of research, tumor-on-chip technology (TOC) has emerged as a promising co-culture system to mimic the mechanical and biochemical properties of the tumor microenvironment. This includes factors such as oxygen and nutrient gradients, extracellular matrix stiffness, and cell-cell interactions. Depending on the complexity of system, TOCs are miniature tumor models in a microfluidic chip allowing researchers to gain a better understanding and controlled cancer environment to effectively test potential drug treatments and study immune cell co-cultures. Champions'TumorGraft3D (CTG3D), established from patient-derived xenografts, is the essential component used to recapitulate tumor microenvironment in the TOC platform which provides an even more powerful tool to gain more insight on the efficacy of various therapeutics. Here, we demonstrate the value in combining microfluidic devices with well characterized CTG3D models at Champions Oncology focused on indications including colorectal, breast, gastric and lung cancer. In brief, we optimized cell seeding conditions in both top (seeded with CTG3Ds) and bottom (seeded with endothelial cells) channels to develop TOCs interfacing epithelial-endothelial cells. These established systems may be applied as a baseline for introducing additional cell types such as autologous tumor-infiltrating lymphocytes (TILs) and studying their effect in the presence and absence of additional treatments. With an initial focus on colorectal cancer, we successfully developed TOC epithelial-endothelial interface using CTG3Ds originated from patients with various clinical backgrounds. We measured the permeability as an initial read-out to prove that although tumor cells do not inherently form a tight barrier, they can still form a non-leaky barrier with distinct organoid-like structures. Next, we extended our study to additional indications featuring unique characteristics and proved the feasibility of applying TOCs as a preclinical tool regardless of the tissue-of-origin. In all cases, the endothelial cells formed mature microvascular structures and to confirm the consistency of formed epithelial-endothelial interface among the replicates of each experimental group, we did Luminex studies to prove high consistency in secreted proteins. Regarding the functionality of TOCs, we investigated the effect of relevant test agents to each indication and showed that that the combination of DRAQ7 dye and high-content imaging may be a reliable read-out to detect the response and viability of cancer cells pre- and post-treatment. In summary, our established tumor-on-chip system proves to be a robust and powerful tool for studying the effect of microenvironmental factors in drug testing and immune cells in cancer progression.

#4286 Proteolytic degradation of BIGH3 can be quantified non-invasively in serum with biomarker potential for patients with non-small cell lung cancer.

R. S. Pedersen, M. Karsdal, N. Willumsen;
Nordic Bioscience, Herlev, Denmark

Introduction: Transforming growth factor beta induced protein ig-h3 (BIGH3/TGFBI) is expressed widely by multiple cell types, including macrophages and fibroblasts, and is participating in various biological processes including adhesion, migration, angiogenesis and wound healing. BIGH3 is known to bind multiple collagens and are often embedded in the matrix where it seems to function as a linker between ECM and cell surfaces. The increased proteolytic activity found in non-small cell lung cancer (NSCLC) may degrade BIGH3 that affect this interaction as well as generate small peptide fragments that can serve as novel non-invasive biomarker targets if released to circulation. The aim of this study is to develop a tool to quantify degraded BIGH3 non-invasively and explore its potential as a biomarker in NSCLC.

Methods: An ELISA, named nordicBIGH3M-N targeting a cleaved fragment of BIGH3 was developed to reflect BIGH3 degradation and enable serological quantification. We incubated recombinant BIGH3 with and without collagenase to confirm that nordicBIGH3M-N only measured degraded BIGH3. In addition, we generated matrixes from normal fibroblasts and cancer associated fibroblasts (CAFs) grown with or without tgf-b. These matrixes were cleaved with collagenase to confirm that NordicBIGH3M-N could be generated from degradation of matrix. nordicBIGH3M-N was also measured in serum from 39 patients with NSCLC (18 patients with adenocarcinoma and 21 patients with squamous cell carcinoma) and 35 healthy controls. BIGH3M-N levels in serum from patients with the two subtypes of NSCLC and healthy controls was compared using Dunn’s multiple comparison test and area under receiver operation characteristic curves (AUROC).

Results: BIGH3M-N was only detectable after incubating recombinant BIGH3 and fibroblasts matrices with collagenase. A 7-fold increase of BIGH3M-N levels was seen between the collagenase degraded matrix from tgf-b treated fibroblasts compared to the degraded matrix from untreated fibroblasts. No difference in BIGH3M-N levels was observed between degraded matrix from tgf-b treated or untreated CAFs. BIGH3M-N was significantly elevated in patients with squamous cell carcinoma compared to healthy controls ($p = 0.006$, AUROC = 0.73) and patients with adenocarcinoma ($p = 0.022$, AUROC = 0.78). However, there was no significant difference between BIGH3M-N levels in serum from patients with adenocarcinoma and healthy controls ($p>0.99$, AUROC = 0.51).

Conclusion: Degradation of BIGH3 can be reflected by non-invasive quantification of the cleaved fragment of BIGH3, BIGH3M-N, in serum. BIGH3M-N is a promising biomarker in NSCLC with potential for discriminating between subtypes. Moreover, BIGH3M-N is connected to fibroblast matrix biology so the optimal use for this biomarker might be in combination with other ECM biomarkers.

#4287 Serological quantification of fibroblast activation protein (FAP) cleaved type III collagen: A biomarker for FAP activity.

R. S. Pedersen, M. Karsdal, N. Willumsen;
Nordic Bioscience, Herlev, Denmark

Introduction: Fibroblast activation protein (FAP) has unique proteolytic activity with very low expression in healthy tissues, while being upregulated in diseased tissues including many types of cancer for example non-small cell lung cancer (NSCLC). The disease specific expression and unique proteolytic activity have made FAP an interesting protein to be utilized for drug targeting purposes. Therefore, it is important to identify the patients with FAP activity. The aim of the study was to develop a tool to non-invasively quantify FAP activity and investigate its potential as a biomarker for patients with NSCLC.
Methods: We developed an ELISA (named C3F), with monoclonal antibodies raised against a FAP generated fragment of type III collagen that was identified by MS, to quantify FAP-mediated cleavage of type III collagen in serum to reflect proteolytic activity of FAP. We confirmed that the biomarker reflects proteolytic activity of FAP by incubating type III collagen with or without FAP and measured C3F. In addition, we confirmed elevated FAP expression in NSCLC (adenocarcinoma and squamous cell carcinoma) compared to healthy tissue and correlation between FAP and COL3A1 expression using data from The Cancer Genome Atlas (TCGA). The comparisons between FAP expression in healthy and cancer tissue was done using one-way ANOVA and correlation between FAP and COL3A1 was done using Spearman correlation. Lastly, C3F was measured in serum samples from patients with NSCLC (n = 109) and healthy controls (n = 42) and the two groups was compared using Mann Whitney test and area under receiver operating characteristic curves (AUROCs).
Results: A C3F signal only appeared after type III collagen incubation with FAP, supporting that C3F reflects FAP proteolytic activity. C3F was significantly elevated in serum from patients with NSCLC compared to healthy controls ($p < 0.0001$, AUROC = 0.78). In support, FAP expression (TCGA) was significantly elevated in NSCLC tissue compared to normal lung tissue ($p < 0.0001$) and FAP expression correlated with expression of COL3A1 (persons $r = 0.83$).
Conclusion: The FAP-cleavage mediated type III collagen fragment C3F reflects FAP activity and can be quantified non-invasively in serum. In this study we show C3F as promising diagnostic biomarker in NSCLC, however as the biomarker reflects FAP activity the optimal use is more is potentially as a predicter of treatment response from FAP-based drug delivery systems.

TUMOR BIOLOGY: Tumor Evolution Models and Technologies
Poster Session

#4291 Bai1 inhibition promotes ferroptosis of breast cancer cells to prevent tumor growth in human xenograft tumor models.

F. K. Noubissi[1], O. Odubanjo[1], H.-C. Huang[1], B. Ogle[2], P. Tchounwou[3];
[1]Jackson State University, Jackson, MS, [2]University Of Minnesota-Twin Cities, Minneapolis, MN, [3]Morgan State University, Baltimore, MD

The adhesion G-protein coupled- receptor 1 ADGRB1/Bai1 was identified as a phosphatidylserine receptor that cooperates with ELMO/Dock180/Rac to promote maximal engulfment of apoptotic cells. This function of Bai1 was also shown to promote myoblasts fusion. Cell-cell fusion has been demonstrated to occur in normal physiological functions as well as in diseases. Studies have shown in cancer that cell-cell fusion increases tumor heterogeneity, drug resistance, and metastasis as hybrids acquire new properties that allow them to migrate and proliferate at new sites. Activation of ELMO-Dock signaling pathway has been associated with breast cancer metastasis. Moreover, ELMO1 has been identified as a modifier of breast cancer risk for BRCA mutation carriers. Rac1 was also shown to be overexpressed in proliferative breast disease, preinvasive and invasive breast carcinoma as well as lymph node metastases. Our recent studies showed that breast cancer cell fusion with bone marrow-derived mesenchymal stem cells was modulated by hypoxic conditions and promoted by apoptosis. Our hypothesis is that hypoxia stress induced apoptosis activates the phosphatidylserine receptor Bai1, and it signals through the ELMO/DOCK180/Rac to promote breast cancer cell fusion-driven tumor heterogeneity and metastasis. In this study, we determined the ability of Bai1 depleted breast cancer cells to induce tumor growth in immunocompromised mice. We used Bai1 sgRNA to inhibit Bai1 expression in the breast cancer cell MDA-MB-231. These cells ($1x\ 10^6$) together with bone marrow-derived mesenchymal stem cells (MSCs) ($1x\ 10^6$) were injected into the fat pad of the breast of 15 NOD SCID female mice. Control mice (15) received the same cells with no inhibition of Bai1. The mice were monitored for eight weeks. We found that Bai1 inhibition significantly reduced tumor growth in these mice in the course of time ($P<0.05$). The average tumor weight was also significantly reduced when Bai1 was inhibited ($P<0.001$). RNA sequencing of tumors generated from these mice revealed a significant increase in the expression of genes driving ferroptosis and a reduction in critical oncogenes in the experiment group compared to the control group. These findings will be helpful in the development of new classes of drugs effective in breast cancer treatment.
Grant Support The NIH/ NIMHD grant 5U54MD015929-03, the Society for Investigative Dermatology (SID) Freinkel Diversity Fellowship, and NSF Award Notice for Award ID 2142465 (awarded to FNK).

#4292 Unraveling the interplay of aging, smoking, and mutation-driven clonal expansions in lung cancer evolution: A multifaceted approach.

A. N. Briggs, J. DeGregori;
University of Colorado Anschutz Medical Campus, Aurora, CO

Despite the well-established link between tobacco use and lung cancer, military personnel face additional risks due to heightened smoking rates and exposure to various environmental contaminants. Aging further amplifies susceptibility to lung cancer, contributing to elevated incidence rates among Veterans compared to non-Veterans. Our studies aim to elucidate the intricate relationship between aging, smoking, and mutation-driven clonal expansions in lung tissue, examining their impact on lung function and cancer evolution. Using cell culture and mouse models, we introduce mutations identified in human lung tissue into airway epithelial cells. Using CRISPR, base editing, and genetically engineered mouse models, we assess the effects on barrier function, cell differentiation, and gene expression. Ultimately, we are investigating the interaction between induced mutations, aging, and smoking, exploring how mutation-driven clonal expansions contribute to lung dysfunction and pre-malignant phenotypes, potentially forming a feedforward loop. This research addresses critical gaps in understanding the complex interplay of aging, smoking, and mutation-driven clonal expansions in lung cancer evolution. Findings have the potential to unveil novel insights into the development of lung dysfunction and malignancy, paving the way for safe and accessible interventions to reduce cancer risk and enhance lung health.

#4293 Chromosomal instability causes epigenetic aberrations in cancer.

Albert S. Agustinus[1], Duaa Al-Rawi[1], Bhargavi Dameracharla[2], Ramya Raviram[3], Bailey S. C. L. Jones[4], Stephanie Stransky[5], Lorenzo Scipioni[6], Jens Luebeck[2], Melody Di Bona[1], Danguole Norkunaite[1], Robert M. Myers[3], Mercedes Duran[1], Seongmin Choi[7], Britta Weigelt[8], Shira Yomtoubian[9], Andrew McPherson[7], Eleonore Toufektchan[10], Kristina Keuper[11], Paul S. Mischel[12], Vivek Mittal[9], Sohrab P. Shah[7], John Maciejowski[10], Zuzana Storchova[11], Enrico Gratton[6], Peter Ly[13], Dan Landau[3], Mathieu F. Bakhoum[4], Richard P. Koche[14], Simone Sidoli[5], Vineet Bafna[2], Yael David[15], Samuel F. Bakhoum[1]

[1]Human Oncology and Pathogenesis Program, Memorial Sloan Kettering Cancer Center, New York, NY,[2]Computer Science, University of California, San Diego, La Jolla, CA,[3]New York Genome Center, New York, NY,[4]Ophthalmology and Visual Science, Yale University School of Medicine, New Haven, CT,[5]Biochemistry, Albert Einstein College of Medicine, New York, NY,[6]School of Engineering, University of California, Irvine, Irvine, CA,[7]Epidemiology and Biostatistics, Memorial Sloan Kettering Cancer Center, New York, NY,[8]Pathology and Laboratory Medicine, Memorial Sloan Kettering Cancer Center, New York, NY,[9]Cell and Developmental Biology, Weill Cornell Medicine, New York, NY,[10]Molecular Biology Program, Memorial Sloan Kettering Cancer Center, New York, NY,[11]Molecular Genetics, University of Kaiserslautern, Kaiserslautern, Germany,[12]Pathology, Stanford University School of Medicine, Stanford, CA,[13]Pathology, University of Texas Southwestern Medical Center, Dallas, TX,[14]Center for Epigenetics Research, Memorial Sloan Kettering Cancer Center, New York, NY,[15]Chemical Biology Program, Memorial Sloan Kettering Cancer Center, New York, NY

Chromosomal instability and changes in the epigenome are defining features in most metastatic cancers. Our research links chromosomal missegregation, their containment in micronuclei, and subsequent rupture of the micronuclear envelope to histone post-translational modification aberrations. This relationship was across all tested human and murine cancer cell lines, as well as non-transformed cells. Furthermore, we discovered that the observed changes in histone PTMs were caused by either micronuclear rupture or the persistence of histone PTM status during cell division. Moreover, we revealed substantial chromatin accessibility differences in micronuclei. Notably, there is a distinct bias in chromatin accessibility between promoter regions compared to distal and intergenic regions of the genome, which aligned well with observed changes in histone modifications. The induction of chromosomal instability leads to widespread, heterogeneous, and heritable abnormalities in the epigenetic landscape of cancer cells. Therefore, on top of genomic copy number changes, chromosomal instability causes epigenetic reprogramming, which adds another layer to cancer heterogeneity.

#4294 The emerging role of deubiquitinase enzymes in lung cancer plasticity.

Juntae Kwon[1], Jinmin Zhang[2], Boram Mok[1], Samuel Allsup[2], Cecil Han[1]

[1]Department of Oncology, Georgetown University School of Medicine, Washington, DC, [2]Department of Biochemistry and Molecular & Cellular Biology, Georgetown University School of Medicine, Washington, DC

Lung cancer is characterized by a high degree of genetic and molecular heterogeneity. Lineage plasticity has emerged as a source of intratumoral heterogeneity and drug resistance, resulting in poor prognosis and treatment failure. The molecular mechanisms driving lung cancer plasticity remain unclear. Ubiquitin-Specific Peptidase 13 (USP13), a deubiquitinating enzyme, is one of the most amplified genes in lung squamous cell carcinoma (LUSC). We developed a USP13 knock-in overexpressing mouse model in *Kras*$^{LSL\text{-}G12D/+}$; *Trp53*$^{fl/fl}$ (KP) background (KPU mice). USP13 overexpression resulted in aggressive tumorigenesis and a shortened survival in *Kras*/*Trp53*-driven lung cancer. Notably, while KP mice developed lung adenocarcinoma (LUAD), KPU mice developed LUSC and LUAD. LUSC in KPU mice faithfully recapitulated the key pathohistological, molecular features, and cellular pathways of human LUSC. Bulk RNA-sequencing analysis showed that KPU tumors were heterogeneous and enriched in lineage reprogramming pathways including basal cell signaling, stem cell pluripotency, and epithelial-mesenchymal transition (EMT). Using cell-type-restricted adenoviral Cre to target cells expressing surfactant protein C (SPC) or club cell antigen 10 (CC10), we identified bronchiolar secretory club cells as the predominant cell origin of LUSC. USP13 altered the levels of lineage transcription factors such as TTF-1 and SOX2 in club cells during early tumorigenesis. Altered expression of these factors reinforced the fate of CC10+ club cells to squamous carcinoma development rather than adenocarcinoma. In addition, USP13 directly acted on the K48-linked ubiquitination of c-Myc and increased its protein stability, contributing to the elevation of squamous gene expression (SOX2, CK5, P40) in the primary mouse and advanced human lung cancer cells. These results suggest that USP13 promotes lineage plasticity in club cells during the early stage of cancer development and drives reprogramming into LUSC. We also found a potential functional association between USP13 and EMT pathway. Notably, irrespective of cell origin, USP13 overexpression enhanced EMT marker expression including N-cadherin, SNAI1, and ZEB1 in lung cancer cells, promoting cell migration and invasion. USP13 increased tumorigenic and metastatic abilities of lung cancer cells in 3D organoid culture and syngeneic mouse models. Collectively, our research highlights the pivotal significance of USP13 in unleashing lineage plasticity during lung cancer progression, suggesting the potential role of deubiquitinase enzymes in regulating lineage plasticity, which may lead to novel therapeutics for treating lung cancer.

#4295 Apoptotic DNase DFFB-induced DNA damage within cancer persister cells underlies acquired resistance to targeted therapies across multiple tumor types.

A. F. Williams[1], D. A. G. Gervasio[1], C. E. Turkal[1], A. E. Stuhlfire[1], M. X. Wang[1], B. E. Mauch[1], A. H. Nguyen[1], M. H. Paw[1], M. Hairani[1], C. P. Lathrop[1], S. H. Harris[1], J. L. Page[2], M. J. Hangauer[1];

[1]UC San Diego, La Jolla, CA, [2]Salk Institute for Biological Studies, La Jolla, CA

Cancer acquired drug resistance contributes to a large proportion of patient deaths. A major obstacle to the development of effective therapies which prevent resistance is our lack of understanding of the relevant fundamental molecular adaptive processes. Here we report the discovery that tumor cells rely upon sublethal engagement of apoptotic death machinery and apoptotic DNase DFFB to acquire resistance to targeted therapies in multiple tumor types in cell culture and in vivo. We found that while DFFB wild type tumor cells readily acquire resistance to targeted therapies by escaping from the quiescent “persister” state into proliferating resistant cells, persister cells lacking functional DFFB remain indefinitely in a quiescent state on treatment. Mechanistically, we found that DFFB, which is activated by apoptotic caspases in surviving cancer persister cells, induces persistent DNA damage which promotes resistance through acquired mutations and nongenetic resistance through suppression of growth-arresting interferon signaling. During drug treatment acute interferon induction arises from sublethal mitochondrial outer membrane permeabilization and cytoplasmic exposure of mitochondrial nucleic acids which activate pattern recognition receptors. However, during longer treatments we found that DFFB knockout persister cells exhibit strikingly elevated levels of STAT1 and STAT2 and interferon stimulated gene sets. This interferon signaling is growth arresting because treatment of DFFB knockout persister cells with a JAK1/2 inhibitor rescues their ability to regrow. Furthermore, in DFFB wild type persister cells we found that DFFB-dependent DNA damage activates stress response transcription factor ATF3 which blocks the transcriptional activation of interferon stimulated genes following initial interferon induction. This is consistent with prior data in other contexts demonstrating that ATF3 is induced by DNA damage and that ATF3 directly binds to promoters of multiple interferon genes repressing their expression. These findings reveal that DFFB activation in persister cells prevents chronic interferon signaling and enables escape into proliferating drug resistant tumor cells. Therefore, DFFB-mediated interferon suppression represents a novel mechanism that is fundamental to acquired drug resistance. In addition, high expression of DFFB and ATF3 correlates with worse overall survival in a pan-cancer analysis and DFFB knockout mice develop normally indicating DFFB is a nonessential gene in normal tissue. Therefore, we propose that DFFB is a promising therapeutic target to prevent acquired resistance to targeted therapy.

#4296 Investigating metabolic sensitivity and organization of renal cell carcinoma: To enhance effective therapies and patient survival.

M. Patankar[1], J. Albeck[1], S. Gulati[2];

[1]University of California Davis, Davis, CA, [2]UC Davis Comprehensive Cancer Center, Sacramento, CA

Background: Renal cell carcinoma (RCC) is the 6th most common cancer in men and the 9th most common in women in the United States. RCC tissues are metabolically dysfunctional, often resulting from loss of von-Hippel Lindau (VHL) and consequent upregulation of hypoxia-inducible factor (HIF1/2). HIF1a is a transcription factor that upregulates glycolytic gene expression. Current therapies, including immune checkpoint inhibitors and tyrosine kinase inhibitors, have shown improvements in the outcomes of RCC patients, however, there are no biomarkers clinically available to predict the efficacy of these drugs. While genomic data and transcriptomic signatures have been investigated, they are not used in clinical practice due to lack of prospective validation. Understanding additional pathways pertaining to metabolic features of RCC, is critical. Our bulk gene expression analysis of primary RCC samples from TCGA-KIRC show a predominance of genes expressing mitochondrial ribosomal proteins and electron transport chain in tumors that relapsed early after nephrectomy, warranting further validation.

Aim: We aim to investigate changes in metabolic adaptation in RCC cells from kidney cancer cell lines (VHL mutant) and primary cells from human-matched primary and metastatic kidney cancer sites. Using a novel biosensor-based technique developed in the Albeck lab, we aim to identify the dependence of live RCC cells on specific metabolic pathways and test the effect of standard-of-care (SOC) pathway inhibitors such as tyrosine kinase, HIF pathway, metabolic pathway inhibitors impacting tumorigenicity.

Methods: To examine functional metabolic behavior in single cells, we generated immortalized cell lines (MCF10A, 184A1, FL83B and HBE-1) stably transfected with biosensors for the activity of AKT, glycolysis, mTOR and AMPK pathway. Data from Live-cells treated with metabolic inhibitors were collected and analyzed using our MATLAB-based pipeline. We have extended the analysis to RCC cell lines (786-O cell lines) and primary cells collected from nephrectomy specimens and matched metastatic biopsy samples, using current SOC pathway inhibitors (including sorafenib, sunitinib, belzutifan) and investigational metabolic drugs (metformin, IACS-010759, niclosamide).

Results & Conclusion: Our preliminary results show an association of high OX-PHOS with primary tumors from early relapse after nephrectomy than the relapsed late tumors. Our biosensor single cell data show that even genetically homogeneous cell populations can vary in their usage of OXPHOS and glycolysis to supply ATP for cell growth. Tumor gene expression profile coupled with biosensor data, will address mechanism behind this metabolic shift in RCC tumors in primary cells isolated from primary and metastatic sites. Our research will improve tumor prognosis and allow designing therapeutic trials.

#4297 Interrogating metabolic heterogeneity and cooperation in lung cancer collective cell invasion.

I. E. Robinson[1], V. Matsuk[2], M. Shanmugam[2], J. K. Mouw[2], A. I. Marcus[2];

[1]Georgia Institute of Technology/Emory Winship Cancer Institute, Atlanta, GA, [2]Emory Winship Cancer Institute, Atlanta, GA

Tumor heterogeneity contributes to tumor progression and a variable response to treatment. We have previously shown that tumor heterogeneity - including metabolic, transcriptional and mutational - underlies non-small cell lung cancer (NSCLC) collective invasion. Using stable subpopulations derived with our Spatiotemporal Cellular and Genomic Analysis (SaGA) technique, we found that two distinct subpopulations of the H1299 NSCLC line cooperate during collective tumor invasion *in vitro*; while H1299 pack leaders are heavily dependent on oxidative phosphorylation, H1299 pack followers are more reliant on glycolysis. To further dissect how intratumoral heterogeneity enables cancer progression to metastasis, we incorporate high resolution imaging, stable fluorescent labeling, gene editing, and *in vitro* tumor invasion models to interrogate mechanisms of metabolic cooperation between heterogeneous NSCLC subpopulations. We hypothesize that cooperation and communication between these distinct metabolic subpopulation drives metastatic tumor progression. To determine mechanisms of metabolic cooperativity between subpopulations, we stably transduced our subpopulations to fluorescently label either the mitochondria (through TOM20 labeling) or a key enzyme in glycolysis (through glucose 6-phosphate isomerase GPI labeling), cultured labeled subpopulations with unlabeled subpopulations, and observed metabolic changes and exchange via time-lapse, fluorescence microscopy and flow cytometry in 2D culture conditions. Next steps include visualizing the metabolic cooperation that occurs in conditions mimicking the tumor microenvironment (i.e., 3D invasion assays) using super-resolution microscopy. Taken together, we have developed a method of temporally visualizing metabolic exchange with high spatial resolution between NSCLC subpopulations to investigate the underlying mechanisms enabling successful cell invasion in a variety of tumor microenvironments. Thus far, we have discovered multiple broad mechanisms of exchange including tunneling nanotubes and extracellular vesicles, both of which are inducible with certain stressors common to the tumor microenvironment.

#4298 Predicting tumor evolution from digital histology using AI.

C. E. Spencer[1], A. Camara[2], A. Riou[2], L. Au[1], J. I. Lopez[3], Z. Tippu[1], C. Maussion[2], K. Ho[1], A. Strange[1], E. Nye[1], V. Birault[1], L. Van-praet[2], K. Edmonds[4], E. Carlyle[1], S. Hazell[4], S. Rudman[5], J. Larkin[1], S. Turajlic[1];

[1]The Francis Crick Institute, London, United Kingdom, [2]Owkin, Paris, France, [3]Biocruces Bizkaia Health Research, Biaritz, Spain, [4]The Royal Marsden Hospital, London, United Kingdom, [5]Guys and St Thomas' Hospital NHS Trust, London, United Kingdom

Diverse clinical presentations of clear cell renal cell carcinoma (ccRCC) confound clinical decision making, leading to over and undertreatment. Clonal evolution of ccRCC proceeds through distinct trajectories characterised by differing levels of genomic intratumoral heterogeneity (gITH) and chromosomal complexity (weighted genomic instability index, wGII). However, accurate evaluation of these indices requires multiregional profiling of fresh tumour; cost prohibitive and logistically challenging in the clinical setting. Clinical histopathology workflows routinely capture multiple tumour areas enabling the use artificial intelligence (AI) to predict tumour evolutionary features directly from clinical grade H&E whole slide image (WSIs). ccRCC displays profound genetic and histological ITH but the link between these entities remains unclear. We leverage the TRACERx Renal cohort, comprising 1485 WSIs from 81 tumours to predict WGII and gITH and to gain insights into the relationship between genetic and histological ITH. Critically, each WSI is associated with a wGII and gITH label derived from a closely linked fresh tumour sample. For both prediction tasks, we extracted meaningful features for each WSI using self-supervised representation learning “MoCo”. Since high wGII confers poor prognosis we focussed on predicting binary stratification label of high wGII or low wGII (relative to the cohort median). First we predicted wGII as a continuous variable using a supervised multiple instance learning regression model trained on the MoCo features, and then classified the predicted wGII into “high” or “low” achieving 0.80 AUROC. To predict gITH we postulated that the degree of gITH would correlate with histological ITH. Using an unsupervised clustering of refined MoCo features we defined 24 histological clusters. The number of computationally derived histological clusters within a single tumour positively correlated with gITH (pearson’s 0.56). We used the number of clusters to classify WSIs into prognostic binary groups of high or low gITH (relative to the cohort median) achieving an AUROC of 0.80. To understand the biological relationship between histological and genetic ITH we pathologically characterised the histological clusters: a pathologist annotated WSIs with tumour architecture and cytomorphology. Image tiles were associated with the annotations using spatial coordinates, illuminating phenotypic traits of different evolutionary trajectories and providing an interpretability framework for our AI pipelines. Since the tumour evolutionary course dictates disease progression tempo, applying evolutionary classification in clinic can fundamentally improve patient care. Here, for the first time, we provide a framework to translate fundamental evolutionary principles underpinning tumour biology and clinical progression into a prognostic computational pathology biomarker possible to clinically implement.

#4299 A lineage-specific role of oncogenic protein kinase Cι in lung adenocarcinoma.

D. T. Nguyen, N. Yin, C. R. Weems, L. Jamieson, K. Meneses, Y. Liu, N. R. Murray, A. P. Fields;
Mayo Clinic Florida, Jacksonville, FL

Lung adenocarcinoma (LUAD), the most prevalent subtype of lung cancer, can arise from two different cell populations: alveolar type 2 (AT2) cells and bronchiolar club cells. By utilizing genomic data from the cancer genome atlas program, human LUAD cell lines, and the well-characterized *LSL-Kras*^{G12D}/*Trp53*$^{-/-}$ (*KP*) mouse model, we demonstrated that tumors arising from club cells are much more aggressive and follow a different trajectory of tumorigenesis when compared to those arising from AT2 cells. Intriguingly, our data strongly suggest that expression and signaling activity of protein kinase C iota (PKCι) can profoundly affect the cell of origin and oncogenic signaling pathways employed by resultant tumors. Specifically, *KP*-mediated transformation of club cells appears to be dependent on PKCι-ELF3-NOTCH3 and PKCι-YAP1 signaling axes, while AT2 cell malignancy is dependent on the PKCι-independent WNT signaling. In addition, club-cell-origin tumors exhibit an enrichment of cancer stem cells and increased infiltration of immunosuppressive myeloid cells in comparison to AT2-cell-origin tumors. This results in accelerated progression and increased likelihood of metastasis by LUAD tumors that originate from club cells. Taken together, our results indicate that PKCι expression and signaling activity can profoundly influence the cells of origin, tumor trajectories, and therapeutic vulnerabilities of LUAD tumors.

#4300 Large-scale, low-cost, and accurate measurement of cancer evolutionary dynamics from clinical patient samples.

C. Gabbutt[1], M. Duran-Ferrer[2], H. Grant[1], D. Mallo[3], F. Nadeu[2], J. Househam[1], N. Villamor[2], O. Krali[4], J. Nordlund[4], T. Zenz[5], E. Campo[2], A. Lopez-Guillermo[2], J. Fitzgibbon[6], C. P. Barnes[7], D. Shibata[8], J. I. Martin-Subero[2], **T. A. Graham[1]**;

[1]Institute of Cancer Research, London, United Kingdom, [2]Fundacio de Recerca Clinic Barcelona-Institut d'Investigacions Biomediques August Pi i Sunyer, Barcelona, Spain, [3]Arizona State University, Tempe, AZ, [4]Uppsala University, Uppsala, Sweden, [5]University Hospital and University of Zurich, Zurich, Switzerland, [6]Barts Cancer Institute, London, United Kingdom, [7]University College London, London, United Kingdom, [8]University of Southern California, Los Angeles, CA

Introduction: Cancer is a dynamic evolutionary process; thus, the evolutionary history of a cancer should strongly influence its future trajectory and so the clinical outcome of patients. However, accurately assessing an individual cancer's evolutionary history in a scalable and clinically relevant manner is currently an open problem. To address this, we introduce a novel methodology (EVOFLUx) to quantitively infer the history of a cancer from single time-point bulk samples using inexpensive, standard methylation arrays.

Description of Methodology: We recently identified fluctuating CpGs (fCpGs), which are CpGs that neutrally and stochastically change methylation state over time in individual cells, uniquely barcoding cells and thus enabling high temporal-resolution lineage tracing approaches. In a bulk population of cancer cells, the distribution of fCpG methylation is determined by the evolution of the population and thus encode a cancer's past clonal dynamics. Here, we have developed a general computational approach to model how the patterns of fCpGs vary according to the evolutionary history of a growing cancer, and a Bayesian inference method to infer these parameters from data.

Results We applied EVOFLUx to quantify the evolutionary dynamics of 1,976 lymphoid cancers, finding that the tumor growth rates, malignancy age and epimutation rates varied by orders of magnitude across disease types.

In addition, EVOFLUx allowed us to test for the presence of ongoing subclonal selection and validated our inference with matched whole exome sequencing data. Alongside characterizing the evolutionary dynamics within single bulk samples, fCpGs also allow for the inference of the phylogenetic relationships between longitudinal samples, which we validated with whole genome sequencing.

Within cancer types, more aggressive subtypes typically had elevated growth rates. In our clinically annotated cohort of chronic lymphocytic leukemia (CLL) samples, we found that patient-specific evolutionary dynamics are strongly associated with outcome.

Conclusions: Hence, we present a powerful new method that uses widely available, low-cost bulk DNA methylation data to precisely measures cancer evolutionary dynamics in patient samples with clinical implications.

#4301 Increasing the therapeutic vulnerability of heterogenous cell phenotypes within prostate cancer.

A. I. Paxson[1], L. H. Chang[2], K. D. Marr[1], J. M. C. Gard[1], C. S. Nelson[1], A. Kapoor[2], W. L. Harryman[1], J. J. Marugan[2], M. J. Henderson[2], T. W. Sanchez[2], A. E. Cress[1];

[1]University of Arizona, Tucson, AZ, [2]National Institutes of Health, Rockville, MD

Phenotype heterogeneity is a hallmark of prostate adenocarcinoma and is a major source of recurrent disease. We tested pre-clinical therapies to eradicate phenotypically distinct cell populations derived from the parental DU145^{WT} prostate cancer cell line. The derived cell lines are called DU145^{AA}, DU145^{J7}, and DU145^{G6}. The DU145^{AA} variant is a non-aggressive cell population while the DU145^{J7} and DU145^{G6} are aggressive phenotypes that invade through muscle and metastasize to bone. Flow cytometry analysis documented the phenotypic plasticity of the DU145 cell variants since DU145 aggressive lines expressed 1.3-fold increases in matrix metalloprotease 14 surface expression and a 2-fold increase in tri-methyl Histone H3 at lysine 27 as compared to the DU145^{WT} parent line. The DU145^{AA} non-aggressive line expressed an epithelial cell-cell lineage phenotype with up to 2-fold increases in E-cadherin, claudin 4, claudin 7, and a unique cytokeratin 6A expression and a 2-fold loss of Zinc finger E-box-binding homeobox 1, EVL, and Kindlin 2. A collaboration with the National Center for Advancing Translational Science (NCATS) resulted in the identification of pharmacological agents active in eradicating DU145^{J7} and DU145^{G6} cells as compared to the DU145^{WT} population. The agents were selected from a quantitative high-throughput screen of 10,677 combined investigative and approved anti-cancer agents using the Cell Titer-Glo Luminescent Cell Viability assay. We independently validated 31 compounds from the assay that have 2-fold, or greater, differences in concentration to inhibit 50% cell growth (IC_{50}) between the wild-type and aggressive variants of DU145 cells. The top 10 hits were tested for the efficacy of different combinations to eradicate defined admixtures of aggressive and non-aggressive phenotypes, including the DU145^{AA} cells, to model tumor heterogeneity. Tested compounds with differential sensitivity between aggressive and non-aggressive cells were those inhibiting histone deacetylase (vorinostat, fimepinostat, and pracinostat), proteasomes (bortezomib, delanzomib, ixazomib), topoisomerases (gimatecan and daunorubicin), and other compounds identified independently by us targeting nicotinamide phosphoribosyl transferase (FK866) and DNA (bleomycin). Using admixtures of tumor cell phenotypes, we determined optimal combinations of compounds that would selectively eradicate the sub-populations. The results suggest that determination of phenotypes within tumor populations may eliminate the heterogenous tumor and prevent recurrent disease. Funding was provided by the University of Arizona Cancer Center (NCI-P30 CA23074 and NCI-R01 CA159406) and by the Partnership in Native American Cancer Prevention at the University of Arizona (U54CA143924) and Northern Arizona University (U54CA143925). Collaborators at NCATS were supported by the intramural research program.

#4302 ONECUT2 activates diverse resistance drivers of androgen receptor-independent heterogeneity in prostate cancer.

C. Qian[1], Q. Yang[1], M. Rotinen[2], R. Huang[3], H. Kim[1], B. Gallent[1], Y. Yan[1], R. M. Cadaneanu[3], B. Zhang[3], S. Kaochar[4], S. J. Freedland[1], E. M. Posadas[1], L. Ellis[5], D. Di Vizio[1], C. Morrissey[6], P. S. Nelson[7], L. Brady[7], R. Murali[1], M. J. Campbell[1], W. Yang[8], B. S. Knudsen[9], E. A. Mostaghel[10], H. Ye[1], I. P. Garraway[3], S. You[1], M. R. Freeman[1];

[1]Cedars-Sinai Medical Center, Los Angeles, CA, [2]Public University of Navarre, Pamplona, Spain, [3]UCLA, Los Angeles, CA, [4]Baylor College of Medicine, Houston, TX, [5]National Cancer Institute, Bethesda, MD, [6]University of Washington, Seattle, WA, [7]Fred Hutchinson Cancer Center, Seattle, WA, [8]Stony Brook University, New York, NY, [9]University of Utah, Salt Lake City, UT, [10]U.S. Department of Veterans Affairs Puget Sound Health Care System, Seattle, WA

Androgen receptor- (AR-) indifference is a mechanism of resistance to hormonal therapy in prostate cancer (PC). Here we demonstrate that ONECUT2 (OC2) activates resistance through multiple drivers associated with adenocarcinoma, stem-like and neuroendocrine (NE) variants. Direct OC2 targets include the glucocorticoid receptor (GR) and the NE splicing factor *SRRM4*, which are key drivers of lineage plasticity. Thus, OC2, despite its previously described NEPC driver function, can indirectly activate a portion of the AR cistrome through epigenetic activation of GR. Mechanisms by which OC2 regulates gene expression include promoter binding, enhancement of genome-wide chromatin accessibility, and super-enhancer reprogramming. Pharmacologic inhibition of OC2 suppresses lineage plasticity reprogramming induced by the AR signaling inhibitor enzalutamide. These results demonstrate that OC2 activation promotes a range of drug resistance mechanisms associated with treatment-emergent lineage variation in PC and support enhanced efforts to therapeutically target OC2 as a means of suppressing treatment-resistant disease.

#4303 Enrichment of nonadherent prostate cancer stem cell populations using simulated microgravity bioreactor.

K. Khazaw, S. Unlu, A. M. Dwead, B. Cinar;
Clark Atlanta University, Atlanta Georgia, GA

Prostate cancer is the most prevalent and the leading cause of cancer-related death among men, particularly African Americans. The cellular and molecular mechanisms contributing to this deadly disease remain largely unknown. As such, there are no effective strategies to treat metastatic cancer and improve patient outcomes. Anchorage-independent growth of circulating prostate tumor cell clusters is essential for developing cancer metastasis. However, there is no model system to study the molecular and functional characteristics of prostate tumor cell clusters reminiscent of the bloodstream in a laboratory setting. In addressing this need, we have established nonadherent LNCaP cell clusters, LN-G2 and LN-G3, under androgen-depleted growth conditions in a simulated microgravity bioreactor called Slow Turning Lateral Vessel (STLV). Our quantitative PCR analysis repeatedly demonstrated that LN-G2 and LN-G3 cell populations expressed high levels of the well-characterized CD44 and CXCR4 cancer stem cell maker, respectively, compared to the LNCaP parental. In addition, our functional analysis indicates that, unlike the LNCaP cell, LN-G2 and LN-G3 cells showed superior clonogenic and growth behaviors in response to androgen depletion and enzalutamide-treatment under adherent monolayer and nonadherent conditions. These observations suggest that cancer stem cell-like cell clusters that survived under microgravitational stress confer distinctive molecular and functional properties associated with superior survival and contribute to castration-resistant prostate cancer. Furthermore, the STLV bioreactor could help enrich cancer stem cell populations and enhance our understanding of the underlying mechanisms of lethal cancer, which may lead to novel therapeutics to improve patient outcomes.

#4304 Chromosome 3 dosage-loss informs on the unique biology underlying ultra high-risk uveal melanoma.

J. L. Rose[1], S. Srinivasan[1], M. He[1], R. Minelli[1], C.-Y. Liu[1], C. Terranova[1], J. Gay[1], J. R. Daniele[1], L. Dmitriy[1], M. Peoples[1], M. Soeung[1], V. Ramamoorthy[1], P. Shah[1], S. Soni[1], C. Bristow[1], F. Wang[1], A. Lopez[1], C. Deckard III[1], B. Meyers[1], L. Perelli[1], K. Wani[1], N. Feng[1], C. P. Vellano[1], J. Marszalek[1], A. J. Lazar[1], A. Futreal[1], G. F. Draetta[1], S. E. Woodman[1], T. Heffernan[1], G. Genovese[1], A. Carugo[2], V. Giuliani[1];
[1]UT MD Anderson Cancer Center, Houston, TX, [2]IRBM, Rome, Italy

Uveal melanoma (UM) is a rare and lethal tumor characterized by mutually exclusive activating mutations in *GNAQ* and *GNA11*, secondary mutations in *EIF1AX*, *SF3B1* and *BAP1*, and a late-stage chromosome 3 copy-number (CN) loss event. Importantly, chromosome 3 CN loss is associated with BAP1 loss-of-function (LOF) and corresponds with tumor metastasis and poor patient prognosis. Understanding the biology underlying this chromosome 3 CN loss event is critical to informing on metastatic UM. To this end, we leveraged CRISPR-based centromere targeting to engineer multiple clones exhibiting chromosome 3 CN loss. We determined that dosage-loss of chromosome 3 was sufficient to develop multiple isogenic clones exhibiting genomic features of “ultra high-risk” UM, independent of BAP1 LOF. Leveraging this isogenic system, we evaluated *in vitro* and *in vivo* profiling, demonstrating site-specific liver metastasis only in orthotopic HR tumors, along with a significantly increased fitness in the liver. Next, we sought to inform on differential signaling pathways and therapeutic sensitivity between LR and HR models. Characterization of established UM oncogenic pathways identified a clear disengagement from classical MAPK and non-canonical Hippo signaling in the HR clones. These findings also correlate with a significant decrease in sensitivity to MEK and FAK inhibitors. In addition, we observed a PKC isoform swap from PKCε and PKCδ to PKCα, a feature observed in late-stage UM patient tumors. Interestingly, we also observed an increase in the expression of PRAME and NBS1 in HR models, both markers for poor prognosis in patients. Genome-anchored transcriptomic analysis also captured distinct profiles between the LR and HR clones, highlighting a significant increase in MYC associated targets upon chromosome 3 dosage-loss. This increase in MYC signaling coincides with site-specific 8q amplifications across the HR clones, implicating MYC as a core fitness driver in high-risk UM and a potential contributor to poor patient prognosis in monosomy 3 patients. Leveraging engineered models of chromosome 3 CN loss, and the subsequent induction of “ultra high-risk” UM, provides a unique opportunity to inform on the underlying biology of UM evolution and potential therapeutic strategies.

#4305 Analysis of tumor heterogeneity in syngeneic models; CT26.WT colon carcinoma and 4T1-Luc2-1A4 breast carcinoma in female BALB/cAnNHsd mice.

J. Snider, D. Germain, L. Kucharczyk, A. Zaitouna, S. Barnes, D. Draper, S. Wise;
Laboratory Corporation of America, Ann Arbor, MI

Cancer is a complex disease that involves both malignant cells and the surrounding microenvironment. The tumor microenvironment (TME) is comprised of various components, including cancer-associated fibroblasts, immune cells, blood vessels, and extracellular matrix elements, all of which interact with cancer cells. It is increasingly recognized that the components of the TME are a critical determinant of therapeutic response and resistance, and as such targeting the TME has emerged as a promising strategy in cancer therapy.

Syngeneic models are necessary to study the TME, and more specifically the tumor infiltrating immune cell populations, as these models allow us to monitor various aspects of the immune response. Another important aspect to consider is tumor heterogeneity, which can cause issues during analysis due to immune cell populations not being evenly distributed throughout the tumor. The decision of whether to analyze whole tumors or halved tumors when monitoring changes in immune cell populations is an important consideration. When considering multiple endpoints from a single tumor sample, halved tumors are oftentimes considered as we remain mindful of the 3Rs (replacement, reduction and refinement) in animal research. As such, it is important to understand the effects of splitting samples and how it can affect the data that is generated.

To determine the effects of analyzing whole and halved tumor samples on immune cell subsets, studies were designed to subcutaneously implant either CT26.WT or 4T1-Luc2-1A4 cells into female BALB/cAnNHsd mice and harvest tumor samples after the completion of treatment. Mice were treated with isotype control (Clone MPC-11) or anti-mCTLA-4 (Clone 9D9). At the time of sample collection, tumors were kept whole intact or halved and analyzed via flow cytometry to quantify lymphoid and myeloid immune cell subsets within tumor samples.

The data revealed differences in immune cell subset populations for both isotype vs. anti-CTLA-4 treated tumors and whole vs. halved tumors. Changes in the lymphoid cell compartment were observed for whole vs. halved tumors of ± ~25-100% and ± ~0-40% for isotype treated and of ± ~0-30% and ± ~25-2600% for anti-CTLA-4 treated CT26.WT or 4T1-Luc2-1A4 tumors, respectively. Changes in the myeloid cell compartment of ± ~5-45% and ± ~10-65% for isotype treated and of ± ~15-100% and ± ~0-70% for anti-CTLA-4 treated CT26.WT or 4T1-Luc2-1A4 tumors, respectively, were also observed. Additionally, differences were observed between the two tumor halves, not just between whole and halved tumors.

Taken together, the data support that splitting tumor samples can negatively impact the analysis of the immune cell populations. Tumors can be split if required to perform multiple analyses, however, this should be done with caution, as it can result in trend differences and increases variability within the dataset.

#4306 Label-free melanoma phenotype classification using AI-based morphological profiling.

Evelyn Lattmann[1], **Andreja Jovic**[2], Julie Kim[2], Aizhan Tastanova[1], Tiffine Pham[2], Christian Corona[2], Kiran Saini[2], Zhouyang Lian[2], Senzeyu Zhang[2], Ryan Carelli[2], Kevin B. Jacobs[2], Manisha Ray[2], Vivian Lu[2], Stephane C. Boutet[2], Mahyar Salek[2], Maddison Masaeli[2], Mitchell P. Levesque[1]

[1]Dermatology, University Hospital Zurich, University of Zurich, Schlieren, Switzerland,[2]Deepcell Inc., Menlo Park, CA

Melanoma plasticity and heterogeneity contribute to therapeutic resistance and mortality, and the ability of melanoma cells to switch from melanocytic to mesenchymal phenotypes results in increased invasion and metastasis. Investigating the role of these phenotypic states has been challenging due to limited marker availability for each cell state. High-parameter molecular methods such as RNAseq have produced more descriptive gene signatures of phenotypic states, but these methods are cell-destructive, labor-intensive, expensive, and can take days to weeks to obtain a readout. Different morphologies have been observed for melanocytic and mesenchymal phenotypic states in culture, thus we hypothesized that morphology could provide an orthogonal method to define and study phenotypes. We utilized the Deepcell platform to develop a classifier to predict the phenotype of melanoma cells as melanocytic or mesenchymal based on morphology alone. This method is free of labels and utilizes viable cells, overcoming the technical and practical limitations of traditional, marker-based methods.

We used 20 patient-derived cell lines with known melanocytic or mesenchymal transcription scores to develop the 'Melanoma Phenotype Classifier' to phenotype melanoma cells based on morphology alone. A classifier accuracy of **>88%** was achieved, and morphological analysis of the images revealed distinct morphotypes for each phenotype, highlighting distinct morphological differences. To further link phenotypic state with multi-dimensional morphological profiles, we performed genetic and chemical perturbations known to shift the phenotypic state. The Melanoma Phenotype Classifier successfully predicted shifts in phenotypes driven by these perturbations. These results further demonstrate how phenotype is linked to distinct morphological changes that are detectable by artificial intelligence. Lastly, we applied the Melanoma Phenotype Classifier to dissociated melanoma biopsies, which revealed phenotypic heterogeneity that was confirmed by single cell RNASeq.

This work establishes a link between cellular morphology and melanoma phenotype and lays the groundwork for the use of morphology as a label-free method of phenotyping viable melanoma cells.

#4307 Quantifying the cell-intrinsic and cell-extrinsic growth effects of cancer-causing mutations *in vivo*.

C. D. McFarland, J. Maltas;
Case Western Reserve University School of Medicine, Cleveland, OH

Adaptive driver phenotypes in cancer must confer either a cell-intrinsic (birth minus death) or cell-extrinsic (field) effect on growth. These effects can be summarized by an r/K logistic growth curve, whereby cell-intrinsic effects manifest as a change in the early, exponential growth constant (*r*) of a tumor population while cell-extrinsic effects alter the long-term 'carrying capacity' (*K*). Previously, we developed a novel genetically-engineered mouse model that tracks tumor growth dynamics with unprecedented precision via Tumor Barcoding, termed TuBa-seq[1]. Here, we quantify the growth trajectories of thousands of *Kras*-driven lung tumors over eight months. Median tumor size is best-described by a Gomp-Ex growth law (i.e. N^{ν}/K where $\nu \to +0$), which also characterizes advanced-stage human tumors[2]. Carrying capacities of individual isogenic tumors varied by over four orders of magnitude, suggesting that microenvironmental heterogeneity profoundly impacts growth dynamics. Our approach further allowed us to track the growth effects of eleven canonical tumor suppressor gene knockouts introduced via multiplexed CRISPR/Cas genome-engineering. All but one of these secondary mutations augmented either the exponential growth rate or the carrying capacity of the tumor. However, only three tumor suppressor losses increased both growth parameters (Rb1, Setd2, and Stk11). Hence, the growth benefits of most cancer-causing mutations are missed when growth is measured only at a single time point. Clinically, we find that *r*-promoting and *K*-promoting mutations interact synergistically to create the most aggressive tumors in human patients (HR = 1.71, P-value < 10^{-10}). Collectively, these results support a universal *r*/*K* framework for tumor growth and progression.

References1.Rogers, Z. N. *et al.* A quantitative and multiplexed approach to uncover the fitness landscape of tumor suppression in vivo. *Nat. Methods* **14**, 737-742 (2017).2.Benzekry, S. *et al.* Classical mathematical models for description and prediction of experimental tumor growth. *PLoS Comput. Biol.* **10**, e1003800 (2014).

#4308 Same-section spatial multiomic analyses using MICS technology for investigating the dynamics of the tumor microenvironment.

Dongju Park[1], Emily Neil[1], Rebecca C. Hennessey[1], Michael DiBuono[1], Hanna Lafayette[1], Erica Lloyd[1], Hsinyi Lo[1], Julia Femel[2], Alex Makrigiorgos[1], Shaina Lu[1], John Lee[1], Sameh Soliman[1], Dominic Mangiardi[1], Paurush Praveen[2], Fabian Staubach[2], Ryan Hindman[1], Thomas Rothmann[2], Telma Santos[2], Stefan Borbe[2], Hansueli Meyer[1], Tanya Wantenaar[2], Jinling Wang[1], Werner Muller[2], Robert Pinard[1], Andreas Bosio[2]

[1]Miltenyi Biotec, Waltham, MA,[2]Miltenyi Biotec, Bergisch Gladbach, Germany

The recent increase in image-based, spatially-resolved technologies enables researchers to profile the tumor microenvironment (TME) by capturing gene expression profiles within tissue sections. However, a significant limitation of these technologies is the lack of ability to resolve protein and RNA information in the same section, as well as conveniently analyze multimodal data sets. Here, we report a spatial RNA detection method, RNAsky, using Miltenyi Biotec's MACSima™ Platform as an automated, multiomic approach. Our method integrates spatial proteomics and transcriptomics data to provide in-depth profiling with single-cell resolution on the same tissue section. We demonstrate these capabilities by characterizing key immune-oncology markers across normal and diseased tissues using our specialized MACS® iQ View analysis software. MACS iQ View provides fast segmentation and intuitive gating and clustering strategies to simultaneously assess protein and RNA data. We investigated the impact of clustering using protein, RNA, or the combination of both to evaluate the contribution of different information modalities on TME spatial dynamics. This cutting-edge approach will enable the identification of valuable parameters and new cell types, furthering the discovery and development of predictive and prognostic biomarkers.

#4309 Establishment of intratumor heterogeneity using patient derived lung cancer cells.

T. Funazo[1], H. Ozasa[1], T. Tsuji[2], Y. Shima[1], K. Suminaga[1], K. Hashimoto[1], H. Yoshida[1], T. Ogimoto[1], K. Hosoya[1], H. Ajimizu[1], T. Nomizo[1], H. Yoshida[1], T. Hirai[1];

[1]Kyoto Univ. Graduate School of Medicine, Kyoto, Japan, [2]Graduate School of Medicine, Nagoya University, Nagoya, Japan

Overcoming cancer treatment resistance is a problem that must be solved to improve the prognosis of cancer patients. In recent years, genome analysis has revealed the existence of multiple subgroups with different properties within a single tumor, and intratumor heterogeneity is a cause of treatment resistance. It has also been reported that. However, the mechanism of intratumor heterogeneity remains unclear. Previous research on intratumor heterogeneity has mainly focused on analyzing patient cancer cells, classifying subgroups, and estimating characteristic factors. This method has two drawbacks. One is limitations in including all subgroups as research subjects, and other is lack of verification of whether characteristic factors are actually involved in intratumor heterogeneity in patients. Therefore, it is necessary to use a model of "early intratumor heterogeneity" in which monoclonal cells are divided into subgroups with different properties, and to verify the discovered factors using patient-derived cancer cell lines. In alectinib-resistant cell line (H2228-AR1S) created from monoclonal ALK-positive lung cancer cell line (H2228) by exposing to alectinib *in vitro*, existence of two fractions with different appearances. Using flow cytometry, it was revealed that H2228-AR1S bimodally expresses EpCAM, and the EpCAM-low fraction has high migration ability. In EpCAM-low fraction, epithelial markers were decreased, and mesenchymal markers were increased using immunoblotting. It suggests that EpCAM low subpopulation has undergone epithelial-mesenchymal transition (EMT). Additionally, we established a BRAF-positive lung cancer cell line (KTOR83) collected with consent from patients attending Kyoto University Hospital. Cells after *in vitro* dabrafenib exposure to KTOR83 showed bimodal EpCAM expression, and the EpCAM-low fraction has high migration ability. We established an intratumor heterogeneous model using commercially available cells and a patient-derived lung cancer cell line. Furthermore, we will explore factors common to the two models and examine factors involved in intratumor heterogeneity.

#4310 Impact of drug combination schedules on the evolution of tumor resistance.

M. Stoddard[1], A. Chen[2], **L. Yuan**[1], D. Van Egeren[3], D. Bottino[4], A. Chakravarty[1];
[1]Fractal Therapeutics, Inc., Lexington, MA, [2]Columbia University, Computational Biology, NY, [3]Stanford University, Palo Alto, CA, [4]Takeda Pharmaceuticals, Cambridge, MA

The emergence of drug resistance during treatment is a critical limiting factor for the long-term effectiveness of anticancer therapies. The use of drug combinations limits the emergence of resistance, thereby prolonging their therapeutic utility. The effect of a drug combination is dependent both on the concentration of the individual drugs and the extent of their interaction (synergistic, additive, or antagonistic). Thus, understanding the scheduling implications for efficacy can be valuable for optimizing tumor response and time to resistance for the combination. To examine this more closely, we used a pharmacokinetic/pharmacodynamic (PK/PD) modeling approach, coupling one-compartment PK models of two hypothetical drugs based on set synchronous or asynchronous (offset) schedules with an evolutionary model of tumor clone growth. We simulated four tumor subpopulations representing binary resistance to one or both drugs, using an exponential growth model with growth penalties based on drug concentrations. We used the model to simulate the effects of pairs of antagonistic, synergistic, and additive drugs on the growth of sensitive and resistant populations in a tumor. Final tumor volume and resistant population were used to compare the efficacy of various drug schedules. As expected, the effect of a drug interaction—either synergistic or antagonistic—is greatest when dosing is synchronous, as this results in the greatest simultaneous drug concentration. The effect of a drug interaction is proportional to the sensitive population size, so the effect of drug interactions decreases over time as the sensitive population is eliminated. Intuitively, the final tumor volume decreases as the strength of a synergistic interaction increases until the sensitive population is eliminated. The resistant populations are unaffected by the strength of the interaction for both antagonistic and synergistic combinations. Resistant populations are not affected by interactions between drugs to which they are resistant, so the growth of resistant populations over time is independent of drug interactions. Crucially, for effective drugs—that is, drugs that eliminate the sensitive population—synergy and antagonism converge to additivity as the sensitive population dies out because the remaining resistant populations are not affected by drug interactions. As synergistic and additive drug combinations are equivalent in the long-term, synergy and asynchronous dosing could be used to limit toxicity without sacrificing efficacy. The evolution of resistance also explains why *in vitro* synergy or antagonism may not translate *in vivo*. Taken together, our work provides several unintuitive insights about combination drug scheduling with practical implications for therapeutic design.

#4311 The interplay of SYNCRIP deficiency, APOBEC activity, and extrachromosomal DNA in castration-resistant prostate cancer drug resistance.

X. Li[1], S. Deng[1], C. Wang[1], Y. Wang[2], P. Mu[1];

[1]UT Southwestern Medical Center, Dallas, TX, [2]Cincinnati Children's Hospital Medical Center, Cincinnati, OH

Background: Prostate cancer, particularly in its castration-resistant form (CRPC), frequently develops resistance to androgen receptor (AR)-targeted therapies. This resistance involves complex factors, including tumor mutational burden and heterogeneity. APOBEC proteins, associated with mutagenesis and DNA damage, are implicated in this process. Our study centers on SYNCRIP, a key regulator of APOBEC activity, and investigates its influence on extrachromosomal DNA (ecDNA) in CRPC. Objective: This research aims to explore how SYNCRIP deficiency leads to increased APOBEC activity, and to examine its possible implications for ecDNA formation and its contribution to drug resistance and tumor heterogeneity in CRPC.

Methods: Genomic and transcriptomic analyses, such as whole exome sequencing and single-cell RNA-seq, were performed on CRPC cell lines and patient-derived samples, with an emphasis on SYNCRIP-deficient models. The study focused on understanding the relationship between elevated APOBEC activity due to SYNCRIP deficiency and potential ecDNA changes, evaluating their effect on AR-targeted drug sensitivity and overall tumor behavior.

Results: SYNCRIP was identified as a critical factor in resistance to AR therapy in both *in vitro* and *in vivo* models. Its deficiency resulted in increased therapy resistance and amplified APOBEC-mediated mutagenesis. Functional CRISPR screening identified eight key drivers of resistance in SYNCRIP-deficient tumors. Single-cell RNA sequencing revealed APOBEC-driven mutagenesis as a key factor in promoting intratumoral heterogeneity and resistance. Notably, in SYNCRIP-deficient CRPC samples, increased APOBEC activity and significant DNA damage were observed, prompting an investigation into a possible correlation between resistance and ecDNA presence.

Conclusion: The study uncovers a significant link between SYNCRIP deficiency and increased APOBEC activity in CRPC. While it also hints at a potential connection with ecDNA alterations, further research is necessary to establish this relationship firmly. This interplay contributes to the complexity of drug resistance in CRPC, highlighting the need for novel therapeutic targets. The dynamics among SYNCRIP, APOBEC activity, and ecDNA offer valuable insights into the molecular underpinnings of therapy resistance in prostate cancer, suggesting new directions for treatment strategies.

#4312 KRAS oncogenic activation in *Gramd2*$^{\pm}$ AT1 cells form lung adenocarcinoma with distinct transcriptomic and tumor microenvironment signatures.

Minxiao Yang[1], Jonathan Castillo[1], Edgar Gonzalez[2], Chunli Yan[3], Evanthia Roussos torres[2], Zea Borok[4], Crystal Marconett[1]

[1]Department of Translational Genomics, USC - University of Southern California, Los Angeles, CA,[2]Department of Medicine, USC - University of Southern California, Los Angeles, CA,[3]USC - University of Southern California, Los Angeles, CA,[4]Department of Medicine, University of California, San Diego, San Diego, CA

Lung adenocarcinoma (LUAD) is the most prevalent subtype of lung cancer and presents with a high degree of biological heterogeneity and distinct clinical outcomes. The current paradigm of LUAD etiology recognizes alveolar epithelial type II (AT2) cells as the primary cell of origin, while the role of AT1 cells in LUAD oncogenesis remains relatively unknown. Here, we examined transformation via activation of the oncogenic KRAS^{G12D} mutation in a Gram-domain containing 2 (*Gramd2*)$^{\pm}$ AT1 cell lineage tracing model system, which resulted in multifocal LUAD, primarily of papillary histology. Spatial transcriptomic sequencing revealed significant differences of transcriptomic signatures and signaling activities between *Gramd2*$^{\pm}$ AT1 cell-derived and *Sftpc*$^{\pm}$ AT2 cell-derived LUAD. Single-cell RNA sequencing of macrodissected LUAD lesions demonstrated heterogeneous cell composition of the tumor microenvironment (TME), with *Gramd2*$^{\pm}$ AT1 cell-derived LUAD fostering a proinflammatory, immunoreactive TME and *Sftpc*$^{\pm}$ AT2-derived LUAD presenting with an immunosuppressive TME. Collectively, our study suggests that cell of origin for LUAD is associated with histologic subtype, transcriptomic aberrations, and immune cell composition within LUAD that may influence response to therapy.

MOLECULAR/CELLULAR BIOLOGY AND GENETICS: Autophagy and Other Forms of Cell Death
Poster Session

#4316 Investigation the role of DDI2 in autophagy.
N. Hosseini, H. A. Byers, S. K. Radhakrishnan;
Virginia Commonwealth University, Richmond, VA

Background: The ubiquitin-proteasome system (UPS) and autophagy-lysosomal pathway (ALP) are critical intracellular protein degradation pathways. In response to proteasome dysfunction, cells initiate compensatory autophagy to manage proteotoxic stress, which impacts cancer therapy efficacy. Despite current insights, the exact molecular mechanisms underlying the induction of autophagy due to impaired proteasome function remain unclear. The transcription factor nuclear factor erythroid-2-related factor 1 (NRF1) is the master regulator of proteasome subunit genes, which is activated by the protease DNA damage inducible 1 homolog 2 (DDI2) upon proteasome inhibition. DDI2 also acts as an ubiquitin shuttling factor, and its depletion causes the accumulation of highly ubiquitinated proteins, resulting in increased sensitivity to proteasome inhibition in cancer cells. However, cancer cells might trigger compensatory autophagy in response to DDI2 depletion to degrade ubiquitinated protein aggregates. Here, we demonstrated that DDI2 depletion plays a role in autophagy induction.
Methods: A panel of cell lines of different origins (EW16 and ES1 human Ewing sarcoma, MIA PaCa-2 human pancreatic cancer, and NIH-3T3 murine fibroblasts) either control or DDI2-deficient were examined for autophagy activity following treatment with the autophagy inhibitor chloroquine (CQ). Through total proteome analysis, we identified an increase in cellular communication network factor 1 (CCN1) protein levels in DDI2-depleted cells, which plays a role in autophagy induction. To determine whether CCN1 is required and sufficient to induce autophagy, we applied small interfering RNA (siRNA), and viral constructs to knockdown and overexpress CCN1.
Results: The autophagic flux measurements in four different DDI2-deficient cell lines revealed elevated LC3B-II protein levels, a known autophagy marker, following CQ treatment compared to their control. Western blotting analysis confirmed increased CCN1 protein levels in the same cell lines. The autophagy induction observed in DDI2-deficient cells was diminished by CCN1-siRNA, demonstrating that CCN1 may be required for autophagy induction. Furthermore, overexpressing CCN1 in wild-type cells resulted in increased LC3B-II protein levels, indicating that CCN1 alone is sufficient to induce autophagy.
Conclusion: Targeting autophagy is a promising therapeutic strategy to improve the effects of anti-cancer therapies. We demonstrated that upon depletion of ubiquitin shuttle factor DDI2, secretory protein CCN1 accumulates leading to the subsequent induction of autophagy. These findings improve our understanding of the molecular basis governing DDI2's role in crosstalk between protein degradation pathways. Targeting DDI2 in combination with autophagy inhibition could further potentiate these drugs as anti-cancer therapies.

#4317 The role of autophagy in triple negative breast cancer.

S. Gamal[1], **N. A. El-Nikhely**[1], H. Nematallah[2], H. M. Saeed[1];
[1]Alexandria University, Alexandria, Egypt, [2]Damanhour University, Damanhour, Egypt

Breast cancer (BC) remains a global health concern, being the most common cancer amongst women in the world, and the second-leading cause of cancer related death. Triple-negative breast cancer (TNBC) represents a challenging frontier in oncology, characterized by its aggressiveness and its unique molecular profile devoid of the known receptors. Its elusiveness lies in the inherent heterogeneity within its subtypes, contributing to diverse clinical behaviours and treatment responses. TNBC has also shown elevated basal autophagy level as a pro-survival mechanism to make up for the increased nutrients demand mandated by the high K-RAS signalling. To tackle such tumour, we chose an autophagy blocker in addition to multi-kinase inhibitor. The combination index calculated for the proposed drugs has shown promising results in reduction of cell viability more than each drug separately. Selectivity index proved the safety of our doses on normal fibroblast cells in contrast to two breast cancer cell lines (MDA-MB 231 & MCF7). To further complement the findings, cell cycle arrest was witnessed at S phase which lead to apoptosis seen by flowcytometry and other expression analysis studies. Finally, Imaging studies and expression analysis on protein level have documented the apoptotic effects rendered by autophagy inhibition.Research endeavours continue to unravel the intricate landscape of TNBC, seeking novel avenues for targeted treatments, immunotherapies, and personalized medicine, aiming to transform the paradigm of care for those affected by this enigmatic form of breast cancer. As evident from the results, our combination has also managed to reduce the cells migration effectively which reflects that it can be initiated with aggressive metastatic tumours like TNBC.

#4318 CD24 enhances cisplatin resistance in ovarian cancer by suppressing autophagy.

Y.-L. Chen, T.-M. Hong, Y.-Y. Wen;
National Cheng Kung University, Tainan, Taiwan

Ovarian cancer is one of the most common gynecological cancers with the highest mortality rate. Most patients are diagnosed with advanced disease and will relapse due to chemoresistance. CD24, a highly glycosylated GPI-anchored membrane protein. Recent studies have shown that CD24 expression is significantly up-regulated in ovarian cancer and is associated with chemotherapy resistance, and CD24 also plays an inhibitory role in tumor immunity by binding to Siglec-10 on macrophages. However, the molecular mechanisms of how CD24 affects chemotherapy resistance in ovarian cancer remain unclear. In this study, we used shRNAs to knockdown CD24 and explore the impact and mechanism of CD24 on the chemotherapy resistance of ovarian cancer cells. The results showed that knockdown of CD24 in ovarian cancer cells SKOV3 and TOV21G significantly reduced cell proliferation and arrested the cell cycle in S phase. Knockdown of CD24 also significantly increased the sensitivity of ovarian cancer cells to cisplatin but had no effect on paclitaxol treatment. Further experiments showed that knockdown of CD24 increased cisplatin sensitivity by promoting autophagy-induced cell death. In addition, Gene Set Enrichment Analysis (GSEA) was used to analyze the correlation between the expression of CD24 and its biological functions in the TCGA ovarian cancer dataset. The results showed that CD24 is mostly correlated to cell proliferation and autophagy-related pathways in ovarian cancers. Further mouse xenograft tumor transplantation experiments also confirmed that knockdown of CD24 reduced tumor size and increased sensitivity to cisplatin treatment by increasing cell autophagy. Taken together, these results indicate that CD24 regulates cell growth and chemoresistance in ovarian cancer cells and that inhibition of CD24 may be helpful in the treatment of ovarian cancer.

#4319 HSF1 inhibition induces pancreatic ductal adenocarcinoma autophagy through JNK.

S. Ghai[1], A. Young[2], K.-H. Su[1];
[1]The University of Toledo College of Medicine and Life Sciences, Toledo, OH, [2]Lake Erie College of Osteopathic Medicin, Erie, PA

Background: Pancreatic ductal adenocarcinoma (PDAC) is the third leading cause of cancer-related mortality, with a 5-year survival rate of 12%. Chemoresistance due to autophagy, a natural process of proteotoxic stress response, is the most common chemotherapy challenge for pancreatic cancer. Autophagy, which maintains cellular homeostasis by removing damaged or unnecessary proteins and organelles, is a self-degradation process regulated by the mammalian target of rapamycin complex (mTORC1). Excessive levels of autophagy can be detrimental and lead to cell death. Nevertheless, this dual function of autophagy in regulating pancreatic cancer remains poorly understood. It has been reported that heat shock factor 1 (HSF1), a critical pro-oncogenic transcription factor in the proteotoxic stress response, inhibits c-Jun N-terminal kinase 1/2 (JNK1/2) signaling pathway to maintain mTORC1 activity and control cell size. HSF1 is highly expressed in pancreatic tumors, and inhibition of HSF1 via small molecules enhances the chemotherapy drug effect on PDAC programmed cell death. However, the PDAC autophagy response in HSF1 inhibition is currently not fully understood. Objective: The objective of this study is to investigate the molecular mechanism of HSF1 inhibition in PDAC autophagy.
Methods and Results: In human PDAC cells, Western blotting analysis revealed that HSF1 inhibition via small molecular including CCT361814/NXP800, an HSF1 inhibitor in phase I clinical trials, increased autophagy marker microtubule-associated protein 1A/1B-light chain 3 (LC3) lipidation and decreased expression of phosphorylation of HSF1 at Ser326 and total HSF1 protein, conversely using HSF1 overexpression model reversed this effect. Inhibition of autophagy via 3-methyladenine reversed HSF1 inhibition-induced autophagy. Results from transmission electron microscopy and GFP-LC3 reporter revealed that HSF1 inhibition induced autophagosome formation and accumulation. Furthermore, HSF1 inhibition induced phosphorylation of JNK1/2 at Thr183/Tyr185 and decreased mTORC1 activity, while knockdown JNK1/2 diminished HSF1 inhibition-induced LC3 lipidation. The combination of chemotherapy drugs with HSF1 inhibitors decreased PDAC cell viability. Additionally, blocking autophagy increased HSF1 inhibition-induced apoptosis.
Conclusions: In conclusion, JNK1/2 is involved in HSF1 inhibition-induced PDAC autophagy, targeting autophagy could unveil a novel treatment strategy for pancreatic cancer through targeted HSF1 inhibition.

#4320 Interrogation of autophagy inhibition in anaplastic large cell lymphoma (ALCL).

K. L. Buelow[1], S. Celano[2], G. Poole[2], K. Martin[2], J. MacKeigan[2], D. J. Hoogstra[3];

[1]Corewell Health, Grand Rapids, MI, [2]Michigan State University, Grand Rapids, MI, [3]Helen DeVos Children's Hospital at Corewell Health, Grand Rapids, MI

The objectives of this study are to evaluate if anaplastic lymphoma kinase (ALK) inhibition activates autophagy in ALK+ ALCL cells and to determine if that activation can be mitigated using autophagy inhibition. ALCL is an aggressive T-cell non-Hodgkin lymphoma that often presents as advanced stage disease. With the addition of crizotinib or brentuximab vedotin to the ALCL99 chemotherapy backbone, the recently reported Children's Oncology Group ANHL12P1 study demonstrated a 2-year event-free survival for ALCL patients of 79%. Thus, even with multi-agent chemotherapy combined with targeted therapy, improved therapeutic efficacy is needed. Autophagy is activated when mTORC1 is inhibited, and as ALK signaling is known to promote mTORC1 activity, ALK inhibition is hypothesized to activate autophagy. If present, ALK inhibitor-induced autophagy activation would represent a novel therapeutic opportunity targetable with emerging autophagy inhibitors. An ALK+ ALCL cell line, Karpas 299, was treated with drug combinations for 3 hours, lysates prepared, and proteins separated by molecular weight using standard procedures. ALK inhibitor target engagement was assessed by western blot using phospho-ALK^{Y1604} intensity in 9-point dose response curves. Target engagement of autophagy inhibition (ULK-101 directed against ULK1/2 and hydroxychloroquine (HCQ) targeting the lysosome) was assessed by western blot using phospho-ATG14^{S29} and LC3B-II intensity in 6-point dose response curves. Cell viability was evaluated using a luminescent CellTiter-Glo assay. Karpas299 cells resistant to crizotinib at 50nM (KCrizR50) were generated by gradually increasing crizotinib concentration in the media until cells grew at a rate similar to parental cells. Crizotinib, ceritinib, and lorlatinib all effectively inhibit ALK phosphorylation in Karpas 299 cells with low nanomolar potency. ULK-101 effectively inhibited pATG14^{S29} at 5 μM and HCQ effectively inhibited autophagic flux, as evidenced by increased LC3B-II intensity, at 20 μM. When treated with the lowest ALK inhibitor dose needed to achieve complete pALK inhibition (IC_{99}), pATG14 intensity increased representing increased autophagic activity. When combined with ALK inhibition, ULK-101 effectively decreased pATG14^{S29}, blocking the ALK inhibitor-induced autophagy activation. Decreased viability in Karpas 299 cells was observed after crizotinib, ceritinib and lorlatinib treatments with nanomolar potency. KCrizR50 cells had a potency higher than parental Karpas 299 cells for all three ALK inhibitors. ALK inhibition activates autophagy in ALCL cells and autophagy activation is effectively mitigated through concurrent autophagy inhibition. ALK inhibitor resistance in Karpas 299 cells will be further evaluated to determine whether autophagy contributes to the resistant phenotype.

#4321 The oncogenic DMTF1β splice variant promotes autophagy-dependent cancer cell motility.

M. P. Tschan, J. Xu, A. M. Bill;
University of Bern, Bern, Switzerland

The oncogenic isoform DMTF1β, which is generated by alternative splicing of the DMTF1 tumor suppressor gene is associated with increased cell proliferation and tumorigenesis. Despite these correlative findings little is known about the DMTF1β mechanism of action. In order to decipher the oncogenic DMTF1β signaling pathway, we performed RNA sequencing of DMTF1β depleted prostate cancer cells and analyzed the DMTF1β-specific protein interactome in these cells. Interestingly, autophagy-related pathways belonged to the most downregulated networks in DMTF1β knockdown cells. Moreover, we found that predominantly DMTF1β, but not a protein lacking the β-specific domain interacts with the key autophagy ULK1-ATG13 protein complex. These interactions were confirmed by co-immunoprecipitation and proximity ligation assays. Importantly, DMTF1β binding to ULK1 stabilized this key autophagy protein. Accordingly, knocking down DMTF1β significantly lowered autophagic flux in breast and prostate cancer cells as assessed by LC3-dependent and independent autophagy assays. Since published data show an important role for autophagy in migration and invasion of cancer cells, we next investigated whether DMTF1β is regulating these cellular processes. Indeed, DMTF1β depleted breast and prostate cancer cells displayed significantly decreased wound closure, trans-well invasion and metastatic foci formation in a zebra fish xenograft model. Importantly, pharmacological inhibition of ULK1 kinase activity or knocking down ULK1 reversed DMTF1β-mediated cancer cell migration. In agreement, decreased cell motility in DMTF1β knockdown cancer cells could be rescued by ectopic expression of the VPS34 complex member Beclin-1. In summary, we identified a novel DMTF1β-ULK1 signaling pathway that activates aberrant cancer cell migration most probably by increasing basal cell autophagy. Targeting autophagy using ULK1 inhibitors may represent a promising strategy to lower metastatic activity of tumor cells.

#4322 Inhibition of ULK and KRAS^{G12C} control tumor growth in preclinical models of lung cancer.

P. Ghazi[1], K. O'Toole[1], S. Boggaram[1], M. Scherzer[1], M. Bogdan[2], B. Smith[2], D. Flynn[2], C. Kinsey[1], M. McMahon[1];
[1]University of Utah, Salt Lake City, UT, [2]Deciphera Pharmaceuticals, Waltham, MA

Approximately 30% of lung cancers are driven by mutationally activated KRAS. The recent FDA approval of sotorasib, a direct pharmacological inhibitor of KRASG12C, marks a critical milestone in the treatment of this important subset of lung cancer. However, a major obstacle in treating lung cancer is resistance to current therapeutic treatments. In response to cellular stresses such as RAS pathway-targeted therapeutics, RAS-mutated cancer cells have been demonstrated to increase autophagy, an intracellular recycling pathway. However, the mechanism(s) underlying treatment-induced autophagy is not well understood. Here, we demonstrate that KRASG12C-driven lung cancer cells increase autophagy in response to treatment with sotorasib. Currently, the only therapeutics in clinical use to inhibit autophagy are lysosomal inhibitors (hydroxy)chloroquine. High concentrations of these compounds are needed to achieve modest inhibition of autophagy, suggesting that the potency of these compounds may limit clinical responses. ULK kinases are serine/threonine kinases that are necessary for the initiation of autophagy. DCC-3116 is a potent inhibitor of the ULK1/2 protein kinases, master regulators of autophagy. Treatment with sotorasib and DCC-3116 led to superior anti-tumor effects in preclinical models of lung cancer. Additionally, about 30% of lung cancer patients with KRAS mutations also have deletions or inactivating mutations in LKB1, a protein involved in the regulation of nutrient sensing and autophagy. In other KRAS-driven cancers, the LKB1-AMPK-ULK1 signaling axis is a proposed mechanism as to how autophagic flux increases following KRAS pathway inhibition. However, our preliminary data demonstrates that LKB1 is dispensable for sotorasib-induced autophagy, suggesting the mechanism(s) of autophagy induction in KRASG12C-driven lung cancer may be different from those detected in other KRAS mutated cancers. Consequently, we have generated genetically engineered mouse models (GEMMs) of KRASG12C-driven lung cancer in which LKB1 is silenced to further investigate the role of LKB1 in the autophagy response of KRASG12C-driven lung cancers to pathway-targeted blockade of oncogenic KRAS signaling. We have treated KRASG12C-driven GEMMs with sotorasib and/or DCC-3116 to test the sensitivity of lung tumors to these treatment options.

#4323 Deletion of the lipid kinase PIKfyve in Kras-driven pancreatic genetically engineered mouse model.

S. N. Yee, X. Jiang, C. Cheng, A. Korkaya, R. Mannan, R. Mehra, Y. Qiao, A. M. Chinnaiyan;
University of Michigan Medical School, Ann Arbor, MI

Background: Pancreatic ductal adenocarcinoma (PDAC) accounts for 95% of all pancreatic cancers and, as one of the most lethal cancers, has a five-year survival rate of approximately 6%. Autophagic processes have been reportedly elevated in PDAC; thus, the inhibition of autophagy leads to decreased tumor growth. Autophagic processes are catabolic mechanisms that recycle cellular components. Cells in stressful conditions, such as starvation, have elevated autophagy to redistribute energy to sustain cell survival; however, this can also lead to cell death when attempts to maintain cell viability fail. In addition, autophagy is known to promote immune evasion by tumors and cancer progression and appears to be required for the optimal development of PDAC. The lipid kinase PIKfyve converts phosphatidylinositol-3-phosphate to phosphatidylinositol 3,5-bisphosphate and is required in the late stage of the autophagic pathway. Blocking PIKfyve disrupts autophagic processes. However, the role of PIKfyve in PDAC development has not been fully understood. We investigated the role of PIKfyve in the progression of PDAC using a genetically engineered mouse model. Given the poor clinical outcomes of pharmacological inhibition of autophagy by chloroquine, we have evaluated the PIKfyve inhibitor ESK981 in the context of PDAC progression.
Methods: The pancreatic-specific deletion of PIKfyve was established on a Kras G12D, Tp53 R172H, and p48 Cre (KPC) or Kras G12D and p48 Cre (KC) background. The ratio of pancreatic mass to body weight was monitored at various time points. Histopathology evaluations were conducted based on hematoxylin and eosin staining and immunohistochemistry of cytokeratin 19 staining. Pharmacological inhibition of PIKfyve was performed on KPC mice using ESK981 monotherapy. Four weeks after vehicle or ESK981 treatment, pancreatic tissues were collected intact and weighed. Histopathology evaluations were performed to evaluate the lesion.
Conclusion: We demonstrated that the deletion of PIKfyve in pancreatic tissue significantly reduces the pancreatic mass weight compared to the PIKfyve wildtype counterpart and is coupled with less pancreatic intraepithelial neoplasia (PanIN) and PDAC development in KPC and KC mice. Compared to the vehicle treatment, pharmacological inhibition of PIKfyve by ESK981 on KPC mice resulted in a significant increase in the percentage of normal pancreatic tissue and reduced pancreatic lesion development.

#4324 IL6ST increases sorafenib-resistance in hepatocellular carcinoma by regulating BECN1-mediated mitophagic cell death.

H. Ma, **Y.-S. Roh**;
Chungbuk National University, Cheong-Ju, Korea, Republic of

Introduction: Sorafenib resistance is often seen in patients with late-stage hepatocellular carcinoma (HCC) and it is a serious concern for the treatment of these patients. Lethal mitophagy plays an important role in anti-tumorigenic mechanisms by inducing mitochondrial dysfunction and mitophagic cell death. Sorafenib resistance is associated with the activation of IL6ST signaling, inhibiting mitochondrial quality. However, how lethal mitophagy regulates sorafenib resistance through IL6ST and mitochondrial dysfunction in HCC is not fully understood.
Experimental procedures: Hepatocyte-specific TAK1 deleted (TAK1ΔHep) and TAK1/ IL6STΔHep were used for in vivo study. Histology, immunoblots, qPCR, microscopy, FACS, and seahorse bioanalyzer were used for analyzing liver and tumor tissues and Hep3B cells.
Results: We identified that sorafenib suppressed IL6ST signaling and that IL6ST signaling was activated in sorafenib-resistant HCC. The number and maximum size of spontaneous HCC in 9-month-old TAK1ΔHep mice were decreased when hepatocyte IL6ST was additionally deleted. Expression of pro-carcinogenic H-19, c-SRC, and MDM2 was increased in 1-month-old TAK1/IL6STΔHep mice compared to TAK1ΔHep mice. An additional IL6ST deletion induced decreases in mitochondrial membrane potential and glycolysis, suggesting that IL6ST protects against mitochondrial dysfunction. Interestingly, IL6ST deletion increases PRKN and BECN1 interaction and translocation to normal mitochondria and subsequent degradation, hereafter referred to as lethal mitophagy. Furthermore, inhibition of BECN1 restores IL6ST deletion-induced lethal mitophagy in HCC, suggesting that IL6ST-mediated lethal mitophagy is dependent on BECN1. Mechanistically, IL6ST inhibited BECN1-lethal mitophagy through STAT3(S705) phosphorylation independently of mTORC1 activation. Notably, enhanced BECN1 through a combination of sorafenib and inhibition of IL6ST increased mitophagic cell death, reducing sorafenib resistance and tumor growth. In addition, enhanced lethal mitophagy through inhibition of GP130 effectively killed sorafenib-resistant HCCs by silencing sorafenib resistance. We further defined the relationship between IL6ST, BECN1, and PRKN expression and sorafenib resistance in terms of HCC patients, RNA sequencing datasets.
Conclusion: These results provide the importance of IL6ST in the development of sorafenib resistance and could be an innovative treatment strategy for sorafenib-resistant patients by regulating the IL6ST/STAT3/BECN1 axis-regulated lethal mitophagy.

#4325 CX-4945 (Silmitasertib) induces cell death through impairment of lysosomal utilization in *KRAS* mutant cholangiocarcinoma cell lines.

C. Kim[1], D. Lee[1], M. Han[2], S. Lee[3], K.-p. Kim[1], C. Yoo[1];
[1]Asan Medical Center, Seoul, Korea, Republic of, [2]University of Ulsan College of Medicine, Seoul, Korea, Republic of, [3]University of Ulsan Digestive Diseases Research Center, Seoul, Korea, Republic of

Purpose: Macropinocytosis is a non-selective endocytosis that uptakes extracellular substances such as nutrients and macromolecules into the cells. In *KRAS*-driven cancer such as pancreatic ductal adenocarcinoma, the macropinocytosis and following lysosomal utilization are enhanced to overcome metabolic stress. In this study, we investigated the role of CK2 in micropinocytosis and the following metabolic process in the *KRAS* mutant CCA cell line.
Materials and Methods: The BSA uptake indicating micropinocytosis was performed by flow cytometry using the HuCCT1, cholangiocarcinoma cell line harboring *KRAS* mutation. To validate macropinosome, the Rab7 and LAMP2 were labeled and analyzed via immunocytochemistry and Western blot. The CX-4945, CK2 inhibitor, was used to investigate the role of CK2 in micropinocytosis and following lysosomal metabolism.
Results: The HuCCT1, a *KRAS* mutant CCA cell line, showed micropinocytosis. Although CX-4945, a CK2 inhibitor, induced morphological changes accompanied by accumulation of intracellular vacuoles and cell death rate, the level of micropinocytosis was not changed. The vacuoles accumulated in the cell were identified as late macropinosomes representing Rab7 before fusion with lysosomes. In addition, the CX-4945 suppressed LAMP2 expression following inhibition of the Akt-mTOR signaling pathway which interrupts mature macropinosome and lysosomal metabolic utilization.
Conclusion: These results support the utilization of micropinocytosis as an energy source even in CCA cell line harboring *KRAS* mutation. The inhibition of CK2, the regulator of macropinosome maturation, by CX-4945, alters lysosome dependent metabolism and leads to cell death in *KRAS* mutant CCA cell lines.

#4326 CDK7/CDK9 mediates transcriptional regulation to prime cancer cell paraptosis.

L.-C. Chang[1], S.-K. Chiang[2], S.-E. Chen[2];

[1]China Medical University Hospital, Taiwan, Taichung, Taiwan, [2]National Chung Hsing University, Taiwan, Taichung, Taiwan

The mechanisms underlying progression in cell paraptosis are largely unknown. CPYPP, cyclosporin A, and curcumin incited cytoplasmic vacuolization and induced paraptosis in breast cancer cells. The paraptotic program evolved with reactive oxygen species (ROS) provocation and overactivation of proteostatic dynamics to elicit transcriptional regulation involved in redox homeostasis and proteostasis. Pharmacological and genetic approaches suggested that cyclin-dependent kinase (CDK) 7/9 drives paraptotic progression in a reciprocally-dependent manner with heat shock proteins (HSPs). Proteostatic stress as accumulated cysteine-thiols, HSPs, ubiquitin-proteasome system, endoplasmic reticulum stress, and unfolding protein response, as well as ROS provocation primarily within the nucleus enforced CDK7/CDK9-Rpb1 (RNAPII subunit B1) activation by potentiating its interaction with HSPs and protein kinase R (PKR) in a forward loop to amplify the transcriptional regulation and thereby exacerbate proteotoxicity leading to overt paraptosis. Xenograft mouse with OECM-1 cells further confirmed the paraptotic induction against tumor growth. A novel regulatory paradigm that activation of CDK7/CDK9-Rpb1 by nuclear proteostatic stress mediates transcriptional regulation to prime cancer cell paraptosis therefore was concluded.

#4327 Development of bioluminescent biosensors to monitor the interaction betweenGSDMD and caspase-1 in living cells.

T. Kelly;
Queen's University, Kingston, ON, Canada

Gasdermin D (GSDMD) is the key executioner of pyroptosis, an inflammatory form of programmed cell death implicated in various inflammation-driven diseases, including cancer, heart failure and strokes. The interaction between GSDMD and caspase-1 (CASP1) orchestrates the critical pathway of GSDMD-mediated pyroptosis. During pyroptosis, pyroptosis stimuli activate CASP1, which subsequently binds to and cleave GSDMD between GSDMD's N- and C-terminal domains. The free N-terminal domains oligomerize and translocate to the cell membrane, forming pores and releasing proinflammatory cytokines and causing cellular lysis. Key interaction sites have been identified for GSDMD recognition and engagement by CASP1; therefore, blocking functionally significant residues presents a new therapeutic strategy for inhibiting CASP1-induced GSDMD cleavage and pyroptosis. Currently, there is no small molecule capable of specifically disrupting the GSDMD and CASP1 interaction. In response, the ongoing pursuit of identifying potential inhibitors is a driving force for developing a biosensor capable of monitoring this interaction and their roles in downstream pyroptotic effects. In this study, we utilized the NanoLuc Binary Technology (NanoBiT) to construct several bioluminescent biosensors comprising two NanoLuc luciferase enzyme fragments (LgBiT and SmBiT) fused to GSDMD and CASP1, respectively, in various combinations. Further validation of these biosensors by luciferase assays in living cells identified a GSDMD-CASP1 biosensor with highest luciferase activity. This newly developed biosensor paves the way for high-throughput screens to identify novel small molecule inhibitors disrupting the GSDMD-CASP1 interplay. These small molecule inhibitors will effectively impede GSDMD-mediated pyroptosis, holding promise for novel therapies of various human diseases.

#4328 Erlotinib suppresses autophagy in colorectal cancer.

A. Siegman[1], A. Shaykevich[1], I. Silverman[1], S. Goel[2], R. Maitra[1];
[1]Yeshiva University, New York, NY, [2]Rutgers Cancer Institute of New Jersey, New Brunswick, NJ

Introduction: Oncogenic *KRAS* mutation is prevalent in approximately 45% of colorectal cancer (CRC) patients. Limited targeted therapies are available to inhibit the detrimental effects of *KRAS* mutation primarily pertaining to its unique structural intricacies. Erlotinib is an EGFR inhibitor which inducing autophagy in lung cancer cells. In this study, we followed the effects of Erlotinib treatment in mutant and wild-type colorectal cancer (CRC) cells. We report that Erlotinib exhibits selectivity between mutated *KRAS* and wild type, significantly modulating the expression of autophagy proteins ATG5, ULK1, Beclin1, and LC3A.
Methodology: The 2 cell lines used in this study were HCT116 (*KRAS* mutant) and Hke3 (*KRAS* wild type). These cells were treated with Erlotinib for 24 hours and 48 hours, A cell viability assay was performed and subsequently followed by protein extraction. The expression of autophagy proteins ATG5, ULK1, Beclin1, and LC3A was determined. The TCGA COAD-READ patient dataset was utilized using GEPIA 2 software. A correlation was found between the autophagy proteins and the *KRAS* gene expression.
Results: The cell viability assays showed that there was significantly more cell death in *KRAS* wild-type cells compared with *KRAS* mutant at time points ranging from 24 to 48 hours ($p = 0.036$). The experiment also showed that treatment of Erlotinib with concentrations of 20 uM, 35 uM, and 50 uM and significant down regulatory fold changes ($p < 0.05$). Both *KRAS* mutated and wild-type cells treated with Erlotinib expressed significant downregulation of ATG5, ULK1, Beclin1, and LC3A proteins at 48 hours ($p < 0.05$). The 20 uM treatment demonstrated a significance of $p < 0.05$ for all proteins. The 20 uM treatment resulted in fold changes of the *KRAS* mutated cells for ATG5, ULK1, Beclin1, and LC3A to be 1.42, 1.42, 1.81, and 2.09 respectively. A strong *KRAS* correlation was found with ATG5, ULK1, Beclin1, and LC3A using COAD & READ tumor and COAD & READ normal ($R > 0.75$, $p < 0.05$).
Conclusion: This study highlights the effects of Erlotinib as a treatment for *KRAS* mutated CRC. Our results confirmed that Erlotinib had the opposite effect on CRC cells in relation to the expression of the autophagy proteins when compared to lung cancer cells. There were distinct effects of Erlotinib between *KRAS* wild-type and mutant cells in both cell viability and the expression of autophagy-related proteins. In both *KRAS* cell types, there was significant downregulation of autophagy proteins, however, the *KRAS* wild type had significantly more downregulation than the *KRAS* mutant. This data suggests that there is a relationship between *KRAS* mutation and the expression of the autophagy proteins. Our analysis of the patient datasets confirmed the strong correlation between *KRAS* mutation and the expression of autophagy proteins. These findings emphasize the need to explore further how Erlotinib can be augmented into the current treatment regimen as a benefit to CRC patients.

MOLECULAR/CELLULAR BIOLOGY AND GENETICS: Characterization of Mutational Processes and Drivers in Cancer Development and Evolution Poster Session

#4331 Machine learning-based classification of tissue origin of cancer using methylation profiles.

Marco A. De Velasco, Kazuko Sskai, Seiichiro Mitani, Yurie Kura, Shuji Minamoto, Takahiro Haeno, Hidetoshi Hayashi, Kazuto Nishio

Kindai University Faculty of Medicine, Osaka-Sayama, Japan

Cancer of unknown primary (CUP) is a malignancy with poor prognosis and an unknown primary site and histologically unknown metastasis. Most patients receive empiric chemotherapy including platinum-taxane therapies but experience short survival times. Patients with poor prognosis CUP could benefit from optimizing drug therapy based on primary organ estimation. We constructed and evaluated an ensemble learning model to accurately determine the primary organ using methylation profiles of tumor tissues. Methylation data from 890 samples representing 10 types of cancer from TCGA were analyzed. After data preprocessing, we extracted the top 10,000 CpGs sites based on ANOVA and Gain Ratio or 100 CpG sites from a Gradient Boosting classifier. Performance was evaluated using several machine learning models. Unsupervised analysis was carried out to determine the relationships between the CpG sites selected by Gradient Boosting. Methylation profiling by ANOVA and Gain Ratio yielded favorable performance when using various machine learning models. Using gradient boosting as a feature selector reduced the number of CpG sites by 100-fold without compromising model performance. The training and validation sets showed favorable results for the classification of primary organs with ensemble models. In validation, classification accuracy was 91.2%, 93.5%, 89.7%, and 87.7% for Extreme Gradient Boosting, CatBoost, Random Forest, and Gradient Boosting, respectively. Further profiling of the selected methylation regions was correlated with cancer types and even revealed subgroups within breast and lung cancers. Gradient Boosting as a feature selector for DNA methylation profiling was highly effective in accurately determining tissue origin. Our study has outlined an approach whereby we used an embedded machine learning algorithm to identify a select set of informative features from complex high-dimension data to train and predict cancer type.

#4332 Isoform-level transcriptome-wide analyses identify extensive genetic mechanisms for breast cancer risk undetectable on the gene-level.

A. Bhattacharya[1], Y.-H. Chang[2], B. Pasaniuc[2], S. Lindstroem[3],

[1]UT MD Anderson Cancer Center, Houston, TX, [2]University of California, Los Angeles, Los Angeles, CA, [3]University of Washington, Seattle, WA

Genome-wide association studies (GWAS) have identified over 170 genetic variants associated with breast cancer risk. Integrative methods, like colocalization and transcriptome-wide association studies (TWAS), can identify potential biological mediators for genetic associations but, to date, have only contextualized a fraction of GWAS loci. This reduced discovery is due to an overreliance on reference transcriptomic panels of total gene expression, which ignore widespread alternative splicing that gives rise to multiple transcript-isoforms of the same gene with differing effects on tumorigenesis and progression. However, integrating highly correlated transcript-isoforms with phenotypic associations from genome-wide association studies (GWAS) requires methodological innovations.Here, we first introduce isoTWAS, a multivariate, machine learning method to integrate genetics, isoform-level expression, and phenotypic associations in a step-wise testing framework, and present its advantages over traditional gene-level methods.We then apply isoTWAS to multiomic data from non-cancerous breast samples from the Genotype-Tissue Expression Project (GTEx) and breast cancer risk GWAS summary statistics from the Breast Cancer Association Consortium. In total, we generated strong predictive models for 70,816 isoforms across 12,103 genes and estimated isoform associations for overall and subtype-specific breast cancer risk. We observed 570 associated isoforms across 384 unique genes (compared to 141 associated genes out of 14,613 genes tested in a gene-level TWAS with the same GWAS) at FDR and FWER-corrected P < 0.05. Critically, isoTWAS prioritized isoform associations within 1 Megabase of 66 independent GWAS-significant loci compared to 22 from gene-level TWAS. Of these isoforms within 1 Megabase of a GWAS locus, 19 associated isoforms had a significantly associated risk variant within the gene body. Of note, we find a negative association between the *ESR1* isoform ENST00000488573 and overall breast cancer risk ($P = 3.35 \times 10^{-9}$). Previous studies using breast tissue have not prioritized *ESR1* expression as a potential mediator, despite strong SNP associations at this locus. We are currently updating transcriptomic annotations using long-read RNA-sequencing data to improve the precision and specificity of GTEx isoform-level quantifications. We will then expand our isoTWAS analysis to other related tissues (connective, adipose, and immune-related tissues) to identify causal susceptibility transcripts for overall and subtype-specific risk. Our study underscores the wealth of information remaining in bulk RNA-seq datasets that sophisticated methods like isoTWAS can leverage to identify genetic risk mechanisms for breast cancer that is missed with traditional gene-centric measurements and methods.

#4333 Identification of glucose-6-phosphate dehydrogenase dependency in IDH1 mutant glioma cells using functional genomics.

K. M. Paras, P. Patel, P. Choi, W. R. Wilson, T.-W. Lee, S. M. F. Jamieson, **D. C. Singleton**;
University of Auckland, Auckland, New Zealand

Astrocytoma and oligodendroglioma are most commonly initiated by missense mutations at the arginine 132 codon of isocitrate dehydrogenase 1 (*IDH1*). Biochemically the mutant IDH1 protein acquires neomorphic activity: reductive NADPH-dependent catalysis of α-ketoglutarate (αKG) to (*R*)-2-hydroxyglutarate [(*R*)-2-HG]. (*R*)-2-HG interferes with the function of αKG-dependent epigenetic modifiers, resulting in extensive epigenetic remodeling that impairs cellular differentiation and promotes gliomagenesis. Strategies for selectively targeting *IDH1*-mutant cells offer promise for improved treatment over the standard modalities of surgery, chemotherapy and radiotherapy.

Whole-genome CRISPR/Cas9 knockout screens were conducted to identify gene dependencies in isogenic *IDH1*-mutant and wild-type (WT) U-87 MG cells. Cells were transduced with the Brunello single guide RNA (sgRNA) library, grown for 21 days, then sgRNA distributions were assessed by amplicon sequencing. Gene dependencies were identified using CRISPRcleanR and BAGELR pipelines. We discovered that glucose-6-phosphate dehydrogenase (G6PD), a pentose phosphate pathway (PPP) enzyme, was needed for viability of *IDH1*-mutant cells, but was dispensable for U-87 MG WT cells. The PPP is the main producer of cytosolic NADPH that is required for de novo lipogenesis, maintenance of antioxidants and production of (*R*)-2-HG by mutant IDH1. Previous reports demonstrated that *IDH1*-mutant cells increase PPP flux to support these processes.

We have validated this dependency using G6PDi-1, a cell-active inhibitor of G6PD. Growth inhibition (IC_{50}) assays demonstrated that *IDH1*-mutant U-87 MG cells were threefold more sensitive to G6PDi-1 with IC_{50} of 23 μM and enhanced cell death (increased propidium iodide uptake), compared with WT U-87 MG cells with IC_{50} of 67 μM. *G6PD* knockout was then conducted to further validate this dependency. Nucleofection of *IDH1* WT U-87 MG cells with *G6PD* multi guide RNA-Cas9 ribonucleoproteins resulted in highly efficient knockout of *G6PD* at day 5 (99-100%), which was maintained at day 21 (96-98%). In contrast, efficient *G6PD* knockout in *IDH1*-mutant U-87 MG cells at day 5 (98-100%) was lost following 21 days culture (0-5%), indicating death of almost all edited cells within the culture. Finally, Kaplan-Meier analysis of *IDH1*-mutant patients in the TCGA lower grade glioma dataset demonstrated that higher *G6PD* expression correlated with worse median overall survival (7.3 versus 9.5 years; log-rank p=0.01), but was not prognostic in the *IDH1* WT TCGA glioblastoma multiforme dataset.

These findings demonstrate that a cell line model of *IDH1*-mutant glioma is highly dependent on *G6PD* for survival. This observation builds on the recognized importance of the PPP in the metabolic biology of *IDH1*-mutant malignancy by establishing G6PD as a targetable dependency in this disease.

#4334 Insight into the structure of breakage fusion bridge events and chromothripsis in cancer cell lines using long-read sequencing.

I. Rodriguez[1], N. Rossi[1], A. Kesus[2], Y. Xie[1], T. Ahmad[2], A. Bryant[2], H. Lou[3], J. Godinez Paredes[1], R. Milano[1], M. Kolmogorov[2], S. Tulsyan[1], J. Bess[1], V. Mukhina[4], D. Gaykalova[4], L. Malik[5], K. J. Billingsley[5], C. Blauwendraat[5], L. Mirabello[1], M. Dean[1];

[1]National Cancer Institute, National Institute of Health, Rockville, MD, [2]National Cancer Institute, National Institute of Health, Bethesda, MD, [3]Frederick National Laboratory for Cancer Research, National Cancer Institute, Frederick, MD, [4]University of Maryland School of Medical Center, Baltimore, MD, [5]National Institute on Aging, National Institute of Health, Bethesda, MD

Cervical cancer is caused by human papillomavirus (HPV) infection and is the most common cause of cancer death in low-resource countries. We characterized 18 cervical and 4 head and neck cancer cell lines using long-read DNA and RNA sequencing and identified the HPV types, HPV integration sites, and cancer driver mutations. This cell line panel represents the major molecular subtypes of cervical cancer. Structural variation analysis revealed recurrent chromosomal alteration and telomeric deletions associated with DNA inversions resulting from breakage-fusion-bridge (BFB) cycles. BFB is a common mechanism of chromosomal alteration in cancer that has not been studied using long-read sequencing. Analysis of the inversion sites revealed staggered ends consistent with exonuclease deletion of the DNA after breakage. Some BFB events are complex, involving interchromosomal or intrachromosomal insertions or rearrangements. In total, there were three different types of BFB events: Type I, II, and III. Type I BFB events have staggered ends but no additional insertion at the fusion site. Type II BFB events have an insertion of DNA from another chromosome at the junction, and Type III has an insertion of sequences from the same chromosome as the BFB. BFB cycles are thought to resolve with the addition of a telomere. However, a search for telomeric sequences did not identify any on chromosomes impacted by BFB. In many cancers, BFB events co-occur with chromothripsis; however, in our cervical cancers, only 1 out of 13 had chromosomal shattering near the BFB event, indicating that the mechanism of chromosome rearrangement may be different in cervical cancers. Five cell lines have a Chr11q BFB event, with YAP1/BIRC2/BIRC3 gene amplification. Analysis of 911 publicly available cervical cancer exomes showed that YAP1 amplification is associated with a 10-year earlier age of diagnosis of cervical cancer (x2, p<0.0001) and is three times more common in African Americans (x2=12, p=0.003). Therefore, cervical cancer patients with YAP1/BIRC2/BIRC3 amplification, especially those of African American ancestry, might benefit from anti-YAP1/BIRC2/BIRC3 therapies. Our panel provides models for all the major HPV types and subtypes of cervical cancer that will aid in developing new therapeutic approaches. In summary, we uncovered novel insights into the mechanisms and consequences of BFB cycles in cervical cancer using long-read sequencing. We are expanding long-read sequencing to other cancer cell lines to gain knowledge of events associated with BFB.

#4335 High-resolution characterization of age-specific cell type composition changes and signaling events in HPV-negative HNSCC tumors.

L. Kroehling[1], A. Spinella[1], M. Kukuruzinska[2], X. Varelas[1], S. Monti[1];
[1]Boston Univ. School of Medicine, Boston, MA, [2]Boston Univ. School of Dental Medicine, Boston, MA

This study is aimed at testing the hypothesis that increased patient age fosters conditions that are favorable for head and neck squamous cell carcinomas (HNSCC) of the oral cavity development. There is a well-documented increase in cancer incidence with age observed across diverse cancer types, where elderly patients exhibit diminished survival outcomes compared to their younger counterparts. While the convergence of aging and cancer hallmarks offers valuable insights, further work is needed to elucidate the age-specific mechanisms influencing HNSCC, beyond the shared characteristics of these biological processes.

To this end, we have assembled a high-quality human single-cell RNA-sequencing HNSCC atlas profiling more than 230,000 cells across more than 50 patients with ages ranging between 18 and 89, which provides a resource to investigate age-associated changes in the disease heterogeneity. For this library, we integrated six publicly available single-cell RNAseq datasets from 54 HPV-negative patients to create the atlas. Cells were clustered, classified, characterized by gene set enrichment analysis, both in the epithelial cell compartment and in the tumor microenvironment (TME). Differential cell type proportion analysis was performed to identify cell types enriched in young (<49 years) or old (>70 years) patients. Cell-cell communication analysis was performed to identify signaling events occurring between different populations, and how these and specific ligand-receptor pairs differed in patients of different ages. CNV analyses were performed to identify cancer subclones and assess level of variation across tumors. Interestingly, we identified distinct cell populations and signaling events that associate with age, and we were able to compare, validate and recapitulate these observations in the 4MOSC1 OSCC isograft tumor model in old and young mice. Additional notable findings include a differential enrichment for cytotoxic CD8 T cells over dysfunctional CD8 T cells in young patients when compared to old, suggesting younger patients have a more effective immune TME. We also found an enrichment for cancer-associated fibroblast populations in old patients (myCAFs) that send collagen signals to malignant epithelial cells, a result we have recapitulated using the 4MOSC1 model, and hypothesize may play a role in ECM stiffening, EMT, and metastasis. Further analyses are ongoing, and we plan to validate the hypotheses generated, specifically the presence of differential abundance of specific cell populations, and age-specific ligand-receptor signaling events that lead to tumor growth.

#4336 Homologous recombination repair deficiency, and not recurrence, determines mutational burden and clonal dynamics in high grade serous ovarian cancer.

M. A. Diaz[1], N. Gull[1], P.-C. Peng[1], K. Lawrenson[1], B. J. Rimel[1], J. Lester[2], B. Karlan[2], S. A. Gayther[1], M. R. Jones[1];
[1]Cedars-Sinai Medical Center, Los Angeles, CA, [2]University of California, Los Angeles, Los Angeles, CA

High grade serous ovarian cancer (HGSOC) is the most lethal gynecologic malignancy, killing more than 9,000 women each year in the United States. Nearly 80% of patients with HGSOC will experience recurrence within 5 years, but little is known about the mechanisms that drive this process. Up to 60% of the genome in an HGSOC tumor is impacted by structural variant mutations and pronounced intratumoral heterogeneity. Intratumor heterogeneity is believed to be a key feature of recurrence and therapy resistance with some evidence indicating diverse and complex mechanisms of the seeding of metastatic sites and recurrent tumors. We included 35 HGSOC patients for whom paired chemo-naive and chemoresistant tumors as well as germline DNA was available. Whole genome sequencing was used to identify somatic single nucleotide variants (SNV) insertion/deletion variants (indels), and structural variants (SVs) in each tumor. The number of somatic SVs and indels was higher in tumors with homologous recombination repair deficiency (HRD; P=0.000252 SVs, P=0.00385 Indel) but was not affected by recurrent status (P=0.826 SV, P=0.145 SNV/indel). Clonal composition and dynamics were measured using SNVs/indels as tumors progressed from chemo-naïve primary samples to recurrent chemo-resistant tumors. Surprisingly, few changes were observed in clonal abundance and complexity through progression. When this analysis was repeated with SVs homologous recombination repair proficient tumors tend to be polyclonal while HRD tumors tend to be monoclonal. Five *denovo* structural variant signatures were identified in our cohort and led to three distinct structural variant classes tumors defined by deletion, tumors defined by duplication, and tumors defined by copy number neutral changes (inversions, translocations and balanced complex events). Patients with tumors defined by deletions and copy number neutral changes carry pathogenic SVs correlating with reduced survival (P=0.00023), while DNA gains are less subject to pathogenic alterations. Each class displayed distinct regions of the chromosome that was frequently affected by large scale SV events (>5Mb), which was also observed in the HRP/HRD status. Although no regions were notably altered across recurrence, GO analysis revealed that recurrent tumors have a significantly reduced immune response, which was not seen in the primary tumors. Within a subset of tumors, we are plan to utilize Oxford Nanopore Technologies ultra long read sequencing which will allow for confirmation of SVs observed in the WGS as well as identification of more complex events that cannot be deciphered using WGS techniques.

#4337 Illuminating the complex rearrangement landscape of sarcoma.

S. Waise[1], T. Lesluyes[1], J. Demeulemeester[2], M. Tarabichi[3], A. Flanagan[4], N. Pillay[4], P. Van Loo[5];
[1]The Francis Crick Institute, London, United Kingdom, [2]KU Leuven, Leuven, Belgium, [3]Universite Libre de Bruxelles, Brussels, Belgium, [4]University College London, London, United Kingdom, [5]MD Anderson Cancer Center, Houston, TX

Structural rearrangements and in particular, gene fusions, are key mutational processes in bone and soft tissue tumors, used for both disease classification and as biomarkers. However, the mutational processes and rearrangement processes underlying many of these events remain poorly characterized. Recent data indicate that sarcomas show particularly high frequencies of complex rearrangement events, including patterns which do not fit those of known mutational mechanisms. As the largest whole genome sequencing (WGS) cohort of sarcomas to date, the Genomics England (GE) 100,000 Genomes project represents a unique dataset in which to profile these events.

Structural variants (SVs) were identified in whole genome sequencing data for 978 samples from the Genomics England 100,000 Genomes Project using an optimized approach based on 5 specialized SV callers. SVs identified by at least 2 callers were filtered to retain only those which passed the quality filter, and to remove variants present in either matched germline samples or >1% of a panel of normal variants. Chromothriptic events, extrachromosomal DNA (ecDNA) and genes enriched for SVs were identified using established algorithms.

The prevalence of SVs varies across sarcoma, in keeping with previous reports, with particularly high rates observed in myxofibrosarcoma and liposarcoma. As described previously, liposarcomas showed the highest rates of chromothripsis. We have examined some tumor types at higher granularity than previously available, demonstrating directly that the rates of complex rearrangement events vary across subtypes. For example, chromothriptic events are identified in 100% of well-differentiated liposarcomas, but less than 10% of myxoid liposarcomas. Similarly, the presence of ecDNA varies by tumor type, with the novel observation of particularly high rates in angiosarcoma. Using these data, we have catalogued the rearrangement patterns generating canonical gene fusions in fusion-driven soft tissue tumor types.

Despite more recent advances in histological classification, survival for patients with sarcoma has remained largely unchanged for 40 years. Characterization of the mutational processes underlying these rearrangements will shed light on the pathogenesis of these tumors.

#4338 A pan-cancer single-cell analysis of intratumoral copy number diversity and evolution.

H. Ye[1], T. McDonald[2], E. Sei[1], D. Conterno Minussi[1], M. Hu[1], C. Tang[1], J. Wang[1], K. Wang[1], A. Casasent[1], H. Chen[1], F. Michor[2], N. Navin[1];
[1]UT MD Anderson Cancer Center, Houston, TX, [2]Harvard University, Boston, MA

Aneuploidy is a hallmark of human cancers and studies have shown that cancer patients harbor many differences in their copy number aberrations (CNAs) reflecting interpatient heterogeneity (IPH). While IPH has been studied extensively, the intratumoral heterogeneity (ITH) of CNAs within a tumor remains understudied. Here, we conducted a pan-cancer analysis of 94 human tumor samples at single cell genomic resolution, representing seven major cancer types: bladder, breast, colon, glioblastoma, kidney, lung, and ovary. In total, 62,646 aneuploid cells were analyzed by single cell copy number profiling and bulk exome sequencing was performed. In most cancer types, increased subclonal diversity was associated with higher CNA burden, whole genome doubling (WGD) events, and *TP53* mutations. In all tumors, our data show that cancer cells share a clonal set of truncal CNAs or mutations, suggesting these tumors evolved from a single ancestral cell. In 18/94 cases we identified subclonal WGD events, which resulted in a higher number of copy number losses after tetraploidization. Macro-spatial sampling showed that increased clonal diversity also correlated with increased spatial geographical diversity. We found that many cancers evolved CNAs in short punctuated bursts of evolution, and that this was not restricted to a specific cancer type. Collectively, these data show that copy number ITH is universally associated with molecular features across these human cancer types.

#4339 Chromatin landscapes of colorectal cancer development and cfDNA fragmentation.

N. A. Vulpescu[1], Z. H. Foda[1], P. H. A. Wisse[2], J. E. Medina[3], V. Adleff[1], R. J. A. Fijneman[2], R. B. Scharpf[1], G. A. Meijer[2], B. Carvalho[2], V. E. Velculescu[1]; [1]Johns Hopkins University School of Medicine, Baltimore, MD, [2]Netherlands Cancer Institute, Amsterdam, Netherlands, [3]Delfi Diagnostics, Baltimore, MD

Introduction: The stepwise progression of colorectal cancer from healthy epithelium, to premalignant adenoma, to cancer is accompanied by genome-wide epigenetic reprogramming. However, current analyses of these processes have been hampered by complex mixtures of cells in normal, adenoma and cancer tissue samples, as well as absence of suitable adenoma model systems. Cultured colorectal organoids, comprised of pure epithelial cells, could enable insights on the epigenetic changes leading to progression from healthy tissue to cancer.

Methods: Using 43 patient-derived colorectal organoids derived from healthy, adenoma, and cancer tissues, we examined the chromatin landscape of tumor progression using transposase accessible chromatin analyses with next generation sequencing. We defined a consensus set of nucleosome depleted regions for each disease stage and used principal component analyses to identify peaks that contributed the most variation across the collection of organoids. Consensus regions were linked to genes they overlapped, and intergenic consensus regions were linked to the nearest gene within 1 Mbp. Subsequently, we performed a gene set enrichment analysis to assess pathways affected by differential chromatin accessibility. To identify the transcription factor drivers of regulatory reprogramming, the DNA sequences within the consensus peaks were analyzed for enrichment of characteristic binding motifs. We analyzed regions of consensus peaks for fragmentation characteristics in the circulating cell-free DNA (cfDNA) of 250 healthy individuals and 51 patients with stage IV colorectal cancer.

Results: Across all organoid samples, we identified >35 million nucleosome depleted regions that we coalesced into a consensus set of 61,755 regions. We excluded 13,040 regions that had low variation across the organoid tissues, leaving 48,715 regions that could potentially define tissue-specific signatures of chromatin accessibility. As 78% of these regions could be linked to genes, we assessed whether these signatures identify known pathways involved in colorectal cancer. We identified unique signatures of healthy tissues, adenomas, and cancers comprising genes of known and novel pathways, including those involved in WNT, hippo, and RAS signaling. We found that changes in chromatin accessibility can be detected in circulating cfDNA profiles and were associated with independent circulating tumor DNA abundance by droplet digital PCR ($R=0.78$, $p<0.0001$).

Conclusions: These analyses highlight important targets of chromatin remodeling in colorectal tumorigenesis and provide an avenue for evaluating these through genome-wide analyses of cfDNA fragmentation.

#4340 Profiling the evolutionary history of giant cancer cells in sarcomas: Hopeful monsters or an evolutionary dead end?.

A. Bowes[1], T. Lesluyes[1], S. Waise[2], A. Verfaillie[3], A. Flanagan[4], J. Demeulemeester[5], M. Tarabichi[6], N. Pillay[7], P. Van Loo[8],
[1]The Francis Crick Institute, London, United Kingdom, [2]Cancer Sciences, University of Southampton, Southampton, United Kingdom, [3]Genomics Core, UZ / KU Leuven, Belgium, Belgium, [4]Genetics and Cell Biology of Sarcoma, UCL Cancer Institute, London, United Kingdom, [5]VIB Centre for Cancer Biology, Leuven, Belgium, Belgium, [6]Institute for Interdisciplinary Research, Universite Libre de Bruxelles, Brussels, Belgium, United Kingdom, [7]Sarcoma Biology and Genomics Group, UCL Cancer Institute, London, United Kingdom, [8]The University of Texas MD Anderson Cancer Centre, Houston, United Kingdom

Background: As tumors evolve, they accumulate somatic mutations that serve as an archeological record of their evolutionary past. Undifferentiated pleomorphic sarcomas (USARCs) are malignant soft tissue tumors that often contain scattered giant cancer cells, or potential 'hopeful monster cells', histologically. As USARCs frequently undergo whole genome doubling (WGD) and chromothripsis (Steele *et al*, 2019), both mutational events are likely to contribute to the formation of giant cancer cells, which frequently display atypical nuclear features such as polyploidy, micronuclei and extrachromosomal DNA. Giant cancer cells are also a common histological finding in other sarcoma types, such as dedifferentiated liposarcomas.
Aims: This study aims to leverage single cell sequencing approaches to determine the evolutionary history and genomic landscape of giant cancer cells in sarcomas.
Methods: 112 giant cancer cells identified in 8 USARCs, 1 dedifferentiated liposarcoma (DDLPS) and 1 myxofibrosarcoma by histology (i.e. nuclear size and shape, as well as multi-nucleation) were isolated via laser capture microdissection thereby retaining important spatial and morphological information. Once isolated, single cell DNA was extracted and amplified using the Ampli1 whole genome amplification (WGA) kit and underwent WGS. DNA was also estimated at a single cell level in one USARC using FACS. Once sorted into different ploidy populations, single nuclei also underwent WGS. Allele specific copy number aberrations (CNAs) were inferred in all single cells. Bulk tumour and normal WGS was also performed.
Results: LCM isolated giant cancer cells exhibited extreme sub-clonal heterogeneity with some demonstrating *de novo* chromothripsis events that was not present in bulk WGS. FACS analysis and copy number inference of single cancer cells in one USARC also revealed the presence of three ploidy populations, including a haploid, a near diploid and a WGD population. Single cell WGS and copy number profiling demonstrated that following near genome scale haploidisation, multiple haploid cells underwent successive rounds of WGD.
Conclusions: Chromothripsis and WGD emerges as major contributors to intra-tumor heterogeneity in sarcoma giant cancer cells. Single cell LCM and WGS revealed that some giant cancer cells contained *de novo* chromothripsis events that were not observed in bulk WGS. Multiple sub-clonal WGD events also permitted one USARC to continue to explore its fitness landscape contributing to ongoing tumor heterogeneity and lethality.

#4341 Non canonical mitochondrial hotspot mutations in cancer.

S. Boscenco[1], J. Tait-Mulder[2], M. Kim[1], C. Tang[1], M. Zucker[1], T. Park[1], W. Wei[3], P. F. Chinnery[3], P. A. Gammage[2], E. Reznik[1];
[1]Memorial Sloan Kettering Cancer Center, New York, NY, [2]Cancer Research UK Beatson Institute, Glasgow, United Kingdom, [3]Medical Research Council Mitochondrial Biology Unit, Cambridge, United Kingdom

The vast majority of recurrent somatic mutations arising in tumors affect protein-coding genes in the nuclear genome. Here, through population-scale analysis of 15,619 whole tumor genomes, we report the discovery of highly recurrent mutations affecting both the small (12S, *MT - RNR1*) and large (16S, *MT - RNR2*) RNA subunits of the mitoribosome. In total, we identified 70 recurrent, hotspot mutations affecting either subunit of the mitoribosome. Compared to non-hotspot positions, rRNA hotspots preferentially affect positions participating in Watson-Crick base pairing, and tend to arise at positions under strong purifying selection in the germline. Consistent with their putative selection, hotspot rRNA alleles arose at higher heteroplasmy than silent mutations under neutral selection. Transcriptional and metabolomic profiling of the m.1227G>A *MT - RNR1* hotspot revealed a heteroplasmic dosage-dependent shift in energy generation towards glycolysis. Mutations disrupting the mitoribosome therefore represent a novel class of functional mutations under positive selection in cancer genomes.

#4342 Breast cancer multi-omic single cell profiling identifies key progressive disease markers.

H. Russell, M. Rao, G. Duclos, R. Aguilar, N. Barkas, M. Callahan, O. Chaudhary, P. Gathungu, C. Rands, V. Shankarappa, D. Stetson, A. Rotem, M. Scaltriti, B. Dougherty;
AstraZeneca US, Waltham, MA

Breast cancer is one of the most diagnosed cancers and has a complex tumor microenvironment (TME). Breast tumors are subtyped by receptor expression, and all have a high degree of cellular heterogeneity. We analyzed tumors from 8 individuals with early-stage breast cancer. The patients had either triple negative breast (TNBC) or an estrogen receptor (ER) positive cancer. The tumors and normal adjacent tissue were profiled by single-nuclei gene expression (GEX) and ATAC data using the 10X multi-ome methodology. Gene set analysis identified specific epithelial clusters associated with the estrogen early/late response, epithelial mesenchymal transition, and several key cytokine pathways. From those epithelial cells, a subset highly proliferative in nature emerged. It consists of both ER positive and TNBC tumor types enriched for specific DNA transcriptional motifs including those for stem cell (Yamanaka) factors and other cellular proliferation motifs. GEX proliferation markers such as MKi-67 were also highly expressed. Overlaying GEX and ATAC data, it was possible to filter the numerous differentially expressed genes and peaks into a subset of genes specific to progressive breast cancer within the proliferative cluster. Those genes included ESRP1, POP4, CCNE1, and AAMDC all of which are associated with progressive breast cancer. To further elucidate the complexity of the TME, we examined clusters of fibroblasts from our dataset. A difference in cancer associated fibroblast marker gene expression was related to the level of ER expression expressed in the tumor epithelium. In general, ER-low tumor fibroblasts had higher expression of immune cancer associated fibroblasts (iCAFs) markers while ER-positive and TNBC tumors had greater expression of extracellular matrix associated markers (emCAFs). Specific clusters were enriched for emCAFs and iCAFs representing another critical part of the TME. In conclusion, using a multi-modal single-cell approach to the TME allowed the identification of an aggressive cluster of epithelial cells marked by genes for cellular proliferation and noted therapeutic targets while also characterizing other critical TME components especially, CAFs.

#4343 Revealing ovarian cancer copy number variation in single cells.

Y. Jin[1], R. Bassiouni[1], L. D. Gibbs[2], J. Qian[2], S. Rotimi[2], M. G. Webb[1], S. Rajpara[2], D. W. Craig[1], L. D. Roman[2], J. D. Carpten[1];
[1]Beckman Research Institute of The City of Hope, Duarte, CA, [2]University of Southern California, Los Angeles, CA

The mortality rate associated with ovarian cancer (OvCa) is disproportionately high in comparison to its incidence rate. This is partly due to the heterogeneous nature of the disease, which reduces treatment efficacy and contributes to high rates of relapse and chemotherapy resistance. Most OvCa are epithelial in origin and can be classified into four main subtypes: serous, mucinous, endometrioid, and clear cell. Of these, high grade serous ovarian cancer (HGSOC) is the deadliest. Epithelial ovarian carcinomas (EOC) typically exhibit widespread chromosomal and arm-level copy number abnormalities across most of the genome; in HGSOC, focal amplifications and microdeletions are especially prevalent and indicative of high genomic instability. To understand the heterogeneity of aneuploidy in EOC and HGSOC, we performed shallow single-cell whole genome sequencing on four EOC samples: two HGSOC, one clear cell, and one mixed clear cell and endometrioid. All samples were late stage and treatment naïve, and one sample had a known *BRCA2* mutation. Sequencing data was processed by two complementary methods to call copy number alterations. First, we used the Cell Ranger DNA pipeline (10x Genomics) to align cell-identified sequencing reads to human reference genome GRCh38 for coverage-based copy number estimation. Resulting copy number calls were cleaned up for mappability, quality, and noisiness. Each sample was then subject to clustering and subclustering analysis using maximum likelihood genetic clustering algorithms. All samples exhibited a high level of aneuploidy, including characteristic alterations known to be associated with EOC. Two tumors contained readily distinguishable clonal populations, and all samples contained main tumor clones that could be further divided by unique subclonal characteristics. Evidence of polyploidy was also seen in all four specimens, with some tumor clusters exhibiting triploid and tetraploid baselines. In parallel, sequencing data was analyzed by the Copy-number Haplotype Inference in Single-cell by Evolutionary Links (CHISEL) algorithm. CHISEL utilizes both binned read depth ratio and B-allele frequency data to determine allele- and haplotype-specific copy numbers in single cells. Results from CHISEL confirmed the copy number calls from Cell Ranger DNA, and revealed widespread loss of heterozygosity in all samples. These findings were corroborated with allele-specific copy number data derived from matched tumor-normal whole exome sequencing. Furthermore, CHISEL detected polyploidy in one-third of the tumor cells with no preference for the A or B alleles. Overall, our findings highlight that the known heterogeneity of ovarian cancer extends to the level of aneuploidy and CNAs, shedding light on factors which pose significant barriers to effective personalized medicine implementation.

#4344 Comprehensive analysis of LINE-1 transposable elements in colorectal cancer.

R. de Wit[1], S. Lakbir[2], C. Buranelli[2], G. A. Meijer[3], S. Abeln[4], R. J. A. Fijneman[3];

[1]Dept. Information and Computing Sciences and Dept. Biology, Utrecht University, Utrecht, Netherlands, [2]Dept. Computer Science, Vrije Universiteit Amsterdam, Amsterdam, Netherlands, [3]Netherlands Cancer Institute, Amsterdam, Netherlands, [4]Utrecht University, Utrecht; VU Bioinformatics Group, Vrije Universiteit Amsterdam, Amsterdam, Netherlands

Background: Colorectal cancer (CRC) is the third most frequent cancer worldwide, and approximately a third of patients die from the disease. There is therefore an urgent need to better understand CRC biology. A particular feature in (colorectal) cancer is the activation of LINE-1 (L1) retrotransposons: DNA fragments which propagate to other places in the genome through an RNA intermediate. Per genome, about 100-150 genomic L1 copies are still retrotransposition-competent, but repressed in most somatic tissues. Their role in tumor development is currently unknown. Recently, the PCAWG consortium characterized the landscape of somatic L1 retrotranspositions in a series of primary cancers of different origin, and identified 124 recurrently active L1 source regions. However, only a limited number of these concerned CRC.

Aim: This study aims to perform a comprehensive analysis of L1 activity in a large cohort of metastatic colorectal cancer.

Methods: To this end, we retrieved data from the Hartwig Medical Foundation, comprising deep (106x) whole genome sequencing (WGS) data from metastatic CRC (n=745), to compare to breast (n=888) and lung cancer samples (n=640). We determined L1 activity as the number of somatic L1 insertions reported by the HMF DNA analysis pipeline and used the activity of each of the 124 L1 sources as previously reported by the PCAWG consortium.

Results: 99% of mCRC samples (n=741) displayed at least 1 somatic L1 retrotransposition, with at least 10 retrotranspositions in 89% of samples. L1 retrotransposition is more prevalent in mCRC than in metastatic lung and breast cancer, in which only 40% and 20% had at least 10 retrotranspositions per sample, respectively. Each cancer type showed a unique profile of active L1 sources. We did not observe a clear preference of L1 insertions for a single genomic region. However, in CRC, the gene most frequently affected in an *exon* was APC (n=13), an important tumor-suppressor gene. An analysis of somatic SNVs and SVs confirmed an association of mutations in some known L1 regulators such as TP53 with increased L1 activity, whereas mutations in others showed no change in the number of somatic retrotranspositions.

Conclusions: We conclude that somatic L1 retrotranspositions are highly prevalent in metastatic colorectal cancer. Presence of L1 insertions in APC suggests retrotranspositions start very early in CRC development and prompts further investigation into earlier CRC stages.

#4345 Evaluation of the prevalence and impact of molecular variation in the three-prime repair exonuclease 1 TREX1 across mammalian species and in human malignancies.

M. M. Konate, M. Shekfeh, J. Krushkal;
National Cancer Inst - Shady Grove Campus, Rockville, MD

The three-prime repair exonuclease 1, TREX1, degrades cytosolic DNA to prevent aberrant immune activation. Inactivation of TREX1 results in DNA accumulation in the cytosol and subsequent induction of the cGAS-STING DNA sensing pathway, downstream interferon-mediated innate immune signaling, and inflammation. Correspondingly, germline pathogenic mutational defects in the TREX1 gene lead to hereditary autoimmune and autoinflammatory disorders. While TREX1 mutations are also reported in some tumors, their consequences in cancer remain poorly understood. To assess the functional importance of amino acid residues in TREX1, we analyzed protein sequences of the functional TREX1 isoform, TREX1b, from 168 mammalian species. We also conducted a survey of genomic variant databases COSMIC, ClinVar, TCGA, LOVD, Decipher, and gnomAD for disease-associated TREX1 mutations. Finally, we modeled TREX1 mutations occurring in human tumors to evaluate predicted impact on protein stability and function using structure-based approaches FoldX and INPS-3D, and compared results to available predictions from AlphaMissense and COSMIC-3D. In the Cancer Genome Atlas (TCGA), 16 out of 32 cancer histologies have tumor samples bearing protein-altering TREX1 variants, with bladder cancer and melanoma having the highest frequency of TREX1 variants at 2.7% of tumor samples. Moreover, all 32 cancer types have some samples with loss of one or both copies of TREX1; frequencies of heterozygous loss range from 0.6% (thymoma) to 86% (kidney clear cell and lung squamous cell carcinomas). We also observed TREX1 copy gain with lower frequency than instances of copy loss, but also occurring in 31 out of 32 studies. Multiple tumors have a combination of a TREX1 protein sequence variant and copy number gain or loss, suggesting that their potential interplay may increase functional impact of TREX1 variants. Out of 15 cancer-associated TREX1 variants, 5 (33%) were predicted to be pathogenic by AlphaMissense. For FoldX and INPS-3D mutagenesis modeling, we used the published experimental 3D crystal structure of the wild type (WT) human TREX1 (PDB: 7TQQ). The changes in Gibbs free energy of folding ΔΔG between WT and mutant predicted by FoldX and INPS-3D both correlated strongly with the AlphaMissense pathogenic probability scores (Pearson r=0.69 and 0.73, respectively). We will discuss implications of TREX1 variation and conservation across mammalian species and potential effects of germline TREX1 variants in hereditary autoimmune and autoinflammatory disorders and on somatic and germline TREX1 variants in human cancer cells and tumor samples.

*The first two authors contributed equally.

#4346 Deciphering the landscape of extrachromosomal DNA in gastric cancer and its potential impact on cancer dynamics.

D. Seol[1], S. Kang[2], S. Kim[2], J. Lee[1], M. Yoo[1], D. Hwang[1], S. Kang[1], C. Bang[1], Y. Park[1], S.-H. Ahn[1], H.-H. Kim[1], H. Kim[2], Y.-S. Suh[1];
[1]Seoul National University Bundang Hospital, Seongnam, Korea, Republic of, [2]Sungkyunkwan University, Suwon, Korea, Republic of

Extrachromosomal DNA (ecDNA) drives substantial copy number increases in focal regions harboring oncogenes and its non-Mendelian inheritance during mitosis contributes to cancer heterogeneity and a poor prognosis across multiple cancer types. However, the prevalence and function of ecDNA in gastric cancer (GC) are still largely unknown. Here, we profiled ecDNA by whole-genome sequencing analysis from 76 GC patients and explored its functional attributes through whole-transcriptome sequencing from the same tissues. Focal somatic copy number amplification (fSCNA) was detected in 27 patients (35.5%), of which 17 (22.4%) had at least one circular form of focal amplification (ecDNA$^{\pm}$/fSCNA$^{\pm}$). Most of the patients carrying one or more ecDNA were classified as TCGA-CIN subtype (n=12; CIN: chromosomal instability). The fSCNA hotspots were observed at 17q12 and 19q12, where *ERBB2* and *CCNE1* are located, respectively. Amplifications at both loci occurred in seven patients and were formed into ecDNA in four and two patients, respectively. The ecDNA amplicons carried more oncogenes with significantly higher copy numbers than other amplicons (one-tailed Mann-Whitney *U* test, p=3.9e-03), and 44.4% (12 of 27) of ecDNA amplicons regions were overlapped with tandem duplication or chromothripsis, known causes of ecDNA formation. Oncogenes such as *ERBB2* and *MIEN1*, residing on ecDNA, exhibited significantly increased expression compared to matched normal tissue as well as patients with the corresponding genes located on their chromosome only, suggesting that the ecDNA-induced copy number increases contribute to elevated expression levels. On the other hand, *MYC* showed higher expression in the ecDNA$^{\pm}$/fSCNA$^{\pm}$ group, irrespective of its fSCNA status ($padj$=0.028 and 4.24e-06 against the ecDNA^{-}/fSCNA$^{\pm}$ and ecDNA^{-}/fSCNA^{-} group, respectively). We further explored gene clusters that were associated with the ecDNA$^{\pm}$/fSCNA$^{\pm}$ group using weighted gene co-expression network (WGCNA) analysis. One module was distinct from ecDNA^{-} patients, consisting of genes associated with the “protein processing in endoplasmic reticulum” and “spliceosome” pathways, inferring that transcription and translation are more active in ecDNA$^{\pm}$ patients. Moreover, the overall survival analysis of 76 GC patients revealed that ecDNA$^{\pm}$/fSCNA$^{\pm}$ patients were significantly associated with poor prognosis (log-rank test, p=0.014). In conclusion, ecDNA may be a main source of high expression of oncogenes that influence GC development, and subsequently upregulated global transcription activity will make GC more aggressive.

#4347 Cell-type specific transcriptional regulation of APOBEC3A in cancers.

D. Yesudhas, B. Lone, K. Butler, A. Chakraborty, A. Banday;
NIH-NCI, Bethesda, MD

APOBEC3s (A-H) are a family of seven cytosine deaminases that inactivate viruses as part of the innate immune response. However, APOBEC3A and APOBEC3B have been found to mediate mutagenesis in tumor genomes by deaminating ssDNA that transiently arise during transcription and DNA replication. The mechanisms that trigger these enzymes to generate high mutation burdens in some cancers and affect disease progression and clinical outcomes are largely unknown. Here, we explored cell-type-specific transcriptional regulation of APOBEC3s using single-nucleus/cell RNA-seq (sn/scRNA-seq) data (>100 samples and >300,000 cells) from four tumor types - bladder, lung, breast, and kidney - that display different levels of APOBEC-induced mutation burden. Our analyses revealed that among seven members of the APOBEC3 family, *APOBEC3A* is expressed in a cell-type-specific manner. The expression was predominant in KRT13 and CDH12 epithelial cell-types and inflamed macrophages. The APOBEC3A+ epithelial cell populations were abundant in the bladder, moderate in the lung and breast, and nearly absent in the kidney tumors. *APOBEC3A* expression correlated with interferon and pro-inflammatory signaling in KRT13+ cells. Transcription factors ELF3 and ATF3 were significantly upregulated in APOBEC3A+ KRT13 cells. Pseudotime analysis of sn/scRNA-seq data revealed that *APOBEC3A* cells are in epithelial-mesenchymal transition. Finally, several gene markers defining APOBEC3A+ KRT13 cell types were identified. Ongoing analyses include investigations into clinical correlates, cell-type-specific mutation burdens, and validation through *in vitro* functional approaches. Our results propose that *APOBEC3A* is turned on in specific epithelial cell types by multiple signaling pathways during tumorigenesis, thereby driving tumor heterogeneity, particularly in high mutation-burden cancers.

#4348 *TP53*-regulome and *TP53*-effectome are frequently altered in Epstein-Barr virus-associated nasopharyngeal cancer.

T. Law[1], Y.-K. Ng[1], J. Wen[1], J.-H. Ng[2], M. Wong[2], P. Tse[2], V. Lui[1];
[1]Augusta University, Augusta, GA, [2]University of California San Diego, La Jolla, CA

Dysregulation of p53 signaling is central to oncogenesis. As revealed by the Cancer Genome Atlas (TCGA), mutation of tumor suppressor *TP53* is the most frequent single somatic event found across human cancers. In Epstein-Barr Virus (EBV)-associated nasopharyngeal cancer (NPC), an aggressive head and neck cancer prevalent in Southeast Asia, our recent study showed that only 9% cases harbored *TP53* mutation. Studies in NPC demonstrated that EBV infection alone was not sufficient to attenuate p53 signaling in EBV(+)NPC cells. As p53 signaling and function are intricately regulated by multiple pathway components, aberrations of the p53 regulatory network may also off-set p53 signaling, thus facilitating EBV(+)NPC tumorigenesis. Here, we hypothesized that in addition to *TP53* aberrations, *TP53*-regulome (genes direct regulate *TP53* expression and function), and *TP53*-effectome (genes responsible for executing biological functions of p53 signaling in cells) may also be genomically altered in NPC during oncogenesis. Here, we assembled the most updated *TP53*-regulome/-effectome genelists, including newly identified p53 regulatory components, to enable characterization of *TP53*-regulatory network in EBV(+)NPC patient tumors. Among the subclasses of *TP53*-regulome, mutations of genes regulating p53 acetylation and ubiquitination were significantly co-occurred, while *TP53*-effectome genes involved in p53-mediated DNA repair and p53 metabolism were co-mutated with statistical significance, for instance. Analysis of the 111 whole-exome sequenced EBV(+)NPC samples first demonstrated that 40.5% and 26.1% was affected by *TP53*-regulome and *TP53*-effectome mutations respectively, while only 9.0% cases carried *TP53* mutation. In total, 55% of EBV(+)NPC harbored p53-related somatic mutations, which may implicate a wider *TP53*-associated genomic defect for NPC tumorigenesis. Among the 10 cases of *TP53*-mutated EBV(+)NPC, 5 of them co-harbored *TP53*-regulome mutations while 5 cases co-harbored *TP53*-effectome mutations. Subsequent in-depth allele frequency analysis revealed that in 4 out of 7 *TP53*, *TP53*-regulome and *TP53*-effectome co-mutated cases, the allele frequencies of *TP53*-regulome or *TP53*-effectome mutant genes were higher than that of *TP53*, implicating likely earlier events of these genetic defects than *TP53* mutation during NPC tumorigenesis. In conclusion, p53 regulatory network mutations are far more frequent than *TP53* mutations in this virally associated HNC, and functional study of such a wide array of p53-network mutations on p53 signaling in NPC tumorigenesis are warranted.
Acknowledgments: VWYL is supported by the Start-up Fund from the Georgia Cancer Center, USA.

#4349 Characterization of a centrosome loss-induced tumorigenic signature in prostate epithelial cells.

J. Yang, D. de Oliveira Pessoa, J. M. Ryniawec, E. Loertscher, A. E. Cress, M. Padi, G. C. Rogers;
University of Arizona, Tucson, AZ

Prostate cancer (PCa) stands as the second leading cause of cancer death in American men, with overtreatment being common given the difficulty in distinguishing between indolent and aggressive cases. Unlike many cancers, PCa lacks hallmark mutations in key oncogenes and tumor-suppressor genes. Instead, PCa exhibit extensive genomic rearrangements and chromosomal instability (CIN). CIN occurs during PCa progression, producing ETS gene family fusions, PTEN loss and androgen receptor amplification. Importantly, the mechanism underlying CIN in PCa remains unclear.

Previously, we found that cell within early-grade human primary prostate adenocarcinomas (PRAD) frequently lack centrosomes, and this frequency correlates with tumor grade. We demonstrated that transient removal of centrosomes within non-tumorigenic human prostate epithelial cells (hPrEC) induces CIN and was, strikingly, sufficient to transform subpopulations of cells capable of producing xenograft tumors in mice. To unravel the molecular mechanisms underlying this path to tumorigenesis, we isolated DNA and RNA from parental hPrECs, clonal lines subjected to transient centrosome loss, and xenograft tumor cells and performed whole genome sequencing (WGS) and bulk RNA-seq. This allowed us to characterize the genomic profiles induced by centrosome loss and to identify an associated mutational signature.

We used MUTECT2 to identify single nucleotide variants. Kataegis loci were observed on multiple chromosomes in all transient centrosome removal samples. Copy number variations were also detected in these samples using FACETS and SEQUENZA. Next, we extracted the copy number (CN) signature with SigProfiler and Sigminer, comparing it to COSMIC CN signatures and WGS data from PRAD patients. Our results revealed that the transient centrosome loss signature bears similarity to CN signatures associated with chromothripsis, loss of heterozygosity, and homologous recombination repair deficiency. Patients with PRAD displaying the centrosome loss CN signature had a poorer prognosis. Additionally, our CN analysis discovered that centrosome loss induced mosaic loss of chromosome Y in our samples. To detect structural variations, we employed DELLY, MANTA, SVABA, revealing a high occurrence of both non-clustered and clustered translocations in transient centrosome loss samples. These translocations were validated in our RNA-seq data using STAR-Fusion. Ongoing analyses include inferring CNV from PCa scRNA-seq data, and determining cell populations with the centrosome loss CN-signature and their associated transcriptome features.

This work unveils a comprehensive genomic profile stemming from centrosome loss and demonstrates its role in driving oncogenesis in PCa. These findings have the potential to establish centrosome loss as a hallmark in PCa stratification, and lead to a significant advancement in prostate tumor treatment.

#4350 Characterization of PUF60 splicing activity that is essential for the survival of triple negative breast cancer.

A. Tankka, T. Gomberg, C. Zhou, V. Pham, G. Yeo;
University of California San Diego - UCSD, La Jolla, CA

Alternative splicing driven by RNA-binding proteins (RBPs) plays a significant role in TNBC, however, pharmacological modulators of core spliceosomal proteins can disrupt early stages of spliceosome assembly and lead to toxic effects in normal tissues, limiting their utility as safe therapeutics. Here, we used *in vivo* CRISPR-Cas9 screening to evaluate RBP dependencies in TNBC and identified 17 splicing regulatory candidates that are essential in TNBC but dispensable for normal cell growth and survival. Within this cohort, the alternative splicing factor, PUF60, was the most significantly upregulated candidate in patient TNBC tumors. We found that depletion of PUF60 induced apoptosis in human TNBC cell lines and impeded xenografted tumor growth *in vivo* while upregulation of PUF60 expression increased TNBC cellular proliferation. Although PUF60 has been shown to also bind DNA and influence transcription, TNBC cells constructed with a previously characterized mutation (L140P) required for 3' splice site recognition displayed significantly decreased cellular proliferation compared to cells containing wild type PUF60. Integrated eCLIP and KD RNA-sequencing revealed that PUF60 selectively regulates the splicing of mRNAs in TNBC that contribute to essential processes including DNA repair, replication and cell cycle progression. RNA-seq following L140P-mediated inhibition of 3' ss recognition revealed a cohort of splicing events within genes enriched for similar processes following knockdown of endogenous PUF60 including cell cycle and histone modification. Altogether, our study highlights a critical role for PUF60-mediated splicing in the maintenance of genomic integrity in TNBC as well as the therapeutic potential of identifying and targeting splicing effector RBPs only responsible for TNBC survival.

#4351 Differential dependency mapping of chimeric RNAs across cancer reveals a new landscape of functional fusion transcripts.

S. Lalani, S. Gadh, J. Elfman, S. Singh, H. Li;
University of Virginia, Charlottesville, VA

Chimeric RNAs are RNA transcripts containing sequences originating from multiple distinct genetic loci and can form through a variety of mechanisms such as DNA rearrangement, cis-splicing of adjacent genes, or RNA trans-splicing. Chimeras have long been known to be a hallmark of cancer and due to their unique properties are promising targets for precision medicine. Appropriately, fusion proteins transcribed from chimeras such as *BCR-ABL1* and *TPM3-NTRK1* have been shown to be effective targets. Due to these past successes, there exists an opportunity to identify new chimeras as therapeutic targets. While modern chimera prediction software allows for the fast and accurate identification of chimeric RNAs from RNA sequencing data, investigations separating therapeutically relevant transcripts from “transcriptional noise” remain lacking. In this study we performed an *in-silico* functional screen of chimeras across cell lines representing a wide variety of cancers. We used state-of-the-art chimeric RNA prediction software to create a database of chimeric RNAs across 1017 cell lines from The Cancer Cell Line Encyclopedia. For each chimera we assessed factors such as frequency, recurrence, breakpoint coordinates, frame, and coding potential. To identify specific functional transcripts, we integrated publicly available shRNA knockdown data with our predictions and developed an in-silico functional analysis pipeline comparing differential knockdown effects between chimera and corresponding parental transcripts. For each transcript we assessed the average fold change of chimera-mapping probes, a function score defined as the difference between the fold change of chimera-mapping and parent-specific probes, and a p-value assessing the confidence of our functional score. From our initial screen of 127,819 transcripts, we identified 1088 high-confidence functional chimeras. We successfully identified nearly all known functional chimeras screened including *PAX3-FOXO1*, *EWSR1-FLI1*, and *TCF3-PBX1*. We also identified previously unknown chimeras that that we predict have a function in cell growth and proliferation. Overall, the results of our study reveal a new landscape of functionally relevant chimeric transcripts in cancer. Follow-up studies can further investigate these transcripts to determine their potential as therapeutic targets.

#4352 A high rate of episomal HPV16 is present in head and neck squamous cell carcinoma tumors by long-read whole genome sequencing.

Sonam Tulsyan[1], Vera Mukhina[2], Isabel Rodriguez[1], Subhendu R. Choudhury[2], Erin Allor[2], Kyle Hatte[3], Michael Dean[1], Daria A. Gaykalova[4]

[1]Laboratory of Translational Genomics, Division of Cancer Epidemiology and Genetics, National Cancer Institute, Rockville, MD,[2]University of Maryland School of Medicine, Institute for Genome Sciences, Baltimore, MD,[3]Department of Otorhinolaryngology-Head and Neck Surgery, Marlene & Stewart Greenebaum Comprehensive Cancer Center, University of Maryland Medical Center, Baltimore, MD,[4]Department of Oncology, Sidney Kimmel Comprehensive Cancer Center, Johns Hopkins University, Baltimore, MD

Persistent Human Papillomavirus (HPV) infection causes an increased risk of Head and Neck Squamous Cell Carcinoma (HNSCC). However, a comprehensive understanding of the intricate molecular events within virus-positive tumors remains a critical knowledge gap. Therefore, we used long-read sequencing to study the intricacies of HPV integration events within the genomic landscape of HPV+ HNSCC tumors. A total of 16 tissue biopsies, including 10 tumors and 6 matched adjacent normal tissues from histopathologically confirmed HNSCC subjects were sequenced by LSK114 chemistry of Oxford Nanopore Technology with an average coverage of 30X and 10X, respectively. The predicted mitochondrial haplotype from Mitomaster confirmed that the tumor/normal pair was from the same individual. The HPV integration status was determined by aligning fastq_pass files at the Cancer Genomics Cloud and viewing the breakpoints in the Integrated Genome Viewer. HPV lineage and sub-lineage classification was determined using ClustalOmega. We detected HPV16 in 8/10 tumors, with sublineages A1 and A2 accounting for 38% (3/8) and D3 for 25% (2/8). One tumor sample had a very low HPV load with only one HPV16 sequence read and low detection by PCR. Interestingly, we found that 5/8 HPV positive tumors had episomal HPV16 with different states. So, two tumors had intact HPV episomes, two more had either a small deletion or an insertion in the episomal HPV, and the last one had a rearranged episomal multimer (Table 1). The remaining three tumors had integrated HPV16: one with type 1 integrations at 11q12.13 and two others with type 2 integrations at chr1q42.12 and chr14q21.1. Our results indicate that episomal HPV16 is more prevalent than integrated HPV16 in primary HPV+ HNSCC samples. These findings provide new insights into the molecular mechanisms and consequences of HPV infection in HNSCC. Table 1: HPV characterization in HNSCC studied tissue biopsies.

Patient ID	Race	HPV status	HPV sublineages	Predicted Haplotype	HPV pattern
#PID_1	Caucasian	HPV16 +	A2	T2b (T2b)	Type 2 Integration (chr1q42.12)
#PID_2	-	HPV-	-	I1a (I1a1b)	-
#PID_3	Caucasian	HPV16 +	A1	H1q (H1q)	Episomal (rearranged multimer)
PID_4	African American	HPV16 +	A1	-	Episomal (deletion of 636bp from 4892 to 5528)
#PID_5	-	HPV16 +	A2	H1 (H1+16189)	Type 1 Integration (complex chr11q12.13)
*#PID_6	Caucasian	HPV16 +	-	T2b (T2b)	-
PID_7	Caucasian	HPV16 +	D3	-	Episomal
#PID_8	African American	HPV16 +	D3	L1c (L1c3a)	Type 2 Integration (chr14q21.1)
PID_9	African American	HPV16 +	A2	-	Episomal (insertion of 257bp from 7310-7567)
PID_10	Caucasian	HPV16 +	A1	-	Episomal

*Very weakly HPV16 positive; #Tumor-normal pair

#4354 Long noncoding RNA DUXAP10 serves as a putative driver of carcinogenic transformation in anaplastic thyroid cancer.

N. R. DeSouza, M. Carnazza, D. Quaranto, T. Jarboe, K. Kopec, R. Suriano, K. Nielsen, A. Moscatello, H. Islam, J. Geliebter, R. K. Tiwari;
New York Medical College, Valhalla, NY

Anaplastic Thyroid Cancer (ATC) is the most aggressive thyroid cancer subset, with a <4% five-year survival rate. ATC is completely refractory to traditional therapy and newer immunotherapeutic options. Unlike other lethal cancers, ATC has a low mutational burden, warranting the need for a comprehensive study of differential gene expression patterns. Transcriptomic regulators known as long non-coding RNAs (lncRNA) have been described as pivotal orchestrators of gene expression and drivers of carcinogenic patterns. Thus, we present the role of novel lncRNAs in shaping the ATC genotype and phenotype. Publicly available ATC vs. normal thyroid tissue transcriptomic datasets (Gene Expression Omnibus; GSE33630, GSE85457) were investigated to identify genomic transcripts that are differentially expressed in ATC samples using GEO2R. Bioinformatic analysis identified Double Homeobox A Pseudogene 10 (DUXAP10), as a highly upregulated lncRNA in ATC patient tissue samples in both databases (40-fold and 20-fold). Gene Expression Profiling Interactive Analysis statistically correlated high DUXAP10 expression with decreased survival in thyroid cancer patients. DUXAP10 expression was similarly upregulated in ATC cell line, T238, compared to immortalized “normal” thyroid epithelial cell line, Nthy-ori-3-1. Our T238-CRISPRi knockdown model of DUXAP10 was evaluated in vitro to assess consequences of overexpression. CRISPRi knockdown of DUXAP10 in T238 significantly reduced its migratory capabilities by 50%, invasion index by 30%, clonogenicity by 70%, cell viability by 67%, 60%, and 50% at 24, 48, and 72 hours, respectively, proliferation by 28%, 45%, and 36% at 24, 48, and 72 hours, respectively, and global transcription rate by 65%. Further, our DUXAP10-CRISPRi knockdown exhibited a downregulation of N-Cadherin and mediators of beta-catenin signaling- confirming a role in regulatory cross-talk of central carcinogenic pathways. We are currently evaluating proteins and miRNAs bound to and “sponged” by DUXAP10 in vitro utilizing RNA-centric methodology. These data reveal the novelty of DUXAP10, and that its over-expression may increase the negative consequences of ATC metastasis. Thus, we have identified DUXAP10 as a putative determinant for ATC diagnosis, prognosis, and therapeutic targeting.

#4355 Characterizing HRD in ovarian cancer: Insights from copy number signatures.

A. Hawari[1], A. Tapinos[1], C. J. H. Kramer[2], A. J. Gruber[3], R. Houlston[4], J. Brenton[1], **D. Wedge**[1],
[1]University of Manchester, Manchester, United Kingdom, [2]Leiden University Medical Center, Leiden, Netherlands, [3]University of Konstanz, Konstanz, Germany, [4]The Institute of Cancer Research, London, United Kingdom

Copy number changes are defining features in ovarian cancers. Two distinct methods by Steele et al. and Drews et al., published back-to-back in 2022, detail features and categories of copy number signatures. However, these methods have not been benchmarked for ovarian cancer. Mutational signatures are pivotal in understanding cancer biology and serve as predictive and prognostic biomarkers. This study aims to examine the landscape of copy number signatures to characterize the diversity of Homologous Recombination (HR) impairment within ovarian cancer. While assessing Homologous Recombination Deficiency (HRD) is crucial for targeted treatments, current HRD tests lack clarity. Using signature extraction tools SigProfilerExtractor and CINSignature, we analyzed whole-genome sequencing data (mean depth 100x) from 416 ovarian cases from Genomics England (GeL), employing both copy number signature methods. Among the signatures extracted, HRD signature CN17 from Steele et al. methodology was identified in 37% of the samples and primarily found in the high-grade serous ovarian cancer (HGSOC) subtype (77%). Additionally, higher exposure levels (median of 0.4 in n=154 compared to median of 0.29 in n=416) of Drews et al. methodology's most complex HRD signature, CX3, was detected in samples exhibiting CN17 activity. This ongoing exploration of the copy number signatures landscape works towards identifying the spectrum of HR impairment, aiming to benchmark these two methods for a standardized diagnostic tool. This study contributes to our understanding of the mutational landscape of ovarian cancer and its potential implications for prevention and personalized treatment strategies.

#4356 An isoform-resolution transcriptomic atlas of colorectal cancer from long-read single-cell sequencing.

Z. Li[1], B. Zhang[1], **J. Chan**[2], H. Tabatabaeian[2], Q. Tong[2], X. Chew[2], X. Fan[2], C. Chan[2], P. Driguez[1], F. Cheong[2], S. Wang[3], B. Siew[4], I.-W. Tan[3], K.-Y. Lee[3], B. Lieske[3], W.-K. Cheong[3], D. Kappei[2], K.-K. Tan[3], X. Gao[1], Y. Tay[2];

[1]King Abdullah University of Science and Technology, Thuwal, Saudi Arabia, [2]Cancer Science Institute of Singapore, National University of Singapore, Singapore, Singapore, [3]National University Health System, Singapore, Singapore, [4]Yong Loo Lin School of Medicine, National University of Singapore, Singapore, Singapore

Colorectal cancer (CRC), a complex and molecularly heterogenous disease that lacks robust predictive markers and targeted therapies, is the second leading cause of cancer death worldwide. In recent years, technological advances in short-read single-cell RNA sequencing (scRNA-seq) have been instrumental in deciphering tumor cell heterogeneities. However, most studies have focused on gene-level expression quantification without considering alterations in transcript structures arising from widespread alternative end processing and/or splicing which are frequently dysregulated in cancer. Here, we combined short- and long-read scRNA-seq of CRC patient samples to build the first isoform-resolution CRC transcriptomic atlas. We identified 394 dysregulated transcript structures in tumor epithelial cells, including 299 derived from the coupling of multiple alternative splicing events. Additionally, we characterized genes and isoforms associated with different colon epithelial lineages and tumor cell subpopulations exhibiting varying levels of stemness and differentiation, as well as their distinct prognostic implications. Finally, we built an algorithm by integrating mass spectrometry data and novel peptides derived from predicted open reading frames of recurrent tumor-specific transcripts to curate a panel of recurring neoepitopes. Overall, this study unveils the transcriptomic landscape of CRC and may drive the identification of neoantigens based on full-length transcriptomic atlases to aid future development of more universal neoantigen-based cancer vaccines.

#4357 Examining the role of end-stage kidney as a potential intermediate stage in the development of renal cell carcinomas; understanding the pathogenesis allowing for early detection.

M. Wan[1], V. Castillo[1], R. Saleeb[2],
[1]University of Toronto, Toronto, ON, Canada, [2]St. Michael Hospital, Toronto, ON, Canada

Introduction: Clear cell renal cell carcinoma (CCRCC) and papillary renal cell carcinoma (PRCC) are both thought to arise from the renal proximal tubules. End stage renal disease (ESRD) patients have an increased incidence of developing PRCC and CCRCC. Some studies showed a progenitor cell population that is inherently present in renal tubules, and is significantly increased after renal injury. The studies have also illustrated similarities between these progenitor cells and PRCC & CCRCC; hypothesizing that they are the cell of origin of these tumors. This trend was not observed in other renal cell carcinomas such as chromophobe renal cell carcinoma (chRCC). This study aims to further examine the possible role of ESRD in the development of PRCC and CCRCC to understand this initial step of renal cell carcinoma pathogenesis.

Methods: A cohort of n = 39 PRCC, 25 CCRCC, 63 normal, 10 end-stage and 18 chRCC cases were selected. RNA sequencing was performed and differential-gene-expression analysis was conducted between normal, ESRD and tumor using DESeq2 software. Pathway analysis was performed using GSEA. Genes from oncogenic pathways that have been studied to be involved in renal cancer development were selected to perform consensus clustering analysis on Genepattern.

Results: Oncogenic and developmental pathways enriched in ESRD are consistently overlapping with that of CCRCC and PRCC tumors. 50% of end-stage developmental pathways are found in both CCRCC and PRCC but only 4.5% in chRCC. 62.4% and 46.4% of end-stage oncogenic pathways are found in CCRCC and PRCC respectively but only 16% in chRCC. Clustering analysis showed ESRD cases clustered together with CCRCC and PRCC groups and not with chRCC. Overall, the ESRD cases exhibited a gene expression profile more closely resembling that of CCRCC and PRCC than chRCC.

Conclusion: Our findings support the hypothesis that ESRD provides a favorable environment for tumor growth promoting pathogenesis of both PRCC and CCRCC. The enrichment of the same developmental pathways in both ESRD and the tumors suggests that the progenitor cell population in the renal tubules, mentioned above, could be the origin of both PRCC and CCRCC lesions. Further analysis would allow the uncovering of the pathways that lead to tumor progression from these cells of origin, and can be used to determine biomarkers for early detection of CCRCC and PRCC. This is of particular benefit for those with increased risk as the ESRD patients.

#4358 Genomic profiling of residual kidney structures in dialysis patients.

Kosuke Ieiri[1], Nobuyuki Kakiuchi[2], Tomonori Hirano[3], Koichi Watanabe[3], Hirona Maeda[3], Hiroko Tanaka[4], Satoru Miyano[4], Dai Takamatsu[1], Takashi Matsumoto[1], Keisuke Monji[1], Masaki Shiota[1], Junichi Inokuchi[1], Hideki Makishima[3], Masatoshi Eto[1], Seishi Ogawa[3]

[1]Kyushu Univ. Graduate School of Medical Sci., Fukuoka, Japan,[2]The Hakubi Center for Advanced Research, Kyoto University, Kyoto, Japan,[3]Department of Pathology and Tumor Biology, Kyoto University, Kyoto, Japan,[4]Department of Integrated Analytics, M&D Data Science Center, Tokyo Medical and Dental University, Tokyo, Japan

Background: Chronic kidney disease is frequently associated with persistent inflammation, which results in fibrosis in the stroma, a reduced number of renal tubules, the formation of multiple cystic lesions, ultimately terminating in renal failure and hemodialysis. The high incidence of renal cell carcinoma (RCC) in hemodialysis patients suggests a relationship between tissue remodeling by chronic inflammation and carcinogenesis. However, little is known about the genetic background of cancer development from remaining tubules and cystic lesions in hemodialysis patients.

Methods: We enrolled 5 patients under hemodialysis who were accompanied by acquired cystic kidney disease and who underwent total nephrectomy for renal cancer. Surgical specimens were fixed with alcohol-based solution and paraffin-embedded, and after H&E staining, subjected to laser capture microdissection (LCM) to collect remaining tubules and cysts containing approximately 200 cells. DNA was extracted and analyzed for somatic mutations and copy number alteration by whole-exome sequencing.

Results: In total, we collected 161 LCM samples, including 118 from proximal tubules, 17 from collecting ducts, and 26 from cysts. The median variant allele frequencies of detected mutations were 0.237 in proximal tubules, 0.133 in collecting duct, and 0.381 in cysts, indicating larger clonal expansion in proximal tubules and cysts than in collecting ducts. Proximal tubules and cysts contained recurrent mutations in *FAT1* (11% and 8%, respectively), *STAG2* (5% and 8%), and *PTEN* (3% and 4%), whereas no recurrent driver mutations were identified in collecting ducts. In copy number analysis, 26% of proximal tubules, 35% of collecting ducts, and 80% of cysts had copy number alterations. Of note, samples from cysts had more copy number alterations compared to remaining tubules (on average, 2.3 vs. 1.1). Proximal tubules had recurrent copy number gains of chromosomes 3, 7, 10, 18, and 20, and loss of chromosome 22 and samples from collecting ducts showed gains of chromosome 7 and loss of chromosome 18. In cysts, gains of chromosomes 2, 3, 7, 10, 12, and 16 and loss of chromosomes 15, 16, 21, and 22 were frequently observed. Copy number profile in cysts was similar to that of papillary RCC and acquired cystic disease-associated RCC.

Conclusion: In the end-stage cystic kidney, both proximal tubules and cysts exhibited an enrichment of driver mutations commonly found in papillary RCC and RCC with acquired cystic disease, reflecting the fact that the incidence of these two types of RCC increases as the duration of dialysis becomes longer. In addition, clear cell RCC drivers, such as *VHL* mutation and loss of chromosome 3, were not observed, possibly explaining the rare occurrence of clear cell RCC in hemodialysis patients. Since cysts had more frequent copy number alterations than remaining tubules, cysts in the end-stage kidney might be precursor lesions of RCC.

#4360 Integrative analysis of multiplex interphase FISH copy number with whole exome sequencing identifies tumor evolution in Stage II colon cancer.

S. Yaghoubi[1], K. Heselmeyer-Haddad[1], I. Archilla[2], C. Parra[3], D. Wangsa[4], G. Castellano[3], J. Zhu[1], D. Yaghoubi[5], S. Lahoz[3], V. Pablo-Fontecha3[6], D. Hirsch[7], W.-D. Chen[1], T. Ried[1], M. Cuatrecasas[8], P. S. Meltzer[1], J. Camps[3];

[1]Genetics Branch, CCR, National Cancer Institute, NIH, Bethesda, MD, [2]2 Pathology Department, Centro de Diagnostico Biomedico, Molecular Biology CORE, Hospital Clinic, Tumour Bank-Biobank, IDIBAPS, University of Barcelona, Barcelona, Spain, [3]Translational Colorectal Cancer Genomics, Gastrointestinal and Pancreatic Oncology Team, Institut D'Investigacions Biomediques August Pi i Sunyer (IDIBAPS), Hospital Clinic de Barcelona, Barcelona, Spain, [4]National Center for Advancing Translational Sciences, NIH, Bethesda, MD, [5]Campus Pierre et Marie Curie, Faculty of Science and Engineering, Sorbonne University, Paris, France, [6]3 Translational Colorectal Cancer Genomics, Gastrointestinal and Pancreatic Oncology Team, Institut D'Investigacions Biomediques August Pi i Sunyer (IDIBAPS), Hospital Clinic de Barcelona, Barcelona, Spain, [7]Molekularpathologie, Universitat Regensburg, Regensburg, Germany, [8]Pathology Department, Centro de Diagnostico Biomedico, Molecular Biology CORE, Hospital Clinic, Tumour Bank-Biobank, IDIBAPS, University of Barcelona, Barcelona, Spain

Colon cancer ranks as the second leading cause of cancer-related death worldwide. Although standard therapies are highly effective in stage II lymph-node negative colon cancers, about 10-15% of these patients show disease relapse within the next 5-year period after intended curative surgery. Extensive prior research has highlighted the role of intratumor heterogeneity, arising from genomic instability, as a leading contributor to metastasis in colon cancer. In the current study, we pioneered the integration of Multiplex Interphase FISH (miFISH) and Whole Exome Sequencing (WES) data aiming to depict intratumor heterogeneity and delineate the landscape of genetic aberrations that underlie the early metastatic potential in stage II colon cancer patients. To this aim, we have showcased the genome-wide copy-number alterations and single nucleotide mutations derived from WES analysis of samples obtained from primary stage II colon tumors and their patient-matched liver metastases of nine patients using multi-region sampling. miFISH was employed for the concurrent quantification of copy-numbers for nine genes relevant to colon cancer and a centromeric control probe in intact tumor nuclei derived from archival patient material allowing us to establish ploidy baselines and gain and loss patterns for the genes analyzed. Our study was revealing of several copy number alterations, such as gains of chromosomes 1q, 7, 8q, 13q and 20, and losses affecting chromosomes 17p and 18, which were confirmed by miFISH. Based on our SNV data, most frequently mutated genes were *APC, TP53, KRAS*. We were able to show several mutations in genes belonging to specific pathways most commonly altered in colorectal cancer, such as *APC*, *TCF7L2*, *AXIN2*, *FBXW7* in WNT signaling, *SMAD4* in TGF-ß signaling, *PIK3CA* and *PTEN* in PI3K signaling and *KRAS* in RTK-RAS signaling pathways. In nearly all cases, subclones that led to metastasis were already present in the primary cancer, indicating a direct progression from the primary to metastatic disease. However, the divergence from the primary tumor to metastasis enabled us to uncover several potential genetic aberrations present in the metastasis but not observed in the primary tumor. Moreover, in one of our cases, despite harboring *APC* and *TP53* mutations in both the primary and metastatic tumor, unique mutations for these genes along with several distinct mutations in the metastasis were identified. These observations suggest that the metastasis might not be related to the primary tumor analyzed and may have arisen from an independent lesion. In conclusion, applying miFISH and WES to decipher the mutational and copy number landscape in metastatic stage II colon cancer provided comprehensive insights into the complex and heterogenous nature of primary colon cancer and the clonal evolution leading to subsequent liver metastases.

MOLECULAR/CELLULAR BIOLOGY AND GENETICS: Deregulated Signaling in Tumor Development and Progression
Poster Session

#4364 Molecular insight of non-canonical Gsk3β-Gli-AR axis: Therapeutic implications of truncated-Gli3 in castration-resistant prostate cancer.

J. B. Kaushal[1], P. Raut[1], S. Seshacharyulu[1], Z. W. Alsafwani[1], G. Sharma[1], A. M. Khan[1], S. Halder[1], S. Rachagani[2], S. K. Batra[1], J. A. Siddiqui[1];
[1]University of Nebraska Medical Center, Omaha, NE, [2]University of Missouri, Missouri, CA

The aberrant activation of the hedgehog (Hh) signaling pathway causes the progression of therapy-resistant castration-resistant prostate cancer (CRPC). In this study, we aimed to unravel the biological significance of Gli-family proteins and their functional involvement of Gsk3β-mediated regulatory mechanism(s) in CRPC. We have discovered a novel function of the truncated form of Gli (t-Gli3) in advancing CRPC. This was accomplished through *in silico* analysis, *in vitro* experiments, PCa patient clinical data, and *in vivo* PCa MYC overexpression mouse models. Our investigation into the Gli3 regulation, typically influenced by receptor-mediated ciliary localization, uncovered a Smo-independent mechanism. Surprisingly, despite the lack of a transactivation domain in t-Gli3, we found a specific requirement for an androgen receptor variant 7 (AR-V7) for its action, as evidenced by co-immunoprecipitation and chromatin immunoprecipitation assays. Mechanistically, Gsk3β activation leads to the t-Gli3 generation, and inhibition of Gsk3β supported the accumulation of full-length Gli3 through a non-canonical mechanism. Knockdown of Gsk3β (Gsk3β KD) reduces CRPC cell proliferation in *2-D* and *3-D* culture models, inhibiting key proliferative signaling pathways and inducing apoptosis via mitochondrial fragmentation. These findings were supported using an orthotropic PCa mouse model. RNA-seq analysis also showed upregulated phenotype enrichment of the apoptosis, P53, and glycolysis pathway genes in 22Rv1Gsk3β KD cells. Compared to scramble, a lower OCR/mitochondrial respiratory rate is evident in 22Rv1Gsk3β KD cells. Next, our exploration of potential therapies for PCa showed that individually targeting Smo or Gli1 is insufficient to inhibit cell viability. Interestingly, we uncovered that solely targeting Gli3 was sufficient to inhibit the growth of CRPC cells. In conclusion, our study provides the significance of Gli-family proteins and novel insights into the interplay of Gsk3β, t-Gli3, and AR, offering therapeutic implications in CRPC.

#4365 Mechanistic effects of N361 glycosylation in epidermal growth factor receptor protein.

D. Lam, A. N. Liberchuk, B. Arroyo, A. L. Wolfe;
Hunter College, New York, NY

Glycosylation is a tightly regulated post-translational modification where structured sugar groups are added to protein amino acid backbones, most commonly on asparagine for N-glycosylation. The glycosylation-regulating metabolic enzyme uridine diphosphate-glucose pyrophosphorylase 2 (UGP2) is required in oncogene-transformed cancer cells, but not in normal cells. UGP2 heavily regulates glycosylation of epidermal growth factor receptor (EGFR) at asparagine 361 (N361), a key site near the ligand binding domain. EGFR is a transmembrane tyrosine kinase receptor that promotes cell proliferation via growth cascades. Mutations and amplifications in EGFR account for a significant fraction of non-small cell lung carcinomas and breast adenocarcinoma, with L858R being the most common oncogenic hotspot. Other glycosylation sites on EGFR have been implicated in ligand binding, dimerization, and phosphorylation of downstream targets. Molecular dynamic simulations suggested that N361 may be important for dimerization or ligand binding. However, the functional relevance of how glycosylation of EGFR at N361 impacts EGFR protein and cellular behaviors remains unclear. To determine the functional relevance of glycosylation at N361, we created glycosylation-defective EGFR N361A mutant, with or without an additional oncogenic EGFR L858R mutant. We expressed these constructs in MCF10A and 293T cells, which do not have pre-existing activation of this pathway. Immunofluorescence and flow cytometry showed that the mutants were each well expressed at the cell membrane. Proximity ligation assays measuring dimerization of EGFR in cells showed that EGFR N361A greatly increased dimerization relative to wildtype controls. Loss of glycosylation of EGFR N361 impacted cell viability when grown in dose courses of its high affinity ligand EGF or lower affinity ligand amphiregulin. Furthermore, EGFR N361A desensitized cells expressing the oncogenic EGFR L858R to inhibitors targeting the extracellular domain, possibly because the mutation alters the antibody binding interface. N361A sensitized EGFR L858R to inhibitors targeting the cytoplasmic domain of EGFR. These findings help us understand the intricate relationship between EGFR and N-glycosylation, reinforcing the critical functional relevance of post-translational modifications on oncogenes.

#4366 Loss of *EP300* triggers IL-1α signaling and subsequent activation of the IL-6/JAK/STAT3 axis to drive oncogenesis in bladder cancer.

J. A. Rodrigues, J. Luo, A. R. Sabel, Z. Chen, X. Tang, F. Kuo, H. Al-Ahmadie, K. Kim, E. Pietzak, G. Iyer, D. B. Solit, S. P. Gao;
Memorial Sloan Kettering Cancer Center, New York, NY

Bladder Cancer (BLCA) is the sixth most common cancer in the United States with 81,180 new cases and 17,100 deaths in 2022. Next Generation Sequencing of BLCA has revealed an enrichment of alterations in genes classified as chromatin modifiers compared to other solid tumors. Among these is *EP300*, the gene encoding the p300 histone acetyltransferase, which is mutated in ~12% of BLCA with the majority putative loss of function frameshift and nonsense mutations. To investigate the biological role of *EP300* loss-of-function in BLCA pathogenesis, we generated isogenic *EP300* null RT112 bladder cancer cells using a 2-step CRISPR knockout (KO) and knockin strategy. *EP300* KO cells demonstrated increased proliferation, anchorage independent cell growth, tumor formation in mice, and enhanced invasive potential. To investigate the mechanism(s) whereby *EP300* loss-of-function enhances oncogenicity, we performed an unbiased Tandem Tag Mass Spectrometry (TMT MS) screen to identify pathways dysregulated in *EP300* KO versus parental cells. *EP300* loss-of-function was found to induce IL-6/JAK/STAT3 signaling via upregulated expression of IL-1α, a canonical pro-inflammatory cytokine. Knock down of *IL1A* gene expression was sufficient to downregulate STAT3 activation in *EP300* KO cells, whereas ectopic stimulation using IL-1α increased STAT3 activation in parental RT112 cells, suggesting that IL-1α was the predominant upstream activator of JAK/STAT3 signaling in our model. Pharmacological inhibition of downstream targets of IL-1α signaling such as IRAK1/4 were also able to inhibit STAT3 signaling in *EP300* KO cells in a dose and time dependent manner. Further investigations indicated that activated IL-1α signaling not only drove transcriptional upregulation of IL-6 but also the production of soluble IL-6R, activating IL-6 trans signaling. Finally, to elucidate how IL-1α upregulation is triggered by *EP300* loss-of-function, we performed immunoprecipitation and immunofluorescence assays, which revealed that IL-1α binds directly to p300. Additionally, ectopic p300 expression in *EP300* KO clones dramatically reduced IL-1α protein expression, indicating that p300 acts as a negative regulator of IL-1α in a bladder cancer context. In summary, *EP300* loss-of-function relieves p300's transcriptional and/or physical-tethering inhibition on IL-1α signaling, subsequently activating the IL-6/JAK/STAT3 pathway to drive oncogenesis in BLCA.

#4367 PTEN/AKT signal promotes cholangiocyte fate in liver tumorigenesis by inducing SOX9 overexpression and crosstalk with Notch activation.

Q. Tang, J. Chen, N. Zeng, L. He, S. Chopra, D. Alhousari, P. Nguyen, G. Zhang, B. L. Stiles;
USC - University of Southern California, Los Angeles, CA

Cholangiocarcinoma (CCA) is the second most dominant primary liver malignancy next to hepatocellular carcinoma (HCC), and among the most mortal among human cancers. The PI3K/AKT signaling pathway was considered a permissive signal for the development of CCA. To explore how the PI3K/AKT signal contributes to CCA development, we deleted *Pten*, the lipid phosphatase that negatively regulates the PI3K/AKT signal in the liver. The Lv-PTEN (*PtenloxP/loxP*; Alb-Cre^{+}) mice developed a mixed HCC and CCA tumor phenotype with all mice developing CCA by 12-month age. Treatment of Lv-PTEN mice with DDC at 3 months to obstruct the bile duct leads to an earlier CCA oncogenesis. Deletion of *Akt2* in the Lv-PTEN mice (Lv-DM, *Akt2*$^{loxP/loxP}$; *PtenloxP/loxP*; Alb-Cre^{+}) significantly attenuates tumor development. Compared with the Lv-PTEN mice, loss of AKT2 in Lv-DM mice robustly and significantly reduced the expression of SOX9, a cholangiocyte gene. This data suggests that the AKT signal may permit a cholangiocyte fate by inducing SOX9 expression. Supporting the role of PTEN/AKT in permitting a cholangiocyte fate, SOX9 expression is also induced in the livers of mice where *Pten* deletion is targeted to the hepatocytes via injection of AAV8-TGB-Cre (Hp-PTEN, *PtenloxP/loxP*; *R26RYFP*; AAV8-TBG-Cre). Similar to the Lv-PTEN mice, treatment with DDC induced early onset of CCA development in the Hp-PTEN mice. We next explore Notch signal for its crosstalk with PTEN loss that permits CCA development. Notch signal is robustly induced in the tumors of the Lv-PTEN mice and induced with DDC treatment in both Lv-PTEN and Hp-PTEN livers. We showed that exposure to Jag1 ligand-coated extracellular matrix or expression of NICD also induced the expression of SOX9 while DAPT time-dependently attenuated the expression of SOX9. In the Hp-Pten mice treated with DDC, inhibiting the Notch pathway with DAPT attenuated ductal reaction and led to downregulation of SOX9 in the Lv-PTEN livers, suggesting a positive regulatory role of Notch on SOX9. These data support that Notch activation regulates SOX9 and collaborates with PTEN loss to drive cholangiocyte fate and CCA development.

#4368 USP36 SUMOylates EXOSC10 and Las1L to promotes their function in rRNA processing.

M. Dai, Y. Li, Y. Yang, X.-X. Sun;
OHSU, Portland, OR

Eukaryotic ribosome biogenesis is a highly regulated multistep process to generate ribosomes, including transcription of pre-ribosomal RNA, rRNA processing, ribosome subunit assembly and export. Dysregulation of ribosome biogenesis is associated with various human diseases, including ribosomopathies and cancer. Therefore, it is crucial to understand how ribosome biogenesis is regulated during normal cell homeostasis and how it is deregulated in human diseases. Here, we report that the ubiquitin-specific protease USP36 acts as a novel SUMO ligase to promote nucleolar protein SUMOylation. Using affinity purification, we found that USP36 associates with a large number of nucleolar and ribosome biogenesis-related proteins, including all 10 components of the nucleolar RNA exosome complex, EXOSC1 to EXOSC10, as well as the Las1L-Nol9 endonuclease-kinase complex. We showed that USP36 interacts with the RNA exosome through EXOSC10 and SUMOylates ECOSC10 at Lys 583. Mutating K583 impaired the binding of EXOSC10 to pre-rRNAs and the K583R mutant failed to rescue the defects in rRNA processing and cell growth inhibition caused by knockdown of endogenous EXOSC10. Likewise, USP36 interacts with the Las1L-Nol9 complex and promotes Las1L SUMOylation at K565. In addition, USP36 deubiquitinates Las1L and Nol9 and regulates their protein stability. Mutating K565 does not affect the levels of Las1L and the formation of the Las1L-Nol9 endonuclease-kinase complex. However, induced expression of a K565R mutant of Las1L failed to rescue the defects in rRNA processing and cell growth inhibition caused by knockdown of endogenous Las1L. Together, these results suggest that USP36 plays an important role in regulating ribosome biogenesis by post-translationally regulating the function of RNA exosome and Las1L-Nol9 complexes.

#4369 CYP3A5 promotes aggressive and therapeutically resistant prostate cancer by modulating AR and Wnt signaling: Implications for racially disparate clinical outcomes.

J. McLean[1], A. P. Singh[2], E. Oh[1], **R. Mitra**[3];
[1]University of Nevada Las Vegas, Las Vegas, NV, [2]University of South Alabama, Mobile, AL, [3]Roseman Univ. of Health Sciences, Las Vegas, NV

Prostate cancer (PC) is the second leading cause of cancer-related death in American men, which disproportionately affects Black/African American (AA) men. The androgen receptor (AR) signaling plays a pivotal role in PC development and is a primary target for intervention in patients with advanced disease. Aberrant activation of AR is also suggested to play a significant role in castration-resistant prostate cancer (CRPC). Despite advancements in anti-androgen therapies with new targeting agents, such as enzalutamide, metastatic CRPC (mCRPC) remains incurable. CYP3A5, a monooxygenase expressed in the prostate, liver and intestine, is involved in drug metabolism and steroid biosynthesis. We earlier reported that intratumoral CYP3A5 activated AR signaling by facilitating its nuclear translocation of AR. More notably, we found a higher CYP3A5 expression in AAs, attributed to the *1 CYP3A5 variant, as compared to non-Hispanic White Americans (NHWA) possessing the *3 variant. Analysis of RNA-seq data using patient tumor samples revealed that elevated CYP3A5 in AA PC patients was associated with Wnt-β catenin signaling activation via TCF4 overexpression. Here, we investigated the role of CYP3A5 in enzalutamide resistance and Wnt signaling by generating enzalutamide-resistant PC cell lines of NHWA (low CYP3A5-LNCaP) and AA-origin (high CYP3A5-MDAPCa2b). RT-qPCR assay was used to examine the changes in AR and CYP3A5 expression between the parental and the enzalutamide-resistant cell lines. The data show heightened CYP3A5 expression in enzalutamide-resistant cells of AA origin (MDAPCa2b/EnzR) but not of NHWA origin (LNCaP/EnzR). Interestingly, MDAPCa2b/EnzR exhibited no change in AR levels whereas it was increased in LNCaP/EnzR cells relative to parental lines. A loss of function assay was performed for siRNA-mediated silencing of CYP3A5 to study its effect on Wnt signaling. RNA sequencing results show that CYP3A5 inhibition in MDAPCa2b downregulated Wnt pathway genes (Wnt5A, Wnt10B, Wnt11, Fzd2, and Dvl3). These observations align with our previous RNA seq results using patient samples where we observed upregulated Wnt-β catenin signaling in high CYP3A5 expressing patient tumor samples. Western analysis post-CYP3A5 inhibition in LNCaP and MDAPCa2b cells revealed upregulated Axin and downregulated LRP6 and Dvl-3, signifying CYP3A5's regulation of the canonical Wnt-β catenin pathway. Additionally, MDAPCa2b saw downregulated Wnt 5A and Wnt 10B, known to influence the Wnt non-canonical pathway. Altogether, our data suggest that *1 CYP3A5 variant in AAs likely contributes to aggressive behavior and therapeutic resistance of PC and serves as a molecular determinant of disparate clinical outcomes.

#4370 Functional characterisation of a novel mutation in PRKCA, a major driver of chordoid gliomas.

C. Bellamy[1], H. Tovell[2], F. Dingli[3], D. Loew[3], S. Liva[4], S. Schwaighofer[5], E. Stefan[5], A. Newton[2], M. Sanson[6], F. Bielle[6];
[1]Paris Brain Institute (ICM), Paris, France, [2]Department of Pharmacology, University of California, San Diego, La Jolla, CA, [3]CurieCoreTech Mass Spectrometry Proteomics, Institut Curie, PSL Research University, Paris, France, [4]Inserm, U900, Institute Curie, Paris, France, [5]Institute of Molecular Biology and CMBI, University of Innsbruck. Tyrolean Cancer Research Institute (TKFI), Innsbruck, Austria, [6]Sorbonne Universite, Inserm, CNRS, UMR S 1127, Paris Brain Institute - Institut du Cerveau (ICM), AP-HP, Hopitaux Universitaires La Pitie Salpetriere - Charles Foix, Service de Neurologie 2-Mazarin, Paris, France

Chordoid gliomas (ChG) are a rare low-grade brain tumor, believed to be derived from tanycytes. An analysis by the team identified a novel mutation present in all ChGs: *PRKCA* p.D463H. This mutation involves a D463H substitution at the kinase domain of the Protein kinase C alpha (PKCα), it is not found in any other cancer, and represents the hallmark of ChG. The aim of the project is to identify novel and biologically relevant $PKC\alpha_{D463H}$ signaling pathways, which will demonstrate the involvement and the role of this mutated kinase in cellular functions implicated in the development of ChGs. The D463H mutation affects a critical residue of the kinase domain of PKCα, suggesting that such a change modifies substrate affinity. Following the purification of $PKC\alpha_{D463H}$, we have shown its inactivation via *in vitro* kinase assays and peptide array. *In cellulo* fret-based activity reporter assays have shown that $PKC\alpha_{D463H}$ has a dominant negative effect over $PKC\alpha_{WT}$. Through co-immunoprecipitation we have shown that the mutant protein can bind the WT form and also colocalizes in the cell. Our results also show that the mutation affects the tertiary structure of the protein, resulting in a more open, unstable protein compared to the WT. Phosphoproteomic analysis of HEK cells overexpressing $PKC\alpha_{D463H}$ show a decrease of phosphorylation specifically on proteins involved with cell-cell adhesion, including functionally relevant phosphosites. This is in line with our Co-IP mass spectrometry data which shows a decrease in interaction of $PKC\alpha_{D463H}$ with proteins involved in cell junctions. The cell of origin, tanycytes, are highly specialized cells that contain important cell-cell junctions and therefore their perturbation could be a potential route of tumorigenesis. By understanding these changes integrated with our snRNAseq and bulk RNAseq of ChGs, and exploration in cellular models, we hope to elucidate the mechanism by which the mutation leads to the development of Chordoid Glioma.

#4371 ERBB4 heterodimers appear to drive *BRAF*WT melanoma cell lines.

V. Dwivedi, L. M. Lucas, J. Davis, K. O'Daniel, R. H. Cooke, J. N. Woggerman, E. N. Wilson, M. N. Ingrao, D. J. Riese II;
Auburn University, Auburn, AL

Purpose of The Study: To determine whether heterodimerization of ERBB4 with EGFR or ERBB2 drives the proliferation of *BRAF* WT melanoma cell lines.
Introduction: Metastatic melanomas that possess wild-type (WT) *BRAF* alleles are just as aggressive as melanomas that harbor gain-of-function (e.g., V600E) *BRAF* alleles. Moreover, no targets for effective chemotherapeutic intervention (other than immune checkpoint inhibitors) have been identified for these tumors. Thus, our goal is to identify candidate targets for therapeutic intervention in *BRAF* WT melanomas. ERBB4 (HER4) is a receptor tyrosine kinase that is closely related to the epidermal growth factor receptor (EGFR/ERBB1/HER1), ERBB2 (Neu/HER2), and ERBB3 (HER3). We have previously demonstrated that *ERBB4* is both sufficient and necessary for the proliferation of *BRAF* WT melanoma cell lines. However, the constitutively homodimerized *ERBB4* Q646C mutant inhibits the proliferation of *BRAF* WT melanoma cell lines. We have also previously demonstrated that ERBB4-EGFR and ERBB4-ERBB2 heterodimers stimulate proliferation and other oncogenic phenotypes in a variety of tumor model systems. Hence, here we test the hypothesis that ERBB4-EGFR or ERBB4-ERBB2 heterodimers drive *BRAF* WT melanomas.
Experimental Approach: We are testing whether wild-type *EGFR* or *ERBB2* alleles stimulate the proliferation of four different human *BRAF* WT melanoma cell lines. We are testing whether the dominant-negative *EGFR* (K721A) or *ERBB2* (K753A) mutant alleles inhibit the proliferation of these cell lines. Likewise, we are testing whether *EGFR* or *ERBB2* shRNAs inhibit the proliferation of these cell lines. Finally, we are testing whether *EGFR* or *ERBB2* enables *ERBB4* mutant alleles found in *BRAF* WT melanoma samples to drive greater levels of proliferation in 32D cells than wild-type *ERBB4*.
Unpublished Results: Wild-type *ERBB2* causes a significant increase in the proliferation of the MEL-JUSO and IPC-298 *BRAF* WT female melanoma cell lines. The *ERBB2* dominant-negative allele causes a significant decrease in the proliferation of these cell lines. Finally, preliminary data suggest that the *EGFR* and *ERBB2* dominant-negative alleles inhibit the proliferation of the MeWo *BRAF* WT male melanoma cell line.
Preliminary Conclusions: Our data suggest that ERBB2-ERBB4 heterodimers drive two female *BRAF* WT melanoma cell lines, whereas ERBB2-ERBB4 and EGFR-ERBB4 heterodimers drive a male *BRAF* WT melanoma cell line. Thus, we predict that FDA-approved ERBB2 inhibitors (and in some cases, EGFR inhibitors) may be effective in *ERBB4*-dependent, *BRAF* WT melanomas. Moreover, ERBB4 heterodimerization with ERBB2 or EGFR may account for the gender disparities observed in *BRAF* WT melanomas.

#4372 Epithelial-to-mesenchymal transition-driven secretory program underlies vulnerabilities in lung cancer.

K. L. Fulp, O. E. Obaleye, G.-Y. Xiao;
University of Kentucky, Lexington, KY

Epithelial-to-mesenchymal transition (EMT) is a driving force behind lung adenocarcinoma (LUAD) progression. Although substantial evidence has been attained in the involvement of EMT and its regulatory mechanisms in cancer, few effective EMT-targeted therapies have been available in the clinic thus far. It is urgent to develop new therapeutic strategies for improving patient outcomes. We have identified RAB6A as a master regulator of EMT-driven secretory trafficking, which coordinates cancer cell invasion and immunosuppression in LUAD. We found that RAB6A expression was associated with a poor prognosis in LUAD patients and that RAB6A inhibition in our LUAD models reversed resistance to immune checkpoint inhibition with PD-L1 blockade, an emerging clinical problem. Thus, RAB6A machinery is a therapeutic target of interest in EMT-driven cancers. Screening approaches to identify selective RAB inhibitors are in their infancy, a challenge that can be overcome only by obtaining insights into the regulation of RAB6A. RAB6A is a small GTPase whose activity is controlled by guanine nucleotide exchange factors (GEFs) like RIC1 and RGP1, and GTPase activating proteins (GAPs) like RABGAP1, as well as other effector proteins. While these GEFs, GAPs, and effectors are all known regulators of RAB6A function and are frequently amplified in different cancer types, their specific functions in cancer progression are still unknown. To establish the causal relationship between these proteins and EMT-driven LUAD progression, we utilize human and murine LUAD cell lines that have been characterized with respect to EMT status. Our findings here show that the intervention of RAB6A activity via depletion of these regulators impairs the recruitment of RAB6A to the Golgi. We demonstrate that knocking down the GEFs, RIC1 and RGP1, significantly decreases invasion while having negligible effects on the migrative and proliferative abilities of these cells. RABGAP1 depletion, on the other hand, reduces cell proliferation but has no effects on the migration and invasion of the cells. Consistent with these results, inactivation of RAB6A abolishes the EMT-dependent pro-metastatic secretion. Mechanistically, the EMT activator, ZEB1, upregulates RGP1 via silencing miR-148a that targets this GEF to activate RAB6A. These findings elucidate the regulatory mechanisms underlying the EMT-driven secretory program, providing a foundation for therapeutic intervention to prevent the progression of LUAD.

#4373 Molecular interactions of human receptor tyrosine kinase oncogenic fusions.

G. Dashi, M. Varjosalo;
University of Helsinki, Helsinki, Finland

Oncogenic fusions (OFs) play a critical role in cancer development. Despite the exponential increase in identifications, only a small number have been extensively characterized functionally. In this study, we are focused on receptor tyrosine kinase OFs (RTK-OFs) prevalent in aggressive cancers. Our primary objective is to elucidate the underlying molecular mechanisms of 182 in-frame RTK-OFs identified in The Cancer Genome Atlas.

An automated high-throughput PCR technique will be used to clone individual gene fusions using the sequences obtained from RNA-Seq data sourced from the TCGA dataset. These clones will be used to establish an RTK-OF-expressing isogenic cell line library. Multiple Approaches Combined (MAC)-tag workflow combining Affinity Purification (AP) and proximity biotin-dependent (BioID) purification within a single construct will be used. Subsequent high-throughput EvoSep One Liquid Chromatography coupled to ultra-fast TimsTOF Pro 2 Mass Spectrometry sample processing enables sensitive and robust analysis. These methods enable the capture of stable protein complexes and transient interactors associated with RTK-OFs. In our proof of concept study, we have identified four in-frame variants of FGFR3::TACC3 oncogenic fusions.FGFR3, part of the fibroblast growth factor (FGF) RTK family, activates cellular proliferation and growth through FGF binding and receptor dimerization. In FGFR3-TACC3 OFs, diverse isoforms are observed, with prevalent rearrangements linking FGFR3 exon 17 to various TACC3 exons. TACC3 is vital for mitotic microtubule organization and stabilizes kinetochore fibers and the mitotic spindle through its conserved C-terminal coiled-coil domain (TACC domain). TACC3 contributes to the fusion with varying sizes of the C-terminal coiled-coil domain which all constitutively activate the FGFR3 tyrosine kinase. In our studies, we show that FGFR3::TACC3 variants have a different localization to their wild-type counterparts. While FGFR3 and TACC3 are found in the cytoplasm all the OF variants strongly localize around the nucleus. Our identified high-confidence interactors represent a comprehensive FGFR3::TACC3 interaction network and reveal central pathways and key interactors related to microtubule assembly and possible deregulation of the cell cycle.

The resultant data from these advanced technologies enable the construction of comprehensive interaction networks, shedding light on critical signaling pathways and subnetworks relevant to RTK-OFs. Further in-depth analysis of 182 RTK-OFs may uncover actionable pathways and druggable interactors within these networks. Our multi-faceted research strategy holds significant promise for advancing targeted drug discovery, ultimately contributing to improved cancer treatment strategies.

#4374 PP2A-B56α in nutrient scavenging: Tipping the balance from macropinocytosis to cell death in pancreatic cancer..

G. Baral, C. M. Pfeffer, I. Doraivel, S. N. Filippelli, B. L. Allen-Petersen;
Purdue University, West Lafayette, IN

Pancreatic Ductal Adenocarcinoma (PDAC) is the fourth leading cause of cancer related deaths in the US, with the lowest five-year survival rate of all major cancers. Nutrients in the PDAC microenvironment are commonly depleted, with the vital amino acid glutamine among the most deficient metabolites. To circumvent this deprivation, PDAC cells initiate KRAS dependent macropinocytosis, an actin-driven nutrient scavenging pathway. Macropinosomes fuse with lysosomes in a process mediated by the kinase PIKfyve. It allows cells to replenish the nutrients required for survival. As glutamine is essential for PDAC cell survival, therapeutic inhibition of macropinocytosis represents a novel strategy to suppress nutrient acquisition and drive cell death.

Protein phosphatase 2A (PP2A) is a heterotrimeric Serine/Threonine phosphatase known to inhibit downstream targets of the KRAS signaling cascade and is implicated in macropinocytosis regulation. PP2A holoenzyme comprises of A, B and C subunits, where the regulatory B subunit provides substrate specificity to the enzyme. Using high molecular weight TMR-Dextran, we demonstrate that overexpression of PP2A-B56α subunit or pharmacological activation by DT061 promotes macropinosome accumulation in cells. Macropinosome accumulation was caused by the inability of macropinosomes to fuse with lysosomes, leading to cell death. The cell death caused by DT061 was significantly rescued when treated with a Rac family inhibitor. To understand if B56α regulates the process of macropinosome-lysosome fusion, we performed co-immunoprecipitation and established the interaction of B56α with PIKfyve. Further, pharmacological PIKfyve inhibition with Apilimod phenocopies DT061 induced vesicle accumulation in cells, suggesting that B56α likely inhibits PIKfyve to promote aberrant macropinocytosis.

Prevention of lysosomal fusion will impact nutrient uptake through macropinocytosis. Our metabolomics study confirmed the deprivation of glutamine with activation of PP2A-B56α. This regulation can be therapeutically leveraged to metabolically stress cells with a combination of DT061 and glutamine transport inhibitor V-9302. Combination drug treatment was found to be synergistic in a panel of PDAC cells. Together, these findings indicate that activation of PP2A in late stage PDAC promotes aberrant macropinocytosis by preventing lysosomal fusion through PIKfyve regulation and establishes a novel role of PP2A-B56α in nutrient scavenging and cell death. These pathways can be further exploited to identify potential combination therapeutics in PDAC.

#4375 ALPPL2 is involved in MAPK signal pathway of pancreatic cancer.

K. Gong, B. Hamid, K. W. Castro, M. S. McDermott, F. Epstein, K. Chau, C. Hu, J. Zhang, M. Lu, B. G. Hoffstrom, **N. A. O'Brien**, D. J. Slamon;
UCLA - University of California Los Angeles, Los Angeles, CA

Background: Alkaline phosphatase placental-like 2 (ALPPL2) is a member of the alkaline phosphatase family. ALPPL2 is currently being investigated as a novel therapeutic target due to its cancer-specific expression. However, our knowledge of ALPPL2 biological function in cancer is limited. Here we describe an interaction between ALPPL2 and MAPK signaling pathway in pancreatic cancer.
Materials and Methods: ALPPL2 mRNA expression in a panel of 27 pancreatic cell lines was determined by RNAseq. Protein expression and phosphorylation were measured by Western blot. ALPPL2 or ALPP were overexpressed in pancreas cell lines through a Lentiviral packaging system. MEK inhibitor (trametinib) activity was assessed in the same panel of cell lines using a 6-day cell proliferation assay on a Synentec Cellavista imaging system. MEK inhibitor resistant cell lines were developed by culturing cells in increasing concentrations of MEK162.
Results: We hypothesized that pancreatic cancer cells with high ALPPL2 expression may be less sensitive to MEK inhibition. Our study from a panel of 27 pancreatic cancer cell lines showed that there was no correlation between ALPPL2 expression and response to trametinib. Western blot showed that the level of phospho-ERK was reduced in PANC1 and HPAC cells at 6 hours after trametinib treatment. Signaling rebounded at 24 and 48 hours, though it remained below baseline. Surprisingly, ALPPL2 expression increased at 24 and 48 hours after trametinib treatment, however, the mRNA of ALPPL2 and ALPP was down-regulated in three pancreatic cancer cell lines conditioned to be MEK inhibitor resistant. To understand the role of ALPPL2 in the MAPK signaling pathway in response to MEK inhibition, ALPPL2 and ALPP were overexpressed in 2 pancreatic cancer cell lines: YAPC and PSN-1 whose ALPPL2 and ALPP were undetected by Western blot prior to transfection. Overexpression of ALPPL2 or ALPP in YAPC cells resulted in more ERK phosphorylation with no change in total ERK, it also resulted in increased total and phospho-S6, and decreased phospho-STAT3 with no change in total STAT3. The amount of total and phospho-ERK were not changed in PSN-1 with overexpression of ALPPL2 or ALPP, however, it did result in increased total and phospho-S6, decreased phospho-STAT3. Interestingly, the expression of ALPPL2 and ALPP in YAPC cells with ALPPL2 or ALPP overexpression was increased at 48 hours after trametinib treatment.
Discussion: To our knowledge, this is the first study to report that ALPPL2 interacts with the MAPK signaling pathway in pancreatic cancer cells. The activated MAPK signaling pathway appears to control ALPPL2 expression. The MAPK signaling pathway may regulate ALPPL2 expression through transcription and protein metabolism. We have also shown that ALPPL2 expression can activate MAPK signaling pathway. Our findings that ALPPL2 expression can be increased after trametinib treatment provide further rationale for targeting ALPPL2 in cancer.

#4376 The pseudokinase PTK7 is a negative regulator of EPHA2 in colorectal cancer.

J.-P. Borg, C. Dessaux, L. Camoin, S. Audebert, E. Baudelet, A. Daulat;
Centre de Recherche en Cancerologie de Marseille (CRCM), Marseille, France

Colorectal cancer (CRC) remains a major public health issue. Identification of biomarkers predicting high risk of recurrence and discovery of novel targets for therapy are urgently needed[1]. The cell surface receptor PTK7 is a poorly described evolutionary conserved member of the receptor tyrosine kinase superfamily that was first identified in human colon carcinoma and melanoma[2-3]. Accumulated data highlighted the implication of PTK7 in diverse cancer-related signaling pathways[4-6] and, despite the lack of kinase activity, anti-PTK7 inhibitors are currently in development at preclinical and clinical stages[7-9]. The dual aim of this project is to increase the basic knowledge about PTK7 and to evaluate its role in CRC in order to propose in the future novel therapeutics directed against PTK7. With the aim to discover novel PTK7 associated pathways, we used a proximity biotinylation strategy coupled to mass spectrometry in CRC cells. Among the partners identified, we found that the pseudokinase PTK7 interacts with the active receptor tyrosine kinase EphrinA2 (EPHA2). Similarly to PTK7, EPHA2 expression correlates with poor prognosis in CRC[10]. In this work, we also demonstrate that PTK7 acts as a negative regulator of EPHA2 activation through the promotion of distinct oligomeric protein complexes and the modulation of EPHA2 phosphorylation. We also shed in light on the role of PTK7 in EPHA2 K63-linked ubiquitination and its subsequent endosomal sorting and lysosomal degradation.

References 1 Punt CJ *et al, Nat. Rev. Clin. Oncol.*, 2016; 2 Lhoumeau AC *et al, Cell Cycle,* 2011; 3 Lhoumeau AC *et al, PLoS One,* 2015; 4 Puppo F *et al, EMBO reports*, 2011; 5 Martinez S *et al, J. Biol. Chem.*, 2015; 6 Daulat AM and Borg JP, *Trends in Cancer*, 2017; 7 Damelin M *et al, Sci. Transl. Med.*, 2017; 8 Jie Y *et al, Front. Immunol.*, 2021; 9 Maitland ML *et al, Clin. Cancer. Res.*, 2021; 10 Dunne P *et al, Clin. Cancer. Res.*, 2016; 11 Cioce M and Fazio VM, *Cancers*, 2021.

#4377 AT rich interaction domain 5a promotes gastrointestinal tumorigenesis by regulating YAP and STAT3 pathways.

K. Taniguchi, K. Hamada, S. Tanaka, H. Kurosu, I. Kawakita, K. Kumagai, K. Nakazono, S. Iwasaki, S. Tanaka;
Hokkaido University, Sapporo, Japan

Background: Chronic inflammation and an inflammatory cytokine, interleukin(IL)-6, play important roles in gastrointestinal tumorigenesis and metastasis. Recently, autocrine IL-6 has been reported to promote cancer development and progression in gastrointestinal cancer. However, it is still unknown how IL-6 level is regulated in gastrointestinal cancer cells. RNA-binding proteins (RBPs) are known to be one of the regulatory mechanisms of cytokine production, including IL-6, especially in immune cells. AT rich interaction domain 5a (Arid5a), one of the RBPs, has been reported to bind to *IL6* 3'UTR and regulates its stability and expression. Therefore, we aimed to elucidate the role of Arid5a in gastrointestinal cancer, especially gastric and colon cancer.
Methods: Human gastric and colon cancer cell lines were used in this study. Arid5a knocked-down gastric and colon cancer cells were generated with lentiviral transduction of shRNAs targeting Arid5a and their phenotypes were investigated by several assays including MTT, apoptosis and sphere formation assays. Bulk RNA-seq analysis was performed using Arid5a knocked-down gastric and colon cancer cells.
Results: In both human gastric and colon cancer cell lines, Arid5a knockdown suppressed cancer cell proliferation and spheroid formation, and increased apoptosis. Unexpectedly, IL6 mRNA expression was not correlated with Arid5a expression level. We found that Arid5a knockdown suppresses the activation of YAP and STAT3 by western blot analysis. We identified several new Arid5a target genes by bulk RNA-seq analysis.
Conclusion: Arid5a plays an important role in the regulation of cancer cell proliferation, apoptosis and stemness in human gastric and colon cancer cells, perhaps independently of IL-6. Arid5a regulates YAP and STAT3 pathways by unknown mechanisms. We are now investigating how Arid5a regulates YAP and STAT3 pathways by focusing new Arid5a target genes.

#4378 Identification of novel TXNIP-dependent antitumor pathways in breast cancer.

J. Singh, B. Sah, R. Clarke, L. Liu;
The Hormel Institute, University of Minnesota, Austin, MN

Thioredoxin-interacting protein (TXNIP) plays a critical role in glucose metabolism and redox signaling. TXNIP has recently emerged as a potent tumor suppressor in various cancer models. In previous studies, we found TXNIP was activated by UNC0642, an inhibitor of histone methyltransferase, in MDA-MB-231 breast cancer cells. TXNIP activation was coupled with significant suppression of cell proliferation and tumor growth. In contrast, TXNIP knockdown increased MDA-MB-231 cell proliferation and in tumor growth and metastasis in vivo. TXNIP-reconstitution in TXNIP-deficient HCC1954 cells reduced cell proliferation and migration coupled with increased reactive oxygen species production. TXNIP-reconstitution also significantly decreased mitochondrial respiration, mitochondrial membrane potential and glycolysis in HCC1954 cells. To understand the mechanisms underlying TXNIP's antitumor activity, we performed co-immunoprecipitation and proteomic analyses to uncover TXNIP-interacting proteins. We identified calpastatin (CAST) as a novel TXNIP-interacting protein in breast cancer cells. CAST is an endogenous inhibitor of calpains, a family of calcium-activated cysteine proteases. Intriguingly, CAST association with TXNIP was readily detectable in TXNIP-low, but not in TXNIP-high breast cancer cells. The disassociation of CAST from TXNIP in TXNIP-high cells might allow CAST to inhibit calpain activity to augment TXNIP's antitumor function. Through RNAseq analysis, we identified a positive correlation between TXNIP expression and IL-24 activation in various breast cancer cells, which were also confirmed by western blotting. IL-24 has emerged as an important cancer therapy target because of its role in promoting cancer-specific apoptosis. Our data also demonstrated that TXNIP upregulated the level of IL-24 and downregulated STAT-3. Moreover, TXNIP exerts multifaceted effects on BC development through the IL24-STAT3 signaling axis, deepening our understanding of its complex role in the disease. Taken together, these studies identified novel TNXIP-dependent pathways and their potential new mechanisms in breast cancer pathogenesis with significant clinical implications.

#4379 RING1, a novel E3 ubiquitin ligase for CIP2A, negatively regulates smoking-induced lung tumorigenesis.

I.-h. Jeong[1], C.-W. Peter Lee[1], H. Lim[2], S. Park[2], J. Hyun[2];
[1]Asan Medical Center, Seoul, Korea, Republic of, [2]Korea Research Institute of Chemical Technology, Daejeon, Korea, Republic of

Lung cancer is the second incidence rate of all new cancer diagnoses and the leading cause of cancer-related deaths globally. To develop novel diagnostic and therapeutic targets for lung cancer, there are emerging needs for molecular biological research on the occurrence and progression. Among the targets, CIP2A has been studied for promoting various cancer types, but detailed underlying mechanisms are needed to be further investigated. In this study, it was verified that CIP2A is overexpressed in lung cancer tissues, particularly amongst those with a smoking history, compared to adjacent normal tissues. CIP2A knockdown in lung cancer cells efficiently reduced cell proliferation and migration capacity. Through the mass spectrometry analysis on A549 cells overexpressing CIP2A, RING1 was identified as a candidate for E3 ligase of CIP2A. The interaction of the two proteins and ubiquitin chain regulation by RING1 was verified by immunoprecipitation. RING1 knockdown enhanced proliferation and migration of lung cancer cells, and these effects result from the upregulation of CIP2A and its downstream molecules, c-Myc and cyclin B1. To further study a trigger for RING1 expression changes in lung tumorigenesis, cigarette smoke extract (CSE) was applied for the following experiments. CSE treatment depleted RING1 mRNA, including protein expression. Decreased RING1 level led to upregulation of CIP2A and c-MYC. Collectively, these results reveal novel roles of the RING1 and CIP2A in lung cancer progression caused by smoking and propose a potential biomarker candidate for the therapeutic and diagnostic targets.

#4380 Role of kindlin-2 in prostate cancer progression and metastasis.

L. El Khalki[1], W. Wang[2], N. A. Yousaf Zai[1], J. Szpendyk[2], E. Pluskota[3], K. Bialkowska[3], E. F. Plow[3], L. R. Languino[4], D. C. Altieri[5], K. Sossey-Alaoui[1]; [1]Case Western Reserve University School of Medicine, Cleveland, OH, [2]Metrohealth System, Cleveland, OH, [3]Cleveland Clinic, Cleveland, OH, [4]Thomas Jefferson University, Philadelphia, PA, [5]The Wistar Institute, Philadelphia, PA

Prostate cancer (PC) is the leading type of cancer in men accounting for more than 25% of all newly reported cancer cases and remains the second leading cause of cancer-related deaths in men in USA in 2023. The success of early treatments has resulted in a 98% 5-year survival rate for early-stage PC. However, resistance to androgen ablation can lead to metastatic castration-resistant prostate cancer (mCRPC), with a significant drop in the survival rate to ~30%. The metastatic cascade involves changes in adhesive, metabolic and signaling properties of PC cells, allowing them to survive, proliferate and thrive in their new microenvironment. Kindlin-2 (K2), a cytoskeletal adapter protein, is highly expressed in cancer, including PC cells and tumors, contributing to their tumorigenic properties. The present study focuses on three K2 functions relevant to PC metastasis: 1)Reduction in K2 levels, achieved through CRISPR/Cas9, profoundly affected the tumorigenic properties of PC cell lines LNCaP (androgen dependent), DU145, and PC3 (both androgen independent), influencing colony formation, invasion, and adhesion to integrin ligands. While reduction in K2 was observed, K1 and K3 levels in these cell lines was not altered by K2KO. 2)The E3 ubiquitin ligase, Parkin, known for its role in Parkinson's disease, has emerged as a tumor suppressor inhibiting various cancer hallmarks. Our recently published studies showed that Parkin induces ubiquitination of specific lysines in K2, leading to the hypothesis that Parkin acts as a tumor suppressor by targeting K2 for degradation. Stable over-expression of Parkin inhibited adhesion to fibrinogen (Fg), while loss of function Parkin mutants failed to do so, supporting a role of Parkin in K2 turnover and its impact on mitochondrial dynamics. We are currently investigating the effect of K2-lysines mutants as well as loss of function Parkin mutants on the progression and metastasis of PC tumors in vivo.3)K2's established function is the regulation of integrin activation, affecting adhesion receptors' transition from low to high affinity/avidity states. The K2-integrin axis is pivotal for understanding oncogenic responses, and its role in the prostate microenvironment in PC progression and metastasis is under exploration using our newly established K2-floxed mouse. The K2-floxed mice are currently being crossed with mice harboring prostate-epithelial specific cre under control of the probasin (Pbsn) promoter. These animal studies will shed light on K2's contribution to PC development and progression in vivo, providing insights into its role in the prostate microenvironment. To sum up, this study emphasizes the crucial role of K2 in the tumorigenic properties of PC cells and tumors. By incorporating CRISPR/Cas9 and innovative mouse models, the study seeks to shed the lights on the mechanisms through which K2 contributes to PC development and progression.

#4381 Role of Kindlin-2 in the regulation of integrins and TBR1 signaling in TNBC.

N. A. Yousaf Zai, L. El Khalki, W. Wang, J. Szpendyk, K. Sossey-Alaoui;
Case Western Reserve University School of Medicine, Cleveland, OH

Background: Kindlins are a small gene family of FERM domain-containing adaptor proteins that function as essential drivers of integrin activation. Kindlin-2 (K2) is the most widely expressed member of the Kindlin family; its homozygous deletion in mice is embryonically lethal, K2 expression is also dysregulated in several human cancers, including the breast. We established K2 as a major driver of TNBC tumors progression and metastasis through the regulation of several hallmarks of cancer. A well-established pathway whereby K2 regulates TNBC oncogenic behavior is through the regulation of integrin inside-out signaling by directly binding to the cytoplasmic tail of integrin β subunit. Interestingly, our recent studies found K2 to play a major role in activating the TGF-β-mediated regulation of the CSF1/EGF signaling through macrophage polarization to the M2 tumorigenic state and their increased tumor infiltration, as well as inhibiting tumor infiltration of cytotoxic lymphocytes, therefore, driving tumor immune evasion. Here we present novel findings involving K2 in the stabilization of the β1-Integrin:TβRI complexes by establishing a physical bridge that links β1-Integrin to TβRI. Loss of K2 results in the degradation of this protein complex and therefore, the inhibition of the oncogenic pathways downstream of these two major regulators of several hallmarks of cancer.
Methods: We applied a combination of in vitro assays; CRISPR/Cas9 gene editing, cell migration, 3D tumor-sphere, solid binding, co-immunoprecipitation, cell adhesion and spreading, as well as western blot and flow cytometry analyses with MDA-MB-231 and 4T1 TNBC cell lines. We also used preclinical in vivo mouse models of TNBC tumor progression and metastasis to support or investigations.
Results: We found that the K2/β1-Integrin direct interaction is mediated through the C-terminal F3 domain of K2, while the K2/TβRI direct interaction is mediated through the F2 domain of K2. Disruption of this bridge, via CRISPR/Cas9-mediated knockout of K2, leads to β1-Integrin and TβRI degradation, and inhibition of the oncogenic pathways downstream of both β1-Integrin and TβRI, and inhibited tumor growth and metastasis in levels comparable to loss of expression of either β1-Integrin and TβRI. Treatment of the K2-deficent cells with the proteasome inhibitor MG-132 restored expression of both β1-Integrin and TβRI, confirming that K2 is required for the stabilization of the β1-integrin/TβR1 complexes at the protein level. Rescue of K2 expression in the K2-KO cells restored their oncogenic activities both in vitro and in vivo.
Conclusion: We identified K2 to play a novel and major in the stabilization of the β1-integrin/TβR1 complexes and the regulation of their downstream oncogenic signaling. These studies have a significant translational impact as they may identify new therapeutically targeted pathways that are desperately needed for the treatment of TNBC tumors.

#4382 PKC-ι/ζ signaling is crucial for apoptosis/pyroptosis inhibition and invasiveness of glioblastoma cells through upregulation of β-catenin, PDK1/Akt1 and Smad cascades via 14-3-3.

L. Lajmi[1], W. S. Ratnayake[1], K. M. Khalid[1], S. Breedy[1], A. Todman[1], T. Smalley[2], C. A. Apostolatos[1], R. Hill[1], M. Acevedo-Duncan[1];
[1]University of South Florida, Tampa, FL, [2]Moffitt Cancer Center, Tampa, FL

Glioblastoma (GB) is an aggressive form of brain cancer derived from astrocytes. Poor predictability of patient outcomes has limited the development of current therapeutic treatments of GB mainly due to the development of drug resistance. Comparative over-expression of atypical protein kinase C-iota and zeta (aPKC-ι/ζ) in GB cells and tissue samples were previously reported. This study establishes the downstream effects of PKC-ι/ζ attenuation on key cellular signaling which governs apoptosis, pyroptosis, survival, proliferation and epithelial-mesenchymal transition (EMT). Our data suggested that aPKC knockdown of expression induces apoptosis and works as an antecedent of pyroptosis. Data also suggested that involvement of Akt1 and PDK1 in aPKC maturation process weakened due to aPKC attenuation. aPKC attenuation downregulated Ras/Erk1 and canonical β-catenin pathways which resulted in reduced transcriptional activities of Stat3, c-Myc, c-Jun and β-catenin. In addition SNAIL1, SLUG, and PRRX1 were diminished that have been known to stimulate EMT. Proteins 14-3-3 and Smad2/3 acted as molecular adaptors between these pathways. A PKC-ι specific inhibitor 5-amino-1-(2,3-dihydroxy-4-(hydroxymethyl)cyclopentyl)-1H-imidazole-4-carboxamide (ICA-1S) and a PKC-ζ specific inhibitor 8-hydroxy-1,3,6-naphthalenetrisulfonic acid (ζ-Stat) were used to conduct *in-vivo* experiments using mouse models. Intravenous and oral administration of ICA-1S resulted in the reduction of tumor growth by approximately 30% in athymic nude mice for U-87 xenografts. Taken together, these results suggest that not only do aPKCs play a central role in GB progression, invasiveness, and cell survival, but that effective therapeutics can be developed to specifically target oncogenic aPKCs.

#4383 Atypical protein kinases C-ζ and ι-inhibitors impede the growth of malignant gastric cancer cells.

Abiral Hasib Shourav, Mahfuza Marzan, Khandker Mohammad Khalid, Wishrawana Sarathi Ratnayake, Mildred Acevedo-Duncan

Chemistry, University of South Florida, Tampa, FL

Currently, the global data on gastric cancer demonstrate that it is the fifth most common type of cancer and as far as cancer-related death is concerned, it is the third most common type. The high mortality of gastric cancer can be attributed to the fact that it is mostly diagnosed when the disease has progressed to the advanced stage. While the bacterium *Helicobacter pylori* is known to be the most common cause of gastric cancer, other notable risk factors also include high salt intake, age and diets lacking in fruits and vegetables. Demographic data have revealed that the regions of East Asia, Eastern Europe and South America are notable hotspots of this type of cancer. Endoscopic resection is considered as the major treatment procedure for early detected gastric cancer while those diagnosed in later stages are treated with surgeries such as D2 lymphadenectomy. Previously, the Atypical Protein Kinases C (aPKCs) - ζ and ι - have been documented to play significant roles in elevated cell proliferation in various cancer types. Here, we employed two inhibitors, ICA-1S (5-amino-1-((1R,2S,3S,4R)-2,3-dihydroxy-4-methylcyclopentyl)-1H-imidazole-4-carboxamide and ζ-stat (8-hydroxy-1,3,6- naphthalenetrisulfonic acid), that specifically inhibit aPKC-ι and-ζ respectively on a gastric cancer cell line (i.e., AGS) to observe their effects on cell proliferation. In separate trials, AGS cells were treated with ICA-1S and ζ-stat for 72 hours (about 3 days). An assortment of drug concentrations for each of the inhibitors were tried and the analysis of the cell count demonstrated that the cell proliferation decreases were statistically significant for both drugs in all concentrations. In case of ICA-1S, the highest decrease in cell proliferation was observed at 20 μM ($p < 0.0001$), whereas in case of ζ-stat, the highest decrease was observed at 10 μM ($p < 0.0001$). Our previous research have revealed that these aPKC inhibitors downregulate the aPKCs-ι and-ζ and interfere with established cancer pathways to cause cell deaths. Based on that and the results from the preliminary data on this project, it can be hypothesized that these two aPKC inhibitors have the potential to lead to Gastric Cancer cell deaths, which could potentially open a new door for Gastric Cancer therapeutics. Henceforth, the Western Blot analysis of AGS cells treated with ζ-stat have demonstrated the downregulation of the aPKC-ζ protein. Likewise, a downregulation of the apoptosis-related markers, Survivin and Caspase-3, was also illustrated in ζ-stat treated cells. Current, investigations include how these aPKC inhibitors, ICA-1S and ζ-stat, play into some of the well-established gastric cancer pathways to lead to cell deaths with techniques such as Western Blot analysis, Immunoprecipitation Assays and Flow cytometry.

#4384 Differential epitope tagging of oncogenic GNAQ mutants produces distinct effects on downstream signaling of GNAQ.

C. Jagadan Ushakumari[1], A. Manglik[2], B. Bastian[1], X. Chen[1];

[1]UCSF - Helen Diller Family Comprehensive Cancer Center, San Francisco, CA, [2]UCSF - School of Pharmacy, San Francisco, CA

GNAQ Q209P and Q209L are common driver mutations in uveal melanoma, leading to constitutive activation of downstream signaling of GNAQ. It is not fully understood whether the two GNAQ mutants have similar effects on downstream signaling pathways. Due to lack of available specific GNAQ antibody, epitope tagging is a well-established tool for protein interaction studies using mass spectrometry. Several studies used an epitope tag inserted into an internal region or the c-terminus of GNAQ to study its function. However, the functional consequences of these modalities on effector engagement are not fully elucidated. Here, we engineered both GNAQ wild-type and GNAQ mutants (Q209L and Q209P) without epitope tag as well as three different commonly used tagging modalities. A 3xflag tag of 22 amino acids was inserted after residue 122 of GNAQ. A MYC/DDK tag consisting of 18 amino acids was incorporated before the stop codon of GNAQ. An internal Glu-Glu epitope tag (EE tag) of 6 amino acids was introduced internally by mutating residues AYLPTQ(171-176) of GNAQ to EYMPTE. To assess the impact of the different modalities on the function of GNAQ mutants, we introduced them into 293FT cells and examined the known oncogenic signaling outputs downstream of GNAQ: MAPK, PKC and FAK signaling. We found that all three tags of both $GNAQ^{Q209L}$ and $GNAQ^{Q209P}$ activated MAPK signaling at similar levels as the corresponding untagged GNAQ mutants as evidenced by increases of pERK and pp90RSK level compared to GNAQ wild-type controls. By contrast, both $GNAQ^{Q209L}$ and $GNAQ^{Q209P}$ tagged with MYC/DDK induced lower p-PKD (a readout of PKC) and p-FAK (a readout of FAK activation) compared to EE-tagged or untagged, suggesting that MYC/DDK tag fused to the c-terminus of GNAQ affects specific effectors downstream of GNAQ. Furthermore, $GNAQ^{Q209P}$ with the 3xflag tag induced lower levels of p-PKD and p-FAK than 3xflag tagged $GNAQ^{Q209L}$ did, indicating that $GNAQ^{Q209P}$ may have a different three-dimensional conformation compared to $GNAQ^{Q209L}$ with different downstream effectors engagement. Moreover, the GNAQ/11 inhibitor YM-254890 inhibited phosphorylation of ERK, PKD, FAK in a concentration dependent manner in 293FT cells transfected with GNAQ mutants tagged with MYC/DDK but had no effect on MAPK, PKC and FAK signaling in cells expressing EE-tagged GNAQ mutants. These data suggest that EE tag has no effect on the function of GNAQ , but interferes
with YM-254890 binding. Our findings highlight unappreciated consequences of epitope-tagging of the oncogene GNAQ that are relevant for studies on the interactome of mutant GNAQ and drug response.

#4385 ZCCHC3 and Efp are prognostic factors for triple-negative breast cancer and potentially modulate cell division-related pathway.

A. Fujimoto[1], K. Ikeda[1], T. Takeiwa[2], K. Kinowaki[3], T. Ogura[3], H. Kawabata[3], A. Osaki[1], K. Horie[1], S. Inoue[2];
[1]Saitama Medical University, Saitama, Japan, [2]Tokyo Metropolitan Institute of Gerontology, Tokyo, Japan, [3]Toranomon Hospital, Tokyo, Japan

Triple-negative breast cancer (TNBC) is an aggressive subtype of breast cancer with poor prognosis and limited therapeutic strategies, lacking expression of estrogen receptor, progesterone receptor, and human epidermal growth factor receptor 2. We previously demonstrated that estrogen responsive finger protein (Efp)/TRIM25 functions as a ubiquitin ligase that degrades cell cycle checkpoint 14-3-3 sigma and promotes cell growth of ER-positive breast cancer [Urano et al., Nature 417:871-875, 2002]. In TNBC cells, we further showed that Efp regulates cell cycle-related gene expression and promotes cell proliferation [Sato et al., Biochem Biophys Res Commun 624:81-88, 2022]. Efp also exerts a distinct function to activate cellular RNA sensors such as RIG-I (retinoic acid inducible gene I), which plays a role in the innate immunity [Gack et al., Nature 446:916-920, 2007]. Another immune-related gene zinc finger CCHC domain-containing protein 3 (ZCCHC3) was recently suggested as Efp interactor, although its pathological relevance in breast cancer remains elusive. We here aimed to clarify the role of ZCCHC3 in TNBC. Immunohistochemical analysis of TNBC tissues from over 100 Japanese patients showed that a positive ZCCHC3 immunoreactivity (IR) was significantly associated with shorter disease-free survival (DFS) and positively correlated with Efp IR. Notably, patients with both ZCCHC3 and Efp IR positivity showed much shorter DFS than those with ZCCHC3 positivity alone. Functional analysis of ZCCHC3 by siRNA silencing demonstrated that ZCCHC3 promotes the proliferation, migration, and cell cycle progression of MDA-MB-231 TNBC cells. We established long-term culturable TNBC patient-derived cells (TNBC-PDC) using spheroid culture technique and revealed that the spheroid growth was suppressed by ZCCHC3-specific siRNA treatment. Moreover, ZCCHC3-specific siRNA injection suppressed in vivo tumor growth of MDA-MB-231 cells inoculated in immunodeficient mice. RNA sequencing analysis of ZCCHC3-silenced TNBC cells showed that cell division-related pathway was enriched among downregulated genes, including non-structural maintenance of chromosomes condensin I complex subunit H (NCAPH). NCAPH silencing inhibited the proliferation of TNBC-PDCs and MDA-MB-231 cells. Overall, ZCCHC3 and Efp are potential poor prognostic factors and can be applied to alternative therapeutic options for TNBC.

#4386 Androgen hormone signaling regulates the association between the hippo pathway component YAP1 and RNA binding protein NPM1.

A. M. Dwead[1], M. M. Al-Mathkour[2], B. Cinar[1];
[1]Clark Atlanta University, Atlanta, GA, [2]University of Miami, Miami, FL

Prostate cancer represents a major health concern for men in the United States and globally, disproportionately affecting men of African descent. Despite recent advances, the precise etiology and molecular mechanisms underpinning fatal prostate cancer in humans remain inadequately understood. RNA binding proteins (RBPs) regulate various aspects of RNA biology, and when their regulation is disrupted, they can lead to human diseases, including cancer. However, the comprehensive alterations in RBP-mRNA interactions in prostate cancer have not been explored. In this study, we investigated the dynamics of RBPs and their interactions with polyadenylated mRNA in the castration-sensitive LNCaP and castration-resistant C4-2 prostate cancer cell lines. Using an enhanced RNA interactome capture assay in combination with mass spectrometry, we discovered that LNCaP and C4-2 cells showed distinct RBP-mRNA interaction patterns in steady-state growth conditions and in response to androgen treatment. Additionally, we investigated the interplay between the oncogene Yes-associated protein 1 (YAP1) and the RNA-binding protein nucleophosmin (NPM1). We identified NPM1 as a component of the YAP1 protein complex through mass spectrometry-based proteomics. Our proximity ligation assay demonstrated that androgen signaling could regulate the interaction between YAP1 and NPM1. Also, our GST-pulldown revealed that NPM1 binds to the proline-rich domain of YAP1 in LNCaP cells, while the WW/SH3 domain of YAP1 mediates the interaction with NPM1 in C4-2 cells. Genetic and pharmacological inhibition of NPM1 activity reduced prostate cancer cell growth in culture by modulating cell cycle progression. Furthermore, our computational and immunological analysis of prostate tumor tissues indicated that the upregulation of NPM1 might be associated with the clinical advancement of human prostate cancer. These findings underscore the critical role of the molecular functional connection between YAP1 and RBPs and the global changes in RBP and RNA interaction patterns, in the progression and recurrence of prostate cancer.

#4387 Interplay of Notch1 and Notch3 signaling regulates pancreatic neuroendocrine tumor proliferation.

R. Guenter, W. Chen, Y. Golivi, M. Robledo, C. Adams, R. Jaskula-Sztul, H. Chen, J. Rose;
University of Alabama at Birmingham, Birmingham, AL

Background: The 5-year survival rate for patients with advanced pancreatic neuroendocrine tumors (pNETs) is less than 30%. Notch signaling is a transmembrane receptor pathway with four receptor isoforms and five different ligands. Binding between a receptor and ligand triggers pathway activation and is linked to cellular differentiation, cell fate, proliferation, and viability. Both Notch1 and Notch3 signaling have been shown to be dysregulated in pNETs. Notch3 activation has been shown to repress Notch1 activity in other cancers. We hypothesize that activation of Notch3 can reduce Notch1-mediated proliferation in pNETs.

Methods: Genetic deletion of Notch1 (N1-KO) in a pNET cell line (BON) was achieved using CRISPR/Cas9 to create a compound heterozygous knockout at exon 3. An inducible Notch1 overexpression cell line was generated by stably transfecting BON with a plasmid construct containing the Notch1 active form (N1ICD) under a Tet-On regulator. A constitutively active Notch3 cell line was generated by lentiviral transduction of BON with a plasmid overexpressing the Notch3 active form (N3ICD). Real-time quantitative PCR was used to measure mRNA transcript levels, and western blot was used to measure protein expression. Two-dimensional (2D) viability was measured by MTT assay, and three-dimensional (3D) proliferation was measured by spheroid size.

Results: Genetic knockout of Notch1 (N1-KO) reduced the expression of Notch3 at both mRNA and protein levels. N1-KO had reduced proliferation compared to (WT) BON. Increased cell density (ligand availability) or treatment with valproic acid (known Notch1 inducer) led to increased N3ICD in WT BON but not in N1-KO. Overexpression of N1ICD was associated with increased expression of a known downstream target Hes1, as well as Notch3. In contrast, forced overexpression of N3ICD led to increased Notch1 expression, but not Hes1 when compared to a BON cell line transfected with an empty vector. Functionally, N1-KO and N3ICD overexpression cells both had reduced proliferation in both 2D and 3D cell culture.

Conclusions: The Notch1 and Notch3 receptors produce signaling cascades that regulate growth in pNET cells through distinct mechanisms. Reduction of Notch1 signaling suppresses growth, while the same effect can be achieved with Notch3 overexpression. Thus, specifically upregulating Notch3 may be a strategy to block Notch1-mediated proliferation in pNET cells.

#4388 Tumor-associated RhoA mutants interact with effectors in both GDP- and GTP-bound states.

Y. Lin[1], T. A. Ramelot[2], S. Senyuz[3], A. Gursoy[4], H. Jang[5], R. Nussinov[5], O. Keskin[4], Y. Zheng[1];
[1]Cincinnati Children's Hospital Medical Center, Cincinnati, OH, [2]Rensselaer Polytechnic Institute, Troy, NY, [3]Koc University, Istanbul, Turkey, [4]Koc Univeristy, Istanbul, Turkey, [5]National Cancer Institute, Frederick, MD

RhoA is the founding member of the Ras-homology (Rho) small GTPase family and is a master regulator for multiple cell functions. Recurrent RhoA mutations have been identified in several human cancers, particularly in leukemia/lymphoma and gastric cancer. Intriguingly, both gain-of-function and loss-of-function mutations of RhoA are present, suggesting that RhoA GTPase may have a more sophisticated role in cancer and requires more rigorous investigations. Here, we have focused on two of the gain-of-function RhoA mutations identified in Adult T cell Leukemia/lymphoma (ATLL) at residue A161 (A161P and A161V) and aim to reveal the underlying mechanistic basis for their function by biochemical and structural analyses. We found that in contrast to conventional gain-of-function RhoA mutants such as $RhoA^{G14V}$ and $RhoA^{Q63L}$ which affect the GTP-hydrolysis activity, $RhoA^{A161P}$ and $RhoA^{A161V}$are both fast-cycling with drastically increased nucleotide dissociation and association rates, but only slightly reduced GTP-hydrolysis activity. We solved the crystal structures of GDP-bound $RhoA^{A161P}$ and $RhoA^{A161V}$ and saw that while $RhoA^{A161P}$ displays impaired solvent-mediated interactions to the bound nucleotide, $RhoA^{A161V}$ has a more exposed nucleotide binding pocket compared to $RhoA^{WT}$ and $RhoA^{A161P}$. Interestingly, $RhoA^{A161P}$ and $RhoA^{A161V}$can interact with effector targets in the GDP-bound states. Further ^{1}H-^{15}N HSQC NMR study provides evidence of the active population in GDP-bound $RhoA^{A161V}$. Molecule dynamics (MD) simulations show that the dynamic properties of RhoA switch regions are affected differently by the two mutations. Thus, $RhoA^{A161V}$ and $RhoA^{A161P}$ are fast-cycling mutants with distinct mechanisms, and both likely endow their GDP-bound state towards an active conformation. These findings provide a better understanding of the oncogenic role of RhoA mutations in cancer and shine light on how changes in RhoA protein dynamic properties caused by mutations may affect its function.

#4389 The role of Rab5 in epithelial growth factor stimulated E-cadherin internalization in spheroid growth of colon cancer cells.

Y.-C. Wang, Y.-C. Ching, H.-C. Chen, C.-P. Cheng, C.-E. Ku, S.-R. Lee, W.-T. Chao;
Tunghai University, Taichung, Taiwan

In epithelial based cancer formation, such as colon cancer, the tumor growth is accompanied with malfunction of cell-cell contact inhibition which is regulated by E-cadherin. However, the dynamics of E-cadherin is complicated, the underlying mechanism in tumor nest growth and collective cell migration is still not clear. Rab5 is the endocytic vesicle protein for the membrane receptor internalization into early endosome. Therefore, this study is to investigate the role of Rab5 in E-cadherin turnover of spheroid formation in colon cancer cells. HT-29 colon cancer cells were used in this study. The cells with less anchorage ability were isolated for spheroid formation. The distribution of Rab5, E-cadherin and focal adhesion kinase were observed by immuno-confocal microscopy. The molecular expressions were analyzed by western blot. HT-29 cells showed well defined epithelial phenotype. In the result of immunostaining, Rab5 was distributed in the cytosol and the cell-cell contacts where it colocalized with E-cadherin. Rab5 was also observed in the cell leading edge, however, not much associated with focal adhesions. When HT-29 cell clusters were stimulated with epidermal growth factor, Rab5 was found abundant in the cell-cell contacts. In cell spheroid that derived from HT-29 cells, Rab5 and E-cadherin co-localization at cell-cell contacts was also increased. Furthermore, when cells were treated with Nocodazole, the tubulin inhibitor blocking tubulin-mediated endocytosis, Rab5 accumulated and colocalized with E-cadherin in the cell leading edge. The results of this study demonstrated Rab5 plays the novel role in E-cadherin turnover upon epidermal growth factor stimulation in the progress of spheroid formation and Rab5 may mediate E-cadherin endocytosis through the cell leading edge.

#4390 IGFBP-6 is induced by progesterone to regulate progesterone receptor expression in breast cancer cells.

F. J. Lariz, P. Botero, K. Houston;
New Mexico State Univ. - Las Cruces, Las Cruces, NM

Insulin-like growth factor binding protein-6 (IGFBP-6) is induced by progesterone (P4) in T-47D breast cancer cells. IGFBP-6 regulates insulin-like growth factor 2 (IGF2) by sequestering it to inhibit receptor binding and extend its extracellular half-life. IGF2 binds to insulin-like growth factor 1 receptor or insulin receptor A to promote breast cancer cell proliferation and survival. Progesterone is an ovarian steroid hormone which has complex roles in breast cancer through the actions of progesterone receptor A and B (PR-A and B). Progesterone antagonizes the actions of estradiol (E2), another steroid hormone which promotes proliferation and survival in breast cancer. T-47D cells treated with both P4 and E2 exhibit significantly reduced proliferation compared to treatment with E2 alone. To better understand the role of IGFBP-6 in progesterone signaling, T-47D cells which over-express IGFBP-6 were treated with P4, E2, or both. Overexpressing cells exhibited stronger antagonism compared to controls when co-treated with P4 and E2. RNA-interference was performed to knockdown IGFBP-6 induction in the presence of P4 and E2. Knockdown of IGFBP-6 in the presence of P4 and E2 decreases the antagonistic effects of P4. Expression of both PR-A and PR-B decreases by about 50% when IGFBP-6 is knocked down. These results indicate that IGFBP-6 increases PR expression in response to P4 stimulation.

#4391 The UBE2F-CRL5^{Asb11}-DIRAS2 axis is an oncogene and tumor suppressor cascade in pancreatic cancer cells.

Y. Sun[1], Y. Chang[1], Q. Che[1], H. Li[2], j. Xu[2], M. Tan[2], X. Xiong[1];
[1]The Second Affiliated Hospital of Zhejiang Univercity School of Medicine, Hangzhou, China, [2]University of Michigan, Ann Arbor, MI

UBE2F is a neddylation E2 that couples with RBX2/SAG E3 to promote CUL-5 neddylation and Cullin-RING ligase-5 (CRL5) activation. Whether and how UBE2F regulates pancreatic tumorigenesis is previously unknown. Here we showed that UBE2F is growth essential for pancreatic cancer cells with KRAS mutant in culture. In *Kras^{G12D}* mouse PDAC model, *Ube2f* deletion suppresses cerulein-induced pancreatitis, and progression of acinar-to-ductal metaplasia (ADM) and pancreatic intraepithelial neoplasia (PanIN). Mechanistically, *Ube2f* deletion inactivates the Mapk-c-Myc signal pathways via blocking ubiquitylation and degradation of Diras2, which is a new substrate of Cul5^{Asb11} E3 ligase. Biologically, DIRAS2 suppresses growth and survival of pancreatic cancer cells with KRAS mutant, and *Diras2* deletion largely rescued the phenotypes induced by *Ube2f* deletion, indicating its causal role. Collectively, Ube2f or Diras2 plays a tumor-promoting or tumor-suppressive role in Kras^{G12D} PDAC model, respectively. The Ube2f-CRL5^{Asb11} axis could serve as a valid target for pancreatic cancer, whereas the levels of UBE2F or DIRAS2 may serve as prognostic biomarkers for PDAC patients.

#4392 Neuropeptide Y system in glioblastoma.

Nouran Abualsaud[1], Jason Tilan[2], Bahauddeen M. Alrfaei[1], Harrison Glor[2], Taylor Polk[2], Ewa Izycka-Swieszewska[3], Joanna Kitlinska[4]

[1]Blood and Cancer Research, King Abdullah International Medical Research Center, Riyadh, Saudi Arabia, [2]Department of Human Science, School of Health, Georgetown University, Washington, DC,[3]Department of Pathology and Neuropathology, Medical University of Gdańsk,, Gdańsk, Poland,[4]Department of Biochemistry and Molecular & Cellular Biology, Georgetown University Medical Center, Washington, DC

Gliomas constitute the most common primary cerebral tumors of the central nervous system (CNS), with glioblastoma (GBM) representing the most aggressive subtype. Neurotransmitters are important players in maintaining physiological processes in CNS and abnormal levels of their expression is pathogenic, leading to different processes, including neoplasia. Neuropeptide Y (NPY) is one of the neurotransmitters that is found to play a pivotal role in several malignancies. NPY, acting via its cognate receptors Y1, Y2 and Y5 (Y1R, Y2R and Y5R), has been shown to stimulate cancer cell proliferation, migration, invasiveness and dissemination, as well as tumor vascularization in various malignancies including neuroblastoma, Ewing sarcoma, colon, breast, prostate and liver cancers. Thus, the goal of this study was to determine if the NPY system is involved in glioma biology. Our immunohistochemistry staining of NPY, Y1R, Y2R, and Y5R in human GBM tissues revealed positive staining for NPY and Y2R in GBM cells. No expression of Y1R and Y5R was detected in GBM neoplastic population. To further elucidate the association between NPY and its receptors with GBM tumor stage and patients' survival, we used the available clinical data from the Cancer Genome Atlas Program (TCGA) database to analyze the gene expression of the NPY system. Y2R expression was increased in high-grade gliomas, while mRNA levels of NPY, Y1R and Y5R inversely correlated with the degree of glioma malignancy. Moreover, high Y2R expression was associated with worse survival in GBM patients. Importantly, endothelial Y2R is also responsible for angiogenic effects of NPY, suggesting its role in GBM vascularization. Altogether, these data suggest the involvement of NPY/Y2R axis in glioma progression toward more aggressive phenotype. Further functional studies are required to determine the role of the Y2R axis in this process.

#4393 Expression levels of T-cell factor-4 variants in hepato-gastrointestinal cancer cells and tissues.

H. Koga[1], Y. Imamura[2], T. Sudo[2], H. Suzuki[1], T. Tanaka[1], T. Sakaue[1], A. Masuda[1], H. Iwamoto[1], T. Nakamura[1], H. Yano[1], T. Kawaguchi[1];
[1]Kurume Univ. School of Medicine, Kurume, Japan, [2]Kurume Univ. Research Center for Innovative Cancer Therapy, Kurume, Japan

Background: We previously identified 14 variants of T-cell factor (TCF)-4, a key transcriptional factor in the canonical Wnt signaling pathway, from human liver cancer cell lines (Exp Cell Res 2011). The functional analysis of the variants demonstrated that the SxxSS motif played crucial roles in high tumorigenicity, resistance to hypoxia (PLoS ONE 2012), and EMT (Liver Int 2013). These findings suggest that expression levels and patterns of TCF-4 variants tightly regulate diverse phenotypes of cancer cells. Currently, we developed a novel RT-PCR system to quantitatively evaluate TCF-4 variant expressions by using the peptide nucleic acid (PNA)-directed PCR clamping method.
Aim: To assess mRNA expression levels of TCF-4 variants in hepato-gastrointestinal cancer cell lines and colon cancer tissues, focusing on TCF-4J and TCF-4K with the presence (K) or absence (J) of the SxxSS motif.
Methods: Thirteen cell lines used in this study were as follows: seven liver cancer; one fetus-derived immortalized hepatocyte; one gastric cancer; two pancreatic cancer; and two colon cancer cell lines. The liver cancer cell lines HAK-1A and HAK-1B are clonally sister cell lines. Sets of three forward primers and four reverse primers were used to generate templates for quantitative PCR (qPCR), and three fluorescence (FAM and Cy5)-tagged primers were applied to detect each variant. Thirty-nine resected human cancer and non-cancerous tissue pairs were used in the IRB-certified study (No. 19192).
Results: All TCF-4 variants except TCF-4M and TCF-4X were specifically and reproducibly detected and quantified. Cancer cells derived from the colon and stomach highly expressed the TCF-4 variants, showing the highest expression in TCF-4J, while cancer cells from the liver and pancreas expressed relatively lower levels. There was no remarkable difference in the expression profile of TCF-4 variants between HAK-1A and HAK-1B. In colon cancer tissues, TCF-4J was significantly more expressed than TCF-4K.
Conclusion: Although the variants had been identified from liver cancer cells, they were universally expressed in cells of other organs. TCF-4J, a variant responsible for aggressive cell phenotype, was prominently found in cancer cells of the digestive tract, where the canonical Wnt signal pathway is known to be constitutively active. A similar variant profile between two liver cancer cell lines with identical clonal origin suggests that the variant pattern in the cells reflects organ-specific traits rather than dynamic phenotypic changes during cancer cell dedifferentiation.

MOLECULAR/CELLULAR BIOLOGY AND GENETICS: Epigenetics and Cancer Biology
Poster Session

#4397 Alpha-Ketoglutarate is a master regulator of epigenetic reprogramming in pancreatic ductal adenocarcinoma progression.
K. Sherman, J. Cheng, W. Zhou, H. Ji, M. Maeda, A. P. Feinberg;
Johns Hopkins University, Baltimore, MD

Most cases of Pancreatic Ductal Adenocarcinoma (PDAC) are diagnosed after metastasis has occurred, making it crucial to find effective treatments for late-stage disease. Previously, our group found widespread epigenetic reprogramming during PDAC metastasis in the absence of additional driver mutations. These cells develop dependence on glucose metabolism through the oxidative pentose phosphate pathway (oxPPP). Inhibition of oxPPP with 6-aminonicotinamide (6AN) reverses the chromatin changes and restores cells to a less malignant state (McDonald *et al. Nat Gen*, 2017). To identify a clinically actionable mechanism for restoration, we hypothesized that oxPPP dependence leads to downstream metabolic changes that mediate chromatin state. Using untargeted metabolomic analysis, we found that alpha-ketoglutarate (AKG), a cofactor of lysine and histone demethylases, was downregulated by oxPPP inhibition ($p=0.033$) in a patient-derived xenograft lung metastasis cell line, A13Lg. Treatment of cells with 6AN and a cell permeable precursor of AKG largely reversed the chromatin changes seen on a western blot. Given that AKG is mainly produced by glutamine metabolism, we inhibited glutaminolysis with glutamine deprivation (Gln(-)) or the glutamine antagonist JHU083. Both treatments decreased AKG (Gln(-) $p=0.002$, JHU083 $p=0.038$) and prevented cell growth (Gln(-) $p<0.0001$, JHU083 $p=0.0002$). Glutamine-deprived cells showed decreased ability to form colonies ($p=0.004$), and JHU083 treated cells showed impaired migration in a Boyden chamber assay ($p=0.003$). Western blots showed a decrease in H3K27 acetylation, a marker of euchromatin, and an increase in H3K9 and H3K27 methylation, markers of heterochromatin, in response to both treatments. Further, homogenized time-resolved fluorescence (HTRF) assays on glutamine-deprived cells showed that H3K9 di- ($p=0.0016$,) and tri- ($p=0.0003$) methylation was increased. Adding cell permeable AKG to media without glutamine largely negated both the phenotypic and epigenetic changes. Using CUT&RUN against H3K27Ac, we found that acetylation was depleted at promoters involved in tumor cell proliferation, invasion, and migration. Bulk RNA-sequencing also showed decreased expression of genes involved in these pathways. Epigenetic and phenotypic changes were not as apparent after treatment with CB839, a glutaminase 1 inhibitor, suggesting that broad inhibition of glutamine metabolism is necessary for chromatin restoration. Together, these data suggest that decreasing AKG in PDAC distant metastasis cells, through glutamine deprivation or JHU083, leads to chromatin changes that specify less malignant phenotypes, providing a rationale for targeting glutamine metabolism as a therapy for late-stage PDAC. *APF and MM are co-corresponding authors.

#4398 *TET2* accelerates clonal hematopoiesis in an age-dependent manner.

S. Karmakar[1], Y. Liu[1], E. Motakis[1], K. Sengupta[1], T. Roeder[2], K. Mujica[3], J. Trowbridge[3], H. Oguro[2], S. Li[1];
[1]The Jackson Laboratory for Genomic Medicine, West Hartford, CT, [2]University of Connecticut Health Center, Farmington, CT, [3]The Jackson Laboratory, Bar Harbor, ME

Aging is a process of systemic deterioration and the most significant risk factor for cancers. Clonal hematopoiesis (CH) commonly occurs with aging and links to higher mortality, leukemia risk, and cardiovascular diseases. Age-related CH involves the abnormal clonal expansion of hematopoietic stem cells (HSCs) bearing somatic mutations in genes frequently mutated in leukemia, including genes encoding epigenetic regulators, such as the DNA demethylase TET2. While such mutations are known to alter the HSC epigenome, the mechanisms through which these mutations drive HSC self-renewal, myeloid transformation, and inflammatory response remain elusive.

In this study, we hypothesize that aging and CH mutations cooperatively reshape the HSC transcriptomic landscape and enhancing HSC competitive advantage that facilitates clonal expansion. Recently, *TET2*-mutant CH in humans has been strongly associated with epigenetic age acceleration. Using single-cell multi-omic analyses and flow-cytometric phenotyping, we demonstrated, for the first time, that HSC aging processes at transcriptomic, epigenomic, and cellular levels are accelerated by *Tet2* deficiency in mice, in an age-dependent manner. *Tet2*-deficient HSCs increase the HSC aging scores at an older age of greater than or equal to 16 months, but not at a young or mid-age, based on gene expression and chromatin accessibility at a single-cell resolution. This age acceleration was further validated by epigenetic clock analysis of DNA methylation mapping. Moreover, we found that *Tet2* deficiency drives a significant expansion of HSCs, a cellular hallmark of HSC aging, in an age-dependent manner. Specifically, we observed increased expression of *S100a6, Cdk6, Egr1* in *Tet2*-deficient HSCs from older mice, suggesting that *Tet2* deficiency hijacks the HSC expansion strategy during HSC aging by enhanced self-renewal. We also observed that the differentially expressed genes between *Tet2*-deficient older HSCs and control older HSCs are associated with open chromatin accessibility. Many of these genes are enriched in the targets of specific transcription factors (TFs), such as Egr1, Creb1, Stat family and Hoxb8. These target genes play critical roles in inflammatory pathways and HSC functions. In conclusion, our findings reveal that *Tet2* deficiency significantly contributes to the acceleration of HSC aging, and hijacks the HSC expansion strategy (e.g., self-renewal) during HSC aging, which exacerbates age-related clonal hematopoiesis. By elucidating the transcriptomic and epigenomic alterations in *Tet2*-deficient HSCs, our study provides novel insights into how age and somatic mutations collaborate to promote the pathogenesis of age-related hematological diseases. These discoveries not only enhance our understanding of HSC aging mechanisms but also offer potential biomarkers for early detection and targets for therapeutic intervention in age-associated clonal disorders.

#4399 HMGA1 is an epigenetic regulator and plays a critical role in melanoma recurrence.

H. Mou, K. DeRosa, V. Yakovishina, Y. Chen, A. Reynolds, M. Xiao, M. Thomas, M. Herlyn;
The Wistar Institute, Philadelphia, PA

Among various genetic mutation in melanoma, $BRAF^{V600E}$ is one of the key drivers of melanoma initiation and progression and has become the frontline target in clinical trials. Although BRAF/MEK inhibitors show very promising therapeutic outcomes, recurrence or relapse is still a major challenge and its underlying mechanisms are still poorly understood. We hypothesized that survival of recurrent tumors is BRAF independent and relies on epigenetic reprogramming. To test our hypothesis, we used either pharmacological inhibition of BRAF/MEK or CRISPR/Cas9 mediated knockout of BRAF to create cell/tumor models of BRAF-independent survival. Cut&Run sequencing was then used to identify epigenetic alterations regulated by H3K4me3 or H3K27Ac in a genome scale and capture the landscape of epigenetic alterations of BRAF-independent cell survival. Combining regular bulk RNAseq, we narrowed down our top candidates and focused on one of the functionally validated candidates, HMGA1. Interestingly, CRISPR/Cas9 mediated HMGA1 knockout cells show significantly slower growth in both *in vitro* colony formation assays and *in vivo* xenografts assay in BRAF/MEK resistant Patient-Derived-Xenograft (PDX) tumor models resembling melanoma recurrence. Furthermore, we selected CRISPR/Cas9 single knockout cells of HMGA1, which is a pure genetic depletion model, and confirmed the phenotype of impaired tumor growth of HMGA1 knockout cells. We then performed RNAseq and ChIPseq, and identified downstream targets of HMGA1 and elucidated mechanisms by which HMGA1 reprograms epigenetics of recurrence. Utilizing the single knockout cell, we re-introduced HMGA1 in the pure knockout cells, and anticipated that restoration of HMGA1 in pure HMGA1 knockout cells rescues impaired tumor growth and confer cells resistance to BRAF/MEK inhibition. Finally, we subcutaneously injected the HMGA1 single knockout cells into humanized mice and tested whether epigenetic alterations perturb the immune microenvironment and sensitize cells to immunotherapy. In conclusion, this study sheds new lights on how melanoma cells reprogram the epigenome to develop mechanisms of recurrence. Identification of HMGA1 and its upstream or downstream targets provides potential druggable targets of overcoming relapse after BRAF/MEK inhibitor therapy.

#4400 Transcriptional dysregulation of chromosomes localized into the micronucleus.

D. Norkunaite, D. Al-Rawi, S. Bakhoum;
Memorial Sloan Kettering Cancer Center, New York, NY

Chromosomal Instability (CIN) is a characteristic of the most aggressive and drug-resistant cancers. Chromosomally unstable cells form micronuclei (MN), a structure with an unstable nuclear membrane that spontaneously surrounds missegregating chromosomes upon mitotic exit. Several studies have demonstrated that CIN drives drug resistance and metastasis through the karyotypic diversity caused by copy number alterations. Beyond facilitating karyotypic diversity, CIN has recently been demonstrated to cause durable epigenetic alterations including reduction of the activating histone H3K27ac mark in chromosomes localized to micronuclei. This reduction in histone H3K27 acetylation persists after the relocalization of the missegregated chromosome to the primary nucleus (PN). Given the loss of transcription-associated epigenetic modifications, we hypothesized that MN would exhibit transcriptional impairment. Indeed, by using nascent RNA assays and immunofluorescence, we found that chromosomes localized into the MN are less transcriptionally active and exhibit lower levels of active RNA polymerase II (RNAP2). Transcriptional inhibitors targeting RNAP2 largely abrogate MN transcription. Conversely, class-specific histone deacetylase inhibitors (HDACi) cause increased hyperacetylation of the MN relative to the PN, which persists beyond MN reincorporation into the PN. We also hypothesized that transcription in MN depends on the manner of MN biogenesis. Preliminary data shows that MN formed from breakage-fusion-bridge (BFB) events may cause less transcriptionally active MN than ones generated from treatment with the MPS1 inhibitor, reversine. To better understand the mechanisms that regulate transcription in the MN, our ongoing work is focused on an unbiased investigation of the micronuclear transcriptome.

#4401 GATA6 is a novel regulator of gene expression and 3D genome in colorectal cancer.

H. Lyu, X. Chen, Y. Cheng, T. Zhang, P. Wang, J.-y. Wong, J. Wang, L. Stasiak, L. Sun, G. Yang, L. Wang, F. Yue;
Northwestern University - Chicago, Chicago, IL

Colorectal cancer (CRC) is one of the most lethal and prevalent malignancies with elusive molecular causes. While the abnormal activity of transcription factors has been reported as a vital component of cancer progression, the mechanism through which they function remains unclear. Here, through the analysis of primary human CRC tissue data, we identified GATA6 as a CRC specific regulator, whose expression upregulation is potentially associated with promoter hypomethylation. In the human genome, GATA6 showed preferential binding at tumor specific active enhancers. Through both auxin-inducible degron (AID) and CRISPR knockout, we showed that GATA6 depletion severely impaired clonogenicity and proliferation. GATA6 depletion caused the loss of CRC specific open chromatin, suggesting a specific regulatory role of GATA6 in CRC pathogenesis. Interestingly, we also discovered the co-occupancy of GATA6 with CTCF and its direct involvement in promoter enhancer loops, suggesting the possibility that GATA6 mediate transcriptional regulation through 3D genome. The loss of GATA6 led to alterations in E-P chromatin interactions of a panel of oncogenes, accompanied by the oncogene downregulation. Finally, we showed that GATA6 loss is detrimental to the xenograft tumor growth and thereby rescued mice survival. Taken together, we unrevealed a novel mechanism by which GATA6 contributes to CRC.

#4402 A genomic insertion/deletion variant activates immune escape and tumor promoting programs in breast cancer.

P. Betancur, C. DiBenedetto, **D. Acenas**, A. Rodriguez, A. Thach;
UCSF School of Medicine, San Francisco, CA

Purpose: Despite all the knowledge we have concerning cancer cells' immunesuppressive ability, we still don't understand whether the mechanisms upregulatingimmune suppression in cancer cells are patient specific. This information is critical forthe generation of tailored treatments that recruit the immune system for the eradicationof cancer disease. In the past, we showed that super-enhancers, composed of cluster ofenhancers spanning over long genomic regions characterized by having potent generegulatory activity, are critical for the upregulation of immune suppressive genes,including CD47, within the tumor. Recently we found a DNA insertion/deletion variant (8bp in size) within a super-enhancer located between the CD47 and Linc00636 genes,that is present more often in European (53%) than Asian (12%) populations and whichassociates with breast cancer. Moreover, sequence analyses of patient-derived breasttumors (44) and gynecological tumor samples (23) demonstrated a significantassociation of this insert with breast cancer and not with gynecological cancer. Thus, wehypothesize that the insertion variant regulates genes that drive immune escape andbreast cancer specifically in patient populations that carry the insert version.

Methods: To test this, we CRISPR deleted the variant's insertion and CRISPR-VP64induced its activation and quantified its effect on target genes and encoded proteinsusing high throughput RNA sequencing and immunofluorescence flow cytometryanalyses respectively.

Results: CRISPR-VP64 induction of the 8bp insertion confirmed that the insertion issufficient to regulate gene expression of CD47 and of an anti-tumor, long intergenicnon-coding RNA (Linc00636) in breast cancer cells. Furthermore, we observed thatCRISPR deletion of the 8bp insertion increases CD47 levels, while dramaticallyincreasing expression of Linc00636 and reducing the expression of CD44, CXCL14,MUC1 genes involved in invasion and migration. Our work shows that the insertion ofan 8bp is responsible for stabilizing upregulation of CD47 (an immune suppressivesignal), downregulating Linc00636 (a modulator of tumor metastasis), and upregulating,as a result, the expression of cell surface receptors involved in metastasis andtumorigenesis.

Conclusions: Here we found a genomic insert within a super-enhancer that unleashesthe upregulation of Linc00636 and of a program that promotes breast cancer, mostlikely in populations of patients carrying this variant. Our findings are important tounderstand patient specific genomic bifunctional modulators of immune suppressionand tumor progression for the design of more personalized treatments geared towardprecision medicine.

#4403 The crosstalk between the tumor microbiome and epigenomic changes in penile squamous cell carcinoma.

J. Viera-Vera[1], Y. Roque-Reyes[1], D. Santiago-Negron[1], M. Sanchez-Vazquez[1], Y. Ortiz Maldonado[1], G. Borges-Velez[1], J. Figueroa-Diaz[2], C. Rivera-Lopez[2], N. Zacharias Millward[3], M. Marcos-Martinez[2], F. Godoy-Vitorino[2], A. Puras-Baez[2], J. Dutil[1], J. Perez-Santiago[1], M. Martinez-Ferrer[1];

[1]University of Puerto Rico Comprehensive Cancer Center, San Juan, PR, [2]University of Puerto Rico School of Medicine, San Juan, PR, [3]The University of Texas MD Anderson Cancer Center, San Juan, PR

Penile squamous cell carcinoma (PSCC) is approximately three times more prevalent in Puerto Rico when compared to other ethnic groups in the United States. Moreover, the mortality rate for PSCC among Puerto Rican men is significantly higher when compared to the US population. Infection with human papillomavirus (HPV) has been identified as a risk factor for an average of 48% of PSCC cases in Puerto Rico. The molecular etiology of $HPV^{\pm}$ and HPV^{-} PSCC remains poorly understood. To date, the role of the microbiota in the pathogenesis of PSCC is unknown, as there are no studies that characterize the microbiome in association with penile cancer. Furthermore, the role of DNA methylation, which is an epigenetic alteration that can be found in cancer cells that can lead to changes in gene expression and cellular function, is also unknown. Therefore, there is an urgent need to address this knowledge gap. This study aims to analyze the DNA methylation patterns and bacterial communities in HPV-positive and HPV-negative PSCC tissues from Puerto Rican men. DNA was extracted from twenty-one fresh PSCC tissue samples from Puerto Rican patients. HPV status and genotyping were determined using the DNA ELISA kit HPV SPF10 protocol. DNA methylation assay was performed using the Infinium Methylation EPIC v2.0 BeadChip Kit to identify and compare average DNA methylation levels (%) in 7 HPV-positive and 14 HPV-negative penile cancer samples. Microbiota analyses were performed using 16S rRNA genes with the Illumina MiSeq platform. Demultiplexed data was deposited in QIITA for quality control and bioinformatic analyses and downstream analyses were done in R and Qiime2. Our results demonstrated that 45 loci methylation patterns were significantly different between HPV-positive and HPV-negative samples, with an adjusted p-value <0.1 (Benjamini-Hochberg method). Three loci methylation patterns were significantly affected by species diversity and richness. The abundance of Firmicutes, Proteobacteria, Bacteroidetes, Fusobacteria, and Actinobacteria was individually associated with number of affected loci (27, 19, 12, 6, and 3, respectively). We found that HPV status is associated with methylation patterns and microbiome in PSCC in Puerto Rican men. Both changes may be involved in triggering inflammatory responses and oncogenesis. Although many challenges must be overcome to dissect the specific interactions of coinfecting bacteria and methylation patterns during the penile cancer infectious process, our findings demonstrate that microbes may be involved in these cellular processes.

#4404 EZH2 modulates mRNA splicing in chronic myeloid leukemia through the repression of splicing factors and exerts part of its oncogenic function through the regulation of CELF2.

R. Brunmeir, Y. Li, B. Lin, L. Zheng, H. Yang, W. Chng;
Cancer Science Institute of Singapore, Singapore, Singapore

The polycomb protein EZH2 is a commonly deregulated or mutated transcriptional regulator in various cancers. In Chronic Myeloid Leukemia (CML) it has been reported to be upregulated and associated with transcriptional reprograming, rendering CML leukemic stem cells (LSCs) sensitive to EZH2 inhibitor treatment. Mechanistically this seems to be linked to the silencing of apoptotic target genes by EZH2-mediated histone H3 lysine 27 tri-methylation (H3K27me3). We hypothesized that the regulation of apoptotic genes is not the only pathway responsible for its oncogenic function, and that EZH2 might also act as a modulator of the mRNA splicing landscape. To test this, we treated the CML cell line K562 with the EZH2 inhibitors GSK126 and EPZ-6438 and performed RNA-seq followed by splicing analysis. Using two different bioinformatics tools, we detected differential splicing of several hundreds of splicing events. However, differentially spliced genes were not associated with increased EZH2 or H3K27me3 signals, suggesting an indirect mechanism of splicing regulation. Indeed, we found 11 splicing factors transcriptionally upregulated upon EZH2 inhibitor treatment. CELF2 was identified as top candidate to mediate part of the EZH2 inhibitor induced phenotype. Upon overexpression, we observed 1) reduced cell growth, viability, and colony formation of K562 cells, 2) a change in the splicing landscape, significantly overlapping with EZH2 inhibitor induced changes, 3) the downregulation of cMYC signaling, also found upon EZH2 inhibitor treatment. To test if CELF2 is indeed acting as EZH2-regulated tumor suppressor in CML, we extended our study to CML patient samples: we performed RNA-seq followed by splicing and gene expression analysis in seven CML patient-derived CD34+ samples and eight healthy donor-derived CD34+ samples, as well as three CML patient samples transduced with CELF2-containing expression constructs. While we found Celf2 mRNA downregulated in CML derived samples, overexpression led to decreased colony formation and cMYC signaling, validating our findings from K562 cells. We also performed an analysis of CML associated splicing changes and found hundreds of deregulated splicing events, of which a significant portion overlapped with CELF2 overexpression mediated changes, suggesting direct regulation by CELF2. Based on this data we propose a novel role of EZH2, where it exerts part of its oncogenic function in CML through the transcriptional repression of splicing factors, in particular CELF2, leading to splicing deregulation, increased cMYC signaling, and enhanced cell growth and viability. Finally, data from other publicly available EZH2 inhibitor treated cancer models suggests that splicing modulation by EZH2 might not be restricted to CML.

#4406 Single cell multiomic analysis reveals how genomic, epigenomic and transcriptomic events drive progression of multiple myeloma precursor states.

R. Canevarolo, P. Sudalagunta, M. Silva, M. Meads, R. Baz, M. Alsina, K. H. Shain, **A. Siqueira Silva**;
H. Lee Moffitt Cancer Center, Tampa, FL

In this study we have leveraged Moffitt Cancer Center's cohort of over 1,000 bone marrow (BMBX) aspirates from normal donors, MM precursor diseases (MGUS, SMOL), active therapy naïve disease (NDMM), as well as early (post 1-3 lines of therapy, ERMM) and late-relapse (3+ lines of therapy, LRMM) MM patients, characterized clinically, cytogenetically (FISH), genetically (WES), and transcriptomically (RNA-seq).Transcriptomic analysis identified a subset of cancer hallmarks differentially expressed between MGUS and NDMM samples (e.g. cell identity, adhesion and inflammatory signaling, etc.).Dimensionality reduction analysis, followed by unsupervised segmentation, identified clusters of co-expressing genes across this dataset. Enrichment analysis of aforementioned gene clusters, differentially expressed between MGUS and NDMM states, identified a number of putative transcription factors (GATA1/2, SUZ12, RUNX1, SOX2, TP63, NFE2L2, FOXM1 and NANOG), as well as polycomb complex and H3K27me3 as main drivers. Single cell ATAC-seq in 11 BMBX (4 SMOL, 4 NDMM, 1 ERMM, 2 LRMM) and single cell multiomics (simultaneous scATAC-seq/scRNA-seq) in additional 10 BMBX (2 healthy, 3 MGUS, 3 SMOL and 2 NDMM) confirmed that the H3K27me3 putatively regulated gene clusters were the only ones with significant chromatin accessibility changes. Single cell analysis confirmed differential expression and accessibility of cancer hallmarks identified in larger cohort, as well as putative driver TFs. Correlation between TF expression and motif accessibility produced an additional list of pioneer TFs putatively involved in progression from MM precursor states (ZEB1, EBF1, SPI1, PAX5, etc.).Investigation of scMultiomic data demonstrated that NDMM and SMOL samples contain subpopulations of cells in MGUS and normal "states" (cell clusters in scMultiomics UMAP), confirming intra-sample heterogeneity, and that divergence within the multiomic plane occurs in the transition between MGUS and SMOL. Through pseudotime and single cell copy number analysis (epiAneufinder/scATAC-seq and inferCNV/scRNA-seq) we were able to reconstruct how MM FISH cytogenetic abnormalities alter the multiome of these cells, creating aforementioned intra-sample heterogeneity. Despite different initiating events, all samples shared a common biology putatively regulated by epigenetic dysregulation, suggesting polycomb complex hijacking as a therapeutic opportunity for precursor MM.

#4407 Simultaneous spatial epigenomic and transcriptomic analysis of gastric adenocarcinoma reveals regulatory patterns governing tumor and microenvironment architecture at the cellular level.

K. J. Noronha, J. M. Garbarino, D. Massucci, A. R. Tyree, C. Ng;
AtlasXomics, Inc., New Haven, CT

Recent advances in spatial transcriptomics and spatial proteomics have enabled increasingly complex questions on the nature of gene regulation and expression in cellular subtypes in tumor tissue and the tumor microenvironment. However, most spatial omics techniques do not profile the epigenomic landscape responsible for downstream gene expression. Furthermore, current spatial technologies have yet to profile the epigenome and transcriptome simultaneously, and thus it remains a challenge to correlate multi-omics data across sections of extremely heterogenous tumor tissue. Recently, co-profiling of spatial epigenomics and transcriptomics using principles of Deterministic Barcoding in Tissue for spatial omics sequencing (DBiT-seq) has been demonstrated on normal brain tissue. Joint spatial profiling of chromatin states and whole transcriptome in tissue allows for parallel characterization of gene regulation programs across all cell types, while preserving the tissue architecture for greater understanding of the cellular environment. Here we present the first application of spatial ATAC-seq and spatial transcriptomics on the same tissue section to characterize the tumor microenvironment of an invasive gastric adenocarcinoma (GAC) and adjacent normal tissue. GAC is the fifth most common cancer and commonly exhibits mutations in epigenetic modifiers, including ARID1A and MLL1-4. Distinct spatial clusters representing different cell subtypes were identified via both spatial chromatin accessibility and spatial transcriptomics. Spatial ATAC-seq profiling of accessible regulatory elements correlated well with RNA expression of target genes. Spatial patterns of transcription factor motif accessibility also correlated well with the observed transcriptional program of tumor tissue. When compared to adjacent normal tissue, spatial co-profiling of chromatin accessibility and the transcriptome revealed that the epigenetic landscape is significantly altered in tumorigenesis of GAC. Future work will focus on development of co-profiling of histone modifications and the transcriptome to enable the study of another layer of the epigenomic landscape, especially as targeting epigenetic modifiers such as EZH2 has been identified as a potential therapeutic strategy in GACs. Overall, we present a solution to profile multiple layers of gene regulation and expression with spatial context, which can be applied to most tumor types for better understanding of tumorigenesis and the consequences of new targeted therapies.

#4409 *FBXW7* and *BCL9L* altered pathways as hallmarks of early-onset colorectal cancer.

R. Mikaeel[1], D. Bellomo[2], S. Rajpara[3], D. Buckley[3], M. Yagle[2], B. Kerimoglu[2], C. Thorne[2], M. Padi[2], B. Salhia[3], N. A. Ellis[2], X. Llor[4], R. Xicola[4];
[1]Yale Medical of Medicine, New Haven, CT, [2]University of Arizona Cancer Center, Tucson, AZ, [3]University of Southern California, Los Angeles, CA, [4]Yale School of Medicine, New Haven, CT

Background: The incidence of early-onset colorectal cancer (EO-CRC) has been alarmingly increasing, particularly among non-Hispanic Whites (NHWs), resulting in similar rates to ones in African Americans (AAs). Overall, the median age of diagnosis has decreased from 72 to 66 years. The molecular features that could potentially distinguish this phenotype are still not well-established. This study aimed to identify genetic, epigenetic, and transcriptomic factors associated with EO-CRC.

Methods: 510 patients with microsatellite-stable tumors analyzed for somatic mutations, targeting 20 cancer driver genes. We included a cohort of 175 AAs from the Yale New Haven Health System, a previously studied cohort of 51 AAs from the Chicago Colorectal Cancer Consortium, and the publicly available molecular data from TCGA COAD-READ PanCancer cohort (50 AAs and 229 NHWs). We analyzed the transcriptomic and methylation profiles from the Yale cohort using Tempo-Seq™ and Illumina EPIC array, respectively.

Results: Of the 510 patients, 18% were diagnosed with EO-CRC. Using a multiple variant analysis, adjusting for sex, race, tumor location, and stage, EO-CRC patients were less likely to be male (OR = 0.59, 95% CI: 0.37-0.94, p-value = 0.03), their tumors lacked mutations in *APC* (OR = 0.37, 95% CI: 0.22-0.63, p-value = 0.0002), and they were more likely to have mutations in *FBXW7* (OR = 3.1, 95% CI: 1.60-6.00, p-value = 0.0007) and *BCL9L* (OR = 3.1, 95% CI: 1.00-8.72, p-value = 0.04). We compared tumors with and without mutations in *FBXW7* or *BCL9L* in two independently analyses. Combining transcriptomics and methylation data, we identified 10 candidate genes that showed significant gene downregulation with hypermethylation or upregulation with hypomethylation. Among FBXW7 mutant tumors, we found the Cartilage oligomeric matrix protein (COMP) gene was significantly downregulated and hypermethylated. In CRC, COMP has been associated with a crosstalk between the TGF-β pathway and immune cell infiltration. Moreover, inactivation of FBXW7 resulted in the accumulation of phosphorylated TGIF1 molecules and repression of TGFβ-dependent transcription in cancer cell lines. Deficiency of *FBXW7* is a key element in the phosphorylation-dependent ubiquitination and subsequent proteasome degradation of oncoproteins, such as c-MYC, NOTCH, and Cyclin E. Among *BCL9L* mutant tumors, keratin 20 (KRT20), the intermediate filament protein and marker of intestinal differentiation in CRC, was downregulated and hypermethylated. *BCL9L* plays an important role in tumorigenesis induced by aberrant Wnt signaling or aneuploidy tolerance.

Conclusion: Our findings further demonstrate the importance of specific etiologic mechanisms in EO-CRC at the level of somatic alterations, providing new ways to understand the biology of EO-CRC and prospects for the development of targeted therapies.

#4410 The CpG island methylator phenotype is closely associated with prognosis in patients with oral squamous cell carcinomas.

M. Abe[1], S. Yamashita[2], T. Ushijima[3], K. Hoshi[1];
[1]Graduate School of Medicine and Faculty of Medicine, The University of Tokyo, Tokyo, Japan, [2]Maebashi Institute of Technology, Maebashi, Japan, [3]Hoshi University, Tokyo, Japan

Few abnormalities are known to be closely associated with prognosis in OSCC cases. In this study, genomic abnormalities of cancer-related genes and epigenomic abnormalities of genes methylation-silenced in OSCCs were analyzed to identify abnormalities associated with prognosis. Thirty-nine OSCC cases and their surgical materials were analyzed for the presence of mutations using next-generation sequencing. Methylation status of promoter CpG islands of five genes was analyzed by methylation-specific PCR. Mutations in CRG, *TP53* and *PIK3CA* were observed in 64.1%, 38.5%, and 33.3%, respectively, of the cases. However, no significant association between mutation status and overall survival (OS) was observed. Aberrant methylation of *CMTM3*, *NKX2-3*, *RBP4*, *EGFLAM*, and *MAP6* were observed in 51.3%, 41.0%, 66.7%, 38.5%, and 41.0%, respectively. Methylation of *NKX2-3*, *EGFLAM*, and *MAP6* were significantly associated with OS in OSCC cases (p=0.006, 0.006, and 0.012, respectively). Cases with methylation of *CMTM3* and *RBP4* showed a trend toward poor prognosis (p=0.052 and 0.059, respectively). Methylation profiles of the five genes indicated the presence of the CpG island methylator phenotype (CIMP), and the CIMP-positive cases showed poor prognosis (HR=20.5, p<0.001). In conclusion, CIMP was closely associated with the prognosis of OSCC cases.

#4411 Enhancing scalability and consistency in clinical multiomics via an optimized fixed cell ATAC-seq method.

D. Alves Winders, R. Graham, X. Mao, I. De Vito, A. O'Hara, L. Turner, H. Latif;
Azenta Life Sciences, South Plainfield, NJ

ATAC-seq has an emerging role in decoding mechanisms of gene regulation, offering valuable insights into pathology and treatment response in disease models. However, clinical adoption of ATAC-seq methods has been limited by logistical hurdles, including time-sensitive processing of fresh samples and compromised viability of cryopreserved cells. These constraints, compounded by changes in open chromatin regions (OCRs) following cryopreservation, introduce unintended bias and pose significant obstacles for the translational impact of ATAC-seq experiments.

Here, we introduce an optimized fixed-cell ATAC-seq approach to overcome these limitations and unlock new sample types for ATAC-seq analyses. Our solution improves and simplifies the workflow from sample collection to clinical deliverable. This method enables ATAC-seq investigation of a diverse range of samples and facilitates the execution of complex experimental designs, including time course studies and high throughput screening.To demonstrate the effectiveness of this method, we compared our optimized fixed-cell method with traditional ATAC-seq preparations in both fresh and cryopreserved GM12878 cells in parallel. Human GM12878 cell line was obtained from Coriell Institute for Medical Research5. Remarkably, we observed consistent genome-wide patterns of OCR enrichment at key regulatory elements across the three sample preparation methods. We observed consistent OCR enrichment across the promoter region of known highly-expressed B-cell genes including *CD48* and *LCP1*, underscoring this assay's ability to detect chromatin changes at key genes in human disease models.

To investigate the potential for multiomic analysis using this method, we prepared RNA-seq libraries from fixed-cell samples in parallel to ATAC-seq. We observed significantly elevated gene expression related to B-cell function and B-cell diseases, demonstrating our method's compatibility with RNA-seq data collection and integration. This optimized fixed-cell ATAC-seq approach offers enhanced scalability and consistency over conventional methods and presents new opportunities for the multiomic analysis of chromatin and transcriptional activity genome-wide from a single sample in both clinical and research settings.

#4412 Defining chromatin alterations in liver cancer at single cell resolution.

Miguel Ramirez[1], Tabea Stephan[2], Daivd Schaeffer[3], Pamela Hoodless[1]

[1]Medical Genetics, University of British Columbia, Vancouver, BC, Canada,[2]University of British Columbia, Vancouver, BC, Canada,[3]Pathology and Laboratory Medicine, University of British Columbia, Vancouver, BC, Canada

Hepatocellular carcinoma (HCC) is the most common liver cancer and arises from the malignant transformation of hepatocytes. HCC tumors often express genes critical for hepatocyte development but the regulatory mechanisms driving aberrant expression remain unclear. Recent evidence indicates that epigenetic alterations contribute to HCC progression with nearly 50% of cases associated with mutations in chromatin modifiers. Thus, it is imperative to understand how chromatin is altered in HCC and identify the DNA regulatory sequences associated with HCC tumorigenesis. Our study aims to map the chromatin landscape and transcriptome in HCC tumors using a multiomic approach at single cell resolution. Single-cell ATAC- and RNA-seq will be conducted in HCC tumors, matched controls and normal livers to identify regulatory sequences and their target genes critical for HCC tumor progression. We will characterize these regulatory sequences in the context of liver development using genetic manipulation and epigenomic datasets generated from human pluripotent stem cells differentiated to hepatic lineages. Our goal is to elucidate how epigenetic alterations in HCC drive cancer progression and how they relate to a dedifferentiated state.

#4413 Identifying genome-wide histone profiles in patient derived models of AML for predictive biomarker development.

A. Simmons[1], E. Oswald[2], G. Kuales[2], M. Keogh[1], V. U. Kumary[1], E. Brill[1], M. W. Cowles[1], B. Venters[1], **J. B. Schueler**[2];
[1]Epicypher, Durham, NC, [2]Charles River Laboratories, Inc., Freiburg, Germany

Acute myeloid leukemia (AML) is a complex disease with highly individualized treatment plans for patients. Mostly these are based on genetic and phenotypic markers of the disease, but the patient's overall condition is playing a significant role as well. To develop innovative drugs for a broad patient cohort, it is essential to understand the biological implications of these differences and to model them preclinically. In this study, we are assessing the utility of EpiCypher's CUT&Tag-FFPE platform to characterize the epigenome of AML PDX samples. CUT&Tag-FFPE is an epigenome profiling assay that is compatible with Formalin-Fixed Paraffin-Embedded (FFPE) samples, enabling robust genome-wide profiling of histone modifications from limited clinical samples. We derived PDX model LEXFAM 2799 (NPM1 wt; FLT3 wt, t(8;21)) and LEXFAM 2966 (NPM1 mut; FLT3 wt) from treatment naïve patients and established in immunocompromised NSG mice. LEXFAM 2799 is a fast-growing model with passaging times of 33 days, whereas LEXFAM 2966 displays a passaging time of 140 days. We next treated with Standard of Care (SoC) agents Decitabine, Cytarabine and all-trans-retinoic acid (ATRA): LEXF 2966 was highly sensitive towards Decitabine leading to complete remission. Cytarabine induced a partial remission and ATRA had only minor effect on tumor growth. In contrast LEXFAM 2799 was resistant towards treatment with ATRA and showed only partial remission under treatment with Cytarabine or Decitabine. Using the CUT&Tag-FFPE platform we are analyzing FFPE slides from the above mentioned two AML PDX models to investigate differences in the genome-wide histone profile that relate to the different growth behavior as well as sensitivity towards SoC treatment. The goal of these studies is to identify tumor model specific profiles that correlated specifically with the sensitivity towards the hypomethylating agent Decitabine. In addition, we plan to analyze additional untreated as well as treated AML PD models to validate the identified signatures confirming them as predictive biomarkers for sensitivity towards current standard of care and prospectively as well innovative compounds.

#4414 Genome-wide DNA methylation classifier diagnoses pancreatic ductal adenocarcinoma in CUP setting.

Teodor G. Calina[1], Eilis Perez[2], Simon Schallenberg[3], Horst David[3], Erik Knutsen[4], David Capper[2], **Mihnea P. Dragomir**[3]

[1]TGC Ventures UG, Berlin, Germany,[2]Neuropathology, Charite - University Medicine Berlin, Berlin, Germany,[3]Pathology, Charite - University Medicine Berlin, Berlin, Germany,[4]Medical Biology, UiT-The Arctic University of Norway, Tromso, Norway

Introduction: The metastasis of a pancreatic ductal adenocarcinoma (PAAD) is a diagnosis of exclusion and one of the most common causes of cancer of unknown primary (CUP). We have recently developed a genome-wide DNA methylation-based neural network classifier that can accurately differentiate between liver metastasis of a PAAD and intrahepatic cholangiocarcinoma (iCCA) (*PAAD-iCCA-Classifier*). Therefore, the aim of our study was to test whether our *PAAD-iCCA-Classifier* can be extended to be used to correctly diagnose PAAD metastases from other sites in CUP setting.

Methods: For this purpose, we enhanced the anomaly detection layer of the classifier by incorporating ten mimicker carcinomas to be excluded by this layer. We used a validation set 1 (n=3786) including primary PAAD (n=242), PAAD liver metastases (n=20), iCCA (n=151) and 10 other mimicker carcinomas (n=3373) and a validation set 2 (n=26) including primary PAAD from a real-life clinical cohort from an independent institution to validate the classifier. Next, we tested the classifier on 16 PAAD initially considered CUP samples (test set) from different sites: peritoneum, lung, liver, and lymph node. The clinical history and diagnostic imaging of these samples were used to confirm PAAD as the most probable origin. We further performed differentially methylated probes (DMP) and copy number alterations (CNA) analysis of primary PAAD and metastatic PAAD from different locations.

Results: The improved version of the *PAAD-iCCA-Classifier* achieved an accuracy of 98.43% on the validation set 1 and was able to exclude most of the mimicker carcinomas. On validation set 2, the classifier achieved an accuracy of 88.46%. Medical history, imaging and immunohistochemical analysis of the test set samples confirmed the diagnosis of PAAD. The DNA methylation classifier correctly labeled 15/16 PAAD metastatic samples as PAAD (93.75% accuracy). We observed that the classifier performance was negatively affected by a high $CD3^{+}$ immune infiltrate and positively affected by high tumor purity and high proliferation rate. CNA revealed that PAAD liver metastases have a distinct CNA profile characterized by chromosome 6, 9 (*CDKN2A/B*) and 18q (*SMAD4*) deletions. DMP analysis showed that PAAD liver metastases have global hypomethylation of both promoter- and enhancer-associated CpGs compared to primary PAAD and PAAD peritoneal carcinomatosis. Finally, gene ontology analysis revealed that different epithelial-mesenchymal transition pathways are activated in PAAD liver metastases compared to PAAD peritoneal carcinomatosis.

Conclusion: Our tool performs well in classifying metastatic PAAD samples and could be of great clinical use when a PAAD origin is suspected in the case of a CUP. DMP and CNA profiles show that PAAD liver metastases may have a distinct DNA methylation and copy number profile compared to primary and peritoneal carcinomatosis PAAD.

#4415 Utilization of MBD-seq to elucidate differentially methylated regions in cfDNA across healthy and cancer patients.

C. Michelon, B. Egan, **B. Delatte**;
Active Motif, Carlsbad, CA

5-Methylcytosine (5-mC) is the most abundant epigenetic DNA modification in eukaryotes. The presence of 5-mC alters gene expression and genome metabolism, and its deregulation is associated with many human diseases. Cell-free DNA (cfDNA) released from apoptotic cells has recently gained attention, as mutations or epimutations (*e.g.* 5-mC variations) detected in cfDNA were shown to have high diagnostic potential to assess the presence, stage and outcome of several cancers. However, 5-mC detection in cfDNA remains a challenge as input material is often very scarce. MBD-Seq is a method that leverages the ability of Methyl-CpG-binding domain protein 2 (MBD2) to capture and detect highly methylated regions of DNA genome-wide. We evaluated MBD-Seq for the detection of aberrant methylation patterns in cfDNA from healthy and diseased patients. We found MBD-seq on cfDNA to be specific (over 100-fold mC:C detection ratio) and sensitive (5 ng of input cfDNA). Applying MBD-seq to samples from healthy vs colorectal and breast cancer patients showed striking differences in methylation of key tumor-associated genes. Hence, MBD-Seq can elucidate aberrant methylation patterns from cfDNA, highlighting its potential as a diagnostics tool for the detection of cancer.

#4416 Rapid, low-input, targeted NGS workflow for DNA methylation.

Loni Pickle[1], Andrew Hatch[1], Gokhan Yavas[1], Melanie Spears[2], Louis Gasparini[2], Vida Talebian[2], Anna Ying-Wah Lee[2], Mathieu Lariviere[1], Jane Bayani[2], Seth Sadis[3], Jeffrey M. Smith[1]

[1]Thermo Fisher Scientific, Carlsbad, CA,[2]MaRS Centre, Ontario Institute for Cancer Research, Toronto, ON, Canada,[3]Thermo Fisher Scientific, Ann Arbor, MI

DNA methylation is a fundamental epigenetic process that regulates human gene expression. In cancer, methylation changes promote proliferation networks and metastasis. Development of biomarkers for methylation will be enabled by flexible, fast, low-input next generation sequencing workflows. We describe the first Ion AmpliSeq™ Methylation targeted panel and protocol on the turn-key Genexus™ Integrated Sequencer as part an ongoing collaboration with Ontario Institute for Cancer Research (OICR) to detect and predict response in early stage breast cancer and improve diagnostics for Black and Asian women. A 2-pool Ion AmpliSeq™ Methylation Panel for Breast Cancer Research was developed as a demonstration of design, workflow, and reporting for targeted, low-input methylation assessment in a multiplex setting across a variety of samples sources including FFPE. The panel contains 327 amplicons and was designed to target both strands and 10ng DNA input into bisulfite conversion was used for controls. A complete workflow begins at bisulfite conversion and progresses through the Genexus™ Integrated Sequencer which combines library construction, template preparation, and sequencing into a single run. The bioinformatics pipeline provides DNA methylation calls on both Watson and Crick strands at single base resolution and methylated:unmethylated ratios for each CpG. The entire end-to-end workflow was completed in 2 days, including a full analysis software solution. The panel was evaluated using 2 control gDNA samples. The first had an expected average methylation state across all CpGs of >98% and the second <5%. An equal mixture of these two samples was also tested. The Methylation Panel for Cancer Research performed well on control samples. The single lane Loading, Total Bases, Final Reads, and Raw Read Accuracy were >92%, >1G, >14 Million, and >90% respectively. The workflow was also demonstrated on research FFPE cancer samples. This Methylation Panel protocol offers a 2-day, end-to-end workflow with high resolution, targeted and quantitative methylation analysis from DNA input as low as 10ng into bisulfite conversion. The option to design custom methylation panels for interrogation of targets of interest without the need for whole genome methylation is now available. <For Research Use Only. Not for use in diagnostic procedures. Early access materials were provided by Thermo Fisher Scientific™ to OICR in support of this abstract, but no other financial support. This study was conducted with the support of the Ontario Institute for Cancer Research through funding provided by the Government of Ontario.

#4417 Development of biochemical screening assays to facilitate drug discovery in RNA m6A modification regulators.

S. F. AbdulSalam, S. Oh, B. P. Lee, J. J. Ferry, J. R. Ries, K. Y. Horiuchi;
Reaction Biology Corporation, Malvern, PA

Over the recent years, knowledge of RNA modifications and their regulation has expanded extensively, providing novel insights and strategies to explore potential therapeutics for pathogenesis of various diseases, including cancer. Several chemical modifications in RNA have been identified so far, among these N^6-methyladenosine (m6A) modification is the most abundant and well-studied epitranscriptomic marker found in mRNA and long noncoding RNA. Abnormal m6A expression is proven to be associated with tumorigenesis, cancer stemness and drug resistance of cancers. Methylation in 6-Adenosin of RNA is a dynamic and reversible process tightly regulated by its writer, m6A methyltransferase complex and erasers, FTO and ALKBH5. m6A methyltransferase complex contains METTL3-METTL14-WTAP as core components. METTL3 is the catalytic component, which is activated by heterodimer formation with METTL14. High METTL3 expression is found in several cancers such as breast, lung, liver, gastric, colorectal, AML and a METTL3 catalytic inhibitor is found to delay AML progression in mouse models. Protein that binds RNA m6A modification to execute it signaling are known as m6A readers. Readers are categorized into three main classes, YTH domain proteins, IGF2 mRNA-binding proteins and heterogeneous nuclear ribonucleoproteins. YTH family readers are found to have oncogenic roles in several cancers including AML, breast, lung, CRC and glioblastoma. Recent studies suggest inhibition of m6A binding of individual YTH family proteins is a promising therapeutic strategy however, potent inhibitors are yet to be identified. This poster summarizes current assays we have developed to facilitate cancer therapeutic discovery in m6A related protein targets. We present development and validation of an assay suitable identify in METTL3 catalytic inhibitors using our proprietary hotspot technology. We also show development of HTRF based biochemical assays for all five YTH family protein YTHDF1-3 and YTHDC1-2, to screen for molecules that disrupt protein-m6A interaction. We further study the selectivity of an FDA approved drug Tegaserod, a reported YTHDF1 inhibitor by a structure based virtual screening, between YTH family proteins.

MOLECULAR/CELLULAR BIOLOGY AND GENETICS: Metabolomics
Poster Session

#4421 Intracellular cytomatrix actin and the Warburg effect.
T. E. Shaiken;
Baylor College of Medicine, Houston, TX

Introduction: The cytoplasm of living cells is dynamic and the motion arising from fluctuating forces in cells is an active process, rather than being thermally induced. Motor proteins could be the primary causative force of intracellular movement. However, which motor protein is involved in the intracellular dynamics, what process requires fluctuational intracellular activity, and where the energy source comes from is unknown. To address the impact of intracellular motion in cellular processes, we chemically separated the viscous fluid (cytosol) and elastic solid (cytomatrix) phases of cytoplasm. The multiomic analysis was used to dissect the compositional differences between the liquid and solid phases. LC-MS/MS-based proteome analysis was used to identify the composition of the HCT-15 colon cancer cell cytomatrix. The mRNA translation was measured by Ribosome footprinting.
Results: Since the kinesis of the solid phase can trigger liquid phase flux, the composition of the cytomatrix was the primary focus of the study of cytoplasmic motion. The systemic analysis of the cytomatrix constituency allowed the identification of a diverse functional group of proteomes that included cytoskeletal and structural elements of organoids, metabolic enzymes, and normal- and proto-oncogenic signaling pathways. The two-phase system elucidated how diverse chemical reactions can occur simultaneously within the cell cytoplasm. Namely, the immobilization of catalytic complexes on the solid cytomatrix physically segregates biochemical reactants, thereby overcoming spatial impediments and allowing diverse metabolic reactions to coincide. Actomyosin and other actin-binding proteins of cytomatrix were the most abundant and diverse proteome, indicating that the primary machinery driving cytomatrix mobility consists of actomyosin, actin-binding, and actin-regulating proteins of cytomatrix. The cytomatrix dynamics trigger the cytosolic motion that carries substrates to immobilized catalytic complexes of the cytomatrix, thereby increasing product output, which appears to be a more intense process in cancer cells due to genetic and epigenetic aberrations. Under normal physiological conditions, mitochondrial respiration can deliver the energy requirements of cytomatrix micromechanics, but in cancer cells, additional energy of ATP is supplied by the aerobic glycolysis known as the Warburg effect to provide the ATP surplus for actomyosin mechanics.
Conclusion: The intracellular motion is supported through non-muscle actomyosin action of the solid phase (cytomatrix), permitting increased glycolytic pathway activity in tumor cells. This novel concept of cancer links the Warburg effect with the bioenergetics of cytomatrix micromechanics and the dynamics of metabolic processes in tumors. Thus, two of the mysteries in cancer cell biology, how chemical reactions occur in the cytoplasm and energy is generated by tumor cells, have now been linked.

#4422 Metabolic adaptations of glioblastoma in hypoxia is mediated by acox-1.

A. Bhattacharya[1], L. Caflisch[1], H. Balinda[1], A. Lodi[2], M. Zhou[1], M. Li[1], J. Chiou[2], R. Pandey[2], G. R. Sareddy[1], S. Tiziani[2], Y. Chen[1], R. K. Vadlamudi[1], A. J. Brenner[1];

[1]UT Health Science Center at San Antonio, San Antonio, TX, [2]The University of Texas at Austin, Austin, TX

Background: Glioblastoma (GBM) is a recurrent, chemoresistant, malignant brain tumor. Hypoxia is a major factor contributing to resistance in GBM which develops due to aggressive tumor growth and chronic anti-angiogenic therapy. Thus, under limited oxygen supply it is unlikely that the high energy consuming pathways are solely able to provide the energy requirement of GBM cells. Thus, based on our metabolomics data stated below we hypothesize that GBM cells adapt to chronic hypoxia utilizing alternate metabolic pathways such as peroxisomal fatty acid oxidation (FAO). Here we have explored the role of Acyl coenzyme A oxidase (ACOX-1), a rate limiting enzyme for peroxisomal FAO in the metabolic adaptations to hypoxia and as a potential drug target.
Methods: U251 CRISPR dox inducible ACOX1 (KO) cells and patient derived primary GBM were grown under normoxic and hypoxic conditions (2%O2, 5%CO_2, 70% humidity). Metabolic analysis was done using UHPLC-MS and LCMS analysis. RNAseq was done using TopHat2 (genome alignment), HTSeq, and DEseq to study the differential gene expression at cut-off of 2-fold change, and $p<0.05$. GSEA was used to interpret biological pathways. NCr/SCID (Severe Combined Immunodeficiency) mice (n=5) inoculated with U251 ACOX1 knockout cells expressing luciferase were used and treated with anti-angiogenic agent pazopanib at 30 mg/kg, 5 days a week. The U251 luciferase-labeled tumors were imaged starting weekly for tumor volumes using the IVIS (In Vivo Imaging System) Lumina.
Results: In patient derived primary GBM cell lines alterations in metabolites in chronic hypoxia compared to normoxia, such as decrease in citric acid cycle metabolites, increase in glycolytic metabolites, and dysfunctional mitochondrial metabolites. In RNA seq downregulation of genes PCK1, SCD, SREBF1, and PIPOX ($p<1x10^{8}$) involved in PPAR and lipid metabolism pathways in hypoxia versus normoxia were noted. Inhibition of ACOX-1 displayed increased survival in mice administered ($p=6.7E-04$) with pazopanib compared to the U251 parental control group.
Conclusion: There is metabolomic reprogramming in ACOX-1 KO cells channeled predominantly through FAO as seen through the downregulation of genes downstream of the PPAR signaling pathway, mediated through SREBF1 the master regulator of lipid metabolism. Thus, these genes could be future targets for therapy in combination with anti-angiogenic therapies that aggravate hypoxia in GBM.

#4423 Cholesterol and arachidonic acid promote the tumor growth of epithelial ovarian cancer via MAPK signaling pathway.

H. Sakaguchi-Mukaida, K. Hiramatsu, M. Kakuda, S. Nakagawa, T. Kimura, Y. Ueda, T. Kimura;
Osaka University, Suita City, Osaka, Japan

Introduction: Previously, we reported that VLDL promoted cell proliferation of epithelial ovarian cancer (EOC) cells in vitro. In vivo, we also confirmed that High-Fat Diet (HFD) strongly promoted the tumor growth of EOC. These results suggest that lipid molecules in HFD might contribute to cell proliferation of EOC cell. In this study, we performed metabolome analysis and analyzed the metabolomic profile of lipid molecules of HFD fed mouse serum. Finally, we demonstrated that some lipid molecules promoted the cell proliferation of EOC cells in vitro and vivo.
Methods: We obtained the serum of HFD and normal diet (ND) fed mouse (non-tumor bearing) and performed metabolome analysis to identify the lipid molecules which associate with cell proliferation. In addition, we demonstrated that the lipid molecules promoted cell proliferation and activated signaling pathway of EOC cells in vitro. Moreover, we evaluated that the lipid molecules-rich diet promoted the tumor growth of EOC in vivo.
Results: The tumor growth of EOC (EOC cell line; KURAMOCHI and RMG-I) was significantly promoted by HFD compared to ND in vivo ($p < 0.05$, respectively). Metabolome analysis using the serum of HFD and ND fed mouse (non-tumor bearing) detected 210 metabolites, and principal component analysis showed obvious different metabolic profiles of HFD fed mouse serum compared to ND. Partial least squares-discriminant analysis revealed cholesterol and arachidonic acid (AA) as the lipid molecules with high VIP score in the serum of HFD fed mouse. In vitro, cholesterol and AA significantly promoted cell proliferation, respectively ($p < 0.05$) through the activation of MAPK signaling pathway. In vivo, we also confirmed that cholesterol and AA-rich feed promoted the tumor growth of EOC, respectively ($p < 0.05$).
Conclusions: Cholesterol and AA significantly promoted the tumor growth of epithelial ovarian cancer through the activation of MAPK signaling pathway.

#4424 Differential metabolic response of triple-negative and estrogen receptor-positive breast cancer cells to abemaciclib, a CDK4/6 inhibitor.

J. Jiang[1], X. Bao[1], Y. Jiang[1], Y. Yue[1], M. Huettemann[2], **J. Li**[1];
[1]Karmanos Cancer Institute, Detroit, MI, [2]Wayne State University, Detroit, MI

Background: Inhibition of the cell cycle kinases CDK4/6 is the standard-of-care for advanced hormone receptor-positive breast cancer. The clinical efficacy of CDK4/6 inhibitors in triple-negative breast cancer remains uncertain. Mechanisms of sensitivity and resistance are not fully understood. This study comprehensively investigated the metabolic response of triple-negative and estrogen receptor-positive breast cancer cells to abemaciclib (Abe), with the aim of providing metabolic insights for resistance mechanisms.
Methods: MCF-7 (MCF) and MDA-MB-231 (MDA) cells were treated with Abe (0, 100, and 500 nM) for 1, 2, or 7 days. Cell cycle and cell senescence analyses were performed to assess drug effects. Cellular metabolism was investigated using the Seahorse assay, LC-MS/MS based targeted metabolomics, and stable isotope-assisted metabolic flux analyses with [U-^{13}C]glutamine, [1,2-^{13}C]glucose, and [U-^{13}C]glucose as the tracers.
Results: Abe induced cell cycle arrest at G0/G1 in both cell lines, more pronounced in MCF. Dose- and time-dependent cell senescence occurred in both treated cell lines, more pronounced in MDA. The Seahorse assay indicated that energy metabolism (assessed by oxygen consumption rate and extracellular acidification rate) was reduced in both treated cell lines. Targeted metabolomics revealed that post Abe treatment, intracellular lactate significantly decreased in both cell lines; intracellular TCA intermediates significantly decreased in MCF while being unchanged in MDA; intracellular deoxynucleotides decreased in both cell lines, to a lesser extent in MDA; cellular energy levels (assessed as the ratios of ATP/AMP, ATP/ADP, CTP/CMP, CTP/CDP) were significantly lower in MCF while remaining unchanged or increased in MDA; intracellular levels of many amino acids significantly increased in MDA while decreasing in MCF. [U-^{13}C]glutamine flux revealed a significant decrease of intracellular glutamine-derived TCA intermediates in both treated cell lines. [1,2-^{13}C]glucose flux indicated an enhanced oxidate pentose phosphate pathway (PPP) activity and increased de novo syntheses of purine nucleotides (ATP and GTP) in treated MDA (but not MCF). [U-^{13}C]glucose flux suggested that while both cell lines responded to Abe with decreased anaerobic glycolysis (pyruvate converting to lactate), MDA (but not MCF) showed an enhanced capability of utilizing glucose-derived carbon to replenish TCA intermediates and increased amino acid synthesis.
Conclusion: Adaptive cellular metabolism, characterized by enhanced utilization of glucose-derived carbon to replenish TCA intermediates and increased PPP activity, thus promoting biosynthesis of amino acids and purine nucleotides to maintain cellular energy and redox balance, may contribute to the intrinsic resistance of triple-negative breast cancer to CDK4/6 inhibitors.

#4425 Metabolic vulnerabilities of dedifferentiated liposarcoma.

J. O. Brett[1], J. Han[2], C. Kim[3], L. P. Kelley[2], S. Han[2], D. Boone[3], J. Crowley[2], S. Joshi[2], C. P. Raut[4], A. Greka[3], M. C. Haigis[2];
[1]Dana-Farber Cancer Institute, Boston, MA, [2]Harvard Medical School, Boston, MA, [3]Broad Institute of MIT and Harvard, Cambridge, MA, [4]Brigham and Women's Hospital, Boston, MA

Dedifferentiated liposarcoma (DDLPS) is a rare, life-threatening malignancy in the family of adipocytic sarcomas. DDLPS, which usually arises in the retroperitoneum of middle-aged adults, has a poor prognosis. This is due to the propensity of DDLPS to metastasize and recur locally, combined with a dearth of effective systemic therapies. A longstanding curiosity is that DDLPS has non-lipogenic morphology and no lipid droplets, while its less aggressive sister sarcoma, well-differentiated liposarcoma (WDLPS), resembles benign adipose tissue and contains large lipid droplets. How DDLPS metabolizes lipids and the metabolic vulnerabilities of DDLPS in patients, which may form new therapeutic targets, are unknown. In our project, we investigate the metabolism of DDLPS versus WDLPS using patient samples and cell lines. Snap-frozen tissues from patients were obtained from the Dana-Farber/Harvard Cancer Center specimen bank of DDLPS and WDLPS. We performed metabolomics and lipidomics on these samples. We complemented these results with publicly available transcriptional profiles of separate cohorts of DDLPS, WDLPS, and other cancers. In vitro, we made use of a panel of multiple DDLPS-derived cell lines, WDLPS-derived cells, benign preadipocytes, and benign adipocytes. We measured mitochondrial function and the cellular effects of perturbing various metabolites in screens in culture. Overall, our initial results indicate strong alterations in mitochondrial metabolism in DDLPS in patients. In culture, DDLPS is susceptible to multiple metabolic perturbations related to mitochondrial dysfunction. These metabolic vulnerabilities of DDLPS provide potential therapeutic opportunities. Work is ongoing to optimize the targeting of these vulnerabilities in vivo, elucidate the molecular roles of specific metabolites, and complete a blueprint of DDLPS metabolic weaknesses in patients.

#4426 Targeting MCT1 and PFKFB3 provokes synthetic lethality in small cell lung cancer.

A. H. Prabhu[1], K. Scott[1], P. Stewart[1], D. Grass[1], M. Fernandez[1], D. Ercan[1], J. Koomen[1], T. Bannister[2], C. Rudin[3], G. DeNicola[1], E. Haura[1], J. Cleveland[1]; [1]Moffitt Cancer Center, Tampa, FL, [2]The Herbert Wertheim UF Scripps Institute, Jupiter, FL, [3]Memorial Sloan Kettering Cancer Center, New York, NY

Small cell lung cancer (SCLC) is the third most common lung cancer and is extremely aggressive and highly metastatic. SCLC responds to radiation and standard platinum-based chemotherapy, yet this is invariably followed by relapse and the rapid emergence of lethal chemoresistant disease. Hence, SCLC has been declared a recalcitrant malignancy by NCI, and there is an urgent need to identify new and actionable therapeutic vulnerabilities. Unbiased metabolomic and shotgun and activity-based proteomic analyses of NSCLC and SCLC patient derived tumor tissues, PDX and a panel of cell lines revealed marked upregulation of glycolytic and nucleotide metabolic pathways in SCLC. Further, unbiased screens with metabolic inhibitors revealed selective sensitivity of SCLC cells to the MCT1 lactate transporter inhibitor SR13800 and to the PFKFB3 inhibitor PFK15, and that combined treatment provokes rapid apoptosis. Metabolic, flux and molecular analyses revealed that MCT1 inhibition (MCT1i) or loss in SCLC cells impairs glycolysis and triggers rapid increases in intracellular lactate that then diminish, and this is driven by the induction of lactate dehydrogenase-B (LDH-B) that oxidizes lactate into pyruvate. This is accompanied by a marked shift in the $NAD^{\pm}$ to NADH ratio towards NADH, and increased pyruvate dehydrogenase (PDH) activity and OXPHOS. Further, MCT1 inhibition provoked increases in the Aspartate-Malate and DHAP-SnG3P shuttles, which restored the NAD^{+}/NADH balance in the cytosol. In contrast, treatment of SCLC cells with PFKFB3 inhibitors (PFKFB3i) leads to inhibition of PDH activity, a collapse in OXPHOS and increases in lactate efflux that are due to flux of glucose through pentose phosphate pathway and re-entry into glycolysis via 3-phosphoglygerate (3-PGA). Combined MCT1/PFKFB3 inhibition amplifies metabolic alterations provoked by both MCT1i and PFKFB3i, triggering a collapse in both glycolysis and OXPHOS. Similarly, inhibition or silencing of enzymes that drive the Aspartate-Malate and DHAP-SnG3P shuttles, or inhibition of the mitochondrial pyruvate transporter, provoked metabolic collapse and cell death following inhibition or loss of MCT1. Finally, SCLC xenografts and primary SCLC CDX treated with a combination of SR13800 and PFK15 showed improved survival compared to vehicle or monotherapy treatments. Thus, co-targeting adaptive metabolic circuits provoked by inhibition of MCT1 and PFKFB3 provokes synthetic lethality in SCLC, supporting the notion that inhibition of these metabolic chokepoints will be an effective strategy for treatment of this lethal malignancy.

#4427 Do changes in lipid metabolism link obesity to pancreatic cancer?.

R. Ghosh, D. Ajit, J. Woodworth, D. Fritze, F. G. Cigarroa, G. A. Halff, **A. P. Kumar**;
UT Health Science Center at San Antonio, San Antonio, TX

The near equal incidence and mortality rates of pancreatic cancer, combined with projections that pancreatic cancer will become the second-most common cancer-related deaths by 2050, underscore the need to identify patients with early disease and interrupt this trajectory. Obesity, weight gain and waistline have been implicated in increasing the risk of pancreatic cancer. Although metabolomic analyses of pancreatic cancer patients have established correlations between phospholipids, lysophospholipids with treatment outcomes, the association between metabolites, obesity, and pancreatic cancer remains largely understudied. The objective of this pilot study was to determine differences in serum metabolites in obese and overweight pancreatic cancer patients compared with healthy non-obese subjects. Our long-term goal is to develop serum marker(s) that may be used to prevent advanced pancreatic cancer and thus improve outcomes for these patients. Serum was obtained from healthy subjects (n=11; BMI range from 18-25), overweight (n=9; 25-30) and obese (n=7; >30) pancreatic cancer patients from an IRB approved study. Males (n=12) and females (n=15) were represented in the study. Global metabolic profiles were determined using Ultrahigh performance liquid chromatography-tandem mass spectroscopy. Raw data was extracted, peaks were identified and processed at Metabolon using the Laboratory Information Management System. Comparison between overweight pancreatic cancer patients and healthy controls identified 403 biochemicals (111 upregulated and 292 downregulated; $p < 0.05$) and 93 biochemicals (40 upregulated and 53 downregulated; $0.05<p<0.10$). Comparison of the differences in biochemicals between obese pancreatic cancer patients and healthy controls showed changes in 293 biochemicals (71 upregulated and 222 downregulated; $p <0.05$) and 123 biochemical changes at $0.05<p<0.10$ (42 increased and 81 decreased). 38 ($p <0.05$) and 47 ($0.05<p<0.10$) differential levels of biochemicals were identified when obese and overweight pancreatic cancer patients were compared. Random forest analysis showed that the 30 top ranking biochemicals were involved in lipid metabolism, amino acid metabolism, nucleotide metabolism, peptide, xenobiotics, and carbohydrate metabolism. These data suggest an association between changes in lipid metabolism may be another link between obesity and pancreatic cancer. This project was funded in part by VA-Merit Award (I01 BX003876).

#4428 Integrated multi-omics analysis reveals systemic and localized metabolic disruptions in colorectal cancer.

G. Patti[1], E. Stancliffe[2], A. Richardson[2], A. Mehta[2], M. Gandhi[2], K. Cho[1];
[1]Washington University in St. Louis, St. Louis, MO, [2]Panome Bio, St. Louis, MO

Despite technological advances in molecular medicine over the last 30 years, no single approach has proven to be sufficient to meet the diagnostic needs in cancer care. Here we use a multiomic approach leveraging proteomic, metabolomic, and transcriptomic technologies to study the metabolic shifts that occur during colorectal cancer (CRC) progression. Our integrated analysis identified systemic changes to beta oxidation pathways and localized changes to tyrosine metabolism within the tumor, creating a mechanistic, actionable description of the core CRC metabolic program. We conducted untargeted proteomics and metabolomics profiling on serum samples from CRC patients (n=10) and healthy controls (n=10). Our serum proteomics data is generated through sample enrichment on the Seer Proteograph system followed by LC/MS analysis with the Thermo Orbitrap Astral. Our metabolomics approach employs LC/MS assays for unbiased profiling of the serum metabolome, exposome, and lipidome. We supplemented this discovery work with both targeted serum and tumor-specific approaches including targeted proteomics to quantify select targets, inflammatory profiling with Alamar proteomics, public transcriptomics data from TCGA, and in vitro metabolic flux data. These large and diverse datasets were then integrated through joint pathway analysis and network integration. The global serum proteomics and metabolomics profiles generated show distinct separation between healthy and diseased individuals. Joint pathway analysis of these discovery datasets highlighted enrichment in beta oxidation pathways and tyrosine metabolism, among others. Interestingly, the Alamar inflammatory panel revealed that many of the analytes in the tyrosine metabolism pathway were well correlated with inflammatory status, while the beta oxidation signature had a lower correlation. To determine the relationship of these systemic findings from serum to tumor metabolism itself, we integrated tumor-specific transcriptomics data and found alterations to tyrosine metabolism with differences in tyrosine aminotransferase expression. The beta oxidation related genes, on the other hand, were not concordant with the serum findings. However, our in vitro metabolic flux studies have shown beta oxidation in CRC cells is upregulated to provide additional fuel for oxidative phosphorylation. This result suggests that beta oxidation may not be transcriptionally regulated in the tumor but rather a consequence of organismal metabolic rewiring. The results of this work, which is currently expanding into a larger and more diverse patient population, underscores the power of multiomic profiling for enhancing our understanding of metabolic dysregulation in CRC. Ultimately, a comprehensive model of the molecular alterations in CRC will yield a better understanding of tumor phenotypes and inform better diagnostics and therapies.

#4429 Plasma metabolic profiles in association with subsequent risk of colorectal cancer in the UK Biobank cohort.

F. Yuan, G. Jia, W. Wen, W. Zheng;
Vanderbilt University Medical Center, Nashville, TN

Background: Dysregulation of metabolic processes contributes to colorectal cancer (CRC) etiology. We aimed to comprehensively evaluate the prospective associations between pre-diagnostic metabolic biomarkers and CRC risk in 230,420 UK Biobank participants.
Methods: A total of 249 metabolic biomarkers were measured by nuclear magnetic resonance spectroscopy from baseline plasma samples. Cox proportional hazard models were used to estimate hazard ratios (HRs) and 95% confidence intervals (CIs) for the associations of metabolic biomarkers with CRC risk after adjusting for potential confounders. Subgroup analyses were performed by sex and CRC subsites (i.e., proximal colon, distal colon, rectum). We also conducted factor analyses to identify latent factors and examined their associations with CRC risk.
Results: During a median follow-up time of 9.7 years, 2,410 incident primary CRC cases were identified after excluding participants diagnosed with CRC within two years after blood collection. After correcting for multiple testing, 50 metabolic biomarkers, including lipids and lipoproteins, fatty acids, ketone bodies, and inflammation, were significantly associated with incident CRC risk. No statistically significant differences were observed for the biomarker-CRC associations by sex and CRC subsite. In the sensitivity analysis, excluding cholesterol-lowering medication users did not alter the main findings. In factor analyses, we identified a significant association of CRC risk (HR = 1.08; 95% CI = 1.04-1.13; *P*-value = 6.89×10^{-5}) with a metabolite pattern which was positively correlated with triglycerides and inversely correlated with relative concentrations of omega-6 fatty acids and polyunsaturated fatty acids.
Conclusion: We identified multiple metabolic biomarkers and a metabolite pattern associated with CRC risk in a large prospective cohort. These findings suggest lipid metabolism may contribute to carcinogenesis of the colorectum.

#4430 Metabolic reprogramming by ASPSCR1::TFE3 and VCP.

R. Patel[1], A. Pozner[1], K. Dunlap[2], L. Carroll[1], J. Brown[1], G. Ducker[2], K. Jones[1];
[1]Huntsman Cancer Institute, Salt Lake City, UT, [2]University of Utah, Salt Lake City, UT

Alveolar soft part sarcoma (ASPS) is a lethal soft tissue malignancy typically incident among adolescents and young adults, distinguished by the t(X;17) ASPSCR1::TFE3 fusion gene (AT3). Conventional chemotherapy has shown limited efficacy against ASPS, necessitating exploration of alternative strategies. Previous investigations have shown the pivotal role of the fusion gene in sarcomagenesis in mice, particularly in lactate-rich environments. This study aims to elucidate the metabolic alterations actuated by the AT3 fusion gene, both in vitro and in vivo. To model in vitro metabolic profiles, ASPS (ASPS-1) and renal cell carcinoma (FU-UR1) cell lines, each expressing AT3, were employed. Utilizing siRNA-mediated gene silencing, AT3 and VCP, a cofactor, were targeted in vitro. Metabolomic profiling through GC-MS analyzed the impact of depletion of AT3 or its transcriptional co-factor, VCP. C13-labeled metabolites were introduced and traced in vitro and in vivo to enhance comprehension of carbon utilization in aerobic respiration. While metabolic activity and O2 consumption differed between cell lines, inhibition of AT3 and VCP led to similar metabolite alterations. Significant changes in amino acid metabolism, notably glutamate, aspartate, and alanine were observed in both cell lines. There was notable diversion of glucose carbon utilization away from typical entry into the tricarboxylic acid (TCA) cycle, with minimal carbon incorporation beyond alpha-ketoglutarate. Despite prior data indicating heightened mitophagy activity in AT3 driven cells, inhibition of lysosomal activity did not yield significant changes in cellular respiration or O2 consumption.

#4431 Steroid hormone metabolites and mammographic breast density in premenopausal women.

K. A. Matthew[1], G. K. Vanapali[1], K. R. Getz[1], M. S. Jeon[1], C. Luo[1], X. Guo[2], J. Luo[1], **A. T. Toriola[1]**;
[1]Washington University School of Medicine in St. Louis, St. Louis,, MO, [2]Vanderbilt Epidemiology Center, Vanderbilt-Ingram Cancer Center, Vanderbilt University School of Medicine, Nashville, TN

Background: Steroid hormones influence breast tissue development and play a role in breast carcinogenesis. Their associations with mammographic breast density (MBD), an established risk factor for breast cancer, are less clear. We, therefore, investigated the associations of steroid hormone metabolites with MBD in premenopausal women.
Methods: Our study population consists of 705 premenopausal women recruited during their annual screening mammogram at the Washington University School of Medicine, St. Louis, MO. We assessed volumetric percent density (VPD), dense volume (DV), and non-dense volume (NDV) using Volpara. We assayed 54 steroid hormone metabolites from fasting blood samples at Metabolon. Linear regression models were used, after adjusting for covariates, to estimate the least square means of VPD, DV, and NDV across tertiles (T) of each metabolite. Sensitivity analysis was performed among the subset of participants with a history of oral contraceptive use (OCP). We used the Benjamini-Hochberg procedure to correct for multiple tests to control the false discovery rate (FDR) at a 5% level.
Results: Five androgen metabolites (androstenediol (3beta,17beta) monosulfate 2, androstenediol (3beta,17beta) disulfate 1, 5alpha-androstan-3alpha,17beta-diol monosulfate 2, 5alpha-androstan-3alpha,17beta-diol disulfate, and 5alpha-androstan-3beta,17beta-diol disulfate) and two corticosteroid metabolites (tetrahydrocortisone glucuronide 5, and cortolone glucuronide 1) were inversely associated with VPD. Androstenediol (3beta,17beta) disulfate 1, and 5alpha-androstan-3alpha,17beta-diol disulfate displayed the strongest associations with VPD. The mean VPD decreased across tertiles of androstenediol (3beta,17beta) disulfate 1 from 9.0% in T1 to 8.5% in T2, and 7.5% in T3 (FDR p-value=0.02). Similarly, the mean VPD decreased from 8.8% in T1 to 8.4% in T2, and 7.6% in T3 of 5alpha-androstan-3alpha,17beta-diol disulfate (FDR p-value=0.03). Progestin steroid metabolites appeared to be positively associated with VPD but only 5alpha-pregnan-3beta,20alpha-diol monosulfate 2 was marginally significant after FDR correction (7.5% in T1, 8.3% in T2, and 8.8% in T3; FDR p-value=0.06). Four metabolites (three corticosteroids and one androgenic steroid) were positively associated with NDV. No metabolite was associated with DV. In sensitivity analysis limited to OCP users, mean VPDs were lower but the directions of associations were similar to those observed in the overall analysis.
Conclusion: We report novel associations of corticosteroids and androgen metabolites with breast density in premenopausal women. Our findings shed important new insights into hormonal biomarkers and MBD.

#4432 Molecular biomarkers of non-Hodgkin lymphomas and subtypes identified by mass spectrometry-based metabolomics.

F. Choueiry, S. Singh, L. Sehgal, **J. Zhu**;
The Ohio State University Wexner Medical Ctr., Columbus, OH

Non-Hodgkin lymphomas (NHLs) constitute a diverse collection of lymphoid neoplasms, each characterized by distinct biological features. Approximately 90% of all lymphomas in the United States stem from B lymphocytes, with the remainder originating from T cells. The therapeutic approach for NHLs hinges on the neoplastic histology and the tumor stage, guiding the determination of whether radiotherapy, chemotherapy, or a combination thereof represents the most effective treatment strategy. Following an indolent phase, 50% of patients experience disease transformation into an aggressive form of lymphoma, leading to rapid deterioration and patient demise. While extensive efforts have been directed towards understanding the genetics of transformation, the contribution of altered tumor metabolism, induced by these genetic lesions, to disease aggressiveness remains unclear. Therefore, there exists an urgent need to better understand the metabolic changes during lymphoma transformation and treatment. Given the metabolic adaptations supporting bioenergetics, biosynthesis, and redox in malignant cells, here in this study we aimed to identify unique metabolic signatures in prominent lymphoma subsets—diffuse large B-cell (DLBCL), mantle cell (MCL), and follicular lymphomas (FL). Employing unbiased mass spectrometry-based metabolomics, we screened sera samples from n=30 patients with lymphoma and n=25 aged and BMI-matched healthy controls for molecular biomarkers that may be indicative of the subtypes. Principal component analysis revealed distinct clustering of the disease and control groups, indicating unique metabolic profiles induced by lymphoma presence. A total of 36 metabolites, including adenine, trans-aconitic acid, and citric acid, were significantly deregulated between groups (FC > 2, FDR $p < 0.05$). Functionally, enriched pathways included tryptophan metabolism and the tricarboxylic cycle (FDR $p < 0.05$), supporting our previous findings that lymphomas rely on oxidative phosphorylation for sustained proliferation. Comparing metabolic profiles of different lymphomas subtypes demonstrated unique clustering, emphasizing the distinct metabolic flexibility of each malignancy. Interestingly, cystine was the primary metabolite driving separation of the groups in our partial least squares discriminant analysis (PLS-DA), with DLBCLs demonstrating the highest abundance of this amino acid. In summary, our research uncovered that there are distinctive metabolic shifts resulting from the transformation of lymphomas. The findings stemming from our unbiased metabolic screening enables a better understanding of the complex metabolic intricacies in lymphomas and paves the way for prominent biomarker detection for improved patient outcomes.

#4433 Secondary electrospray ionization mass spectrometry for volatile analysis of lung cancer.

J. Zhu, F. Choueiry;
The Ohio State University Wexner Medical Ctr., Columbus, OH

Lung cancer remains a leading cause of cancer-related mortality globally, necessitating innovative approaches for early detection and improved understanding of its metabolic landscape and consequences. Secondary Electrospray Ionization Mass Spectrometry (SESI-MS), an innovative analytical technique, has emerged as a powerful tool for the analysis of volatile organic compounds (VOCs) associated with various diseases, from metabolic disorders to bacterial infections. In this proof-of-concept study, we first utilized SESI-MS analyses of four representative lung cancer cells of both non-small cell lung cancer (NSCLC) and small cell lung cancer (SCLC) to demonstrate its capability to profile VOCs released by lung cancer cells. The technique allows for real-time, non-invasive analysis of the headspace above cultured cells, enabling the detection of unique VOC signatures associated with different lung cancer subtypes. Meanwhile, SESI-MS also facilitated the discrimination specific cells based on distinct VOC patterns. Furthermore, we also performed cisplatin treatment experiments and observed the metabolic signature shift post drug treatment. These results collectively offered potential applications in early diagnosis and personalized treatment strategies. Next, we continued with in vivo investigations to further extend the utility of SESI-MS in lung cancer research. Animal models, mimicking human lung cancer pathophysiology, have been subjected to SESI-MS analysis to identify volatile biomarkers indicative of tumor development and progression. Several representative cancer drug treatments were performed to the lung cancer mice model, and the drug-induced responses were also monitored via SESI-MS breath analyses. The in vivo SESI-MS approach detected many interesting breath VOC features that could provide valuable insights into the dynamic changes in VOC profiles during various stages of lung cancer, and therefore has the potential to offer a deeper understanding of the disease's metabolic alterations and potential avenues for targeted therapeutic interventions. In conclusion, SESI-MS-based volatile analysis presents a robust and versatile approach for investigating lung cancer, and our ongoing work has the potential to bridge the gap between in vitro and in vivo models for better translational research outcomes. The detection of unique VOC signatures associated with lung cancer cells and tumors holds significant promise for early detection, subtype classification, and monitoring of treatment responses. As technology continues to advance, SESI-MS stands poised to play a pivotal role in transforming the landscape of lung cancer diagnostics and research.

#4434 Cancer cell-derived adrenomedullin downregulates Zeb1 in adipocytes to induce adipolysis and promote breast cancer progression.

L. Cao, X. Chen, Y. Shi, S. Yang;
Nankai University, Tianjin, China

Background: Once breast carcinoma in situ breaks through the basement membrane, it preferentially invades the lipid-rich microenvironment around the mammary gland, which indicates a poor prognosis. However, the detailed mechanisms of this interaction remain elusive. Here, we describe bidirectional communication between breast cancer cells and cancer-associated adipocytes (CAAs). Different from the common hormone-driven mechanism of lipolysis of adipocytes, we found that CAAs perform a unique lipolysis program, and Zeb1 plays an important role in this lipolysis process.

Methods: Fabp4-cre;Zeb1$^{-/-}$ as adipose tissue-specific Zeb1 gene knockout homozygous mice and Fabp4-cre;Zeb1 tg as adipose tissue-specific Zeb1 gene overexpression mice were constructed to study mammary gland development and perform orthotopic tumor transplantation experiments. Tetracycline-induced Zeb1-overexpressing stable cells were constructed from mouse preadipocytes 3T3-L1 to study phenotypes of lipolysis. Single-cell sequencing, targeted lipidomics, and RNA sequencing analysis were used to investigate the interaction between cancer cells and adipocytes. Western blotting and immunohistochemical staining assays were used to detect the expression Zeb1 at the cellular level, in mouse models and in patient tissue samples.

Results: Our results indicated that breast cancer cell-derived adrenomedullin (ADM) significantly down-regulates Zeb1 expression in adipocytes, which drives downstream gene expression of Pnpla2/HSL/SCD1 and induces adipocyte lipolysis into CAA, a process that results in the release of excess palmitoleic acid. Consequently, we proved that palmitoleic acid could replace arachidonic acid (ARA) in the phospholipid sn-2 position of breast cell membrane, which enhances the fluidity and invasiveness of cancer cells. In addition, overexpression of Zeb1 in adipocytes reduces the ability of cancer cells to induce adipolysis and inhibits the malignant progression of cancer cells.

Conclusion: These results indicate that Zeb1 plays a pivotal role as core transcriptional factor in CAA lipolysis. The interaction between breast cancer cells and adipocytes leads to the reprogramming of metabolism within their tumor microenvironment, which may become a new target for breast cancer treatment.

#4435 Taurine metabolism as a marker for pancreatic cancer.

H. Nam[1], W. Lee[2], H. T. Nguyen[1], L. X. Mai[1], S. Kim[2], S. Park[1];

[1]Seoul National University, Seoul, Korea, Republic of, [2]University of Ulsan College of Medicine, Asan Medical Center, Seoul, Korea, Republic of

Pancreatic ductal adenocarcinoma (PDAC), known for its aggressive nature and poor prognosis, presents a significantly altered metabolic landscape compared to normal pancreatic tissue, a feature that has been the focus of recent research but remains underexplored in actual pancreatic tissues. In this study, we undertook an untargeted metabolomics analysis to compare the metabolic profiles of PDAC with matched normal tissues, revealing a notable elevation in taurine levels in PDAC. This increase was further validated through immunohistochemistry in separate PDAC and normal tissue samples. To delve deeper, we conducted a comprehensive bioinformatics analysis, integrating transcriptomic and proteomic data, which identified the taurine metabolism pathway as significantly altered, with *ADO* emerging as a pivotal gene in this process. Further investigations, including gene modulation and xenograft models, demonstrated that *ADO* knockdown curtails cancer cell proliferation and tumor growth, potentially impacting the Raf-MEK-ERK signaling pathway. Clinically, the ADO-Taurine axis was found to have substantial prognostic significance, correlating with recurrence rates and survival in PDAC patients. These insights collectively suggest that the ADO-Taurine axis, through its modulation of taurine metabolism, presents as a promising biomarker for PDAC prognosis and a potential avenue for therapeutic development.

#4436 Phenotypic heterogeneity in pancreatic ductal adenocarcinoma revealed by single-cell lipidomics.

M. Trajkovic-Arsic[1], J. Delafiori[2], M. Shahraz[2], C. Munch[3], S. Lueong[3], S. Liffers[3], D. Hellerschmied[4], T. Alexandrov[2], **J. T. Siveke**[1];

[1]German Cancer Consortium (DKTK), partner site Essen/Dusseldorf, a partnership between DKFZ and University Hospital Essen, Essen, Germany, Essen, Germany, [2]European Molecular Biology Laboratory - EMBL, Metabolomics Core Facility, Heidelberg, Germany, Heidelberg, Germany, [3]University Hospital Essen, Bridge Institute of Experimental Tumor Therapy- West German Cancer Center, University of Duisburg-Essen, Essen, Germany, Essen, Germany, [4]Faculty of Biology, Center of Medical Biotechnology, University Duisburg-Essen, Essen, Germany, Essen, Germany

Introduction: The high chemoresistance of pancreatic ductal adenocarcinoma (PDAC) is partly attributed to the phenotypic plasticity and high adaptability of PDAC cells to the challenges of the harsh microenviroment. Phenotypic presentation of the PDAC cell is also determined by the lipid composition of the plasma membrane and lipid species that organize the rigid or more flexible lipid bilayer and determine the cellular mobility and plasticity. Lipids are also important energy and signaling molecules that contribute to the aggressiveness of the cell. Here we focus on differences in lipid profile of PDAC cells in epithelial and mesenchymal cell state using single-cell lipidomics approach (SpaceM).

Methods: Lipid profile of 2D cultures of eight conventional and ten primary patient derived cell lines of different source (patient derived xenograft, ascites, primary tumor, organoid derived) was investigated. Epithelial (E) or mesenchymal (M) cell state was evaluated by gene and protein expression of EMT markers. Matrix-Assisted Laser Desorption/Ionization (MALDI)-imaging MS was used for data acquisition on positive ion mode at 25 µm step size and m/z range of 600-1000. For annotating lipids in MALDI-imaging data, we used the METASPACE cloud software. For constructing single-cell lipidomic profiles we used the SpaceM method. In total, around 150.000 cells were analyzed and 1400 lipid ions detected.

Results: Gene expression analysis suggested prominent metabolism of structural lipids in the conventional epithelial cells. In UMAP analysis of single cell lipidomics data, each cell line, conventional and primary, presented a unique lipid fingerprint with however prominent clustering into the two phenotypes, epithelial and mesenchymal. We detected enrichment of alkyl-acyl phosphatidylcholines, alkyl-acyl phospatidylethanolamines, ceramides and sphingolipids in the epithelial phenotype. Mesenchymal phenotype was enriched for lipids involved in lateral diffusion and low bilayer thickness supporting the increased fluidity of the mesenchymal cell membrane. Furthermore, mesenchymal phenotype was enriched for lipid droplets and energy storing triacylglycerols, also confirmed by histological lipid droplet staining.

Conclusions: Using the single cell lipid information, a successful grouping to epithelial or mesenchymal subtype could be performed regardless of sample source, suggesting a conserved lipid profile typical for the two states. Further detailed investigation of single cell lipidomics data aims to unveil the prominent epithelial-mesenchymal state lipid markers and open a niche for functional investigations of cell-state specific markers and potential cell-state targeting.

#4437 Dysregulated lipid metabolism and high-fat diet influences prostate cancer (PCa) progression.

Saurav Subedi[1], Federico La Manna[1], Katja Ovchinnikova[1], **Wanli Cheng**[1], Eugenio Zoni[1], Nicola Zamboni[2], Bahtiyar Yilmaz[3], George N. Thalmann[4], Marianna Kruithof-de Julio[1]

[1]Department for BioMedical Research, Urology Research Laboratory, University of Bern, Bern, Switzerland,[2]Institute of Molecular Systems Biology, ETH Zurich, Zurich, Switzerland,[3]Department of BioMedical Research, Systems biomedicine of cellular development, University of Bern, Bern, Switzerland,[4]Department of Urology, Inselspital, Bern, Switzerland

Dysregulation of lipid metabolism is observed during the development and progression of various types of cancer including prostate cancer (PCa). Systemic metabolic changes driven by genetic alterations in conjunction with obesity and a high-fat diet have been demonstrated to induce PCa progression. In this study, we aimed to investigate the impact of high- and low-fat diets on the progression and morbidity of prostate cancer, utilizing inducible genetically engineered mouse models (GEMMs) that mimic different grades of prostate cancer. The mice were initially placed on a standard diet until week 6, after which they were randomly assigned to either a low-fat or high-fat diet. At week 8, the Cre recombinase enzyme was activated to induce the desired phenotype in the GEMMs, effectively mimicking the initiation and progression of prostate cancer. The experimental design allowed us to gain insights into the interplay between dysregulated lipid metabolism, diet, and the pathogenesis of prostate cancer. Two groups of mice were taken for the study, with one group being fed a low-fat diet and the other group being fed a high-fat diet. The mice were maintained on their respective diets for a period of 1, 3, and 5 months. At each endpoint, tissue samples were collected. Samples were taken from the prostate, plasma, and liver tissues. These samples were then subjected to various analyses to investigate the changes occurring at the molecular and cellular level. Blood was collected to determine lipidomic content in response to high and low-fat diet and the relation of tumour progression. Finally, faecal samples were collected throughout the duration of the experiment to perform metagenomic studies. The consumption of a high-fat diet significantly increased the body weight of the mice which corresponded to increased liver weight. Furthermore, we identified that the consumption of a high-fat diet significantly correlated with an increase in prostate weight at 3 and 5 months after initiation. Preliminary metabolomic analysis of the plasma revealed a distinct clustering of samples based on the consumed diet. Metagenomic analyses conducted at 1 and 3 months indicated a visible shift in the composition and diversity of gut microbiota in mice fed either a high- or low-fat diet. In conclusion, our study will shed light on the influence of dietary factors on prostate cancer development, providing valuable information for the development of targeted therapeutic strategies to combat this disease.

#4438 Time restricted eating improves antitumor immune responses via modulation of insulin-like growth factor 1 in patients with head and neck cancer.

M. Eysha[1], C. A. Galindo[1], J. Muzaffar[2], J. Mine[1], R. Chauriogonzalez[1], M. Baig[3], L. Lopez-bailon[1], M. Alhomsi[1], M. Hathout[3], J. Wang[1], W. Zhang[1], D. Rizvi[1], A. Huang[1], K. Lee[1], D. Kye[1], A. Sen[1], J. Conejo-Garcia[1], S. Bari[2];

[1]Duke University School of Medicine, Durham, NC, [2]Duke Cancer Institute, Durham, NC, [3]Duke University shcool of medicine, Durham, NC

Background- Treatment of metastatic head and neck cancer remains an area of unmet need with median survival less than a year. We tested the efficacy of a novel circadian aligned fasting intervention called “time restricted eating” (TRE), to improve ICB response in tumor bearing head and neck syngeneic mice models (MOC1), and showed significant reduction in tumor growth, which we then recapitulated in a pilot, open labeled, interventional clinical trial in 30 metastatic head and neck cancer patients. We noted significant improvement in median progression free survival (5 months vs not reached (NR), HR-0.2, p-0.0008) and overall survival (8 months vs NR, HR-0.00000045) in patients observing TRE vs those who did not. The favorable effect of TRE was mediated via modulation of gut microbiome, microbial tryptophan metabolome, and insulin signalling, specifically reduction in circulating insulin-like growth factor 1 (IGF1). We hypothesized that IGF1 mediates ICB resistance via protecting tumor cells from cytotoxic T cell activity.

Methods- We performed in vitro luciferase cytotoxicity assays using HLA-A2^{+}NY-ESO^{+} squamous cell cancer 4 (SCC-4) human cancer cells as targets, and HLA-A2-restricted NY-ESO-1-specific T cell receptor (TCR) -transduced T cells. We co-cultured the tumor cells and the T cells for 24 hours under different conditions of IGF-1 concentration (100 ng, 50 ng, and 10 ng) and T cell-to-tumor cell ratio (1:5, 1:10, and 1:20). We also treated the tumor cells with IGF-1 alone to assess its direct cytotoxic effect.

Results We observed that IGF-1 impaired the ability of the T cells to kill the tumor cells in a dose-dependent manner, while IGF-1 had no cytotoxic effect on the tumor cells in the absence of T cells.

Conclusion- While the role of IGF1 in treatment resistance has been described, its role and mechanism in antitumor immune response is largely unknown. We, for the first time demonstrate the role of IGF1 in impairing T cell mediated antitumor activity in a dose dependent fashion, thus contributing to ICB resistance. Further work will help us develop alternative strategies to modulate IGF1 and improve ICB resistance, in patients who are unable to tolerate TRE.

#4439 Decoding the metabolic symphony TP53 mutation-driven rewiring of cellular metabolism in non-small cell lung carcinoma.

J. Khan, Sr., A. Rehman, Sr., A. Mathur, Sr., Naveen Kumar Bhatrajuc, Anannya Tulid, Divya Rajput, Mohammad Askandar Iqbal, D. Saluja, Sr.;
University Of Delhi (North Campus), New Delhi, India

TP53 is a critical regulator of major metabolic pathways. Metabolic reprogramming is one of the "hallmarks of cancer" and drives tumorigenesis. Frequent p53mutations not only eradicate tumour suppressor capacities but also confer various activities that impact the alteration of metabolic pathways now regarded as central for tumour development and progression. We selected three hotspot mutants (R175H, R273H and R249S) and wtp53 to evaluate the effects in the human non-small cell lung carcinoma cell line (NCI-H1299). Differential expressions of p53 mutants were observed in normal and glucose/glutamine starvation. However, WTp53 expression was not found to be affected. Under both the glucose and glutamine starvation, inhibition of the cell growth and migratory potential of mutant cells was observed which was more prominent in glutamine starvation. Basal respiration and ATP production in $p53^{-/-}$ R273H and R249S significantly increased under glucose starvation. However, Non-mitochondrial oxygen consumption and maximal respiration were found to be decreased in all the cell lines. Importantly, the cells harbouring mutation R175H increase the glycolysis and TCA cycle. The metabolic intermediates of the urea cycle were found to be increased by nearly fourfold in R273H cells. Indicating increased utilization of the urea cycle instead of the TCA cycle, which has been known to be fueled by glutamine for anaplerosis. This study demonstrates that mutp53 influences several metabolic processes and has an influence on cancer cell aggression under starvation of main carbon sources (Glucose and Glutamine). In starved conditions, cells with p53 mutations enhance mitochondrial activity and use alternative pathways in non-small cell lung cancer cells. This might provide a foundation for the development of more effective targeted therapeutics/pharmacological approaches toward variants of mutant p53.

#4440 Topographical investigation of metabolites in excised squares (TIMES^2): Comprehensive cross-sectional metabolite quantification of pancreatic cancer *in vivo*.

P. Yu[1], R. Banh[1], A. Sohn[1], S. Martis[2], D. Biancur[1], K. Yamamoto[1], E. Lin[1], A. Kimmelman[1];

[1]NYU Grossman School of Medicine, New York, NY, [2]Memorial Sloan Kettering Cancer Center, New York, NY

Purpose: Pancreatic cancer is a lethal malignancy characterized by complex intratumoral metabolic reprogramming and intercellular nutrient sharing between cells in the tumor microenvironment (TME) that promote pancreatic cancer progression. However, this crosstalk, as well as regional variation in perfusion and oxygenation, can lead to metabolic heterogeneity that has not been appreciated by metabolomics of whole tumors. Here we quantify amino acids and tricarboxylic acid cycle (TCA) intermediates using a novel methodology that allows us to portray global tumor metabolite heterogeneity in a tumor.

Methods: Human PaTu-8902 or murine HY19636 (from female KPC mice LSL-KrasG12D; p53 L/+, Ptf1a-Cre+) pancreatic cancer cell lines were orthotopically injected into pancreata of NCr nude mice (n=3) or C57BL/6 mice (n=2). Mice were euthanized after 3-5 weeks and tumors were harvested. Tumor slices were further sectioned into 1mm x 1mm x 1mm cubes using a custom-made multisectional slicing device and each cube location was recorded. Each cube was extracted using methanol, water, and chloroform with labelled amino acid standards, derivitized, and resolved using gas chromatography-mass spectrometry (DB-35MS column with Agilent 7890B gas chromatograph coupled to a single quadrupole 5977B mass spectrometer). 22 metabolites (15 amino acids, 5 TCA intermediates, lactate, and pyruvate) were identified by unique fragments and retention time compared to known standards. Peaks were picked using OpenChrom and analyzed using MATLAB. Data was analyzed using Graphpad Prism. Principal Component Analysis (PCA) was visualized using Python on a Jupyter notebook.

Results: Both orthotopic human and murine pancreatic tumors demonstrated striking levels of intratumoral metabolite heterogeneity. Glycine, glutamine, and proline were the amino acids with the highest coefficient of variance, while leucine, isoleucine, and serine had the lowest coefficient of variance. α-ketoglutarate and succinate were the TCA intermediates with highest coefficient of variance. Lactate had the lowest coefficient of variance among all examined metabolites. Spatial mapping of each metabolite demonstrated distinct regions with varying abundance levels of metabolites. PCA demonstrated 75% of variance was carried by PC1 and 10% carried by PC2.

Conclusions: This study reveals insights into the degree of intratumoral heterogeneity present in pancreatic tumors that illustrate the difficulty of *in vivo* metabolomics analysis and suggest that high-resolution (single cell) metabolomics techniques will be critical to study metabolism in the complex TME.

#4441 The epigenetic factor BMI1 regulates metabolism and tumorigenesis in human pancreatic cancer cells.

J. N. Mills[1], D. Awad[1], H. K. Schofield[1], J. K. Thompson[1], H. Watkoske[1], D. Sutton[1], N. Nedzesky[1], D. Drouillard[2], Z. Nwosu[3], C. Espinoza[1], Y. Zhang[1], A. Del Vecchio[4], C. J. Halbrook[5], M. Pasca di Magliano[1], C. A. Lyssiotis[1], F. Bednar[1];

[1]University of Michigan, Ann Arbor, MI, [2]Medical College of Wisconsin, Milwaukee, WI, [3]Cornell University, Ithaca, NY, [4]Memorial Sloan Kettering, New York, NY, [5]University of California, Irvine, Irvine, CA

Dysregulation of epigenetic factors is a key component of tumorigenesis. BMI1, a member of the polycomb repressor complex 1 (PRC1), is an oncogenic factor studied in many types of cancer, including pancreatic ductal adenocarcinoma (PDAC). PDAC is the third most common cause of cancer-related death in the United States and investigation of the biology involved in transformation is critical for improving outcomes in this devastating disease. In PDAC, BMI1 is required for initiation of pancreatic cancer in mice and enhances *in vitro* growth of human and murine tumor cell lines. CRISPR-mediated knock out of BMI1 results in reduced subcutaneous and orthotopic tumor growth in mice and decreased expression of genes related to metabolism, specifically glycolysis, and cell proliferation. BMI1 has also been implicated in regulation of metabolism in other epithelial tumor types, including ovarian cancer. Given these preliminary findings, we hypothesized that loss of BMI1 in multiple human PDAC cell lines would result in altered metabolic activity, reducing the growth and tumorigenic properties of these cells. We demonstrated that BMI1 expression is higher in PDAC cell lines compared to normal pancreatic epithelial cells and normal human donor pancreatic tissue. Following CRISPR-mediated BMI1 knock out in human PDAC cell lines, we investigated the alterations to metabolism using metabolic flux analysis. Loss of BMI1 resulted in lower basal and compensatory rates of glycolysis and increased oxygen consumption rates compared to wild-type cells. Metabolomic analysis demonstrated reduction in all the enzymes involved in the glycolysis pathway with loss of BMI1. Cell growth was reduced by loss of BMI1 *in vitro*, and orthotopic injection into mice of human cells with BMI1 knock out resulted in decreased tumor size compared to wild-type, recapitulating these findings *in vivo*. Together, these data identify a role of BMI1 in promotion of tumor growth through regulation of metabolism in pancreatic cancer. Experiments are ongoing to determine the underlying mechanism of this regulation and implications on therapeutic targeting with BMI1/PRC1 complex inhibitors in conjunction with traditional chemotherapy.

#4442 Associations between pre-diagnostic plasma metabolites and biliary tract cancer risk in the prospective UK Biobank cohort.

V. Gunchick, G. Gia, W. Zheng;
Vanderbilt University Medical Center, Nashville, TN

Background Annually, approximately 200,000 people are diagnosed with biliary tract cancer (BTC). Most present with metastatic disease which encompasses a 5-year survival rate of <5%. Etiology is poorly understood though some studies suggest metabolic dysregulation may contribute to development. Previous evaluations of metabolites and BTC risk have primarily been limited to case-control studies, few metabolites, or post-diagnostic blood samples.
Methods We evaluated 248,285 adult participants with metabolite data in the UK Biobank, a prospective cohort study. Participants were excluded (6.2%) primarily due to a baseline history of cancer. To reduce potential influences of reverse causation, those who developed cancer or died within one year after baseline blood collection were also removed. Metabolites were trimmed to two standard deviations, log-transformed (ln[x+0.5]), z-scored, and evenly divided into tertiles. Cox proportional hazards regression was implemented to evaluate associations of BTC risk per 1-standard deviation (SD) and across tertiles with hazard ratios (HR) and 95% confidence intervals (95% CI). Models were adjusted for age, sex, education, income, fasting time, and statin use. A p-value of 0.001 was considered statistically significant after multiple comparison adjustment (0.05 divided by 50, the number of independent tests).
Results The analyzed cohort includes 232,781 UKB participants with a median age of 58, a median follow-up time of 11.8 years, and 268 first primary incident BTC cases. Multiple metabolites were significantly associated with BTC risk using continuous variables (per 1-SD increment). High triglyceride to total lipid ratios were associated with higher BTC risk, and the strongest association was for intermediate-density lipoproteins (the HR (95% CI) was 1.33 (1.15-1.54), p=0.0001). On the other hand, high cholesterol to total lipid ratios were associated with lower BTC risk, and the strongest association was for the free cholesterol to total lipids in small very-low-density lipoproteins (VLDL) (0.76 (0.66-0.88), p =0.0002). High glutamine was associated with lower BTC risk (0.68 (0.69-0.89), p =0.0003) as was the phospholipid to total lipid ratio in small VLDL (0.75 (0.65-0.87), p =0.0002). Analysis by tertile identified additional significant associations, including a higher polyunsaturated fatty acid to total fatty acid ratio being associated with lower BTC risk (the HR (95% CI) comparing the highest to lowest tertile, 0.50 (0.35-0.71), p-trend=0.0001). Notably, within polyunsaturated fatty acids, a higher omega-6 to omega-3 ratio trended toward higher risk (1.32 (0.94-1.85), p-trend=0.11).
Conclusion These findings indicate circulating metabolites may be biomarkers for BTC and suggest that triglycerides, cholesterols, fatty acids, phospholipids, and glutamine may be involved in BTC etiology.

#4443 Trans-population two-sample Mendelian randomization study of circulating metabolites and prostate cancer risk.

H. Fuller[1], R. Rohde[2], H. Highland[2], J. Shen[3], B. Yu[4], E. Boerwinkle[4], M. Grove[4], K. E. North[2], D. V. Conti[3], C. A. Haiman[3], K. Young[2], B. F. Darst[1]; [1]Fred Hutchinson Cancer Center, Seattle, WA, [2]University of North Carolina at Chapel Hill, Chapel Hill, NC, [3]University of Southern California, Los Angeles, CA, [4]The University of Texas Health Science Center, Houston, TX

While prostate cancer (PCa) is highly heritable, mechanisms underlying disease risk and PCa disparities are not well understood. Here, we conducted a two-sample Mendelian randomization (MR) to assess whether serum metabolites are causally associated with PCa risk in European, African, and Hispanic populations.

MR analyses were performed on metabolite quantitative trait loci (mQTLs) for 250 metabolites quantified by untargeted mass spectroscopy via the Metabolon platform for 1,498 European and 1,740 African ancestry individuals from the Atherosclerosis Risk in Communities (ARIC) cohort and for 711 metabolites measured in 3,166 Hispanic individuals from the Hispanic Community Health Study/Study of Latinos (SOL). PCa GWAS summary statistics were obtained for men from European (122,188 cases, 604,640 controls), African (19,391 cases, 61,608 controls) and Hispanic (3,931 cases, 26,405 controls) populations from the PRACTICAL Consortium. Within each population, QTLs associated with metabolites at the genome-wide significance level ($P<5x10^{-8}$) were included in instruments upon removing rare (minor allele frequency≤0.01) or correlated (R^2≥0.2) SNPs calculated in ancestry-matched TOPMed populations. Inverse variance weighted (IVW) random effect models are presented as primary results. Sensitivity analyses were utilized to assess assumption violations (weighted mode, weighted median and MR egger). MR were conducted separately in each population, and fixed effect meta-analyses were conducted across population-specific MR results to identify trans-population associations. A false discovery rate was implemented to account for multiple testing.

In total, 22, 4 and 1 metabolites significantly associated with PCa risk in Hispanic, European and African populations, respectively. Of these, 13 metabolites had a MR instrument in ≥1 population, 12 of which were significant following a trans-population meta-analysis, including 5 fatty acids, 3 lysophospholipids, 1 amino acid, 1 carbohydrate, 1 nucleotide and 1 xenobiotic. All fatty acids were associated with decreased PCa odds (2%-10%), as were 4 other metabolites (amino acid 3-methyoxytyrosine, nucleotide 5-methyluridine and lysophospholipids 1-archidonoyl-GPC (20:4n6) and 1-archidonoyl-GPE (20:4n6), 4%-9%). The 3 remaining metabolites, erythritol, 1-linoleoyl-GPE (18:2) and mannose, were found to increase PCa odds by 10%, 6% and 4%, respectively. Additional metabolite harmonization efforts are underway to conduct trans-population analyses metabolome-wide.

This study provides evidence of associations between metabolites, such as fatty acids and lysophysopholipids, and PCa across diverse populations. These findings point to mechanisms that could inform preventive or therapeutic strategies pending functional investigations. Multivariable and bidirectional MR are ongoing to further assess findings.

MOLECULAR/CELLULAR BIOLOGY AND GENETICS: Signaling Pathways That Regulate Metabolism 2
Poster Session

#4447 ZC3H18: A novel regulator of NAD^+ metabolism in high-grade serous ovarian cancer.
B. Wilson, N. Wilson, X. Chen, S. Zhang, C. Wang, L. M. Karnitz, S. H. Kaufmann, **A. Kanakkanthara**;
Mayo Clinic, Rochester, MN

ZC3H18 is a multifunctional regulator of gene expression that is lost in a subset of high-grade serous ovarian cancers (HGSOC). Our prior studies have established that the loss of ZC3H18 diminishes BRCA1 levels, leading to the disruption of homologous recombination DNA repair (HR) and heightened sensitivity of HGSOC cells to PARP inhibitors. Here we show an additional facet to ZC3H18's impact, showing that its loss also induces a reprogramming of energy metabolism in HGSOC. Our findings demonstrate that the depletion of ZC3H18 results in reduced mRNA and protein levels of the NAD^+-biosynthetic enzyme, NMNAT1, in HGSOC cells. Mechanistic studies uncovered that ZC3H18 occupies the *NMNAT1* promoter, facilitating *NMNAT1* transcription by recruiting CDK12 onto the promoter. Consistent with this mechanism, loss of ZC3H18 led to a reduction in CDK12 levels on the *NMNAT1* promoter, diminishing NMNAT1 abundance and subsequently causing a decline in cellular NAD levels. These observations unveil a previously unknown role for ZC3H18 in HGSOC, shedding light on its involvement in the regulation of energy metabolism. Importantly, our findings provide valuable insights into potential therapeutic pathways that leverage the metabolic changes linked to ZC3H18 deficiency.

#4448 Effects of adagrasib on cholesterol, lipid and glucose gene expression regulation in tumor xenograft models and patient samples.

F. Shelton[1], N. Hoffman[1], D. Trinh[1], X. M. Helu[1], A. Calinisan[1], A. Hebbert[1], L. Yan[1], D. M. Briere[1], L. Hover[2], J. Fernandez-Benet[2], K. Anderes[1], J. G. Christensen[1], **J. Hallin**[1], P. Olson[1];

[1]Mirati Therapeutics, San Diego, CA, [2]Monoceros Biosystems LLC, San Diego, CA

Introduction: Clinically active $KRAS^{G12C}$ inhibitors have represented a key research breakthrough and led to novel treatment options for lung, colorectal and other cancer patients harboring this mutation. While treatment with $KRAS^{G12C}$ inhibitors are clinically active in the majority of patients, the depth and duration of response is variable and most patients ultimately progress. This variation in therapeutic response highlights the need for a better understanding of drug mechanism of action and the identification of rational combination strategies. Oncogenic *KRAS* mutations hyperactivate the MAPK pathway, create an immunosuppressive tumor microenvironment, and promote glycolysis even in the presence of oxygen commonly known as the Warburg effect. This altered metabolic state is marked by increased glucose uptake and lactate production, providing necessary substrates for rapid tumor growth.

Results: Pharmacological inhibition of $KRAS^{G12C}$ with a potent and selective $KRAS^{G12C}$ inhibitor, adagrasib, revealed marked alterations of metabolic gene expression programs in tumor samples collected from mouse xenograft studies and repeat biopsies provided by patients enrolled on adagrasib clinical trials. Upregulation of genes involved in reverse cholesterol transport including ApoE, NR1H3 (LXRa) and ABCA1 was observed across both preclinical tumor xenografts and patient samples following adagrasib treatment. Additionally, decreased expression of Glut1 and low-density lipoprotein receptor (LDLR) genes were also observed in both tumor models and patients suggesting that adagrasib treatment results in an extensive shift in uptake and utilization of cholesterol, lipid, and glucose. The impact of adagrasib treatment on circulating metabolic parameters in tumor xenograft-bearing mice were investigated in follow up studies.

Conclusions: Taken together, these data suggest adagrasib modulates cholesterol efflux, glucose and lipid pathways and alters tumor and systemic metabolic regulation. Additional research may yield a targetable collateral vulnerability and rational combinatorial strategy.

#4449 Hepatic steatosis induced by bioactive lipids.

M. Alba[1], I. Slarve[1], B. Ebright[1], Y. Zhou[1], W. Cohn[2], Y. Jia[1], E. Elton[3], J. Khan[1], A. Datta[1], L. He[1], Q. Tang[1], P. Pammidimukkala[1], T. Tu[1], P. Nguyen[1], J. Katz[3], J. Whitelegge[2], S. Louie[1], B. Stiles[1];

[1]USC - University of Southern California, Los Angeles, CA, [2]UCLA, Los Angeles, CA, [3]Ellison Institute of Technology, Los Angeles, CA

Introduction: HCC is the most common form of liver cancer and is the sixth most common cancer globally. Despite the clinical advancement of immune checkpoint inhibitors, median survival continues to be less than twenty months and most patients develop resistance making it one of the deadliest malignancies. The rate of liver cancer continues to rise, which is coupled to the high prevalence of steatosis and steatohepatitis that accounts for about 25% in the general population. Pathologically, 80% of liver cancer occurs in patients with an underlying liver disease that displays liver steatosis. Thus, it is paramount to better characterize the transition from steatosis to HCC.

Methods: Utilizing a *Pten* deleted mouse model (*Pten*$^{loxP/loxP;\ Alb\text{-}Cre^{\pm}}$) that recapitulates HCC progression, protein and lipid fractions were isolated to explore differentially expressed proteins and their correlations with bioactive lipid metabolism. Global untargeted differential proteomics was done with fractionation using a qExactive. Lipid fractions were analyzed using a Sciex 6500 for targeted lipidomic analysis. In addition, genetic knockout hepatocyte cell lines of each AKT isoform were used to explore the involvement of the PI3K/AKT signal. Further, a phosphoproteomic enrichment was performed to discover downstream signaling targets.

Results: The PTEN regulated PI3K/AKT signal is induced in 54% of all liver cancers and represents the dominant signaling pathway regulating liver cancer progression. Untargeted differential proteomic analysis of *Pten* deleted mice livers revealed significant dysregulation in oxidative stress and eicosanoid metabolism among the top enriched disease and biological functions when the phenotype progressed from steatosis to HCC. Analysis of publicly available liver cancer patient samples from the NCI Proteomic Data Commons further shows strong correlation between PTEN protein abundance and the expression of enzymes involved in eicosanoid metabolism. Our analysis using a bio-active lipid multi reaction monitoring panel of *Pten* deleted mouse livers further validates significant decreases in resolving eicosanoid levels along with increases in proinflammatory eicosanoid precursors as steatosis progress to HCC. These data suggest a potential hepatic AKT-dependency in regulating the shift towards proinflammatory eicosanoids. Primary isolated hepatocytes from mouse livers lacking either AKT1 or AKT2 were analyzed to elucidate AKT's regulatory role in hepatic eicosanoid metabolism. Proteomic and lipidomic analysis of these hepatocytes supported a unique AKT isoform specific role in the regulation of eicosanoids via potential isoform specific signaling interactions with MAPK.

Conclusion: Eicosanoid metabolism dysregulation plays a key role in the progression from steatosis to HCC and appears to be regulated in an AKT isoform specific manner via interactions with MAPK signaling.

#4450 MYC upregulates MCT4 expression and promotes metabolic reprogramming and enhanced lactate utilization in LKB1-deficient NSCLC.

Y. Qian[1], D. Molkentine[1], Y. Kong[1], Q. Huang[1], C. Yang[2], A. Poteete[1], A. P. Guimaraes[1], P. Jiang[1], F. Skoulidis[1], A. Reuben[1], J. D. Minna[2], R. J. DeBerardinis[2], J. V. Heymach[1];

[1]UT MD Anderson Cancer Center, Houston, TX, [2]UT Southwestern Medical Center, Dallas, TX

STK11, which encodes the serine/threonine kinase LKB1, is the second most commonly altered tumor suppressor in non-small cell lung cancer (NSCLC). LKB1 loss is frequently co-mutated with *KRAS* and associated with primary resistance to immunotherapy, which is partially due to MCT4-dependent lactate secretion. However, the mechanisms driving MCT4 elevation and metabolic reprogramming remains unclear. We hypothesized that increased MYC expression, which is associated with LKB1 loss, plays a pivotal role in metabolic alterations, promoting lactate incorporation and maintaining redox homeostasis. To explore the impact of lactate on tumor cells with LKB1 loss, we performed metabolic profiling on KRAS mutant (K) murine lung cancer cells with or without LKB1 knockout (KL) treated with either glucose or lactate as the carbon source. PLS analysis indicated that there was no notable difference between K and KL cells after glucose treatment. However, we observed significant changes in metabolites between K and KL cells when treated with lactate. Differentially altered metabolites included TCA-related components such as acetyl-CoA and glutamate, indicating enhanced lactate utilization in KL tumor cells. We also noticed that KL cells showed increased oxidative phosphorylation (OXPHOS) with the addition of lactate, with increased GSH/GSSH and NADPH/NADP+ ratios, suggesting that, as compared to LKB1-intact cells, LKB1-deficient cells had an enhanced ability to utilize OXPHOS and maintain redox homeostasis with lower levels of ROS generation when utilizing lactate as an energy source. However, in KL cells, MYC knockout (KO) or MCT4 KO partially abolished the lactate-induced OXPHOS and increased ROS. Moreover, [U-13C]lactate tracing revealed that isotopologues were significantly enriched in TCA components in KL cells, and this was reversed by either MYC KO or MCT4 KO, suggesting that MYC and MCT4 were critical for lactate reutilization in KL tumor cells. We observed that MYC could directly bind to the promoter region and transcriptionally activate MCT4 expression, and restoring MCT4 in MYC KO cells enhanced lactate incorporation and decreased ROS levels. Finally, we injected KL murine tumor cells with or without MYC/MCT4 KO into mice and infused [U-13C]lactate to detect the isotopologues distribution in vivo. KL tumors showed significantly enhanced lactate incorporation as compared to K tumors, while MYC KO or MCT4 KO reversed these phenotypes. Collectively, our data indicates that in LKB1-deficient tumors, upregulation of MYC promotes MCT4 expression and increases lactate incorporation and utilization, and that can be inhibited by targeting MYC or MCT4. These findings provide insight into the mechanisms driving the metabolic reprogramming and aggressive phenotype of KRAS-mutant LKB1-deficient tumors and identify a novel therapeutic strategy for this recalcitrant subgroup.

#4451 Regulation of lipid metabolism and ferroptosis by DAXX.

W. Yang, N. Awasthee, Q. Chen, S. Hale, **D. Liao**;
University of Florida College of Medicine, Gainesville, FL

Intracellular lipid production in cancer cells supplies lipids to synthesize cell membranes and signaling molecules during rapid cell proliferation and tumor growth. Cancer cells also utilize fatty acid oxidation (FAO) to generate ATP to meet their energy demand. Notably, lipid metabolites can inhibit and trigger ferroptosis due to iron-dependent oxidation of polyunsaturated fatty acids (PUFAs). Therefore, identifying regulators that maintain the intricate balance of lipid biosynthesis required for cell proliferation and survival is critical in cancer biology and therapy. Lipid metabolism is regulated by two oncogenic signaling pathways: the RAS-RAF-MEK-MAPK and the mammalian target of rapamycin (mTOR) pathways. About 30% of all cancers harbor constitutively active mutations in KRAS, HRAS, or NRAS, resulting in hyperactive RAS-RAF-MEK-MAPK signaling to drive tumorigenesis, metastatic progression, immune evasion, and resistance to therapy. KRAS regulates lipid uptake, lipid synthesis, and FAO. mTOR is a serine/threonine kinase acting as a key intracellular signaling hub to regulate nutrient homeostasis, metabolism, protein synthesis, and autophagy. The mTORC1 complex promotes lipogenesis. The RAS and mTOR signaling pathways exhibit both positive and negative cross-regulation. The coordinated activity of both pathways is critical to sustained tumor growth. Notably, mTORC1 signaling inhibition enhances RAS-RAF-MEK-MAPK signaling to promote cancer cell survival and proliferation. Furthermore, constitutive mTORC1 signaling induces cell death when the supply of unsaturated FAs is limited. However, the molecular link for coordinating the activity of the RAS and mTOR signaling pathways remains poorly defined. Death domain-associated protein (DAXX) is essential for mouse embryonic development and has ill-defined pro-cell survival functions. Our lab has a long-standing interest in deciphering DAXX's complex biological functions. Our recent study shows that DAXX drives tumorigenesis by promoting lipogenic gene expression and lipid synthesis through interacting with sterol regulatory element-binding proteins SREBP1 and SREBP2 (SREBP1/2) (Mahmud et al., 2023, PMID 37045819). Unexpectedly, our new data reveal that DAXX inhibits ferroptosis. Significantly, phosphorylation via RAS signaling appears to regulate DAXX's activity in lipid synthesis and resistance to ferroptosis. Remarkably, disruption of DAXX-mediated lipid synthesis potentiates ferroptosis due to mTORC1 activity. Based on these observations, we propose that stimulated by the RAS-RAF-MEK-MAPK oncogenic signaling, DAXX promotes tumorigenesis through upregulating genes for lipid synthesis and resistance to ferroptosis, and that the lack of DAXX-mediated lipid synthesis leads to sensitization of cells to ferroptosis due to mTORC1's proliferative effects. (Supported by FDOH grant 23K03).

#4452 The macropinosome: Uncovering the molecular anatomy of an oncogene-driven organelle.

A. Manceau, K. M. O. Galenkamp, C. M. Galapate, C. Commisso;
Sanford Burnham Prebys Medical Discovery Institute, San Diego, CA

As an integral aspect of the metabolic reprogramming that occurs in cancer, oncogenic KRAS mutations drive the stimulation of macropinocytosis, a type of endocytosis that mediates nonselective fluid-phase uptake. Using KRAS-driven models of pancreatic ductal adenocarcinoma (PDAC), we were the first to demonstrate that macropinocytosis functions in tumor cells as a nutrient acquisition pathway. Macropinocytosis triggers the internalization of extracellular proteins via discrete endocytic vesicles called macropinosomes. The incoming protein cargo is targeted for lysosome-dependent degradation, causing the intracellular release of amino acids. These protein-derived amino acids support metabolic fitness by contributing to the intracellular amino acid pools, as well as to the biosynthesis of central carbon metabolites. In this way, macropinocytosis represents a novel amino acid supply route that tumor cells use to survive the nutrient-poor conditions of the tumor microenvironment. While the tenets of the signal transduction events that drive macropinocytosis in cancer have emerged, a detailed picture of the macropinosome itself is not yet available. With the aid of nanotechnology, we have developed a methodology to isolate a pure fraction of macropinosomes from PDAC cells. Using a large-scale proteomic approach, we have been able to generate a list of proteins that reside in macropinosomes. The specificity of this approach was confirmed through the identification and validation of proteins known to specifically localize to these organelles in different contexts, such as Rab5 or SDC1. Thanks to this innovative method, we have demonstrated the involvement of two calcium channels, ATP2B1 and ATP2B4, in the formation of macropinosomes. By elucidating the molecular anatomy of KRAS-driven macropinosomes, we will gain further insight into the regulation and function of macropinocytosis in cancer. Moreover, having a clearer picture of the macropinosome will make us better positioned to exploit this pathway therapeutically and deliver breakthroughs to patients.

#4454 Manipulation of the amino acid metabolism promotes therapeutic efficacy through targeting lysosome in glioblastoma.

Y. Jing, M. Kobayashi, A. Hirao;
Kanazawa University Cancer Research Institute, Kanazawa, Japan

Nutrients are converted by the body to smaller molecules, which are utilized for both anabolic and catabolic reactions. Cooperative regulation of these metabolic processes is critical for maintaining tissue homeostasis. Based on these findings, our group has been focusing on how the regulation of nutrient-driven metabolism controls the malignancy of cancer cells. Metabolic regulation has been considered crucial for cellular adaptation to environmental changes and promoting survival and proliferation. Recent studies showed the successful applications of targeting specific nutrients for cancer therapy. In this study, we developed a new lysosome-targeting therapeutic strategy, centered around the manipulation of the amino acid metabolism for GBM. Using patient-derived GBM cells, we found that lysosomal proteolytic activity is a unique metabolic biomarker representing malignant phenotypes of GBM and that it is closely correlated with the efficacy of current conventional therapy for GBM patients. Furthermore, the MiT/TFE family members, TFEB and TFE3, which are the master regulators of lysosomal biogenesis, controlled malignant progression and therapeutic efficacy in vitro and vivo. Combinatory analyses with clinical patient samples and xenograft models demonstrated that the MiT/TFE family plays a crucial role as a regulator of malignant properties in GBM. Analysis of The Cancer Genome Atlas (TCGA) glioma dataset, which includes data from patients with Grade 2, 3, and 4 (GBM) gliomas, showed that higher expression of the MiT/TFE family was significantly associated with shorter survival. Interestingly, we discovered that an essential amino acid controls lysosomal biogenesis and membrane integrity by regulation of nitric oxide signaling pathway. Finally, we screened the potential anti-cancer drugs, including temozolomide, exhibiting the synergy effect in amino acid-restriction conditions by conducting a drug screening using a clinically available anti-cancer drug library. Our study demonstrated that lysosomal function, supported by amino acid metabolism, plays a critical role in the regulation of GBM malignant status and proposed precision nutrition as a promising therapeutic approach.

#4455 Metabolic stress induces a double positive feedback loop between AMPK and p62 conferring dual activation of AMPK and NRF2 to synergize antioxidant defense.

Eun-Ji Choi[1], Hyun-Taek Oh[2], Seon-Hyeong Lee[3], Chen-Song Zhang[4], Mengqi Li[4], Soo-Youl Kim[3], Sunghyouk Park[2], Tong-Shin Chang[2], Byung-Hoon Lee[2], Sheng-Cai Lin[4], **Sang-Min Jeon**[2]

[1]Ajou University, Suwon, Korea, Republic of,[2]Seoul National University, Seoul, Korea, Republic of,[3]National Cancer Center, Goyang, Korea, Republic of,[4]Xiamen University, Fujian, China

Co-occurring mutations in KEAP1 in LKB1-mutant NSCLC activate NRF2 to compensate losing LKB1-AMPK activity during metabolic adaptation and survival. Here, we investigated the regulatory crosstalk between LKB1-AMPK and KEAP1-NRF2 pathways during metabolic stress. We found that metabolic stress activates NRF2 through the expression and phosphorylation of p62, causing the autophagic degradation of KEAP1. Intriguingly, the induction of p62 during metabolic stress is also required to activate AMPK by promoting AXIN-LKB1-AMPK complex formation and recruiting it to the lysosomal membrane. Importantly, the p62-driven dual-activation of AMPK and NRF2 was critical for tumour growth by synergizing antioxidant defences. In turn, the induction of p62 also required LKB1-AMPK activity, suggesting a double positive feedback loop between AMPK and p62. Mechanistically, the increase in lysosomal pH caused by low glucose metabolism and AMPK-dependent reduction of proton generation induced PP2A-dependent dephosphorylation of TFEB/TFE3 which increased the expression of p62. The increase of ROS caused by metabolic stress induced lysosomal MCOLN1-Ca^{2+} dependent activation of TAK1 which increased p62 phosphorylation. Protons provided by lactic acid abrogated all the effects caused by metabolic stress. This positive feedback loop between AMPK and p62 that activates AMPK and NRF2 can potentially explain why co-occurring mutations in LKB1 and KEAP1 occur and further provide promising therapeutic strategies for lung cancer.

#4457 Skeletal muscle-infiltrating CD8 T cells exacerbate muscle atrophy in a syngeneic lung cancer cachexia mouse model.

S.-Y. Park[1], B. Kim[1], M. Lee[2], H. Lee[2], N.-Y. Song[1];

[1]Yonsei University, Seoul, Korea, Republic of, [2]Pusan National University, Busan, Korea, Republic of

Cancer-associated cachexia (CAC) is a devastating syndrome of irreversible body weight loss and muscle wasting. CAC has been reported to often lead to poor outcomes of immune checkpoint inhibitors (ICIs), emerging as a standard treatment for various types of cancer. Previously, we have demonstrated that KRAS-mutant lung tumor tissues display an immunosuppressive microenvironment with decreased CD8 T cells and increased regulatory T cells (Tregs). In this orthotopic lung cancer mouse model, treatment with an anti-PD-L1 antibody, a representative ICI, reduced tumor burden, whereas accelerated loss of body weight and skeletal muscle mass. We thus assumed that CD8 T cells could facilitate skeletal muscle wasting in lung tumor-bearing mice, a key feature of CAC. First, we established a syngeneic CAC mouse model through orthotopic transplantation of murine lung cancer cells. At 7 weeks post-injection, these mice developed CAC, displaying over 20 % body weight loss, almost total loss of epididymal fats, and profound skeletal muscle wasting. In line with our assumption, CAC mice showed an increased number of CD8 T cells but a reduced number of Tregs in skeletal muscles, compared to tumor-free control mice. We then investigated whether skeletal muscle-infiltrating CD8 T cells directly induce muscle atrophy indeed. In CAC mice, CD8 neutralization led to restoration of muscle mass and downregulation of muscle atrophy markers, but was not able to significantly affect lung tumor burden. Moreover, direct co-culture with splenic CD8 T cells exacerbated C2C12 myotube atrophy in a conditioned medium from lung cancer cells, further supporting the involvement of CD8 T cells in CAC. To elucidate its underlying mechanism, RNA sequencing analysis was conducted in both skeletal muscles and lung tumors of CAC mice. Based on the differently expressed gene analysis, *Cxcl13* was upregulated in skeletal muscles of CAC mice, while downregulated in lung tumors. It is well documented that CXCL13 can mediate recruitment of CD8 T cells. In this regard, CXCL13 might be a plausible regulator in CD8 T cell-induced skeletal muscle atrophy, which requires further investigation to fully understand the molecular mechanism.

#4459 Metabolic liabilities of iron-dependent ferroptosis mediated through NRF2/GPX4 axis in osteosarcoma.

M. Abdullah, D. Lee, R. Li, J. Kim;
University of Florida, Gainesville, FL

Osteosarcoma is an aggressive bone malignancy that predominantly affects adolescents and young adults. Despite recent advancements in treatments, the challenges of recurrence and chemoresistance persist. Ferroptosis is a form of regulated cell death driven by iron-dependent lipid peroxidation, and emerging evidence suggests significant roles for NRF2 and GPX4 in iron metabolism, regulating tumor cell functions. In osteosarcoma, however, the molecular mechanisms of the NRF2/GPX4 axis and its therapeutic potential remain unknown. In this study, we first determined GPX4 and xCT expression levels and cellular responses to RSL3, a GPX4 inhibitor, and Erastin, an xCT inhibitor in osteosarcoma cells. A total of seven osteosarcoma cell lines, consisting of five human cell lines (HOS, 143B, Saos-2, MG-63, U2OS) and two canine cell lines (COS31 and DOUG), were used. Our results revealed that the IC50 values ranged from 0.02 uM to 1.01 uM in cells treated with RSL3 and from 0.35 uM to 1.41 uM in cells treated with Erastin, respectively. These values were proportional to GPX4 and xCT levels across the cell lines. Then, U2OS, as the most sensitive, and Saos-2, the least sensitive based on their IC50 values, were selected to examine the iron regulatory machinery. In U2OS cells, RSL3 treatment significantly decreased NRF2 and GPX4, while increasing ferroportin-1 and ferritin. GPX4 knockdown also led to comparable changes in NRF2, ferroportin-1, and ferritin expression. NRF2 appears to mediate iron metabolism, ferroportin-1 acts as an iron exporter, and ferritin stores intracellular iron. Therefore, our findings suggest that GPX4-mediated ferroptosis is regulated by iron metabolic pathways, potentially to prevent ferroptotic cell death. We also found that Ferrostatin-1, a lipid peroxidation inhibitor showed no changes in ferroportin-1, ferritin, and NRF2. In Saos-2, RSL3 induced a remarkable reduction in GPX4 expression, akin to U2OS. However, no significant change was found in NRF2, ferroportin-1, and ferritin. Instead, Ferrostatin-1 restored the decreased GPX4 and increased NRF2, ferroportin-1, and ferritin levels. In addition, Z-VAD (a pan-caspase inhibitor), Necrosatin-1s (a RIPK1 inhibitor), and Ferrostatin-1 were capable of preventing Saos-2, COS31, and DOUG cells from RSL3-induced cell death at lethal doses. Such protection was undetected in U2OS. These data suggest that metabolic pathways controlling intracellular iron are crucial for NRF2/GPX4-mediated ferroptosis in osteosarcoma cells. Furthermore, we generated RNA-seq and LC-MS/MS data to identify novel molecular targets governing the metabolic pathways of ferroptosis in osteosarcoma. Our ongoing work includes downstream molecular and functional assays following gene modifications in osteosarcoma cells (overexpression and knockout) and assessing metabolic vulnerabilities by targeting iron-mediated ferroptosis in xenografts.

#4460 Investigating a non-canonical role for SHP2 in pancreatic ductal adenocarcinoma metabolism and response to dietary modifications.

R. Walsh, J. L. Jack, A. E. Eades, B. A. Bye, M. T. Ruckert, J. Ambrose, M. N. VanSaun;
University of Kansas Medical Center, Kansas City, KS

Pancreatic ductal adenocarcinoma (PDAC) is predicted to be the second leading cause of cancer death in the US by 2025, with rising incidence. Mutant KRAS in >90% of PDAC cases promotes activation of the MAPK pathway, yet targeting the MAPK pathway clinically has failed to improve patient outcomes. SHP2 canonically promotes KRAS activation and is essential for PDAC development in mouse models. Because targeting MAPK is insufficient, yet SHP2 loss blocks PDAC development, we hypothesized SHP2 has both MAPK dependent and independent functions. Initial studies revealed that SHP2 inhibition with SHP099 in murine KPC [K8484: $KRAS^{G12D/+}$, $p53^{R172H/+}$, $Pdx1^{Cre/+}$] cells required concentrations exceeding 50 μM to elicit a minimal ERK inhibition. This led us to predict that there may be a tumor suppressive mechanism of SHP2 inhibition that is KRAS/MAPK independent. We utilized available RNAseq data (NCBI GEO: PRJNA558508) of PDAC MiaPaCa2 cells treated with the MEK inhibitor, Trametinib, or SHP099 to compare the direct effects of inhibition on transcriptional outcomes. We identified inositol phosphate signaling as a candidate target, whose downstream consequence is Ca^{2+} flux. We measured IL-1β induced Ca^{2+} flux in a panel of human PDAC cells exposed to MEK or SHP2 inhibition. Trametinib treated cells showed no effect on Ca^{2+} flux, however, SHP099 led to a drastic depletion of free Ca^{2+} and response to stimulus. We then validated the Ca^{2+} response to IL-1β stimulus in Crispr-Cas9 SHP2-knockout K8484 cells. While we did not observe a difference in basal free calcium, we still found a reduction in response to IL-1β stimulus. Because Ca^{2+} is an important co-factor for mitochondrial metabolism, we then interrogated metabolic effects. We tested mitochondrial function using a Seahorse Mito-Stress test and found that while MEK inhibition failed to affect mitochondrial metabolism, SHP2 inhibition ablated it. A Glycolysis-Stress Test revealed that SHP2 inhibition led to glucose consumption primarily through anaerobic respiration. TMT-labeled phospho-proteomic analysis comparing SHP2KO and MEK inhibited K8484s revealed SHP2 dependent deficiencies in mitochondrial proteins, among others, involved in mitochondrial fission and lipid metabolism. Western diets have been shown to promote tumor progression in GEM models of PDAC, so we used $KRAS^{G12D/+}$, $SHP2^{fl/fl\ or\ wt./wt}$, $Ptf1a^{Cre/+}$ (SKC and KC) mice to demonstrate that while diet-induced obesity affects KC tumor burden, the lack of SHP2 in SKCs prevents the diet associated discrepancy in tumor progression. Collectively, these data led us to conclude that while SHP2 has been studied as a contributor to KRAS signaling in PDAC, the outcomes of its role specifically on mitochondrial metabolism have yet to be appreciated or thoroughly investigated, opening the path for a new approach to its contribution to tumor progression.

#4461 Unveiling the links between methionine metabolism and epigenomic reprogramming in upper aerodigestive squamous cell carcinoma.

C. Nam;
Herman Ostrow School of Dentistry, University of Southern California, Los Angeles, CA

Upper aerodigestive squamous cell carcinoma (UASCC) presents as a prevalent and aggressive malignancy, posing challenges in terms of effective therapeutic interventions. In this study, we explored the intricacies of amino acid metabolism within UASCC, revealing an unexpected observation that distinguishes UASCC among all human cancers, having the highest methionine levels, driven by the overexpression of its transporter LAT1. Notably, LAT1 exhibits peak expression levels in UASCC, regulated at the transcriptional level by UASCC-specific promoters and enhancers, co-regulated by SCC master regulators TP63/KLF5/SREBF1.Surprisingly, our unbiased bioinformatic screen identifies EZH2 as a pivotal downstream target of the LAT1-methionine pathway, establishing a direct link between methionine metabolism and epigenomic reprogramming. This cascade emerges as crucial for the survival and proliferation of UASCC patient-derived tumor organoids. Furthermore, we find that LAT1 expression closely correlates with cellular sensitivity to inhibition of the LAT1-methionine-EZH2 axis.Significantly, the newly discovered LAT1-methionine-EZH2 cascade emerges as a promising target for intervention, with effective outcomes achievable through both pharmacological approaches and dietary interventions *in vivo*. In summary, this research unveils a novel mechanistic crosstalk connecting epigenomic reprogramming with methionine metabolism, revealing its biological significance in UASCC. Moreover, it identifies a unique tumor-specific vulnerability, providing avenues for exploitation through both pharmacological and dietary strategies

#4463 Metabolic reprogramming through Notch1 signaling promotes a survival advantage in pancreatic neuroendocrine tumor cells.

R. Guenter, W. Chen, B. Herring, Y. Golivi, M. Sammy, J. Whitt, R. Jaskula-Sztul, H. Chen, J. Rose;
University of Alabama at Birmingham, Birmingham, AL

Background: Cancer cells utilize both oxidative phosphorylation (OXPHOS) and glycolysis to generate energy. Switching between OXPHOS and glycolysis can promote tumor progression. The mechanisms governing oncogenic metabolic reprogramming are largely unknown, but recent data has suggested that Notch1 dysregulation in cancer cells can contribute to altered metabolic phenotypes. We hypothesized that Notch1 signaling supports metabolic reprogramming in pancreatic neuroendocrine tumor (pNET) cells.

Methods: We established a Notch1-knockout pNET cell line (BON-N1-KO) by deleting Notch1 at exon 3 in a pNET cell line (BON) using CRISPR/Cas9. Proliferation over time was measured using a trypan blue exclusion test. Seahorse Glycolytic Rate Assay and Mitochondria Stress Test were used to measure the glycolytic and mitochondrial activities of cells. A glycolysis deprivation assay was employed to determine cell viability at varying glucose concentrations. Single end RNAseq was performed using the Illumina NGS platform, to a read depth of 50M.

Results: Over time, pNET cells lacking Notch1 (BON-N1-KO) proliferated slower than wildtype (WT) cells (p=0.034). Compared to WT BON, the BON-N1-KO cells had reduced basal oxygen consumption rate (28.2 ± 1.3 vs. 40.7 ± 1.4; p=0.02, ATP production (21.9 ± 1.0 vs. 29.6 ± 0.98; p=0.04), and maximal respiration (39.4 ± 1.7 vs. 63.7 ± 2.1; p=0.004). BON-N1-KO cells also had a reduction in basal glycolysis, as measured by proton efflux rate, compared to WT (48.7 ± 2.6 vs. 57.7 ± 6.2; p=0.2). To further test metabolic reprogramming, WT and BON-N1-KO cells were starved of glucose (0mM), compared to normal glucose (17.5mM) and viability was measured over time. By day 5, the BON-N1-KO group had a viability of 0%, whereas 12.8% of WT cells were alive (p=0.038). To determine if Notch1 loss was associated with altered expression of established metabolic genes, we performed RNAseq. Differential gene expression analysis found that OXPHOS-related genes (*UQCC2, COX15, COX20*) and glycolysis-related genes (*Slc1a1, Slc2a4, Hk1, Hk2*) were significantly down-regulated in BON-N1-KO cells.

Conclusions: Our study shows that Notch1 signaling facilitates metabolic reprogramming as a survival advantage in pNET cells. Targeting Notch1 signaling to mediate cellular metabolism may be a novel therapeutic strategy in pNETs.

#4464 Ferredoxin 1 is essential for embryonic development and lipid homeostasis.

Jin Zhang, Sharkur Mohibi, Xinbin Chen, Vivian Perng, Yanhong Zhang

UC Davis, Davis, CA

Mammalian ferredoxin 1 and 2 (FDX1/2) belong to an evolutionary conserved family of iron-sulfur cluster containing proteins and act as electron shutters between ferredoxin reductase (FDXR) and numerous proteins involved in critical biological pathways. FDX1 is involved in biogenesis of steroids and bile acids, Vitamin A/D metabolism, and lipoylation of tricarboxylic acid (TCA) cycle enzymes. FDX1 has been extensively characterized biochemically but its role in physiology and lipid metabolism has not been explored. In this study, we generated Fdx1-deficient mice and showed that knockout of both alleles of the Fdx1 gene led to embryonic lethality. We also showed that like Fdxr+/− mice, Fdx1+/− mice had a shorter life span and were prone to steatohepatitis. However, unlike Fdxr+/− mice, Fdx1+/− mice were not prone to spontaneous tumors. Additionally, we showed that FDX1 deficiency led to lipid droplet accumulation possibly via the ABCA1-SREBP1/2 pathway. Specifically, untargeted lipidomic analysis showed that FDX1 deficiency led to alterations in several classes of lipids, including cholesterol, triacylglycerides, acylcarnitines, ceramides, phospholipids and lysophospholipids. Taken together, our data indicate that FDX1 is essential for mammalian embryonic development and lipid homeostasis at both cellular and organismal levels.

#4465 Galectin-1 regulates CD147 and downstream pathways critical for glioma progression.

M. R. Guda, A. J. Tsung, S. Asuthkar, K. Velpula;
University of Illinois College of Medicine, Peoria, IL

Galectin-1 (Gal-1) is an important protein for glioma progression and glioma stem cell maintenance. Gal-1 may act through CD147, a potential Gal-1 receptor. CD147, also known as Basigin or extracellular matrix metalloproteinase inducer (EMMPRIN), is a transmembrane glycoprotein highly expressed in various cancer cells. An analysis utilizing the Gliovis database and encompassing 667 Glioblastoma Multiforme (GBM) patients segregated based on median CD147 expression levels delineated cohorts with above-median (n=339) and below-median (n=328) CD147 expression. Kaplan-Meier survival curves unveiled a significant association between heightened CD147 expression and reduced overall survival (OS) in this patient population. Experimental approaches employing immunoblotting and immunohistochemistry techniques on shGal-1 treated cell lysates and mouse brain samples exhibited decreased CD147 expression compared to respective controls. Additionally, immunocytochemical studies corroborated an augmented colocalization of Gal-1 and CD147, with a subsequent reduction in this association following shGal-1 treatment. Next, we used AC-73, a selective CD147 inhibitor, to determine the levels of CD147 and Gal-1. Treatment with 20μM AC-73 and siRNA for CD147 showed reduced CD147 levels in GSC33 and GSC20 cells while maintaining unaltered Gal-1 expression. Inhibiting CD147 did not affect Gal-1 levels, further suggesting Gal-1 acts upstream. CD147 activates matrix metalloproteinase-9 (MMP9), and CD147 knockdown reduced MMP9 levels, elucidating a Gal-1-CD147-MMP9 pathway. Overall, Gal-1 appears to act upstream of CD147 to regulate MMP9, integrins, and other factors important for glioma progression. Further elucidation of these pathways will provide insights into glioma biology and potential therapeutic targets.

#4466 Omega-3 fatty acid-induced ferroptosis in 4T1 breast cancer through CD36/FABP5 axis.

A. Avellino, J. Hao, M. Yorek, J. Yu, B. Li;
University of Iowa, Iowa City, IA

Mammalian cells utilize energy from many different sources, and fatty acids are one of these sources. Dietary fats contain various structures of fatty acids, each impacting cell lipid metabolism in unique ways. Omega-3 fatty acids are known to induce breast cancer cell death through ferroptosis. However, the specific molecular mechanisms by which omega-3 fatty acids trigger ferroptosis have yet to be fully elucidated. Fatty acid binding proteins (FABPs) constitute a family of evolutionarily conserved lipid chaperones, facilitating the transport and utilization of fatty acids within cells. Notably, FABP5 is highly expressed in breast cancer, especially in the most aggressive form, triple-negative breast cancer. We hypothesized that FABP5 acts as a lipid sensor, mediating the ferroptosis induced by omega-3 fatty acids in triple-negative breast cancer cells. To test this, we created Fabp5 stable knockout cell lines in 4T1 and MDA-MB-231, two commonly used triple-negative breast cancer cell lines, using CRISPR/Cas9 technology. When treated with docosapentaenoic acid (DPA), these Fabp5-knockout cells exhibited reduced ferroptosis compared to their wild-type counterparts. Interestingly, blocking the surface protein CD36, either with inhibitors or antibodies, also reduced DPA-induced ferroptosis. Furthermore, mutations in Fabp5 decreased maximal mitochondrial respiration in both 4T1 and MDA-MB-231 cells, suggesting a crucial role for FABP5 in mediating oxygen consumption and reactive oxygen species (ROS) production during DPA-induced ferroptosis. Additionally, mice fed a high-fat diet rich in omega-3 fatty acids showed reduced tumor size and lung metastasis. Collectively, our data indicate that FABP5 is a key molecular sensor mediating oxygen consumption and ROS production, thus contributing to ferroptosis induced by omega-3 fatty acids in triple-negative breast cancer.

#4468 Elucidating the phosphoinositide-modulatory function of INPP5B in regulating cancer stemness and tumorigenesis in liver cancer.

L. Liu, Y. Wang, Y. Xie, M. Tong;
The Chinese University of Hong Kong, Shatin, NT, Hong Kong

Hepatocellular carcinoma (HCC) represents a major global health challenge, characterized by its heterogeneity and aggressive nature. Solid evidence has now suggested that tumor growth is driven by subpopulations of tumor cells with less differentiated cell states, called cancer stem cells (CSCs), which govern therapeutic resistance and tumor recurrence. Therefore, characterization of CSCs and their associated oncogenic signaling pathways is crucial to the development of more specific and sensitive HCC prognostic markers and to the design of novel targeted therapies against CSCs for HCC treatment. In search of the altered genes and pathways that are tightly associated with cancer stemness trait in HCC, we exploited the stemness and oncogenic dedifferentiation signature to mine the HCC dataset of the Cancer Genome Atlas. Phosphoinositide signaling was identified to be enriched and downregulated in the transcriptomes of HCC patients with strong stemness and dedifferentiated signature. Subsequent clinical correlation analysis found inositol polyphosphate-5-phosphatase B (INPP5B) to be the top downregulated gene in phosphoinositide signaling with its expression correlated with poor survival in HCC patients. Functional studies showed that INPP5B overexpression reversed the oncogenic and stemness properties while INPP5B knockout promoted tumor growth in immunocompetent mice. Subsequent RNA sequencing and molecular assays revealed INPP5B deregulation to be associated with lipid metabolism remodeling. Collectively, our results suggest an intricate relationship between phosphoinositide signaling and lipid metabolism through the regulation of INPP5B in HCC. The findings may open new avenue for future research aimed at devising targeted therapies to interfere with liver CSCs and enhance the prognosis of HCC patients.

CHEMISTRY: Drug Design and in Silico Screening
Poster Session

#4472 Discovery of potential RAF-selective back pocket as a promising biological target for BRAF inhibitors in the treatment of resistant melanoma: Design, synthesis, biological evaluation and *in silico* studies.

Usama Ammar[1], Mahmoud Gamal[2], Mohammed Abdel-Maksoud[2], Eslam Ali[3], Zeyad Mahmoud[4], Kim Deug[5], Park Jun[5], **Soo Lee**[6], Chang Oh[4]

[1]School of Applied Sciences, Edinburgh Napier University, Edinburgh, United Kingdom,[2]Medicinal & Pharmaceutical Chemistry Department, National Research Centre, Giza, Egypt,[3]School of Pharmacy and Pharmaceutical Sciences, UC Irvine, Irvine, CA,[4]Center for Biomaterials, Korea Institute of Science and Technology (KIST), Seoul, Korea, Republic of,[5]CTCBIO Inc., Gyeonggi-do, Korea, Republic of,[6]Department of Oncology/Hematology, Kyungpook National University, Daegu, Korea, Republic of

The mutated BRAF kinase (V600E) is considered the key component in the MAPK signaling pathway that was reported to be significantly contributed to melanoma disease. Vemurafenib and dabrafenib are examples of drugs that were approved by FDA to treat melanoma through inhibition of mutated BRAF kinase (V600E). However, drug resistance was reported after 6 - 7 months of treatment using these drugs due to activation of this signaling pathway through another RAF kinase (CRAF). As a Drug Discovery research group, we were interested to study and identify the possible biological target to inhibit this resistant form of cancer. We run molecular modelling simulation to study the key features of the active sites of RAF kinases and we taken vemurafenib as a starting point to design our compounds. We identified a selective back pocket in the active site of RAF kinases that can be targeted to enhance the inhibition of these kinases to overcome the drug resistance in the resistant melanoma. We designed a library of compounds based on imidazothiazole core scaffold decorated with different hydrophobic substituents to target the selectivity back pocket. Among the designed and synthesized series, KS16, that showed potent biological profile against RAF kinases compared to vemurafenib as a standard. In the cellular level, KS16 showed the same potencies against mutated BRAF-based melanoma cell line (A375) as that of vemurafenib. To evaluate the selectivity profile of KS16, kinase panel assay against 60 kinases has been investigated that showed high selectivity profile of KS16 (98 - 100% inhibition against ^{WT}BRAF, CRAF and ^{V600E}BRAF). In addition, KS16 was submitted to National Cancer Institute (NCI) to be tested against 60 human cancer cell lines in 5-point assay. It showed selective cytotoxic inhibition against melanoma cell lines compared to the other types of cancer cell lines. To evaluate the efficacy of KS16 against resistant melanoma, both KS16 and vemurafenib were tested against resistant melanoma cell line (A375R). The results revealed that KS16 showed the capability to inhibit the growth of resistant melanoma cell line in contrast to vemurafenib which failed to exhibit the same inhibition profile. The drug-candidate cardiac safety profile of KS16 was emphasized in this current project. KS16 was tested against hERG using E4031 (IC_{50} = 0.025 µM) as positive control to set up the hERG channel binding assay. The results revealed that KS16 showed relatively weak binding to hERG (% inh 64%) compared to that of the potent positive control (E4031, % inh 97%). The results revealed that KS16 is a potential drug candidate with minimal cardiotoxic effect. Further pharmacokinetic studies are being performed to KS16 to investigate and develop the ADME profile of KS16 to be a potential selected drug candidate against resistant melanoma disease.

#4473 Targeting matrix metalloproteinase-3 (MMP-3) in high-grade serous ovarian cancer.

V. G. Reyes-Burgos[1], E. Hernandez-O'Farrill[1], L. E. Vazquez Quinones[2], M. Flores-Colon[1], F. Valiyeva[3], P. E. Vivas-Mejia[1];
[1]University of Puerto Rico Medical Sciences Campus, San Juan, Puerto Rico, [2]Interamerican University of Puerto Rico, Arecibo, Puerto Rico, [3]University of Puerto Rico Comprehensive Cancer Center, San Juan, Puerto Rico

High-Grade Serous Ovarian Cancer (HGSOC) is the most aggressive and lethal gynecological malignancy. Surgery and chemotherapy (with platinum compounds) are the main treatments. Many patients relapse and develop chemotherapy resistance, limiting the therapeutic utility of these therapies. This persistent resistance makes HGSOC treatment difficult. Cisplatin-resistant ovarian cancer cells upregulate Matrix Metalloproteinase-3. MMP3 is an enzyme involved in active tissue remodeling and extracellular matrix protein breakdown during dynamic physiological processes. The structure of MMP3 includes the prodomain, the catalytic domain and the hemopexin domain. We showed that MMP3 protein levels are higher in cisplatin resistant as compared with cisplatin sensitive HGSOC cells. Our research team showed that small interference RNA (siRNA)-mediated MMP3 knockdown reduced cisplatin-resistant ovarian cancer cell growth and invasion. This data indicates that MMP3 may be a promising HGSOC treatment target. Targeting MMP3 with small chemical inhibitors (SCI) could represent a better option than siRNA because SCI are more stable and easier to deliver. The purpose of this project is to design SCI of MMP3 in the propeptide, catalytic, and hemopexin domains of MMP3. We used in silico methods to identify MMP3 inhibitors in these domains. The ZINC20 database of commercially compounds was used for virtual screening using Python Prescription (PyRx) software. We identified 25 ligands out of 370,000 with the greatest affinity for each MMP3 functional domains. SwissADME was then used to evaluate in silico absorption, distribution, metabolism, pharmacokinetics, drug-likeliness, and medicinal chemistry. This research lays the groundwork for HGSOC therapeutic strategies to improve treatment efficacy, especially for chemotherapy-resistant patients.

#4474 Novel analogs of 4-substituted pyrrolo[2,3-*d*]pyrimidines as dual-targeted mEGFR/AURKA inhibitors for lung cancer.

S. Kurup[1], G. Carpenter[1], S. Satawa[1], F. Amissah[1], E. Lisabeth[2], M. Giletto[2], E. Ellsworth[2];
[1]Ferris State University, Big Rapids, MI, [2]Michigan State University, East Lansing, MI

Small molecule, mutant epidermal growth factor receptor kinase (mEGFR) inhibitors such as osimertinib and erlotinib constitute the recommended therapy for mEGFR-positive non-small cell lung cancer (NSCLC). However, mEGFR inhibitors are ineffective in NSCLC over time due to mutations within mEGFR and redundant signaling pathways such as mutant KRAS (mKRAS) that bypass mEGFR inhibition. Simultaneous inhibition of multiple kinases has been suggested to provide synergistic effects on tumor growth inhibition and tumor resistance. Studies have shown that resistance to mEGFR inhibitors was overcome when mEGFR inhibitors were combined with aurora kinase (AURK) inhibitors. Additionally, mEGFR inhibitors were found to retain their anticancer effects in mKRAS-positive NSCLC cells if given concurrently with AURK inhibitors. Kurup *et al.* previously reported a series of 4-substituted pyrrolo[2,3-*d*]pyrimidines as dual mEGFR/AURKB inhibitors. Novel analogs of **1-5** have been designed to incorporate AURKA inhibition while maintaining mEGFR inhibition. Molecular modeling was utilized to guide selectivity for AURKA over AURKB. This study led to the identification of novel dual-targeted mEGFR/AURKA inhibitors with demonstrated inhibition of mKRAS+ NSCLC and mEGFR+ NSCLC. The design, synthesis, kinase inhibitory activities, and anticancer effects for these novel analogs will be presented. Structure-activity relationships for dual mEGFR/AURKA inhibition will be defined.

#4475 Discovery of an oral tricyclic STING agonist with superior pharmacokinetic properties and potent in vivo efficacy.

Hong-Yi Zhao, Zhongwei Liu, Shuai Mao, Miao He, Meilin Wang, Bo Wen, Wei Gao, Duxin Sun

University of Michigan, Ann Arbor, MI

Stimulator of interferon genes (STING) plays a pivotal role in regulating immune microenvironment for cancer immunotherapy. However, the use of most STING agonists has been hindered by the necessity for intra-tumoral or intravenous administration, underscoring the challenge in developing an orally bioavailable STING agonist with favorable pharmacokinetic (PK) properties. In this study, we discovered oral STING agonists featuring a novel tricyclic benzo[4,5]thieno[2,3-c]pyrrole-1,3-dione scaffold, thus achieving both superior PK properties and potent in vivo efficacy. Our lead compound, ZSA-51, exhibited nanomolar cellular STING activation activity (EC_{50} = 100 nM) in THP1 cells, surpassing the reported oral STING agonist MSA-2 by 32-fold (EC_{50} = 3200 nM). Furthermore, ZSA-51 demonstrated superior PK properties with an oral bioavailability of 49%, and robust in vivo antitumor activity both in colon and pancreatic cancers model upon oral administration. Notably, ZSA-51 displayed preferential distribution to the lymph nodes and spleen, enhancing its systemic immune-stimulating effects. The specificity of ZSA-51 was further confirmed by a comparison with a negative control compound (ZSA-52NC2) that was unable to stimulate in vitro and in vivo STING activity. Molecular docking and MD simulation confirmed that the active form of ZSA-51 stably bound to STING dimer with validated hydrogen bond network. Taken together, our findings suggest ZSA-51 as a promising oral STING agonist characterized by superior PK properties and potent in vivo efficacy, holding potential for future development for cancer immunotherapy.

#4476 Novel auristatins with improved tolerability and unique bystander activity profile.

P. N. Moquist, N. M. L. Eng-Duncan, T. Bovee, K. Snead, J. Wright, K. Smith, T. Blevins, B. Blackburn, M. Ulrich, F. Magunda, J. Simmons, P. D. Senter, S. O. Doronina;
Seagen, Bothell, WA

Auristatins are a class of clinically validated payloads used extensively in antibody-drug conjugate (ADC) technology. There are currently 4 FDA approved ADCs utilizing the vedotin drug linker to treat an array of solid tumors and lymphomas and several more in clinical trials. Auristatin payloads have several desirable properties, including strong anticancer cytotoxicity, bystander activity, and induction of immunologic cell death. While auristatin-based ADCs have been remarkably successful, there remain opportunities to further understand and improve payload properties. Bystander activity is one such property that can greatly impact the balance between efficacy and tolerability. Herein, we present a medicinal chemistry investigation into a series of auristatins with similar tubulin binding and biochemical potency that differ in lipophilicity and ability to cross the cell membrane. This design enabled us to focus on and characterize the impact of bystander activity while maintaining all other parameters. Ultimately, this effort resulted in ADCs with similar on-target in vitro cytotoxicity but differed in the extent of off-target bystander activity. Evaluation of in vivo efficacy, in vivo bystander activity, and rodent tolerability afforded a lead drug linker that was well-tolerated as an ADC and exhibited strong antitumor growth delay.

#4477 The development of a small molecule dual inhibitor of CXCR4 and Mcl-1 to target bortezomib resistant and stem-like cells in multiple myeloma.

W. O. Elbezanti[1], O. S. Al-Odat[2], S. C. Jonnalagadda[2], T. Budak-Alpdogan[1], M. K. Pandey[3];
[1]Cooper Univ. Hospital, Camden, NJ, [2]Rowan University, Camden, NJ, [3]Cooper Medical School of Rowan University, Camden, NJ

Multiple myeloma (MM) is a malignant plasma-cell illness defined by clonal growth of malignant plasma cells within the bone marrow (BM) microenvironment. Despite the availability of many therapeutic alternatives, MM remains consistently lethal, demanding the development of novel techniques. The intimate relationship between myeloma cells and the BM microenvironment is a distinguishing hallmark of MM. The chemokine stromal cell-derived factor-1 (SDF-1) and its receptor CXCR4 enhance the homing of MM cells to the BM, which has important functional implications. The BM microenvironment secretes a variety of hormones and cytokines that activate several signaling pathways, resulting in enhanced production of the anti-apoptotic Mcl-1 protein, boosting the proliferation, survival, and migration of MM cells and conferring resistance to standard chemotherapy. As a result, we created GA-A, a hybrid molecule in which we coupled an aralkyl carboxylic acid moiety, known to preferentially inhibit Mcl-1, to gambogic acid, which has previously been demonstrated to inhibit CXCR4 in MM. Our western blot has shown that this unique hybrid compound successfully suppressed CXCR4 and Mcl-1. Interestingly, using qPCR we found that CXCR4 was observed to be higher expressed in CD138- versus CD138+ cells, while GA-A inhibited CXCR4 in both subpopulations. In addition, using annexin-V flow cytometry staining we found that GA-A increased the apoptotic effect of bortezomib in MM stem-like cells while inhibiting the viability of bortezomib resistant cells. Using human cytokine array we found that GA-A activates some of proinflammatory cytokines that can activate the immune system such as GM-CSF, IFN gamma, IL-2 and IL-12. In summary, our findings indicate the successful creation of a novel dual CXCR4-Mcl1 inhibitor that demonstrates efficacy against the stem cell-like population and bortezomib resistant cells and enhances the effectiveness of bortezomib.

#4478 Development and characterization of kinase sparing TPX2-tethering Aurora kinase A ligands for cancer therapy.

A. Moschopoulou[1], M. Henning[1], B. Wagner[2], D. Flotgen[2], J. Reiner[2], Y. Skliarenko[1], S. Zwirner[1], C. Hinterleitner[1], M. Seehawer[1], L. dArtista[1], E. Rist[1], T. Pantsar[3], T. Kronenberger[2], D. Dauch[1], C. Gehring-Khav[1], A. Poso[3], L. Andreeva[1], M. Schwab[4], M. Forster[2], W. Albrecht[1], S. Laufer[2], **L. Zender**[1]; [1]University Hospital Tubingen, Tubingen, Germany, [2]University of Tubingen, Tubingen, Germany, [3]University of Eastern Finland, Kuopio, Finland, [4]Dr Margarete Fischer-Bosch Institute of Clinical Pharmacology, Stuttgart, Germany

A major limitation in the treatment of cancer is the limited therapeutic index of currently available chemotherapies or molecularly targeted therapies. Drug related toxicities often necessitate restricted drug dosing regimens, resulting in subtotal tumor remissions, which represent an important cause for tumor recurrences and the development of therapy resistance. Following up on previous work suggesting Aurora kinase A (AURKA) as a promising therapeutic target for the treatment of *TP53* altered liver carcinomas (Dauch D. et al., *Nat. Med*., 2016) and *TP53*; *RB1* altered small cell lung carcinomas (Gong X. et al., *Cancer Discovery*, 2019), we here report on the development and characterization of first in class kinase sparing AURKA ligands, which selectively kill *TP53* deficient liver cancer cells and *TP53*; *RB1* deficient small cell lung cancer cells by tethering AURKA to its binding partner TPX2 in mitotic cells. Small molecule mediated stabilization of AURKA/TPX2 complexes resulted in formation of multipolar spindles and subsequent cell death through mitotic catastrophe. Mechanistically, we were able to show that the hypersensitivity of *TP53* deficient liver cancer cells and *TP53; Rb1* deficient small cell lung cancer cells towards AURKA ligands is due to low expression levels of the antiapoptotic protein MCL1, which is necessary for survival of cancer cells in prolonged mitosis. Our novel AURKA ligands do not affect the kinase function of AURKA and thus, in contrast to conventional AURKA kinase inhibitors, can be administered continuously to mice without inducing toxicity related to inhibition of kinase related non-canonical (non-mitotic) functions of AURKA in normal cells or *TP53* and *RB1* wildtype cancer cells. Preclinical therapy studies in cell-line derived xenograft (CDX) tumor models of small cell lung cancer (SCLC) and orthotopic models of *TP53* altered hepatocellular carcinoma and *TP53;Rb1* altered SCLC demonstrated marked monotherapeutic efficacy of AURKA ligands. Conceptually, our herein provided data suggest that small molecules designed to stabilize protein-protein interactions represent powerful anti-cancer drugs with exceptional therapeutic window and thus open a venue towards the development of novel cancer therapies.

#4479 Design, synthesis, and evaluation of amino acid conjugated niclosamide prodrugs as a PepT1 substrate.

Alaina C. McDonough[1], Jeffery Y. Cheng[1], Shabber Mohammed[1], Pui-Kai Li[1], Yangzom Bhutia[2]

[1]Ohio State Univ. College of Pharmacy, Columbus, OH,[2]Department of Cell Biology and Biochemistry, Texas Tech University, Lubbock, TX

The anthelmintic drug, Niclosamide, has a multitude of promising anticancer properties including inhibition of key signaling pathways involved in tumorigenesis, disruption of mitochondrial function, degradation of the overexpressed androgen receptor, and more. However, a key limitation of the clinical use of Niclosamide in cancer treatment is its low solubility and cellular uptake, which result in poor pharmacokinetic properties and dose-limiting GI toxicities at concentrations lower than the therapeutic threshold of the drug. To overcome this, we hypothesized that we could use amino acid conjugated niclosamide prodrugs to improve cellular uptake by creating a substrate of the PepT1 transport protein. The overexpression of the PepT1 transport protein that is involved in many hormonal cancers is being used to our advantage. Our study involved first synthesizing a group of niclosamide and niclosamide analogs conjugated with polar or nonpolar amino acids. Next, we conducted a Glycine-Sarcosine assay measuring changes in the uptake of the dipeptide glycyl-sarcosine (Gly-Sar). Our initial step was to examine if our conjugates could disrupt the absorption of Gly-Sar. The active conjugate will be tested whether they are substrates or inhibitors of the transporter. For the future, we have plans to determine the half-maximal inhibitory concentration (IC50) of niclosamide conjugates in various cancer cell lines and to quantify cleavage of the prodrugs intracellularly.

#4481 Enhancing AOH1996 through structure activity relationship exploration for caPCNA inhibition.

P. Haratipour, M. Zangi, M. Yaghoubi, L. Gu, J. Jossart, J. J. P. Perry, L. H. Malkas, R. J. Hickey;
Beckman Research Institute of City of Hope, Duarte, CA

Recently, we have developed AOH1996, a small molecule PCNA ligand currently in phase I clinical trial, designed to selectively inhibit the functions of cancer-associated PCNA (caPCNA). Seeking to enhance the potency and selectivity of AOH1996, we conducted an exhaustive Structure-Activity-Relationship (SAR) investigation. Over 100 analogues of AOH1996 were synthesized, systematically modifying its three main components: the naphthyl group, glycine linker, and diphenyl ether. The glycine linker underwent substitution with various natural and unnatural amino acids, while the 1-naphthyl group saw replacements with diverse monocyclic and bicyclic aromatic groups, including quinoline and isoquinoline derivatives. The diphenyl ether moiety was extensively explored by substituting the bridging oxygen with different functional groups (sulfonyl, imido, sulfur, amide), substituting both phenyl rings with various functional groups (fluorine, chlorine, hydroxy, methoxy, methyl, trifluoromethyl), and adopting a nitrogen-walk approach on the terminal phenyl ring to evaluate critical ligand/caPCNA-binding positions. This meticulous effort resulted in the identification of several analogues, such as AOH1160S (featuring a diphenyl thioether group), AOH1996S-4CH3 (with a methyl group at the para-position of the terminal thiophenyl ring), and AOH1996-3CH3 (incorporating an m-methoxy function in the terminal phenyl ring and bridging oxygen), exhibiting similar or superior potency compared to AOH1996. The target binding of these analogues was verified by capturing the binary complex of the more polar version of these analogues in the crystal structure. The synthesis, characterization, and detailed biological activities of these promising AOH analogues will be thoroughly described.

#4482 Development of small molecule inhibitors of lipocalin 2 for the treatment of aggressive cancers.

M. Flores-Colon[1], C. A. Pena-Vazquez[2], E. Hernandez-O'Farril[1], L. E. Vazquez-Quinones[3], P. E. Vivas-Mejia[1];
[1]University of Puerto Rico Medical Sciences Campus, San Juan, PR, [2]University of Puerto Rico Rio Piedras Campus, San Juan, PR, [3]Interamerican University, Arecibo, PR

Lipocalin-2 (LCN2), a secreted protein pivotal in iron homeostasis, immune responses, siderophore transport, and epithelial cell differentiation. LCN2 is highly abundant in aggressive forms of many cancers including breast, pancreatic, ovarian, and esophageal cancer. Elevated LCN2 levels in aggressive tumors correlate with heightened cancer cell motility, proliferation, angiogenesis, invasion, and metastasis. After the protein folds it makes a barrel structure which encloses a three-calyx pocket that can bind and transport molecules. A first generation of small molecule inhibitors (SMIs) targeting LCN2 demonstrated efficacy in attenuating the proliferative capacity of Inflammatory breast cancer (IBC) cells. IBC stands as a rare and highly aggressive variant, accounting for 1 to 5% of all BC cases, with 20-30% presenting as de novo metastatic disease. In the previous studies the concentration of LCN2 inhibitors to reduce cell proliferation in 50% was around 10 µM. In pursuit of better LCN2 SMIs, we conducted in-silico analysis using a library of 369,000 ligands. Through the High-Performance Computer Facility at UPR Río Piedras, we employed AutoDock Vina for virtual screening, targeting the LCN2-calyx with Lys134 as the central coordinate. Docking protocols, predicting binding affinities, identified 8,162 out of 327,638 ligands that have been docked already with values below -9.6 kcal/mol for further consideration. The next phase involves subjecting these potential inhibitors to the SwissADME tool for a comprehensive evaluation of absorption, distribution, metabolism, and excretion parameters, as well as pharmacokinetics, drug-likeness, and medicinal chemistry considerations. The parameters to be evaluated are the Lipinski rules, which states that an orally active drug may have a maximum of one violation and the pann-assay interference compounds (PAINS) alerts tool, a source of false positives for biologically active compounds. The top candidates, exhibit binding affinities within the range of -11.5 to -12.2. After SwissADME filtering, we will re-rank the ligand list, identifying 30 commercially available candidates for subsequent cell viability assays in SUM149 (TNBC) and SUM190 (HER2+) cell lines. This multifaceted approach integrates computational methodologies with rigorous experimental validation, paving the way for potential therapeutic interventions in IBC treatment.

#4483 New drug development opportunities for PARP1.

P. Iglesias, D. Moreiras, L. Porres-Ventin, L. Gonzalez-Rendo, J. A. Zumalave, **V. M. Arce**, J. A. Costoya;
Universidad Santiago de Compostela, Santiago De Compostela, Spain

Personalized therapies allow, not only the increase of its therapeutic efficiency, but also the reduction of the secondary effects associated to the treatment of cancer. Data obtained in our group suggest that PARP1 could play a key role in the cell cycle regulation through its interaction with E2F1 transcription factor. Considering that most oncogenic processes is associated with cell cycle deregulation, the disruption of this interaction would provide a new therapeutic target of great interest and wide spectrum of indications. Therefore, our goal was to find molecules that interfere its role in cell-cycle regulation without affecting its function on DNA repair. The identification of novel compounds disrupting the PARP1/E2F1 interaction was carried out by combining *in silico* and *in vitro* screening, using a rational drug design. The virtual screen was performed using a molecular library of several million compounds at the selected target site, using AtomNet® (Atomwise), the first deep learning neural network for structure-based drug design and discovery. Since there is no complete structural information of the PARP-1/E2F1 protein-protein interaction, a homologous structure of BRCT domain of BRCA1 complex with the phospho-peptide (PDBID: 1T2V) was utilized to identify the potential binding interface of BRCT domain of PARP-1 (PDBID: 2COK) and the E2F1 protein. Top scoring compounds were clustered and filtered to arrive at a final subset of 83 compounds, library that were incorporated to our in vitro screening, which included both transcriptional (E2F1 activity) and survival studies. Twelve compounds were finally selected, based upon their higher capacity of inhibiting E2F1 activity.This work was supported by Agencia Estatal de Investigación (AEI/10.13039/501100011033), Xunta de Galicia (GPC GI-1862, ED431B 2020/26; ED431G 2019/02) and European Regional Development Fund-ERDF. AIMS Awards Program - Project A19-513, Atomwise Inc.

#4484 Discovery of a potential first-in-class Za targeted small molecule inhibitor of ADAR1 p150 which demonstrates strong anti-tumor efficacy.

A. Goswami[1], S. Goyal[1], K. Singh[1], P. Khurana[1], B. Deb[1], **A. Kulkarni**[2];
[1]Aten Porus Lifesciences, Bangalore, India, [2]Avammune Therapeutics, King of Prussia, PA

Background: Adenosine deaminase, RNA specific (ADAR1), catalyzes the hydrolytic deamination of adenosine (A) to inosine (I) in double-stranded (ds) RNAs. ADAR1 has two isoforms: p110 in the nucleus and p150 in the cytoplasm. Both isoforms alter the coding and non-coding sections of self-dsRNA. The ADAR1 p150 isoform is expressed from an interferon (IFN)-response promoter and has a Z-DNA/Z-RNA binding domain at the N-terminus. ADAR1 has been implicated in promoting cell survival and resistance to immune response in several cancer types like multiple myeloma, breast, lung, liver, and skin cancer. Inhibition of ADAR1 p150 has the potential to enhance anti-tumor efficacy as monotherapy and in combination with other therapeutic modalities. The Zα domain of ADAR1 p150 provides exclusivity to p150 compared to the other isoforms. Herein, we outline the discovery of a potential first-in-class Zα targeted ADAR1 p150 inhibitor and degrader for cancer immunotherapy.

Methods: AVA-ADR-001 was identified through a high throughput p110 knockout cell-based assay. The ability of AVA-ADR-001 to induce interferons was confirmed in various cell lines. The anti-tumor efficacy of AVA-ADR-001 was evaluated in B16F10 syngeneic melanoma mice model as monotherapy and in combination with anti-PD-1. PROTAC AVA-ADR-703 was used to demonstrate selective degradation of the ADAR1 p150 protein.

Results: We have discovered AVA-ADR-001, a novel small molecule inhibitor of ADAR1 which significantly increases the IFN response in vitro in an MDA5-dependent manner. In vitro binding studies confirm that AVA-ADR-001 binds to the Zα domain of ADAR1 with low nM potency. AVA-ADR-001 demonstrates anti-tumor efficacy 1.5X superior to anti-PD1 ICB non-responsive tumor models. In addition, the AVA-ADR-001 monotherapy and combination groups showed a significant upregulation of numerous interferon-stimulated genes, including IFIH1, IFN-β, and CXCL-10. Finally, targeted protein degradation of ADAR1 p150 while sparing ADAR1 p110 was confirmed when cells were treated with AVA-ADR-703 with nM DC_{50}, the PROTAC variant of AVA-ADR-001.

Conclusions: To our knowledge, AVA-ADR-001 and AVA-ADR-703 are the first selective Zα-targeted small molecule inhibitor and degrader of ADAR1 p150 respectively to be disclosed. As a powerful and targeted first-in-class ADAR1 inhibitor, AVA-ADR-001 has demonstrated a strong induction of interferon (IFN) in a number of cancer cell lines and *in vivo*. AVA-ADR-001 has also demonstrated strong *in vivo* anti-tumor efficacy as monotherapy and in combination with anti-PD1. Furthermore, AVA-ADR-703 demonstrates selective and highly efficient degradation of ADAR1 p150 while sparing ADAR1 p110. Given that ADAR1 has a pro-metastatic and immune-suppressive role, AVA-ADR-001 and AVA-ADR-703 have significant potential to emerge as strong cancer immunotherapy candidates.

#4485 Identification of novel lead compounds and repurposing FDA approved drugs as telomerase inhibitors using structure-based drug designing approach and their evaluation using in-vitro and ex-vivo assays.

D. Kaur, M. Chopra, D. Saluja;
Dr. B.R. Ambedkar Ctr. for Biomedical Res., Delhi, India

Introduction: Upregulated telomerase activity is an established hallmark in about 85-90% of cancer malignancies making it an attractive therapeutic target. However, the development of approved small-molecule telomerase inhibitors has been impeded by a lack of structural ambiguity for decades. In our study, we have employed a molecular dynamics approach to validate the binding site of BIBR1532, an approved telomerase inhibitor in the hTERT thumb domain followed by a structure-based drug designing approach to repurpose FDA-approved drugs and identify novel lead compounds targeting the enzyme.
Material and Methods: Due to the unavailability of a co-crystalized structure of BIBR1532 with the catalytic hTERT thumb domain, we employed a Molecular dynamics-based method to identify and validate the exact binding site of the inhibitor. Two pharmacophore models were generated for the putative and newly identified binding pockets which were screened virtually through an anti-cancer library and Drug Bank database. The models were validated on the basis of the fit value of the BIBR1532 and selectivity value indicating the favorable feature set required. The top hits obtained were filtered using drug-likeliness parameters like Lipinski, ADME, and TOPKAT followed by redocking into their binding site. Finally, lead molecules that were able to dock in the new pocket were validated using Molecular Dynamics (MD)simulation studies and their binding free energy was calculated using MM-PBSA calculations followed by their evaluation using in-vitro TRAP assay.
Results: Structural investigation, molecular docking studies, and confirmatory molecular dynamics revealed that the exact binding site of BIBR1532 is 8.4 Å away from the reported FVYL pocket strikingly with clinically relevant and characteristic interactions conserved. We have identified five lead compounds and four lead compounds from DrugBank and the anti-cancer library respectively, that were stable in the new binding pocket based on their MD trajectory analysis, and parameters like RMSD, RMSF, H-bonds and Radius of Gyration as well as their MM-PBSA scores. The lead compounds are being evaluated in vitro using TRAP assay and ex-vivo assays.
Conclusion: The study identified five existing FDA-approved drugs in the market for other diseases as potential telomerase inhibitors alongside four novel compounds that can be used for the treatment of cancer in the future after further validation studies.

#4486 Characterization of a novel mutant selective, EGFR sparing, ErbB2 inhibitor with activity across activating mutations in systemic and CNS tumors.

J. Fulton, T. Bettendorf, A. Blandon, K. Bouhana, R. K. Brizendine, L. Cable, M. J. Chicarelli, M. Crow, B. Fell, J. Fischer, A. Guarnieri, M. Hillman, R. Jalluri, V. Kumar, C. A. Malinky, R. Rieger, J. Robinson, L. Stunkard, F. Sullivan, J. I. Trujillo, S. Winski, Y. Zhou;
Cogent Biosciences, Inc., Boulder, CO

Alterations in ErbB2, including amplification, overexpression, insertions, and point mutations, are established oncogenic drivers in many solid tumors. These mutations are found in approximately 3-4% of breast cancers and 3% of advanced lung cancers and have emerged as mechanisms of acquired resistance to targeted therapies. ErbB2 alterations are also found in metastatic breast and lung cancers that have advanced to the brain and remain a major clinical challenge with limited therapeutic options. Currently approved ErbB2 tyrosine kinase inhibitors have inferior potency against these mutations and lack sufficient brain penetration to be an impactful treatment option for patients. Herein, we describe advanced preclinical profiling of our candidate series of brain-penetrant EGFR-sparing ErbB2 inhibitors with activity against prevalent point mutations and exon 20 YVMA insertions.

#4487 Simple modifications of 3-HPT for improved *in-vivo* activtiy.

R. E. B. Kern, S. Huang, U. Arunsi, A. Oyelere;
Georgia Institute of Technology, Atlanta, GA

One of the key targets in the treatment of castration resistant prostate cancer is HDAC6. HDAC6 removes acetyl groups from Heat shock protein 90 (HSP90), which is a protein chaperone that folds the androgen receptor. By inhibiting HDAC6 it is possible to prevent the expression of mutated androgen receptors, that are no longer responsive to androgen deprivation therapy, treating castration resistant prostate cancer. The Oyelere lab has previously demonstrated that 3-Hydroxypyridin-2-thione (3-HPT) can serve as a scaffold for HDAC6 inhibitors. While the unaltered 3-HPT has been shown on its own to inhibit HDAC6 in enzyme specific assays. The unaltered 3-HPT had no effect in whole cell assays. This work investigated simple modification of the 3-HPT scaffold to improve the in-vivo activity of 3-HPT. This work is an extension of work previously done in the Oyelere lab. The aim of this work is to apply simple modifications to the 3-HPT scaffold to improve the in-vitro activity. Previously 3-HPT was shown on its own to inhibit HDAC6 with an IC_{50} of 681nM but have no effect on cell assays. The hypothesis was that by converting the secondary amine into a tertiary amine the pharmacokinetic-properties of 3-HPT allowing can be improved focusing on cellular entry. The specific modification was the addition of alkanes and fluorinated alkanes at the secondary amine. This addition should improve the charge of the compounds improving the invitro activity. Based on molecular docking studies using Autodock vina, the introduction of fluorines improves the binding to HDAC6 by interacting with a hydrophilic pocket near the zinc ion. The preliminary in-vivo results in LnCAP and DU145 cells demonstrate that the addition of fluorinated alkanes has substantially improved the IC_{50} compared to the base 3-HPT compound. The base 3-HPT compound has an IC_{50} of greater than 100μM while the compounds with fluorinated alkanes have IC_{50} values in the range of 2-15μM. this data indicates improved drug likeness.

Preliminary IC50 values of compounds in prostate cancer cell lines

Compound Name	**LNCaP IC_{50}** (μM)	DU145 **IC_{50}** (μM)	Vero **IC_{50}** (μM)
SH-1-78	>100	>100	>100
SH-1-94	2.50	19.29	22.53
RK-1-187	96.95	95.45	88.57
SH-1-110	1.27	21.47	17.41
RK-2-16	2.09	62.86	18.76
RK-2-17	>100	>100	>100
RK-2-64	78.36	>100	76.45
RK-2-67	14.19	26.95	11.38

#4488 Newly developed organoiridium(III) complexes containing N,P-ligands possess antiproliferative activity in selected cancer cell lines.

R. Hezova[1], J. Hosek[1], N. Strakova[1], P. Simeckova[1], J. Masek[1], S. Kajabova[1], P. Starcha[2];
[1]Veterinary Research Institute, Brno, Czech Republic, [2]Palacky University Olomouc, Brno, Czech Republic

In conventional cancer treatment, platinum-based cytostatics are considered as standard therapy; however, they possess severe side effects. This fact leads to a constant effort to develop new non-platinum metallodrugs with different mechanism of action (MoA). In our study we developed new half-sandwich organoiridium(III) complexes, of general formulas $[Ir(\eta^5\text{-}Cp^*)Cl(L^{NP})]PF_6$ (1-3) and $[Ir(\eta^5\text{-}Cp^{ph})Cl(L^{NP})]PF_6$ (4-6) involving three different N,P-donor phosphinoalkylamines (L^{NP}), which we tested on 2D and 3D cancer models; HCp* = pentamethylcyclopentadiene, HCp^{ph}= (2,3,4,5-tetramethylcyclopenta-2,4-dien-1-yl)benzene. The most effective complexes 3 and 6 bearing 3-(diphenylphosphanyl)propan-1-amine had the highest cytotoxic effect against various cancer cell lines (THP-1, HeLa, SW982, A549, MOR) including a cisplatin-resistant lung carcinoma cell line (MOR/CPR) with IC_{50} values between 3.1 and 9.1 µM for specific cell lines. The cytotoxic effect was further demonstrated on 3D spheroids of lung cancer cells that revealed anti-cancer and anti-migration potential of complexes 3 and 6. Cell cycle and cell death analysis showed a different mechanism compared to the effect of cisplatin. Moreover, complex 3 did not decrease cell viability of non-cancerous cells (peripheral blood mononuclear cells and porcine chondrocytes) under 50% at a concentration of 20 µM. In addition, we report for the first time that organoiridium complexes showed high cytotoxic activity on cancer cell lines, including cisplatin-resistant cell line, with different MoA from cisplatin. They trigger expression of stress-related genes associated with oxidative stress, DNA damage, and endoplasmic reticulum stress and, moreover, complex 3 showed cytotoxic selectivity towards cancer cells. *This work was supported by the Czech health research council of the Ministry of Health of the Czech Republic (AZV Project NU22-08-00236).*

#4489 Developing dual FLT3/MNK inhibitors to overcome sorafenib resistance in FLT3-ITD AML cells.

L. Zhao[1], S. Zuo[1], K. Xing[1], X. Yue[1], H. Zhang[1], J. Zhang[1], S. Waxman[2], Y. Jing[1];

[1]Shenyang Pharmaceutical University, Shenyang, China, [2]Icahn School of Medicine at Mount Sinai, New York, NY

Acute myeloid leukemia (AML) patients with FLT3-ITD mutations are associated with poor prognosis. FLT3-ITD inhibitors developed only result in transient disease remission with disease relapse and resistance. Agents overcoming FLT3-ITD inhibitor resistance need to be developed. Sorafenib is one of FLT3-ITD inhibitors used in clinic. Using FLT3-ITD AML MOLM-13 cell line, we established a sorafenib resistant subclone MOLM-13/Sor, explored the resistance mechanism and revealed the overactivated mTOR signaling. MNK as one of the alternative mTOR signaling pathways is activated. MNK inhibitor eFT508 could overcome sorafenib resistance. Previously we developed a dual pyrido[3,2-*d*]pyrimidine MNK/PIM inhibitor 21o. Through optimization of 21o we obtained two new compounds H104 (IC_{50} values: MNK1 19 nM; MNK2 8 nM; FLT3-ITD 46 nM; PIM1 1388 nM) and H118 (IC_{50} values: MNK1 35 nM; MNK2 21 nM; FLT3-ITD 25 nM; PIM1 518 nM) with selective inhibition of MNK and FLT3 and losing PIM inhibition ability. H104 and H118 show better antiproliferative efficacy in FLT3-ITD MOLM-13 cells (GI_{50}: 1.07±0.04 μM and 0.99±0.08 μM) than non-FLT3-ITD HL-60 cells (GI_{50}: 7.04±0.15 μM and 4.78±0.31 μM). More intriguingly H104 and H118 exhibit superior antiproliferative effects in sorafenib resistant MOLM-13/Sor cells (GI_{50}: 0.44±0.05 μM and 0.24±0.06 μM). H104 and H118 decreased the levels of p-eIF4E, c-myc and Mcl-1, the downstream substrates of FLT3-ITD and MNK. Our data indicate that the activated MNK is one mechanism of FLT3-ITD resistance and the dual MNK/FLT3 inhibitors have advantage for FLT3-ITD AML treatment.

#4490 Targeting NQO1 with Episesaminol: A new therapeutic option identified for colorectal cancer using integrated systems biology and structural biology-based approach.

Sohini Chakraborty[1], Gaurav Sharma[1], Sricheta Karmakar[1], Prarthana Chatterjee[1], Saptarshi Sinha[2], Pradipta Ghosh[2], Satarupa Banerjee[1]

[1]Department of Biotechnology, Vellore Institute of Technology, Vellore, India, [2]Department of Cellular and Molecular Medicine, University of California San Diego, San Diego, CA

Introduction: Colon and/or rectal cancer together constitute colorectal cancer (CRC), the 2nd most lethal and the 3rd common cancer worldwide. Drug resistance to modern chemotherapies results in decreased therapeutic efficacy and CRC treatment failure. Herein, multi-layered strategies are used for a better identification of the newer therapeutics.

Methodology: Different publicly available datasets were used for the identification of the differentially expressed genes (DEGs) between normal and CRC tissues. miRNAs, lncRNAs and small molecules interacting with those DEGs were mined from various databases. A complex network of interacting mRNA-miRNAs-lncRNAs-small molecules was created using the Cytoscape. Hub RNAs, significant modules and cliques were identified using Cytohubba and MClique plugins. The mRNAs from the top 30 cliques were analyzed by expression, oncoprint, survival and gene ontology. Polyphenols from the PhenolExplorer database were also assessed for their druggability and toxicity properties to finally obtain druggable polyphenols (DPs). A two-step molecular docking was done using PyRx for mRNAs from top 30 cliques and DPs and the top ten complexes were docked again using AutoDock. Molecular dynamics simulation (MDS) is performed for the best fit protein-proposed DP vs protein-known drug using GROMACS.

Results: 1915 DEGs, 2609 miRNAs, 1411 lncRNAs and 8790 small molecules (other than selected DPs) interactions were considered for generating a comprehensive interaction network. The 27 mRNAs from the top 30 cliques were subjected to an array of analyses. NCAPD2, CDK4 and FASN were found to be involved in different stages of CRC. IRF2BPL, CMPK1, CCNF and UST were found as survival biomarkers, whereas FAT4 was found to be the only genetically altered mRNA. Functional enrichment supported the analysis revealing significant CRC-associated gene ontology as well as pathways. 56 DPs when docked with the DEGs, the two-step docking revealed NQO1-Episesaminol to be the best target-drug complex. Results of docking were comparable when MDS was performed for NOQ1•Episesaminol Vs NQO1•Doxorubicin (approved drug).

Conclusion: In the current interaction network and MDS-based integrated analysis, significant druggable CRC biomarkers and their newer therapeutic solutions were identified. MDS reveals NQO1•Episesaminol as a potential target•drug combination for CRC.

#4491 Development of IRE-1 inhibitors for B cell cancer therapy.

A. Shao[1], C.-H. A. Tang[1], J. R. Del Valle[2], **C.-C. A. Hu[1]**;
[1]Houston Methodist Research Institute, Houston, TX, [2]University of Notre Dame, Notre Dame, IN

In response to the endoplasmic reticulum (ER) stress, the IRE-1 kinase/RNase splices the mRNA of the XBP-1 gene, resulting in the spliced XBP-1 (XBP-1s) mRNA that encodes the functional XBP-1s transcription factor. XBP-1s is critically important for the growth and survival of B cell leukemia, lymphoma, and multiple myeloma. When compared with other inhibitors targeting IRE-1, the tricyclic chromenone-based inhibitors B-I09 and D-F07, prodrugs harboring an aldehyde-masking group, emerged as the very reliable inhibitors for potent suppression of the XBP-1s protein. Protection of the aldehyde as a 1,3-dioxane acetal led to strong fluorescence emitted by the coumarin chromophore, enabling both B-I09 and D-F07 to be tracked inside the cell. We installed a photolabile structural cage on the hydroxy group of D-F07 to generate PC-D-F07. Such a modification significantly stabilized the 1,3-dioxane acetal protecting group, allowing for specific stimulus-mediated control of the inhibitory activity. Upon photoactivation, the re-exposed hydroxy group triggered the aldehyde-protecting 1,3-dioxane acetal to slowly decompose, leading to the inhibition of the RNase activity of IRE-1. Since chemical modifications of the hydroxy group could be used to tune 1,3-dioxane prodrug stability, we installed reactive oxygen species (ROS)-sensitive boronate cage groups onto B-I09 (BC-B-I09) and D-F07 (BC-D-F07) to achieve stimuli-responsive activities and improve tumor-targeting efficiency based on that cancerous B cells indeed produced higher levels of ROS than normal B cells. These boronate caged compounds could be further combined with the FDA-approved Auranofin, a thioredoxin reductase inhibitor, to achieve synergistic cancer-killing effects. These results led us to further develop a novel prodrug, TC-D-F07, in which a thiol-reactive dinitrobenzenesulfonyl (Dns) cage was installed onto the hydroxy group of D-F07. The electron-withdrawing Dns group in TC-D-F07 similarly stabilized the neighboring 1,3-dioxane acetal, allowing for stimulus-mediated control of its inhibitory activity. TC-D-F07 exhibited high sensitivity to intracellular thiols produced by cancerous B cells. In addition, when TC-D-F07 was decomposed into D-F07, we observed that a dinitrophenyl cysteine adduct resulting from cleavage of the Dns group could induce the ER stress, causing cancerous B cells to increase the expression of XBP-1s. However, the accumulated levels of D-F07 from TC-D-F07 and its gradual decomposition into the active IRE-1 inhibitor could eventually deprive cancer cells of all XBP-1s, leading to more severe apoptosis in TC-D-F07-treated than in D-F07-treated cells. Thus, TC-D-F07 with both ER stress-inducing and XBP-1s-inhibiting activities represents an IRE-1-targeting caged prodrug that can be used to treat B cell cancer effectively.

#4492 Deferiprone optimization for the treatment of triple-negative breast cancer.

A. Johnston, A. K. Oyelere;
Georgia Institute of Technology, Atlanta, GA

Triple-negative breast cancer (TNBC) is the leading cause of new cancer cases and the second leading cause of cancer deaths in American women disproportionately affecting Black and Hispanic women under 40. Currently, there is no targeted therapy for TNBC and treatment options to manage this lethal disease include surgery, adjuvant chemotherapy and radiotherapy. Among the chemotherapy agents, combination of the PARP inhibitors with DNA-damaging results in a more promising anti-tumor effect. A better understanding of TNBC etiology has aided in unraveling the roles of two additional cellular targets - androgen receptor (AR) and histone lysine demethylase (KDM) - in the viability and survival of TNBC. Interestingly, AR overexpression is the most important driver of prostate cancer (PCa). A class of current medications used to treat PCa act as androgen receptor (AR) antagonists (or antiandrogens). Antiandrogens are under investigation in the clinic as potential therapies for luminal AR (LAR) subtypes of TNBC, a particularly worrisome subtype that frequently metastasizes to regional lymph nodes and bones. Although LAR TNBC constitutes 15-20% of TNBCs, it is characterized by minimal response to chemotherapy and aggressiveness. It is therefore plausible to repurpose and optimize antiandrogens, in the context of designed multiple ligands; to obtain a TNBC-targeting therapy effective against several subtypes of this heterogenous disease, including the basal subtype that is responsible for ~80% of TNBC incidence. The proposed therapeutics are dual-acting antiandrogen-KDM inhibitors. The antiandrogen moiety of these agents will enable TNBC cell-targeting and translocation of the drug into the nucleus where inhibition of KDM will prevent transcription of KDMs that promote tumor growth. The three pharmacophores of these agents are (i) an AR binding group, (ii) a linker, and (iii) an iron-binding group. Two functional classes of these compounds, alkyl- and aryl-derivatives, vary in the design of the AR binding moiety. To optimize these agents, the methylene linker length is varied in each class for in vitro determination of the optimal length for increased drug efficacy. The compounds are tested on TNBC cell lines (MDA-MB-231, low AR+; and MDA-MB-453, high AR+), and ER+ BCa (MCF-7) while PCa cell lines (LNCaP PCa, AR+; and DU 145, PCa, AR-) serve as controls for AR dependency of the compounds. Longer linker length compounds exhibited low micromolar cytotoxicity and selectivity for AR+ TNBC and PCa cell lines. Further analysis of lead compounds in TNBC cells aided in understanding the effects on targets, transcriptomic effects via RNA sequencing analysis and the mechanism of action. Thus far, the designed dual-acting therapeutics have potential to revolutionize the design of anticancer drugs and improve treatment outcome for TNBC patients.

#4493 Protein structure inspired drug discovery.

F. Qiao[1], T. Binkowski[2], W. Anderson[3], W. Chen[1], G. Schiltz[4], K. Scheidt[4], A. Natarajan[1], R. Bergan[1];
[1]UNMC Eppley Institute, Fred & Pamela Buffett Cancer Center, Omaha, NE, [2]The University of Chicago, Chicago, IL, [3]Northwestern University, Chicago, IL, [4]Northwestern University, Evanston, IL

Introduction: Drug action is mediated by a small molecule therapeutic binding to a specific structural motif on a protein. As structure determines function, it follows that unique structural motifs are enriched for sites of unique function and high therapeutic target value. We hypothesized that protein structure constitutes high value *primary* information that can drive the discovery of novel therapeutic agents.
Method: We developed a unique physics-based protein structure analysis platform scaled to run on a supercomputer, allowing us to consider dynamic protein flexibility and the influence of solvent upon protein structure, and to probe large protein libraries as a primary source of structure information that can support up-front structure-based screens. We developed and then probed a high resolution protein x-ray crystallographic library, created and curated by us. From a 60 million compound library, we conducted virtual screens for docking to identified sites. 8-day colony formation assays were conducted on a panel of 8 human breast, prostate, lung and colon cancer cell lines, as well as 8- and 14-day trilineage hematopoietic colony formation assays on human cord blood stem cells.
Findings: From the first 180 deposited protein structures, we screened for unique protein surface structure. Structures were deemed unique if they were not otherwise known to be associated with any particular functional roles and were not the binding site of known therapeutics. Further selection included those that were clefts and possessed physical characteristics compatible with binding small chemicals whose properties have been linked to effective therapeutics. For each of 8 sites on 6 different proteins, a suite of analytics probed docking solutions from the compound library, generating a ranked list of 100 compounds for each site. Based on factors inclusive of availability and low potential for toxicity, compounds were acquired and used in in-parallel selection and de-selection functional assays. Cancer cell growth inhibition was a positive selection criterion, with additional ranking based on greater potency and broader efficacy. Bone marrow toxicity is limiting for most drugs, and inhibition of bone marrow stem cell growth was as a deselection criterion. Multiple compounds clustered around 2 sites on 2 different proteins. One compound, Dxr2-017, exhibited very high relative efficacy against colon and breast cancer cells. Evaluation of Dxr2-017 in the NCI-60 panel corroborated these findings, and showed even higher efficacy against melanoma. We demonstrated that Dxr2-017 inhibited melanoma growth with low nanomolar efficacy, while concentrations of over 2300-fold higher had only limited inhibitory effects on bone marrow stem cells.
Conclusions: This study provides proof-of-principle that protein structure constitutes high value primary information that can support identification of novel therapeutics. This approach is widely applicable and expandable.

#4494 Cryo-EM structure-based small molecule inhibitor drugs targeting CSPG4/NG2 in glioblastoma.

L. Neset, M. Nilsen, V. S. Arnesen, K. A. Alam, M. Chekenya, M. A. Rahman;
University of Bergen, Bergen, Norway

Background: Glioblastoma (GBM) is the most malignant primary brain tumor with a median survival of 15 months despite aggressive multimodal treatment. There is an urgent need for novel drug discovery for GBM. CSPG4/NG2 transmembrane proteoglycan is a validated target, upregulated in 50% of GBM patient tumours, drives malignant progression and is independently prognostic for poor survival. We have recently identified a cancer specific 13 bp frameshift deletion in the CSPG4/NG2 gene (CSPG4/NG2del13), which leads to reduced protein expression and slowed cell growth *in vitro* and tumor take *in vivo*. The 3D structure of CSPG4/NG2 has not yet been solved, and unsuited for structure prediction by AlphaFold2 due to its size and PTMs. The structure of CSPG4/NG2 domain 1 (residues 411-547), containing the site of the 13 bp deletion, has been solved using cryo-EM and can be useful for new drug design. We hypothesize that a small-molecule inhibitor that binds to this 13 bp region of the CSPG4/NG2 proteoglycan, might induce the same phenotype as the 13 bp deletion.
Methods: Using the published structure of domain 1, we performed *in silico* analysis to predict binding sites and docked 1280 compounds from the Prestwick Chemical library's database of FDA-approved drugs to these sites. The high ranked hits were further tested *in vitro* in GBM cells. Clonogenic survival, cell proliferation and scratch-wound assays were performed in patient derived P3, A172 and in CSPG4/NG2del13 heterozygous (HZ) GBM cells, that served as controls.
Results: Three binding sites were found in the close proximity to the 13 bp deletion region within the N-terminal domain 1 of CSPG4/NG2. Docking analysis revealed multiple drug candidates bound to the predicted binding site, three of which were further analyzed. Dopamine is found to closely interact with CSPG4/NG2 domain 1, near the 13 bp deletion site, forming hydrogen bonds with Glu413 and Glu521. Pyrazinamide forms two hydrogen bonds with Glu521. 5-Azacytidine fits well into active site 1, establishing hydrogen bonds with key residues Gly475, Glu482, Val472 and Thr473. The *in vitro* functional assays showed that the top hits have a dose dependent negative effect on colony formation and cell proliferation in P3 and A172 GBM cells ($P < 0.0001$). The treatment with the same drug IC_{50} doses led to a growth rescue in the CSPG4/NG2del13 HZ cells compared to the WT cells ($P < 0.001$). 5-Azacytidine showed a significant inhibitory effect ($P < 0.0001$) on cell migration in P3, A172 GBM cells and also in HZ cells, ($P < 0.001$).
Conclusion: The residues spanning the site of 13 bp deletion have chemical motifs that are salient for docking small molecule inhibitors that disrupt CSPG4/NG2 function. N-terminus domain 1 and full-length CSPG4/NG2 proteins for Cryo-EM 3D structure determination are being used to interrogate biochemical kinetics and identify new target regions.

#4495 Structure-based screening for potential ROR1 inhibitors and their potential as antitumor agents in pancreatic cancer cells.

I. K. Singh[1], S. R. Gupta[1], P. Mittal[2], S. Soni[2], J. H. Lo[2], F. Battaglin[2], Y. Yang[2], L. Torres-Gonzalez[2], S. Algaze[2], P. Jayachandran[2], K. Ashouri[2], A. Wong[2], W. Zhang[2], J. Millstein[2], H. J. Lenz[2];

[1]Deshbandhu College, University of Delhi, New Delhi, India, [2]USC - University of Southern California, Los Angeles, CA

Background: The identification of novel compounds that specifically target cancer cells while sparing normal tissues is crucial. The orphan tyrosine kinase-like receptor 1 (ROR1) is one such target expressed exclusively in various human malignancies, including pancreatic cancer, but not in normal adult tissues. Inhibiting ROR1 signaling shows promise in halting pancreatic cancer cell proliferation and invasion. In this study, lead compounds CSF1R-IN-1 and MCULE-8715589337 were found as potential inhibitors of the ROR1 and were further evaluated for its potential effect on pancreatic cancer cell viability.

Method: We curated a compound library of 6 million from PubChem, 2 million lead-like compounds from ZINC15, and 2 million compounds from diverse vendors. Employing Glide's HTVS followed by XP, we refined the selection based on docking scores lower than the reference molecule, Ponatinib. Compounds were shortlisted by pre-simulation MMGBSA calculations with Schrödinger Prime MM-GBSA module, focusing on compounds with energies below -100 kcal/mol. Then we performed MD simulation for 100ns. Post-simulation MMGBSA on the last 1 ns of simulation assessed change in ligands' binding energies. The selected leads underwent further validation utilizing two pancreatic cancer cell lines, MiaPaCa-2 and PANC-1. Half-maximal inhibitory concentration (IC50) was assessed using MTS cell viability assay.

Result: Comparing pre- and post-simulation MMGBSA energies, the reference compound showed increased, while CSF1R-IN-1 and MCULE-8715589337 exhibited decreased energies. The reference ligand's RMSD showed stability with fluctuations of 3 to 3.5 Å, whereas CSF1R-IN-1 and MCULE-8715589337 had stable and lower RMSD values (approximately 3 Å and 2.4 Å). Test compounds, CSF1R-IN-1 and MCULE-8715589337 showed better molecular interactions with ROR1 compared to reference. The reference compound formed hydrogen bonds with ILE555 and ASP633, along with pi-pi stacking with PHE552. CSF1R-IN-1 forms a hydrogen bond with ILE555 and ASP633, pi-pi stacking with PHE552, and interaction with SER632 through a water bridge. Additionally, compound MCULE-8715589337 forms hydrogen bonds with ASP633, SER632, LYS506, and GLU523. CSF1R-IN-1 notably inhibited proliferation in MiaPaCa-2 cells (IC50: 1.29 µM) while no efficacy in PANC-1 cells (IC50: 78.41 µM). MCULE-8715589337 showed relatively similar IC50 values of 39.06 µM and 37.73 µM in MiaPaCa-2 and PANC-1 cells, respectively.

Conclusion: The reduction in MMGBSA energies, low RMSD values, and a higher number of interactions highlight the better characteristics of both compounds compared to the reference. Our findings show CSF1R-IN-1 and MCULE-8715589337 have efficacy in pancreatic cancer cells, but further studies are required to validate and to understand the mechanism of action.

#4496 A computational initiative to determine the role of dietary polyphenols against oncogenic KRAS mutants.

P. Chatterjee[1], R. Karn[1], S. Chakraborty[1], S. Sinha[2], P. Ghosh[2], S. Banerjee[1];
[1]Vellore Institute of Technology, Vellore, India, [2]University of California San Diego, San Diego, CA

Introduction: Two oncogenic driver mutants (G12C and G14D) of KRAS have been reported to drive tumorigenesis in several cancers and targeting the switch I/II domain of mutant KRAS oncoprotein can be an efficient strategy for inhibiting the mutated KRAS-driven tumors. Modern clinical therapeutics are often associated with several adverse side effects and the eventual development of multi-drug resistance. Herein, exhaustive computational strategies are employed in designing dietary polyphenol-based small molecule inhibitors against such oncogenic KRAS tumors.
Methodology: Integrated bioinformatics strategies such as pharmacokinetic property prediction, analysis of medicinal chemistry profile, density functional theory (DFT) study, molecular docking, molecular dynamics simulation (MDS) and principal component analysis were performed to screen 930 dietary polyphenols to identify potent inhibitors against the G12C and G14D mutants. Sotorasib, an FDA-approved KRAS chemotherapeutic inhibitor was used as a reference drug in this study.
Results: Out of the 930 dietary polyphenols screened, based on the properties of pharmacokinetic descriptors and medicinal chemistry profile, 512 molecules were shortlisted for further studies. Five dietary polyphenols viz. Quercetin, Luteolin, Peonidin 3-O-glucoside, Myricetin, and Kaempferol identified via DFT and MDS exhibited the highest binding affinity and optimum energy profiles with our selected mutants G12C and G14D. An all-atom MDS study executed over 200 ns each revealed that Quercetin, Luteolin, and Peonidin 3-O-glucoside show favorable thermodynamic stability with significantly less conformational perturbations with G12C mutant. By contrast, mutant G12D complexed with Kaempferol and Myricetin exhibited the least thermodynamic flexibility and stable backbone trajectory, when compared to clinically standardized KRAS inhibitor Sotorasib. The efficient and higher binding stability of the polyphenols targeting the KRAS mutants, G12C and G14D switches I/II is mainly attributed to the formation of hydrogen bonds and other hydrophobic interactions at the molecular level. All five evaluated polyphenols qualified the parameters of cell-line cytotoxicity hinting at remarkable chemotherapeutic efficacy.
Conclusion: Computer-aided drug designing performed here aided the identification of natural dietary polyphenolic inhibitors as potential drug candidates exhibiting stable binding dynamics like Sotorasib, which thus awaits validation through further *in-vitro* analyses in inhibiting KRAS-driven tumorigenesis.

CHEMISTRY: Targeted Protein Degradation
Poster Session

#4500 A high-throughput approach to discover and characterize glueable ligase-target pairs.
A. Sen, P. Burke, R. Bansal, D. Krayushkina, D. Noble, K. McGowan, N. Seelam Murakowska, P. Reed, J. Barrett, **R. Lopez**;
A-Alpha Bio, Seattle, WA

Targeted protein degradation can be induced with monovalent small molecules, termed molecular glues, that modify the substrate-binding interface of E3 ligases and reroute them to novel targets. Despite there being over 600 E3 ligases encoded in the human genome, most glues have focused on only a few. Expanding to additional ligases and targets is challenging due to the low probability of successful 'glueing.' Many have suggested that a weak basal interaction between a ligase and neo-substrate is an important prerequisite for the function of a molecular glue, but such weak interactions are challenging to discover. To address this need, we have harnessed AlphaSeq, a synthetic biology platform that measures protein-protein interactions at scale and with high sensitivity, to identify and characterize novel E3-target pairs. Our approach is twofold. First, we test for novel weak interactions (~100nM to 10uM) between a panel of E3 ligases and a library of disease relevant target proteins. Second, starting from a weakly interacting protein pair, we build mutational libraries of both proteins and measure their binding strengths. Mutations that strengthen binding serve to validate the weak interaction, provide structural insights into the nature of binding, and help to inform subsequent small molecule discovery. Here, we present our approach to discover and evaluate glueable ligase-target pairs using AlphaSeq, validation through proof-of-concept experiments involving a known interaction agonized by small molecules, and examples of novel glueable ligase-target pairs that we have recently discovered.

#4501 First reported PIM kinase degraders: Design, profiling & optimization.

C. Legros[1], P. Ratcliffe[2], V. Porkolab[3], M. Modugno[4], O. Mirguet[1];

[1]Eurofins Discovery, Celle Levescault, France, [2]Eurofins Discovery, Ongar, United Kingdom, [3]Eurofins Cerep, Celle Levescault, France, [4]Eurofins DiscoveryOne, Ongar, United Kingdom

The PIM serine/threonine kinases (PIM1/PIM2/PIM3) are downstream effectors of ABL, JAK2 and Flt-3 oncogenes and are required for tumorigenesis. Overexpression has been reported in hematological and solid tumors, myeloma, lymphoma, leukemia and adenocarcinoma. The first generation of PIM inhibitors to make it to the clinic, including SGI-1776, AZD1208 and PIM447, are known to be pan-PIM inhibitors, while the aim of this project was to identify novel & selective PIM3 inhibitors. To this end, several Hit-finding approaches were employed to rapidly generate novel chemical matter, which were then assessed for their activity against PIM3 using a robust ADP-Glo™ assay. In parallel to this Hit-findings activity, we used AZD1208 scaffold as a starting point to generate PIM3 bifunctional protein degraders and designed a specific screening cascade in order to profile such modalities. The PIM degrader library, synthetized using Automated Robotics Lab, was characterized using ADP-Glo assays. It was then screened on our binding and activity kinase platforms, KINOME*scan*® and KinaseProfiler™, and then fully profiled including ternary complex formation with biophysics and *in vitro* Safety Pharmacology Profiling Panels. One example is the AZD1208 derivate degrader, i.e. EC108154-1, which showed nanomolar range affinity for PIM3 and the E3-ligase CRBN-DDB1, and its affinity range was also confirmed with the ternary complex in SPR and MST-TRIC. This comprehensive screening cascade ensures an in-depth characterization and optimization of protein degraders, with the possibility of monitoring the ternary complex formation with biophysics methods. It is a good illustration of how this combination of tests can be instrumental in selecting the best degraders to progress to the next step of drug discovery.

#4502 Design, synthesis, and evaluation of next-generation EGFR degraders to overcome osimertinib-resistance.

M. Baig[1], J. Bok[2], D. Kim[3], S. D. Nale[4], Y. Jo[1], C. Kim[5], T. Park[4], **J. Dong**[1], B. Moon[3];
[1]Yonsei University College of Medicine, Seoul, Korea, Republic of, [2]Handok. Inc., Seoul, Korea, Republic of, [3]Handok. Inc, Seoul, Korea, Republic of, [4]BNJbiopharma. Inc., Seoul, Korea, Republic of, [5]Catholic University, Seoul, Korea, Republic of

The occurrence of C797S mutation in epidermal growth factor receptor (EGFR) is a leading mechanism of clinically acquired resistance to third-generation EGFR inhibitors, including Osimertinib. L858R/T790M/C797S and del19/T790M/C797S are commonly observed tertiary EGFR mutants identified in Osimertinib-resistant tumors. As of now, no clinically approved treatment exists that specifically targets these mutants. Here, we report the design and synthesis of a series of highly effective next-generation EGFR degraders effectively degrading EGFR C797S-containing triple mutants. Most compounds demonstrated antiproliferation activity in the subnanomolar range when tested on Ba/F3$^{L858R/T790M/C797S \text{ and } del19/T790M/C797S}$ cells. Not only C797S but our designed degraders also degraded a wide range of EGFR mutants, including Exon19Del and L858R/T790M (DC50 <100nM). One representative Compound, HDBNJ2812, strongly degrades L858R/T790M/C797S and del19/T790M/C797S with DC50 of 34 nM (Dmax 88.5%) and 14 nM (Dmax 99.7%), respectively. This compound potently inhibits the proliferation of Ba/F3L858R/T790M/C797S (GI50 64 nM) and del19/T790M/C797S (GI50 40 nM). HDBNJ2812 demonstrated high inhibitory potential on HCC827 (del19) and H1975 (L858R/T790M) cell lines (GI50 18.9 and 85 nM, respectively). Furthermore, this degrader demonstrates weak cytotoxicity on non-mutant EGFR-expressing cells, such as A431, WI-26 (human lung fibroblast cells), and CHO-K1 (Chinese hamster ovary cells). Additionally, the *in vivo* PK/PD findings complement this compound's potential to be considered further. HDBNJ2812 may serve as a lead compound to render the greater therapeutic window for treating resistant non-small cell lung cancer patients with EGFR C797S mutants.

#4503 Preclinical characterization of PRT7732: A highly potent, selective, and orally bioavailable targeted protein degrader of SMARCA2.

A. Shvartsbart, K. Ito, J. Rager, M. Hulse, A. Agarwal, K. Vykuntam, J. Burtell, M. Wang, J. Kurian, M. Cowart, J. Cote, N. Stahl, M. Sivakumar, A. Reichelderfer, J. Carter, A. Grego, C. Bachner, A. Moore, N. Bhagwat, R. Kuskovsky, S. Ganesan, S. Ruepp, T. Emm, P. Pitis, C. Basch, K. Bersch, Y. Pan, S. Mei, R. Leal, J. Rose, D. Roth, C. Xu, G. Cao, K. Vaddi, S. Lee, S. Geeganage, A. Combs, P. Scherle;
Prelude Therapeutics, Wilmington, DE

SWI/SNF (BAF) complexes play an important role in controlling gene expression by remodeling chromatin. SMARCA2 (BRM) and SMARCA4 (BRG1) are the core catalytic subunits of the SWI/SNF complexes, containing an ATPase domain and a bromodomain. SMARCA4 protein expression is lost in some cancers due to loss-of-function (LOF) mutations and homozygous deletions, and SMARCA4-deleted cancer cells are highly dependent on its paralog gene SMARCA2 for their survival. Therefore, targeting SMARCA2 in SMARCA4-deficient cancers using selective SMARCA2 degraders induces synthetic lethality while sparing SMARCA4 wild type (WT) normal cells. We have recently identified a series of orally bioavailable SMARCA2 selective degraders that demonstrate robust efficacy in pre-clinical animal models with favorable pharmacokinetic properties and safety profiles. Our nomination candidate PRT7732 exhibits >1000x selectivity for SMARCA2 over SMARCA4 in cell-based assays, with DC_{50} values in cancer cell lines in the low nanomolar range. The PRT7732-induced SMARCA2 degradation was rescued by a proteasome inhibitor and neddylation inhibitor, indicating ubiquitin-proteasome dependent degradation. Furthermore, PRT7732 does not change levels of known CRBN ligand neo-substrates such as IKZF2/3, GSPT1 and SALL4. PRT7732 inhibits only SMARCA4-deficient cancer cell proliferation with IC_{50} values ranging from 5.0-50 nM, but not SMARCA4 WT cells in vitro. Oral administration of PRT7732 resulted in near-total degradation of SMARCA2 protein with complete selectivity over SMARCA4 protein in a SMARCA4 WT lung cancer model in mice, consistent with the SMARCA2 degradation kinetics-based pharmacodynamic prediction model. PRT7732 oral daily administration showed significant tumor growth inhibition of SMARCA4-deficient lung cancer xenograft models at well tolerated doses. The treated tumor tissues show robust SMARCA2 protein reduction for 24h post dosing. In summary, our orally bioavailable SMARCA2 degraders induce synthetic lethality in SMARCA4-deficient cancers in vitro and in vivo. Efforts to further evaluate these compounds in additional models and in combination with other agents are ongoing.

#4504 Discovery of CBPD-409 and CBPD-268 as highly potent and orally efficacious CBP/p300 PROTAC degraders for the treatment of castration-resistant prostate cancer.

Z. Chen[1], M. Wang[1], D. Wu[1], L. Zhao[1], T. Xu[1], H. Metwally[1], Y. Wang[1], D. McEachern[1], W. Jiang[1], L. Bai[1], J. Luo[2], M. Wang[1], R. Li[1], J. Takyi-Williams[1], L. Wang[1], Q. Li[1], B. Wen[1], D. Sun[1], A. M. Chinnaiyan[2], S. Wang[1];

[1]University of Michigan, Ann Arbor, MI, [2]University of Michigan Medical School, Ann Arbor, MI

Prostate cancer remains the leading cause of cancer-related death globally in men. While current AR-targeted therapies are effective for the treatment of prostate cancer and improve patient survival, resistance in patients typically develops within 18 months. CBP/p300 are AR transcriptional co-activators and are promising therapeutic targets for the treatment of castration-resistant prostate cancer (CRPC). We developed a series of highly potent, selective, and orally efficacious CBP/p300 PROTAC degraders, with CBPD-409 being the best compound. CBPD-409 induces robust CBP/p300 degradation with DC_{50} 0.2-0.4 nM and displays strong anti-proliferative effects with IC_{50} 1.2-2.0 nM in VCaP, LNCaP and 22Rv1 AR+ cell lines. It has a favorable oral pharmacokinetic profile and achieves 50% of oral bioavailability in mice. A single oral administration of CBPD-409 at 1 mg/kg achieves >95% depletion of CBP/p300 proteins in the VCaP tumor tissue at 3 h and 24 h time points. CBPD-409 exhibits strong and dose/schedule-dependent tumor growth inhibition and is more potent and efficacious than two CBP/p300 inhibitors CCS1477 and GNE-049 and the AR antagonist Enzalutamide. To further improve the degradation potency and the oral bioavailability in rats, we developed a new class of CBP/p300 degraders based on our optimized CRBN ligand TX-16. Our efforts led to the discovery of CBPD-268 as an exceptionally potent, effective, and orally efficacious degrader of CBP/p300 proteins. In the VCaP, LNCaP and 22Rv1 cell lines, CBPD-268 induces consistent and robust CBP/p300 degradation with DC_{50} of ≤0.03 nM and D_{max} >95%, leading to potent cell growth inhibition. CBPD-268 has excellent oral bioavailability in both mice and rats and has a good ADME profile. Oral administration of CBPD-268 at 0.3-3 mg/kg resulted in profound and persistent depletion of CBP and p300 proteins in tumor tissues and achieved strong antitumor activity in the VCaP and 22Rv1 xenograft tumor models in mice, including tumor regression in the VCaP tumor model. CBPD-268 was well tolerated in mice and rats and displayed a therapeutic index of >10. Taken together, CBPD-409 and CBPD-268 are highly promising CBP/p300 degraders for further extensive evaluations for the treatment of CRPC and other types of human cancers.

#4505 Discovery of a cebrelon-based PTPN1/PTPN2 dual targeting degrader for cancer immunotherapy.

Z. Qu, Y. Bai, J. Dong, Z. Zhang, B. Huang, Y. Miao, A. W. Tao, P. S. Low, Z.-Y. Zhang;
Purdue University, West Lafayette, IN

Cancer immunotherapy has achieved notable clinical success, yet its broader application is impeded primarily by immune evasion mechanisms, predominantly stemming from factors such as tumor antigen loss, intrinsic low antigen presentation, and the inherent impermeability of current macromolecules, including cells, antibodies, and proteins. Consequently, there exists a pressing demand for more permeable agents that target intracellular components as viable alternatives. Among the various molecular players involved in immune evasion, PTPN1 and PTPN2, two protein tyrosine phosphatases (PTPs), play a non-redundant role in regulating tumor antigen presentation. They achieve this by modulating the JAK/STAT signaling pathway within tumor cells, with their deletion having been demonstrated to enhance MHC-I presentation across various cell types. Furthermore, PTPN1 and PTPN2 also negatively regulate T cell receptor (TCR) signaling in T cells, as supported by genetic studies. Consequently, these two proteins present as promising targets for the development of innovative cancer immunotherapies due to their dual impact on both tumor cells and T cells. Addressing the intrinsic impermeability challenges associated with macromolecules, we embarked on the development of small molecule agents that specifically target PTPN1 and PTPN2, culminating in the successful creation of a low-nanomolar proteolysis targeting chimera (PROTAC), designated as X1. PROTAC X1 exhibits sustained low-nanomolar binding affinity and exceptional selectivity toward PTPN1 and PTPN2 in in vitro settings. Furthermore, it has demonstrated a nano-molar half-maximal degradation concentration (DC50) in Jurkat T cells and numerous cancer cell lines, while concurrently exhibiting efficacy in eliciting TCR signaling and enhancing MHC-I presentation. Additionally, X1-treated CAR-T cells exhibited augmented cytotoxicity through increased IFN-γ secretion, thereby reinforcing its efficacy in T cell activation. To ascertain the anti-tumor efficacy of X1, we administered X1 to C57BL/6 mice bearing MC38 tumors, resulting in a significant retardation of tumor progression. Subsequent investigations revealed that X1 treatment induced an inflammatory response in the tumor microenvironment, characterized by enhanced T cell infiltration and the activation of CD8+ T cells. Notably, no discernible adverse effects, such as autoimmune symptoms, were observed during treatment. Collectively, these findings indicate that X1 represents a potent and safe agent for cancer immunotherapy. This study not only elucidates the mechanism of action of PTPN1B/TC-PTP pharmacological degradation as a viable approach for cancer treatment but also solidifies the potential of PTPN1B/TC-PTP degradation as a novel avenue for cancer immunotherapy.

#4506 Discovery of potent, highly selective and orally efficacious SMARCA2 degraders.

Lingying Leng, Lin Yang, Wenbin Tu, Rohan Rej, Srinivasa Rao Allu, Liyue Huang, Wei Jiang, Yu Wang, Jeanne Stuckey, Farzad R Sarkari, Meilin Wang, Lu Wang, Bo Wen, Duxin Sun, Shaomeng Wang

University of Michigan, Ann Arbor, MI

In human non-small cell lung cancer, melanoma and other types of human cancers, the mammalian SWItch/Sucrose Non-Fermentable (SWI/SNF) helicase SMARCA4 is frequently mutated, which leads to inactivation of its functions. SMARCA2, a close homologous protein of SMARCA4, is an attractive synthetic lethality target for human cancers with SMARCA4 deficiency. Herein, we report the discovery and biological evaluation of potent, highly selective, orally efficacious SMARCA2 PROTAC degraders exemplified by UM-SMD-8801. UM-SMD-8801 has DC_{50} <10 nM and Dmax >90% against SMARCA2 and >1,000-fold degradation selectivity over SMARCA4. Consistently, UM-SMD-8801 potently inhibits cell growth in SMARCA4 mutated cancer cell lines with low nanomolar IC_{50} values and shows >100-fold weaker activity in SMARCA4 wild-type cancer cell lines. UM-SMD-8801 has a good overall pharmacokinetic profile and an excellent oral bioavailability in mice. Oral administration of UM-SMD-8801 is highly effective in reducing SMARCA2 protein by >90% in tumor tissues in mice, while having minimal effect on SMARCA4 protein. UM-SMD-8801 represents a very promising SMARCA2 degrader for extensive evaluation as a potential new therapy for the treatment of SMARCA4-deficient human cancers.

#4507 Discovery of a smart molecular glue: A small-molecular compound selectively degrades Nrf2 in KEAP1-mutated tumor cells, by restoring the broken KEAP1 mutant/Nrf2 interaction.

X. Tian[1], T. Aboulkassim[1], Q. Liu[2], M. Hancock[3], J. Wu[1], G. Batist[1];

[1]Lady Davis Institute, Jewish General Hospital, McGill University, Montreal, QC, Canada, [2]Lady Davis Institute, Jewish General Hospital, Montreal, QC, Canada, [3]McGill University, Montreal, QC, Canada

Overcoming therapeutic resistance without incurring prohibitive normal tissue toxicity is a great challenge in anticancer therapies. Transcription factor NRF2 is a master regulator of cellular protective response, which provides protective effects in normal tissues. KEAP1, the endogenous NRF2 inhibitor, binds NRF2 and redirect it towards proteasome-dependent degradation. KEAP1/NRF2 interaction is therefore critical for maintaining NRF2 at a basal level. Accumulated studies revealed cancer cells could hijack NRF2 pathway to confer drug resistance. A number of clinically-relevant KEAP1 mutations were shown to disrupt the KEAP1/NRF2 interaction, leading to elevated NRF2 level and confer drug resistance. Here, by structure-based drug design approach, we discovered a small-molecule NRF2 inhibitor, R16, which selectively binds KEAP1 mutants and restores their NRF2-inhibitory function in tumor cells. We performed in silico screening against the NCI-open database. Top-ranking candidates were initially evaluated by ARE-luc reporter assays, leading to discovery of R16. Effect of R16 in restoring interaction between KEAP1 mutants and NRF2 were evaluated by BRET2 assays. Among 14 KEAP1 mutations that result in disruption of KEAP1/NRF2 interaction, R16 is active against 11 of them. A variety of assays, including tryptophan quenching, cellular target engagement, BRET[2] and GST-pull down assays, indicated that R16 selectively engage KEAP1 mutants and restore their interaction with NRF2, leading to NRF2 degradation. R16 at 0.5 uM substantially sensitizes KEAP1-mutated tumor cells to cisplatin and gefitinib, with no obvious effect in wild-type KEAP1 cells. Importantly, R16 showed significant in-vivo efficacy in sensitizing A549 xenograft bearing KEAP1 G333C mutation to cisplatin, while it has no effect on xenograft with wild-type KEAP1. KEAP1-mutated tumors are emerging as a sub-group with severe resistance to currently available therapies. Here, we have identified a KEAP1 mutant-selective NRF2 inhibitor, which potently sensitizes KEAP1-mutated cells/tumors to anticancer agents, with little effects on the WT-KEAP1. Our work demonstrated it is feasible to restore the NRF2-inhibitory function of KEAP1 mutants, by targeting the mutants with compounds to repair the disrupted KEAP1 mutant/NRF2 interactions. The KEAP1 mutant-selectivity is critical, as NRF2 is a master regulator of cellular defense response in WT-KEAP1 normal tissues.

#4508 Defining PIM kinase protein regulation and PROTAC for pre-clinical testing.

H. Liou[1], J. Brognard[2], R. Swenson[3], P. Torres-Ayuso[4], N. Warfel[1];
[1]University of Arizona, Tucson, AZ, [2]NIH/CCR, Frederick, MD, [3]NHLBI, Rockville, MD, [4]Temple University, Philadelphia, PA

The PIM kinase family are serine/threonine kinases known to be overexpressed in castration-resistant prostate cancer (CRPC). PIM1, an isoform of PIM, is known to regulate cell survival, migration, and proliferation. Uniquely, PIM kinases are constitutively active due to the lack of a regulatory domain. Therefore, PIM protein levels are reflected in PIM activity and are regulated by protein degradation and synthesis. PIM inhibitors have been developed, targeting the PIM kinase activity and inhibiting phosphorylation of downstream targets, but have had limited efficacy. Our lab and others demonstrate that PIM inhibitor treatment increases total PIM protein levels, suggesting that PIM kinases control protein stability via autophosphorylation. To elucidate the mechanism of autophosphorylation dependent regulation of PIM1, we used phospho-proteomics to identify potential autophosphorylation sites on PIM1. We have identified overexpression of deubiquitinase USP28 inhibiting degradation of PIM1, leading to the investigation of the role of F-box protein Fbw7 in regulating PIM1. Dominant-negative expression of Fbw7 results in increased PIM1 total protein. Additionally, coimmunoprecipitation of Fbw7 knockdown cells resulted in decreased PM1 ubiquitination compared to control. Therefore, we have identified Fbw7 as a putative E3 ligase responsible for PIM1 degradation. To address the limited efficacy of PIM inhibitors, we have developed the first PIM-PROTAC (PIMTAC) with our collaborators. Proteolysis targeting chimera (PROTAC) is a promising approach to eliminating the pro-tumorigenic effects of PIM. The PIMTAC selectively targets PIM kinases for degradation and we have demonstrated *in vitro* efficacy. PIMTAC successfully maintains degradation of all isoforms of PIM for over 72 hours. In vitro assessment of anti-tumor efficacy demonstrated increased apoptotic death with PIMTAC alone compared to PIM inhibitor or docetaxel. Furthermore, dual treatment of PIMTAC and docetaxel had more apoptotic death compared to PIM inhibitor with docetaxel. We aim to develop the PIMTAC for pre-clinical testing.

#4509 Discovery of potent and highly efficacious STAT3 PROTAC degraders capable of achieving long-lasting tumor regression.

R. K. Acharyya, L. Bai, H. Zhao, D. Wu, M. Hoda, M. Donna, W. Bo, D. Sun, S. Wang;
University of Michigan, Ann Arbor, MI

STAT3 (signal transducer and activator of transcription 3) is a transcription factor and a promising therapeutic targets for cancer and other human diseases. We have previously reported the discovery of SD-36 and SD-91 as potent, selective and highly efficacious STAT3 degraders. In the present study, we report the discovery of highly potent, selective and efficacious new STAT3 degraders. These STAT3 degraders were designed using our high-affinity STAT3 ligands and high-affinity VHL-1 ligands, with UM-STAT3-3100 being the best. In direct comparison, UM-STAT3-3100 is >10-times more potent than SD-36 and SD-91 in inducing STAT3 degradation in cells and are highly selective over other STAT members *in vitro* and *in vivo*. A single intravenous administration of UM-STAT3-3100 resulted in complete and long-lasting depletion of STAT3 protein for >48 hrs in tumor and native tissues. Weekly administration of UM-STAT3-3100 at 10 mg/kg achieved complete and long-lasting tumor regression in animal models of human cancer without any signs of toxicity. UM-STAT3-3100 is a promising compound for extensive evaluation for the treatment of human cancers and other human diseases in which STAT3 plays a key role.

#4510 Potent and orally efficacious PROTAC degraders of estrogen receptor α (ERα).

R. K. Rej[1], Z. Chen[1], R. K. Acharyya[1], D. Wu[1], B. Hu[1], G. Xu[2], R. Nagilla[2], H. Metwally[1], Y. Wang[1], B. Wen[1], D. Sun[1], L. Bai[1], S. Wang[1];
[1]University of Michigan, Ann Arbor, MI, [2]Proteovant Therapeutics, Philadelphia, PA

The estrogen receptor α (ER*α*) plays a crucial role in hormonally driven breast cancer, making it a clinically validated oncology target. Over the past 30 years, SERMs, SERDs, and AIs have been the mainstay of endocrine therapy for ER+ breast cancer, but relapse and resistance remains a significant challenge for metastatic breast cancer, leading to cancer recurrences, metastasis, and mortality. We report the discovery and extensive evaluations of potent and orally efficacious ERα degraders using the PROTAC technology through extensive optimization of the cereblon ligands, the linker and ER ligands. Our lead compounds (UM-ERD-3111 and UM-ERD-4001) achieved sub-nanomlar DC_{50} values in ER degradation and demonstrate excellent oral bioavailability. Oral administration of these ER degraders effectively reduces the ER wild-type and ER mutated proteins in tumor tissues in mice. Both ERD-3111 and UM-ERD-4001 are capable of inducing tumor regression *in vivo* and are more efficacious than ARV-471, a PROTAC ER degrader currently in phase 3 clinical development. UM-ERD-3111 and UM-ERD-4001 are highly promising compounds for extensive evaluations as potential new therapies for the treatment of ER+ human breast cancer.

#4511 Discovery of the first-in-class G9a/GLP PROTAC degrader.

J. Velez, Y. Han, H. Yim, P. Yang, Z. Deng, K.-S. Park, M. Kabir, H. Kaniskan, Y. Xiong, J. Jin;
Icahn School of Medicine at Mount Sinai, New York, NY

G9a and GLP are lysine methyltransferases that catalyze dimethylation of histone H3 lysine 9 (H3K9me2), a transcriptionally repressive mark. Aberrantly expressed G9a/GLP has been implicated in numerous cancers, including prostate, lung, and leukemia. The oncogenic activity of G9a/GLP is attributed to both its catalytic and non-catalytic functions, such as forming co-activator complexes with p300, CARM1, GRIP1, and Mediator to positively regulate gene transcription. As such, current G9a/GLP enzymatic inhibitors display limited anti-cancer activity. As an alternative therapeutic strategy, PROTAC degraders harness the ubiquitin-proteasome system (UPS) to effectively eliminate oncoproteins and abrogate all catalytic and non-catalytic functions. Here, we present the first-in-class G9a/GLP PROTAC degrader, MS8709, which potently degrades G9a and GLP in a time-, concentration-, and UPS-dependent manner. Moreover, MS8709 induces superior cell growth inhibition compared to its parent inhibitor in prostate, lung, and leukemia cell lines. Overall, MS8709 is a useful chemical tool to investigate G9a/GLP biology and offers a novel approach for the treatment of G9a/GLP-dependent cancers.

#4512 Discovery of highly potent, selective, and orally bioavailable IKZF2 degrader and its anti-tumor activity in syngeneic mouse models.

S. Park[1], J. Moon[1], G. Lee[1], H. Kim[2], J.-H. Kim[1], **J. Hwang**[2];
[1]Korea Research Institute of Bioscience and Biotechnology (KRIBB), Daejeon, Korea, Republic of, [2]Korea Research Institute of Chemical Technology (KRICT), Daejeon, Korea, Republic of

Molecular glue degraders (MGDs) are emerging as innovative therapeutic modalities, owing to their efficacy in targeting previously undruggable targets. MGDs induce close proximity between the target protein and E3 ligase, resulting in the degradation of the target protein. In the wake of the remarkable success of PD-1/PD-L1 inhibitors, various approaches to modulate the activity of regulatory T cells (Tregs) activity have been explored. Tregs represent the primary immune suppressor and significantly impede antitumor immune responses. IKZF2, a marker of stable suppressive Treg, is essential for maintaining the stable Treg cell phenotype. Depletion of IKZF2 can induce a transition from Treg to effector T cell (Teff) phenotypes, thereby enhancing anti-tumor responses. Leveraging an Immunomodulatory drug (IMiD), Novartis has developed the IKZF2 degrader DKY709, which is currently undergoing Phase I clinical trials, both as a monotherapy and in combination with a PD-1 immune checkpoint inhibitor. In this presentation, we present the preclinical results of the best-in-class IKZF2 degrader, PRT-101. PRT-101 elicits rapid and robust degradation of IKZF2, demonstrating subnanomolar DC_{50} and achieving 100% D_{max} in a proteasome- and CRBN-dependent manner. However, PRT-101 does not induce the degradation of well-known neosubstrates, including IKZF1, IKZF3, SALL4, and CK1a. Global proteomic analysis reveals that PRT-101 exclusively facilitates IKZF2 degradation. The degradation of IKZF2 by PRT-101results in an increase in IL-2 secretion, a marker of T effector function. Furthermore, oral administration of PRT-101 exhibits excellent pharmacokinetics, concurrent with IKZF2 degradation, yielding superior anti-tumor effects compared to DKY709 in the MC38 mouse syngeneic model. In conclusion, our findings underscore the potential of the novel IKZF2 degrader as a promising immuno-oncology target for the treatment of solid tumors.

#4513 Exploration degradation of intrinsically disordered protein YAP induced by PROTACs.

C. Zhou[1], C. Sun[2], L. Pi[2], C. Li[1];
[1]University of Florida, Gainesville, FL, [2]Tulane University, New Orleans, LA

Yes-associated protein (YAP), a potent oncogene and a key player in the Hippo tumor suppression pathway, has long been considered challenging to target due to its partially intrinsically disordered nature. However, recent advancements in High-throughput Screening (HTS) have yielded a breakthrough, as several YAP binders have been identified, igniting new possibilities in the quest to combat YAP-driven malignancies. Building upon this progress, a novel approach utilizing Proteolysis-Targeting Chimera (PROTAC) technology was employed to design and synthesize a series of YAP degraders. Here, our degraders were created by linking NSC682769, a previously reported YAP binder, with either VHL ligand 2 or pomalidomide using various linkers of different lengths and types. Among these degraders, YZ-6 emerges as the most promising, inducing rapid and sustained YAP degradation via promoting its ubiquitination-proteasome-dependent proteolysis. This process effectively suppressed YAP/TEAD-led transcription in both YAP-dependent NCI-H226 and Huh7 cancer cell lines. In addition to its degradation capabilities, YZ-6 also exhibited antiproliferative activity in both cell lines. Importantly, YZ-6 efficiently suppressed tumor development in the Huh7 xenograft mouse model, accompanied by a remarkable decrease in YAP levels, without adverse effects on the mice. These findings highlight the potential of PROTAC-mediated degradation as a viable strategy for reducing oncogenic YAP levels and attenuating downstream signaling in cancer cells. Moreover, the development of PROTACs based on NSC672869 holds promise for treating YAP-driven malignancies, opening new avenues for cancer therapy.

#4514 Discovery of potent and orally bioavailable degraders of HPK1 based on a novel HPK1 binder.

Z. Zhang, M. Wu, L. Wang, X. Yang, Z. Zhang, L. Guo, H. Pan, M. Zhao, L. Wang, S. Liu, Z. Dong, C. Jiang, H. Zheng, **D. Liu**;
Huadong Medicine, Hangzhou, China

Background: Proteolysis targeting chimeras (PROTACs) are novel structures designed to target a protein of interest (POI) for ubiquitination and degradation, leading to the selective reduction in the expression levels of the POI. Hematopoietic progenitor kinase 1 (HPK1) is considered a promising target for tumor immunotherapy. PROTAC-involved disruption of HPK1 protein activity enhanced the treatment efficacy of CAR-T-cell-based immunotherapies in different solid tumors and mouse models. Thus, targeting HPK1 by PROTAC to restore T-cell activity is an attractive approach to induce a greater immune responses in cancer.

Results: We designed and synthesized a series of HPK1 degraders by tethering our previously discovered novel HPK1 inhibitor with CRBN binder through various linkage. The most potent PROTAC effectively degrades HPK1 proteins in the Ramous cell in a dose-dependent manner and achieves DC_{50} value <50 nM. The maximum degradation (D max) values achieved are >90%. Our PROTAC showed EC_{50} value <100 nM for IL-2 and IFNγ production. PK studies revealed a low clearance, high plasma exposure and oral bioavailability in mice and rats. Furthermore, our PROTAC is shown to induce robust and statistically significant tumor growth inhibition in the MC38 and CT26 syngeneic model with increased T cell signatures observed within the tumor. The PROTAC in combination with anti-PD1 also resulted in robust anti-tumor activity with TGI > 90%. The 14 days DRF experiment shows that the compound has a great safety window(>200 folds).

Conclusion: We show here that a potent oral HPK1 degrader demonstrates strong immune cell activation and robust anti-tumor activity in mouse syngeneic tumor models, as a single agent and in combination with anti-PD1. Further evaluation of these potent degraders in additional in vivo studies will continue to build upon our mechanistic understanding of HPK1 degradation as a novel immunomodulatory approach for anti-tumor immunity.

#4515 Orally bioavailable PROTAC based MDM2 degrader.

A. Aguilar, J. Yang, Y. Li, D. McEachern, S. Wang;
University of Michigan, Ann Arbor, MI

Activation of the tumor suppressor p53, through inhibition of the MDM2 protein, has been pursued as a cancer therapeutic strategy and has produced many distinct inhibitors that are in clinical trials. A limitation arising from inhibiting the MDM2-p53 interaction is the upregulation of MDM2, itself a target gene of p53, and this attenuates the activation of p53 and efficacy of the inhibitors. To circumvent this limitation, we previously reported the first PROTAC based MDM2 degraders. These induced and sustained robust degradation of MDM2, achieved stronger p53 activation, and more potent anticancer activity than MDM2 inhibitors thus representing a new therapeutic strategy for targeting MDM2. Currently, all the PROTAC based MDM2 degraders are all dosed intravenously. Here we describe our design, synthesis, and optimizations that led to the discovery of the first orally bioavailable PROTAC based MDM2 degrader and our investigation of its therapeutic potential and mechanism of action. Consistent with its design to effectively degrade MDM2, our PROTAC effectively induces rapid degradation of MDM2 resulting in accumulation of wild-type p53 protein and activates p53 transcriptional activity in leukemia cells without accumulation of MDM2 protein. Consequently, it potently inhibits cell growth and induces apoptosis at low nano-molar concentrations in ALL and AML cell lines >10-100 times more potent than MDM2 inhibitors; and, after 50 mg/kg oral dose, 5 days/week for 3 weeks, it increased the median survival by 26 days of mice with disseminated RS4;11 cancer.

#4516 Inhibiting YAP activity in cancers by targeted degradation of TEAD.

H. Chen[1], A. Gridnev[2], N. Schlamowitz[2], G. Zheng[1], J. Misra[2];
[1]University of Florida, Gainesville, FL, [2]University of Texas at Dallas, Richardson, TX

The oncogenic transcriptional coactivators YAP/TAZ function as the terminal effectors of the Hippo signaling pathway and are dysregulated in many human cancers, where they promote cancer cell proliferation, survival, stemness, and resistance to targeted therapies, and thus provide a critical point for therapeutic targeting. YAP/TAZ activity is regulated by phosphorylation mediated by the kinase cascade of the Hippo signaling pathway, where phosphorylation causes cytoplasmic retention. Aberrantly activated Hypo/unphosphorylated YAP/TAZ translocates into the nucleus, where it exerts its oncogenic activity by associating with the TEAD1-4 transcription factors and inducing expression of genes encoding pro-proliferative and antiapoptotic factors. Since YAP/TAZ cannot be directly therapeutically targeted, its oncogenic transcriptional activity can be controlled indirectly by targeted degradation of TEAD. Here we report on the development of Proteolysis Targeting Chimeras that potently induces degradation of TEAD and inhibits YAP transcriptional activity and cell proliferation in YAP-dependent cancers.

#4517 Novel chemical degraders targeting NSD2 in head and neck squamous cell carcinoma (HNSCC).

A. Ismail[1], E. Roshchina[2], I. Topchu[2], G. Schiltz[3], Y. Boumber[1];
[1]The University of Alabama At B, Birmingham, AL, [2]Northwestern University, Chicago, IL, [3]Northwestern University, Evanston, IL

Head and neck squamous cell carcinoma (HNSCC) is the sixth most common cancer worldwide. Despite advances in treatments and significant efficacy of immunotherapy drugs in HNSCC, no effective targeted therapies have been approved in this disease yet. NSD2 is a histone lysine methyltransferase, which is overexpressed in HNSCC and is implicated in tumor growth, cell cycle regulation, epithelial-mesenchymal transition (EMT) and metastasis not only in HNSCC, but also in many other solid tumors. Development of inhibitors to the catalytic activity of NSD2 has been rather limited to date, which necessitates an alternative approach. To target NSD2, we have recently developed a series of novel proteolysis targeting chimeras (PROTACs), which chemically degrade NSD2 utilizing native cellular machinery - ubiquitin-proteasome system - with VHL as an E3 ligase. A series of >40 compounds were tested in HNSCC cell lines (JHU-011 and FaDu) and NSD2-dependent multiple myeloma cell line (KMS11) for degradation activity against NSD2 protein, and H3K36me^2 chromatin mark reduction, using Western blot. We also tested their anti-proliferative activity in cell viability assay (CTB) and clonogenic assay. Compounds NUCC-0227381, NUCC-0227384, NUCC-0227414 and NUCC-0227383 show promising results by reducing NSD2 and H3K36me^2 levels. NUCC-0227383 compound was highly promising, as it was the most potent in reducing NSD2/K36me^2 levels without affecting NSD1/NSD3 levels and had profound effects on HNSCC cell growth. Lead compound NUCC-0227383 was chosen for further testing and in preliminary testing, showed a dose-dependent, VHL-mediated, and proteasome dependent function. Proteomics analysis, testing for specificity of NUCC-0227383 against a panel of histone methyltransferases, and in vivo testing of this promising compound against HNSCC is planned.

#4518 Proteolysis targeting chimera (PROTAC)-driven internalization of antibodies targeting oncogenic cell surface receptors.

E. J. Tolosa[1], L. Yang[1], J. Ayers-Ringler[1], J. Mallareddy[2], J. Schaefer-Klein[1], F. Kosari[1], A. Natarajan[2], A. S. Mansfield[1];
[1]Mayo Clinic College of Medicine and Science, Rochester, MN, [2]University of Nebraska Medical Center, Omaha, NE

Antibody-drug conjugates (ADCs) are increasingly being used in clinic, and many novel ADCs are being tested in clinical trials. Most ADCs act by delivering cytotoxic payloads into target cells. The activity of most ADCs is predicated upon internalization to release the cytotoxic payloads intracellularly to act on the malignant cells. The degree of ADC internalization is incomplete or absent for many cell surface targets, limiting the activity of ADCs. PROTACs are heterobifunctional molecules that result in the polyubiquitylation of their targets by inducing proximity with E3 ligases. The proteasome then recognizes the poly-ubiquitin chains and degrades these targets. We hypothesized that PROTACs that act on the same targets as ADCs could improve the internalization and efficacy of these ADCs.

Using multiple cell lines derived from breast, lung or pancreatic cancers that express the oncogenic cell surface proteins EGFR (ERBB1), HER2 (ERBB2) or MET (HGF), we measured antibody internalization with live cell imaging. Antibodies were labeled with a pH sensitive reagent that fluoresces red (640 nm) upon exposure to acidic environments. Fluorescence was measured over time to create an area under the curve which was compared between the cell lines that were treated with and without PROTACs. Antibody internalization was observed in all cell lines that expressed the targets recognized by the antibodies. The addition of PROTACs targeting the same oncogenic cell surface proteins as the antibodies significantly increased antibody internalization beyond that observed without PROTACs. Internalization of antibodies was confirmed by measuring intracellular immunoglobulins by Western blot. Antibody internalization with PROTACs was dose-dependent, increased over time and was blocked by either the clatharin inhibitor Dyngo4a or the proteasome inhibitor MG132. In the case of HER2 for which there are FDA-approved anti-HER2 ADCs, the cytotoxicity of trastuzumab emtansine (TDM1) significantly increased with the addition of a HER2-targeting PROTAC across a range of doses.

PROTACs that target the same oncogenic cell surface proteins as antibodies improve antibody internalization and ADC cytotoxicity, in a process dependent upon clatharin and the proteasome. This novel application of PROTACs may impact the use of ADCs, and provides a rationale to combine these agents in clinical trials.

#4519 Discovery of highly potent, selective and efficacious STAT3 PROTAC degraders capable of achieving complete tumor regression.

H. Zhou, **D. Wu**, L. Bai, R. K. Acharyya, H. Metwally, D. McEachern, B. Wen, D. Sun, S. Wang;
University of Michigan, Ann Arbor, MI

STAT3 (signal transducer and activator of transcription 3) is a transcription factor and a promising therapeutic targets for cancer and other human diseases. We have previously reported the discovery of SD-36 and SD-91 as potent, selective and highly efficacious STAT3 degraders. In the present study, we report the discovery and extensive evaluation of highly potent, selective and efficacious new STAT3 degraders designed using novel cereblon ligands and novel STAT3 ligands. Our most potent STAT3 degraders are >10-times more potent than SD-36 in inducing STAT3 degradation in cells and demonstrates >100-fold degradation selectivity over other STAT members. They achieve nanomolar IC_{50} values in leukemia and lymphoma cancer cell lines with activated STAT3. A single intravenous dose of these STAT3 degraders reduces the STAT3 protein for >48 hrs in xenograft tumor and native tissues, without reducing another other STAT members. Weekly administration of these STAT3 degraders is capable of achieving complete tumor regression in xenograft tumor models without any signs of toxicity. Taken together, these STAT3 degraders are promising lead compounds for extensive evaluation for the treatment of the treatment of human cancers and other human diseases in which STAT3 plays a key role.

#4521 Investigating bAP15, a new inhibitor of UCHL5/USP14 deubiquitinating enzymes, as a potential treatment for chondrosarcoma: A comprehensive *in vivo* and *in vitro* study.

K.-L. Kuo[1], F.-S. Hsu[2], S.-J. Chang[3], S.-M. Liao[1], W.-C. Lin[3], T.-Y. Ke[1], T.-T. Liu[3], K.-Y. Huang[4];
[1]National Taiwan University College of Medicine and Hospital, Taipei, Taiwan, [2]YangMing Branch of Taipei City Hospital, Taipei, Taiwan, [3]National Taiwan University Hospital, Taipei, Taiwan, [4]National Cheng Kung University Hospital, Tainan, Taiwan

Chondrosarcoma, a highly resilient cancer characterized by limited effective treatment options, represents a significant therapeutic challenge. bAP15, a novel inhibitor of deubiquitylating enzymes (DUBs), has emerged as a promising therapeutic agent, exhibiting anti-tumor activity in various cancer models. This study investigated the efficacy of bAP15 against chondrosarcoma in vitro and in vivo. To evaluate bAP15's effects on chondrosarcoma cells, the SW1353 and JJ012 cell lines were employed. Cell viability, apoptosis, and cell cycle progression were assessed using MTT assay and flow cytometry. Western blotting was utilized to analyze apoptosis, cell stress, and endoplasmic reticulum (ER) stress. Additionally, a xenograft mouse model was established to examine the in vivo anti-tumor potential of bAP15. Compared to normal cartilage tissue, chondrosarcoma cells exhibited significantly higher expression of the DUB UCHL5, suggesting its potential involvement in chondrosarcoma development. Treatment with bAP15 effectively induced apoptosis in chondrosarcoma cells by activating caspases and cleaving PARP. Furthermore, bAP15 enhanced ER stress by activating caspase-4 and CHOP. In the xenograft mouse model, bAP15 demonstrated remarkable anti-tumor efficacy with minimal toxicity. These findings highlight the potential of bAP15 as a therapeutic strategy for chondrosarcoma. Its ability to induce ER stress and cell cycle arrest, coupled with its in vivo anti-tumor activity, provides compelling evidence for its further development as a novel treatment option for this challenging cancer.

EXPERIMENTAL AND MOLECULAR THERAPEUTICS: DNA Reactive Agents
Poster Session

#4525 Discovery of a highly potent and selective PARP1 inhibitor with superior PK and safety profiles.
y. wei, w. Li, z. li, m. li, k. kang, z. wen, t. yin, K.-L. Yu, G. Zhao, h. Yuan;
Acerand Therapeutics US, Carmel, IN

PARP inhibitors have been an effective treatment option for cancers deficient in homologous recombination repair, such as ovarian, breast, prostate, and pancreatic cancers, particularly those harboring BRCA mutations. However, their severe overlapping hematological and gastrointestinal toxicities have limited their clinical use, especially in the combination therapies with other anti-cancer agents. More recently, studies have shown that inhibiting PARP1 mainly drives anti-tumor activity while inhibiting PARP2 contributes to the hematological toxicity such as anemia due to its essential role in the survival of hematopoietic stem and progenitor cells. Thus, there is an urgent need for developing a selective PARP1 inhibitor. In this study, we report the discovery and characterization of a unique PARP1 inhibitor, ACE-86225106. This molecule is highly selective at inhibiting PARP1 over PARP2 as demonstrated in biochemical (72x) and DNA-trapping (131x) assays. It demonstrates potent anti-proliferative activities against BRCA mutant cancer cell lines (IC_{50} = 1-9 nM) but not against BRCA wild type cancer cells (IC_{50} >30,000 nM). As compared to the BRCA mutant cancer cells, this molecule is much less active at inhibiting the differentiation of $CD34^{+}$ hematopoietic stem cells (IC_{50} ≈ 450-1,400 nM), *i.e.*: erythroid, myeloid and megakaryocyte. The results of these studies show that ACE-86225106 is a highly potent and selective PARP1 inhibitor. This molecule has a unique PK profile characterized by its long half-life and low volume of distribution. As such, it demonstrates robust efficacy at low dose (1 mg/kg) with a less frequent dosing schedule (once a week). Importantly, there was no significant body weight loss observed in the treatment group even at much higher doses (10 mg/kg), but there was a significant body weight gain. The GLP toxicology studies have confirmed its superior safety profile as the maximum recommended safe starting first-in-human dose was >5-fold higher than the predicted human efficacious dose. Taken together, ACE-86225106 is a highly potent, selective PARP1 inhibitor with excellent PK and safety profile and expected to have a better safety profile, deeper and more durable clinical responses, and broader utility in the clinic as a preferred combination partner with other anti-cancer therapies. A phase 1 clinical trial to evaluate its safety, PK, and clinical utility is to begin in early 2024.

#4526 Inhibition of RNA Pol I transcription and induction of nucleolar stress in cancer cells treated with the experimental alpha-adrenergic receptor antagonist JP-1302.

S. Saproo, S. Papadaki, J. A. Espinoza, J. Bartek, **M. S. Lindstrom**;
Karolinska Institutet, Stockholm, Sweden

The inhibition of ribosome biogenesis through pharmacological means has drawn attention as a potential strategy in cancer therapy. In our previous study we highlighted a novel property of the FDA-approved antimalarial drug amodiaquine, demonstrating its ability to dose-dependently inhibit ribosomal RNA (rRNA) transcription, a critical step in ribosome biogenesis (Espinoza JA, et al Cell Death Diff, 2020). Amodiaquine was found to induce the degradation of the catalytic subunit of RNA polymerase I, known as POLR1A (RPA194), and resulting in nucleolar stress and the stabilization of p53. Notably, RNA Pol I shutdown occurred independently of DNA damage. Motivated by these findings, we sought to find additional inhibitors of ribosome biogenesis. Acridine derivatives display anti-cancer properties. The activity of acridines is mainly attributed to the planarity of these structures, which can intercalate within the DNA structure, and inhibition of chromatin associated protein targets including topoisomerases. JP-1302 is an experimental drug, on a 9-aminoacridine structural scaffold, acting as a selective alpha-2 adrenergic receptor antagonist. It was recently shown that JP-1302 inhibits transcription, blocking RNA Pol II phosphorylation and inhibiting p21 expression at a concentration of 10 µM (Mitchell DC, et al Nat Biotech, 2023). Given JP-1302's structural similarity to other acridine derivatives such as aminacrine, ethacridine, and the experimental compound BMH-21, all known to inhibit RNA Pol I transcription, we hypothesized that JP-1302 might share similar properties. The purpose of our new study was to evaluate JP-1302´s effect on ribosome biogenesis, p53, and cancer cell growth. We show here that JP-1302 acts as an inhibitor of RNA Pol I transcription. Treatment with JP-1302 induced a rapid decrease in the levels of POLR1A, cessation of rRNA synthesis and nucleolar stress already within six hours and at a concentration of 0.5 µM. JP-1302 treatment stabilized wild type p53 and enhanced p21 expression in the osteosarcoma line U2OS. RNA Pol I shutdown occurred in the absence of DNA damage response, as determined by gH2A.X staining. JP-1302 impaired the growth of both p53 wild type and p53 null HCT116 cells with GI50 values of around 0.6 µM, as well as in U2OS cells at 0.8 µM, as determined after 48 hours. Paradoxically, at very low concentrations JP-1302 appeared to transiently stimulate RNA synthesis, a phenomenon that will require further investigation. In conclusion, we identified JP-1302 as a novel inhibitor of ribosomal RNA synthesis, exerting this effect at concentrations that do not induce DNA damage, and independently of p53. Given that JP-1302 passes the blood-brain barrier in rodents, and accumulating in different brain regions, it is of future interest to evaluate this drug in brain tumor models.

#4527 TNG348 is synergistic with PARP inhibitors in tumor models with elevated replication stress.

A. Simoneau, H.-J. Wu, C. Pratt, G. Comer, S. Liu, S. Meier, T. Khendu, A. Choi, H. Zhang, B. Shen, D. Whittington, S. Sudsakorn, W. Zhang, Y. Yu, Y. Chen, B. Haines, A. Crystal, J. N. Andersen, J. Maxwell, S. Throner;
Tango Therapeutics, Boston, MA

Defective maintenance of genomic integrity is a hallmark of cancer cells that can result from oncogene-induced replication stress and by loss of DNA repair mechanisms. DNA repair deficiencies and elevated replication stress present targetable vulnerabilities for cancer treatment. Notably, BRCA1/2 mutant and homologous recombination deficient (HRD) tumors cannot repair double-strand breaks by homologous recombination and rely on alternative pathways of DNA repair. PARP inhibitors (PARPi), which are a standard of care in many BRCA1/2 mutant tumors, cause synthetic lethality with BRCA1/2 mutation by inhibiting the DNA base excision repair pathway. Despite the clinical benefit of PARPi, they are not effective in every HRD tumor and the acquisition of PARPi resistance limits long-term response. TNG348, a selective allosteric inhibitor of the deubiquitinating enzyme USP1, was specifically designed to target HRD vulnerabilities through an alternative mechanism. We previously showed that the anti-tumor activity of USP1 inhibition results from disruption of the translesion synthesis DNA damage tolerance pathway, a mechanism of action that is functionally distinct from base excision repair targeted by PARPi. Our preclinical studies show that TNG348 is active in HRD models and strongly synergizes with PARP inhibitors to drive strong anti-tumor responses. We have identified replication stress as a predictive biomarker of TNG348 response using cell line profiling and genome-wide CRISPR screens. For example, overexpression of oncogenes known to induce replication stress sensitized to the TNG348 and PARPi combination both in vitro and in vivo. These data indicate that cancer-specific elevated DNA replication stress could contribute to tumor sensitivity to TNG348 and provide additional patient stratification strategies and opportunities for indication expansion.

#4528 Improving carboplatin therapy: A novel albumin-targeted platinum(IV) prodrug with superior anticancer activity *in vivo*.

H. Schueffl[1], R. Weinmuellner[2], N. Sommerfeld[2], B. Keppler[3], W. Berger[1], C. Kowol[3], P. Heffeter[1];
[1]Medical University of Vienna, Vienna, Austria, [2]P4 Therpeutics GmbH, Vienna, Austria, [3]University of Vienna, Vienna, Austria

Platinum(II)-based chemotherapeutics are among the most commonly used anticancer drugs and are part of nearly every second treatment scheme. However, they lack in tumor specificity, causing severe sides effects, dose-dependent toxicity as well as drug resistance development. Due to their higher tolerability, platinum(IV) prodrugs are currently in the focus of interest. However, comparable to their platinum(II) counterparts, they show insufficient tumor accumulation and are frequently prematurely activated. A promising strategy to improve tumor targeting of anticancer drugs is to exploit the enhanced consumption and accumulation of albumin in the malignant tissue. Thus, we developed a new albumin-targeted maleimide-containing platinum(IV) prodrug, which releases carboplatin in a highly tumor-specific manner. The maleimide moieties enable the drug to selectively bind the endogenous albumin via its free thiol of cysteine 34. The aim of this study was to in-depth characterize the pharmacological behavior and anticancer activity *in vivo* of the new prodrug. To this end, several xenograft and allograft experiments were performed. To investigate tissue distribution and pharmacokinetics serum, urine, tumor and organ samples of mice were collected after drug treatment and were evaluated by (size-exclusion chromatography) inductively-coupled plasma mass spectrometry and immunohistochemistry (e.g cleaved caspase-3). These experiments revealed that the new prodrug fast and selectively binds to the serum albumin after intravenous injection, leading to an enhanced plasma half-life and an increased tumor accumulation in comparison to its corresponding platinum(II) drug carboplatin. Additionally, the new complex resulted in superior anticancer activity and prolonged overall survival based on the distinctly improved pharmacokinetic profile and enhanced apoptosis induction. In conclusion, these data support that albumin binding is a potent tool to increase the tumor specificity of platinum(IV) drugs and prevent their premature activation in other body compartments. Consequently, this very promising prodrug will be further developed towards clinical phase I testing.

#4529 Characterization of PARP inhibitor combination therapies in triple-negative breast cancer.

Elicia Fyle, Djihane Abdesselam, **Mallory Frederick**, Saima N. Hassan

University of Montreal, CRCHUM, Montreal, QC, Canada

Introduction: Triple-negative breast cancer (TNBC) is the most aggressive type of breast cancer, with limited targeted treatment options. TNBC patients can, however, benefit from targeted drugs known as Poly (ADP-Ribose) Polymerase inhibitors (PARPi). PARPi disrupt DNA repair pathways by targeting tumors with germline *BRCA1/2* mutations (*BRCA-MUT*) via synthetic lethality and PARP-DNA trapping mechanisms. Only 15-20% of the TNBC patient population are *BRCA-MUT* and can thus benefit from PARPi. However, preclinical studies and clinical trials have suggested that PARPi can also be effective in *BRCA1/2* wild-type (*BRCA-WT*) cancer cells that have genomic phenotypes similar to *BRCA-MUT* cells, a phenomenon known as BRCAness. Previously, we used whole transcriptome analysis in a panel of TNBC cell lines to identify a 63-gene signature for BRCAness. The 63-gene signature was shown to predict response to PARPi with an accuracy of 86% in patient-derived xenografts, and was present in 45% of TNBC patients. We hypothesize that targeting genes in this 63-gene signature can enhance the sensitivity of PARPi in *BRCA-WT* and *BRCA-MUT* TNBC cells. Our aim is to identify and target genes from this signature that are involved in DNA synthesis and repair pathways, to identify effective combination strategies with PARPi.

Methods: Using a PARPi-resistant TNBC cell line, MDAMB231, we carried out an siRNA screen of six genes from the 63-gene signature (*BARD1, BUB1, RRM2, FEN1, EXO1, and USP1*), chosen based on DNA repair functions and small-molecule inhibitor availability. The gene knockdowns were combined with the application of a potent PARPi, talazoparib, to determine the impact on DNA damage and cell death in TNBC cell lines. We then focused on targeting FEN1 function with the inhibitor LNT1. Using the Chou & Talalay combination index, we combined LNT1 with talazoparib to determine drug synergy in TNBC cell lines.

Results: The individual siRNA knockdowns of *BARD1*, *BUB1*, *FEN1*, *EXO1*, and *USP1*, in combination with talazoparib, led to increased γ-H2AX and cleaved-caspase 3 levels, indicating augmentation of DNA damage and apoptosis. In particular, the FEN1 inhibitor, LNT1 demonstrated efficacy as a single-agent and synergy in combination with talazoparib in both *BRCA-WT* and *BRCA-MUT* TNBC cell lines.

Conclusions: The siRNA screens, in combination with talazoparib, show that there are indeed targets within the 63-gene signature that can be used with PARPi that enhance DNA damage and cell death. The drug synergy shown between LNT1 and talazoparib in both *BRCA-WT and BRCA-MUT* TNBC cells suggests that LNT1 with PARPi could be an effective targeted combination approach, with great potential for TNBC patients.

#4530 Nuclear export inhibitor cooperates with PARP inhibitor to suppress the growth of metastatic castration resistant prostate cancer *in vivo*.

M. Uddin, A. Aboukameel, H. Y. Khan, S. F. Bannoura, F. Cackowski, R. Beydoun, G. Dyson, S. Kim, J. Boerner, V. Shidham, R. M. Mohammad, B. C. Pasche, A. S. Azmi, E. I. Heath;
Karmanos Cancer Institute, Wayne State University, Detroit, MI

Background: Aberrant nuclear protein transport, often observed in cancer, causes mislocalization-dependent inactivation of critical cellular proteins. Earlier we showed that overexpression of nuclear export protein exportin 1 (XPO1) is linked to higher grade and Gleason score in metastatic castration resistant prostate cancer (mCRPC). The network topology computational approach (NTCP) determined a higher synthetic lethal score between XPO1 and poly (ADP-ribose) polymerase (PARP1). We showed that selective inhibitor of nuclear export (SINE) could synergized with PARP inhibitors in mCRPC cell lines. Here we evaluated the efficacy of SINE and PARP inhibitor (PARPi) combination in cell line derived as well as patient derived xenograft (CDX and PDX) models and deciphered the mechanism of synergy.
Methods: For CDX model, the 22rv1 mCRPC cells were grown as subcutaneous xenografts in ICR-SCID male mice. For PDX model, tissue was collected from Champions Oncology (CTG-3581) and grown subcutaneously in CEIA/NOG male mice. SINE dosed orally at 10-15 mg/kg twice a week and PARPi dosed orally at 50 mg/kg daily. For *in vitro* mechanistic study, 22rv1 cells were subjected to RNAseq and proteomic analysis after treatment. Data analysis was performed using iPathwayGuide (advaitabio.com).
Results: The CDX and PDX showed pronounced anti-cancer efficacy by this combination compared to single agents without any significant weight loss. Survival analysis in CDX model demonstrated enhanced benefits to the mice of combination group. Immunohistochemistry (IHC) revealed apoptotic cell death in the combination group which is evident from cleaved caspase 3 staining and terminal deoxynucleotidyl transferase dUTP nick end labeling (TUNEL). To decipher the mechanism of synergy we performed transcriptomic (RNAseq) and proteomic analysis *in vitro*. We observed downregulation of DNA replication related gene minichromosome maintenance complex component 6 (MCM6) and cell division cycle 6 (CDC6) in the combination treatment. Gene set enrichment analysis (GSEA) also showed low enrichment scores for DNA replication. Proteomic analysis revealed a down regulation of DNA replication modulators such as HMGB2 and DNAJC9 which work on DNA coiling and histone respectively.
Conclusions: Taken together, this study revealed the therapeutic potential of SINE-PARPi combination via targeting DNA damage response pathway in mCRPC. Further evaluation of molecular synergy in the xenograft models are underway through RNA interference (RNAi) technique and Digital Spatial Profiling (DSP).

#4531 The synergistic potential of PARP inhibitors and irinotecan in small cell lung cancer.

Songji Oh[1], Miso Kim[2], Soyeon Kim[1], Bhumsuk Keam[2], Jeonghwan Youk[2], Tae Min Kim[2], Dong-Wan Kim[3], Dae Seog Heo[4]

[1]Cancer Research Institute, Integrated Major in Innovative Medical Science, Seoul National University College of Medicine, Seoul, Korea, Republic of,[2]Cancer Research Institute, Seoul National University Hospital, Seoul National University College of Medicine, Seoul, Korea, Republic of,[3]Cancer Research Institute, Integrated Major in Innovative Medical Science, Seoul National University Hospital, Seoul National University College of Medicine, Seoul, Korea, Republic of,[4]Cancer Research Institute, Seoul National University, Seoul, Korea, Republic of

Background: Small cell lung cancer (SCLC) is highly aggressive and associated with a poor prognosis. While effective treatment is limited after a relapse from platinum-based chemotherapy, recent research has identified novel pathway targets including DNA damage repair (DDR) pathway. Poly (ADP-ribose) polymerase inhibitors (PARPi) have been currently evaluated for their efficacy as a monotherapy and in combination with other agents, such as immunotherapy.
Methods: We evaluated the efficacy of combining PARPi and irinotecan in ten SCLC cell lines with diverse genetic backgrounds in the DDR genes. After treating the cells with three different PARPi in combination with irinotecan, we assessed cell viability and the combination effects. Furthermore, we confirmed protein changes in the DDR pathway through western blotting and measured the number of apoptotic cells using Annexin V staining.
Results: In our experiments, talazoparib had the most potent effect at low concentrations, while olaparib and venadaparib showed more pronounced synergistic effects (average fold change of IC_{50}: olaparib, 1649±4049; talazoparib, 25±34.21; venadaparib, 336±596.01; see Table). The combination of talazoparib or venadaparib with irinotecan led to a reduction of IC_{50} values to below 10 nM in 7 out of 10 tested cell lines. Three cell lines carrying *BRCA* mutations displayed a strong sensitivity to PARPi, whereas no significant correlation found with alterations in other DDR genes. The combined use of both drugs increased p-chk1 and p-p53 proteins, along with apoptosis signaling. Additionally, venadaparib alone did not induce cell toxicity but significantly increased apoptosis when combined with irinotecan, even at very low concentrations.

IC50 values of PARP inhibitors in SCLC cells w/ or w/o irinotecan 50 nM

	IC_{50} (nM)	Olaparib		Talazoparib		Venadaparib	
BRCA or *PTEN* status	Irinotecan 50 nM	-	+	-	+	-	+
BRCA1 deletion	NCI-H1694	5,933	148.9	52.38	2.19	>10,000	1.02
BRCA2 deletion	NCI-H211	392.8	37.20	2.28	0.99	3.82	0.94
BRCA2 deletion	NCI-H1048	1,704	282.7	9.74	2.36	62.01	3.02
PTEN deletion	NCI-H1341	>10,000	6,880	452.9	83.9	>10,000	>10,000
PTEN deletion	DMS 79	2,382	221.9	18.55	3.4	175.16	3.07
no mutation	NCI-H841	5,099	6,202	529.5	380.5	>10,000	>10,000
no mutation	NCI-H2029	>10,000	>10,000	478.2	56.16	>10,000	>10,000
no mutation	NCI-H2227	3,407	827.5	52.03	2.17	>10,000	0.69
no mutation	NCI-H146	5,094	3.31	56.11	0.86	1,295	0.93
no mutation	NCI-H209	579.2	0.05	5.24	0.05	8.18	0.04

Conclusions: The combination of a PARPi with irinotecan significantly inhibited cell growth more than the use of either agent alone. Our findings indicate that clinical trials are warranted to confirm the effectiveness of combining PARPi with irinotecan in patients with SCLC.

#4532 Discovery of DAT-1000A, a potent Polθ inhibitor that significantly enhances anti-tumor efficacy in combination with PARP inhibitor in homologous-recombination-deficient tumors.

D. Yan, Y. Zhang, Y. Zhang, J. Zhang, B. Wang, H. Chen, J. Shi, X. Lin, J. Zhuo, K. Zhou;
Danatlas Pharmaceuticals Co., Ltd., Beijing, China

Cancers exhibiting homologous recombination (HR) repair deficiencies due to mutations in genes like BRCA1 or BRCA2 rely on alternative DNA damage response (DDR) pathways to uphold genomic integrity. This vulnerability allows for the targeted disruption of these pathways through synthetic lethality approaches. DNA polymerase theta (Polθ, encoded by *POLQ*) assumes a crucial role in mending DNA double-strand breaks (DSB) via microhomology-mediated end-joining (MMEJ), one of the principal pathways for repairing DNA DSB. Notably, Polθ expression is minimal in normal tissues but becomes upregulated in HR-deficient cancer cells, positioning Polθ as a prime target for synthetic lethality in HRD cancers. Reversion mutations in HR-related genes frequently employ micro-homology deletion mechanisms. Consequently, the inhibition of Polθ holds the potential to thwart the emergence of PARPi resistance, primarily driven by BRCA reversion mutations. In this context, we introduce DAT-1000A, a novel small-molecule Polθ inhibitor exhibiting potent activity with a single-digital nanomolar IC_{50} value. Its efficacy in MMEJ functional assays validates its on-target cellular activity. Assessments of cell viability in HR-deficient BRCA2-KO DLD-1 cells, compared to their parental counterparts, reveal a striking synthetic lethality window exceeding 500-fold. Additionally, DAT-1000A displays synergistic anti-proliferative effects when combined with PARP inhibitors in BRCA1/2-mutated cells. In BRCA1/2-mutated xenograft models, DAT-1000A demonstrates robust and sustained tumor regression, as evidenced by the level of γH2AX, a common marker for double-strand breaks, which closely correlates with anti-tumor efficacy. Importantly, high-dose DAT-1000A treatment in mice elicits no significant abnormalities, underscoring its excellent tolerability. Collectively, DAT-1000A emerges as a novel Polθ inhibitor, offering both potent activity and a favorable safety profile, and holds promise for advancing therapeutic options in the realm of HRD cancer treatment.

#4533 Identification of DAT-2000A, a novel potent PARG inhibitor that selectively inhibits PARPi-resistant and homologous-recombination-deficient tumors.

D. Yan, Y. Zhang, Z. Yu, Y. Zhang, J. Zhang, B. Wang, H. Chen, J. Shi, Z. Bao, X. Lin, J. Zhuo, K. Zhou;
Danatlas Pharmaceuticals Co., Ltd., Beijing, China

A significant portion of patients with homologous recombination repair deficiencies(HRD) do not respond to PARP inhibitors, and even among those who initially respond, resistance often develops after PARP inhibitor treatment. This underscores the unmet clinical need to address the challenges in the treatment of HRD patients. Poly (ADP-ribose) glycohydrolase (PARG) plays a key role in hydrolyzing PAR chains from PARylated protein substrates, such as PARP1, serving as a critical checkpoint in DNA damage repair and the control of DNA replication stress. Therefore, PARG has emerged as a promising target for cancer therapy. Cancer cells experiencing replication stress, such as HRD breast cancer cells and those resistant to PARPi, exhibit sensitivity to PARG inhibition. DAT-2000A is a potent, selective, orally bioavailable small-molecule inhibitor of PARG, which directly binds to the catalytic domain of PARG, inducing the accumulation of poly-PAR chains at DNA lesions, and exhibits notable anti-proliferative activity across a wide range of HRD tumors both *in vitro* and *in vivo*. Biochemical assays confirm DAT-2000A's high potency and selectivity as an inhibitor of PAR-chain hydrolysis. In cellular assays, DAT-2000A demonstrates selective sensitivity in HRD cells, distinguishing itself from PARPi across various indications. Preclinical studies involving CDX and PDX xenograft models reveal that DAT-2000A exerts robust anti-tumor effects in both PARPi-sensitive and -resistant settings. Furthermore, it induces a dose and time-dependent accumulation of PAR chains, which may serve as a reliable pharmacodynamic biomarker indicative of PARG target engagement. In conclusion, DAT-2000A represents an innovative targeted therapy that warrants further investigation in clinical trials for the treatment of HRD cancers and beyond.

#4534 HSK40495, a highly selective PARP1 inhibitor with improved hematopoietic safety for the treatment of HRD cancers.

F. Li[1], X. Gou[2], L. Chen[2], Q. Meng[1], Y. Li[2], H. Dong[2], P. Tang[2], **J. Wang**[1], P. Yan[2];

[1]Haisco Pharmaceutical Group Co., Ltd., Shanghai, China, [2]Haisco Pharmaceutical Group Co., Ltd., Chengdu, China

It is well known that several PARP inhibitors have been approved for tumors with homologous recombination repair deficiencies (HRD), such as BRCA mutations. However, the common side effect of these inhibitors is hematologic toxicity, which limits their therapeutic index and combination potential with first-line chemotherapies. One possible reason is that currently approved PARP inhibitors do not specifically target PARP1, and might also affect other PARP family members. Recent studies have shown that the synthetic lethality caused by PARP trapping with HRD is mainly dependent on PARP1 inhibition, but not other PARP family members. Accordingly, we developed a selective PARP1 inhibitor that effectively inhibits tumor growth with less hematologic toxicity. HSK40495 is a potent PARP1 inhibitor with highly selectivity of PARP2. HSK40495 inhibited PARP1 enzymatic activity with a single digit nanomolar potency and with greater than 5000-fold selectivity against PARP2 in the protein binding assay. In addition, HSK40495 exhibited potent anti-proliferation activity in both DLD1(BRCA KO) cell and MDA-MB-436 cell, while had minimal effects against BRCA-WT DLD1 cell up to 30 μM in an anti-proliferation assay. In a subcutaneous MDA-MB-436 xenograft tumor model, HSK40495 administered orally once daily achieved excellent tumor growth inhibition of 100% at 3mg/kg. HSK40495 demonstrated significant PARylation inhibition in tumor tissues. Importantly, in CD34+ human bone marrow progenitor cell, HSK40495 showed improved cytotoxicity when compare to first-generation PARP inhibitor, Talazoparib. Meanwhile, in a lineage-specific hematotoxicity assay, HSK40495 exhibited improved cytotoxic safety in the process of differentiation of myeloid, erythroid and megakaryocyte compared with Talazoparib treatment. In summary, HSK40495, a highly selective PARP1inhibitor over other PARP family members, exhibits excellent pharmacological and safety properties, and also has the favorable pharmacokinetics profile in preclinical studies. All these findings suggest that HSK40495 has the great potential to be a promising PARP1 inhibitor for further development in the patients with HRD tumors.

#4535 JAB-26766: A small-molecule, orally bioavailable PARP7 inhibitor with high potency and selectivity.

Di Kang, Yanping Wang, Xin Sun, Man Yan, Haijun Li, Mingming Chen, **Yiwei Lin**, Wei Long

Jacobio Pharmaceuticals Co., Ltd., Beijing, China

Background: PARP7 (also referred to as TIPARP or ARTD14) is a mono-ADP-ribosyl transferase that inhibits type I interferon (IFN) signaling. Targeting PARP7 to restore antitumor immunity represents a promising treatment strategy. We have developed JAB-26766, an orally bioavailable, highly potent, and selective PARP7 inhibitor.

Methods: A time-resolved fluorescence energy transfer (TR-FRET) assay was applied to determine the binding and inhibition of PARP7 by JAB-26766. IFN-β secretion assay, STAT1 phosphorylation assay, and ISG (interferon stimulated gene) mRNA assay were performed to evaluate the inhibitory activities of JAB-26766 on the downstream signaling of PARP7. CellTiter-Glo assay was performed to evaluate cell viability upon treatment of JAB-26766. *In vivo* PK-PD study was conducted to evaluate the relationship between JAB-26766 concentration and the level of tumor STAT1 phosphorylation. The antitumor activity of JAB-26766 either as a single agent or in different drug combinations was evaluated in multiple mouse models.

Results: High potency of JAB-26766 on PARP7 inhibition as well as >1800-fold selectivity over PARP2 was observed through biochemical assays. At the cellular level, JAB-26766 induced IFN-β secretion, up-regulated ISG mRNA levels, increased phosphorylation of STAT1, and inhibited cell viability of multiple tumor cell lines (with most IC_{50} values below 50 nM). JAB-26766 combined with a STING agonist resulted in synergistic activation of STING pathway, as evidenced by increased CXCL10 secretion, and inhibited tumor cell proliferation. *In vivo* PK-PD study showed that JAB-26766 exposure in plasma and tumor has good correlation with induction of tumor STAT1 phosphorylation. Furthermore, JAB-26766 showed potent antitumor activity and good tolerability either as monotherapy or combined with STING agonist or anti-PD-1 antibody in mouse models of non-small cell lung cancer, breast cancer and colorectal cancer.

Conclusions: JAB-26766 is an orally bioavailable, highly potent, and selective PARP7 inhibitor that shows early promising anti-tumor activities.

#4536 MTAP loss alters the epigenetic landscape and demonstrates superior therapeutic sensitivity to concomitant PRMT5 and PARP inhibition in cholangiocarcinoma.

Pooja A. Shah, Ajay Kumar Saw, William Padron, Ming Zhao, Argun Akcakanat, Kurt Evans, Funda Meric-Bernstam, Milind Javle, Jordi Rodon, Kunal Rai

UT MD Anderson Cancer Center, Houston, TX

5'-methylthioadenosine phosphorylase (*MTAP*), is deleted in 15% of all cancers (estimated 100,000 patients per year in the United States), including 12-15% of cholangiocarcinoma (CCA) cases. MTAP deficiency accumulates 5'-methylthioadenosine (MTA) that subsequently binds protein arginine methyl transferase 5 (PRMT5) and inhibits its activity. This renders selective targeting of MTAP null tumors with agents (MRTX1719, AMG193, TNG462, TNG908) targeting MTA bound PRMT5 (PRMT5:MTA), while sparing surrounding normal *MTAP* wild-type (WT) tissue. Early signs of clinical activity was seen with MRTX1719, including objective responses in patients with *MTAP* loss tumors, including biliary tract cancer from the phase I/II study (NCT05245500). Despite these advances, prolonged targeted therapy poses the risk of development of acquired resistance demanding the need for better therapeutic strategies. To address this pressing need, we co-treated CCA cell lines with MRTX1719 and PARP inhibitor olaparib. We hypothesize that since PRMT5 is a critical regulator of splicing and DNA damage pathways, inhibition of PRMT5 disrupts these downstream processes creating an additional vulnerability to DNA damage inducing agents such as PARP inhibitors. Our preliminary data combining MRTX1719 with olaparib in three *MTAP* loss CCA cell lines (RBE, YSCCC, TFK1) show synergy (combination index; CI<1), and significant reduction in cell viability as well as colony formation ability when compared to monotherapy *in vitro*. To further gain mechanistic insights into the biology of *MTAP* loss, we stably expressed MTAP in *MTAP* null CCA cell line, RBE and demonstrated that *MTAP* loss drives tumorigenesis *in vivo* highlighting its tumor suppressor function in CCA. Mass spectrometry-based profiling of histone modifications from the isogenic RBE cell lines showed heightened methylation and reduced acetylation marks in the absence of MTAP. We also noted substantial differences in the distribution of splicing events, with increased intron retention, 3' alternative splicing and decreased exon skipping as a result of *MTAP* loss. Similar differences in proportion of splicing events were also observed in *MTAP* loss CCA patient derived xenografts as compared to WT models. Collectively, these data implicate MTAP to be a crucial player in modulation of the chromatin and splicing events that may drive therapeutic response to PRMT5 inhibition.

#4537 VB15010 is a potent PARP1 selective inhibitor and durable trapper with improved pharmacological activities.

D. D. Fang, Y. Liu, Y. Liu, H. Zhang, J. Wu, J. Wei, W. Sha, C. Z. Ding;
Shenzhen Yangli Pharmaceutical Technology Co., Ltd., Shenzhen, China

PARP inhibitors have become the backbone of therapy for patients bearing cancers with homologous recombination deficiency (HRD). Currently approved PARP inhibitors, such as olaparib, are pan-PARP inhibitors targeting PARP1, PARP2, and other PARP family members. Emerging evidence suggests that targeting PARP1 is sufficient to exert antitumor effect, whereas targeting PARP2 causes hematological toxicity. Consequently, these pan-PARP inhibitors often lead to dose reduction and treatment discontinuation in clinics. Therefore, developing PARP1 selective inhibitors becomes advantageous to improving patient outcomes and broadening the applications of the targeted therapy. To this end, multiple PARP1 selective inhibitors are currently in preclinical or early clinical development worldwide. We report herein preclinical investigation of a novel, potent PARP1 selective inhibitor and durable DNA trapper, VB15010, which demonstrates improved pharmacokinetic (PK) and pharmacodynamics (PD) properties, and antitumor activity in comparison with an advanced agent in clinical development. Comparatively, VB15010 exhibited higher selectivity for PARP1 over other PARP family members (30 to 8,000-fold) in enzymatic assays, and superior selectivity for PARP1- over PARP2-DNA trapping (>1700-fold) in DNA trapping assays. Genetic knockout of *PARP1*, but not *PARP2*, abolished inhibition of PARylation by VB15010 in *PARP1/2* wild type cells, further validating its PARP1 selectivity. Besides, VB15010 induced substantially more durable PARP1-DNA trapping when compared to the reference agent. In addition, VB15010 demonstrated potent antiproliferative activity in *BRCA*m or HRD-positive cancer cell lines (IC_{50} < 100 nM), as well as induced an increase in DNA damage, cell cycle arrest in G2 phase, and apoptosis in *BRCA2*-deficient cells *in vitro*. *In vivo*, VB15010 showed excellent bioavailability in preclinical animal models. Moreover, VB15010 exerted substantial antitumor activity at a dose range from 0.1 to 30 mg/kg, leading to tumor regression at as low as 0.3 mg/kg in *BRCA*m human cancer cell line-derived and HRD-positive patient-derived mouse xenograft models with an excellent PK-PD correlation. Tumor-to-plasma ratios of drug exposures indicate that VB15010 displayed a preferable tumor tissue distribution compared with the reference agent. Collectively, with improved PK-PD properties, including durable DNA trapping capability, higher apoptosis-inducing potency, and favorable tumor-to-plasma distribution ratio, as well as potent antitumor activity, VB15010 may achieve enhanced clinical efficacy and reduced hematological toxicity with a higher therapeutic index in patients. Its IND filing is expected in the first quarter of 2024.

#4538 Brigatinib induces synergy with PARP inhibitors through dual inhibition of FAK and EphA2 in high-grade serous ovarian carcinoma.

J. R. Duffield, X. Hou, I. K. McKeon-Makki, A. M. Huehls, B. W. Wilson, A. Prasad, X. Wu, S. H. Kaufmann, L. M. Karnitz, J. J. Weroha, A. Kanakkanthara; Mayo Clinic, Rochester, MN

PARP inhibitors (PARPis) have now become a standard of care for high-grade serous ovarian cancer (HGSOC), especially for those with defects in homologous recombination (HR) DNA repair. However, the innate and acquired PARPi resistance in HGSOC poses a significant concern, necessitating the exploration of novel treatment options and strategies. Here we investigated the potential of combining brigatinib—a second-generation anaplastic lymphoma kinase (ALK) inhibitor approved for treating lung cancer—with PARPis as way to enhance PARPi activity in HGSOC. Clonogenic cell survival assays revealed that brigatinib synergizes with PARPis in HR-proficient and -deficient HGSOC cell lines. In subsequent proteomics approaches and cell-based confirmatory studies, we found that brigatnib suppressed tyrosine kinases FAK and EphA2 with reduction in downstream signaling. Follow-up pharmacologic and gene-silencing techniques demonstrated that dual FAK and EphA2 inhibition additively reduces PI3K/Akt and MAPK/ERK cell survival signaling to levels conferring PARPi sensitivity. Additionally, the efficacy of this therapeutic approach on tumor size reduction was assessed in HGSOC patient-derived xenograft (PDX) models, with combination treatment inducing tumor regression more effectively than either agent alone. Overall, our studies unveil a beneficial ALK-independent effect of brigatinib that may offer new avenues for considering its repurposing as a HGSOC therapy.

#4539 ZM-2311 a novel and highly potent Polθ inhibitor demonstrates synergistically anti-tumor activities in combination with different therapeutics.

F. Zhou[1], L. Liu[2], L. Jiang[2], S. Qian[2], L. Xue[1], M. Li[2], Z. Li[1], Z. Li[2], J. Li[2], R. Tang[1];
[1]State Key Laboratory of Neurology and Oncology Drug Development, Simcere Zaiming Pharmaceutical Co, Ltd., Shanghai, China, [2]Simcere Zaiming Pharmaceutical Co, Ltd., Shanghai, China

Homologous recombination (HR) is a high-fidelity DNA double-strand break (DSB) repair pathway, and its dysfunction leads to cell genome instability and can result in tumorigenesis. In the situation of HR deficiency, DNA polymerase theta (Polθ) mediated microhomology-mediated end joining (MMEJ) is up-regulated to serve as a backup pathway for DSB repair. Several studies have proved that the inhibition of Polθ causes synthetic lethality with HR deficiency, and Polθ emerges as a potential DNA damage repair (DDR) target for the treatment of HR deficient tumors. In addition, there is evidence showing that the depletion of Polθ improves the sensitivity of some other DDR-related targeted therapies, chemotherapy, and radiotherapy. Here we identify a novel small molecular Polθ inhibitor, ZM-2311, which inhibits Polθ activity with an IC_{50} of 24 nM, and strongly inhibits cellular MMEJ pathway with a single nanomolar IC_{50}. ZM-2311 illustrates a robust potency against tumor growth in a MDA-MB-436 SHLD2-/- xenograft model, suggesting potential monotherapy application in BRCA1 mutation patients with TP53BP1/Shieldin complex deficiency. Besides monotherapy, ZM-2311 elicits strong synergetic anti-proliferation activities in combination with PARP inhibitors on $BRCA2^{-/-}$ DLD-1 and endogenous HR deficient tumor cells *in vitro* and *in vivo*. Tumor regression is observed even at a low dosage, indicating a high potency of ZM-2311. As reversion mutation of HR genes such as BRCA1/2 mediated by the MMEJ pathway is reported to be a mechanism of PARP inhibitor resistance, ZM-2311 is evaluated and demonstrates its potential to overcome the resistance to PARP inhibitors. Furthermore, the combination of ZM-2311 with other DDR agents, such as ATR inhibitors, induces fatal DNA damage to HR deficient cells. Considering a low risk of hematotoxicity of Polθ inhibition, ZM-2311 may provide a new combination option for DDR agents. Besides, ZM-2311 was assessed in combination with different therapies respectively which functionally induce DNA damage, such as radiotherapy and chemotherapy. ZM-2311 renders tumor cells more sensitive to radiotherapy in both HR deficient cells and proficient cells *in vitro*, accompanying with the upregulation of Polθ expression after radiotherapy and an enhanced phosphorylation level of H2AX in the combination treatment. Similarly, ZM-2311 also achieves a robust synergetic effect in combination with chemotherapy in cell lines with different HR statuses. These results indicate a potential application expansion of ZM-2311 to HR-proficient tumors, which is expected to bring better efficacy and reduced hematotoxicity. Taken together, ZM-2311 has proved to be a highly potent Polθ inhibitor and has promising combination potential with multiple therapy strategies.

#4540 SY-7021, a novel DNA-PK inhibitor, exhibits significant anti-tumor activity *in vitro* and *in vivo*.

K. Zhang, Z. Liu, Y. Gao, C. Lu, S. Cheng, X. Liu, **H. Luo**, Y. Sun;
Shouyao Holdings Co., Ltd, Beijing, China

Cancer therapies such as ionizing radiation or topoisomerase II inhibitors (for example, doxorubicin) induce DNA double-strand breaks (DSBs), which can subsequently be repaired by homologous recombination or non-homologous end joining (NHEJ). DNA-dependent protein kinase (DNA-PK), a nuclear serine/threonine protein kinase complex, is a pivotal component of the NHEJ process that maintain genome integrity. The critical role of DNA-PK in DNA damage response (DDR) and the dysregulated DNA-PK expression in cancer make it an intriguing therapeutic target for cancer, especially when combined with DSBs agents. Here, we identified a highly potent and selective DNA-PK inhibitor, SY-7021, with an IC_{50} value of 0.242 nM on DNA-PK kinase and high selectivity on ATM and ATR (greater than 400-fold) in biochemical assays. In a reporter assay for NHEJ repair, SY-7021 was able to dose-dependently reduce cellular NHEJ efficiency. Functionally, SY-7021 inhibited cell proliferation in multiple cancer cell lines alone or combined with doxorubicin. Basically, combination of SY-7021 and doxorubicin induced significant G2/M phase arrest and cell apoptosis, as well as enhanced the phosphorylation on Ser139 of γH2AX, Tyrosine 68 of CHK2 and Serine15 of p53 in MDA-MB-468 cells. In a subcutaneous NCI-H1703 xenograft tumor model, SY-7021 administered orally twice daily achieved dose-dependent tumor growth inhibition *in vivo*, with a tumor growth inhibition (TGI) of 105.6% at 60 mg/kg and no significant weight loss was observed. In addition, SY-7021 demonstrates good PK properties and acceptable safety profiles in *in vivo* studies. Collectively, SY-7021, a potent and selective DNA-PK inhibitor, shows significant inhibition on tumor growth in *in vitro* and *in vivo* studies, providing a rationale treatment for multiple tumors in monotherapy or in combination with other agents.

EXPERIMENTAL AND MOLECULAR THERAPEUTICS: Drug Combinations
Poster Session

#4546 Pegargiminase and melphalan as a novel drug combination strategy for uveal melanoma.

I. Pavlyk[1], J. Carpentier[1], E. A. Szlosarek[1], P. Y. Chan[2], J. S. Bomalaski[3], P. W. Szlosarek[1];

[1]Queen Mary University of London, London, United Kingdom, [2]The Wellcome Sanger Institute, London, United Kingdom, [3]Polaris Pharmaceuticals, Inc., San Diego, CA

Uveal melanoma (UM) is a hard-to-treat arginine auxotrophic cancer with approximately 50% of patients succumbing to metastases predominantly to the liver with a median overall survival of 19-22 months and a 5 year survival of around 10%. Novel drug strategies are urgently needed beyond the currently available immunotherapies that provide durable disease control in a small subset of patients. Arginine deprivation with pegylated arginine deiminase (ADI-PEG20; pegargiminase) is a novel anti-metabolite therapy which demonstrated activity in early phase trials in patients with UM, and more recently, increased survival in patients with the aggressive arginine-dependent cancer, non-epithelioid mesothelioma in the global phase 3 trial, ATOMIC-Meso. Here, we investigated the preclinical rationale for combining pegargiminase with melphalan, a drug which is delivered directly to the liver using an FDA-approved device from Delcath for patients with hepatic-centric UM disease. Two of four uveal melanoma cell lines were negative for expression of the rate-limiting enzyme for arginine production, argininosuccinate synthetase 1 (ASS1) and were submitted for drug evaluation accordingly. ADI-PEG20 treatment of ASS1-deficient cell lines 91.2 and MP41 demonstrated sensitivity to ADI-PEG20 (500ng/ml) compared to MP38 and MP46 ASS1-proficient cell lines. Moreover, the combination of ADI-PEG20 and melphalan (0.77µM) had at least an additive effect on ASS1 negative cell lines in 2D assay (92.1 p-value 0.0061; MP41 p-value is 0.0053). UM cell line proliferation was decreased by 50% in the combination group compared to ADI-PEG20 alone by 6 days of culture. Experiments to assess cytotoxicity and cell death analysis are ongoing. This drug combination therapy has the potential to improve outcomes in patients with uveal melanoma. Based on the good tolerability and safety of both drugs in patients, a clinical trial of pegargiminase with melphalan is planned for 2024 (ATOMIC-UM).

#4547 A novel drug combination with improved therapeutic efficacy over sorafenib in multiple preclinical models of hepatocellular carcinoma.

A. Chambers, S. Shrestha, A. Ladd, S. Duarte, A. Zarrinpar;
University of Florida Health Shands Cancer Hospital, Gainesville, FL

Introduction: Due to the heterogeneity of hepatocellular carcinoma (HCC), the incidence of resistance and toxicity to first-line therapy sorafenib is high. Combinations of drugs can be used to exploit synergistic effects to reduce adverse events, while improving efficacy and survival. *In-vitro* studies performed by our team identified irinotecan and sonidegib to have potential for synergistic therapeutic effects in combination with sorafenib. Follow up *in-vivo* dose optimization studies in a murine NASH induced HCC found this 3-drug combination to be more effective than sorafenib-alone at arresting tumor development and progression. In this study, we tested the *in-vivo* efficacy of the combination in two separate preclinical cell-line derived xenograft (CDX) models.

Experimental Procedure: HCC CDX models were generated by injecting two distinct HCC cell lines, Huh7 and HepG2, subcutaneously in the flank of male NOD.Cg-Prkdc^{scid}IL2rg^{tm1Wjl}/SzJ (NSG) mice. Mice were administered either vehicle, sorafenib, or a 3-drug combination, and mouse tumor volumes and weights were tracked for duration of study. Mice were all euthanized at study endpoint and tissues collected for analysis, including the assessment of tumor weights, differentiation, grade, necrosis, and proliferation status. Serum collected from endpoint blood was measured for human alpha fetoprotein (AFP) and alanine transaminase (ALT) levels. Changes in protein expression of tumors were assessed by western blot analysis.

Results: Huh7 and HepG2 tumors were both sensitive to sorafenib-alone treatment. However, Huh7 tumors treated with the 3-drug combination had a significant decrease in tumor volume and weight at endpoint compared to the vehicle and sorafenib-alone. HepG2 tumors treated with the combination also had a significant decrease in tumor volume and weight at endpoint compared to the vehicle. Though the difference in tumor volume and weight was not statistically significant for the combination compared to sorafenib, a trend towards decrease was observed. This was further confirmed by significantly reduced AFP levels in the combination compared to the vehicle and sorafenib in HepG2 and Huh7. Drug toxicities, measured by mouse weights and ALT levels, were not significantly different. Histological and immunohistochemical assessment of tumors showed necrosis and Ki67 staining to be significantly elevated in vehicle and sorafenib-alone compared to the 3-drug group. The targets for all three drugs present in the combination were downregulated in the combination compared to the vehicle and sorafenib-alone.

Conclusion: This study provides strong evidence that a novel 3-drug combination of irinotecan, sonidegib, and low dose sorafenib can significantly reduce tumor proliferation and burden in multiple independent pre-clinical *in-vivo* HCC models compared to high dose sorafenib monotherapy.

#4548 Discovering novel ALK-lung carcinoma therapeutic strategies by identifying combinations with Alectinib from ALK-positive lung carcinoma cell lines.

H. Madhi, H. Serhan, N. M. Vandecan, Z. Qin, A. Liu, A. Udager, S. D. Merajver, M. B. Soellner, N. Merrill;
University of Michigan, Ann Arbor, MI

Background: The therapeutic landscape for chromosomally rearranged anaplastic lymphoma kinase (ALK) has focused on the development of Tyrosine-kinase inhibitors (TKI) that specifically target ALK activity. However, as patients progress on first- and second line TKIs, over 50% of resistance is due to non-mutational resistance via compensatory pathways, also known as ALK-non dominant resistance. Alterations in other drivers such as EGFR, KRAS, MET account for some of the resistance mechanisms. Thus, here we explore the therapeutic activity of drug combinations that pair an ALK inhibitor with a drug that targets a "second driver". We describe our high-throughput drug screening platform that combines Alectinib, a selective blocker of ALK, with a panel of hundreds of chemical compounds curated to be active against a diverse array of pathways involved in cellular functions dysregulated in cancer. In this work, we identified several synergistic combinations that further increased the sensitivity of five ALK-positive lung cancer cell lines (DFCI 032, NCI-H3122, NCI-H2228, SNU2535, SNU324) to Alectinib in comparison to single treatment with the final goal of targeting resistance, before it emerges.
Methods: ALK-positive cancer cell sensitivity to different compounds was assessed by generating the IC50 curves in the presence and absence of Alectinib. Cells were characterized by bulk-RNAseq, bulk-DNA seq, Reverse-phase protein array, and Mass spectrometry to identify perturbed RNA pathways, DNA mutations, and proteome alterations.
Results: In this study, we present for the first time, a group of compounds, such as Gilteritinib, Trametinib, Dinaciclib, WYE-125132, Cenisertib, SN-38 which exhibit the capacity to induce cytotoxic effects in ALK-positive lung cancer cells, when combined with Alectinib. Our findings demonstrate a novel sensitivity of ALK driven by non-conventional parallel signaling, apart from conventional targets previously described, such as phosphoinositol-3kinase (PI3K)/Akt, signal transducer and activator of transcription 3 (STAT3), and extracellular signal-regulated kinases (ERK).
Conclusions: Through the integration of different multiomic approaches on five ALK-positive lung cancer cell lines, we have pinpointed a novel role of MAPK, CDK, and mTOR, pathways and their regulators, as a promising avenue for advancing treatment strategies for ALK-positive lung cancer. These findings, along with the identification of several other significant targetable elements illustrate a new approach towards the discovery of new drug combinations and targetable pathways to tackle ALK TKI resistance in ALK-positive patients before it emerges. We have previously generated Alectinib-resistant models and are in the process of screening to identify any resistant pathways that may align with those identified in the sensitive lines.

#4549 Combinations of ciclopirox olamine and metformin exert synergistic antitumor activity in triple-negative breast cancer.

Y. Wu[1], H. Lyu[1], C. Tan[1], M. Larsen[1], S. Huang[2], B. Liu[1];

[1]Departments of Interdisciplinary Oncology and Genetics, Stanley S. Scott Cancer Center, School of Medicine, Louisiana State University Health Sciences Center, New Orleans, LA, [2]Department of Biochemistry and Molecular Biology, Louisiana State University Health Sciences Center, Shreveport, LA

Introduction: Triple-negative breast cancer (TNBC) represents a challenging subtype of breast cancer because of its limited treatment options. Recent research has highlighted the potential benefits of combining pharmacological agents to enhance therapeutic outcomes. Studies show that Ciclopirox olamine (CPX), an off-patent anti-fungal drug, induces cell cycle G1-phase arrest and activates the intrinsic apoptosis pathway by downregulating the anti-apoptotic proteins. Meanwhile, metformin, a safe and first-line drug for the treatment of type II diabetes, has been shown to induce cell cycle S-phase arrest and activates the extrinsic apoptosis pathway via induction of endogenous TRAIL in TNBC cells. However, whether the combinations of CPX and metformin would exert potent antitumor activity against TNBC remains unclear.

Methods: Cell proliferation (MTS) assays and LIVE/DEAD cell imaging were used to determine the combined inhibitory effects on TNBC cells. IC50s and the combination index (CI) were calculated. Flow cytometry assays were carried out to analyze if the combinations are more potent to block cell cycle progression. Apoptotic-specific ELISA and flow cytometry analysis of Annexin V-PI staining were performed to assess if the combinations are significantly more effective to induce apoptosis. Western blot assays were used to examine if the combinations markedly induced the expression of TRAIL and cleavages of PARP and caspases. Tumor xenograft models will be established to test the in vivo antitumor activity of CPX and metformin either alone or in combinations.

Results: Data indicated that both CPX and metformin independently inhibited the proliferation of TNBC cells. A synergistic effect was observed when CPX and metformin were used in combination, resulting in a more potent inhibition of TNBC cell proliferation. The combinatorial treatment effectively suppressed colony formation of TNBC cells. Synergy between CPX and metformin was partially linked to the enhanced activation of the AMPK-mTOR pathway, as the combination significantly enhanced the phosphorylation of AMPKα. The combinations also induced enhanced apoptosis in TNBC cells through both the intrinsic and extrinsic pathways. The combinatorial effects of CPX and metformin on in vivo tumor growth are under investigation.

Conclusions: Combinations of CPX and metformin show synergistic effects on inhibiting TNBC cell proliferation. Our studies suggest a potential therapeutic strategy for TNBC, with the combinations of these agents exhibiting an enhanced antitumor activity. Further investigation is warranted to validate the results and explore their clinical applications.

Key words: Triple-negative breast cancer, Ciclopirox olamine, Metformin, Combination, Apoptosis

#4550 Synergistic combinations of lurbinectedin with ONC212 in pancreatic cancer.

T. Tummala, A. S. Sevilla Uruchurtu, N. R. Liguori, A. E. Abbas, C. G. Azzoli, W. S. El-Deiry;
Legorreta Cancer Center at Brown University, Providence, RI

Pancreatic cancer is a devastating disease with a poor five-year survival rate of approximately 12%. Given the poor prognosis of the disease, there is urgent need for novel therapeutic regimens. Lurbinectedin is chemotherapeutic compound that stalls and degrades RNA Polymerase II after binding to guanine-rich sequences in the minor groove of DNA. This stalls transcription machinery and leads to single- and double- stranded breaks in DNA and subsequent apoptosis. Our group recently described lurbinectedin's potency as both a single agent and combinatorial agent with irinotecan and 5-fluorouracil in pancreatic cancer cell lines. We also recently discovered a synergistic interaction between lurbinectedin and ONC201/TIC10, a novel compound that induces the TRAIL apoptotic pathway, in small cell lung cancer cell lines. Synergy was accompanied by an activation of p-Chk1 and the integrated stress response. We now demonstrate a synergistic combination of lurbinectedin and ONC212, an imipridone and chemical derivative of ONC201, results in highly efficient killing of pancreatic tumor cells at sub-nanomolar concentrations of lurbinectedin and sub-micromolar concentrations of ONC212. We hypothesize that the integrated stress response underlies lurbinectedin and ONC212 synergy. We further hypothesize a combination of lurbinectedin and ONC212 will sensitize the tumor cells to CD8+ T-cell killing, which will be examined via co-culture assays. Our results are developing insights into a novel combinatorial therapeutic regimen while investigating the molecular mechanisms underlying synergism.

#4551 A novel MET antibody-drug conjugate based combination therapy to overcome colorectal cancer plasticity and drug resistance.

S. Subramanian[1], T. A. Posey[2], J. Jacob[1], A. Aldana[3], K. S. Carmon[1];

[1]The University of Texas MD Anderson Cancer Center UTHealth Houston Graduate School of Biomedical Sciences, Houston, TX, [2]The University of Texas MD Anderson Cancer Center, Houston, TX, [3]The University of Texas Health Science Center at Houston, Houston, TX

Despite therapeutic advancements, colorectal cancer (CRC) remains the second deadliest malignancy in the United States. Challenges encountered in CRC treatment may be attributed to cancer stem cells (CSC), an immortal tumor cell population. CSCs potentiate tumor relapse by exploiting its infinite replicative potential and inherent drug resistance. Moreover, CSCs exhibit plasticity, allowing them to transition between differentiated and undifferentiated states in response to environmental cues to evade therapy and drive metastatic progression. MET is a receptor tyrosine kinase frequently upregulated in CRCs. We previously demonstrated that treatment with chemotherapies or antibody-drug conjugates (ADCs) targeting the CSC marker LGR5 led to the loss of LGR5 expression with concomitant MET-STAT3 pathway activation in therapy-resistant CRC cells. Further, we showed that LGR5 couples to the scaffold protein IQGAP1, which correlates with poor prognosis in several cancer types. Interestingly, our new data revealed that LGR5 knockdown enhances IQGAP1 interaction with MET and STAT3 via co-immunoprecipitation assays, suggesting a role for IQGAP1 in mediating MET-STAT3 activation and plasticity of $LGR5^{+}$ CRC cells. To overcome therapy-induced plasticity, we generated MET-targeting ADCs conjugated to DNA-crosslinking payloads. First, we cloned and produced MET monoclonal antibodies (mAbs) and evaluated them for specificity and binding in a panel of CRC cell lines expressing different MET protein levels. MET mAbs demonstrated high selectivity for MET-expressing CRC cells and internalized to lysosomes, which is necessary for ADC payload release. To generate MET ADCs, we employed a site-specific conjugation methodology to attach cleavable peptide linker-drug moieties to the highest affinity MET mAb. MET ADCs were evaluated for cancer cell-killing efficacy *in vitro* in parallel with MET mAb, non-targeting control mAb (cmAb), and control ADC (cADC). Our MET ADC displayed high potency and efficacy in MET-expressing CRC cells, whereas MET mAb, cmAb, and cADC had minimal effects. MET ADCs were then tested in combination with chemotherapies or other targeted therapies. The combination of MET ADCs with 5-fluorouracil showed a synergistic effect *in vitro*. Future work involves investigating the safety and efficacy of MET ADCs alone and combined with chemotherapies in xenograft models of CRC. These findings present a mechanism underpinning CRC plasticity and the rationale for a novel treatment modality to potentially overcome CRC resistance and relapse.

#4552 EGFR inhibitors increase LGR5 expression and enhance potency of LGR5 antibody-drug conjugates targeting colorectal cancer stem cells.

Peyton C. High[1], Zhengdong Liang[2], Kendra S. Carmon[2]

[1]The University of Texas MD Anderson Cancer Center UT Health Houston Graduate School of Biomedical Sciences, Houston, TX, [2]The University of Texas Health Science Center at Houston, Houston, TX

Colorectal cancer (CRC) is the second leading cause of cancer-associated deaths in the United States. One of the primary challenges in treating CRC is therapy resistance thought to be mediated by cancer stem cells (CSCs), a subpopulation of cancer cells with infinite replicative potential that can differentiate to drive tumorigenesis and disease relapse. Antibody-drug conjugates (ADCs) are amongst the fastest growing classes of anticancer drugs and utilize the specificity of monoclonal antibodies (mAbs) to hone cytotoxic payloads to cancer cells. We generated ADCs directed against leucine-rich repeat-containing G protein-coupled receptor 5 (LGR5), a well-defined biomarker of CSCs that is highly overexpressed in CRCs. LGR5 ADCs demonstrated high specificity and efficacy in CRC cells and xenograft models, though tumor relapse after treatment withdrawal was a major obstacle. Interestingly, FDA-approved therapy targeting epidermal growth factor receptor (EGFR) has been shown to increase *LGR5* mRNA expression levels in patient-derived models of CRC. This study aims to determine the mechanism of EGFR-mediated regulation of LGR5 expression and evaluate the therapeutic efficacy of combination treatments targeting EGFR and LGR5 for the improved treatment of CRC. To first analyze the effect of EGFR inhibition on LGR5 expression, a panel of CRC cell lines of different KRAS and PI3CKA mutational statuses were treated with FDA-approved EGFR-targeted mAbs or small molecule inhibitors. LGR5 protein expression was shown to be upregulated by EGFR-targeted therapies in a dose- and time-dependent manner, independent of mutation status. Notably, treatment with EGF, MEK1/2 inhibitor trametinib, and EGFR-directed siRNA all resulted in concomitant reduction in EGFR and LGR5 protein levels, suggesting EGFR and LGR5 are co-degraded. Co-immunoprecipitation and immunocytochemistry experiments identified a novel EGFR-LGR5 interaction and co-internalization mechanism in CRC cells, respectively. Furthermore, we showed EGFR-LGR5 interaction is enhanced by treatment with the EGFR-targeting mAb, cetuximab (CTX). To evaluate efficacy of combination therapies targeting EGFR and LGR5, CRC cells were treated with LGR5 ADCs with or without CTX. Importantly, we showed CTX significantly enhanced the potency of LGR5 ADCs incorporating different classes of cytotoxic payloads. These results suggest combining LGR5 ADCs with EGFR inhibitors may be a more effective approach for the treatment of CRC and eliminating CSCs to overcome resistance and relapse.

#4553 DXC004A, a novel EGFR antibody-tubulysin analog conjugate demonstrated potential to broaden therapeutic opportunities for non-small cell lung cancer.

X. Cai, M. Cao, H. Guo, Q. Yang, Y. Chen, X. Kong, Y. Du, Z. Ye, Z. Guo, L. Zhang, L. Bai, J. Jia, Y. Zheng, W. Zheng, J. Zheng, W. Li, Y. Huang, Z. Fan, B. Chen, M. Dai, **R. Y. Zhao**;
Hangzhou DAC Biotechnology Co., Ltd., Hangzhou City, China

EGFR is a member of the epidermal growth factor receptor (HER) family, and the over-expression of EGFR plays an important role in the growth and progression of various tumors, including non-small cell lung cancer. Monoclonal EGFR antibodies, such as cetuximab and panitumumab, have proven efficacy in various types of cancer. However, treatment with the anti-EGFR agents can be associated with toxicities of the skin, nails, hair, and eyes. Nimotuzumab (Nimo) is the first humanized monoclonal antibody targeting EGFR and has been granted approval for use in squamous cell carcinoma of head and neck (SCCHN), glioma and nasopharyngeal cancer in different countries. In contrast to cetuximab, Nimotuzumab is distinguished by achieving higher or similar complete remission rate (CRR) or overall remission rate (ORR) of the primary tumor in clinical applications but much less toxicity, resulting in a better safety profile, which has been attributed to its about 10-fold lower affinity. Paclitaxel combined with cisplatin is the first-line chemotherapy regimen for non-small cell lung cancer. A phase 2 clinical trial has confirmed that Nimotuzumab combined with concurrent chemoradiation therapy (radiation concurrent with docetaxel and cisplatin, CCRT) was well tolerated for locally advanced squamous cell lung cancer. However, the combination strategy of Nimo-CCRT has only demonstrated similar OS and PFS to those in the CCRT group. DXC004A is an ADC drug targeting EGFR, in which a Nimotuzumab derivative and a Tubulysin B analog is conjugated by a functional linker. DXC004A is in phase I clinical trial and has demonstrated clinical activity in advanced non-small cell lung cancers and good tolerability. In vitro and in vivo results had confirmed that DXC004A monotherapy had better anti-tumor activity than the combination of Nimotuzumab and Tubulysin analog in HCC827 cell lines with high EGFR expression. Meanwhile, a single injection of low-dose DXC004 (2.5 mg/kg) in HCC827 xenograft model showed very good durable anti-tumor effect. Moreover, the combination of DXC004A with Cisplatin exhibited significantly better activities than that of Nimo-CCRT combination, DXC004A or cisplatin alone, in vitro and in vivo, which might solve the predicament of poor efficacy of Nimo-CCRT combination therapy. This synergy results suggested that DXC004A plus cisplatin would possibly be a new adjuvant therapy for non-small cell lung cancer in further clinical studies.

#4554 Novel combination therapy for treating proteasome inhibitor-resistant multiple myeloma.

B.-G. Kim[1], S. Choi[1], H. Nguyen[1], F.-S. Liang[1], S.-J. Kim[2], J. Letterio[1], A. Huang[1];
[1]Case Western Reserve University School of Medicine, Cleveland, OH, [2]MedPacto, Seoul, Korea, Republic of

Multiple myeloma (MM) is an incurable plasma cell malignancy characterized by osteolytic bone disease and immunosuppression. Proteasome inhibitors (PIs) have remarkably improved the survival of MM patients, but dose-limiting toxicities and the development of drug resistance limit their long-term utility. Elevated TGF-β levels in MM patient sera correlate with drug resistance, disease progression, metastasis and poor prognosis. Therefore, we evaluated the anti-MM therapeutic potential of a TGF-β type I receptor kinase inhibitor, Vactosertib. *In vitro* treatment of Vactosertib synergistically inhibited the growth of bortezomib (BTZ)-resistant MM cells in combination with either BTZ or ixazomib (IXZ) by suppressing TGF-β activation of Smad2/3 and expression of *PSMB5,* which encodes the proteasome 5 catalytic subunit targeted by PIs. Oral administration of Vactosertib as a single agent decreased MM progression and mortality of the mice bearing BTZ-resistant MM. Vactosertib alone also attenuated PSMB5 expression and proteasome activity, reduced the expansion of $CD11b^{+}Gr\text{-}1^{+}$ myeloid derived suppressor cells (MDSCs) in bone marrow (BM) tumor microenvironment (TME), and diminished the population of $Foxp3^{+}$ regulatory T cells (Treg) in the spleen. Combination therapy of Vactosertib plus PI (BTZ or IXZ) exhibited a synergistic anti-myeloma effect when compared to either Vactosertib or PI alone by greatly prolonged survival and significant a reduction in both MDSCs and Tregs. Furthermore, therapy of $BCMA^{+}$ CAR T cells in combination with Vactosertib exhibited a synergistic anti-tumor effect, compared to either CAR T cells or Vactosertib. Taken together, our data provide the rationale for clinical evaluation of Vactosertib in MM and demonstrate proof-of-concept that combination of Vactosertib and either PI or cell therapy may overcome drug resistance and enhance durable patient responses.

#4555 c-Met/AXL crosstalk in mediating therapeutic resistance in renal cell carcinoma.

A. Sabarwal[1], L. Rawat[1], J. Wedel[1], M. Balan[1], G.-S. M. Lee[2], T. K. Choueiri[2], S. Pal[1];
[1]Boston Children's Hospital, Boston, MA, [2]Dana-Farber Cancer Institute, Boston, MA

Receptor Tyrosine Kinase (RTK), c-Met, is overexpressed in renal cancer and correlates with a decreased survival rate. Upon binding with its specific ligand, Hepatocyte Growth Factor (HGF), c-Met activates pro-tumorigenic signaling. c-Met/RTK inhibitors are used for the treatment of advanced renal cell carcinoma (RCC). However, acquired therapeutic resistance is a major clinical problem and the underlying mechanisms are largely unknown. Hence, novel therapeutic targets are needed to overcome the clinical hurdles; and the RTK, AXL, can be a potential target. AXL is overexpressed and a poor prognostic marker in RCC. AXL overexpression drives wide-ranging processes, including epithelial-to-mesenchymal transition (EMT), tumor angiogenesis, and resistance to chemotherapeutics. Cabozantinib (XL184/Cabo), is approved for advanced-stage RCC and can inhibit c-Met and VEGFR2 activation (including AXL and a few other RTKs); however, it is not a specific/potent inhibitor of AXL. Hence, inhibiting c-Met alone may not be sufficient when AXL remains active. Therefore, the pro-tumorigenic role of AXL and its cross-talk with c-Met in renal cancer need to be thoroughly investigated. We compared the expression of c-Met and AXL in TCGA and found significantly high expression of both c-Met and AXL in primary renal tumor tissues compared to normal tissues. Our data showed that AXL forms a complex with c-Met and may have a significant cross-talk which can be involved in therapeutic resistance. We have also found that prolonged treatment of c-Met inhibitor Cabo, (including Crizotinib and PF-4217903) induced c-Met and AXL overexpression in RCC cells. Interestingly, c-Met inhibitor(s)-induced overexpressed c-Met can also be increasingly phosphorylated (at low concentrations) in the presence of HGF, which may cause enhanced downstream tumor-promoting signaling. To understand the role of AXL in tumor-promoting pathways and therapeutic resistance, we have generated CRISPR/Cas9-mediated AXL knock-out cells (AXL-KO) and found that silencing AXL can prevent c-Met-inhibitor(s)-mediated c-Met overexpression. Furthermore, to identify the effect of AXL-KO on pro-tumorigenic signaling, transcriptional profiles of control clones and AXL-KO cells were compared. The gene set enrichment analysis (GSEA) showed that genes involved in ‘EMT’, ‘Hypoxia’, and ‘K-Ras’ signaling pathways were significantly downregulated. We have also utilized an AXL-specific small molecule inhibitor, TP-0903, in combination with Cabo and validated our data. We have also generated a Cabo-resistant cell line (Caki-1) and found high expression of c-Met and AXL in these cells. Furthermore, either silencing of AXL (using siRNA) or inhibiting AXL (using TP0903) induced significant apoptosis in these Cabo-resistant cells. Together, our data suggest that inhibition of AXL along with c-Met can be beneficial in preventing acquired therapeutic resistance in RCC.

#4556 USP51-GRP78-ABCB1 axis promotes chemoresistance of triple negative breast cancer by decreasing the accumulation of doxorubicin in cells.

Y. Ou, K. Zhang, q. shuai, C. Wang, H. Hu, L. Cao, C. Qi, M. Guo, Z. Li, J. Shi, Y. Liu, S. Zuo, X. Chen, Y. Wang, M. Feng, H. Wang, Y. Shi, G. Yang, S. Yang; Nankai University, Tian Jin, China

Background: Resistance to chemotherapy remains an obstacle for triple-negative breast cancer (TNBC) patients. The core components of the ubiquitin-proteasome system have been demonstrated to regulate chemoresistance of TNBC. As a novel deubiquitinase (DUB), ubiquitin-specific peptidase 51 (USP51) plays a pivotal role in chemotherapeutic resistance in multiple malignancies. Herein, we sought to better understand how USP51 performs a cell-intrinsic role in mediating chemotherapeutic resistance in TNBC.

Methods: Western blotting, RNA-sequencing and CCK8 assays were used to identify the DUBs for chemoresistance of breast cancer. Coimmunoprecipitation, GST-pulldown, protein deubiquitination and immunohistochemistry assays were then used to determine the biological phenotypes of ectopic USP51 in TNBC chemoresistance and associated signaling pathways in several different cell lines, mouse models and patient tissue samples. Ubiquitin-7-amido-4-methylcoumarin (Ub-AMC)-based deubiquitinase activity, cellular thermal shift and surface plasmon resonance (SPR) analyses were performed to investigate the activity of USP51 inhibitors.

Results: To identify the critical DUBs involved in breast cancer chemoresistance, we established doxorubicin-resistant Cal51 and MDA-MB-231 TNBC cell lines by multiple dose exposure. We found ectopic USP51 in doxorubicin-resistant cells compared with their parental cells. Moreover, USP51-interfered chemoresistant tumor cells exhibited impaired cell viability as well as increased DNA damage and cell apoptosis upon treatment with doxorubicin. On the contrary, overexpression of USP51 performed the opposite effects to enhance cell viability but decrease DNA damage and apoptosis in response to doxorubicin; however, these outcomes were not shown for its catalytically inactive mutant $USP51^{C372S}$. At the molecular level, GRP78 was identified as a bona fide substrate of USP51. Importantly, knockdown USP51 increased doxorubicin-induced DNA damage and apoptosis, which was rescued by overexpression of GRP78 *in vitro* and *in vivo*. In addition, the activity of ABCB1, the main efflux pump of doxorubicin, was enhanced by GRP78. Consistently, the expression of USP51, GRP78 and ABCB1 were correlated with chemoresistant phenotypes in TNBC patients. Of note, we also explored a small molecular inhibitor of USP51, WCY-4-1, which conferred chemosensitization in TNBC.

Conclusion: These findings collectively indicated that ectopic USP51 enhances the activity of ABCB1 by deubiquitinating and stabilizing GRP78, which leads to decreased accumulation of doxorubicin as well as decreased DNA damage and cell apoptosis in TNBC. Our results also revealed that specific inhibition of USP51 significantly impairs doxorubicin-resistance in TNBC.

#4557 Overexpressed CPAP promotes cancer stemness and enhances chemo-resistance in HCC.

L.-Y. Hung;
National Cheng Kung University, Tainan, Taiwan

Hepatocellular carcinoma (HCC) is the most common type of primary liver cancer and is highly resistant to chemotherapy and targeted therapy. It was reported that HCC cancer stem cells (CSCs) are involved in chemo-drug resistance by regulating multidrug resistance (MDR) gene expression, such as ABC transporters. Our previous reports indicated that CPAP, a centrosomal protein, can promote HCC progression by up-regulating NF-κB and STAT3 transcriptional activities. Here, we demonstrated that overexpressed CPAP can increase cancer stemness features and CSCs-derived sorafenib resistance in HCC by up-regulating the transcriptional activities of NF-κB and β-catenin. Importantly, CPAP stably expressed HCC spheroids are significantly resistance to sorafenib in vitro and in vivo. Our results suggested that CD24 and ABCG2 are two potential downstream effectors in CPAP overexpressed HCC. CPAP can transcriptionally up-regulate CD24 and ABCG2 expression via Wnt/β-catenin and NF-κB signaling pathways, respectively; high CPAP/ABCG2/CD24 expression levels are negatively correlated with disease-specific survival rates in HCC patients. Combined treatment with sorafenib and Wnt/β-catenin pathway inhibitor PRI-724 significantly inhibited CPAP-overexpressing Hep3B spheroids-derived tumor growth in a xenograft mouse model. Our study highlights the oncogenic role of CPAP in promoting CSCs-induced sorafenib resistance in HCC and provides insights into potential therapeutic strategies.

#4558 A triterpenoid derivative has strong antitumor activities in gemcitabine-resistant advanced bladder cancer models and promotes immune cell infiltration in a high grade murine syngeneic model.

J. R. Seremak, K. Gupta, S. S. Panda, B. L. Lokeshwar;
Augusta University, Augusta, GA

Bladder cancer (BC) presents a formidable challenge in treatment and patient survival, requiring particular attention to advanced stages, such as muscle-invasive stage (MIBC), due to its potential for rapid progression and substantial impact on patient morbidity and mortality. The five-year survival rate for MIBC is a meager 30%, which drops further down to 8% once tumors metastasize. Advanced bladder cancers (High grade T1) are treated with intravesical therapy with Gemcitabine and Cisplatin (G+C) combination and Stage T2 are treated neoadjuvant with G+C and cystectomy, thereby decreasing the quality of life for patients with BC. Furthermore, tumors progress beyond responding to other chemotherapy regimens such as dose-dense treatment with Methotrexate +Vinblastine + Adriamycin and Cis-platin (MVAC), all of which will further decrease the quality of life with persistent adverse toxicity. Our laboratory has developed a novel compound derived from the pentacyclic triterpenoid, Ursolic acid, termed N-methyl piperazine conjugated-Ursolic acid, or UA4, and have demonstrated its antitumor activities against both Gem-Sensitive (Gem-S) and Gem-Resistant (Gem-R) human advanced BC cell lines, T24 and 5637. We tested the combination of Gem, UA4 and Gem + UA4 in a murine non-MIBC model (MB49) to investigate the role of immune cell infiltration during tumor development and treatment response. UA4 treatment was equally effective in chemo-sensitive and chemo-resistant cell lines at dosages between 4-5µM. Previous *in vitro* mechanistic studies on UA4 and UA4+Gem combination treatments revealed cell death occurred through apoptosis and autophagy, along with a highly selective form of mitochondrial-mediated autophagy (mitophagy). These findings were confirmed with transmission electron microscopy ultrastructural analysis, cell cycle phase analyses, excess, changes in mitochondrial membrane potential and reactive oxygen species measurements. Gem-S and Gem-R xenografts in athymic mice further supported UA4's efficacy *in vivo*, demonstrating a significant reduction in both tumor weight and volume following oral gavage (100mg/kg), with mice exhibiting no signs of systemic toxicity. Combination treatment with UA4 and Gem synergistically increased antiproliferative activity. MB49 syngeneic mice model further supported UA4 as an effective therapy, and immunofluorescence assays with immune-related markers, suggested an anti-inflammatory effect *in vivo*. Overall, we demonstrate UA4 has a potential to be used as an efficacious, non-toxic compound for further adjuvant use in clinical settings.

#4559 SMAD3 mediates oxaliplatin resistance in esophageal adenocarcinoma.

F. Ballout, H. Lu, N. Bhat, L. Chen, D. Peng, Z. Chen, A. Zaika, O. McDonald, W. El-Rifai;
University of Miami Miller School of Medicine, Miami, FL

Background: Resistance to conventional treatments is a significant barrier to esophageal adenocarcinoma (EAC) therapy. TGF-β signaling appears to be important for EAC tumorigenesis; however, its role in EAC chemoresistance remains understudied. This study investigates the role of SMAD3 in EAC resistance to the frontline chemotherapeutic drug oxaliplatin.
Methods: Publicly available datasets were analyzed to determine SMAD3 expression in EAC versus normal samples. Western blot, quantitative real-time polymerase chain reaction, immunofluorescence staining, and flow cytometric analyses were utilized to validate bioinformatic results. Human EAC cell lines (OE33 and OE19) were treated with pharmacologic inhibitors or transfected with small interfering RNA and assessed for DNA damage and apoptotic cell death. Patient-derived organoids and patient-derived xenograft models of EAC were used to confirm our findings in vivo.
Results: SMAD3 was significantly upregulated in EAC versus normal tissue samples. Total and phosphorylated SMAD3 protein levels were upregulated in EAC tissues accompanied by increased expression of several genes regulated by SMAD3. Notably, oxaliplatin-resistant EAC cells exhibited overexpression of SMAD3. Chemotherapy non-responding patients showed enrichment of SMAD3 gene expression when compared to responders in the clinical dataset GSE165252. Knockdown or inhibition of SMAD3 hindered DNA repair and sensitized EAC cells to oxaliplatin treatment in vitro and in vivo. Mechanistically, SMAD3 promoted ATM phosphorylation by interacting with protein phosphatase 2A (PP2A) and sequentially inhibiting the binding of PP2A to ATM.
Conclusion: Our results reveal a pivotal role for SMAD3 in mediating oxaliplatin resistance in EAC and thus hold a significant potential in guiding future drug development and combination strategies.

#4560 Assessing cancer drug combination efficacy across 900+ PRISM cell lines in a multiplexed screening assay.

A. Bino George, S. Nair, M. Kocak, E. Nguyen, A. Kalathungal, A. Fazio, C. Ponsi, A. Golabi, M. A. Ronan, M. G. Rees, J. A. Roth;
Broad Institute of MIT and Harvard, Cambridge, MA

Combination therapies are crucial in cancer care, yet identifying which combination will benefit a specific patient is challenging. The vast array of clinical, investigational, and tool anticancer agents and diverse cancer contexts makes investigating many drug combinations over a large number of cell lines infeasible. Here, we describe a multiplexed screening approach using the PRISM assay, where drug combinations are screened on >900 DNA-barcoded cancer cell lines. We analyze cell viability data in drug combinations and single agents using established metrics to describe the combined effects such as additivity, synergy, and antagonism. Quantifying and classifying combined effects will help prioritize specific combinations for follow-up investigations and provide biological and mechanistic insights, thus enabling rationally designed combination therapies. We illustrate our methodology through data from three drug combinations that exemplify synergy and antagonism. In the first combination, temozolomide+O6-benzylguanine (alkylating agent + MGMT inhibitor), we found that cell lines expressing MGMT were sensitized to temozolomide in the presence of O6-benzylguanine, thus illustrating synergy. In the second combination, we screened two anti-apoptosis compounds A-1331852+AZD5991 (BCL-xL + MCL1 inhibitor) and found that BCL-xL and MCL1 inhibition were also synergistic. In the third combination, ML210+ferrostatin-1 (GPX4 inhibitor inducing ferroptosis + ferroptosis inhibitor), we found that ferrostatin-1 antagonized the effects of ML210. Our analysis also reveals the importance of appropriate dose selection and analytical metrics for reliably measuring combined effects. In conclusion, the PRISM platform's multiplexed cell line screening is a robust method for characterizing rationally designed drug combinations, offering a systematic approach to enhance the precision of combination therapy development in cancer care.

#4561 Mechanism of histone H3K27me3 demethylase therapy for restoring cisplatin sensitivity in refractory testicular cancer.

D. N. Shokry, R. Singh, M. Khan, Z. Fazal, R. Boyd, C. Powell, S. J. Freemantle, M. J. Spinella;
Department of Comparative Biosciences, College of Veterinary Medicine, Carle Illinois College of Medicine, Carl R. Woese Institute for Genomic Biology, and Cancer Center of Illinois, University of Illinois Urbana-Champaign, Urbana, IL

Testicular germ cell tumors (TGCTs) can be cured at a high rate with standard cisplatin-based chemotherapy, but 15% of metastatic patients are cisplatin resistant/refractory and die from progressive disease. In prior work, we used *de novo* pharmacogenetic approaches leveraging a series of unique cisplatin resistant cell models that uncovered an important role for polycomb and histone H3K27me3 methylation in mediating TGCT sensitivity and resistance to cisplatin. Importantly, we demonstrated that pharmacological inhibition of H3K27 methylation with the EZH2 inhibitor GSK-126 conferred cisplatin resistance to parental cells while induction of H3K27 methylation with the histone lysine demethylase inhibitor GSK-J4 resulted in a high degree of cisplatin sensitization of TGCT tumors including cisplatin resistant TGCT cells. In order to elucidate mechanisms that account for the remarkable cisplatin sensitization effects of GSKJ4 in TGCTs, we used two distinct cisplatin resistant TGCT cell lines 2102EP-C1 and NT2D1-A4. Cells were pretreated for three days with either vehicle control or 1μM GSK-J4 to modulate H3K27me3 followed by treatment with vehicle control or 0.5μM cisplatin for 6 hours. RNA was extracted from cells after 24 hours of cisplatin removal. This treatment protocol was designed to capture “early” transcriptional responses to GSKJ4 sensitization before the onset of cell death. RNA-seq transcriptomic profiling and differential gene expression analysis revealed as expected a severely attenuated transcriptional response to cisplatin in cisplatin refractory cells that was restored with GSKJ4 pretreatment. Interestingly GSKJ4 alone resulted in a robust transcriptional response with a large overlap with gene changed with cisplatin alone, despite the fact that GSKJ4 alone did not affect cell proliferation or survival. However, GSKJ4 uniquely regulated a subset of genes and uniquely restored cisplatin response to a subset of genes which are candidates for driving the remarkable cisplatin sensitizing effects of GSKJ4 in TGCTs. Further enrichment and biological classification analysis of these distinct gene subsets are ongoing and will be presented. In summary, our data suggests mechanisms to account for why directly targeting H3K27 methylation with GSKJ4 appear highly effective in treating cisplatin resistant/refractory TGCTs and may provide biomarkers for future clinical investigation of this strategy.

#4562 Activity of PARP1-selective inhibitor SNV-001 in models of HRD cancers as monotherapy and in combination.

Z. Li, Q. Fan, M. Gao, J. Pan, L. Wu, W. Yao, P. C. C. Liu;
Synnovation Therapeutics, Inc., Wilmington, DE

Current FDA approved poly (ADP-ribose) polymerase inhibitors (PARPi) inhibit both PARP1 and PARP2. Genetic studies indicate that loss of PARP1 is synthetic lethal with homologous recombination deficiency (HRD), including BRCA1/2 mutations, and PARP2 depletion may be linked to hematologic toxicity. To date, no first generation PARPi has been successfully combined with standard of care (SoC) agents in the clinic without significant reduction in dosing intensity because of overlapping toxicities. A selective inhibitor could potentially improve the therapeutic index and provide additional opportunities in combination strategies especially with drugs that are prone to myelosuppression. SNV-001 potently and selectively inhibits PARP1 in biochemical and cellular assays. SNV-001 inhibits PARylation in the low nanomolar range with over 500-fold selectivity against PARP2. SNV-001 did not inhibit any other PARP family member tested up to 10 uM in biochemical assays confirming its selectivity for PARP1. In human erythroid and myeloid colony formation assays, the IC50s of SNV-001 for both lineages were approximately 100-times higher than the target efficacious concentration based on the IC95 for inhibition of DLD1 (BRCA2 -/-) colony formation. In a subcutaneous MDA-MB-436 (BRCA1mut) xenograft model, oral administration of SNV-001 once daily resulted in a dose-dependent tumor regression. SNV-001 showed greater efficacy at lower doses compared to olaparib at 100 mg/kg or at equivalent doses of AZD9574. SNV-001 showed promising synergy with SoC chemotherapies or DDR inhibitors in cell proliferation assays. SNV-001 enhanced cytotoxicity of the DNA-damaging agent topotecan or carboplatin in Capan-1 (BRCA2mut) and HCC1395 (BRCA1mut) cells. Synergy was seen between SNV-001 and cell cycle check point inhibitors camonsertib (ATRi) or adavosertib (WEE1i) in DLD1 (BRCA2 -/-) and UWB1.289 (BRCA1mut) cells, as DNA damage induced by PARP1 trapping relies on cell cycle modulation for repair. Combination of SNV-001 with polymerase theta inhibitor ART558 or USP1 inhibitor KSQ4279 exhibited synergistic effects in DLD1 (BRCA2 -/-) or UWB1.289 (BRCA1mut) cells. These results suggest that inhibition of microhomology-mediated end-joining and translesion synthesis pathways may further exacerbate SNV-001-induced DDR in certain cellular contexts.In summary, the PARP1 selective inhibitor SNV-001 demonstrates potent antitumor activity and shows promising synergy between SoC chemotherapies or DDR inhibitors. Current data highlight a potential strategy for improving treatment efficacy and overcoming resistance. Further clinical investigations are warranted to validate this combination strategy.

#4563 Ferroptotic mechanism of drug induced toxicity of PARPi and AurKi in prostate cancer.

A. John, K. Luo, Z. Lou, L. Wang;
Mayo Clinic, Rochester, MN

BACKGROUND: Cancer is typically treated with a combination of drugs rather than monotherapy stratagems, but identification of synergistic drug combinations for the treatment of cancers is challenging. Here we present the combination of PARP and Aurora Kinase inhibitors synergize through induction of the ferroptosis pathway of cell death.
METHODS: We identified these drugs through an unbiased screen of enriched drug class response correlations. We then validated a synergistic cell killing effect of multiple drugs of each class by in vitro drug screening. Next, we performed reversal experiments using a ferroptosis inhibitor and lipid peroxide staining to confirm ferroptosis is a relevant cell death pathway. We performed Western immunoblot analysis in cells overexpressing putative Aurora Kinase phospho-substrates in the relevant pathway of interest, and performed site directed mutagenesis experiments to show the relevant amino acid altered by kinase activity. We also performed a series of qPCR and co-IP experiments to show PARPi effect on the antioxidant signaling pathway.
RESULTS: We validated and identified synergy in a prostate cancer specific context. Next, we found Talazoparib and Alisertib induced ferroptosis after synergy was reduced with a ferroptosis inhibitor and lipid peroxides increased accumulation. We found a novel mechanism action for Alisertib, wherein Aurora Kinase inhibitors can alter the phospho-status and activity of the iron reduction enzyme Steap3.We also found that PARP inhibitors can affect the Nrf2-driven antioxidant signaling pathway on a transcriptional level.
CONCLUSION: Aurora Kinase inhibitors and PARP inhibitors for the treatment of prostate cancer was identified and was validated as synergistic, which revealed new functional roles of both drugs in the context of cell killing. These findings represent a new clinical combination of drugs in prostate cancer and reveal a novel role for this drug class in ferroptosis.

#4564 Therapeutic potential of SOS1 and KRAS inhibitors in malignant peripheral nerve sheath tumors.

O. Yuce Petronczki, L. Pisarsky, P. L. Szabo, J. Brunmair, A. Geyer, N. Kraut, D. McConnell, I. Waizenegger;
Boehringer Ingelheim RCV GmbH & Co KG, Wien, Austria

Neurofibromatosis type 1 (NF1) is a genetic disorder that affects the nervous system. It is caused by mutations in the NF1 gene. NF1 loss of function leads to elevated RAS signaling, which plays a crucial role in cell growth and proliferation. Due to the dysregulated RAS signaling, individuals with NF1 are prone to the development of neurofibromas. These neurofibromas are typically benign and called Plexiform Neurofibromas (PNFs), in some cases, they can transform into malignant peripheral nerve sheath tumors (MPNSTs). MPNSTs are highly aggressive and invasive cancers that contribute to a significant proportion of soft tissue sarcomas. The exact mechanisms behind this transformation are not fully understood, however it involves additional genetic mutations and alterations in cellular signaling pathways. With limited effective targeted therapies available, surgical removal remains the primary treatment option. However, due to tumor size and location, surgery may not always be feasible. The MEK inihibitor, selumetinib, has received approval for the treatment of PNFs, however some patients who were treated with selumetinib continued to develop MPNSTs suggesting that MEK inhibitors may have limitations in addressing MPNSTs. To target the RAS pathway and mitigate the effects of NF1 gene alterations, we aim to explore the therapeutic potential of two novel, potent and orally bioavailable small molecule inhibitors targeting SOS1 (BI 1701963) or KRAS ($KRAS^{multi}$ inhibitor BI 3706674), as alternative treatment options for MPNSTs. The $KRAS^{multi}$ inhibitor BI 3706674 binds non-covalently to the KRAS wild type allele as well as multiple KRAS mutant alleles in the GDP-bound state and thereby disrupts KRAS signaling. Therefore, we hypothesize that both inhibitors will work in NF1 models by reducing activated KRAS levels. In this study, a series of *in vitro* and *in vivo* experiments were conducted to evaluate the efficacy of BI 1701963 and BI 3706674 inhibitors, both individually and in combination. The studies were done in comparison to the MEK inhibitor selumetinib. *In vitro* analysis revealed a synergistic anti-proliferative effect when combining BI 1701963 and BI 3706674 inhibitors both in 2D and 3D growth conditions, which led to the downregulation of the RAS pathway, specifically the MAPK and PI3K signaling cascade, and an increase in apoptosis. The *in vivo* efficacy of either BI 1701963 or BI 3706674 inhibitor alone or in combination was tested in four different *in vivo* MPNST models. We observed significant tumor growth stabilization as well as tumor regression in all tested models *in vivo*. In-depth pathway modulation and pharmaco-dynamic studies are ongoing. In conclusion, this study highlights the combined effects of SOS1 (BI 1701963) and KRAS (BI 3706674) inhibition in MPNSTs. The combination therapy of these novel therapeutics may hold promise as a potential treatment strategy for patients with MPNSTs.

#4565 Reckless mitotic entry as a chemosensitization approach for alkylating agents.

F. Lang, J. A. Cornwell, K. Kaur, M. I. Aladjem, M. Aregger, S. D. Cappell, C. Yang;
National Cancer Institute, Bethesda, MD

The cell cycle is tightly regulated by checkpoints, playing a vital role in controlling its progression and timing. Cancer cells exploit the G2/M checkpoint, which serves as a resistance mechanism against genotoxic anti-cancer treatments, allowing for DNA repair prior to cell division. Therefore, manipulating cell cycle timing has emerged as a potential strategy to augment the effectiveness of DNA damage-based therapies such as alkylating agents and radiation. In this study, we conducted a forward genome scale CRISPR/Cas9 chemogenomic screening with repeated exposure to the alkylating agent temozolomide (TMZ) to investigate the mechanisms underlying tumor cell survival under genotoxic stress. Our findings revealed that canonical DNA repair pathways, including ATM/Fanconi and mismatch repair, determine cell fate under genotoxic stress. Notably, we identified the critical role of the membrane-associated tyrosine- and threonine-specific cdc2-inhibitory kinase, known as Myt1 (encoded by PKMYT1), in ensuring cell survival. Analysis on patient cohort demonstrated that *PKMYT1* is not only highly presented in malignancy, but also predisposes an unfavorable disease outcome. Genetic depletion of PKMYT1 led to overwhelming TMZ-induced cytotoxicity in cancer cells. Isobologram analysis demonstrated potent drug synergy between TMZ and other clinically used alkylating agents, such as carmustine, busulfan, and dacarbazine, when combined with a novel Myt1 kinase inhibitor, RP-6306. Mechanistically, inhibiting Myt1 forced G2/M-arrested cells into an unscheduled transition to the mitotic phase without complete resolution of DNA damage, as indicated by a substantial increase in γH2AX-positive cells in mitosis. Moreover, RP-6306 dramatically altered cell cycle timing, reducing the threshold time for mitotic entry. This forced entry into mitosis, along with persistent DNA damage, resulted in severe mitotic abnormalities, including unaligned and partially condensed chromosomes, lagging chromosomes, chromosome bridges, and multipolar spindles. Ultimately, these aberrations led to mitotic exit with substantial apoptosis. Importantly, preclinical animal studies demonstrated that the combination regimen involving TMZ and RP-6306 prolonged the overall survival of glioma-bearing mice. Collectively, our findings highlight the potential of targeting cell cycle timing through Myt1 inhibition as an effective strategy to enhance the efficacy of current standard cancer therapies, potentially leading to improved disease outcomes.

#4566 Synergistic anticancer activity of cannabinoids and beta caryophyllene in xenograft mouse model of triple negative breast cancer.

M. Aare, I. Khan, A. Nathani, B. Boirie, A. Bagde, M. Singh;
Florida A&M University College of Pharmacy & Pharmaceutical Sciences, Tallahassee, FL

Combination therapy, a treatment modality that studies the effect of two or more drugs is the most common strategy used to overcome drug resistance in cancer. Cannabinoids have been proven to be potential anticancer agents. Terpenes have also been demonstrated to exhibit anticancer activity. The purpose of this study was to evaluate the effect of combinations of various cannabinoids and terpenes against drug resistant lung and breast cancer. Several cannabinoids and terpenes such as cannabidiol (CBD), cannabichromene (CBC), cannabidiolic acid (CBDA), cannabidivarin (CBDV), cannabinol (CBN), cannabigerol (CBG) and β-caryophyllene (BC), bisabolol, myrcene, linalool, limonene, geraniol, neralidol, α-pinene, α-terpineol, γ-terpinene respectively were screened for their anticancer activity against MDA MB 231 DOX RT, H1975 OSM RT, PDX Lung cancer cell lines using 2D cytotoxicity and 3D spheroids assay. It was found that the cytotoxic potential of combinations of cannabinoids with BC increased by 10 folds in comparison to their individual anticancer activity. The combinations that exhibit synergistic action were determined from combination index (CI) values using compusyn software. Other assays such as colony formation, wound healing, apoptotic assay, cell cycle analysis by flow cytometry elucidated the possible mechanism underlying the synergism of the combinations investigated. CBC+BC was proven to be the most potent combination from all the *in-vitro* studies and hence was further evaluated in *in-vivo tumor* xenografts. Briefly, 5 million MDA MB 231 DOX RT cells were injected by S.C route in the right flank region of BALB/c nude mice. The animals were treated after the tumor volume reached 180-200mm^3. The animals were administered CBC (15mg/kg, i.p.), BC (100mg/kg, i.p.) and CBC+BC thrice a week for two weeks. The tumor volume in the combination group was reduced by 2 folds relative to individual treatments and 4 folds relative to control. Western blot analysis of tumor xenografts showed downregulation of apoptotic markers such as PARP, mTOR, pAMPK, Survivin, autophagy markers such as LC 3, Glypican 5 and migration markers such as vimentin and Integrin. Immune check point proteins such as PD-L1 and PD-1 were also downregulated by combination treatment. This was further validated by qPCR. In conclusion, CBC induces programmed cell death in tumors and induces autophagy whereas BC inhibits migration and thus this combination was able to overcome resistance than individual therapies in a synergistic fashion.

#4567 Dual targeting of HSP70 and AURKA improves treatment in neuroendocrine prostate cancer.

P. Xu[1], J. C. Yang[1], B. Chen[1], S. Ning[1], L. Wang[1], C. Nip[1], C. P. Evans[1], M. A. Dall'Era[1], A. C. Gao[1], J. Gestwicki[2], C. Liu[1];
[1]UC Davis, Sacramento, CA, [2]UCSF, San Francisco, CA

Background: Neuroendocrine prostate cancer (NEPC) is the most aggressive type of prostate cancer with no effective treatments. Therefore, there is an urgent need to develop new treatment strategies. N-Myc plays a key role in driving NEPC progression, and Aurora kinase A (AURKA) prevents N-Myc degradation by interact with N-Myc and disallowing the intervention of ubiquitin ligases. The AURKA inhibitor Alisertib inhibits NEPC tumor growth by disrupting N-Myc signaling, but it is failed in a phase II clinical trial. In this study, we tested the synergy of novel HSP70 allosteric inhibitor JG231 and Alisertib in NEPC cells, organoids, and patient derived xenograft (PDX) models, which will provide new therapeutic strategies for the NEPC treatment.
Methods: RT-PCR, western blotting, or immunohistochemistry (IHC) were used to determine the expression of N-Myc, neuroendocrine maker (NSE, SYP, CHGA, etc) in different prostate cancer cell lines and PDX tumors. After the knockdown of HSP70 and AURKA by siRNA transfection, cell proliferation and N-Myc expression were assessed by using cell viability assay, RT-PCR and Western blotting respectively. The co-immunoprecipitation assay was performed to detect the N-Myc ubiquitination. RNA-sequencing, gene set enrichment analysis was employed to determine the changes of JG231 on gene programs. The effects of JG231 and Alisertib on the proliferation were examined in NEPC cell lines and PDX organoids models.
Results: We determined that PC3, CWR22Rv1, H660 cell lines, LuCaP49, and LuCaP93 PDX tumors had significantly increased the expression of N-Myc and neuroendocrine makers. Knockdown of HSP70 or using the HSP70 inhibitor, JG231, significantly inhibit the growth of H660 and CWR22Rv1 cells and leads to a synergistic effect with Alisertib ($p<0.001$). JG231 combined with Alisertib also inhibits growth and induces the death of LuCaP93 and H660 tumor derived organoids in a dose-dependent manner ($p<0.001$). Mechanistically, JG231 inhibits the protein expression of N-Myc through the ubiquitin-proteasome system and promote STUB1 to enter the nucleus to bind to N-Myc.
Conclusions: JG231, a novel HSP70 inhibitor, can improves the treatment efficacy of AURKA inhibitor Alisertib against NEPC through the regulation of N-Myc protein homeostasis.

#4568 Rational targeting of BCL-xL and/or mTOR enhance the efficacy of KRAS^{G12D} inhibitor in pancreatic cancer.

S. Khan[1], L. Cao[1], V. Vudhata[2], Y. Yang[1], P. Zhang[3], G. Zheng[3], J. G. Trevino[2], D. Zhou[1];

[1]UT Health Science Center at San Antonio, San Antonio, TX, [2]Virginia Commonwealth University Massey Comprehensive Cancer Center, Richmond, VA, [3]University of Florida, Gainesville, FL

Background: Pancreatic cancer (PaCa) is a highly aggressive malignancy with a very low five-year survival rate secondary to late diagnosis, limited treatment options and resistance to existing therapies. While the emergence of mutant-selective KRAS^{G12D} (G12D) inhibitors brings promise for treating PaCa patients carrying these mutations, their effectiveness as single agents is expected to be limited as evident from the clinical efficacy of KRAS^{G12C} inhibitors.

Experimental Design: First, multiple G12D-mutated PaCa cell lines were treated with a G12D inhibitor (MRTX1133) and subjected to immunoblot analysis for the expression of KRAS effectors and BCL-2 family proteins. Next, a proteolysis-targeting chimera (PROTAC)-based platelet-sparing BCL-xL degrader (DT2216) and/or an mTOR inhibitor (everolimus) were evaluated in combination with MRTX1133 for viability, clonogenicity and apoptosis. Subsequently, mechanistic investigations were carried out using immunoblotting, senescence-associated β-galactosidase staining and qPCR. Finally, therapeutic efficacy and safety of the combinations were evaluated in cell-derived and patient-derived xenograft models.

Results: MRTX1133 treatment creates apoptotic vulnerabilities by inducing aberrations in BCL-2 family proteins, with elevated BIM levels and decreased NOXA levels, in G12D-mutated PaCa cells. Furthermore, DT2216 and everolimus were shown to release BIM and stabilize NOXA, respectively, and their combination with MRTX1133 synergistically killed G12D-mutated PaCa cells in vitro and caused significant tumor growth inhibition or regression compared to single agents in vivo. Additionally, MRTX1133 treatment led to induction of senescence in a fraction of PaCa cells. These senescent cells were found to be dependent on BCL-xL and MCL-1 for their survival and were effectively killed with a combination of DT2216 and everolimus through BCL-xL degradation and NOXA-mediated MCL-1 inhibition, respectively.

Conclusions: Our findings suggest that the single agent efficacy of MRTX1133 is limited due to apoptosis inhibition and complimentary senescence induction, and therefore its combination with DT2216 and/or everolimus is synergistic, which can potentially overcome resistance, by enhanced apoptosis and clearance of senescent cells.

#4569 APG-2449, a novel focal adhesion kinase (FAK) inhibitor, inhibits metastasis and enhances the antitumor efficacy of PEGylated liposome doxorubicin (PLD) in epithelial ovarian cancer (EOC).

Z. Yu[1], E. Liang[2], D. Liu[1], B. Wu[1], X. Yao[1], Y. Ji[1], D. Yang[1], Y. Zhai[1];
[1]Ascentage Pharma (Suzhou) Co., Ltd., Suzhou, China, [2]Ascentage Pharma Group Inc., Rockville, MD

Ovarian cancer is the leading cause of cancer-related death in women and most cases are diagnosed at later stages, with distant metastasis. Standard-of-care therapy is surgery followed by platinum and paclitaxel; however, most patients who initially respond to therapy eventually relapse after developing metastatic disease and chemoresistance. FAK overexpression or activation occurs in a substantial proportion of EOCs and is predictive of poor clinical outcomes. Recent studies have reported that FAK plays an important role in cell migration and chemoresistance, rendering FAK inhibition a promising treatment approach to reduce metastasis of tumor cells and sensitize them to chemotherapy. The aim of this study was to evaluate the antitumor efficacy of investigational APG-2449, a novel FAK inhibitor, combined with PLD, a commonly used chemotherapy, in relapsed or refractory ovarian cancer. Four EOC cell lines (OVCAR-3, SK-OV-3, A2780, and Kuramochi) were used for *in vitro* experiments. Cell proliferation was measured by CellTiter-Glo assays. Cell migration ability was assessed by wound healing assays. OVCAR-3 xenograft and luciferase-tagged ID8 (ID8-Luc) peritoneal syngeneic models were established to evaluate the synergistic antitumor efficacy of combined APG-2449 and PLD *in vivo*. APG-2449 combined with doxorubicin showed synergistic antiproliferative effects in both platinum-resistant (OVCAR-3 and SK-OV-3) and platinum-sensitive (A2780 and Kuramochi) cell lines. In wound healing assays, FAK inhibition via APG-2449 alone attenuated migration of ovarian cancer cells (SK-OV-3, OVCAR-3, and ID8-Luc) in a dose-dependent manner. In the OVCAR-3 xenograft model, combined APG-2449 and PLD demonstrated enhanced antitumor effects compared with either APG-2449 or PLD monotherapy (synergistic index, 1.33). In the ID8-Luc peritoneal syngeneic model, the combination regimen outperformed PLD or APG-2449 monotherapy in tumor growth inhibition. This inhibitory effect persisted more than 1 month after stopping combination treatment, whereas the monotherapy groups experienced rapid disease relapse. The combination group also exhibited the longest ascites-free and survival times compared with PLD or APG-2449 monotherapy groups. Overall, our data suggest that inhibition of FAK by APG-2449 enhances the antitumor effect of PLD in EOC cell lines and the OVCAR-3 xenograft mouse model. The combination regimen can also prolong ascites-free and survival times, as shown in the ID8-Luc peritoneal syngeneic model. These promising results support future clinical development of this combination treatment for ovarian cancer.

#4570 Prostate-specific membrane antigen targeted chemo-photodynamic therapy for the treatment of prostate cancer.

X. Wang, A. Shirke, S. Chavali, L. Zhang, E. Walker, G. Ramamurthy, J. Basilion;
Case Western Reserve University, Cleveland, OH

Introduction: Prostate cancer is the most prevalent cancer among men in the United States and is their second leading cause of cancer death. During initial screen, about 17-31% of patients are diagnosed with non-metastatic high-risk localized prostate cancer. These patients have an increased risk of treatment failure and oncological progression. The contemporary treatment paradigm of high risk localized prostate cancer is moving toward a multidisciplinary integrated approach of systemic and local therapy. In addition, incorporation of molecular biomarkers can also improve the risk stratification and treatment of prostate cancer. Among the biomarkers for prostate cancer, prostate specific membrane antigen (PSMA) has been proven to be an excellent target for diagnosis and treatment of prostate cancer. We have generated a PSMA-targeted photodynamic therapy (PDT) agent, PSMA-1-Pc413, and a PSMA-targeted chemotherapeutic agent, PSMA-1-MMAE. The objective of this study is to generate a new molecule that combines PDT and chemotherapy to achieve improved antitumor activity.

Methods: Using a bifunctional PSMA ligand, a novel theranostic PSMA-targeting conjugate was synthesized, which integrated both the photosensitizer Pc413 and the microtubular inhibitor monomethyl auristatin E (MMAE) in one simple molecule, PSMA-1-MMAE-Pc413. This molecule was first tested for in vitro uptake and cytotoxicity studies using PSMA-positive PC3pip and PSMA-negative PC3flu cells. The conjugate was then tested for in vivo fluorescence imaging using mice bearing both PC3pip and PC3flu tumors. Finally, the antitumor activity of PSMA-1-MMAE-Pc413 was tested in mice with PC3pip tumors with and without light irradiation.

Results: In *in vitro* uptake studies, the uptake of PSMA-1-MMAE-Pc413 in PC3pip tumor was about 3-fold higher than that in PC3flu cells. In *in vitro* cytotoxicity studies, when exposed to 5 J/cm^2 of 672nm light, PSMA-1-MMAE-Pc413 demonstrated a synergistic effect leading to greater cytotoxicity for PC3pip cells (IC_{50}=2.77nM) when compared to PSMA-1-Pc413 with light irradiation (IC_{50}=372nM) or PSMA-1-MMAE-Pc413 without light irradiation (IC_{50}=12.6nM). In *in vivo* imaging studies, PSMA-1-MMAE-Pc413 demonstrated selective uptake in PC3pip tumors. Further, antitumor activity studies showed that PSMA-1-MMAE-Pc413 with light irradiation significantly inhibited PC3pip tumor growth and prolonged survival time as compared to mice receiving equimolar amounts of PSMA-1-Pc413 with light irradiation or PSMA-1-MMAE-Pc413 without light irradiation.

Conclusion: We have synthesized a new theranostic agent PSMA-1-MMAE-Pc413 that combines imaging, chemotherapy and PDT. The new molecule dramatically improves the treatment effect as compared to each single treatment alone. (The work is supported by NIH 1RO1CA255925-01A.)

#4571 Combination of FOLFIRI (5-FU, Leucovorin, and Irinotecan) and ProAgio on colon cancer growth and metastasis.

P. N. Ganji[1], J. B. Foote[1], M. S. Saddala[2], F. Mishra[3], S. Sarvesh[1], M. Malla[1], A. Masood[4], Z.-R. Liu[3], B. F. El-Rayes[1];
[1]University of Alabama at Birmingham, Birmingham, AL, [2]University of California, Irvine, CA, [3]Georgia State University, Atlanta, GA, [4]Indiana University School of Medicine, Indianapolis, IN

Background/Objective: One of the common mechanisms of resistance of solid tumors, including colon cancers, is activation of integrins on endothelial cells (ECs) and cancer-associated fibroblasts (CAFs). ProAgio is a small molecule developed to target integrin alpha V beta 3 (αvβ3), located on surface of abnormal ECs and CAFs. ProAgio enhances apoptosis and inhibits angiogenesis via targeting αvβ3. The aim of the current study is to evaluate the ProAgio combination with FOLFIRI on the immune profile and tumor growth of colon cancer.
Material and Methods: Female BALB/CJ and male NSG (NOD.Cg-Prkdcscid Il2rgtm1Wjl/SzJ) mice were acquired from the Jackson Laboratory, and experiments were performed under the approval of The University of Alabama at Birmingham-Institutional Animal Care and Use Committee. For orthotropic tumor efficacy studies, BALB/CJ mice were injected with 2×10^5 CT-26 wild type and CT26.CL25 cells in 30ul 1:1 Matrigel Matrix and PBS into the Cecum. PDX (10mg) was orthotopically implanted into the NSG mice cecum. At Day five, mice were divided into four treatment groups: including 1) sterile water (vehicle), 2) ProAgio (15mg/kg; IP; once daily for nine days), 3) FOLFIRI (5-FU: 30mg/kg; Leucovorin 50mg/kg; Irinotecan; 20mg/kg - once every three days intraperitoneal) or 4) combination of ProAgio and FOLFIRI. The study completed on day 15, tumor weight was noted, and tumors were processed for histology and flow cytometry.
Results: ProAgio plus FOLFIRI significantly ($p<0.001$) reduced tumor weight in both models compared to individual treatments and vehicles. Combination-treated mice showed a significant ($p<0.001$) reduction in T-cell exhaustion ($CD8^{\pm}$ T cells that are positive for PD-1, TIM-3, and CTLA-4). Analysis of the myeloid compartment showed a significant ($p<0.001$) increase in the M1 macrophages that express F4/80 as well as CD86, MHC-II and a decrease in the M2 macrophage in the mice treated with ProAgio plus FOLFIRI. The combination therapy exhibited a significant ($p<0.001$) increase in the dendritic cell infiltration into the tumor microenvironment. Histology analysis showed that ProAgio treatment reduced the incidence of organ site metastasis (disseminated and locoregional spread) such as liver, pancreas, and diaphragm.
Conclusion: Our study offers encouraging observations that ProAgio plus FOLFIRI can suppress colon cancer growth and metastasis by inhibiting αvβ3 preclinically and may provide a novel therapeutic combination for the management of colon cancers.

#4572 Ginsenoside Rh3 increases the susceptibility of regorafenib-mediated cancer cell death by inhibiting the JAK/STAT3 signaling pathway in hepatocellular carcinoma.

Y. Jeon[1], H. Kwon[1], Y. Park[2], D.-Y. Woo[1], T. Kim[1], J. Ham[1], **Y.-J. Kim**[1];

[1]Korea Institute of Science and Technology (KIST), Gangneung, Korea, Republic of, [2]Yonsei University College of Medicine, Seoul, Korea, Republic of

Ginsenosides, bioactive compounds derived from Panax ginseng, exhibit diverse pharmacological effects, including anti-cancer properties. Regorafenib, a potent multi-kinase inhibitor, is employed as a second-line therapy for advanced hepatocellular carcinoma (HCC). However, the modest survival benefits observed in treated patients may be attributed to drug resistance. In this study, we screened a panel of 40 ginsenosides for their activity in combination with regorafenib in HCC cell lines and investigated their underlying cellular mechanisms. Synergistic effects were evaluated using the WST-8 assay, and optimal drug concentrations were determined through synergy scoring. A phospho-kinase assay was conducted to elucidate the mechanism of action, and in vivo experiments validated our findings. Ginsenoside Rh_3 emerged as a promising candidate, enhancing the sensitivity of HCC cells to regorafenib-induced anticancer effects by promoting apoptosis. The phospho-kinase array revealed that the combined treatment's apoptotic effect was associated with the inhibition of signal transducer and activator of transcription 3 (STAT3) activation through the Janus kinase pathway. *In vivo* results demonstrated the combination treatment's inhibitory effects on tumor growth. Our study proposes a novel treatment strategy, highlighting the potential efficacy of combining regorafenib and ginsenoside Rh_3 for HCC treatment.

#4573 Pre-clinical evaluation of small molecule CHK2 inhibitor, ART446, pre-IND candidate that enhances the olaparib and irinotecan.

T. Baik[1], Y. Kang[1], H. Lee[1], J. Kim[1], A. Jeong[1], J. Kim[2], W.-Y. Kim[3];

[1]Arum Therapeutics Inc., Seoul, Korea, Republic of, [2]Yeungnam University, Gyeongsan, Korea, Republic of, [3]Sookmyung Women's University, College of Pharmacy, Seoul, Korea, Republic of

Background: Poly (ADP-ribose) polymerase (PARP) plays a pivotal role in DNA damage repair. Tumors with DNA Damage Response (DDR) defects exhibit increased susceptibility to drugs targeting PARP. The drugs induce DNA damage like Irinotecan (a Topoisomerase I inhibitor) are widely used in clinic as well. However, intrinsic resistance remains a significant obstacle, leading to frequent treatment failures. Chk2 is activated in response to these DNA damage inducing agents and hold the cell cycle. We developed pre-IND candidate ART446, with the aim of exploring its therapeutic potential in sensitizing DNA damage-targeting reagents.

Results: In the radiometric HopSpot Kinase Assay, ART446 demonstrated significant inhibition of Chk2 (IC_{50}, 9 nM). In HT-29 colon adenocarcinomas, co-treatment with SN38 and ART446 exhibited a synergistic therapeutic effect in vitro, with a subsequent in vivo tumor growth assay demonstrating a remarkable combined effect (TGI: Irinotecan, 46%; ART446, 16%; combined, 83.4%). Further extending our investigation to triple-negative breast adenocarcinoma MDA-MB-436, characterized by a BRCA1 mutation, we explored the sensitization potential of ART446 to PARP inhibitors. Strikingly, the combination therapy with a PARP inhibitor, Olaparib surpassed monotherapy outcomes, resulting in complete tumor growth inhibition (TGI: Olaparib, 73%; ART446, 20%; combined, 102%). Mechanistic insights revealed an increase in gamma H2AX levels by ART446 and a decrease in active forms of Chk2 which were activated by Olaparib affirming that Olaparib-induced Chk2 inhibition contributed to the sensitization effect.

Conclusions: The pre-IND candidate ART446 exhibits promising potential in enhancing the therapeutic effects of Olaparib and Irinotecan. These findings provide a robust foundation for further clinical development, offering a strategic approach to overcome resistance in cancer treatment.

#4574 Next generation nuclear export blocker KPT8602 synergizes with KRAS^{G12D} inhibitor MRTX1133 resulting in improved antitumor effects against pancreatic ductal adenocarcinoma.

H. Y. Khan[1], A. Aboukameel[1], M. Uddin[1], S. F. Bannoura[1], K. Keffri[1], M. Jasti[1], R. Virga[1], S. Motorwala[1], K. Choucair[1], T. Hadid[1], M. Al-Hallak[1], E. Beal[1], M. Tobon[1], R. Beydoun[1], G. Dyson[1], S. Kim[1], M. Nagasaka[2], P. A. Philip[3], B. El-Rayes[4], H. Chen[4], A. Shields[1], R. Mohammad[1], B. Pasche[1], A. Azmi[1];
[1]Barbara Ann Karmanos Cancer Institute, Detroit, MI, [2]University of California Irvine School of Medicine, Orange, CA, [3]Henry Ford Health, Detroit, MI, [4]School of Medicine, University of Alabama, Birmingham, MI

Introduction: A novel KRAS inhibitor, MRTX1133, specifically targeting the G12D isoform, prevalent in pancreatic ductal adenocarcinoma (PDAC), holds promise for a substantial PDAC patient population. Nevertheless, given the clinical experience with sotorasib (a KRAS^{G12C} inhibitor) in lung cancer, it's anticipated that resistance to the KRAS^{G12D} inhibitor will eventually emerge in most PDAC patients. This underscores the need to identify strategies that can enhance the efficacy of KRAS inhibitors in PDAC. Emerging evidence suggests that the nuclear export protein exportin 1 (XPO1) is a druggable vulnerability in KRAS mutant cancers. XPO1 plays a pivotal role in shuttling various critical tumor suppressors, genome surveillance proteins, and transcription factors out of the nucleus and is frequently overexpressed in various cancers, including PDAC. In this study, we employed both *in vitro* and *in vivo* models to assess the potential of KPT8602, an investigational and next-generation selective XPO1 inhibitor, to synergize with the KRAS^{G12D} inhibitor MRTX1133 and sensitize MRTX1133-resistant PDAC cells.

Methods: We examined the cytotoxic and molecular effects of KRAS^{G12D} inhibitor MRTX1133 in combination with nuclear export blocker KPT8602 in KRAS^{G12D} mutant 2D and 3D cellular/spheroid models. The preclinical antitumor efficacy of the combination was evaluated in a KRAS^{G12D} mutant PDAC cell derived xenograft (CDX) model.

Results: KPT8602 synergized with MRTX1133 *in vitro* yielding suppressed proliferation of KRAS^{G12D} mutant PDAC cells. Similar synergistic effects were also seen in 3D cultures of KRAS^{G12D} mutant PDAC cancer cell lines and patient derived primary tumor cells where the combination suppressed spheroid formation and reduced spheroid viability. Also, the combination inhibited the clonogenic potential of KRAS^{G12D} mutant PDAC cells. In addition, we developed a PDAC cell line resistant to MRTX1133 and observed that such MRTX1133-resistant cell line was acutely sensitive to treatment with KPT8602. Mechanistically, KPT8602 and MRTX1133 combination led to reduction in protein expression of KRAS downstream effectors and cell cycle markers. Furthermore, a combined administration of KPT8602 and MRTX1133 at sub-optimal doses resulted in remarkable tumor growth inhibition in a KRAS^{G12D} mutant HPAC CDX mice model. Moreover, KPT8602 as a maintenance therapy also prevented tumor relapse.

Conclusion: This is the first study demonstrating that nuclear export blocker KPT8602 can synergize with KRAS^{G12D} inhibitor MRTX1133 and has the potential to target MRTX1133-resistant PDAC cells. This study provides a rationale for combining MRTX1133 with KPT8602 for the treatment of PDAC patients with KRAS^{G12D} mutant tumors.

#4575 FGFR3 altered bladder cancer exhibits a lineage-dependent vulnerability.

M. Koleilat, Y. Zhu, L. Kwong;
UT MD Anderson Cancer Center, Houston, TX

Fibroblast Growth Factor 3 (FGFR3) genomic alterations are oncogenic drivers in ~15% of bladder cancer patients. A novel FGFR inhibitor, Erdafitinib, was FDA approved in 2019 based off a Phase II trial with an overall response rate of 40%. However, the majority of patients rapidly relapse at a median of 6 months, requiring combination therapies to prevent drug resistance. We hypothesized that a genome-wide CRISPR screen would identify Erdafitinib-sensitizing co-targets. We screened UM-UC-14, an S249C FGFR3 mutated bladder cancer cell line, and identified Cyclin C as a top hit in addition to known MAPK effectors such as ERK2 and SHP2. Cyclin C is a non-cell cycle related cyclin and part of the CDK8/19 kinase module of Mediator. Pharmacological validation in 4 FGFR3 altered cell lines confirmed a high degree of synergy between Erdafitinib and the CDK8/19 inhibitor Sel120, while no effect was seen in 2 wildtype cell lines, suggesting strong specificity. Moreover, the synergy in FGFR3-mutant cells was superior to that of SHP2 inhibitor SHP099 or the ERK inhibitor BVD-523. Similarly, GATA3 and PPARG also scored highly in our CRISPR screen. These transcription factors have been shown to be sufficient to enforce a luminal identity but not necessarily to maintain it. We validated these 3 genes as sensitizers and show in luminal cells that loss of either GATA3 or PPARG leads to loss of luminal markers and gain of basal markers. In contrast, cells treated with Sel120 showed, on RNAseq, an increase in basal markers without loss of luminal markers. Interestingly, our data suggests that the gain of basal markers, commonly associated with a worse prognosis, is associated with a strong sensitization to FGFR inhibition in FGFR3 alteration driven bladder cancer. We conducted a xenograft experiment confirming that mice responded well to single agent Erdafitinib, but without frank tumor regression. By contrast, Sel120+Erdafitinib induced complete responses in 8/10 mice compared to 6/10 mice for SHP099+Erdafitinib. Remarkably, after 60 days of daily drugging and a 20-day washout, the tumors did not grow back in the complete responders. Importantly, no loss of body weight or other signs of morbidity were found. Our results suggest an immediate and promising benefit in combining either CDK8/19 or SHP2 inhibitors with Erdafitinib in treating patients with FGFR3 alteration driven bladder cancers. Furthermore, we identified a strategy in targeting lineage modulators as sensitizers to existing therapies.

EXPERIMENTAL AND MOLECULAR THERAPEUTICS: HDAC and Methyltransferase Inhibitors
Poster Session

#4579 DNMT1 determines the sensitivity of Class I HDAC inhibitor Psammaplin A to induce apoptosis and DNA damage in hematological malignant cells.

Y. Bao[1], D. Liu[1], Z. Wu[1], Y. He[1], P. Gong[1], S. Waxman[2], Y. Jing[1];
[1]Shenyang Pharmaceutical University, Shenyang, China, [2]Icahn School of Medicine at Mount Sinai, New York, NY

Histone deacetylases (HDACs) and DNA methyltransferases (DNMTs) are overexpressed in cancer cells associated with dysregulated gene expression and tumor progression. DNMT1 partnered with Class I HDAC as complex to inhibit gene transcription. Several pan-HDAC inhibitors have been approved for T-cell lymphoma with evident side effects. More selective HDAC inhibitors need to be developed. Psammaplin A (PsA), a symmetrical bromotyrosine-derived disulfide dimer isolated from the *Psammaplysilla sponge*, is a selective Class I HDAC inhibitor. We tested its cell growth inhibition and apoptosis induction in 12 hematological malignant cell lines with 8 lines sensitive (more than 50% growth inhibition at 1 μM) and 4 lines insensitive (less than 20% growth inhibition at 1 μM). PsA induces acetylation of H3, but not α-tubulin, supporting the Class I HDAC inhibition selection. In the sensitive cell lines, PsA induces apoptosis with down-regulation of c-Flip and upregulation of NOXA as well as DNA damage detected by γ-H2A.X. RNA sequence analysis results confirm the regulation of PsA on *NOXA*, *c-Flip* and *p21* gene expression. The four insensitive cell lines express high levels of DNMT1 with resistance to apoptosis induction. Silencing DNMT1 with siRNA sensitizes PsA-induced apoptosis with induction of NOXA and γ-H2A.X. Azacytidine, the DNMT1 degrader, in combination with PsA induce synergistic cell growth inhibition and apoptosis in vitro. PsA (20 mg/kg) plus Azacytidine (2.5 mg/kg) synergistically inhibit tumor growth in insensitive mantle cell lymphoma Jeko-1 xenografts, without detected toxic signs in organ pathological analysis. We find a new mechanism of DNMT1 controlling the sensitivity of Class I HDAC inhibitor PsA and provide a rationale of PsA with azacytidine for combination therapy.

#4580 Selective HDAC3 inhibition e-sensitizes PARPi-resistant ovarian cancer cells to olaparib.

B. E. Fashemi[1], V. Gupta[1], M. Akande[1], Y. Ota[1], S. Mitra[1], B. Bitler[2], D. Khabele[1];

[1]Washington University School of Medicine in St. Louis, St. Louis, MO, [2]Colorado School of Medicine, Aurora, CO

High-grade serous ovarian cancer is a rare but deadly disease. Platinum-based therapy along with poly ADP ribose polymerase inhibitors (PARPi) maintenance therapy, is recommended to 80% of patients. However, acquired PARPi resistance is an ongoing clinical problem and there is a growing need for the development of more targeted therapies. We have previously shown that the class I histone deacetylase inhibitor (HDACi), entinostat, which is selective for HDAC1/2, resensitizes ovarian cancer cells to PARPi. Here, we propose to examine whether selective inhibition of HDAC3 will induce a synthetic lethality in PARPi-resistant ovarian cancer cells. BRD3308 is an HDACi that is a potent and highly selective inhibitor of HDAC3 and of HDAC1/2 to a lesser extent. To investigate these effects, we used two mouse ovarian cancer epithelial lines ID8 TP53-/-/BRCA2-/- (ID8) and an olaparib resistant line ID8 TP53-/-/BRCA2-/--OR (ID8_OR). We performed cell viability assays (MTS) by treating both cell lines with increasing concentrations of olaparib (0-40uM), BRD3308 (0-2uM), and in combination. When ID8_OR cells were treated with olaparib 5uM and 0.25uM of BRD3308 in combination, cell proliferation was significantly reduced when compared to olaparib treatment alone (p= 0.0077). We did not observe a significant differences in cell proliferation between olaparib alone and in combination with BRD3308 in the ID8 cells. Olaparib and BRD3308 treatment in the ID8_OR cells were found to be synergistic at four out of the five drug concentrations tested, with concentrations 2.5uM olaparib and 0.125 uM of BRD3008 scoring the highest (22, Loewe Synergy Score). In the presence of BRD3308, the olaparib EC50 reduced ~13-folds in the ID8_OR cells compared to only a 2-fold reduction in the ID8 cells. We hypothesizes that inhibition of HDAC3 induces apoptosis by downregulating homologous recombination repair in response to DNA damage. To examine these, we irradiated both ID8 cell lines and treated with olaparib (10 uM), BRD3308 (0.5uM) and in combination, for 24 hours, followed by western blot analysis. Rad51 expression was reduced following combination treatment when compared to control or olaparib alone. Lastly, our clonogenicity data revealed colony formation in both ID8 cell lines were reduced when treated with olaparib (5uM) and BRD3308 (0.25uM). Interestingly, BRD3308 alone reduced colony formation in the ID8_OR cells, but not in the ID8 cells. In conclusion, selective HDAC3 inhibition in combination with olaparib may be an effective therapy in the treatment of acquired PARPi resistant ovarian cancers.

#4581 Identifying class 1 HDACs as a vulnerability for aggressive uveal melanoma.

G. Yenisehirli[1], A. Zuniga[1], S. Rodriguez[1], E. V. Adis[1], G. Quintana[2], S. Borges[2], S. Lopez[2], K. Lopez[1], S. Braun[1], C. H. Volmar[1], J. W. Harbour[3], S. Kurtenbach[1];

[1]University of Miami Miller School of Medicine, Miami, FL, [2]University of Miami, Miami, FL, [3]University of Texas Southwestern Medical Center, Miami, FL

Uveal melanoma (UM) is the most common primary intraocular cancer in adults, with a strong propensity to metastasize, primarily to the liver. Metastatic UM is notoriously unresponsive to existing therapies, rendering it almost uniformly lethal. Virtually all UM tumors have activating mutations in the Gq signaling pathway, predominantly in GNAQ/11, and around half of tumors have additional loss-of-function mutations in the tumor suppressor BAP1. Mutations in the epigenetic modulator BAP1 are the most significant clinical marker of metastatic risk. The limited efficacy of current treatment options necessitates an urgent exploration of novel therapeutic approaches to improve patient prognosis. Thus, we conducted a large epigenetic compound library screen with the currently most well characterized, focused epigenetic library available, which consisted of 960 potent, cell permeable, medically active, epigenetic-directed small molecule modulators (TargetMol, L1200). We screened BAP1-mutant as well as BAP1-wildtype uveal melanoma cell lines and followed up with comprehensive dose-response and synergy tests. Our lead compounds were highly efficient in reducing viability of UM cells. We find that inhibitors with high specificity for class 1 HDAC inhibition are especially cytotoxic to UM cells. Together, our results reveal a possible mechanism of interfering with UM progression and identify lead compounds to be tested in clinical trials.

#4582 HDAC6 inhibition reshapes the epigenome of cancer *via* P300 stabilization.

M. Gottardi Zamperla[1], B. Illi[2], V. Barbi[1], C. Cencioni[3], S. Gagliardi[4], M. Garofalo[4], G. Zingale[5], I. Pandino[5], D. Sbardella[5], L. Cipolla[6], S. Sabbioneda[6], A. Farsetti[3], C. Ripamonti[7], G. Fossati[7], C. Steinkuhler[7], S. Atlante[3], C. Gaetano[1];

[1]Istituti Clinici Scientifici Maugeri Spa Societa' Benefit, Pavia, Italy, [2]Consiglio Nazionale delle Ricerche-Istituto di Biologia e Patologia Molecolari, Roma, Italy, [3]Consiglio Nazionale delle Ricerche-Istituto di analisi dei sistemi ed informatica, Roma, Italy, [4]IRCCS Fondazione Mondino,, Pavia, Italy, [5]IRCCS Fondazione G.B. Bietti,, Roma, Italy, [6]Istituto di Genetica Molecolare "Luigi Luca Cavalli-Sforza", Pavia, Italy, [7]Italfarmaco Group, Cinisello Balsamo, Italy

Introduction: Histone deacetylases (HDACs)are crucial in regulating gene expression, DNA synthesis, and metabolic processes, including cancer, in various cellular environments. The unique structural and functional attributes of class IIb HDAC6 position it as a key player in influencing protein stability and chromatin dynamics. While its role in cancer progression and immunomodulation is well-recognized, the in-depth mechanisms following HDAC6 inactivation, particularly its influence on chromatin remodeling and gene regulation, are not thoroughly understood. This knowledge gap represents a critical area of investigation, given the potential of HDAC6 as a therapeutic target in oncology. This study aims to elucidate HDAC6 inactivation-dependent epigenetic effects of, exploring the possibility to exploit these latter for therapeutic purposes in cancer. This aim includes an examination of the stabilization of the lysine acetyltransferase P300 and its implications for chromatin structure and function.

Methods & Results: In this study, ITF3756 and CRISPR/Cas9 were employed to inactivate HDAC6 across a variety of cancer cell lines (Jurkat, MDA 231, HCC1806, 4T1, and B16F10 melanoma). ATAC-seq and H3K27Ac ChIP-seq were used to investigate changes in chromatin accessibility, revealing significant alterations, particularly in introns and distal intergenic regions. Gene Ontology (GO) analysis further supported this alteration in the chromatin landscape, which indicated a differential expression of genes involved in critical cellular processes like cell proliferation, adhesion, migration, and apoptosis. A notable outcome of this study was the stabilization of P300 following ITF3756 treatment, an effect that was paralleled by changes in the expression of critical genes, including AKT1, ITGB3, GAS6, SOX9, NF1, TGFB2, and CASP7. These genes are integral to cellular survival mechanisms, and their modulation emphasizes the role of HDAC6 in cancer cell physiology.

Conclusions: This research shows that the chemical or genetic inactivation of HDAC6 impacts cancer cell proliferation and chromatin architecture, underscoring the potential of HDAC6 as a target in cancer therapeutics.. A critical finding of this study is the stabilization of P300, which offers new perspectives on HDAC6's functionality and its role as an epigenetic modifier in cancer cells. This study contributes to the field by suggesting therapeutic strategies focusing on HDAC/HAT pharmacological targeting, thereby advancing our understanding of the role of HDAC6 in regulating cancer cell behavior and epigenetic landscape.

#4583 Development of selective HDAC6 inhibitors to improve cancer immunotherapy.

Nithya Gajendran[1], Manasa Suresh[1], David Quiceno[1], Xintang Li[1], Marie Durr[1], Sebastian J. Marquez Rodriguez[2], Mario A. Noboa[2], Sruthi Mohan[2], Barbora Havlinova[3], Julia Kudlacova[3], Satish Kumar Reddy Noonepalle[1], Cyril Barinka[3], Duncan J. Wardrop[2], Alejandro Villagra[1]

[1]Department of Oncology, Georgetown University Medical Center ,Lombardi Comprehensive Cancer Center, Washington, DC,[2]Department of Chemistry, University of Illinois at Chicago, Chicago, IL,[3]Institute of Biotechnology of the Czech Academy of Sciences, Prumyslova, Czech Republic

Histone Deacetylases (HDACs) are enzymes that modify histones and non-histone proteins. Our group has previously demonstrated that HDAC6 inhibitors (HDAC6is) modulate multiple immune pathways, including those that suppress the antitumoral M2 phenotype, leading to improved antitumor immunity. Despite the potential of HDAC6is, current inhibitors have poor selectivity and off-target effects and only work at micromolar concentrations. In this work, we designed a screening pipeline of HDAC6i, considering selectivity, potency, capacity to prevent the protumoral phenotype of macrophages, and low cytotoxicity on macrophages and other immune cells. This approach has not been tested before, as the standard screening method for antitumoral HDACis has focused on its cytotoxic effect on cancer cells. We initially designed in silico 980 compound derivatives from previously reported HDAC6i, such as SS208, Nexturastat A, and Suprastat. Twenty-four compounds with a high capacity to bind HDAC6 and chemical stability were screened by their ability to inhibit HDAC6 in cell-free conditions. Sixteen compounds demonstrated high potency and were further evaluated in murine macrophages by their cytotoxic effect using CellTox. The capacity to impede tubulin deacetylation was assessed by western blot and deacetylase activity by HDAC-Glo. The top six candidates were then evaluated by their selectivity compared to other HDAC members and by their effect on repressing the expression of protumoral M2 macrophages Arginase 1 and Fizz1, and activation of antitumoral markers TNFa and iNOS by western blot and qRT-PCR. The best three candidates were then evaluated at nanomolar concentrations to explore their immunomodulatory potential of M1 against M2 by performing antigen presentation (SIINFEKL presentation) and phagocytic capacity using microscopy. Two of these compounds, SM-06-09 and SM-05-947, will be further tested in syngeneic murine melanoma models for their ability in tumor regression and antitumor immunity. This study has yielded important insights into developing new and improved HDAC6is with minimal cytotoxicity, and we believe our work will help advance cancer research and ultimately lead to better patient outcomes.

#4584 Novel YAP1/TAZ pathway inhibitors identified through phenotypic screening with potent anti-tumor activity via blockade of GGTase-I and Rho-GTPase signaling.

Keith Graham[1], Philip Lienau[2], Benjamin Bader[1], Stefan Prechtl[1], Jan Naujoks[1], Ralf Lesche[1], Barbara Nicke[1], Wilhelm Bone[1], Sven Golfier[1], Krzysztof Brzezinka[1], Stefan Kaulfuss[1], Charlotte Kopitz[1], Holger Steuber[1], Nico Braeuer[1], Katrin Nowak-Reppel[1], Carlo Stresemann[1], Patrick Steigemann[1], Julia Kuehnlenz[2], Lisette Potze[1], Francesca Zanconato[3], Anna Montebaur[2], Sabine Pilari[2], Sikander Hayat[2], Atanas Kamburov[2], Andreas Steffen[2], Andreas Schlicker[2], Philipp Buchgraber[2], Nuria Aiguabella Font[2], Tobias Heinrich[2], Lara Kuhnke[2], Annette O. Walter[2], Simona Blotta[2], Matthias Ocker[2], Ashley Lakner[2], Dominik Mumberg[2], Knut Eis[2], Stefano Piccolo[3], **Martin Lange**[1]

[1]Nuvisan ICB GmbH, Berlin, Germany,[2]Bayer Pharma AG, Berlin, Germany,[3]University of Padua, Padua, Italy

YAP1/TAZ have been shown to be aberrantly activated oncogenes in several human solid tumors, resulting in enhanced cell proliferation, metastasis and provision of a pro-tumorigenic microenvironment, making YAP1/TAZ targets for novel cancer therapies. Yet, the development of effective inhibitors of these potent oncogenes has been challenging. In this work, we break new ground in this direction through the identification of novel inhibitors of YAP1/TAZ activity. This study describes the identification and target deconvolution of novel small molecule inhibitors of oncogenic YAP1/TAZ activity with potent anti-tumor activity in vivo. A high-throughput screen (HTS) of 3.8 million compounds was conducted using a cellular YAP1/TAZ reporter assay. HTS hits that selectively inhibited TEAD-luciferase, but not TK-Renilla-luciferase (n = 3.994) were subsequently assessed regarding their ability to induce translocation of YAP1 from the nucleus to the cytoplasm in MDA-MB-231 cells, which is the physiological mechanism of inactivation. Out of these, 392 hits showed activity to induce translocation of YAP1. Finally, selected hits active in both assays (n = 96) were assessed regarding their effect on endogenous YAP1/TAZ target genes. The small molecule BAY-856 demonstrated the most consistent YAP1/TAZ inhibitory activity of all selected hits, which warranted further exploration of the unknown direct drug target. Target deconvolution studies identified the geranylgeranyltransferase-I (GGTase-I) complex, as the direct target of YAP1/TAZ pathway inhibitor BAY-856. BAY-856 and close analogs with improved in vitro potency blocked the activation of Rho-GTPases, leading to subsequent inactivation of YAP1/TAZ and inhibition of cancer cell proliferation in several tumor types in vitro. Multi-parameter optimization resulted in BAY-593, an in vivo probe with favorable PK properties. BAY-593 demonstrated anti-tumor activity in solid tumor models and blockade of YAP1/TAZ signaling *in vivo*. BAY-593 is a novel tool compound to explore Rho-GTPase signaling and downstream YAP1/TAZ biology in vitro and in vivo.

#4585 Discovery of ETS-006, a highly potent YAP/TEADs PPI inhibitor with broad anti-tumor activity as a single agent.

J. Lu, M. Gao, W. Du, X. Fan, J. Li, M. Wang, L. Feng, Y. Li, J. Yao, J. Lu, W. Cui, Q. Zheng, **J. Zhu**;
ETERN Therapeutics Co., Ltd., Shanghai, China

The transcription co-activators YAP, pairing with the TEAD family of transcription factors, serve as essential effectors of the conserved Hippo signaling pathway. Hippo kinase cascade controls YAP nuclear entry and binding with TEADs by modulating its phosphorylation and stability. Overexpression and activation of YAP/TAZ are frequently observed in a variety of cancers. It has been well established that YAP aberration contributes to cancer development, metastasis, immunosurveillance escape and drug resistance. Disruption of YAP/TEADs PPI is an effective approach to inhibit YAP transcriptional activity. We previously have reported the identification of YAP/TEADs PPI hit compound through the fragment-based screen and advanced the hit to lead compound ETS-003. Here we reported the preclinical candidate of YAP/TEADs PPI inhibitor ETS-006 with much more potent anti-tumor activity and favorable safety profile. Compared to TEAD palmitoylation inhibitor, ETS-006 could completely disrupt the interaction of YAP/TEADs, resulting in a more profound downregulation of YAP target gene expression. ETS-006 demonstrated more robust anti-tumor activity than the competitor's YAP/TEADs PPI inhibitor in MPM CDX model with favorable ADME properties. Notably, ETS-006 showed promising efficacy across multiple solid tumor types, including head and neck squamous cell carcinoma, osteosarcoma, and triple-negative breast cancer with urgent unmet clinical needs. In conclusion, ETS-006 is a highly potent and orally available YAP/TEADs PPI inhibitor with broad anti-tumor activity as a single agent.

#4586 ITF3756 increases NKG2D expression and cytotoxic activity of activated human CD8 T cells.

C. Ripamonti, V. Spadotto, C. Steinkuhler, G. Fossati;
Italfarmaco S.p.A., Cinisello Balsamo, Italy

Effector cytolytic CD8 T cells play a major role in the recognition and killing of cancer cells. These cells are short living due to the loss of their self-renewal capacity and rapid exhaustion. Enduring antitumor immune response relies on the capacity of regenerating effector cells upon antigen re-encounter by memory cells. Focusing on molecules that could modulate the differentiation of T cells towards a memory subset with a prolonged anti-tumor activity is strategic for an efficient anti-tumor immunotherapy. Thus, we developed a selective HDAC6 inhibitor currently in Phase I clinical trial, ITF3756, which *in vitro* drives the differentiation of human CD8 T cells towards a central memory phenotype with reduced expression of exhaustion markers and higher expression of IFNγ and Granzyme b upon tumor cells coculture. This suggests that ITF3756-treated CD8 T cells could have a greater tumor killing activity. Moreover, if this augmented cytotoxic activity is directed not only towards tumor cells expressing MHC I but also towards MHC I negative cells, the anti-tumor efficacy could be improved. We thus selected the MHC I negative K562 leukemic cell line as target in an in vitro model of CD8 T cell killing assay. CD8 T cells were stimulated with anti CD3CD28 beads with or without ITF3756, and then co-cultivated with K562 cells for 4h. ITF3756 treatment improved significantly CD8 mediated K562 killing over this short period of time. However, since the effectiveness of memory cells is based on their capacity of maintaining a long-lasting immune response, we monitored the cytolytic activity over a period of 2 weeks. After 14 days of co-culture, ITF3756 treated CD8 T cells showed a higher cytotoxic capacity compared to control cells. These results indicate that ITF3756-treated CD8 T cells can kill a target tumor cell in a more efficient way independently of MHC I restricted tumor recognition, both after short and long term in vitro co-culture. Since it has been described that CD8 T cells can also kill MHC I-negative tumor cells through the NKG2D-NKG2DL axis, we assessed if ITF3756 could modulate the expression of NKG2D on CD8 T cells. Indeed, ITF3756-treated CD8 T cells had a significantly higher expression of NKG2D compared to untreated cells. In conclusion, we show that ITF3756 promotes the differentiation of cells that possess better effector activity when co-cultured with tumor cells for both short and long periods of time. ITF3756 increased the expression of NKG2D and this could be a driver of the increased cytolytic activity. One mechanism of tumor immune escape is the downregulation of MHC I. Our results suggest that ITF3756 could be used to improve the efficacy of T cell therapy by enhancing the cytolytic activity even in the absence of MHC I.

#4587 Development of highly selective, potent, orally available PIM1 inhibitor BLX0631 shows a therapeutics potential in multiple myeloma models.

Z. Li, C. Lin, D. J. Bearss, **H. Vankayalapati**;
Biolexis Therapeutics Inc., American Fork, UT

Background: The Proto-oncogenic PIMs family are nuclear and cytoplasmic Ser/Thr kinases (PIM1, PIM2, and PIM3) that are constitutively active and play a vital role in proliferation and survival in Multiple Myeloma (MM). Activated PIM1 kinase can induce progression of the cell cycle, inhibition of apoptosis, and modulation of other signal transduction pathways.

Methods: BLX-0631 and a few analogs evaluated against a panel of MM cell lines (EJM, IM-9, L-363, LP-1, MM-1R, MM.1S, MOLP-2, NCI-H929, OPM-2, RPMI8226 and U-266) and primary MM patient samples by CellTiter-Glo® (CTG) assays. Cellular apoptosis, Cell cycle analysis, Flow Cytometry, and bone marrow microenvironment experiments on the most sensitive cells were performed. PIM1 and downstream targets by western blot, cell migration, and invasion on our lead PIM1 inhibitor BLX-0631 along with, kinome selectivity, ADME-Tox, PK, and in vivo MM.1S efficacy experiments were conducted.

Results: The application of our empirical MolecuLern™ fragment library, PIM1 crystal structure, scaffold hopping, and the enumeration features of MolecuLern™ in combination with 3, 6, and 7-group analysis on pyridazine, lead to a synthesizable potential new lead series, representing Med Chem tractability and developable characteristics. Further, the consensus scoring, binding energies, and MolecuLern tractability filters were applied and led to the discovery of the BLX-0631 series that inhibits the PIM1 kinase. The active compounds, with their binding modes and lead optimization strategies, lead to the synthesis and testing of over 60 novel entities as PIM1 kinase inhibitors. Thus, based on our previous chemotype series and scaffold hopping method, the impact of changing the 3, 6, and 7 positions, while retaining the pyridazine core led to the discovery of BLX-0631 and its series of compounds exhibiting <5 nM potency. BLX-0631 in CTG assay demonstrated 100% cell growth inhibition across all MM cell lines tested. The lead compound BLX-0631 is a very potent inhibitor with an IC_{50} of 5.0/17/5.0 nM when tested against PIM1, PIM2, and PIM3 kinases respectively, and selective against a panel of 468 kinase panels. Dosing through IV and PO delivery routes, formulations, salt forms of BLX-0631 in mice, PK properties along with ADME-Tox, P450, and hERG results will be presented. *In vivo* MM.1S mouse xenograft models of BLX-0631 at 15, 30 and 45 mg/Kg, p.o, QD demonstrated TGI of 16.28%, 31.81% & 35.16% dose-dependently.

Conclusions: The present study demonstrates that PIM1 plays a vital role in the proliferation and survival of Multiple Myeloma. BLX-0631 induces full inhibition of all MM cell lines, suppresses cancer cell proliferation *in vitro,* and exhibits promising efficacy in MM tumor models. BLX-0631, a nominated IND candidate can serve as a novel targeted agent for treating Multiple Myeloma patients.

#4588 Combination of MTA-cooperative PRMT5 inhibitor and direct mutant-selective KRAS inhibitors as a novel therapeutic approach for MTAP-deficient pancreatic cancer.

K. Drizyte-Miller[1], W.-H. Chang[1], A. M. Waters[2], C. A. Stalnecker[3], J. Wang[4], A. J. Aguirre[4], A. D. Cox[3], C. J. Der[3],
[1]UNC Lineberger Comprehensive Cancer Center, University of North Carolina at Chapel Hill, Chapel Hill, NC, [2]University of Cincinnati, Cincinnati, OH, [3]UNC Lineberger Comprehensive Cancer Center, Chapel Hill, NC, [4]Broad Institute of MIT and Harvard, Boston, MA

KRAS is mutationally activated in 95% of pancreatic ductal adenocarcinoma (PDAC) patients. Direct KRAS inhibitors are under intense preclinical and clinical development, with two $KRAS^{G12C}$ mutant-selective inhibitors (G12Ci) now approved. However, treatment-associated resistance to KRAS inhibitors has been reported in the clinic highlighting an urgent need to identify both additional therapeutic targets and novel combination treatment strategies with KRAS inhibitors. To that end, we performed a CRISPR/Cas9 loss-of-function screen using a library targeting ~2,500 druggable genes in $KRAS^{G12C/D}$-mutant PDAC cell lines. We identified multiple genes that were essential for PDAC cell growth and selected PRMT5, a protein arginine methyltransferase, to assess as a novel therapeutic target for pancreatic cancer. We found that suppression of PRMT5 activity using two distinct first-generation clinical candidate small molecule inhibitors (JNJ-64619178 and GSK3326595) demonstrated single agent activity and reduced PDAC cell growth. We further assessed a mechanistically distinct MTA-cooperative clinical candidate PRMT5 inhibitor, MRTX1719, that is selective for *MTAP*-deleted tumors, which occur in ~25% of PDAC patients. We determined that MRTX1719 exhibited low nanomolar GI_{50} activities in *MTAP*-deficient but not *MTAP* wild-type KRAS-mutant cell lines. Unexpectedly, PDAC cells treated with MRTX1719 exhibited a paradoxical activation of ERK, suggesting that combined inhibition of PRMT5 and KRAS might be therapeutically advantageous. In support of our hypothesis, we demonstrated that combination treatment with MRTX1719 and mutant selective KRAS inhibitors (G12Ci/MRTX849 and G12Di/MRTX1133) further sensitized $KRAS^{G12C/D}$-mutant PDAC cells to KRAS inhibition in short- and long-term growth assays as well as *in vivo* xenograft studies. Our ongoing studies are evaluating the consequences of co-targeting PRMT5 and KRAS on gene expression changes using RNA-Seq and cancer cell signaling pathways using RPPA analyses. In summary, our data support concurrent inhibition of PRMT5 and KRAS as a promising therapeutic strategy for MTAP-deficient KRAS-mutant pancreatic cancer.

#4589 Synergistic effects of EZH1/2 dual inhibition and cisplatin on lung cancer cell lines with loss of *SMARCA4* and *SMARCA2*.

J. Lee[1], B. Keam[2], S. Kim[1], J. Youk[2], M. Kim[2], T. Kim[2], D.-W. Kim[2], H. Dae Seog[1];
[1]Seoul National University Cancer Research Institute, Seoul, Korea, Republic of, [2]Seoul National University Hospital, Seoul, Korea, Republic of

Purpose: *SMARCA4* mutations are observed in approximately 10% of non-small cell lung cancer (NSCLC) cases and are implicated in various biological functions. Lung cancers harboring these mutations are associated with poor prognosis and often exhibit resistance to conventional chemotherapies, highlighting the urgent need for innovative therapeutic strategies. We evaluated the efficacy of a novel EZH1/2 dual inhibitor, HM97662, and its synergistic potential with cisplatin in *SMARCA4*-deficient lung cancer cell lines.

Experimental Design: CCLE datasets were employed to identify cell lines harboring truncated mutations in the *SMARCA4* gene. Immunoblotting was conducted to verify the inactivation of *SMARCA4* and to check for the expression of SMARCA2. We assessed cellular viability and colony-forming capabilities of lung cancer cell lines
(NCI-H1975, PC9, A549, HCC15, NCI-H522, NCI-H1581, NCI-H1048, NCI-H841) to determine the cytotoxic effects of an EZH1/2 dual inhibitor as well as cisplatin, both as single agents and in combination.

Results: Immunoblotting showed distinct lung cancer cell lines characterized by three profiles: proficient SMARCA4 expression, absent SMARCA4 but present SMARCA2 expression, and concurrent loss of both SMARCA4 and SMARCA2. After 14 days of treatment with the EZH1/2 dual inhibitor HM97662, there was a significant reduction in cell proliferation, particularly in the both *SMARCA4*- and *SMARCA2*-loss cell lines. Furthermore, colony-forming assays demonstrated a significant decrease in colony-forming ability upon HM97662 treatment, an effect exclusive to the both SMARCA4 and SMARCA2 loss cell lines. Pre-treatment with 1 μM of HM97662 for 7 days potentiated the cytotoxicity of cisplatin compared to untreated controls in the SMARCA4/2 loss cell lines, as indicated by a lower IC50 value.

Conclusion: The novel EZH1/2 dual inhibitor, HM97662, exhibits antitumor activity and a synergistic effect with cisplatin in lung cancer cell lines with concomitant loss of *SMARCA4* and *SMARCA2*. These findings suggest the potential utility of EZH1/2 dual inhibition as a targeted therapeutic approach in lung cancers characterized by the dual loss of SMARCA4/2.

#4590 Antitumor effects of histone deacetylase inhibitors on breast cancer cell viability and mammosphere formation.

G. Asaadi Tehrani, B. Kubick, M. Datta;
University of Notre Dame, South Bend, IN

Histone deacetylases (HDACs) are overexpressed in various types of primary human cancer and have become attractive targets for cancer therapy. This study aimed to evaluate the cytotoxic properties of three HDAC inhibitors (suberoylanilide hydroxamic acid (SAHA, or Vorinostat), Valproic Acid (VPA) and CAY10603) and compare them to Paclitaxel (PTX), a chemotherapy agent used to treat Triple Negative Breast Cancers (TNBCs). In the present study, drug response in the MDA-MB-231, MDA-MB-468, and MCF-10A cell lines was evaluated by cell viability assays. Apoptosis and cell cycle distribution were analyzed by flow cytometry. Mammospheres generated from MDA-MB-231 and MDA-MB-468 breast cancer cells were also subjected to drug treatment; their response was assessed under both normoxic and hypoxic conditions.

We found that SAHA and CAY10603 inhibited breast cancer cell viability without significantly affecting MCF-10A cells. SAHA, CAY10603, and VPA all arrested a significant percentage of MDA-MB-231 cells at G2/M phase after 24h compared to controls. TNBC cells experienced an increase in both early and late apoptosis following treatment with the most effective concentrations of SAHA, CAY10603, and VPA (1.8μM, 2μM, and 0.4mM, respectively). SAHA proved to be the most effective drug for induction of apoptosis compared to the control, followed by CAY10603 (8.26% and 6%, 3.67%). In both TNBCs and mammospheres under hypoxic conditions, SAHA and CAY10603 down regulated *HIF-1α* expression significantly, but PTX did not. In contrast, VPA and PTX down regulated *CTNNB1* gene expression.

This study indicates that epi-drugs exert an anti-tumor effect on TNBCs, suggesting a potential role for HDAC inhibitors as novel therapeutics for breast cancer patients.

#4591 PH020-2: an MTA-cooperative PRMT5 inhibitor with excellent selectivity and brain-penetration capability that targets MTAP-deleted tumors.

F. Gao[1], B. Liu[1], J. Wang[1], L. Jing[2], Y. Wu[2], P. Zhang[1], Y. Gao[1], Z. Li[3], Y. Guo[1];
[1]Puhe Biopharma, Beijing, China, [2]Gongkang Bio, Suzhou, China, [3]Shiyu Children Foundation, Beijing, China

Background: Methylthioadenosine phosphorylase (MTAP) gene deletion is highly prevalent across many cancer types such as brain, pancreatic and lung cancer. Accumulated MTA in MTAP loss cells competes with S-adenosylmethionine (SAM, the methyl donor) and leads to partial inhibition on protein arginine methyltransferase 5 (PRMT5), resulting in the sensitivity of these cells to PRMT5 inhibition. On this basis, MTA cooperative PRMT5 inhibitors (such as MRTX1719 and TNG908) have been designed to stabilize the binding of PRMT5 to MTA, but not SAM, resulting in further improvement of selectivity window. The clinical data showed that MRTX1719 has the capability to inhibit MTAP-loss tumor growth while avoid hematology toxicity observed with first generation PRMT5 inhibitors.

Methods: A pair of HCT116 isogenic cell lines (MTAP-/- and MTAP+/+) were used to determine the effects of PH020-2 on cell proliferation and intracellular symmetric dimethylarginine (SDMA) content. Human CD34+ hematopoietic stem cells (HSCs) were collected to evaluate hematological toxicity. Intravenous injection of PH020-2 in rats were performed to assess the brain-penetration capability. The *in vivo* efficacy was tested in cell derived xenograft (CDX) mouse models with tumor harboring MTAP gene deletion. The *in vitro* and *in vivo* pharmacokinetic (PK) and safety properties were assessed with corresponding assay methods.

Results: PH020-2 dramatically decreased SDMA content and inhibited proliferation in HCT116 MTAP-/- cells (IC_{50}, SDMA, 0.31 nM; proliferation, 5.9 nM), but had very weak effect on HCT116 WT cells (IC_{50}, SDMA, 296.2 nM; proliferation, 1381 nM), suggesting an excellent selectivity (proliferation, 253×). In comparison, IC_{50} of MRTX1719 and TNG908 on MTAP-/- cell viability was 8.38 and 52.75 nM, respectively, generating a selectivity of 118× and 28×, respectively. PH020-2 mildly inhibited CD34+ HSC (IC_{50}=807.1 nM), compared to the test on MRTX1719 (IC_{50}=481.9 nM). The tests on a panel of cancer cells confirmed activity and selectivity of PH020-2. PH020-2 possessed excellent PK profiles in all species with absolute bioavailability of 98% in dogs. At the same time, PH020-2 showed outstanding brain penetration in rats (Kp, 0.67). In three CDX models (H838, H2170, Hup-T4), PH020-2 at a dose of 25 mg/kg BID potently inhibited tumor growth, and tumor regression was observed at higher doses in all tested models. Methyltransferase screening (44 targets) showed that PH020-2 potently inhibits PRMT5, but not others. Safety panel assays covering 47 targets demonstrated excellent safety profiles of PH020-2. All other *in vitro* and *in vivo* tests showed favorable results and supported for preclinical development.

Conclusion: The data suggest that PH020-2 is an MTA-cooperative PRMT5 inhibitor with excellent brain-penetration that selectively targets MTAP-deleted tumors.

#4592 Preclinical characterization of ATG-042-198, a novel MTAP ^{null}-selective PRMT5 inhibitor.

Y. Kong[1], M. Zhang[1], L. Jiang[1], R. Xu[2], B. Jiang[1], G. Dai[1], Y. He[1], H. Liu[2], J. Mei[3], B. Hou[3], **B. Shan**[3];
[1]Antengene Corporation Co., Ltd., Shanghai, China, [2]Antengene Biologics, Hangzhou, China, [3]Antengene Corporation Co., Ltd., Shaoxing, China

Background: PRMT5 inhibitors are considered as a promising approach for cancer therapy due to their crucial role in the initiation and progression of many types of malignancies. Nevertheless, the crucial involvement of PRMT5 in controlling hematopoiesis, even in normal cells, resulted in significant on-target-off-tumor hematological toxicity when using first-generation, non-selective PRMT5 inhibitors in clinical settings, which hampered the clinical development of these drugs. The MTAP gene is deleted in around 10-15% of all human malignancies. As a result, the loss of MTAP leads to the buildup of MTA, which can bind to PRMT5 and partially inhibit PRMT5 activity. Inhibitors targeting the PRMT5-MTA complex become a promising strategy for treating MTAP^{null} cancer in a synthetically lethal manner. Herein, we report the preclinical feature of ATG-042-198, a novel MTAP^{null}-selective PRMT5 inhibitor.

Methods: The in vitro activity and MTAP selectivity of ATG-042-198 on cell proliferation and cellular symmetric dimethylarginine (SDMA) expression were profiled using HCT116 MTAP wild type (wt) cells and HCT116 MTAP knock out (ko) cells, as well as in five MTAP^{null} cell lines. The in vivo efficacy was tested in cell derived xenograft (CDX) mouse models with HCT116 MTAP wt cells, HCT116 MTAP ko cells and LU99 cells (MTAP^{null}). The in vitro and in vivo pharmacokinetic properties were assessed with corresponding assay methods.

Results: ATG-042-198 demonstrated potent and selectively inhibitory effect on HCT116 MTAP ko cells' proliferation (IC_{50}=44nM) and SDMA expression (IC_{50}=0.146nM), but very weak effect on HCT116 MTAP wt cells' proliferation (IC_{50}=4550nM) and SDMA expression (IC_{50}>500nM). Consistently, ATG-042-198 showed excellent anti-proliferation activities on multiple endogenous MTAP^{null} cell lines (A549, IC_{50}=2nM; LU99, IC_{50}=6nM; U87MG, IC_{50}=11nM; NALM-6, IC_{50}=37nM; MIA PaCa-2, IC_{50}=43nM). ATG-042-198 demonstrated high permeability (Caco2 assay, ER=2), good metabolic stability (Human liver microsomes assay, T1/2>145min), and low risk of drug interaction (CYP inhibition assay, 3A4/2C19/2D6, all IC_{50}>10μM). In vivo PK study showed that ATG-042-198 was well absorbed, with a dose-dependent increase in plasma distribution and high oral bioavailability (F=108%). Plasma free drug concentrations were continuously higher than the IC_{50} of cell proliferation inhibition within 24 hours after 30mpk administration. In three CDX models (HCT116 MTAP wt, HCT116 MTAP ko and LU99), ATG-042-198 at a dose of 30 mg/kg QD potently and selectively inhibited tumor growth (TGI=-1%, 89% and 106%) without inducing body weight loss.

Conclusions: In summary, ATG-042-198 is an oral MTAP ^{null}-selective PRMT5 inhibitor with potent efficacy against MTAP^{null} tumor. It also demonstrated good tolerability and preclinical PK profiles.

#4593 A synergy between MDM2 and AURKB pathways in driving cell cycle and cell survival in lung cancer cells.

U. Natarajan, A. Rathinavelu;
Barry and Judy Silverman College of Pharmacy, Nova Southeastern University, Davie, FL

Lung cancer is the leading cause of cancer-related deaths worldwide and non-small cell lung cancer (NSCLC) is the most prevalent type among lung cancers, contributing to the high mortality seen with this deadly disease. Despite aggressive treatments, the 5-year survival rate for lung cancer is only 23.7% in the United States. MDM2 and AURKB are two cancer-driving genes that are highly expressed in a broad range of cancer types including lung cancers. Furthermore, MDM2 overexpression can positively impact AURKB expression and contribute to oncogenesis and cancer progression. Therefore, blocking MDM2 with specific inhibitors has become a promising strategy for the restoration of p53 function that could be used for the treatment of different types of cancers including lung cancers. In this regard, both MDM2 and AURKB inhibitors have shown promising antitumor activity against NSCLC. Therefore, the main objective of this study was to understand the molecular mechanisms linking MDM2 and ARKB using RG7388, CM272, BMS-582949 (p38 inhibitor), and Ralimetinib (p38 inhibitor) in A549 and H460 lung cancer cells. We analyzed the individual or combination treatment effects of these drugs on epigenetic modifications, cell cycle arrest, and cell death mechanisms, using the *in vitro* experimental model. When RG7388 was used individually, or in combination with BMS-582949 or Ralimetinib, a significant increase in the cytotoxic effect was observed in A549 and H460 cells. Induction of cell cycle arrest by RG7388 in cancer cells was evidenced by elevated p21 expression levels. In addition, RG7388 and combination treatments in NSCLC cells showed significant upregulation of p53, p27, Bax, cleaved PARP, phospho-FOXO3a and down-regulation in DNMT3a, DNMT1, FOXM1, AURKB, CDC25, and CDK4 levels. It appears that during treatments with a combination of MDM2 with DNMT or p38 inhibitor, two pathways might be blocked simultaneously, which could lead to increased cancer cell death. RG7388 appears to induce cell death in a p21-dependent manner and CM272, BMS-582949, and Ralimetinib seem to induce cell death *via* a p21-independent manner by inhibiting a downstream pathway. However, further studies are needed to fully understand the intracellular link between MDM2 and AURKB that is disrupted by the anti-cancer agents used in our study. (This project was supported by the PFRDG Grant of Nova Southeastern University and by the Generous support from the Royal Dames of Cancer Research Ft. Lauderdale, FL)

#4595 HSK41959-2: An oral MTA-cooperative PRMT5 inhibitor for MTAP deleted cancer.

P. Yan[1], **J. Wang**[2], M. Qian[1], X. Yu[1], Y. Li[1], H. Zhang[1], L. Tao[1], R. Kou[1], T. Hu[1], P. Tang[1], H. Dong[1], A. Wu[1], M. He[1];
[1]Haisco Pharmaceutical Group Co., Ltd., Chengdu, China, [2]Haisco Pharmaceutical Group Co., Ltd., Shanghai, China

Methylthioadenosine phosphorylase (MTAP) homozygous deletion occurs in 10-15% of all human cancers. Loss of MTAP result in methylthioadenosine (MTA) accumulation. PRMT5, which is a type II arginine methyltransferase that regulates multiple essential cellular functions via symmetric dimethylation of arginine (SDMA) in target proteins, was identified as a synthetic lethal target for MTAP del cancers. MTA-cooperative PRMT5 inhibitors may exhibit better safety profiling compared to first generation PRMT5i (which observe limiting heme-related toxicities in clinical), which preferentially inhibiting PRMT5 in MTAP del cancer cells to normal cells. HSK41959-2 is a MTA-cooperative PRMT5 inhibitor, which could selectively inhibits PRMT5 in the present of MTA with IC_{50} was 0.80 nM. In HCT116 MTAP Deleted cell line, HSK41959-2 significantly inhibits the cell proliferation with GI_{50} of 19.89 nM, which was around 45-fold selectivity in HCT116 cell line. In SDMA assay, HSK41959-2 also showed high potency in HCT116 MTAP-del cell line with IC_{50} was 3.39 nM, and much weaker in HCT116 MTAP-WT cell line with IC_{50} was 499 nM, around 147-fold selectivity. In vitro CD34+ Hematopoietic stem cell cell proliferation assay was used for evaluate the heme-related toxicities. HSK41959-2 weakly inhibited the cell proliferation with IC_{50} of 544 nM while the first generation PRMT5i with IC_{50} was 35.39 nM. This results indicated HSK41959-2 may has lower heme-related toxicities compared with the first generation PRMT5i. In the HCT116 MTAP-del xenograft model, daily orally administrated with 25 mpk and 100 mpk HSK41959-2 showed significant tumor growth inhibition, with TGI were 62% and 88%, and PRMT5-dependent SDMA protein inhibition were 89% and 95%, respectively. Meanwhile in the HCT116 MTAP-WT xenograft model, HSK41959-2 did not show tumor growth inhibition at 100 mpk. In conclusion, HSK41959-2 is a promising oral MTA-cooperative PRMT5 inhibitor, it was nominated as a development candidate.

#4596 Targeting arginine methylome in *9p21*/*MTAP*-deleted malignant cancers with a next generation PRMT5-specific inhibitor CTS3497.

Y. Liu[1], L. Wang[1], H. Shi[1], Y. Liu[1], Q. Ouyang[1], X. Fu[1], M. Wang[1], J. Guo[1], Y. Wang[2], Y. Wang[1], G. Xu[2], Y. Mi[1], H. Wu[1];
[1]CytosinLab Therapeutics Co., Ltd., Shanghai, China, [2]Center for Excellence in Molecular Cell Science, Chinese Academy of Science, Shanghai, China

It remains largely challenging to treat cancer patients with chromosome 9p21-deletion which occurs in approximately 15% of human cancers. Recently, specific targeting of protein arginine methyltransferase 5 (PRMT5), a key member of the type-II PRMT family and a master epigenetic modulator of arginine methylome essential for cancer progression, has emerged as a promising therapy in various hematological and solid tumors with *MTAP* deletion serving as a precision biomarker. To optimize the potential of targeting PRMT5, we developed CTS3497, a potent, brain-penetrable, orally bioavailable MTA-cooperative PRMT5 inhibitor, using our EpigenPLUS^{TM} platform. The overall excellent drug-like properties of CTS3497 support fast track IND application, and it is anticipated to enter Phase 1 trials in 2024. CTS3497 demonstrated potent PRMT5 inhibitory activity in cellular pharmacodynamics (PD) assays, evidenced by the suppression of symmetric dimethylarginine (SDMA). Additionally, it exhibited profound cell growth inhibition with a low single-digit nM IC50 and 171-fold high selectivity for *MTAP*^{null} over isogenic *MTAP*^{wt} cell lines. Moreover, CTS3497 displayed strong inhibitory effects on cell growth across diverse panels of *MTAP*^{null} cancer cell lines and patient-derived xenograft organoids (PDXOs) spanning various lineages. *In vivo*, oral administration of CTS3497 resulted in significant tumor regression in multiple *MTAP*-deleted xenograft models, notably *MTAP*^{null} brain tumors. The observed anti-tumor activity correlated with PRMT5 modulation, as indicated by reduced SDMA levels. Impressively, sustained tumor growth inhibition led to the complete tumor regression, with no regrowth even after discontinuation of CTS3497 treatment. The brain penetration property of CTS3497 underscores its therapeutic potential for both primary brain tumors, and brain metastases arising from specific cancers like lung cancer. At the molecular level, PRMT5 inhibition by CTS3497 induced substantial and distinctive RNA splicing defects and differentially expressed gene signatures, impacting key cellular activities downstream of arginine and epigenetic reprogramming in *MTAP*^{null} cancer cells. Furthermore, a synergistic anti-tumor effect was observed in multiple *MTAP*-deleted tumors when combining PRMT5 inhibition with CTS2190, an investigational type-I PRMT inhibitor currently in phase I/II clinical trials. In summary, CTS3497, a PRMT5 inhibitor selectively targeting *MTAP*^{null} tumor cells, demonstrated robust and durable anti-tumor responses both *in vitro* and *in vivo* across diverse lineages of *MTAP*-deleted tumors. Its superior ADME properties and favorable safety profiles observed in preclinical studies mark a breakthrough in the next generation epigenetic therapy. CTS3497 emerges as a promising therapeutic option for patients with *MTAP*-deleted malignancies.

#4597 RNA m^1A methyltransferase TRMT61A induces MAPK/ERK signaling and is a therapeutic target in colorectal cancer.

X. Zhang, N. Qin, F. Ji, H. Su, H. Chen, H. Shang, **H. Chen**;
Chinese University of Hong Kong (CUHK), Hong Kong, Hong Kong

The widespread presence of N1-methyladenosine (m^1A) modifications controls RNA metabolism and is pivotal to fundamental biological processes. However, the understanding of RNA m^1A involved in cancer is still minimal. Here we reported the oncogenic role and the therapeutic targeting of RNA m^1A methyltransferase TRMT61A in colorectal cancer (CRC). We observed consistent elevation of TRMT61A expression and RNA m^1A levels in primary CRC tissues, which was significantly associated with poor patient survival in two independent cohorts (both $P<.001$). CRISPR/Cas9 screenings revealed that TRMT61A is the most essential gene among m^1A regulators. TRMT61A facilitates the growth and metastasis of CRC cells by increasing the stability of mRNA of crucial targets, such as ONECUT2, which leads to the activation of MAPK/ERK signaling in an m^1A-dependent manner. Notably, depletion of ONECUT2 or inhibition of MAPK/ERK could abrogate the tumor-promoting role of TRMT61A, implying that TRMT61A induces ONECUT2-MAPK/ERK axis to facilitate CRC. Inhibiting TRMT61A with nanoparticle-encapsulated siTRMT61A or our recently identified small molecule compound PGG shows promising anti-CRC effects in vitro and in vivo. Together, our study reveals the promoting role of TRMT61A-induced m^1A modification in MAPK/ERK signaling and highlights the potential of targeting TRMT61A as a promising therapeutic approach in CRC treatment.

#4598 Discovery of novel MTA-cooperative PRMT5 inhibitors as targeted therapeutics for MTAP-deleted cancers.

A. Radzimierski, A. Bobowska, A. Stachowicz, K. Kuś, K. Kozłowska-Tomczyk, A. Ludwig-Słomczyńska, P. Podkalicka-Gołda, A. Gołas, M. Żukowska, P. Lebed, P. Wyrębek, D. Szukiel, M. Stefaniak, O. Popika, J. Krzywik, S. Sasmal, P. Niedziejko-Ćwiertnia, K. Korta-Piątek, K. Fijołkowska, A. Więckowska, M. Olszak-Płachta, S. Nipunge, M. Świrski, M. Wronowski, H. Pawlik, Q. Vũ, K. Łagosz-Ćwik, M. Stoszko, S. Woroszyło, I. Tomczyk, E. Gabor-Worwa, N. Gaud, A. Kowal-Chwast, D. Gogola, M. Miodek, R. Starczak, A. Dudek, J. Faber, B. Winnik, S. Novak-Ratajczak, A. Świrska, K. Gluza, P. Guzik, K. Banaszak, N. Boutard, G. Ćwiertnia, K. Brzozka, M. Nowak, A. Bartosik, **D. Pez**;
Ryvu Therapeutics, Krakow, Poland

Homozygous deletions of the p16/CDKN2a (cyclin dependent kinase inhibitor 2A) locus, which is responsible for regulating the cell cycle, are commonly found in cancer and often involve the deletion of adjacent genes. One such adjacent gene is methylthioadenosine phosphorylase (MTAP), involved in metabolism, located on chromosome 9p21 in close proximity to the p16/CDKN2A tumor-suppressor locus. Co-deletion of MTAP is observed in approximately 80-90% of tumors with homozygous deletion of CDKN2A, representing 10-15% of all human tumors. These tumor types, including non-small cell lung cancer, pancreatic adenocarcinoma, glioblastoma, and mesothelioma, have a poor prognosis, highlighting the significant unmet medical need in this area.
Deletion of MTAP leads to a significant accumulation of methylthioadenosine (MTA) in cells. MTA, at high concentrations, selectively inhibits the PRMT5 methyltransferase enzyme, competing with the substrate S-adenosylmethionine (SAM) required for methylation reactions. As a result, the overall level of symmetric arginine dimethylation throughout the proteome is reduced. This heightened sensitivity to modulation of methylosome activity makes cells with MTAP deletion more susceptible to therapeutic targeting of PRMT5. Hence, selective targeting of PRMT5 in cancers with homozygous MTAP deletion represents a promising strategy for specifically eliminating cancer cells with this genetic alteration. Ryvu has developed MTA-cooperative PRMT5 inhibitors characterized by good drug-like physicochemical properties and inhibition of methyltransferase activity with IC50 values in the low nanomolar range. A structure-based lead optimization delivered compounds coming from two independent series with high selective potency in MTAP-deleted cell lines and DMPK profiles allowing an oral administration. The antitumor activities were compared in vitro and in vivo to MRTX1719 and AMG193 in MTAP null tumors such as HCT116 MTAP KO, DoHH-2 and Lu99. The correlation between compound exposure and on-target effect was confirmed in PK/PD and efficacy studies. Taken together, these studies confirm that MTA cooperative PRMT5 inhibitors exert strong synthetic lethal phenotype in MTAP deleted cancers and offer an exciting therapeutic opportunity for a large patient population.

#4599 A novel small molecule inhibitor targeting MYC oncogenic signaling as an enhancer of HDAC inhibitors for the treatment of high-risk medulloblastoma.

S. Ng, S. Gadde, Q. Wang, B. B. Cheung, G. M. Marshall;
Children's Cancer Institute Australia, Sydney, Australia

Background: Medulloblastoma (MB) is the most prevalent malignant childhood brain tumour. Although prognosis has improved over time, 95% of children with high-risk or relapsed MB eventually succumb to the disease. A key driver gene in high-risk MB is the c-*MYC* oncogene, for which there are currently no approved inhibitors. Histone deacetylases (HDACs) are transcriptional repressors that are dysregulated in many cancers, making them an attractive therapeutic target. Although several HDAC inhibitors have been FDA-approved for cancer treatment, they have been associated with high toxicity and limited efficacy as single agents. Therefore, simultaneously targeting c-*MYC* and HDACs may result in synergistic effects that could overcome drug resistance in high-risk MB.
Methods and Results: We previously reported a novel pyrido-benzimidazole analogue, SE486-11, which enhanced the therapeutic effect of HDAC inhibitors in MYCN-driven cancers. We recently developed analogues (UNSW-SC compounds) with more potent activity (IC_{50}: 0.017 to 3.70 μM). Here, we showed that these compounds significantly reduced cell viability and induced apoptosis in MB cells. MYC status was a key determinant of sensitivity of UNSW-SC compounds, with more than 3-fold higher cytotoxicity in high MYC compared to low MYC MB cells. The lead compound, UNSW-SC-22, was shown to reduce MYC protein expression and was found to be highly synergistic in enhancing the efficacy of HDAC inhibitors in MB cells. Most importantly, we demonstrated that UNSW-SC-22 was able to freely cross the blood brain barrier, reaching a concentration of 10.8 μM, with a half-life of 1.22 hours. UNSW-SC-22 directly bound to c-MYC and MYCN proteins at low micromolar equilibrium dissociation constant (KD) values which was demonstrated by surface plasmon resonance assay. In a MYCN-driven MB mouse model, we found that UNSW-SC-22 as a single agent at 90 mg/kg decreased tumor growth and prolonged survival. Through RNA-sequencing, we identified 512 differentially expressed genes after in vitro treatment with UNSW-SC-22. Importantly, GSEA analysis revealed MYC targets and cell cycle pathways as highly downregulated pathways, and upregulation in the p53 pathway. Several genes, such as MELK and USP1 were validated as down-stream targets of UNSW-SC-22. As UNSW-SC-22 is a first-in-class anticancer drug, which we are currently testing extensively in other MYC-driven MB mice models.
Conclusion: Collectively, our data strongly suggest that c-Myc and MYCN are the molecular targets of UNSW-SC compounds, and these compounds have strong potential to serve as specific targeted therapy to treat subgroup 3 and 4 of MB patients with c-Myc and MYCN overexpression and amplification.

EXPERIMENTAL AND MOLECULAR THERAPEUTICS: Mechanisms of Drug Resistance and Novel Combinations
Poster Session

#4603 Single-cell and spatial dissection of the effect of combined PD-L1 and TGFb blockade by bintrafusp alfa from the ICING window-of-opportunity trial in resectable locally advanced HNSCC patients.

C. Hoffmann[1], J.-T. Werle[2], J. Gal[3], P. Sirven[2], J. Klijanienko[2], J. Mesple[2], B. Demaille[2], W. Zeitouni[4], O. Choussy[2], G. Marret[2], N. Badois[2], A. Dubray-Vautrin[2], G. Dolivet[5], L. Geoffrois[5], M. Kamal[2], I. Bieche[2], L. Monard[6], C. Simon[6], C. Le Tourneau[2], H. Salmon[2];
[1]Owkin, Paris, France, [2]Institut Curie, Paris, France, [3]Centre Antoine Lacassagne, Nice, France, [4]Genosplice, Paris, France, [5]Institut de Cancerologie de Lorraine Alexis Vautrin, Vandouvre-les-Nancy, France, [6]Unicancer, Paris, France

Despite high tumor mutational burden, immune checkpoint blockade has shown limited efficacy in head and neck squamous cell carcinoma (HNSCC), highlighting the need for additional therapeutic targets. TGFb signaling has been associated with an immunosuppressive tumor microenvironment as well as a lack of response to anti-PD(L)1 therapy, which led to the development of combined therapeutic approaches. ICING is a prospective (NCT04428047) open label, multicenter, phase II, window-of-opportunity preoperative, single-agent trial. The primary objective was to evaluate the efficacy and biological activity of pre-operative combined PD-L1 and TGFb blockade by bintrafusp alfa in patients with untreated resectable stage III/IV locally advanced HNSCC and its effect on the tumor microenvironment (TME). Tumor samples were harvested at baseline prior to immunotherapy and at surgery after two doses (1200mg; D1 and D15) for pre- and post-treatment comparison. Treatment efficacy was assessed using the pathological response (PathR) with a 10% threshold for response as primary endpoint. Changes in the TME were determined by single-cell RNA sequencing (scRNAseq) and multiplexed imaging. Seven patients were included and six received the full treatment scheme (5 oral cavity and 2 oropharyngeal, all HPV-negative; median age = 61y, range 34y-74y). Four patients had a PathR exceeding 10%, including one with a major PathR above 50%. The TME pre-treatment of this major responder did not differ from the other samples, but this sample was set apart by the presence of proliferative, p16+, HPV-negative tumor cells with mildly higher genomic alterations whilst still classified as low tumor mutational burden. Regardless of treatment response, we report several changes in post-treatment samples: (i) the remodeling of the stromal architecture concomitant with a phenotypic shift in cancer-associated fibroblasts (CAF) with a reduction in activated LRRC15+ CAF and an increase in CD10+IL24+ CAF; (ii) a reduction of TGFb-induced genes in both stromal and cancer cells; (iii) a reduction in both conventional and regulatory CD4+ T cells; (iv) an increase in CD8+ T cell infiltration in previously excluded tumors; (v) an interferon gamma-mediated activation of monocytes, macrophages and dendritic cells expressing CXCL9 and CXCL10. Collectively, our study deciphers the effects of bintrafusp alfa both molecularly and spatially at unprecedented granularity, which is of major importance for the many combined PD(L)1 and TGFb blockade therapeutic approaches currently under clinical development.

#4604 Imipridones ONC201 and ONC212 exhibit anti-tumor activity in biliary tract cancers and synergy when combined with trametinib and olaparib *in vitro*.

G. Sun[1], A. J. Lannigan[1], J. Chan[1], M. Schwermann[1], V. V. Prabhu[2], L. Zhou[1], W. S. El-Deiry[1], A. G. Raufi[1];
[1]Brown University, Providence, RI, [2]Chimerix, Durham, NC

Background: Biliary tract cancers (BTCs) are an aggressive group of malignancies affecting 220,000 new individuals globally each year. Despite advances in immunotherapy and targeted therapies, 5-year survival remains at 2% for those with metastatic disease. Thus, new therapies are desperately needed. The novel imipridone class of antineoplastic agents show promising activity in preclinical pancreatic ductal adenocarcinoma models; however, have not been investigated in BTC. Dordaviprone (ONC201) is a dopamine receptor D2 and mitochondrial protease ClpP modulator that induces apoptosis in cancer cells through both upregulation of tumor necrosis factor-related apoptosis-inducing ligand (TRAIL) and the integrated stress response. ONC212 is a second-generation imipridone that targets orphan GPCR 132 and ClpP, leading to reduced oxidative phosphorylation from ClpX suppression. We hypothesized that the ONC201 and ONC212 would demonstrate antitumor effects in BTCs, both alone, and in combination with MEK and PARP inhibition.
Methods: Two established BTC cell lines, RBE and HuCCT1, were used for these experiments. Sensitivity of RBE and HuCCT1 cells to ONC201, ONC212, MEK inhibition (trametinib), and PARP inhibition (olaparib) was assessed using CellTiter-Glo® luminescent cell viability assay. Each cell line was plated on 96-well plates and treated with ONC201 concentrations ranging from 0uM to 40uM for RBE and 0uM to 32uM for HuCCT1; ONC212 ranging from 0nM to 752nM for RBE and 0nM to 640nM for HuCCT1; trametinib ranging from 0nM to 24nM for RBE and 0nM to 16nM for HuCCT1; and olaparib ranging from 0uM to 256uM for RBE and 0uM to 124uM for HuCCT1. Results were analyzed after 72 hours of incubation. Synergy studies were conducted in both cell lines, combining each imipridone with either trametinib or olaparib, and SynergyFinder® was used to evaluate synergy. Western blotting was performed on lysates generated from treated cell lines.
Results: Both ONC201 and ONC212 demonstrated antineoplastic effects in two BTC cell lines. Half maximal inhibitory concentrations (IC50) of ONC201 in RBE and HuCCT1 cell lines were 2.5uM and 2.0uM, respectively. The IC50 of ONC212 in RBE and HuCCT1 was 47nM and 39nM, respectively, which was similar to IC50s demonstrated with cytotoxic chemotherapy (gemcitabine IC50 = 7.57nM (RBE) and 9.84nM (HuCCT1)). Both lines also demonstrated sensitivity to trametinib (IC50 = 5.9nM (RBE) and 3.7nM (HCCT1)), and to a lesser extent olaparib (IC50 = 64uM (RBE) and 31uM (HuCCT1)). Although synergy was noted with several combinations, this was most striking with the combination of ONC212 and either trametinib or olaparib. Further analysis of key signal transduction pathways, including MAPK and PI3K, as well as analysis of mechanisms of cell-death through apoptosis, autophagy, ferroptosis, and necroptosis is underway

#4605 AZD4573 in combination with CHOP increases combination benefit in preclinical peripheral T-cell lymphoma models.

D. S. Potter[1], I. Ott[1], J. Saeh[1], R. Olsson[2], S. Fawell[1], L. Drew[1], J. E. Roderick[1];

[1]AstraZeneca Oncology, Waltham, MA, [2]AstraZeneca Oncology, Gothenburg, Sweden

Peripheral T-cell Lymphoma (pTCL) makes up about 10% of non-Hodgkin's lymphoma in the United States. Patients with relapsed/refractory pTCL have limited treatment options and poor prognosis. Current standard of care for pTCL revolves around the chemotherapy regimens CHOP/E. Here we examine the efficacy of CDK9 inhibition for the treatment of pTCL. CDK9 regulates transcription through phosphorylation of RNA polymerase II. AZD4573 is a highly potent and selective CDK9 inhibitor; acute inhibition with AZD4573 downregulates short-lived proteins such as MCL-1, BFL-1, and c-MYC, which are often overexpressed in hematologic tumors. It has been shown that the expression pattern of the anti-apoptotic BCL-2 family members in pTCL cell line models closely resembled the expression patterns in pTCL patient samples (Koch *et al.* 2019). Expression of BCL-2 family members is highly heterogeneous in pTCL, with MCL-1 being the most universally expressed. Using MCL-1 inhibitor AZD5991, we showed statistically significant benefit in survival when combined with CHOP in MCL-1 dependent preclinical pTCL PDX models (Koch *et al.* 2019). In addition, we have previously reported the importance of the anti-apoptotic protein BFL-1 in cell survival in NHL, including a subset of pTCL (Boiko *et al* 2021). AZD4573 treatment showed a range of activity across the panel of 18 human pTCL cell lines, in a 6-hour caspase-3/7 activation assay. 14 of the cell lines were sensitive, with EC_{50} values less than 100 nM, and 13 reached a max caspase activation of over 40%. pTCL subtypes that responded to AZD4573 treatment included ALCL, NK-TCL, and PTCL-NOS and CTCL. Acute AZD4573 treatment resulted in decreased pSer2-RNAP2 and reduced protein levels of c-MYC and MCL-1. To determine what was driving the apoptotic phenotype, we used ribonucleoprotein (RNP) mediated CRISPR knock out (KO) of *MYC* and *MCL1* genes. While pTCL cell lines were dependent on c-MYC and MCL-1 for viability after KO, only MCL-1 KO impaired AZD4573 treatment, suggesting that efficacy is mediated through MCL-1 in ALCL pTCL cell lines assessed. To determine if combining AZD4573 with CHOP improved efficacy, we tested 5 pTCL cell lines in a 6x6 combination dosing matrix and measured viability after 24-72 hours using RealTime-Glo after 24hr exposure to CHOP with AZD4573 added for the last 6hrs. Adding AZD4573 to CHOP *in vitro* increased the efficacy in pTCL ALCL cell lines with MCL-1 dependency, but not in CTCL cell line with BCL-xL dependency and resistance to AZD4573. CHOP treatment *in vitro* resulted in a decrease in c-MYC levels but not MCL-1, suggesting that combination benefit may be driven through c-MYC. This data suggests that treatment with AZD4573 as a monotherapy or in combination with CHOP regimen would be an effective therapeutic strategy in pTCL.

#4606 Combinatorial effects of a sequence of trabectedin (T) and CD13-targeted tissue factor tTF-NGR on human vascular endothelial cells (HUVEC) and in soft tissue sarcoma (STS) models.

C. Brand, S. Pavelka, K. Hessling, H. Hintelmann, A. F. Berdel, S. Baumer, N. Baumer, G. Lenz, C. Schliemann, **W. E. Berdel**, C. Schwoppe;
University of Munster, Muenster, Germany

Trabectedin represents a standard treatment option for relapsed or refractory soft tissue sarcomas. CD13 is a neutral aminopeptidase expressed on remodeling and invasive endothelial cells such as in the tumor vasculature. CD13-targeted tissue factor (tTF-NGR) is a recombinant pro-coagulatory fusion protein which accumulates in the tumor vasculature leading to tumor vascular occlusion and ultimately to tumor infarction. Giving both compounds in sequence could trap trabectedin inside tumors and thus increase its efficacy. This *vice versa* can optimize the activity of tTF-NGR. To prepare a multicenter clinical trial of a combination of trabectedin and tTF-NGR in patients with advanced soft tissue sarcomas refractory to 1st line systemic therapy (TRABTRAP), preclinical experiments on the mechanism of action of this combination, its efficacy and pharmacokinetics (PK) were performed. We first tested the pro-apoptotic function of trabectedin on human vascular endothelial cells (HUVEC) and human HT1080 sarcoma cells *in vitro*. Trabectedin significantly ($p<.0001$) increased the presence of phosphatidylserine (PS) on the outer leaflet of the phospholipid bilayer of the cell membrane in a dose- and time-dependent manner. The resulting optimized phospholipid milieu significantly potentiated the pro-coagulatory efficacy of tTF-NGR within the factor X:factor VIIa:tTF-NGR:CD13 complex on the outer cell membrane when compared to cultures without trabectedin ($p<.05$). This effect was specifically dependent on the presence of PS as it could be abolished by masking PS via preincubation with annexin V, whereas corticosteroids had no effect on the pro-coagulatory response of HUVEC in the presence of tTF-NGR. In an *in vivo* HT1080 human sarcoma xenograft model in athymic mice, systemic combination treatment of trabectedin followed by tTF-NGR (n=11) inhibited tumor growth to a greater extent than either compound alone (trabectedin n=9, tTF-NGR n=9) and compared to a saline control (n=8). The terminal half-life of tTF-NGR infused intravenously over 1 hour, was 9 hours (phase I trial). To further characterize the duration of tTF-NGR presence upon binding to the endothelial cell surface molecule CD13, we performed flow cytometry and fluorescence labeling experiments with tTF-NGR and HUVEC *in vitro*. After coincubation with HUVEC, the cells rapidly internalized the tTF-NGR:CD13 complex into the cytoplasm of the cells (approx. 50% of the labeled tTF-NGR after 3 h at 37^{o}C), a process which exposed the protein to intracellular degradation. The multicenter TRABTRAP trial is actively recruiting patients (EudraCT 2020-005858-21).

#4607 Targeted nanoparticle delivery of irinotecan and Ewing sarcoma-specific siRNA is an effective combination therapy for Ewing sarcoma.

S. A. Mitra[1], J.-H. Parmentier[1], H.-G. Kang[1], T. J. Triche[2];
[1]Children's Hospital Los Angeles, Los Angeles, CA, [2]University of Southern California, Los Angeles, CA

Background: Ewing sarcoma (ES) is an aggressive bone and soft tissue tumor affecting children and adolescents with an overall survival rate of 50%. Irinotecan (IR) is an effective chemotherapeutic agent but is associated with significant toxicity. Using an anti-CD99 targeted hybrid polymerized lipid nanoparticle containing IR, NV103, in pre-clinical mouse xenograft model of the disease, tumor ablation was achieved at 2mg/kg of IR versus 50mg/kg for free IR. All ES harbor a chromosomal translocation resulting in expression of a fusion EWS-FLI1 protein or equivalent. This chimeric gene is a transcriptional regulator that upregulates the FEZF1 and FEZF1-AS1 genes. Both EWS-FLI1 and FEZF1-AS1 genes are unique to ES and are not expressed in normal adult tissues. EWS-FLI1 promotes cell growth while the FEZF1-AS1 complex promotes tumor metastasis, a hallmark of ES. *In vitro* RNAi targeting of EF and FEZF1-AS1 results in tumor cell death. We hypothesized that combining EWS-FLI1 and/or FEZF1-AS1 targeted RNAi therapy with NV103 cytotoxic therapy would be more effective than any single modality therapy.
Methods: NV103 was provided by NanoValent Pharmaceuticals. siRNA containing lipid nanoparticles (LNP-siRNA) were generated using PreciGenome NanoGenerator. siRNA was quantified using the ribogreen assay. Nanoparticles were analyzed for size and particle numbers by NanoSight. siRNA was used to target the following genes- EWS-FLI1, FEZF1, FEZF1-AS1, or GFP. A673 cells expressing GFP were used for this *in vitro* study. Various doses of IR and siRNA were used in combination and cell growth/death was imaged live using Incucyte. ATP assay was used to confirm live cells and to determine minimum effective dose (MED) over 72 hours of treatment.
Results: LNP-siRNA, mean diameter 70nm and PDI<0.2, encapsulated 90% of the siRNA in solution. LNP are stable at 4°C for at least 4 weeks with minimal-to-no loss of activity. NV103 had a MED of 1μM. MED of various siRNA was 30 to 50nM. Combination of NV103 and LNP-siRNA reduced MED of IR to 250nM. One treatment dose of LNP-siRNA followed by NV103 treatment three days later maintained significant cell death over 10 days post treatment initiation. Control cells were 97% more confluent than NV103/ EWS-FLI1 siRNA treated ones, 85% more than NV103/ FEZF1 siRNA cells and 92% more than NV103/ FEZF1-AS1 treated cells. siRNA combinations of EWS-FLI1 and FEZF1 or FEZF1-AS1 along with NV103 added no further benefit.
Conclusion: Combination nanoparticle therapy of IR and ES-specific siRNA reduces IR MED by four-fold. LNP delivery of siRNA enables tumor-specific gene targeting. Most have no available small molecule therapy. Targeting ES cells with both a low dose (250nM) of IR and 30-50nM of siRNA against unique tumor biomarkers results in increased cell death with no IR toxicity. Further animal studies are required to determine the effectiveness of such therapy *in vivo*.

#4608 Combinations of Cdc-like kinase (CLK) inhibitors with targeted oncology agents or standard chemotherapy in patient-derived multi-cell type tumor spheroids.

T. S. Dexheimer[1], T. Silvers[1], **N. P. Coussens**[1], S. D. Gore[2], J. H. Doroshow[2], B. A. Teicher[2];
[1]Frederick National Laboratory for Cancer Research, Frederick, MD, [2]National Cancer Institute, Bethesda, MD

The alternative splicing of mRNA precursors allows one gene the capacity to yield multiple protein isoforms, each with distinct functions. Although this intricate process is subject to stringent regulation under normal physiological conditions, aberrant alternative splicing can generate atypical proteins and contribute to various diseases, including cancer. By activating splicing factors, Cdc-like kinases (CLKs) serve as pivotal regulators of alternative splicing and are considered promising therapeutic targets for various tumors. In this study, we investigated the activity of two CLK inhibitors, cirtuvivint (SM08502) and CC-671, in combination with precision oncology agents or conventional chemotherapeutics. Thirty highly characterized patient-derived cancer cell lines were selected from the National Cancer Institute's Patient-Derived Models Repository (https://pdmr.cancer.gov/models/database.htm). The cell lines were derived from a range of cancer types including head and neck, bladder, pancreas, endometrial, colon, and melanoma, and contained clinically relevant variants of KRAS (G12C, G12D). Multi-cell type tumor spheroids were grown from a ratio of 6:2.5:1.5 malignant cells, endothelial cells, and mesenchymal stem cells, respectively. Following three days of growth, the spheroids were treated with single agents or combinations at concentrations up to their clinical C_{max} value, if reported. After seven days of continuous drug exposure, cell viability was assessed using the CellTiter-Glo 3D assay. As a single agent, cirtuvivint showed concentration-dependent activity in all spheroid types with 1 – 3 logs of cytotoxicity, whereas CC-671 did not show activity in all spheroid types and achieved no more than 1 log of cytotoxicity. Among the standard chemotherapeutic drugs, doxorubicin and SN-38 demonstrated additive and greater-than-additive cytotoxicity in various spheroid types when combined with either CLK inhibitor. Several of the targeted oncology drugs exhibited noteworthy additive and greater-than-additive cytotoxicity when combined with a CLK inhibitor. These agents included the XPO1 inhibitor, eltanexor, the MCL-1 inhibitor, tapotoclax, the α-isoform-specific PI3K inhibitor, inavolisib, and the pan-PI3K inhibitor, copanlisib. Notably, combinations of the CLK inhibitors with the KRAS G12D variant-specific inhibitor, MRTX-1133, showed selective activity against all tumor cell lines harboring this genetic variant. Interestingly, a strong antagonistic interaction between paclitaxel and CC-671 was observed in all thirty spheroid types, while no such interaction was observed with cirtuvivint. This project was funded in part with federal funds from the NCI, NIH, under contract no. HHSN261201500003I.

#4609 Plixorafenib (plixo) synergizes with MEK inhibitors (MEKi) in MAPK pathway inhibition in BRAF V600 and non V600 alterations, with higher potency compared to early generation BRAFi and pan-RAFi.

G. Tarcic[1], L. Cohen[1], **S. P. Shepherd**[2], N. Filippov Levy[1], H. Billauer[1], L. Birnbaum[1], S. Gasasa[1], R. Maor[1], R. Abu-Liel[1], E. Goldfarb[1]; [1]Fore Biotherapeutics Inc., Ness Ziona, Israel, [2]Fore Biotherapeutics Inc., Philadelphia, PA

The efficacy of BRAFi in V600 mutated tumors is established and requires effective inhibition of the MAPK pathway. However, the use approved BRAFi leads to paradoxical MAPK pathway activation associated with toxicities and to acquired resistance. Therefore, these inhibitors were combined with MEKi to mitigate toxicities, which has been shown to be more effective than monotherapy in some settings. Although effective, these combinations result in bothersome side effects, a high discontinuation rate, and risk of secondary malignancies, indicating a continued unmet need. Also, ~35% of all BRAF mutations occur outside the V600 codon, composed of a wide array of missense mutations, fusions, and in-frame deletions, which are not targeted by the earlier generation BRAFi. By design, plixo (FORE8394; PLX8394), a clinical stage BRAFi, binds the monomeric form of BRAF and inhibits its dimerization, while sparing the WT form, avoiding paradoxical MAPK pathway activation. We hypothesized that the combination of plixo with a MEKi will improve its efficacy and potency through maximal suppression of the MAPK pathway. Using ForeSight assay, a unique platform for testing MAPK signaling, we tested the efficacy of plixo and 4 MEKi (trametinib, cobimetinib, binimetinib and mirdametinib) across a cohort 18 BRAF alterations (V600E, 2 class II and 15 fusions) as single agents and in combinations. The combinations of plixo with the different MEKi were synergistic across all BRAF alterations tested. Furthermore, we compared the potency of a combination of plixo with binimetinib (bini) to that of another BRAFi (vemurafenib) or pan-RAFi's (tovorafenib and lifirafenib) with bini in 2 class I, 3 class II and 7 BRAF fusions using the foresight assay. The IC:50 of BRAF V600E expressing cells treated with plixo + bini was 6nM compared with 57nM, 103nM and 190nM for the tovorafenib, vemurafenib, and lifirafenib combinations with bini respectively. A similar trend was shown in 9 of 11 additional alterations tested, indicating the potency of the combination of plixo + bini. Results were validated using western blot analysis and cell viability assays of both melanoma and CRC V600E mutated cell lines. Western blot correlated with ForeSight results both in single agents and combination treatment. Cells treated with plixo + bini showed complete growth inhibition while the same drug concentrations of vemurafenib + bini and tovorafenib + binimetinib showed no growth inhibition beyond the effect of bini single agent. These results indicate the improved efficacy of plixo + bini combination in inhibiting MAPK signaling and cancer cell proliferation. Overall results support that maximal suppression of the MAPK pathway with plixo is more potent in combination with a MEK inhibitor in BRAF V600 and non-V600 nonclinical models compared to BRAF or pan-RAF combinations.

#4610 Dual inhibition of CDK4/6 and IL-6 pathways as a novel therapeutic approach for triple-negative breast cancer cells.

K. Caroland[1], C. Shi[1], H.-W. Lo[2], J. Lin[1];

[1]University of Maryland, Baltimore, Baltimore, MD, [2]Department of Neurosurgery and the University of Texas McGovern Medical School at Houston, Houston, TX

Triplenegative breast cancer (TNBC) is highly aggressive and associated with poor clinical outcomes. TNBC stands as a major cause of death among breast cancer patients and offers only a few therapeutic options. Abemaciclib, a cyclin dependent kinase 4/6 (CDK4/6) inhibitor, has received FDA approval for use in hormone receptor-positive, HER2-negative, and metastatic breast cancers. However, acquired resistance to CDK4/6 inhibitors in treating TNBC is becoming an increasing concern. Our recent results indicated that CDK4/6 inhibitors can induce IL-6 levels in TNBC cells as a potential resistance mechanism by augment IL-6 signaling axis, and that targeting IL-6 signaling can sensitize TNBC cells to CDK4/6 inhibitor therapy. In this study, combination of Abemaciclib with an IL-6/GP130 inhibitor (bazedoxifene) was tested in TNBC cells. We examined the effect of the combination on cell viability, cell migration, and invasion of human and mouse TNBC cell lines. Our data demonstrated that the bazedoxifene and abemaciclib combination treatment synergistically inhibited TNBC cell viability, cell migration, and invasion *in vitro*. These results support dual inhibition of CDK4/6 and IL-6 as a novel therapeutic approach for TNBC.

#4611 The co-targeting of PLK1 and FoxM1 contributes to synergistic antitumor effects in PTC.

P. Poyil, A. K. Siraj, D. Padmaja, S. K. Parvathareddy, S. Thangavel, S. Al-Sobhi, F. Al-Dayel, K. S. Al-Kuraya;
King Faisal Specialist Hospital and Research Center, Riyadh, Saudi Arabia

Polo-like Kinase 1 (PLK1) plays a key role in cell proliferation with vital regulatory functions in mitosis and cell survival. We investigated the expression of PLK1 protein in a large cohort of PTC patient's samples and explored its functional role in PTC cell lines *in vitro* and *in vivo*. PLK1 overexpression was observed in 54% of all PTC and was significantly associated with aggressive clinico-pathological parameter and it was found to be independent prognostic marker for recurrence-free survival. PLK1 inhibition indeed inhibited cell proliferation and induced cell cycle arrest and apoptosis in PTC cell lines. Importantly, silencing of PLK1 decreases the self-renewal ability of spheroids generated from PTC cells. Immunoprecipitation analysis shows that PLK1 binds to FoxM1 and vice versa *in vitro*. Mechanistically, PLK1 knockdown suppresses FoxM1 expression, whereas inhibition of FoxM1 does not affect PLK1 expression, which suggests that PLK1 acts through the FoxM1 pathway. The combined inhibition of PLK1 with volasertib and FoxM1 with thiostrepton synergistically attenuated PTC cell growth *in vitro* and *in vivo*. Our findings suggest that co-targeting of PLK1 and FoxM1 could be a viable therapeutic strategy for treating patients with an aggressive subtype of PTC.

#4612 Inhibition of BCL2 and XPO1 demonstrates synergistic effects in triple-negative breast cancer cell lines.

M. M. Jackson, S. G. Smoots, A. T. A. Dominguez, E. Dus, S. Bagby, C. Binns, T. M. Pitts, J. R. Diamond;
University of Colorado Anschutz Medical Campus, Aurora, CO

Background: Triple-negative breast cancer (TNBC) is an aggressive subtype of breast cancer, accounting for about 15-20% of all breast cancers. Characterized by a lack of estrogen and progesterone receptors and non-amplified HER2, treatment options are limited compared to other breast cancer subtypes. The aim of this study was to evaluate eltanexor (Elta), an XPO1 inhibitor, in combination with venetoclax (Ven), a Bcl-2 inhibitor to promote apoptosis in TNBC models.

Methods: CellTiter-Glo Cell Viability Assay was utilized to determine cell viability in 6 TNBC cell lines after 72-hour exposure to no drug, Elta, Ven or the combination. Synergy scores were determined using the Bliss model in SynergyFinder+, scores 10 or above indicating synergy. Apoptosis (by Annexin V) was assessed after 24- and 48-hour exposure to drug via flow cytometry. Immunoblots were used to assess the mechanism of action in cell lines treated for 24 hours.

Results: CellTiter Glo displayed greater anti-proliferative activity in combination versus single agent exposure. Synergy was observed in CAL-120, BT-20, and MDA-MB-468 cell lines, with synergy score values ranging from -13.22 - 25.07. Additive effects were observed in other cell lines. An increase in apoptosis was observed in CAL-51 and MDA-MB-231 cells after 24- and 48-hour treatment that was greater with the combination. CAL-51 cells exposed to single agent Ven or Elta [0.5 µM] for 24 hours had significantly less apoptosis than those exposed to the combo ($p = <0.0001$). After a 48-hour exposure, CAL-51 cells exposed to single agent Ven had less apoptosis than in combination with Elta [0.1 µM] ($p = 0.0431$) or Elta [0.5 µM] ($p = 0.0036$ µM]. Additionally, single agent Elta [0.5 µM] resulted in less apoptosis than the combination ($p = 0.0067$). Similar results were observed in MDA-MB-231 cells. We observed an increase in apoptotic markers with the combination in all cell lines treated. In all cell lines, DNA-damage marker pH2Ax increased with Ven and the combination. In the CAL-51 cells, p53 increased following Elta or combination exposure. In the MDA-MB-231 cells, a decrease in the anti-apoptotic protein MCL1 was observed with Elta or combination.

Conclusion: The combination of Elta and Ven resulted in increased apoptosis and antiproliferative activity in TNBC cell lines. Combined, the two drugs synergistically functioned to increase DNA damage and promote apoptotic cell death. This work supports the continued evaluation of Elta and Ven in TNBC.

#4613 Tumor-derived interleukin 35 facilitates the gemcitabine resistance in pancreatic adenocarcinoma by mediating the dissemination of chemoresistance among PDAC cells.

C. Huang, H. Sun, A. Chang, J. Hao;
Tianjin Medical Univ. Cancer Inst. & Hospital, Tianjin, China

Rapid drug resistance after chemotherapy is a key cause of treatment failure in human pancreatic ductal adenocarcinoma (PDAC). Here, we found that tumor-derived interleukin 35 (IL-35) mediated the rapid resistance of PDAC to gemcitabine (GEM). The role of IL-35 in GEM resistance was determined by molecular and cell biology approaches in PDAC cells and in patient-derived tumor xenograft (PDX) models. We used whole genome RNA sequencing, molecular cloning and other molecular biological methods to study the molecular mechanism of IL-35 mediated GEM resistance. An anti-IL-35 neutralizing antibody was used in mouse models to investigate the feasibility of targeting IL-35 to overcome drug resistance in pancreatic cancer. We observed the phenomenon that GEM resistance could spread from GEM resistant PDAC cells to GEM sensitive ones. The results of sequencing and experiments confirmed that the IL-35 secretion is responsible for the dissemination of chemoresistance. IL-35 secreted from GEM resistant cells activated the IL35 expression in GEM sensitive cells and upregulated SOD2 expression via GP130-STAT1 signaling, which scavenges reactive oxygen species (ROS) and then leads to GEM resistance.Furthermore, we found that a neutralizing antibody against IL-35 significantly enhanced the tumor suppressive effect of GEM. These findings collectively reveal that IL-35 plays crucial roles in mediating GEM resistance in pancreatic cancer. Moreover, IL-35 might serve as a promising therapeutic target for combating PDAC chemoresistance.

#4614 Inhibition of NEK2 promotes chemosensitivity and reduces primary effusion lymphoma burden.

M. C. White, J. P. Wong, B. Damania;
UNC Lineberger Comprehensive Cancer Center, Chapel Hill, NC

Non-Hodgkin lymphoma (NHL) is a common cancer in both men and women, and represents a significant cancer burden worldwide. Primary effusion lymphoma (PEL) is a subtype of NHL infected with Kaposi sarcoma-associated herpesvirus (KSHV). PEL is an aggressive and lethal cancer with no current standard of care, owing largely to its propensity to develop resistance to current chemotherapeutic regimens. Here, we report a reliance of PEL on the mitotic kinase, NEK2, for survival. Genetic and pharmacologic targeting of NEK2 resulted in caspase 3-mediated apoptotic cell death of PEL. Furthermore, inhibition of NEK2 significantly prolonged survival and reduced tumor burden in a PEL mouse model. We also report that the ABC transporter proteins, MDR1 and MRP, are most active in PEL and that NEK2 inhibition of PEL reduced the expression and activity of these ABC transporter proteins, which are known to mediate drug resistance in cancer. Additionally, NEK2 inhibition sensitized both viral and non-viral NHL to other chemotherapeutic agents such as rapamycin, resulting in enhanced cancer cell death. Overall, these data offer insight into the mechanisms underlying PEL survival and drug resistance, and suggest that NEK2 is a viable therapeutic target for PEL.

#4615 HC-7366, a potent GCN2 activator, complements belzutifan, a HIF-2α antagonist, by providing combination benefit in belzutifan-sensitive models and monotherapy activity in belzutifan-resistant models.

M. E. Stokes, F. Tameire, P. Wojnarowicz, S. Fujisawa, **C. Dudgeon**, S. Huang, N. Collette, B. Harrison, A. LaCayo, X. Qiu, T. Kangas, W. Zhang, J. Drees, D. Surguladze, E. S. Lightcap, N. Bose;
HiberCell, Roseville, MN

Recent approval of the HIF-2α antagonist belzutifan (Welireg) for patients with *VHL* disease has enabled the clinical opportunity to target the HIF-2 axis in cancer. This is particularly important for patients with clear cell renal cell carcinoma (ccRCC), in which 90% of tumors are *VHL* deficient, and approximately one in four primary tumors express HIF-2α exclusively. Clinical studies to date suggest an overall response rate (ORR) of 20-25% for belzutifan monotherapy, highlighting the need for a rational combination strategy to improve patient outcomes. This has led to multiple clinical trials testing belzutifan in combination with diverse therapeutic agents, including immune-checkpoint inhibitors, VEGFR-TKIs, and CDK4/6 inhibitors.

HiberCell is developing a first-in-class GCN2 activator currently undergoing Ph1 clinical evaluation in patients with solid tumors (NCT05121948). GCN2 activation by HC-7366 drives the Integrated Stress Response (ISR), resulting in translation inhibition and delayed cell cycle progression in cancer cells. In preclinical studies, HC-7366 demonstrated significant antitumor activity associated with HIF suppression across diverse tumor models, including ccRCC (70% TGI), head and neck (33% regression), sarcoma (84% TGI) and prostate (100% TGI). Analysis of tumor samples revealed that HC-7366 inhibited both HIF-1α and HIF-2α, as well as multiple cell cycle regulators. Given the mechanistic link between HIF-2 and cell cycle regulation, and the noted combination benefit reported when CDK inhibitors are combined with belzutifan, we hypothesized that HC-7366 would enhance the antitumor effects of belzutifan in RCC.

Combination studies in HIF-2 dependent 786-O and A-498 RCC xenografts demonstrated that HC-7366 improved the antitumor effects of belzutifan at clinically relevant doses. The combination of HC-7366 and belzutifan in A-498 drove robust tumor inhibition (~90% TGI). In 786-O, HC-7366 increased the number of complete responses from 2 of 8 tumors in the belzutifan-treated animals to 6 of 8 in the combination group. When tested in two belzutifan-resistant PDX models, HC-7366 resulted in significant monotherapy activity, achieving 17% regression as a maximal response, and inhibiting both HIF and cell cycle markers.

Belzutifan is currently being tested in indications beyond RCC, so we evaluated the combination in *VHL*wt endometrial cancer model, MFE-280. Consistent with RCC models, the combination of HC-7366 and belzutifan resulted in tumor stasis with activation of ISR, enhanced inhibition of HIF and cell cycle markers in the combination vs belzutifan monotherapy.

Together, these findings suggest that HC-7366 enhances belzutifan activity and serves as a rationale supporting clinical evaluation of this therapeutic combination.

#4616 TBK1 and GSK3 mediated TRAF2 phosphorylation confers resistance to PI3K-AKT inhibition in breast cancer cells.

H. Habelhah, L. Zhang;
University of Iowa, Iowa City, IA

Breast cancer (BC) is the most frequently diagnosed malignancy and the second leading cause of cancer mortality in Western women. As is the case for most other solid tumors, metastasis and drug resistance are the main causes of death. In ~80% of BC cases, the PI3K-AKT pathway is aberrantly activated, due to the alterations in genes encoding the pathway components, such as Ras, Her2, PTEN, PIK3C and AKT. Consequently, over 100 clinical trials are currently underway worldwide to evaluate the therapeutic efficacy of PI3K and AKT inhibitors in BC; however, initial data revealed that inhibition of this pathway is either not effective or often results in development of resistance and relapse of the disease. Thus, identification of additional targets and therapeutic combinations are urgently needed. We previously reported that TBK1-mediated TRAF2 Ser-11 phosphorylation enhances NF-κB activation to promote cancer cell survival under conditions of cellular stresses. Recently, we discovered that GSK3β directly phosphorylates TRAF2 at Thr-7 upon Ser-11 phosphorylation by TBK1, and that phosphorylation of both Thr-7 and Ser-11 is essential for sustained NF-κB activation and BC cell resistance to PI3K-AKT inhibition. TBK1 and its close homologue IKKε are overexpressed in ~70% of BC and play critical roles in BC cell survival. GSK3β is a constitutively active kinase activity in unstimulated normal cells, but its activity is suppressed in most cancer cell types by AKT-mediated phosphorylation. These published reports and our new findings suggest that inhibition of AKT in BC cells leads to increased phosphorylation of TRAF2 by TBK1 and GSK3β, which confers resistance to PI3K-ATK inhibition. Bioinformatic analyses revealed that TRAF2 and GSK3β are also overexpressed in invasive BC, and significantly correlate with poor prognosis. As expected, inhibition of both AKT and TBK1 or GSK3b synergistically induced apoptosis in BC cell lines *in vitro* and significantly suppressed xenograft BC tumor growth *in vivo*. Thus, our data suggest that further investigation of the efficacies of combined PI3K/AKT and TBK1/GSK3β inhibition in PDX models of BC has the potential to develop new strategies for BC treatment.

#4617 Fisetin, a multi-kinase inhibitor enhances chemotherapeutic sensitivity in head and neck cancer.

D. Tailor[1], D. Mishra[2], S. V. Malhotra[1], **R. P. Singh**[2];

[1]Knight Cancer Institute, Oregon Health & Science University, Portland, OR, [2]Jawaharlal Nehru University, New Delhi, India

Background: The limitations of chemotherapeutic applications are often imposed by dose-related toxicity and the emergence of therapeutic resistance. Fisetin, a naturally occurring flavonoid, has demonstrated anticancer properties in various cancer types. Despite its proven effectiveness against cancer, the molecular target of fisetin remains unknown.

Methods: Our study focused on understanding how fisetin and chemotherapy work together to inhibit the growth and survival of human HNC. We conducted *in silico, in vitro* and *in vivo* investigations. We employed target prediction, kinase profiling, transcriptome analysis and tumor xenograft to identify the chemosensitivity efficacy and mechanism of fisetin.

Results: *In-silico* target prediction suggested that fisetin might target multiple kinases. Based on this lead, we have screened fisetin for different kinase inhibition activities and found that it inhibits multiple CDKs including CDK1, 2, 4, 5 and 6 at nanomolar concentration. To test its cellular activity, we have selected the head and neck cancer (HNC) model and found that fisetin treatment strongly inhibited cell proliferation and arrested the HNC cells in G1 phase followed by apoptotic cell death. In tumor xenograft experiment, we found that oral fisetin treatment inhibited the FaDu and SAS tumor growth in the athymic mouse model. Transcriptome analysis on FaDu and SAS cell lines indicated that fisetin treatment significantly modulates pathways associated with cell cycle progression and regulation. These pathways include cellular assembly, DNA replication, cell death, and cell morphology. Pretreatment of HNC cells with fisetin improved the effectiveness of chemotherapy drugs including cisplatin, 5-fluorouracil, and docetaxel. Consistent with this, fisetin pre-treated cells showed elevated levels of cellular and mitochondrial ROS followed by the activation of caspases and apoptosis induction when compared with that in control cells after cisplatin, 5-FU, or docetaxel treatment.

Conclusion: These results imply that fisetin has the potential to be utilized as a multi-kinase inhibitor in cancer cells. The study revealed that fisetin has a strong potential for increasing the sensitivity of cancer cells to chemotherapy.

#4618 PIM kinases drive cell adhesion mediated drug resistance in prostate cancer.

C. Flores, S. Chauhan, C. Miranti, A. Cress, G. Rogers, N. Warfel;
University of Arizona, Tucson, AZ

Introduction: Castration-resistant prostate cancer (CRPC) is an incurable and lethal progression of the disease that does not respond to any treatment options. Cell adhesion to the extracellular matrix (ECM) activates survival pathways, allowing cancer cells to evade anti-cancer therapy, a phenomenon known as cell adhesion-mediated drug resistance. Bone, which is the primary site of prostate cancer metastasis, is known to be enriched in laminin, a ubiquitous ECM protein. In addition, laminin binding integrins, α6β1 and α3β1, are the major integrins expressed in CRPC, suggesting that laminin-dependent adhesion provides a survival advantage. Based on these findings, activation of the laminin-binding integrin, α6β1, is an intriguing factor mediating resistance to therapy in CRPC. PIM1 is an oncogenic Ser/Thr kinase that is elevated in CRPC and is known to promote resistance to therapy. In contrast, to many pro-survival kinases, PIM kinases do not possess any obvious regulatory domains. Current evidence suggests that PIM1 is constitutively active when it is expressed, so PIM1 expression level directly correlates with its catalytic activity. Despite this fact, little is known about the internal and external mechanisms that dictate PIM1 protein levels and spatial activation in cancer cells. Here, we identify PIM1 as a key survival signal that contributes to cell adhesion-mediated drug resistance.
Experimental procedures: Supporting the importance of this signaling axis in human tumors, multiplex IHC of a TMA containing prostate adenocarcinoma and CRPC bone metastases to show that integrin α6 and PIM1 are coexpressed and spatially correlated in primary and metastatic prostate cancer. To examine the spatiotemporal dynamics of PIM1 during cell adhesion, We developed a kinase activity reporter (PIMKAR) to monitor PIM catalytic activity in live cells. Because we observed PIM was highly localized to the membrane in patient tumors, we tagged PIMKAR with a myristylation sequence to specifically measure PIM activity at the membrane vs cytosol. Immunofluorescence and biochemical techniques were used to demonstrate the effect of PIM1 on mitophagy and oxidative stress.
Conclusions: We demonstrate that activation of integrin α6β1 downstream of cell adhesion stabilizes PIM1 by blocking its proteasomal degradation. The resulting upregulation of PIM1 serves to reduce oxidative stress through complementary mechanisms reducing mitochondrial fragmentation and increasing the removal of damaged mitochondria by increasing mitophagy. Mechanistically, PIM1 upregulates BNIP3 to enhance mitophagy and thereby reduce oxidative stress in the cell. Together, these results expand our understanding of the mechanisms regulating PIM1 activation and provide evidence for the use of PIM inhibitors in bone mCRPC and other cancers where laminin is a major component of the ECM

#4619 Prolonged inhibition of androgen receptor signaling induces expression of Nuclear ErbB3 which renders prostate cancer cells susceptible to targeted inhibitors.

M. K. Jathal, M. M. Mudryj, P. M. Ghosh;
UC Davis, Sacramento, CA

Objective: Nuclear expression of the receptor tyrosine kinase (RTK) ErbB3/HER3 increases in highly aggressive prostate cancer cells, but its nuclear transport mechanism is currently unknown. Prostate tumors rely on the androgen receptor (AR), whose activation transcriptionally controls ErbB3 expression, but its role in ErbB3 nuclear localization had not previously been reported. Here, we investigated the mechanism by which subcellular localization of ErbB3 was altered in prostate cancer.

Methods: ErbB3 localization was investigated in the human prostate cancer tumor progression model LNCaP, C4, C4-2 and C4-2B. ErbB3 was stimulated with heregulin-1β (HRG). Nuclear translocation was tested with a nucleocytoplasmic transport inhibitor panel (chlorpromazine, filipin III, amiloride and Leptomycin B) LNCaP and C4 cells were continuously cultured with the AR activation inhibitor abiraterone acetate (AbiAc) or ethanol (VEH) or treated with the AR inhibitors enzalutamide, darolutamide and apalutamide. ErbB3 activity and subcellular localization were analyzed using confocal microscopy/subcellular fractionation/immunoblot. Cell viability was determined by MTT assay. Proliferation and apoptosis were determined by flow cytometry. Invasive potential was investigated by crystal violet staining of cell colonies. ErbB3 expression was reduced by siRNA technology.

Results: The ratio of nuclear to cytoplasmic ErbB3 increased in untreated cells from LNCaP<C4-2<C4<C4-2B. In all four lines, nuclear localization of ErbB3 peaked at 30 minutes after HRG treatment, with a rapid return to the cytoplasm in LNCaP cells (at 1 hour), slower in C4 cells (at 4 hours), and continued accumulation in the nucleus in C4-2 and C4-2B 8 hours following HRG treatment. Treatment with the transport inhibitor panel showed that nuclear accumulation of ErbB3 was prevented by the clathrin-dependent endocytosis inhibitor Chlorpromazine (CPZ) but not by the others. In LN-VEH and C4-VEH cells, HRG induced nuclear translocation of ErbB3 but not in LN-AbiAc or C4-AbiAc cells. Accordingly, HRG increased ErbB3 phosphorylation at Y1328 and nuclear Akt phosphorylation at S473 in VEH but not AbiAc cells. C4 cells, which had high baseline nuclear ErbB3, were more sensitive to the AR inhibitors and showed decreased viability and invasive potential compared to LNCaP cells.

Conclusions: These results indicate that (1) ErbB3 nuclear localization required clathrin-dependent endocytosis (2) ligand binding of ErbB3 as well as the presence of an active AR is necessary for ErbB3 nuclear localization and (3) the presence of nuclear ErbB3 increases sensitivity to AR inhibitors.

#4620 Exploring the role of GHRH antagonist MIA-602 in overcoming doxorubicin resistance in acute myeloid leukemia.

S. I. Gaumond[1], J. Costoya, Jr.[1], A. V. Schally[2], J. J. Jimenez[1];

[1]University of Miami Miller School of Medicine, Miami, FL, [2]Veterans Affairs Medical Center, Miami, FL

Acute Myeloid Leukemia (AML) is characterized by the uncontrolled proliferation of immature hematopoietic progenitors, often associated with a poor prognosis. Conventional therapies involve chemotherapy and bone marrow stem cell transplantation. The growth hormone releasing hormone receptor (GHRH-R) antagonist MIA-602 has exhibited inhibitory effects on the growth of various human cancer cell lines, including AML cells. This study aimed to investigate the impact of MIA-602 alone and in combination with doxorubicin on three doxorubicin-resistant AML cell lines, K-562, U-937, and KG-1A. Initial examinations confirmed the presence of GHRH receptors in both wild-type and doxorubicin-resistant cell lines through western blot analysis. Doxorubicin was administered at concentrations of 0.005, 0.01, and 0.05 µg/ml, while MIA-602 was used at 5 µmol/L. Subsequent experiments involved culturing both wild-type and doxorubicin-resistant clones with MIA-602 at concentrations ranging from 0.05 µmol/L to 5 µmol/L for 24 and 48 hours. The results revealed a significant, dose- and time-dependent reduction in cell proliferation across all six cell lines. Both wild-type and doxorubicin-resistant clones exhibited a comparable decrease in cell proliferation when exposed to MIA-602 at concentrations greater than 0.05 µmol/L ($p < 0.05$) after 24 and 48 hours. In conclusion, our study demonstrates that these three AML cell lines and their doxorubicin-resistant clones remain susceptible to GHRH antagonist MIA-602. These findings may pave the way for the development of novel therapies or drug combinations using GHRH antagonists such as MIA-602 for treating AML. This is of particular interest for those who are resistant to conventional chemotherapy, further broadening the spectrum of treatment options available. Additional investigations are warranted to progress these findings to *in vivo* xenograft models.

#4621 Dual targeting as an effective therapeutic strategy for malignant brain tumors.

E. Y. Magnan, K. Gourishetti, S. Thomas, D. Bhere;
University of South Carolina, School of Medicine - Columbia, Columbia, SC

Glioblastoma, a type of brain cancer known for its aggressive nature and resistance to traditional treatments, remains a significant challenge for the medical community. Despite advances in surgical, radiation, and chemotherapy strategies, patients with glioblastoma typically have a poor prognosis, with a median survival time of only 15 months. While temporary symptom relief may be possible for some patients, complete tumor remission is often not achieved. Given the complexity of this disease, effective treatment options for glioblastoma are highly sought after. In this study, we have evaluated the effectiveness of a combinatorial approach using stem cell-derived exosomes enriched with miR-124 cargo paired with viral oncolysis for treating glioblastoma.

Human Umbilical Cord Stem cells (hUCs) are genetically modified with specific miR plasmids, and then cultivated in a specialized medium that has been depleted of exosomes. The exosomes (exo) that contain the target miR are subsequently extracted, purified, quantified, and characterized. These exosomes are then utilized for all subsequent investigations. Using a combination of cell viability assays and microscopy, the overall effect of the exo-miR-124 and oncolytic virus on both established and patient-derived primary GBM cells is analyzed. Additionally, a time course western blot analysis is conducted to comprehend the molecular mechanisms underlying the effects of the miR modification and viral oncolysis on cell proliferation and death pathways. Orthotopic animal models of GBM will be utilized to assess the effects of miR modulation and viral oncolysis *in vivo.*

Our research has shown that stem cell-derived exosomes are an effective way to deliver microRNA to specific cells, including tumor cells. This is because they can evade the immune system and target cells directly. Our experiments have shown that combining miR modulation paired with viral oncolysis as a promising approach for treating glioblastoma. Specifically, we have found that miR modulation and viral oncolysis can halt tumor cell proliferation in vitro by targeting multiple pathways involved in GBM growth and progression.

#4622 Anti-tumor activity of CDK2 inhibitor BLU-222 in combination with CDK4/6 inhibitors for overcoming resistance in HR positive and triple negative metastatic breast cancers models.

L. Luo[1], Y. Wang[1], T. Bui[1], M. Li[1], S. Kim[1], J. Navarro-Yepes[1], N. M. Kettner[1], D. Tripathy[1], K. K. Hunt[1], K. Faia[2], K. Keyomarsi[1];
[1]UT MD Anderson Cancer Center, Houston, TX, [2]Blueprint Medicines Corporation, Cambridge, MA

Background: Cyclin-dependent-kinase-4/6 inhibitors (CDK4/6is) plus endocrine therapy (ET) are standard of care first-line treatment for patients with hormone receptor (HR)-positive, HER2-negative metastatic breast cancer (mBC). However, the emergence of resistance to CDK4/6is plus ET presents a clinical challenge with few treatment alternatives. The effectiveness of CDK4/6is in patients with triple-negative (TN) breast cancer remains uncertain, although the potential synergy with other targeted therapies is currently under investigation. Our study demonstrates the enhanced and synergistic activity of BLU-222, a selective CDK2 inhibitor, when combined with CDK4/6is in preclinical models of both HR+/HER2- and TN breast cancer resistant to CDK4/6is. Methods: Palbociclib resistant (PR) HR+/HER2- (MCF7 and T47D) and TN (MDA-MB-231 and BT-20) breast cancer cell lines were generated by escalating palbociclib concentrations in culture. Using SynergyFinder, we assessed the effect of BLU-222 alone and in combination with palbociclib in the highest single-agent model in vitro. The effectiveness of BLU-222, alone or in combination with palbociclib, was further evaluated in four patient-derived xenograft (PDX) models from HR+/HER2- patients whose tumors progressed after palbociclib plus ET, two TN PDX models, and a TN breast cancer transgenic model driven by tumor-specific forms of cyclin E. Results: The PR HR+/HER2- and TN breast cancer cell lines, unresponsive to palbociclib, exhibited significantly increased sensitivity to BLU-222. The combination of BLU-222 and palbociclib in all four cell lines revealed a robust synergistic effect in PR cells, inducing enhanced apoptosis and cell cycle alterations in G1 or G2/M phases. Treatment with BLU-222 and palbociclib demonstrated substantial antitumor activity in all six PDX models and the cyclin E high TN transgenic models, surpassing the effects of individual treatments in each model. This combination led to lasting tumor regression and extended survival, even after treatment discontinuation. Mechanistically, treatment with BLU-222, alone or combined with palbociclib, induced the expression of p21 and/or p27 in all in vivo models, which we hypothesize sensitizes tumors to palbociclib. In vitro, the CRISPR knockout of p21 or p27 in MCF-7 PR cells abolished the synergistic activity of BLU-222 and palbociclib, confirming the crucial involvement of p21 and p27 in influencing the treatment's effectiveness. Conclusions: We found robust activity of the CDK2 inhibitor, BLU-222 when combined with CDK4/6is in resistant HR+/HER2- and TN breast cancer cell lines and in vivo models. These results support the potential clinical utility of BLU-222 in combination with CDK4/6is for the treatment of both subtypes of breast cancer.

EXPERIMENTAL AND MOLECULAR THERAPEUTICS: Molecular Classification of Tumors for Diagnostics, Prognostics, and Therapeutic Outcomes Poster Session

#4626 A kit targeting detection of *ESR1* mutations from circulating exosomal RNA and cell-free DNA supports longitudinal studies into endocrine therapy resistance in a broadly accessible RT-qPCR format.

J. T. Brown[1], J. R. Thibert[1], L. Chen[1], M. Church[1], H. Dale[1], J. Myers[1], E. Hallmark[1], M. Yociss[1], J. Sanchez[2], K. Franzen[2], J. Skog[2], G. Latham[1], B. Haynes[1], **S. Statt**[1];

[1]Asuragen, a Bio-Techne Brand, Austin, TX, [2]Exosome Diagnostics, a Bio-Techne Brand, Austin, TX

Introduction: The most prevalent subtype of breast cancer is HR+/HER2- (positive for hormone receptor, negative for human epidermal growth factor receptor 2). For metastatic breast cancer (mBC), a frequent occurrence is resistance to the aromatase inhibitors used in endocrine therapy (ET). Resistance is mediated through mutations in the ligand binding domain of estrogen receptor 1 (*ESR1*). Approval of elacestrant, a second-line agent for HR+/HER2-/*ESR1* mutated mBC , underscores the need for early detection of ESR1 resistance mutations. We have developed sensitive RT-qPCR reagents for targeted longitudinal studies into the emergence of *ESR1* resistance mutations in plasma. This all-inclusive kit analyzes circulating exosomal RNA (exoRNA) and cell-free DNA (cfDNA) to accurately identify low copy number mutations with a rapid turnaround time.

Methods: Challenge panels were constructed using blends of synthetic nucleic acids of known mutational status in a background of partially fragmented wild-type DNA from cell lines. Additionally, plasma samples collected from subjects with stage IV mBC (HR+/HER2-) on active aromatase inhibitor therapy, +/- CDK 4/6 inhibitor for a minimum of one year, were subjected to an in-house method optimized to co-enrich exoRNA and cfDNA. Multiplex RT-qPCR-based target enrichment performed on 11 *ESR1* mutations and an internal control were evaluated on widely used thermal cycler and qPCR instruments.

Results: We developed technology that interrogates 11 key *ESR1* mutations associated with ET resistance in HR+/HER2- mBC cases. Earlier studies performed in simplex analyzed plasmid-based *ESR1* mutations with detection of 10 or fewer mutant copies, estimating analytical sensitivity of at least 0.1% (5 mutant copies in a background of 5,000 WT copies). Herein, we describe the subsequent work to complete the methodology employed in the kit, including the incorporation of an endogenous control, external batch run control materials (positive, negative), deeply optimized reagents (RT, pre-amplification, qPCR), and automated analysis. We report on the results of studies into the kit's performance characteristics against their targets: analytical sensitivity of the equivalent of 5 copies of mutation per mL plasma, high precision across replicates at 0.1% allele fraction, analytical specificity of ≥90% negative results in mutation-negative replicates, as well as workflow attributes (reduced pipetting steps and turnaround time).

Conclusion: Our solution to detect *ESR1* resistance mutations facilitates the generation of nucleic acid sample to results within one day using liquid biopsy samples and a multiplexed RT-qPCR. Enhancing mutation detection sensitivity by complementing cfDNA with exoRNA will facilitate future research into breast cancer treatment options.

#4627 Metastatic renal cell carcinoma with occult primary: Clinical and biological evidence for a new entity of cancers of unknown primary that beneficiates from tissue-tailored treatment.

Nicolas Jacquin[1], Julien Masliah-Planchon[2], Guillaume Grisay[3], Ronan Flippot[3], Riwan Brillet[4], Celia Dupain[5], Maud Kamal[5], Isabelle Guillou[5], Nadege Gruel[1], Nicolas Servant[6], Pierre Gestraud[6], Jennifer Wong[7], Vincent Cockenpot[8], Andreia Goncalves[8], Janick Selves[9], Helene Blons[10], Etienne Rouleau[11], Oliver Delattre[1], Christophe Le Tourneau[5], Ivan Bieche[2], Yves Allory[8], Laurence Albiges[3], Sarah Watson[1]

[1]INSERM U830, Diversity and Plasticity of Childhood Tumors Lab, Institut Curie Hospital, Paris, France,[2]Department of Genetics, Institut Curie Hospital, Paris, France,[3]Department of Cancer Medicine, Institut Gustave Roussy, Villejuif, France,[4]Clinical Bioinformatic Unit, Department of Diagnostic and Theranostic Medecine, Institut Curie Hospital, Paris, France,[5]Department of Drug Development and Innovation, Institut Curie Hospital, Paris, France,[6]INSERM U900, CBIO-Centre for Computational Biology, Institut Curie Hospital, Paris, France,[7]Somatic Genetic Unit, Department of Genetics, Institut Curie Hospital, Paris, France,[8]Department of Pathology, Institut Curie Hospital, Paris, France,[9]Department of Pathology, University Hospital of Toulouse (IUCT), Toulouse, France,[10]Department of Biochemistry, Georges Pompidou European Hospital, Paris, France,[11]PRISM Center for Personalized medicine, Institut Gustave Roussy, Villejuif, France

Background: Cancers of unknown primary (CUP) is a heterogenous group of malignancies characterized by distant metastases in the absence of detectable primary. Specifics subgroups of CUP that share similarities with cancers of known primary beneficiate from tissue-tailored therapeutic strategies. The objective of this study was to characterize the clinical and biological presentation of a cohort of patients with suspected CUP of renal origin (rCUP) and to evaluate their optimal therapeutic management.

Methods: All Patients with rCUP identified prospectively between 2020 and 2023 within the French National Multidisciplinary Tumor Board for CUP were included. Centralized pathological review and immunohistochemical stainings were performed. Whole Exome Sequencing (WES), whole transcriptomic sequencing (RNAseq) and application of the deep-learning based algorithm TransCUPtomics for prediction of tissue of origin, and DNA methylation analysis were performed and compared to public renal cell carcinomas (RCC). Progression Free Survival (PFS) and Overall Survival (OS) were calculated using Kaplan-Meier estimates.

Results: 23 patients were included. The median age at diagnosis was 57 yo and 17/23 were male. The most common metastatic sites were the bones (N=17) and the lymph nodes (N=14). 19/23 patients presented with at least two distinct distant metastatic sites. Genomic analyses performed in 10 patients led to the identification of recurrent inactivating mutations in genes commonly altered in RCC, including NF2 (N=7), SETD2 (N=3), or VHL (N=1). 10/11 samples analyzed by RNAseq were predicted as RCC by the TransCUPtomics classifier based on their gene expression profiles. DNA methylation profiling performed in 7 samples showed major similarity with known RCC subtypes.Centralized pathological review and integration of molecular characteristics led to the final diagnoses of papillary RCC (N=2), clear cell RCC (N=7), renal medullary carcinoma (N=1), TFEB-amplified RCC (N=1) and unclassified RCC (N=12). 20/23 patients received at least one line of systemic treatment based on the renal origin, including anti-angiogenic TKI, anti-PD1/PDL1 antibody, anti-CTLA4 antibody or mTOR inhibitor. The median PFS under the first renal-oriented systemic treatment was 5 months and 10 patients remained progression-free for more than 6 months under tailored-treatment. The median OS was 31 months, and 11 patients are still alive in October 2023.

Conclusions: This study shows that rCUP represent a new entity within CUPs that shares major similarities with classical RCC despite the more frequent presentation of unfavorable prognostic factors. Prolonged survival can be observed with renal-tailored systemic treatment, supporting the individualization of these patients within CUP.

#4628 Validation of an automated, scalable comprehensive genomic profiling assay for hematologic malignancies.

Grant Hogg[1], Tong Liu[1], Helen Cao[1], Adib Shafi[1], Ashraf Shabaneh[1], Jon Williams[1], John Howitt[2], Amanda Williamson[2], Rachel Dango[2], Xiaojun Guan[1], Heidi Hoffmann[3], Michael Mooney[2], John Pruitt[2], Scott Parker[2], Henry Dong[4], Stan Letovsky[3], Li Cai[2], Eric A. Severson[2], Shakti H. Ramkissoon[2], Anjen Chenn[2], Marcia Eisenberg[5], Brian Caveney[5], Eyad Almasri[1], Taylor J. Jensen[1]

[1]Labcorp, San Diego, CA,[2]Labcorp, Durham, NC,[3]Labcorp, Westborough, MA,[4]Labcorp, New York, NY,[5]Labcorp, Burlington, NC

Optimal diagnosis, prognosis, and treatment selection for hematologic malignancies requires assessment of somatic mutations across a subset of clinically relevant genes. Here we present the analytical validation results of an expanded targeted next generation sequencing (NGS) panel of 141 clinically relevant genes for myeloid and lymphoid malignancies. Based on review of clinical guidelines, 141 genes including 79 myeloid and 84 lymphoid associated genes were selected. The expanded hematological panel interrogates all coding exons of the 141 genes to detect single nucleotide variants (SNVs) and insertions/deletions (indels). The panel also identifies copy number aberrations (CNAs) in 16 genes, *FLT3* internal tandem duplicates (ITDs), select non-coding pathogenic variants, and patient sex. The custom hybrid capture-based assay utilizes genomic libraries created from 250 ng gDNA extracted from peripheral blood, bone marrow, or cell suspensions, followed by sequencing on Illumina® instruments. Concordance studies were performed on clinical samples previously assessed using an orthogonal NGS-based laboratory developed test for SNVs/indels/*FLT3*-ITDs or digital multiplexed ligation-dependent probe amplification for CNAs. In total, 308 patient samples were evaluated and included 72 (23.4%) acute myeloid leukemia and 58 (18.8%) myelodysplastic syndromes samples among other indications, of which 240 (77.9%) were bone marrow specimens. Analysis of concordance demonstrated a positive percent agreement (PPA) of 99.7% for SNVs (750/752), 99.5% for indels <25bp (206/207), and 95.7% for indels ≥ 25bp (22/23). Variants were from 45 genes including *TP53*, *NPM1*, and *IDH1/2*. PPA was 100% for *FLT3*-ITDs (38/38; size range 18-300 bp) and sex (294/294). For CNAs, PPA was 96.4% (132/137) and negative percent agreement (NPA) was 98.3% (931/947). Assay precision was determined using three replicates of 15 clinical samples for both intra and inter-assay precision using multiple operators, instruments, and reagent lots. 100% concordance was observed for SNVs (36/36), indels (11/11), a 24 bp *FLT3*-ITD (1/1), CNAs (24/24), and sex (15/15). Analytical specificity was assessed using 5 replicates of NA12878 showing specificity >99.99% for SNVs/indels with variant allele frequency ≥ 3%, and >99.99% for CNAs with copy number ≤0.85 or ≥1.15. Dilution series to determine analytical sensitivity are in progress. This study highlights the analytical validation of the expanded NGS panel for the detection of clinically informative genomic alterations in hematologic malignancies. Results from this validation study, when complete, will include at least 576 samples plus orthogonal testing. These data describe the performance of the assay to enable a comprehensive evaluation of genomic alterations using a single sample, further facilitating the use of broad NGS assays in patients with hematologic malignancies.

#4629 QClamp™ Plex VEXAS syndrome UBA1 mutation detection assay: A noval XNA based assay to simultaneously detect eight UBA1 somatic mutations associated with VEXAS syndrome.

Y. Ma;
DiaCarta, Inc., Pleasanton, CA

VEXAS syndrome (acronym for Vacuoles, E1 enzyme, X-linked, Autoinflammatory, Somatic) is a monogenic disease discovered in December 2020. It is an adult-onset systemic inflammatory disorder genetically characterized by somatic mutation of the UBA1 gene which encodes the ubiquitin like modifier activating enzyme 1. VEXAS patients have overlapping rheumatologic and hematologic manifestations, including increased risk for myelodysplastic syndrome (MDS). It is critically important to diagnose VEXAS syndrome, but UBA1 mutation test is still not commercially available. The three most frequent mutations of UBA1 gene are p.M41T(122T>C), p.M41V (c.121A>G), and p.M41L (c.121A>C) in codon 41 of exon 3. Other mutations including splice site mutations at exon 3 (c.118-2A>C, c.118-1G>C and c.118- 9_118-2del), p.S56F (c.167C>T) in codon 56 of exon 3, and p.S621C (c.1861A>T) in codon 621 of exon 16 have been reported. Based on XNA technology, we developed a QClampTM Plex platform to detect all the eight mutations in a single reaction with Luminex system. XNA technology enriches mutant target sequence in a PCR reaction by using synthetic DNA analog XNA (xenonucleic acid) to block wild type DNA. With spiking synthetic mutant DNA in GM24385 cell line DNA, we determined that this assay can detect mutations with a detection limit of variant allele frequency (VAF) for M41T at 0.1%, M41V at 0.1%, M41L at 0.25%, c.118-2A>C at 1%, c.118-1G>C at 1%, c.118- 9_118-2del at 1%, S56F at 0.25% and S621C at 1%, respectively, and specificity of 100% for all mutations. We tested saved DNA samples extracted from whole blood previously collected from suspected VEXAS patients and tested at the National Cancer Institute by Sanger sequencing, including 13 positive and 20 negative samples. Our assay detected all corresponding UBA1 mutations in the 13 positive patient samples, and did not detect UBA1 mutation in 18 of the 20 negative patient samples. Two of the 20 negative samples were also tested positive for UBA1 M41T and M41L on our assay, respectively, due to its significantly higher sensitivity than the Sanger sequencing platform, which has a detection limit of 15-20% VAF.

#4630 Clinical and epidemiological profile of neuroendocrine differentiation- A hospital-based retrospective study.

Y. Wen, S. Shi;
Cancer Hospital Chinese Academy of Medical Sciences, Beijing, China

Background: Neuroendocrine differentiation (NED) in carcinomas is poorly studied globally, despite its distinct clinical features, disease progression, pathology, treatment outcomes, and poor prognosis. Therefore, it is imperative to conduct further analysis utilizing extensive clinical samples to unveil the clinical and epidemiological profile of NED.
Methods: A retrospective study was conducted to analyze the histopathological samples of patients diagnosed with malignant tumor using immunohistochemical techniques for NED markers, such as ChrA, Syno and CD56. The morbidity and prognosis of NED patient would be analyzed subsequently. Eligible patients must have pathologically confirmed gastric cancer, colorectal cancer, lung cancer, esophageal cancer and prostate cancer with no prior neoadjuvant chemotherapy or radiotherapy received before surgery. Patients aged 18-75 years with normal organ functions were enrolled.
Results: Between January 2017 and June 2018, over 450 cases were enrolled. Preliminary analysis focused on 36 esophageal cancer (EC) and 44 prostatic cancer (PC) samples. NED markers were expressed in 4 (11.1%) of 36 EC patients, including 4 cases positive for Syno, 1 case positive for ChrA, and 2 cases positive for CD56. Meanwhile, NED markers were expressed in 15 (34.1%) of 44 PC patients, including 10 cases positive for Syno, 15 cases positive for ChrA, and 2 cases positive for CD56.
Conclusion: Neuroendocrine differentiation is obviously observed in EC and PC. The encouraging prevalence rate of NED may have clinical implications for individualized treatment. Further research is needed to explore this area in more detail.

#4631 Evaluation of the impact of homozygous MTAP truncations on the activity and selectivity of MTA-cooperative PRMT5 inhibitors.

M. R. Tonini, A. A. Mignault, D. A. Whittington, S. A. Lombardo, B. Shen, H. Stowe, S. Yoda, S. Liu, M. Zhang, K. M. Cottrell, S. R. Meier, H. Rego, J. Morawiak, E. Hooper, Y. Yu, H. DiBenedetto, A. S. Crystal, T. Teng, **K. Briggs**;
Tango Therapeutics, Boston, MA

Homozygous deletion of the MTAP gene occurs in 10-15% of all human cancers. To benefit this large and diverse patient population, MTA-cooperative PRMT5 inhibitors, including TNG908 and TNG462, have been developed to leverage the synthetic lethal relationship between MTAP deletion and PRMT5 inhibition. MTA-cooperative PRMT5 inhibitors selectively bind the PRMT5-MTA complex driving selective inhibition of PRMT5 in MTAP-deleted cancers while sparing normal, MTAP-proficient cells. Our PRMT5 inhibitors are currently in Phase I/II clinical trials (NCT05275478 and NCT05732831), and eligibility is restricted to patients with tumors with confirmed MTAP loss either detected by next-generation sequencing (NGS) or immunohistochemistry.
MTAP gene loss occurs in cancers because of its chromosomal proximity to one of the most common genetically altered tumor suppressor genes, CDKN2A, but the chromosomal 9p breakpoints for the co-deletion are not uniform. Indeed, while clinical NGS testing and preclinical data confirm that homozygous intragenic MTAP breakpoints occur, the functional consequence of any given breakpoint on MTAP enzymatic activity and protein function remains unknown. Given the potential implications for homozygous intragenic MTAP deletions to impact the clinical response to MTA-cooperative PRMT5 inhibitors, we have started to evaluate the loss-of-function phenotype of various MTAP truncations to determine whether they retain MTAP activity. Here, we present our initial functional genomics analysis of this important diagnostic biomarker using in vitro cDNA reconstitution approaches for MTAP activity combined with analysis of PRMT5 inhibitor sensitivity. Ultimately, these data may help refine patient enrollment on clinical trials to drive the maximum benefit for patients with MTAP-deleted cancers.

#4632 Lineage plasticity as a determinant of antibody-drug conjugate target expression in urothelial bladder cancer.

J. Luo[1], S. P. Gao[1], F. Kuo[1], G. Gokturk Ozcan[1], M. Basar[1], F. Koll[1], J. E. Tallman[1], S. M. Alam[1], C. E. Chu[2], Z. Chen[1], E. J. Pietzak[1], G. Iyer[1], J. E. Rosenberg[1], D. B. Solit[1], H. Al-Ahmadie[1];

[1]Memorial Sloan Kettering Cancer Center, New York, NY, [2]University of California, San Francisco, San Francisco, CA

Bladder cancers display a wide spectrum of morphologies that frequently co-exist within individual tumors. Several histologic variants, including plasmacytoid, neuroendocrine, and micropapillary subtypes, are associated with an increased bladder cancer recurrence risk and cancer-specific mortality. The molecular basis and therapeutic implications of this phenotypical plasticity remain poorly understood. Enfortumab vedotin (EV), an antibody-drug conjugate targeting Nectin-4, has also emerged as a new standard-of-care for metastatic bladder cancer patients, but the association between lineage plasticity as manifested by morphologic heterogeneity in bladder cancer, Nectin-4 expression and ADC response remains poorly defined. Previous DNA-based molecular profiling studies of histologic variants revealed that *CDH1* mutations were the pathognomonic molecular alteration in plasmacytoid urothelial carcinoma, but no recurrent driver mutations have been found to be unique to the aberrant histology regions of other mixed histology subtypes. Thus, to explore the molecular basis for the lineage plasticity of bladder cancers with aberrant histology and to define the association between lineage plasticity manifested as morphologic heterogeneity and the expression of Nectin-4, HER2 and other potential ADC targets, we performed RNA-seq of pure urothelial carcinomas (n=118, not otherwise specified, UC-NOS) and bladder tumors with divergent differentiation or histologic subtypes (n=199). Our cohort included a subset of tumors in which RNA-seq was performed on microdissected UC-NOS and variant histology regions of the same tumor. Tumors with neuroendocrine, sarcomatoid and squamous histology had the lowest Nectin-4 expression, whereas histologic subtypes that retained a luminal transcriptional profile such as micropapillary, plasmacytoid and nested histology had higher levels of Nectin-4 expression. In mixed histology tumors, Nectin-4 and/or HER2 expression was often restricted to only one of the two histologic components. Gene Set Enrichment Analysis noted enrichment of distinct oncogenic pathway gene sets in different histologic variants. Preliminary investigation into the mechanism(s) of Nectin-4 regulation using bladder cancer cell lines and patient-derived organoids (PDOs) has identified targetable pathways which when inhibited revert lineage plasticity and induce Nectin-4 expression. In sum, lineage plasticity manifested as heterogenous histomorphologies was associated with heterogeneous Nectin-4 expression in some but not all histologic variants of bladder cancer. Ongoing studies using PDOs from bladder cancer patients with mixed histology will seek to identify molecular pathways whose inhibition leads to increased expression of Nectin-4 or other ADC targets such as HER2 and thus increased sensitivity of ADCs targeting these cell surface proteins.

#4633 Differentiation driver gene HOXD4 as a potential prognostic indicator and therapeutic target in anaplastic thyroid cancer.

K. Kopec, T. Jarboe, N. R. DeSouza, H. K. Islam, J. Geliebter, R. K. Tiwari;
New York Medical College, Valhalla, NY

Anaplastic thyroid cancer (ATC) is always diagnosed as stage IV with a 5 year survival rate of less than 3% due to its aggressive metastatic phenotype. ATC lacks differentiation and loses its thyroid-like functions making it a difficult cancer to treat due to its lack of targetable genetic lesions and unresponsiveness to conventional treatments. Therefore, we investigated genes that had aberrant expression in ATC in relation to differentiation. Using NCBI Gene expression omnibus (GSE33630, GSE85457), which provides publicly available transcriptomic datasets, and bioinformatics software, GEO2R, we found that Homeobox D4 (HOXD4) has 12.5FC higher expression in ATC vs. normal tissue (p=0.000552) and 4.36FC higher in ATC vs. papillary thyroid cancer (PTC) in human patients (p=6.69e-08). HOXD4 is a transcription factor that plays a crucial role in cell differentiation and has been associated with a worse prognosis in cancers such as ovarian serous carcinoma. As loss of differentiation is essential to ATC's refractory nature and therapeutic resistance, we are exploring modulation of differentiation by all-trans retinoic acid (ATRA). ATRA was used to induce differentiation in ATC cell line T238 therefore abrogating the aggressive phenotype of this cancer. T238 treated with ATRA had a 26% decrease in proliferation at 24 hours, 46% at 48 hours, and 87% at 72 hours measured using a trypan blue exclusion assay. T238 treated with ATRA also had a 44% decrease in migratory capacity at 24 hours and 24% at 48 hours measured by a cell scratch wound assay. Immortalized normal thyroid cell line NTHY-ori-3-1 did not have a significant decrease in either proliferation or migratory capacity when treated with ATRA. T238 cells treated with ATRA for 24 hours had a 30% decrease in HOXD4 protein levels. Lastly, immunohistochemistry staining of HOXD4 in human patient tissue samples confirmed the over-expression of HOXD4 in ATC (19.5% staining) vs. normal tissue (2.5%) and PTC (7.5%). Overall, we hypothesize that the aberrant expression of HOXD4 in ATC plays a crucial role in the aggressive metastatic phenotype and therefore differentiation agents such as ATRA can target this biomarker to modulate the ATC phenotype. Therefore, HOXD4 can be used as a potential prognostic indicator for early detection of ATC. Future studies will involve CRISPRi based knockdown of HOXD4 in vitro and validation of these results in animal in vivo models.

#4634 Inhibitory-κB kinase alpha as a biomarker and therapeutic target in colorectal cancer.

K. A. F. Pennel[1], M. McKenzie[1], G.-Y. Lian[1], J. A. Quinn[1], S. Samir Foad Al-Badran[1], C. S. D. Roxburgh[1], S. P. Mackay[2], J. Birch[1], J. Edwards[1];
[1]University of Glasgow, Glasgow, United Kingdom, [2]University of Strathclyde, Glasgow, United Kingdom

Introduction/Aims: Colorectal cancer (CRC) remains a leading cause of cancer-related mortality. The canonical NF-κB pathway driven by IKKβ has been implicated in CRC development and progression, however less research has focused on non-canonical NF-κB signaling, regulated by inhibitory-κB kinase alpha (IKKα). This project aimed to assess IKKα, phospho-IKKα (pIKKα^{s176}) and IKKβ expression in a retrospective CRC cohort to establish association with survival outcomes. Subsequently, this project aimed to determine the effect of abrogating IKKα activity without perturbing the canonical NF-κB pathway controlled by IKKβ using a first-in-class selective IKKα inhibitor in vitro/ex vivo.

Methods: Immunohistochemical staining for IKKα/pIKKα ^{s176}/IKKβ was performed using tissue microarrays from a CRC patient cohort (n=787). QuPath® software was used to semi-quantitively assess expression levels and scores were analyzed for association with cancer-specific survival (CSS). CRC cell lines (n=3), patient-derived organoids (PDOs; n=5) and patient-derived explants (n=5) were treated with novel IKKα inhibitor SU1644 and assessed for cell viability and proliferation.

Results: Positive staining for IKKα, pIKKα^{s176} and IKKβ was detected in tumor specimens. High cytoplasmic expression of IKKα within tumor cells was associated with reduced CSS in patients with right-sided colon cancer (HR=3.091, 95%CI; 1.128-9.467, log rank p=0.021). Conversely, high IKKβ expression was a marker of good prognosis (HR=0.627, 95%CI; 0.457-0.861, log rank p=0.004). A high ratio of IKKα to IKKβ was associated with reduced CSS in the full cohort (HR=1.404, 95%CI; 1.050-1.879, log rank p=0.021) and this was potentiated in right-sided colon cases (HR=1.772, 95%CI; 1.107-2.837, log rank p=0.016). Selective inhibition of IKKα using 1μM SU1644 in vitro caused a significant reduction in HT29 colony formation (p=0.012) and cell viability (p=0.039). PDOs showed altered cell morphology, reduced cell viability and proliferation when treated with SU1644. In the patient-derived explant model, Ki67 expression was reduced in tumor explants treated with SU1644.

Conclusions: These data establish high cytoplasmic IKKα expression within tumor cells as a marker of poor prognosis in CRC and conversely high IKKβ expression as a marker of good prognosis. This highlights the importance of development of selective IKKα inhibitor SU1644. IKKα inhibition using SU1644 demonstrated anti-cancer activity in recapitulative CRC disease models.

#4635 RNF208: A novel diagnostic and prognostic biomarker for colorectal cancer and key regulator of malignant behavior.

Fangyue Guo, Shanfeng Zhang, **Pei Li**

Basic Medical Experimental Center, School of Basic Medical Sciences, Zhengzhou University, Zhengzhou, Henan, China

Background: RNF208, a member of the RING finger protein family, has been implicated in ubiquitin-mediated degradation of Vimentin, regulating invasion in breast cancer, and serves as a prognostic factor in uveal melanoma. However, its diagnostic and prognostic value in colorectal cancer (CRC), as well as its role in regulating malignant behavior in CRC, remains unclear. This study aims to reveal the potential of RNF208 as a diagnostic and prognostic marker for CRC and its function in regulating malignant behavior in CRC through bioinformatics analysis and experimental validation.

Methods: In this study, based on the ExoRbase2.0 human plasma exosome database (CRC=35; Healthy=118) and TCGA-COAD dataset (CRC=478; Healthy=41), we conducted bioinformatics analysis of the transcriptomic differences in plasma exosomes between CRC patients and normal individuals using ExoRbase2.0. Survival data from the TCGA-COAD dataset were integrated to select key molecules for CRC diagnosis and prognosis. Plasma samples from 39 CRC patients and 16 normal individuals were collected from hospital, and exosomes were isolated and purified using a reagent kit. qPCR was employed to validate the levels of RNF208 in plasma exosomes, confirming the results of bioinformatics analysis. Biological behavior was assessed through CCK-8 proliferation assays, flow cytometry experiments, and Transwell migration assays to investigate the relationship between RNF208 and malignant behavior in the HCT116 colorectal cancer cell line.

Results: Bioinformatics analysis revealed a significant correlation between elevated RNF208 expression in plasma exosomes and the incidence of CRC, as well as poor prognosis. The qPCR results from clinical samples further confirmed this correlation, and ROC curves demonstrated high sensitivity and accuracy, suggesting RNF208's potential as a diagnostic and independent prognostic factor for CRC. CCK-8 experiments showed that RNF208 knockdown suppressed proliferation activity in HCT116 cells, flow cytometry indicated that RNF208 knockdown promoted apoptosis in HCT116 cells, and Transwell migration assays demonstrated that RNF208 knockdown inhibited the migration of HCT116 cells.

Conclusion: RNF208 serves as a novel diagnostic and prognostic biomarker for colorectal cancer, promoting the proliferation and migration of colorectal cancer cells and contributing to the further deterioration of the disease.

#4636 Genome-wide drug anchor screens identify CAAP1 and AKAP17A as regulators of PRMT5 inhibitor sensitivity.

S. Yoda, M. R. Tonini, H. E. Nicolson, S. Poleretzky, S. Fenoglio, S. Lombardo, L. Grove, S. R. Meier, A. Choi, Y. Yu, K. M. Cottrell, J. P. Maxwell, T. Teng, J. N. Andersen, K. J. Briggs;
Tango Therapeutics, Boston, MA

MTA-cooperative PRMT5 inhibitors are an emerging treatment option for patients with one of the 10-15% of all human cancers harboring MTAP homozygous deletion. To identify potential regulators of sensitivity to PRMT5 inhibitors, we performed genome-wide CRISPR knockout screens in the presence and absence of an MTA-cooperative PRMT5 inhibitor. Knockout of CAAP1 and AKAP17A were among the strongest sensitizing hits across multiple MTAP-deleted cancer cell lines representing different histologies. Strikingly, the CAAP1 gene co-localizes with MTAP and CDKN2A on chromosome 9p21. Co-deletion of CAAP1 is reported in 20 percent of MTAP-deleted cancers in the TCGA PanCancer Atlas. CAAP1 or AKAP17A knockout in MTAP-deleted cancer cell lines sensitized the cells to PRMT5 inhibitors including the clinical stage MTA-cooperative inhibitors, TNG908 and TNG462, and the non-MTA-cooperative inhibitor, GSK3326595. Moreover, we discovered that CAAP1 and AKAP17A protein levels are interdependent, as knockout of either gene caused decreased protein levels for the other. Consistent with this finding, CAAP1 reconstitution in CAAP1-deleted cell lines led to increased AKAP17A levels. Endogenous CAAP1 and AKAP17A protein levels are positively correlated across a panel of cancer cell lines and MTAP-deleted patient-derived xenograft models. Consistent with a previous report (Ni et al., 2023), exogenous CAAP1 and AKAP17A co-immunoprecipitation studies suggest that the proteins form a protein complex. AKAP17A and CAAP1 are not well-characterized proteins, but PRMT5 inhibitors induce global alternative splicing events (ASEs) in cancer cells, and based on preliminary studies a possible function for the CAAP1/AKAP17A complex could be to mitigate ASEs induced by PRMT5 inhibition. Collectively, these data indicate that CAAP1 and AKAP17A exist interdependently and mediate sensitivity to PRMT5 inhibitors. The colocalization and 20 percent incidence of CAAP1 deletion in the setting of MTAP deletion may suggest that such patients will have improved responses to PRMT5-targeted therapy. S. Yoda and M. R. Tonini contributed equally.

#4637 National multidisciplinary tumor board improves diagnostic stratification and therapeutic management in cancers of unknown primary.

C. Dupain[1], N. Jacquin[1], I. Guillou[1], E. Rouleau[2], J. Masliah Planchon[1], I. Soubeyran[3], C. De La Fouchardiere[4], C. Tlemsani[5], H. Blons[6], L. Marisa[6], A. Patrikidou[2], F. Escande[7], P. Blanc[8], J. Wong[1], P. Saintigny[9], S. Boyault[9], A. Buisson[9], Y. Allory[10], A. Vincent-Salomon[1], V. Cockenpot[1], J. Selves[11], I. Bieche[1], M. Kamal[1], C. Le Tourneau[1], S. Watson[1];

[1]Institut Curie, Paris, France, [2]Gustave Roussy, Villejuif, France, [3]Institut Bergonie, Bordeaux, France, [4]Institut Paoli Calmettes, Marseille, France, [5]APHP Institut Cochin, Paris, France, [6]APHP Hopital Europeen Georges Pompidou, Paris, France, [7]CHRU Lille, Lille, France, [8]Laboratoire SeqOIA, Paris, France, [9]Centre Leon Berard, Lyon, France, [10]Institut Curie, Saint-Cloud, France, [11]IUCT Oncopole, Toulouse, France

Introduction: With the increasing complexity of current diagnostic investigations, the integration of clinical, pathological and genomic characteristics is crucial for the management of patients (pts) with cancers of unknown primary (CUP). A national multidisciplinary tumor board (NatCUPMTB) was created in July 2020 in France to discuss the diagnostic and therapeutic management of CUP pts. The objective of this study was to evaluate the diagnostic, prognostic and therapeutic impact of this NatCUPMTB after 39 months of activity.

Methods: This was a multicenter retrospective study with prospective follow-up. All pts discussed at least once in the NatCUPMTB between July 2020 and October 2023 were included. Pts and tumors characteristics, pathological and genomic analyses including WGS, WES and transcriptome analysis performed on the two PFMG2025 (French Genomic Medecine Plan 2025) national sequencing laboratories, multidisciplinary tumor board (MTB) conclusions, and follow-up after MTB were collected.

Results: 244 pts were included. The median age at diagnosis was 60 yo, 53% were female, and the majority of patients had an OMS status <2. The median number of metastatic sites at diagnosis was 2, with a majority located in the lymph nodes (62%). The median time between diagnosis and first MTB presentation was 3 months (1-20). At the time of analysis, NatCUPMTB conclusions were available for 129 pts with a second MTB presentation. MTB investigations enabled to identify a likely primary origin in 89/129 (69%) pts, the most frequent being breast carcinoma (N=15), renal carcinoma (N=13) and lung carcinoma (N=13). The most frequently molecular alterations found were in *TP53 (37%), KRAS (19%), CDKN2A (18%), NF2 (12%), KMT2C (10%), CDKN2B (9%), PBRM1 (9%)* genes. MTB diagnoses were based on the combination of clinical, pathological and genomic investigations in 51/89 (59%) of pts. Importantly, a personalized therapeutic strategy was recommended by NatCUPMTB in 91/129 (71%) of pts. Among these recommendations, 72/91 (79%) were based on the diagnosis of tissue of origin (TOO), 9/91 (10%) on an actionable molecular alteration validated in the TOO indication, 8/91 (9%) on an actionable molecular alteration not validated in the TOO indication and 2/91 (2%) based on a druggable alteration only independently from the TOO. After a median follow-up of 1.5 months, the median overall survival (OS) was 17.7 months from the 2nd MTB presentation.

Conclusion: NatCUPMTB provides significant diagnostic in 69% of pts with CUP and a therapeutic strategy recommendation for 71% of pts.

#4638 Integrated proteogenomic characterization of longitudinal glioblastoma.

S. Migliozzi[1], K.-H. Kim[2], H. Koo[2], J.-H. Hong[2], S. M. Park[2], H. J. Kwon[2], L. Garofano[1], Y. T. Oh[1], F. D'Angelo[1], C. I. Kim[2], A.-L. Di Stefano[3], F. Bielle[4], J. Yin[2], M. Sanson[4], D.-H. Nam[5], J. K. Sa[6], A. Lasorella[1], J. B. Park[2], A. Iavarone[1];

[1]Univ. of Miami Sylvester Comprehensive Cancer Ctr., Miami, FL, [2]National Cancer Center, Goyang, Korea, Republic of, [3]Ospedali Riuniti di Livorno, Livorno, Italy, [4]Pitie Salpetriere Hospital, Paris, France, [5]Sungkyunkwan University School of Medicine, Seoul, Korea, Republic of, [6]Korea University College of Medicine, Seoul, Korea, Republic of

Glioblastoma multiforme (GBM) is the most aggressive form of primary brain tumor, with no curative treatment options and median patient survival time of almost one year. Despite multi-modal therapy including surgery, irradiation and chemotherapy, all patients experience tumor progression and recurrence. Our group proposed and validated the first single cell guided functional classification of primary GBM in four tumor-intrinsic cell states which informed clinical outcome and delivered therapeutic options. However, recurrent GBM remains therapeutically unresolved due in part to the diffusely invasive nature and in part to marked cellular heterogeneity of the tumor.The evolutionary trajectory of glioblastoma after therapy is a multifaceted biological process that extends beyond discrete genetic alterations alone. Here, we profiled by multi-omics platforms the largest dataset of matched primary and recurrent GBM including 123 longitudinal glioblastoma pairs, temporally separated by standard-of-care treatment. Genomics, proteomics, and phosphoproteomics all independently captured the loss of proliferative-progenitor characteristics and a significant upregulation of specialized neuronal and synaptic signaling programs in recurrent GBM. Proteomic and phosphoproteomic analyses revealed that the molecular transition from proliferative to neuronal state at recurrence is marked by coherent post-translational activation of the WNT/PCP signaling pathway and the BRAF protein kinase. Multi-omic analysis of Patient-Derived Xenograft (PDX) models mimicked the patterns of evolutionary trajectory, consisting of marked activation of neuronal signaling programs in recurrent patients. Inhibition of the BRAF kinase with small molecule inhibitors impaired both neuronal transition and migration capability of recurrent glioblastoma cells, which are the phenotypic hallmarks of glioblastoma progression after therapy. Accordingly, combinatorial treatment of temozolomide with BRAF inhibitor, vemurafenib, significantly prolonged the survival of mouse PDX models. This work provides comprehensive insights into the biological mechanisms of glioblastoma evolution and treatment resistance and highlights new therapeutic opportunities to effectively counter them in the clinic.

#4639 Unraveling the oncogenic network of USP37 and USP14 in gynecological cancers: Decrypting the molecular landscape of chemoresistance.

R. Chauhan[1], A. Gupta[1], G. Dagar[1], L. Malhotra[2], E. Rai[3], M. A Macha[4], A. A Bhat[5], E. A Samath[1], M. Singh[1];
[1]All India Institute of Medical Sciences (AIIMS), New Delhi, India, [2]Sri Venkateswara College, University of Delhi, New Delhi, India, [3]Jawaharlal Nehru University, New Delhi, India, [4]Islamic University of Science and Technology, Pulwama, India, [5]Sidra Medicine, Doha, Qatar

Background: Gynecological cancers (GC) involve female reproductive system malignancies, and acquired chemoresistance is a challenge in the treatment of GC. Protein deubiquitination, mediated by deubiquitinating enzymes (DUBs) like ubiquitin-specific proteases (USPs), holds therapeutic promise in cancer treatment. This study delves into the mechanistic understanding of DUBs, particularly in acquired chemoresistance in GC.
Methodology: We initially examined TCGA database to assess the impact of Ubiquitin Specific Proteases (USPs), specifically USP37 and USP14, on prognosis in Gynaecological Cancers (GCs). Subsequently, we evaluated their expression in various GC cell lines at both protein and RNA levels. Cell proliferation and metastasis assays were performed to analyze the effect of depleting these USPs on survival and metastasis in GC cells under replication stress. Proteomics analysis was conducted on cells with altered expression of USP37 and USP14 to identify interacting proteins regulating proliferation and metastasis. To investigate DUBs role in chemoresistance, we generated chemoresistant (CR) cell lines with cisplatin exposure, characterized their viability and proliferation, conducted cell cycle and apoptosis analyses, and performed proteomic profiling to explore the USP37 and USP14 specific interactome in chemoresistant cell lines.
Results: Examination of TCGA database revealed an association between elevated USP37 and USP14 expression and poor Overall Survival (OS) and Disease-free Survival (DFS) in Gynaecological Cancers (GC) cohort. Increased expression of USP37 and USP14 at RNA and protein levels was observed in GC cell lines. Inhibiting USP37 and USP14 reduced GC cell proliferation under replication stress and hindered metastasis. Proteomics analysis identified proteins linked to replication (PCNA), DNA damage (Chk-1), cell cycle, and metastasis. Cisplatin-resistant GC cell lines were successfully established, demonstrating prolonged survival and increased proliferative capacity after cisplatin treatment compared to chemosensitive (CS) cell lines. FACS analysis indicated altered cell cycle distribution and increased proliferation in CR cells. Comparative interactome analysis revealed altered protein sets associated with USP37 and USP14 in CR and CS GC cells.
Conclusion: This study provides evidence that supports the participation of USP37 and USP14 in the onset of gynecological cancers (GC). We present evidence of alterations in the oncogenic network linked to USP37 and USP14 in GC. Additionally, we elucidate the roles of these deubiquitinating enzymes (DUBs) in chemoresistant cell lines.

#4640 Pan-cancer analysis of the influence of ERBB2 alteration on HER2 expression.

T. Lee, S. Shin, H. Song, S. Park, S. Pereira, D. Yoo, J. Ro, J. Moon, S. Cho, C. Ahn, C.-Y. Ock, S. M. Ali;
Lunit, Seoul, Korea, Republic of

Introduction: HER2 (ERBB2) is a target for various anti-cancer therapies, including large (Trastuzumab deruxtecan) or small molecules (Neratinib). Quantitative assessment of HER2 expression at the cellular level may improve therapeutic efficacy prediction. While ERBB2 mutations are known oncogenic drivers, their impact on tumor cell HER2 expression is unclear. In this study, we focused on common ERBB2 mutations, and analyzed HER2 expression via AI-powered image analysis in pan-cancer tumor specimens to identify possible mutation-expression correlations.

Methods: We analyzed 183,292 pan-cancer samples from AACR GENIE, and 10,967 from TCGA. A set of 156 cases with both ERBB2 mutation status and HER2 4B5 IHC WSIs was obtained (Neogenomics). An AI-powered HER2 analyzer (Lunit SCOPE HER2) was previously developed using 1,133 HER2 IHC-stained WSIs of breast cancer stained with 4B5. Single-cell HER2 intensity was analyzed and aggregated, reported based on breast ASCO/CAP criteria. ERBB2 RNA levels were analyzed for mutations and amplification.

Results: We identified 2,735 cases with ERBB2 mutations (2,603/183,292 [1.4%] in GENIE and 132/10,967 [1.2%] in TCGA). These mutations were categorized for analysis based on their highest frequency and previous characterization: exon 20 insertions (ex20ins, including Y772dup (YVMA) and G776InsVC), S310x, and other pathogenic mutations. In the dataset, ex20ins cases were predominantly non-small cell lung cancer (NSCLC, 381/482 [79.0%]) and S310x cases were enriched in urothelial, NSCLC, and breast cancers (269/683 [39.4%], 64/683 [9.4%], and 47/683 [6.9%], respectively). Of the 156 ERBB2-mutated cases with HER2 IHC images, 59 had ex20ins, 24 had S310x, and 73 had other mutations. AI analysis in each case type indicates a significantly higher proportion of HER2 3+ tumor cells in S310x and ex20ins cases than other mutations (median, 7.5% vs. 6.1% vs. 2.8%, p = 0.003). As such, high HER2 expression was observed in S310x and ex20ins cases compared to other mutation cases (HER2 3+ 10/24 [41.7%], 22/59 [37.3%], and 14/73 [19.2%]). Additionally, in NSCLC, ex20ins and S310x cases exhibited a modest enrichment for high HER2 expression relative to other mutation cases (21/56 [37.5%], 3/9 [33.3%], and 5/20 [27.6%]). RNA analyses from TCGA showed higher levels for ex20ins (median 13.6; interquartile range 13.1-13.7 in log2 scale), compared to S310x (12.4; 11.9-13.6) and other mutations (12.6; 12.1-13.3), but lower than that of amplified ERBB2 (15.5; 13.8-17.0).

Conclusion: An AI-powered pan-cancer image analysis of HER2 IHC of tumor cells in conjunction with genomic data reveals a positive correlation between ex20ins and S310x ERBB2 mutation and protein expression. This correlation is also seen at the RNA level, but the lesser levels relative to ERBB2 amplified cases suggests the effect may be mediated at the protein level.

#4641 Preclinical evaluation of the novel curcumin Analogue AKT-100 demonstrates therapeutic effectiveness in p53-mutated cancer cells.

K. K. Leslie, J. L. Padilla, G. L. Williams, H.-Y. Fan, C. G. Bologa, E. R. Prossnitz, J.-Y. Choe, L. E. Smith, A. Goss, R. J. Lake, A. D. Sahu;
University of New Mexico Health Sciences Ctr., Albuquerque, NM

Among the myriad of molecular alterations associated with cancer, loss of the normal tumor suppressive functions of p53, the “guardian of the genome,” is the most consistent. Thus, the possibility of targeting oncogenic, mutant p53 proteins has long been a therapeutic goal. However, that aspiration has not been fully realized, leaving patients vulnerable to aggressive disease that is resistant to chemotherapy and to targeted agents such as PARP inhibitors and immunotherapy owing to the loss of wild type p53 functionality and the gain of new oncogenic functions when mutant p53 is expressed. An effective therapeutic strategy is urgently needed for p53 mutant cancers, and our team is developing novel analogues of curcumin with the potential to convert mutant p53 to a wild type conformation and restore its tumor suppressive functions. In this study, we investigated the effects of AKT-100, which was developed from the parent molecule and curcumin analogue HO-3867. Effects were compared to another drug believed to reactivate p53 functionality, APR-246, using CyQUANT IC50 cell proliferation assays and bulk and single cell RNA sequencing. Structural analyses are underway investigating the specific sites of interaction of AKT-100 with various mutant forms of p53. Our findings indicate that, *first*, AKT-100 exhibits impressive cell killing in multiple ovarian and serous endometrial cancer cells at concentrations ranging from 100-300 nM and is synergistic with the PARP inhibitor olaparib. *Second*, RNA sequencing demonstrates the reactivation of wild type p53 genes associated with normal cell cycle regulation (induction of *CDKN1A* encoding p21 and *GADD45A*), apoptosis (induction of *PMAIP1* encoding Noxa and *DR5* encoding Death Receptor 5), and the inhibition of DNA replication and multiple alternative mechanisms of DNA repair employed by malignant cells. *Third*, RNA sequencing indicates that AKT-100 acts through both p53-dependent and independent pathways to inhibit cancer cell proliferation. Gene expression is impacted in ways that portend a therapeutic effect as well as highlight potential resistance pathways (e.g. significant induction of *PLK5* encoding polo like kinase 5) that can be further targeted to create synthetic lethal drug combinations with AKT-100 chosen specifically to target the various mutant forms of p53. Taken together, these results identify novel curcumin analogues in early development with the potential to improve therapy for p53 mutant cancers. Through this strategy it is also possible to identify and block resistance pathways that are activated by different forms of mutant p53 in response to AKT-100 and to create synthetic lethal precision drug combinations.

#4642 Fatty acid synthase as a novel prognostic biomarker and a potential therapeutic target in diffuse malignant peritoneal mesothelioma.

V. Doldi[1], S. Martini[1], C. Ciniselli[1], A. Beretta[1], M. Deraco[1], S. Kusamura[1], D. Baratti[1], P. Gandellini[2], P. Verderio[1], N. Zaffaroni[1];
[1]Fondazione IRCCS Istituto Nazionale dei Tumori, Milan, Italy, [2]University of Milan, Milan, Italy

Diffuse malignant peritoneal mesothelioma (DMPM) is a rare and locally aggressive tumor with a dismal prognosis. The availability of new therapies and biomarkers for patients' selection is still an urgent need. Altered lipid metabolism, which has been reported in several tumors, has not yet been studied in DMPM. By comparatively analyzing gene expression profiles of tumors form relapsed (n=18) and non-relapsed (n=18) DMPM patients, we initially found that fatty acid synthase (FASN) was up-modulated in relapsed tumors, with a significant linear correlation between FASN expression and shorter patient relapse-free survival (RFS), suggesting a potential role of FASN in DMPM progression. The prognostic significance of FASN was further assessed in a cohort of 80 DMPM patients who underwent cytoreductive surgery combined with hyperthermic intraperitoneal chemotherapy. Our results indicated that high FASN staining was significantly associated with reduced RFS (hazard ration (HR): 1.930; p=0.014) and Overall Survival (OS) (HR: 1.854; p=0.032) as assessed by immunohistochemistry in tissues microarray samples. The prognostic value of FASN, along with Ki67 staining and patient age, was also maintained in multivariate analysis in terms of both RFS (HR: 2.240; p=0.007) and OS (HR: 2.246; p=0.014). To validate FASN as a therapeutic target, we investigated the cytotoxic effects of non-selective (orlistat) and selective (cerulenin and C75) FASN inhibitors on patient-derived DMPM cell lines, both as single agents and in combination with selinexor -a selective inhibitor of the exportin chromosome maintenance protein. FASN pharmacological inhibition in DMPM cells resulted in a significant reduction of cell proliferation, especially upon C75 exposure. In combination experiments, we observed a synergistic activity of FASN inhibitors and selinexor, as determined by Chou and Talalay method. Through western blotting and flow cytometry analysis, we gained further insight into the mechanisms by which FASN inhibitors and selinexor synergize to reduce DMPM cell proliferation. Compared to single agents, the combined treatments resulted in increased apoptosis response and cell cycle impairment, as indicated by caspase-dependent apoptosis activation and cell accumulation in the G2-phase. Overall, our results support the relevance of FASN as a prognostic biomarker for DMPM patients and underscore its potential as a novel therapeutic target.

#4643 A novel epigenomic profiling assay reveals disease biology and therapeutic targets in gastro-esophageal cancer from 1 ml of plasma.

J. Beagan[1], **A. Gorthi**[1], A. D'Ippolito[1], T. Clark[1], M. Coyne[1], T. Tamakloe[1], A. Donahue[1], B. Tran[1], H.-H. Jeong[1], K. Cibulskis[1], H. Sawaengsri[1], C. A. Painter[1], J. Chmielecki[1], J. Barrett[1], M. F. Afreen[2], A. Pandey[2], I. Schechter[3], M. S. Taylor[2], M. R. Strickland[2], M. Eaton[1], S. J. Klempner[2];

[1]Precede Biosciences, Inc., Boston, MA, [2]Massachusetts General Cancer Center, Boston, MA, [3]Massachusetts General Hospital, Harvard Medical School, Boston, MA

INTRODUCTION: Gastro-esophageal adenocarcinoma (GEA) is an aggressive and heterogeneous disease with a poor prognosis. Targeted therapies have failed largely due to challenges associated with biopsy collection, tumor antigen heterogeneity, and accurately distinguishing transcriptionally distinct esophageal, GE junction or gastric tumor types. We developed a novel, multimodal liquid biopsy assay that profiles genome-wide transcriptional activation. Here, we deploy this assay to define clinically relevant insights in a cohort of GEA patients.

METHODS: 1 ml of plasma from whole blood samples was used to assess genome-wide enhancer, promoter and DNA methylation loci in 11 GEA patients (Stage III: 1, Stage IV: 10) and 7 healthy volunteers. 6 patients were confirmed as HER2+ based on standard tissue IHC/ISH methods. ctDNA estimation was performed using the ichorCNA algorithm on low pass whole genome sequencing data. A multimodal HER2 classifier developed previously using genome-wide features including HER2 was used to predict HER2 status of the GEA samples.

RESULTS: Epigenomic profiling and comparison of GEA and healthy volunteer plasma samples revealed distinct genome-wide transcriptional activation patterns associated with gastroesophageal adenocarcinoma, including (i) the characteristic upregulation of HER2, FGFR2 and VEGF (ii) SOX2, KLF4, GATA6 transcription factor circuitry, and (iii) DNA methylation at the CHFR and MGMT promoters. We then explored if epigenomic profiling of liquid biopsies could infer the activation status of antibody-drug conjugate (ADC) targets currently under investigation in GEA cancers. Simultaneous examination of multiple target genes including HER2, HER3, TROP2, CLDN18, CEACAM5 and MET demonstrated patient-specific differences and dynamic range in transcriptional activation of a subset of these target genes. Finally, we investigated if HER2 status could be assigned accurately and quantitatively from a liquid biopsy using the multimodal HER2 classifier. HER2 positivity by IHC was predicted accurately in 8/11 samples corresponding to an area under the ROC curve (AUC) greater than 0.85. Discordance between plasma and tissue HER2 calls could be partially attributed to variability associated with tumor site/section used for tissue collection, IHC staining, and time between biopsy collection and blood draw.

CONCLUSIONS: We demonstrate the feasibility of comprehensive epigenomic profiling from low input volume of 1ml of plasma to provide a snapshot of the tumor's transcriptional state to derive clinically actionable insights. The HER2 classifier overcomes several of the challenges with IHC profiling by providing a uniform and quantitative measurement of HER2 activation. This non-invasive assay provides an accurate reflection of tumor transcriptional biology that can inform optimal patient selection strategies.

#4644 Single strand DNA GAP accumulation as a functional biomarker for USP1 inhibitor sensitivity in ovarian cancer patient-derived organoid models.

A. B. Da Costa, O. Somuncu, R. Ravindranathan, S. Mukkavalli, D. Martigneti, H. Nguyen, Y. Jiao, B. Lamarre, G. Sadatrezai, L. Moreau, J. Liu, D. Iyer, J.-B. Lazaro, G. Shapiro, K. Parmar, A. D. D'Andrea;
DFCI/Harvard Medical School, Boston, MA

Recent studies suggest that PARP inhibitors and POLQ inhibitors confer synthetic lethality in BRCA1-deficient tumors by accumulation of single-stranded DNA gaps (ssDNA gaps) at replication forks. Loss of USP1, a deubiquitinating enzyme, is also synthetic lethal with BRCA1 deficiency, and USP1 inhibitors are now undergoing clinical development for these cancers. Here, we show that USP1 inhibitors also promote the accumulation of ssDNA gaps during replication in BRCA1-deficient cells. USP1 inhibition increased monoubiquitinated PCNA at replication forks and resulted in accumulation of ssDNA gaps in BRCA1-deficient cancer cells. Knockdown of RAD18, the E3 ubiquitin ligase known to ubiquitinate PCNA, caused USP1 inhibitor resistance and suppression of ssDNA gaps. ssDNA gap accumulation induced by USP1 inhibition correlates with drug sensitivity of *BRCA1*-mutated cancer cells and overcomes PARP inhibitor resistance in cell line and xenograft models. Furthermore, USP1 inhibition was synergistic with PARP and POLQ inhibition in *BRCA1*-mutant cells, with enhanced ssDNA gap accumulation. A set of patient-derived ovarian cancer organoids (PDOs) were used to confirm the sensitivity of *BRCA1*-deficient cells to USP1 inhibition. Five PDOs were derived from patients with high grade-serous ovarian cancer (HGSOC). Among the five PDOs, two of them were from tumors harboring germline *BRCA1* pathogenic mutations. *BRCA1*-mutant PDOs, but not *BRCA1*-WT PDOs, were sensitive to a USP1 inhibitor and to PARP inhibitor monotherapies. The accumulation of ssDNA gaps after treatment with a USP1 inhibitor or a PARP inhibitor correlated with the sensitivity to these drugs in all the models tested. Moreover, the combination of a PARP inhibitor and a USP1 inhibitor showed synergy in a *BRCA1*-WT model, which was resistant to both monotherapies. Interestingly, ssDNA gaps accumulated with the combination treatment and not with monotherapy in this model. Ovarian cancer PDOs therefore provide a powerful tool for rapid *in vitro* sensitivity testing. The detection of ssDNA gap accumulation may be a useful predictive biomarker for response to USP1 inhibition as monotherapy or in combination in ongoing clinical trials.

EXPERIMENTAL AND MOLECULAR THERAPEUTICS: New Compounds and Drug Targets
Poster Session

#4648 Metabolic vulnerabilities of drug-resistant melanoma with therapeutic potential.

Y. Yu[1], L. Huang[1], W. Chen[2], G. Merlino[1];
[1]National Cancer Institute, Bethesda, MD, [2]National Institutes of Health, Bethesda, MD

Melanoma has been at the center of revolutions in both targeted BRAF therapy and immune therapy. However, the resistance to current therapeutic drugs has been a formidable obstacle to continuing benefit to patients. Overcoming resistance and new therapeutic agents and strategies are the primary goals of current cancer research. We currently found that metabolic pathways altered significantly in BRAFi-resistant melanoma. We hypothesized that BRAFi-resistant melanoma rewires its metabolic routes to reach its needs in energy and biosynthetic precursors, both essential for escaping the BRAFi attack. We found that five amino acids transporters and metabolic enzymes (ASNS, slc7a11, slc7a5, slc3a2, slc4a7) were the significant increase in resistant melanoma. Knockdown by shRNA or knockout by crispr/cas9 of these amino acids transporters or/and metabolic enzymes enhanced the sensitivity of BRAFi resistant melanoma to BRAFi. In contrast, overexpression of these amino acid transporters or/and metabolic enzymes promoted the ability of resistance of BRAFi in parent melanoma cells. Moreover, the inhibition of these amino acid transporters and metabolic enzymes by small molecular inhibitors significantly attenuated the resistance of the BRAFi-resistant melanoma whereas less affected the parent melanoma. Notably, we confirmed that blocking these amino acid transporters and metabolic enzymes by shRNA and/or small molecular inhibitors could rescue the sensitivity of resistant melanoma cells and inhibit resistant-melanoma cell growth in the preclinical mouse model in vivo. Importantly, we found that overexpression of slc7a11, slc7a5 and slc3a2 correlated with worse survival in melanoma in SK-TCGA data. Our findings uncovered the mechanism of how metabolic reprogramming fueled melanoma cell growth and proliferation for escaping drug attacks and offered a rational strategy to guide clinical treatment. The identified novel molecular proteins represented a promising therapeutic target for BRAF mutant melanoma patients with resistance to current therapy.

#4649 BLX-3030, a potent, selective, orally available small molecule CDK9 inhibitor for aggressive variant prostate cancers.

Z. Li, C. Lin, K. Medley, H. Vankayalapati, D. J. Bearss;
Biolexis Therapeutics Inc., American Fork, UT

Background: The use of novel, potent targeted therapies in prostate cancers has led to the development of highly aggressive variant cancers, including neuroendocrine prostate cancer (NEPC). Gene amplification of N-MYC and C-MYC oncogenes leads to its overexpression in NEPC and mCRPC patients, highly prevalent in these lethal subtypes of cancers detected in 2% of all Prostate Cancers (PCa) and over 10-17% of mCRPC patients. N-MYC is a transcriptional target of CDK9, which acts as an oncogenic driver sufficient to transform human-derived prostate cancer to take on NEPC phenotypic changes resulting in a more aggressive disease identified in late-stage human PCa patients. Additionally, N-MYC and C-MYC are required for tumor drug resistance, and their downregulation through CDK9 inhibition lowers tumor growth. Our efforts have demonstrated that targeting both N-MYC and C-MYC as a driver of NEPC and mCRPC with highly selective CDK9 inhibitor BLX-3030 is a viable approach for therapeutic intervention of mCRPC and NEPC.

Materials and Methods: Our empirical data-driven AI/ML MolecuLern™ fragment library, workflows, LigEdit design strategies, and hit2-lead optimization methods are employed. I*n vitro* experiments include kinase glo, cell titer glo, selectivity profiler, ADME-Tox, FACS/apoptosis, cell migration, live cell imaging, immunofluorescent, western blot, combination studies and *in vivo* experiments including PK, prostate tumor models, 7-day tox, BLX-3030 non (GMP) scaleup and safety pharmacology experiments conducted.

Results: We synthesized a series of novel small molecule CDK9 inhibitors that reversibly bind to CDK9, competitively block the ATP site with an IC_{50} of 1.06 nM, and elicit pharmacological responses in N-MYC, C-MYC, and other prostate cancer cells *in vitro* and *in vivo*. We studied the CDK9 N-MYC expression detected in PC-3, DU-145, LNCaP, and in LASCPC-01, NCI-H660, and 22RV1 cell lines. BLX-3030 exhibited potent cellular efficacy with an IC_{50} of 22 to 590 nM in PC cell lines and in N-MYC expressed cells had an activity of 76, 470, and 132 nM respectively, and reduced *p*CDK9, C-MYC, Mcl-1, N-MYC and its downstream RNA Pol II (Ser-2) and *p*AR (Ser-81) dose-dependently. BLX-3030 exhibits in vivo antitumor activity in LASCPC-01, 22RV1, and C4-2 prostate cancer mouse models. Several ADME-Tox, MTD, dose range finding, hERG and other in vivo safety pharmacology experiments have advanced BLX-3030 to the IND enabling studies.

Conclusions: BLX-3030 is currently being investigated in non-clinical toxicology, toxicokinetic, and core battery of safety pharmacology studies including the assessment of effects on cardiovascular, central nervous, and respiratory systems.

#4650 RalBP1, a novel approach for ovarian cancer therapy.

S. S. Singhal[1], S. Ramisetty[1], A. Mohanty[1], P. Kulkarni[1], D. Horne[1], S. Awasthi[2], R. Salgia[1];
[1]City of Hope National Medical Center, Monrovia, CA, [2]CTMH Doctors Hospital in Cayman Islands, George Town, Cayman Islands

Ovarian cancer (OC) is the most devastating gynecologic cancer. The ever-climbing incidence rate of OC makes it the most lethal female reproductive disorder. Triggering apoptosis is one of the potential strategies to overcome chemoresistance. Recent evidence suggests that the failure of drug-induced apoptosis may be an underlying cause of drug-resistance. Molecular mechanisms of failed apoptosis in chemoresistant OC cells include p53 mutations, abnormal expression of the Bcl2 family proteins, and upregulation of other inhibitors of apoptosis that block caspases and stabilize the mitochondrial permeability pore. RalBP1 (Ral-binding protein) is a required stress-defense protein for OC, and its specific depletion or inhibition will cause apoptosis in cancer cells expressing RalBP1. RalBP1 is a multifunctional 76 kDa protein encoded as a splice variant in the human *RALBP1* gene (18p11.22). RalBP1 is an ATP dependent efflux transporter for glutathione (GSH) conjugates (GS-E) of products of oxidative stress, like 4HNE and GSH-conjugates of chemotherapy drugs. Our recent studies indicate that upon depletion/inhibition of RalBP1, malignant cells are significantly more sensitive to apoptosis than non-malignant cells, suggesting that the stress-protective, anti-apoptotic activity of RalBP1 is necessary for malignant cells. This differential sensitivity to RalBP1 translates into tumor regression, a lack of toxicity, and the prolonged survival of mice bearing subcutaneous OC cells in which RalBP1 is inhibited by anti-RalBP1 IgG or depleted using RalBP1 antisense oligonucleotides. These studies demonstrate that inhibition or depletion of RalBP1 exerts anti-neoplastic effects in OC and indicate that this GS-E and xenobiotic transporter occupies an important position in the hierarchy of stress defense mechanisms necessary for cancer cell survival. Overall, the present research focuses on hypothesis-driven studies to define novel relationships between RalBP1 and signaling pathways, and to determine the suitability of RalBP1 as an anticancer target for OC.

#4651 A macrocyclic kinase inhibitor overcomes the compound mutations that cause the resistance to all approved EGFR inhibitors in EGFR-positive lung cancer.

R. Katayama, K. Uchibori, M. Nishio, N. Fujita;
Japanese Foundation for Cancer Research, Tokyo, Japan

EGFR mutant cancers account for 20-30 % of non-small cell lung cancers and show marked sensitivity to EGFR tyrosine kinase inhibitors (TKIs). However, the tumor almost inevitably relapses due to acquired resistance. To date, several EGFR-TKIs have been approved, and the third-generation EGFR-TKI, osimertinib, has been widely used both as first-line therapy and for patients with the EGFR-T790M mutation after 1st or 2nd generation EGFR-TKI therapy. However, the EGFR-T790M+C797S compound mutation confers resistance to all approved EGFR-TKIs. In our previous study, we experimentally demonstrated that brigatinib with anti-EGFR antibody was effective against osimertinib-resistant EGFR-C797S and EGFR-T790M+C797S mutants, and is currently undergoing clinical studies. However, the tumor would relapse because of the acquisition of additional resistance mutations. Here, we first demonstrated the binding mode of brigatinib to the EGFR-T790M/C797S mutant by crystal structure analysis and predicted brigatinib-resistant mutations through a cell-based assay, including N-ethyl-N-nitrosourea (ENU) mutagenesis. We found that clinically reported L718 and G796 compound mutations appeared, consistent with their proximity to the binding site of brigatinib, and brigatinib-resistant quadruple mutants, such as EGFR-activating mutation/T790M/C797S/L718M, were resistant to all clinically available EGFR-TKIs. BI-4020, a fourth-generation macrocyclic EGFR inhibitor plus anti-EGFR antibody, overcomes the quadruple and major EGFR-activating mutants in vitro and in vivo, but not the minor mutants such as L747P. Microsecond molecular dynamics simulations revealed the binding mode and affinity between BI-4020 and the EGFR mutants. This study identified potential therapeutic strategies using new-generation macrocyclic EGFR inhibitor to overcome the emerging resistance mutants.

#4652 Combined inhibition of MCL-1 and MEK reduces tumor growth in a triple-negative/inflammatory breast cancer, MEK-resistant xenograft mouse model.

M. Mughees[1], A. Tan[1], L. Iles[1], M. White[2], D. Tripathy[1], S. Krishnamurthy[1], J. Wang[1], W. A. Woodward[1], G. Bartholomeusz[1], C. Bartholomeusz[1];
[1]UT MD Anderson Cancer Center, Houston, TX, [2]AstraZeneca, Waltham, MA

Background: Triple-negative breast cancer (TNBC) and inflammatory breast cancer (IBC) are highly aggressive subtypes of invasive breast cancer. Our previous work showed that the MEK inhibitor (MEKi) selumetinib (AZD6244) prevents lung metastasis in a xenograft model. However, clinical studies have shown that MEKi's as single agents have only modest activity against solid tumors. Using a genome-wide synthetic lethal siRNA screening, we identified myeloid cell leukemia-1 (*MCL1*) as a potential contributor to selumetinib resistance. MCL-1 is an anti-apoptotic protein associated with cell immortalization, transformation, and chemoresistance in numerous cancers. We hypothesized that MCL-1 promotes MEKi resistance in TNBC/IBC and inhibition of MCL-1 in the presence of AZD6244 overcomes this MEKi resistance.

Methods & Results: To understand MCL1's role in MEKi resistance, we established two AZD6244 -resistant TNBC/IBC cell lines: MDA-MB-231-R and SUM149-R. These cells showed increased cell viability, colony formation, migration, cells in G1 phase, $CD44^{+}CD24^{low}$, mammosphere count, anchorage-independent growth and high MCL-1 expression. MCL-1's biological role was evaluated by transient and stably knock down (KD) of MCL-1 in the resistant cells which showed decreased cell viability, colony formation, and increased apoptosis. To understand the mechanism mediating apoptosis, we examined the expression of MCL-1's binding partners in the MCL-1-KD-R cells in the presence of AZD6244. These cells showed a high expression of the PUMA, NOXA, BAK, and BAX in the presence of AZD6244. Further, we treated resistant cells with MEKi AZD6244 and an MCL-1i (AZD5991) that confirmed restoration of MEK sensitivity in both resistant cell lines, resulting in decreased cell viability, colony formation and increased apoptosis. We compared tumor formation capability between SUM149 parental and SUM149 resistant cells by injecting them in *nu/nu* mice and observed a time-dependent increase (avg. 4-fold) in tumor growth with SUM149-R cells compared to parental cells ($P \leq 0.0001$). Moreover, IHC analysis showed high expression of MCL-1 ($P \leq 0.01$), Ki67 (ns), CD44 ($P \leq 0.0001$), and ALDHA1 ($P \leq 0.0001$) in the mammary gland tumor tissues of SUM149-R-injected mice compared to SUM149-P-injected mice. Next, we evaluated the therapeutic effect of AZD6244 in mice harboring SUM149-R - MCL-1-deficient tumors. AZD6244 treatment significantly reduced tumor development in mice harboring SUM149-R - MCL-1-KD tumors compared to control mice ($P<0.0001$), suggesting that MCL-1 mediates MEK resistance in triple-negative/inflammatory breast cancer.

Conclusion: Our results suggest that MCL-1 is important for inducing acquired MEK resistance and combining an MCL-1i with a MEKi could improve treatment outcomes of patients with TNBC or IBC who have developed resistance to single-agent MEKi.

#4653 Unraveling the vulnerabilities of targeted therapy-tolerant persister cells in NSCLC.

D. Kim[1], D. Kuchenov[1], A. Zaman[1], N. Bennett[2], E. Ramos[1], K. Nakamura[2], A. P. Wiita[1], S. Bandyopadhyay[1], T. Bivona[1];
[1]UCSF - University of California San Francisco, San Francisco, CA, [2]Gladstone Institutes, San Francisco, CA

Genetic profiling and the development of targeted therapy has improved survival of many cancer patients, but resistance to targeted therapy remains a major barrier to long-term patient survival. To develop more pro-active strategies to improve clinical outcomes, our research focuses on drug-tolerant persister cells that constitute a reservoir of cancer cells that survive and adapt during the initial stage of therapy. These cells typically display therapy resistance in a reversible manner and set the stage for the subsequent emergence of cells with full acquired resistance. We utilized quantitative proteomics to characterize persister cells generated from EGFRmut, KRASmut, and ALKmut non-small cell lung cancer (NSCLC) cell lines after treatment with osimertinib, sotorasib, and lorlatinib, respectively. Integrating proteomics data with network analysis revealed a decrease in the signaling network associated with cell cycle regulation and DNA replication. Meanwhile, persister cells exhibited an enrichment in proteins linked to lysosomes, amino acids, and fatty acid metabolism. The data revealed a consistent metabolic shift in persister cells, with an increased dependence on oxidative phosphorylation (OXPHOS) for ATP generation. Small-scale drug screening was performed based on findings from proteomics and confirmed that persister cells are vulnerable to inhibitors of OXPHOS mitochondrial complexes. Combination treatment of OXPHOS inhibitors and each targeted therapy delayed the emergence of resistance. One complex V inhibitor, Gboxin, selectively inhibited the growth of persister cells. The therapeutic potential of complex V was further validated by CRISPR-based genetic knockdown studies. The metabolic transition in drug tolerant persister cells may serve as a critical adaptive resistance mechanism to provide a survival advantage under targeted therapy-induced stress. Understanding this metabolic shift may lead to new treatments that aim to prevent or delay the onset of acquired resistance in NSCLC.

#4654 Targeting poly-resistant stem cells in high-grade serous ovarian cancer via synthetic lethal drugs.

Wa Xian[1], Frank McKeon[1], Christopher Crum[1], Jaffer Ajani[2], Peter Davies[3], Matthew Vincent[4], William Bachovchin[5], Hung-Sen Lai[5], Shuang Pan[5], Melina Khorrami[1], Melika khorrami[1], Raul caballero Montes[1], Paria Mosaffa[1], Ashley Hoffman[1], Amber Su[1]

[1]University of Houston, Houston, TX,[2]MD Anderson Cancer Center, Houston, TX,[3]Texas A&M, Houston, TX,[4]Tract Bio, Houston, TX,[5]Tufts University, Boston, MA

High-grade serous ovarian cancer (HGSOC) is remarkably responsive to chemotherapy and yet recurs at high rates as resistant disease. Using novel technology that selects for rare clonogenic cells which recapitulate HGSOC in immunodeficient mice, we have identified, in therapy-naive HGSOC, a minor population of clones that are intrinsically resistant to paclitaxel/carboplatin as well as to a broad spectrum of oncology drugs. These intrinsic "polyresistant" cells are a common, albeit minor, component of clonogenic cells in all therapy-naive tumors analyzed. Importantly, the polyresistant clonogenic cells share a gene expression signature distinct from the majority of clonogenic cells that are exquisitely sensitive to paclitaxel/carboplatin, and this gene signature of polyresistant cells extends to all polyresistant clones within a patient and across HGSOC cases. We have exploited these polyresistant clones to perform high-throughput screening of small molecule "bioactive" libraries to identify compounds that circumvent this resistance. While single agent "hits" were obtained, these showed minimal therapeutic windows relative to normal stem cells of the liver and gastrointestinal tract. Adaptations of synthetic lethal strategies have yielded lead drug combinations that eliminate polyresistant clones from all four cases tested at low nanomolar concentrations *in vitro*. We have improved these combinations via the synthesis of new chemical entities that show potent effects against both subcutaneous and peritoneal tumor models in immunodeficient mice derived from polyresistant HGSOC clones. Clonogenic analyses of these treated and untreated xenografts support the notion that these drug combinations are targeting the stem cell populations within these tumors. We anticipate that these drug combinations will assist in preventing or treating recurrent HGSOC.

#4655 Targeting FAK improves the tumor penetration of antibody-drug conjugates to strengthen the anti-cancer responses.

B. Zhang[1], Z. Zhang[2], J. Gao[1], S. Lu[1], R. Pang[1], D. Li[2], X. Huang[2], N. Qin[1], L. Liu[1], Z. Wang[1];
[1]InxMed (Shanghai) Co., Ltd., Shanghai, China, [2]WuXi AppTec, Shanghai, China

Antibody-drug conjugates (ADCs) such as HER2 ADC Enhertu and TROP2 ADC Trodelvy have been proved to be the promising therapeutic agents in portion of cancer diseases. However, there are still numerous patients refractory to the therapy, indicating that the efficacy of ADCs may need to be further optimized. Here, we report that the excessive cancer-associated fibroblasts (CAFs) can serve as a fibrotic barrier, to the detriment of anti-tumor effects from ADCs by alleviating their tissue penetration. Mechanistically, the cancer cells can transform the normal fibrotic cells into CAFs which are featured by the hyperactivated focal adhesion kinase (FAK) signaling. The fast-growing CAFs would decrease the tumor uptake of the big molecules, conferring drug resistance of ADCs to the cancer cells. Targeting FAK with a small molecule inhibitor IN10018 is capable to reduce CAFs associated tumor barrier, elevating the tissue penetration of different types of ADCs regardless their respective targets. The combination regimen comprising IN10018 and the ADCs targeting either HER2 or TROP2 outperformed each monotherapy with respect to antitumor outcomes in different animal experiments. The preclinical evidence for the dual regimen of IN10018 and ADCs warrants a further validation in clinical settings.

#4656 Novel mitochondria-based targeting overcomes resistance in prostate cancer.

Yan Ou[1], Adrian Lim[1], Ning Zhai[1], Mouad Edderkaoui[1], Stephen Pandol[1], Ruoxiang Wang[1], Yi Zhang[2]

[1]Department of Medicine, Cedars Sinai Medical Center, Los Angeles, CA,[2]Department of Biomedical Sciences, Cedars Sinai Medical Center, Los Angeles, CA

Background: Prostate cancer (PC) is a major contributor to cancer-related mortality in men, with metastatic castration-resistant PC (mCRPC) presenting a significant obstacle due to its resistance to standard treatments. Current therapies, including nonsteroidal antiandrogens and chemotherapy drugs, provide limited effectiveness and are often accompanied by severe side effects. Recently, statins have gained attention as antitumor agents, demonstrating chemopreventive effects on a range of human cancers while maintaining a well-established safety profile. However, the use of statins as standalone treatment is limited by insufficient cancer cell targeting.

Methods: We synthesized a DZ-simvastatin (DZ-SIM) conjugate that combines a near-infrared heptamethine carbocyanine dye (DZ) with simvastatin for selective tumor cell targeting. Cancer cell survival was measured by crystal violet and MTT assay. Co-localization of DZ-SIM with mitochondria and lysosome in cells was detected under confocal microscope using Mitotracker and Lysotracker. Cellular and mitochondrial cholesterol levels were detected by LC-MS. Male nude mice were inoculated subcutaneously with 22Rv1-Luc cells as a prostate cancer xenograft mouse model. We used Swiss-PDB and Rosetta algorithms to model the structure of the OATP1B3 channel. Oxygen consumption rate and extracellular acidification rate were measured by Seahorse assay. After treatment with DZ-SIM, differentially expressed genes profiling of prostate cancer cells was performed using RNAseq.

Results: Our research demonstrates the conjugate's ability to effectively kill androgen-independent and metastatic PC cells without harming normal cells. Furthermore, DZ-SIM has been shown to kill multiple human PC cell lines, regardless of androgen receptor status or therapeutic resistance. DZ-SIM has been shown to inhibit growth in human prostate cancer cell line xenograft models. NIR fluorescence imaging showed specific localization of DZ-SIM to cancer, but not to normal cells and tissues. It could localize into cancer cells by binding the transmembrane transporter OATP to primarily target subcellular organelle mitochondria, decreasing the OCR and ECAR of cancer cells. DZ-SIM can bind to multiple cytosolic and mitochondrial proteins as detected by NIRF imaging. Cholesterol levels also decrease in whole cells and mitochondria. Ingenuity Pathway Analysis (IPA) of RNAseq showed that the four signaling pathways in the DZ-SIM treatment group are significantly enriched in genes related to cholesterol synthesis.

Conclusion: DZ-SIM specifically targets PC cells and their mitochondria, resulting in loss of mitochondrial function and consequent cell death. With a unique subcellular targeting strategy, the conjugate holds the potential to outperform existing chemotherapeutic drugs.

#4657 PHI-501 is a novel potent next-generation pan-RAF/DDRs inhibitor, and overcomes resistance to RAF or MEK inhibitor in melanoma via dual inhibition of RAF and DDR1/2 signaling.

Sue Min Kim[1], Sungmin Cho[1], Gi-Jun Sung[2], Ky-Youb Nam[2], June Han[2], Sang Joon Shin[3]

[1]Yonsei University College of Medicine, Seoul, Korea, Republic of,[2]Pharos iBio CO., Ltd., Anyang, Korea, Republic of,[3]Division of Medical Oncology, Department of Internal Medicine, Yonsei Cancer Center, Yonsei University College of Medicine, Seoul, Republic of Korea, Seoul, Korea, Republic of

Background: The prevalent mutation of BRAF (~50%) and NRAS (~30%) in malignant melanomas has led to the aggressive development of RAF and MEK inhibitors as anticancer drugs. However, the major hurdle of targeted therapies for melanoma is resistance to RAF or MEK inhibitors, either intrinsic- or acquired-resistance. PHI-501 is an orally bioavailable and highly effective pan-RAF inhibitor. PHI-501 has dual inhibition activity against pan-RAF and discoidin domain receptor (DDR), a collagen-activated receptor tyrosine kinase. In this study, we evaluated the ability of PHI-501 to overcome drug-resistance to RAF or MEK inhibitors in melanoma harboring NRAS or BRAF mutations.

Methods: Three drug-resistant cell lines were established by long-term treatment of belvarafenib in SK-MEL-2 (SK-MEL2BR) and each of dabrafenib and trametinib in SK-MEL-3 (SK-MEL3DR and SK-MEL3TR, respectively). RNA-seq of each resistant cell line and in-depth analysis of sequencing data was conducted, including GSEA. The anti-proliferative activity and signaling inhibition of PHI-501 were evaluated by CCK-8 assay and western blots. A long-term clonogenic assay was performed to confirm cell survival upon PHI-501 treatment. In vivo efficacy was evaluated in SK-MEL-3DR cell line xenograft models.

Results: PHI-501 demonstrated significant anti-proliferative effects (GI50 < 1 μM, Mean GI50: 0.3 μM) in all 12 melanoma cell lines tested in this study. PHI-501 exerted cell growth inhibitory activities at least 3 to 50 times stronger than other RAF or MEK inhibitors in each of the resistance cell lines. Moreover, PHI-501 doses of less than 100 nM, significantly inhibited the colony formation of drug-resistant cells. Western blot revealed that PHI-501 retained strong inhibition of both ERK and AKT phosphorylation through downregulating pDDRs. In the SK-MER3DR xenograft mouse model, treatment of PHI-501 alone induced a rapid tumor reduction (TGI 72.1%), whereas the vehicle or dabrafenib did not display an anti-melanoma effect (TGI -7.4%). A comprehensive pathway analysis showed the TNFA-NFKB, IL6-JAK-STAT3, and KRAS signaling enriched in drug-resistant cells compared to the parental cells. PHI-501 treatment effectively downregulated those pathways in all three drug-resistant cells. In particular, PHI-501 downregulates the geneset in epithelial-mesenchymal transition (EMT) signaling more effectively in SK-MEL2BR, SK-MEL3DR, and SK-MEL3TR (Adjusted P=<.0001, and NES: -2.01, -1.72, -2.30, respectively).

Conclusion: Novel pan-RAF/DDR dual inhibitor PHI-501 has greater anti-tumor activity in RAF or MEK inhibitor-resistant melanoma, which is through downregulation of MAPK signaling and EMT-related genesets and promoting apoptosis. These data support that the clinical development of PHI-501 for melanoma refractory to MAPK inhibitors.

#4658 Genome wide CRISPR/Cas9 library screening identifies aurora kinase A as a regulator of elraglusib sensitivity in pancreatic cancer.

L. Ding[1], E. Maeder[1], C. Zhang[1], T. Weiskittel[1], D. Schmitt[2], A. Mazar[2], H. Li[1], D. Billadeau[1];

[1]Mayo Clinic, Rochester, MN, [2]Actuate Therapeutics, Inc, Fort Worth, TX

Pancreatic ductal adenocarcinoma (PDAC) is a deadly malignancy with a dismal 5-year survival rate, highlighting the urgent need to improve drug response and overcome primary or acquired (secondary) resistance to conventional chemotherapy. Glycogen synthase kinase 3β (GSK-3β) is a target in PDAC and the GSK-3 inhibitor, elraglusib, has been shown to improve chemosensitivity of PDAC and survival in preclinical cancer models. In addition, data from phase II clinical trials in patients with previously untreated metastatic pancreatic cancer is demonstrating preliminary evidence of clinical benefit in patients receiving a combination of gemcitabine/nab-paclitaxel. While this early evidence is highly encouraging, the biological determinants of elraglusib response are unknown. Using genome wide CRISPR/Cas9 library screening, we identify aurora kinase A (AURKA), an oncogenic kinase with major roles in mitosis, as a critical regulator for elraglusib sensitivity. Elraglusib treatment activates AURKA by inducing a G2/M cell cycle arrest. We show that knocking out AURKA reduces the phosphorylation of polo like kinase 1 (PLK1), arresting cells in mitosis, and leading to mitotic catastrophe and significant apoptosis after elraglusib treatment. Strikingly, the AURKA inhibitor, alisertib, works synergistically with elraglusib to inhibit PDAC cell line growth and induce apoptosis. In summary, our results demonstrate that targeting AURKA is an effective approach to sensitize PDAC tumors to elraglusib.

#4659 A genome-wide CRISPR screen identifies *ARID1A* as a potential resistance marker of IDH1 inhibitor in *IDH1*-mutant cholangiocarcinoma cell.

T. Kondo[1], O. Kikuchi[2], Y. Wang[1], Y. Nakai[1], T. Ida[1], Y. Cao[1], T. H. N. Vu[2], Y. Kondo[1], T. Sunami[1], Y. Yamamoto[1], T. Saito[1], S. Kataoka[1], A. Yamada[1], M. Kanai[1], S. Ohashi[1], M. Muto[1];

[1]Kyoto University Graduate School of Medicine, Kyoto, Japan, [2]Kyoto University Center for Immunotherapy and Immunobiology, Kyoto, Japan

Background: Isocitrate dehydrogenase 1 (*IDH1*) mutations have been identified in approximately 20% of intrahepatic cholangiocarcinoma cases. These predominant gain-of-function mutations at codon 132 lead to abnormal production of the oncometabolite D-2-hydroxyglutarate. Targeted pharmacological disruption of the *IDH1* mutation demonstrates tumor growth inhibition in *IDH1*-mutated cholangiocarcinoma. However, the efficacy of an IDH1 inhibitor (AG-120) as monotherapy for *IDH1*-mutated cholangiocarcinoma has been proven clinically insufficient, suggesting a need for investigating predictive biomarkers. In this study, we employed a genome-wide CRISPR screen to pursue resistance mechanisms to pharmacological IDH1 inhibition.

Methods: The screening utilized SNU1079 cells harboring the *IDH1* R132C mutation and the Brunello genome-wide CRISPR knockout (KO) pooled library (Addgene #73178, Broad Institute GPP, 4 guides/gene). The read couns of sgRNAs were normalized to reads per million, and then log2 was transformed. The log fold change (LFC) of each sgRNA of the AG-120-treated group was determined relative to that of the DMSO-treated group. Hypergeometric distribution was used to determine statistical significance. P values per gene were calculated as the average -log10(P value) of individual sgRNAs. We validated the CRISPR screening outcomes *in vitro* using both *IDH1*^{R132C} mutant (SNU1079) and *IDH1*^{R132S} mutant (RBE) cells by WST-1 assays, clonogenic assay and competition assay. (Tsujino T et al. *Nat Commun*. 2023) In competition assay, GFP was constitutively expressed in *ARID1A*-knockout cells and cultured together with *ARID1A* intact cells, under treatment with 1 μM AG120 or DMSO for 21 days. Relative cell numbers of GFP-positive (*ARID1A*-KO) cells in comparison with GFP-negative (*ARID1A* intact) cells were quantified using a BD LSRFortessa Analyzer (BD Biosciences).

Results: Based on a volcano plot analysis, we identified three genes (*SMCHD1*, *ARID1A*, and *PGP*) with LFC > 1.5. Following a recent report of frequent *ARID1A* alteration (20%; 84/412) in a clinical study (Boerner, et al. *Hepatology*. 2021), we focused our research on *ARID1A* (LFC = 1.531; $-\log_{10} P = 3.75$). WST-1 assays and clonogenic assays as short-term (3-7 days) assays failed to validate the results of CRISPR screening; however, in competition assays under treatment with AG120, cells with *ARID1A*-KO exhibited significantly greater proliferation in comparison with *ARID1A* intact cells in two different cell lines (SNU1079, RBE).

Conclusions: The results demonstrated that ARID1A disruption reduced the efficacy of the IDH1 inhibitor against *IDH1*-mutatedcholangiocarcinoma cells. Based on these findings, we are planning comprehensive analyses employing *in vivo* models and clinical data to substantiate these observations.

#4660 Characterization of a nicotinamide-based kinase inhibitor HSN748 for inhibition of RET-driven tumors.

U. Khatri[1], N. Dayal[2], T. Shen[1], X. Hu[1], H. Sintim[2], J. Wu[1];
[1]University of Oklahoma Health Sciences Center, Oklahoma City, OK, [2]Purdue University, West Lafayette, IN

Rearranged during transfection (RET) is a protein tyrosine kinase that is aberrantly activated by gene fusions or mutations in many types of human cancer including thyroid cancer and non-small cell lung cancer (NSCLC). Selpercatinib (LOXO-292) and pralsetinib (BLU-667) are FDA approved RET-selective tyrosine kinase inhibitors (TKIs) being used to treat RET-altered cancer. However, these tumors develop selpercatinib/pralsetinib-resistance via acquisition of RET(G810C/R/S) mutations located at the solvent front of the ATP binding pocket. The overall goal of our research is to discover next-generation of RET kinase inhibitors to inhibit selpercatinib/pralsetinib-resistant RET solvent-front mutants. In this study, we characterized one of the nicotinamide-based RET kinase inhibitor, HSN748, *in vitro* and *in vivo*. HSN748 was able to inhibit selpercatinib/pralsetinib-resistant RET(G810C/R) solvent-front mutations. In BaF3/KIF5B-RET(G810C) tumor xenograft experiment, HSN748 treatment resulted in tumor regression. In immune competent transgenic mice, KIF5B-RET-induced lung tumors regressed after HSN748 treatment by oral gavage for one month (10-15 mg/kg, QD) without affecting body weight. These results identify HSN748 as an orally available RET inhibitor capable of inhibiting KIF5B-RET and its solvent-front mutant-driven tumors.

#4661 A dual degrader of HER2 and EGFR obliterates oncogenic signaling, overcomes therapy resistance, and inhibits metastatic lesions in HER2-positive breast cancer models.

L. Yang[1], A. Bhattacharya[1], D. Peterson[1], Y. Li[1], X. Liu[2], E. Marangoni[3], V. Robila[1], Y. Zhang[4];
[1]Virginia Commonwealth University, Richmond, VA, [2]Roswell Park Comprehensive Cancer Center, Buffalo, NY, [3]Institute of Curie, Paris, France, [4]Massey Comprehensive Cancer Center, Virginia Commonwealth University, Richmond, VA

Background: HER2 is an oncogenic receptor tyrosine kinase (RTK) implicated in several types of human cancer. It is strongly expressed in about 20% of breast cancer (BC), known as HER2-positive BC (HER2+ BC), due to gene amplification. HER2 amplification or overexpression is a strong predictor of poor disease prognosis. HER2-targeted therapies are the linchpin of treating HER2+ BC. However, drug resistance is common. The main resistance mechanism is unknown. We exploited cell lines and mouse models (orthotopic patient-derived xenografts, and metastatic lesions in the brain and lung of therapy-resistant HER2+ BC) for experiments of genetic and pharmacologic depletion of HER2 and its family member EGFR, analysis of RTKs and no-RTKs, and evaluation of cell and tumor growth, to delineate the mechanism of HER2+ BC resistance to HER2 inhibitors and assess the therapeutic activity of $PEPD^{G278D}$. $PEPD^{G278D}$, a recombinant human protein, is the first-in-class dual degrader of HER2 and EGFR.
Results: Trastuzumab-resistant HER2+ BC cells and tumors are highly vulnerable to targeted degradation of HER2 and EGFR. Trastuzumab is the most commonly used HER2 inhibitor in the clinic. Targeted degradation of HER2 and EGFR by $PEPD^{G278D}$, which binds to their extracellular domains, causes extensive inhibition of oncogenic signaling proteins in HER2+ BC cells resistant to trastuzumab. This is accompanied by strong growth inhibition of cultured cells, orthotopic patient-derived xenografts, and metastatic lesions in the brain and lung of trastuzumab-resistant HER2+ BC. siRNA knockdown shows that eliminating both HER2 and EGFR is important to maximize therapeutic outcome. Collectively, our results reveal the key vulnerability of trastuzumab-resistant HER2+ BC and shows a promising strategy that overcomes trastuzumab resistance by targeting this vulnerability.
Conclusions & Therapeutic Relevance: This study identifies a key therapeutic vulnerability of drug-resistant HER2+ BC and shows that an agent that targets this vulnerability is highly effective in overcoming drug resistance in this disease. The findings provide new insights and innovations to advance treatment of drug-resistant HER2+ BC that remains an unmet problem.

#4662 High-throughput screening identifies potential combinatorial therapies to overcome lenvatinib resistance in liver cancer.

K. Chau, M. S. J. McDermott, K. Gong, D. J. Slamon;
UCLA - University of California Los Angeles, Los Angeles, CA

Liver cancer has seen an increase in mortality rate over recent decades due to limited targeted therapies and growth in specific etiologies. Lenvatinib, a multi-TKI inhibitor, is used as a first-line therapy for liver cancer patients who cannot receive immunotherapy, which is a component of the current standard of care. Unfortunately, lenvatinib efficacy is short. Understanding why liver cancers become resistant and identifying interventions to restore sensitivity can help prolong the clinical efficacy of lenvatinib. A panel of 20 liver cancer lines was screened to identify four lenvatinib-sensitive lines. These lines were subsequently conditioned to grow under increasing lenvatinib concentrations to generate lenvatinib-resistant (LR) models. One such model, Hep3B LR, exhibited a stable resistance to lenvatinib for up to 12 weeks in culture. Hep3B LR showed cross-resistance to selective inhibitors of FGFR4 and FGFR1 but not of MAPK14 and PDGFR, suggesting that the resistance phenotype may result from FGFR dysfunction. Unlike parental Hep3B, Hep3B LR exhibited a 3.4X increase in migration. Western blot detected an increase in pAKT, a survival marker. Additionally, proteins associated with cancer drug resistance were higher in Hep3B LR cells: Notch receptors and ligands, pStat3, and Axl. To identify means of overcoming lenvatinib resistance in Hep3B LR, a Cell-Titer Glo high-throughput assay was developed to measure the growth inhibition of candidate drugs in the presence and absence of lenvatinib. Preliminary results from the first 24 drugs screened reproduced known drug sensitivities associated with lenvatinib resistance (i.e., MEK/ERK, EGFR, GPX4 inhibition) but also identified novel sensitivities to inhibition of PKMYT1 or γ-secretase, the latter a cleavage enzyme involved in Notch signaling activation. Validation of these candidate hits using a grid-based titration of both drugs showed additive growth inhibition of lenvatinib in combination with ERK, EGFR, or GPX4 inhibitors but not with PKMYT1 or γ-secretase inhibitors in resistant cells. Interestingly, EGFRi and lenvatinib were substantially synergistic in parental cells, suggesting that an upfront combination of these inhibitors could potentially be used before the emergence of lenvatinib resistance in liver cancer. We have established a lenvatinib-resistant liver cancer cell model and validated a drug screening assay to identify potential combinatorial therapies to overcome lenvatinib resistance in liver cancer.

#4663 Establishing the role of PRMT5 in lung cancer tumorigenicity and modulation of expression in smokers.

Syed N. Ali, Meet Patel, Bamby Dieng, Cody Lund, Neelu Puri

University of Illinois College of Medicine Rockford, Rockford, IL

Studies show that PRMT5 (protein arginine methyl transferase 5) is responsible for increased tumorigenicity by activation of the PI3K/Akt signaling pathway promoting increased cancer cell proliferation. However, the role of PRMT5 in modulating EGFR TKI resistance is minimally studied. We hypothesize that over-expression of PRMT5 could promote tumorigenesis and TKI resistance by activating PI3K-Akt-mTOR signaling pathways. Hence, modulating this key biomarker may help reduce tumorigenicity and overcome TKI resistance. We performed qPCR to study the expression of PRMT5 in normal lung cells and NSCLC cell lines. We also compared the expression of these biomarkers in erlotinib resistant (ER) and Osimertinib resistant (OR) cells using Western blotting. PRMT5 was inhibited using GSK591 (PRMT5i) to evaluate its sensitivity to EGFR TKIs (ER and OR). PRMT5 expression in normal lung cells and NSCLC cells treated with Cigarette smoke extract (CSE) were also studied and correlated with immunostaining results from smoker and non-smoker lung tumor tissue samples. Changes in PRMT5 expression were analyzed in WT-EGFR lung cancer cell lines (H358, H2170), mutant EGFR lung cancer cell lines (H3255, H1975, PC9) and normal lung fibroblast cells (HLF). PRMT5 expression was upregulated by 1.6-2.1 fold in HLF, H2170 and H358 cells after 1 week of treatment with CSE. CSE treatment also upregulated expression of inflammatory cytokines (IL-1β, IL-8 and TNF-α) in H358 cells by 1.6-7 fold as analyzed by qPCR. PRMT5 expression was upregulated in EGFR-TKI resistant cell lines, by 1.5-1.9 fold in PC9ER, PC9OR and H2170ER cells, compared to parental cells. Similar results were found using qPCR, with 1.6-2.3 fold increase in PRMT5 mRNA expression in H2170OR, PC9ER/OR and H3255OR cells compared to parental cells. An MTT assay was done to assess percentage viability of cells after treatment of PRMT5i. While 2μM PRMT5i treatment of PC9OR cells decreased cell viability by 42%, an inhibitory effect that was more than additive was seen with a combination of 2μM of PRMT5i and 21nM of OR. Similar results were also observed in H2170ER cells. Migratory properties of OR resistant cells, were studied by wound healing assays. Percentage wound area in PRMT5i treated PC9OR cells was 29.3% as compared to 6.1% and 10.5% in diluent and OR treated cells respectively after 48 hrs. Combination treatment of PRMT5i and OR further inhibited cell migration with higher wound area of 41.7%. Immunostaining of lung tumor sections from smokers and non-smokers showed high expression of PRMT5 localized in the cytoplasm and nucleus. Microscopic analysis of 20 tumor sections from smokers showed higher expression of PRMT5 ($p<0.05$) compared to non-smokers. We can conclude that PRMT5 is upregulated in TKI resistant cells causing tumorigenesis. Modulation of PRMT5 can prove to be groundbreaking and revolutionary, as it may increase the efficacy of EGFR TKIs.
[S.N.A. and M.P. contributed equally to this work.]

#4664 Therapeutic targeting of *TP53*-mutated acute myeloid leukemia by inhibiting cell cycle checkpoint.

D. Gwak, D. Kim, H. Jang, J. Liu, S. Min, J. Byun, Y. Koh, J. Hong, S.-s. Yoon, D.-Y. Shin, Department of Internal Medicine, Seoul National University Hospital, Seoul, Korea, Republic of;
Seoul National University, Seoul, Korea, Republic of

Acute myeloid leukemia (AML) is a hematological malignancy characterized by various somatic mutations leading to abnormal proliferation and differentiation of hematopoietic cells. Mutations on the *TP53* gene occur in 5% to 10% of patients with *de novo* AML, with higher frequency in patients with relapsed and refractory (R/R) AML. Patients with *TP53*-mutated AML typically exhibit a poor response to conventional induction therapy and have a short overall survival (OS) rate, with a median duration of 5-9 months. Although various target agents have been developed for the treatment of AML, treatment options for *TP53*-mutated AML remain limited. Here, we have discovered a novel drug combination that can enhance the efficacy of the conventional therapeutic regimen for *TP53*-mutated AML patients. For *in vitro* analysis, we used the human AML cell line Kasumi-1(AML-M2), which harbors a homozygous *TP53* R248Q mutation. We treated kasumi-1 cells with a combination of cytarabine and Idarubicin to produce drug tolerant persisters (DTPs) which is a minor population that survived the drug treatment. The Kasumi-1 DTPs displayed temporal G2/M phase cell cycle arrest and significant resistance to further repeated drug treatment. To discover drug candidates targeting *TP53*-mutated DTPs, we first examined the differentially expressed genes (DEGs) of *TP53*-mutated AML patients using patients' RNA expression data deposited in the cancer genome atlas (TCGA) database. Using selected DEGs, drug candidates potentially affecting *TP53*-mutated AML cells were extracted from the connectivity map (CMap build 02) database. In addition, through a literature search, drugs with the ability to reactivate mutant p53, drugs that directly target mutant p53, synthetic lethal partners with mutant p53, and drugs that target leukemia stem cells were selected as candidate groups. As a result, we selected 46 drug candidates that would be effective for *TP53*-mutated AML through *in silico* analysis and therapy strategies targeting p53. Using *in vitro* cytotoxicity assay, we screened 46 candidate compounds at multiple doses and confirmed several drugs that effectively eliminate DTPs. The drug screening showed that cell cycle checkpoint inhibitors not only resulted in a significant reduction of G2/M phase arrested cells but also induction of apoptotic cells at the subG1 phase. Furthermore, the zero interaction potency (ZIP) model of SynergyFinder (https://synergyfinder.fimm.fi) analysis showed that cell cycle checkpoint inhibitors synergistically enhanced the cytotoxic effect of cytarabine on Kasumi-1 DTPs. Collectively, this study suggests that novel combination treatment of cell cycle checkpoint inhibitors with conventional drugs selectively inhibits *TP53*-mutated AML DTPs.

#4665 USP18 promotes anlotinib resistance in medullary thyroid carcinoma by stabilizing aurora B kinase.

X. Qin[1], X. Wan[1], D. Li[1], Y. Liu[1], X. Ruan[1], F. Luan[2], K. Xu[2], J. Li[2], R. Xiang[2], Y. Piao[2], Y. Shi[2], X. Zheng[1];
[1]Tianjin Medical Univ. Cancer Inst. & Hospital, Tianjin, China, [2]Nankai University, Tianjin, China

Targeted therapy resistance is the main cause of disease progression in advanced medullary thyroid carcinoma (MTC). However, the key molecules and mechanisms remain unclear. We previously performed a genome-wide in vitro screen of Anlotinib resistance-related genes in human MTC cell line TT using CRISPR-dCas9-SAM system and identified ubiquitin-specific protease 18 (USP18) as a key molecule mediating Anlotinib resistance in MTC. However, its downstream mechanism needs further clarification. Based on the high-throughput DNA sequencing results of the control group and the Anlotinib screening group, a group of key genes related to Anlotinib resistance in MTC was screened through the MAGeCK algorithm and the enrichment ratio of sgRNA in the Anlotinib screening group. Among them, USP18 ranked first in the enrichment results. Analysis of the correlation between the expression level of USP18 in MTC patient specimens and survival revealed that patients with high USP18 expression in tumor cells had poorer prognosis. Overexpression of USP18 in MTC tumor cells significantly promoted the growth of subcutaneous xenograft tumors in NOD/SCID mice treated with Anlotinib. In vitro cell experiments also showed that overexpression of USP18 promoted the proliferation of MTC tumor cells and significantly inhibited the proportion of cell apoptosis after Anlotinib treatment. Further research found that USP18, as a deubiquitinating enzyme that can specifically remove ISG15-like ubiquitin-like proteins from substrate proteins, can improve the kinase stability of Aurora B by removing ISG15-like ubiquitin modification and promote MTC tumor cell proliferation through the activation of PI3K-Akt signaling regulated by Aurora B kinase. Application of Aurora B kinase inhibitor in Anlotinib-resistant MTC cell lines significantly inhibited tumor cell proliferation, and Aurora B kinase inhibitor significantly increased the proportion of cell apoptosis in MTC tumor cells overexpressing USP18. In the subcutaneous xenograft tumor model of MTC in NOD/SCID mice, the growth of xenograft tumors in the Anlotinib combined with Aurora B kinase inhibitor treatment group was also significantly inhibited. In summary, overexpressed USP18 can activate PI3K-Akt signaling and promote tumor cell proliferation by increasing the stability of Aurora B kinase, ultimately leading to the formation of Anlotinib resistance in MTC patients. Combined use of Aurora B kinase inhibitor is a potentially effective combined treatment strategy for Anlotinib-resistant MTC patients.

#4666 HC-7366, a potent GCN2 kinase activator, augments osimertinib therapy to delay resistance in EGFR mutant NSCLC models.

C. Dudgeon, S. Fujisawa, O. Funk, F. Tameire, T. O. Kangas, W. Zhang, E. S. Lightcap, D. Surguladze, N. Bose;
HiberCell, Roseville, MN

Despite the efficacy seen with EGFR tyrosine kinase inhibitors (TKIs) in the treatment of EGFR mutant NSCLC, the long-term prognosis remains unfavorable due to resistance. Osimertinib is used as the first- and second-line treatment for EGFR exon 19 deletion, L858R mutation, and acquired T790M mutation. Resistance is driven by both EGFR-dependent and independent events, such as gene amplification and upregulation of HIF1α. Metabolic events also drive resistance by increasing oxidative phosphorylation (OXPHOS) caused by osimertinib-induced glycolysis inhibition. HiberCell has developed HC-7366, a GCN2 activator currently being investigated in a Ph1 clinical trial in patients with solid tumors (NCT05121948). GCN2 activation by HC-7366 drives the integrated stress response (ISR) by inducing the expression of ATF4. This results in translation inhibition, cell cycle arrest, HIF1α suppression, and apoptosis in cancer cells. Our preclinical data suggest HC-7366 can reduce glycolysis, TCA cycle metabolites, and OXPHOS, thereby causing mitochondrial dysregulation. We hypothesized that combination of HC-7366 with osimertinib could reduce resistance by evading the adaptive resistance mechanisms. We treated the NCI-H1975 xenograft model with HC-7366, a clinically relevant dose of osimertinib, and the combination for 21 days and then followed for tumor regrowth. At day 21, the HC-7366 group showed efficacy with tumor growth inhibition (TGI) of 55%, while osimertinib resulted in tumor regression of 97% with 8/10 CRs and 2/10 PRs. The combination had tumor regression of 99% with 10/10 CRs. After treatment cessation for 74 days, tumors in the osimertinib group quickly regrew with 6/10 tumors progressing and 4/10 mice tumor-free. In contrast, the combination group had only 2/10 tumors regrow with 8/10 mice tumor-free. In an EGFR-dependent resistance model NCI-H1975 (EGFR C797S), combination achieved 63% TGI versus 31% with osimertinib. In an EGFR-independent resistant PDX with EGFR exon 19 deletion, combination benefit was seen at 70% TGI compared to 40% for osimertinib, while a PDX with EGFR L858R showed a trend for combination benefit. To understand the mechanism of action, we examined osimertinib-resistance pathways to determine how GCN2 activation could affect them. Combination with HC-7366 reduced the expression of short-lived proteins involved in osimertinib resistance, including HIF1α, MET, cyclin D1, and CDK4. Combination decreased TIM17A and TIM23, proteins essential for mitochondrial protein translocation, potentially causing mitochondrial dysfunction. We found a proliferation reduction by Ki67 and an increase in apoptotic proteins CHOP, PUMA, and cleaved caspase 3. Taken together, these data reveal that combination of HC-7366 and osimertinib, and potentially other EGFR TKIs, may be an effective treatment strategy at targeting adaptive resistance mechanisms.

#4667 HDAC9 as a potential regulator of lenvatinib resistance in hepatocellular carcinoma.

Y. Xie[1], M. Zhang[1], Y. Liu[1], L. Liu[1], A.-L. Cheng[1], S. Ma[2], M. Tong[1];

[1]The Chinese University of Hong Kong, Shatin, NT, Hong Kong, [2]The University of Hong Kong, Pok Fu Lam, Hong Kong Island, Hong Kong

Lenvatinib is used as the first-line therapy for advanced hepatocellular carcinoma (HCC) patients. However, poor response and compromised therapeutic effect with prolonged treatment are frequently observed in HCC patients. To elucidate the underlying mechanisms, lenvatinib responsive and non-responsive stages were modeled in liver tumor-bearing immunocompetent mice which were divided into lenvatinib and vehicle control treatment groups. Tumor tissues after short and prolonged lenvatinib treatment were harvested for single-cell RNA sequencing. Results from single-cell RNA sequencing revealed heterogenous tumor cell sub-populations associated with tumor differentiation and identified an upregulated expression of class IIa histone acetylase HDAC9 in lenvatinib-treated tumor at the non-responsive stage. Upregulation of HDAC9 was similarly observed in lenvatinib-resistant human patient-derived xenograft (PDX). Functional studies suggested that suppressing HDAC9 could re-sensitize lenvatinib response in both in vitro and in vivo models. In sum, we identified a potential regulator of lenvatinib treatment response in HCC.

#4668 Characterization of fourth-generation EGFR inhibitors in binding experiments with C797S mutant EGFR and cell-based assays with osimertinib-resistant non-small cell lung cancer cell lines.

J. J. T. Melis[1], K. Kevenaar[1], J. J. Kooijman[1], Y. Grobben[1], J. Ytsma[1], J. Bertran-Alamillo[2], M.-A. Molina-Vila[2], N. Willemsen-Seegers[1], G. J. R. Zaman[1]; [1]Oncolines B.V., Oss, Netherlands, [2]Pangaea Oncology, Barcelona, Spain

Osimertinib is a third-generation epidermal growth factor receptor (EGFR) tyrosine kinase inhibitor that inhibits the EGFR kinase domain by irreversible binding of the cysteine-797 residue (C797). Osimertinib was originally designed to target the T790M mutation, which is clinically the most frequently observed resistance mechanism to treatment with first- or second-generation EGFR inhibitors. Osimertinib has a high selectivity for the classical EGFR driver mutations (exon 19 deletion and L858R) compared to wild-type EGFR. Due to this favorable selectivity profile, osimertinib has become the standard first-line therapy for non-small cell lung cancer (NSCLC).

Common resistance mechanisms following osimertinib treatment are *MET* oncogene amplification, and cysteine-to-serine substitution at position 797 (C797S) of EGFR, which precludes binding of osimertinib. Fourth-generation EGFR inhibitors and combinations with other targeted agents are potential strategies to overcome osimertinib resistance or to increase its efficacy.

Three fourth-generation EGFR inhibitors were profiled in biochemical and cell-based assays: BDTX-1535, BLU-945, and JBJ-09-063. The binding kinetics for wild-type and C797S mutant EGFR were determined in surface plasmon resonance binding experiments on a Biacore 1S+ (Cytiva). The effect on osimertinib-resistant cells, generated using two different approaches, was studied in cell viability assays. In the first model, subclones of the NSCLC cell line PC-9, harboring an exon 19 deletion activating EGFR mutation, were selected for osimertinib resistance by *in vitro* drug selection [1]. In the second model, the EGFR C797S mutation was introduced into the NSCLC cell line NCI-H1975, which expresses both the L858R activating mutation and the T790M resistance mutation, by gene-editing with CRISPR-Cas9. Synergies with fourth-generation EGFR inhibitors were determined by profiling combinations in a 6-by-6 matrix, and quantifying synergistic effects using the Excess over Bliss score.

We will present a detailed comparison of the binding kinetics of the three fourth-generation EGFR inhibitors on wild-type and C797S-mutant EGFR, and their ability to compete with osimertinib for binding to the kinase domain of EGFR. The different fourth-generation inhibitors show various selectivities for the various EGFR mutants and differences in their ability to spare wild-type EGFR. Profiling results of the three fourth-generation EGFR inhibitors in the osimertinib-resistant cell lines and on a panel of more than one hundred human cancer cell lines will be presented.

Reference: [1] Bertran-Alamillo *et al.* Nature Communications 10, 1812; 2019

#4669 Differential preclinical activity of Bruton tyrosine kinase inhibitors (BTKis) against *BTK* resistance-associated mutations.

M. S. Davids[1], I. E. Ahn[1], J. J. Riehm[2], M. Acar[2], V. Girardi[2], S. Patel[2], T. Gururaja[2], J. Woyach[3], L. T. Lam[2], E. Szafer-Glusman[2];
[1]Department of Medical Oncology, Dana-Farber Cancer Institute, Boston, MA, [2]AbbVie, North Chicago, IL, [3]Ohio State University Comprehensive Cancer Center, Columbus, OH

Background: Differences in profiles of acquired mutations of resistance to BTKis might have implications for treatment sequencing. We evaluated preclinical activity of BTKis (ibrutinib [Ibr], acalabrutinib [Acala], zanubrutinib [Zanu], and pirtobrutinib [Pirto]) against multiple clinically relevant *BTK* mutations and report on the clinical impact of *BTK* C481S in patients (pts) treated with Ibr.
Methods: Inhibition of kinase activity by BTKis was evaluated in a cell-free kinase activity assay (Nanosyn). Cell-killing activity on CRISPR-generated *BTK* mutant knock-in TMD8 cells was assessed after 3 days of BTKi treatment. Time from first detection of C481S mutation to progressive disease (PD) was evaluated in pts treated with Ibr with previously untreated (n=247) or relapsed/refractory (R/R; n=172) CLL using pooled data from 5 clinical trials.
Results: In vitro kinase activity was highest for Ibr compared with Acala or Zanu against C481S (Ibr IC_{50}: 26.3 nM; Zanu: 84.8 nM; Acala: 338 nM) and T474I (Ibr: 1.2 nM; Zanu: 4.4 nM; Acala: 43.6 nM). Ibr maintained cell-killing activity against all tested *BTK* mutants, whereas limited activity was seen with Acala against C481S and A428D; with Zanu against C481S, L528W, and A428D; and with Pirto against T474I, L528W, V416L, and A428D (Table). In pts treated with Ibr, C481S was detected prior to clinical PD in 3 previously untreated pts and in 26 pts with R/R CLL; median (range) time from first detection of C481S to PD in these pts was 17.0 mo (11.2-34.3) and 10.0 mo (2.6-35.7), respectively.
Conclusion: This study demonstrates activity of Ibr against all evaluated *BTK* variants, which are associated with resistance to covalent and noncovalent BTKis. Clinical data shows that pts who develop C481S mutations continue to derive benefit from Ibr for several months before PD. Together, these data suggest a role for Ibr in the treatment of pts with a broad spectrum of *BTK* variants.

Table. Cell-killing activity of BTKis against wild type and mutant BTK

EC_{50} (nM)	***BTK***					
	Wild type	**C481S**	**T474I**	**L528W**	**V416L**	**A428D**
Ibr	0.6	414.0	1.9	181.4	0.5	205.3
Acala	3.9	2973.8	43.3	3.5	106.3	3000.0
Zanu	0.7	2322.0	11.7	3000.0	0.6	1726.0
Pirto	8.2	12.6	2727.5	3000.0	1898.0	3000.0

#4670 KS18, an Mcl-1 inhibitor, triggers cell death and enhances the therapeutic efficacy of venetoclax in bortezomib-resistant multiple myeloma cells.

O. Al Odat[1], O. Aloudat[2], E. Nelson[1], T. Budak-Alpogan[3], S. Jonnalagadda[1], Y. Chen[4], M. Pandey[2];
[1]Rowan University, Glassboro, NJ, [2]Cooper Medical School of Rowan University, Camden, NJ, [3]Cooper University Hospital, Camden, NJ, [4]College of Science and Mathematics, Rowan University, Glassboro, NJ

A critical clinical challenge in the management of multiple myeloma (MM) is the development of both innate and acquired resistance to the treatment with bortezomib. Our prior research showed that the overexpression of the anti-apoptotic Bcl-2 family protein Mcl-1 can result in resistance to the chemotherapy drugs bortezomib and venetoclax. In order to overcome the issues posed by resistance, this study investigates the possibility of a small chemical called KS18, a novel Mcl-1 inhibitor. KS18 outperforms other Mcl-1 inhibitors such as S63845, VU661013, and AZD5991, according to the findings of our research, which shows that it is extraordinarily effective against MM cells that have become resistant to bortezomib. We establish the selectivity of KS18 through tests employing Mcl-1 knock-down (KD), and we find that it is both effective and efficient. In addition, we used immunoprecipitation (IP) and protein-protein interaction analysis (PPIs) to investigate the dynamic connections that exist between Mcl-1 and pro-apoptotic proteins. The KS18 therapy exhibits an outstanding ability to cause complete apoptosis, as seen by the remarkable 88.8% apoptosis rate recorded in MM patient samples. Not only does KS18 restore apoptosis in bortezomib-resistant MM cells, but it also synergizes with venetoclax to enhance the apoptotic response. This is an important finding. It has been demonstrated through both *in vitro* and *in vivo* research that KS18 can re-sensitize MM cells to the effects of bortezomib, which represents a potential step forward in the treatment of the disease. In bortezomib-resistant MM cells, treatment with KS18 led to a remarkable 92% reduction in colony formation compared to untreated controls. *In vivo* experiments that were performed on mice models that were resistant to bortezomib provide additional evidence that KS18 is effective. The extraordinary reduction in tumor weight of 55% that occurred as a direct result of treatment with KS18 at a dose of 1 mg/kg for a period of 15 days exemplifies the powerful anti-resistance characteristics of this compound. These intriguing findings highlight the potential value of KS18 as an adjunct to therapies aimed at overcoming bortezomib resistance in MM and other associated cancers. Bortezomib-resistant malignancies provide a challenge for patients, but additional research into the clinical value of KS18 holds the potential to improve treatment outcomes and broaden the range of therapeutic alternatives available to these patients.

#4671 Efficacy and mechanism of mebendazole for ovarian cancer therapy.

R. Rai[1], D. Penta[1], D. Dey[1], D. Benbrook[1], L. Wang[2], M. Bieniasz[2], L. Dockery[1];
[1]University of Oklahoma Health Sciences Center, Oklahoma City, OK, [2]Oklahoma Medical Research Foundation, Oklahoma City, OK

Introduction: Ovarian cancer (OvCa) is the most lethal gynecological malignancy. Although most OvCa patients initially respond to frontline platinum-based therapies with approximately 80% of patients experiencing remission, approximately 75% of those women experience a recurrence with only approximately 50% of patients alive 5 years following diagnosis. There is a critical need to develop novel therapeutic agents or methods to overcome chemoresistance and toxicities experienced with conventional chemotherapy regimens used for OvCa patients. Repurposing drugs is a promising strategy to safely and more rapidly evaluate potentially effective treatment regimens. Over the past two decades, Mebendazole (MBZ), an anti-parasitic drug, has gained much attention in oncology due to its favorable biosafety profile and potent anti-cancerous activity seen in several human malignancies. Therefore, we examined the efficiency and mechanism of MBZ against OvCa.

Methods: The *in vitro* efficacy of MBZ was evaluated in cisplatin-resistant (CPR) and parent (WT/sensitive) OVCAR-8 cell lines as well as in ascites samples collected from chemo-resistant OvCa patients by using 2D and/or 3D cell viability assay and invasion assay. The *in vivo* efficacy of MBZ was assessed in orthotopic animal models, utilizing CPR-OVCAR8 spheroids, and patient-derived xenograft (PDX) animal models with specimens from chemo-resistant ovarian cancer patients. Molecular mechanisms were investigated through western blot and immunofluorescence analysis.

Result: Our results confirmed that MBZ efficiently decreased cell viability, spheroid size, and the invasion ability of OvCa cell lines and ascites samples. OvCa cells treated with MBZ demonstrated downregulation of proliferation markers and upregulation of apoptosis markers indicating inhibition of cell proliferation and induction of apoptosis. Mechanistically, MBZ inhibited the Wnt/β-catenin signaling pathway by downregulating the expression and nuclear localization of β-catenin and epithelial-mesenchymal transition (EMT) markers. Preclinical studies showed that MBZ at 50 mg/kg/day dose for 28 days significantly reduced tumor growth in PDXs and orthotopic tumor models without any evidence of toxicity.

Conclusion: Collectively, our study strongly supports the therapeutic potential of MBZ against OvCa particularly, which warrants further clinical studies.

#4673 Genome-scale metabolic models identify gene targets that enhance drug response of drug-resistant breast cancer cells.

H. Jung[1], J. Lim[1], H. Ryu[2], Y. Kim[1], H. Kim[1];

[1]Korea Advanced Institute of Science and Technology, Daejeon, Korea, Republic of, [2]Seoul National University Hospital, Seoul, Korea, Republic of

Adaptive drug resistance poses a significant therapeutic challenge in treatment of breast cancer patients. Metabolic reprogramming in cancer cells is one of the major mechanisms associated with drug resistance. In this study, we aim to identify gene targets that enhance the drug response of drug-resistant breast cancer cells through downregulation. We hypothesized that metabolic perturbation in drug-resistant breast cancer cells could revert their metabolic features to those of drug-sensitive cells. To predict such gene targets, we used a computational model known as a genome-scale metabolic model (GEM). A GEM simulates the entire metabolic reaction fluxes of a cell under varying genetic and/or environmental conditions. We specifically targeted two engineered MCF7 breast cancer cell lines: one resistant to doxorubicin and the other to paclitaxel. First, we generated proteome data from drug-sensitive and drug-resistant MCF7 cell lines, and used them to construct the cell-specific GEMs. Subsequently, single-gene knockout simulation was conducted using these cell-specific GEMs. The initial list of the gene knockout targets was subjected to pathway analysis involving proteome and metabolome data to finalize the gene targets. The final gene targets were expected to lead to metabolic features similar to those of drug-sensitive MCF7 upon the downregulation. *In vitro* experiments using inhibitors were conducted to validate these predicted gene targets. This study provides a computational approach that can also be applied to other types of drug-resistant cancer cells.

#4674 Reserpine analog modulates transport function of ABCG2.

S. Ohnuma[1], S. Kokubo[1], N. Sugisawa[1], M. Murakami[2], Y. Hatsuzawa[1], M. Kobayashi[1], T. Kajiwara[1], H. Suzuki[1], H. Karasawa[1], K. Watanabe[1], T. Doi[3], S. V. Ambudkar[2], T. Kamei[1], M. Unno[1];

[1]Tohoku University Hospital, Sendai, Japan, [2]National Cancer Institute, National Institutes of Health, Bethesda, MD, [3]Graduate School of Pharmaceutical Sciences, Tohoku University, Sendai, Japan

Backgrounds: Reserpine is an agent that is used for the treatment of hypertension. ABCG2 also known as breast cancer resistance protein (BCRP) is a member of the ABC transporters associated with multidrug resistance (MDR). Our high-throughput screening assay has revealed that reserpine analog inhibits transport function of ABCG2.

Aim: To investigate the effect of reserpine analog on ABCG2 function.

Results: Flow cytometry assay showed that reserpine analog blocked the efflux of Pheophorbide a (PhA: fluorescent substrate of ABCG2) from ABCG2-expressing HCT-116/BCRP colon cancer cells in a concentration-dependent manner. Furthermore, cell proliferation assay (MTS assay) revealed that 5 and 10 μM reserpine analog sensitized HCT-116/BCRP cells to SN38 with IC50 value 0.61 + 0.12 μM and 0.22 + 0.036 μM, respectively. Finally, reserpine analog did not stimulate ABCG2-mediated ATP hydrolysis, but rather inhibited it (concentration required for 50% inhibition = 2.7 μM), suggesting that reserpine analog might prevent conformational changes required for ATP hydrolysis.

Conclusion: Reserpine analog could be developed as a potent modulator to overcome ABCG2-mediated MDR in cancer cells.

#4675 Reduction in NSCLC tumorigenesis by targeting sphingosine kinase 2.

Ayesha Khan, Bamby Dieng, Namrata Dube, Mohammad Fazle Alam, Neelu Puri

University of Illinois College of Medicine (Rockford), Rockford, IL

Lung cancer will account for 21% of US cancer deaths in 2023 with 238,340 cases and 127,070 deaths. Treatment with EGFR-TKI (epidermal growth factor receptor tyrosine kinase) inhibitors initially decrease tumor growth, but often leads to TKI resistance. According to studies, non-small cell lung cancer (NSCLC) tumors express more SphK2 (Sphingosine kinase 2) than normal lung tissue and patients with overexpression have worse survival chances. However, SphK2's role in TKI resistance is unclear. We hypothesize that inhibiting/downregulating SphK2 could reduce tumorigenicity and overcome ER (Erlotinib) and OR (Osimertinib) resistance. We studied the expression of SphK2 in both drug-resistant (OR/ER) and drug sensitive (parental) H358, H2170, H3255, and PC9 NSCLC cell lines using Western blotting, qRT-PCR, and immunofluorescence. H3255OR cells were also bioprinted with GelMA hydrogel using an R-Gen 200 bioprinter to mimic the physiological tumor environment and treated with SphK2 siRNA or ABC294640 (SphK2i). Immunoblotting was done to analyze changes in the expression of SphK2 in H358 (WT-EGFR) and H3255 (mutant EGFR- L858R) parental and OR-resistant cell lines. Results indicated a 1.5-1.8-fold upregulation of SphK2. Increased SphK2 gene expression was observed using qPCR in TKI-resistant H3255OR (4.3-fold), PC9ER/OR with mutant EGFR (E746-A750del) (1.8-3.3-fold), and H2170ER/OR with WT EGFR (1.3-1.5-fold) compared to parental cells. Immunofluorescence studies showed increased fluorescence of SphK2 in H3255OR (2.6-fold), H358 ER (2.4-fold) and OR cells (2.3-fold) compared to parental cells. Spheroids formed from single cancer cells can "re-create" the growth of a tumor. The spheroid count of H3255OR was reduced by 73.98% and 56%, respectively, when SphK2i was added to the 3D-cell culture with Matrigel, compared to the diluent and OR alone ($p \leq 0.01$). We used 3D bioprinting to precisely stack cells on biological scaffolds to recreate lung tumors from patients and boost the therapeutic efficacy of these findings. When bioprinted spheroids of H3255OR were treated with SphK2i in combination with OR, the number of spheroids per microscopic field were reduced by 87.3% compared to OR alone. Bioprinted H3255OR spheroids treated with SphK2 siRNA and OR revealed a 75.8% and 84% reduction of spheroid count, respectively, compared to treatments with siRNA alone or OR alone ($p \leq 0.05$). This data supports the hypothesis that SphK2 suppression or downregulation can assist in mitigating oncogenesis. We also used H3255OR transwell migration assays to examine how SphK2 inhibition affects cell migration. Combining OR with SphK2i resulted in a 94.7% and 91.4% decrease in cell migration compared to diluent and OR alone ($p \leq 0.01$). In H358OR-resistant cells, combining OR with SphK2i resulted in a 94.97% inhibition compared to diluent ($p \leq 0.01$). These results suggest that targeting SphK2 could be a valuable approach for treating lung cancer.
[A.K. and B.D. contributed equally to this work.]

#4676 11α-O-2-methylbutanoyl-12β-O-tigloyl-tenacigenin B (MT2) is a novel paclitaxel chemosensitizer to inhibit growth in Taxol non-resistant and Taxol resistant cancers.

Ka Ming Cheng[1], Gui yun Wu[2], Kowk Kuen Cheung[1], Xiao-Ling Shen[2], Ying-Jie Hu[2], **Ki Lui**[3]

[1]Department of Rehabilitation Sciences, Hong Kong Polytechnic University, Hunghom, Hong Kong,[2]Science and Technology Innovation Center, Guangzhou University of Chinese Medicine, Guang Zhou, China,[3]School of Nursing and Health Studies, Hong Kong Metropolitan University, Ho Man Tin, Hong Kong

11α-*O*-2-methylbutanoyl-12β-*O*-tigloyl-tenacigenin B (MT2) is a single molecule isolated from a traditional Chinese Medicinal herb *Marsdenia tenacissima* (MT). Recently, our group has isolated a few single molecules from the MT herb, they have shown significant anti-tumor activity in vitro and MT2 has the highest potential among all. We have performed MTT viability assay and clonogenic assay to demonstrate that MT2-alone is non-cytotoxic, but the cytotoxicity of the paclitaxel+MT2 combination treatment was more significant than that of paclitaxel, a microtubule stabilizing chemotherapeutic agent. The underlying mechanism of such growth inhibition is contributed by the down-regulation of the pro-survival signaling and up-regulation of the apoptotic signaling such as an increase in cleaved caspase 3 and decrease in anti-apoptotic Bcl-2 proteins when cancer cells are co-treated with MT2+paclitaxel. More importantly, intraperitoneal administration of the combination treatment 5 times of MT2+paclitaxel (30mg/kg, 8mg/kg) has a more significant anti-tumor effect than the paclitaxel-alone (8mg/kg) or MT2-alone (30mg/kg) treatments using the wild-type hepatic HepG2 xenograft model in nude mice. Besides the wild-type HepG2 cancer cells, we have further demonstrated that MT2 is able to resensitize paclitaxel-resistant HepG2 cancer cells by inhibiting the activity of p-glycoprotein (Pgp), a key drug efflux transporter in chemotherapy resistance cancer cells. Also, the combination treatment has shown a significant anti-tumor effect in HepG2/DOX Pgp-overexpressed xenograft in nude mice. Taken together, MT2 is a novel chemosensitiser in combination use with paclitaxel to treat cancer. It enhances cancer apoptosis by suppressing the anti-apoptotic and survival signaling pathways in cancer cells.

#4677 Characterizing resistant and metastatic phenotypes to pharmacological ascorbate in pancreatic cancer.

A. N. Pope, B. R. O'Leary, J. Du, G. R. Buettner, M. D. Henry, J. J. Cullen;
Carver College of Medicine, University of Iowa, Iowa City, IA

Background and purpose: Pharmacological ascorbate (P-AscH) is a prooxidant that oxidizes to produce high levels of hydrogen peroxide. It is currently being investigated as an anti-cancer neoadjuvant for pancreatic cancer (PC). In phase I clinical trials, P-AscH has generated encouraging results in terms of efficiency and safety. However, 50% of patients do not respond to P-AscH suggesting that resistance occurs in a subset of patients. We have generated PC cell lines resistant to P-AscH to characterize mechanisms of resistance.
Methodology: PANC-1 and MIA PaCa-2 PC cell lines were treated with a stepwise progression of increasing concentrations of P-AscH until 10-fold IC_{50} concentration was fully tolerated (AscR, ascorbate resistant) as determined by clonogenic survival. Once resistance was achieved, various redox enzyme protein expression and activity were measured to determine their role in resistance to P-AscH. Proliferation and cell cycle analysis were conducted on resistant and sensitive cells. An RNA sequencing screen was conducted as an unbiased approach to identify potential candidates crucial for resistance. Finally, phenotypes associated to increased metastatic potential, including collagen invasion and in vivo tumor colonization were explored for characterization.
Results: PANC-1 and MIA PaCa-2 AscR cells developed unique mechanisms to tolerate high levels of P-AscH. PANC-1 AscR cells almost exclusively rely on catalase to detoxify H_2O_2 generated during P-AscH treatments, while MIA PaCa-2 AscR cells do not. It is interesting to note that not every redox enzyme was upregulated in response to P-AscH treatments, including GPx1/4. The AscR cell lines also differed in growth rates. PANC-1 AscR cells developed a faster proliferation rate, whereas MIA PaCa-2 AscR cells significantly decreased their growth. This is consistent with a shortened G1/G0 cell cycle phase and an accumulation in G2/M, respectively. The RNA sequencing screen revealed a metastatic signature in association with resistance to P-AscH, including upregulation of the PI3K/AKT axis. We observed a significant increase in collagen matrix invasion, as well as metastatic colonization in vivo. Additionally, we have observed increased expression of active AKT in both AscR cell lines, indicating a potential mechanism for the increased metastatic phenotype.
Conclusion: Our findings demonstrate distinct mechanisms for AcsR cells to tolerate high doses of P-AscH. Although catalase has demonstrated to be a key factor in controlling redox flux, it may not be necessary for all cell types. Not only can P-AscH resistance alter redox enzyme expression, but we have also observed substantial increase in metastatic potential to drive invasion and tumor colonization. In summary, our data indicate a potential route for PC to tolerate high levels of P-AscH and may explain how some patients do not respond to this treatment regimen.

EXPERIMENTAL AND MOLECULAR THERAPEUTICS: New Targets, Technologies, and Drug Delivery Systems
Poster Session

#4681 Unlocking the anticancer potential of calix[4]arene-based Cu(I) ionophores *in vitro* and *in vivo*.

P. Lelievre[1], C. Nogier[1], N. Renier[2], J.-L. Coll[1], I. Jabin[2], L. Sancey[1], H. Valkenier[1], A. Deniaud[3], **B. Busser**[1];
[1]Institute for Advanced Biosciences, Grenoble, France, [2]Universite libre de Bruxelles, Bruxelles, Belgium, [3]CEA Grenoble, Grenoble, France

Introduction: Cuproptosis is a novel programmed cell death pathway triggered by increased intracellular Copper (Cu) levels. This process offers promising avenues for cancer therapy and underscores the pivotal role of Cu-targeting molecules, such as chelators and ionophores. Despite the progress made, there is still a critical need for novel molecules capable of disrupting copper homeostasis within cancer cells.
Methods: We developed and patented a novel class of Cu(I) ionophores characterized by calix[4]arene structures. The anticancer effects of these compounds were evaluated through proliferation assays (IC50), cell cycle assays, and the mechanisms of cell death were explored, including apoptosis, senescence, autophagy, and cuproptosis. To elucidate the mechanisms of action, we conducted proteomic and phosphoproteomic analyses in three different lung adenocarcinoma cell lines (A549, H322, and PC9). Intracellular concentrations of Zn, Fe, and Cu were determined by Inductively Coupled Plasma Mass Spectrometry (ICP-MS). Animal experiments were conducted on nude mice bearing subcutaneous A549 lung cancer xenografts.
Results: Our lead compound, Cuphoralix, demonstrated potent cytostatic effect across a panel of 60 cancer cell lines. This effect was attributed to an early and irreversible blockade of the cell cycle initiation at 24 hours post-treatment. Cuphoralix treatment did not induce senescence or apoptosis. Proteomic analyses confirmed the differential regulation—both upregulation and downregulation—of over 500 proteins and phosphopeptides following treatment with Cuphoralix. Notably, Cuphoralix treatment resulted in decreased expression levels of proteins implicated in cell cycle progression and DNA replication. We discovered that Cuphoralix induced cuproptosis and autophagy, as evidenced by the overexpression of LC3B-II. Intracellular Cu level was significantly increased after treatment with Cuphoralix, suggesting the initiation of cuproptosis. In vivo, the toxicity of liposomal Cuphoralix was assessed following three intravenous injections / week for 4 weeks. Animal weights remained stable, with no observed toxicity or signs of neurological or functional impairment. The anticancer efficacy of Cuphoralix, both alone and in combination with other treatments, was corroborated in vivo by measuring the volumes of subcutaneous xenografts.
Conclusions: Our novel Cu(I) ionophore, Cuphoralix, has demonstrated significant potential in inducing cuproptosis and disrupting copper homeostasis, presenting a novel approach to cancer therapy. The compound's capacity to initiate an early and irreversible cell cycle blockade and to modulate the expression of key proteins underscores its therapeutic promise. The profound in vitro and in vivo anticancer effects observed encourage further development and investigation of cuproptosis as a targeted cancer treatment strategy.

#4682 Membrane protein expression and activity following inhibition of B-cell receptor-initiated signaling by WBMP-4, a therapeutic antibody for leukemia/lymphoma.

R. S. Welt[1], D. Kostyal[2], V. Raymond[3], J. M. Lobo[1], S. Welt[1];
[1]Welt Bio-Molecular Pharmaceutical, Briarcliff Manor, NY, [2]ARDL, Akron, OH, [3]Biogent Consultants, LLC, Armonk, NY

The B-cell Receptor (BCR), comprising membrane Ig (mIg) and CD79a/b, controls normal signaling in B-cells, but dysregulation of this signaling is the dominant driver of leukemia/lymphoma. The class-specific mIg subunit of the BCR is a rational drug target for B-cell malignancies. It plays a critical role in the functioning of these cells, and allows for restricted targeting of only B-cells expressing an Ig class, offering a more tumor-specific approach than current pan-B-cell treatments. We developed a first-in-class antibody, WBMP-4, to the mIgM-BCR, which inhibits cell growth and induces apoptosis via widespread down-regulation of tyrosine kinase activity. Given the potent inhibition of intracellular signaling induced upon WBMP-4 binding to the mIgM-BCR, we expect that translation of membrane proteins will be impacted. Here we investigate the expression and phosphorylation profile of cell surface proteins following treatment of malignant B-cells with WBMP-4.

Using western blot and flow cytometry, we measure levels of CD79a/b, CD19, CD20, CD21, CD22, CD32a, CD81, and CXCR4 at 6, 24, and 48 hours after low (5ug/mL) and high (20ug/mL) dose WBMP-4 treatment, as compared to control, untreated Burkitt lymphoma (CA46) cells. We analyze phosphorylation levels of those surface proteins that serve as kinases in this system (CD79a/b, CD19, CXCR4, etc.). Using these same methods, we also examine the expression and phosphorylation of key B-cell transcription factors (e.g. NF-kB, c-MYC, STAT5, PAX5, EBF1, FOXO, and BCL-2).

Preliminary analyses show a complete absence of CD79a protein (western blot), and decreased phospho-kinase activity of CD79b (Pamgene phosphokinase array) following treatment of Burkitt lymphoma cells with WBMP-4, as compared to untreated cells. While the effect of an antibody binding to mIg may be most pronounced for CD79a/b relative to other proteins, as mIg and CD79a/b form a complex, we expect that the absence of CD79a/b is a result of WBMP-4-induced mIgM inhibition modulating downstream signaling and transcription factor activity. By examining cell surface markers, we may gain insight into how WBMP-4 impacts a cell's interaction with the tumor microenvironment, and this information is valuable for diagnostic and patient monitoring purposes, and to determine drug combination strategies. This work will be considered in the context of our ongoing research on WBMP-4's inhibition of intracellular signaling pathways, and the resulting biologic effects, and will contribute to the continued development of WBMP-4 by providing an understanding of the effects achieved (cell growth inhibition, cell differentiation, apoptosis) at different dosages and if these effects are maintained over time. As a novel, efficacious, and low toxicity treatment strategy for B-cell leukemia and lymphoma, WBMP-4 has significant clinical potential.

#4683 Suppression of ARL6ip1 inhibits malignant phenotypes of human colorectal cancer cells in vivo and > in situ.

Y. Lin, S. Karnan, H. Ito, K. Umezawa;
Aichi Medical Univ., Nagakute, Japan

Introduction: Conophylline is an alkaloid isolated from the leaves of the Thai plant, *Ervatamia microphylla*. We isolated conophylline as an inhibitor of K-Ras functions and an activator of pancreatic β-cell differentiation. It ameliorates various disease models in animals, including cancer, diabetes mellitus, NASH, and hepatic cirrhosis. On the other hand, its molecular target was determined to be ADP-ribosylation factor-like 6-interacting protein 1 (ARL6ip1) using a conophylline-biotin conjugate. ARL6ip1 is located in the endoplasmic reticulum (ER) membrane, and conophylline binds to the cytoplasmic portion of ARL6ip1. Known functions of ARL6ip1 include inhibition of apoptosis, inhibition of glutamate transporter, and modulation of the ER structure. Previously, we knocked out ARL6ip1 in human colon carcinoma cells by CRISPR-Cas9 and found that either deletion of ARL6ip1 or addition of conophylline inhibited migration, invasion and tumorigenicity in cultured cancer cells. In the present research we have studied the in vivo anticancer effect of conophylline and ARL6ip1 knockout, and the mechanism of anticancer activity in cultured cells.

Materials and Methods: Conophylline was isolated from the leaves of *Ervatamia microphylla*. We employed HCT116 and DLD1 cell lines as human colorectal cancer cells. Cellular migration was measured by a wound-healing assay. The activity of Akt was measured by the phospho-Akt antibody. BALB/cSlc-nu/nu mice were used for the animal experiment.

Results: Colon adenocarcinoma tissue microarray comparing tumor and adjacent normal tissues revealed that ARL6ip1 expression was significantly higher in cancer than in normal tissues. Intraperitoneal administration of conophylline and knockout of ARL6ip1 both inhibited the growth of HCT116 in mice. Neither influenced the bodyweight of animals. Conophylline and deletion of ARL6ip1 both inhibited the migration. Rescue of ARL6ip1 canceled the effect of ARL6ip1 deletion on migration in HCT116 and DLD1 cells. As the mechanism, either conophylline or ARL6ip1 knockout inhibited the Akt activity, which was canceled by the rescue of ARL6ip1 in both cell lines.

Conclusion: ARL6ip1 was found to be highly expressed in the tumor tissue in colorectal cancer. CRISPR-Cas9 knockout of ARL6ip1 showed a similar anticancer activity as treatment with conophylline in the animal experiment. It is likely that the anticancer activity of conophylline would be mediated by Akt. Thus, ARL6ip1 would be a useful molecular target for the treatment of cancer.

#4684 A comprehensive platform for identification of KRAS-specific synthetic lethal targets using patient-derived cells.

M. Dulęba[1], E. Zimoląg[1], J. Szuszkiewicz[1], M. Serocki[1], J. Szklarczyk[1], O. Dracz[1], Z. Kurzejamska[1], D. Coelho[1], M. Combik[1], O. Bryzghalov[1], J. Krawczyk[1], A. Stachowicz[1], M. Mikula[2], K. Brzozka[1], R. Dziadziuszko[3], T. Rzymski[1], **A. Mazan**[1];

[1]Ryvu Therapeutics, Krakow, Poland, [2]Maria Skłodowska-Curie Institute of Oncology, Warsaw, Poland, [3]Medical University of Gdańsk, Gdańsk, Poland

Colorectal cancer (CRC) remains a global health concern, constituting a large portion of cancer incidence and mortality. Despite advances in comprehending the genetic and epigenetic landscape of CRC and progress achieved in developing KRAS-specific inhibitors poised for clinical evaluation, a significant unmet medical need persists. This underscores the necessity for innovative therapeutic interventions in this field, as effective therapeutic strategies targeting specific molecular vulnerabilities are currently lacking. Our study aims to address this gap by focusing on the identification of synthetic lethal (SL) inhibitors specific to the KRAS pathway. We have established a platform utilizing human intestinal stem cell (hISC)-derived CRC model cells, patient-derived xenografts (PDXs), and clinical samples for genomic and functional analyses. Employing CRISPR/Cas9 technology, we introduced common CRC mutations into hISCs, generating isogenic CRC model cells with diverse mutational backgrounds including KRAS G12D. Additionally, we developed PDXs from CRC patients and collected biopsy samples from primary and metastatic tumors. Through RNA-seq and whole-exome sequencing (WES), we identified molecular signatures and pathways associated with different mutational variants. Our innovative platform enables high-throughput screening, incorporating both small molecule screening and CRISPR/Cas9 dropout screening with a genome-wide library on CRC model cells. Notably, our focus on KRAS-specific SL inhibitors distinguishes our approach, aiming for targeted therapies tailored to specific CRC subtypes. Validation of driver mutations, such as APC, KRAS, and TP53, in patient-derived material showcased the relevance of our model. High-quality screening results, meeting industry-standard QC criteria, allowed us to identify essential and tumor suppressor genes critical for CRC. Importantly, the use of normal hISCs enabled the identification of genes crucial only for transformed cells. The platform serves as a powerful tool for target discovery and validation in CRC, emphasizing the significance of primary material-derived cells. Beyond CRC, our findings have broader implications for other cancer types and personalized medicine approaches. By focusing on the identification of KRAS-specific SL inhibitors, our research contributes to the development of novel therapies for CRC, addressing the urgent need for targeted interventions in this heterogeneous malignancy.

#4685 The identification of new therapeutic targets in mucinous ovarian carcinoma.

S. Petrella, M. Colombo, M. Marabese, C. Grasselli, A. Panfili, I. Craparotta, M. Barbera, G. Cassanmagnago, M. Bolis, G. Damia;
Istituto di Ricerche Farmacologiche Mario Negri IRCCS, Milano, Italy

Background: Epithelial ovarian cancer (EOC) is the second cause of death among gynaecological cancersworldwide. Mucinous ovarian carcinoma (mEOC) accounts for 3-5% of all EOCs, and when diagnosed at anadvanced stage its prognosis is very poor mainly for its limited chemosensitivity. PLK1 is a member of thewell-conserved serine/threonine kinase family, that plays a key role in the progression of mitosis, in the G2/Mcheckpoint regulation, DNA damage replication, stress response, and cell death pathways. mEOC has beenshown to be sensitive to PLK1 inhibition both with siRNA and small molecule inhibitor (onvansertib). Giventhis background and the need for new therapeutic approaches in mEOC, the purposes of this work were toidentify new therapeutic targets in mEOC using CRISPR/Cas9 lentivirus libraries and to find synthetic lethalpartners with the PLK1 inhibitor onvansertib.
Methods: We used three different mucinous cell lines: MCAS,EFO27, TOV2414, overexpressing Cas9 gene. We evaluated the Cas9 expression through Western Blotanalysis, and the Cas9 activity through a Fluorescent Activated Cell Sorter- based-GFP assay. We used twodifferent lentiviral gRNAs Libraries (Bassik Library Human CRISPR Deletion Library - Apoptosis and cancer(Addgene #101926)/Drug targets, kinases, and phosphatases (Addgene #101927)). The EFO27 Cas9 cells wereused for the screening experiment. Cells were infected with the lentiviral libraries at MOI of 0.3 and put inpuromycin selection. Six days after puromycin addition (Time point 0) 30x10^6 cells were collected forsequencing. The remaining 30x10^6 cells were split in two: control cells and cells treated with a subtoxic doseof onvansertib (IC30). After 7 days (Time point 1) 30x10^6 cells for each condition were collected forsequencing. The infection of libraries was performed alone and in combination with sub-toxic onvansertibtreatment, to identify genes important for mucinous carcinoma cell survival, and those genes in syntheticlethality with onvansertib.
Results: Bioinformatic analyses comparing control cells (time 1 vs time 0) andPLK1 treated and non -treated cells (time 1) allowed the generation of a gene ranking list, including genesinvolved in survival of EFO27 cells like ZC2HC1C, RPA2, POLE3, KIN, TUBG1, SMC2, CDC26, CDC42, HOXA9,TAF10, DCLRE1C, SENP1, MRPS31, COPS2; and genes in synthetic lethality with PLK1 treatment, like JUND,CARD9, BCL2L2. Validation experiments are ongoing and will be presented and discussed.
Conclusion: Using a CRISPR-based approach, we identified genes that either alone or in combination with PLK inhibitioncould have therapeutic value in mEOC.

#4686 Identification of ART3 as a novel synthetic lethal partner of the BRCA1 mutation in breast cancer.

H. Neiger[1], X. Pei[2], A. Nguyen[1], W. Wang[1], E. L. Siegler[1], J. Zhou[1], K. Lau[1], A. Tan[1], **Y. Shi**[3];
[1]California Northstate University, Elk Grove, CA, [2]City of Hope, Duarte, CA, [3]California Pacific Medical Center Research Institute, San Francisco, CA

Breast cancer (BC), the most prevalent malignancy in women, ranks fourth in cancer mortality as of 2022. Mutations in the BRCA genes significantly elevate BC risk and are associated with markedly reduced survival compared to non-carriers. These genes are crucial in homologous recombination, a mechanism essential for error-free DNA repair. Despite advancements, treatment options for BRCA mutation-driven cancers remain limited. Synthetic lethality (SL) has emerged as a promising strategy, with poly(ADP-ribose) polymerase inhibitors (PARPi) being the first developed drugs based on this principle. However, PARPi's effectiveness is limited, as nearly 40% of BRCA-mutated BCs are unresponsive, and resistance often develops in initial responders. Therefore, novel mutation-specific targeted therapies are urgently needed. In this study, we employed the novel computational method 'Mining Synthetic Lethals (MiSL)' to analyze TCGA pan-cancer primary tumor data, identifying ART3 as a potential SL partner of the BRCA1 germline mutation. Our approach focused on the intersection of genetic interactions and cancer vulnerabilities, providing a unique insight into SL relationships. siRNA-mediated silencing of ART3 in BRCA1-mutated cells consistently led to decreased cell viability, apoptosis induction, and G2/M cell cycle arrest. Following stable transfection with an inducible ART3 shRNA construct, we confirmed significant reduction in cell viability in BRCA1-deficient cells through colony formation assays. RNA sequencing of ART3 knockdown cells revealed transcriptional changes in genes involved in cell cycle progression, apoptosis, and growth and proliferation pathways compared with control cells. Immunofluorescent staining revealed increased DNA damage foci with decreased DNA repair in ART3 knockdown BRCA1-deficient cells. In conclusion, our study identifies ART3 as a novel SL partner of the BRCA1 mutation in BC. This discovery paves the way for developing new therapeutic strategies for BRCA1-mutated breast cancers and novel chemoprevention approaches for individuals carrying germline BRCA1 mutations. Future research will focus on further elucidating the molecular mechanisms underlying this SL interaction and exploring its therapeutic potential in clinical settings.

#4687 Primary study on the anticancer role of BAM15 in lung cancer cells.

M.-y. Zhang, Y.-N. Wang, Y.-F. Zhou, S.-C. Wang, S.-J. Mai, H.-Y. Wang;
State Key Laboratory of Oncology in South China, Guangdong Provincial Clinical Research Center for Cancer，Sun Yat-Sen University Cancer Center, Guangzhou, China

Background: Lung cancer remains the leading cause of cancer-related death worldwide. Non-small cell lung cancer (NSCLC) accounts for about 80-85% of all lung cancer cases. BAM15, a mitochondrial uncoupler, is a potential therapeutic agent for many diseases, including obesity, diabetes, nonalcoholic fatty liver disease, Sepsis and cancers. However, there is no report on the anti-tumor role of BAM15 in NSCLC.
Methods: To investigate the direct anti-cancer effects of BAM15 in NSCLC, we examined its inhibitory role on cell proliferation of NSCLC cells using the Cell Counting Kit-8(CCK8), colony forming assays and EdU staining assays. The impact of BAM15 on the cell cycle and cell apoptosis of NSCLC cells was analyzed by flow cytometric. A xenotransplanted NSCLC model in mice were used to test the anticancer role of BAM15.
Result: Using the CCK8 assay, we found that the inhibitory role of BAM15 on the proliferation and colony formation of NSCLC cells is dose-dependent. The half maximal inhibitory concentration (IC50) values for cell proliferation were 2.71, 4.74, and 9.50 μM for A549, PC9, and H1299 NSCLC cells, respectively. The EdU staining assay demonstrated that BAM15 treatment significantly inhibited DNA synthesis in NSCLC cells. Flow cytometric analysis revealed that BAM15 arrested cell cycle at G2 phase in NSCLC cells and caused a striking increase in the percentage of apoptotic cells in NSCLC cells. The xenotransplanted NSCLC experiment indicated that BAM15 could significantly suppressed the growth of NSCLC tumors compared with the control tumors.
Conclusions: Our study demonstrates that BAM15 significantly inhibits cell proliferation and promotes apoptosis in NSCLC cells, indicating that BAM15 is a potential therapeutic candidate for the treatment of NSCLC.

#4688 EC359, A new therapeutic drug for the treatment of low grade serous ovarian cancer.

Y. Lyons[1], W. C. Arnold[1], B. Ebrahimi[1], B. Santhamma[2], E. R. Kost[1], H. B. Nair[2], S. Viswanadhapalli[1], R. K. Vadlamudi[1];
[1]UT Health Science Center at San Antonio, San Antonio, TX, [2]Evestra Inc., San Antonio, TX

Background: Ovarian cancer (OCa) is the deadliest of all gynecologic cancers in the United States. About 10% of all cases of serous ovarian cancer have the unusual histology named low-grade serous carcinomas (LGSOC), that has a distinct clinical behavior with a unique molecular landscape. LGSOC is characterized by a younger age at diagnosis, indolent progression, and chemotherapy resistance. BRAF and KRAS mutations occur in 33% and 35% of LGSOC cases, respectively. LGSOC is frequently detected when the malignancy is in advanced stage and LGSOC relapses in about 70% of patients with advanced disease. Therefore, new targeted therapies are required. Since LGSOC uniquely expresses mutations of either BRAF or KRAS, and because Leukemia Inhibitor Factor (LIF) expression is induced by oncogenes such as KRAS, we reason that the LIF/LIFR axis represents a unique target for treating LGSOC. The objective of this study is to test the utility of blocking LIF/LIFR axis using LIFR inhibitor EC359 in treating LGSOC.
Methods: The expression of LIF and its receptor LIFR was profiled using multiple established LGSOC cells and primary LGSOC model cells. The effects of EC359 on LGSOC cells were evaluated using cell viability, colony formation, and apoptosis assays. Mechanistic investigations were conducted with Western blotting, reporter assays and RT-qPCR analysis. The *in vivo* efficacy of LIFR inhibitor EC359 as a targeted therapy was investigated using LGSOC cell-based xenografts.
Results: Western blot analysis confirmed expression of LIFR and LIF in established LGSOC and primary LGSOC cells and functional autocrine loop of LIF/LIFR signaling. The treatment with the LIFR inhibitor EC359 significantly reduced LGSOC cell viability, cell survival, and increased apoptosis. The activation of downstream LIFR signaling including STAT3, mTOR, AKT, and p42/44 MAPKs markedly decreased by EC359 treatment. EC359 enhanced the efficacy of trametinib, a currently used medication of LGSOC. EC359+trametinib as a combination therapy showed more efficacy over monotherapy of EC359 or trametinib in reducing cell viability and colony formation. Using cell-based xenograft and PDX models, we demonstrated that the EC359 at 5mg/kg dose significantly reduced the LGSOC xenograft growth compared to the vehicle control.
Conclusions: Together, our findings support the existence of LIF/LIFR autocrine loops, and EC359 is a viable treatment option for LGSOC.

#4689 4HF CancerDataMiner platform accelerates target discovery and evaluation.

H.-H. Fiebig, A.-L. Peille, M. Schmitz, V. Vuaroqueaux, T. Metz;
4HF Biotec GmbH, Freiburg, Germany

For the management of metastasized cancer, tumor-targeted chemotherapies with improved therapeutic index are urgently needed. Over the last 25 years, antibody drug conjugates (ADCs) targeting cancer-associated proteins have emerged as a promising new treatment modality. While the first ADCs were registered for the treatment of acute leukemias and lymphomas, more recently at least six ADCs were approved by the FDA for solid tumors. Despite these successes, clinical development of ADCs remains a risky exercise as evident from the failure of more than 20 pivotal clinical phase III trials. A narrow therapeutic index due to excessive toxicity of potent payloads, little therapeutic activity, and difficulties in chemistry, manufacturing, and controls were among the limiting factors. Meanwhile, ADC technology and production have advanced substantially. More than 100 ADCs are currently in clinical development in approximately 600 clinical trials, with some of the investigated ADCs being close to approval. While issues related to ADC linkers and payloads have been extensively investigated and many problems have been solved, the choice of molecular targets for ADCs remains challenging. This is, in part, due to a lack of information about candidate targets: while knowledge about generally accepted cancer targets such as ERBB2 is abundant, data about many novel targets is still scarce. In particular, reliable information about expression in normal tissues, subcellular localization and protein function is often missing. 4HF Biotec has established the CancerDataMiner, an *in-silico* platform dedicated to cancer data mining by integrating large OMICS datasets that are connected and aligned. It allows molecular analyses of all human genes in >12,000 tumor samples and >14,000 normal tissues, using proprietary tools and widgets for visualization and statistics. Target evaluations are performed at the DNA, RNA and protein levels and employ complementary tools such as pathway analysis and literature search to obtain a comprehensive picture of candidate targets. Using this approach, we recently reviewed the molecular targets of all ADCs that either have already received approval or are in clinical development. As proof-of-concept for the CancerDataMiner, here we analyze targets of ADCs and compare our findings with the clinical data obtained for those ADCs. The profiles of selected ADC targets will be discussed, among them CD79B and CD33 for hematologic malignancies and FOLR1 and Claudin 18.2 for solid cancers. We will demonstrate that proteins with very diverse profiles can make good ADC targets. In conclusion, the 4HF CancerDataMiner is a platform which has proven its value for the identification and characterization of cancer-associated targets for ADC development for all tumor types.

#4690 SC-2882, a novel QPCTL inhibitor, with anti-tumor activity in solid tumor models.

J. Mullenders, M. Scheepstra, M. R. Faas, A. B. Galler, B. Evers, J. U. Wuerthner;
Scenic Biotech B.V., Amsterdam, Netherlands

Background: SC-2882 is an orally administered first-in-class small molecule inhibitor of glutaminyl-peptide cyclotransferase like (QPCTL). QPCTL is an intracellular enzyme that modifies several proteins containing an N-terminal glutamine or glutamate, resulting in pyroglutamylated amino acids. Pyroglutamylation can alter protein function in different ways and dependent on context. Key substrate proteins include the “don’t eat me” signal protein CD47 and several chemokines (CCL2 and CCL7) (Nat Med 2019, Nat Imm. 2022). Previously, we have shown activity of SC-2882 in a murine model of diffuse large B-cell lymphoma (Di Siervi, 2023). Here we report for the first time, the evaluation of SC-2882 in several preclinical mouse models for solid tumors.
Methods: Potency of SC-2882 was evaluated in a cell-based assay in several human and mouse tumor cell lines: SIRPα binding to CD47 in response to increasing concentrations of SC-2882 was measured in a flowcytometry-based assay. Several syngeneic mouse tumor models were evaluated for their response towards SC-2882 as a single agent and in combination with either a murine anti-PD-L1 antibody or cisplatin. Animals were dosed orally with SC-2882 once daily for the duration of the experiment.
Results: In all human and mouse cancer cell lines tested, SC-2882 was able to reduce SIRPα binding to CD47 significantly. This reduction was equivalent to the reduction observed in QPCTL genetic knockouts created in the same cell line. In the same experiments, no differences in CD47 expression were observed. From anti-tumor efficacy studies, we learned that SC-2882 was well tolerated in mice as a single agent and in combination with anti-PD-L1 or cisplatin for at least 4 weeks (this was the maximum period tested). No clinical signs or changes in body weight were observed, even over prolonged periods of treatment. Tumor growth inhibition and tumor shrinkage by SC-2882 was observed in 5 different syngeneic mouse tumor models. In two out of these five models, SC-2882 was able to reduce tumor growth as a single agent. In the other three models, tumor growth inhibition was observed in combination with either anti-PD-L1 or cisplatin.
Conclusions: SC-2882 is an orally administered small molecule inhibitor with a favorable PK profile. Preclinical studies show that SC-2882 was well tolerated in mice. In several mouse tumor models, SC-2882 reduced tumor growth in either single agent treated animals or in combination with anti-PD-L1 or cisplatin. SC-2882 is currently in IND enabling studies and scheduled to enter the clinic in 2024.

#4692 A novel ceramide synthase 2 agonist and its implication in triple-negative breast cancer therapy.

H. Alatawi[1], N. Koo[1], I. Mahmud[1], H. Nair[1], A. Singh[2], T. J. Garrett[1], A. K. Sharma[2], S. Hong[1], **S. Narayan**[3];
[1]University of Florida, Gainesville, FL, [2]University of Florida, Hersey, PA, [3]Narayan (Individual), Gainesville, FL

Based on the biological/molecular markers, breast cancer can be classified into five subgroups: Luminal A (ER+/PR+/HER2-), Luminal B (ER+/PR-/HER2- or ER+/PR+/HER2+, triple-positive), ER-/PR-/HER2+, and ER-/PR-/HER2- (triple-negative). Significant progress has been made in treating hormone-responsive and HER2-expressing breast cancer. However, the targeted therapies are limited for triple-negative breast cancer (TNBC) due to lack of well-defined druggable targets. Additionally, all breast cancer subtypes can quickly develop resistance to current treatments. Thus, there is an urgent need for therapeutic strategies targeting pathways common to all subtypes, irrespective of receptor status. In this effort, we have synthesized a novel biisoquinoline-derivative, DH20931 (US Patent ID: US9914733B2) that induces cytotoxicity in breast cancer cells, including TNBC cells. The spatial molecular modeling and enzymatic assays show that DH20931 interacts with and stimulates ceramide synthase 2 (CerS2) activity, reduces the growth of hormone-responsive, HER2-expressing, and TNBC cells in monolayer and 3D spheroid culture models. DH20931 treatment increases the level of very long chain fatty acid (VLCFA) containing ceramides, induces lipotoxic endoplasmic reticulum (ER) stress, and ATF4/CHOP/PUMA pathway of apoptosis. Based on Swiss-ADME analysis, DH20931 possess all the properties of a druggable molecule and obeys the Lipinski-rule-of-five. Thus, DH20931 can be developed as a novel targeted therapeutic agent independent of ER, PR and HER2 status that potentially may reduce the morbidity and mortality for women with breast cancer.

#4693 A Phase 1b study of BYL719 (Alpelisib) in combination with androgen receptor inhibitor (enzalutamide) in patients with androgen receptor (AR)-positive and PTEN-positive metastatic breast cancer.

M. Karuturi[1], T. Fuji[2], N. Ueno[3];
[1]UT MD Anderson Cancer Center, Houston, TX, [2]National Caner Insttitute, Bethesda, MD, [3]University of Hawaii Cancer Center, Honolulu, HI

Background: Novel combination therapies treatment of Hormone Receptor (HR)+/HER2- metastatic breast cancer, with a high incidence of AR expression, remains to be a priority in modern-day clinical trials. The PI3K pathway, a crucial regulator of cell processes, has been closely linked to AR signaling, with the interplays between the AR and PI3K pathways leading to emerging interest in exploring combination that target both pathways. Several studies have hinted at concordance between AR expression and PI3K pathway aberrations in breast cancer. therapies.
Methods: We conducted a phase 1b clinical trial of BYL719 in combination with enzalutamide for patients with AR-positive (defined as ≥ 1% of nuclear staining) , PTEN-positive (defined as >0% of nuclear staining), HER2-negative metastatic breast cancer (MBC). The primary objective was to determine the recommended dose of the 2 drugs for a phase II study (RP2D), in addition to the toxicity/safety profile of the combination. A conventional 3+3 dose escalation design was applied.
Results: A total of 18 patients were enrolled, with 17 ultimately treated (12 in dose-finding and 5 in dose-expansion). The median age was 57 (28-77 y/o). Two of the 17 were classified as having metastatic TNBC, and the remainder ER and/or PR+ MBC. Patients received a median of 2 prior endocrine therapies (range 0-5) and a median of 2 prior chemotherapies (range 0-4). Dose-limiting toxicities (DLTs) established a dose of BYL719 of 200 mg in combination with enzalutamide 160 mg. 4 patients experienced DLTs at the higher dose of BYL719 of 250 mg PO daily (4 with a maculopapular rash ranging from grade 1-3, 1 additionally with allergic reaction and lung infection categorized as grade 3). Three patients experienced SAEs, 2 at a higher dose of BYL 719 (fever, maculopapular rash, infection, allergic reaction) and 1 at the 200 mg dose, thought to be unrelated. The most common AEs attributed to enzalutamide included anemia (6 total, 3 grade 3, 3 grade 2), headache (6 total, 4 grade 1, 2 grade 2), and nausea (6 total, 3 grade 1, 3 grade 2). The most common AEs attributed to alpelisib included diarrhea (8 total, 5 grade 1, 2 grade 2, 1 grade 3), hyperglycemia (14 total, 7 grade 1, 4 grade 2, 3 grade 3) and rash (7 total, 1 grade 2, 6 grade 3). Clinical benefit rate was observed at 16 weeks, 6.7% partial response, 26.7% stable disease, and 60% progressive disease. Overall survival in the total cohort was 19.4 month (95% CI 4.11-NA), with a median time to progression of 2.07 months (95% CI 1.81-NA).
Conclusions: The Phase 1b study of BYL719 in combination with enzalutamide provides valuable insights into the safety and tolerability of the combination in AR/PTEN-positive MBC, including RP2D. Further studies are needed to evaluate their treatment efficacy fully.

#4694 In charge: Targeting neddylation of UBE2M for anticancer therapy.

A. G. Batrouni[1], J. P. Matson[1], A. L. Mota[1], A. Ravi[1], M. O'Hara[1], M. D. Smith[2], J. C. Smith[3], V. K. Vishnudas[1], A. Thakurta[1], S. Gesta[1], M. D. Nastke[1]; [1]BPGbio Inc., Framingham, MA, [2]University of Tennessee, Knoxville, TN, [3]Oak Ridge National Laboratory, Oak Ridge, TN

Post-translational modification of proteins with ubiquitin and ubiquitin-like molecules orchestrates a vast number of processes in the cell. Consequently, post-translational modification pathways are considered major targets for therapeutic intervention of many diseases, including cancers. Neddylation is a post-translational mechanism like ubiquitination, but instead of ubiquitin, NEDD8 is conjugated to protein targets via an E1-E2-E3 multi-enzymatic cascade. Neddylation is upregulated in multiple cancer types and the development of therapeutics targeting neddylation pathways are gaining increasing popularity. UBE2M, one of the two E2 neddylation conjugation enzymes, takes part in two types of reactions: transthiolation-transfer of NEDD8 from a thioester to a thiol group and aminolysis-transfer of NEDD8 from a thioester to an amino group. These activities require both a 26-residue N-terminal docking peptide and a conserved E2 catalytic core domain, which is the basis for the transfer of NEDD8. Here, we describe findings in the quest to understand the UBE2M interaction with NEDD8 and effects on cancer cells by modifying UBE2M at the N-terminal docking peptide or at the catalytic site. Cancer cells were transfected with ΔN or catalytic site UBE2M mutant constructs and analyzed by immunoprecipitation for charging of NEDD8 onto UBE2M. The catalytic site mutants are deficient in charging (C111A) or discharging (C111S) of UBE2M by NEDD8, which leads to a decrease in neddylation of downstream substrates, such as CULLIN family members. Elimination of the N-terminal docking peptide by introduction of catalytically competent ΔN UBE2M mutant constructs resulted in reduced reaction kinetics. Structural modeling suggests that the loss of the N-terminal docking region likely weakens protein-protein interactions between UBE2M and the UBA3-APPBP1 E1 complex. Interestingly, ΔN UBE2M mutants were observed to be slightly charged with NEDD8, but appeared to have a defect in NEDD8 discharge, resulting in reduced neddylation of substrates. Moreover, further phenotypic evaluation of UBE2M mutant transfected cancer cells revealed a divergence in phenotypic effect: while both mutant types led to a deficiency in NEDD8 charge or discharge from UBE2M, only the manipulation of the active site of UBE2M led to a DNA re-replication phenotype with subsequent cell death. These observations reveal the complexity of the neddylation cascade and raise the question if slowing down discharge of NEDD8 from UBE2M is a more viable therapeutic option than slowing down the charging of UBE2M.

#4695 Effect of fully human anti-PTGFRN antibody drug conjugate on head neck cancer cells and patient derived xenografts.

J. Marquez[1], J. Dong[1], M. Oshimura[2], J. Hayashi[3], **G. Serrero[1]**;

[1]A&G Pharmaceutical, Inc., Columbia, MD, [2]Trans Chromosomics, Inc., Yonago, Japan, [3]Precision Antibody, Columbia, MD

Prostaglandin F2 Receptor Negative regulator, or PTGFRN, also known as FPRP is a 175 kDa transmembrane protein associated with metastatic characteristics of certain cancer types and a member of the tetraspanin family. PTGFRN expression is undetectable to low in normal tissues whereas it is elevated in several cancers such as head and neck, mesothelioma and medulloblastoma. PTGFRN has also been reported to be upregulated in many different types of cancer, increasingly so in metastatic cancer cells, compared to their non-metastatic counterparts PTGFRN expression has been reported to be a poor prognostic factor for glioblastoma making it a potential novel cancer therapeutic target. We have previously shown that PTGFRN is an internalizable cell surface protein making it suitable for targeting by antibody drug conjugate (ADC). We have developed fully human monoclonal antibodies to PTGFRN by immunizing humanized transgenic TC mice with human PTGFRN. Within 60 days from the start of immunization we were able to select several fully human anti-PTGFRN monoclonal antibodies that were examined by several functional assays that included flow binding, internalization, affinity determination and cell killing as antibody drug conjugates. Several monoclonal antibodies were selected and evaluated for their ability to inhibit tumor formation in several cancers. Selected antibodies were then conjugated to duocarmycin by a cleavable linker. The present study proposed to examine the effect of one such anti-PTGFRN ADC on head and neck cancer cell lines and patient derived xenografts that had been analyzed for their PTGFRN expression by western blot analysis using anti-PTGFRN antibody. Cells lines and PDX that were positive for PTGFRN expression were used to examine the effect of anti-PTGFRN ADC on their in vitro and in vivo proliferation. The data show that anti-PTGFRN ADC inhibits tumor formation in a dose-dependent fashion. These data also establish PTGFRN as cancer druggable target and the selected fully human anti-PTGFRN antibody as an attractive antibody for the development of new antibody drug conjugate in Oncology. These data also emphasize the potential of humanized transgenic TC mice for the development of fully human monoclonal antibodies, thus bypassing the need for humanization and affinity maturation required by other humanized mice or phase display.

#4696 ERBB2 signaling and inhibition in bladder cancer.

C. Caparas-Spaugy, C. Stubben, K. Boucher, B. Feng, A. Atkinson, D. Nix, B. Cairns, S. Gupta;
University of Utah Huntsman Cancer Institute, Salt Lake City, UT

The role of human epidermal growth factor receptor-2 (HER2) protein and the inhibition of its oncogenic signaling pathway, ERBB2, is well defined and found to be beneficial in combination with standard chemotherapies in breast and certain gastro-intestinal cancers. Targeting the ERBB2 pathway has had unclear or inconsistent results in early trials in bladder cancer (BLCA) and the efficacy of its combination with cisplatin, a standard BLCA chemotherapy, is not known. In this study, we identify the transcriptomic oncogenic signatures that correlate with ERBB2 signaling in BLCA, explore how HER2 expression in BLCA cell lines correlates with treatment response *in vitro*, and evaluate the potential of ERBB2 inhibition in combination with cisplatin for BLCA.

We analyzed the tumor transcriptome from the Cancer Genome Atlas (TCGA) study of BLCA with single sample Gene Set Enrichment Analyses (ssGSEA) for Hallmark and Oncogenic gene sets. We performed multiple Pearson correlation analyses of HER2 protein levels and ERBB2 signaling with other signaling pathways in the TCGA BLCA tumors and adjusted the significance for multiple comparisons using the Benjamini-Hochberg method. Immunoblotting was used to assess HER2 protein levels across a panel of bladder cancer cell lines. We then assessed cell viability and colony formation upon exposure to the specific ERBB2 inhibitor, tucatinib. Synergy between cisplatin and tucatinib in BLCA cell lines was evaluated using the Chou-Talalay method.

In the TCGA BLCA dataset, HER2 protein positively correlates with ERBB2 signaling with a Pearson correlation coefficient of 0.45 and an adjusted p-value of 1.73E-17. ERBB2 signaling has multiple significant positive and negative correlations. ERBB2 signaling negatively correlates with the DNA repair gene set with a Pearson coefficient of -0.5 and an adjusted p-value of 1.40E-22. HER2 protein expression varies greatly between bladder cancer cell lines: HT-1197 and UMUC3 have lower HER2 expression, with HT-1376, T24, RT4, 5637, and SW780 showing higher HER2 expression. HT-1197 and RT4 had the lowest IC50s for tucatinib and showed a strong response to low doses of tucatinib in the colony formation assay. Cisplatin and tucatinib have synergetic growth inhibition (combination index <1) at low concentration levels in the HT-1197 and SW780 cell lines.

Multiple oncogenic pathways coexist with ERBB2 signaling in BLCA. The varied response to specific ERBB2 inhibition and the lack of correlation of the response with HER2 protein level in cell lines alludes to alternative oncogenic pathways. A strong negative correlation of ERBB2 signaling with the DNA response pathway in the TCGA BLCA dataset, combined with preclinical evidence of synergy between tucatinib and cisplatin, indicates a potential for development of the combination as a clinical treatment strategy and warrants further study.

#4697 Surface localization of enolase-1 (ENO-1) as an attractive theranostic target in docetaxel-resistant neuroendocrine-like prostate cancer cells.

K. R. Santiago Torres, C. A. Casiano, F. Almaguel, A. Duran, K. Whitley;
Loma Linda Univ. School of Medicine, Loma Linda, CA

Prostate cancer (PCa) is American men's second most common cancer. Although taxane-based chemotherapy is the last line of defense for Metastatic Castration Resistant Prostate Cancer (mCRPC), it invariably fails due to chemoresistance. The protein-specific membrane antigen (PSMA) has been an effective target for the imaging and therapy of mCRPC. Although PSMA radioligand therapy (PSMA-RLT) is a theranostics option for men with advanced PCa, about 30% have a limited response due to neuroendocrine-like PCa (NEPC), which lacks PSMA expression. Enolase (ENO) is a promising theranostic alternative due to its cell surface localization in many human tumors. We observed that chemosensitive PCa cell lines expressing NEPC markers express both ENO-1 and ENO-2; however, docetaxel-resistant NEPC-like cells only express ENO-1 and have a metabolic vulnerability due to the loss of ENO-2. We hypothesize that ENO-1 is expressed on the surface of NEPC-like cell lines and can be targeted with small molecule inhibitors (SMIs) that could potentially be used as theranostics agents. Additionally, we have observed changes in the expression and localization of ENO-1 in NEPC-like cell lines under different glucose concentrations. Our data show that under high glucose conditions, found on metabolically active metastatic tumors, ENO-1 is highly expressed on the cell surface, making it a promising candidate target for theranostics. However, low glucose conditions inhibit the activity of the c-MYC oncogene resulting in ENO-1 downregulation and upregulation of MBP1, the small splice variant of ENO1 that blocks the transcriptional activity of c-MYC. Our efforts to confirm ENO-1 surface expression on NEPC-like cell lines entailed using confocal microscopy, cell fractionation analysis followed by Western blotting, and Flow cytometric cell surface staining. We also evaluated the cytotoxicity of SMIs designed to target ENO-1 in chemoresistant NEPC-like cell lines using MTT viability assays, clonogenic assays, and Hoffman Modulation microscopy imaging. Our long-term goal is to identify an alternative treatment for patients with NEPC by establishing ENO-1 as a novel theranostics target.

#4698 Measuring cellular PARylation to gain insight in PARP / PARG-targeted drug discovery.

C. Pilo, M. Awad, V. T. Baron, F. Martins, J. Mikolosko, S. Plouffe, Z. Tao, K. Zientara-Rytter, H. Zhu, P. Shashkin;
BPS Bioscience, San Diego, CA

Inhibitors of poly (ADP-ribose) polymerases (PARPs) have revolutionized cancer therapy by highlighting the potential of synthetic lethal drugs to target the DNA damage response (DDR) network. More recently, the development of PARG inhibitors was spurred by the discovery that inhibiting PARG (poly (ADP-ribose) glycohydrolase) results in the accumulation of poly ADP-ribose on DDR proteins and induces cell death. Adding PARG or PARP inhibitors to a cell of interest and quantifying the resulting levels of PARylation can provide valuable insight on compound membrane permeability and target engagement in a cellular context. Nevertheless, assessing PARylation (poly-ADP-ribosylation in which multiple ribose units are added in linear or branched forms) in cells is difficult compared to biochemical assays, impeding the progress of candidate drug development. A sandwich ELISA-based assay was developed to analyze the total protein PARylation present in cellular extracts. Experimental protocols were optimized to discern differences in cellular PARylation levels resulting from activating the DDR and from exposure to PARP inhibitors and/or PARG inhibitors. It is worth noting that our assay specifically detects PARylation, measuring the effects associated with PARP family members 1 to 5, as other family members primarily catalyze MARylation (mono-ADP ribosylation in which a single ADP-ribose unit is added). Titration of known PARP inhibitors and PARG inhibitors was performed to validate the assay. 1) PARG inhibitor PDD00017273, used in combination with DNA damaging agent H_2O_2, increased the level of cellular PARylation, exhibiting a similar IC_{50} value across the four cell lines tested. This is consistent with the notion that PARG is the major de-PARylating enzyme in most cells. The potency of other known PARG inhibitors PDD00017272 and PDD00017238 ranked the compounds as expected from published results (PDD00017272< PDD00017273< PDD00017238). 2) Titration of the three PARP1/2 inhibitors Talazoparib, Olaparib and AZD5305, in combination with a DNA damage agent and PDD00017273 inhibitor, shows a dose-dependent reduction in cellular PARylation in HEK293 cells, as expected since PARP1 is activated in response to DNA damage and this activation is blocked by the inhibitors (IC_{50} values, Olaparib = 0.013 µM, AZD5305 = 0.0024 µM, Talazoparib = 0.0016 µM). These IC_{50} are consistent with published values and underscore the usefulness of the assay in measuring dose response effects, allowing accurate determination of compound IC_{50} in living cells. In summary, our optimized experimental cell treatment protocols and ELISA-based assay allow quantification of total cellular PARylation and accurately rank candidate drugs targeting PAR erasers or PAR writers in a high-throughput format, using living cells.

#4699 Evaluating extracellular matrix invasion and cytotoxicity of natural killer cells in a novel co-culture assay.

J. Thyagabhavan Mony, X. Zhang;
Agilent Technologies, Inc., San Diego, CA

Background: The complex tumor microenvironment (TME) in solid tumors presents unique challenges for lymphocytes used in cancer immunotherapy. The extracellular matrix (ECM) in TME can limit the recruitment of lymphocytes and restrict access to cancer cells. This study utilized Matrigel to study the kinetics of natural killer cell invasion and cytotoxicity. We hypothesized that the kinetics of tumor cell killing by the NKs would depend on the distance for invasion and rely on matrix-metalloproteinases (MMPs) for remodeling the ECM.
Methods: Increasing volumes (50-100 µL/well) of Matrigel (6 mg/mL) representing increasing distance for invasion was layered over MCF7-red target tumor cells expressing nuclear-localized mKate2 (red fluorescent protein). NK92 (Creative Bioarray) or eGFP-NK92 (BPS Bioscience) were seeded over the solidified Matrigel layer at E:T of 3:1. The broad spectrum MMP inhibitor, Ilomostat (GM6001, 2 µM and 10 µM), was added to the wells to investigate to role of MMPs. Label-free impedance and live cell imaging data was collected in real time on xCELLigence RTCA eSight to evaluate NK cell invasion and cytotoxicity. Percent cytolysis was calculated on the RTCA software from normalized cell impedance readings and imaging data using the formula [(1-(treated/untreated)*100].
Results: Impedance reading increases as the MCF7-red cells settle, attach, and proliferate. The readings plateau as the cells reach confluence. The addition of Matrigel modulates the impedance signature of MCF7 cells. Importantly, Matrigel delays cytolysis by NK92 cells added at 24h. The delay increases with increasing volume of Matrigel representing increasing invasion distance. The time to achieve 60% killing with respect to controls (KT60) was 67, 76 and 89 hours for 50, 75 and 100 µL/well, respectively. Consistent with the role of MMPs in invasion, percent cytolysis calculated independently from normalized impedance readings and live cell imaging data confirmed both delayed and reduced target cell killing by GFP-NK92 cells in the presence of Ilomostat. Interestingly, only a few GFP-NK92 were detected by live cell imaging when there was increased target cell death. These included highly active NK cells that made multiple contacts with different MCF7 red targets in clusters suggesting serial killing activity.
Conclusions: The observations that only a few NK92 cells are detected during the killing of susceptible target cells and that cytolysis is not abrogated by the inhibition of MMPs suggest a potential role for distal effectors like cytokines, independent of invasion. This is a novel 2.5D assay that demonstrates the potential of RTCA eSight platform for studying the invasion and cytotoxicity function of various immune cells through both real-time impedance recording and live-cell time-lapse imaging simultaneously. (For Research Use Only. Not for use in diagnostic procedures. RA45236.3472453704)

#4700 Induced phenotype targeted ADC by using caspase enzymatic cleavable peptide linker to overcome tumor heterogeneity.

H. Lee[1], B. Kim[1], H. Chang[2], S. Kim[3], Y. Byun[1];

[1]Seoul National University, Seoul, Korea, Republic of, [2]University of Ulsan College of Medicine, Seoul, Korea, Republic of, [3]Pharosgen Co., Seoul, Korea, Republic of

Antibody-drug conjugates (ADCs) have ushered in a new era of precision cancer therapy, and the caspase-3-cleavable linker has demonstrated its potential as a game-changing addition to the ADC toolkit. The DEVD peptide, specifically cleaved by caspase and lysosomal enzymes, in combination with the KG peptide, provides the necessary flexibility to achieve targeted cancer cell apoptosis. This research explores the key attributes and actions of the linker, aiming to highlight its potential for revolutionizing ADC therapy. The caspase-3-cleavable linker operates through caspase-3 activation during apoptosis. After targeting cancer cells with specific antigens, the ADC is internalized into the cells, and the linker is cleaved by caspase-3, releasing the drug and initiating apoptosis. The specificity of caspase-3 extends the drug's effect to neighboring cells, even those lacking the target antigen. This cascade effect ensures the continuous activation of ADCs until all cancer cells are eradicated. Firstly, it overcomes tumor heterogeneity by activating the drug outside of the cell. Traditional bystander killing effects rely on internalization followed by drug release and penetration of neighbor cancer cells. However, this linker's unique mechanism ensures that the drug is activated by caspase-3 outside the cell without the need for internalization, effectively targeting all cancer cells within the tumor tissue. This is achieved through the induced phenotype targeting effect (IPTE), which involves caspase-3 cleavage of the linker, inducing a phenotype in the tumor tissue that targets all cancer cells, regardless of their specific markers. Secondly, it maintains therapeutic efficacy even as the target antigen decreases. Current targeted therapies face a challenge as target antigens may diminish during treatment, leading to reduced drug effectiveness. However, the unique mechanism of the linker ensures that the drug continues to be activated as long as there is caspase-3 secretion, resulting in continuous activation of ADCs in the tumor, with a feedback amplification loop that ensures therapeutic efficacy until all cancer cells are eliminated. Lastly, the linker's superior physicochemical properties allow for a maximum drug-to-antibody ratio (DAR). Its hydrophilic nature enables independent drug conjugation, increasing therapeutic potential and mitigating aggregation issues. This innovation addresses the current limitations in ADC conjugation technologies. In summary, the caspase-3-cleavable linker represents a significant leap forward in the field of ADCs. Its unique attributes offer promising prospects for more effective and targeted cancer treatments. This linker is poised to revolutionize the landscape of targeted cancer therapy, bringing us one step closer to the dream of eradicating cancer cells with precision and efficiency.

#4701 A novel microtubule disruptor exerts broad anticancer efficacy with a tolerable safety profile.

H. Lelie[1], I. Brandsma[2], G. Hendriks[2], L. R. Cavedine[3], B. A. Epkins[3], S. M. Garner[3], A. J. Cook[3], M. Renganathan[3], Y. Zhao[3], A. J. King[3], P. Y. Chan[4], A. Risinger[4], **M. Koutsioumpa**[1];

[1]Australis Pharmaceuticals, Inc., Simi Valley, CA, [2]Toxys B.V., Oegstgeest, Netherlands, [3]Eurofins Discovery, St. Charles, MO, [4]University of Texas Health Science Center at San Antonio, San Antonio, TX

Initial evaluation of the prenylated hydroxy-stilbene isolated from bee propolis, AUS_001, in the NCI 60 human cell line anticancer screen showed significant growth inhibitory effects with the most robust being observed in leukemia, central nervous system and breast cancer cell lines. The aim of the current study was to further assess the potency of AUS_001 *in vitro* and investigate its safety profile and mechanism of action. A commercially available cell-based profiling screen (OncoPanel®) identified significant AUS_001-induced growth inhibition in 273 out of 280 cancer cell lines with a concentration causing 50% cell growth inhibition in the range of 0.021-0.94 µM, while non-neoplastic cells required an average of 20x higher concentration to generate similar efficacy. These findings indicate that AUS_001 exerts a high degree of potency across 30 cancer types with a selectivity for cancer versus normal cells. Maximum tolerated dose studies in mice illustrated that orally administered AUS_001 is well tolerated at doses 4 times greater than those that conferred antitumor efficacy, with no myelosuppression or other overt toxicities observed. Predictive toxicology and safety screening indicated that AUS_001 exerts a strong safety profile as evidenced by absence of mutagenic potential in the Ames test using up to 100 µM drug doses and low hERG-blocking liability with a half-maximal inhibitory concentration of 65 µM. Notably, AUS_001 is a poor substrate of the drug efflux transporter, P-glycoprotein 1 (Pgp), as it does not inhibit drug-stimulated Pgp ATPase activity and retains efficacy in high Pgp-expressing models *in vitro*. Subsequently, the effects of AUS_001 were explored in the ToxTracker® assay, consisting of a panel of mammalian stem cell lines that contain fluorescent reporters for the exploration of DNA damage, oxidative stress, and protein damage using flow cytometry. Robust activation of the Rtkn genotoxicity reporter under low cytotoxicity conditions, in combination with accumulation of cells in G_2/M phases of the cell cycle within 4 h and an increase in aneuploid cells after 24 h of drug treatment, suggested an aneugenic mode of action, typically caused by tubulin-targeting agents or mitotic kinase inhibitors. Biochemical tubulin polymerization assays then revealed that AUS_001 acts as a direct tubulin destabilizing agent and monitoring microtubule dynamics in GFP-tubulin reporter cells provided evidence that AUS_001 blocks microtubule assembly. Our studies have elaborated the mechanism of AUS_001 as an inhibitor of tubulin polymerization. The favorable safety profile of AUS_001, along with its ability to circumvent Pgp-mediated multidrug resistance, provides potential for efficacy against multiple cancers where microtubule destabilization is proven to be an effective target.

#4702 MediLink's TMALIN ADC linker technology: Tumor microenvironment specific extracellular and intracellular double cleavage mechanism for better efficacy and expanded target space.

T. Xue[1], L. Xiao[1], Q. Liu[1], S. Song[1], A. Shan[1], X. Zhang[1], S. Stann[2], **J. Cai**[1];
[1]MediLink Therapeutics (Suzhou) Co., Ltd., SuZhou, China, [2]MediLink Therapeutics USA, INC., Boston, MA

Antibody-drug conjugates (ADC) are a type of the fastest growing anticancer drug modalities. However, the traditional ADC technologies constrain on therapeutic development, requiring overexpressed targets, high internalizing antigens and efficient intracellular processing. To this end, MediLink's TMALIN platform was developed, with an irreversible pyrimidine coupling anchor and a valyl dipropyl-lysyl glycinamide-methylene (-VK*G-$NHCH_2$-O-) cleavable sequence. The TMALIN platform is featured as a high hydrophilicity linker-payload, remarkable stability in circulation, coupled with an efficient payload release mechanism which is achieved through the cleavage both extracellularly in the tumor microenvironment and intracellularly within lysosomes. A site-specific and homogeneous conjugation using TMALIN platform provides highly stable ADC in circulation. It is evidenced by less than 2% payload drop-off after a 21-day incubation in plasma under physiological conditions in vitro. This feature is observed in over 7 ADCs developed using the TMALIN platform. Additionally, the high stability was also illustrated by the pharmacokinetic profiles in NHP studies and clinical trials, with the overlapped curves of ADC and TAb in all TMALIN platform-based ADCs. Apart from the stability, a battery of *in vitro* and *in vivo* studies showed the linker-payload efficiently releases the payload in both tumor cells and the tumor microenvironment. Due to the high stability in circulation and efficient cleavage within tumors, the TMALIN platform ADCs have shown promising efficacy and good safety windows in preclinical studies. In xenograft mouse models, including those with low antigen expression, these ADCs have demonstrated tumor regressions and good tolerability. This highlights the potential of the TMALIN platform in improving the efficacy of ADCs and expanding their therapeutic applications. Furthermore, favorable safety profiles have been observed in clinical trials and/or pivotal non-human primate (NHP) studies for ADCs developed using the TMALIN platform. No drug-related adverse effects in organs were identified including the lungs, liver, or kidneys for those ADCs. In summary, the TMALIN platform addresses the unmet need of ADCs by releasing the payload extracellularly in tumors and tumor microenvironments on top of the known intracellular lysosomal cleavage mechanisms. This enables the advancement of ADC development, and has the potential to expand the field of ADC therapy and improve patient outcomes.

#4703 Automated 42 PDX 3D *in vitro* tumor models of the TME screen immuno-oncology and targeted compounds and biologics for antitumor effects and MOA.

B. Xue[1], C. Harrod[1], L. Le[1], J. Schuler[2], **K. C. Hribar**[1];
[1]Cypre Inc., San Francisco, CA, [2]Charles River Laboratories, Freiburg im Breisgau, Germany

High throughput screening has been widely utilized for its efficiency in testing novel therapeutic agents. However, the conventional screening using 2D culture of cancer cell lines lacks the biological complexity of the tumor microenvironment or the immune compartment which limits their application in testing immune-oncology therapies. Particularly with the passing of the FDA Modernization Act 2.0, it is critical to create more biologically relevant 3D in vitro models that can be used to reduce, refine and ultimately replace preclinical animal models. Here we have developed a highly automated 3D high throughput screening platform comprised of 42 patient-derived xenograft models in coculture with fibroblasts in engineered extracellular matrix hydrogels that resemble tumor stromal microenvironment. The PDX models cover a diverse range of tumor and histological types including NSCLC, CRC, gastric, TNBC, RCC, bladder, ovarian, melanoma, pancreatic, and others. Moreover, PBMCs or other immune cells can be incorporated into the system for evaluating immuno-oncology drugs. The panel has been tested against chemotherapy drug cisplatin and the immunotherapy biologic, Solitomab, an EpCAM/CD3 bispecific antibody. The endpoint analyses for antitumor effects include the dose response of tumor size and tumor cell death percentage based on high content imaging analysis. In addition, immune cells and supernatant in the IO assay can be recovered from the wells and used for flow cytometry profiling and cytokine assays. In summary, the novel 42-PDX panel described here offers a unique and powerful tool for rapidly generating preclinical data and a better understanding the drug activity at the pharmacology stages, opening the door for faster and more human relevant drug discovery for cancer patients.

#4704 Biochemical and cell-based assay platforms for development of RAF inhibitors against human cancers.

J. Wu, Y. Wan, S. Liang, P. Gallagher, L. Liang, C. Loch, H. Ma;
Reaction Biology Corporation, Malvern, PA

The RAF protein kinases are key intermediates in cellular signal transduction, functioning as direct effectors of the RAS GTPases and as the initiating kinases in the ERK cascade. In human cancer, RAF activity is frequently dysregulated due to mutations in the RAF family members (ARAF, BRAF, and CRAF) or to alterations in upstream RAF regulators, including RAS and receptor tyrosine kinases. The first and second generations of RAF inhibitors have yielded dramatic responses in malignant melanomas containing BRAF mutations; however, their overall usefulness has been limited by both intrinsic and acquired drug resistance. In addition, cancers with hyperactive RAS exhibit intrinsic resistance to these drugs. In particular, issues related to the dimerization of the RAF kinases can impact the efficacy of these compounds and are a primary cause of drug resistance. We have established biochemical HotSpot™ kinase assay, NanoBRET™ and NanoBIT™ cell assay platforms for High Through Screening of kinase inhibitors. Here, we demonstrate that the 3rd generation of pan-RAF inhibitors LY3009120, LXH254, and Belvarafenib inhibit ARAF, BRAF, CRAF, BRAF(V600E), and CRAF(R391W) kinase activity in biochemical HotSpot™ assay. Our NanoBRET™ target engagement and NanoBIT™ cellular assay data show that LY3009120, LXH254, and Belvarafenib bind to KRAS(G12C) primed BRAF and CRAF, and block BRAF and CRAF dimerization. Furthermore, our results show these inhibitors can block the downstream ERK phosphorylation in cellular HTRF assay and induce caspase-3/7 activation in Western blot assay in the triple negative breast cancer MDA-MB-231 cells. Taken together, our results indicate the biochemical HotSpot™ kinase activity assay, and NanoBRET™ target engagement and NanoBIT™ cellular assays can serve as great platforms to facilitate RAF drug discovery against human cancers.

#4705 Repetitive membrane potential oscillations enhance metformin's antiproliferative effect in glioblastoma stem cells.

Ivan Verduci, Gaetano Cannavale, **Guido Rey**, Francesca Cianci, Alessandro Fantin, Michele Mazzanti

University of Milan, Milano, Italy

Glioblastoma (GB) is the most common and lethal brain tumor and there is a general agreement that GB stem cells (GSCs) are primarily responsible for its high aggressiveness and recurrence. It was recently reported that GSCs are enriched in the transmembrane form of CLIC1 protein (tmCLIC1) and its inhibition was shown to impair tumor growth both *in vitro* and *in vivo*. IAA94 hampers tmCLIC1 function but could not be used in clinics. However, tmCLIC1 is also sensitive to metformin, the most used drug to treat type-2 diabetes. Metformin has been demonstrated to have the same effect as IAA94 in *in vitro* experiments, resulting in an antitumoral action on cancer cells. Moreover, GB orthotopic mouse model treated with metformin shows a 50% survival compared to control animals, even if metformin concentration in the mice brain resulted in the nanomolar range. In this scenario, the main aim of this work is to enhance the effect of metformin able to reach the brain, improving its antitumoral activity in GB. The interaction between metformin and tmCLIC1 occurs only when this protein is in its open state. TmCLIC1 has the peculiarity of being a voltage-dependent ion channel that opens at depolarized voltages. Thus, our strategy is to apply electromagnetic field (EMF) stimulation to induce repetitive membrane depolarization, increasing metformin-tmCLIC1 binding. Our results show that EMF stimulation induces the close-to-open transitions of tmCLIC1, resulting in a 10-fold decrease of the operative concentration of Metformin. This was verified initially *in vitro* with GSC culture and spheroids model and afterward confirmed also in an *in vivo* model. The project's long-term goal is to combine transcranial stimulation and metformin administration in patients as an adjuvant therapy able to target cells that are resistant to chemotherapy and drive tumor relapse.

#7249 Enhancing mRNA- lipid nanoparticles formulations to improve transfection efficiency in macrophages and dendritic cells in cancer immunotherapy.

Yasir Alshehry, Matthew Fernandez, Raneem Aldaqqa, Asma Al-Terawi, Douglas Sweet, Sandro da Rocha

Department of Pharmaceutics and Center for Pharmaceutical Engineering and Sciences, Virginia Commonwealth University, Richmond, VA

Cancer poses a global health challenge, driving the quest for innovative therapies. Messenger ribonucleic acid (mRNA) lipid nanoparticles (LNPs) are a promising strategy in cancer immunotherapy. However, a major obstacle lies in efficiently transfecting immune cells like macrophages and dendritic cells (DCs) with LNPs. This study seeks to improve cancer immunotherapy by optimizing mRNA-LNP formulations. Therefore, we systematically evaluated three components of LNPs, namely ionizable lipids, phospholipids, and sterols, and fine-tuned the components and their molar ratios. A comprehensive screening process was conducted to determine the efficiency of LNPs, involving in vitro experiments on macrophages and DCs, as well as in vivo assessments. Among six ionizable lipids assessed in different cell lines (RAW264.7 and DC2.4), SM-102 significantly enhanced the transfection efficiency in macrophages and DCs. Subsequently, we evaluated these LNPs in an in vivo setting. We quantified the bioluminescence signal after administering LNPs loaded with luciferase mRNA. The results demonstrated a significant increase in luciferase expression when using SM-102 and ALC-0315 lipids. To validate this finding, we conducted a T cell response study, which revealed an increased percentage of CD8+ T cells with SM-102-based LNPs compared to other formulations. Having identified SM-102 as a potent ionizable lipid, we proceeded to evaluate three phospholipids in vitro. The results indicated a significant enhancement in transfection efficiency with DOPE lipids compared to DSPC. Consequently, we selected DOPE as the phospholipid for subsequent screening. Lastly, we explored different types of sterols with varying molar ratios in macrophages and DC cells. Our findings unveiled a notable improvement in mRNA delivery, particularly in DCs, when the molar ratio of β-sitosterol was increased to 19.5%, while concurrently decreasing the molar ratio of cholesterol to 19% within the same formulation. It is noteworthy that the addition of β-sitosterol alone led to reduced transfection efficiency in DCs but resulted in a significant enhancement in macrophages. Lastly, we evaluated the top four formulations in vivo, and the results demonstrated a significant increase when β-sitosterol was added to the formulation with cholesterol, at molar ratios of 19.5% and 19%, respectively. Overall, altering lipid composition and their molar ratios profoundly impact mRNA-LNP transfection. The optimized formulations, comprising SM-102, DOPE, and cholesterol with or without β-sitosterol, outperformed the alternatives. These refined formulations hold promise for clinical applications, potentially enhancing passive therapeutic agent delivery into macrophages and DCs, offering promising prospects for advancing cancer immunotherapy.

EXPERIMENTAL AND MOLECULAR THERAPEUTICS: Other Cellular Mechanisms for Anticancer Drug Action
Poster Session

#4708 Potency and selectivity of ERBB2-targeting antibody drug conjugates in vitro.

A.-L. Peille[1], K. Holtorf[2], P. Anton Garcia[1], N. Obier[2], D. Feger[2], T. Metz[1], S. Dempe[2], H.-H. Fiebig[1], J. Ehlert[2], V. Vuaroqueaux[1];
[1]4HF Biotec GmbH, Freiburg, Germany, [2]Reaction Biology Europe GmbH, Freiburg, Germany

Previously we have reported on the relevance of the joint ProLiFiler and Cancer DataMiner platforms when studying the antitumor efficacy of novel antibody-drug conjugates (ADCs), such as Sacituzumab govitecan. In this study, we use our platforms to investigate and compare the selectivity of two FDA-approved Trastuzumab-based ADCs targeting ERBB2: Kadcyla, the first-in-class ADC employing a microtubule inhibitor bound via a non-cleavable linker, and Enhertu, which combines a topoisomerase inhibitor with a protease-cleavable linker. We performed a cell proliferation and survival assay using the ProLiFiler™ (Reaction Biology) to characterize the in vitro antitumor effects of Enhertu, Kadcyla, and their individual cytotoxins, deruxtecan & mertansine on 160 human cancer cell lines (CLs). The resulting data were uploaded to 4HF´s Cancer DataMiner platform for data analysis. First, we confirmed high potency and limited selectivity of mertansine, as it displayed an IC_{50} < 250 nM (mean: 27.3 nM) in 95% of cell lines (CLs). A COMPARE analysis confirmed that mertansine data correlated best with those of other microtubule inhibitors in our drug databases (e.g., MMAE, Spearman rho = 0.79, p=9.6E-27). Conversely, a paired analysis showed that CLs were less sensitive to Kadcyla than to mertansine except for CLs overexpressing ERBB2. The 160-CL panel included a total of nine CLs (six mammary, two gastric, one ovarian) with strong ERBB2 overexpression (Affymetrix data >10), mostly associated with ERBB2 gene amplification; seven of them were the most sensitive CLs to Kadcyla (IC_{50} < 6 nM). Focusing solely on breast cancer cell lines (breast cancer is the approved indication for Kadcyla), we observed a strong correlation between sensitivity to Kadcyla and ERBB2 expression (Spearman r = -0.78, p = 0.003). Interestingly, in line with published data, the ERBB2-overexpressing cell lines SNU-216 (stomach cancer) and JIM-T1 (breast cancer) were less sensitive to Kadcyla. In non-ERBB2-amplified CLs, Kadcyla sensitivity did not correlate with ERBB2 expression levels. Focusing on ERBB2-negative CLs such as hematological CLs, we unexpectedly observed consistent cell inhibition (mean IC_{50} =33 nM) with Kadcyla, suggesting that the ADC was cleaved, and the payload released into the medium. Overall, this study has demonstrated the relevance of our platforms to study and compare newly developed ADCs. Cytotoxic activities recorded for conjugates and free payloads, along with molecular data for the test cell lines, provides insight in the mode of action of conjugates and their target cell populations and hence can support the development of ADCs. Investigations are underway with Enhertu and its payload deruxtecan, and results will be compared with those obtained for Kadcyla and mertansine.

#4709 The RAS^{MULTI}(ON) inhibitor RMC-7977 blocks downstream MAPK and PI3K pathway activation in KRAS^{G12X} mutant cancers.

P. S. Bapat, K. Seamon, A. Gould, D. Wildes;
Revolution Medicines, Inc., Redwood City, CA

Oncogenic RAS binds to multiple effector proteins to activate downstream signaling pathways, including the MAPK and PI3K axes. While RAS-mediated MAPK activation has a well-validated role in driving cancer progression, the contribution of PI3K activation has been more difficult to assess. Understanding the degree to which different KRAS-mutant genotypes stimulate PI3K activity may inform biomarker and combination strategies for RAS inhibitors currently undergoing clinical evaluation.RMC-7977 is a RAS^{MULTI}(ON) inhibitor that targets GTP-bound RAS(ON) and blocks effector protein binding. RMC-7977 exhibits similar potency for wild-type and oncogenic mutant RAS and is a powerful preclinical tool, representative of the investigational RAS^{MULTI}(ON) inhibitor RMC-6236, for comparing how RAS-mutant genotypes differ with respect to signal activation. MAPK signaling proceeds through a protein phosphorylation cascade that is readily detectable using standard cell biology methods, but PI3K is a lipid kinase whose activity is not amenable to protein characterization techniques. An assay of phosphatidylinositol (3,4,5)-trisphosphate (PIP3) was developed to directly measure the activity of PI3K in the context of RAS inhibition.In isogenic LIM1215 cell lines expressing different KRAS^{G12X} mutants (KRAS^{G12D}, KRAS^{G12V}, KRAS^{G12C} and KRAS^{G12R}), RAS inhibition by RMC-7977 completely suppressed PI3K activity in cells with wild-type KRAS and KRAS^{G12D}, had a moderate inhibitory effect in KRAS^{G12C} and KRAS^{G12V}, and had no effect in KRAS^{G12R}. To confirm that this inhibition is dependent on a direct interaction between RAS(ON) and PI3K, CRISPR engineering was used to introduce mutations in *PIK3CA* to perturb the RAS-binding domain. In cells with disrupted RAS-PI3K interactions, the basal levels of PIP3 are significantly reduced and no longer change in response to treatment with RMC-7977.Based on the isogenic cell line results, KRAS^{G12D} and KRAS^{G12R}-mutant pancreatic cancer cell lines were profiled for their response to RAS inhibition. RMC-7977 decreased the levels of MAPK signaling in both KRAS^{G12D} and KRAS^{G12R} genotypes, but PI3K activity was only inhibited in KRAS^{G12D} lines. MEK inhibitors only inhibited MAPK signaling and had no effect on PI3K activity in either genotype. The simultaneous inhibition of MAPK and PI3K signaling by RMC-7977 led to deeper suppression of cyclin D levels and a more pronounced G1 cell cycle arrest as compared with MAPK inhibitors.We demonstrate that the coupling between RAS activation and PI3K signaling varies between oncogenic mutants, with KRAS^{G12D} showing the greatest degree of PI3K stimulation. In KRAS^{G12D}-mutant pancreatic cancer cell lines, a RAS^{MULTI}(ON) inhibitor suppresses both PI3K and MAPK signaling. These preclinical results may be used to inform potential, rational, mechanism-based combination treatment strategies for RAS(ON) inhibitors.

#4710 The polymeric AMD3100 based drug PAMD-Ch17 induces its anti-leukemic effects in a CXCR4 independent mechanism.

C. Lam, J. Chinmay, E. Kapoor, S. Tang, S. Romanova, D. Oupicky, K. Hyde;
University of Nebraska Medical Center, Nebraska, NE

Background: Acute myeloid leukemia (AML) and acute lymphoblastic leukemia (ALL) are devastating blood cancers associated with 5-year survival rates of ~50% each in adults. We recently developed a new class of polymeric drugs called PAMDs based on the CXCR4 inhibitor AMD3100 (plerixafor). PAMDs have the potential to be more effective and less toxic therapeutics than the standard of care high-dose chemotherapy. We tested one variant (PAMD-Ch17), and found that unlike AMD3100, PAMD-Ch17 has several novel anti-leukemic effects. To understand the potential mechanism(s) for these new activities, we performed the following study.

Methods: To test the role of CXCR4 in PAMD-Ch17's activities, we generated *CXCR4* knockout cells via Crispr/Cas9. We used PrestoBlue, 7-AAD, and Annexin V staining to assay viability and apoptosis. To identify pathways deregulated by PAMD-Ch17, we performed whole transcriptomic sequencing (RNA-Seq). To investigate if PAMD-Ch17 mediates its activities by inducing oxidative stress, we performed SeaHorse assays, and dihydroethidium (DHE), Mitosox, and Bodipy C11 staining. To investigate whether PAMD induces programmed cell death pathways, we used ferrostatin and deferoxamine to inhibit ferroptosis, necrostatin-1 against necroptosis, and Z-VAD-FMK against apoptosis.

Results: We found that PAMD-Ch17 induces cell death in a dose dependent manner in human AML and ALL cell lines and, mouse primary leukemia cells, but not healthy mouse bone marrow cells. Surprisingly, PAMD-Ch17 induces equivalent levels of cell death in both wild type and CXCR4 knockout Jurkat cells, indicating that the only known target of the polymer is not required for its anti-leukemic effects. By RNA-Seq, we found altered expression of genes related to mitochondrial function, suggesting that PAMD-Ch17 could be targeting the mitochondria. To test this, we performed SeaHorse assays and found that PAMD-Ch17 induces a significant decrease in mitochondrial respiration. Consistent with this, we found that PAMD-Ch17 induces a significant increase in superoxide production, as well as lipid peroxidation. Using inhibitors of programmed cell death pathways, we found that preventing necroptosis, apoptosis, or ferroptosis caused only subtle effects on PAMD-Ch17 induced cell death, implying that the polymer's anti-leukemic activity is likely not entirely dependent on these pathways.

Conclusions: These results indicate that PAMD-Ch17 induces cell death in leukemia cells but not healthy bone marrow via a CXCR4 independent mechanism. We also found that PAMD-Ch17 induces reactive oxygen species, potentially explaining its selectivity for leukemia cells compared to healthy blood cells. Continued investigation of PAMD-Ch17 will not only further development of this new class of drugs, but also provide much needed insight into leukemia biology.

#4711 Evaluation of effect of autophagy inhibition by SAR405, a selective Vps34 inhibitor, on proliferation of pleural mesothelioma cells.

Y. Kuwabara, K. Sakai, S. Ishi, S. Yokosuka, M. Abe, T. Takahashi, Y. Kawano, H. Nishimura, M. Toda-Sasaki, Y. Kobayashi-Ogawa, S. Kikuchi, Y. Hirata, H. Kyoyama, G. Moriyama, N. Koyama, K. Uematsu;
Saitama Medical University Saitama Medical Center, Saitama, Japan

Pleural mesothelioma is a poor prognostic malignancy because the efficacy of therapies remains limited; thus, there is an urgent need to elucidate the pathophysiology leading to newer treatment modalities. Macroautophagy (hereafter referred to as autophagy) is an intracellular degradation system in which cytoplasmic components are degraded by the lysosome. Autophagy plays pivotal roles in various physiological processes, including adaptation to starvation, preimplantation embryonic development, elimination of intracellular pathogens, and regulation of innate and adaptive immunity. In cancer cells, autophagy may have the potential to function protectively for the cells and, alternatively, to work suppressively. It can promote tumor growth in established cancers through autophagy-mediated intracellular recycling, providing substrates for metabolism and maintain that the functional pool of mitochondria. On the other hand, it may lead to a cytotoxic effect called autophagy-dependent cell death. Several reports have demonstrated that autophagy has cytoprotective effects on pleural mesothelioma cell lines. In this study, we assessed effects of inhibition of autophagy using SAR405, which specifically inhibits Vps34 in an early step of autophagy, on pleural mesothelioma cells. Additionally, we investigated whether SAR405 could enhance the growth suppression induced by cisplatin in these cells. Mesothelioma cell lines, including NCI-H28 (H28), NCI-H2452 (H2452), and MSTO-211H (211H), were cultured with 0.1-50 μM SAR405 or 1.0-5.0 μM cisplatin for cell viability analysis using water-soluble tetrazolium salt-8, and cell cycle analysis. For the assessment of autophagy, a plasmid, pMRX-IP-GFP-LC3-RFP-LC3ΔG, was stably transfected into mesothelioma cells. Transfected cells generate GFP-LC3-RFP-LC3ΔG, and it is cleaved into GFP-LC3 and RFP-LC3ΔG by inherent ATG4. GFP-LC3 levels are decreased by autophagy activation, while RFP-LC3ΔG serves as an internal control. SAR405 dose-dependently suppressed cell viability, accompanied by a significantly increase in the proportions of cells in the G2/M phase. The IC50 of SAR405 at 72 hours was 11.5 μM for H28, 16.7 μM for H2452, and 14.9 μM for 211H. SAR405 inhibited autophagy 24 hours after treatment at 2.5 μM for H28 and 211H, and at 5.0 μM for H2452. Furthermore, cisplatin induced autophagy at 5.0 μM for H28, 0.5 μM for H2452, 1.0 μM for 211H. The combination of 2.5-10 μM SAR405 and 0.5-5.0 μM cisplatin exhibited additive or synergistic effects on cell growth inhibition in all plural mesothelioma cell lines. In conclusion, Vps34 inhibition by SAR405 suppressed cell growth in pleural mesothelioma cells, accompanied by autophagy inhibition. The combination of SAR405 and cisplatin resulted in a synergistic inhibition of cell proliferation.

#4712 GPCR panel establishment and application in drug discovery.

X. Wang, N. Sui, D. Hu, Z. Zhang, **T. Bing**;
ICE Bioscience, Inc., Beijing, China

G protein-coupled receptors (GPCRS) are the largest family of membrane proteins of cell surface receptors. It can be activated by various stimuli and play an important role in various physiological and pathological processes such as cell growth, proliferation, differentiation, metabolism, and homeostasis. Abnormal regulation of GPCR is associated with various human diseases, such as metabolic diseases, cardiovascular diseases, and eye diseases. G protein contains three subunits: α, β, and γ, which form a trimer. When extracellular ligands are bound to GPCRs which activate G protein and GTP phosphorylates Gα subunits, leading to the dissociation of Gα subunits from the trimer and dissociation from the β and γ subunits. In addition, Gα different subtypes of Gαs, Gαi and Gαq have different biological effects after activation, Gαs-coupled receptors activate adenylyl cyclase (AC) to increase cAMP. In contrast, Gαi-coupled receptors activated adenylyl cyclase (AC) to inhibit cAMP. Gαq coupled receptors promote phospholipase C (PLC) to produce IP3, and IP3 can increase intracellular Ca^{2+} concentration. GPCR Panel With high general availability, which provides over 150 GPCR targets, covering wide families like 5-Hydroxytryptamine, adrenoceptors, Acetylcholine, dopamine, glucagon, and opioid receptors and having the selectivity of multiple species. It can conduct similar GPCR poly-link interaction and screening, used to study new GPCR drug development technology, detect the expression properties of GPCR receptors, reveal new GPCR structure and function, and screen GPCR drugs. We also constructed different assay platforms, including cAMP assay, Ca2+ flux assay, IP3 assay, β-arrestin recruitment assay and reporter assay to detect the different second messengers produced by G protein submits and GPCR-mediated multiple signaling pathways. This research constructed stable cell lines expressing GPCRs and provided related assays, which could be used to detect compounds' effects on GPCR targets successfully. In addition, the GPCR panel was applicable to both activating and inhibitory models, and the establishment of this platform provides a powerful tool for drug development of GPCR-related targets.

#4713 Chlorpromazine affects glioblastoma bioenergetics by interfering with pyruvate kinase M2: A route for drug repurposing in glioblastoma.

C. Abbruzzese[1], S. Matteoni[1], P. Matarrese[2], M. Signore[2], B. Ascione[2], E. Iessi[2], A. Gurtner[1], A. Sacconi[1], A. Pace[1], V. Villani[1], A. Polo[3], S. Costantini[3], A. Budillon[3], G. Ciliberto[1], **M. G. Paggi**[1];

[1]IRCCS Regina Elena National Cancer Institute, Rome, Italy, [2]Istituto Superiore di Sanita, Rome, Italy, [3]Istituto Nazionale Tumori-IRCCS-Fondazione G. Pascale, Naples, Italy

Glioblastoma, the most common and deadly brain tumor, remains a critical unmet medical need due to the limited effectiveness of current treatments. Drug repurposing has recently emerged as a promising strategy to improve glioblastoma outcomes. Antipsychotic drugs, with their established safety profile and potential to disrupt tumor-neuron interactions, have drawn particular attention. Among these, chlorpromazine, a well-tolerated medication included in the 2021 WHO Model List of Essential Medicines, holds promise due to its therapeutic effects in psychiatric disorders stemming from its non-specific interference with various CNS neurotransmitter receptors. Our recent studies have demonstrated chlorpromazine's ability to inhibit several molecular and cellular processes in glioblastoma cells, suggesting its potential as a novel treatment option for this challenging disease.To elucidate chlorpromazine's mechanism of action as a potential anticancer drug, we employed two proteomics approaches: Reverse-Phase Protein microArrays to evaluate its impact on signal transduction pathways and Activity-Based Protein Profiling followed by mass spectrometry to identify novel molecular targets.Our data revealed that chlorpromazine significantly modulates major signal transduction pathways and implicates pyruvate kinase (PK) M2 as a drug target. PKM2, a PK variant characteristic of many cancers, plays a crucial role in orchestrating metabolic alterations, exemplified by the Warburg effect – the high glucose consumption and lactate production by cancer cells even under oxygen-rich conditions. PKM2 functions as a tetramer in the glycolytic pathway, while its dimeric form acquires nuclear localization, protein kinase activity, and interacts with various transcription factors, contributing to its pro-tumorigenic activity.Consistent with its ability to target PKM2, chlorpromazine promoted PKM2 tetramerization in glioblastoma cells, leading to significant alterations in glioblastoma energy metabolism. Notably, RPE-1 non-cancer neuroepithelial cells showed a reduced response to the drug. Additionally, silencing PKM2 diminished the effects of chlorpromazine. 3D modeling revealed that chlorpromazine interacts with the PKM2 tetramer at the same site involved in binding other small-molecule activators that stabilize the PKM2 tetramer.These findings suggest that chlorpromazine counteracts the Warburg effect and, consequently, malignancy in glioblastoma cells, while sparing non-cancerous RPE-1 cells. This preclinical evidence supports the rationale behind our recently completed multicenter Phase II clinical trial investigating the role of chlorpromazine in glioblastoma treatment. The study is registered as EudraCT #2019-001988-75 and ClinicalTrials.gov Identifier #NCT0422444.

#4714 Mechanisms by which the Rac & Cdc42 inhibitor MBQ-167 overcomes the adverse effects of paclitaxel in TNBC.

Nilmary Grafals-Ruiz[1], Patricia Sanchez-Orive[2], Anamaris Torres-Sanchez[3], Ailed Cruz-Collazo[1], Derealise Garcia-Almedina[2], Stephanie Dorta-Estremera[4], Suranganie Dharmawardhane[1]

[1]Biochemistry, University of Puerto Rico - Medical Sciences Campus, San Juan, PR,[2]Natural Sciences, University of Puerto Rico - Rio Piedras Campus, San Juan, PR,[3]Biology, University of Puerto Rico - Rio Piedras Campus, San Juan, PR,[4]Microbiology and Medical Zoology, University of Puerto Rico - Medical Sciences Campus, San Juan, PR

Triple-negative breast cancer (TNBC) is the most aggressive, recurrent, and metastatic type of BC. Since there are limited targeted therapies available, the standard treatment is taxane-based chemotherapy, which still results in recurrence and metastasis. Therefore, we developed MBQ-167, a clinical-stage Rac/Cdc42 inhibitor that reduces tumor progression and metastasis in TNBC mouse models. In vitro studies show that PXL increased Rac activation, which MBQ-167 reduced in combination with PXL. In mouse models of TNBC, we found that PXL increases metastasis and that MBQ-167 prevents it. Therefore, this study aimed to identify potential mechanisms to explain the antimetastatic effects of MBQ-167 in combination with PXL. Previous studies suggest that PXL may act as an agonist to the Toll-Like 4 Recceptor (TLR4) and activate NfkB signaling to promote metastasis. We hypothesize that MBQ-167 chemosensitizes TNBC cells to PXL and reduces metastasis by blocking Rac/Cdc42 and TLR4/NF-kB signaling. Treatment of SCID mice with orthotopic MDA-MB-468 TNBC tumors with MBQ-167, PXL, or the combination increased lung metastases in mice treated with PXL, which MBQ-167 suppressed. Flow cytometry of spleens harvested from the mice with or without tumors demonstrated increased M2 immunosuppressive macrophages (F480+, CD206+) compared to M1 macrophages (F480+, CD206-), where macrophage differentiation has been implicated with TLR4 signaling. To determine the role of TLR4 signaling, we treated MDA-MB-231 cells stably expressing scrambled or TLR4 shRNA with MBQ-167, PXL, or the combination. Treated cells were evaluated for cell viability, apoptosis, migration, mammosphere assay, and NF-kB p65 activation. Results show that MBQ-167 reduced cell viability stem-cell-like features and increased apoptosis comparable to vehicle or PXL. TLR4 knockdown (kd) did not change cell viability, apoptosis, or migration in vehicle-treated cells. However, TLR4 kd further reduced the decreased cell viability and increased apoptosis in response to MBQ-167, PXL, or the combination, indicating that PXL effects on cell growth are at least partially dependent on TLR4. PXL treatment did not affect cell migration in the control cells but reduced migration in TLR4 kd cells. TLR4 kd exacerbated the inhibitory effects of MBQ-167 or the combination. MBQ-167, but not PXL, reduced LPS-induced (i.e., TLR4-regulated) NfkB translocation to the nucleus, with a similar effect as the combination. Therefore, MBQ-167 may prevent PXL-induced metastasis by partially inhibiting the NF-kB pathway in TNBC tumors and reducing inflammation and immunosuppression from M1 and M2 macrophages *in vivo*.

#4715 Azathioprine and Z36 induced cell death in human colorectal cancer HCT-116 and HCT-15 cells.

Y. Tahir Ali, M. Fatima, M. Ahmed, H. Siddiqi, A. Hussain, **M. Rehman**;
Aga Khan University, Karachi, Pakistan

Rationale and Objectives: Cancer accounts for a huge global health burden and is the third highest cause of death across the globe. Cancer cells are known to have higher basal reactive oxygen species (ROS) levels, owing to their higher metabolism and proliferation. Higher basal ROS in cancer cells made them susceptible to exogenous ROS stimuli that lead to cell death. Therefore, in the present study, we have analyzed the effects of Azathioprine, a glutathione (GSH) inhibitor and an intracellular ROS producer. The effect of Azathioprine was analyzed alone or in combination with a BCL-2 family protein inhibitor Z36, on human colorectal cancer cell lines HCT-116 and HCT-15.

Methods: The effects of the drugs have been investigated using various methods including cell viability assay, DNA fragmentation assay, and Annexin V-FITC/PI apoptosis assay. In addition, morphological changes evident in cell death were detected by Giemsa staining. Combination dosage for drug synergistic effects was computed through the use of CompuSyn software. Western blot was performed to detect changes in the expression of cell death-related proteins following drug treatments.

Results and conclusion: Azathioprine at a dose of 5 μM has been demonstrated to induce cell death in both HCT116 and HCT15 cells in a concentration and time-dependent manner. On the contrary, Z36, a novel BCL_{XL} inhibitor, has demonstrated similar cell viability results at an even lower dose of 2.5 μM. When both drugs were combined at lower doses, no significant effects were observed on the cell viability of either cell line, demonstrating that the combined treatment has no synergistic or additive effects. This suggests that both drugs do not augment each other and might induce cell death via upregulation of ROS using a similar mechanism.

#4716 First-in-class peroxiredoxin 3 (PRX3) inhibitor RSO-021 triggers mesenchymal-to-epithelial transition in mesothelioma.

T. Messier[1], V. Gibson[1], D. J. Seward[1], E. Y. Baitei[2], P. Jordan[2], C. Poile[2], J. Dzialo[2], A. Bzura[2], K. Kutywayo[2], A. Nakas[3], G. N. Naumov[4], D. A. Fennell[2], **B. Cunniff**[1];

[1]Larner College of Medicine at The University of Vermont, Burlington, VT, [2]University of Leicester and University Hospitals of Leicester, Leicester, United Kingdom, [3]University Hospitals of Leicester, Leicester, United Kingdom, [4]RS Oncology, Cambridge, MA

Mesothelioma, a lethal cancer associated with asbestos exposure, lacks effective drug therapy particularly in the relapsed treatment setting. Epithelial-to-mesenchymal transition (EMT) confers an aggressive sarcomatoid phenotype capable of invasion, metastasis, and drug resistance. Pharmacological targeting of EMT could favorably alter the progression and treatment of mesothelioma. We identified a geospatial transcriptomic gradient between adjacent epithelioid and sarcomatoid regions in patient-derived biphasic mesotheliomas involving hypoxia tolerance, TGF-β, mitochondrial oxidative phosphorylation, and EMT. Mesothelioma cells rely on buffering of mitochondrial oxidative stress through the expression and activity of mitochondrial peroxiredoxin 3 (PRX3), which is covalently inactivated by the first-in-class inhibitor RSO-021, now under investigation in the phase 1/2 MITOPE clinical trial (NCT05278975). To better understand the pharmacodynamics of RSO-021, transcriptomic profiles of drug sensitive and resistant biphasic mesothelioma cell lines were generated. Differential analysis revealed that RSO-021 induced up-regulation of ROS response and apoptosis signaling, while down-regulating TGF-β and EMT markers, WNT signaling, and TEAD target genes. Additionally, we observed altered expression of the mesothelioma specific EMT genes Col5A2, mesothelin and VISTA. Resistance to RSO-021 conferred significant proliferative defects and was reversible upon RSO-021 removal, however the down-regulation of EMT genes was conserved, suggesting an irreversible mesenchymal-to-epithelial transition. In summary PRX3 is a clinically actionable drug target, inhibition of which correlates with EMT modulation. This activity suggests a mechanism to alter mesothelioma progression and prevent the emergence of the most aggressive mesothelioma phenotype.

#4717 Small molecule modulation of PP2A selectively induces oncogenic cytotoxicity through chronic and irreversible integrated stress response.

R. A. Avelar, R. Gupta, G. Carvette, F. da Veiga Leprevost, J. Colina, J. Teitel, G. Narla, A. DiFeo;
University of Michigan, Ann Arbor, MI

High-grade serous cancer (HGSC) is the most lethal gynecological malignancy and accounts for approximately 70% of all ovarian carcinomas. Despite recent advancements in drug discovery and a deeper understanding of the genetic mechanisms that drive HGSC oncogenesis, the mortality rate has remained stagnant over the past three decades, with a 5-year survival rate below 30%. Due to the prevalence of homologous recombination defects (HRD) in over 50% of HGSC tumors, the clinical management of patients harboring these genetic vulnerabilities has vastly relied on PARP inhibitors (PARPi). Nonetheless, about 80% of these patients ultimately relapse with refractory resistant and more aggressive disease, having no effective therapeutic alternatives currently available. Therefore, there is an urgent need for novel targeted therapies to be tailored towards the treatment of HGSC. Recently, we unveiled that 95% of HGSC tumors present with a widespread loss-of-heterozygosity in genes essential to form the tumor suppressor Protein Phosphatase 2A (PP2A) heterotrimer, second only to *TP53*. These deleterious alterations have been established to inhibit PP2A function, preventing it from counteracting oncogenic signatures that drive tumorigenesis. Our studies revealed that a Small Molecule Activator of PP2A (SMAP) synergizes with PARPi to induce synthetic lethality in HGSC cells while displaying favorable tolerability profiles in normal tissues. Mechanistically, SMAP activates distinct translational responses and stress signatures depending on the cellular context, driving selective oncogenic cytotoxicity through a chronic and irreversible integrated stress response (ISR), independent of PERK activation. In malignant contexts, SMAP-mediated activation of PP2A specifically drives the dephosphorylation of TFE3 to transcriptionally activate ATF4 and CHOP. Consequently, as cancer cells are incapable of activating adaptive homeostatic recovery mechanisms in response to SMAP, chronic ISR is induced, ultimately leading to cell death. Conversely, non-transformed cells leverage their intrinsic ISR plasticity to adapt, thereby restoring basal functions that allow cell survival under SMAP-mediated stress conditions. Collectively, our data highlights a new role of PP2A in HGSC and further underscore SMAP's selective cytotoxicity in cancer cells, independent of oncogenic genetic vulnerabilities or HRD profiles, by leveraging ISR plasticity and intrinsic adaptive homeostatic mechanisms. Thus, this class of PP2A modulators holds tremendous promise for broader therapeutic applications across diverse patient populations and tumor histological subtypes beyond HGSC, while mitigating standard-of-care therapy-associated toxicity.

#4718 Reclaiming a dirty drug: What is the context of vulnerability to arsenic trioxide in glioblastoma?.

C. Shaffer IV[1], N. Tang[1], Y. Hao[1], K. Fink[2], G. Snipes[2], B. Mickey[2], M. Berens[1];
[1]TGen (The Translational Genomics Research Institute), Phoenix, AZ, [2]Baylor Scott & White Research Institute, Dallas, TX

Glioblastoma (GBM) is the most prevalent type of malignant tumor within the central nervous system. There is a growing demand to develop and adapt new therapeutic options in order to combat the five-year survival rate of 6.8% and improve patient quality of life. Arsenic trioxide (ATO) is the standard of care for myelodysplasia and relapsed or refractory acute promyelocytic leukemia. While currently being classified to have an idiopathic mechanism of action, two specific cytotoxic consequences of ATO have emerged: MNK1 activity and oxidative stress. Across six GBM PDX models a 20-fold difference in sensitivity manifests, indicative of underlying innate sensitivity or resistance to ATO. To correlate this to the proposed mechanisms of action, we observed ATO's effect on MNK1 activity through eIF4E phosphorylation and glutathione (GSH) levels following treatment. A subset of GBM models exhibited a marked upregulation of eIF4E phosphorylation following treatment with 2 uM ATO. Of the six models, three were chosen to undergo further testing to observe whether this upregulation showed a consistent dose-dependent relationship across the models and correlated with vulnerability to ATO. Combination therapy with the MNK1 inhibitor, ETC-206, displayed mild to moderate synergy on overall cell viability and strong synergy when observing its effects on the glioma stem cell population. This preferential effect on the GSC populations suggests that MNK1i based combination strategies may show greater effectiveness *in vivo* than indicated by our previous *in vitro* studies. Nutraceuticals targeting GSH synthesis, Chrysin and Silibinin, displayed a 0.95 to 1.4-fold decrease in ATO IC_{50} values across all 6 models. To observe whether each nutraceutical impacted GSH levels consistently across all of the tested models, we measured GSH levels following treatment for each individual compound and their combination treatments. These findings further implicate MNK1 activity and cellular response to oxidative stress as markers of ATO sensitivity, however they are not the sole determinates of response. Understanding of the mechanism of action for idiopathic compounds may allow for the discovery of molecular signatures of sensitivity, improving patient selection for clinical trials and the development of new combination approaches to combat resistance in other tumor types.

#4719 Modulation of HR-HPV viral protein E7 by SHetA2 in cervical cancer.

J. Garland[1], S. Hussain[2], D. M. Benbrook[1];
[1]University of Oklahoma Health Sciences Center, Oklahoma City, OK, [2]ICMR-National Institute of Cancer Prevention & Research, Noida, India

Introduction: The purpose of this study is to determine the effect of the chemotherapeutic sulfur heteroarotinoid A2 (SHetA2) on high-risk human papillomavirus (HR-HPV) proteins and the modulation of cell survival and proliferation in cervical cancer. Cervical cancer is caused by persistent HR-HPV infection. HR-HPV tumorigenesis is driven by its early 6 and 7 (E6, E7) oncoproteins, which increase cell proliferation and survival. Cellular pathways regulated by E6 and E7 are counter-regulated by the investigational new drug SHetA2, which is currently in phase 1 clinical trial for advanced and recurrent cancers. SHetA2 disrupts complexes of 70-kDa heat shock protein (HSP70) family members, hsc70, GRP78, and mortalin, with their client proteins. We hypothesized that SHetA2 reduces E6 and E7 levels and their binding to HSP70 chaperones in association with the reduction of cervical cancer cells and tumor growth.
Methods: SHetA2 effects on specific genes and proteins in HR-HPV-positive cervical cancer cell lines and xenograft tumors were assessed by western blot, quantitative polymerase chain reaction, immunofluorescence ligation assays, and coimmunoprecipitation assays.
Results: SHetA2 significantly reduced E6 and E7 mRNA, and protein levels of E7 and the E7-regulated p16, but not E6 in cervical cancer cells and xenograft tumors. MG132 inhibition of proteasome function attenuated the E7 reduction. HSP70/hsc70 proteins bound E7 and SHetA2 disrupted these complexes.
Conclusions/Implications: SHetA2 reduces E7 proteins in cervical cancer cells through a mechanism that involves proteasomal degradation in association with disruption of HSP70/E7 complexes, p16 reduction, and decreased cell and tumor growth. This is the first demonstration of HSP70/E7 complexes. SHetA2-induced release of E7 from HSP70s could be causing increased susceptibility of E7 to proteasomal degradation. This data supports the development of SHetA2 and HSP70 inhibitors for cervical cancer.

#4720 Effects of removing heat and nourishing yin prescription on malignant phenotype and PI3K/AKT signaling pathway of human esophageal carcinoma cells.

F. Si[1], W. Zhao[1], G. Si[2], X. Song[1];
[1]Henan University of Chinese Medicine, Henan, China, [2]Peking University Third Hospital, Beijing, China

Introduction: Esophageal carcinoma (EC) ranks eighth in the incidence of malignant tumors and the sixth mortality worldwide. This study aims to screen out the Chinese herbs with strong inhibitory effects on the proliferation of four kinds of EC cells EC9706, EC-1, TE-1 and Eca109 from 366 Chinese herbs produced in Henan Province, and study the effect of composed Removing Heat and Nourshing Yin Prescription(RHNYP) on the proliferation, migration, invasion and PI3K/AKT signaling pathway of four EC cells.
Methods: MTT and orthogonal design was applied to screen out the best effective Chinese herbs and determine the optimal dosage ratio of prescription on EC9706, EC-1, TE-1, Eca109 cells from 366 Chinese herbs alcohol extracts, the effects of this prescription on the proliferation, migration, invasion, clone formation, cell cycle and apoptosis of four EC cells were investigated by MTT, RTCA, soft agarose colony forming test, flow cytometry and western blot analysis. Then exploring the effects of RHNYP on EC related signaling pathways and key genes expression by western blot and RT-PCR assay.
Results: Rhizoma Fagopyri Dibotryis(Jinqiaomai), Rhizoma Anemarrhenae(Zhimu), Asparagus Cochinchinensis(Tiandong), and Carpesium Abrolanoides Linne(Heshi) were screened out and composed Removing Heat and Nourshing Yin Prescription(RHNYP) according to their efficacy and orthogonal design. RHNYP could obviously inhibit the proliferation of EC9706, TE-1, EC-1, ECa109 cells with dose-effect and time-dependent manner. IC50 values of Jinqiaomai, Zhimu, Tiandong, Heshi in RHNYP for EC9706 cell were 27.639μg/ml, 40.015μg/ml, 9.044μg/ml, 11.208μg/ml respectively; for EC-1 cell were 24.575μg/ml, 56.991μg/ml, 9.361μg/ml, 13.584μg/ml respectively; for TE-1 cell were 23.534μg/ml, 25.862μg/ml, 6.788μg/ml, 8.911μg/ml respectively; for ECa109 cell were 33.990μg/ml, 33.604μg/ml, 19.873μg/ml, 15.227μg/ml respectively. RHNYP could effectively inhibit the proliferation, migration, invasion, cloning ability, cell cycle and reduce apoptosis of four EC cells. PI3K/AKT/mTOR pathway had closely relationship with the occurrence and development of EC and RHNYP could effectively regulate the proteins expression on the pathway. CDCK3, KIF4A and RAD51AP1 genes were negatively correlated with the overall survival of EC patients and RHNYP could significantly inhibit their expression in four EC cells.
Conclusion: RHNYP can effectively inhibit EC cell proliferation, migration, invasion and cell cycle, induce apoptosis, which may be related to the regulation of PI3K/AKT/mTOR pathway.

#4721 Cell death induction via CB2 receptor and TRPV receptor in cannabichromene (CBC) treated human pancreatic cancer cells.

Y.-N. Hwang, **K.-C. Kim**;
Kangwon National University, Chuncheon, Korea, Republic of

Cannabichromene (CBC: $C_{21}H_3O_2$, M.W.: 314.46g) is one of the most abundant nonpsychotropic phytocannabinoids extracted from Hemp species (*Cannabis sativa),* and can extract using either a hexane/florisil extraction method. Phytocannabinoids contain Δ9-tetrahydrocannabinol (Δ9-THC), cannabidiol (CBD), cannabigerol (CBG), cannabichromene (CBC), and other compounds. CBC can cause strong anti-inflammatory effects in animal models of edema through non-CB receptor mechanisms, but there is little pharmacological study in cancer disease models. In this study, we investigated the molecular mechanism on anti-cancer activity of CBC treatment in human pancreatic cancer cells. MTT assay was performed to determine concentrations for inducing pharmacological effects of CBC in human pancreatic cancer cells. FACS and Annexin V/PI staining analysis showed the increase dead cells by CBC treatment, and Western blot analysis also showed the changes in expression of cell death related proteins by CBC. Moreover, CBC treatment increased expression of CB2 receptor and TRPV receptor, but the anti-cancer effect was restored by double inhibition with SR144528 for CB2 receptor and capsazepine for TRPV receptor, respectively. mRNA-seq analysis showed that 1206 genes were upregulated and 1145 genes were down-regulated by CBC treatment, indicating that some of ferroptosis related genes (HMOX1, CHAC1, GPX4 and NFE2L2) were regulated by CBC treatment. qPCR analysis showed that those genes are increased by CBC treatment in time dependent manner. It was also confirmed that HMOX1 protein expression was increased using Western blot analysis. Therefore, we suggest that CBC induces multiple cell death mechanism including ferroptosis via CB2 receptor and TRPV receptor in human pancreatic cancer cells.

#4722 Enhanced phenotypic screening: A kinetic, multiplexed approach to analyzing drug effects using Incucyte® Live-Cell Analysis System.

K. McBain[1], G. Lovell[1], J. Trigg[1], N. Bevan[1], D. Appledorn[2];
[1]Sartorius, Royston, United Kingdom, [2]Sartorius, Ann Arbor, MI

Phenotypic screening is a valuable tool for analysis of the complex mix of effects that drug treatment has on cells. Traditionally image-based screening uses fixed cells stained with reagents at a pre-chosen end point, however our technique combines kinetic, label-free readouts with non-perturbing fluorescence reporters to enable information-rich quantification of compound effects. A549 lung cancer cells were treated with a library of over 800 FDA-approved drugs while images were acquired in the Incucyte® Live-Cell Analysis System every two hours for four days. Cell growth and viability were measured using label-free readouts of confluence and dead cell count while cell cycle, cell death and Akt pathways were investigated using multiplexed fluorescent readouts. Cytotoxicity was measured using label-free Incucyte® AI Cell Health Analysis Software Module which uses two neural networks to segment individual cells and classify them as live or dead. Assay robustness was quantified using the time course of positive and negative controls (camptothecin and vehicle, respectively). Z' reached a maximal value >0.9 between 48h and 72h; at 72h 4.4% of the compounds within the library induced >50% cell death. Correlation between % Live cells and % Confluence indicated 3 types of effect: cytotoxic (low viability, low confluence), cytostatic (high viability, low confluence), and none (high viability, high confluence). Morphological changes were observed in a multitude of wells with 29 compounds inducing cell enlargement >1800 μm^2, suggesting induction of senescence. Hits from fluorescent readouts were identified as the compounds which perturbed the quantified readout more than 3 standard deviations away from the mean value of the vehicle. Mechanisms of cell death were examined by correlative analysis of the total dead cell population (label-free cell death identification), caspase-active (caspase 3/7-reagent positive) and Annexin V positive cells. This enabled rapid identification of compounds which induced apoptosis by caspase-independent pathways, including the serotonin-selective reuptake inhibitor Sertraline. Kinetic plots of cell cycle stage (% S|G2|M or G1) revealed contrasting mechanisms. Mycophenolic acid induced cell cycle arrest, observed as a consistent increase in the percentage of cells in G1 over time. However flumazenil displayed repeated, transient peaks in the percentage of cells in S|G2|M over the same 72h period, indicating synchronisation behavior. Incucyte® Live-Cell Analysis System as a phenotypic screening platform provides valuable kinetic data from cells within the physiologically relevant environment of a standard incubator. Label-free readouts yield direct cellular information and can be combined with fluorescent data to provide vastly more information than a single endpoint readout.

#4723 Target engagement sheds light on difference in drug efficacy in breast cancer cell lines.

Tomas Friman, Tuomas Tolvanen, Merve Kacal, Victoria Brehmer, Stina Lundgren, Laurence Arnold, Daniel Martinez Molina

Research & Development, Pelago Bioscience AB, Solna, Sweden

Breast cancer is a serious disease that affects millions of women worldwide, and 700,000 people succumb to the disease annually. Breast cancers are divided into several functional subgroups based on molecular characteristics and growth pattern: Luminal A and B, HER2 positive (HER2+) and triple negative. The subgroups are important from a clinical perspective as they partially guide treatment strategies. In this study we wanted to investigate the difference in target engagement with four drugs indicated for treatment of different types of breast cancer: Alpelisib, Neratinib, Vinorelbine, and Docetaxel. Five different human breast cancer cell lines were included, representing Luminal A (MCF-7, T-47D), HER2+ (SK-BR-3, BT-474), and triple negative (BT-20). We used CETSA® (CEllular Thermal Shift Assay) coupled to mass spectrometry detection to assess proteome wide changes in protein thermal stability in intact breast cancer cell lines. CETSA is unique as a target engagement detection modality as it allows for target engagement assessment in intact cells with unaltered drug molecules. Also, as biology is intact in live cells it is possible to follow compound induced downstream signaling or phenotypic events that result in changed thermal stability of proteins. In addition to assessing protein thermal stability with CETSA, which is a short treatment of 1 h, we also subjected cells in culture to prolonged drug exposures, ≤72 h, in order to measure viability. This was done to correlate early changes in protein thermal stability to the viability phenotype that manifested later. In general, responses both in protein thermal stability and cell viability was heterogenous among the cell lines. The most homogenous response in viability was observed for the Phosphatidyl Inositol 3' kinase inhibitor Alpelisib, which reduced viability to 20 - 40% in all cell lines. In contrast, partial resistance was shown to the other drugs by at least one of the cell lines. For Alpelisib, the amount and type of proteins that were thermally shifted correlated with the effect on viability. The covalent HER2 inhibitor Neratinib was most effective in inhibiting viability in HER2+ cells and proteins of the HER2 pathway were thermally shifted in these cells, which was not observed for the other cell lines. Viability of the other cell lines were also affected by Neratinib, but only at higher concentrations. Both microtubule inhibitors induced thermal stabilization of tubulins, but that did not always translate into efficacy in the viability assay. However, sensitive cell lines showed thermal shifts of tubulins at lower concentrations of compound. In oncology drug development it is important that effects on viability are driven by on-target efficacy and not by off-target effects. Here we show the benefit of connecting knowledge of target engagement and phenotypic readouts; what targets are engaged, at which concentrations, and what is the corresponding phenotype.

#4724 Optimizing 500 pooled PRISM cell lines for a 10-day assay to elucidate viability effects and mechanism of action for slower-acting therapeutics.

M. Ronan, B. C. Ip, E. Nguyen, U. Widocki, T. Sangpo, A. Kalathungal, N. Diaz-Gallegos, A. Fazio, A. Golabi, M. Naim, A. Bino George, Y. Liu, M. Kocak, R. Puram, M. G. Rees, J. Roth;
Broad Institute of MIT and Harvard, Cambridge, MA

PRISM (Profiling Relative Inhibition Simultaneously in Mixtures), using DNA-barcoded cell lines cultured as ~25 cell line pools, has been an effective drug discovery screening platform to rapidly test large numbers of potential therapeutics on over 900 different cancer cell lines. However, the conventional 5-day assay may be too short to offer the resolution needed to identify the full cellular response for slower-acting therapeutics such as those directed against epigenetic pathways. Here, we describe development of the PRISM 10-day extended assay with ~500 adherent solid tumor cancer cell lines to overcome this challenge. We found that the ranges of cell line growth rates within the standard PRISM pools were too large and not amenable for a long-term assay beyond 6 days—after 10 days of growth, slower cell lines dropped below the limit of barcode detection as faster cell lines overtook the pools. We therefore regenerated pools to reduce the range of growth rates within a pool. We show that this re-pooling, coupled with seeding density optimization, enables recovery of > 98% of cell lines at day 10 in vehicle-treated wells, with acceptable data variability. The average estimated number of cell doublings across our cell lines, 7, is significantly greater than the number of doublings in the PRISM standard 5-day assay (~3 doublings). Importantly, we observe greater drug effects on day 10 versus day 6 when cells are treated with slow-acting DNA methyltransferase inhibitors such as decitabine; this also results in increased sensitivity to identify cellular biomarkers underlying differential response. In summary, we have successfully engineered a PRISM 10-day assay in ~500 adherent cell lines, where the extended duration can be beneficial in elucidating the effects and mechanism of action for epigenetic drug candidates.

#4725 Phenotypic single-cell analysis of nuclear stress responses in drug-treated prostate cancer cells.

E. Batnasan, M. Karkkainen, S. Koivukoski, P. Ruusuvuori, **L. Latonen**;
University of Eastern Finland, Kuopio, Finland

Chemotherapy with anti-cancer drugs aims to stop the growth of cancer cells either by killing them or by stopping them from dividing. The different specificities in inducing cellular damage responses are incompletely understood currently and may underlie the preferential effectiveness of anti-cancer drugs against different types of cancer cells. Better understanding and tools to measure drug-induced phenotypes *in vitro* may aid in assessing cellular heterogeneity of responses, determining potential effectiveness, estimating amount and types of adverse effects, and predicting likelihood of surviving populations for residual disease. To measure the types and extent of nuclear stress responses to cancer drugs, we studied nuclear organelle, namely nucleolar and Cajal body, phenotypes to drug-induced stress in prostate cancer cells. We utilized organelle-specific markers NPM, Fibrillarin, Coilin, and SMN1 in immunofluorescence staining to determine suitable markers for nuclear organelle stress. We used three different prostate cancer cells lines representing different biological types of advanced prostate cancer (AR positive, AR negative, and expressing AR transcript variant). Based on initial assessments, NPM and coilin immunostaining were selected for automated phenotypic analysis screening for drug effects. Using AI-assisted nuclear segmentation and feature-based single-cell phenotypic analysis, we demonstrated quantitative effects on nuclear morphology, nucleoli, and Cajal bodies with drug treatments. A proof-of-principle study with platinum-based chemotherapeutic agents in clinical use demonstrated heterologous responses to the platinum drugs that are associated with prostate cancer cell types with different AR status. Further, we have defined the corresponding quantitative responses for androgen deprivation therapy (ADT) drugs enzalutamide and bicalutamide in AR-positive prostate cancer cells. Our findings evidence variability of prostate cancer cells' response to chemotherapy and have implications in future therapy regimen considerations. Furthermore, we have developed a fluorescence light microscopy-based method to assess nuclear stress response phenotypes in prostate cancer cells that can be used for high throughput drug screening.

#4726 Identification of efficacy biomarkers for therapies targeting miR-10b.

A. Halim, N. Al-Qadi, S. K. Mondal, E. Kenyon, N. Savan, H. Mackie, A. Moore;
Michigan State University, East Lansing, MI

Breast cancer stemness is one of the drivers of metastatic spread and presents a key target in the battle against metastatic disease, especially in triple-negative breast cancer (TNBC). Existing treatment options for TNBC are limited due to recurrence and resistance, representing a major unmet clinical need. MicroRNA-10b (miR-10b) is one of the major drivers of breast cancer cell migration and invasion. In our earlier studies, we discovered that miR-10b is also responsible for metastatic cell viability. With the goal of translation of this finding to the clinic, we developed a novel therapeutic, or "nanodrug," that targets miR-10b, consisting of antisense anti-miR-10b oligonucleotides conjugated to magnetic nanoparticles (MN) that serve as delivery vehicles. Administration of the nanodrug in mice bearing metastatic MDA-MB-231 TNBC tumors prevents the development of metastases and stops the growth of pre-existing metastases. Additionally, combination treatment with adjuvant doxorubicin induced a stable regression of metastases in immunocompromised and immunocompetent mouse models of metastatic TNBC. A limitation of our previous studies is the lack of understanding of the molecular basis for the therapeutic effect of MN-anti-miR10b. To address this gap in knowledge, we performed RNA sequencing on MDA-MB-231 cells treated with the nanodrug or controls. Functional enrichment analysis of differentially expressed genes (DEGs) between cells treated with the nanodrug versus controls (PBS or bare MN) identified a significant overrepresentation of genes associated with cell differentiation. It has been suggested that miR-10b confers stem cell-like properties such as self-renewal and drug resistance onto cancer cells. Our RNA sequencing findings led us to hypothesize that MN-anti-miR10b functions by inhibiting these stem-like cancer cell (CSC) features that are critical to cancer survival. Here, we present preliminary data showing that miR-10b is overexpressed in MDA-MB-231 cells expressing a CSC-associated surface marker phenotype (CD44+/CD24-, compared to CD44-/CD24- cells) and that this trend is not universal among other miRNAs. Furthermore, we found that the nanodrug interferes with the ability of cells to assemble as spheroids, a property associated with CSCs. With our recent observation that the nanodrug inhibits miR-10b in metastases *in vivo* in as little as one dose after 72 hours, our next steps are to determine whether the cell differentiation-associated DEGs identified in RNA sequencing results can be used as biomarkers of nanodrug efficacy *in vivo*. Understanding the changes in gene expression induced by MN-anti-miR10b as a function of time will be critical for guiding treatment regimens in future preclinical and clinical trials.

#4727 Large scale drug response comparison across different neuroblastoma cell model systems.

S. Park[1], **E. Liu**[1], A. Los[1], B. Seashore-Ludlow[1], P. Ostling[1], J. Molenaar[2], O. Kallioniemi[1], J. Stenman[1], K. Karlsson[1];
[1]Karolinska Institutet, Stockholm, Sweden, [2]Princess Maxima Centre, Utrecht, Netherlands

Traditionally neuroblastoma research has predominantly used 2D cell lines, which, despite their simplicity, often fall short in mirroring the physiological complexity of actual tumors. Recently, 3D models like patient-derived tumor organoids (PDO) and patient-derived xenografts (PDX) have emerged as superior alternatives, offering more realistic predictions of patient treatment responses. This study aims to discern the differences in drug response between conventional 2D cell lines and the more advanced 3D neuroblastoma models - specifically, patient-derived organoids (nPDO) and patient-derived xenograft organoids (nPDXO). Employing high-throughput drug screening of 528 cancer drugs, we evaluated the drug responses across traditional 2D cell lines, nPDOs, and nPDXOs. Additionally, focused experiments with 29 selected drugs were conducted to determine the influence of culture topology on drug efficacy. The findings were compared to a study by Hansson et al.[1] that used nPDXO. Our study discovered a pronounced difference in drug sensitivity between 2D cell lines and 3D models, with 3D models showing heightened sensitivity. Interestingly, 2D cell cultures had a more heterogenous drug response compared to 3D models. The drug response correlation between nPDOs and nPDXOs was relatively high (Spearman ~0.8), indicating consistent responses across these models. Our comparison underscores the impact of model system choice on drug response studies in neuroblastoma. The study highlights important differences in drug response between neuroblastoma 2D and 3D cell culture models. However, only subtle differences were found between PDO and PDX-derived organoid lines, despite differences in treatment centers and media compositions. This suggests that while the choice of cell culture topology greatly impacts drug response, PDO and PDX derived lines can largely be used interchangeably for drug screening experiments.

References: 1. Hansson et al, *Therapeutic targeting of KSP in preclinical models of high-risk neuroblastoma*, *Science Translational Medicine*(2020)

#4728 Circ-EGFR enhances cetuximab efficacy by regulating miR-942-3p/GAS1 signaling axis in colorectal cancer.

S. Sui[1], C. Xu[1], Y. Li[1], W. Wei[2], J. Maurel[3], M. Li[4], A. Goel[1];

[1]Beckman Research Institute of The City of Hope, Monrovia, CA, [2]Harvard Medical School, Boston, MA, [3]Hospital Clinic of Barcelona, Barcelona, Spain, [4]the Second A, Dalian, China

Background: Cetuximab, an epidermal growth factor receptor (EGFR)-targeting IgG1 monoclonal antibody (mAb), results in beneficial, yet limited, clinical improvement in metastatic colorectal cancer (mCRC) patients with wild-type (WT) KRAS gene. Numerous studies have shown that circRNAs are aberrantly expressed in tumors and play crucial roles in tumor growth and metastasis in various human malignancies, including colorectal cancer (CRC). One such circRNA, circ-EGFR, has been identified as having associations with tumor progression and chemotherapy response in diverse cancer types. However, exploring the functional role and underlying mechanisms of circ-EGFR in the context of the response to EGFR-targeted therapy may offer new therapeutic avenues for mCRC.

Methods: The expression level of circ-EGFR (hsa_circ_0080229) was evaluated in cetuximab-sensitive and resistant RAS and BRAF WT CRC cell lines by using real-time quantitative reverse transcription polymerase chain reaction (RT-qPCR). The biological function of circ-EGFR was investigated by loss- and gain-of-function assays in cultured cells and an animal model. The potential targets of circ-EGFR were identified through in-silico analysis, and the circ-EGFR/miR-942-3p/GAS1 axis pathway was verified using the luciferase reporter assay and RT-qPCR. The association of circ-EGFR expression with clinical prognosis in mCRC patients with different cetuximab responses was analyzed by Kaplan-Meier survival analysis.

Results: The expression of circ-EGFR was remarkedly higher in sensitive (DiFi and SW48) compared with resistant cell lines (CaCO2 and SNU-C1) after exposure of cells to cetuximab (sensitive vs. resistant: $p < 0.001$). Biologically, genetic depletion of circ-EGFR significantly enhanced cell proliferation, migration [DiFi: sh-circ-EGFR vs. shNC: Foldchange (FC) = 1.97, $p < 0.001$; SW48: FC = 1.96, $p < 0.001$], and invasion (DiFi: sh-circ-EGFR vs. shNC: FC = 2.23, $p < 0.001$; SW48: FC = 1.78, $p < 0.001$) after 24-48 hours of cetuximab treatment in DiFi and SW48 cell lines, and its overexpression suppressed tumor growth *in vivo* under cetuximab treatment. Mechanically, we identified circ-EGFR as a sponge for miR-942-3p to regulate the expression of Growth Arrest Specific 1 (GAS1), which promoted sensitivity to cetuximab treatment in CRC. Notably, our findings identified circ-EGFR as a promising therapeutic indicator in clinical applications.

Conclusion: Our study illustrated that circ-EGFR plays a vital role in affecting cetuximab efficacy by regulating the miR-942-3p/GAS1 axis in CRC. This holds promise for improving patient selection and management in this malignancy.

#4729 Incorporation of the antitumor compound 2OHOA and its metabolite into cell membranes.

R. Beteta-Gobel[1], R. Rodriguez-Lorca[1], P. Fernandez-Garcia[1], P. V. Escriba[1], V. Llado[2];
[1]Laminar Pharma, Inc., Palma de Mallorca, Spain, [2]Laminar Pharma, Inc., Boston, MA

The compound 2-hydroxyoleic (2OHOA) is a bioactive lipid molecule that has demonstrated an anti-tumor effect and high safety in cellular and animal models of glioblastoma multiform (GBM), considered the most aggressive and lethal of primary tumors of the central nervous system. Due to the poor prognosis of patients, with a median survival of 15 months, it is of great importance to develop new therapeutic strategies that improve the efficacy and safety of treatments to achieve complete remission of GBM. Granted orphan designation for the treatment of glioma in both the European Union and the United States, 2OHOA completed a phase I/IIA study on advanced solid tumors in adults (NCT01792310) showing pharmacological efficacy and safety. It is currently undergoing a phase IIB/III clinical trial on glioma patients (NCT04250922) in combination with the standard of care for glioma and a pediatric study on glioma and other solid tumors (NCT04299191).Here, we seek to define the mechanism of action of 2OHOA which is based on Membrane Lipid Therapy, an innovative approach that proposes the use of new molecules designed to modify the composition and lipid structure of the membrane and reverse a pathological lipid state. Therefore, we further investigated the effect of 2OHOA on membrane lipid composition when applied to human glioblastoma cell line by gas chromatography. In addition, we defined the 2OHOA's effect on different components of the cell signaling pathway by Western Blot and PK in glioma patients.Our results demonstrated that 2OHOA is mostly incorporated in glioma cell membranes and poorly integrated in non-tumor cells, which would explain its specific effects and low side effects in GBM treatment. Moreover, we observed that after its incorporation, 2OHOA is metabolized to produce the compound C17:1n-9 by α-oxidation pathway, a key process for its anti-tumor effect in glioma cells. In addition, the C17:1n-9 metabolite impairs cell growth, reinforcing the 2OHOA activity. Finally, we examined this metabolite as a biomarker to predict and trace 2OHOA treatment, studying the pharmacokinetics of glioma patients treated with the drug in phase I/IIA and its accumulation in mice xenograft tumors. In conclusion, 2OHOA shows a different incorporation into cell membranes between tumor cells and non-tumor cells. Moreover, both 2OHOA and its metabolite C17:1n-9 have an antiproliferative effect and exhibit an appealing potential in the treatment of patients that develop GBM with unmet effective therapy.

#4730 Pharmacodynamic determinants of anti tumor activity of SHMT2 inhibitors.

M. J. Schneider[1], C. O'Connor[1], X. Bao[1], M. Nayeen[2], Z. Hou[1], J. Li[1], A. Gangjee[2], L. Matherly[1],
[1]Wayne State University School of Medicine, Detroit, MI, [2]Duquesne University, Pittsburgh, PA

These studies investigate factors that impact the antitumor activity of SHMT2 targeting including drug accumulation, metabolism, expression of one carbon (C1) related enzymes, and tumor hypoxia. Mitochondrial C1 metabolism is upregulated in a variety of cancer types including leukemias and solid tumors. The mitochondrial C1 enzymes serine hydroxymethyltransferase (SHMT) 2 and 5,10-methylene tetrahydrofolate (THF) dehydrogenase 2 (MTHFD2) are among the top 5 overexpressed metabolic enzymes in tumors vs normal tissues in a wide range of tumor types. Thus, SHMT2 and MTHFD2 are potential therapeutic targets for cancer, sparing normal tissues that are less reliant on mitochondrial C1 metabolism. SHMT2 metabolizes serine and THF to produce glycine and 5,10-methylene THF; MTHFD2 metabolizes 5,10-methylene THF to NADH and 10-formyl THF which is converted to formate by MTHFD1L. Thus, mitochondrial C1 metabolism is the principal source of C1 units for cellular biosynthesis and provides the majority of glycine for protein, purine and glutathione synthesis. We previously discovered novel 5-substituted pyrrolo[3,2-*d*]pyrimidine antifolate compounds which exhibit primary inhibition at mitochondrial SHMT2 along with cytosolic SHMT1 and *de novo* purine biosynthesis at glycinamide ribonucleotide and 5-aminoimidazole-4-carboxamide ribonucleotide formyltransferases. The lead compound AGF347 is taken up into cells by the facilitative transporters reduced folate carrier (SLC19A1) and the proton coupled folate transporter (SLC46A1) and like folate cofactors is metabolized to polyglutamate (PG) forms by folylpolyglutamate synthase (FPGS) which promotes retention in cytosolic and mitochondrial compartments and target enzyme engagement. We investigated the impact of folate transporter expression on metabolism to PGs for SHMT2 targeted antifolates. Folate transporter expression inversely correlated with anti-tumor efficacy of SHMT2 targeted antifolates and overexpression of FPGS resulted in dramatically increased sensitivities. However, for pyrazolopyran inhibitors of SHMT2 (e.g. SHIN1) which enter cells by diffusion and are not metabolized to polyglutamates, increased transporter and FPGS levels dramatically decreased anti-tumor activity. As SHMT2 is a target of HIF1α, we studied the impact of multitargeting SHMT2 and purine biosynthesis by pyrrolo[3,2-d]pyrimidine antifolates under hypoxic conditions. Our results establish that multi-targeting SHMT2 and purine biosynthesis preserves anti-tumor activity under hypoxia. Collectively, our results demonstrate that SHMT2 targeted pyrrolo[3,2-*d*]pyrimidine antifolates exhibit increased antitumor efficacies in cells expressing low folate transporter expression and is further enhanced by increased FPGS activity. Additionally, we find multitargeting of SHMT2 and *de novo* purine biosynthesis manifests as antitumor activity even under hypoxic conditions.

#4731 Targeting Lon protease as novel strategy to treat aggressive IDH mutant diffuse malignant astrocytoma.

C. Douglas, **S. Jain**, N. Lomeli, T. Vu, J. Pham, D. A. Bota;
UC Irvine, Irvine, CA

While isocitrate dehydrogenase (IDH) wild-type and mutant malignant astrocytoma (IDH*wt*, IDH*mt*) are diffuse CNS tumors that have a high degree of parallelism with one another, including microvascular proliferation and necrosis, the IDH*wt* tumors clinically presents with a higher tumor grade and thus poorer prognosis and survival rate. Isocitrate dehydrogenase mutation (IDH) hinders the hypoxia response in gliomas and promotes an advantageous reduction in both tumor growth and treatment resistance. Since recurrence is high, adequate characterization and identification of potential novel molecular targets in IDH*mt* mutant diffuse glioma is integral for developing new therapeutic strategies for better control of tumor burden and, thus, improved outcomes. Our previous published work has shown that the hypoxia responsive LONP1 mitochondrial protease is involved in glioma growth and treatment resistance and that LONP1 inhibitors can augment the effect of chemotherapy in IDH*wt* models. Here, we highlight the downstream activity of LONP1 via the NRF2 pathway and how synergistically, along with the IDH mutation, LONP1 overexpression can promote the subsequent proneural to mesenchymal transition (PMT) induced by stress and other tumor microenvironment signals. By characterizing the interplay between LONP1 and IDH mutation in *in-vitro* models, we demonstrate that oxidative stress modulates both PMT and TMZ drug resistance. When translated to an i*n-vivo* patient-derived, intracranial orthotopic xenograft model, LONP1 overexpression is associated with decreased survival.Based on our findings, future clinical translation includes the possibility of using LONP1 as a novel target to optimize the standard of care treatment in IDH mutant diffuse astrocytoma.

EXPERIMENTAL AND MOLECULAR THERAPEUTICS: Reversal of Drug Resistance 1
Poster Session

#4736 Evaluate the potential sensitization effect and underlying mechanism of lenvatinib on cisplatin resistance oral squamous cell carcinoma.

Y.-T. Chen[1], Y.-T. Tsai[2], F.-T. Hsu[2], H.-F. Tu[1];

[1]Department of Dentistry, National Yang Ming Chiao Tung University, Taipei City, Taiwan, [2]Department of Biological Science and Technology, China Medical University, Taichung City, Taiwan

Oral squamous cell carcinoma (OSCC) is a prevalent form of cancer that develops in the oral cavity, globally recognized as the eighth most commonly diagnosed cancer. Despite the application of standard surgical techniques or concurrent chemoradiotherapy, the prognosis for OSCC patients remains unsatisfactory. Initially, cisplatin, the primary and most frequently used chemotherapy agent for treating OSCC, demonstrates effectiveness in therapy. Nonetheless, chemoresistance frequently arises, leading to treatment failure, and this is intricately associated with the activation of hypoxia-inducible factor 1α (HIF-1α) signaling. Recent research has brought to light heightened levels of HIF-1α-mediated vascular endothelial growth factor (VEGF) and BCL-2 in OSCC tumor sites, which play crucial roles in regulating angiogenesis and anti-apoptotic processes within cancer cells. Additionally, interventions aimed at targeting anti-apoptotic molecules or augmenting the expression of pro-apoptotic molecules may represent promising strategies to overcome chemoresistance in OSCC. Therefore, HIF-1α/VEGF/BCL-2 axis could be considered a potential target for the development of chemopreventive and chemotherapeutic strategies for OSCC. Lenvatinib is a targeted multi-kinase inhibitor that can inhibit tumor growth and angiogenesis by blocking the activation of vascular endothelial growth factor receptor (VEGFR) 1-3, fibroblast growth factor receptor (FGFR) 1-4, platelet-derived growth factor receptor (PDGFR) α, as well as the proto-oncogenes RET and KIT. However, whether lenvatinib may sensitizes OSCC to cisplatin remains unclear. In our study, we used the MTT assay to prove the cytotoxicity of OSCC cells (SAS and MOC1 cells) was induced by cisplatin and lenvatinib. We employed flow cytometry to verify that the combination of lenvatinib and cisplatin can indeed trigger both extrinsic and intrinsic apoptotic pathways in OSCC cells. Furthermore, our demonstration revealed that the induction of apoptosis pathways by the combination of lenvatinib and cisplatin is associated with mitochondrial-dependent apoptosis and death receptor-dependent apoptosis. Then, transwell invasion and migration assay results proved the inhibition effect of lenvatinib combined with cisplatin in SAS and MOC1 cells. Furthermore, we indicated that the combination of lenvatinib and cisplatin can effectively inhibit angiogenesis and anti-apoptotic mechanisms mediated by the HIF-1α/VEGF/BCL-2 axis in OSCC cells. In summary, our results demonstrate that the combined treatment with lenvatinib and cisplatin enhances the response of OSCC cells under hypoxic conditions. Additionally, it aims to mitigate the negative impact of hypoxia on cisplatin's therapeutic effectiveness and increase the sensitivity of OSCC cells to cisplatin.

#4737 The combination of the BET inhibitor JQ1 and gemcitabine induces regressions in gemcitabine resistant patient-derived xenograft models of pancreatic cancer.

A. L. Miller, S. C. Fehling, E. J. Brown, E. O. Heard, T. L. Gamblin, R. B. Vance, **K. J. Yoon**;
University of Alabama at Birmingham, Birmingham, AL

Efforts to develop targeted therapies for drug resistant tumors have been relatively unsuccessful. The 5-year survival for patients with advanced pancreatic cancer is ~3%. Gemcitabine is usually combined with nab-paclitaxel as a standard of care for treatment of locally advanced or metastatic pancreatic ductal adenocarcinoma (PDAC). However, no chemotherapeutic regimens thus far evaluated have been curative. We developed the first PDAC patient-derived xenograft (PDX) models in which resistance against gemcitabine was acquired *in vivo*. We used RNA-seq and ingenuity pathway analysis to compare expression profiles of paired parent vs gemcitabine resistant PDX models. This comparison suggested a previously unreported mechanism for gemcitabine resistance, involving aberrations of cholesterol biosynthesis and lipid metabolism pathways. We also made the unexpected observation that gemcitabine-resistant PDAC models derived from primary tumors have high levels of 3-hydroxy-3-methylglutaryl-CoA synthase 2 (HMGCS2), an enzyme essential to cholesterol biosynthesis and rate limiting in ketogenesis. Notably, the BET bromodomain inhibitor JQ1 decreases HMGCS2 levels; and BET inhibitors + gemcitabine exert synergistic cytotoxicity in gemcitabine-resistant PDAC cells. We determined that the BET bromodomain inhibitor JQ1 + gemcitabine induces regressions of two *in vivo* gemcitabine-resistant tumor models which we developed directly from primary human tumor tissue. These mechanism-based studies suggest that inhibiting HMGCS2 represents a novel approach to therapy for PDAC. We propose that combining gemcitabine with agents that decrease levels of HMGCS2 comprises effective treatment for patients with drug resistant PDAC.

#4738 Overcoming therapy resistance in rhabdomyosarcoma by targeting the PI3K-MAPK pathway.

Y. Wang, E. Chen;
Univ. of Washington School of Medicine, Seattle, WA

Rhabdomyosarcoma (RMS) is a devastating pediatric cancer. There has not been any significant change in the treatment options for the last 4 decades, especially for relapsed or advanced disease. There is an urgent need to identify alternative treatment options to improve survival outcomes of RMS patients. RMS is comprised of two major subtypes as defined by the presence or absence of PAX3/PAX7-FOXO1 gene fusion. Fusion-negative RMS (FN RMS) is characterized by alterations in the RAS-PI3K-MAPK pathway in >90% of the cases. However, the role of the PI3K-MAPK pathway in therapy resistance and disease relapse remains poorly characterized. We have generated two FN-RMS lines, RD and SMS-CTR, with resistance to the standard-of-care chemotherapeutic agent, vincristine, through long-term culturing in incrementally increased concentrations of the drug. By RNA sequencing, vincristine-resistant RD and SMS-CTR cells demonstrated increased expression of genes in the RAS-PI3K-MAPK pathway compared to the parental lines. We hypothesize that increased activity of the PI3K-MAPK pathway contributes to therapy resistance in FN RMS. To test the hypothesis, we first showed that targeted disruption of PIK3CA by shRNA inhibited the cell growth of vincristine-resistant FN RMS cells. The same cells also showed increased sensitivity to the MEK inhibitor, trametinib, as well as the PIK3Cα inhibitor, alpelisib, compared to the parental cells. We then showed that zebrafish FN-RMS tumors treated with the combination of vincristine and alpelisib significantly inhibited tumor growth compared to the treatment with each agent alone. Through integrative analysis of RNA sequencing and ATAC-seq data, we identified MYOD1 and NFATC2 as among the top candidate upstream regulators. Targeted disruption of either MYOD1 or NFATC2 by CRISPR/Cas9 reduced cell growth of vincristine-resistant FN RMS cells and altered expression of the genes in the PI3K-MAPK pathway, implicating MYOD1 and NFATC2 in driving abnormal activity of this pathway. To assess the relevance of our findings in the clinical settings, we showed that selective components in the PI3K-MAPK pathways are up-regulated in 3 matched primary-recurrence/metastasis paraffinized tissue samples of human FN RMS by the NanoString GeoMx Digital Spatial Profiler (DSP) platform. Our findings indicate that targeting the PI3K-MAPK pathway is a promising targeted therapy option for overcoming therapy resistance in RMS.

#4739 Targeting resistance to BET inhibitors in Fusion-Positive Rhabdomyosarcoma.

M. Cassandri[1], E. Ferraro[1], L. D'Archivio[1], F. Aiello[1], H.-C. Chou[2], Y. K. Song[2], B. E. Gryder[3], J. S. Wei[2], S. Sidoli[4], R. G. Hawley[5], R. Rota[1], F. Locatelli[1], J. Khan[2], **S. Pomella**[1];

[1]Bambino Gesu Children's Hospital, Rome, Italy, [2]National Institute of Health, National Cancer Institute, Bethesda, MD, [3]Case Western Reserve University School of Medicine, Cleveland, OH, [4]Albert Einstein College of Medicine, New York, NY, [5]GW Cancer Center, Washington DC, DC

Rhabdomyosarcoma (RMS) is the most frequent pediatric soft tissue sarcoma. Fusion-positive (FP-)RMS expressing the oncogenic chimeric transcription factor (TF) PAX3-FOXO1 (P3F) is at high risk of recurrence. FP-RMS cells show survival dependency on P3F. Despite P3F, as a TF, is considered undruggable, we and others demonstrated that P3F levels/functions can be epigenetically modulated. The BET protein and epigenetic reader BRD4 binds super-enhancers (SEs) to foster oncogenic transcription in cancer. We showed that P3F rewires the RMS enhancer landscape by recruiting BRD4 on oncogenic SEs. Accordingly, JQ1, a BET inhibitor (BETi) shuts down P3F functions halting tumor growth in vitro and in vivo. Therefore, BRD4 inhibition in FP-RMS results in a tumor subtype-specific vulnerability. Nonetheless, as for other targeted therapies, cancer cells can acquire resistance to BETi, thus, we investigated whether FP-RMS cells could develop BETi resistance. Therefore, we established resistant cells from two sensitive FP-RMS cell lines chronically exposed to escalating doses of JQ1, as a model of naturally acquired resistance. Our data show that the two established FP-RMS cell lines, acquired resistance by increasing JQ1 IC50 over the sensitive cells both in 2D and 3D settings. Compared to the sensitive ones, both the resistant cell lines show cross-resistance to other monovalent and bivalent BETi and degraders. Resistant cells also maintain the ability to form colonies in a clonogenic assay and to invade in a 3D Matrigel assay in the presence of JQ1. Moreover, conversely to sensitive cells, JQ1 treatment is unable to down-regulate P3F, MYCN and BCL2 (P3F target) levels in resistant cells. Furthermore, integration of transcriptomic and proteomic data reveals differentially modulated subset of genes/proteins among which MYCN and P3F targets, suggesting a restored activity of the TFs circuitry in resistant cells. Accordingly, MYCN silencing completely halts growth of resistant cells. In line, MYCN protein levels are reduced by JQ1 in a dose-dependent manner in sensitive but not in resistant cells and its half-life is 3 folds longer in resistant than in sensitive cells. Being MYCN protein stability affected by specific post-translational modifications among which the phosphorylation at Ser62 by ERKs, we evaluated the expression of phosphorylated MYCN and the activated form of ERK (pERK) and found both of them increased in resistant cells. In agreement, resistant cells are more sensitive to MEK-ERKs pathway inhibition, showing a lower IC50 of Trametinib (MEKi) compared to sensitive cells. Moreover, Trametinib and JQ1 co-treatment downregulates MYCN protein levels in resistant but not in sensitive cells, suggesting that ERKs overactivation could participate to BETi acquired resistance by stabilizing MYCN, thus representing an acquired vulnerability. The study has received funding from Ministero della Salute to SP.

#4740 Acid ceramidase inhibition enhances venetoclax sensitivity in preclinical models of acute myeloid leukemia.

J. Ung[1], S.-F. Tan[1], J. J. P. Shaw[1], T. E. Fox[1], M. Taori[1], D. F. Claxton[2], K. H. Fisher-Wellman[3], M. C. Cabot[3], D. J. Feith[1], T. P. Loughran, Jr.[1]; [1]University of Virginia School of Medicine, Charlottesville, VA, [2]Pennsylvania State University College of Medicine, Hershey, PA, [3]East Carolina University, Greenville, NC

Acute myeloid leukemia (AML) is an aggressive hematologic malignancy in urgent need of improved therapeutic strategies. AML blasts frequently rely on the anti-apoptotic protein, Bcl-2, for survival. The specific Bcl-2 inhibitor, venetoclax (VEN), is FDA-approved in combination with low-dose cytarabine (LDAC) or azacitidine for patients unfit for intensive induction chemotherapy. Unfortunately, responses are transient due to upregulation of compensatory survival proteins (e.g., Bcl-xL or Mcl-1) or resistance characterized by reprogrammed mitochondrial bioenergetics. Our research aims to improve current AML treatments and understanding of AML pathogenesis by targeting dysregulated sphingolipid metabolism. Ceramides are tumor-suppressor sphingolipids that mediate therapy-induced cell death. Sphingolipid dysregulation that results in decreased ceramide content and/or enhanced ceramide catabolism is an emerging AML hallmark. We've previously shown that acid ceramidase (AC), a ceramide catabolizing lysosomal enzyme, is overexpressed in AML and contributes to drug resistance. Here, we demonstrated that AC inhibition enhanced VEN cytotoxicity. Combining the AC inhibitor/ceramide analog, SACLAC, with VEN resulted in synergistic lethality in multiple AML cell lines in cell viability and apoptosis assays. Genetic inhibition of AC also improved VEN cytotoxicity. The SACLAC+VEN combination achieved Bliss scores (SynergyFinder 2.0) between 22 and 32 in cell lines, which indicate a highly synergistic combination. SACLAC+VEN efficacy was comparable to the FDA-approved combination of VEN+LDAC when tested in 67 primary AML patient samples. Pharmacological inhibition of AC also increased the efficacy of the VEN+LDAC combination. Mechanistically, the observed synergistic lethality was independent of changes to Bcl-2, Mcl-1, and Bcl-xL protein levels. Combined AC and Bcl-2 inhibition resulted in synergistic ceramide accumulation, integrated stress response (ISR) activation, and caspase-dependent apoptosis characterized by impaired mitochondrial function. Pretreatment with the pan-caspase inhibitor, zVAD-FMK, or ISR inhibitor, ISRIB, significantly rescued cell death. Ongoing studies aim to further characterize mitochondrial impairment and ISR activation induced by inhibiting AC and Bcl-2. Taken together, these results detail the first report of ISR activation and mitochondrial defects elicited by combined AC and Bcl-2 inhibition as contributory to cytotoxic impact (mechanism) and warrant additional studies of AC inhibitors with frontline AML therapeutics.

#4741 Targeting sorafenib-resistant HCCs by protein X-armed T cell immunotherapy.

M.-H. T. Ngo, M. Chen, P.-C. Lan, K.-H. Chuang, Y.-H. Huang;
Taipei Medical University, Taipei, Taiwan

Hepatocellular carcinoma (HCC) is the most common type of liver cancer globally, ranking fourth according to the World Health Organization's GLOBOCAN database. Sorafenib and lenvatinib are single-drug therapies used for advanced HCC, but only around 30% of patients benefit from them, and drug resistance typically develops within a few months. Our previous study has demonstrated the specific IL-6-IGF-1R-YAP signaling in regulating the stemness expressions, tumor metastasis, and drug-resistance of the sorafenib resistant HCC (2015 Clinical Cancer Res, 2019 J Exp Clinical Cancer Research, 2021 Cancers, 2023 Cancers). In advance our previous study, this study aims to develop a novel immune therapeutic strategy for sorafenib-resistant HCC treatment. We found, when compared to peri-tumor tissues, the immunohistochemical staining showed a high co-expression of both protein X and PD-L1 in liver tumor tissues (6.25%, n=32 versus 28.125%, n = 64, respectively). To further confirm this observation, we used in vitro cell line models with sorafenib-naïve HCCs (HepG2215_N, Hep3B_N, Huh7_N, and PLC5_N) and sorafenib-resistant HCCs (HepG2215_R, Hep3B_R, Huh7_R, and PLC5_R) in this study. As PD-L1 on tumor cells can dampen T cell cytotoxicity, we generated CD3/protein X bispecific antibodies, which can bind to both CD3 and protein X, and coupled them to T cells (Arm-T cells) and normal T cells (N-T cells). We tested their cytotoxic effects on sorafenib-resistant HCCs using the sorafenib-resistant HepG2215_R cells, co-cultured with Arm-T cells and N-T cells for 24 hours. Our results showed that Arm-T cells exhibited a significantly stronger cytotoxic effect on sorafenib-resistant HepG2215_R cells, with several notable findings: (1) The binding time of Arm-T cells to HepG2215_R cells was significantly longer than that of N-T cells (248.9 ± 146.6 minutes, n=23 versus 28.3 ± 13.49 minutes, n=24); (2) The cytotoxicity of Arm-T cells was significantly higher than that of N-T cells (29.7 ± 2.3% versus 13.6 ± 3.3%); and (3) The secreted levels of INFγ and TNFα by Arm-T cells were significantly higher than those of N-T cells (138.1 ± 7.2 ng/ml and 34.6 ± 0.7 ng/ml versus 31.4 ± 2.5 ng/ml and 3.6 ± 1.1 ng/ml, respectively). These findings were also consistent when using Hep3B-R cells (data not shown). To summarize, our study shows that Arm-T cells possess strong cytotoxic abilities against sorafenib-resistant HCC. These findings have implications for developing effective immuno-therapeutic strategies for patients with sorafenib-resistant HCCs.

#4742 Targeting the RNA-binding protein LARP1 overcomes therapeutic resistance in ovarian cancer.

A. M. Elsayed, P. Amero, E. Bayraktar, A. K. Sood, G. Lopez-Berestein, **C. Rodriguez-Aguayo**;
UT MD Anderson Cancer Center, Houston, TX

La-related protein 1 (LARP1) is an RNA-binding protein that plays a pivotal role in regulating mRNA on a post-transcriptional level. Overexpression of LARP1 has been detected in multiple cancers substantiating the critical role of LARP1 as a driver for cancer progression. This study aims to investigate the downstream target pathways regulated by LARP1 and to determine the impact of LARP1 targeting on the resistance to cisplatin and olaparib therapy in ovarian cancer (OC). Analysis of The Cancer Genome Atlas OC dataset, reverse phase protein array, *in vitro* functional and mechanistic experiments, and a xenograft OC mouse model using OVCAR8 cell line were executed. Our results revealed that overexpression of LARP1 is negatively correlated with progression-free survival in OC patients. Furthermore, LARP1 knockdown using two independent small interfering RNAs (siRNAs) suppressed cell growth, invasion, and migration, and ameliorated cisplatin resistance *in vitro*. Mechanistic analyses identified AXL as a target of LARP1 and this finding was further supported clinically in which co-overexpression of LARP1 and AXL is associated with poor prognosis in OC. Furthermore, LARP1 knockdown resulted in reduced phosphorylation of mTOR, AKT, and SRC with no significant effect on FAK. *In vivo*, administration of 1,2-dioleoyl-sn-glycero-3-phosphatidylcholine (DOPC) nanoparticles loaded with LARP1-siRNA suppressed tumor growth and improved the response to cisplatin and olaparib in a xenograft OC mouse model. In conclusion, LARP1 acts as an oncogenic RNA-binding protein in OC, and targeting LARP1 may represent an innovative therapeutic approach for ameliorating resistance to chemotherapy and targeted therapy in OC.

Keywords: RNA-binding proteins; cisplatin resistance; olaparib resistance; chemotherapy resistance; LARP1; ovarian cancer.

#4743 Targeting a novel TWIST1-Hexokinase II pathway to overcome MET TKI resistance in NSCLC.

P. H. Rumde[1], K. R. Cargill[1], V. Kumar[1], P. Devadassan[1], J. Chen[1], L. McGraw-Sapp[1], X. Wu[1], S. Dacic[2], R. Bao[1], B. Sivakama[1], E. S. Goetzman[1], S. Agnihotri[1], S. J. Mullett[1], S. G. Wendell[1], L. P. Stabile[1], T. F. Burns[1];

[1]University of Pittsburgh, Pittsburgh, PA, [2]Yale School of Medicine, New Haven, CT

Non-small cell lung cancer (NSCLC) is the most common primary tumor to metastasize to the brain, with up to 40% of NSCLC patients developing brain metastases (BM). These BM portend a poor prognosis, even when extracranial disease is well-controlled. While targeted therapy and immunotherapy have improved lung cancer survival, there are no therapies specifically targeting NSCLC BM. Our lab identified a significant enrichment of *MET* amplification in lung adenocarcinoma (LUAD) BM (16%) compared to primary NSCLC (3%) and liver metastases (5%). MET, a receptor tyrosine kinase, and its ligand, hepatocyte growth factor (HGF), promote proliferation, epithelial-mesenchymal transition (EMT), angiogenesis, and metastasis. Although MET tyrosine kinase inhibitors (TKIs) are approved for use in *MET*altered NSCLC, half of patients with *MET* alterations fail to respond or inevitably acquire TKI resistance. We have found that MET pathway activation by *MET* alterations leads to increased expression of TWIST1, an EMT transcription factor required for tumorigenesis in MET-dependent NSCLC. Together, the HGF/MET/TWIST1 axis promotes cancer survival and metastasis. We found that *MET* amplified BM had distinct transcriptional signatures reflecting increased glycolysis. A similar shift toward glycolysis was observed in the *MET* amplified metastatic LUAD cell line (H1993) compared to the *MET* wild type primary LUAD line (H2073) derived from the same patient. Furthermore, LUAD cell lines with high MET expression demonstrated increased expression and activity of glycolytic enzymes, as well as increased susceptibility to glucose deprivation and glycolytic inhibitors (2DG, PFK158, AT-101, V-9302). Conversely, treatment of *MET* amplified cells with MET TKI, capmatinib, reduced glycolysis and oxidation phosphorylation to the levels observed in *MET* wild type LUAD lines. Activation of the MET pathway with HGF or TWIST1 overexpression specifically increased the mRNA and protein expression of the key glycolytic enzyme, Hexokinase II (HK2), compared to other glycolytic pathway proteins. Conversely, inhibition of the MET pathway with capmatinib or the TWIST1 inhibitor, harmine, decreased HK2 protein expression through a MYC-independent pathway. However, TWIST1 was required for MET-dependent transcriptional upregulation of HK2. Remarkably, in two novel *MET* altered models (cell line and patient derived xenograft) of acquired MET TKI resistance, TWIST1 and HK2 expression were increased at the time of resistance. Both models remained sensitive to pharmacologic inhibition of either TWIST1 or glycolysis at the time of acquired resistance to MET TKIs. These findings suggest that continued upregulation of the TWIST1-HK2 axis is required for acquired MET TKI resistance. In summary, these studies suggest a targetable, metabolic reprogramming in *MET* altered LUAD BM mediated through a novel TWIST1-HK2 pathway.

#4744 Overcoming MK1775 resistance in upper gastrointestinal cancers with combined WEE1 and CHK1 inhibition.

K. Thangaretnam, M. Islam, H. Lu, D. Peng, N. Bhat, M. Soutto, E.-R. Wael, Z. Chen;
University of Miami, Miami, FL

Background: Upper gastrointestinal cancers (UGC), encompassing esophageal and gastric cancers, rank among the top causes of cancer-related deaths globally, with esophageal cancer being the sixth and gastric cancer the fourth leading cause. Esophageal adenocarcinoma (EAC), predominant in the western world, shares histopathological and molecular characteristics with gastric cancer (GC). Despite these similarities, treatment challenges persist, exemplified by the limited efficacy of the WEE1 inhibitor MK1775 in clinical trials due to drug resistance. Our study investigates novel mechanisms underlying this resistance in UGC.

Methods and results: RNA sequencing and immunohistochemistry staining demonstrated notable overexpression of WEE1 in over two hundred human EAC and GC samples compared to normal tissues. Concurrently, Western blot analysis revealed a positive correlation between WEE1 and CHK1 overexpression across 16 UGC cell lines. To categorize UGC cells based on their sensitivity to MK1775, we conducted ATP-glo cell viability assays, determining their half-maximal inhibitory concentration (IC50) values. Utilizing nuclear-cytosol separation, our data intriguingly uncovered, for the first time, that in MK1775-resistant cells, MK1775 treatment induces the abnormal translocation of phosphorylated CHK1 (p-CHK1) from the nucleus to the cytoplasm, a shift not observed in MK1775-sensitive cells. Further analysis through Western blot suggested that the cytoplasmic presence of p-CHK1 might trigger the activation of oncogenic STAT3 following MK1775 treatment. This activation appears to stimulate the expression of genes that promote cancer cell survival and drug resistance by enhancing cell survival and inhibiting apoptosis. Notably, combining the WEE1 inhibitor with the CHK1 inhibitor CHIR124 effectively inhibited CHK1 kinase activity and abrogated STAT3 phosphorylation, DNA binding, and transcriptional activity in UGC cells. Our findings strongly indicate that a combined therapy of WEE1 and CHK1 inhibitors could be a promising strategy to overcome MK1775 resistance in UGC cells. Our ongoing research will employ human-derived UGC organoids, patient-derived xenografts (PDXs), and human tissue samples to further validate these findings.

Conclusions: Our study underscores the potential of combining WEE1 and CHK1 inhibitors to effectively combat MK1775 resistance in UGC, offering a promising direction for improved treatment strategies and patient outcomes in these challenging malignancies.

#4745 A novel combination therapy targeting RAF, MEK and FAK to overcome skin cutaneous melanoma treatment resistance.

S. Lubrano[1], F. Faraji[2], R. Cervantes-Villagrana[1], S. Ramirez[3], N. Arang[1], A. Officer[1], D. C. Rigiracciolo[1], P. Y. Anguiano Quiroz[1], A. Bacchiocchi[4], R. Halaban[4], S. Coma[5], S. Holmen[6], C. Martini[7], J. Pachter[5], A. Aplin[8], **J. Gutkind**[1];

[1]UCSD Moores Cancer Center, La Jolla, CA, [2]University of California, San Diego School of Medicine, La Jolla, CA, [3]La Jolla Institute for Immunology, La Jolla, CA, [4]Yale School of Medicine, New Haven, CT, [5]Verastem Oncology, Boston, MA, [6]University of Utah School of Medicine, Salt Lake City, UT, [7]University of Pisa, Pisa, Italy, [8]Thomas Jefferson University, Philadelphia, PA

Metastatic melanoma is the most aggressive malignancy of the skin and $BRAF^{V600E}$ mutation is the most common genetic alteration in skin cutaneous melanoma (SKCM). Despite the advent of immune checkpoint inhibition (ICI) immunotherapy, only 40% of patients show long-term responses. As such, combined therapy with BRAF and MEK inhibitors (BRAFi + MEKi) remains the standard of care for $BRAF^{V600E+}$ SKCM. In the present study, transcriptome analysis of $BRAF^{V600E+}$ SKCM tumors derived from patients revealed that activation of extracellular matrix signaling, including focal adhesion signaling, is highly enriched in patients who experienced disease progression on BRAFi + MEKi therapy. Consistent with these results, we found increased activation of focal adhesion kinase (FAK) in human $BRAF^{V600E+}$ SKCM A375 cells treated with BRAFi, MEKi or the RAF/MEK clamp avutometinib. Mechanistically, we discovered that avutometinib-mediated inhibition of the RAF/MEK/ERK pathway decreased RhoE/Rnd3 expression, thereby unleashing RhoA/FAK/AKT signaling. Thus, we hypothesized that FAK activation represents a resistance mechanism to BRAFi + MEKi and that FAK inhibition (FAKi) might overcome resistance to BRAFi/MEKi. Indeed, avutometinib demonstrated synergistic antiproliferative and proapoptotic activity when combined with FAKi in human $BRAF^{V600E+}$ SKCM A375 cells. Importantly, we found that the combination of FAKi + avutometinib overcame resistance to BRAFi + MEKi in SKCM xenografts and patient-derived cells from SKCM-resistant lesions. Finally, we showed that while $BRAF^{V600E+}$ SKCM YUMM 1.7 syngeneic tumors failed to respond to ICI therapy, avutometinib ± FAKi inhibited tumor growth. We observed that tumors treated with avutometinib as single agent eventually developed resistance and escaped growth inhibition, but those treated with combined avutometinib and FAKi displayed durable treatment responses, often with complete tumor regression. These findings provide a rationale for the clinical development of avutometinib with defactinib (FAKi) in patients with $BRAF^{V600E+}$ cutaneous melanoma following progression on BRAFi + MEKi and/or ICI therapy.

#4746 PIM kinase inhibition synergizes with a MERTK inhibitor to treat osimertinib resistant *EGFR*-mutant non-small cell lung cancer.

D. Yan[1], X. Wang[2], S. V. Frye[2], H. Earp III[3], D. DeRyckere[4], D. K. Graham[4];
[1]Emory University, Atlanta, GA, [2]Chemical Biology and Medicinal Chemistry, Chapel Hill, NC, [3]UNC Lineberger Comprehensive Cancer Center, Chapel Hill, NC, [4]Aflac Cancer and Blood Disorders Center, Children's Healthcare of Atlanta, Atlanta, GA

There is an unmet need for effective treatment in the setting of acquired osimertinib resistance in EGFR-mutant non-small cell lung cancer (NSCLC) patients and MERTK tyrosine kinase is a potential therapeutic target in this context. Treatment with the MERTK inhibitor MRX-2843 was sufficient to abrogate downstream PI3K-AKT and MAPK-ERK signaling, cell expansion, and colony formation in osimertinib-resistant EGFR-mutant NSCLC cell lines, suggesting dependence on MERTK signaling for tumor cell proliferation/survival. Further, two structurally distinct PIM kinase inhibitors, SGI-1776 and PIM447, provided synergistic inhibition of cell expansion and colony formation in osimertinib-resistant cell line cultures when combined with MRX-2843 treatment. Mechanistically, treatment with MRX-2843 in combination with either PIM kinase inhibitor decreased downstream PI3K-AKT and MAPK-ERK signaling more effectively than single agents. Furthermore, knockdown of PIM kinases (PIM1, 2, 3) using nine sets of siRNAs led to various changes in expression of TAM receptor family members (TYRO3, AXL, MERTK), indicating a role for PIM kinases in regulation of TAM kinase expression. These studies suggest a novel treatment strategy for osimertinib-resistant EGFR-mutant NSCLC using a first-in-class MERTK kinase inhibitor that is currently under evaluation in multiple Phase I clinical trials.

#4747 Novel targets for BRAF^{V600E} and BRAF^{V600E}RAC1^{P29S} drug resistant melanoma.

C. Uribe-Alvarez, D. Araiza-Olivera, A. Cannon, J. Chernoff;
Fox Chase Cancer Center, Philadelphia, PA

The most common mutational drivers in malignant melanoma are the oncogene *BRAF*$^{V600E/K}$ (60%), *NRAS*$^{Q61L/R}$ (30%) and the RHO GTPase RAC1$^{P29S/L}$ (9%). BRAF$^{V600E/K}$ melanoma standard of care comprises the use of checkpoint inhibitors (CPIs) such as anti-PD1 or anti-CTLA-4 in combination with targeted therapies against BRAF and MEK kinases. BRAF mutant melanomas develop intrinsic, acquired, or after treatment resistance to BRAF and MEK inhibitors : around half of targeted therapy combination treatments with anti-PD1 and 70% with anti-CTLA-4 will be unsuccessful due to melanoma intrinsic resistance. Among other causes, intrinsic drug resistance can be associated with additional genome mutations, such as the activating Rac1^{P29S} mutation present in 6% of patients with BRAF positive melanoma. A deeper understanding on the biology, progression, and tumor microenvironment of drug resistant melanomas is needed to aid in the search of novel targets and to increase the effectivity of proposed treatments.

We generated 3 sets of isogenic BRAF^{V600E} and BRAF^{V600E}/RAC1^{P29S} cell lines by transfecting 501mel, 451Lu and YUMM1.7 cell lines with Rac1^{P29S}. We then exposed them for 3 months to increasing concentrations of PLX4720 to generate drug resistant cell lines (DR). Rac1^{P29S} -transfected and PLX4720 resistant cell lines had an increase in the Mek/Erk signaling pathway. A differential analysis using a kinome and an epigenome drug screening library in the 501mel cell lines (501mel, 501mel Rac1^{P29S}, 501mel-DR, 501mel Rac1^{P29S} -DR) showed that BRAF^{V600E}/RAC1^{P29S} and the DR melanoma cell lines growth can be inhibited with mTor, PI3K, cdk9 and BRD4 inhibitors. BRD4 is an epigenetic regulator that recruits P-TEFb to stimulate RNA polymerase II elongation. BRD4 also interacts with SMAD3 and CDK9 to regulate transcription through eIF4G increasing oncogenic c-Myc and increasing Mek/Erk signaling pathways. We tested 501mel, 451Lu and YUMM1.7 isogenic cell line series against Rapamycin to confirm mTORC1 as an effective target. Drugs that target different subunits of the eIF4F complex (CR-1-31-B, Ribavirin and Briciclib) also decrease BRAF^{V600E}/RAC1^{P29S} and the DR melanoma cell lines growth specifically. Furthermore, silencing of eIF4A1 and Raptor genes reduces cell growth in the BRAF^{V600E}/RAC1^{P29S}, and the DR cells when compared to the parental cell lines. Silencing Rictor had no effect on cell growth on any cells. When tested in a syngraft model, CR-1-31-B and rapamycin reduced tumor size when using YUMM1.7, YUMM1.7- RAC1^{P29S} and YUMM1.7 RAC1^{P29S}-DR cell lines. Next, we sought to investigate the effect of inhibiting mTOR and eiF4F in the PD-1/PD-L1 axis in tumor cells and tumor associated dendritic cells and macrophages, and how targeting these modifies the tumor microenvironment.

#4748 Aronia berry overcomes gemcitabine resistance by regulating the MYD88/NF-kB/P-glycoprotein pathway in pancreatic ductal adenocarcinoma.

Y. Li[1], C. Xu[1], H. Han[2], A. Goel[1];

[1]Beckman Research Institute of The City of Hope, Monrovia, CA, [2]The Translational Genomics Research Institute, Phoenix, AZ

Background: Pancreatic ductal adenocarcinoma (PDAC) is lethal, which is partly due to the limited efficacy of Gemcitabine (Gem)-based chemotherapy, resulting from the development of acquired resistance to this regimen. Aronia berry extract (ABE) is a natural source of phenolic compounds known for its anti-cancer properties. Previous research has highlighted the ability of ABE to help overcome chemoresistance to conventional chemotherapies in various cancers. In this study, we interrogated the ability of ABE to overcome Gem-resistance (Gem-R) in PDAC and identify specific pathway(s) responsible for this anti-cancer efficacy. Methods: We performed a series of in-vitro experiments in Gem-R cells to evaluate the synergistic effect of combined treatment with Gem and ABE. Furthermore, we conducted a genomewide transcriptomic analysis to identify the critical regulatory pathways associated with chemoresistance and potential therapeutic targets of ABE in Gem-R PDAC cells. The cell culture findings were validated in patient-derived 3D organoids. Results: The combined treatment with ABE and Gem in Gem-R cells exhibited significant synergistic anticancer effects on cell viability, proliferation, migration, and invasion. The transcriptomic analysis revealed that the NF-κB signaling pathway was associated with Gem-R ($p<0.05$), with a significant upregulation of MYD88. Additionally, MYD88 was significantly associated with overall survival in PDAC patients in the TCGA cohort (HR=1.58, P=0.045). The MYD88/NF-κB signaling is associated with chemoresistance as it can upregulate the efflux transporters like P-glycoprotein (P-gp). Our results confirmed that combined treatment inhibited the NF-κB signaling pathway by suppressing MYD88 and downregulating P-gp expression to overcome Gem-R. Finally, the combined treatment demonstrated superior anti-cancer activity in 3D organoids by reducing both their number and size (P<0.05). Conclusion: We provide novel insights into the potential of ABE in overcoming Gem-R in PDAC cells by targeting the MYD88/NF-κb/P-gp axis, which offers a safe and inexpensive approach for improving therapeutic outcomes in this fatal malignancy.

#4749 Acrivon predictive precision proteomics (AP3) uncovers mechanism of resistance to ACR-368, a clinical-stage CHK1/2 inhibitor, and identifies rational combination treatment.

H. Nilsson[1], L. Shi[2], M. E. Jakobsson[1], J. Baddour-Sousounis[2], S. Rafiei[2], U. Muralitharan[1], Z. Best[2], V. Siino[1], F. J. Santana[2], I. Arribas Diez[1], K. Singh[2], P. Lombardo[2], W. Dahlberg[2], S. Kumar[2], A. Youssef[2], R. Improgo[2], C. Xu[2], J. Jung[2], J.-M. Lee[3], A. Murshid[2], M. Shipitsin[2], J. V. Olsen[4], K. Masson[2], D. A. Proia[2], C. Wigerup[1], P. Blume-Jensen[2];

[1]Acrivon Therapeutics, Lund, Sweden, [2]Acrivon Therapeutics, Watertown, MA, [3]National Cancer Institute, Bethesda, MD, [4]University of Copenhagen, Copenhagen, Denmark

ACR-368 (prexasertib) is a clinically advanced CHK1/2 inhibitor which has demonstrated durable activity across a proportion of patients with advanced solid tumors. Genomic biomarkers have proven unsuccessful in predicting response to ACR-368, limiting its clinical success. Using AP3, we previously developed a response-predictive proteomics-based test for ACR-368 (ACR-368 OncoSignature) for the identification of patients sensitive to ACR-368 monotherapy treatment as demonstrated in blinded preclinical studies. A Phase 2 clinical trial is ongoing where patients are treated with ACR-368 monotherapy based on OncoSignature-predicted sensitivity (NCT05548296). Here, we demonstrate the utility of AP3 for the identification of a key druggable resistance mechanism to ACR-368 and how to overcome that with low dose gemcitabine (gem), providing OncoSignature negative patients with a new potential therapeutic option. Five ovarian cancer cell lines were rendered durably resistant to ACR-368 by culturing in the presence of clinically relevant concentrations of ACR-368. Matched parental and ACR-368 resistant cell line pairs were profiled using AP3 mass spectrometry. Comprehensive pathway reconstitution and kinase activity analyses were performed to identify drug resistance mechanisms in an unbiased manner. Downregulation of DNA damage repair pathway activity was causally linked to the ACR-368-resistant phenotype, suggesting agents that restore replication stress around the CHK1/2 signaling axis may re-sensitize to ACR-368. To test this, a panel of ovarian cancer cell lines with intrinsic or drug-induced resistance to ACR-368 were screened for cell growth inhibition by ACR-368 combined with gem. Gem synergized with ACR-368 in 12/13 cell lines at low doses (1-40 nM). Moreover, Western blot analysis demonstrated protein markers of replication stress were induced by low dose gem (3-30 nM), suggesting a correlation between gem-induced replication stress and synergy with ACR-368. Comet assays showed that DMSO, gem (3 nM), or ACR-368 (100 nM) had minimal impact (4.4%, 4.5%, and 11.4%, respectively) on % comet tail DNA in ACR-368 resistant cells, while the gem combination led to 35% comet tail DNA ($p<0.001$). Finally, in a human tumor xenograft mouse model, low dose gem demonstrated a dose-dependent increase in replication stress markers (Cyclin E, pCHK1 S345) from 0.3-3 mg/kg, which allometrically scales to 1-10 mg/m2 in humans. These data supported a dose escalation Phase 1b/2 clinical study of low dose gem with ACR-368 to evaluate the efficacy and safety of the combination in ACR-368 OncoSignature negative patients (NCT05548296). This shows the potential of AP3 for unbiased elucidation of actionable drug resistance mechanisms and rapid clinical implementation in our trials, which have recently confirmed clinical activity.

#4750 The MNK inhibitor EB1 sensitizes AR-V7 positive castration-resistant prostate cancer to enzalutamide.

S. Garcia-Ortega[1], L. Suarez-Cabrera[1], J. Morote[1], O. Mendez[1], M. Cano-Galietero[2], E. Muro-Blanc[1], J. I. Borrell[3], A. Santamaria[1], S. Ramon y Cajal[1], S. Hummer[1];

[1]Vall d'Hebron Research Institute (VHIR), Barcelona, Spain, [2]Spanish Biomedical Research Network Centre in Oncology (CIBERONC), Madrid, Spain, [3]IQS School of Engineering, Barcelona, Spain

Introduction: Resistance to androgen receptor signaling inhibitors (ARSI) like Enzalutamide is frequent in castration resistant prostate cancer (CRPC). The mechanisms driving drug resistance include the overexpression of androgen receptor (AR) and the presence of splice variants like androgen receptor splice variant 7 (AR-V7). Clinical studies (PROPHECY) have demonstrated that AR-V7 positive CRPC patients treated with Enzalutamide show poorer overall survival and thus lack an effective targeted line of treatment. Recently, AR signaling and the regulation of protein translation via the translation initiation factor 4E (eIF4E) and MAPK-interacting kinases (MNKs) have been shown to depend on each other and targeting eIF4E has been proposed to increase the efficacy of ARSI.
Objectives: We have recently described EB1 as the first in class non-ATP competitive inhibitor of MNK1/2 (Bou-Petit et al. JMC, 2022) and have now tested its applicability in CRPC. In this work we describe the impact of EB1 on the efficacy of Enzalutamide treatment in CRPC.
Methodology: Cell lines 22RV1 and LNCaP-95 were used as AR-V7 positive models of CRPC. Effects of EB1 and Enzalutamide alone and in combination on cell growth were studied through crystal violet assay. Drug combination Index was calculated following Chou-Talalay method using CompuSyn Software. Cell death was studied through propidium iodide (PI) staining. AR transcriptional activity was assessed through RT-qPCR of AR canonical target genes like PSA. A head-to-head study with eFT-508 (Tomivosertib, eFFECTOR Therapeutics, Inc.) as the most advanced Type I MNK inhibitor was performed. Lastly, spheroids obtained through centrifugation in ultra-low attachment plates were used for validating drug interaction in 3D growth and viability studies. Spheroid viability was assessed through PI and Calcein AM staining as well as MTT assay.
Results: In vitro results demonstrate strong to moderate synergistic inhibition of cell growth through the induction of cell death by the combination of Enzalutamide and EB1 in AR-V7 positive CRPC cell lines, as well as reduction of AR transcriptional activity (PSA). Drug combination also reduced growth and viability of spheroids, indicating good tumor penetrating properties in 3D models and giving in vitro proof-of-concept for in vivo applications. Furthermore, drug synergy with Enzalutamide could only be observed with EB1 and not with Type-I MNK inhibitors like eFT-508, indicating that MNK1/2 functions beyond its kinase activity might be relevant for cancer progression.
Conclusion: Here we demonstrate that the novel MNK inhibitor EB1 shows promising in vitro results, which cannot be obtained with Type-I MNK inhibitors. The combination of EB1 with the standard of care Enzalutamide provide a novel therapeutic opportunity for the treatment of CRPC, particularly in AR-V7 positive patients.

#4751 The antiviral, Daclatasvir, downregulates Tribbles 2 pseudokinase and reverses enzalutamide resistance in prostate cancer.

J. Monga, R. Guddeti, C. Rogers, S. Gadgeel, D. Chitale, **J. Ghosh**;
Henry Ford Health System, Detroit, MI

Background: FDA-approved enzalutamide is commonly prescribed for advanced prostate cancer. However, enzalutamide-resistant prostate cancer (ERPC) invariably develops, which leads to aggressive, lethal disease. Recently, we found that the Tribbles 2 (TRIB2) pseudokinase is overexpressed in ERPC cells and confers resistance to enzalutamide by promoting lineage plasticity to neuroendocrine differentiation. Though TRIB2 emerged as an excellent molecular target for ERPC, suitable inhibitors are not commercially available for effective targeting.

Methods: Compounds were tested using a luciferase-tagged TRIB2 fusion protein-based assay system. Binding of drugs with TRIB2 protein was analyzed by thermal shift assays and by advanced computer-based homology modeling. Degradation of TRIB2 protein was measured by Western blot. Drug effects on re-sensitization of ERPC cells and synergy with enzalutamide were determined through cell viability and apoptosis assays. To gauge the *in vivo* effects of Daclatasvir (DCV), ERPC tumor xenograft-bearing mice were treated with varying doses of DCV via oral gavage. Tumor growth was calculated by measuring volumes and molecular markers in tumors were analyzed by immunohistochemistry.

Results: By designing a luciferase-tagged TRIB2 fusion protein-based assay system, we screened a library of about 1,600 FDA-approved compounds and found that DCV, effectively inhibits the TRIB2-luciferase activity (more than 70% inhibition in 24 hours at 10 micromolar) but does not inhibit the activity of free luciferase. Notably, DCV directly binds to pure TRIB2 protein, leading to its destabilization and a reduction in the half-maximal melting temperature *(Tm)* from 41^{o}C to 37^{o}C, as confirmed by thermal shift assays. Interestingly, we found that DCV degrades TRIB2 proteins via activation of proteasomes and re-sensitizes ERPC cells to enzalutamide. DCV downregulates the master neuronal transcription factor, BRN2, and the stemness factor, SOX2, and synergizes with enzalutamide at lower, sub-lethal doses to decrease the viability of prostate cancer cells by inducing apoptosis. Finally, DCV was found to effectively inhibit the growth of ERPC tumors and decrease the protein level of TRIB2 in mice when delivered via oral gavage.

Conclusion: These findings indicate that DCV effectively downregulates TRIB2 both *in vitro* and *in vivo* and suggest that further testing of DCV may help design an innovative therapeutic approach for management of enzalutamide-resistant, aggressive, lethal prostate cancer.

#4752 Enhancer of zeste homolog 2 inhibitors overcome glucocorticoid resistance in acute lymphoblastic leukemia by augmenting pro-apoptotic signaling.

M. Dalal[1], J. Yi[2], J. Li[3], A. Shobh[1], D. DupereRicher[1], R. Bennett[1], J. Licht[1];
[1]University of Florida College of Medicine, Gainesville, FL, [2]Baylor College of Medicine, Houston, TX, [3]Thomas Jefferson University, Philadelphia, PA

Introduction Relapsed acute lymphoblastic leukemia (ALL) portends a poor prognosis. Glucocorticoids (GCs) are a central component of a multi-agent regimen to treat ALL. GCs mediate ligand-dependent global transcriptional changes activating feedback loop that increases GC receptor (GR) expression and pro-apoptotic signaling. GC resistance is a common mechanism in relapsed/refractory ALL. Altered function of Enhancer of Zeste Homolog 2 (EZH2), a histone methyl transferase (HMT), including increased expression and activating mutations have been reported in ALL. Previously, EZH2 inhibitors have been shown to increase GC efficacy in non-ALL B-cell lymphoid malignancies including non-Hodgkin lymphoma. Furthermore, EZH2 inhibitors reversed GC resistance and increased efficacy of GCs in an ALL subtype with an activating point mutation in an HMT called nuclear set domain 2. Overcoming GC resistance by novel therapeutic strategies may help improve outcomes in relapsed/refractory ALL.

Hypothesis EZH2 inhibitors may enhance GC efficacy by augmenting downstream effects of GCs.

Methods We performed in-vitro studies of EZH2 inhibitors, EPZ-6438 and CPI-1205, at graded doses in GC resistance human-derived B-cell (SUPB15) and T-cell (SUPT1, KOPTK1, PEER) ALL cell lines followed by graded doses of dexamethasone (dex). Cell viability was performed using CellTiter-Glo assay. Induction of apoptosis was measured with Annexin V flow cytometry. Pro-apoptotic BIM mRNA and protein levels were measured using real-time PCR and immunoblot. Global H3K27me3 protein levels were assessed using immunoblot.

Results GC resistant B-cell ALL and T-cell ALL treated with EZH2 inhibitors for 3-7 days followed by the addition of dex for 48-72 hours led to decreased cell viability and increased apoptosis of the ALL cells compared to cells treated with vehicle (DMSO) and dex alone. EZH2 inhibitors on their own did not cause apoptosis. SynergyFinder revealed Bliss synergy scores between 23- 31 in B-cell ALL and T-cell ALL cell lines with greater than 10 considered a synergistic drug interaction. Immunoblotting of cells treated with EZH2 inhibitors alone showed an increase in pro-apoptotic protein, BIM. BIM level was further enhanced when dex was added in combination with EZH2 inhibitors compared to vehicle and dex alone suggesting that EZH2 inhibitors were augmenting BIM expression. Further assessment of the mechanism of how EZH2 inhibitors lead to improved GC efficacy will be performed by integrating transcriptomic and epigenomic profiling in the presence and absence of EZH2 inhibitors. Furthermore, in-vivo testing of EZH2 inhibitors in patient derived xenografts will be performed.

Conclusion EZH2 inhibitors can overcome GC resistance in ALL posing as a potential novel therapeutic agent to treat relapsed/refractory ALL.

#4754 Targeted inhibition of the HNF1A/SHH axis by triptolide overcomes paclitaxel resistance in non-small cell lung cancer.

P. Li, L. Li, L. Yang, L. Liu, **X. Zhao**;
The Second Hospital of Shandong University, Jinan, China

Paclitaxel resistance is commonly associated with a poor prognosis in non-small cell lung cancer (NSCLC) patients, and there are no promising pharmacological treatments for paclitaxel resistance. Here, we constructed human NSCLC-derived paclitaxel-resistant cell lines as an effective tool to explore the mechanisms of chemoresistance. We discovered that triptolide, a monomer compound extracted from Tripterygium wilfordii Hook F, was able to reverse paclitaxel resistance by reducing ABCB1 expression in vivo and in vitro. Through high-throughput sequencing, we found that the SHH-initiated Hedgehog signaling pathway played an important role in this process. More importantly, triptolide could directly target HNF1A, a transcription factor of SHH, and inhibited HNF1A/SHH expression, ensuing in attenuation of Hedgehog signaling. Clinically, we found a positive correlation between HNF1A and SHH expression in both NSCLC tumor tissue microarrays and cancer network databases. These findings illuminated a novel molecular mechanism through which triptolide effectively targets and inhibits HNF1A, thereby impeding the activation of the Hedgehog signaling pathway and reducing the expression of ABCB1. This finding indicated the potential clinical application of triptolide and provided promising prospects in targeting the HNF1A/SHH pathway as a therapeutic strategy for NSCLC patients with paclitaxel resistance.

#4755 Extracellular GRP78 inhibition reverses drug and immune resistance in cancer cells.

D. J. Davidson, J. Zelek, E. Stolarik, M. Thigpen, A. Davidson, DPT;
Creative BioTherapeutics, Gurnee, IL

CBT300 was created from Creative BioTherapeutics' discovery that drug resistant recurrent cancer cells up-regulate a survival pathway that results in the expression of extracellular Glucose-Regulated Protein 78 (ecGRP78) in the tumor microenvironment (TME). This TME ecGRP78 binds to cancer and immune cell surfaces, which induces a cascade of events to increase drug resistance, immune suppression, and cancer stem cell (CSC) formation. CBT300 targets surface bound ecGRP78 that has been found on breast, lung, ovarian, prostate, melanoma, multiple myeloma, colon, pediatric and adult brain tumors. We can now show that inhibition of ecGRP78 can a) induce apoptosis of drug resistant tumor cells, b) eliminate drug and immune resistance showing synergistic effects with chemotherapy and immunotherapy, c) decrease the amount of chemotherapy about 90% in combination with CBT300. Recent publications show that ecGRP78 is found on many types of tumor cell surfaces but not on normal cell surfaces. In fact, cell surface bound ecGRP78 is important for many aspects of cancer development, including cell survival, proliferation, chemoresistance, angiogenesis, metastasis formation, immune suppression, and stem cell formation. Recently, it has been shown that increased ecGRP78 expression in metastatic breast cancer, glioblastoma and multiple myeloma patients was significantly associated with later stage, increased distant metastasis, increased aggressiveness, shorter disease-free survival, and decreased overall survival. In studies to help understand how ecGRP78 causes tumor progression and drug and immune resistance, we discovered a novel ecGRP78 binding transmembrane protein on TNBC, and brain cancer cells called Receptor Tyrosine Kinase Orphan Receptor-1 (ROR1). Using the GRP78 binding domain from ROR1 and a human Fc domain, we created a biologic fusion protein that is a potent and specific ecGRP78 inhibitor called CBT300. We now show that CBT300's elimination of csGRP78 destabilizes and removes oncofetal proteins ROR1, and Cripto, and checkpoint protein PD-L1 from tumor cell surfaces resulting in reversal of chemoresistance, reduction in immune suppression, inhibition of stem cell phenotype and increased tumor cell apoptosis. Our results with CBT300 demonstrate proof of concept data in vitro and in vivo for our novel ecGRP78 inhibitor on several drug resistant cancers demonstrating the potential to provide a major advance in the treatment of drug resistant cancers either alone or in combination with lower doses of chemotherapy. Exploiting a novel mechanism of action with a non-toxic, efficacious and cost effective biologic therapy that has shown increased survival in recurrent cancers will bring new hope for these patients.

#4756 Targeting DNA topoisomerase II to manage acquired resistance to third generation EGFR tyrosine kinase inhibitors in the treatment of EGFR mutant NSCLC.

Z. Chen[1], K. A. Vallega[1], D. Wang[1], Z. Quan[2], S. Fan[2], Q. Wang[3], T. A. Leal[1], S. S. Ramalingam[1], **S.-Y. Sun**[1];
[1]Emory University, Atlanta, GA, [2]The Second Xiangya Hospital, South Central University, Changshai, China, [3]Henan Cancer Hospital, Zhengzhou, China

Development of effective strategies to manage the inevitable acquired resistance to osimertinib, a 3rd generation EGFR inhibitor with proven clinical efficacy in prolonging survival of patients with EGFR mutant (EGFRm) non-small cell lung cancer (NSCLC), is an urgent and critical area of unmet need in the clinic. Effort toward this direction led us to find that the DNA topoisomerase II (Topo II) inhibitors, doxorubicin and etoposide (VP-16), but not other chemotherapeutic agents, synergistically decreased the survival of osimertinib-resistant cell lines when combined with osimertinib. The combination of osimertinib with either doxorubcin or VP-16 effectively induced DNA damage and apoptosis in osimertinib-resistant cells, suppressed the growth of osimertinib-resistant tumors, and delayed the emergence of acquired resistance to osimertinib. Mechanistic studies found that osimertinib as well other EGFR-TKIs effectively decreased Topo IIα levels in EGFRm NSCLC cells by facilitating its proteasomal degradation and induced DNA damage; these effects were lost in cell lines with osimertinib acquired resistance that possessed elevated basal levels of Topo IIα. In the majority of EGFRm NSCLC tissues relapsed from EGFR-TKI treatment, Topo IIα levels were substantially increased. Enforced expression of ectopic *TOP2A* genes in sensitive EGFRm NSCLC cells conferred resistance to osimertinib in inducing DNA damage and apoptosis, whereas knockdown of *TOP2A* in osimertinib-resistant cell lines restored their responses to undergo osimertinib-induced DNA damage and apoptosis. Together, these results reveal a previously undiscovered essential role of Topo IIα modulation in regulating the responses of EGFRm NSCLC cells to osimertinib, providing scientific rationale for targeting Topo II to manage acquired resistance to osimertinib and possibly other third generation EGFR-TKIs, thus warranting clinical validation of this strategy. (This study was supported by NIH/NCI R01 CA223220 and UG1 CA233259 and Emory Winship Cancer Institute lung cancer research pilot funds).

#4757 Combining PARP inhibitor with TACC3 inhibition overcomes PARP inhibitor resistance in ovarian cancer.

Y. Wu[1], Q. Wang[2], C. Deng[3], M. Li[1], **Y. Xiao**[1];

[1]Peking University Third Hospital, Beijing, China, [2]Peking University, Beijing, China, [3]Peking University People's Hospital, Beijing, China

The treatment of ovarian cancer (OC) presents a significant challenge due to the emergence of resistance to poly (ADP-ribose) polymerase inhibitors (PARPi). Transforming acidic coiled coil containing protein 3 (TACC3) belongs to the TACC family, characterized by its coiled-coil domains. TACC3 plays a crucial role in cell division, particularly in the formation and stability of the mitotic spindle, which is essential for proper chromosome segregation. Mutations or changes in TACC3 have been associated with various cancers, making it an increasingly attractive target for anticancer therapy in recent years. Here, we demonstrated a significant upregulation of TACC3 in OC, correlating with adverse clinical outcomes. Notably, PARPi-resistant OC cells exhibited a marked sensitivity to TACC3 inhibition. This was evidenced by the induction of spindle defects and mitotic catastrophe in PARPi-resistant cells upon TACC3 suppression, achieved either genetically or pharmacologically. Moreover, we explored the therapeutic efficacy of combining TACC3 inhibitor with PARPi, specifically BO-264 with olaparib or niraparib. This combination exhibited a synergistic effect, markedly reducing cell viability in vitro and tumor growth in PARPi-resistant tumor xenograft models. Our study suggests a promising new method for treating ovarian cancer, especially for those resistant to current PARPi treatments, by simultaneously targeting TACC3 and PARPi, enhancing treatment efficacy and potentially improving patient outcomes.

#4758 Targeting cellular pH as a novel therapeutic strategy in CDK4/6 inhibitor resistant breast cancer.

E. R. Scheidemann, D. M. Demas, A. N. Shajahan-Haq;
Georgetown Lombardi Comprehensive Cancer Ctr., Washington, DC

Cyclin dependent kinase 4 and 6 inhibitors (CDK4/6i) are part of standard of care therapy in combination with antiestrogens for the treatment of metastatic estrogen receptor positive (ER+) breast cancer. Of the three major CDK4/6i, only ribociclib and abemaciclib, but not palbociclib, have shown significant improvement in overall survival in the clinic. However, resistance to CDK4/6i is prevalent and advanced metastatic ER+ breast cancer remains incurable. Other studies have focused on cell cycle or growth factor alterations in resistant tumors but targeting these pathways have not been clinically validated. Beside inhibiting the cell cycle, CDK4/6i are known to induce lysosomes in sensitive cells but the role of lysosomes in CDK4/6i resistance remains elusive. Recently, we have shown that CDK4/6i resistant breast cancer cells gain metastatic potential relative to sensitive cells and this is potentially due to deregulated lysosomes, which can be targeted with lysosome destabilizers. Here we show that all three CDK4/6i induce rapid lysosomal acidification in sensitive cells, which suggests a role of cellular pH in CDK4/6i-mediated cell death. However, in resistant cells, lysosomal acidification following CDK4/6i treatment was diminished. Therefore, we hypothesize that cellular pH is tightly regulated in CDK4/6i resistant cells and this pathway can be targeted to inhibit cell viability. Interestingly, protein levels of carbonic anhydrase IX (CA9), an important regulator of cellular pH, is significantly elevated in resistant cells. Increased CA9 levels correlate with impaired overall survival in breast and other cancers. Small molecule inhibitor of CA9, S4 or clinical-grade SLC-0111, inhibits growth of resistant cells when combined with CDK4/6i plus antiestrogens. Thus, our study highlights the role of pH changes in CDK4/6i resistant breast cancer and offer therapeutic strategies to treat this incurable disease.

#4759 Targeting slow-cycling persisters in EGFR mutant non-small cell lung cancer.

M. Thiruvalluvan[1], S. Billet[1], Z. Liu[2], J. Lownik[1], G. Gonzales[1], H. Kim[1], A. L. Villamejor[1], L. Milshteyn[1], K. Sankar[1], E. M. Posadas[1], J. Lopategui[1], S. You[1], K. Reckamp[1], N. A. Bhowmick[1];

[1]Cedars-Sinai Medical Center, Los Angeles, CA, [2]Radiation Effects Research Foundation, Hiroshima, Japan

Activating mutations in the epidermal growth factor receptor (EGFR) gene in non-small cell lung cancer (NSCLC) patients are associated with clinical benefit in the metastatic and adjuvant settings when treated with EGFR inhibitors, such as osimertinib. Despite its dramatic efficacy, most patients are partial responders and refractive disease leave limited treatment options. The objective was to dissect the mechanism of osimertinib resistance in EGFR mutant NSCLC models to identify a means of re-sensitization. Imaging mass cytometric analysis of 76 NSCLC patients demonstrated EGFR expression was inversely correlated to CD105 membrane expression. CD105 is a transforming growth factor beta (TGF-β) family co-receptor that promotes bone morphogenic protein (BMP) signaling and inhibits TGF-β signaling. Significant elevation in cell surface CD105 by osimertinib was furthered by EGFR knockdown in two NSCLC lines with EGFR activating mutations. These lines were subjected to a program of increasing osimertinib concentrations to generate isogenic resistant lines. Heterogeneous drug-tolerant persister cells had significantly higher mutational load, increased CD105 cell surface expression as well as greater expression of bypass signaling factors such as ERK, PI3K, and BMP ligands compared to their parental counterparts. Single cell RNA-seq analysis of parental NSCLC revealed a small population of cells that shared elevated endothelial and pyrimidine metabolism, with a slow-cycling signature that was enriched in the osimertinib-resistant cells. Combining osimertinib with a CD105 neutralizing antibody, carotuximab, reduced the slow-cycling population and restored osimertinib sensitivity in resistant cell lines. The knockdown of CD105 had a more pronounced decrease in cell viability when combined with osimertinib. The osimertinib-resistant lines demonstrated more condensed chromatin and glycolytic state compared to the respective parental lines by ATAC-seq and Single Cell ENergetIc metabolism profiling, respectively. The addition of carotuximab reversed the chromatin and metabolic reprograming of osimertinib resistance. Carotuximab was discovered to initiate CD105 interaction with EGFR and its dominant active variant, EGFRv3. Ultimately, combination therapy of carotuximab and osimertinib resulted in significantly reduced tumor expansion compared to mice treated with either drug alone. Paradoxically, the small tumors from combination therapy had greater mitosis compared to the larger tumors of the osimertinib single agent treated mice. Inhibition of CD105 with carotuximab can overcome resistance to osimertinib and inhibit NSCLC tumor progression. This is a first-in-class pre-clinical foundation for a novel synthetic lethality treatment strategy resulting from the observation of global changes in EGFR-antagonist resistance as opposed to individual mutations identified in tumor subpopulations.

#4760 Inhibition of FASN postpones development of resistance to BRAF inhibitors in colorectal cancer.

M. Geisen, J. weber-Tessmann, C. Kelson, D. He, C. Wang, A. Faisal, J. Kolesar, Y. Zaytseva;
University of Kentucky, Lexington, KY

Introduction: Mutations in proto-oncogene BRAF occur in about 10-15% of CRC patients and $BRAF^{V600E}$ is the most common. For patients who undergo BRAF-targeted therapy, resistance develops 4-6 months after treatment initiation and results in more aggressive disease. We found that development of resistance to BRAF inhibitors (BRAFi) is associated with an increase in lipid metabolism and expression of fatty acid synthase (FASN). FASN is a key enzyme of lipid synthesis overexpressed in CRC. Therefore, our hypothesis is that inhibition lipid metabolism via FASN will postpone development of resistance to BRAFi.
Methods: We established CRC cells resistant to PLX8394, a novel BRAFi. To evaluate differences in parental and resistance cells, CellTiterGlo 2.0, PrestoBlue, CytoSelect™ Invasion Assay, Triglyceride Assay, Seahorse XF, and confocal microscopy were used. Combination of PLX8394 and TVB3664 or C75 (FASN inhibitors) was tested on cell viability, colony formation, and synergy studies in parental and BRAFi resistant cells.
Results: The development of resistance to BRAFi promotes cellular proliferation and increases cyclin D and survivin expression *in vitro* and *in vivo*. BRAFi resistance is also associated with an increase in invasive properties and loss of E-cadherin expression. Metabolic changes include an increase in lipid metabolism, oxidative phosphorylation, and triglycerides storage. RNAseq and western blot analysis show significant upregulation of FASN in BRAFi resistant cells. Using cell viability and soft agar colony formation assays, we show that combined PLX8394 and TVB3664 treatment leads to a significantly higher decrease in cell viability and colony formation as compared to each drug alone in parental cells but not in BRAFi resistant cells. The calculation of a Bliss synergy score confirms that combination treatment with C75 and PLX8394 has synergetic effect in $BRAF^{V600E}$ cells. To further confirm that FASN contributes to resistance to BRAFi, we show that HT29 FASN shRNA cells are more susceptible to PLX8394 treatment as compared to control cells. Importantly, our data show that the long-term treatment with PLX8394 in combination with TVB3664 postpones development of resistance to BRAFi as compared to cells treated with PLX8394 alone.
Conclusion: Our study demonstrates that resistance to BRAFi is associated with a significant increase in proliferation, metastasis, and lipid metabolism. We demonstrate that combination of FASN inhibitors and BRAFi postpones development of resistance in $BRAF^{V600E}$ cells. However, FASN inhibition does not sensitize cells to BRAFi in already resistance cells, suggesting that this approach cannot be used to overcome acquired resistance to BRAFi. In summary our data suggest that an addition of TVB3664 at the beginning of BRAF treatment regimen could be an efficacious treatment strategy for $BRAF^{V600E}$ CRC patients.

#4761 Understanding three-drug combinations: optimizing scheduling while avoiding toxicity.

M. Stoddard[1], **L. Yuan**[1], D. Van Egeren[2], A. Chen[3], D. Bottino[4], A. Chakravarty[1];
[1]Fractal Therapeutics, Inc., Lexington, MA, [2]Stanford University, Palo Alto, CA, [3]Columbia University, New York, NY, [4]Takeda Pharmaceuticals, Cambridge, MA

The promise of combination therapies in managing tumor resistance is constrained by the therapeutic window (the difference between efficacious and toxic doses). We have sought to understand the impact of dose scheduling on the emergence of resistance, using a mathematical model-based approach linking pharmacokinetics (PK) to a parsimonious evolutionary model of tumor growth incorporating the emergence of drug resistance. Here, we analyze the potential of a three-drug combination to minimize toxicity while preventing the emergence of resistance. We simulated eight tumor subpopulations representing resistance to one, two or three hypothetical drugs, using an exponential growth model with growth penalties based on drug concentrations. We used the model to simulate the effects of pairs of antagonistic, synergistic, and additive drugs on the growth of sensitive and resistant populations in a tumor. Final tumor volume and resistant population were used to compare the efficacy of various drug schedules. We assumed an overlapping neutropenia-like toxicity as the dose-limiting toxicity for the three drug combination, which we have previously shown to be proportional to the peak moving average drug concentration over 18 days. Final tumor volume and peak toxicity were used to compare the effectiveness of various dosing strategies and interaction combinations. Synchronous dosing results in the greatest drug interaction effect between any two drugs. When all interactions between the three drugs are either antagonistic or synergistic, the greatest effect is observed when all drugs are dosed simultaneously. The drugs are most toxic when all three are dosed simultaneously or nearly simultaneously. Our work shows that time sensitivity—that is, the magnitude of the changes in efficacy associated with small changes in schedule—varies with phase offset. Scheduling is most time sensitive when all drugs are dosed simultaneously or nearly simultaneously; dosing of two drugs simultaneously is less time sensitive. Three-drug combinations are an effective means of preventing complete resistance. While simultaneous dosing of two or more drugs confers the greatest efficacy, such simultaneous dosing results in greater peak toxicity because of higher simultaneous drug concentrations. A potential compromise is the simultaneous dosing of two of the three drugs, which results in an intermediate toxicity. Dosing of two drugs simultaneously is also less time sensitive, advantageous in a practical sense as it is more robust to patient dosing error. While the approach used here is based on hypothetical drug properties, it provides a framework that is readily applicable to real-world drug combinations, with the potential for practical insights to guide the framing of the Target Product Profile for three-drug combinations.

#4762 Tumor treating fields (TTFields) increase cancer cell membrane permeability and improve sensitivity to doxorubicin in vitro and in vivo.

B. Koltun, **T. Voloshin**, T. Kan, C. David, L. Koren, Y. Porat, A. Volodin, N. Kaynan, A. Klein-Goldberg, R. Paz, B. Brant, Y. Barsheshet, E. Zemer-Tov, A. Haber, M. Giladi, U. Weinberg, Y. Palti;
Novocure Ltd, Haifa, Israel

Background: Tumor Treating Fields (TTFields) are electric fields that disrupt cellular processes critical for cancer cell viability and tumor progression. While the mechanism of action of TTFields has been associated with an antimitotic effect and impaired DNA damage repair mechanisms, the application of TTFields has also been shown to increase the membrane permeability of glioblastoma cells. The current study examined whether increased cell membrane permeability is relevant in other tumor types and may be leveraged to facilitate uptake of the anticancer agent doxorubicin (DOX).
Methods: Breast mammary carcinoma (4T1), breast adenocarcinoma (MCF-7), uterine sarcoma (MES-SA), lung fibroblasts (MRC-5), and brain endothelial (HBMVEC) cells were treated with TTFields using the inovitro™ system. Intracellular 7-aminoactinomycin D (7-AAD) accumulation and cell count were measured using flow cytometry to determine membrane permeability and cytotoxicity, respectively. TTFields (300 kHz) together with DOX were applied to 4T1 cells DOX-sensitive (4T1-S) and DOX-resistant (4T1-R, generated by repeated DOX exposure of the 4T1-S cells), followed by flow cytometry analysis of DOX accumulation (24 h treatment) and cell survival using cell count (72 h treatment). For proof of concept, mice were orthotopically inoculated with 4T1-S cells, followed by TTFields treatment for 72 h and injection of DOX (5 mg/kg) 24 h before ending TTFields treatment. DOX fluorescence was measured by flow cytometry in single-cell tumor suspension and whole tumor in vivo imaging system (IVIS). For the efficacy studies, mice were orthotopically inoculated with 4T1-S or 4T1-R cells. Tumors were allowed to grow, and then the mice were treated with TTFields (300 kHz) or sham-heat continuously for 8 days, with DOX (1 mg/kg for 4T1-S cells; 5 mg/kg for 4T1-R cells) or vehicle 2- and 6-days following treatment initiation. Tumor volumes were measured using caliper.
Results: TTFields increased 7-AAD accumulation in cancer but not normal cells. Maximal TTFields-induced cellular permeability was identified at 300 kHz for 4T1 cells, whereas TTFields-induced cytotoxicity was the highest at 150 kHz. The application of TTFields allowed DOX accumulation to the same extent in both DOX-resistant and DOX-sensitive cells and sensitized both cell types to DOX cytotoxicity. A 2- to 3-fold higher DOX accumulation was observed in tumors isolated from mice treated with TTFields relative to control mice. Significantly lower tumor volume was observed in mice treated with TTFields and DOX relative to control or mice treated with DOX alone.
Conclusions: TTFields increased cancer cell permeability, resulting in enhanced intracellular accumulation of DOX. Concomitant treatment with TTFields and DOX can improve treatment efficacy in DOX-resistant tumors and sensitize DOX-sensitive tumors to lower DOX concentrations.

PREVENTION / EARLY DETECTION / INTERCEPTION: Biomarkers and Molecular Targets for Cancer Prevention
Poster Session

#4765 Tumor, serum and plasma metabolome in patients with high-grade bladder cancer.

M.-M. Tsamouri[1], A. Karthikeyan[2], C. A. Lucchesi[3], B. P. Durbin-Johnson[2], M. A. Dall'Era[1], **P. M. Ghosh**[1];
[1]UC Davis, Sacramento, CA, [2]UC Davis, Davis, CA, [3]VA Northern California, Mather, CA

Introduction: Bladder cancer (BlCa) ranks as the sixth most prevalent cancer in the world. A number of urine based BlCa detection tests have recently been approved for clinical use, including the NMP22 tests and the bladder tumor antigen (BTA) tests for both detection and monitoring of patients with known bladder cancer. The FDA have approved them both for surveillance in BlCa only in conjunction with cystoscopy. Unfortunately, the sensitivity and specificity of these tests are poor, and cannot distinguish between aggressive and non-aggressive tumors. This project aims to identify alternate markers that can overcome these drawbacks.
Methods: We characterized the global metabolome of 47 bladder tumors retrieved by radical cystectomy (RC) or TURBT, including 14 specimens with matching plasma and serum samples. All specimens were subjected to untargeted metabolomic approaches with gas chromatography- time-of-flight mass spectrometry (GC-TOF MS) to profile primary metabolites, hydrophilic interaction liquid chromatography MS (HILIC-QTOF MS) to profile biogenic amines, and liquid chromatography charged surface hybrid MS (LC-CSH-QTOF MS) to characterize complex lipids. Differentially expressed metabolites were analyzed with respect to grade, stage, metastases, and the use of neoadjuvant chemotherapy. For selected metabolites, area under the ROC curve (AUC) is calculated as % sensitivity vs. 100% specificity. Expression of highly discriminatory metabolites were then validated in the plasma and serum samples to determine which forum would provide greater specificity.
Results: We first assembled a discovery cohort of 33 patients who did not have matching blood specimen for primary metabolites, biogenic amines and complex lipids. Comparison of high vs low grade tumors yielded two lipids, a sphingomyelin (SM (d38) and a phosphatidylcholine PC(p-38), that were significantly different (adjusted p-value<0.05, $\log_2$fold change>2.5). These results were validated in the 14-sample cohort with matching plasma and serum of which the latter showed significant correlation between tumor and plasma (Spearman R=0.872, adj p=0.03).
Conclusions: Our results indicate that certain sphingomyelins and phosphatidylcholines may be useful as plasma markers of high grade BlCa. Further analyses are required to evaluate whether these markers are more discriminatory compared to existing urinary markers.

#4766 Androgen deprivation in mice is linked with cognitive impairment.

S. S. Verma[1], D. Swain[2], V. Singh[2], E. Shankar[2], Z. Lee[2], S. Gupta[2];
[1]Case Western Reserve University School of Medicine, Cleveland, OH, [2]Case Western Reserve University, Cleveland, OH

Androgens play a neuroprotective role in maintaining the normal physiological functions of the brain. It also plays a pivotal role in prostate cancer development and progression. Advance-stage prostate cancer treatment is primarily based on androgen deprivation therapy (ADT) that blocks the male hormone testosterone. Moreover, prostate cancer patients who undergo ADT develop cognition impairment such as loss of memory, learning, reasoning, and decision-making. Several studies have shown a positive association between ADT and the risk of cognitive impairment. Currently, there are no clinical markers to identify patients at-risk to ADT-mediated cognition. This demands a need for biomarkers that can help distinguish the vulnerability of patients toward cognitive impairment undergoing ADT. We utilized a in-vivo model to identify biomarkers and the impact of ADT in different regions of the brain. Sixteen-week-old BALB/c mice were gavage 50 mg/kg/day of enzalutamide (mimicking ADT) for 5 days per week (0.2 ml of vehicle consisting of 0.5% methylcellulose and 0.025% Tween 20) for a total of 8 weeks. Control animals received 0.2 ml vehicle per day for the same time period. Mice were observed for behavioral changes post-enzalutamide treatment and brain PET scans were generated. The experiment was terminated, the brain was excised for cortex, cerebellum, and hippocampus, and subjected to mass spectroscopic (MS) analysis. Differentially expressed proteins were identified and validated using qRT-PCR in the mice blood. Enzalutamide treatment for 8 weeks resulted in a modest weight gain and lack of attention and letharginess in these mice. Examination of PET scan and H&E sections of mice brain from control group by light microscopy showed a normal morphology of neurons in the cortex. Enzalutamide treatment showed lower neuron density and signs of neuron injury, as well as cytoplasmic swelling of the astrocytes. MS analysis identified a number of differentially expressed proteins that were validated in the blood. These include ABCB10, CAB, DAZAP1, DCU, DERL1, FBXO, MBNL, PUM2, SERL1, SLC8A3, SLC9A, TCF20, VIM, and ZYXIN. Among them, the expression of SLC8A3, PUM2, and SERL1, were significantly higher than others in the enzalutamide-treated group. Taken together, our findings suggest that enzalutamide treatment in mice leads to cognitive impairment like that observed in men on ADT protocol. Our study highlights that blood-based markers can be developed for ADT-mediated cognition which can lead to the identification of new strategies for prevention and early intervention to improve the quality-of-life of patients suffering with advance-stage prostate cancer.

#4767 Changes in the NSE and S100B levels following treatment with peripheral neuropathy-inducing drugs.

P. R. Vontikommu[1], S. Selvakumar[1], U. Natarajan[2], A. Rathinavelu[2];

[1]Rumbaugh-Goodwin Institute for Cancer Research, Nova Southeastern University, Davie, FL, [2]Rumbaugh-Goodwin Institute for Cancer Research, Barry & Judy Silverman College of Pharmacy, Nova Southeastern University, Davie, FL

Neo-adjuvant chemotherapy is considered the standard of care for patients with multiple myeloma (MM). Peripheral neuropathy (PN) is one of the most common chemotherapy-induced side effects that impact 50% of all patients who receive chemotherapy and can lead to discontinuation of drug treatment. Treatment with Bortezomib (BTZ), Cisplatin (CIS), and Vincristine (VIN) has been established as the most common trigger of ChemotherapyInduced Peripheral Neuropathy (CIPN) among cancer patients. Since CIPN can lead to disabling long-term adverse effects, many cancer patients discontinue or limit their treatment regimen once they see signs or symptoms of CIPN. Therefore, it was hypothesized that developing diagnostic/prognostic biomarkers that can accurately predict the onset or progression of CIPN would help to determine the chemotherapy eligibility with the above-mentioned drugs and proactively prepare for protective care. Hence, our initial goal was to elucidate the molecular mechanisms underlying the onset and progression of CIPN that would allow for the identification of suitable biomarkers that can be used for monitoring before or during chemotherapy with BTZ, CIS, and VIN. Initially, we conducted *in vitro* studies to identify the underlying molecular mechanisms activating CIPN related pathways. We used neuronal Schwann cells (RT4), for testing the neurotoxic effects of BTZ, CIS, and VIN that might precede or coincide with the onset of CIPN in an *in vivo* condition. Interestingly, the BTZ treatment was able to significantly reduce the intracellular level of NSE and S100B in RT4 cells compared to the untreated controls, when they were measured using an immunofluorescence assay and Western blot. Furthermore, we conducted an *in vivo* study to determine the CIPN using rats. We used the sciatic nerve (SN) from drug-treated animals to check the S100B level using the ELISA method. Our preliminary results showed that levels of S100B in the SN of Rats were reduced following 8 weeks of treatment with the PN-inducing chemo drugs. We anticipate that this study will enrich our understanding of how chemotherapy medications induce PN in cancer patients and guide us to identify reliable biomarkers (This project was supported by the PFRDG grant of the Nova Southeastern University, Ft. Lauderdale Florida, and the Royal Dames of Cancer Research Inc., Ft. Lauderdale, Florida).

#4768 Differential expression of triptolide gene targets in human papillomavirus positive and negative head and neck squamous cell carcinomas.

W. E. Kamm, L. J. Mortenson, F. G. Ondrey;
University of Minnesota Medical School, Minneapolis, MN

Head and neck squamous cell carcinoma (HNSCC) is the fifth most common cancer in the US. HPV represents a more recent risk factor for which treatment may be individualized. HPV expresses viral E6 and E7 oncoproteins which downregulate wild type p53 and Rb respectively. Triptolide, a derivative of a traditional Chinese medicinal herb, has been shown to inhibit viral E6, thereby reactivating wild type p53. Therefore, triptolide may target HPV positive HNSCC as a putative treatment. To explore this, we compared mutation, methylation, and expression of triptolide gene targets between HPV positive and HPV negative samples from The Cancer Genome Atlas (TCGA) program.

Patient data was queried from the TCGA PanCancer Atlas for HNSCC using cBioPortal. This included a total of 523 patients with 487 meeting inclusion criteria. 415 patients were HPV (-) and 72 were HPV (+).Differences in direct genomic alterations, DNA methylation, mRNA expression, and protein expression of the 34 known triptolide targets were compared between these two groups using the Benjamini-Hochberg Procedure with a significance level of $q < 0.05$. Significant differences of the studied genes ($q < 0.05$) are shown in Table 1. There were no significant differences in protein expression.

Of the 34 known triptolide targets, HPV positive and negative samples show variable enrichment. Triptolide targets exhibit greater methylation and mRNA expression in HPV positive samples supporting triptolide's efficacy in these samples. However, other triptolide targets are the differentially expressed and methylated in HPV negative samples, so the compound may have a beneficial effect in this context as well. Further studies are required to test efficacy of triptolide against HPV positive and HPV negative HNSCC in vitro and in vivo models.

Table 1. Significant genomic differences between HPV (+) and HPV (-) samples shown.

Enriched in HPV (+)				**Enriched in HPV (-)**			
	Gene	Log2 ratio	q-value		Gene	Log2 ratio	q-value
DNA methylation				Direct genomic mutations			
	VEGFA	0	5.85E-03		*TP53*	3.08	4.53E-29
	BCL2	0.07	9.78E-18	DNA methylation			
	JUN	0	4.89E-02		*RELA*	0.07	5.06E-04
	CD80	0.06	2.56E-02		*STAT3*	0.24	3.19E-20
	BIRC3	0.01	1.29E-04		*TNF*	0.07	4.31E-04
	CD274	0.07	4.40E-03		*XIAP*	0.07	8.02E-06
	CCR7	0.11	3.56E-08		*CXCR4*	0.04	3.58E-03
	CD1A	0.10	2.36E-05		*CD40*	0.06	1.00E-05
	C3	0.06	6.91E-03		*CD14*	0.04	8.12E-03
	CD86	0.03	2.45E-02	mRNA expression			
mRNA expression					*RELA*	0.16	1.90E-03
	STAT3	0.25	4.22E-03		*CDKN1A*	0.28	3.00E-02
	BCL2	1.95	1.68E-14		*PLAU*	1.37	3.24E-12
	CASP3	0.45	2.55E-07		*CXCL8*	1.05	1.51E-04
	TP53	1.45	3.16E-25		*MCL1*	0.23	3.59E-04
	IL2	0.52	2.13E-06		*TGFB1*	0.77	3.27E-11
	INFG	1.15	2.08E-05		*DEFB4A*	1.10	1.77E-02
	CXCR4	1.18	8.03E-07				
	BIRC3	1.20	6.14E-06				
	IL23A	0.77	3.88E-04				
	CCR7	1.18	2.10E-06				
	CD40	0.54	2.27E-04				

#4769 Phospho-YAP (Ser127) overexpression is associated with sporadic advanced adenomas: The Tennessee Colorectal Polyp Study.

L. Fan[1], X. Guo[1], M. K. Washington[1], J. Shi[1], R. M. Ness[1], Q. Liu[2], W. Wen[1], X. Liu[2], Q. Cai[1], W. Zheng[1], R. J. Coffey[1], M. J. Shrubsole[1], T. Su[1]; [1]Vanderbilt University Medical Center, Nashville, TN, [2]Vanderbilt University, Nashville, TN

About 70-80% of sporadic colorectal cancers (CRCs) harbor APC mutations. Whether specific characteristics of APC mutation or APC-related signaling pathways contribute to tumor initiation, advanced progression, and recurrence in the precancerous lesions remain to be elucidated. This study included145 sporadic precancerous adenomas from the Tennessee Colorectal Polyp Study. Expression of six APC-related proteins (β-catenin, p-YAP, CtBP, EB1, Asef, and N-terminal APC) in adenoma and non-tumor tissues (n=22) were quantitatively detected by immunohistochemistry. Targeted sequencing of APC was done for 108 adenomas. Metachronous adenoma status was obtained from chart review. *YAP*-correlated genes and their functional enrichment analysis were conducted using gene expression data of 326 adenomas from the Gene Expression Omnibus database. We found that nuclear β-catenin and p-YAP overexpression only existed in adenoma tissue, correlated with each other (r=0.26, *P*=0.0018), and associated with APC mutations (*P*=0.05). P-YAP was strongly associated with odds of large adenomas (OR=14.25, 95%CI=3.32-61.18, *P* trend<0.0001), villous growth pattern (OR=58.71, 95%CI=10.49-328.61, *P* trend<0.0001) and advanced adenomas (OR=12.62, 95%CI 4.57-34.86, *P* trend<0.001), and showed a significant interaction with nuclear β-catenin on advanced tumor (OR=16.82, 95%CI 4.41-64.08, *P*<0.0001). After adjusting for selected covariates and mutually adjusting for biomarkers with *P*<0.20 in crude models, p-YAP overexpression remained significantly associated with advanced adenomas (OR=12.31, 95% CI=3.78-40.10, *P* trend<0.0001). YAP-correlated genes were significantly enriched in autophagy, unfolded protein response, and sirtuin pathways with predominantly pro-tumorigenic alterations. APC mutation and selected biomarkers were not significantly associated with metachronous adenoma. In conclusion, p-YAP overexpression might be a promising biomarker for high-risk sporadic adenoma. In addition to its synergistic effect with nuclear β-catenin, p-YAP may play tumorigenic roles through interaction with other cancer pathways in human sporadic adenoma. This study provided new evidence for oncogenic effects of p-YAP in human sporadic adenomas and shed light on the complex network of Hippo, Wnt, and other oncogenic signaling pathways.

#4771 Assessment of Ki67 proliferation index in pre-malignant colonic adenomas: Implication for new biomarker testing to predict metachronous disease (The INCISE project).

G. P. Lynch[1], A. Ammar[1], C. Bigley[1], M. Johnstone[1], J. Jawny[2], H. Morgan[1], J. Hay[3], N. Maka[2], S. McSorley[1], J. Edwards[1];
[1]University of Glasgow, Glasgow, United Kingdom, [2]NHS Greater Glasgow and Clyde, Glasgow, United Kingdom, [3]The Francis Crick Institute, London, United Kingdom

Approximately 40% of patients are found to have polyps at bowel screening colonoscopy, which are associated with a higher risk of developing future polyps or colorectal cancer. The British Society of Gastroenterology 2020 (BSG20) guidelines stratify patients into high/low risk of metachronous disease, using the size, dysplasia, and number of polyps found at index colonoscopy. This study aims to explore the prognostic significance of Ki67 proliferation percentages in adenomatous polyps, with metachronous disease. Tissue microarray (TMA) was constructed from 1201 index adenomatous polyps with representative cores of basal and luminal adenomatous epithelia. 67% patients were identified as high risk at index colonoscopy. The median time to detect metachronous polyps was 55 months (range 6-72 months) with 56% of patients developing metachronous polyps by the end of follow-up. TMA was stained for Ki67 using immunohistochemistry. Ki67 proliferation percentages in adenomatous epithelia was quantified using QuPath. Data was split into training (n=830) and test (n=371) datasets. The Ki67 proliferation cutpoint was made using Survmine R package using the training dataset. X^2 test was used to study associations with clinicopathological criteria and Kaplan survival analysis was used to assess Ki67 association with metachronous lesions. Ki67 percentages were higher in lumina than in basal adenomatous epithelium (median Ki67 were 63% & 48%; respectively). Total Ki67 percentages were computed by averaging luminal and basal values. Thresholds of 70%, 64% and 59% were employed to classify patients into low/high categories based on luminal, basal or total percentages; respectively. In the training cohort, high luminal, basal or total Ki67 were associated with metachronous lesions (p values 0.032, <0.001 and 0.006; respectively). Other associations were significant between luminal or total Ki67 and location of index polyps (p=0.017 & p=0.044; respectively), histology (p=0.019) and advanced future lesion status (p=0.002 & p<0.001; respectively). In multivariate cox regression analysis, high Ki67 was an independent prognostic factor for metachronous polyps (luminal Ki67 HR=1.28, CI: 1.052-1.560, p=0.014; basal Ki67 HR=1.639, CI: 1.313-2.046, p<0.001; total Ki67 HR=1.344, CI: 1.105-1.635, p=0.003) when adjusted to number of index polyps and BSG20 risk score. BSG20 risk score stratification of patients in terms of metachronous disease was improved when combined with luminal, basal or total Ki67 in the training datasets (all p<0.05). Prediction of metachronous disease by the combined groups was validated in the test cohort for luminal, basal and total Ki67 (all p<0.05). High Ki67 proliferation rates in adenomatous polyps are independently associated with the development of metachronous polyps and may help improve the BSG20 criteria.

#4772 Metabolic phenotype, age acceleration, and obesity-related cancer risk in Women's Health Initiative and Atherosclerosis Risk in Communities cohorts.

Prasoona Karra[1], Garnet L. Anderson[2], Mary C. Playdon[3], Sheetal Hardikar[3], Aladdin Shadyab[4], Kari E. North[5], Anne E. Justice[6], Elizabeth A. Platz[7], Jan Bressler[8], Anna Prizment[9], Weihua Guan[9], Dominique S. Michaud[10], Eric A. Whitsel[11], Brock C. Christensen[1], Lucas A. Salas[1]

[1]Department of Epidemiology, Geisel School of Medicine, Dartmouth College, Lebanon, NH,[2]Division of Public Health Sciences, Fred Hutchinson Cancer Center, Seattle, WA,[3]3Cancer Control and Population Sciences, Huntsman Cancer Institute, Salt Lake City, UT,[4]Herbert Wertheim School of Public Health and Human Longevity Science, University of California, San Diego, CA,[5]Gillings School of Global Public Health, University of North Carolina, Chapel Hill, NC,[6]Dept. Population Health Sciences, Geisinger Health, Danville, PA,[7]Johns Hopkins Bloomberg School of Public Health, Baltimore, MD,[8]The University of Texas Health Science Center, Houston, TX,[9]University of Minnesota, Minneapolis, MN,[10]Tufts University School of Medicine, Boston, MA,[11]Department of Epidemiology, Gillings School of Global Public Health, University of North Carolina, Chapel Hill, NC

Introduction: While normal physiologic aging causes metabolic decline, metabolic dysregulation owing to excess nutrient intake, physical inactivity, and obesity may drive accelerated aging. However, the relationship of accelerated aging with metabolic dysfunction across different levels of BMI (i.e., metabolic obesity phenotype) and whether it may mediate the relationship with obesity-related cancer (ORC) risk is not well established.
Methods: To test this hypothesis, we are leveraging existing blood-based DNA methylation (DNAm) data within the Women's Health Initiative (WHI) and the Atherosclerosis Risk in Communities (ARIC) cohorts. Weight, height and blood pressure were measured by trained technicians in the respective cohorts and fasting blood glucose, triglycerides and HDL cholesterol were quatified by standard clinican assays. Metabolic obesity phenotypes are classified as metabolically healthy normal weight (MHNW), metabolically unhealthy normal weight (MUNW), metabolically healthy overweight/obese (MHO), and metabolically unhealthy overweight/obese (MUO) when defined by ATP III criteria. Age acceleration was measured as a residual from regressing pan-tissue Horvath's DNAmAge on chronological age.
Results: The mean baseline age was 64 ± 6.6 years and 54 ± 5.7 year among WHI and ARIC participants, respectively and the age acceleration was measured at an mean follow-up time of 16 years from baseline for WHI and 3.5 years from baseline for ARIC cohort. The outcome of interest, ORC incidence was observed among 474 participants of which 387 were women. The median time for cancer diagnosis from baseline was 25 year and from DNAm measurement was 18.6 years. Of the 4341 (70% women) participants included in the analysis, 23.9% were MHNW, 3.2% MUNW, 39% MHO, and 33.5% MUO. A 31.5% of MHNW, 40.4% of MUNW, 28.7% of MHO, and 35.2% of MUO showed age acceleration. MUNW (OR 1.47, 95% CI: 1.03-2.11) and MUO (OR 1.18, 95% CI: 1.00-1.40) individuals at baseline had increased odds of experiencing age acceleration at a follow-up visit. The risk of all ORC combined was significantly elevated among MUO (HR 1.63, 95% CI: 1.27-2.09) compared to MHNW. Age acceleration at the follow-up visit was not significantly associated with ORC risk (HR 0.91, 95% CI: 0.75-1.11). These analyses were not adjusted for confounders.
Conclusions: MUNW and MUO individuals had increased odds of age acceleration at a follow-up visit. Furthermore, MUO individuals were at an elevated risk of ORC, compared to individuals with MHNW. Accelerated aging does not appear to mediate this association, as accelerated aging was not associated with ORC.

#4773 Interferon regulatory factor 8 (IRF8) as a biomarker for early detection and prevention of axillary lymph node-positive breast cancer.

M. Rossi[1], N. Cruz-Reyes[1], M. L. Stallings Mann[1], B. M. McCauley[2], T. L. Hoskin[2], R. A. Vierkant[2], S. J. Winham[2], A. C. Degnim[2], M. E. Sherman[1], D. C. Radisky[1];

[1]Mayo Clinic, Jacksonville, FL, [2]Mayo Clinic, Rochester, MN

Breast cancer (BC) remains a leading health concern worldwide and is often undetected until the cancer metastasizes. Early detection can limit the need for aggressive treatments and improve prognosis. We analyzed early immune and molecular markers in benign breast disease (BBD) biopsies prior to BC development to identify women at elevated risk of developing node-positive invasive BC, which might direct surveillance and prevention efforts aimed at reducing incidence of this disease. Utilizing the Mayo Clinic BBD cohort, we compared women who developed node-positive BC following their BBD biopsy (cases; n=42) with those who remained cancer-free (controls; n=37), matched on patient age and biopsy date. We used NanoString nCounter system to identify differentially expressed genes (DEGs) between cases and controls. We also developed a multiplex immunofluorescence (mIF) approach using Opal system by Akoya Biosciences for comprehensive marker detection in FFPE tissue, enabling correlation of cells expressing DEGs with innate and adaptive immune cells. Digitized images were segmented, and cell phenotyping, and spatial relationships were compared between cases and controls. Our findings revealed significantly increased expression levels of IRF8 (interferon regulatory factor 8, a factor involved in immune cell differentiation) in controls as compared to cases and found that increased IRF8 expression in cases is correlated with delayed cancer onset. Additionally, controls exhibited higher frequencies of CD4+, CD8+, CD68+, CD20+ and CD11c+ immune cells, and lower frequency of Ki67+ staining, with a notable increase of CD11c+/CD68+ cells, a marker for M1 type macrophages, indicating a pro-inflammatory, antitumorigenic immune microenvironment polarization. Furthermore, our mIF analyses offer new insights into spatial biomarker localization, enhancing prognostic accuracy. Our findings suggest that decreased numbers of immune cells in BBD biopsies may be associated with increased risk of developing axillary node-positive BC. This research underscores the importance of dissecting molecular and immune interactions in BBD for assessing the risk of this disease. Our results have the potential to improve individualized risk assessment, leading to more targeted surveillance and informed screening, potentially reducing BC incidence and mortality through early intervention. This study not only contributes to our understanding of BC pathogenesis but also opens avenues for developing novel preventive strategies.

#4774 Inhibition of pancreatic acinar ductal metaplasia by novel YAP/TAZ inhibitor, CV-4-26.

C. M. Perkins[1], C. Zhou[1], M. Campbell-Thompson[1], Y. Mao[2], K. R. Atanasova[1], J. Jiang[1], R. Ratnayake[1], H. Luesch[1], J. Ali[3], C. Li[1], T. D. Schmittgen[1]; [1]University of Florida, Gainesville, FL, [2]Florida Agricultural and Mechanical University- Florida State University, Tallahassee, FL, [3]Florida Agricultural & Mechanical University- Florida State University, Tallahassee, FL

Current challenges for pancreatic ductal adenocarcinoma (PDAC) treatment include overcoming the disease's fibrous tumor microenvironment with limited cytotoxicity- in which tissue stiffening is believed to occur even pre-disease onset. Acinar to ductal metaplasia (ADM), the transdifferentiation of acinar cells into duct-like cells, is a predisposing event to PDAC development that is also linked to Hippo signaling, a major pathway involved in fibrosis and inflammation. Hippo activation is initiated by the yes-associated protein (YAP) in conjunction with the PDAZ binding motif (TAZ) and TEA domain (TEAD) transcription factor. Thus, the synthesis of the novel covalent TEAD autopalmitoylation inhibitor, CV-4-26, presented an opportunity to therapeutically target ADM. CV-4-26 binds to the TEAD lipid binding pocket, which, in turns, hinders TEAD palmitoylation, thereby leading to the inhibition of the Hippo pathway. Utilizing our 3D organoid p48Cre/+LSL-KRASG12D/+ (KC) mouse model, we demonstrated pronounced phenotypic and molecular inhibition of ADM by CV-4-26, resulting in a conserved acinar phenotype, as well as downregulation of downstream markers of the YAP/TAZ complex. The compound did not reverse ADM to the acinar state once ducts were visibly formed. Yet, CV-4-26 demonstrated a lack of cytotoxicity (up to 25 μM) as determined by Calcein AM staining. Biomechanical measurements of extracellular matrix stiffness acquired through calculations of fluorescent nanoparticle displacement further displayed decreased moduli as a response to inhibition treatment. Moreover, a 56-fold downregulation of collagen (COL1A1, COL1A2) mRNA, markers for PDAC development, was observed. However, less reduction in the collagens and extracellular matrix stiffness was observed in the ADM reversal treatments, corroborating our morphology and gene expression results. Our data suggest that combining CV-4-26 by ADM inhibition with standard of care therapies for PDAC may enhance the penetration of small molecules through the tumor's extracellular matrix.

#4775 Unveiling caveolin-1's crucial role in breast cancer progression and metastasis: A molecular perspective.

R. Begum[1], S. Thota[1], D. Singh[2], N. Chintala[1], A. Pandit[1], B. Sapkota[1], J. Francis[1];
[1]Louisiana State University, Baton Rouge, LA, [2]Indiana University Health, Indiana, IN

Background: Breast cancer, particularly its metastatic form, constitutes a significant portion of oncological mortality. Caveolin-1 (Cav-1), a caveolae structural protein, has been implicated in cellular processes such as proliferation, apoptosis, autophagy, and cellular motility (aberrant in breast cancer). With its dual role as a tumor suppressor and promoter, Cav-1's function in breast cancer pathophysiology requires elucidation for potential therapeutic targeting.
Methods: We utilized a syngeneic mouse model to engineer Cav-1 deficient 4T1 murine mammary carcinoma cells which mirror the characteristics of stage IV breast cancer to investigate Cav-1's role in tumor growth and metastasis. We assessed cellular proliferation and lung metastasis, compared with wild-type controls, and performed molecular analyses to evaluate epithelial and mesenchymal marker expression, stemness-related markers, and autophagy-related gene expression.
Results: Cav-1 ablation corresponded with a marked decrease in tumor proliferation and lung metastasis, indicating a suppressive role in tumor progression. Molecular characterization revealed downregulated epithelial markers (E-cadherin, β-catenin), transcription factors (TWIST1/2), and stem cell markers (NANOG, OCT4, SOX2, c-MYC, SALL4), with concurrent upregulation of the mesenchymal marker vimentin. Enhanced expression of autophagy-related genes (Beclin-1, ATG5, ATG16) was also observed, suggesting a disruption in autophagic pathways.
Conclusion: Our findings underscore the critical role of Cav-1 in breast cancer progression, specifically its function in suppressing metastasis and modulating cellular phenotypes. Targeting Cav-1 could represent a novel therapeutic strategy to mitigate breast cancer growth and dissemination. Further research is warranted to explore the therapeutic potential of modulating Cav-1 in breast cancer treatment.

#4776 The role of angiogenesis in gastric tumorigenesis.

V. Akkanapally, S. BASU;
The Ohio State University, Columbus, OH

Introduction: Gastric or stomach cancer remains one of the most lethal malignancies, with an estimated 1,089,103 new cases and 768,793 deaths worldwide in 2020. In the United States, it is estimated that there were 26,500 new cases and 11,130 deaths from stomach cancer in 2023. Unfortunately, despite improved treatment in recent years, ~65% of gastric cancer patients present with aggressive metastatic disease, and they die within one year of diagnosis. Therefore, the identification of newer and effective therapies to target the precancerous stages of the disease promises possibilities for the prevention of gastric cancer in patients harboring these lesions. Gastric metaplasia and dysplasia are precancerous lesions that often progress to gastric cancer. Since anti-VEGF-A anti-angiogenic agents have shown efficacy in advanced gastric cancer patients, we hypothesized that VEGF-A-mediated angiogenesis has a functional role in the pathogenesis of gastric metaplasia and dysplasia.

Experimental Procedures: The Initial experiments were undertaken in human gastric metaplasia and dysplasia tissues and murine gastric metaplasia and dysplasia tissues collected from a well-established *Helicobacter felis* (*H. felis*) induced murine model of gastric tumorigenesis simulating human patients to detect angiogenesis (CD31/MVD) and identify angiogenic pathways using GeoMx DSP Spatial Proteomics and NanoString nCounter assay. Thereafter, further experiments were undertaken in the *H. felis*-induced murine model of gastric metaplasia and dysplasia, simulating human patients using VEGF-A hypo mice to determine the role of VEGF-A-induced angiogenesis in the progression of these lesions.

Results and Conclusion: Although our results indicated angiogenesis and VEGF-A expression in both human and mouse gastric metaplasia and dysplasia, inhibition in the progression of the precancerous gastric lesions was observed in only 40% of the VEGF-A hypo mice, thereby suggesting that VEGF-A induced angiogenesis might not be the major angiogenic pathway in these precancerous lesions in every patient. A similar phenomenon is also seen in some gastric cancer patients.

#4777 A small-molecule SMUG1 activator enhances repair of 5-hydroxymethyl-2'-deoxyuridine-mediated pyrimidine lesions in DNA.

L. A. McPherson, Y. Gao, S. Adimoolam, S. Suresh, D. L. Wilson, I. Das, E. R. Park, C. S. C. Ng, Y. Jun, J. M. Ford, E. T. Kool;
Stanford University, Stanford, CA

Background: Pharmacological upregulation of DNA repair pathways presents a potentially promising approach for cancer prevention in populations that are genetically high-risk. SMUG1, an enzyme involved in base excision repair, removes uracil and certain oxidized bases from DNA to mitigate adverse genotoxic and mutagenic effects and represents a promising target for cancer therapy. A growing body of evidence suggests that SMUG1 is involved in tumorigenesis, and deficiency of SMUG1 correlates with poor prognosis in several cancers. We hypothesize that upregulation of SMUG1 by a small molecule activator may be a viable strategy for reducing tumorigenesis in at-risk populations. We report on the properties of SU0547 - a SMUG1 activator that was derived from the EGFR inhibitor drug gefitinib - which shows reduced kinase inhibition and potent activation of SMUG1 both in vitro and in human cell lines.
Methods: MTT proliferation assays were used to screen for toxicity and to determine the effect of SU0547 on 5-hydroxymethyl-2'-deoxyuridine (5-hmdU)-treated cell lines. The effect of the compound on SMUG1 expression was determined by Western blot and RT-qPCR while its effect on DSBs via γH2AX expression in 5-hmdU-treated cells was determined by immunofluorescence and Western blot.
Results: SU0547 activates SMUG1 by 347 ± 50% in vitro at 100 nM, with an AC_{50} of 2.55 ± 0.62 μM. We examined whether it can modulate SMUG1 activity in a panel of human cell lines by artificially inducing DNA damage with the native SMUG1 substrate 5-hmdU and treating cells with the activator. In all five human cancer cell lines tested, SU0547 caused the cells to become significantly more resistant to 5-hmdU by factors of 2.1 to 5.3-fold. A series of CRISPR-Cas9 generated SMUG1 KO cell lines showed resistance to 5-hmdU and SU0547 had no effect on these treated cells, confirming that this activator acts on endogenous SMUG1. To determine the effect of the activator on double-strand breaks (DSBs), cells were treated with 5-hmdU with or without the compound and DSBs were visualized and quantitated by examining γH2AX foci. 5-hmdU treatment induced γH2AX foci while SU0547 treatment significantly reduced these foci to near or below baseline levels. These results were confirmed using Western blot quantitation of γH2AX.
Conclusions: We envision that this activator will serve as a useful tool for further studying the role of SMUG1 in mediating 5-hmdU toxicity and will enable the testing of our hypothesis that enhancing DNA repair processes may serve to inhibit mutagenesis and slow progression of pre-neoplastic lesions to invasive cancers associated with genomic instability.

#4778 Development of self-amplifying RNA vaccines targeting prostate tissue-restricted and tumor-associated antigens.

R. H. Shoemaker[1], J. H. Erasmus[2], P. Berglund[2], J. D. Marshall[3], Y. Koboziev[3], B. M. Beckman[3], B. D. Cholewa[1], S. G. Reed[2];
[1]National Cancer Institute, Bethesda, MD, [2]HDT Bio, Seattle, WA, [3]Frederick National Laboratory for Cancer Research, Frederick, MD

Prostate cancer is the most frequent cancer type in men, with increasing incidence at advanced age. As this cancer is frequently slow growing, opportunities for cancer interception exist, particularly among men with low-grade tumors who frequently undergo active surveillance. A well-tolerated vaccine intervention would be ideal for this population. Self-amplifying RNA (saRNA) vaccines built on a replication-deficient alphavirus backbone such as VEEV, offer several advantages for vaccine development. Sequences for relatively large antigens can be encoded and efficiently expressed, at low vaccine doses. Practical and efficient delivery of the saRNA is possible with advanced nanoparticles such as cationic inorganic lipid nanoparticles (LION). Among candidate antigens for a prostate cancer interception vaccine, we selected prostein (SLC45A3), a protein whose natural expression is restricted to the prostate gland and prostate cancer and ERG, a member of the ETS family of transcription factors frequently involved in chromosomal translocations in prostate cancer. We generated saRNA constructs with several design strategies and demonstrated that upon in vitro transfection, both antigens are expressed as assessed by mass spectrometry and Western blot analysis. This was achieved using commercial transfection reagents and LION. Prostein expression was particularly notable in that this eleven-transmembrane protein could be detected in HEK-293 cells using flow-cytometry and cell-surface staining. Nearly 50% of the cell population stained positively. Immunogenicity of the vaccines was tested in mice. Following formulation with LION particles i.m. injection and boosting, saRNAs coding for prostein elicited strong cellular immunity as demonstrated by IFN-γ ELISPOT analysis. Detailed analysis of intracellular cytokine expression indicated a strong CD8 response. saRNAs coding for ERG also showed antigen-specific ELISPOTs. Using commercially available recombinant ERG protein, an ELISA was developed and a strong humoral response to the ERG saRNA vaccine was demonstrated. The saRNA vaccines will be further credentialled with additional preclinical studies including cancer preventive efficacy studies in genetically engineered mouse models of prostate cancer.

#4779 The effects of glutamine deprivation on ovarian cancer initiation and progression.

S. Ferri-Borgogno[1], K. Lu[1], B. T. Gamal[1], C. Au Yeung[1], E. Seeley[2], J. A. Gomez[1], A. Basi[1], J. K. Burks[1], O. Animasahun[3], D. Nagrath[3], S. C. Mok[1];
[1]UT MD Anderson Cancer Center, Houston, TX, [2]University of Texas at Austin, Austin, TX, [3]The University of Michigan, Ann Arbor, MI

High-grade serous ovarian cancer (HGSC) is the most common subtype of ovarian cancer. Most patients with HGSC are diagnosed at advanced stage diseases. Despite the high response rate to platinum/taxane-based chemotherapy, most of these patients will develop recurrent chemoresistant disease. Recent studies showed the cancer associated fibroblasts (CAFs) in the tumor microenvironment (TME) play an important role in modulating the malignant phenotypes of HGSC. CAFs are primarily responsible for producing factors such as cytokines and growth factors to modify the TME niche to promote the malignant phenotypes of cancer cells. Recently, we have identified a previously unrecognized mechanism in which metabolism of reactive CAFs is reprogrammed through an upregulated glutamine anabolic pathway in HGSC. This dysfunctional CAF metabolism confers atypical metabolic flexibility and adaptive mechanisms in CAFs, allowing them to harness carbon and nitrogen from noncanonical sources to synthesize glutamine in nutrient-deprived conditions existing in the TME. Our preliminary data show that tumors developed from syngeneic fallopian epithelial cell-derived cancer cells injected IP into C57BL/6 mice, which started to be fed with normal diet two weeks before tumor cells injection had significantly higher tumor burden than those fed with the glutamine-deprived diet. Moreover, tumor-bearing mice treated with glutaminase inhibitor for 3 weeks demonstrated significantly lower tumor burden than those treated with the control vehicle. These findings suggest that the interplay between CAFs and HGSC cells enriches glutamine in the ovarian TME; and glutamine depletion can not only suppress ovarian tumor growth but also prevent the development of advanced progressive diseases. In addition to the direct promoting effect of glutamine on the glutamine addicted HGSC cells, increased CAF-derived glutamine can also affect the activity of other stromal cell types such as immune cells in the TME, which subsequently modulate HGSC cell growth. Imaging mass cytometry (IMC) and Mass Spectrometry Imaging (MSI) were performed on serial tissue sections of tissue microarrays generated from the abovementioned murine samples. Mice fed with a glutamine-deprived diet or treated with the glutaminase inhibitor not only have a significantly lower tumor burden but also induced dramatic changes in the cellular and molecular composition within the TME. In particular, mice fed with a glutamine-deprived diet had greater B-cell-related immune response, reduced stemness, and EMT of ovarian cancer cells, and more activated CAFs, which may result in increased stiffness of the ECM and subsequently enhance the malignant phenotype of HGSC cells. Further studies to delineate the molecular mechanisms by which spatial cellular and metabolic profiles modulate HGSC pathogenesis and progression are warranted.

#4780 TRAIL-inducing imipridone ONC201/TIC10 demonstrates anti-neoplastic effects in colonic adenoma-derived organoids.

A. J. Lannigan[1], J. Chan[1], M. Schwermann[1], L. Zhou[1], V. V. Prabhu[2], M. Dame[3], D. Brenner[3], W. S. El-Deiry[1], A. G. Raufi[1];
[1]Brown University, Providence, RI, [2]Chimerix Inc., Durham, NC, [3]University of Michigan, Ann Arbor, MI

Background: Colorectal cancer (CRC) is the second leading cause of cancer-related death inthe United States and screening is the most effective method to reduce mortality. Chemoprevention, which aims to prevent CRC through eradication or prevention of precursor colonic adenomas, represents an alternative strategy to address this problem. The imipridone dordaviprone (ONC201) has been shown to induce apoptosis in cancer cells through both upregulation of tumor necrosis factor-related apoptosis-inducing ligand (TRAIL) and the integrated stress response. More recently, we have shown that ONC201 induces TRAIL and apoptosis in a dose-dependent manner and reduces adenoma formation in the *Apc*$^{min/+}$ CRC mouse model. We hypothesized that ONC201 would similarly enhance human colonic adenoma cell death through both TRAIL-dependent and TRAIL-independent mechanisms. We therefore evaluated the effects of ONC201 in two adenoma-derived organoid lines: one developed from an adenoma obtained from an individual with familial adenomatous polyposis (FAP) and the second from a sessile serrated adenoma (SSA).
Methods: Sensitivity of the FAP and SSA organoid lines to ONC201 was assessed using CellTiter-Glo® luminescent cell viability assay. Organoids were plated in triplicates and treated with ONC201 (concentration ranging from 0 uM to 20 uM). Results were analyzed after 72 hours of incubation. Western blotting was performed on lysates generated from organoids treated with either 1.69 uM DMSO, 1.69 uM ONC201, or 3.38 uM ONC201 for FAP and 1.23 uM DMSO, 1.23 uM ONC201, or 2.46 uM ONC201 for SSA for 0, 24, or 48 hours. Co-culture experiments were performed with the adenoma-derived organoids (dyed using blue CMAC dye) and human NK-92MI cells (dyed with green CMFDA dye) treated with either 845 nM DMSO, 845 nM ONC201, or 1.69 uM ONC201 for FAP and 615 nM DMSO, 615 nM ONC201, or 1.23 uM ONC201 for SSA. Fluorescent images following administration of red live/dead dye were performed using DAPI, FITC, and cherry red channels on ImageXpress® at 0, 24, 48, and 72hours.
Results: ONC201 demonstrated antineoplastic effects in adenoma-derived FAP and SSA organoids. Half maximal inhibitory concentrations (IC50) of ONC201 in FAP and SSA organoids were 1.69 uM and 1.23 uM, respectively. As was noted in rodent studies, the mechanism of action of ONC201 appears to be mediated through modulation of multiple pathways including the TRAIL pathway (TRAIL and DR5 were both upregulated) and the integrated stress response (ATF4 was upregulated). Co-culture with NK cells revealed an increase in NK-mediated organoid cell death. The ability of ONC201 to enhance NK-mediated killing is still being evaluated. Further analysis of the effects of ONC201 on stemness markers and on T-cell-mediated organoid cell killing are currently underway and may reveal other potential biomarkers and chemopreventive strategies for ONC201.

#4781 Evaluation of a TP53 biomarker for lung cancer risk in nasal brushings and peripheral blood.

E. L. Crawford[1], D. J. Craig[1], P. T. Gorman[1], M. Omballi[1], R. Ahmad[1], E. L. Grogan[2], S. A. Deppen[2], **J. C. Willey**[1];
[1]University of Toledo, Toledo, OH, [2]Vanderbilt University Medical Center, Nashville, TN

Background and Purpose: Early detection of lung cancer through annual screening with low-dose computed tomography (LDCT) scans enables potentially curative surgical or stereotactic body radiation therapy (SBRT) treatment and thereby significantly reduces mortality. However, LDCT screening among those currently eligible based primarily on age and smoking criteria yields a large number of false-positive findings and many lung cancers occur among individuals who currently are ineligible. A biomarker that identifies lung cancer risk independent from that caused by age and cigarette smoking might increase specificity and increase the number of people eligible for LDCT screening. Recently we demonstrated that a biomarker measuring TP53 somatic mutations in bronchial brush biopsy specimens from grossly normal airway epithelium was significantly associated with cancer status independent of age and smoking status. Additionally, the TP53 biomarker was synergistic with traditional risk score models (e.g. $PLCO_{M2012}$ risk score). The goal of this pilot study was to test the TP53 biomarker in nasal brush biopsy specimens, a potential surrogate tissue obtained using less invasive collection methods. **Methods:** Nasal brushings from 10 lung cancer and 11 control subjects were collected at the University of Toledo and Vanderbilt University Medical Center under approved institutional protocols. Genomic DNA (gDNA) was extracted with the Qiagen AllPrep DNA/RNA kit using a modified protocol. Amplifiable copies of gDNA were measured using quantitative PCR. For each test a sample comprising 25,000 amplifiable copies of gDNA was combined with 50,000 copies of a TP53 internal standard and a complexity control, then PCR amplified, purified and barcoded. Samples were pooled to create two NGS libraries, each with approximately equal numbers of cases and controls, and sequenced on an Illumina MiSeq (Two V3 flow cells, 2 x 250 paired-end). Bioinformatic analysis was conducted using Qiagen CLC Workbench. Variants were called using the Basic Variant Detection Tool. Poisson Exact Test was utilized to determine the significance of endogenous variants relative to internal standard variants at the same base position and a Bonferroni correction was applied to minimize false discovery. Comparison of variant numbers between cases and controls was conducted using an f-test followed by a paired t-test. **Results and Conclusions:** Consistent with previous results in airway epithelium, in this pilot study the TP53 mutation biomarker measured in nasal brushing was associated with lung cancer ($p=0.0085$). Measurement of the TP53 biomarker in nasal brush specimens in a larger case-control study currently is underway along with a pilot study in gDNA from peripheral blood.

PREVENTION / EARLY DETECTION / INTERCEPTION: Population-Based Screening
Poster Session

#4784 PATHFINDER 2: A prospective study to evaluate safety and performance of a multi-cancer early detection test in a population setting.

K. V. Giridhar[1], M. J. Demeure[2], R. H. Kim[3], J. A. Chen[4], S. Gadgeel[5], D. Kurbegov[6], M. Lopatin[4], R. Matthews[7], M. Matrana[8], C. McDonnell[9], D. Richards[10], B. Rybicki[5], G. Stipec[11], N. Nabavizadeh[12];

[1]Mayo Clinic, Rochester, MN, [2]Hoag Memorial Hospital Presbyterian, Newport Beach, CA, [3]University Health Network, Toronto, ON, Canada, [4]GRAIL, LLC, Menlo Park, CA, [5]Henry Ford Health, Detroit, MI, [6]Sarah Cannon Research Institute, Nashville, TN, [7]Morehouse School of Medicine, Atlanta, GA, [8]Ochsner Clinic Foundation, New Orleans, LA, [9]Sutter Institute For Medical Research, Sacramento, CA, [10]Texas Oncology, Tyler, TX, [11]Long Beach Memorial Medical Center, Long Beach, CA, [12]Oregon Health & Science University, Portland, OR

Background: Multi-cancer early detection (MCED) tests are being established as a novel approach to screen for multiple cancer types with one test. A blood-based MCED test using cell-free DNA targeted methylation patterns to detect a shared cancer signal and predict a cancer signal origin (CSO) has demonstrated feasibility. An initial return of results study (PATHFINDER; NCT04241796) reported performance of a refined version of the MCED test, including a 43.1% positive predictive value (PPV), 98.5% negative predictive value (NPV), 99.5% specificity, and 88.0% CSO accuracy. To build on this work, the PATHFINDER 2 study (NCT05155605) will evaluate safety and performance of the MCED test in larger, more diverse populations.

Methods: PATHFINDER 2 is a prospective, multicenter, interventional study. Participants ≥50 years of age will be enrolled, with specific targets to improve diversity (age, sex, race/ethnicity) and few exclusions due to comorbid conditions. Exclusion criteria include current clinical suspicion of cancer or recent cancer/treatment (within 3 years). Participants will undergo blood draw for MCED testing, followed by return of results (cancer signal detection and CSO) to the investigator and diagnostic evaluations if a cancer signal is detected. A confirmatory PET-CT scan will be performed when CSO-directed workups do not result in a cancer diagnosis. Participants will be followed for approximately 3 years. Primary endpoints include 1) MCED test safety in terms of diagnostic testing triggered by a positive result (number/type of procedures and adverse events) and 2) test performance (PPV, NPV, specificity, sensitivity, CSO accuracy, cancer detection rate and number needed to screen). Secondary endpoints include participant reported outcomes (eg, anxiety), utilization of guideline-recommended cancer screening, and cancer detection rate of confirmatory PET-CT, amongst others.

The study plans to enroll approximately 35,000 participants across North America. Sites were selected based on geographic location, catchment area demographics, and practice setting (academic vs non-academic). Enrollment targets for age, sex and race/ethnicity (White [non-Hispanic] 72%; Hispanic or Latino 11%; African American or Black 11%; Asian, Native Hawaiian or Other Pacific Islander 6%; American Indian/Alaska Native 1%) were derived from US Census data. Strategies to promote diverse recruitment include translation of participant-facing documents across multiple languages, participant and healthcare provider educational material, and site-led community outreach campaigns.

MCED testing is an emerging, potentially paradigm-changing strategy in cancer screening, and PATHFINDER 2 is designed to characterize the safety, performance, and clinical implementation of the MCED test as a screening tool in a broad and representative population.

#4786 Colorectal cancer screening rates among deaf, deafblind, and hard of hearing adults aged 45 to 75 years old.

R. M. Wang[1], S. R. Rao[2], **E. J. Bergeron**[3], E. C. Perrodin-Njoku[3], P. Kushalnagar[3];
[1]University of California at San Diego Health, San Diego, CA, [2]Boston University, Boston, MA, [3]Gallaudet University, Washington, DC

Background: Deaf, deafblind, and hard of hearing (DDBHH) individuals who use American Sign Language (ASL), a subpopulation of the disability, experience disparities concerning cancer screening and cancer-related health outcomes. For this study, we explored colorectal cancer screening rates among DDBHH survey respondents in comparison to rates found in the hearing population.
Materials and Methods: Using the National Cancer Institute Health Information National Trends Survey in ASL (Kushalnagar et al., 2015), we surveyed participants 18+ years old using the Center for Deaf Health Equity at Gallaudet University's database of over 2,500 DDBHH participants from all over the USA, including Hawaii and Puerto Rico. We used the U.S. Preventive Services Task Force (USPSTF) guidelines' age cutoffs to assess adherence to colorectal cancer screenings.
Results: Survey response rate within three weeks of mail out in July 2023 was 12%. A total of 405 DDBHH adult participants answered screening questions for colorectal cancer in ASL and English. Overall, 43.7% self-reported screening adherence for age-eligible (45-75 years) colorectal cancer screening; 54.7% reported never having a colorectal cancer screening. Similarly-aged hearing adults reported 58.7% adherence in the English version of the National Health Interview Survey (NHIS).
Discussion: With the 43.7% adherence rate, the DDBHH community is lagging behind colorectal cancer screenings compared to the general population of hearing adults. Estimating the colorectal cancer screening rates among the DBHH community and understanding the reasons for these existing disparities is important to achieve screening adherence of 68.3%, the target set by the Healthy People 2030. Such research will aid the Center for Deaf Health Equity to actively work with the community to improve strategies to increase colorectal cancer screening.

#4787 Preference for multi-target stool DNA for colorectal cancer screening among Alaska Native people in rural/remote communities.

D. Redwood;
Alaska Native Tribal Health Consortium, Anchorage, AK

Background: The Alaska Tribal Health System is working on increasing colorectal cancer (CRC) screening rates among Alaska Native people, who have the highest CRC rates in the world. Most remote Alaska Native communities are not connected to the road system, which severely limits access to screening colonoscopy. As part of a clinical trial, Alaska Native patients were offered either colonoscopy or the at-home multi-target stool DNA test (mt-sDNA; Cologuard®). Patients had never been offered mt-sDNA before and it was unknown what they would think about the new test option. Both tests were provided at no cost to patients.
Methods: From April 2022 to July 2023, 194 patients who chose mt-sDNA for screening received a follow-up phone survey asking whether they were aware that they could have had colonoscopy instead, their reasons for choosing mt-sDNA, and the factors influencing their choice of mt-sDNA over colonoscopy. Patients answered the survey before receiving results of their mt-sDNA test in order to capture initial screening test preferences.
Results: A total of 115 (59%) Alaska Native patients participated in the survey; 56% men and 44% women. About 70% were ages 45 to 60 years while the remaining 30% were 61 to 75 years old. The majority (80%) were aware that they had the option to undergo colonoscopy for CRC screening instead of mt-sDNA. Key themes for mt-sDNA preference included not having to travel, less time commitment, and greater convenience. Many patients expressed financial concerns arising from the costs of air travel and accommodation required to access screening colonoscopy even though the procedure itself was covered. Additionally, patients highlighted existing obligations such as childcare and work responsibilities which made the use of mt-sDNA at home more appealing. Many respondents also shared negative perceptions of colonoscopy procedure including fear, embarrassment, and discomfort as reasons why they preferred mt-sDNA instead.
Conclusions: These findings demonstrate the multifaceted factors influencing the preference for at-home mt-sDNA CRC screening among Alaska Native individuals. Challenges such as limited access to medical facilities, financial burdens, and personal commitments have significant bearing on the screening decision-making process. Moreover, the emotional aspect of fear and discomfort associated with colonoscopy plays a role in shaping these preferences. CRC screening programs need to be aware of patient needs and preferences when deciding which screening methods to offer to increase screening rates and result in improved colorectal health outcomes.

#4788 Noninvasive longitudinal monitoring of residual disease in chemotherapy-treated colorectal cancer patients.

Alison D. Tang, Rebecca Gupte, Victoria Cheung, Tao Qing, Austin Cauwels, Emily Leff, Kimberly Walter, Ehsan Tabari, Alex Lovejoy, Jimmy C. Lin

Freenome, Inc., South San Francisco, CA

Noninvasive monitoring of cancer shows great promise in assessing therapy response and improving patient outcomes. Recently, various groups have developed methods that detect circulating tumor DNA (ctDNA) in the plasma to measure minimal or molecular residual disease (MRD). Aberrant DNA methylation patterns are a hallmark of cancers, and robust signals can be detected by sensitive ctDNA assays. Here, we present a methylation-based approach for longitudinal monitoring of tumor burden that is tumor-naive, i.e., with no reliance on prior characterization of tumor molecular characteristics. We assess the effectiveness of our approach in a cohort of colorectal cancer (CRC) patients receiving chemotherapy with or without additional targeted agents.
Longitudinal blood samples were collected from patients (n = 57) while on therapy, which averaged 4.9 months, for a total of 239 sample collection time points (median per patient = 5). Based on RECIST status, 16 patients were classified as complete responders (CR) at the end of treatment.
We generated plasma cell free DNA-derived libraries for methylation sequencing targeting regions relevant to CRC. Next, we computed a disease burden score for each sample and related these scores to clinical response (CR vs. non-CR). We trained a classifier on an independent cohort of CRC and healthy donor plasma cfDNA samples, and used this classifier to check for residual disease at the end of treatment for each of our 57 patients. The classifier detected residual disease in only 3/16 CRs (19%) but 35/41 non-CRs (85%).
Two of the non-CR patients were initially assessed as CRs at earlier time points. In both cases, our method successfully detected residual disease at or prior to the CR assessment and consistently showed residual disease in all follow up samples. This suggests improved sensitivity relative to RECIST and highlights the potential of using noninvasive blood tests for continuous monitoring of CRC patients receiving therapy.*Authors contributed equally to the work

#4790 Hospitalization as an opportunity to improve lung cancer screening in high-risk patients.

E. M. Nielsen, J. Zhang, J. Marsden, C. Bays, W. P. Moran, P. D. Mauldin, L. A. Lenert, B. A. Toll, A. D. Schreiner, M. Heincelman;
The Medical University of South Carolina (MUSC), Charleston, SC

Background: Lung cancer screening with annual low-dose computed tomography (LDCT) in high-risk patients with exposure to smoking reduces lung cancer-related mortality, yet the screening rate of eligible adults is low. As hospitalization is a critical moment to engage patients in their overall health, it may be an opportunity to improve rates of lung cancer screening. Prior to implementing a hospital-based lung cancer screening referral program, this study assesses the association between hospitalization and completion of lung cancer screening.
Methods: A retrospective cohort study of evaluated completion of at least one LDCT from 2014-2021 using electronic health record data using hospitalization as the primary exposure. Patients aged 55-80 who received care from a university-based internal medicine clinic and reported cigarette use were included. Univariate analysis and logistic regression models evaluated the association of hospitalization and completion of LDCT. The secondary outcome was completion of any CT of the chest.
Results: Of the 1,935 current smokers identified, 47% had at least one hospitalization, and 21% completed a LDCT during the study period. While a higher proportion of patients with a hospitalization had a LDCT (24%) compared to patients without a hospitalization (18%, $p<0.001$), there was no association between hospitalization and completion of a LDCT after adjusting for potentially confounding covariates (95%CI 0.680 - 1.149). Of cohort patients, 38% completed any CT of the chest and hospitalization was associated with increased odds of receiving chest CT imaging in the adjusted model (OR 1.72; 95%CI 1.37 - 2.17).
Conclusions: In a cohort of patients at risk for lung cancer, only 1 in 5 completed lung cancer screening with LDCT and hospitalization events were not associated with LDCT completion. A hospitalist driven lung cancer screening program has the potential to increase the suboptimal rates of lung cancer screening in high-risk patients.

#4791 Characterizing interventions to reduce disparities in lung-cancer screening uptake by state Medicaid expansion status: A scoping review.

M. J. Reid, C. Washington, M. Wheeler, L. Adkins, D. Braithwaite, R. Salloum;
University of Florida College of Medicine, Gainesville, FL

Background: Lung cancer is the leading cause of cancer-related deaths in the United States, and yet, lung cancer screening rates remain persistently low. Many interventions are being developed to address the low rates of lung cancer screening (LCS), including interventions that address the additional barriers faced by historically marginalized racial and ethnic populations as well as low-income and rural populations. However, the impact of Medicaid expansion on the types of interventions developed in non-expansion states and the efficacy of those interventions is not well understood.
Methods: A research librarian conducted searches in MEDLINE via PubMed, Web of Science, and Embase. Results were screened and evaluated for eligibility by three reviewers in Covidence. Data was extracted from included studies after full-text review and analyzed using both a thematic analysis and a descriptive numerical summary of studies. The chosen framework was based on scoping review guidelines by Levac et al. and Preferred Reporting Items for Systematic reviews and Meta-Analyses extension for scoping reviews (PRISMA-ScR).
Results: Of 4696 studies found through the initial search, 53 met inclusion criteria. This includes 34 studies in Medicaid expansion states (M) and 17 studies in non-Medicaid expansion states (NM). Two additional studies compared interventions implemented in a Medicaid expansion state to a similar intervention implemented in a non-expansion state. Studies in both groups were primarily focused on addressing disparities by race and ethnicity (M=74%; NM=65%), with fewer studies focusing on rurality (M=9%; NM=12%), income (M=9%; NM=0%), or multiple disparities (M=9%; NM=24%). In non-expansion states, the most common interventions were patient navigation (29%) and community outreach (24%). While in Medicaid expansion states, the most common interventions were EHR algorithms (24%) and decision aids (21%). The intervention setting for both Medicaid expansion and non-expansion states were most commonly in a hospital/health system (M=53%; NM=47%) or community setting (M=24%; NM=47%). Interventions in both groups typically showed some improvement in uptake of LCS, though the degree of impact was variable between studies.
Conclusion: Due to continued barriers to access posed by inadequate insurance coverage, there is a critical need for interventions to reduce disparities in lung cancer mortality in states that have not expanded Medicaid. Interventions focused on patient navigation and community outreach have been effective in multiple settings in these states and could fill that gap.

#4792 Nationwide patterns of incidence and surveillance of second primary lung cancer among long-term lung cancer survivors using SEER Medicare data.

Chloe C. Su[1], Eunji Choi[2], Julie T. Wu[3], Allison W. Kurian[1], Michelle C. Odden[1], Manisha Desai[4], Leah M. Backhus[5], Heather A. Wakelee[6], Ann N. Leung[7], Joel W. Neal[6], Summer S. Han[2]

[1]Epidemiology and Population Health, Stanford University School of Medicine, Palo Alto, CA,[2]Quantitative Sciences Unit, Stanford University School of Medicine, Palo Alto, CA,[3]Veterans Affairs Palo Alto Healthcare System, Palo Alto, CA,[4]Biomedical Data Science, Stanford University School of Medicine, Palo Alto, CA,[5]Department of Cardiothoracic Surgery, Stanford University School of Medicine, Palo Alto, CA,[6]Division of Oncology, Stanford University School of Medicine, Palo Alto, CA,[7]Department of Radiology, Stanford University School of Medicine, Palo Alto, CA

Background: With advances in screening and therapy, the number of lung cancer (LC) survivors is rapidly increasing, with over half a million as of 2019. Prior studies demonstrated that the incidence of second primary lung cancer (SPLC) among LC survivors is 4-6 times that of initial primary lung cancer (IPLC) in the general population. However, the incidence of SPLC and surveillance strategies using computed tomography (CT) have not been examined in long-term LC survivors with over 5-year survival. We aim to estimate SPLC incidence among long-term survivors and the effectiveness of annual surveillance CT exams.
Methods: We used data from SEER-Medicare with a cohort of 1,232,338 LC patients from the SEER cancer registry followed till death or last follow-up, who were also enrolled in Medicare in 1999-2020. The study cohort included 12,948 patients who were long-term survivors (≥ 5-year survival from IPLC) by age 65, received curative therapy for IPLC, and were continuously enrolled in Medicare 1 year prior to 5 years after IPLC diagnosis. The primary outcome was the 10-year cumulative SPLC incidence accounting for competing risk of death in the full study cohort and by receipt of surveillance CTs post-5-year survival, defined using detailed billing and LC-related ICD codes. To qualify as surveillance CTs, two annual CTs 9-18 months apart is required. Cox regression was used as exploratory analysis to examine the association between LC-specific survival (LC as cause of death) and the receipt of two CTs post-5-year survival as a binary variable, adjusting for SPLC diagnosis, age, sex, marital status, race, IPLC stage, income, education, and poverty.
Results: Of 12,948 long-term LC survivors, 46% (n=6,015) were male, 90% (n=11,476) had early-stage disease, 77% (n=9,945) had undergone surgery for initial curative treatment, and 3.8% (n = 486) received two surveillance CTs initiated within 18 months post-5-year survival. The 10-year cumulative incidence of SPLC was 5.06% [95% CI: 5.00-5.12%] in the SEER cohort but was substantially higher among long-term LC survivors at 13.6% [13.0-14.2%]. Those who received two annual surveillance CTs after 5-year survival had a significantly higher 10-year SPLC incidence (23.3% [19.4 - 27.2%]) than those who received one or no CT (13.2% [12.6 - 13.8%]). The adjusted hazard ratio of the association between LC-specific survival and receipt of two CTs was 0.67 [0.59-0.80, $p < 0.0001$].
Conclusions: The high cumulative risk of SPLC among long-term LC survivors warrants tailored surveillance strategies. Our exploratory analysis showed a high SPLC detection rate among those who received two annual surveillance CTs vs. those who did not, with significantly higher LC-specific survival in the former. Future work will include extensive analysis accounting for time-varying exposure of multiple surveillance CTs using rigorous causal inference methods.

#4793 Effects of treatment delays on lung cancer survival.

P. Guzman Montero[1], S. Segura Cordero[2];
[1]National Cancer Institute, Bethesda, MD, [2]Universidad Internacional de las America, San Jose, MD

Background: Previous studies have established a link between treatment initiation delays and reduced overall survival in individuals diagnosed with lung cancer. These delays are often influenced by diagnostic complexities, logistical hurdles, and patient-related factors. However, the association between treatment delays and survival outcomes has yet to be extensively investigated using data from a large national cohort. This study aims to fill this research gap and provide unique insights into the relationship between treatment delays and lung cancer survival by utilizing data from a substantial national cohort.
Methods: The study population consisted of 3,723 lung cancer patients participating in the NCI PLCO Cancer Screening Trial. Cox Proportional Hazards (PH) Regression analyses examined the time between cancer diagnosis and treatment initiation using several measures including intervals from tumor doubling/stage progression time models by Spratt et al. (1964) and Detterbeck et al. (2008). Analyses controlled for patient and clinical characteristics including age, sex, race/ethnicity, smoking status, histopathologic type, cancer stage, and treatment modality. Data analysis was conducted using Microsoft Excel, STATA, and IBM SPSS software.
Results: PH Regression analyses demonstrated a clear association between longer time intervals from diagnosis to treatment initiation and increased risk of mortality. Patients with time intervals exceeding 20 days exhibited a hazard ratio (HR) for mortality of 1.21 ($p < 0.001$, 95% confidence interval [CI] 1.1158-1.3176). The Spratt tumor progression model, considering intervals exceeding 88 days, revealed a HR of 1.22 ($p = 0.03$, 95% CI 1.0146-1.4885). On the other hand, the Detterbeck model, which considered intervals exceeding 118 days, did not show a statistically significant association with increased mortality risk. Furthermore, PH analysis identified cigarette smoking status, marital status, and tumor grade as significant predictors of mortality risk.
Conclusions: Data from a large national cohort study indicate that delays in lung cancer treatment initiation have detrimental impacts on survival. Treatment initiation shortly after diagnosis had the most significant differential impact on mortality risk. Timely initiation of treatment is of utmost importance and should be prioritized in lung cancer care. By addressing factors contributing to treatment delays, it is likely possible to improve the survival rates of patients with lung cancer.

#4794 Impact of prior upper endoscopy on gastric cancer stage and survival.

S. Wagner[1], J. S. Ferris[1], J. Soddano[1], J. Yoon[2], S. D. Rustgi[1], H. Zylberberg[1], J. Yang[1], Y. Huang[3], L. Chen[3], C. Hur[1];
[1]Columbia University Irving Medical Center, New York, NY, [2]Icahn School of Medicine at Mount Sinai, New York, NY, [3]Columbia University College of Physicians and Surgeons, New York, NY

Background: While gastric cancer (GC) incidence in the US has decreased, 5-year survival remains at 34.5%. Early diagnosis offers curative or treatable options, yet many cases are detected at an advanced stage with poor prognosis. In high-incidence East Asian countries with established screening programs, endoscopic screening demonstrates stage shift towards early GC diagnosis and reduced GC-related mortality. Analyses of these programs have reported benefit of endoscopic screening up to 36 months prior to diagnosis. This study explores the impact of esophagogastroduodenoscopy (EGD) in this timeframe on GC stage at diagnosis and survival in an older US population.

Methods: The SEER-Medicare database was queried from 2000 to 2017 for patients 68 years of age or older with histologically confirmed GC with continuous Medicare enrollment for at least 36 months prior to GC diagnosis. We excluded patients with prior cancer history and those diagnosed by autopsy or death certificate. Medicare claims files were searched for EGD claims 6-36 months prior to GC diagnosis. We excluded claims in the 6 months prior to diagnosis to avoid capturing potential diagnostic EGD. We defined the exposed group as patients with an EGD claim 6-36 months prior to GC diagnosis (Prior EGD) and the unexposed group as patients with no EGD claim in this period (No Prior EGD). Propensity score analysis balanced baseline differences for patients with and without Prior EGD using covariates sex, age and year of diagnosis, race and ethnicity, rural/urban, comorbidity, SES, and marital status. The primary outcome was in situ/local-stage GC (early) at diagnosis compared to regional/distant-stage (advanced). Secondary outcomes were 5-year overall and GC-specific survival. The adjusted odds of having in situ/local-stage GC diagnosis compared to regional/distant-stage was estimated using logistic regression, and survival analysis was done using the Kaplan-Meier method.

Results: In 10,572 patients with GC (57.5% male, mean age 78.8 years), 16.4% had Prior EGD (n=1,736). Patients with Prior EGD had a significantly higher proportion of GC diagnosed in local stage compared to patients with No Prior EGD (45.7% vs. 30.2%, $p < 0.001$). After controlling for confounders, Prior EGD group had two-fold increased odds of GC diagnosis at early-stage compared with No Prior EGD (OR=1.99, 95% CI: 1.88-2.10). Compared with No Prior EGD, Prior EGD was associated with higher overall survival (5-year survival 32.1% vs. 22.7%, $p<0.001$) and GC-specific survival (5-year survival 46.0% vs. 31.1%, $p\leq0.001$), both driven by early-stage disease.

Conclusions: Our analysis demonstrates that EGD up to 36 months prior to the diagnosis of GC is associated with earlier stage at diagnosis and improved overall and GC-specific survival. This study of an older population suggests that endoscopic screening may be beneficial even in a low-incidence country such as the US and warrants further study.

#4795 Social capital and screening mammography rates in the United States.

Tracy Huang, Christine Ekenga

Emory University, Rollins School of Public Health, Atlanta, GA

Background: Social capital may play a role in screening mammogram utilization by influencing individuals' access to information and providing social support for healthy behaviors. However, few studies have examined associations between community-level social capital and screening mammography use. The purpose of this study was to examine the association between county-level social capital and screening mammography rates in the United States (U.S.).
Methods: We conducted a cross-sectional study of social capital and screening mammography rates across 2,613 U.S. counties for 2014. We obtained county-level data on (1) screening mammography rates for female Medicare enrollees aged 67-69 years and (2) social capital (Penn State Social Capital Index). Multivariable regression models were used to evaluate associations between social capital quartiles and mammography screening rates. Models were adjusted for county-level socioeconomic, demographic, and access to care factors.
Results: Average county-level screening mammography rates were 60.5% ± 8.3% (range 26%-88%). Across all U.S. counties, social capital was associated with county-level mammography rates, after adjusting for covariates ($p < 0.001$). This association did not vary by urban-rural classification. In analyses by region, associations between social capital and screening mammography rates were strongest in the West region ($p<0.001$).
Conclusions: In this nationwide study, social capital was significantly associated with screening mammography. Our findings suggest that there are regional variations in the association between social capital and mammography rates. The relationship between social capital and cancer screening behaviors warrants further investigation, particularly in the U.S. West.

#4796 Improving cancer screening performance for women with dense breast tissue.

M. Smith, M. Wang, A. Carson, B. Lee, M. Salmans, B. Leatham;
Genece Health, Inc., San Diego, CA

Breast cancer is the most common cancer in women in the United States. To reduce mortality, screening by mammography in females is recommended by the United States Preventive Services Task Force, successfully reducing mortality by 15 - 32% in women aged 40 - 69 years. This is partially due to the high compliance rate (60 - 80%) among the candidate population. Mammography increases early-stage disease detection, which is correlated with better outcomes. While mammography has been largely successful, this screening method has limitations. Overall, mammography has false-negative and false-positive rates estimated at 12 - 20% and 7 - 12%, respectively. Consequently, annual mammograms result in 50 - 60% of women having a false-positive result within a 10-year span. Additionally, high breast density, found in approximately 50% of females over the age of 40, increases susceptibility to false positive and negative results. For this reason, in 2023 the FDA required that dense breast tissue status, an independent risk factor for cancer, be disclosed to mammogram recipients. The subsequent diagnostic pathway for women with dense breast tissue is not well defined for the care provider. Alternative imaging options have performance issues or are less accessible. Here we describe a liquid biopsy test to complement mammography in women with dense breast tissue to help resolve ambiguity in results. Blood from early- and late-stage breast cancer patients was prospectively collected in Streck cfDNA BCT Devices (n=100) or retrospectively acquired (n=100); and blood from presumed normal samples was collected (n=200). cfDNA was extracted and converted into libraries for low-pass whole genome sequencing (LP-WGS). Sequenced reads were analyzed to generate fragment end-motif and size (FEMS) and fragment coverage dataframes for classification using Genece Health's proprietary analysis pipeline and machine-learning (ML) algorithm. 150 breast cancer samples distributed across stages and 150 presumed normal samples were selected to create a training cohort. Performance was tested using a 5-fold cross validation strategy. The best performance was observed using a convolution neural network (CNN) ML model with >80% sensitivity when specificity was set at 85%. The remaining 50 breast cancer samples and 50 presumed normal samples were used as an external test set. The performance in this cohort was comparable to the training cohort, with both specificity and sensitivity >80%. Genece presents an early proof of concept breast cancer screening liquid biopsy assay that uses LP-WGS fragmentomics and ML to detect cancer from a single blood sample. Continuing development with additional cohorts and optimization will yield even greater performance. The Genece liquid biopsy test has the potential to be paired with mammography, especially in women with dense breast tissue, to improve screening sensitivity, specificity, and overall outcomes.

#4797 Impact of COVID-19 pandemic on breast cancer screening and diagnosis stage in a large midwestern United States academic medical center.

K. J. Johnson, R. Waken, C. P. O'Connell, D. Brown;
Washington University in St. Louis, St. Louis, MO

Background: Access to breast cancer screening mammogram services decreased in association with the COVID-19 pandemic. There is also evidence for increases in late-stage breast cancer diagnoses. Our objectives were to determine: 1) the COVID-19-affected period on mammogram screening, 2) the proportion of pandemic-associated missed or delayed mammogram screening visits overall and by race/ethnicity and age group, and 3) evidence for pandemic-associated shifts in diagnosis stage.
Methods: Screening mammogram encounter data between 1-1-2019 and 12-31-2022 were extracted from EPIC for females ≥ 40 years old for the screening analysis. We used Bayesian state space models to describe weekly screening mammogram counts, modeling an interruption that phased in and out from 3-1-2020 to 9-1-2020. We used the posterior predictive distribution to simulate differences between a predicted, uninterrupted process and the observed screening mammogram counts. Breast cancer diagnoses at ≥ 21 years from the tumor registry between 12-1-2018 and 11-30-2021 were included in the stage analysis. We used logistic regression models to estimate late-stage diagnosis odds comparing matched three-month periods during the pandemic to before the pandemic.
Results: A total of 319,492 encounters among 146,644 women were included. Model-estimated screening mammograms dropped by 98.8% (95% CI 95.1 to 100) between 3-15-2020 and 5-24-2020, returning to pre-pandemic levels or higher after this period. Drops in screening mammogram encounters did not vary significantly by race/ethnicity or age group ($p > .75$). Among 4,669 breast cancer diagnoses, we found no significant differences in the odds of late-stage diagnoses for any period vs. the same period before the pandemic (Table).
Conclusions: These data suggest a short-term pandemic effect on screening mammograms. Evidence for increases in late-stage diagnoses is limited. These results may inform future pandemic planning.

OR (95% CI)	Period comparison
1.19 (0.74 to 1.91)	3/2020 to 5/2020 vs. 3/2019 to 5/2019
1.05 (0.69 to 1.60)	6/2020 to 8/2020 vs. 6/2019 to 8/2019
1.14 (0.73 to 1.78)	9/2020 to 11/2020 vs. 9/2019 to 11/2019
0.92 (0.60 to 1.41)	12/2020 to 2/2021 vs. 12/2019 to 2/2020
1.08 (0.71 to 1.65)	3/2021 to 5/2021 vs. 3/2019 to 5/2019
0.89 (0.59 to 1.33)	6/2021 to 8/2021 vs. 6/2019 to 8/2019
1.31 (0.84 to 2.04)	9/2021 to 11/2021 vs. 9/2019 to 11/2019

#4798 MRI screening for brain metastases (BrM) versus SYMptom-directed brain imaging for patients with triple negative (TN) or HER2+ metastatic breast cancer (MBC): An ad-hoc interim analysis of a randomized phase II pilot study.

K. J. Jerzak[1], M. Shum[1], G. Pond[2], O. Freedman[3], G. Chandhoke[3], T. Conrad[1], P. Brastianos[4], G. Stanisz[5], A. Sahgal[1], E. Warner[1];
[1]University of Toronto, Toronto, ON, Canada, [2]McMaster University, Toronto, ON, Canada, [3]Lakeridge Health, Oshawa, ON, Canada, [4]Harvard Medical School, Boston, MA, [5]Sunnybrook Research Institute, Toronto, ON, Canada

Background: Patients with HER2+ or TN MBC are at high risk of developing BrM, but the role of MRI screening for early detection of asymptomatic BrM has not yet been established.
Methods: We conducted a multicentre phase II pilot study, which randomized patients with TN or HER2+ MBC to 1 year of BrM screening (contrast enhanced brain MRI at baseline, 4, 8, and 12 months) versus a control arm of symptom directed brain imaging (MRI only if symptoms of BrM develop). The primary goal was to determine the feasibility of a future randomized trial of BrM screening versus symptom-directed imaging in this patient population. Key inclusion criteria were age ≥18; TN MBC diagnosed ≤12 weeks prior to study entry or HER2+ MBC with no restrictions regarding time of diagnosis; no symptoms of BrM or known asymptomatic BrM; ECOG ≥ 1 and no MRI contraindications. Overall (EORTC QLQ BN20) and neurologic-specific (FACT-BR tools) quality-of-life as well as cancer-related anxiety (NCI PRO-CTCAE) were assessed at baseline, 6 and 15 months. Criteria rendering a future trial “not feasible” were defined a-priori as: <30% of eligible patients enroll in the study, <50% complete the study protocol, and/or >50% of patients allocated to the control arm during the 1 year study period are screened for asymptomatic BrM with CT or MRI.
Results: Between 2018 and 2023, 44 patients from 3 participating centres enrolled in the study. Thirty-five participants (80%) had HER2+ and 9 (20%) had TN MBC. Of the 22 patients randomized to each of the study arms; 3 patients (8%) in each arm withdrew prior to study completion. Reasons for withdrawal included claustrophobia (n=3) or discontent with their randomised arm (n=3) or follow-up requirements (n=1). Metrics regarding the proportion of eligible patients who enrolled in the study were only collected from the Sunnybrook Odette Cancer Centre site; of 91 patients approached, 38 (42%) enrolled in the study. Within the 12-month study period, the incidence of BrM among patients in the screening arm was n=3 (14%) versus n=4 (18%) in the control arm. To-date among patients in the study arm, 11 (50%) completed the 12-month screening protocol, 5 (23%) remain on study and 6 (27%) did not complete the protocol due to either death or early study withdrawal. Among patients in the control arm, 10 (45%) completed 12-month follow-up, 4 (18%) remain on study and 8 (36%) did not complete follow-up due to either death or early study withdrawal. In total, 13 patients (59%) in the control arm had brain imaging, 4 in the absence of neurological symptoms.
Conclusion: A large randomized trial to investigate the utility of MRI-based surveillance for asymptomatic detection of BrM in the proposed patient population is likely feasible, although episodic brain imaging in the control arm was common. Analysis of patient reported outcomes is ongoing.

#4799 Hidden epidemics: The gender divide in HCV and cancer screenings among the unhoused.

Talal Al-Assil[1], Claire Kalina[1], Madison Laird[1], Nataly Dawood[1], Raven Riordan[1], Neya Suresh Kumar[1], Ryan Olivier[1], Cheryl Dickson[2], Gitonga Munene[3]

[1]Western Michigan University Homer Stryker M.D. School of Medicine, Kalamazoo, MI,[2]Department of Diversity, Equity, and Inclusion, Western Michigan University Homer Stryker M.D. School of Medicine, Kalamazoo, MI,[3]Department of Surgery, Western Michigan University Homer Stryker M.D. School of Medicine, Kalamazoo, MI

Background & Methodology: In the United States, the unhoused population experiences disproportionately higher rates of cancer incidence and mortality—double that of the general populace. Despite these startling statistics, there is a notable dearth of research on this topic within medical literature. Our medical student-led pilot study aimed to bridge this knowledge gap by evaluating the uptake of cancer screenings and identifying the barriers faced by the unhoused in Southwest Michigan. Our objective was to enhance the understanding of cancer care disparities and identify factors that hinder access to cancer screenings for this marginalized group. Utilizing questionnaires distributed in homeless shelters, we collected data on the prevalence and impediments to screenings for hepatitis C virus (HCV), and lung, breast, colon, and cervical cancers in a local community.

Results: The study encompassed 143 participants, revealing that women reported a shorter median duration of homelessness (5 months) than men (18 months). The primary barriers to cancer screening were access to services and lack of awareness, rather than insurance coverage. Gender disparities were evident in HCV screening, with an overall rate of 55%; however, willingness to screen was higher among women (83%) compared to men (49%). Colon cancer screening showed no significant gender disparity, standing at 45% uptake. The prevalence of smoking was high at 78%, yet a higher proportion of men were amenable to lung cancer screening. Interestingly, Pap smear uptake surpassed national averages, while mammogram rates were below expected at 40%.

Discussion & Conclusion: While the discrepancies between genders may not be immediately apparent, our data shows that developing targeted interventions and tailoring the delivery of adequate cancer screenings to the unhoused require consideration of gender as a key factor. Women's perceived barriers differ slightly from men's, and generally-speaking, they undergo more cancer screenings per year compared with men. The reluctance among male participants to engage in HCV screening has been observed in other studies as well and as our study demonstrates, it may be related to informational barriers. Although preliminary, our findings shed light on the critical health care issues faced by the unhoused and serves as a steppingstone towards improving our understanding on their challenges in hopes of improving their health outcomes. Comprehensive research is imperative to unravel the complex causes of these gender-based discrepancies. In the interim, the implementation of a navigator social worker system could prove beneficial in facilitating the unhoused with the logistics of screening processes, overcoming transportation hurdles, and reinforcing the importance of ongoing health management.

#4800 Reducing health disparities for prostate adenocarcinoma by integrating multi-omics data via a multi-modal transfer learning approach.

L. Li, J. Wang, S. Wan;
University of Nebraska Medical Center, Omaha, NE

Prostate adenocarcinoma (PRAD) is the most common subtype of prostate cancer, which is the second leading cause of cancer death in American men. Although significant progress has been made to improve PRAD prognosis, existing studies indicated that Black American men have disproportionately high incidence and mortality rate in prostate cancer compared with non-Hispanic White American men. With artificial intelligence (AI) and machine learning (ML) being increasingly applied to PRAD research and clinical decision-making, PRAD data disparities would introduce bias to AI/ML models and further enhance negative impacts on healthcare towards underrepresented groups. Transfer learning has shown potential to reduce racial disparities in PRAD. However, its performance may be deteriorated due to: (1) its model requires large-scale training samples which are difficult to obtain in clinical settings, and (2) it only uses single-omics data without integrating multi-omics information. To address these concerns, we propose to develop a multi-modal transfer learning model to integrate multi-omics data for reducing health disparities. Specifically, we first investigated two multi-modal ensemble methods, Pearson Correlation Coefficient (PCC) based patient-pairwise similarity, and variational autoencoder (VAE) to integrate different types of omics data. Then, we leveraged a transfer learning model based on domain adaptation to pre-train the model on the majority group (White Americans) and fine-tune the model using the minority group (Black Americans). To further address the imbalanced data among ethnic groups, we explored implementing a data augmentation method, Synthetic Minority Oversampling Technique (SMOTE), to increase the size of minority group data. We evaluated our model on multi-omics data (mRNA, miRNA and methylation) of PRAD from The Cancer Genome Atlas (TCGA) database. Results suggested that our proposed approach achieved better performance of reducing health disparities for Black Americans compared with the mixture model and the independent model as well as the conventional transfer learning model in predicting progression-free interval (PFI) prognosis for PRAD patients. Furthermore, we also demonstrated that SMOTE alleviated the data imbalanced problem and improved the performance of the prognosis classification for ethnic minority groups. In summary, our results demonstrated that our proposed multi-modal transfer learning approach could effectively reduce the performance gap between majority and minority groups in PRAD prognosis, thereby mitigating health disparities. We expect that our proposed multi-model transfer learning framework can be customized and extensible to reduce health disparities in other types of cancer.

#4801 Clinical polygenic model to stratify risk of any, metastatic, and fatal prostate cancer in a randomized controlled trial of precision screening.

A. M. Dornisch[1], R. Karunamuni[1], K. N. Maxwell[2], J. Lynch[3], I. P. Garraway[4], A. Kibel[5], C. A. Brunette[6], M. E. Danowski[6], K. M. Lee[3], S. L. DuVall[3], J. M. Gaziano[7], B. S. Rose[8], R. L. Hauger[8], J. L. Vassy[7], T. M. Seibert[8];

[1]UC San Diego, La Jolla, CA, [2]University of Pennsylvania, Philadelphia, PA, [3]VA Salt Lake City Healthcare System, Salt Lake City, UT, [4]Greater Los Angeles Veterans Affairs Healthcare Center, Los Angeles, CA, [5]Brigham and Women's Hospital, Harvard Medical School, Boston, MA, [6]Veterans Affairs Boston Healthcare System, Boston, MA, [7]VA Boston Healthcare System, Boston, MA, [8]VA San Diego Healthcare System, San Diego, CA

Introduction: Lifetime risk of prostate cancer (PCa) is strongly associated with three factors: ancestry, family history, and genetics. We previously developed a polygenic hazard score (PHS) for PCa comprised of 290 common genetic variants (PHS290). When accounting for family history and ancestry (self-reported or genetically determined), PHS290 remained a powerful independent predictor of age at PCa diagnosis, metastatic PCa diagnosis, and PCa death. Additional variants associated with PCa susceptibility or benign elevation of prostate-specific antigen (PSA) have since been published. Here, we evaluate their impact on lifetime risk predictions for metastatic and fatal PCa and develop an updated polygenic score. This score will inform the design of the Prostate Cancer, Genetic Risk, and Equitable Screening Study (ProGRESS, ClinicalTrials.gov ID NCT05926102), a nationwide randomized controlled trial evaluating precision PCa screening in the VA healthcare system.

Methods: We utilized a machine learning approach to update the PHS. Over 450 variants associated with PCa, aggressive PCa, benign prostatic hyperplasia, or benign PSA elevation were evaluated for inclusion. First, we identified pairs of variants with highly correlated genotype (defined as $R^2 > 0.95$) and utilized univariable Cox proportional hazards models (using age at diagnosis of PCa) to exclude one variant from each pair. We then evaluated all remaining candidate variants for inclusion in a new PHS using a LASSO-regularized Cox proportional hazards model. We combined the new PHS with clinical predictors (ancestry and family history) to create a comprehensive, quantitative polygenic score in a diverse, population-based cohort of n=590,750 (Million Veteran Program). Both self-reported and genetic ancestry (based on 2,309 ancestry informative markers) were assessed. We estimated hazard ratios (HRs) to compare men with high versus low polygenic score and evaluated absolute predictions of any, metastatic, and fatal PCa.

Results: The updated polygenic score included 356 variants, as well as family history and genetic ancestry. When comparing the highest to the lowest quintile of the population for polygenic score, the HRs for any PCa, metastatic PCa, and fatal PCa were 5.6, 5.8, and 5.2 respectively. These HRs are all greater than those achieved with PHS290, which yielded 5.2, 4.9, and 4.4 respectively. Risk stratification improved within each ancestry group, including within the >100,000 participants of African ancestry—a group known to have elevated risk of fatal PCa. Absolute risk prediction was accurate for both metastatic and fatal PCa.

Conclusion: The polygenic score accurately predicts risk of metastatic and fatal PCa in multiple ancestry groups. A clinical polygenic model has potential utility for precision PCa screening and will now be evaluated prospectively in the ProGRESS trial.

#4802 Accuracy of the GALAD serologic model in the diagnosis of hepatocellular carcinoma in Ghanaian patients.

Y. A. Nartey[1], J. Yang[2], T. Zemla[3], J. Ayawin[4], S. Osei Asibey[5], M. El-Kassas[6], S. A. Bampoh[7], A. Duah[8], A. Agyei-Nkansah[9], Y. A. Awuku[10], M. Yeboah Afihene[11], H. Yamada[12], J. Yin[13], A. Plymoth[14], L. R. Roberts[3];

[1]Cape Coast Teaching Hospital, Cape Coast, Ghana, [2]Cedars-Sinai Medical Center, Los Angeles, CA, [3]Mayo Clinic, Rochester, MN, [4]Komfo Anokye Teaching Hospital, Kumasi, Ghana, [5]Kumasi Technical University, Kumasi, Ghana, [6]Helwan University, Helwan, Egypt, [7]Greater Accra Regional Hospital, Accra, Ghana, [8]University of Ghana Medical Center, Accra, Ghana, [9]University of Ghana Medical School, Accra, Ghana, [10]University of Health and Allied Sciences, Ho, Ghana, [11]Kwame Nkrumah University of Science and Technology, Kumasi, Ghana, [12]FUJIFILM Corporation, Tokyo, Japan, [13]Moffitt Cancer Center, Tampa, FL, [14]European Centre for Disease Prevention and Control (ECDC), Stockholm, Sweden

Background: Hepatocellular carcinoma (HCC) is one of the leading causes of cancer-related mortality worldwide. In sub-Saharan Africa, HCC is the second most common cancer in men and the sixth in women. African patients present with HCC at a young age and at advanced stage of disease. Improved surveillance can increase early HCC detection. The GALAD score has good sensitivity in the diagnosis of HCC in Asia, Europe and North America, however, it has not been validated in an African cohort. The aim of this study was to assess the performance of the GALAD score in the diagnosis of HCC in Ghanaian patients.

Methods: Clinical data from patients with cirrhosis (n=93) or HCC (n=78) from out-patient hepatology clinics at 3 teaching hospitals in Ghana were abstracted, and serum samples analyzed. A logistic regression model predicting HCC status based on GALAD score was constructed to obtain the Receiver Operating Characteristics (ROC) curve for GALAD. The area under the curve (AUC) with 95% confidence interval was calculated and used to assess the performance of the GALAD score in surveillance for HCC.

Results: The median AFP (5010.2 vs. 3.4), L3% (28.3 vs. 0.3) and DCP (507.6 vs. 0.2) levels were all significantly higher among HCC cases than the controls ($p<0.0001$). The median GALAD score was also higher among HCC patients (8.0 vs. -4.1, $p<0.0001$). The AUC of the GALAD score in the diagnosis of HCC was 0.86 (95% CI 0.79 - 0.92). At a cut-off value of -0.37, the GALAD score had a sensitivity of 0.81 and a specificity of 0.86. In a re-fit of the logistic regression model, the most significant factors in the GALAD model in our cohort were AFP-L3% and log(DCP). The AUC of the new GALAD model after model selection was 0.89.

Conclusion: The GALAD score can be used to detect HCC in Ghana and has the potential to improve HCC surveillance in low-resource settings in sub-Saharan Africa.

#4803 Cancer screening, knowledge, and fatalism among Chinese, Korean, and South Asian residents of New York City.

I. I. Curro[1], C. A. Teasdale[1], L. Wyatt[2], Y. Yusuf[2], V. Foster[2], S. Sifuentes[2], P. Chebli[2], J. A. Kranick[2], S. C. Kwon[2], C. Trinh-Shevrin[2], M. N. LeCroy[2];
[1]The City University of New York Graduate School of Public Health and Health Policy, New York, NY, [2]NYU Grossman School of Medicine, New York, NY

Background: Asian New York City (NYC) residents have the lowest screening rates by race across cancer type. Past studies indicate heterogeneity within the Asian American population, yet few have examined differences in screening uptake and related factors among Asian ethnic subgroups in NYC. Further, cancer screening knowledge and cancer fatalism have been found to impact cancer screening uptake, and effects vary by race, ethnicity, immigration status, and cancer type.
Objective: Our study aimed to examine differences in cancer screening uptake, knowledge, and fatalism among Chinese, Korean, and South Asian NYC adults and to examine the effects of cancer screening knowledge and cancer fatalism on cancer screening uptake.
Methods: We used data from NYU Langone Perlmutter Cancer Center's Cancer Community Health Resources and Needs Assessment survey. The survey was developed and distributed in 10 languages in collaboration with 23 community partners. Data were collected from NYC adults with recruitment strategies focused on immigrant and non-English language preference communities from Oct. 2021 - Dec. 2022. Multivariable logistic and multinomial regression analyses were used to examine differences in breast, cervical, and colorectal cancer (CRC) screening uptake; breast and CRC screening knowledge; and cancer fatalism between Chinese, Korean, and South Asian (Bangladeshi, Pakistani, Asian Indian, and Nepali) adults; and to examine the effects of breast and CRC screening knowledge on breast and CRC screening uptake and cancer fatalism on breast, cervical, and CRC screening uptake (n=1,045). Analyses were restricted by age and sex using United States (U.S.) Preventive Services Task Force guidelines.
Results: The sample was 60.0% female with a mean age of 45.7 years; 83.1% of participants were born outside of the U.S., 49.9% of participants were Chinese, 22.8% were Korean, and 27.3% were South Asian. Korean women had 0.52 (95%CI: 0.31, 0.88) times lower odds of Pap test uptake than Chinese women; South Asian adults had 0.44 (95%CI: 0.24, 0.80) times lower odds of CRC screening uptake than Chinese adults. Korean adults had 1.68 (95%CI: 1.17, 2.41) times higher odds of knowing the correct age to begin having mammograms compared to Chinese adults; South Asian adults had 0.66 (95%CI: 0.46, 0.94) times lower odds of knowing the correct age to begin CRC screening compared to Chinese adults. Korean adults had a 0.39 (95%CI: 0.25, 0.63) and 0.22 (95%CI: 0.13, 0.37) times lower odds of some and high cancer fatalism, respectively, compared to Chinese adults. No associations were found between cancer screening knowledge or cancer fatalism and cancer screening uptake.
Conclusions: Our study adds to the current literature on the diversity of cancer needs, beliefs, and behaviors among Asian Americans. The findings indicate the need for ethnic-specific cultural tailoring for future cancer screening interventions.

#4804 Prevalence of anal HPV infection in women attending a gynecology and colposcopy clinic: Assessing the potential impact of HPV vaccination..

A. Dominicci-Maura[1], A. P. Ortiz[2], J. Romaguera[3], F. Godoy-Vitorino[1];
[1]University of Puerto Rico - Medical Sciences Campus, San Juan, PR, [2]Comprehensive Cancer Center - University of Puerto Rico, San Juan, PR, [3]School of Medicine, University of Puerto Rico - Medical Sciences Campus, San Juan, PR

Human papillomavirus (HPV) accounts for over 80% of anal cancer cases. In the effort to prevent HPV-related cancers, the 9-valent HPV vaccine emerged as a crucial intervention, targeting HPV types 6, 11, 16, 18, 31, 33, 45, 52, and 58; the previous 4-valent (types 6,11,16,18) and 2-valent (types 16, 18). This study involved 213 women aged 21-50 attending gynecology and colonoscopy clinics in San Juan, Puerto Rico. The study assessed anal HPV prevalence and analyzed vaccination status-related differences. Anal swabs were collected for HPV testing using the ATILA AmpFire, targeting 17 HPV types. This method identified 15 high-risk HPV types (16, 18, 31, 33, 35, 39, 45, 51, 52, 53, 56, 58, 59, 66, and 68) and two low-risk HPV types (6 and 11). Prevalence of any HPV, HR-HPV, and LR-HPV, and of specific HPV types were calculated by overall and vaccination status. Differences were assessed for statistical significance ($p<0.05$) using Fisher's exact or Pearson $\chi 2$ test. The mean age of women was 36.0 ± 5.9 years. Overall, 19.7% (n=44) had received the HPV vaccine; among them, 52.2% (n=23) had received the 4-valent vaccine, 2.3% had received the 2-valent vaccine, 2.3% had received the 9-valent vaccine, and 43.2% were uncertain about their specific HPV vaccine type. The prevalence of anal HPV infection was 68.5% for any HPV, 61.5% for HR-HPV, and 15.0% for LR-HPV. The most prevalent HR-HPV types were HPV 56 (13.2%), HPV 68 (11.7%), and HPV 66 (11.2%). There were no statistically significant differences in the prevalence of any HPV, HR-HPV, and LR-HPV between vaccinated and unvaccinated women. The most common HR-HPV type among vaccinated were HPV 66 (20.5%), HPV 31 (18.2%), HPV 56 (15.9%), while the most common among unvaccinated women were HPV 56 (12.4%), HPV 68 (12.4%), and HPV 16 (12.4%). Additionally, when evaluating as a grouped variable, the HPV genotypes covered by the 4-valent, unvaccinated women had a significantly higher prevalence of these types as compared to those vaccinated (28.9% vs. 13.6%, respectively, p-value =.03). The unvaccinated women showed a lower prevalence for HPV types covered by the 9-valent vaccine compared to the vaccinated cohort (43.2% vs. 45.5%). However, this difference was not statistically significant. We found a high prevalence of anal HPV among these women, with lower prevalence of 4-valent and 2-valent HPV types among vaccinated women, evidencing the pivotal role of HPV vaccination. Future research should assess the 9-valent vaccine's long-term effectiveness against more HPV types. Funding: Research Centers in Minority Institutions (RCMI), University of Puerto Rico (NIMHD # 2U54MD007600-36), and CAPAC Research Training Program (NCI #R25CA240120).

#4805 Identifying neighborhood hot spots of HPV-associated cancers for targeted interventions of HPV vaccination uptake in underserved communities of South Florida.

M. Lee[1], S. Parrott[2], R. Kaiser[1], R. Vyas[1], D. Gabuzda[1], A. Vazquez[1], D. Flores Quetant[1], N. Elliott[1], V. Bethel[1], A. Rivera[1], B. Mahal[1], R. Balise[1], E. Franzmann[1], E. Kobetz[1];

[1]University of Miami Miller School of Medicine, Miami, FL, [2]University of Miami, Miami, FL

Background: Although the incidence of cervical cancer in the US has declined, the incidences of other HPV-associated cancers are on the rise. HPV vaccination is an important primary prevention strategy for reducing the burden of HPV-associated cancers. In South Florida (population over 6 million), the percentage of adolescents aged 13-15 years who completed the recommended HPV vaccine series is 54%, which lags significantly behind the Healthy People 2030 target of 80%. In addition, vaccination disparities exist in South Florida by races/ethnicities and sexes, with non-Hispanic black males having the lowest rate at 27%. To address HPV cancer disparities, we performed a geospatial analysis on the incidence of HPV-associated cancers by sex and races/ethnicity to identify communities in South Florida with high incidence of HPV-associated cancer to target interventions that may improve HPV-vaccine uptake via community outreach and engagement.

Methods: The average annual (2010-2019) incidence of HPV-associated cancers in women (cervical, oropharyngeal, vulva, vaginal, and anal) and men (oropharyngeal, penile, and anal) were calculated for Hispanics, Non-Hispanic Whites (NHWs) and Non-Hispanic Blacks (NHB) at the census tract level across South Florida using data from the Florida Cancer Data System (FCDS), the state incident cancer registry. Geospatial hot spot analyses were used to identify clusters of census tracts with high HPV cancer incidence by sex and race/ethnicity. Socioeconomic and cervical screening data of the hot spots were analyzed to identify other neighborhood risk conditions that may be associated with high HPV cancer risk.

Results: For Hispanics and NHBs in South Florida, census tract hot spots for male and female HPV cancers appear to overlap in low-income neighborhoods; however, hot spots for NHW males are mostly in medium to higher income areas and do not overlap with hot spots observed for NHW females, likely given that NHW females generally report higher cervical screening rates.

Conclusion: There is a positive association between male and female HPV cancer incidence in Hispanic and NHB communities of South Florida, justifying the need for increased HPV vaccination and screening programs in these neighborhoods. While increasing cervical screening rate in the hot spot neighborhoods is urgent for cervical cancer control, increasing gender-neutral HPV vaccination uptake in these communities will not only reduce the incidences of male HPV cancers but also help to accelerate cervical cancer elimination by reducing HPV infection.

#4806 The potential impact of a Von Hippel-Lindau clinical care center for patients at the University of Illinois Chicago.

N. Hippalgaonkar[1], K. Drabek[1], A. Aseem[1], T. Maga[1], L. Balay[1], V. Pan[1], P. Ganschow[2], K. Tawagi[1], N. Awati[1], N. Reizine[1];
[1]University of Illinois at Chicago, Chicago, IL, [2]University of Illinois Cancer Center, Chicago, IL

Introduction: Von Hippel-Lindau (VHL) is an inherited autosomal dominant cancer syndrome causing early-onset tumors in various organs. It poses high risks of renal cell carcinoma, hemangioblastomas, pheochromocytomas, and paragangliomas among others. VHL can be clinically diagnosed based on the Danish, international, or Dutch guidelines, or through molecular diagnosis by identifying a pathogenic variant in the VHL gene. There is now an FDA-approved HIF-2 alpha inhibitor that is effective for the treatment of VHL-related manifestations, and the identification of eligible patients is paramount to receive this benefit. In addition, the screening recommendations for VHL are extensive and result in significant burden on patients. We suspect that VHL is under-diagnosed in the clinical setting, and we further hypothesize that this burden may contribute to care gaps and disparities in access to VHL-related care.
Methods: This is a single-institution, retrospective study conducted at the University of Illinois Health and Hospitals System (UIH). We assessed the prevalence of patients with VHL-related tumors by examining ICD diagnosis codes from 2010 to 2023. Additionally, we analyzed the subset of these patients who underwent germ-line genetic testing. Furthermore, we examined our cohort of VHL patients more closely to explore the burden of VHL-related care. We examined the time to germ-line genetic and cascade testing from first clinical touchpoint at UIH, as well as the total number of clinical departments accessed at UIH. Demographics, clinical characteristics, germ-line genetic testing results, and information on clinical visits were also collected from those with a molecular or clinical diagnosis of VHL.
Results: We found 9,875 patients with at least one VHL-associated tumor. Among them, 1,379 had two or more VHL-associated tumors, with <2% undergoing germline genetic testing. We identified 10 individuals diagnosed with VHL. Of the ten patients, 30% were black, 30% were white, and 40% self-identified as other. Age of onset for VHL-related screening ranged from 10 to 37 years. All patients diagnosed with VHL underwent germ-line genetic testing, with 60% opting for cascade testing of at-risk family members. Patient care was fragmented, with on average, each VHL patient seeking care from five different UIC clinical departments (range 1-11) and receiving care from multiple separate institutions (range 1-4).
Conclusion: Our data revealed that most patients with VHL-associated tumors did not receive genetic testing, demonstrating a potential missed opportunity for early diagnosis and interventions to improve outcomes for VHL-related disease. Furthermore, our data highlights the clinical burden of VHL, and supports the potential impact of a coordinated care program for these patients.

#4807 Gaucher disease treatment reduces the progression of smoldering myeloma.

R. Shukla[1], A. Parekh[2], V. Leshchenko[1], K. Barley[1], D. Vatti[3], D. Verina[1], M. Balwani[1], S. Parekh[1];
[1]Icahn School of Medicine at Mount Sinai, New York, NY, [2]Ardsley High School, New York, NY, [3]New york university, New York, NY

Background: Gaucher disease (GD), a hereditary condition characterized by glucocerebrosidase deficiency, results in the impaired degradation of glucocerebroside (GL1) and its deacetylated form, lyso-GL1 (LGL1). This leads to the accumulation of these substrates primarily in the bone marrow (BM), liver, and spleen. Notably, individuals with GD face an increased risk of plasma cell dyscrasias (PCD) by approximately nine-fold. We present two compelling cases of the regression of smoldering multiple myeloma (SMM) following GD treatment, substantiated by biochemical evidence of lipid-reactive clonal paraproteins (PP) in both patients.

Methods: Peripheral blood samples were obtained with IRB approval from patients with concurrent SMM and GD at the Icahn School of Medicine at Mount Sinai. Utilizing C-18 beads coupled with gly-sphingosine-coated liposomes and Sphingosine-1 phosphate bead liposome-based pulldown, we established the binding of glycolipids to serum PP.

Results: In a 66-year-old male, hepatosplenomegaly and pancytopenia revealed compound heterozygous N370S/V394L mutations and reduced β-glucosidase activity, confirming Type 1 GD. Laboratory findings included substantial pancytopenia (WBC 2.5 k/μL, Hgb 12.1 g/dL, platelet 44 k/μL) and myeloma markers (M spike 1.58 g/dL, monoclonal IgA λ). A BM biopsy indicated 30% λ-restricted plasma cells. PET-CT showed hepatosplenomegaly without FDG avid lytic lesions, consistent with SMM. Imiglucerase enzyme therapy improved GD biomarkers, decreased hepatosplenomegaly, and blood count improvement (WBC 4.7 k/μL, Hgb 13.6 g/dL, platelet 66 k/μL). Notably, myeloma burden significantly reduced (M-spike 0.94 g/dL, IgA 1373 g/dL and free lambda 26.1 mg/L). Similarly, a 41-year-old female with mild fatigue, Hgb levels of 10.9 g/dL, a platelet count of 169 k/μL, M spike of 0.9 g/dL, IgG κappa on immunofixation, and IgG levels at 1730 mg/dL, indicating SMM. GBA analysis showed homozygous N370S mutation and reduced beta-glucosidase activity consistent with Type 1 GD. Substrate reduction therapy with eliglustat alleviated fatigue, reduced GD biomarkers, normalized cytopenias, and gradually decreased myeloma markers. Laboratory results indicated an M spike of 0.5 g/dL, IgG levels at 1295 mg/dL, and free kappa at 31.3 mg/L. To explore the interaction between clonal immunoglobulins (Ig) and lyso-lipids, we utilized Gly-sphingolipids (see methods) and demonstrated a robust interaction with IgA (patient 1) and IgG (patient 2) paraprotein by western blotting.

Conclusion: Our experimental findings confirm specific clonal Ig binding in SMM and GD patients and demonstrate potent and timely benefits from addressing GD in managing SMM patients. This holds significance amid ongoing clinical trials exploring aggressive interventions for SMM, including bispecific and CAR-T therapies.

#4808 Small intestinal leiomyosarcoma in a young adult.

A. A. Guo, B. H. Bentley, A. L. Ellington, H. Lu, W. C. Lippert;
Wake Forest University School of Medicine, Winston Salem, NC

Objectives: • Outline the epidemiology of leiomyosarcoma•Identify the immunohistochemistry of a leiomyosarcoma

Introduction: Primary small intestinal malignancies are rare malignancies as compared with other malignancies of the gastrointestinal tract. Here, we present a case of a jejunal leiomyosarcoma in a young adult.

Case Presentation: A 23-year-old Caucasian male with GERD presented with five months of abdominal pain, intermittent nausea with non-bloody emesis, and a 20-pound weight loss. Presenting vital signs were within normal limits. Physical exam revealed conjunctival pallor with epigastric tenderness to palpation. Serology demonstrated iron deficiency anemia, hemoccult positive stool, negative CEA, CA19-9, and AFP tumor markers. HIV antigen antibody and EBV-PCR were non-reactive. CT of the abdomen and pelvis revealed markedly thickened heterogenous jejunal loop in the left hemiabdomen with associated mesenteric adenopathy and small volume pelvic ascites. EGD with push enteroscopy revealed a single, malignant appearing and ulcerated mass in the proximal jejunum. PET-CT showed a hypermetabolic, multilobulated, ill-defined mass involving multiple loops of jejunum. He underwent exploratory laparotomy with resection of a proximal jejunal mass (10x8 x7 cm), mesenteric lymphadenectomy, and a jejunojejunostomy creation. Pathology demonstrated leiomyosarcoma (pT2aN0MoG3), and he was initiated on cyclophosphamide and doxorubicin.

Discussion: Primary small intestinal malignancies are rare malignancies with an incidence of less than 5% of all GI malignancies. 56 cases of GI leiomyosarcoma in adults were identified between 2000-2012 with a peak incidence between 55-59 years of age (Aggarrwal 2012). Leiomyosarcomas are soft tissue sarcomas arising from bones, tendons, blood vessels, or muscles with a spectrum of disease ranging from low-grade cutaneous lesions to aggressive lesions of internal organs with significant potential for metastasis (Pipe 2002). Diagnosis is based on immunohistochemical positivity for SMA, desmin, and h-caldesmon, and negativity for CD117, CD34, and DOG1.1, notably lacking *KIT* and *PDGFRA* mutations (Aggarwal 2012). Treatment involves surgical resection and a cost benefit analysis of adjuvant chemotherapy with (Reynolds, 2014). This case of a 23 year old, without significant risk factors, diagnosed with a jejunal leiomyosarcoma presents as one of the youngest cases ever to be reported and emphasizes the importance of recognizing the cancer in a broader range of the adult population.

POPULATION SCIENCES: Cancer Disparities 2: Survivorship Research Addressing Cancer Disparities
Poster Session

#4812 Evaluating racial and ethnic differences in advanced-stage laryngeal cancer treatment and outcomes in Florida: Unmasking the inequities.
C. J. Washington, C. Lattimore, D. Braithwaite, K. Fredenburg, S. Karanth;
University of Florida, Gainesville, FL

Purpose: To evaluate the association between race/ethnicity, treatment, and mortality among individuals with advanced-stage laryngeal cancer in Florida.
Methods: We obtained data from the Florida Cancer Data System (FCDS) on non-Hispanic (NH)-White (the reference group), Hispanic, and NH-Black patients with advanced-stage (regional and distant) laryngeal cancer from 2009 to 2020. Sociodemographic factors were obtained from FCDS (age, marital status, and insurance) and the United States Census at the county level (education, household income, and rurality). Treatment strategies included chemoradiation, surgery followed by chemoradiation, chemotherapy, radiation, surgery, and surgery followed by chemotherapy. The primary outcome was overall mortality. Multivariable Cox proportional hazard models were used to calculate hazard ratios (HR) and 95% confidence intervals (95% CI) and to examine the association of race/ethnicity with treatment and survival, while adjusting for sociodemographic factors.
Results: There were 4,522 participants with advanced-stage laryngeal cancer (57.9% <65 years, 79.5% male, 75.4% NH-White, 13.1% Hispanic, and 11.5% NH-Black) included in the analysis. Compared to NH-White patients, NH-Black patients were less likely to be married, have private insurance, and live in an urban county. Moreover, NH-Black individuals were less likely to receive chemoradiation alone and were more likely to receive surgery followed by chemoradiation. Government insurance was highly associated with chemoradiation receipt. In age-adjusted models, NH-Black patients with advanced-stage laryngeal cancer had a higher risk of death compared to NH-White patients (HR: 1.19; 95% CI: 1.06, 1.32), while Hispanic patients had a lower risk of death compared to NH-White patients (HR: 0.80; 95% CI: 0.71, 0.89). After adjusting for sociodemographic factors, there was no statistically significant difference in overall mortality in NH-Black patients compared to NH-White patients (HR: 1.07; 95% CI: 0.96, 1.20). However, among individuals who received chemoradiation, NH-Black patients had a higher risk of mortality, even after adjusting for sociodemographic factors, compared to NH-White patients (HR: 1.27; 95% CI: 1.04, 1.55).
Conclusions: Among patients with advanced-stage laryngeal cancer in Florida, NH-Black patients experienced a higher risk of overall mortality compared to other racial and ethnic groups, but this discrepancy was primarily among those who received chemoradiation, even after accounting for sociodemographic factors. This study emphasizes the urgency of expanding laryngeal cancer care access for NH-Black individuals and investigating possible biological variations in their response to chemoradiation and subsequent survival outcomes.

#4813 Demographic, treatment, and survival patterns in Hispanic vs. non-Hispanic patients with lymphoplasmacytic lymphoma/Waldenstrom macroglobulinemia: A national retrospective analysis from the National Cancer Database.

Maria Elena Fierro[1], Heidi Latiolais[2], Qianquian Liu[3], Joel Michalek[4], Adolfo Enrique Diaz Duque[5]

[1]Internal Medicine, University of Texas Health Science Center at San Antonio, San Antonio, TX,[2]Hospital Medicine, University of Texas Health Science Center at San Antonio, San Antonio, TX,[3]Epidemiology and Biostatistics, University of Texas Health Science Center at San Antonio, San Antonio, TX,[4]University of Texas Health Science Center at San Antonio, San Antonio, TX,[5]Hematology-Oncology, Mays Cancer Center UT Health San Antonio MD Anderson, San Antonio, TX

Background: Lymphoplasmacytic lymphoma (LPL) is a rare type of non-Hodgkin B cell lymphoma. Waldenstrom macroglobulinemia (WM) is a form of LPL that presents with overproduction of IgM monoclonal protein. The understanding and treatment of LPL/WM has improved. However, few studies analyze LPL/WM in Hispanic (HI) patients specifically. This study aims to evaluate demographics, treatment, and survival patterns in HI vs. Non-Hispanic (NH) patients with LPL/WM.

Methods: Data were analyzed on LPL/WM patients in the US reported to the NCDB from 2004-2019. Demographic and treatment characteristics were compared between ethnic groups. Kaplan-Meier and Cox regression analyses were used to compare overall survival (OS) between HI and NH. Multivariate analysis and propensity score matching were performed with adjustment for age, stage, co-morbidity score, insurance status, type of facility and great circle distance (GCD).

Results: 17,915 patients were identified. 92% were NH, 3% were HI. Most patients were male in both NH and HI ($p = 0.120$). The median age at diagnosis for HI was 68 vs. 71 for NH ($p < 0.001$). Most HI and NH were white (87% HI, 91% NH $p < 0.001$). More HI were uninsured (8% HI, 1% NH $p < 0.001$) and were less likely to have government sponsored insurance (60% HI, 66% NH $p < 0.001$). Regarding income, most NH (42%) were in the $63,000+ bracket while most HI were in the $48,000-$62,999 bracket. Regarding education, reported in percent quartiles with no high school degree, most HI (41%) were in the > 21% bracket while most NH (35%) were in the 7-12.9% bracket ($p < 0.001$). Most HI (43%) were treated at academic/research programs; most NH were treated at comprehensive community cancer programs (38.4%, $p < 0.001$). Regarding comorbidities score, 9% of HI scored ≥ 2 vs 8% of NH (p 0.029). Regarding GCD, the median distance in miles between the patient's residence and the hospital that reported the case, HI lived at a median of 6.7 miles vs 9 miles for NH ($p < 0.001$). Regarding treatment, 68% of HI were given treatment vs. 62% of NH ($p < 0.001$). There was no difference in mortality between HI vs. NH (30 day mortality $p = 0.322$; 90 day mortality $p = 0.217$). On survival analysis, the survival probability at 2, 5 and 10 years of HI vs NH were 81% vs 83%, 69% vs 68%, and 52% vs 46%, respectively. The median survival time (MS) was 10.6 years for HI vs 9 years for NH. There was no OS difference between HI vs. NH ($p = 0.47$). On multivariate analysis, there were no independent variables associated with better or worse OS. The propensity matched analysis showed no MS difference between HI vs NH (8.96 y vs. 8.74 y).

Conclusion: We identified ethnic differences in age, race, insurance, education, income, location of treatment, GCD, staging, and treatment patterns. However, there was no statistically significant ethnic difference in MS or OS.

#4814 Pediatric radiation treatment adherence in LMIC.

A. Joseph[1], A. Akinsete[2], U. Fakile[3], C. Agbakwuru[1], L. Keno[4], O. O. Adisa[3], A. Oladipo[1], O. Fagbemide[1], M. Habeebu[1], W. Ngwa[5];
[1]NSIA - LUTH Cancer Center, Lagos University Teaching Hospital, Lagos, Nigeria, [2]University of Lagos, Lagos, Nigeria, [3]Lagos University Teaching Hospital, Lagos, Nigeria, [4]Johns Hopkins University School of Medicine and The University of Scranton, Baltimore, MD, [5]Johns Hopkins University School of Medicine, Baltimore, MD

Background: Radiation therapy plays a significant role in the treatment of pediatric cancer. However, there have been documented challenges and difficulties encountered by patients while accessing care for cancer and it has been postulated that travel distance contributes to treatment breaks and abandonment.
Objectives: The objective of this study was to determine the prevalence of treatment breaks, assess the travel burden of patients receiving radiotherapy for pediatric cancers at a high-volume center in Nigeria and to determine the impact of travel burden on treatment breaks and treatment completion.
Materials and Methods: A retrospective cross-sectional study design was utilized. Data was extracted from the electronic medical records of all pediatric patients referred to the center for radiation therapy between June 2019 and June 2023. Data was analyzed using Microsoft Excel and the results were presented in descriptive statistics. Association between data were analyzed using chi-square test with the level of significance (p) set at <0.05. **Results:** A total of 210 pediatric cancer patients were enrolled with an average age of 10.9 years. Children aged 0-14 years accounted for 69.05% while 30.95% were between the age of 15 and 19 years. Brain tumors were the most predominant diagnosis, representing 28.10% of cases. Treatment intent was predominantly radical or curative (81.69%). 61.43% (129) of the patient population came from the within the state with an average travel distance of 19.3 km. Of all the 210 patients, 44.29% of patients did not commence RT. The reasons for this were mostly financial constraints but were not explored in this study. Of those who did commence RT, 54.70% had breaks, and 45.30% did not have breaks. Also, 75.21% of patients completed their treatment; however, 24.79% were unable to complete their treatment. Travel distances varied, with the average distance to the treatment center being 165.3 km and the median at 28.5 km. The study categorized travel distance into quartiles: short (0-16 km), medium (>16 km to 28.5 km), long (>28.5 km to 302 km), and very long (>302 km to 1387 km). Chi-square test did not reveal a significant association between travel distance and treatment completion (p=0.57), nor between travel distance and treatment breaks (p=0.20).
Conclusion: These findings highlight the complex interplay of demographic factors, disease profiles, and socioeconomic barriers affecting treatment continuity and completion among pediatric oncology patients in a resource-limited setting. These findings suggest that in this low - resource context, other variables such as socioeconomic status and financial barriers may play a more pivotal role than travel distance in treatment commencement, adherence and completion. As such, more detailed investigation of the obstacles through a comprehensive and targeted strategy could lead to more favorable outcomes in pediatric cancer radiation therapy adherence.

#4815 Time to lung cancer treatment in West Virginia and patient survival.

A. R. Lumadue[1], **S. O. Nduaguba**[2];
[1]West Virginia University School of Pharmacy, Morgantown, WV, [2]Mary Babb Randolph Cancer Center and School of Pharmacy at West Virginia University, Morgantown, WV

Background: Patients from rural areas typically have poor access to healthcare. Studies have shown varying results on the relationship between time to lung cancer treatment and patient survival. We aimed to examine the association of rurality with timely receipt of lung cancer treatment and survival in West Virginia (WV).
Methods: A retrospective study was conducted using WV Cancer Registry data to identify persons diagnosed with NSCLC in WV between 1993 and 2021 who received treatment (surgery, radiation, systemic therapy, other). Participants were classified by rurality (rural vs non-rural), and time to treatment from diagnosis was dichotomized as early treatment (<35 days) or delayed treatment (≥35 days). Descriptive statistics and survival analysis (with univariate and multivariate Cox regression controlling for age, sex, race/ethnicity, marital status, Charlson comorbidity index, cancer stage, and treatment type) were used to address study objectives.
Results: Of 10,463 participants, 678 (6.5%) were rural residents. The majority were male (58.1%), married or partnered (59.9%), and non-Hispanic white (97.5%). 61% received early treatment. 45%, 38%, and 16% received systemic therapy, surgery, and radiation, respectively. There were significantly more non-Hispanic white (99.6% vs 97.3%, p<0.004) patients residing in rural areas compared to non-rural areas, and fewer rural residents were diagnosed at stages 1 (29.4% vs 34.3%) or 2 (10.0% vs 11.6%) (p<0.5). Rurality was not associated with time to treatment but was associated with 9% increase in hazard of death (HR=1.09, 95% CI=1.00-1.18, p<0.05). Significant covariates associated with increasing hazard of treatment included being male (HR=1.08, 95% CI=1.04-1.13, p<0.0001) and cancer stage (HR range=1.19-2.38, while being Black and receiving surgery (0.43, 0.30-0.62, p<.0001), radiation (0.48, 0.33-0.68, p<.0001), or systemic therapy (0.33,0.23-0.47, p<.0001) (compared to other treatment) were each associated with reduced hazard of treatment. Significant covariates associated with hazard of death include increasing age (HR=1.01, 95% CI= 1.01-1.02, p<.0001), increasing CCI (HR=1.07, 95% CI=1.05-1.09, p<.0001), being male (HR=1.21, 95% CI=1.16-1.26, p<.0001), increasing cancer stage (HR range=1.58-4.79) while being married (HR=0.92, 95% CI=0.88-0.96, p<.001), receiving surgery (HR=0.16, 95% CI=1.11-0.22, p<.0001), radiation (HR=0.34, 95% CI=0.24-0.49, p<.0001), or systemic treatment (HR=0.17, 95% CI=0.12-0.24, p<.0001), and delayed treatment (HR=0.82, 95% CI=0.78-0.85, p<.0001) were each associated reduced hazard of death.
Conclusion: Rurality affects lung cancer outcomes in WV increasing risk of death for NSCLC patients by 9%.

#4816 Racial disparities in adjunctive supportive care medication use in pancreatic cancer patients.

Olga M. Trejos Kweyete[1], Yi Guo[2], Sherise C. Rogers[2], Lisa Scarton[2], David L. DeRemer[2], Chardae L. Whitner[3], Diana J. Wilkie[2], John M. Allen[1]

[1]University of Florida, Orlando, FL,[2]University of Florida, Gainesville, FL,[3]University of Florida, Jacksonville, FL

Background: Beyond its well-known lethality, pancreatic cancer (PC) is associated with a wide variety of physical and psychological complications. These complications collectively lead to an increase in symptom burden experienced by patients with PC, as compared to other cancer types, leading to lower health-related quality of life (HRQoL) and worsened clinical outcomes. Reducing symptom burden is often achieved through the use of supportive care medications (SCM). Racial disparities have been described in the use of pain and psychiatric medications but limited research has explored potential disparities in access to and utilization of other SCM among diverse racial and ethnic groups. The goal of this study was to illustrate the presence of racial/ethnic disparities in the treatment patterns of supportive care medications in end-of-life care of PC patients

Methods: We used data from the Surveillance, Epidemiology, and End Results (SEER)-Medicare-linked database from 2005 to 2017. Participants were identified using ICD9 and ICD10 diagnostic codes. Patients diagnosed with PC and have died in 2005-2007 with more than 1 year of Medicare enrollment before death were included. Logistic regression models to assess the association between use of supportive care medications and race, adjusting for covariates (sex, race, age, marital status, education, income, residence, CCI, year of diagnosis of PC, cancer stage).

Results: After the application of the inclusion/exclusion criteria, 74,309 patients were included in the final analysis (White: 72.53%, Black 11.01%, Hispanic 9.60%, Asian/Pacific Islander 6.58%) Racial and ethnic disparities in the use of multiple SCM drug classes were identified. The results are summarized in Table 1.

Conclusion: Disparities in the use of SCM were found in patients with PC. Minorities had significantly less use of sleep aids and headache aids, and increased use of cognitive aids and appetite stimulants. AAs also had lower uses of anti-emetics.

	AA		**Hispanic**		**Asian**	
SCM Drug Class	**aOR**	**95% CI**	**aOR**	**95% CI**	**aOR**	**95% CI**
Anti-emetics	*0.77*	*(0.73, 0.81)*	0.98	(0.93, 1.03)	1.01	(0.95, 1.08)
Appetite stimulants	*1.06*	*(1.01, 1.11)*	1.01	(0.96, 1.06)	*1.28*	*(1.20, 1.36)*
Cognitive aids	*1.38*	*(1.25, 1.53)*	1.04	(0.93, 1.17)	1.11	(0.97, 1.26)
Headache aids	*0.68*	*(0.63, 0.74)*	*0.81*	*(0.74, 0.87)*	*0.85*	*(0.77, 0.93)*
Sleep aids	*0.71*	*(0.67, 0.75)*	*0.87*	*(0.82, 0.92)*	*0.87*	*(0.81, 0.93)*

#4817 Patterns and predictors of opioid dispensing among older cancer patients from 2008 to 2015.

Y. Chen[1], Y.-E. Shin[2], S. Spillane[1], M. Shiels[1], A. Coghill[3], L. Enewold[1], R. Pfeiffer[1], N. Freedman[1];

[1]National Cancer Institute, Rockville, MD, [2]Seoul National University, Seoul, Korea, Republic of, [3]Moffitt Cancer Center, Tampa, FL

Introduction: Understanding factors associated with opioid dispensing in cancer patients is important for developing tailored guidelines and ensuring equitable access to pain management. We examined patterns and predictors of opioid dispensing among older cancer patients from 2008 to 2015.

Methods: We analyzed data from the Surveillance, Epidemiology, and End Results (SEER) database linked to Medicare claims. We included the most common cancer types among patients aged 66-95 years. Opioids dispensed within 30 days before and 120 days after cancer diagnosis were assessed. We used logistic regression models to examine trends, adjusted odds ratios (aORs), and 95% confidence intervals (CIs) for opioid dispensing, considering patient demographics, geography, cancer stage, comorbidities, and treatment options.

Results: A total of 211,759 cancer patients aged 66-95 years were included in the study. Moreover, opioid dispensing increased from 16.4% within 30 days pre-diagnosis to 59.8% within 120 days post-diagnosis. Variations were observed across cancer types, with the largest increase among female breast cancer patients (74.9%, n=44,544). We observed significant increases over calendar time in opioid dispensing within120 days post-diagnosis in both women (p=0.02) and men (p=0.001). For all cancers combined, non-Hispanic Black men had a significantly lower likelihood of receiving opioids during the 120 days post-diagnosis (aOR=0.9, 95% CI=0.8-0.9) compared to non-Hispanic White men. Factors such as pre-diagnosis opioid dispensing, age, geography, cancer stage, comorbidities, and type of cancer treatment were associated with opioid dispensing during the 120 days post-diagnosis. Surgery had the strongest association, with men undergoing surgery being 4.4 times more likely to receive opioids within 120 days post-diagnosis (aOR=4.4, 95% CI=4.2-4.6), while women had an odds ratio of 2.7 (95% CI=2.6-2.8). Chemotherapy and radiotherapy were also positively associated with opioid dispensing, though the associations were less pronounced. Moreover, compared to urinary bladder cancer, patients with kidney cancer (women, aOR=1.6, 95% CI=1.5-1.8; men, aOR=1.7, 95% CI=1.5-1.8), lung cancer (women, aOR=1.4, 95% CI=1.3-1.5; men, aOR=1.5, 95% CI=1.4-1.6), and female breast cancer (aOR=1.8, 95% CI=1.6-1.9) were more likely to receive opioids within the 120 days post-diagnosis.

Conclusion: This population-based study reveals significant variations in opioid dispensing among cancer patients over age 65 across cancer types and demographic and clinical factors. Further research is needed to address disparities and optimize opioid dispensing in older cancer patients, ensuring tailored guidelines and improving patient care.

#4818 Cancer disparities in Chile: Unveiling the impact of educational disparities and regional variances on mortality rates.

Paz Cook[1], Fabio Paredes[2], Jorge Jimenez de la Jara[3]

[1]Center for Cancer Prevention and Control (CECAN), Santiago, Chile,[2]Estadisticas, Pontificia Universidad Catolica de Chile, Santiago, Chile,[3]Salud Publica, Pontificia Universidad Catolica de Chile, Santiago, Chile

Differences in education not only influence our access to good-quality and timely healthcare but also impact our ability to make healthy decisions, access nutritious food, and inhabit healthy and safe physical and psychological environments. Consequently, these factors have contributed to an increase in cancer incidence and mortality among individuals with lower levels of education. To assess the mortality rate based on education, we utilized census data and the national mortality register, comparing the cancer mortality rate between those with more than 12 years of education and those with less than 8 years. We employed a Poisson regression model, with the number of deceased individuals as the dependent variable and age, along with gender, region of residence, and education level as covariates. The natural logarithm of the population served as an offset. The exponential of the estimated betas in this regression represents the Relative Index of Inequality (RII), comparing individuals with a low educational level to those with a high educational level. We conducted the analysis using SPSS version 17.0 and SAS version 9.4, considering values with p-values less than or equal to 0.05 as significant, with a confidence interval of 95%. Our findings indicate that two cancer sites are particularly affected by these educational differences, gallbladder (RII(95%CI): 5.43 (4.0-7.5)) and gastric (RII(95%CI): 4.09 (3.5-4.8)) with additional disparities when comparing by gender (RII gallbladder in women (95%CI): 7.06 (5.0-10.9)). Interestingly, even though Chile is a relatively small country, there are significant variations of mortality by geographical region (RII(95%CI): 1.3 (1.1-1.5) to 3.1 (2.3-4.0)), in terms of magnitude and cancer sites, suggesting the influence of environmental factors. The results of this study should serve as a basis for decentralization and the development of a cancer policy that considers territorial differences in resource allocation and plans specific screening and early detection strategies tailored to the epidemiologic and sociodemographic profile. We also conducted a mortality analysis comparing education levels across age intervals. Our findings reveal that, up to the age of 60, mortality is significantly higher among individuals with less than 8 years of schooling. However, beyond the age of 60, the group with higher mortality comprises individuals with 9-12 years of education. This suggests that they may be more capable of affording health services and accessing screening and diagnosis compared to the less educated group but are still diagnosed at later stages when curative treatment is not feasible. In addition, this group has the highest tobacco consumption in the country.

#4820 Comparison of Black and White patients in treatment for papillary thyroid cancer in an equal access health system.

Y. L. Eaglehouse, S. Darmon, C. D. Shriver, K. Zhu;
Murtha Cancer Center Research Program, Uniformed Services University of the Health Sciences, Bethesda, MD

Introduction: In the U.S., Black patients with papillary thyroid cancer (PTC) are less likely to receive treatment than non-Hispanic White patients. Access to care and insurance status may be related to these disparities. We aimed to compare Black and White patients in receipt of cancer care for PTC in the equal access Military Health System.

Materials and Methods: We used the MilCanEpi database to identify a cohort of men and women aged 18 or older who were diagnosed with PTC between January 1, 1998 and December 31, 2014. Patients were assessed for treatment by surgery (e.g., lobectomy, thyroidectomy), adjuvant radioactive iodine (RAI), or active surveillance. Treatment appropriate for risk status (low-risk or high-risk) was compared between non-Hispanic White and Black patients using multivariable logistic regression and expressed as adjusted odds ratios (aOR) with 95% confidence intervals (CIs).

Results: Among 3,511 patients with PTC, 65.0% White and 65.5% Black received surgical treatment (aOR 0.97, 95% CI 0.80-1.18 for Black vs. White). For patients with low-risk PTC, overall receipt of either surgery or active surveillance (aOR 0.86, 95% CI 0.67-1.10 for Black vs. White) was similar between races. For patients with high-risk PTC, overall receipt of surgery (aOR 1.19, 95% CI 0.71-2.01) or adjuvant RAI (aOR 1.44, 95% CI 0.60-3.44) was similar for Black compared to White patients.

Conclusions: In an equal access health system, there were no overall racial differences in receipt of surgical treatment for PTC. Further, in analysis by risk status, there were no significant racial differences in receipt of active surveillance for low-risk PTC nor receipt of adjuvant RAI for high-risk PTC. This suggests the role of access to care in reducing racial disparities in treatment for PTC observed in the general U.S. population.

Funding and Acknowledgement: The authors thank the Joint Pathology Center (JPC) for providing the DoD cancer registry data and the Defense Health Agency (DHA) for providing the MHS data repository (MDR) data. This project was supported by the Murtha Cancer Center Research Program (MCCRP) of the Department of Surgery, Uniformed Services University of the Health Sciences (USUHS) under the auspices of the Henry M. Jackson Foundation for the Advancement of Military Medicine (HJF, Inc.), grant numbers HHU0001-16-2-0014 and HU0001-18-2-0032 awarded to C.S.

#4821 Lung cancer survival disparities by ethnicity in Guam, 2001-2020.

C. Aurienne, L. J. Dulana, R. Teria, G. Badowski;
University of Guam, Mangilao, GU

Background: Lung cancer is the leading cause of cancer-related deaths in Guam, with a significantly higher mortality rate compared to the United States (46.9 vs 40.2 per 100,000), despite a lower incidence rate (50.9 vs 52.6 respectively, for the years 2013-2017). There are significant ethnic disparities in lung cancer incidence and mortality rates, with CHamoru (indigenous people) and Micronesian (immigrants from other Micronesian Islands) populations being disproportionately affected compared to other ethnic groups. This study aims to assess lung cancer survival rates in Guam and explore how demographic and other factors impact these rates.

Methods: This study included 1171 patients diagnosed with invasive lung cancer and reported to the Guam Cancer Registry from 2001-2020. Five-year and 10-year survival rates were calculated using the Kaplan-Meier method and were compared using the log-rank test across different ethnic groups: CHamoru (N = 613), Filipino (N = 245), Asian (N = 74), Micronesian (N = 110), and Caucasian (N = 82). The Cox proportional hazards regression was used to investigate the effects of sex, age, year of diagnosis, ethnicity, lung cancer staging, and cancer treatment status on the risk of all-cause mortality.

Results: Mean age at diagnosis was 65.75 years. Of the cases, only 10.8% were identified at an early stage, 43.1% at a late stage, and 46.0% unstaged. Significant differences in the 5-year and 10-year survival rates were found across ethnic groups. CHamoru had the lowest 5-year (15.6%) and 10-year survival rates (13.2%) followed by Micronesian (18.7% and 17.2%, respectively). All-cause mortality was higher among CHamoru (HR = 1.54, 95% CI: 1.28, 1.85) and Micronesian (HR=1.51, 95% CI: 1.15, 1.98) compared with Filipino after adjusting for age, sex, year of diagnosis, staging, and cancer treatment status. There were no statistically significant differences in all-cause mortality between Asian and Caucasian patients and Filipino patients. Cancer staging also indicated a significantly higher hazard rate for late-stage patients (HR = 1.78, 95% CI: 1.41, 2.25) and un-staged patients (HR = 1.51, 95% CI: 1.18, 1.94) compared to early-stage patients. Additionally, patients who did not receive any treatment (HR = 1.46, 95% CI: 1.22-1.74) and those with unknown treatment status (HR = 1.40, 95% CI: 1.17-1.68) experienced higher hazard rates than those who received at least one form of treatment.

Conclusion: The predominance of late-stage or unstaged diagnoses in this study highlights a significant gap in early lung cancer detection in Guam. Survival rates for the CHamoru and Micronesian populations are notably lower than those observed in the U.S. These findings underscore the critical need for expanded lung cancer screening initiatives in Guam to facilitate earlier diagnosis and potentially improve survival outcomes.

Acknowledgement: This study was supported by the PIPCHE/U54 Grant (U54CA143728).

#4822 Disparities in receiving non-surgical therapy impact outcomes in non-metastatic gastric cancer in Louisiana.

C. D. Hartupee, K. Maupin, D. M. Danos, O. Moaven;
Louisiana State University Health Sciences Center, New Orleans, LA

Background: Given the history of evolving medical therapies and advancements in cancer treatments over the last decades, resectable gastric cancer has presented multiple strategies for care. Previous literature indicates historically decreased use of multimodal therapies in minority populations. This study aims to evaluate Louisiana patient populations for rates of definitive treatment, inequities in access to care, and evaluating its impact on the outcomes of minorities and underserved population.

Methods: Patients with non-metastatic primary invasive gastric cancer, with T2-4 or any T status with positive lymph nodes, were identified in the Louisiana Tumor Registry using ICD-O codes and AJCC staging system. Receipt of non-surgical therapy was modeled using logistic regression. Overall survival (OS) was modeled using a Cox proportional hazards model.

Results: The study included 561 patients, of which 37.6% (n=211) did not receive surgical treatment and 16.2% (n=91) did not receive non-surgical therapy. A subset of the cohort received no definitive treatment, (6.8%, n=38). In a demographic only multivariable model, adjusting for age, sex, and race, age 70 and over [OR (95%CI) =0.18 (0.08-0.42), p<0.001] and female sex [OR (95%CI) =0.48 (0.28-0.85), p=0.011] was associated with decreased rates of non-surgical therapy. Black [OR (95%CI) = 0.54 (0.31-0.93), p=0.027] and Hispanic [OR (95%CI) = 0.38 (0.13-1.08), p=0.070] race was associated with decreased receipt of non-surgical therapies. However, after adjusting for domestic partner, insurance status, rurality, area poverty, and surgery status, racial disparities were no longer significant compared to whites: Black [OR (95% CI) = 0.59 (0.33-1.06), p=0.075]; Hispanic [OR (95% CI) = 0.52 (0.17-1.66), p=0.272]. In multivariable analyses, receipt of surgery [HR (95% CI) = 0.3 (0.23 - 0.38), p<0.001) and any non-surgical therapy [HR (95% CI) = 0.43 (0.31 - 0.60), p<0.001) were associated with increased overall survival.

Conclusion: A significant number of patients did not receive all modalities of the multidisciplinary treatment that is recommended for patients with non-metastatic gastric adenocarcinoma. Black patients and females are less likely to receive non-surgical modalities for gastric cancer in Louisiana, which is, at least, partially driven by socioeconomic determinants. Identifying patients with these risk factors is a crucial step in allocating resources to increase access the care and improve outcomes.

#4823 Survival outcomes similar in T-cell/histiocyte-rich large B-cell lymphoma between Hispanics and non-Hispanics within the United States.

I. Mines, D. Urueta-Portillo, Q. Liu, J. Michalek, A. E. Diaz Duque;
The University of Texas Health Science Center At San Antonio, San Antonio, TX

Background: T-cell/histiocyte-rich large B-cell lymphoma (THRLBCL) is a rare variant of large B-cell lymphoma with features that overlap with Nodular lymphocyte-predominate Hodgkin lymphoma (NLPHL). (**Blood** *PMID: 32871584*, **PLoS One** *PMID: 24244368*,**Haematologica** *PMID: 20207840*). Unlike NLPHL, which has a good prognosis. THRLBCL's prognosis is worse (**Leuk Lymphoma** *PMID: 31287335*). Given its rarity and difficulty to diagnose, limited studies explore prognostic factors for it. This study aims to explore clinical, demographic, and survival outcomes differ in Hispanic (HI) versus non-Hispanic (NH) patients with THRLBCL in the United States (US).

Methods: Data were analyzed on THRLBCL patients in the US and reported to the National Cancer Database (NCDB) between 2004 and 2019. Demographic and treatment characteristics were compared between ethnic groups. Kaplan-Meier and Cox regression analyses compared OS between HI and NH. Multivariate analysis and propensity score matching was performed with adjustment for age, stage, co-morbidity score, insurance status, type of facility, and great circle distance.

Results: Of 1252 THRLBCL patients, 7% were HI and 93% NH. 67% of HI were male, compared to 68% of NHHI pts were younger at diagnosis 55 vs 57 (p=0.471); the majority of HI and NH were <65, 64% and 66% respectively (p=0.574)Most of HI and NH were white (88% vs 74%). When examining stage, most of HI and NH were stage (IV) (50% vs 57%) (p=0.600)Regarding insurance type, Government-sponsored was the most prevalent in HI (52%), while private insurance was most prevalent for NH (51%) (p=0.001). The most non-Insured group was HI (11% vs 3%).Regarding Census Median Income (2008-2012), the most prevalent bracket (39.5%) for HI was $48,000 - $62,999, and for NH (31%) $>63,000. Charlson-Deyo Score (comorbidities score), HI had a 10% =/> 2 score, vs NH 7%. Regarding treatment facility type Academic/Research Programs were the most prevalent for HI (44%) and NH (38%).The median distance in miles between the patient's residence and the hospital that reported the case (Great Circle Distance), HI lived at a median of 10 miles, vs NH at a median of 11 miles. On survival analysis, the survival probability at 2, 5, and 10 years of HI vs NH were 83% vs 83%, 77% vs 75%, and 69% vs 62%. The median survival time (MS) was not reached for HI or NH. There was no overall survival difference (OS) between HI/NH (p=0.8). Independently, on multivariate analysis, ethnicity was not associated with worse OS (HR 1.2, CI 0.67-2.17, p=0.54).

Conclusion: The MS and OS between HI and NH with THRLBCL within the US were similar. However, due to the rarity of THRLBCL, the size of both populations was small, which reduces the confidence that there are no
differences in the outcomes of these two populations. Because of this, more data is needed to evaluate further the clinical and socioeconomic factors that play a role in the survival outcomes of THRLBCL.

#4824 Multi-level intervention to increase minority cancer patient enrollment to clinical treatment trials- Study design considerations and baseline characteristics from the ACTWONDER2S Study.

D. E. Rollison[1], R. P. Amorrortu[1], L. N. Fuzzell[1], M. A. Garcia[1], E. S. Tapia-Kwan[1], Y. Zhao[1], S. A. Eschrich[1], B. R. Gore[1], B. S. Mittman[2], N. B. Stanley[1], S. T. Vadaparampil[1];

[1]Moffitt Cancer Center, Tampa, FL, [2]Kaiser Permanente, Tampa, FL

Introduction: Black/African American (AA) and Hispanic cancer patients are underrepresented in cancer clinical trials (CCTs). Disparities stem from multiple factors, thus, comprehensive, multi-level interventions (MLI) are needed. Presented here is a conceptual framework for selecting the appropriate study design for MLIs using ACTWONDER[2]S, a multi-level intervention (MLI) aimed to increase Black/AA and Hispanic patient participation into CCTs, as an illustrative example. Baseline characteristics of the ACTWONDER[2]S target populations are also provided.

Methods: ACTWONDER[2]S integrates community health educator and digital tools into an MLI targeting community residents and physicians in the Moffitt Cancer Center (MCC) catchment area, as well as MCC patients, physicians and CCT coordinators. A literature review of the relative strengths and weakness of 5 candidate designs for MLIs was conducted, and a cluster stratified randomized design was selected. Geospatial analytics were used to identify clusters of census tracts ("priority zones") with high Black/AA and Hispanic populations for intervention deployment. Baseline characteristics of the priority zones were described using US Census data and other sources.

Results: 14 priority zones were identified, which were matched on population characteristics and randomized into intervention (n=7) and control (n=7) zones. There were no statistically significant differences between the intervention and control priority zones in total population size (paired t-test p-value=0.63), proportions of Black/AA (p=0.133) and Hispanic populations p=0.17), and distance (in miles) from MCC (p=0.64). Approximately 35.8% and 16.5% of the intervention priority zones were Hispanic or Black/AA, respectively. Average distance to MCC, cancer cases, referral and CCT enrollment rates were also similar between groups.

Conclusion: Decision frameworks for MLI study design selection are lacking. The framework provided here for ACTWONDER[2]S can be applied to other studies seeking to evaluate MLIs. Furthermore, the randomization of the priority zones produced optimal target populations for testing the efficacy of the MIL within ACTWONDER[2]S.

#4825 Addressing financial toxicity in cancer clinical trial participation: Barriers and facilitators of enrolling in a reimbursement program for out-of-pocket travel costs.

E. Ramos[1], V. Nguyen[2], A. Santaniello[3], D. Dornsife[4], R. G. Johnson[4], P. E. Wileyto[3], R. H. Vonderheide[3], C. E. Guerra[3];
[1]University of Pennsylvania, Philadelphia, PA, [2]Sidney Kimmel Medical College at Thomas Jefferson University, Philadelphia, PA, [3]Abramson Cancer Center, Philadelphia, PA, [4]Lazarex Cancer Foundation, Danville, CA

Financial toxicity has been associated with adverse outcomes for patients with cancer. Out-of-pocket (OOP) costs contribute to the high financial toxicity (FT) experienced by patients with cancer. Cancer clinical trial (CCT) participants face significant extra OOP expenses presenting a barrier to participation and retention. To address FT in CCTs, the Lazarex Foundation created the Improving Patient Access to Cancer Clinical Trials (IMPACT) Program, a financial reimbursement program (FRP) for OOP travel and lodging costs associated with therapeutic CCT participation. Our study aimed to quantify the FT experienced by patients in CCTs and understand their experience to determine the barriers and facilitators of enrolling in the Lazarex IMPACT Program. Patients enrolled in a CCT were referred to the IMPACT team to determine eligibility. Patients were eligible for IMPACT if they were active on a therapeutic CCT and their household income was less than 700% of the most recent HHS federal poverty guidelines. Patients who enrolled in the program were invited to participate in a brief semi-structured interview via telephone call. We used grounded theory techniques of analysis to identify themes of barriers and facilitators to enrollment in the Lazarex IMPACT program at our cancer center. Table 1 shows the emerging themes from the interviews as barriers and facilitators of enrolling in IMPACT. As a part of the interview process, patients also completed the COST-FACIT questionnaire, a patent reported outcomes measure to evaluate the degree of FT associated with cancer. COST scores in our cohort (n=39) ranged from 14-39.6, mean=27.12, median=27.5; SD=7.96. Following enrollment in the program, patients on average had COST scores indicating low degrees of financial distress. Taken altogether, our results have the potential to inform the development of FRPs for patients with cancer to facilitate their participation in CCTs.

Table 1: Emerging themes from grounded analysis of semi-structured interviews and their frequency

Barrier to enrolling in FRP program.	No. of Participants	Facilitator of enrolling in FRP program	No. of Participants
Patients wanted to be made aware of program earlier in their CCT timeline	4	Enrollment process was easy and straightforward	17
Patients made aware of program after their CCT started	3	IMPACT team contacted patients to offer program	13
CCT Team unaware of program availability	3	Patients learned about the program through their CCT team	8
Patients reported difficulty with technology access and literacy	3	Patients reported sufficient technology access and literacy	4
Patients reported hesitancy sharing financial information	2	Cancer foundation was timely and helpful in enrollment process	2
Patients reported difficulty navigating vast resources at cancer center	1	Cancer Center social workers provided connection to program	1

#4826 Cancer mortality attributable to area-level socioeconomic inequalities in Japan from 2015 to 2020.

Y. Ito[1], T. Nakaya[2], M. Inoue[3], T. Sobue[4], H. Nakagama[3],

[1]Educational Foundation of Osaka Medical and Pharmaceutical University, Takatsuki-shi, Japan, [2]Tohoku University, Sendai-shi, Japan, [3]National Cancer Center, Chuo-ku, Tokyo, Japan, [4]Osaka University, Suita-shi, Japan

Background: In the 3rd Healthy Japan 21 and the 4th National Cancer Plan, the government focused on reducing health inequalities. However, current monitoring of socioeconomic inequalities in cancer is still insufficient to set the targets for the plan. To prioritize strategy aimed at reducing socioeconomic inequalities in cancer mortality, we estimated the population attributable risk fraction (PAF) and excess death due to socioeconomic inequalities, by sex, age group and cancer site.

Method: We used the areal deprivation index (ADI) to establish area-based socioeconomic status. We categorized municipalities to ADI quintile weighted by the size of population, Q1 is the least deprived and Q5 the most deprived group. Excess death due to socioeconomic inequalities was calculated by the difference between observed number of deaths and expected death of Q2 to Q5 group with Q1 as standard population. We used cancer mortality data obtained from vital statistics in 2015-2020.

Results: In total, about 12000 male and 2800 female excess deaths per year due to socioeconomic inequalities were estimated; that is 5.5% and 1.8% as PAF. PAF due to socioeconomic inequalities limited to premature death, less than 75 years old, was estimated as 7.6% in men and 3.3% in women. By age group, the 0-39 years group showed the largest PAF at 15.7% in men and 16.6% in women. In men of all age groups, except 0-39 years, lung cancer was the highest excess death due to socioeconomic inequalities. For women, some cancer sites (breast, ovary, esophagus) showed an opposite association, Q1 was the highest mortality group. Therefore, total excess death was lower than in men. In women of all ages, the highest rate of excess death due to socioeconomic inequalities was gallbladder cancer. For the 0-39 years group, a high rate of excess death in stomach, leukemia, and cervical cancer was observed.

Discussion: Excess death and PAF due to socioeconomic inequalities differed by sex and age group. A greater impact of socioeconomic inequality on cancer mortality was observed in men than in women. Among women, further attention should be paid to areal variation of cancer death related to socioeconomic inequalities, based on the different area-based indices.

#4827 Financial toxicity among cancer survivors during the COVID-19 pandemic.

T. Srivastava, S. Shariff-Marco, S. L. Washington III, C. Miaskowski, J. M. Chan;
UCSF - University of California San Francisco, San Francisco, CA

Background: Financial toxicity (FT), the financial impact of cancer and its treatments on patients' employment, income, and health insurance, can have significant short- and long-term consequences for cancer survivors. With significant increases in cancer survivorship and the changing demographics of the United States, a need exists to identify those most susceptible to FT. This study evaluated FT prevalence during the COVID-19 pandemic and identified factors associated with greater FT risk.

Methods: Data were collected from 1,147 cancer survivors recruited from previous National Cancer Institute-funded studies, from electronic health record searches for patients with cancer diagnoses at University of California, San Francisco (UCSF) and Mount Sinai Medical Center and Columbia University Medical Center in New York City, and the Dr. Susan Love Foundation for Breast Cancer Research. Adults, diagnosed with cancer and proficient in English, completed an online survey via the Research Electronic Data Capture (REDCap) system between May 27, 2020 and February 21, 2021. FT was assessed for the past 14 days using the validated 11-item COmprehensive Score for financial Toxicity (COST) measure. Patients were categorized by score: no FT (COST scores >25), mild FT (14-25), and moderate/severe FT (0-13). Using Pearson's chi-square test of independence, and univariate ordinal logistic regression, the study evaluated sociodemographic and clinical characteristics associated with FT, including age, race and ethnicity, gender, household income, education, marital status, health insurance status, and cancer site.

Results: The COST measure had excellent reliability for the sample (Cronbach's alpha = 0.911). Overall, 9% of respondents reported moderate/severe FT (MSFT), 16% mild. Race/ethnicity, education level, annual household income, cancer site, and years from diagnosis (p-values ≤ 0.035) were associated with FT. Current health insurance coverage was not associated with FT (p=0.456). 18% Black, 13% Asian American, 17% mixed, and 20% other races/ethnicities reported MSFT, while 8% non-Hispanic White and 5% Hispanic respondents reported the same. 31% of survivors with annual household income <$40,000 reported MSFT vs. 7% with ≥$40,000 income. 14% of survivors with less than a college degree reported MSFT vs. 8% amongst those with a college degree or higher. For men, the odds of having FT (mild or MSFT) were 0.60 (95% CI 0.40, 0.90) times that of women. Survivors <50 years old at diagnosis had 7.53 (95% CI 4.09, 13.83) times the odds of FT (mild or MSFT) vs. those aged ≥75 years.

Conclusions: These preliminary analyses from this cross-sectional study characterizes the prevalence and determinants of FT experienced by cancer survivors during the COVID-19 pandemic. The next steps will include multivariable analysis and comparison with pre-pandemic data, to identify those at greatest risk and inform interventions.

#4828 Effect of county-level income and rurality on cardiovascular disease mortality among Asian and Pacific Islander breast cancer survivors in the US, 2000-2018.

K. L. Ho[1], C. Ramin[2], J. Z. Shing[3], K. Taparra[4], J. B. Vo[3];
[1]Johns Hopkins Bloomberg Sch. of Public Health, Baltimore, MD, [2]Cedars-Sinai Medical Center, Los Angeles, CA, [3]National Cancer Institute, Bethesda, MD, [4]Stanford Medicine, Palo Alto, CA

Purpose: To examine differences in cardiovascular disease (CVD) mortality by county-level income and rurality for Asian versus Pacific Islander (PI) breast cancer survivors.
Background: Asian and PI individuals experience varying cancer burden, and prior studies have reported disparities in treatment-related CVD mortality among breast cancer survivors by socioeconomic status and race and ethnicity. However, the impact of county-level income and rurality on CVD mortality among Asian and PI breast cancer survivors, separately, are not well described.
Methods: We included 60,184 Non-Hispanic Asian and PI women diagnosed with first primary, invasive breast cancer between 2000-2017 in the U.S. Surveillance, Epidemiology, and End Results program (aged 18-84, survived 12+ months, and received initial surgery). We estimated the hazard ratio (HR) of CVD mortality using Cox proportional hazard models assessing the impact of county-level income (median household income: low = <$75,000; high [ref] = ≥$75,000) and rurality (urban [ref] = metropolitan counties, population ≥ 250,000; rural = nonmetropolitan counties), separately for Asian and PI breast cancer survivors. Models adjusted for continuous age, stage (localized, regional/distant), and year of breast cancer diagnosis (2000-2004, 2005-2009, 2010-2017). We calculated 10-year cumulative CVD mortality for Asian and PI women accounting for competing risks (e.g., non-CVD deaths).
Results: Of 55,602 Asian and 4,582 PI breast cancer survivors, 1,114 Asian and 178 PI women died from CVD through 2018 (median follow-up, Asian = 6.0 years; PI = 5.5 years). PI women had a higher median age at breast cancer diagnosis (57 vs. 55 years) and more advanced stage (37% vs. 33%) than Asian women. Among Asian breast cancer survivors, low county-level income was associated with elevated CVD mortality (HR = 1.17, 95% CI = 1.04, 1.31), but not rurality (HR = 1.20, 95% CI = 0.91, 1.58). For PI breast cancer survivors, there were no significant associations observed for low county-level income (HR = 0.83, 95% CI = 0.60, 1.14) or rurality (HR = 1.11, 95% CI = 0.76, 1.61). At 10 years after breast cancer diagnosis, 1 in 40 Asian women and 1 in 20 PI women died of CVD.
Conclusion: Asian breast cancer survivors living in low-income counties had heightened risk of CVD mortality compared with those living in higher income counties, highlighting potential healthcare access barriers to cancer survivorship care. Although PI women did not experience significant differences in CVD mortality across groups of county-level income and rurality, they had twice as high absolute risk of CVD mortality than Asian women, warranting further investigation. Future studies that disaggregate Asian and PI individuals into more diverse and granular ethnicity groups are needed to understand heterogeneity in breast cancer survivorship outcomes.

#4829 Pre-diagnostic comorbid conditions and survival among black women with ovarian cancer.

Alicia Richards[1], Courtney E. Johnson[2], Anthony J. Alberg[3], Elisa V. Bandera[4], Melissa Bondy[5], Michele L. Cote[6], Theresa A. Hastert[7], Kristen Haller[2], Jeffrey R. Marks[8], Edward S. Peters[9], Paul D. Terry[10], Andrew B. Lawson[11], Joellen M. Schildkraut[2], Lauren C. Peres[1]

[1]Moffitt Cancer Center, Tampa, FL,[2]Emory University, Atlanta, GA,[3]University of South Carolina, Columbia, SC,[4]Rutgers Cancer Institute of New Jersey, New Brunswick, NJ,[5]Stanford University, Stanford, CA,[6]Indiana University, Indianapolis, IN,[7]Wayne State University, Detroit, MI,[8]Duke Medical Center, Durham, NC,[9]University of Nebraska Medical Center, Omaha, NE,[10]University of Tennessee, Knoxville, TN,[11]Medical University of South Carolina, Charleston, SC

Introduction: Black women with epithelial ovarian cancer (EOC) have worse survival compared to other racial groups, and the causes of these poor outcomes remain unclear. Compared to other racial groups, Black women are disproportionately affected by comorbid conditions which can adversely impact cancer care and outcomes. Thus, we examined the association of pre-diagnostic comorbid conditions and their associated medications with survival among Black women with EOC.

Methods: Using data from Black women with EOC in the African American Cancer Epidemiology Study, we evaluated the self-reported Charlson comorbidity index (CCI) and three cardiometabolic comorbidities (diabetes mellitus, hypertension, and hyperlipidemia). We also characterized whether women with each cardiometabolic condition were using medication for their condition. Kaplan-Meier survival curves and log-rank tests were used to examine survival by the CCI, each cardiometabolic comorbidity, and medication use. Cox proportional hazards regression models were used to examine the association of comorbid conditions and medications with survival while adjusting for age at diagnosis, stage, histotype, and study site.

Results: Among 592 Black women with EOC, 35% had a CCI ≥2, and the prevalence of diabetes, hyperlipidemia, and hypertension was 19%, 31%, and 62%, respectively. Among women with each cardiometabolic condition, the prevalence of medication use for diabetes, hypertension, and hyperlipidemia was 73%, 78%, and 60%. In bivariate analyses, women with a higher CCI, diabetes, hyperlipidemia, and hypertension had worse survival compared to women without these conditions (P<0.05). However, when adjusting for prognostic factors, only a high CCI (≥2 vs. 0) and diabetes were significantly associated with higher hazard of death (HR=1.36, 95% CI=1.06-1.74 and HR=1.40, 95% CI=1.08-1.81, respectively). Investigating the independent associations of each condition included in the CCI with survival revealed that diabetes was largely driving the association of CCI with survival. When considering medication use, women with diabetes, irrespective of medication use, women with hypertension not on medication, and women with hyperlipidemia on medication had worse survival compared to women without these conditions in bivariate models (P<0.05). Compared to women without diabetes, women with diabetes on medication and women with diabetes not on medication had a statistically significant higher hazard of death in multivariable models (HR=1.39, 95% CI=1.02-1.88 and HR=1.63, 95% CI=1.04-2.57, respectively). No associations with survival were observed when considering medication use for hypertension and hyperlipidemia after adjusting for prognostic factors.

Conclusion: Similar to prior studies among White women with EOC, diabetes, regardless of medication status, was strongly associated with poorer survival among Black women with EOC.

#4830 Predicting drug treatment response in African American lung cancer patients who smoke.

M. Ray[1], I. Osei-Gyening[2], K. Acheampong[3], M. Riebesell[4], **K. A. Mitchell**[5];

[1]Penn State College of Medicine, Hershey, PA, [2]Memorial Sloan Kettering Cancer Center, New York, NY, [3]Bristol Myers Squibb, Princeton, NJ, [4]Lafayette College, Easton, PA, [5]Fox Chase Cancer Center, Philadelphia, PA

Background: Lung cancer is the third most commonly diagnosed cancer in the US and the leading cause of cancer-related death. African Americans (AAs) have higher lung cancer incidence and mortality rates, and lower survival rates, when compared to their European American (EA) counterparts. It is widely known that cigarette smoking is the strongest risk factor for lung cancer development, but it also plays a significant role in clinical outcome. Cigarette smoking after lung cancer diagnosis (up to 30% patients) comes with several risks, including increased secondary tumors and mortality rates (by 20%), as well as poor treatment outcomes (higher radiation and chemotherapy failure and higher drug clearance). There are limited transcriptomic studies that describe molecular characterizations of AA smokers with lung cancer to predict treatment outcomes.

Hypothesis: Cigarette smoking leads to greater drug resistance-related gene expression in AA lung cancer patients.

Methods: mRNA expression changes in an AA (NCI-H2172) and EA (NCI-H1944) lung cancer cell line pair exposed to liquid cigarette smoke condensate (CSC) were profiled. The cell lines were matched based on age (62 years), sex (female), histology (lung adenocarcinoma, LUAD, the most common subtype), and culture properties (adherent). The CSC was derived from Murty Pharmaceuticals and prepared by smoking University of Kentucky's 3R4F Standard Research Cigarette on an FTC Smoke Machine. A total of 500,000 cells per well were treated for one hour under standard incubation conditions (37°C, pH 7.0, 5% CO_2). Cells were pelleted, RNAs were isolated, treated with DNAse-I to remove contaminating genomic DNA, quantified, and sent for bulk mRNA-sequencing (Novogene Co). Three biological replicates and technical triplicates were performed. Partek Flow and Partek Genomics Suite workflows were used to identify population-specific differentially expressed gene (DEG) signatures and pathway enrichment after CSC exposure. DEG were profiled in LUAD tissues from current smokers in an AA and EA TCGA cohort (n = 18 AAs, 86 EAs).

Results: Population-specific gene expression changes were discovered (n = 52 AA DEGs, n = 31 EA DEGs; $P < 0.001$). All of the DEGs were mutually exclusive with no overlap. Some pathways were shared between both populations and others were unique. PI3K/Akt/mTOR signaling pathway enrichment was unique in AA LUAD cells and ECM receptor interactions were distinct in EA LUAD cells. AKT2 (which activates mTOR) had significantly higher expression in LUAD tumor tissues from current AA smokers compared to current EA smokers.

Conclusion: Population-specific PI3K/Akt/mTOR pathway alterations may help explain drug resistance in LUAD tumors from AA patients. PI3K signaling is considered a significant cause of resistance to chemotherapy, targeted therapy, and immunotherapy.

Future Directions: Expose AA and EA LUAD cell lines to CSC and PI3K/Akt/mTOR pathway inhibitors.

#4831 Racialized economic segregation and disparities in late-stage diagnosis, treatment and mortality among patients with non-small cell lung cancer.

P. Shrestha, M. Lian, Y. Liu;
Washington University In St. Louis, St. Louis, MO

Importance: Little is known about the impact of residential segregation on early detection, treatment, and prognosis among patients with non-small cell lung cancer (NSCLC), a predominant type of lung cancers.
Objective: To examine the associations of racialized economic segregation with the risks of late-stage diagnosis, non-adherence to guideline-recommended treatment, and mortality among non-Hispanic White (NHW) patients and non-Hispanic Black (NHB) patients with NSCLC.
Methods: This population-based retrospective cohort study included patients with NSCLC as a first primary malignancy diagnosed at age 20 and older between January 2007 and December 2015, followed through December 2016, and identified from the Surveillance, Epidemiology, and End Results (SEER) dataset released in April 2019. County-level racialized economic segregation was estimated using the Index of Concentration at the Extremes (ICE). We used multilevel logistic regression and multilevel Cox regression accounting for county-level clustering to estimate odds ratios (ORs) for late-stage diagnosis and non-adherence to guideline-recommended treatment, and hazard ratios (HRs) for overall mortality and lung cancer-specific mortality.
Results: Of 203, 441 patients, 85.8% were NHW and 14.2% were NHB. Compared with patients living in the most privileged (lowest ICE quintile—segregated, high-income NHW) counties, patients living in the least privileged (highest ICE quintile—segregated, low-income NHB) counties had higher risks of late-stage diagnosis (OR=1.09, 95% CI: 1.02-1.16; P_{trend} <.001), non-adherence to guideline-recommended treatment (OR=1.28, 95% CI: 1.16-1.41; P_{trend} <.0001), lung cancer-specific mortality (HR=1.10, 95% CI: 1.07-1.14; P_{trend} <.0001), and overall mortality (HR=1.12, 95% CI: 1.09-1.16; P_{trend} <.0001). The association of segregation with treatment underutilization was stronger in NHW patients than NHB patients ($P_{interaction}$ =0.02). There was no significant difference in the segregation-related risk of late-stage diagnosis, lung cancer-specific mortality, or overall mortality between NHW and NHB patients.
Conclusions: Living in segregated, low-income NHB counties was associated with increased risks of late-stage diagnosis, suboptimal treatment, and mortality among patients with NSCLC. Future research should investigate contributors to the adverse impact of residential segregation on lung cancer care and outcomes.

#4832 The impact of neighborhood-level disadvantage on the patient-reported outcomes of primary brain tumor patients.

Z. A. Karim, K. Reinhart, O. Celiku, Y. Kim, H. Miller, E. Vera, J. B. Vo, T. S. Armstrong, M. L. Stockdill;
National Institutes of Health (NIH), Bethesda, MD

There is increased recognition that social determinants of health may impact well-being and health in those with various cancers, but they have not been systematically evaluated in primary brain tumor (PBT) patients. Here, we examined the association between Area Deprivation Index (ADI), a measurement of sociodemographic neighborhood disadvantage, and patient-reported outcomes (PROs) in a cohort of adult PBT patients enrolled in a large National Institutes of Health observational trial (NHS, NCT02851706, PI: Armstrong). We utilized linear regression to assess the relationship between ADI (less advantaged [ADI≥40, n=153, 24%], more advantaged [ADI<40, n=490, 76%]) and patient symptom burden (MDASI-BT), anxiety, and depression (PROMIS Short Forms v1.0 8a). Logistic regression was used to evaluate the association between ADI and health-related quality of life using the 5 dimensions of the EQ-5D-3L. Models were adjusted for age, sex, race/ethnicity, tumor grade, Karnofsky Performance Score (KPS), and tumor recurrence. A sub-analysis stratifying by tumor grade (low, high) was completed. Among 643 PBT patients, the majority resided in more advantaged areas (n=490; 76%) and had high-grade tumors (n=448; 70%). Those who were less advantaged reported more symptom severity (β=1.10, SE=1.05, *P*=0.041), more activity-related interference (β=1.11, SE=1.05, *P*=0.03), and had 4.68 times the odds of having moderate-severe difficulty completing self-care tasks (95% confidence interval [1.46, 14.96], *P*=0.009) compared to those who were more advantaged. KPS was a significant predictor for all three outcomes, and age at diagnosis was significant for PBT symptom severity. Among patients with low-grade tumors, those who were less advantaged reported higher symptom interference (β=1.24, SE=1.10, *P*=0.020), affective symptoms (β=1.24, SE=1.08, *P*=0.007), treatment-related symptoms (β=1.21, SE=1.08, *P*=0.021), general disease symptoms (β=1.26, SE=1.10, *P*=0.016), activity-related interference (β=1.26, SE=1.09, *P*=0.006), mood-related interference (β=1.20, SE=1.09, *P*=0.039), and anxiety (β=1.03, SE=1.02, *P*=0.023), with KPS being a significant predictor for all outcomes except anxiety. Overall, less advantaged PBT patients reported worse symptom severity and activity-related interference, and those with low-grade tumors experienced more affective symptoms, including fatigue, general disease and treatment-associated symptoms, and symptoms of anxiety, but not neurologic or cognitive symptoms. Living in less advantaged areas may lead to barriers to care access, symptom management medications, or other neighborhood resources that could alleviate PBT patient symptom burden but may compound over time for those with poor performance status or low-grade tumors. These results highlight the need for targeted supportive interventions for PBT patients living in less advantaged areas.

#4833 Impact of poverty in surrounding neighborhoods in cancer mortality in the US: A nationwide study among US women.

I. Nwigwe, M. Desjardins, K. Visvanathan;
Johns Hopkins Bloomberg Sch. of Public Health, Baltimore, MD

Background: Poverty at the individual and county levels is known to lead to worse cancer outcomes. We believe the relationship between poverty and cancer may involve individual-level factors including tumor biology, socioeconomic status, and community measures that alter cancer outcomes such as death. We aim to understand to what extent poverty in the surrounding neighborhood may identify counties at the highest risk of cancer mortality and whether it is modifiable.
Methods: This study used data collected by SEER to examine the association between neighborhood effects of poverty on the top three sites of cancer mortality among women. We included women >= 20 years of age diagnosed with breast, lung, and colorectal cancer between 2005-2009 and 2010-2014 who survived more than one year after diagnosis. We determined county-level neighborhood poverty environments using local spatial autocorrelation (LISA) analysis with Local Moran's I of five-year county-level poverty estimates from the American Community Survey. US counties with poverty estimates above or below the national median were defined as high (H)- or low (L)- poverty counties, respectively. We defined neighborhood poverty environments as H-counties among H-counties (HH), L-counties among L-counties (LL), H-counties among LL-counties (HL), and L-counties among HH-counties (LH). We used a Poisson regression model adjusting for age at diagnosis, race/ethnicity, cancer stage, year of diagnosis, treatment, and cancer type to assess county-level neighborhood poverty environment effects on cancer mortality. We also used stratified analyses to explore the effect of cancer type, stage, and race/ethnicity strata on the association between neighborhood poverty environments and cancer death.
Results: Our analysis includes 36,481 women with 4,740 cancer deaths. In total 7,182 women were in HH counties; 21,112 women were in LL counties; 6,476 women were in HL counties; and 1,711 women were in LH counties. Women in HH, LH, and HL counties had a respective 1.23 [95%CI:1.14,1.32], 1.20 [95%CI:1.05,1.36], and 0.95 [95%CI: 0.88,1.03] relative risk (RR) of cancer death when compared to deaths in LL counties. In our stratified analyses, women with breast cancer in HH and HL counties had higher cancer deaths (RR = 1.21 [95%CI:1.03,1.42] and 1.37 [95%CI:1.13,1.65], respectively) when compared to women with lung cancer. We also observed higher cancer deaths from counties that were LL in 2005-2009 and changed to HH counties in 2010-2014 (RR = 1.60 [95%CI:0.85,2.68]) when compared to unchanged LL counties.
Conclusion: We used LISA spatial clustering to demonstrate the effects HH and LH environments have on cancer mortality. We also demonstrate the impact that changes in neighborhood environments can have on cancer mortality. Our findings suggest that prioritization of resource allocations to HH neighborhoods could improve the burden of women with cancer.

#4834 Racial disparities in pain and psychiatric medication use in patients with metastatic colorectal cancer.

J. M. Allen[1], O. M. Trejos Kweyete[1], Y. Guo[2], S. C. Rogers[2], L. Scarton[2], D. L. DeRemer[2], C. Whitner[3], D. J. Wilkie[2];
[1]University of Florida, Orlando, FL, [2]University of Florida, Gainesville, FL, [3]University of Florida, Jacksonville, FL

Background: In the United States, colorectal cancer (CRC) is a public health concern, as it is the second leading cause of cancer-related death, accounting for over 50,000 deaths annually. In addition to its high mortality, CRC is associated with significant comorbidities including pain and psychiatric symptoms, particularly in late-stage disease. Supportive care medications (SCM) are frequently used for symptom management and improving health-related Quality of Life (HRQoL). Racial disparities in clinical outcomes including HRQoL have been reported in CRC. While racial disparities have been described in the use of SCM for some cancer types, no investigation of SCM use in late-stage CRC have been performed. The purpose of our study was to explore the relationship between SCM use and race/ethnicity in patients with metastatic CRC.

Methods: We used the National Cancer Institute Surveillance Epidemiology and End Results (NCI SEER)- Medicare-linked database to analyze all patients with a CRC diagnosis and a newly initiated outpatient prescription claim for an SCM of interest from 2009-2018. Patients on SCM before cancer diagnosis or who had non-metastatic CRC at diagnosis were excluded. We assessed six SCM classes: opioids, non-opioid analgesics, skeletal muscle relaxants, antidepressants, anxiolytics, and antipsychotics.

Results: After application of inclusion/exclusion criteria, 28, 212 patients were included in the final analysis (White: 72.8%, Black: 12.7%, Hispanic: 9.5%, Asian: 4.6%, Native American: 0.4%). After controlling for socioeconomic factors and compared to non-Hispanic White patients, there were significant differences across multiple SCM drug classes. When considering pain medications, these differences were bi-directional. Black patients were less likely to receive opioids (adjusted Odds Ratio [aOR] 0.86, 95% CI: 0.80-0.93), while Hispanic patients were more likely to receive opioids (aOR: 1.12, 95% CI: 1.03-1.22) and non-opioid analgesics (aOR 1.22, 95% CI: 1.06-1.40). Asian patients were more likely to receive non-opioid analgesics (aOR 1.71, 95% CI: 1.45-2.03), but less likely to receive skeletal muscle relaxants (aOR 0.60, 95% CI: 0.43-0.82). When considering psychiatric medications, decreased use among all racial groups was noted for antidepressants (Black: aOR 0.53, 95% CI: 0.50-0.60; Hispanic: aOR 0.82, 95% CI: 0.75-0.90; Asian: aOR 0.48, 95% CI: 0.42-0.56), and anxiolytics (Black: aOR 0.43, 95% CI: 0.38-0.49; Hispanic: aOR 0.76, 95% CI: 0.67-0.85; Asian: aOR 0.45, 95% CI: 0.37-0.55). Among antipsychotics, only Asian patients had less use compared to non-Hispanic White patients.

Conclusion: Racial disparities in the use of pain and psychiatric medications among patients with late-stage CRC were present, even after controlling for multiple confounders. Further investigation is needed to understand drivers and their impact on HRQoL outcomes.

#4835 Demographic factors and risk of persistent opioid use in a diverse cohort of breast cancer survivors.

L. Chen[1], R. C. Hechter[1], J. Shi[1], Z. Gu[1], M. Brady-Rogers[2], R. T. Chlebowski[3], R. Haque[1];
[1]Kaiser Permanente Research, Pasadena, CA, [2]Alive & Well Women, South Pasadena, CA, [3]The Lundquist Research Institute for Biomedical Innovation at UCLA-Harbor, Torrance, CA

Background: Persistent opioid use (POU), in breast cancer survivors after they have completed active cancer treatment is an emerging area of concern. We examined rates and identified risk with POU in breast cancers survivors in the year after active cancer treatment going forward, and if these risks differed by race/ethnicity.
Methods: We assembled a cohort of female breast cancer survivors diagnosed in 2009-2019 treated for early-stage disease (in situ, local, regional), and had at least two opioid prescriptions after one year of survivorship in a large health plan in southern California. Data were captured from the tumor registry, electronic health records, and pharmacy databases. The primary outcome was POU defined as continuously receiving at least 90 days supplied of opioids during follow-up. Patients were followed through the date once they met POU criteria, died, disenrolled from health plan, or reached study's end (12/31/2021), whichever came first. We calculated rates as the number of patients who experienced POU per 1,000 person-years (PY). We identified the predictors and estimated hazard ratios (HR) associated with POU using multivariable proportional hazard regression and stratified by race/ethnicity.
Results: The cohort included 14,347 breast cancer survivors who used opioids followed for a maximum of 12 years (median: 6.6 years). Overall, the cohort was diverse: 9% Asian/Pacific Islander (API); 14% Black; 22% Hispanic; and 54% White women. Out of 14,347 patients who used opioids, 2,285 (16%) patients developed POU. POU rates was the highest in Whites (36.2 per 1,000 PY) compared other race/ethnicity groups including Blacks, Hispanics, APIs (30.7, 17.3, 10.6 per 1,000 PY, respectively). Patients who developed POU had longer annualized median opioid duration, especially in Black patients (175.0 vs. 5.3 days) and were prescribed stronger opioids (median maximum daily morphine milligram equivalent 83.7 vs 50.0), compared to those who did not develop POU. In adjusted analyses of POU risk, Black (HR, 0.81; 95% CI: 0.72-0.92), API (HR, 0.59; 95% CI, 0.52-0.66), and Hispanic women (HR, 0.59; 95% CI, 0.52-0.66) were less likely to develop POU compared to White women. Patients with older age, Elixhauser Comorbidity Index ≥3, smoking, breast cancer stage (regional); type of opioid (Oxycodone); and who used other psychiatric and pain medications had significantly greater POU risk. In stratified analysis, the POU risk was 2.6 times greater (HR, 2.61; 95% CI, 1.32-5.15) in Hispanic patients aged≥65 vs <40 years. The highest HR was in APIs who were current smokers (HR, 4.26; 95% CI, 1.77-10.29) compared with non-smokers.
Conclusion: The findings suggest that patients who are older, current smokers, with more comorbidities, and diagnosed with higher cancer stage were most vulnerable to developing POU.

#4836 Race differences in symptom burden and medication adherence among women with breast cancer on adjuvant endocrine therapy: A post hoc analysis of a randomized control trial.

X. Hu[1], R. A. Krukowski[1], E. Stepanski[2], L. S. Schwartzberg[3], G. A. Vidal[4], I. Graetz[5];

[1]University of Virginia School of Medicine, Charlottesville, VA, [2]Ovation.io, Cambridge, MA, [3]Renown Institute for Cancer and University of Nevada, Reno, NV, [4]West Cancer Center and Research Institute, Germantown, TN, [5]Emory University, Rollins School of Public Health, Atlanta, GA

Background: Adjuvant endocrine therapy (AET) reduces breast cancer recurrence, but racial differences in nonadherence remains a concern. Differential symptom burden may contribute to disparities in AET adherence.

Method: We conducted a post hoc analysis by race among women with breast cancer starting AET who were randomized in THRIVE Study (NCT03592771) to investigate remote symptom monitoring intervention vs. usual care from 11/2018 to 06/2021. Participants completed surveys at baseline, 6- and 12-month. Outcomes were symptom burden measured by FACT-Endocrine Subscale, and adherence measured by electronically monitored pillbox (>80% Proportion of Days Covered). We estimated symptom differences by race using linear regression with and without adjusting for baseline characteristics. To examine whether symptom burden contributed to racial differences in adherence, we conducted multivariable regression for adherence with and without controlling for symptom burden, and Blinder-Oaxaca decomposition.

Results: Among 102 (34%) Black and 194 (66%) White women who were randomized, retention was 88% at 12-month. Compared to White participants, Black participants were younger (55 vs. 60 years), more likely to be at poverty (10.8% vs. 4.1%), and had lower health literacy (18.9% vs. 13.4%; *p-values*<.01). While symptom burden did not differ by study arm, Black participants had worse symptoms than White at baseline (60.8 vs. 64.5, *p*=.002). This gap became smaller at 6-month (59.7 vs. 61.2, *p*=.30), but diverged again at 12-month (56.9 vs. 61.8, *p*<0.01). Differences at 12-month diminished after controlling for baseline characteristics (-1.6, 95%CI=-4.4 to 1.2). Notably, being at poverty and younger age were associated with higher symptoms. Adherence was lower among Black participants at 6-month (0.69 vs. 0.78, p=.13) and 12-month (0.44 vs. 0.60, p=.014) than White participants. Unadjusted differences in adherence at 12-month (-16.0 percentage points [ppts], 95%CI=-28.9 to -3.3, p=.01) attenuated after adjusting for baseline symptoms, symptom changes to 12-month, and other baseline characteristics (-10.4 ppts, 95%CI=-25.6 to 4.8, p=.18). Lower baseline symptoms were associated with better adherence (0.8 ppts, 95%CI=0.1 to 1.4, p=.03). Decomposition indicates that 9.1 ppts (95%CI=-4.8 to 23.0, 57%) of the difference in 12-month adherence was explained by symptoms and baseline characteristics, and remaining unexplained difference was 6.9 ppts (95%CI=-12.6 to 26.4, 43%).

Conclusion: Our results add to increasing evidence that Black women with breast cancer have lower AET adherence, which may be partially attributed to worse symptoms than White women. These results highlight the need for new strategies to promote equitable symptom management and adherence strategies between Black and White women to reduce disparities in outcomes.

#4837 Perceived discrimination, medical mistrust, and their associations with ovarian cancer mortality among women in the African American Cancer Epidemiology Study.

L. J. Collin[1], C. Johnson[2], M. Akonde[3], M. Kan[2], E. V. Bandera[4], L. Peres[5], A. Alberg[6], T. Hastert[7], J. Schildkraut[2];

[1]University of Utah Huntsman Cancer Institute, Salt Lake City, UT, [2]Emory University, Atlanta, GA, [3]University of South Carolina, Charleston, SC, [4]Rutgers Cancer Institute, New Brunswick, NJ, [5]Moffit Cancer Center, Tampa, FL, [6]University of South Carolina, Charlston, SC, [7]Wayne State University, Detroit, MI

Background: There are pronounced racial disparities in ovarian cancer mortality wherein Black women are on average 30% more likely to succumb to their disease than White women. Factors that contribute to these disparities are complex and multifactorial. Racial discrimination is hypothesized to affect cancer health disparities through three distinct pathways including the impact on socioeconomic inequities, chronic stress, and restricted access to goods and services. In this study, we examined the role of perceived discrimination and medical mistrust on all-cause mortality among ovarian cancer patients.

Methods: Using data from the African American Cancer Epidemiology Study (AACES), we included 592 ovarian cancer patients who self-identified as Black or African American and completed a telephone interview. Perceived discrimination was measured with a modified version of the 5-question Williams Everyday Discrimination scale. Medical mistrust was measured with the Trust in Physician scale (ranged 0-48 based on a combination of 12 questions). We used Cox proportional hazard models to compute hazard ratios (HR) and 95% confidence intervals (CIs) associating perceived discrimination and medical mistrust with all-cause mortality, adjusting for age, stage, and histotype.

Results: Nearly two-thirds of the cohort passed away by the end of follow-up (mean follow-up 5.5 years, ranging 0.5-12 years). We observed that 231 participants patients (39%) reported experiencing discrimination in at least one of the domains assessed. Reporting any experience of discrimination was associated with lower all-cause mortality (HR=0.78, 95% CI: 0.62, 0.97). In multivariable adjusted models, higher trust in physicians (above vs. below the median of 35) was associated with a decreased risk of mortality (HR=0.87, 95% CI: 0.70, 1.08).

Conclusion: In our preliminary results, we observed an association between any experience of discrimination and better survival, and that a higher trust in physicians was associated with better survival. Further work on this project will try to understand the paradoxical association with perceived discrimination, and evaluate the associations of discrimination and medical mistrust with ovarian cancer treatment, leading to more insight into drivers of racial disparities in ovarian cancer mortality.

#4838 Impact of social determinants of health (SDH) on systemic therapy and survival in young women with breast cancer.

N. J. Reed, F. Ahmed, C. Schepel, L. Hadzikadic-Gusic, J. Fisher, A. R. Tan, A. L. Heeke;
Levine Cancer Institute, Charlotte, NC

Introduction: Health disparities are often influenced by SDH. Breast cancer patients (pts) with negative SDH may experience less access to treatment, which can impact outcomes. This study evaluated the association between SDH, utilization of medical therapy, and outcomes in young pts with early breast cancer.
Methods: We performed a retrospective review of female pts 18-40 years old in the Young Women's Breast Cancer Database at a single institution with non-metastatic breast cancer diagnosed from 2011-2020. Predefined SDH were recorded along with clinical characteristics at diagnosis. Descriptive statistics and logistic regression analyses were performed. Survival analyses were conducted using Kaplan-Meier and Cox Proportional Hazard model.
Results: 1,061 pts were eligible for analysis; 67% were White, 27% Black, 4% Asian, and 3% Other. Additional demographic and clinical characteristics are shown in Table 1. Pts with Medicaid received chemotherapy (chemo) more often than pts with private insurance (OR 2.04, p=0.003), as did self-pay/uninsured pts (OR 1.74, p=0.003). Divorced/separated/widowed pts were more likely to receive chemo than married pts (OR 1.85, p=0.049). Pts living in 1st quartile of area deprivation index (ADI) received chemo less than those in the 4th ADI quartile (OR 0.45, p=0.003). Divorced/separated/widowed pts with HR+ disease were less likely to receive endocrine treatment than married pts (OR 0.48, p=0.039). Worse overall survival (OS) was seen for Black vs White pts (HR 1.72, p<.001); pts with Medicaid or self-pay/uninsured vs privately insured (HR 1.67, HR 1.92; p=0.025); and unemployed vs employed pts (HR 2.49, p<.001) adjusted for chemo use and clinical stage.
Conclusions: Young pts experiencing negative SDH were more likely to receive chemo, less likely to take endocrine therapy if indicated, and suffered from worse OS. These findings may highlight the influence of a pt's social network on access to care and treatment completion.

Table 1: Demographics & clinical characteristics in young women with early-stage breast cancer

Demographic Characteristics				
	Overall, N=1061			
Race	Asian: 40 (3.9 %)	Black or African American: 270 (26.6 %)	Other: 29 (2.9 %)	White or Caucasian: 677 (66.6 %)
Ethnicity	Hispanic or Latino: 86 (8.4 %)	Non-Hispanic or Non-Latino: 939 (91.6%)		
Insurance Type	Private: 824 (77.7 %)	Medicare: 16 (1.5 %)	Medicaid: 145 (13.7 %)	Self-pay/Uninsured: 75 (7.1 %)
Area Deprivation Index (ADI) Quartile*	Q1= 1-25: 215 (20.3 %)	Q2= 26-50: 375 (35.4 %)	Q3= 51-75: 315 (29.7 %)	Q4= 76-100: 155 (14.6 %)
Median Household Income	<45000: 44 (4.1 %)	45000-79,999: 600 (56.6 %)	80000-119,999: 304 (28.7 %)	≥120,000: 112 (10.6 %)
Employment status	Unemployed: 224 (21.1 %)	Employed: 657 (61.9 %)	Unknown: 180 (17.0 %)	
Marital Status	Married: 631 (59.8 %)	Single: 355 (33.6 %)	Separated/ Divorced/ Widowed: 70 (6.6 %)	
Clinical Characteristics				
Clinical AJCC Stage	Stage 0: 149 (14.3 %)	Stage I: 335 (32.1 %)	Stage II: 430 (41.2 %)	Stage III: 129 (12.4 %)
Receptor Status	HR+/HER2+: 174 (19.9 %)	HR+/HER2-: 519 (59.3 %)	HR-/HER2-: 182 (20.8 %)	
Utilization of Chemotherapy	Yes: 702 (67.1 %)	No: 344 (32.9 %)		
Utilization of Endocrine Therapy	Yes: 451 (43.3 %)	No: 590 (56.7 %)		
Recurrence Status	Yes: 111 (10.5 %)	No: 942 (89.5 %)		
Survival Status	Alive: 868 (81.8 %)	Dead: 101 (9.5 %)	Lost to follow-up: 92 (8.7 %)	
*Higher score correlates with greater disadvantage				

#4839 Ethnicity dictates survival benefit in Hispanics diagnosed with diffuse large B-Cell lymphoma survival: A national cancer database analysis.

C. Velez-Mejia[1], E. Toro Velez[1], D. Rosas[2], Q. Liu[1], J. E. Michalek[1], E. Diaz Duque[1];

[1]UT Health Science Center at San Antonio, San Antonio, TX, [2]Memorial Healthcare, Hollywood, FL

Background: Diffuse Large B-Cell Lymphoma (DLBCL) is the most common Non-Hodgkin lymphoma in the United States (US) but there is limited evidence showing ethnic disparities affecting overall survival (OS) (***Blood***10.1182/blood-2022-159201, ***Blood***10.1182/blood-2021-151816). This is the largest nationwide cancer registry analysis evaluating ethnic differences for HI vs Non-Hispanics (NH) with DLBCL in the US.

Methods: Data were analyzed using the National Cancer Database from 2004-2019. Sociodemographic characteristics were compared between ethnic groups. Kaplan-Meier and Cox regression analyses were used to compare OS between HI and NH. Multivariate analysis and propensity score matching were performed with adjustment for age, stage, comorbidity score, and insurance status, type of facility, and great circle distance

Results: 239,391 patients (HI n=18,290, NH n=221,101) were diagnosed with DLBCL. Male sex predominated for both and the majority of patients were Whites. HI were diagnosed at a median age of 62 years (y) vs 68 y for NH [p<0.001]. For HI and NH, most of the patients were diagnosed from 2016-2019.

For both groups, the majority of patients had a Charlson-Deyo Score of 0, stage IV at diagnosis and unknown HIV status. The primary payer at diagnosis was government sponsored for HI and NH. In HI the median income based on the Median Income Quartile for 2000 corresponded to the highest level of >$46,000 and from 2008-2012 it was similarly distributed. For NH, for both time periods the majority of the patient were in the highest bracket. Most patients in the HI and NH were located in metropolitan area and were more likely to be treated at a comprehensive cancer center with a great circle distance (miles) of 7.3 for HI and 9.7 for NH.

The median survival for HI was 11 y vs 6.8 y for NH. The survival probability at 2, 5 and 10 y for HI corresponded to 69%, 61% and 52%, while for NH it was 66%, 55% and 41%, respectively. The OS probability at 10 y was statistically significant favoring HI [p<0.0001]. Independently, on multivariate analysis, not insured status was associated with worse OS (HR 1.2, CI 1.13-1.28, [p<0.01]) and private insurance type was associated with better OS (HR 0.81, CI 0.77-0.84, [p<0.01])

Conclusion: This nationwide cancer registry study identified better OS in HI diagnosed with DLBCL in the US. Both cohorts had similar sociodemographic and clinical results; however, HI were diagnosed at younger age. This finding may not only help to explain a unique trait towards development of cancer at an earlier age, but also an enhanced response to therapy. Regarding median income there wasn't a tendency noted for HI, which support the unique complex interactions in socioeconomic status. Further studies examining intrinsic biologic differences are needed to better understand improved OS for HI, which could also help the rational development of targeted therapies.

#4840 Creating a culturally sensitive manual to increase clinical trial participation among African Americans and African Nationals.

Carolina Aristizabal, Eduardo Ibarra, **Lourdes A. Baezconde-Garbanati**

Keck School of Medicine of USC, Los Angeles, CA

Background: Racial and ethnic minorities are immensely underrepresented in clinical trial studies in the United States. Black/African Americans, Latinos/as, Asians, American Indians, and Pacific Islanders make up roughly 30% of all clinical trials (CT) participation across all race groups. Being inclusive of all populations in CT ensures that everyone has access to modern medicines and treatments, but also, that these latest treatments work and react well to all people.
Methods: We developed a manual on clinical trials with a target focus to African Americans and African Nationals. We hosted two focus groups with Blacks/African Americans in which we found they are more comfortable getting cancer related information through trusted community services, such as coming from churches. We have connected with over 80 Pastors who agreed to collaborate in clinical trials education.
Results: Through outreach and engagement to African American churches in Los Angeles County, we have distributed a copy of this clinical trials educational manual to 90 churches to be disseminated during their services. Our office of Community Outreach and Engagement (COE) regularly attend community health and resource events and provide hard copies of the clinical trials manual at tables/booths designated for our participation. We have attended 50 community events and have disseminated about 1,900 copies of the CT manual so far this year 2023. This manual is also available for free download on our cancer center's website, in which over 100 toolkits have been downloaded within the last year.
Conclusions: By creating a culturally sensitive and adapted educational manual and partnering with trusted services in the community such as faith-based organizations, we can begin to break down barriers to clinical trials participation among all race and ethnic minority groups.

POPULATION SCIENCES: Descriptive Epidemiology and Statistical and Epidemiological Methodology
Poster Session

#4844 Epidemiology of bone and soft-tissue sarcomas: A two-decade analysis of the surveillance, epidemiology, and end results program.

Marc El Beaino[1], **Rachel Baum**[1], Katherine M. Connors[1], Karim Masrouha[2], Santiago A. Lozano-Calderon[3], Patrick P. Lin[4]

[1]Department of Orthopaedic Surgery and Rehabilitation Medicine, State University of New York, Downstate Health Sciences University, Brooklyn, NY,[2]School of Public Health, State University of New York Downstate Medical Center, Brooklyn, NY,[3]Department of Orthopaedic Surgery, Harvard Medical School, Boston, MA,[4]Department of Orthopaedic Surgery, New York University Langone Health, New York, NY

In the United States, ~15000 cases of bone and soft-tissue sarcomas are diagnosed annually, representing roughly 1% of all incident cancers. While several studies have analyzed independent predictors of outcomes for these sarcomas, small samples and confounding bias have limited their ability to establish reliable conclusions. The present analysis provides a comprehensive epidemiological description of patients with any of 16 distinct bone and soft-tissue sarcomas by querying the Surveillance, Epidemiology, and End Results database between 2000 and 2020. Incidence, prevalence, incidence-based mortality, survival rates, and case-fatality ratios were computed. Using patient age, sex, race, and ethnicity, as well as tumor size, grade, and stage as covariates, multivariable survival Cox proportional hazards regression analyses were performed to model hazard ratios (HRs) and identify independent predictors of worse prognosis. Only patients with myosarcoma and fibrous histiocytoma witnessed a decrease in the prevalence of their disease over time (both, $p<0.05$). The incidence of chondrosarcoma and synovial sarcoma increased in White and Asian patients but decreased in Black individuals (both, $p<0.001$), while their case-fatality rates remained constant and increased, respectively, regardless of race and ethnicity (all, $p<0.05$). Case-fatality rates only declined significantly for White and Non-Hispanic patients with solitary fibrous tumor (both, $p<0.05$). Aside from alveolar soft-part sarcoma and clear cell sarcoma, a 10-year increase in age of patients with bone and soft-tissue sarcomas resulted in 18% to 61% higher likelihood of death (all, $p<0.05$). For most malignancies, having a tumor size greater than 5 cm yielded a 37% to 189% higher likelihood of death. While incidence trends suggest improvements in diagnostic techniques and early tumor detection, survival and case-fatality trends indicate potential for advancement in treatment for most bone and soft-tissue sarcomas.

#4845 Evaluating racial disparities in immune checkpoint inhibitor survival and autoimmunity.

K. L. Nunes, P. Llerena, P. Kaki, S. Mandloi, A. Moroco, E. Mastrolonardo, D. M. Cognetti, A. J. Luginbuhl, J. M. Curry;
Thomas Jefferson Univ. Hospital, Philadelphia, PA

Introduction: In recent years, immune checkpoint inhibitors (ICI) have revolutionized the landscape of treatment across a variety of cancers. Potential concerns regarding racial disparities in ICI access and therapeutic efficacy have been well documented. Recent studies have indicated improved ICI access and response outcomes in White patients compared to minority groups with head and neck cancer (HNC) and melanoma patients. In contrast, patients diagnosed with lung cancer have been mixed, with some research suggesting black patients may fare better with ICI therapy. Existing literature is largely limited to retrospective studies with small population sizes, and lacks comparisons of racial disparities across malignancies. We aim to describe and compare racial inequities in ICI outcomes in HNC, melanoma, and lung cancer.

Methods: The TriNetX US Collaborative Network database was queried for patients >18 years-old with a diagnosis of head and neck cancer, melanoma or lung cancer that were treated with ICIs. Malignancy cohorts were defined by race: non-Hispanic White (NHW) and Black. Race cohorts were 1:1 propensity score matched (PSM) for comorbidities, oncologic stage, and chemoradiation treatment. Demographic differences in cohorts were evaluated prior to matching. Following PSM, overall survival and rates of autoimmunity were assessed at 5 years.

Results: 19,443 NHW and 2,827 Black patients treated with ICI were identified. At a baseline, the Black patient cohorts had significantly higher rates of comorbidies ($p<0.02$). Across all malignancies, the geographic distribution of NHW patients was more equally distributed compared to Black patients (majority south). With PSM, black HNC patients had significantly lower survival rates compared to NHW [HR: 1.4 (1.2, 1.6), $p=0.0002$]. In melanoma, the same trend was present, though not significant [HR: 1.3 (0.95, 1.7), $p=0.1$]. In contrast, in lung cancer, Black patients had significantly higher survival rates compared to NHW patients [HR 0.78 (0.70, 0.86), $p<0.0001$]. In HN and lung cancer, NHW patients had significantly higher rates of autoimmune conditions after ICI therapy compared to Black [OR: 2.0 (1.4,2.8), 1.2 (1.0, 1.4), respectively].

Conclusion: This study represents the most extensive analysis of racial disparities on ICI outcomes across malignancies. This study found that black patients treated with ICIs had decreased survival rates at 5 years compared to NHW patients in HNC and melanoma, but increased survival rate in lung cancer. This disparity persisted following PSM, matching cohorts for comorbidities, oncologic stage and adjuvant therapy. Black patients also had significantly lower rates of autoimmunity in HN and lung cancer. Noted differences in survival may be a reflection of geographic practice differences, access to care and/or socioeconomic status. Further investigation is required to elucidate the underlying etiologies of these trends.

#4846 Geographic and physician-level variation in the use of hypofractionated radiotherapy for breast cancer in the U.S.: A cross-classified multilevel analysis.

Y. Sun, L. Saulsberry, C. Liao, D. Hedeker, D. Huo;
University of Chicago, Chicago, IL

Hypofractionated whole-breast irradiation (HF-WBI), a radiotherapy with a larger dose per fraction and a shorter schedule for early-stage breast cancer patients post breast-conserving surgery, shows equivalent safety and efficacy compared to conventionally fractionated whole-breast irradiation (CF-WBI) regarding local recurrence and disease-free survival. While several countries have set HF-WBI as the preferred standard of care for these patients, its uptake in the U.S. has lagged behind expectations. We used the Health Care Cost Institute (HCCI) database 2008-2017, covering a third of the U.S. employer-sponsored insurance population, to identify early-stage breast cancer patients. Patients were clustered at different geographic levels (Census region, state, core-based statistical area (CBSA), hospital referral region of Dartmouth Atlas, and zip code) and the radiation oncologist level. These two levels are cross-nested. We used a Bayesian cross-classified multilevel logistic model to simultaneously model the geographic units variability and physician-level variability in HF-WBI use across the U.S. Variation metrics included intracluster correlation coefficient (ICC) and median odds ratios (MOR). ICC with a value of 0 is equivalent to MOR of 1, indicating identical outcomes across all levels. After accounting for these variations in the cross-classified multilevel model framework, we evaluated the association between HF-WBI use and clinical and demographic factors.Our study included 79,747 women (74.0%) who underwent CF-WBI and 27,999 (26.0%) who received HF-WBI. HF-WBI adoption increased over time (2008-2017). Variability across radiation oncologists (ICC = 0.272, MOR = 2.88) was notably larger than geographic areas variability. Variability across CBSA (ICC = 0.097, MOR = 1.76) was the strongest among all the geographic levels. The variation in HF-WBI use was mainly attributed to physician-level variability (ICC=0.222, MOR=2.59) based on the cross-classified multilevel model. No substantial differences were found between young (aged 64 or younger with commercial health plans) and older patients (aged 65 or older with Medicare Advantage plans) in terms of both geographic and physician-level variations. After accounting for variability in radiation oncologists and CBSAs, older age, non-reception of chemotherapy, and several community-level factors, including longer distance from home to facility and higher community education level, were associated with a higher likelihood of HF-WBI use. These results may lend insights into potential facilitators/barriers to HF-WBI uptake. Future studies can further investigate the impact of the 2018 American Society for Radiation Oncology (ASTRO) guideline and the Covid-19 pandemic on HF-WBI use, which would illuminate potential improvements of healthcare practices.

#4847 Diverging global incidence trends of early-onset and later-onset cancers.

M. Terashima[1], H.-Y. Lee[2], Y. Tsukumo[3], S. Ugai[4], M. Song[5], N. Sasamoto[6], I. Kawachi[4], T. Ugai[6];
[1]Okayama University Medical School, Okayama, Japan, [2]Graduate School of Public Health and Healthcare Management, The Catholic University of Korea, Seoul, Korea, Republic of, [3]Boston University, Boston, MA, [4]Harvard T.H. Chan School of Public Health, Boston, MA, [5]National Institute on Aging, Baltimore, MD, [6]Brigham and Women's Hospital, Boston, MA

Background: The global increase of the incidence of early-onset cancers (defined as cancers diagnosed at 20-49 years) is a serious public health problem. However, it is understudied whether the incidence of early-onset cancers has increased in parallel with that of later-onset cancers (defined as cancers diagnosed at 50 years or above) or only the incidence of early-onset cancer has increased worldwide. We therefore evaluated the recent global trends of the incidence of early-onset cancers and later-onset cancers.
Method: We retrieved sex-stratified age-standardized incidence rates of early-onset cancer and later-onset cancer diagnosed between 2000 and 2012 in 39 countries where data was available from the GLOBOCAN database. Using joinpoint regression models, we assessed average annual percentage change (AAPC) by cancer types and countries, with statistical significance corresponding to a 95% CI that does not include zero.
Results: We observed statistically significant positive AAPCs for early-onset cancers (AAPC [95% CI], 1.9% [1.8%, 2.1%] for females, 0.7% [0.6%, 0.9%] for males in all available countries combined) in many early-onset cancer types, including colorectal, esophagus, gallbladder, kidney, liver, multiple myeloma, pancreas, prostate, stomach, testis, thyroid and uterine cancer in many parts of the world. There were variations in many later-onset cancer types depending on cancer types and countries. Notable cancer types that have significantly increased in early-onset cancers but have decreased or showed no change in later-onset cancers include colorectal (5 countries in females and 6 countries in males), uterine (4 countries), and thyroid cancers (5 countries in females and 3 countries in males). In particular, early-onset colorectal cancer has increased but later-onset colorectal cancer has decreased among both sexes in Canada (AAPC [95%CI], early-onset: 1.6% [0.9%, 2.7%], later-onset: -0.8% [-1.0%, -0.5%] for females; early-onset: 1.8% [1.0%, 2.6%], later-onset: -1.2% [-1.5%, -0.9%] for males), USA (Early-onset: 2.0% [1.5%, 2.5%], later-onset: -2.7% [-2.9%, -2.6%] for females; early-onset: 1.6% [1.1%, 2.2%], later-onset: -3.2% [-3.7%, -2.6%] for males), Australia (Early-onset: 1.8% [0.7%, 2.9%], later-onset: -1.0% [-1.5%, -0.6%] for females; early-onset: 1.4% [0.7%, 2.4%], later-onset: -1.5% [-1.9%, -0.9%] for males).
Conclusion: Our study highlights differences in cancer incidence trends between certain early-onset and later-onset cancer types in many parts of the world. Notably, early-onset colorectal, uterine, and thyroid cancers have significantly increased but corresponding later-onset cancers have decreased or showed no change in many countries. Different patterns in cancer incidence trends of early-onset and later-onset cancers in different regions should be further investigated to better understand and prevent the increase in the incidence of early-onset cancers.

#4848 An analysis of black women in the Deep South with triple negative breast cancer and the social determinants of health.

L. K. Evans, I. T. Jubilee II, K. P. Lemieux;
Xavier University of Louisiana, New Orleans, LA

Background: Triple negative breast cancer (TNBC) has a higher incidence both of diagnosis and mortality among Black women. This research aims to identify specific social determinants of health among African American women in the Deep South with breast cancer. The biological presentation of disease accounts for approximately forty percent of the Experience with the health care providers, access to greenspace, and the quality of infrastructure, such as sidewalks and streetlights evaluate environmental trends associated with the outcomes of Black women in the Deep South who have been diagnosed with TNBC.
Methods: Survey data was derived from the All of Us Research Program Database with inclusion criteria of Black women from Alabama, Georgia, Mississippi, and Louisiana who are 18 or older, born a female, and have been diagnosed with TNBC. Selected questions from the SDoH survey examined infrastructure, interactions with healthcare providers, and perceptions of community dynamics. Participants were identified via the cohort selection tool and further subdivided based on zip codes within the target states. Python was used in Jupyter Notebook to analyze the data the AoURP Workbench, responses were organized according to their corresponding survey questions. Participant responses were then extracted and quantified, facilitating the interpretation of respondents' answers on a larger scale.
Results: Three hundred and twenty women met the criteria of being born female, being black, being diagnosed with TNBC, and living in the Deep South. Of the topics examined, infrastructure was the area where participants' feedback indicated the largest socioeconomic deficit. Forty-eight and 49%, respectively. Indicated that did not have access to greenspace nor did not live within 10-15-minute walking distance of a transit stop. Thirty percent reported that their doctor or nurse does not listen to what they are saying.
Conclusion: Quality of life and interaction with members of the health care team associated with poorer health outcomes for Black women in the Deep South. These preliminary results indicate that those diagnosed with TNBC are impacted by the social determinants of health, specifically, proximity to public transportation, quality healthcare, recreational facilities, and infrastructure which suggests that basic needs are not met.

#4849 Mosaic chromosomal alterations in a prospective cohort of Mexican Americans for cancer risk and genetic insights.

Jessica Valdebenito[1], Justin Wong[1], Dahwei Chang[1], Henry Gomez[1], Kevin T Nead[1], Yasminka Jakubek[2], Paul Scheet[1]

[1]Epidemiology, University of Texas MD Anderson Cancer Center, Houston, TX,[2]Internal Medicine, College of Medicine, University of Kentucky, Lexington, KY

Introduction: In this study, we aim to explore mosaic chromosomal alterations (mCA) and their implications in cancer risk among Mexican Americans (MA) - an expanding yet historically underrepresented ethnic minority in the U.S. In addition, we propose to develop a novel method that identifies high mutant cell fraction (MCF) copy-neutral Loss of heterozygosity (cn-LOH). At sufficiently high MCF, these will look like runs of homozygosity (ROH) and may be missed by current mCA detection techniques that rely on identified germline heterozygote genotypes. Our preliminary findings revealed frequent and widespread homozygosity across the genome, predominantly in short regions (<10 Mb), although some exceeded 100 Mb. Our objective is to advance mCA detection techniques, differentiating cn-LOH from ROH, to deepen our understanding of mCA.

Methods: We analyzed SNP array data from blood and saliva samples of 1657 individuals, focusing on cancer and chronic disease risk ages, from the *Mano a Mano* Mexican American Cohort Study. We applied hapLOH and MoChA, both haplotype-based methods, to detect mCA. To identify high-MCF cn-LOH, we first scanned for observed ROH using PLINK. Separately, we develop a statistical framework through simulations to differentiate high-MCF cn-LOH from ROH. We considered multiple methods; initially, we built a statistical framework using a hypothesis-testing approach (H_0: ROH; H_1: cn-LOH), where we compared the “B allele” frequency information within observed ROH. To split this information and obtain our groups, we used population genetic principles. Secondly, we classified our events, calculating the likelihood ratio of our statistical hypotheses. Finally, we explored a haplotype-based imputation approach that leverages flanking diploid region information.

Results: We identified numerous mCA, predominantly in individuals without cancer. Simulations showed effective classification in larger homozygosity regions (>10 Mb), guiding our methodological focus on detecting shorter high-MCF regions. Not surprisingly, extremely high MCFs (0.99-1) presented challenges in accurate identification.

Conclusion and Future Directions: To improve our mCA results description, we will thoroughly characterize and study their association with cancer phenotypes and environmental exposures. We are in the process of genotyping the entire cohort, which consists of over 25,000 participants. To date, our cohort includes 909 cancer cases, of which 262 are hematological malignancies. We sought to design a unique method that differentiates high-MCF cn-LOH from observed ROH, improving current mCA discovery. Our focus is on small regions as they provide limited information to infer event types. Our next step is to characterize and validate our results, especially in pathologically normal samples, as a way of identifying potential biomarkers of interest.

#4850 Sex differences in cancer incidence: Prospective analyses in the UK Biobank.

M. Khan, K. Papier, K. Pirie, J. Atkins, T. Key, R. Travis;
Oxford Population Health, University of Oxford, Oxford, United Kingdom

Background: Exploring the underlying sex differences in cancer incidence and the potential reasons for the differences may provide insights into cancer aetiology. We aimed to examine the differences in incidence of cancer between men and women in the UK Biobank and to assess the extent to which any disparities persisted after accounting of established risk factors for those cancers.
Methods: Prospective analyses were performed in the UK Biobank to examine associations between sex and risk of 15 cancers (and 13 subtypes) common to both sexes using minimal and multivariable-adjusted Cox proportional hazards regression models.
Results: Over an average of 10.5 (SD 2.2) years of follow-up, 46,081 incident cancers were identified in 470,771 individuals (aged 37 to 73 years at recruitment); 24,634 cancers (53.5%) diagnosed in women and 21,447 (46.5%) in men. While some differences in cancer risk between the sexes were attenuated in the comprehensively multivariable-adjusted models, men compared to women remained at greater risk of cancers at eight sites. Compared to women, men had higher risks of oesophageal adenocarcinoma (hazard ratio 5.45; 95% confidence interval, 4.17-7.12), gastric cardia (3.65; 2.48-5.38), bladder (3.47; 2.85-4.24), oral (2.06; 1.69-2.51), liver (1.91; 1.48-2.47), kidney (1.77; 1.51-2.09), rectum (1.7; 1.47-1.96), and leukaemia (1.43; 1.21-1.69); while women had higher risks of cancers of the breast, thyroid (0.36; 0.26-0.49), anus (0.41; 0.26-0.64), gallbladder (0.56; 0.31-0.99), and lung adenocarcinoma (0.72; 0.62-0.84).
Conclusion: Further studies of unexplained sex differences may provide insights into cancer aetiology.

#4851 Burden and inequality of early-onset tracheal bronchus, and lung cancer in US, China, and India: A trend and comparison analysis.

Wenxuan Li, Guojin Si, Yacong Zhang, Zhangyan Lyu, **Kexin Chen**

Tianjin Medical Univ. Cancer Inst. & Hospital, Tianjin, China

Background: For tracheal, bronchus, and lung (TBL) cancer, the leading cause of cancer morbidity and mortality worldwide, guaranteeing quality health care for all populations is a critical component of achieving universal health coverage. Little is known about the burden and inequality of early-onset TBL cancer in countries with different economic development levels. This study aimed to compare the trends of TBL cancer burden among adults in the United States (US), China and India.

Methods: Early-onset TBL cancer age was defined as 15-49 years old. We used Joinpoint regression to evaluate the average annual percentage change (AAPC) and its 95% confidence intervals (CIs) to quantify trends in incidence, mortality, and disability-adjusted life years (DALY) based on the Global Burden of Disease 2019 database. We also used the Gini coefficient (GC) to measure the age-standardized DALY rate (ASDR) inequalities across three countries.

Results: The incidence, mortality, and DALY rates for early-onset TBL cancer among Americans. population from 1990 to 2019 declined from $7.81/10^5$ to $4.23/10^5$, $5.95/10^5$ to $2.96/10^5$, and $270.54/10^5$ to $133.41/10^5$, respectively. However, among the Chinese and Indian populations, the incidence (China: $5.30/10^5$ to $7.47/10^5$; India: $0.99/10^5$ to $1.38/10^5$), mortality (China: $4.73/10^5$ to $5.82/10^5$; India: $0.90/10^5$ to $1.23/10^5$) and DALY (China: $227.94/10^5$ to $270.26/10^5$; India: $42.89/10^5$ to $58.64/10^5$) rate of early-onset TBL cancer show upward trend from 1990 to 2019. The AAPC in incidence (China: 1.14, 95%CI: 0.87 to 1.40; India: 1.17, 95%CI: 0.85 to 1.49), mortality (China: 0.68, 95%CI: 0.45 to 0.91; India: 1.17, 95%CI: 0.81 to 1.52) and DALY (China: 0.50, 95%CI: 0.18 to 0.86; India: 1.11, 95%CI: 0.78 to 1.43) rates for early-onset TBL cancer from 1990 to 2019 in both Chinese and Indian populations showed an increasing trend and the increasing trend was higher than the 50-74 age group. While the AAPC in American populations presented a decreasing trend of early-onset TBL cancer (incidence: -1.76, 95%CI: -2.14 to -1.37, mortality: -2.33, 95%CI: -2.56 to -2.10, DALY: -2.35, 95%CI: -2.59 to -2.12). The AAPC in incidence mortality and DALY rates for early-onset TBL cancer from 1990 to 2019 in both the Chinese and Indian female populations showed a higher trend than the male population. The GC value of ASDR for TBL cancer showed a downward trend, from 0.32 in 1990 to 0.24 in 2019; but for early-onset TBL cancer, it showed an upward trend, from 0.28 in 1990 to 0.31 in 2019, across three countries.

Conclusions: Compared to the US, early-onset TBL cancer burden in China and India has been rising annually. The inequality in ASDR for early-onset TBL cancer remains high across all three countries. Redistributing attention and resources to help adults in low or middle socioeconomic-level countries, especially the female population, may help hold back the expanding inequality for TBL cancer.

#4852 High brain relapse rates in stage III triple negative inflammatory breast cancer are independent of systemic therapy.

Azadeh Nasrazadani, Rebecca Slack Tidwell, Megumi Kai, Rachel Layman, Vicente Valero, Sadia Saleem, Bisrat G. Debeb, Anthony Lucci, Susie X. Sun, Swetha Bopparaju, Hope E. Murphy, Angela Alexander, Angela N. Marx, Michael C. Stauder, Bora Lim, Wendy A. Woodward

MD Anderson Cancer Center, Houston, TX

Background - Inflammatory breast cancer (IBC) is an aggressive subtype of invasive breast carcinoma that confers a comparatively poorer prognosis owing to consistently observed inferior responses to systemic therapies as compared to non-IBC cases. Triple negative (TN) breast cancer which is characterized by lack of estrogen receptor (ER) and progesterone receptor (PR) expression, as well as by lack of HER2 amplification portends particularly poor outcomes including high rates of brain failure. Here we reviewed our prospective IBC registry data for contemporary TNIBC patients to assess current outcomes and brain failure risk in the context of standard neoadjuvant immunotherapy.

Methods - Given the change to the inclusion of pembrolizumab in addition to chemotherapy in the neoadjuvant setting in 2020, we reviewed records from 2016-2023 for Stage III TNIBC patients who presented to MD Anderson Cancer Center (MDACC) prior to receiving other therapy. TNIBC was defined as ER <1%, PR <1%, HER2 IHC 0/1+ or ISH-. N = 38. We examined PCR and brain mets as first failure by regimen (KN522, ACT, AC/TC) and compared using descriptive statistics. Log rank statistic was used to compare overall survival (OS) by PCR. Patients with stage III TNIBC who started the KN522 regimen achieved a pCR rate of 35% (N= 20) and pCR was less frequent in postmenopausal KN522 patients (1/7 PCRs. P = 0.016). Among this cohort, 20% of patients experienced relapse in the CNS as a site of first failure including two patients who achieved a PCR, and 25% had any brain failure at a median follow up post-surgery of 8M. Among 9 patients treated with AC/T 22% achieved pCR with 22% brain metastasis relapse rate as site of first failure and 33% overall was observed at a median follow up of 14M post-surgery. In 9 patients receiving AC/TC, the PCR was 44% and any brain relapse rate was 22%, 1/2 was a site of first failure, median follow up 38M. Despite similarities in brain relapse rates, achieving pCR nonetheless correlated with improved overall survival, P < 0.05. For comparison, among 11 stage IV TNIBC patients treated with neoadjuvant systemic therapy pre-KN522, median follow up 22M from initial diagnosis, 6/11 patients developed brain involvement, 5/6 as a site of first failure. Given small numbers it is difficult to compare PCR by regimen, however we note the PCR in KN522 is lower than expected, and the rate of brain metastases particularly as a site of first failure is consistently high across regimens regardless of PCR. It is critical to consider brain penetrance of neoadjuvant systemic therapies, brain staging and even prophylaxis of brain metastasis in patients with non-metastatic and metastatic TNIBC. Current efforts are ongoing to determine molecular signatures which may aid in prognostication and potentially study design to incorporate prophylactic therapies with the overarching goal of improving outcomes in patients with triple negative IBC.

#4853 Impact of different therapeutic strategies on survival in laryngeal squamous cell carcinoma (LSCC).

S. Alshwayyat[1], A. Erjan[2], M. Rawashdeh[3], T. Abdulsalam[1], M. Alshwayyat[1];

[1]Jordan University of Science & Technology, Irbid, Jordan, [2]King Hussein Cancer Foundation, Amman, Jordan, [3]King Abdullah University Hospital, Irbid, Jordan

Background: LSCC has seen a rise in cases and deaths over the past 30 years. Considering advancements in the treatment landscape, therapeutic options for patients with LSCC were evaluated to assess their efficacy in improving survival rates.

Methods: Data were retrieved from the Surveillance, Epidemiology, and End Results (SEER) (2000-2020) for localized/regional-stage cancer only, including the glottis (GC), supraglottic (SuGC), and subglottic (SC). Patients with a histologically confirmed diagnosis, no other malignancies, and complete data were included. Eight therapeutic groups were identified: surgery (Sx), chemotherapy (CTX), radiotherapy (RT), Sx + adjuvant radiotherapy (ART), Sx + CTX, Sx + RT, Sx + CTX + RT, and CTX + RT. T-tests and chi-square tests were used to compare variables, while Kaplan-Meier, log-rank tests, and Cox regression were used to identify prognostic factors for overall survival (OS) and cancer-specific survival (CSS).

Results: 68,282 patients were included (43,434 GC, 24,010 SuGC, and 838 SGC). 12.8% underwent Sx, 0.8% CTX, 0.3% Sx + CTX, 17.1% Sx + ART, 35.3% RT, 1.5% Sx + RT, 5.1% Sx + CTX + RT and 21.5% CTX + RT. 80.8% were males and 63.5% were over 60 years old and white (n=56,171). The median age was 64 years, and median tumor size was 3.2 cm. 36.5% underwent surgery with local tumor excision in 23.9 % and total laryngectomy in 5.7%. White race, regional stage, large tumor size, and CTX were poor prognostic factors for GC. Asian, white race, and total laryngectomy were good prognostic factors for SuGC, whereas male sex and older age were poor prognostic factors. In terms of SCG, Sx + ART was associated with a better prognosis, while regional and white race were associated with a poor prognosis.

Conclusion: This study shows survival differences among treatment groups and identifies factors for personalized treatment. It is the first study on all types of laryngeal tumors with a large sample size. Further research is necessary to validate and expand these results.

The 5-year survival rates (as a percentage of OS/CSS) for each therapeutic group

Cancer Type	Sx	CTX	Sx + CTX	RT	Sx + RT	CTX + RT	Sx + CTX + RT	Sx + ART
GC	91.9/75.5	79.8/77.3	89.2/81.8	89.8/78.1	89.5/85.3	87.8/83	79.1/90.1	90/78.1
SuGC	54.7/56.5	12.9/46.7	25.6/56.2	43.1/51.9	33.5/56.4	45.7/49.7	50.5/59.4	49.3/59.3
SGC	42.2/42.2	75/75	17.7/17.7	53/53	44.4/44.4	47.2/47.2	44.1/41.1	58.7/58.7

#4854 Breast cancer incidence trends in Ukraine 2010-2019: Rising incidence at young ages.

N. Verovkina[1], O. Sumkina[2], L. Syvak[3], W. El-Diery[1];

[1]Legorreta Cancer Center at Brown University, Providence, RI, [2]National Cancer Institute, Kyiv, Ukraine, Kyiv, Ukraine, [3]National cancer institute, Kiev, UA, Kyiv, Ukraine

Background. BC commonly affects women of older age, however, in developing countries around 20-25% cases of BC presented in young woman. Age-specific clinical characteristics or outcomes data for young women are lacking. Most of the standard treatments used in this subpopulation currently are derived from older patients. Early onset BC is often defined aggressive in nature. Several research have attributed this to a hidden unique biology. However, findings remain controversial.

Purpose: The aim of this study is to describe recent trends for BC incidence in Ukraine since 2010 by age groups and interpret them to seek clue for improvement.

Methods: We analyzed records from the NCR on 143420 BC cases (C50, International Statistical Classification of Diseases and Related Health Problems, 10th Revision (ICD-10)) diagnosed in 2010-2019 in female Ukrainian population. The data were submitted on the beginning of 2022. We calculated annual age-standardized incidence rates (ASRWs) for three age groups. The estimated annual percent change (EAPC) of the rates was calculated using the generalized linear regression. The difference of the rates with its statistical significance was determined with the standardized rate ratio.

Results: During 2010-2019, the proportion of BC in all cancers detected at the age of 20-44 increased from 21.7% to 25.9%, while the frequency of BC detection at the age of 45+ did not change and ranged 19.3-20.2%. During the study period, the BC incidence rate has increased significantly (≤0.01): the ASRW of females aged 0-85+ grew with EAPC=0.6% amounting to 42.4-45.7 per 100,000 population, the incidence rate of women aged 45+ grew with EAPC=0.3% ranging from 130.0 to 139.6 per 100,000 population, while the incidence rate of women aged 20-44 grew with EAPC=1.8% amounting to 22.8-27.8 per 100,000 population. In age group 20-44 years, EAPC of BC incidence (1.8%) significantly exceeds the EAPC of the incidence for all cancers combined (0.2%). The dynamics of stage distribution showed increasing proportion of BC cases detected in women aged 20-44 in stage 1 (by 4.1% from 2010 to 2019) and its decreasing for BC cases detected in stage 2 by 4.5%; the proportion of cases diagnosed in stage 4 decreased by 0.5% along with increase in number of cases with undefined stage by 0.6%.

Conclusions: The obtained results indicate trends for increasing the incidence of Early Onset BC in Ukraine and justify need for the further research elucidating prognosis and validating novel biomarkers for customizing therapy for this patient group .

#4855 Identifying hot spots of breast cancer and industrialized areas in Hermosillo, Sonora, Mexico.

D. E. Villa-Guillen[1], A. A. Mata-Valenzuela[2], H. Tecuanhuey-Tlahuel[2], A. M. Galvez-Arevalo[3], K. L. Garcia-Castellon[4], Y. E. Guzman-Hernandez[4], K. S. Ortega-Landa[5], F. Y. Pelayo-Rodriguez[6], J. R. Silva-Rivera[4], R. A. Urena-Acosta[7], D. O. Garcia[1], J. A. Villa-Carrillo[5];
[1]The University of Arizona, Tucson, AZ, [2]IMSS UMF No. 37, Hermosillo, Mexico, [3]Universidad Autonoma de Occidente, Los Mochis, Mexico, [4]Universidad Autonoma de Nayarit, Tepic, Mexico, [5]Universidad de Sonora, Hermosillo, Mexico, [6]Universidad de Guadalajara, Guadalajara, Mexico, [7]Universidad Autonoma de Sinaloa, Culiacan, Mexico

Background: Sonora, a state in Mexico, has the highest rates of breast cancer in the country and has a history of industrial pollution. These factors may contribute to an increased risk of breast cancer. Hermosillo, the state capital, exhibits both of these characteristics. Given these conditions, it is important to further evaluate the prevalence of breast cancer hotspots and the potential links between breast cancer and industrialized areas.
Objective: Identify breast cancer hot spots and their association to industrialized areas in Hermosillo, Sonora, Mexico.
Methods: This study collected clinical data on breast cancer cases (current, survivors, deceased) from hospital files in Hermosillo that were 10 years old. The primary unit of analysis was neighborhoods. The study estimated breast cancer prevalence by analyzing the number of females per neighborhood, based on data reported by INEGI Census 2020. The data was categorized by age groups (age group no. 1 of 18 to 59 years old, no. 2 of 60 to 64 years old, and no. 3 of 65 years old or older). The estimated prevalence was depicted on a map using ArcGIS software, version 10.8.2. Hot spot analysis was used to identify neighborhoods with high breast cancer prevalence. The study also categorized neighborhoods as industrialized areas if they contained at least six hazard-generator industries.
Results: A total of 1394 cases of breast cancer were gathered from hospitals. Location information for 3697 industries was provided by INEGI. Out of the 756 neighborhoods studied, 95 (12.6 %) were found to be industrialized areas, while 661 (87.4 %) were non-industrialized. Four neighborhoods in Hermosillo's southeast were observed to have breast cancer hot spots (unadjusted). After adjusting for age, one hot spot was found in the southeast for age group no. 1 (one neighborhood), while hot spots for group no. 2 (three neighborhoods) and no. 3 (33 neighborhoods) were in Hermosillo's northwest. The hot spots were related to industrialized areas (unadjusted OR = 6.94, 95% CI (0.94, 50.8), p-value = 0.05). After age adjustment, this association was statistically significant for group no. 3 (OR = 2.70, 95% CI (1.27, 5.72), p-value = 0.009), but not for group no. 1 (OR = 1.69, 95% CI (0.06, 41.74), p-value = 0.748) or group no. 2 (OR = 2.56, 95% CI (0.23, 28.46), p-value = 0.44).
Conclusions: Our research found a link between industrialized areas and high breast cancer rates. We also found hotspots for women aged 65+ in Hermosillo, with 33 affected neighborhoods in the city's northwest. This is the first comprehensive study examining breast cancer prevalence in Hermosillo over a ten-year period. More extensive studies are needed in other cities in Sonora, Mexico, to confirm our findings.

#4856 Sex differences in childhood leukemia genomics.

Lindsay A. Williams[1], Lauren J. Mills[2], Sofia Barragan[2], Peter M. Gordon[2], Jenny N. Poynter[2]

[1]University of Minnesota, Woodbury, MN,[2]University of Minnesota, Minneapolis, MN

Males have higher ALL and AML incidence and worse ALL survival using population-based data. Somatic genetics may play a role in ALL survival disparities and highlight potential sex specific treatment strategies for future study. Therefore, we evaluated sex differences in gene expression (RNA seq), copy number variation (CNV), and somatic mutation in ALL and AML. We stratified by cytogenomic subtypes in publicly available data from clinical cohorts using St. Jude PeCan (subtypes in Table 1). Then, we explored survival differences by sex within cytogenetic subtypes in publicly available data collected from Children's Oncology Group patients in the NCI TARGET dataset (ALL n=387, 63% male; AML n=151, 51% male). Differentially expressed genes by sex were identified for ALL adjusting for subtype (n=214) and within subtypes (Table 1). There were no sex differentially expressed genes shared across subtypes and pathways identified from sex differentially expressed genes were few. In *ETV6-RUNX1,* there was as suggestion of worse 10-year survival for males (n=44, 61% male; Log-Rank p=0.068). Differentially expressed genes by sex were identified for AML adjusting for subtype (n=537) and within subtypes (Table 1). There were no differentially expressed genes by sex shared across AML subtypes. *KMT2A* had the highest number of pathways identified from sex differentially expressed genes (Table 1). There were no sex differences in AML survival. In ALL and AML subtypes there were no sex differences in CNVs (all t-test p>0.05) or somatic mutations (all Fisher's Exact p>0.05). There were no sex differences in AML survival in TARGET, in agreement with population-based studies, and few differentially expressed genes identified in PeCan by subtypes. Sex differences in ALL survival were subtype specific and not heavily dependent on differentially expressed genes, CNVs, or somatic mutation. Sex differences in ALL survival may depend on treatment received, response to therapy, or other characteristics.

Table 1. Select characteristics from leukemia cases

PeCan ALL SubtypeTotal n=247, 58% male	N (% male)	Number of differentially expressed autosomal genes by sex (male-female expression) in PeCan	Number of biologic pathways identified from differentially expressed genes (Reactome)
BCR-ABL1	76 (68)	48	8
DUX4-IGH	54 (57)	218	0
ETV6-RUNX1	50 (52)	86	1
hyperdiploid	14 (64)	3,199	2
iAMP21	12 (50)	120	0
KMT2A	41 (51)	216	0
AML SubtypeTotal n=149, 51% male			
CBFB-MYH11	34 (55)	7	0
KMT2A	44 (50)	422	19
RUNX1-RUNX1T1	61 (46)	30	1

#4857 Contemporary hospital-based study examining demographics, treatment patterns and survival outcomes of primary effusion lymphoma in the United States, with a specific emphasis on Hispanics..

S. A. Vallejo Avila, J. Michalek, Q. Liu, A. E. Diaz Duque;
UT Health Science Center at San Antonio, San Antonio, TX

Background: Primary effusion lymphoma (PEL) is a rare and aggressive non-Hodgkin lymphoma associated with HIV and human herpesvirus 8 (HHV-8). (***Blood*** *PMID: 8695812).* Without treatment, patients typically survive only two to three months (***Oncol Res Treat*** *PMID: 28253516*) Limited research has been conducted on PEL, particularly in minorities in the United States. Limited research, especially in minority populations (***Blood*** *PMID: 30154110*), has prompted a nationwide study comparing demographics, clinical characteristics, treatment patterns, and survival outcomes between Hispanic (HI) and Non-Hispanic (NH) PEL patients.

Methods: Data on PEL patients from the National Cancer Database (NCDB) between 2004 and 2019 were analyzed in the US. Demographics and treatment characteristics were compared across ethnic groups. Kaplan-Meier and Cox regression analyses were used to compare overall survival (OS) between HI and NH populations. Multivariate analysis and propensity score matching were conducted, adjusting for age, stage, co-morbidity score, insurance status, type of facility, and great circle distance.

Results: Of 459 PEL patients, 18% were HI, and 79% were NH. Both groups had mostly male patients (87% vs. 86%). HI patients were younger at diagnosis (mean 49 years vs. 57 years, p=0.163). Diagnoses were mostly from 2014-2019, and the majority were white (87% vs. 69%). Government-sponsored insurance was more prevalent in both groups (62% vs. 66%). HI had a higher percentage of uninsured individuals (8% vs. 5% NH) (p-value=0.01). The median income bracket was over $46,000 for both cohorts, HI 34% and NH 37%. Advanced comorbidities were similar between HI 50% and NH 43% based on Charlson-Deyo Score. The survival probabilities at 2, 5, and 10 years for HI vs NH were (40% vs 40%), (34% vs 289%), and (34% vs 24%), respectively. The median survival time (MS) was 0.8 years for HI and 0.9 years for NH. There was no overall survival (OS) difference (p-value=0.51). On multivariate analysis, there were no independent variables associated with better or worse OS. The propensity-matched analysis showed no MS difference between HI and NH (0.80 vs 0.71 years).

Conclusion: This hospital-based analysis confirmed low survival rates and revealed no statistical differences in MS or OS among HI and NH individuals with PEL. Interestingly, the disease was more prevalent in high-income subjects in both cohorts, despite HI individuals having lower insurance rates. A better understanding of intrinsic disease characteristics and biological variables can offer valuable insights into how to unveil potential targets of better and hopefully meaningful therapies that could improve survival outcomes.

#4858 Examining state- and race-specific five-year prostate cancer mortality rates (2016-2020) and their association with prostate-specific antigen screening.

H. E. Guard[1], J. B. Vaselkiv[1], E. Ecsedy[1], F. Kuechen[1], N. Minassian[1], J. Dun Rappaport[1], Z. Qian[2], M. O. Sodipo[1], K. L. Penney[3], K. H. Stopsack[4], L. A. Mucci[1];

[1]Harvard T.H. Chan School of Public Health, Harvard University, Boston, MA, [2]Brigham and Women's Hospital, Harvard Medical School, Boston, MA, [3]Brigham and Women's Hospital and Harvard Medical School, Boston, MA, [4]Massachusetts General Hospital and Harvard Medical School, Boston, MA

Background: In 2023, 34,000 US men will die from prostate cancer. The impact of prostate cancer mortality varies greatly across states. Racial differences in state populations may explain some but not all of this variability. This study examined prostate cancer mortality rates by state and race and their associations with state-level prostate-specific antigen (PSA) screening prevalence.

Methods: We obtained race-specific, state level five-year average age-standardized prostate cancer mortality rates from 2016-2020 from the NCI State Cancer Profiles. Data on race-specific, state level PSA screening prevalence in 2010 were obtained from the Behavioral Risk Factor Surveillance System. We compared mortality rate ratios (RR, 95% confidence intervals [CI]) of state level prostate cancer mortality rates of Black, Hispanic, Asian/Pacific Islander, and American Indian/Alaskan Native men to White men. We generated descriptive statistics (median and range) on state level mortality rates to quantify the variability within racial/ethnic groups. We fit univariable Poisson regression models to explore associations between prostate cancer mortality rates and PSA screening prevalence, for White, Black, and Hispanic men, but omitted Asian and American Indian men due to sparse data.

Results: Mortality data were available for 50 states and the District of Columbia (D.C.) for White, 40 states and D.C. for Black, 36 states for Hispanic, 24 states for Asian, and 11 states for American Indian men. The US average prostate cancer mortality rate was 18.8 deaths per 100,000 per year. As expected, rates were higher among Black than White men (RR 2.07; 1.90, 2.24), while rates among Hispanic (RR 0.75; 0.68, 0.84) and Asian (RR 0.48; 0.41, 0.56) men were lower. Rates among American Indian men were slightly higher than White men (RR 1.12; 0.96, 1.29). Variability of state-level mortality rates within each race was quite high, with largest ranges for Black and American Indian men. Black men had a median (range) state-level prostate cancer mortality rate of 37.9 (23.9 to 49.2), and American Indian men had a median rate of 20.4 (7.7 to 28.9). Median (range) rates were 17.7 (11.3 to 22.3) for White, 8.3 (4.3 to 17.4) for Asian, and 13.5 (8.9 to 22.5) for Hispanic men. Associations between a 5-percentage point increase in PSA screening prevalence and prostate cancer mortality rates were RR 0.92 (95% CI: 0.84, 0.99) in White, RR 0.96 (0.88, 1.05) in Black, and 0.98 (0.90, 1.07) in Hispanic men.

Conclusion: There is considerable variability in prostate cancer mortality rates across states, both between and within racial/ethnic groups, highlighting complexity of racial disparities. PSA screening may weakly contribute to this variability, but other factors such as health care access, social determinants, and lifestyle factors that vary between states should be considered in future studies.

#4859 Mental health of early-onset and late-onset cancer survivors.

J. H. Lee[1], J. An[2];
[1]Jayden Lee (Individual), South Pasadena, CA, [2]Kaiser Permanente, Pasadena, CA

Background: Psychiatric disorders such as anxiety and depression are shown to be common when diagnosed with early-onset cancer, often defined as cancers diagnosed in adults <50 years of age. We hypothesize that the mental health of early-onset cancer survivors is negatively affected compared to late-onset cancer survivors.
Methods: We identified cancer survivors in the Medical Expenditure Panel Survey 2021 Full Year Consolidated Data File. We categorized cancer survivors as early-onset (≤ 50 years of age) and late-onset (> 50 years of age). We examined the proportion of mood and anxiety disorders, and the proportion of antidepressant and antianxiety medication use among the early and late-onset cancer survivors. We conducted chi-square tests and multivariable logistic regression models by adjusting for sex and race.
Results: We identified 291 early-onset cancer survivors (mean age 41 years, 71% female) and 2556 late-onset cancer survivors (mean age 71 years, 56% female). Among the early-onset cancer survivors, 18% had mood disorders (17% took antidepressants) and 20% had anxiety disorders (6% took antianxiety medication). In comparison, 12% late-onset cancer survivors had mood disorders (21% took antidepressants) and 13% had anxiety disorders (8% took antianxiety medication). Early-onset cancer survivors were more likely to develop mood (Adjusted Odds Ratio (aOR)=1.45; 95% CI=1.06 - 1.99) and anxiety (aOR=1.42; 95% CI=1.05 - 1.92) disorders compared to late-onset cancer survivors. However, there were no differences in receiving antidepressants (aOR=0.79; 95% CI=0.57 - 1.09) or antianxiety (aOR=0.69; 95% CI=0.41 - 1.16) medication between early and late-onset cancer survivors when adjusting for sex and race.
Conclusion: Early-onset cancer survivors had an elevated risk of acquiring psychiatric disorders such as mood and anxiety disorders than late-onset cancer survivors, but treatment was suboptimal. Clinician and patient awareness can help narrow the gaps of treatment for early-onset cancer survivors.

Table 3. Odds Ratio for early-onset vs. late-onset cancer survivors (*Sex and Race adjusted)

Variables	Crude Odds Ratio	Adjusted Odds Ratio *
Mood Disorders	1.48 (1.09 - 2.00)	1.45 (1.06 - 1.99)
Anxiety Disorder	1.52 (1.13 - 2.03)	1.42 (1.05 - 1.92)
Antidepressants	0.80 (0.59 - 1.10)	0.79 (0.57 - 1.09)
Antianxiety	0.70 (0.42 - 1.17)	0.69 (0.41 - 1.16)

#4860 Recommendations for enhancing inclusion and management of esophagus cancer clinical trials: Insights on mortality of esophagus cancer as a second primary malignancy.

H. Zhou[1], J. Leng[1], H. Qiu[1], Q. Huang[1], J. Zhang[2], **Z. Jiang**[3];

[1]Guangdong Provincial People's Hospital (Guangdong Academy of Medical Sciences), Southern Medical University, Guangzhou, China, [2]Pingxiang People's Hospital, Pingxiang, China, [3]University of California, Berkeley, Berkeley, CA

Background: Esophagus cancer as a second primary malignancy (esophagus-2) is increasingly common, but its prognosis is poorly understood. This study aims to examine the overall, non-cancer related and cancer-specific survival of patients diagnosed with esophagus-2 compared to the first primary esophagus cancer (esophagus-1).

Methods: We included primary esophagus cancer patients diagnosed from 1975 to 2020 in the Surveillance, Epidemiology, and End Results program. Esophagus-2 was identified in patients with a previous diagnosis of non-esophageal primary malignancy. Hazard ratios of overall, esophagus cancer-specific and non-cancer related mortality were estimated among patients with esophagus-2 compared to esophagus-1, adjusting for age, sex, tumor stage and other demographic and clinical characteristics.

Results: A total of 74521 and 14820 patients were identified as esophagus-1 and esophagus-2. Esophagus-2 patients suffered lower risk of esophagus cancer-specific mortality in initial 5 years but similar risk thereafter, independent of tumor characteristics and treatment. In the first 5 years after diagnosis, patients with esophagus-2 had similar risk of overall mortality with those with esophagus-1 but increased risk thereafter. As for non-cancer related mortality, esophagus-2 patients had higher risk all along.

Conclusion: Patients diagnosed with esophagus-2 face a favorable esophagus cancer-specific survival within the early period after diagnosis. However, patients with esophagus-2 are more liable to die of non-cancer cause. A conservative approach to manage esophagus-2 solely based on malignancy history is not supported but effort should be put into surveillance, prevention and management of the comorbidities and complications for the first malignancy.

#4861 Incidence rates of bladder and kidney cancers among U.S. military servicemen: Comparison with the rates in the general U.S. population.

J. A. Bytnar[1], K. A. McGlynn[2], S. Q. Kern[1], C. D. Shriver[1], K. Zhu[1],

[1]Murtha Cancer Center Research Program, Uniformed Services University Walter Reed Surgery, Henry M. J, Bethesda, MD, [2]National Cancer Institute, Bethesda, MD

Background: The military population may differ from the general population in factors related to the incidence of bladder and kidney cancers. However, incidence rates of these cancers have not been systematically compared between the two populations. This study compared incidence rates of bladder and kidney cancers and their trends between active-duty servicemen and men in the general U.S. population.

Methods: Data were obtained from the Department of Defense's (DoD) Automated Central Tumor Registry (ACTUR) and the National Cancer Institute's Surveillance, Epidemiology and End Results (SEER) database. Patients were active-duty servicemen in ACTUR and men in SEER who were diagnosed with malignant bladder and kidney cancers and 18-59 years at diagnosis from 1990-2013. Age-adjusted rates, incidence rate ratios (IRR), and their 95% confidence intervals (95% CI) were compared between the two populations by age, race, and cancer stage. Trends in the incidence were also compared.

Results: Incidence rates were lower in ACTUR than SEER for bladder cancer overall (IRR=0.55, 95% CI=0.48-0.62) and by age, race, or tumor stage. However, for 50-59-year-old men, the rates did not differ between the populations. Trend analysis showed bladder cancer incidence decreased more in ACTUR than SEER over the study period. Kidney cancer incidence rates were marginally lower overall (IRR=0.92, 95% CI=0.84-1.00) and significantly lower for 30-49-year-old Black men in the military than the general population. For kidney cancer, the trends were similar between the two populations with increased incidence from 1999 to 2013.

Conclusion: Lower bladder and kidney cancer incidence in ACTUR, notably in younger individuals, may be primarily associated with healthier status and better health care. The lack of differences in bladder or kidney cancer incidence among 50-59-year-old men between the populations might result from more cumulative military-related exposures in this age group, which effects were offset by healthier status and better medical care. Disclaimer: The contents of this publication are the sole responsibility of the authors and do not necessarily reflect the views, opinions or policies of NCI, USUHS, HJF, the DoD or the Departments of the Army, Navy or Air Force. Mention of trade names, commercial products or organizations does not imply endorsement by the US Government.

#4862 Rural-urban disparities in early-onset breast cancer amongst US women aged 20-49, trends from 2000-2020.

K. L. Ho, A. Connor;
Johns Hopkins Bloomberg Sch. of Public Health, Baltimore, MD

Purpose: To characterize rural-urban disparities of breast cancer (BC) incidence among younger women by stage and race/ethnicity.
Background: Cancer incidence in younger adults is increasing, but trends and disparity patterns in early-onset BC are not well-described for women aged <50 years. Current screening guidelines recommend against routine screening until age 40 for various perceived harms that outweigh benefits which can lead to delayed diagnosis and more aggressive stage when BC is identified among younger women. It is unclear how BC incidence patterns such as stage at diagnosis and race/ethnicity differ by rurality, as rural residents may experience geographic isolation, lower socioeconomic status (SES), higher rates of cancer risk behaviors, and limited access to healthcare, compared to urban residents.
Methods: We used incidence data from the North American Association of Central Cancer Registries to identify trends in early-onset BC among women aged 20-49 from 2000-2020, stratified by rurality (2013 USDA Rural-Urban Continuum Codes) and to explore patterns by stage and race/ethnicity. We extracted age-adjusted incidence rates (IR) [adjusted to 2000 US Standard Population] for each year and detected significant increasing or decreasing trends over time using the Joinpoint Regression Program. The annual percentage change (APC) for IR trends were calculated.
Results: Of the 854,590 patients, 88% lived in urban areas (12% rural). Cumulatively over 2000-2020, we observed similar average APCs for early-onset BC both in urban (IR = 68.8 per 100,000; avg. APC +0.37, 95% CI 0.23, 0.50) and rural areas (IR = 65.1 per 100,000; avg. APC +0.35, 95% CI 0.14, 0.57). Rural areas did not significantly trend upwards until 2010-2020 (APC +0.71, 95% CI 0.38, 1.05). Rates for localized stage increased from 2000-2020 (APC +0.69%, 95% CI 0.48, 0.89) for urban areas, but declined in rural areas between 2000-2008 (APC -0.77, 95% CI -1.33, -0.20), only to increase again from 2008-2020 (APC +1.01, 95% CI 0.68, 1.34). In rural areas, there is a corresponding dramatic increase in distant stage BC diagnosed between 2000-2007 (APC +5.99%, 95% CI 2.29, 9.93) but slowed in the period after (2007-2020 APC +1.35, 95% CI 0.22, 2.51). While the rate remained stable for Hispanics living in both urban and rural areas, Non-Hispanic Whites (2000-2020 APC +0.59, 95% CI 0.46, 0.72), Non-Hispanic Blacks (2000-2009 APC +0.85, 95% CI 0.33, 1.37), and Other Non-Hispanic racial groups (2000-2020 APC +1.27, 95% CI 1.16, 1.58) saw significant increased rates in urban areas over time.
Conclusions: Overall, early-onset BC has risen over the past 20 years in both urban and rural areas, but clear differences exist by stage at diagnosis and race/ethnicity. More research is needed to understand how SES, healthcare access, screening recommendations, and additional cancer risk factors can modulate BC incidence and disparities among younger women.

#4863 A retrospective study characterizing 1714 cases of epithelioid cell melanoma.

M. Al Kurnas, X. Wu, A. Mubin, P. T. Silberstein;
Creighton University School of Medicine, Omaha, NE

Introduction: Epithelioid cell melanoma (ECM) is a variant of cutaneous melanoma (CM) typically characterized by large malignant cells with abundant, glassy cytoplasm and large nuclei. ECMs are aggressive neoplasms and tend to have worse prognosis than other subtypes of CM with a higher risk of metastasis[1]. Few studies have explored the demographic features of ECM and their effects on outcomes. Using data from the National Cancer Database (NCDB), we hope to fill this gap.

Methods: This is a retrospective study of patients diagnosed with ECM(ICD-8771) between 2004 and 2020 in the National Cancer Database (NCDB) describing demographic features associated with and tumor characteristics of ECM (N = 1714). Descriptive statistics were collected for all patients with ECM and CM (N = 827623) and were compared using Pearson Chi-Square test. Overall survival was determined by the Kaplan-Meier test. Cox regression analysis was used to determine which factors led to decreased survival in ECM. All statistical tests were evaluated for a significance of $P < 0.05$. Exclusion criteria included missing data.

Results: The cases of ECM were composed mainly of White (96%) males (58.9%), and most had private insurance as the primary payor at diagnosis (50.1%). Greater than half of ECM cases had a primary site of skin on the trunk, upper limbs, or shoulders. Cox regression analysis revealed that patients with ECM treated at integrated network cancer programs had a HR of 0.46 when compared to community centers (95% CI 0.257 - 0.831, $P < 0.05$). Those with ECM treated at academic programs and comprehensive community cancer programs had hazard ratios of 0.41 (95% CI 0.239 - 0.701, $P < 0.05$) and 0.49 (95% CI 0.288 - 0.845, $P < 0.05$) respectively when compared to community programs. Only patients with ECM who had private insurance as primary payor at diagnosis had better outcomes when compared to non-insured with an HR of 0.40 (95% CI 0.225 - 0.714, $P < 0.05$). In addition, patients with ECM were more likely to be treated at academic centers than patients with CM (55.48% vs 46.95%, $P < 0.05$). The mean survival of patients with ECM was 12.3 months less than those with CM (141.1 months versus 153.4 months.)

Conclusion: Overall survival for patients was better at academic centers, integrated network cancer programs, and comprehensive community cancer programs when compared to community centers. In addition, only patients who had private insurance were found to have better outcomes than those who were uninsured. These findings help shed light on the effects of certain socioeconomic and factors on outcomes in ECM. We hope this study will be a launching point for further inquiry into the causal relationships these factors have on outcomes in this rare cancer.

1. (Russo A, Avitabile T et al. Iris Melanoma: Management and Prognosis. Appl Sci 2020; 10: 8766).

#4864 Epidemiological characteristics and treatment strategies of gastric cancer with neuroendocrine differentiation (NED).

Z. Huang, J. Wei, Y. Shen, **J. Zhang**;
The First Affiliated Hospital of Chongqing Medical University, Chongqing, China

Background: Gastric cancer with neuroendocrine differentiation (NED) occurs in 10% to 40% of cases, a significant proportion that is under-researched. The lack of clinical guidelines for this subgroup necessitates the development of effective treatment protocols.
Methods: This study enrolled 149 gastric cancer patients, analyzing retained surgical wax blocks via immunohistochemistry for syn, CgA, and CD56 expressions. Patients were categorized into NED-positive and NED-negative groups for analysis, employing continuous variable analysis, categorical variable analysis, clustering, principal component analysis (PCA), feature importance analysis, heatmap analysis, and survival prognosis. Moreover, the clinical efficacy and safety of first-line (surufatinib + SOX + anti PD-1 antibody, n=3) and second-line (surufatinib + anti PD-1 antibody, n=3) treatments were observed in six advanced gastric cancer with NED patients, exploring the epidemiological characteristics, feasibility, and importance of clinical treatments for NED.
Results: The study revealed a 10.1% incidence of NED positivity in gastric cancer patients. NED-positive patients exhibited a rapid decline in early survival probability, with a median relapse-free survival of 32.4 months compared to 41.5 months in NED-negative patients, indicating a poorer prognosis for NED-positive patients. In-depth analysis suggested significant correlations between NED status and factors such as gender, tumor location, pathological type, and AJCC staging, with the most significant associations observed in males, stage IIIA, and gastric angle location. In the six advanced gastric cancer with NED cases, effective tumor reduction was observed in both first-line (100% tumor shrinkage rate, ORR 66.7%, DCR 100%) and second-line treatments (66.7% tumor shrinkage rate, ORR 33.3%, DCR 100%), showing sustained partial responses (PR) exceeding 10 months in two patients and 7 months in one patient, respectively. The major grade 3 or higher TEAEs being neutropenia and thrombocytopenia in the first-line, and hypertension and proteinuria in the second-line therapy.
Conclusion: This study provides pivotal epidemiological and clinical treatment evidence for gastric cancer with NED, underscoring the necessity of personalized treatment strategies for this subgroup. Future research should focus on refining treatment protocols to enhance the quality of life and overall prognosis for these patients.

#4865 Income dynamics and the risk of hepatocellular carcinoma in individuals with type 2 diabetes: A nationwide population-based cohort study.

J. Baek[1], B. Amick III[1], C. Brown[1], M. Schootman[1], M.-R. Narcisse[1], S.-H. Ko[2], P. McElfish[1], M. Thomsen[1], S.-S. Lee[2], K. Han[3], **Y.-M. M. Park[1]**; [1]University of Arkansas for Medical Sciences, Little Rock, AR, [2]The Catholic University of Korea, Seoul, Korea, Republic of, [3]Soongsil University, Seoul, Korea, Republic of

Introduction: Type 2 diabetes (T2D) is associated with over 2 times increased risk of hepatocellular carcinoma (HCC). Low-income status is associated with a higher risk of developing HCC, more advanced stage, and mortality. Evidence is limited on whether income dynamics are associated with the risk of developing HCC in individuals with T2D who are susceptible to income changes. We examined whether income levels and income changes are associated with HCC risk.
Methods: Using representative data from the Korean National Health Insurance Service (NHIS), 2,227,893 adults with T2D (aged ≥ 20 years) without a cancer history were included between 2015-2016. Income levels were measured based on health insurance premiums and categorized into 4 levels (quartiles [Q], 1 [low income], to 4 [high income]). These quartiles excluded the very low-income individuals who qualified as Medical Aids beneficiaries (MAB), which comprised a 5th income category. To identify income change, income levels were collected annually from the baseline year backward 4 years. The incident HCC, defined based on ICD-10 codes and special reimbursement codes, was identified until December 2020. Hazard ratios (HRs) and 95% confidence intervals (CIs) were estimated to assess the association between income parameters and HCC after adjusting for sociodemographic factors, comorbidities, and diabetes duration and treatment. Income parameters included 1) the baseline income status, 2) the cumulative number of years being in each income level, and 3) changes in income level between the two time points (4 years ago vs. baseline).
Results: During follow-up (median, 3.9 years), 9,887 HCC cases developed. Individuals who had experienced at least one episode of MAB during the five years showed a significantly higher HCC risk than those who had never qualified as MAB (HRs ranging from 1.52 to 2.01). In contrast, individuals who had experienced high-income status (Q4) during the five years had a lower HCC risk than those who had never experienced (HRs ranging from 0.79 to 0.92; $HR_{n=5\ years\ vs.\ n=0\ years}$ 0.79, 95% CI 0.75-0.83; *P* for trend <0.05). Individuals in the low-income status (MAB-Q1) at the first assessment (4 years ago) but experienced increased income had a reduced risk of HCC, which linearly declined with increasing income rise. Also, those who experienced a substantial increase in income up to the top quartile (Q4) had the lowest HCC risk (HR 0.73, 95% CI 0.60-0.88; P for trend<0.05) than those who maintained the low-income status.
Conclusions: Experiencing any very low- or high-income state was independently associated with increased or decreased HCC risk. Improved income levels among those in the low-income status had an inverse linear association with reduced HCC risk. Our findings underline the need for increased public policy awareness of the impact of income dynamics on HCC risk in adults with T2D.

#4866 To weight or not to weight? Studying the effect of selection bias in three EHR-linked biobanks with applications to colorectal cancer.

M. Salvatore[1], R. Kundu[1], X. Shi[1], C. R. Friese[1], S. Lee[2], L. G. Fritsche[1], A. M. Mondul[1], D. Hanauer[1], C. L. Pearce[1], B. Mukherjee[1];
[1]University of Michigan, Ann Arbor, MI, [2]Seoul National University Graduate School of Data Science, Seoul, Korea, Republic of

The use electronic health record (EHR)-linked biobanks, including All of Us (AOU), the Michigan Genomics Initiative (MGI), and the UK Biobank (UKB), has become increasingly common in cancer research. However, each has a different participant recruitment strategy resulting in non-probability samples, which can lead to selection bias. An unanswered question is whether researchers should use selections weights when analyzing these data. Using colorectal cancer as the test case, we investigate the impact of using such weights on descriptive and analytic tasks in these three biobanks.

We curated sociodemographic and clinical diagnosis data for 726,841 individuals (n = 244,071, 81,243, and 401,167, in AOU, MGI, and UKB, respectively). EHR ICD (diagnosis) code data were mapped to broader 2,042 codes, called phecodes, using the new phecode X mapping table developed by researchers at Vanderbilt University. Selection weights were constructed in AOU and MGI to make them more representative of the US adult population, using data from the 2019 National Health Interview Survey; previously described weights for the UKB were used. We estimated phenomewide prevalences, pairwise correlations, and phenome dimensionality (via principal components analysis). To investigate the role of weighting on conclusions from hypothesis testing and association estimation, we conducted a colorectal cancer phenomewide association study and estimated the sex-colorectal cancer log-odds ratio, respectively.

We found that phecode prevalences in AOU and MGI decreased following weighting (median prevalence ratio [MPR]: 0.82 and 0.61, respectively) while those in UKB increased (MPR: 1.06). MGI is enriched for phecodes compared to AOU (MPR: 1.15) and UKB (MPR: 6.28). Weighting PCA had minimal impact on phenome dimensionality (e.g., 732 PCs explaining 95% of cumulative variation in AOU vs. 711 after weighting). Weighted PheWAS for colorectal cancer identified 21 hits not identified in unweighted PheWAS, but only one was from a new disease category. Weighted estimates of the female-colorectal cancer log-odds ratio overlapped with the benchmark range in MGI and UKB though resulted in a null association in AOU.

Weighting had limited impact on dimensionality estimation and hypothesis testing but were important to consider for prevalence and association estimation. Results from untargeted analyses should be followed up with targeted analyses using curated weights. The importance of weights depends on the estimates obtained and inference
goals and can improve the representativeness of results for cancer-related outcomes based on EHR-linked biobank data. Importantly, EHR-linked biobanks should be explicit in reporting recruitment and selection mechanisms and when possible, supply selection weights to researchers for population-based inference along with a clear definition of the target population.

#4867 Longitudinal latent class analysis to further understand trajectory of density over time and risk of breast cancer.

G. A. Colditz, D. L. Bennett, S. Jiang;
Washington University School of Medicine in St. Louis, St. Louis, MO

Background: It is clinically important to refine strategies to manage women with dense breasts as they represent approximately 50% of all women screened. Change in breast density is related to risk of breast cancer.[1] We also must understand this change in density over time in women with dense and non-dense breasts. While population level data have been reported to estimate decrease in density with age, this has largely used digitized film images.[2] Expanding use of digital mammography and repeated screening generates a large library of images for each woman, offering the potential to use more of the image data.
Methods: We use longitudinal latent class analysis to cluster women and estimate their change in density over time. To evaluate the groups of women with different patterns of change in density we fit latent class models to our previously published data.[1] This includes 289 pathology confirmed cases of breast cancer and 658 controls among women followed from November 3, 2008 to October 31, 2020.
Results: Among women with dense breasts, there are 107 who developed breast cancer during follow-up and 267 control women who remained free from breast cancer. In the women without dense breasts, 173 cases and 383 controls were evaluated and showed similar age and BMI within the controls as seen in women with dense breasts. Prevalence of family history and history of benign breast biopsy did not differ between the two groups. We observe this latent class and trajectory of density phenomenal separately for dense and non-dense groups in our data. We show that the data define 2 classes, those who have decrease in density over time and those who have increase over time. The odds ratio (OR) for cancer comparing decline vs. incline is 4.9 in women with dense breasts (BI-RADS C, D) and 6.17 on women with non-dense breasts (BI-RADS A, B).
Discussion: To refine our understanding of patterns of change in breast density over time in relation to breast cancer risk we fit latent class models. Longitudinal change matters as reflected in the 2-class model. This is independent of starting density and confirms that a one-time measure of density is not enough to define level of risk for subsequent breast cancer. Further work is needed to better define the drivers and inhibitors of decline in breast density over time given this change over time as women age is a universal phenomenon.[2]

1. Jiang S, Bennett DL, Rosner BA, Colditz GA. Longitudinal Analysis of Change in Mammographic Density in Each Breast and Its Association With Breast Cancer Risk. JAMA Oncol 2023;9(6):808-814. (In English). DOI: 10.1001/jamaoncol.2023.0434.
2. Burton A, Maskarinec G, Perez-Gomez B, et al. Mammographic density and ageing: A collaborative pooled analysis of cross-sectional data from 22 countries worldwide. PLoS Med 2017;14(6):e1002335. DOI: 10.1371/journal.pmed.1002335.

#4868 Avoiding the pitfalls in developing and validating prediction models for rare outcomes in nested case-control.

B. Rentroia-Pacheco[1], D. Bellomo[2], I. M. Lakeman[3], M. Wakkee[1], L. M. Hollestein[1], D. van Klaveren[4];
[1]Erasmus MC Cancer Institute, Erasmus University Medical Center, Rotterdam, Netherlands, [2]SkylineDx, Rotterdam, Netherlands, [3]Leiden University Medical Center, Leiden, Netherlands, [4]Erasmus University Medical Center, Rotterdam, Netherlands

Background: Molecular-biomarker-based prediction models, whether based on statistics or artificial intelligence, are becoming increasingly popular in the medical community as an alternative or complement to more traditional prediction tools, such as staging systems. Population-based cohorts are the preferred study design for building and validating such models, but they are generally expensive and frequently unfeasible, particularly, when the outcome of interest is rare, and when the collected data include expensive or difficult-to-obtain molecular biomarkers. As such, studies often develop or validate risk models in cohorts obtained based on data availability, rather than on the representativeness of a target population. Nested case-control (NCC) is an efficient study design for building and validating such models in a rare outcome setting, but it requires a fully enumerated source population, and appropriate methodologies to accommodate the under-sampling of the controls and any matching. Unfortunately, these methodologies are not systematically described in a form easily accessible to clinicians.
Methods: We systematically characterized how to correctly develop and evaluate the performance of prediction models in NCC cohorts, by weighing the subjects based on sampling probabilities to account for the sub-cohort sampling. We illustrated the use of weighted metrics for the NCC, with a validation of a model that predicts breast cancer development - BOADICEA version 5 - in the population-based Rotterdam study. We used the C-index, threshold-based metrics, observed-to-expected events ratio (O/E ratio), calibration slope, and decision curve analysis as performance metrics. We compared the metrics obtained in the full cohort with those obtained in NCC cohorts sampled from the Rotterdam study, with and without a matched design.
Results: NCC cohorts of 326 women were derived from the full cohort of 4,377 women from the Rotterdam Study. Performance metrics without weight adjustment were biased on the NCC cohorts: the unweighted C-index of the BOADICEA model was 0.61 (0.58-0.63) for the unmatched design. However, with weight adjustment, the C-index in the NCC cohorts (0.65 (0.61-0.69)) corresponds to
the C-index in the full cohort (0.65 (0.62-0.69)), despite the NCC cohort being much smaller in size. Similarly, weighted adjustments of O/E ratio, threshold-based metrics, and net benefit for decision curves were unbiased estimates of the corresponding metrics in the full cohort, while the corresponding unweighted metrics were biased.
Conclusions: We provided a practical guide for clinicians on how to develop and validate prediction models in NCC cohorts. We showed that this study design is an efficient solution, in case of expensive or difficult-to-obtain biomarkers, and when the outcome is rare; but the performance metrics must be appropriately adjusted to the sampling procedure.

#4869 Efficient study design for the discovery of a gene expression signature predicting metastasis in cutaneous squamous cell carcinoma.

B. Rentroia-Pacheco[1], L. Pozza[2], Y. Chen[2], D. Huigh[2], C. J. Eggermont[1], O. F. Steijlen[1], S. Alex[2], J. Dwarkasing[2], D. Bellomo[2], H. J. van de Werken[1], A. L. Mooyaart[1], M. Wakkee[1], L. M. Hollestein[1];

[1]Erasmus Medical Centre, Rotterdam, Netherlands, [2]SkylineDx, Rotterdam, Netherlands

Background: The StepIdent study aims to develop a gene signature predicting metastasis in patients with cutaneous squamous cell carcinoma (cSCC) to improve risk stratification, thus enabling personalized decisions about follow-up schedules and treatment options. Here we describe the unique characteristics, challenges, and best practices for an efficient design of a discovery cohort for a rare outcome (metastasis prevalence: 2-5%); for retrieving, curating, and linking the clinical and pathological data through nationwide databases; and for measuring gene expression through sequencing of archived Formalin-Fixed Paraffin-Embedded (FFPE) primary tumor samples.

Methods: Following a predefined protocol, we identified a nested-case control cohort (NCC) of 305 cases and 305 controls from a nationwide cohort of 19,120 patients with a first cSCC in the Netherlands from 2007 to 2009, followed up until 2020. We chose an NCC design since it is an efficient study design in a rare outcome setting (weighting is needed to accommodate the under-sampling of the controls). Patients were identified from the Dutch National Cancer Registry (NCR) and the clinical information was retrieved from the NCR which is linked to the nationwide registry of histo- and cytopathology (PALGA). Tumor blocks were requested from PALGA, and pathological characteristics were assessed by dermatopathologists. We matched controls to cases, based on a risk score estimated by a clinicopathological model. Gene expression was measured using the Illumina RNA Prep with Enrichment kit combined with the whole exome panel and paired-end sequenced on the NextSeq 550.

Results: Tissue slides for 541 samples were retrieved for sequencing. 151 samples were excluded after pathology review or due to low pre-library concentration. The final cohort includes 195 case-control pairs (n=390). The median sequencing depth was 43M (Q1-Q3: 35-52M); the median Q30 was 85% (Q1-Q3: 83-87%); the median GC content was 51% (Q1-Q3: 50-52%); a median of 1.8% of base pairs (Q1-Q3: 1.4-2.1%) was trimmed prior to the mapping/alignment; a median of 69% (Q1-Q3: 65-74%) of reads were aligned as protein-coding and a median of 7% (Q1-Q3: 6-10%) as rRNA; a median of 95% (Q1-Q3: 93-96%) of reads were aligned by STAR. Two samples were excluded based on quality control.

Conclusion: We described an efficient design and implementation of a nationwide discovery study in cSCC, involving the retrieval of clinicopathological data, the collection of FFPE materials, and the execution of omics measurements. This study presents the largest cohort to date, incorporating omics measurements of primary cSCC samples, combined with simultaneous access to well-curated clinical and pathological information and follow-up data. Our findings can provide guidance for similar studies involving a rare clinical endpoint, where an efficient study design is a necessity.

#4870 Defining metabolically healthy and unhealthy obesity in relation to cancer risk: A prospective cohort study by using a machine learning approach in comparison with conventional definitions in the UK Biobank.

Z. Zhou[1], S. Parra-Soto[1], Y. Lu[2], Z. Fang[2], K. Wang[2], A. Bever[2], L. Tao[2], F. Petermann-Rocha[1], J. Boonpor[1], N. Sattar[1], C. Celis-Morales[1], J. P. Pell[1], F. K. Ho[1], M. Song[2],

[1]University of Glasgow, Glasgow, United Kingdom, [2]Harvard T.H. Chan School of Public Health, Boston, MA

Background: The definition of metabolically healthy and unhealthy obesity for cancer risk remains uncertain and controversial. This study proposed a novel classifier based on biomarkers selected using machine learning (ML) and compared its risk stratification with the conventional definition.

Methods: A prospective cohort study was conducted of 317,569 UK Biobank participants who were free of cancer and with body mass index (BMI) ≥18.5 kg/m^2 at baseline. Individuals were classified into metabolically healthy and non-obese (MHNO), metabolically unhealthy and non-obese (MUNO), metabolically healthy and obese (MHO), and metabolically unhealthy and obese (MUO), according to body mass index (BMI) and six metabolic criteria. For the ML approach, LASSO regularization was used to select a subset from seventeen metabolic biomarkers to optimize C index. Clinical cut-off value was applied to this subset to define MHO. Multivariable Cox proportional hazards models were used to estimate hazard ratios (HRs) of total, obesity-related, type two diabetes (T2D)-related, and 23 site-specific cancers according to the conventional and ML definitions.

Findings: Of 21 biomarkers, 17 were selected using LASSO. Compared with MHNO, individuals with MHO had higher risk of obesity-related cancer ($HR_{conventional}$ 1.22, 95% CI 1.15-1.29; HR_{ML} 1.23, 95% CI 1.16-1.30) and T2D-related cancer ($HR_{conventional}$ 1.25, 95% CI 1.19-1.39; HR_{ML} 1.27, 95% CI 1.20-1.34) after adjusting for sociodemographic and lifestyle factors. ML-defined metabolic status better-stratified individuals with normal weight for risk of total cancer ($HR_{conventional}$1.02, 95% CI 0.99 -1.06; HR_{ML} 1.06, 95% CI 1.02 - 1.10) and some site-specific cancers, e.g., hepatocellular carcinoma ($HR_{conventional}$ 0.89, 95% CI, 0.53-1.48; HR_{ML} 2.52, 95% CI, 1.85-3.45).

Interpretation: Compared with the conventional definition of metabolic health, a broader array of metabolic markers may help better stratify individuals for cancer risk.

Keywords: Obesity, cancer, metabolically healthy obesity, hepatocellular carcinoma.

#4871 Colorectal cancer incidence and overall survival by race, stage, and age: A SEER database analysis, 2009-2020.

A. C. McDonald, S. Joo, J. Ma, M. M. Amonkar, C. Shao, K. Desai, A. C. Deitz;
Merck & Co., Inc., Rahway, NJ

Introduction: In the United States, colorectal cancer (CRC) is the fourth most common cancer and the second leading cause of cancer-related deaths. Although incidence rates of CRC have been decreasing overall, recent studies suggest a shift in demographics, specifically an increase in the number of new CRC cases among younger individuals and a higher incidence among those who identify as non-Hispanic Native American/Alaska Native. To examine the latest trends in incidence and overall survival (OS) among adults with CRC in the United States, we conducted an observational study using the Surveillance, Epidemiology, and End Results (SEER) Program database.

Methods: Patients aged ≥18 years with newly diagnosed CRC between January 1, 2009, and December 31, 2020 were identified in the SEER 17 database. Age-adjusted incidence rates for CRC were calculated by race/ethnicity and age groups (18-49, 50-64, and ≥65 years) from 2009 to 2020. Kaplan-Meier curves were generated to examine 5-year OS by race/ethnicity, stage, and age groups.

Results: There were 429,218 CRC cases identified with a median age of 67 years. Most were male (52.4%) with stage 0-II CRC (51.4%). Most patients identified as non-Hispanic White (66.3%), followed by non-Hispanic Black (11.5%), non-Hispanic Asian/Pacific Islander (8.9%), non-Hispanic Native American/Alaska Native (0.7%), and Hispanic of any race (12.7%). The age-adjusted incidence rate between 2009 and 2020 was 51.9 per 100,000 persons; incidence decreased from 59.5 per 100,000 persons in 2009 to 44.2 per 100,000 persons in 2020, with male patients having a higher incidence rate than female patients. By 2020, non-Hispanic Native American/Alaska Native patients had the highest incidence rate (54.5 per 100,000 persons) followed by non-Hispanic Black patients (50.6 per 100,000 persons). CRC incidence rates increased slightly for age <50 years (10.5 to 12.9 per 100,000 persons) and decreased for ages 50-64 (74.6 to 63.9 per 100,000 persons) and ≥65 years (222.4 to 136.1 per 100,000 persons). Non-Hispanic Black patients (53%), age ≥65 years (47%), and those with stage III-IV CRC (41%) had a lower 5-year OS from 2015 to 2019 compared to patients who were non-Hispanic White (57%), aged 50-64 (68%) and <50 years (70%), and with stage 0-II CRC (77%).

Conclusion: Our results confirm a slight increase in CRC incidence among younger (<50 years) individuals over the 2009-2020 time period. Patients who were non-Hispanic Native American/Alaska Native had the highest CRC incidence rate and patients who were non-Hispanic Black had the poorest OS. Targeted preventative efforts such as CRC screening programs in addition to improved access to care/treatment may be needed to reduce the number of new cases and improve outcomes among historically underserved groups.

#4872 Elevated colorectal cancer incidence among American Indian/Alaska Native persons in Alaska compared to other populations worldwide.

D. Haverkamp[1], D. Redwood[2], E. Roik[2], S. Vindigni[2];
[1]Centers for Disease Control & Prevention, Atlanta, GA, [2]Alaska Native Tribal Health Consortium, Anchorage, AK

Background: Colorectal cancer (CRC) is a leading cancer worldwide. Incidence varies greatly by country and racial group. We present recent CRC incidence and mortality rates among American Indian/Alaska Native (AI/AN) persons in Alaska and compare them to rates among other racial groups in Alaska and AI/AN persons in other regions of the United States, and to published CRC incidence rate estimates for other countries around the world.
Methods: To calculate CRC incidence in the United States, we used U.S. Cancer Statistics data, which includes cancer registry data from the Centers for Disease Control and Prevention's (CDC) National Program of Cancer Registries and the National Cancer Institute's Surveillance, Epidemiology, and End Results Program. Cancer data for AI/AN persons in Alaska came from the Alaska Cancer Registry as well as the Alaska Native Tumor Registry. Death data came from the CDC's National Death Index, which was linked with the Indian Health Service patient registry database to address race misclassification in AI/AN populations, to create the United States Cancer Statistics American Indian and Alaska Native Mortality Database. This database was used to calculate CRC mortality rates for AI/AN persons in this study. Rates were age-adjusted using the World Health Organization's World Standard Population (2000-2025), so that rates for AI/AN persons in the United States could be more comparable to rates that have been estimated for countries around the world. Estimates of worldwide CRC incidence came from the International Agency for Research on Cancer Global Cancer Observatory GLOBOCAN 2020 database.
Results: AI/AN persons in Alaska (males and females combined) had the highest CRC incidence rate (58.4 per 100,000 people) in the year 2020, when compared to AI/AN persons in every other region of the United States. Within Alaska, AI/AN persons had a higher CRC incidence rate than persons of any other racial group. When compared with published CRC incidence rates worldwide, the rate for AI/AN persons in Alaska was higher than the rates reported for any country in the world in 2020. The country with the highest recorded CRC incidence rate in 2020 was Hungary (45.3 per 100,000 people). AI/AN persons in Alaska also had the highest CRC mortality rate (27.1 per 100,000 people) in 2020. Worldwide, the country with the highest recorded CRC mortality rate in 2020 was Slovakia (21.0 per 100,000 people).
Conclusions: This review of CRC incidence and mortality rates from populations in the US and worldwide showed that AI/AN persons in Alaska had the highest documented incidence and mortality rates of CRC in the world in 2020. Health systems serving AI/AN persons in Alaska could implement policies and interventions that support colorectal cancer screening, to reduce the burden of this preventable disease.

BIOINFORMATICS / COMPUTATIONAL BIOLOGY / SYSTEMS BIOLOGY / CONVERGENT SCIENCE: Application of Bioinformatics to Cancer Biology 4 Poster Session

#4876 Data-driven discovery of cancer-specific targets for hepatocellular carcinoma using spatial transcriptomics.

Sungwoo Bae[1], Dongjoo Lee[2], Daeseung Lee[2], Kwon Joong Na[2], Suk Kyun Hong[3], YoungRok Choi[3], Nam-Joon Yi[3], Kwang-Woong Lee[3], Kyung-Suk Suh[3], Hongyoon Choi[2]

[1]Institute of Radiation Medicine, Medical Research Center, Seoul National University, Seoul, Korea, Republic of,[2]Portrai, Inc., 78-18, Dongsulla-gil, Jongno-gu, Seoul, Korea, Republic of,[3]Department of Surgery, Seoul National University College of Medicine, Seoul, Korea, Republic of

Background: Hepatocellular carcinoma (HCC) is frequently diagnosed in advanced stages, with limited options available for systemic treatment. Given the significant investment of time, the high costs, and the notable failure rates involved in developing new drugs, it is crucial to identify appropriate cancer-specific surface targets, especially aiming at antibody drug conjugates and radioligand therapy. This study aims to propose a pipeline utilizing spatial transcriptomics (ST) to prioritize potential cancer-specific surface targets for HCC.

Methods: Visium ST samples were collected from fresh-frozen tissues of HCC patients undergoing hepatectomy. The spots with over 500 expressed genes and a mitochondrial gene percentage below 20% were selected. Counts were normalized with sctransform, and the tumor cell proportion in each spot was predicted using CellDART. Cancer region-specific genes were identified based on three criteria: high topological overlap with tumor cell distribution (using STopover), a high correlation coefficient with tumor cell proportion, or significantly higher expression in the tumor cell cluster compared to others in single-cell RNA-sequencing dataset. Genes identified through these methods were pooled and filtered based on average expression in the whole tissue using human normal cell atlas data and surface proteins. To select drug candidates with low normal organ toxcity, Tabula Sapiens datasets were used. Genes expressed in over 50% of cells and with an average expression above 1 in any critical organs were excluded.

Results: One ST sample was obtained from each of the 7 HCC patients. The topology, correlation, and single-cell-based criteria resulted in 42, 15, and 7 genes, respectively, with only 1 gene (*P4HB*) overlapping across all three methods. After filtering genes with high expression in normal organs based on Tabula Sapiens, 25 genes remained. In the GEPIA databases, *GPC3* exhibited the highest log fold change in RNA expression between HCC and normal liver (6.280), followed by *TM4SF4* (2.156), *EFNA1* (0.581), *GJB1* (0.498), and *IRS1* (0.391). To externally validate the results, 17 ST datasets from 5 patients provided by HCCDB were used. Among the selected genes, only *GPC3* and *EFNA1* had higher average expression in the tumor compared to other compartments (normal, stromal, and immune) in at least 3 out of 5 patients.

Conclusion: The proposed platform prioritizes cancer-specific surface targets for HCC, focusing primarily on spatial gene expression profiles obtained from ST and gene expression data from external databases. This analytical tool can be further utilized to identify molecular targets for developing antibody drug conjugates or radioligand therapies, which are designed to specifically deliver therapeutic agents to the tumor.

#4877 Morphological detection of chemotherapy resistance in cancer cell lines using AI-based analysis.

A. Jovic[1], M. Ray[1], R. Carelli[1], K. Saini[1], T. Pham[1], C. Corona[1], S. C. Boutet[1], C. Johnson[1], M. Salek[1], M. Masaeli[1], M. Barnes[2], C. Y. Ramathal[2]; [1]Deepcell Inc., Menlo Park, CA, [2]Abbvie, Chicago, IL

Chemoresistance can develop during the course of treatment of many cancers, which can limit the utility of standard therapeutics and lead to poor outcomes. The mechanism by which resistance arises is not well understood, and developing models to study resistance can be challenging. Resistance can spontaneously arise in cell lines, however, it is difficult to separate resistant from sensitive cells using traditional biomarkers, hampering their utility for studying mechanisms. Morphology presents another modality to examine resistance, independently of protein markers, and may solve a previously intractable problem of separating resistant from sensitive cells for further study.

Here we sought to study the mechanism of chemoresistance in cell lines using multi-parameter morphology in combination with gene expression and other standard molecular approaches. We induced resistance to specific chemotherapeutic drugs in parent cancer cell lines from lung, ovarian, and melanoma cancers. IC-50s of each drug increased by ≥1 order of magnitude in the resistant cells. Whole exome sequencing and bulk RNAseq were performed to examine differentially expressed genes and pathways between the parent and resistant cell lines.

Each cell line was analyzed using multi-dimensional morphology using the Deepcell platform, which extracts >100 morphological features from images of unlabeled single cells using artificial intelligence (AI), advanced imaging, and microfluidics. The morphology features represent both Deep Learning (DL)-derived features and human-interpretable morphometric features, such as size and shape. Unique morphotypes were observed differentiating each combination of parent and resistant cell lines, with notable changes in granularity distinguishing them. A subset of images was used to train a random forest classifier to predict the resistant state of each cell image, which performed with up to 85% accuracy on independent cell images. Strikingly, the combination of DL plus morphometric features outperformed the use of morphometric features alone, demonstrating the increased utility of combined analysis. The top gene pathways and top morphological features were examined to infer potential mechanisms underlying chemoresistance.

This work demonstrates that morphology alone can be used to distinguish drug resistant vs. parent populations without the use of markers. Morphology analysis can be applied to understanding complex phenotypes, and future platform improvements will enable sorting of these resistant populations to better identify molecular pathways in both cell lines and in primary tumor samples.

#4878 Enhancing non-invasive detection of urothelial carcinoma through combined cytology and methylation profiling of urinary cell-free DNA.

H. Zhao[1], **H. Dong**[2], H. Tang[2], Z. Zhang[1], N. Wei[3], J. Xu[3], P. Du[2], S. Jia[2], T. Xiao[4], H. Guo[1];

[1]National Cancer Center/National Clinical Research Center for Cancer /Cancer Hospital, Chinese Academy of Medical sciences and Peking Union Medical college, Beijing, China, [2]Huidu (Shanghai) Medical Sciences, Ltd., Shanghai, China, [3]the First Affiliated Hospital of Zhengzhou University, Zhengzhou, China, [4]National Cancer Center/National Clinical Research Center for Cancer/Cancer Hospital, Chinese Academy of Medical Sciences and Peking Union Medical College, Beijing, China

Detection of urothelial carcinoma (UC) faces a significant challenge in sensitivity due to the limitations of existing methodologies such as cytology. Identifying tumors through epigenetics pattern presents a promising advancement in diagnostic precision. This study aims to explore a non-invasive and more sensitive strategy by analyzing urinary cell-free DNA (ucfDNA) methylation profiles in conjunction with traditional urine cytology. The cohort for this study were collected from 20 patients with UC and 17 patients with benign or non-tumor lesions which histopathologic and cytopathologic results were reviewed by pathologist. Additional 16 cancer samples and 40 healthy donor samples were collected from independent research centers. We employed PredicineEPIC, a comprehensive whole-genome methylation assay, to investigate the DNA methylation characteristics in urine samples. The dataset was splited into 1:2 proportions for modeling and validation. The methylation signals were fed to three machine learning algorithms for determining the most effective classification model. Differentiating cancer and benign samples through urinary cytology has high specificity (1.0) but low sensitivity (0.3). Then we examined differentially methylated regions and implemented four most abnormally methylated regions as classify features. We found that the Gradient Boosting Machine (GBM) model achieved optimal performance in the validation set, with an AUC of 0.93, sensitivity of 0.81 (21/26), and specificity of 1.0 (36/36). The combination of methylation- and urine cytology-based models raised 2% prediction accuracy without reducing precision, suggesting that this assay could be applied to augment the cytology testing for UC detection. This study proposes a new and promising approach, leveraging cytology combined with epigenetic profiles of urinary cell-free DNA, for the precise diagnosis of urothelial carcinoma.

#4879 Delineating lymphocyte aggregates from tertiary lymphoid structures using spatial transcriptomics.

J. Krull, A. Byappanahalli, Y. Jiang, A. Gunderson, Q. Ma;
The Ohio State University, Columbus, OH

Tertiary Lymphoid Structures (TLSs) are ectopic lymphoid structures that form in chronically inflamed non-lymphoid tissue. The presence of TLSs in tumors is largely associated with favorable outcomes among patients and also exhibit positive associations with response to immune checkpoint blockade. Although mainly comprised of lymphocytes (B cells and T cells), they are considered a separate entity from lymphocyte aggregates within tissue. Lymphocyte aggregates are fairly routine to identify in H&E stained tissue sections, but delineating TLSs from simple lymphocyte aggregates is subjective and not clearly defined. Additionally, the definition of TLSs is only recently being elucidated, so a clear molecular definition of both TLSs and lymphocyte aggregates is needed. To address this problem, we leveraged open-source spatial transcriptomics (ST) data from 17 samples across 7 cancer types. High resolution H&E images were manually evaluated for lymphocyte aggregates by identifying dense pockets of lymphocytic-appearing nuclei. Suspected aggregates were detected in 10 of 17 samples. We then applied a visium spot-level signature scoring method for 4 well published TLS signatures. Of the spots identified, 62% had enhanced signature expression for at least 2 of the signatures, although most of the incorrect annotations came from the lone gastric cancer sample. Differential expression between a TLS-sig- suspected lymphoid aggregate and a TLS-sig+ region not identified by H&E enriched primarily for B cell identity genes, suggesting B-cell-rich TLSs may not always appear as lymphoid aggregates in histology. [AG1] Strikingly, ST revealed strongly positive enhancements in the TLS signatures, where no annotations were made, and no obvious lymphoid aggregation was present, suggesting manual annotation from H&E is inadequate for identifying TLSs. Together, these results demonstrate that literature derived TLS signatures can correctly identify lymphoid aggregates as TLSs and that cellular and molecular differences between standard lymphoid aggregates and TLSs may be smaller than is currently accepted.

#4880 Identification and clinicopathological analysis of potential p73-regulated biomarkers in colorectal cancer via integrative bioinformatics.

C. Bareja, K. Dwivedi, A. Uboveja, A. Mathur, N. Kumar, D. Saluja;
University of Delhi, New Delhi, India

This work aims to decipher p73-regulated biomarkers for a prompt diagnosis of colorectal cancer (CRC) by employing a combination of integrative bioinformatics and expression profiling technologies. Transcriptome profile of HCT116 cell line p53−/− p73+/+ and p53−/− p73 knockdown was performed to identify differentially expressed genes (DEGs) followed by cross-checking with three CRC tissue expression datasets available in Gene Expression Omnibus. KEGG and Gene ontology were performed on differentially expressed transcripts obtained via the transcriptome profile and intersected genes. The PPI network was constructed via Cytoscape to extract hub genes. KM plots assisted in investigating the prognostic significance of the hub genes. The clinicopathological relevance was explored using the GEPIA and UALCAN databases. Finally, machine/deep learning algorithms were employed to perform TNM-stage classification. Transcriptome profiling revealed 1,289 upregulated and 1,897 downregulated genes. When intersected with employed CRC datasets, 284 DEGs were obtained. The analysis of gene ontology and KEGG showed enrichment of the DEGs in metabolic process, fatty acid biosynthesis, etc. The PPI network constructed using these 284 genes assisted in identifying 20 hub genes. Kaplan Meier, GEPIA, and UALCAN analyses uncovered the prognostic and diagnostic relevance of these hub genes. Conclusively, the deep learning model achieved TNM-stage classification accuracy of 0.78 and 0.75 using 284 DEGs and 20 hub genes, respectively. This is a novel study utilizing transcriptomics, publicly available tissue datasets, and machine learning to unveil key CRC-relevant genes. These genes are found relevant regarding the patients' prognosis and diagnosis. The unveiled biomarkers are also found robust in TNM-stage prediction. This is the first study where transcriptomics, publicly available tissue datasets, and machine learning are altogether employed to reveal key genes in CRC pathogenesis. Our research highlights the robust analysis of four independent data sets to find the key hub genes, further predicting the performance of the key genes in stage-wise classification.

#4881 Detecting cancer microbiota using unmapped RNA reads on spatial transcriptomics.

Jeongbin Park[1], Seo Hye Park[1], Dongjoo Lee[1], Jae Eun Lee[1], Daeseung Lee[1], Kwon Joong Na[2], Hongyoon Choi[3], Hyung-Jun Im[4]

[1]Portrai, Inc., Seoul, Korea, Republic of,[2]Department of Thoracic and Cardiovascular Surgery, Seoul National University Hospital, Seoul, Korea, Republic of,[3]Department of Nuclear Medicine, Seoul National University Hospital, Seoul, Korea, Republic of,[4]Department of Molecular Medicine and Biopharmaceutical Sciences, Graduate School of Convergence Science and Technology, Seoul National University, Seoul, Korea, Republic of

Background: Recently, the study of microbiota has emerged as a novel area in cancer research. While next-generation sequencing (NGS) technologies are becoming more prevalent in the area, the acquisition of spatial information in microbiota is still challenging. Despite the possibility of detecting microbial RNAs on Visium (10X genomic, USA), methods depending on predefined host and microbial references cannot reliably capture microbial RNA reads, since Visium inherently lacks the ability to capture RNAs that are missing poly-A tails. Therefore, a reference-independent microbial RNA detection method needs to be developed for more trustworthy research on cancer microbiota on Visium.
Methods: Initially, we reconstructed Visium data from a public raw dataset (Project: PRJNA811533, European Nucleotide Archive) derived from colorectal cancer (CRC) and oral squamous cell carcinoma (OSCC). BAM files were obtained by running Space Ranger on a human reference, GRCh38. These BAM files were firstly separated according to spatial barcodes with samtools and xargs. Then, microbial scores for each barcode were obtained using PathSeq. On the other hand, barcode-wise unmapped reads were extracted from the original BAM files simply by remaining unmapped reads, sorting them by spatial barcodes, and counting the number of reads. Then, the unmapped reads originating from host RNA reads were eliminated by regression analysis, remaining the microbial RNA reads. Subsequently, we conducted a comparison of microbial RNA reads from two different techniques.
Results: By filtering out the unmapped reads associated with the host, microbial reads could be isolated. While these remaining microbial RNA reads show a significant correlation with the PathSeq scores, the unmapped reads were significantly higher than the PathSeq scores, increasing the statistical power for the downstream analysis with unmapped reads. Additionally, tissue regions with low PathSeq scores and high volumes of non-human unmapped reads were identified. These regions may indicate the presence of microbial sequences or RNA species that were not detected in the PathSeq analysis.
Conclusion: The use of unmapped reads enables us to capture a greater number of RNA transcripts compared to PathSeq to indirectly analyze cancer microbiota. This means that we can observe hard-to-identify RNA variants, such as unstable RNAs or new species originating from the interaction between microbial RNAs and host RNAs. Our methods can provide plausible explanations for the existence of microbial RNAs on Visium, and we suggest a reference-independent detection of cancer microbota reads by utilizing unmapped reads.

#4883 *NFE2L3* regulates the expression of *BHLHE40* in triple-negative breast cancer.

S. Modi, T. Andey, G. Acquaah-Mensah;
Massachusetts Col. of Pharmacy & Health Sci., Worcester, MA

Introduction: Breast Cancer (BrCA) is one of the most common cancers, causing mortality in women worldwide. Among the subtypes of breast cancer, triple-negative breast cancer (TNBC) is the most aggressive due to the absence of three major receptors: estrogen receptor (ER), progesterone receptor (PR), and human epidermal growth factor receptor-2 (HER-2). Treatment options for TNBC are limited because of the lack of these molecular targets. We hypothesized that the identification and characterization of novel transcriptional regulatory relationships in TNBC will provide etiologic insights, enhance therapeutic outcomes, and improve patient survival. Overexpression of *NFE2L3* in BrCA has inhibited cell proliferation and metastasis while overexpression of *BHLHE40* has produced an inverse effect. This study aims to characterize the relationship between *NFE2L3* and *BHLHE40* in TNBC cells.
Methods: Patient data from the two groups of our focus from the Cancer Genome Atlas BrCA RNAseq gene expression dataset were examined: triple-positive breast cancer (TPBC) and TNBC. Differentially expressed genes (DEGs) between these groups were identified using DESeq2. Pathways over-represented among the DEGs were determined using enrichR. For their impact on biological interactions, those DEGs were mapped to curate protein-protein interactions - the STRING database. Additionally, DEGs were superposed on two network inference algorithm-generated transcriptional regulatory networks (TRNs). Virtual Inference of protein activity by Enriched Regulon analysis was applied to the generated TRN to identify master regulators driving gene expression differences between TPBC and TNBC. Of the master regulators observed, the activity of NFE2L3 was explored in TNBC cells. The TRNs indicate that NFE2L3 regulates the expression of BHLHE40. This regulatory relationship was explored in TNBC cells by RNA interference, qRT-PCR, immunoblotting, and co-immunoprecipitation assays to investigate *NFE2L3* and *BHLHE40* gene and protein expression and interaction.
Results: Among 12,000 DEGs (5% FDR), over-represented pathways included "*mitotic signaling"* and *"G1/S transition*". Master regulators with higher expression in TNBC included NFE2L3, HMGA1, TP53, FOXC1, and SOX9; those with lower expression included FOXA1, BHLHE40, AR, XBP1, and ESR1. On silencing the cells of *NFE2L3* and performing qRTPCR analysis, the expression of *BHLHE40* was decreased in the TNBC cells. The protein-protein interaction between NFE2L3 and BHLHE40 was also validated.
Conclusion: DEGs up-regulated in TNBC participate in cell cycle signaling. And there is a novel transcriptional regulatory relationship between *NFE2L3* and *BHLHE40* in TNBC cells.

#4884 Evaluating the utility of *in silico* variant annotation tools for cancer driver detection.

M. Madhumita, Z. Sondka, J. Teague;
Wellcome Sanger Institute, Cambridge, United Kingdom

In cancer genomics, precise variant annotation is crucial for clinical decisions, drug development, and research. The burgeoning genomic data offers an opportunity to use data-driven approaches to generate knowledge that supports clinical decisions. Particularly machine learning (ML) and Deep learning (DL), are becoming essential, as their application is fast, scalable, simple to implement, and generates reproducible results. The methods ranging from simple sequence-based alignment scoring to advanced algorithms like Logistic regression, Support vector machine, and Recurrent neural networks, have been employed by multiple variant annotation tools. This study compares *in-silico* methods available in Ensembl's Variant Effect Predictor (VEP) using a test dataset with COSMIC annotations.

ML/DL success relies on robust training sets with comprehensive genomic variants features, including effects on transcription/translation, genomic context, annotation resources, *in silico* pathogenicity predictions, and population allele frequency. The training set, composed of known benign or pathogenic variants, serves as a reference for these algorithms to classify new and unseen variants. Our analysis reveals a limited concordance between the prediction algorithms. Despite comparable true/false positives/negatives, discrepancies persist in variant classification. Certain algorithms exhibit a propensity to over or under-call deleterious mutations. Some demonstrate a tendency to classify random variants in non-cancer genes as deleterious. Challenges include the absence of consensus on informative features, diverse training datasets, and restriction to well annotated proteins/transcripts.

Balancing the sensitivity and false positives in detecting cancer drivers is crucial. Integrating individual prediction scores with ML algorithms enhances tool performance but comes with risk of error propagation, and limited accuracy. The study emphasises the need for context-specific variant classification tools, as many variants' impacts are cancer-type specific, and some may drive disease synergistically. Existing tools, designed for a "one variant - one score approach," struggle to capture complex associations, especially those dependent on changes in the tumour microenvironment.

Highlighting areas for improvement, the study addresses the "black box" problem in decision processes. While limited interpretability might not hinder practical applications, tools should evolve to assess more complex associations guided by biology. Formal consensus, reference training datasets, and standards are deemed essential for developing next-generation tools. The envisioned context-dependent tools aim to streamline feature complexity, thereby mitigating the black box problem and advancing the accuracy and interpretability of cancer variant annotation.

#4885 Integrating mutational profiles and transcriptional data with *ASTUTE* to elucidate the key molecular functions involved in the pathogenesis of cancer.

V. Crippa, D. Fontana, I. Civettini, L. Mologni, R. Piazza, C. Gambacorti-Passerini, D. Ramazzotti;
University of Milano-Bicocca, Monza, Italy

Cancer is a highly heterogeneous disease characterized by genomic and phenotypic changes that differ among tumor subtypes. A comprehensive understanding of the molecular heterogeneity is crucial for identifying molecular biomarkers and developing targeted therapies. While recent years have seen significant progress in genomic studies and advancements in next-generation sequencing technologies, elucidate the impact of individual genomic alterations on the transcriptome landscape of cancer cells remains essential. This knowledge is crucial for developing personalized therapies. To integrate mutational profiles and transcriptional data, we have developed a novel computational framework named ASTUTE (Association of SomaTic mUtaTions to Expression). ASTUTE establishes associations between somatic mutations and gene expression profiles, quantifying the results as fold changes and comparing the effects of individual mutations. In particular, ASTUTE leverages LASSO regularized regression for feature selection, identifying the most relevant mutated genes that exhibit a strong association with expression levels. Our goal is to create a valuable resource for identifying diagnostic markers and advancing the development of targeted therapies in cancer. To this end, we applied ASTUTE to two published bulk RNA-seq datasets of adult acute myeloid leukemia (AML) patients from the Beat AML program and the TCGA study to verify the capacity of our approach to identify genes whose expression correlates with the presence of specific somatic mutations. The first dataset comprises 585 samples, while the second one includes 173 specimens, both of them contain mutations and RNA-seq data. We executed ASTUTE on the two datasets independently, considering all genes for RNA-seq data and the alterations in the top 10 most mutated genes. We considered the associations consistently discovered in both cohorts. Our analysis revealed a strong association between NPM1 mutations and the expression of HOX genes. Specifically, HOXB6, HOXB5, HOXB3, HOXA5, HOXB2, and HOXA10 exhibited a log2 fold change higher than 1.5. The upregulation of these genes has been reported in association with NPM1 mutations in AML adult patients. Additionally, ASTUTE identified HOXA6, HOXA7, HOXA4, and HOXA9, whose expression has been described to be upregulated in the presence of NPM1 mutations in AML pediatric samples. Finally, we identified a robust relationship between NPM1 mutations and the expression of PBX3, MEIS, and ITM2A. The first two genes are upregulated in the presence of NPM1 mutations, while the third one is downregulated. Our analysis showcases ASTUTE's capability to identify potential markers and underscores the possibility to apply ASTUTE to different tumors datasets, with the aim to better characterize cancer heterogeneity and develop targeted therapies.

#4886 An in-depth single-cell map of inflammatory breast cancer reveals wide-scaled restructuring associated to an immunosuppressive and inflammation-like microenvironment.

P. Schwerd-Kleine[1], T. Cheytan[1], R. Wurth[1], E. Gutjahr[2], L. Michel[3], V. Thewes[4], P. Lichter[4], A. Schneeweiss[3], A. Trumpp[1], M. Sprick[1];
[1]German Cancer Research Center (DKFZ), Heidelberg Institute for Stem Cell Technology and Experimental Medicine (HI-STEM gGmbH), German Cancer Consortium (DKTK), Heidelberg, Germany, [2]Institute of Pathology, University of Heidelberg, German Cancer Research Center (DKFZ), Heidelberg Institute for Stem Cell Technology and Experimental Medicine (HI-STEM gGmbH), German Cancer Consortium (DKTK), Heidelberg, Germany, [3]Division of Gynecological Oncology, National Center for Tumor Diseases (NCT), Heidelberg, Germany, Heidelberg, Germany, [4]Division of Molecular Genetics, German Cancer Research Center (DKFZ), National Center for Tumor Diseases (NCT) Heidelberg, Germany, Heidelberg, Germany

Inflammatory Breast Cancer (IBC) has increasingly been recognised as a distinct form of breast cancer, that is characterised by its distinctive clinical presentation, as well as its fast onset and poor prognosis. Despite previous efforts, the underlying molecular heterogeneity of IBC remains poorly understood. We used single-cell transcriptomics to dissect the transcriptional landscape of IBC at single-cell resolution, and elucidate differences to non-inflammatory breast cancer (non-IBC), of which we created and curated a subtype-matched comparison dataset. Our analysis revealed a previously underappreciated role of the microenvironment in driving the immune suppressive and angiogenic phenotype of IBC. Furthermore, we identified key transcriptional signatures associated with IBC aggressiveness, including dysregulated pathways across all major cell compartments. Within each compartment, we used a combination of approaches to assign functional roles to subsets of cells, including expression of marker genes, gene programmes and projection onto thoroughly annotated reference-spaces. We thus identify cell populations present in significantly different proportions between IBC and non-IBC. Interestingly, among the populations enriched in IBC we identified iCAFs, pro-inflammatory M1-like myeloid cells as well as regulatory T cells. In non-IBC on the other hand, enriched cell types include myCAFs, M2-like myeloid cells and cytotoxic T cells.In addition to differences in the cell composition, we also find differences in the expression of certain markers and gene programmes. A pseudo-time analysis of T cells reveals a shift towards an exhausted T cell phenotype in IBC, in line with a lower expression of HLA genes in its epithelial compartment. In agreement with the known angiogenic phenotype, we also see an enrichment in mitogenic signatures in IBC-associated endothelial cells. In summary, our data describe an immunosuppressive environment, highlighted by the presence of cell types with an inflammation-like phenotype, signs of immune evasion and exhaustion and angiogenesis. Our comprehensive and unique single-cell transcriptomic dataset of this rare form of breast cancer provides valuable insights into the complex cellular composition of IBC, offering a foundation for further functional exploration of involved pathways, and finally development of new targeted therapy approaches. Our study contributes to a deeper understanding of IBC biology and pathology, enabling future identification of direly needed biomarkers and therapeutic approaches for this hard-to-treat breast cancer type.

#4887 Unveiling the functional impact of glioma non-coding germline variants using large language models.

M. Alvarez-Torres, X. Fu, R. Sagatelian, A. Buendia, R. Rabadan;
Columbia University, New York, NY

Efforts to identify the risk for developing gliomas through Genome-Wide Association Studies (GWAS) face relevant challenges, such as accurately pinpointing the genomic positions of germline variants, primarily found in non-coding regions, with unclear functional implications in glioma development. In this context, the GET method, a large language model designed to unveil regulatory grammars across 213 human cell types, emerges as a valuable tool for elucidating the mechanisms of non-coding mutations.

Our aims include: I) Validate the efficacy of the GET method using a well-documented case and prioritize relevant variants for analysis; II) Refine the genomic positions of these variants and exploring their linkage disequilibrium (LD); III) Identify potential motifs and genes that might be influenced by these high-impact variants.

After examining published GWAS, 39 non-coding SNPs in gliomas were found. Adding 316 variants in high LD (R2 > 0.8) expanded the dataset to 355 variants for analysis. Using the GET method, we calculated impact scores (ISs) for each variant, considering changes in motif binding score (ΔBM) and motif gradient (GM) across human astrocytes. We focused on rare variants (risk allele frequency <0.25) with the higher odds ratios (OR).

The table presents GET results for a well-known case-control, showing its role in increasing glioma risk through OCT4 motif disruption and enhanced MYC expression, as previously was confirmed experimentally. Moreover, it details results concerning the 5 rare germline variants exhibiting the highest ISs, including precise genomic positions and the most affected motifs and genes that could potentially be impacted by each variant.

	Variant ID	**Genomic Position**	**Altered Motif**	**Affected Gene**	**Ref allele**	**Alt allele**
Case-control	rs55705857	Chr8:129633445	OCT4+SOX2:POU	MYC	A	G
H-I variant #1	rs78378222	Chr17:7668433	HD/18	PER1	T	G
H-I variant #2	rs518394	Chr9:22019673	KLF/SP/2	CDKN2A	G	C
H-I variant #3	rs79495512	Chr15:76199995	KLF/SP/2	LINGO1	T	C
H-I variant #4	rs78185702	Chr15:76317893	SMAD	LINGO1	C	T
H-I variant #5	rs2538067	Chr7:54907724	CTCF	EGFR	G	A

Using a large language model, this study overcomes the challenge of mere variant identification, aiming to establish a framework for uncovering the underlying mechanism of risk variants. While further validation is essential, this is a promising approach to explore the impact of germline mutations.

#4888 Multi-modal knowledge graphs enhance patient stratification & biomarker discovery.

M. Goncalves[1], J. Cohen-Setton[1], I. Kagiampakis[2], B. Sidders[1], K. Bulusu[1];
[1]AstraZeneca UK Limited, Cambridge, United Kingdom, [2]AstraZeneca, San Francisco, CA

Background: Multi-modal analysis is crucial for deeper understanding of disease subtypes and more meaningful patient selection. We developed a flexible Knowledge Graph (KG) framework that enables deep multi-omic analysis. It can be used to uncover the interrelationships between the layers of data in a population to inform patient selection or biomarker discovery. We present an application of our framework to non-small cell lung cancer (NSCLC) to identify and separate communities of patients based on their survival and identify the associated biomarkers. We identified potentially mislabeled patients that do not share all the characteristics of the cancer subtype to which they are assigned: either lung adenocarcinoma (LUAD) or lung squamous cell carcinoma (LUSC). Crucially, the community-based biomarkers for poor or long survivors were validated on the whole population.
Methods: Our KG framework was leveraged by applying supervised community detection to NSCLC data from TCGA, specifically RNA expression and DNA methylation, with overall survival (OS) as the endpoint (n=999 subjects). Biomarkers associated to each community were ranked based on their prevalence inside against their prevalence outside the community.
Results: We obtained 3 communities (391 + 229 + 379 patients) that are all significantly separated by their OS ($p<0.05$). While KG-derived communities largely overlapped with histology-labelled LUAD or LUSC (concordant LUAD (n=330) / concordant LUSC (n=342)), a small number of patients did not (discordant LUAD (n=37) / discordant LUSC (n=61)). Discordant LUAD patients had significantly lower OS than concordant LUAD ($p=0.0198$), despite being both labeled as LUAD. Many of the discordant LUSC lacked the 3q26 amplification commonly seen in LUSC and other squamous cell carcinomas. The results from our KG framework highlight its increased sensitivity in relation to existing tools (Cline, *Sci Rep* 3, 2652 (2013)) as we identified a discordant LUAD group in addition to a discordant LUSC group. Moreover, our tool can select the biomarkers most prevalent in each community, and these significantly separated long from poor survivors on the whole population ($p=3.53e-5$). Some of these KG-identified biomarkers are known regulators of progression and survival in NSCLC, whereas others are still not extensively studied. This highlights another advantage of our approach in prospective target discovery.
Conclusions: Our KG framework allowed the observation of potential misclassifications of tumor subtypes in NSCLC (TCGA). This approach is a proof-of-concept of the value KGs have in identifying signals in muti-omic data that may improve patient stratification and uncover associated biomarker signatures. Our flexible end-to-end framework can take any type of ‘omic data and can be applied to any tumor type for such findings, which represents an alternative to pre-defined KG architectures with defined relationships.

#4889 Integrative multi-omic analysis reveals novel prognostic biological entities in pediatric medulloblastoma.

K. Rathi[1], V. Kesherwani[1], A. S. Naqvi[1], Y. Zhu[1], A. Sickler[1], X. Huang[1], B. Zhang[1], B. Rood[2], A. C. Resnick[1], **A. A. Kraya**[1];
[1]Children's Hospital of Philadelphia, Philadelphia, PA, [2]Children's National Hospital, Washington, DC, DC

Medulloblastoma is a cerebellar tumor for which relapses are associated with poor survival rates of less than 5%. Molecular heterogeneity and dose-limiting toxicities that occur with standard of care approaches, which include surgical resection, craniospinal irradiation, and chemotherapy, complicate the treatment of both primary and recurrent medulloblastoma due to adverse long-term sequela. While the integration of molecular analyses into the histopathology of pediatric medulloblastomas has changed the way these diseases are diagnosed, classified, and treated, there remains an unmet need to further understand the underpinnings of the disease to improve clinical outcomes and minimize neuronal, cognitive, and hormonal toxicities that occur with standard-of-care therapies. We therefore aimed to investigate novel subgroups of pediatric medulloblastoma as a basis for further defining biological properties and targets for the disease through multi-omic characterization. We derived single-nucleotide variant, copy number variant, expression, alternative splicing, and methylation array data from pediatric medulloblastomas profiled as part of the Children's Brain Tumor Network (CBTN) and the Open Pediatric Cancer (OpenPedCan) projects. Using non-negative matrix factorization across the five datasets derived from genomic, transcriptomic, and epigenomic profiling, we identified 14 clusters found to be prognostically significant by Kaplan-Meier analysis of overall survival ($p < 0.0001$). Our model further subdivided sonic hedgehog (SHH) and Group 3/4 tumors, but not Wnt-driven tumors, suggesting that the latter forms a homogeneous molecular subgroup. Among our subgroups, we recapitulated the four classically defined medulloblastoma subtypes known to be associated with mutations in *KDM6A, KMT2C, CTNNB1, PTCH1, TP53, KBTBD4, MYC,* and *MYCN*. Cascading biological relationships across the copy number, methylation, and expression domains were observed among novel subgroups, potentially driving migratory, immuno-regulatory, GPCR-related, growth factor-related, and histone methylation biological programs. A comparison of subgroup expression profiles to transcriptional signatures from the Library of Integrated Network-Based Cellular Signatures (LINCS) program identified canonical oncogenic pathways unique to each subgroup as potentially targetable, including, but not limited to, MAPK, VEGFA, inflammatory, fatty acid metabolic, and PI3K/AKT signaling. Our work uncovers novel biological entities in pediatric medulloblastoma potentially driven by higher order mechanisms across the genome, transcriptome, and epigenome, with the possibility of informing novel precision medicine approaches for the disease.

#4890 *In silico* study of enzymes involved in heparan sulfate catabolic process in cancer resistant mammals.

F. Oliveri Payet, **C. Machicado Rivero**;
Universidad Peruana Cayetano Heredia, Lima, Peru

Some mammals such as elephants, bats, whales, and blind mole rats (*Spalax*) are resistant to cancer. One of the cancer protective mechanisms present in such species includes a reduced degradation of heparan sulfate (HS), an important component of the extracellular matrix (ECM), present in *Spalax*. Such effect occurs due to a splicing variant of heparanase, called variant 36, that lacks enzymatic activity. Consequently, both HS and ECM are very stable in Spalax's tissues. If HS is stabilized, in cancer resistant mammals, due to the decrease of heparanase or other enzymes involved in HS catabolic process is unknown. We studied total of 9 enzymes (HPSE2, GusB, IDUA, IDS, NAGLU, SGSH, GNS, Sulf-2, HGSNAT) that regulate HS catabolism and homologs in 9 mammals. Multiple sequence alignments were done by MEGA to identify substitutions present in cancer resistant species in comparison with cancer susceptible animals. Such amino acid variants were further analyzed and both their energy stability and their functional effects were predicted by using online *in silico* tools including MAESTROweb, Condel, PANTHER, REVEL, and CADD. Finally, homologs with deleterious predicted variants were modelled with SWISSMODEL and their 3D structures were analyzed with Pymol and ChimeraX to identify structural features likely related to its loss of function. We found two loss of function missense variants, K264Q and W626L, in Alpha-L-iduronidase (IDUA) of *Spalax*. In addition, most of Brandt's bat enzymes and the N-sulphoglucosamine sulphohydrolase (SGSH) of the bowhead whale were very energy destabilizing enzymes with positive and higher ΔΔG values compared to human homologs. In the other hand, although some catalytic residues in the study enzymes are conserved in cancer resistant animals, their spatial arrangement and conformation in the 3D structure are different compared to human homologs, including E182 of IDUA which is one of the catalytic residues. In general, the secondary structure is conserved across the 9 enzymes studied but some differences were observed in cancer resistant animals including one of the beta strands near the catalytic domain in human and mice IDUA that appears as a loop in *Spalax*. In summary, HS stabilization could raise in cancer resistant mammals through the existence of lack of enzymatic activity not only in heparanase but also in other enzymes that participate in HS catabolic process, via a set of loss of function variants and changes in secondary and tertiary structure as well as a reduction of energy stabilization. More interestingly, such mechanism could be present in other cancer resistant mammals such as bats and bowhead whales. This study demonstrates that computational approaches are useful to study biological mechanisms of cancer resistance present in some mammals. This knowledge could be translated to humans and HS catabolic process could offer a new source of therapeutic anticancer targets.

#4891 Discovery of novel biomolecular condensate drug targets in oncology using *in silico* predictive tools.

K. L. Saar[1], M. Rebmann[1], M. Kanchwala[2], S. Qamar[1], P. Radhakrishnan[2], J. Cornish[1], J. Doh[2], J. Cattin[1], A. Rotem[2], M. Ghandi[2], A. Seeber[2], R. C. Centore[2], S. A. Teichmann[3], T. Knowles[1], **S. Arora**[2];

[1]Transition Bio, Cambridge, United Kingdom, [2]Transition Bio, Watertown, MA, [3]Wellcome Sanger Institute,, Cambridge, United Kingdom

Biomolecular condensates play a crucial role in maintaining cellular homeostasis by regulating various cellular processes, such as signaling, gene expression, DNA repair, and stress response. Dysregulation of condensate function has been implicated in the onset and progression of several cancer types, highlighting the potential of targeting condensates as a therapeutic approach.

To establish a pipeline for discovering and prioritizing new oncology targets that function *via* biomolecular condensates, we developed *in silico* models that link protein condensate formation to its sequence. Leveraging publicly available data and neural network based protein language models, we built predictive models for protein phase separation and for their localization into heteromolecular condensates.

With these models, we mapped the condensation character of the full human proteome, including disease variants of genes/proteins. Our results suggested that approximately half of the proteome has the potential to localize into condensate systems. We identified a broad array of chromosomal rearrangements that lead to pathological condensation (e.g., EML4-ALK fusions in lung cancer) and several instances where disease specific isoforms suppressed condensation (e.g., BARD1 mutations in breast cancer and DAXX mutations in melanoma). To identify cases where commonly occurring missense mutations lead to abnormal condensation we analyzed omics data from patients and healthy volunteers, focusing on two mechanisms: (i) condensation due to protein overexpression and (ii) altered condensation characteristics of disease variants compared to wild type protein. We investigated 18 TCGA oncology indications and identified several targets where mutations were predicted to cause aberrant condensation. The identified targets presented a wide range of biological classes, with transcription factors, co-activators, and epigenetic modulators being the most prominent. We prioritized CTNNB1 (βcatenin) for experimental validation and successfully demonstrated both the phase separation ability of the reconstituted protein and the presence of CTNNB1 condensates in colon carcinoma cells with mutated WNT pathway.

Notably, many of our predicted targets contain extended intrinsically disordered regions (IDRs), which have remained challenging to target using conventional drug discovery approaches due to their lack of a well-defined 3D structure. To identify compounds that modulate IDR containing proteins we are utilizing our PhaseScan™ platform, which can screen tens of thousands of compounds against our predicted targets within condensates and measure their modulation potential. Subsequent cellular profiling of active compounds in the predicted disease models will allow us to validate the predictions made by our *in silico* models and ultimately unlock drugging novel targets within biomolecular condensate.

#4892 MicroRNA signature and telomere genes in kidney cancer survival.

S. Yerukala Sathipati, R. Sharma, S. Hebbring;
Marshfield Clinic Research Institute, Marshfield, WI

Introduction: Kidney cancer ranks among the top 10 most prevalent cancers in the United States, clear cell renal cell carcinoma (ccRCC) has the worst disease specific survival histology. MicroRNAs (miRNAs) have emerged as potential prognostic indicators in various cancers, including kidney cancers. Telomerase, a biomarker associated with uncontrolled cancer cell growth, plays a crucial role in the human kidney cortex's telomere shortening over time. However, the link between miRNAs and telomeres in kidney cancer survival remains underexplored. Our study aims to uncover a miRNA signature capable of predicting 5-year survival in ccRCC patients and to investigate the biological relevance of this signature, particularly its shared pathway enrichment mechanisms with telomere genes.

Methods: We extracted miRNA expression profiles from The Cancer Genome Atlas database, comprising 166 patients with ccRCC. To identify a robust miRNA signature predicting 5-year survival in ccRCC, we established an Evolutionary Kidney Survival Estimator (EKSE) using an optimal feature selection algorithm and support vector regression. Additionally, we conducted bioinformatics analyses to uncover common biological pathways between miRNAs and telomere genes using Kyoto Encyclopedia of Genes and Genomes (KEGG) and Gene Ontology (GO) categories, encompassing biological processes, molecular functions, and cellular components.

Results: EKSE identified a robust signature consisting of 37 miRNAs, achieving a mean correlation coefficient and mean absolute error of 0.82±0.01 and 0.65±0.18, respectively between actual and estimated survival times. The top 10 ranked miRNAs in the signature, including hsa-miR-26a-1-3p, hsa-miR-28-5p, hsa-miR-3913-5p, hsa-miR-3170, hsa-miR-148a-5p, hsa-miR-671-3p, hsa-miR-224-3p, hsa-miR-10a-5p, hsa-miR-29b-1-5p, and hsa-miR-106b-5p, also showed promise in diagnosing ccRCC with AUC values ranging from 0.56 to 0.91. Furthermore, bioinformatics analysis revealed that the miRNA signature targeted well known telomere-associated genes such as TERT, DKC1, CTC1, and RTEL1. Notably, miRNA signature and telomere genes shared several common pathways, including cellular senescence (hsa04218) and proteoglycans in cancer (hsa05205). They also had overlapping GO-Molecular functions, such as DNA-binding transcription factor activity (GO:0003700), histone deacetylase binding (GO:0042826), and promoter-specific chromatin binding (GO:1990841).

Conclusions: Our findings suggest an association between microRNAs and telomere genes, potentially playing significant roles in the survival of patients with ccRCC. The identified miRNA signature robustly predicts 5-year survival in ccRCC. The shared biological pathways between these miRNAs and telomere genes offer new insights into the mechanisms driving ccRCC, signaling potential for therapeutic targets and improved prognostic markers in kidney cancer.

#4893 Role of MGMT expression in the genomic landscape and immunogenicity in human colorectal carcinomas.

B. Rajendran[1], J. Zhang[1], S. Desai[1], J. Gibson[1], J. DiPalermo[1], P. LoRusso[1], Y. Kong[2], H. Zhao[2], M. Cecchini[1], K. A. Schalper[1];
[1]Yale University School of Medicine, New Haven, CT, [2]Yale School of Public Health, New Haven, CT

Introduction: Colorectal cancer (CRC) is second most common cause of cancer-related mortality in the USA and most patients with advanced tumors lack effective therapeutic options. Epigenetic silencing resulting in reduced expression of O^6-methylguanine-DNA methyltransferase (*MGMT*) has been described in diverse tumor types including CRC and it is linked with reduced DNA repair capability and increased sensitivity to alkylating agents such as temozolomide. However, the potential role and clinical significance of MGMT overexpression in cancer cells has not been studied.
Methods: We used spatially resolved multiplex quantitative immunofluorescence (mQIF) analysis to concurrently measure the levels of MGMT protein, γH2AX and CD8+ tumor infiltrating lymphocytes (TILs) in a cohort of 111 CRCs and paired non-tumor colorectal mucosa from the same patient represented in tissue microarray format. To assess the genomic and immunologic context of MGMT expression, we studied the methylome, mutation profiling and mRNA expression of 526 CRCs from TCGA. The immunologic landscape of tumors was studied using GSEA and multiple transcriptomic-based tumor immune infiltration scores such as TIMER, CIBERSORT, etc. Finally, the genomic alterations and immunogenicity of SW620 human CRC cells (with baseline *MGMT* hypermethylation) with or without MGMT transfection were studied using *in vitro* co-culture preparations coupled to ultra-deep DNAseq and flow cytometry analysis.
Results: On mQIF analysis, cancer-cell MGMT protein upregulation was identified in 73.9% of CRCs and was associated with reduced levels of γH2Ax in malignant cells and lower CD8+ TILs. 26.1% of cases showed MGMT protein downregulation. The genomic analysis of the TCGA cohort revealed that the mean nonsynonymous mutational load was significantly lower in MGMT-high than low tumors with marked differences in the type of variants and frequency of oncogenic mutations. The transcriptomic analysis revealed that MGMT overexpressing tumors showed lower immune infiltration than the MGMT-low group and reduced representation of immune associated signatures including interferon gamma response and TNF-alpha signaling. In contrast, DNA repair, *TP53* pathways, were enriched. The exogenous expression of MGMT in
SW620 cells reduced the number of nonsynonymous mutations by 15.6% (141 vs 119 mean mutations) and was also associated with low T-cell activation (CD69+/CD8+ T-cells) and cancer-cell elimination on allogenic co-cultures with human PBMCs.
Conclusion: MGMT protein upregulation is common in human CRCs and is associated with reduced DNA damage response, distinct genomic features, and adaptive immune evasion. To our knowledge, this study is the first to report the biological and clinical characteristics of CRCs with *MGMT* overexpression that could support diagnostic and therapeutic developments.

#4894 Multi-omic approach for drug repurposing in the poor prognosis CMS4 subtype of colon cancer.

T. M. Marvulli, D. Traversa, R. Di Fonte, L. Maurmo, A. Azzariti, L. Porcelli, C. A. Coppola, C. Saponaro, E. Mattioli, F. A. Zito, R. Fasano, S. Serrati, D. Quaresmini, O. Brunetti, S. Tommasi, R. Massafra, **S. De Summa**;
IRCCS Istituto Tumori Giovanni Paolo II, Bari, Italy

Introduction: Colon cancer (CC) is one of the deadliest malignancy in developing countries. Key drivers considered for the clinical management are RAS, BRAF alterations together with TNM staging and microsatellite status (MS). With the advancement of sequencing technologies and bioinformatic approaches, various molecular classifications of CC have been proposed. Guinney et al. proposed a transcriptomic-based molecular subtyping, the so-called four Consensus Molecular Subtypes (CMS). CMS4 patients have the worst prognosis. Biologically, CMS4, also known as mesenchymal, shows high expression of genes related to EMT, matrix remodelling, TGFb signaling, and inflammatory-related system and a peculiar enrichment in stromal cells. Thus, in the present study we are focusing on CMS4 subgroup in order to identify drugs to be repurposed in such a clinical setting through a multi-omic approach.
Methods: Using *TCGAbiolinks* R package, we retrieved STAR Counts transcriptome profiling data, for COAD and READ. CMSclassifier was used to determine the CMS of the samples. We separated the coding genes from the long noncoding RNAs (lncRNAs) using annotation databases generated from Ensembl. We estimated the fraction of cell populations throughout the CIBERSORTx. Features selection approaches was performed both for coding genes and lncRNA. Data normalization has been carried out through variance stabilizing transformation for read count data. To identify CMS and potential biomarkers, we adopted *mixOmics* N-integration method. Our independent validation cohort consists of 100 patients, locally enrolled, upon local Ethical Committee approval. Features contributing to CMS4 subtype have been extracted and use to construct drug-gene interaction network.
Results: To set-up the classification model the DIABLO approach was used, reaching a mean AUCROC of 0.9022. Contributing features related CMS4 subtypes included nine coding genes, six lncRNAs and, regarding CibersortX deconvolution, Macrophage M0 and M2.The drug-gene interaction network includes six subnetworks centered to ALOX5, KCNMA1, AQP9, TGFB3, THBS4 and DPYSL3. The role of TGFb pathway was confirmed, considering the contribution to classification. Interestingly, we found interactions with Non-Steroid Anti-Inflammatory Drugs (NSAIDs), such as Mesalazine. Moreover, THBSA gene, involved in cell-to-cell, cell-to-matrix and stromal response, could also be targeted.
Conclusions: The results of our drug repositioning approach have been biologically corroborated considering, as mentioned above, the peculiar enrichment of CMS4 subtype for TGFb pathway and stromal cells. The chance to modulate the macrophagic activity in the tumor microenvironment through NSAIDs could be evaluated. Experimental validation on patient-derived organoids (PDOs), related to samples included to local validation cohort, is ongoing.

#4895 Optical genome mapping analysis across multiple solid tumor types in Bionano VIATM software.

S. I. Al-Saffar, B. Clifford, A. Raksi, A. Hastie, N. Miller, A. Chaubey;
Bionano Genomics, San Diego, CA

Solid tumors can show highly complex somatic structural and copy number variants (CNVs) of multiple classes. These variants can reveal mechanisms behind carcinogenesis, including the amplification of oncogenes, deletion or inactivation of tumor suppressor genes, and fusions to create new oncogenes. High degrees of heterogeneity within solid tumors can complicate analysis.

Optical Genome Mapping (OGM) is a comprehensive technology which combines the resolution of molecular-level data with the scale of cytogenomic analysis. ≈5-15mg sections of freshly frozen tumor are homogenized in buffer to release ultra-high molecular weight DNA. Long fragments are then labeled at a regular 6mer, then linearized and imaged with native long-range structure (≥150kbp) preserved. In silico molecules are assembled into maps and aligned to a reference genome to detect structural variants with sensitivity to ≥5% allele fraction. Bionano VIATM software provides tools for visualization and interpretation of structural variants detected with OGM. VIA also provides CNV calling and detection of Absence of Heterozygosity (AOH) and allelic imbalance using SNP-FASST3, a segmentation algorithm for detecting mosaic events in OGM and other types of data. VIA calculates a B-Allele frequency (BAF) distribution from OGM data and adds a genome-wide BAF track to the applications suite, enabling calling of allelic imbalance events such as AOH. Visualized together, the overlay of structural variant information on copy number data provides context for chromosome fusions underlying copy number change. Additionally, balanced fusions are revealed consistently in cases where the impact is copy neutral. To demonstrate the utility of integrative analysis of structural, copy number, and allelic imbalance variants in solid tumor datasets, we processed a pilot set of six diverse solid tumors through Bionano software. Brain, breast, kidney, lung, ovarian, and prostate tumor data which had undergone previous analysis in Bionano Solve 3.7 were freshly analyzed in Solve 3.8 and VIA 7.0. In the lung tumor dataset there are clear allelic imbalance segments spanning most of chromosome 4 with no concomitant copy number change. In VIA, these segments can be merged on examination, converted to AOH calls, and further specified to reflect mosaic copy neutral loss of heterozygosity (CN-LOH). In the complex kidney tumor dataset, it is difficult to resolve ploidy state based on copy number data alone. This ambiguity is resolvable with VIA, by leveraging the copy number and BAF-based allelic imbalance distributions and recentering probes to a manually defined diploid region. The comprehensive OGM data approach facilitated by VIA can streamline analysis in challenging solid tumor datasets. Structural variant visualization, CNV detection and AOH detection are available in VIA 7.0.

#4896 A high throughput method of identifying cells with increased genomic content across diverse cancer tissues.

S. Priyadarsini Nair, K. J. Pienta, S. R. Amend;
Johns Hopkins University School of Medicine, Baltimore, MD

Cancer cells with increased genomic content have been associated with recurrence and poor patient outcomes. The current manual identification of these rare cells by pathologists is time-consuming and labor intensive, given their scarcity within tissue samples. This study introduces a robust methodology for the automated identification of cancer cells with increased genomic content within prostate cancer tissues. Leveraging Qupath software integrated with the Stardist extension, our approach combines precise nuclear segmentation with threshold setting using a Python script. This methodology enables the specific identification of noncancerous small cells, cancerous cells, and those exhibiting genomic content significantly surpassing the average cancer cell (3x to 5x), complemented by thresholds based on hematoxylin intensity for enhanced result accuracy. Thus, our methodology offers an efficient solution to streamline the identification processes for these challenging cells.

We have extensively validated our method across diverse models, including animal and human models, transgenic and subcutaneous models, and Human Tissue Microarrays (TMAs), to identify cancer cells with increased genomic content. The rarity of these cells within tissue samples underscores the practical significance of our research, providing a solution to the current difficulties faced by researchers and clinicians in their identification.

The integration of this methodology aims to improve efficiency in cancer tissue analysis. Ongoing efforts are directed towards the evaluation of this high-throughput methodology using animal models and TMAs with known outcomes, further substantiating its applicability and potential clinical relevance.

#4897 Personalized cell surface target identification from pan-cancer RNA-seq and proteomics profiling of tumors.

G. B. Marino[1], E. Z. Deng[1], D. J. Clarke[1], W. Ma[1], P. Wang[1], A. C. Resnick[2], A. Ma'ayan[1];
[1]Icahn School of Medicine at Mount Sinai, New York, NY, [2]The Children's Hospital of Philadelphia, Philadelphia, PA

In its third phase, the Clinical Proteomic Tumor Analysis Consortium (CPTAC) program collected pan-cancer data from 1,069 patients profiling the transcriptome, proteome, and phospho-proteome of tumors and adjacent tissues from ten cancer types. To identify potential immunotherapeutic candidates from this CPTAC cohort, we searched for cell-surface proteins that are highly expressed in tumor subtypes compared to their expression in normal tissues and cell types from ARCHS4 and the Genotype-Tissue Expression (GTEx) resources. For each cancer type, tumor samples were first clustered into subtypes based on RNA-seq data, and then cell surface targets were prioritized for each cluster. These targets were subsequently confirmed for high protein expression in the tumor subtypes. Tumor samples were also processed by their classification into immune subtypes to identify targets specific to hot (CD8+/IFNG+) and cold (CD8-/IFNG-) tumors of each cancer type. For each cancer type, the computational pipeline identified ~30 cell surface proteins that are highly expressed in the tumor and lowly expressed across tissues and cell types in both the ARCHS4 and GTEx backgrounds. Many of these targets are also robustly differentially expressed at the proteome level. Several targets were shared across tumor types, including VTCN1 and TMPRSS4. Altogether, this rational approach to identify potential targets demonstrates a pipeline that can be applied for personalized cancer diagnosis and therapeutic development.

#4898 Highly accurate profiling of leukocyte composition from bulk peripheral blood with targeted digital cytometry.

A. Nakao[1], A. M. Newman[2], A. A. Alizadeh[2], M. Diehn[2], M. Ghosh[3], M. Aliminati[3], J. Ghosh[3], K. Stephenson[3], **A. Ashutosh**[3];
[1]CiberMed Inc., Saratoga, CA, [2]Stanford University, Stanford, CA, [3]Agilent Technologies, Inc., Santa Clara, CA

Background: Cell profiling methods such as flow/mass cytometry and single-cell RNA-sequencing are powerful tools for quantifying immune composition from healthy and neoplastic tissues. However, only a modest number of markers can be interrogated by the former and the latter remains cost prohibitive for large-scale analysis. Here we demonstrate robust, accurate, and reproducible enumeration of immune cell subsets from 36 whole blood samples using SureSelect XT HS2 RNA sequencing combined with CiberMed's iSortTM digital cytometry solution. Enrichment of genes in the LM22 signature matrix, a well-established collection of reference profiles for deconvolving 22 human immune subsets, was achieved with two new targeted sequencing panels—Agilent SureSelect CD CiberMed Heme and Agilent SureSelect CD CiberMed Heme + HiRes. Both panels were assessed for their ability to profile leukocyte subsets with CiberMed's iSortTM Fractions software, an optimized and standardized version of CIBERSORTx with novel enhancements.
Methods: Whole blood samples were freshly collected from 36 healthy donors and split into two fractions—one was immediately processed for complete blood count (CBC) and flow cytometric enumeration of major leukocyte populations; the other was stored in PAXgene Blood RNA tubes for subsequent RNA sequencing. A Sysmex system was employed for CBC quantification and a Becton Dickinson 6-color TBNK MultiTest in vitro diagnostic (IVD) assay was employed for enumerating B cells, CD8 T cells, CD4 T cells, NK cells. These data were used as ground truth to assess iSortTM deconvolution performance from targeted and whole-transcriptome bulk RNA sequencing data. RNA-seq expression values were used as input to iSortTM Fractions to deconvolve 22 immune subsets in each sample.
Results: Across 7 major populations, cell type fractions determined by iSortTM Fractions were highly concordant with ground truth fractions determined by clinical grade standards (r□0.96) and exhibited strong reproducibility across technical replicates (r□0.98). Furthermore, targeted enrichment using the SureSelect CD CiberMed Heme panel reduced the sequencing requirement by nearly 50-fold compared to whole-transcriptome sequencing, while also improving accuracy.
Conclusion: These new panels for digital cytometry are being released through the Agilent Community Design program to enable focused, reliable, and high-throughput analysis of cell type composition from peripheral blood samples.

#4899 Interface-guided phenotyping of coding variants in the transcription factor RUNX1.

K. Ozturk[1], R. Panwala[1], J. Sheen[1], K. Ford[1], N. Jayne[1], D.-E. Zhang[1], S. Hutter[2], T. Haferlach[2], T. Ideker[1], P. Mali[1], H. Carter[1];
[1]UC San Diego, La Jolla, CA, [2]Munich Leukemia Laboratory GmbH, Munich, Germany

Understanding the consequences of single amino acid substitutions in cancer driver genes remains an unmet need. Perturb-seq provides a tool to investigate the effects of individual mutations on cellular programs. Here we deploy SEUSS, a Perturb-seq like approach, to generate and assay mutations at physical interfaces of the RUNX1 Runt domain. We measured the impact of 115 mutations on RNA profiles in single myelogenous leukemia cells and used the profiles to categorize mutations into three functionally distinct groups: wild-type (WT)-like, loss-of-function (LOF)-like and hypomorphic. Notably, the largest concentration of functional mutations (non-WT-like) clustered at the DNA binding site and contained many of the more frequently observed mutations in human cancers. Hypomorphic variants shared characteristics with loss of function variants but had gene expression profiles indicative of response to neural growth factor and cytokine recruitment of neutrophils. Additionally, DNA accessibility changes upon perturbations were enriched for RUNX1 binding motifs, particularly near differentially expressed genes. Overall, our work demonstrates the potential of targeting protein interaction interfaces to better define the landscape of prospective phenotypes reachable by amino acid substitutions.

#4900 Spatial Atlas of Human Anatomy (SAHA): A subcellular, multiscale spatial odyssey of immune and gastrointestinal tissues and tumors.

J. Park[1], R. Gregorio[1], E. Hissong[1], S. Patel[1], B. Robinson[1], F. Socciarelli[1], E. Metzger[2], Y. Liang[2], J. Reeves[2], J. Beechem[2], O. Elemento[1], A. Alonso[1], S. Houlihan[1], R. Schwartz[1], C. E. Mason[1];

[1]Weill Cornell Medicine, New York, NY, [2]NanoString Technologies, Seattle, WA

The Spatial Atlas of Human Anatomy (SAHA) is a foundational effort to map 250 million cells and transcriptomes and proteomes of 30 non-diseased organs from healthy adults at two spatial scales: whole transcriptome of histological features (50 µm to 2 mm), and 1,000-plex RNA and 64-plex protein panels at spatial subcellular resolution (50 nm across 1 cm2). The project aims to establish and validate best practices in experimental design, sample processing, data analysis, and data standards for high-content spatial analysis across multiple human organs at whole transcriptome and proteome levels. The profiled samples will capture variability across genders and ancestries. All results, including raw and processed data, will be made available to the scientific community through the SAHA data portal and AtoMxTM Spatial Informatics Platform.

Here we present the part of Phase I data collected specifically around immune (bone marrow and lymph node) and gastrointestinal tissues (ileum, appendix, colon, and liver), and compare these data to colon and liver cancer samples. On serial sections, we perform spatial whole transcriptome data (with GeoMx® Digital Spatial Profiler) and 1,000-plex RNA profiles and 64-plex protein profiles collected by the CosMx™ Spatial Molecular Imager (SMI) matched to the exact shape of functional histological organ features from H&E and immunofluorescence stainings. Our data, which spans ~1.5 million cells collected across ~1,100 fields of view, enables the highest-ever subcellular resolution maps of cell types, lineage states, metabolic capacity, cellular neighborhoods, subcellular movements of organelles, and spatially resolved (and novel) ligand-receptor interactions across normal and cancer tissues. Through comparing these data to several cancer samples collected across multiple spatial platforms, we show how spatial organ atlasing at multiple scales can uncover unique insights into organ development, health, and cancer. We also show how the SAHA data can serve as a benchmark reference for spatial precision medicine.

#4901 High-resolution spatial transcriptomics identifies candidate genes facilitating perineural invasion.

D. G. Olgun[1], P. L. Wang[2], R. Zhao[2], D. H. Gong[2], W. L. Hwang[2];

[1]University of Virginia, Charlottesville, VA, [2]Massachusetts General Hospital and Harvard Medical School, Boston, MA

Perineural invasion (PNI), or the invasion of cancer to the space surrounding nerves, is associated with poor prognosis, but the underlying molecular factors that drive its initiation and progression are poorly understood. To explore this systematically, we applied a 6000-plex spatial transcriptomic panel with subcellular resolution to curated microarrays from 5 pancreatic ductal adenocarcinoma (PDAC) patients spanning different stages of tumor-nerve involvement. With this preliminary cohort, we explored malignant cell signatures associated with invasion and adaptation to the intraneural environment. Strikingly, we observed enrichment of a classical-like malignant transcriptional program marked by genes involved in glucose and lipid metabolism in nerve-invading malignant cells. Despite the known association of chemoresistance with serine dependence, these cells also exhibited upregulation of genes involved in serine biosynthesis, suggesting that intraneural invasion may offer an orthogonal path of treatment evasion. Overall, our findings indicate that nerve-invasive cancer cells adopt a unique transcriptomic signature within the neuronal microenvironment. Further studies will aim to uncover the relevance of these signatures to survival within the nerve environment and treatment resistance.

BIOINFORMATICS / COMPUTATIONAL BIOLOGY / SYSTEMS BIOLOGY / CONVERGENT SCIENCE: Artificial Intelligence and Machine/Deep Learning 3
Poster Session

#4905 Multimodal transformer model improves survival prediction in lung cancer compared to unimodal approaches.

A. Tripathi[1], A. Waqas[1], Y. Yilmaz[2], G. Rasool[1];
[1]H. Lee Moffitt Cancer Center, Tampa, FL, [2]University of South Florida, Tampa, FL

Integrating multimodal lung data including clinical notes, medical images, and molecular data is critical for predictive modeling tasks like survival prediction, yet effectively aligning these disparate data types remains challenging. We present a novel method to integrate heterogeneous lung modalities by first thoroughly analyzing various domain-specific models and selecting the optimal model for embedding feature extraction per data type based on performance on representative pretrained tasks. For clinical notes, the GatorTron models showed the lowest regression loss on an initial evaluation set, with the large GatorTron-medium model achieving 12.9 loss. After selecting the top performers, we extracted robust embeddings on the full lung dataset built using the Multimodal Integration of Oncology Data System (MINDS) framework. MINDS provides an end-to-end platform for aggregating and normalizing multimodal patient data. We aligned the multimodal embeddings to a central pre-trained language model using contrastive representation learning based on a cosine similarity loss function. To adapt the language model to the new modalities, we employed a parameter-efficient tuning method called adapter tuning, which introduces small trainable adapter layers that leave the base model weights frozen. This avoids catastrophic forgetting of the pretrained weights. We evaluated our multimodal model on prognostic prediction tasks including survival regression and subtype classification using both public and internal lung cancer datasets spanning multiple histologic subtypes and stages. Our aligned multimodal model demonstrated improved performance over models utilizing only single modalities, highlighting the benefits of integrating complementary information across diverse lung data types. This work illustrates the potential of flexible multimodal modeling for critical lung cancer prediction problems using heterogeneous real-world patient data. Our model provides a strong foundation for incorporating emerging data types, modalities, and predictive tasks in the future.

#4906 Biopsy free virtual histology to discriminate benign from malignant squamous neoplasms.

N. Kokikian[1], R. Wahhab[1], J. Li[1], S. Martin[2], D. P. Beynet[2], A. Ozcan[1], P. O. Scumpia[1];
[1]University of California, Los Angeles, Los Angeles, CA, [2]Veterans Affairs Greater Los Angeles Healthcare System, Los Angeles, CA

Reflectance confocal microscopy (RCM) is a noninvasive optical imaging modality that allows for cellular-level resolution, in vivo images of skin without performing a traditional skin biopsy. RCM image interpretation currently requires specialized training to interpret the grayscale output images that are difficult to correlate with tissue pathology. Here, we use a deep learning-based framework that uses a convolutional neural network to transform grayscale output images into virtually-stained hematoxylin and eosin (H&E)-like images allowing for the visualization of various skin layers, including the epidermis, dermal-epidermal junction, and superficial dermis layers. To train the deep-learning framework, a stack of a minimum of 7 time-lapsed, successive RCM images of excised tissue were obtained from epidermis to dermis 1.52 microns apart to a depth of 60.96 microns using the Vivascope 3000. The tissue was embedded in agarose tissue and a curette was used to create a tunnel through which drops of 50% acetic acid was used to stain cell nuclei. These acetic acid-stained images were used as “ground truth” to train a deep convolutional neural network using a conditional generative adversarial network (GAN)-based machine learning algorithm to digitally convert the images into GAN-based H&E-stained digital images. We used the already trained machine learning algorithm and retrained the algorithm with new samples to include squamous neoplasms. Through further training and refinement of the algorithm, high-resolution, histological quality images can be obtained to aid in earlier diagnosis and treatment of cutaneous neoplasms. The overall goal of obtaining biopsy-free virtual histology images with this technology can be used to provide real-time outputs of virtually-stained H&E skin lesions, thus decreasing the need for invasive diagnostic procedures and enabling greater uptake of the technology by the medical community.

#4907 RanBALL: Identifying B-cell acute lymphoblastic leukemia subtypes based on an ensemble random projection model.

L. Li, H. Xiao, J. D. Khoury, J. Wang, S. Wan;
University of Nebraska Medical Center, Omaha, NE

As the most common pediatric malignancy, B-cell acute lymphoblastic leukemia (B-ALL) has multiple distinct subtypes characterized by recurrent and sporadic somatic and germline genetic alterations like chromosomal alteration, transcription factor rearrangement or kinase inhibition. The treatment of B-ALL patients is personalized based on specific subtypes, as the treatment responses for different B-ALL subtypes may vary considerably. Identification of B-ALL subtypes can facilitate risk stratification and enable tailored therapeutic approaches. Existing methods for B-ALL subtyping primarily depend on immunophenotypic, cytogenetic and genomic analyses, which would be costly, complicated, and laborious in clinical practice applications. To overcome these challenges, we present RanBALL (an Ensemble Random Projection-Based Model for Identifying B-Cell Acute Lymphoblastic Leukemia Subtypes), an accurate and cost-effective model for B-ALL subtype identification based on transcriptomic profiling only. RanBALL leverages random projection (RP) to construct an ensemble of dimension-reduced multi-class classifiers for B-ALL subtyping. Specifically, the transcriptomic profiling features were projected onto low-dimensional spaces by random projection matrices whose elements conform to a distribution characterized by zero mean and unit variance. To ensure reliable and robust performance, we selected 20 subspace dimensions ranging from 600 to 2500, with intervals of 100. The transformed low dimensional data matrix was used for training an ensemble of multi-class support vector machine (SVM) classifiers, each corresponding to one of the RP matrices of various dimensions. The predicted probabilistic scores of each B-ALL subtype were integrated for determining the final decision. Results based on 10 times 10-fold cross validation tests for >1700 B-ALL patients demonstrated that the proposed model achieved an accuracy of 93.7%, indicating promising prediction capabilities of RanBALL for B-ALL subtyping. Furthermore, the 30% held-out tests suggested that the model was robust and consistent to maintain high confidence levels for accurate predictions. The high accuracies of RanBALL suggested that our model could effectively capture underlying patterns of transcriptomic profiling for accurate B-ALL subtype identification. To extend the impact of RanBALL, we have established a free and publicly available python package for RanBALL available at https://github.com/wan-mlab/RanBALL. We believe RanBALL will facilitate the discovery of B-ALL subtype-specific marker genes and therapeutic targets, and eventually have consequential positive impacts on downstream risk stratification and tailored treatment design.

#4908 Comprehensive tool for pan-cancer consensus data mining of drugs, targets and biomarkers.

S. Yoon;
Sookmyung Women's University, Seoul, Korea, Republic of

The rapid increase in collateral omics and phenotypic data has enabled data-driven studies for the discovery of drug targets and biomarkers. For this purpose, we have developed a convenient tool, Q-omics software, for general researchers and cancer scientists to carry out customized data mining without bioinformatics background. Q-omics provides a comprehensive interface and smart functions for facilitating pan cancer-wide association studies on mutations, RNA expression, protein abundance, shRNA/CRISPR efficacy, drugs, tumor-infiltrating cells, patient survival, clinical info. etc. Furthermore, consensus scores on associated data pairs from heterogeneous samples, help to predict the reproducibility of data mining results. Q-omics (download: http://qomics.io) improves the utility of cancer omics big data for non-computational scientists at all levels of cancer research.

#4909 An RNA-based model for tertiary lymphoid structure (TLS) prediction and classification in pancreatic adenocarcinoma (PDAC).

A. Livanova, A. Tyshevich, A. Kravets, S. Kurpe, N. Lukashevich, D. Ivchenkov, D. Dymov, A. Belozerova, K. Kryukov, A. Sarachakov, V. Svekolkin, V. Kushnarev;
BostonGene Corporation, Waltham, MA

Although TLS status possesses prognostic significance in PDAC and can potentially affect chemotherapy outcomes, there is currently a notable lack of RNA sequencing (RNA-seq) models that specialize in TLS identification and classification in PDAC. Here, we developed a model for predicting TLS status (high or low) based on RNA-seq data.

Design: Hematoxylin and eosin (H&E) whole slide images of PDAC samples from The Cancer Genome Atlas (TCGA, n = 118) and Clinical Proteomic Tumor Analysis Consortium (CPTAC, n = 129) were used to detect intratumoral and borderline TLSs followed by TLS density measurements (units/mm^2) by an experienced pathologist. The samples were then stratified into TLS-high and TLS-low groups based on median density values. Next, we used deconvolution by Kassandra algorithm to identify cell subtypes enriched in each TLS group based on gene expression (RNA-seq) data. Calculation of ssGSEA scores for gene signatures corresponding to cell subtypes and TLS structures was performed, along with survival analysis. Differential expression analysis between TLS-high and TLS-low samples, followed by functional enrichment ($|logFC| > 2$; $padj < 0.01$), was conducted. The LightGBM gradient boosting classifier was then trained on ranked expression data with sequential feature selection to predict TLS-high and TLS-low groups. We trained the model with H&E staining annotations and ranked RNA expression data from TCGA or CPTAC samples (total n = 167). The remaining 80 were designated as hold-out samples. The weighted F1 score was computed as a performance metric.

Findings: Median density of detected TLSs in the TCGA and CPTAC samples was 0.012 units/mm^2. Kassandra deconvolution revealed B-cell enrichment, but fibroblast and M2 macrophage depletion in the TLS-high group. Our calculated ssGSEA scores of previously described TLS gene signatures, along with those of different B-cell subtypes and follicular dendritic cells, showed significant association with the TLS-high group. Genes associated with B-cell proliferation, differentiation, and signaling (*CD19, CD22, CD79A, CD79B*, and *CR2*) were also upregulated in this group. Comparing the performance of our RNA-based model on the validation dataset with manual TLS
classification by a pathologist, we obtained an F1 weighted score of 0.72 and ROC-AUC score of 0.77. Thus, the TLS predictions by our model concurred with the TLS classification based on H&E annotations and pathological evaluation. Moreover, patients in the predicted TLS-low group had worse overall survival (OS) compared to the TLS-high group ($Log(HR) = 0.76$; 95% CI [0.04; 1.48]; $p<0.05$).

We present an RNA-based model that stratifies PDAC samples as TLS-high or TLS-low, with predictions that conform to pathological findings. We also found TLS-low samples to associate with worse OS, thus offering an objective means to predict prognoses of PDAC patients based on TLS status.

#4910 AI predicts drug response from the genomic features of cells and the kinase activity changes induced by compounds.

R. Janssens[1], K. Rizzolo[1], E. Artin[1], J. Wagner[1], M. Riester[1], J. Korn[1], **J. Park**[2],
[1]Novartis Biomedical Research, Cambridge, MA, [2]Novartis Biomedical Research, San Diego, CA

Human protein kinases are playing an important role in various biological activities including tumorigenesis and cancer progression, and for this reason, many kinase inhibitors have been developed as promising targeted therapies for cancer. To date, there are 72 FDA-approved treatments targeting about two dozen different protein kinases; 3 of them were approved in 2022. However, there are still critical challenges that can be addressed to improve the robustness and selectivity of the kinase inhibitors such as drug resistance, toxicity and compromised efficacy. To gain a deeper understanding of the biological mechanisms underlying the resistance to kinase inhibitors, we hereby design and train an artificial intelligence (AI) model that predicts in-vitro cell response to various kinase inhibition from the integration of the genomic features of cancer cell lines and the biochemical profiles of kinase activities. The inner-working of an optimized model provides important insights on the relevant kinase activities for the cell response. A major challenge for training such a model is that the training data for biochemical kinase activity is very sparse; the kinase panels are not consistent across different sources and each dataset contains many missing values. To address this, we train a secondary AI model to predict all the missing values for the kinase activity in our training data using the combination of the compound chemical structure and the kinase structure. The secondary model is independently validated to ensure the quality of the training data for the drug response prediction model. An investigation of the secondary model's inner mechanism sheds light on the kinase binding sites and which chemical substructures are important for its inhibition. The model accurately predicts the cell response to different CDK inhibition. A focused analysis of the model characterizes off-target effects of the CDK inhibitors which may be linked to the drug resistance mechanisms, suggesting ways to improve the inhibitors or potential targets for combination therapies.

#4911 PAIRWISE: Deep learning-powered personalized medicine approach identifies actionable drug combinations in B cell lymphoma.

C. Xu[1], J. Cohen-Setton[2], Z. Shen[3], M. Milo[2], I. US[1], B. Sidders[2], J. Fitzgibbon[2], H. Pan[4], O. Elemento[1], K. Bulusu[2];
[1]Weill Cornell Medicine, New York, NY, [2]AstraZeneca, Cambridge, United Kingdom, [3]Memorial Sloan Kettering Cancer Center, New York, NY, [4]Peking University Third Hospital, Beijing, China

Combination drug therapies offer promise for improving cancer treatment. However, identifying actionable drug combinations for specific cancer subtypes and individual patients remains challenging due to the vast number of possibilities. Existing approaches like high-throughput screening (HTS) and rule-based drug additions have limitations in their ability to predict clinically translatable synergistic combinations. Therefore, advanced machine learning focused on patient-centric modelling have the potential to optimize combination therapies.

PAIRWISE is a patient-centric deep learning-powered drug combination recommendation platform. Given gene expression along with chemical structures and targets from a set of two drugs being applied, the output is the binary combination outcome. PAIRWISE introduces a new approach of representing tumor genomics using the unsupervised pretraining design on 11K TCGA tumors. The power of PAIRWISE is derived from knowledge-guided transfer learning by learning from in vitro experiments with drug-drug-cell interactions and cellular heterogeneity. PAIRWISE can accurately predict combination synergy with area under the curve (AUC) > 0.85 across 10 tissue types in a large dataset of 200K in vitro drug combinations and significantly outperform all state-of-the-art methods.

Diffuse large B cell lymphoma (DLBCL) is the most common B cell non-Hodgkin lymphoma and remains incurable in around 40% of patients. Finding optimal combination therapy for each DLBCL patient is a critical unmet need. As independent validation, we applied PAIRWISE to an external HTS study of Bruton Tyrosine Kinase inhibitor (BTKi) combinations (Griner et al., 2014), confirming the reproducibility and accuracy of high-confidence predictions (AUC = 0.72).

PAIRWISE was also applied to transcriptomic data of 29 DLBCL cell lines (Bal et al., 2022) and predicted BTKi-containing combinations across ABC subtypes with higher synergy scores than GCB ($P = 0.02$). This is consistent with expected better overall efficacy of BTK inhibitors in ABC subtype (Younes et al., 2019; Davis et al., 2010; Wilson et al., 2015).

To predict opportunities in DLBCL, PAIRWISE was used to identify BTKi partners for an additional 211 anti-cancer drugs using 562 published ex vivo DLBCL samples (Schmitz et al., 2018). PAIRWISE effectively identified novel DLBCL sub-population with significantly higher response scores for predicted BTKi combinations and favorable survival. Notably, patients predicted as responsive had significantly better outcomes upon first-line chemotherapy treatments than non-responsive ones ($P < 0.0001$).

Collectively, we demonstrate that PAIRWISE is a highly efficient and generalizable framework that enables confident predictions of pairwise drug combinations at disease subtype level, with the potential of informing treatment options and clinical trial design.

#4912 Unsupervised detection of stromal phenotypes with distinct fibrogenic and inflamed properties in NSCLC.

N. Patel, N. Le, T. Nguyen, F. Najdawi, S. Srinivasan, A. Stanford-Moore, D. Kartik, J. Zhang, J. Brosnan-Cashman, R. Egger, J. Lee, M. Bronnimann; PathAI, Inc., Boston, MA

Background: Understanding the composition of cancer-associated stroma (CAS) is vital, as the number and location of immune cells and fibroblasts, as well as the degree of extracellular matrix deposition, have implications for cancer progression and response to treatment, including in non-small cell lung cancer (NSCLC). Manual analysis of CAS does not fully describe the stromal milieu, especially from a spatial perspective, and is highly subjective. To this end, we have developed an unsupervised machine learning (ML) model to characterize the CAS in NSCLC from hematoxylin and eosin (H&E) stained whole slide images (WSI) at scale.

Methods: PathExploreTM models were deployed to predict stromal tissue and cell types, while another ML model was used to detect collagen fibers from H&E stained WSIs from the TCGA LUAD (N=536) and LUSC (N=464) datasets. Stroma was divided into small regions (median = 0.02 mm2), and 88 features characterizing cell distribution, tissue composition and fiber density were extracted from each region. Graphs were generated connecting neighboring regions (nodes), and an unsupervised variational graph auto-encoder (VGAE) model was trained to learn 8 latent features through dimensionality reduction. Stromal phenotypes were then derived from the latent features using k-means clustering. The fraction of each phenotype in the stroma was correlated against immune- and stroma-related gene expression signatures (GES) and overall survival (OS).

Results: Deployment of VGAE on LUAD and LUSC WSIs revealed three distinct stromal phenotypes - P0, P1 and P2. Fibroblast density was elevated in P0 and P1 regions ($p<0.001$), immune cell density was elevated in P2 regions ($p<0.001$), and collagen fiber intensity was highest in P1 regions ($p<0.001$). P2 enrichment was correlated with elevated expression of the T cell-inflamed gene expression profile (TGEP; Spearman $\rho = 0.43$ in LUAD; $\rho = 0.27$ in LUSC) and with improved OS (HR = 0.696; 95% CIs: 0.571-0.847 in LUSC). Conversely, P1 enrichment was positively associated with a transforming growth factor-β-induced cancer associated fibroblast GES (TGFβ-CAF: $\rho = 0.19$ in LUAD and $\rho = 0.12$ in LUSC) and poor OS (HR = 1.358; 95% CIs: 1.149-1.603 in LUSC). These phenotypes are consistent with fibroblast-enriched, collagen-depleted stroma (P0), collagen-rich, fibroblast-enriched tumor-promoting stroma (P1), and immune cell-enriched, tumor-suppressive stroma (P2).

Conclusions: We describe an unsupervised, data-driven method of predicting stromal regions with discrete patterns of cell composition and collagen deposition in NSCLC. This approach identified three phenotypes of NSCLC stroma. These results highlight the ability of ML models to characterize and find meaningful patterns within the cell, tissue, and matrix components of a tumor. This work provides further evidence of the potential of ML to discover novel precision medicine biomarkers in NSCLC.

#4913 Morphological feature discrepancies in wild-type vs. BRCA1/BRCA2 mutated high-grade serous ovarian cancer.

J. Lee[1], **H. Kim**[1], Y. Lee[1], Y.-L. Choi[2], K. Jung[2], T.-Y. Kwak[1], S. Kim[1], H. Chang[1];

[1]Deep Bio Inc., Seoul, Korea, Republic of, [2]Samsung Medical Center, Seoul, Korea, Republic of

Introduction: The understanding of morphological heterogeneity at the cellular level in High-Grade Serous Ovarian Cancer (HGSOC), particularly in relation to BRCA1 and BRCA2 mutations, is still an ongoing area of research. This study aims to elucidate the morphological features that distinguish wild-type (WT) tumors from those with BRCA1/BRCA2 mutations using deep learning models.

Methods: A total of 300 H&E stained HGSOC slides were collected in a patient-wise manner and tumor areas were annotated by an expert pathologist. We used a convolutional neural network model with spatial attention pre-trained on pathological images to extract features from slides, and the features were clustered into 96 groups. Subsequently, a nuclei segmentation model was employed for precise cell segmentation, followed by measurement of cellular features including cell shape (area, eccentricity) and cell texture (dissimilarity, correlation). The assessment of cell texture evaluates the variation and uniformity in gray-level intensity across the cell. We performed independent t-tests on samples of 100 patches from each cluster, comparing cells of selected patches from the top-N clusters representing the highest proportion of each label.

Results: H&E slides (n=300) include 69 (23%) BRCA1 mutants and 50 (16.7%) BRCA2 mutants. In Table1, negative t-statistics suggest that WT carcinoma cancer cells exhibit lower values for the measured features compared to BRCA mutants, whereas positive values denote higher values in WT. BRCA1 and BRCA2 mutant carcinoma cancer cells showed significantly larger areas and higher eccentricity than WT carcinoma cancer cells in all top-N clusters settings (N=3, 5, 10, 30). Furthermore, WT carcinoma cancer cells showed higher dissimilarity and reduced correlation compared to BRCA1 mutant carcinoma cells in four settings.

Conclusions: Our observations in BRCA-mutated HGSOC cells enrich our understanding of tumor cell morphology with BRCA mutations.

Table1. Comparison of cell features between WT and BRCA mutants

cell feature	comparison	top-3 clusters (t-statistics, p-value)	top-5 clusters (t-statistics, p-value)	top-10 clusters (t-statistics, p-value)	top-30 clusters (t-statistics, p-value)
area	WT vs BRCA1	-37.41, <0.001	-50.2, <0.001	-37.53, <0.001	-85.95, <0.001
	WT vs BRCA2	-42.14, <0.001	-50.61, <0.001	-16.57, <0.001	-51.98, <0.001
eccentricity	WT vs BRCA1	-24.40, <0.001	-34.14, <0.001	-38.02, <0.001	-37.40, <0.001
	WT vs BRCA2	-26.77, <0.001	-30.46, <0.001	-29.47, <0.001	-47.64, <0.001
dissimilarity	WT vs BRCA1	55.17, <0.001	52.73, <0.001	103.57, <0.001	166.78, <0.001
	WT vs BRCA2	-38.15, <0.001	-24.75, <0.001	0.2, <0.001	107.73, <0.001
correlation	WT vs BRCA1	1.94, <0.001	-2.46, <0.001	-50.24, <0.001	-65.96, <0.001
	WT vs BRCA2	87.62, <0.001	90.83, <0.001	52.6, <0.001	-48.90, <0.001

#4914 Mapping the cancer immune landscape in colorectal adenocarcinoma using multiplexed imaging and AI based analysis.

Vasundhara Agrawal[1], Lisa Arvidson[2], Michael J. Smith[1], Katie O. White[1], Richard A. Heil-Chapdelaine[1], Samuel Jensen[2], **Arindam Bose**[1]

[1]Leica Microsystems, Waltham, MA,[2]Cell Signaling Technology, Danvers, MA

Colorectal cancer is a high burden cancer in the United States, leading to the second highest cause of cancer deaths. Despite chemotherapeutic intervention and surgical resection, recurrent disease may occur in some patients and typically, has a poorer prognosis. Thus, there is a demand for advanced therapies such as immunotherapies for improved clinical outcomes. An in-depth understanding of the colon cancer microenvironment is necessary to improve outcome in this subset of patients. Spatial biology approaches are well positioned to comprehensively uncover the molecular and biological mechanisms of cancer cell aggression in colorectal cancer. Here, we visualized nearly 30 biomarkers in colon adenocarcinoma (CAC) tissue using the Cell DIVE multiplexed imaging workflow and validated antibodies from Cell Signaling Technology (CST®). Using this approach, we were able to probe multiple pathways of interest in cancer progression, such as vascularization of tumor tissue, immune cell responses, and cell proliferation. Together, these data allow the creation of a spatial map of tumor cell aggression and offer predictive value for the progression of the disease. Deep molecular and architectural insights on this level are possible only with a spatial biology approach and offer multiple downstream hypotheses to further understand cancer progression and interrogate the heterogeneity within the tumor microenvironment.

#4915 Identification and validation of novel prognostic genetic markers in HER2-negative advanced gastric cancer (AGC) by artificial intelligence (AI) deep learning and machine learning algorithm.

S. Park[1], S.-J. Heo[2], C.-K. Lee[3], Y. Lee[2], W. Kwon[1], J. Che[4], M. Kim[2], H. Chung[3], S. Rha[3];

[1]Song-Dang Institute for Cancer Research, Yonsei University College of Medicine, Seoul, Korea, Republic of, [2]Yonsei University College of Medicine, Seoul, Korea, Republic of, [3]Division of Medical Oncology, Department of Internal Medicine, Yonsei Cancer Center, Yonsei University College of Medicine, Seoul, Korea, Republic of, [4]Pharos iBio Co., Ltd., Seoul, Korea, Republic of

Introduction: Despite advances in anticancer treatments, there has been urgent need to identify novel prognostic markers for HER2-negative AGC. We propose AI based deep learning and machine learning pipeline to explore genetic markers that predict patient response to chemotherapy in HER2-negative AGC.
Methods: We retrospectively assessed 179 stage IV HER2-negative AGC patients who have been treated with first-line chemotherapy in Yonsei Cancer Center, Korea between 2015 and 2021. In-house targeted sequencing panel data (CancerSCAN^{TM} and CancerMaster) were used to identify candidate prognostic markers. DeepSurv was mainly used to analyze the progression-free survival (PFS), which is a deep learning algorithm that can investigate prognostic roles. The SHapley Additive exPlanations (SHAP) method was applied to open the deep learning models' black-box and calculate the importance ranking of gene features. Machine learning models-random survival forest, elastic-net, and lasso-were also investigated to identify potentially meaningful gene variants. To rank the gene features, we calculated variable importance (VIMP) for random survival forest, and penalized regression coefficients for elastic-net and lasso. All deep learning and machine learning models were trained using 5-folds cross-validation in 1,000 iterations of re-sampling bootstrapping with hyperparameter tuning by grid search. To classify responder or non-responder related genetic markers to chemotherapy, we used the signs of averaged penalize coefficients obtained from elastic-net and lasso. Based on the median linear predictor with candidate gene features, patients were classified into high-risk and low-risk group.
Results: A total of 7,824 common variants were analyzed and 20 prognostic genetic markers were identified based on the top average values of SHAP, VIMP, and penalized regression coefficients. The top 10 non-responder genetic markers are included as follows: PARP4(p.S873N), CHUK(p.V268I), BARD1(359_365del), CREBBP(p.Y1125F), BARD1(p.P24S), PHLPP2(p.R1312Q), FAT3(p.Q3375R), CASP5(p.T106A), PHLPP2(p.I544V), and PTCH2(p.T988M). Otherwise, the top 10 responder genetic markers are defined as follows: IL7R(p.I66T), NOTCH4(L16delinsLL), FGFR3, BCL2A1(p.G82D), ZNF217(p.T548I), BRCA1(p.K1183R), FANCA(p.A412V), ADGRA2, CDKN2B, and FANCM(p.S175F). The high-risk group had worse PFS compared with low-risk group (median PFS 4.1 vs. 9.1 months; *P*-value <0.0001).
Conclusion: This study showed the potential of AI deep learning and machine learning pipeline that employs an innovate prognostic genetic markers for HER2-negative AGC. Current ongoing analyses of larger cohort with more comprehensive clinical data will be presented.

#4916 Enhancing multi-organ frozen section cancer discrimination model by sharing cancer discrimination and organ classification task.

J. Lee[1], **J. Cho**[1], J. Lee[1], Y.-L. Choi[2], K. Jung[2], T.-Y. Kwak[1], S. Kim[1], H. Chang[1];
[1]Deep Bio Inc., Seoul, Korea, Republic of, [2]Samsung Medical Center, Seoul, Korea, Republic of

Introduction: Frozen section(FS) testing is an important method that removes part or all of a patient's tissue of a suspected tumor during surgery and microscopic examination to determine a diagnosis and surgical method that requires a rapid and accurate diagnosis. In this study, we developed a deep learning model to determine the presence of cancer and the type of organ in H&E FS whole slide images(WSIs) of 5 organs such as Breast(BR), Lung(LU), Stomach(ST), Breast Sentinel Lymph Node(LN), and Prostate(PR).
Design: In this study, we utilized a dataset comprising 19,881 H&E FS WSIs and 11,985 H&E-stained formalin-fixed paraffin-embedded (FFPE) WSIs to enhance generalization. The dataset included FS and FFPE WSIs from 33 different organs sourced from The Cancer Genome Atlas (TCGA) and additional FS and FFPE WSIs from a domestic hospital and the Camelyon 16 dataset, respectively. For the FS dataset, 20% was set aside for performance evaluation, while the remaining was randomly split into a 3:1 ratio for train and validation. In our methodology, we utilized instance-based multi-instance learning (MIL) to identify patches (1024*1024 pixels, 20x mag) with a high likelihood of cancer presence in each WSI. Then, we implemented multi-task learning (MTL) to predict the presence of cancer and the organ simultaneously.
Result: The table shows the WSI level performance through the 5 organs. The top 5 rows show results of MIL that only discriminate cancer. In comparison, the bottom 5 rows show results of MIL with MTL that share features from the cancer discrimination and organ classification. MIL with MTL make higher roc/auc than MIL only.
Conclusion: This study explores the automated analysis of H&E-stained FS WSIs using a deep-learning to discriminate cancer and classify organs. We could figure out that training cancer discrimination and organ classification simultaneously can make general features, and it leads to increased diagnostic performance.

Performance Table Between MIL vs MIL + MTL

Method	Organ	F1-score	Sensitivity	Specificity	ROC/AUC	Organ Accuracy
MIL	**LN**	0.9358	0.9669	0.6170	0.7919	NaN
	ST	0.9458	0.9583	0.8302	0.8943	
	LU	0.9577	0.9457	0.9275	0.9366	
	BR	0.9902	0.9895	0.9757	0.9826	
	PR	0.9346	0.9328	0.8786	0.9057	
MIL + MTL	**LN**	0.9448	0.9448	0.7872	0.8660	0.8816
	ST	0.9771	0.9697	0.9623	0.9660	0.7595
	LU	0.9700	0.9721	0.9203	0.9462	0.9509
	BR	0.9932	0.9910	0.9877	0.9894	0.8979
	PR	0.9480	0.9515	0.8913	0.9214	0.9803

#4918 Cancer mutations converge on a constellation of molecular assemblies to predict resistance to replication stress agents.

X. Zhao, A. Singhal, S. Park, J. Kong, R. Bachelder, T. Ideker;
University of California, San Diego, La Jolla, CA

Rapid proliferation is a hallmark of tumor cells, associated with sensitivity to therapeutics that cause DNA replication stress (RS). Many tumors exhibit drug resistance, however, via molecular pathways that are incompletely understood. Here, we develop an ensemble of predictive models that elucidate how cancer mutations impact the response to common RS-inducing (RSi) agents. The models implement recent advances in deep learning to facilitate multi-drug prediction and mechanistic interpretation. Instead of associating individual genetic alterations with RSi drug responses directly, the strategy is to project these alterations on a map of protein complexes and larger molecular assemblies associated with cancer. Initial studies in tumor cells identify 41 molecular assemblies that integrate alterations in hundreds of genes for accurate drug response prediction. These cover roles in transcription, repair, cell-cycle checkpoints, and growth signaling, of which 30 are shown by loss-of-function genetic screens to regulate drug sensitivity or replication restart. The model translates to cisplatin-treated cervical cancer patients, highlighting an RTK-JAK-STAT assembly governing resistance. This study defines a compendium of mechanisms by which mutations affect therapeutic responses, with implications for drug selection and combination.

#4919 AI-enabled hit selection of drug screening on human pancreatic cancer organoids.

Z. Tong[1], A. Lim[1], M. Meyer[2], M. Claples[3], O. Sirenko[1], N. Brandenberg[3];
[1]Molecular Devices, LLC (Moldev), San Jose, CA, [2]DOPPL SA, Lausanne, Switzerland, [3]SUN bioscience SA, Lausanne, Switzerland

Cancer remains one of the leading causes of death in the 21st century. Despite the latest advances in oncology, most cancer patients lack tailored therapeutic approaches with lasting benefit. Measuring the impact of anticancer compounds and their combinations is only possible on *ex vivo* assays. To this end, patient-derived organoids (PDOs) have been proposed as viable and efficient models for ex vivo testing. PDOs show long-term expansion potential while retaining tumor histopathology as well as cancer gene mutations. However, the translation of organoids in screening applications has so far been hampered by the lack of homogeneity and difficulties in handling and automation. Moreover, organoids are typically randomly distributed across the culture which complicates imaging and images analyses. To overcome these challenges, we set up a compound screening workflow with PDOs using Gri3D platform, comprising plates with micro-cavities suitable for high-throughput and reproducible organoid culture. Based on a standard 96 microtiter plate, each well contains a microwell array patterned in a cell repellent hydrogel. On Gri3D®, organoids are robustly generated in the microwells and are located in the same imaging plane. This greatly facilitates quantitative analyses in high content image-based screens. Furthermore, the pipetting port enables automation of cell seeding, media exchange and compound incubation with liquid-handlers, thus increasing assay reproducibility. In the presented work, we exposed human pancreatic cancer PDOs to a panel of anti-cancer compounds at different doses and followed their response to the drugs using viability dyes Calcein AM (live stain) and Ethidium Homodimer-1 (dead stain) with high-content confocal imaging. Using an AI-based approach, we efficiently detected each single organoid and extracted phenotypic features from all three channels (TL, live stain and dead stain) which correlate with cytotoxicity. The extracted features (more than 100) were first dimensionally reduced to 3 components using either PCA or UMAP, the treatments were then visualized in 3D scatter plots, ranked and clustered using machine learning. The data suggests that the compound treatment Palbociclib 50uM has significant cytotoxicity effects similar to the positive control, which is consistent with the traditional live/dead analysis. The AI approach demonstrates feasibility to perform drug screening in a robust and un-biased data analysis approach.

#4920 A nanopore sequencing approach characterizes cell-free DNA methylation-fragmentomics profiles indicative of breast cancer in a large cohort.

X. Bai, B. T. Lau, A. Almada, S. Grimes, T. Chen, H. Lee, H. P. Ji;
Stanford University School of Medicine, Stanford, CA

The detection of breast cancer from cell-free DNA (cfDNA) offers a new approach with the potential to benefit individual screening and early detection. However, identifying breast cancer from cfDNA remains a major challenge when one uses conventional short-read sequencing. Methylation and DNA fragmentation characteristics provide highly informative biomarkers for detecting and monitoring cancer. To characterize these genomic features from cfDNA, we developed an approach using single molecule Nanopore sequencing. Single cfDNA molecules are sequenced intact with the methylation and fragment size directly extrapolated from Nanopore data. Moreover, our approach requires small amounts of cfDNA to discern specific genomic features from individual molecules. Thus, the use of Nanopore sequencing provides both methylation and fragment size as directly measured from native cfDNA without the use of any chemical processing or other molecular manipulation. We studied an extended breast cancer cohort with in total 1080 of samples, consisting of 440 untreated breast cancer patients and 640 healthy controls. Nanopore sequencing analysis of these cfDNA samples identified a range of 1 to 4 million CpG sites from 1 ml of plasma. Leveraging the cohort, we developed an ensemble classifier for breast cancer detection based on cfDNA methylation and fragmentation. The classifier leveraged a leave-one-out cross-validation (LOOCV) to generate predicted probability. We created nucleosome-specific methylation scores as the input features to the classifier, which scores quantified the similarity of each sample's methylation profile to a training set on a selected set of CpG sites associated with cancers. Furthermore, we also identified DNA fragmentation features, revealing distinct mono-nucleosome and di-nucleosome patterns that distinguish cancers from healthy controls. Aggregating the DNA nucleosome-specific scores and fragmentation features, we built an ensemble LOOCV random forest model. We applied the model to the breast cancer cohort and achieved a detection specificity of 74%, a sensitivity of 71%, and an overall accuracy of approximately 73%. The area under the receiver operating characteristic curve (AUROC) reached 80%. We validated the classifier with two external independent cohorts. Validation cohort 1 demonstrated as a specificity of 85%, a sensitivity of 80%, and overall accuracy of 83% with AUROC of 90%. Validation cohort 2 without controls demonstrated that the classifier achieved a sensitivity of 94%. Both validation sets confirm that our model can achieve excellent performance for early breast cancer detection. In summary, our findings demonstrate that nanopore sequencing provides cfDNA methylation and fragment profiling that enables breast cancer detection. This approach holds the potential to improve cancer diagnosis and treatment outcomes.

#4921 A user-friendly R Shiny web app for predicting cancer genetic dependencies using deep learning.

M. J. Kasper, L.-J. Wang, M. Ning, Y. Huang, Y.-C. Chiu;
UPMC Hillman Cancer Center, Pittsburgh, PA

Understanding the genetic vulnerabilities (*i.e.*, genetic dependencies) of cancer cells is crucial for developing novel anti-cancer treatments. The Cancer Dependency Map (DepMap) projects, conducted by the Broad Institute and Wellcome Sanger Institute, have performed comprehensive genome-wide CRISPR-Cas9 knockout screens across diverse cancer cell lines. These data resources have enabled computational biologists to glean insights into cancer genetic dependencies using sophisticated computational models. As different genomic mechanisms govern tumorigenesis and genetic vulnerability, the relationship between cancer genomics and genetic dependencies is nonlinear, making the prediction of genetic dependencies challenging. Addressing this challenge, we previously developed a deep learning model, namely DeepDEP, to predict cancer genetic dependencies using multi-omic profiles (Chiu *et al.* DOI:10.1126/sciadv.abh1275). DeepDEP has a transfer learning scheme that integrates genomic representations captured from unlabeled tumor samples of the Cancer Genome Atlas (TCGA) and genomic features that are predictive of genetic dependencies in cell lines. Such a design enables the application of DeepDEP to both cell lines and tumors. The model demonstrated superior performance compared to various conventional machine learning methods. Prediction results were validated using independent cell-line datasets and patient clinical data. Here, we developed an intuitive web application for DeepDEP which allows users to easily utilize the model on their in-house data. Users can simply indicate whether the query sample is derived from a cancer cell line or a tumor, upload any combination of mutation, gene expression, DNA methylation, and copy number alteration datasets, and view the predicted dependencies of 1,298 cancer-relevant genes. Along with the genetic dependency predictions, users are provided with model performance metrics, detailed gene annotations, and links to useful resources such as Ensembl and COSMIC. Our web application features a variety of interactive visualizations to guide users to interpret the results at the levels of individual genes and pathways. The tool has two supplemental modules to enhance its functionality. One allows users to search for similar cell lines to the query sample within the DepMap project or for similar tumors within the TCGA project. The other supplemental module provides data exploration tools for pre-calculated predictions across all TCGA tumors. In summary, this user-friendly web application provides researchers with access to deep learning predictions of cancer genetic dependencies with various interactive visualization and analysis tools. It is anticipated that this application will facilitate the study of cancer genetic dependencies and enhance the efficiency of anti-cancer drug discovery.

#4922 Unraveling sarcomatoid features in clear cell renal cell carcinoma with RNA-seq.

K. Kryukov, S. Davitavyan, D. Stupichev, A. Sharun, A. Love, M. Kleimenov, S. Kuznetsov, A. Tkachuk, V. Kushnarev;
BostonGene, Waltham, MA

Introduction: Sarcomatoid clear cell renal cell carcinoma (ccRCC) represents a challenging and aggressive subset of kidney cancers with poor prognosis and resistance to conventional treatments. Recent studies have shown the benefit of checkpoint inhibitors (CPIs) for patients with sarcomatoid components; therefore, precise and objective evaluation of sarcomatoid differentiation is essential for CPI selection. Here, we developed a predictive model to identify sarcomatoid features in ccRCC.

Methods: The machine learning-based transcriptomic sccRCC model was developed on 512 samples from publicly available datasets: TCGA-KIRC and CPTAC-ccRCC. Samples were excluded with the following criteria: inconsistent with ccRCC, less than 10% sarcomatoid component, or <20% tumor neoplastic cellularity. Sarcomatoid features for each case were assessed by 3 pathologists. The meta-cohort was divided into training (n = 348) and validation (n = 164) cohorts.The model was tested on a publicly available cohort of ccRCC patients from Sato et al. (n = 100). Clinical validation was performed using an additional prospective cohort that received BostonGene's Tumor PortraitTM test (n = 32) with RNA-seq and whole exome sequencing (WES). The JAVELIN Renal 101 cohort was used to uncover differences in progression-free survival (PFS) associated with a predicted sarcomatoid component in advanced or metastatic ccRCCs treated with a combination of CPIs and tyrosine kinase inhibitors (TKIs).

Results: H&E analysis of the TCGA, CPTAC, and BostonGene cohorts identified zones with sarcomatoid features in 129 out of 556 (23.2%) samples. The sarcomatoid predictive model demonstrated robust performance, with weighted F1-scores of 0.85 when applied to the test cohort (Sato et al.) and 0.70 for the prospective clinical cohort. The model accurately classified 9 out of 10 total sarcomatoid samples in the prospective clinical cohort, highlighting its potential for real-world clinical applications. When applied to TCGA validation samples, sarcomatoid patients identified by the transcriptomic model exhibited median overall survival (mOS) of 55 months, whereas sarcomatoid patients based on H&E assessment had a mOS of 67 months, indicative of the model's superior performance when detecting sarcomatoid features for OS prediction. Moreover, the sarcomatoid ccRCCs predicted by transcriptomic model that were treated with a combination of CPIs and TKIs had statistically (p=0.0001) improved PFS compared to the TKI-treated group.

Conclusion: The developed transcriptomic model effectively differentiated sarcomatoid from non-sarcomatoid ccRCC samples with robust performance metrics. With additional investigation, the predictive value of the sarcomatoid ccRCC transcriptomic model can be leveraged to guide CPI and TKI selection.

#4923 A systematic framework for predicting adverse drug reaction signals using medical data.

J. Jeon, E. Hong, H. Kim;
Korea Advanced Institute of Science and Technology, Daejeon, Korea, Republic of

Prescribing a combination of medications is a common strategy to enhance the effectiveness of disease treatment. While this approach aims to improve therapeutic outcomes, it may lead to unintended adverse drug reactions (ADRs) due to interactions between prescribed drugs and individual factors. Recognizing the importance of ADRs, various machine learning models have been developed. However, these models face limitations, particularly in predicting reactions induced by three or more drugs and in accounting for individual patient factors, such as age and medical history. To address these limitations, we propose a systematic framework that leverages medical data for predicting ADR signals. In the framework, the MIMIC-IV database was systematically preprocessed, and a series of machine learning models were developed that predict the ADR signals. The model predictions were validated using the eICU collaborative research database. The machine learning models process multiple inputs, including information on administered drugs, age, gender, ethnicity, and underlying medical conditions to predict ADR signals. The ADR signals are determined by classifying abnormalities in 20 specific laboratory test values, such as hematocrit, creatinine, and hemoglobin. The machine learning models developed in this study hold promise as a valuable tool for assessing potential risks, such as ADRs, associated with the concurrent use of multiple drugs.

#4924 Assessing microsatellite instability dominance in colorectal cancer phenotype: A multi-study initiative using multi-target transformers for genomic biomarker prediction.

M. Gustav[1], M. van Treeck[1], Z. I. Carrero[1], C. M. L. Loeffler[1], N. G. Reitsam[2], B. Markl[2], A. Rabasco Meneghetti[1], L. A. Boardman[3], A. J. French[3], E. L. Goode[3], A. Gsur[4], S. Brezina[4], M. J. Gunter[5], N. Murphy[5], P. Limburg[3], S. Thibodeau[3], S. Foersch[6], R. Steinfelder[7], T. Harrison[7], U. Peters[7], A. Phipps[7], J. N. Kather[1];

[1]Technische Universitat Dresden, Dresden, Germany, [2]University of Augsburg, Augsburg, Germany, [3]Mayo Clinic, Rochester, MN, [4]Medical University of Vienna, Vienna, Austria, [5]World Health Organization, Lyon, France, [6]University Medical Center Mainz, Mainz, Germany, [7]Fred Hutchinson Cancer Center, Seattle, WA

We used deep learning (DL) to predict multiple genetic biomarkers of colorectal cancer (CRC) from routine histopathology images, aiming to identify morphological changes associated with the mutational profile of tumors.

A new Transformer-based prediction model was developed which can simultaneously predict multiple biomarkers from a single histopathology image. We compared the performance of the multi-target approach to conventional single-target models. We analyzed five patient cohorts from the Genetics and Epidemiology of CRC Consortium (GECCO) with colorectal cancer (N=1,385 patients). Our model was trained on an internal data set (N=739) to predict the presence of >200 genetic alterations, focusing on genes with non-silent mutations and mutational signatures, which were assessed using targeted sequencing. We used a 7-fold cross validation and validated the model on an independent, external data set (N=646). Morphological features of microsatellite instability (MSI) are detectable by DL models in histopathology images, making MSI a potential confounding factor. Thus, we also assessed whether our model can predict genetic alterations regardless of MSI status, or whether the model identifies the MSI phenotype.

For the majority of biomarkers, the multi-target transformer reached a higher prediction performance as measured by the mean Area Under the Receiver Operating Characteristic (AUROC) Curve and lower standard deviation than single-target DL models. For the external validation set, the mean AUROC of the multi-target versus the single-target model was 0.78 (+/- 0.01) versus 0.72 (+/- 0.06) for BRAF mutations, 0.88 (+/- 0.01) versus 0.86 (+/- 0.03) for hypermutation status, 0.94 (+/- 0.01) versus 0.91 (+/- 0.02) for MSI, 0.86 (+/- 0.01) versus 0.80 (+/- 0.05) for RNF43 mutations and 0.72 (+/- 0.02) versus 0.69 (+/- 0.05) for TP53 mutations, respectively. However, our analysis of the individual prediction scores suggests that the model does not identify the phenotype of the alterations themselves. Instead, the model seems to determine the status of specific genetic alterations based on their correlation with MSI. Consequently, biomarkers which are associated with microsatellite stability have prediction scores negatively correlated with predicted MSI scores. Conversely, biomarkers which are associated with MSI have prediction scores positively correlated with predicted MSI scores.

Our results demonstrate potential benefits of multi-target DL models in improving the predictive power and efficacy of histology-based biomarker extraction compared to single-target DL models. However, our results crucially highlight the importance of considering potential confounders, such as MSI status in CRC, and emphasize the need for extensive analysis beyond AUROC in studies focusing on DL-based biomarker detection.

#4925 Spatial heterogeneity of tumor boundary in mammograms is prognostic of recurrence in triple negative breast cancer (TNBC).

S. Ghose[1], C. Davis[1], S. Cho[1], Y. Polar[2], F. Ginty[1], S. Badve[2],
[1]GE Healthcare, Waukesha, WI, [2]Emory University School of Medicine, Atlanta, GA

Introduction: Despite standard-of-care therapies, at least 25% of all TNBC patients will develop recurrence or metastasis within 3-5 years and die due to breast cancer. Early prediction of recurrence in TNBC patients from clinical mammograms would allow more aggressive intervention for higher risk patients. The tumor boundary represents the heterogeneous invasive front where malignant cells interface extracellular matrix (ECM) and contribute to invasion. In this study, we investigated role of the irregular infiltration of the normal tissue by tumor in heterogeneity of radiomics features at the boundary of the tumor.

Method: Surgically treated patients with pathologically confirmed diagnosis of TNBC of any tumor size were included. All cases had node negative status and were treated with adjuvant chemotherapy. Patients with node positive or metastatic TNBCs at diagnosis, receiving neo-adjuvant chemotherapy or non-chemo regimens were excluded. Manually segmented breast lesions in mammograms from a cohort of 29 patients with 5-year outcomes were used to automatically determine the tumor boundary as a zone of 1 mm from both intra-tumoral and peritumoral regions in concordance with prior studies. Over 2000 radiomics features from the tumor boundary and the central regions of the tumor were extracted to quantify heterogeneity, obscure margins, spiculations, texture, breast fat percentage, shape, and size of the tumor. Recursive feature elimination using random forest classifier was used to reduce feature dimensionality to prevent over-fitting and predict recurrence in TNBC patients.

Results: We observed that tumor boundary heterogeneity as quantified by continuous gradient magnitude features at pixel level was significantly better at predicting lethality for TNBC patients when compared to usual radiomic features (gradient, texture, and shape features) extracted from the entire tumor, as done in prior radiomics analyses. Continuous gradient magnitude features quantifying spatial heterogeneity of the tumor boundary were found to be superior to texture features in providing estimation of local changes in pixel-level heterogeneity. In a three-fold validation framework, continuous gradient features were associated with a mean AUC of 0.82 (std 0.17) and better differentiated patient lethality risk *as compared to* gradient, texture, and shape features of the *entire tumor* (mean AUC of 0.27 (std 0.11)).

Conclusions: To the best of our knowledge, this is the first time that heterogeneity features of a tumor quantified by continuous gradient magnitude features from tumor boundary, as observed in routine clinical mammograms, have been shown to predict TNBC lethality. This model will be validated in a larger cohort in future studies.

#4926 Advancements in somatic variant calling from UG100 whole genome and whole exome sequencing data.

D. Shem-Tov[1], M. Levy[1], G. Hornung[1], I. Soifer[1], H. Benjamin[1], A. Jaimovich[1], A. Blattler[2], W. Brandler[2], R. Sugar[2], I. Kinde[2], O. Barad[1], D. Lipson[1];
[1]Ultima Genomics, Fremont, CA, [2]Exact Sciences Corporation, Madison, WI

Somatic variant calling involves the identification of genomic alterations that occur in somatic cells, requiring deep coverage to enable high sensitivity for low-frequency variants. Characterizing somatic variants across the entire genome therefore benefits from novel cost-efficient sequencing platforms, such as UG100. Here, we present optimization of variant calling tools for short and structural variants on WGS and WES data from UG100.

For calling short variants, we optimized DeepVariant (DV) for somatic calling using data from matched tumor-normal sample pairs, improving both variant calling accuracy and pipeline running time (up to 10-fold). We defined the task of somatic variant calling as deciding if the pileup image containing reads from the tumor and normal samples represents a true somatic variant (vs a germline variant or artifact).

The challenge of robust variant calling using deep learning models is exacerbated in somatic calling, where sequencing depth and coverage variability are typically high. Our optimized DV overcomes these challenges by several data sampling strategies. First, allele-frequency preserving down-sampling reduces randomness of read sub-sampling in high coverage regions. Second, alternative allele prioritization samples alt-allele supporting reads first allowing to call variants at very high coverage loci without sacrificing sensitivity and computational efficiency. Finally, a Panel-of-Normals based on targeted WES data provides an additional improvement of precision for this assay type. We used these strategies to train two models, one for tumor characterization using WGS (T/N coverage: 40x-150x/40x-100x), and one for deep WES (T/N coverage: >500x/>120x).

We called variants on simulated tumors using the WGS model. For VAF>10% the model showed SNV recall >98% and indel recall >95% with false-positive rate of 0.2/Mb. For VAF range of 5-10%, indel recall was 67% and SNV recall was 86%. To demonstrate the utility of our somatic variant calling, we applied the models to call somatic variants from well characterized cancer cell lines: COLO829, HCC1395 and HCC1143. Results showed F1>90% for variants with VAF>10%. The WES model was used to reliably call variants at VAF>5% on simulated tumors with average SNV recall of 99% with precision >99% and indel recall >86% with precision >94%.

To analyze structural and copy-number variations, we optimized the assembly engine of GRIDSS to enable fast calling of structural variations and demonstrate that Control-FREEC can be used to call copy number variants. SV calling on COLO829/COLO829BL achieved sensitivity >95%.

In conclusion, our research highlights the utility of UG100 within the field of oncology, demonstrating its capacity for comprehensive and precise somatic variant detection, both on WGS and WES data.

#4927 Combining single-cell ATAC and RNA sequencing for supervised cell annotation.

Jaidip Gill[1], **Abhijit Das Gupta**[2], Brychan Manry[2], Natasha Markuzon[3]

[1]School of Public Health, Imperial College, London, United Kingdom,[2]AstraZeneca US, Gaithersburg, MD,[3]AstraZeneca US, Waltham, MA

Background: Analysis of samples at the single-cell level offers insights into cellular heterogeneity and cell function. Cell type annotation is the first critical step for performing such an analysis. While current methods primarily utilize single-cell RNA sequencing (scRNA-seq) for annotation, several studies have demonstrated improved classification accuracy by combining scRNA-seq with transposase-accessible chromatin sequencing (ATAC-seq) using unsupervised methods. However, the utility of ATAC-seq features for supervised cell-type annotation has not been explored.

Aims/Objectives: The objective of this study was to evaluate the relative performance of supervised cell-type classification using scRNA-seq alone vs. in multimodal combination with ATAC-seq; and how these data interplay with choice of classification and dimensionality reduction methods.

Methods: A peripheral-blood mononuclear cell multi-omic dataset from a single, healthy female donor wasanalysed in this study. Ground truth annotations were generated using unsupervised annotation with the weighted nearest neighbour clustering method. Two dimensionality reduction methods (principal component analysis (PCA), single-cell Variational Inference (scVI) autoencoder) and four classification models (logistic regression, random forest, support vector machine (SVM)) were implemented and performance metrics (F1 score, precision, and recall) were compared over 10 bootstrap samples.

Results: ATAC-seq features improved annotation quality and prediction confidence when using scVI embeddings, independent of the classifier. The best-performing model (SVM with scVI embeddings) showed an increase from a median macro F1 score of 0.907 (IQR = [0.902, 0.910]) using scRNA-seq alone to 0.946 (IQR = [0.940, 0.949], $p < 0.05$) with ATAC-seq added. For PCA embeddings, improvements in macro F1 score were insignificant.

All cell types (B, T, monocytes, natural killer and dendritic cells) showed significant improvements when using ATAC-seq with scVI embeddings. CD4 T effector memory cells showed the largest gain in F1 score (0.112, $p < 0.01$), whilst type-2 conventional dendritic cells showed the smallest improvement (0.006, $p < 0.05$). Prediction confidence was improved in B cells, monocytes, natural killer cells, CD4 and CD8 naïve cells, CD4 T central memory cells and CD8 T effector memory cells. Improvements in F1 scores were lost when only classifying major cell types rather than subtypes.

Conclusions: Employing ATAC-seq embeddings with scVI autoencoder enhances supervised annotation quality over scRNA-only methods. Further studies should explore the use of ATAC to improve the annotation of highly heterogeneous tissues such as tumours.

#4928 REFINE Method: Novel strategy for signal enhancement.

M. Wang[1], J. Ahn[2], J. Lee[2], D. Kim[2], E.-H. Cho[2], B. Lee[1], A. Carson[1];
[1]Genece Health, Inc., San Diego, CA, [2]GC Genome, Yongin, Korea, Democratic People's Republic of

Fragmentomics has emerged as a powerful tool in the detection of early cancer malignancies. One of the challenges for fragmentomics is the low signal to noise ratio in early stage cancer samples. Fragmentomic sequencing data is also inherently noisy and susceptible to batch effects. Common strategies to address these challenges include using normalization methods, such as frequency or Z-score normalization, to scale data. However, these existing methods struggle to differentiate true signals from noise and are susceptible to experimental bias. To address the need for a strategy that removes noise and batch effects, Genece Health is employing a novel normalization technique, the REFINE method, to improve the results of fragmentomic cancer detection. Whole genome sequencing (Illumina) fragmentomic data were generated at an average 2.5x coverage from 3,669 normal and 1,346 cancer samples. Six different cancer types were represented: colorectal, esophageal, liver, lung, ovarian, and pancreatic. Fragment end-motifs and fragment sizes (FEMS) data were then extracted from the sequence data. REFINE first establishes a baseline FEMS signal from a representative and random panel of normals (PoN) comprised of 100 healthy samples. This baseline, which represents the normal background FEMS noise in healthy donors, is subsequently decomposed using truncated singular value decomposition. Next, REFINE then eliminates this decomposed baseline FEMS signal from the raw FEMS data in all other samples using linear regression. A convolutional neural network (CNN) was trained (2,206 normal and 1,000 cancer samples) using frequency normalized data versus REFINE normalized data using 5-fold cross validation. The performances of both models were then assessed using the remaining 1,463 normal with 346 cancer samples. With a training dataset specificity threshold of 90%, REFINE significantly improves the sensitivity performance of the CNN model >30% (from 50.4% to 83.0%). REFINE also improves the auROC from 0.753 to 0.944. We also show that increasing the size of the PoN to 812 samples and including hyper-parameter optimizations further improves the sensitivity to 85.9% (with an auROC of 0.955). The REFINE method demonstrates a dramatic enhancement in the detection of ctDNA from fragmentomic data, overcoming the limitations of conventional normalization techniques. REFINE effectively enhances the signal to noise ratio, facilitating more accurate cancer detection. Future work will focus on validating the REFINE method across diverse datasets and exploring its application in other areas of oncology.

#4930 Identification of CBX7 and PCDHB18 as novel prognostic biomarkers of cervical cancer: RNA-sequencing and machine learning analysis.

G. Pourali[1], M. Zeinali[2], M. Arastonejad[3], N. Khalili-Tanha[4], E. Nazari[5], G. Khalili-Tanha[6], A. T. Toriola[1];

[1]Washington University in St. Louis, Saint Louis, MO, [2]Islamic Azad University Khomeinishahr Branch, Isfahan, Iran, Islamic Republic of, [3]Virginia Institute for Psychiatric and Behavioral Genetics, Virginia Commonwealth University, Richmond, VA, [4]Western College of Veterinary Medicine, University of Saskatchewan, Saskatoon, SK, Canada, [5]School of Allied Medical Sciences, Shahid Beheshti University of Medical Science, Tehran, Iran, Islamic Republic of, [6]School of Medicine, Mashhad University of Medical Sciences, Mashhad, Iran, Islamic Republic of

Background- Cervical cancer, ranking fourth in prevalence among women worldwide, is highly preventable when diagnosed early. The advent of innovative technologies including bioinformatics and machine learning, is revolutionizing the discovery and development of novel biomarkers for cancer. Our study uniquely integrates artificial neural networks with RNA-sequencing data of cervical cancer patients. This combination enhances the accuracy and reliability of biomarker predictions, providing a better understanding of the potential clinical utility of the identified biomarkers.

Methods- RNA-sequencing data and clinicopathological details of 304 Cervical Squamous Cell Carcinoma and Endocervical Adenocarcinoma (CESC) were obtained from the GDAC database (https://gdac.broadinstitute.org/). Differentially expressed genes (DEGs) were identified ($P<0.05$, $|\log2 \text{ fold change (FC)}| > 1.5$, false discovery rate (FDR) < 0.05). Pathway enrichment analysis was performed and protein-protein interactions of DEGs were constructed using the STRING database. Prognostic biomarkers were identified using Kaplan-Meier and Cox proportional hazard methods adjusted for potential confounders such as age, disease stage, and comorbidities ($HR<1$, $p<0.05$). Deep learning algorithms were applied for predictive marker identification, utilizing Weight by Correlation feature selection. The model used AUC (Area Under the Curve), accuracy, MSE (Mean Squared Error), and R2 (R-squared) as evaluation metrics in a 70-30 training-test split. A combined ROC curve assessed diagnostic biomarkers, validated externally with a GEO dataset on cervical cancer patients.

Results- In our study, 4153 DEGs were identified. Pathway analysis revealed that key dysregulated genes play a pivotal role in extracellular matrix organization. The survival analysis identified that six upregulated genes (CT62, SLC7A5P1, C10orf110, FDPSL2A, TNFSF15, and TTLL13) and seven downregulated genes (BAI3, CBX7, DKFZp566F0947, PCDHB18, GRAPL, PCDHB19P, and C4orf38) decreased the overall survival in patients. The machine learning model demonstrated high predictive accuracy (AUC=1, accuracy=99.02%, R2=0.99), identifying twenty genes with a positive correlation to cervical cancer risk. Notably, CBX7 emerged as a prognostic and diagnostic biomarker (AUC=0.99, sensitivity=0.93, specificity=1.00).

Conclusion- Our study uncovers the prognostic significance of two novel genes in cervical cancer: CBX7, a vital regulator of tumor suppression, and PCDHB18, a member of the protocadherin beta gene cluster functioning as a cell adhesion molecule. Downregulation of these genes is associated with decreased overall survival. Further functional analyses and validation of these candidate biomarkers are crucial to fully assess their potential clinical value in cervical cancer.

#4931 The Cancer Proteome Atlas: Expanded datasets and empowered with an AI-driven chatbot.

H. Liang, W. Liu, J. Li, Y. Tang;
UT MD Anderson Cancer Center, Houston, TX

Reverse-phase protein arrays (RPPAs) represent a powerful functional proteomic approach to elucidate cancer-related molecular mechanisms and develop novel cancer therapies. To facilitate community-based investigation of the large-scale protein expression data generated by this platform, we have developed a user-friendly, open-access bioinformatic resource, The Cancer Proteome Atlas (TCPA, http://tcpaportal.org), which contains several applications. The first one focuses on RPPA data of patient tumors, which contains >8,000 samples of 32 cancer types from The Cancer Genome Atlas (TCGA) and other independent patient cohorts. The second application focuses on the RPPA data of >1,500 cancer cell lines with publicly available, high-quality DNA, RNA and drug screening data. The third one focuses on perturbed RPPA profiles of >14,000 samples given drug treatments. We recently expanded our RPPA protein set from 200 to 500 proteins Importantly, this highly selected set is enriched in therapeutic targets and biomarkers and covers key oncogenic pathways such as PI3K/AKT, RAS/MAPK, Src/FAK, TGFβ/SMAD, JAK/STAT, epithelial-mesenchymal transition, DNA damage repair, Hippo, Notch, cell cycle, apoptosis, and immune-oncology. Using this upgraded RPPA platform, we generated an harmonized, expanded RPPA dataset of 8000 TCGA patient samples and 1000 CCLE cell line samples. To further address the informatic challenges of analyzing such large, diverse datasets, in addition to the GUI interfaces, we recently developed a chatbot through which users can analyze the RPPA data through human nature languages and obtain the results and related analytic reports without a learning curve. Such a chatbot empowers a broad research community to explore high-quality RPPA datasets and generate testable hypotheses in an effective and intuitive manner, representing the direction of next-generation data analytics.

#4932 UltiAnalyzer.AI: An automatic and robust AI-Driven tool for the quantification of multiplex immunofluorescence whole slide images.

R. Cardenes[1], D. Wood[1], M. Schulze[2], J. Lee[1], L. Rognoni[1];
[1]Ultivue, Inc., Cambridge, MA, [2]Slash-m GmbH, Harth-Pollnitz, Germany

Introduction: Whole slide multiplexed immunofluorescence (mIF) facilitates in-depth study of the tumor microenvironment with multi-channel images resulting in an enormous amount of protein expression and spatial data across millions of single cells. Therefore, it has become crucial to process this huge amount of data automatically and reliably. Here we introduce UltiAnalyzer.AI, a software tool that integrates a set of artificial intelligence (AI) models specifically designed for the analysis of whole slide mIF slides, that is fully automatic, highly accurate, highly efficient, and fully scalable.
Methods: UltiAnalyzer.AI processes are specialized for 1) tissue segmentation, in which tissue regions are identified using a semantic segmentation AI model on low magnification versions of the DAPI channel, 2) tiling, where slide images are divided into 512x512 overlapping tiles for efficient image processing and lower memory requirements, 3) tumor region segmentation based on a semantic segmentation AI model, 4) nucleus segmentation using the open-source StarDist model, and 5) marker-positive cell detection, in which AI object detection models are employed to classify nuclei as positive or negative in each marker channel using the Faster R-CNN architecture. Here, we take advantage of the full 16-bit dynamic range of images produced using Ultivue InSituPlex® amplification technology, although our approach could be applied to other platforms. Intensity thresholding is no longer necessary, and identification of a positive cell mainly considers the morphology of the cell in the context of its cellular neighborhood.
Results: Trained on over 60 mIF slides and validated with manual annotations, UltiAnalyzer.AI has demonstrated strong performance, achieving f1-scores between 0.8 to 0.91 for cell detection, and average correlations of 0.9 for cell counts across 15 markers. Processing time is around 3s per tile, enabling the processing of large slides in under an hour. It has been tested on over 1000 slides, and in a comparative study, it matched a VisioPharm-based quantification with 0.95 correlation in positive counts for 8 markers. Cloud deployment allows for processing thousands of slides simultaneously and in considerably less time.
Conclusions: UltiAnalyzer.AI represents a significant advancement in the field of whole-slide mIF analysis, offering high accuracy and scalability using fully automated processes. By utilizing the full dynamic range of Ultivue's mIF technology and avoiding traditional thresholding methods, the tool also increases robustness and reproducibility. The incorporation of cutting-edge AI technology and scalable cloud computing capabilities positions UltiAnalyzer.AI as a leading-edge solution for mIF analysis in digital pathology.

#4933 A workflow for cloud-based AI development of multiplex IF image analysis using the OMERO Plus platform.

R. Cardenes[1], E. Diel[2], D. Wood[1], J. Lee[1], A. Vasaturo[1], M. Schulze[3], L. Rognoni[1];
[1]Ultivue, Inc., Cambridge, MA, [2]Glencoe Software. Inc,, WA, Seattle, WA, [3]Slash-m GmbH, Kockritz, Harth-Pollnitz, Germany

Background: The advancement of AI in digital pathology is essential for analyzing image data containing billions of cells. This is true for digital pathology workflows using bright-field images, but this is even more critical for multiplex immunofluorescence (mIF) whole-slides due to the increased number of fluorescent channels and bit-depth per pixel. These complexities necessitate improved data management, and efficient visualization for both the mIF image and AI-based analysis results. We present a workflow using OMERO Plus, AWS SageMaker, and Ultivue software for AI model development in mIF. *Method*: Images were uploaded to AWS S3 and imported to the data management system OMERO Plus, where they were organized into training and validation groups.
Annotations: PathViewer was used to place rectangular fields of view (FOV) in locations selected by the pathologist where all positive cells for each target marker were manually annotated.
Data Preparation: Using the OMERO Plus API, annotation coordinates, image tiles, and image metadata were extracted and formatted for model training. All training data is under a version control system using Gitlab and Data Version Control tools using AWS S3. Additionally, strict quality checks were performed to ensure data integrity.
Training: For both semantic segmentation and cell object detection, the training data was used in a customized training workflow using AWS SageMaker, including modern deep learning architectures, data augmentation, training logging, evaluation, and deployment. All AI models were trained using Pytorch and deployed with the open model format ONNX.
Results Visualization: AI segmentation results of cells and regions are visualized using PathViewer as overlays on the original images by converting them to the OME-NGFF label image format that uses Zarr multidimensional arrays. *Results*: We utilized 58 and 24 mIF images for training and validation, respectively, on 15 markers using ISP Ultivue technology with 1681 and 296 FOVs, encompassing over 60K cells. Using this data and methodology we trained 3 semantic segmentation models and over five object detection models suitable for all twenty-four OmniVUE markers. For instance, the CD3 positive cell detection model, trained with 390 FOVs, achieved highly accurate results: f1-score of 0.915 evaluated on 34 FOVs.
Conclusions: The combination of OMERO Plus, PathViewer, AWS SageMaker, and internal tools can successfully address mIF Big Data data management complexities in a cloud environment for digital pathology. The architecture is highly scalable, cost effective, and reliable, enabling a very efficient AI workflow.

BIOINFORMATICS / COMPUTATIONAL BIOLOGY / SYSTEMS BIOLOGY / CONVERGENT SCIENCE: Integrative Computational Approaches 1 / Analytic Pipeline Optimization
Poster Session

#4936 An ultrahigh-throughput synergy screening platform enables discovery of novel drug combinations.
W. C. Wright, P. Geeleher;
St. Jude Children's Research Hospital, Memphis, TN

The battle against many cancers and infectious diseases has long been hindered due to the complexity of finding potent and effective drug combinations. With each new drug considered, the number of combinations to potentially test increases exponentially, posing substantial challenges in screening throughput. These challenges further intensify when accounting for the number of doses of each drug that need to be tested in a drug combination matrix (known as matrix density). There is a pressing need to screen large amounts of combinations at sufficient density to discover new therapies for diseases like cancer, but this has traditionally been out of reach. However, the recent widespread adoption of acoustic liquid handling robots has shown promise to overcome these obstacles by allowing for intricate drug screening template designs which were previously not possible to make. Despite these advances, the throughput achieved by these technologies has been limited due to lack of broadly accessible protocols and analytical tools for drug combination screening.
We present Combocat, an end-to-end platform that allows for substantial increases in throughput of drug combination screens by combining experimental protocols that can be deployed for acoustic liquid handlers, machine learning algorithms for data imputation, and software that allows for in-depth analysis of results. We first generated a reference dataset of over 250,000 unique drug combination measurements in multiple cancer cell lines. The combination data were collected in a dense format (10×10 combination matrices) using a novel drug-drug template and achieved a dramatic increase in throughput compared to conventional methods. We then used this dataset to build a computational model which allowed us to accurately estimate drug combination effects using sparse measurements and imputing non-measured values with machine learning. The sparse measurements are collected in 1536-well microplates and substantially boost the throughput capabilities of drug-drug screens. As proof-of-concept, we used our method to screen a preclinical model of neuroblastoma with 9,045 drug combinations. This represents 10% the scale of the largest drug combination studies ever reported, achieved using a fraction of the resources, and in dense formats. We validated our findings by re-screening top hits using the fully-measured, non-imputed method and demonstrate the accuracy of our platform.
The Combocat platform’s documentation and codebase is open-source, and we also make a GUI available for interactive exploration of screening results. By integrating advanced experimental and computational methods, we provide a generalizable pipeline that will expedite synergy screens and the drug combination discovery process for many diseases.

#4937 Potential therapeutic targets with anti-inflammatory activity spectrum(COX-2/PGE2) of compounds associated with anti-cancer activityagainst oral and colorectal cancers.

S. Sampoornam Pape:
Kalinga Institute of Industrial Technology (KIIT), Bhubaneswar, India

Introduction: COX-2 and PGE2 are prevalent inflammatory cytokines that exert influence on several cancer-related pathways throughout the gastrointestinal tract, spanning from oral cancers to colorectal cancers. One of the tactics being developed for the treatment of oral and colorectal malignancies is the identification of drugs that can selectively target receptors associated with COX-2 and PGE2.
Materials and Methods: The objective was to identify potential therapeutic targets for oral cancer and colorectal cancer, specifically focusing on drugs that act as inhibitors or antagonists of the COX2/PGE2 pathway and its related receptor. A method for systematic data mining was created with a total of 32 targets associated with the COX-2/PGE2 pathway which were identified using the KEGG database. These targets were shown to be linked to both the oral cancer pathway and the colorectal cancer pathway. The compounds of interest were obtained from the Chembl25 database and their similarity was assessed using the Tanimoto similarity index, which was generated based on the Morgan fingerprints. The study employed molecular docking techniques to examine the interaction between the chosen drugs and the anticipated targets. A systematic data mining approach and computational methodology were devised utilizing the KNIME platform.
Results: A total of 16,900 compounds were extracted for a set of 32 targets. Following the implementation of rule-based filters, the number of compounds was reduced to 13,800. The compounds that have a similarity index greater than 0.7 were chosen for inclusion in final analysis. Among various targets examined, empirical evidence was found to support the inhibition of expected target for PI-3 kinase-mTOR, GSK-3CD1, GSK3-AKT and PI3kinase-AKT pair. However, no evidence was found to support the inhibition of GSK3-Ikappa B-kinase. In order to examine the likelihood of the compound's interaction with anticipated target, molecular docking was employed to explore the interaction of one inhibitor compound for each pair. This investigation was conducted in contrast to the existing inhibitor compound and the subsequent findings were analyzed and discussed.
Conclusion: The implemented data mining technique has demonstrated a notable decrease in the duration needed for comparable investigations, enabling the execution of experiments including numerous targets and a substantial number of ligands within a cumulative timeframe of 30 minutes. The findings of this study have the potential to be utilized in the identification of targets and the discovery of lead compounds for the purpose of managing oral as well as colorectal malignancies.

#4938 Prediction of gene mutation from colorectal adenocarcinoma whole slide images via integrated deep learning pipeline.

G.-Y. Tien[1], L.-C. Lai[2], T.-P. Lu[3], M.-H. Tsai[4], H.-H. Chen[5], E. Y. Chuang[1];

[1]Graduate Institute of Biomedical Electronics and Bioinformatics, National Taiwan University, Taipei, Taiwan, [2]Graduate Institute of Physiology, College of Medicine, National Taiwan University, Taipei, Taiwan, [3]Institute of Health Data Analytics and Statistics, National Taiwan University, Taipei, Taiwan, [4]Institute of Biotechnology, National Taiwan University, Taipei, Taiwan, [5]Institute of Computer Science and Information Engineering, National Taiwan Normal University, Taipei, Taiwan

Colorectal cancer (CRC) stands as one of the deadliest cancer types worldwide. Identifying specific gene mutations crucial for targeted therapy is pivotal for CRC treatment. However, the current genetic testing method involves liquid biopsy, which is often cumbersome and cost-intensive. Histopathological whole-slide images (WSIs) are routinely generated for diagnostic purposes and can offer valuable insights into cellular heterogeneity. In this study, we aim to develop an integrated deep learning pipeline for predicting TP53 mutations in CRC, one of the most frequently mutated genes in CRC.

We commenced by collecting 424 diagnostic WSIs from the TCGA-COAD cohorts. Each WSI was split as small patches at a resolution of 0.5 micrometers per pixel for following analyses. Quality control was implemented using Otsu thresholding and Gaussian blur filtering, both at the slide-level masking and patch-level filtering stages. Additionally, we applied the Macenko algorithm for color normalization to eliminate systematic errors. Following image preprocessing, we constructed a tissue-type classification model based on VGG19, which was trained and tested using the NCT-CRC-HE-100K and CRC-VAL-HE-7K datasets, both containing pixels with tissue types labeled by human experts. The trained classifier was then used to identify adenocarcinoma epithelium patches from TCGA-COAD. Subsequently, we applied multiple pre-trained Convolutional Neural Network (CNN) models, including ResNet-101, DenseNet-201, and Inception-ResNet-v2, to predict TP53 mutations for the identified adenocarcinoma epithelium patches from TCGA-COAD. A novel integration approach was employed to aggregate patch-level predictions into slide-level outcomes.

We evaluated the trained models using various metrics, including accuracy, precision, recall, F1 score, AUC (Area Under the Curve), and Cohen's Kappa coefficient. The tissue-type classification model exhibited robust performance, achieving an overall accuracy of 94.7%, a Cohen's Kappa coefficient of 94%, a precision of 95.3%, a recall of 99.76%, and an F1 score of 97.48% for identifying adenocarcinoma epithelium patches. Regarding the TP53 mutation prediction models, ResNet-101, DenseNet-201, and Inception-ResNet-v2 exhibit the predictive ability to both patch level (AUC=65%) and slide level (AUC=70%).

In summary, the proposed deep learning pipeline offers an efficient way to acquire gene mutation information from WSIs. Moreover, it demonstrates a capability to discover potential molecular aberration from the clinical images.

#4939 Computational pathology approach for prognostic advancements and therapeutic benefits in gastrointestinal cancer: A multi-centric retrospective study.

T. Zhang[1], Z. Sun[1], Z. Li[2], M. Ahmad[3], M. Islam[3], F. Yang[4], Z. Li[5], **Y. Jiang**[6];

[1]Southern Medical University, Guangzhou, China, [2]Northwestern Polytechnical University, XIAN, China, [3]Stanford University School of Medicine, Palo Alto, CA, [4]Wake Forest University, Winston Salem, NC, [5]Yunnan Cancer Hospital, Kunming, China, [6]Wake Forest University School of Medicine, Winston Salem, NC

Background: The current cancer staging methods cannot accurately predict survival and therapeutic benefits in cancer patients. Digital pathomics is an emerging field with potential to revolutionize disease evaluation. The present study aims to develop and validate a deep learning pathomics signature from digital hematoxylin-eosin (H&E) staining slides to predict the survival of pan-gastrointestinal cancer, and further investigated its associations with chemotherapy and immunotherapy response. P

atients and Methods: This international multicenter study included 2,463 patients with pan-gastrointestinal cancer from twelve cohorts of seven cancer centers, among which 1653 patients were diagnosed with GC. We proposed a deep learning pathomics signature (DLPS) by integrating information on three scales from the whole slide images (WSIs) of H&E, including pathomics nucleus, pathomics microenvironment, and single-cell spatial distribution features. Next, we evaluated the predictive accuracy of DLPS for prognosis, chemotherapy response, and immunotherapy response. To interpret the predictive ability of the DLPS, we analyzed multi-omics data and employed the Shapley value strategy to provide its biological insights and importance ranking.

Results: The DLPS was significantly associated with overall survival in patients with GC (hazard ratio range: 1.203-2.717, all $p < 0.001$), which was further validated in other gastrointestinal cancers (all $p < 0.02$). The DLPS remained an independent predictor of prognosis in multivariable analysis (all $p < 0.001$). Furthermore, a nomogram incorporating the DLPS and TNM stage shows significantly improved accuracy in predicting cancer prognosis compared to that with TNM stage alone (all $p < 0.05$). Shapley value analysis highlighted DLPS as the strongest predictor for prognosis. Importantly, GC patients with a low-DLPS (but not those with a high-DLPS) exhibited substantial benefits from adjuvant chemotherapy (all $p < 0.05$). Furthermore, we found the objective responses of anti-PD-1 immunotherapy is significantly higher in the low-DLPS group (29.6%) than in the high-DLPS group (8.3%, $p < 0.05$). Upon analyzing multi-omics data, we found that a higher DLPS was positively correlated with tumor promoting, chemotherapy resistance, immune tumor microenvironment and metabolic signaling.

Conclusion: The DLPS enabled improved assessment on prognosis, and has the potential to identify patients who will benefit from adjuvant chemotherapy and immunotherapy, which can further be extended to many gastrointestinal cancers or other solid tumors.

#4940 Unraveling ctDNA features in high-grade serous ovarian carcinoma and insights from genomic and transcriptomic integration.

Mai TN Nguyen[1], Jaana Oikkonen[1], Yilin Li[1], Daria Afentave[1], Veli-Matti Isoviita[1], Anni Virtanen[1], Johanna Hynninen[2], Sampsa K. Hautaniemi[1]

[1]University of Helsinki, Helsinki, Finland, [2]Department of Obstetrics and Gynaecology, University of Turku and Turku University Hospital, Turku, Finland

High-grade serous carcinoma (HGSC) is often diagnosed at advanced stages with less than 40% of patients surviving for five years after diagnosis. Circulating tumor DNA (ctDNA) is a minimally invasive technology that can provide crucial insights into tumor biology. Unique features from ctDNA, fragment patterns and nucleosome footprints at transcription start sites (TSS), complement genomic variants. Our study explored ctDNA features in HGSC, integrating with tumor biopsies' genomic and transcriptomic profiles. We focus on two aspects in HGSC: understanding how ctDNA features assist genomic profiling and track dynamic changes during treatment and exploring the biological factors impacting ctDNA release. We used 500+ longitudinal plasma and 400+ pretreatment tissue samples from HGSC patients in the DECIDER study (NCT04846933). Shallow whole-genome sequencing (sWGS) with 0.4x average coverage was conducted on plasma. Integration of DNA and RNA pretreatment tissue data was performed for 98 and 91 patients with available plasma before treatment, respectively. Plasma samples underwent analysis for fragment patterns and TSS signals. Somatic mutations and mutational signatures were retrieved for patients with available WGS tissue data. Pathway enrichment analysis was applied to diverse gene expression profiles. WGS data from 29 healthy individuals (Zhu, G. et al. (2023)) served as controls. DNA fragment profiles and TSS signals distinguish ctDNA from healthy samples. The ability to cluster sample phases based on ctDNA features facilitates tracking longitudinal changes. Integrating tissue DNA and RNA data reveals a positive correlation between high ctDNA release and mutational burden, single-base substitution signature SBS1 as a marker for cell division/mitotic clock and doublet-base substitution signatures linked to late replication. These mechanisms help explain why high ctDNA release group (n=40) is associated with a shorter progression-free survival. Additionally, transcriptomics data indicates associations with proliferation pathways in cancer cells and ctDNA release. The concordance in results from DNA and RNA points to a higher proliferation rate in patients with high ctDNA release, suggesting the need for alternative treatment compared to those with low ctDNA release. In conclusion, our results provide a multifaceted perspective on ctDNA in HGSC. The identification of longitudinal ctDNA features signifies the capability to stratify sample states and show the potential findings through fragment profiles and the discernment of key TSS regions. The proposed aetiologies and enriched pathways associated with ctDNA release, mutation burden and proliferation, shed light on potential treatment avenues. These findings contribute to our understanding of ctDNA in HGSC and offer insights for personalized treatment strategies and monitoring approaches.

#4942 Unraveling a prognostic and predictive 8-gene signature related to cuproplasia in pan-cancer.

V. Pham[1], T. Jue[1], J. Bell[1], F. Luciani[1], F. Michniewicz[1], G. Cirillo[2], L. Vahdat[3], C. Mayoh[4], O. Vittorio[1];
[1]UNSW Sydney, Sydney, Australia, [2]University of Calabria, Rende, Italy, [3]Dartmouth-Hitchcock Medical Center: Lebanon, New Hampshire, NH, [4]Children's Cancer Institute, Sydney, Australia

This study aims at identifying a cuproplasia-related gene signature to predict outcome for cancer patients based on gene regulatory networks. Copper is a vital micronutrient involved in many biological processes. Copper influences tumor growth through a process called cuproplasia, defined as abnormal copper-dependent cell-growth and proliferation. Copper-chelation therapy targeting this process has demonstrated efficacy in several clinical trials against cancer. While the molecular pathways associated with cuproplasia are partially known, genetic heterogeneity across different cancer types has limited the understanding of how cuproplasia impacts patient survival. We proposed a novel framework based on gene regulatory networks to identify critical cuproplasia-related genes (CCGs) across different cancer types. Utilizing RNA-sequencing data from The Cancer Genome Atlas (TCGA) and the Genotype-Tissue Expression (GTEx) datasets, we generated gene regulatory networks for 23 different cancer types. We applied a network control method to discover critical genes in these networks and combined with copper metabolism related genes to identify CCGs across 23 cancer types. We then performed a comprehensive analysis on the identified CCGs to better understand their potential roles and associations with cancer patient survival. We discovered 30 CCGs which were enriched in pathways related to a wide range of biological processes supporting cancer progression and immune evasion processes. The specific processes related to the identified CCGs include autophagy, cell cycle regulation, cell proliferation, kinase signaling pathways, immune infiltration, and immune checkpoint regulation. From this, we identified a novel 8-CCG signature significantly associated with survival pan-cancer, including CDK1, AP1S1, CASP3, MAP1LC3A, SNCA, TMPRSS6, MAPT, and GSK3B. Although some of these genes are known for their important roles in various malignancies and are associated with poor survival, this is the first study defining their connection with high copper levels in cancer cells. Furthermore, in keeping with previous studies that have used metal regulatory genes to predict outcomes in a specific cancer type, we specifically used low grade glioma (LGG), a cancer type highly impacted by intracellular copper level, as an example to explore the role of CCGs in a specific cancer type. Through our proposed gene regulatory network methodology, we identified a 3-gene signature that overlapped with a 6-gene prognostic risk score model for LGG patients. These 6 genes included ALB, CASP3, CDK1, CP, CYP1A1, and MT-CO1. To our knowledge, this is the first pan-cancer analysis for genes related to cuproplasia. The findings from our study highlight the use of gene regulatory networks to identify CCGs which could be used to develop novel targeted therapeutic strategies.

#4943 Benchmarking unpaired single-cell RNA and single-cell ATAC integration.

J. Chen, W. Xiao, E. Zhang, X. Chen;
St. Jude Children's Research Hospital, Memphis, TN

The integration of single-cell RNA-sequencing (scRNA-seq) and single-cell ATAC-sequencing (scATAC-seq) data offers a unique opportunity to gain a comprehensive view of cellular identity with defining features and to infer gene-regulatory relationships. Despite the emergence of technologies that simultaneously capture both the gene expression and chromatin accessibility of individual cells (paired data), the practical challenges of these approaches (e.g., the unavailability in previous samples and prohibitive cost) have led researchers to turn to the existing trove of single-modality data generated from independent biological samples (unpaired data). Various computational tools have been developed to integrate these unpaired single modality datasets. However, the comparative performance of these tools has not been comprehensively evaluated, and a standard benchmark pipeline is still lacking. To address these challenges, we used pseudo-unpaired scRNA-seq and scATAC-seq data derived from publicly available paired single-cell multi-omics datasets to benchmark 14 publicly available integration methods. The primary goal of unpaired single-cell multi-omics integration is to narrow the omics gap while preserving cell type diversity. We therefore focused on pair-wise cell distance and cluster performance in the joint latent space constructed by various integration tools in our benchmarking pipeline. To ensure the robustness of these computational approaches, we examined their stability across a variety of scenarios, including variations in cell number, cell types, and biological and technical batch effects. A number of the integration methods tested produced promising results. While the widely used Seurat package was recently reported to have the best performance (Lee et al., Genome Biology 2023), other computational tools such as scVI, Cobolt, scJoint, scglue and scBridge performed equally well or better in reducing omics differences and facilitating the identification of cell clusters. Notably, scglue and Cobolt demonstrated strong performance in aligning the same cell from different modalities, and discrete clusters emerged in the joint latent space using scJoint and scBridge. These findings suggest that it may not be strictly necessary to use paired multi-omics data to guide integration to achieve favorable results. Our freely available benchmarking pipeline will empower researchers to identify the optimal data integration methods for their specific data, facilitate the benchmarking of new methods, and contribute to future method development in the field.

#4944 Divergent proteogenomic gene expression is driven by microenvironment across tumor types.

J. LaMorte[1], N. Bateman[2], T. Conrads[1], R. F. Browning, Jr.[1], C. D. Shriver[1], R. L. Kortum[1], **M. D. Wilkerson**[1];
[1]Uniformed Services University, Bethesda, MD, [2]Uniformed Services University; Henry M. Jackson Foundation, Bethesda, MD

Solid tumors develop through a complex series of genome and downstream expression alterations that interact with the local tissue microenvironment, leading to a transformed cell and malignant phenotype. With massive multi-omic data, recent proteogenomics studies have jointly analyzed RNA and protein expression to uncover new gene regulatory relationships; however, many of these studies focused on single tumor types and lack a generalizable view of joint RNA and protein expression. Here, we present the first pan-cancer analysis of sample-wise RNA to protein correlation (SRPC). We re-analyzed over 1,000 tumors across 10 tumor types from published proteogenomic data from the Clinical Proteomic Tumor Analysis Consortium (CPTAC) and the Applied Proteogenomics OrganizationaL Learning and Outcomes (APOLLO) Research Network. We identified a wide range of SRPC across all tumors (ρ range: -0.08 to 0.70, median: 0.45). We then analyzed tumor pathologic and molecular characteristics versus the range of SRPC. High SRPC tumors had high tumor purity by pathology review, by somatic DNA whole exome sequencing, and by RNA and protein purity scores. In contrast, low SRPC tumors had high immune cell and stromal cell expression scores as inferred by either protein or RNA based signatures. We observed marked differences in cell type populations estimated by expression in different SRPC tumor tranches (low SRPC: macrophages, endothelial cells, cancer-associated fibroblasts; high SRPC: CD4+ Th2 cells). Tumors expressed signaling pathways depending on their SRPC (low SRPC: hypoxia, inflammatory response, and KRAS signaling; high SRPC: DNA repair and E2F targets). SRPC also stratifies tumors with distinct somatic DNA alterations (low SRPC: HRAS and NF2; high SRPC: TP53, MEN1, high Tumor Mutational Burden and high DNA chromosomal instability). Finally, we found that cancer driver genes displayed divergent gene-wise RNA to protein correlations (GRPC) among tumor types with a median absolute deviation interquartile range of 0.1 - 0.2, suggesting tumor-type-specific regulation. In summary, divergent RNA and protein expression is driven, in part, by tumor microenvironment composition across tumor types. Tumors with a diverse cellular microenvironment display a summation of RNA and protein expression resulting from this cell type diversity leading to a low SRPC, while tumors predominated by tumor cells display coordinated RNA and protein expression levels resulting from a pure clonal or cell type leading to a high SRPC. This first deep analysis into sample-wise RNA to protein correlation represents a large proteogenomic community resource for informing biomarker analysis by modality and by tranches of tumor microenvironment. The views expressed in this abstract are solely of the authors and do not reflect the official policy of the Departments of Army/Navy/Air Force, Department of Defense, USUHS, HJF, or U.S. Government.

#4945 Computational modeling-based discovery of novel anticancer drug candidates targeting centromere-associated protein E.

P. Lu[1], R. Kamata[2], M. R. Weil[1], N. Ohashi[1], A. Ohashi[2], E. A. Stahlberg[1];

[1]Frederick National Laboratory for Cancer Research, Frederick, MD, [2]National Cancer Center Japan, Kashiwa, Japan

Purpose: Centromere-associated protein E (CENP-E), a mitotic motor protein, is crucial for cell division. Inhibition of CENP-E can lead to chromosome misalignment and aneuploidy. Our recent studies revealed that the CENP-E inhibitor (CENP-Ei), Compound A, induces aneuploid-mediated cGAS-STING pathway activation in cancer cell lines, which is expected to trigger innate immune response and induce immunological conversion of the tumor microenvironment from cold to hot. However, known CENP-Eis exhibited limited efficacy, and none have gone beyond phase I trials since 2012. The aim of this study is to develop a workflow integrating structure and artificial intelligence-based modeling approaches to accelerate the discovery of novel CENP-Eis with improved efficacy and overcome related challenges.

Method: The inhibitor-bound CENP-E structure was modeled using chimeric homology modeling followed by induced fit docking with known CENP-Eis. Structure-based virtual screening (VS) was performed on large compound libraries in Enamine REAL, Synthetically Accessible Virtual Inventory, and MolPort databases. Consensus scoring methods were applied by averaging ranks of individual molecules obtained from VS against different CENP-E conformations. An active learning-enhanced VS pipeline was developed using ATOM Modeling PipeLine (AMPL) to find the best-ranked ligands more efficiently. CENP-E ligand candidates were further filtered based on their safety properties predicted by machine learning models trained with curated databases of adverse drug reactions using AMPL. The success of this study was measured by its ability to reveal novel chemotypes that could modulate CENP-E in kinesin ATPase assays.

Result: Conformations of CENP-E's ligand binding site were predicted for VS using the homology model. Structure-based VS was performed to select high-ranked compounds based on consensus scoring. The active learning-enhanced VS pipeline achieved 75% accuracy in ranking the top 20% of hit compounds. The graph convolutional network model with a ROCAUC, 0.76, was created using AMPL to filter ligand candidates based on their predicted safety properties. Seventy-three potential CENP-E ligands computationally prioritized from the Molport database were experimentally tested using kinesin ATPase assays from which 4 potential inhibitors and 8 potential activators were identified indicating overlapping binding sites of inhibitors and activators.

Conclusion: Our integrated workflow is effective in discovering novel CENP-E modulators. The discovery of CENP-E activators provides an opportunity to identify novel therapeutics in hepatocellular carcinoma malignancies known to experience decreased CENP-E activity leading to aneuploidy. The predictions generated by computational models combined with experimental validations could further accelerate anticancer drug discovery.

#4946 ssTimiGP: Equip the TimiGP system with a single-sample module, facilitating the cell-cell interaction inference of the tumor microenvironment in any sample.

C. Li[1], J. Zhang[1], C. Cheng[2],

[1]The University of Texas MD Anderson Cancer Center, Houston, TX, [2]Baylor College of Medicine, Houston, TX

Understanding the tumor microenvironment (TME) is essential in cancer treatment and risk assessment. While single-cell RNA-seq (scRNA-seq) offers in-depth insights into the TME, its expensive cost results in limited data sets and size. In contrast, microarray and RNA-seq provide rich datasets from larger cohorts, but they yield bulk data with lower resolution. To leverage the strengths of both approaches and comprehensively study the TME, we developed the computational framework TimiGP (Tumor Immune Microenvironment Illustration through Gene Pairs). It is inspired by the dynamic balance of the immune system and extended to the entire TME. TimiGP utilizes scRNA-seq to define cell type of interest, and bulk transcriptomic profiles to deduce clinically relevant cell-cell interaction networks and cell functions. Our recent release includes both prognosis and response modules to study the association between TME and the corresponding clinical outcomes. However, their applicability is constrained by the necessity for paired clinical information.

In response to this limitation, we present a significant enhancement, a single sample module slightly modified from the TimiGP framework (ssTimiGP). This upgraded version enables TME analysis in any individual sample, requiring only bulk RNA-seq data and cell-type markers. It exports a cell-cell interaction network representing the relative expression of functional markers and the abundance of cells. This optimization expands the utility of TimiGP, making it more accessible across diverse samples and species.

We have further expanded the application of ssTimiGP from solid tumors to liquid samples (e.g., peripheral blood). To validate its performance, we conducted a comparative analysis between the interactions of eight immune cell types observed in experimental results using FACS and the computational results derived from ssTimiGP based on paired RNA-seq data. As a result, ssTimiGP not only successfully identified interactions between different cell types that exhibited a significant correlation with experimental findings (e.g., CD4+ naïve T cells → Monocyte, R=0.75, p< 0.001, accuracy = 0.8), but also demonstrated its capability to achieve higher resolution in capturing interactions between immune cell subpopulations (e.g., CD4 naïve T cells → activated CD4+ memory T cells, R=0.57, p=0.008, accuracy = 1.0). In our benchmark analysis, ssTimiGP demonstrated superior performance compared to CIBERSORTx (e.g., CD4+ naïve T cells → Monocyte, R=0, Accuracy=0.3).

In summary, ssTimiGP signifies an expansion of the TimiGP system, enabling the inference of the TME in individual solid tumors and liquid samples at various resolutions by integrating the strengths of both scRNA-seq and bulk RNA-seq. This approach offers substantial potential for advancing personalized cancer treatment.

#4947 Uncovering the molecular basis for clinically relevant sphingolipidomic subtypes in acute myeloid leukemia.

B. Paudel[1], S.-F. Tan[1], J. Ung[1], D. Claxton[2], D. J. Feith[1], T. P. Loughran, Jr.[1], K. A. Janes[1];
[1]University of Virginia, Charlottesville, VA, [2]Penn State Cancer Center, Hershey, PA

Acute myeloid leukemia (AML) has been extensively studied at the genomic level, resulting in various genomic classifications. Despite the progress, three key challenges remain: 1) a significant proportion of patients lack identified genomic features, 2) a discrepancy exists between genomic risk classification and clinical outcomes, and 3) many mutated targets remain non-druggable. There is an urgent need for an enhanced AML risk classification that goes beyond genomic aberrations to guide effective therapeutics. Recent research, including our own, has increasingly linked AML pathogenesis and therapeutic resistance with dysfunctional sphingolipid metabolism, a family of bioactive molecules crucial for cellular functions. In a recent manuscript, we identified two robust sphingolipidomic clusters in AML, characterized by reciprocal abundances of hexosylceramide (Hex) and sphingomyelin (SM) species (HexloSMhi, HexhiSMlo). These clusters correlate with latent transcriptional states and stratify patient groups in multiple independent datasets such as TCGA, and BeatAML, with the HexloSMhi cluster representing a high-risk subgroup associated with poor clinical outcomes. These findings underscore the role of sphingolipids in refining AML risk assessment and creating avenues for discovery and therapeutic intervention. However, the signaling states driving these sphingolipidomic clusters and the mechanisms elevating risk in the HexloSMhi cluster require further investigation. To identify regulatory genes for the AML subtypes, we constructed gene regulatory networks using differentially expressed genes. Focusing on the high-risk subtype, we identified highly connected genes ranked by connectivity, including KDM1A, GSK3β, LCK, and STAT5A. We found that higher STAT5A abundances in the HexloSMhi subtype, particularly correlated with pro-survival Bcl-xL proteins. Furthermore, we identified STAT5 protein abundance as a key variable associated with drug sensitivity from pharmacological screening with sphingolipid pathway inhibitors and AML therapeutics 30 AML cell lines and patient samples. This is encouraging as STAT5 is druggable as evidenced in the NIH-Pharos druggable genome database, and several small-molecule inhibitors are currently in clinical trials. Analysis of gene expression data suggest that STAT5 inhibition, through genetic or pharmacological means, downregulates cell cycle-related genes and significantly alters sphingolipid gene expression. Recent work by others indicates that sphingolipid-catalyzing enzymes regulate STAT5 activity in leukemias, with ceramides acting as a second messenger in cells. Taken together, this suggests a possibility of a positive feedback loop between sphingolipid homeostasis and activity of STAT5; the details of this interaction require further investigation.

#4948 Automated tumor microenvironment analysis for multiple samples by image-based spatial transcriptomics on tissue microarray.

Dongjoo Lee[1], Seungho Cook[1], Yeonjae Jung[1], Myunghyun Lim[1], Jae Eun Lee[1], Hyung-Jun Im[2], Daeseung Lee[1], Hongyoon Choi[3]

[1]Portrai, Inc., Seoul, Korea, Republic of,[2]Department of Molecular Medicine and Biopharmaceutical Sciences, Graduate School of Convergence Science and Technology, Seoul National University, Seoul, Korea, Republic of,[3]Department of Nuclear Medicine, Seoul National University Hospital, Seoul, Korea, Republic of

Introduction. Tissue Microarrays (TMAs), widely utilized in the field of pathology, have now found a powerful ally in Image-based Spatial Transcriptomics (ST). By analyzing various gene expression data with high resolution, image-based ST data on TMA can provide the heterogeneous patterns of tumor microenvironment in multiple samples. However, an efficient method for processing multiple samples post-data acquisition is still under development. A streamlined process would expedite the discovery of spatial gene expression patterns, thereby enhancing our understanding of the tumor microenvironment and its implications for cancer diagnostics and treatment strategies.

Methods. Our automated pipeline is initiated by automatic segmentation of every core in the whole TMA, derived from the processed output of the MERSCOPE or Xenium platform. Then, it subsequently removes QC failed cells unrelated to any core. Each core receives sequential naming and undergoes automated cell type mapping utilizing a reference single-cell RNAseq data. Additionally, the pipeline computes neighborhood enrichment between cell types, providing a nuanced comprehension of spatial relationships and interactions among diverse cell populations within the tissue microenvironment from multiple samples on the TMA.

Results. The automated pipeline we've developed provides several key advantages. It enables the simultaneous analysis of multiple tissue cores, effectively minimizing batch effects and ensuring the reliability of results across diverse tissue samples. Furthermore, by automating core separation, labeling, and cell type mapping, our pipeline significantly streamlines the time and effort required for TMA data analysis. This cost-effective approach allows researchers to optimize resource allocation, making our automated pipeline a valuable tool in cancer research. It facilitates the exploration of gene expression patterns within specific tissue regions, ultimately contributing to the advancement of our understanding of cancer biology.

Conclusion. By seamlessly integrating TMA data with image-based ST technologies such as Xenium and MERSCOPE, we can perform comprehensive spatial transcriptomics analyses and provide detailed statistical information on cell type proportions within the tumor microenvironment. This automated pipeline not only ensures robust and reliable results across diverse tissue samples but also optimizes resource allocation by minimizing batch effects and reducing analysis time. This cost-effective solution empowers researchers to delve deeper into spatial gene expression patterns, enhancing our comprehension of the tumor microenvironment.

#4949 Multimodal analysis of metals, spatial transcriptomics, and histological structures in colorectal cancer.

A. Srivastava[1], N. Shaik[2], Y. Lu[3], M. Chan[3], A. Diallo[4], S. Han[3], R. Steiner[4], T. Punshon[4], B. Jackson[4], L. Vahdat[3], L. Vaickus[3], J. Hoopes[4], F. Kolling IV[4], J. Marotti[3], J. Levy[5];

[1]Grafton High School, Yorktown, VA, [2]Basis Independent Silicon Valley, San Jose, CA, [3]Dartmouth Health, Lebanon, NH, [4]Dartmouth College, Hanover, NH, [5]Cedars Sinai Medical Center, Los Angeles, CA

Colorectal Cancer (CRC) accounts for nearly 10% of all cancer cases and is the second-leading cause of cancer-related deaths worldwide. The increased incidence of CRC in younger demographics underscores the need for improved screening and prognostication. These enhancements are crucial to augment staging practices which focus on accurate evaluation of local lymph node involvement and distant metastasis. Essential trace elements such as copper and iron within the tumor microenvironment (TME) present novel therapeutic strategies- e.g., copper in cell proliferation/signaling and iron in pro-tumorigenic pathways, amongst other multifaceted roles. Despite advancements in spatial imaging/sequencing for detailed mapping of elemental abundance and gene expression profiles at near-subcellular resolution, the understanding of metal signaling and transport pathways in tumors is limited. This gap highlights the need for sophisticated informatics software for data integration and analysis. We developed a computational workflow for spatial multimodal analysis of elements, genes, cell-types, and histological features, applied to a unique CRC case (pT3) as proof-of-concept. Elemental imaging at 5-micron resolution was performed using laser ablation inductively coupled plasma time-of-flight mass spectrometry (LA-ICPTOF-MS). The 10x Genomics Visium spatial transcriptomic (ST) CytAssist assay captured spatial variation in gene expression within 55-micron spots, with 40X H&E-stained whole slide imaging (Leica Aperio GT450). Cell type proportions within spots were determined through integration of single cell RNASeq. Regions within, around and away from tumor were annotated by a pathologist. ST and LA-ICPTOF-MS were integrated through co-registration software developed at Biomedical National Elemental Imaging Resource. Local Getis-Ord spatial statistics defined hotspots with high elemental concentration. Wilcoxon tests were used to perform differential expression analysis based on metal hotspots, followed by identification of associated biological pathways through Enrichr with Bonferroni adjustment. Preliminary findings revealed distinct trace element distributions in the TME. For instance, Copper was localized within tumor, correlating with pathways related to immune response and activation (overlap=10/89, $p<0.0001$). Iron was found concentrated at the proliferative front of the tumor, associated with the epithelial to mesenchymal transition pathway and extracellular matrix remodeling (overlap=25/291, $p<0.0001$), as well as with a mesenchymal phenotype ($W=11.7$, $p<0.0001$), identified through cell type deconvolution. Future work will expand on these findings across multiple tissue contexts as means to capture biological processes governing tumor metastasis, recurrence and survival for biomarker discovery and therapeutics development.

#4950 Applying fragmentomics profiles of plasma cell-free DNA for breast cancer detection.

Y. Liu[1], S. Gan[2], **H. Dong**[2], H. Tang[2], N. Wang[1], X. Gui[1], A. Zhu[1], R. Zhang[1], P. Du[2], S. Jia[2];
[1]Peking University Cancer Hospital & Institute, Shanghai, China, [2]Huidu (Shanghai) Medical Sciences, Ltd., Shanghai, China

The liquid biopsy approach focusing on DNA molecules supports the non-invasive diagnosis of breast cancer. Low-pass whole genome sequencing(lpWGS) for breast cancer detection has been validated for accuracy and cost-effectiveness, especially with copy number variant (CNV) analysis. However, detecting breast cancer with cell-free DNA (cfDNA) CNV was limited by tumor fraction. Utilizing cell-free DNA fragmentation characteristics for cancer detection has shown potential in plasma with high precision and applicability with low tumor fraction. In this study, 217 patients with breast cancer and 10 healthy individuals were enrolled. The cfDNA was extracted and performed using PredicineSCORE, a low-coverage whole genome sequencing assay to identify tumor-specific features. The cfDNA fragmentomics profiles including the coverage at specific regions, length and end-motif of fragment were implemented. We also investigated the copy number variation and the inferred tumor fraction which was adjusted by the Expectation-Maximum (EM) algorithm. Combining, an ensembled machine learning model was constructed for the classification of breast cancer and normal control. We observed a high correlation between tumor fraction and features. The absolute correlation coefficient scores between tumor fraction with the LYL1, MAF, FOXA1, and GRHL2 bonding sites' relative depth were over 0.82, 0.71,0.89,0.87. The insert size ratio of short reads and the CCCA end motif were over 0.77 and 0.72, respectively. We then diluted the tumor samples of tumor fraction at 0.1% to 50% by manually mixing reads from tumor samples into normal samples. By applying the XGBoost algorithm, the performance (F1 score > 0.95) showed a promising ability to distinguish tumors from normal samples. The limit of detection (LOD) was less than 1% which is more sensitive than previously proposed models. Those samples detected mutations with high through panel which can confirm the accuracy of the assay. Our results discovered that profiling the cell-free DNA fragment could facilitate the way of non-invasively detection of breast cancer with high precisions.

#4951 Integrative multi-omic machine learning model predicts neoadjuvant immunotherapy response using molecular data and deep learning-derived features from digital pathology.

L. V. M. Leek[1], V. Botha[1], V. A. Baxi[2], J. Teuwen[1], H. M. Horlings[1], S. D. Chasalow[2], J. van de Haar[1], C. U. Blank[1], L. F. A. Wessels[1], A. DebRoy[2], E. E. Voest[1];

[1]Netherlands Cancer Institute, Amsterdam, Netherlands, [2]Bristol Myers Squibb, Princeton, NJ

Background: Over the past decade, there has been an exponential accumulation of digital patient data through molecular profiling and digitization of pathology slides. However, integrating this to advance diagnostics and cancer patient care remains a significant challenge. By integrating information from diverse modalities to capture aspects of the tumor microenvironment (TME) and immune landscape, we aim to improve patient stratification for immunotherapy.

Methods: We collected data from baseline biopsies from patients with palpable melanoma stage III (*n*=195) who received neoadjuvant immunotherapy followed by surgical resection of largest lymph node metastasis. The different modalities included clinical information, whole-genome sequencing (WGS), RNAseq, laboratory tests of blood, haematoxylin and eosin (H&E) images, and PDL1 immunohistochemistry (IHC) images. Cell detection and classification models were trained to identify tumor-infiltrating lymphocytes and tumor cells on H&E whole-slide images (WSI), deriving spatial features to quantitatively describe the tumor-immune interaction. Various biomarkers, including tumor mutational burden, BRAF status, expression of inflammatory gene signatures, systemic neutrophil-to-lymphocyte ratio, and tumor-lymphocyte spatial measures, were collectively integrated using machine learning models (random forest, elastic-net regularized logistic regression, CatBoost, support vector machine (SVM), and an ensemble classifier combined from the other models) within a 5x5-fold nested cross-validation scheme to predict pathologic response.

Results: Pathologic response to immunotherapy is associated with multi-omics biomarkers which were integrated using machine learning. The ensemble approach showed that when all modalities were combined a higher AUC (AUC=0.69, 0.61-0.77) could be achieved than for the clinical modality alone. RNA plus clinical emerged as the most predictive standalone modality with an AUC of 0.62 (0.50-0.75). The overall highest AUC was achieved using a SVM (AUC=0.72, 0.66-0.82).

Conclusions: Immunotherapy efficacy depends on diverse tumor microenvironment components, which were comprehensively assessed through data integration. A multi-omic predictive model holds promise for refining personalized and effective immunotherapy strategies.

#4953 A proposal to extend standardized organ mapping antibody panels (OMAPs) to integrate protein and RNA analysis in spatial biology.

Werner Muller[1], **Julia Femel**[1], Emily Neil[2], Dongju Park[2], Rebecca C. Hennessey[2], Eric C. DiBiasio[2], Michael DiBuono[2], Hanna Lafayette[2], Erica Lloyd[2], Hsinyi Lo[2], Alex Makrigiorgos[2], Sameh Soliman[2], Dominic Mangiardi[2], Paurush Praveen[1], Silvia Ruberg[1], Fabian Staubach[1], Ryan Hindman[2], Thomas Rothmann[1], Hansueli Meyer[2], Tanya Wantenaar[1], Jinling Wang[2], Robert Pinard[2], Andreas Bosio[1]

[1]R&D, Miltenyi Biotec, Bergisch Gladbach, Germany,[2]R&D, Miltenyi Biotec, Waltham, MA

The HubMap consortium has developed a new standard to report on normal histological samples using multicolor immunofluorescence imaging. An Organ Mapping Antibody Panel (OMAP) currently describes in a table the antibodies used, the cycle number assigned to a given reagent, and provides the rationale for using a particular antibody to better understand features of the tissue. This table is accompanied by antibody validation templates that show example images from the tissue described for the OMAP table. In addition, links to existing databases, gene symbols, the antibody features and colors are included. For each tissue, a further table called "Anatomical Structures, Cell Types, plus Biomarkers" (ASCT+B), which contains structures of the tissue, cell types in a given tissue structure, key RNA transcripts for a given cell type, and antibody stains as used in the OMAP table, is created. So far, this process has not been established for spatial multiomic datasets including protein and RNA detected on the same tissue section.

We have extended spatial biology methodology to combine cyclic RNA transcript detection with cyclic antibody-based protein detection using the MACSima Imaging Cyclic Staining (MICS) technology as well as H&E-staining on the same tissue section. For such datasets, the current OMAP data table needs to be extended by adding information on the RNA detection, cycle IDs and RNA validation templates, demonstrating the correct performance of a given RNA probe detection.

This poster will demonstrate a proposal to extend the OMAP table structure on an extended version of the “tonsil OMAP (OMAP-10)”, which was published on the Zenodo data repository page (https://zenodo.org/records/7875938). In addition, we will apply this extended OMAP to a colorectal cancer sample, to highlight the applicability and relevance of the OMAP structure for tumor tissue.

#4954 Improving microbial detection in cancer tissue samples with computational host depletion using the pangenome.

C. Guccione[1], L. Patel[1], D. McDonald[1], C. Martino[2], A. Gonzalez[1], G. D. Sepich-Poore[3], R. Knight[1], K. Curtius[1],
[1]University of California San Diego - UCSD, San Diego, CA, [2]Leaven Foods, San Diego, CA, [3]Northwestern University, Chicago, IL

Sensitive removal of host genetic information (i.e., host depletion) is a key first step towards accurate classification of potential microbial DNA sequences in low-biomass samples, such as human tumors. Inadequate filtration of human reads prior to microbial classification can cause false positives, biasing biological conclusions. Previous computational host depletion pipelines predominantly employed the human reference genome GRCh38 (hg38), which lacks genetic diversity of the human population and excludes substantial portions of the Y-chromosome. To address these deficiencies, we constructed a pipeline to maximally remove human reads that incorporates hg38, the first complete genome build T2T-CHM13v2.0 (T2T), and the 47 diploid genomes from the Human Pangenome Reference Consortium (HPRC) [1]. Reads passing maximal host depletion and quality control are considered sufficiently cleaned for downstream microbial analyses.

We first evaluated the specificity of our pipeline by simulating Illumina whole genome sequencing (WGS) data from 10 heldout HPRC humans, whose genomes were excluded from the host depletion pipeline. We found significant improvement in the median number of human reads remaining across successive host depletion methods (hg38, 0.05369%; hg38+T2T, 0.00535%; hg38+T2T+HPRC, 0.00093%). For sensitivity, we applied our pipeline to simulated data from 962 microbes in the FDA-ARGOS dataset and found minimal removal of true microbial reads (median 99.9390% reads retained). As a real world example, we evaluated our pipeline on 583 metastatic colorectal cancer tissue (WGS) samples from the Hartwig Medical Foundation (HMF) database (median 106X coverage)[2] and found successive decreases in median number of reads retained (hg38, 185,135; hg38+T2T, 92,951; hg38+T2T+HPRC, 10,314). Using Woltka for taxonomic classification against database RefSeq210, we assessed biological sex similarity across the HMF samples using Robust Aitchison PCA (RPCA). Notably, microbial data following hg38-only host depletion showed significant microbial differences between male and female-labeled samples ($p=0.00001$), which was biologically unexpected. However, our updated pipeline (hg38+T2T+HPRC) removed the false sex-based separation in the microbial data ($p=0.1837$).

Thus, utilization of diverse sets of complete human genomes for computational host depletion can mitigate artifactual bias, enabling more sensitive and specific host-microbe conclusions in cancer research.

[1] Liao, et al. *Nature* 617, 312-324 (2023).
[2] Priestley, et al. *Nature* 575, 210-216 (2019).

#4955 An analytic pipeline of neoantigen selection for both MHC-I and MHC-II pathways.

Ko-Han Lee, Timothy Sears, Andrea Castro, Maurizio Zanetti, Hannah Carter

University of California San Diego, La Jolla, CA

Background: Accurate neoantigen selection is pivotal for assessing mutation burden and optimizing cancer vaccine formulation thereby playing a crucial role in cancer immunotherapy. The concurrent activation of CD4+ and CD8+ T cells engenders a robust immune response, which is key to effective treatment. However, currently analytic tools predominantly focus on the MHC-I pathway, typically relying on metrics such as gene expression level and MHC-binding affinity of mutated peptides. To address this gap, our study presents a comprehensive pipeline that encompasses both MHC-I and MHC-II pathways and integrates three critical dimensions of immune response: neoantigen abundance, presentation, and immunogenicity.

Methods: We estimated mutated peptide abundance by analyzing genomic allelic frequency, transcriptomic allelic frequency, and RNA expression level. Antigen presentation was assessed using the patient harmonic binding rank (PHBR, a composite binding score for all potential MHC-peptide pairs) and MHC diversity (the variety of MHC alleles involved in peptide binding), with additional consideration for the loss of heterozygosity of MHC-I alleles, potentially indicative of immune escape. For immunogenicity, we factored in agretopicity (comparison of MHC-binding affinity between mutated and wild-type peptides), foreignness (similarity to immunogenic foreign antigens), and dissimilarity (sequence disparity with self-peptides, reflecting T cell negative selection process).

Results: Implementing our pipeline on a dataset from Parkhurst et al. (2019), we analyzed immune reactivity in relation to 11,537 somatic mutations from 75 gastrointestinal cancer patients. Key metrics—RNA expression, transcriptomic allelic frequencies, PHBR, and MHC diversity—demonstrated significant correlations with both CD4+ and CD8+ activity ($p<0.05$). Notably, genomic allelic frequency was a significant factor in CD8+ reactivity, whereas agretopicity was crucial for CD4+ reactivity.

Conclusion: Our pipeline elucidates the necessity for implementing both MHC-I and MHC-II pathway analyses to effectively select neoantigen candidates for CD8+ and CD4+ T cells respectively. The study confirms that abundance and antigen presentation metrics are robust indicators of neoantigen immunogenicity, supporting their use as potential markers in crafting more effective cancer vaccines. The findings highlight the critical role of this dual-pathway selection approach in generating a comprehensive immune response through neoantigen vaccination.

#4956 A fast and efficient bioinformatics analysis workflow for processing reads from single-cell multiomics assays captured on a microwell-based platform.

R. Padmanabhan, B. Weichel, A. Radenbaugh, Y. Jiang, C. Weeks, T. McCarthy, Y. Kim, A. Berno, D. Jensen;
Becton Dickinson & Company, San Jose, CA

Here, we present a significant update: version 2.0 of our sequencing analysis, it is a comprehensive primary analysis workflow that is up to 7X faster and consumes 2X less disk space than the previous release. We used it to process a library with 20,000 human PBMCs sequenced to a depth of 1.2 billion reads in 2.5 hours of wall-clock time. The pipeline can be used with reads from single-cell whole transcriptome, targeted mRNA, surface antigens (AbSeq), TCR/BCR and Sample Tag libraries captured on the BD Rhapsody™ System platform. The major processing steps include Quality Filtering, Cell Barcode Identification, Read Alignment, Feature Assignment, UMI Error Correction, Identification of Putative Cells, Sample De-Multiplexing, Dimensionality Reduction for Visualization and VDJ Contig Assembly and Annotation. Output files and metrics are available in easy-to-digest formats, including an html report with dynamic visualization. Integrated outputs in Seurat and Scanpy formats combine expression matrices and all cell annotation metadata (e.g., predicted cell type, sample assignment, TCR/BCR sequence and gene segments). These pre-generated files are ready to load into popular single-cell analysis tools. The pipeline uses CWL as the workflow manager and makes use of custom code written in C++ and Python along with various open-source packages for data processing. The pipeline can also process reads from non-human species and includes built-in support for specifying and building custom reference genome indices. In support of high-throughput multiomic discovery studies enabled by the BD Rhapsody™ HT Xpress System, this pipeline has been tested with datasets containing more than 800,000 putative cells and 14.5 billion reads.

#4957 DNA quality control metrics in cryopreserved tissue outperform DNA extracted from FFPE tissue.

Jared James Barrott[1], Nikole O'Neal[2], Jeffrey Okojie[1], David Booker[3], Ken Dixon[3]

[1]Brigham Young University, Provo, UT,[2]Idaho State University, Pocatello, ID,[3]Specicare, Inc, Gainesville, GA

Personalized cancer care requires molecular characterization of neoplasms. While the research community accepts frozen tissues as the gold standard analyte for molecular assays, the source of tissue for testing of tumor tissue in clinical cancer care comes primarily from formalin-fixed, paraffin-embedded tissue (FFPE). Specific to genomics assays, numerous studies have shown significant discordance in genetic information obtained from FFPE samples and frozen samples. To explain the discordance between FFPE samples and cryopreserved samples, a head-to-head comparison between FFPE and cryopreserved tissues was performed to analyze the DNA yield, DNA purity and DNA quality in terms of DNA length. Additionally, short-read sequencing was performed on matched samples and quality control metrics were compared between the two sample types. Matched human tumors (n = 50) were processed either by formalin fixation and paraffin embedding or placed in cryovials containing cryopreservation medium. These cryovials were cooled slowly to -80°C and stored in liquid nitrogen. DNA was extracted using the same protocol for both tissue types with the exception that tissues embedded in paraffin were first dewaxed followed by a multistep rehydration protocol. Samples were weighed and calibrated for mass. After the column purification and elution, sample concentration and purity were measured. DNA fragment length was measured on a fragment microelectrophoresis analyzer. Graded amounts of tumor tissue were used to determine the lowest starting material needed to extract 200 ng of DNA. The average of all the samples reached the minimal threshold of 200 ng. However,74% of FFPE specimens failed to meet the minimum 40 ng/mg, whereas only 21% were below the threshold in the cryopreserved samples. In the cryopreserved group, the average DNA yield was 222.1 ng/mg, whereas 52.8 ng/mg was obtained from FFPE tissue. For DNA purity in cryopreserved tissues, the 260/280 ratio was 1.76, and in FFPE tissues the mean was 1.78. The DNA Quality Number (DQN) is a measurement of DNA fragment length and the percentage that exceeds the threshold of 300 bp. For FFPE, the DQN was 4.4 compared to a DQN of 9.8 for the cryopreserved samples. Setting a higher threshold of DNA length to 40,000 bp and measuring the area under the curve (AUC), it was observed that cryopreserved samples were 9-fold higher in fragments greater than 40,000 bp. Cryopreserved cancer tissue provides superior quality assurance measurements of DNA over FFFPE. Treatment decisions based on molecular results demand accuracy and validity. The pathology community should support efforts to cryopreserve cancer biospecimens in the clinical setting to provide valid molecular testing results. The automatic pickling of tumor specimens in formalin is no longer an acceptable default.

#4958 Optimizing transcriptome-based synthetic lethality predictions to improve precision oncology in breast cancer: BC-SELECT.

Y. Kim[1], M. Nagy[2], R. Pollard[3], N. U. Nair[1], L. Ray[1], E. Ruppin[1], P. S. Rajagopal[1];

[1]National Institutes of Health (NIH), Bethesda, MD, [2]Boston Children's Hospital, Boston, MA, [3]Maret High School, Washington DC, DC

Introduction: Precision oncology currently focuses on targeting specific mutations in cancer driver genes as predictors of treatment response. Clinical application of tumor transcriptomics is similarly limited to using specific RNA-based fusions for using therapy. SELECT (Lee et al, Cell 2021) is a computational tool that characterizes synthetic-lethal and/or synthetic-rescue genetic interactions of potential drug targets by using expression data, then uses these interactions to predict drug response in cancer patients. SELECT was initially developed using pan-cancer data from The Cancer Genome Atlas (TCGA), with limited evaluation on agents in breast cancer. We therefore sought to optimize SELECT for patients with breast cancer in an adaptation named BC-SELECT.
Methods: The standard SELECT comprises two steps: (1) Using an in-vitro screen, a patient tumor data screen, and a phylogenetic screen to build a library of clinically relevant candidate synthetic-lethal / synthetic-rescue gene partners; and (2) Generating scores based on gene partners' expression levels in a given sample. Scores are then used to predict the likelihood of response to a given therapy. For BC-SELECT, we modified this framework as follows: We incorporated the METABRIC dataset, comprising 1,989 samples and used only the breast cancer-specific TCGA dataset (1,075 samples) (which outperformed training on pan-cancer TCGA). To enhance the survival screening process, we include up to 5 clinical covariates for each training dataset, and prioritized gene pairs based on survival. Furthermore, we introduced new scoring controls to confirm prediction accuracy. All parameters have been standardized to optimize performance.
Results: BC-SELECT predicted treatment response in our initial cohort of breast cancer trials with immunotherapy or targeted therapy and expression data, where the same treatment / treatment target was present in more than one trial. BC-SELECT prediction was more accurate for immunotherapy and PARP inhibitors compared to trastuzumab. The AUC ranges for immunotherapy are between 0.67 and 0.83. For PARP inhibitors, the AUC ranges from 0.5 to 0.78, and for trastuzumab, it falls between 0.5 and 0.75.
Discussion: BC-SELECT advances transcriptome-based synthetic lethality prediction for translational use in patients with breast cancer. This tool demonstrates analytic and clinical validity to begin to improve therapy stratification and prioritization in patients.

#4959 Immunopipe: A comprehensive and flexible scRNA-seq and scTCR-seq data analysis pipeline.

P. Wang[1], H. Dong[2], Y. Yu[2], S. Zhang[2], Z. Sun[2], J.-P. A. Kocher[2], J. Wang[3], L. Yi[2], Y. Li[4];
[1]Mayo Clinic, Scottsdale, AZ, [2]Mayo Clinic, Rochester, MN, [3]The University of Hong Kong, Hong Kong, Hong Kong, [4]Mayo Clinic, Jacksonville, FL

Introduction: Single-cell RNA-sequencing (scRNA-seq) pairing with single-cell T-Cell-Receptor-sequencing (scTCR-seq) enables profiling of gene expression and TCR repertoires in individual T cells, elevating our understanding of T-cell-mediated immunity. Here, we present immunopipe, a comprehensive and flexible pipeline (https://github.com/pwwang/immunopipe) for analyzing the paired data. Besides the command-line tool, it offers a user-friendly web interface that allows users with varying programming expertise to configure, initiate, and monitor the pipeline. By combining extensive functionality with ease of use, immunopipe empowers users to unlock valuable insights from the data, which notably advances our understanding of immune response and fosters the development of innovative immunotherapies.

Results: *Immunopipe* is a comprehensive analytical pipeline for scRNA-seq and scTCR-seq data, offering various modules leveraging existing tools and novel methods to ensure data quality and enable downstream analytics. It performs quality control for scRNA-seq data, clusters cells based on gene expression to facilitate the identification of cell populations and provides insights into T-cell heterogeneity and functional diversity through T-cell selection and clustering. Enrichment analysis identifies markers and pathways for T-cell characterization. Our automated T-cell annotation tool annotates cell types accurately and hierarchically. For scTCR-seq data, *immunopipe* analyzes TCR clones, including clonality, diversity, gene usage, and repertoire overlap. Clone residency analysis examines the presence of clones across samples. Integrative analyses combine scRNA-seq and scTCR-seq data, providing a comprehensive understanding of the cellular landscape. *Immunopipe* incorporates diverse cell group information to analyze T-cell populations, which enables granular perspectives of the data for comprehensive insights. *Immunopipe* offers a flexible platform, allowing users to customize the analyses as needed. It supports both core and optional analyses through configuration, where users have control over the adjustable parameters. The pipeline relies on cell grouping information that can be referenced from metadata or modified to generate new variables for analysis and data filtering. *Immunopipe* can be executed locally or on scheduler platforms, and a docker image is provided for compatibility and simplified installation. It also offers a web interface that facilitates configuration, execution monitoring, and access to results.

Conclusion: *Immunopipe* is a flexible and user-friendly pipeline for analyzing scRNA-seq and scTCR-seq data. It empowers researchers to gain valuable insights that could enhance the understanding of immune responses and facilitate the development of innovative immunotherapies.

#4960 PIONEER initiative: Providing patient access to functional precision medicine.

Ken Dixon[1], Jared James Barrott[2], David Booker[3]

[1]Specicare, Inc, Gainesville, GA,[2]Brigham Young University, Provo, UT,[3]Specicare, Gainesville, GA

Eighty-five percent of patients receive medical care in cancer centers without National Cancer Institute (NCI) designation or significant ongoing research. The ability to access fresh tumor tissue for immediate functional testing is now available with appropriate logistical coordination. Cryopreservation of these tissues also allows testing to be done at a later date. We hypothesize that patient access to and ownership of each individual's tissues will facilitate personalized testing, thus bridging the chasm between research and the clinical cancer care for the individual patient. The PIONEER Initiative stands for Precision Insights On N-of-1 Ex vivo Effectiveness Research. In this Initiative we save cancerous tissue for any patient at any location, with subsequent cryopreservation and functional testing as needed and as able within an environment in which neither are standard. Our endpoint was to determine if this process serves to alter care for individual patients, and to what degree. The SpeciCare PIONEER Initiative: Precision Insights On N-of-1 Ex Vivo Effectiveness Research Based on Individual Tumor Ownership Trial (MYCT001) received human subjects IRB approval (Approval Number: 33943/1) from Quorum Review. The PIONEER Initiative is our lead clinical trial designed to provide the foundation for subsequent adaptive trials. Our mission with this trial was to demonstrate the utility of carrying out functional precision medicine in that cohort of patients who receive local cancer care at institutions that do not have significant research capabilities or are not NCI-designated cancer centers. Most cancer patients (~85%) are in this category. It is imperative to open the possibility of the best-in-class functional precision medicine testing to these patients. Core aspects of the PIONEER Initiative involve scaling up this process to approximately 200 patients, showing that our proof of concept in a more limited set of patients can ultimately scale to arbitrarily large numbers of patients. We see this capacity filling an important unmet need within the cancer community. The primary endpoint was the return of actionable information to positively impact care as assessed by the patient's clinical team and the patient. The underlying basic assumption of the PIONEER Initiative is that the ability to receive the best in cancer care should not come with restriction as to location, age, or medical condition. The PIONEER Initiative design facilitates inclusion of subjects across all these divides, thus providing beneficence to all participants. Among the 60 patients whose tumors had ex vivo drug testing performed, none of the data was included in the clinical decision making of the healthcare team. We conclude that physicians are not adequately prepared to use ex vivo drug testing data and the more likely acceptance of molecular characterization is primarily driven by genomic sequencing.

#4961 Large-scale CyTOF data modeling of leukemia patient cohorts.

G. Kong, T. Vu, E. Lind, **O. H. Nikolova**;
OHSU, Portland, OR

Introduction: Cytometry by Time-of-Flight (CyTOF) is a single-cell proteomic assay that uses antibody-lanthanide metal conjugates to tag surface or intracellular proteins, quantified via mass spectrometry. Compared to flow cytometry, CyTOF significantly reduces overlapping signals and increases the maximum protein features from 8 to 50. CyTOF data is commonly analyzed with the 'gating' workflow, which is the iterative process of plotting cells by two protein features to select discrete cell populations. While CyTOF can comprehensively profile nuanced cell types, gating does not scale well in the number of features. Biases in gating often arise from the forced discretization of cell populations, subjectivity of gate boundaries, and intrinsic sample-sample variation. Contemporary challenges in CyTOF data analysis can be attributed to data volume and gating bias, which can lead to oversight of disease-related cell populations while hindering reproducibility.

Methods: We developed a computational platform that enables the processing and analysis of large-scale CyTOF data. Our workflow includes modular components for data harmonization, normalization, transformation, batch correction, quality control, subsampling, and dimensionality reduction via UMAP of input sample files in Flow Cytometry Standard (FCS) format. Further, additional analytical modules are currently being integrated to deploy large-scale machine learning models for cell type identification. We use the results of these models as input for multi-scale analysis, where we aim to link single-cell CyTOF data with clinical outcomes. We test our workflow on previously published datasets and apply it to new leukemia patient cohorts of blood and bone marrow samples and a variety of marker panels.

Results: We tested our workflow on previously published datasets of 4.7 M peripheral blood mononuclear cells from healthy donors (N= 20) and T cells (N = 8). We observed that samples mixed well upon integration and separated into major cell types like monocytes, CD4+/CD8+ T-cells, naïve/mature B-cells, and natural killer T-cells. We then applied it to a bone marrow cohort of healthy donors (N = 10), where we observe good mixing of samples but less clear separation of cell types. Finally, we applied our workflow to 9.3 M cells from 51 chronic lymphocytic leukemia (CLL) patients and 4 healthy donors, using a lymphocytic marker panel. Here, we observed a clear resolution of a major clonal B-cell population and immune T-cells. We are in the process of applying it to Acute Myeloid Leukemia (AML) patient data with myeloid and immune marker panels.

Conclusions: We developed a computational platform that facilitates the simultaneous analysis of large-scale CyTOF data, both in the number of samples and cells per sample, a variety of marker panels, while minimizing gating biases common in traditional gating analysis.

CLINICAL RESEARCH: Artificial Intelligence and Data Science on Real World Data
Poster Session

#4965 Detection of status of cancer in radiology notes using artificial intelligence.
A. Arya, A. Niederhausern, N. S. P. Bahadur, N. J. Shah, C. Nichols, A. Chatterjee, J. Philip;
Memorial Sloan Kettering Cancer Center, New York City, NY

Introductory Statement: The goal is to use an AI model to replicate the human curator's response on cancer status in radiology notes of ~20,000 cancer patients.
Introduction: MSKCC currently has ~100,000 patients with genomic testing (IMPACT) and continues to accrue more. Clinicians use this genomic data for research but lack clinical structured data to analyze alongside the genomic data. We use a vendor called VASTA Global to manually curate unstructured paragraph text. Depending on the data model, we found that a patient's full cancer history can take up to 8 hours to curate. Therefore, we want to implement AI to automate the curation of this data to save time and cost.
We hope to achieve a faster curation process that allows us to accomplish more than 1 patient a day to catch up to the 100,000 MSK-IMPACT cohort. To decrease the average curation time per patient, we investigated the use of an NLP model to replicate manual curation of the PRISSMM™ ontology field for change in cancer status from radiology reports. Manual curation of radiology reports is time intensive due to curators understanding their cancer status and the volume of scans patients undergo.
Methods:A pre-trained Bidirectional Encoder Representations from Transformers (BERT) model is fine-tuned using training data using GPUs in IBM Cloud Pak for Data (CPD) platform. The hyperparameters were adjusted using accuracy and F_1 metric of evaluation data. Using one vs. rest approach the model is evaluated on held out test data with results shown in table 1.Table 1 includes class 1-5: Progressing/worsening/enlarging, stable/no change, improving/responding, not stated/indeterminate or mixed.
Summary: The weighted AUCROC ~ 0.97, F1 ~ 0.85 and accuracy ~ 93%. These metric scores improve by choosing notes with higher class probabilities only.
Conclusion: Due to the above 0.9 calculated accuracy this NLP model is successful in replicating the curated results of cancer status and the next steps will be to run this model on a new cohort of patients not yet curated.

Cancer Status Metrics

Class	Prevalence	Precision	Recall	F_1 Score	AUCROC	Accuracy
1	38.9%	88.7%	87.0%	87.9%	96.5%	90.7%
2	24.7%	89.9%	88.2%	89.1%	98.3%	94.6%
3	15.9%	87.6%	90.7%	89.1%	98.7%	96.5%
4	15.7%	77.0%	72.6%	74.7%	94.4%	92.3%
5	4.8%	68.1%	74.4%	71.1%	97.9%	97.1%
Weighted Average		85%	86%	85%	97%	93%

#4966 Machine learning and large language model approach to pancancer data elements.

A. Niederhausern[1], N. S. P. Bahadur[1], G. Wallace[2], G. E. Saadawi[2], **J. Philip**[1];
[1]Memorial Sloan Kettering Cancer Center, New York City, NY, [2]Realyze Intelligence Healthcare Solutions, Pittsburgh, PA

Introductory Statement: The goal is to use machine learning (ML) and large language model (LLM) to augment the manual curation of cancer data elements.
Introduction: Memorial Sloan Kettering Cancer Center (MSKCC) has ~100,000 cancer patients and counting with genomic testing. Clinicians use genomic data for research but lack clinical data to analyze together. We use a vendor, VASTA Global to hire curators to manually curate cancer patient's core clinical data elements (CCDE) within unstructured/paragraph text in electronic medical record (EMR) notes.
CCDE encompasses 122 data elements that include a patient's full cancer history that can take up to 1 working day to curate. We collaborated with the Realyze Intelligence Healthcare Solutions vendor to use their AI pipeline to generate the manual curated dataset.
Realyze generated the CCDE data elements such as histology, pathology site, MMR, TNM staging, ECOG, and KPS for a pilot lung cancer cohort of 150 patients. We manually validated the generated data for 74 out of 150 patients.
Methods:The Realyze platform uses a combination of LLMs, ML algorithms and standard terminologies to create a cancer patient model. These models are flexible enough to address the unique needs and challenges of a pan-cancer oncology model. By using standardized FHIR export, results were delivered to a data lake solution and written into a REDCap database to enable human review.
Summary: We manually assessed 74 patients. The NLP gave concordant values for MMR, KPS and TNM staging for 100% of the instances. For MMR these were all null values with false negative (FN) of 100% accuracy. Pathology site had 92.15% accuracy while histology has 97.5% accuracy.
Conclusion: Will work on refining pathology site and histology's ICDO3 list to increase the percentage of accuracy. Once Realyze refines their model for these data elements we will re-run it on a larger cohort of cancer patients and calculate the accuracy.

Accuracy Results

Clinical data elements	74 patients assessed: Accuracy %
ECOG	98.6
KPS	100
T (path)	100
T (clinical)	100
N (path)	100
N (clinical)	100
M (path)	100
M(clinical)	100
MMR	100
Histology (path)	97.5
Path site	92.15

#4967 Predicting progression-free survival (PFS) in first-line (1L) immune checkpoint inhibitor (ICI)-treated patients (pts) with advanced non-small cell lung cancer (aNSCLC): Machine learning (ML) application in real-world data.

D. K. Hathi[1], J. Harnett[1], N. Wu[1], Z. Xu[2], W. Pan[2], T. G. Hager[1], R. G. W. Quek[1], S. Aggarwal[1], Y. Kim[1], P. Rietschel[1], F. Seebach[1], F. Wang[2], Y. Li[1]; [1]Regeneron Pharmaceuticals, Inc., Tarrytown, NY, [2]Cornell University, New York, NY

Introduction: Anti-programmed cell death (ligand)-1 ICIs are the standard of care 1L treatment for pts with aNSCLC without actionable oncogenic driver mutations. Heterogeneity in ICI utilization and outcomes is observed in real-world pts. By leveraging ML in electronic health records (EHRs), we identified predictors influencing key clinical outcomes, and developed a nomogram to predict likelihood of median PFS in 1L ICI-treated aNSCLC pts for potential risk stratification for interventions.

Methods: 1L ICI-treated aNSCLC pts without *ALK*/*ROS1*/*KRAS*/*BRAF*/*EGFR* alterations were identified in a US oncology EHR database (ConcertAI; Jan 2015-Feb 2023). Survival ML models were trained on 112 clinical and demographic features with 5-fold nested cross-validation. The top predictors, determined by the best-performing ML model through SHapley Additive exPlanations and clinical judgement, were used to create a Cox proportional hazard (CPH) nomogram of median PFS. All models were evaluated using the concordance index (c-index). Patients were categorized as having high and low risk of progression/death at median PFS according to median risk predicted by the nomogram.

Results: The study cohort had 4668 pts (median PFS: 6.1 months; 3811 events). The CPH nomogram predicting 6-month PFS had a c-index of 0.60 with the top 10 predictors identified using the XGBoost model (c-index: 0.62). Nomogram predictors included increased number of metastases, ECOG PS, cough suppressant use, WBC counts, and NLR (**Table**). Median probability of 6-month PFS for low- and high-risk groups was 35.9% and 19.4%, respectively.

Conclusions: Future research should validate these findings and evaluate the opportunity to guide clinical practice to optimize outcomes in aNSCLC pts treated with 1L ICIs.

Summary of top 10 clinical predictors at baseline

	Mean HR (95% CI)	Max nomogram points
Total metastases, n	1.15 (1.11-1.19)	100
ECOG PS, ordinal	1.14 (1.10-1.19)	55
Basophils, %	0.81 (0.73-0.90)	52
Albumin, g/dL	0.81 (0.75-0.87)	46
Chloride, mmol/L	0.98 (0.97-0.99)	46
Cough suppressants/expectorants, n	1.08 (1.03-1.14)	42
NLR	1.03 (1.02-1.05)	33
WBC counts, 10^3 cells/mL	1.02 (1.01-1.03)	29
PD-L1 expression, %	1.00 (1.00-1.00)	28
Presence of liver metastases	1.26 (1.15-1.39)	24
ECOG PS, Eastern Cooperative Oncology Group performance status; NLR, neutrophils-to-lymphocytes ratio; PD-L1, programmed cell death-ligand 1; WBC, white blood cell.		

#4968 Discovery of cancer-associated factors in 293.5 million diagnosis records using statistical machine learning analysis.

M. Alam, N. Duesbery, D. Daniel Fort;
Ochsner Health System, New Orleans, LA

Cancer, a leading global public health issue, ranks as the second leading cause of death in the United States, with projections indicating 1,958,310 new cases and 609,820 deaths in 2023. Accurately quantifying specific pre-disease diagnosis factors associated with cancer, as well as predicting cancer through disease trajectories and imaging modalities, presents a complex and formidable challenge. A comprehensive temporal trajectory analysis of cancer diseases, using disease trajectories as an insight within large cohorts in the USA, has not yet been developed. Our analysis used a comprehensive EHR dataset stretching back to 1999, encompassing 293,501,891 records and involving 3,019,978 patients within Ochsner Health, a large integrated health system across the State of Louisiana. According to our investigation, those diagnosed at the ICD chapter level with diseases of the genitourinary system (genitourinary diseases, ICD-10 Chapter 14, relative risk (RR=1.65)) or endocrine nutritional and metabolic diseases (obesity, ICD-10 Chapter 4, RR=1.35) have an elevated risk of being diagnosed with cancer in the subsequent five years. The top four individual diagnosis ICD-10 codes associated with increased risk are N60 (Benign Mammary dysplasia, RR=7.80), M34 (Systemic sclerosis, RR=7.72), R43 (Disturbances of smell and taste, RR=6.93), and R92 (Abnormal and inconclusive findings on diagnostic imaging of the breast, RR=6.59). Furthermore, in our investigation of specific types of cancer risk across 17 cancer types (Breast, Skin, Prostate, Lung, Pancreatic, etc.), we observed that the most common diseases associated with breast and skin cancer involved immune mechanisms (RR=8.35 and 8.68), genitourinary issues (RR=4.13 and 2.48), obesity (RR=3.42 , 3.35), and cardiovascular conditions (ICD-10 Chapter 9, RR=1.73 and 2.19). For prostate cancer, associations were found with obesity (RR=3.50), human immunodeficiency virus (HIV, ICD-10 Chapter 1, RR=2.39). Across lung cancer, involvement with chronic viral hepatitis (ICD-10 Chapter 1, RR=4.00), cardiovascular issues (RR=3.52), genitourinary problems (RR=4.13), and obesity (RR=3.42) were indicated. Our comprehensive analysis has the potential to contribute to the early detection, diagnosis trajectories, and improved understanding of the pathological processes underlying cancer in patients worldwide.

#4969 Investigating digital pathology tumor microenvironment features for immunotherapy outcome in patients with advanced non-small cell lung cancer.

E. M. Ebot, K.-T. Chen, M. Biggs, D. I. Lin, J. A. Elvin, G. M. Frampton, J. J. Pao;
Foundation Medicine, Inc., Cambridge, MA

Introduction
The composition of the tumor microenvironment (TME) has been shown to influence response to immunotherapy (IO). In this study, we investigated digital pathology TME features of IO outcomes among patients with non-squamous, non-small cell lung cancer (NSCLC) within a real-world dataset.
Methods
From the nationwide de-identified Flatiron Health-Foundation Medicine NSCLC clinico-genomic database, a cohort of 50 *EGFR*/*ALK*-negative, non-squamous NSCLC patients treated with first-line pembrolizumab monotherapy (mono-IO) or pembrolizumab in combination with carboplatin/cisplatin and pemetrexed (chemo-IO) that had available whole slide images of H&E-stained tissue resection specimens were included. The de-identified data originated from approximately 280 US cancer clinics (~800 sites of care). AI-powered TME characterization models developed by PathAI (Boston, MA; commercially available as PathExplore™) were deployed on scanned H&E slides to extract a panel of cell- and tissue-level human interpretable features (HIFs). Cox proportional hazards regression was used to identify digital pathology features or HIFs associated with overall survival.
Results
17 HIFs were associated with better survival and 19 HIFs were associated with worse survival among patients treated with mono-IO ($p < 0.05$). Lymphocyte features were among the HIFs associated with favorable survival, including density of lymphocyte cells in cancer epithelium (hazard ratio (HR) per unit standard deviation (SD) = 0.46 [0.24, 0.88], p-value = 0.02) and proportion of lymphocyte cells relative to total immune cells in cancer epithelium (HR per unit SD = 0.61 [0.39, 0.95], p-value = 0.03). Cell-level features associated with worse survival included density of fibroblast cells in stroma (HR per unit SD = 1.51 [1.01, 2.25], p-value = 0.05). These associations remained after adjusting for tumor mutational burden (TMB) (N = 29 low, 21 high) and PD-L1 status (N = 0 negative, 1 low-positive, 17 high-positive, 32 unknown). Additionally, similar associations were not observed among patients treated with chemo-IO. High lymphocyte density was associated with better survival compared to low lymphocyte density in mono-IO treated patients (adjusted HR per unit SD = 0.36 [0.18, 0.74], p-value = 0.01) but not in chemo-IO treated patients (adjusted HR per unit SD = 1.10 [0.76, 1.60], p-value = 0.6).
Conclusion
These results indicate that the composition of TME assessed via digital pathology may have utility in identifying NSCLC patients that will respond to first-line immune checkpoint inhibitors beyond the established IO biomarkers.

#4970 Multi-modal machine learning approaches for predicting cancer type and Gleason grade leveraging public TCGA data.

C. Wohlfart[1], E. Klaiman[1], J. Witkowski[2], M. King[1], J. Gildenblat[3], O. Etz-Hadar[3], M. Ashtari[4], **A. Vladimirova**[5];
[1]Roche Information Solutions, Penzberg, Germany, [2]Roche Information Solutions, Warsaw, Poland, [3]DeePathology.ai, Ra'anana, Israel, [4]Roche, Toronto, ON, Canada, [5]Roche Information Solutions, Santa Clara, CA

Introduction: To better understand the complex and challenging nature of diseases such as cancer and for improved diagnosis, it may require the combination of multiple data modalities, such as histopathological images and omics data such as RNA-seq. By integrating these heterogeneous but complementary data, a multimodal approach unites both worlds and could achieve better synergistic results compared to using a single modality. The growing availability of large datasets such as The Cancer Genome Atlas (TCGA) with more than 10000 patients made it possible to combine different modalities to train machine learning algorithms which offers great potential to address challenging cancer related research. In this proof of concept initiative we use machine learning approaches within an open-source framework in order to leverage the potential of multimodality (Histopathology Whole Slide Images (WSI) and Genomics/RNA-seq) to build predictive AI models for cancer type and prostate Gleason score, and provide a potential to develop a quality control step.
Method: We used matched WSI and RNA-Seq profiles from TCGA, including 11093 samples and 30 cancer types to develop a pancancer classification model using both modalities. For prostate Gleason score prediction 401 patients were available. Both datasets were split into a train (70%) and test (30%) components. We used a late fusion approach where we combined the RNA-seq model (linear SVM) with the WSI model (Resnet18) by multiplying the probability scores of each single-modality model. Model performance was measured with the F1 metric.
Results: For cancer type prediction, the multimodality model achieved an F1 score of 0.95 on the test set. About 40% of the cancer types benefited from a synergistic effect by combining the two modalities. Cancer types and percent increase in F1 scores, respectively, that benefit most by combining modalities are: Cervical squamous cell carcinoma and endocervical adenocarcinoma (4.23%), Cholangiosarcoma (6.66%) and Uterine carcinosarcoma (4%). Interestingly, in other cancer types the combination did not result in improved predictive scores compared to a single modality model, e.g. in Rectum adenocarcinoma, Sarcoma or Stomach adenocarcinoma. For Prostate cancer grading, Gleason score prediction of patterns 3/4/5, combined multi modality model earned 0.73 F1 outperforming the single modality models.
Conclusion: By combining histopathology imaging and omics modalities we demonstrated synergistic effects in predictive power for both cancer-related research questions. We show improved predictive performance in 40% of the classified cancer types by taking both modalities. Imaging or omics modalities alone can be sufficient in some cases and their strengths are very problem-specific.

#4971 Integrating artificial intelligence and functional precision oncology for individualized cancer therapies.

F. Eguiarte-Solomon, R. Prendergast, B. Carapia, J. Rodriguez, K. Buck, D. Gorospe, E. Valencia, J. Lopez-Ramos, I. Gutierrez, R. Pippa, Y.-H. Chien, W. Andrews, L. Do, J. Sperry, **J. K. Nakashima**;
Certis Oncology Solutions, San Diego, CA

Precision oncology seeks to tailor cancer treatments to individual patients. Patient-derived xenografts (PDXs) have emerged as a promising platform for selecting efficacious, personalized therapies and developing new oncology drugs. Here, we present a workflow for selecting and validating treatments for patients with colorectal cancer (CRC) that integrates orthotopic PDX (O-PDX) models, molecular profiling, machine learning, and in vivo pharmacological validation. Of the nine tumor biopsies collected, seven were successfully developed into O-PDX models (78%) with a median time to establishment of 119 days. Models were molecularly profiled for gene expression and were serially passaged to perform orthotopic pharmacology studies to validate test agents selected by oncologists as well those suggested by CertisAI™, a novel ensemble of machine learning models for the prediction of drug response in human cancers. The correlation between CertisAI's predicted therapy responses and the actual observed tumor growth inhibition (TGI) was r = 0.7, encompassing 37 distinct treatments across studies from six patients. This research collectively illustrates that the integration of artificial intelligence with functional in vivo assays offers a powerful platform for precision oncology, enabling the identification and validation of tailored treatments for individual cancer patients.

#4972 Bioinformatic analysis of an annotated genomic database is clinically useful in a private cancer center.

C. E. Zuazo, S. Darabi, D. R. Braxton, P. Stafford, M. J. Demeure;
Hoag Family Cancer Institute, Newport Beach, CA

Background: Sequencing of patient solid tumor tissue is not a common service provided by community cancer centers. Our community cancer center has collected and sequenced over 5,000 tumor tissue samples from patients with various types of cancer. Since April 2019, we have conducted whole-exome and whole-transcriptome sequencing and stored this data in an internal genomics database. To analyze large patient cohorts, we must first optimize bioinformatic workflows on a smaller scale, which can then be applied to studies of larger populations. Previous studies have shown *BRAF* mutations are associated with an increased activation of the mitogen-activated protein kinase (MAPK) pathway. We analyzed transcriptomes of a cohort of 30 patients with thyroid cancer, 15 with V600E *BRAF* mutations and 15 wild-type for *BRAF*, for MAPK Pathway Activation Scores (MPAS). MPAS serves as a transcriptomic measure of the activation state of the MAPK pathway and has been shown to be a reliable prognostic biomarker of MAPK activity.
Method: We conducted a retrospective analysis of data from FFPE tumor samples sent to a commercial CLIA-certified laboratory from April 2019 to October 2023. Samples were profiled by whole exome, whole transcriptome sequencing and immunohistochemistry (IHC). Whole transcriptome sequencing (WTS) was executed using Illumina NovaSeq along with the Agilent SureSelect Human All Exon V7 bait panel. Resulting data were reported in transcripts per million (TPM) using the Salmon expression pipeline. MPAS was calculated using the expression profile of 10 MAPK-associated genes.
Results: There was no significant difference in *BRAF* expression levels or MAPK activation between patients with *BRAF* mutant and *BRAF* wild-type thyroid cancer (median MPAS scores: -0.09 vs. 0.11, p=0.9). This analysis workflow will be repeated with a larger patient population of patients with melanoma in the future; however, the consistency of expression between the groups, the rank-order, and the low variability per group suggest that expression changes related to this *BRAF* mutation may occur upstream or via differential regulation of an indirect pathway. Rank-order statistics and percentiles become more precise as data per tumor type grows.
Conclusions: Our community cancer center began building an internal genomics database including whole-exome and whole-transcriptome sequencing since 2019. This resource facilitates analysis of patient samples for tumor mutational burden, gene fusions, transcriptomic data, and other important characteristics which could reveal patterns or trends that inform cancer diagnosis and prognosis of other patients. Analysis of expression data for patients with advanced solid tumors who have mutations in genes of interest could inform on potential targeted treatments in the future. This study represents a single example of the potential of our internal clinically annotated genomics database.

#4973 Impact of technology on quality of thoracic multidisciplinary cancer conferences.

O. Ibekwe, C. Gaudioso, K. M. Attwood, S. Pokharel, C. L. Roche, C. E. Nwogu;
Roswell Park Comprehensive Cancer Center, Buffalo, NY

Background: Complex cancer cases require discussion at Multidisciplinary Cancer Conferences (MCCs) to determine the best management. The study aim was to assess the impact of navify® tumor board solution (NTBS) technology on the quality of information presented, case discussions, and care plans at thoracic MCCs.

Methods: Between September 2020 and February 2022, using a before-after study design, we prospectively collected data through direct observation of thoracic MCCs at an academic cancer center. The NTBS technology was introduced in March of 2021. Additionally, we reviewed medical records to assess several factors including the rate of change in care plans as decided by the MCC, compliance of all care plans with national guidelines, and concordance of treatment received with MCC recommendations. Observational data was collected via a validated tool “Metric for the Observation of Decision-Making". We used SAS v9.4 (Cary, NC) for statistical analyses.

Results: We identified 151 and 166 thoracic cancer cases before and after implementation of NTBS, respectively. The overall quality of case presentation and discussion, represented by a mean composite score (the summation of individual variables scored on a 1-5 scale, poor to excellent), increased from 56.8 to 82.0 ($p<.001$). This improvement was also observed across multiple sub-components of the composite score including case history (3.4 vs 4.6), reason for presentation (3.2 vs 4.6), comorbidities/performance status/psychosocial information (2.8 vs 4.2), patient views (1.2 vs 3.3), radiology and pathology presentations (3.5 vs 4.8 and 3.2 vs 4.4, respectively), and contribution from surgical, medical, and radiation oncologists (3.9 vs 4.3, 3.3 vs 3.8, and 3.5 vs 3.8, respectively), as well as the moderation by the MCC chair (4.9 vs 5.0). All these results were statistically significant with $p<.001$. There was no statistically significant difference between the two cohorts in rate of change in care plans by the MCC, care plan compliance with national guidelines, and concordance of treatment received with MCC recommendations.

Conclusion: Technology improves the quality of information and discussion at tumor boards. However, this study did not demonstrate an impact on compliance with practice guidelines. Practitioners should explore the available tumor board technology platforms to optimize the conduct of MCCs in their respective institutions.

#4974 Development of an ovarian cancer diagnosis score using electronic health records.

M. Phung[1], K. McLean[2], G. E. Hanley[3], C. Pearce[1];

[1]University of Michigan, Ann Arbor, MI, [2]Roswell Park Comprehensive Cancer Center, Buffalo, NY, [3]University of British Columbia, Vancouver, BC, Canada

Background: Diagnosis of invasive epithelial ovarian, fallopian tube, and primary peritoneal cancers (hereafter referred to as ovarian cancer) is often delayed, worsening both survival and quality of life for ovarian cancer patients. Diagnosis is delayed in ovarian cancer both because there is no effective screening method and because the symptoms commonly associated with ovarian cancer (i.e., abdominal/pelvic pain, bloating, loss of appetite, urinary symptoms) are non-specific to the disease. It would be beneficial to develop a flag in the electronic health record (EHR) when a patient's healthcare utilization indicates further investigation for possible ovarian cancer is warranted. Thus, we used EHR data to develop a diagnosis score that identifies people who should be further assessed for potential ovarian cancer.

Methods: EHR data from 211,123 female patients, including 135 ovarian cancer patients, at the University of Michigan Medical System during 2012-2023 were analyzed. Time-varying Cox proportional hazard models were fit to identify the association between ovarian cancer and the diagnostic codes recorded for healthcare visits in the EHR, including the temporal sequence of the diagnostic codes. The beta coefficients for the diagnosis codes from the Cox models were summed to create a weighted diagnosis score for each patient. The weighted diagnosis score was tested for association with ovarian cancer in the same population.

Results: A total of 79 diagnostic codes were statistically significantly associated with ovarian cancer after applying a Bonferroni correction ($p<9x10^{-5}$). The temporal sequence of the diagnoses was not associated with ovarian cancer. There were 11 pairs of diagnosis codes that were correlated (correlation coefficient ≥0.25); the diagnosis code with the higher p-value was excluded from further consideration. The remaining 68 codes were used to construct the diagnosis score. There was a statistically significant trend of increasing rate of ovarian cancer per quartile of the diagnosis score (hazard ratio=3.75, 95% confidence interval 3.50-4.03).

Conclusion: A score for ovarian cancer diagnosis was developed based on 68 diagnostic codes in the EHR. The next step is to validate the diagnosis score in an external dataset. This validation is underway using administrative data from British Columbia, Canada.

#4975 Stretching the boundary of Oncotype DX testing.

Z. Al-Saheli, V. Dabak;
Henry Ford Health System, Detroit, MI

Background: The predictive value of Oncotype DX in early-stage breast cancer had been well established. Strongest data support the use of chemotherapy for Recurrence Score (RS) > 30, with 25-30 deriving some benefit. Those with intermediate RS 16-25 are thought to have a small benefit from chemotherapy, especially premenopausal patients. Tumor size >5 cm is viewed as a high-risk feature regardless of RS. Our goal is to investigate how patients with uncertainty regarding their anticipated recurrence risk were managed at our institution.
Methods: We conducted a retrospective analysis to explore the management of non-metastatic HER-2 negative hormone sensitive breast cancer patients diagnosed between 01/2018 &12/2020 stratifying them into the following study groups of interest: premenopausal (age <50), RS 16-25 compared to RS 26-30 and tumor size >5cm. Patients were compared based on whether they received adjuvant chemotherapy or not. The primary endpoint was the rate of local recurrence.
Results: The results of our analysis are illustrated in the table. Studying the premenopausal group, 91.3% had RS < 16; yet 35% of them received chemotherapy. Patients with RS > 25 represented 3.2% of the premenopausal group, 12.5% of which did not receive chemotherapy. The six recurrences in the premenopausal group were all from the RS <16 subgroup. Comparing the RS 26-30 to the RS 16-25 group, patients were on average older with tumors being on average smaller, yet more patients were treated with chemotherapy; and there were no recurrences noted in both subgroups. Finally, in the tumor size >5 cm group, 91.4% had RS <16, almost all were premenopausal with many patients being lymph node negative, yet more than half received chemotherapy.
Conclusions: In our study we demonstrate that in certain subgroups of early-stage breast cancer there is inconsistency in clinical practice when prescribing chemotherapy to patients factoring in their Oncotype DX scores. There is need for larger trials to guide clinicians on using Oncotype DX in those subgroups of patients.

Characteristics, Treatment Pattern and Outcomes of Patient Groups of Interest

Characteristics	**Premenopausal (N=506)**	**RS 16-25 (N=28)**	**RS 26-30 (N=36)**	**Tumor Size >5 cm (N=47)**
Age, Mean (SD)	42.65 (5.46)	44.71 (3.85)	63.56 (9.65)	42.02 (6.14)
Age, Range	19 - 49	36 - 49	45 - 79	28 - 57
Mean Tumor Size, mm (SD)	29.66 (52.21)	29.57 (33.88)	16.88 (11.19)	83.61 (37.52)
Lymph Nodes Positive, n (%)	91 (18.0%)	2 (7.1%)	0 (0.0%)	16 (34.0%)
Received Chemotherapy, n (%)	184 (36.4%)	7 (25.0%)	13 (36.1%)	25 (53.2%)
Local Recurrence, n (%)	6 (1.2%)	0 (0.0%)	0 (0.0%)	0 (0.0%)
Mean Follow- Up, months (SD)	19.28 (8.20)	19.39 (7.07)	21.21 (11.04)	19.26 (8.93)

#4976 The impact of obesity on survival in epithelial gynecological tumors.

A. Badran[1], M. Elshenawy[1], W. Fallatah[2], A. K. Hinkston[2], S. S. Ali[2], M. Ali Omar[2], A. M. Alaklabi[2], H. M. Abdalla[2], T. Z. Arabi[2], **B. N. Sabbah**[2], H. Alhusaini[1]; [1]King Faisal Specialist Hospital and Research Centre, Riyadh, Saudi Arabia, [2]Alfaisal University, Riyadh, Saudi Arabia

Background: The impact of obesity on the survival of patients with epithelial gynecological tumors is not yet clear. We aim to elucidate the impact of body mass index (BMI) on epithelial gynecological tumors in a large tertiary center at Saudi Arabia.
Methods: We retrospectively reviewed the medical files of all patients with pathologically confirmed epithelial gynecological tumors at our center. Then, we assessed the difference in overall survival (OS) according to primary tumor location, BMI, stage at presentation, and performance status (PS) at presentation using log-rank tests.
Results: 400 patients were included in the analysis. The mean age at diagnosis was 56.1±13 years. 242 (60.5%) patients were diagnosed with uterine carcinomas, 137 (34.3%) with ovarian carcinomas, and 21 (5.3%) with cervical carcinomas. 278 (69.5%) patients were obese at presentation, 74 (18.5%) were overweight, 43 (10.8%) were within normal range, and 7 (1.8%) were underweight. The PS at presentation was 0, 1, 2, 3, and 4 in 351 (87.8%), 17 (4.3%), 10 (2.5%), 16 (4%), and 6 (1.5%) patients, respectively. Cervical cancer was associated with long OS, while ovarian cancers demonstrated poor prognosis ($p=0.0159$). There was no difference in OS between different BMI groups ($p=0.072$). Patients with stage 4 cancers had significantly shorter OS ($p<0.0001$). Patients with PS 4 at presentation was associated with the worst prognosis ($p<0.0001$).
Interpretation: Shorter OS was associated with ovarian carcinomas, advanced staging, and poor PS at presentation. BMI classification had no impact on OS. Further studies are needed to confirm our findings.

#4977 The prevalence of key oncogenic driver mutations in stage I-III non-small cell lung cancer: Results from the AACR GENIE BPC dataset.

K. Zu, J. Ma, C. Chen, C. Pierce;
Merck & Co., Inc., Rahway, NJ

Background: While there is growing interest in targeted therapy for non-small cell lung cancer (NSCLC) in perioperative settings, data on key oncogenic driver mutations is limited in early-stage NSCLC. This real-world database study aims to evaluate the prevalence of select genomic alterations in stage I-III NSCLC.
Methods: From the American Association for Cancer Research (AACR) Project Genomics Evidence Neoplasia Information Exchange (GENIE) Biopharma Collaborative (BPC) V2.1-consortium dataset, we included adult patients with a confirmed diagnosis of NSCLC who had genomic testing using stage I-III NSCLC tissue samples. Descriptive statistics were used to summarize baseline characteristics and the prevalence of select genomic alterations.
Results: A total of 465 patients were included in this study, of whom 61% were female, 85% were white, 19% were never smokers, and 77% had adenocarcinoma. Less than 2% of the study population had BRAF V600E, HER2 activating mutations, HER2 amplification, MET amplification, HER3 amplification, RET fusion, ALK fusion, or ROS1 fusion. Among genomic alterations with a prevalence of 2% or higher, such as EGFR sensitizing mutations, KRAS G12C, MET exon 14 skipping, STK11, KEAP1, and TP53, some variations in prevalence were observed across baseline patient and disease characteristics such as race, smoking status, and histology (Table 1).
Conclusion: The prevalence of key oncogenic drivers and its relationship to select baseline disease characteristics among patients with early-stage NSCLC are similar to those of advanced NSCLC observed in other real-world clinico-genomic databases.

Table 1. Prevalence of Select Genomic Alterations in Stage I-III NSCLC (N=465)

	Prevalence of Positive Biomarker Status (%)					
	EGFR	KRAS G12C	MET Exon 14 Skipping	STK11*	KEAP1*	TP53
Overall	17.6	12.7	4.5	16.0	11.0	52.7
Gender						
Male	7.1	9.3	5.5	18.5	18.5	59.6
Female	24.5	15.9	3.9	14.3	6.3	48.2
Race						
White	15.6	14.1	4.5	16.5	12.0	53.7
Black	15.0	5.0	5.0	22.2	11.1	60.0
Asian	44.0	4.0	8.0	8.3	4.2	44.0
Smoking Status						
Never smoker	41.4	1.2	6.9	4.7	1.2	36.8
Former smoker	13.7	16.0	4.6	17.4	12.9	52.4
Current smoker	5.7	12.9	1.4	23.9	15.4	72.9
Histology						
Adenocarcinoma	20.1	14.3	4.6	18.1	10.4	46.0
Squamous cell carcinoma	0	2.9	4.4	4.6	14.1	86.8
*The numbers of patients tested for STK11 and KEAP1 were 457 and 445, respectively.						

#4978 Genomic characterization of metastatic pancreatic cancer according to tumor sample sites.

S. Y. Goksu[1], M. Ozer[2], B. Bacik Goksu[3], N. N. Sanford[4], A. Jones[4], N. Verma[4], S. Kazmi[4];

[1]West Suburban Medical Center, Oak Park, IL, [2]Dana Farber Cancer Institute, Harvard Medical School, Boston, MA, [3]University of Illinois at Chicago, Chicago, IL, [4]UT Southwestern Medical Center, Dallas, TX

Background: Our research aimed to evaluate and compare the genetic variations in the primary and metastatic sites of patients with metastatic pancreatic cancer.

Methods: In this study, we selected individuals with metastatic pancreatic cancer from the data provided by the American Association for Cancer Research Project GENIE (version 14.1). The comparison of genetic mutations between primary and metastatic tumor sites was conducted using the Fisher exact test, augmented with the Benjamini-Hochberg adjustment technique.

Results: In a study of 3,108 patients with metastatic pancreatic cancer, 38.9% had metastatic site tumor samples, while 61.1% had samples from the primary tumor. The most frequent mutations were KRAS (89.4%), TP53 (72.9%), SMAD4 (21.2%), and CDKN2A (17.4%). Metastatic samples showed higher rates of CDKN2A, CDKN2B, and MTAP mutations compared to primary site samples (40.1% vs. 29.1%; 20.3% vs. 10.4%; and 20.8% vs. 8.9%, respectively, all with $p<0.001$ and $q<0.001$). In patients with young-onset pancreatic cancer (younger than 50 years), there was no notable difference in gene mutations between the two sample groups.

Conclusion: Our findings corroborate the notion that identifying the precise genes that contribute to the development of metastatic pancreatic cancer is vital for gaining a more comprehensive understanding of the biological mechanisms. Moreover, genomic profiling could be a key in pinpointing potential biomarkers for diagnosis and therapy.

#4979 Genomic profiling of early-onset metastatic colorectal cancer based on tumor sample location.

M. Ozer[1], S. Y. Goksu[2], B. Bacik Goksu[3], N. N. Sanford[4], A. Jones[4], N. Verma[4], S. Kazmi[4];
[1]Dana Farber Cancer Institute, Harvard Medical School, Boston, MA, [2]West Suburban Medical Center, Oak Park, IL, [3]University of Illinois at Chicago, Chicago, IL, [4]UT Southwestern Medical Center, Dallas, TX

Background: Here, we describe analyses towards identifying and comparing genetic variations between the primary and metastatic sites in early-onset metastatic colorectal cancer patients.
Methods: We selected patients with early-onset metastatic colorectal cancer (under 50 years old) using data from the American Association for Cancer Research Project GENIE (version 14.1). We used the Fisher exact test to compare genetic mutations between the primary tumor and metastatic sites, complemented by the Benjamini-Hochberg adjustment method.
Results: In a total of 1,791 patients with early-onset metastatic colorectal cancer, 27.1% had tumor samples from metastatic sites, while the majority, 72.9%, were from the primary tumor location. The most common mutations found were in the TP53 gene (77.6%), followed by APC (76.0%), KRAS (42.4%), and PIK3CA (19.0%). Notably, the metastatic samples had a significantly higher occurrence of SMAD4 mutations compared to their primary site counterparts (20.8% vs. 14.0%, $p<0.001$, $q<0.001$). Conversely, the primary tumor samples exhibited higher frequencies of TCF7L2 and ARID1A mutations (16.9% vs. 10.6%, $p<0.001$, $q<0.001$, and 13.0% vs. 6.4%, $p<0.001$, $q<0.001$, respectively).
Conclusion: Determining the specific genes responsible for the formation of metastatic tumors is crucial for a deeper understanding of the disease's underlying biology in early-onset metastatic colorectal cancer. Such genomic details are crucial to pave the way to the discovery of potential biomarkers for diagnosis and the development of new cancer therapeutics.

#4980 Genomic and clinical characteristics of advanced pancreatobiliary cancer, stratified by KRAS mutation status.

H. Miyashita, P. S. Shah, G. A. Brooks;
Dartmouth Cancer Center, Lebanon, NH

Mutations in KRAS are common in pancreatobiliary cancer, occurring in 90% of advanced pancreatic ductal adenocarcinomas (PDAC) and 20% of advanced cholangiocarcinomas (CCA). We analyzed clinico-genomic databases to evaluate the hypothesis that KRAS mutation status defines subsets of PDAC and CCA with similar genomic characteristics and clinical behavior. Using the genomic data of PDAC and CCA from AACR Project GENIE Cohort version 14.0-public, we analyzed the genomic landscape of four cohorts of pancreatobiliary cancer: KRAS mutated PDAC, KRAS wild-type PDAC, KRAS mutated CCA, and KRAS wild-type CCA. Excluding KRAS mutations, there were 53 gene alterations observed in ≥2.5% of cases in at least one of the four cohorts. The three most common gene alterations in each cohort were; TP53, SMAD4, and CDKN2A mutations (KRAS mutated PDAC), TP53, ARID1A, and SMAD4 mutations (KRAS wild-type PDAC), TP53 mutation, CDKN2A deletion and SMAD4 mutation (KRAS mutated CCA), and TP53, ARID1D and IDH1 mutations. (KRAS wild-type CCA) The similarity of gene alteration patterns was evaluated by principal component analysis (PCA) 3D plot and calculation of average Euclidean distance. The PCA plot suggested heterogeneous genomic profiles in KRAS wild-type CCA in contrast to relatively monotonous profiles in KRAS mutated PDAC. The average Euclidean distance between KRAS mutated CCA and KRAS wild-type CCA was significantly longer than that between KRAS mutated CCA and KRAS mutated PDAC (2.00 vs. 1.89, $p < 0.001$), suggesting that KRAS mutated CCA is more genomically related to KRAS mutated PDAC than KRAS wild-type CCA. The average Euclidean distance between KRAS mutated PDAC and KRAS wild-type PDAC was significantly shorter than that between KRAS wild-type CCA and KRAS wild-type PDAC. To compare the clinical characteristics of the four cohorts, we evaluated the data of patients with stage IV pancreatobiliary cancer, using cBioPortal. The number of cases in each cohort was 1544 (KRAS mutated PDAC), 121 (KRAS wild-type PDAC), 91 (KRAS mutated CCA), and 459 (KRAS wild-type CCA). Median overall survival (OS) was 14.7, 21.5, 10.7, and 15.4 months, respectively. Compared to KRAS wild-type CCA, KRAS mutated CCA had a significantly shorter OS (hazard ratio [HR] = 1.45, 95% confidence interval [CI] = 1.12 - 1.89). The OS of KRAS mutated CCA was shorter than KRAS mutated PDAC (HR 1.32, 95% CI 1.03 - 1.68). KRAS wild-type PDAC had a significantly longer OS compared to KRAS mutated PDAC. (HR 0.72, 95% CI 0.57 - 0.92) In conclusion, KRAS mutated CCA has a poor OS and a genomic landscape distinct from KRAS wild-type CCA; it is genomically more similar to KRAS mutated PDAC. KRAS wild-type PDAC has a better OS than KRAS mutated PDAC, though it was not genomically similar to KRAS wild-type CCA. Therapeutic approaches stratified by KRAS mutation status should be considered for pancreaticobiliary cancers.

CLINICAL RESEARCH: Chemotherapy, Radiation, and Vaccine Mediated Immunity
Poster Session

#4984 TCR-CD3 bispecifics kill tumor cells in a caspase- and gasdermin-dependent manner by inducing multiple cell death pathways.

S. Varadarajan, A. Raczka, S. Khakoo, L. Collins, A. Benlahrech;
Immunocore Ltd., Abingdon, United Kingdom

Background:ImmTAC® (immune-mobilizing monoclonal T cell receptor against cancer) molecules are soluble bi-specific TCR molecules that redirect T lymphocytes to kill tumor cells. Tebentafusp, which targets the melanocyte lineage gp100, is the first ImmTAC molecule approved for the treatment of HLA-A*02:01 adult patients with metastatic uveal melanoma.[1] While the roles of Granzyme B and Perforin in the anti-tumor activity of CD3 T cell engagers are well described, the contribution of other apoptotic pathways, e.g. pyroptosis (inflammatory apoptosis), is poorly understood. For this reason, we explored apoptosis mechanisms induced by ImmTACs *in vitro* and their relevance to the anti-tumor activity of tebentafusp in a Phase 2 clinical trial.
Methods: Cell lines derived from different malignancies, MP41 (uveal melanoma), MEL624 (cutaneous melanoma) and NCI-H1755 (non-small cell lung carcinoma) were co-cultured with PBMC and ImmTAC molecules for defined time periods, followed by cytolysis measurements (xCelligence) and protein expression analysis (western blotting). Relevant cell death pathways were targeted by genetic (CRISPR knockout) or pharmacological inhibition. Translational relevance of *in vitro* experiments was assessed using RNAseq of tumor biopsies at baseline (N=70) and matched on-treatment at 16 days post treatment [N=35] or at progression [N=14]) from a Phase 2 trial of tebentafusp in HLA-A*02:01^{+} mUM patients (NCT02570308). Clinical data cut-off: 17-Oct-2022.
Results: ImmTAC-mediated tumor killing *in vitro* occurred in a caspase-dependent manner and accompanied a profound induction of several apoptotic, necroptotic and pyroptotic proteins, such as GZMB, Caspases 8 and 7, RIPK3, MLKL and GSDMD in several cell lines. In NCI-H1755 cells, genetic knockout of GSDMD significantly diminished ImmTAC-mediated cytolysis (92% reduction), thereby confirming the involvement of pyroptosis in ImmTAC-mediated tumor killing in these cells. In agreement, RNAseq analysis of tumor biopsies from mUM patients after 3 doses of tebentafusp revealed enhanced expression of genes involved in different cell death pathways, including Caspase 7, RIPK3, MLKL and GSDMD (fold changes of 1.2-2). In addition, patients exhibiting above-median tumor expression of GSDMD at progression had longer overall survival (Hazard ratio = 0.074 95% C.I. 0.01-0.64).
Conclusions: ImmTAC redirection of T cells resulted in a caspase-dependent, pyroptotic cell death of tumor cell lines and enhanced gene expression of necroptotic and pyroptotic pathways in tumor biopsies. GSDMD, induced during ImmTAC-mediated cytolysis, also correlated with better overall survival in tebentafusp-treated patients. Induction of multiple cell death pathways, particularly pyroptosis, helps to explain the anti-tumor activity of tebentafusp.
References: 1. Nathan, P. *et al. New Engl J Med* 385, 1196-1206 (2021).

#4985 Pivotal roles for cancer cell-intrinsic mPGES-1 and autocrine EP4 signaling in suppressing anti-tumor immunity.

N. Markosyan[1], I. Kim[1], C. Arora[2], N. Cheng[1], E. Schechter[1], J. W. Tobias[1], B. Z. Stanger[1], R. H. Vonderheide[1];
[1]University of Pennsylvania, Philadelphia, PA, [2]University of Pittsburg, Pittsburg, PA

Tumor cell-derived prostaglandin E2 (PGE_2) is a tumor cell-intrinsic factor that supports immunosuppression in the tumor microenvironment (TME). Using a genetically engineered mouse model of pancreatic ductal adenocarcinoma, we demonstrate that deleting the terminal PGE_2 synthesis enzyme or disrupting autocrine PGE_2 signaling through cognate EP4 receptors on tumor cells reverses the T cell-low, myeloid cell-rich TME to activate T cell immunity and suppress tumor growth. Knockout (KO) of *Ptges* (the gene encoding PGE_2 synthesis enzyme mPGES-1) or the EP4 receptor gene (*Ptger4*) in KPCY (*Kras*^{G12D}/*P53*^{R172H}/*Yfp*/*Cre*^{Pd}) pancreatic tumor cells abolished growth of implanted tumors in a T cell-dependent manner (KO vs control $p<0.0001$ for both). Blockade of the EP4 receptor in combination with immunotherapy, but not immunotherapy alone, induced complete tumor regressions and immunological memory. Mechanistically, *Ptges* and Ptger4 KO tumor cells exhibited altered T and myeloid cell attractant chemokines, became more susceptible to TNF-α killing, and exhibited reduced adenosine synthesis. In hosts treated with an adenosine deaminase inhibitor, *Ptger4* KO tumor cells accumulated adenosine and gave rise to tumors. These studies reveal an unexpected role for autocrine mPGES1-PGE_2-EP4 signaling axis in pancreatic cancer cells, nominating mPGES-1 inhibition and EP4 blockade as immune-sensitizing approaches in cancer therapy.

#4986 Single-cell multimodal characterization of ovarian cancer microenvironment under neoadjuvant niraparib treatment informs an effective therapeutic strategy of suppressing HRD-dependent eTreg hyper-expansion.

Y. Luo[1], Y. Xia[2], D. Liu[2], X. Li[3], H. Li[2], Y. Zhao[4], D. Ma[2], Y. Fang[2], H. Liang[1], Q. Gao[2];

[1]UT MD Anderson Cancer Center, Houston, TX, [2]Tongji Hospital, Tongji Medical College, Wuhan, China, [3]Central Hospital of Wuhan, Tongji Medical College, Wuhan, China, [4]Precision Scientific (Beijing) Co., Ltd., Beijing, China

Homologous recombination deficiency (HRD) is a widespread hallmark in cancer, rendering tumors susceptible to PARP inhibition. Despite this well-established tumor-intrinsic vulnerability, the effects of HRD and related therapies on the tumor microenvironment (TME) remain poorly understood. In this study, utilizing single-cell RNA and T cell receptor profiling (scRNA/TCR-seq), we characterized 79 high-grade serous ovarian cancer (HGSOC) samples, both pre- and post-treatment, from 46 patients treated with neoadjuvant niraparib or chemotherapy in a phase II clinical trial (NCT04507841). This effort established the most comprehensive HGSOC TME atlas to date, encompassing over 700,000 cells. By integrating multiplex immunofluorescence imaging, flow cytometry, and bulk TCR-seq data from additional tumors and matched peripheral blood samples, we systematically assessed HRD-induced and treatment-perturbed dynamics of tumor-infiltrating and circulating immune cells. Surprisingly, among over 120 cell states across 10 cell types, effector regulatory CD4$^{\pm}$ T cells (eTreg) exhibited the strongest enrichment in treatment-naïve HRD tumors and a marked treatment-induced reduction. Further analyses of transcriptional states and clonal kinetics revealed HRD-driven functional coordination between eTregs and exhausted CD8$^{\pm}$ T cells (Tex), both displaying uniquely heightened tumor reactivity signatures and clonal co-expansions. The intra-population heterogeneity analysis of Tregs and Texs further demonstrated an effectiveness gradient, wherein the terminal subsets had a greater presence in HRD and were reversed by both niraparib and chemotherapy treatments. Delineating the clonal evolution of Tregs and Texs, we identified their notable crosstalk with other tumor-infiltrating T cell populations while remaining remarkably isolated from the peripheral blood repertoire, in line with their terminally differentiated status. Furthermore, we observed widespread, chronic activation of interferon signaling across TME components, downstream of HRD. This orchestrated CD4$^{\pm}$ T cell anergy induction into Tregs, mainly through direct engagement by cancer cells that upregulated MHC-II molecules but lacked essential co-stimulatory ligands. Finally, we experimentally validated a therapeutic strategy to conjunctively and effectively break down these factors in HGSOC by combining PARP inhibition and eTreg deletion through a humanized therapeutic anti-CCR8 antibody in multiple syngeneic HGSOC mouse models. Our study unravels a key immunoregulatory role of eTregs in the HGSOC TME amplified by HRD. These findings underscore the underappreciated value of eTreg-focused therapeutics as novel immunotherapies for HGSOC and other genomically unstable cancers.

#4987 TREM2 is a radiation-induced target for immunomodulation of tumor-associated macrophages in the prostate cancer tumor microenvironment.

J. A. Villa-Pulgarin[1], U. Chan[1], F. Khani[1], F. Socciarelli[1], J. Wu[1], R. Carelli[2], J. Kraynak[1], S. C. Formenti[1], L. Marchionni[3], M. Loda[1], H. Nagar[1], **A. E. Marciscano**[4], C. E. Barbieri[1];

[1]Weill Cornell Medical College, New York, NY, [2]Replit, New York, NY, [3]Weill Cornell Medical College, Boston, MA, [4]Harvard Medical School/Massachusetts General Hospital, Boston, MA

Background: The prostate cancer (PCa) tumor microenvironment (TME) is characterized by a predominance of myeloid cells that may have a key role in immunosuppression and disease progression. Stereotactic Body Radiation Therapy (SBRT) is utilized for treatment of localized and metastatic PCa and promotes inflammatory remodeling of the TME. We analyzed human PCa specimens at acute post-SBRT timepoints to identify radiation-induced targets in the PCa TME and used *in vitro* and *in vivo* models to test and validate our findings.

Methods: We performed 10X single-cell RNA sequencing (scRNA-seq) on prostatectomy specimens from men with high-risk localized PCa; 12,988 cells from 4 patients that underwent pre-operative SBRT and 47,314 cells from 6 patients that underwent prostatectomy alone. THP-1 monocytes polarized into macrophage (Mϕ) states [M0, M1, M2 and tumor-associated macrophages (TAM), were used to characterize TREM2 expression and immune responses to radiation or conditioned media (CM) derived from irradiated PC3 cells. In vivo studies with C57BL/6 mice inoculated with MC38 flank tumors or $PTEN^{-/-}$ $SPOP^{mut}$ $CHD1^{del}$ mouse prostate organoid line were used to analyze intratumoral myeloid populations in response to SBRT (37.5Gy in 5 fractions).

Results: scRNA-seq analysis (Cell Ranger 7.1.0 pipelines; Seurat v5 R package) revealed enrichment of a cluster of myeloid cells defined by a damage-associated Mϕ gene signature (TREM2, APOE, SPP1, LGALS3, CD9) in response to SBRT compared with non-irradiated specimens (35.6% vs 5.7%). TREM2 expression was significantly upregulated in THP-1 cells polarized in M2 ($p<0.001$) and TAM ($p<0.001$) conditions, compared to M1 conditions. Irradiation (20Gy x1) of THP-1 cells significantly increased TREM2 expression in M0 ($p<0.01$), M1 ($p<0.001$), and TAM ($p<0.01$) conditions. Proliferation of PC3 cells exposed to CM from irradiated TAMs was significantly increased ($p<0.0001$) compared to CM from non-irradiated TAM. Alternatively, CM derived from irradiated PC3 cells significantly increased ($p<0.05$) TREM2 expression in M0-polarized Mϕ. In vivo studies, in MC38 and organoid models, noted a significant reduction ($p<0.0001$) in tumor volume at day 7 post-SBRT. Multi-parametric flow cytometry demonstrated robust myeloid infiltration in response to SBRT dominated by $CD11b^{+}F4/80^{+}$ TAMs in irradiated tumors. Among irradiated tumors, TREM2 expression was markedly elevated in TAMs (organoid and MC38, $p<0.0001$).

Conclusion: Preliminary data in human irradiated PCa and validation studies in preclinical models suggest TREM2 expression on myeloid cells is a radiation-induced target. Further studies are underway to understand the functional and immunological implications of SBRT-induced TREM2 expression on TAMs and whether this can be therapeutically targeted to enhance anti-tumor immunity in PCa.

#4988 Responders to combination radiation and PD-1 blockade demonstrate reduced myeloid immunosuppression and enhanced interferon signaling in oligometastatic prostate cancer patients.

Z. Fan[1], D. Y. Oh[1], A. Wong[1], K. Shinohara[1], H. Nguyen[1], C. Hwang[1], H. Chang[1], A. Starzinski[1], T. Li[1], C. De Leon[1], M. Gin[1], E. Van Allen[2], L. Zhang[1], R. R. Aggarwal[1], T. W. Friedlander[1], E. J. Small[1], F. Y. Feng[1], L. Fong[1];

[1]University of California San Francisco, San Francisco, CA, [2]Center for Cancer Genomics, Dana-Farber Cancer Institute, Boston, MA

Background: Prostate cancer is unresponsive to current immunotherapies such as checkpoint inhibitors. Overcoming this “cold” environment requires rational combination of therapeutic modalities that can prime anti-tumor immunity. Radiation is a potential candidate; however it remains unclear how it should be most productively combined with immunotherapies.

Methods: We completed an investigator-initiated clinical trial of newly diagnosed men with oligometastatic, hormone-sensitive prostate cancer (mHSPC, NCT03007732). Patients were randomized to receive anti-PD-1 x 13 cycles (pembrolizumab, Arm 1, n=12), or anti-PD-1 with intraprostatic injections of TLR9 agonist SD-101 (Arm 2, n=11). All patients received SBRT to the prostate tumor during cycle 1, and concomitant hormonal therapy with a GnRH agonist and abiraterone. Response was assessed as PSA < nadir + 2 ng/mL at 15 months after ceasing all cancer therapies. For unbiased correlative immune interrogation of these patients, fresh paired biopsies of primary prostate tumor and PBMCs both before and after radiation and immunotherapy were analyzed by multi-omic single-cell genomics to assess changes with treatment, including T cell repertoire changes.

Results: Fourteen of 21 evaluable patients responded by PSA criteria with 3 patients not yet reaching 15 months of post-treatment follow-up. Adverse events included expected IRAEs from anti-PD-1, and flu-like symptoms from SD-101, with no unexpected AEs. Single-cell analysis of tumor biopsies reveals treatment-induced decreases in cytotoxic T cell populations and increases in both immunostimulatory LAMP3+ dendritic cells and immunosuppressive SPP1+ myeloid populations. Treatment increased interferon (IFN) signaling in most myeloid subsets while strongest in LAMP3+ DCs. Compared to non-responders, responders showed less immunosuppression at baseline with depletion of myeloid cells and enhanced IFN activity on LAMP3+ DCs, and treatment-induced IFN activity on cytotoxic T cells. TLR9 agonism also specifically enhanced IFN responses, persistence of cytotoxic T cell clonotypes, and enhanced antigen presentation in tumor cells. Circulating T cells in blood detected shared clones with tissue showing enrichment in cytotoxic phenotype and association with responders.

Conclusions: Responders to combination radiation and anti-PD-1 blockade have decreased myeloid immunosuppression and enhanced IFN activity prior to treatment in oligometastatic prostate cancer. This may identify patients likely to respond, and baseline immune setpoints that can be enhanced with improved immunotherapy strategies.

Acknowledgements: This work was supported by the Prostate Cancer Foundation and Merck. Merck Sharp & Dohme LLC, Rahway, NJ, USA provided drug and financial support for the study.

#4989 Targeting IL-1β mitigates radiation induced MDSC expansion & improves survival in glioblastoma.

S. Ghosh[1], J. Huang[2], D. DeNardo[2], D. Hallahan[2], J. Jaboin[1], D. Thotala[1];

[1]Stephenson Cancer Center, The University of Oklahoma, Oklahoma City, OK, [2]Washington University School of Medicine in St. Louis, St. Louis, MO

Background: Our previous research demonstrated that radiation therapy (RT) for glioblastoma (GBM) induces aberrant myelopoiesis, increasing production of myeloid derived suppressor cells (MDSCs) and exacerbating T-cell suppression. However, the precise biological mechanisms underlying this phenomenon remain unclear. This study aims to elucidate the role of the pro-inflammatory cytokine interleukin-1beta (IL-1β) in RT-induced myelopoiesis and its correlation with poor prognosis in GBM patients.

Methods: We conducted an extensive analysis of circulatory immune cells and pro-inflammatory cytokines in GBM patients treated with chemoradiotherapy. Using an orthotopic mouse model of GBM, we investigated the impact of IL-1β on myelopoiesis and survival. Functional assays were employed to examine MDSC expansion. Multi-color flow cytometry was used for immune profiling.

Results: We found that RT elevated the plasma IL-1β concentration in both GBM patients and GBM-bearing mice, which also corresponded with an increase of MDSC in blood. In the murine GBM model, RT appeared to promote hematopoietic stem (HSPC) differentiation towards myelopoiesis. This led to increased MDSC precursor cells in the bone marrow, elevated circulating MDSCs in blood, and more infiltration of MDSCs in the tumor microenvironment (TME). Similar effects were observed in GBM-bearing mice following the administration of exogenous IL-1β. In contrast, inhibition of IL-1β using anti-IL-1β antibody during RT led to reduced myelopoiesis. When anti-IL-1β antibody was combined with functional inhibition of MDSCs using phosphodiesterase-5 inhibitor-tadalafil during RT, we observed decreased MDSC infiltration and increased CD8+ T cell infiltration in the TME. The combination approach also extended the survival of GBM-bearing mice after RT longer than either drug alone.

Conclusions: Irradiation of GBM appears to induce IL-1β to promote aberrant myelopoiesis and MDSC expansion. A multi-pronged approach to inhibit MDSC production using IL-1β inhibitor and MDSC function using tadalafil during RT may be a promising approach to overcome the immune-suppressive TME of GBM.

#4990 Genotoxic chemotherapy impedes antibody-mediated complement dependent cytotoxicity (CDC), via a Chk1-CD59 axis.

Allison S. Y. Chan[1], Patrick W. Jaynes[1], Nurulhuda B. Mustafa[2], Akshaya A. Anbuselvan[1], Charmaine Z. Y. Ong[1], Anand D. Jeyasekharan[1]

[1]National University of Singapore, Cancer Science Institute of Singapore, Singapore, Singapore,[2]Department of Pharmacology, Yong Loo Lin School of Medicine, National University of Singapore, Singapore, Singapore

Monoclonal antibodies such as rituximab exert targeted tumor cell lysis via complement dependent cytotoxicity (CDC). These antibodies are often combined with chemotherapy in clinical treatment protocols. However, the impact of chemotherapy on cell-intrinsic pathways that regulate antibody-mediated CDC is not known. Through a phage display screen, we identified that genotoxic stress caused upregulation of a membrane complement regulatory protein (mCRP), CD46, prompting further investigation into its implications and mechanism.

Using cell lines from diffuse large B cell lymphoma (DLBCL) as our model, we confirmed that genotoxic chemotherapy upregulates CD46, as well as other mCRPs such as CD55 and CD59. We hypothesized that upregulated mCRPs could impede Rituximab-mediated CDC. We assessed this in-vitro using rituximab and complement human serum. Aligned with our hypothesis, chemotherapy treatment of DLBCL cells significantly impeded rituximab-induced CDC. Using blocking antibodies to each mCRP, reversal of the effect of chemotherapy on CDC only occurred after co-treatment with a CD59 blocking antibody, suggesting that CD59 is a key player for chemotherapy-invoked resistance to CDC.

To further elucidate the underlying cellular pathway, we performed a high-throughput small molecule screen using rituximab-induced CDC as a readout, with or without cotreatment of a genotoxic chemotherapeutic (etoposide). We identified Chk1 inhibitors as consistent top rescuers. qPCR and flow cytometry revealed that Chk1 inhibition prevented the upregulation of mCRPs transcriptionally. Sp1 is a known transcription factor driving constitutive CD59 expression. Inhibiting Sp1 similarly prevented chemotherapy-induced upregulation of CD59 and resistance to CDC. However, CHIP-qPCR showed no increased binding of total Sp1 protein to the CD59 promoter after chemotherapy. Instead, positive co-immunoprecipitation of pATM and p300 with Sp1 only with etoposide and not with co-treatment of Chk1 inhibitor suggests Chk1-mediated activation of Sp1. Mechanistically, we have found that chemotherapy-activated Chk1 modulates Sp1-mediated CD59 transcription and that the induced upregulation of CD59 is able to prevent antibody-mediated CDC.

Overall, these results indicate novel immune regulation by DNA damage response, particularly in the context of complement regulatory proteins. Our results advocate consideration when using simultaneous administration of chemotherapy with CDC-inducing monoclonal antibodies, and suggest Chk1 blockade as a possible therapeutic addition.

#4991 Radiotherapy-induced immunological and therapeutic response depends on stem-like TCF-1$^{\pm}$PD-1$^{\pm}$CD8$^{\pm}$ T-cells.

H. Koksal, M. Herbst, N. Marti, M. van den Broek;
Universitat Zurich, Zurich, Switzerland

Radiotherapy is a frequently used treatment for cancer. Recent data, including ours, showed that radiotherapy promotes an inflammatory response in the tumor that supports tumor-specific immunity, and in fact, the efficacy of radiotherapy in pre-clinical models depends on CD8$^{\pm}$ T-cells. According to our preliminary data, the response to radiotherapy is independent of de novo recruited CD8$^{\pm}$ T-cells, suggesting that radiation drives differentiation and proliferation of preexisting intratumoral CD8$^{\pm}$ T-cells. Intratumoral CD8$^{\pm}$ T-cells are heterogeneous concerning phenotype and function. Under conditions of chronic stimulation by antigen, a subset of CD8$^{\pm}$ T-cells expressing PD-1 and the transcription factor TCF-1 was described. These so-called stem-like CD8$^{\pm}$ T-cells, which give rise to effector cells, were shown to be essential for the clinical response to PD-1 blockade. How radiotherapy influences the different CD8$^{\pm}$ T-cell subsets in the tumor microenvironment has not been comprehensively investigated. We propose that the efficacy of radiotherapy depends on the presence of stem-like CD8$^{\pm}$ T-cells, presumably by giving rise to effector cells. To address this, we selectively depleted TCF-1$^{\pm}$ cells from tumor-bearing mice immediately before radiotherapy. Subsequently, we correlated tumor regression with the immunological response using single-cell analyses of intratumoral CD8$^{\pm}$ T-cells. In the absence of TCF-1$^{\pm}$ cells, we found a reduced efficacy and reduced number of intratumoral effector cells after radiotherapy. We currently analyze our single-cell RNA-sequencing data and expect to discover novel radiotherapy-induced pathways in CD8$^{\pm}$ T-cells that contribute to therapeutic efficacy.

#4992 Baseline and alteration in pre vs post standard of care management serum-derived inflammatory markers are associated with radiation treatment volumes and patient outcomes in patients with GBM in a large-scale proteomic panel.

S. V. Jagasia[1], T. Joyce[1], S. Chappidi[2], E. Tasci[1], T. Cooley Zgela[1], M. Mackey[1], M. Sproull[1], K. Camphausen[1], A. V. Krauze[1];
[1]National Cancer Institute, Bethesda, MD, MD, [2]National Cancer Institute / University of Cambridge, Bethesda, MD / Cambridge, United Kingdom

Glioblastomas (GBM) are the most aggressive central nervous system tumors with near universal recurrence following resection and chemoradiation (CRT). Inflammation plays a multifaceted role in GBM development and progression through disruption of the brain barrier, immunosuppression, angiogenesis, and release of inflammatory mediators. Previously established serum inflammatory markers (IM) have been studied in baseline measures obtained prior to surgical resection, making it difficult to establish patterns for potential treatment-induced alteration of IM. We tested the hypothesis that serum-derived IM measured post-resection, prior to and following completion of CRT, may be related to residual tumor burden and response to treatment. IM was analyzed in serum collected pre and post-CRT from 82 individuals with a pathologic confirmed diagnosis of GBM using aptamer-based SOMAScan® proteomic assay. Clinical variables were collected or derived from electronic health records and included RT (radiation therapy) gross tumor volumes GTVT1 (enhancing tumor volume on T1 gadolinium MRI pre CRT), GTVT2 (T2 FLAIR tumor volume on MRI pre CRT), the volume receiving the higher prescribed RT dose (60Gy) (PTVHD) and lower dose (46Gy) (PTVLD), and outcomes (overall survival (OS), progression-free survival (PFS)). Cox regression analyses were performed with pre and post IM levels significant associations ($p<0.05$) were identified. GTVT1 and PTVHD correlated positively with pre-CRT Fibrinogen level and negatively with alteration in CD23. GTVT2 and PTVLD correlated negatively with Kininogen alteration ($p<0.05$ for all). GTVT1 correlated positively with pre IL-6 level. PTVLD correlated negatively with pre TNFb level and PTVHD with CD14 alteration. High alteration in Albumin and a2-HS glycoprotein, lower pre HLA-G and pre IL-6, high pre IgE, pre PD-1 and pre TNF-b and lower altered TNF-b were all associated with longer OS ($p<0.05$). Accounting for age, tumor volumes and RT volumes, fibrinogen was the most prevalent signal associated with outcomes, the pre CRT level associated with OS (*HR: 0.66, p: 0.04*) and pre, post, and alteration significant for PFS (pre (*HR : 0.60, p : 0.01*), post (HR: 1.6, p: 0.01), alt (*HR : 1.52 , p < 0.005*). SAA pre CRT level was associated with OS (*HR : 1.46, p: 0.02*) and its alteration with PFS (*HR : 1.62, p : 0.02*). Additional IM alterations associated with OS CRP (*HR: 0.57, p: 0.01*), PD-1 (*HR : 3.52, p , 0.005*) and PFS, post CRT IL-10 level (*HR : 0.04 , p : 0.02*). GTVT1/PTVHD, GTVT2/PTVLD have distinct IM correlates in serum. Serum IM are associated with OS ad PFS and tumor volumes. Potential associations of previously literature-described inflammatory markers including Fibrinogen, SAA, IL-6, TNF-b and PD-1, were identified and are undergoing further analysis.

#4993 CJRB-101 induces immune responses through the GUT-TME axis in immune cell-driven mechanism in lung cancer models.

A. Min[1], B.-e. Kwon[1], S.-s. Kang[2], S. Baek[3], J. Yang[1], H. Park[1], J. Im[1], H. Kim[1], J. Kim[1], J. Kwon[1], D. Kim[3], J. Lee[3], H. Oh[1], S. Yang[3], Y. Han[3], M. Kim[3], H. Han[3], K. Na[3], Y. Kim[3], M. Yun[3], J. Kim[3], Y. Byeon[3], Y. Kim[3], M. Hong[3], S. Lim[3], K.-H. Pyo[3], B. Cho[3];

[1]CJ Bioscience Inc., Suwon, Korea, Republic of, [2]JEUK Co, Seoul, Korea, Republic of, [3]Yonsei University College of Medicine, Seoul, Korea, Republic of

Background Live biotherapeutic products (LBPs) are known to enhance immune responses through the GUT-TME axis. Here, we investigate the GUT-TME-related immune cell profiling and signals associated with the anti-cancer effects of CJRB-101.

Methods Tumors from NSCLC patients (anti-PD-1 refractory) were transplanted in Hu-CD34-NSG to establish humanized patient-derived xenograft (PDX) models. CJRB-101 was administered at $1x10^9$ CFU (*p.o.*, BID) or combination with anti-PD-1 (10 mpk, *i.p.*, BIW). TME was analyzed using multiplex IHC, flow cytometry and scRNA sequencing. Samples were collected from C3PQ syngeneic mice at multiple timepoints for GUT-TME immune cell profiling. For depletion assay, immune cells were individually depleted during the combination treatment. TLR4-mediated mechanism was evaluated using ex vivo and in vivo assay treated with CJRB-101 or cell membrane of CJRB-101.

Results CJRB-101 combined with pembrolizumab effectively suppressed tumor growth in anti-PD-1 resistant PDX models. Further analysis revealed a correlation between the activity of NK cells and angiogenesis inhibition. Abundance of NK/NKT was higher in the CJRB-101 treated group compared to the vehicle group in multiple PDX models. The expression of GZMB and IFNG in NK/NKT cells was significantly higher in the CJRB-101 treated group compared to the vehicle group in YHIM2014 ($p<0.001$). CJRB-101 treated group showed significantly higher expression of antiangiogenic IL1B ($p<0.001$) while the expression of pro-angiogenic VEGFA ($p=0.002$) was lower compared to the vehicle group in YHIM2014 cancer cells. Macrophages in the intestine were increased at Day 3 in the CJRB-101 group compared to anti-PD1, while NK cells, granulocytes, $CD3^{\pm}$, $CD4^{\pm}$, $CD8^{\pm}$ T cells increased at Day 10 in the syngeneic model. Depletion assay confirmed that macrophages, $CD8^{\pm}$ T cells and neutrophils were pivotal in the anti-cancer effects of CJRB-101. We observed that TAK242 and MD2 reduced the IL-6 secretion of Raw264.7 in a dose-dependent manner. The cell membrane played a key role in increasing BMDM M1 polarization and repolarization of M2 to M1, and that inhibition of TLR4 resulted in a decrease in BMDM repolarization. TLR inhibition also demonstrated that TGI decreased from 34% to 20% when treated with cell membrane + TAK242 compared to cell membrane monotherapy.

Conclusions This study showed that macrophages were the dominant immune population in the early stages then T cells (CD3, CD4, CD8), NK cells and granulocytes became more active in the latter stages of the GUT-TME-axis immune response. In vivo results indicated that anti-cancer efficacy of CJRB-101 is immune-cell driven by TLR4-dependent stimulation of key immune cell populations (macrophages, CD8+ T cells, neutrophils) modulated by the cell membrane of CJRB-101. CJRB-101 is currently undergoing clinical investigation for treatment of patients with advanced NSCLC.

#4995 Impact of radiotherapy on extracellular vesicle mediated anti-tumor immunity in oligometastatic prostate cancer.

C. J. Uzendu[1], Y. Kim[2], R. R. Lavoie[2], H. Dong[2], S. Park[2], F. Lucien-Matteoni[2];
[1]Mayo Clinic Graduate school of biomedical Sciences, Rochester, MN, [2]Mayo Clinic, Rochester, MN

Metastasis-ablative radiotherapy is a new therapeutic approach that prolongs survival in patients with advanced cancers. Tumour irradiation can elicit an immunogenic cell death resulting in the expansion of tumour-reactive T cells and eradication of both irradiated and distant non-irradiated metastases, referred to as the “abscopal effect”. This abscopal response, nevertheless, is observed in a minority of patients suggesting uncharacterized mechanisms that prevent robust systemic anti-tumor immune response. Tumour-derived extracellular vesicles (TdEVs) have recently emerged as mediators of antitumor immunity but their immunomodulatory role in response to radiotherapy remains largely unknown. Recent clinical studies by our lab have demonstrated that circulating levels of tumour-derived extracellular vesicles (tdEVs) are elevated in response to radiotherapy and high tdEV concentrations are associated with reduced levels of peripheral cytotoxic CD8+ T cells and higher risk of disease recurrence in advanced prostate cancer. Based on our findings, we hypothesize that radiotherapy induces the release of tumor-derived EVs that suppress anti-tumor immunity. Prostate cancer cells (PC3 and DU145) were irradiated with clinically used doses of ionizing radiation (20Gy x 1 or 10Gy x 3 fractions) and tdEVs were co-cultured with human CD8+ T cells to measure their proliferation and cytotoxic activity. Increased levels of tdEVs were released by tumour cells treated with radiotherapy. A higher frequency of impaired T cell cytotoxic activity and a reduction in CD8 T cell proliferation was found in the 10Gy x 3 radiation regimen. Proteomic analysis and western blot showed an increased expression of the immune checkpoint molecule B7-H3 on the tumour cell surface and tdEVs in response to radiotherapy. While coculture of CD8 T cells with B7-H3 depleted tdEVs led to recovery of T-cell cytotoxic ability, overexpression of the B7-H3 in tdEVs inhibited cytotoxic activity. This study provides a rationale for future studies in which we will test the immune-mediated effects of radiotherapy-induced tdEVs in immunocompetent mouse models and investigate B7-H3 blockade as a therapeutic approach to boost abscopal response in the treatment of advanced prostate cancer.

#4996 Analysis of the effect of eribulin on tumor immunity against triple-negative breast cancer.

S. Tadafumi, T. Oba, K.-i. Ito;
Division of Breast and Endocrine Surgery, Department of Surgery, Shinshu University School of Medicine, Matsumoto, Japan

Purpose: Chemotherapeutic agents may induce immunomodulatory effects on immune cells and cancer cells in patients with triple negative breast cancer (TNBC). Recent studies have demonstrated that absolute lymphocyte count in peripheral blood can predict response to eribulin in patients with breast cancer, suggesting that eribulin have some favorable effects on immune cells. However, there have been no reports demonstrating the mechanisms of how eribulin affects the immune cells of patients with breast cancer. This study aimed to analyze the effect of eribulin on T cells *in vitro* and *in vivo*.

Materials & Methods: Using human peripheral blood mononuclear cells (PBMCs) from healthy donors and patients with TNBC, we investigated the effects of eribulin on proliferation of these cells, changes in the expression of surface markers, and antitumor effects on TNBC cells. Three TNBC cell lines (MDA-MB-231, Hs578T, MDA-MB-157) were used in this study. Human PBMCs were activated by CD3/CD28 stimulation *in vitro* for six days and analyzed for T-cell surface markers by flow cytometry. For three patients with TNBC who underwent eribulin treatment, blood was collected at baseline and on days 8, 22, and 64 after treatment, and PBMCs were isolated, and analyzed by flow cytometry.

Results: The proliferation of activated $CD8^+$ T cells from healthy donors and patients was facilitated when cultured with 1nM of eribulin compared to the control. Moreover, eribulin significantly decreased CD4/8 ratio in T cells ($p< 0.05$). In PBMCs from healthy donors, the frequency of $CD45RA^+$ $CD45RO^-$ cells and $CCR7^+$ cells in $CD8^+$ T cells was significantly increased by eribulin treatment ($p< 0.05$). Furthermore, eribulin significantly increased $CD127^+$ $KLRG1^-$ cells (memory precursor effector cells) and $TCF1^+$ cells in $CD8^+$ T cells ($p< 0.01$). Furthermore, the anti-tumor effect of activated T cells from PBMCs of healthy donors and patients with TNBC was enhanced when cultured with eribulin in all three TNBC cell lines compared to control, and $IFN\gamma^+$ $CD8^+$ T cells were significantly increased by eribulin treatment ($p< 0.05$). However, in TNBC patients treated with eribulin in clinical practice, there were no significant changes in the CD4/8 ratio, the frequency of $CD45RA^+$ cells or $CCR7^+$ cells in $CD8^+$ T cells before and after treatment of eribulin.

Conclusions: Our findings suggest that eribulin can facilitate the proliferation of $CD8^+$ T cells and potentiates T cell-mediated anti-tumor activity against triple-negative breast cancer cells *in vitro*. Further analysis of the effects of eribulin on TNBC cells and immune cells *in vivo* is required, and we continue to analyze immunomodulation in patients treated with eribulin.

#4997 Auranofin enhances the efficacy of anti-PD1 immunotherapy.

Zichen Zhao[1], Shichuan Hu[2], **Yan Zhang**[1]

[1]Lung Cancer Center, West China Hospital, West China School of Medicine, Sichuan University, Chengdu, China,[2]State Key Laboratory of Biotherapy, West China Hospital, West China School of Medicine, Sichuan Univeristy, Chengdu, China

Anti-PD-1 immunotherapy brings hope for the treatment of malignant tumors, but its overall response rate is low. Therefore, how to sensitize anti-PD-1 therapy to make more patients benefit from immunotherapy is an urgent clinical demand. PKCι, a classical oncogene that affects cell proliferation and differentiation, has recently been found to be involved in the recruitment of immunosuppressive cells MDSCs and Tregs, which leads to anti-PD1 immunotherapy resistance. Our study is consistent with previously reported results that interfering with PKCι expression in tumor cells significantly enhances the anti-tumor effect of anti-PD1 therapy. Immunological mechanistic analyses demonstrated that the inhibition of PKCι expression significantly reduced the infiltration of tumor-associated macrophages (TAMs) rather than MDSCs or Tregs. Further studies revealed that PKCι enhanced the expression of macrophage chemokine CCL7 by promoting the formation of the YAP1/TEAD transcriptional complex. Interference in vitro and pharmacological inhibition of PKCι in tumor cells both significantly reduced CCL7 expression and TAMs invasion. Auranofin is a commonly used anti-inflammatory agent in clinical practice, which has been recently found that it directly induces tumor death by modulating the cellular redox system in tumor cells and remodels the tumor immunosuppressive microenvironment by specifically inhibiting PKCι expression. The results of our study showed that the anti-tumor effect of Auranofin combined with anti-PD1 therapy was superior to that of monotherapy in lung adenocarcinoma. Auranofin exerted synergistic anti-tumor effects with anti-PD1 immunotherapy by inhibiting the expression of PKCι-YAP1/TEAD-CCL7, reducing the recruitment of TAMs, and promoting the infiltration of effector CD8+ T cells. In summary, Auranofin is a potent candidate for sensitizing anti-PD-1 immunotherapy, reversing immunotherapy blunting by remodeling TIME, which provides new ideas and theoretical basis for immunotherapy of sensitizing malignant tumors.

#4998 Pralsetinib induces opportunistic infection in RET fusion-positive NSCLC patients via inhibition of IL-2 production by blocking Jak3-Stat5 activation.

S. Yoon[1], H.-M. Ryu[2], S.-W. Kim[1], **K.-S. Park**[1], D. Lee[1];

[1]Asan Medical Center (AMC), Seoul, Korea, Republic of, [2]University of Ulsan College of Medicine, Seoul, Korea, Republic of

Background: Oncogenic alteration in RET, representing 1-2% of non-small cell lung cancer (NSCLC), is one of the important targets. Pralsetinib is a selective RET inhibitor that targets RET fusions. We present a case series on opportunistic infections and the mechanism of immunosuppression.
Methods: From October 2021 to March 2022, we administered pralsetinib to a total of 15 patients with NSCLC harboring RET fusion. We retrospectively analyzed the clinical efficacy and adverse event related to pralsetinib. To investigate the potential impact of pralsetinib on T-cells, we examined cytokine release from Jurkat T (JT) cells after pralsetinib treatment. To test if Stat5 bind to IL-2 promotor, we conducted Chromatin Immunoprecipitation (ChIP).
Results: Out of a total of 18 patients with measurable disease, 14 patients (93%) achieved a partial response. With the median follow-up duration of 8.7 months, four cases of opportunistic infections were occurred. Notably, three patients (16.6%) experienced invasive pulmonary aspergillosis, and one patient (5.5%) experienced cytomegalovirus pneumonia. To mimic conditions akin to activated T cells, we treated JT cells with PMA and ionomycin, inducing IL-2 release through the binding of NFAT, AP-1, and NF-κB to the IL-2 promoter. Following approximately two weeks of pralsetinib treatment, a decrease of IL-2 releases, the inhibition of Jak3 and the reduced-expression of JunB and c-Jun was observed. Additionally, to investigate the direct correlation between Jak3 and IL-2 release, JT cells were treated with ritlecitinib, the Jak3-selective inhibitor, for approximately two weeks. Like pralsetinib, a reduction in IL-2 release was observed. Furthermore, based on the evidence that Stat5 inhibition leads to reduced IL-2 release, we also showed that the transcription factor Stat5, a direct downstream signaling component of Jak3, binds to the IL-2 promoter during the activation of Jurkat T cells.
Conclusion: Pralsetinib inhibits additional IL-2 production by blocking Jak3/Stat5 activation triggered by IL-2 released during early T cell activation. As a result, the Jak3 inhibition induced by pralsetinib leads to a decrease in JunB/c-Jun expression and blocking Stat5 activation by reducing IL-2 release. Consequently, Pralsetinib-related opportunistic infections may be caused by inhibition of the JAK3 pathway and IL-2 release.

#5000 Low dose ionizing radiation elicits the extrusion of neutrophil extracellular traps.

Alvaro Teijeira, Ana Martinez-Riano, Beatrice Pinci, Almudena Manzanal, Paula Molero, Maria E. Rodriguez- Ruiz, Ignacio Melero

Center for Applied Medical Research (CIMA), Pamplona, Spain

The majority of cancer patients undergo radiotherapy interventions at some point in their clinical management with unintended irradiation of blood vessels. We show that very low γ-irradiation doses (0.5-1 Gy) of human and mouse neutrophils elicit neutrophil extracellular trap (NET) formation in a manner dependent on oxidative stress, NADPH oxidase activity and autocrine interleukin-8. Radiation-induced NETs interfere with NK- and T-cell cytotoxicity-repelling effector lymphocytes away from tumor cells. As a consequence, pre-injection of irradiation-induced NETs increases the number of successful metastases in mouse tumor models. Increases in circulating NETs are readily detected in series of patients following radiotherapy interventions. Our results reveal new mechanisms whose knowledge may help to improve the efficacy and safety of radiotherapy, especially when used in combination with immunotherapy approaches.

#5001 Personalized neoantigen/cancer-testis antigen nanovaccine for advanced solid tumors, a single-arm, open-label pilot study.

J. Wei, Q. Liu, L. Zhu, J. Shao, J. Yang, G. Xu, N. Wu, H. Wang, R. Li, H. Sha, Q. Xu, J. Shen, L. Xie, L. Wang, J. Du, L. Cen, M. Tian, L. Yu, B. Liu; Department of Oncology, Nanjing Drum Tower Hospital, Affiliated Hospital of Medical School, Nanjing University, Nanjing, China

Background: Neoantigens, derived from somatic mutations in tumor cells, have been identified as promising targets of immunotherapy. A personalized neoantigen/cancer-testis antigen (CTA) nanovaccine (PNVAC) platform has been established by us previously, and demonstrated its feasibility, safety and efficacy in preventing recurrence of high-risk resected gastric/gastroesophageal junction (G/GEJ) cancer in both preclinical and clinical studies. This study aims to explore the universality of PNVAC monotherapy or combined with anti-angiogenesis drugs or anti-programmed death 1 (PD-1) in patients with multiple advanced solid malignancies.

Methods: Patient-specific neoantigens were selected based on tumor-specific mutations identified by whole-exome sequencing (WES) and RNA sequencing of paired blood and tumor tissues. Bioinformatic analysis for neoantigen prediction, including sequencing read filtering, human leukocyte antigen (HLA) typing and neoantigen filtering was performed. PNVAC is an amphiphiles nanovaccine loaded with multiple personalized neoantigens designed to induce specific T cell responses. PNVAC is administrated to patients with metastatic solid tumors on days 1, 4, 8, 15, 22, 43 (prime phase) and 64, 85 and 169 (boost phase) alone, or combined with anti-angiogenesis or anti-PD-1 drugs. Safety, immunogenicity and clinical efficacy are evaluated.

Results: Of the 30 enrolled patients, no treatment-related severe adverse events (AEs) occurred and the vast majority of AEs were limited to grade 1-2, only 1 patient developed grade 3 thrombocytopenia. The objective response rate (ORR) was 26.7% (8/30), including 2 cases of complete response (CR) and 6 cases of partial response (PR), and a disease control rate (DCR) of 66.7% achieved. The median progression-free survival (PFS) was 9.90 months (95% CI, 3.46-16.34 months), while the median overall survival (OS) was not reached (range, 0.80-43.53 months), and the estimated 1- and 2-year survival rates were 86.2% and 60.6%. Notably, among the 21 patients who had relapsed disease after previous ICB and/or anti-angiogenesis, disease control was asserted in 14 (66.7%) of them (7 of SD, 5 of PR, 2 of CR). ORR of this set was 33.3% (7/21), higher than that of all the enrolled patients (26.7%), and the set without prior ICB and/ or anti-angiogenesis treatment (11.1%). For immune analysis, PNVAC elicited robust and persistent immune responses against neoantigens/CTAs. Additionally, peripheral T cells with a cytotoxic phenotype tended to increase after vaccination, and immune memory was also detected in some representative patients.

Conclusions: These data supported the safety, immunogenicity, and efficacy of this regimen in patients with advanced solid malignancies, thus broadening the application and combined strategies of neoantigen-based vaccines. Clinical trial information: ChiCTR1800017319.

#5002 Next-generation mRNA-LNP vaccine prototype achieves tumor clearance in a GBM mouse model.

R. Nechanitzky[1], S. Snelling[2], K. Ellestad[2], X. Lun[2], K. Olsen[1], Y. Wu[1], Y. Karpov[1], J. Liu[1], M. Gold[1], H. Menon[1], R. Krishnan[1], R. Georgantas[1], P. S. Ohashi[3], D. J. Mahoney[2], J. A. Chan[2], N. Martin-Orozco[1];

[1]Providence Therapeutics Inc, Calgary, AB, Canada, [2]University of Calgary, Calgary, AB, Canada, [3]Princess Margaret Cancer Centre, Toronto, ON, Canada

Glioblastoma (GBM) is the most prevalent and aggressive primary brain tumor type with an abysmal prognosis, featuring an immunologically dampened tumor microenvironment and limited neoantigen production. Novel therapeutic strategies are urgently needed. A well-characterized GBM-associated mutation that can elicit an anti-tumor immune response is EGFRvIII mutation. The cancer-driver mutation is detected in approximately 30% of patients at the time of diagnosis and plays a pivotal role in the emergence of GBM. EGFRvIII is an in-frame epidermal growth factor receptor (EGFR) deletion generating a constitutively active oncogenic protein. Its highly immunogenic nature represents an ideal focal point for cutting-edge mRNA-LNP candidate therapeutics. To evaluate proprietary lipid nanoparticle (LNP) compositions for their capacity to induce anti-GBM immunity, we developed a murine transplantable GBM tumor model by neonatal electroporation. The somatically engineered glioblastomas harbor two targeted CRISPR knockouts and stably overexpress EGFRvIII to yield transplantable cell lines for orthotopic tumor initiation. One week after intracranial tumor cell implantation of 6-8 week-old female mice (day 0; n=10), half the animals were administered either buffer (control cohort) or our novel anti-EGFRvIII mRNA-LNP vaccine (experimental cohort). The regimen involved four intramuscular injections before monitoring tumor progression by MRI on day 30. The imaging revealed a high tumor burden in all control group animals, compared to no detectable tumor cells in vaccine-protected mice. All control group animals were humanely euthanized by day 38 due to symptoms associated with the growing brain tumor mass. The asymptomatic experimental animals received a fifth anti-EGFRvIII vaccination before MRI-based examinations on day 43 and day 78 confirmed that no tumor cells could be detected in vaccine-protected mice. The results highlight the potency and potential of our proprietary anti-EGFRvIII mRNA-LNP vaccine as a novel anticancer therapeutic. In addition, the established tumor model represents a valuable tool to test future mRNA-LNP designs. Outstanding cellular and molecular investigations will reveal vaccine-mediated mechanistic insights, allowing for the co-advancement of the tumor model and next-generation multi-target mRNA-LNP vaccine candidates.

#5003 Efficacy of the STC-1010 a new allogenic cancer vaccine in different colorectal cancer models.

G. Alzeeb[1], C. Gongora[2], C. Richard[3], R. Boidot[3], T. Fortin[4], Y. Wang[5], A. Bessede[6], B. Pinteur[1], L. Chalus[1], C. Tortorelli[1], P. Bravetti[1], F. Ghiringhelli[7]; [1]Brenus Pharma, Lyon, France, [2]INSERM U1194, Montpellier, France, [3]CNRS 6302, Dijon, France, [4]Anaquant, Lyon, France, [5]Inovotion, La Tronche, France, [6]Explicyte, Bordeaux, France, [7]Inserm 1231, Dijon, France

Colorectal cancer (CRC) is the 2nd cause of cancer-related death worldwide. Recent tremendous progress has installed immunotherapy as a treatment option and opened multiple ways to address therapeutic challenges for CRC patients. Accordingly, Brenus-Pharma developed a therapeutic cancer vaccine, based on stimulating tumor cells (STC) technology with physical (irradiation and heat shock) or chemical (chemotherapy) stress, coupled to haptenization making vaccine more immunogenic. We first validated STC technology using a “one cell line” mouse surrogate vaccine in CT26 mouse model showed an efficacy of the combination of stress plus haptenization. We next prepared a mouse surrogate vaccine using three murine tumoral cell lines the mSTC-1010 (CT26, CMT93 and LTPA), and confirmed the value of using 3 cell lines to increase the antigenicity. In addition, mSTC-1010 associated with immunostimulant (cyclophosphamide and mGM-CSF), combined or not with chemotherapy (FOLFOX or FOLFIRI) led to a significant decrease of tumor volume, a M1-oriented macrophage response (immunohistochemical, iNOS/CD163 >1), and an increase of T lymphocyte infiltration. Following, we confirmed these proofs-of-concept with the human vaccine, STC-1010, composed of 6 drug substances (DS) derived from 3 CRC human cell lines (HCT116, HT29 and Lovo), stressed physically or chemically and then haptenized. Transcriptomic analysis showed the induction of stress-related pathways with a certain specificity for each DS, allowing their quantification in the STC-1010 by deconvolution strategy. Moreover, proteomic analysis showed specific protein expression modification of each DS and confirmed the rationale of using 3 cell lines with 2 stresses to cover the CRC heterogeneity. More than 200 cancer-related proteins from the Atlas proteins’ database were identified in theSTC-1010 including CRC-specific proteins, tumor plasticity and tumor-associated antigens. In ex vivo model, the efficacy of the vaccine was shown, through that CD8+ T cells primed by the STC-1010 treated DCs (versus control), induced massive apoptosis of cancer cells ($p<0,001$). In chicken embryo Chorio-Allantoid Membrane (CAM) model, STC-1010 significantly increased IL-12, IL-2 and IFN-gamma expression (versus control $p<0.02$). Results from this immune reactive model showed a significant increase of tumor necrosis ($p=0,0267$), metastasis regression (-49%), and increased infiltration of CD4+, CD8+ (versus control). The good tolerability and reproducible efficiency of the STC-1010 vaccine in these different clinical models allow to plan a first-in-human phase I/II clinical trial for metastatic CRC(mCRC) patients. A dose-escalation and cohort extension phase I followed by a phase IIa with STC-1010 plus immunostimulant, associated to mFOLFOX6 w/o bevacizumab, will be performed for MSS mCRC patients to evaluate the safety and preliminary effectiveness in human.

#5004 Oncolytic Jurona-driven systemic and intratumoral immunotherapy combined with immune checkpoint blockade boost immune response and survival in hepatocellular carcinoma models.

M. Z. Tesfay, K. U. Ferdous, A. Cios, R. S. Shelton, C. C. Simoes, S. R. Post, T. J. Kelly, M. J. Cannon, A. Basnakian, B. M. Nagalo;
University of Arkansas for Medical Sciences, Little Rock, AR

The members of the vesiculovirus genus have recently become attractive immunotherapeutic agents due to their natural selectivity for tumors and lack of toxicity in humans. Here, the research shows Intratumoral (IT) or Intraperitoneal (IP) injection of JURV was found to induce dynamic tumor regression in human hepatocellular carcinoma (HCC) xenografts and syngeneic models. Furthermore, IT injections of JURV were also shown to recruit and activate cytotoxic T lymphocytes and decrease tumor-associated macrophage infiltration, resulting in the delay of tumor growth in both local and distant murine HCC tumors established in a syngeneic model. Additionally, the concurrent use of JURV and anti-PD-1 antibodies was found to synergistically modulate the tumor microenvironment (TME) via increased tumor-infiltrating CD4+ T cells and depleted CD8+ PD-1+ and NK cells. Furthermore, using RIL-175, an aggressive metastatic HCC tumor mouse model, we show that intraperitoneal (IP) (systemic) administration of JURV and anti-PD1 significantly improved long-term survival (90%) compared to the (20%) JURV or anti-PD1 alone. Through proteogenomic analysis, the activation of different effectors of the immune system was observed to cooperate to alter the TME to a favorable anti-tumor immune state. These findings further support the development of JURV as an immunovirotherapy platform for HCC, with the potential to induce abscopal effects via the activation of several tumor suppressor genes and the mechanism regulating the T helper cell responses.

#5005 Safety and tolerability of multi-epitope HER2 peptide vaccines in combination with trastuzumab emtansine in HER2-positive breast cancer patients with residual disease after neoadjuvant chemotherapy.

S. Chumsri[1], S. Giri[2], A. J. Ness[2], D. W. Hillman[2], N. Norton[1], D. Cogen[1], B. M. Necela[1], A. Nassar[1], D. W. Northfelt[3], P. Advani[1], R. Rao[1], K. Sideras[1], A. Moreno-Aspitia[1], B. J. Ernst[3], K. J. Ruddy[2], M. P. Goetz[2], K. L. Knutson[1];

[1]Mayo Clinic Florida, Jacksonville, FL, [2]Mayo Clinic, Rochester, MN, [3]Mayo Clinic Arizona, Phoenix, AZ

Background: Residual disease after neoadjuvant chemotherapy (NAC) in breast cancer (BC) confers poor outcomes. Trastuzumab emtansine (T-DM1) is approved for HER2+ patients with residual disease after NAC. However, many patients still develop recurrence. H2NVAC is a multi-epitope CD4 helper T cell activating vaccine that includes a pool of 4 degenerate HER2-derived HLA-DR epitopes admixed with GM-CSF. Our previous phase I trial showed that this vaccine was safe and generated robust, long-lasting T and B cell immune responses.

Method: We conducted a safety run-in phase of H2NVAC in combination with T-DM1 in stage II-III HER2+ BC with residual disease after NAC. Patients were treated with H2NVAC and T-DM1 for 6 cycles, followed by 2 boosters at 3 and 12 months. Dose-limiting toxicity (DLT) was defined as any grade (G) ≥ 3 toxicity occurring within 21 days after the first vaccination.

Results: 20 patients were enrolled (median age 51; 27-69 years), including 80% White and 15% Black. 90% had hormone receptor-positive disease. There was no DLT observed in the safety run-in cohort. All adverse events (AEs) during the DLT period were grades 1 and 2, with fatigue being the most common (60% G1, 5% G2), followed by peripheral sensory neuropathy (55% G1, 5% G2), and injection site reaction (50% G1). Across all treatment cycles, the 10 most common AEs that were at least possibly related to treatment in all cycles are summarized in the table below. The injection site reaction was the most common AE, with 85% G1 and 15% G2.

Conclusion: H2NVAC, in combination with T-DM1, was safe, with a favorable side effect profile. There was no DLT observed. The most common AE was injection site reaction, with the majority being G1. A multicenter, randomized, placebo-controlled, phase II trial of H2NVAC vs. placebo in combination with trastuzumab emtansine is currently ongoing through the ACCRU consortium (NCT04197687).

Adverse Events	**Grades**			
1	**2**			
N	**%**	**N**	**%**	
Injection site reaction	17	85.0	3	15.0
Aspartate aminotransferase increase	13	65.0		
Alanine aminotransferase increase	9	45.0		
Fatigue	7	35.0	2	10.0
Peripheral sensory neuropathy	7	35.0	2	10.0
Alkaline phosphatase increase	8	40.0		
Nausea	7	35.0	1	5.0
Arthralgia	7	35.0		
Myalgia	5	25.0	1	5.0
Platelet count decrease	6	30.0		

#5006 Discovery of immunogenic neo-peptides from actionable RNA fusions for developing cancer vaccines.

S. Rankothgedera[1], M. Castillo[1], S. Thevasagayampillai[1], C. Woody[1], A. Kandasamy[1], A. Diaz III[2], M. Wick[2], P. Gunaratne[1];
[1]University of Houston, Houston, TX, [2]XenoSTART, San Antonio, TX

The global surge in cancer cases, with a staggering 20 million new instances reported in 2023 alone, underscores an urgent demand for advanced and reliable cancer therapeutics. Immunotherapies centered around neoantigens have emerged as a promising avenue for enhancing treatment efficacy and have become a focal point in cancer research. We hypothesize that the tumor cells present a rich neoantigenic repertoire and the immunogenic neoantigens arising from the junctions of proteins translated from chimeric RNAs present viable targets for peptide and mRNA vaccines, offering a promising approach to impede tumor progression. To validate our hypothesis, we acquired a dataset of RNA fusions detected through RNAseq of tissue extracted from patient-derived xenograft (PDX) models established by XenoSTART, a global non clinical oncology contract research organization. This comprehensive dataset encompassed 985 PDX models across 27 cancer types, revealing three fusions associated with the neuregulin-1 (NRG1) gene. NRG1 gene fusions have been identified as a clinically actionable target for multiple solid tumors as they result in ErbB-mediated pathway activation. CD74-NRG1 has emerged as the most frequently reported NRG1 fusion across many cancers such as pancreatic ductal adenocarcinoma, triple negative breast cancer and ovarian cancer. The CD74-NRG1 fusion was identified in two PDX models harboring lung cancer (ST2891 and ST3204) and in an ovarian cancer model (ST088). The lung cancer PDXs displayed a notable abundance of fusion junction-crossing reads. We generated the CD74 (Exon 1-6) -NRG1 (Exon 6-12) fusion transcript model, where the first 6 exons of CD74 fused to exon 6 of NRG1 leading to an in-frame fusion. Validation of this fusion in PDX tissue was accomplished through PCR and Sanger sequencing of the PCR product. We assessed the affinity of the 9-mer neo peptide sequences formed by the translated junction of CD74-NRG1 to Major Histocompatibility Complex (MHC) Class I molecules using the in-silico prediction pipelines MHCNuggets and MixMHCPred-2 and found HLA-A*68:23 to be the MHC allele with highest binding affinity. HLA-Arena was used to investigate the binding affinity between the peptides and the MHC molecules via molecular docking, which revealed 4 peptides to be strong binders to HLA-A*68:23.The immunogenicity of these neoantigenic peptides to HLA-A*68:23 matched Peripheral Blood Mononuclear Cells (PBMCs) will be assessed by the IFN-γ Enzyme Linked Immunosorbent Spot (ELISpot) assay. To elucidate the specific T-cell clonotypes responding to the neo peptides, the 10X Genomics single-cell 5’ Gene Expression Assay, coupled with T Cell Receptor mapping, will be employed. The objective of the study is to establish a robust combinatorial therapeutic strategy leveraging peptide and mRNA vaccine technology to support an effective framework for personalized cancer treatment.

#5007 *Ex vivo* evaluation of mRNA lipid nanoparticle cancer vaccines.

Tommy Lidstrom, Mara Blanco Arauzo, Nickolas Karlowatz, Mikael Johansson, Mattias Forsell, Jonas Nilsson

Radiation sciences/Oncology, Umea University, Umea, Sweden

Lipid nanoparticle vaccines have recently been developed broadly against pathogens and recently, in precision medicine targeting mutations in different tumors. Evaluating vaccine candidates typically require animal models using orthotopic or allogenic transplantations to evaluate efficiency. Evaluating vaccine efficacy using ex vivo systems is faster and less technically demanding. Here we aim to develop individualized cancer vaccines based on neoantigen identified within established human organoids or directly from patient tissue. The selected neoantigens are enriched for epitopes identified on gene fusions. Identified gene fusions encoding predicted immunogenic proteins are inserted into a vaccine backbone and used to make mRNA lipid nanoparticle vaccines. The neoantigen candidates are then evaluated in a personalized ex vivo testbed. Within the *ex vivo* testbed personal tumor neoantigens are tested on the patients own isolated CD8+ T cells and monocytes. Monocytes are *in vitro* differentiated into monocyte derived dendritic cells (moDCs), which specialize in antigen cross presentation. The moDCs are inoculated with mRNA lipid nanoparticle vaccines or loaded with peptides. The moDCs are then co-cultured with syngeneic T cells. Vaccine candidates are evaluated based on CD8+ T cell activation and cytotoxicity in the co-culture ex vivo testbed. Our pipeline offers a fast and efficient means of evaluating individualized vaccine candidates. Effective vaccines developed through this process can be administered as a standalone therapy or in combination with checkpoint inhibitors, to generate a strong durable immune response against a variety of solid tumor types.

#5009 Deciphering anticancer mechanisms of oncolytic virus-loaded stem cells.

M. Hammad[1], A. Seth[1], Y.-C. Yuan[1], H. Ngai[1], R. Mooney[1], J. Lara[1], Y. Kang[2], I. Minev[2], D. Nguyen[2], B. Minev[2], A. Santidrian[2], K. Aboody[1];
[1]City of Hope National Medical Center, Duarte, CA, [2]Calidi Biotherapeutics, San Diego, CA

Background: Oncolytic viruses (OVs) selectively trap, replicate, and eradicate tumor cells without endangering healthy cells. However, any virus that enters the body will be found and rendered inactive by our immune system. Therefore, cancer-killing viruses don't function properly when given by themselves. Loading therapeutic viruses into stem cells is a promising solution since they shield the OVs from the immune system until they reach tumor cells and eventually destroy them. Stem cells are potent immunomodulators and, apart from protecting and delivering the cancer-killing viruses may release additional cell factors that may regulate tumor microenvironment favoring the effect of the therapy. In this study, we analyze these factors secreted by clinically relevant stem cells loaded with oncolytic viruses CLD-101 (Neuronova platform) and CLD-201 (Supernova platform)
Method: In our studies, we loaded neural stem cell line (NSCs) with tumor-selective oncolytic adenovirus CRAD-s-PK7 (CLD-101) and adipose-derived stem cells (AD-MSC) with tumor-selective oncolytic adenovirus vaccinia virus CAL1 (CLD-201), and studied their secretome transcriptomic and proteomic profile.
Results: The transcriptomic analysis demonstrated that immunomodulatory cytokines, chemokines, and their receptors are induced after three and twenty-four hours of OV infection. The proteomic analysis of the virus-loaded stem cells revealed a notable distinction from the naive stem cells indicating a potential immunotherapeutic role of the stem cells in addition to the delivery and protection of the OVs.
Conclusions: Our findings suggest that the enhanced therapeutic efficacy of stem cells loaded with OV is, at least partially because of qualitative and quantitative alterations in stem cells' secretome (including immunostimulatory cytokines and chemokines), These findings advance our knowledge of the molecular mechanisms underlying the immunostimulatory role of OV-loaded stem cells and specifically help to understand the mechanism of action of the promising clinical immunotherapies CLD-101 and CLD-201.

#5010 Development of a universal cancer vaccine using common cancer antigens cocktail that targets various cancer patients and overcomes the heterogeneity of individual cancer.

T. Nakatsura, K. Takenouchi, H. Kinoshita, N. Tsukamoto, K. Ohnuki, T. Suzuki;
National Cancer Center, Kashiwa, Japan

In clinical trials of the glypican-3 (GPC3)-derived peptide vaccine targeting hepatocellular carcinoma (HCC), hepatoblastoma, etc., peptide-specific CTL were detected in many patients. There have been some partial response advanced cancer cases, and it is expected to be effective in prolonging the prognosis after HCC surgery. Five children with refractory hepatoblastoma who had repeated relapses and remissions are all surviving for more than 9 years without relapse by only peptide vaccine therapy. On the other hand, several patients have experienced recurrence of hepatocellular carcinoma that does not express GPC3 despite the detection of a large number of peptide-specific CTLs in the blood after administration of peptide vaccines. GPC3 is highly expressed in many hepatocellular carcinomas, but there are GPC3-negative cancer cells, so it is difficult to prevent recurrence of hepatocellular carcinoma with a single type of GPC3 peptide vaccine. In other words, to cure cancer, it is necessary to combine multiple common cancer antigens. Through immunohistochemical analysis, we identified 10 common cancer antigens, including GPC3, that are frequently expressed in various solid cancers but rarely expressed in normal tissues. Five of these antigens are membrane protein antigens, and we have confirmed that at least one of these antigens, and often more than one, is expressed in many cancers investigated. We synthesized peptides predicted to be presented at HLA-A*24:02 or HLA-A*02:01 from the full-length amino acid sequences of 10 types of common cancer antigen proteins. These peptide vaccines were administered to HLA-A*24:02 or HLA-A*02:01 transgenic mice once a week for a total of three times, and a number of peptide-reactive CTLs were identified in the splenocytes. These peptides have better CTL-inducing ability than the peptides of the GPC3 peptide vaccine used in clinical trials. Among these 10 types of common cancer antigens, we will use 5 types of membrane protein common cancer antigens in particular to develop a cocktail mRNA vaccine with the goal of preventing cancer recurrence after surgery. Of course, it is also possible to develop cocktail peptide vaccines. At the same time, we are developing a cocktail CAR/TCR-T cell therapy targeting these common cancer antigens for the treatment of advanced cancer.

CLINICAL RESEARCH: Circulating Nucleic Acids 4
Poster Session

#5014 Analytical validation of a complete system for detection and characterization of genomic aberrations in circulating tumor DNA.

E. Stamper[1], W. Shen[1], A. Pruthi[1], C. Nagel[1], M. Piechota[2], K. Tomala[2], Q. Wei[1], D. Willoughby[1];
[1]Frontage Laboratories, Inc., Deerfield Beach, FL, [2]Intelliseq, Inc., Krakow, Poland

Cell-free DNA (cfDNA) fragments are readily detected at a low concentration in the human blood stream. In healthy patients cfDNA is primarily derived from apoptosis of hematopoietic cells. In cancer patients circulating DNA derived from tumor cells (ctDNA) undergoing apoptosis, shedding, and necrosis contribute to total cfDNA. Next generation sequencing (NGS) of cfDNA isolated from patient plasma can be used to fully characterize cancer driven changes in the tumor DNA including the relative contribution of cfDNA, single nucleotide variants (SNVs), small insertions and deletions (Indels), larger deletions, regions of amplified DNA, and structural rearrangements.

Frontage has developed a complete lab system for analysis of circulating cfDNA including automated sample extraction, preparation and sequencing of libraries targeting exon sequences of 293 oncology-related genes, and a bioinformatic reporting system. The Frontage sample extraction process uses a post-extraction size selection step to remove high molecular weight DNA derived from lysed blood cells in the plasma sample to increase the sensitivity of detection of ctDNA. The NGS platform couples hybridization-based selection of genomic DNA fragments derived from protein-coding exons with deep sequencing to ~4,000X gross coverage on the NextSeq 2000. The bioinformatic pipeline integrates unique molecular barcode-based generation of consensus reads for each template molecule, somatic variant calling with GATK Mutect2 and FreeBayes, and removal of false positive variants by comparison to a 60 samples healthy patient data set.

Analytical validation was performed for each component of the system. For verification of the sample extraction process, cfDNA was extracted in duplicate from four lots of pooled K2 EDTA plasma of healthy patients as well as individual K2 EDTA plasma of colorectal cancer (CRC) patients in four independent extraction runs. The mean yields of cfDNA from healthy samples ranged from 2.3 - 4.2 nanograms per ml plasma and all 32 of the isolated cfDNA aliquots from healthy patient plasma showed a prominent peak around 167 nt with minimal contamination from high molecular weight DNA. For validation of the NGS and bioinformatics platform a set of 8 different reference cfDNAs were processed through four independent runs of library preparation, sequencing, and analysis. For each of the validation runs, greater than 97% of 208 SNVs and Indels with expected allele frequencies (AF) between 2-3% were detected by the platform with higher levels of accuracy for variants at above 3% AF. Two or less false positive variants per run were detected out of 278,000 nucleotides of verified non-mutated sequence that overlapped with the 293 gene panel. Four known DNA amplification events were detected in each of the validation runs. Data from characterization of CRC and other clinical samples with the system will be presented.

#5015 Genomic profiling of colorectal cancer - insights from liquid biopsy comparisons between U.S. and China cohorts.

H. Tang[1], C. Jia[1], F. Xie[1], Y. Zhang[1], X. Dong[2], Y. Huang[2], S. Jia[2];

[1]Huidu (Shanghai) Medical Sciences, Ltd., Fengxian District, Shanghai, China, [2]Predicine, Inc., Hayward, CA

Background: Molecular characteristics play a pivotal role in cancer diagnosis, treatment selection, and disease monitoring across various tumor types. While previous research has elucidated the molecular classification of colorectal cancer using tissue NGS, limited investigation has explored the molecular profile of colorectal cancer through liquid biopsy, especially across diverse human races. This study presents a comprehensive genomic profiling analysis of colorectal cancer patients, using a globally harmonized liquid biopsy assay to compare patient cohorts from both the U.S. and China.

Methods: The prospective study is part of Predicine's Phoenix Program, a global molecular biomarker screening initiative across multiple solid tumors. At present, the study has enrolled 57 patients in the U.S. and 62 patients in China, all presenting with advanced colorectal cancer. A 10ml blood sample was collected from each patient and tested using PredicineCARE, an NGS-based liquid biopsy assay, to profile somatic mutations, copy number variations, and gene fusions among these patients.

Results: The assay, validated in both the U.S. and China using the same reference materials, achieved a LOD of 0.25% mutation allele frequency, with a positive predictive value exceeding 99%. Subsequently, the assay was applied to profile molecular aberrations in colorectal patients in both the U.S. and China. Among U.S. patients, the most commonly altered genes were APC (60%), KRAS (56%), TP53 (54%), MYC (25%), PIK3CA (16%), and EGFR (14%). In Chinese patients, the predominant altered genes were TP53 (48%), APC (42%), KRAS (32%), GNAS (21%), EGFR (16%), and PIK3CA (11%). The prevalence of GNAS variations was significantly higher in China than in the U.S. ($p < 0.05$), while the prevalence of APC ($p < 0.05$), KRAS ($p < 0.01$), and MYC ($p < 0.001$) variations was significantly higher in the U.S. than in China.

Conclusions: This study reveals the extensive mutational landscape in advanced colorectal cancer patients through liquid biopsy. Distinct prevalence patterns in certain genes between the U.S. and China cohorts offer novel biomarkers for clinical diagnosis and provide insights for targeted therapy mechanism studies.

#5016 Building better contrived samples to properly evaluate Next-generation MRD and LBx assays.

P. Labrousse[1], H. Russell[1], D. Shera[1], D. Stetson[1], B. Nuttall[1], B. Dougherty[1], D. Hodgson[2], J. Hadfield[2];
[1]AstraZeneca R&D Boston, Waltham, MA, [2]AstraZeneca R&D, Cambridge Biomedical Campus, United Kingdom

Circulating tumor DNA (ctDNA) is a component of cell-free DNA (cfDNA) that originates from tumor tissue in the plasma of cancer patients. Although ctDNA is a broadly applicable tumor biomarker, the absolute amount of ctDNA varies across indication and stage, with the level of ctDNA present reflective of tumor volume. As novel methods for the characterization of ctDNA develop, there is need to evaluate these assays with appropriate samples. But current commercial reference standards, generated from modified cell lines or oligonucleotides lack important features such as DNA methylation, fragmentation pattern and nucleosome positioning, whilst clinical trial samples lack the required volume to perform multiple tests and often lack proper consent. We have created a framework for generating contrived samples containing the biological features of clinical samples and the attributes of a reference standard. The *plasma-in-plasma* contrived samples are generated from commercially purchased and fully consented matched tumor and plasma from cancer patients with age and gender matched healthy donor plasma. Samples are characterized by an internally validated 700 gene NGS panel to identify somatic variants and copy number alterations, which establishes 'ground truth'. A contrived plasma dilution range based on the mean variant allele frequency (VAF) of the concordant somatic variants identified is generated. Using these methods, we have been able to generate sample sets for pan-cancer and disease specific evaluations. We have tested these samples through many novel high sensitivity assays that utilize both tumor-informed and tumor agnostic methods. We have confirmed that *plasma-in-plasma* contrived samples are amenable to all evaluated assays to date. The FFPE tumor tissue provide results matching clinical trial samples and the extraction yields of cfDNA are within the range of plasma samples from clinical trial data. Each dilution can be generated with replicates for reproducibility metrics. Current models of the sample dilutions have been generated to increase the number of replicates at relevant levels of tumor burden (i.e., 0.01% VAF). Negative samples consisting of the background plasma were also generated for each sample used. These *plasma-in-plasma* contrived samples have greater commutability to clinical samples than other commercial reference standards, however there are limitations. The complexity of generating these samples restrict the number of unique patients that can be utilized. Also, due to the volume of healthy plasma used as diluent, it is difficult to generate volumes greater than 4ml. To our knowledge, this is the first report examining the generation and usage of a contrived sample set that can be applied to evaluating novel high sensitivity MRD assays with clinical sample commutability.

#5017 Analytical performance of contrived samples for validation of liquid biopsy assays.

A. E. Harvey[1], C. K. Maddox[1], S. O. Dillon[1], O. T. Khawar[1], E. L. Verner[1], A. Greer[1], K. C. Valkenburg[1], B. J. Caveney[2], S. Ramkissoon[2];
[1]Labcorp, Baltimore, MD, [2]Labcorp, Durham, NC

Introduction: Cell-free DNA (cfDNA) extracted from plasma is critical for the analytical validation of liquid biopsy assays. cfDNA is comprised of genetic material from tumor and non-tumor cells, which can be highly variable across tumor types and disease stage. Relative to tumor tissue, cfDNA yield is lower and may not always capture all clinically relevant variants (e.g. gene fusions). Supplementing analytical validation studies with contrived samples prepared from cell line derived DNA to mimic the features of cfDNA allows for more robust testing of rare variants in clinical samples. To determine the commutability of contrived sample DNA to clinical plasma sample cfDNA, a retrospective analysis of sensitivity studies using two methods of contrived sample preparation was performed.
Methods: The PGDx elio Plasma Focus assay was used to compare sample base size post library preparation and limit of detection (LoD) of clinically relevant variants. Both methods used fragmented cell line DNA with a variant of interest and for method #1, cell line DNA was spiked into noncancerous donor plasma, which was then extracted resulting in a cfDNA and cell line DNA mixture. This contrived sample was diluted using wild-type (WT) DNA extracted from noncancerous donor plasma to obtain a target variant allele frequency (VAF). Method #2 used fragmented cell line DNA diluted with fragmented WT cell line DNA to obtain a target VAF. This retrospective data analysis will include a minimum of 28 samples run in replicate (3-20) across multiple studies.
Results: Data obtained from a DNA fragment analyzer post library preparation show similarities between fragmented cell line DNA spiked into plasma, fragmented cell line DNA, and clinical plasma cfDNA, with fragment peaks ranging from 290-320 base pair (bp). The median LoDs across the three sample types (n=28) were also similar for single nucleotide variants (SNVs) at VAFs of 0.70%, 0.76%, 0.72%, indels at VAFs of 0.70%, 1.0%, 0.78%, amplifications at folds of 1.4, 1.3, 1.5, and translocations at fusion read fractions of 0.5%, 0.61%, 0.55%. When comparing the same variants in a contrived sample functional characterization study, the call rates of various dilution levels were similar. A Fisher's Exact Test of the Hit Rate showed no significant difference for *KRAS G12V* SNV, *ERBB2* amplification, and *RET* translocation between cell line DNA and clinical cfDNA.
Conclusions: This data demonstrates that contrived samples perform with general equivalence to and may be an appropriate substitute for clinical plasma samples, though certain DNA sources may influence overall performance. Overall, fragmented cell line DNA spiked into plasma and fragmented cell line DNA diluted with WT fragmented cell line DNA performed similarly to clinical cfDNA samples representative of the intended use population.

#5018 Evaluation of whole blood fractionation conditions for optimal liquid biopsy NGS applications.

M. JASTI, S. Hernandez, N. Siepert, L. Kodandaramaswamy, T. Jayaweera, J. Schageman, A. Cheng, S. Lopez, M. Chen;
Thermo Fisher Scientific, Austin, TX

"For research use only. Not for diagnostic procedures."

Introduction: Liquid biopsy is a non-invasive alternative to tissue biopsies for cancer profiling using cell-free total nucleic acids (cfTNA; including cell free DNA (cfDNA) and cell free RNA (cfRNA)), the biological analytes derived from tumor cells floating in blood. However, it is crucial to optimize the whole blood fractionation workflows, since limited access to a suitable centrifuge at blood collection sites poses a challenge to this critical fractionation step, causing delays in processing the blood, leading to decreased sensitivity of variant detection and increased occurrence of false positives. Current study shows a systematic comparison of the effects of 8 different blood fractionation conditions for spin speeds, temperatures and duration on the levels of cfTNA derived from K2-EDTA-derived blood from multiple healthy and non-small cell lung cancer (NSCLC) donors, using next generation sequencing (NGS).

Methods: CfTNA from K2-EDTA derived plasma was isolated using the MagMAX™ Cell-Free Total Nucleic Acid kit and the Genexus™ Cell free total nucleic acid kit, utilizing the KingFisher™ Flex and Genexus™purification systems. Yield and integrity of cfTNA isolated was evaluated by Qubit™, Agilent Tapestation and quantitative real time PCR (qRT-PCR). Furthermore, the impact of these test conditions on quality control specifications of DNA and RNA was assessed by performing sequencing on an Ion Torrent™ Genexus™ sequencing instrument using the AmpliSeq™ HD target amplification assay, that reports sequence variations in DNA for 42 cancer related genes and RNA in 7 cancer related genes.

Results: Results showed comparable performance for all the 8 blood fractionation conditions tested, for yield and cfDNA profiles compared to control condition, indicating that there is no significant impact of these conditions on either yield or integrity of the cfDNA isolated. In addition, NGS data also showed that on target reads and median molecular coverage for DNA are comparable for all the conditions tested. However, sequencing data demonstrated that one test condition showed significantly better performance for RNA quality control specifications in terms of RNA mapped reads and molecular coverage for process controls used in the assay, compared to all other conditions tested.

Conclusion: Data suggests that one of the whole blood fractionation conditions tested impact the cfRNA recovery from plasma without negatively affecting the yield, and integrity of isolated cfDNA and shows increased sensitivity for RNA process controls in NGS.

#5019 Comprehensive pan-cancer analysis of cfDNA methylation marks in tumors reveals complex epigenetic regulatory circuits and diagnostic biomarkers.

S. S. Lueong[1], M. Metzenmacher[2], G. Zaun[2], G. L. Mayer[3], E. J. Hemmer[1], K. Luckerath[1], K. Pomykala[4], B. Hegedus[5], P. A. Horn[6], M. Trajkovic-Arsic[1], T. Szarvas[1], R. Varaljai[7], C. Keup[3], I. Tinhofer[8], S. George[8], S. Kasimir-Bauer[3], S. Pena-Llopis[9], A. Roesch[7], C. Kurten[10], L. Boosfeld[10], K. Bruderek[11], C. Darr[12], T. Hilser[2], V. Grunwald[13], S. Brandau[11], B. Hadaschik[12], H. Neubauer[14], I. Irene Esposito[15], T. Fehm[16], C. Olah[12], A. Csizmarik[17], F. Thangarajah[3], L. Reetz[18], G. Jamal[19], B. K. Thakur[19], H. Kalkavan[2], A. Schramm[20], M. Schuler[13], **J. T. Siveke**[1];

[1]German Cancer Consortium (DKTK), partner site Essen/Dusseldorf, a partnership between DKFZ and University Hospital Essen, Germany, Essen, Germany, [2]Department of Medical Oncology, West German Cancer Center, University Hospital Essen, Essen, Germany, [3]Department of Gynecology and Obstetrics, University Hospital Essen, Essen, Germany, [4]Institute for Artificial Intelligence in Medicine, University Hospital Essen, Essen, Germany, [5]Department of Thoracic Surgery, University Medicine Essen - Ruhrlandklinik, Essen, Germany, [6]Institute for Transfusion Medicine, University Medicine Essen, University Hospital Essen, University Duisburg-Essen, Essen, Germany, [7]Department of Dermatology, University Hospital Essen, West German Cancer Center, University Duisburg-Essen and the German Cancer Consortium (DKTK), Essen, Essen, Germany, [8]Department of Radiooncology and Radiotherapy, Charite-Universitatsmedizin Berlin, Corporate Member of Freie Universitat Berlin, Humboldt-Universitat zu Berlin, and Berlin Institute of Health, Berlin, Germany, [9]Translational Genomics in Solid Tumors, Department of Ophthalmology, University Hospital Essen, Essen, Germany, [10]Department of Otorhinolaryngology, Head and Neck Surgery, University Hospital Essen, University Duisburg-Essen, Essen, Germany, [11]Experimental and Translational Research, Department of Otorhinolaryngology, University Hospital Essen, Essen, Germany, [12]Department of Urology, University Hospital Essen, University of Duisburg-Essen, Essen, Germany, [13]National Center for Tumor Diseases (NCT) West, Campus University Hospital Essen, Essen, Essen, Germany, [14]German Cancer Consortium (DKTK), partner site Essen/Dusseldorf, a partnership between DKFZ and University Hospital Essen, Germany, Dusseldorf, Germany, [15]Institute of Pathology, Heinrich-Heine University and University Hospital of Dusseldorf, Dusseldorf, Germany, [16]Klinik fur Geburtshilfe und Frauenheilkunde, Universitatsklinikum Dusseldorf, Dusseldorf, Germany, [17]Department of Urology, Semmelweis University, Ulloi ut 78/b, Budapest, Hungary, [18]20Department of Pediatrics III, University Hospital Essen, Essen, Germany, [19]Department of Pediatrics III, University Hospital Essen, Essen, Germany, [20]Laboratory of Molecular Oncology, Department of Medical Oncology, West German Cancer Center, University Hospital Essen, Essen, Germany

Early detection of tumor activity in clinically asymptomatic patients has the potential to improve quality of life and prevent unnecessary exposure to toxic therapies. DNA methylation is one of the most studied, stable, and fundamental epigenetic marks and represents a prominent alteration in most cancers. Analysis of DNA methylation, particularly in liquid biopsies has been introduced in cancer diagnosis and risk stratification. Despite indisputable achievements, translation into clinical practice is lagging behind, primarily due to 1) challenges associated with the analysis of DNA methylation, 2) the fragmented nature of cell-free DNA (cfDNA), aggravated by bisulfite treatment, 3) lack of clinical validation of reported cfDNA methylation marks, and 4) the paucity of knowledge about the functional consequences of cfDNA methylation marks within tumors. Using a sample pooling strategy, complemented with robust whole genome and reduced representation methylation sequencing, we establish a pan-cancer cfDNA methylation resource encompassing 12 cancer entities with diverse clinical phenotypes and treatment modalities. We built this compendium using a robustly performing whole genome and reduced representaion enzymatic methylation sequencing of more than 150 cfDNA and tumor DNA. We complement our data by analyzing DNA methylation data from 15 cancer entities (more than 7,000 patients) within the TCGA. We developed an enzymatic digital PCR (dPCR) approach for pan-cancer but also entity-specific analysis of cfDNA methylation at single base-resolution. Using this dPCR assay, we analyzed cfDNA and tumor DNA samples from more than 400 patients and compared enzymatic digestion with bisulfite treatment. We demonstrate that this resource can allow for the identification of entity-agnostic and specific markers, and that cfDNA methylation patterns are mirrored in tumor samples. The approach can be applied for methylation profiling of yet unanalyzed entities. Finally, we demonstrate unconventional epigenetic regulation of gene expression by methylated DNA-binding transcription factors whose activities are tissue- and context-specific and dosage-dependent. This work, therefore, provides a reference resource to identify minimally invasive, entity-specific and pan-cancer markers applicable for diagnostics, surveillance and patient stratification. It also sets the stage for further investigation of tissue- and context-specific epigenetic regulation of gene expression in health and disease by methylated DNA-binding transcription factors.

#5020 Pre-analytical characterization of cell-free DNA to enable liquid biopsy for solid tumors.

R. J. Summersgill[1], J. M. Fox[1], J. S. Dickey[1], L. T. Cox[1], C. D. Palumbo[1], K. C. Valkenburg[1], B. J. Caveney[2], S. Ramkissoon[2], J. B. Jackson[1];
[1]Labcorp, Baltimore, MD, [2]Labcorp, Durham, NC

Background: The integration of liquid biopsy in oncology has transformed clinical management of patients with cancer. Cell-free DNA (cfDNA) represents extracellular nucleic acid fragments shed during cellular apoptosis, necrosis, or secretion, and can be extracted from whole blood. PGDx elio plasma focus analyzes cfDNA to enable non-invasive genomic profiling with next-generation sequencing. In this study, we characterized the cfDNA fraction (%) and yield (ng) across multiple tumor types and stages.

Methods: cfDNA fraction was obtained using automated electrophoresis (Agilent 4200 TapeStation System) to assess a region of 50-700 bp across 293 clinical plasma samples (tumor stages I - IV). The fraction of cfDNA to total DNA present was then calculated to determine overall cfDNA percentage. The overall DNA yield (ng) was quantified via Qubit fluorometer immediately following extraction from plasma and normalized to volume of plasma (ng of cfDNA/mL of plasma). In addition, data was evaluated from 100 clinical plasma cases with strict extraction conditions allowing for yield normalization to plasma volume. Sequencing metrics were evaluated for all clinical cases with a recommended input of 25 ng DNA using PGDx elio plasma focus.

Results: Average cfDNA fraction for individual tumor types ranged from 78.0% - 91.4%, with a mean (n=293) of 84.8%. When examining the yield normalized cohort (n=206), the average yield was 23.4 ng of cfDNA/mL of plasma. cfDNA yield and fraction varied across tumor types and increased with cancer stage. Despite these differences, the majority of cases (99.7%) yielded sufficient cfDNA to proceed with PGDx elio plasma focus testing. No statistical differences in sequencing performance (variants reported and coverage for each tumor type) were observed and the PGDx elio plasma focus assay success rate was 97%. There was a slightly higher failure rate (17.6% (3/17)) for samples below 60% cfDNA, indicating that high amounts of contaminating genomic DNA from white blood cells may obscure the number of available cfDNA fragments for analysis.

Conclusions: These data characterize pre-analytical factors that impact performance of PGDx elio plasma focus using cfDNA isolated from plasma of patients with solid tumors. We showed cfDNA yield and fraction varied across tumor types and increased with cancer stage. The overall success rate for testing was 97% while failed samples were associated with higher levels of genomic DNA contamination.

#5021 Circulating mutated and methylated tumor DNA detection for colorectal cancer diagnosis.

P. K. Bains, M. Kulak, Z. Cui, A. Babu, S. Tran, A. Zhang, M. Sha;
DiaCarta, Inc., Pleasanton, CA

Introduction: Detection of mutation and methylation patterns in liquid biopsies has emerged as a promising approach for screening early-stage cancers. We have developed a targeted next-generation sequencing (NGS)-based assay "OptiSeq™ Colorectal Cancer Detection Panel", a combined platform for assessing mutation and methylation in both low-quantity (plasma cfDNA) and low-quality formalin-fixed paraffin-embedded (FFPE) tissue for colorectal cancer (CRC) detection.

Methods: The OptiSeq™ Colorectal Cancer Detection Panel targets 442 SNVs and 434 CpG sites to detect circulating tumor DNA (ctDNA) in early-stage patients. With this panel, we profiled 6 early-stage and 6 metastatic CRC samples (matching cfDNA and FFPE) along with 2 primary colon specimens with adjacent normal tissue DNA. We also profiled 2 matching cfDNA and FFPE samples from precancerous adenomas (advanced adenomas (AA)) and 6 AA FFPE tissue DNA. In addition, we characterized the mutation and methylation pattern in 10 CRC fresh-frozen tissue DNA samples. For healthy individuals, we profiled 12 normal colon FFPE samples and 10 plasma cfDNA. The clinical performance for the CRC detection panel was calculated using AA, CRC, and cancer-free individuals.

Results: For CRC early and metastatic matching cfDNA and FFPE samples, clinical samples testing showed that the CRC detection panel had a sensitivity of 100% (95% CI: 69.8-100.0) and specificity of 100% (95% CI: 81.5-100). For precancerous AA FFPE tissues, combined DNA mutation and methylation increased the CRC detection sensitivity to 100% (95% CI: 51.6-100.0) and specificity to 100% (95% CI: 61.8-100). More clinical samples testing is underway.

Conclusion: We have developed the targeted NGS-based panel to detect clinically relevant mutation and methylation patterns and demonstrate its potential using the combined genetic and epigenetic markers making it a highly sensitive assay for early CRC diagnosis.

#5022 MEDOCC-CrEATE trial: Feasibility of measuring circulating tumor DNA after surgery to guide adjuvant chemotherapy in stage II colon cancer patients.

I. Franken[1], S. Schraa[1], K. van Rooijen[1], D. van der Kruijssen[1], C. Rubio-Alarcon[2], S. Ketelaars[2], S. van Nassau[1], T. Snetselaar[1], B. Adriaans[1], J. Phallen[3], S. Angiuoli[4], A. Greer[4], E. Verner[4], V. Coupe[5], H. Verkooijen[1], M. van Dongen[2], L. Bosch[2], M. Lanfermeijer[2], D. van den Broek[2], G. Meijer[2], V. Velculescu[3], M. Sausen[4], M. Koopman[1], R. Fijneman[2], G. Vink[6], on behalf of the PLCRC-MEDOCC group;

[1]UMC Utrecht, Utrecht, Netherlands, [2]Netherlands Cancer Institute, Amsterdam, Netherlands, [3]Johns Hopkins University School of Medicine, Baltimore, MD, [4]Personal Genome Diagnostics (LabCorp), Baltimore, MD, [5]Amsterdam UMC, Amsterdam, Netherlands, [6]Netherlands Comprehensive Cancer Organisation (IKNL), Utrecht, Netherlands

Introduction: Patients with stage II colon cancer not classified as high risk (pT4 microsatellite stable) do not receive adjuvant chemotherapy (ACT) according to Dutch guidelines. However, 15-20% of patients with stage II colon cancer experience a disease recurrence, indicating that there is an unmet clinical need to identify patients who could benefit from adjuvant treatment. Observational studies demonstrate that postoperative circulating tumor DNA (ctDNA) is indicative of minimal residual disease (MRD) and a strong prognostic biomarker for disease recurrence.

Aim: The MEDOCC-CrEATE trial aims to assess 1) the proportion of stage II colon cancer patients with detectable postoperative ctDNA accepting ACT and 2) whether ctDNA-guided ACT reduces 2-year recurrence rate (RR).

Methods: MEDOCC-CrEATE is an interventional trial following the 'trial within cohorts' design. Participants of the Prospective Dutch Colorectal Cancer cohort with stage II colon cancer and no indication for ACT randomized to the intervention arm undergo postoperative tumor-informed ctDNA testing using next-generation sequencing of 33 genes through the PGDx elio™ liquid biopsy assay. If ctDNA is detected, they are offered 4 cycles of adjuvant capecitabine plus oxaliplatin. Patients in the intervention arm who test ctDNA negative and patients in the control arm receive standard of care follow-up. For all patients, blood is collected every 6 months for 3 years to monitor disease recurrence.

The primary endpoint is the proportion of patients with detectable postoperative ctDNA willing to receive ACT. Secondary endpoints include 2-year RR, disease-free and overall survival, quality of life and cost-effectiveness of ctDNA-guided ACT. The study is powered for 2-year RR, randomizing 660 patients to each study arm in order to treat 30 patients in the intervention arm with detectable postoperative ctDNA, assuming 5% ctDNA detection and 10% noncompliance.

Results: Logistics for timely multicenter collection of tumor tissue and blood have been optimized across 28 Dutch hospitals. At present, 240 patients have been randomized. Of the 119 patients in the intervention arm, 98 provided consent for immediate postoperative ctDNA analysis (82%). Of the 92 currently available results, 5 (5 %) had detectable ctDNA. The median time from surgery to blood collection was 15 days (IQR 11-19), with a median turnaround time from surgery to ctDNA result of 47 days (IQR 39-54).

Conclusion: Multicenter postoperative tumor-informed ctDNA testing for MRD is operationally and technically feasible within the clinically relevant 8-12 week window to start ACT. The observed ctDNA detection rate is in accordance with expectations and the study design. Upon study finalization, the results will be used for health technology assessment to demonstrate the putative clinical utility of ctDNA-guided ACT in stage II colon cancer.

#5023 Analytical validation of the Oncomine™ Dx Express Test using liquid biopsy samples as an IUO assay in a CAP/CLIA lab.

J. C. Espinoza[1], R. Ramsamooj[2], A. Yuki[1], J. Williamson[1], D. Hassell[3], M. Jasti[3], S. Salazar[1], D. Ginzinger[1];
[1]Thermo Fisher Scientific, West Sacramento, CA, [2]Consultant, West Sacramento, CA, [3]Thermo Fisher Scientific, Austin, TX

Introduction: The Oncomine™ Dx Express Test (ODxET) is a next-generation sequencing (NGS) test. It can be used as an investigational use only (IUO**) test to detect somatic DNA and RNA alterations in human cell-free total nucleic acid (cfTNA) isolated from plasma samples. This study outlines the analytical validation of the ODxET for relevant single nucleotide variants (SNV) and insertion/deletions (INDEL) in liquid biopsy specimens. The Ion Torrent Genexus™ platform has a short turnaround time with minimal operator input. This study was performed in a College of American Pathologists (CAP™) accredited and Clinical Laboratory Improvement Act (CLIA) licensed laboratory.

Methods: Forty-seven unique samples (39 clinical, 3 derived, 2 reference and 3 commercially available DNA controls) were analyzed. All experiments began with sample extraction, except the lower input limit of detection (LLOD). We evaluated limit of detection, variant calling accuracy, and precision. Two control NIST™ samples were sequenced with 3 technical replicates each for INDEL and SNVs analytical accuracy. The LOD was evaluated at both the target input of 2ng/µl (40ng), and the minimum input,0.33ng/µl (6.6ng) with allele frequency (AF) levels at 1%, 0.5%, and 0.25%. The 39 clinical plasma samples were used for variant calling accuracy. Inter-assay reproducibility was assessed by sequencing DNA controls across four runs by different operators over multiple days/systems. Intra-assay repeatability was assessed by sequencing 4 samples in replicate on the same run by one operator on the same day/system.

Results: The analytical accuracy and NPV was 100% for SNV/INDEL variants. The 40ng input LOD sensitivity was 96% for SNVs at 0.5% AF and 100% for INDELs at 0.25% Minimum AF. The lower input LOD sensitivity was 89% for SNVs and 100% for INDEL at 1% AF. Variant calling accuracy on samples with pre-characterized data was 100% for the 13 positive samples. Specificity was >99% for all samples including both healthy donor and positive samples. Repeatability was 100% for INDELs and >96% for SNVs, reproducibility was 100% for both variant classes.

Conclusion: This validation study to estimate analytical accuracy, limit of detection, variant calling accuracy and precision has demonstrated that the ODxET assay is highly robust in detecting SNV and INDEL mutations in plasma samples and is suitable for use in a CAP/CLIA laboratory as an IUO assay.**=In Vitro Diagnostic use only. Not available in all regions including North America.

#5024 Analytical performance of a genome-wide methylome enrichment platform to detect minimal residual disease from plasma-derived cell-free DNA.

S. Shen[1], I. Cirlan[1], F. Vincelli[1], B. Brown[2], J. Min[2], J. Burgener[1], J. Zhang[1], Y. Newton[2], M. Gruca[2], A. Licon[2], J. Zhang[2], A.-R. Hartman[2], A. Williams[2], **H. Mellert**[2], D. D. De Carvalho[1];

[1]Adela, Inc., Toronto, ON, Canada, [2]Adela, Inc., Foster City, CA

Introduction: Plasma-derived cell-free DNA (cfDNA) can be used to identify cancer signals, including minimal residual disease (MRD), in patients who have undergone curative cancer treatments. The cell-free methylated DNA immunoprecipitation and high-throughput sequencing (cfMeDIP-seq) methodology is combined with custom algorithms that leverage differentially methylated regions (DMRs) found in cfDNA to distinguish between cancer and non-cancer signals. This novel non-degradative, tissue-agnostic approach was developed to bypass the limitations of bisulfite-sequencing and tissue-informed methods used in other liquid biopsy technologies. Here we present preliminary analytical performance metrics of an algorithm in development for detecting MRD.

Methods: In the genome-wide methylome enrichment platform, plasma-derived cfDNA is subjected to standard library preparation, combined with DNA filler, denatured, and immunoprecipitated using an anti-5-mC antibody. Captured DNA is amplified and sequenced. For this study, a candidate algorithm comprised of differentially methylated regions (DMRs) and 12 cancer types was used to quantify cancer-specific methylation. Control samples from 12 non-cancer donors were used to establish a selected 95% true negative rate threshold. This threshold was used to determine assay sensitivity, which was evaluated using contrived cancer samples intended to mimic low-level circulating tumor DNA (ctDNA) representative of MRD. Samples were contrived by titrating fragmented DNA from three immortalized tumor-derived cell-lines into plasma-derived cfDNA in a titration series targeting <1% ctDNA levels. Cell-lines were of non-small cell lung cancer and head and neck squamous cell carcinoma origin; titration series were replicated for a total of 65 tests.

Results: All non-cancer and contrived cancer samples met in-process quality control metrics. This included ≥98.5% methylation specificity and ≥80 million unique molecules. Limit of detection calculations at 95% sensitivity (LoD95) were <0.1%.

Conclusions: Tissue-agnostic approaches for detecting cancer signals from plasma have significant benefit, especially in settings where tissue is not accessible for evaluation. However, these tests must have highly sensitive methods of cancer signal detection for clinical applications. Our preliminary analytical data demonstrates the use of a blood-based, tissue- agnostic genome-wide methylome enrichment platform utilizing non-degradative methodology combined with specific algorithms and DMRs for MRD quantification and prognostic prediction, using treatment-naïve plasma samples. Future studies in post-treatment and longitudinal samples are ongoing to evaluate the utility of this genome-wide methylome enrichment platform for cancer management.

#5025 Extracellular vesicle DNA as a potential biomarker for cancer detection: A comparative analysis with ctDNA.

T. Wu, T. Tsering, Y. Chen, A. Nadeau, J. V. Burnier;
McGill University Health Centre Research Institute, Montreal, QC, Canada

Background: Liquid biopsy testing has been implemented in clinical practice because of recent advancements in detecting and characterizing circulating tumor DNA (ctDNA). The Food and Drug Administration (FDA) has approved three ctDNA liquid biopsy tests that detect mutations in cancers, which can aid clinicians in choosing the most effective treatments. While ctDNA has been validated for clinical applications, the same is not true for extracellular vesicle (EV)-associated DNA, which is another promising biomarker. Previously, our laboratory developed the Extracellular Vesicle-Associated DNA Database (EV-ADD) to provide validated experimental details and data extracted from peer-reviewed published literature on EV-DNA. The aim of our study was to investigate the potential clinical utility of EV-DNA in liquid biopsy for tumor detection by surveying studies on EV-ADD that compared ctDNA and EV-DNA.
Methods: We searched the entire EV-ADD to selectively identify studies that compared cell-free DNA (cfDNA) or ctDNA and EV-DNA in cancer patients (inclusion criteria). The sensitivity and specificity of cancer detection, the concentrations of DNA, and the methods of detection were compared between ct/cfDNA and EV-DNA. We define sensitivity as the ability to detect mutations in ctDNA/EV-DNA from patient blood when the mutations are known. Specificity is defined as the proportion of true negatives from the sum of true negatives and false positives. A true negative case occurs when no driver mutation is detected in ctDNA/EV-DNA of a patient whose tumor does not have the mutation either. A false positive case occurs when a driver mutation is detected in ctDNA/EV-DNA of a patient whose tumor does not have the mutation.
Results: Of 97 studies in the database, 20 met our inclusion criteria. From 12 studies that matched our definition of sensitivity, the sensitivity of EV-DNA and ctDNA ranged from 19% to 95% and 14% to 97%, respectively. From the same 12 studies, the specificity of EV-DNA and ctDNA ranged from 89% to 100% and 80% to 100%, respectively. Other studies that met our inclusion criteria but did not match our definition of sensitivity either calculated sensitivity differently (2 studies), calculated sensitivity the same way in pleural effusions (2 studies), in bronchoalveolar lavage fluid (2 studies), analyzed mitochondrial DNA (1 study), or did not calculate sensitivity (1 study). The concentrations of EV-DNA and ctDNA in blood ranged from 0.8 - 118.4 ng/ml and 4.0 - 236.5 ng/ml, respectively. Digital droplet PCR (ddPCR) and sequencing were the most common methods (45% and 35%, respectively) for detecting cancer mutations.
Conclusions: Since EV-DNA performed comparably to ctDNA in detecting cancer DNA in the blood of patients, EV-DNA should be seriously considered as a potential biomarker and complementary tool for detecting and monitoring cancer tumors.

#5026 Microfluidic capillary electrophoresis optimization of high-throughput cfDNA and pDNA measurements for enabling cancer diagnostics and gene therapy development.

James Geiger[1], Dipti Mehta[1], Gayatri Gautam[1], Adriana Coll de Pena[2], Menel Ben Frej[1], Anubhav Tripathi[2], James White[1]

[1]Applied Genomics, REVVITY, Hopkinton, MA,[2]Biomedical Engineering, Brown University, Providence, RI

Rapid and accurate electrophoresis characterization can be an important tool for cancer researchers and therapy manufacturers. Advances in NGS of low molecular weight cfDNA for diagnostics may benefit from high-throughput checks of cfDNA sample quality with ultra-low quantities of sample. On the other hand, high molecular weight pDNA characterization and separation of supercoiled, linear and open-linear conformations aids in quality control of these payloads for personalized medicine and in particular cancer vaccines and gene therapies. This work shows optimization of established microfluidic capillary electrophoresis to enable the measurement of cfDNA and pDNA. cfDNA study was completed on plasma reformatted from whole blood tubes using Janus G3 Blood iQ workstation. The cfDNA samples were extracted using commercial cfDNA extraction kits. Using a LabChip GX Touch Biologics Characterization system: gel optimization, marker solution dilution, and inclusion of a low molecular weight DNA standard improved the sensitivity of cfDNA detection. This afforded a new electrophoresis assay with linear dynamic range of 50-1000 pg/uL and sensitivity of <25 ng/uL. pDNA, supercoiled DNA and linear DNA standards were prepared according to published procedures and measured on the LabChip GX Touch Biologics Characterization system. A new ladder system was developed along with gel optimization to develop a new High Sensitivity Assay platform capable of baseline resolving each conformation and providing fragment DNA sizing and purity information. Taken together, this work provides researchers new tools to leverage automated microfluidic capillary electrophoresis for DNA analysis in both upstream and manufacturing processes.

#5027 Simplified selective electrochemical detection of ctDNA differentiates between cancer progression and regression.

M. J. Russo[1], K. Arnold[1], S. Tunney[1], S. Wright[1], F. Taub[1], C. S. Henry[2];
[1]aiGENE, Inc., Aurora, CO, [2]Colorado State University, Fort Collins, CO

Advanced cancers therapies, including personalized ones, often fail. Rapid evaluation of treatment efficacy is therefore critical to reduce medical and financial side effects and, most importantly, facilitate the implementation of a therapy most appropriate for that individual. Current approaches for evaluating treatment are too slow and expensive to rapidly modify therapy. The previously documented selective affinity of DNA to Au surfaces, albeit cumbersome, unsuitable for point-of-care (PoC) applications and having poor discrimination ability, suggested a solution to this clinically important problem. Methods presented herein potentially solve the problem as first illustrated by a studies of plasma from those with and without cancers. Multiple improvements, most notably optimized buffer conditions dramatically changed and enhanced the difference in adsorption between ctDNA and normal cfDNA drastically improving assay performance. The enhanced sensitivity of this Therascape™ assay was not only able to better detect the difference between healthy and cancer cfDNA but demonstrated potential for the monitoring of cancer treatment efficacy. De-identified clinical samples of the few patients that the Scripps Biorepository and University of Colorado supplied had samples before and after treatment, and were known to have progressed or responded in the interim, were analyzed. This initial group included 6 lymphoma patients and two NSCLC patients (in one case the cfDNA was isolated from urine). One of the patient samples taken before initiating therapy was in the healthy range and considered ineligible for the assay. Ten before and after pairs were then evaluated in a blinded fashion. TheraScape correctly correlated with the change in cancer burden in each pair (10/10 times, p = 0.00016, paired t-test). In some cases the “after” specimen was ~1 month after therapy began. The presentation will include additional patients. The CVs of repeat electrodes were less than 10%, interoperator variability did not increase this. The novel method of detecting cfDNA using disposable electrodes presents a significant advancement in monitoring the efficacy of treatments for advanced cancers, and may be particularly critical for immunotherapy. This approach reduced expenses by 10 to 50 times compared to current reimbursement rates for sequence dependent methods, even more critical is the same day turn around would allow rapid, truly individualized, patient therapy optimization.

#5028 Detection of non-small cell lung and bladder cancer signatures in peripheral blood using a novel antibody-free chromatin capture assay.

K. Lai, K. Dilger, R. Cunningham, T. Barnes, K. Truong, K. Lam, R. Boquiren, **M. C. Louie**, D. Abdueva;
Aqtual Inc., Hayward, CA

Immune checkpoint inhibition (ICI) via anti-PD-1/PD-L1 has improved clinical outcomes for multiple cancers, including bladder and non-small cell lung cancer (NSCLC). Yet, the response rates remain low highlighting a significant knowledge gap in the mechanisms driving response and resistance. While the expression of PD-L1 has been established as a predictive biomarker of ICI response, other features, including molecular tumor burden, tumor microenvironment (TME), and the host's immune mechanisms may contribute to overall response. The complex interactions between a tumor and the immune system underscore the need for a more comprehensive approach to explore novel biological and immunological insights of cancer progression.

Circulating tumor DNA assays, while integral to contemporary decision-making in oncology, fall short in delineating the transcriptional programs that dictate cancer phenotypes and their evolution over the disease trajectory. To bridge this gap, we have developed a plasma-based active chromatin capture method that enables the comprehensive epigenetic and transcriptomic interrogation of both tumor and immune components.

In this study, we quantified epigenetic profiles from plasma samples (n=100) of patients with bladder cancer (n=20) and NSCLC (n=24) undergoing ICI therapy, along with samples (n=70) from healthy individuals (n=5). As expected, the total cfDNA yield (ng) of lung (1.7x, p=2.3e-08) and bladder (1.98x, p=1.6e-11) cancer samples were higher than those of healthy individuals. More Interestingly, the longer cfDNA fragments derived from regulatory-active chromatin, also showed a significantly higher abundance in plasma samples from both lung (2.0x, p=2.5e-09) and bladder (3.2x, p=3.2e-14) cancer patients. Furthermore, the patterns of epigenetic regulations across cancer and healthy conditions showed distinct and stable clusters, consistent between gene bodies and transcription start sites, highlighting the epigenetic changes that may be driving cancer progression. We also observed a common enrichment of immune epigenetic signatures in both lung and bladder cancer samples, likely attributed to shared mechanisms associated with the modulation of the tumor microenvironment and immune interactions. Understanding these changes at an epigenetic level could provide insights into novel therapeutic approaches that target the tumor microenvironment and the immune interactions.

#5029 VAF in ctDNA correlated with advanced breast cancer tumor burden and prognosis.

J. Zhong[1], H. Li[1], B. Shao[1], H. Jiang[1], X. Liu[1], H. Tang[2], S. Jia[2];

[1]Key Laboratory of Carcinogenesis and Translational Research (Ministry of Education/Beijing), Department of Breast Oncology, Peking University Cancer Hospital & Institute, Beijing, China, [2]Huidu (Shanghai) Medical Sciences, Ltd., Shanghai, China

Purpose: In patients with first-line advanced breast cancer (ABC), the correlation between ctDNA variant allele frequency (VAF) and tumor disease burden, and its prognostic value remains poorly investigated.

Methods: This study included patients with ABC diagnosed at Peking University Cancer Hospital who performed ctDNA test before receiving first-line treatment. Baseline plasma samples were collected for assessing ctDNA alterations and VAF with next-generation sequencing. The sum of tumor target lesion diameters (SLD) was measured with imaging methods according to RECIST 1.1 criteria.

Results: The final cohort included 184 patients. The median age of the cohort was 49.4 (IQR: 42.3-56.8) years. The median VAF was 15.6% (IQR: 5.4%-33.7%). VAF showed positive correlation with SLD in patients with relatively large tumor lesions ($r = 0.314$, $p = 0.003$), but not in patients with small tumor lesion ($p = 0.226$). VAF was associated with multiple metastasis sites ($p = 0.001$). Multivariate Cox regression analysis showed that high VAF was associated with shorter overall survival (OS) (HR: 3.519, 95% confidence interval (CI): 2.149-5.761), and first-line progression-free survival (PFS) (HR: 2.352, 95%CI: 1.462-3.782).

Conclusion: ctDNA VAF associated with tumor disease burden, and was a prognostic factor for patients with ABC. A combination of ctDNA test and radiographic imaging might enhance tumor burden evaluation, and improve prognosis stratification in patients with ABC.

#5030 Evaluation of different blood collection tubes for liquid biopsy NGS applications.

N. Siepert, E. Ostrowska, L. Qu He, M. Jasti, K. Lea, T. Jayaweera, A. Cheng;
Thermo Fisher Scientific, Austin, TX

Intro: Liquid biopsy is fast becoming a standard practice in oncology research due to recent advancements in Next Generation Sequencing (NGS). To detect genetic variants, whole blood samples are collected in blood collection tubes (BCTs) and fractionated to obtain plasma which is then used to isolate cell free nucleic acid (cfNA) for analysis. While the limited availability of cfNA is a challenge in liquid biopsy, storage condition and duration between blood collection and fractionation have a significant impact on the quantity and quality of the cfNA due to degradation and genomic DNA and RNA contamination. There are several BCTs available on the market offering stabilization of cfNA profiles to overcome the above challenges.

Methods: Here we compare the NGS performance of cfNA derived from three commonly used BCTs on the market, BD Vacutainer™ K_2EDTA Tubes, Streck™ Cell-Free DNA, and PAXgene® Blood ccfDNA tubes. Matched whole blood samples collected in the above-mentioned tube types were obtained from commercial vendors which were derived from 38 healthy donors as well as 6 cancer research samples. Whole blood samples were fractionated as per manufacturer recommendations and cfNA was isolated and quantified using Genexus™ Cell-Free Total Nucleic Acid Purification Kit on Genexus™ purification system. Isolated cfNA was then sequenced using Ion Ampliseq™ HD target amplification assay on Genexus™ Integrated sequencer.

Results: Data shows that K_2EDTA collected samples contain slightly higher amounts of cfNA compared to PAXgene® and Streck™ samples. When the cfDNA profiles were analyzed by Agilent™ BioAnalyzer™, K_2EDTA derived cfDNA showed varying degrees of genomic DNA contamination which can inflate the cfDNA concentration. However, both Streck™ and PAXgene® derived cfDNA showed little to no detectable genomic DNA contamination. As a result, a higher percentage of PAXgene® and Streck™ samples did not meet the minimum input requirement (5ng) for the sequencing assay. Sequencing data for DNA showed that K_2EDTA samples had higher total reads and median molecular coverage compared to the other two BCT types. However, all samples had passing QC metrics, and mean read length, on target reads, and uniformity were comparable between the three tube types. When DNA variant detection was evaluated using cancer research samples, no significant difference was observed in performance between K_2EDTA and PAXgene® samples. Interestingly, sequencing data for RNA shows that PAXgene® samples had slightly higher mapped reads on average, and significantly higher internal process control coverage compared to both K_2EDTA and Streck™ samples. Whereas Streck™ samples had significantly lower internal process control coverage.

Conclusion: In summary, this study demonstrates the advantages and disadvantages of using different BCTs for liquid biopsy applications, in terms of cfNA yields, isolated DNA profiles, and sequencing performance.

#5031 Identification of predictive/prognostic biomarkers in metastatic castration-resistant prostate cancer patients using plasma cell-free total RNA-sequencing.

G. Gurioli, M. Urbini, A. Virga, C. Casadei, E. Giunta, N. Brighi, M. Cortesi, M. Zanoni, S. Bravaccini, G. Martinelli, P. Ulivi, U. De Giorgi;
IRCCS Istituto Romagnolo per lo Studio dei Tumori (IRST) "Dino Amadori", Meldola, Italy

Background Metastatic castration-resistant prostate cancer (mCRPC) is a heterogeneous disease that is still lacking an optimal patient selection strategy and a validated sequence of therapies. Therefore, there is an urgent need to identify non-invasive biomarkers to guide treatment choice in a perspective of personalized medicine. Plasma cell-free RNA profiling has emerged as a tool to investigate potential liquid biopsy biomarkers. In this study, we aimed to evaluate a method to capture total RNA content deriving from plasma and to identify potential biomarkers for mCRPC.
Methods Plasma samples of 41 mCRPC patients treated with first line Abiraterone or Enzalutamide and 7 healthy donors were collected and stored from 2015 to 2022. Plasma cell-free RNA was purified using miRNeasy Serum/Plasma Advanced Kit (Qiagen) with DNase treatment. Bioanalyzer (Agilent) was used for the evaluation of RNA content and integrity profile of the samples. Sequencing libraries were generated using SMARTer Stranded Total RNA-Seq Kit v3 - Pico Input Mammalian (Takara Bio). An average of 80 millions reads pairs were sequenced on Novaseq 6000 (Illumina) using 100 bpx2 approach. After demultiplexing, reads were trimmed and aligned on hg19. Sequencing metrics were evaluated using Picard. Kallisto was used for gene expression analysis.
Results A median of $10x10^9$ bases per sample were aligned on hg19, of which a mean of 45% were located on coding or UTR regions. Storage time was investigated as a potential variable for RNA content and sequencing metrics, but no difference related to the year of storage was found. Unsupervised principal component analysis confirmed the absence of batch effects (including storage and sequencing analysis). PC1 seemed to reflect the different tumor RNA content of each sample, in which healthy donors and cancer patients were distinguished. Higher androgen receptor (AR) gene expression was found in mCRPC patients compared to healthy donors.
Conclusions Despite enormous interest in extracellular nucleic acids, RNA-sequencing methods for total RNA content outside cells are rare and not standardized. In this study, we found a method to identify plasma non-invasive RNA biomarkers in mCRPC samples, retrieving coding and non-coding RNAs. Case series enlargement and differential gene expression analyses are ongoing.

#5032 Analysis of analytical variables in the cancer detection assay utilizing cfDNA fragmentomics.

J. Lee, **J.-w. Kim**, J. Kim, S. Oh, D. Kim, J. Park, J. Lee, C.-S. Ki, E.-H. Cho;
GC Genome, Yongin, Korea, Republic of

Introduction: Recent studies have increasingly employed the fragmentation pattern of cfDNA-WGS to enhance the cancer detection rate. The control of experimental variables can exert a significant influence on the outcomes. In this study, our objective was to assess the stability of cfDNA from a fragmentomics standpoint in practical experiments involving diverse scenarios. Utilizing our proprietary fragmentomics-based algorithm, we conducted data analysis, confirming the stability of plasma cfDNA in blood across various storage periods. Furthermore, we assessed the robustness of fragmentomic profiles concerning the library's storage duration.

Method: To confirm the stability of cfDNA in plasma within Streck tubes, two experiments were conducted. In Experiment 1, three samples were stored at 4°C and room temperature (0, 3, 7, 14 days). Experiment 2 involved eight samples stored at room temperature (1, 2, 3, 4 days). To validate the stability of the library based on its storage period, 17 samples were sequenced using the library stored at -80°C for a period ranging from 3 to 88 days. All samples and libraries were utilized to generate low-depth whole-genome sequencing (WGS) using Novaseq, and the data were analyzed using our algorithm, which incorporates fragment size and end motifs.

Result: Regardless of the storage temperature of the Streck tube, the insert size exhibited less than a 3bp difference up to 7 days, but a rapid increase in insert size was observed on day 14 under room temperature conditions. The heatmap of 256 end-motif frequencies showed consistent patterns up to 7 days. The difference in insert size according to the library storage period was less than 2bp, and the analysis of density distribution based on fragment size confirmed no significant differences between the data. The heatmap of 256 end-motif frequencies showed similar patterns up to 88 days regardless of the library's storage period.

Conclusion: Results of this study showed that cfDNA of end motifs and size in Streck tubes remained stable for up to 7 days at both room temperature and 4°C, and libraries were stable for up to 88 days when stored at -80°C.

#5033 Sub-0.01% KRAS G12C dPCR variant detection by mutation specific blocker (MSB) cassettes.

A. Beams, K. Lee, S. Addison, N. Riccitelli;
Navigate BioPharma, Carlsbad, CA

Purpose: Kirsten rat sarcoma viral oncogene homologue (KRAS) is one of the most well-known oncogenes and is found commonly mutated in numerous cancer subtypes. Despite its prevalence as a driver of disease state, until recently KRAS-targeting therapeutics have proven difficult to develop due to lack of specificity (Huang 2021). Now, several treatments have been approved for KRAS mutated cancers that are driven specifically by the G12C variant, and additional compounds are under investigation. Enrollment on these therapies is conditional on the G12C mutation presence, and thus accurate, sensitive detection of G12C is critical. Herein, we describe the development of KRAS G12C-targeting MSB dPCR assays capable of detecting G12C variants down to less than 0.01% variant allele frequency in whole blood, FFPE, and cfDNA samples.

Methods: Multiple KRAS G12C MSB cassettes were developed, composed of four components: a mutation-specific forward primer with an engineered penultimate nucleotide mismatch, a non-extendable blocking oligo for the wild-type (WT) KRAS G12 sequence, a TaqMan probe, and a standard reverse primer. Initial cassette performance was assessed using synthetic KRAS G12C and KRAS G12 WT sequences inserted into an IDT plasmid backbone and tested directly or spiked into whole blood or extracted genomic DNA obtained from healthy donors prior to testing. Data obtained with the MSB cassettes across multiple matrices was compared to a BioRad off-the-shelf KRAS G12C droplet digital PCR (ddPCR) assay for accuracy. Cassette designs achieving the desired specificity and sensitivity were subsequently run on cell-free DNA samples possessing KRAS G12C, KRAS G12D, and WT sequences to evaluate performance in patient material.

Results: The enhanced WT suppression design of the assay allowed the lower limit of detection and limit of blank to remain at 6 copies/reaction (cps/rxn) and 3 cps/rxn, respectively, across 30 ng/rxn to 350 ng/rxn gDNA background. At the theoretical maximum input of 200,000 cps/rxn, the assay can achieve 0.003% frequency detection in a single well, with robust detection down to 5 ng/rxn input, making it ideal for samples with limited availability. The assay demonstrated high accuracy, with a correlation coefficient ≥ 0.95 to known values and the BioRad reference assay, and high precision, with less than 10% coefficient of variation among allele frequencies of the same sample.

Conclusion: With the emergence of targeted therapies for KRAS G12C driven cancers, detection of this mutation has become crucial in the diagnosis. While multiple methods are available for variant identification, MSB cassettes represent a powerful approach to achieve a sensitivity of molecular detection not possible with other techniques. This enhanced sensitivity directly impacts patient access to potentially life-saving therapies, ensuring all possible options are available to diagnose the patients sensitively and early.

#5034 Analytic validation of an ultra-sensitive tumor-informed circulating tumor DNA assay based on whole genome sequencing.

J. Northcott, G. Bartha, J. Harris, S. Ma, M. Hong, Q. Zhang, R. Chen, J. Lyle;
Personalis, Inc., Fremont, CA

Monitoring of circulating tumor DNA (ctDNA) levels has demonstrated utility in the detection of residual and recurrent disease after tumor resection, and as a prognostic indicator of patient outcome following initial therapy, in a wide range of cancers. Here we describe the analytic validation of the NeXT Personal® assay, an ultra-sensitive, quantitative, tumor-informed ctDNA assay for use in patients diagnosed with solid tumors. NeXT Personal utilizes whole genome sequencing (WGS) of tumor and normal samples and advanced noise suppression to accurately identify somatic variants and generate a patient-specific diagnostic panel based on up to ~1,800 single nucleotide variants. This personalized panel is used to test for the presence of ctDNA in the patient's blood samples. The NeXT Personal validation was performed using 123 matched tumor, normal and plasma clinical sample sets representing 9 cancer types. The assay achieved 100% specificity on donor normal plasma samples with an in silico approach giving us a confidence interval of 99.87% to 100%. The analytical range measurements were performed using two paired tumor and normal cell lines, one of which is a commercially available MRD control. The detection threshold for the analytical range measurement was 1.68 parts per million (PPM) with a limit of detection at 95% (LOD95) of 3.52 PPM. Furthermore, NeXT Personal showed linearity over a range of 0.8 PPM to 300,000 PPM (Pearson correlation coefficient= 0.9998) with a limit of quant (LOQ) of 10 PPM. The assay also demonstrated strong performance across varying cfDNA input amounts from 2 ng to 30 ng. These studies demonstrate that NeXT Personal is an ultra-sensitive, highly specific, quantitative and robust assay, giving it the potential to detect residual disease and recurrence earlier than less sensitive assays.

#5035 Use of Streck nucleic acid BCT with plasma nucleic acid next-generation sequencing workflows.

N. M. George, L. Bartron;
Streck Laboratories, Inc.R, La Vista, NE

Introduction: Liquid biopsies, which interrogate body fluids in search of analytes released by cancer cells, are becoming increasingly common in clinical oncology. Foremost among the technologies used are those that employ nucleic acids, such as cell-free DNA (cfDNA) and cell-free RNA (cfRNA). Currently, many NGS-based tests perform near the limit of assay detection, making the identification of critical mutations, fusions, or expression patterns like finding a needle in a haystack. Further hindering successful assay development is the variability in analyte availability and detectability that can occur prior to analysis due to blood collection, transport, and storage. Here, we demonstrate that Nucleic Acid BCT stabilizes draw-time levels of plasma nucleic acids for downstream use with NGS-based assays.

Methods: Blood from self-proclaimed healthy donors was drawn into EDTA and Nucleic Acid BCT and stored at ambient temperature for up to 7 days before plasma isolation with a general double-spin protocol and storage at -80 °C. Plasma nucleic acids were isolated using the MAGicBead cfDNA Kit (Zymo, cfDNA) or the QIAamp Circulating Nucleic Acid Kit (QIAGEN, cfRNA). Library prep for cfDNA was carried out with added synthetic mutant spike-in oligonucleotides using the Illumina TruSight Tumor 15 kit (Illumina). cfRNA library prep was done with the NEBNext Ultra II RNA Library Prep Kit for Illumina with upfront rRNA depletion (New England Biolabs). Sequencing was performed using an Illumina NextSeq 500 system, and all data were saved in and analyzed with Illumina BaseSpace applications.

Results: When blood samples were stored in EDTA tubes for up to 7 days, spiked mutant alleles ($EGFR^{L858R}$, $EGFR^{del19}$, $KRAS^{G12D}$, and $PIK3CA^{E545K}$) were no longer detected, likely due to a dilution of the spiked DNA concentration following the release of genomic DNA containing wildtype alleles during white blood cell degradation. In contrast, equivalent blood samples stored in Nucleic Acid BCTs displayed mutant allele frequencies reflective of draw-time levels. Interrogation of plasma RNA expression patterns in samples stored in Nucleic Acid BCT versus EDTA revealed similar results, where differentially expressed plasma transcripts in blood samples stored in EDTA were found at high levels (>1,000 transcripts) versus donor-matched blood samples stored in Nucleic Acid BCT (<50 transcripts).

Conclusions: Our data demonstrate that Nucleic Acid BCT maintains mutant allele frequencies and the plasma transcriptome profile of blood samples during ambient temperature storage. This provides precious sample integrity during whole blood storage and transport, offering laboratories and assay developers reduced preanalytical variability for NGS-based analysis of gene mutations, fusions, indels, and the plasma transcriptome. Nucleic Acid BCT is for Research Use Only. Not for use in diagnostic procedures.

#5036 Analytical and clinical validity of Northstar Select, a quantitatively enhanced liquid biopsy assay for comprehensive genomic profiling of solid tumors.

X. Bower, J. Wignall, J. Zhu, N. Searle, M. Varga, E. Rosas-Linhard, J. Luong, E. Lin, M. Simon, J. ten Bosch, W. Zhou;
BillionToOne, Inc., Menlo Park, CA

Background: Liquid biopsy assays have emerged as vital tools in precision oncology. Among these assays, Comprehensive Genomic Profiling (CGP) tests in particular have improved treatment selection for late-stage solid tumor cancer patients by allowing for the detection via circulating tumor DNA (ctDNA) of somatic mutations in the tumor, many of which have corresponding targeted therapies. However, technical restrictions in the performance of such tests have limited their utility when ctDNA signal is low. BillionToOne's Northstar Select assay is a new CGP test that achieves increased performance by addressing these limitations.
Innovation: By using Quantitative Counting Template (QCT) technology, Northstar Select is able to track the yield of multiple processing steps, contributing to the higher sensitivity of the assay by maximizing the number of decoded molecules after sequencing. In addition, it employs chemistry and panel design optimizations, as well as novel algorithms for SNV, indel, CNV, fusion, and MSI calling to increase sensitivity and specificity.
Analytical Performance: The performance of Northstar Select surpasses that of other commercially available tests for multiple mutation types, detecting more pathogenic and actionable mutations at low tumor DNA fraction while maintaining similarly high specificity. In analytical validation (N=103), limit of detection was determined to be 0.13-0.16% variant allele fraction (VAF) for SNVs and indels, 2.11 copies for copy number amplifications, 1.8 copies for copy number losses, 0.35% VAF for fusions, and 0.07% tumor fraction for MSI.
Clinical Performance: Northstar Select was determined to have high clinical utility as well, with a study of clinical samples (N=481) from a variety of tumor types yielding <2% of reports with 0 mutations detected. A head-to-head comparison with other commercial liquid biopsy assays on a subset of the clinical samples (N=192) showed that the assay detected 115 additional pathogenic mutations in total, leading to a higher proportion of patients with at least one pathogenic mutation detected (90%) compared to comparators (79%).
Conclusion: These results demonstrate that the Northstar Select assay is an innovative and high-performing diagnostic for treatment selection in oncology, leveraging quantitative approaches in process design, chemistry, and bioinformatics to offer superior analytical and clinical performance compared to the current landscape of liquid biopsy CGP tests.

#5037 Development of multiplexed Absolute Q digital PCR assays to rapidly quantify EGFR and KRAS genotype in advanced non-small cell lung cancer (NSCLC) patients' plasma.

B. Hanna, S. Xu, C. P. Paweletz, **Y. Kuang**;
Dana-Farber Cancer Institute, Boston, MA

Introduction: There are needs to identify and serially monitor driver and resistance mutations (muts) in therapy-treated cancer patients (pts). Quantitative liquid biopsy in cell-free (cf)DNA has been widely adopted. We have developed and clinically validated droplet digital PCR (ddPCR) assays to detect common driver/resistance muts such as *EGFR* del19, L858R, T790M and *KRAS* G12X in the cfDNA of advanced NSCLC pts. We have established ddPCR assays for 30+ driver/resistance muts in multiple genes (*BRAF, MET, ESR1,* etc.) relevant to melanoma, breast, and colorectal cancer. Our assays use tumor/cell line DNA as positive controls and serve as benchmarks to develop newer assays such as plasma NGS. In this study, we converted existing/validated *EGFR* and *KRAS* G12X ddPCR assays to the QuantStudio Absolute Q digital PCR (dPCR) system. The selected mutations maximize actionable clinical information and are designed to study oncogenic and resistance mutations in NSCLC efficiently. dPCR's accuracy and efficiency enables target multiplexing, providing comprehensive information from limited materials and contributing to liquid biopsy research progress.

Methods: Plasma from pts with tumors harboring *EGFR* and *KRAS* muts was collected at progression with advanced disease following consent to protocol DFCI #14-147. We designed a multiplex dPCR assay that identifies the most common and therapy-relevant *KRAS* muts in NSCLC, G12C/D/V, and detects other G12X using a drop-off probe. We also designed 2 *EGFR* kits, one identifying driver muts, the other resistance muts.

Results: To validate assay performance, we used gDNA derived from cell lines with *EGFR* or *KRAS* muts. We serially diluted mut gDNA samples in background wt gDNA (16 ~ 1000 mut copies in 1000 wt copies) and performed *KRAS* and *EGFR* dPCR assays. We detected 16 mut copies with sensitivities similar to those of ddPCR assays. We then studied 48 cfDNA samples from plasma of NSCLC pts with tumor confirmed *KRAS* G12X or *EGFR* L858R, del19, T790M muts. No samples had both *EGFR* and *KRAS* muts detected, suggesting our assays are specific. We detected muts in samples with an allele frequency median of 0.9% for *KRAS* mut, 11.9% for *EGFR* driver mut, 2.9% for *EGFR* T790M. The concordance rate is 91.3% between dPCR and ddPCR results. Our findings suggest these assays are as sensitive and specific as our validated ddPCR assays. Multiplexed Absolute Q dPCR saves cfDNA and cuts turnaround time (TAT) to 90 min for *KRAS* assay and 3hr for *EGFR* assays.

Conclusions: We developed rapid, sensitive and specific quantitative dPCR assays for *KRAS* and *EGFR* muts on the QuantStudio Absolute Q platform to quantify plasma genotyping in NSCLC. We will clinically pilot our validated rapid genotyping approach and quantify TAT advantage of multiplexed genotyping in NSCLC pts undergoing standard-of-care tumor genotyping.

#5038 Validation of a comprehensive next-generation sequencing liquid biopsy assay for clinical diagnostics and clinical trial applications.

X.-X. Tan, T. Peters, M. Berry, K. Barber, K. Jeter, B. Lovell, P. Elizondo, Y. Mou, B. Thomas, H. Xie, J. Guo;
NeoGenomics Laboratories, Inc., Houston, TX

Liquid biopsy next generation sequencing (NGS) provides a powerful non-invasive approach to detect solid tumor derived somatic variants in a massively parallel manner. Liquid biopsy NGS has rapidly become an invaluable choice of testing technologies for clinical utility where invasive tissue biopsy is inaccessible and/or inadequate for molecular characterization. We present here a targeted NGS gene panel assay designed and validated specifically for liquid biopsy characterization. The assay was designed to test cell free DNA and cell free RNA from blood plasma for detection of single nucleotide variants (SNV), insertion/deletion (Indel), copy number variants (CNV), and gene fusions present in 52 most commonly mutated genes in cancers. The validation was performed to assess assay accuracy, specificity, sensitivity, repeatability, and reproducibility, with including pre-characterized reference controls, retrospective plasma samples from cancer patients, and prospectively-collected clinic blood specimen. Triplicates were included and testing was performed at different times and by different operators to assess the assay precision. Over 100 clinic blood specimens were collected in Streck cfDNA tubes from multiple trial centers, including treatment naïve phase III-IV patients with solid tumor (lung cancer, breast cancer, brain cancer, prostate cancer, kidney cancer, melanoma, etc) as well as heathy donors, processed within 7 days for plasma separation and total nucleotide acid (TNA) extraction, and assessed by the NGS assay for mutation detection. The identified mutations and wild-types were verified with orthogonal ddPCR. Assay sensitivity as low as 0.1% for SNV and Indel, 1.3 fold change for CNV, and 10 copies for gene fusion were observed, with near-perfect assay specificity (>99.99%) at these sensitivity levels. In conclusion, a targeted NGS liquid biopsy assay was analytically validated under medical oversight, with a demonstrated rigor of the test by its high sensitivity/specificity and robust reproducibility. The validated assay has been utilized for clinical diagnostics and to support research and development efforts in clinical trials.

#5039 Preanalytical workflow enabling cfDNA analysis from urine samples.

D. Mancarella, J. Rutsch, L. Erkelenz, M. Meyer, L. Witthaus, M. Rath, T. Voss;
QIAGEN GmbH, Hilden, Germany

Introduction: Urine has become an important source of information in the liquid biopsy field. In contrast to blood, specifications for the collection, storage, transport and processing of urine intended for molecular examination are not widely established. Preanalytical specifications were published for urine cell-free DNA (cfDNA) only recently (CEN/TS 17811:2022). In this study, we investigated post-collection changes to cfDNA profiles in urine samples and present the performance of an optimized preanalytical workflow for cfDNA analysis.
Methods: Urine from apparently healthy, consented female individuals was spiked with processed cell-free male urine or with a cfDNA standard containing PIK3CA mutations (SensID). The urine was stabilized with a urine collection/ stabilization solution under development at PreAnalytiX or was left unstabilized. Urine samples were stored for varying durations at different temperatures in a time course experiment to simulate different urine storage conditions. After storage, urine samples were centrifuged to remove cells and cfDNA was isolated from the supernatant via the QIAsymphony® platform (QIAGEN). Autosomal and male-specific targets were quantified using the Rotor-Gene® Q instrument and the therascreen® PIK3CA qPCR Kit (both QIAGEN) or the QIAcuity® Digital PCR System and a dPCR LNA PIK3CA Mutation Assay (both QIAGEN). Fragment size distribution was determined by TapeStation® Cell-free DNA ScreenTape® (Agilent Technologies).
Results: Analysis of cfDNA profiles in unstabilized urine stored for varying durations and temperatures highlighted changes which create artificial cfDNA profiles. The yield of cfDNA drastically decreases over time. Furthermore, the size distribution of cfDNA isolated from unstabilized urine was impacted by release of gDNA as well as DNA degradation. Urine stabilization minimized cfDNA degradation and gDNA release and allowed isolation of cfDNA that was analyzed with qPCR and dPCR even after urine storage. Analysis of isolated cfDNA revealed positive detection of PIK3CA mutations in spiked urine samples.Conclusions: Changes in post-collection cfDNA profile can hinder downstream analysis, resulting in artificial or failed outcomes. Urine stabilization with a collection/stabilization solution under development at PreAnalytiX minimized DNA degradation and gDNA release. It enabled urine storage, allowed analysis of urine cfDNA and target detection by qPCR and dPCR.

#5040 Evaluation of commercially available cell free DNA extraction kits using biosynthetic reference materials.

D. Ruminski Lowe, S. Jamindar, A. Anfora, D. Merriam, C. Huang, R. Garlick, B. Anekella;
LGC Clinical Diagnostics, Gaithersburg, MD

Extraction of cell free DNA (cfDNA) from a patient's blood sample is a crucial preanalytic step of the liquid biopsy process. Whether testing is being performed for early disease diagnosis, therapy selection, or disease and treatment surveillance, the input material must be of sufficient quantity as well as high quality to return informative data. In addition, accurate capture of the full cfDNA content from a sample is necessary to evaluate tumor growth or recurrence. Fragmentomics is an emerging field that can indicate tumor origin among other information, and again, accurate and precise cfDNA content is critical. The cfDNA content in patient plasma is highly variable, and sample mass is quite limited compared to that of resected tumors. Healthy donor plasma, though abundant, varies in cfDNA levels batch to batch and should not contain any somatic variants relevant to liquid biopsy assay development or validation. Despite the challenges associated with cfDNA isolation and ctDNA analysis there are few reference materials available to optimize laboratory process for these preanalytic challenges. Here we evaluate various commercially available extraction kits using novel Seraseq® cfDNA Extraction Reference Materials. Genomic DNA from the GM24385 cell line was blended with 4 biosynthetic DNA EGFR variants targeted at 1% allele frequency and verified using the Bio-Rad QX-200 Droplet Digital PCR (ddPCR) System. The mixed DNA was fragmented and size selected to create ctDNA-like size profiles. The ctDNA was mixed into a synthetic plasma matrix to simulate native cfDNA samples and diluted to three distinct concentrations (20, 50, and 80 ng/mL). Verification of concentration was performed using the QIAGEN QIAamp Circulating Nucleic Acid Kit for extraction. The final materials were also extracted with other kits: the Maxwell RSC ccfDNA Plasma Kit, the MagMAX Cell-Free DNA Isolation kit, the Zymo MAGicBead™ cfDNA Isolation Kit, and the Takara NucleoSnap cfDNA Kit. Yields were measured with Qubit dsDNA BR assay and EGFR variants were measured using Bio-Rad ddPCR. Other sites evaluated the materials as well, using various kits. The kits showed variable yields, but there was a clear difference between the cfDNA extracted from each reference material correlating with the intended increasing concentration. The EGFR variants were all present at ~1% regardless of the cfDNA concentration and the kit used for extraction. Seraseq ctDNA Plasma Reference Materials serve to evaluate extraction of cfDNA in liquid biopsy testing workflows without having to source donor plasma, which is limited and variable in cfDNA content. The consistency and availability of these biosynthetic materials allow for optimization without risking patient samples.

#5041 Next generation liquid biopsy reference material performance across NGS assays and platforms.

D. Ruminski Lowe, S. Jamindar, Y. Konigshofer, A. Anfora, K. Nahilk, D. Xia, E. S. Davis, D. Merriam, C. Huang, R. Garlick, B. Anekella;
LGC Clinical Diagnostics, Gaithersburg, MD

Liquid biopsy testing has grown to support early disease diagnosis, therapy selection, and disease and treatment surveillance in cancer survivors. Recent advances in next generation sequencing (NGS) have enabled larger panel sizes, pan-cancer target sets, and wider ranges of genomic alterations. More inclusive analytical validation materials are needed to assess assay sensitivity, specificity, and limit of detection of all variant types to serve the expanded utility of liquid biopsy testing. Here we describe the development and multisite evaluation of expanded Seraseq® ctDNA Mutation Mix v4 reference materials. Genomic DNA from the GM24385 cell line was blended with 93 clinically relevant biosynthetic DNA variants including single nucleotide variants (SNVs), insertions and deletions (indels), structural variants (SVs), copy number variations (CNVs), and mono- and dinucleotide biomarkers for microsatellite instability (MSI). Variant allele frequency (VAF) was targeted to 0.5% and total copy number for CNVs was targeted to 2.5 and verified using the Bio-Rad QX-200 Droplet Digital PCR (ddPCR) System. The DNA mix was fragmented and purified to create ctDNA-like size profiles. Wild-type (WT) material was prepared for comparison and identification of background variants. Agilent Bioanalyzer High Sensitivity DNA and TapeStation Cell-free DNA ScreenTape analyses were used to assess fragment size. The ctDNA mixes were analyzed with the Illumina TruSight™ Oncology 500 (TSO 500) ctDNA assay, the Thermo Oncomine™ Precision assay, and additional assays. All biosynthetic SNVs, indels, SVs, and CNVs in the 0.5% ctDNA mix were detected near target values. The average fragment size was about 190 bp, similar to native ctDNA. The VAFs and CNVs observed in the TSO 500 data correlated well with those that were obtained by dPCR. Variants reported by all evaluation site assays showed good concordance of VAF values. The two sites that tested the materials with TSO 500 revealed consistency in both VAF and total copies with an average CV of 16.1% and 2.5%, respectively. The sequencing performance of the reference material was similar to patient samples and showed comparable levels of background noise. The performance of the Seraseq ctDNA v4 mutation mix across NGS assays, supported by robust digital PCR data, demonstrated that these materials will allow for assessment of complex and sensitive liquid biopsy tests. Comparing data measured at different sites highlights the variability in liquid biopsy assay performance and the importance of highly multiplexed and consistent reference materials. Remnant samples are typically not an option due to limited yields from a standard blood draw, thus contrived standards are especially needed. Expanded variant content and improvements in the methods used to produce the Seraseq ctDNA Mutation Mix v4 materials will enable advancements in the blood-based NGS clinical diagnostics space.

#5042 Urine as a non-invasive proxy for plasma in prostate cancer-related liquid biopsy applications.

Nafiseh Jafari[1], Jason Saenz[1], Lauren Lee[1], Carlos Hernandez[1], Andrew Dunnigan[1], Amit Arora[2], Rafal Iwasiow[2], Mayer Saidian[1]

[1]nRichDX, Irvine, CA,[2]DNA genotek, Ottawa, ON, Canada

Introduction: The non-invasive collection of urine renders it an attractive and pragmatic substitute for plasma in liquid biopsy applications, fostering the creation of diagnostic methods that are more patient-friendly and less cumbersome for clinicians. This study investigates the feasibility of urine-derived cfDNA as a non-invasive option for acquiring vital diagnostic insights, further enhancing the liquid biopsy field.

Methods: Paired male first void urine (FVU) and venous blood samples were collected from healthy donors (n=40) using Colli-Pee UAS devices (Novosanis) and BD K2EDTA Vacutainer tubes, respectively. Out of these, 20 paired urine and blood samples were spiked with 10 ng of cfDNA reference standard containing the KRAS p.G12V mutation. ~35 ml of urinary cell-free supernatant and ~3.5 ml of plasma were obtained after centrifugation of FVU and blood sample, respectively, and used as input material for cell-free nucleic acids extraction using the nRichDX Revolution Max20 cfDNA Isolation Kit. The extracted cfDNAs profile was assessed on 4200 TapeStation System, Agilent, using cfDNA ScreenTape. Extracted nucleic acids from urine samples were subjected to a qPCR assay to quantify endogenous human cfDNA content using 2X iTaq Universal SYBR Mastermix (Bio-Rad). Human cfDNA quantity was assessed using Ct values obtained from the qPCR assay. The actionable cfDNA molecules recovery was determined by qPCR mutation detection assay using TaqMan Genotyping.

Results: Male FVU collected in Colli-Pee UAS device showed the presence of 100-250 bp cell-free DNA fragments similar to plasma obtained from whole blood collected in 10 ml vacutainer tubes as demonstrated by the Agilent cfDNA ScreenTape analysis. The cfDNA yield was similar when comparing one tube of blood (~3.5 mL of plasma) to one Colli-Pee of urine (~35 mL) shown by endogenous cfDNA qPCR assay. Additionally, the amplifiability of the KRAS G12V mutation was consistent in both plasma and urine samples, with comparable Ct values.

Conclusion: The nRichDX Revolution Sample Prep System demonstrates the ability to extract cfDNA from both plasma and urine samples, with comparable extraction efficiency observed between matched samples from the same donor. This study provides evidence supporting the viability of first void urine samples as a non-invasive alternative for prostate cancer-related liquid biopsy applications. It indicates that cfDNA can be recovered from a sample collected with a single BCT or Colli-Pee UAS urine collection device. Future investigations will be required to assess clinical samples and biomarkers to establish a robust correlation between cfDNA levels and various cancer types and stages. This study reinforces the utility of first void urine samples as a reliable proxy for blood-based liquid biopsy applications.

#5043 Achieving sensitivity of 0.1% variant allele frequency (VAF) in plasma and urine with the nRichDX revolution sample prep system evaluated on the the MassARRAY system.

Nafiseh Jafari[1], Mayer Saidian[1], Jason Saenz[1], Lauren Lee[1], Andrew Dunnigan[1], Carlos Hernandez[1], Jessica Mendoza[2], Francisco Hernandez[2], Darryl Irwin[2]

[1]nRichDX, Irvine, CA,[2]Agena Bioscience, San diego, CA

Introduction: Achieving high sensitivity in detecting cancer variants is essential for accurate diagnosis and monitoring of diseases. In this study, we explore the effectiveness of the nRichDX Revolution Sample Prep System in conjunction with the MassARRAY System for enhancing sensitivity and achieving 0.1% VAF in plasma and urine samples. The ability to detect such low-frequency variants is significant in clinical applications.

Methods: Whole blood from healthy donors was collected in K2EDTA tubes. Plasma aliquots were extracted from 5mL (6) and 20mL (6) inputs using the Revolution Max20 cfDNA Extraction Kit. Replicate samples were extracted using the QIAamp Circulating Nucleic Acid kit from QIAGEN. Urine from healthy donors was extracted from 10mL (3) and 20mL (3) inputs using the Revolution Max20 cfDNA Extraction kit. (12) Replicate samples were extracted using a MagMAX cfDNA Isolation kit from Thermo Fisher Scientific. All the samples were spiked with a cfDNA standard containing a KRAS p.G12V mutation at 0.1% VAF. The quantity and quality of extracted cfDNA were determined using the LiquidIQ Pro Panel on the MassARRAY System, which measures amplifiable cfDNA copies. Recovery and frequency of the spiked ctDNA standard were performed with the UltraSEEK LungPanel v2.0, capable of detecting variants as low as 0.1% VAF.

Results: The spiked KRAS mutation was recovered consistently by all nRichDX 5mL plasma samples with an accepted mutation frequency and high mutation significance z-score (z-score>10). However, 3/6 of the QIAGEN 5mL plasma samples did not detect the mutation. The spiked KRAS mutation was recovered consistently by all nRichDX 10 and 20mL urine samples with an accepted mutation frequency and high mutation significance z-score. However, all the MagMAX 10 and 20mL urine samples did not pass the QC (5) or detect the mutation (1). The amplifiable copies of cfDNA recovered from nRichDX 20mL plasma samples are significantly higher than Qiagen ($p < 0.0001$). The amplifiable copies of cfDNA recovered from nRichDX 10 and 20mL urine samples are significantly higher compared to MagMAX ($p < 0.0063$.)

Conclusion: The evaluation of the nRichDX Revolution Sample Prep System on the MassARRAY System has demonstrated its effectiveness in achieving 0.1% VAF detection in plasma and urine samples. The nRichDX System extracts cfDNA and ctDNA with consistently high yields. Two sample T-Test analysis shows that the nRichDX System performed significantly better than the QIAGEN and Thermo Fisher Scientific extraction kits. The results demonstrate the capability of the nRichDX system to recover more amplifiable copies with consistent cfDNA quality and ctDNA frequency with high z-scores. This advancement in sensitivity enhances our ability to detect rare cancer variants, leading to the potential for better patient outcomes in precision medicine.

CLINICAL RESEARCH: Molecular Biology in Clinical Oncology: Genetics and Beyond
Poster Session

#5047 Identifying genomic features associated with pathologic lymph node metastasis in lung adenocarcinoma patients.

S. Wang[1], **Z. Zhou**[1], S. Wang[2], R. Guo[2], Z. Ma[1], D. Zhao[1], L. Wang[1], Y. Liu[1], Y. Ma[1], J. Zhang[1], S. Wang[2], Y. Chen[2], H. Tang[2], Q. Ou[2], J. Chen[1];
[1]Peking University Cancer Hospital & Institute, Beijing, China, [2]Nanjing Geneseeq Technology Inc., Nanjing, China

Introduction: Lymph node metastasis evaluation in solid tumors is mainly complicated by the diagnostic yield of standard imaging modalities and tumor size contradictions. Exploring clinical/molecular features that complement the use of radiologic and bronchoscopy findings may provide significant values for a more accurate pathologic determination of nodal metastasis.
Methods: We analyzed surgery-resected tumor samples from 72 treatment-naïve lung adenocarcinoma (LUAD) patients via whole-exome sequencing (WES). Mutational profiles of patients categorized based on their pathologic lymph node metastasis (pN) status were assessed, and the association between metastatic-driving features and overall survival (OS) was then explored in both the study cohort and the Cancer Genome Atlas Program (TCGA) external cohort.
Results: Among all 72 patients, 41 (56.9%) were pathologically confirmed as positive for lymph node metastasis (pN-positive), while 31 (43.1%) were categorized as pN-negative. The most frequently mutated gene was *TP53* in both subgroups (54.8% and 53.7%, respectively), and the aberrant KEAP1-NRF2 signaling pathway was found significantly more enriched in pN-negative patients. Copy-number variant analysis showed that chromosome 7p amplifications (X7p_amp) at the arm level and *EGFR* amplifications at the focal gene level were more frequently identified in pN-positive patients (P=0.008 and P=0.004, respectively). Importantly, these amplifications were associated with worse OS in both the study cohort and the TCGA external dataset. Consistent with the unfavorable prognosis, pN-positive patients demonstrated a higher chromosome instability score (CIS) (median: 0.32 vs. 0.14, P=0.14) and a lower tumor mutation burden (TMB) (median: 1.83 vs. 3.85 muts/Mb, P=0.048) compared to pN-negative patients.
Conclusion: Our findings suggest that X7p_amp, particularly *EGFR* amplification, might be associated with pathologic involvement of lymph nodes and an unfavorable prognosis in LUAD patients. Our study highlights the importance of integrating clinical and genomic data into conventional radiologic modalities for a more accurate determination of pathologic nodal involvement.

#5048 NF2 mutations are enriched in FH deficient renal cell cancer.

K. Bin Satter, L. Xi, C. Rickets, W. M. Linehan, M. J. Merino;
National Cancer Institute, Bethesda, MD

Introduction: NF2 is a tumor suppressor gene in charge of producing a protein called Merlin that controls cell growth and division. Mutations in the NF2 gene affect predominantly the nervous system causing the development of benign tumors. NF2 mutations have been reported in Renal cancers with morphologically specific tumor types and in aggressive tumors. We studied a cohort of 16 cases of RCC in which the NF2 mutation was identified and describe other molecular changes as well as morphology and clinic-pathological correlation.

Materials and Methods: Sixteen patients had been consented and treated for renal masses in protocols of the UOB division of the NCI. Next generation sequencing was performed with tumor DNA from FFPE tissue using the Illumina TruSight Oncology 500 Kit (TSO500) NextSeq 550DX. TSO500 assay was designed to detect single nucleotide variations, small insertions/deletions, copy number variations from 92 genes, TMB and MSI. Morphology and IHC stains were performed.

Results: Nine patients were female and 7 males, ranging in age from 21 to 87 years. Fourteen patients underwent partial or total nephrectomies, one case had a biopsy and in 1 case a metastatic tumor to a lymph node was studied. Morphologically, nine cases were diagnosed as HLRCC, three clear cells, two cases with clear and papillary cell, one medullary and one oncocytoma. Genetic findings revealed mutations in NF2, FH,VHL, SMARCB1, HOBB13, ARID1B, B2M, EP300, BCORL1 and MGA. Concurrent coexistence of NF2 and FH mutations was present in 9 cases. Three patients with concurrent FH and NF2 mutations died of the disease.

Conclusions: NF2 mutations have been identified in a variety of morphologic types of Renal cell cancer. However, we were surprised by the number of cases with NF2 mutation in tumors that also harbor the FH (HLRCC) mutation. NF2 tumors have been reported to have an aggressive behavior, and FH cancers are also known to have poor survival. Genomic studies of renal cancers is recommended since some genetic alterations are targetable and may provide adequate therapies that will lead to longer survivals.

#5049 Detecting chromosomal copy number variations and point mutations in Glioma using a single assay; sparing tissue while significantly reducing testing time and cost.

M. L. Mimosa[1], J. T. Simpson[1], K. Boissinot[2], M. Tiab[2], R. Fattouh[1], R. M. Saleeb[1];
[1]University of Toronto, Toronto, ON, Canada, [2]St. Michael's Hospital, Toronto, ON, Canada

We aimed to develop a single streamlined assay to detect all Glioma biomarkers. The current diagnosis of Gliomas incorporates molecular biomarkers that include whole chromosomal copy number variations (CNVs) and single nucleotide variations (SNVs). Testing CNVs and SNVs are traditionally done using different large platforms and are performed in large genomic facilities that have the suitable infrastructure. This creates delays in testing, where samples undergo lengthy referrals and the tissue is often split between institutions, which also adds substantially to the costs. We have previously used Nanopore sequencing to develop an assay to detect *IDH* SNVs from formalin-fixed paraffin-embedded (FFPE) tissue. Nanopore sequencing platform uses small inexpensive tools and can test for both CNVs and SNVs. However, combining both targets efficiently in FFPE tissue remains a challenge.
While nanopore whole genome sequencing can detect CNVs, it does not allow for enough coverage to accurately detect small SNVs. Also, raw FFPE DNA is not compatible with the nanopore technology. To fix both challenges we used a PCR based approach that allows enrichment of the SNV targets, as well as creates new nanopore compatible DNA copies. To counteract the bias that PCR creates with uneven amplification, we used a SNP based method to call chromosomal gains and losses. Statistical analysis of probability showed that targeting 15 heterozygous SNPs per chr arm is sufficient for accurate CNV detection (error rate <0.1%). A total of 57 amplicons targeting CNVs on Chr 1,7, 10, 19, and *EGFR* gene; and *IDH1 and IDH2* SNVs were pooled together in one assay and tested on 4 Glioma samples. Variant calling was performed with a custom Python script.
All CNV targets were accurately detected on all samples. Losses in chr 1p, 19q and chr 10 were evident with a loss of heterozygosity (LOH) pattern on the SNP analysis. The gain in chromosome 7 was also observed as an allele gain 2:1 SNP pattern on the corresponding samples. The SNV statuses of these samples were also accurately detected when compared to reference results. Finally, the SNV and CNV calling analysis were streamlined using custom shell script, further reducing total turnaround time (including sequencing and data analysis) to less than a day for the entire batch of samples. Initial cost analysis shows <50% of the traditional testing costs for the assay.
This work is the first to develop a streamlined single test to detect CNVs and SNVs in Gliomas using FFPE DNA on the nanopore sequencing platform. The shorter testing time, streamlined workflow, and low assay/capital cost could positively influence the care of brain cancer patients. Notably, nanopore-based sequencing tools can also be implemented in other types of tumor diagnosis, especially by smaller labs, helping to overcome many of the existing diagnostic challenges.

#5050 Germline variants in *CDKN2A* wild-type melanoma prone families.

S. Knappskog[1], G. T. Iversen[1], M. Loeng[2], A. L. Holth[2], P. E. Lonning[1], J. Geisler[2];
[1]University of Bergen, Bergen, Norway, [2]Akershus University Hospital, Lorenskog, Norway

The presence of germline pathogenic variants in *CDKN2A* is a well-established underlying cause of familial malignant melanoma. While pathogenic variants in several other genes have also been linked to melanoma development, many familial cases remain unexplained. We analyzed for pathogenic germline variants in a panel of 360 cancer related genes in a set of 56 Norwegian melanoma prone families. The index cases and families were selected based on familial history of melanoma and/or multiple primary melanomas in the same individual, along with previous negative tests for pathogenic *CDKN2A* variants. We found 6 out of 56 index individuals to carry germline pathogenic or likely pathogenic variants. These variants were found in *BRCA2*, *MRE11*, *ATM*, *MSH2*, *CHEK2* and *AR*. In addition, one family member with a melanoma diagnosis (not index case) carried a pathogenic variant in *MAP3K6*. In genes typically linked to xeroderma pigmentosum, we found a high fraction of variants previously considered benign and/or as variants of uncertain significance. In particular the XPC^{L48F} variant was found in 8 out of 56 indexes, thus, the allele fraction (0.07) was significantly higher than in comparable healthy populations (p-values from 0.007 to 0.014). Similarly, we found presumed benign or uncertain variants in *MC1R* to be significantly enriched or numerically higher in index cases versus comparable healthy populations (p-values from 0.009 to 0.1). The common $MC1R^{Arg151Cys}$ variant was highly enriched in our cohort (p=0.001).In conclusion, we found that several melanoma prone families harbored pathogenic variants in genes not usually linked to melanoma.

#5051 Evolutionary characterization and refinement of copy-number high endometrial carcinoma.

C. J. H. Kramer[1], D. Ruano[1], A. Hawari[2], F. Blanc-Durand[3], C. D. de Kroon[1], J. R. Kroep[1], G. Ortoft[4], E. Hogdall[5], A. Leary[3], C. L. Creutzberg[1], M. P. G. Vreeswijk[1], N. Horeweg[1], D. N. Church[6], D. C. Wedge[2], T. Bosse[1];

[1]Leiden University Medical Center (LUMC), Leiden, Netherlands, [2]Manchester Cancer Research Centre, Manchester University, Manchester, United Kingdom, [3]Institute Gustave Roussy, Villejuif, France, [4]Copenhagen University Hospital, Rigshospitalet, Copenhagen, Denmark, [5]Copenhagen University Hospital, Herlev and Gentofte Hospital, Copenhagen, Denmark, [6]University of Oxford, Oxford, United Kingdom

Copy-number (CN)-high endometrial carcinoma (EC) is characterized by abundant CN-alterations, thought to be driven by *TP53* aberrations, and is the subgroup with the poorest prognosis. CN-high EC exhibit substantial heterogeneity in histotypes, molecular markers, and mutational profiles. Here, we aimed to refine this subgroup by assessing the evolution and identifying CN-signatures (Drews et al. Nature) to establish CN-clusters. We used whole-genome sequencing (WGS;100X) data from 146 CN-high cases from Genomics England (GeL) as discovery cohort. We then performed shallow WGS (sWGS;0.1X) of FFPE tumor DNA of *n*=307 CN-high EC from (non-)trial cohorts. Timing of canonical driver mutations by MutationTimer in CN-high GeL revealed that *TP53* mutations were: (i) not ubiquitous and (ii) not consistently identified as early clonal events (Table), challenging conventional belief that *TP53* inactivation is necessary for initiation of CN-high EC. Evolutionary analyses (Plackett-Luce) are ongoing to identify carcinogenesis trajectories and assess how driver mutations other than *TP53* influence CN-phenotypes. Unsupervised clustering of 307 EC by CN-signatures identified five clusters (E1: 19%; E2: 2%; E3: 20%; E4: 19%; E5: 40%), characterized by CN-signatures linked to biological phenomena. Clusters E1/E4 reflect homologous recombination deficiency (CX3), while cluster E5 seems driven by chromosomal missegregation (CX1). Notably, there was no one-to-one relationship between CN-clusters and histotypes, suggesting CN-evolution is independent of morphology. In conclusion, we have identified *TP53*-dependent and -independent pathways in CN-high EC evolution. Potentially clinically relevant CN-clusters were identified using cost-effective sWGS. sWGS of additional *n*=475 CN-high EC are ongoing. Furthermore, we will analyze in-depth clinicopathological relationships of clusters, including prognosis/prediction, using PORTEC trials prior to the meeting.

Table. Timing of canonical driver mutations in CN-high EC

	Clonal - early	Clonal - late	Subclonal	Clonal - NA	Total
1. *TP53*	87 (67%)	4 (3%)	3 (2%)	36 (28%)	130 (100%)
2. *PIK3CA*	42 (76%)	1 (2%)	1 (2%)	11 (20%)	55 (100%)
3. *PPP2R1A*	18 (47%)	1 (3%)	2 (5%)	17 (45%)	38 (100%)
4. *PTEN*	17 (59%)	1 (3%)	2 (7%)	9 (31%)	29 (100%)
5. *PIK3R1*	11 (46%)	0 (0%)	3 (13%)	10 (42%)	24 (100%)
6. *FBXW7*	14 (61%)	0 (0%)	0 (0%)	9 (39%)	23 (100%)
7. *KRAS*	9 (64%)	0 (0%)	2 (14%)	3 (21%)	14 (100%)
Abbreviation: NA, timing not applicable.					

#5052 Novel drug resistance mechanisms and drug targets in *BRAF* mutated peritoneal metastasis from colorectal cancer.

C. Lund-Andersen[1], A. Torgunrud[1], C. Kanduri[2], V. J. Dagenborg[1], I. S. Froysnes[1], M. M. Larsen[2], B. Davidson[1], S. Larsen[1], K. Flatmark[1];
[1]Norwegian Radium Hospital, Oslo University Hospital, Oslo, Norway, [2]University of Oslo, Oslo, Norway

Objective: Patients with peritoneal metastasis (PM) from colorectal cancer (CRC) have inferior prognosis and respond poorly to chemotherapy compared to other metastatic locations. This study aims to identify the molecular explanation for the observed clinical behavior and suggest novel treatment strategies in PM-CRC.

Design: Tumor samples from a Norwegian national cohort of 230 patients undergoing surgery and hyperthermic intraperitoneal chemotherapy (HIPEC) with mitomycin C (MMC) for PM-CRC were subjected to targeted DNA sequencing, and associations between molecular findings and clinical data were analyzed. mRNA sequencing was conducted on a subset of thirty samples to compare gene expression in tumors harboring mutations in the *BRAF* or *KRAS* oncogenes and wild-type tumors.

Results: Almost one-third of the patients had mutations in the *BRAF* oncogene, which were associated with *RNF43*/R-Spondin aberrations and low expression of negative Wnt regulators (ligand dependent Wnt activation). This molecular profile, with high abundance in PM, could be an underlying mechanism promoting aggressive tumor biology that facilitates metastasis to the peritoneal cavity, and could contribute to the observed poor overall survival of this patient subgroup. *BRAF* mutations were also associated with gene expression changes in transport solute carrier proteins and drug metabolism enzymes that could influence the efficacy of MMC and irinotecan, commonly used in PM-CRC treatment. *BRAF*-mutated tumors exhibited increased expression of BTN immune checkpoint molecules, and targeting these checkpoints in addition to ligand dependent Wnt activation could be two novel targeted therapy approaches.

Conclusion: *BRAF* mutations were associated with particularly poor survival in this cohort, possibly related to altered drug transport and metabolism conferring resistance to MMC and irinotecan. Two potential novel therapeutic approaches were identified, suggesting specific targeting of BTN immune checkpoint molecules and the use of inhibitors to target ligand-dependent Wnt activation.

#5053 Clinicopathologic and molecular genetic features of STAT3-mutated myeloid neoplasms.

M. T. Ye, Z. Zuo, S. Calin, F. Ye, H. He, W. Kamata, M. You;
UT MD Anderson Cancer Center, Houston, TX

STAT3 is a key transcription factor that can mediate cancer progression through phosphorylation or gain-of-function mutations. *STAT3* mutations have been mainly associated with large granular lymphocytic T-cell leukemia. Whereas STAT3 activation is common in myeloid neoplasms, it is primarily mediated through STAT3 phosphorylation. *STAT3* mutation has only rarely been reported in myeloid neoplasms. We assessed the clinicopathologic and molecular genetic features of 32 *STAT3*-mutated myeloid neoplasms. Twenty (62.5%) cases were classified as acute myeloid leukemia (AML), 7 (21.9%) as myelodysplastic syndrome (MDS), and 5 (15.6%) as chronic myelomonocytic leukemia (CMML). It is of note that *STAT3* mutation was not detected in myeloproliferative neoplasms (MPN). *STAT3* mutations were detected at the initial diagnosis in 22 of 25 (88%) cases, suggesting *STAT3* mutation is an early event in pathogenesis. However, *STAT3* mutations represented the dominant clone in only 6 (18.8%) cases, all classified as AML. Most are missense mutations, located at the SH2 domain. The median variant allele frequencies were 6.8%, 4.6% and 3.1% for AML, MDS and CMML, respectively, and in a case of CMML, the VAF increased from 2.4% to 34.8% upon leukemic transformation. *STAT3* mutation was accompanied by co-existing mutations in all cases, with *SRSF2* (40.6%), *TET2* (40.6%), *ASXL1* (37.5%), and *SETBP1* (34.4%) being most common. Cases with *STAT3* mutations were usually associated with morphologic dysplasia and increased blasts. Monosomy 7/del7q was the most common cytogenetic abnormality, seen in 11 (34.4%) cases. With a median follow-up of 24.5 months, 21 patients died, 6 had persistent disease, and 5 achieved complete remission. We summarize that *STAT3* mutation is present in a variety of myeloid neoplasms, but not seen in MPN. It is often an early events and always with concurrent mutations. It may play an important role in the pathogenesis and progression of myeloid neoplasms by activating JAK-STAT pathway, and may serve as a potential therapeutic target.

#5054 Optimization and evaluation of an FFPE dual extraction protocol for next-generation sequencing applications.

R. Hong[1], J. Chu[2], S. Hsiao[1], D. Whang[1], S. P. Rivera[2], H. Xie[1], J. Guo[2];
[1]NeoGenomics, San Diego, CA, [2]NeoGenomics, Aliso Viejo, CA

Formalin-fixed paraffin-embedded (FFPE) biopsies are highly valuable and widely used tissue specimens for clinical diagnostics. However, obtaining sufficient and high-quality nucleic acid material from limited FFPE samples presents a challenge for downstream molecular analysis, such as next-generation sequencing (NGS). We present an optimized sequential extraction method that generates high-quality DNA and RNA from a single set of input tissues that is automatable and operation-friendly. This workflow performs well with reduced FFPE tissue input and efficiently supports various high-throughput clinical NGS applications. The DNA/RNA yield, quality, purity, and impacts on NGS assay performances were on par or better than an existing validated comparator extraction method. With comparable FFPE input, the new method demonstrated a superior extraction performance with significantly higher yield, quality, and purity. For DNA, NGS libraries were made with two different library preparation methods: a TA-ligation-based method and a single-strand-based method, followed by hybrid capturing and sequencing. The DNA from the new extraction method demonstrated a superior library conversion rate and improved target enrichment uniformity with both chemistries. This provides the potential of reduced input requirements, allowing very limited tissue, such as fine needle aspirate or core needle biopsy, for clinical NGS testing. The sequencing results were highly concordant between the existing and new extraction methods when the extracted DNA was subjected to a validated comprehensive genomic profiling (CGP) clinical test, demonstrating the quality and robustness of the extraction. For RNA, NGS libraries were made following the validated CGP clinical test with hybrid capturing, and the results were comparable between the two extraction methods. In conclusion, an FFPE extraction method was optimized to allow more clinical biopsy samples to be tested with different NGS workflows, providing a better diagnostic value for patient care.

#5055 Genetic background of recurrent uterine leiomyomas.

S. Khamaiseh[1], A. Ayravainen[1], M. Arffman[1], S. Reinikka[1], A. Pasanen[1], R. Butzow[1], P. Harkki[2], P. Vahteristo[1];
[1]University of Helsinki, Helsinki, Finland, [2]Helsinki University Hospital, Helsinki, Finland

Uterine leiomyomas, also known as fibroids, are common benign smooth muscle tumors in women of reproductive age. Leiomyomas can cause symptoms that can significantly reduce the quality of life. Treatment mainly involves hysterectomy or myomectomy, the latter for women who wish to preserve their uterus. Most leiomyomas harbor one of the three driver mutations affecting either *MED12*, *HMGA2*, or *FH*. Recently identified rare subtypes include tumors with mutations in genes linked to the neddylation of the Cullin 3-RING E3 ligase or SRCAP complex. Recurrence of leiomyomas is poorly understood in relation to their clonal origins and molecular factors. The aim of this study was to characterize the mutational profiles of leiomyomas from recurrent operations and to identify the frequency of clonally related tumors. We utilized a retrospective cohort of 234 women who underwent laparoscopic or open abdominal myomectomy, with 46 (20%) of them experiencing multiple procedures related to leiomyomas. We examined the mutation profiles of 133 leiomyomas (62 index and 71 recurrent tumors) from 33 patients who required multiple tumor removal surgeries. We screened the tumors for the three primary leiomyoma drivers—*MED12* mutations, HMGA2 overexpression, and FH-deficiency—to identify potentially clonal tumors. We found that 21 out of 33 (64%) patients had tumors from multiple operations with identical leiomyoma driver alterations. To further assess the clonal relationship, we executed whole exome sequencing on these 52 tumors. We identified three patients with two clonally related tumors each through shared somatic copy number alterations and point mutations. The clonally related tumors included HMGA2, FH, and wild-type tumors. Notably, leiomyomas with *MED12* mutations—the most common molecular leiomyoma subtype—were not found among the clonally related tumors. Three patients harbored numerous FH-deficient tumors from recurrent operations. In all those patients, we found *FH* germline mutations, characteristic of Hereditary Leiomyomatosis and Renal Cell Cancer syndrome (HLRCC). Moreover, we identified somatic mutations in *YEATS4*, a member of the SRCAP complex, in four recurrent tumors from three patients. Interestingly, all *YEATS4* mutations were different, and the tumors were not clonally related. Further research is required to elucidate the role of *YEATS4* in leiomyoma recurrence. In conclusion, our systematic study confirms that reinterventions are common after myomectomy, and while uterine leiomyomas typically develop independently, some share a clonal origin. Additionally, we show that recurrence may be due to genetic predispositions, such as germline *FH* mutations.

#5056 Molecular characterization of microsatellite stable (MSS) colorectal cancer (CRC) patients with a BRAF V600E mutation.

Y. van der Pol[1], B. Yilma[1], V. K. Morris[2], C. Chao[1], M. Harris[1], J. Guinney[1], S. Kopetz[2];
[1]Tempus Labs, Chicago, IL, [2]MD Anderson Cancer Center, Houston, TX

Introduction: A $BRAF^{V600E}$ mutation is an unfavorable prognostic biomarker for CRC and is associated with short-lived treatment response to BRAF and EGFR blockade. Anti-PD-1 therapies are ineffective in MSS CRC but demonstrate efficacy in combination with BRAF + EGFR inhibition for MSS $BRAF^{V600E}$ CRC. A comprehensive characterization of MSS $BRAF^{V600E}$ CRC as an immunologically distinct subpopulation of MSS CRC has not been performed. Here, we characterize the clinicopathological and transcriptomic features of MSS $BRAF^{V600E}$ CRC patients, relative to $BRAF^{WT}$ MSS CRC patients.Methods: De-identified records of 12,009 MSS CRC patients were retrospectively analyzed from the Tempus clinicogenomic database. CMS subtypes were derived using the CMScaller algorithm. Survival was assessed using Kaplan-Meier survival analysis with risk set adjustment (RSA) method; log-rank test was used to compare survival. Categorical and continuous variables were compared using chi-squared test and Wilcoxon rank sum test, respectively.
Results: $BRAF^{V600E}$ was found in 5% (n=630) of the patients. Demographics and clinicopathological features varied significantly between the $BRAF^{WT}$ and $BRAF^{V600E}$ cohorts (Table 1). Relative to the $BRAF^{WT}$ cohort, $BRAF^{V600E}$ tumors were enriched for the immune-activated CMS1 signature (53% vs 11%, p< .001), PD-L1 detection (9.5% vs 3%, p<0.001), and CD8+ T-cell infiltration (4.6% vs. 2.5%, p<0.001). CMS4 was linked to an unfavorable prognosis in the $BRAF^{WT}$ cohort (HR=0.58 compared to CMS1, p=0.026), yet this was not observed in the $BRAF^{V600E}$ cohort (HR=2.60 compared to CMS1, p=0.083).
Conclusions: $BRAF^{V600E}$ MSS CRC exhibited immune activation characteristics that were not observed in the $BRAF^{WT}$ group, including greater CMS1 status, PD-L1 expression, and CD8-T cell infiltration. Our findings support investigation of novel immune-based therapeutic strategies of MSS $BRAF^{V600E}$ CRC as an immunologically distinct subpopulation of MSS CRC.

Cohort characteristics

			$BRAF^{WT}$	$BRAF^{V600E}$	P-value
Demographics	Age (median)		60 (51,69)	65 (55,74)	<0.001
	Ethnicity	Not Hispanic or Latino	3,444 (83%)	200 (93%)	0.001
		Hispanic or Latino	699 (17%)	16 (7.4%)	
	Gender	Female	4,771 (42%)	345 (55%)	<0.001
		Male	6,608 (58%)	285 (45%)	
	Race	White	5,050 (75%)	318 (87%)	<0.001
		Black or African American	888 (13%)	19 (5.2%)	
		Other	517 (7.7%)	20 (5.4%)	
		Asian	297 (4.4%)	10 (2.7%)	
Clinicopathology	TNM stage	I	61 (0.7%)	0 (0%)	0.1
		II	388 (4.6%)	17 (3.2%)	
		III	1,130 (13%)	88 (17%)	
		IV	6,941 (81%)	424 (80%)	
	Laterality	Right	777 (15%)	89 (39%)	<0.001
		Transverse	193 (3.8%)	27 (12%)	
		Left	2,326 (46%)	73 (32%)	
		Rectum	1,761 (35%)	37 (16%)	
	CMS	CMS1	1,077 (11%)	307 (53%)	<0.001
		CMS2	3,067 (31%)	6 (1%)	
		CMS3	1,777 (18%)	71 (12%)	
		CMS4	3,920 (40%)	199 (34%)	
Immunology	CD8 T-cell infiltration (median, IQR)		2.5% (0.0, 7.7)	4.6% (0.0, 9.4)	<0.001
	PD-L1		127 (3%)	22 (9.5%)	<0.001

#5057 microRNA profiling in combination with whole exome sequencing reveals insights into long-term recurrence patterns in chordoma.

S. R. Ullmann[1], F. Karras[1], J. Schreier[1], K. Korber-Ferl[2], D. A. Ullmann[3], S. Franke[1], A. Roessner[1], D. Jechorek[1];

[1]Otto von Guericke Univ. of Madgeburg, Magdeburg, Germany, [2]Martin-Luther-Universitat Halle-Wittenberg, Halle, Germany, [3]Berufgenossenschaftliches Universitatsklinikum Bergmannsheil Bochum, Bochum, Germany

While few studies on miRNA profiling in primary chordomas have been published, there is no data on the miRNA landscape of long-term recurrences. Therefore, we performed a miRNA analysis and whole exome sequencing (WES) investigating four patients with multiple recurrences over seven to 16 years and eight patients with non-recurrent tumors (NRTs), conventional, sacral chordomas in order to compare both groups as well as the recurrence cases (RCs) to each other. Our aim was to find typical miRNA patterns distinguishing the recurrences from the NRTs. After histopathological classification, immunohistochemical and morphometric analysis, DNA and miRNA were extracted from formalin-fixed-paraffin-embedded tissue samples and analyzed by WES and Nanostring. The microRNA regulation patterns showed similarities within RCs differing from NRTs. In unsupervised clustering there is a tendency of recurrences clustering apart from the NRTs. The differential expression between cases developing recurrences and NRTs showed highly significant differences between both groups with 32 miRNAs upregulated in the RCs being downregulated in NRTs. The miRNA expression of long-term recurrences of each patient are quite homogenous differing only from their primary tumor. Comparing NRTs with primary tumors that would later develop long-term recurrences showed significant up-regulation of 5 miRNAs in the RCs. This suggests a pivotal molecular difference between singular and long-term recurring chordomas. Our WES analysis confirmed known and revealed possible new driver genes. Recurring tumors had a higher number of mutations classified as pathogenic as well as increased proliferation rates and pleomorphic changes. Recurrences displayed a change in mutational distribution, showing considerably more disturbances in embryonic signaling and our proposed driver genes. Intriguingly, our study found a progress in number of alterations throughout the recurrences most of all affecting chromatin regulation and the new drivers.

Less disruption of these pathways in primary cases than in recurrences implies their pivotal role not only in chordoma formation, but also in recurrence evolution. The miRNA alterations were correlated with the genomic differences. Validated affected genes of miRNAs deregulated primarily in the recurrences are involved in those pathways as well. As current targeted therapy options are only sporadically altered in few patients, the progress in number of pathogenic mutations throughout the recurrences as well as the drastic change in miRNA expression could present new research approaches for chordomas with long-term recurrences. Combined clinical and molecular studies of miRNA patterns and genetic alterations could expand the understanding of recurrence development leading to new therapeutic targets inhibiting or delaying recurrence formation.

#5058 Genomic alterations predictive of outcome in early staged cervical cancer: *A translational investigation from the SENTICOL III trial*.

M. El Gani[1], S. Ibadioune[2], Z. El Beaino[3], A. Hamza[2], S. Vacher[2], E. Jeannot[2], J. Masliah-Planchon[2], A. Salomon[2], A. Degnieau[2], A.-S. Bats[4], M. Koskas[5], V. Fourchotte[2], E. Wafo[6], N. Bourdel[7], R. Fauvet[8], M. Plante[1], P. Mathevet[9], **M. Kamal**[2], F. Lecuru[10], I. Bieche[2];

[1]CHU de Quebec, Universite Laval, Quebec, QC, Canada, [2]Institut Curie, Paris, France, [3]Hopital St Joseph, Paris, France, [4]Hopital Europeen Georges Pompidou, Paris, France, [5]Hopital Bichat Claude Bernard, Paris, France, [6]Grand Hopital de l'Est Francilien, Jossigny, France, [7]CHU Estaing, Clermont Ferrand, France, [8]CHU Cote de Nacre, Caen, France, [9]CHUV - Centre Hospitalier Universitaire Vaudois, Lausanne, Switzerland, [10]Universite Paris, Institut Curie, Paris, France

Background: The risk of relapse in patients with early-stage cervical cancer (ESCC) ranges from 4-14% (LACC study). Risk-factors for recurrence are mainly derived from histopathological factors. Senticol III is a large multicenter international randomized prospective study aims to validate sentinel lymph node biopsy in the surgical management of ESCC. Our objective is to characterize prognostic and actionable biomarkers in ESCC.

Methods: FFPE-fixed tumoral slides of the first 150 randomized patients were analyzed based on SEDLIS criteria. We characterized TIL's infiltration, PD-L1 expression and HPV status. Sequencing of tumor DNA was carried out using an in-house targeted next-generation sequencing panel (571 genes). Relapse-free survival (RFS) was defined as the time between randomization and relapse of any type. We performed Fisher's exact test and Student's t-test to compare distributions of categorical variables and Log Rank test.

Results: The sequencing quality control criteria were met for 135 samples. *PIK3CA* was the most commonly altered gene (17%). Loss-of-function variants in *KMT2*-family genes (*KTM2C* 9%, *KMT2D* 6%, *KMT2A* 1%) were found in 16% of samples. The loss-of-function variant of *ARID1A* was mostly non-sense mutation (6%). Activations of *ERBB2* (5%) were 3 focal amplifications and 4 hotspot missense mutations. Two samples were found to have microsatellite instability due to an alteration of *MLH1*. The Pik3/AKT/mTOR (26%) and the chromatin remodeling (23%) pathways were the most altered pathways. The median follow-up period was 20 months. There were 6 relapses, of which 80% were considered as low risk based on SEDLIS criteria. Recurrences were local and occurred 9-23 months following surgery. Multiparity was the only clinical feature associated with RFS ($p < 0,001$). Tumor size, histological subtypes, PD-L1 status, number of TIL's, presence or absence of lymphovascular emboli and deep stromal invasion were not associated with RFS in our cohort.*KMT2C* ($p=0,018$) and *ARID1A* ($p < 0,001$) pathogen variants were significantly associated with RFS. The pathway chromatin remodeling ($p=0,063$) showed a trend toward association with RFS. We found 32% of genomic alterations actionable for a target therapy including mutations of PIK3CA, ERBB2, ARID1A, PTEN, BRCA2, KRAS, BRAF, CDK12, FGFR2, NF1, AKT1, BRCA1, TP53 and MSI-high.

Conclusion: Our prospective, randomized and multicentric study suggests a genomic profile from a homogeneous cohort of 150 patients. We identified genes involved in chromatin remodeling (*ARID1A* and *KMT2C*) as prognostic biomarkers of clinical interest and suggesting the relevance of epidrugs in ESCC. Theranostic annotations of variants identify a matched to target therapy for 32% of alterations. Those targets represent multiple tracks for personalized therapy in ESCC.

#5059 Robust single sample consensus molecular subtype classification for primary and metastatic colorectal cancer.

A. J. Sedgewick, T. Chandra, T. Taxter, J. Guinney;
Tempus Labs, Chicago, IL

Introduction Consensus Molecular Subtypes (CMS) represent a well-established molecular stratification framework for colorectal cancer (CRC). Existing methods for CMS classification rely on a representative input cohort as a preprocessing step (CMScaller) or have difficulty generalizing to metastatic samples (CMSclassifier). We developed Tempus CMS to overcome these limitations. Our method normalizes gene expression data from input samples to a static reference cohort to enable single sample classification of both primary and metastatic tumors. We evaluated the performance of this classifier on a large, de-identified CRC cohort comprising 8,489 samples from primary and metastatic sites.

Methods To normalize input data, our method shifts and scales each gene expression value based on the mean and standard deviation of the expression of that gene in the reference cohort (n=2,787 primary and metastatic CRC). CMS calls are then generated via nearest template prediction similar to CMScaller (Eide et al., 2017). The analysis cohort was selected from clinical biopsies within 30 days of primary or metastatic diagnosis excluding reference cohort samples. CMS calls were assessed by comparing subtype prevalence to reported rates and by testing for known enrichments of pathways and genomic markers.

Results Subtype prevalences for lower gastrointestinal (GI) biopsies and resections (n=5,090) were comparable to reported rates for primary CRC tumors: CMS1 - 12%, CMS2 - 28%, CMS3 - 19%, and CMS4 - 33% with 7.6% no calls. Biopsies from metastatic tissue showed site-specific changes in prevalence: CMS2 increased to 43% in liver samples (n=1,715) and CMS4 was identified in 49% of samples from metastatic sites excluding the liver (n=1,684). In addition, we found that purity had an effect on prevalence: in lower GI tumors with ≥ 50% tumor purity rates of CMS2 and CMS4 were 34% and 26%, respectively, while rates in tumors with purity between 20% and 50% were 20% CMS2 and 41% CMS4.

Across all tissue groups, pathway enrichment showed significant associations, including TGF-□ signaling in CMS4 (adj *P* ≤ 4.4e-15) and cell differentiation in CMS3 (adj *P* ≤ 3.0e-27). Expected enrichments of CMS markers were also observed: *BRAF* mutations and microsatellite instability in CMS1 and *KRAS* mutations in CMS3. In liver tissue, higher *KRAS* mutation rates were noted in CMS1 (57%) and CMS3 (83%) compared to GI tissue (35% and 67%, respectively).

Conclusions In this study, we developed an enhanced, single sample CMS-calling algorithm optimized for primary and metastatic sites. Application of this algorithm in a large cohort recapitulated known biology, which suggests that the tool can be used to support clinical studies requiring robust molecular stratification.

#5060 Role of molecular driver mutations in recurrence of early stage laryngeal cancer following narrow field definitive radiotherapy.

Aaron Segura[1], Emily Nissen[2], Chris Lominska[3], Ryan Morse[4], Deri Morgan[3], Prakash Neupane[5], Dong Pei[2], Devin Koestler[2], Randall Kimple[6], Umamaheswar Duvvuri[7], Kevin Sykes[8], Sufi Thomas[8], Rohit Nallani[8], Lisa Shnayder[8], Kiran Kakarala[8], Andres Bur[8], Emrullah Yilmaz[9], Gregory Gan[10]

[1]Department of Internal Medicine, Division of Radiation Oncology, University of New Mexico Health Sciences Ctr., Albuquerque, NM,[2]Department of Biostatistics & Data Science, University of Kansas Medical Center, Kansas City, KS,[3]Department of Radiation Oncology, University of Kansas Medical Center, Kansas City, KS,[4]Department of Radiation Oncology, University of North Carolina, Chapel Hill, NC,[5]Division of Medical Oncology, Department of Internal Medicine, University of Kansas Medical Center, Albuquerque, KS,[6]Deparment of Human Oncology, University of Wisconsin School of Medicine and Public Health, Madison, WI,[7]Department of Otolaryngology, Head and Neck Surgery, NYU Grossman School of Medicine, New York, NY,[8]Department of Otolaryngology, Head & Neck Surgery, University of Kansas, Kansas City, KS,[9]Department of Hematology and Medical Oncolgy, Cleveland Clinic, Cleveland, OH,[10]University of Kansas Cancer Center, Kansas City, KS

PURPOSE/OBJECTIVES

Recurrent early-stage laryngeal cancer poses profound clinical and prognostic dilemmas. The primary endpoint of this study was to identify patient exome differences between early-stage laryngeal cancer patients who responded or rapidly progressed following definitive, narrow field radiotherapy. Our study offers the first exploration of mutation patterns in early-stage laryngeal head and neck squamous cell carcinoma (HNSCC) patients receiving curative radiation therapy.

MATERIALS/METHODS

We identified 36 early-stage laryngeal (T1 = 8, T1a = 4, T1b = 2, T1c = 1, T2 = 20, NA =1) HNSCC patients from the University of Kansas Medical Center treated with definitive narrow field radiotherapy to 63-70 Gray (gy) dose. Whole exome sequencing was performed in all patients. Patients were stratified into “responders” (never failed, N=14) and “non-responders” (recurrence <12 months, N=21). Most non-responder patients with local recurrence underwent total salvage laryngectomy (TSL, N=18). All patients underwent whole exome sequencing. The Genome Analysis Toolkit (GATK) was used for pre-processing and functional annotation of variants. Cancer driver genes were detected for each group using the OncodriveCLUST algorithm. Differentially mutated genes were assessed using Fisher’s exact or exact McNemar’s test at $P < 0.05$. Tumor mutational burden (TMB) comparisons employed the Wilcoxon rank-sum test with the same threshold. For pathway analysis in Reactome and Ingenuity, a $P < 0.1$ was used for exploratory significance.

RESULTS

Mutation analysis identified distinct cancer driver genes between responders, (N=3), non-responders (N=36), and post-TSL (N=4). Among 75 genes with significant pre-treatment mutation differences between responders and non-responders, KCNT2 and AGAP6 were exclusively mutated in non-responders (OR=0, P=0.005 and OR=0, P=0.027, respectively). ADAMTS7 was solely mutated in responders (OR=inf, P=0.019), and PLEC showed more mutations in responders (OR=11.6, P=0.006). Pathway analysis showed these genes were involved in the RND2 GTPase cycle, protein O-glycosylation related diseases, and apoptotic pathways. Post-treatment analysis indicated an enrichment of mutations in apoptosis regulation pathways, with genes like PLEC being more frequently mutated in responders than in non-responders or TSL patients. In addition, we observed in non-responders that they trended towards higher median pre-treatment TMB compared to responders (7.98 vs 6.16, P=0.072). There was no significant difference in TMB between TSL patients and responders or non-responders pre-treatment.

CONCLUSION

Our analysis reveals distinct mutation patterns in early-stage laryngeal cancer patients by response to radiotherapy and the potential role of these mutated genes in apoptosis related pathways.

#5061 Improved survival and unique mutational signatures in small cell lung cancer arising in patients with limited tobacco use.

K. Concannon[1], M. Sahu[2], W. Lewis[1], H. Tran[1], L. Diao[1], Y. Xi[1], B. Morris[1], S. Heeke[1], X. Tang[1], J. Stewart[1], I. Valiev[3], G. Raso[1], J. Wang[1], K. Sasaki[1], C. Gay[1], J. Heymach[1], L. Byers[1];

[1]The University of Texas MD Anderson Cancer Center, Houston, TX, [2]The University of Texas Health San Antonio Long School of Medicine, Houston, TX, [3]BostonGene LLC, Waltham, MA

Small-cell lung cancer (SCLC) remains the deadliest histologic lung cancer subtype with a median survival of only 12.3 months among trial-eligible patients with extensive-stage (ES-SCLC) disease, as demonstrated in the IMPower133 trial. Heavy tobacco use, >40 pack-years, is strongly associated with developing SCLC, which near universally harbors *RB1* and *TP53* co-mutations. However, there is a paucity of information regarding SCLC tumors that occur in patients with minimal tobacco use. This represents an unmet need given an increasing appreciation for low pack-year and never-smoker SCLC with some studies, like the CAPSTONE-1 trial, demonstrating an incidence of never-smoking SCLC >20%. To address this, we clinically characterized the treatments and outcomes of a 164 SCLC patient cohort with ≤10 pack year smoking histories treated at the University of Texas MD Anderson Cancer Center; 22 of which underwent whole-exome sequencing (WES).

The overall survival of limited-stage (LS-SCLC) and extensive-stage (ES-SCLC) disease in the low pack-year cohort were 33.6 and 16.6 months, respectively (P=0.003); superior to historic medians of roughly 17.0 and 12.3 months, respectively. Among those with ES-SCLC, those who reported 1-10 pack-years had significantly improved median overall survival as compared to never-smokers; 19.5 vs 15.8 months, respectively (P=0.02). This trend was observed in LS-SCLC as well with 1-10 pack-year and never-smokers demonstrating median overall survivals of 88.6 vs 26.2 months, respectively (P=0.2). Demographic differences including age were similar across these cohorts.

WES of tumors from 22 patients demonstrated significantly fewer mutations in *RB1* and *TP53* than was observed in previously reported cohorts of SCLC from smokers. Among the low-pack year cohort, 7/22 (32% vs 98.2%:P<0.001) harbored an *RB1* alteration, 7/22 (32% vs 90.9%: P<0.001) harbored a *TP53* mutation, and 4/22 (18% vs 90.9%: P<0.001) had co-occurring *RB1/TP53* mutations. No patients harbored mutations in *EGFR, HER2*, or *RET*. Mutations in potentially targetable pathways were observed throughout the cohort including the DNA-damage repair pathways, RTK/RAS, and PI3K.

Taken together, these data demonstrate that patients with low pack-year SCLC have improved overall survival compared to historic averages for SCLC patients with a history of heavy tobacco use. Paradoxically, however, light-smokers with SCLC live longer than never-smokers, and these patients may harbor a higher frequency of targetable alterations than typical SCLC patients, highlighting the importance of molecular profiling in SCLC patients with minimal tobacco use.

#5062 Evaluation of genetic mutations in non-small cell lung cancer patients.

M. Rothstein[1], P. Broughton[1], E. Markalunas[2], A. Funkhouser[1], L. Allen[3], J. Martin[3], W. Edenfield[3], A. V. Blenda[1];
[1]Univ. of South Carolina School of Medicine Greenville, Greenville, SC, [2]Brown University, Providence, RI, [3]Prisma Health, Greenville, SC

Lung cancers represent the second most common cancer and Non-Small Cell Lung Cancer (NSCLC) constitutes 80-85% of all lung cancers. Genes within several cellular pathways have been previously evaluated for their clinical impact in NSCLC. In this investigation, we evaluate genetic mutations found in 50 cancer-critical genes implicated in the signaling pathways RTK/RAS/MAP, TGFβ, PI3K, Wnt, GPCR, p53, JAK/STAT, Notch, and the cell cycle pathway. Some of these mutations have not yet been described or have not been described in NSCLC. The intent of our study is to evaluate these mutations and allow further research into their impact, specifically highlighting mutations that are involved in clinically important pathways.

We evaluated mutations found in 59 NSCLC patients at the Prisma Health Cancer Institute. These mutations are part of 2,800 COSMIC (Catalogue of Somatic Mutations in Cancer) hotspot mutations in 50 cancer-critical genes. Each mutation was investigated further using the ClinVar database to identify whether it had been described in NSCLC or other cancers/conditions, its genetic consequence, pathogenesis, possible variations, and origin.

A total of 73 unique mutations in 59 NSCLC patients were evaluated. Of the 73 mutations, 17 had not been described at all, 40 had been described in other cancers/conditions, and 16 had been previously described in NSCLC. The known mutations' effects in other cancers/conditions were categorized as pathogenic, likely pathogenic, likely benign, benign, or uncertain. Novel mutations were found in genes that provide a druggable target, help predict treatment response, are under investigation for their ability to predict treatment response or confer additional clinical utility.

Medical management of cancer has benefitted greatly from studies of genetic mutations. Most mutations identified in our patient population had not been described in NSCLC, and a smaller number of those had not been described at all. Further elucidation of these mutations may lead to additional discoveries relevant to NSCLC prognostication and treatment.

#5063 Exploring the mutational landscape of *KRAS* and *NRAS* in tumors with non-V600 *BRAF* mutations.

C. L. Mukonoweshuro, E. Rousselle, A. A. N. Rose;
Lady Davis Institute at Jewish General Hospital, Montreal, QC, Canada

Background: BRAF, a key modulator of the Mitogen-Activated Protein Kinase (MAPK) pathway, is observed in 7% of all cancers. Therapeutic response to MAPK inhibition (MAPKi) often relies on molecular distinctions between members of varying classes: Class 1 (V600), Class 2 and 3 (non-V600) BRAF mutants. Preliminary data indicates that co-occurring *RAS* mutations in non-V600 BRAF mutant cancers are less responsive to MAPKi treatment. This emphasizes the need to investigate the characteristics of *RAS* co-mutations in non-V600 BRAF mutant tumors.

Methods: Genomic data was obtained from a cohort of 183,292 patients provided by the AACR GENIE database (v14.1). Patient samples were clustered according to their *BRAF* mutation status and co-occurring *K/NRAS* mutations: WT BRAF (n=60,845) vs. non-V600 *BRAF* (n=1009). Samples were grouped based on cancer type: melanoma (n=3841), colorectal (n=15,434), and non-small cell lung cancer (n=14640) and were further categorized according to key biochemical features of RAS GTPase function and overall GTPase activity.

Results: This dataset revealed a diverse array of allelic variants of *K/NRAS* between cancer types and their underlying *BRAF* mutation status (Table 1). Non-V600 BRAF mutant cancers showed an enrichment for *KRAS* mutations linked to amplified nucleotide exchange (37.9% vs. 13.4%; p<0.0001) and hydrolysis-impairing *NRAS* mutations (41.9% vs. 23%; p<0.0001), compared to WT BRAF cancers. Rare allelic variants including *KRAS* L19F, *KRAS* A146T, and *NRAS* G60E were seen in Class 2/3 BRAF mutants.

Conclusion: This data suggests that non-V600 BRAF mutant tumors are characterized by a unique distribution of *RAS* mutations. More research into the difference in downstream effectors of *RAS* mutants overrepresented in non-V600 BRAF mutant tumors could provide important insights into how these tumors develop and resist targeted therapies.

Table 1. Classification of *KRAS* and *NRAS* mutations in WT BRAF vs. non-V600 BRAF mutant tumors

	Cancer Type		**All cancers**			**NSCLC**			**Colorectal**			**Melanoma**		
	BRAF mutation		**WT**	**non-V600**	**p-value**	**WT**	**non-V600**	**p-value**	**WT**	**non-V600**	**p-value**	**WT**	**non-V600**	**p-value**
GTPase Function	**KRASmutation class**	**Impaired hydrolysis**	n=20731 (79.8%)	n=167 (51.9%)	<0.0001	n=6068 (86.1%)	n=60 (56.6%)	<0.0001	n=4799 (68.2%)	n=16 (29.1%)	<0.0001	n=38 (48.1%)	n=13 (50.0%)	0.4047
		Nucleotide Exchange	n=3475 (13.4%)	n=122 (37.9%)		n=530 (7.5%)	n=36 (34.0%)		n=1842 (26.2%)	n=36 (65.5%)		n=30 (38.0%)	n=12 (46.2%)	
		Hybrid	n=1765 (6.8%)	n=33 (10.2%)		n=446 (6.3%)	n=10 (9.4%)		n=395 (5.6%)	n=3 (5.5%)		n=11 (13.9%)	n=1 (3.8%)	
	NRAS mutation class	**Impaired hydrolysis**	n = 974 (23.0%)	n=78 (41.9%)	<0.0001	n=29 (18.7%)	n=9 (39.1%)	0.0196	n=188 (32.6%)	n=17 (68.0%)	<0.0001	n=86 (5.5%)	n=22 (27.8%)	<0.0001
		Nucleotide Exchange	n=459 (10.8%)	n=22 (11.8%)		n=5 (3.2%)	n=2 (8.7%)		n=48 (8.3%)	n=4 (16.0%)		n=93 (5.9%)	n=10 (12.7%)	
		Hybrid	n=2811 (66.2%)	n=86 (46.2%)		n=121 (78.1%)	n=12 (52.2%)		n=341 (59.1%)	n=4 (16.0%)		n=1385 (88.6%)	n=47 (59.5%)	
GTPase Activity	**BRAF mutation**		**WT**	**non-V600**	**p-value**	**WT**	**non-V600**	**p-value**	**WT**	**non-V600**	**p-value**	**WT**	**non-V600**	**p-value**
	KRASmutation class	**Intermediate activity**	n=14408 (55.3%)	n=142 (44.4%)	0.0001	n=5082 (72.3%)	n=54 (50.5%)	<0.0001	n=3540 (49.9%)	n=17 (31.5%)	0.0089	n=46 (56.8%)	n=13 (50.0%)	0.6516
		High activity	n=11630 (44.7%)	n=178 (55.6%)		n=1947 (27.7%)	n=53 (49.5%)		n=3552 (50.1%)	n=37 (68.5%)		n=35 (43.2%)	n=13 (50.0%)	
	NRAS mutation class	**Intermediate activity**	n=1364 (32.2%)	n=101 (55.8%)	<0.0001	n=36 (23.4%)	n=12 (54.5%)	0.0041	n=239 (41.8%)	n=20 (87.0%)	<0.0001	n=190 (12.3%)	n=34 (43.0%)	<0.0001
		High activity	n=2868 (67.8%)	n=80 (44.2%)		n=118 (76.6%)	n=10 (45.5%)		n=333 (58.2%)	n=3 (13.0%)		n=1357 (87.7%)	n=45 (57.0%)	

#5064 Wild type *KRAS* amplification as *de novo* oncogenic driver in non-small cell lung cancer.

B. Ricciuti[1], S. V. Michelina[2], J. Alessi[1], X. Wang[3], F. Pecci[1], A. Di Federico[1], M. Gandhi[1], G. Lamberti[1], E. Patrucco[1], L. Sholl[1], A. Aguirre[1], C. Ambrogio[1], M. M. Awad[1];

[1]Dana-Farber Cancer Institute, Boston, MA, [2]University of Turin, Turin, MA, [3]Harvard T.H. Chan School of Public Health, Boston, MA

Introduction: Oncogenic *KRAS* mutations define subsets of non-small cell lung cancer (NSCLC) with unique clinicopathologic and genomic features, and the recent development of direct KRAS inhibitors has changed the treatment landscape of these patients (pts). However, whether *KRAS* amplification is oncogenic and defines unique subset of potentially targetable NSCLCs is currently unknown.

Methods: Clinicopathologic and genomic data were abstracted from multiple independent cohorts of NSCLCs which underwent tumor genomic profiling at the Dana-Farber Cancer Institute (Cohort 1), AACR-GENIE v.13, TCGA, and other 212 studies (Cohort 2). Whole transcriptome sequencing and quantitative proteomics data from the The Cancer Genome Atlas (TCGA) and the Cancer Cell Lines Encyclopedia (CCLE) were used to correlate *KRAS* amplification with KRAS RNA levels and protein expression. KRAS doxycycline-inducible models were generated to determine *in vitro* and *in vivo* oncogenicity of wild-type KRAS overexpression.

Results: Among 15,341 pts with NSCLC identified, *KRAS* amplification was identified in 355 (2.4%) cases. Compared to *KRAS* not amplified cases, pts with *KRAS* amplified NSCLC were more likely to be males (52.4% vs 45.6%, p=0.01), have a history of smoking (82.1% vs 64.2%, p<0.01), and higher median pack-years (35 vs 23.5, p<0.01). *KRAS* amplification was also associated with higher median aneuploidy levels (as fraction of genome altered) (30.4% vs 14.3%, p<0.01), tumor mutational burden (p<0.01), and increased median PD-L1 expression (20% vs 5%, p=0.01). KRAS amplified cases were enriched with *KRAS*, *POLE2*, *SLC34A2* and *PALB2* mutations, while *EGFR* mutations were mutually exclusive (Q<0.1). Among NSCLC samples with transcriptomic and proteomic profiling from the TCGA and CCLE cohorts, *KRAS* amplification was associated with significantly increased KRAS mRNA (p<0.01) and protein expression (p<0.01), compared to *KRAS* diploid samples. Among pts with clinical outcomes data available (N=9,335), median overall survival (OS) from the date of diagnosis was significantly shorter in pts with *KRAS* amplified vs *KRAS* diploid genotype in both KRAS mutant (HR: 0.71, P=0.02) and KRAS WT (HR: 0.74, P=0.02) NSCLCs. In KRAS doxycycline-inducible models (BEAS-2B cells) we demonstrated increased cell proliferation and MAPK activation upon doxycycline-induced KRAS expression. *In vivo*, sustained expression of KRAS in animals constantly fed with doxycycline-diet triggered tumor formation and development of metastasis, indicating that WT KRAS overexpression is oncogenic.

Conclusion: *KRAS* amplification defines a novel subset of NSCLCs characterized by distinct clinicopathologic and genomic features, and worse survival. Developing novel therapeutic strategies to target *KRAS* amplification may improve outcomes in pts with NSCLC.

#5065 Integrating blood based liquid biopsies with TNM stage improves survival prediction model for non-small cell lung cancer.

L. Schmalz[1], C. Urtis[1], L. Liu[1], E. Forbes[1], F.-C. Hsu[1], N. Steuerwald[2], A. de Hoyos[1], T. Lycan[1], J. Ruiz[1], W. Petty[1], W. Zhang[1];
[1]Atrium Health Wake Forest Baptist, Winston Salem, NC, [2]Levine Cancer Institute, Charlotte, NC

Introduction: Stage is the most important prognostic factor for survival in non-small cell lung cancer (NSCLC). The current TNM (Tumor, Node, Metastasis) staging system for NSCLC uses physical exam, histology, imaging, and surgical findings to define the extent and spread of a patient's cancer. Despite advances in molecular testing which can impact treatment and prognosis for NSCLC patients, the current system does not incorporate molecular data into staging. We proposed a novel predictive model for survival analysis which integrates molecular analysis of liquid biopsies (B) into the TNM staging system (1). In this study, we tested this new staging system and our predictive model shows TNM + B (TNMB) provides a better predictive model for survival compared to TNM alone.

Methods:176 patients were identified at Atrium Health Wake Forest Baptist with Guardant 360 liquid biopsies sent at diagnosis for NSCLC. Clinical data was obtained through retrospective chart review. Molecular analysis was performed on 81 genes across all Guardant 360 liquid biopsies. Using Cox proportional hazards model, we identified significant gene mutations or genes with significant magnitude of variant allele frequency (VAF) that improved survival prediction. We then designed a novel staging system incorporating whether a patient had a positive liquid biopsy test (B1), defined by the presence of these impact gene variables, to TNM stage.

Results: Three impact genes STK11 (p=0.0253), NFE2L2 (p = 0.0025), TP53 (p=0.0129) and one gene with a magnitude of VAF, ARID1A (p=0.0082) was identified which significantly improved the predictive model for survival. Patients with negative liquid biopsy test, B0, had improved survival compared to patients with a positive liquid biopsy test, B1 (p<0.005). In our cohort, TNM staging alone did not show a significant survival difference between stage II and III (p = 0.19). Whereas TNMB staging showed a significant survival difference between stage II, III and IV.

Conclusions: While TNM stage remains a major prognostic factor for NSCLC patients, it fails to incorporate molecular data which has a critical impact on management and prognosis. We designed a novel method to analyze molecular data obtained by liquid biopsy to identify significant gene mutations and gene magnitude of VAF that impacts survival prediction. In our cohort, we showed 4 impact genes which we used to create a new TNMB staging system which led to improved survival prediction compared to TNM alone.

Acknowledgments: Research partly supported by NIH T32 Grant (T32CA247819) and Cancer Center Support Grant (P30CA012197)

Reference: (1) Yang M, Forbes ME, Bitting RL, O'Neill SS, Chou PC, Topaloglu U, Miller LD, Hawkins GA, Grant SC, DeYoung BR, Petty WJ, Chen K, Pasche BC, Zhang W. Incorporating Blood-based Liquid Biopsy Information into Cancer Staging: Time for a TNMB System? Ann Oncol. 2018 Feb 1;29(2):311-323.

#5066 Integrating spatial and single cell transcriptomics to identify and characterise biologically driven subgroups in invasive lobular carcinoma.

M. Serra[1], A. Papagiannis[1], M. Rediti[1], F. Lifrange[2], N. Occelli[1], L. Collet[1], D. Vincent[1], G. Rouas[1], D. Fimereli[1], L. Craciun[1], D. Larsimont[1], D. Venet[1], M. Vikkula[3], F. P. Duhoux[4], F. Rothe[1], C. Sotiriou[1];

[1]Institut Jules Bordet, Bruxelles, Belgium, [2]University Hospital Center of Liege, Liege, Belgium, [3]de Duve Institute, Universite Catholique de Louvain, Bruxelles, Belgium, [4]Institut Roi Albert II, Cliniques universitaires Saint-Luc and Institut de Recherche Experimentale et Clinique (pole MIRO), Bruxelles, Belgium

Background: Invasive lobular carcinoma (ILC) is the second most common histological breast cancer subtype; however, little is known about its tumor microenvironment (TME). Here, we aimed to identify and to characterise ILC subgroups based on TME heterogeneity by combining spatial transcriptomics (ST) and single cell RNA-sequencing (scRNA-seq).

Methods: We performed ST (Visium 10x Genomics) on frozen tumor samples from 41 primary hormone receptor positive (HR+), HER2-negative (HER2-) ILCs. Information coming from the morphological annotation of ST slides and the gene expression-based clustering of ST spots was integrated and used as input for a patient level classification (using intNMF algorithm). Subgroups of patients were annotated using morphology, gene set enrichment analysis and ST deconvolution based on scRNA-seq data (CARD software). SCAN-B bulk RNA-seq dataset was used as validation set (HR+, HER2- ILC samples, n = 853).

Results: Four subgroups of patients were identified: proliferative (P, n = 12, enriched in tumor cells and proliferation-related pathways), normal-stroma enriched (NSE, n = 10, enriched in fibroblasts, stroma-related pathways and showing an higher level of colocalization between invasive and in situ carcinoma), metabolic (M, n = 9, enriched in metabolic related-pathways) and metabolic-immune enriched (MIE, n = 10, enriched in adipocytes, metabolic and immune-related pathways). Deconvolution of ST spots with single cell data revealed matching results with morphology (in terms of cell types). We observed an enrichment of myofibroblasts in NSE, an enrichment of cancer epithelial in P and, interestingly, an enrichment of endothelial cells in M subgroup (fdr < 0.25). MIE was characterized by perivascular like-endothelial cells and myeloid cells (monocytes and macrophages, fdr < 0.25). Of note, at the level of the ST slide, myeloid cells in MIE subgroup were more present in the adipose tissue compartment (fdr < 0.25) compared to the rest of the slide. NSE subgroup showed a trend for association with better prognosis. Gene signature-based assignment identified the same four subgroups in SCAN-B: GSEA analysis and comparisons among the four subgroups showed matching results between our dataset and SCAN-B. Of note, in SCAN-B, we observed differences in prognosis among the subgroups, with NSE showing better, M and MIE intermediate and P worse prognosis for overall survival and relapse free interval (p < 0.01).

Conclusions: Four subgroups of ILC based on TME heterogeneity and showing differences in prognosis were identified and validated in external cohort. Of note, two of these groups were related to metabolism, highlighting the value of such process in ILC biology. Importantly, myeloid cells were the predominant immune cell types in ILC, and they showed a specific compartmentalization inside the TME. Further validation is needed.

#5067 Exploring the genomic landscape of de novo neuroendocrine prostate cancer: Insights for innovative therapies from spatial gene expression analysis.

R. Watanabe[1], N. Miura[1], M. Kurata[1], R. Kitazawa[2], T. Kikugawa[1], T. Saika[1];
[1]Ehime University Graduate School of Medicine, Toon, Japan, [2]Ehime University Hospital, Toon, Japan

Introduction & Objectives Neuroendocrine prostate cancer (NEPC) accounts for less than 1% of all prostate cancers but has a worse prognosis than androgen receptor-positive prostate adenocarcinoma (ARPC). Rare cases exist where both de novo NEPC and ARPC are found in the same tissue sample. Our study examines one such unique case: a 78-year-old male treated at Ehime University Hospital who was diagnosed with both ARPC and adjacent de novo metastatic NEPC. This case provides an excellent opportunity for studying gene expression in these two types of prostate cancer. Materials & Methods We used Visium CytAssist Spatial Gene Expression technology from 10x Genomics to analyze formalin-fixed, paraffin-embedded (FFPE) tissue samples from this unique patient. Results We observed elevated expression levels of specific neuroendocrine markers like PEG10, DLL3, NCAM1, SYP, and CHGA in de novo NEPC regions. In contrast, androgen receptor markers such as KLK3, ACPP, TMPRSS2, and NKX3.1 were more prevalent in ARPC areas. Furthermore, genes like Chek1, BRCA1/2, TOP2A, and FANCA were also elevated in NEPC, suggesting that PARP and TOP2 inhibitors could be effective. Expression levels of Rbfox3 and SFRTM2 were lower in NEPC areas, implying possible roles in epithelial-mesenchymal transition (EMT) and Wnt signaling pathways. Additionally, fibrotic markers like HGF, HMOX1, ELN, and GREM1 were upregulated, suggesting that de novo NEPC tumors might be 'immune cold,' thus requiring treatments to boost the effectiveness of immune checkpoint inhibitors. Conclusion The data from additional cases could open the door for new treatment options for NEPC and improve survival rates for castration-resistant prostate cancer patients. Our research serves as a pioneering application of Visium CytAssist on FFPE samples and is the first to examine gene expression in both ARPC and de novo NEPC. A subset of these findings was published in the International Journal of Molecular Science (IJMS) in May 2023.

#5068 Clonal Hematopoiesis of indeterminate potential (CHIP) in patients with advanced solid tumors treated with immune checkpoint blockers (ICB) as monotherapy: Analysis of the PREMIS study.

J. E. Rodriguez, F. X. Danlos, A. Larive, A. Marabelle, Y. Loriot, C. Robert, L. Albiges, M. Frelaut, M. Aldea, B. Besse, M. Ducreux, C. Even, J. B. Micol, S. Ponce, C. Marzac, N. Chaput, C. Massard, C. Baldini;
Gustave Roussy, Villejuif, France

Introduction: Clonal Hematopoiesis of indeterminate potential (CHIP) is a clonal expansion of mutations affecting genes involved in hematologic malignancies in patients without a hematological disease per se. It has emerged as a significant risk factor for cardiovascular events via skewing innate immune cells towards a pro-inflammatory state. Recently studies have shown its potential detrimental impact on overall survival in patients treated with chemotherapy. However, its impact on patients treated with immune checkpoint blockers in monotherapy remains unclear.
Objective: Our aim is to evaluate CHIP prevalence in a prospective cohort of patients treated with ICB for advanced solid tumors and its impact on patient outcomes.
Materials and methods: We performed a Next-Generation Sequencing (NGS) panel of 74-genes dedicated to hematological alterations on DNA extracted from whole blood collected before first administration of an ICB for an advanced solid tumor, within the PREMIS trial (NCT03984318). CHIP prevalence was assessed according to a variant allele frequency (VAF) threshold ≥ 2%.
Results: We included 127 pts in the analysis; 88 pts (69%) were male with a median age of 70 years [range 37-100]. Most common tumor locations were skin (29%), genitourinary (25%) and lung (19%). ICB setting was 1°L in 40% of patients; 2°L in 43%; > 3°L in 17%, and the most used ICB was Nivolumab in 39% of patients. At least 1 CHIP mutation was found in 55 pts (43%). The most frequent mutations were found in *DNMT3A* (40%), *TET2* (18%) and *PPM1D* (13%). Co-mutations were found in 20% of patients. Median PFS was 7.7 months (m) for CHIPm patients compared to 5.7 m in non-CHIPm patients (p=2.2) and median OS was 16.2 m in CHIPm patients compared to 14.9 m in non-CHIPm patients (p= .5). No pts developed hematological disease during the follow up.
Conclusion: CHIP is commonly found in pts with solid tumors, with a prevalence in our cohort of 43% with no statistical significance neither in PFS nor in OS in the CHIP-mutated population.

#5069 Retrospective analysis of acute myeloid leukemia using next generation cytogenomics identifies variants missed at diagnosis.

S. Eacker[1], M. Malig[1], M. Wood[1], A. Muratov[1], O. Sala-Torra[2], I. Liachko[1], C. Yeung[2], J. Radich[2];
[1]Phase Genomics, Inc., Seattle, WA, [2]Fred Hutchinson Cancer Center, Seattle, WA

Cytogenetics forms the cornerstone of diagnostic genetic testing in leukemia, providing both prognostic and diagnostic information to help guide treatment. Currently, standard-of-care cytogenetics in acute myeloid leukemia (AML) is composed of a combination of karyotyping, FISH testing, and in some cases chromosomal microarray analysis, each test offering a unique combination of advantages and weaknesses. A particular challenge for this combination of tests is the delivery of results in a timely and comprehensive manner. To overcome these limitations, we have developed OncoTerra, a proximity-ligation-sequencing based method which can rapidly detect all classes of variants detected by cytogenetics tests in a single assay. We applied OncoTerra to a cohort of more than 100 samples from a SWOG AML trial (S0106), benchmarking sensitivity and specificity of the variants. We observed an overall >0.95 sensitivity and a specificity of 1 for the variants identified by cytogenetics and identified numerous cryptic variants. Overall, we identified variants that changed the diagnostic risk stratification of 15% of the patient involved in the trial based on the ELN 2022 criteria. This translated into better overall prediction of outcomes of patients in the trial and has identified both known and novel variants missed by standard-of-care tools.

#5070 Landscape of clonal hematopoiesis prior to PARP inhibitor treatment in patients with ovarian cancer.

A. Asare, S. Corvigno, J. Yao, L. Zhao, N. D. Fleming, J. Celestino, R. A. Hajek, M. S. Kim, A. Flores Legarreta, K. H. Lu, K. Takahashi, P. A. Futreal, A. A. Jazaeri, S. N. Westin, A. K. Sood, S. Lee;
UT MD Anderson Cancer Center, Houston, TX

Background: Poly (ADP-ribose) polymerase inhibitors (PARPi) are an important tool for treatment of ovarian and other cancers, particularly for those with mutations in BRCA1 or 2 genes or homologous recombination deficiency. The risk of developing secondary hematologic malignancy, particularly myelodysplastic syndrome or acute myeloid leukemia (MDS/AML), is substantially higher (4-12%) after PARPi maintenance or treatment in the second line and beyond in patients with ovarian cancer. This elevated risk necessitates additional investigation into the pathogenesis of PARPi-related secondary malignancy. Clonal hematopoiesis of indeterminate potential (CHIP) has been associated with the development of therapy-related myeloid neoplasms. We aim to understand the patterns of CHIP in patients with high grade serous ovarian carcinoma who receive PARPi therapy.
Methods: We performed ultra-high-depth whole exome sequencing of plasma derived cfDNA or white blood cells (WBCs) barcoded with unique molecular identifiers from patients with high grade serous ovarian carcinoma who were treated with multiple lines of chemotherapy (n=6) or with PARPi in addition to chemotherapy (n = 10). Using spike-in mutated DNAs as positive controls, we detected variant alleles as low as 1% variant allele frequency. Gene set enrichment analysis was performed on identified groups.
Results: We identified 7162 recurrent variants among our patients. We began by comparing quantities of CHIP between the samples from patients who eventually receive PARPi and those who do not. Samples contained a median of 2030 recurrent CHIP variants and 4300 total variants. No differences in total CHIP quantity or mutation type was discernable among samples from patients who will receive PARPi (BRCA1/2 enriched) vs those who will not. Among our 16 patients, 14 ultimately developed secondary hematologic malignancy (t-MN+ Comparison of t-MN+ (n=14) and t-MN- (n=2) defined a group of 14 variants enriched in the t-MN+ population and a group of 85 variants depleted in the t-MN+ population. The t-MN+ enriched variants we identified were not previously associated with CHIP and had significant overlaps with alkyl transferase activity (FDR q val < 0.01) and nucleotide binding gene sets (FDR q val < 0.01).
Conclusions: We used a novel methodology to identify unbiased low variant mutational changes in the hematopoietic system. These results suggest that baseline clonal hematopoiesis variants are similar among patients newly diagnosed with ovarian carcinoma. We have also identified a signature potentially related to future risk of leukemia requiring further validation.

#5071 Minimal residual disease (MRD) status by peripheral blood mononuclear cells (PBMCs) and circulating tumor DNA (ctDNA) demonstrates rapid, deep, and sustained response in patients (Pts) with relapsed/refractory follicular lymphoma (R/R FL) treated with subcutaneous (SC) epcoritamab monotherapy in the pivotal phase 1/2 EPCORE™ NHL-1 trial.

D. Soong[1], I. Altıntaş[2], J. Karavitis[1], K. M. Linton[3], W. Jurczak[4], C. Thieblemont[5], K. Zhao[6], E. Szafer-Glusman[6], D. Hoehn[1], E. Favaro[7], M. Sacchi[1], M. Jure-Kunkel[1];

[1]Genmab, Plainsboro, NJ, [2]Genmab, Utrecht, Netherlands, [3]The Christie NHS Foundation Trust and Manchester Cancer Research Centre, Manchester, United Kingdom, [4]MSC National Research Institute of Oncology, Krakow, Poland, [5]Assistance Publique & Hopitaux de Paris (APHP), Hopital Saint-Louis, Hemato-oncologie, Universite de Paris, Paris, France, [6]AbbVie Inc, South San Francisco, CA, [7]Genmab, Copenhagen, Denmark

Introduction: Outcomes in high-risk R/R FL are poor. Epcoritamab SC, a CD3xCD20 bispecific antibody, demonstrated promising efficacy with a manageable safety profile in pts with R/R FL after ≥2 prior lines of therapy (phase 1/2 EPCORE NHL-1; NCT03625037). Here we evaluated MRD with PBMCs and ctDNA in pts with R/R FL and correlated the results with clinical findings.

Methods: Adults with R/R FL 1-3A enrolled in EPCORE NHL-1 received epcoritamab SC in 28-day cycles. MRD analysis was performed on longitudinal plasma and PBMC samples collected at prespecified timepoints (clonoSEQ assay, Adaptive Biotechnologies). Screening tumor biopsies were used to identify trackable tumor clones; samples were quantified as tumor clones detected per mL plasma for ctDNA and per one million nucleated cells for PBMC. Overall response and progression-free survival (PFS) were assessed using Lugano criteria by independent review committee.

Results: Of 128 pts in the R/R FL 1-3A cohort, 91 with PBMC data and 100 with ctDNA data were MRD evaluable. Overall MRD negativity was achieved in 67.0% [95% CI: 56.4-76.5] of pts per PBMC and 68.0% [95% CI: 57.9-77.0] of pts per ctDNA. Concordance of subject-level MRD status was high (79 of 89 with PBMC and ctDNA data; 88.8%). In most pts, MRD negativity was reached prior to radiographic complete response (PBMC, 76.4%; ctDNA 58.5%). MRD negativity by PBMC preceded ctDNA (median days to MRD negativity, 28 [PBMC] vs 57 [ctDNA]), suggesting a difference in methodology in detecting tumor DNA. Pts who became MRD negative had prolonged PFS (median not reached). Baseline MRD levels were not associated with clinical outcomes (PBMC; Wilcoxon *P*=0.59, ctDNA *P*=0.39). PFS was similar in pts achieving MRD negative status (median not reached, PBMC and ctDNA), independent of high-risk/difficult-to-treat disease (≥4 prior lines, Ann Arbor stage III-IV, bulky disease, double refractory, FLIPI 3-5, and POD24). The overall MRD negativity rate was also similar in high-risk pts, except those with ≥4 prior lines of therapy.

Conclusions: Based on the EPCORE-NHL-1 study, one of the first pivotal studies to report MRD in pts with R/R FL, epcoritamab drives rapid, deep, and sustained responses as supported by MRD assessment by both PBMC and ctDNA. MRD results correlate with clinical outcome, and achieving MRD negativity is associated with longer PFS. PFS was similar among all pts who achieved MRD negativity, including those with high-risk disease.

#5072 Multi-omic, multi-scale characterisation of colorectal cancer defines spatiotemporal patterns of recurrence.

C. S. Wood[1], J. Da Silva Filho[2], A. Cameron[1], A. Legrini[1], H. Leslie[1], T. Zhang[1], Y. Doncheva[1], C. Kennedy-Dietrich[1], M. Marti[2], J. Edwards[1], P. Horgan[1], C. Roxburgh[1], C. Steele[1], N. Jamieson[1];

[1]University of Glasgow - Institute of Cancer Sciences, Glasgow, United Kingdom, [2]University of Glasgow - Institute of Infection, Immunity and Inflammation, Glasgow, United Kingdom

Aim: Patients who undergo intended curative resection of colorectal cancer (CRC) have a 20-25% chance of metachronous recurrence, the site and timing of which are unpredictable and resistant to current treatment. The biological basis for such heterogeneous disease behavior remains to be elucidated. Bulk transcriptomic profiling and subsequently single-cell RNAseq have provided insight in the epithelial subtypes and immune microenvironment. Recently spatially resolved transcriptomic assessment allow molecular profiling of tissue while preserving tissue architecture. Utilizing ST technology we sought to perform deep characterization of a large cohort of patients with primary CRC with the intention to decipher the biological determinants of spatio-temporal patterns of recurrence.

Methods: 750 patients who underwent resection of CRC with mature follow up were studied. Bulk transcriptomic, genomic and multiplex immune characterization was performed using a TMA format. Of these, 28 patients were assessed using single cell spatial transcriptomics (Nanostring CosMx Spatial Molecular Imager (SMI, 1000plex gene panel)), 120 tumors underwent regional whole transcriptome profiling of epithelium and TME (Nanostring GeoMx Digital Spatial Profiler using FFPE tissue). We used image analysis and bioinformatics to integrate these complex datasets in over 120000 single-cells in the context of their spatial tissue architecture and clinicopatholgical outcome and recurrence data.

Results: Using the CosMx SMI we characterized cells with complete topographic detail and defined 2 unique epithelial cell states defined. Each epithelial state had distinct spatial properties including cell size and morphology, average distance to nearest lymphocyte, neighboring cell types and stromal neighborhood. This epithelial signature was integrated in GeoMx samples and were found to predict recurrence ($p<0.05$). The Epithelial, Fibroblast and Immune GeoMx transcriptomic compartments were expanded and grouped using unsupervised clustering. Each compartment demonstrated groups of patients where specific spatially derived signatures could predict site and time of recurrence ($p<0.05$).

Conclusions: By maintaining the tissue structure, we have directly measured cellular interactions and captured cells commonly missed during dissociative studies whilst defining novel molecular subtypes of CRC with clinical relevance. Novel platforms such as CosMx allow deeper characterization of unique cell types and cellular interactions that may pave the way for novel therapeutics and precision medicine for patients with CRC.

#5073 Advancing precision oncology: Insights from pan-cancer proteogenomic signatures.

Y. Li, N. V. Terekhanova, M. C. Wendl, F. Chen, L. Ding;
Washington University School of Medicine in St. Louis, St. Louis, MO

Somatic mutations in cancer genomes arise from diverse mutational processes, leaving distinct mutational signatures. However, the proteogenomic implications of these signatures and their connections to environmental influences and immune interactions remain largely unexplored. In this study, we comprehensively investigated these signatures from a broader proteogenomic perspective to further discern their genetic, proteomic, phosphoproteomic, and environmental ramifications. The harmonized dataset of 1064 samples across ten cancer types from the Clinical Proteomics Tumor Analysis Consortium (CPTAC) pan-cancer resource was utilized for this investigation. Beyond genetic alterations and mutational signatures, we harnessed high-throughput multi-omics data to detect critical changes and infer expression signatures associated with the transitions to seven tumor-linked phenotypes: aging, Apolipoprotein B mRNA Editing Catalytic Polypeptide (APOBEC), Homologous Recombination Deficiency (HRD), Microsatellite Instability (MSI), Polymerase Epsilon (POLE), smoking, and ultraviolet (UV) light exposure at the pan-cancer level. We prioritized the top differentially expressed markers uniquely found at the protein and phosphoprotein levels and developed a quantitative score predicting each phenotype status, such as MSI. Respectively, we pinpointed potential candidates as actionable therapeutic targets by linking the identified markers to druggable databases. This offers additional cues to optimize therapeutic options for patients. Specifically, directing attention to genes up-regulated in HRD tumors treated with PARP1 inhibitors shows potential promise in overcoming resistance. Moreover, we explored environmental exposure-related tumor proteogenomic signatures and their association with immune infiltration levels and phenotypes. Notably, smoking strongly influenced the tumor microenvironment (TME) and prognosis in lung cancer. In summary, our identification of expression signatures facilitates phenotype prediction and unveils their molecular mechanisms. We anticipate clinical utility in classifying samples using proteogenomics, particularly in cases where a solely genomic assessment is inconclusive.

#5074 Profiling the splicing landscape in solid tumors in a large, real-world dataset.

M. G. Rosasco, A. J. Sedgewick, J. Guinney, M. M. Stein;
Tempus, Chicago, IL

Introduction Aberrant pre-mRNA splicing is common across cancers. Molecular regulation of splicing is an attractive drug target and clinical trials are currently evaluating splice-targeted therapies (STTs). Due in part to the complex and pleiotropic nature of splicing regulation, molecular biomarkers to identify patients who may benefit from STTs are lacking. While mutations in splicing factors (SFs) are promising biomarkers, these are rare, leaving many patients with unmet need. In this study, we identified and characterized splicing patterns (SPs) in a large, multi-cancer cohort.

Methods De-identified patient records with splicing data from the Tempus xR whole transcriptome assay were extracted from the Tempus clinicogenomic database (N=2918). A total of 1052 alternative splicing events were detected in at least 90% of the samples with at least 10 supporting reads. Leiden clustering was applied to the percent spliced-in (PSI) values of these events to identify SPs. Fisher's exact test was used to assess clinical and molecular enrichment in SPs, and Cox proportional-hazards models were used to assess associations with rwOS and derive hazard ratios (HRs).

Results From a list of 404 SF genes 7.7% of patients had one or more pathogenic or likely pathogenic (P/LP) SF variants, and 2.2% had variants in the key biomarker SF genes *SF3B1*, *SRSF2*, or *U2AF1*. Clustering revealed 15 SPs containing 43 to 353 samples. One SP had a significant enrichment of SF variants (19.7% of SP, P < 0.0005). SPs were associated with significant differences in rwOS, and many were enriched for samples from a single cancer type, biopsy, or histology - principally by prostate cancer (97.5% of SP), melanoma (94.3% of SP), urothelial carcinoma (93.4% of SP), and renal clear cell carcinoma (93.0% of SP), as well as samples collected from liver biopsies (93.9% of SP). In contrast, colorectal and lung adenocarcinoma samples were present in a wide variety of SPs. One SP was enriched for squamous histologies (66.6% of SP, P < 0.0005) and associated with shorter rwOS (HR = 1.33, 95% CI [1.11, 1.59], P < 0.0005). This association remained after controlling for squamous histology (HR = 1.45, 95% CI [1.02, 2.05], P = 0.04). Samples in this SP were characterized by increased expression of *MYC*- and proliferation-related genes, and lacked enrichment for SF variants (P = 0.51, 6.6%).

Conclusions Mutations in SFs were rare in our cohort, highlighting the need for additional biomarkers related to STTs. This work revealed the presence of multiple SPs - characterized by distinct clinical and molecular traits. Further work will be able to contextualize STT response data using SPs to facilitate STT biomarker discovery.

#5075 Transcriptomic landscape of tumor microenvironment in gastric cancer in treatment with different types of cancer drugs.

H. Yamashita[1], J. G. Zhang[2], C. Mashima[3], R. Kamata[3], T. Yamamori[3], I. Nakayama[1], A. Kawazoe[1], K. Shitara[1], T. Yano[1], Q. Xu[2], A. Ohashi[3], T. Saito[2]; [1]National Cancer Center Hospital East, Kashiwanoha, Kashiwa, Chiba, Japan, [2]Astellas Pharma Global Development, Inc, Northbrook, IL, [3]National Cancer Center, Kashiwanoha, Kashiwa, Chiba, Japan

Gastric cancer (GC) in the fifth-leading types of cancer and the third-leading cause of death from cancer. Characterization of tumor microenvironment (TME) in GC is important not only to comprehensively understand tumor biology in GC but also to develop a novel cancer therapeutics targeting TME. In this study, we conducted multi-omics analyses of single-cell RNA sequencing (scRNA-seq), bulk RNA sequencing (bulk RNA-seq), and whole exome sequencing (WES) using biopsied tumor samples through endoscopy from 23 GC patients: 3 treatment-naïve patients, 7 patients in treatment with chemotherapy (Chemo), 5 patients in combination treatment with chemotherapy and immune checkpoint blockade (Chemo+CPI), 3 patients in combination treatment with chemotherapy and Her2-antibody targeted therapy (Chemo+Her2i), and 5 patients in third-line or later treatment. We initially classified the GC samples into 4 molecular subtypes (CIN, GS, MSI, and EBV) using datasets of WES, bulk RNA-seq and scRNA-seq, showing that our samples were mainly composed of CIN (n=7) and GS (n=16) types. In scRNA-seq, we revealed that drug treatments profoundly modulated not only proportions of TME components but also their molecular characteristics. For instance, Chemo+CPI treated patients showed higher proportion of CD8+ cytotoxic T cells with activation and/or exhaustion markers. Combination treatments with Chemo+Her2i, in addition, resulted in higher Trail and Estrogen signaling pathways in epithelial cells of TME components. These findings suggest that interventions with certain cancer therapeutic drugs could substantially convert transcriptome landscape and reconstitute GC TME components. High-resolution of GC TME analyses should provide a clue for developing a next generation of cancer therapeutic drugs.

CLINICAL RESEARCH: Novel Immunotherapies and Immune Modulation
Poster Session

#5079 Comparative studies of chemotherapy and immuno-oncology combinations in multiple mouse syngeneic tumor models.
E. Park, M. Hinton, M. Cai, M. A. Gil, G. Hebert, L. Cui, D. Linn, B. J. Long, E. R. Barry;
Merck, Boston, MA

The development of immune checkpoint inhibitors (ICIs) and combinations of immuno-oncology therapies with standard-of-care (SoC) chemotherapeutic agents has shifted therapeutic paradigms for patients with multiple cancer indications. For many patients, these combinations have shown a beneficial effect on clinical outcomes and disease management. However, additional combination therapies are still needed. Preclinically, a comparison of responses from SoC chemotherapies and ICI combinations in multiple disease models may be helpful in identifying optimal treatment combinations in the clinic. Here we report the results of multiple SoC/ICI in vivo combination efficacy studies in a large panel of mouse syngeneic models spanning seven tissue origins: 1) Colon: CT26, MC38; 2) Breast: EMT6, 4T1; 3) Kidney: Renca; 4) Bladder: MB49, MBT2; 5) Skin: B16F10, CM3; 6) Lung: TC1, LL/2, M109; 7) Brain: GL261. The advantage of using syngeneic models is not limited to the rapid and reproducible tumor growth, but importantly that the animals also have an intact immune system and clinically relevant tumor microenvironment, which are required for ICI combination studies. We tested > 10 chemo SoC combinations with a murinized anti-PD-1 antibody (DX400) in 14 syngeneic mouse models. We found that multiple SoC regimens combined well with DX400 treatment, including FOLFIRI, FOLFOX (colon), Carboplatin/Paclitaxel, Carboplatin/Pemetrexed (lung), Capecitabine/Docetaxel, Cisplatin/Gemcitabine (bladder), Cisplatin/5-FU/or capecitabine, and Oxaliplatin/5-FU/ or capecitabine (gastric). Specifically, we observed that the SOC/ICI combinations resulted in enhanced antitumor activities compared to single-agent treatments in many of the models. These data, particularly specific SoC combination regimens that combine well with ICIs in each disease, are useful for optimizing promising combination approaches for clinical development and will be presented here.

#5080 Antibody drug conjugate trastuzumab deruxtecan suppresses leptomeningeal brain metastasis cells and is potentiated by addition of immune check point inhibitor.

E. C. Smith, S.-Y. Wu, R. P. Deshpande, A. Tyagi, K. Watabe;
Wake Forest University School of Medicine, Winston Salem, NC

Leptomeningeal disease (LMD) is defined by dissemination of metastatic cancer cells into the subarachnoid space with subsequent involvement of the cerebrospinal fluid and leptomeninges. LMD is an aggressive, late-stage development of cancer, which is increasing in prevalence as improved treatments for systemic malignancies are discovered. It leads to significant neurological morbidity and mortality, and outcomes remain poor despite improving cancer treatment strategies. There is a large population of patients with human epidermal growth factor receptor 2 (HER2) expressing cancers, such as breast and lung cancers, who suffer from leptomeningeal metastasis. There has been evolving research looking at antibody drug conjugates for treatment of these primary pathologies, such as Trastuzumab Deruxtecan (TDxd), which shows improved progression free survival and overall survival in those with HER2 expressing primary cancers, as well as in intraparenchymal brain metastasis. However, as of yet there has been no study of its utility in LMD. Additionally, use of immune check point inhibitors (ICI) for treatment of LMD has been studied, showing some efficacy, but less robust response than that in intraparenchymal brain metastasis. Given the significant population of patients who continue to be affected by leptomeningeal metastasis, there is significant need for an improved treatment regimen. We hypothesize that TDxd will have a killing effect on HER2 expressing LMD cells, which can be further potentiated by the addition of ICIs. To test this hypothesis, we developed breast and lung cancer cell lines (SKBrM-LMD, and H2030BrM-LMD) that express HER2 and preferentially metastasize to leptomeningeal space. These cell lines were also labeled with luciferase. We then treated these cell lines with TDxd and found that TDxd had significant growth inhibitory effect on these cells *in vitro* when compared to the control. Furthermore, we educated human T Cells against the SkBrM-LMD cells and treated these cells with the aforementioned T cells plus the ICI Anti-PD1. Our results showed that ICI had significant killing effect when compared to the control. We have also created an *in vivo* LMD model by performing intraventricular injection of HER2 expressing tumor cells into a mouse model, which can be used for testing the efficacy of TDxd and ICI by intrathecal injection. In conclusion, our results indicate that TDxd and ICI have significant killing activity against HER2 expressing LMD cells, and therefore intrathecal administration of these drugs is a promising treatment modality that will be demonstrated using a mouse LMD model.

#5081 Immune sensitization of melanoma to checkpoint inhibitor therapy using acoustically active nanoparticles.

M. I. Henderson, L. Xiang, S. Drennan, X. Yi, J. Fischer, A. Yildirim;
Cancer Early Detection Advanced Research (CEDAR), Knight Cancer Institute, Oregon Health & Science University, Portland, OR

Advanced melanoma remains the most fatal form of skin cancer with novel therapeutic approaches required to treat inoperable metastatic lesions. While immunotherapies have shown promise in improving long-term melanoma survival, its treatment efficacy is limited, with only 50% of patients responding. Focused ultrasound (FUS) offers as a non-invasive strategy for targeted tumor ablation, thereby strengthening immunotherapy efficacy by release of tumor associated materials. However, control over tumor material release through FUS, without causing excessive thermal damage to surrounding healthy tissue remains challenging. To address this challenge, our group has previously developed acoustically active nanoparticles (AANPs) responsive to low intensity ultrasound for mechanical tumor ablation by generating strong and durable acoustic cavitation in the tumor tissue. Building upon previous success with AANPs, our current work focuses on sensitizing melanoma tumors to checkpoint inhibitor therapy by releasing tumor antigens into circulation using AANPs and FUS. Our findings revealed sensitization of an immunologically cold B16-F10 metastatic melanoma tumors following treatment, which resulted in a notable 12-day stall in tumor growth. When combined with immune checkpoint inhibitors α-PD-L1 and α-CTLA-4, this approach showed a complete response in B16-F10 bearing mice with impressive memory immune response upon a tumor rechallenge. Herein, these novel AANPs represent a promising advancement to enable accurate immune surveillance by boosting the release of tumor antigens and offers new strategies for improved immunotherapy of melanoma and other solid tumors.

#5082 Novel TSHR CAR T therapy for targeting oncocytic carcinoma.

J. J. Gleba[1], A. Alasonyalilar-Demirer[1], M. Pawlush[1], C. Manriquez-Roman[2], E. L. Siegler[2], R. C. Smallridge[1], A. Zubair[1], H. W. Tun[1], S. S. Kenderian[2], J. A. Copland III[1];

[1]Mayo Clinic Cancer Center, Jacksonville, FL, [2]Mayo Clinic, Rochester, MN

Oncocytic carcinoma (Hurthle cell carcinoma) has the highest incidence of metastasis among the differentiated thyroid cancers. Metastatic disease is reported at the initial diagnosis in 10-20% of patients and 34% overall. Thyroid-stimulating hormone receptor (TSHR) expression is limited to the thyroid gland. It is abundantly expressed on thyroid tumor cells, making TSHR a compelling target for advanced thyroid cancer diagnostics and therapeutics. We developed a potent anticancer strategy for treating oncocytic carcinoma using a novel thyroid hormone stimulating receptor (TSHR)- targeted (chimeric antigen receptor) CAR T cell therapy. TSHR CAR T was generated by transducing T cells derived from healthy donors. *In vitro* effector functions (cytotoxicity, proliferation, degranulation) were tested in TSHR+ tumor models, and subsequent *in vivo* studies using NSG mice were performed to assess anti-tumor activity efficacy. We observed strong anti-tumor activity against metastatic oncocytic carcinoma cell line XCT.UC1 using the TSHR CAR T therapy *in vivo*. Re-challenging treated mice with XCT.UC1 cells reactivated TSHR CART cells with enhanced proliferation and complete suppression of tumor growth of the newly injected tumor cells. Our work represents a promising strategy to improve treatment outcomes of patients with metastatic oncocytic carcinoma that may provide a durable response.

#5083 Discovery of an asymmetric IgG-like bispecific ADC targeting EGFR/HER3.

L. Chen[1], S. Peng[2], C. Wang[1], X. Miao[1], Y. Yan[1], J. Xing[1], W. Huang[2], A. Tsun[1], Y. Xu[1], X. Liu[1], **Y. Luo**[1];
[1]Biotheus Inc., Zhuhai, China, [2]Biotheus (Suzhou) Co., Ltd., Suzhou, China

Background: The epidermal growth factor receptor (EGFR) family, consisting of EGFR, HER2, HER3, and HER4, plays a critical role in tumorigenesis and tumor progression. Inhibition of ERBBs using either monoclonal antibodies (mAb) or small-molecule tyrosine kinase inhibitors have been approved for use for the treatment of various types of cancers. Despite relative success, many patients acquire resistance to long-term benefit due to alternative compensatory signaling pathways. Accordingly, activating mutations or overexpression of HER3 has been reported in many cancers, such as breast, ovarian, lung, colorectal, melanoma, head and neck, cervical and prostate cancers. Here, we report the discovery of a humanized anti-EGFR x HER3 IgG-like bispecific antibody-drug conjugate (ADC). The ADC takes a asymmetric 1+1 form through HC-HC and HC-LC charge-based heterodimerization, which is then conjugated to a topoisomerase 1 inhibitor (TOP1i) payload via a cleavable linker. The affinity of EGFR and HER3 was optimized to improve the therapeutical window, and has shown potent anti-tumor efficacy in various tumor models with limited toxicity supporting further development in clinic.
Methods: An anti-EGFR x HER3 bispecific ADC (PM1300) was generated by introducing unique mutations to the CH1-CL domains of each binding arm to avoid HC-LC mispairing. KIH mutations were also introduced to each CH3 domain to support HC/HC heterodimerization and generate an IgG-like bispecific with one arm binding to EGFR and the other to HER3. TOP1i payload was conjugated to the IgG-like bispecific by the endogenous cysteine residues at DAR 8 via a clearable linker.
Results: Through affinity optimization, PM300 was found to preferentially bind to EGFR/HER3 double-positive cells rather than EGFR single-positive cells. PM1300 showed significantly increased internalization and anti-proliferation activity against EGFR/HER3 double-positive cells, with limited activity towards single positive-cells. PM1300 used an optimized linker for better payload release and serum stability. PM1300 induced a potent anti-tumor efficacy in various CDX models representing different EGFR and HER3 expressing levels and mutations. Importantly, PM1300 exhibited a good safety profile in NHP consistent with the optimal affinity for EGFR and HER3. These results demonstrate that PM1300 has a promising efficacy/safety therapeutical window in preclinical models supporting further development in the clinic.
Conclusion: A bispecific ADC targeting EGFR x HER3 was discovered, named PM1300, which has an asymmetric 1+1 IgG-like structure and optimized affinity. This allows for preferential binding to EGFR/HER3 double-positive cancer cells, rather than EGFR single-positive cells. This may significantly contribute to minimizing safety risk that is common for EGFR-targeting agents.

#5084 A first-in-class bispecific antibody CPL976 with a dual PD-L1/AXL mechanism of action that promotes common biological antitumor effects in *in vitro* and *in vivo* models.

D. Popiel, D. Kołakowski, A. Bojko-Matuszek, K. Lacek, A. Jabłońska, A. Sowińska, F. Mituła, M. Bojko, B. Wiernicki, A. Mikołajczyk, T. Kornatowski, K. Flis, M. Skupińska, J. Hucz-Kalitowska, E. Mroz, M. Choroś, M. Wieczorek, J. Pieczykolan, O. Abramczyk;
Celon Pharma SA, Kazun Nowy, Poland

Background: Bispecific antibodies emerged as a leading drug class for cancer therapy and are becoming increasingly interesting for the therapeutic applications. The Gas6/Axl signaling pathway contributes to the immunosuppressive tumor microenvironment by increasing the expression of PD-L1 and tumor-derived chemokines. This results in increased infiltration of macrophages, monocytes, and myeloid-derived suppressor cells, but decreased infiltration of CD4+ and CD8+ T cells and dendritic cells in the tumor bed. The PD-1/PD-L1-mediated signaling pathway is a well-known mechanism responsible for T-cell inhibition, consequently disrupting their ability to eliminate tumor cells. In addition, AXL and PD-L1 are concurrently highly expressed in many tumors. Therefore, bispecific antibody that inhibits both axes seems like a promising therapeutic strategy engaging anti-proliferative effect by AXL inhibition, and cytotoxic properties of effector T cells by breaking the PD-1/PD-L1 axis.
Materials and Methods: Bispecific antibody CPL976 was designed as a VHH-Fc-VHH format, with two VHHs raised against PD-L1 and two against AXL. Activity, selectivity, and potential for internalization and degradation of targets were studied on cancer cell lines with different expression levels of the targets. In addition, CPL976 efficacy was verified in syngeneic mouse models, when antibodies were administered intravenously at different doses for 3 weeks.
Results: We confirmed the CPL976's innovative mechanism of action based on the strong and simultaneous engagement of both therapeutic targets, and potential internalization and degradation of target proteins in cancer cell lines with different expression levels of AXL and PD-L1 (MDA-MB 231, A375, A549, H1299). Potent and dose-dependent in vivo antitumor activity was observed in the syngeneic mouse model, where at a dose of 15mg/kg remission of the tumor was observed in 5/8 compared to 0/8 in the control group.
Conclusions: CPL976 is the bispecific antibody that combines the effects of cancer inhibition by interacting with AXL and immunotherapy by disrupting the PD-1/PD-L1 axis. The use of the bispecific antibodies simultaneously targeting PD-L1 and AXL provokes internalization of the targets to maximize the biological effect of the inhibition of the receptor/ligand complexes (AXL/cGAS6, PD-1/PD-L1) formation. Simultaneous action on both therapeutic targets may help achieve an enhanced immune response against cancer cells and lead to tumor eradication and overcoming the primary and secondary resistance to PD-1/PD-L1 targeted therapies.

#5085 Preclinical development of NaPi2b-PL2202, a novel camptothecin-based antibody-drug conjugate targeting solid tumors expressing NaPi2b.

E. Horsley[1], A. Jabeen[1], N. Veillard[1], K. Havenith[1], N. Janghra[1], P. Alves[1], C. Oblette[1], I. Kirby[1], P. W. Hogg[1], F. Zammarchi[2], L. de Haan[1], **P. v. Berkel**[1]; [1]ADC Therapeutics, London, United Kingdom, [2]Myricx Bio, London, United Kingdom

NaPi2b, encoded by the SLC34A2 gene, is a multi-transmembrane, sodium-dependent phosphate transporter expressed at high levels in tumors and low levels in normal tissues. Functionally, it is involved in trans-cellular flux of phosphate in the small intestine and in the synthesis of surfactant in lung alveoli. NaPi2b is reported to be expressed at a high frequency in ovarian carcinoma as well as in NSCLC, bladder, endometrial and papillary thyroid carcinoma[1], and its expression is associated with poor prognosis [2, 3]. The purpose of this study was to characterize the *in vitro* and *in vivo* anti-tumor activity and tolerability of NaPi2b-PL2202, an antibody-drug conjugate (ADC) composed of a humanized, Fc-silenced IgG1 antibody directed against human NaPi2b, to which PL2202, a novel payload containing a valine-alanine cleavable linker and a camptothecin warhead, has been site-specifically conjugated with a drug to antibody ratio of 6. In addition, the level of NaPi2b expression in selected human tumor specimens was evaluated by immunohistochemistry (IHC). *In vitro*, NaPi2b-PL2202 showed good binding affinity for mouse, rat, cynomolgus monkey and human NaPi2b, and displayed highly potent, targeted cytotoxicity against various NaPi2b-expressing tumor cell lines. NaPi2b-PL2202 also exhibited strong *in vitro* bystander activity. *In vivo*, intravenous (IV) administration of a single dose of NaPi2b-PL2202 at 6.6 mg/kg resulted in substantial tumor regression in the OVCAR-3 ovarian carcinoma xenograft model, with 3/10 partial responders (PR) and 7/10 complete responders (CR), and all CRs being tumor-free at the end of the study (Day 44). In the G-402 renal leiomyoblastoma xenograft model, administration of a single IV dose of NaPi2b-PL2202 at 3.3 mg/kg was associated with durable antitumor activity and resulted in 1/10 CR, with this animal remaining tumor-free by the end of the study (Day 42). With respect to toxicity, in single dose studies in male rats, NaPi2b-PL2202 was tolerated up to 300 mg/kg IV. Furthermore, in a dose-range finding study in male cynomolgus monkeys, NaPi2b-PL2202 was well tolerated up to 40 mg/kg IV given on Day 1 and 22. Finally, cell membranous NaPi2b expression was confirmed by IHC in a panel of tissue microarrays including ovarian, lung, bladder and endometrial cancers. In conclusion, NaPi2b-PL2202 demonstrated specific and potent *in vitro* and *in vivo* anti-tumor activity, and was tolerated at high doses in toxicity studies in rats and cynomolgus monkeys, indicating a good therapeutic index. Together, these observations support future clinical development of NaPi2b-PL2202 for the treatment of NaPi2b-expressing cancers. 1- Bodyak N. D. et al., 2021 2- Valsenkova R. et al., 2021 3- Hakim S. A. et al., 2021

#5086 Functional profiling in lung tumor explants show contributions of the tumor microenvironment to response of Dato-DXd*ex vivo*.

S. Yasuda[1], E. V. Ivanova[2], H. V. Vo[2], S. Kivlehan[2], I. Gjeci[2], M. Ha[2], P. Lizotte[2], R. Bueno[3], D. A. Barbie[2], **C. P. Paweletz**[2];
[1]Daiichi Sankyo, Baskin Ridge, NJ, [2]Dana-Farber Cancer Institute, Boston, MA, [3]Brigham and Women's Hospital, Boston, MA

Background: Antibody drug conjugates (ADCs) have demonstrated significant antitumor activity against multiple treatment refractory cancers. While Trastuzumab deruxtecan, a HER2 directed ADC, has shown impressive clinical activity in HER2-expressing cancers, the ability to predict responses of ADCs by IHC has been limited. Dato-DXd is a TROP2 directed ADC that is currently being studied in a number of registrational phase 3 trial incld. TROPION-Lung01. In the phase 1b TROPION-Pan tumor 01 trial (TP01) response to Dato-DXd did not correlate to TROP2 IHC expression. Here we investigate molecular determinants of sensitivity to Dato-DXd using short-term microfluidic culture of patient derived organotypic tumor spheroids (PDOTS).
Methods: Surgical NSCLC cases collected from Brigham and Women's Hospital and St. Elizabeth's Medical Center under an IRB approved protocol were studied. PDOTS were generated as previously described. *Ex vivo* response was assessed by live/dead imaging, TROP2 antigen density on EPCAM+ cells by flow cytometry (FCM) and by immunofluorescence (IF). T cell and myeloid cell populations were analyzed by FCM of CD45+ cells isolated during tumor preparation. For a subset of samples single cell RNA sequencing (scRNAseq) was performed.
Results:Eleven NSCLC explants were studied. Two specimens were excluded due to excess of fibrotic material. Response to Dato-DXd was measured by change in raw live cell area compared to control samples. Median response to Dato-DXd was -48.5% (ranging from +33.9% to -77.8%). Using a cut-off of -40%, four cases were characterized as non-responders (NR) and 5 as responders (R). Tumor TROP2 expression by IF ranged from 0 to 3+ with no relationship between TROP2 expression and response being observed. TROP2 staining positivity by IF didn't correlate to Dato-DXd sensitivity *ex vivo*. TROP2 FCM, on the other hand discriminated between responsive and non-responsive models in 100% of the cases, using a cutoff of MFI >13000. Furthermore, we observed an increase of tumor CD8 abundance in Dato-DXd R compared to NR (median %CD8 in R 10.3% (range 5.1%-62.5%); median %CD8 of live cells in NR 2.3% (range 1.2%-3.7%) p-value 0.029). Conversely, we also observed a trend of higher granulocytic myeloid-derived suppressor cells abundance in NR compared to R (NR median %gMDSC of CD15+ cells 84.1% (range 73.4%-90.2%) ; R median %gMDSC 61.7% (range 54.3%-90.6%); p-value 0.069). In 2 cases with high and low TROP2 MFI available scRNAseq data showed TROP2 expression exclusively in tumor cells, with further analysis ongoing.
Conclusion: By functionally profiling NSCLC PDOTS that retain immune cells, we correlated multiple parameters with *ex vivo* response to Dato-DXd. Our results have important implications for precision deployment of ADCs and suggest that target tumor antigen density in conjunction with addition immune cell features may refine patient selection strategy.

#5087 ILB-3101, a novel B7H3-targeting ADC with Eribulin as payload, demonstrates strong tumor killing activities and favorable PK/TOX profile in preclinical evaluation.

Y. Shang, J. Qiu, Y. Xin, M. Zhao, Q. Liu, Z. Wang, X. Gong, **Y. Xu**, Y. Li, M. Xia, R. Chen;
Innolake Biopharm, Hangzhou, China

B7H3, a B7 family member of immune checkpoint proteins, is overexpressed in a broad spectrum of malignant tumors. It has become an attractive target for cancer therapies in recent years. ILB-3101, a potential best-in-class ADC, was constructed by conjugating a potent mitotic inhibitor Eribulin to a proprietary anti-B7H3 mAb through a proprietary linker. This ADC molecule has been developed and preclinically evaluated as both the 1st line ADC treatment with B7H3 expressed patients in Eribulin sensitive cancer types and the later line treatment for patients whose cancer are B7H3 positive but TopoI inhibitor resistant.
The humanized antibody of ILB-3101 is IgG1 type and shows high affinity to both human and monkey B7H3 proteins. It also shows better internalization than benchmark antibodies such as that of DS-7300 analog. The DAR value of ILB-3101 is 3.5. ILB-3101 has potent and dose-dependent cytotoxicity to B7H3-positive tumor cells and shows better activities than DS-7300 analog as positive control. *In vivo* studies based on xenograft tumor models reveal that ILB-3101 has potent anti-tumor activities in various tumor types including TNBC, sarcoma, ovarian cancer and AML etc., which are superior or comparable to DS-7300 analog. Furthermore, ILB-3101 shows strong anti-tumor activity on Dxd based ADC resistant tumors in xenograft tumor models. The PK study of ILB-3101 in cynomolgus monkeys shows dose-dependent exposure and desirable PK profile. ILB-3101 was well tolerated in cynomolgus monkeys with HNSTD at 6 mg/kg. No serious adverse events were observed, and the main safety findings were limited and reversible hematological and immunological effects, which are consistent with the safety profile of Eribulin as an approved chemotherapy.
The *in vitro* and *in vivo* preclinical results above demonstrate that ILB-3101 has good efficacy and safety profile and it is a promising and potentially best-in-class B7H3 targeting ADC drug candidate. ILB-3101 is worthy of further translational research and clinical trials. Its IND application has been submitted in China, followed by US FDA filing soon.

#5088 Evaluating TNF-receptor associated factor 2 (TRAF2) as a targetable driver of immune resistance in LKB1 deficient non-small cell lung cancer.

Bahareh Nourmohammadi[1], Joseph M. Amann[1], Rahul Shivahare[1], Qin Ma[2], Zihai Li[1], David P. Carbone[1], Jacob Kaufman[1]

[1]Division of Medical Oncology, Department of Internal Medicine, The Ohio State University Comprehensive Cancer Center, Columbus, OH,[2]Department of Biomedical Informatics, The Ohio State University College of Medicine, Columbus, OH

STK11 is a serine-threonine kinase and tumor suppressor lost in about 25% of NSCLC. It potently regulates a network of downstream effector kinases in the AMPK family, thereby exerting major effects on cell signaling, metabolic activity, and epigenetic patterning. Clinically loss of STK11 in NSCLC is associated with poor response to immune checkpoint blockade. Several mechanisms of immune resistance have been identified involving both tumor intrinsic pathways as well as changes in the immune microenvironment. Dysregulation of cellular inhibitor of apoptosis proteins, specifically cIAP1 has been identified as a specific resistance mechanism, which was shown to also influence the STING pathway in the context of STK11 loss. However, there is a gap in understanding how loss of STK11 influences cIAP1 signaling.We evaluated cIAP1, its TRAF family member binding partners, and downstream NF-kB and immune signaling using a multiomic approach. Using CPTAC multiomic data of 110 lung adenocarcinomas, we observe discordance between protein vs mRNA expression for cIAP1, which shows no significant association with STK11 loss in mRNA, but is significantly over-expressed at the protein level (P<1e-4). Conversely, we identify TRAF2 as the only TRAF member whose expression is increased in STK11-deficient NSCLC, with concordant increase in both mRNA (P<1e-8) and protein (P<1e-10). Further, on the protein level TRAF2 and cIAP1 levels were highly correlated (P<1e-12), strongly suggesting that TRAF2 is the proximal factor driving dysregulation of cIAP1 signaling in these tumors. We also observe a correlated pattern of phosphorylation sites within cIAP1, TRAF2, and other NF-kB signaling members that we putatively link to STK11 loss. We confirm that TRAF2 mRNA is consistently over-expressed in STK11 deficient NSCLC across multiple additional transcriptomic datasets together comprising >2000 tumors. Across this large dataset we observe that among STK11-deficient tumors, TRAF2 is anti-correlated with NF-kB signaling and immune infiltration signatures, a relationship that is strikingly absent among the STK11-WT subset. Using GEMM cell lines (KRAS, TP53, STK11 GEMM; Winslow lab, Stanford), we derived STK11 mutant vs WT isogenic pairs and performed T-cell co-culture experiments using ovalbumin antigen and OT-I CD8 T-cells. This showed that inhibition of cIAP1 using birinapant was synergistic to CD8 cytotoxicity, as previously known, but the synergy was much more pronounced in STK11 mutant vs STK11-WT context (Bliss index 38, P<1e-10). Together, these data demonstrate that the link between STK11-loss and cIAP1 dysregulation is likely through over-expression of TRAF2, and support the strategy of targeting TRAF2/cIAP1 to overcome immune resistance STK11-deficient NSCLC.

#5089 Therapeutically targeting endometrial cancer by ICAM1 antibody-drug conjugates.

H. Xie[1], L. Sun[2], S. Yao[3], P. Guo[3], Y. Zhang[2];

[1]Postgraduate training base Alliance of Wenzhou Medical University, HangZhou, China, [2]Zhejiang Cancer Hospital, Hangzhou, China, [3]Hangzhou Institute of Medicine (HIM), Chinese Academy of Sciences, HangZhou, China

Background: Endometrial cancer is the most frequently occurring gynecologic cancer in developed countries and the third leading cause of cancer deaths among women. It remains one of the few malignant tumors with rapidly increasing mortality and morbidity. Patients with recurrent or metastatic endometrial cancer continue to experience poor outcomes. Antibody-drug conjugates (ADCs) represent a class of targeted therapeutic modalities that offer biomarker-based therapeutic options for patients with endometrial cancer. In this study, we proposed to identify a novel molecular target for the preclinical development of an ADC for endometrial cancer-targeted therapy.

Methods: Firstly, to determine the level of target expression within endometrial cancer tissue components as well as differences, we performed immunohistochemical staining of human endometrial cancer and paracancerous tissue. Secondly, the expression of the target on the cell membrane surface was quantitated and qualitatively verified using flow cytometry and single-photon confocal microscopy. In the third step, an endocytosis assay was used to verify the endocytosis of the target antibody by EC cells. Confocal imaging can directly observe the endocytosis of the target antibody, and flow cytometry can be analyzed and quantified. Co-localization experiments with antibody fluorescence can verify the specific site where the target antibody is endocytosed into cancer cells. We then designed and characterized two targeted ADCs. Next, the *in vitro* inhibitory activities of these ADCs against endometrial cancer cell lines and normal cells were evaluated using the CCK8 assay. Finally, we established a cell line-derived xenograft (CDX) model of endometrial cancer to validate the *in vivo* efficacy and bio-safety of the ADCs.

Results: We have determined a correlation between ICAM1 overexpression and EC, and IHC staining of patient tissues showed significantly higher levels of ICAM1 expression in endometrial cancer tissues than in paracancerous tissues. The high cell surface expression of ICAM1 was verified in a panel of various human endometrial cancer cell lines. Moreover, two ICAM1 ADCs were established using clinically-approved ADC linker and payload combinations. It was visually confirmed that ICAM1 ADCs selectively recognize endometrial tumors and efficiently enter endometrial cells via antigen-mediated endocytosis. We compared the anti-tumor activity of ICAM1 ADCs with standard-of-care chemodrugs, and ICAM1 ADCs outperformed chemodrugs in the CDX model of endometrial cancer without toxicity.

Conclusion: We identified that ICAM1 is a promising ADC target for endometrial cancer and confirmed the potent anti-tumor activity and biosafety of ICAM1 ADCs *in vitro* and *in vivo*, warranting further pre-clinical and clinical investigations.

#5090 Development of HSPG2 targeted glycoengineered antibody-drug conjugates.

X. Li, S. Prabha;
Temple Univ, Lewis Katz School of Medicine, Philadelphia, PA

Ovarian cancer is associated with poor outcomes and aggressive behaviors. Although surgical removal of tumors and chemotherapy can initially eradicate cancer, many patients eventually experience relapse with chemotherapy-resistant tumors, resulting in poor long-term outcomes and chemotherapy complications. Antibody-drug conjugates (ADCs) are formed by integrating the tumor specificity provided by antibodies (Ab) and small molecule cytotoxicity drugs and can facilitate highly targeted delivery with minimal toxicity to normal tissues. Our group has identified that the overexpression of a novel target, heparan sulfate proteoglycan 2 (HSPG2), is associated with poor prognosis and survival of high grade serous ovarian cancer (HGSOC) patients. We have developed a monoclonal antibody (AM6) that effectively targets HSPG2-expressing tumors. In this study, we used a novel glycoengineering strategy to introduce artificial azide groups at the N-glycan sites of AM6 without affecting its antigen affinity and intracellular localization. The azide groups were then used for site-specific conjugation of the cleavable dibenzyl cyclooctyne - monomethyl auristatin E (DBCO-PAB-MMAE) linker (drug conjugate) to form an AM6 antibody-drug conjugate (AM6 ADCs). Hydrophobic interaction chromatography (HIC) and liquid chromatography/quadrupole time-of-flight/mass spectrometry (LC/Q-TOF/MS) confirmed the successful conjugation of the DBCO-PAB-MMAE to the AM6. In-vitro cytotoxicity studies of AM6 ADCs in OVCAR8 (high HSPG2 expression) and CAOV3 (regular HSPG2 expression) showed the cell line dependent response with lower IC50 in OVCAR8. These results suggest that the effectiveness of AM6 ADCs is proportional to the HSPG2 expression levels of the cells. Future studies will be aimed at the in-vivo evaluation of optimized antibody-drug conjugates.

#5091 Response to neoadjuvant chemoimmunotherapy in resectable locally advanced oral squamous cell carcinoma: a single-center retrospective observational study.

Jinsong Li, Bowen Li, Shule Xie, Haotian Cao, Zhaoyu Lin, Qunxing Li, Song Fan

Sun Yat-Sen Memorial Hospital of Sun Yat-Sen University, Department of Oral and Maxillofacial Surgery, China

Background: This study aims to investigate the effectiveness of neoadjuvant chemoimmunotherapy (NACI) regimens in treating advanced oral squamous cell carcinoma (OSCC).
Methods: We analyzed clinicopathologic features of advanced OSCC patients who received PD-1 inhibitors in combination with carboplatin and paclitaxel before surgical tumor resection between 2020 and 2022. The Response Evaluation Criteria in Solid Tumors (RECIST, version 1.1) and pathologic response were used to evaluate the efficacy of the NACI treatment. Adverse events apparently related to NACI treatment were graded according to the Common Terminology Criteria for Adverse Events, version 4.0. Disease-free survival (DFS) and overall survival (OS) were calculated using the Kaplan-Meier survival curves and compared using the log rank test. Additionally, we calculated the area under curve (AUC) to compare the predictive value of PD-L1 expression with baseline serum lipid biomarkers for patient response.
Results: Our analysis involved 104 advanced OSCC patients who received NACI. Notably, the top three grade 1-2 treatment-related adverse events (TRAEs) were Alopecia (104; 100%), Anemia (81; 77.9%) and Pruritus (62; 59.6%). Only one patient developed grade 3-4 TRAEs due to increased aminotransferases. The pathological complete response (PCR) rate was 47.1%, and the major pathological response (MPR) rate was 65.4%. Importantly, patients achieving MPR exhibited higher CPS. The diagnostic value of CPS as a biomarker for NACI efficacy was enhanced when combined total cholesterol (TC) level. Our findings from DFS and OS suggested that patients who underwent NACI before surgery experienced improved survival compared to those who accepted the surgery alone.
Conclusions: The data from this study proved evidence that NACI treatment is safe and encouragingly efficacious in treating advanced OSCC patients.

#5092 Development of a priming approach to enhance antigen-directed therapies in hematological malignancies and solid tumors.

K. E. Vanderlaag, A. Dhar, M. Volkman, E. Werner, T. Nguyen, K. Ali;
Eigen Therapeutics Inc., Redwood City, CA

Clinical success of antigen-directed therapies in cancer has been limited by heterogeneous antigen expression and a narrow therapeutic window. In many patients, failure of antigen-directed therapies such as CAR T-cell therapies, antibody-drug conjugates (ADC) or radioligand therapies (RLT) has less to do with a lack of potency or specificity of the agent and more to do with variable and suboptimal antigen expression in the patient. We are developing combination therapies that introduce a priming agent designed to optimize antigen expression in the patient and improve the therapeutic window of existing antigen-directed therapies. Our high-throughput platform utilizes machine learning and automation to scale functional combinatorial screening for small molecule priming agents using cell lines and patient samples. Using this platform, we are identifying priming therapies for CD123, CD33, CD22, and CD19 in hematological malignancies including acute myeloid leukemia (AML), and HER2, HER3, and TROP2 in solid tumors including breast cancer.For our CD123 program, we have identified priming agents that selectively upregulate CD123 expression ≥2-fold on AML cells without increasing expression on normal myeloid progenitor cells, which also express CD123. AML cells treated with a CD123 priming agent in combination with a CD123 ADC showed greater tumor-cell killing compared to the ADC alone. In comparison, normal myeloid progenitor cells from healthy bone marrow treated with the same CD123 priming-ADC combination treatment did not show an increase in ADC-mediated cell killing. From our mechanistic studies, we have identified a somatic mutation associated with CD123 upregulation that may lead to selective upregulation on cancer cells and not on normal cells. Additionally, this marker can be used for patient selection. We have also observed CD123 upregulation in vivo using mouse models of AML and are currently conducting additional in vivo proof of concept studies to demonstrate that CD123 priming therapy enhances efficacy.There are two distinct advantages of a priming approach paired with an antigen-directed therapy, which include: (1) improving the durability of patient responses and (2) expanding the patient population. Our priming combination approach has the potential to overcome antigen heterogeneity and thereby improve the clinical success of antigen-directed therapies.

#5093 Analysis of protein expression in head and neck cancers as therapeutic targets for antibody drug conjugates.

J. T. Moyers[1], S. L. Smith[1], M. M. Mora[1], R. Carmagnani Pestana[2];

[1]The Angeles Clinic and Research Institute, A Cedars-Sinai Affiliate, Los Angeles, CA, [2]Hospital Israelita Albert Einstein, Sao Paulo, Brazil

Introduction: Antibody Drug Conjugates (ADCs) represent a new category of therapeutic molecular targeting for solid tumors. To date 6 ADCs have been approved in solid tumors against 5 targets (HER2/ERBB2, Folate alpha, Tissue Factor, Nectin-4, and Trop-2). Thus far, no ADCs have been approved for head and neck cancers.

Methods: We queried protein expression data from a publically available consortium of datasets (TNMPlot.com) containing protein expression data from over 56,000 tumor and normal samples from GEO, GTex, TCGA, and TARGET databases. Genes examined for protein targets, included those with ADC targets of both presently approved and investigational drugs from clinical trials.The level of overexpression was determined as the percent of tumors over the 75th percentile of expression in normal tissue.

Results: Protein expression data were available for 99 HNSCC samples. Among targets with ADCs available, increased protein expression was seen in HNSCC for 0% of ERBB2 (n=0/99), 38% of FOLR1 (n=38/99), 0% of TACSTD2 (n=0/99), and 42% of F2 (n=42/99) genes.Among gene targets with investigational ADCs, increased protein expression was seen in HNSCC for 35% of of AXL (n=35/99), 13% of B7H3/CD27 (n=12/99), 50% of EGFR (n=50/99), 63% of VTCN1 (n=63/99), 10% of MSLN (n=10/99), 77% of CDH3 (n=76/99), and 39% of PDGFRA (n=39/99).

Conclusion: Increased protein expression for approved ADC targets were infrequent in HNSCC. However, increased protein expression is seen for several ADCs under clinical investigation supporting the potential therapeutic approaches for investigational ADC targets.

#5094 Immunotherapy in advanced cutaneous non-melanomatous spindle cell neoplasms.

L. S. McLean[1], A. M. Lim[1], C. Angel[1], R. J. Young[1], A. Pizzolla[1], S. Archer[2], A. A. Thai[1], B. Solomon[1], J. Lewin[1], D. Rischin[1];
[1]Peter MacCallum Cancer Centre, Melbourne, Australia, [2]Monash Bioinformatics Platform, Melbourne, Australia

Background: Non-melanomatous cutaneous spindle cell neoplasms (NMCSpC) are a rare group of malignancies including pleomorphic dermal sarcoma (PDS) and spindle-cell cutaneous squamous cell carcinoma (SpSCC). They present a diagnostic challenge with overlapping morphological features and variable patterns of immunohistochemical (IHC) staining. There is a lack of consensus on how to best manage advanced NMCSpC and limited reports of immunotherapy (IO) responses. This study reviews the efficacy of IO in NMCSpC and performs comprehensive tumor profiling to identify biological rationale for IO use in this rare group of tumors.

Methods: We performed a single-center retrospective review of all locally-advanced or metastatic NMCSpCs treated with IO. Blinded histopathology reviews occurred to confirm each diagnosis. Overall response rates (ORR) were collected as per Response Evaluation Criteria in Solid Tumors 1.1 or Positron Emission Tomography Response Criteria 1.0. Comprehensive tumor profiling included whole exome sequencing for tumor mutational burden (TMB) and ultraviolet(UV)-signatures, and IHC for immune-cell infiltration (CD103/CD4/CD3/CD8/CD20) and immune-checkpoint expression (PD-L1/TIGIT/LAG3).

Results: 7 patients were identified. Median follow up was 18.1 months (range: 5.3-34.7). ORR 86% (6/7) with five complete responses (CR). One patient who achieved stable disease progressed. Responses were durable with two patients in CR >30 months after IO commencement. Blinded pathological review identified 3 SpSCC, 2 PDS and 2 spindle cell tumors of unclear sub-classification. All patients had high TMB and UV-signatures. One patient had PD-L1 100% (combined positive score) with abundant immune-cell infiltration and LAG3 expression (Table 1).

Conclusion: In advanced NMCSpC, excellent responses to IO with durable disease control was observed. IO is worthy of further exploration in these patients. UV-signatures and high TMB could be used to help select patients for treatment.

Immunohistochemistry (IHC)^, tumor mutational burden and ultraviolet signatures

Patient	T-cell markers				B-cell marker	Immune-checkpoints			Tumor mutational burden (mutations/megabase)	Ultraviolet-mutational signature	Best response assessment#
	CD103	CD4	CD3	CD8	CD20	PD-L1	TIGIT	LAG3			
1	1	20	1	1	0	7	0	0	17.94	Yes	Stable metabolic response
2	1	20	30	10	0	100	0	10	35.34	Yes	Complete metabolic response
3	1	10	10	5	0	5	0	0	104.87	Yes	Complete metabolic response
4	1	0	1	0	0	0	0	0	74.04	Yes	Partial metabolic response
5*	NA	NA	NA	NA	NA	NA	NA	NA	29	Yes	Complete metabolic response
6	1	0	0	5	0	0	0	4	12.02	Yes	Complete metabolic response
7	1	0	5	1	0	0	0	0	41.17	Yes	Complete response

^IHC scores are % of positively stained cells, except for PD-L1 which is combined positive score (CPS). *Insufficient tissue for IHC on Patient 5. #As per PERCIST 1.0 on FDG-PET/CT or RECIST1.1 on CT.

#5095 Characteristics of patients with advanced renal cell carcinoma (aRCC) who received first-line (1L) nivolumab plus cabozantinib (NIVO+CABO), pembrolizumab plus lenvatinib (PEM+LEN), or nivolumab (NIVO) monotherapy in the real-world (RW) setting.

K. K. Zarrabi[1], B. Miron[2], X. Yin[3], L. Rosenblatt[3], S. B. Guttenplan[3], W. John[4], T. A. Miller[4], P. Asgarisabet[4], P. Pathak[4], M. Ahlquist[4], Y. Gash[4], D. M. Geynisman[2];

[1]Thomas Jefferson University, Philadelphia, PA, [2]Fox Chase Cancer Center, Philadelphia, PA, [3]Bristol Meyers Squibb, Princeton, NJ, [4]Cardinal Health, Dublin, OH

Background: Recent advances in immunotherapy have introduced new treatment modalities for aRCC. In absence of guideline recommendations, it is unclear what factors drive providers in selecting 1L treatments for aRCC. To address this gap, we described the baseline demographic and clinical characteristics of patients with aRCC who received 1L NIVO+CABO, PEM+LEN, or NIVO monotherapy in the RW setting.

Methods: In this retrospective cohort study, treating oncologists from a US nationally representative network abstracted electronic health record data from patients with aRCC who initiated 1L NIVO+CABO or NIVO monotherapy (off-label in the US) between 2/1/2021 and 6/12/2023, or PEM+LEN between 9/1/2021 and 6/12/2023. Patient demographic and clinical characteristics were summarized descriptively.

Results: Compared with patients who received NIVO+CABO (n = 200) or PEM+LEN (n = 100), patients who received NIVO (n = 147) were relatively older at 1L initiation (Table). Sex, race, and region of residence were comparable across cohorts. Patients who received NIVO were more likely to have an ECOG PS score of ≥ 2 (59.2%) compared with NIVO+CABO (14.5%) or PEM+LEN (20%) cohorts. The distribution of MSKCC or IMDC risk scores at 1L initiation was comparable across cohorts . Grade 3 or 4 tumors were reported among 56.5%, 41.0%, and 43.5% of those who received NIVO+CABO, PEM+LEN, and NIVO, respectively.

Conclusions: This study suggests that 1L treatment for aRCC using IO monotherapy may be more likely to be considered than IO-TKI therapy for older patients and those with poorer ECOG PS, possibly reflecting perceived tolerability of TKI combinations in these patient populations. Further research is needed to understand the impact of these 1L treatment selection patterns on outcomes.

Table: Key patient characteristics at 1L initiation.

	PEM+LEN	**NIVO+CABO**	**NIVO**
	n = 100	**n = 200**	**n = 147**
Mean age, year (standard deviation)	64.4 (7.9)	66.3 (7.4)	74.1 (9.6)
Male, n (%)	93 (63.3)	122 (61.0)	93 (63.3)
Race, n (%)			
White	61 (61.0)	127 (63.5)	91 (61.9)
Non-white/unknown	39 (39.0)	73 (36.5)	56 (38.1)
Region of residence, n (%)			
Northeast	23 (23.0)	44 (22.0)	37 (25.2)
Midwest	22 (22.0)	53 (26.5)	27 (18.4)
South	20 (20.0)	34 (17.0)	33 (22.4)
West	35 (35.0)	69 (34.5)	50 (34.0)
MSKCC or IMDC risk score, n (%)			
Favorable	13 (13.0)	28 (14.0)	22 (15.0)
Intermediate	57 (57.0)	100 (50.0)	74 (50.3)
Poor	28 (28.0)	68 (34.0)	41 (27.9)
ECOG-PS, n (%)			
0 or 1	80 (80.0)	171 (85.5)	60 (40.8)
≥2	20 (20.0)	29 (14.5)	87 (59.2)
Grade of tumor differentiation, n (%)			
Grade 1	3 (3.0)	10 (5.0)	16 (10.9)
Grade 2	56 (56.0)	77 (38.5)	67 (45.6)
Grade 3	36 (36.0)	98 (49.0)	55 (37.4)
Grade 4	5 (5.0)	15 (7.5)	9 (6.1)

#5096 Clinical feature of immune checkpoint inhibitor-induced pancreatic injury.

J. Itani, T. Ishikawa, T. Doi, D. Sone, R. Morita, N. Iwai, R. Hirose, K. Inoue, O. Dohi, N. Yoshida, K. Uchiyama, T. Takagi, H. Konishi, Y. Itoh;
Kyoto Prefectural University of Medicine, Kyoto, Japan

Immune checkpoint inhibitors(ICIs) cause multiple adverse inflammatory reactions known as immune-related adverse events(irAEs), but ICI-related pancreatic injury(ICI-PI) is rare. ICI-PI ranges from asymptomatic hyperamylasemia to acute pancreatitis(ICI-AP), and its clinical features are not fully understood. We investigated the frequency and clinical features of ICI-PI and ICI-AP as well as their possible risk factors. Of the 186 consecutive cases who received ICI for GI cancers in our hospital from January 2020 to May 2022, 185 could be evaluated for serum amylase(AMY) levels pre- and post- ICI treatment. We retrospectively examined the clinical features and predictors of ICI-PI. Hyperamylasemia of grade 2 or higher according to CTCAE(v.5.0) was considered ICI-PI, and cases with other obvious factors were excluded. In the case of ICI-AP, we analyzed the pathological features of the tissues collected by EUS-FNA as well as the clinical features. The median of ICI doses was 6.0(range, 1-64), and the median duration of observation was 236 days(range, 17-1162). There were 25 cases of hyperamylasemia (higher than ULN) before starting ICI treatment. After starting ICI treatment, 14 patients(7.6%) developed ICI-PI, in all cases grade 2. The median time to onset of ICI-PI was 37.5 days(7-715). No cases discontinued ICI dosing due to ICI-PI, and no cases developed obvious pancreatic endocrine or exocrine insufficiency during the observation period. Overall survival was significantly longer in cases with ICI-PI than in those without ICI-PI(MST; 855 vs. 347days, p=0.029) and there was a trend toward longer PFS(MST; 160 vs. 96 days, p=0.057). Multivariate analysis revealed that only pretreatment serum AMY level(≥80 U/L) was a significant independent predictor of developing ICI-PI(HR: 5.00, 95% CI: 1.057-23.668, p=0.04). ICI-AP occurred in 2 cases(1.1%), both of them discontinued ICI treatment. Both cases showed enlarged pancreas on CT scan, negative serum IgG4 level, and responded well to steroid therapy. Pathological findings showed lymphoplasma cell infiltration, flower-like fibrosis, and obstructive phlebitis, which were similar to type 1 autoimmune pancreatitis(AIP) in one case. In the other case, neutrophil infiltration was observed in the stroma and epithelium, similar to type 2 AIP. The best overall response was PR in both cases with ICI-AP. The findings of this study indicate that higher pretreatment serum AMY levels may increase the probability of ICI-PI. ICI-PI cases without pancreatitis did not show any pancreatic endocrine or exocrine insufficiency during the observation period without interruption of ICI treatment and had favorable prognosis, but a more long-term evaluation of the impact on pancreatic function is needed. The clinical implications of ICI-related hyperamylasemia and its differences from ICI-AP remain uncertain and need to be explored in the future.

#5097 Effectiveness and safety of atezolizumab plus bevacizumab in unresectable hepatocellular carcinoma: A multicenter, retrospective real-world study in China.

H. Zhang, M. Shao, B. Tan, Y. Fu, Y. Yuan, H. Chen;
Southwest Hospital, Third Military Medical University, Chongqing, China

Background: Atezolizumab plus bevacizumab (Atezo+Bev) has shown better benefits than sorafenib as the first-line treatment for unresectable hepatocellular carcinoma (uHCC) in IMbrave 150. However, the real-world evidence of Atezo+Bev in uHCC is limited, especially in China. We aimed to investigate the real-world effectiveness and safety of Atezo+Bev in Chinese patients with uHCC.

Methods: Patients with uHCC treated with Atezo+Bev were included at 5 centers in China from Jan. 2021 to Jan. 2023. Overall response (ORR), organ-specific response rate (OSRR), disease control rates (DCR), time to disease progression (TPP), progression-free survival (PFS), metastasis-specific PFS and overall survival (OS) were calculated.

Results: Among 48 patients, the median age was 58.4 years with 85.4% being male. A total of 35 and 13 patients received Atezo+Bev as 1st and 2nd line treatment, respectively. The median number of treatment cycles were 8, and 27 (56.3%) patients received locoregional therapies. Detailed treatment response is in the Table. The overall ORR and DCR assessed by mRECIST were 60.4% and 75.0%, while the intra- and extrahepatic OSRR were 59.4% and 62.5%, respectively. With a median follow-up of 14.5 months, the median PFS was 8.5 months (95%CI: 4.4, 11.2) in 1st line setting and 5.1 months (95%CI: 2.1, 7.9) in 2nd line setting. Median intra- and extrahepatic metastasis-specific PFS were 7.9 and 7.6 months, respectively. Median overall TTP was 7.6 months. The median OS was not reached. A total of 36 patients (75%) experienced any grade adverse events, most commonly being thrombocytopenia (27.1%, n=13), lymphopenia (25%, n=12) and abnormal liver function (14.6%, n=7).

Conclusion: This study confirmed effectiveness and safety of Atezo+Bev in the 1st line treatment of uHCC, and observed its potential in 2nd line in a real-world setting. Further studies are warranted to confirm these observations and refine treatment strategies.

Table. Treatment response

N (%)	Response Evaluation Criteria in Solid Tumors (RECIST) 1.1(N=48)	Modified RECIST(N=48)
Complete response (CR)	7 (14.6)	9 (18.8)
Partial response (PR)	12 (25.0)	20 (41.7)
Stable disease (SD)	15 (31.2)	7 (14.6)
Progressive disease	11 (22.9)	12 (25.0)
Not evaluated	3 (6.2)	0
ORR (CR+PR)	19 (39.6)	29 (60.4)
DCR (CR+PR+SD)	34 (70.8)	36 (75.0)

#5098 Second-line treatment outcomes in Extensive Stage Small Cell Lung Cancer (ES-SCLC) patients after first-line immuno-chemotherapy.

R. Wan, L. Fan, J. Zhong, J. Duan, Z. Wang, X. Hao, J. Wang;
Cancer Hospital Chinese Academy of Medical Sciences, Beijing, China

Background: First-line immune checkpoint inhibitors (ICIs) has significantly improved overall survival (OS) of ES-SCLC. However, second-line treatment options are still controversial with limited overall survival. This study aims to evaluate the efficacy of different second-line regimens for relapsed ES-SCLC after first-line immuno-chemotherapy.

Patients and Methods: We retrospectively reviewed 96 ES-SCLC patients receiving first-line immuno-chemotherapy in Cancer Hospital Chinese Academy of Medical Sciences, from Jan 2019 to Dec 2022. Clinical data were collected from electronic medical records. The clinical outcomes, including objective response rate (ORR), progression-free survival (PFS) and overall survival (OS) were assessed by Kaplan-Meier method and standard log-rank test.

Results: From January 4, 2019 to December 18, 2022, a total of 96 ES-SCLC patients received first-line immuno-chemotherapy and 49 of them went through second-line treatment in our center. Patient characteristics were listed as follows : median age 63 (31-79), male 76 (79.2%) , heavy smoker 59 (61.5%), liver metastasis 40 (41.7%), brain metastasis 33 (34.4%) and refractory recurrence 58 (60.4%). Second-line treatments included immunotherapy crossover and combination with chemotherapy (n=40), anlotinib with or without chemotherapy (n=5), chemotherapy alone (n=4). ORR of the whole group in the second-line setting was 22.4%. Median PFS was 3.23 months (95% CI 1.96-4.50). Cross-line immunotherapy failed to improved survival for relapsed ES-SCLC compared with those without ICIs (mPFS 3.23 vs 3.13m, *p*=0.829). Anlotinib based treatment showed numerically superior PFS for relapsed SCLC compared with those without anlotinib therapy (mPFS 6.00 vs 3.13m, p=0.089).

Conclusion: This retrospective study indicated cross-line ICIs failure to improve clinical outcome for relapsed ES-SCLC, and implied the potential benefits of anlotinib in second-line setting.

#5099 Prevalence of fibroblast growth factor receptor (*FGFR*) alterations (alts) and programmed death-ligand 1 (PD-L1) expression (exp) in Chinese solid tumor patients (pts).

M. Qing[1], F. Yang[1], X. Chen[1], X. Lyu[1], A. Wang[2], Y. Yu[2], S. Thomas[3], **L. Zhou[1]**;

[1]Janssen Research & Development, Shanghai, China, [2]OrigiMed Co., Ltd, Shanghai, China, [3]Janssen Research & Development, Spring House, PA

Background: PD-L1 expression drives anti-PD(L)-1 treatment decisions across many cancer indications. *FGFR* inhibitors have been approved for the treatment of metastatic urothelial cancer (UC) and cholangiocarcinoma with *FGFR* alts. BALVERSA (erdafitinib), a selective pan-*FGFR* kinase inhibitor, has shown clinical activity against *FGFR* altered solid tumors in pts who exhausted standard treatment options. It is important to understand the prevalence of *FGFR* alts and relationship between *FGFR* alts and PD-L1 expression levels in different cancer types.

Methods: In this real-world study, 9937 Chinese solid tumor pts with the PD-L1 (22C3) immunohistochemistry and OrigiMed 450-gene next-generation sequencing panel results were selected. Chi-square test and Fisher test were used to explore the association between the *FGFR* alts and PD-L1 expression.

Results: *FGFR1-4* somatic alts were found in 9.0% of Chinese cancer pts evaluated. *FGFR1* amplification (amp) was the most prevalent alts identified (1.9%). There were no significant differences in frequency of FGFR alts between the Chinese cohort and MSK-IMPACT cohort in each cancer type tested. Up to 40.6% of pts evaluated were PD-L1 positive (CPS ≥1 or TPS ≥1%). The PD-L1 positive rate (TPS ≥1%) in SCLC (12.4%, n=121) and NSCLC adenocarcinoma tumors (LUAD) (26.1%, n=2902) was relatively low. In few tumor types, higher expression of PD-L1 in FGFR altered samples was observed compared with FGFR unaltered samples in pan-tumor (mean TPS 14.8% vs.8.6%, *P*=6.0*E-9; mean CPS 6.3 vs. 6.1, *P*=3*E-4). Those includes LUAD (mean TPS 14.2% vs. 7.4%, *P* = 1.7*E-16), colorectal tumor (mean CPS 4.6 vs. 3.9, *P* = 4.6*E-8), and uterine tumor (mean CPS 8.1 vs. 6.5, *P* = 9.6*E-5). While PD-L1 expression is lower in FGFR altered samples than FGFR unaltered samples in UC (n=154; mean CPS 3.9 vs. 6.8, *P* = 0.004). No relationship was observed between FGFR alts and PD-L1 expression in cholangiocarcinoma (n=610). Specific *FGFR* alts eligible for erdafitinib UC treatment were further investigated in UC and observed with rate 10.4%, including *FGFR3* short variants (9.7%) as main alts. Specific FGFR altered tumors showed similar trend with lower PD-L1 expression than *FGFR* unaltered tumors in UC. The inverse relationship between *FGFR* alts and PD-L1 expression in UC compared to other solid tumors may explain variable role of *FGFR*s since the predominant *FGFR* alt types vary among different cancer types (*FGFR3* short variants enriched in UC vs no such predominant *FGFR* alt types in other cancer types).

Conclusion: The large Chinese solid tumor cohort analysis showed comparable *FGFR* alts prevalence between Chinese and Western population. Differences in relationship between *FGFR* alts and PD-L1 expression across tumor types reflect the differential role of predominant *FGFR* types in each tumor type.

#5100 Multimodal real world data reveals immunogenomic drivers of acquired and primary resistance to immune checkpoint blockade.

M. Keddar[1], S. Carrasco Pro[2], K. Burke[2], A. Camelo Stewart[1], M. Cobbold[3], R. Stewart[1], S. Khosla[1], B. Sidders[1], S. Hammond[4], D. C. Palmer[4], J. Dry[2], **M. L. Miller**[1];

[1]Astrazeneca, Cambridge, United Kingdom, [2]Tempus Labs Inc, Boston, MA, [3]Astrazeneca, Waltham, MA, [4]Astrazeneca, Gaitherburg, MD

Background: Why some patients fail or have short lived response to immune checkpoint blockade (ICB) immunotherapy remains largely unknown. While baseline molecular assessments have provided clues to prognostic factors, insights into resistance drivers remains elusive. This is partially due to the difficulty in getting access to post progression samples from patients that were either primary resistant or developed acquired resistance after an initial response to ICB. Thus, the tumor-intrinsic and -extrinsic features that are selected for during progression and potentially drive primary and acquired resistance to immunotherapy remain underexplored.

Methods: To compare clinical features and immunogenomic drivers of acquired and primary resistance to ICB across major cancers, we analysed and annotated de-identified patient records in the Tempus real-world database. We built an immuno-oncology cohort consisting of >2500 multimodal (DNA, RNA and clinical outcome data) pre-treatment baseline with >1500 post-treatment tumour biopsy samples from mainly NSCLC, TNBC, HNC and Bladder cancer patients. We used bulk RNA-seq data to estimate activation of the hallmark oncogenic pathways and immune cell composition and used panel DNA-seq data (>500 genes) to quantify mutation selection at the gene and pathway levels using *dndscv*.

Results: Compared to acquired, primary resistant patients tended to have a higher observation of liver lesions at progression. Post-ICB, acquired resistant NSCLC and HNC patients showed a significantly inflamed tumour microenvironment (TME) characterised by higher estimation of infiltration of T cells and myeloid cells and higher activation of interferon gamma (IFNg) signalling as compared to primary resistant patients. In addition, in post-ICB acquired resistance in NSCLC we observed selection for mutations in genes involved in known immunomodulatory pathways, including loss-of-function mutations in *B2M*. Consistently, acquired resistance patients showed stronger selection for mutations in Hedgehog and Notch pathways as compared to primary resistance patients across NSCLC, HNC and TNBC post-ICB.

Conclusions: Acquired and primary ICB resistant patients have distinct clinical and molecular features at progression. Their tumours' TME is fundamentally different with acquired resistance TMEs being infiltrated with immune cells albeit escaped post progression. In addition, ICB selects mutations that potentially activate pathways such as Notch and Hedgehog. This multi-modal Real-World Data with post therapy biopsies has given insights for patient selection strategies and provides rational into combination treatment options for acquired resistant patients.

#5101 Comparative genomic analysis reveals distinctive immune profiles in MET exon 14 mutated and MET amplified lung cancer.

S. Javeri[1], R. Minne[1], S. Ramesh[1], A. Baschnagel[1], R. Kimple[1], L. Lamb[2], S. Tomlins[2], B. Johnson[2], N. Khazanov[2];
[1]University of Wisconsin-Madison, Madison, WI, [2]STRATA Oncology, Ann Arbor, MI

Background: In non-small cell lung cancer (NSCLC), the MET tyrosine kinase receptor can be mutated or amplified resulting in dysregulation of receptor function leading to tumor proliferation. MET exon 14 (METEx14) mutated and MET amplified NSCLC tumors have shown varied response to immunotherapy. Therefore, we sought to compare the genomic and immune landscape of MET-altered NSCLC.
Methods: The genomic profiles of 3,821 NSCLC tumors sequenced using the Strata Select assay on the Strata Oncology Platform were analyzed. Tumors were sorted based on METex14 mutations, MET amplification (METamp) defined as copy number gain (CNG) ≥6 and MET wild-type (METwt). The RNA expression of 19 immune regulatory genes, tumor mutation burden (TMB), Strata Immunotherapy Response Signature (IRS) score and the frequency of gene co-alterations were compared across groups. Statistical comparisons of medians were done with Kruskal-Wallis testing and categorical comparisons with Chi square using R Studio version 4.3.2.
Results: 122 (3.2%) METex14, 70 (1.8%) METamp, and 3,629 (95.0%) METwt were identified. Patients with METex14 were older and more frequently female. MET gene expression was found to be higher in METamp (median 14.4) compared to METex14 (median 12.3) ($P<0.01$). TMB was lowest in METex14 (median 2.7) group compared to METamp (median 7.1) and METwt (median 5.1) ($P<0.001$). High PD-L1 expression occurred in 71.4% of METamp, 68.0% of METex14 and 41.3% of METwt ($P<0.001$). Overall, METamp tumors had a greater proportion of high IRS scores (52.9%) compared to METex14 (35.2%) and METwt (45.4%) ($P<0.01$). mRNA expression of immune checkpoints CTLA4, PD-1, LAG3, IDO1, TIGIT and HAVCR2 were all higher in METex14 compared to METamp and METwt ($P<0.001$ for all). METex14 tumors also exhibited higher gene expression of CD4, CD8A and FOXP3 compared to METamp and METwt ($p<0.001$). METex14 had higher prevalence of MDM2 amplification (34% vs 3% vs 4%) and lower prevalence of alterations in EGFR (0.8% vs 22% vs 21%), KRAS (0.8% vs 10% vs 26%), CDKN2A (17% vs 29% v 28%) and TP53 (34% vs 87% vs 64%) compared with METamp and METwt tumors, respectively ($p<0.05$).
Conclusion: METex14 and METamp tumors harbor distinct immune-gene expression profiles and co-occurring gene alterations that distinguish themselves from each other and METwt tumors. Further analysis must be conducted to determine how these variations impact immunotherapy in MET-altered NSCLC.

CLINICAL RESEARCH: Pediatric CNS Tumors, Leukemia, and Neuroblastoma: Translational
Poster Session

#5105 Aberrant CLK1 splicing is a key dependency factor in pediatric high-grade gliomas.

A. S. Naqvi, P. Seghal, R. Corbett, K. Rathi, B. Ennis, B. Zhang, M. Brown, D. Miller, A. Kraya, J. Dybas, K. E. Hayer, S. Arif, Z. Geng, A. Chroni, A. Lahiri, K. Conkrite, M. Hollawell, S. Diskin, P. Madsen, J. B. Foster, M. P. Koptyra, A. Thomas-Tikhonenko, A. Resnick, P. J. Storm, Jr., J. Rokita;
Children's Hospital of Philadelphia, Philadelphia, PA

Pediatric brain cancer is the leading cause of disease-related mortality in children. With a paucity of therapeutically targetable alterations, there is a pressing need to identify effective strategies for many of these tumors. In this study, we systematically examine aberrant alternative splicing in pediatric brain tumors from the Open Pediatric Brain Tumor Atlas, and additional tumors from the Children's Brain Tumor Network and the Pacific Pediatric Neuro-Oncology Consortium (n = 1831). Notably, high-grade gliomas (HGGs), including those with and without H3 histone mutations, were enriched in the upper quartile of all tumors with high splicing burden (SB). HGGs demonstrated the greatest SB heterogeneity of all tumor types and we identified a total of 19,229 aberrant splicing events in 8,577 genes in midline tumors compared to non-tumor brainstem controls (ΔPSI >= |.20|, p < 0.05). We next integrated protein annotations from the UniProt Knowledgebase to assess and prioritize differential alternative splicing events affecting protein function. This approach led to the discovery of 3,754 splice variants in 5,036 genes resulting in the gain or ablation of functional sites. The protein kinase *CDC-like kinase 1 (CLK1)*, a recognized master splicing factor and cell-cycle modulator, exhibited aberrant splicing of exon 4, whereby inclusion promoted the gain of two known phosphorylation sites. Additionally, we observed a strong correlation between *CLK1* splicing, its own RNA expression and proteomic activity of the Serine/Arginine-rich (SR) family of splicing factors. The distribution of exon 4 splicing was significantly different (p = 0.019) between tumors with low vs high splicing burden; tumors with high splicing burden had increased exon 4 inclusion. Further, we performed experimental modulation of *CLK1* exon 4 aberrant splicing in the brain tumor cell line KNS42 and demonstrated that forced exon 4 skipping leads to reduced CLK1 protein abundance and significantly reduces cell proliferation (p < 0.01 vs. control). Following bulk RNA-Seq analysis of these cell lines, we identified that forced *CLK1* exon 4 skipping resulted in 4,518 dysregulated genes enriched for known cancer pathways such as mitotic spindle, E2F targets, and G2M checkpoint. Our data suggest a role for *CLK1* in driving transcriptional dysregulation in pediatric high-grade gliomas and uncover a potential therapeutic vulnerability.

#5106 Pharmacological targeting of LSD1 prolongs animal survival times in patient derived orthotopic xenograft models of posterior fossa ependymoma in combination with fractionated radiation.

M. M. Suarez Palacios[1], S. Zhao[2], H. Zhang[2], L. Qi[2], H. Lindsay[2], M. Kogiso[2], F. Braun[2], A. M. Adesina[2], Y. Du[2], Y. Song[2], X.-N. Li[2];
[1]Northwestern University - Chicago, Chicago, IL, [2]Baylor College of Medicine, Houston, TX

Background: Posterior Fossa Group A Ependymoma (PFA EPN) constitute one of the most aggressive and highly recurrent molecular subtypes of childhood Ependymomas. We recently performed a comprehensive genome-wide DNA methylation analysis in recurrent pediatric EPN tumors from patients that were followed up for over 13 years. Integrative analysis between tumor DNA methylation and histone modification identified LSD1 as a druggable driver of PFA EPN recurrence. In this study, we examined the therapeutic efficacy of our newly developed LSD1 inhibitor SYC-836 in PDOX models of recurrent PFA EPN.
Methodology: To determine the *in vitro* anti-tumor activities of SYC-836, paired PFA EPN xenograft cell cultures (monolayer and 3D neurospheres) were treated with SYC-836 at 8 concentrations (0.02-25 µM) and examined for changes of cell proliferation every 3-4 days through day 14. To validate the drug's *in vivo* efficacy, two established posterior fossa EPN PDOX models, ICb-4423EPN and ICb-2002EPN, were utilized. Forty 8-week old SCID mice of both genders received intra-cerebellar tumor cell implantation and were divided into 4 treatment groups (n=10 per group): 1) control, 2) radiation (2 Gy/day x 5 days), 3) SYC-836 (15 mg/kg, daily intra-peritoneal injection for 28 days), and 4) combination (radiation + SYC-836). Animal survival times were analyzed using log-rank analysis. Changes in LSD1 protein expression and histone lysine methylation were examined through western hybridization.
Results: SYC-836 strongly suppressed PFA EPN cell growth *in vitro,* in both, a time- and dose-dependent manner. While there was no survival benefit with either SYC-836 only (P=0.186) or XRT only (P=0.205); combining SYC-836 with XRT significantly (P=0.04) prolonged the median survival time of ICb-4423EPN, from 46 days in the untreated group to 59 days; and in ICb-2002EPN, even more prominent, from 136 days to 180 days (P=0.007). SYC-836 was well tolerated in mice with no loss of body weight or other toxicities. Changes in LSD1 protein expression and H3K4me2 were detected through western hybridization during and after SYC-836 treatment.
Conclusion: Our data support LSD1 as a druggable driver of PFA recurrence and highlights strong anti-tumor activities of SYC-836 in combination with radiation, a standard therapy of pediatric EPN. SYC-836 may have a role in the clinical setting by either reducing radiation dosages or be an adjuvant agent to other chemotherapy drugs in our treatment approach for ependymoma.

#5107 Targeting CTPS1 and nucleotide biosynthesis pathways as a novel therapeutic approach in MYC-amplified medulloblastoma.

M. Hathaway[1], H. Jagana[1], M. Meechan[1], J. Hemenway[1], **K. E. Gadek**[1], A. Miyaki[1], I. Terrones[1], B. Slusher[2], S. Pattwell[1], N. Vitanza[1], M. K. Evans II[1];
[1]Seattle Children's Research Institute, Seattle, WA, [2]Johns Hopkins School of Medicine, Baltimore, MD

Although leukemia is the leading pediatric oncology diagnosis, brain tumors are the leading cause of pediatric cancer-related death. Medulloblastoma is the most common pediatric brain tumor, representing approximately 20% of all diagnoses. Of all four defined subgroups, MYC-amplified Group 3 medulloblastoma (G3 MB) tumors are the deadliest, with a < 50% 5-year overall survival rate. High risk patients receive large doses of chemo- and radio- therapy (CT/RT) with most survivors experiencing debilitating neurological and cognitive sequelae making the identification of novel targets of the utmost importance. Utilizing whole-genome CRISPR screening from the Pediatric Cancer Dependency Map, we identified the enzyme CTPS1 as a strong G3 MB-specific vulnerability. Recent studies corroborate our findings and suggest a dependence on the *de novo* pyrimidine biosynthesis pathway in MB. Targeted knockdown of CTPS1 restricts sphere formation and reduces proliferation of G3 MB tumor lines. We confirmed this genetic approach using a specific CTPS1 inhibitor, which also reduced proliferation but did not induce cell death, suggesting a cytostatic mechanism. Strikingly, we demonstrate that G3 MB is only dependent upon de novo pyrimidine synthesis and not de novo purine synthesis, despite regulation of both pathways by oncogenic MYC signaling. Previous work has shown that triggering an imbalance in pyrimidine and purine levels leads to replication stress and activation of the ATR/CHK1 pathway. Both genetic and pharmacologic inhibition of CTPS1 leads to CHK phosphorylation, allowing for cell survival despite lack of dNTPs. Previously, the CHK1 inhibitor, prexasertib, demonstrated robust brain accumulation and targeting of G3 MB in pre-clinical models. Dual inhibition of CHK1 and CTPS1 synergizes to significantly reduce cell viability *in vitro* and tumor growth *in vivo*. We further demonstrated robust synergy of CHK1 inhibition with either glutamine antagonists or other inhibitors of the *de novo* pyrimidine synthesis pathway, prolonging *in vivo* survival in an orthotopic xenograft G3 MB model. The results of this investigation confirm CTPS1 as a novel target in G3 MB, pinpoint a dependency on *de novo* pyrimidine rather than purine biosynthesis, and identifies a novel rational combination for treatment in MYC-amplified MB patients.

#5108 Immunomodulatory and anti-tumor effect of radiation and induced telomere damage to treat pediatric high-grade gliomas.

U. Banlanjo[1], S. Senthil Kumar[1], S. Gryaznov[2], **R. Drissi**[1];
[1]Nationwide Children's Hospital, Columbus, OH, [2]MAIA Biotechnology Inc., Chicago, IL

Pediatric high-grade gliomas (pHGGs), including diffuse intrinsic pontine glioma (DIPG) are among the most treatment refractory cancers in children. Despite multimodal therapy, prognosis is dismal with survival of <1 year for DIPG and a 5-year overall survival <10% for other pHGGs. Radiotherapy remains the only standard of care for DIPG that extends the survival by few months. In recent years, immunotherapy is emerging as a potential alternative treatment option. However, several factors have hindered the use of immunotherapy for pHGGs including “cold” immune environment with lack of immune cells infiltration, low tumor mutational burden, and lack of neo-antigen expression that prevents tumor recognition by the immune system. Therefore, novel therapies that activate the immune system while evading the tumor immunosuppression are highly needed. Here, we aim to demonstrate the immunomodulatory anti-tumor effects of THIO (6-thio-2’deoxyguanosine), a nucleoside analog and a telomerase-dependent telomere targeting agent, in DIPG mouse models. Our preclinical *in vitro* and *in vivo* data have demonstrated the efficacy of THIO in inducing telomeric damage, G_2/M cell cycle arrest, and apoptosis in high-risk medulloblastoma and DIPG. Importantly, we have demonstrated that THIO crosses the blood-brain barrier and specifically targets tumor cells in an orthotopic mouse model of DIPG. THIO was shown to induce anti-tumor immunity through micronuclei formation leading to cGAS-STING pathway mediated activation of the innate and adaptive immune response in colon, lung, and hepatocellular carcinoma tumor models. Our preliminary data demonstrate the THIO-dependent induction of micronuclei formation co-localizing with cGAS and leading to STAT1 activation in DIPG cell lines. We have also shown that THIO synergistically sensitizes DIPG cells to ionizing radiation (IR), significantly decreasing cell proliferation. We are currently testing the combination of THIO+IR in an orthotopic mouse model for DIPG. We will present results on the potential of THIO and IR treatments to stimulate anti-tumor immunity through the activation of STING pathway in a syngeneic mouse model of DIPG. These preclinical studies will support the potential use of THIO and IR to treat children with high-risk pediatric brain tumors.

#5109 Novel acylfulvene LP184 shows single agent and combinatorial efficacy with PARP inhibitors in atypical teratoid rhabdoid tumors.

Abigail Tindall, Hyuk J. Kwon, Istabraq Musa, Tyler Findlay, Su Chan Lee, Charles Eberhart, Eric Raabe

Pediatric Oncology, Johns Hopkins University School of Medicine, Baltimore, MD

Atypical Teratoid Rhabdoid Tumor (AT/RT) is an aggressive form of pediatric brain cancer that spreads quickly and leads to survival rates of less than 40%. Current treatments are insufficient at reducing this poor prognosis. A hallmark feature of ATRT is a SMARCB1 mutation. Illudins are a class of cytotoxic compounds with activity against pediatric solid tumors, including AT/RT. LP-184 is a novel synthetic illudin with improved brain penetration and activity against adult high-grade glioma orthotopic xenografts. We tested LP-184 against a battery of AT/RT cell lines including BT37, CHLA06, CHLA05, and CHLA266. LP-184 decreases viability at nanomolar concentrations with IC50s ranging from 9.91nM - 23.92nM. LP-184 decreased proliferation as measured by immunofluorescence and confirmed by western blots (BT37 p=0.0001, CHLA06 =0.0001, CHLA05=0.033). LP-184 also induced apoptosis as demonstrated in immunofluorescent images and western blots (BT37 p=0.0001, CHLA06 =0.0001, CHLA05=0.0015, CHLA266 p=0.002). Furthermore, LP-184 shows strong synergy with the PARP inhibitor Rucaparib, suggesting that inhibition of DNA repair potentiates LP-184 activity. LP-184 reduces viable cell count by as much as 50% and combination with Rucaparib further decreases viability by 75% (BT37=0.0001, CHLA06=0.0002, CHLA05=0.0077). The dual therapy also demonstrates cytostatic and cytotoxic effects as confirmed by immunofluorescence and western blots (BT37 BrdU = 0.0004, BT37 CC3 = 0.0002, CHLA06 BrdU = 0.0033, CHLA06 CC3 = 0.0117 compared to control). Further studies *in vivo* are being conducted to test single agent and combination therapies of LP-184 and Rucaparib in ATRT, as our data indicates that the two could provide a compelling treatment option for patients with this poor prognosis brain tumor.

#5110 Exploring the effects of Indirubins in pediatric diffuse high grade glioma models.

J. S. Clark[1], J. Jimenez-Macias[1], P. Vaughn-Beaucaire[1], S. Zhang[1], W. El-Deiry[1], R. Lulla[2], S. Lawler[1];
[1]Legorreta Cancer Center at Brown University, Providence, RI, [2]Hasbro Children's Hospital, Providence, RI

Diffuse midline glioma (DMG) is an invasive pediatric brain tumor which grows in the pons of the brainstem. The current course of treatment is focal radiation however, DMG continues to have a very poor prognosis with a median survival of less than 10 months. A major barrier for chemotherapeutic treatment of DMG is the blood brain barrier (BBB) which tightly controls access of molecules to the brain. This limits the efficacy of drugs to treat brain cancer and other diseases of the central nervous system. Previous studies from the Lawler lab and others have shown that the indirubin derivative, 6-bromoindirubin-3′-acetoxime(BIO-acetoxime/BIA), has anti-invasive properties and can enhance survival in glioblastoma xenograft models. Here, we investigated the effects of BIA on pediatric glioma models using a range of relevant assays. In an *in vitro* collagen migration assay, BIA was observed to significantly slow cell migration at a concentration of 1μM in DIPG 36 cells, over 72 hours. Furthermore, we have also shown that BIA modulates the tumor vasculature, which could limit tumor growth, and improves drug delivery to tumors by targeting tight junctions in tumor associated endothelium. The effect on BBB drug penetration was assessed in a multicellular 3D *in vitro* BBB model and effects of BIA on endothelial barrier functions was determined using trans-endothelial resistance assays (TEER). BIA treatment increased dextran uptake into 3D BBB models, and also lowered endothelial cell permeability *in vitro* via a reduction in the expression of tight junction proteins as shown by staining and a decrease in TEER values. In order to assess potential synergistic interactions, a drug screen was performed on a panel of distinct pediatric glioma cell lines (DIPG 36 and KNS42). This identified several FDA approved drugs that combine well with BIA. From this screen, BIA was shown to synergize with DNA damaging chemotherapy to enhance toxicity and in combination with cisplatin promote DNA damage in pediatric glioma cell lines. Other drugs identified in the screen are currently under investigation and details will be reported. Thus, our hypothesis is that BIA may provide an effective approach for further development as a DMG therapeutic through targeting invasion and enhancing drug potency and delivery via modulation of endothelial cell tight junctions. Interrogating the mechanisms involved and developing drug formulations informed by the drug screen for *in vivo* studies to determine the translational potential of this approach is our focus for future studies.

#5111 Rational synergistic radiosensitization strategies for group 3 medulloblastoma.

J. Povilaikaite, K. Stitz, N. Austin, V. Ramaswamy;
The Hospital for Sick Children, Toronto, ON, Canada

Medulloblastoma (MB) is the most common malignant pediatric brain tumor. MB is comprised of 4 groups, termed Wnt, Shh, Group 3 and Group 4, each characterized by distinct molecular and clinical profiles. *MYC*-amplified Group 3 MB is associated imminent fatal metastatic relapse following standard treatment approaches, which currently include surgery, craniospinal irradiation and chemotherapy, highlighting an urgent need for identification of therapeutic vulnerabilities for these tumours. As such, using 4 novel patient-derived models of Group 3 MB that faithfully recapitulate the molecular and histological tumor characteristics, we characterised response to radiation of Group 3 MB *in vitro* to show that these tumors do not possess intrinsic radiation resistance. Furthermore, cumulative radiation experiments do not increase bulk radiation resistance in MB cells, highlighting the contribution of dynamic cell states to radiation response. In contrast, exposure to radiation leads to changes in cell clonogenic capacity as measured by limited dilution assays. Furthermore, RNA-seq data uncovered altered transcriptomic programs in response to cumulative radiation treatment. In particular, we observe differential regulation of genes encoding potassium ion channels and their regulators as well as genes encoding ECM and cell adhesion proteins. As part of our goal to evaluate the current multimodal treatment strategy of MB, we also show that a set of standard chemotherapeutic agents (etoposide, thiotepa and lomustine) currently used in the clinic do not produce a potent response at optimal doses *in vitro*, potentially accounting for abysmal survival outcomes seen in chemotherapy treated MB patients. As such, we conducted a screen of 144 FDA approved cancer drugs and identified therapeutics that selectively target Group 3 MB cells in contrast to normal tissue controls (foetal neural stem cells) in the low nanomolar dose range. In particular, topoisomerase inhibitor topotecan produces a potent response specific to MYC-amplified Group 3 MB, and sensitizes 2 patient-derived MB models to gamma irradiation. Altogether, our data characterizes Group 3 MB molecular and cellular responses to current treatment modalities and provides rationale for new clinical strategies to sensitize patients to radiation that will potentially allow to reduce the required radiation doses to treat these aggressive tumors, reduce the incidence of radiation treatment-related morbidity as well as improve cure rates.

#5112 Discovery of nuclear envelope mislocalization in *MYC*-driven group 3 medulloblastoma.

Y. Suk[1], J. Ibanez-Vega[2], I. Chaudhry[1], M. Rossotti[3], M. Subapanditha[1], P. Miletic[1], S. Custers[1], L. Escudero[1], A. Delaidelli[4], T. Nakashima[5], Y. Xiao[6], J. Moffat[6], H. Suzuki[5], P. Sorensen[4], K. Henry[3], C. Venugopal[1], G. Krenciute[7], S. Singh[1];

[1]McMaster University, Hamilton, ON, Canada, [2]St. Jude Children's Hospital, Memphis, TN, [3]National Research Council Canada, Ottawa, ON, Canada, [4]University of British Columbia, Vancouver, BC, Canada, [5]National Cancer Center Research Institute (Japan), Tokyo, Japan, [6]University of Toronto, Toronto, ON, Canada, [7]St. Jude Children's Research Hospital, Memphis, TN

Medulloblastoma (MB) is the most common malignant pediatric brain tumor, comprised of four distinct molecular subgroups (WNT, SHH, Group 3, and Group 4). A subset of Group 3 MB tumors harbor focal amplifications of the *MYC* oncogene and are particularly prone to tumor recurrence and leptomeningeal spread which currently remains incurable. Therefore, there is an urgent need for the development of therapeutic modalities that can spare the vulnerable, developing brain while having potent antitumor efficacy against recurrent MB. Through proteomic profiling of cyclophosphamide-resistant patient-derived *MYC*-driven Group 3 MB cell line SU_MB002, we identified nuclear envelope (NE) proteins to be highly abundant and enriched in Group 3 MB compared to normal tissue. We discovered that LBR, an inner nuclear transmembrane protein, while present in all cells at the NE, is aberrantly presented to the cell surface in *MYC*-driven Group 3 MB cell lines. Immunohistochemistry analysis of LBR on MB patient tumor samples identified that positive LBR staining correlated with a significantly worse prognosis and was also identified to be enriched in recurrent tissue compared to their matched primary samples. Cell surface expression flow cytometry analysis identified highly abundant cell surface expression in all MYC-driven Group 3 MB cell lines with low to no expression in human neural stem cells and other MB subgroups. Mechanistically, high resolution microscopy of endogenously HALO-tagged LBR reveals LBR cell surface presentation to be linked to ER or ER-like vesicles that are directly trafficked to the cell surface. Transcriptomic analysis of LBR cell surface positive and negative cells identify that cell surface positivity is significantly linked to cell division and mitotic processes (cell cycle process, mitotic cell cycle process, chromosome segregation, cell division, nuclear division). LBR mislocalization stems from mitosis at the time of nuclear envelope dissolution and is enriched in the hyperproliferative, therapy-resistant subpopulation of MB cells following exposure to chemotherapy and radiation *in vitro* and *in vivo* and may act as a marker for the brain tumor initiating cells that seed recurrence. Therefore, we demonstrate that LBR is an ideal therapeutic target for patients facing relapsed or treatment-refractory MB and have generated single domain antibodies in an effort to engineer LBR-specific CAR T cells. The development of therapies against NE proteins like LBR may provide patients a novel therapeutic opportunity that may be able to treat therapy-resistant, hyperproliferative *MYC*-driven Group 3 MB cells.

#5113 Fractionated radiation therapy alters energy metabolism and induces cellular quiescence exit in patient-derived orthotopic xenograft models of high-grade glioma.

Z.-L. Huang[1], Z.-G. Liu[2], Q. Lin[1], Y.-L. Tao[3], X. Li[1], P. Baxter[2], J. Su[2], A. Adesina[4], C. Man[2], M. Chintagumpala[2], W. Teo[2], Y.-C. Du[1], Y.-F. Xia[3], X.-N. Li[1]; [1]Program of Precision Medicine PDOX Modeling of Pediatric Tumors, Ann & Robert H. Lurie Children's Hospital of Chicago; Department of Pediatrics, Northwestern University Feinberg School of Medicine, Chicago, IL 60611., Chicago, IL, [2]Texas Children's Cancer Center and Department of Pediatrics, Baylor College of Medicine, Houston, TX, houston, TX, [3]State Key Laboratory of Oncology in Southern China, Department of Radiation Oncology, Sun Yat-Sen University Cancer Center, Guangzhou 510060, China, Guangzhou, China, [4]Department of Pathology, Texas Children's Hospital, Houston, TX, houston, TX

Radiation is one of the standard therapies for pediatric high-grade glioma (pHGG), of which the prognosis remains poor. To gain an in-depth understanding of the biological activities beyond the classic DNA damage, we treated 6 patient-derived orthotopic xenograft (PDOX) models, including one with DNA mismatch repair (MMR) deficiency, with fractionated radiations (2 Gy/day x 5 days). Extension of survival time was noted in 4/6 PDOX models (P<0.05) and widespread γH2AX positivity in >95% tumor cells in tumor core and >85% in the invasive foci, accompanied by ~30% apoptotic and mitotic catastrophic cell death. The model with DNA MMR (IC-1406HGG) was the most responsive to radiation with a reduction of Ki-67(+) cells. Altered metabolism, including mitochondria number elevation, COX IV activation and reactive oxygen species buildup, were detected together with the accumulation of $CD133^{\pm}$ tumor cells. The latter was caused by the entry of quiescent G_0 cells into cell cycle and the activation of self-renewal (SOX2 and BMI1) and epithelial mesenchymal transition (fibronectin) genes. These novel insights about the cellular and molecular mechanisms of fractionated radiation in vivo should support the development of new radio-sensitizing therapies.

#5114 Deciphering the implications of THOC7 in medulloblastoma: Unraveling its role in tumor growth and progression.

S. M. Abdulsahib, S. Timilsina, S. Nirzhor, D. Medina, P. V. Pitta, P. Subbarayalu, M. K. Rao;
UT Health Science Center at San Antonio, San Antonio, TX

Background: Medulloblastoma (MB) is the most common malignant brain cancer in children. Despite the progress made in treating MB, the 5-year survival rate for high-risk tumors remains poor and risk of recurrence within 2 years of treatment is still high. Unfortunately, patients who do survive have reduced quality of life because of the highly toxic side effects of radiation and chemotherapy. Those facts underline the importance of identifying new drivers of MB and understanding the mechanism by which those drivers may promote MB. Using CRISPR-based dependency analysis, we discovered THO Complex Subunit 7 Homolog (THOC7) as one of the highly differentially expressed genes that may uniquely provide survival advantage to MB cells. THOC7 is a component of the THO subcomplex of the TREX complex, which is known to couple mRNA transcription, processing and nuclear export associated with spliced mRNA.
Methods: To understand the role of THOC7 in MB, we silenced the expression of THOC7 using siRNAs in multiple MB cell lines. The knockdown efficiency was confirmed by western blot and qPCR. The effect of THOC7 silencing on the viability of MB cells was assessed by short-term viability and long-term colony formation assays. The effect of THOC7 silencing on MB cell proliferation was measured using an IncuCyte. To assess whether THOC7 may affect MB progression, we performed Transwell migration assay. To understand the mechanism by which THOC7 may play a role in medulloblastomogenesis, we measured the effect of THOC7 silencing on the cell cycle progression and apoptosis. As presence of cancer stem cells is linked to relapse and makes MB refractory to radiation therapy, we asked whether THOC7 may support MB stem cell proliferation using neurosphere assay.
Results: Our analysis revealed that MB is highly addicted to THOC7. Importantly, higher expression of THOC7 is strongly correlated with lower overall survival of MB patients. We showed that depletion of THOC7 inhibited the short- and long-term viability as well as proliferation of MB cells. In addition, silencing of THOC7 inhibited migration/invasion of MB cells. THOC7 depletion led to cell cycle arrest and increased apoptosis of MB cells. Furthermore, our neurosphere assay demonstrated that silencing of THOC7 blocked the MB stem cell proliferation.
Conclusion: Our results suggest that THOC7 may be a novel driver of MB growth and progression. Inhibition of MB stem cell proliferation in THOC7 depleted cells indicates that THOC7 inhibition may sensitize refractory MB to radiation therapy. Experiments are currently underway to understand the mechanism by which THOC7 may support MB growth and progression. In conclusion, our results showing no effect of THOC7 silencing on normal cell viability suggest that approaches aimed at silencing THOC7 may be a safe and viable approach for treating MB.

#5115 Designing targeted approaches for recurrent medulloblastoma.

J. Rodriguez Blanco;
The Medical University of South Carolina (MUSC), Charleston, SC

Designing targeted therapies for recurrent medulloblastomaPediatric brain tumors are the leading cause of cancer-related death in children, with medulloblastoma (MB) being the most common type. Despite significant progress in the field, approximately 30% of children with MB will relapse. Recurrent MB is commonly metastatic and virtually none of these patients will live beyond the one-year hallmark. These sobering statistics highlight the significant unmet need for effective therapies for recurrent MB. The likely underlying cause of the constant failure of our current clinical approaches, which are based on data obtained from disease models recapitulating primary tumors, is the disparity in genomic and transcriptomic data between primary and relapsed disease. Because of these disparities, we hypothesize that by conducting mechanistic studies and drug screens in relapse disease models, we can improve the outcomes for children with recurrent MB. Our data, obtained through a bioinformatics mining approach to predict tumor response, enabled us to identify a clinically relevant candidate drug for the treatment of recurrent MB: Minnelide. This compound acted on MYC to reduce tumor growth and the metastatic dissemination of tumors with the genetic background often found in relapsed MB patients. Additionally, to further support the translational relevance of our data, Minnelide increased the efficacy of adjuvant therapeutics used in the clinical management of MB. Our findings not only highlight the potential for repurposing Minnelide to treat children with recurrent MB, but also the potential of our research approaches aimed at identifying novel therapeutics for relapsed cancers.

#5116 Stress-induced AMPK interactome analysis reveals novel protein-protein interactions associated with chromatin remodeling in acute lymphoblastic leukemia..

A. Shvab, G. J. Leclerc, J. C. Barredo;
University of Miami, Miami, FL

Acute lymphoblastic leukemia (ALL) is a leading cause of cancer-related death among children, adolescents and young adults. We previously reported that ALL cells are vulnerable to metabolic stress conditions following AMP-activated protein kinase (AMPK) activation, leading to cell death. AMPK is the master metabolic regulator, and we and others have reported it interacts with chromatin-associated proteins to regulate gene expression in response to metabolic stress. To investigate AMPK's mechanistic role in epigenetic gene regulation under metabolic stress, and identify new AMPK partners, we performed a comprehensive interactome analysis using TurboID-based proximity labeling proteomics. We generated HEK293T cells stably expressing TurboID fused to the AMPKα1, AMPKα2, AMPKβ1 or AMPKγ1. Following treatment with the allosteric AMPK activator PF-06409577 (PF064) for 1h, to mimic the cell's rapid response to energy/metabolic stress, the samples underwent mass spectrometry-based proteomics. Proteomics data analysis identified novel altered (enhanced or reduced) AMPK protein-protein interactions (PPI) following PF064 treatment. The GO analysis of proteins interacting with AMPK showed that metabolic stress enhances PPIs involved in regulating gene expression, cellular metabolic processes, DNA repair, chromatin organization, histone modifications, etc. More importantly, we identified that AMPK interacted with members of the non-canonical Polycomb repressive complex 1 (PRC1.1) such as PCGF1, RING1, KDM2B, BCORL1, USP7. PRC1 is a known epigenetic regulator that monoubiquitinylates histone H2A at Lys119 (H2AK119ub) to control transcription and regulate gene expression. Using Co-IP, we confirmed these interactions in KASUMI-2 (Bp-ALL) and KE-37 (T-ALL) cells. When cells were treated with PF064 or 991 (another AMPK activator), we found that the interactions of AMPK with the catalytic core of PCR1.1 (PCGF1, RING1) were increased compared to untreated cells. To examine the effect of activated AMPK on PCR1.1 activity, we determined the level of H2AK119ub in ALL cells treated with PF064 and 991 for 1h. We found that the level of H2AK119ub protein expression was increased in ALL-treated cells indicating the PRC1.1 was activated. Together, these data suggest that stress-induced AMPK activation increased the catalytic activity of the PRC1.1 via PPI in ALL. Our findings are consistent with our previous published RNA-Seq and ChIP-Seq data indicating an epigenetic role for AMPK in altering gene expression examined under metabolic stress (two thirds exhibited downregulation), and provide insights into the AMPK-driven mechanism(s) involved. Further elucidation of the uncovered PPIs and its mechanistic role(s) may lead to potential epigenetic-based strategies to overcome resistance/refractoriness in ALL and other malignancies.

#5117 CK2 inhibiton exhibits synergistic effect in acute lymphoblastic leukemia.

Daniel Gary Bogush, Joseph Schramm, Katarina Dovat, Yali Ding, Chingakham Singh, Sinisa Dovat

Penn State College of Medicine, Hershey, PA

Survival for pre-B cell Acute lymphoblastic leukemia (B ALL) has improved greatly, however. High risk (HR) subgroups continue to result in significant mortality and morbidity of pediatric oncology patients. Pediatric T-cell acute lymphoblastic leukemia (T-ALL) is a lethal disease, often associated with high-risk clinical features. T-ALL therapy has made less improvement than B ALL and continues to represent a significant number of high-risk outcomes. Novel treatment strategies are required to overcome chemotherapy resistance and improve morbidity for HR B ALL. The development of treatments that can overcome chemotherapy resistance is essential for improving survival in T-ALL. Deletions of *IKZF1,* resulting in decreased IKAROS function, are present in High-risk ALL patients. Casein kinase 2 (CK2), a protein kinase upregulated in ALL, phosphorylates IKAROS preventing DNA binding reducing transcriptional regulation in ALL patients. Past studies have shown that pharmacologic inhibition of CK2 with CX-4945 rescues IKAROS function as a transcriptional regulator. Receptor tyrosine kinase c-KIT is transcriptionally regulated by IKAROS and is often upregulated in cancer. The purpose of this study was to determine whether restoration of IKAROS via CX-4945 would act in a synergistic manner with c-KIT inhibitor imatinib in ALL.Methods/results B-ALL Nalm6 cells were treated with imatinib over 72-hours to establish the half-maximal inhibitory concentration (IC_{50}). The IC_{50} was used to determine the concentration range of imatinib to be used in combination with CX-4945 in a 72-hour synergy analysis of cytotoxicity.. Cell viability was measured using WST-1 cell proliferation assay. The data were analyzed using Calcusyn and synergy was defined as a combination index below 0.85. The study was repeated to determine a more precise range of synergy. The cytotoxicity of single drug c-KIT inhibitor, Imatinib, in Nalm6 B-ALL yielded an IC_{50} of 25uM while CK2 inhibitor CX-4945 resulted in 4uM. When a combination was administered with a constant dose of CX-4945 at 4uM and varying concentrations of imatinib, synergy was observed at multiple dose combinations. Conclusion: The data shows that CK2 inhibitor, CX-4945, and c-KIT inhibitor, imatinib, exhibit a synergistic therapeutic effect. Imatinib is indicated for use in Philadelphia positive (Ph+) acute lymphoblastic leukemia so future studies will include testing CX-4945/imatinib synergy in Ph+ BALL where we expect to see more potent synergistic effect.

#5118 Neuroblastoma extracellular vesicles present GPC2 and activate GPC2 CAR T cells in an antigen-dependent manner.

A. M. Giudice, S. Matlaga, G. Pascual-Pasto, P. M. Schuerch, G. Rouin, B. McIntyre, V. P. Zecchino, K. R. Bosse;
Children's Hospital of Philadelphia, Philadelphia, PA

Glypican 2 (GPC2) chimeric antigen receptor (CAR) T cells are safe and efficacious in neuroblastoma and are currently being tested in a first-in-human Phase 1 clinical trial at the Children's Hospital of Philadelphia. Tumor-derived extracellular vesicles (TEVs) are nanosized vesicles secreted by cancer cells, often enriched with glypicans. However, the presence of GPC2 on neuroblastoma TEVs and any interaction with GPC2 CAR T cells has not been explored. High-levels of GPC2 were found on TEVs isolated from neuroblastoma preclinical models [7 cell lines, circulating EVs from 6 patient-derived xenograft (PDX)-bearing mice] and from the peripheral blood of 16 neuroblastoma patients, but not on circulating EVs from 7 non-tumor bearing mice or 12 healthy human donors. The level of circulating GPC2+ EVs isolated from the peripheral blood of PDX-bearing mice positively correlated with PDX size ($R=0.96$; $P<0.0001$) and parent PDX GPC2 expression. To evaluate how GPC2 on EVs modulates CAR T cell functionality, we generated EVs with varied levels of GPC2 (Hi/Lo/Neg) and co-incubated each EV subset with GPC2 CAR T cells. Here using immunofluorescence and flow assays we found that EVs bind GPC2 CAR T cells proportional to the amount of GPC2 on their surface. Further, $GPC2^{Hi}$ EV-CAR T cell synapses induced potent T cell activation shown by CD69/Granzyme B expression and release of IL-2/IFN-γ. $GPC2^{Hi}$ EV pre-incubated CAR T cells also displayed enhanced target neuroblastoma cell cytotoxicity, inducing 4-fold more specific cytotoxicity than CAR T cells incubated with control $GPC2^{Neg}$ EVs. *In vivo* we observed that injection of $GPC2^{Hi}$ EVs into $GPC2^{Lo}$ neuroblastoma SK-N-AS xenografts genetically altered to have significantly decreased endogenous EV production (via *RAB27A* knock-out) greatly enhanced the efficacy of co-infused GPC2 CAR T cells ($p<0.05$). Similarly, in an isogenic SK-N-AS-GPC2 xenograft murine model treated with a limiting number of GPC2 CAR T cells concurrently with the EV-inhibiting drug GW4869, GPC2 CAR efficacy was dependent on the presence of $GPC2^{Hi}$ EVs. Here, pharmacologic EV inhibition in mice decreased GPC2 CAR efficacy which could be rescued by intratumoral injection of $GPC2^{Hi}$ EVs. In both *in vivo* models, the presence of intratumoral $GPC2^{Hi}$ EVs resulted in a significantly enhanced tumor infiltration of activated (CD69+/CD25+) GPC2 CAR T cells ($p<0.05$).
Taken together, $GPC2^{Hi}$ EVs are selectively secreted from neuroblastomas and bind and activate GPC2 CAR T cells enhancing their anti-tumor cytotoxicity. To further capitalize on these findings, we engineered $GPC2^{Hi}$ EVs to have an extended circulation half-life through albumin binding or tumor targeting via GD2 binding that are currently being tested *in vivo* and results will be reported. EVs offer a versatile platform for CAR antigen presentation and should be further validated as a strategy to enhance CAR T cell efficacy for solid tumors.

#5119 Exploring the relationship between metabolism and the epigenome in *MYCN*-amplified neuroblastoma.

K. M. Dalton, T. L. Lochmann, C. Coon, M. L. Calbert, M. Dozmorov, L. Shock, J. Koblinski, A. C. Faber;
Virginia Commonwealth University, Richmond, VA

Background: Neuroblastoma (NB) is the most common cancer of infancy and is responsible for the most cancer-related deaths in children under the age of five. The transcription factor MYCN is the most studied oncogene in NB and automatically confers high-risk. MYCN drives numerous effects in the cell, including metabolic changes that are critical for oncogenesis. NB has also been demonstrated to be a highly methylated cancer, with DNA methyltransferases (DNMTs) largely responsible for these modifications. Epigenetics and metabolism are closely connected, with oncogene-driven metabolic rewiring modifying the epigenetic landscape through increases of metabolites that are critical for the activities of epigenetic enzymes, and conversely the enhanced epigenetic activity further regulating the activity of metabolic enzymes.
Aims: As metabolism is believed to be a key regulator of the epigenome, the objective of this proposal is to understand the connection between MYCN-DNMT1-driven epigenetic alterations and dysregulated metabolism in *MYCN*-amplified NB.
Methods: RNA-seq and mass spectrometry analyses were performed to explore the MYCN-driven metabolome in NB and changes that occur with DNMT1 inhibition. The efficacy of DNMT1 inhibition in *MYCN*-amplified NB was tested in vivo.
Results: Our data demonstrate that sensitivity to DNMT1 inhibition is linked to MYCN status in NB. We found that MYCN indeed dysregulates metabolism in NB, and DNMT1 inhibition led to a global decrease in oxidative phosphorylation and exacerbated mitochondrial dysfunction in *MYCN*-amplified NB. Expression of MYCN was linked to an increase in methionine and subsequently SAM, the universal methyl donor, further supporting reliance on DNMT1. Most importantly, we have found that treatment with DNMT1 inhibitors in vivo inhibited tumor growth, even after treatment had stopped.
Conclusion: We have found a correlation between MYCN and metabolism that supports DNMT1 activity. This relationship allows for a potential treatment for a high-risk disease in which there is few clinically actionable targets.

#5120 Direct targeting of the COMPASS complex inhibits neuroblastoma growth by inhibiting cancer stem cells.

Rameswari Chilamakuri, **Saurabh Agarwal**

St. John's University, College of Pharmacy and Health Sciences, Queens, NY

Epigenetic regulator COMPASS Complex, a histone H3K4 methyltransferase has recently been shown to be involved in multiple cancers and attaining focus as a novel therapeutic target. High-risk neuroblastoma (NB) is a heterogeneous pediatric cancer with high mortality and relapse rates. The relapse of refractory cancer is shown to be driven by cancer stem cells (CSCs), which are maintained by epigenetic malfunctions. In the present study, we determined the effects of inhibiting the COMPASS complex on NB CSCs and overall NB growth. A high-throughput shRNA screening of methyltransferases and demethylases reveals the role of COMPASS complex partners MLL1 and Menin in NB proliferation. We found that both MLL1 and Menin are overexpressed in our previously identified CD114+ NB CSCs. Further, *MEN1* (gene coding Menin) expression showed an inverse correlation with overall NB patient survival and cancer progression in a comprehensive analysis of 1235 primary NB patient data. Our ChIP results show that the *CSF3R* gene which codes for CD114 and maintains CD114+ NB CSCs, is regulated by the presence of high H3K4me3 activating marks. Further, we used MI-503 to inhibit MLL1-Menin interaction and also developed *MEN1* stable knockdown and found that both strategies significantly inhibit H3K4me3 activity in NB, particularly at the *CSF3R* gene promoter. This led to decreased *CSF3R* expression and NB CSC levels. MI-503 significantly inhibits proliferation in different NB cell lines and primary patient-derived xenograft (PDX) lines, with minimal effect on non-cancerous fibroblasts. MI-503 significantly inhibits NB cell cycle progression at the S phase, induces apoptosis, and inhibits NB 3D spheroid growth and development. Interestingly, we overserved differential selectivity of MI-503 in inducing apoptosis and in blocking the cell cycle in NB CSCs in contrast to non-CSCs. *MEN1* knockdown also inhibits NB proliferation and 3D spheroid growth. Furthermore, MI-503 in a dose-dependent manner synergistically sensitizes NB to chemotherapy doxorubicin and significantly inhibits NB proliferation and spheroid growth compared to either agent alone. Further, by using the NB xenograft *in vivo* tumor model, we established that MI-503 significantly inhibits NB tumor growth and tumor metastasis by directly inhibiting tumor NB CSCs, without any observed toxicities. Similar results of significantly reduced tumor growth, metastasis, and NB CSCs were shown by the *MEN1* knockdown *in vivo*. Overall, our data show that the MLL1-Menin of the COMPASS complex directly activates the *CSF3R* gene to maintain NB CSCs and drive NB pathogenesis. Our data show that MI-503 or *MEN1* knockdown leads to significant inhibition of NB growth by directly inhibiting NB CSCs in both *in vitro* and *in vivo* tumor models. Further developing these epigenetic-based therapeutic strategies and combining them with current therapies will pave the way for effectively managing NB.

#5121 Next-generation immunocompetent and humanized neuroblastoma murine models for the discovery and validation of novel immunotherapies.

T. T. Spear[1], E. Posthill[1], D. Groff[1], A. M. Giudice[1], K. R. Bosse[1], L. Ma[2], S. P. Schoenberger[3], J. M. Maris[1];
[1]Children's Hospital of Philadelphia, Philadelphia, PA, [2]Perelman School of Medicine at the University of Pennsylvania, Philadelphia, PA, [3]La Jolla Institute for Immunology, La Jolla, CA

The success of CD19-directed chimeric antigen receptor (CAR)-T cell therapy for ALL has yet to be matched in solid pediatric malignancies. Moreover, immune checkpoint blockade has shown limited benefit in pediatric cancer. Despite this unmet need, there is a lack of reliable preclinical models to facilitate novel target discovery, validate therapeutic benefit, anticipate on- or off-target toxicity, and understand mechanisms of resistance.

Syngeneic murine model systems are a critical intermediate for preclinical translation, preserving the complex and heterogenous immune landscape and host-immunotherapy interactions. However, model interpretation and validity are limited as expression and function of murine targets and immune effector cells are not always conserved. We have developed a syngeneic immunocompetent C57BL/6 neuroblastoma system to study CAR efficacy, toxicity, and mechanisms of resistance, as well a variety of vaccination strategies. Specifically, we have built two murine CAR T constructs containing a 100% conserved antigen-directed scFv joined to orthologous murine TCR signaling machinery. In parallel, we engineered the murine neuroblastoma cell line 9464D to stably express surface antigen Gpc2 (Bosse, *Cancer Cell* 2017), or a novel chimeric single chain trimer of a 9mer peptide from intracellular oncoprotein PHOX2B discovered on HLA-A*24:02 (Yarmarkovich, *Nature* 2023) as Phox2b/A24*02/H2-k^{b} to generate tumor-bearing B6 or B6-A24-Tg mice. We are currently using this system to demonstrate how vaccination approaches enhance the persistence and potency of CART directed to both targets and are extending our syngeneic murine constructs to additional TH-MYCN allograft models.

To further study the innate and adaptive immune response to various therapeutics, we have developed peripheral blood mononuclear cell (PBMC) humanized models. Our autologous humanized PDX mouse models of neuroblastoma use immunocompromised NSG mice engrafted with a PDX and humanized with patient-matched PBMCs to evaluate personalized vaccines *in vivo.* We have shown the ability to stably engraft both lymphoid and myeloid populations in various human cytokine transgenic NSG variants (i.e. SGM3, Flt3L), allowing for T/B cell and APC crosstalk, thus providing a robust means to study targeted interventions. We are currently using this autologously humanized PDX model to test the ability of multivalent, personalized neoantigen vaccines developed specific to the neoantigen landscape of individual PDXs, with a focus on endogenous T cell responses of patient PBMC against their own PDX *in vivo.*

#5122 Modulating anti-GD2 immunotherapy via dual DFMO and TGF-β inhibition in neuroblastoma.

O. H. Gandhi, C. S. Turn, K. Liu, A. T. Vu, H. Bassiri, M. D. Hogarty;
Children's Hospital of Philadelphia/Perelman School of Medicine at the University of Pennsylvania, Philadelphia, PA

Neuroblastoma (NB) is an often-lethal childhood solid tumor. Anti-GD2 immunotherapy improves survival but not all responses are durable. Transforming growth factor-beta (TGFβ) has been implicated in solid tumor immunoresistance. High-risk NBs harbor activated *MYC or MYCN* to coordinately expand intratumoral polyamines (PA), oncometabolites with immunomodulatory roles, to support tumor progression. Difluoromethylornithine (DFMO) is an inhibitor of ornithine decarboxylase, the rate-limiting enzyme in PA synthesis, and has shown activity in preclinical NB models, including *TH-MYCN*$^{+/+}$ transgenic mice, and is in clinical trials in children. We sought to augment anti-GD2 therapy using DFMO and the small molecule TGFβ-receptor inhibitor, galunisertib. We randomized *TH-MYCN*$^{+/+}$ mice in two experiments (10 therapy arms; n=6-10 mice/arm) to receive combinations of DFMO, galunisertib, and anti-GD2 antibody m14G2a and to assess impact on survival. We measured 770 genes using nCounter Immuno-Oncology 360 (Nanostring), 36 cytokines using xMap bead-arrays (Luminex), and tumor-infiltrating leukocytes using flow cytometry in harvested tumors. Cell line TGFβ signaling was evaluated in tissue culture. In vitro, galunisertib consistently suppressed the upregulated TGFβ-Smad2/3 signaling cascade in *MYCN*-amplified neuroblastoma cell lines. In vivo, DFMO alone extends mouse survival and increases intra-tumoral neutrophils and natural killer (NK) cells. These NK cells increased surface expression of activation receptors like NKG2D ($p<0.05$), while tumor cells increased surface expression of NK-ligands. Tumor cells also expressed increased latency-associated peptide (LAP; $p<0.05$), a TGFβ precursor, suggesting NK cells were poised to kill but restrained by TGFβ. Cytotoxicity assays showed reversal of this inhibition with TGFβR1 inhibitor galunisertib in vitro. In a proof-of-concept trial, DFMO and galunisertib (DFMO/gal) demonstrated a clinical anti-tumor synergistic effect. DFMO/gal treated tumors had upregulated NK cell activity genes and downregulated TGFβ signaling genes. Cytokine analysis confirmed DFMO induced upregulation of TGFβ1 and TGFβ2 ($p<0.01$) that was modulated by galunisertib. IL6, GCSF, and GMCSF were markedly downregulated in tumors treated with both DFMO and galunisertib ($p<0.05$). An expanded trial showed DFMO/gal added to m14G2a showed no significant survival benefit over the DFMO and m14G2a combination. Ultimately, DFMO creates a pro-inflammatory cellular and cytokine milieu in *TH-MYCN*$^{+/+}$ NBs. DFMO and TGFβR1 inhibition via galunisertib activate NK cells further and decrease the anti-inflammatory cytokine IL6. Ongoing studies are further characterizing the gene expression and cytokine levels of the NB TME under these treatment conditions.

#5124 A CRISPR-drug perturbational map for identifying compounds to combine with commonly used chemotherapeutics.

W. C. Wright, P. Geeleher;
St. Jude Children's Research Hospital, Memphis, TN

Combination chemotherapy is crucial for successfully treating cancer. However, the enormous number of possible drug combinations means discovering safe and effective combinations remains a significant challenge. To improve this process, we conduct large-scale targeted CRISPR knockout screens in drug-treated cells, creating a genetic map of druggable genes that sensitize cells to commonly used chemotherapeutics. We prioritize neuroblastoma, the most common extracranial pediatric solid tumor, where ~50% of high-risk patients do not survive. Our screen examines all druggable gene knockouts in 18 cell lines (10 neuroblastoma, 8 others) treated with 8 widely used drugs, resulting in 94,320 unique combination-cell line perturbations, which is comparable to the largest existing drug combination screens. Using dense drug-drug rescreening, we find that the top CRISPR-nominated drug combinations are more synergistic than standard-of-care combinations, suggesting existing combinations could be improved. As proof of principle, we discover that inhibition of PRKDC, a component of the non-homologous end-joining pathway, sensitizes high-risk neuroblastoma cells to the standard-of-care drug doxorubicin in vitro and in vivo using patient-derived xenograft (PDX) models. Our findings provide a valuable resource and demonstrate the feasibility of using targeted CRISPR knockout to discover combinations with common chemotherapeutics, a methodology with application across all cancers.

CLINICAL RESEARCH: Predictive Biomarkers 3
Poster Session

#5128 Circulating H3K27me3 modified nucleosomes as a biomarker to monitor anti EZH2-based treatment in advanced solid tumour patients: Translational analyses from CAIRE trial.

Francesca Salani[1], Mark Eccleston[2], Lola-Jade Palmieri[3], Simon Pernot[4], Sophie Cousin[3], Gianluca Masi[5], Francesco Crea[6], Antoine Italiano[7]

[1]LHCS (The Open University), The Open University Milton Keynes, Universita di Pisa and Scuola Superiore Sant'Anna, Pisa, Italy,[2]Belgian Volition SRL, Isnes, Belgium,[3]Department of Medicine, Institut Bergonie, Bordeaux, France,[4]Department of Medical Oncology, Institut Bergonie, Bordeaux, France,[5]Ricerca Traslazionale e Delle Nuove Tecnologie in Medicina e Chirurgia, Universita di Pisa, Pisa, Italy,[6]Cancer Research Group-School of Life Health and Chemical Sciences, The Open University, Milton Keynes, United Kingdom,[7]Faculty of Medicine, University of Bordeaux, Bordeaux, France

CAIRE is a phase 2 umbrella study which assessed activity of combined anti-EZH2 tazemetostat and anti-PDL1 durvalumab (T+D) in advanced pretreated pancreatic, colorectal and sarcoma cancer patients. The are currently no plasma biomarkers for anti-EZH2 treatment monitoring or outcome. EZH2 catalyzes tri-methylation of Lysine 27 (K27me3) on nucleosomal histone 3 (H3, H3K27me3). Circulating, cell free H3K27me3 modified nucleosomes are thus a potential biomarker for tazemetostat activity. We evaluated the concentration of circulating H3K27me3 modified nucleosomes normalized to H3.1 nucleosomes (the most common isoform of H3) in T+D treated patients, irrespective of the tumor primary site, to determine target engagement during anti-EZH2 treatment. Plasma from patients receiving T+D was collected before the first cycle administration (C1D1), on the following two cycles administration (C2D1, C3D1) and at end of treatment (EOT). H3.1 and H3K27me3 containing nucleosomes were quantified by Nu.Q®-H3.1 and Nu.Q®-H3K27me3 Chemiluminescent Immunoassays. Concentrations are reported as ng/ml and the comparison of their median values at the different timepoints were tested with Kruskal-Wallis and Mann Whitney (independent samples) or Wilcoxon tests (paired samples), with SciPy.stat package (1.6.2). Bonferroni correction was applied to multiple comparisons. Of 197 total samples, 191 were evaluable for both biomarkers (6 higher than top standard after 5x dilution): 69 at C1D1, 63 at C2D1, 50 at C3D1 and 9 at EOT. For 58 patients paired C1D1 and C1D2 levels were available, 46 from C1D1 to C3D1 and 8 from C1D1 to EOT. The normalized Nu.Q®-H3K27me3 C1D1 median value (0.56) was significantly higher than C2D1 (0.31, p: e^{-12}), C3D1 (0.31, p: e^{-12}) and EOT ones (0.28, p: 0.001). Conversely, Nu.Q®-H3.1 levels were similar from C1D1 to C3D1 (range of the medians: 122.16-133.25 ng/ml) and increased at EOT (290.09 ng/ml), but with no significant difference between pairwise timepoints. Regarding paired-samples comparison, the normalized Nu.Q®-H3K27me3 was significantly higher at C1D1 than at C2D1 (p: e^{-8}) and C3D1 (p: e^{-9}) and at EOT (p: 0.02). Conversely, H3.1 concentration was significantly higher at EOT than at C1D1 (p: 0.02), at C2D1 (p: 0.02) and C3D1 (p: 0.05).In conclusion, we described for the first time that normalized circulating nucleosomal H3K27me3 values significantly decrease during T-based treatment in metastatic solid tumor patients, irrespective of the primary disease site, supporting its potential role as a pharmacodynamic biomarker for EZH2 inhibition. Moreover, total nucleosomal H3.1 seems to represent a surrogate of disease burden in metastatic pancreatic, colorectal and sarcoma cancers, as suggested previously in other hematological malignancies.

#5129 Subcellular MLH1 protein as first in class biomarker for CDK4/6 response in endocrine resistant ER+/HER2- breast cancer.

A. Mazumder, E. Oropeza, N. Punturi, S. Haricharan;
Sanford Burnham Prebys Med. Discovery Inst., La Jolla, CA

Over 175,000 diagnoses of estrogen receptor-positive breast cancer are made every year in the US. Of these, >40,000 patients will go on to die of their disease. We recently identified defects in a principal mismatch repair (MMR) gene, MLH1, as a driver of resistance to standard-care treatment and poor patient outcomes. Moreover, we demonstrated increased sensitivity to palbociclib, a CDK4/6 inhibitor, in experimental model systems *in vitro* and *in vivo* and in clinical trial data. MLH1 is mutated in 5-10% of treatment-resistant tumors, i.e., 4,000 patient tumors every year. However, most of these mutations are missense and variants of unknown significance (VUS). The impact of these mutations on mismatch repair capability and on treatment resistance remains uncertain. Here, we use experimental model systems to phenotype MLH1 VUS´ *in vitro* and *in vivo* using xenograft systems.Specifically, we use nuclear localization of MLH1 and repair of mismatches through a mismatch repair deficiency assay to test for mismatch repair capability in ER+ breast cancer cells engineered to express mutations in MLH1 that are found in patient tumors associated with poor survival. Second, we assess the ability of variants of MLH1 to induce activation of G1/S cell cycle checkpoints by activating Chk2. Lastly, we directly test the ability of variants in MLH1 to induce resistance to standard-care endocrine therapies and sensitivity to palbociclib, using 2D and 3D growth assays and xenograft experiments. Results from these experiments serve to systematically catalog VUS´ in MLH1 based on their predictive potential. We identified for the first-time specific mutation in MLH1 that induces resistance to endocrine therapy by stalling nuclear translocation of MLH1 which inhibits Chk2 activation. Cells with impaired Chk2 activation maintain a high CDK4/6 levels and are therefore more sensitive to CDK4/6 inhibition. Currently, there are few tests available in the clinic to predict response to therapies early in the timeline of ER+ breast cancer patients. Due to the nature of the disease, this can result in years of overtreatment. Overtreatment comes at great financial, physical, and emotional cost to patients and their families. Simultaneously, a lack of predictive markers can result in missed opportunities of presenting patients likely to relapse on standard care with personalized alternative therapeutic strategies. Based on our findings, cytoplasmic MLH1 may serve as first in-class biomarker for CDK4/6 response in ER+/HER2- patients.

#5130 Phospho-proteomic dynamics reveal DNA damage and repair signatures of drug sensitivity.

G. Arad, A. Hay-Koren, N. Simchi, D. Kovalerchik, D. Daitchman, A. Manor, O. Givton, E. Lezmi, I. Alchanati, Y. Katzenelenbogen, S. Herman, A. Shtrikman, G. Otonin, E. Seger, **K. Pevzner**;
Protai, Tel Aviv, Israel

There are numerous drug development efforts of DNA damage response (DDR) targets, such as PARP, ATR, ATM, CHK1, where the ability to accurately identify responsive sub-populations for monotherapies and combinations is a major challenge. Patients are routinely assigned to these drugs based on BRCA mutation, or BRCAness profile, encompassing homologous recombination deficiencies (HRD) which do not always represent the responsive sub-populations. Since DNA replication and DNA repair mechanisms are dominated by signaling events, we hypothesized that HRD extends beyond the genomic status, and is manifested also in the level of protein expression and protein modification.
To that end, we created a harmonized data atlas consisting of phenotypic drug sensitivity and basal and dynamic phosphoproteomics of multiple cell lines before and after treatment of multiple DDR drugs. Proteogenomic analysis of cell lines showed that some cell lines are sensitive to DDR drugs despite being DDR-proficient at the genomic level. Proteomic analysis of these cell lines showed that at least a third of them exhibit proteomic DDR deficiency, explaining DDR sensitivity beyond mutation status. We then utilized our proteogenomic atlas and computational platform to address challenging clinical needs, namely discovery of a predictive ATR biomarker and identifying potential combination treatments to overcome ATRi resistance. Using basal state and protein dynamics of ATR coupled with ATRi sensitivity, we developed a novel predictive ATR biomarker, and tested it using two independent validation datasets. Our ATR biomarker exhibited improved precision and recall compared to genomic biomarkers represented by mutations commonly used in the clinic, and was not confounded by mutations. In addition, integrated analysis of basal and dynamic data of multiple cell lines treated with ATRi, highlighted both known (e.g. ATM) and novel resistance mechanisms and suggested potential drug combinations.
Altogether, we demonstrate here the benefit of utilizing (phospho)-proteomic data to tackle clinical challenges in DDR drug development, such as predictive biomarkers and combination strategies. We provide a proteomics-based framework that would enable future patient selection in DDR clinical trials.

#5131 TYMS overexpression - but not copy number alteration - is associated with cancer aggressiveness in urothelial bladder cancer.

H. Plage[1], S. Hofbauer[1], K. Furlano[1], S. Weinberger[1], A. Franz[1], A. Fendler[1], F. Ro?ner[1], S. Schallenberg[1], S. Elezkurtaj[1], A. Frericks[2], M. Lennartz[2], A. H. Marx[3], H. Samtleben[3], M. Fisch[2], M. Rink[4], M. Slojewski[5], K. Kaczmarek[5], T. Ecke[6], S. Koch[6], N. Adamini[7], R. Simon[2], G. Sauter[2], H. Zecha[7], J. Weischenfeldt[8], T. Klatte[6], S. Minner[2], D. Horst[1], T. Schlomm[1], **M. Kluth**[2];

[1]Charite - Universitatsmedizin Berlin, Corporate Member of Freie Universitat Berlin, Humboldt-Universitat zu Berlin and Berlin Institute of Health, Berlin, Germany, [2]University Medical Center Hamburg-Eppendorf, Hamburg, Germany, [3]Academic Hospital Fuerth, Fuerth, Germany, [4]Marien Hospital Hamburg, Hamburg, Germany, [5]Pomeranian Medical University, Szczecin, Poland, [6]Helios Hospital Bad Saarow, Bad Saarow, Germany, [7]Albertinen Hospital, Hamburg, Germany, [8]Charite - Universitatsmedizin Berlin, Corporate Member of Freie Universitat Berlin, Humboldt-Universitat zu Berlin and Berlin Institute of Health, Berlin, Germany, Biotech Research & Innovation Center (BRIC), University of Copenhagen, Copenhagen, Denmark

Background: Thymidylate Synthetase (TYMS) is an import enzyme in the early stage of DNA biosynthesis. It is coded by the TYMS gene at 18p11.32, a region which has been found amplified in urothelial carcinoma. TYMS is a target enzyme for 5-fluorouracil (5-FU) and methotrexate. Elevated TYMS expression has been associated with poor prognosis and unfavorable therapy response in different cancer types. The aim of this study was to clarify the clinical relevance of TMYS expression in urothelial carcinoma and to determine the relationship between TYMS expression and gene amplification.

Design: TYMS expression was analyzed by immunohistochemistry and TYMS copy number status was determined by fluorescence in-situ hybridization on a tissue microarray (TMA) containing more than 2,700 urothelial carcinomas of the urinary bladder including >600 patients who had undergone cystectomy for muscle-invasive disease and for which follow-up data were available.

Results: TMYS immunostaining was detectable in 83.1% of 1,799 analyzable bladder cancers, including 56.4% with weak, 14.4% with moderate, and 12.3% with strong staining. The rate of strongly TMYS positive cancers increased markedly from pTaG2 low (0.3%) to pTaG2 high (4.1%), and pTaG3 cancers (11.8%; p<0.0001) and was even somewhat higher in pT2-4 cancers (16.7%; p=0.6401; pTaG3 vs pT2-4). In muscle-invasive cancers, the frequency of strong TMYS immunostaining increased with tumor stage (p=0.0011) and grade (p=0.0007) but was lower in lymph node positive cancers (p=0.0018). No association was found between TYMS expression and patient prognosis. TYMS amplification was found in 3.1% and TMYS deletion in 1.2% of 1,775 analyzable bladder cancers. The rate of TYMS amplification increased from pTa (0.6%) to pT2-4 (3.7%; p<0.0001) cancers whereas TYMS deletion was only found in pT2-4 (1.4%) cancers. In muscle invasive-cancers, TYMS copy number alterations were unrelated to tumor phenotype and patient prognosis. Strong TYMS positivity was significantly associated with TYMS amplification (p=0.0096) but only 28.6% of 42 amplified cancers showed a strong TMYS staining and only 7.2% of strongly TYMS positive cancers had a TYMS amplification.

Conclusion: The significant association between TYMS overexpression and parameters of aggressive phenotype are consistent with a role of TYMS in bladder cancer progression. The incomplete association between TYMS amplification and overexpression demonstrates that TYMS is not the critical target of 18p11 amplification in bladder cancer and that TYMS upregulation is in most cases due to other mechanisms than amplification.

#5132 Multi-omics analysis uncovers predictive biomarkers for the efficacy and outcomes of immune checkpoint inhibitor in combination with chemotherapy in advanced unresectable biliary tract cancers.

J. Ying[1], Q. Xu[1], J. Ni[1], H. Chen[2], C. Li[3], Y. Xie[4], Q. Zheng[5], J. Jin[6], J. Yan[2], X. Wu[2], Q. Ou[2], L. Yuan[1], W. Zhuo[7], **H. Tang**[2];

[1]Zhejiang Cancer Hospital, Hangzhou Institute of Medicine, Chinese Academy of Sciences, Hangzhou, China, [2]Nanjing Geneseeq Technology Inc., Nanjing, China, [3]Wenzhou Medical University, Wenzhou, China, [4]Lishui Municipal Central Hospital, Lishui, China, [5]Quzhou Affiliated Hospital of Wenzhou Medical University, Quzhou People's Hospital, Quzhou, China, [6]Taizhou Hospital of Zhejiang Province, Taizhou, China, [7]Zhejiang University School of Medicine, Hangzhou, China

Background: Biliary tract cancer, typically diagnosed at advanced stages with a poor prognosis, has witnessed a glimmer of hope in the progress of immune checkpoint inhibitors (ICIs). Yet, their limited response rates necessitate the search for effective biomarkers to refine patient selection.

Methods: A total of 125 patients with a confirmed histological diagnosis of unresectable advanced or metastatic biliary tract cancers (BTC) who received first-line ICIs in combination with chemotherapy (chemoimmunotherapy) were prospectively enrolled. All baseline samples from 125 patients underwent targeted DNA sequencing, with an additional 62 patients undergoing RNA sequencing, and 85 patients had accessible mIHC data. The associations between molecular characteristics and the response to chemoimmunotherapy, progression-free survival (PFS) and overall survival (OS) were evaluated.

Results: The cohort had a median age of 63 years (range from 34 to 82) and 52.8% (66/125) were male, including 54 with gallbladder cancer, 57 with intrahepatic cholangiocarcinoma, and 14 with extrahepatic cholangiocarcinoma. The median duration of follow-up was 14.8 months for the entire cohort, with the median PFS and OS of 6.9 months (95%CI: 6.2-7.9) and 11.8 months (95%CI: 10.3-14.8), respectively. The most mutated genes were *TP53* (64/125, 51.2%), *KRAS* (34/125, 27.2%), *ERBB2* (18/125, 14.4%), and *ARID1A* (17/125, 13.6%). Mutations of *TP53* (51.2%, p = 0.042), *BRCA2* (4.8%, p = 0.002), cytokine genes (6.4%, p = 0.004), and high tumor mutation burden (p = 0.072) demonstrated significant correlation with chemoimmunotherapy response. *KRAS* G12D mutations (PFS: P < 0.001; OS: P = 0.034) and *ARID1A* loss-of-function mutations (PFS: P = 0.009; OS: P = 0.012) were adverse survival factors, while high *CXCL9* or *CTLA4* expression was associated with response (*CXCL9*, P = 0.014; *CTLA4*, P = 0.067), improved PFS (*CXCL9*, P = 0.018; *CTLA4*, P = 0.008), and longer OS (*CXCL9*, P = 0.010; *CTLA4*, P = 0.008) under chemoimmunotherapy. Patients were classified into three subtypes using the identified survival biomarkers. Among them, Type I patients, characterized by the absence of *KRAS* G12D or *ARID1A* mutations but expressing high levels of *CTLA4* or *CXCL9*, demonstrated the best outcomes under chemoimmunotherapy. Interestingly, further RNA analysis suggested that elevated *CXCL9* expression correlated with heightened immune checkpoint expressions, including *CTLA4*, *PD-L1*, and *PD-1* (all P < 0.001), as well as increased tumor microenvironment immune activity, findings validated in two additional independent patient cohorts both internal and external.

Conclusions: Our study revealed predictive biomarkers relevant to the response and efficacy of immune checkpoint inhibitors in combination with chemotherapy in advanced biliary tract cancer.

#5133 Gastric cancer carrying FAT4 mutations associated with favorable prognosis in comparison to wild-type: Results from Real-World Cohorts.

S. Wang[1], H. Wang[1], Y. Ma[1], Y. Wang[1], Y. Zhao[1], C. Peng[1], W. Duan[2], F. Zhao[2], **J. Yang**[1];

[1]Department of Digestive Surgery, Xi Jing Hospital, The Fourth Military Medical University, Xi'an, Shaanxi, China, Xi'an, China, [2]3D Medicines Inc., Shanghai, China, Shanghai, China

Introduction: Gastric cancer (GC) is a complex and heterogeneous disease with variable clinical outcomes. Identifying prognostic factors that can reliably predict patient outcomes is crucial for personalized treatment strategies. In this study, we aimed to investigate the impact of mutations in the FAT4 gene as potential prognostic factors in gastric cancer.

Methods: We conducted a comprehensive analysis of genomic data from a cohort of 236 gastric cancer patients to identify mutations in the FAT4 gene and validated it using the TCGA cohort. The mutational landscape of FAT4 was analyzed using next-generation sequencing (NGS) techniques. Clinical data, including patient demographics, tumor characteristics, and survival outcomes, were collected and correlated with the presence of FAT4 cadherin mutations.

Results: In the real-world cohort, the occurrence of mutations of FAT4 was 19.1% (45/236), while in the TCGA cohort, it was 21.0% (89/423). Specifically, the mutation rates in the single cadherin functional domain of FAT4 were 10.2% (24/236) in the real-world cohort and 8.0% (34/423) in the TCGA cohort. The mutation rates for multiple cadherin sites were 2.5% (6/236) and 2.1% (9/423) in the real-world and TCGA cohorts, respectively. Survival analysis revealed that patients with FAT4 mutations had a significantly better prognosis compared to those with wild-type FAT4 ($p=0.0357$). Patients with multiple cadherin mutations had a better prognosis compared to those with single cadherin mutations in real-world cohorts ($p=0.0651$). No significant difference was observed in the TCGA cohort between single and multiple cadherin mutations ($p = 0.2003$), although FAT4 mutations exhibited a significant improvement in prognosis compared to wild-type patients in the TCGA cohort ($p = 0.0226$).

Conclusion: Our findings indicate that FAT4 mutations confer a favorable prognosis in gastric cancer patients. The presence of FAT4 mutations was associated with improved survival compared to patients with wild-type FAT4. These findings underscore the potential value of FAT4 mutation status as a prognostic factor, guiding personalized treatment approaches for individuals with gastric cancer.

#5134 Immunohistochemistry expression of membrane targets for novel therapeutic agents in RET-rearranged NSCLC.

A. Marinello[1], M. Ghigna[1], W. Zrafi[1], M. Mandarano[2], I. Monnet[3], C. Genova[4], A. Russo[5], S. Terrisse[6], G. Metro[7], J. Remon[1], A. Gazzah[1], F. Barlesi[1], D. Planchard[1], J.-Y. Scoazec[1], B. Besse[1], M. Aldea[1];

[1]Gustave Roussy, Villejuif, France, [2]University of Perugia, Perugia, Italy, [3]Centre Intercommunal Hospitalier de Creteil, Creteil, France, [4]IRCCS Policlinico San Martino, Genova, Italy, [5]Centro Oncologico Ospedale Papardo, Messina, Italy, [6]St Louis Hospital APHP, Paris, France, [7]Ospedale Santa Maria della Misericordia, Perugia, Italy

Background: *RET* fusions are found in 1-2% of patients (pts) with advanced non-small cell lung cancer (aNSCLC). RET inhibitors (RETi) are effective, but resistance occurs. Scarce data are available on treatment after progression (PD) to RETi. Antibody-drug conjugates and bispecific antibodies are promising therapies in NSCLC, possibly employed at resistance. Data on the expression of membrane targets and the impact of novel agents are lacking.
Methods: This is a multicentric retrospective study of 6 European centers. We collected archival tissue samples from pts with RET+ aNSCLC, treated or not with RETi. Membrane expression of cMET/TROP2/HER2/HER3/EGFR was centrally evaluated by immunohistochemistry (IHC). Expression was scored from 0 to 3+. cMET was assessed with EP1454Y clone, TROP2 with EPR20043, HER2 with 4B5, HER3 with D22C5, EGFR with DAKO EGFR pharmDx kit. IHC 2+ and 3+ were considered as high expression. cMET FISH testing was performed on cMET 3+ cases with available tissue. PFS was calculated from RETi start to PD or death, OS from diagnosis to death/last follow up in pts treated with RETi.
Results: 52 pts were included. Median age was 65 years, 63% were female, 92% had adenocarcinoma, median PD-L1 expression was 10% (IQR 0-62.5). All samples were collected before RETi start. IHC 2/3+ scores were observed in 80% of evaluable cases (25/31) with TROP2, 60% (30/50) with cMET, 39% with HER3 (19/48), 31% with EGFR (15/48), and 4% (2/48) with HER2. 31 patients had more than 1 highly expressed target, mostly TROP2/cMET (n=17) and cMET/HER3 (n=13). FISH testing was negative for *MET* amplifications (N=5). PFS and OS of pts with low vs high target expression are presented in the Table.
Conclusion: cMET and TROP2 were frequently expressed in RET+ aNSCLC, EGFR and HER3 were present in a lower proportion, HER2 was rarely found. These markers were not associated with a prognostic or predictive impact on RETi outcomes. The activity of novel therapeutic agents should be evaluated in this setting.

PFS and OS of pts with low versus high target expression.

Marker	cMET	TROP2	HER2	HER3	EGFR
Treated with RETi, n	Total=38 low=17 high=21	Total=22 low=4 high=18	Total=36 low=34 high=2	Total=37 low=24 high=13	Total=36 low=27 high=9
PFS of low vs high, median in months	12.88 vs 15.05 (HR 0.90, 95%CI 0.34-2.05, p=0.77)	3.99 vs 6.06 (HR 2.44, 95%CI 0.54-11.3, p=0.10)	13.96 vs 10.10 (HR 0.57, 95%CI 0.91-3.63, p=0.445)	7.55 vs 17.12 (HR 1.54, 95%CI 0.65-3.67, p=0.356)	12.88 vs 13.96 (HR 1.29, 95% CI 0.47-3.52, p=0.64)
OS of low vs high, median in months	38.75 vs 51.6 (HR 1.29, 95%CI 0.53-3.14, p=0.55)	22.17 vs 51.6 (HR 2.09, 95%CI 0.50-8.71, p=0.19)	NE	51.5 vs 62.6 (HR 1.31, 95%CI 0.50-3.46, p=0.59)	51.6 vs 62.45 (HR 0.97, 95% CI 0.32-2.96, p=0.96)

#5135 Tertiary lymphoid structures and T-cell aggregates signal a robust anti-tumor immune response in a subset of leiomyosarcoma patients.

Aditya Suru, Alexandre Maalouf, Lingling Chen, Ada Tam, William Villasi, Kaushal Sharma, Lindy Zhang, Christian Meyer, Jonathan Greer, Fabian Johnston, Carol Morris, Sophia Strike, Adam Levin, Daniel Rhee, Brian Ladle, Kornel Schuebel, Yan Zhang, Rulin Wang, Srinivasan Yegnasubramanian, John Gross, Robert Anders, Andrew Pardoll, Nicolas Llosa

Johns Hopkins, Baltimore, MD

Cancer immunotherapy has ushered in a new era for treatment of many difficult to treat cancers such as Leiomyosarcoma (LMS), one of the most common subtypes of sarcomas. There are few biomarkers which can be used to identify patients who might benefit from immunotherapy. There is an urgent need to discover novel biomarkers which might be prognostic of a strong anti-tumor response. We thus sought to comprehensively profile the microenvironment of LMS tumors to identify features which might be suggestive of an active immune response and molecular features prognostic of response to immunotherapy. We began our analysis by classifying the LMS tumors from The Cancer Genome Atlas (TCGA) into 4 subtypes based on previously identified molecular features and comparing the enrichment of various immune gene signatures. Two of the subtypes had a high expression of various immune gene signatures including B Cells, M2 macrophages and Cytotoxic T cells. Visual inspection of the Hematoxylin and Eosin-stained tissue slides available with TCGA pointed to a presence of lymphoid aggregates or Tertiary lymphoid structures (TLS) in 10-15% of the tumors - predominantly belonging to one of the two subtypes. This subtype displayed features of smooth muscle differentiation and was also associated with improved survival. To validate our findings, we performed immunohistochemistry (IHC) and bulk RNA sequencing of LMS specimens (n=66) obtained from surgical resections from the Johns Hopkins Hospital. We identified mature CD21+ TLS in 15% of these cases and non-germinal center T cell aggregates present in more than 30% of the cases and these features were associated with improved survival. We digitally merged the different IHC sections to study if the markers were spatially correlated. Interestingly, spatial analysis showed that these CD8 T cells aggregates co-localized with neighborhoods of high density of PD-L1+ cells, hinting at the possibility of immune mediated upregulation of PD-L1 as means of immune suppression. The deconvolution of the transcriptome of these samples showed a marked presence of cytotoxic CD8 T cells and plasma B cells in this subset of patients, an enrichment of pathways related to T cell trafficking, activation and proliferation. Single cell RNA sequencing of tumor infiltrating immune cells showed an oligoclonal expansion of B and T cells. Taken together, this study shows that a subset of LMS patients have a strong anti-tumor immune response which is characterized by the presence of Tertiary Lymphoid Structures and patches of high density of PD-L1 expressing cells. These features might serve as biomarkers in screening LMS patients which might benefit from immunotherapy.

#5136 Development of a highly specific NAPRT monoclonal antibody for the detection of tumors sensitive to pharmacological inhibition of NAMPT.

J. Spurrier[1], E. S. Burgos[1], M. R. Lundquist[1], K. Tanaka[1], S. Brook[1], M. Gozzi[1], J.-S. Yi[1], J. Edmonds[2], M. Raponi[1];
[1]Alphina Therapeutics, Inc., New Haven, CT, [2]Yale School of Medicine, New Haven, CT

Introduction: A key component of targeting synthetic lethality in cancer is identifying specific biomarkers, such as sources of NAD+ synthesis, that differentiate between healthy and diseased tissue. In mammals, NAD+ can be synthesized from nicotinamide via nicotinamide phosphoribosyltransferase (NAMPT) or from nicotinic acid (niacin, NA) via nicotinic acid phosphoribosyltransferase (NAPRT). NAPRT loss has been identified across tumor indications as a synthetic lethal sensitizer to small molecule inhibitors of NAMPT. Given the reliance of cancer cells on NAD+ synthesis, blocking NAD+ production is a compelling target for anti-cancer therapeutics. However, identifying tumors with NAPRT loss has been a challenge as NAPRT can be expressed by as many as 14 transcripts, only some of which code for the active enzyme. This complicates transcript-based analyses and necessitates proteomic assessment. Here, we have developed a mouse monoclonal antibody (4A5D7) to specifically detect active NAPRT and to identify indications enriched for NAPRT loss in patients through an IHC-based assay. We further confirm that loss of NAPRT makes cells susceptible to NAMPT inhibition, and ultimately show that our antibody can identify patient-derived xenograft (PDX) models that respond to NAMPT inhibition.
Methods We utilized a hybridoma system to produce antibodies against epitopes in the NAPRT active site; clones were subsequently screened for their ability to selectively recognize active NAPRT. After identifying clone 4A5D7, we validated our proprietary antibody against FFPE specimens across multiple cancer indications (TNBC, NSCLC, SCLC, CRC, gastric, ovarian, and prostate). Stained samples were scored by a pathologist and assessed for percent of positive tumor cells, nuclear and/or cytoplasmic staining, and staining intensity. CCLE and TCGA datasets were mined for indications enriched for suspected NAPRT-loss and sensitivity to NAMPT inhibitors. We then selected cell lines and pan-tumor PDX tissue microarrays (TMAs) from indications of interest and characterized samples by western blot and IHC to determine NAPRT status. Cell lines and PDX tumor tissue were exposed to increasing ranges of NAMPTi in the presence or absence of NAPRT-substrate NA to validate our approach.
Results: We validated that our proprietary NAPRT monoclonal antibody clone 4A5D7 only detects functional NAPRT and demonstrated improved performance over previous antibodies. We used our antibody to characterize cell lines and PDX tumor samples, and subsequently show that NAPRT-null cell lines and tumor samples are susceptible to NAMPT inhibition, while samples with functional NAPRT can be rescued by NA.
Conclusion: Our proprietary antibody can identify NAPRT null tumors and identify samples that will respond to NAMPT inhibition, a critical advancement for patient selection in clinical trials.

#5137 BRAF mutations in primary central nervous system tumors.

J. B. Blaquier, F. D'Angelo, D. Tejera, R. A. Nasany, G. Saigal, A. Iavarone, M. I. de la Fuente;
Univ. of Miami Sylvester Comprehensive Cancer Ctr., Miami, FL

Background: *BRAF* alterations are present in a variety of primary central nervous system (CNS) tumors from 3% in glioblastomas to 60% in pleomorphic xanthoastrocytomas. BRAF V600E mutation is the most common *BRAF* alteration found in tumors and has been successfully targeted by combining BRAF/MEK inhibitors in different tumor types, including gliomas. We aimed to describe the clinical and genomic features of primary CNS tumors harboring BRAF alterations and real-world data on BRAF-targeted therapy including our experience sequencing BRAF-directed therapies (BDI) in gliomas.
Methods: Single-center retrospective analysis of patients with diagnosis of primary CNS tumors with NGS testing. Clinical, histological and molecular characteristics were analyzed.
Results: 44 patients with *BRAF* mutant primary CNS tumors were included. 28 (64%) were male. 24 (55%) had histology consistent with high-grade glioma (HGG), 14 (32%) low grade glioma (LGG), 4 (9%) low grade neuroepithelial tumors and 2 (4%) others. Missense mutations were found in 77%, followed by amplifications (9%), fusions (9%) and in/del alterations (5%). V600E was the most common mutation (63%), followed by class 2 (16%) and 3 (7%) mutations and amplifications (9%). Co-occurring mutations were found in *CDKN2A/B* (22), *TERT* (20) and *MTAP* (12). median TMB was 2 mut/mb and only 2 patients had high TMB. 4 patients had commuted *IDH1* (3 R132H), non-concurring with a V600E mutation. For patients with HGG, median age at diagnosis was 47 years and 16 (66%) were male. Lesions were more frequent in left hemisphere (70%) and temporal lobe (54%). V600E was found in 50% of cases. KIAA1549-BRAF fusion was found in 1 case. Median follow-up was 40 months (95% CI 11-68) and median overall survival (OS) was 22 months (3.4-40) for the whole population, and 56 (4-109) months for patients treated with BDI (n=4). All 4 patients had an OS >30 months. In the LGG cohort, median age at diagnosis was 34 years (IQR 24-46). 8 (57%) were male. 50% of the lesions were in the left side and 21% of the tumors were in the posterior fossa. 78% had a V600E mutation, with no statistical difference with HGG cohort (p=.082). Median follow up was 11 months, median OS was not reached. For 5 patients treated at recurrence with BDI, median PFS was 15 months (3-27).5 patients were treated with plixorafenib (PLX8394) on clinical trial achieving disease control (PR +SD) in 4 cases. Upon progression, 4 were rechallenged with dabrafenib + trametinib and 1 with another BDI. 4 patients had a partial response with duration of response >6 months in 3 cases.
Conclusion: BRAF mutant CNS tumors are a heterogeneous disease. Longer survival was observed in the small group of HGG patients treated with BDI compared to SoC (56 months vs 22months). BDI rechallenge showed durable responses in heavily pretreated patients. Further molecular characterization of these patients is ongoing. The best therapeutical sequencing strategy for BDI remains uncertain.

#5138 Proteomic analyses of the urothelial cancer landscape reveal highly distinct prognostic and predictive subtypes.

F. F. Dressler[1], F. Diedrichs[1], D. Sabtan[1], S. Hinrichs[2], P. Mackedanz[2], M. Schlotfeldt[2], C. Krisp[3], M. Hennig[2], H. Schlueter[3], U. Wetterauer[4], R. Zubarev[5], D. Horst[1], S. Perner[2], P. Wolf[4], A. Vegvari[5],

[1]Charite - University Medicine Berlin, Berlin, Germany, [2]University Medical Center Schleswig-Holstein, Luebeck, Germany, [3]University Medical Center Hamburg-Eppendorf, Hamburg, Germany, [4]University of Freiburg - Medical Center, Faculty of Medicine, Freiburg, Germany, [5]Karolinska Institutet, Stockholm, Sweden

Introduction: Urothelial cancer (UC) is a challenging disease with a wide tumor-biological spectrum. Most molecular classifications cover only muscle-invasive bladder cancer and are transcriptome-based, relating only indirectly to the therapeutically relevant and more stable protein level. Also, the recent introduction of antibody-drug conjugates (ADCs) requires quantitative data about the tumor specificity of their target proteins. We turned to the proteome to address these questions.

Methods: We performed deep proteomic profiling of a comprehensive cohort by optimized tandem mass tag-labelled liquid chromatography-coupled tandem mass spectrometry. Data acquisition was validated internally with immunoblotting and externally by bioinformatic reclassification within existing, filtered transcriptomic data. After bioinformatics, the top cluster defining proteins were quantified immunohistochemically under real-world conditions. Protein profiles were individualized and separately evaluated with drug repurposing libraries. Cell viability assays were performed for a panel of twelve UC cell lines to validate these predictions in vitro.

Results: We analyzed 434 samples with 242 tumors and 192 paired normal mucosae, covering all stages of UC. 9542 proteins were quantified and revealed five distinct proteomic subtypes. These were validated internally and externally, showing relevant survival stratification also in the TCGA dataset. The proteomic subtypes were independent from pathological groups with relevant stratification of progression- free and overall survival (low vs. high-risk: median 103 vs. 27 months). Tumor specificity of all proteins was highly heterogeneous across stages and subtypes. As an example, the ADC target NECTIN4 was generally overexpressed mainly in non-muscle-invasive UC. Drug repurposing revealed several new candidate drugs, each specific to different proteomic subtypes. In vitro data showed increased sensitivity by subtype in line with four out of seven representative predictions.

Conclusions: Proteomic subtypes add independent prognostic information and carry predictive value for several newly identified adjuvant drug candidates. The actual tumor specificity of biomarkers and ADC targets is highly dependent on stage and subtype and calls for individualized patient-specific predictive testing.

#5139 PD1-PDL1 interaction as a superior predictor for response to immune checkpoint therapy in NSCLC patients.

P. Micke[1], A. Lindberg[1], R. Artursson[1], L. Hellberg[1], H. Yu[1], M. Backman[1], J. Botling[1], H. Brunnstrom[2], A. Mezheyeuski[3], J. Isaksson[1], **C. Strell**[1];
[1]Uppsala University, Dept of Immunology, Genetics and Pathology, Uppsala, Sweden, [2]2Department of Clinical Sciences Lund, Division of Pathology, Lund University, Lund, Sweden, [3]Molecular Oncology Group, Vall d'Hebron Institute of Oncology, Barccelona, Spain

Background: Immune checkpoint therapies (ICT) are now widely introduced in clinical oncology and most often guided by PDL1 expression in diagnostic biopsies. However, the predictive value of this testing is only modest, leading to over- and undertreatment. Conceptually, the prevention of binding of ligand PDL1 to PD1 receptor is decisive for the efficacy of ICT. Therefore, directly detecting the spatial PD1-PDL1 interaction would provide more predictive information.

Methods: A second-generation *in situ* proximity ligation assay (isPLA; Navinci Diagnostics) was established to detect PD1-PD-L1 interactions in diagnostic patient samples and linked to an automated analysis pipeline (QuPath). For basic validation, we used pan-cancer tissue microarrays (TMA) including 16 solid tumor types, and a non-small cell lung cancer (NSCLC) TMA (359 ICT-naïve surgically treated patients). In addition, we analyzed diagnostic tissue biopsies from 75 advanced NSCLC patients treated with anti-PD1-PDL1 regiments.

Results: The pan-cancer analysis revealed varying levels of PD1-PDL1 interaction among the solid cancer types, with the lowest levels detected in liver cancer and the highest in testicular cancer. A general positive association was observed between the literature-reported objective ICT response rate (ORR) per tumor type and its corresponding PD1-PDL1 interaction status. Conventional immunohistochemical analysis of the ICT-naïve, surgically treated NSCLC cohort revealed variable protein expression level for both, PDL1 and PD1, for 200 cases, but only 108 (54%) of them demonstrated a detectable PD1-PDL1 interaction with our isPLA assay. EGFR mutated cases showed generally lower PD1-PDL1 interaction scores (p=0.01). PD1-PDL1 interaction was not associated with survival (p=0.46). A subsequent analysis of the ICT-NSCLC cohort revealed a significant positive association between PD1-PDL1 interaction status and prolonged overall survival upon ICT (median survival 14.8 vs 32.3 months; p=0.022). The standard tumor proportional score (TPS) of membranous PDL1 expression did not correlate with ICT-specific survival (p=0.40).

Conclusions: The second generation isPLA successfully distinguishes a previously difficult-to-define patient subset with positive PD1-PDL1 interaction status. Our data suggest that the PD1-PDL1 interaction is a superior clinical biomarker for patient selection for ICT in NSCLC. The interaction analysis is applicable to sections from minute diagnostics biopsies and accessible by light microscopy either semi-quantitatively by a pathologist or by an automated image analysis program. Thus, the assay holds great potential to be integrated into routine clinical pathological workflow to stratify cancer patients for ICT.

#5140 ITGB6 as a predictive biomarker for overall prognosis and PD-(L)1 immune checkpoint blockade response in various cancer types.

W. J. MacDonald, P. R. Srinivasan, M. Pinho-Schwermann, V. Tajiknia, C. Purcell, L. Carlsen, W. S. El-Deiry;
Legorreta Cancer Center at Brown University, Providence, RI

Our previous work studying the effects of integrin αvβ6 knockdown in cancer cells demonstrated αvβ6 as a method of T cell suppression in a co-culture model. ITGB6, the gene encoding the β6 subunit of αvβ6, is a potent prognostic marker across multiple cancer types. As a major activator of latent TGFβ, αvβ6, and consequently, ITGB6, has considerable therapeutic implications due to the immunosuppressive effect that activated TGFβ has on the tumor microenvironment. A Human Protein Atlas search of ITGB6 expression surveyed the upregulation of ITGB6 across cancer types. Cancer ITGB6 expression was then compared to expression in paired adjacent normal tissue using the TNMplot tool (Bartha, 2021) on a concatenated set of GEO, GTex, TCGA, and TARGET RNA-seq databases. Kaplan-Meier curves were generated using TCGA mRNA data through the cBio portal, splitting the cohorts according to an ITGB6 mRNA expression threshold of one standard deviation above the mean (z-score ± 1.0). ITGB6 expression and immune checkpoint blockade (ICB) response were evaluated with the Kaplan-Meier Plotter tool (Kovacs, 2023). ITGB6 expression levels between ICB responders and non-responders were quantified using the ROC Plotter tool (Fekete, 2023), and the figures were generated using Matplotlib in Python. Lung, bladder, head and neck, pancreatic, and cervical cancer all demonstrated high expression of ITGB6. Head and neck squamous cell carcinoma (median fold change 2.70, $p<0.0001$), bladder urothelial carcinoma (FC 2.41, $p<0.001$), cholangiocarcinoma (FC 5.33, $p<0.01$), and esophageal carcinoma (FC 2.72, $p<0.03$) showed strong upregulation of ITGB6 compared to normal tissue. Interestingly, lung adenocarcinoma (FC 0.77, $p<0.04$) and lung squamous cell carcinoma (FC 0.55, $p<0.0001$) showed downregulation of ITGB6 compared to normal tissue. Survival data revealed that ITGB6 was a potent marker of a poor prognosis in pancreatic adenocarcinoma (high ITGB6 median survival 16.79 mos, vs. low ITGB6 21.88 mos, $p<0.004$) and head and neck squamous cell carcinoma (high ITGB6 30.06 mos vs. low ITGB6 57.42 mos, $p<0.03$). However, no significant prognostic difference was observed in non-small cell lung cancers. Finally, high pan-cancer expression of ITGB6 led to poorer response to αPD-1 (high ITGB6 Hazard Ratio 1.37, $p<0.05$) and αPD-L1 (high ITGB6 HR 1.50, $p<0.001$). In vitro and in vivo experiments to validate the benefit of ITGB6 as a biomarker and as a therapeutic target are underway.

#5141 Autoantibody profiling for predictive biomarkers for immune-related adverse events and clinical benefit in rare tumors treated with anti-PD-1 therapy.

M. H. Derbala[1], J. Hajjar[2], B. Stephen[1], S. A. Gurses[1], E. Kwiatkowski[1], P. Budde[3], H.-D. Zucht[3], M. Brautigam[3], A.-S. Schubert[3], B. Ahangarianabhari[3], E. Rodriguez[1], M. Gouda[1], L. Castillo[1], A. Zarifa[1], J. A. How[1], J. T. Moyers[4], D. S. Hong[1], F. Meric-Bernstam[1], A. Naing[1];
[1]The University of Texas MD Anderson Cancer Center, Houston, TX, [2]Baylor College of Medicine, Texas Children's Hospital, Houston, TX, [3]Oncimmune Germany GmbH, Dortmund, Germany, [4]Angeles Clinic and Research Institute, Cedars-Sinai Affiliate, Los Angeles, CA

Background: Immune checkpoint inhibitors (ICIs) have changed the cancer treatment paradigm; however, with high frequency of immune-related adverse events (irAEs) and limited response rates in select patients. This underscores the unmet need for the development of biomarkers predictive for the development of irAEs and ICI response. Herein, we conducted autoantibody (AAb) profiling to assess baseline (BL) AAb associations with clinical benefit (CB) and irAEs in patients (pts) with rare tumors (RT) treated with programmed cell death protein 1 (anti-PD-1) therapy.
Methods: AAbs against 1168 antigens were analyzed using the SeroTag antibody discovery technology. The study included 41 pts with RT who received anti-PD-1 therapy. We conducted a Significance Analysis of Microarray (SAM) to analyze the association between BL AAbs with irAEs and CB (defined as pts achieving complete response (CR), partial response (PR), or stable disease (SD) for ≥4 months by Response Evaluation Criteria in Solid Tumors (RECIST) v1.1). AAb biomaker candidates were discovered based on filtering for SAM hits with $p < 0.05$ and a delta score $|D| > 2$.
Results: Table 1 outlines patients' demographics. CB and irAEs were observed in 34% and 39% of patients, respectively. Eighteen BL AAbs were significantly associated with CB such as DNA ligase III (LIG3) and small nuclear ribonucleoprotein polypeptide (SNRPA) ($p = 0.002$ and $p = 0.003$, respectively). Likewise, 13 BL AAbs showed significant associations with any-grade irAEs, particularly AAbs to breast cancer 2 (BRCA2) DNA repair associated antigen and chromatin-modifying protein 4A (CHMP4A) ($p = 0.001$ and $p = 0.003$, respectively).
Conclusion: The predictive potential of autoantibodies as biomarkers is promising. Further evaluation in larger cohorts is needed for validation of our findings and understanding the underlying mechanism.

Table 1. Patients' demographics

Total patients		n=41
	Median age in years (range)	66 (35-84)
	Male	n=19
	Female	n=22
Tumor type	Carcinoma of unknown primary	n=13
	Squamous cell carcinoma of the skin	n=9
	Small cell malignancies of non-pulmonary origin	n=7
	Adrenocortical carcinoma	n=6
	Vascular sarcoma	n=5
	Other rare histology	n=1
Clinical benefit	CR, PR, or SD ≥ 4 months	n=14
	SD <4 months or progressive disease (PD)	n=23
	Not evaluable	n=4
irAEs	Yes	n=16
	No	n=25

#5143 Molecular investigation of a polymorphic variant in *JMJD1C* that associates with chemoradiotherapy outcomes in locally advanced rectal and head and neck cancer.

Adria Hasan[1], Elena V. Demidova[1], Philip Czyzewicz[1], Shreya M. Shah[1], Karthik Devarajan[2], Thomas J. Galloway[3], Margret B. Einarson[4], Barbara Burtness[5], Erica A. Golemis[6], Joshua E. Meyer[3], Sanjeevani Arora[1]

[1]Cancer Prevention and Control Program, Fox Chase Cancer Center, Philadelphia, PA,[2]Program in Biostatistics and Bioinformatics, Fox Chase Cancer Center, Philadelphia, PA,[3]Department of Radiation Oncology, Fox Chase Cancer Center, Philadelphia, PA,[4]Program in Cancer Signalling and Microenvironment, Fox Chase Cancer Center, Philadelphia, PA,[5]Department of Internal Medicine, Yale Cancer Center, Yale School of Medicine, New Haven, CT,[6]Department of Cancer and Cellular Biology, Lewis Katz School of Medicine, Temple University, Philadelphia, PA

Background: Neoadjuvant chemoradiotherapy (nCRT) is standard therapy for locally advanced rectal cancer (LARC). While only a minority of patients are expected to have a complete response, all are at risk of toxicity. Currently no biomarkers reliably predict response to nCRT in LARC. Further, standard therapy in locally advanced head and neck squamous cell carcinoma (HNSCC) is adjuvant CRT. A major cause of poor outcomes in HNSCC is regional persistence or recurrence post-CRT. No biomarkers, apart from HPV, predict CRT response in HNSCC. CRT causes double-strand breaks (DSBs) and methylation of histones on lysine residues is known to affect chromatin, influencing DSB repair. We hypothesized that single nucleotide polymorphisms (SNP) in the histone 3 lysine 9 (H3K9) demethylase-encoding *JMJD1C* influenced CRT response.

Methods: LARC patients (n=84) were divided into poor (PoR) and complete (CR) responders based on Neoadjuvant Rectal score. Lymphocyte DNA was sequenced, and LARC patient-derived cells were treated with DSB-inducing agents to assess viability. Sequencing was confirmed in an independent cohort of CRT-treated HNSCC patients (n=90) divided into: disease-free (n=30), recurrent disease (n=28), and never-disease-free (n=32). HNSCCs were in the larynx or oral cavity. Not all patients received HPV-testing; p16 expression was positive for 19/43 tumors. CRISPR/Cas9 editing of HPV-negative HNSCC lines (SCC9, Cal27) generated JMJD1C WT or SNP isogenic pairs. Bulk RNA-sequencing, colony survival, and immunofluorescence studies were performed.

Results: In LARC patients, CRs were enriched for a coding, missense germline SNP in *JMJD1C* versus PoRs (discovery n=30, p<0.00001; validation n=54, p=0.001, Fisher's Exact). When subjected to DSB, LARC patient-derived cells with the SNP displayed greater sensitivity than their WT counterparts (n=12, p<0.001, Mann-Whitney). In HNSCC, a correlation was identified between the same *JMJD1C* SNP and no recurrence (p=0.0003, Fisher's Exact). HNSCC SNP cells showed changes in mRNA levels of DNA repair and immune response genes versus HNSCC WT cells (q-value<0.05). Upon irradiation, kinetics of foci resolution of the DNA damage response protein MDC1, specific to DSBs, were slower in SNP versus WT HNSCC cells (p<0.05, Mann Whitney). Further, there was reduced colocalization of BRCA1 with RAP80, a crucial factor for homology-directed DSB repair, in SNP versus WT HNSCC cells (p<0.01, Mann-Whitney).Targeted introduction of the SNP into HNSCC cell lines reduced viability and radiation response.

Conclusion: Our study identifies a polymorphic coding variant in *JMJD1C*, as a predictive biomarker for CRT effectiveness in LARC and HNSCC, and defines a DNA repair mechanism by which JMJD1C influences response to irradiation.

#5145 Association of a ctDNA biomarker of treatment response with clinical outcomes in a real-world pan-cancer cohort treated with tyrosine kinase inhibitors.

A. Mitra[1], J. Guittar[1], R. Schwind[1], T. Driessen[1], M. Berginski[1], C. Lo[1], M. M. Stein[1], J. Freaney[1], S. Won Hyun[1], C. Sangli[1], K. Sasser[1], H. Nimeiri[1], A. Chaudhuri[2];

[1]Tempus Labs, Chicago, IL, [2]Washington University in St. Louis, St Louis, MO

Clinical evidence suggests that early changes in circulating tumor DNA tumor fraction (ctDNA TF) is predictive of patient response to immune checkpoint inhibitors, but the extent to which this approach can be used for patients on Tyrosine Kinase Inhibitors (TKIs) is not known. Here, we use xF Monitor to estimate ctDNA TF in patients that received TKIs and show that changes in circulating TF correlate with outcomes in a real-world pan-cancer cohort.

Tempus xF Monitor is a ctDNA assay that measures quantitative molecular changes in ctDNA TF by utilizing diverse genomic events, dynamically weighting somatic variant allele frequencies and copy number variants, while using germline information to inform these estimates and providing single nucleotide variant (SNV) results on 105 genes. Molecular responders (MR) were defined as patients with ≥50% reduction in ctDNA TF between baseline and on-treatment time points, consistent with our previously established threshold. Deidentified patient records from the Tempus multimodal database were analyzed if patients had an xF test ≤ 15 weeks prior to the start of their first TKI regimen and an xF test 15 -180 days post-TKI initiation. Patients received TKI agents as classified in the Tempus Medical Ontology, which assigns a unique ID to key clinical concepts, validated and harmonized across industry standard terminologies. The TKI list was further validated using the NCI Metathesaurus (https://ncim.nci.nih.gov/ncimbrowser/) TKI concept (NCI Code C1967). Clinical endpoints were defined from TKI start to the first progression event or death (rwPFS) or death (rwOS), both censored on the last follow-up in event-free patients. Kaplan Meier analysis and Cox proportional hazard models were fitted to compare MR status and survival outcomes on TKI.

The evaluable pan-cancer cohort N=69, median age = 61.5 yo, advanced/metastatic disease = 72%, 65% were female, consisted of > 10 cancer diagnoses (35% NSCLC, 26% BC), 41% 1L. In this cohort, 49% of patients received a TKI combination regimen, 21% with CT, 18% with ICI. 68% of patients with NGS testing received matched targeted mutation therapies based on NCCN guidelines. Patients classified as MR based on xF Monitor results had improved survival outcomes with a median rwOS of 951 days (vs 439 days for non-MRs). MR patients had significantly longer rwPFS (HR = 0.383, p = 0.005, CI = 0.12 - 0.75) and rwOS (HR = 0.205, p = 0.004, CI = 0.07 - 0.61) than non-MRs.

xF Monitor is a novel tumor naive serial quantitative ctDNA TF algorithm off the Tempus xF assay that has the potential to be used clinically as a monitoring biomarker to stratify patients who are likely to benefit from TKI therapy. xF monitor can be used as a strategy to identify patients at a high risk of progression who could benefit from early switch or intensifying therapy. Results need to be prospectively validated in a larger cohort.

#5146 Clinical significance of inter-assay discrepancy in PD-L1 expression evaluation for the efficacy of pembrolizumab in advanced NSCLC patients with high PD-L1 expression.

J. Miyakoshi, J. Kashima, M. Shirasawa, M. Torasawa, Y. Matsumoto, K. Masuda, Y. Shinno, Y. Okuma, T. Yoshida, Y. Goto, H. Horinouchi, K. Shiraishi, T. Kohno, N. Yamamoto, Y. Yatabe, Y. Ohe;
National Cancer Center Hospital - Japan, Tokyo, Japan

Introduction: The expression of programmed cell death ligand-1 (PD-L1) is a predictive biomarker for the efficacy of pembrolizumab in advanced non-small cell lung cancer (NSCLC). While several assays have been approved for evaluating PD-L1 expression status, the inter-assay discordances are observed. The clinical significance of these discrepancies is still unclear.

Methods: We retrospectively reviewed treatment-naïve NSCLC patients with available PD-L1 expression status by both 22C3 and SP142 assays. Among these patients, efficacy analysis was performed in those with PD-L1 tumor proportion score (TPS) ≥ 50% (22C3) who received the first-line pembrolizumab monotherapy. Additionally, we conducted RNA-sequence analysis in the patients with TPS ≥ 50% to investigate the distinct immune profiles with the inter-assay discordance.

Results: A total of 611 patients were evaluated for PD-L1 expression status by both assays. Of 198 patients with TPS ≥ 50%, 91 (46%) had TC score ≤ 1 (SP142, i.e., inter-assay discrepancy). In 52 patients who received the first-line pembrolizumab monotherapy, the efficacy in patients with the inter-assay discrepancy was significantly lower than those without the discrepancy (shown in Table). While there was no difference in tumor microenvironments such as the tumor-infiltrating lymphocytes, the transcriptome analysis revealed significantly more *CD274* splicing variants with aberrant 3'-terminal sequences in tumors with the inter-assay discrepancy than those without discrepancy, leading to the suppressed PD-1/PD-L1 pathway in those with the discrepancy.

Conclusion: The inter-assay discrepancy in the PD-L1 expression status on tumor cells between the 22C3 and SP142 assays, reflecting an imbalance of the *CD274* splicing variants, could be a primary-resistance mechanism to the pembrolizumab monotherapy in highly PD-L1-expressing NSCLCs.

PD-L1(22C3)	Discrepancy	Pts.	ORR(%)	p value	Median PFS(months)	95%CI	p value
TPS ≥ 50%	yes	17	18	< 0.001	3.2	0.8–5.5	< 0.001
	no	35	83		8.3	5.7–24.2	

#5147 Identification of pharmacodynamic biomarkers in PBMCs and cancer cells for SIK2 kinase inhibitor therapy.

H. Yang[1], W. Mao[1], P. Rask[1], M. Peter[2], G. Swaminath[2], S. W. Morris[2], Z. Lu[1], R. C. Bast[1];
[1]UT MD Anderson Cancer Center, Houston, TX, [2]Greenfire Bio, Frisco, TX

Salt-inducible kinase 2 (SIK2) is an AMPK family kinase involved in multiple signaling pathways including the LBK1-SIK-HDAC, LKB1-SIK-CRTC/CREB, PI3K-PKA-mTOR and Hippo pathways. The expression of SIK2 is significantly upregulated in fraction of ovarian and breast cancers, and associated with poor prognosis. Inhibition of SIK2 kinase activity suppresses growth of ovarian and breast cancers as well as progression of acute myeloid leukemia. SIK2 inhibitors synergistically enhance sensitivity of ovarian and breast cancer cells to paclitaxel, carboplatin and PARP inhibitors. Utilization of SIK2 inhibitors to treat cancers has been investigated in preclinical studies and in a Phase I clinical trial (NCT04711161). To enable pharmacodynamic (PD) analysis in clinical studies, we have developed biomarkers that measure the effect of GRN-300, a SIK2/3 inhibitor, on SIK2 signaling in ovarian cancer cells. Class IIa histone deacetylases (HDAC4/5/7) are SIK2 substrates in cancer cells; and are also expressed in peripheral blood mononuclear cells (PBMCs). We found that GRN-300 decreased phosphorylated HDAC4/5/7 levels in ovarian and breast cancer cells (Lu et al. J Clin Invest, 2022) and now report that this SIK2 inhibitor also decreases pHDAC4/5/7 in PBMCs *ex vivo* in a dose-dependent manner using Western blot analysis. We also identified three mRNA markers in PBMCs by RNAseq analysis - SEPP1, RNASE1 and MS4A6A - which are up-regulated by GRN-300 in PBMCs isolated from healthy donors. However, these mRNA markers were either expressed at very low levels or not dramatically changed in cancer cells. We identified an additional mRNA marker panel using RNAseq technology by screening seven ovarian and six breast cancer cell lines: A2780, Caov3, IGROV1, OC316, OVCAR3, OVCAR8, SKOv3ip, BT549, Cal51, HCC1937, MDA-MB-231, MDA-MB-436 and MDA-MB-468. mRNA expression of three genes - DDIT4, NUPR1 and IL6 - is upregulated by GRN-300 in more than 9 of 13 cell lines tested. Five genes - ID1, ID2, ID3, ID4 and TGFBI - are down-regulated in response to GRN-300 treatment in more than 10 of 13 cell lines. The decrease in HDAC4/5/7 phosphorylation, and alterations in mRNA markers we discovered could serve as PD biomarkers for clinical trials to evaluate the effects of SIK2 inhibitors and provide insights in the mechanisms of drug action.

#5148 Analysis of HER2 prevalence by RNA expression across solid tumors.

K. Moxley[1], E. Scherrer[2], M. Bontrager[3], S. Whitman[2], N. R. M. Schwartz[2], C. Sangli[3], S. Won Hyun[3], H. Nimeiri[3], J. Ball[3], C. Aggarwal[4]; [1]Oklahoma Cancer Specialists and Research Institute, Tulsa, OK, [2]Seagen, Inc., Bothell, WA, [3]Tempus Labs, Inc., Chicago, IL, [4]University of Pennsylvania, Philadelphia, PA

Background: The frequency of HER2 expression in solid tumors other than breast (BC) and gastric cancer (GC) is not well defined. This study describes the frequency of HER2 expression by correlating HER2 IHC/ ISH and ERBB2 mRNA levels by NGS in tumor samples of patients with locally advanced/metastatic (LA/m) BC or GC and applying those findings to predict HER2 expression in other solid tumors.

Methods: De-identified records from NGS-tested patients with LA/m BC, GC, HNSCC, NSCLC, endometrial, and ovarian cancers in the Tempus database from 2015 - 2021 were analyzed. Patients with BC and GC who underwent HER2 IHC/ISH testing were categorized as: RNA-zero (IHC0), -low (IHC1+, IHC2+/ISH-), and -positive (HER2+; IHC2+/ISH+, IHC3+). To identify thresholds separating HER2 subgroups, a logistic regression model was fit to NGS and IHC status data in BC and GC. These thresholds were applied to other solid tumors to predict the distribution of HER2 expression. HER2 amplification and mutation rates were evaluated in the Tempus NGS data.

Results: Logistic regression modeling used 3,898 samples. HER2+ samples had the highest IHC-to-RNA agreement at 80% (BC) and 81% (GC) compared to HER2 low and zero samples which ranged ~56-75% agreement. When applying thresholds identifying RNA-low and RNA-positive sample to other tumors (N = 4,726), the models predicted up to 33% (BC thresholds) or 56% (GC thresholds) of tumors express HER2 at levels that may be detectable (Table 1).

Conclusions: A notable amount of solid tumors apart from BC or GC have RNA expression that may correspond to HER2 IHC ≥1+. This opens the possibility for novel agents such as HER2-directed antibody drug conjugates to impact patient care in several tumor types. Further IHC testing in these populations are needed to corroborate our results.

Table 1. ERBB2 (HER2) Categories in Solid Tumors

HER2 Status	**HNSCC** (N = 630)	**NSCLC** (N = 2945)	**OC** (N = 855)	**EC** (N = 295)
NGS BC thresholds ERBB2 Log2(TPM+1)				
RNA-Zero	589 (93.5%)	1,974 (67.0%)	626 (73.2%)	205 (69.5%)
RNA-Low	33 (5.2%)	853 (29.0%)	214 (25.0%)	64 (21.7%)
RNA-Positive	8 (1.3%)	118 (4.0%)	15 (1.8%)	26 (8.8%)
RNA-Low + RNA-positive	41 (6.5%)	971 (33.0%)	229 (26.8%)	90 (30.5%)
NGS GC thresholds ERBB2 Log2(TPM+1)				
RNA-zero	492 (78.1%)	1,345 (45.7%)	395 (46.2%)	130 (44.1%)
RNA-Low	124 (19.7%)	1,190 (40.4%)	384 (44.9%)	127 (43.1%)
RNA-Positive	14 (2.2%)	410 (13.9%)	76 (8.9%)	38 (12.9%)
RNA-Low + RNA-positive	138 (21.9%)	1,600 (54.3%)	460 (53.8%)	165 (55.9%)
DNA Amplification				
Unamplified	622 (98.7%)	2,911 (98.8%)	843 (98.6%)	277 (93.9%)
Amplified	8 (1.3%)	34 (1.2%)	12 (1.4%)	18 (6.1%)
DNA mutation				
Wild-Type	623 (98.9%)	2,916 (99.0%)	850 (99.4%)	287 (97.3%)
Mutated	7 (1.1%)	29 (1.0%)	5 (0.6%)	8 (2.7%)

NGS: next-generation sequencing; HNSCC: head and neck squamous cell carcinoma; NSCLC: non-small cell lung cancer; OC: ovarian cancer; EC: endometrial cancer; TPM: transcripts per million

#5149 Extracellular matrix remodeling in metastatic mismatch repair deficient endometrial cancer:Implications for immune checkpoint inhibitor response prediction.

J. Grau[1], C. Aime[2], M. Mehnert[3], E. Yaniz-Galende[1], C. Genestie[1], A. Le Formal[1], E. Edmond[1], A. Lachaud[3], P. Pautier[1], J. Michels[1], S. Gouy[1], A. Maulard[1], E. Colomba-Blameble[1], F. Blanc-Durand[1], M.-C. Schanne-Klein[4], A. Leary[1];

[1]Institut Gustave Roussy, Villejuif, France, [2]Ecole Normale Superieure, PSL University, Sorbonne University, CNRS, Paris, France, [3]Biognosys AG, Schlieren, Switzerland, [4]Ecole Polytechnique CNRS - INSERM - Institut Polytechnique de Paris, Palaiseau, France

Mismatch repair deficient (MMRd) status is a predictive biomarker for Immune checkpoint inhibitors (ICI) in endometrial cancer (EC), however, half of these patients (pts) do not respond. Most studies exploring biomarkers of response to ICI have focused on tumor or immune cell factors. We aimed to describe the extracellular matrix components of the tumor microenvironment (TME) in ICI-Responder (R) versus Non-Responder (NR) MMRd EC pts to identify new predictive biomarkers of response.

Clinical data and outcomes of metastatic MMRd EC pts, treated with ICI (2016-2021), were retrospectively collected. Pts were classified as Rs (CR, PR, or SD ≥12 months) or NRs (PD or SD <12 months). Pre-ICI FFPE tumor samples were subjected to Biognosys UltraDeep TrueDiscovery™ Mass Spectrometry (MS) for identification of differentially regulated protein expression between R and NR. Criteria for protein candidate selection were p-value < 0.01 and average absolute log2 fold change (AVG Log ratio) > 0.58. Collagen was visualized on whole slides using Masson's trichrome and quantified by Qupath. Collagen density was expressed as % positive surface in the intratumoral area. Second-harmonic generation (SHG) microscopy plus polarimetry (p-SHG) was used to estimate collagen content and describe the spatial orientation of fibrillar collagen in the intratumoral area. intraepithelial (ie) and stromal (s) CD3+ and CD8+ cells were quantified by Qupath. Non-parametric t-tests and Spearman's rank coefficient (r) for linear correlation were used.

Twenty-five tumor samples were included in the analysis: 17 from Rs and 8 from NRs. MS identified collagen type V alpha-2 (AVR Log ratio 2.9, p 0.008) and type XXII alpha-1 chains (AVR Log ratio 1.14, p 0.006) as significantly upregulated in NRs. Using spatial imaging, collagen density in the intratumoral area was significantly higher in NRs (median: 14.2% vs 4.6%, p 0.01). Intratumoral collagen density was positively correlated with collagen type V expression (r 0.54, p 0.016), and negatively correlated with ie and s CD3+ cell (r -0.39, p 0.054; r -0.4, p 0.048, respectively) and ie and s CD8+ cell (r -0.39, p 0.053; and r -0.29, p 0.166) infiltration. SHG confirmed that fibrillar collagen content in the tumor area was significantly greater in NRs (p 0.02). p-SHG revealed that NR tumors tended to show a highly disorganized collagen matrix. In contrast, a linear collagen pattern was associated with response to ICI: 89% of tumors displaying this pattern were Rs.

Both MS and two different spatial approaches consistently demonstrated that increased collagen expression or density may serve as a potential predictive biomarker of resistance to ICI in MMRd metastatic EC, contributing to create an immunosuppressive TME. The spatial orientation pattern of collagen fibers may also be crucial in shaping immune TME and influencing the response to ICI.

#5150 An immunohistochemical survey of predictive biomarkers for immunotherapy in ampullary carcinoma identifies strata with unique prognostic signatures.

S. E. Kalloger[1], J. Karasinska[2], J. Topham[2], D. J. Renouf[2], D. F. Schaeffer[2];

[1]University of British Columbia Faculty of Medicine, Vancouver, BC, Canada, [2]Pancreas Centre BC, Vancouver, BC, Canada

Introduction: Carcinomas located in the ampulla of Vater are a low incidence malignancy. Therapeutic options for early stage disease largely consist of pancreaticoduodenectomy followed by adjuvant chemotherapy with or without radiation. We explored the localization of CD8 and CD3 positive cells in addition to PDL-1 staining and mismatch repair deficiency markers to gain insight into the potential applicability of immunotherapy for patients with this disease.
Methods: Excess material from clinically diagnosed cases collected between 1997 - 2013 were used to construct a duplicate 0.6mm core tissue microarray (TMA). All cases were derived from the Vancouver Coastal Health Region. Immunohistochemical staining was performed with the following markers: CD8, CD3, PD-L1, and the mismatch repair (MMR) markers: MSH2, MSH6, MLH1 and PMS2. CD3 and CD8 were quantified using localization within the tissue. PD-L1 was considered positive with >1% of cells stating positive. MMR markers were confirmed using full section and cases with convincing loss of any MMR marker were considered MMR deficient. Univariable disease specific survival analysis was performed to identify unique prognostic signatures and contingency analysis was performed to identify co-expression of the aforementioned biomarkers.
Results: Ninety-eight cases were evaluable for all markers. The median age of the cohort was 69 [41 - 84] years. Forty-two percent were female. Adjuvant chemotherapy was provided to 15% of patients with the remainder undergoing post-surgical observation. Almost 90% were pT3 or pT4 and 48% had regional lymph node metastasis. CD3+ T-cells were either localized in the tumor stroma only (59%) or in both the stroma and epithelial compartments (41%). CD8+ T-cells were principally located in the stroma (66%) and both the epithelial and stroma (24%). Ten percent of cases had no CD8+ T-cells. PD-L1 staining was found in 10% of cases. MMR deficiency was found in 5% of cases. Improved prognostic signatures were found for cases with CD3+ and CD8+ T-cells in both the epithelial and stromal compartments ($p <= 0.02$). A trend towards a negative prognostic signature was observed for MMR deficient cases and for PD-L1 positive cases. The only significant positive association between biomarkers was found for CD3+ and CD8+ in both the epithelial and stromal compartments.
Conclusions: The results of this analysis suggest that enhancement of an immune response yielding an increase CD3+ and CD8+ T-cells in the epithelial compartment may have a beneficial effect on prognosis. The relative scarcity of MMR deficiency in this disease is within the expected prevalence supported by other studies. Further exploration of the potential role of immunotherapy in immune enhanced subgroups of ampullary cancers is warranted.

#5151 High serum kidney injury marker-1 and high baseline tumor PD-L1 protein expression levels are independently associated with treatment effect in adjuvant nivolumab plus ipilimumab vs placebo in localized clear cell renal cell carcinoma.

S. Vemula[1], W. Xu[2], Y. Wang[1], X. Liu[3], J. Somocurcio[3], D. McDermott[3], J. Li[1], R. Bhatt[1], C.-W. Lee[1], B. Simsek[1], S. Gupta[1], R. Motzer[4]; [1]Bristol Myers Squibb, Princeton, NJ, [2]Dana-Farber Cancer Institute, Boston, MA, [3]Beth Israel Deaconess Medical Center, Boston, MA, [4]Memorial Sloan Kettering Cancer Center, New York City, NY

Introduction: CheckMate 914 (CM-914) Part A is a double-blind, phase III randomized trial of the Nivolumab (NIVO) plus Ipilimumab (IPI) vs placebo (PBO) in localized ccRCC. Our prior report from this study suggested a disease-free survival (DFS) benefit for NIVO+IPI among patients with Fuhrman grade 4, TNM stages PT2a and PT4, or sarcomatoid features, although the sample size was limited. It is known that high circulating KIM-1 is associated with worse DFS after nephrectomy. In this exploratory post hoc analysis, we investigated whether high KIM-1 may help identify a subset of patients who benefit from adjuvant NIVO+IPI.

Methods: Patients (n=816) with RCC after nephrectomy were randomized in CM-914 Part A to receive NIVO+IPI or PBO as previously described. Assessment of KIM-1 levels was performed using enzyme linked immunoassay (ELISA) on pre-treatment (n=584) and matched on-treatment blood samples (n=584). We used pre-treatment tumor samples to assess PD-L1% tumor cell expression (%TC) in an PD-L1 IHC 28-8 pharm Dx assay. The association between biomarkers and DFS outcomes was investigated by Kaplan-Meier (KM) and Cox proportional hazards analysis.

Results: Median baseline serum KIM-1 level was 102 (9.9 - 1055.7) pg/mL. Serum KIM-1 levels were higher in males vs females, ≥65 yrs vs <65 yrs, Asian vs white patients, and patients with partial vs radical nephrectomy. In the PBO arm, subjects with highest quartile of pre-treatment KIM-1 had significantly worse DFS than those from the three lower quartiles. In contrast, this DFS risk among the subjects within the highest KIM-1 quartile was mitigated with NIVO+IPI treatment. Among patients within the highest quartile of pre-treatment KIM-1, there was trend for better DFS for NIVO+IPI versus PBO, HR=0.6 (0.34-1.04). Increase in KIM-1 during study therapy was positively associated with higher DFS rate in both arms. Multivariable analysis showed that PD-L1 %TC was predictive at predefined PD-L1 cutoffs (>=1%, >=5%, and >=10%), associating with improved DFS compared to placebo. Subjects with high PD-L1 expression had a DFS benefit from NIVO+IPI independent of KIM-1.

Conclusion: Circulating KIM-1 and tumor PD-L1 expression may enrich for benefit from IO therapy in adjuvant ccRCC and hence holds promise for informing risk stratification and patient inclusion in neoadjuvant or adjuvant clinical trials.

#5152 Co-expression and prognostic significance of HER family members and EGFRvIII in patients with hepatocellular carcinoma.

O. Sherif[1], S. Khelwatty[1], I. Bagwan[2], A. Seddon[1], A. Dalgleish[3], S. Mudan[3], **H. Modjtahedi**[1];

[1]Kingston Univ. London School of Life Sci., Kingston upon Thames, United Kingdom, [2]The Royal Surrey County Hospital, Guildford, United Kingdom, [3]St Gerorge's University of London, London, United Kingdom

Hepatocellular carcinoma is one of the most common type of liver cancer. Despite advances in its treatment including the approval of several targeted agents in the past few decades, many patients do not respond or have a response of short duration to such therapeutic interventions. As a result, liver cancer is the third leading cause of cancer-related deaths worldwide. Therefore, it is essential to identify additional therapeutic targets and to develop more effective therapeutic interventions. In the past few decades, increased expression, and activation of the human epidermal growth factor receptor (HER) family members have been detected in various cancer types and of these, EGFR and HER2 are important therapeutic targets for the treatment of patients with a wide range of cancers, but currently not in liver cancer. In some studies, cross-talk between different members of the HER family has been associated with tumor progression and resistance to therapy with EGFR inhibitors but there has been no comprehensive study of the expression of all members of the HER family in patients with hepatocellular carcinoma. In this study, we examined the relative expression of all members of the HER family, type-III deletion mutant of EGFR (i.e.EGFRvIII), which is a tumor specific antigen, and two putative liver cancer cell biomarkers (i.e. CD44, EpCAM) in 43 patients with hepatocellular carcinoma by immunohistochemistry. The prognostic significance of such antigens was also investigated. Of these, the expression of EGFR, HER2, HER3, HER4 and EGFRvIII was found in tumor specimens from 35%, 58%, 0%, 19%, and 26% of the cases, respectively. Interestingly, at a cut off value of >5% of tumor cells with staining, 23%, 14% and 9% of the patients had co-expression of EGFR with HER2, EGFRvIII, and HER2/EGFRvIII. In addition, 40% and 33% of the cases were CD44 and EpCAM positive. Of these, the expression of EGFRvIII positivity at >5% (HR=3.35, p=0.002) and 20% (HR=7.22, p=0.003) of tumour cells and membranous CD44 (HR=2.12, p=0.04) were associated with a poorer survival in patients with hepatocellular carcinoma. In contrast, the expression of cytoplasmic CD44 was associated with a better overall survival (HR=0.30, p=0.02). These were found to be independent prognostic markers in multivariate analysis. Interestingly, the co-expression of EGFR with EGFRvIII was associated with a poorer overall survival (59.5 vs 21.0 months, p=0.004). Taken together, our results suggest that the expression of EGFRvIII occurs in patients with hepatocellular carcinoma and highlight its importance as biomarker for tumor progression and as a potential target for therapeutic intervention with drugs targeting EGFRvIII and other members of HER family.

#5153 Pyramidobacter-DMMR synergy in colorectal cancer: Unveiling prognostic impact, mechanistic insights, and tumor microenvironment dynamics.

S. LI[1], Y. LI[1], H. Ma[2], S. Qin[2], F. Zhao[3], J. Li[1];

[1]The First Affiliated Hospital of Air Force Medical University, Shannxi, China, [2]Air Force Medical University, Shannxi, China, [3]3D Medicines Inc,, Shanghai, China

Background: Colorectal cancer (CRC) exhibits a heightened presence of intratumoral bacteria, and deficient DNA mismatch repair (dMMR) contributes to nucleotide mismatch accumulation, fostering mutagenesis. However, the combined impact of intratumoral bacteria and dMMR on the tumor immune microenvironment (TIME) in CRC, and its consequential influence on patient prognosis, remains elusive.

Methods: We utilized samples from the Cancer Microbiome Atlas project (TCMA), collecting tumor and matched paracancer tissues from colorectal cancer patients. Phyloseq in R was employed to scrutinize microbial abundance differences. The effects of microbial enrichment on prognosis were assessed through survival analysis, and GSEA enrichment analysis provided mechanistic insights.

Results: A total of 173 samples, including 28 dMMR tumors, 112 proficient MMR (pMMR) tumors, and 22 paired para-cancer tissues, were collected. Following stringent filtration, we analyzed 230 bacterial genera. Notably, 26 genera, including Fusobacterium and Streptococcus, showed significant enrichment in dMMR tumors compared to para-cancer tissues. Furthermore, 18 genera were enriched in dMMR tumors compared to pMMR tumors. Of these, 8 genera like Desulfovibrio and Pyramidobacter consistently exhibited enrichment in dMMR CRC compared to either para-cancer tissues or pMMR tumors. Survival analysis highlighted Pyramidobacter as the only genus significantly associated with prognosis in dMMR CRC. Increased Pyramidobacter abundance correlated with decreased overall survival (OS) (P value: 0.049). Stratifying dMMR CRC patients based on Pyramidobacter abundance further emphasized the significantly worse survival in the Pyramidobacter-High group (HR 0.93, 95%CI 1.03-9.60, log-rank p = 0.015). Exploring the impact of Pyramidobacter infection on tumor progression, we assessed TIME and oncogenic pathways between Pyramidobacter-Low and Pyramidobacter-High groups. While overall immune infiltration was higher in the Pyramidobacter-High group, it primarily stemmed from increased B cell and naive CD8+ T cell infiltration. Importantly, pathways enriched in the Pyramidobacter-High group included inflammatory response, epithelial-mesenchymal transition (EMT), and KRAS signaling, while those enriched in the Pyramidobacter-Low group encompassed IFNα response, IFNγ response, and DNA damage repair. These findings suggest Pyramidobacter's role in inducing inflammation, promoting tumor proliferation and metastasis, and suppressing interferon response.

Conclusion: Pyramidobacter emerges as a key player in the development of dMMR CRC, exerting a pivotal influence on patient prognosis through the induction of inflammatory responses and EMT.

#5154 Bacterium LF-3: A dual player in colorectal cancer, shaping prognosis and immune responses.

K. Du[1], F. Zhao[2], F. Feng[1];

[1]Xijing Hospital, the Fourth Military Medical University, Shannxi, China, [2]3D Medicines Inc, Shanghai, China

Background: Colorectal cancer is distinctive for its heightened intra-tumor bacterial presence. While previous studies concentrated on the genus level, the impact of unclassified bacteria, identified through extensive genome sequencing, has been underexplored.

Methods: Utilizing samples from colorectal cancer patients in the Cancer Microbiome Atlas project (TCMA), we applied phyloseq for a nuanced analysis of microbial abundance disparities between tumor and paracancer tissues. Prognostic implications of microbial enrichment were explored through survival analysis, with mechanistic insights gleaned from Gene Set Enrichment Analysis (GSEA).

Results: We meticulously examined 151 colorectal cancer tumors and 22 corresponding para-cancer tissues, scrutinizing a total of 1217 microbial species. We observed that 240 species exhibited a statistically significant enrichment in tumor samples. A focused investigation involving 22 tumor and para-cancer tissue pairs unveiled 35 species with notable enrichment specifically within tumors. A subset of 25 species, including well-documented entities like Fusobacterium sp. oral taxon 370 and Streptococcus oralis, emerged consistently across both comprehensive and paired analyses. We then delved into the prognostic implications of these enriched bacteria. Strikingly, patients with bacterium LF-3 positivity exhibited significantly improved prognoses compared to those without (HR 0.40, 95% CI 0.18-0.91, log-rank p = 0.024). Considering the pivotal role of Microsatellite Instability (MSI) status in the context of Tumor Immuno-Microenvironment (TIME) and prognosis, our analysis of bacterium LF-3 encompassed both MSI-H and MSS CRC cases, with proportions of 12/28 (43%) and 55/102 (54%), respectively. Even after meticulous adjustments for MSI status, bacterium LF-3 maintained a robust correlation with prognosis (HR 0.42, 95% CI 0.18-0.99, p = 0.048), highlighting its independent prognostic significance. Further exploration among MSS patients (N = 112) unearthed intricate details about the impact of bacterium LF-3 on tumor signaling pathways. TNF-α and IFN-γ pathways were significantly up-regulated in bacterium LF-3-positive cases, while the MYC pathway, PI3K pathway, and various cell cycle-related pathways (G2M checkpoint, The E2 factor [E2F] targets, and mitotic spindle assembly) were down-regulated. As for TIME, bacterium LF-3 positivity correlated with the significant enrichment of CD4+ Th2 cells, suggesting a potential role in modulating immune responses.

Conclusion: Bacterium LF-3 in colorectal cancer reveals a dual role, instigating inflammation and tumorigenesis, yet simultaneously activating the innate immune system and promoting cellular immunity. This dual functionality contributes to improved patient prognosis, highlighting the intricate interplay between microbes, immune responses, and colorectal cancer outcomes.

#5155 CD8$^{\pm}$ T cells and CD4$^{\pm}$central memory T cells as biomarkers of perioperative anti-PD-1 therapy in combination with concurrent chemoradiotherapy for locally advanced G/GEJ adenocarcinoma.

Y. Wang[1], Y. Chen[1], J. Yang[1], X. Zhou[2], Y. Wei[2], Q. Liu[1], Y. Yang[1], W. Guan[3], B. Liu[1], J. Wei[1];

[1]Department of Oncology, Nanjing Drum Tower Hospital, Affiliated Hospital of Medical School, Nanjing University, Nanjing, China, [2]Department of Oncology, Nanjing Drum Tower Hospital Clinical College of Nanjing University of Chinese Medicine, Nanjing, China, [3]Department of General Surgery, Nanjing Drum Tower Hospital, Affiliated Hospital of Medical School, Nanjing University, Nanjing, China

Background: Gastric or gastroesophageal junction (G/GEJ) adenocarcinoma is one of the most common lethal malignancies in the world. Near half of the G/GEJ adenocarcinoma are locally advanced at diagnosis and with poor prognosis. Several clinical trials including SHARED (ChiCTR1900024428), which conducted in our center, demonstrated that perioperative anti-PD-1 therapy in combination with concurrent chemoradiotherapy for locally advanced G/GEJ cancers, could raise the pCR rate over 30%. However, the biomarkers for patients with pCR are nor clear.

Methods: Baseline tumor biopsies and post-treatment surgical tissues were collected for next-generation sequencing (NGS) and mass cytometry (CyTOF). The overall survival (OS) was measured from the date of surgery to the date of death or the last follow-up visit.

Results: 34 patients with locally advanced G/GEJ cancer received anti-PD-1 therapy (Sintilimab) in combination with concurrent chemoradiotherapy in our center. Our results met the pre-specified primary endpoint, with a pCR rate of 38.2% (13/34) and median DFS of 17.0 months. Tumor mutation burden (TMB) analyzed by NGS was higher in the pCR group than those not achieving pCR (non-pCR). Deletion of cytoband 7q35, where TPK1 locates, was significantly enriched in pCR groups. The RNA sequencing data revealed an enrichment of dendritic cells (DC), CD8$^{\pm}$ T cells and cytotoxic cell signatures in the pCR group. Conversely, the signature for CD4$^{\pm}$ central memory T cells (TCM) was observed to be lower in the pCR group. On the other hand, CyTOF data also demonstrated that the proportion of CD8$^{\pm}$ T cells, CD8$^{\pm}$ effector memory T cells (TEM) were both higher in pCR group at baseline, while CD4$^{\pm}$ TCM was lower. Moreover, the proportion of specific subtype characterized by CD127$^{\pm}$CD27$^{\pm}$CD45RO$^{\pm}$CXCR5^{-}CD4$^{\pm}$ TCM was significantly lower in pCR patients and significantly reduced after treatment. As continuous variable, only CD8$^{\pm}$ T cells correlated with OS.

Conclusions: It seemed that CD8$^{\pm}$ T cells and CD4$^{\pm}$ TCM cells could be predictive biomarkers of perioperative anti-PD-1 therapy in combination with cCRT for locally advanced G/GEJ. Furthermore, we found a new CD4$^{\pm}$ TCM subtype defined with CD127$^{\pm}$CD27$^{\pm}$CD45RO$^{\pm}$CXCR5^{-} could be novel biomarkers.

#5156 Is the formation of Stroma AReactive Invasion Front Areas in colorectal cancer driven by characteristic extracellular matrix reorganization processes based on the plasmin/plasminogen system?.

B. Grosser[1], N. G. Reitsam[1], F. Sommer[2], J. Hardt[3], B. Markl[1];

[1]Pathology, Medical Faculty, Augsburg, Germany, [2]General and Visceral Surgery, Medical Faculty, Augsburg, Germany, [3]Laboratory Medicine and Microbiology, Medical Faculty, Augsburg, Germany

Background: As patient stratification still needs to be refined in colorectal cancer (CRC), we established SARIFA (Stroma AReactive Invasion Front Areas) as a novel H&E-based prognostic biomarker that is defined by a direct tumor-adipocyte interaction with a lack of desmoplastic reaction. Even though we could prove the high prognostic relevance of SARIFA now in multiple cohorts in gastric, colorectal, and pancreatic cancer, as well as could link an upregulation of lipid metabolism and immune alterations to this specific aggressive tumor biology, it remains an open question how SARIFAs are formed mechanistically.
Materials/Methods: Based on the results of our recently established SARIFA-scores in the TCGA-CRC (TCGA-COAD & TCGA-READ cohorts; SARIFA-positive n=69, SARIFA-negative n=138) and the corresponding differential gene expression analysis, which are part of a previous study, protein levels (in ng/mL) measured by commercially available uPA and PAI1 enzyme-linked immunosorbent assays (ELISAs) were compared between SARIFA-positive and SARIFA-negative CRC patients (SARIFA-positive n=35, SARIFA-negative n=62). Additionally, immunohistochemistry for FABP4 as a key player in lipid metabolism was performed. Moreover, spatial transcriptomics (digital spatial profiling, DSP) was performed with tumor and stroma section segmentation on a subset of cases.
Results: In TCGA-CRC, *SERPINE1* (PAI1), as well as *PLAU* (uPA), are both significantly upregulated on mRNA level (LFC: 1.14 and 0.74, respectively; both adjusted p-values ≤0.001). Logically, *SERPINE1* and *PLAU* are highly expressed in mesenchymal CMS4 CRCs, which overlap with SARIFA-positivity. This is reflected by an upregulation of matrix metalloproteinases in predicted functional protein networks (*STRING* analysis). In our local cohort, we could now validate this upregulation of uPA in SARIFA-positive CRCs on protein level (p=0.0027). For PAI1, a trend towards higher protein levels in SARIFA-positive CRCs could be observed (p=0.209). Moreover, SARIFA-positive CRCs show a higher number of tumor buds (p=0.013) as well as increased FABP4 expression at the invasion front (p<0.001) in our local cohort. In DSP analysis, the stroma fraction of SARIFA-positive CRCs showed significant changes compared to SARIFA-negative cases.
Conclusion: Our current data shows that the formation of SARIFAs and the consecutive direct tumor-adipocyte interaction with a tumor-promoting increase in lipid metabolism may rely on alterations in the plasmin/plasminogen system, which could be a novel potential drug target in the aggressive subset of SARIFA-positive CRCs.

#5157 Development and evaluation of a high-throughput method for rapid detection of surface antigen expression in fixed cells.

Kaja Holtorf[1], Anne-Lise Peille[2], **Daniel Feger**[1], Vincent Vuaroqueaux[2], Jan Erik Ehlert[1], Nadine Obier[1]

[1]Cellular Pharmacology, Reaction Biology Europe GmbH, Freiburg, Germany,[2]4HF Biotec GmbH, Freiburg, Germany

Cell surface proteins are increasingly considered in the development of novel anticancer agents, as demonstrated by recent clinical successes in the field of immuno-oncology and antibody-drug conjugates (ADCs). These conjugates specifically target antigens present on the surface of tumor cells, enabling the delivery of cytotoxic agents to specific tumor sites. During the preclinical development of such compounds, for example, when they are tested on a wide panel of cell lines, it is essential to have a rapid and reliable method for monitoring target expression and distribution.

Complementing our 160 Cell line panel ProLiFiler™, we report here the development of a novel method named oncoFLOW-Profiler™ which includes steps of cell fixation, micronic storage, staining, and measurement by flow cytometry. This method is applied in a 96-well format, enabling screening of all cell lines in parallel and analysis of the expression of different targets in just one day.

In this proof-of-concept study, we investigated the level of ERBB2 expression across the ProLiFiler panel of 160-cell lines in order to validate this methodology. We first compared the impact of fixation methods and sample storage on knowingly positive and negative control cell lines over a period of several months. ERBB2 measurements from the oncoFLOW-Profiler™ will be analyzed and validated by comparison with various OMICs datasets from the Cancer DataMiner platform (4HF Biotec), including RNA expression, mutational status, and protein expression levels. To determine the expression cutoff of ERBB2 amplified models, results will be analyzed according to gene copy number variation. Finally, the flow cytometry data generated will be investigated for use as a predictor of response to clinically approved ADCs targeting ERBB2: Kadcyla and Enhertu.

Here we present a method that we have demonstrated is feasible for investigating cell surface receptor/antigens during preclinical phase of drug development. Our method has enabled us to successfully assess ERBB2 in biological samples and to identify models sensitive to ADCs targeting ERBB2. We will also discuss the results of ongoing experiments analyzing the applicability of this screen to intracellular targets and carbohydrate-based surface antigens, which cannot be analyzed either by transcriptomics or proteomics.

CLINICAL RESEARCH: Predictive Biomarkers 4
Poster Session

#5160 Evaluation of circulating microRNAs as predictive and prognostic biomarkers for advanced melanoma patients.

G. Durante[1], F. Comito[2], M. Naddeo[2], S. De Matteis[2], M. Bonafe[3], E. Dika[3], A. Ardizzoni[3], **M. Ferracin**[3];
[1]University of Bologna, Bologna, Italy, [2]IRCCS Azienda Ospedaliero-Universitaria di Bologna, Bologna, Italy, [3]University of Bologna, IRCCS Azienda Ospedaliero-Universitaria di Bologna, Bologna, Italy

Introduction Metastatic melanoma is the deadliest form of skin cancer whose incidence has been rising dramatically over the last few decades. The advent of Immune checkpoint inhibitors (ICIs) has strongly improved the survival of melanoma patients. However, a high fraction of patients shows primary resistance or will develop secondary resistance during therapy. For these reasons, it is of utmost importance to develop biomarkers that could predict response or resistance to therapies. Among the most promising biomarkers analyzed in peripheral blood there are circulating microRNAs (miRNAs). The aim of this study is to identify a miRNA signature able to predict prognosis and clinical relapse in advanced melanoma patients treated with ICIs.
Methodology We collected longitudinal blood draws from metastatic melanoma patients treated with ICIs at Bologna University-Hospital (Italy). We separated plasma from whole blood, extracted RNA and determined the absolute levels of miR-155-5p, miR-424-5p and miR-320a using EvaGreen-based droplet digital PCR. Moreover, in the subset of first-line anti-PD-1 treated patients, we performed cytofluorimetric leukocyte analysis.
Results and discussion We found that patients with pre-therapy (baseline) high expression of circulating miR-155-5p, miR-320a and mir-424-5p had longer progression-free survival (PFS), and overall-survival (OS). In patients treated with anti PD-1 as first-line treatment, we found that baseline miR-155-5p levels were significantly higher in patients who responded to therapy, and therefore miR-155-5p could have a predictive value. Moreover, using a flow cytometric approach, we noted that baseline miR-155-5p levels correlated with CD4+Naïve (r:-0.91, p:0.027) and CD4+PD1+ T-cells (r:0.94, p:0.015) in patients treated with first-line anti-PD-1 treatment.
Conclusion These preliminary findings propose baseline circulating miRNAs as potential predictive and prognostic biomarkers in the setting of advanced melanoma patients treated with immunotherapy.

#5161 Integrating patient's derived organoids and liquid biopsy: An exploratory study of early stage pancreatic cancer.

M. Cortesi[1], T. Rossi[1], M. Zanoni[1], S. Bandini[1], C. Pacilio[2], A. Cucchetti[3], M. Valgiusti[1], C. Gallio[1], A. Passardi[1], G. Gurioli[1], S. Bravaccini[1], A. Dubini[4], G. Frassineti[1], P. Ulivi[1], G. Martinelli[1], G. Ercolani[3], I. Rapposelli[1];

[1]Istituto Romagnolo per lo Studio dei Tumori "Dino Amadori" - IRST S.r.l., Meldola, Italy, [2]Morgagni-Pierantoni Hospital, AUSL Romagna, Forli, Italy, [3]Alma Mater Studiorum - University of Bologna; Morgagni-Pierantoni Hospital, Ausl Romagna, Bologna, Italy, [4]GB Morgagni L. Pierantoni Hospital, Forli, Italy

Background: Pancreatic cancer (PC) has a 5-year survival of 12% despite recent therapeutic advancements. There is a desperate need to discover novel ways of treating PC since a large proportion of patients do not benefit from therapy and experience significant toxicity. A major cause of therapy failure is therapy resistance due to tumor heterogeneity. Nowadays, a deeper understanding of tumor heterogeneity could be assisted by the use of patients-derived organoids (PDOs). Furthermore, the use of liquid biopsy may allow for the investigation of circulating factors with predictive value and for disease monitoring over time. Methods: Patients were enrolled in the comprehensive, multiomic study of pancreatic cancer CONTAINER. Patients with early stage PC treated with preoperative chemotherapy or undergoing surgery first were selected for the present study. When possible, a surgical specimen was collected to obtain PDOs. Tissue from resected tumors was dissociated by GentleMACS™ dissociator (Miltenyi Biotec), fragments were embedded in Matrigel™ and cultured in PancreaCult™ human Organoid Media (stemcell technologies). PDO histological features were investigated by H&E staining and IHC. Blood samples were collected before and one month after surgery. From blood samples circulating tumor cells (CTCs) were enriched and isolated, extracellular vesicles (EVs) were isolated from plasma with size-exclusion chromatography and their concentration and size distribution was evaluated with NanoSight NS300. Then, EV surface antigens were characterized by flow cytometry. A panel of inflammatory cytokines was finally evaluated through Ella Automated Immunoassay System. Results: In CONTAINER study 113 patients were enrolled and 30 of them underwent surgery. 21 surgical specimens were received from which 18 PDOs were successfully established. EVs with diameter ≥ 70nm were isolated from plasma, EV mean size was similar before and after surgery whereas individual variations in particle concentration and in surface antigen exposure were observed. Correlation with clinical and pathological characteristics of patients will be performed once reached an adequate sample size for statistical analyses. A panel of inflammatory cytokines (IL1β-, IFNγ, TNFα, IL6, IL8, TGFβ1, CRP and Leptin) was assessed in plasma samples obtained before and after surgery. Except for IL1β, a significant individual variation of circulating cytokines before and after surgery was observed. Conclusions: This study will contribute to unveil mechanisms of disease progression and drug resistance in PC. Possible predictive factors and mechanisms of drug resistance will be investigated taking advantage of the information derived from both in vitro models and circulating tumor-related entities.

#5162 Tumor transcriptional identity as a key predictor of clinical outcome in EGFR-Mutant non-small cell lung cancer.

S. Heeke, M. Nilsson, D. Gibbons, J. Zhang, I. I. Wistuba, K. Park, J. V. Heymach, X. Le;
UT MD Anderson Cancer Center, Houston, TX

Background: EGFR tyrosine-kinase inhibitors (TKIs) produce significant clinical benefit in patients (pts) harboring *EGFR*-activating mutations, however, patient outcomes remain heterogeneous, highlighting the need to identify novel biomarkers for treatment response prediction. We aim to investigate the association of tumor transcriptional identity with clinical outcomes in *EGFR*-mutant NSCLC.

Methods: We used consensus classification to derive unsupervised transcriptionally distinct clusters in *EGFR*-mutant NSCLC from the TCGA (N= 44). Then, we built a predictive model using extreme-gradient boosting to (1) classify an additional 88 surgically resected tumors from the LCCS study and analyzed for overall survival (OS) prediction; (2) classify metastatic *EGFR*-mutant NSCLC from the RELAY trial with available RNAseq data (N = 106) and analyzed for progression-free survival (PFS) with erlotinib treatment.

Results: Consensus clustering revealed two distinct clusters, one associated with more lineage-preserving features and one with more lineage-independent features that could transcriptionally distinguish *EGFR*-mutant lung cancer. No differences in primary *EGFR* mutations were detected across the two clusters. Ingenuity Pathway Analysis revealed TGFB1 as the most significantly enriched pathway in the lineage-independent cluster which was also significantly more mesenchymal (p = 0.0028). For surgically resectioned *EGFR*-mutant NSCLC, OS was consistently shorter in the lineage-independent cluster for TCGA (23.6 vs 58.3 mo; p = 0.049; HR = 0.4) and the LCCS cohort (55.7 vs not-reached; p = 0.0073; HR = 0.27). In the metastatic setting with erlotinib treatment, there was a trend for PFS to be shorter in the lineage-independent cluster (15.2 vs 19.4 mo; p = 0.12; HR = 0.61).

Conclusions: Transcriptional identity in *EGFR*-mutant lung cancer are prognostic of clinical outcome. The lineage-independent tumors have inferior benefit to EGFR TKI as well as inferior OS, indicating that transcriptional biomarkers can be independent of oncogene biomarkers. These transcriptional biomarkers may help identify pts with poor outcome for future intensification of therapies.

#5163 Determining the role of septin expression in response of breast cancer patients to microtubule targeted chemotherapy.

T. Aldawoodi, J. N. Essif, A. Naqvi, L. D. Boyle, D. Urueta Portillo, K. Lathrop, A. L. Risinger;
UT Health Science Center at San Antonio, San Antonio, TX

Drugs that disrupt the microtubule cytoskeleton, including both microtubule stabilizing taxanes and destabilizers like eribulin, are regularly used in the treatment of metastatic breast cancer. However, there are currently no molecular biomarkers to guide their use. Septins, a class of small GTPases, interact with both microtubules and actin to functionally link these cytoskeletal components and regulate cell biological processes shown to be critical for the invasion and migration of cancer cells. In particular, septin 9 (SEPT9) directly interacts directly with microtubules through an N-terminal domain on the longest isoform, SEPT9i1, which is sufficient to promote migration and invasion of breast cancer cells in vitro. We hypothesized that the relative expression of septin9 isoforms in breast tumors could play a role in their response to treatment with microtubule-targeted chemotherapy, particularly in the metastatic setting. A retrospective investigation of the relationship between septin expression and response to taxane chemotherapy was conducted utilizing full transcriptome sequencing data from biopsies of 75 breast cancer patients treated at our NCI-Designated Mays Cancer Center who received molecular profiling through Caris Life Sciences. Levels of total SEPT9 expression as well as the expression of specific variants that encode mechanistically distinct septin9 isoforms, SEPT9v1, v2, and v3, were determined for each sample and correlated with demographic, treatment, and outcome data for these patients. The oncogenic sept9_v1 variant (which produces the septin9_i1 isoform) was detected in over half of tumors and those with the highest total septin9 expression also expressed significantly higher levels of this isoform. Strikingly, the expression of total septin9, as well as the v3 variant, was significantly increased in taxane-treated patients who survived over a year after diagnosis with metastatic breast cancer, suggesting that septin9 expression could be a molecular correlate of response to taxane chemotherapy. We found that the expression of total septin9 and its variants was not significantly correlated with race, ethnicity, or cancer type suggesting that our findings would apply to our patient population as a whole, which is over 50% Hispanic. These data were used to support an ongoing prospective study to determine effect of septin expression on response to taxane chemotherapy in the neoadjuvant setting and determine the effect of taxane treatment on septin expression by comparing samples pre and post treatment. Together this work supports our overall goal of identifying predictive biomarkers to facilitate the use of microtubule targeted chemotherapy in a more personalized manner.

#5164 Deployment of ASPYRE-Lung targeted variant panel across three sites and testing with FFPE tissue and cytology-derived nucleic acid samples.

S. E. Herlihy[1], C. Gentile[1], S. J. Scott[2], B. A. Smith[2], K. A. Stoll[2], K. F. Schilter[2], J. Mordaka[3], R. Palmer[3], C. Xyrafaki[3], E. Gillon-Zhang[3], C. King[3], R. Evans[3], A. Green[3], A.-L. Silva[3], M. Stolarek-Januszkiewicz[3], K. von Bargen[3], I. Turner[3], C. Ho[3], A. Collazos[3], N. Potts[3], D. Nugent[3], J. Jose[3], E. Gray[3], E. Shapiro[3], **W. J. Levin**[3], A. Cooke[3], B. Balmforth[3], R. Osborne[3], H. V. Reddi[3], V. M. Van Deerlin[1];

[1]University of Pennsylvania, Philadelphia, PA, [2]Medical College of Wisconsin, Milwaukee, WI, [3]Biofidelity, Morrisville, NC

While there is no shortage of approved targeted therapeutics to address driver mutations in NSCLC, many patients are not tested for these alterations due to gaps in biomarker testing access. Challenges in NSCLC molecular testing include the need for assessment of multiple variants in both DNA and RNA, samples are often small specimens, cost, and clinical need for rapid turn-around time when patients are deteriorating and require timely treatment initiation. ASPYRE-Lung detects a targeted panel of 114 actionable genomic variants across 11 genes, covering NCCN treatment guideline-recommended biomarkers for samples that are associated with NSCLC. The assay simultaneously analyzes DNA and RNA with inputs of only 20 ng and 6 ng respectively. ASPYRE-Lung is easily adoptable by standard clinical laboratories, requiring only PCR and qPCR thermocyclers, with no specialist bioinformatics skills required for analysis and a run time of 2 days from specimen to result. We established the assay at two external sites and Biofidelity laboratories, with multiple operators at each site. We first determined that the assay had acceptable performance at each site, using a panel of contrived control samples. We then examined 56 matched DNA and RNA samples extracted from clinical FFPE lung tissue specimens. We also tested 29 unmatched samples derived from FFPE tissue (13), fine needle aspirate (FNA, 4), FNA rinse (5), peritoneal fluid (1), pleural effusion (1), pleural fluid (1) and fresh tissue (4), at all 3 sites. Data were analyzed using a simple cloud-based turnkey analysis solution. All samples yielded valid results across all runs. We assessed reproducibility (inter-run precision) using all 85 clinical samples, across new and experienced users, achieving a positive percent agreement (PPA) of 100% and negative percent agreement (NPA) of 99.99%. We then assessed concordance with NGS results, investigating any discrepancies. The 69 FFPE tissue-derived samples (56 matched DNA/RNA, 7 unmatched DNA, and 6 TNA) had PPA 96.55% and NPA 99.98%. The 16 cytopathology-derived samples had PPA 100% and NPA 99.96%. Together, these results demonstrate high concordance of ASPYRE-Lung and NGS across different types of clinical samples, alongside ease of adoption of the ASPYRE-Lung assay with simple training and no specialist expertise required. ASPYRE-Lung promises to enable all patients with NSCLC to start appropriate treatment in a cost-effective and timely manner.

#5165 Development and validation of an assay for the characterization of SSTR2 expression on CTCs from liquid biopsies.

E. G. Bayer[1], R. N. Ponting[1], C. M. Kelly[2], A. Lutfi[3], M. K. Afghan[3], A. B. Ramirez[1], P. M. Kasi[3];

[1]RareCyte, Inc., Seattle, WA, [2]Memorial Sloan Kettering Cancer Center, New York, NY, [3]Weill Cornell Medicine, Cornell University, New York, NY

Background: Expression of Somatostatin Receptor subtype 2 (SSTR2) is observed in multiple cancers, including breast and colorectal cancer. Its role as a prognostic or predictive marker is cancer-type dependent. Recently, there has been renewed interest in assessing this biomarker since it plays a critical role as a target for radiotherapeutics (peptide receptor radionuclide therapy - PRRT) in patients with neuroendocrine tumors (NETs). Blood-based liquid biopsies are a non-invasive tool with proven effectiveness in characterizing cancer biomarker expression in patients. In this study, we describe the development and validation of a novel assay to analyze circulating tumor cells (CTCs) for expression of SSTR2 using the RareCyte platform.

Experimental Procedures: Using AccuCyte®, an unbiased density-based method for collecting nucleated cells from whole blood, we transferred nucleated cells to slides and stained for SSTR2, CD45, and CK/EpCAM to identify CTCs (CK+/EpCAM+, CD45-), and evaluate SSTR2 expression. Slides were imaged with CyteFinder®, an automated multiparameter immunofluorescent (IF) microscopy system that applies machine learning algorithms for rare cell identification. Both clinical and spike-in samples were used for assay validation. Single-cell SSTR2 mean fluorescence intensities (MFI) were analyzed to determine protein expression levels. Colorectal cancer with neuroendocrine features and Merkel cell cancer (neuroendocrine tumor of the skin) patient samples were evaluated for CTC enumeration and SSTR2 expression.

Results: The assay's performance metrics for SSTR2 expression were 90+% accuracy, 85% sensitivity, 100% specificity with repeatability and intermediate precision CVs of 14.4% and 16.4%, respectively. A small cohort of colorectal cancer (1) and Merkel cell cancer (2) patient blood samples were tested using the assay. All 3 patients had high CTC levels (300+ per 7.5 mL). The percentage of SSTR2-positive CTCs ranged from 20-60%, reflective of tumor heterogeneity.

Conclusions: SSTR2 is an important target now in the advent of theranostics - PRRT. Prognostic and therapeutic implications of SSTR2 expression is an area of active clinical research. SSTR2 targeted therapeutics like 177Lu-dotatate illustrate the possible utility of SSTR2 as a predictive biomarker of treatment response. To date, most of the work has been focused on assessing SSTR2 on tissue. Herein, we show how a CTC platform can be adapted to assess a clinically relevant cell surface protein biomarker. This is now included as an important correlative in a clinical trial for Merkel Cell Cancer patients called iPRRT that is actively accruing (NCT05583708).

#5166 A multiplexed immunofluorescence assay to assess Rb and phospho-Rb as predictive biomarkers for CDK4/6 inhibitors in HR+/HER2- breast cancer.

M. Tabassum[1], S. Suresh Kanna[1], W. Cao[1], M. Rimawi[2], G. Miles[2], M. Trivedi[1];
[1]University of Houston, College of Pharmacy, Houston, TX, [2]Baylor College of Medicine, Houston, TX

Introduction: Cyclin-dependent kinases 4/6 inhibitors (CDK4/6i) are used as the first-line treatment of advanced/metastatic or high-risk HR+/HER2- breast cancer (BC) that make up about 60-70% of all cases. However, nearly 50% of patients exhibit drug resistance. Therefore, biomarkers that predict CDK4/6i response are needed to spare patients from toxicities and high costs. Resistance to CDK4/6i [palbociclib, ribociclib, and abemaciclib] is associated with the aberrant or loss of Retinoblastoma (Rb). A decline in phospho-Rb (pRb) levels on therapy is also associated with CDK4/6i response. We aimed to develop a multiplex immunofluorescence (IF) assay to assess Rb and pRb levels that can be used on circulating tumor cells (CTCs) to predict tumor response to CDK4/6i. Here, we report the selection of internal controls for Rb and pRb, assay repeatability and reproducibility, as well as compatibility of the CTC isolation protocol with the assay.
Methods: Rb and pRb expression was evaluated by western blotting (WB) and IF in parental (P), estrogen deprivation-resistant (EDR), palbociclib-resistant (PalboR), and EDR/PalboR derivatives of two HR+/HER2- cell lines (MCF7 and T47D), Rb1 KO cells of MCF7 and T47D, as well as triple-negative cell lines, BT549 and MDA-MB-468. IF-stained cells were imaged using Leica STED SP8 confocal microscope and Zeiss Axioscan 7. The concordance between IF and WB results was assessed using a Bland-Altman plot. Selectivity and specificity of the assay as well as repeatability and reproducibility between investigators were also assessed. Blood from healthy subjects was used to test the compatibility of the ScreenCell® filtration system to isolate CTC with the IF assay.
Results: Our initial approach utilized indirect IF staining for Rb and pRb using the same primary antibodies as WB. On the Bland-Altman plot, most data points were relatively close to the bias line, suggesting that the difference between the two methods was acceptable. The analytical range for mean Rb and pRb staining intensity was 0.744 - 46.779 and 1.001 - 52.919, respectively. Based on WB and IF data, we nominated T47D PalboR and MDA-MB-468 cells as negative controls for Rb and pRb expression. The selectivity and specificity were 100% and 70%, respectively, for the Rb expression and 99% and 61% for pRb, respectively. The IF assay was repeatable and reproducible between two investigators. The ScreenCell® CTC isolation method was not compatible with the assay, as Rb and pRb expression was either not detected or limited when processed using FC2 or PBTFC buffer, irrespective of the antigen retrieval.
Conclusion: We have selected internal cell line controls for Rb and pRb and are in the process of optimizing signal-to-noise ratio and specificity using conjugated antibodies. We are also testing the compatibility of other CTC isolation methods with the IF assay.

#5167 Barriers to tumor mutational burden (TMB) testing in oncology care - U.S. Physician Survey.

G. Jones[1], E. Szamreta[1], B. Jackson[2], N. Ning[2], J. Stephens[2], A. Hussain[3];
[1]Merck & Co., Inc, Rahway, NJ, [2]OPEN Health, Bethesda, MD, [3]University of Maryland, Baltimore, MD

Background: Genomic technologies have become increasingly available in oncology; however, barriers remain in terms of TMB use. This study aimed to identify barriers to physicians' adoption/use of TMB testing.
Methods: A cross-sectional online survey was conducted with a representative sample of U.S. general medical, surgical, and/or gynecologic oncologists, including both users and non-users of TMB testing. Physician demographics, practice characteristics, barriers (reimbursement, knowledge, logistics), and approaches to alleviate barriers were collected. Quotas were put in place to ensure a distribution of diverse physician characteristics such as academic affiliations, geography, TMB use, etc. Descriptive analysis was conducted via SASv9.4.
Results: Three hundred physicians participated (47.6 mean years of age and 15.2 mean years in clinical practice on average; 50% medical oncologists, 31% surgical oncologists, and 19% gynecologic oncologists). Ninety percent of respondents reported using TMB testing. The most common barrier to TMB testing use was test turnaround time (All: 74.3%; TMB users: 72.3%; non-TMB users: 93.1%). Other commonly reported barriers included unawareness of corresponding therapy and/or clinical trials that may benefit a patient with mutation (All: 68.3%; users: 66.1%; non-users: 89.7%), obtaining prior authorizations (All: 65.7%; users: 62.7%; non-users: 93.1%), and difficulty obtaining a biopsy for testing (All: 57.3%; users: 57.6%, non-users: 55.2%). Increased coverage of TMB testing, access to educational content, and the establishment of minimally acceptable technical standards were reported as key approaches to increasing adoption/use of TMB testing.
Conclusions: These results suggest that challenges around reimbursement, knowledge, and logistics are key barriers to use of TMB testing for physicians and provide insights for solutions to alleviate the barriers to TMB testing in oncology.

Table 1. Barriers to TMB Test Adoption Reported by Physicians, %

		All N=300	TMB user N=271	Non TMB user N=29	p-value
Reimbursement	Obtain prior authorizations	65.7	62.7	93.1	0.003
	TMB not covered by insurance	53.7	53.5	55.2	>0.99
	Coverage policy refers to TMB as “experimental”/”unproven”	52.7	51.7	62.1	0.26
	Insurance policy restricts genomic tests to particular lab/test provider	51.3	50.6	58.6	0.79
Knowledge/awareness	Unaware of therapy/clinical trials that may benefit a patient with mutation	68.3	66.1	89.7	0.03
	Unaware of approved indications for TMB	51.3	51.3	51.7	>0.99
	Lack of training on TMB	48.7	47.2	62.1	0.28
Logistics	Test turnaround time	74.3	72.3	93.1	0.02
	Difficulty obtaining biopsy	57.3	57.6	55.2	0.87
	Inaccessibility to personnel/lab	49.0	48.3	55.2	0.84

#5168 Analysis of biomarker and outcomes data: 7-year update from COLUMBUS.

R. Dummer[1], **K. Flaherty**[2], S. Deng[3], T. Xie[3], P. Hamilton[3], N. Pathan[4], C. Robert[5], A. Arance[6], J. W. B. de Groot[7], C. Garbe[8], H. J. Gogas[9], R. Gutzmer[10], I. Krajsova[11], G. Liszkay[12], C. Loquai[13], M. Mandala[14], D. Schadendorf[15], N. Yamazaki[16], P. A. Ascierto[17], A. di Pietro[18], C. B. Davis[3];
[1]University Hospital Zurich, Zurich, Switzerland, [2]Massachusetts General Hospital Cancer Center, Boston, MA, [3]Pfizer, La Jolla, CA, [4]Formerly Pfizer, La Jolla, CA, [5]Gustave Roussy and Paris-Saclay University, Villejuif, France, [6]Hospital Clinic of Barcelona and IDIBAPS, Barcelona, Spain, [7]Isala Oncology Center, Zwolle, Netherlands, [8]University Hospital Tubingen, Tubingen, Germany, [9]National and Kapodistrian University of Athens, Athens, Greece, [10]Department of Dermatology, Ruhr University Bochum Campus, Minden, Germany, [11]General Teaching Hospital in Prague, Prague, Czech Republic, [12]National Institute of Oncology, Budapest, Hungary, [13]University Medical Center of the Johannes Gutenberg University Mainz, Mainz, Germany, [14]University of Perugia, Perugia, Italy, [15]University Hospital Essen, West German Cancer Center and German Cancer Consortium, Partner Site Essen; National Center for Tumor Diseases (NCT)-West, Campus Essen, and Research Alliance Ruhr, Research Center One Health, University Duisburg-Essen, Essen, Germany, [16]National Cancer Center Hospital, Tokyo, Japan, [17]Melanoma Unit, Cancer Immunotherapy and Innovative Therapies, Istituto Nazionale Tumori IRCCS Fondazione Pascale, Naples, Italy, [18]Pfizer, Milan, Italy

Background: In the randomized, 2-part, phase 3 COLUMBUS study (NCT01909453), encorafenib (enco) + binimetinib (bini)—an approved regimen in the US, EU, and other countries—improved 7-year PFS and OS vs vemurafenib (vemu) in patients (pts) with BRAF V600E/K-mutant locally advanced unresectable or metastatic melanoma. We investigated genetic and transcriptional correlates of outcomes in an exploratory biomarker analysis of COLUMBUS Parts 1 and 2.
Methods: In Part 1, 577 pts were randomized 1:1:1 to enco 450 mg QD + bini 45 mg BID, enco 300 mg QD, or vemu 960 mg BID; in Part 2, 344 pts were randomized 3:1 to enco 300 mg QD + bini 45 mg BID or enco 300 mg QD. Baseline tumor samples were analyzed using the ACE ImmunoID NeXT whole exome sequencing/whole transcriptome sequencing (WES/WTS) assays (Personalis). PFS and OS were analyzed (cutoff: Jan 13, 2023) by treatment arm and presence of specific genetic or transcriptomic alterations.
Results: Among treated pts, 668 had WES or WTS data. K-means clustering identified 3 major transcriptional clusters: (1) microphthalmia-associated transcription factor (*MITF*)-low (invasive dedifferentiated tumor cell phenotype), (2) *MITF*-high (proliferative melanocytic phenotype), and (3) immune-high. Cluster assignments were significantly associated with biopsy site ($P<0.001$), with cluster 1 enriched in skin biopsies and cluster 3 in lymph node metastases; biopsy site-independent characteristics were also captured. Improved PFS with enco + bini vs vemu was most pronounced in cluster 3 (Table 1). *ERBB2* expression and *PI3KCA* pathway mutation, previously found to be associated with reduced survival benefit with enco + bini vs vemu, were enriched in clusters 1 and 2 vs cluster 3.
Conclusions: Enco + bini showed benefit across molecular subtypes in BRAF V600E/K-mutant melanoma. The contribution of bini was most pronounced in the immune-high cluster. Improved outcomes in this cluster support ongoing trials of combinations with immune checkpoint inhibitors, such as STARBOARD and PORTSIDE.

Table 1. Hazard ratios of PFS and OS for enco + bini or enco vs vemu by cluster

	HR (95% CI) vs vemu			
	PFS		**OS**	
	Enco + bini	**Enco**	**Enco + bini**	**Enco**
Overall	n=255 vs 100	n=159 vs 100	n=255 vs 100	n=159 vs 100
	0.47 (0.35, 0.63)	0.78 (0.57, 1.07)	**0.66 (0.50, 0.86)**	0.85 (0.63, 1.13)
Clusters				
Cluster 1: *MITF*-low	n=72 vs 34	n=44 vs 34	n=72 vs 34	n=44 vs 34
	0.74 (0.44, 1.26)	0.92 (0.51, 1.66)	**0.63 (0.40, 1.00)**	**0.57 (0.34, 0.96)**
Cluster 2: *MITF*-high	n=120 vs 46	n=76 vs 46	n=120 vs 46	n=76 vs 46
	0.48 (0.32, 0.74)	0.75 (0.48, 1.17)	**0.66 (0.45, 0.97)**	0.86 (0.56, 1.32)
Cluster 3: Immune-high	n=63 vs 20	n=39 vs 20	n=63 vs 20	n=39 vs 20
	0.23 (0.12, 0.44)	0.64 (0.33, 1.21)	0.80 (0.40, 1.59)	1.55 (0.76, 3.15)

Numbers are given as the number of pts included in the treatment arm vs the number of pts in the comparator arm (vemu-treated). Statistical significance ($P<0.05$) is shown by bold font. Bini, binimetinib; enco, encorafenib; MITF, microphthalmia-associated transcription factor; pts, patients; vemu, vemurafenib.

#5169 Circulating levels of ANGPTL3, PCSK9, apoCIII and lipoprotein (a) in high-grade serous ovarian cancer.

E. Wong Chong[1], F.-H. Joncas[1], P. Douville[1], D. Bachvarov[1], F. Calon[1], N. G. Seidah[2], C. Diorio[1], A. Gangloff[1];
[1]CHU de Quebec - Universite Laval, Quebec, QC, Canada, [2]Institut de Recherches Cliniques de Montreal, Montreal, QC, Canada

Background: Ovarian cancers require abundant amounts of lipids for their growth. Recent years have highlighted the role of ANGPTL3, PCSK9, ApoCIII and Lp(a) as key players in lipid metabolism. But circulating levels of these factors in ovarian cancers have not been thoroughly investigated to date.
Objective: We assessed the profiles of plasma ANGPTL3, PCSK9, ApoCIII and Lp(a) in ovarian high-grade serous carcinoma (HGSC).
Methods: Plasma samples collected from women diagnosed with an HGSC (n=31) or a benign ovarian lesion (BOL, n=40) were analyzed for plasma lipid profile (ApoB, total cholesterol, HDL, triglycerides, Lp(a) levels) on a clinical modular platform (Roche). ApoCIII, ANGPTL3 and PCSK9 levels were measured with commercially-available ELISA kits. Differences between HGSC and BOL were assessed by two-group comparisons. Pairwise correlation strength between variables was evaluated with Spearman's rank order tests. Logistic regression modelling was used to further examine the associations between selected variables and HGSC diagnoses.
Results: ANGPTL3 levels increased in HGSC (84.1 ng/ml, SD=29.2ng/ml, n=31) compared to BOL (66.9ng/ml, SD=30.7 ng/ml, n=40; HGSC *vs* BOL p=0.02). Receiver operating characteristic (ROC) curve suggested that plasma ANGPTL3 levels were moderately associated with HGSC (AUC=67.7%, p=0.005 1) and did not increase predictive performance of ovarian tumor biomarkers CA125 and HE4 in multivariable model. Associations between ANGPTL3 levels and cholesterol (HDL, non-HDL, LDL and total) could be observed in the control group but not in the HGSC group. The same dissociation was observed for the inverse correlation between HDL and triglycerides in HGSC. Furthermore, moderate associations were observed between PCSK9 & CA19-9 in the entire cohort (rho=0.34, n=53, p=0.013) and Lp(a) & CA125 in HGSC cases (rho=0.51, p= 0.017).
Conclusion: In this cohort of 71 women, we report increased levels of ANGPTL3 in HGSC with an effect size (Cohen's D) of 0.57. Confirmation of this result in larger cohort studies (minimal n>50 in each group) would warrant further investigation into the roles of circulating ANGPTL3. Its inhibition may allow to tackle deregulated lipid metabolic pathways contributing to ovarian cancer progression.

#5170 Novel dSTRIDE-HR assays can accurately assess DNA repair defects in human cancers and distinguish HR status of tumors.

M. Jarosz[1], Z. Prucsi[1], F. Sierpowski[1], K. Stepien[1], S. Ostrowska-Paton[1], S. Koman[1], N. Riaz[2], S. Powell[2], F. Pareja[2], E. da Silva[2], M. Kordon-Kiszala[1], K. Solarczyk[1];

[1]intoDNA, Krakow, Poland, [2]Memorial Sloan Kettering Cancer Center, New York, NY

Accurate patient stratification is crucial for the successful application of targeted anti-cancer therapeutic approaches. It has been shown that PARP inhibitors are synthetic lethal with defective homologous recombination (HR) repair, with genes such as BRCA1 and BRCA2 identified as conferring therapy resistance or sensitivity, depending on their mutational status. Moreover, there is evidence of patient benefit of carboplatin-based therapy in HR deficient (HRD) tumors. With a growing emphasis on HRD in cancer treatment, efforts have been made to define the HRD phenotype. Nonetheless, the current approaches employed in the clinic, such as Next Generation Sequencing (NGS), HRD score or RAD51 assays have significant limitations and their interpretation can be unclear.

To answer the need for a functional HR-specific biomarker, we have recently developed and introduced two new assays, called collectively dSTRIDE-HR. The assays are based on the STRIDE platform technology that enables direct and sensitive detection of single- or double-strand DNA breaks *in situ* in fixed cells. Novel dSTRIDE-HR explicitly detect double-strand DNA breaks localized in close proximity to RPA (dSTRIDE-RPA) or RAD51 (dSTRIDE-RAD51) proteins. The assays have been shown to be reliable reporters of HR activation in cellular models after exogenous DNA damage induction, yet their potential to predict HR status in an *in vivo* setting has not been tested so far.

To assess the suitability of the dSTRIDE-HR assays for determining the HR status of patients' tumor cells, we applied these assays in FFPE sections from biopsies derived from breast cancer patients with a different mutational status of BRCA1 and BRCA2 genes. The assays showed low dSTRIDE-RPA and dSTRIDE-RAD51 readouts in BRCA1/2 mutated tumors in comparison to wild type tumors, as well as a great concordance of readouts within a given genetic background. Additionally, the cell cycle analysis proved nearly twofold increase in foci numbers of dSTRIDE-RPA and dSTRIDE-RAD51 in G2/S phase.

Our study unveils a potential of dSTRIDE-HR assays to become predictive biomarkers reporting on the status of HR repair in breast tumors, although more patient samples need to be tested to confirm initial findings.

#5171 CD39, CD73 and CD38 as potential biomarkers for monitoring the response to mogamulizumab in Sézary syndrome.

Yuliya Yakymiv[1], **Sara Marchisio**[1], Erika Ortolan[1], Verdiana Pullano[1], Chiara Leso[1], Rebecca Senetta[2], Lorenzo Marega[1], Gabriele Roccuzzo[1], Pietro Quaglino[1], Ada Funaro[1]

[1]Medical Sciences, University of Torino, Torino, Italy,[2]Oncology, University of Torino, Torino, Italy

We demonstrated aberrant expression of CD39 or CD73 and low expression of CD38 in circulating and skin-homing CD4+ T cells in patients with Sézary syndrome (SS), an erythrodermic cutaneous T-cell lymphoma (CTCL) with a leukemic component. The anti-CCR4 monoclonal antibody Mogamulizumab (Moga) has been shown to increase progression-free survival in patients with advanced SS. Here, we longitudinally explored the modulation of the expression of CD39, CD73 and CD38 in circulating CD4+ T cells from SS patients under treatment with Moga. Eight patients with relapsed/refractory SS were included in the study and prospectively followed up for two years (median duration of treatment 9,5 months, range 5-28 months). Seven out of eight (87,5%) patients showed early complete response in the blood and partial (5/7, 71,4%) or near complete response (2/7, 28,6%) in the skin. One patient (12,5%) showed no blood or skin response to the treatment. Flow cytometry analysis highlighted that the clinical response was accompanied by a rapid and remarkable increase in CD38 expression in the residual circulating CD4+ T cells, as well as in CD8+ T cells. Moreover, in six patients carrying the homozygous G/G or heterozygous A/G *ENTPD1* SNP rs10748643 genotypes, permissive to CD39 overexpression in T cells, the increased CD38 expression was paralleled by rapid reduction/loss of CD39. Notably, in one patient carrying the A/A genotype, characterized by low CD39 and high CD73 expression at the baseline, response to treatment was characterized by reduction of CD73 expression. The only one patient with A/A genotype who didn't respond to Moga showed no modulation of CD38 or CD39 expression, while CD73 expression increased. Noteworthy, Moga increases the expression of CD38 in responding patients, and influences the expression of CD39 only in patients with the permissive CD39 genotypes (G/G; A/G), but not in those with the A/A genotype. Two patients showing initial response to Moga experienced skin progression during treatment, which was associated with a significant increase of CD39 and simultaneous decrease of CD38 in residual circulating CD4+ T cells, although there was no evidence of blood relapse. These preliminary results suggest that partial or complete responses to Moga is paralleled by reduced CD39 and/or CD73 expression and increased CD38 expression. Instead, an opposite modulation of these markers is associated with disease progression hinting at the potential clinical utility of CD38, CD39 and CD73 as markers to monitor patients' response to Moga therapy.

#5172 miRNA lncRNA network associated with response to cemiplimab in cutaneous squamous cell carcinoma.

L. Porcelli, S. De Summa, R. Fasano, M. Guida, T. M. Marvulli, T. Rafaschieri, G. De Palma, S. Serrati, R. Di Fonte, I. De Risi, S. Strippoli, S. Tommasi, A. Azzariti;
IRCCS Istituto Tumori Giovanni Paolo II, BARI, Italy

Introduction: For advanced cSCC the use of immunological therapies relies on the biology of the tumor, characterized by high mutational burden. However, although the anti-PD1 cemiplimab showed to be a promising treatment option, future research focusing on the use of biomarkers to predict treatment response are needed. Since increasing number of studies has revealed the crucial roles of non-coding RNAs, such as miRNAs and lncRNAs in the development of SCC, the present study had the purpose to explore the lncRNA-miRNA-mRNA networks associated with response to anti-PD1. For this purpose the experimental procedure envisaged a preliminary in silico analysis followed by the investigation of identified miRNA and lncDNA in liquid biopsy.
Methods: For the in silico study, GSE139505 RNA-sequencing raw data have been retrieved from SRA, including 7 Healthy Samples and 9 cSCC biopsies. Two matrices have been prepared, including coding genes and lncRNAs. Normalized coding gene matrix have been used as input to perform GSEA. Coexpression analysis between lncRNAs and Core enrichment genes resulting from GSEA was performed. Biological network including validated miRNA-gene interactions (TarBase) and lncRNA-miRNA interactions (lncBase) has been built-up through Cytoscape. MCODE analysis to identify subnetwork with the closest relationships was performed. The quantification of identified miRNAs (miR-125a, miR-125b, miR-148a, miR-148b) and lnc (AF131217.1, RP11-362F19.1, PVT1, LINC00665) was performed in pre-therapy plasma samples of 34 cSCC patients, categorized according to clinical response to cemiplimab, in responders and non-responders. miRNA-specific RT primers were used for reverse transcription by ddPCR.
Results: The computational analysis revealed a significant enrichment of two gene sets related to immunotherapy, namely the Reactome_PD1_signaling and WP_Cancer_Immunotherapy_by_PD1_blockade. The coespression analyses highlighted more than 600 correlations gene-miRNA-lncRNA for the two above-mentioned genesets. CD4-miR-125a/b and AF131217.1/RP11-362F19.1 are strongly correlated for the first one; whilst, regarding the latter one, CD274/HLA-A with mir-148a/b and PVT1/ LINC00665 and JUN with mir-125a/b and AF131217.1/RP11-362F19.1 were found. The validation in cSCC plasma samples evidenced the significant correlation between mir-148a/b and PVT1/LINC00665 and an higher expression of all miRNAs in responders respect to non-responders. The longitudinal study assessing the correlation between miRNA expression and response to cemiplimab is ongoing.
Conclusion: Preliminary analysis in pre-therapy plasma samples of cSCC validated the in silico data highlighting the inverse correlation between miR-148a/b and lnc (PVT1 and LINC00665). Further investigation will confirm the role of miR125a/b and miR148a/b as predictors of cemiplimab response.

#5173 TRAIL expression in tumor cells predicts and drives poor response to neoadjuvant immunochemotherapy in esophageal squamous cell carcinoma.

W. Yang[1], F. Wang[1], J. Guo[1], J. Cai[2], Z. Wang[1], Y. Liu[1], Z. Fang[1], W. Chen[1], L. Xu[1], S. Zhang[1], B. Zeng[1], Z. Liu[1], S. Peng[1], S.-C. J. Yeung[3], **C. Cheng**[1]; [1]The First Affiliated Hospital of Sun Yat-sen University, Guangzhou, China, [2]Sun Yat-sen University, Guangzhou, China, [3]The University of Texas MD Anderson Cancer Center, Houston, TX

Background: Neoadjuvant PD-1 blockade combined with chemotherapy has shown promising antitumor efficacy in the therapy of esophageal squamous cell carcinoma (ESCC). However, effective biomarkers and potential mechanisms of resistance to this treatment are still unclear.

Methods: We prospectively collected pre- and post-neoadjuvant treatment ESCC tissues from 40 patients who received PD-1blockade (camrelizumab, 200mg) and chemotherapy (albumin-paclitaxel, 260mg/m^2 and carboplatin, area under the curve = 5). Based on their pathological responses to neoadjuvant immunochemotherapy (NICT), patients were classified into “responder” and “non-responder” groups. All samples were subjected to bulk RNA-sequencing and whole-exome sequencing. Of note, samples from 14 patients in both groups were subjected to single cell RNA sequencing and TCR sequencing. We characterized and validated the changes in the immunological landscape of “responder” and “non-responder” groups using multi-omics sequencing data, multiplex immunofluorescence, *in vitro* and *in vivo* experiments. External validation cohorts of ESCC treated with NICT were analyzed to validate the predictive biomarkers for NICT.

Results: We found that TNF-related apoptosis-inducing ligand (TRAIL) signaling was significantly higher in pre-treatment non-responders than in responders, and was inversely correlated with T cell proliferation and TCR expansion. TRAIL was mainly secreted by tumor cells and bound to its specific receptor DR5 in T cells, thereby inhibiting the activation of T cells. Functional co-culture experiments and T cell cytotoxicity assays revealed that TRAIL$^+$ tumor cells mediated T cell suppression and caused CD8$^+$ T cell dysfunction. Furthermore, TRAIL inhibition could improve the efficacy of anti-PD-1 in a xenografted mouse model. In bulk RNA-seq (n=40), TRAIL expression was associated with worse disease-free survival and overall survival, however, these results were not observed in the ESCC cohort treated with upfront surgery from the TCGA database, suggesting that the predictive value of TRAIL is specific to NICT. In an external validation cohort of ESCC patients treated with NICT (n=81), multivariable Cox regression analysis showed that high TRAIL expression was an independent risk factor for unfavorable outcomes. Importantly, TRAIL expression exhibited a higher accuracy in predicting NICT response compared with PD-L1 expression in ESCC (AUC of ROC curves: 0.886 vs 0.607, respectively P<0.001). Meanwhile, the serum concentrations of TRAIL (measured by ELISA) in pre-NICT ESCC patients were also significantly higher in non-responders (n=58).

Conclusions: TRAIL expression in tumor cells is negatively correlated with the response of ESCC to NICT. TRAIL expression may serve as a promising biomarker to predict NICT response and guide NICT selection in ESCC patients.

#5174 Organoids to predict treatment response in metastatic colorectal cancer (OPTIC).

L. P. Smabers[1], E. Wensink[1], C. S. Verissimo[2], M. Doorn[2], T. Yang[2], T. Voskuilen[2], Y. Abouleila[2], M. A. Huismans[1], L. Valkenburg-van Iersel[3], G. A. Cirkel[4], E. C. Gootjes[5], F. J. Jeurissen[6], G. M. Bol[1], H. H. Nienhuis[1], M. M. N. Braat[1], B. Penning de Vries[1], S. G. Elias[1], E. Cuppen[7], R. G. Vries[2], O. Kranenburg[1], M. Koopman[1], S. F. Boj[2], J. M. L. Roodhart[1];

[1]UMC Utrecht, Utrecht, Netherlands, [2]HUB Organoids B.V., Utrecht, Netherlands, [3]Maastricht University Medical Center, Maastricht, Netherlands, [4]Meander Medical Center, Amersfoort, Netherlands, [5]Radboud University Medical Center, Nijmegen, Netherlands, [6]Haaglanden Medical Center, The Hague, Netherlands, [7]Hartwig Medical Foudation, Amsterdam, Netherlands

Introduction: The inability to predict treatment response results in unnecessary toxicity, decreased efficacy and survival. There is a clinical need for an effective biomarker to select patients for cancer treatment. A promising biomarker for treatment efficacy is response testing on patient-derived organoids (PDOs). For metastatic colorectal cancer (mCRC), larger prospective studies are needed to evaluate the predictive value of standardized PDO screens.

Methods: OPTIC is an ongoing prospective multicenter trial (NL61668.041.17, started 2018) that will evaluate the value of tumor PDOs in therapy response prediction. We establish PDOs for mCRC patients from newly obtained biopsies, prior to the start of treatment. We compare PDO sensitivity (area under drug response curve) with patient response measured by changes in biopsied metastatic lesion size on CT scans. Secondary outcome measures are RECIST response and progression-free survival. We evaluate the feasibility of using PDOs as a biomarker by examining drug screen availability in a clinically relevant timeframe of 4 weeks. From 2020 onwards, we incorporated whole genome sequencing (WGS) on fresh-frozen biopsies to correlate drug response in vitro and in vivo, to genetic tumor characteristics. Additionally, PDO screens with experimental drugs based on genetic alterations identified by WGS could be performed. Trial inclusion will continue until 85 PDOs from clinically evaluable patients for standard of care (SOC) treatment are established, with expected completion in Q1 2024.

Results: Currently, 206 patients were included in 5 hospitals and 180 biopsies were taken. PDO establishment success gradually increased from 22% in 2018-2020 to 75% in 2023, yielding an overall success rate of 50% (n=84 PDOs and 13 in culture). Critical factors in optimizing culture success were replacement of several growth factors in the culture medium, reducing time to processing and more frequent handling of biopsies. We have established PDOs for comparing with patient response for the following treatment categories: 5-fluorouracil (n=4), CAPOX/FOLFOX (n=23), irinotecan/FOLFIRI (n=11), FOLFOXIRI (n=12), trifluridine/tipiracil (n=14), panitumumab (n=14), encorafenib-cetuximab (n=2), non-SOC drugs (n=4). We have successfully screened the first 8 PDOs in consistent technical triplicates and biological duplicates ($R<0.88$, $p<0.02$). WGS succeeded in 76% (n=75), primarily failing when tumor percentage was <20%.

Conclusion: We improved PDO establishment success to 75% which is essential to facilitate the implementation of PDOs in clinical treatment. OPTIC will enhance the clinical application of PDOs by defining thresholds for PDO sensitivity and analyzing the diagnostic power for different treatments. To enable personalized treatment in clinical practice, PDO screening should guide mCRC treatment and result in enhanced chance of response and reduced over- and mistreatment.

#5176 TIGIT expression increases with advancing clinical stages and does not differ across racial groups in resected pancreatic cancer.

M. George, J. Clark, K. Gartrelle, G. Nassif, K. Hartway, D. Long, D. Salas-Escabillas, A. Wombwell, T. Pichardo, H.-J. Wen, S. Benitz, S. Zwernik, R. Shah, H. Park, P. Philip, G. Khan, H. Crawford, D. Kwon, B. Theisen, N. Steele;
Henry Ford Health, Detroit, MI

Pancreatic ductal adenocarcinoma (PDAC) has a dismal 12% 5-year survival rate (SEER) due to a lack of early detection biomarkers and resistance to standard therapeutic options (surgery, chemotherapy, radiation). Black African Americans (BAA) have 20% increased incidence of PDAC compared to those with European Ancestry (EA). TIGIT, an immune checkpoint receptor, is a marker of T cell exhaustion and plays a key role in the inhibition of anti-tumor immune responses. Recent studies have demonstrated that immune checkpoint receptor expression (PD-1 and TIGIT) on specific T cell populations correlates to worse overall survival (OS). TIGIT inhibitors are being explored in clinical trials in pancreatic cancer due to implications of its ligand (CD155) promoting immune evasion. We hypothesize that targeted anti-TIGIT therapy, in conjunction with other therapies targeting the tumor microenvironment, could reverse the immune suppression that is characteristic of PDAC. We performed RNAscope in situ hybridization (ISH) with a probe specific for human TIGIT mRNA (combined with a nuclear counterstain) on 79 tissue samples. The cohort of tissue samples included 8 biopsies (endoscopic-guided fine needle biopsies at time of diagnosis), 66 primary (from surgical resection), and 5 metastatic (liver core biopsies from patients with a primary PDAC diagnosis) formalin-fixed paraffin-embedded (FFPE) tissue sections from patients with histologically confirmed PDAC. After cells were segmented based on nuclear recognition, the presence of TIGIT probe within the cytoplasm of each cell was determined and quantified. Percent positive cell values were then exported for statistical analysis in R. De-identified clinical metadata was obtained from REDCap, a cloud-based HIPAA-compliant database used to compile patient data for research purposes. We tested for associations between %TIGIT present and clinical covariates, using linear regression for continuous outcomes, and logistic regression for binary outcomes. ScRNAseq revealed that TIGIT mRNA is enriched in, but not exclusive to the T/NK cellular compartments in PDAC. Staining analysis showed that TIGIT expression did not differ significantly between racial groups (comparing BAA to non-BAA). The mean percentage of TIGIT positive cells was 64.0%. High expression of TIGIT was associated with clinical stage, where an increase in stage was associated with increasing %TIGIT ($p < 0.05$).The TIGIT biomarker assay can be conducted at time of diagnosis, time of surgical resection, and time of metastatic biopsy. If patients' samples contain high levels of TIGIT expression, these patients may be candidates for anti-TIGIT drug therapy. Considering that TIGIT expression correlates with advancing clinical stage, patients with more advanced staging at diagnosis (stage IIB, III, IV) especially may benefit from anti-TIGIT therapy.

#5177 *Ex vivo* assessment of cellular mass response predicts clinical efficacy in solid tumors.

R. Kimmerling[1], M. Stevens[1], S. Olcum[1], M. Vacha[1], R. LaBella[1], K. Katsis[1], R. Aikens[1], C. Hannah[2], A. Guo[1], J. Fujii[3], Z. Shaheen[3], S. Sundaresan[3], A. Rainey[2], A. M. Blakely[2], J. Hernandez[2], A. Tamrazi[4], C. Reid[1];

[1]TRAVERA, Medford, MA, [2]NIH/NCI, Bethesda, MD, [3]Sequoia Hospital, Redwood City, CA, [4]Palo Alto Medical Foundation, Redwood City, CA

Introduction: Identifying personalized, efficacious therapies for cancer remains an urgent unmet need in oncology. While genomics-based biomarkers have demonstrated significant progress, they are not universally applicable, with most patients still treated using clinical guidelines.

Experimental procedures: We have previously demonstrated broad clinical applicability of a functional precision medicine (FPM) workflow that incorporates high-resolution measurements of single-cell mass changes in response to drugs. As a highly integrative biomarker of cellular state, mass change serves as a rapid and mechanism agnostic readout of drug response, demonstrating an ability to detect signal from over 100 different cytotoxic and targeted therapies within 24 hours of treatment *ex vivo*. As a single-cell assay that requires as few as 10,000 cells to assess drug response, this method does not require any *ex vivo* culture for cell expansion and is compatible with a range of clinically relevant tissue specimen formats. Together, these features have enabled this mass response framework to be implemented in a CLIA-certified laboratory with a reporting turnaround time of just two days.

Summary of the new, unpublished data: Having previously shown that mass response testing is compatible with various solid tumor specimen formats such as malignant fluids, core biopsies and fine needle aspirates, here we present preliminary results that demonstrate compatibility with surgically resected tissue specimens. Specifically, we demonstrate that mass response testing results correlate with clinical response across of broad array of solid tumors. In our cohort of 24 patients, we found that mass response measurements correlated with clinical response to therapy with an accuracy of 83% (OR=19.66, P=0.003). Within this group, we also found clear examples of how mass response testing can serve as a valuable complement to existing genomic approaches to guide therapy. Importantly, we demonstrate both concordant and discrepant results using small molecule inhibitors in the setting of known biomarkers of response, highlighting the need for functional testing in precision cancer medicine.

Conclusions: These results support that mass response testing is feasible and broadly applicable to solid tumor malignancies and may serve as a valuable complementary readout for informing therapeutic selection for cancer patients.

#5178 Guided by a predictive *ex vivo* test: Bringing the PLK1 inhibitor volasertib back into the clinic for venetoclax-HMA relapsed/refractory acute myeloid leukemia patients.

M. D. Lacher[1], G. Michelson[1], A. Ling[1], W. Anderson[1], J. Vinas[1], C. J. Gu[1], C. Leonardi[1], J. Wagner[1], G. N. Mannis[2];
[1]Notable Labs, Foster City, CA, [2]Stanford University, Stanford, CA

INTRODUCTION: Volasertib, a polo-like kinase 1 (PLK1) inhibitor, has a roughly 30% CR/CRi response rate in de novo acute myeloid leukemia (AML) patients when combined with low-dose cytarabine. However, its development was halted due in part to toxicity in a Phase 3 study. We have built a flow cytometry-based, high-throughput predictive precision medicine platform to forecast clinical responses to various treatments. Here, we present our design plan for a Phase 2a clinical trial with volasertib in relapsed/refractory (R/R) AML using a modified protocol to reduce toxicity and the development of a companion diagnostic to predict responders in a follow-up Phase 2b study.

METHODS: We will initiate an open-label clinical trial in AML with volasertib in venetoclax-hypomethylating agent (HMA) R/R patients while co-developing a companion diagnostic to selectively enroll predicted responders in a follow-up, Phase 2b, study. Primary and secondary objectives will focus on efficacy/safety of intravenous volasertib and *ex vivo* responses, respectively. To reduce the toxicity seen in the Phase 3 study, specific strategies like tailored dosing will be implemented. To develop the clinical trial assay, peripheral blood or bone marrow samples were collected from AML patients and treated *ex vivo* with volasertib for 3 days. Surviving blast cells were enumerated by flow cytometry. Using a dynamic separation model restricted to the 35% most sensitive samples, we estimated optimal blast cutoffs for volasertib sensitivity.

RESULTS: In single-agent experiments with 41 primary AML samples (31 de novo, 9 R/R, 1 with disease status unclear), we observed dose-response profiles consistent with volasertib's role as a cell cycle inhibitor. Irrespective of the disease status, median and mean EC_{50} values were about 10 nM (1st-3rd quartile from 7-12 nM). To identify an optimal concentration of volasertib for patient stratification, we compared the *ex vivo* resistant blast fractions at each concentration with the areas under the dose-response curves (AUCs), assuming that in our case, AUCs most accurately reflect clinical responses. At 31.6 and 100 nM, the Pearson correlation coefficients were highest ($r > 0.8$), suggesting that these are optimal stratifying doses. With these concentrations and corresponding blast cutoff values, 32-33% of the de novo and 25% of the R/R patients would have been predicted to be responders were they given volasertib, assuming a positive predictive value of 100%.

CONCLUSION: Volasertib's EC_{50} values clustered within a narrow range, suggesting that EC_{50} may not be a suitable metric to stratify patients into responders and nonresponders, in contrast to AUCs and residual blast fractions at 31.6 and 100 nM of volasertib, which displayed more heterogeneous distributions. Limitations include small sample sizes, especially for the R/R group.

#5179 Tumor microenvironment (TME) biomarkers of TIGIT and PD-L1 immune checkpoint blockade in cervical cancer: An exploratory biomarker analysis from SKYSCRAPER-04 (SKY04) study.

V. Krishnan[1], C.-W. Chang[1], E. Bader[1], R. Salani[2], B. J. Monk[3], Y.-M. Kim[4], S. Ghamande[5], S. L. Hall[6], D. Lorusso[7], L. Barraclough[8], L. Gilbert[9], A. Guzman Ramirez[10], C.-H. Lu[11], D. Berton[12], N. Colombo[13], M. Castro[1], Y. G. Lin[1], M. McCormack[14], L. Molinero[1],

[1]Genentech, Inc., South San Francisco, CA, [2]David Geffen School of Medicine, UCLA, Los Angeles, CA, [3]HonorHealth University of Arizona College of Medicine and Creighton University School of Medicine, Phoenix, AZ, [4]Gynecologic Cancer Center, Asan Cancer Institute, Asan Medical Center, University of Ulsan, Seoul, Korea, Republic of, [5]Georgia Cancer Center, Augusta University, Augusta, GA, [6]National Cervical Cancer Coalition, Research Triangle Park, Durham, NC, [7]Fondazione Policlinico Gemelli and Catholic University of the Sacred Heart, Rome, Italy, [8]The Christie NHS Foundation Trust, Manchester, United Kingdom, [9]Department of Gynecologic Oncology, McGill University Health Centre, Montreal, QC, Canada, [10]Instituto de Investigacion en Ciencias Medicas (ICIMED), San Jose, Costa Rica, [11]Taichung Veterans General Hospital, Taichung, Taiwan, [12]Institut de Cancerologie de l'Ouest, Saint Herblain, France, [13]Department of Medicine and Surgery, University of Milan-Bicocca and Gynecologic Oncology Program, European Institute of Oncology IRCCS, Milan, Italy, [14]Department of Oncology, University College London Hospitals, London, United Kingdom

Introduction: Immune checkpoint inhibitors are active in advanced cervical cancer. SKYSCRAPER-04 (NCT04300647) explored the clinical activity of Tiragolumab (T, anti-TIGIT) plus atezolizumab (A, anti-PD-L1) dual blockade (T+A) in patients (pts) with PD-L1+ cervical cancer. This study aimed to evaluate the histological, transcriptomic and genomic TME biomarkers associated with both immune checkpoint blockade (ICB: combined A and A+T arms) and predictive of T clinical outcome.

Methods: FFPE tumor biopsies were collected from patients with recurrent/persistent PD-L1+ cervical cancer (n=171). Samples were tested for PD-L1 (high [TAP ≥10%] vs low [TAP 5-9%]), stromal tumor infiltrating lymphocytes (sTIL by H&E, n=168), immune phenotypes (inflamed, excluded, desert) and total CD8 T cells by CD8/PanCK dual IHC (n=163), TIGIT IHC (n=166), tumor DNA NGS panel (FoundationOne CDx, n=95), and RNA sequencing (RNA Access, n=168) for biological pathways. Biomarker association with outcome was performed with chi-squared test for ORR and Cox-regression analysis for PFS and OS. Analyses are not adjusted for multiple testing.

Results: Biomarkers associated with PD-L1 and TIGIT biology were evaluated for association to clinical outcome in ICB or T analysis. Pts with PD-L1 high tumors had higher ORR and longer PFS and OS, while IFNg/IFNa pathways (RNA) were associated with higher ORR and TIGIT IHC was only associated with longer ICB OS. In contrast, RNA signatures of highly proliferative tumors were negatively associated with ICB ORR. sTILs (IHC) and PVR (RNA) were numerically linked to higher ORR, PFS and OS in T+A vs A arms. The subgroup of patients analyzed for genomic profile (55% of randomized population) showed that TMB high (≥10 mut/Mb; 26% of pts) had higher ORR for ICB and numerically longer PFS and OS than TMB low (<10 mut/Mb). Mutations (mut) of activated *PTEN/PIK3CA/AKT* pathway was the most prevalent feature (52%) and pts with *PIK3CA*-mut had higher ICB ORR, PFS and OS.

Conclusions: This exploratory analysis suggests that increased tumor immunity and mutation burden (TMB and *PIK3CA*-mut) correlates with improved ICB clinical outcomes. No biomarkers were clearly associated with tiragolumab outcome. These results are hypothesis generating and should be confirmed in an independent dataset.

#5180 Pharmacodynamic biomarker analysis of gastrointestinal cancer patients treated with metronomic chemotherapy in the Italian COMET Trial.

M. L. Manca[1], D. Prospero[2], S. Darvishi[2], A. Bandini[1], M. Banchi[1], P. Orlandi[1], H. Padilla[2], A. Sanchez[2], C. E. I. Perucho[2], N. de Avila[2], H. Padilla[2], B. E. Ortega[2], R. D. Stewart[2], M. Santillan[2], V. Lopez[2], R. Kirken[2], G. Allegrini[1], G. Bocci[1], **G. Francia**[2];

[1]The University of Pisa, Pisa, Italy, [2]The University of Texas at El Paso, El Paso, TX

Metronomic, or continuous low-dose, chemotherapy produces antitumor effects through multiple mechanisms. These include inhibition of angiogenesis and activation of the immune system. At AACR 2017 we presented a small, proof-of-concept, multiplex analysis of 14 cytokines specifically chosen by their association with activation of the immune system. The 14 cytokines were evaluated in 31 out of 38 patients with advanced refractory gastrointestinal tumors, enrolled in a phase II clinical trial of metronomic UFT (a 5-fluorouracil prodrug; 100 mg/twice per day p.o.) and cyclophosphamide (500 mg/mq2 i.v. bolus on day 1 and then 50 mg/day p.o.) plus celecoxib (200 mg/twice a day p.o.); the Italian COMET trial (Clinical Trial ID NCT02926911; Allegrini et al. Angiogenesis 2012: 15(2):275-86). We evaluated baseline (day 0) plasma levels with levels at days 28 and 56, and tested for correlations with observed Progression Free Survival, which we then reported (Valenzuela et al. Clin Exp Med. 2021: 21(1):149-159). We now present a comprehensive analysis of 75 cytokines in 34 of the 38 patients. Furthermore we extend the analysis to include baseline (day 0), days 28 and 56, and days 84 and 112 of the COMET trial, and we also correlated specific cytokines levels with Overall Survival. After an estimation of optimal cut-off points of plasma levels of the cytokines, survival analysis was performed, and log-rank tests and cox regression analyses were applied. We show that pre-treatment plasma level <435.46pg/ml of macrophage-derived chemokine (MDC), was a predictive marker for those patients with better progression-free survival at 3 and 6 months (log-rank test p=0.0046; Cox regression analysis p=0.016). Moreover, baseline plasma levels of three cytokines, including monocyte chemoattractant protein 2 (MCP-2), monocyte chemoattractant protein 4 (MCP-4) and TNF-related apoptosis-inducing ligand (TRAIL), were associated with an improved overall survival. MCP-2 values >26.21pg/ml (log-rank test p=0.0012; Cox regression analysis p=0.007), MCP-4 >72.97pg/ml (log-rank test p=0.012; Cox regression analysis p=0.019) and TRAIL >60.73pg/ml (log-rank test p=0.0059; Cox regression analysis p=0.011) were predictive markers for subjects with a better overall survival at 6 and 9 months. These results indicate that a methodology based on the detection of optimal cut-off points and survival analysis allowed the selection of potential biomarkers, such as MDC or MCPs. We propose that the systematic use of these statistical strategies, aimed at detecting potential biomarkers, could help to identify those patients that are likely to benefit from metronomic chemotherapy schedules. This would allow the stratification of such patients for future metronomic chemotherapy trials, and the potential identification of patients that should instead be offered alternative therapeutic strategies.

#5181 Early activity and biomarker evaluation of NT219 in combination with cetuximab in a Phase 1/2 study of recurrent/metastatic squamous cell carcinoma of the head and neck (R/M SCCHN).

A. J. Rosenberg[1], S. Kato[2], D. Johnson[3], A. Popovtzer[4], V. Chiu[5], R. Geva[6], H. Ben-David[7], T. Meirson[7], M. Schickler[7], **H. Reuveni**[7];
[1]The University of Chicago, Chicago, IL, [2]UCSD Moores Cancer Center, San Diego, CA, [3]Ochsner Health, New Orleans, LA, [4]Hadassa Medical Center, Jerusalem, Israel, [5]Cedars-Sinai, LA, CA, [6]Sourasky Medical Center, Tel Aviv, Israel, [7]Purple Biotech, Rehovot, Israel

Background. NT219 is a novel small molecule, dual inhibitor, that uniquely triggers the degradation of Insulin Receptor Substrates 1/2 (IRS) and the dephosphorylation and suppression of STAT3. These two major oncogenic targets in the tumor and tumor microenvironment (TME) play a key role in drug resistance, particularly to EGFR inhibitors. Previously, we demonstrated synergistic effect of NT219 and cetuximab in multiple SCCHN patient-derived xenograft (PDX) models. HPV-negative R/M SCCHN patients have poor survival and demonstrate IGF1R/IRS and STAT3 upregulation. We report biomarker results from dose escalation of NT219 in combination with cetuximab in patients (pts) with immunotherapy-refractory R/M SCCHN (NCT04474470).
Method. Biopsies from 11 enrolled SCCHN patients treated with different dose levels of NT219 (6, 12, 24 and 50 mg/kg) were obtained and evaluated using Immunohistochemistry and pathological analysis. Evaluation of potential biomarkers included measurements of IRS1/2 levels, as well as IGF1R and STAT3 phosphorylation (pIGF1R, pSTAT3) in tissue biopsies, and H-score was defined for tumor cells, infiltrating immune cells, and fibroblasts in the TME. Membrane completeness (mc) parameter was included in pIGF1R scoring.
Results. NT219 Cmax and AUC demonstrated a dose dependent increase, with 50mg/kg dose mean human AUC reaching Human Equivalent Dose efficacy of animal models. Indeed, at this dose, anti-tumor activity in humans was also demonstrated with 2 confirmed partial responses (PR) reported. At the 50 mg/kg NT219 dose, out of 4 SCCHN pts, for whom pre-treatment biopsies were available, 3 were HPV negative and 2 of them achieved PR. Pretreatment biopsies of these 2 pts demonstrated high activated IGF1R membranal staining (Avg. mcH-score: 285, p-value:) and high activated STAT3 nuclear staining (Avg. H-score: 285), in contrast to the non-responding SCCHN pts (30 and 33, with p-value 0.017, 0.004 respectively). Inhibition of intratumoral IGF1R/IRS and STAT3 was demonstrated in on-treatment biopsies. Analysis will be presented at the conference.
Conclusion. NT219 in combination with cetuximab demonstrated safety and early activity with 2 confirmed PRs at 50mg/kg dose level in R/M SCCHN pts. This dose level was the first dose at which the observed NT219 exposure was within the range of the efficacious dose levels in pre-clinical models. Detection of activated IGF1R and STAT3 in responding pts, compared to the non-responding pts, suggests a potential use of these targets as biomarkers for future patient selection. This notion is further substantiated by the demonstration of NT219 on-target effects in on-treatment tumor biopsies. Upregulation of NT219 targets, IGF1R and STAT3, in HPV-negative SCCHN pts and their response to the NT219+cetuximab treatment, support further evaluation of this patient population.

#5182 Exploiting tumor RNA-sequencing data for prediction of immune checkpoint inhibition response.

P. Mestdagh, P.-J. Van Dam, F. De Baene, C. Fierro, E. Van Hoof, E. Riviere, H. Dangreau, R. Van Cauwenberge, J. Vandesompele;
CellCarta, Antwerp, Belgium

Immune checkpoint inhibitors (ICI) have become the standard of care as a first- or second-line systemic treatment for patients with various cancer types. Unfortunately, many patients do not respond to this treatment and the occurrence of immune-related adverse events varies widely. There is an urgent need for robust predictive biomarkers for ICI response to identify patients with likely clinical benefit from this costly treatment. Several biomarkers, aimed at predicting response to ICI, have been proposed, including PD-L1 expression, tumor mutation burden (TMB), infiltration of cytotoxic T-cells in the tumor, Microsatellite Instability (MSI) and expression of various immune gene signatures. However, these individual biomarkers have suboptimal performance and multiple complementary omics technologies are required to properly quantify them. Integration of these multi-omic biomarkers has proven valuable in increasing the accuracy and robustness of ICI response prediction.We have developed a computational pipeline that determines the expressed mutation burden (eTMB), MSI status, fraction of infiltrating immune cells and various immune gene expression signatures directly from the RNA-sequencing profile of the tumor. Each biomarker is quantified using a dedicated algorithm that applies machine learning (eTMB and MSI) or computational deconvolution (infiltrating immune cells) and integrates external data sources to maximize performance. Algorithm performance has been validated on large cohorts of tumor RNA-sequencing data with matching gold standard quantification of said biomarkers.

As a proof of concept, we applied our pipeline to tumor RNA-sequencing data of 45 gastric cancer patients treated with pembrolizumab. Responders showed significantly higher eTMB scores and were enriched among the MSI-H patients. Fractions of CD8 T-cells and M1 Macrophages, together with interferon gamma and cytotoxic T-cell gene expression signatures, were significantly increased in responders. Notably, integrating these biomarkers into a single prediction model improved prediction of response to checkpoint inhibition therapy compared to predictions based on eTMB or MSI alone.

Taken together, our approach enables the quantification of various ICI response biomarkers from a single omics layer (RNA-sequencing) and can contribute to ICI response prediction.

#5183 Retrospective analysis of CCNG1 expression in tumors, a novel biomarker in development for partnering with DRG-101, a tumor targeted retrovector encoding a CCNG1 inhibitor gene.

N. Omelchenko[1], V. Kumar[1], S. Jeffrey[1], G. Haroun[1], D. Brigham[2], W. H. Isacoff[1], S. Chawla[1];
[1]Sarcoma Oncology Research Center, Santa Monica, CA, [2]Aveni Foundation, Santa Monica, CA

Background: CCNG1, a non-canonical cyclin, is a novel biomarker in development for partnering with DRG-101 (DeltaRex-G), a tumor targeted retrovector encoding a CCNG1 inhibitor gene. Expanded access using DRG-101 is currently open for an intermediate-size population of advanced pancreatic cancer, sarcoma and carcinoma of breast (NCT04091295). Therefore, it is important to identify patients who might respond favorably to DRG-101 gene therapy. Previously, we reported that CCNG1 expression is enhanced in sarcoma tumors (Ann Oncol 34, 1980P, 2023). In this report, we have expanded the analysis to 137 patients with all cancer types and describe patients with known CCNG1 expression levels who have been treated with DRG-101.
Methods: Archived formalin-fixed paraffin-embedded (FFPE) tumor specimens (n=137) from patients who were followed at the Sarcoma Oncology Research Center were collected, processed, and subjected to RNA sequencing. Briefly, RNA-seq libraries were sequenced to generate 50 million reads, aligned using Kallisto v0.42.4 to GENCODE v23 transcripts with default parameters. Only protein-coding, IGH/K/L- and TCR-related transcripts were retained for downstream processing, resulting in 20,062 protein-coding genes. Gene expression levels in patients of the reference cohorts are categorized as low/medium/high, defined by Low = < 17%; Medium-high = 50%-83%; Medium-low = 17%-49%; High = >83%.
Results: Seventy women and sixty-seven men, ranging in age from 16 to 87 years, were studied. All tumors showed enhanced CCNG1 expression. Thirty (22%) tumors exhibited high CCNG1 expression, 53 (39%) showed medium-high CCNG1 expression, 48 (35%) displayed medium-low CCNG1 expression, and six (4%) had low CCNG1 expression. One hundred (73%) patients had metastatic disease, and 37 (27%) had localized disease. There was no correlation between CCNG1 expression and disease stage. As a result of these findings, the FDA-CBER authorized the use of DRG-101 in an Expanded Access program as platform therapy upon which one or more FDA approved cancer drugs/immunotherapies may be added. Historically, one patient with metastatic pancreatic cancer, one with early stage, HR+ HER2+ invasive breast cancer and one with early stage triple negative breast cancer are alive 15, 3 and 2.5 years in sustained remission with DRG-101 therapy, and had 24%, 23% and 74% CCNG1 tumor expression levels respectively. Five patients with advanced pancreatic cancer, sarcoma and breast cancer and known CCNG1 expression levels are currently being treated with DRG-101.
Conclusions:(1) 100% of tumors tested showed enhanced CCNG1 expression at varying levels, and (2) the use of DRG-101 in combination with FDA approved cancer drugs/immunotherapies is on-going for an intermediate size population of advanced pancreatic cancer, sarcoma and carcinoma of breast.

#5184 Biomarker results from PEVENAZA, a randomized phase 2 study of venetoclax and azacitidine +/- pevonedistat in newly diagnosed AML patients unfit for intensive chemotherapy: Increased efficacy in a subset of patients with IDH1/2 mutations and other observations.

R. Ramesh[1], X. Fang[1], S. Li[1], S. Friedlander[1], F. Sedarati[1], L. Ades[2], N. Short[3], C. Papayannidis[4], T. Yeh[1];
[1]Takeda Development Center Americas, Inc (TDCA), Lexington, MA, [2]Hopital Saint Louis & Paris Cite University, Paris, France, [3]The University of Texas MD Anderson Cancer Center, Houston, TX, [4]IRCCS Azienda Ospedaliero-Universitaria di Bologna, Bologna, Italy

Background: Many newly diagnosed patients with AML are ineligible for intensive chemotherapy due to pre-existing comorbidities and older age. VIALE-A, a phase-3 trial with venetoclax (ven) and azacitidine (aza) established this combination as a new standard of care (SOC) for this patient population. The addition of pevonedistat (pevo) to this combination was evaluated in the same patient population in the current trial (NCT04266795). Here we present results of biomarker analyses from baseline and on-treatment bone marrow samples.

Methods: Molecular mutational analysis was performed using a next generation sequencing (NGS) panel on baseline bone marrow samples. Combining this data with cytogenetics allowed centralized assignment of risk category based on ELN2017 guidelines. Longitudinal bone marrow aspirate samples were also examined by multi-color flow cytometry for expression of select surface antigen expression and to identify AML leukemic stem cells (LSCs) from the blast population.

Results: Eleven genes were selected for analyses based on prevalence and scientific interest, including DNMT3A, ASXL1, TET2, FLT3, and IDH1/2. In contrast to other genes and ELN risk categories, we observed a statistically significant increase (p-value 0.013) in CR+CRi rates for IDH1/2 mutant patients when treated with pevo + ven + aza (95%, n=21) compared to ven+aza control arm (62%, n=21). In addition, we evaluated the prevalence of CD33, CD123 and CLEC12a, targets of current AML developmental therapeutics, in both the blast and LSC populations at baseline. The median (n=120 pts) % blast cells expressing CD33, CD123, or CLEC12a were 89.8%, 63.2%, and 66.0%, respectively. The median (n=78 pts) % LSCs expressing CD33, CD123, or CLEC12a were 48.2%, 90.9%, and 32.0%, respectively. Importantly, we did not see any significant difference in median fluorescence intensity (MFI) or % expression in any of the three proteins after treatment with ven and aza (+/- pevo). Finally, no strong associations were observed between expression levels and either mutations or ELN risk categories.

Conclusions: Analyses of biomarker samples as part of the PEVENAZA trial resulted in several insights for not only the pevonedistat program but also for other AML therapeutics in development. The observation that newly diagnosed patients with IDH1/2 mutations may benefit from the addition of pevo to ven+aza is certainly hypothesis-generating but would require further follow-up with higher patient numbers. In addition, baseline CD33, CD123, and CLEC12a expression levels were in line with published studies. Here we have also shown they remain similar after SOC treatment (ven+aza) supporting the development of agents that target these proteins in both first and second line settings for AML.

#5185 A multimodal, spatially defined, nanomechanical signature as predictive biomarker for breast cancer outcome: A 20 year survival study.

S. Nizzero[1], M. Pelaez Soni[2], G. Zaugg[3], Y. Xu[4], L. Zhang[4], J. Zheng[4], L. B. Jordan[5], C. A. Purdie[5], P. R. Quinlan[6], C. Nagi[7], K. A. Sepulveda[7], P. Oertle[3], T. A. Appenzeller[3], M. Loparic[3], S.-H. Chen[4], V. Cristini[4], M. Plodinec[3], A. M. Thompson[7];

[1]ARTIDIS Inc, Houston, TX, [2]Houston Methodist Resarch Institute, Houston, TX, [3]ARTIDIS AG, Basel, Switzerland, [4]Houston Methodist Research Institute, Houston, TX, [5]University of Dundee, Dundee, United Kingdom, [6]University of Nottingham, Nottingham, United Kingdom, [7]Baylor College of Medicine, Houston, TX

Background: With the recent advancement in perioperative treatment protocols, the search for clinical biomarkers that can predict overall response and long-term cancer outcome independent from treatment acquires even more importance. Recently, it has become clear that mechanical properties of the tumor microenvironment in solid tumors play a key role in driving outcome, mediating immune infiltration and activation, and response to therapy. Moreover, a growing body of evidence supports the understanding that mechanical changes induced by a plethora of therapeutic regimens should be leveraged to elicit favorable outcome.

Methods: In this work we propose a dual approach to reveal mechanical biomarkers predictive of long-term outcome in solid cancers. Our first approach is based on a newly developed, 60 channel, biomechanical imaging mass cytometry panel to elucidate biomechanical cues that drive tumor aggressiveness and immune infiltration. Our second approach utilizes the AFM-based Automated and Reliable Tissue Diagnostics (ARTIDIS) investigational device to measure mechanical properties of fresh clinical biopsy samples at a nanoscale resolution. Our analysis was performed on over 300 clinical samples, from routine baseline clinical biopsies collected from both the Breast Clinic, University Hospital Basel, and the University of Dundee, in the UK. Patients in these two cohorts were treated with either adjuvant or neoadjuvant approaches, including radiation, chemotherapy, hormonal, and surgical treatment regimens, with individual patient follow up as long as 20 years.

Results: We demonstrated with two complimentary technologies that biomechanical spatial patterns drive outcome in breast cancer. Our results include a multi-platform elucidation of the biomechanical phenotypes of epithelial to mesenchymal transitions driven by hypoxic environments. Furthermore, we identified several biomechanical subpopulations of cancer associated fibroblasts, and their role in mediating cancer outcome, in relationship with survival time and several clinical variables (e.g. metastasis, nodes, grade). We mechanistically corroborated these results by evaluating the immune modulatory effect of the identified biomechanical microenvironments in breast cancer. Lastly, we correlated the identified biomechanical microenvironments with the ARTIDIS nanomechanical signature as a clinically integrated, rapid, single biomechanics signature at the nanoscale.

Conclusion: Our results further validate the importance of biomechanics in driving tumor response and immune infiltration across a variety of clinical treatment setting. These result support the integration of ARTIDIS nanomechanical signature in clinical settings as a single predictive biomarker able to rapidly and accurately capture biomechanical alterations that drive cancer outcome.

#5186 Spatial single-cell deconvolution of the bone marrow microenvironment to define predictive biomarker for response to immunotherapy in patients treated with a check point inhibitor in smoldering multiple myeloma, phase II trial of nivolumab in combination with lenalidomide and low dose dexamethasone.

Y. Konishi[1], G. Tarantino[1], Y. He[1], R. Sklavenitis-Pistofidis[1], S. Shah[2], K. Towle[3], C. Cea-Curry[3], O. Zavidij[3], R. Carrasco[4], S. Rodig[2], J. Aster[2], D. Liu[1], G. Getz[5], I. Ghobrial[1];

[1]Dana-Farber Cancer Institute/Harvard Medical School/Broad Institute of Massachusetts Institute of Technology (MIT) and Harvard, Boston, MA, [2]Brigham and Women's Hospital, Boston, MA, [3]Dana-Farber Cancer Institute, Boston, MA, [4]Dana-Farber Cancer Institute/Brigham and Women's Hospital, Boston, MA, [5]Massachusetts General Hospital/Harvard Medical School/Broad Institute of Massachusetts Institute of Technology (MIT) and Harvard, Boston, MA

Background:The immune system is critical for response and resistance in all cancer types and therapies. Patients with Smoldering Multiple Myeloma (SMM) have altered immune cell composition in the bone marrow (BM). However, little is known about the role of BM spatial immune profiling in patients treated with checkpoint inhibitors in MM.

Methods: We performed spatial profiling with imaging mass cytometry of trephine biopsies of the BM (n=15; pre-treatment n=7 and post-treatment n=8) from patients with high-risk SMM enrolled in a phase II trial of nivolumab in combination with lenalidomide and low dose dexamethasone (NCT02903381). Patients received 6 cycles of induction therapy of nivolumab (240mg) at days 1 and 15, in combination with lenalidomide (25mg) at days 1-21 and dexamethasone at days 1, 8, and 15. The induction phase was followed by nivolumab (240mg) and lenalidomide (25mg) maintenance for another 6 cycles. A treatment cycle was defined as 28 consecutive days for a total of 12 months period. Event monitoring was performed up to 3 years. The primary efficacy outcome was progression-free survival 2 years after treatment.

Results: Eight patients were enrolled on this study from January 2017 to June 2017. The study was put on hold due to the toxicity of checkpoint inhibitors observed in other trials of MM. The median age for all patients at enrolment was 60 years (range 49 to 81), with 5 males (62%) and 3 females (38%). All patients met criteria for high risk SMM disease. Median follow-up for all 8 patients was 38.7 months. Median overall survival was not reached; median progression-free survival was 33.8 months. Seven total patients had a response of Minimal Response (MR) or better, and 4 patients who initially responded eventually progressed. The total number of patients who were followed for at least two years and remained progression-free was 4 of 8 evaluable patients (50%; 90% CI: 19 - 81%).Spatial profiling with a panel of 37 markers on the pre-treatment samples allowed us to assess the states and abundances of multiple immune subpopulations, including rare regulatory NK cells. To assess the accuracy of our cell type annotation, we correlated the proportion of malignant plasma cells identified per patient with the value determined by pathologists for clinical diagnosis. These measures were significantly positively correlated ($R=0.92$, $p<0.01$). Spatial neighborhood analysis revealed statistically significant interactions enriched in the responders, even with our small sample size (t-test; $p < 0.05$).

Conclusions and future directions: This pilot study suggests that BM spatial immune profiling before receiving immune check point inhibitors can be a biomarker for response in patients with SMM.

#5187 VistaPlex immunofluorescence assay panels provide reliable deep spatial phenotyping for diverse immuno-oncology applications.

A. Christians[1], C. E. Jackson[2], J. Boog[1], M. H. Ingalls[2], A. Northcutt[2], K. E. Cashion[2], J. Rauer[1], K. Kwarta[2], J. S. Schwarz[2], O. Braubach[2];
[1]Canopy Biosciences-A Bruker Company, Hannover, Germany, [2]Canopy Biosciences-A Bruker Company, Saint Louis, MO

Multiplex immunofluorescence (mIF) is a powerful tool that enables deep phenotyping of immune and cancer cells across a wide variety of tissue types. The initial effort and cost required to develop high-plex mIF panels is significant and poses a considerable hurdle for adoption of spatial biology. To streamline high-plex assay development, we developed a process for creating and validating multiplex antibody panels for use in immuno-oncology applications that leverage CellScape™, an automated end-to-end platform for Precise Spatial Multiplexing. Our multiplex assay development was a rigorous, multi-stage, iterative process to evaluate antibodies for suitability, specificity, and reproducibility. These assay panels are formulated as ready-to-use VistaPlex™ assay kits and are intended to enable rapid, reliable spatial phenotyping of key immune populations.

To confirm the utility of VistaPlex, we deployed the Human FFPE Spatial Immune Profiling Panel to stain and image various FFPE tissue samples on the CellScape platform. With CellScape, tissues are mounted in enclosed fluidic chambers while on-instrument staining, imaging and signal erasure are conducted in iterative rounds. The panel presented here contains antibodies against 16 common biomarkers used in immune-oncology applications. Among these are CD3, CD4, CD8, CD20, and CD45 to detect cell lineages, PD-1 and PD-L1, to interrogate immune checkpoints, and markers that inform about cell state and activation. Spatial immune profiling data were obtained from human tonsil, colon, breast, and lung tissue samples. Deep immune phenotyping was performed using unsupervised clustering analysis and AI-assisted cluster labelling, and biomarker distributions were studied in the context of cellular neighborhoods and other proximity analyses. Overall, we identified more than 19 cell phenotypes with varying frequencies and spatial arrangements across tissue samples.

Our data are robust and demonstrate that VistaPlex Assay kits for spatial profiling present an efficient and cost-effective solution for users that want to break into spatial biology.

#5188 Defining PD-1/PD-L1 receptor-ligand interactions in the head and neck cancer tumor microenvironment identifies unique 'immune cell rivers' of cellular interactions.

H. Sadeghirad[1], V. Yaghoubi Naei[1], J. Monkman[1], S. Basu[2], A. Wicher[2], R. Ladwa[1], B. G. Hughes[3], **A. Kulasinghe**[1];
[1]University of Queensland, Brisbane, Australia, [2]Navinci Diagnostics, Uppsala, Sweden, [3]Royal Brisbane and Women's Hospital, Brisbane, Australia

Head and neck squamous cell carcinoma (HNSCC) is the 7th most common cancer globally with a poor 5-year survival rate of ~50%. With the emerging successes with immune checkpoint blockade (ICB) in the metastatic and recurrent setting, there is a need for predictive biomarkers to identify patients likely to achieve clinical benefit. Whilst PD-L1 expression on tumour cells and PD-1 on immune cells have been investigated, these remain inconclusive biomarkers. To better understand and map the PD-L1/PD-1 receptor-ligand interactions, we evaluated a novel in situ proximity ligation assay (is PLA) across whole tissue sections of pre-treatment HNSCC patients to received ICB therapy. Pre-treatment FFPE whole tissue samples were collected from n=25 advanced stage HNSCC patients across two major Queensland Hospitals (Royal Brisbane and Women's Hospital and the Princess Alexandra Hospital). Tissues were stained with multiplex immunofluorescence and the Navinci Diagnostics fluorescent is PLA assay for PD-1/PD-L1. Tissues were incubated with the PD1/PD-L1 antibodies and subsequent incubation with oligonucleotide-tagged secondary probes enabled PLA, which highlights PD1 and PD-L1 interactions. Following the application of secondary probes, the sections underwent a ligation step, then a post-blocking, and an amplification process to enhance the detection of protein interactions. Next, the sections were treated with a detection solution to visualize the amplification product. The PLA assay findings were measured against clinical endpoints (PFS/OS criteria). In n=5/25 HNSCC tissues, positive PD-1/PD-L1 interactions were measured across the tumour microenvironment (TME), specifically in the immune rivers on the immediate tumour periphery. These cells showed highly specific binding of the PLA product. These areas positive by the PLA assay were in stark contrast to the tumour bulk/nests which were absent in PD-1/PD-L1 interactions. Notably, the PLA PD-1/PD-L1 do not correlate with tumour PD-L1 expression or tumour proportion scores (TPS). Rather, our study highlighted the difference in spatially mapping PD-1/PD-L1 interactions which may better recapitulate the tumour-immune recognition and activity in the TME. Taken together, these data provide a novel approach for determining clinically relevant receptor/ligand interactions in the HNSCC TME.

#5189 The potential of minimal residual disease (MRD) in guiding adjuvant therapy (AT) decisions in non-small cell lung cancer (NSCLC).

S. Lei[1], H. Xu[2], Y. Yang[1], L. Tian[1], T. Ma[3], Y. Wang[1];

[1]Department of Medical Oncology, National Cancer Center/National Clinical Research Center for Cancer/Cancer Hospital, Chinese Academy of Medical Sciences and Peking Union Medical, Beijing, China, [2]Department of Comprehensive Oncology, National Cancer Center/National Clinical Research Center for Cancer/Cancer Hospital, Chinese Academy of Medical Sciences and Peking Union Medical College, Beijing, China, [3]Genecast Biotechnology Co, Ltd, Wuxi, China

Background: Circulating tumor DNA (ctDNA)-based minimal residual disease (MRD) detection has become a strong prognostic stratification factor in post-operation non-small cell lung cancer (NSCLC). Here we sought to investigate the guiding potential of MRD in informing adjuvant therapy (AT) decisions.
Methods: Patients with stage IA-IIIB NSCLC who had undergone confirmed R0 resection were enrolled. Blood samples were collected prospectively one month after surgery before initiation of AT (landmark) and longitudinally every 3-6 months since surgery. Postoperative AT was conducted according to the guideline recommendations and regular radiographical examinations were recommended for relapse surveillance. MRD detection was conducted via the MinerVa platform (Genecast Biotechnology Co., Ltd) using a tumor-informed strategy based on a fixed next-generation sequencing (NGS) panel spanning 769 cancer-related genes.
Results: 168 patients were included in this study, with 11 (6.5%) experiencing confirmed relapse. Positive MRD was detected in 10.2% (16/157) of patients at landmark and was associated with a significantly higher risk of shorter disease-free survival (DFS)(HR: 26.2[6.7-102.7], *P*<0.001), irrespective of disease stage or gene alteration. Dynamic changes in ctDNA status further stratified patients into three subgroups with different prognosis. Consistent negative MRD detected at the landmark and all longitudinal timepoints represented the group with the best prognosis, while positive MRD detected at either the landmark or one subsequent timepoint showed a worse prognosis (Neg-Pos vs. Neg-Neg, HR: 37[3.2-438], *P*=0.004; Pos-Neg vs. Neg-Neg, HR: 14[1.2-172], *P*=0.035). The group with the worst prognosis occurred with consistent positive MRD (Pos-Pos vs. Neg-Neg, HR: 50[5.3-473], *P*<0.001). For patients with negative landmark MRD, there was no significant difference between the DFS of patients who received AT and those who didn't(*P*=0.241), and the result was replicated in a highly controversial subgroup: stage I patients with high-risk factors (*P*=0.130). Besides, whether chemotherapy was applied before targeted therapy in the *EGFR*-mutant subgroup showed no influence on DFS provided that landmark MRD was negative (*P*=0.197). In multivariate analysis considering pathological high-risk factors, poor differentiation was identified as an independent risk factor for landmark MRD positivity (HR: 10.6[1.96-168.01], *P*=0.030).
Conclusions: MRD is a strong and steady prognostic factor in post-operative NSCLC. AT may be waved for stage I patients with high-risk factors given that they had negative landmark MRD, same as the adjuvant chemotherapy before targeted therapy for patients with sensitive *EGFR* mutation. More attention should be paid to poorly differentiated tumors, indicative of a high-risk subgroup with potential residual diseases.

CLINICAL RESEARCH: Prognostic Biomarkers 1
Poster Session

#5193 Molecular evolution of chemoresistance acquisition and predictive insights into the progression of bladder cancer.
G.-E. Yang, J.-J. Kim, T. Shin, S.-H. Leem;
Dong-A University, Busan, Korea, Republic of

Cancer heterogeneity arises from cellular features, suggesting that distinct molecular drivers may be latent within cancers diagnosed at different clinicopathological stages. We thoroughly assessed phenotypic traits and molecular alterations linked to chemoresistance and constructed chemoresistant bladder cancer cell lines representing the stepwise transformation. Model cell lines (5637GRCs, gemcitabine-resistant cells) with stepwise gemcitabine resistance representing early, intermediate, and late resistance phases were developed from non-muscle-invasive bladder cancer (NMIBC) cells. Notably, an increase in cell motility was observed at a relatively early phase. The results from the time-course analysis of molecular evolution showed changes in focal adhesion kinase signaling, PI3K-Akt signaling, and TGF-β signaling pathways during the phase of increasing cell motility. As chemoresistance increased, the levels of genes related to differentiation and MAPK signaling gradually increased. A 63-gene chemoresistance-motility (CrM) signature was constructed and weighted according to cell motility, and a strong correlation was observed between cancer metastasis and drug resistance; the signature also showed prognostic relevance in patients with NMIBC. This study affords a significant understanding of the molecular evolution of chemoresistance acquisition and enables prediction of cancer progression during chemotherapy treatment. Moreover, it provides insights into the progression of cells through all chemoresistance stages from NMIBC to MIBC. Therefore, this study proposes the feasibility of utilizing biomarkers correlated with cancer motility to predict cancer progression in the early phase of chemotherapeutic intervention in patients with non-muscle-invasive bladder cancer.

#5194 Pre-operative markers extracted from extracellular vesicles related with lung cancer relapse.

H. Koba, S. Nanjo, S. Yano;
Kanazawa Univ. Hospital, Kanazawa, Japan

Background: Pre- and post-operative immunotherapy have been a new standard of care for lung cancer patients. On the other hand, post-operative Osimertinib; EGFR-TKI therapy had obtained new evidence to the *EGFR* mutant lung cancer patients. Both treatments revealed to make patient survival prolonged. However, there are quite a lot patients who had experienced disease relapse, despite of multimodal therapy. Extracellular vesicles (EVs) have reported to have potent for searching a new target to cancers.
Purpose: Exploration of novel risk factors related with post-operative recurrence of lung cancer.
Methods: We retrospectively examined patient background, disease-free survival, overall survival, and preoperative liquid biopsy analysis in lung cancer patients who underwent surgery at Kanazawa University Hospital between January 2017 and May 2020, in whom preoperative chemotherapy was not administered. EVs were extracted from 500 µl serum within 7 days before surgery using MagCapture Exosome isolation Kit PS Ver.2 (FUJIFILM). First, we focused the six cases that had the 3 phase samples: preoperative, disease free and relapse phase. According to the EV concentrations calculated by BCA method, comprehensive protein assessment of these subjects was performed using shotgun mass spectrometry. Secondly, all cases' prognosis were analyzed in connection with the detected marker using Dot blotting.
Results: All EV samples from primary 6 cases were able to be detected and median concentration of those was 27 µg/ml (9-82). We focused on three factors (LCEV1-3) among the 6 cases analysis, when we disease fluctuation. Among LCEV1-3 examination to all preoperative samples, LCEV2 had been related with disease recurrence.
Discussions: EVs contain amount of information such as cancer biomarker. Not only that, these factors may have a potency for therapeutic target. Further investigations are needed.

#5196 Stepwise molecular mechanisms involved in chemoresistance in bladder cancer cells.

J.-J. Kim, G.-E. Yang, T. Shin, S.-H. Leem;
Dong-A University, Busan, Korea, Republic of

Bladder cancer (BC) is one of the most prevalent genitourinary tumors worldwide, with approximately 573,000 new cases reported. Approximately 80% of BC patients are diagnosed with non-muscle-invasive bladder cancer (NMIBC) with a high five-year survival rate, while the remaining 20% are diagnosed with muscle-invasive bladder cancer (MIBC). Although the surgical operation has been utilized to BC, patients with NMIBC frequently experience disease recurrence, of which about 20% progress to MIBC. However, the response rate of MIBC patients to gemcitabine treatment has been shown to be limited to less than 40% efficacy, and only a small number of patients have potential benefits.Chemotherapy resistance is an obstacle to cancer therapy and is considered a major cause of recurrence. Thus, understanding the mechanisms of chemoresistance is critical to improving the prognosis of patients. Here, we have established a stepwise gemcitabine-resistant T24 bladder cancer cell line to understand the molecular mechanisms of chemoresistance within cancer cells. The characteristics of the stepwise chemoresistance cell line were divided into 4 phases (parental, early, intermediate, and late phases). These four phase cells showed increasingly aggressive phenotypes in vitro and in vivo experiments with increasing phases
and revealed the molecular properties of the biological process from parent cells to phased gemcitabine-resistant cell line (GRC). Taken together, through the analysis of gene expression profile data, we have characterized gene set of each phase indicating the response to anticancer drug treatment. Specifically, we identified a multigene signature (23-genes including GATA3, APOBEC3G, NT5E, MYC, STC1, FOXD1, SMAD9) and developed a chemoresistance score consisting of that could predict eventual responsiveness to gemcitabine treatment. We suggest that our findings improve prognosis by predicting to acquiring of chemotherapy resistance in bladder cancer patients.

#5197 Identification of novel molecular biomarkers for predicting postoperative recurrence of ampulla of Vater carcinoma.

H. Kim[1], J. Choi[1], H.-o. Jeong[2], A. Kim[1], S.-H. Lee[1], K. Lee[1], K. Lee[1], J. Lee [1], S. Lee[2], J. Park [1];

[1]Samsung medical center, Sungkyunkwan University School of Medicine, Seoul, Korea, Republic of, [2]Ulsan National Institute of Science and Technology, Ulsan, Korea, Republic of

Background: Ampulla of Vater (AoV) carcinoma is a rare tumor that accounts for 20 % of periampullary cancers. Surgical resection is the only treatment that can expect cure of disease, and there is still an unmet need to predict postoperative recurrence. In this study, we investigated the novel molecular biomarkers that can predict the risk of recurrence after surgery with AoV carcinoma.

Methods: In this retrospective study, we collected the surgically resected tissue and medical records of patients who were diagnosed with AoV carcinoma at Samsung Medical Center from January 2005 to December 2020. Patients were classified patients according to the initial stage and experience of tumor recurrence. Whole transcriptomic analysis using primary AOV tumor and recurred tumor tissue samples was conducted to identify the molecular biomarker for tumor recurrence.

Results: A total of 40 tumor tissue from primary site in non-recurrence group, 22 tumor tissue from primary site in recurrence group, and paired 22 tumor tissue from recurrence site were analyzed. A total of 1005 genes differentially expressed between primary tumor of non-recurrence group and recurrence group were found. Gene set enrichment analysis showed that pathways related to fatty acid metabolism, adipogenesis, oxidative phosphorylation, and hypoxia were upregulated, and pathways associated with interferon gamma response, and mTOR signaling were downregulated in recurrence group. These pathways were significantly affecting the recurrence free survival which was verified with TCGA data, and we further identified some candidate genes including PIM3, IGFBP4, SLC19A1, HIF1A and CXCL11 to predict tumor recurrence . Moreover, we found candidates for single gene level biomarkers to predict early tumor recurrence in N0 stage. Low expression of UQCC3 and high expression of CLCNKB was related to early tumor recurrence.

Conclusions: We found the candidates for novel molecular level biomarker to predict postoperative recurrence of AoV carcinoma. In the future, it is necessary to develop a predictive model for the risk of recurrence after surgical resection for AoV carcinoma.

#5198 Non-invasive biomarkers of ECM turnover are prognostic for combinations of checkpoint inhibition immunotherapy in solid tumors.

C. N. Bistrup[1], V. Araujo Barbosa de Lima[2], C. Jensen[1], M. A. Karsdal[1], I. Svane[3], U. Lassen[3], **N. Willumsen**[1];
[1]Nordic Bioscience, Herlev, Denmark, [2]Copenhagen University Hospital, Copenhagen, Denmark, [3]Copenhagen University Hospital, Herlev, Denmark

Background: Immune checkpoint inhibitors (ICIs) are investigated in many different combinations (Table 1). As only a fraction of patients responds to ICIs, prognostic biomarkers are needed to assess the likelihood of benefit. High collagen turnover in the tumor microenvironment are closely related to response to ICIs and survival outcomes. In this study, we explored the clinical utility of non-invasive biomarkers of type I collagen (reC1M), type III collagen (PRO-C3), type IV collagen (C4M), type XIX collagen (PRO-C19), type XX collagen (PRO-C20), TGF-β activity in metastatic cancer patients treated with ICIs.
Methods: PRO-C3, PRO-C19, PRO-C20, TGF-β, reC1M and C4M were measured with ELISAs in pre-treatment serum from 33 patients with metastatic disease in a basket trial comprising 14 different tumor types, treated with 8 different checkpoint inhibition regimens (Table 1). The association between biomarker levels and overall survival (OS) outcome was evaluated by Kaplan-Meier analysis and Cox regression analysis after dichotomizing patients at the 75th percentile (Q4).
Results: When evaluating the combined group of cancer patients, high levels (Q4) of PRO-C3 (HR=3.00, 95%CI=1.21-7.44, p=0.018), PRO-C19 (HR=2.49, 95%CI=1.04-5.99, p=0.041), PRO-C20 (HR=2.49, 95%CI=1.04-5.99, p=0.041), TGF-β (HR=2.52, 95%CI=1.05-6.04, p=0.039), reC1M (HR=2.79, 95%CI=1.16-6.67, p=0.021) and C4M (HR=2.52, 95%CI=1.05-6.04, p=0.039) were all associated with poor OS compared to low levels (Q1-Q3). The median OS was 4.7-6.1 months in biomarker-high patients compared to 8.7-11.4 in biomarker-low patients.
Conclusion: Across a diverse cohort of metastatic cancer patients treated with different checkpoint inhibition regimens, non-invasive biomarkers associated with tumor fibrosis and collagen turnover (PRO-C3, PRO-C19, PRO-C20, TGF-β, reC1M and C4M) could identify cancer patients with poor prognosis.

Table 1

Cancer type	**Number of patients**	**Treatment**
Esophageal	1	Nivolumab (Nivo) +Anti-LAG3
Breast	2	Carboplatine+Gemciabine+Pembrolizumab (Pembro)
Ovarian	4	Atezolizumab+BET inhibitor
Parotid	1	Nivo
Gastric	2	Nivo+Anti-LAG3 or Atezolizumab+CD40-agonist
Bladder	3	Pembro
Colorectal	5	Nivo, Pembro, Atezolizumab++bispecific antibody targeting CEA and CD3 or Atezolizumab+CD40-agonist
Hepatocellular carcinoma	3	Nivo+Anti-LAG3
Colorectal	1	Atezolizumab+bispecific antibody targeting CEA and CD3
Mesothelioma	2	Pembro or Atezolizumab+CD40-agonist
Neuroendocrine tumor	1	Pembro
non-small cell	5	Nivo, Pembro or ipilumumab+Nivolumab
Pancreas	1	Atezolizumab+CD40-agonist
Unknown primary	2	Atezolizumab++bispecific antibody targeting CEA and CD3 or Pembro

#5199 Protease-activated CDCP1 as a marker for aggressive primary prostate cancer and castration resistance.

R.-M. Merivirta, T.-P. Lehto, A. Rannikko, T. Mirtti, H. Koistinen;
University of Helsinki, Helsinki, Finland

CUB domain-containing protein 1 (CDCP1) is a type 1 transmembrane protein overexpressed in many cancers, including prostate cancer. CDCP1 has been associated with tumor progression, metastasis, drug resistance and poor prognosis in prostate cancer, making it a potential prognostic biomarker and therapeutic target. It has been shown to be overexpressed in a subset of castration resistant prostate cancers (CRPC) and cooperate with the loss of tumor suppressor PTEN to promote metastatic dissemination. Extracellular serine proteases activate CDCP1 by cleaving it into an N-terminal and C-terminal fragments. Proteolytic cleavage has been associated with the tumor-promoting functions of CDCP1. We studied the expression of full-length and cleaved form of CDCP1 in grade group 2-4 primary prostate cancer tissues and CRPCs using immunohistochemistry. Total CDCP1 staining was observed in 60% of primary prostate cancer samples, while the staining of cleaved CDCP1 was somewhat less frequently observed (45%). The results will be further analyzed regarding the PTEN status and for association with survival of the patients. In conclusion, so far, our results have indicated that cleaved CDCP1, which likely represents activated CDCP1, is detectable in GG 2-4 prostate cancers.

#5200 Multiparametric MRI along with machine learning informs on molecular underpinnings, prognosis, and treatment response in pediatric low grade glioma.

A. Nabavizadeh[1], A. Kraya[2], K. Rathi[2], M. Kim[2], N. Khalili[2], A. Familiar[2], V. Kesherwani[2], H. Anderson[2], D. Gandhi[2], A. Mahtabfar[2], S. Bagheri[1], X. Huang[2], Y. Zhu[2], A. Sickler[2], S. Phul[2], S. Mueller[3], M. Koptyra[2], P. Storm[2], J. Ware[1], Y. Song[2], M. Fisher[2], A. Vossough[2], C. Davatzikos[1], A. Resnick[2], A. Fathi Kazerooni[2];

[1]Perelman School of Med. Univ. of Pennsylvania, Philadelphia, PA, [2]CHOP, Philadelphia, PA, [3]UCSF, San Francisco, CA

We report a comprehensive radiogenomic analysis, including multiparametric MRI and RNA sequencing of 502 tumors across 13 histological types of pediatric low-grade glioma (PLGG). Through an unsupervised analysis of treatment-naïve imaging, we were able to identify 3 distinct imaging clusters that were associated with different molecular pathways according to transcriptomic pathway analysis. Using xCell enrichment scores as input for clustering, we discovered three distinct immunological groups based on immune cell infiltration. The results suggested the presence of an ‘immune-hot” cluster within the tumors with a poorer prognosis, which may potentially benefit from emerging immunotherapies. We subsequently generated a radiomic signature that was able to predict immunological profiles. We also developed a clinicoradiomic predictive model that can assess patients’ risk of progression and predict treatment response. Finally, we evaluated the transcriptomic pathways that were most predictive of clinicoradiomic risk scores and identified the biological pathways most predictive of risk of progression in PLGG, when adjusting for molecular subtype, race, reported gender, age at diagnosis, and the anatomic location of the tumor. This is the first large-scale radiogenomic analysis in PLGG that can aid in prognostication, assessing patients’ risk of progression, predicting treatment response in conventional therapies, and early stratification of patients to identify potential candidates for targeted therapies.

#5201 Characterization of *PDLIM2* in non-small cell lung cancer.

K. Ashouri[1], H. Krause[2], A. Elliott[2], S. V. Liu[3], P. C. Ma[4], B. Halmos[5], Z. Qu[1], G. Xiao[1], A. Vanderwalde[2], J. J. Nieva[1];
[1]University of Southern California, Los Angeles, CA, [2]Caris Life Sciences, Phoenix, AZ, [3]Georgetown University, Washington, DC, [4]Penn State College of Medicine, Hershey, PA, [5]Montefiore Medical Center, Bronx, NY

Introduction: PDZ and LIM domain protein 2 (PDLIM2) acts as tumor suppressor by downregulating NF-κB and STAT3 signaling, modulating inflammation, immune response, and cell survival. Mouse model studies have demonstrated that downregulation of *PDLIM2* leads to PD-1 immune blockade and chemotherapy resistance. We present a large clinical and molecular characterization of *PDLIM2* expression in non-small cell lung cancer (NSCLC).
Methods: NextGen sequencing of DNA (whole exome)/RNA (whole transcriptome) was performed for NSCLC (Total N = 29126; Adenocarcinoma [-A, N = 15765], Squamous [-S, N = 6416]) patient tumors submitted to Caris Life Sciences (Phoenix, AZ). Mutations were defined as pathogenic SNVs/indels. Samples were stratified by PDLIM2 expression quartiles (in transcripts per million [TPM]) for all NSCLC tumors (Q4: H, Q1: L). PD-L1 expression [22C3; Positive (+): tumor proportion score (TPS) ≥1%]was assessed by IHC. High tumor mutational burden (TMB-high) set as ≥10 mutations per Mb. Cell infiltration in the tumor microenvironment was estimated by QuantiSEQ. Gene expression profiles were analyzed for transcriptional signatures predictive of response to immunotherapy (T cell-inflamed). Real-world overall survival was assessed from insurance claims data and Kaplan-Meier estimates were calculated for molecularly defined subpopulations. Mann-Whitney U and X^2/Fisher-Exact tests were applied where appropriate, with P-values adjusted for multiple comparisons ($p < 0.05$).
Results: Median *PDLIM2* expression was higher in NSCLC-A compared to NSCLC-S (15.3 vs 13.6 TPM, $p < 0.001$). *PDLIM2*-A^L had a lower prevalence of *EGFR* mutations than *PDLIM2*-A^H (15.5% vs 19.4%, $p < 0.01$), but the opposite pattern was observed for *STK11* (21.5% vs 11.2%), *RB1* (7.5% vs 3.8%), *TP53* (62.9% vs 52.8%), *KEAP1* (18.4% vs 10.9%), and *SMARCA4* (9.15 vs 4.5%) alterations (all $p < 0.001$). *PDLIM2*-A^L tumors had decreased PD-L1+ (L: 52.4% vs H: 58.4% $p < 0.001$) but increased TMB-High status (L: 40.9% vs H: 28.5%, $p < 0.001$). PD-L1+ and TMB-H frequency did not vary with *PDLIM2* expression in NSCLC-S. In both NSCLC-A and -S tumors, *PDLIM2*^{H} had increased infiltration of NK cells, macrophages, dendritic cells, T cells, neutrophils, monocytes, and B cells compared to PDLIM2^L (all $p < 0.05$), in addition to increased T cell-inflammed scores ($p < 0.001$). *PDLIM2*-A^H was associated with improved overall survival (OS) (median 21.7 vs L: 15.6 months; $p < 0.001$; Hazard ratio [HR] = 0.825, 95% Confidence Interval [CI] 0.765 - 0.889) and time on pembrolizumab treatment (median 6.2 vs L: 5.6 months; $p = 0.009$; HR = 0.825 95% CI 0.714 - 0.953). No difference in OS was observed between *PDLIM2*-S^H vs ^{L} tumors (H: 14.8 vs L: 14.0 months; $p = 0.37$; HR = 0.95, CI 0.85-1.06).
Conclusions: NSCLC-A with high *PDLIM2* expression have a unique mutational profile, increased immune cell infiltration and favorable OS. Therapeutic strategies for targeting PDLIM2 to modulate NF-κB and STAT3 signaling should be further explored.

#5203 Identification of prognostic and predictive biomarkers for palbociclib add-on therapy using cancer panel sequencing of cell-free DNA in patients with HR-positive HER2-negative advanced and metastatic breast cancer with fulvestrant resistance.

T. Takeshita[1], T. Iwamoto[2], N. Niikura[3], K. Watanabe[4], Y. Kikawa[5], K. Kobayashi[6], N. Iwakuma[7], T. Okamura[3], H. Tada[8], S. Ozaki[9], T. Okuno[10], U. Toh[11], Y. Yamamoto[12], M. Tsuneizumi[13], H. Ishiguro[14], N. Masuda[15], S. Saji[16];

[1]Kumamoto City Hospital, Japan, Kumamoto, Japan, [2]Kawasaki Medical School Hospital, Okayama, Japan, [3]Tokai University School of Medicine, Kanagawa, Japan, [4]Hokkaido Cancer Center, Hokkaido, Japan, [5]Kansai Medical University Hospital, Osaka, Japan, [6]Saitama Red Cross Hospital, Saitama, Japan, [7]NHO Kyushu Medical Center, Fukuoka, Japan, [8]Tohoku University Graduate School of Medicine, Miyagi, Japan, [9]Hiroshima Prefectural Hospital, Hiroshima, Japan, [10]Kobe City Nishi-kobe Medical Center, Hyogo, Japan, [11]Kurume University Hospital, Fukuoka, Japan, [12]Kumamoto University Hospital, Kumamoto, Japan, [13]Shizuoka General Hospital, Shizuoka, Japan, [14]Saitama Medical University International Medical Center, Saitama, Japan, [15]Nagoya University Graduate School of Medicine, Aichi, Japan, [16]Fukushima Medical University, School of Medicine, Kumamoto, Japan

Purpose: The combination of cyclin-dependent kinase 4/6 inhibitors with endocrine therapies has shown promise for improving the survival of patients with hormone receptor (HR)-positive/human epidermal growth factor receptor 2 (HER2)-negative advanced and metastatic breast cancer (ABC/MBC). The FUTURE trial (UMIN000029294) demonstrated that adding palbociclib after acquiring fulvestrant resistance is potentially safe and effective. To further identify biomarkers for patient selection, this preplanned translational sub-study aims to use cancer panel sequencing of cell-free DNA (cfDNA) to discover prognostic and predictive biomarkers for additional palbociclib treatment after acquiring fulvestrant resistance in patents with HR-positive/HER2-negative ABC/MBC.

Methods: Herein, we utilized 149 cfDNA samples from 61 patients with disease progression after fulvestrant monotherapy and who subsequently received fulvestrant and palbociclib. Circulating cfDNA was analyzed at the time of palbociclib addition after fulvestrant resistance, on day 15 of cycle one (D15), and at the end of treatment (EOT) using the ThruPLEX ctDNA Assay, which can identify single or multi nucleotide variants, DNA insertions, and deletions in up to 34 cancer-associated genes.

Results: The genetic landscape of patients with BC undergoing palbociclib treatment was dynamic and changed over the course of treatment. Regarding progression-free survival, alterations in *NRAS* (Hazard Ratio (HR): 11.97, P < 0.005)), *MAP3K1* (HR: 6.86, P < 0.005), and *TP53* (HR: 3.6, P = 0.02) were identified in cfDNA on D15 and were linked to poor prognoses. Alterations in *CBFB* at baseline (HR: 5.15, P = 0.01), in *BRCA2* (HR: 7.17, P < 0.005) and *NRAS* (HR: 5.32, P < 0.005) at D15, and *ESR1* (HR: 4.37, P = 0.01) at EOT were also linked to poor prognosis, whereas alterations in *WEE1* (HR: -5.84, P = 0.02) at EOT were associated with a favorable prognosis. Alterations in *ESR1*, *WEE1, CBFB*, and *BRCA2* were prognostic factors at peak frequencies during treatment. Moreover, our research uncovered a novel observation that as treatment progressed, the relationship between prognostic factors focused on alterations in *ESR1* and *TP53* tended to weaken.

Conclusion: Cancer panel testing for cfDNA identified prognostic and predictive biomarkers for palbociclib add-on therapy after acquiring fulvestrant resistance in patients with HR-positive/HER2-negative ABC/MBC. These findings have important implications for patient selection and personalized treatment strategies in such patients.

#5204 Exploring the therapeutic potential of EGFR retreatment: A comprehensive analysis of T790m(+) conversion and prognosis in lung cancer patients.

Joong Jin Ahn[1], Jae Cheol Lee[2], Chang Min Choi[3], In Ae Kim[4], Kye Young Lee[4], Jeong Eun Lee[5], Seung Hoon Jang[6], Seong Hoon Yoon[7], In Jae Oh[8], Sang Hoon Lee[9], Eun Young Kim[9], Juwhan Choi[1], **Sung Yong Lee**[1]

[1]Korea University Guro Hospital, Seoul, Korea, Republic of,[2]Ulsan University Asan Medical center, Seoul, Korea, Republic of,[3]Ulsan University Asan Medical Center, Seoul, Korea, Republic of,[4]Konkuk University Medical Center, Seoul, Korea, Republic of,[5]Chungnam National University Hospital, Daejeon, Korea, Republic of,[6]Hallym University Medical Center, Anyang, Korea, Republic of,[7]Pusan National University Yangsan Hospital, Pusan, Korea, Republic of,[8]Chonnam National University Hwasun Hospital, Jeonnam, Korea, Republic of,[9]Yonsei University Severance Hospital, Seoul, Korea, Republic of

Background: T790M acquired resistance occurs in 30-40% of cases after first- or second-generation EGFR TKI treatment. However, some patients who did not develop T790M mutation are converted to T790M positive through EGFR TKI retreatment. We conducted a Phase II prospective study analyzing T790m (+) conversion and prognosis in patients who were not induced T790M mutation at 2nd biopsy and were re-treated with first-generation EGFR-TKI as the third-line or later therapy.

Methods: We re-administered first-generation EGFR-TKI to 63 patients (gefitinib n=34 or erlotinib n=29) who had previously been treated with first- or second-generation EGFR TKIs and cytotoxic chemotherapy because they were T790M-negative at the 2nd biopsy. Results: Among the 63 patients, a new T790m (+) mutation was identified in 20 patients (32%) with EGFR TKI retreatment. The first EGFR TKI treatment period and EGFR TKI retreatment period were significantly longer in the T790m (+) group than in the T790m (-) group (P-value=0.026, P-value=0.029, respectively). The best response to retreatment was also favorable in the T790m (+) group (P-value=0.038). The median overall survival (OS) in the T790m (+) group was 29.3 months, which was significantly better than the 6.0 months observed in the T790m (-) group (P-value<0.001). In an additional NGS analysis conducted on stored plasma samples from the 24 patients who were negative for T790M in the tumor tissue before retreatment, T790M was detected in five patients. These patients, who were subsequently treated with a third EGFR TKI, demonstrated very favorable overall survival (OS).

Conclusions: EGFR retreatment could induce T790m (+) conversion in approximately one-third of cases, and these patients exhibited favorable prognosis. Through NGS analysis using plasma samples, approximately 20% cases of T790m mutation, which were not detected through routine PCR tests at the tumor tissue, could be identified. Retreatment-EGFR TKI and NGS analysis through blood samples could improve patient prognosis through the additional discovery of T790m (+) mutation.

#5205 Beyond boundaries: ADRB3, a novel prognostic marker in pediatric neuroblastoma.

G. Mattei[1], C. Banella[2], F. Carrozzo[2], A. Pasha[2], A. Tondo[2], C. Favre[2], **M. Calvani**[2];
[1]University of Florence Department of Information Engineering, Firenze, Italy, [2]Meyer Children's Hospital-IRCCS, Firenze, Italy

Introduction: Neuroblastoma (NB) is a pediatric tumor arising from immature nerve cells originating from neural crest cells. This malignancy is characterized by a remarkably early onset, with only 10% of cases occurring beyond 5 years of age. According to the INRG classification, ~50% of patients are classified as low risk (L1/L2). Despite advances in treatment, around 20% of these experienced a relapse within 5 years with a mere 10% survival rate.
Methods: We investigated the role of the adrenoceptor beta-3 (ADRB3) as a prognostic factor for NB. The samples provided by IRCCS Meyer Children's Hospital allowed us to measure cytofluorimetric level expression of ADRB3 in tissue biopsies from 43 NBs, in the circulating tumor cells (CTCs) and in the bone marrow cells (BMCs) at onset and at the end of treatment. Further, to study the role of ADRB3 in NB, we used CRISPR-Cas9 to knock down ADRB3 expression in mice model.
Results: Results indicate that ADRB3 levels in biopsy at the onset are significantly higher (Wilcoxon test, $p = 0.026$) in patients with negative outcome than those who achieved complete remission. The R package survival was used to perform Survival curve analysis to further assess the impact of ADRB3 at the onset in biopsy tissues. Results confirmed a significant separation ($p = 0.031$) between survival curves of patients with high levels and those with low levels, reinforcing its importance as a prognostic factor. Moreover, the same results were found in survival curves ($p = 0.038$) in low-risk patients, corroborating the importance of ADRB3 levels to discriminate between unfavorable or favorable prognosis. Moreover, post-chemotherapeutic treatment analysis, in both residual CTCs and BMCs, indicated statistically differences in ADRB3 levels between fully recovered patients and deceased. Survival curves, stratified by ADRB3 levels in CTCs post-chemotherapy, a favorable prognosis for patients with low levels ($p = 0.0001$). Finally, the expression analysis showed that ADRB3 levels in NB cells led to increment of processes associated with the cellular migration and metastasization and in metabolism.
Conclusion: Our findings suggest that ADRB3 is a significant prognostic factor for NB. Patients with high ADRB3 expression in biopsy at the onset and after the treatment have a higher risk of unfavorable outcome, even for low-risk patients. In conclusion, our results challenge current classification and prognostic paradigms, highlighting ADRB3's crucial role in NB, contributing to refine risk stratification and unveil a new potential target for liquid biopsy of detecting, analyzing and monitoring CTCs.

#5206 High level STING expression in tumor and inflammatory cells is linked to microsatellite instability and favorable tumor parameters in a cohort of 1,900 colorectal cancer patients..

Elena Bady[1], Zhihao Huang[1], Maximilian Lennartz[1], Claudia Hube-Magg[1], Julia Ebner[2], Frank Jacobsen[2], Stefan Steurer[2], Christian Bernreuther[1], Till S. Cauditz[2], Andreas H. Marx[3], Till Krech[2], Eike Burandt[2], Guido Sauter[2], Ronald Simon[2], Sarah Minner[2], **Jan Hendrik Mueller**[1]

[1]University Medical Center Hamburg-Eppendorf, Hamburg, Germany,[2]Department of Pathology, University Medical Center Hamburg-Eppendorf, Hamburg, Germany,[3]Department of Pathology, Clinic Furth, Furth, Germany

Background: The stimulator of interferon genes (STING) is a transmembrane protein expressed on a variety of cell types including epithelial, inflammatory (lymphocytes and macrophages), and endothelial cells. STING expression has been described at variable levels in various tumor types where it might enhance anti-tumoral effects of the immune system and impact tumor angiogenesis. STING activating targeted therapies are currently evaluated in preclinical studies. However, the clinical significance of STING expression in tumor cells as compared to tumor-associated inflammatory cells is not fully resolved.
Methods: To evaluate the potential clinical significance of STING expression in different cell types of colorectal cancer (CRC) tissue (tumor cells, lymphocytes, macrophages and endothelial cells), more than 1.900 patients were analyzed by multiplex fluorescence immunohistochemistry (CKpan, STING, CD45, CD68 and CD31) in a tissue microarray format (TMA) in combination with a deep-learning based algorithm for automated cell detection.
Results: STING expression on colorectal cancer cells varied markedly. Of 1,905 evaluable cancers, 601 (31.5%) showed a strong expression in virtually all tumor cells and 428 (22.5%) lacked STING staining while 478 (25.1%) showed a weak, and 398 (20.9%) a moderate staining. High STING expression on tumor cells was associated with microsatellite instability (MSI, p<0.0001), low tumor stage (p=0.0013), absence of nodal metastasis (pN0, p=0.0003) and tumor localization in the right colon (p<0.0001). A multivariate analysis revealed that these associations were solely driven by the tight relationship between STING expression in tumor cells and MSI. Accordingly, subgroups of tumors with and without MSI lacked significant associations between STING expression on tumor cells and pT or pN categories. While the total number of lymphocytes and macrophages were related to MSI, low pT, and pN0, there were significant associations between a high percentage of STING positive macrophages and lymphocytes to low pT stage (p<0.0001 each) and absence of nodal metastases for high percentage of STING positive macrophages (p=0.0033). STING was regularly expressed on endothelial cells of small vessels. Although the intensity appeared to be variable, there was no link to tumor phenotype.
Conclusion: In summary, the significant link between high STING expression on tumor cells, lymphocytes and macrophages with a favorable tumor phenotype supports the concept of STING representing an enhancer of anti-tumoral effects of the immune system.

#5207 Hypermethylation of SOX17 is an important epigenetic mark in Afro-Brazilian breast cancers.

L. Delgado-Cruzata[1], D. J. Gomes de Paula[2], J. G. Vieira[3], A. L. Christianes[2], T. Simao[3], L. B. Gusmao[3], L. Ribeiro Pinto[2], S. Coelho Soares Lima[2]; [1]John Jay College, New York, NY, [2]INCA, Rio de Janeiro, Brazil, [3]UERJ, Rio de Janeiro, Brazil

Afro-Brazilian women suffer from higher excess breast cancer mortality after adjusting for age, level of education and stage at diagnosis. Limited studies have researched disease characteristics in this population, which can benefit from the identification of molecular markers that can provide an insight into who is at greater risk of mortality. Epigenetic biomarkers represent the combined effect of environmental and genetic factors. Particularly DNA methylation biomarkers can be valuable as biomarkers of breast cancer risk and prognosis. While studies in other populations have identified DNA methylation biomarkers associated with breast cancer and its clinicopathological outcomes, research on Brazilian cohorts has been limited in scope and focused on women of European descent. The goal of this work was to determine the epigenetic makeup of breast cancer in Brazilian women of African descent. To identify epigenetic biomarkers in Brazilian women who self-identified as Black or Brown, we conducted a case-series analysis investigating DNA methylation patterns in tumor (T) and adjacent non-tumor (NT) tissue. For this, we used the Illumina EPIC (850k) arrays to carry out DNA methylation profiling in 48 frozen tissue paired T and NT samples of breast cancer patients treated at the National Cancer Institute Breast Cancer Hospital in Rio de Janeiro, Brazil. We identified a total of 7,749 probes with Benjamini-Hochberg adjusted p-value < 0.0001 and differences between T and NT tissue above |0.3|. Of these, 5,976 or 77.12% had lower DNA methylation in T when compared to NT tissue; while 1,773 (22.88%) had higher DNA methylation. These were used to identify 21 differentially methylated regions (DMRs) that contained a minimum of seven cg sites, a mean difference larger than |0.2| and a maximum difference above |0.4|. DMRs were mostly (12) hypermethylated in T, and included PCDHGA, NKAPL, ZKSCAN4, SPAG6, CA3, DPP6, RGS22, NXPH1, ANK3, OTX2, SOX17, and CDO1. We used pyrosequencing to validate the levels of SOX17 in eighty-eight tumor and non-adjacent tumor tissue DNAs. We found SOX17 to be hypermethylated in T (44.5±19.1% vs 10.2±10.6, p<0.0001). Differences in DNA methylation in T and NT tissue we still observed by race/ethnicity categories, 43.9±18.6% vs 11.0.±13.2% (p<0.0001) for Brown, and 45.1±20.7% vs 8.8±3.0% for Black women (p<0.0001), respectively. Similarly to previously reported, SOX17 hypermethylation was found to be associated with Luminal A and B molecular subtypes (p<0.0001). To our knowledge, this is the first study to use a discovery approach to identify epigenetic biomarkers in Black and Brown Brazilian women. Our findings confirming previously reported data on SOX17 hypermethylation in breast cancer are encouraging. We expect to validate other epigenetic markers unique to this population that can ultimately aid in the molecular characterization of Brazilian breast cancers.

#5208 Dynamic changes in circulating tumor DNA and T cell receptor repertoire predict disease progression in patients with unresectable esophageal squamous cell carcinoma.

Baidong Zhang[1], Xiang Zhan[2], Qiang Li[1], Chenxuan Wang[3], Jiaohui Pang[3], Yaru Zhang[3], Song Wang[3], Qiuxiang Ou[3], **Haimeng Tang**[3], Alei Feng[1], Zhe Yang[4]

[1]Tumor Research and Therapy Center, Shandong Provincial Hospital Affiliated to Shandong First Medical University, Jinan, China, [2]Tumor Research and Therapy Center, Shandong Provincial Hospital, Shandong University, Jinan, China, [3]Nanjing Geneseeq Technology Inc, Nanjing, China, [4]Tumor Research and Therapy Center, Shandong Provincial Hospital, Shandong University, Shandong Provincial Hospital Affiliated to Shandong First Medical University, Jinan, China

Background: Patients with unresectable esophageal squamous cell carcinoma (ESCC) showed variations in their response to treatments and experienced inevitable disease progression. The development of non-invasive and clinically viable biomarkers is urgently needed. Therefore, this study aimed to investigate prognostic value of circulating tumor DNA (ctDNA) and T cell receptor (TCR) repertoire in these patients.

Methods: A total of 21 ESCC patients who underwent definitive chemoradiotherapy, radiotherapy, or immune checkpoint inhibitor (ICI)-combined therapy from October 2020 to March 2022 were retrospectively evaluated. Baseline tumor samples were collected for genomic profiling using targeted NGS. Baseline and post-therapy plasma were collected for genomic and TCR profiling.

Results: We found that ctDNA detection rates were significantly reduced after treatment ($P<0.001$). Post-treatment ctDNA positivity were associated with worse local recurrence-free survival ($P=0.001$) and progression-free survival ($P=0.001$), but not overall survival. Moreover, TCR clonality was significantly increased after treatment, including CDR3 diversity ($P=0.003$), TCR clonotype ($P=0.004$), and VJ pairs ($P=0.010$), indicating an increased T cell expansion and complexity. Specifically, we identified two increased and four reduced VJ rearrangements after treatment, and the four reduced VJ rearrangements (Vβ12-2Jβ2-4, Vβ6-9Jβ1-5, Vβ6-7Jβ1-5, and Vβ6-9Jβ1-1) were significantly associated with worse progression-free survival.

Conclusion: Our findings suggest the prognostic implication of plasma ctDNA and TCR profiles in patients with unresectable ESCC receiving definitive therapy, supporting the future development of non-invasive monitoring of disease progression in these patients.

#5210 The Prognostic value of serum TK1 protein determinations using AroCell TK210 ELISA in DLBCL patients treated with R CHOP.

K. Jagarlamudi[1], G. Hedstrom[2], P. Venge[2], S. Eriksson[3], D. Molin[2], G. Enblad[2];

[1]AroCell AB, Stockholm, Sweden, [2]Uppsala University, Uppsala, Sweden, [3]Swedish Agricultural University, Uppsala, Sweden

Background: Diffuse large-cell B-cell lymphoma (DLBCL) is the most common subtype of non-Hodgkin's lymphomas (NHL) that accounts for approximately 25% of the patients. Earlier studies demonstrated the prognostic value of serum thymidine kinase 1 (STK1) activity determinations in different hematological malignancies. To date, the prognostic value of STK1 protein concentration in patients with DLBCL treated with R-CHOP has not been investigated. The purpose of this retrospective study was to determine the value of high TK levels on Overall survival among DLBCL patients treated with R-CHOP as first-line treatment.
Materials and Methods: The study included 146 patients diagnosed with DLBCL between 2010 and 2016 from the Uppsala-Umeå Comprehensive Cancer Consortium (U-CAN). All patients included were treated using the standard chemotherapy regimen R-CHOP. Serum samples were collected at the time of diagnosis, during the treatment, 1 year after treatment, and after relapse. Non-infected and apparently healthy persons, matched to the DLBCL patients (57 males and 88 females), served as controls. The TK1 protein levels in all serum samples were determined by using AroCell TK 210 ELISA (AroCell AB, Sweden). The TK1 protein concentration was expressed as µg/L.
Results: The TK1 concentrations in sera from DLBCL patients before treatment were significantly higher compared to the concentrations in healthy individuals, median 0.44 µg/L (IQ range 0.22 to 1.06 µg/L) vs. median 0.22 µg/L (IQ range 0.18 to 0.29 µg/L, P<0.00001). Serum TK1 was also significantly higher in patients with more advanced stages (P<0.00001), higher IPI (P<0.00001), and in patients with B-symptoms (P<0.0001). Patients with STK1 protein levels below the cut-off value (0.45 µg/L) had significantly better OS and DFS (P=0.04 and P=0.0006, respectively) compared to patients with STK1 concentration above the cut-off. In multivariate analyses, dichotomized S-TK1 measurements before treatment were found to be significant for the risk of relapse in combination with either aaIPI or IPI (p<0.01).
Conclusions: These results confirmed that STK1 concentration correlates with risk factors such as tumor burden, Ann Arbor stage, and IPI. In conclusion, patients with high TK1 concentrations at the time of diagnosis have short overall survival and STK1 concentrations are apparently a prognostic indicator for survival in patients treated with modern chemo-immunotherapy.

#5211 Somatic copy number variation as prognostic marker for recurrence in never-smokers with early-stage lung adenocarcinoma.

S. Vanstraelen, A. Reiner, B. H. Mastrogiacomo, K. Tan, J. Dycoco, B. J. Park, P. S. Adusumilli, M. J. Bott, D. R. Jones, G. Rocco;
Memorial Sloan Kettering Cancer Center, New York, NY

Objective: Lung cancer in never-smokers has a distinct genomic profile with low tumor mutation burden, more tumor promotor mutations and fewer somatic copy number variations (CNV) than smokers. CNVs have shown to be associated with poor outcome in advanced stage disease. However, the relationship between CNV and clinicopathologic features on prognosis in early-stage lung cancer is undefined. To address this knowledge gap, we assessed the impact of CNV on recurrence in never-smokers who underwent curative resection for pathological stage I-II lung adenocarcinoma using an integrated genomic and clinicopathological analysis.

Methods: We analyzed a cohort of 210 never-smokers with stage I-II lung adenocarcinoma treated from 2014 to 2022 who met the inclusion criteria (no neoadjuvant therapy, pathological stage I-II, complete resection, next-generation sequencing available). The patient cohort was stratified using unsupervised hierarchical clustering of arm-level CNVs. We assessed cumulative incidence of recurrence (CIR) between CNV groups using competing risk regression analysis, adjusting for SUVmax, pathologic stage, lymphovascular invasion, IASLC grade, and tumor mutation burden.

Results: Of the 210 patients, 159 patients were female (76%), and patients were primarily from Caucasian (n=140, 67%) or Asian decent (n=50, 24%). Based on arm-level CNV clustering, the cohort was stratified into three groups: CNV low (n=86, 41%), CNV moderate (n=75, 36%) and CNV high (n=49, 23%). The CNV low tumors were characterized by a low CNV burden. Conversely, the CNV moderate tumors primarily exhibited gains in chromosomes 1q, 5p and 7p, along with loss of heterozygosity in chromosome 9p, 9q and 13. CNV high tumors were characterized by whole-genome doubling. Whole-genome doubling was significantly more common in CNV high tumors (n=33, 66%) compared to CNV low (n=2, 2.3%) and CNV moderate tumors (n=2, 2.7%) (*p<.001*). *EGFR* (n=145, 69%) and *TP53* (n=61, 29%) were the most frequently altered genes, with *EGFR* alterations being significantly more prevalent in CNV high tumors (n=41, 84%) compared to CNV low tumors (n=46, 53%) (*p<.001*). In total, 42 patients (20%) developed recurrences. The CIR was lower in the CNV low group (5y-CIR, 14%, 95%CI: 6.5%-25%) compared to the CNV moderate (5y-CIR, 31%, 95%CI: 18%-44%) and CNV high group (5y-CIR, 48%, 95%CI: 27%-66%) (*p=.004*), with adjusted hazard ratios of 2.3 (95%CI: 0.93-5.71; *p=0.074*) and 2.65 (95%CI: 1.07-6.60; *p=.037*), respectively. The CIR for locoregional (n=11, 5%) and distant recurrence (n=31, 15%) remained lower in the CNV low group compared to the combined CNV moderate & high groups (Gray test *p=.020* and *p=.049*, respectively).

Conclusion: In never-smokers who underwent curative treatment of pathological stage I-II lung adenocarcinoma, copy number status seems a predictor of recurrence, with CNV low tumors associated with the best prognosis.

#5212 Prognostic biomarkers for breast cancer: Metabolic and inflammatory pathways.

A. N. McMahon[1], C. Takita[1], J. L. Wright[2], I. M. Reis[1], E. Lee[3], G. Yang[1], J. J. Hu[1];
[1]University of Miami Miller School of Medicine, Miami, FL, [2]Johns Hopkins University School of Medicine, Washington, DC, [3]University of Central Florida, Miami, FL

Objective: To assess the prognostic significance of molecular biomarkers, particularly metabolic and Inflammatory pathways using samples from a prospective study of breast cancer patients undergoing adjuvant radiotherapy (RT).
Methods: We used ultra-performance liquid chromatography-mass spectrometry (UPLC-MS/MS) for measuring urine metabolites. Following normalization to osmolality, log transformation, and imputation of missing values, we used Welch's two-sample t-test to identify biochemicals that differed significantly by progression status. We measured pre- and post-RT plasma high-sensitivity C-reactive protein (hsCRP) levels. Progression-free survival (PFS) was calculated from the date of diagnosis to the date of disease progression or last follow-up. Univariable and multivariable Cox proportional hazards regression models assessed the associations between hsCRP and PFS.
Results: In 120 breast cancer patients, carbohydrate metabolism, branch-chain amino acid (BCAA) metabolism, phosphatidylcholine metabolism, arginine metabolism, oxidative stress-related metabolites, androgenic steroids, and nucleotide metabolism had the most notable differences in patients with progression versus progression-free cases. In 488 breast cancer patients, RT significantly increased plasma hsCRP levels, and post-RT hsCRP levels were significantly higher in deceased vs. alive patients (p=0.031). In multivariable models, hsCRP had a prognostic value for all-stage and stage 0-II patients.
Conclusions: In our study of breast cancer patients receiving adjuvant RT, multiple metabolite biomarkers and post-RT plasma CRP levels were associated with a worse prognosis. BCAAs and fatty acids regulate cell metabolism by affecting mitochondrial function and inflammation signals. Thus, our findings suggest a potential role of metabolic and inflammatory pathways in breast cancer prognosis. These molecules may have potential utility as prognostic biomarkers for breast cancer patients undergoing adjuvant RT and targets for intervention.
Keywords: breast cancer, metabolomics, inflammation, prognosis

#5213 Evaluation of HER2DX risk-score in residual disease (RD) from HER2-positive (HER2+) early breast cancer (EBC) patients (pts) following neoadjuvant trastuzumab and pertuzumab (HP)-based therapy: An exploratory analysis from the PHERGain trial.

Jose Manuel Perez-Garcia[1], Fara Braso-Maristany[2], Elena Martinez-Garcia[1], Carmen Mora Gallardo[1], Eileen Shimizu[3], Olga Boix Sanchez[1], Jose Rodriguez-Morato[1], **Mario Mancino**[1], Laia Pare[4], Guillermo Villacampa[4], Mercedes Marin-Aguilera[4], Patricia Galvan[2], Ana Vivancos[5], Patricia Villagrasa[4], Joel Parker[6], Charles M. Perou[6], Antonio Llombart-Cussac[1], Javier Cortes[1], Aleix Prat[4]

[1]Medica Scientia Innovation Research (MEDSIR), Barcelona, Spain,[2]Translational Genomics and Targeted Therapies in Solid Tumors, Institut D'Investigacions Biomediques August Pi i Sunyer, Barcelona, Spain,[3]Medica Scientia Innovation Research (MEDSIR), Jersey City, NJ,[4]Reveal Genomics S L, Barcelona, Spain,[5]Cancer Genomics Group, Vall d'Hebron Institute of Oncology (VHIO), Barcelona, Spain,[6]Lineberger Comprehensive Cancer Center, University of North Carolina, Chapel Hill, NC

Introduction:
HER2DX is a prognostic (risk-score) and predictive (pathological complete response-score) genomic assay validated in baseline (BL) tumor samples from HER2+ EBC pts. RD after neoadjuvant anti-HER2-based therapy is associated with worse outcomes. Whether HER2DX risk-score analyzed in RD provides additional prognostic information is unknown.

Methods:
This retrospective analysis included 14 pts from group B of the PHERGain trial (NCT03161353): 6 who developed distant recurrences and 8 matched controls with HER2DX high-risk score at BL who did not. Group B pts had centrally confirmed, stage I-IIIA, HER2+ EBC and were treated with HP (± endocrine therapy), with chemotherapy added for pts without PET response after 2 treatment cycles or pathological complete response (Perez-Garcia et al, Lancet Oncol 2021).HER2DX was evaluated on tumor samples collected at BL and surgery. The primary objective was to determine the association of HER2DX risk-score in RD with the development of distant recurrences. Secondary objectives were to assess gene expression and the HER2DX signatures in BL vs RD and their association with distant recurrences. Cox regression models evaluated the association of variables with distant recurrence. Paired SAM with a false discovery rate <5% identified differences in gene expression between BL and RD samples.

Results:
Median follow-up was 4.04 years. Five (83.3%) of 6 pts with distant recurrences had HER2DX high-risk scores at BL. The 8 control pts had HER2DX high-risk scores at BL but no relapse. In RD, all 6 pts (100%) who relapsed had a HER2DX high-risk score, while 4 (50%) of 8 pts without distant recurrence presented a HER2DX downstaging. Pts with HER2DX low-risk in RD had better 3-year distant disease-free survival than high-risk pts (100% vs 50%; hazard ratio = 4.34 [1.03-18.23], p=0.045). In RD, high expression of the proliferation signature and 15 genes, including proliferation genes, and low expression of 38 genes, including immune and luminal-related genes, were associated with poor prognosis. In paired analyses of BL and RD samples, 118 genes (63.8%) were differentially expressed in pts that did not relapse, while only 3 genes (1.6%) were differentially expressed in pts that relapsed.

Conclusions:
These data suggest that HER2DX risk-score in RD provides additional information on the likelihood of developing distant recurrences. In RD, high expression of immune and luminal genes was associated with a reduced risk, while high expression of proliferation genes was associated with a higher risk. Molecular changes after anti-HER2 therapy were mainly observed in RD of pts that did not relapse. Prognostic impact of HER2DX downstaging merits further evaluation.

#5214 HYAL4 splice variant induces treatment-resistance in advanced bladder cancer.

K. Aguilar, S. Panda, J. Van Der Eerden, L. Lopez, M. Terris, P. Santamaria, B. Lokeshwar, V. B. Lokeshwar;
Augusta University, Augusta, GA

Introduction and Objective: Precision-based treatment approaches could improve the prognosis of patients with bladder cancer (BC). We recently discovered a first-in-class human Chondroitinase (Chase) that degrades chondroitin sulfate. This Chase is a splice variant of HYAL4 (V1) and promotes a malignant phenotype and chemoresistance in BC cells. We evaluated V1/Chase expression and functions in BC and inhibitors to overcome V1/Chase-mediated Gemcitabine (Gem) resistance.

Methods: Cohort 1: 653 voided urine specimens (BC, 160; non-BC, 493); cohort 2: 40 cystectomy specimens from MIBC patients who received adjuvant Gemcitabine plus cisplatin (G+C) treatment. Gene expression was measured by q-PCR and urine was assayed by the Chase test. V1 was expressed in BC cell lines or silenced and the transfectants were analyzed for sensitivity to Gem and Cisplatin. The mechanism of Gem resistance was evaluated in preclinical *in vitro* and *in vivo* models.

Results: In cohort 1, Chase levels were 7-10-fold elevated in patients with BC compared to patients with benign genitourinary conditions, history of BC, or other cancers. Chase test detected BC with 94.4% and 87.4% specificity. Chase test had 84% accuracy in correctly diagnosing the cases with atypical cytology inference. Stem cell marker CD44 was the major substrate of Chase in BC cells. V1's Chase activity induced CD44 cleavage and shedding. Intracellularly, CD44 cleavage induced JAK2/Stat3 pathway and subsequently upregulation of cytidine deaminase. CDA induces Gem metabolism and efflux of dFdU, an inactive Gem metabolite. HPLC analysis showed, V1 transfectants have increased levels of dFdU and higher efflux. STAT3 and CDA inhibitors synergistically re-sensitized V1-expressing cells to Gem. In cohort 2, V1, p-JAK2 and CDA expression predicted failure to G+C treatment ($P<0.0001$). JAK2, STAT3 and CDA inhibitors synergistically re-sensitized V1-expressing cells to Gem. V1-induced muscle invasive tumors that were metastatic. While V1-expressing tumors were resistant, combination of Gem with a CDA or JAK-2 inhibitor abrogated V1 tumor growth with minimal toxicity.

Conclusion: V1/Chase is a potential diagnostic and prognostic biomarker for bladder cancer and drives muscle-invasion, metastasis, and Gem resistance in BC. Inhibitors of the Chase signaling pathway overcome V1-induced Gem resistance, suggesting a precision-based treatment approach to improve treatment response.

Support: 1R01CA227277-05A1; 1R01CA283699-01

#5215 Orphan noncoding RNA (oncRNA) liquid biopsy assay is prognostic for survival in patients with triple-negative breast cancer (TNBC) and residual disease.

R. Yoder[1], J. Yen[2], M. Karimzadeh[2], J. M. Staley[1], I. Fernandez[3], A. C. Heinrich[3], F. Hormozdiari[2], J. Gregg[2], A. K. Godwin[4], I. Acerbi[2], R. Trivedi[2], B. Alipanahi[2], S. R. Stecklein[4], P. Sharma[3],

[1]The University of Kansas Cancer Center, Westwood, KS, [2]Exai Bio, Inc., Palo Alto, CA, [3]University of Kansas Medical Center, Westwood, KS, [4]University of Kansas Medical Center, Kansas City, KS

Introduction: Residual disease (RD) after neoadjuvant systemic therapy is associated with high recurrence risk in patients with TNBC. oncRNAs are a novel category of small RNAs that are largely absent in healthy tissue but enriched in tumors and can be detected using a blood-based assay. This study investigated impact of an oncRNA recurrence risk model on outcomes in TNBC patients with RD.

Methods: Study population included stage I-III TNBC patients with RD and available end-of-treatment (EOT) serum samples who were enrolled in a multisite prospective cohort study. EOT samples were collected after completion of all curative treatment (local/systemic). Small RNAs were isolated from EOT serum, sequenced at average depth of 76.5 ± 12.5 million 50bp single end reads, and annotated using a bespoke bioinformatics pipeline to identify oncRNAs. Cancer risk scores were generated using an oncRNA based tumor detection artificial intelligence model trained on 451 treatment naive breast cancer samples and 470 samples from individuals without known cancer diagnosis. Score cutpoint for high vs low recurrence risk was determined through ROC analysis. Impact of EOT oncRNA risk category on event free survival (EFS) and overall survival (OS) was estimated by Kaplan Meier method and compared by log rank test followed by Cox regression. Residual cancer burden (RCB) was determined according to classification by Symmans et al.

Results: oncRNA isolation/score generation was successful for 79 out of 80 TNBC patients with RD and available EOT serum sample. Median age was 48 years and 39% had node positive disease. RCB class distribution was as follows: RCB I=27%, RCB II=49%, RCB III=18%. Training set (n=39) was used to define oncRNA risk score cutpoint. In the testing set (n=40), 38% were classified as oncRNA high-risk and 62% as oncRNA low-risk. oncRNA risk category was not associated with baseline T stage, nodal status, or RCB class. oncRNA high-risk status was associated with lower EFS and OS; 3y EFS was 47% and 73% (HR 2.76, 95% CI 0.92-9.24, p=0.058) and OS 53% and 76% (HR 3.78, 95% CI 1.19-12.00, p=0.016) in high and low risk groups, respectively. In multivariable analysis including oncRNA risk status, T stage, nodal status, and RCB class, oncRNA high risk status retained significant association with lower EFS (HR 7.70, 95% CI 1.33-44.64, p=0.023) and OS (HR 7.99, 95% CI 1.36-47.00, p=0.022).

Conclusion: EOT oncRNA liquid biopsy assay was independently prognostic for outcomes in TNBC patients with RD. More than half of patients in the oncRNA high-risk group suffered an EFS event by 3 years. oncRNA risk score has potential to provide prognostic utility complementary to clinicopathologic characteristics in patients with TNBC. These findings should be confirmed in other TNBC studies and may provide insights for patient stratification/selection in RD adjuvant therapy intensification trials.

#5216 Peripheral T cell receptor repertoire diversity is associated with outcome in bladder cancer.

A. Kjar[1], N. Kristjansdottir[1], I. Nordentoft[1], R. Juul[1], K. Birkenkamp-Demtroder[1], J. Ahrenfeldt[1], D. Hodgson[2], C. Abbosh[2], H. Aerts[3], M. Agerbak[4], J. Jensen[4], N. Birkbak[1], L. Dyrskjot[1];

[1]Aarhus University, Aarhus, Denmark, [2]AstraZeneca, Cambridge, United Kingdom, [3]Harvard Medical School, Boston, MA, [4]Aarhus University Hospital, Aarhus, Denmark

Bladder cancer is the sixth most common cancer overall, and treatment often involves removal of the bladder, which comes with a significant reduction in quality of life. Within this cancer type, an easily applicable prognostic biomarker may have clinical utility, potentially stratifying patients into bladder-sparing treatments. Expansion of T cell populations targeting cancer-specific neoantigens is an early response to malignancy. To investigate if the T cell receptor (TCR) repertoire could serve as a biomarker for cancer progression, we analyzed the TCR landscape in a cohort of 119 patients with muscle-invasive bladder cancer, treated with neoadjuvant chemotherapy before undergoing radical cystectomy.

Peripheral and tumor TCR repertoires were produced using amplicon-based sequencing of the TCR beta chain. Additionally, T cell fraction was determined from whole exome sequencing data using TcellExTRECT, and latent viral DNA was investigated in plasma whole genome sequencing data using Kraken2. Antigen targets were estimated using GLIPH2. To explore the T cell repertoire subtypes, single-cell sequencing was performed on four fresh blood samples.

In pre-treatment peripheral blood, low-diversity TCR repertoires were associated with worse survival (HR=2.3, p=0.024). Particularly poor outcome was observed in a subset of patients with both low TCR diversity and low fraction of circulating T cells (HR=4.7, p=5e-4). Low-diversity repertoires were dominated by expanded T cell clones. TCR target annotation revealed that expanded T cell clones disproportionately targeted latent viral infections (p=2e-13), and cytomegalovirus DNA detection was strongly associated with decreased TCR diversity (p=5e-5). Additionally, tumor TCR sequencing revealed that expanded clones were rarely found in the tumor. Single-cell sequencing of peripheral blood found that most expanded clones consisted of cytotoxic T cells, while non-expanded clones mostly consisted of naive T cells. This indicates that low TCR diversity may represent a contraction of the naive T cell compartment, resulting in reduced immune competence. Finally, analysis of patient-matched longitudinal samples revealed that chemotherapy and cystectomy reduced TCR diversity in patients with high pre-treatment diversity (p=0.001), indicating that treatment negatively affected the immune system in the most immune-competent patients.

Our results suggest that both low TCR diversity and low T cell fraction represent decreased immune competency. This could be associated with an elevated risk of progression due to a reduced ability to control cancer growth and limit systemic cancer cell dissemination. These findings underline that immune health is an important factor during malignant disease, even when patients are not treated with immunotherapies. Therefore, improving immune health could be a potential future goal for cancer treatment and prevention.

#5217 Genome instability in renal tumors.

Hanbyul Cho, Ginny X. Li, Rahul Mannan, Noshad Hosseini, Yi Hsiao, Yuping Zhang, Aniket Dagar, Chandan Kumar-Sinha, Marcin P. Cieslik, Saravana M. Dhanasekaran, Alexey I. Nesvizhskii, Arul M. Chinnaiyan, Clinical Proteomic Tumor Analysis Consortium

University of Michigan Medical School, Ann Arbor, MI

Genome instability (GI), a recognized cancer hallmark, encompasses CNV burden, tumor mutational burden (TMB), and microsatellite instability and is variably associated with several clinical/ prognostic features in solid tumors. GI and intratumor mutational heterogeneity in clear cell renal cell carcinoma (ccRCC) were associated with poor prognosis in a large multi-site sequencing study. As 10-15% of renal tumors exhibit copy number burden associated GI, the development of proteogenomic biomarkers to identify this subset of tumors will be of high clinical value. In our in-depth analysis of CPTAC renal cancer cohorts namely, ccRCC discovery and rare RCC, we first estimated absolute copy number using CNVEX TPO analysis pipeline. Copy number burden-based genome instability was estimated by calculating whole genome instability index (wGII) from DNA sequencing data, in addition to the estimation of genome ploidy and purity of the tumors. Genome instability was associated with survival outcomes in both ccRCC and rare RCC (Ref. 1 and 2). Differential proteogenomic analysis identified IGF2BP3, IGF2BP1, PYCR1 RNA and protein, to be upregulated among high wGII tumors. High wGII tumors showed upregulation of cell proliferation and other cell cycle/proliferation concepts in gene set enrichment analysis. Interestingly, transcriptional module analysis revealed transcription factors and target genes specifically upregulated in GI cases and this pattern showed certain degree of overlap to 9p loss ccRCC tumors (another molecular ccRCC subset that is also associated with poor prognosis). Differential expression analysis also identified, kinases, phosphosites and co-regulated kinase-substrates that are dysregulated in genome instable renal tumors. IGF2BP3 immunohistochemistry staining showed specific overexpression in high wGII tumors and the high positivity was observed exclusivity in the tumor cells. Prognostic biomarkers IGF2BP3, IGF2BP1, PYCR1, and UCHL1 show great promise to be developed as clinical prognostic assays and warrants additional characterization.

#5219 Loss of chromosome Y is unrelated to the composition of the tumor microenvironment and patient prognosis in muscle-invasive urothelial bladder cancers.

M. Kluth[1], H. Plage[2], S. Hofbauer[2], K. Furlano[2], S. Weinberg[2], A. Franz[2], A. Fendler[2], F. Ro?ner[2], S. Schallenberg[2], S. Elezkurtaj[2], N. C. Blessin[1], M. Lennartz[1], A. H. Marx[3], H. Samtleben[3], M. Fisch[1], M. Rink[4], M. Slojewski[5], K. Kaczmarek[5], T. Ecke[6], S. Koch[6], N. Adamini[7], R. Simon[1], G. Sauter[1], J. Weischenfeldt[8], T. Klatte[6], S. Minner[1], D. Horst[2], T. Schlomm[2], D. Zecha[7];

[1]University Medical Center Hamburg-Eppendorf, Hamburg, Germany, [2]Charite - Universitatsmedizin Berlin, Corporate Member of Freie Universitat Berlin, Humboldt-Universitat zu Berlin and Berlin Institute of Health, Berlin, Germany, [3]Academic Hospital Fuerth, Fuerth, Germany, [4]Marien Hospital Hamburg, Hamburg, Germany, [5]Pomeranian Medical University, Szczecin, Poland, [6]Helios Hospital Bad Saarow, Bad Saarow, Germany, [7]Albertinen Hospital, Hamburg, Germany, [8]Charite - Universitatsmedizin Berlin, Corporate Member of Freie Universitat Berlin, Humboldt-Universitat zu Berlin and Berlin Institute of Health, Berlin, Germany, Biotech Research & Innovation Center (BRIC), University of Copenhagen, Copenhagen, Denmark

Background: Loss of chromosome Y (LOY) occurs commonly in cancers of male patients. It was recently proposed to be associated with cancer aggressiveness and altered T-cell function in bladder cancer and it was found to be linked to poor prognosis in a TCGA bladder cancer patient cohort of 300 patients based on a combined analysis of RNAs from Y-chromosome genes. In this study, we aimed to clarify the clinical relevance of LOY in a large cohort of urothelial bladder cancer patients by using fluorescence in-situ hybridization (FISH).

Design: X and Y chromosomes were analyzed by FISH on a tissue microarray (TMA) containing 1,819 urothelial carcinomas of the urinary bladder from male patients including 487 patients who had undergone cystectomy for muscle-invasive disease and for which follow-up data were available. Data of tumor microenvironment parameters were obtained in a previous study.

Results: LOY was found in 26.0% of 1,479 analyzable cancers. In the subset of non-invasive cancers, the frequency of LOY increased from pTaG2 (14.5%) to pTG3 (28.6%) but these differences were not significant (p=0.1015). In muscle-invasive cancers, the frequency of LOY increased slightly from pT2 (25.4%) to pT4 cancers (32.8%) but this association was again not significant (p=0.1868). Within pT2-4 cancers, LOY was associated with venous invasion (p=0.0010) but unrelated to pT, pN, and L-status, as well as to overall, recurrence-free, and cancer-specific survival. Muscle-invasive urothelial carcinomas with and without LOY did not show significant differences in the number of CD8 positive lymphocytes, the fraction of CD8 positive intraepithelial lymphocytes, the number of macrophages and dendritic cells, as well as the fraction of t helper and t regulatory cells.

Conclusion: FISH is the gold standard for determining LOY. That LOY was neither associated with histopathological parameters of cancer aggressiveness and patient prognosis nor with any parameters describing the tumor microenvironment strongly argues against a driving role of LOY for bladder cancer progression and cancer associated immune reaction. The slight increase of LOY from pTaG2 to pT4 cancers is consistent with a continuous (but clinically irrelevant) loss of the dispensable Y chromosomes during tumor evolution over time.

#5220 Reduced expression of Glutathione peroxidase 2 (GPX2) is an independent predictor of poor prognosis in muscle-invasive urothelial carcinoma of the bladder.

H. Plage[1], S. Hofbauer[1], K. Furlano[1], S. Weinberger[1], A. Franz[1], A. Fendler[1], J. Weischenfeldt[2], F. Ro?ner[1], S. Schallenberg[1], S. Elezkurtaj[1], M. Kluth[3], A. H. Marx[4], H. Samtleben[5], M. Fisch[3], M. Slojewski[6], K. Kaczmarek[6], T. Ecke[7], S. Koch[7], N. Adamini[8], R. Simon[3], G. Sauter[3], H. Zecha[8], T. Klatte[7], S. Minner[3], D. Horst[1], T. Schlomm[1], M. Rink[9], **M. Lennartz**[3];

[1]Charite - Universitatsmedizin Berlin, Corporate Member of Freie Universitat Berlin, Humboldt-Universitat zu Berlin and Berlin Institute of Health, Berlin, Germany, [2]Charite - Universitatsmedizin Berlin, Corporate Member of Freie Universitat Berlin, Humboldt-Universitat zu Berlin and Berlin Institute of Health, Berlin, Germany Biotech Research & Innovation Center (BRIC), University of Copenhagen, Copenhagen, Denmark, [3]University Medical Center Hamburg-Eppendorf, Hamburg, Germany, [4]Academic Hospital Fuerth, Hamburg, Germany, [5]Academic Hospital Fuerth, Fuerth, Germany, [6]Pomeranian Medical University, Szczecin, Poland, [7]Helios Hospital Bad Saarow, Bad Saarow, Germany, [8]Albertinen Hospital, Hamburg, Germany, [9]Marien Hospital Hamburg, Hamburg, Germany

Background: The Glutathione peroxidase 2 (GPX2) is a selenium-dependent glutathione peroxidase with a pivotal role in removing potentially harming reactive oxygen species (ROS) from cells by catalyzing the reduction process of hydrogen peroxide to water. GPX2 is strongly expressed in normal urothelium but can be reduced in urothelial cancer. The aim of the study was to evaluate the potential clinical significance of GPX2 expression in urothelial bladder cancer.
Design: GPX2 was analyzed by immunohistochemistry (IHC) in more than 2,500 urothelial bladder carcinomas in a tissue microarray format. Follow-up data were available for more than 600 patients with muscle-invasive disease.
Results: GPX2 staining occurred in 67.5% of urothelial carcinomas including 11.4% with weak, 11.9% with moderate, and 44.2% with strong staining. While GPX2 staining was always strong in normal urothelium, it decreased markedly during grade and stage progression. Within pTa tumors, GPX2 positivity continuously decreased from pTaG2 low grade (99.4% positive) to pTa G2 high grade (97.2% positive) and to pTa G3 (90.5%; p=0.0013) while there was a marked further drop of GPX2 positivity from pTaG3 to muscle-invasive cancers (56.6%; p<0.0001 for pT2-4 vs. pTa G3). Within pT2-4 carcinomas, low or absent GPX2 staining was significantly linked to poor overall survival (p=0.0140), V1 (p<0.0001), L1 (p=0.0014), and high grade (p=0.0091), but statistically unrelated to pT and pN. In a multivariate analysis, the prognostic impact of reduced GPX2 expression (p=0.0081) was independent of pT (p<0.0001) and pN (p<0.0001) in pT2-4 tumors. GPX2 expression loss was inversely related to the expression of the luminal subtype markers GATA3 (p<0.0001), uroplakin 1b (p<0.0001) and cytokeratin 20 (p<0.0001) in pT2-4 carcinomas.
Conclusion: GPX2 expression loss is a common event during bladder cancer progression which is strongly associated with poor prognosis in patients with pT2-4 urothelial carcinomas. GPX2 expression measurement - optimally together with other markers - could be useful for clinical risk assessment of bladder cancer patients.

#5221 TTF-1 status in early-stage lung adenocarcinoma is an independent predictor of relapse and survival superior to tumor grading.

S. Schallenberg[1], G. Dernbach[1], M. Dragomir[1], G. Schlachtenberger[2], K. Boschung[3], C. Friedrich[1], K. Standvoss[4], L. Ruff[4], P. Anders[5], C. Grohe[6], W. Randerath[3], S. Merkelbach-Bruse[2], A. Quaas[2], M. Heldwein[2], U. Keilholz[1], K. Hekmat[2], J. Ruckert[1], R. Buttner[2], D. Horst[1], F. Klauschen[7], N. Frost[1];
[1]Charite - University Medicine Berlin, Berlin, Germany, [2]University Hospital Cologne, Cologne, Germany, [3]Bethanien Hospital, Cologne, Germany, [4]Aignostics GmbH, Berlin, Germany, [5]Semmelweis University, Budapest, Hungary, [6]Protestant lung clinic Berlin, Berlin, Germany, [7]Ludwig-Maximilian University of Munich, Munich, Germany

Background: Thyroid transcription factor 1 (TTF-1) is expressed in 70% to 80% of lung adenocarcinomas (LUAD). Several papers revealed that TTF-1 expression is associated with better patient outcomes independent of the tumor stage. However, it is unknown whether the prognostic impact of TTF-1 only results from a different growth pattern (tumor grading) or is independently associated with a biologically more aggressive phenotype. Thus, we analyzed a large bi-centric cohort of LUAD to assume the true prognostic value of TTF-1 in relation to the tumor grade.
Methods: We collected a large, real-life cohort of 447 patients with completely resected LUAD from two large-volume German lung cancer centers. TTF-1 status, evaluated by IHC, and tumor grading were correlated with clinical, pathologic, and molecular data, as well as patient outcomes. Kaplan-Meier curves were used for comparison of TTF-1 status and different tumor grades in terms of the DFS. The impact of TTF-1 was measured by univariate and multivariate Cox regression. Finally, a causal graph analysis was performed to identify and account for potential confounders to improve the statistical estimation of the predictive power of TTF-1 expression for DFS in comparison to the tumor grade.
Results: Kaplan-Meier curves revealed that TTF-1 positivity is associated with longer DFS independent of tumor grade, whereas a strong association of DFS with the tumor grade is observed only in TTF-1-positive patients. In univariate analysis, TTF-1 positivity was associated with significantly longer DFS (median log HR -0.83 [-1.43; -0.20]; p=0.018), whereas higher tumor grade showed a non-significant association with shorter DFS (median log HR 0.30 [-0.58; 1.60]; p=0,62 for G1 to G2 and 0.68 [-0.24; 1.89]; p=0,34 for G2 to G3). In multivariate analysis, TTF-1 positivity resulted in a significantly longer DFS (median log HR -0.65 [-1.13; -0.09]; p=0.05) independent of all other parameters, including tumor grade. Applying the adjustment sets suggested by the causal graph analysis, the superiority of TTF-1 (median log HR -0.86 [-1.25; -0.41]) over tumor grade (median log HR 0.31 [-0.32; 1.30]/ 0.61[-0.07; 1.65]) in terms of prognostic power was confirmed.
Conclusion: This study draws three important conclusions: Firstly, it indicates that the prognostic power of tumor grade is limited to TTF-1-positive patients. Secondly, it underlines the independent prognostic value of TTF-1 expression for DFS regardless of tumor grade. Finally, our analyses reveal that the effect size of TTF-1 surpasses that of tumor grade. To transfer the results directly into the clinical area, we recommend distinguishing between TTF-1-positive and TTF-1-negative LUADs in the pathological report. Tumor grading should only be applied to TTF-1-positive LUADs (TTF-1+ / G1-3). TTF-1-negative LUADs should either not be graded or always be classified as high-grade (TTF-1- / G3).

#5222 AI-driven, mIF-based cell-omics reveals spatially resolved cell signature for outcome prediction in NSCLC patients.

S. Schallenberg[1], G. Dernbach[1], S. Ruane[2], C. Bohm[2], L. Ruff[2], K. Standvoss[2], S. Ghosh[2], M. Frentsch[1], M. Dragomir[1], R. Fritz[1], I. Koch[1], C. Friedrich[1], I.-K. Na[1], S. Merkelbach-Bruse[3], A. Quaas[3], N. Frost[1], K. Boschung[4], W. Randerath[4], G. Schlachtenberger[3], M. Heldwein[3], U. Keilholz[1], K. Hekmat[3], J. Ruckert[1], R. Buttner[3], A. Vasaturo[5], D. Horst[1], M. Alber[2], F. Klauschen[6],

[1]Charite - University Medicine Berlin, Berlin, Germany, [2]Aignostics GmbH, Berlin, Germany, [3]University Hospital Cologne, Cologne, Germany, [4]Bethanien Hospital, Cologne, Germany, [5]Ultivue, Cambridge, MA, [6]Ludwig-Maximilian-University of Munich, Munich, Germany

Background: Despite the rapidly increasing number of new targeted and immunotherapeutic options over the past two decades, the prognosis of patients with NSCLC, even with early-stage tumors, is still poor and novel biomarkers are needed to better stratify patients in terms of survival and treatment response. A novel approach is to gain a holistic understanding of the cellular composition and formation of the tumor microenvironment (TME). Therefore, we developed a miF-based, AI-driven approach for spatially resolved TME characterization at the cellular level and used this to successfully predict clinical outcome.

Methods: We assembled a large bicentric real-world sample group of 1168 patients with resected NSCLC from the Charite and the University Hospital Cologne. For tissue microarray construction, four 1.5 mm tissue cores were punched from each formalin-fixed and paraffin-embedded tumor block. Sections were stained with a 12-plex IF panel followed by H&E staining. All stains were scanned and co-registered with single cell accuracy. Next, we trained a H&E-based tissue segmentation model to detect the different tumor regions: carcinoma, stroma, and necrosis. In addition, we developed a nucleus-based cell detection model, and 12 cell classification models to categorize each detected cell by single-miF channels. Different cell phenotypes were derived from the marker-specific cell classifications. Finally, we trained a model on the Charité cohort using the spatially resolved cell readouts, spot-wise phenotype log-density, co-clustering of marker expression, and frequency of co-occurrence of marker expression through Delaunay triangulation, to predict patient survival on the Cologne cohort.

Results: The tissue segmentation model achieved a macro averaged F1 score of 92%. The cell detection model identified a total of 53 million cells that were classified marker-wise with an F1 score of at least 95% on hold-out data. Our final prediction model identified a stable spatially resolved cell signature, consisting of 10 different characteristic cell neighborhood niches, which could be used to predict overall patient survival. The model trained on the Charite cohort was validated with the Cologne cohort and achieved a high performance (C-score of 71). In comparison, the UICC8 stage and the immunoscore ($CD20^{\pm}CD3^{\pm}$/carcinoma cell ratio), which were used as a baseline, achieved C-scores of 63 and 54, respectively.

Conclusions: The combination of our large real-world clinical cohort, multiplex panel, and automated AI approach enabled a broad spatially resolved exploration of the TME in NSCLC at single cell resolution. Our model identified a specific cell neighborhood signature predictive of patient survival outperforming the commonly used prognostic scores, UICC8 stage and immunoscore. This allows for an improved patient stratification with potential implication for therapy selection.

IMMUNOLOGY: Adoptive Cell Therapies 4
Poster Session

#5226 A 3D ECM embedded tumoroid platform for testing antibody drugs and engineered TCRs for immune oncology.
E. H. Danen;
Leiden Univ., Leiden, Netherlands

We developed a screening platform for immune oncology using an assay based on automated image guided injection of tumoroids in wells of multi-well plates preloaded with a collagen-rich ECM. The identical x-y-z position and size of the ECM-embedded tumoroids in each well facilitates automated real time confocal microscopy and quantitative image analysis algorithms. The model is used to generate quantitative data for T cell recruitment to tumoroids and killing of tumoroids by T cells. We have applied this to screening a panel of CD3:Her2 bispecific antibodies (BsAb) binding with different affinities to CD3 or Her2 or displaying high affinity interactions with different epitopes on Her2. Exposure to fresh, non-activated peripheral blood mononuclear cell (PBMC) derived T cells shows an initial phase of random T cell movement throughout the ECM followed by a BsAb-dependent phase of active T cell recruitment to tumoroids (day 2-4) and a subsequent phase of tumoroid killing (day 4-6). We show that the wave of T cell recruitment following initial T cell-tumoroid contact involves chemotactic signaling. Decreased affinity at the Her2 or CD3 arm can be compensated for by increasing BsAb concentrations. However, we detect major differences in efficacy for different high affinity epitopes. I.e., of two BsAbs interacting with high affinity with distinct Her2 epitopes and each causing effective tumor cell killing in 2D co-culture, only one was able to trigger a wave of T cell recruitment and subsequent tumoroid killing in 3D. We have applied the same setup to testing the efficacy of T cells expressing engineered TCRs aimed at application in adoptive T-cell therapy. Kinetics of experiments using these activated engineered T cells are considerably shorter (24 hours instead of ~6 days) but show a similar pattern of T cell recruitment and subsequent tumoroid killing. We demonstrate successful generation of quantitative data for T cell recruitment and tumoroid killing for engineered T cells targeting tumor antigens expressed on TNBC and uveal melanoma tumoroids.

#5227 Gamma-delta (γδ) CAR-T cells lacking the CD3ζ signaling domain enhance targeted killing of AML cells and preserve healthy tissues.

L. Ding, Y. Li, J. Li, M. Ter Haak, L. Lamb, Jr.;
IN8bio, New York, NY

Chimeric antigen receptor T cell (CAR-T) therapy has shown remarkable efficacy against B cell malignancies, offering hope to patients with limited treatment options. However, extending this therapy to myeloid malignancies and solid tumors has proven challenging due to co-expression of targetable antigens on hematopoietic progenitors and healthy tissues. In this context, γδ T cells show promise, as they can directly identify and eliminate malignant cells via recognition of multiple tumor-associated stress antigens rarely expressed on normal tissues. We leveraged the tumor-sensing capabilities of γδ T cells with enhanced tumor localization by employing a non-signaling CAR (nsCAR) that excludes the CD3ζ domain, facilitating targeted tumor cell killing while sparing healthy tissues. We designed second-generation lentiviral constructs for anti-CD33-scfv for *in vitro* evaluation against acute myeloid leukemia (AML) lines HL-60, KG-1a, and MOLM-13 and the chronic myeloid leukemia (CML) line K-562 Additionally, we tested CD33/CD123 dual-targeting nsCAR constructs (ns-dCAR) to determine if the addition of CD123 targeting enhanced the therapeutic index. We also tested whether a secreted IL-15 (sIL-15) would enhance CAR-T cell fitness. We observed significant upregulation of CD69 in Jurkat cells transduced with signaling CARs in co-culture with KG-1a cells but not in those with nsCAR constructs. We also noticed a time-dependent reduction (43%) in the CD3ζ+ CD33CAR+ population over a 7-day extended coculture while the nsCAR+ Jurkat population remained stable, suggesting potential mitigation of activation-induced cell death (AICD). Expanded and activated γδ T cells from healthy donors were then transduced with nsCAR lentiviral vectors. The ns33CAR+ γδ T cells exhibited enhanced killing capability against HL-60 (up to 1.3x) and K-562 (up to 1.6x) compared to unmodified γδ T cells (UTD) in a 24-hour cytotoxicity assay. Incorporation of sIL-15 into the nsCD33 CAR construct also increased killing across all 4 cell lines (up to 1.8x for HL-60, up to 2.6x for KG-1a, up to 2.0x for MOLM-13 and up to 2.0x for K-562). Minimal cytotoxicity (<10%) was observed for nsCARs or UTDs against normal CD33+/CD123+ cells from healthy donor PBMC or CD34+ HPSCs. The ns-dCAR constructs did not improve in vitro AML killing compared to ns33CAR alone, although ns-dCARs generally exhibited lower transduction efficiency. In summary, our findings suggest that combining nsCAR constructs with γδ T cells may widen the therapeutic window to expand the reach of CAR-T therapy to cancers with limited target antigen expression on critical healthy tissues. Further optimization to improve integration and incorporation of membrane-bound IL-15 co-expression holds the potential to enhance both the efficacy and safety profiles of next-generation adoptive cell therapies against a broader spectrum of cancers.

#5228 Engineering CD123-targeting vδ1-enriched γδT cells with enhanced preclinical efficacy and safety profile.

M. Ng, S. L. Hayward, D. Zhang, G. Gu, B. Paulhus, D. Gjuka, C. Crowley, S. McLaughlin, A. Lublinsky, A. Mathew, E. Berreondo Giron, D. Mai, M. Lee, M. Wal, R. Alade, A. Simoes, R. Lytle, J. Gavin, S. Cramer, Z.-h. Yan, T. Hickman, R. Choudhary, C. Abikoff, Y. Wang, I. Kovacs, N. M. Sobhana, L. Cao; Takeda Development Center Americas, Inc, Cambridge, MA

Acute myeloid leukemia (AML) is an aggressive hematological malignancy that, despite advances in treatment, has an overall 5-year survival rate of less than 30%. There is an urgent unmet need for new and effective therapies for AML. Chimeric antigen receptor (CAR)-modified cell therapies are emerging as promising options. However, the selection of suitable antigens is challenging, due to the heterogeneous expression of potential antigen targets in AML. Most antigens, such as CD123, are expressed on both leukemic cells and normal hematopoietic stem and progenitor cells. In addition, conventional autologous or allogeneic T cell therapies present many limitations, such as cytokine release syndrome (CRS) and graft-vs-host disease (GvHD). We therefore evaluated CD123-targeting CAR designs in vδ1-enriched γδT cells, an innate immune cell platform that is inherently non-MHC restricted, has low risks of CRS and GvHD, and is capable of discriminating between malignant and healthy cells in preclinical models.

We engineered vδ1-enriched γδT cells from peripheral blood of healthy individuals to express various CD123-targeting CAR constructs. The CD123-targeting CAR-engineered vδ1-enriched γδT cells expressed high levels of natural cytotoxicity receptors, suggesting capability to target innate receptor ligands on AML cell surface. CD123-targeting CAR-expressing vδ1-enriched γδT cells demonstrated enhanced cytotoxicity in vitro against multiple AML cell lines, in both short-term co-culture and repeated antigen stimulation assays. CD123-targeting CAR-expressing vδ1-enriched γδT cells also showed enhanced efficacy and survival in vivo against mouse models of human AML. Interestingly, attenuation of CAR activity via novel designs preserved the inherent selectivity of vδ1-enriched γδT cells against AML cells relative to normal hematopoietic stem or progenitor cells, which also express CD123.

Together, our results demonstrated through rational CAR designing and engineering in vδ1-enriched γδT cells, an allogeneic cell therapy targeting CD123 can be generated with selective cytotoxicity against AML cells while sparing normal hematopoietic stem cells. Such product designs have the potential to be a transformative therapeutic option for a broad population of AML patients.

#5229 Enhancing solid tumor treatment with engineered blood-derived Vδ1 platform: Safe and effective targeting of mesothelin-expressing tumors with Vδ1 γδT cells.

N. Mohan Sobhana, A. Simoes, S. Edwards, S. Mishra, G. Gu, G. Papadopoulos, S. Kiesgen, R. Alade, L. Li, A. Venuso, J. Kumaran, K. Waddington, T. Huseni, R. Karattil, L. Reynolds, M. Sharif, D. Wotherspoon, C. Tudor, I. Kovacs, M. Rosa Ng, Y. Wang, L. Cao;
Takeda Development Center Americas, Inc., Cambridge, MA

Mesothelin (MSLN) is a solid tumor-associated antigen that has been thoroughly studied and is expressed in several tumor indications that have significant unmet therapeutic needs. Vδ1-enriched γδT cells differentiate themselves from other MSLN-targeted modalities by mitigating the challenges of targeting tumors with heterogeneous MSLN expression through their inherent capability to detect malignant cells while sparing normal cells. The ability to effectively combat cancer cells that express mesothelin is significantly increased by the expression of a chimeric antigen receptor (CAR). Novel armoring is being evaluated to improve engineered Vδ1 persistence in the solid tumor microenvironment. Cytokine armoring, through novel engineering, enhances sensitivity to cytokines and recovers cell fitness that is impaired by 'traditional' cytokine armoring options.

Extensive *in vitro* and *in vivo* safety and efficacy studies were carried out to validate the product's potency. These studies aimed to determine cytotoxicity, expansion, and persistence. MSLN CAR cytokine-armored Vδ1 cells exhibited high post-thaw viability and survival. Furthermore, cytokine-armored Vδ1 cells displayed elevated innate receptor expression and gene-engineered cells maintained their baseline innate phenotype, indicating that they can maintain their 'innate' effectiveness over time. *In vitro* studies demonstrated broad anti-tumor activity against multiple tumor cell lines expressing various levels of mesothelin. Additionally, in long-term cytotoxicity assays, cytokine-armored cells demonstrated improved tumor-clearance capabilities. The effector cells also exhibited an enhanced innate cytotoxic phenotype that equips the cells with the capability to persist and proliferate in response to soluble cytokines and upon cytokine trans-presentation by adjacent cells. *In vitro* studies further revealed that there is a distinction in the killing activity between tumor and normal cells, which is important for ensuring that the product is safe for use in patients. An orthotopic lung tumor-bearing mouse model was developed to confirm their anti-tumor effectiveness *in vivo*. The model's outcomes demonstrated that MSLN CAR cytokine-armored Vδ1 cells exhibit higher *in vivo* efficacy in comparison to their unarmored counterparts at low effector-to-target ratios. With no significant healthy tissue damage found, the histopathology report confirmed an excellent safety profile. Terminal biodistribution studies demonstrated that armored drug candidates preferentially home to and persist in tumor-bearing tissues.

Overall, these findings imply that the product might be highly effective in treating tumors that express mesothelin. This strategy could greatly advance our knowledge of how Vδ1-enriched γδT cells function as a platform against solid tumors.

#5230 A modified FcyRI expressing T cell (SolidT) exhibits profound anti-tumor activity followed by maturation into effector memory t cells that can be reactivated to kill a secondary tumor.

S. Dotan[1], N. Pilpel[1], P. Rider[1], H. Shpilt[1], D. Rasoulouniriana[1], Y. Carmi[2], J. E. Wooldridge[3];
[1]Gilboa Therapeutics Ltd., Rehovot, Israel, [2]Tel Aviv University, Tel Aviv, Israel, [3]Gilboa Therapeutics Inc., Cambridge, MA

We previously described a subset of cytotoxic FcyRI (CD64)-expressing T cells in tumors and inflamed tissues (PMID 31449054). We subsequently expressed an engineered modified CD64 into T cells ("SolidT") and demonstrated that these cells possessed greater specificity for tumor over normal tissues, reduced exhaustion, and attenuated cytokine secretion compared to other engineered cell therapies. SolidT activation correlates with surface tumor antigen density enabling the differentiation between tumor cells and normal cells by use of a specific antibody targeting tumor antigens. We previously showed that SolidT + mAb has anti-tumor activity *in vitro* and *in vivo* in several tumor models, including immunodeficient HER2 xenografts and an immunocompetent syngeneic B16-TYRP1 model (PMID 37070661). In this study, we further assessed the effect of SolidT on HER2+ tumors in a rechallenge model and extended the platform to CD20+ lymphoma models by combining SolidT with rituximab. In an *in vivo* experiment using HER2+, NCI-N87 cells in immunodeficient mice, several mice in the SolidT + trastuzumab group experienced complete tumor clearance. These mice were monitored until day 84, then rechallenged with NCI-N87 cells along with a new control group. After tumor establishment, mice were treated only with trastuzumab weekly for two weeks. While tumors in the control group progressed, the tumors in the rechallenged mice were completely cleared with a trastuzumab boost only, suggesting a SolidT cell memory response. Bone marrow from these rechallenged mice was analyzed and revealed the presence of effector memory SolidT cells. The SolidT model was then studied in a human, CD20+ lymphoma model *in vitro* and *in vivo* in immunodeficient mice. SolidT + rituximab was more potent *in-vivo* against CD20+ lymphoma cells than rituximab. *In vivo*, mice treated with SolidT + rituximab had significantly greater survival, lower tumor burden, and fewer sites of metastases than mice treated with rituximab alone. Bone marrow from these mice was analyzed and revealed the presence of effector memory SolidT cells in mice treated with SolidT + rituximab. We demonstrated that marrow resident SolidT cells developed an effector memory phenotype that positively correlated with outcome in HER2+ and CD20+ xenograft models, consistent with earlier data from a syngeneic B16 melanoma model. We further demonstrated that SolidT cells can be reactivated in a rechallenge model with only the addition of tumor targeting mAb, resulting in the eradication of the recurring tumors. This data further confirms that the SolidT platform can be targeted against different tumor antigens by using different tumor targeting mAbs. The SolidT platform could represent a paradigm shift in the approach to engineered cellular therapy for hematological malignancies and solid tumors.

#5231 NK and T cells armed with EVE16, a novel synthetic immune receptor, mediate robust anti-tumor responses through dual direct cytotoxicity and ADCC with minimal trogocytosis and exhaustion.

A. Ali[1], J. D. Ham[2], F. Zairi[3], V. Patel[3], M. Tarannum[1], K. Dinh[1], Y. Abdulhamid[1], J. Vergara[1], R. Soiffer[1], J. Ritz[1], J. Beadle[3], **N. A. Ivica**[3], J. Chen[4], R. Romee[1],

[1]Dana-Farber Cancer Institute, Boston, MA, [2]Massachusetts Institute of Technology, Cambridge, MA, [3]InnDura Therapeutics, Cambridge, MA, [4]2. Koch Institute for Integrative Cancer Research, Massachusetts Institute of Technology, Cambridge, MA

Despite the major advances, cancer patients treated with targeted chimeric antigen receptor (CAR)- based T and NK cell therapies often face the challenge of frequent disease relapse, and their efficacy in solid tumors is low. This is attributed to the inherent potency of the starting cell material, unique characteristics of CAR engineering resulting in trogocytosis and tonic signaling, and the notable absence of homogenously expressed surface markers, particularly in solid tumors.

To address these limitations, we engineered a novel synthetic immune receptor termed Enhanced-Valency Engineered CD16A (EVE16) and evaluated it in memory-like NK cells and T cells against liquid and solid tumors. We hypothesized that post-activation cleavage of CD16A by ADAM17 plays a crucial role in reducing trogocytosis and tonic signaling. EVE16 utilizes the inherent potential of CD16A to trigger an activation signaling cascade through the endogenous CD3ζ adaptor signaling protein. Unexpectedly, we discovered that, aside from the CD16A transmembrane domain, the Fc-binding domain is essential for proper surface expression. After multiple rounds of optimization, we developed a receptor that surpassed the activation potency of endogenous CD16A and allowed both direct binding to the tumor targets and retained antibody-dependent cellular cytotoxicity (ADCC), and this dual 'CAR-like' and ADCC function opens the potential for combination with clinically approved antibodies to prevent immune escape. Furthermore, in contrast to the conventional CAR(BBζ), the optimized EVE16 receptor exhibited minimal tonic signaling in both T and NK cells. This translated to enhanced sensitivity towards low antigen-density targets, as demonstrated by a cytotoxicity assay performed on polyclonal cancer cells engineered with target antigen knock-down. Additionally, EVE16, but not CAR transduced, protected T and NK cells from trogocytosis and allowed for the efficient disengagement of cytotoxic lymphocytes from cancer targets due to CD16A cleavage by ADAM17 upon immune cell activation. In *in vivo* mouse xenograft models, CD19-targeted EVE16 memory-like NK cells, rapidly manufactured using our approach, demonstrate outstanding performance in terms of robust expansion, prolonged persistence, and effective leukemic clearance, underscoring the effectiveness of our method.

In summary, we here describe a novel synthetic immune receptor called EVE16 which enables both direct (CAR-like) and ADCC functionality while preventing trogocytosis and exhaustion. Clinical trials are being planned for the near future.

#5232 Placental circulating T cells expressing CD16 in combination with trastuzumab demonstrate robust anti-tumor antibody-dependent cellular cytotoxicity (ADCC) against gastric cancer.

K. Karasiewicz-Mendez, J. Gleason, K. Tess, M. Djedaini, S. Lin, C. Huang, S. He, R. Hariri, A. Kilcoyne;
Celularity Inc., Florham Park, NJ

Introduction: Celularity is developing PT-CD16VS as a novel platform for use in combination with approved monoclonal antibodies for the potential treatment of multiple cancers. PT-CD16VS is an allogeneic cell therapy derived from human postpartum placental circulating T (P-T) cells that are genetically modified to express a proprietary CD16 variant and endogenous T cell receptor (TCR) knockout. Here we report the characterization and preclinical evaluation of PT-CD16VS against HER2+ gastric cancer cells in combination with Trastuzumab. *In vitro* safety studies evaluating the potential for on-target/ off-tumor activity of PT-CD16VS against HER2 low expressing lung epithelial cells (LEC) and human dermal fibroblasts (HDF) are also highlighted.
Methods: P-T cells were activated and transduced with a lentiviral vector containing a CD16 construct expressing a high affinity CD16 variant, CD16VS. Following transduction, P-T cells were transfected to knock out the TCR. *In vitro,* the functional activity of PT-CD16VS cells in combination with Trastuzumab was assessed against the HER2+ gastric cancer NCI-N87 cell line in cytotoxicity, cytokine release, and proliferation assays. For on-target/ off-tumor studies, similar assays were utilized to assess activity against the HER2 low expressing LEC and HDF cell lines. *In* vivo, PT-CD16VS with Trastuzumab was evaluated in a subcutaneous NCI-N87 xenograft model in NSG mice. Tumor volume was measured and tumor samples were evaluated for PT-CD16VS infiltration.
Results: High CD16 transduction efficiency (>60%) was achieved across donors. *In vitro*, PT-CD16VS plus Trastuzumab demonstrated potent cytotoxicity against NCI-N87 cells at low E:T ratios (0.625:1) and at 12 hours of co-culture with moderate cytokine secretion at 24-hour of co-culture. PT-CD16VS proliferated following 48-hour incubation with NCI-N87 cells and Trastuzumab, as compared to an IgG1 control. PT-CD16VS in combination with Trastuzumab did not elicit on-target/ off-tumor cytotoxicity or cytokine release in response to low HER2 expression on normal LEC or HDF cells. *In vivo*, PT-CD16VS with Trastuzumab demonstrated significant reduction in tumor volume compared to vehicle, Trastuzumab alone, and the positive control Enhertu groups. In addition, PT-CD16VS infiltration into the tumor was shown to be Trastuzumab dependent, with infiltrating cells expressing high levels of CD16 and Ki67.
Conclusions: Our results show that PT-CD16VS has robust *in vitro* and *in vivo* ADCC activity against gastric cancer tumor cells when combined with Trastuzumab. Furthermore, PT-CD16VS activity is specific to tumor HER2 antigen expression and does not target low HER2 expression on normal healthy cells. PT-CD16VS is being developed in combination with various monoclonal antibodies for the treatment of multiple cancers.

#5233 Engineered NK-like NKG2C+ CD8 T cells mediate superior anti-tumor efficacy over conventional CD8 T cells and NK cells.

K. Lupo, M. Panjwani, A. Daniyan, C. Klebanoff, K. Hsu;
Memorial Sloan Kettering Cancer Center, New York, NY

We have recently characterized a unique CD8 T cell subset that expresses NKG2C, as well as multiple other natural killer cell markers. These NKG2C+ CD8 T cells demonstrate NK-like effector functions against various tumor targets, can be efficiently expanded and engineered using GMP-compatible techniques, and most importantly, display beneficial qualities unique to T and NK cells while minimizing the therapeutic deficits of each. NKG2C+ CD8 cells can be easily expanded using a genetically modified K562 feeder line and can be efficiently engineered via retroviral transduction. We genetically engineered NKG2C+ CD8 T cells to express an anti-CD19-28-z CAR construct to target B cell malignancies and compared effector functions of the CAR-engineered NKG2C+ CD8 T cells against CAR+NKG2C- (conventional) CD8 T cells and CAR+ NK cells in vitro and in vivo. We examined expansion, engineering efficiency, tumor control, and extent of cytokine release syndrome (CRS). We also engineered NKG2C+ CD8 T cells with a transgenic NY-ESO-1 TCR to target melanoma and compared the functional responses and efficacy of TCR-engineered NKG2C+ CD8 T cells against TCR-engineered conventional CD8 T cells. CAR+NKG2C+ CD8 T cells demonstrated superior in vitro effector function when compared to CAR+ conventional CD8 T cells and CAR+NK cells and did not upregulate characteristic T cell exhaustion markers, such as PD-1, TIM-3, and LAG-3. These CAR+NKG2C+ CD8 T cells demonstrated superior control of a CD19+ NALM6 tumor model in NRG mice, which was further enhanced with administration of IL-15. CAR+NKG2C+ CD8 T cells with IL-15 demonstrate dramatic and enhanced persistence, as well as superior cytotoxicity and activation in vivo when compared to CAR+ conventional CD8 T cells and CAR+ NK cells. Using a SCID-beige CRS mouse model, we observed reduced CRS in mice treated with CAR+ NKG2C+ CD8 T cells than in mice treated with CAR+ conventional CD8 T cells, with lower levels of proinflammatory cytokines and minimal expansion of murine myeloid subsets. Similarly, TCR-engineered NKG2C+ CD8 T cells demonstrated enhanced tumor control and in vivo persistence in an A375 melanoma-bearing NRG mouse model compared to TCR-engineered conventional CD8 T cells. We have successfully demonstrated that CAR- or TCR-engineered NKG2C+ CD8 T cells have superior anti-tumor efficacy, in vitro and in vivo, to conventional CD8 T cell and NK cell counterparts due to their innate tumor killing and greater in vivo persistence. These cells mediate less CRS and provide a safer alternative to traditional engineered T cell therapeutics. Ultimately, our NKG2C+ CD8 T cells represent a unique platform for engineered T cell therapies to target both solid tumors and hematologic malignancies, that is easily expanded ex vivo, does not require CD4 T cells for in vivo persistence, and is resistant to exhaustion.

#5234 TGF*beta*-conditioned K-NK cells are able to counter immune suppression in the tumor micro-environment.

A. Kunert[1], A. Oja[1], I. Cesonyte[1], K. Franciszkiewicz[2], S. Sidhu[2], H. Jetani[1], G. Bocconcelli[1], R. Igarashi[1], V. R. Fantin[3];
[1]Sanofi Oncology, Amsterdam, Netherlands, [2]Sanofi Oncology, Vitry, France, [3]Sanofi Oncology, Boston, MA

Recent advances have enabled the use of autologous K-NK cells to treat patients suffering from hematological malignancies. When aiming to treat patients suffering from solid tumors however, the suppressive effects of the tumor microenvironment (TME) and the involvement of other immune cells need to be considered to make a cell therapeutic potentially more effective.
TGFβ-conditioning (TGFβ-c), the co-culture of K-NK cells with low-dose TGFβ while undergoing cytokine-mediated expansion, imbues these cells with unique qualities suitable to mitigate immuno-suppressive effects of the TME, making them more efficacious toward solid tumors. The exposure to TGFβ during expansion results in significant downregulation of SMAD3, rendering these cells insensitive to TGFβ-mediated down-regulation of NK cell receptors. TGFβ-c K-NK cells display enhanced in vitro cytotoxicity towards 2D, 3D cultured cell lines as well as against organoid models derived of various indications. These cells infiltrate into patient-derived tumor organoids at higher frequency and have increased IFNγ secretion upon target-specific activation. The effect of the higher IFNγ output on a complementary anti-tumor immune subset was investigated in complex immune cell cultures and was indeed shown to enhance DC maturation.
In vivo studies revealed prolonged persistence of TGFβ-c K-NK cells in mice while retaining both altered gene-expression and functional hallmarks for up to 28 days, indicating that the conditioning results in a stable phenotype.
In summary, TGFβ-c K-NKs are a platform with enhanced potency to transition cell therapy from treating hematological to solid tumor malignancies.

#5235 Combination STING agonist and NK cellular therapy in patient derived organotypic tumor spheroids.

P. H. Lizotte[1], E. Ivanova[1], S. Park[1], N. Spicer[1], S. Kivlehan[1], I. Gjeci[1], S. Kiesgen[2], V. Appleman[2], L. Talarico[2], M. Y. Tolstorukov[1], R. Bueno[3], D. A. Barbie[1], C. P. Paweletz[1];

[1]Dana-Farber Cancer Institute, Boston, MA, [2]Takeda Pharmaceuticals, Cambridge, MA, [3]Brigham and Women's Hospital, Boston, MA

Background: Increasing the immunogenicity of solid tumors may potentiate durable anti-tumor immunity. Targeting innate pattern recognition receptor signaling is a promising strategy to repolarizing the suppressive tumor immune microenvironment (TME). A potential synergistic approach is the addition of cellular therapy. Tumor models expressing high levels of endogenous STING, but where the pathway is not active, were considered for evaluating STING agonism as a potential intervention. Additionally, prior work has demonstrated that STING induction is toxic to T cells; however, natural killer (NK) cells are unaffected, due to their differential regulation of autophagy. Here we investigate the immunomodulatory properties of STING agonism alone and in combination with NK cells using short-term microfluidic culture of fresh patient-derived organotypic tumor spheroids (PDOTS).

Methods: Surgical cases from Brigham and Women's Hospital under an IRB-approved protocol were studied. PDOTS were generated as previously described. Ex vivo response was assessed by fluorescent live/dead imaging, immunofluorescence (IF), multiplexed cytokine array, and single cell RNA sequencing (scRNAseq). Baseline immune phenotypes were analyzed by FACS from single cells isolated during tumor sample preparation.

Results: Twelve explants were studied. Two specimens were excluded from viability assessment due to excess of fibrotic material and low viability. Using a cut-off of -40%, three cases were characterized as responders (R) and seven as non-responders (NR). We observed significant induction of CXCL10 in all samples treated with STING agonist. IFN-β, IFN-γ, TNF-α, and MIP1-α were also consistently induced by STING agonist treatment. More detailed analysis of two samples by scRNAseq revealed a strong interferon stimulated genes (ISG) signature in STING agonist conditions; the cellular source of CXCL10 secretion in STING agonist treatment was tumor cells and fibroblasts. We also observed profound changes in myeloid biology, indicating that these cells polarized to a more pro-inflammatory and antigen-presenting phenotype with STING agonism. Interestingly, NK-based cell therapy added to PDOTS cultures displayed better persistence and enhanced effector function relative to endogenous NK cells, with and without STING agonism.

Conclusions: Using tumor explants and a variety of orthogonal techniques, we investigated the response to STING agonism and NK cellular therapy ex vivo. Our results indicate that STING agonism remodels the TME, creating a more immune-permissive environment. STING agonism induces secretion of chemoattractant CXCL10 by tumor cells and fibroblasts. STING agonism does not abrogate NK cell effector function and therefore, may synergize with NK cell therapies.

#5236 Adoptive natural killer therapy is effective for synovial sarcoma cell lines..

N. Oike[1], T. Miyazaki[1], Y. Murayama[1], T. Ariizumi[1], A. Ogose[2], M. Baba[1], H. Kawashima[1], C. Imai[3];
[1]Niigata Univ. School of Medicine, Niigata, Japan, [2]Uonumakikan Hospital, Niigata, Japan, [3]Toyama University, Toyama, Japan

Despite the development of multimodal therapy consisting of surgery, radiotherapy, and chemotherapy, the prognosis of patients with metastatic or relapsed synovial sarcoma (SS) remains poor. A novel treatment option including immunotherapy is urgently required. Natural killer (NK) cells are innate immune cells that can recognize and kill tumor cells. The cytolytic activity of NK cells is determined by the balance of signals from both inhibitory and activating receptors expressed on cell surface. Activating receptors include NKp30, NKp44, NKp46, NKG2D, and DNAM-1. Furthermore, tumor cells with low HLA class I expression are potentially even more sensitive to NK-mediated cytotoxic killing due to a lack of inhibitory signals. We previously reported that HLA class I expression was down regulated in one third of patients with synovial sarcoma, suggesting that NK cell therapy may be effective for patients with SS. However, the efficacy of NK cells treatment in SS was not well established. In this study, we evaluated surface ligands for NK cell activation on SS cell lines and demonstrated the effectiveness of activated allogenic NK cells for SS cell lines *in vitro*.The surface expression of ligands for NK cell-activating receptors including NKp30, NKp44, NKp46, NKG2D, and DNAM-1 in three SS cell lines (SYO-I, HS-SY-II, and Yamato-SS) was evaluated using flow cytometry. Peripheral blood from two healthy donors were ficoll-separated to collect peripheral blood mononuclear cells (PBMCs). Then, PBMCs were stimulated with irradiated K562 cells expressing the NK-stimulatory molecules 4-1BB ligand and membrane-bound Interleukin 15 in the presence of human Interleukin-2 in RPMI1640 with 10% FBS. The cells were expanded for 14 days, and the expanded NK cells are CD3-CD56+ NK cells. These expanded cells are reproducible in their function, and we have utilized these cells for *in vitro* cytotoxicity assays. 2x10E4 of SS cell lines (SYO-I, HS-SY-II, and Yamato-SS) were seeded in a 96 well plates and cultured overnight. Then, allogenic NK cells or activated T cells as a control at various tumor effector ratio. The cells were co-cultured with activated T cells or NK cells in the presence of low dose interleukin2. Forty-eight hours later, cell viabilities were measured using WST-8 assay.Ligands for NKp44, NKp30, NK2GD, were expressed in all three SS cell lines. It suggested that SS cells upregulate activating receptor ligands for NK cells. In addition, cytotoxicity of allogenic NK cells for SS cell lines was significantly higher than that of activated T cells. To determine whether cytotoxic activity was effect of allogenic NK cells, CD107a mobilization assay using flowcytometry was performed. CD107a mobilization assay demonstrated degranulation of NK cells, leading us that NK cells had an antitumoral effect on SS cell lines in vitro. Based on these initial findings, we were able to demonstrate that allogenic NK cells may be a promising immune therapy for SS.

#5237 Engineered probiotics direct the antigen specificity of CAR-T cells *in situ*.

R. L. Vincent, F. Li, A. Vardoshvili, C. Gurbatri, N. Arpaia, T. Danino;
Columbia University, New York, NY

Antigen-targeting therapies such as chimeric antigen receptor (CAR)-T cells have achieved unparalleled success in the treatment of hematological malignancies. However, broad success has remained bottlenecked by the lack of targets that are specifically, and uniformly, expressed on heterogenous solid tumors. In contrast, certain strains of bacteria are gaining recognition as a new class of antigen-agnostic cell therapies due to their selective growth within the immuno-suppressive niche of the solid tumor microenvironment (TME). Bridging these approaches, we developed a platform of probiotic-guided CAR-T cells (ProCARs) - in which tumor-colonizing probiotics release synthetic targets that efficiently tag tumor tissue for CAR-mediated lysis. Here, we engineered a well-characterized strain of probiotic bacteria, *E. coli* Nissle 1917, to sustain the intratumoral production of genetically encoded CAR targets and T cell attracting chemokines in multiple xenograft and syngeneic models of human and murine tumors. We design orthogonal CAR targets (Tags) as modified dimers of GFP that broadly anchor to collagens, fibronectins, and heparin sulfates found in high abundance within the solid TME to achieve antigen-agnostic tumor targeting. We demonstrate that Tags robustly coat the surface of cancer cell lines through interaction with cell surface matrix proteins, thus leading to the activation of GFP CAR-T cells and Tag-dependent killing across a panel of genetically distinct target cells. We additionally show that injected probiotics selectively grow within the tumor core and maintain the intratumoral production of Tags and human chemokines - leading to therapeutic efficacy across multiple subcutaneous and orthotopic tumor models. Moreover, we demonstrate a systemic antitumor benefit in immune-competent hosts, whereby unilateral treatment of primary tumors leads to a significant reduction in the growth rate of distal, untreated tumors. Finally, we show that intratumoral bacteria provide natural TLR agonists that trigger substantial activation of human and murine ProCAR-T cells. Our findings highlight the potential of the ProCAR platform to address the critical roadblock of identifying suitable CAR targets by providing an antigen *in situ* that is orthogonal to both healthy tissue and tumor genetics. Altogether, the use of a bacterial delivery platform in the ProCAR system offers a partner organism that naturally enhances CAR-T cell effector function and broadens the scope of CAR-T cell therapy to include previously difficult to target tumors.

#5238 uPAR as a novel immunotherapeutic target in recurrent glioblastoma.

William T. Maich[1], Muhammad Vaseem Shaikh[1], Anish Puri[1], Alisha Anand[1], Chirayu Chokshi[1], Sabra Salim[1], Neil Savage[1], Chitra Venugopal[1], Martin Rossotti[2], Thomas Kislinger[1], Kevin Henry[2], Sheila Singh[1]

[1]McMaster University, Hamilton, ON, Canada,[2]National Research Council, Ottawa, ON, Canada

Glioblastoma (GBM) is the common malignant brain tumor in adults, accounting for approximately 15% of all CNS tumors, and 48.6% of malignant brain tumors, with a median survival of approximately 15 months, and minimal clinical progress having been made in the past two decades. GBM is characterized by extensive inter- and intra-tumoral heterogeneity as well as an extremely immunosuppressive tumor microenvironment. Following Standard-of-Care (SoC) surgical resection and chemoradiotherapy at primary diagnosis, few therapeutic avenues exist at recurrence, owing in part due to a lack of clinically relevant targets. Data from our multi-institutional target pipeline shows that the extracellular urokinase plasminogen activator receptor (uPAR) is significantly upregulated at recurrence on putative GBM brain tumor initiating cells (BTICs), which are believed to drive *de novo* tumor formation, tumor recurrence, and therapeutic resistance. uPAR plays an important role in the plasminogen activation system, and in the context of cancer, has been implicated in numerous pro-tumorigenic processes such as invasion, proliferation, epithelial-to-mesenchymal transition, and therapy resistance. We used CRISPR-Cas9 to genetically delete uPAR from our in-house patient-derived GBM cell lines, and found that *in vitro*, knockout of uPAR expression in recurrent GBM cells significantly reduces proliferation and sphere formation capacity, two stem-like traits associated with BTICs. Additionally, we found that uPAR knockout significantly reduced the frequency of BTICs in a given population. Additionally, uPAR knockout cells display increased sensitivity to standard-of-care chemoradiotherapy, implicating uPAR expression in therapy resistance, as seen in recurrent disease. We orthotopically injected immunocompromised mice to generate patient-derived xenograft models of GBM, and found that knockout of uPAR significantly increases survival, and decreases tumor burden. Further, we generated novel anti-uPAR single domain antibodies (sdAbs) and found that they specifically bind uPAR at low nanomolar concentrations *in vitro*. Using these sdAbs, we created an anti-uPAR CAR T which showed potent cytotoxicity *in vitro*, and drastically reduced tumor burden and extended survival *in vivo*. From this work we believe uPAR to be a clinically relevant target in recurrent GBM, and further investigation into therapeutic strategies to target uPAR-positive GBMs should be investigated further.

#5239 Discovery of AML associated therapeutic targets.

Omar M. Ibrahim, Michael P. Rettig, Reyka G. Jayasinghe, Li Ding, John F. DiPersio

Washington University School of Medicine in St. Louis, St. Louis, MO

Chimeric Antigen Receptor T-cell (CART) immunotherapy has shown significant success in the treatment of hematological malignancies. However, their efficacy in AML is limited due to the disease's genetic diversity and lack of uniform antigen targets. To identify potential AML cell-surface markers, we employed a comprehensive approach that involved the utilization of 3' single-cell RNA sequencing (scRNA-seq), bulk RNA sequencing (RNA-seq), and enhanced whole exome sequencing (eWES). A total of 21 samples were analyzed, comprising 18 distinct AML patients and 3 healthy bone marrow aspirates, serving as controls. We conducted scRNAseq on 21 samples, yielding a total of 185,106 high-quality cells, which were effectively clustered into 38 unbiased groups. Notably, tumor clusters exhibited highest copy number variations and formed separate clusters from other non-tumor immune cells. To uncover key functional pathways, we conducted pathway enrichment analysis comparing tumor cells to non-tumor cells. Our findings demonstrated a significant overrepresentation of cellular processes related to Allograft rejection, IL2/STAT5 signaling, IFN-gamma response and apoptosis. To identify AML specific markers, we performed an unbiased systematic search of the scRNAseq dataset for genes with unique expression patterns in tumor cells compared to the healthy bone marrow controls. Our analysis identified differentially expressed genes, with many genes displaying relative cell and tissue specificity. Notably, among these genes, we unveiled key potential targets with cell surface specificity, including novel markers alongside previously known ones. Noteworthy candidates, such as *ADGRE2, CD33, CD123, CLEC12A*, and *FLT3* and understudied novel markers such as *CD86, CSF1R,* S100 proteins and *VMP1*, were prominently expressed, showcasing their potential significance as targets for engineered immunotherapy. To validate and consolidate our discoveries, we conducted a cross-referencing exercise by comparing our scRNAseq data against bulk RNA data from primary human AML samples and cell lines. Bulk global proteomics, flow cytometry-based and CART generation studies are ongoing to confirm our discoveries. Our rigorous computational and experimental approach provides valuable insights into tumor-specific cell surface proteins, which hold promise as potential targets for innovative and precision immunotherapeutic interventions in the realm of AML treatment.

#5240 Novel CD3-Fusion Receptor enables combination of T-cell engagers and allogeneic CAR T cells to promote enhanced antitumor activity and overcome antigen escape.

D. Lu, **E. Peralta**, H.-Y. Chu, S. Park, M. Tsuda, E. Avramis, M. Denholtz, A. Witty, T. Lee, B. Valamehr;
Fate Therapeutics, San Diego, CA

Chimeric antigen receptor (CAR) T cells have shown remarkable clinical success in the treatment of hematologic malignancies. However, the durability of response of CAR T therapy can be impaired by heterogenous expression of the CAR-specific target antigen (1° Ag) on tumors. In combination with a CAR, T-cell engagers (TCEs) that target additional tumor antigen (2° Ag) can be a unique approach to address tumor heterogeneity and overcome antigen escape. Engineered induced pluripotent stem cell (iPSC) master cell lines are a renewable source material from which iPSC-derived CAR T (CAR-iT) cells can be manufactured and administered in an off-the-shelf manner. In developing allogeneic CAR-iT cells, the T-cell receptor (TCR) must be eliminated to prevent graft-versus-host disease. However, the absence of TCR expression leads to loss of surface CD3 and a corresponding loss of TCE compatibility. Here we discuss a novel CD3ε fusion receptor (CD3-FR) with a modified transmembrane and endodomain, which allows for CD3 surface expression on TCR-less T cells and effective combination of off-the-shelf allogeneic CAR-T cells and TCEs. CAR$^{\pm}$ CD3-FR$^{\pm}$ iPSCs were differentiated into CAR-iT cells, uniformly expressing both modalities (>95% CAR$^{\pm}$, >90% CD3ε$^{\pm}$) and absent of TCR. To demonstrate that CD3-FR$^{\pm}$ CAR-iT cells can elicit TCE-dependent activity, 1° Ag^{-} (CD19^{-}) / 2° Ag$^{\pm}$ (EpCAM$^{\pm}$) target cells were used in cytotoxicity assays. As shown, CD3-FR^{-} CAR-iT cells failed to kill 1° Ag^{-} target cells. In contrast, CD3-FR$^{\pm}$ CAR-iT cells demonstrated potent activity toward the target cells (>80% cytolysis) but only in the presence of the TCE targeting 2° Ag.

To test the ability of CD3-FR$^{\pm}$ CAR-iT cells to mitigate antigen escape, we used a tumor cell population heterogenous for the CAR-specific target (50% 1° Ag^{-}) but homogenous for TCE-specific target (100% 2° Ag$^{\pm}$). In co-culture assays, CD3-FR^{-} CAR-iT cells failed to prevent tumor cell growth due to 1° Ag^{-} tumor escape. However, CD3-FR$^{\pm}$ CAR-iT cells in the presence of TCE exhibited robust control (80% cytolysis) of the heterogenous tumor, mitigating 1° Ag^{-} tumor escape via targeting of 2° Ag. Next, we tested the ability of CD3-FR$^{\pm}$ CAR-iT cells to control heterogeneous tumor *in vivo* in a disseminated leukemia model. As expected, CD3-FR$^{\pm}$ CAR-iT cells exhibited significantly better tumor growth inhibition in the presence of TCE (p-value <0.005) compared to controls lacking the CD3-FR modality. *Ex vivo* analysis of tumor in the bone marrow confirmed 1° Ag^{-} tumor escape in the control treated mice, but not in mice treated with CD3-FR$^{\pm}$ CAR-iT and TCE targeting 2° Ag.

Taken together, these studies present a novel opportunity to leverage a novel CD3 fusion receptor and enable combination of TCEs with engineered off-the-shelf CAR T-cell products, uniquely harnessing two potent therapeutic modalities for improving cancer therapy.

#5241 Generation of allogeneic CAR-T circumvents functional deficits in patient-derived autologous product for glioblastoma.

M. Shaikh[1], S. K. Salim[1], J. Wei[2], W. T. Maich[1], A. A. Anand[1], O. Y. Tang[3], M. K. Subapanditha[1], Y. Suk[1], M. Singh[1], Z. Alizada[1], B. Brakel[1], V. Dimitrov[2], Z. Tabunshchyk[1], K. Brown[2], P. Vora[1], Z. Binder[3], C. Venugopal[1], J. Moffat[2], S. K. Singh[1];

[1]McMaster University, Hamilton, ON, Canada, [2]University of Toronto, Toronto, ON, Canada, [3]Perelman School of Medicine, University of Pennsylvania,, Phildelphia, PA

Glioblastoma (GBM) is the most common malignant primary brain tumor in adults. Despite an aggressive standard of care that includes maximally safe surgical resection, chemo-radiotherapy, median overall survival remains stagnant at 15 months. However, immunotherapeutic strategies have provided an exciting avenue of exploration to meet clinical need. Chimeric antigen receptor T-cell (CAR-T) therapy has shown promising results in liquid malignancies, but clinical trials in GBM targeting various tumor antigens have not shown durable clinical benefit. While this may be attributable to various tumor-intrinsic immune evasion strategies characteristic of GBM, little work has assessed whether the issue is due to the quality of the CAR-T treatment itself. Currently, CAR-Ts for clinical studies are manufactured in an autologous setting wherein T-cells are extracted from patients, engineered ex-vivo, and subsequently re-infused back. However, peripheral T-cells taken from untreated GBM patients have demonstrated qualitative and functional deficits, which may contribute to suboptimal treatment outcomes. Thus, we aimed to establish whether CAR-Ts generated from GBM patients would show reduced efficacy in comparison to healthy donors using our previously validated CD133 CAR-T. In this work, we show that in-spite of no inherent phenotypic differences, patient derived CAR-Ts shows pre-treatment exhaustion and upon preclinical evaluation using an orthotopic xenograft model of human GBM reduced survival advantage in autologous, patient-derived CD133-targeting CAR-T cell products was observed as compared to the controls. Transcriptomic analysis highlighted a decreased panel-wide enrichment in genes related to T cell and lymphocyte activation, lower prevalence of T cells (including Th1 and CD8+) and higher prevalence of exhausted CD8+ cells in T-cells products derived from GBM donors as compared to healthy donors. To overcome the functional and logistical considerations of autologous therapy, we additionally aimed to generate an “off-the-shelf” allogeneic CD133 CAR-T. Using CRISPR gene editing technology, we generated TCR-knockout CAR-T cells with comparable pre-clinical efficacy to our autologous models. In conclusion, this work highlights the need to reassess autologous CAR-T therapy for GBM and considers allogeneic approaches as promising alternatives. By addressing the inherent deficits in patient-derived CAR-Ts, allogeneic CD133 CAR-Ts may offer a more effective and logistically feasible therapeutic option for treating GBM.

#5242 In vitro cytotoxicity assays to support CAR T cell evaluation against solid tumors.

C. N. Castro, V. Bergo, H. Weber, **P. Metzger**;
Reaction Biology Europe GmbH, Freiburg, Germany

CAR T cells are donor/patient-derived T cells genetically engineered to express a chimeric receptor against a specific tumor antigen (TA), which allows an MHC-independent recognition and targeting of tumor cells. While CART cell therapies have been tremendously successful against hematological cancers, with 6 T cell products being approved up to date from the FDA (Sengsayadeth S etal, EJHaem. 2022), the activity on solid tumors is more difficult. Solid tumors remain a unique challenge in part due to trafficking problems of CAR T cells, a hostile TME and heterogenous antigen expression, which limits CART cell capacity to find their target. Several strategies are being developed at the moment with the aim to overcome these hurdles, such as multispecific CART cells, co-therapy with checkpoint inhibitors, or inhibition of DNA methylation enzymes to prevent exhaustion. To offer an in vitro platform to assess the effectiveness of upcoming cellular therapies we developed several pipelines to allow the investigation of cytotoxic potential in 2D and 3D formats.
We show here our results using a CART cell product expressing a coreceptor to enhance its activation potential upon recognition of the target. We next tested the capacity of these cells to kill solid tumor in vitro by coculturing with potential target cells cultured in a monolayer (2D). By measuring the luciferase expression of the target cells, we could track the cytotoxicity exerted by the effector cells. In vitro, the CART cells were able to kill in a dose dependent manner different solid tumor cell lines expressing the cognate antigen for the co-receptor. At Reaction Biology we have developed spheroid-based 3D killing assays in which target cells from solid tumor entities are pre-cultured to form spheroids prior to their coculture with effector cells. Using this technique, we challenged the capacity of these CART cells to recognize their antigen in a 3D format. This 3D assay system can be used as well in combination with co therapies such as PD1 inhibitors, in a sensitive and high throughput manner. Finally, we evaluated the therapeutic capacity of these CART cells in vivo in a subcutaneous THP-1 tumor model. Mice treated with these CART cells showed a marked reduction of tumor volume.
In summary we show here a pipeline to characterize in vitro the effectivity of new T cell products, in particular those designed to overcome some of the hurdles against solid tumors.

#5243 CAR B cells to accelerate antigen presentation in cancer.

M. Molloy, J. Balero, A. Contreras-Sandoval, M. Selby, H. Park, S. Kothakota, K. Boyle, R. Romano, S. Rajendiran, M. Hernandez, A. Pios, R. Williams; Walking Fish Therapeutics, South San Francisco, CA

Engineered B cells hold promise for multiple therapeutic applications. Walking Fish Therapeutics is engineering B cells to produce replacement proteins for deficiency diseases, antibodies of defined specificity and effector function, and Chimeric Antigen Receptor (CAR) B cells with and without therapeutic payloads for use in the oncology setting. B cells are professional antigen presenting cells (APCs) with the ability to present antigen to CD4+ T cells. Recent studies have found the presence of tumor infiltrating B cells are associated with favorable outcomes across multiple cancer types. Adoptive transfer of B cells has demonstrated antitumor activity in a syngeneic mouse model. B cells from OVA-vaccinated transgenic luciferase mice were adoptively transferred to mice bearing EG7.OVA-tumors. We observed B cells migrating to the tumor and tumor draining lymph node (TDLN), locations where B cells can engage with antigen. Further, we observed a strong anti-tumor response in mice receiving B cells from OVA-vaccinated donors. Based on these results, we hypothesized that B cells engineered to target tumor specific antigens may engage and activate the immune system leading to an enhanced antitumor immune response. We generated CAR B cells expressing synthetic BCRs with tumor-antigen specific scFvs fused to designated B cell signaling motifs. Expression of different CAR constructs were confirmed in both human and mouse B cells. Upon antigen engagement CAR B cells release pro-inflammatory cytokines. Importantly, we demonstrate *in vitro* that antigen-specific CAR B cells can recognize cognate cell surface antigen, leading to uptake, processing, and presentation on MHCII as detected by activation of peptide-specific CD4+ T cells. When administered *in vivo* by IV administration, we observed a significant increase in mouse CAR B cells at the tumor site compared to unengineered B cells. We are currently investigating additional CAR formats that may lead to enhanced anti-tumor activity.

#5244 SIRPα knockout iPSC-derived macrophages (iMACs) are resistant to CD47-dependent inhibition of phagocytosis and efficiently kill tumor cells in pre-clinical models.

K. Haake[1], M. Mirenda[2], Q. Bernard[2], P. Hublitz[1], L. Gouxette[2], M. Briscadieu[2], P. Scheinpflug[1], G. Singh[1], A. Hinkelmann[1], T. Schneider[1], M. Esquerre[2], A. Holtzinger[1], M. Epstein[3], D. Sommermeyer[1], M. Paillasse[2], A. Scheel[1], M. Dangl[1], M. Braun[1], **N. Wagner**[1];
[1]Evotec International GmbH, Gottingen, Germany, [2]Evotec France SAS, Toulouse, France, [3]Evotec (UK) Ltd., Abingdon, United Kingdom

The CD47-SIRPα axis is a critical checkpoint that prevents SIRPα-positive macrophages from phagocytosing CD47-expressing solid tumors. Several agents aiming to block this axis have recently entered early clinical trials including anti-CD47 and anti-SIRPα monoclonal antibodies (mAb). These checkpoint inhibitors (CPI) aim to modulate the phagocytotic activity of endogenous tumor associated macrophages (TAMs). However, the adoptive transfer of macrophages resistant to CD47-based inhibition in the tumor microenvironment (TME) could also increase clinical efficacy while avoiding side effects linked to the use of anti-CD47 mAb. Cell therapy based on autologous macrophages have gained increasing attention for cancer treatment due to their ability to infiltrate into the immunosuppressive TME and their unique immunomodulatory characteristics. However, due to required intricate genetic manipulation of autologous macrophage cell product for each patient, optimization and consistency of the cell product remains challenging. In contrast, the use of induced pluripotent stem cell (iPSC)-derived macrophages (iMACs) facilitates the introduction of genetic modifications to further optimize the iMAC cell product and limits the need for combination therapies. The knockout (KO) of the SIRPα gene in iMACs is a promising genetic modification that results in a potent iMAC cell therapy product resistant to phagocytosis inhibition by CD47-expressing tumor cells.

A SIRPα KO was introduced in a fully characterized GMP iPSC line that was then differentiated to iMACs using Evotec's 3D differentiation protocol. The SIRPα KO iMACs were then evaluated for their antibody-dependent cellular phagocytosis (ADCP) capacity in comparison to antibody-loaded wildtype (WT) iMACs when co-cultured with CD47-expressing tumor cells.

SIRPα KO iPSCs showed differentiation potential comparable to WT iPSC and resulted in iMACs expressing typical markers of fully differentiated macrophages. SIRPα KO iMACs exhibited increased phagocytic potency and killing capacity compared to WT iMACs when both cell types were exposed to CD47-positive tumor cells and loaded with the same tumor-targeting mAb. This increased phagocytosis of tumor cells by antibody-loaded SIRPα KO iMACs was also comparable to ADCP observed for WT iMACs in the presence of an anti-CD47 blocking antibody.

Using Evotec's gene editing platform we were able to efficiently generate SIRPα-deficient iPSCs that serve as the starting material to manufacture highly pure, genetically modified iMACs that lack SIRPα expression rendering them resistant to CD47-dependent inhibition of phagocytosis. This novel allogeneic *off-the-shelf* iMAC cell product overcomes the need to combine this cell therapeutic with CD47-SIRPα axis CPIs and provides the basis to develop innovative treatments for solid tumors.

#5245 Anti-CSPG4 CAR-Macrophages synergize with anti-CD47 in melanoma cytotoxicity.

D. Greiner, Q. Xue, T. Waddell, M. Roh-Johnson;
University of Utah School of Medicine, Salt Lake City, UT

While CAR T-cells have been a success in treating liquid tumors, these successes have not been replicated in solid tumors. There are several reasons for these challenges, including physical matrix barriers and increased tumor antigen heterogeneity in solid tumors. Macrophages are frequently found in melanoma tumors, even in those that have low T-cell infiltrate, suggesting macrophages are well equipped to penetrate the physical barriers surrounding solid tumors. Macrophages are also antigen-presenting cells, thus, if macrophages phagocytose the tumor, they will likely present additional antigens to T-cells, potentially enhancing the adaptive immune response in cancer treatment. Thus, we hypothesized that macrophages expressing chimeric antigen receptors (CAR-Macrophages or CAR-Ms) are able to access solid tumors, phagocytose cancer cells, and subsequently re-educate the tumor immune environment by directly polarizing tumor-associated macrophages and by presenting novel antigens to recruit and educate adaptive immune cells. To test these hypotheses, we generated CAR-Ms with primary human macrophages using an scFV specific to chondroitin sulfate proteoglycan 4 (CSPG4), a highly expressed antigen enriched and specific to melanoma tumors, and an intracellular activation domain to promote phagocytosis. We found that anti-CSPG4 CAR-Ms phagocytosed human melanoma cells at high efficiency, however, this phagocytosis did not result in high levels of melanoma cell cytotoxicity. To improve CAR-M-mediated melanoma cell death engulfment, we blocked the anti-CD47/SIRPα (“don’t eat me”) signaling axis with an anti-CD47 blocking antibody, which resulted in additive effects for phagocytosis, and a robust effect on the melanoma cell killing. Preliminary *in vivo* xenograft experiments suggest that anti-CSPG4 CAR-Ms alone delay melanoma growth. We are now testing whether combining anti-CD47 and CSPG4 CAR-Ms therapies *in vivo* can 1) further reduce primary tumor growth and 2) prevent recurrence following surgical resection by treating remnants of the tumor. Our work shows that CSPG4 CAR-M-mediated killing of CSPG4-positive cancer cells is significantly enhanced when in combination with anti-CD47 antibody treatment.

#5246 Therapeutic efficacy of glypican-3 peptide-linked chimeric antigen receptor-macrophages in hepatocellular carcinoma.

W. Leung, O. Leung, T. Wong, K. Lee;
The Hong Kong Polytechnic University, Hong Kong, Hong Kong

Hepatocellular carcinoma (HCC) is the third most lethal cancer and sixth most diagnosed cancer worldwide. Recently, chimeric antigen receptor-T cell (CAR-T) therapy has been demonstrated to be a promising immunotherapy for the treatment of hematologic malignancies such as leukemia. However, its application in solid tumors has proven to be challenging. To overcome this limitation, chimeric antigen receptor-macrophages (CAR-Ms) have emerged as a new immunotherapy against solid cancers, capitalizing on the unique attributes of macrophages in penetrating the tumor microenvironment, promoting antigen presentation, and priming T cells. Traditionally, CAR-M therapy involves the transfer of an edited CAR gene into macrophages via viral infection. However, this method is expensive, involves tedious procedures, and has long-term safety concerns. In the present study, we employed peptides to mimic the genetic approach for producing CAR-Ms to reduce the above uncertainties. To achieve this, we developed a novel bioconjugation method called the phthalaldehydeamine capture (PAC) reaction to produce peptidic CAR-Ms (pCAR-Ms) targeting Glypican-3 (GPC3) in HCC cells. This was achieved by linking GPC3 specific peptides to Raw264.7 murine macrophages. Using an *in vitro* co-culture system, we demonstrated the specificity and efficacy of pCAR-Ms against GPC3, as evidenced by a significant increase in the number of phagocytosed cells with high GPC3 expression when compared to their low-expression counterparts, by flow cytometry and confocal microscopy. The specificity of pCAR-Ms was further proven in GPC3-knockdown HCC cells, with a significant decrease in the phagocytic rate. Using an HCC xenograft model derived from MHCC97L cells, we confirmed the specific homing of pCAR-Ms to tumor sites via intravenous injection of lipopolysaccharide (LPS)-differentiated pCAR-Ms. Strikingly, pCAR-Ms suppressed HCC tumor growth when compared with untagged macrophages and PBS control. In conclusion, we provided evidence of the potency and specificity of non-viral-based pCAR-Ms in targeting HCC with simple and short production time and increased flexibility.

#5247 Reprogramming tumor microenvironment with intratumor macrophage adoptive cell therapy in melanoma.

S. R. Noonepalle[1], N. Gajendran[1], M. Suresh[1], X. Li[1], M. D. G. Hernandez[2], C. Z. Delgado[3], N. Aghdam[4], M. Berrigen[5], T. Knox[1], K. Tan[1], M. Durr[1], E. Sotomayor[6], K. B. Chiappinelli[2], D. Wardrop[7], A. Horvath[2], B. A. Shook[2], N. H. Lee[2], A. Dritschilo[1], R. Fernandes[2], K. Musunuri[8], M. Shibata[2], A. Villagra[1]; [1]Georgetown University, Washington DC, DC, [2]George Washington University, Washington DC, DC, [3]University of Houston, Downtown, Houston, TX, [4]Beth Israel Deaconess Medical Center, Boston, MA, [5]George Wsahington University, Washington DC, DC, [6]Tampa General Hospital, Tampa, FL, [7]University of Illinois, Chicago, IL, [8]Avstera Therapeutics Inc, Malvern, PA

The interplay between tumor cells and immune cells within the tumor microenvironment (TME) dictates protumor or antitumor immune responses. Tumor-associated macrophages (TAMs) respond to signals of the TME and exhibit a spectrum of phenotypes ranging between M1 (antitumor) and M2 (protumor) macrophages. In most tumor types, including melanoma, the balance between M1 and M2 macrophages is critical with a higher M1/M2 ratio favoring antitumor immunity. Therefore, strategies enhancing the M1/M2 ratio can significantly alter the TME towards antitumor immunity. In this study, we administered luciferase and GFP-expressing M1 macrophages as an adoptive cell therapy (ACT) through intravenous (i.v) and intratumor routes respectively, into mice bearing SM1 murine melanoma tumors to determine the effective treatment modality. We reprogrammed antitumor M1 macrophages ex-vivo with HDAC6 inhibitors to lock into the M1 phenotype and administered intratumorally as ACT in the syngeneic SM1 murine melanoma and humanized NSG-SGM3 melanoma models. We performed histological analysis of tumors for macrophage markers, immune phenotyping of infiltrated immune cells, single-cell secretome analysis of tumor macrophages, and single-cell RNA-seq analysis of CD45+ immune cell populations to demonstrate the benefit of macrophage ACT. Tail vein injected, luciferase-expressing M1 macrophages localized in the lungs and spleen, failed to reach the tumor as visualized by IVIS imaging, suggesting that i.v administration is ineffective for macrophage therapy. On the contrary, intratumor M1 macrophage ACT resulted in diminished tumor growth. Single-cell RNA-seq analysis of the CD45+ sorted tumor-associated immune cell population revealed distinct macrophage subsets and a significant M1/M2 macrophage ratio increase. NicheNet cell-cell interaction analysis indicated that M1-like TAMs activated infiltrating T-cells and monocytes through ligand-receptor interactions. Trajectory analysis of infiltrated monocytes indicated differentiation toward inflammatory macrophages in ACT tumors. Flow cytometry analysis corroborated that ACT increased the M1/M2 macrophage ratio and an increase in CD8 effector T-cells. Furthermore, HDAC6i-treated macrophages increased antigen cross-presentation. Single-cell secretome analysis of F4/80+ TAMs by the Isoplexis platform revealed polyfunctionality of HDAC6-treated M1 macrophages secreting inflammatory cytokine Tnfa and T-cell recruiting chemokine Cxcl10. Histological examination of tumor sections for macrophage phenotypic markers suggested that transplanted macrophages retained the M1 phenotype post-ACT in both SM1 murine and NSG-SGM3 melanoma tumor models. We demonstrated the potential of reprogramming macrophages ex vivo with HDAC6 inhibitors as a feasible macrophage cell therapy to treat solid tumors.

#5248 Novel costimulatory domain improves CAR-monocyte activity against tumors.

Kevin Carbajal, Warren Anderson, **Kilsoo Jeon**, Grace Reynolds, Prasanna Ekambaram, Beatrice Breckheimer, Anastasya Birger, Jessica Pafford, Mathew Esquivel, Adam Pecoraro, Sumiti Jain

Inceptor Bio, LLC, Raleigh, NC

Myeloid cells, unlike other immune cells such as T cells or NK cells, are known residents in the solid tumor microenvironment (TME). In the absence of checkpoints and in proinflammatory conditions, myeloid cells (particularly M1 macrophages) are known to be capable of direct phagocytosis of tumor cells and can present tumor-associated antigens to the host immune system. However, the immunosuppressive conditions within the TME restrict and limit the anti-tumor response of tumor associated macrophages (TAMs), including their ability to recruit and activate other immune cells against the tumor. Engineered CAR-Monocytes can serve a unique function in cell therapy by bridging a key gap in the treatment of solid tumors. We are developing an autologous engineered CAR-M cell therapy product targeting Glypican-3 (GPC3) to treat hepatocellular carcinoma (HCC). The CAR serves a dual purpose as a homing ‘GPS’ signal for trafficking directly to the tumor site, and for directing phagocytosis specifically at targeted tumor cells. We have designed a proprietary CAR molecule (M83 CAR) which contains a macrophage-specific costimulatory domain that significantly increases the phagocytosis function of the CAR-M cells. Furthermore, we have demonstrated that the M83 CAR-M cells are not inhibited by the prevalent CD47 checkpoint (‘do not eat me’ signal expressed on tumor cells), which is known to restrict myeloid function in the TME. Effective phagocytosis of engineered CAR-M cells is central to subsequent mechanisms of actions that can elicit robust anti-tumor immunity against patient-specific neoantigens. However, the first barrier to overcome is effective infiltration of engineered CAR-M into the tumor from the periphery. We have demonstrated that our engineered CAR-Monocyte drug product can successfully home to the targeted tumor specifically, from the periphery. Subsequent in situ differentiation of CAR-monocytes into CAR-macrophages (M1) enables robust tumor cell phagocytosis, the central mechanism that can result in the following series of events: 1) proinflammatory shift in the TME milieu, 2) recruitment of innate and adaptive immune cells, 3) activation of T-cells against tumor neo-antigens. This is a unique outcome of the CAR-M mechanism of action that is not capitulated by CAR-T or CAR-NK cells. Leveraging and further enhancing CAR-M function could lead to the rejection of the tumor and its metastases, particularly in combination with other immune-modulating therapies.

#5249 Macrophages expressing synthetic cytokine receptors reverse IL10-mediated immunosuppression within solid tumors and promote adaptive immunity.

C. Sloas, S. Beghi, Y. Huangfu, R. Qureshi, B. Schott, M. Ball, D. Blumenthal, T. Condamine, M. Klichinsky, Y. Ohtani;
Carisma Therapeutics, Philadelphia, PA

Motivation: In solid tumors, anti-inflammatory cytokines such as IL10 and TGFβ support an immunosuppressive tumor microenvironment (TME) and inhibit anti-tumor immunity. Many therapeutic approaches to overcome immunosuppression have used monoclonal antibodies to block cytokine signaling. Instead of silencing TME-associated cytokines, a more powerful strategy may be to leverage them as disease markers and convert them into anti-tumor signals, using a logic-gated cell-based immunotherapy. Here, we engineered macrophages with synthetic cytokine switch receptors (SR) that convert IL10 or TGFβ into pro-inflammatory signals. Macrophages are homeostatic regulators capable of both infiltrating solid tumors and initiating inflammation, and we harnessed this proficiency using SRs that convert prevalent cytokines in the TME into pro-inflammatory responses for TME modulation. We termed this engineered myeloid cell platform “Engineered Microenvironment Converters” (EM-C) and evaluated its ability to overcome cytokine-mediated immunosuppression in solid tumors.
Methods: EM-C were produced by transducing primary macrophages or monocytes with a SR that converts IL10 into an interferon-based signal. The response of EM-C to IL10 was monitored *in vitro* using phenotypic characterization of surface molecules, measurement of secreted factors, and mRNA profiling. The *in vivo* activity of EM-C was evaluated using a subcutaneous tumor model in immunocompetent mice. Murine EM-C were administered to tumor-bearing mice, and their ability to modulate the TME was monitored via immunophenotyping, secretome analysis, and single cell transcriptomics. To demonstrate modularity of the EM-C platform, additional SR were designed to convert TGFβ into interferon or toll-like receptor signals.
Results: EM-C efficiently sequestered IL10 or TGFβ and upregulated pro-inflammatory markers, cytokines, and pathways in a dose-dependent manner *in vitro*. EM-C administered to tumor-bearing mice remodeled the TME immune compartment by increasing the abundance of CD8 T cells and reducing the presence of immunosuppressive Tregs. EM-C furthermore augmented the cytokine/chemokine profile of the TME in a manner that correlated with anti-tumor response. TME modulation by EM-C improved tumor control, as compared to non-engineered macrophages, and had additive efficacy with checkpoint blockade.
Conclusion: We present a versatile immunotherapy platform that harnesses macrophages as “living converters” to locally augment inflammation in solid tumors. EM-C exhibit a modular ability to locally convert IL10 or TGFβ into pro-inflammatory signals without systemic cytokine antagonism. The EM-C platform enables development of target antigen-agnostic myeloid cell immunotherapies for overcoming immunosuppression in diverse solid tumors.

#5250 Chimeric antigen receptor macrophages (MOTO CARs) driving repolarization of macrophages in solid tumors.

Michael Boyer[1], Michelle Townsend[1], Timothy Phares[1], Adam Blaszczak[1], Rachel Garlick[1], Kenneth Katschke[1], Gaju Shrestha[1], Toni Mortimer[2], Ashlin Cowager[1], McCall Jensen[1], **Abigail Cheever**[2], Kim O'Neill[2]

[1]ThunderBiotech, Provo, UT, [2]Microbiology and Molecular Biology, Brigham Young University, Provo, UT

Introduction: Though chimeric antigen receptor (CAR) T cells have been effective in treating hematological cancers, they have lacked in solid tumors. Due to the nature of solid tumors and how macrophages are localized there, we propose that macrophages are a better cell type for targeting solid tumors. In tumors, most of the macrophages are Tumor Associated Macrophages (TAMs) which are M2 polarized and promote tumor growth, angiogenesis, and metastases. If these macrophages could be repolarized to an anti-tumor, M1 phenotype, they could alter the tumor immune microenvironment and facilitate destruction of the tumor by immune cells.

Methods: We hypothesize that CAR macrophages (MOTO-CARs) could infiltrate solid tumors, and affect the tumor immune microenvironment to repolarize (TAMs) from an M2 to M1 phenotype. Over 150 signaling domains from published sequences were cloned into a CAR constructs, comprised of an anti-mesothelin scFv, CD34 hinge, and transmembrane and activation domains from various immune cells. Functional activation assays were preformed in reporter HEK cells lines. Functional constructs were then transduced into THP-1 cells. The function of these MOTO-CARs were evaluated using a flow cytometry based phagocytosis assay (indication of an M1 phenotype) and RT-qPCR repolarization assay.

Results: Of the constructs tested in HEK reporter cell lines, around one third demonstrated significant activation, that is 20% higher than the background control. The phagocytosis assay performed on the functional constructs showed that around one third of these constructs exhibited higher phagocytosis compared with a control construct with no signaling domain. However, it is noteworthy that this no signaling domain control had significantly higher rates of phagocytosis than untransduced controls. The RT-qPCR demonstrated that M2-like THP-1 cells transduced with the CAR constructs exhibited a significant shift in expression towards M1 characteristic genes when stimulated with mesothelin beads, with the TLR4 construct exhibiting the greatest shift.

Conclusion: Several of the MOTO-CAR constructs, including TLR4, showed significant activation, phagocytosis, and ability to repolarize macrophages from M2 to M1 phenotype. Further analysis hopes to prove the functionality of these MOTO-CAR constructs with primary cells as well as in vivo, making MOTO-CARs a valuable treatment option for patients with solid tumors.

#5251 RNA primed SMAR-T cells against multiple driver mutations, all HLA's designed for first line therapy.

A. E. Slanetz, S. Srivatsa, F. Muzaffar, W. Barry, D. Ryan, S. Metri, M. Slanetz;
Geneius Biotechnology, Inc., Natick, MA

Success of immune checkpoint inhibitors (e.g., anti-PD1 antibodies) have revolutionized cancer immunotherapy by demonstrating that a patient's own T-cells recognize and treat cancer. The efficacy of PD-1 blockade is driven by recruitment of new T-cells from blood rather than via activation of pre-existing tumor infiltrating lymphocytes (Yost K.E., et al. Nat. Med. 2019). However, anti-PD1 therapy is most effective in ~5% of malignancies i.e., cancers with high mutational burden. Hence, the challenge of addressing most lower mutational burden cancers (the ~95%) needs an alternate treatment strategy. We address this challenge by using RNA to prime and expand peripheral T-cells to cancer-specific mutations ex-vivo. Using our proprietary, patented, and robust manufacturing method, we can generate T-cell populations reactive to as low as 8 and as high as 40 cancer-specific mutant proteins. In-vitro, these T-cells have cancer mutation-specific cytotoxicity and do not kill the normal cells. Further, the T-cells express homing receptors enabling them to infiltrate tumors and express high levels of TNFα and IFNγ, which are associated with effective tumor cytotoxicity and pro-inflammatory modification of tumor microenvironment (TME). Additional characterization shows these cells to be predominantly CD4+ and CD8+ T-cells bearing central and effector memory phenotypic with negligible regulatory or exhausted T-cells. We believe our T-cells can be used for cellular therapy in conjunction with, or as an alternative to, immune checkpoint inhibitors to treat lower mutational burden cancers present in most patients.

#5252 Expansion of human T cells and NK cells for chimeric antigen receptor based therapies using human platelet lysate.

V. Alonso-Camino, W. Mirsch;
Mill Creek Life Sciences, Rochester, MN

T cells and NK cells expressing chimeric antigen receptors (CAR) have demonstrated potent clinical efficacy in patients with hematological malignancies. One of the issues to overcome in the treatment of solid tumors using CARs is the lack of a process that generates large amounts of CAR-T cells, reduces cell exhaustion and differentiation, and improves long term survival after infusion into patients.

Previously, Torres Chavez et al. demonstrated in a series of *in vitro* and *in vivo* experiments, performed in both hematologic and solid tumor models, the profound qualitative impact on CAR-T cell performance after using human platelet lysate (hPL) as a cell growth supplement. T cells expanded with their hPL showed a good proliferative capacity and enhanced long-term in vivo persistence compared to Fetal Bovine Serum (FBS) or human AB Serum (ABS), resulting in superior anti-tumor effects. Additionally, this group demonstrated that the transduction of T cells to generate the CAR-T cells was significantly improved by the use of hPL.

Mill Creek's human platelet lysate (hPL) is produced using expired human platelets obtained from accredited blood banks in the United States. These platelets were originally intended for use in patient transfusion. The safety of platelets used in transfusion is managed by the U.S. Food & Drug Administration (FDA), as well as the Association for the Advancement of Blood & Biotherapies (AABB). These organizations set standards, including testing for transmissible diseases. The United States record for blood safety is well established, with extremely low rates of disease transmission, making the platelet units used for hPL manufacture low risk. The Covid-19 pandemic has increased awareness of emerging infectious diseases, even though transmission of Covid-19 via blood transfusion has not been documented. For that reason, we developed a gamma irradiated version of our products, which offers an additional safety measure in the clinic.

Our data from experiments performed using human CD3+ and purified NK cells from donor peripheral blood suggests that our human platelet lysates offer an improved cell phenotype and expansion capacities versus serum derived products, but also versus other platelet lysates on the market. PLTGold® and PLTGold®-GI efficiently promote cell expansion, with higher cell yields and lower cell exhaustion rate. Additionally, our hPLs are suitable for suspension culture, potentially facilitating the large-scale expansion of allogeneic CAR cells.

The use of our platelet lysates has the potential of significantly improving CAR-T and CAR-NK manufacture, but also the outcome of the therapy itself by improving the quality and potency of the end product.

#5253 Epigenetic drugs partially restored anti-cholangiocarcinoma activity of dysfunctional CD3+CD56+ cells.

A. Wongkajornsilp[1], P. Chusorn[2], K. Phongkitkarun[3], K. Htwe[1], S. Duangsa-ard[1], K. Kasetsinsombat[1], N. Sawatpiboon[1];
[1]Mahidol University, Faculty of Medicine Siriraj Hospital, Bangkok, Thailand, [2]Faculty of Liberal Arts and Science, Roi Et Rajabhat University, Roi Et, Thailand, [3]Faculty of Engineering, Mahidol University,, Nakhon Pathom, Thailand

The cholangiocarcinoma cell-exposed cytokine-induced killer (CIK) cells or their most efficacious $CD3^{\pm}CD56^{\pm}$ subset displayed weaken anti-tumor cytotoxicity upon subsequent exposure. RNAseq analysis of the resistant phenotype gave rise to a list of drugs that could potentially counter the activity of genes associated with resistance to the anti-tumor activity of CIK cells. The top-ranking drugs appeared to be epigenetic drugs. Sublethal concentration of these drugs were assayed for their synergistic activity with CIK cell or the $CD3^{\pm}CD56^{\pm}$ subset for cytolysis of resistant CCA cells in tissue culture model. These drugs, although in low concentration, contained anti-tumor activity. The tumor cytolysis was greater after the combination with either CIK cells or the $CD3^{\pm}CD56^{\pm}$ subset. An in vivo model of CCA-implanted mice exhibited the synergistic activity of subtherapeutic dose of these drugs and $CD3^{\pm}CD56^{\pm}$ subset in suppressing tumor growth. It is concluded that epigenetic drugs in subtherapeutic dose could prevent the dysfunction of CCA-exposed CIK cells.

#5254 The “off-the-shelf ”CD19-CAR-Vδ1T cells demonstrated an enhanced therapeutic effect on B-cell malignancy models.

D. Chen[1], F. You[1], C. Chen[1], S. Xiang[1], P. Zhang[1], H. Wu[1], Z. Zheng[1], M. Wang[2], X. Wang[3], H. Meng[1], N. Yang[1], B. Zhang[4], **L. Yang**[5]; [1]PersonGen BioTherapeutics, Suzhou, China, [2]PersonGenAnke Cellular Therapeutics Co., Ltd, Hefei, China, [3]Department of Hematology, The First Affiliated Hospital of USTC , Division of Life Sciences and Medicine, University of Science and Technology of China, Hefei, China, [4]PersonGen BioTherapeutics, Suzhou, China;PersonGenAnke Cellular Therapeutics Co., Ltd., Hefei, China, [5]PersonGen BioTherapeutics, Suzhou, China;Cyrus Tang Medical Institute, Soochow University, Suzhou, China

Background: The commercialization of autologous chimeric antigen receptor T cell (CAR-T) is hindered by the expensive and time-consuming manufacturing process, presenting major challenges. The development of allogeneic products is proposed as an alternative strategy to overcome these obstacles. Vδ1T cells, possessing active homing capability, are known to infiltrate tumor tissues and have been linked with favorable patient prognosis due to their direct killing effect via innate immunity and their sensitive T cell receptors that can broadly recognize tumor antigens. Unlike conventional αβ T cells, Vδ1 TCRs are not restricted by major histocompatibility complexes (MHCs), thus preventing the development of graft-versus-host disease (GVHD). Therefore, Vδ1T cells were hypothesized to be a superior candidate for universal CAR-T cells. Nevertheless, the small portion of Vδ1T cells (less than 1%) in peripheral blood posts a significant challenge for CMC and production. Here we present the successful development of CD19-CAR-Vδ1T cells, which demonstrate enhanced therapeutic efficacy on B-cell malignancy models.

Methods: High-purity CD19-CAR-Vδ1T cells were prepared using PersonGen's proprietary platform technology. Multiple CAR structures were tested for cytotoxicity, and the fourth-generation CAR-transduced Vδ1 cells designated as UTAA09 exhibited sustained killing of CD19+ target cells. UTAA09 underwent in-depth research regarding its anti-tumor efficacy and safety.

Results: The Vδ1T cell purity exceeded 95%, while the residual TCRαβ count remained under 1%. The CAR transduction efficiency remained stable across batches, with medium CAR+~30%, and up to 2×10^{11} UTAA09 cells were harvested in compliance with GMP standards. The presence of secreted IL-2 significantly increased the persistence of UTAA09 in vitro, and UTAA09 showed comparable anti-tumor activity and expansion rates to CD19-CAR-αβT cells. Notably, no exhaustion phenotype was detected for UTAA09 after multiple antigen stimulation processes. Moreover, UTAA09 lacked detectable IL-17A, indicating a non-promoting characteristic in tumor growth. In the xenograft model, significant inhibition of tumor growth was observed in all mice, of which 40% achieved long-term disease-free survival ($p<0.01$) . On days 5, 12, and 19 after the administration of UTAA09, Vδ1T cells underwent significant expansion in all 5 mice tested. Subsequent analysis confirmed that the majority of these expanded Vδ1T cells were CAR+ cells, indicating the specific and long-lasting expansion of CD19-CAR+ Vδ1T cells in vivo. Importantly, none of the mice experienced significant weight loss, demonstrating the safety and outstanding in vivo effectiveness of UTAA09.

Conclusion: UTAA09 shows potential as an off-the-shelf allogeneic cellular therapy for the treatment of B-cell malignancies and autoimmune diseases derived from B cells.

#5255 A B7-H3-CAR-modified Vδ1 T cells showed potentanti-solid tumor potential.

L. Jiang[1], C. Qi[2], F. You[1], S. Xiang[1], P. Zhang[3], M. Wang[3], H. Wu[1], K. Yan[1], J. Huang[1], H. Meng[1], N. Yang[1], S. Zhang[4], L. Shen[2], **L. Yang**[5];
[1]PersonGen BioTherapeutics Co., Ltd., Suzhou, China, [2]State Key Laboratory of Holistic Integrative Management of Gastrointestinal Cancers, Beijing Key Laboratory of Carcinogenesis and Translational Research, Peking University Cancer Hospital & Institute, Beijing, China, [3]PersonGenAnke Cellular Therapeutics Co., Ltd., Hefei, China, [4]PersonGen BioTherapeutics Co., Ltd. / PersonGenAnke Cellular Therapeutics Co., Ltd., Suzhou, China, [5]PersonGen BioTherapeutics(Suzhou) Co., Ltd. / Cyrus Tang Medical Institute, Soochow University / PersonGenAnke Cellular Therapeutics Co., Ltd., Suzhou, China

Background: CAR-αβT cells have made limited advancement in treating solid tumors. Vδ1 T cells, a subtype of γδT cells, are rare in human peripheral blood, but they are the main tissue-resident immune cells found in epithelial and mucosal tissues. This suggests that Vδ1 T cells might be a potential modality for treating solid tumors. To explore this possibility, we hypothesized that Vδ1 T cells modified with B7-H3 CAR (B7-H3-CAR-Vδ1 T) could have great potential of anti-solid tumor activity, making them a promising candidate for further development as a universal cellular therapy product.
Methods: A proprietary manufacturing procedure to produce Vδ1 T cells from the leukopak of healthy donors has been established under GMP compliance. The immune checkpoint molecule B7-H3 was selected as the target. The allogeneic B7-H3-CAR-Vδ1 T cells carrying IL-2 (UTAA06), which displayed the most prolonged anti-tumor activity, were chosen for comprehensive functional validation. Single-cell sequencing and mass spectrometry flow cytometry were utilized to characterize the biology of UTAA06. In vivo effectiveness of UTAA06 was confirmed in animal models.
Results: A clinical-grade manufacturing process for Vδ1 T cells is developed. This process results in a purity of over 95% of Vδ1 T cells, with an expansion of more than 20,000-fold, and a CAR lentiviral transduction efficiency of over 50%.žSingle-cell sequencing and mass cytometry analysis both demonstrated that the Vδ1 T cells produced by our approach exhibited high expression levels of natural cytotoxic receptors (including NKG2D, DNAM1, and NKp series receptors), chemokine receptors (such as CXCR3 and CXCR6), anti-tumor related molecules (such as CD27 and CD137), and low expression levels of inhibitory molecules (such as PD1 and LAG3).ž
UTAA06 cells did not produce IL17A, which is a signal protein with pro-tumor activity. Meanwhile, UTAA06 demonstrated significant and specific inhibitory effects on the growth of various solid tumor cell lines.žUTAA06 cells were found to significantly suppress tumor cell growth in solid tumor mouse models. The complete remission (CR) for each tumor model was 83.3% of neuroblastoma (SK-N-AS, N=6), 66.7% of pancreatic cancer (SW1990, N=6), 100% of lung cancer (A549, N=6), and 70% of colorectal cancer (HCT-15, N=10) respectively. In addition, a potent capacity of UTAA06 to penetrate tumor tissues with a favorable safety profile in mice was observed.
Conclusion: UTAA06 exhibited extraordinary anticancer properties both in vitro and in vivo against solid tumors. Additionally, the outstanding manufacturing process of UTAA06 will facilitate the clinical application of this product.

IMMUNOLOGY: Immune Modulating Effects of Chemotherapy and Other Agents
Poster Session

#5259 Mechanistic evaluations of the immunological and cell biological effects that distinguish eribulin from other microtubule-targeted chemotherapeutics.

Z. Hassouneh, N. Wilkinson, L. Takahashi-Ruiz, N. Mukherjee, A. L. Risinger;
UT Health Science Center at San Antonio, San Antonio, TX

Microtubule-targeted agents (MTAs) are some of the most widely used and effective chemotherapeutics and they continue to find utility as the payloads of antibody-drug conjugates and in combination with targeted agents to improve response, including with immune checkpoint inhibitors. While all MTAs have shared antiproliferative effects, over the last decade it has become increasingly clear that individual drugs of this class have distinct effects on microtubule-dependent signaling and trafficking that are critical for their anticancer efficacy. We and others have demonstrated that eribulin is unique from other MTAs in its ability to promote vascular remodeling, reverse epithelial-to-mesenchymal transition (EMT), and increase immune infiltration into tumors both in animal models and in the clinic. However, the mechanism linking eribulin-mediated microtubule destabilization to these phenotypes, which are associated with improved overall survival of eribulin-treated patients, is unclear. We found that acute eribulin treatment at clinically relevant concentrations promotes the production of antitumor cytokines in both immune and cancer cells and synergizes with direct STING agonists to promote enhanced immune infiltration and improved antitumor efficacy in vivo in both breast and bladder cancer models. This effect was shown to involve activation of natural killer cells and is associated with TBK1-mediated IRF3 phosphorylation, which is regulated downstream of the microtubule associated GTPase GEF-H1. Intriguingly, GEF-H1 release from destabilized microtubules has also been shown to enhance the formation of focal adhesions and promote the differentiation of mesenchymal cells to a more epithelial phenotype. We show that eribulin is indeed sufficient to promote the formation and activation of focal adhesion complexes in mesenchymal triple-negative breast cancer cells, which was not observed when cells were subjected to treatment with microtubule stabilizing chemotherapeutics. Both genetic and pharmacological inhibitors of GEF-H1 were utilized to interrogate the relationship between eribulin-mediated microtubule destabilization and TBK1/IRF3-dependent immunological activation as well as the formation of RhoA-dependent focal adhesions and reversal of EMT-associated phenotypes. Together, our data provide a mechanistic rationale for unique effects of eribulin as compared to other classes of MTAs that could inform on the use of these widely used, but mechanistically underappreciated drugs in a more personalized manner and inform on their rational combination with targeted agents, including immunotherapy.

#5260 Combination activity of eribulin liposomal formulation and anti-PD-1 antibody after tumor regrowth during anti-PD-1 antibody treatment in mice.

M. Tamura, Y. Niwa, T. Semba;
Eisai Co., Ltd., Tsukuba, Japan

Eribulin (ERI) has been reported a microtubule dynamics inhibitor with unique tumor microenvironment modulations such as vascular remodeling activity. In the previous meeting (AACR2022, 2023), we reported that ERI and liposomal formulation of ERI (ERI-LF) also have immunomodulatory activity that induces $CD8^{\pm}$ T cells via its vascular remodeling activity and ERI-LF showed more potent immune modulation and combination activities with anti-PD-1 antibody (PD-1 Ab) than ERI in syngeneic mice models and humanized mice models. Although immune-checkpoint inhibitors (ICI) are using as a key drug for various types of cancers in clinical setting, several clinical questions regarding suitable therapies after ICI therapy and efficacy of ICI rechallenge are remaining. In this study, we evaluated anti-tumor activities of combination of ERI-LF and PD-1 Ab in two syngeneic transplantation models using mouse non-small lung cancer cells, P-glycoprotein-knockout (Pgp-KO) KLN205 cells and Pgp-KO LL2 cells. As a result, combination of 1mg/kg ERI-LF (Q7D×2) with PD-1 Ab (200 ug/head, twice a week ×2 weeks) showed significant stronger antitumor activity compared with each monotherapy in only Pgp-KO KLN205 model, in which ERI-LF increased intratumoral microvascular density as a vascular remodeling activity, not in Pgp-KO LL2 model. We next conducted continuous treatment of PD-1 Ab in Pgp-KO KLN205 model to investigate tumor regrowth during treatment of PD-1 Ab. In this model, tumor growth was inhibited by PD-1 Ab until about two weeks after initiation of the treatment and then this inhibitory activity disappeared after two weeks even by continuous treatment of PD-1 Ab. We performed flow cytometry analysis (FCM) for tumor-infiltrating immune cells and RNAseq analysis using regrowing tumors compared with non-treatment tumors. Expressions of mRNA of several immune inhibitory receptors were upregulated in tumors with regrowth, although $CD4^{\pm}$ cells and $CD8^{\pm}$ cells were also increased in FCM using tumor samples. Furthermore, we investigated anti-tumor activity of combination of ERI-LF and PD-1 Ab against tumors which changed from inhibitory phase to regrowth phase during PD-1 Ab treatment in Pgp-KO KLN205 model. The combination of ERI-LF at 1mg/kg (Q7D×3) and PD-1 Ab (200 ug/head, twice a week ×3 weeks) also showed potent anti-tumor activity against tumors with regrowth by prior PD-1 Ab treatment as well as PD-1 Ab-naïve tumor, suggesting that this combination therapy might be effective after prior ICI therapy. Currently, Phase 1b/2 clinical trial of ERI-LF plus nivolumab in patients with selected solid cancers (NCT04078295) is underway. Patients with or without prior ICI therapy were enrolled in a small cell lung cancer cohort of this clinical study. Our preclinical results might provide a scientific rationale for a uniqueness of ERI-LF as a post ICI therapy.

#5261 Immunologic signatures of peripheral blood cells in patients with advanced pancreatic cancer under lenvatinib-pembrolizumab maintenance therapy.

V. Chung, F. Kos, E. Manual, S. Dempsey, D. J. Diamond;
City of Hope, Duarte, CA

Background: The treatment of pancreatic cancer is limited by chemotherapy toxicities which impacts quality of life. This is a phase 2 clinical trial of lenvatinib and pembrolizumab as maintenance therapy in patients with advanced pancreatic cancer. We observed preclinical activity of this combination in pancreatic mouse models. We hypothesize that this combination may address unmet needs to minimize toxicities associated with standard treatments, stimulate anti-tumor T cell immunity, and improve the progression free and overall survival. Exploratory studies aim to characterize immune-related systemic changes in peripheral blood over the course of therapy and to identify global changes in expression of tumor-related genes in needle biopsy samples of liver metastatic lesions.
Methods: Multiplex gene expression analysis of unsorted peripheral blood mononuclear cells (PBMC) was performed using PanCancer Immune Profiling Panel on NanoString nCounter platform. PBMC samples from pre- through week 32 of treatment were assessed for differential expression of 730 immune profiling genes defining T cell functions and associated immune categories.
Results: PBMC immune profiling from 4/5 patients show a distinctive pattern of increased activation of T cells during the first 9 weeks of treatment followed by a sharp inhibition starting at weeks 9-12 after 3-4 cycles of treatment (CD3E, CD247, LCK, TBX1, TCF7, STAT4, IL2RG). Subsequent upregulation of macrophage-derived scavenger, inflammatory, and immunosuppressive gene expression patterns continued for the remainder of treatment (CD14, MSR1, MARCO, CD68, TGFB1, IL10RA). The median PFS of first 10 patients was 21.5 (9-32) weeks.
Conclusions: Immunotherapy resistance may be related to rapidly developing terminal differentiation and unresponsiveness of T cells in parallel with upregulation of macrophage-derived inflammatory and immunosuppressive processes. Studies are on-going to prevent inhibition of the T-cells.

#5262 MBO enhances anti-tumor immunity in pancreatic ductal adenocarcinoma by inducing immunogenic apoptosis.

S. R. Gaikwad, S. K. Srivastava;
Texas Tech University Health Sciences Center, Abilene, TX

Pancreatic ductal adenocarcinoma (PDAC) poses significant therapeutic challenges due to its aggressive nature and limited treatment options. In this study, we explored the anti-cancer potential of MBO, a compound selected through drug repurposing strategy based on its cytotoxic ability and modulation of key survival pathways in PDAC. Our preliminary in vitro experiments demonstrated MBO's potent cytotoxicity against various PDAC cell lines, inhibiting cellular growth and clonogenicity. MBO induced G1 phase cell cycle arrest in a concentration-dependent manner. In the next step, in vivo, studies using xenograft and orthotopic mouse models confirmed MBO's ability to suppress tumor growth and increase CD8+ T cell infiltration. MBO demonstrated a favorable tumor suppressive activity wherein it suppressed tumor growth by approximately 49% and 56% in xenograft and orthotopic models, respectively. A CD8+ T cell depletion experiment revealed partial dependence on CD8+ T cells for MBO's overall anti-tumor efficacy. Further, combining MBO with anti-PD1 therapy exhibited a synergistic effect, enhancing overall T cell infiltration, particularly CD8+ T cells. Our mechanistic studies revealed that MBO induced immunogenic apoptosis, as evidenced by increased expression of immunogenic cell death markers (HSP90 and calreticulin) and apoptotic markers. To further delineate the mechanism, we performed RPPA profiling. RPPA analysis indicated MBO's impact on mitochondrial gene expression and stress response pathways, suggesting its involvement in disrupting cellular survival mechanisms along with stress-induced immunogenic marker expression. Overall, this study demonstrates MBO as a promising anti-cancer agent with the potential to serve as an immune adjuvant. Particularly, in combination with immunotherapies, MBO can serve as a potential option to improve immunotherapeutic response in PDAC tumors providing valuable insights for developing novel therapeutic strategies in PDAC.

#5263 The impact of MRTX1133 on anti-tumor immunity in lung cancer with KRAS^{G12D} mutation.

Kunihiro Shono[1], Satoshi Watanabe[1], Takaaki Masuda[1], Ryo Suzuki[2], Tomoya Wakabayashi[1], Tomoki Sekiya[1], Susumu Tanaka[1], Aya Ohtsubo[1], Tomohiro Tanaka[1], Koichiro Nozaki[1], Rie Kondo[1], Yu Saida[1], Satoshi Hokari[1], Naohiro Yanagimura[1], Masashi Arita[1], Riuko Ohashi[3], Kenjiro Shima[1], Yosuke Kimura[1], Nobumasa Aoki[1], Yasuyoshi Ohshima[1], Toshiyuki Koya[1], Toshiaki Kikuchi[1]

[1]Department of Respiratory Medicine and Infectious Diseases, Niigata University Graduate School of Medical and Dental Sciences, Niigata, Japan,[2]Sado General Hospital, Sado, Japan,[3]Division of Molecular and Diagnostic Pathology, Niigata University Graduate School of Medical and Dental Sciences, Niigata, Japan

Background: To date, there have been no clinical molecules that are selective for KRAS^{G12D} mutant tumors. Although immune checkpoint inhibitors (ICIs) have improved the survival for patients with lung cancer, inferior efficacy of ICIs has been reported in KRAS^{G12D} mutant NSCLC. MRTX1133 is a selective KRAS^{G12D} inhibitor, which has been investigated in early clinical studies. In this study, we aimed to reveal the immune status using preclinical murine model of KRAS^{G12D} mutated lung cancer. In addition, we investigated whether MRTX1133 effects the anti-tumor immunity in mice bearing lung cancer with KRAS^{G12D}.
Method: CCSP-rtTA/TetO-Cre mice were crossed with LSL-KRAS^{G12D} knock-in mice to obtain CCSP-rtTA/TetO-Cre/LSL-KRAS^{G12D} conditional mutant mice (KRAS^{G12D} mice). These mice were fed an autoclaved rodent diet supplemented with 0.0625% doxycycline when the mice were about 8~12 weeks old. Mice were treated with 10 mg/kg MRTX1133 in vehicle once daily by intraperitoneal injection for 4 or 8 days. After administration of MRTX1133, the lungs and spleens were harvested, and single cell suspensions were labeled with fluorophore-conjugated antibodies for FACS analyses.
Results: More regulatory T cells (Tregs) infiltrated the tumors of lung of mice treated with doxycycline for a longer period of time. The expression of immune checkpoint molecules (ICMs), including PD-L1, PD-1, TIGIT, TIM-3, LAG-3, were also upregulated on CD4^{+} and CD8^{+} T cells in the KRAS^{G12D} mice. Treatment with MRTX1133 strongly inhibited KRAS^{G12D} tumor progression, reduced the percentage of Tregs and downregulated the expression of PD-1 on CD4^{+} and CD8^{+} T cells infiltrating in lung cancers. The expression of the other ICMs remained high after MRTX1133 administration. In addition, MRTX1133 tended to increase the percentage of tumor-specific CD8^{+} effector T cells infiltration in lung tumors. Conclusion: T cells were exhausted in mice with KRAS^{G12D} mutant lung cancer. MRTX1133 demonstrates the therapeutic efficacy in preclinical murine KRAS^{G12D} mutated lung cancer model. This efficacy is more likely to relate not only signal inhibition but also enhances the anti- tumor immune responses. Our findings could aid in developing an alternative immunotherapy strategy in patients with KRAS^{G12D} mutant lung cancer.

#5264 KRAS^{G12C} inhibition synergizes with checkpoint blockade in KRAS^{G12C}-mutated tumor model.

L. Hua, S. Li, C. Nie, C. Zhang, L. Bourre, **J. Wang**;
Crown Bioscience, Inc., San Diego, CA

Introduction: The KRAS^{G12C} mutation is found in 14% of non-small cell lung cancer (NSCLC) and 3% of colorectal cancer (CRC). Sotorasib (AMG510), which covalently binds to the mutated cysteine 12 of KRAS^{G12C} protein, became the first KRAS^{G12C} inhibitors approved by the FDA for KRAS^{G12C}-mutated NSCLC treatment. AMG510 not only increased apoptosis in cancer cells harboring KRAS^{G12C} mutation, but also re-modelled tumor microenvironment. Thus, to evaluate novel therapeutic strategies for treating KRAS^{G12C}-mutated tumors, we established a CT26-KRAS^{G12C} tumor model and explored the combination of AMG510 with anti-PD1 therapy.

Methods: We knocked in KRAS^{G12C} mutation in murine CT26 colorectal cancer cells using CRISPR/Cas9 to generate CT26-KRAS^{G12C} cells. The mutation was confirmed by PCR sequencing. *In vitro*, CT26-KRAS^{G12C} cells were treated with AMG510 for 2h or 72h, and then p-ERK and cell viability were analyzed. *In vivo*, 3×10^5 CT26-KRAS^{G12C} cells were subcutaneously injected into BALB/c mice, and the tumor bearing mice were treated with AMG510 (30 mg/kg or 100 mg/kg, *QD*×21), anti-PD-1 (10 mg/kg, *BIW*×3) and combination of AMG510 and anti-PD-1. On day 5 after randomization, the composition of immune cells, including CD4^{+} T cells, CD8^{+} T cells, dendritic cells (DC), and natural killer (NK) cells in tumors were analyzed by flow cytometry. The mice with complete tumor regression were re-challenged with bilateral tumors of CT26-KRAS^{G12C} (3×10^5) and unrelated mouse breast tumor cells, 4T1 (3×10^5) to evaluate the effect on tumor growth.

Results: Following confirmation of KRAS^{G12C} mutation, AMG510 treatment decreased p-ERK expression by ~50% and impaired the cell growth with IC50 value of 0.1802 μM in CT26-KRAS^{G12C} cells. *In vivo*, single treatment of AMG510 at 30 mg/kg or 100 mg/kg significantly inhibited tumor growth with TGI of 60% or 99% on day 15 after randomization, respectively (both $p<0.001$). Combined treatment of AMG510 (30 mg/kg or 100 mg/kg) and anti-PD-1 also led to significant tumor inhibition with TGI of 64% or 99% on the same day, respectively (both $p<0.001$), although PD-1 blockade didn't show anti-tumor effect alone. Noticeably, combined treatment of AMG510 (100 mg/kg) and anti-PD-1 induced complete tumor regression in 3 of 10 mice, which remained cured 124 days later. Moreover, the combined treatment significantly improved survival compared to the AMG510 treatment alone. Notably, all 4T1 tumors grew, but none of the CT26-KRAS^{G12C} tumors were palpable in the cured mice after the re-challenge. In the control group, all tumors were well established. Additionally, combined treatment of AMG510 (100mg/kg) and anti-PD-1 markedly increased the infiltration of CD4^{+} T cells, DC, and NK cells in the tumors.

Conclusion: The successfully established CT26-KRAS^{G12C} model is a useful tool for investigating therapeutic strategies to combine KRAS^{G12C} inhibitors with immunotherapy.

#5265 Targeting mtDNA dynamics enhances immunogenicity and sensitizes *KRAS* mutant cancers to PD-1 blockade.

K. Tanaka, Y. Adachi, M. Yoshiya, T. Owari, T. Yamamori-Morita, A. Ohashi, S. Kobayashi, S. Koyama, H. Nishikawa;
National Cancer Center, Chiba, Japan

Mitochondrial DNA (mtDNA) can stimulate an innate immune response that potentiates the efficacy of cancer immunotherapy. However, mtDNA-targeting therapy has not been developed to enhance this innate immune system in specific cancer subtypes efficiently. Here we discover that mtDNA is enriched in *KRAS* mutant tumors where the DNA sensor machinery cGAS-STING signaling is primed for innate immune activation. Intriguingly, MEK inhibitor induces cytosolic mtDNA release to potently activate the cGAS-STING signaling, which in turn induces PRKN-mediated mitophagy in response to mitochondrial stress in *KRAS* mutant cancer cells. During the process of mitophagy, PRKN, as an E3 ubiquitin ligase, degrades BAX protein and attenuates mitochondrial pore formation, which is essential for mtDNA efflux upon MEK inhibition. Combined MEK and mitophagy inhibitors efficiently stimulate type I IFNs in both mtDNA- and STING-dependent manners, and this combination enhances the efficacy of PD-1 blockade in *Kras* mutant murine syngeneic tumors. In the clinic, PRKN is associated with a ‘cold tumor’ phenotype among *KRAS* mutant tumors. Together, targeting mtDNA dynamics by co-inhibition of MEK and mitophagy represents a promising strategy to convert ‘cold to hot tumor’ in mtDNA-enriched *KRAS* mutant cancers.

#5266 Deciphering the systemic immune effects of abemaciclib in recurrent metastatic breast cancer: A multicenter, prospective study.

Y. Fukui[1], K. Kawaguchi[1], Y. Maeshima[1], Y. Fujimoto[1], H. Ishiguro[2], K. Yamagami[3], S. Takahara[4], H. Suwa[5], M. Torii[6], S. Nagai[7], Y. Sagara[8], W. Tsuji[9], H. Yamashiro[10], T. Kotake[10], S. Fukuda[11], K. Saito[12], Y. Yamamoto[12], M. Kataoka[1], Y. Himoto[6], A. Yonezawa[1], Y. Nakamura[1], W. Li[1], S. Tanaka[1], S. Morita[1], M. Takada[1], M. Toi[1];

[1]Kyoto University Hospital, Kyoto, Japan, [2]Saitama Medical University International Medical Center, Saitama, Japan, [3]Shinko Hospital, Kobe, Japan, [4]Kitano Hospital, Tazuke Kofukai Medical Research Institute, Oosaka, Japan, [5]Hyogo Prefectural Amagasaki General Medical Center, Amagasaki, Japan, [6]Japanese Red Cross Wakayama Medical Center, Wakayama, Japan, [7]Saitama Prefectural Cancer Center, Kitaadachigun, Japan, [8]Sagara Hospital, Kagoshima, Japan, [9]Shiga General Hospital, Moriyama, Japan, [10]Tenri Hospital, Tenri, Japan, [11]Keio University, Tsuruoka, Japan, [12]Fujita Health University, Toyoake, Japan

Background: Abemaciclib, a CDK4/6 inhibitor, stands as a cornerstone for managing hormone receptor-positive, HER2-negative advanced or metastatic recurrent breast cancer. It is known to modulate the tumor immune microenvironment, enhancing anti-tumor responses. Yet, its systemic immunological impact remains to be elucidated. This investigation aims to delineate the influence of abemaciclib on both the gut microbiota and the systemic immune landscape in patients with breast cancer.

Methods: A multicenter, prospective clinical trial was conducted involving 40 patients with hormone receptor-positive, HER2-negative advanced or metastatic recurrent breast cancer, scheduled for abemaciclib therapy. The trial's primary objectives were to evaluate the duration of treatment efficacy and the severity of gastrointestinal toxicity. Secondary objectives included assessing the interplay between circulating immune profiles, gut microbiota, and clinical outcomes. Patient samples, including peripheral blood mononuclear cells (PBMCs) for single-cell RNA sequencing and stool for 16S rRNA gene analysis, were collected at baseline and after 90 days of treatment initiation.

Results: This interim report presents findings from 39 patients. We examined 75 PBMC samples and 78 stool samples. Preliminary analysis indicated that abemaciclib precipitated an upregulation of cytokines pivotal for anti-tumor immunity, notably IL-7 and IP-10, alongside an activation of circulating innate immune cells such as CD4-positive T cells and dendritic cells. Concurrently, gut microbiota analysis revealed a post-treatment reduction in alpha diversity, with notable shifts in microbial populations implicated in innate immune activation.

Discussion: This study presents novel insights into the systemic immunomodulatory effects of abemaciclib. Our results suggest that abemaciclib's therapeutic efficacy may partially derive from its ability to alter the circulating immune profile and gut microbiota. These findings could pave the way for innovative immunotherapeutic approaches, integrating gut microbiome considerations into the treatment of hormone receptor-positive, HER2-negative breast cancer.

#5268 Targeting DHX9 triggers interferon response and replication stress in small cell lung cancer.

T. Murayama[1], J. Nakayama[2], K. Q. Cai[1], K. Miyata[3], A. Efimov[1], Y. Tan[1], Y. Zhou[1], K. S. Campbell[1], Y. Yang[1], S. Balachandran[1], I. Canadas[1];
[1]Fox Chase Cancer Center, Philadelphia, PA, [2]National Cancer Center Research Institute, Tokyo, Japan, [3]Japanese Foundation for Cancer Research, Tokyo, Japan

Small cell lung cancer (SCLC) is the most lethal type of lung cancer. The uniqueness of this tumor consists of an initial exquisite response to chemotherapy. However, at relapse, which occurs nearly in all patients, the tumor is resistant to all available therapies, causing a premature death of the patient. Despite the addition of immune checkpoint blockade (ICB) therapy to standard chemotherapy, response rates are modest and only a very small fraction of SCLC patients responds to these therapies because of immunologically “cold” microenvironment. Activating innate immunity in cancer cells through cytoplasmic nucleic acid sensing pathways, a phenomenon known as “viral mimicry”, has emerged as an effective strategy to convert immunologically “cold” tumors into “hot”. Here, through a curated CRISPR-based screen of RNA Helicases, we identified DExD/H-box helicase 9 (DHX9) as a potent repressor of double-stranded RNA (dsRNA) in SCLC cells. Depletion of DHX9 induced accumulation of cytoplasmic dsRNA, which mainly derived from repetitive sequences of short interspersed nuclear elements (SINEs) and long interspersed nuclear elements (LINEs), and triggered tumor-intrinsic innate immunity. Intriguingly, ablating DHX9 also induced the aberrant accumulation of R-loops (DNA/RNA hybrids), which resulted in an increase of DNA damage-derived cytoplasmic DNA and replication stress in tumor cells, selectively killing them. In vivo, DHX9 deletion in SCLC tumor cells promoted a decrease in tumor growth while inducing a more immunogenic tumor microenvironment (TME), invigorating responsiveness to immune checkpoint blockade (ICB). These findings suggest that DHX9 is a crucial repressor of tumor-intrinsic innate immunity and replication stress, and represents a promising and unexplored target for SCLC and other “cold” tumor types where replication stress and genomic instability contribute to pathology.

#5269 Evaluation of mitotic spindle inhibitors as cell autonomous inflammatory stimulants in MYC overexpressing breast cancers.

M. Jacobo Jacobo, A. Goga;
UCSF - University of California San Francisco, San Francisco, CA

The oncogenic transcription factor MYC is overexpressed in most cancer types, including difficult to treat human malignancies such as receptor triple-negative breast cancers (TNBC). MYC overexpression induces aneuploidy and suppresses anticancer immunity. Elevated levels of MYC can induce mitotic spindle assembly defects and chromosomal instability (CIN) events, exemplified by an increase in cells with micronuclei. These defects are partially mitigated by concomitant upregulation of various mitotic spindle genes. Micronuclei result in cytosolic DNA which can activate cGAS-STING signaling, activating an interferon regulatory transcriptional program responsible for mounting an inflammatory immune response that potentially enhances immune cell recognition. We hypothesized that pharmacological inhibition of specific MYC deregulated mitotic spindle genes will further exacerbate mitotic defects in MYC high cells resulting in synthetic-lethal cell death and additional CIN to activate robust cGAS-STING activation. Interferon activation can increase surface expression of antigen presentation machinery, such as MHC-I, restoring the immunogenicity of MYC high cells. Here, we used mouse breast tumor cells in which MYC expression is conditionally expressed as well as human breast cancer cell lines with different levels of MYC expression. We assessed the anti-proliferative and cytotoxic effects of 9 mitotic small molecular inhibitors that affect spindle function. cGAS-STING activation in inhibitor treated and untreated samples was measured by immunoblotting for pathway proteins phosphorylated TBK1, total TBK1, and IFIT1. Differences in MHC-I cell surface expression was quantified using flow cytometry. Our findings revealed that inhibition of kinesin-like protein KIFC1 and transforming acidic coiled-coil-containing protein 3 (TACC3) induced greater levels of apoptosis in MYC high models. Moreover, inhibition of KIFC1 robustly triggered cGAS-STING activity in MYC high cells as evidenced by increased protein abundance of phospho-TBK1 and IFIT1 in a dose-dependent manner. In addition, sublethal KIFC1 inhibition resulted in increased levels of MHC-I surface expression in MYC high models. Our findings suggest that inhibition of MYC regulated mitotic spindle genes, specifically KIFC1, can serve to preferentially eliminate MYC overexpressing aggressive cancers. Furthermore, sublethal concentrations of a KIFC1 inhibitor can stimulate a tumor cell-intrinsic inflammatory-pathway. Future studies will determine if targeting KIFC1 can enhance the response of MYC high cancers to immunotherapy.

#5270 Androgen receptor blockade in macrophages primes NLRP3 inflammasome-mediated phagocytosis and tumor clearance in advanced prostate cancer.

K. Chaudagar[1], S. Rameshbabu[1], S. Mei[2], T. Hirz[2], Y.-M. Hu[3], A. Argulian[1], B. Labadie[1], K. Desai[1], S. Grimaldo[1], D. Kahramangil[1], R. Nair[1], S. DSouza[1], D. Zhou[1], R. Chen[1], J. Shafran[1], M. Loyd[1], Z. Xia[3], D. Sykes[2], A. Moran[3], **A. Patnaik**[1];

[1]University of Chicago, Chicago, IL, [2]Center for Regenerative Medicine, Massachusetts General Hospital Cancer Center, Boston, MA, [3]Knight Cancer Institute, Oregon Health and Science University, Portland, OR

Immune-based therapies induce durable remissions in subsets of patients across multiple malignancies. However, there is limited efficacy of immunotherapy in metastatic castrate-resistant prostate cancer (mCRPC), manifested by an enrichment of immunosuppressive (M2) tumor-associated macrophages (TAM) in the tumor immune microenvironment (TME). Therefore, therapeutic strategies to overcome TAM-mediated immunosuppression are critically needed in mCRPC. Our single-cell RNA sequencing analysis in human tumors revealed that NLR family pyrin domain containing 3 (NLRP3), an innate immune sensing protein, is differentially expressed in TAM from metastatic PC patients treated with standard-of-care androgen deprivation therapy (ADT), relative to other tumor types and untreated primary PC. Furthermore, bulk RNA sequencing analysis in human mCRPC samples revealed an inverse relationship between NLRP3 expression and AR activity, with high NLRP3 expression associated with an M1 signature and a favorable clinical response to ICI in mCRPC. Based on these findings, we hypothesized that androgen axis blockade could enhance NLRP3 expression and potentiate innate immune tumor control in advanced PC. Critically, we discovered that blockade of TAM-intrinsic androgen receptor (AR) activity enhanced NLRP3 expression, but not inflammasome activity in the immunosuppressive (M2) TAM. In contrast, anti-tumor (M1) TAM exhibited high de novo NLRP3 expression, regardless of AR activity. The combination of AR blockade and NLRP3 agonism significantly enhanced phagocytosis of cancer cells by M2 TAM, whereas NLRP3 agonist treatment alone was sufficient to induce phagocytosis in M1 TAM. Following AR blockade/NLRP3 agonist combination treatment, all TAM acquired a distinct phenotype with high PD-L1 and CD86 expression, indicative of phagocytic TAM. Critically, NLRP3 agonism in combination with ADT resulted in significant tumor control in an aggressive c-myc driven advanced PC model, with 55% of mice achieving complete tumor clearance, which was abrogated by concurrent clodronate treatment (which systemically depletes phagocytic macrophages), thus demonstrating TAM-mediated phagocytosis enhancement as a major driver of the observed anti-tumor response. Collectively, our results identify NLRP3 as an AR-regulated “macrophage phagocytic checkpoint” that can be inducibly expressed and activated in TAM following ADT and NLRP3 agonist treatment, respectively, the combination resulting in TAM-mediated phagocytosis and tumor control.

#5271 Pseudohypoxia by HIF-PHD inhibitors activates tumor immune response for MSS colorectal cancer.

T. Ohara, Y. Chen, Y. Hamada, S. Nishimura, H. Kawai, K. Noma, H. Tazawa, T. Fujiwara, A. Matsukawa;
Okayama Univ. Graduate School of Med., Okayama, Japan

Purpose: Microsatellite-stable (MSS) colorectal cancer is resistant for immune therapy, necessitating the exploration of novel modalities for its conquest. Recent revelations have revealed the genetic upregulation of HIF-1α as a potential activator of CD8+ T-cells, enhancing an anti-tumor effect. Pseudohypoxia, characterized by normoxic upregulation of Hypoxia-Inducible Factor (HIF-1α), is known to be induced by iron chelators, including HIF-PHD inhibitors. In this study, we aimed to examine whether pseudohypoxia by HIF-PHD inhibitor can enhance immune response and elucidate the underlying mechanism.
Method: Colon 26, SW480 and HT29 were used as murine and human MSS colorectal cancer model. Human and murine CD8+ T-cells were represented by Jurkat cells and isolated splenic CD8+ T-cells, respectively. HIF-PHD inhibitors Roxadustat and Vadadustat were used in the study, and a subcutaneous Colon 26 tumor model was established in BALB/c WT and nude mice. Hypoxic culture conditions were maintained for 48 hours at 2% O_2.
Results: Roxadustat and Vadadustat did not suppress the proliferation of cancer cells under conditions marked by HIF-1α upregulation. Roxadustat and Vadadustat suppress the colon 26 subcutaneous tumor growth in WT mice, the effect was cancelled in the nude mice. The treatment regimen was associated with an augmentation in the total number and effector-like subtypes of CD8+ T-cells (T_{ex}) infiltrating the tumor. Combination therapy involving Roxadustat and PD-1 antibody synergistically inhibited tumor growth and was accompanied by an increase in PD-1^{lo}, Ly108^{-}, TIM-3^{+} CD8+ T-cells within the tumor microenvironment. Immunohistochemistry revealed that Interleukin-2 (IL-2) expression of murine spleen was stronger in Roxadustat than control group. Interestingly, HIF-PHD inhibitors induced the secretion of IL-2 from isolated CD3+ T-cells of murine spleens in ELISA, a phenomenon uniquely observed under pseudo-hypoxic conditions created by HIF-PH inhibitors, rather than actual hypoxia. This result indicates that pseudo-hypoxia may induce more robust hypoxic response than real hypoxia.
Conclusion: The induction of pseudohypoxia by HIF-PHD inhibitors activates the tumor immune response for MSS colorectal cancer via induction of splenic IL-2.

#5272 APL-1202 enhances anti-tumor immune response through induction of cellular stress signaling and immunogenic cell death pathway in cancer cells.

Rakesh BAM[1], Jingmin Guan[2], Neetha Nanoth Vellichirammal[1], Murli Manohar[1], David Mulholland[3], John Sfakianos[3], Qiaoling Sun[2], Zuoan Yi[1], Alice Chen[1]

[1]Asieris Pharmaceuticals, Inc., Palo Alto, CA,[2]Asieris Pharmaceuticals, Shanghai, China,[3]Mount Sinai School of Medicine, New York, NY

Introduction: Treatment approach combining cancer cell targeted therapy and immunotherapy is an effective strategy to trigger robust tumor-specific immune responses. The aim of this study is to determine the impact of APL-1202, a clinical-stage drug candidate (NCT04813107), on cellular stress-driven immunogenic outcomes in bladder cancer cells.

Methods: RNA-seq analysis was performed using bladder cancer and endothelial cell lines (A56, J82, T24, HUVEC) treated with APL-1202. Key determinants of immunogenic cell death pathway were measured by cell-surface translocation of calreticulin (flow cytometry), extracellular ATP release assay (bioluminescence) and HMGB1 secretion (ELISA) in the supernatants of cancer cells after APL-1202 treatment. Effects on the innate immune effector function was measured by flow cytometry-based phagocytosis assay consisting of Far-Red dye-stained, pre-treated bladder cancer cell lines (UMUC3, T24) in coculture with THP1-derived macrophages/immature dendritic cells or human monocyte-derived dendritic cells. *In vivo*, tumor end-point immune cell analysis, tumor weight and mouse survival were compared in chemically induced (BBN: N-butyl-N-(4-hydroxybutyl)-nitrosamine) orthotopic bladder cancer mice treated with APL-1202 and anti-PD1 antibody.

Results: Pathway analysis of RNA-seq data from APL-1202 treated cells suggested upregulation of cellular stress-related gene signatures (oxidative stress, autophagy, P53) and pro-inflammatory responses (IL-6, IL-8, HMGB1 signaling). Conversely, downregulation of cell cycle (E2F targets, G2-M checkpoint) and IL-10 signaling suggested increased genomic stress and inflammatory switching in the treated cancer cells. Acute exposure to APL-1202 increased cell-surface translocation of calreticulin as well as extracellular release of ATP and HMGB1 in the treated T24 and UMUC3 cells. Higher percentages of phagocytic activities were detected in both THP-1-derived macrophages/immature dendritic cells and human monocyte-derived dendritic cells after coculture with APL-1202 treated T24 and UMUC3 cells compared to coculture with DMSO treated control cells. Immune phenotyping in tumors derived from BBN bladder cancer mouse model revealed increased infiltration of NK cells and CD8+ T cells. Furthermore, APL-1202 enhanced the anti-tumor effects of a therapeutic anti-PD1 antibody in mice as reflected by significantly decreased tumor weights and increased survival in a combination group with APL-1202 treatment compared to the anti-PD-1 antibody alone treatment group.

Conclusion: APL-1202 may improve the efficacy of immune-checkpoint blockade therapies in bladder cancer patients by enhancing cancer cell immunogenicity and subsequent anti-tumor effector immune cell processes, particularly in tumors with deficits in antigen-specific immunity.

#5273 A novel immunogenic cell death that exploits the cancer-specific overexpression of Rad51.

Maria Soloveychik, Charly Chahwan

SyntheX, San Francisco, CA

Overexpression of the Homologous Recombination (HR) DNA repair pathway is often correlated with poor prognosis and metastatic disease. SyntheX developed STX100, a small, stabilized peptide that is able to disrupt the function of Rad51 - a crucial component of HR. STX100 exhibits low nanomolar affinity to the target, cell permeability, and proteolytic stability. STX100 has acute mono-agent activity that is selective towards HR-overexpressing cancer cells. Interestingly, STX100-mediated cell killing is independent of canonical cell death mechanisms (apoptosis, necroptosis, pyroptosis, ferroptosis, etc.). Rather, the elevated abundance of Rad51 in cancer cells relative to healthy tissues underlies the selective cytotoxicity resulting from an acute calcium surge upon STX100-mediated target engagement. The mechanism translates to in vivo models, where a single dose can achieve sustained survival when administered locally as a mono-therapy or in combination with an immune checkpoint blockade agent.

#5274 Targeting retinoblastoma protein in tumor-associated macrophages suppresses ovarian cancer progression.

E. N. Tcyganov[1], T. Kwak[1], X. Yang[1], A. N. R. Poli[1], C. Hart[1], A. Bhuniya[1], J. Cassel[1], A. Kossenkov[1], N. Auslander[1], P. Sharma[1], M. G. Cadungog[2], S. Jean[2], S. Chatterjee-Paer[2], D. Weiner[1], L. Donthireddy[1], B. Bristow[2], R. Zhang[3], J. M. Salvino[1], L. J. Montaner[1];

[1]The Wistar Institute, Philadelphia, PA, [2]Christiana Care Health System, Wilmington, DE, [3]University of Texas MD Anderson Cancer Center, Houston, TX

Ovarian cancer is characterized by an immunosuppressive tumor microenvironment (TME) maintained by tumor-associated M2-like macrophages (TAMs) hindering anti-tumor responses and immunotherapy efficacy. An effective approach to target TAMs in ovarian cancer treatment is currently not available, but would be expected to release immunosuppressive pressure, enable a robust T cell response and improve immunotherapy outcomes. Retinoblastoma protein (Rb) is a well-known tumor suppressor and regulator of tumor cell proliferation. Accumulating evidence demonstrates its role in immune cells, in myeloid cells, in particular. However, these mechanisms remain poorly understood.

Based on our previous data on Rb role in myeloid cell viability, we decided to test the effects of Rb modulation in macrophages. We used the small molecule, AP-3-84 compound, and newly developed analogs which bind the LxCxE motif of Rb and disrupt Rb interaction with its binding adaptor proteins. AP-3-84 induced cell death preferentially in macrophages, but not in T cells or tumor cells (without effects on cell proliferation). Gene and protein expression analysis revealed that Rb targeting induced major intracellular stress response programs and p53/mitochondria-related cell death pathways in TAMs. Moreover, we found that M2 type polarized macrophages expressed higher levels of Rb compared to M1 macrophages. In agreement with that, M2 type macrophages were significantly more sensitive to AP-3-84 treatment than M1 polarized cells. Next, we demonstrated that low dose therapeutic use of AP-3-84 in mice bearing ovarian cancer significantly re-shaped the immune composition of the TME by depleting TAMs and inducing remarkable T cell infiltration. Importantly, these AP-3-84 effects were immune-mediated, since identical AP-3-84 treatment in NSG immunodeficient mice had no effect on tumor growth. Similarly, anti-CD4/CD8 depletion also reverted AP-3-84 effects on cancer inhibition. An analysis of activation and differentiation markers in myeloid and T cell subsets in the TME showed a shift of the remaining macrophages towards an M1-like cell type accompanied by activation of T cells. Using ovalbumin-overexpressing ovarian cancer cell line, we documented the accumulation of antigen-specific T cells in the TME associated with a substantial delay of ovarian cancer upon AP-3-84 therapeutic Rb targeting.

Ex vivo, we observed an analogous cell death induction by AP-3-84 treatment in TAMs from post-surgery ascites from ovarian cancer patients. Using available datasets, we further documented that an increase in Rb expression in the TME myeloid cells is associated with poorer prognosis.

Overall, our data supports that therapeutic targeting of the Rb LxCxE motif is a promising approach for ovarian cancer treatment due to depletion of TAMs and re-shaping the ovarian cancer TME.

#5275 Celecoxib and chloroquine enhance the antitumor effect of immune checkpoint blockade therapy, in a syngeneic mouse model for pancreatic cancer.

J. Moore[1], D. Chand[2], D. Levey[2], D. Von Hoff[1], H. Han[1];

[1]TGen (The Translational Genomics Research Institute), Phoenix, AZ, [2]Agenus Inc., Lexington, MA

Immune checkpoint inhibitors (ICIs) have shown impressive clinical activities in some cancer types, but they have yet to demonstrate any meaningful clinical benefit in patients with pancreatic ductal adenocarcinoma (PDAC) except those with microsatellite instability high (MSI-H) tumors. Several recent studies showed that concomitant use of NSAIDs such as celecoxib by patients with certain cancers could improve the survival benefit of ICI treatment (e.g., Sebastian et al, Clin Lung Cancer, 2023;). Furthermore, autophagy inhibitors such as chloroquine were also reported to sensitize pancreatic tumors to the treatment of ICIs in mouse models for PDAC (Yamamoto, et al, Nature, 2020). We recently reported that the combination of chemotherapy (triple combination of nab-paclitaxel + gemcitabine + cisplatin) and a mouse surrogate of the IFc-enhanced anti-CTLA-4 antibody botensilimab, showed significantly improved antitumor activity in immune competent KPC syngeneic mouse model for PDAC [Tanne, et al, Cancer Res (13_Supplement), 2020]. In this study, we sought to determine whether or not the addition of celecoxib and/or chloroquine further improve the antitumor activity of triple chemotherapy and ICI in the syngeneic KPC model. We first found that celecoxib (30mg/kg P.O. QDx21) significantly enhanced the tumor growth inhibition when added to triple chemotherapy (Gemcitabine 70mg/kg I.P., Cisplatin 4mg/kg I.P., Nab-paclitaxel 25mg/kg I.V. days 1,4 and 7) plus the murine equivalents of botensilimab (100ug I.P. BIW for three weeks) and balstilimab (200ug I.P. BIW for three weeks) ($p=0.004$, N=10). We then performed a pilot study to assess if adding chloroquine could further improve the activity. While adding chloroquine (60mg/kg I.P. QDx21) alone did not significantly affect tumor growth the addition of both chloroquine and celecoxib greatly improve the tumor growth inhibition compared to just the triple chemotherapy and ICIs ($p=0.009$, N=5). Overall, our data showed that celecoxib or the combination of celecoxib and chloroquine could substantially sensitize the mouse pancreatic tumors to the treatment of chemotherapy and ICIs. (This work was supported in part by the Seena Magowitz Foundation and the Purple Pansies)

#5276 Immunomodulatory activity of intermittent low-dose erlotinib plus sulindac: Implications for hereditary and sporadic colorectal cancer.

C. Tripathi[1], **J. E. Tovar Perez**[1], S. Kapoor[1], A. Muhsin[1], W. Dashwood[1], Y. Demirhan[1], M. Demirhan[1], A. Shapiro[1], A. Mohammed[2], S. Sei[2], P. H. Brown[3], M. I. Savage[3], E. Vilar[3], P. Rajendran[1], R. H. Dashwood[1];

[1]Texas A&M University, Houston, TX, [2]National Cancer Institute, Rockville, MD, [3]The University of Texas MD Anderson Cancer Center, Houston, TX

A once-weekly optimized dosing regimen of erlotinib (ERL) in the polyposis in rat colon (Pirc) model [1] was a reliable predictor of antitumor efficacy in familial adenomatous polyposis (FAP) patients [2]. Pirc rats are increasingly used as a translational tool for FAP studies. Based on transcriptomic data from FAP patients receiving ERL plus sulindac (SUL) vs. placebo [3], we determined the timing of changes in interferon-γ signaling in Pirc adenomas, while performing additional dose titration. In rats that were given ERL administered at 5 mg per kilogram of body weight through oral gavage (two times a week) and that received a diet containing 125 parts per million of SUL, a regimen referred to as SUL125+ERL5x2, significant suppression of tumor growth was observed. This combination represented half of the standard of care SUL dose and about one-quarter of the ERL dose in FAP patients. In adenomas collected after one year of treatment from SUL125+ERL5x2 treated rats, the expression of genes related to the major histocompatibility complex (MHC) class I (β2m, Cnx, Psmb8 and Tap1) and MHC class II (RT1-A2, Cd74, RT-1Bb, Cd74, and Ciita) was increased, compared to vehicle controls, excluding a subset of adenomas that remained resistant. Through the use of multiplex mass cytometry (CyTOF), an increase in tumor-infiltrating CD4+ T cells was observed in adenomas from the SUL125+ERL5x2 treatment group. Administration of single or combined agents increased CD68+ cells and reduced the presence of Foxp3+ and Arg1+ cells in Pirc adenomas. The natural history of adenomatous colon polyps indicated an increase in MHC gene expression as tumors increased in size; however, this trend reversed markedly in fully occluding lesions. Additionally, expression of MHC-related factors increased in Pirc colon adenoma and murine colon carcinoma cells treated with ERL±SUL, resulting in enhanced CD8+ T-cell activation and IL-2 secretion. In conclusion, treatment with intermittent low doses of ERL±SUL increased MHC gene expression and induced changes in the immune cell component in the tumor microenvironment of Pirc rat adenomas. A subset of non-responsive adenomas could benefit from additional immunopreventive approaches, with implications for possible clinical applications in both hereditary and sporadic colorectal cancer.

References:1.- Ulusan AM et al., Cancer Prev Res (Phila) 2021;14(3):325-336. 2. Samadder NJ et al., Gut. 2023;72(2):256-263. 3.- Delker DA et al., Cancer Prev Res (Phila). 2018;11(1):4-15.

Funding: This work was supported by the NCI Prevent Program 75N91019D00021, Task Order 75N91019F00130

#5277 The ROCK-2 inhibitor belumosudil exerts a direct antimyeloma effect and improves isatuximab-mediated cytotoxicity against multiple myeloma cells.

M. Meloni[1], P. Perrin[1], C. Nouguier[1], S. Poirier[2], M. Bouaboula[2], K. Bisht[2], H. Van de Velde[2], A. Virone-Oddos[1], M. Chiron[1];
[1]Sanofi, Vitry-sur-Seine, France, [2]Sanofi, Cambridge, MA

Multiple myeloma (MM) is a plasma cell malignancy characterized by clonal accumulation of malignant plasma cells in the bone marrow. Isatuximab (Sarclisa®) is a monoclonal antibody used for the treatment of MM. Isatuximab binds to CD38 (highly expressed on MM cells) and induces tumor cell killing via several mechanisms including antibody dependent cellular cytotoxicity (ADCC) and direct apoptosis. Belumosudil (Rezurock™) is a ROCK2 inhibitor that is approved for the treatment of chronic graft versus host disease (cGVHD). Recent reports suggest that inhibition of ROCK2 induces apoptosis and prevents growth of MM cells. Here, we investigated the potential antimyeloma effect of belumosudil alone or in combination with isatuximab with different readouts of viability, apoptosis and cytotoxicity.

The potential cytotoxic effect of belumosudil (as single agent or in combination with isatuximab) against MM cells was assessed *in vitro* by flow cytometry apoptosis assay, CellTiter-Glo® luminescent cell viability assay or long-term cytotoxic assay (Incucyte). The effect of belumosudil on healthy donor-derived NK cells viability was also assessed by flow cytometry.

Belumosudil reduced the number and viability of several MM cell lines without affecting healthy donor NK cell number and viability. Moreover, belumosudil induced apoptosis of MOLP-8 MM cells in a dose-dependent manner and further increased MOLP-8 cell apoptosis when combined with isatuximab after 2, 3 and 4 days of *in vitro* treatment. Belumosudil induced killing of MM cells in a dose-dependent manner over time (up to 4 days), independently of the presence of NK cells, as measured by Incucyte-based cytotoxicity assay. In addition, the combination of belumosudil (3.3 µM) with isatuximab (10 µg/ml) in presence of NK cells enhanced the killing of different MM cell lines over time compared to single agents.Finally, the expression of CD38 on MM cells has been documented to be decreased after treatment with anti-CD38 antibodies. Interestingly, analysis of CD38 expression on MM cells indicated that belumosudil induces an increase of CD38 on the surface of MOLP-8 MM cells and prevents isatuximab-induced decrease of CD38 expression.

These data suggest that belumosudil has a direct antimyeloma effect and increases isatuximab-mediated cytotoxicity against MM cells, without affecting the viability of NK cells. Taken together, this study provides evidence of the therapeutic potential of belumosudil in combination with isatuximab in the setting of MM.

#5278 Immunological control by PARP inhibitors for successful immunotherapy in metastatic ovarian carcinoma.

P. Holicek[1], S. Vosahlikova[1], I. Moserova[1], S. Orsulic[2], R. Mikyskova[3], M. Hensler[1], L. Kasikova[1], T. Lanickova[1], O. Novotny[3], M. Reinis[3], J. Drozenova[4], A. Ryska[5], J. Laco[5], L. Rob[4], M. Halaska[4], D. Cibula[6], R. Spisek[1], J. Fucikova[1];

[1]SOTIO Biotech, Inc., Prague, Czech Republic, [2]University of California, Los Angeles, CA, [3]Institute of Molecular Genetics of the Czech Academy of Sciences, Prague, Czech Republic, [4]3rd Faculty of Medicine and University Hospital Kralovske Vinohrady, Prague, Czech Republic, [5]Charles University, Faculty of Medicine and University Hospital Hradec Kralove, Hradec Kralove, Czech Republic, [6]Gynecologic Oncology Center, Prague, Czech Republic

Epithelial ovarian carcinoma (EOC) is among the top five causes of cancer-related death in women. Most women with EOC achieve indeed complete remission after primary or interval cytoreductive surgery combined with chemotherapy based on a platinum-taxane doublet. Homologous recombination (HR) defects imposed by germline or somatic BRCA1 DNA repair-associated (BRCA1) or BRCA2 mutations are not only key determinants of platinum sensitivity in EOC patients but also provide a strong rationale for maintenance therapy based on poly(ADP-ribose) polymerase (PARP) inhibitors, which is generally associated with improved progression-free survival (PFS). Besides direct cytotoxic and cytostatic properties, PARPi have been shown to mediate multipronged immunostimulatory effects, largely reflecting their ability to inhibit DNA repair in malignant cells and indicating the possibility to synergy with immune-check point inhibitors (ICIs). Here, using multiparametric flow cytometry, multiplex immunostaining, single cells transcriptomics and functional studies in experimental syngeneic BR5$^{Brca1-/-}$ mouse model and EOC tumor samples, we discuss PARPi immunomodulatory activity, with a specific focus on molecular and cellular pathways that can be harnessed to develop superior combinatorial regimens for clinical management. Thus, PARPi might enhance the mutational load of EOCs as consequence of unrepaired DNA damage and DAMPs exposure, favoring T cell infiltration, but also appear to drive robust type I IFN secretion downstream of cyclic GMP-AMP synthase and stimulator of IFN response cGAMP interactor 1 activation. In addition, the combination of PARPi with ICIs positively regulate the balance between adaptive anti-tumor immunity and innate myeloid components and significantly improve the cytotoxic T cell profile as shown in both experimental mice model and HGSOC tumor samples. We surmise that rationally designed combinations of PARPi and immunotherapeutic agents might be critical to unlock immunosuppression in the EOC microenvironment in support of clinical efficacy.

#5279 Sequential treatment with PARPi and WEE1i minimizes T cell DNA damage and enhances its immune response.

X. Jiao[1], J. Liu[1], W. Mu[1], L. Zhu[1], X. Zhao[1], G. B. Mills[2], Q. Gao[1], **Y. Fang**[1];

[1]Tongji Hospital, Tongji Medical College, Huazhong University of Science and Technology, Wuhan, China, [2]Oregon Health and Sciences University; Knight Cancer Institute, Portland, OR

Background: DNA damage response (DDR) targeted therapy, like PARP inhibitors (PARPi) and WEE1 inhibitors (WEE1i), have demonstrated potent anti-cancer activity and are pronounced to activate the cytosolic immunity pathway. Our previous work showed that sequential inhibition of PARP and WEE1 could kill tumor cells as effective as their concurrent application, with ameliorated toxicity to normal cells, suggesting high clinical translational potential of this regimen. However, the effect of sequential treatment on T lymphocytes and anti-cancer immunity remains largely unknown.

Methods and results: T cells were treated with 25 μM olaparib, or 250 nM AZD1775, or olaparib combined with AZD1775 (concurrent group) for 48h, or olaparib for 24h followed by AZD1775 for 24h (sequential group) in vitro. AZD1775 and concurrent treatment reduced the T cell viability to 19% and 14.3%, while sequential treatment maintained the viability to 58.6%, closed to olaparib monotherapy (61.6%). And the most potent proliferation capacity accompanied with the lowest apoptosis level were both recorded after sequential treatment, manifested by the increasing of Ki67 and EdU and the decreasing of cleaved caspase-3. Reverse-phase protein arrays (RPPA) analyses identified relieved DNA damage in T cells receiving sequential treatment. Alkaline comet assay and detecting of γH2AX further confirmed that the T cell DNA damage caused by PARPi and WEE1i was obviously alleviated after sequential therapy. Furthermore, sequential treatment activated cGAS-STING pathway effectively and upregulated the production of CCL5, CXCL10 and IFNβ of downstream type I interferon response compared with monotherapy and concurrent treatment in ovarian cancer cell lines (SKOV3, OVCAR8, A2780). We also evaluated an ID8 intraperitoneal syngeneic immunocompetent mouse model. T cells isolated from tumors, ascites, spleen and peripheral blood in sequential group were presented with the highest proliferation potential and the lowest level of DNA damage. And the tumor burden of mice in sequential group was obviously subsided, which was comparable to that in concurrent group.

Conclusions: This study demonstrated that targeting PARP and/or WEE1 impaired the T cell viability and led to DNA damage. However, administrating PARPi and WEE1i sequentially diminished this inhibitory effect on T cells on the premise of ensuring their anti-tumor effect. These data provide strong rational for the further investigation on exploring the clinical significance of sequential treatment with PARPi and WEE1i.

#5280 Minimizes T cells DNA damage induced by PARP inhibitors and enhances its anti-tumor efficacy.

Jiahao Liu[1], Xiaofei Jiao[1], Wei Mu[2], Huayi Li[1], Li Zhu[2], Xuejiao Zhao[1], Gordon B. Mills[3], Qinglei Gao[1], **Yong Fang**[1]

[1]Department of Gynecological Oncology, Cancer Biology Research Center, Tongji Hospital, Tongji Medical College, Huazhong University of Science and Technology, Wuhan, China,[2]Department of Hematology, Tongji Hospital, Tongji Medical College, Huazhong University of Science and Technology, Wuhan, China,[3]Department of Cell, Development and Cancer Biology, Oregon Health and Sciences University; Knight Cancer Institute, Portland, OR

Background: Poly (ADP-ribose) polymerase (PARP) inhibitors have emerged as promising targeted therapies for ovarian and breast cancer. The sustained remission induced by PARP inhibitors largely depends on T cell activity. However, the direct effects of PARP inhibitors on T cells, as well as their precise impact on T cell DNA integrity and subsequent anti-tumor immune responses, have not been fully elucidated.
Method & Result: Following treatment with 25 μM olaparib or 15 μM niraparib for 48 hours, T cell viability decreased by 39.20% and 41.89%, respectively. Reduced proliferation and increased cell death were also observed, as indicated by reduced Ki-67 and elevated cleaved Caspase-3 levels. RNA sequencing further revealed a significant enrichment of DNA damage pathways in T cells after olaparib treatment, which was validated by elevated γH2AX levels in T cells using western blots and immunofluorescence. To assess PARP inhibitor-induced DNA damage in clinical settings, paired ovarian cancer samples pre- and post-niraparib monotherapy were obtained from the NANT trial (NCT04507841). Post-treatment tumor samples exhibited a higher number of γH2AX+ T cells compared to their pre-treatment counterparts. To identify the key protein mediating T cell inhibition induced by PARP inhibitors, a whole genomic CRISPR knock-out screening was conducted in human T cells, revealing an enrichment of sgRNAs targeting PARP1 after PARP inhibitor treatment. This outcome was further confirmed by the knockout of PARP1 in human T cells in vitro, leading to the restored viability and reduced levels of DNA damage after olaparib treatment. Importantly, following cytosine base editors (CBEs) of PARP1 in CAR-T cells, improved anticancer activity was observed both in vitro and in two ovarian cancer patient-derived xenografts (PDX) models when combined with PARP inhibitors.
Conclusion: This study observed that PARP inhibitors can cause significant DNA damage in human T cells, resulting in cell death, inhibited proliferation, and impairment of anti-cancer immunity. PARP1 was identified as the target for PARP inhibitor-induced T cell death, and its knockout or point mutation led to improved anticancer efficacy of T cells when used in combination with PARP inhibitors. [JH Liu and XF Jiao contributed equally as co-first authors.]

#5281 5-Fluorouracil decreases MDSC and the development of osteolytic bone metastases from breast cancer in mice.

P. G. Fournier[1], P. Almeida Luna[1], D. Arellano[1], S. Jimenez[1], F. Olvera[2], P. Juarez[1];

[1]Centro de Investigacion Cientifica y de Educacion Superior de Ensenada, Ensenada, Mexico, [2]Instituto de Biotecnologia Universidad Nacional Autonoma de Mexico, Cuernavaca, Mexico

Bone metastases are a highly debilitating complication in more than 70% of patients with advanced breast and prostate cancer. Currently approved treatments fail to cure bone metastases or increase patient survival. Although immunotherapies can cause a durable response in some patients, it seems that their efficacy is limited in bone metastases, which could be due to a cold metastatic microenvironment. Our aim was to identify immunosuppressive factors in bone metastases and target them using a drug-repositioning type approach. We used a syngeneic model in which 4T1 triple-negative breast cancer cells derived from a Balb/C mouse are inoculated in the left cardiac ventricle of Balb/C mice to cause osteolytic bone metastases. Using flow cytometry, we found that the bone marrow of mice with 4T1 bone metastases is enriched in large cells with a high SSC index that could be myeloid-derived suppressor cells. We confirmed that the inoculation of 4T1 cells increased the amount of $CD11b^{+}$ $Ly6G^{+}$ $Ly6C^{lo}$ ROS^{hi} and $CD11b^{+}$ $Ly6G^{-}$ $Ly6C^{hi}$ NO^{hi} cells. Both cell types were isolated from bone metastases and prevented the proliferation of $CD8^{+}$ T cells *ex vivo*, confirming they were polymorphonuclear- (PMN-) and monocytic-MDSCs (M-MDSCs), respectively. In addition, both types could differentiate into osteoclasts that cause bone loss. Reviewing the current literature, we found that FDA-approved sildenafil (a PDE-5 inhibitor), zoledronic acid (a bone resorption inhibitor), and 5-fluorouracil (5-FU, a chemotherapeutic agent) can decrease MDSCs in other cancer models. However, sildenafil (20mg/kg, i.p., every 2 days) and zoledronic acid (25µg/kg, s.c., 3x/week) did not decrease the amount of MDSCs in 4T1 bone metastases. 5-FU (i.p., 4 inoculations) at 50mg/kg prevented the 4T1-induced splenomegaly and the increase of PMN- and M-MDSCs but seemed to decrease the number of T cells in bone metastases. Thus, we tested the efficacy of a lower number of inoculations. A single inoculation of 5-FU was not efficient, while 2 or 3 inoculations of 5-FU (50mg/kg) prevented the splenomegaly and the histological damage due to extramedullary hematopoiesis in the spleen. In 4T1 bone metastases, there was a decrease of PMN-MDSCs and an increase of the number of $CD4^{+}$ and $CD8^{+}$ T cells. On radiographs, 2 or 3 inoculations of 5-FU (50mg/kg) significantly decreased the area of the osteolytic lesions caused by 4T1 cells (-57% and -60%, respectively, compared to placebo, $P<0.005$). In conclusion, our results show that functional PMN- and M-MDSCs can increase and accumulate in the microenvironment of breast cancer bone metastases and that an optimized treatment with 5-FU can prevent this expansion of MDSC, increasing T cell infiltration in bone metastases and decrease the associated bone lesions. Treatment with 5-FU could then contribute to turning bone metastases from a cold to a hot microenvironment and increase the efficacy of immunotherapies in patients.

#5282 Sulindac modulates the response of triple negative breast cancer to anti-PD-L1 immunotherapy.

B. Yi, R. Ma, Y. Xi;
University of Georgia, Athens, GA

Triple-negative breast cancer (TNBC) is a heterogeneous tumor, and there is a lack of effective therapies. Immune checkpoint inhibitors (ICIs) therapy has been widely used to treat a variety of human cancers including TNBC. Despite the FDA's approval of therapies like Atezolizumab (anti-PD-L1) and Pembrolizumab (anti-PD-1) for certain TNBC cases, more than half of all TNBC patients, especially those with low PD-L1 levels and in advanced stages, remain unresponsive. Therefore, there is urgent clinical need to find other innovative combination therapy strategy for these TNBC patients. In this study, we examined the efficacy of sulindac to enhance the response of TNBC to anti-PD-L1 immunotherapy. We utilized a 4T1 syngeneic mouse tumor model to compare the inhibitory effects of PD-L1 antibody, sulindac, and their combination on 4T1 tumor growth. We found that mice treated with combination therapy showed a significant reduction in tumor volume, along with increased infiltration of activated T lymphocytes (Granzyme B+/CD8+ T cells) in the tumor tissues. We also established a PBMC humanized mouse model to further confirmed that combination therapy could significantly reduce the tumor size of TNBC patient-derived xenografts (56S) and the combination group were found to have the most infiltrating activated human T lymphocytes (Granzyme B+/CD8+ T cells) in the tumor tissues. Immunofluorescent staining of organoids also confirmed that organoids from combination group have more CD8+ T cell and the results of organoid cell viability assay *in vitro* indicated that combination of sulindac with PD-L1 antibody together with activated human PBMC significantly reduce 56S organoid cell viability, which is consistent with *in vivo* study. When investigating the mechanism of action, first we found sulindac could downregulate exosomal PD-L1 by decreasing expression of nsMase2 which is a major regulator in production of exosomal PD-L1. Second, we demonstrated that sulindac could downregulate PD-L1 by blocking Stat3 signaling and enhancing the expression of miR-570-3p which can potentially target PD-L1, which in turn led to a further decrease in exosomal PD-L1. Previous study showed that PD-L1 antibody could be bound and consumed by exosomal PD-L1 in the blood circulation. Therefore, in combination therapy, sulindac downregulating exosomal PD-L1 leads to increased availability of PD-L1 Ab, which potentially improves the overall efficacy of anti-PD-L1 therapy. In conclusion, our findings provide unique insights into the mechanism of action and efficacy for sulindac as an immunomodulatory agent in combination with anti-PD-L1 therapy for the treatment of TNBC.

#5283 Polyamine blockade therapy: A strategy to block immunosuppression in pancreatic cancer.

J. A. Goode;
University of Central Florida, Orlando, FL

Pancreatic ductal adenocarcinoma (PDAC) is lethal in 88% of patients and is characterized by a dense tumor microenvironment (TME) which impedes tumor entry of immune cells and delivery of therapeutics. Immunosuppressive myeloid populations of PDAC, including myeloid-derived suppressor cells (MDSCs) and tumor-associated macrophages (TAMs), are known to not only support PDAC development but also impede the anti-tumor immune response elicited by therapeutic agents. To improve prognosis while maintaining tolerability, this study aims to target polyamine metabolism that is upregulated in the immunosuppressive myeloid populations and cancer cells to disrupt their contribution to PDAC progression and the immunosuppressive TME. We previously demonstrated that polyamine blockade therapy (PBT), via blocking biosynthesis with difluoromethylornithine (DFMO) and transport with a novel inhibitor (Trimer44NMe), elicits an anti-tumor response and improves median survival in PDAC engrafted immunocompetent mice. In the current study, PBT was found to lead to a selective reduction of the dominant MDSC subtype in PDAC, polymorphonuclear (PMN) MDSCs. Upon co-culturing of MDSCs with CD8+ T cells, PBT dampened MDSC-mediated suppression of T cell activity. These findings were corroborated by tracking Arginase 1, a driver of MDSC-mediated immunosuppression, which exhibited a significant decrease in response to PBT at both the activity and gene expression level. Ex-vivo generated M2 macrophages and TAMs treated with PBT also demonstrated a shift from the M2 pro-tumor phenotype towards the anti-tumor M1 macrophage phenotype. In summary, these findings support that PBT is effective at reducing myeloid-mediated immunosuppression through subtype specific modulation and supports the use of PBT for treatment of PDAC in combination with other immunomodulatory therapeutics.

#5284 Immune surveillance of chemotherapy-induced mutant subclones in CRC.

P. Vitiello[1], P. Battuello[1], R. Chila[2], V. Battaglieri[2], V. Amodio[2], G. Grasso[1], F. Di Nicolantonio[1], G. Crisafulli[2], G. Germano[1], A. Bardelli[1];
[1]University of Turin, Torino, Italy, [2]IFOM ETS - The AIRC Institute of Molecular Oncology, Milano, Italy

Molecular alterations generated by DNA repair deficiencies and DNA damaging agents can be detected by the host immune system and this can restrict cancer growth. We have previously reported that temozolomide (TMZ) is able to induce MMR defects and hypermutability leading to immunotherapy clinical benefit in the subset of CRCs characterized by inactivation of O6-methylguanine methyltransferase (MGMT). We reasoned that combination of chemotherapeutic agents could similarly impair DNA repair function, increase mutational burden and trigger cancer immunogenicity in the larger group of MMR proficient (MMRp) / MGMT wild type (MGMTwt) CRCs. For this reason, we investigated the impact of treatment with TMZ and cisplatin (CDDP), as well as other commonly used cytotoxic agents in CRC such as 5-fluorouracil, irinotecan and oxaliplatin, on the immunogenomic features of murine CRC cells. We performed a two-step experiment: first, murine CRC models were exposed *in vitro* to chemotherapy agents used alone or in combination in a pulsatile schedule in order to mimic drug exposure in the clinical setting (priming phase); second, the cells were challenged *in vivo* with subcutaneous injection in immune-deficient and -proficient syngeneic mice (editing phase). Whole exome sequencing (WES) was performed at baseline and after both the priming and the editing phases to identify mutational signatures, predict neoantigens and assess immunoediting. We found that combinatorial treatment of MMRp / MGMTwt CRC cells with CDDP and TMZ causes clonal and subclonal hypermutability, eventually leading to tumor rejection in syngeneic mice. By following the fate of chemotherapy-induced mutations and predicted neoantigens in primed tumors grown in immunocompromised or immunocompetent mice we found that the majority of chemo-induced mutant clones were immunologically deleted in the CDDP-TMZ combination arm. The same effect was not observed when CDDP and TMZ were administered as monotherapy or when CRC cells were primed with the 5-fluorouracil-oxaliplatin-irinotecan (FOLFOXIRI) triplet. Mutational signature profiling of the immunologically deleted mutations was consistent with the previous exposure to chemotherapy in the priming phase. Moreover, the extent of the immunoediting was related to the clonality of the chemo-induced mutations, underlining the relevance of clonal abundance of immunogenic mutations in immune recognition and surveillance. These results indicate that rational combinations of commonly used cytotoxic agents can be exploited to promote cancer cell subclonal and clonal hypermutability. This approach can be used to promote cancer immunogenicity with implications for the design of new chemo-immunotherapy strategies in CRC.

#5285 DKK1 blockade inhibits progression of bone metastases via multiple mechanisms and synergize with zoledronate treatment.

T. Shi, K. Liang, Y. Zhang, X. Zhou, B. Liu, J. Wei;
Department of Oncology, Nanjing Drum Tower Hospital, Affiliated Hospital of Medical School, Nanjing University, Nanjing, China

Background: Despite the important breakthroughs of immune checkpoint blockade (ICB) therapy in multiple primary cancers, responses of ICB therapy in bone metastases remain extremely poor, largely due to the highly immunosuppressive bone metastasis microenvironment. However, the current understanding of bone metastasis microenvironment is still incomplete, and specific treatment targets for patients with bone metastasis are still lacking.
Methods: Transcriptome sequencing data of gastric and breast cancer bone metastasis samples from The TCGA and GEO databases were obtained. The correlation between DKK1 expression and prognosis, intertumoral immune infiltration of bone-metastatic patients was analyzed. Mouse bone metastasis models from gastric, breast and lung cancer were established, and *in vivo* treatment efficacy of DKK1 and/or zoledronic acid was evaluated by micro-computed tomography (CT), micro-magnetic resonance imaging (MRI) and immunohistochemistry (IHC) staining. The changes of immune components wthin bone-tumor microenvironment were explored via flow cytometry, CyTOF and scRNA-seq analysis. The impact of DKK1 on different immune cell types was analyzed via *in vitro* co-culture models.
Results: Serum detection of gastric cancer patients from our center showed that compared with non-metastatic patients, DKK1 concentration in patients with bone metastasis was the significantly increased ($p<0.0001$); and compared with other metastatic sites of breast cancer patients, bone metastases had the highest level of DKK1 mRNA expression ($p<0.05$). Using multiple bone metastasis mouse models, we found that DKK1 blockade significantly controlled the tumor burden of bone metastases. Results of micro-CT and TRAP staining showed that the bone destruction and osteoclast activity within bone lesions were significantly inhibited after DKK1 blockade. In addition, results of flow cytometry and immunofluorescence staining on bone metastasis samples showed that both innate and adaptive anti-immune responses were obviously improved after DKK1 blockade, including increased infiltration of $CD8^{\pm}$ T cells, M1 macrophages and decreased infiltration of M2 macrophages. Mechanistically, DKK1 directly induced inhibition of $CD8^{\pm}$ T cell activation, M2 polarization of macrophages and maturation of osteoclasts, which all contributes to the immune suppression in the bone metastasis microenvironment. Finally, combined therapy of DKK1 blockade and zoledronic acid had synergistic treatment effects in bone metastases.
Conclusion: Our study provides novel insights into the multiple role of DKK1 in the bone metastasis immune microenvironment. DKK1 is a potential immunotherapeutic target for bone metastases, and dual blockade of DKK1 and zoledronic acid is a promising combination immunotherapy strategy for patients with bone metastasis.

#5286 M2 to M1 repolarization of tumor-associated macrophages via the lysosomal effect of itraconazole.

Y. Takimoto, **H. Tsubamoto**, K. Sakata, R. Isono-Taniguchi, T. Ueda, H. Shibahara;
Hyogo Medical University, Nishinomiya, Japan

Objective: Itraconazole (ITZ), an antifungal agent, has been reported to have tumor agnostic anticancer effects. Previous reports have shown prolonged survival in patients with lung and ovarian cancer who received ITZ. The anticancer mechanisms vary depending on the cancer type and stromal cells. Based on our previous studies, we focused on tumor-associated macrophages (TAMs).
Methods: Anti-tumorigenic M1 and pro-tumorigenic M2 macrophages were established from THP-1 cells and their phenotypes were determined based on morphology, cell surface antigens by Western blotting, and secreted proteins by ELISA. Bulk proteomic analysis of cell proteins was conducted using liquid chromatography-tandem mass spectrometry. The viability of CaSki cervical cancer cells was evaluated both in culture with the supernatant and co-culture with M2 macrophages after treatment with ITZ (10^{-5} M). Single-cell RNA sequencing (scRNA-seq) with surface labeling of M2 macrophages with and without the ITZ was performed. Using LoupeBrowser (10x Genomics, Inc.), ITZ-treated M2 macrophages were divided into two groups, one with newly emerged clusters after ITZ treatment (group 1) and the other (group 2). Differentially expressed genes between group 1 and group 2 were identified based on a two-fold and a 0.05 adjusted p value and were subjected to Reactome pathway analysis. Significant pathways were identified based on both p value < 0.05 and FDR <0.3. A triple-labeling immunofluorescence study was conducted to detect cholesterol, IL-1β, and organelles (the endoplasmic reticulum, phagosome, and lysosome).
Results: ITZ changed M2 macrophages to M1-like morphology and protein expression. While co-culture with M2 macrophages promoted cancer cell proliferation, both culture with the supernatant and co-culture with ITZ-treated M2 macrophages significantly inhibited CaSki cell growth. scRNA-seq identified newly emerged clusters (group 1) among M2 macrophages following ITZ treatment. Group 1 had elevated mRNA expression of M1 markers, including IL1β, IL6, CD86, TL4, GAPDH, and RKM, compared to group 2. Group 1 expressed the CD86 and TLR4 surface antigen proteins. Pathway analysis identified 176 significant pathways including lysosome vesicle biogenesis. Immunofluorescence analysis showed that M1-like macrophages in ITZ-treated M2 macrophages had enlarged lysosomes containing cholesterol.
Conclusion: ITZ repolarized THP-1 derived M2 macrophage to an M1-like phenotype. The mechanism of repolarization involves intracellular cholesterol accumulation via lysosomal dysfunction.

#5287 Ex vivo pharmacologic inhibition of STAT3 effectively targets tumor and tumor associated suppressor cells in high-grade glioma 3D spheroids.

K. A. Lassahn, A. K. Elrod, T. M. DesRochers, **K. M. Appleton**;
Kiyatec, Greenville, SC

Gliomas, a type of brain tumor originating from glial cells, comprise a heterogenous group of neoplasms. High-grade gliomas, in particular, present significant therapeutic challenges in the clinic. Unlike other solid tumors, the heterogenous glioma microenvironment is heavily enriched with tumor associated suppressor cells including myeloid-derived suppressor cells (MDSCs) and tumor-associated macrophages (TAMs), which can account for 30-40% of the cellular composition[1]. These pro-tumorigenic myeloid cells are thought to contribute to the resistance of glioma to immunotherapy. Efforts to target the suppressive nature of these dominating cell types are in development to yield more therapeutic options for patients with these devastating diseases. Constitutive activation of STAT3 in gliomas has been associated with increased tumor progression and reduced immune response. We have observed in other cancer models that a phenotypic switch occurs from STAT3 pathway activation in 3D spheroid culture to STAT3 inactivation when cultured in 2D. Therefore, we sought to determine the role of STAT3 activation and its role in the interplay between glioma and their immune suppressive environment using a 3D spheroid model. We modified our commercially available test platform, 3D-Predict™ Glioma, such that it is conducive to monitoring immune cell function. Newly diagnosed treatment naive primary samples from HGG patients were dissociated and cryogenically preserved and banked. Samples were profiled for the abundance of tumor associated suppressive myeloid cells using flow cytometry. We determined that relative proportions of tumor suppressor cells were detectable and varied across HGG primary patient samples with TAMs being the predominate immune cell type identified. Pro-tumorigenic TAM markers including CD163 and CD206 were correlated with temozolomide response and were associated with poor patient prognosis. When we evaluated the role of p-STAT in HGG primary samples, p-STAT was detected at baseline and abundance was related back to the presence of tumor associated immune suppressor cells. The impact of STAT3 signaling blockade by the inhibitor WP1066 was determined *ex vivo*, and efficacy was related back to MGMT promotor methylation status and patient clinical outcome. We detected shifts in cytokine signatures following treatment of HGG 3D spheroid models with WP1066 which are known to target tumor associated suppressor cell functions. This work demonstrates the critical role suppressive immune cells play in HGG clinical response. Given p-STAT can be altered in 2D culture compared to 3D culture, *ex vivo* therapeutic response profiling of HGG samples is necessary using the more physiologically relevant spheroid culture model.

1.Hambardzumyan et al. The role of microglia and macrophages in glioma maintenance and progression. *Nat. Neurosci.* **19**, 20-27 (2016).

#5288 Soy isoflavone genistein reboosts targeted therapy sensitivity in triple negative breast cancer.

T. Bankole, Z. Li, **Y. Li**;
University of Maryland, College Park, College Park, MD

Triple-negative breast cancer (TNBC) is a very aggressive type of breast cancer that does not expression important proteins called estrogen, progesterone and HER2. This makes TNBC hard to treat because it does not respond to common targeted treatments. However, recent treatments using the immune system to target key immune proteins such as PD-1 and PD-L1 have been successful in many types of cancer. This form of immunotherapy works by blocking PD-1/PD-L1 pathway and leads to stimulating the body's own immune system to recognize and attack cancer cells, thus providing a potential new treatment option for TNBC patients. Nevertheless, only approximately 30% of TNBC patients may respond to these drugs, suggesting the majority of TNBC patients would not benefit from these innovative immunotherapies. It is believed that low levels of immune cells and PD-L1 expression in tumors are the primary reasons for the lack of response or resistance to anti-PD-1/PD-L1 treatments. The use of nontoxic and healthy food and nutrition to increase treatment response is an emerging field of cancer research. Our studies showed that adding genistein (GE), a bioactive dietary component found in soybean products such as soy milk, soy protein and tofu, could significantly enhance the efficacy of anti-PD-1 immunotherapy in a TNBC mouse model that was previously not responsive to the treatment. Our research also found that soybean GE can increase tumor immune response by significantly recruiting active immune cells into the tumor and increasing PD-L1 expression. Our studies will help to establish a novel nutrition-based intervention targeting TNBC patients who might not qualify for this treatment initially. Eventually, we will develop a novel strategy of administering a tailored dietary plan to resensitize these patients to emerging anti-PD-1/PD-L1 immunotherapies.

IMMUNOLOGY: Immune Modulation Employing Agonist or Co-Stimulatory Approaches
Poster Session

#5292 CD28 humanized mouse model for efficacy and safety assessment of CD28-targeting therapies.
F. Sonego, A. Pappalardo, G. Martin, Y. Cherifi, P. Isnard-Petit, K. Thiam;
genOway, Lyon, France

Agonist antibodies targeting CD28 have proven to be effective against cancer, but also faced challenges due to severe adverse events triggered by its activation. Human (hCD28) and mouse CD28 (mCD28) have different signaling responses, with CD28 ligands and superagonists inducing pro-inflammatory cytokines upon stimulation in absence of TCR ligation in humans, but not in mice. Expression of CD28i amplifier isoform, which is thought to enhanced the production of cytokines in humans, could partially explain this difference, as it is not expressed in mice. In addition, evidence suggests that the different signaling between hCD28 and mCD28 relies on one amino acid change in the intracellular domain (ICD)[1]. Herein, we describe a CD28 humanized mouse model for assessment of CD28-targeting agents. To improve translatability, we decided to keep the expression of both canonical and CD28i human isoforms to avoid undermining the biological effects of the testing agents. Although keeping the human ICD could favor the evaluation of cytokine production and therefore the safety of the test agents, we decided to keep the mouse ICD to enable a proper interaction of CD28 with its signaling partners, allowing a physiological stimulation of CD28 in efficacy studies. The hCD28 model expresses a chimeric protein, with the whole human extracellular domain, and mouse intracellular domain. Human CD28 is expressed at physiological levels on T cells, and these cells can be activated and proliferate in response to hCD28 ligands and agonist antibodies. Tumor growth inhibition and complete tumor regressions are achieved in a MC38-TAA colorectal cancer model following prophylactic treatment with CD28-TAA bispecific antibody in combination with anti-PD-1. Extension of this study and re-challenged of the tumor-free surviving animals shows that re-challenged hCD28 mice have enhanced survival compared to naïve hCD28 mice inoculated with MC38-TAA, suggesting tumor immunological memory. Furthermore, TGN1412 administration in CD28 mice induces cytokine release, and a slightly body weight loss, but no major change in body temperature. Although the model does not fully reproduce the ability of human CD28 to produce cytokines upon activation due to the mouse ICD, the expression of the amplifier isoform CD28i might contribute to the response to TGN1412. Altogether, data suggest that hCD28 model enables assessment of efficacy and safety of CD28-targeting agents. The hCD28 model was intercrossed with CD3 humanized models to enable assessment of combination therapies and bispecific antibodies targeting both CD3 and CD28.
[1] Porciello N, Grazioli P, Campese AF, et al. A non-conserved amino acid variant regulates differential signalling between human and mouse CD28. Nat Commun 2018; 9:1-16

#5293 Preclinical development of NI-3201, a PD-L1xCD28 bispecific antibody mediating CD28 costimulation upon PD-L1 blockade.

S. Majocchi[1], N. Anceriz[1], A. Viandier[1], A. Lesnier[1], L. Cons[1], L. Nouveau[1], E. A. Pace[2], B. L. Millard[2], B. Daubeuf[1], V. Moine[1], S. Salgado-Pires[1], J. Saro[1], L. Shang[1], K. Masternak[1], W. G. Ferlin[1];

[1]Light Chain Bioscience - Novimmune SA, Plan-les-Ouated, Geneva, Switzerland, [2]Residual Dynamics, LLC, Camano Island, WA

NI-3201 is a PD-L1xCD28 bispecific antibody generated on the κλ body platform that blocks the PD-L1/PD-1 immune checkpoint pathway and conditionally provides T cell activation “signal 2” when engaging PD-L1+ tumor or immune cells (e.g., antigen-presenting cells). By combining two distinct mechanisms of action into a single molecule, NI-3201 overcomes two major immune suppression mechanisms commonly observed in a variety of solid tumors, namely: [1] suppression of T cell response (induced by PD-L1+ cells engaging PD-1 on T cells) and [2] restricted/limited T cell activation (due to the lack of costimulatory signal associated to the scarcity of CD28 ligands in the TME). Importantly, NI-3201 was designed to require primary T cell stimulation (“signal 1”) to afford its activity: in the absence of TCR engagement, NI-3201 is unable to activate T cells, thus preventing unintended systemic inflammation.

The single agent pharmacological activity of NI-3201 was assessed *in vitro* through a Cytomegalovirus (CMV) recall assay in which CMV+ PBMCs were cocultured with PD-L1+ cancer cell lines ectopically loaded with CMV-specific MHC-I peptides, thus providing “signal 1”. NI-3201 induced the activation and proliferation of CMV-specific T cells which resulted in killing of the target tumor cells. *In vivo*, the single agent activity of NI-3201 was shown in immunocompetent huCD28-transgenic mice engrafted with huPD-L1-expressing murine colon adenocarcinoma MC38 cells, a model in which NI-3201 induced durable anti-tumor immunological memory response. In humanized mouse models where T cell engagers (TCEs) were ineffective, NI-3201 was able to synergize with TCEs to control tumor growth, even inducing tumor regression in one model. The pharmacokinetics (PK) and tolerability of NI-3201 were investigated in non-human primates (NHP) after single and repeated-dosing. NI-3201 demonstrated favorable PK with close to dose-proportional concentrations being achieved. Upon repeated NI-3201 administration, no hypercytokinemia was observed; only a mild and transient IL-6 release and associated increase in C-reactive protein (CRP) levels were seen, with no clinical signs reported. The favorable profile seen in NHP was supported by data generated *in vitro* further de-risking the cytokine release syndrome (CRS) potential. Quantitative systems pharmacology (QSP) modelling integrating both *in vitro* and NHP data predicted a drug concentration required for optimal NI-3201 activity in the TME, and preliminary data suggests optimal patient activity at Q2W-Q3W dosing schedule.

The anti-tumor activity as a single agent or as universal combination partner for TCEs, shown *in vitro* and *in vivo*, together with the favorable safety profile of NI-3201, support its clinical development planned to start in Q1 2025.

#5294 Conditionally active CD28xVISTA bispecific antibodies induce myeloid-driven tumor-specific T-cell co-stimulation for improved cancer immunotherapy.

T. Thisted, Z.-G. Jiang, Z. Biesova, A. Onumajuru, Y. Kleschenko, K. Malhotra, V. Saxena, A. Mukherjee, F. Smith, E. H. van der Horst;
Sensei Biotherapeutics, Rockville, MD

Introduction: Tumor-specific recruitment of co-stimulatory bispecific antibodies (bsAbs) has emerged as a promising therapeutic strategy. Here, we investigated pH-selective CD28xVISTA bsAbs to act selectively within the acidic tumor microenvironment (TME). Our CD28xVISTA bsAbs are designed for tripartite "*trans*-activation" of CD28 in the TME, aiming for enhanced T-cell-mediated cancer cell killing while minimizing systemic T-cell activation and Cytokine Release Syndrome (CRS) risk.

Experimental Procedures: We evaluated various CD28xVISTA bsAbs, focusing on a prototype 1+2 format with monovalent CD28 binding, bivalent VISTA binding and Fc receptor interaction null mutations (BS2). BS2 was tested for T-cell *trans*-activation using Jurkat-IL-2-luciferase reporter cells in the presence of HEK293 cells expressing membrane bound OKT3-scFv and CHO cells expressing human VISTA. BS2's potency was further evaluated in an xCelligence-based human T-cell killing assay that dynamically monitors growth of LNCaP prostate cancer cells co-cultured with VISTA$^{\pm}$ Kasumi-3 cells, alone or in combination with a CD3xPSMA bispecific T-cell engager. T-cell activation and proliferation were also measured using flow cytometry with CD3, CD4, CD8 and CD25 markers. Additionally, we modified BS2 to introduce pH-selective VISTA binding, limiting its activity to the TME, and tested this version in a syngeneic mouse model in combination with anti-murine PD-1 (anti-mPD-1). Finally, cytokine release from human PBMCs, co-cultured with human umbilical vein endothelial cells (HUVECs) and treated with the pH-selective BS2 (or TGN1412 as a positive control), was measured using a bead-based multiplex immune assay.

Results: Our data show that the combination of anti-mPD-1 and our prototype CD28xVISTA bsAb (BS2) with pH-selective VISTA binding significantly inhibited tumor growth *in vivo*. *In vitro*, CD28xVISTA co-stimulation in *trans* by BS2 potentiated the activity of a CD3xPSMA bispecific T-cell engager in our human T-cell killing assay. Cytokine release assessments demonstrated negligible induction of inflammatory cytokines, indicating a favorable safety profile for this antibody.

Conclusion: Our study demonstrates the feasibility of *cis* and *trans* CD28 co-stimulation using a CD28xVISTA bsAb (BS2). This approach, which bypasses the need for tumor-associated antigens (TAAs) required by other CD28xTAA bispecifics in development, suggests a potentially safer alternative for T-cell engagement and stimulation. Moreover, our novel myeloid-directed TME-selective co-stimulation strategy with a CD28xVISTA bsAb may broaden the potential for T-cell engagement approaches in solid tumors by enabling rational combinations with existing CD3xTAA T-cell engagers without competing for the same target.

#5295 Tumor targeted-CD28 bispecific antibody with optimized potency, robust anti-tumoral activity and stringent CD3-dependence.

Xiguang Zhang, Shiqi Cao, Li Li, Shuaixiang Zhou, Yao Xiong, Dian Kang, Feifei Wang, Jie Ren, Keke Fei, Jianglu Wang, Jinchang Lu, **Huizhong Xiong**

Innovent Biologics, Suzhou, China

CD28 is an essential co-stimulatory signal (Signal 2) for optimal T cell function upon TCR/CD3 activation (signal 1). However, clinical development of CD28 agonist antibodies has been confounded by toxicities presumably from CD3-independent and/or tumor non-specific activation. Here we report a rationally screened CD28 agonist antibody with optimized potency, from which a PSMAxCD28 bispecific was made. The bispecific antibody had several unique features: (1) minimal activity in the absence of CD3, even under stringent conditions, (2) superior tumor killing *in vivo* alone and in combination with anti-PD1 antibody, (3) requirement of abundant level of PSMA for activation, sparing $PSMA^{low}$ cells, and (4) extended half-life in human-CD28 KI mice. To summarize, our anti-CD28 bispecific antibody enhances dependence on TCR/CD3 (Signal 1), induces selective killing of PSMA high expressing cancer cells, and elicits robust tumor eradiation *in-vivo* with extended PK. These features may translate to further improvements in efficacy and safety for tumor-targeted CD28 bispecific antibodies.

#5296 Enhancing the strength and durability of vaccine-induced anti-tumor immunity with CD27 agonism of CD4+ T cells.

B.-J. Hwang[1], E. Crosby[1], T. Trotter[1], L.-C. Tsao[1], T. Wang[1], C. Liu[1], X. Yang[1], G. Lei[1], J. Wei[1], X. Ma[1], B. Liu[1], A. Hobeika[1], M. Morse[1], T. Keler[2], L.-Z. He[2], H. K. Lyerly[1], Z. Hartman[1];

[1]Duke University, Durham, NC, [2]Celldex Therapeutics, Hampton, NJ

Despite encouraging early phase clinical trials, decades of research have yet to yield effective cancer vaccine immunotherapies. To determine potential markers for success, we performed a follow-up study of a HER2-pulsed dendritic cell cancer vaccine Phase I trial performed in advanced HER2+ cancer patients. Surprisingly, we found that all treated patients were alive at over 18 years post-treatment. These patients still possessed significant HER2-specific memory T cell responses, typified by CD27 expression. The expansion of HER2-specific CD27+ memory T cells was also observed in patients from a separate clinical trial, who received a HER2-expressing viral vaccine. To validate these clinical responses, we vaccinated human CD27 transgenic mice with a HER2 viral vector again observing HER2-specific CD27+ memory T cells, suggesting the significance of this axis in eliciting and maintaining effective vaccine-specific memory T cell responses. We hypothesized that CD27 expression was not just a marker of memory T cells, but represented a critical activation pathway during memory formation. To determine the potential impact of CD27 agonism in vaccination, we combined HER2 vaccination with an anti-CD27 agonist antibody (Varlilumab). The combination treatment elicited a robust increase in HER2-specific CD4+ memory T cell responses that was maintained for at least 300 days post-vaccination. Using therapeutic HER2 vaccination in combination with anti-CD27 of HER2+ tumor bearing mice, we show significantly increased anti-tumor efficacy and further enhancement in combination with PD1 inhibition. The anti-tumor response was triggered by anti-CD27 antibody during the vaccine priming phase, which enhanced HER2-specific CD4+ T cells. Critically, we found that HER2 specific CD4+ T cell responses allowed for anti-tumor responses that persisted after CD8+ T cell depletion, indicating a direct role for antigen-specific CD4+ T cells independent of CD8+ T cells. Collectively, our results support a central role for antigen-specific CD27+ CD4+ T cells in cancer vaccination. These data support the addition of CD27 agonism to improve the therapeutic index of cancer vaccines and potentially enhance responses to immune checkpoint blockade in refractory cancers.

#5297 CLN-619, a clinical stage MICA/B-specific hIgG1 monoclonal antibody, engages multiple immune effector cells to promote anti-tumor activity.

K. A. Whalen, C. C. Henry, K. Rakhra, K. Meetze, J. S. Michaelson, P. A. Baeuerle;
Cullinan Oncology, Inc., Cambridge, MA

CLN-619 is a humanized IgG1 monoclonal antibody that targets MICA and MICB (MICA/B) and is currently in phase 1 clinical development in cancer patients (NCT05117476). MICA/B serve as activating signals on target cells for recognition by the NKG2D receptor, which is expressed on NK cells and a subset of T cell populations. MICA/B expression is induced in response to stressed conditions, thereby enabling NKG2D-mediated elimination of target cells. On NK cells, NKG2D is one of many receptors in the complex network of activating and inhibitory receptors, whereby NKG2D pathway activation results in cytokine production, enhancement of ADCC and target cell death. On CD8 T cells, the NKG2D axis plays a costimulatory role in lowering the threshold for lysis upon TCR engagement, and may also drive direct CD8-mediated killing following prior TCR activation. MICA/B is expressed broadly on a range of solid and hematological malignancies. However, tumor cells evade NKG2D-mediated elimination by shedding MICA/B ligand from the cell surface via proteases present in the tumor microenvironment (TME). CLN-619 functions by binding to MICA/B and preventing shedding, thereby increasing MICA/B cell surface expression to restore the NKG2D-MICA/B axis to promote tumor cell killing by NK cells and T cells. Additionally, CLN-619 can mediate ADCC and ADCP by NK cells and macrophages. In preclinical xenograft models, doses as low as 0.03 mg/kg inhibited tumor outgrowth. We investigated the effects of CLN-619 on a variety of primary immune cells including NK cells, T cells and macrophages. In the evaluation of NK cells, we measured CLN-619 modulation of cytokine production and cytotoxicity in the presence of MICA/B expressing target cells. In addition, we demonstrated the contribution of Fc-mediated functions of CLN-619. In the context of T cells, we explored the requirement of TCR co-stimulation or prior antigen exposure in the activation of the NKG2D pathway by CLN-619. In the context of macrophages, we measured the ability of CLN-619 to mediate ADCP against MICA/B-expressing target cells. These data highlight the potential of CLN-619 to engage multiple immune cell types within the TME, which may lead to greater and broader efficacy compared to IO therapies targeting a single immune cell type.

#5298 BSI-093, a best-in-class anti-BTN3A monoclonal antibody for cancer immunotherapy by activation of Vg9Vd2 T cells.

W. Dai[1], J. Li[1], J. Liu[1], H. Li[1], X. F. Liu[2], S. Xia[1], Q. Lyu[1], H. M. Davis[2], **M. Chen**[1], Z. Peng[1];
[1]Biosion, Inc., Nanjing, China, [2]Biosion USA, Inc., Newark, DE

Background: Gamma delta T (γδ T) cells are potent anti-cancer effectors with the potential to target tumors broadly, independent of patient-specific neoantigens or human leukocyte antigen background. Among tumor-infiltrating lymphocytes, the presence of γδ T cells is the most favorable prognostic marker for overall survival of patients with various solid and hematologic tumors. Vγ9Vδ2 T cells are the predominant γδ T cells in peripheral circulation. Butyrophilin 3A (BTN3A) members, widely expressed in tumors, have emerged as novel molecules modulating the function of Vγ9Vδ2 T cells. Targeting BTN3A for activation of Vγ9Vδ2 T cells provides an alternative strategy for cancer immunotherapy.

Experimental procedures: BALB/c mice were immunized with recombinant BTN3A1-ECD-Fc. The Biosion proprietary H^3 (High-throughput, High-content and High-efficiency) antibody discovery platform was used to identify an anti-BTN3A monoclonal antibody lead candidate - BSI-093. The target binding specificity, binding activity, and affinity of BSI-093 were evaluated by protein-based ELISA, cell-based FACS and Biacore-based SPR. *Ex vivo* assays were used to evaluate the cellular bioactivity of BSI-093 on activating Vγ9Vδ2 T cells for killing activity of various tumor cells. B-NDG mice bearing Jurkat-GFP-Luc tumors were used to evaluate the tumor inhibitory activity of the anti-BTN3A antibody.

Summary: BSI-093 is a humanized monoclonal antibody with the following critical properties: (1) binds to all BTN3A members (BTN3A1, BTN3A2 and BTN3A3) with high affinity; (2) has potentially longer half-life and silenced Fc-effector function by Fc-engineering; (3) exhibits cross-reactivity to rhesus BTN3A members; (4) demonstrates strong activity on activating Vγ9Vδ2 T cells to kill a variety of natural cancer cells in *ex vivo* assays; and (5) shows significant anti-tumor efficacy in a CDX model.

Conclusion: BSI-093 demonstrates potential best-in-class biophysical properties and functional characteristics, supporting the initiation of development activities including manufacturing and IND-enabling studies.

#5299 A novel anti-4-1BB antibody with no liver toxicity and its application in a bi-specific antibody.

Jen-Kuan Chang, Jie Xue, Chen Dong, An Ju, Toya Baral, Julie Yoo, Yanling Wang, Marco Muda, Qiang Liu, Wenfeng Xu, Weidong Jiang, Lixin Feng

Henlius USA, Milpitas, CA

4-1BB (CD137, TNFRSF9) is a co-stimulatory receptor initially identified on T cells, belonging to the tumor necrosis factor receptor superfamily. Primarily expressed on activated CD8+ T cells, it plays a crucial role in immune activation. Moreover, the intracellular domain of 4-1BB is leveraged to enhance the proliferation and cytotoxicity of Chimeric Antigen Receptor-T (CAR-T) cells. However, the development of 4-1BB agonist antibodies has encountered challenges, with limited clinical efficacy (e.g., utomilumab) or dose-dependent liver toxicity (e.g., urelumab). Consequently, there is a significant demand for the development of next-generation 4-1BB agonist antibodies, leading to numerous ongoing preclinical R&D efforts and clinical trials. Here, we introduce a novel fully humanized anti-4-1BB antibody, HLX25, and discuss the development of HLX34, a bispecific antibody targeting both 4-1BB and Her2. HLX25 boasts a unique binding epitope distinct from first-generation 4-1BB antibodies and demonstrates multiple cross-species reactivities. Additionally, HLX25 incorporates an engineered Fc region to enhance intratumoral clustering while reducing toxicity. In vitro studies reveal that HLX25 exhibits activity similar to natural 4-1BB ligands. In contrast, utolimumab shows inadequate activity, and urelumab displays superior activity, suggesting a correlation between efficacy and safety. As reported previously, (As been profiled in our Lab,) HLX25 exhibits robust dose-dependent anti-tumor activity in the MC38/h4-1BB KI mouse model. Noteworthy is the superior safety profile of HLX25 in the h4-1BB KI model, where both HLX25 and utolimumab induce no significant AST and ALT upregulation, unlike urelumab, which demonstrates such upregulation in vivo. A comparative analysis of HLX25 with other second-generation anti-4-1BB antibodies in clinical trials in vivo reveals that HLX25 provides superior tumor inhibition without observed toxicity within the effective dose range. Furthermore, we've developed HLX34, a Her2x4-1BB bispecific antibody, derived from Trastuzumab and HLX25. Its format underwent optimization using a reporter assay, indicating superior in vitro activity. Validation through a cytokine release assay with primary PBMCs in vitro and confirmed in vivo activity in animal models, without observed toxicity, strongly supports the efficacy and safety of HLX34 in Her2-positive tumors. These results provide evidence that our novel anti-4-1BB antibody activates proper 4-1BB signaling through tumor-enriched FcgRIIB or tumor-associated antigen-mediated clustering, inhibiting tumor growth with good safety in both in vitro and in vivo settings. This underscores HLX34 as a promising alternative therapeutic strategy for next-generation cancer immunotherapy.

#5300 BH3120, PD-L1 X 4-1BB bispecific antibody, plus PD-1 antagonist results in synergistic anti-tumor efficacy with excellent safety profile.

Jun Wang, Jing Wang, Yang Liu, **Jiangcheng Xu**, Jiawang Liu, Kyoungwoo Lee

Beijing Hanmi Pharm. Co. Ltd., Beijing, China

BH3120 is a clinical stage PD-L1 binding dependent 4-1BB agonist with moderate affinity against 4-1BB. In multiple preclinical evaluations, BH3120 decoupled T cell modulation in TME from that in normal tissues, indicating potential decoupling of efficacy from safety concerns.
4-1BB agonism improves T cell functions in TME, combining BH3120 and PD-1 antagonist shows dose dependent and complete control of established tumor burden with bi-directionally synergistic mechanism: Blockade of PD-1 increases the expression and exposure of surface PD-L1, providing BH3120 more chance to form immune clusters in the tumor environment. In the meantime, increased PD-1 induced by BH3120 can be blocked by PD-1 antagonist.
This bi-directional mechanism results in rapid eradication of tumor tissues shortening the time to regression, indicating potentially fast control of tumor burden and associated symptoms. With the characteristics decoupling co-stimulatory activity in TME from that in normal tissues, BH3120 either as a monotherapy or in combination with PD-1 antagonist was not associated with liver toxicity and other concerns in relation to excessive modulation of immune cells systemically.
Safety profile and clinical signs with BH3120 are being investigated in early-stage clinical trials as a monotherapy and in combination with a PD-1 antagonist.

#5301 Tumor-targeted activation of CD137 using *Bicycles*: New insights into mechanism of action and discovery of BT7455, a clinical candidate for the treatment of EphA2-expressing cancers.

J. Lahdenranta[1], K. Hurov[1], H. Cohen[1], L. Luus[1], C. Bray[1], P. Brown[2], A. Devlen[1], C. Campbell[1], M. Gray[2], M. Kelly[2], G. Mudd[2], P. Upadhyaya[1], S. Battula[1], K. Zhang[1], A.-S. Dugast[1], K. McDonnell[1], P. Brandish[1], N. Keen[1];

[1]Bicycle Therapeutics, Cambridge, MA, [2]Bicycle Therapeutics, Cambridge, United Kingdom

Introduction: Clinical studies in cancer patients have validated CD137 agonism as an activator of the immune system to enable tumor rejection. We have demonstrated that small, chemically synthetic bicyclic peptides can drive tumor-localized agonism of CD137 and anti-tumor immunity in mouse models. Here, we report the next stage of our work - delving into the mechanism of action of these novel agents and extending our program to serve patients whose tumors express EphA2. Experimental Procedures: MultiOmyx™ hyperplexed immunofluorescence assay was used to evaluate the expression of CD137 and EphA2 in head and neck squamous cell carcinoma samples. Human PBMC/tumor cell co-culture assays were used to assess CD137 *Bicycle* TICA™ in vitro bioactivity and syngeneic mouse tumor models were used to evaluate CD137 *Bicycle* TICA anti-tumor activity as mono- or combination therapies. Pharmacodynamic activity was evaluated by transcriptional profiling using NanoString assays or single cell RNA sequencing.

Summary of the Data: Studies utilizing a syngeneic mouse model and deep RNA sequencing of tumors from CD137 *Bicycle* TICA-treated mice implicated intratumoral dendritic cells in addition to T cells as early responders to localized CD137 agonism and potential contributors to the anti-tumor response. Furthermore, a mouse efficacy model demonstrated synergy with checkpoint inhibitor therapy. Multiplex imaging revealed that EphA2 and CD137 are co-expressed in human tumors of high unmet medical need and therefore, using our highly modular *Bicycle* platform, we discovered BT7455, a *Bicycle* TICA that engages EphA2 and CD137 with high affinity, resulting in potent EphA2-dependent activity in vitro and robust anti-tumor activity in vivo with intermittent dosing in mouse models. Gene expression profiling of tumors revealed that BT7455 led to increased production of cytokines and chemokines known to drive T cell infiltration, the extent of which differentiated it from both a checkpoint inhibitor and an anti-CD137 monoclonal antibody agonist. BT7455 was well tolerated in preclinical species and liver function tests indicated no evidence of hepatic toxicity.

Statement of Conclusions: In summary, we have identified EphA2 as a promising target to pair with a CD137 agonist. In addition to CD8+ T cells, tumor-resident dendritic cells are a likely contributor to anti-tumor immunity following treatment with *Bicycle*® TICAs, supporting utility for *Bicycle*® tumor-targeted CD137 agonists in solid tumors beyond those that are highly T cell-infiltrated. We have advanced a clinical development candidate, BT7455, to realize this potential for patients with EphA2-expressing cancers.

#5302 CB699: A novel mesothelin-binding Humabody® CD40 and CD137 dual-agonist for enhancing immune cell responses against MSLN+ tumors.

A. J. Pierce, P. M. Brailey, S. Archer, H. Spencer, M. Song, T. Wong, P. D. Bartlett, K. Williams, L. Jasaitis, P. Bland-Ward;
Crescendo Biologics, Cambridge, United Kingdom

INTRODUCTION: CD137 is a TNF receptor superfamily (TNFRSF9) costimulatory receptor expressed by T cells and NK cells. Clustering-mediated CD137 signaling enhances immune cell survival, proliferation, cytokine production and memory formation. CD40 (previously TNFRSF5) is a related superfamily member expressed primarily on B cells and antigen-presenting cells (APCs) which upon clustering is also a key modulator of T cell responses. Mesothelin (MSLN) is highly upregulated on tumor cells in ovarian and pancreatic cancer and select other solid tumour histologies. To avoid systemic toxicity, CB699 is designed to be immunologically active in the presence of any two of its three binding targets, thus enhancing both immune-immune and tumour-immune crosstalk. We present here the preclinical pharmacology of CB699.

EXPERIMENTAL PROCEDURES: Binding of CB699 to CD40, CD137 or MSLN was measured by surface plasmon resonance and by flow cytometry. CD137 and/or CD40 agonism, immune cell activation and cytokine secretion were evaluated *in vitro* using reporter gene assays and primary cell coculture assays in the presence/absence of MSLN-expressing tumor cells. The ability of CB699 to enhance tumor cell killing was characterized in 3D spheroid cocultures. CB699 toxicology and toxicokinetics was assessed in a dose range-finding study in cynomolgus macaques. CB699 was also assessed *in vivo* with a human CD34+ cell engrafted mouse model.

RESULTS: CB699 binds to primary and immortalized cells that express CD40, CD137 or MSLN, with low nanomolar affinity. CB699 also binds to cells from primary disaggregated human solid tumors. CB699 induces CD137 reporter cell activity in cocultures containing cells expressing either CD40 or MSLN. Additionally, CB699 induces CD40 reporter cell activity in cocultures containing cells expressing either CD137 or MSLN. CB699 induces IL-2 secretion and upregulation of CD86 on B cells in primary cocultures containing healthy human PBMCs and MSLN expressing cancer cells. Enhanced tumor cell killing was observed in spheroid cultures containing CB699 and was coupled with immune cell expansion. CB699 showed significant pharmacology *in vivo* with immune cell engrafted mice. Finally, CB699 was well tolerated in a dose range finding non-human primate toxicology study.

CONCLUSIONS: CB699 is a novel MSLN-binding CD137 and CD40 dual agonist that selectively enhances immune cell activity by enhancing both T cell and APC signaling axes. CB699 is positioned to enter clinical development.

#5303 A novel TIGIT and 4-1BB bispecific antibody, ABL112, exhibits potent in vitro and in vivo antitumor activity through dual immune modulation.

W. Son, Y. Lee, Y. Park, J. Won;
ABL Bio, Inc., Sungnamsi, Korea, Republic of

T cell immunoreceptor with Ig and ITIM domains (TIGIT) is an immune checkpoint molecule responsible for delivering inhibitory signals that suppress immune activation. Due to its inhibitory role in the immune response, TIGIT has emerged as a potential therapeutic target for various malignancies, with several clinical trials exploring the use of anti-TIGIT blocking antibodies with anti-PD-(L)1 therapies. Recent reports have indicated elevated expression of 4-1BB within intra-tumoral Tregs. Therefore, we hypothesized that a dual targeting approach involving both TIGIT and 4-1BB could effectively enhance intra-tumoral immunity. ABL112, a First-in-Class bispecific antibody targeting TIGIT and 4-1BB, demonstrated the induction of T cell activation by blocking the TIGIT signaling and TIGIT dependent 4-1BB clustering. By having intact Fc, ABL112 bound to FcγRI and its crosslinking with 4-1BB also induced 4-1BB activation. ABL112 selectively depleted Treg cells but not other T cells *in vitro*, potentially through antibody-dependent cell-mediated cytotoxicity.
ABL112 demonstrated superior efficacy in tumor regression compared to anti-TIGIT monoclonal antibody across various mouse tumor models. Additionally, combining ABL112 with pembrolizumab significantly inhibited tumor growth better than combining anti-TIGIT monoclonal antibody with pembrolizumab. According to immune cell depletion assay, ABL112-mediated tumor suppressive activity was predominantly driven by $CD8^{+}$ T cells, with a partial tumor reduction by $CD4^{+}$ T cell or NK cell depletion. Mice with complete remission (CR) were further protected from the tumor re-challenge after 3 months of cessation of ABL112 treatment, and the proportion of tumor-specific memory T cells in the blood increased, suggesting long-term immunological memory has been established. In conclusion, ABL112 exhibited potent in vitro and in vivo anti-tumor activity through multiple mode of action including TIGIT inhibition and 4-1BB activation. These results strongly suggest that ABL112 is an innovative and promising therapeutic option with the combination of anti-PD-(L)1 therapies for cancer patients.

#5304 ABL407, a LILRB4x4-1BB bispecific antibody with a wild type Fc, exhibits potent antitumor activity by modulating immune system in multiple ways involving T cells, myeloids, and regulatory T cells.

M. Seon, Y. Lee, H. Youn, Y. Park, S. Kim, K. Park, J. Won;
ABL Bio, Inc., Gyeonggi-Do, Korea, Republic of

Tumor-associated myeloid cells such as myeloid-derived suppressor cells (MDSC) accumulate in the tumor microenvironment (TME) and suppress anti-tumor immune responses in a broad range of cancers. LILRB4 (Leukocyte Immunoglobulin-Like Receptor Subfamily B Member 4), an emerging myeloid target, is specifically expressed in tumor-associated myeloid cells and suppresses the immune response, thus promoting cancer progression and metastasis. ABL407 is a First-in-Class bispecific antibody designed to simultaneously target LILRB4 and 4-1BB, enabling LILRB4 expression-dependent 4-1BB activation. By antagonizing LILRB4 signaling, ABL407 inhibited LILRB4 mediated immunosuppression, restoring T cell activity. In addition, ABL407 inhibited fibronectin, a potential LILRB4 ligand, -mediated suppression of myeloid cells. To evaluate the efficacy of ABL407, we established EL4 murine tumor model overexpressing LILRB4 (EL4/LILRB4) in h4-1BB transgenic mice and hLILRB1/4-h4-1BB triple transgenic mice. We observed LILRB4 was overexpressed in M-MDSC in the blood and liver-metastasized tumors. A significant decrease of M-MDSC population and tumor growth inhibition was observed in mice treated with anti-LILRB4 antibody and ABL407. ABL407 treatment resulted in a proportion increment of T cells. However, the percentage of Treg cells and M-MDSC in the liver and blood was reduced by ABL407 treatment in hLILRB1/4-h4-1BB triple transgenic mice. Mice with complete remission (CR) were further protected from the rechallenge of previously exposed tumor after 3 months of cessation of ABL407 treatment, implicating that immunological memory might be generated. In conclusion, our findings suggest that ABL407, LILRB4x4-1BB bispecific antibody, may be a promising strategy for the treatment of cancer. It can be applied as a "LILRB4 antagonist" as well as a "LILRB4-dependent 4-1BB agonist" across a broad spectrum of cancers.

#5305 M9657, a tumor-targeted anti-CD137 agonist, induced significant antitumor immunity in combination with anti-PD-1 antibody.

C. Xu, S. Yalavarthi, H. Zhang, U. Gundra, C. Bourin, L. Helming;
EMD Serono Research & Development Institute, Billerica, MA

Background: M9657, a first-in-class tumor-targeted conditional immune agonist, was developed to boost antitumor immune responses in the tumor microenvironment (TME) by targeting CD137. The immune agonism potency of M9657 was validated through *in vitro* assays and *in vivo* efficacy studies in syngeneic tumor models using the surrogate antibody FS122m. Combining CD137 agonists and antiPD(L)-1 antibodies presents a novel therapeutic strategy to overcome immune checkpoint inhibitor (ICI) resistance and enhance antitumor activity via complementary mechanisms. Anti-PD-(L)-1 antibodies can reverse the suppressive immune signals, and CD137 agonists can boost T cell activation, improving antigen presentation and cytokine release.
Methods: The antitumor immunity of M9657 + pembrolizumab (anti-PD-1 antibody) combination therapy was assessed using in-vitro luciferase and ex-vivo functional assays. In vivo antitumor efficacy was investigated with the M9657 surrogate (FS122m) and anti-mPD-1 in syngeneic tumor models expressing Mesothelin (MSLN).
Results: The combination of M9657 and pembrolizumab displayed dose-dependent immune agonism potency and significantly enhanced tumor cell cytotoxicity and CD8+ T cell cytokine release relative to single agent treatments. In various syngeneic tumor models, the combination of FS122m with antimPD1 significantly increased antitumor efficacy relative to monotherapies, with more mice achieving complete tumor regression and prolonged median survival. Tumor-cured mice after combination treatment exhibited resistance to the primary tumor rechallenge, indicating the generation of tumor antigen-specific antitumor immunity and long-term immune protectivity.
Conclusion: The combination of M9657 with anti-PD-(L)1 could overcome primary ICI therapy resistance and improve the antitumor efficacy of current anti-PD-(L)1 therapy in the clinic. Our findings support a combination strategy to combine M9657 with anti-PD-(L)1 in a clinical setting, potentially leading to enhanced antitumor immunity and improved patient outcomes. Future studies should investigate the safety and efficacy of this combination therapy in human patients.
Sponsored by the healthcare business of Merck KGaA, Darmstadt, Germany (CrossRef Funder ID: 10.13039/100009945)

#5306 PTPN22 targeting partners with 41BB/OX40 costimulation to overcome anti-PD1 resistance in pancreatic ductal adenocarcinoma.

S. Charmsaz[1], N. E. Gross[1], J. W. Lee[1], J. Lin[2], A. G. Hernandez[1], E. M. Coyne[1], S. M. Shin[1], C. Cannon[1], X. Yuan[1], Z.-Y. Zhang[2], E. M. Jaffee[1], W. Ho[1]; [1]Johns Hopkins University School of Medicine, Baltimore, MD, [2]Purdue University, West Lafeyette, IN

Background: The pancreatic ductal adenocarcinoma (PDAC) tumor microenvironment (TME) is notable for a scarcity of cytotoxic T cells and an overabundance of immunosuppressive myeloid and regulatory T cells. Checkpoint immunotherapies targeting PD/L1 or CTLA4 have shown efficacy in immunogenic cancers but remain ineffective in PDAC, highlighting a need for novel approaches. Abrogating protein tyrosine phosphatase non-receptor type 22 (PTPN22), a phosphatase in the TCR signaling cascade, has been shown to modulate multiple mechanisms of immune resistance. Furthermore, 41BB costimulatory pathway has recently been investigated as a potential strategy to enhance immunotherapy against PDAC. Using immune-resistant murine models of PDAC, we investigated PTPN22 as an immunotherapeutic target in combination with 41BB co-stimulation and PD1 inhibition against PDAC.

Methods: We employed a well-characterized murine PDAC cell line expressing mutant *Kras*^{G12D} and *Trp53*^{R172H} under the *Pdx1*-cre promoter (KPCY 6419c5). This tumor line is resistant to combination immuno- and chemotherapies. To determine treatment efficacy, PTPN22 deficient mice (KO) were inoculated with KPCY6419c5 cells either subcutaneously or orthotopically into the pancreas. To extend the translatability of PTPN22 targeting, we also injected PTPN22 competent mice with the same tumor cells and treated them with our novel PTPN22 inhibitor L1. Harvested tumors were processed for FFPE and mass cytometry (CyTOF) analysis to track changes in the immune compartment.

Results: When PTPN22 was abrogated, treatment with anti-PD1 and 41BB agonism led to a 10-day delay in substantial tumor formation and roughly 75% reduction in tumor volume by 21-days post treatment. These tumors showed elevated levels of OX40 and OX40L primarily in the setting of PTPN22 KO/PD1/41BB therapy. In a subsequent in vivo experiment using an OX40L neutralizing antibody, we found that OX40 signaling is essential for the efficacy of PTPN22 KO/PD1/41BB therapy. Furthermore, combining OX40 agonist with anti-PD1 in PTPN22 KO sufficiently mimicked the efficacy seen with the anti-PD-1 and 41BB combination. CyTOF analysis indicated that OX40 expression is enriched in Tregs and OX40L is enriched in myeloid derived suppressor cells (MDSCs). Moreover, combination therapy efficacy was reproduced using the PTPN22 inhibitor L1.

Conclusions: PTPN22 abrogation enhances the success of PD-1 inhibition given with either OX-40 or 41BB agonist therapies. In addition, PTPN22 abrogation together with PD1 inhibition and 41BB costimulation reduces MDSC and Treg suppression of effector T cells via the OX40L-OX40 axis. Finally, PTPN22 can be blocked by a small molecule inhibitor strengthening its candidacy as a therapeutic target.

#5307 Preclinical evaluation of a potential FIC 4-1BB/CD24 bispecific antibody IBD0333.

X. Jiang, C. Wu, Z. Chen, **L. Yin**;
SUNHO (China) BioPharmaceutical Co.,Ltd., Nanjing, China

Background: This study demonstrates the preclinical evaluation of a novel 4-1BB/CD24 bispecific antibody IBD0333. 4-1BB's activation triggers a signaling cascade that activates both innate and adaptive immune systems. Due to the hepatotoxicity of current anti-4-1BB monoclonal antibodies, tumor-associated antigens (TAA) targeting to specifically activate immune cells in the tumor microenvironment (TME) is expected to enhance its safety profile. CD24 is highly expressed in many cancers, such as ovarian and breast cancer and its high expression is often related to poor prognosis. The signaling pathway of CD24/Siglec-10 triggers a "don't eat me" signal that facilitates immune escape of tumor cells. Therefore, IBD0333 was designed to target CD24 overexpressed tumor cells and activate CD8+ T cells to induce T cell mediated antitumor immunity in TME of the targeted tumor tissue. To further reduce the toxicity risk, the anti-4-1BB moiety is designed to activate the signaling pathway only when IBD0333 binds to the tumor cells that overexpress CD24.
Methods: For CD24 terminus, we applied virus like particle (VLP) as antigen for immunization to obtain functional CD24 antibodies. For 4-1BB terminus, competitive ELISA/FACS analysis as well as amino acid point mutation binding ability analysis based on the receptor crystal structure were performed to characterize the binding epitope. The in vivo mice efficacy and toxicity study, as well as cynomolgus monkey toxicity study were also conducted to describe the anti-tumor activity and safety profile. For IBD0333, we verified binding affinity by FACS to cancer cells and the 4-1BB activity in reporter-gene assay. IL2 and INF-γ secretion assay were performed to evaluate the PBMC activation. C57BL/6J-h4-1BB humanized mice bearing MC38-hCD24 colon cancer cells were used to validate the anti-tumor efficacy of IBD0333. Preclinical PK and toxicity study was also performed in cynomolgus monkeys to describe the safety profile of IBD0333.
Results: IBD0333 showed excellent binding and PBMC stimulation activities. In toxicology studies of IBD0333, no obvious abnormality in mice or cynomolgus monkeys administered with IBD0333 was observed. The MTD was estimated to be greater than 200 mg/kg with no severe side effects observed in the study, showing that IBD0333 has great potential to achieve significantly improved safety profile. As to efficacy, IBD0333 showed excellent tumor inhibition activities in mice model with 99% tumor growth inhibition at 1 mg/kg and 100% at 3 mg/kg.
Conclusion: IBD0333 is a clinical stage, potential first-in-class, 4-1BB/CD24 bsAb that simultaneously stimulates both innate and adaptive immunity to achieve strong synergistic effects with reduced hepatotoxicity. The IND approvals from the FDA and the NMPA have been obtained and the Phase I clinical trial of IBD0333 in locally advanced/metastatic solid tumors or non-Hodgkin's lymphoma is currently on-going.

#5308 Ifngr1 signaling on tumor-specific CD4 T cells is required to mitigate Treg differentiation during CD40 agonist and anti-PD-L1 immunotherapy in pancreatic ductal adenocarcinoma.

E. Cruz-Hinojoza, A. Burrack, Z. Schmiechen, C.-L. Lonetree, E. A. Miller, M. Patterson, J. Williams, T. Dileepan, I. Stromnes;
University of Minnesota, Minneapolis, MN

Pancreatic ductal adenocarcinoma (PDA) is a particularly lethal malignancy that lacks effective therapeutic strategies. A promising therapeutic modality that can elicit transient antitumor responses in a subset of metastatic PDAs is chemotherapy + CD40 agonist +/- anti-PD-1. A deeper understanding of the cellular mechanisms that mediate the initial responses will inform new strategies to enhance the durability of this therapy. Our prior studies demonstrated that tumor-specific CD4 T cells are critical for mitigating tumor growth in a syngeneic KPC orthotopic tumor model of PDA that expresses a model neoantigen, click beetle red luciferase (CBR). CD4 T cells direct tumor antigen recognition by tumor-associated macrophages and host interferon-gamma receptor (Ifngr1) signaling. Here, we demonstrate that CD4 T cells are required for the antitumor effects of anti-CD40 agonist indicating that this therapy fails to compensate for a lack of CD4 T cell help. We sought to test the hypothesis that host Ifngr1 signaling acts in a CD4 T cell intrinsic manner to promote antitumor responses. As such, we develop and validate a novel MHC class II tetramer (CBR54-62:I-Ab) to track the fate of endogenous CD4 T cells during tumor growth. We demonstrate that tumor-specific CD4 T cell abundance and Th1 polarization is decreased in orthotopic tumors, particularly between day 14 and day 21 post tumor implantation. Combination agonistic anti-CD40 + anti-PD-L1 maintained tumor-specific CD4 T cell numbers in the spleen and pancreas-draining lymph nodes of tumor-bearing mice. Intriguingly, Th1 polarized tumor-infiltrating CD4 T cells were decreased by aPD-L1, but were restored by anti-CD40, a finding further corroborated by single-cell RNA sequencing. Further, agonistic anti-CD40 + anti-PD-L1 alone or in combination robustly decreased Treg polarized tumor-specific CD4 T cells. Using a mixed bone marrow chimeric approach, we show immunotherapy's Treg-depletion effect is dependent on Ifngr1 on antigen-specific CD4 T cells. In contrast, Ifngr1 signaling on tumor-specific CD8 T cells appeared inconsequential to CD8 T cell fate following immunotherapy. To our knowledge, this is the first study to interrogate tumor-specific CD4 T cells in PDA and uncover novel interplay between CD4 T cells, CD8 T cells, and myeloid cells that are critical for immunotherapy response.

#5309 ATOR-4066, a Neo-X-Prime™ bispecific antibody targeting CD40 and CEACAM5, induces tumor localized immune cell activation in preclinical *in vivo* tumor model.

Hampus Andersson[1], Ida Uddback[1], Mona Celander[1], Maria Johansson[1], Lill Ljung[1], Anneli Nilsson[1], Amulya Krishna Shetty[1], David Gomez Jimenez[1], Mattias Levin[1], Sara Fritzell[1], Laura von Schantz[1], Malin Lindstedt[2], Karin Hagerbrand[1], Anette Sundstedt[1], Peter Ellmark[1]

[1]Alligator Bioscience AB, Lund, Sweden,[2]Department of Immunotechnology, Lund University, Lund, Sweden

ATOR-4066 is a preclinical stage bispecific antibody targeting CD40 and CEACAM5, based on Alligator's novel Neo-X-Prime™ antibody technology platform. ATOR-4066 induces a neoantigen specific T-cell response by simultaneous binding to CD40 on myeloid cells such as antigen presenting cells (APCs) and to CEACAM5 on tumor cells. CEACAM5 is a tumor-associated antigen highly expressed on several cancer indications such as colorectal and gastric cancer, as well as on tumor-derived material. ATOR-4066 treatment results in (1) CEACAM5-conditional CD40-mediated activation of APCs and (2) enhanced uptake of tumor-derived material, leading to cross-presentation of neoantigen and priming of neoantigen-specific T cells, resulting in enhanced tumor cell killing. We have previously shown evidence of a potent anti-tumor effect of ATOR-4066 *in vivo*, superior to the effects observed with the corresponding CD40 mAb. Moreover, we have demonstrated CEACAM5-dependent activation of CD40-expressing cells *in vitro*, and an ability to mediate co-localization of CEACAM5-expressing tumor debris and CD40 expressing APCs. In addition, ATOR-4066 was shown to induce CEACAM5-conditional activation of tumor-infiltrating CD40-expressing immune cells in dissociated primary human tumor material from colorectal and gastric cancer patients. Here we present data further elucidating the mode of action of ATOR-4066 *in vivo*. Following ATOR-4066 treatment, tumors and lymph nodes were isolated from human CD40 transgenic mice bearing MC38 tumors expressing human CEACAM5. Flow cytometry analysis shows an increased number of tumor-infiltrating immune cells in mice treated with ATOR-4066 compared to treatments with CD40 mAb or vehicle. The study also reveals upregulation of co-stimulatory molecules such as CD86 on DCs and macrophages after treatment with ATOR-4066 compared to groups treated with CD40 mAb or vehicle. The effect was localized to the tumor microenvironment and not observed in tumor draining lymph nodes, confirming previous *in vitro* results demonstrating CEACAM5-conditional immune activation. Moreover, RNA-sequencing of tumor samples displayed distinct transcriptomic alterations following ATOR-4066 treatment vs. CD40 mAb or vehicle treatment *in vivo*. In contrast, RNA-sequencing of peripheral blood in ATOR-4066 treated mice showed only small transcriptomic differences compared to the vehicle treated group, but distinct from mice treated with a CD40 mAb, further demonstrating the CEACAM5 dependent response of ATOR-4066. In summary, these preclinical data demonstrate that ATOR-4066 activates infiltrating myeloid cells resulting in increases in activated tumor infiltrating T cells, thus creating a pro-inflammatory tumor microenvironment, which strongly supports further development and clinical testing of ATOR-4066.

#5310 KK2269, an epithelial cell adhesion molecule-targeted CD40 agonist, demonstrates antitumor effects in combination with standard therapies for NSCLC.

Y. Tezuka, K. Kawasaki, Y. Sumitomo, M. Saito, A. Yao, M. Ando;
Kyowa Kirin Co., Ltd., Tokyo, Japan

CD40 is a key molecule expressed on antigen presenting cells (APCs), whose signaling activates APCs and generates antitumor immune responses. Although CD40 agonists have been investigated in clinical trials, systemic toxicities have limited their full potential in providing adequate antitumor effects. To overcome this limitation, we developed KK2269, a bispecific antibody, using REGULGENT™ technology. KK2269 binds to CD40 and tumor-expressed epithelial cell adhesion molecule (EpCAM) to allow activation of CD40+ APCs only at EpCAM+ tumor sites, thus avoiding systemic toxicity. EpCAM is overexpressed in many types of epithelial cancers, including non-small cell lung cancer (NSCLC). KK2269 exerts synergistic antitumor activity and tumor-specific immune responses in combination with docetaxel, a common chemotherapy for NSCLC, in an EpCAM-expressing tumor mouse model. Hence, we aimed to evaluate KK2269 for the treatment of NSCLC. Docetaxel is used as a combination therapy with ramucirumab, an anti-VEGF receptor 2 (VEGFR2) antibody, for previously treated advanced NSCLC. In addition, many clinical studies are evaluating the add-on effects of PD-1/PD-L1 blockade combined with standard chemotherapies (including docetaxel) in NSCLC, which may become the standard of care for advanced NSCLC in the future. Therefore, we investigated the antitumor effect of KK2269 in combination with docetaxel + anti-mouse VEGFR2 (study 1) and with docetaxel + anti-mouse PD-1 (study 2) using a mouse EpCAM-expressing B16F10 tumor-bearing human CD40 transgenic mouse model. The prolongation of TTP5X (the day on which the tumor volume is observed to be ≥5-fold of that observed on day 0) was evaluated. In study 1, the median TTP5X (95% confidence interval [CI]) with the control, docetaxel + anti-VEGFR2, and triple combination (KK2269, docetaxel, anti-VEGFR2) was 10.0 days (7.0, 10.0), 26.0 days (17.0, 28.0), and 52.0 days (42.0, not calculable), respectively. The TTP5X was significantly prolonged with the triple combination compared with the control ($p=0.000007$, log-rank test) and docetaxel + anti-VEGFR2 ($p=0.000004$, log-rank test). In study 2, the median TTP5X (95% CI) was 7.0 days (not calculable), 9.0 days (6.0, 11.0), 16.0 days (7.0, 18.0), and 26.5 days (7.0, 32.0) with the control, KK2269, docetaxel + anti-PD-1, and triple combination (KK2269, docetaxel, anti-PD-1), respectively. TTP5X was significantly prolonged with the triple combination compared with the control, KK2269, and docetaxel + anti-PD-1 ($p<0.0001$, $p=0.0003$, and $p=0.0023$, respectively, log-rank test). Thus, a significant antitumor effect was demonstrated when KK2269 was added to the standard treatment of NSCLC (docetaxel + anti-VEGFR2 antibody) and to docetaxel + anti-PD-1 antibody. Our findings strongly suggest that KK2269 provides improved treatment options for patients with NSCLC.

#5311 KK2269, an epithelial cell adhesion molecule-targeted CD40 agonist, stimulates anti-tumor immunity resulting in sustained anti-tumor effect against mouse intrahepatic tumor without hepatotoxicity.

Y. Sumitomo, K. Kawasaki, Y. Tezuka, M. Saito, A. Yao, M. Ando;
Kyowa Kirin Co., Ltd., Tokyo, Japan

Several anti-CD40 agonist antibodies have been evaluated in clinical trials based on their preclinical antitumor activity via generation of antitumor innate and adaptive immunity through activation of antigen-presenting cells. However, conventional monospecific anti-CD40 agonist antibodies have faced limitations in terms of safety margins and clinical efficacy. To address this problem, we developed KK2269, a novel bispecific antibody (REGULGENT™ format) that binds to both CD40 and epithelial cell adhesion molecule (EpCAM), which is highly expressed in several types of tumors. KK2269 demonstrated EpCAM-dependent activation of CD40 signals both in vitro and in vivo, confirming that it is a tumor-targeting CD40 agonist. Liver metastasis is common in EpCAM-positive cancers, including colon, stomach, and lung cancers. Intrahepatic tumors can attenuate the efficacy of immune checkpoint inhibitors due to the liver tumor-specific suppressive immune milieu. Although CD40 agonists are expected to overcome the immunosuppressive environment, non-tumor-targeting CD40 agonists cause hepatotoxicity. In the present study, we used a syngeneic intrahepatic tumor model to examine whether KK2269 exhibits antitumor efficacy without causing hepatotoxicity. Firstly, we confirmed that KK2269 administration did not increase aspartate aminotransferase (AST) or cause pathological abnormalities in the liver despite Il12b induction in the EpCAM-positive tumor. Additionally, gene expression analysis of peritumoral normal liver revealed that KK2269 did not induce inflammatory cytokines. In contrast, a conventional anti-CD40 agonist antibody increased AST, caused pathological abnormalities, and upregulated inflammatory cytokines in peritumoral normal liver, as reported in the clinical setting. Secondly, the antitumor effect of KK2269 in combination with docetaxel was evaluated. The combination therapy synergistically reduced intrahepatic tumor volume, and the effect persisted even 21 days after the administration. Gene expression analysis revealed a lower immune infiltration in the intrahepatic tumor versus subcutaneous tumor and that KK2269 in combination with docetaxel increased T-cell infiltration and activation even in the immunosuppressive intrahepatic tumor. In summary, our study demonstrated that KK2269 activated dendritic cells in an EpCAM-positive tumor in the liver but did not affect peritumoral normal liver tissues. In addition, KK2269 in combination with docetaxel showed potent antitumor effect accompanied by T-cell infiltration and activation against the intrahepatic tumor, which has a lower immune infiltration. These results suggest that the combination therapy of KK2269 and docetaxel is promising for metastatic EpCAM-positive tumors.

#5312 Agonist CD40 engineered smart immunosomes induced anti-tumor immunity, reduced associated toxicities and showed tumor free survival in murine glioblastoma model.

V. Gaur[1], W. Tyagi[2], S. Das[2], S. Ganguly[3], J. Bhattacharyya[4];

[1]Indian Institute of Technology Delhi (IIT Delhi), New Delhi, India, [2]National Institute of Immunology, New Delhi, India, [3]Jamia Hamdard University, New Delhi, India, [4]Indian Institute of Technology Delhi, New Delhi, India

CD40 agonist antibodies (αCD40) have proven great potential as an anti-cancer immunotherapeutic by showing promising anti-tumor response in both preclinical and early clinical studies. However, it has been observed that the systemic administration of αCD40, even at low dose, is associated with serious immune- and hepato- toxicities. In addition, αCD40 showed low tumor retention and induced PD-L1 expression which makes tumor microenvironment (TME) immunosuppressive. To overcome these issues, in this study, we have developed an immunosome where αCD40 is conjugated on the surface and VJ23, a small molecule immune-modulator was encapsulated inside it . Immunosome showed higher tumor accumulation till 96 hr of administration and displayed sustained release of αCD40 *in vivo*. Immunosome significantly delayed tumor growth and showed tumor free survival in mice bearing GL-261 glioblastoma tumor by increasing the population of $CD45^{+}CD8^{+}$ T cells, $CD45^{+}CD20^{+}$ B cells, $CD45^{+}CD11c^{+}$ DCs and $F4/80^{+}CD86^{+}$M1 macrophage in TME. In addition, Immunosome significantly reduced the population of T-regulatory cells, M2 macrophage, and MDSCs and lowered the expression of PD-L1 to modulate immunosuppressive TME. Moreover, Immunosomes significantly enhanced the level of pro-inflammatory cytokines (IFN-γ, IL-6, IL-2) and lowered anti-inflammatory cytokines (IL-4 and IL-10) level which supported anti-tumor response. Most interestingly, Immunosomes averted the *in vivo* toxicities associated with free αCD40 by lowering the levels of alanine aminotransferase (ALT), aspartate aminotransferase (AST), IL-6, IL-1α and reduced the degree of liver damage. Our results suggested that this novel formulation can be further explored in clinics to improve the *in viv*o anti-tumor efficacy of αCD40 while reducing the associated toxicities.

#5313 CB307: A dual targeting costimulatory Humabody® V_H therapeutic for treating PSMA-positive tumors.

S. Archer[1], P. M. Brailey[1], M. Song[1], P. D. Bartlett[1], I. Figueiredo[2], B. Gurel[2], C. Guo[2], V. Brucklacher-Waldert[1], H. Thompson[1], J. Akinwale[1], S. E. Boyle[1], C. Rossant[1], N. R. Birkett[1], J. Pizzey[1], M. Maginn[1], J. Legg[1], R. Williams[1], C. M. Johnston[1], P. Bland-Ward[1], J. S. de Bono[2], A. J. Pierce[1];
[1]Crescendo Biologics, Cambridge, United Kingdom, [2]Institute of Cancer Research, London, United Kingdom

INTRODUCTION: CD137 is a T and NK cell costimulatory receptor involved in consolidating immunological responses. The potent CD137 agonist urelumab has shown clinical promise as a cancer immunotherapeutic but development has been hampered by on-target off-tumour toxicities. A CD137 agonist targeted to the prostate-specific membrane antigen (PSMA), frequently and highly expressed on castration-resistant metastatic prostate cancer (mCRPC) tumour cells, could bring effective immunotherapy to this immunologically challenging to address disease.
EXPERIMENTAL PROCEDURES: We designed and manufactured CB307, a novel half-life extended bispecific costimulatory Humabody® V_H therapeutic to elicit CD137 agonism exclusively in a PSMA-high tumour microenvironment (TME). The functional activity of CB307 was assessed in cell-based assays and in syngeneic mouse anti-tumour pharmacology studies. Non-clinical toxicology and toxicokinetic properties of CB307 were assessed in a good laboratory practice (GLP) compliant study in cynomolgus macaques.
RESULTS: CB307 provides effective CD137 agonism in a PSMA-dependent manner, with anti-tumour activity both in vitro and in vivo, and additional activity when combined with checkpoint inhibitors. A validated novel PSMA/CD137 immunohistochemistry (IHC) assay demonstrated a higher prevalence of CD137-postive cells in the PSMA-expressing human mCRPC TME with respect to primary lesions. CB307 did not show substantial toxicity in non-human primates and exhibited a plasma half-life supporting weekly clinical administration.
CONCLUSIONS: CB307 is a first-in-class immunotherapeutic that triggers potent PSMA-dependent T cell activation thereby alleviating toxicological concerns against unrestricted CD137 agonism.

#5314 Improved breast cancer tumor control with addition of CD40 agonist and Flt3 ligand to pegylated liposomal doxorubicin is only partially mediated by CD8 T cells.

P. L. Mylabathula, S. Nooka, A. Alkhani, J. Zhu, A. Vu, R. Ali, V. Ramasamy Balasubramanian, I. Chan, **S. M. Reddy**;
UT Southwestern Medical Center, Dallas, TX

Background: There is a need for improved immunotherapy strategies beyond current FDA approved treatments for triple negative breast cancer. Defective antigen presentation has been shown to play a contributory role in deficient anti-tumor immunity in breast cancers. Flt3 ligand (Flt3L) is a growth factor that increases differentiation into DC1 dendritic cells. CD40 agonist (CD40a) activates all 3 classes of antigen presenting cells - DCs, B cells, and macrophages. Synergy with chemotherapy and CD40a has been seen in other cancers but not explored in breast cancers.

Methods: C57BL/6 mice (aged 6-8 weeks) were injected with 150,000 E0771 breast cancer cells within the mammary fat pad. Tumors were allowed to grow to a volume of ~50 mm^3 before randomization into treatment groups. Mice were treated with triplet therapy of pegylated liposomal doxorubicin (PLD) via tail vein followed by Flt3L intraperitoneal (IP) daily for 5 days and CD40a IP 1 week later as well as monotherapy and doublet therapy controls. Tumor growth and survival were monitored throughout the experiment. Tumors were harvested for single cell RNA sequencing (scRNAseq) and immunohistochemistry. To further study subset specific effects on efficacy of the immunotherapy, CD8 and CD4 T-cells were systemically depleted with anti-CD8 and anti-CD4 antibodies administered IP every 4 days starting 2 days before PLD treatment.

Results: Triplet therapy led to improved tumor control compared to no treatment, monotherapy, and doublet controls ($p<0.0001$). Increased tumor infiltration with CD8 T cells was observed with triplet therapy via immunohistochemistry. scRNAseq showed increased cDC1 subset with Flt3L treatment. Contrastingly, CD40a decreased DC subsets likely due to activation and emigration out of the tumor, remodeled macrophage populations, and decreased T regulatory cells. CD8 depletion led to faster tumor growth whereas CD4 depletion reduced tumor growth. Triplet therapy maintained efficacy over PLD with both CD8 and CD4 depletion but showed reduced magnitude of benefit with CD8 T cell depletion suggesting a partial CD8 mediated process. CD4 T cell depletion did not hinder triplet therapy efficacy compared to PLD but depletion further enhanced tumor control in combination with triplet therapy, with 20% (2/10) of animals achieving complete regression.

Conclusion: Triplet therapy with PLD, Flt3L, and CD40a improved tumor control and survival in syngeneic E0771 breast cancer mouse model. Added benefit of immunotherapy to PLD is partially CD8 T cell mediated. CD4 depletion further enhances tumor control in combination with triplet therapy. Experiments to explore the interactive effect of triplet therapy with other pertinent immune subsets are ongoing. A clinical trial with this combination in metastatic triple negative breast cancer patients is open and recruiting (NCT05029999).

#5315 Bispecific antibody discovery platform for IND enabling studies: Case study of HER-2/NKG2D bispecific antibody.

L. Ratcliffe, R. Pooley, K. Carr, H. Janbazacyabar, D. Cobeta Lopez, D. Bruce, S. L. Martin, M. Benson, J. White, B. Quist, S. Vermond, **G. Moiset**, S. Hill, R. Feldman, P. Wan, E. Oswald, F. Verkaar, M. Aspinall-O'Dea, J. Schueler, N. Jayanth;
Charles River Laboratories, Inc., Leiden, Netherlands

There has been a surge in the number of therapeutic antibody modalities primarily attributable to the increasing array of antibody engineering platforms. Among these, the emergent class of bispecific antibodies has exhibited remarkable potential compared to conventional monoclonal antibodies, marked by their targeting precision, expanded therapeutic scope, and personalized medicine prospects. Presently, eight bispecific antibodies are approved, with over 100 in varying clinical trial phases. Using a bispecific targeting HER-2 and NKG2D, we outline a comprehensive end-to-end platform for bispecific antibody discovery and characterization, designed to facilitate the progression of novel bispecific antibodies through the antibody discovery pipeline. To secure the most optimal binders tailored to specific targets, our methodology capitalizes on an extensive repertoire of phage display libraries. This strategy is instrumental in the identification of antibody candidates with exceptional binding affinity, broad cross-species compatibility, and enhanced drug-like properties. From the anti-HER2 chimeric antigen receptor ML39 and anti-NKG2D Fab KYK2.0, we synthesized four distinct bispecific formats by fusing single-chain variable fragments (scFv) to immunoglobulin G (IgG) molecules. These formats varied in terms of valency and scFv positioning, allowing us to assess their impact on antibody expression, binding kinetics, and functional efficacy. Subsequently, the bispecific antibodies underwent comprehensive in vitro efficacy and safety characterization, employing multiple innovative technologies. Utilizing a distinctive label-free approach with the xCELLigence system, we elucidated the kinetics of immune cell-mediated target cell killing upon antigen-antibody complex recognition in specific cancer cells. Safety assessments, with a focus on on-target/off-tumor effects, were conducted using the Retrogenix platform. Furthermore, cytokine profiling was utilized to evaluate potential risks associated with enhanced cytokine levels, reinforcing the specificity and safety profile of the bispecific antibody. Finally, pertinent in vivo models, including peripheral blood mononuclear cells (PBMC) and immune cell transfer models, facilitated the translation of preclinical bispecific antibody evaluations into clinically relevant contexts. This comprehensive platform for bispecific antibody discovery and functional characterization serves as a robust foundation for supporting Investigational New Drug (IND) applications, thus facilitating the transition of novel bispecific antibodies from the pre-clinical to the clinical phase of the drug discovery process.

#5316 SM2256: A bispecific conditional CD40 and 4-1BB dual agonist for enhanced solid tumor immune response.

W. Song, S. Yang, Y. Wei, S. Lu, H. Geng, X. Liu, H. Zhou, S. Xie, X. Zhang, S. Zhou, **Y. Liang**;
Beijing StarMab BioMed Technology, Ltd., Beijing, China

Background: Monoclonal antibodies targeting the co-stimulatory receptors CD137 (4-1BB) and CD40 have displayed encouraging activity against a wide range of solid tumors in preclinical animal models. However, their clinical development as monotherapy has been hindered by dose-related liver toxicity, leading to limited efficacy at safe doses. To address this challenge and bolster tumor-specific immunity by orchestrating the interaction between dendritic cells (DCs) and cytotoxic T cells, we introduce SM2256 - a bispecific conditional CD40 and 4-1BB dual agonist. SM2256 physically bridges DCs and T cells, enhancing T cell priming and reactivation. In preclinical animal studies, SM2256 exhibited both excellent tolerability and potent anti-tumor activity.
Methods: SM2256 was engineered by fusing high-affinity, non-ligand-blocking VHH domains targeting 4-1BB and CD40 to a silenced IgG1 Fc backbone. This fusion resulted in a tetravalent bispecific antibody capable of conditionally activating CD40 and 4-1BB upon mutual receptor binding. We assessed the binding specificity and affinity of SM2256 to human CD40 and 4-1BB using ELISA and flow cytometry. The target-dependent activation of CD40 and 4-1BB was confirmed via reporter assays and co-culture systems using primary DCs and T cells. In vivo safety and anti-tumor efficacy were evaluated in a syngeneic transplantation model using the MC38 cancer cell line in B-h41BB/B-hCD40 double humanized mice.
Results: SM2256 exhibited sub-nanomolar binding affinity to recombinant human and cynomolgus monkey CD40 and 4-1BB, activating 4-1BB-NFκB-luc and CD40-NFκB-luc reporter cell lines at picomolar concentrations in a strictly target-dependent manner. Furthermore, SM2256 physically facilitated the interaction between DCs and T cells, leading to increased expression of DC co-stimulatory ligands and elevated secretion of cytokines by T cells in mixed lymphocyte cultures. In a syngeneic tumor transplantation model, SM2256 significantly restrained the growth of MC38 tumors in B-h41BB/B-hCD40 double humanized mice.
Conclusions: SM2256 is a novel conditional CD40 and 4-1BB dual agonist that demonstrates promising preclinical efficacy against solid tumors while boasting an improved safety profile when compared to existing monoclonal antibodies.

#5318 SM2275, A tetraspecific, dual EGFR and PD-L1-targeting, conditionally activating co-stimulatory CD28 and simultaneously blocking PD-1/PD-L1 signaling to promoting fully activated T cell killing effects on tumor cells.

S. Lu, X. Liu, S. Zhou, W. Song, H. Geng, S. Yang, H. Zhou, S. Xie, Y. Wei, X. Zhang, **Y. Liang**;
Beijing StarMab BioMed Technology, Ltd., Beijing, China

Background: T cells require both signal 1 TCR engagement and signal 2 co-stimulatory signal to achieve complete activation and tumor recognition. CD28 is a signal 2 co-stimulatory receptor and activating CD28 increases T cell sensitivity, cytokine production and T cell survival. PD-1/PD-L1 signaling attenuates the T cells functional activity by inhibiting CD28 co-stimulation in the presence of TCR stimulation. Therefore, we developed SM2275, a tetraspecific VHH antibody against EGFR, PD-L1, CD28 and HSA, for the treatment of EGFR+/PD-L1+ solid tumors. Preclinical study demonstrated promising efficacy and favorable safety profile via a unique mechanism of action.
Methods: SM2275 was developed using StarMab's proprietary Quadbody multifunctional VHH antibody platform. It features two monovalent, low-affinity binding domains for EGFR and PD-L1, along with nanomolar low affinity CD28 binding domains arranged in a tandem format, followed by a half-life extending HSA binding domain. Differential binding affinities of SM2275 to EGFR/PD-L1 single-expressing versus double-expressing cell lines were analyzed by flow cytometry. Avidity-enhanced blockade of PD-1 on EGFR+PD-L1+ double-positive compared to PD-L1+ single-positive cells was analyzed via competitive binding assay and Jurkat PD1 NFAT Luciferase reporter assay. EGFR/PD-L1 dual-target-dependent CD28 activation was confirmed using a primary human T cell IL2 & IFN-γ release assay in the presence of TCR stimulation. In vivo efficacy against EGFR+/PD-L1+ double-positive human tumors were evaluated using a syngeneic tumor transplantation model of MC38-hEGFR/hPDL1 cell line into hPD-L1/hCD28 humanized mice.
Results: SM2275 displays dramatically increased affinity for cancer cells co-expressing EGFR/PD-L1 compared to single-expressing cells. This leads to an avidity-enhanced PD-L1 blockade specifically on the surface of EGFR+PD-L1+ double-positive cancer cells, enabling localized reactivation of tumor-infiltrating T cells without systemic immune toxicity. Simultaneously blocking the PD-L1 signaling unleashed the inhibition of CD28 co-stimulation for the full T cell activation. In the presence of SM2275, EGFR /PD-L1 double-positive cancer cells induce significantly enhanced CD28 activation and cytokine secretion compared to single-antigen-expressing cells. In a syngeneic tumor transplantation model, SM2275 effectively inhibits the growth of MC38-hEGFR/hPDL1 tumors in hPD-L1-hCD28 humanized mice, with no apparent cytokine release and immune toxicity.
Conclusions: SM2275 is a novel dual-EGFR & PD-L1-targeting, conditional CD28 agonistic antibody. It demonstrated promising efficacy and favorable safety profile in preclinical studies via a unique mechanism of action.

IMMUNOLOGY: Inflammation in Tumor Initiation and Progression
Poster Session

#5321 Chronic use of tobacco products promotes breast cancer progression through α7 nAChR/STING pathway activation.
S. Mugisha, S. Baba, S. Labhsetwar, R. Klemke, J. Desgrosellier;
University of California San Diego - UCSD, San Diego, CA

Tobacco-use is associated with an increased risk of developing aggressive breast cancer, however the cause remains unclear. While there is a dose-dependent decrease of patients' overall survival due to tobacco-use, the risk persists even after cessation. Here we show that chronic treatment with of breast cancer cells with low-dose nicotine significantly increases tumorsphere formation, self-renewal and tumor growth, while the acute treatment has little effect. Interestingly, these outcomes were noted even weeks after nicotine treatment was stopped. Mechanistically, this was attributed to α7 nAChR, previously described as an essential regulator of inflammation. In fact, α7 nAChR knock-out prevented activation of the STING antiviral pathway by reducing the nicotine-induced mRNA expression of STING, CCL5, CXCL10 and STAT3. Overall, these findings highlight long-term impact of nicotine on cancer progression through α7 nAChR/STING pathway. This may inform new biomarkers for diagnosis and potential new treatment strategies to combat tobacco-related breast cancers.

#5322 Discovery of CRD1601, a potent and selective HPK1 inhibitor with robust *in vivo* anti-cancer activity.

M. Banerjee[1], R. Shrivastava[1], D. Pryde[2], S. Middya[1], S. Debnath[1], A. Middya[1], D. Yadav[1], N. Rawat[1], R. Ghosh[1], M. Padaliya[1], S. Basu[1], A. Surya[1];
[1]Curadev Pharma, Noida, India, [2]Curadev Pharma, Sandwich, United Kingdom

Background: Haematopoietic Progenitor Kinase (HPK-1, MAP4K1) is a member of the STE20 family of serine/threonine kinases, expressed predominantly in hematopoietic cells. HPK-1 functions as a negative regulator of T-cell and B-cell receptor activation by triggering proteasomal degradation and disrupting signalosome complexes downstream of TCR and BCR. HPK1 inhibition is a novel IO strategy that could combine with existing chemotherapies and immunotherapies.
Methods: Curadev used a pharmacophore based approach to discover novel small molecule HPK-1 inhibitors using in vitro enzymatic and phenotypic cellular screens using primary cells. CRD1601, the clinical candidate was selected based on its ability to enhance human T-cell proliferation through the induction of IL2 and IFNγ. Syngeneic tumor models were used to assess anti-tumor activity of selected compounds as a monotherapy or combination therapy.
Results: CRD1601 is a potent HPK1 inhibitor with a single digit nanomolar IC50 value in enzymatic assay and potent cellular activity in the SLP76 assay. A single dose of CRD1601 in mice treated with an anti-CD3 antibody caused systemic enhancement of pro-inflammatory cytokines such as IL2, IFN gamma and reduced pSLP76 levels in the spleen. Further, CRD1601 reversed the immunosuppressive effect of PGE2 and NECA. CRD1601 demonstrated significant single agent activity in murine tumor models while also synergizing with chemotherapy and immunotherapy.
Conclusions: Inhibition of HPK-1 is a promising therapeutic modality that could augment the effects of existing anti-cancer treatments including immunotherapy. CRD1601 is a potent and selective HPK-1 inhibitor with favorable drug like properties that has been selected from a rich portfolio of active compounds and shows promising in vivo activity in tumor models.

#5323 Inflammation drives lineage plasticity and a club cell-like phenotype in prostate epithelial cells.

M. Hess[1], H. Song[2], J. Hicks[1], L. Mummert[1], A. De Marzo[1], F. W. Huang[2], K. Sfanos[1];
[1]Johns Hopkins University School of Medicine, Baltimore, MD, [2]University of California, San Francisco, San Francisco, CA

Background: Club cells are a type of bronchiolar epithelial cell that serve a protective and antimicrobial function in the lung. An epithelial cell population in adult human prostates was recently identified as sharing a similar transcriptomic profile and morphology to lung club cells. Club-like epithelial cells were identified in the prostatic urethra, collecting ducts, and rarely in the peripheral zone of normal organ donor prostates. However, we recently reported that cells expressing club cell markers (*CP, LTF, MMP7, PIGR, SCGB1A1*) are present in the peripheral zone of radical prostatectomy specimens. Here, expression of club cell markers was restricted to luminal epithelial cells in an inflammation-associated lesion termed proliferative inflammatory atrophy (PIA). We also demonstrated that these club-like cells within PIA express the same markers as intermediate cells, a proposed prostate cancer progenitor cell. We now aim to identify exogenous factors that drive the club cell phenotype *in vitro*. Our ultimate goal is to understand how club cell gene expression affects the oncogenic and metastatic potential of prostate epithelial cells.
Methods: We characterized the expression of club cell genes in prostate cell lines (LNCaP, PREC, and PREC-AR-Myc) following exposure to inflammatory stimuli (TNFα, hydrogen peroxide, uropathogenic *Escherichia coli*) *in vitro*. We performed quantitative reverse transcription PCR (RT-qPCR) to measure expression of club cell markers (*LTF, MMP7, PIGR*) and intermediate cell markers (*AR, NKX3.1, SMOX*). Additionally, we used chromogenic RNA *in situ* hybridization (RISH) to visualize *LTF*, *MMP7*, and *PIGR* expression following exposure to inflammatory stimuli.
Results: We report that TNFα exposure *in vitro* increased expression of club cell genes (*LTF, MMP7, PIGR*). Surprisingly, TNFα exposure induced *LTF* expression in LNCaP cells, despite prior findings that *LTF* is silenced by CpG island hypermethylation in prostate cancer and in LNCaP cells. This finding was confirmed by both RT-qPCR and RISH. Additionally, we found that TNFα exposure altered intermediate cell markers (*AR, NKX3.1, SMOX*) expression consistent with the previously reported gene expression pattern of luminal epithelial cells in PIA.
Conclusions: Overall, our results suggest that TNFα-mediated signaling drives the expression of club cell markers associated with lineage plasticity. Our next step will be to analyze inflammation-driven alterations to methylation and chromatin accessibility around loci associated with club cell genes, proton-oncogenes, and tumor suppressor genes.

#5324 Key antiviral response genes mediate the impact of chromosomal instability on breast cancer stemness.

S. A. Baba, S. Mugisha, S. Iabhsetwar, R. klemke, J. Desgrosellier;
University of California San Diego - UCSD, San Diego, CA

Chromosomal instability (CIN) is a recognized hallmark of cancer, pivotal in tumor evolution and metastasis. Our research unveils CIN as a stress during tumor initiation, uniquely tolerated by activated breast cancer stem cells (aCSCs). Elevated CIN, specific to tumors from aCSCs, contrasts with baseline levels akin to non-stem cell types. This transient increase in CIN, observed in low burden aCSC tumors, diminishes in established disease, suggesting a dynamic induction during initiation. Consist wit this we have observed increase in CIN tolerance in stem-like vs basal-like cells suggesting heterogeneity in response. CIN triggers a specific response, activating proinflammatory cancer autonomous immune signaling. We identified several CIN-induced proinflammatory stem cell-specific genes from our overlap studies. Knockdown assays targeting RSAD2 and PLAU showed a significant decrease in tumorsphere properties, emphasizing their functional relevance for cancer progression. AXL did not show any effect on tumorsphere but was important to tolerate CIN induced due to reversine. Mechanistically, AXL expression was induced by c-Jun stress signaling activation in aCSCs. These antiviral CIN-induced proinflammatory markers, emerge as a vital player in breast cancer progression. This study establishes a foundation for investigating antiviral genes as crucial contributors to cancer.

#5325 Cytokine CCL9, new downstream target of oncogene Kras to modulate acinar-to-ductal metaplasia during pancreatic cancer initiation.

Geou-Yarh (Stancy) Liou[1], Justin K. Messex[2], Crystal J. Byrd[3]

[1]Center for Cancer Research & Therapeutic Development; Biological Sciences, Clark Atlanta University, Atlanta, GA,[2]Center for Cancer Research & Therapeutic Development, Clark Atlanta University, Atlanta, GA,[3]Biological Sciences, Clark Atlanta University, Atlanta, GA

Pancreatic ductal adenocarcinoma (PDAC) is one of the most lethal types of cancer with a current five-year survival rate at 12% in the US, and is dominated by oncogenic Kras mutations. Accumulating evidence showed that PDAC can be originated from acinar-to-ductal metaplasia (ADM). In this process, pancreatic acini harboring oncogenic Kras mutations are transdifferentiated to a duct-like phenotype that further progresses to become pancreatic intraepithelial neoplasia (PanIN) lesions, giving rise to PDAC. Although ADM formation is commonly observed in $Kras^{G12D}$ transgenic mouse models of PDAC, the exact mechanisms of how oncogenic $Kras^{G12D}$ modulates this process remain unclear. Here, we unveil a new downstream target of oncogenic Kras, cytokine CCL9 during ADM formation. Either exogenously treating primary pancreatic acini with recombinant CCL9 or ectopically expressing CCL9 in primary pancreatic acini resulted in ADM formation in a 3D organoid culture system. Furthermore, knockdown of CCL9 in $Kras^{G12D}$-expressed acini reduced $Kras^{G12D}$-induced ADM. Higher levels of reactive oxygen species (ROS) were detected in the $Kras^{G12D}$-expressed pancreatic acini, and knockdown of CCL9 in these acini decreased ROS levels. Overexpression of CCL9 in primary pancreatic acini elevated cellular ROS of pancreatic acinar cells. Furthermore, depletion of ROS in 3D organoid culture of CCL9-expressed acini reduced CCL9-induced ADM formation. In transgenic mice of $p48^{cre}$;$Kras^{G12D}$, blockade of CCL9 through its specific neutralizing antibody attenuated ADM formation as well as PanIN structures. Altogether, our results indicated oncogenic $Kras^{G12D}$ initiates PDAC through a new downstream target molecule, CCL9, to enhance ROS levels of pancreatic acinar cells.

#5326 Selective deletion of estrogen receptor β in lung epithelium suppresses K-ras mutant lung tumorigenesis.

M. J. Clowers[1], A. L. Thompson[2], C. I. Rodriguez Reyna[1], S. Deng[1], S. Moghaddam[1];
[1]UT MD Anderson Cancer Center, Houston, TX, [2]Mississippi State University, Starkville, MS

Although lung cancer is the most prolific cause of global cancer-related deaths, outcomes by sex have gained traction as a means to stratify patients and tailor therapies accordingly. In recent years, females have begun to shoulder a greater burden of lung cancer diagnoses, specifically within the lung adenocarcinoma (LUAD) subtype; conversely, mortality is worsened for males. However, other sex-dependent effects in lung cancer are harder to predict. For example, hormone replacement therapy for post-menopausal women has been shown to predict better survival in some cohorts while auguring worse outcomes in others. Similar controversy exists regarding menopausal status, gender affirming care, and castration/oophorectomy status. However, there is consensus that these differential effects relate to a patient's sex hormone composition. Estrogen, a sex hormone abounding in females, boasts well-described pro-tumor signaling in breast cancer. Unfortunately, its role in lung cancer remains elusive. Estrogen is reported to exert inflammatory properties in the lung environment, to drive immune function, and to induce proliferation of lung cancer cells. This functional antagonism has led to questions about how these compartment-specific effects are balanced. In the lung, estrogen signaling occurs mainly via estrogen receptor beta (ERβ), a nuclear hormone receptor highly expressed in lung tissue and lung tumors. ERβ is understudied relative to its sibling ERα, a well-known oncogene in breast cancer. While it is tempting to analogize ERα oncogene function to ERβ, the literature lacks consensus on the role of ERβ in lung cancer, with some authors classifying it as an oncogene and others as a tumor suppressor. In LUAD, Kras mutations encompass a quarter of driver mutations, and interaction of Kras with ERβ is understudied. Here, we tested the effects of genetic ablation of ERβ in a murine model of Kras mutant LUAD (KM-LUAD) termed $CCSP^{Cre}$/LSL-$Kras^{G12D}$ (CC-LR). Esr2 floxed mice were crossed with CC-LR mice to create a lung epithelial-specific conditional knockout of ERβ (LR/$Esr2^{\Delta/\Delta}$). LR/$Esr2^{\Delta/\Delta}$ mice show significant decrease in tumor burden and total lung immune infiltration, indicating reduced tumor development and tumor-promoting inflammation. Of note, this effect manifests regardless of sex. RNA and protein-level analysis further suggest that ERβ deletion alters the balance of inflammatory transcription factors, resulting in skewing from STAT3- to NF-κB-driven inflammation and a net anti-tumor response. These data suggest that ERβ offers a promising early target in nascent KM-LUAD tumors with therapeutic intervention possible regardless of sex-specific effects. Acknowledgement: supported by NIH/NCI grant awarded to Seyed Javad Moghaddam (R01 CA225977); Michael J Clowers partly supported by NIH/NCI (F31 CA261121); Annamarie L Thompson supported by CPRIT Research Training Award (RP210028).

#5327 Interleukin-1 upregulates dual oxidase 2 expression and ROS production in human pancreatic cancer cells.

David J. Mallick[1], Yongzhong Wu[2], Mariam M. Konate[1], Becky Diebold[2], Smitha Antony[1], Jennifer L. Meitzler[2], Guojian Jiang[2], Jiamo Lu[2], Krishnendu Roy[1], James H. Doroshow[1]

[1]Division of Cancer Treatment and Diagnosis, National Cancer Institute, Bethesda, MD,[2]Developmental Therapeutics Branch, National Cancer Institute, Bethesda, MD

Chronic pancreatitis increases the risk of developing pancreatic ductal adenocarcinoma (PDAC) and is associated with enhanced expression of the NADPH oxidase (NOX) isoform dual oxidase 2 (DUOX2). Interleukin-1 (IL-1) is a major upstream pro-inflammatory cytokine secreted by malignant or microenvironmental cells that supports pancreatic inflammation, tumorigenesis, invasiveness, and tumor heterogeneity. Previously, our laboratory demonstrated that the expression of DUOX2, one of seven NADPH oxidase (NOX) family members, is significantly enhanced by a wide variety of pro-inflammatory cytokines, and that DUOX2-related ROS production may contribute to the development of an oxidative, pro-angiogenic microenvironment in PDAC. In the current studies, we have shown that DUOX2 is upregulated and expressed along with its maturation factor, DUOXA2, in several human pancreatic cancer cell lines following exposure to both IL-1α and IL-1ß, two major agonists of IL-1 signaling. Administration of the anti-inflammatory antibody anakinra (an IL-1R1 antagonist) either in conjunction with or after prolonged treatment with IL-1 *in vitro* ablated induction of DUOX2/DUOXA2 and of IL-8 (CXCL8), a chemokine essential for neutrophil recruitment and a potent promoter of angiogenesis. Increased expression of other NOX family members following IL-1 exposure was not observed. Using CRISPR/Cas9-mediated DUOX2 knockout models, we report that DUOX2 is the major contributor to IL-1-mediated ROS production in PDAC cells. In a panel of PDAC lines, siRNA knockdown of proximal IL-1 signaling nodes, such as MYD88, significantly decreased expression of DUOX2/DUOXA2 and of CXCL8. However, knockdown of IRAK1 or IRAK4, two critical signaling kinases downstream of MYD88, as well as known downstream mediators of IL-1-related transcription (such as NF-κB, STAT1, MEK/ERK), did not affect IL-1-induced DUOX2/DUOXA2 upregulation, suggesting that alternative pathways of IL-1 signaling might be involved in the enhancement of DUOX2 expression by the cytokine. Because IL-1 signaling is known to affect various acetylation/methylation events in epithelial cells, we evaluated the effect of administering the histone acetyltransferase (HAT) inhibitor A-485 with IL-1; we found that A-485 significantly diminished cytokine-induced DUOX2/DUOXA2 upregulation; however, CXCL8 induction was unchanged. These studies suggest that epigenetic modulation of PDAC cells by IL-1 could contribute to DUOX2-induced ROS production and ROS-related inflammatory stress in the PDAC microenvironment.

#5328 Dual role of Kupffer cell secreted CXCL5 in hepatocellular carcinoma.

T. Tu, H. Hong, L. He, M. Alba, T. Qi, C. T. Okamoto, B. L. Stiles;
USC - University of Southern California, Los Angeles, CA

Hepatocellular carcinoma (HCC) is hallmarked by inflammatory cell infiltration. Chemokines secreted during inflammation are crucial at directing immune cell infiltration during cancer development. We screened patient dataset from different etiologies including HBV, HCV, alcohol and non-alcoholic steatohepatitis (NASH) and identified CXCL5 as the only chemokine consistently upregulated in HCC. Immunohistochemistry (IHC) of patient liver tumor tissues further showed the production of CXCL5 by tumor surrounding non parenchymal cells. Using a mouse model ($Pte^{loxP/loxP}$; Alb-$Cre^{\pm}$, *Pten* null) which recapitulates human liver disease progression from non-alcoholic fatty liver disease (NAFLD) to NASH to liver cancer, we found that CXCL5 was expression was gradually increased during disease progression. Further analysis using IHC and flow cytometry analysis showed that CXCL5 is predominantly expressed by Kupffer cells in *Pten* null livers bearing tumors. Furthermore, we found that LPS stimulated the expression and secretion of CXCL5 in Kupffer cells, but not other macrophages including peritoneal macrophage and macrophage cell line Raw264.7 cells. We hypothesized that the Kupffer cell-secreted CXCL5 in response to LPS promotes tumor progression by promoting HCC cell proliferation and regulating HCC associated immune cell infiltration. To investigate whether CXCL5 increases tumor cell proliferation, we treated wild type and *Pten* null hepatocytes with various concentrations of CXCL5. Our results showed that CXCL5 increased hepatocytes viability in a dose dependent manner. BrdU incorporation assay further confirmed that CXCL5 treatments induces HCC cell proliferation through its receptor CXCR2. We further demonstrated that CXCR2 knockdown led to reduced xenograft tumor growth using HepG2 cells. Additionally, we injected *Pten* null mice with CXCR2 inhibitor to block CXCL5 signal and observed partial response. We analyzed the immune cell profile of the responder mice vs. non-responder mice and showed that tumor inhibition is correlated with T cell infiltration. To test whether Kupffer cells regulate T cells through CXCL5, we isolated primary Kupffer cells from murine livers. We performed transwell migration assay using immune cells from murine spleens. Our results indicate that LPS stimulation in Kupffer cells reduced the ratio of migrated CD4+ T cells, while blocking CXCL5 using a CXCL5 antibody significantly increased $CD4^{\pm}$ T cell recruitment to the LPS-stimulated Kupffer cells and moderately decreased neutrophil recruitment. Consistently, we found that recombinant CXCL5 protein reduces $CD4^{\pm}$ T cell migration independent of neutrophils. In summary, our study suggests that Kupffer cell secreted CXCL5 reduces liver $CD4^{\pm}$ T cell recruitment and increases liver cancer cell proliferation.

#5329 Ovarian cancer predisposes neutrophils to form neutrophil extracellular traps(NETs).

G. Yamamoto, M. Kawano, M. Bun, K. Shimura, A. Toda, K. Nakamura, Y. Kinose, M. Kodama, K. Hashimoto, K. Sawada, T. Kimura;
Osaka University, Osaka, Japan

Objective: Neutrophil extracellular trap (NETs) are neutrophil-derived extracellular DNA released in response to inflammation. In contrast to their primary host-defensive role, NETs have been recently reported to promote cancer progression. The aim of this study is to investigate the role of NETs in ovarian cancer progression.
Method: The clinical data of ovarian cancer patients who underwent primary surgery at Osaka University Medical Hospital were retrospectively reviewed (n=340). The relationship between neutrophilia, peritoneal dissemination and prognosis were analyzed. Prior to initial treatment, peripheral blood was obtained from newly diagnosed ovarian cancer patients and examined for CBC and granulocyte-colony stimulating factor (G-CSF) concentration by ELISA. To evaluate NETs formation capacity, isolated neutrophils were stimulated with G-CSF and incubated in vitro to monitor NETs formation. The ascites was collected at the initial surgery and assessed for G-CSF concentration and for neutrophils population using flow cytometry. The omental tissues were pathologically examined for NETs using H&E-staining and immunostaining with anti-Citrullinated Histon3 (CitH3) antibody. To test NETs induction capacity, we treated human peripheral blood neutrophils with the conditioned media from 20 ovarian cancer cell lines and the serum from ovarian cancer patients. Then human ovarian cancer OVCAR8 cells were co-cultured with NETs to evaluate the effect of NETs on cancer cell adhesion.
Results: Neutrophilia (neutrophils>7000/μl) was found in 39 patients (39/340,11.5%). Patients with neutrophilia were associated with advanced disease accompanied by peritoneal dissemination and compromised survival compared to patients without neutrophilia (5-year PFS 40.0 vs 59.9 %, p 0.0027). In these patients, serum G-CSF was upregulated. Neutrophils from ovarian cancer patients formed NETs significantly earlier than those from benign tumor patients. Ovarian cancer patients with neutrophilia showed elevated G-CSF concentration and increased neutrophils proportion in their ascites. Omental tissues from patients with neutrophilia showed NETs foci close to the disseminated lesions. G-CSF strongly induced neutrophils to form NETs in vitro, which was observed in some conditioned media from ovarian cancer cell lines and serum from ovarian cancer patients as well. The adhesion of ovarian cancer cell was increased by co-incubation with NETs.
Conclusion: Neutrophilia is associated with peritoneal dissemination and poor prognosis in ovarian cancer. One of the underlying mechanism of neutrophilia is upregulated G-CSF, which stimulate neutrophils to form NETs. NETs may have a causative effect on ovarian cancer dissemination.

#5330 Intestine-specific homeobox edits macrophage polarization in the disease microenvironment by activating inflammasome activity.

L.-T. Wang[1], S.-H. Hsu[2];

[1]National Taiwan Normal University, Taipei, Taiwan, [2]Kaohsiung Medical University, Kaohsiung, Taiwan

Inflammasome activity has a pivotal role in the innate immune system, highlighting its importance in the development of various inflammatory diseases, including cancers. However, the specific impact of inflammasome-produced cytokines from tumor cells on disease progression remains uncertain. In this study, we show that the expression levels of inflammasome-related genes (NLRP1 and NLRP3), combined with levels of the intestine-specific homeobox (ISX), significantly correlate with factors like lesion count, disease stage, and lymph vascular invasion. Tumor cells enhance the secretion of key cytokines such as IL-1β and IL-18, exacerbating disease progression via the ISX-TWIST1 complex. In terms of mechanism, transcriptomic analysis and molecular evidence reveal that ISX interacts with the basic helix-loop-helix (bHLH) domain of TWIST1 through its homeobox domain. This interaction forms a transcriptional complex that activates inflammasomes by directly binding to the conserved sequence "-GGDWYR-" in promoter regions of several NF-κB and inflammasome-related genes (NFKBs, RELs, NLRP1, NLRP3, NEK7, AIM2, and ASC). Elevated levels of IL-18, induced by active inflammasomes, lead to the shift of M0 macrophages into the M2-like phenotype within the hepatic microenvironment. In mice with liver-specific ISX mutations, inflammasome-related genes and activities were eliminated, stopping disease progression in an acute hepatic disease model. These findings underscore the critical role of the ISX-TWIST1 complex in liver disease and tumor progression on both mechanistic and clinical levels. They also offer new insights for potential preventive and therapeutic targets in liver disease.

#5331 Spatial resolution of immune cell lineages in the tumor microenvironment of plasma cell dyscrasias.

M. A. Dillon[1], L. Arvidson[2], C. G. Phalen[1], J. R. Ishibashi[1], J. B. Johanneson[1], Z. J. Thomson[1], P. A. Zhao[1], J. Malone[1], M. S. Kopp[1], M. Norton[2], G. Spang[2], S. A. Ludmann[1], A. K. Savage[1], C. E. Gustafson[1], M. Glass[1], E. L. Kuan[1], T. Peng[1], L. T. Graybuck[1], X.-j. Li[1], T. R. Torgerson[1], P. J. Skene[1], A. W. Goldrath[1], S. Jensen[2], S. Anover-Sombke[1], **M. L. Angus-Hill**[1];

[1]Allen Institute for Immunology, Seattle, WA, [2]Cell Signaling Technology, Danvers, MA

Plasma cell dyscrasias (PCDs) are diseases of the hematologic system, with Multiple Myeloma as the most common disease. Less common PCDs include primary and secondary extramedullary plasmacytomas (EMP), which occur in soft tissues. EMPs are typically solitary and infrequent, often localized in the upper aerodigestive and gastrointestinal tracts, lung, and lymph nodes among other organs, and can convert to Multiple Myeloma. Secondary extramedullary plasmacytomas are often noted in advanced disease following multiple rounds of therapy and are commonly associated with poor prognosis. Studies aimed at gaining a better understanding of soft tissue EMPs, whether solitary plasmacytomas with undiagnosed multiple myeloma or in the context of recurrent or metastatic EMP disease, are limited. In this study, we employ a comprehensive approach using multiple modalities, including dissociated CITE-seq, spatial transcriptomics, and multiplexed spatial immuno-fluorescence imaging to interrogate the tumor and immune landscape in EMP disease. Importantly, the use of the same biomarker antibodies across these modalities provides a cross-data-framework for a deep contextual understanding of the immune and tumor cell organization and cell-to-cell signaling in EMP. Ultimately, this study provides new insights into patient-to-patient and tumor location variability, tumor and immune cell microenvironment heterogeneity, and possible future therapeutic strategies for EMP.

#5332 ST316, a clinical peptide antagonist of beta-catenin, induces anti-tumor immune responses by multiple mechanisms of action.

C. Scuoppo, K. Mendelson, R. Ramirez, M. Koester, J. Diehl, E. Gallagher, S. Leong, J. Gonzales, Z. Mattes, L. Ghamsari, G. Merutka, B. J. Kappel, A. Vainstein-Haras, J. A. Rotolo;
Sapience Therapeutics, Inc., Tarrytown, NY

Wnt/β-catenin plays several important roles in cancer, including driving oncogenesis via cell proliferation, survival and metabolic reprogramming of cancer cells, and enhancing immune-desertification of the tumor immune microenvironment (TIME). ST316 is a clinical stage cell-penetrating peptide antagonist of the interaction of β-catenin with its co-activator BCL9, selectively impairing a subset of Wnt target genes and demonstrating potent anti-tumor activity against Wnt-driven tumors in vivo. ST316 is currently being evaluated in a Phase 1-2 study (NCT05848739) enrolling patients with selected advanced solid tumors likely to harbor abnormalities of the Wnt/β-catenin signaling pathway. Here we explore the potential of ST316 to activate the TIME and provide data to support combination treatment with anti-PD-1 and anti-TIGIT therapies. Macrophages derived from human peripheral blood mononuclear cells (hPBMCs) were activated by LPS and IFNγ (M1) or IL-4 (M2) in the presence of ST316 or control and were immunophenotyped by expression of CD80 and CD163 to assess M1 and M2 macrophages, respectively. ST316 induced marked repolarization of hPBMC-derived M2 macrophages to the M1 identity in vitro, as shown by increased CD80 and decreased CD163 staining. Increasing concentration of ST316 in co-cultures of M2 cells with CD8+ T cells induced up to a three-fold increase in IFN-γ expressing cells relative to controls. Additionally, ST316 exposure increased CD155/PVR expression on 4T1 Triple Negative Breast Cancer (TNBC) cells, but not MV411 TNBC that are not Wnt-dependent. When combined with anti-TIGIT treatment, ST316 led to increased T cell activation in an ex vivo assay where 4T1 cells were co-incubated with syngeneic splenic CD8+ cells and frequency of IFN-γ producing cells was assessed. In in vivo experiments, Balb/C mice bearing syngeneic 4T1 TNBC orthotopic tumors were treated with vehicle, ST316, anti-PD-1 or combination. Sub-pharmacologic ST316 enhanced anti-PD-1 suppression of 4T1 tumor growth and induced a substantial decrease of the M2 marker CD209 (DC-SIGN) in the Tumor Associated Macrophage (TAMs). These data support two novel mechanisms of action for the β-catenin antagonist peptide ST316. First, ST316 exposure results in macrophage repolarization towards an immune-active M1 program, both in vitro and in vivo, and increases T-cell activation in co-culture assays. Second, ST316 induced CD155/PVR upregulation and T-cell activation in the presence of anti-TIGIT antibody. Collectively these results suggest a novel immune-modulatory role for ST316 in the TIME and provide rational for combination therapy with checkpoint inhibitors.

#5333 NeoMab: A novel platform for fully human therapeutic antibody development.

M. Zhang, C. Ju, S. Li, J. Peng, J. Zhao, X. Gao;
Gempharmatech Co., Ltd., Nanjing, China

Antibodies and antibody containing therapeutics, such as multivalent antibodies, chimeric antigen receptors (CARs), and antibody directed conjugates (ADCs), have been proven to be highly prominent in cancer treatment. However, challenges such as immunogenicity stemming from non-human or unnatural sequences and limitations in preclinical animal study systems still impede the rapid development of antibody drugs.

To overcome these hurdles, GemPharmatech has created a novel antibody gene humanized model, the NeoMab mouse, to develop fully human antibodies. The NeoMab model was established via large genomic fragment knock-in technology, retaining native mouse constant region encoding genes and regulatory elements, while incorporating human variable gene repertoires into the endogenous loci. Developed in the BALB/c background, the NeoMab mouse carries fully functional MHC molecules, potentially enhancing antigen presentation. These mice sustain a competent immune system with a B cell development and maturation pattern, immune cell profile, and serum immunoglobulin levels comparable to those of BALB/c mice.

NeoMab mice exhibit a robust humoral immune response, with a rapid increase in antigen-specific serum titers upon immunization using different antigens, such as recombined protein, plasmids, and overexpressing cell lines. Utilizing human V(D)J genes to encode immunoglobulins at a human-like frequency and diversity, antibodies derived from NeoMab mice demonstrate affinity and functional activity comparable to, or even surpassing, FDA-approved drugs.

In conclusion, the NeoMab mouse model in the BALB/c background has been rigorously validated to elicit a robust response to specific antigen immunization, producing antibodies with high affinity, diversity, and functional activity. GemPharmatech's extensive drug-target gene humanized mouse library (comprising over 800 targets) and diverse disease models in oncology and other fields facilitate a seamless connection between in vitro antibody screening and in vivo animal studies. The integration of NeoMab, target humanization animals, and disease models enables GemPharmatech to provide an integrated solution, reducing time and costs while elevating the quality of antibody discovery in the field.

#5334 Humanization of NOG mice and next-generation NOG strains to induce lineage-specific differentiation of immune cells for assessment of novel immune cell therapies, check point inhibitors, and immune cell engagers for translational immuno-oncology research.

M. Stecklum[1], L. Baskin[2], **J. Hoffmann**[1];
[1]EPO GmbH, Berlin, Germany, [2]Taconic Biosciences, Inc., Rensselaer, NY

Background: The preclinical evaluation of novel immune therapies requires humanized immune system (HIS) mouse models. In previous studies we have demonstrated that either peripheral blood mononuclear cells (PBMC), subsets of PBMCs like T and NK cells or CD34+ hematopoietic stem cells (HSC) can be used to establish a HIS model. With the development of next-generation NOG mice, lineage-specific differentiation of immune cell sub-populations of interest can be supported. Transplantation of cell line-derived (CDX) or patient-derived (PDX) tumor xenografts on HIS mice provides a full model for human tumors for the investigation of checkpoint inhibitors (CPI), as well as novel cell therapies and immune cell engagers.
Methods: HSC-humanized mice were generated by i.v. transplantation of CD34+ stem cells to immunodeficient mice. For humanization, NOG mice and next-generation NOG strains were used: NOG, NOG-EXL, hIL-2 NOG, hIL-6 NOG and FcResolv™ NOG mice were compared to each other for lineage-specific differentiation using single donors or a mixed HSC donor pool. Engraftment of immune cells was monitored by FACS analysis of blood every four weeks. In humanized NOG mice, CDX and PDX from different entities were s.c. transplanted and used to evaluate CPI.
Results: Humanized hIL-2 NOG mice showed significantly decreased survival after HSC transplantation in comparison to the other mouse strains and had to be sacrificed within the first 6-8 weeks after HSC transplantation. In the other mouse strains, transplanted HSCs engrafted and differentiated mainly into B and T cells. NOG-EXL mice displayed the highest engraftment, with up to 80% of human cells in the blood, including a higher portion of myeloid cells. In humanized hIL-6 NOG mice a higher portion of monocytes could be determined. FcResolv™ NOG mice lack murine Fc gamma receptors in order to reduce confounding interactions between residual murine immune cells and antibody-based therapies, and they engraft and differentiate human HSCs similarly to the parent NOG strain. In humanized NOG mice, selected CDX and PDX tumors successfully engrafted without significant differences in tumor growth compared to non-humanized mice. CPI treatments induced tumor growth delay in selected models.
Conclusions: Next-generation NOG mouse strains are characterized by a lineage-specific differentiation of immune cells depending on integrated human cytokines. Furthermore, we established a human tumor-immune-cell model for NOG mice using different entities of CDX or PDX in combination with CPI. Our human tumor-immune cell models allow preclinical translational studies on tumor immune biology as well as evaluation of new therapies, drug combinations and biomarker identification and validation.

#5335 Immune cell population variations in the livers of commonly used mouse strains.

Francisco J. Rodriguez-Matos, Patrick Huang, Rajiv Trehan, Benjamin Ruf, Chi Ma, Tim F. Greten

Thoracic and GI Malignancies Branch, NIH/NCI, Bethesda, MD

Previous studies have shown that the distribution of major immune cell populations differ across mouse strains in peripheral blood and hematopoietic organs at baseline. Additionally, variations in immune responses exist between mouse strains in *Leishmania spp.* and Melanoma models, but these studies in the context of liver diseases including Non Alcoholic Fatty Liver Disease (NAFLD) and Hepatocellular Carcinoma (HCC) have not been carried out. With the effort to state if these variations exist within the liver, we performed comprehensive spectral flow cytometry analysis on the liver and spleens of three female mouse strains commonly used in cancer research (BALB/c, C57BL/6, and FVBN). NAFLD was induced by providing mice with a methionine choline deficient diet. To promote HCC, a single genotype (myc/p53$^{+/-}$) was induced by administering transposon-based vectors to overexpress Myc-Luc and CRISPR/Cas-9 vectors to knock down p53 via hydrodynamic tail-vein injection. To confirm vector integration and monitor tumor growth (luciferase activity), in vivo imaging was performed at different time points. As a result, we confirm throughout this study that differences exist within immune cell populations of the liver and spleen at baseline. Moreover, we depict differences in the shift of immune cell populations across mouse strains in the pathologic states included. In NAFLD, there is an increase of dendritic cells (DCs), macrophages, NK cells, ILC1s, T regulatory cells (Tregs), T_H1, and T_H2, and a decrease of CD4+ T cells, B cells, γδ-T cells, and NKT cells in the liver across all mouse strains, when compared to controls. However, the population of neutrophils in BALB/c decreases, and the population of CD8+ T cells increases in C57BL/6 mice, which differs from the patterns of change seen in the other mouse strains. Moreover, in spleens, NAFLD promotes an increase of T_H1 and NK cells, and a decrease of T_H2 and NKT Cells across the mouse strains included in the study, whereas the patterns of change differ between mouse strains among the remaining immune cell types. When evaluating liver immune cell population shifts on our HCC model, BALB/c mice showed a decrease in macrophages and ILC1s, C57BL/6 mice showed a decrease in γδ-T cells, prominent shifts across Neutrophils, T_H1, and NKT cells, and null changes in T_H2 and CD4+ T cell shifts, and FVBN mice had a less prominent decrease of B cells, which differed from the shifts observed in the mouse strains used for comparison. Immune cell populations in the spleens of our HCC mouse model also presented with differences across the mouse strains studied. In conclusion, we highlight that key differences in immune profiles exist across commonly used mouse strains for cancer research in the presence of liver pathology including HCC, suggesting that mouse strains could be possible confounders in the study of immune oncology of HCC.

#5336 Establishment and characterization of a novel inducible *Apoc2* knockout mouse model to study the roles of Apoc2 in normal hematopoiesis.

X. Zhang, R. Chandwani, M. Pospiech, Y. Meng, K. Dhuri, B. Thakker, A. Ali, S. M. Kadam, Y.-C. Wei, H. Alachkar;
USC - University of Southern California, Los Angeles, CA

Apolipoprotein C2 (Apoc2) is upregulated in acute myeloid leukemia and presents a viable therapeutic target. Whether this gene plays a role in normal hematopoiesis remains unknown. To investigate the impact of targeting *Apoc2* on normal hematopoiesis, we established and characterized an inducible *Apoc2* knockout mouse model. Homozygous floxed *Apoc2* mice (*Apoc2*$^{fl/fl}$) were obtained from the NIH (Dr. Remaley's lab) and were crossed with homozygous R26-CreERT2 mice. After three generations, *Gt(ROSA)26Sor*$^{Cre/Cre}$, *Apoc2*$^{fl/fl}$ mice were generated and confirmed by genotyping. Male (M) and female (F) mice were injected with tamoxifen (TAM: 20mg/mL dissolved in corn oil) intraperitoneally (75mg/kg per day for 5 days) to induce *Apoc2* knockout (*Apoc2*-KO). The control wild type (WT) group included *Gt(ROSA)26Sor*$^{wt/wt}$, *Apoc2*$^{fl/fl}$ mice, and CD45.2^{+} WT mice injected with TAM, or *Gt(ROSA)26Sor*$^{Cre/Cre}$, *Apoc2*$^{fl/fl}$ mice injected with corn oil.No obvious abnormal phenotypes were observed in Apoc2-KO mice. The average increase of body weight 3 weeks post TAM or corn oil injections of 5-week-old *Gt(ROSA)26Sor*$^{Cre/Cre}$, *Apoc2*$^{fl/fl}$ siblings was not statistically significantly different (*Apoc2*-KO (n = 2M + 2F) vs WT (n = 2M + 2F) = 2.450g vs 2.125g, P = 0.63). Analyses of *Apoc2*-KO (n = 5M + 3F) and WT (n = 4M + 2F showed no significant difference in livers and spleens weight when normalized to mice age. The percentage of knockdown in liver (99.96%), spleen (77.32%), bone marrow (BM, 83.56%) and blood (82.02%) was confirmed by qPCR. In-vitro cell expansion was performed in the presence of thrombopoietin and stem cell factor for BM cells and IL-2 and PHA for T cells. *Apoc2*-KO BM cells exhibited similar in vitro expansion to that of control mice (*Apoc2*-KO vs WT: Day 10/ Day 6: 1.22 fold vs 1.57 fold; Day 10/Day 1: 57.26% vs 72.34%; P > 0.05; and Cell Trace assay: mean fluorescence intensity (MFI) of Day 9 normalized to Day1: *Apoc2*-KO vs WT = 0.37 vs 0.39; P > 0.05). Also, the colony forming ability was not significantly different between *Apoc2*-KO and WT BM cells (*Apoc2*-KO vs WT = 79.09 units vs 81.47 units, P = 0.62). In-vitro T cell expansions of splenocytes were not significantly different between *Apoc2*-KO and WT mice (*Apoc2*-KO vs WT: Day 10/ Day 4: 1.73 fold vs 1.83 fold; Cell Trace: mean MFI of Day 9 normalized to Day1: *Apoc2*-KO vs WT = 0.6208 vs 0.7088; P > 0.05). Hematology analysis assessing white blood cell count, red blood cell count, hemoglobin count, neutrophil, lymphocytes, showed no significant difference between the groups.Here we report the first inducible *Apoc2* knockout mouse model and demonstrated that *Apoc2* knockout has limited impact on normal hematopoietic cells in mice. On-going research using this model will assess the impact of *Apoc2* knockout on ageing related phenotypes and leukemia progression.

#5337 Profiling of human CD34+ donors in a myeloid-supportive HIS model provides increased predictability and facilitates study design for evaluation of immuno-oncology therapeutics.

J. R. Richardson[1], M. M. MacBride[1], E. Andino[1], E. Sack[1], N. Smith[1], P. Y. Ho[2], F. Xiao[2], K. A. McEachin[2], D. T. Omstead[2], R. Grgich[2], M. N. Alonso[2], J. A. Kenkel[2], S. E. Ackerman[2];

[1]Taconic Biosciences, Inc., Rensselaer, NY, [2]Bolt Biotherapeutics, Redwood City, CA

Background: Humanized immune system (HIS) mice are critical immuno-oncology tools for *in vivo* evaluation of therapeutic target engagement and efficacy. HIS mice require a human donor source of CD34+ hematopoietic stem cells to provide the human immune cell system. However, variance across donors complicates study design and hypothesis testing. To determine if parameters critical to drug discovery are consistent across batches of HIS mice from the same donor, we evaluated two independent cohorts of human tumor xenograft-bearing mice made using a common set of five different CD34+ cell donors. Our study included evaluation of tumor growth kinetics, human immune reconstitution and phenotype, and the pharmacokinetics and anti-tumor efficacy of a therapeutic monoclonal antibody directed against a human target expressed on tumor-associated macrophages (TAMs).

Method: HIS NOG-EXL (huNOG-EXL) mice were created using CD34+ cells from five donors in two independent cohorts (~12 weeks apart). Baseline immune reconstitution in blood was assessed at 10 weeks post engraftment. MDA-MB-231 cells were inoculated bilaterally and mice were randomized into groups for immune profiling, pharmacokinetics, and efficacy studies. Body weight, clinical observations, endogenous hIgG levels, and tumor growth were measured. For efficacy, tumors grew to ~100 mm^3 and mice were dosed intraperitoneally every five days (6 doses total). Separate cohorts of mice were used for immune phenotyping and the single-dose PK study.

Results: Donor consistency was seen for some of the parameters assessed but not all. The overall health outcomes for a given donor appeared to have an impact on the consistency of important parameters (e.g. efficacy). Donors that had poor health outcomes (body condition scores [BCS] <3) showed less consistency than those that experienced good (BCS=3) outcomes. The health trajectory, peripheral human immune cell engraftment, and PK profiles were similar across experiments for a given donor. Total human immune cell infiltration in tumors was similar across experiments, but there were notable shifts in immune cell composition. Whereas mice in the first cohort showed a dominant TAM phenotype within the tumor (~>50% of all hCD45+ cells), mice across donors in the second cohort had reduced TAMs and corresponding increases in several T cell subsets. Efficacy was consistent in donors with good health outcomes (Donors 1 and 4) and was inconsistent in those with poor outcomes (Donors 3 and 5).

Conclusion: Our study demonstrates that a return-to-donor approach can provide information that is reproducible across cohorts to help build a donor profile. An understanding of this profile should afford greater predictability and facilitate study design for drug discovery applications.

#5338 Evaluation of checkpoint inhibitor efficacy in a humanized immune system mouse model lacking murine Fc gamma receptors.

N. Smith[1], M. Buczek[1], M. MacBride[1], E. Andino[1], E. Sack[1], D. Freer[1], M. Vedder[1], K. Bott[1], L. Baskin[1], D. France[2], F. Bichat[2], C. Mignard[2], J. Richardson[1];
[1]Taconic Biosciences, Inc., Rensselaer, NY, [2]Oncodesign Services, Dijon, France

Humanized immune system (HIS) mice are critical immuno-oncology tools for evaluating antibody-based therapeutic target engagement and efficacy in a human-like context. Most antibody-based therapeutics have an IgG backbone and thus engage Fc gamma receptors. Traditional HIS mice retain murine immune cells such as neutrophils and macrophages which can interact with human IgG-based therapeutics and confound preclinical results. To determine whether knockout of murine Fc gamma receptors (FcγRs) in a super-immunodeficient mouse model would alter anti-PD1 efficacy compared to the parent strain, we studied tumor growth kinetics, human reconstitution, and tumor infiltrating leukocytes (TILs) in each strain engrafted with HCC827 lung adenocarcinoma tumor cells treated with pembrolizumab or vehicle. Methods: HIS NOG (huNOG) or HIS FcγR knockout NOG mice (FcResolv™ huNOG) were created using identical protocols with CD34+ cells from three human donors shared across both strains. Baseline reconstitution was evaluated in naïve animals via flow cytometry. HCC827 cells were inoculated in remaining animals. Animals were randomized on day 7 post-tumor implantation into 12 groups. Body weight, clinical observations, and tumor growth were measured. Mice received treatment from D7, dosed twice weekly for four weeks, and were then euthanized for FACS analysis, collecting blood, spleen, and tumor samples. Results: For a given donor, no significant differences were seen between strains in human immune reconstitution and kinetics. Pembrolizumab treatment showed significant tumor growth inhibition in one donor in FcResolv huNOG, but not in donor-matched huNOG mice. Evaluation of human TILs in pembrolizumab-treated animals showed significant differences between the strains across all donors, with FcResolv huNOG mice showing increased CD8+ T cells and decreased tumor-associated macrophages compared to vehicle-treated mice, and no significant differences in huNOG. Evaluation of murine TILs revealed differences in murine macrophage populations, regardless of treatment, with $Ly6C^{lo}$ dominant in FcResolv huNOG and $Ly6C^{hi}$ dominant in huNOG. In the presence of pembrolizumab, the murine myeloid and granulocyte population within the spleen is significantly decreased in FcResolv huNOG mice whereas no change was seen in huNOG. Conclusions: Our study demonstrates when treated with anti-PD1, FcResolv huNOG mice show expected pharmacodynamic changes and donor-dependent efficacy whereas, despite identical donors and creation protocols, pembrolizumab-treated huNOG mice showed neither. These differences are due to the presence or absence of murine FcγRs and their impact on antibody IgG-based therapeutics.

#5339 Establishment of a humanized IL5/IL5RA mouse model to evaluate modulators of eosinophilic inflammation *in vivo*.

S. Zhao[1], S. Zhang[1], Z. Chen[1], L. Yang[1], **M. Kuraguchi**[2], J. Yuan[1], H. Shen[1];
[1]Biocytogen Pharmaceuticals (Beijing) Co., Ltd., Beijing, China, [2]Biocytogen Boston Corp, Waltham, MA

IL-5/IL-5R signaling plays a key role in the maturation, activation, survival, and recruitment of eosinophils to sites of inflammation. Targeting this pathway is an attractive therapeutic strategy for certain inflammatory diseases, such as asthma. Here, we generated a novel humanized IL5/IL5RA model (B-hIL5/hIL5RA) to examine the utility of human IL-5/IL5R-targeting therapeutic candidates. Specifically, the entire murine *Il5* coding region was replaced by the corresponding human *IL5* sequence, and the human *IL5RA* sequence coding the extracellular domain was inserted to replace the corresponding murine sequence. Successful generation of the model was confirmed by expression of human IL-5 by ELISA and IL5RA by flow cytometry. Furthermore, the proportion of eosinophils in the blood of B-hIL5/hIL5RA mice increased after stimulation with human IL5 recombinant protein, indicating that the humanized IL5RA protein is functional. Next, the ability of the humanized mice to establish asthma-like disease was tested using ovalbumin: following a 14 day sensitization period, mice were challenged with nebulized OVA daily from day 21 until the endpoint; treatment with mepolizumab or benralizumab analog was performed. Flow cytometric analysis of the bronchioalveolar fluid indicates that treatment with mepolizumab or benralizumab analog significantly lowered the number of eosinophils when compared to the isotype control in homozygous B-hIL5/hIL5RA mice. Blood counts and quantification of lung H&E sections also confirm that the treatments lowered the number of eosinophils in circulation and lung tissue, respectively. Taken together, these data indicate that B-hIL5/hIL5RA mice are a suitable preclinical model to test novel modulators of human IL-5/IL-5RA signaling.

#5340 NK-humanized mouse models for the *in vivo* evaluation of NK cell-based therapies in solid tumors.

P. Rettman, S. Benhamouche-Trouillet, M. Pelat, K. Franciszkiewicz, G. Azar, L. Blot, L. Calvet, **S. Sidhu**, C. Nicolazzi;
Sanofi, Vitry-sur-Seine, France

Novel immunotherapeutic strategies targeting Natural Killer (NK) cells using monoclonal or multi-specific antibodies and immune modulator molecules are under development and suitable mouse models are needed to evaluate these therapeutics. We developed and characterized robust *in vivo* models that allow the engraftment and long-term maintenance of fully functional human NK (huNK) cells in immunodeficient transgenic mice for human cytokines (IL15). In efficacy studies, we confirmed that huNK cells are recruitable by NK cell-based therapies including therapeutic antibodies or multi-specific biologics and able to control tumor growth in these models.To establish a more relevant model for better clinical translatability for Fc-competent therapeutics evaluation, we optimized the model by validating a mouse strain with a functional knock-out of murine Fcγ receptors (FcgR-KO) to minimize the confounding impact of mouse immune cells. We characterized huNK cells kinetics and profile by flow cytometry compared to NOG-huIL15 mice. In efficacy studies with the FcgR-KO strain, therapeutic antibodies are inactive in non-NK-humanized mice, whereas in NK-humanized mice huNK cells can be recruited by the therapeutic antibody to control tumor growth by ADCC, in B cell lymphoma or multiple myeloma bearing mice.We also report the development of NK-humanized models for the evaluation of NK-based therapies in solid tumors. We characterized huNK intratumoral infiltration in several subcutaneous tumor xenograft models and evaluated the impact of tumor environment on the expression of functional NK markers (NKp46, NKG2D, Tim3, CD69) by flow cytometry and IHC studies.In summary, we have developed and optimized robust murine models sustaining fully functional huNK cells that can be proficiently recruited *in vivo* by various NK-based therapeutics. These models can also be used to evaluate the efficacy of combination therapies.

#5341 Novel FcγR humanized mouse model enables assessment of PK/PD of therapeutic antibodies.

F. Sonego[1], A. Pappalardo[1], G. Martin[1], R. Courtois[2], S. Augier[2], Y. Cherifi[1], A. Morel[2], P. Isnard-Petit[1], K. Thiam[1];
[1]genOway, Lyon, France, [2]Innate Pharma, Marseille, France

Therapeutic antibodies have revolutionized the way we treat cancer. Enhanced activity of therapeutic IgG can be achieved by the modulation of Fc binding to Fcγ receptors (FcγR), which will consequently modulate the Fc-effector functions triggered upon crosslinking of target and effector cells by these antibodies. Assessment of therapeutic antibodies pharmacodynamic (PD) in preclinical models is challenging, as the FcγR are different from mice to human, as well as their expression pattern. FcRn is involved in the recycling and transport of IgG and is a key determinant of the pharmacokinetics (PK) of IgG. We report here a novel mouse model expressing human FcγR with a human-like expression pattern, in which human FcγRI, FcγRIIA, FcγRIIB, FcγRIIIA, FcγRIIIB are expressed and replace their mouse orthologs. The model was intercrossed with the hSA/hFcRn mouse model (Viuff *et al*., 2016), which has shown to improve translatability of PK assessment of therapeutics with extended half-life via FcRn recycling and/or HSA binding. Investigation of FcγRI, FcγRIIA, FcγRIIB, FcγRIIIA, FcγRIIIB expression on DC, monocytes, granulocytes, NK, T and B cells shows that expression pattern in hFcγR mice is consistent with their expression on human PBMC, with a few exceptions. These receptors are functional, as a human IgG1 targeting mouse CD20 induces approximately 50% of B-cell depletion in blood and liver, after a single iv administration in hFcγR mice. This depletion is Fc-mediated, as it is abrogated when hFcγR mice are treated with an anti-mouse CD20 human IgG1 with a Fc-null mutation. Assessment of antibody-dependent cell cytotoxicity (ADCC) *ex vivo* to investigate FcγR functionality in NK cells shows that Rituximab, an anti-human CD20 chimeric IgG1 with regular Fc, induces higher ADCC efficacy in NK cells from hFcγR than in NK cells from WT mice. Obinutuzumab, an anti-human CD20 featuring an optimized Fc portion to enhance binding to FcγRIII, shows higher tumor cell lysis than Rituximab in NK cells from hFcγR mice, suggesting this model enables ranking of antibodies. Moreover, assessment of activity of Fc-engineered anti-influenza IgG antibodies also shows that anti-Flu antibody with enhanced Fc binding outperforms the WT antibody, improves protective activity, and demonstrates effector function in influenza challenge model, following prophylactic treatment. Conversely, hFcγR mice treated with an Fc-null version of the anti-Flu antibody shows reduced protective activity and survival compared with the WT antibody. Therefore, the model reported here is a novel tool for testing efficacy of Fc-engineered therapeutic antibodies. We are currently investigating the PK profile of therapeutic antibodies in the hFcγR/hSA/hFcRn model. This novel tool is being improved to enable tolerability to human IgG1, biodistribution to the central nervous system, and flexibility of test of therapeutics through expression of human immune checkpoints.

#5342 Evaluation of autologous and allogeneic T cell-based therapies in *ex-vivo* and *in-vivo* xenograft tumor models.

S. Liu, J. Borroel, C. Sunico, E. Eastwood, B. Corcoran, B. Carapia, J. Sperry, J. Nakashima, R. Shrimali;
Certis Oncology Solutions, San Diego, CA

The field of adoptive T cell-based immunotherapy, including tumor-infiltrating lymphocytes (TILs), T cell receptor (TCR) & Chimeric antigen receptor (CAR) - T cells, has undergone unprecedented growth, specifically later in delivering effective and durable clinical response. Notable success with CAR-T cells is limited to hematological malignancies while clinical gains with solid tumors is still a challenge. Solid tumors' heterogenous target expression and loss, T cell status and metabolic fitness, T cell trafficking into the tumor, and the hostile immunosuppressive tumor microenvironment (TME) have hampered T cell efficacy in the patients. There is a lack of clinically relevant solid tumor models for the translation of T cell-based therapies into the clinic.

We report the development of translational *ex-vivo* and *in-vivo* platforms for evaluating cell line-derived and patient-derived xenografts (CDX and PDX) models (BarneyOI™ model), validated with hCD3 T-cells, autologous TILs and/or allogeneic 3rd generation CAR-T cells (scFv(HER2)-CD28-4-1BB-CD3zeta CAR-T). Anti-hPDL1 but not anti-hPD1 significantly enhanced hCD3 T-cell and autologous TIL-mediated killing of tumor cells in an *ex-vivo* co-culture assay using Incucyte-based live cell imaging. Also, a dose-dependent killing of HER-2 expressing CDX (A549 & Colo205) and PDX was observed with HER-2 targeting CAR-T cells in an *ex-vivo* co-culture assay. This was in concordance with the activation, effector function, and differentiation status of the CAR-T cells, immune phenotype by Cytek aurora spectral flow cytometry. Further, to imitate the patient population and the effect of solid TME, HER-2 targeting CAR-T cells were assessed for their *in-vivo* efficacy and immune response differences in the subcutaneous and orthotopically implanted HER-2 expressing PDX in immunodeficient NOG mice. Our findings highlight the importance of testing T cell-based immune therapies in the appropriate translational tumor models with better certainty of clinical outcome.

#5343 Depletion of gut microbiota with broad spectrum antibiotics drives *Pten*-null prostate cancer growth in mice.

Marco A. De Velasco, Yurie Kura, Kazuko Sakai, Mitsuhisa Nishimoto, Yasunori Mori, Kazuhiro Yoshimura, Kazutoshi Fujita, Kazuto Nishio, Hirotsugu Uemura

Kindai University Faculty of Medicine, Osaka-Sayama, Japan

Gut microbes have the potential to be either promoters or inhibitors of cancer. Use of antibiotics during cancer therapy can lead to dysbiosis, which may affect treatment outcomes. Here, we examine the effects of broad-spectrum antibiotics on cancer progression in mice with *Pten*-null castration resistant prostate cancer (CRPC). After five or eight weeks, orchiectomized conditional *Pten*-null knockout (KO) mice aged 50 and 90 weeks were given two biweekly cycles of a broad-spectrum antibody cocktail (BSAbx), respectively. The effects of BSAbx on tumor burden were compared, and molecular and immunological responses were analyzed by quantitative IHC (qIHC) and qRt-PCR at week four after antibiotic treatment. BSAbx treatment resulted in tumor burdens of 1.2 and 2.4-fold higher than in control mice in mice aged 50 and 90 weeks, respectively. qIHC analysis of KI67 showed increased proliferation in stromal and cancer cells. Additionally, androgen receptor (AR) protein and gene expression levels of *Ar* and *Ar* target genes (*Fkbp5*, *Tmprss2*, and *Timp4*) were elevated in tumors of BSAbx-treated mice. Restoring gut microbiota by fecal microbiota transplantation (FMT) from KO mice CRPC after BSAbx restored AR transcriptional activity to basal levels and lessened tumor growth. FMT from non-castrated KO with castration-naïve prostate cancer or heathy wildtype mice further reduced AR Transcriptional activity. Moreover, altering the gut microbiota of CRPC mice with FMT from heathy mice resulted in a tendency for lower tumor burden, 21% reduction versus control mice. Immunologically, BSAbx treatment resulted in decreased CD11b+/GR1+ cells in tumors and were associated with decreased interferon-gamma (IFN-gamma), dendritic cell functions and T cell-mediated cytotoxicity gene signatures. Mice that received FMT form health mice showed enhanced T cell mediated immunity as demonstrated by higher IFN-gamma signatures and tumor abundances of CD8+ T cells expression IFN-gamma, TNF-alpha and the cytotoxic granule granzyme B. Our study shows that broad spectrum antibiotics caused dysbiosis and promoted prostate cancer growth in mice with *Pten*-null prostate cancer. The effects were partly mediated through the upregulation of AR signaling and the impairment of neutrophil and T cell-mediated immune responses in tumors.

#5344 Myeloid populations upregulated in prostate cancer are associated with colitis induced colorectal cancer.

Yurie Kura, **Marco A. De Velasco**, Kazuko Sakai, Mamoru Hashimoto, Syogo Adomi, Takafumi Minami, Kazuhiro Yoshimura, Kazutoshi Fujita, Kazuto Nishio, Hirotsugu Uemura

Kindai University Faculty of Medicine, Osaka-Sayama, Japan

Chronic systemic inflammation caused by diseases like ulcerative colitis (UC) and Crohn's disease (CD) increases the risk of developing colorectal cancer (CRC). Research indicates that patients with UC are more susceptible to prostate cancer (PCa) and individuals with PCa may also be at a higher risk for developing CRC. However, these relationships are not well defined. Here, we explored these relationships using preclinical mouse models of dextran sulfate sodium (DSS)-induced colitis (DSS-UC) and in young and aged healthy wild-type mice and conditional transgenic mice harboring *Pten*-deficient (KO) or *Pten/Trp53-deficient* (DKO) PCa. After a 25-week follow-up, DSS-induced UC caused more severe colitis in prostate tumor-bearing DKO compared to healthy WT mice. None of the DSS WT mice developed tumors, whereas 75% (3/4 mice) of DSS DKO mice did, including two out of four mice that developed multiple tumors. Overall, DKO mice with prostate tumors had increased levels of $CD11b^{\pm}/Gr1^{\pm}$ in peripheral blood, prostate, and colon compared with WT mice. Quantitative immunohistochemical analyses revealed that DKO mice with prostate tumors had a significantly higher 2.8-fold increase in the levels of Gr1+ cells in the colon compared to heathy WT mice. Overall, DSS-induced colitis further increased Gr1+ cells in the colon of WT and DKO mice by 2.5- and 2-fold, respectively. Gr1+ cells comprised 3.0%, 4.7%, and 10.1% of cells in normal colon from control WT mice and inactive and active regions of the colon in DSS-exposed WT mice, respectively. In DKO mice, Gr1+ cells comprised 7.0%, 19.2%, and 23.6% of cells in normal colon from control mice and inactive and active regions of the colon in DSS-exposed mice, respectively. CD68+, which corresponds to M1 polarized macrophages comprised 0.9%, 1.8%, and 20.6% of cells in normal colon from control WT mice and inactive and active regions of the colon in DSS-exposed WT mice, respectively. However, in DKO mice CD68+ cells comprised 3.0%, 2.8% and 1.6% of cells in normal colon from control mice and inactive and active regions of the colon in DSS-exposed mice, respectively. Our study suggests that Gr1 cells that were abundant in PCa-bearing mice were also present in colons and could have contributed to CRC. Moreover, CD68+ macrophages in the colons of healthy mice may have decreased tumor promoting effects of DSS. This study provides preclinical evidence showing that systemic inflammation in the presence of an existing malignancy increases the risk of a second malignancy, in this case linking PCa to colitis-induced-CRC.

#5345 Development and validation of humanized HLA mouse model platforms for preclinical evaluation of novel peptide vaccines.

Zhenlan Niu[1], Xuan Yu[1], Zhiyuan Shen[1], Jing Guo[1], Qingcong Lin[2], **Veronika Chromikova**[2], Hui Xu[1]

[1]Biocytogen Pharmaceuticals (Beijing) Co., Ltd., Beijing, China,[2]Biocytogen Boston Corp, Waltham, MA

The human leukocyte antigen (HLA) class I major histocompatibility complex (MHC) plays an integral role in immune surveillance by presenting intracellular antigen peptides on the cell surface, enabling recognition by cytotoxic T cells and subsequent elimination. Harnessing this intrinsic process for cancer immunotherapy is a promising therapeutic strategy; thus, developing preclinical models to evaluate the efficacy of novel peptide vaccines *in vivo* and *ex vivo* is critical. Previously, we developed a humanized MHC I mouse model (B-HLA-A2.1 mice), in which we successfully demonstrated efficacy of peptide vaccines as assessed by splenocyte IFN-γ production measured via ELISpot. Here, we provide evidence that B-HLA-A2.1 mice can also mount immune responses to NY-ESO-1 and WT1-Db126 peptides using the same assay. Additionally, immunization with WT1-Db126 at 7, 14, and 21 days prior to tumor inoculation with WT1-expressing MC38 colon cancer cells significantly reduced tumor volume. Additionally, we have generated two new humanized HLA models: B-HLA-A11.1 mice and B-HLA-A24.2 mice. Flow cytometric data demonstrate successful expression of the human HLAs on the cell surface of splenocytes isolated from both strains. Compared to wild-type C57BL/6 mice, analysis of leukocyte and lymphocyte subpopulations in the humanized mice indicates that the CD4/CD8 ratio is altered in favor of CD4+ T cells in both strains, similar to what was observed in B-HLA-A2.1 humanized mice. Despite these observed alterations, B-HLA-A24.2 mice were able to mount an immune response to peptide SART2 93-101, which was measured by splenocyte IFN-γ production. In summary, our data indicate that humanized HLA-A mice provide a powerful preclinical model for *in vivo/ex vivo* evaluation of novel peptide vaccines.

#5346 A novel humanized CD16A model to evaluate efficacy of human antibody therapeutics in triggering ADCC.

Xiao Liu[1], Zhenlan Niu[1], Ruili Lv[1], Qingcong Lin[2], **Mari Kuraguchi**[2], Qingqing Xu[1]

[1]Biocytogen Pharmaceuticals (Beijing) Co., Ltd., Beijing, China,[2]Biocytogen Boston Corp, Waltham, MA

Antibody-dependent cellular cytotoxicity (ADCC) is a mechanism by which immune effector cells engage the Fc portion of antibodies bound to antigen on the surface of another cell, thereby targeting that cell for destruction. In mice, the Fcgr4 receptor is primarily responsible for triggering ADCC, while the FCGR3A receptor (CD16A) mediates this function in human NK cells, which are an attractive target cell type for cancer immunotherapy. Given these differences, we sought to generate humanized CD16A preclinical models to evaluate the efficacy of antibodies in triggering human CD16A-mediated ADCC *in vivo*. Previously, we established humanized CD16A mice on immunocompetent backgrounds for evaluating efficacy of novel antibodies in preventing growth of syngeneic tumor models. Here, we introduce a novel humanized CD16A mouse on the CB-17-SCID background, in order to inoculate human tumor cells for therapeutic efficacy testing. We confirmed expression of CD16A in human NK cells and monocytes/macrophages, but not granulocytes in the model; expression of murine Fcgr4 was no longer detectable, indicating successful generation of the model. Assessment of leukocyte populations in the humanized model indicated no significant alterations in the percentages of NK cells, dendritic cells, granulocytes, monocytes and macrophages in the spleen or blood of the humanized mice compared with wild-type CB-17 SCID mice. Subsequently, the ability of these mice to grow human tumor cells was evaluated: B-hHep3B-Luc, HC116, K-562, and NCI-N87 tumors were all successfully established. Finally, efficacy of an anti-human CLDN18.2 antibody was evaluated against B-hCLDN18.2 BxPC-3 tumors in the humanized mice, which showed modest anti-tumor efficacy at 30 mg/kg when compared to isotype control-treated mice. In summary, humanized B-hCD16A mice (CB-17-SCID) provide a suitable model for evaluating the ability of antibody candidates to induce ADCC.

IMMUNOLOGY: Tumor-Induced Immune Suppression 2: Intrinsic Factors
Poster Session

#5350 Decr2 regulates tumor cell ferroptosis and immunotherapy efficacy.
S. Li, J. Shapiro, H. Shah, E. F. Higgs, L. Xie, Y. Zha, J. Trujillo, A. Cabanov, T. A. Jones, B. Flood, K. Hatogai, J. Kline, T. F. Gajewski;
University of Chicago, Chicago, IL

Checkpoint blockade therapies have transformed the landscape of cancer care. Durable clinical responses have been observed in a subset of patients. However, many patients do not respond, and understanding the mechanisms that determine tumor resistant to checkpoint blockade drugs could potentially benefit more patients. Ferroptosis is a relatively newly described form of regulated cell death distinct from apoptosis and necroptosis. Recently, T cell-promoted tumor ferroptosis was shown to be an anti-tumor mechanism and targeting this pathway could be a potential therapeutic approach. To identify genes critical to immunotherapy resistance, B16.SIY cells were transduced with a genome-scale gRNA lentivirus to generate loss of function mutants. *In vitro*-primed $CD8^{\pm}$ T cells isolated from $2C/Rag2^{-/-}$ TCR transgenic mice specific for the SIY antigen were co-cultured with transduced B16.SIY tumor cells. Resistant mutants were identified by deep sequencing of survival clones. The gene encoding Decr2, a peroxisomal 2,4-dienoyl-CoA reductase, was identified. Decr2 mutants were relatively resistant to $CD8^{\pm}$ T cell killing *in vitro*. Consistent with this resistance to $CD8^{\pm}$ T cell killing, Decr2 knock-down tumors showed minimal response to anti-PD-L1 therapy *in vivo*. Tumor microenvironment analysis in Decr2 knockdown B16.SIY tumors showed failed antigen specific $CD8^{\pm}$ T cells' expansion and less IFN-γ production after anti-PD-L1 treatment. Knock-down of Decr2 resulted in diminished ferroptosis, triggered either by pharmacologic inducers or antigen-specific $CD8^{\pm}$ T cells. Mechanistic studies revealed that Decr2 knockdown resulted in diminished induction of polyunsaturated ether phospholipids (PUFA-ePLs), which is due to reduced polyunsaturated ether phospholipids synthesis rate . Analysis of melanoma tumors from human patients revealed that up-regulation of Decr2 was associated with anti-PD-1 efficacy. Our results proved Decr2 knock down suppressed tumor ferroptosis and confer tumors resistance to anti-PD-L1 therapy by reducing the polyunsaturated ether phospholipids (PUFA-ePLs) synthesis.

#5351 Tumor PKC-Delta induces immune exclusion in non-small cell lung cancer.

X. Fan;
Macau University of Science and Technology, Macao, Macao

The recruitment of a sufficient number of immune cells to induce an inflamed tumor microenvironment (TME) is a prerequisite for effective response to cancer immunotherapy. The immunological phenotypes in the TME of EGFR-mutated lung cancer were characterized as non-inflamed, for which immunotherapy is largely ineffective. To orchestrate host immunity against lung tumors, we proposed that PKCδ, a gatekeeper of immune homeostasis with kinase activity, is responsible for the un-inflamed phenotype in EGFR-mutated lung tumors. It promotes tumor progression by stimulating extracellular matrix (ECM) and PD-L1 expression which leads to immune exclusion and assists cancer cell escape from T cell surveillance. Ablation of PKCδ enhances the intratumoral penetration of T cells and suppresses the growth of tumors. Furthermore, blocking PKCδ significantly sensitizes the tumor to immune checkpoint blockade (ICB) therapy (αPD-1) in vitro and in vivo models. These findings revealed that PKCδ is a critical switch to induce inflamed tumors and consequently enhances the efficacy of ICB therapy in EGFR-mutated lung cancer. This opens a new avenue for applying immunotherapy against recalcitrant tumors.
This work was funded by the FDCT project grant to Dr. Xing-Xing Fan (Grant no. 0058/2020/A2).

#5352 SOX9-dependent immune microenvironment remodeling drives KRAS-induced lung adenocarcinoma progression.

Dinoop Ravindran Menon[1], Hua Zhong[2], Shridar Ganesan[2], Hatim Sabaawy[1], Sharon Pine[1]

[1]Division Of Medical Oncology, University of Colorado, Aurora, CO,[2]Rutgers Cancer Institute of New Jersey, New Brunswick, NJ

Interactions between tumor intrinsic factors and tumor microenvironment play a vital role in disease progression and treatment response. SOX9, a transcription factor crucial for tissue development and homeostasis, has been linked to the advancement of tumor growth. However, its specific role as a driver in lung adenocarcinoma (LUAD) is not well-defined. Additionally, the impact of SOX9 on the tumor microenvironment has not been previously explored. We here identify SOX9 transcription factor to play a critical role in defining tumor immune microenvironment and driving disease progression. We employed CRISPR/Cas9 and Cre-LoxP gene knockout methods within the *Kras* G12D-induced mouse model of lung adenocarcinoma (LUAD). Our objective was to investigate the mechanisms through which SOX9 contributes to the development and advancement of lung adenocarcinoma. To substantiate our findings, we conducted immune profiling, gene expression analyses, RT-qPCR, and immunohistochemistry assessments in the *Kras* G12D-driven murine LUAD. These results were subsequently validated by examining bulk and single-cell gene expression profiles, as well as immunohistochemistry, in human lung adenocarcinoma. Our studies indicated that SOX9 played a very important role by enhancing lung tumor development, burden, and progression, leading to lower overall survival. SOX9. SOX9 consistently facilitated the growth of organoids in vitro. However, the promotion of tumor growth by SOX9 was notably reduced in immunocompromised mice compared to syngeneic mice. SOX9 demonstrated a suppressive effect on immune cell infiltration, particularly affecting the functionality of tumor-associated CD8+ T cells, natural killer cells, and dendritic cells. CD8+ T cells in the SOX9 overexpressing tumors showed upregulation of exhaustion markers. SOX9-mediated tumor growth advantage could not be observed in the CD8 knockout mice model, suggesting a CD8+ T cell-dependent role. In addition, SOX9 significantly upregulated collagen-related gene expression, leading to a substantial increase in collagen fibers possibly affecting the migration of immune cells into the tumor microenvironment. Together, our studies indicate that SOX9 plays a very critical role in modulating tumor microenvironment by controlling immune cell infiltration and CD8+ T cell exhaustion driving *Kras* G12D- driven lung tumor progression.

#5354 High-resolution analysis of immune checkpoint activation utilizing a combined PD1/PD-L1 *in situ* proximity ligation assay (isPLA) and multiplex immunofluorescence (mIF) imaging approach.

A. Christians[1], J. Boog[1], C. E. Jackson[2], M. H. Ingalls[2], J. S. Schwarz[2], S. Bodbin[3], A. Z. Wicher[3], S. Basu[3], O. Braubach[2];
[1]Canopy Biosciences-A Bruker Company, Hannover, Germany, [2]Canopy Biosciences-A Bruker Company, Saint Louis, MO, [3]Navinci Diagnostics, Uppsala, Sweden

The immune checkpoint involving PD-1 and PD-L1 generates suppressive signals in T cells, which help to prevent autoimmunity by inducing a state of immune exhaustion. In the context of the tumor microenvironment (TME), however, cancer cells can manipulate these pathways to camouflage themselves from an immune attack. Blocking these checkpoints has thus emerged as a key immunotherapeutic tactic. Nonetheless, the success rate of immune checkpoint inhibitors (ICIs) has been mixed, even for patients who test positive for relevant diagnostic biomarkers. Patient stratification currently depends on immunohistochemical staining for checkpoint proteins like PD-L1, but these tests do not provide adequate stratification. A more comprehensive stratification, one that includes immune profiling of the TME plus an evaluation of immune checkpoint interactions, might provide better patient stratification and ICI responsiveness. Here we describe mIF that is augmented with a PD-1 and PD-L1 protein-protein interaction assay.

Human formalin-fixed, paraffin-embedded (FFPE) tissue sections were subjected to standard histological processing and then incubated with primary antibodies against PD1 and PD-L1. Sections were then treated with oligonucleotide-modified secondary probes suitable for *in situ* Proximity Ligation Assay (isPLA), enabling the detection of PD1 and PD-L1 interactions. The PLA protocol utilized a fluorescent probe complementary to amplified nucleic acid to enhance the visibility of the protein interactions. The sample was then mounted in a closed microfluidic chamber and imaged on the CellScape™ platform for Precise Spatial Multiplexing. After imaging of the isPLA signal, the CellScape cyclic multiplex mIF staining approach was used to iteratively stain immune and structural markers on the tissue sample utilizing the VistaPlex™ Spatial Immune Profiling Assay Kit.

This proof-of-concept study demonstrates that high-plex mIF can be augmented with an isPLA on human FFPE samples. The combined application of both methods allows visualization of PD1/PD-L1 protein-protein interactions and integrates this interaction within the spatial context of the surrounding cell populations. This approach allows for a more comprehensive insight into the interplay of different immune cell and non-immune cell populations during checkpoint activation processes in normal and neoplastic tissues.

#5355 A novel subset of Treg-like MDSCs expressing LAG-3 found in advanced gastric cancer.

T. Iwasawa[1], S. Yamauchi[2], T. Fukunaga[3], H. Orita[3], T. Ito[4], K. Kazunori[1];

[1]Toyo Univ., Bunkyo-ku, Japan, [2]Johns Hopkins Univ., Dept. Surg., MD, [3]Juntendo Univ., Bunkyo-ku, Japan, [4]Juntendo Univ., Nagaoka, Japan

The development and progression of cancers are frequently promoted by immunosuppressive cells, such as Treg and myeloid-derived suppressor cells (MDSCs) mediated by various immune checkpoint molecules. Therefore, MDSCs are potential diagnostic and therapeutic targets in cancer. However, the definitive cell surface markers for defining MDSC and the subset that correlates with cancer progression are not clear. In our previous studies, there was no difference in the amount of total granulocyte MDSCs (G-MDSCs) between early and advanced gastric cancer. We inferred that there is a novel subset of G-MDSCs involved in cancer progression rather than the previous marker-based classification. The purpose of this study is to analyze MDSCs in gastric cancer patients at different stages of progression and to identify subsets of G-MDSCs that are involved in cancer progression. As a result, we identified a subset of novel G-MDSCs that correlate with cancer progression by expressing LAG-3. LAG-3 is a molecule that is expressed in Tregs and causes strong immunosuppression, suggesting that it is involved in the immunosuppressive potential of MDSCs.

#5356 Wild type Kirsten rat sarcoma (Kras) activation drives evasion of interferon-mediated immunity in hepatocellular carcinoma.

M. Lei, T. Lee;
Hong Kong Polytechnic University, Hong Kong, Hong Kong

Background: Immune checkpoint inhibitors (ICIs) exhibit heterogeneous efficacy in patients with advanced hepatocellular carcinoma (HCC). Currently, there are no effective biomarkers to select patients who could benefit the most from ICIs or to predict response outcomes. Increasing evidence indicates that oncogenic pathway activation is associated with the generation of an unfavorable tumor microenvironment, with consequent immunotherapy resistance. Therefore, an understanding of the immune evasive mechanism of HCC is urgently needed.
Methods: Utilizing the antigen-expressing c-Myc^{OE}/Tp53^{KO} HCC mouse model, a critical oncogenic signaling pathway in immune evasion was identified by data-independent acquisition mass spectrometry (DIA-MS) proteomics. Potential downstream pathways were investigated by scRNA-seq, immune profiling, western blot, and multiplexed immunofluorescence staining. We also examined the therapeutic potential of targeting wild-type Kras using the Kras inhibitor MRTX0902 and the MEK inhibitor trametinib to enhance the efficacy of immunotherapy in HCC.
Results: We identified a significant upregulation of wild-type Kras in immune-escaped tumors, with concurrent activation of its ligand-driven EGFR and its downstream MEK/ERK signaling. Likewise, endogenous Kras overexpression in this model resulted in increased tumor burden with reduced survival time in mice, implicating the regulatory role of Kras signaling in immune evasion. Clinically, wild-type Kras showed elevated expression in HCC at both the mRNA and protein levels, and was associated with tumor recurrence and poorer patient survival. Through scRNA-seq analysis, we demonstrated that Kras hindered dendritic cell recruitment, leading to compromised Cd8^{+} T cell activity via the suppression of interferon-mediated Cxcl9. Wild-type Kras activation further impaired HCC recognition by T cells via the downregulation of MHC-I expression. Notably, the combination therapy of MRTX0902, trametinib, and anti-PD-1 effectively enhanced intratumoral Cd8^{+} T cell infiltration and demonstrated a favorable response in survival outcomes.
Conclusion: This study showed that wild-type Kras, via the activation of its downstream MEK/ERK signaling, acts as a crucial immune evasive mechanism in HCC and contributes to resistance to anti-PD-1 therapy. It also provided new insights into the therapeutic potential of targeting wild-type Kras to enhance the efficacy of anti-PD-1 therapy, providing a foundation for further exploration and potential clinical applications in HCC.

#5357 The tumor-intrinsic RNA binding protein HuR is essential for anti-tumor immunity in PDAC.

Y. Guo, J. M. Finan, A. Q. Bartlett, J. R. Brody, R. Eil;
OHSU, Portland, OR

Immunotherapies have shown limited effectiveness in pancreatic ductal adenocarcinoma (PDAC), despite having success in other cancers. The RNA-binding protein HuR is known to play a critical role in the oncogenesis of PDAC by regulating key mRNA transcripts. Our lab has shown that tumor-intrinsic HuR is overexpressed in PDAC and regulates the tumor microenvironment composition, altering multiple tumor cytokines to release. Thus, we hypothesized that HuR plays a role in immune evasion of PDAC. We disrupted the locus encoding HuR (*Elavl1*) using CRISPR Cas9 in Kras-p53 mutant-driven (KPC) murine PDAC to assess its function in tumor immune evasion. Here, we report that HuR, a known pro-survival factor for PDAC, has a role in tumor immune evasion by suppressing T cell infiltration and T cell activation. Specifically, HuR-knockout (KO) KPC tumors grew slower compared to KPC wildtype (WT) tumors in an orthotopically implanted model (p-value < 0.0001), even though human PDAC cell lines with HuR-WT and HuR-KO grew at the same rate in NRG mice (in an immune-compromised environment). Accordingly, HuR-KO tumors had more T cell infiltration and activated T cells compared to HuR-WT tumors (p-value = 0.0047). Importantly, T cell depletion (both CD4+ and CD8+) partially rescued the size of HuR-KO tumors. Next, we rescued the expression of HuR in the HuR-KO cell line, and the re-expression partially rescued the tumor size in vivo. This observation validates a HuR-mediated dependent mechanism. Collectively, these data support the hypothesis that HuR suppresses T cell activation and prevents T cells from infiltrating into the PDAC microenvironment, leading to PDAC immune evasion. Ongoing experiments will transduce KPC cell lines with ovalbumin (OVA) antigen, which will selectively activate CD8+ OT-I T cells through their transgenic TCR, to measure the ability of KPC HuR-WT or HuR-KO OVA cells in directly activating CD8+ OT-I T cells. We will also investigate HuR's impact on immune cells' cytokine release and how that will impact the cytotoxicity of T cells. These findings support the ongoing concept that HuR plays an important pro-survival role in PDAC in vivo, and targeting strategies against HuR being developed (e.g., siHuR nano-therapies and small molecule inhibitors) could potentially enhance PDAC sensitivity to immune-based anti-cancer therapies, such as checkpoint blockade and T cell transfer.

#5358 The influence of extracellular vesicles on immune cells in PDAC.

C. S. Mundry, Y. Huang, P. M. Grandgenett, M. A. Hollingsworth;
University of Nebraska Medical Center, Omaha, NE

Introduction: Pancreatic Ductal Adenocarcinoma (PDAC) is bad. The tumor microenvironment consists of an abundance of immunosuppressive immune cells and anti-inflammatory cytokines that contribute to local and systemic immunosuppression in PDAC. Tumor cells can influence the tumor microenvironment and, with that, the present immune cells through the secretion of cytokines or chemokines or the secretion of extracellular vesicles (EVs). EVs are a media of communication among the tumor cells themselves, but also with other cells of the body, with the goal to promote tumor expansion and metastasis and decrease any anti-tumor-directed forces of the immune system. Our lab has shown that those EVs play a significant role in tumor growth and metastasis in PDAC. We have found MUC1 to be an important marker for tumor-derived EVs (tdEVs), associated with their activity and influence on cell proliferation and tumor growth *in vitro* and *in vivo*. Determining which immune cell populations are most targeted and impacted by tdEVs is essential to improving our understanding of the role of EVs in PDAC.

Methods: TdEVs were isolated from murine pancreatic cancer cell lines through differential ultracentrifugation. EVs were then labeled with a membrane dye, which allows tracking of the EVs in the mouse. We designed an *in vivo* study to investigate the effects that tdEVs have on different immune cell populations, as well as tumor growth and metastasis. This study has two distinct phases: a 3-week “Pre-Education Phase”, with injection of either $MUC1^{\pm}$ or MUC1KO EVs, is followed by orthotopic implantation of tumor cells in the pancreas.

Data: We hypothesized that tdEVs impact effector immune cells in PDAC, leading to phenotypic, transcriptional, and functional changes that result in a decreased anti-tumor immune response. The highest uptake of EVs was found in macrophages and dendritic cells (DCs). Furthermore, most immune cells preferably take up $MUC1^{\pm}$ as compared to MUC1KO EVs. After three weeks of EV education, RNA sequencing of the liver showed differential gene expression in a variety of genes related to processes associated with B cells. Treatment with $MUC1^{\pm}$ EVs downregulated B cell-related processes in the liver, B cell differentiation, proliferation and activity are reduced. Several genes coding for immunoglobulin parts were affected as well. Immune cell profiling of the blood and spleen showed that $MUC1^{\pm}$ EVs reduce NK and macrophage numbers in the spleen as compared to MUC1KO EV treatment after three weeks. Additionally, EV-treatment increased $CD8^{\pm}$ T cell numbers in the blood but decreased $CD8^{\pm}$ T cells in the spleen.

Conclusion: We have shown that tdEVs induce phenotypic and transcriptional changes in immune cell populations and alter immune cell frequencies *in vivo*. Ongoing research in our lab involves analysis of phenotypic and transcriptional changes after tumor implantation as well as functional differences in EV-treated immune cells *in vitro* and *in vivo*.

#5359 Targeted engineering mRNA 3′UTR length enhances immunotherapy response in prostate cancer.

F. Huang[1], F. Yuan[1], Y. Cui[2], L. Li[2], K. Li[1], Z. Cui[1], J. Yan[3], Q. Chen[4], C. Nicchitta[4], W. Ye[2], Y. Zhang[3], W. Hankey[1], J. Everitt[1], M. Chen[1], J. Huang[1], H. Wang[1], X. Lu[5], E. Wagner[6], Y. Dong[3], W. Li[2], Q. Wang[1];

[1]Department of Pathology and Duke Cancer Institute, Duke University School of Medicine, Durham, NC, [2]Division of Computational Biomedicine, Department of Biological Chemistry, School of Medicine, University of California, Irvine, CA, [3]Division of Pharmaceutics & Pharmacology, College of Pharmacy, The Ohio State University, Columbus, OH, [4]Department of Cell Biology, Duke University School of Medicine, Durham, NC, [5]Department of Biological Sciences, Boler-Parseghian Center for Rare and Neglected Diseases, Harper Cancer Research Institute, University of Notre Dame, Notre Dame, IN, [6]Department of Biochemistry & Biophysics, University of Rochester School of Medicine and Dentistry, Rochester, NY

Background: Global mRNA 3′untranslated region (3′UTR) shortening through alternative polyadenylation (APA) has been widely observed in most cancers; however, it has not been demonstrated whether targeted interference of specific oncogenic mRNA 3′UTR lengths can inhibit tumor growth and potentiate immunotherapy response in prostate cancer.

Methods: DaPars algorithm was applied for *de novo* identification of dynamic alternative polyadenylation (APA) during prostate cancer progression to the lethal phase; 3′UTR polyadenylation site (PAS) locations and usages were identified by Poly(A)-ClickSeq (PAC-seq) and 3′RACE; APA transcripts were quantified by RHAPA assay; a 3′UTR CRISPR/dCas13 Engineering System (3′UTRCES) was developed to manipulate the length of desired 3′UTRs; RIP-qPCR and PAR-CLIP-qPCR assays were used to determine the mechanistic basis of 3′UTRCES in APA editing; RNA-seq was utilized to evaluate the off-target effects; TT3 Lipid-like nanoparticles (LLN) were applied for intratumoral delivery of 3′UTRCES RNA molecules for targeted 3′UTR therapy. Quantitative proteomics and immunoprecipitation assays were conducted to investigate how major histocompatibility complex class I (MHC-I) substrates were recognized by SPSB1-containing ubiquitin ligase complex for degradation; Flow cytometry and T cell cytotoxicity assays were performed to evaluate MHC-I level and killing of tumor cells by antigen-stimulated $CD8^{\pm}$ T cells.

Results: 3′UTR globally shortens during prostate cancer progression to castration-resistance. Through blocking the proximal PASs, 3′UTRCES efficiently and specifically reverses the 3′UTR shortening of novel APA-linked, clinically-relevant prostate cancer oncogenic mRNAs, such as *SPSB1*, leading to reduced *SPSB1* mRNA translation and prostate cancer cell proliferation. Intratumoral injection of TT3 LLN encapsulating 3′UTRCES RNA molecules effectively and safely inhibits prostate tumor growth in engrafted and transgenic mouse models. Notably, downregulation of SPSB1 protein by 3′UTRCES disrupts the interactions of SPSB1-containing ubiquitin ligase complex, leading to compromised ubiquitination-mediated MHC-I degradation and increased stability and abundance of MHC-I protein. Consistently, 3′UTRCES enhances MHC-I-regulated antigen presentation and thereby augments $CD8^{\pm}$ T cell-mediated cytotoxicity, which suggest the potentials of 3′UTRCES to sensitize prostate cancer to immune checkpoint therapies. Importantly, 3′UTR shortening of *SPSB1* mRNA is significantly associated with decreased MHC-I expression, reduced cytotoxic T-cell infiltration and activation in castration resistant prostate cancer patients.

Conclusions: Our results establish the concept of “3′UTR targeted therapy” for treatment of prostate cancer with broad applications to other cancers and other 3′UTR-related diseases.

#5360 Relief of chromosomal instability-induced cGAS-STING signaling sensitizes *STK11*-mutant non-small cell lung cancer to immune checkpoint blockade.

L. A. Caprio[1], C. Hong[2], A. D. Amin[1], S. Tagore[1], M. Duran[2], M. Rogava[1], L. Cai[1], L. Ebel[1], J. Melms[1], H. Hibshoosh[1], S. Bakhoum[2], B. Izar[1];
[1]Columbia University Irving Medical Center, New York, NY, [2]Memorial Sloan Kettering Cancer Center, New York, NY

Non-small cell lung cancers (NSCLCs) harboring deletions or inactivating mutations in *STK11* (encoding LKB1) are associated with poor prognosis and immune evasion, but the underlying mechanisms are poorly understood. Through integrative analyses of >10,000 molecular profiles from public data sources and an additional ~15,000 new patient data profiles, we find identify *STK11*-deficient NSCLC as an archetypical chromosomally unstable tumor. Using high-content imaging, we show that both human and murine *STK11*-mutant models have a higher rate of micronuclei and chromosome mis-segregation events, confirming their high degree of chromosomal instability (CIN). We show that CIN-induced tonic activation of the cGAS-STING pathway results in impaired type I interferon expression, thus, turning the physiological function of this pathway on its head. We show that temporary relief of tonic CIN-induced signaling reprogrammed cancer cells towards production of type I interferons. We achieved this through orthogonal routes, including genetic suppression of CIN by overexpression of mitotic centromere-associated kinesin (MCAK), rescue of wild-type *STK11* (but not its kinase-dead) allele, genetic deletion or pharmacological inhibition of cGAS. Relief through any of these approaches re-sensitized cells to acute STING agonism with its endogenous ligand (cGAMP) or pharmacological stimulation. Using otherwise isogenic, syngeneic *KRAS*-mutant *Stk11*/Lkb1$^{-/-}$ (KL) and *KRAS*-mutant *p53* mutant (KP) murine models, we show that cGAS KO sensitized otherwise highly resistant KL models to immune checkpoint blockade (ICB), while an increase in CIN (through overexpression of dominant-negative MCAK) in KP conferred resistance in this otherwise ICB-sensitive model. In summary, we define *STK11*-mutant as archetypical chromosomally unstable form of NSCLC, provide mechanistic basis that correlates with poor clinical outcomes, and demonstrate how relief of tonic CIN-induced changes may be therapeutically leveraged.

#5361 Aberrant glycosylation in mPDAC is associated with increased epithelial-mesenchymal transition and recruitment of immunosuppressive cells.

S. Brookens[1], D. Degaramo[1], K. Wilson[2], W. Condori Obregon[3], P. Nagarkatti[2], M. Nagarkatti[2], A. Posey Jr.[1];
[1]University of Pennsylvania, Philadelphia, PA, [2]University of South Carolina, Columbia, SC, [3]Gettysburg College, Gettysburg, PA

The tumor-associated glycan Tn antigen (GalNAc-α-O-Ser/Thr) is associated with poor prognosis in various solid tumors. However, the mechanisms that Tn antigen promotes tumorigenesis are incompletely understood. Here, we generated Tn antigen-expressing murine pancreatic ductal adenocarcinoma (mPDAC) tumor cell lines through CRISPR/Cas9-mediated knockout of the *C1galt1c1* gene. Tn antigen expressing mPDAC cell lines exhibited increased *in vitro* proliferation and migration compared to parental controls. RNA sequencing revealed that loss of *C1galt1c1* in mPDAC cells correlated with increased expression of genes associated with epithelial-mesenchymal transition, myeloid recruitment, and extracellular matrix deposition. Consequently, knock-down of elevated genes using CRISPR interference dampened *in vitro* cell proliferation of *C1galt1c1* knockout mPDAC cells to the growth rate of parental controls. Additionally, *C1galt1c1* knockout mPDAC cells implanted into mice led to accelerated tumor growth and increased tumor infiltration of myeloid-derived suppressor cells and neutrophils as determined by flow cytometry and scRNAseq. Interestingly, surface expression of a binding partner of Tn antigen, macrophage galactose-type lectin 2 (Mgl2), was altered in the immune infiltrate of *C1galt1c1* knockout tumors suggesting a role for the Mgl2-Tn interaction in tumor progression. Mgl2-deficient mice exhibit increased T effector cells in the draining lymph nodes of tumors highlighting a potential mechanism for promoting the influx of immune cells in ordinarily cold tumors. Together, our data indicate that truncated O-glycans expressed commonly on tumor cells promotes tumorigenesis through creating an immunosuppressive microenvironment in mPDAC.

#5362 Targeting IRE1α alleviates the immunosuppressive tumor microenvironment in prostate cancer.

B. Unal[1], O. F. Kuzu[1], Y. Jin[1], D. C. O. Hurtado[1], M. L. Kuijjer[1], M. Daugaard[2], H. Z. Oo[2], J. B. Patterson[3], F. Saatcioglu[1];
[1]University of Oslo, Oslo, Norway, [2]Vancouver Prostate Centre, Vancouver, BC, Canada, [3]Orinove Inc, Newbury Park, CA

Unfolded protein response (UPR) is a central stress response pathway in normal cells that is hijacked by tumor cells for their survival. However, how activation of UPR in cancer cells shapes the tumor microenvironment (TME) remain largely unexplored. Here, we investigated the role of IRE1α-XBP1s pathway on modulation of TME dynamics in prostate cancer (PCa). We found that IRE1α is increased in PCa patients and genetic or pharmacological inhibition of IRE1α signaling in the immunocompetent syngeneic mouse PCa model dramatically reduced tumor growth. Multiomics analysis of tumor samples upon IRE1α deletion in cancer cells showed significantly potentiated interferon (IFN) response and activation of immune system related pathways in the TME. Single-cell RNA sequencing (scRNA-seq) analysis revealed that the abundance of immunosuppressive cells, such as tumor-associated macrophages (TAMs) and T regulatory cells were markedly reduced in the IRE1α deficient tumors. Analysis of differentially expressed genes in the annotated cell types in the TME demonstrated that expression signatures associated with IFN responses were significantly enriched in TAMs, cancer cells, and dendritic cells. In addition, a novel scRNA-seq derived TAM gene signature is strongly associated with poor PCa survival. Furthermore, IRE1α inhibition by the small molecule MKC8866 (ORIN1001) that is in clinical trials significantly enhanced anti-PD-1 checkpoint inhibitor therapy in mice. Our findings indicate that IRE1α not only promotes cancer cell growth and survival, but it also strongly inhibits anti-tumor immunity in the PCa TME.

#5363 New targeted therapy on SOCS1-related immune-response in triple-negative breast cancer.

Shigeru Imoto[1], Tomohiro Chiba[2], Hirohito Seki[1], Yoshiharu Ishizaka[1], Ai Tsuchiya[1], Tomoko Kitaoka[1]

[1]Department of Breast Surgery, Kyorin University Hospital, Mitaka city, Japan,[2]Department of Cytology, The Cancer Institute Hospital, Japanese Foundation for Cancer Research, Tokyo, Japan

Background: Triple-negative breast cancer (TNBC) is heterogenous, which includes basal-like, immunomodulatory, mesenchymal, mesenchymal stem cell and luminal androgen receptor subtypes. In addition to chemotherapy, PARP inhibitors and immune checkpoint inhibitors are effective for TNBC with *BRCA*-mutated and PD-L1-positive cases. However, overall survival of TNBC remains unfavorable. To explore new targeted therapy in TNBC, we reported previously that SOCS1 (suppressor of cytokine signaling 1), IL-13 and several genes were predicted as interactive targets of miRNA in TNBC from the microarray expression analysis (Agilent Technologies, Inc.) of small RNA extracted from 11 breast cancer specimens (AACR2020, #1709). Thus, we investigated SOCS1-related immune-response under co-culture of TNBC and monocyte cell lines with or without paclitaxel exposure.
Materials and Methods: MDA-MB-231, MDA-MB-468, RAW264.7 cell lines were used with co-culture system (Falcon® Cell Culture Inserts, Corning, NY, USA). SOCS1-expression vector and siSOCS1 were transfected into TNBC cell lines with polyethylenimine (PEI Max; Polysciences, Inc., Warrington, PA). RAW264.7 was activated with lipopolysaccaride (5ug/ml) and IFNγ (10ng/ml) for 2 days before co-culture. Relative cell viability of TNBC cell lines with vehicle control (DMSO) or paclitaxel exposure was measured with WST-8 (Cell Counting Kit-8; Dojindo, Japan) using TC20 Automated cell counter (Bio-Rad Laboratories, Inc., Japan) after 2 days' co-culture of TNBC and RAW264.7 cells under several conditions of SOCS1 overexpression and /or RAW264.7 activation.
Results: First, paclitaxel inhibited cell growth of MDA-MB-231 and MDA-MB-468 in a dose-dependent manner (at 1nM~100nM). Second, at paclitaxel exposure of 10 nM and 50 nM, relative cell viability of MDA-MB-468 decreased with co-culture of activated RAW264.7. The tendency was enhanced with SOCS1 overexpression in breast cancer cell lines. Similar results were observed in MDA-MB-231 cells.
Discussions: SOCS1 is well known as a negative regulator of JAK-STAT pathway. SOCS1 is also related to suppression of T cell activation and modulation of M1 macrophage. At AACR2020, we reported that SOCS1 gene amplification in cancer tissues after neoadjuvant chemotherapy was relatively lower in 6 cases with pathologically partial or complete response than in 11 cases with no pathological response. In vitro, paclitaxel-toxicity in TNBC cells was augmented by activated monocyte (M1 macrophage) and more sensitized with SOCS1 overexpression in TNBC cells. These results suggest that proinflammatory cytokines from M1 macrophage influence cell viability of TNBC.
Conclusion: SOCS1 is a promising molecular target to modulate immune-response in TNBC.

#5364 Progesterone receptor modulates the antigen processing and presentation machinery decreasing MHC class I expression on tumors.

J. Tinoco[1], L. Werner[1], E. Chowanec[1], H. Saunders[1], S. Xiaopeng[2], J. Gertz[3], J. Balko[4], Z. C. Hartman[5], C. Hagan[1];
[1]University of Kansas Cancer Center, Kansas City, KS, [2]Vanderbilt University, Nashville, TN, [3]University of Utah, Salt Lake, UT, [4]Vanderbilt University Medical Center, Nashville, TN, [5]Duke University School of Medicine, Durham, NC

Hormone receptor (HR) positive breast cancers, which account for approximately 75% of all breast cancers and express both estrogen receptor (ER) and progesterone receptor (PR), have been the subject of much research. As such, successful anti-estrogen/ER-based therapies have been very successful in the treatment of HR+ breast cancer. Despite this success, over 1/3 of patients will eventually progress on current ER/estrogen-targeted therapies, underscoring the need for new targeted therapies in HR+ breast cancer. Unlike ER, the role of PR in breast cancer progression has received far less attention. In a previous study, we found that a mouse mammary tumor cell line E0771, modified to express the mouse progesterone receptor (mPR) and the OVA peptide, demonstrated decreased T cell-mediated cell death when treated with progesterone compared to the control group. Progesterone-mediated protection from T-cell death was only observed in mPR+ cell lines. Flow analysis of the E0771-Ova-mPR cells also revealed a decrease in MHC Class I presentation in progesterone-treated cells compared to a vehicle control. To further explore the role of the machinery required for antigen processing and presentation of MHC Class I molecules, we conducted additional experiments using the E0771 cell line. Our results showed that treatment with progesterone led to a reduction in RNA levels of all the machinery required for antigen processing and presentation (APP). Based on these findings, we hypothesize that activation of the progesterone receptor by progesterone may decrease MHC Class I expression by regulating APP. Our results showed that treatment with progesterone resulted in a reduction in RNA levels of Tap1, Tap2, Tapbp, Nlrc5, B2m, and Psmb8, which are essential for APP. We therefore propose that activation of the progesterone receptor by progesterone may decrease MHC Class I expression by directly modulating the APP pathway. The findings of this study may have significant implications for our understanding of how breast cancer cells evade T-cell mediated cytotoxicity.

#5365 Characterizing signaling in macrophage-GBM cell coculture.

A. D. D'Souza, R. Mukkamala, R. Ahn, F. M. White;
MIT, Cambridge, MA

Macrophages are a type of immune cell that play a crucial role in the tumor microenvironment. In tumors, macrophages can be polarized towards a pro-inflammatory phenotype, referred to as M1, or towards an anti-inflammatory and tumor-promoting phenotype, referred to as M2. M2 macrophages promote tumor growth by secreting cytokines that increase tumor proliferation, angiogenesis, and dampen the immune response from other immune cells such as T cells and dendritic cells. The balance between M1 and M2 macrophages in the tumor microenvironment is critical in determining the outcome of cancer progression and response to therapy. By understanding the pathways that lead to macrophage polarization, we can develop therapeutics that inhibit this process and support an anti-tumor macrophage response. Co-culture is a powerful model to study interactions between different cell types. We created co-cultures with macrophages and glioblastoma multiforme (GBM) cells to understand how these cell-cell interactions can lead to altered cell phenotype. Several studies have looked at the interaction of two populations using a transwell system where one cell population is placed in a well with a permeable membrane and the other population is placed below, allowing for the exchange of soluble factors. However, this does not account for an important mode of cell-cell interaction, which is physical contact. Therefore, we tested how macrophages derived from primary monocytes polarized in the context of conditioned media (supernatant), cell lysate, and direct co-culture. We used U87-MG as a model GBM cell line. We assayed the M2 phenotype by using flow cytometry with CD163 as a marker. Our findings show that direct co-culture is crucial for promoting macrophage M2 polarization. Using our in vitro model for tumor-induced macrophage polarization, we conducted phosphoproteomic analysis to characterize signals associated with this phenotypic change. To study how co-culture induced differential signaling in tumor populations and macrophages, we devised a method to fix cells to preserve cell signaling, followed by separation using flow cytometry and LC-MS/MS analysis of individual cell populations. We created co-cultures of U87-MG tumor cells and macrophage-differentiated THP-1 cells, a monocyte cell line. We then tested whether our method could reliably separate the different populations, whether we could detect altered signals due to co-culture, and showcase how separating cell populations yields information that could not be gathered from bulk analysis of co-cultures. Our data shows that the analysis was highly reproducible and that the signaling from cells separated from co-culture was highly similar to signaling in cells that were grown individually. However, some phosphorylation residues were uniquely upregulated in the co-culture condition, pointing to signaling that may occur in response to tumor interaction.

#5366 ATR promotes extracellular matrix stiffness mediated cytoskeleton remodeling and immunosuppression.

X. Tu, Z. Lou, R. Mutter;
Mayo Clinic, Rochester, MN

The stiffening of the extracellular matrix (ECM), a phenomenon that often promotes metastasis and immunosuppression in many cancers, is a process that is not yet fully understood. Our study reveals that ATR, a molecule primarily recognized for its role in maintaining the genome, plays a crucial role in ECM stiffness-induced immune evasion and metastasis in triple negative breast cancer (TNBC) through DNA repair independent manner. In response to ECM stiffness, ATR activates SUN2, a component of the linker of nucleoskeleton and cytoskeleton (LINC) complex. This activation enhances the interaction of SUN2 with outer nuclear membrane proteins KASH1 and KASH2. The interaction between SUN2 and KASH1/2 facilitates the nuclear localization of β-catenin, which in turn promotes epithelial mesenchymal transition (EMT) and reduces the expression of E-cadherin. E-cadherin is essential for attracting CD103+ immune cells that perform anti-tumor immunity. Interestingly, inhibiting ATR reduces EMT in tumor cells, leading to an increase in CD103+ dendritic cell infiltration while decreasing neutrophil and polymorphonuclear myeloid-derived suppressor cell (PMN-MDSC) infiltration. Further, we found that ATR levels are inversely correlated with immunotherapy response rates in patients. The alteration in immune cell composition sensitizes tumors to immunotherapy, thereby suppressing tumor growth and metastasis. In conclusion, the role of ATR in remodeling the immune environment could be crucial for optimizing the clinical use of ATR inhibitors. This makes ATR a promising target for overcoming immunotherapy resistance. We suggest early or prolonged treatment with an ATR inhibitor to potentially reduce metastasis rates and improve the prognosis of TNBC patients. Furthermore, we suggest using ATR levels as a marker to predict response rates and prognosis in TNBC patients. For patients with higher ATR expression levels, combination treatment with ATR inhibitors and immunotherapy may yield better outcomes. Enhanced anti-tumor immunity could increase the chances for patients to eliminate cancer cells and help end breast cancer. Finally, our research suggests the combined treatment of ATR inhibition and immunotherapy for patients without necessarily applying DNA damage stimulation. This approach could potentially reduce toxicity while still benefiting patients.

#5367 Single cell resolution spatial transcriptomics reveals genetic driver and TME interaction in clear cell renal cell carcinoma.

I. Strunilin, W. Caravan, A. Abedin-Do, A. Houston, Y. Li, Y. Song, S. Cao, C.-K. Mo, S. Chen, R. Pachynski, F. Chen, L. Ding;
Washington University in St. Louis, Saint Louis, MO

BAP1 mutations are associated with increased T cell and tumor-associated macrophage infiltration in clear cell renal cell carcinoma (ccRCC) and are predictive of poor prognosis. BAP1 mutations have also been found to be associated with T-cell infiltration in peritoneal mesothelioma and uveal melanoma. Because BAP1 mutations are known to be associated with aggressive disease and poor survival, we hypothesize that these mutations lead to a more immunosuppressive microenvironment. Using single nucleus RNA sequencing and high-resolution spatial transcriptomics, we confirmed that BAP1 mutant tumors are immune hot with a high fraction of Treg, exhausted CD8+ T cells, CD4+ T cells, and macrophages. At the same time, these tumors have a lower proportion of endothelial cells and pericytes. Evident of pro-tumor microenvironment we have found BAP1 mutations to be associated with the upregulation of SPP1, CD163, and MARCO immunosuppressive genes in tumor-associated macrophages. Here we propose a mechanism by which BAP1-mutant cancer cells induce an immunosuppressive microenvironment: through activation of the complement system and TGF-β signaling to attract macrophages. Taken together, our results suggest that BAP1 mutations contribute to poor ccRCC outcomes not only through cell-intrinsic effects, but also by promoting infiltration of Tregs and tumor-associated macrophages and polarizing infiltrated macrophages towards immunosuppressive phenotype.

#5368 Targeting tumor-intrinsic S100A1 augments antitumour immunity and potentiates anti-PD-1 efficacy.

Y. Guo, **R. Wan**, H. Bai, J. Wang;
National Cancer Center, National Clinical Research Center for Cancer, Cancer Hospital, Chinese Academy of Medical Sciences & Peking Union Medical College, Beijing, China

Immune-checkpoint blockade (ICB) has revolutionized cancer treatment. However, only a minority of patients achieve the long-term, durable response to ICB, and the response rates in most advanced tumors is limited to 10%-25%. The unsatisfactory overall response to ICB and the great variation in response among individuals highlight the necessity for developing predictive biomarkers and overcoming ICB resistance. A potential mode of resistance is tumor-mediated immunosuppression leading to inhibition of T cell-mediated infiltration and immunity. Here, combining single-cell and bulk transcriptomic analysis with liquid biopsy of tumor patients, we showed that S100 calcium binding protein A1 (S100A1) was closely related to ICB response, and that detecting plasma S100A1 level could help predicting the response to ICB, implying that tumor-intrinsic S100A1 may contribute to immunosuppressive tumor microenvironment (TME) and resistance to ICB. Importantly, endogenous *S100a1* knockdown (*S100a1*^{KD}) promoted anti-tumor immunity, conferred tumor regression, and sensitized tumors to anti-PD-1 immunotherapy in multiple syngeneic murine models. By characterizing the immune landscape of *S100a1*^{KD} syngeneic murine tumor models and non-small cell lung cancer (NSCLC) clinical samples, we demonstrated a negative relationship between tumor-intrinsic S100A1 expression and infiltration of M1-like macrophage and CD8^{+} T cells. Single cell and spatial transcriptomic analyses, together with functional studies, have revealed that ablation of tumor-intrinsic S100A1 exerts profound impacts on the M1-like polarization of macrophages and cytotoxicity of CD8^{+} T cells. Moreover, the conditioned medium from *S100a1*^{KD} tumor cells promoted M1 polarization of both bone marrow-derived macrophages (BMDMs) and Raw264.7 cells, which in turn reinvigorated tumor-specific T cell immunity both *in vitro* and *in vivo*. Of note, as a secreted protein, introducing recombinant S100A1 into the medium from *S100a1*^{KD} tumor cells could not reverse the effects on T cells and macrophages, suggesting that these effects were independent of extracelluar S100A1 secretion and that S100A1 may act as an intracellular signaling molecule. Mechanistically, S100A1 affects deubiquitination of NF-κB through interacting with the ubiquitin-like (Ubl) domains of ubiquitin specific protease 7 (USP7), leading to upregulated granulocyte-macrophage colony-stimulating factor (GM-CSF) expression. Collectively, these data identified the S100A1/USP7/p65/GM-CSF inhibitory axis as a critical immune suppressor on M1-like macrophage polarization and T cell immunity for the promotion of tumor progression and resistance to ICB. Our findings demonstrated the potential of plasma S100A1 expression in predicting the response to ICB, and provide a rationale for combining GM-CSF and anti-PD-1 immunotherapy in tumors with high S100A1 expression.

#5369 Mapping a T cell-cold phenotype to the colorectal cancer genome to identify POFUT1 as a driver of CD8+ T cell inhibition.

C. J. Wagner, E. D. Routh, R. Rutledge, L. D. Miller;
Wake Forest University School of Medicine, Winston-Salem, NC

CD8+ T cells are a critical anti-cancer immune subset; however, most colorectal cancer (CRC) patients have inadequate levels of CD8+ T cells in their tumor microenvironment (TME), contributing to poor survival and increased CRC aggression. While current immune checkpoint inhibitors are able to elicit anti-cancer CD8+ T cell responses in some patients, a majority of patients are still nonresponsive, and have minimal levels of tumor-infiltrating CD8+ T cells. This effect is potentially due to still-unrecognized cancer-driven mechanisms of immunosuppression. To identify candidate genes with roles in CD8+ T cell exclusion, we used a T cell gene signature (Tsig) to quantify CD8+ T cell infiltration in tumors profiled by RNA-seq. Partial Spearman correlation adjusted for tumor purity was performed for all annotated genes (N=20501) in the TCGA CRC RNA-seq data set (N=373) to identify genes most inversely correlated with Tsig. A locus at chromosome 20q was identified as the region of the genome most inversely correlated with Tsig - both by copy number analysis and by RNA expression. Interestingly, this region is the most copy number-amplified region in CRC tumors, and the genes at this locus are among the most highly expressed genes in CRC tumors. Within this region, the amplified and overexpressed gene Protein O-Fucosyltransferase 1 (POFUT1) had the strongest inverse correlation to Tsig. POFUT1 function is essential to canonical NOTCH signaling, and CRC-expressed NOTCH is implicated in increased CRC secretion of immunosuppressive factors IL-6, TGF-β and VEGF, and reduced CD8+ T cell secretion of IFN-γ and IL-2. POFUT1 overexpressing (OE) CT26 and MC38 cell lines were generated, and confirmed by Western Blot to have elevated levels of both cleaved NOTCH1 (NICD1), and NOTCH pathway transcriptional target, HES1. Murine CD8+ T cells were stimulated *in vitro* with CD3/CD28 microbeads and IL-2 in conditioned medium (CM) from vector or POFUT1-OE lines. CD8+ T cells cultured in CM from POFUT1-OE lines had significantly lower levels of activation markers (CD45 (p=0.0022), CD8 (p=0.0095), CD25 (p=0.0069, CD69 (p=0.0099)), reduced proliferation (CFSE, p=0.1281), and generated less ATP (Cell-Titer Glo, p=0.0003) than CD8+ T cells cultured in vector CM. In pan-cancer correlational analyses, POFUT1 is in the top 5% of genes most inversely correlated with Tsig in 12/24 solid tumor types annotated in TCGA (SKCM, THCA, COAD, READ, LUSC, CESC, KIRC, STAD, HNSC, KIRP, LIHC, UCEC p<0.0001). POFUT1 is robustly negatively correlated with T cell infiltration in many cancer types. We observed a positive association in CRC between POFUT1 and NOTCH signaling, and observed that POFUT1 expression reduced CD8+ T cell activity, potentially through upregulation of extracellular factors (in progress). Our findings fit a model where POFUT1 amplification in CRC promotes CD8+ T cell dysfunction as a mechanism of immune escape.

#5370 Tumor-intrinsic cGAS-STING activation promotes anti-tumor inflammatory response in osteosarcoma.

E. P. Young, C. Johnson, A. G. Lee, E. A. Sweet-Cordero;
UCSF - University of California San Francisco, San Francisco, CA

A “cold” tumor microenvironment (TME) is often seen in patients with osteosarcoma (OS). Genomic instability, characteristic of OS, can stimulate the cGAS-STING pathway and activate the innate immune system. Tumor-intrinsic STING pathway silencing mechanisms can link genomic instability to immune evasion in OS. We hypothesize that dysregulation of the cGAS-STING pathway suppresses an innate immune response to genomic instability and plays a key role in tumor progression through establishing an immunosuppressive TME in OS. Using a novel panel of 11 OS patient-derived cell lines, we have identified two groups in terms of capacity for tumor-intrinsic STING activation, and we aim to unravel the mechanism of STING repression in a subset of OS tumors. To investigate the effects of tumor-intrinsic STING activation on macrophage polarization we employed tumor conditioned media (TCM) assays with murine-derived macrophages and tumor lines treated with cGAS-STING agonism. Tumor-intrinsic STING activation resulted in a significant increase in pro-inflammatory macrophages in a manner dependent on tumor STING. Lastly, we performed bulk RNA seq of OS PDX cell lines treated with STING agonist, defining for the first time the OS-specific STING activation signature. We then evaluated primary patient samples for evidence of this signature by single sample GSEA and performed survival analysis after stratifying samples as high or low for this signature, which demonstrated a significant protective effect of the STING activation signature on progression-free and overall survival. We have defined two subtypes of OS in terms of responsiveness to STING activation and demonstrated that STING activation has a protective effect in the human disease, which is the foundation of current efforts to identify targetable mechanism to reverse STING unresponsiveness and activate immune surveillance in this cancer.

#5371 Multimodal CRISPR activation screens reveal new mechanisms to sensitize cancer cells to targeted T cell mediated elimination.

R. V. Akana, C. Sun, Y. Kim, Y. Cai, S. Kim, J. Yoe, O. Laveroni, L. Jerby-Arnon;
Stanford University, Palo Alto, CA

Cell autonomous resistance mechanisms can protect cancer cells from targeted T cell elimination, resulting in resistance to a broad range of immunotherapies. High-throughput gene knockout and gene inhibition screens have been instrumental in identifying key drivers of such mechanisms, yet often uncovering gene activity that is essential but not sufficient for response. Here we set out to leverage gene activation as an orthogonal approach to identify novel regulators of the cancer-immune interface. First, we performed CRISPR activation screens in melanoma cells co-cultured with antigen-specific primary CD8+ T cells. Our findings revealed a collection of novel genes that substantially sensitize melanoma cells to targeted T cell-driven elimination when activated, including DNA damage and unfolded protein response genes (e.g., ETS1, TSPYL2), Wnt ligands (e.g., WNT3A, WNT1), and others that are deleterious only in combination with targeting T cells. Among the resistance genes we found regulators of insulin signaling (e.g., HGF, TCF7L2) and numerous glycoproteins (e.g., PDPN, CD44). Second, we validated top novel hits in 2D and in 3D spheroid models, using optical readouts to investigate their impact on cancer cell elimination and cancer-T-cell spatial dynamics. Third, we performed a Perturb-seq screen to stratify dozens of hits into functional groups based on the transcriptional readouts in the cancer cells. Lastly, we developed an in situ Perturb-Seq method, where we combine high-plex spatial transcriptomic readouts at subcellular resolution with in situ detection of genetically modified cells, and applied it to track the impact of the (de)sensitizing perturbations not only on the cancer cells themselves, but also on T cell recruitment and suppression. Taken together, our study provides a catalog of immune evasion mechanisms and an array of novel targets, demonstrating that synthetic gene activation can diminish immune evasion and open novel avenues for development of agonist-based and RNA-based interventions.

#5372 KITENIN leads immunosuppression in the glioblastoma microenvironment via CCL20.

E.-J. Ahn[1], N. Kim[1], S. Kim[1], J.-H. Lee[1], J. Rhee[1], K.-K. Kim[1], H. Kim[2], K.-H. Lee[1], **K.-S. Moon**[1];
[1]Chonnam National University Medical School, Hwasun, Korea, Republic of, [2]Sunchon National University, Sunchon, Korea, Republic of

Background: Glioblastoma (GBM) is characterized by an immunosuppressive tumor microenvironment (TME), limiting the effectiveness of existing treatments. The author investigated the role of KAI1 COOH-terminal interacting tetraspanin (KITENIN) in mediating this immunosuppression, focusing on its effect on cytokine secretion and tumor-infiltrating lymphocyte (TIL) profiles in the TME.
Materials and Methods: Using cytokine array and Luminex multiplex assays, the author evaluated cytokine secretion in KITENIN-modulated GL261 cells. The author further isolated TILs from an orthotopic mouse model implanted with these cells and induced in vitro differentiation of myeloid cells. The effect of neutralizing antibody for target cytokine, was assessed in vivo, and clinical relevance was investigated using GBM patient data from our cohort and TCGA.
Results: Employing cytokine array and Luminex multiplex assays, we found increased level of CC chemokine ligand 20 (CCL20) within KITENIN-overexpressed (KIT-HA) GL261 cell supernatants. Immunohistochemical analyses using GBM samples confirmed that both KITENIN and CCL20 expressions co-directionally increased and this was associated with decreased survival by TCGA analysis. Myeloid-derived suppressor cells (MDSCs), macrophages, and $CD4^{\pm}Foxp3^{\pm}$ regulatory T cells (Tregs) were observed to be higher in brain tumor implanted with KIT-HA GL261. Furthermore, KIT-HA GL261 conditioned medium expanded $CD45^{\pm}CD11b^{\pm}Gr1^{-}Ly6c^{\pm}$ monocytic MDSCs (M-MDSCs), an effect that was abrogated by CCL20 downregulation. In vivo neutralization of CCL20 resulted in reduced tumor volume, prolonged survival, and decreased M-MDSCs, thus affirming the role of CCL20 in mediating immunosuppression.
Conclusion: These findings underscore the KITENIN-CCL20 axis as a promising target for alleviating the immunosuppressive TME in GBM, potentially unlocking new avenues for GBM immunotherapy.

#5373 Decoding the role of intrinsic pancreatic cellular signaling in shaping the immunosuppressive tumor microenvironment.

Bushangqing Liu, Ethan Agritelley, Daniel Nussbaum, Junping Wei, Gangjun Lei, Melissa Gajda, Zachary Hartman

Duke University School of Medicine, Durham, NC

Background: Pancreatic ductal adenocarcinoma (PDAC) has the highest mortality rate among major cancers, with over 50% of patients having liver metastases at diagnosis. Conventional T-cell-based immunotherapies are ineffective against PDAC liver metastases due to the intricate hepatic tumor microenvironment (TME) that hinders effective immune responses. Thus, it is vital to promote the influx of cytotoxic lymphocytes and prime antitumor immunity. PDAC cells exhibit plasticity and intrinsic cellular heterogeneity, leading to varying immune cell infiltrates and immune responses. Concurrently, early metastases to the liver create an immunosuppressive environment. Our study employs multiple PDAC models, originating from a congenic array of distinct PDAC cell clone tumors with varying degrees of T cell infiltration to delineate the signaling pathways that lead to immunosuppression in the pancreas and liver.
Methods: The compendium of congenic PDAC murine cell clones mirrors immune heterogeneity observed in tumors, spanning from low to high T cell infiltration. To overcome a scarcity of tumor-specific neoepitopes in PDAC, we engineered PDAC cell clones expressing chicken ovalbumin (OVA) for antigen-specific T and B cell responses. By subcutaneous and intraportal vein injection of PDAC cell clones into mice, we induce primary pancreatic and metastatic liver tumors to explore immune phenotypes and assess anti-tumor adaptive immune responses, including myeloid and lymphoid cell subsets.
Results: In vivo engraftment of PDAC clones showed varied CD4+/CD8+ T cells and polymorphonuclear myeloid-derived suppressor cells, accentuated with immunogenic OVA antigen expression. While all OVA+ PDAC lines elicited antigen-specific immune responses, only ‘TIL high’ tumors were eradicated, while ‘TIL low’ clones persisted in vivo. Additionally, ‘TIL low’ clones formed liver metastases upon intraportal injection, despite OVA expression. RNAseq unveiled differential expression in IL-1 family cytokines and receptors, chemokine-like factor gene superfamily, parathyroid hormone relevant function and metabolism. Current investigations include altering these pathways to re-program the tumor microenvironment and induce local immune suppression.
Conclusion: Using diverse PDAC models, we created tumors with immune heterogeneity and altered transcriptional profiles. We identified validated differentially expressed immune altering cytokines, such as CXCL1 and CSF3, and potential novel IL-1 family genes and parathyroid signaling genes. The altered TME conferred protection against tumor antigen-specific immunity in certain clones, both in subcutaneous and liver metastasis models. Ongoing studies will assess the impact of these genes in the distinct environments, offering avenues for immunotherapeutic strategies targeting pancreatic cancer liver metastasis.

#5374 Novel mouse models to study the role of the docking protein GAB2 in general and in cancer.

M. Angel[1], V. Klappstein[1], J. Schrimpf[1], M. Langhammer[1], K. Shoumariyeh[1], C. Miething[1], U. Kloz[2], B. Armstrong[2], F. van der Hoeven[2], T. Brummer[1], S. Halbach[1];

[1]Albert-Ludwigs-Universitat Freiburg, Freiburg im Breisgau, Germany, [2]German Cancer Research Center (DKFZ), Heidelberg, Germany

The docking protein GAB2 binds to growth factor, cytokine and antigen receptors via the adaptor GRB2. Thereby, GAB2 amplifies the signaling output of the SHP2/Ras/ERK, PI3K/AKT and STAT5 pathways, leading to survival, proliferation and migration. Beside these physiological functions, GAB2 is often overexpressed or hyperphosphorylated in different types of cancer, in particular melanoma, breast cancer and various leukemia entities. Previous studies demonstrated that mice with constitutive *Gab2* deficiency are protected against breast cancer, acute and chronic myeloid leukemia driven by HER2, BCR::ABL1 and FLT3-ITD, respectively. While these studies support a critical role in tumor initiation, nothing is known about the relevance of GAB2 for tumor maintenance and progression. To this end, we have developed two novel conditional loss- and gain-of-function mouse models to further analyze the role of GAB2 in cancer.
In the first model, the transgenic GAB2 mouse, GAB2 is expressed under the control of the TET-O promotor, allowing the tetracycline dependent expression in tissues expressing a tetracycline trans activator (tTA). We have already started by crossing in the SCLtTA mouse, in which tTA is expressed under the control of the murine stem cell leukemia 3' enhancer. Here we show that the expression of transgenic GAB2 is tightly regulated by tetracycline and restricted to hematopoietic cells. This system is now perfectly suited to analyze the role of GAB2 in hematologic malignancies. By expressing tTA under different promotors, we propose that GAB2 overexpression can be directed to other organs or cell types. Combining this mouse line with cancer mouse models will allow to study the role of GAB2 in different cancer entities.
With the second mouse model, the conditional *Gab2* KO mouse, it is possible to study the therapeutic potential of GAB2 impairment *in vivo*. In this mouse, exon three of the *Gab2* gene is flanked by LoxP sites. This allows for its CRE recombinase mediated deletion, leading to GAB2 deficiency. The combination of this mouse model with inducible and tissue specific CRE strains will allow to analyze the role of GAB2 in various cancer mouse models. To demonstrate the efficient conditional deletion of exon 3, we first crossed in the tamoxifen inducible ROSA26 CreERT2 mouse line. So far, we were able to show the functionality of this system *in vitro* in mouse embryonic fibroblasts (MEFs) generated from the conditional *Gab2* KO mouse. In a next step we will verify the results *in vivo* and will cross this mouse line with a mouse model for Chronic Myeloid Leukemia (CML) to investigate the therapeutic potential of GAB2 in CML.
In summary, we are convinced that these two novel mouse models will help to identify GAB2 as a potential target or biomarker in various cancer entities. In particular, the conditional approach will allow to alter GAB2 expression in already established tumors, thus mimicking pharmacological targeting.

#5376 Quantitative profiling of HLA class I and class II antigens and neoantigens in tissue biopsy and PBMC samples using an optimized mass spectrometry-based workflow.

I. Shapiro, M. Tognetti, T. Temu, O. Bernhardt, **D. Redfern**, Y. Feng, R. Bruderer, L. Reiter;
Biognosys AG, Schlieren, Switzerland

Major histocompatibility complex (MHC) molecules play a central role in orchestrating immune responses by presenting antigenic peptides derived from both self and foreign proteins. In the context of cancer, understanding the repertoire of tumor-associated antigens (TAAs) presented by MHC molecules (or HLA molecules in human) is crucial for deciphering how the immune system recognizes and responds to malignant cells. The identification of neoantigens, unique to individual tumors due to somatic mutations, has become a focal point in immunopeptidomic studies. One significant hurdle in systematic immunopeptidomics analysis is the high input material requirement. Here, we present a semi-automated workflow to robustly identify and quantify immunopeptides from reduced amounts of clinical tissue biopsy and peripheral blood mononuclear cell samples. At the core of immunopeptidomics is the enrichment of HLA-associated peptides, followed by identification using mass spectrometry and bioinformatics tools. We optimized the native lysis and a sequential immunoprecipitation workflow for both class I and class II immunopeptides while ensuring scalability and reproducibility. Leveraging the magnetic properties of the beads, 1,000 samples can be processed within a week by a single operator. For both tissue and PBMC samples, we performed a systematic ramping experiment starting with as little as 2.5mg tissue or 5 million PBMCs. In all experiments, The established sample preparation offers high reproducibility and identifications of good quality: 1) Class-I immunopeptides: >60% of the peptides identified are 9-mers, >80% predicted strong binders, and the expected amino acids are enriched at the anchor positions; 2) Class-II immunopeptides, >50% of the peptides identified are 14-to-16-mers, and >50% are predicted strong binders. Furthermore, the pipeline is highly sensitive as we could still identify over 2,800 class-I immunopeptides when processing 2.5 mg fresh frozen tissue and 2,000 - 3,000 class-I immunopeptides when starting from 5 million PBMCs. Furthermore, the developed immunopeptidomics workflow was deployed to profile a cohort of 12 cancerous and matched healthy lung tissue samples. Their Class-I immunopeptidomes clearly displayed a pattern where matched tissues from each subject cluster together, further underlining the fact that the intricate immune-tumor interface is highly personalized. Overall, we established a robust pipeline for for class-I and II immunopeptidome profiling from clinically relevant sample types. Taking advantage of the nature of mass spectrometry-based methods, customized targeted assays can be developed without the need for affinity reagent, allowing specific and absolute quantification of any immunopeptide of interest.

#5377 Investigating human leukocyte antigen (HLA) class 1 leukemogenic pathways in acute myelogenous leukemia.

P. Sackstein[1], S. Mudra[1], L. Williams[1], G. Diltz[1], R. Zemel[1], S. Teegavarapu[2], M. Mims[2], C. Lai[3], K. Doucette[1], A. Renteria[1], O. Timofeeva[1], G. A. Rivero[1]; [1]Georgetown Univ. School of Medicine, Washington, DC, [2]Baylor College of Medicine, Houston, TX, [3]University of Pennsylvania, Philadelphia, PA

Background: Aging, smoking and germline predisposition are known to accelerate leukemogenesis. However, the the ability for myeloid clonal pathogenic variants (MCPV) to elicit an antigen-driven host antileukemia immune response is not well characterized. A better understanding on how cellular immunity selectively discriminates leukemia-related “neopeptides” could uncover mechanisms supporting tumor genome evolution.

Methods: 122 patients with acute myelogenous leukemia (AML) were included and 111 had available protein coding sequences. A neopeptide library was created using protein FASTA coding extracted for individual myeloid clonal mutations via National Center for Biotechnology Information (NCBI). Patient class 1 HLA typing was obtained through Tempus, and Genomic Testing Cooperative laboratories. Prediction of number and strength of AML neopeptide bindings to MHC class I molecules were obtained via NetMHCPan-1. Analysis was performed with K-means algorithm assigning age at diagnosis, detected MCPV, number of neopeptides binding (as continuous variable), overall survival (OS) and event-free survival (EFS) as variables. Unsupervised data input allowed 3 cluster partitions for differential survivals allowing HLA class 1 peptide binding aggregation with potential roles in leukemogenesis and patient outcome. Descriptive statistics were performed with SAS.

Results: Sixty-six different MCPV were detected. Of 111 patients, 70 (63%) with available MCPV produced at least 1 MHC I neopeptide binding. Frequently observed variants were *P53* (13%), *FLT3* (9.2%), *WT1* (7%), *DNMT3A* (6.5%), *RAS* (5%), *ASXL1* (4.3%), *RUNX1* (4.2%), *NPM1* (4.2%) and *IDH1/2* (2.6%). Cluster 2 demonstrated a lack of favorable and higher proportion of adverse ELN 2022 subgroups. Cluster 3 exhibited a higher of *P53* [p=0.03] and MDS-related mutations. OS was 79, 239, and 1551 days for cluster 2,1 and 3, respectively [p=0.0001]. EFS was 134, 363 and 451 days for cluster 2,1 and 3, respectively [p=0.0001]. Interestingly, Cluster 2 and 3 assembled the highest probability for peptide binding [1 v 2 v 3 = 1.76% v 36.6% v 62%, p=0.01]. Lastly, albeit in low frequencies, higher diversity of DNA repairing enzymes was seen in cluster 2.

Conclusions: Different MCPV arising in AML genome are variably immunogenic and leukemia-related neopeptide binding’s ability is differentially expressed in our 3 clusters. Frequent neopeptide bindings in clusters 2 and 3 may reflect higher AML immunogenicity resulting in genomic instability. It is possible that less “edited” genomes in cluster 1 preserve higher chemosensitivity resulting in better OS, while highly edited genomes in cluster 2 and 3 are less chemo-sensitive and circumvent host immunosurveillance. Further expansion of cluster 2 is necessary to better understand the role of DNA repairing enzymes in younger patients’ outcomes, especially when genomic instability is observed.

#5378 Spatially resolved human leukocyte antigen (HLA) expression correlates with motif neoepitope expression and durable response to immune checkpoint blockade (ICB) in non-small cell lung cancer (NSCLC).

Lucas Goldman, Sarah Gorbatov, Collin Shen, Alexa Berezowitz, Edward Garon, **Amy Lauren Cummings**

UCLA - University of California Los Angeles, Los Angeles, CA

Background: We previously showed electrostatic interactions enhance binding between “motif” neoepitopes and HLA and predict advanced NSCLC ICB benefit, suggesting optimal neoantigen presentation drives effective anti-tumor immune response (Cummings 2020). However, not all cases with motif neoepitopes exhibit favorable ICB outcomes.

Methods: As proof-of-concept, participants from our published NSCLC ICB cohort with available pre-treatment archival tissue were selected based on HLA supertype B44, predicted motif neoepitopes, and best response of progressive disease (PD) vs partial/complete response (PR/CR). Whole exome sequencing, HLA typing and neoepitope prediction were previously performed (Cummings 2020). GeoMx slides were prepared, hybridized with RNA probes and stained with antibodies to cytokeratin (CK), nuclear material and CD45 per manufacture instructions (Geiss 2008). Antibody to CD8 (Novus) was optimized at 1:50 dilution. Twelve regions of interest (ROI) were selected per sample including the following compartments: CK+CD8+, CK+CD8-, CK-CD8+ and CK-CD8- (negative control). Each ROI included ~150 nuclei selected using GeoMx Digital Spatial Profiler. Sequencing was performed on Illumina Novaseq 6000 (50bpx2) demultiplexed using Illumina Bcl2fastq v2.19.1.403. Raw reads were normalized and compared using paired student’s T-tests with Tukey’s correction via R v4.1. Neoepitope (non/motif) comparisons used matched numbers per sample selected by highest expression.

Results: Seven participants (3 PD, 3 PR, 1 CR) were included, each exhibiting 1-7 motif neoepitopes without HLA loss of heterozygosity. 84 ROI included 24 CK+CD8+, 24 CK+CD8-, 24 CK-CD8+ and 12 CK-CD8- with at least one ROI per category per participant. PD samples had fewer CD8+ ROI (12 vs 36) and lower CXCL9 ($p=0.011$) and CD274 ($p=0.014$). HLA-A/B/C expression followed a gradient with highest expression in CK+CD8+ ROI with limited detection in CK-CD8- ROI. Among HLA, HLA-B had highest median expression (A: 226, B: 650, C: 202; $p<0.001$). In CK+ ROI, motif neoepitope expression was detectable for all participants but not statistically different from non-motif expression ($p=0.23$). HLA-A/B/C all exhibited lower expression in PD CK+ ROI ($p<0.001$).

Conclusion: HLA expression may modify prediction of clinically meaningful neoepitopes and response to ICB. Validation in a larger, prospective cohort is planned.

#5379 Inhibition of ULK1/2-mediated autophagy augments antigen processing and presentation in STK11 mutant NSCLC.

S. C. Schwager, E. Park, A. Van Abbema, Y. Guan, C. Rosen, S. Cho, M. Black, I. Kurilyak, J. Jeffrey, J. Fung, S. L. Paprcka, E. Fernandez-Salas; Arcus Biosciences, Inc., Hayward, CA

BACKGROUND: Inactivating mutations and deletions in STK11 are present in 9-20% of NSCLC and result in immunologically cold tumors that respond poorly to therapy, despite having a high tumor mutational burden and neoantigen load. STK11 mutations in NSCLC are associated with higher levels of ULK1/2-mediated macroautophagy, resulting in localization of MHC-I to autophagosomes and lysosomes leading to its degradation and decreased antigen presentation. Knockdown of ULK1/2 can restore surface MHC-I in highly autophagic cell lines. Here, we show that inhibition of ULK1/2 decreases macroautophagy, resulting in increased antigen processing and presentation (APP) and MHC-I levels in cancer cells, supporting the hypothesis that inhibition of ULK1/2 will restore antigen presentation in NSCLC STK11mut tumors.

METHODS: TCGA datasets were analyzed to determine transcriptional differences in autophagy and APP between STK11 WT and mutant NSCLC tumors. CRISPR was used to stably knockout STK11 in multiple human NSCLC cell lines to generate isogenic pairs. mRNA and protein levels of APP machinery in NSCLC cell lines were assessed using qPCR, western blots, and flow cytometry. CRISPR was additionally used to knockout ULK1 and ULK2 in human STK11 mutant A549 cells. ULK1/2 tool compounds were synthesized based on existing patent literature. Effects of the combination of ULK1/2 inhibition with low levels of IFNγ on surface MHC-I levels were evaluated in several NSCLC cell lines by flow cytometry.

RESULTS: NSCLC tumors with loss of function mutations or deletion of STK11 display increased transcription of genes in the ULK complex and reduced transcription of genes necessary for APP. STK11mut and KO NSCLC cell lines also display lower levels of APP at the mRNA and protein levels. Double knockout of ULK1 and ULK2 in A549 cells is not cytotoxic and results in decreased autophagy as well as increased immunoproteasome components and cell surface MHC-I. ULK inhibition reduces autophagy and restores APP at the protein level, but not at the transcriptional level, in all NSCLC cell lines evaluated. Combination of very low concentrations of IFNγ with ULK inhibition demonstrates additive increases in MHC-I greater than either single-agent treatment alone.

CONCLUSIONS: STK11mut/del is associated with poor prognosis in NSCLC and leads to increased ULK-induced autophagy and decreased APP. ULK inhibition increases APP and surface MHC-I levels in STK11mut cell lines. In the presence of low concentrations of IFNγ, ULK1/2 inhibition restores APP in NSCLC STK11mut cell lines to the levels seen in NSCLC STK11 WT cell lines. The data presented here provides a rationale for targeting ULK1/2 to amplify immune recognition in immunologically cold tumors with high autophagy to increase responses to immunotherapies.

TUMOR BIOLOGY: Angiogenesis in Cancer
Poster Session

#5384 The hypoxia-alleviating agent ITPP restores vascular function in zebrafish xenografts of pancreatic cancer.

R. Abou Khouzam[1], F. Amorim[2], A. Rifath[1], H. Nawafleh[1], V. Povoa[2], R. F. Zaarour[1], J. M. Lehn[3], R. Fior[2], P. Limani[4], S. Chouaib[5];
[1]Gulf Medical University, Ajman, United Arab Emirates, [2]Champalimaud Foundation, Lisbon, Portugal, [3]University of Strasbourg, Strasbourg, France, [4]University Hospital Zurich, Zurich, Switzerland, [5]Gustave Roussy, Villejuif, France

Pancreatic cancer mostly manifests as pancreatic ductal adenocarcinoma (PDAC) and is characterized by a highly hypoxic microenvironment that is associated with worse patient survival and resistance to therapy. Hypoxia induces angiogenesis and the resulting leaky and unstructured vessels fail to reoxygenate the tumor mass, thus exacerbating hypoxia and its downstream impact on tumorigenesis. Myo-inositol trispyrophosphate (ITPP) is a non-toxic allosteric effector of hemoglobin shown to reduce tumor growth and enhance survival in mice and rat models of different tumor types. Herein the aim is to assess for the first time the ability of ITPP to effectively treat PDAC tumors *in vivo* in zebrafish xenografts and to investigate its impact on vascular normalization. To that aim, four PDAC cell lines, AsPC1, Capan1, MIA PaCa2, and PANC1 were included, as well as the angiogenic breast cancer cell line, Hs578t. Cells were grown in appropriate conditions and on injection day, labeling was done with deep red. Labeled cells were then injected in the perivitelline space of anesthetized larvae. The following transgenic larvae were used: those having labeled blood vessels only (*Tg(kdrl:DsRed)*), labeled blood and lymphatic vessels (*Tg(fli1:eGFP)*), and double transgenics with labeled gata+ erythrocytes (*Tg(fli1:eGFP;gata:dsRed)*). One day post injection (dpi) xenografts were sorted based on size and treated by immersion for three consecutive days with control medium or ITPP at a concentration selected based on the maximum tolerated dose assay. Treatment was refreshed daily, and at 4dpi live confocal imaging was conducted on select *Tg(fli1:eGFP;gata:dsRed)* xenografts. All xenografts were then fixed and subjected to whole mount immunofluorescence. Nuclei were stained with DAPI and anti-Caspase3^{Asp175} was used as a marker for apoptosis. Imaging was performed using the Zeiss LSM confocal microscope and tumor size, apoptosis and mitotic figures were quantified with ImageJ. Vascular function was defined as the presence of gata+ cells within tumor-related vasculature, while vessel density and infiltration were determined in ImageJ by calculating the percentage of GFP area in the tumor. Thus far results from AsPC1-derived xenografts demonstrate that ITPP leads to a significant decrease in mitotic figures ($p=0.0132$) and an increase in apoptosis ($p=0.0025$), with no change in tumor size. Preliminary data reveal a trend of increased functional vasculature in both the AsPC1- and Hs578t- derived xenografts upon ITPP treatment. A trend of decreased vasculature infiltration could also be observed in the ITPP-treated Hs578t-derived xenografts. Based on these results, the zebrafish model could be an appropriate alternative for assessing the anti-tumorigenic activity of ITPP in PDAC in a short turnaround time and could potentially enable the visualization of ITPP's impact on angiogenesis at single cell resolution.

#5385 Synthetic disulfide derivative of vitamin B1, fursultiamine, prevents VEGF-induced angiogenesis.

S. Tran, Z. Frost, K. Ramana;
Noorda College of Osteopathic Medicine, LLC, Provo, UT

Angiogenesis is a process in which new blood vessels are formed from the existing blood vessels required to supply nutrients and oxygen to various tissues. Angiogenesis plays a significant role in the growth and spread of many cancers, and several anti-angiogenic agents act as chemotherapeutic agents. Recent studies have shown that fursultiamine (thiamine tetrahydrofurfuryl disulfide), a lipid-soluble synthetic disulfide derivative of thiamine, possesses viable antineoplastic and antiviral effects. However, its role in preventing angiogenesis is not known. We hypothesize that fursultiamine, with its potent antioxidative actions, prevents VEGF-induced angiogenesis in vitro and in vivo. Human umbilical vein endothelial cells (HUVECs) were treated with VEGF in the absence and presence of fursultiamine (0-100 uM) in a time and dose-dependent manner. Cell viability was determined by MTT assay and in vitro angiogenesis by tube formation assays. The expression of various pro-angiogenic, anti-angiogenic and inflammatory markers will be determined by specific antibody arrays. Our results indicate that fursultiamine prevents VEGF-induced endothelial cell growth in a dose-dependent manner. Further, fursultiamine prevents the in vitro tube formation as determined tube formation assays. Further, fursultiamine also regulated the VEGF-induced expression of various angiogenic markers such as VEGF, PDGF, EGF, Ang1, Ang2, angiogenin, and FGF, inflammatory markers such IL-1b, GM-CSF, TGF-b, MMPs, and others such as TIMPs, PTX3 and CF-III. Based on our in vitro data, we suggest that fursultiamine could prevent VEGF-induced angiogenesis, and this compound as a potent anti-angiogenic agent that could prevent cancer growth and metastasis.

#5386 Increased sprouting angiogenesis in a microphysiological model of cisplatin-resistant recurrent lung cancers.

E. Olsen, G. Kpeli, O. Ahmad, M. Mondrinos;
Tulane University, New Orleans, LA

Non-small cell lung cancer (NSCLC) constitutes 85% of total lung cancer cases and first-line therapies still often employ the platinum-based agents. Cisplatin therapy for NSCLC often leads to relapse of aggressive tumors with high metastatic potential after a period of dormancy. We hypothesize that cisplatin-resistant tumor cell phenotypes will increase features of aggressivity including sprouting angiogenesis in microphysiological models of NSCLC. First, we engineered various TME configurations using A549 cell spheroids and cancer associated fibroblasts (CAF) to establish a baseline of tumor cell proliferation, ECM deposition, and expression of proangiogenic and proinflammatory genes. Next, we generated cisplatin-resistant (Cis-R) A549 sub-lines to test the hypothesis that 3D tumor models engineered using these drug-resistant cells will capture hallmarks of highly aggressive recurrent tumors such as increased expression of progression-associated genes, increased induction of local stromal reactions and more profound angiogenesis. We treated parent A549 with 25 μM cisplatin for 96 hours followed by at least 14 days of recovery to generate Cis-R A549 cells. Interestingly, Cis-R spheroids exhibited significantly lower rates of proliferation ($P<0.01$) relative to parent A549 spheroids as measured by Ki67 index. Cis-R cells and spheroids exhibit increased genetic expression for genes involved in inflammation, EMT, proliferation and chemoresistance. Furthermore, Cis-R cells in 2D displayed a mesenchymal-like morphology and further exhibited dysmorphic spheroid morphology in 3D. We then developed a membrane free microphysiological system (MPS) comprised of two adjacent and contiguous tissue layers to investigate cancer mediated angiogenesis. We seeded one layer with lung fibroblasts and endothelial cells, which formed a vascularized network, while the other lane was cultured with no cells (control), parent A549 spheroids, or Cis-R A549 spheroids. Media void of VEGF was used throughout the duration of the experiment to isolate the effect of TME-derived factors. We measured increased angiogenetic sprouting induced by Cis-R tissues relative to parent using the following metrics: sprout density (Cis-R = 49.86 ± 10.93 $\mu m/\mu m^2$, parent = 13.73 ± 4.12 $\mu m/\mu m^2$, blank = 14.76 ± 4.22 $\mu m/\mu m^2$), sprout length (Cis-R = 15006 ± 5507 μm, parent = 2466 ± 639.1 μm, blank = 4749 ± 1547 μm), and sprout area fraction (Cis-R = 0.10 ± 0.028, parent = 0.041 ± 0.010, blank = 0.032 ± 0.0095). Thus, the creation of drug resistant tumor cell sub lines enables the construction of more aggressive engineered tumor microenvironments. Future iterations of our MPS model will be used to investigate angiogenesis in the context of additional cancers, including breast and colon, while transitioning to the use of patient-derived organoids.

#5387 Host-derived CCL2 drives prostate cancer bone metastasis *via* CCND2/STAT3 pathway.

J. Meng[1], M. Chang[2], S. Qin[2], X. Huang[2], W. Liang[2], H. Tong[3], **J. Zhang**[2];

[1]Liuzhou Worker's Hospital, Liuzhou, Guangxi , China, Liuzhou, China, [2]Southern University of Science and Technology, China, Shenzhen, China, [3]University of Macau, Taipa, Macao SAR, China

Overexpression of tumor-derived CCL2 has been shown to partially promote prostate cancer (PCa) bone metastasis, but the function of host-derived CCL2 is not fully understood. We first developed a mouse model using intracardiac injection and obtained highly metastatic PCa cell subclones through *in vivo* selection. The highly metastatic tumor cells were injected intracardially into CCL2 knockout (CCL2 KO) mice and wild-type (WT) controls, and the tumor cell growth and metastasis were monitored weekly by bioluminescence imaging. The osteolytic lesions were evaluated by radiography, micro-computed tomography (microCT) and immunohistochemistry (IHC) staining. The cells in the bone microenvironment were analyzed by flow cytometry. Also, RNA sequencing (RNA-seq) analysis was performed on the cells either from CCL2 KO mice or WT controls. We found that a loss of host-derived CCL2 significantly retarded tumor growth in bone and prolonged mouse survival. In addition, bone density analysis revealed a decrease in osteolytic lesion in CCL2 KO mice, compared to WT controls. Systemically, CCL2 deficiency reduced the proportion of granulocyte-myeloid-derived suppressor cell (G-MDSC) populations with immunosuppressive function and decreased the PCa conditioned medium (CM)-induced osteoclast formation. The enrichment analysis revealed that the dysregulated genes in bone metastatic cells from CCL2 KO mice were significantly enriched in several biological processes, including vitamin metabolism, monoatomic anion homeostasis, immune response, and bone growth. Additionally, we also confirmed that the CCND2/STAT3 pathway is apparently suppressed in the cells from CCL2 KO mice. This study demonstrated that targeting the host-derived CCL2 might be a novel potential anti-metastatic approach. Supported by the NSFC projects (81972766, 81972420, 82173336), as well as grants from the Science and Technology Project of Shenzhen (JCYJ20190809161811237, JCYJ20210324104214040).
Key words Host-derived CCL2; Prostate cancer; Bone metastasis; osteoclast; CCND2

#5388 FOSL1 promotes glioma tumorigenesis and stemness through NF-κB and STAT3 pathways.

M. Liu[1], V. Ramar[1], A. Khedri[1], B. Hudson[1], S. Guo[2];
[1]Morehouse School of Medicine, Atlanta, GA, [2]Xavier University, New Orleans, LA

Background: Glioblastoma multiforme (GBM) is the most common and malignant primary brain tumor, GBM's inevitable recurrence suggests that glioblastoma stem cells (GSC) render these tumors persistent. Our previous work showed that FOSL1, which is transactivated by the STAT3 gene, functions as a tumorigenic gene in glioma pathogenesis and is a diagnostic marker and potential drug target for glioma patients. Accumulating evidence shows that STAT3 and NF-κB cooperate to promote the development and progression of various cancers. The link between STAT3 and NF-κB suggests that NF-κB can also transcriptionally regulate FOSL1 and contribute to gliomagenesis.
Methods: 1). To investigate downstream molecules of FOSL1, we analyzed the transcriptome after overexpression of FOSL1 in a PDX-L14 line, characterized by very low FOSL1 expression 2). We conducted immunohistochemical staining for FOSL1 and p65 using rabbit polyclonal anti-FOSL1 and p65 in glioma tissue microarrays (TMA) derived from 76 glioma patients and 10 normal individuals. 3). Mutants of the human FOSL1 promoter, featuring mutations in essential binding sites for NF-κB and STAT3, were generated using a Q5 site-directed mutagenesis kit. Subsequently, we examined luciferase activity in glioma cells and compared it to the wild-type FOSL1 promoter. 4). We explore the mutual regulation between NF-κB signaling and FOSL1 by modulating the expression of NF-κB or FOSL1. Subsequently, we assessed the activity of FOSL1 and NF-κB. 5) To understand the role of FOSL1 in cell growth and stemness, we conducted a CCK-8 assay, cell cycle analysis, assessing apoptosis and GSC markers, ALDH1 and CD133 under varying FOSL1 expression conditions.
Results: 1) Transcriptome analyses of downstream molecules of FOSL1 show that NF-κB signaling pathways are regulated by FOSL1. 2) p65 protein expression correlates to the expression of FOSL1 in glioma patients. 3) NF-κB is a crucial transcription factor activating the FOSL1 promoter in glioma cells. 4) Mutual regulation between NF-κB and FOSL1 contributes to glioma tumorigenesis and stemness through promoting G1/S transition and inhibition of apoptosis.
Conclusion: The FOSL1 molecular pathway is functionally connected to NF-κB and STAT3 activation, enhances stemness, and FOSL1 is a novel GBM drug target.

#5389 Development of T-cell exclusion in melanoma.

Ha-Ram Park, Hee Won Yang, Minah Kim

Columbia University Irving Medical Center, New York, NY

Immune checkpoint inhibitors (ICIs), which prevent immune cell exhaustion and boost an antitumor response, have shown remarkable treatment efficacy in patients with advanced melanoma. However, its efficacy is limited by the emergence of resistance associated with an immunosuppressive tumor microenvironment (TME). The contribution of abnormal tumor vasculature to limited immune cell infiltration into the tumor core has been reported but the mechanisms of its development are still elusive. We analyzed how tumor angiogenesis affects the immune cell exclusion at different time points of primary melanoma using syngeneic murine melanomas. The spatial distribution of various immune cell populations and vascular integrity were analyzed in whole tumor cross-sections via multiplex immunofluorescence staining. We found that the exclusion pattern of CD8+ T cells was less evident with a balanced distribution across the whole tumor regions at the early stage. However, as the tumor grows, there is a pronounced accumulation of CD8+ T cells at the tumor periphery with a conspicuous absence in the core. Tumor blood vessels were structurally uniform and functionally stable in the early developmental tumor but became unstable and leaky as the tumor progressed, which was associated with the development of CD8+ T-cell exclusion. To understand the mechanism underlying vascular regulation of immune exclusion during tumor progression, we will investigate the expression of genes related to tumor angiogenesis using spatial transcriptomic analysis and RNA sequencing of endothelial cells (CD45+CD31-) sorted from the murine melanomas. These results highlight the contribution of spatial tumor vascular destabilization to the T-cell exclusion development, implying the potential of targeting tumor vasculature to enhance immune activation and the therapeutic efficacy of ICI in melanoma.

#5390 Exploring signaling pathways of tumor-nerve interactions in prostate and breast cancer.

B.-J. Hwang[1], G. J. Edwards[2], C. Knoblich[3], K. Rezvani[2], V. Odero-Marah[1];
[1]Morgan State Univ., Baltimore, MD, [2]Claflin University, Orangeburg, SC, [3]Sanford School of Medicine, Vermillion, SD

A significant portion of prostate cancer (PCa) and breast cancer (BCa) patients develop bone metastatic disease. In some cases, cancer spreads through the nervous system, a process known as perineural invasion (PNI). Neurite outgrowth is believed to be a precursor to PNI. Snail is an important gene which regulates the epithelial-mesenchymal transition (EMT) process in which tumor cells at the invasive front undergo this transition to promote invasion, migration, and subsequent metastasis. We recently published that Snail promotes neurite outgrowth in PCa cells. We hypothesize that Snail expression will stimulate neurite outgrowth in both PCa and BCa cells through extracellular vesicles from cancer cells interacting with neurons. To test this hypothesis, we first collected conditioned media from PCa and BCa cells expressing Snail and isolated exosomes. Exosomal markers were detected using western blot to confirm the isolated exosomes. Additionally, we used Transmission Electron Microscopy (TEM) to observe the secretion of exosomes. Proteomics was performed to analyze proteins expressed within exosomes of LNCaP Snail overexpressing or C4-2 Snail knockdown PCa cells. Our results showed that Snail-expressing cells secrete exosomes containing Talin1, specifically, the proteolyzed C-terminal rod domain, while full-length Talin1 is found in whole cell lysates from Snail-expressing cells. Talin1 has previously been associated with neurite outgrowth. Neurite outgrowth assays were then performed using conditioned medium collected from C4-2 PCa cells with Snail knockdown and MCF-7 BCa cells with Snail overexpression. Increased neurite outgrowth is observed in PC-12 cells and NPC (Induced Pluripotent Stem Cells differentiated neuronal progenitor cells) when cultured with conditioned medium collected from PCa and BCa cells expressing high levels of Snail. AKT activation was observed in the neuronal cells in response to conditioned media from Snail-expressing cells. Furthermore, we found that mH_4, a proprietary small molecule inhibitor of Talin1, reduces Snail-mediated neurite outgrowth and AKT activation (p-AKT Thr308 and Ser473). Overall, we have uncovered a pathway whereby Snail transcription factor promotes secretion of exosomes containing Talin1 which promotes AKT signaling in neuronal cells and neurite outgrowth. Talin1 small molecule inhibitor shows promise for therapeutic targeting of tumor-nerve interactions.
Acknowledgements: The authors acknowledge the use of core facilities supported by the National Institute on Minority Health and Health Disparities through grant number 5U54MD013376 and 1U54GM128729-01-DaCCoTA Scholars Program (PI: Rezvani) National Institute of General Medical Sciences (NIGMS).

#5392 Plasma levels of Matrix metalloproteinases 9, an angiogenic promoting protein, are persistently elevated three weeks after minimally invasive colorectal resection (MICR) for cancer which may support residual tumor metastasis.

Chandana S. K. Herath Mudiyanselage, Anuj R. Sharma, Neil Mitra, Aashutosh Sah, Xiaohong Yan, Pablo Palacios, Vesna Cekic, Richard L. Whelan

Department of Surgery, Lenox Hill Hospital, New York, NY

Introduction: The Matrix metalloproteinases (MMPs) family are a collection of zinc and calcium-dependent endopeptidases. MMP-9 is instrumental in modifying the extracellular matrix (ECM) and generating bioactive molecules which influence a range of physiological functions. Cellular TNF-a, IL-8, VEGF, and FGF-2 can stimulate the production of MMP-9 in endothelial cells (EC), a process that controls healthy and disease-related angiogenesis. MMP-9 facilitates tumor metastasis and also is involved with wound healing. MMP-9 is generated by white blood cells, ECs, and several other cells. There's a significant increase in plasma MMP-9 levels in patients suffering from colorectal cancer (CRC). The aim of this study was to assess plasma MMP-9 levels before and during the first month following MICR for CRC.

Method: CRC patients enrolled in an IRB approved data/plasma bank who had undergone MICR for whom plasma samples were available from the following time points were deemed eligible for this study; preoperatively (PreOp) and on Postoperative Day (POD) 1, POD 3 and at least 1 later postop timepoint (POD 7-41). The demographic, clinical operative and pathology reports were reviewed. Blood specimens were collected, processed, and frozen. MMP-9 levels were measured in duplicate via ELISA. The Wilcoxon paired t-test was used for analysis and significance set at $p<0.05$.

Results: 86 CRC MICR patients (69% colon,31% rectal; laparoscopic 69%, hand-assisted 31%; 47 males, 39 females; mean age 63.9± 14.3 years), met the entry criteria. The mean hospital stay was 6.5±3.0 days. The cancer stages were distributed as follows: stage I; (n=26), II; (n=25), III; (n=30), and IV; (n=4). Compared to the mean preop MMP-9 plasma levels (155.3±132.1,n=86; ng/ml), there was a significant increase on postoperative day (POD) 1 (292.6± 213.0; n=86, $p<0.001$), POD3 (232.1±205.9,n=78, $p<0.01$), POD7-13 (217.8±171.2, n=63, $p<0.01$), POD14-20 (228.7± 109.1,n=24,p=03). No difference was found at the POD 21-41 time points vs preop results. Non-significant increases in plasma MMP-9 levels were noted in the hand-assisted surgery group during the POD 3-27 period compared to the laparoscopic group.

Conclusion: Postop plasma MMP-9 levels were significantly elevated (20% - 88%) vs preop levels for 3 weeks after MICR for CRC. The increased MMP-9 levels in the early postoperative period may be due to the acute inflammatory response, including increases in IL-1 and TNF mediated activation of neutrophils and macrophages. However, the spike during weeks 2-3 may be related to wound healing given MMP-9's role in angiogenesis. This persistent elevation for 3 weeks after surgery may also enhance angiogenesis in residual cancer deposits postoperatively. Further studies are needed.

#5393 Characterization of small ubiquitin-like modifier (SUMO) protein complex expression in human cancer cells to identify novel therapeutic targets.

M. A. Salih, R. Williamson, S. Kantamneni;
University of Bradford, Bradford, United Kingdom

SUMOylation is a post-translational modification where a number of small ubiquitin-like modifier proteins (SUMO) are conjugated to lysine residues of the target proteins and contribute to various cellular functions essential for cancer cell survival and proliferation. The unique behaviors, phenotypic and molecular adaptations found in the naked-mole rat (NMR) suggest a high stability and effective functioning of the molecular machinery that counteracts damage accumulation in its genome. NMR can reach 32 years, shows no signs of ageing, and possesses a very efficient mechanism of resistance to cancer. This study aims to investigate the regulation of SUMOylation machinery between NMR tissues in comparison to human cancer cells, to find novel targets for cancer therapy. Gene expression of SUMO isoforms between NMR and humans, were investigated through qRT-PCR. The data suggests a significant low expression level for most SUMO machinery (except PIAS4) in NMR brain and intestine tissues compared to MCF-7, DLD-1, SH-SY5Y, and MCF-10A cells. Western blotting analysis also revealed high protein expression of PIAS4 in NMR compared to SENP1 and Ubc9. Also, SUMO machinery expression levels from NMR are recapitulated in cancer cells either silencing (hUBE2I: shRNA, hSENP1: shRNA) or overexpression (Myc/hPIAS4: Exp). Further, cytotoxicity assay was analyzed in relevance to Doxorubicin in MCF-7, 5-Fluorouracil in DLD-1 and Methotrexate in SH-SY5. The functional assays such as clonogenic and invasion assays were performed including apoptotic mechanisms (Bcl-2, and BID). In conclusion, the data revealed important differences in SUMOylation machinery between NMR and human cancer cells, which provides a future therapeutic path for cancer treatment.

#5394 Nicotine-induced exosomal miR-3157-3p from prostate cancer cells promotes angiogenesis.

S. Singh, M. Khan, S. Anand, S. Saranyutanon, S. Srivastava, S. Singh, A. P. Singh, K. Vikramdeo;
Mitchell Cancer Institute, University of South Alabama, Mobile, AL

Nicotine is a psychoactive component of cigarette smoke responsible for addictive properties of tobacco and is shown to promote cancer pathogenesis. We earlier reported that exosomes released from nicotine-treated prostate cancer cells played a key role in tumor angiogenesis, a process necessary to maintain the supply of nutrients and oxygen to the fast proliferating cancer cells. Here, we examined the molecular mechanisms underlying the exosome-mediated effect of nicotine on angiogenesis. For this, we screened the expression of angiogenesis-related miRNAs in the exosomes derived from LNCaP and C4-2 cells treated with vehicle or nicotine (400 nM). Highest and most differential abundance of miR-3157-3p was found in exosomes derived from nicotine-treated prostate cancer cells. Furthermore, the expression of TIMP-2 and KLF-2, established targets of miR-3157-3p, was also downregulated in endothelial cells transfected with exosomes derived from nicotine-treated prostate cancer cells or miR-3157-3p mimics. Studies are currently underway to establish direct targeting of TIMP-2 and KLF-2 by miR-3157-3p and confirm that their suppression is indeed associated with observed changes in endothelial cell growth, migration and capillary-forming ability.

#5395 The influence of hyperthermia on epigenetic signaling in dysbiotic tumor vasculature.

H. Kristian, S. Jenkins, R. Griffin, **R. P. Dings**;
UAMS Winthrop P. Rockefeller Cancer Institute, Little Rock, AR

The overall use of antibiotics has increased significantly in recent years. Although they resolve infections, oral antibiotics (ABX) severely alter the gut microbiota, disrupting commensal bacteria crucial for maintenance of various homeostatic processes. ABX-induced microbial imbalance, or dysbiosis, has systemic and long-lasting deleterious effects on the host. For example, we and others have shown that distal, non-GI tract solid tumors show accelerated progression during dysbiosis due to vascular immune suppression. Localized hyperthermia has been increasingly recognized to elicit various cellular responses, yet the epigenetic effects of hyperthermia on the tumor vasculature during ABX-induced dysbiosis are unknown. The balance of histone acetylation and deacetylation plays a critical role in the regulation of gene expression and thereby cellular processes. Therefore, we assessed which histone deacetylases (HDACs) are expressed and their abundance in endothelial cells of various sources with or without dysbiotic stress and/or hyperthermia to understand the utility of thermal medicine to promote normal functioning of the vasculature in dysbiotic patients. We found that HDAC expression levels differed among endothelial origins and that hyperthermia (60 min of either 41.5 °C or 43 °C) influenced the HDAC levels differentially. Especially HDAC 2, 3 and 8 were inhibited by hyperthermia. Additionally, we found that the vasculature receptors for endogenous HDAC inhibitors, GPR41, GPR43, and GPR109a are less abundant intrinsically on dysbiotic than orthobiotic tumor endothelial cells and that hyperthermia increased this expression. Although further studies are warranted, these results demonstrate that hyperthermia exerts epigenetic effects and is capable of overcoming the dysbiosis-induced phenotype. Since anti-cancer treatment with HDAC inhibitors has shown promise in the clinic but is hindered by systemic toxicities, localized hyperthermia may become a viable alternative in the future.

#5396 Vascularized gastric cancer 3D co-culture model using a microphysiological system as an oncolytic virus testing platform.

Y. Kim[1], Y. Song[2], Y. Choi[2], J. Jang[2], S. Kim[2], T.-L. Liu[2], K. Baek[2], K. Oh[3], S. Ma[4], T. Kim[5], W. Kwon[5], S. Yoo[2], J. Kim[1], S. Rha[6];
[1]Gangnam Severance Hospital, Yonsei University College of Medicine, Seoul, Korea, Republic of, [2]Qureator, San Diego, CA, [3]Research Center, SillaJen Inc., Seongnam-si, Korea, Republic of, [4]SillaJen Bio., San Francisco, CA, CA, [5]Song-dang Institute for Cancer Research, Yonsei University College of Medicine, Seoul, Korea, Republic of, [6]Yonsei Cancer Center, Yonsei University College of Medicine, Seoul, Korea, Republic of

Introduction: Angiogenesis is a critical aspect of cancer growth and metastasis. Consequently, inhibiting angiogenesis has garnered substantial attention in oncology research. JX-594 (pexastimogene devacirpvec; Pexa-Vec®), engineered from the Wyeth vaccine strain, has emerged as an attractive oncolytic virotherapy and demonstrated oncolytic, immunotherapeutic, and tumor vasculature-disrupting capacities. In our previous study, we found that JX-594 reduced the amount of vasculature in gastric tumors using a xenograft mouse model. In the present study, we investigate the effect of JX-594 on tumor vasculature using an *in vitro* human cell 3D co-culture model of vascularized gastric cancer, to determine if this tool provides improved accuracy in evaluating the mechanism of action and biological activity of JX-594 as compared to traditional animal models.
Methods: The Curio-Spheroid chip is a Microphysiological System (MPS) that can grow tumor organoids or spheroids in 3D using physiologically relevant hydrogels and culturing them with other human cell types such as fibroblasts, endothelial cells, and immune cells. We evaluated nine human gastric cancer cell lines (YCC-18, YCC-19, YCC-22, YCC-30, YCC-32, YCC-38, Hs746T, NUGC-3, SNU-620) for their ability to form spheroids and induce angiogenesis inside Curio-Spheroid chips. We selected YCC-32 for the oncolytic virus testing. Serial increases of M.O.I (multiplicity of infection) of JX-594 disrupted the tumor-induced angiogenesis in a dose-dependent manner.
Results: JX-594 treatment of the YCC-32 spheroid resulted in decreased levels of Ki-67 and cytopathic effects in a dose-dependent manner inside the Curio-Spheroid MPS system. Angiogenesis was observed surrounding the spheroid when co-cultured with endothelial cells and fibroblasts. JX-594 decreased YCC-32 spheroid-induced angiogenesis in a dose-dependent manner in the vascularized gastric cancer 3D co-culture model.
Conclusion: JX-594 had an inhibitory effect on tumor-induced angiogenesis in our vascularized gastric cancer *in vitro* 3D human cell co-culture model, demonstrating the utility of the platform as a tool to interrogate the effects of an oncolytic virus on both tumor cell killing and tumor-induced angiogenesis.

#5397 Characteristics of cancer associated fibroblasts isolated from refractory colorectal cancer using RNA sequence.

H. Kasashima, Y. Fukui, K. Yonemitsu, K. Kitayama, Y. Miki, M. Yoshii, T. Fukuoka, T. Tamura, M. Shibutani, T. Toyokawa, S. Ree, M. Yashiro, K. Maeda; Osaka Metropolitan University, Osaka, Japan

Primary tumor location of colorectal cancers (CRCs) is emerging as an important prognostic factor owing to distinct biological features. In fact, the patients with right-side CRCs (R-CRCs), in which primary tumors were resected in our department and followed by systemic chemotherapy, have a poorer prognosis in 2-year overall survival and progression-free survival than those with left-side CRCs (L-CRCs). Furthermore, cancer-associated fibroblasts (CAFs) promote tumor malignancy, but the precise transcriptional mechanisms regulating the acquisition of the CAF phenotype are not well understood. Here, we isolated the CAFs and normal counterparts from 10 CRCs which were performed radical resection, including 5 L-CRCs and 5 R-CRCs, and analyzed transcriptomic profile of CAFs by RNA-sequencing. Gene Set Enrichment Analysis (GSEA) was performed and inflammatory signatures, such as "HALLMARK IL2 STAT5 SIGNALING"(NOM p-value<0.001, FDR q-value=0.146), "HALLMARK IL6 JAK STAT3 SIGNALING"(NOM p-value=0.014, FDR q-value=0.162), "HALLMARK INTERFERON GAMMA RESPONSE"(NOM p-value=0.032, FDR q-value=0.1726), were enriched in the CAFs isolated from R-CRCs (R-CAFs). In addition to sidedness of CRCs, based on gene expression profiles from bulk tumors, CRCs were classified into four consensus molecular subtypes (CMS1-4). Among them, The fibrotic CMS4 subtype portends poor relapse-free survival. We identified 4 CMS4-CRCs, which have the characteristics of stromal activation and the worst prognosis among other CRCs. GSEA showed that the signature of "HALLMARK TNFA_SIGNALING_VIA_NFKB" (NOM p-value=0.023 FDR q-value=0.207), "HALLMARK GLYCOLYSIS" (NOM p-value=0.036 FDR q-value=0.239) were upregulated in the CAFs isolated from CMS4-CRCs. These results indicated that CAFs isolated from refractory CRCs have unique phenotypes and the elucidation of these mechanisms might lead to a promising treatment for refractory CRCs.

#5398 Single-cell transcriptomic analysis of partial endothelial-to-mesenchymal transition in sprouting angiogenesis.

K. Thapa[1], C. J. Hatch[2], C. Hughes[2], J. S. Fang[1];

[1]Tulane University, New Orleans, LA, [2]University of California, Irvine, CA

Endothelial-to-mesenchymal transition (EndoMT) is a process of morphological, functional, and molecular shift of endothelial cells (EC) towards a mesenchymal identity. This process is critical for embryonic development, and knockout animals lacking copies of the individual master EndoMT transcription factors – including Slug, Snail, and Twist – exhibit significant cardiovascular defects. We previously showed that while Slug knockout animals have a modest developmental vascular phenotype, there is a striking loss of tumor angiogenesis in these animals. Based on these and other data, we hypothesize that sprouting angiogenesis involves transient acquisition of an intermediate state of the EndoMT program –i.e., partial EndoMT (pEndoMT). To test this hypothesis, we used single cell RNA sequencing at day 2 and day 6 following TGF-β activation to map the transcriptomic changes associated with complete endothelial-to-mesenchymal transition. In parallel, we sequenced EC activated to undergo sprouting angiogenesis *in vitro* at the same timepoints. We show that angiogenic EC transiently acquire a transcriptomic profile of the pEndoMT state, but then later reacquire the transcriptomic profile of committed EC rather than transition completely into mesenchymal cells. We further use this dataset to identify several candidate genes that appear to be regulated by Slug and associated with the pEndoMT state. Future work will use *in vitro* and *in vivo* angiogenesis models to identify how pEndoMT is regulated in angiogenesis, and how this regulation may differ in the presence of tumor stroma.

#5400 CD160 regulates angiogenesis in activated human endothelial cells.

A.-i. AZIZ;
Mohammed VI Polytechnic University, Ben Guerir, Morocco

Angiogenesis, the process of forming new blood vessels from pre-existing ones, plays a pivotal role in various physiological and pathological conditions. CD160, a cell surface receptor known for its modulatory function in the immune response, has recently garnered attention as a surface marker for activated endothelial cells. In this study, we investigate the anti-angiogenic effects of a novel anti-CD160 antibody. Using the tube formation assay, we evaluated the novel anti-CD160 antibody's ability to inhibit neovascularization potential in activated Human umbilical vein endothelial cells (HUVEC) *in vitro*. Our results revealed a significant reduction in total tube length, the number of branches, and closed networks, indicating the antibody's efficacy in impeding neovascularization. In addition, we explored the molecular mechanisms underlying CD160's anti-angiogenic properties, showing its ability to selectively decrease fibroblast growth factor-2-induced angiogenesis. Furthermore, we assessed the safety profile of our new anti-CD160 antibody by examining its impact on endothelial cell apoptosis. Encouragingly, our findings demonstrated no induction of apoptosis, suggesting the antibody's selective targeting of angiogenic processes without compromising endothelial cell viability, thus supporting CD160's vascular normalization properties. In conclusion, our research provides compelling evidence for the anti-angiogenic effects of the CD160 antibody, as evidenced by its inhibition of tube formation without inducing apoptosis in activated endothelial cells. These findings hold promising therapeutic implications for targeting angiogenesis in various pathological conditions, warranting further exploration for potential clinical applications.

Keywords: CD160, Angiogenesis, Endothelial cells. HUVECs.

#5401 Vasculogenic mimicry: A three-step progress to form lumen-containing and fluid-conducting tubular structures *in vitro*.

G. I. Owen[1], N. Santander[1], G. Mingo[1], P. Gonzalez[1], V. George[1], N. Babbitt[1], A. Espinioza[1], I. Vega[1], C. Canales[1], C. Ibanez[1], R. Gejman[1], J. Roa[1], F. Nualart[2], A. Ravasio[1], C. Bertocchi[1];

[1]Pontificia Universidad Catolica de Chile, Santiago, Chile, [2]Universidad de Concepcion, Concepcion, Chile

Introduction: Vasculogenic mimicry (VM) is a clinical phenomenon by which cancer cells can form vessel-like structures in an endothelial-free (CD31-) fashion. VM presence in tumors correlates to poor patient prognosis. In our laboratory we have established an *in vitro* model where cancer cells from either cell lines or primary culture form lumen-lined and fluid-conducting tubular structures when grown on laminin-rich Matrigel over a four-day period. Given the duration of formation and the complexity of these structures, we hypothesize that VM *in vitro* is a multistep process, where each stage requires spatio-temporal organization of adhesive proteins, stemness and EMT (suggesting the need for epithelial to mesenchymal transition) signaling.

Methods: Using our *in vitro* models, we analyzed by siRNA, immunostaining and live cell imaging with Airyscan the distinct phases and the corresponding spatio-temporal organization of selected proteins.

Results: We show that VM *in vitro* has three distinct phases that are characterized by (1) alignment and migration, (2) contraction, proliferation and bridge formation, and (3) tubular structure closure and lumen formation. These steps require spatio-temporal distribution of ZEB1 and E-cadherin (suggesting gain and loss of epithelial to mesenchymal transition), the presence of Integrin β1 and laminin 111, and the distinct localization of Laminin and CD44.

Conclusion: A better characterization of VM may lead to the identification of a clinically useful marker to predict poor patient prognosis and shed light on a druggable pathway to treat this subgroup of aggressive cancer.

#5402 Understanding the role of exercise in lymphatic vessel regulation in melanoma.

P. Tirumala[1], J. Lee[2], K. L. Schadler[2];
[1]Rice University, Houston, TX, [2]University of Texas MD Anderson Cancer Center, Houston, TX

Exercise has been demonstrated to be an effective method to remodel tumor blood vessels and to improve immune cell infiltration in multiple tumor models in mice. However, it is unclear whether aerobic exercise alters lymphatic vasculature in tumors. The lymphatic system plays an important role in tumor growth and metastasis because it regulates interstitial fluid pressure via lymph flow and immune cell trafficking, in conjunction with blood vessels. Lymphatic vessels are particularly important during metastasis because tumor cells frequently escape the primary tumor through lymphatic vasculature to establish the first site of metastasis in the lymph nodes. Here, we evaluated the effect of aerobic exercise on lymphatic vessels and lymphatic endothelial cell junctions in melanoma in male C57BL/6J mice. BP melanoma cells derived from transgenic mice with *Braf*$^{V600E/+}$ and *Pten*$^{-/-}$ mutations were injected subcutaneously. Mice were assigned to no exercise and exercise groups when tumors reached ~30 mm^3. The exercise group completed treadmill running at 12 meters/minute for 45 minutes for 5 consecutive days with 2 days of rest per week for 2 weeks before tumor harvest. Tumor lymphatic endothelial cells were identified by LYVE-1, endothelial tight junctions by ZO-1, and nuclei were identified by DAPI using immunofluorescence staining on frozen tumors. The number of total lymphatic vessels, elongated vessels(>100 µm), open lumens, and co-localization of ZO-1 with LYVE-1 was quantified on 6 random images per tumor using NIH Image J software. ANOVA and t-test were used to conduct statistical analysis ($p < 0.05$). Tumors from exercised mice had higher lymphatic vessel density ($p=0.002$) and more open lumens ($p=0.001$). Surprisingly, tumors from exercised mice had fewer ZO-1 positive vessels ($p=0.015$) and lower co-localization of ZO-1 and LYVE-1 ($p = 0.0185$) than tumors from non-exercised mice, suggesting fewer stable endothelial cell junctions in lymphatic vessels. The higher lymphatic vessel density and higher number of open lumens present in tumors from exercised mice may contribute to an exercise-induced improved anti-tumor immune response, which has been previously reported. However, the lower ZO-1 expression on lymphatic endothelial cells in tumors from exercised mice may indicate lymphatic vasculature dysfunction and/or hyper-permeability. Further work is needed to assess the functional changes in tumor lymphatic vasculature by exercise, and how these changes impact the anti-tumor immune response and metastasis.

#5403 Meeting the Physical Activity Guidelines is associated with increased CD8+ T-cell density in the tumor microenvironment of breast cancer patients.

R. Cannioto[1], A. Omilian[1], E. Davis[1], L. Mendicino[1], S. Abrams[1], B. Qin[2], C.-C. Hong[1], E. Bandera[2], S. Yao[1], C. Ambrosone[1];
[1]Roswell Park Comprehensive Cancer Center, Buffalo, NY, [2]Rutgers Cancer Institute of New Jersey, New Brunswick, NJ

Background: Our current understanding of how physical activity (PA) is associated with immunity in breast cancer (BC) patients is based on pre-clinical evidence gleaned from mouse models or immune cells in the circulating blood, which may not be reflective of the tumor immune microenvironment (TIME). Whether self-reported PA is associated with immune cell infiltration in the breast TIME, the most relevant site for prognosis, remains a fundamental gap in knowledge. Herein, we examined the association of self-reported PA in the year before BC diagnosis with CD8+ T-cell density in the breast TIME. As prior evidence from healthy adults suggests the relationship between exercise and immunity is not linear, we hypothesized that patients reporting the highest PA level would not have the highest $CD8^{\pm}$ T-cell density in their tumor.

Methods: We leveraged data and tumor samples from 685 women with BC (548 self-identified Black and 137 self-identified White) enrolled in the Women's Circle of Health Study and the Women's Circle of Health Follow-Up Study. $CD8^{\pm}$ T-cell density per square millimeter of tumor tissue was derived from IHC staining of tissue microarrays. Weekly PA in the year before diagnosis was categorized as inactive; low active (<7.5 MET hours/week); moderately active [7.5-14.9 MET hours/week, the equivalent of meeting the minimum PA Guidelines (PAG)]; or high active (≥15.0 MET-hours/week, exceeding the minimum PAG). Log transformed mean $CD8^{\pm}$ T-cell densities were compared by PA level using t-tests and multivariable linear regression with adjustment for age, race, estrogen receptor status, and tumor grade.

Results: Meeting the minimum PA Guidelines was associated with significantly higher $CD8^{\pm}$ T-cell density in the breast TIME [120.4 (353.6)] in comparison to inactivity [62.0 (154.5), p=0.02]. Although there were also distinct differences in T-cell density between moderate and low-active patients [120.4 (353.6) versus 69.5 (172.6), p=0.10] and moderate and high-active patients [120.4 (353.6) versus 80.7 (223.3), p=0.051], associations were shy of significance. Multivariable linear regression analyses confirmed that moderately active patients had significantly higher $CD8^{\pm}$ T-cell density in comparison to inactive patients, overall (p=0.029), and among Black patients (p=0.021).

Conclusions: In comparison to inactivity, BC patients meeting the PAG (moderate activity) had significantly increased $CD8^{\pm}$ T-cell density in their tumor, which is associated with better survival outcomes. This new translational knowledge suggests exercise-induced immunomodulation may be an important molecular mechanism underlying the association of PA with improved BC survival. As the immune system is a key player in treatment response and efficacy, further study of the role that PA ancillary to therapy may play in improving treatment and survival outcomes is warranted.

TUMOR BIOLOGY: Invasion and Motility
Poster Session

#5407 Temozolomide promotes matrix metalloproteinase 9 expression through p38 MAPK and JNK pathways in glioblastoma cells.
C. Jung, H. D. Thanh, S. Lee, K.-S. Moon;
Chonnam National University Medical School, Hwasun-gun, Korea, Republic of

Glioblastoma multiforme (GBM) is a highly aggressive and deadly brain cancer. Temozolomide (TMZ) is the standard chemotherapeutic agent for GBM, but many patients experience recurrence and invasion of tumor cells. We investigated whether TMZ treatment of GBM cells regulates matrix metalloproteinases (MMPs), which have main function to promote tumor cell invasion. TMZ effectively killed GL261, U343, and U87MG cells at a concentration of 500 μM, and surviving cells upregulated MMP9 expression and its activity but not those of MMP2. TMZ also elevated levels of *MMP9* mRNA and *MMP9* promoter activity. Subcutaneous graft tumors survived from TMZ treatment also exhibited increased expression of MMP9 and enhanced gelatinolytic activity. TMZ- mediated-MMP9 upregulation was specifically mediated through the phosphorylation of p38 and JNK. This then stimulates AP-1 activity through the upregulation of c-Fos and c-Jun. Inhibition of the p38, JNK, or both pathways counteracted the TMZ-induced upregulation of MMP9 and AP-1. This study proposes a potential adverse effect of TMZ treatment for GBM: upregulation of MMP9 expression associated with increased invasion and poor prognosis. This study also provides valuable insights into the molecular mechanisms by which TMZ treatment leads to increased MMP9 expression in GBM cells.

#5408 SERPINB3 impact on cervical cancer cell mobility and migration.

M. L. Campos Guerrero, L.-Y. Chen, S. Markovina;
Washington University In St. Louis, St. Louis, MO

Cervical cancer is the fourth most common cancer in women, with 311,000 deaths worldwide in 2018. About two thirds of patients with cervical cancer exhibit elevated serum levels of squamous cell carcinoma antigen (SCCA), also known as SERPINB3. SERPINB3 is associated with advanced stage and lymph node metastasis and we have previously shown it has a protective role against radiation treatment and chemotherapy induced cell death. We have also shown that SERPINB3 promotes tumor growth in both immunocompromised and immune competent murine models, yet the molecular mechanism is unknown. We have recently shown that SERPINB3 expression results in activation of signal transducer of transcription 3 (STAT3) and extracellular signal regulated kinase (ERK) in cervical cancer cells. These signaling cascades promote cell proliferation, survival, invasion, and metastasis. Proximity labeling using biotin-ligase fused to SERPINB3 revealed STAT3 and ERK as potential interacting partners. We aim to identify the molecular mechanism by which SERPINB3 promotes tumor progression, and determine if SERPINB3 drives invasion and metastasis in-vivo. We hypothesized that SERPINB3 directly interacts with and activates STAT3 and ERK leading to downstream signaling promoting invasion and metastasis. To test this hypothesis, we used cervical tumor cell lines engineered with SERPINB3 or empty vector control and determined migration by wound healing assay and downstream activation of STAT3 and ERK. Co-immunoprecipitation (co-IP) with western blot was performed to determine an interaction between SERPINB3 and STAT3 and ERK. E6/E7-expressing TC-1, and Lewis Lung Carcinoma cells, LL2, to develop a method for injecting the cervix of immunocompetent c57BL/6 albino mice (no available murine cervical carcinoma line). Wound healing assays revealed that knocking out SERPINB3 shows a decrease in wound closure in both SW756 and HT3 cervical cancer cells compared to control cells, respectively. Co-IP of STAT3 in HT3 cells revealed the presence of SERPINB3, providing further evidence for an interaction between STAT3 and SERPINB3. We were able to grow tumors in the cervix of the C57/BL6 mice and identified potential metastatic deposits in the lung. Moving forward, we plan to identify the minimal functional domain of the interaction between SERPINB3 and STAT3/ERK using a step-wise genetic approach for protein domain deletion. To determine the role of SERPINB3 on metastasis in vivo, we will use, LL2 and TC-1 engineered with the mouse orthologue mSERPINB3a to determine effect of SERPINB3 on invasion and metastasis. Conducting this study will provide insights as to how SERPINB3 may function in a pro-tumor role in cervical cancer and allow the development of SERPINB3-targeted drugs.

#5409 Phosphorylated focal adhesion kinase by mild reduction of cell surface proteins inhibits integrin α5β1-dependent patient- derived cancer cell migration and invasion.

J. Kim[1], L. D. Anggradita[1], S. Hur[1], J. Park[2], S.-H. Kim[3], M. Ban[2], Y. Hwang[1];

[1]Soonchunhyang Institute of Medi-bio Science, Cheonan-si, Korea, Republic of, [2]Soonchunhyang University Cheonan Hospital, Cheonan-si, Korea, Republic of, [3]Korea Institute of Science and Technology, Seoul, Korea, Republic of

Although head and neck squamous cell carcinomas (HNSCCs), including tongue, vocal cord, and buccal cancers, are one of the most common cancers worldwide with a mortality rate of more than 40%, there have been no solid standard biomarkers for effectively diagnosing HNSCCs at early stages and no effective protocols available to support in vitro expansion of HNSCC cells. To establish a cell culture method to support in vitro self-renewal of HNSCC cells, patient-derived tumor was enzymatically digested, and the tongue cancer epithelial cells were seeded onto feeder cells with the Rho kinase inhibitor (Y-27632). Additionally, to test our hypothesis that free thiol groups in the cells, generated by a mild reduction of cell surface proteins using the reducing agent tris(2-carboxyethyl) phosphine hydrochloride (TCEP), would modulate cancer cell adhesion and migration, we assessed the expression levels of integrins, focal adhesion kinase (FAK), and phosphorylated FAK (pFAK) of tongue cancer epithelial cells cultured on both soft and rigid polyacrylamide (PAAm) hydrogel-based cell culture substrates. Patient-derived tongue cancer epithelial cells exhibited self-renewal ability and maintained cancerous phenotypes, with high expressions of P53, Ki67, E-cadherin, CD44, and AHDH1A1. Treatment with the reducing agent (TCEP) increased the degree of cell adhesion through the significantly upregulated integrin α5β1-mediated phosphorylation of FAK, resulting in inhibited single-cell and collective cell migration as well as invasion. Additionally, when these cells were cultured on stiff PAAm hydrogels mimicking the tumor microenvironment, the cells exhibited accelerated cell migration behaviors, compared to cells on soft hydrogels. These results highlight the synergetic contributions of feeder cells and Rho kinase inhibitor to support long-term self-renewal of tongue cancer patient-derived epithelial cells.

#5410 Unveiling PAI-1 as a new player in chemoresistant melanoma in aged human skin reconstructed in vitro.

R. Oliveira da Silva[1], L. A. C. Carvalho[2], D. E. M. Camarena[1], J. R. Silva[1], I. H. Y. Noma[1], M. O. Moraes, Jr.[1], P. C. Pennacchi[3], S. S. Maria Engler[1];
[1]University of Sao Paulo, Sao Paulo, Brazil, [2]Moffitt, Tampa, FL, [3]Vivia Biotech,, Madrid, Spain

The impact of advanced glycation end products (AGEs) accumulation is associated with the development and exacerbation of many degenerative processes and disorders, including aging and cancer. AGEs accumulation in the skin leads to stiffness and loss of elasticity by building up in the connective tissue during aging process. This process has implications of the extracellular matrix, affecting the adhesion, migration, and invasiveness potential of melanoma cells. Furthermore, tumor invasiveness is correlated with mechanical stiffness, contributing to the high metastatic capacity of melanoma. To address this research gap, our study aimed to evaluate the invasive potential of chemoresistant melanoma using an in vitro model of reconstructed aged human skin modified by glycation. Glycated skin exhibited distinct features indicative of aging, including positive pentosidine fluorescence and elevated CML labeling and expression, well-established biomarkers of aging. Furthermore, glycated skin with resistant melanoma demonstrated reduced expression of differentiated keratinocytes (CK-10) and increased expression of undifferentiated keratinocytes (CK-14). Overall, in glycated skin with resistant melanoma, decreased proliferation and increased tumor invasion were observed, associated with changes in the expression of key markers, such as reduced MITF and SOX-10 and increased AXL. Downregulation of MITF in skin with resistant melanoma resulted in decreased Melan-A expression, implying altered pigmentation of melanoma cells. Additionally, resistant melanoma in glycated skin showed enhanced inflammation, as indicated by higher levels of IL-8 and IL-1α. Gene screening showed upregulation of the PAI-1, ABL-1, COL1A1, SPARC genes. Among these genes, PAI-1 (Plasminogen activator inhibitor-1) was upregulated in resistant melanoma compared to naïve melanoma both in glycated skin. PAI-1 may play a critical role in the development of aging-associated pathological changes. In addition, PAI-1 is recognized as a marker of senescence and a key member of a group of proteins collectively known as the senescence-messaging secretome. It also performs protumorigenic functions, such as promoting vasculature, increasing growth, motility and protecting tumor cell apoptosis. Overall, this work demonstrated that skin aged by glycation when associated with i-Braf resistant melanoma exhibited a more invasive and less proliferative profile (low MITF and SOX10, elevated AXL), more inflammatory (elevated IL-8 and IL-1α) and with a greater number of immature keratinocytes (elevated ck-14). PAI-1 overexpression may be a promising target to expand studies caused by oncogenes in the model of aged skin by glycation with resistant melanoma.

#5411 Effect of different fatty acids on ccRCC behavior and metabolism.

I. Ramos de Andrade, D. Wang, S. Welford;
University of Miami Miller School of Medicine, Miami, FL

Introduction: Clear Cell Renal Cell Carcinoma (ccRCC) is the most common type of kidney cancer, presenting with defining characteristics of increased lipid droplets formation, loss of the VHL tumor suppressor, and low levels of fatty acid oxidation (FAO). Obesity is associated with an increase in ccRCC incidence, although obese patients respond better to different therapies, a phenomenon called as obesity paradox. The consumption of diets rich in lipids and leading to obesity has been increasing, but how the dietary composition affects ccRCC progression, or could be modulated in combination with other therapies for better responses is still unclear. In the present study, we aimed to evaluate how different fatty acids (FAs) affect ccRCC behavior and metabolism.
Methods: We used 786-O and 769-P ccRCC cell lines. Palmitic acid (PA), oleic acid (OA), and linoleic acid (LA), which are saturated, monounsaturated, and polyunsaturated fatty acids, respectively were used as stimuli for the cells at 50 or 200μM. All stimuli were diluted in culture media with 5% FBS. Lipid droplets were evaluated by Oil Red O staining; viability was assessed by MTT; protein expression was tested by Western Blotting; Oxygen Consumption rate (OCR) by Seahorse; survival was quantified by clonogenic assay; and mRNA was measured by RT-qPCR.
Results: All FAs increased the amount of lipid droplets compared to the control, but OA was the most potent. PA impaired the growth rate for cells compared to control, and other FAs in both cell lines, and did not increase the expression of cleaved caspase-3. PA, even in a lower concentration [50μM], impaired the formation of colonies for both cell lines compared to control and other FAs. LA impaired colony formation only in the higher concentration [200μM], while OA only induced a difference for 769-P cells at the smaller concentration, increasing the number of colonies. OA, and mainly PA, decreased 769-P cells migration, at the time of 6 and 12 h, while only PA decreased migration for 786-O cells, at the time of 12 h. LA, and mainly PA, increased CPT1a mRNA levels in 786-O cells but did not induce a significant difference to 769-P, and all FAs decreased FASN in both cell lines.
Conclusion: It was demonstrated that OA was a potent inducer of lipid droplet formation, which can be protective in avoiding lipid peroxidation. On the other hand, PA and LA induced fewer lipid droplets probably because they are going to FAO, as we observed increased mRNA CPT1a levels, which is the rate-limiting enzyme in FAO. PA impaired potentially the formation of colonies and growth rate, and it is important to highlight that it was without inducing caspase 3-dependent programmed cell death. Taken together our data suggest that PA could be a target therapy for ccRCC, but it is still necessary for more studies in vitro and in vivo to evaluate how PA and enriched lipid diet can impact a better outcome for patients.

#5412 In vitro plasticity profiling of metastatic cancer cells with an imaging-based pipeline.

Saba Sameri[1], Durdam Das[2], Stefanie Michaelis[3], Joachim Wegener[3], Hedayatollah Hosseini[1], Martin Hoffmann[2]

[1]Experimental Medicine and Therapy Research, University of Regensburg, Regensburg, Germany,[2]Fraunhofer Institute for Toxicology and Experimental Medicine ITEM, Regensburg, Germany,[3]Fraunhofer Institute for Electronic Microsystems and Solid State Technologies EMFT, Regensburg, Germany

Different types of cancer cells exhibit varying levels of invasiveness, migration behavior and ability to resume growth at distant sites. In order to classify cell lines for these fundamentally important traits of metastasis, we sought to generate an image-based *in vitro* assay that quantifies morphological and functional features of cancer cell plasticity. We developed an Imaging-Based Pipeline as an R Package for *in vitro* cell monitoring using the breast cancer cell lines MDA-MB-231 and MCF-7 that represent high-metastatic and low-metastatic cells *in vivo*, respectively, to identify relevant feature variables. Live cell imaging via the zenCELL owl system captured images for labeling and segmentation. Pre-trained neural network models from Cellpose, combined with user-calibrations, accurately segmented cells for tracking. The tracking pipeline calculated similarity coefficients, Jaccard index, between consecutive frames for cell trajectory analysis. Geometric and morphological features, speed, and distance measurements were derived for assessing structural motility and proliferation-associated changes. The analysis of two cell line models revealed significant variations in morphological changes, with MDA-MB-231 showing more rapid changes between round and elongated shape compared to MCF-7 cells. Moreover, the analysis of cell motility, consistent with the morphological changes, revealed that TGF-beta1 induced migration in MDA-MB-231 cells much stronger than in MCF-7 cells. Likewise, differences in proliferation induction upon addition of growth factor was monitored, showing that MCF-7 cells are more responsive to the growth stimulation than MDA-MB-231 cells. Consequently, the morphological plasticity of cancer cells, closely linked to the epithelial-to-mesenchymal transition (EMT) state, emerges as a defining factor for the *in vitro* plasticity of these cells. Quantified proliferation rate and migration speed of the cells was then used to establish an *in vitro* "plasticity index" that captures a cell line's ability to switch between migration and proliferation. This index will undergo validation using cell lines with well-established metastatic propensities.
In conclusion, we developed an Imaging-Based Pipeline that can effectively explore cancer cell plasticity in vitro and monitor the impact of genetic or pharmacologic perturbations on this critical characteristic of aggressive cancer cells.

#5413 *In vitro* modeling of the migration ability of lung adenocarcinoma cell lines under hypoxic conditions.

S. E. Surguta[1], M. Baranyi[2], L. Svajda[1], I. Ranđelović[1], M. Cserepes[1], J. Tovari[1];
[1]National Institute of Oncology, Budapest, Hungary, [2]KINETO Lab Ltd., Budapest, Hungary

Hypoxia is a common condition in the tumor microenvironment that contributes to tumor cell migration, invasion, and metastasis, partly through inducing epithelial-mesenchymal transition (EMT). One of the key proteins in this process is hypoxia-inducible factor 1 (HIF-1), which regulates the expression of various genes as transcription factor and is vital for the cellular response in tissue hypoxia. Several studies have investigated the causation between hypoxic conditions and increased *in vitro* tumor cell motility and the role of potential regulatory signaling pathways. Understanding the precise molecular mechanisms underlying hypoxia-induced responses is crucial for better targeting tumor progression. However, establishing sound and predictive models is urgently needed to achieve this.In this study, we investigated the migration ability of four non-small cell lung cancer cell lines carrying different mutations of the growth factor pathway (H1975: EGFR T790M, PF901: BRAF V600E, PF139: KRAS G12C mutant, and H838: triple WT) under normoxic, hypoxic, and hypoxia-mimicking $CoCl_2$-treated conditions. The motility of the cells was investigated by 48 h video microscopy (single cell random migration) and 72 h scratch assay. We analyzed the expression of crucial genes and proteins, including HIF-1α, as well as molecules associated with epithelial-mesenchymal transition (*vimentin, n-cadherin*, and *e-cadherin*), proliferation (PCNA), and apoptosis (PARP), using Western blot and qPCR techniques. Our work showed no change in cellular motility between any of the cell lines following treatment with $CoCl_2$ compared to normoxic conditions. However, PF139 and PF901 cell lines showed a significant decrease in single-cell motility upon hypoxia. Interestingly, immunoblot analysis revealed stabilization of HIF-1α in response to both $CoCl_2$ and hypoxia in the meantime. Additionally, we observed cell line-dependent changes in EMT marker expression upon $CoCl_2$ treatment and hypoxia. Our work complements previous results published by our group and others on the tumor-promoting role of hypoxia, demonstrating that short-term exposure to hypoxia may act as an acute stressor for tumor cell lines. Our work suggests that the tumor progression-promoting effects are tissue-specific and should be investigated using long-term hypoxia models.
Acknowledgments: This work was supported by the Hungarian Thematic Excellence Program (TKP2021-EGA-44) and the National Laboratories Program - National Laboratory for Tumor Biology (NLP-17). Sára Eszter Surguta is a grantee of the ITM-NKFIA funded Cooperative Doctoral Program (1018567).

#5414 BDNF/TrKB signaling may lead to higher incidence of perineural invasion in men with prostate cancer.

G. J. Edwards[1], V. Odero-Marah[2];
[1]Claflin University, Orangeburg, SC, [2]Morgan State University, Baltimore, MD

Perineural invasion (PNI) is a crucial mechanism facilitating prostate cancer metastasis. PNI encompasses perineural, circumferential, and intraneural invasion, with cancer cells closely interacting with nerves. Evidence suggests that cancer cells utilize the nervous system for metastasis through signaling pathways. PNI is associated with poor prognoses in various cancers, but its role in prostate cancer remains unclear. PCa primarily metastasizes through systemic routes, such as lymphatic and circulatory systems. Metastasizing cancer cells undergo epithelial-mesenchymal transition (EMT), enhancing their motility. SNAIL1, a transcriptional repressor, induces EMT and promotes cancer cell migration, including towards nerves, termed neurite outgrowth. Neurite outgrowth involves intricate signaling between tumor cells and nerves, possibly facilitating cancer cell infiltration into nerve sheaths and PNI. Our lab has shown SNAIL1 in interactions with neurotrophic factors like Brain-Derived Neurotrophic Factor (BDNF) and Tyrosine Kinase Receptor Beta (TrkB), modulating cancer cell behavior. TrkB is overexpressed in various cancers, while BDNF signaling contributes to EMT via the Twist-Snail axis. BDNF may also play a role in PNI pathogenesis. **Our hypothesis posits the BDNF-TrkB axis drives aggressive prostate cancer and PNI.** This study employed prostate cancer cell lines for comprehensive analysis. We assessed BDNF expression in different cell lines, particularly those with high Snail levels, and analyzed BDNF transcript levels via real-time quantitative PCR following RNA extraction and reverse transcription. We explored whether BDNF overexpression enhanced cancer cell migration towards nerves, employing migration assays. Our findings indicated heightened migration in BDNF-high cell lines, C42, PC3, and MDA-2b, compared to BDNF knockdown cells. Additionally, a TrkB inhibitor, K252a, attenuated migration due to BDNF-induced TrkB phosphorylation. Our study establishes that BDNF/TrkB signaling promotes prostate cancer cell migration towards nerves, a phenomenon reversible with K252a, offering a potential strategy to impede prostate cancer progression and metastasis.

#5415 Fibroblast mediated head and neck tumor cell invasion in 3D culture is independent of partial epithelial to mesenchymal transition.

P. Park, M. M. Alexander, J. M. Curry, A. J. Luginbuhl, A. P. South;
Thomas Jefferson University, Philadelphia, PA

Head and neck squamous cell carcinoma (HNSCC) is the sixth most common cancer worldwide, with a five-year-survival of 61-64%. Recent studies have demonstrated tumor keratinocytes with features of a partial transition from epithelial to a mesenchymal phenotype, also known as partial-EMT (pEMT), at the edge of invading tumor islands associates with metastatic disease. As such, pEMT likely results from direct interactions between tumor cells and their surrounding microenvironment. To test if specific secreted factors or cell interactions drive the acquisition of pEMT, we first analyzed a series of primary and established HNSCC cell populations to determine TGF-β1 responsiveness since TGF-β1 is a known driver of pEMT. Of the eight populations tested, six displayed an increased level of pSMAD3 upon incubation with 5 ng/mL of TGF-β1 ($p < 0.0001$). To determine if this TGF-β1 response leads to an increase in pEMT phenotype, a pEMT-score (derived from mRNA expression of 9 pEMT markers) for each HNSCC population was determined following TGF-β1 treatment. As expected, the two non-responsive HNSCC populations showed no increase in pEMT-score, whilst five of the six TGF-β1-responsive HNSCC populations demonstrated a significant increase in pEMT-score ($p = 0.006$). To assess if TGF-β induced pEMT phenotype correlates with increased invasive potential, we produced 3D skin equivalent models using the eight HNSCC keratinocyte populations, in the presence or absence of primary fibroblasts and/ or TGF-β1 treatment. TGF-β1 treatment alone caused a significant increase in invasion of all five TGF-β1-induced pEMT HNSCC populations ($r^2 = 0.449$, $p = 0.0045$), whilst the three populations previously shown to be pEMT unresponsive to TGF-β1 treatment showed no increase. Interestingly, addition of primary fibroblasts without TGF-β1 treatment caused a universal dramatic increase in invasion in 3D organ culture ($p = 0.0064$, 34-fold increase), regardless of the previously determined TGF-β1-induced pEMT status. Unexpectedly, TGF-β1 treatment in the presence of fibroblasts caused no significant increase in invasion in 3D cultures ($r^2 = 0.00001$, $p = 0.9906$). We next compared levels of pEMT markers in 3D cultures using immunofluorescence and observed a significant increase in PDPN in six of the eight HNSCC populations ($p = 0.0136$) with the addition of fibroblasts suggesting that factors independent of TGF-β1 contributes to pEMT marker expression and invasion in 3D culture. Overall, these data demonstrate fibroblasts induce HNSCC keratinocyte invasion regardless of the population's ability to respond to TGF-β1-induced pEMT and that pEMT may be driven by factors independent of TGF-β1 in 3D culture.

#5416 Purinergic P2Y6 receptor antagonists as potential anti tumor agents.

K. Ghimeray, S. Sharma, R. S. Akundi;
South Asian University, New Delhi, India

Introduction: Cancer places a tremendous strain on society in both developed and economically less developed nations. It remains the most recurring and deadliest disease despite rapid advances in treatment modalities. The major contributors are the prevalence of known risk factors, urbanization, population growth and ageing. Cancer resurgence depends on the organ in which the tumor first appears, immune response, patient's characteristics, disease stage and tumor microenvironment (TME). Among the several inflammatory molecules found within the TMEs, the levels of adenosine triphosphate (ATP) has been found to be high. In healthy tissue, the concentration of ATP in the extracellular space (eATP) is negligible and does not accumulate significantly due to the activity of ectonucleotidases. However, tissue injury, cellular stress and chemotherapy mediated cell death can increase the levels of ATP in the TME. The eATP exerts its effect mainly through purinergic P2 receptors expressed by most malignant cells. We have previously shown that eATP promoted migration and invasion of cancer cells in vitro through increased expression of the enzyme cyclooxygenase 2 (COX-2) (Sharma et al., 2021). We showed that eATP mediated COX-2 expression is through P2 receptors (Akter et al., 2021). Accordingly, we hypothesized that blocking the P2 receptors would abolish the COX-2-mediated migration of tumor cells and tested the same in an animal model.

Methodology: Tumors were generated in 8-15-week-old male C57BL/6 mice (20-25 g weight) through subcutaneous injection of syngeneic EL4 lymphoma cells in the left flank of the mice. When tumors were palpable around day 10, saline or P2 receptor, antagonists were directly injected into the center of the tumor and mice were divided into three groups: saline (vehicle control), suramin (broad-spectrum P2 receptor antagonist), and MRS 2578 (P2Y6 receptor-specific antagonist). Drugs were chosen based on prior in vitro research and a vernier caliper was used to assess the growth of the tumor every day. Behavioral tests were performed on day 8 (prior to P2 receptor injections) and days 11, 14 and 17 post-tumor injection. Mice were continuously monitored for their health and were sacrificed on day 18 with deep CO_2 anesthesia and cervical dislocation.

Results: We found that suramin-injected tumors had a substantial reduction in tumor volume when compared to saline-injected ones. Intra-tumoral injections of P2 receptor antagonists such as MRS-2578 also resulted in similar outcomes as suramin. In tumors treated with P2 receptor antagonists, the expression of COX-2, cell cycle proteins and epithelial-to-mesenchymal (EMT) markers, which aid in metastasis, were significantly downregulated, indicating a suppressive effect. Therefore, we propose that P2 receptor-dependent anti-inflammatory drugs (PBAIDs) could be considered a potential alternative therapeutic option for preventing cancer recurrence.

#5417 PHGDH expression level impacts tumorigenesis and metastasis in human breast cancer.

J. Baik[1], J. Kim[2], S. Lee[1], A. Park[3], K. Shin[4], S. Kwon[4], H. Lee[5], W. Han[3];

[1]Integrated Major in Innovative Medical Science, Seoul National University Graduate School, Seoul, Korea, Republic of, [2]Biomedical Research Institute, Seoul National University, Seoul, Korea, Republic of, [3]Interdisciplinary Programs in Cancer Biology Major, Seoul National University Graduate School, Seoul, Korea, Republic of, [4]Department of Electrical and Computer Engineering, Seoul National University, Seoul, Korea, Republic of, [5]Department of Surgery, Seoul National University College of Medicine, Seoul, Korea, Republic of

Background: Phosphoglycerate dehydrogenase (PHGDH) is a metabolic enzyme, which is associated with the first step of serine synthesis. The gene encoding this enzyme is often elevated in some types of human cancer, including breast cancer. There are some researches that High-PHGDH expression promotes cancer cell proliferation and tumorigenesis. However, latest study showed that although breast tumors with high expression levels of PHGDH had more possibility to undergo primary-tumor growth, were less likely to metastasize than tumors with low expression of PHGDH by using mouse cell derived mouse models and PDX models. Nevertheless, the applicability of these outcomes to human breast cancer cell lines remains uncertain.
Methods: The survival analysis according to PHGDH mRNA expression was analyzed in METABRIC datasets of breast cancer and the whole-transcriptome sequencing data of 120 breast cancer patients. To investigate the effect of PHGDH in human TNBC cell lines, PHGDH overexpressing MDA-MB-231 cell lines and PHGDH knockdown MDA-MB-468 cell lines were established. Subsequent functional experiments were performed to explore the influence of PHGDH on breast cancer tumorigenesis and metastasis.
Results: In the analysis using METABRIC datasets, overall survival and disease-free survival were reduced in patients with high PHGDH expression and basal type breast cancer showed the highest mRNA level of PHGDH. Using whole-transcriptome sequencing data of 120 breast cancer patients, we also found PHGDH expression level was higher in cancer tissue(n=120) than normal tissue(n=90). In particular, triple-negative breast cancer indicated higher PHGDH level than luminal type breast cancer. We also used this data to perform analysis of overall survival, disease-free survival, metastasis free survival of non-TNBC patient and it resulted in reducing survival rate when patient showed high-PHGDH expression. However, TNBC patients demonstrated diametrical results in the identical analysis. We examined the impact of PHGDH overexpression in MDA-MB-231 cells and PHGDH knockdown in MDA-MB-468 cells, observing increased proliferation and decreased migration in breast cancer cells with elevated PHGDH levels. Conversely, PHGDH knockdown exhibited opposing effects. Subsequently analysis of markers associated with epithelial-mesenchymal transition revealed a correlation with PHGDH expression.
Conclusions: Our data suggest that a potential role for PHGDH in breast cancer as a marker of reduced survival in triple-negative breast cancer, and as a regulator of cancer cell proliferation and metastasis.

#5418 Lamellipodial protrusions induced by hypoxia depend upon kindlin-2 in prostate cancer cells.

C. Nelson[1], D. Hernandez-Cortes[2], K. D. Marr[1], J. M. Gard[1], A. I. Paxson[1], W. L. Harryman[1], N. K. Seppanen[1], J. M. Ryniawec[1], A. E. Cress[1];
[1]University of Arizona, Tucson, AZ, [2]University of California San Fransico, San Fransico, CA

Hypoxia is a physiologically relevant feature of the prostate microenvironment that promotes migration and invasion resulting in extracapsular extension, the first step toward metastatic progression. Prostate cancer invasion depends on integrins as mechanosensing membrane receptors during creation of membrane lamellipodial protrusions and focal adhesions (FAs). The objective of this study was to determine the molecular events that promote membrane protrusions under hypoxia and whether this was dependent upon kindlin-2, an essential integrin adapter that marks activated β1 integrin heterodimers. DU145 cells depleted of one copy of FERMT2$^{+/-}$ (50% kindlin-2 expression) by CRISPR/Cas9 or DU145 FERMT2^{wt} (normal kindlin-2 expression) were grown under acute exposure to hypoxia (1% O_2) and compared to cells grown under normal tissue culture conditions. Immunofluorescence microscopy experiments were performed to analyze the spatial temporal expression of kindlin-2 complexes. Kindlin-2 complexes were confirmed by immunoprecipitation using an anti-kindlin-2 3A3-antibody from Sigma-Aldrich. Colocalization was determined by obtaining 2D immunofluorescence microscopy images analyzed using ImageJ 2.1.0/1.53c and Nikon NIS-Elements 5.30.04. Under hypoxic conditions, analysis over four time points (4h, 8h, 12h & 16h) increased the number and area of FAs (marked by paxillin (PXN)) containing kindlin-2 in a time-dependent manner by 2-fold and 1.5-fold, respectively, but not in DU145 FERMT2$^{+/-}$ cells. Additionally, hypoxia increased membrane area, perimeter, and the plasma membrane intensity of kindlin-2 exclusive of FAs in DU145 FERMT2^{wt} cells which was maximal after 8 hours of hypoxia. Interestingly, limiting the kindlin-2 expression in FERMT2$^{+/-}$ cells resulted in a loss of hypoxia-induced lamellipodial protrusions (marked by lamellipodin (RAPH1)) containing kindlin-2 while hypoxia-induced kindlin-2 FA changes were preserved. The current working hypothesis is that lamellipodial protrusions are dependent upon kindlin-2 expression whereas the established FAs are stable under conditions of reduced kindlin-2 expression in hypoxia. This data suggests that an early stage of migration, lamellipodial extensions are sensitive to kindlin-2 availability. Further studies are required to determine the dynamic interplay between protrusive events and focal adhesions in relation to kindlin-2 for prostate cancer cells to migrate and invade.

#5419 Claudin-7 mediates Rab25-induced suppression of colon cancer cell invasion.

S. Cho[1], B. Jeong[2], S.-H. Yoon[1], C. Park[1], H. Lee[1];
[1]Konyang Univ. College of Medicine, Daejeon, Korea, Republic of, [2]Oregon Health Science University, Portland, OR

Ras-related protein 25 (Rab25) is a member of small GTPase, and growing evidence demonstrates the context-dependent roles of Rab25 in cancer progression. While Rab25 aggravates cancer cell invasion in ER-positive breast, ovarian, and gastric cancers, Rab25 is under-expressed and suppresses colon and triple-negative breast cancer progression. Claudins are major components of tight junctions, and disruption of claudins is implicated in tumorigenesis. Among 27 known members of the claudin family, claudin-7 is suggested to suppress colon cancer progression. Previously, we identified that Rab25 induces endothelial-mesenchymal transition (EMT) and invasiveness of several types of cancer cells through activating the β1 integrin/epidermal growth factor receptor (EGFR)/Snail signaling cascades. However, little is known about the underlying mechanism of Rab25-induced tumor suppression. In the present study, we identify the critical role of claudin-7 in Rab25-induced suppression of colon cancer invasion. 3D Matrigel and modified Boden chamber were used to assess the invasiveness of colon cancer cells. Wound-healing assay was used to analyze colon cancer cell migration. 3D Matrigel was used to analyze tumor growth. Immunoblotting was used to assess the protein expression. Rab25 induced claudin-7 expression in colon cancer cells through protein stabilization. In addition, the enforced expression of claudin-7 not only reduced the EGFR/ Ras signaling activity and Snail expression but also attenuated colon cancer cell invasion. However, silencing of claudin-7 expression rescued the tumor suppressive role of Rab25, thereby increasing colon cancer cell invasiveness. Collectively, our data demonstrate for the first time that Rab25 reduces the EGFR/ Ras/ Snail signaling activity and inhibits colon cancer cell invasion by upregulating claudin-7 expression.

#5420 NLRX1 involves in prostate cancer cell growth, survival and migration.

W.-W. Lin, V. Rathore;
National Taiwan University College of Medicine, Taipei, Taiwan

Prostate cancer (PCa) is one of the most common male cancer and is the second leading cause of death in men. The basic working components about its cause and progression are not surely known in the research as well as the practitioner community. The current curing therapies such as surgery, radiation therapy, cryotherapy, and hormone therapy are not very encouraging. Subsequently, there is a need to investigate new potential targets for focused treatment. NLRX1 (NOD9 or NLR family member X1) is one member among the NLRs and is a non-inflammasome forming NLR sub-group localized in mitochondria. Previous studies showed that NLRX1 is involved as a tumor suppressor in colorectal cancer and hepatocellular carcinoma. However, NLRX1 serves as tumor promoter in breast cancer and head and neck cancer sarcoma. The present study focuses on the role of NLRX1 in prostate cancer cells under stress conditions including serum-free and hydrogen peroxide (H_2O_2) to understand cell regulation and functions of NLRX1. We used human prostate cancer PC3 and LNCaP cell lines as the models and the following methods, including Annexin V/PI staining for cell viability, BrdU incorporation for cell proliferation, mitoSOX staining for mitochondrial ROS, wound healing assay for cell migration and Boyden chamber for cell invasion. First, we assessed the TCGA database via UCSC Xena and found that prostate cancer tumors have high NLRX1 expression than normal tissues. Next, we knock down the NLRX1 through lentivirus transduction. We found that silencing NLRX1 expression can decrease cell proliferation in PC3 cells. Furthermore, silencing NLRX1 can significantly decrease cell viability under H_2O_2 in PC3 cells and serum-free condition in both cancer cell lines. In addition, we found that H_2O_2-induced cell death is reversed by necroptosis inhibitor Nec-1. Moreover, NLRX1 silencing reduces cell migration in both PC3 and LNCaP cells and can inhibit cell invasion in both cell lines at 24 h. These results suggest that NLRX1 is a positive regulator of cell growth, migration and invasion in prostate cancer cells, and NLRX1 provides a cell-protective role in response to H_2O_2 and serum-free stress. Thus, this study will provide a potential target for the development of a therapeutic strategy for prostate cancer.

#5421 Characterizing functional cell migration states with highly multiplexed immunofluorescence imaging.

W. D. Leineweber, A. Finkelstein, E. Lundberg;
Stanford University, Stanford, CA

Cancer cell migration is a necessary step in the metastatic cascade, but there are heterogeneous cellular mechanisms to achieve this behavior. This study leveraged live-cell tracking and end-point spatial proteomics to better characterize what underlying molecular states drive migration heterogeneity. U2OS osteosarcoma stably expressing the FUCCI cell cycle reporter system were tracked for 20 hours on a Leica DMI8 widefield microscope. Immediately after, cells were fixed and prepared for highly-multiplexed immunofluorescence imaging on a Canopy CellScape instrument. Initial results from these experiments demonstrate that transferring the sample between these two systems is feasible and results in minimal loss of cells despite the multiple staining cycles. Unlike standard marker panels intended to differentiate between cell types, the initial panel used in this study includes markers that differentiate between migration modes. Even within one cell line, unsupervised clustering identified cell clusters for vimentin high/ E-cadherin low and E-cadherin high/ vimentin low, indicated an epithelial to mesenchymal transition (EMT) axis in the dataset. Furthermore, the spatial relationships between the cell neighborhoods show largely heterogeneous distributions of cell states, with clusters of more homogeneous cell states arising in more densely-packed regions of the coverslip. Further analysis of how single cell trajectories correlate to these cell states, as well as how cell cycle dynamics impact both migration and molecular cell states are in progress. Results from these analyses will shed new light on the “go vs. grow” hypothesis by directly testing how cell speed, persistence, and overall invasion correspond to cell cycle stage and progression. Furthermore, the high-resolution detail from the multiplexed imaging will allow for subcellular profiling of dynamic proteins, such as beta catenin, and directly link it to a larger protein and migration state. Overall, this experimental approach represents an important bridging between functional measurements and end-point omics technologies that will be crucial to gain actional insights amid the boom in multiomics.

#5422 Identification of ZEB1-regulated circular RNAs in lung cancer cells.

S. Cho, J.-A. Choi, Y.-H. Ahn;
Ewha Womans University, Seoul, Korea, Republic of

ZEB1 is a master transcription factor playing a crucial role in promoting epithelial-mesenchymal transition (EMT), as well as the progression and metastasis of lung cancer. The progression of lung cancer is regulated by non-coding RNAs, including microRNAs, long non-coding RNAs, and circular RNAs (circRNAs). In this study, we aimed to identify circRNAs under the regulation of ZEB1 and elucidate their functions within lung cancer cells. Through RNA sequencing and subsequent CIRI-full analysis in ZEB1-overexpressing lung cancer cells, we identified 25 circRNAs displaying differential expression compared to control cells. Among these circRNAs, we targeted circDennd1b, which showed down-regulation in ZEB1-overexpressing cells. We used siRNAs to target the back-splicing junction of circDennd1b, resulting in its knockdown and consequently promoting the invasion of lung cancer cells. Now, we are studying how circDennd1b affects the progression and metastasis of lung cancer. In summary, the circRNAs modulated by ZEB1 are anticipated to play a key role in the invasion, progression, and metastasis of lung cancer.

#5423 Selective inhibition of glucose transporter 3 (GLUT3) suppresses triple-negative breast cancer cell migration by modulating actin cytoskeleton and cell mechanics.

T.-H. Kim[1], A. Qadir Bhat[1], C. V. Iancu[2], J.-Y. Choe[2];
[1]University of New Mexico Health Sciences Center, Albuquerque, NM, [2]University of New Mexico, Albuquerque, NM

Studies have reported clear clinical observations indicating that obesity and diabetes, which often accompany hyperglycemia, are linked to a poor prognosis across various types of cancer. Specifically, multiple clinical studies involving breast cancer patients have demonstrated that hyperglycemia (>7 mM) is associated with an unfavorable prognosis. Despite the evident correlation between elevated glucose levels and cancer metastasis, the causality remains unclear, and the underlying molecular mechanisms are largely unknown.

In both normal and diseased physiology, a broad range of tissue glucose levels has been documented, ranging from normal blood circulation (5.5 mM) to normal tissues (1 - 3 mM) and to tumor tissues (<0.5 mM). Consequently, during the early stages of metastasis, cancer cells undergo a significant increase in extracellular glucose levels.

The capacity of cancer cells to deform and exert contractile force, collectively known as cell mechanics, plays a crucial role in various stages of metastasis. In our previous work, we demonstrated that elevated extracellular glucose levels boost glycolysis and activate the RhoA signaling pathway. This leads to heightened cell stiffness and increased contractility in human triple-negative breast cancer (TNBC) cells. Furthermore, the modified cell mechanics are associated with enhanced cell migration and invasion.

In this study, we present findings indicating that the inhibition of glucose transporter 3 (GLUT3) significantly diminishes the motility of human TNBC cells, including MDA-MB-231 and its highly metastatic variant, MDA-MB-231/HM cells. Mechanistic investigations reveal that GLUT3 inhibition, facilitated by a well-characterized potent GLUT3-selective inhibitor (G3iA), results in reduced glucose uptake and glycolysis. The diminished glycolysis, induced by GLUT3 inhibition, activates 5' AMP-activated protein kinase (AMPK) and enhances the phosphorylation of Yes-associated protein (YAP). Moreover, GLUT3 inhibition leads to a decrease in non-muscle myosin II activity and induces alterations in F-actin rearrangement by influencing actin-binding proteins such as VASP and cofilin. These changes are associated with a reduction in cell migration.

In summary, our results suggest that inhibiting GLUT3 modifies the mechanics of TNBC cells, leading to a decrease in cell motility. Given that GLUT3 is notably elevated in TNBC and is linked to metastatic progression and a poor prognosis in breast cancer patients, our findings underscore the need for further in vivo studies to validate G3iA as a potential anti-metastatic drug in hyperglycemic TNBC animal models.

#5424 Respiratory function linked to *in vivo* metastatic lung cancer progression.

P. Bisoyi, Y. Sei, N. Bennett, K. Nakamura, J. L. Nakamura;
UCSF - University of California San Francisco, San Francisco, CA

Metastases are a major cause of morbidity and mortality in patients with cancer. How metastatic tumors employ metabolic programs to successfully colonize diverse microenvironment is poorly understood. Using an orthotopic xenograft mouse model of lung cancer that develops metastases and recapitulates metastatic lung cancer spread, we injected GFP-LUC-expressing human H1975 lung tumor cells into the left lungs of mice. In vivo bioluminescence imaging was used to visualize tumor growth and metastatic spread for 30 days. Animals were then euthanized and primary and metastatic tumors were collected from different anatomical sites of the body (left lung, right lung, mediastinum, abdominal metastases). Tumor samples were analysed by RNA sequencing analysis. The transcriptomes of lung metastases demonstrated a significant reduction in the expression of genes encoding respiratory pathway protein as compared to the primary lung tumors, suggesting metabolic reprogramming of their respiratory metabolism. CRISPRi-mediated silencing of genes encoding components of respiratory function in human lung cancer cells was associated with significantly increased metastatic spread *in vivo*. These studies suggest the functional importance of respiratory metabolism on modulating *in vivo* disease spread.

#5425 MITF/TFE regulatory programs in neural crest migration are co-opted in melanoma metastasis.

J. Chang[1], K. Campbell[1], R. Moore[1], R. Cornell[2], C. Kenny[1];

[1]University of Iowa Hospitals & Clinics, Iowa City, IA, [2]University of Washington, Seattle, WA

Introduction: Microphthalmia-associated transcription factor (MITF) is a critical regulator of melanocyte differentiation and melanoma oncogenesis. Melanoma expression profiling has revealed a strong trend between low MITF expression levels and invasive behavior. However, it is unclear how low levels of MITF are connected to invasive behavior. Preliminary data from our lab has identified transcription factor E3 (TFE3), a MITF paralog, as a transcriptional regulator in MITF-low melanoma states. We hypothesize that in melanoma cells with low MITF levels, TFE3 promotes invasion. To assess the possibility that the antagonistic regulatory interaction between MITF and a paralog was coopted from the embryo, we examine migratory behavior of neural crest cells in zebrafish embryos that are wild-type, *mitfa* loss-of-function (LOF) mutants, *tfec* (TF3 ortholog) LOF mutants, or *mitfa/tfec* double LOF embryos.
Methods: We evaluated TFE3 levels by Western blot in a panel of melanoma cell lines known to express a range of MITF expression levels. We mutated *TFE3* exon 4, which encodes the DNA binding domain, using a single guide RNA, and assessed cellular invasive potential using an *in vitro* transwell invasion assay. CUT&RUN sequencing was used to profile TFE3 genomic binding. Zebrafish embryos were generated in which the *mitfa* promoter drove expression of RNA encoding green fluorescent protein (GFP), and of the genotypes mentioned above. From transgenic wild-type and *mitfa* LOF mutant embryos we isolated GFP-expressing cells and conducted single cell-RNA sequencing. We assessed migration of GFP-labeled cells by fluorescent microscopy in 20-48 hour post fertilization zebrafish embryos of all genotypes mentioned above.
Results: We found that melanoma cell lines with high levels of *MITF* (SKMEL3 and SKMEL28) had low levels of TFE3 protein, and those with low levels of *MITF* (A375 and RPMI 7952) had high levels of TFE3 protein. The TFE3-high cell lines were more invasive *in vitro* than the TFE3-low cell lines. TFE3-high cell lines depleted of TFE3 were less in invasive *in vitro* than parental cells. CUT&RUN profiling of TFE3 demonstrates that TFE3 binds mesenchymal-like enhancers in MITF-low cell lines. Single cell RNA sequencing revealed that in a melanocyte precursor cluster present in both wild types and in *mitfa* mutants, expression of *tfec* was higher in the latter. Finally, migration of GFP-expressing cells was higher in *mitfa* LOF mutant embryos than in *mitfa/tfec* double LOF mutant embryos.
Conclusion: These data indicate that reduction of MITF expression up-regulates TFE3 expression in melanoma and *tfec* in zebrafish melanocytes, although the mechanism of this regulation is unclear. They also show that TFE3 and Tfec promote migration of metastatic melanoma and melanocyte precursors, respectively. Because regulatory mechanisms in cancer are often coopted from embryonic cells, studying the embryo may illuminate cancer pathogenesis.

#5426 SMC2 orchestrates non-small cell lung cancer proliferation, invasion, and metastasis by modulating the ERK/AKT/NF-κB pathways.

Y. He[1], Z. Luo[2], Y. Wang[2], S. Xiong[2], **R. Wan**[1], X. Zhang[1], H. Bai[1], J. Wang[1];

[1]CAMS Key Laboratory of Translational Research on Lung Cancer, State Key Laboratory of Molecular Oncology, Department of Medical Oncology, National Cancer Center/National Clinical Research Center for Cancer/Cancer Hospital, Chinese Academy of Medical , Beijing, China, [2]Southwest Medical University, Luzhou, China

Chromatin instability has been associated with the expression of structural maintenance of chromosomes (SMC) family members and is a common feature in many tumors. SMC family members have been associated with poor outcomes in several cancer types. However, little is known about their functions and mechanisms in promoting cancer progression, particularly in non-small cell lung cancer (NSCLC). Here, we evaluated the expression of SMC family members in the tumor microenvironment of NSCLC specimens using single-cell RNA sequencing analyses. After a survival analysis, it was found that the sole factor associated with a poor prognosis for NSCLC was member SMC2 expression. Immunohistochemistry was used with data from the Human Protein Atlas, the Cancer Genome Atlas, and the Gene Expression Omnibus databases to confirm the overexpression of SMC2 in NSCLC. We demonstrated that SMC2 regulates not only the fluctuations in the critical states of tumor cells, which are defined by different transcriptome and metabolic properties but also coordinates the immunological components and cell-to-cell communications of the immune milieu, potentially through the pleiotrophin and the Galectin pathways. In vitro and in vivo evidence support the pro-metastatic role of SMC2 in NSCLC. Subsequent investigations showed that SMC2 increases NSCLC progression and metastasis via modulating the ERK/AKT/NF-κB pathway and the epithelial-mesenchymal transition process. Our research clarifies the role and potential mechanisms of SMC2 in NSCLC, providing new treatment options and valuable insights for the management of NSCLC.

TUMOR BIOLOGY: Mechanisms of Cancer Cell Stemness and Resistance
Poster Session

#5430 Discovery of CYP26A1 as a link between WNT and retinoic acid signaling pathways that modulates retinoid-induced differentiation of *APC*-mutant colorectal cancer cells.

C. O. B. Facey, V. O. Hunsu, C. Zhang, B. T. Osmond, L. M. Opdenaker, B. M. Boman;
Helen F. Graham Cancer Center & Research Institute, Newark, DE

APC mutation is the main driver mechanism of CRC development and leads to constitutively activated WNT signaling, overpopulation of ALDH+ stem cells (SCs), and incomplete differentiation. We previously reported that retinoic acid (RA) receptors are selectively expressed in ALDH+ SCs, which provides a way to target cancer SCs with retinoids to induce differentiation. We hypothesize that a functional link exists between WNT and RA pathways, and *APC* mutation generates a WNT:RA imbalance that decreases retinoid-induced differentiation and increases ALDH+ SCs. Accordingly, to restore parity in WNT:RA signaling, we induced *wt-APC* expression in *APC*-mutant CRC cells and assessed the ability of all-trans-retinoic acid (ATRA) to induce differentiation. Notably, ATRA substantially increased expression of the WNT-target gene, *CYP26A1*, and inducing *wt-APC* reduced this expression by 50%. Thus, RA and WNT pathways crosstalk to modulate *CYP26A1* metabolism of retinoids and retinoid agents. We found that inducing *wt-APC* augments ATRA-induced cell differentiation by: *i*) decreasing cell proliferation; *ii*) suppressing ALDH1A1 expression; *iii*) decreasing ALDH+ SCs; and *iv*) increasing neuroendocrine cell differentiation. NanoString profiling and bioinformatics also identified a novel *CYP26A1*-based network that links WNT and RA signaling. Moreover, in an effort to translate manipulation of the WNT/RA imbalance as a therapeutic approach *in vitro*, we treated HT29, SW480, and HCT116 CRC cells with inhibitors against CYP26A1 enzyme activity and WNT signaling. We found that CYP26A1 inhibitors sensitized CRC cells to the anti-proliferative effect of drugs that downregulate WNT signaling. Furthermore, decreased CYP26A1 expression in tumor vs normal tissue was determined to be a predictor of patient survival in patients who have *wt-APC*. Thus, by inducing *wt-APC* expression and exogenously activating RA signaling, we found a way to increase differentiation of SCs along the NEC (and other) lineage(s). Translating this strategy *in vivo* might lead to new, more effective treatments involving retinoids for CRC patients.

#5431 Identification of serine/threonine kinase 39 (STK39) as a driver for multidrug resistance in hepatocellular carcinoma.

C. Leung, **T.-W. Lee**;
Hong Kong Polytechnic University, Hong Kong, Hong Kong

Hepatocellular carcinoma (HCC) is a common type of cancer globally and is associated with a poor prognosis due to its high recurrence rate and resistance to treatment. Solid evidence showed the existence of cancer stem cells (CSCs) that are crucial for therapeutic resistance. However, there are only a few kinase inhibitors that have been found to specifically target liver T-ICs for the HCC treatment. To understand the regulatory mechanism of liver CSCs, we employed RNA-Seq analysis to compare the gene expression profiles, with a particular focus on protein kinases, between (1) sorted CD133$^{\pm}$ liver CSCs and CD133- differentiated cells extracted from two HCC cell lines (Huh7 and PLC8024), as well as cultured hepatospheres and adherent differentiated cells of HCC cell line PLC/PRF/5. Our analysis identified Serine/Threonine kinase 39 (STK39) as a commonly up-regulated protein kinase in both CD133$^{\pm}$ liver CSCs and CSC-enriched hepatospheres. Based on our analysis of the TCGA data, a positive correlation has consistently been observed between STK39 mRNA expression and the expression of liver CSC markers, including CD24, CD133, and CD47. Utilizing publicly available transcriptome datasets from the NCBI Gene Expression Omnibus (GEO), including GSE14520 and GSE25097, we found that overexpression of STK39 is detected in HCC tumor tissues ($p<0.001$) and is significantly associated with poorer overall survival and disease-free survival. Through the use of lentiviral based overexpression and knockdown approaches, we have demonstrated the role of STK39 in regulating liver CSC properties, including self-renewal, tumorigenicity, cell invasiveness, and the expression of liver CSC markers. STK39 expression was found to be significantly elevated in in HCC cells that were resistant to both sorafenib and lenvatinib, and its inhibition resulted in increased sensitivity of HCC cells to these treatments. To identify the downstream target of STK39 for regulation of cancer stemness, tandem affinity purification coupled with mass spectrometry was employed. The analysis led to the identification of PARP1 as a novel protein binding partner of STK39. Upon suppression of STK39 in HCC cells, it was observed that the phosphorylation of PARP1 at Threonine 368 (T368) was significantly inhibited, indicating its role as a downstream effector of STK39-mediated liver CSC functions. Interestingly, STK39-mediated PARP1 phosphorylation led to development of resistance to PARP1 inhibitor, rucaparib. Additionally, STK39 plays a critical role in regulating PARP1-mediated chromatin decondensation, which enables it to open chromatin structure at the promoter regions of SOX2/OCT4. In summary, treatment of molecular targeted drugs including rucaparib and lenvatinib with STK39 inhibitor may be a potential therapeutic strategy for treatment of this deadly disease.

#5432 The role of nuclear factorκB-inducing kinase in ovarian cancer stem cells, chemoresistance, and relapse.

Cassidy C. Lucht, Mikella Robinson, Samuel F. Gilbert, Omar Lujano Olazaba, Carrie D. House

San Diego State University, San Diego, CA

Ovarian cancer is the most lethal gynecological cancer in the United States, largely due to its high relapse rates. Research suggests these high relapse rates are due to cancer stem-like cells (CSCs), a subpopulation of tumor cells that are resistant to chemotherapy and have enhanced tumor-initiation capacity. Post-treatment, CSCs self-renew to re-establish new tumors, leading to recurrent disease that is now resistant to chemotherapy. Given that over-expression of NF-κB has been linked to CSCs, cancer progression, and chemoresistance in various tumors, including ovarian, studies uncovering the mechanisms of this pathway are needed to develop novel therapeutics for ovarian cancer treatment. The upstream activator of the alternative NF-κB pathway, Nuclear Factor κB-inducing Kinase (NIK), could be an enticing target for eliminating CSCs, however its function in these cells is not established. In our current studies, we show that HGSOC cells grown as CSC-enriching 3D spheroids have increased NIK expression and activity relative to monolayer cultured cells. Moreover, cells expressing CSC markers (CD117+/CD133+), have increased NIK gene expression, further supporting an association between NIK and CSC maintenance. Upon treatment with chemotherapies carboplatin and paclitaxel, NIK gene expression increased in the surviving population, indicating a role in chemoresistance. Knockdown of NIK using siRNA led to changes in alternative NF-kB transcriptional activity and higher sensitivity to carboplatin and paclitaxel relative to vehicle controls. Current studies are evaluating the role of NIK in tumor-initiation capacity, asymmetric division, proliferation, and changes in expression of stemness genes. Lastly, an *in vivo* relapse model will test the feasibility of using a NIK inhibitor following chemotherapy to prevent relapse and prolong survival. Findings from this work will further define the role of NF-kB pathway components in facilitating CSCs survival and re-establishment of tumors and identify a new potential target for eliminating CSCs in ovarian cancer.

#5433 Functional involvement of ribosomal protein L9 to colorectal cancer stemness.

E.-H. Jeon[1], K. Park[1], H.-M. Ryoo[2], I. Hwang[1], Y.-H. Lee[1];

[1]Keimyung University Dongsan Medical Center, Daegu, Korea, Republic of, [2]Daegu Catholic University, Daegu, Korea, Republic of

We have previously demonstrated that targeting of ribosomal protein L9 (RPL9) suppresses the growth of colorectal cancer (CRC) via the inactivation of Id-1/NF-κB signaling axis which is known to augment tumor stemness. Thus we aimed in this study to investigate whether the function of RPL9 was associated with CRC stemness properties. It was initially evidenced that inhibition of RPL9 expression reduces the migration and invasion abilities of HT29 parental cell population. We have then sorted out $CD133^{\pm}$ cancer stem cells (CSCs) from HT-29 parental cell culture and treated RPL9-specific siRNAs to the isolated CSCs to observe the effect of RPL9 targeting on stemness. As results, knockdown of RPL9 significantly suppressed the proliferation potential and sphere forming capacity of $CD133^{\pm}$ HT29 CSCs accompanying with the reduction in CD133 and Id-1 levels. Reflecting these molecular alterations, targeting RPL9 also inhibited the abilities of migration and invasion in $CD133^{\pm}$ HT29 CSCs population. Taken together, these findings suggest that RPL9 could be a therapeutic target for both primary CRC treatment and the prevention of metastasis and/or recurrence.

#5434 A novel combination therapy for lung squamous cell carcinoma.

D. Alqasrawi[1], R. Argo[1], C. Ratliff Rang[1], P. Pandya[1], S. Klinge[1], J. Lindemann[2], N. Searl[3], A. Fields[1], V. Justilien[1];
[1]Mayo Clinic Florida, Jacksonville, FL, [2]University of North Florida, Jacksonville, FL, [3]Stanton College Preparatory School, Jacksonville, FL

Lung cancer is the leading cause of cancer deaths in the US. Non-small cell lung cancer (NSCLC) accounts for ~80% of lung cancer cases and is further classified into adenocarcinoma (LUAD), squamous cell carcinoma (LUSC), and large cell carcinoma. New approaches targeting pathways in NSCLC have emerged, resulting in encouraging new treatments that benefit LUAD patients, but very few advances have been made in the treatment options for LUSC which accounts for ~30% of lung cancer cases. NSCLCs, including LUSCs, contain a sub-population of cells that exhibit properties of cancer stem cells (CSCs) and are responsible for tumor initiation, maintenance, therapeutic resistance, and relapse. Therefore, CSCs must be effectively targeted to elicit long lasting therapeutic results in LUSC patients. Our studies have shown that: *1)* PKCι is an oncogene and prognostic marker in LUSC; *2)* copy number gains (CNGs) of the PKCι gene (*PRKCI*) drives overexpression of PKCι in 90% of LUSCs; *3)* PKCι phosphorylates SOX2, and controls SOX2-mediated transcriptional activation of Hedgehog Acyl Transferase, resulting in Hedgehog (Hh) pathway activation that drives a CSC phenotype in LUSC cells; and *4)* the FDA approved compound Auranofin (ANF) is a potent inhibitor of oncogenic PKCι. In this study, we assessed the effect of ANF in combination with the Hh pathway inhibitor, LDE225, on LUSC CSCs and tumor growth. Cell viability, sphere formation and soft agar assays were used to assess the effects of ANF and LDE225 alone or in combination on the growth of LUSC CSCs with *PRKCI* CNGs or LUAD and LUSC CSCs without *PRKCI* CNG to determine if *PRKCI* CNG can be used to predict response to ANF and LDE225 and test the selectivity of response for LUSC. The effects of ANF and LDE225 on the levels of PKCι-Hh signaling components was assessed by qPCR and western blotting. Finally, the efficacy of ANF and LDE225 in combination was evaluated in human primary LUSC patient-derived xenograft (PDX) models that harbor *PRKCI* CNGs and the ability of PKCι-Hh signaling intermediates to serve as biomarkers of PKCι-Hh pathway inhibition was validated *in vivo*. We observed a dose-dependent decrease in cell proliferation, clonal expansion and transformed growth in CSCs treated with ANF and LDE225 alone. ANF and LDE225 combined treatment of LUSC CSCs with *PRKCI* CNGs (but not LUAD or LUSC CSCs without *PRKCI* CNG) synergistically inhibited CSC phenotypes based on results of combination index analysis. Furthermore, treatment of LUSC PDX models with ANF and LDE225 in combination had a synergistic effect on tumor growth inhibition. Lastly, ANF and LDE225 treatment led to inhibition of PKCι-Hh signaling intermediates demonstrating the on-target effects of treatment. Our data indicate that a PKCι-Hh vertical blockade strategy of combined ANF and LDE225 effectively targets LUSC CSCs and blocks tumor growth *in vivo* and provides compelling rationale to develop this novel combination strategy further in clinical trials.

#5435 CUEDC2 involved in the inhibitory effect of dandelion on triple-negative breast cancer stem cells.

X. Deng, Y. Jiao, H. Hao, Z. Guo, D. Xue, **S. Han**;
Peking University Cancer Hospital, Beijing, China

Background: Cancer stem cells (CSCs) exert a substantial influence on the initiation, progression, and metastasis of triple-negative breast cancer (TNBC). Dandelion has exhibited encouraging outcomes in impeding the proliferation of TNBC cells. Nevertheless, the extent of investigation regarding the efficacy of dandelion in targeting CSCs remains restricted.
Purpose: The aim of this study was to investigate the impact of dandelion extract (DE) on CSCs properties.
Methods: *In vitro* experiments were conducted using TNBC cell lines. Mice bearing TNBC tumors were established for *in vivo* investigations. Biochemical analysis and cell biological assay were carried to evaluate the effect of dandelion and the underlying mechanisms.
Results: DE treatment significantly decreased the proportion of ALDH+ cells, mammosphere formation ability, and CSCs-related markers. CUEDC2 is highly expressed in ALDH+ TNBC cells, and its overexpression increased the expression of markers related to CSCs. Conversely, the tumor growth was impeded in CUEDC2 KO mice and the markers related to CSCs also were also reduced. CUEDC2 overexpression reversed the inhibitory effect of DE on TNBC CSCs properties. Mechanistically, CUEDC2 related pathway involved in the inhibitory effect of DE on TNBC CSCs properties.
Conclusion: CUEDC2 played a crucial role in maintaining the stem cell properties of TNBC. DE inhibit the self-renewal of TNBC stem cells by regulating the CUEDC2 related signaling pathway.
Keywords: Dandelion; CUEDC2; Triple-negative breast cancer; Cancer stem cell.

#5436 A therapeutically targetable dysadherin/YAP axis promotes cancer stem features and tumor aggressiveness in hepatocellular carcinoma.

S.-E. Jeon, T.-Y. Jang, C.-J. Lee, H.-J. Yun, Y.-H. Cho, D.-Y. Lim, J.-S. Nam;
Gwangju Institute of Science & Technology, Gwangju, Korea, Republic of

Hepatocellular carcinoma (HCC) remains one of the most challenging tumors to treat. Cancer stem-like cells (CSCs) are believed to be important in HCC development, immune evasion, and treatment resistance. Dysadherin is a cell membrane glycoprotein linked to cancer progression by endowing HCC with CSC features. However, the underlying mechanism of increasing CSC characteristics in refractory advanced HCC is not entirely understood. A comprehensive bioinformatics study revealed that dysadherin-expressing HCC cells were associated with cancer stemness and the YAP signaling activation. Dysadherin knockdown or overexpression in liver cancer cell lines attenuated or increased cancer stemness and aggressiveness via YAP signaling, respectively. Correspondingly, dysadherin deficiency lowered cancer stemness and aggressiveness in the HCC mouse model by blocking the YAP pathway. Mechanistically, dysadherin promoted YAP nuclear localization, which activated stem cell transcription factors such as OCT4, KLF4, and MYC. Of note, our comprehensive gain and loss of function studies in CSCs demonstrated that targeting the dysadherin/YAP axis could boost sorafenib's therapeutic effect and suppress PD-L1 expression, which helps tumor cells escape from immune surveillance. Thus, our results highlight that the dysadherin/YAP axis drives the aggressive phenotype of HCC, providing a potential therapeutic strategy for HCC.

#5437 Chemoproteomics-enabled discovery of covalent inhibitors targeted at AGPAT4: Unravelling tumor lineage plasticity to overcome drug resistance in hepatocellular carcinoma.

K.-Y. Ng[1], T.-Y. Koo[1], T.-L. Fong[1], Y. Gao[1], T.-L. Wong[1], Y. Gao[2], J.-P. Yun[3], X.-Y. Guan[1], M. Liu[4], C. Y. Chung[1], **S. Ma**[1];
[1]The University of Hong Kong, Hong Kong, Hong Kong, [2]Fourth Military Medical University, Xian, China, [3]Sun Yat-Sen University Cancer Centre, Guangzhou, China, [4]Guangzhou Medical University, Guangzhou, China

The liver is a unique organ that is responsible for many metabolic functions. During hepatocellular carcinoma (HCC) development, these metabolic machineries are extensively reprogrammed to support the insatiable nutrient requirements of HCC. Tumor lineage plasticity, a recognized hallmark of cancer, is a phenomenon in which tumor cells co-opt developmental pathways to attain cellular plasticity, enabling them to evade targeted therapeutic interventions. Cancer cells can reprogram their metabolic pathways to match their increased metabolic needs for cancer cell survival under adverse conditions. Identifying novel metabolic targets related to stemness can offer promising strategies for targeting cancer stemness roots and hence to kill and control their growth. Through pathway enrichment analysis of genes that linked metabolism and stemness, we identified an aberrant glycerophospholipid metabolism signature, with AGPAT4 ranking as the top-hit. AGPAT4 upregulation in HCC is strongly correlated with aggressive clinical features, including survival, metastasis, and stemness signatures. AGPAT4 expression peaked during early liver progenitor development, decreased during hepatocyte maturation and progressively increased from well-differentiated to poorly differentiated HCCs. Enrichment of AGPAT4 in HCC is mediated by promoter binding of SOX9 to drive AGPAT4 transcriptional activity. AGPAT4 inhibition can mitigate tumor initiation, self-renewal, metastasis, and sorafenib resistance. Mechanistic studies revealed an AGPAT4-mediated phosphatidic acid production axis that promotes HCC through the regulation of mTOR signaling. Inhibition of Agpat4 by AAV8 shRNA reduced tumorigenicity and stemness, and sensitized HCC tumors to sorafenib. AGPAT4 overexpression can predict sorafenib response in clinical settings. Through chemoproteomics screening of a cysteine-reacting compound library using activity-based protein profiling, a cysteine-reacting compound with high binding affinity and selectivity towards AGPAT4 was identified and found to work synergistically with sorafenib to suppress HCC, as demonstrated in HCC patient-derived tumor xenograft (PDTX) models. Toxicity analysis through histological examination of organs, body weight measurements, and biochemical tests revealed minimal toxicity associated with the covalent inhibitor. In conclusion, AGPAT4 is a novel metabolic driver of oncogenic stemness, dedifferentiation, and metastasis in HCC. AGPAT4-induced tumor lineage plasticity may represent an Achilles heel for HCC treatment, and inhibition of AGPAT4 may widen the therapeutic window for sorafenib treatment in the clinic.

#5438 Circulating tumor cells exhibit a tumor stemness defense phenotype in Head and Neck cancer subjects undergoing cisplatin based chemotherapy.

L. Pathak[1], B. Pal[2], J. Talukdar[1], P. J. Saikia[1], S. Sandhya[1], W. Tasabehji[3], H. Li[3], J. Phukan[4], A. Bhuyan[5], S. Patra[6], B. Das[1];
[1]KaviKrishna Laboratory, Indian Institute of Technology Research Park, Guwahati, India, [2]Thoreau Laboratory for Global Health, UMass, Lowell, MA, USA, Lowell, MA, [3]Forsyth Institute, Cambridge, MA, USA, Cambridge, MA, [4]Guwahati Medical College, Guwahati, India, Guwahati, India, [5]KaviKrishna Telemedicine Care, Sualkuchi, Assam, India, Guwahati, India, [6]Indian Institute of Technology, Guwahati, Guwahati, India

Introduction: We have proposed that tumor has its own defense mechanism similar to an organism having its own defense at the population level. We also proposed that the center of this tumor defense is the hypoxic niche of cancer stem cells (CSCs). Our lab has previously characterized the hypoxic niche of CSCs, and demonstrated that these CSCs reprogram to a highly inflammatory, aggressive and embryonic stemness phenotype during oxidative stress (1). These reprogrammed CSCs, the tumor stemness defense (TSD) phenotype is transient, and exert altruistic defense against bacterial invasion in SCC-25 cell line (2). Further, VEGF/VEGFR1 autocrine signaling was found in cisplatin induced TSD phenotype (4) and Myc/Hif2alpha stemness pathway was found in TSD phenotype of a leukemia stem cell model (3). We hypothesize that the platinum-induced stress may also activate TSD phenotype in the dormant CSC fraction of head and neck squamous cell carcinoma (HNSCC), which may mobilize to the distant tissue via circulation as circulating tumor cells (CTCs).
Methods: To test the hypothesis, we isolated EpCAM+/ABCG2+ CTCs (blood, n=14) and EpCAM+/ABCG2+ CSCs (tumor tissue, n=6/14) of HNSCC subjects under cisplatin treatment. CTCs were collected from peripheral blood mononuclear cells (PBMNC) by the immunomagnetic sorting of EpCAM+ cells, and then cells were expanded in a defined serum free media that we used to maintain the hypoxic CSCs (1). We evaluated the EpCAM+/ABCG2+ CTCs and EpCAM+/ABCG2+ CSCs for TSD phenotype by performing qPCR gene expression, Boyden chamber assay of invasion, clonogenic assay and serial transplantation assay in NOD/SCID mice. Data was compared with the EpCAM+/ABCG2- cell population. We also developed a pre-clinical model of cisplatin-induced reprogramming of HNSCC derived CSCs to understand the molecular mechanisms.
Results: In 8/14 patient derived EpCAM+/ABCG2+ CTCs and EpCAM+/ABCG2+ CSCs showed TSD phenotype associated gene expression, high migration/invasion, self sufficiency (ability to form spheroid when grown in serum free media without growth factors), enhanced secretion of protumorigenic growth factors; VEGF, SDF-1, PIGF, and HMGB1. These CTCs and CSCs have shown tumor formation with significant CSC frequency, when injected to NOD/SCID mice. Finally, using a SCC-25 cell line derived pre-clinical model, we demonstrated that cisplatin therapy reprogram CSCs to TSD phenotype.
Conclusion: Our work indicates that CTCs with TSD phenotype may indicate the interaction between cisplatin and CSC niche defense. Using the pre-clinical model, the TSD phenotype based CSC niche defense mechanism may be further explored to develop markers for therapy response, metastasis or recurrence in HNSCC.
References: 1. Das B et al, 2008, PMID:18467664, 2. Bhuyan et al, 2022, PMID: 36248858, 3. Das B et al, 2019, PMID: 31266772, 4. Tsuchida R et al, 2008, PMID:18332870

#5439 Metastasis-enhancing protein KITENIN confers temozolomide resistance in glioblastoma with unmethylated MGMT via upregulation of cancer stem cell makers.

E.-J. Ahn[1], Y. Kim[1], T.-Y. Jung[1], J.-H. Lee[1], J. Rhee[1], K.-K. Kim[1], S. Kim[1], N. Kim[1], H. Kim[2], K.-S. Moon[1], **K.-H. Lee**[1];
[1]Chonnam National University Medical School, Jeollanam-do, Korea, Republic of, [2]Sunchon National University, Sunchon, Korea, Republic of

Background: Elevated expression of cancer stem cell (CSC) markers is linked with progression, poor survival, and treatment resistance in glioblastoma (GBM). Our prior work identified KAI1 COOH-terminal interacting tetraspanin (KITENIN) as key to GBM progression. We investigated its influence on temozolomide (TMZ) resistance in GBM through modulation of CSC markers.
Methods: We examined KITENIN and CSC markers in TMZ-resistant GBM cells and patient-derived GBM cells, and assessed therapeutic responses to TMZ in mice implanted with KITENIN-modulated GBM cells. The correlation of these markers with clinical outcomes was analyzed using our cohort and The Cancer Genome Atlas (TCGA) data.
Results: High KITENIN expression correlated positively with elevated CSC marker levels in human GBM samples and KITENIN-modulated GBM cells. Inhibition of KITENIN using usnic acid reduced tumor progression by decreasing CSC marker expression. Our data and TCGA analyses linked co-directional increase of these factors with tumor recurrence and shorter survival in GBM patients with unmethylated MGMT. This increase was also observed in TMZ-resistant cell lines with unmethylated MGMT. Implantation of KITENIN-overexpressing cells led to TMZ resistance in our mouse model, associated with co-directionally increased CD44 and ALDH1A1 expression. The link between KITENIN and CD44/ALDH1A1 could be inhibited by DKC2511, a novel KITENIN inhibitor, and T5244, a c-Fos/AP-1 inhibitor.
Conclusion: KITENIN might contribute to TMZ resistance in GBM patients with unmethylated MGMT, potentially through AP-1 activation and subsequent upregulation of CSC markers. Hence, targeting KITENIN could provide a novel strategy to overcome TMZ resistance in GBM patients with unmethylated MGMT.

#5440 TM4SF1 maintains cancer stemness in cholangiocarcinoma.

X. Zhu[1], J. Golino[1], X. Wang[2], C. Xie[3];
[1]NIH/NCI, Bethesda, MD, [2]Albert Einstein College of Medicine, New York City, NY, [3]NIH/NCI/CCR, Bethesda, MD

Cholangiocarcinoma (CCA) is an aggressive liver malignancy with increased incidence globally but poor prognosis. Cancer stemness plays critical roles on tumor initiation, recurrence, and resistance to therapy. However, the mechanism of stemness maintenance in CCA has been less explored. Previously, we have reported TM4SF1 is associated with poor survival in CCA and high expression of TM4SF1 tends to promote tumorigenesis. In this study, we found that the expression of TM4SF1 gene is upregulated in tumor tissues compared to adjacent normal tissues in CCA based on bulk RNA sequencing dataset from The Cancer Genome Atlas (TGCA) CCA cohort. There is a positive correlation between the expression of TM4SF1 and stemness genes, ITGB3, SOX9, ALDH1A3, and ITGB1. Interestingly, knockdown of TM4SF1 with siRNA in CCA cell line HuCCT-1 cells demonstrated a decrease in expression of cancer stem cell surface markers, CD24 and Prom1. Furthermore, with a CRISPR-based lentivirus construct to knockdown TM4SF1 gene in HuCCT-1 cells *in vitro*, we found that spheroid formation in TM4SF1 knockdown was attenuated in comparison to TM4SF1 wild type. In addition, the results from flow cytometry and RT-PCR showed a corresponding decrease in CD24 and CD133 expression with TM4SF1 knockdown when comparing to TM4SF1 wild type. In conclusion, TM4SF1 is associated with the stemness of CCA and could be a therapeutic target for CCA therapy to overcome therapy resistance in future.

#5441 Down regulation of cysteine glutamate antiporter in ALDH1A1 expressing oral and breast cancer stem cells induced oxidative stress triggered ferroptosis.

R. Bellala;
Gitam University, Visakhapatnam, India

Background: Sulfasalazine, an xCT inhibitor, is being used as a repurposed antineoplastic drug to induce ferroptosis. Ferroptosis is a regulated necrotic cell death pathway that is dependent on iron reserves. Interestingly, cancer stem cells (CSCs) that are regarded as major drivers of resistance to conventional therapies accompanied with tumor relapse and recurrence have bulk amount of iron reserves in the form of ferritin. This suggests that inducing ferroptosis might disrupt stemness and drug resistant mechanisms in cancer stem cells, thereby reducing the risk of drug resistance, cancer recurrence, and relapse.
Materials & Methods**:** In the present study, ALDH1A1 expressing oral (OCSCs) and breast (BCSCs) cancer stem cells were sorted and used to investigate the role of sulfasalazine to induce ferroptosis. To check the self-renewability of CSCs spheroid formation assay was performed and the resultant CSCs were treated with sulfasalazine (SAS) and subjected to gene expression analysis RT PCR and flow cytometry. FACS was performed to check stem cell marker expression, cell cycle arrest, and apoptosis.
Results**:** Our results suggest that the cells showed a gradual increase in sphere formation till S3 in the case of OCSCs and S2 in the case of BCSCs, with a gradual decrease in sphere forming efficiency from the respective generations. When treated with 0.6mM SAS, these cells induced ferroptosis by downregulating stem cell markers like ALDH1A1, SLC7A11, ferritin, and GPx 4 with a concomitant increase in transferrin and STEAP 3. Flow cytometry studies revealed that the cells have undergone mitochondrial dysfunction characterized by loss of membrane potential and the cell cycle progression was halted in the G2/M phase.
Conclusion**:** In the present study, we demonstrate that SAS potentially induced ferroptosis accompanied with oxidative stress in both OCSCs as well as BCSCs by lowering GPx 4 activity, a key enzyme that scavenges the products produced as a result of oxidative stress.

#5442 Tert^{high}cells: key players in salivary gland homeostasis and regeneration after radiation therapy in adult mice.

L. Guan[1], V. Viswanathan[1], S. V[1], H. Cao[1], Y. Jiang[1], J. Zhao[2], D. R. C. Colburg[1], P. T. Neuhoefer[1], Y. Xu[1], E. E. Laseinde[1], S. Artandi[1], Q.-T. Le[1]; [1]Stanford University, Stanford, CA, [2]Columbia University, New York, NY

Salivary gland homeostasis and regeneration post-radiotherapy depend significantly on stem/progenitor cells. However, the lineage of SMG progenitor cells is not as well defined as in other normal organs, and better understanding of this population would be important for their future clinical application for tissue regeneration. Using a mouse strain expressing regulated CreERT2 recombinase from the endogenous Tert locus, we identify a distinct Tert^{high} cell population that are located in the ductal region throughout the submandibular gland (SMG), express ASCL3 (another progenitor cell marker) and can give rise to ductal cells during homeostasis. In contrast, Tert^{high} cells are found to repopulate both ductal and acinar cells at one year of tracing after radiotherapy. Tert^{high} cells from adult SMG retain self-renewal capacity when subjected *in vitro* culture, are resistant to radiation cell kill, and display enhanced proliferative activity post-radiation. Similarly, primary human SMG cells with high Tert expression display enhanced cell survival after radiotherapy. RNA sequencing reveals upregulation of the cell cycling and oxidative stress response pathways these cells after radiation. Mechanistically, Tert appears to modulate cell survival and ROS level in SMG spheres following radiation damage. Collectively, these data suggest that Tert^{high} cells constitute a novel subset of SMG progenitor cells located throughout the ductal region of the gland that can help to repopulate both ductal and acinar cells after RT damage.

#5443 Identifying key regulators of glioblastoma cancer stem cells.

T. Wang, X. Xie, L. F. Parada;
Memorial Sloan Kettering Cancer Center, New York, NY

Glioblastoma multiforme (GBM) has a dire prognosis that has had little progress over the past three decades. The existence of a unique population of stem-like gene signature baring quiescent cells (GSCs) within GBM are important for GBM tumorigenesis, therapy-resistance and recurrence. Our lab has developed one of the most faithful genetically engineered mouse models, encompassing a *Nestin* promoter-enhancer driven CreER^{T2}-H2BeGFP-hDTR cassette (hereafter as *CGD*), that allows us to accurately capture and isolate GSCs in mouse GBM. The next logical step is to leverage these tools to uncover therapeutic vulnerabilities of GSCs and make a meaningful impact on GBM patient outcomes. To our knowledge, very few studies have explored the functional regulators of GSCs using a CRISPR/Cas9 screening approach. Our GSC signature provides a strong foundation for performing targeted *in vitro* or *in vivo* screens. In this study, to identify functionally important genes that may regulate GSC self-renewal and tumorigenic properties, an *in vitro* CRISPR knockout screens using a gene library derived from the GSC signature. The viral library was applied to low passage primary cultures of FACS sorted CGD_GFP+ and CGD_GFP- GBM cells developed from *CGD; Nf1*$^{f/+}$*;Trp53*$^{f/f}$*;Pten*$^{f/+}$ mice, respectively. The result of our *in vitro* CRISPR knock-out screen demonstrated guide depletion of *Atp1b2*-sgRNA in CGD_GFP+ but not in CGD_GFP- cells. The main objective of this study is to utilize *in vitro* and *in vivo* functional assays to test the difference between *Atp1b2* WT and *Atp1b2* KO GSCs and *Atp1b2* WT vs KO GSC-derived tumors. Having a targeted candidate gene list is also particularly helpful for designing an *in vivo* CRISPR knockout screen, which is more physiological relevant. Therefore, I propose to use the candidate gene list derived from the *in vitro* screen as a starting point. The in vivo screen can provide valuable insights for the selection of the most optimal candidates for anti-GSC therapies.

#5444 EGFR missense mutation(s) induce OLIG2 expression to regulate glioma stem cells maintenance and therapeutic resistance.

S. Weaver[1], A. Miller[1], M. Blomquist[1], J. McNamara[2], K. Orndorff[2], C. Sereduk[1], J. Kloss[1], J. Loftus[1], S. Mehta[2], N. L. Tran[1];
[1]Mayo Clinic Arizona, Scottsdale, AZ, [2]Barrow Neurological Institute, Phoenix, AZ

Glioblastoma (GBM) tumors contain a subpopulation of glioma stem cells (GSC) which can escape therapeutic effects through self-renewal and invasion. Epidermal growth factor receptor (EGFR) mutations are the most common alteration in GBM (50%). One example includes extracellular domain missense mutations like G598V, A289V, and R108K (10-15%). These extracellular domain missense mutations increase ligand binding affinity, inducing a highly active receptor. Earlier reports have shown these EGFR missense mutations exhibit therapeutic resistance; however, the molecular mechanism of these missense mutations in GBM remains unknown. In this study, we show high oligodendrocyte transcription factor 2 (OLIG2) expression in GSCs with EGFR-G598V and EGFR-A289V missense mutations. OLIG2 is universally expressed in glioma and essential for reprogramming GBM cells into stem-like tumor cells. Here, we report GSCs with these point mutations display increased self-renewal, growth, invasion, and therapeutic resistance. In addition, EGFR-G598V and EGFR-A289V trigger distinct downstream signaling pathways in GSCs to regulate OLIG2 function. These missense mutation(s) also represent different pathway-based GBM subclassifications, where A289V induces a Neuronal subtype and G598V induces a Glycolytic/Plurimetabolic subtype. We hypothesize that GBM tumors harboring EGFR missense mutations (G598V, A289V) influence stem cell properties *via* multiple pathways to evade therapeutic effects and inhibiting these different signaling pathways will decrease therapeutic resistance in GBM. Understanding the mechanism of these EGFR mutations may lead to improved therapeutic strategies for GBM patients.

#5445 Unravelling the molecular mechanisms of stemness in small cell lung cancer using an iPSC-based approach.

S. Gara[1], H. Wang[1], A. Singh[1], T. Tolunay[1], V. Shukla[2], R. Wang[1], M. Zhang[1], S. Shiffka[1], D. S. Schrump[1];
[1]National Cancer Institute, Bethesda, MD, [2]FDA, White Oak, MD

Introduction: The cancer stem cell hypothesis explains the heterogeneity, drug resistance, and metastatic potential of Small Cell Lung Cancer (SCLC). To address limited surgical tissue availability, we developed an induced pluripotent stem cell (iPSC) model for investigating SCLC stemness mechanisms and potential novel therapies. Cigarette smoke condensates (CSC) have previously been linked to stem cell activation in lung epithelial cells. We aimed to transform normal lung iPSCs (Lu-iPSC) through prolonged CSC exposure to identify candidate genes in the transition to cancer stem cells.
Methods: Four Lu-iPSC clones derived from normal human small airway epithelial cells (SAEC) of two healthy donors were exposed to CSC at different concentrations for short- (7 days) and long-term (6 months) periods. RNA-seq was performed to identify differentially expressed genes (DEGs) relative to respective SAEC. Gene expression data of 23 SCLC cell lines and 38 NSCLC from the public databases was extracted and analyzed relative to SAEC. In vitro tri-lineage differentiation studies, drug sensitivity assays, and phenotypic characterization by flow cytometry was performed in this study.
Results: Gene expression profiles of Lu-iPSCs closely resembled those of SCLC rather than NSCLC. Short-term CSC exposure reduced Lu-iPSC proliferation while increasing the expression of key stemness markers such as SALL1 in a dose-dependent manner. Concurrently, CSC exposure downregulated the expression of nodal and its inhibitors, LEFTY1 and LEFTY2, which can be considered as the earliest signs of differentiation events in Lu-iPSC. Long term CSC exposure induced expression of epithelial mesenchymal transition markers including ZEB1 and ZEB2. In-vitro trilineage differentiation studies revealed that CSC particularly decreased expression of endodermal lineage specific markers (GATA4, SOX17, and FOXA2) without affecting mesodermal and ectodermal markers. Importantly, CSC induced the phenotypic expression of several lung cancer stem cell markers (CD44, CD133, and CD338) along with resistance to cisplatin and topotecan. RNA seq analysis of long-term CSC exposed Lu-iPSCs identified 92 common DEGs (53 up and 39 down) relative to their controls. Gene set enrichment analysis on DEGs indicated upregulation of Notch signaling, IGFBPs, TGF beta receptor signaling, and NCAM1 interactions while GABA receptor activation and GPCR signaling were downregulated. Comprehensive RNA seq analysis of CSC exposed and unexposed Lu-iPSCs relative to SCLC and NSCLC, identified potential candidate genes associated with SCLC stemness.
Conclusion: Our findings suggest that this iPSC model shows promise for investigating mechanisms mediating stemness in SCLC and identifying candidate genes and their associated pathways as potential targets for preclinical development of novel treatment regimens for these highly lethal neoplasms.

#5446 The role of snoRNAs in GBM cells, GSCs, neuronal precursor cells (NPCs), astrocytes, and normal brain tissues.

S. Chatterjee[1], S. Kuersten[1], C. Middle[1], M. Roos[1], P. A. F. Galante[2], G. Guardia[2], L. Penalva[3];
[1]Illumina, Inc., San Diego, CA, [2]Instituto Sirio-Libanes de Ensino e Pesquisa, Sao Paulo, Brazil, [3]UT Health San Antonio, San Antonio, TX

rRNA modification are a crucial step in ribosome assembly and function. Small nucleolar RNAs select which nucleotides in rRNAs get modified. Typically, C/D box snoRNAs are implicated in 2'-O-ribose methylation (2'Omet) while H/ACA box snoRNAs are responsible for pseudo-uridylations. Alterations in snoRNA expression have been described in multiple tumor types while distinct snoRNAs have been linked to cancer-relevant phenotypes. Our initial study on snoRNA expression using a dedicated Ampliseq platform revealed a specific glioma stem cell (GSC) signature. We propose this snoRNA signature creates a unique rRNA modification pattern that shapes the ribosome, favoring the translation of genes in pathways critical for GSC growth and survival. We will expand our study and characterize the expression profile of snoRNAs and 2'Omethylation in a large panel of GBM cells, GSCs, neuronal precursor cells (NPCs), astrocytes, and normal brain tissues. Next, we will select snoRNAs displaying differential expression in GSCs and determine if changes in their levels affect proliferation, viability, response to temozolomide and radiation, and translation. We and others have observed that the integrity of protein complexes that regulate ribosomal biogenesis depends on PolyADP-ribosylation (PARylation)and PAR-binding. In agreement, genomic screenings determined that multiple genes regulating ribosome biogenesis confer sensitivity to PARP inhibitors. These findings offer a therapeutic opportunity. We will investigate the functional impact of PARylation on rRNA modification by determining the effect of PARP inhibitors on snoRNP assembly and 2'Omethylation. Finally, we will test the hypothesis that PARP and ribosome biogenesis inhibitor combinations would be more effective than PARP inhibition alone in treating GBM.

#5447 Microtubule-associated protein MAP2 promotes drug resistance and cancer stemness in hepatocellular carcinoma through integrin dysregulation.

Ut Kei Lou[1], Ka-Hei Lam[1], Huajian Yu[1], Jia Jian Loh[1], Ki-Fong Man[1], Lei Zhou[2], Yuan Gao[3], Tin-Lok Wong[1], Cheng-Han Yu[1], Stephanie Ma[1]

[1]School of Biomedical Sciences, Li Ka Shing Faculty of Medicine, University of Hong Kong, Hong Kong, Hong Kong,[2]Precision Medicine Institute, The First Affiliated Hospital, Sun Yat-Sen University, Guangzhou, China,[3]State Key Laboratory of Cancer Biology, Biotechnology Center, School of Pharmacy, Fourth Military Medical University, Xi'an, China

Integrins are adhesion molecules that mediate mechanical and chemical signal transduction pathways to support cell survival and proliferation. Dysregulated integrin signaling empowers tumor cells to drive oncogenic stemness functions, including tumor initiation, epithelial plasticity, metastatic reactivation, and resistance to therapies. However, the interplay between cancer stemness and integrin signaling in hepatocellular carcinoma (HCC) remains poorly understood. HCC cells marked by CD133 represent an important functional subset of HCC tumors, displaying a dedifferentiated status with stem cell traits. In this study, transcriptome profiling reveals specific downregulation of integrin α family genes and integrin signaling in 'HCC' CD133^{+} cells isolated from NRAS+AKT-driven HCC, but not epithelial-specific 'normal' CD133^{+} cells isolated from regenerating liver. Of note, one of the most differentially upregulated genes identified in CD133^{+} HCC cell profiling, microtubule-associated protein MAP2, demonstrates the ability to suppress integrin expression. MAP2 overexpression is frequently observed in HCC and correlates with aggressive clinical and stemness features, including survival, tumor stage, and stemness signatures. Epigenetic modifications by H3K27Ac contribute to MAP2 upregulation. Functionally, MAP2 promotes cancer stemness and cell invasion, and confers resistance to the targeted therapy sorafenib. Mechanistically, the inhibition of collagen-binding integrin α subunits by MAP2 subsequently ablates integrin β1-mediated cell adhesion and FAK signaling. Estramustine Phosphate (EMP), previously reported to inhibit the interaction of MAP2 with actin filaments, attains a synergistic effect in suppressing tumor initiation and growth of HCC cell lines, HCC patient-derived organoids and NRAS+AKT HCC mouse model when used in combination with sorafenib. In summary, MAP2 inhibition may represent a potential novel therapy for HCC by targeting its cancer stemness roots and altering integrin signaling. Ongoing work is focused on the study of MAP2 regulation of integrin signaling and cell behaviours in the maintenance of a more stemness state in HCC.

#5448 Malignant RNA editing by inflammation-responsive RNA editase ADAR1 drives T-cell leukemia relapse via attenuating dsRNA sensing.

M. D. Rivera[1], H. Zhang[1], Q. Zhou[1], J. Pham[1], J. Isquith[1], R. Sasik[1], A. Mark[1], S. Enlund[2], F. Holm[2], M. Wenxue[1], K. Fisch[1], D. Kuo[1], C. Jamieson[1], Q. Jiang[1];

[1]UC San Diego, San Diego, CA, [2]Karolinska Institutet, Stockholm, Sweden

Leukemia-initiating cells (LICs) play a crucial role in leukemia research and treatment, being considered the source of relapse and resistance, posing a substantial challenge for successful management of the disease. It's crucial to identify the key factors that drive LIC self-renewal to develop targeted methods for eliminating LICs and preventing relapse. In this study, we demonstrate that the RNA editing enzyme ADAR1 plays a vital role as a determinant of stemness, promoting LIC self-renewal by reducing the detection of abnormal double-stranded RNA (dsRNA). As a result, ADAR1-knockdown significantly impairs the ability of LICs to self-renew and extends survival in T-ALL PDX models. We performed RNA-seq studies on enriched T-ALL LICs (CD34+Lin-). The lentivirus-to-cell ratio was optimized to achieve a 50% reduction in ADAR1, resulting in differential expression of 661 genes, with downregulation of critical self-renewal genes in ADAR1-deficient leukemia-initiating cells. Importantly, additional data indicated that ADAR1 likely influences self-renewal gene expression independently of A-to-I RNA editing, revealing novel regulatory mechanisms in leukemia. Knockdown of MDA5 and ADAR1 in patient-derived xenograft (PDX) T-ALL leukemia-initiating cells (LICs) revealed diverse rescue effects on self-renewal in different PDX models. The differential response was associated with variations in gene expression patterns in Rig-I-Like signaling and cytosolic sensing pathways, suggesting intrinsic differences in IFN signaling properties among patients. Moreover, the study proposes a patient-specific reliance on the ADAR1 p150-MDA5 axis for promoting self-renewal, as evidenced by differential rescue effects and varying expression levels of ADAR1 isoforms and MDA5 in T-ALL patient samples and cell lines. ADAR1, beyond its role in RNA editing, acts as a dsRNA binding protein, exerting RNA editing-independent functions to suppress aberrant IFN signaling and promote cancer progression. Using Jurkat cells with high intrinsic MDA5 levels, an ADAR1 knockout (KO) was generated, revealing that ADAR1 is upregulated by IFN treatment, predominantly the p150 isoform. We explored the dual roles of ADAR1—RNA editing-dependent and -independent—in suppressing IFN-induced apoptosis, demonstrating the necessity of both for optimal function. Additionally, ADAR1 was found to suppress cytoplasmic dsRNA sensing pathways, such as RIG-I and PKR, and its RNA editing-independent activity contributes significantly to the suppression of interferon-stimulated gene (ISG) expression in T-ALL. In summary, our findings reveal that ADAR1 acts as a factor that promotes self-renewal while limiting the recognition of naturally occurring dsRNA. Therefore, targeting ADAR1 emerges as a safe and effective therapeutic approach for eradicating LICs in T-ALL.

#5449 Exploring signaling pathways essential for stemness and metastasis of colorectal cancer cells.

T. Fujishita[1], M. M. Taketo[2], **M. Aoki**[1];
[1]Aichi Cancer Center Research Institute, Nagoya, Japan, [2]Kyoto University Hospital-iACT, Kyoto, Japan

The prognosis of colorectal cancer (CRC) patients with distant metastasis remains poor, requiring elucidation of molecular mechanisms and identification of therapeutic targets. While cancer stem cells have been implicated in metastasis, recurrence, and drug resistance, our understanding of the regulatory mechanisms governing the stemness of CRC stem cells remains largely incomplete. In this study, we utilized an innovative autochthonous metastatic mouse model of CRCs generated by the introduction of sporadic mutations in *Ctnnb1*, *Kras*, *Trp53*, and *Smad4* genes (CKPS mice) and CRC cell lines derived from the mice (CKPS cells). Our investigation revealed that the cAMP/PKA/CREB and TGFβ/SMAD4 pathways play a positive and negative role, respectively, in the sphere-forming and metastasis-initiating ability of CRC cells. Treatment with the CREB inhibitor 666-15 or the genetic knockout of CREB significantly reduced the spheroid-forming and metastasis-initiating potentials of CKPS cells. Intriguingly, we observed that the irinotecan treatment induced CREB phosphorylation in liver metastases, and co-treatment of 666-15 greatly potentiated the inhibitory effect of irinotecan on liver metastasis. Furthermore, we found that the transition from 2D to 3D spheroid culture of CKPS cells led to the induction of RhoC expression. Notably, RhoC knockout in CKPS cells effectively suppressed spheroid formation *in vitro* and inhibited metastasis formation in an intrasplenic injection liver metastasis assay. Potential therapeutic implications of these findings will be discussed.

#5451 FOXC2 influences EMT-induced stem cell properties through regulation of FABP4 in breast cancer.

B. R. Demestichas[1], V. Shivakumar[2], E. Ramirez-Pena[2], J. Taube[3], P. den Hollander[1], S. A. Mani[1];
[1]Brown University, Providence, RI, [2]MD Anderson Cancer Center, Houston, TX, [3]Baylor University, Waco, TX

Cancer stem cells (CSCs) pose a significant clinical challenge due to their inherent resistance to therapies and prevalence in cancer recurrence. CSCs have the ability for self-renewal and to adapt to different microenvironments during dissemination and seeding into distal organs, and these properties are critical in metastasis. We and others have shown that epithelial to mesenchymal transition (EMT) drives the acquisition of stem cell properties, particularly via the forkhead box protein C2 (FOXC2) transcription factor. FOXC2 is a master regulator of EMT and is necessary for the induction and maintenance of CSC properties. Importantly, FOXC2 is not expressed in most adult tissues except adipocytes, in which it dictates several aspects of lipid metabolism. Additionally, metabolic changes during EMT can equip cancer cells with enhanced survival mechanisms during tumor progression and metastasis. We hypothesized that FOXC2 regulates metabolism in EMT-induced cells, facilitating stem cell properties and metastatic competence.

To determine the downstream metabolic genes regulated by FOXC2 and that enhance stemness properties in cancer cells, we performed gene expression profiling and identified fatty acid binding protein 4 (FABP4), which is known to be involved in lipid metabolism, especially in adipocytes and macrophages. We demonstrate that inhibition of FOXC2 expression using shRNA in EMT-induced cells markedly reduces FABP4 expression. In agreement with this, we found that the overexpression of FOXC2 expression rescues the expression of FABP4. In addition, FOXC2 binds to the FABP4 promoter and regulates its expression suggesting that FABP4 is a direct target of FOXC2. We demonstrate that both lipid uptake and CSC formation is inhibited in a dose-dependent manner using a FABP4-specific small molecule inhibitor. Additional experiments are underway to assess the role of FABP4 in CSC formation in vivo and in contributions to metastasis, using our small molecule inhibitor in mouse models of metastatic breast cancer.

Overall, our data indicate that FABP4 is a key regulator of stemness in breast cancer cells and targeting the FOXC2—FABP4 axis may provide therapeutic benefits for breast cancer. This work also provides insights into the metabolic shifts that occur during EMT and CSC formation, which warrants further investigation into these mechanisms.

#5452 AXIN2 differentially modulates stem cell subpopulations providing a potential therapeutic opportunity for targeting colorectal cancer stem cells.

C. Zhang, C. O. B. Facey, L. M. Opdenaker, B. M. Boman;
Helen F. Graham Cancer Center & Research Institute, Newark, DE

Constitutively activated WNT-signaling promotes stem cell (SC) overpopulation which drives most colorectal cancer (CRC) development. It is not known, however, how WNT-signaling activity regulates different SC sub-populations. We previously reported that SC population size decreases as AXIN2 is knocked down, and increases when AXIN2 is overexpressed. Changes in cell cycle and apoptotic rate were also observed. Here, we present our recent results on changes between different SC subpopulations (ALDH+ *vs.* LGR5+) that occur due to AXIN2 modulation. We *hypothesize* that modulation of AXIN2 promotes differential expansion between different CRC SC subpopulations (ALDH+ and LGR5+). We observed that AXIN2 not only increases LGR5+ SC population size, but also expands the ALDH+ SC population to a greater extent as shown by an increased ALDH+-to-LGR5+ SCs ratio. This indicates that AXIN2, via WNT signaling, regulates SC population size, particularly ALDH+ SCs. Since the ALDH SC marker is also a key component in the retinoic acid (RA) signaling pathway, we surmised that increased AXIN2 would not only lead to elevated ALDH levels, but also upregulate the RA-signaling pathway components in CRC cells. To this end, we conducted NanoString mRNA profiling to study the effects of *AXIN2* knockdown and overexpression in HT29 and SW480 CRC cells. The results showed that increased AXIN2 significantly up-regulated several key components of the RA-signaling pathway. Taken together, our results indicate that AXIN2 drives a shift in SC subpopulation sizes favoring the ALDH+ SCs. It also promotes the RA-signaling component expression - a pathway known to regulate SC differentiation. As a potential treatment strategy for CRC, therapeutically inducing high levels of AXIN2 could shift the balance between SC populations towards ALDH+ SCs, which may provide a way to target cancer SCs with retinoids to induce their differentiation.

TUMOR BIOLOGY: Pediatric Cancer Microenviroment, Tumor Heterogeneity, and Targeted Therapeutics
Poster Session

#5456 Identifying the role of tissue factor in osteosarcoma metastasis.
C. C. Treinen, A. Gross, M. Cam, B. Kerlin, R. Roberts;
Nationwide Children's Hospital, Columbus, OH

Patients with osteosarcoma who develop metastasis face very poor prognoses. Even when treated with the most effective medical and surgical interventions available, about forty percent of osteosarcoma patients will eventually succumb to lung metastasis. Despite the relevance of metastasis to clinical outcomes, we understand little about the mechanisms that drive these tumor cells into the lung and facilitate their metastatic growth. Consequently, there are no approved antimetastatic agents for osteosarcoma and outcomes have not improved in more than 40 years. Tissue factor is a tightly regulated physiologic initiator of coagulation with functions in inflammation, cytokinesis, angiogenesis, apoptosis, and growth factor secretion. These functions are divided between two separate pathways: initiation of the coagulation cascade via activation of factors VII and X, and propagation of cell signaling pathways via PAR activation. It is aberrantly expressed in many cancers and has been associated with metastatic behavior and inferior outcomes by affecting metastatic vascularity, growth, and migration. Osteosarcoma has been shown to also aberrantly express tissue factor, with descriptive studies suggesting similar effects on metastatic behavior. We hypothesized that tissue factor expressed on the surface of disseminated osteosarcoma cells activates procoagulant pathways and PAR signaling, and that both facilitate pulmonary metastasis. To test this, we first established and quantified expression of tissue factor across six osteosarcoma cell lines using Western blot, flow cytometry, and confocal microscopy in both monoculture and in coculture with human bronchial epithelial cells. PAR1 and PAR2 were also discovered to be expressed in osteosarcoma cells. RNA sequencing performed suggests that both tissue factor and PAR1 expression in osteosarcoma increase over the metastatic period, as does FVII expression by alveolar macrophages; this implies that tissue factor activation during metastasis is dynamic and dependent on host interactions. Ongoing work includes functional assays of osteosarcoma tissue factor and PARs activity as well as preclinical testing of tissue factor inhibition in a murine xenograft model of osteosarcoma. To define how tissue factor propagates metastasis, we are separately inhibiting its coagulant and cell signaling pathways after murine tail vein injection using apixaban or pathway-specific antibodies. We will also use an inducible F3 knockout to alter tumor expression of tissue factor. If we find that manipulation of tissue factor expression changes metastatic behavior across cell lines, this will suggest that tissue factor plays a crucial, mechanistic role in osteosarcoma metastasis. Varying effectiveness of coagulation or signaling pathway inhibition on metastasis will implicate tissue factor's mechanism of metastatic propagation.

#5457 Inflammatory paracrine loops established between metastasis-initiating cells and alveolar epithelium drive interactions between tumor cell subtypes that are essential for osteosarcoma lung colonization.

Amy C. Gross[1], James B. Reinecke[1], Amanda Saraf[2], John Hinckley[3], Maren Cam[1], Matthew V. Cannon[1], Sophia Vatelle[1], Ryan D. Roberts[1]

[1]Nationwide Children's Hospital, Columbus, OH,[2]Riley Children's Health, Indianapolis, IN,[3]Battelle, Columbus, OH

Introduction: The development of lung metastasis drives the poor outcomes experienced by children and young adults with osteosarcoma. The mechanisms that facilitate metastatic colonization remain poorly understood. We previously determined that IL6 and CXCL8 are two osteosarcoma derived cytokines that are required for metastasis, though roles played by these cytokines have not been identified.
Methods: To explore the interactions that drive cytokine expression, the role these factors play in tumor cell trafficking, and the mechanisms that facilitate metastatic niche development, we utilized transwell and co-culture systems together with a panel of metastatic osteosarcoma mouse models that allowed tumor cell manipulation via lentiviruses, CRISPR-based gene editing, and pre-clinical therapeutic evaluation approaches.
Results: While metastatic osteosarcoma cells produced small amounts of IL6 and CXCL8 at baseline, lung epithelial cells markedly upregulated IL6/CXCL8 production. Ligand-receptor analysis utilizing single-cell transcriptomic data identified IL1 as an epithelial derived ligand that drives tumor IL6/CXCL8 production. Interestingly, IL6/CXCL8 production was limited to a small subset of hypo-proliferative osteosarcoma cells that have metastasis-initiating capacity. Utilizing CRISPR-mediated ablation of IL1R1 signaling within osteosarcoma cells and pharmacological inhibition with recombinant IL1R antagonist (anakinra), we elucidated that formation of pulmonary lesions in multiple mouse models of metastatic osteosarcoma required IL1 signaling. Recent work from our lab has demonstrated that osteosarcoma metastases are defined by marked phenotypic heterogeneity, though the mechanisms by which metastatic heterogeneity occurred were unclear. We hypothesized that hypo-proliferative metastasis-initiating cells may recruit circulating cells with higher proliferative capacity to establish phenotypic heterogeneity. Transwell migration assays showed that tumor cells induced the chemotactic recruitment of other tumor cells in an IL6/CXCL8-dependent manner. To test this hypothesis *in vivo*, we injected mice with GFP-tagged osteosarcoma cells, then injected the same mice 14 days later with RFP-labeled tumor cells from the same culture. Lungs harvested 14 days later exhibited RFP-dominant lesions surrounding a small core of GFP-labeled cells.
Conclusions: Collectively, these data suggest that cytokines expressed by a subgroup of hypo-proliferative tumor cells upon interaction with lung epithelium drive the trafficking of highly proliferative circulating tumor cells into developing metastatic lesions and that disrupting these signaling networks can prevent metastatic colonization.

#5458 Plasticity of CAF-like states in Ewing sarcoma is mediated by TGF-beta.

E. Wrenn[1], A. A. Apfelbaum[2], K. Braun[1], E. R. Rudzinski[3], X. Deng[3], A. Miyaki[1], T. Lipson[4], N. M. Garcia[1], V. J. Hoglund[1], E. R. Lawlor[1];
[1]Seattle Children's Research Institute, Seattle, WA, [2]Dana Farber Cancer Institute, Boston, MA, [3]Seattle Children's Hospital, Seattle, WA, [4]University of Washington, Seattle, WA

Transcriptional plasticity of cancer cells promotes tumor progression and treatment resistance via generation of phenotypically distinct cell states. We previously showed that Ewing sarcoma (EwS) cells exhibit inter- and intra-tumoral transcriptional heterogeneity and that they undergo state changes in response to cues from the tumor microenvironment (TME). More recently, we identified phenotypically distinct EwS tumor cell subpopulations in vivo that deposit pro-tumorigenic extracellular matrix (ECM) proteins, adopting similar functions to cancer-associated fibroblasts (CAFs). Here, we sought to identify the upstream regulators of these CAF-like EwS cells with the goal of defining molecular mechanisms that control EwS plasticity and creation of ECM-remodeling states. Integration of single cell proteogenomic sequencing (CITE-seq) with immunofluorescence and digital spatial profiling of cell line xenografts and patient tumors validated the cell-surface protein CD73 (*NT5E*) as a biomarker of ECM-secreting EwS cell subpopulations in vitro and in vivo. The transcriptomes of CD73+ CAF-like cells were compared to isogenic CD73- cells (n=9 cell lines) and highly significant enrichment of gene ontology terms related to TGF-beta signaling (p.adj = $<4.4x10^{-14}$) was noted. EwS cells were previously reported to be non-responsive to TGF-beta due to profound transcriptional repression of the TGF-beta type 2 receptor (*TGFBR2*) by EWS::FLI1. In support of this, *TGFBR2* expression was low in bulk measurements of EwS cells. However, *TGFBR2* mRNA and surface protein expression were significantly increased in CD73+ subpopulations. Exposure of EwS cells to TGF-beta ligands (TGFB1 or TGFB2) strongly induced the CAF-like gene signature, including ECM genes *BGN, COL1A1, SPARC,* and *TNC* (p. adj < $8.5x10^{-5}$), and this was augmented in CD73+ cell populations. Transduction of EwS cells with dominant negative-TGFBR2 inhibited both basal and TGF-beta-induced expression of CAF-like signature genes and blocked SMAD2 phosphorylation. To test the functional significance of the TGF-beta response, unsorted EwS cells were plated in 2D or as tumor spheroids in collagen I-rich 3D cultures and exposed to TGFB1 or SB-505124, a TGF-beta inhibitor. TGFB1 treatment had no effect on cell viability or proliferation in 2D but increased invasion into collagen in 3D. Inhibition of TGF-beta reduced CAF-like gene expression in 2D cultures and diminished both viability and invasion in 3D. Finally, our studies revealed that *NT5E* (CD73) is a TGF-beta induced target in EwS cells and that CD73+ cells upregulate expression of *TGFB2.* Thus, an autocrine signaling circuit is created in which TGF-beta activity in CAF-like tumor cell subpopulations is sustained by CD73+ tumor cell-derived ligand. Together these studies demonstrate that TGF-beta is a key determinant of cell plasticity and ECM remodeling in EwS.

#5459 Inflammatory gene-based subtyping of osteosarcoma patients reveals the association of inflammation in tumor microenvironment with better survival.

L. Yang[1], Y. Sheng[1], S. Qiao[1], D. Hu[2], D. Chowdhury[1], H. Yip[1], Z. Chen[1], Y. He[1], A. Lu[1], F. Li[1];
[1]Hong Kong Baptist Univ. School of Chinese Med., Hong Kong, China, [2]Huazhong University of Science and Technology, Wuhan, China

Introduction: Inflammation has a significant impact on the tumor microenvironment (TME) of osteosarcoma (OS). Nevertheless, due to the high heterogenecity and variable inflammatory characteristics among OS patients, it is still unclear which inflammatory factors or immune/stroma cell types are crucially associated with OS prognosis. Therefore, it is essential to explore the immune infiltration pattern and the related core inflammatory genes in OS. **Method:**We combined bulk RNA-seq data of 88 osteosarcoma (OS) patients from the TARGET database and single cell RNA-seq data in GSE152048 from the NCBI Gene Expression Omnibus. Firstly, we calculated the inflammatory gene expression matrix of bulk RNA-seq data by combining 80 inflammatory gene sets (3427 genes in total) from the MSigDB using the gene set variation analysis (GSVA). Secondly, consensus clustering was executed to evaluate the stability of clustering for the above matrix. Furthermore, the overall survival and differential expression analyses were used to screen for core inflammatory genes. Immune infiltration patterns among groups were profiled with CIBERSORT. Finally, we employed the scRNA-seq series to evaluate cell-level information to identify the survival-associated cell subpopulations using the Seurat package. The t-SNE was used for dimensionality reduction and cluster identification. **Results:**88 osteosarcoma (OS) patients were clustered into two distinct groups according to the consensus clustering of our formed GSVA inflammatory gene expression matrix. Group 1 (43 patients) exhibited evident inflammation features, while Group 2 (45 patients) displayed limited inflammation features. Patients from Group 1 had significantly better overall survival than those from Group 2. The difference in immune infiltration pattern of two groups were examined using bulk RNA-seq data. Group 1 showed a higher population of macrophages and CD8+ T cells compared to Group 2, implying high inflammatory features might lead to a better immune activation of TME in patients. To explore the factors and cell types that contributes to restricted immune infiltration and activation in OS TME, scRNA-seq data of 11 OS patient tissues were analyzed. Consistently with bulk RNA seq analysis, the 338 up-regulated genes from Group 1 were mainly expressed in immune cells including macrophages and myeloid cells. Interestingly, the 64 up-regulated genes from Group 2 were found nearly uniformly expressed in two type of non-immune cells: myoblasts and chondroblastic cells. **Conclusion:**Inflammatory gene-based subtyping of osteosarcoma (OS) patients reveals that the inflammation in TME led by myeloid-derived immune cells including macrophage is associated with better prognosis. Furthermore, myoblasts and chondroblastic cells might contribute to the limited inflammation response in OS TME.

#5460 Discovery and validation of effective combination therapies targeting cell state-specific master regulator vulnerabilities by network-based protein activity inference in diffuse midline glioma.

E. Calvo Fernandez[1], L. Tomassoni[1], X. Zhang[1], A. Obradovic[1], P. Laise[1], A. T. Griffin[1], L. Vlahos[1], J. Wang[2], H. E. Minns[1], D. V. Morales[1], C. Simmons[1], M. Gallito[1], H.-J. Wei[1], Z. Zhang[1], R. Gartrell[1], L. Szalontay[1], S. Zacharoulis[1], C.-C. Wu[1], A. Califano[1], J. Pavisic[1];
[1]Columbia University Irving Medical Center, New York, NY, [2]University of California LA, Los Angeles, CA

Diffuse Midline Glioma (DMG) are fatal pediatric brain tumors with no effective systemic therapies. We leveraged network-based methodologies to dissect tumor heterogeneity, discover Master Regulators (MR) representing pharmacologically accessible vulnerabilities of distinct DMG cell states, and validated candidate MR-reversing drugs predicted by the NYS CLIA-certified OncoTarget and OncoTreat algorithms (Cancer Discov 2023) *in vivo*.

We first interrogated single cell DMG regulatory networks generated by ARACNe (Nat Genet 2005) with publicly available gene expression signatures from 3,039 tumor cells across 6 patients using VIPER (Nat Genet 2016) to infer single cell regulatory protein activity. Clustering of cells by protein activity defined 7 patient-independent cell states with distinct MR profiles reflecting known glial lineage markers (OPC-like-S1, OPC-like-S2, OC-like-S1, OC-like-S2, Cycling, AC-like, and AC/OPC-like). We then generated drug-induced differential protein activity from RNAseq profiles following perturbation with 372 oncology drugs in two DMG cell lines that together recapitulate the MR signatures of the cell states and used this to identify drugs that invert tumor MR activity profiles using OncoTreat. Candidate drugs predicted by OncoTarget (inhibitors of individual MRs) and OncoTreat were distinct across the cell states, and we selected five drugs targeting the OPC/cycling-like cells (Trametinib, Dinaciclib, Avapritinib, Mocetinostat, and Etoposide), and four drugs targeting the AC-like cells (Ruxolitinib, Venetoclax, Napabucasin, Larotrectonib) for further validation as these states comprised most tumor cells across patients.

We generated single-cell RNAseq for 95,687 cells after 5 days of treatment with either vehicle control (n = 4) or candidate drug (n = 2-3/drug) in subcutaneous SU-DIPG-17 mouse models. We show this model recapitulates cell states seen in patients and confirm reduction in tumor growth and significant depletion of either OPC/cycling-like cells or AC-like cells in line with our drug predictions for 8/9 candidate drugs. We then treated a syngeneic (DIPG4423) orthotopic DMG model with each drug and demonstrate significant differences in survival with Avapritinib, Dinaciclib, and Trametinib. Notably, the combination of drugs targeting OPC/cycling-like and AC-like cells (*i.e.* Trametinib+Ruxolitinib and Avapritinib+Venetoclax) showed significantly lower tumor volumes after 2 weeks of treatment as compared to vehicles or each drug alone, and significant survival differences for some combinations. This work provides a precision medicine platform to nominate much-needed novel drug combinations addressing DMG tumor heterogeneity for further study to improve outcomes in this devastating disease.

#5461 Antecedent STING agonist therapy improves tumor response to chemotherapy in murine models of osteosarcoma.

E. E. Resch, E. Kulp, M. Doucet, A. Recho, B. H. Ladle;
Johns Hopkins University, School of Medicine, Baltimore, MD

Little improvement has been made in outcomes for pediatric patients with osteosarcoma in decades. Cytotoxic chemotherapy alone is insufficient for cure and upfront complete surgical resection is usually required to achieve long-term survival. Better systemic therapies are needed. Osteosarcoma is characterized by a high degree of genomic instability that would suggest these tumors have sufficient neoantigen burden to be immunogenic and responsive to immunotherapy, but trials of immune checkpoint inhibitors in osteosarcoma have shown poor effectiveness. Although immunotherapy drugs targeting the adaptive immune system have worked poorly, we hypothesize that an innate immune adjuvant - stimulator of interferon response cGAMP interactor 1 (STING) agonist - in combination with cytotoxic chemotherapy would improve chemotherapy effectiveness and immune-mediated tumor clearance, particularly given the abundance of innate immune cells in the microenvironment of these tumors. Using two different immune-competent *in vivo* murine models of osteosarcoma (K7M2 in BALB/c mice and F420 in C57BL/6 mice), we challenged mice with tumor cells via subcutaneous or intratibial injection. In all experimental replicates, we observed improved tumor regression in mice treated with intratumoral STING agonist followed by intraperitoneal treatment with carboplatin. Responses included complete tumor response in up to 40% of treated mice. Treatment with STING agonist alone or carboplatin alone only delayed tumor growth compared to untreated controls. Additionally, mice treated first with carboplatin and then with STING agonist demonstrated an initial modest response to treatment, but ultimately exhibited tumor progression, suggesting an importance to the sequence of STING agonist administration. *In vitro* treatment of K7M2 and F420 cells with STING agonist showed a tumor-intrinsic transient increase in expression of pro-inflammatory mediators Cxcl10, Ccl5, and Ifnb 4 hours after STING exposure. Flow cytometry analysis of K7M2 tumors demonstrated increased infiltration of STING/carboplatin-treated tumors with $CD8^{+}$/$IFN\gamma^{+}$ lymphocytes and $CD11b^{+}$/$MHCII^{+}$/$F480^{+}$ tumor-associated macrophages. Interestingly, these tumors also demonstrated an increased quantity of $CD11b^{+}$/MHCII^{-}/F480^{-}/$Ly6G^{lo}$/$Ly6C^{+}$ myeloid-derived suppressor cells despite their favorable clinical response. Our findings suggest that intratumoral STING agonist therapy stimulates tumor-intrinsic and tumor-extrinsic pro-inflammatory mediators that improve the tumor response to treatment with carboplatin. Ongoing studies are further investigating the tumor-intrinsic and extrinsic mediators that are driving this improved response to therapy.

#5462 Single-cell spatial proteomic analysis to explore the spatial heterogeneity of desmoplastic small round cell tumors.

D. Truong, S. Krishnan, C. Agyemang, D. Ingram, R. Lascano, A. Basi, J. Gomez, J. Burks, A. Lazar, J. Ludwig;
UT MD Anderson Cancer Center, Houston, TX

Desmoplastic small round cell tumor (DSRCT) is a rare and usually incurable aggressive sarcoma subtype. All malignant cells harbor a pathognomonic EWSR1::WT1 fusion protein (FP). However, FP-targeted agents are nonexistent; less than 20% of patients survive beyond five years. The spatial organization of DSRCT, consisting of tumor nests surrounded by desmoplastic stroma, is a hallmark of this disease. Given this context, we seek to understand the spatial heterogeneity within DSRCT and the tumor-stroma interactions to reveal potential therapeutic vulnerabilities. We generated a 20-panel marker developed to interrogate the cellular constituents of the tumor microenvironment (TME) and to characterize the multilineage expression DSRCT, including androgen receptor (AR) and neuroendocrine signatures (NE). The following markers were used: DSRCT (ST6GALNAC, pan-Cytokeratin), Fibroblasts (Collagen, α-smooth muscle actin), Endothelial Cells (CD31, α-smooth muscle actin), T-cells (CD45, CD4, CD8), Macrophages (CD45, CD68, CD163, CD11c), AR/NE markers (AR, neural-specific enolase, synaptophysin). We explored the expression of these markers in a nine-patient cohort from 9 x 9 mm^2 tissue sections imaged by the Lunaphore COMET. We used a deep learning model in Visiopharm to extract high-quality areas and segment cells based on their nucleus. The spatial image data was converted into matrix data, which could be further analyzed in R. We confirmed that the tumor nests are surrounded by dense desmoplasia by collagen expression. We identified tumor cells, fibroblasts, immune cells, and endothelial cells by thresholding for classical cell markers. ST6GALNAC, a sialyltransferase that was found to be highly expressed in DSRCT based on RNA-seq data, marked the tumor nests. Previous data from single-nucleus RNA-sequencing (snRNA-seq) showed that DSRCT exhibited three possible subtypes: AR+/NE-, AR-/NE+, and Hybrid AR+/NE+. We found concordance between the prior transcriptomic signatures and the proteomic markers. In tumor nests that were positive for AR, we found AR localized to the nucleus, suggesting downstream activation of this pathway. High AR expression was also correlated with positive expression of pan-cytokeratin in the tumor nests. Future work will focus on quantifying spatial relationships and patterns. This includes characterizing the spatial distribution of all cell types found in DSRCT, including fibroblasts, endothelial cells, and immune cells. We will also address whether tumor nest characteristics are associated with cell phenotype or DSRCT subtype.

#5463 Germline *DICER1* loss promotes rhabdomyosarcoma via innate immune system.

R. Larsen IV, J. Hanna, K. Reed, H. Jin, W. Kimbrough, K. Vuong, M. Evans, C. Langdon, C. Drummond, M. Garcia, D. Finkelstein, P. Schreiner, J. Rehg, M. Hatley;
St. Jude Children's Research Hospital, Memphis, TN

DICER1 syndrome is a cancer predisposition syndrome where affected patients have increased risk of neoplasms including pleuropulmonary blastoma, Sertoli-Leydig cell tumor, and fusion-negative rhabdomyosarcoma (FN-RMS). This syndrome is defined by germline heterozygous loss of function mutations in the gene *DICER1*, but it remains unclear exactly how these mutations predispose children to develop cancer. One would expect the germline loss of one allele to provide a sensitized background in the tumor cell to acquire a second hit mutation. To gain insight into the role of *Dicer1* loss in FN-RMS, we deleted the *Dicer1* gene both globally in the germline and conditionally in the tumor cell in our previously established mouse model of FN-RMS. Surprisingly, we observed faster tumor onset and increased penetrance in mice with germline heterozygous *Dicer1* loss (*Dicer1*$^{+/-}$) but not in mice where *Dicer1* loss was restricted to the tumor cells, demonstrating that *Dicer1* functions as a non-cell autonomous haploinsufficient tumor suppressor. Single cell RNA sequencing (scRNA-Seq) revealed massive expansion of immature neutrophils in *Dicer1*$^{+/-}$ tumors, which were enriched for proteases associated with neutrophil extracellular traps (NETs). NETs are webs of chromatin and proteases released when neutrophils undergo NETosis in response to inflammatory stimuli. These NETs are known to cause significant damage to the local extracellular matrix (ECM) and have been implicated in tumor promotion. In addition to the neutrophil enriched immunophenotype, we found that *Dicer1*$^{+/-}$ tumors show significant ECM remodeling and are enriched for C5a, the potent neutrophil chemoattractant and NET-priming factor. Taken together, these results suggest NETosis is upregulated in *Dicer1*$^{+/-}$ FN-RMS tumors. Performing iTALK ligand-receptor pair analysis on the scRNA-Seq data revealed a putative interaction between a NET-derived ligand and EGFR and IGF1R on tumor cells, suggesting direct tumor promoting signaling from NET-to-tumor. We validated this novel FN-RMS promotion mechanism in vitro using human FN-RMS cell lines and observed that this NET-derived ligand promoted FN-RMS growth in a dose-dependent manner and could function through both EGFR and IGF1R signaling. Finally, we incorporated a *Padi4*$^{-/-}$ allele into our tumor model to genetically block NETosis and observed complete rescue of the accelerated tumor onset and increased penetrance observed in *Dicer1*$^{+/-}$ mice, demonstrating that NETosis promotes the growth of *Dicer1*$^{+/-}$ FN-RMS tumors. Importantly, these findings may be applicable to many *DICER1* syndrome-associated cancers, as neutrophils which get converted to tumor promoters by heterozygous *DICER1* loss are present in *DICER1* syndrome patients regardless of tumor type.

#5464 Galectin-3 expression in Ewing sarcoma: Modulation of the immune microenvironment in an immunocompetent model.

Y. Maharjan, S. Dey, E. Mukherjee, J. Daley, K. M. Bailey;
University of Pittsburgh School of Medicine, Pittsburgh, PA

Objective: Ewing sarcoma is an aggressive cancer of adolescents. Patients with metastatic Ewing sarcoma often receive radiation as part of their treatment protocol. We have demonstrated that both Ewing tumor cells and T cells infiltrating Ewing tumors express Galectin-3 (*Gal3*), an immunosuppressive protein in the tumor microenvironment. Here, we utilize an immunocompetent, humanized mouse model of Ewing sarcoma to investigate the role of Galectin-3 in the Ewing tumor immune microenvironment both at baseline and following radiation. Specifically, we sought to determine the influence of Galectin-3 on post-radiation inflammation in Ewing sarcoma.

Methods: Human Ewing cells -/+ *Gal3* expression were generated using CRISPR/Cas 9 technology. Cells -/+ *Gal3* were orthotopically injected into humanized mice and allowed to established tumors over ~3 weeks. Tumors were then treated with radiation (or no radiation controls). To also address immune cell expression of Gal3, galectin inhibitors were utilized. Tumors were analyzed by bulk RNA sequencing and flow cytometry analysis (Cytek Aurora) for human CD45, CD3, CD4, CD20, CD8, CD56, CD14, CD16, etc. Peripheral blood controls were also collected and analyzed to ensure consistent baseline immune reconstitution.

Results: CHLA10 and TC32 Ewing sarcoma cell lines both demonstrate Gal3 expression at baseline by western blot. CRISPR/Cas 9 knock-out of *Gal3* in both cell lines showed successful knock down. Impact on growth and sensitivity to radiation *in vitro* was assessed by live cell Incucyte assays. Tumors in humanized mice were established utilizing these cells (or *Gal3* expressing non-targeting controls) and changes in the post-radiation transcriptional profiles were assessed. Immune cells infiltrating these tumors were also quantified. Ongoing work focuses on additional characterization of these tumor infiltrating immune cell populations following radiation therapy and the impact of broader galectin inhibition on this effect.

Conclusion: This work contributes to the understanding of radiation-induced tumor inflammatory responses in Ewing sarcoma by defining the role of tumor and T cell galectin-3 expression inn Ewing immunobiology. Next steps will explore translational opportunities based on these findings.

#5466 *In vivo* characterization of neuroblastoma intratumoral heterogeneity.

W. R. Squires, A. Weiss, S. Cohen-Gogo, A. Shlien, D. Kaplan, M. S. Irwin, M. N. Hayes;
The Hospital for Sick Children, Toronto, ON, Canada

Background: Neuroblastoma is a pediatric solid tumor that arises from neural crest-derived progenitor cells of the peripheral sympathetic nervous system (PSNS). Neuroblastoma patients display a significant level of genetic and phenotypic heterogeneity, with amplification of the *MYCN* oncogene associated with poor clinical outcomes. To better understand underlying genetic mechanisms associated with aggressive neuroblastoma, our group incorporated patient-relevant loss-of-function mutations into the established MYCN-driven zebrafish model of neuroblastoma (Tg(*dbh*:EGFP-MYCN)), which resulted in increased tumor penetrance and a highly metastatic phenotype.
Aims & Methods: We aimed to investigate metastases-associated intratumoral heterogeneity *in vivo* using our patient-relevant metastatic zebrafish models, with functional validations performed using human neuroblastoma cell lines.
Results: Single-cell RNA sequencing of metastatic zebrafish neuroblastoma tumors revealed intra-tumor cell heterogeneity, with a subset of cells highly expressing markers of more differentiated adrenergic-like cell fates (*th*, *dbh*, *phox2a*) while others enriched for markers of less differentiated mesenchymal-like progenitor cells (*prrx1a*, *vim*, *fn1a*). Differential cell labeling in zebrafish neuroblastoma suggests distinct tumor cell populations for follow-up validation and characterization throughout metastatic progression.
Conclusion: Single-cell RNA sequencing of zebrafish metastatic neuroblastoma showed evidence of intratumoral heterogeneity that warrants further investigation. We are characterizing neuroblastoma intratumoral heterogeneity in our *in vivo* metastatic zebrafish models to examine the association between neuroblastoma tumor composition and metastatic potential. Altogether, this work aims to improve our understanding of the evolution of tumor cell heterogeneity associated with neuroblastoma metastasis and uncover novel therapeutic opportunities to improve patient outcomes.

#5467 Identification of possible new treatment options for rare pediatric CNS tumors using a panel of validated and characterized PDX models.

E. Oswald[1], D. Lenhard[1], K. Lashuk[1], O. Delattre[2], D. Surdez[2], J. Gojo[3], D. Lotsch-Gojo[3], W. Berger[3], S. Pfister[4], **J. B. Schueler**[1];
[1]Charles River Laboratories, Inc., Freiburg, Germany, [2]Institut Curie, Paris, France, [3]Medical University, Vienna, Austria, [4]DKFZ, Heidelberg, Germany

Central nervous system (CNS) malignancies are the most frequent group of childhood solid tumors. While pediatric mortality due to CNS tumors has decreased over the past 40 years, however, there has been no significant change in brain and other CNS tumor mortality in children and adolescents since 2007*. Advances in research and innovative therapies are crucial to improving outcomes and reducing mortality. Collaborative efforts between researchers, healthcare professionals, and the pharmaceutical industry play a pivotal role in developing more effective treatments for these indications. One important piece in this endeavor is the availability of well characterized preclinical models for rigorous preclinical testing. In the framework of the ITCCP4 consortium (www.ITCCP4.eu) our group determined the pharmacological profile of ten orthotopically implanted pediatric brain tumor PDX models. The panel comprises amongst others four CNS-BCOR models, one ZFTA::RELA ependymoma model and two models of PFA ependymoma. We tested the models in a single mouse trial format with 16 arms covering standard of care therapy including radiation as well as targeted agents. All tumors were intracranially implanted into immune-compromised NSG mice. Tumor load was determined using a fluorescence based *in vivo* imaging technology based on the lentiviral transient transduction of PDX cells with iRFP713 prior to implantation into the brain. In addition, body weight and neurological scoring were monitored to determine the overall condition of the animals. At the end of the study brain tissue was harvested and tumor load confirmed by immunohistochemistry. Vismodegib, a first in class inhibitor of the hedgehog signaling pathway, was the most efficacious treatment with a significantly extended overall survival (Log Rank, $p< 0.001$) and a reduced tumor load compared to untreated control arms. The effect was most prominent in the subclass of CNS-BCOR models leading to growth delay or stable disease. Several targeted agents such as Ipatasertib (AKT inhibitor), Idasanutlin (MDM2-antagonist) and standard of care such as Carboplatin and Radiotherapy induced stable disease as well but had no significant effect on overall survival. The positive results for Vismodegib, Ipatasertib as well as Idasanutlin will be validated in a smaller subset of models in a conventional set-up to confirm the current dataset. In summary, the single mouse trial format using intracranially implanted PDX models proved to be a feasible tool to identify most promising drug candidates for pediatric ependymoma. *Ostrom QT, Price M, Ryan K, Edelson J, Neff C, Cioffi G, et al.. CBTRUS statistical report: pediatric brain tumor foundation childhood and adolescent primary brain and other central nervous system tumors diagnosed in the United States in 2014-2018. Neuro-Oncology (2022) 24(Supplement_3):iii1-38.

#5468 Pediatric Preclinical In Vivo Testing (PIVOT) data portal enables access to 15 years of retrospective treatment study data in support of prospective study design.

S. E. Acevedo[1], T. M. Stearns[2], P. Webster[1], V. Philip[2], M. W. Lloyd[2], A. Srivastava[3], S. Neuhauser[2], D. Begley[2], D. M. Krupke[2], E. L. Jocoy[4], C. J. Bult[2], J. H. Chuang[3], D. A. Dean II[1];

[1]Velsera, Charlestown, MA, [2]The Jackson Laboratory, Bar Harbor, ME, [3]The Jackson Laboratory, Farmington, CT, [4]The Jackson Laboratory, Sacramento, CA

The PIVOT program (https://preclinicalpivot.org) is a National Cancer Institute (NCI) funded initiative in support of the RACE Act that funds collaborations between academic centers and industry partners to test the efficacy of targeted cancer treatments developed for adult oncology for potential application in diverse pediatric cancers, including cancers of the central nervous system, leukemia, osteosarcoma, sarcoma, and neuroblastoma. In support of the PIVOT program, we have harmonized more than 15 years of data collected during two previous preclinical pediatric testing programs. To disseminate the data and results of these programs broadly we designed and implemented the PIVOT Data Portal.

The PIVOT Data Portal is an R Shiny App that makes treatment efficacy data from PIVOT accessible on the web. The data are harmonized which supports comparison of treatment results across different cancer types. The data from the portal are freely available and downloadable. The portal includes study summaries within and across cancer models, statistical reports, tables, and tools for the visualization of treatment results. Data summary tables include entries for objective response measures (ORM), mean outcome, number of tumor studies, and p-value as appropriate. Visualizations include relative tumor volume plots for solid tumors; CD45 plots for leukemia; and survival curves to compare survival time across treatment groups. Treatment study visualizations and data summaries with their related metadata can be generated and downloaded within the Shiny App, allowing researchers to perform further downstream analysis.

The portal collectively contains data for 52 agents, 45 drug targets, 34 drug classes (including ADCs, small molecular inhibitors, protein degraders, BiTEs, etc.), and 167 models, with a total of 245,926 data points. Currently, 44% of agents have been tested on 2 or more cancer types. Among the solid tumor models tested, 10 had at least one treatment that resulted in an ORM of maintained complete response (MCR), while 29 leukemia models had an ORM of MCR. Similarly, 48% of agents tested had an ORM of MCR for at least one cancer type.

The PIVOT Data Portal makes pediatric cancer model treatment data available without restriction to support retrospective analyses and design of prospective studies. We are working to link cancer model data within the portal to molecular data. Merging outcome data with genomics data will facilitate computational approaches for molecular target identification, personalized treatment, and treatment optimization.

#5469 ITCC-P4, a preclinical proof-of-concept drug testing platform as a tool for pharmacological screening in pediatric tumor models.

E. Indersie[1], S. Branchereau[2], B. Fresneau[3], C. Chardot[4], D. Surdez[5], A. Saint-Charles[5], M. Marques da Costa[6], A. M. Carcaboso[7], K. Scotlandi[8], M. Moro[9], H. Kovar[10], J.-H. Klusmann[11], K.-M. Debatin[12], S. Bomken[13], L. Chesler[14], C. Jones[15], B. Schafer[16], M. Wachtel[16], J. Gojo[17], W. Berger[18], C. Guttke[19], M. Hattersley[20], F. Colland[21], A. Strougo[22], D. Gurgen[23], J. Hoffmann[23], J. Schueler[24], P. M. Aviles[25], M. Guillen[25], A. Federico[26], A. Gopisetty[26], J. Wierzbinska[27], A. Schlicker[27], S. Colombetti[28], O. Heidenreich[29], F. Iradier[30], N. Huebener[31], N. Jager[26], J. Koster[32], M. Kool[26], G. Schleiermacher[5], J. J. Molenaar[29], B. Geoerger[3], D. J. Shields[33], H. N. Caron[34], L. F. Stancato[30], S. M. Pfister[26], G. Vassal[3], E.-M. Rief[35], **O. Deas**[1];

[1]Janvier Group, Evry-Courcouronnes, France, [2]Bicetre Hospital, Le Kremlin Bicetre, France, [3]Gustave Roussy Cancer Center, Villejuif, France, [4]Necker Enfants Malades Hospital, Paris, France, [5]U830 Inserm, RTOP Translational Research in Pediatric Oncology, Paris, France, [6]Gustave Roussy Cancer Campus, INSERM U1015, Universite Paris-Saclay, Villejuif, France, [7]Institut de Recerca Sant Joan de Deu, Barcelona, Spain, [8]IRCCS-Istituto Ortopedico Rizzoli, Experimental Oncology Laboratory, Bologna, Italy, [9]Department of Experimental Oncology, Epigenomics & Biomarkers of Solid Tumors Unit, Milano, Italy, [10]St. Anna Children?s Cancer Research Institute, Vienna, Austria, [11]Martin-Luther-University Halle-Wittenberg, Halle, Germany, [12]Ulm University Medical Center, Ulm, Germany, [13]Wolfson Childhood Cancer Research Centre, Translational and Clinical Research Institute, Newcastle upon Tyne, United Kingdom, [14]Centre for Paediatric Oncology Experimental Medicine, The Institute of Cancer Research, London, United Kingdom, [15]Institute of Cancer Research, London, United Kingdom, [16]University Children's Hospital, Children's Research Center, Zurich, Switzerland, [17]Department of Pediatrics and Adolescent Medicine, Comprehensive Center for Pediatrics, Medical University of Vienna, Vienna, Austria, [18]Center for Cancer Research and Comprehensive Cancer Center, Medical University Vienna, Vienna, Austria, [19]Johnson & Johnson Innovative Medicine R&D, Spring House, PA, [20]AstraZeneca R&D, Waltham, MA, [21]Institut de Recherches Servier, Croissy-sur-Seine, France, [22]Sanofi, R&D, Amsterdam, Netherlands, [23]Experimental Pharmacology and Oncology Berlin-Buch GmbH, Berlin, Germany, [24]Charles River Germany, Freiburg, Germany, [25]PharmaMar S.A., Madrid, Spain, [26]Hopp Children's Cancer Center (KiTZ), Heidelberg, Germany, [27]Bayer AG, Pharmaceuticals, Research & Early Development Oncology, Berlin, Germany, [28]Roche Innovation Center Zurich, Roche Pharma Research and Early Development (pRED), Schlieren, Switzerland, [29]Princess Maxima Center for Pediatric Oncology, Utrecht, Netherlands, [30]Eli Lilly and Company, Indianapolis, IN, [31]Charite - Universitatsmedizin Berlin, Berlin, Germany, [32]Center for Experimental and Molecular Medicine, Amsterdam University Medical Centers, Amsterdam, Netherlands, [33]Pfizer Centers for Therapeutic Innovation, Pfizer Inc, New-York, NY, [34]Hoffman-La Roche, Basel, Switzerland, [35]ITCC-P4 gGmbH, Heidelberg, Germany

Cancer remains the main cause of disease-related death in childhood. Pediatric tumors are characterized by a low mutational burden and high intertumoral heterogeneity, with multiple subtypes compared to their adult counterparts. The lack of access to many innovative therapies remains one of the main challenges in the pediatric oncology, especially for the 25% of patients who experience relapses. In this context, the need for the development of a well characterized collection of pediatric models, to provide large scale preclinical testing, is capital for the subsequent identification and prioritization of promising novel therapeutic options. The EU funded “Innovative Therapies for Children with Cancer-Pediatric Preclinical Proof-of-Concept Platform” (ITCC-P4) consortium is a unique public-private collaborative project consisting of academic and industrial partners that aimed at establishing a collection of >400 patient-derived xenograft (PDX) models representing the most common high-risk pediatric cancers. The project involved various aspects of model development including the thorough molecular and pharmacological characterization. XenTech’s participation was focused on the development and preclinical in vivo drug testing of Ewing sarcoma (n=17), hepatoblastoma (n=10), rhabdoid tumors (n=6), synovial sarcoma (n=2), rhabdomyosarcoma (n=2) and other tumors (n=6), as part of overall cohort. PDXs were obtained by transplantation of post-surgery tumor specimens, either by grafting tumor fragments into the interscapular region or subcutaneously in the right flank of nude, NOD-Scid or NOD-Scid gamma mice. Tumor xenografts were amplified by serial transplantation, and tissue samples were retained at early passages for molecular characterization. Fragments from established PDX models where frozen to generate a revivable ITCC-P4 PDX collection. Then, proof-of-concept drug testing was conducted, in a single mouse trial format: each tumor type (n=X PDX models) was treated with a dedicated panel of Standard-of-Care (SoC;n=3) and novel targeted therapies (n=6), or combinations of 2 or 3 novel targeted therapies; for each PDX model n=1 mouse being included per treatment. All molecular and drug-testing data obtained by the different partners are being centralized in the R2 repository (https://r2.amc.nl), providing a powerful tool for data integration, visualization and interpretation of the results. A unique collection of well characterized pediatric PDX models derived from the most relevant pediatric tumor types was enabled by a strong public-private collaborative project. This large cohort is now available for preclinical testing of novel therapeutic agents within a non-for-profit spinoff company, ITCC-P4 gGmbH (www.itccp4.com), offering new perspectives to the identification of promising treatment options for children with cancer.

#5470 ONC206 inhibits tumour growth and is a potential novel therapeutic strategy for refractory medulloblastoma.

T. Tzaridis[1], J. Liu[2], V. Prabhu[3], R. Wechsler-Reya[4], T. MacDonald[2];
[1]Sanford Burnham Prebys Med. Discovery Inst., La Jolla / San Diego, CA, [2]Department of Pediatric Oncology, Emory University School of Medicine, Children's Healthcare of Atlanta, Atlanta, GA, [3]Chimerix, Durham, NC, [4]Department of Neurology and Herbert Irving Comprehensive Cancer Center, Columbia University Medical Center, New York, NY

Medulloblastoma is the most common malignant pediatric brain tumor with a for certain molecular subgroups very low overall survival and therefore an urgent need for novel treatment approaches. Dordaviprone (ONC201) and its chemical derivative with nanomolar potency ONC206 are inhibitors of the dopamine receptor 2 (DRD2) and more importantly induce apoptosis of cancer cells by activation of the mitochondrial caseinolytic protease P (ClpP). ONC201 has shown objective responses in patients with diffuse midline gliomas and is currently being evaluated in the Phase 3 ACTION study. ONC206 is currently in Phase I clinical trials for pediatric and adult patients with primary brain tumors. In this study, we evaluated the preclinical therapeutic effects of ONC206 in medulloblastoma *in vitro* and *in vivo* and investigated the molecular mode of action for this imipridone. We found evidence for high expression of ClpP at both the RNA and protein level in medulloblastoma tumours, compared to very low expression in normal brain and normal cerebellum. In addition, we saw a pronounced reduction in cell viability of human Group 3 and Group 4 and murine medulloblastoma cells treated with ONC206 with extremely low IC-50s (range: 14nM - 2µM).After treatment with ONC206, we observed a significant downregulation of mitochondrial electron transport chain complexes I and III and mitochondrial hyperpolarization, as well as an induction of the ATF4 pathway, thereby implying that ONC206 induces an integrated stress response and mitochondrial damage. In order to test the efficacy of ONC206 *in vivo,* we used murine models of SHH-driven and Group 3 medulloblastoma as well as Group 3 patient-derived xenografts (PDXs). ONC206 led to a significant prolongation of survival in both murine models, with the SHH mice demonstrating a remarkable survival benefit. Mice from both Group 3 PDXs also responded to ONC206, with 25% of ONC206 treated animals exhibiting long-term tumor-free survival. Our results highlight ONC206 as a novel attractive therapeutic option for patients with relapsed medulloblastoma and importantly pave the way for a clinical trial testing the efficacy of ONC206 in the treatment of these patients.

#5471 Ribosome heterogeneity and RNA poll inhibition in osteosarcoma heterogeneity.

Marc Baud'huin[1], Elvina Colleville[2], Rose Anne Thepault[2], Emilien Orgebin[2], Francois Lamoureux[2], Benjamin Ory[2]

[1]CRCI2NA / INSERM UMR 1307 / CNRS UMR 6075 / Nantes Universite /CHU de Nantes, Nantes, France,[2]CRCI2NA / INSERM UMR 1307 / CNRS UMR 6075 / Nantes Universite, Nantes, France

Osteosarcoma is the most common primary bone tumour in adolescents and young adults, with an incidence rate of 3.8 per million. These tumors affect the long bones of the body such as femur. Current standard therapy includes tumour resection associated with multi-drug chemotherapy. The 5-year survival rate can reach 65% but is significantly reduced to 30% when pulmonary metastases are detected at the time of diagnosis. As this rate has not improved in the last 50 years, it is necessary to identify new therapeutic strategies. Inhibition of ribosomal biogenesis is one of the strategies developed in many cancer studies. This can be obtained by inhibition of RNA pol I, and in particular by BMH-21. The objective of this study was to analyze the complexity and heterogeneity of osteosarcomas through the ribosomal spectrum. The effect of BMH-1 on survival was also studied in osteosarcoma cell lines. The data obtained showed that there was no difference in ribosome protein composition in the “core” ribosome in different osteosarcoma cell lines. In addition, BMH-21 decreased cell viability in all osteosarcoma and chemoresistant cell lines. However, any activation of the apoptotic pathway by caspases was detected, nor any impact on the formation of new colonies after treatment with BMH-21. These results suggest a rather cytostatic mechanism. Moreover, a G0/G1 arrest in cell cycle was shown for U2OS cells. Finally, BMH-21 does not appear to have any impact on migration in HOS and U2OS cells. The different molecular mechanisms involved in the regulation of proliferation need to be further investigated.

#5472 Direct cytotoxicity of hu14.18K.322A in high-risk neuroblastoma.

M. Gnanamony, M. Thomas, T. Nguyen, A. M. D'Souza, P. de Alarcon;
University of Illinois College of Medicine (Peoria), Peoria, IL

Background: Neuroblastoma is a childhood cancer of the sympathetic nervous system and is associated with disialoganglioside GD2 overexpression. The main goal of this study is to investigate the involvement of GD2 targeting humanized antidisialoganglioside monoclonal antibody hu14.18K.322A (hu14) in high-risk neuroblastoma direct cell cytotoxicity, assess for synergy with induction chemotherapy agents, and delineate the mechanisms involved in cell death.
Methods: For this study, we used a panel of GD2 expressing cell lines [SK-N-BE (2), SK-N-BE (1), LAN5, CHLA15] and a GD2 non-expressing cell line LAN6. We measured surface expression of GD2 and performed cell cycle analysis using flow cytometry. The role of hu14 in neuroblastoma cell death was assessed using cell viability assays, proliferation assays, real time PCR and western blot analysis. We measured synergy between hu14 and induction phase chemotherapy drugs. Further, we employed next generation sequencing (NGS) to analyze the transcriptomic changes in human neuroblastoma cell lines in response to hu14 treatment to understand the pathways involved and the molecular mechanisms of hu14-mediated cellular response.
Results: Using a cell viability assay, we found that CHLA15 and SK-N-BE (1) cell lines were sensitive to hu14 treatment whereas SK-N-BE (2), LAN5, LAN6 were resistant. Hu14 treatment resulted in a dose dependent reduction in cell proliferation in these cell lines. We also found that hu14 treatment resulted in increased expression of apoptotic and autophagy pathway proteins, but not ferroptosis or necroptosis pathways proteins. Hu14 induced cell death was partially inhibited by a pan-caspase inhibitor, confirming that caspase-dependent pathways are involved. Western blot analysis also showed decreased levels of p53 phosphorylation in both sensitive cell lines upon hu14 treatment suggesting an important control mechanism centered on the p53 pathway. Hu14 treatment reduced the surface expression of GD2 in the sensitive cells suggesting direct inhibition of the GD2 synthesis pathway. However, PCR analysis of GD2 synthesis genes did not show any significant difference upon treatment suggesting posttranscriptional control of these genes. Furthermore, NGS analysis revealed alterations in several pathways, but these changes were distinct between the cell lines reconfirming the complexity of therapy response in high-risk Neuroblastoma.
Conclusion: Taken together, our findings suggest that hu14.18K322A induces direct cell cytotoxicity in a subset of high-risk Neuroblastoma and synergizes well with standard chemotherapy drugs. Furthermore, our research highlights the complex nature of signaling pathways involved in hu14-mediated cytotoxicity that can be harnessed towards targeted therapy.

#5473 Combined inhibition of MDM2 and PARP lead to a synergistic anti-tumoral response in p53 wild-type rhabdomyosarcoma.

G. Pons[1], G. Gallo-Oller[1], L. Garcia-Gilabert[1], P. Zarzosa[1], J. Sansa-Girona[1], N. Navarro[1], P. Cabre-Fernandez[1], M. Segura[1], J. Sanchez de Toledo[2], S. Gallego[2], L. Moreno[2], J. Roma[1];

[1]Vall d'Hebron Research Institute (VHIR), Barcelona, Spain, [2]Hospital Universitari Vall d'Hebron, Barcelona, Spain

Targeting MDM2-p53 interaction to enhance p53 activity represents an attractive antitumoral strategy for p53 wild-type tumors. However, early-phase clinical trials in hematological and solid cancers have shown limited efficacy of MDM2 inhibitors highlighting the necessity for exploring more effective combinations with additional agents. In this study, we provide results from a 22-drug combination screening demonstrating the therapeutic potential of combining Siremadlin (MDM2 inhibitor) and Olaparib (PARP inhibitor) for treating p53 wild-type rhabdomyosarcoma (RMS). Cell survival, cell death and apoptosis analysis revealed synergistic effects when combining Siremadlin and Olaparib *in vitro*. Combination of both drugs resulted in a significant increase of p53 activity as evidenced by p53 accumulation and K382 acetylation along with an increased expression of p53 targets. Finally, combination of both drugs resulted in significant reduction of tumor growth and increased overall survival outperforming individual treatments and control groups. In summary, our study demonstrates, for the first time, the synergistic effect of the combination between Siremadlin and Olaparib in the inhibition of p53 wild-type RMS tumor growth *in vitro* and *in vivo*. These findings advocate for the exploration of this drug combination in clinical trials and underscore the need for further investigation in tumors sharing similar molecular features.

#5474 Biorepository yields potential for personalized medicine approach in pediatric brain cancer patients.

A. Pronina, E. Nasajpour, C. Tran, T. Schouten, E. Gibson, J. Nirschl, L. M. Prolo, K. Mahaney, H. Vogel, C. K. Petritsch;
Stanford University, Palo Alto, CA

Childhood brain cancer, with a 12% mortality rate, stands as the most lethal cancer among children. Out of the annual 4,000 diagnoses, 30% involve low-grade gliomas, with a troubling 10% progressing to lethal high-grade gliomas within 2 years. While surgery can often cure the remaining 90%, 50% necessitate adjuvant therapies like chemotherapy and molecular targeting, with radiation sparingly used. Alarmingly, 66% of survivors grapple with long-term health, mental, and cognitive issues due to treatment toxicity, emphasizing the urgent need for innovative biological therapies in pediatric glioma treatment.Our proposed strategy involves the acute analysis of freshly discarded tissue from brain cancer craniotomies, departing from the use of FFPE-preserved tissue, which may exhibit suboptimal quality. All patients provided informed consent, and by prospectively preserving viable tissue, we enable its utilization in ten or more subsequent analyses. These encompass cell-culture-based assays, viability assays, bulk, single cell, and single nucleus RNA sequencing, DNA sequencing, single-cell proteome analyses, flow cytometry, and immunofluorescence.Our findings highlight a direct correlation between surgical sample size and analysis feasibility. Bulk RNA sequencing proves valuable in acutely isolated surgical tissue and cryostored or flash-frozen tissue for identifying novel therapeutic targets in individual patients. Viable cells retrieved from cryopreserved tissue of the same patient allow ex vivo functional validation of therapeutic targets, eliminating the need for establishing patient-derived cell lines and xenografts, particularly challenging for low-grade gliomas. These findings establish the feasibility of a personalized bedside-to-bench approach, contingent on an adequate supply of surgical material.Expanding this approach to encompass all childhood brain cancer types, we plan to investigate using our comprehensive biorepository, housing viable tissue and single-cell suspensions from 122 childhood brain cancer patients. Among these, 51 cases yielded tissue for single-cell RNA-seq and viable cryoprotection. The most common tumor histology identified was low-grade glioma (32), primarily pilocytic astrocytoma (19), followed by embryonal (12) and ependymal tumors (4).In summary, we developed a standard operating procedure for analyzing fresh and cryopreserved surgical discards, identifying novel targets in childhood brain cancer tissue, and functionally validating them in patient-matched samples. This personalized medicine approach holds promise in circumventing the tedious development of patient-derived models.

#5475 Development of high-throughput 3D bioprinted pediatric models for precision medicine.

V. Poltavets[1], M. Jung[1], J. Skhinas[1], K. Kimpton[1], A. Kamili[1], G. Tax[1], J. Mao[1], L. Cui[1], M. Wong[1], M. J. Cowley[1], L. Lau[1], E. M. M. Dolman[1], J. J. Gooding[2], M. Kavallaris[1];

[1]Children's Cancer Institute, Randwick, Australia, [2]University of New South Wales, Sydney, Australia

Childhood cancer patients with high-risk disease have poor prognosis. Therapies given to treat these patients are often highly toxic and determined empirically, exposing children to damaging and ineffective therapies. Precision medicine is a promising strategy for these patients. However, tumor biopsies often lack sufficient sample for phenotypic drug screening, requiring cell expansion via primary cell culture or development of patient-derived xenograft models - a slow process with variable success rates. There is an unmet need for sensitive, predictive, and timely drug testing models. Dynamic interactions between cells and the extracellular matrix (ECM) impact cellular signaling and response to cancer therapy. The development of patient-derived tumor models that are reflective of the patient sample and achieved in a clinically relevant timeframe will be game changing. In-silico analysis of 265 ECM gene expression from a high-risk neuroblastoma and sarcoma patient cohort (n=145) identified collagens and fibronectin to be the most abundantly expressed ECM genes in the tumor samples. To reflect this environment, we developed tuneable tissue ECM-like bioinks where cells are embedded within the bioink that mimics growth constraints within a tumor [1]. Specifically, we functionalized the bioinks with peptides of collagen I, fibronectin, and laminin to mimic the ECM environment and combined this with HTP 3D bioprinting technology to create patient-derived tumoroids. In this proof-of-concept study, we identified conditions that enable the growth and expansion of the neuroblastoma and sarcoma cells in a 3D ECM-like environment. The tumor samples proliferate in the bioinks and HTP drug screening was used to determine drug sensitivity. Importantly, the bioprinted cells reflect the genetic and phenotypic characteristics of the original patient tumors and retained their tumorigenic capacity in vivo. Collectively, we have successfully generated preclinical models that reflect patient tumors and are directly compatible with preclinical drug testing. Importantly, our 3D bioprinting platform has the potential to advance cancer precision medicine in a clinically relevant timeframe. These findings have broader applications for a range of cancer types for preclinical testing, drug discovery and cancer biology.1. Utama, RH, et al. *Macromolecular Bioscience*, 2021. 21(9):e2100125

TUMOR BIOLOGY: Spatial Resolution of the Tumor Microenvironment
Poster Session

#5479 Spatially resolved molecular features in the tumor-immune microenvironment of germline BRCA1/2 mutated versus BRCA wild type high grade serous ovarian cancers.

J. Qian[1], L. D. Roman[1], R. Bassiouni[2], S. Rajpara[1], M. Neuman[1], V. Khetan[1], D. W. Craig[2], J. W. Carlson[1], J. D. Carpten[2];
[1]Keck School of Medicine, University of Southern California, Los Angeles, CA, [2]City of Hope, Duarte, CA

High-grade serous ovarian cancer (HGSC) is the most common and aggressive subtype of epithelial ovarian cancer. Importantly, germline mutations in BRCA1/2 give rise to HGSC. Because most HGSC are diagnosed at stage III/IV, outcomes are poor and more effective therapies are needed. Although immune checkpoint inhibitors show promise for a number of cancer types, efficacy has been variable in HGSC. To help provide new clues to the molecular features of HGSC, we set out to elucidate the tumor microenvironment of HGSC using spatial transcriptomics approaches. Specifically, we applied 10x Genomics Visium Spatial Transcriptomics (ST) technology to 48 samples representing primary HGSC tumors from 24 patients, including 15 BRCA1/2 mutated cases and 9 BRCA non-mutated cases. In addition to individual sample analysis, we normalized data from 64,784 total features across all sections and performed an integrated cluster analysis to get an overall picture of the cellular architecture of HGSC, but to also directly investigate differences in the tumor microenvironment based on BRCA mutation status. The resulting 17 integrated clusters were subjected to molecular annotation using GSEA, ESTIMATE, and CIBERSORTx, which revealed feature clusters representing important cell types defined by marker genes. Analysis of the entire dataset identified a primary tumor cluster defined by the expression of known ovarian cancer genes including *WFDC2* and “don’t eat me” marker genes *CD24* and *CD47*. However, the predominant tumor cell population in BRCA mutated cases was marked by the expression of *MUC1, EPCAM, CLDN3*, and *CD24*, while BRCA non-mutated tumor cell cluster was marked by *EFNA1, ID1, LSR*, and *CD9*. Importantly, both groups revealed the presence of a specialized monocyte derived macrophage cluster defined by the expression of *LYZ* and genes involved in cholesterol metabolism including *APOE* and *APOC1*. These lipid-associated macrophages are M2 polarized and shown to be associated with poor outcome. Additional analyses are underway to determine spatial dependencies of various tumor and immunological cell compartments. These data provide novel insights into the HGSC tumor microenvironment that may influence HGSC’s vulnerability to immunological therapies.

#5480 Single cell and spatial transcriptomic profile of appendiceal tumour peritoneal disease.

M. C. Strach[1], N. Yeung[2], E. Apostolov[2], T. Wang[2], H.-M. Lin[2], N. Ansari[3], C. Koh[1], J.-S. Shin[3], J. Kench[3], A. Swarbrick[4], L. Horvath[5], **K. L. Mahon**[5]; [1]University of Sydney, Camperdown, Australia, [2]Garvan Institute of Medical Research, Darlinghurst, Australia, [3]Royal Prince Alfred Hospital, Camperdown, Australia, [4]Garvan Institute of Medical Research, Camperdown, Australia, [5]Chris O'Brien Lifehouse, Camperdown, Australia

Introduction: Appendiceal tumors (AT) are rare and often develop peritoneal disease (PD), with 5 year survival of 15-63% for high grade adenocarcinomas (HG) and 46-96% for low grade mucinous neoplasms (LG). While the mainstay of treatment is cytoreductive surgery and heated intraperitoneal chemotherapy (CRS/HIPEC), the role of systemic chemotherapy is less clear with limited biological characterization of AT and its tumor microenvironment (TME). The purpose of this study was to evaluate the TME of AT PD. Here we present an atlas of AT PD cells alongside a spatially resolved transcriptomic profile comparing HG and LG.

Methods: We collected tissue from 29 patients with AT PD during CRS prior to HIPEC (18 LG, nine HG and two no tumor control). We performed comprehensive single-cell RNA sequencing (38224 cells) on fresh tissue specimens from nine patients (four HG, five LG), and whole transcriptome spatial analysis (>18000 genes) using the GeoMx Digital Spatial Profiler on formalin-fixed paraffin-embedded tissue from 22 patients (five HG, 13 LG). In the spatial profiling, we used anti-CK20, anti-CD45 and SYTO 83 as morphology markers to select areas of interest (AOIs): tumor (CK20), immune (CD45) and stroma (non-CK20/CD45). Analyses were performed with R and a false discovery rate threshold of 0.05.

Results: Single-cell RNA sequencing showed that both LG and HG have a preponderance of T-lineage cells including CD8, CD4 and NK T-cells. Both LG and HG tumors display association of mesothelial cells with cancer-associated fibroblasts (CAF), and CAF subsets expressing genes of epithelial-mesenchymal transition (EMT). LG and HG tumors display different patterns of mucin gene expression - epithelial cells of HG express the secreted mucin *MUC20* in addition to *MUC2* and *MUC5B* also expressed in LG; a subset of mesothelial cells in LG but not HG express the transmembrane mucin genes *MUC1, MUC3A, MUC12* and *MUC16*. Spatial analysis of tumor AOIs revealed HG compared to LG had increased expression of genes associated with MYC targets, oxidative phosphorylation, anti-tumor immune pathways (IFNα/γ response, intestinal immune network for IGA production), cell cycle pathways (E2F targets, G2M checkpoint) and EMT. LG compared to HG had increased expression of genes associated with inflammation-mediated disease (TNFα signaling via NFKB, inflammatory response), regulation of tumor growth (P53), hypoxia and early cell cycle (estrogen response) and glycosylation pathways. Immune and stromal AOIs did not have significant transcriptomic differences between LG and HG.

Conclusion: This study provides novel insights into the biological profile of AT PD by describing TME cell types, immune function, tumor growth and cell cycle pathways. These findings may be used to identify clinically relevant biomarkers and new therapeutic targets.

#5481 Spatial multiplex proteins profiling of tumor microenvironment to decipher d*e novo* metastasis in nasopharyngeal carcinoma.

Larry Ka-Yue Chow, Ying Wang, Lanqi Gong, Siqi Xu, Zhaozheng Hou, Xinyuan Guan, Dora Lai-Wan Kwong, Victor Ho-Fun Lee, Wai Tong Ng, Anne Wing-Mui Lee, Zhonghua Liu, Yunfei Xia, **Wei Dai**

The University of Hong Kong, Hong Kong, Hong Kong

Background: Nasopharyngeal carcinoma (NPC) has a high incidence rate in Southeast Asia, where more than 90% of NPC cases are associated with Epstein-Barr virus (EBV). Although NPC patients are generally sensitive to radiotherapy and chemotherapy, about 20-30% of patients have treatment failure due to the development of distant metastasis, i.e. *de novo* metastasis. In this study, we utilized GeoMx Digital Spatial Profiler (DSP), a multiplex and high-throughput sequencing platform designed for spatially- and morphologically resolved protein expression profiling to investigate the intra-tumoral and inter-tumoral heterogeneity of tumor microenvironment (TME) and identify the mechanisms underlying distant failure in NPC.
Methods: We utilized GeoMx Protein Assays consisting of 147 proteins from 15 functional modules to compare the difference between NPC cases developing distant failure (DF) (n=21) and stage-, age-, gender- and treatment-matched NPC cases without developing distant failure (noDF) (n=15) within five years of treatment. Two fluorescent morphological markers including PanCK and CD45, were used for delineating the structural architecture of the tissues, identifying cell types, and selecting regions of interest (ROIs), followed by sequencing for protein expression quantification. NanoString GeoMx DSP Analysis Suite was used for quality control and data normalization. The NPC TME heterogeneity was further investigated by the 10X Visum platform for spatial transcriptome. The public single-cell RNA sequencing (scRNA-Seq) and bulk RNA sequencing datasets were obtained for the downstream analyses.
Results: By analyzing protein expression profiles, the study revealed the intratumoral and intertumoral heterogeneity associated with EBV latent infection in the TME of NPC. Regions with high EBV latent gene expression exhibited a noticeable reduction in T cell infiltration, indicating an "immune cold" phenotype, whereas regions with low EBV latent gene expression displayed heavy T cell infiltration, indicating an "immune hot" phenotype. Moreover, the study identified a panel of autophagic and anti-apoptotic proteins that were significantly upregulated in the cancer cells of NPC cases developing distant failure after treatment. This observation, supported by the single-cell RNA sequencing datasets, further implicated EBV latent infection for the upregulation of autophagic and anti-apoptotic genes. Notably, the study also demonstrated that the genes upregulated in the immune cells in NPC cases with distant failure were associated with poor progression-free survival in an independent NPC cohort.
Conclusions: These findings shed light on the crucial role of EBV latent infection in TME heterogeneity and highlight the potential involvement of autophagy and anti-apoptosis in *de novo* metastasis in NPC.

#5482 Spatial and multi-omic interrogation of the primary and recurrent glioblastoma microenvironment.

J. R. Clemenceau, P. Suarez-Meade, A. Quinones-Hinojosa, T. Hwang;
Mayo Clinic Florida, Jacksonville, FL

Glioblastoma remains as one of the deadliest malignancies with most cases likely to recur. Recent work has focused on characterizing not only glioma cells, but the tumor microenvironment via single-cell and spatial transcriptomic technologies. This has improved our understanding of the high heterogeneity of this disease and described potential tumor domains. However, there is still a need to further understand the changes that occur between the primary and the recurrent lesion. We propose that a spatial, multi-omic characterization of matched primary and recurrent glioblastoma can yield insights into recurrence mechanisms occurring throughout the tumor microenvironment. We collected 22 IDH-WT glioblastoma samples from 12 patients (11 primary, 11 recurrent, 10 matched pairs) from the Mayo Clinic Neuroscience Biobank. We performed single-nucleus RNA sequencing (15 samples, 10 patients, 5 matched pairs) and proteomics (16 samples, 6 matched pairs) from fresh-frozen tissue, as well as spatial transcriptomics with 10x Visium (14 samples, 8 patients, 6 matched pairs) and 10x Xenium in-situ molecular imaging (6 samples, 2 matched pairs). Using spatial transcriptomics data, we identified regional subsets present in different proportions and distributions between primary and recurrent glioblastoma. These clusters were characterized with gene set and gene ontology analysis, identifying regions enriched with known glioma subtypes and cellular activity. Spatial-based cluster genes were consistent with significantly differentially expressed proteins. We used single-nucleus RNAseq and in-situ molecular imaging data from matched tissue samples to further interrogate relevant cell populations and location in the tumor micro-environment. We identified regions with enriched extra cellular matrix interaction and remodeling signatures to be highly expressed in recurrent glioblastoma. Primary glioblastoma was enriched with oligodendrocyte-like regions with high cell communication and extracellular vesicle signatures. This study will further our understanding of the changes in the mechanisms at play in the complex ecosystem of glioblastoma as it recurs.

#5483 Macrospatial ecotype heterogeneity in early-stage breast cancer identified by spatial nucleus barcoding.

K. Wang*[1], **Z. Xiao***[1], Y. Lin[1], R. Wei[1], S. Bai[1], J. Ye[1], R. Ye[1], M. Hu[1], A. Thennavan[1], E. Sei[1], A. Thompson[2], S. Krishnamurthy[1], N. Navin[1];
[1]UT MD Anderson Cancer Center, Houston, TX, [2]Baylor College of Medicine, Houston, TX

Ductal carcinoma *in situ* (DCIS), the predominant form of early-stage breast cancer and a precursor to invasive breast cancer, remains inadequately understood in terms of spatial microenvironment reprogramming. In this study, we developed a Spatial Nucleus Barcoding (SNuBar) approach for single-nucleus RNA sequencing (SNuBar-RNA) that utilizes a single oligonucleotide adaptor to preserve spatial information. The accuracy and scalability of SNuBar was validated using cell line mixture experiments. We then applied SNuBar-RNA to investigate the macrospatial ecotype heterogeneity in early-stage breast cancer. By analyzing single cells from different macrodissected spatial regions in normal breast tissues, matched normal and DCIS tissues, we identified 13 major cell types and 43 distinct cell states, co-localizing in diverse combinations across four primary topographic areas (adipose-enriched, normal epithelial, activated stroma and tumor). Spatial analysis revealed the reprogramming of vascular and myoepithelial cells in localized zones near premalignant cells, while fibroblasts, T-cells, and myeloid cells exhibited reprogramming across broader fields. Validation using the MERSCOPE assay confirmed stromal heterogeneity between tumor and normal areas. Collectively, our data shows that many diverse cell types are reprogrammed in spatially-defined areas in the early-stage breast cancer microenvironment, relative to the normal breast tissue regions.

#5484 Spatial transcriptomic profiling reveals characteristic gene expression patterns of cancer-associated fibroblasts in lung adenocarcinoma with interstitial pneumonia.

C. Inoue[1], Y. Miki[1], Y. Aoyama[1], S. Shibata[2], Y. Okada[2], T. Suzuki[1];
[1]Tohoku University Graduate School of Medicine, Sendai, Japan, [2]Institute of Development, Aging and Cancer, Tohoku University, Sendai, Japan

Background: Interstitial pneumonia (IP) is a risk factor for lung cancer (LC). LC, a significant contributor to mortality, shows improved prognosis with molecular targeted drugs. However, LC combined with IP (LC with IP) has a poor prognosis because of acute exacerbations. Therefore, developing effective drugs for LC with IP is necessary. Cancer-associated fibroblasts (CAFs), influencing cancer progression through interactions with the microenvironment are anticipated as a new therapeutic target. Therefore, we hypothesized that CAFs in LC with IP, having undergone repeated destruction and regeneration, exhibit distinct characteristics from those in LC without IP and exert varied influences on carcinogenesis and cancer progression.
Methods: Six cases of lung adenocarcinoma, the predominant type of LC, were enrolled in this study. Spatial profiling was performed on FFPE specimens from three LC with IP and three LC without IP cases, using GeoMx whole-transcriptome atlas assay. Immunostaining for α-SMA, a major CAFs-marker, and pan-cytokeratin (CK), an epithelial marker, were employed to identify regions of interest (ROIs). In LC with IP, two ROIs were designated for cancerous and non-cancerous areas, respectively, whereas in LC without IP, two ROIs were selected for cancerous areas. Each ROI was segmented for epithelium and cancer (CK+/α-SMA -) and α-SMA-positive stroma (CK-/α-SMA +) areas of illumination. NGS data were analyzed using the edgeR to compare mRNA expressions in cancerous (LC-IP) and non-cancerous (NC) areas of LC with IP. Additionally, comparisons were made between LC-IP and cancerous areas of LC without IP (LC-nonIP) for mRNA expression.
Results: Analysis of α-SMA-positive stroma revealed 86 differentially expressed genes (DEGs) in LC-IP vs. NC. Notably, COTL1 and NFKB2 increased, whereas TNC and MMP7 were decreased in LC-IP α-SMA-positive stroma. Pathway Enrichment analysis indicated activation of the response to cytokines. Between LC-IP and LC-nonIP, 151 DEGs were detected. CXCL8 and NFKB2 were elevated, whereas ACAN and ELN decreased in LC-IP α-SMA-positive stroma. KEGG pathway analysis demonstrated inactivated ECM-receptor interactions. Analysis of CK-positive regions showed 710 DEGs in LC-IP vs. NC, and KEGG pathway analysis indicated inactivated ECM-receptor interaction. In LC-IP vs. LC-nonIP, 321 DEGs were detected, with KEGG pathway analysis suggesting inactivation of ECM-receptor interaction and activation of a chemokine signaling pathway and cytokine-cytokine receptor interaction.
Conclusion: These findings suggest that inflammatory factors may play a more critical role than extracellular matrix in the interaction between α-SMA-positive stroma and CK-positive cancer cells in LC with IP. Future plans include conducting *in vitro* experiments, as well as immunohistological studies.

#5485 Spatial characterization of the immunosuppressive tumor microenvironment in estrogen receptor positive breast cancer at single cell level.

J. Tessier[1], S. Curras-Alonso[2], J. Lee[1], F. Delahaye[2], H. Ma[1], K. Malley[1], D. Bangari[1], D. Jackson[1], A. Hadjipanayis[1];
[1]Sanofi, Cambridge, MA, [2]Sanofi, Vitry-sur-Seine, France

We characterized immune cell exclusion in estrogen receptor positive (ER+) breast cancer through the study of spatial relationships among various subsets of cancer-associated fibroblasts (CAFs), tumor-associated macrophages (TAMs), and other immune cells using a novel in-situ spatial transcriptomic technology. ER+ breast cancer is the most common breast cancer subtype. While endocrine therapy and immune checkpoint inhibitors have considerably reduced relapse and mortality for breast cancer patients, tumor resistance to treatment remains a major challenge. The tumor microenvironment (TME) plays an important role in this mechanism of resistance. Our previous spatial proteomic analysis of ER+ breast FFPE samples demonstrated the intricate relationship between tumor and immunosuppressive cells such as CAFs and TAMs via the CXCR4-CXCL12 axis associated with the exclusion of CD8 T cells from the TME. However, the limited number of antibodies in the panel made it challenging to investigate the diversity of those CAF and TAM populations and better understand their contribution to T cell exclusion. For this purpose, we further characterized the TME of 4 human ER+ breast cancer FFPE cores using the Xenium in-situ transcriptomic platform with a breast cancer-focused panel of 280 genes from 10x Genomics plus 100 additional genes selected from literature and publicly available single cell datasets to delineate CAF and TAM sub-populations. Image analysis enabled the quantification and spatial mapping of the target genes within each cell boundary. Cells were manually annotated through unsupervised clustering of over 1 million cells. The cell phenotyping analysis allowed us to annotate major cell types including tumor cells, macrophages, T cells and fibroblasts. With our curated panel, we further characterized CAF and TAM sub-populations by identifying myofibroblastic CAFs (myCAFs), inflammatory CAFs (iCAFs), and antigen-presenting CAFs (apCAFs) in addition to M1 and M2-like macrophages as reported in the literature. We then performed spatial neighborhood analysis based on the similarity of the cell type composition in the vicinity of each cell. The results showed that myCAFs and M2-like macrophages are found in proximity to tumor cells and may play a role in T-cell exclusion. In addition, iCAFs mainly express CXCL12, a chemokine known to attract immunosuppressive cells such as regulatory T cells and M2-like macrophages as well as repel cytotoxic T cells from infiltrating the tumor via the CXCR4-CXCL12 axis. Overall, our work shows the potential of spatial transcriptomics to elucidate the spatial distribution of cells and their contribution to the immunosuppressive TME, which may enable researchers to improve understanding of tumor biology and drug target discovery efforts.

#5486 Spatial profiling reveals unique immune-transcriptomic features of tertiary lymphoid structures in melanoma.

Manoj Chelvanambi[1], Brenda Melendez[2], Elise F. Nassif[3], Rossana N. Lazcano[4], Matthew J. Lastrapes[5], Bharat S. Bhushan[2], Sarah B. Johnson[2], Khalida Wani[4], Davis R. Ingram[4], Y. David Seo[1], Beth A. Helmink[1], Michael G. White[6], Russell G. Witt[7], Laurence P. Diggs[1], Golnaz Morad[1], Monika Zelazowska[8], Somnath Paul[8], Florentia Dimitriou[1], Ashish V. Damania[2], Matthew C. Wong[2], Neeta Somaiah[3], Nadim J. Ajami[2], Emily Z. Keung[1], Wolf H. Fridman[9], James P. Allison[10], Padmanee Sharma[11], Kevin M. McBride[8], Tina Cascone[12], Christina L. Roland[1], Alexander J. Lazar[4], Jennifer A. Wargo[1]

[1]Surgical Oncology, UT MD Anderson Cancer Center, Houston, TX,[2]Genomic Medicine, UT MD Anderson Cancer Center, Houston, TX,[3]Sarcoma Medical Oncology, UT MD Anderson Cancer Center, Houston, TX,[4]Translational Molecular Pathology, UT MD Anderson Cancer Center, Houston, TX,[5]Epidemiology, UT MD Anderson Cancer Center, Houston, TX,[6]Colon and Rectal Surgery, UT MD Anderson Cancer Center, Houston, TX,[7]University of Virginia School of Medicine, Charlottesville, VA,[8]Epigenetics and Molecular Carcinogenesis, UT MD Anderson Cancer Center, Houston, TX,[9]Cordeliers Research Centre, Paris, France,[10]Immunology, UT MD Anderson Cancer Center, Houston, TX,[11]Genitourinary Medical Oncology, UT MD Anderson Cancer Center, Houston, TX,[12]Thoaric Head and Neck Medical Oncology, UT MD Anderson Cancer Center, Houston, TX

Background: Previous studies have shown that intratumoral immune aggregates called tertiary lymphoid structures (TLS) are associated with exceptional response to immune checkpoint blockade (ICB) in several cancer types. However, the specific mechanisms through which TLS contribute to ICB-response remain poorly characterized in part due to technical limitations with isolating TLS. Here, we use the NanoString GeoMx digital spatial profiler to interrogate TLS with deep spatial and transcriptional resolution and identify cellular and molecular features of response-associated TLS in melanoma.
Methods: Twelve neoadjuvant ICB-treated high-risk resectable melanoma patients [NCT02519322] with formalin-fixed paraffin embedded (FFPE) surgical resections were included in this study. Major pathologic response (MPR) defined as <10% viable tumor at time of surgery was used to evaluate response (R – responder; NR – non-responder). TLS were sampled (via H&E) using 1mm core punches and assembled into a tissue microarray (TMA). The TLS TMA was probed using the human whole transcriptome atlas (huWTA) and the human T-cell receptor (huTCR) atlas. Melanoma (S100B) and immune markers (CD45 and CD20) were used to guide region-of-interest (ROI) selection of classical TLS. Differential gene expression was calculated using a linear mixed model and corrected with Benjamini-Hochberg. Immune deconvolution was performed using CIBERSORTx with FDR cutoff of < 0.25.
Results: Fifty percent (6/12) of patients included in this study demonstrated MPR following treatment with neoadjuvant ICB. Principal component analysis of huWTA probes revealed distinct transcriptional states of R TLS vs NR TLS, with PC1 strongly correlating with response status ($r=0.88$, $p<0.0001$). Differential immune analysis showed that R TLS harbored more CD8+ T-cells ($p<0.001$), NK cells ($p=0.004$), γδ T-cells ($p=0.017$) and memory B-cells ($p=0.026$) and preferentially upregulated inflammatory genes such as pattern recognition receptors (TLR8 and KLRC2) and immune-stimulatory markers (CD27 and CD103). Immune-repertoire analysis revealed a trend towards increased TCR diversity in R TLS ($p = 0.3$) and distinct TCR signatures in R TLS underscored by elevated expression of TRDJ4 ($p<0.001$), TRGJ1/2($p<0.001$), TRGV4($p<0.001$) and TRAV1-2($p=0.018$) genes amongst others.
Conclusions: These findings demonstrate that, although melanomas from both R and NR patients contain TLS, the immune-phenotype of R TLS is more cytotoxic and characterized by a more diverse TLS-resident T-cell population. These findings present new insights into the therapeutic underpinnings of TLS in cancer and will inform future investigations evaluating their formation/function in solid tumors.

#5487 Improved spatial biology analysis of the tumor microenvironment with the next generation of the MultiOmyx™ platform.

M. Lazare, H. Nunns, F. Jelvhei Moghaddam, X. Jin, C. Todorov, E. Leones, M. Thio, F. Sahafi, E. Parnell, Q. Au;
NeoGenomics, Aliso Viejo, CA

Multiplexed Immunofluorescence is a powerful tool for spatially characterizing and phenotyping cells within the tumor microenvironment. MultiOmyx has been one of the leading platforms for generating multiplexed immunofluorescence data to support translational and clinical research for more than 10 years. However, MultiOmyx and other similar platforms are often hampered by a limited imaging area due to either restricted staining areas or being cost prohibitive due to excessive imaging times. Here, we demonstrate the capabilities of an improved MultiOmyx platform which can be used to generate whole-tissue data from the iterative MultiOmyx multiplexing process using the CyteFinder® II microscope and a customized software package developed by RareCyte, Inc. The new NeoLYTX image analysis pipeline in conjunction with the whole-tissue image output allows for improved interaction with pathologists, better histological context, and unbiased spatial analysis. In this study we utilized a 16-marker panel consisting of CD3, CD4, CD8, FoxP3, CD20, CD68, CD163, HLA-DR, PD-1, PD-L1, CTLA-4, CD34, Vimentin, SOX10, Ki67, and PanCK to generate immune profiles for colorectal carcinoma, prostate carcinoma, non-Small cell lung cancer, and triple negative breast cancer samples. We showed concordance with the current MultiOmyx imager - the IN Cell 2200 - for each of the markers in the panel. Additionally, we demonstrated that the updates made to the proprietary NeoLYTX image analysis pipeline are able to facilitate the significantly larger data sets that will be generated with the new MultiOmyx platform. This study successfully demonstrates the capability of the improved MultiOmyx system to characterize the distribution of T-cell and myeloid phenotypes in the tumor microenvironment using the proven MultiOmyx workflow, now enhanced by whole slide images and analysis.

#5488 AI-enhanced spatial proteomics reveals B-cells & FoxP3+ cells interactions in HPV(+) oropharyngeal squamous cell carcinoma Progression.

S. Nakkireddy[1], R. David[2], K. Bartemes[2], D. Ma[2], T. Hwang[1], K. Van Abel[2], C. Nimeh Abdel-Halim[2];
[1]Mayo Clinic Florida, Jacksonville, FL, [2]Mayo Clinic, Rochester, MN

Background: Analyzing interactions and the microanatomical distribution of the tumor immune microenvironment (TIME) is essential for a comprehensive understanding of tumor progression. Imaging Mass Cytometry (IMC) is a high-dimensional tissue imaging system that enables the deeper and multiparametric *in situ* exploration of tumor microenvironments at a single-cell level. This study describes a pipeline for analyzing 39-plex IMC images of human HPV(+) oropharyngeal squamous cell carcinoma (OPSCC) tumor sections, elucidating immune cells' nature, functions, and interactions with tumor cells. The IMC data analysis provides valuable information for clinical studies that could be used for the identification of prognostic biomarkers and mechanisms of resistance to current immunotherapies.

Methods: A retrospective study was conducted on (N=20) patients (10 progressors and 10 non-progressors) with HPV(+) OPSCC. The dataset comprises paired hematoxylin and eosin (H&E) images with IMC data from multiple Regions of Interest (ROIs) (N=82), enabling the in-situ profiling of 39 proteins in primary tumor tissue. Cell segmentation was followed by employing original images and their segmentation masks for cell phenotype identification using a probabilistic neural network method to spatially profile cancer cells, macrophages, NK-M cells, B-cells, and distinct T-cell populations. We identified protein expression at single-cell resolution and investigated the impact of multicellular spatial organization on the disease progression. The spatial neighborhood interaction score of tumor cells with various other cells was computed for all the ROIs across the two groups.

Results: The markers showed varying expression levels of intensity distribution, likely due to differences in tissue sample composition. Specifically, CD3, CD4, CD8, CD19, CD20, and CD68 showed significantly higher intensity in non-progressors. Interestingly, FoxP3 also had a significantly higher intensity level in non-progressors. Cell phenotyping emphasized that non-progressors generally have increased levels of NK-M cell markers. Spatial analysis revealed a significant increase in interaction between CD3 cells and tumor cells in non-progressors (p-value=0.07, Mann-Whitney U test). Furthermore, a significant rise in the interaction between B-cells and FoxP3+ cells was observed in non-progressors (p-value<0.05, Mann-Whitney U test) suggesting a coordinated suppression of tumor growth.

Conclusion: We developed a deep learning-based pipeline to analyze spatial relationships in the TIME of IMC data, demonstrating its clinical relevance in predicting disease progression. Our findings emphasize the importance of spatial relationships in the TME for response and suggest that proximity between either CD3+ T-cells to cancer cells or B-cells to FoxP3+ cells are candidate biomarkers.

#5489 The spatial landscape of early-stage lung adenocarcinoma.

Junbum Kim, Hiranmayi Ravichandran, Liron Yoffe, Bhavneet Binder, Timothy McGraw, Nasser K. Altorki, Vivek Mittel, Olivier Elemento

Weill Cornell Medicine, New York, NY

Cellular and molecular basis of ground-glass opacities (GGO), which has been used as a screening indicator for lung cancer, remains a gray area. Our aim was to investigate the tumor-immune microenvironment (TIME) in a cohort of early-stage lung adenocarcinomas (LUAD) through imaging mass cytometry, enabling us to examine the TME spatial composition of nodules at single-cell resolution. We collected 354 imaging mass cytometry (IMC) regions of interest (ROI) from 135 early-stage lung adenocarcinoma patients to investigate the spatial and molecular profiles of early stage LUAD. Specifically, we gathered 27 solid (S), 39 part-solid (PS), 74 pure non-solid (PNS) patients and 89 matched adjacent-normal cases to profile the phenotype of 2.24 million cells across the two IMC panels to characterize the cellular and molecular composition of GGO nodules. Comparing progression from adjacent normal, pure non-solid, part-solid, to solid, we observed consistent reduction in RAGE+ AT1 cells ($p^*<1.6E-7$) and a reciprocal increase in SFTPC+ AT2 cells ($p^*<1.3E-8$) and PanCK+Ki67+ proliferative epithelial cells ($p^*<2.8E-7$). We also report fibrogenesis and an increase in immune cell populations such as regulatory ($p^*<1.4E-5$), CD4 ($p^*<0.0024$), CD8 T ($p^*<0.017$) cells, B ($p^*<5.5E-9$) cells, and macrophages. Spatially, we quantify an upregulation of tumor-tumor and tumor-fibroblast interaction, and a downregulation of tumor-immune interaction. We believe this evidence suggests the role of fibroblasts as liner for tumors, barricading immune infiltration and harvesting uninterrupted tumorigenesis. In summary, we performed a highly multiplexed IMC data to analyze the TIME spatial profiles of GGO nodules in early-stage LUAD at a single-cell level. Spatial analysis of this integrated multidimensional omics dataset provides insight into the pivotal role of fibroblasts in early-stage LUAD in immune suppression, evasion, tumorigenesis, and potentially metastasis.

#5490 Spatial profiling of inflamed tumor microenvironment of clear cell renal cell carcinoma.

T. Pellinen[1], L. Luomala[1], K. Mattila[2], J. Saila[1], A. Hemmes[1], K. Valimaki[1], O. Bruck[1], L. Paavolainen[1], H. Nisen[1], P. Jarvinen[1], O. Kallioniemi[1], P. Vainio[2], P. Jaakkola[2], T. Mirtti[1],

[1]University of Helsinki, Helsinki, Finland, [2]University of Turku, Turku, Finland

Clear cell renal cell carcinoma (ccRCC) presents a distinctive tumor microenvironment (TME) characterized by extensive vascularization and immune infiltration. This unique TME makes ccRCC an attractive target for anti-angiogenesis and immune checkpoint blockade (ICB). To better understand the complexity of ccRCC and the associated cell types and states involved in disease progression, we conducted high-throughput single-cell immunofluorescence imaging on tissue sections from 437 localized tumors that were surgically resected. These samples included regions from the tumor center, tumor edge, and adjacent benign areas (TMA cores, n=1859). Our primary focus was on tumors with elevated immune cell enrichment ($CD45^{high}$), as these tumors are known to be aggressive and may respond well to immunotherapy. Our study reveals the intricate interactions between tumor, vascular, stromal, and immune cells within ccRCC. We find that $CD45^{high}$ tumors, upon losing epithelial marker expression, acquire tumor cell PD-L1 and mesenchymal markers such as Fibroblast activation protein (FAP). This shift is indicative of the epithelial-mesenchymal transition (EMT) process. These $CD45^{high}$ and EMT^{high} tumors are enriched with changes in TME, including elevated FAP+ cancer-associated fibroblasts (CAFs) and subsets of immune suppressive T cells and macrophages. We report that ccRCC patients with high tumor PD-L1 expression or abundant FAP+ CAFs are associated with earlier metastasis and, in sunitinib-treated patients, shorter progression-free survival. This study illuminates the intricate connection between immune cell infiltration, stromal biology, and EMT in ccRCC, offering a deeper understanding of the disease's complex biology and potentially guiding future therapeutic approaches and strategies.

#5491 Mapping ovarian cancer spatial organization uncovers immune evasion drivers at the genetic, cellular, and tissue level.

K. Aguirre, C. Yiwen-Yeh, O. Laveroni;
Stanford University School of Medicine, Stanford, CA

Immune exclusion and evasion are central barriers to the success of immunotherapies and cell therapies in solid tumors. Here we applied single cell spatial and perturbational transcriptomics alongside clinical,histological, and genomic profiling to elucidate immune exclusion and evasion in high-grade serous tubo-ovarian cancer (HGSC). Using high-plex spatial transcriptomics we profiled more than 1.3 million cells from 95 tumors and 60 patients, revealing generalizable principles in HGSC tumor tissue organization.Our data demonstrates that effector T cells resist stroma-mediated trapping and sequestration. However, upon infiltration into the tumor, T cells, as well as Natural Killer (NK) cells, preferentially co-localize only with a subset of malignant cells that manifest a distinct transcriptional cell state. The latter consists of dozens of co-regulated genes and is repressed under various copy number alterations. Performing CRISPR Perturb-seq screens in ovarian cancer cells, we identified functionally diverse genetic perturbations - including knockout of the insulin sensing repressor PTPN1 and the epigenetic regulator ACTR8 - that de-repress the proposed immunogenic malignant cell state identified in patients and indeed sensitize ovarian cancer cells to T cell and NK cell cytotoxicity. Taken together, our study uncovered a profound connection between somatic genetic aberrations, malignant cell transcriptional dysregulation, and immune evasion at the cellular and tissue level, allowing us to identify targets that reprogram malignant cell states as an avenue to unleash anti-tumor immune responses.

#5492 Spatial organization and cellular composition of immunity hubs in human colorectal cancer.

Mukta G. Palshikar[1], Maxwell Spurrell[2], Jack Demaray[3], Han Chen[3], Scott Engels[3], Roopa Madhu[4], Milan Parikh[5], Izabella Zamora[6], Arnav Mehta[6], Nicolas Fernandez[7], Colles Price[7], Jiang He[7], Sonia Cohen[6], Karin Pelka[3], Nir Hacohen[5], Jonathan Chen[6], Ilya Korsunsky[1]

[1]Harvard Medical School/Brigham and Women's Hospital, Boston, MA,[2]Massachusetts General Hospital (MGH) Krantz Family Center for Cancer Research, Boston, MA,[3]Gladstone-UCSF Institute of Genomic Immunology, Gladstone Institutes, San Francisco, CA,[4]Immunology, Harvard Medical School, Boston, MA,[5]Broad Institute of Massachusetts Institute of Technology (MIT) and Harvard, Cambridge, MA, USA, Cambridge, MA,[6]Broad Institute of Massachusetts Institute of Technology (MIT) and Harvard, Cambridge, MA,[7]Vizgen, Inc, Cambridge, MA

Background: Among colorectal cancer (CRC) tumors, mismatch repair deficient (MMRd) tumors have more immunogenic neo-antigens, hence more cytotoxic T-cell mediated anti-tumor immunity than mismatch repair proficient (MMRp) tumors. Previously[1], we transcriptionally profiled over 300,000 cells from 62 MMRd and MMRp CRC tumors and found an MMRd-unique network of immunologically active transcriptional states enriched in interferon-stimulated genes (ISGs). With 4-color imaging, we showed that this program arises from spatially organized hubs of at least 3 cell types: IFNã-secreting T and interferon-responsive CXCL9/10/11+ myeloid and tumor cells. To characterize the breadth of cells involved in tumor immunity hubs, we must simultaneously measure the expression of 100s of genes *in situ*.

Methods: To describe the cellular composition, structural organization and intercellular spatial interactions of these immunity hubs, we profiled primary untreated resection specimens from 17 CRC donors (n=12 MMRd, 5 MMRp) using multiplexed error-robust FISH (MERFISH) mRNA microscopy. Efforts were made to sample both the tumor body and the invasive border of the tumor. We designed a panel of 479 genes to capture key transcriptional programs from our single-cell atlas[1]. We wrote analytical pipelines to segment transcripts into cells, select high-quality cells, and organize cells into distinct zones in tissue. To leverage the rich information in the scRNA-seq atlas[1], we designed a robust label transfer analysis to assign cell state labels to MERFISH cells by comparison to scRNAseq cells.

Results: We profiled 7.5 million high quality MERFISH cells across 21 CRC tissue sections and labeled the cells into 7 major lineages: 63.19% epithelial, 22.52% stromal, 7.75% myeloid, 3.72% T/NK/ILCs, 1.45% plasma, 1.2% B, and 0.17% mast cells. We visualized the spatial location of these cell types. T cells aggregated into 3 distinct regions of tissue: tertiary lymphoid structures (TLS) outside the tumor, and smaller clusters near the invasive border and in the tumor center. We identified immunity hubs defined by colocalized *CXCL9/10/11* expressing cells and T cells near the invasive border and in the center of MMRd tumors. As expected, we found enrichment of *CXCL13*, *IFNG*, and ISGs such as *CD74* and *MHCII* genes at these locations. In contrast, we found evidence of *CCL17+CCL19+LAMP3+* activated dendritic cells and B cells enriched in the TLS. These results support a distinct composition and localization of immunity hubs in tumors, in contrast to TLS outside tumors.

Conclusions: Our study defines the composition, spatial organization, and intercellular interactions of immunity hubs, shedding light on the anti-tumor immune response in CRC.

Ethics Approval: Approved by the DF/HCC Institutional Review Board (protocol #02-240).(1) Pelka, K. et al. Spatially organized multicellular immune hubs in human colorectal cancer. Cell 184, 4734-4752.e20 (2021)

#5493 Digital spatial profiling of MC38 colon carcinoma following checkpoint inhibition.

P. Singh, D. Saims, **S. Barnes**, D. Draper;
Labcorp Drug Development Inc., Ann Arbor, MI

Immunotherapy aims to bolster the immune response within the tumor microenvironment (TME). However, checkpoint inhibitors utilized in the treatment of colon carcinoma have demonstrated efficacy only in certain patients. To develop more effective therapeutics, strategies that navigate the heterogeneous nature of the TME must be employed. The MC38 tumor model, known for its immunologically active characteristics and responsiveness to certain immunotherapies, is widely used for preclinical drug development. Furthermore, elevated levels of pan-cytokeratin (PanCK) expression in tumors have shown an association with diminished survival rates among colon carcinoma patients. In this study, we used the GeoMx® DSP platform (NanoString Technologies) to investigate the spatial expression profile of PanCK in MC38 tumors and analyze the impact that PanCK expression exerts on anti-PD-1 induced gene expression in tumor and immune cells. To this end, C57BL/6J female mice were implanted with MC38 cells, enrolled into groups, and treated with anti-PD-1 antibody. Tumor growth was monitored by caliper measurements and anti-PD-1 produced minimal responses with a Day 22 median % Delta T/C value of 88%. For DSP analysis, tumors were collected 10 days post-treatment, formalin fixed for paraffin embedding, and then sectioned for PanCK and CD45 protein visualization. Regions of interest were drawn to create a matrix analysis that defined regions with high or low PanCK expression, that were proximal or distal to CD45+ immune rich regions of the tumor. A segmentation algorithm was applied to examine gene expression within each region using the GeoMx Mouse Whole Transcriptome Atlas. Cluster analysis revealed an enrichment of apoptosis and autophagy gene sets in tumor cells that were proximal to immune rich regions. In the CD45+ segment, immune cells adjacent to high PanCK-expressing cells contained 318 genes with significantly increased expression levels when compared to low PanCK-expressing cells, and only 11 genes with decreased expression levels. The upregulated genes were enriched for numerous biomarkers of T cell recruitment and activation, including cd3, cd8, cxcr3, ccl5, cxcl9, icos, and cd27. Next, we conducted a linear mixed model analysis to examine the impact of PanCK expression on anti-PD-1 induced gene regulation. Notably, an enrichment of genes that code for T cell exhaustion biomarkers was observed in immune cells near PanCK high expressing cells, including ctla4, slamf7, tigit, and lag3. In summary, the most pronounced transcriptomic changes occurred within immune cells situated near tumor cells displaying high PanCK expression and suggest that PanCK expression correlates directly with T cell recruitment and activation but also exhaustion. Furthermore, these data emphasize the significance of spatial analysis as a valuable component of preclinical research, as demonstrated in MC38 tumor model.

#5494 Spatial organization between claudin and the tumor microenvironment in head and neck squamous cell carcinomas.

K. Maclean, L. Chandramohan, M. Rohafza, H. Nunns, E. Parnell, Q. Au, A. Juncker-Jensen;
NeoGenomics, Aliso Viejo, CA

Background: Head and neck squamous cell carcinoma (HNSCC) is the sixth leading form of cancer worldwide and one of the most difficult and challenging malignancies, with a high level of heterogeneity and a wide range of treatment responses. Oral squamous cell carcinoma (OSCC) is the most common head and neck cancer and accounts for over 90% of cancers that develop within the mucosal epithelium of the oral cavity. Additional carcinogenic risk factors, including tobacco, alcohol and HPV infection are also associated with the pathogenesis of oral carcinogenesis. Unfortunately, today the failure of standard treatment modalities, such as surgery, radiotherapy, and chemotherapy underscore the need to identify better biomarkers of this disease. Advances, especially in spatial technology have created unprecedented opportunities to identify cell types and biomarkers of disease processes, revealing important relationships within the tumor microenvironment (TME) that allow a detailed characterization of specific cell phenotypes defined by co- or lack of expression of multiple markers that may help in predicting clinical responses and mechanisms of resistance to therapy. Recent findings indicate that abnormal expression of claudins (CLDNs) is closely related to the occurrence, progression and prognosis of many solid tumors. Specifically, CLDN6 is expressed in numerous tumors but rarely found in adult normal tissues making it a potential therapeutic target in head and neck tumor types. To investigate this further, expression of CLDN6 and the its relationship with changes within the TME of cohort OSCC tumors was determined using a proprietary comprehensive spatial workflow and gene expression analysis.

Methods: A retrospective analysis was performed on biopsied Formalin-Fixed Paraffin-Embedded (FFPE) samples from OSCC patients with and without a history of smoking and treated +/- chemotherapy. Patient samples representing matched normal tissue to serve as controls were compared to samples derived from OSCC tumors. In order to perform a comprehensive expression profiling of the TME from OSCC tumors we used the spatial MultiOmyx™ immunofluorescence (IF) multiplexing assay with transcriptomic information from bulk mRNA gene expression acquired using the NanoString nCounter® PanCancer IO 360™ panel that includes the Tumor Inflammation Signature (TIS), as well as targets that characterize immune hot, desert, and cold regions in the stroma and tumor epithelium.

Results: We characterized the expression of CLDN6 across the different cohorts of OSCC samples and further investigated the relationship within the tumor immune microenvironment coupled to genes related to the prognosis of OSCC. A better understanding of the TME and gene expression profiling of OSCC tumors and the effect of smoking will allow us to tailor the treatment of patients to continue to improve outcomes.

#5495 Multiplexed analysis across cancers of diverse origins to unravel spatial interactions within the tumor microenvironment.

V. Agrawal[1], L. Arvidson[2], M. J. Smith[1], K. O. White[1], R. A. Heil-Chapdelaine[1], S. Jensen[2], **A. BOSE**[1];
[1]Leica Microsystems, Waltham, MA, [2]Cell Signaling Technology, Danvers, MA

The tumor microenvironment (TME) is heterogeneous and is primarily composed of fibroblasts, extracellular matrix, immune cells, and blood vessels. Importantly, the tumor immune microenvironment (TIME) is a major source of cancer heterogeneity and influences both disease progression and response to therapeutic interventions. Malignant cells typically recruit various cell types such as vascular endothelial cells, cancer-associated fibroblasts (CAFs), and tumor-associated macrophages (TAMs) to promote tumor growth. Therefore, studying such a complex interplay among tumor, stromal cells, and immune cells within the TME necessitates a multiplexed analytical approach to investigate cancerous tissues from diverse origins, to ultimately predict clinical outcomes and design novel therapies. While numerous studies have been focused on investigating the expression patterns of immune-oncology markers within specific tissues, the extent to which such marker expression patterns are shared across tumors originating from various tissues is not adequately understood. In this study, we analyzed a large panel of Cell Signaling Technology (CST®) antibodies that are targeting immune, stromal, epithelial, and vascular markers in cancer tissues derived from various origins including lung, colon, and pancreas. Using multiplexed Cell DIVE imaging, key spatial interactions in the tumor microenvironment that are (1) tissue-specific, and (2) shared across tumors irrespective of origin were determined. Specifically, cluster analysis of a common panel of markers across tissues of different origins uncovered molecular signatures that are common to all cancer tissue types as well as those that are unique to specific tissue types to advance our understanding of the disease, and its progression, shedding light on the intricate interactions within the TME.

#5496 Multi-omic spatial analysis of the tumor microenvironment in gliomas.

D. Klymyshyn[1], V. Jain[2], L. Whaley[2], E. Hocke[2], B. Ben Cheikh[1], A. Smith[2], K. Abramson[2], N. Nelson[3], D. Satterfield[4], E. Thomas[4], G. Lopez[4], S. Hariharan[4], M. Brown[4], N. Jhaveri[1], R. McLendon[5], D. Ashley[4], M. Waitkus[4], S. Gregory[4];

[1]Akoya Biosciences, Menlo Park, CA, [2]Duke Molecular Genomics Core, Duke Molecular Physiology Institute, Durham, NC, [3]Abcam, Cambridge, United Kingdom, [4]The Preston Robert Tisch Brain Tumor Center at Duke, Brain Tumor Center, Durham, NC, [5]Duke Cancer Center Brain Tumor Clinic, Durham, NC

Introduction: The diverse tumor environment of high-grade glioma, which remains refractory to treatment, demands new innovative, multi-omic approaches to characterize tumor heterogeneity and expression profiles associated with progression and therapeutic response.

Approach: We have applied an integrated, multi-omic approach using paired spatial *in situ* sequencing (Xenium) and protein profiling (PhenoCycler® Fusion) of glioma tissue to identify distinct glioma cellular phenotypes, activation states and metabolic pathways at true single cell resolution. Our multi-omic approach used hundreds of phenotypic RNA target probes and >50 antibodies in an unbiased single-cell analysis of primary, recurrent, and IDH1 mutant/wild type tumors with a range of heterogeneity.

Summary: We were able to distinguish differentially regulated genes and pathways between aggregated primary and recurrent GBM, including cell cycle pathways being upregulated in primary vs recurrent GBM glial cell clusters and a down regulation of ERBB4 signaling in vascular cell clusters in primary GBMs. Our data also suggests that SOX11, known to be involved in tumorigenesis, is >2-fold upregulated in annotated tumor cells in primary compared to recurrent tumors. We were also able to quantitatively localize the expression of Epidermal Growth Factor Receptor, variant III (EGFRvIII) to specific tumor-cell sub-types, which is important given its association with therapeutic resistance. Further, we have been able to establish the cellular neighborhoods and cell-cell and receptor-ligand relationships within the tumors. Our spatial protein analysis identified distinct tumor and immune phenotypes with varying abundance of myeloid and lymphoid populations in IDH1 wt and mt tumors. Moreover, spatial proximity analyses and cellular neighborhood analyses revealed differences in higher order organizational landscapes that may contribute to the differential outcomes across wt and mt tumor subtypes.

Conclusion: Multiomic spatial analysis enables deeper characterization of the glioma cellular and functional landscape to broaden our understanding of the key TME features that contribute to disease pathogenesis and prognoses. Our study provides an analytical framework to combine RNA and protein-based spatial data for a holistic investigation into a variety of glioma subtypes and aid in the identification of novel biomarkers, spatial neighborhoods, and functional states that drive glioma progression.

#5497 Towards a drag and drop spatial biology workflow: Introducing sample reinterrogation as a conduit for the progressive development and on-line analysis of high parameter spatial biology data.

M. H. Ingalls[1], X. Meshik[1], C. E. Jackson[1], K. E. Cashion[1], A. Christians[2], A. Brix[2], M. Boettcher[3], J. S. Schwarz[1], O. Braubach[1];
[1]Canopy Biosciences-A Bruker Company, St. Louis, MO, [2]Canopy Biosciences-A Bruker Company, Hannover, Germany, [3]Canopy Biosciences-A Bruker Company, Leipzig, Germany

The potential for spatial biology in cancer research is understood and edified. With it we can understand the tumor microenvironment, unravel responsiveness to drug treatments and cell therapies, and ultimately stratify patients for targeted treatment and clinical trial enrollment. Yet, researchers exploring spatial biology may be discouraged by what can be a resource intensive exercise, and most importantly, a commitment of high value patient samples. Furthermore, the design of reagent panels used to study samples is not trivial, and a specimen's unique biomarker expression profile may require adjustments. Here we present a novel solution that permits sample re-interrogation and in-flight adjustments of reagent panels in our spatial biology workflow.

The CellScape™ platform for Precise Spatial Multiplexing paired with VistaPlex™ Assay Kits provide a ready-to-use cyclic multiplex immunofluorescence (IF) solution to interrogate fresh frozen and FFPE tissue samples. Tissues are mounted in enclosed fluidic chambers, while staining and imaging are conducted on the CellScape instrument. The experiment requires no additional autostainer equipment and is divided into separate staining and imaging rounds. The end user may therefore pause between rounds and conduct *inter-round* analyses, which can then guide decisions of whether and how to continue the experiment. To illustrate the benefit of this approach, we present a use case in which we applied VistaPlex antibody panels to reveal the spatial distribution of major immune cell populations. *Inter-round* analysis and conclusions were then drawn from this preliminary phenotype map before successive rounds of rationally planned staining were conducted to further deepen the depth and breadth of spatial phenotyping.

The CellScape sample reinterrogation feature is a pragmatic spatial biology solution that optimizes the use of precious resources, whilst allowing researchers to generate informed decisions about antibody panel designs almost in real time. This enhanced utility may reduce the resistance to spatial biology among researchers working with samples that are limited or irreplaceable.

#5498 Multi-modal examination of spatial heterogeneity in the astrocytoma microenvironment.

J. Moffet, J. Kriel, T. Lu, L. Freytag, J. Whittle, S. Best, **S. Freytag**;
The Walter & Eliza Hall Institute of Medical Research, Parkville, Australia

Astrocytoma is a diffuse tumor that infiltrates the brain. Despite post-operative therapy including radiation and chemotherapy, 52% of patients' tumors recur within five-years of surgery. These tumors are characterized by mutations in the IDH1 or IDH2 gene that confer metabolic alterations, most notably the production of the onco-metabolite 2-hydroxyglutarate. To reveal the metabolic alterations and their upstream regulation across the tumor microenvironment, we applied spatial metabolomics and spatial transcriptomics to sequential sections from resected tumor samples of patients with low grade astrocytoma. This necessitated extensive optimization of atmospheric-pressure MALDI-TOF, including the establishment of a custom automated computational pipeline with abilities to identify metabolic niches. Additionally, using sequential sections of the same tumor, we also compared all commercially available imaging-based spatial transcriptomic technologies (10x Genomics Xenium, Nanostring CosMx, Vizgen MERSCOPE) to evaluate their suitability with regards to building a multi-modal model of metabolic activity and regulation across the tumor microenvironment. We found that 10x Genomics Xenium was most suited for this task as image registration across sequential sections was comparatively straight-forward. Combining spatial transcriptomics generated with 10x Genomics Xenium and spatial metabolomics across 8 matched sequential slices of the same tumor, we identified metabolic niches associated with distinct cell type composition and transcriptional regulation.

#5499 Spatially-resolved transcriptomics analyses of liver cancer.

Liang Wu

University of Chinese Academy of Sciences/BGI-Shenzhen, Shenzhen, China

Dissecting and understanding the cancer ecosystem, especially that around the tumor margins, which have strong implications for tumor cell infiltration and invasion, are essential for exploring the mechanisms of tumor metastasis and developing effective new treatments. Using a novel tumor border scanning and digitization model enabled by nanoscale resolution-SpaTial Enhanced REsolution Omics-sequencing (Stereo-seq), we identified a 500 μm-wide zone centered around the tumor border in patients with liver cancer, referred to as “the invasive zone”. We detected strong immunosuppression, metabolic reprogramming, and severely damaged hepatocytes in this zone. We also identified a subpopulation of damaged hepatocytes with increased expression of serum amyloid A1 and A2 (referred to collectively as SAAs) located close to the border on the paratumor side. Overexpression of CXCL6 in adjacent malignant cells could induce activation of the JAK-STAT3 pathway in nearby hepatocytes, which subsequently caused SAAs’ overexpression in these hepatocytes. Furthermore, overexpression and secretion of SAAs by hepatocytes in the invasive zone could lead to the recruitment of macrophages and M2 polarization, further promoting local immunosuppression, potentially resulting in tumor progression. Clinical association analysis in additional five independent cohorts of patients with primary and secondary liver cancer (n = 423) showed that patients with overexpression of SAAs in the invasive zone had a worse prognosis. Further in vivo experiments using mouse liver tumor models in situ confirmed that the knockdown of genes encoding SAAs in hepatocytes decreased macrophage accumulation around the tumor border and delayed tumor growth. The identification and characterization of a novel invasive zone in human cancer patients not only add an important layer of understanding regarding the mechanisms of tumor invasion and metastasis, but may also pave the way for developing novel therapeutic strategies for advanced liver cancer and other solid tumors.

#5500 Single cell sequencing reveals cancer associated fibroblast heterogeneity at the core of the tumor microenvironment in brain metastasis.

T. Simon[1], D. N. Buckley[1], B. Y. Tew[1], M. Salomon[1], Z. Yang[1], G. C. Gooden[1], S. A. Toms[2], G. Zada[1], B. Salhia[1];
[1]University of Southern California, Los Angeles, CA, [2]The Warren Alpert Medical School of Brown University, Providence, RI

Introduction: Brain metastasis (BM) remains incurable with a dismal 2-year survival of less than 2%. BM are surrounded by a complex tumor microenvironment (TME) comprised of a meshwork of extracellular matrix (ECM) proteins and an assemblage of cell types including cancer-associated fibroblasts (CAFs), the most prominent cell type within the TME. We have previously shown that patient-derived BM CAFs can either support or inhibit tumor growth *in vivo*, suggesting that BM CAFs are heterogenous. Yet, there remains a dearth of data on the functional and mechanistic underpinnings of CAFs in the BM TME.
Methods: To explore both the molecular profiles of CAFs and their heterogeneity in the BM TME, we performed a single cell Multiome (RNA and Assay for Transposase-Accessible Chromatin (ATAC)) sequencing (scMultiome-seq) analysis of 9 human BM tissue samples and 4 BM patient-derived CAF cell lines, from both lung and breast primary cancers. Next, we investigated the tumor supportive or inhibitory capabilities of BM CAF cell lines on the growth of BM tumor cells *in vitro*.
Results: ScMultiome-seq analysis of BM tissue samples identified 4 distinct CAF subpopulations, that we termed desmoplastic, immune, contractile, and neural CAFs, in the BM TME. These CAF subpopulations are respectively involved in either regulating the ECM organization, orchestrating the neuroimmune response, triggering tissue contraction or regulating neural components upon BM growth. CellPhoneDB analysis revealed that CAFs had more cell-cell interactions with other cells than any other cell types in the BM TME. Pseudotime analysis demonstrated the potential cell of origin of each BM CAF subpopulation and the cell state transition they undergo. We observed that the end cell state of the desmoplastic CAFs expressed high levels of immunoglobulin superfamily containing leucine rich repeat (ISLR). ISLR was also observed to be highly expressed in a BM patient-derived CAF cell line which was previously reported by our lab to restrain tumor growth *in vivo*, suggesting that desmoplastic CAFs with high ISLR expression (ISLR-CAFs) might be tumor inhibitory. ScMultiome-seq analysis of BM CAF cell lines validated that tumor inhibitory CAF cell lines were primarily of the desmoplastic ISLR-CAF subpopulation. Conditioned media obtained from ISLR-CAFs containing high levels of ISLR inhibited tumor cell viability *in vitro* compared to controls.
Conclusion: Our study is the first to describe the heterogeneity of CAFs and their potential central roles in the BM TME. We also identify that CAF subpopulations are dynamic and can transition to tumor inhibitory cell states, such as ISLR-CAFs. These data have potential to help design therapeutic strategies that selectively target tumor supportive CAFs whilst protecting tumor inhibitory ones.

#5501 Novel whole slide imaging modes for imaging mass cytometry unveil extensive cellular heterogeneity in human gliomas.

N. Zabinyakov, Q. Raza, **T. D. Pfister**, N. Parsotam, D. Howell, L. Lim, C. Loh;
Standard BioTools, Markham, ON, Canada

Gliomas present a complex form of cancer that is challenging to diagnose and treat, with a median survival of just over one year after diagnosis for primary glioblastoma (GBM). GBM can occur as multi-lesion, remote, or diffuse tumors, and often contains a tumor microenvironment (TME) that is devoid of peripheral immune cells. Additional hallmark features of GBM include necrosis, hemorrhage, and pseudo palisades, making it a highly heterogeneous disease requiring further investigation. Identification of the cellular and spatial level composition of the TME is vital for interpretation of GBM disease origin, progression, prediction, and treatment.

A 40-plus-marker neuro-oncology Imaging Mass Cytometry™ (IMC™) antibody panel was used to determine the cellular and structural landscape of the brain TME. We applied the panel on a tissue microarray (TMA) containing dozens of human glioma cores and uncovered the spatial distribution of over 40 distinct molecular markers. We performed imaging using two new features of the Hyperion XTi™ Imaging System that provide whole slide scanning capabilities. Ultrafast preview mode was applied to rapidly screen tumor cores for expression signatures associated with tumor immuno-oncology processes. This enabled biomarker-guided selection of areas in tumor tissue that were imaged at higher resolution and analyzed using single-cell analysis. In parallel, a high-throughput tissue mode was applied to perform a detailed scan of the brain tumor TMA followed by pixel-based analysis to unravel the spatial composition of the TME. Using tissue mode imaging, we successfully mapped the spatial location of cell populations making up human gliomas, such as neurons, astrocytes, microglia, and oligodendrocytes, across the entire TMA. Various tumor cell phenotypes, resident and infiltrating cells, and resting and activated microglia were detected across all TMA cores. Subsequent single-cell analysis of select regions of interest provided a quantitative assessment of the cellular composition of the brain TME. We classified the distinct states of neurons and quantified myeloid and lymphoid immune cell infiltration across normal, astrocytoma, and GBM tissues. Striking cellular and protein heterogeneity was observed between acquired cores, indicating the complexity of each case that is impossible to capture with low-plex visualization techniques. Therefore, IMC is a highly relevant tool capable of quantitative spatial evaluation of the high-plex protein composition in the brain TME without the complications of autofluorescence, tissue degradation, and spectral overlap. Empowered by the neuro-oncology panel and new whole slide imaging modes, IMC accelerates neurological research and provides insights into the spatial complexity of gliomas and other tumors.

For research purpose only. Not for use in diagnostic procedures.

#5502 Multiplex data utilizing a single-step staining and imaging workflow for the investigation of multiple sample types.

S. Larkin, T. George, E. Kaldjian;
RareCyte, Inc., Seattle, WA

Background: Tissue consists of heterogenous cell types, each with diverse functions and functional states, where spatial organization can impact patient health status. Resolving this complexity at the subcellular level has historically been challenged by image resolution, the number of targets that can be simultaneously assessed, and throughput. Such barriers can be broken using high plex and whole slide biomarker imaging data, in one single cycle thus also mitigating issues that arise with multiple cyclic rounds.
Methods: A range of whole slide healthy and diseased tissue types were stained with 15 to 18-plex validated biomarker panels. The tissues' inherent autofluorescence was isolated into discrete fluorescence channels for enhanced information about each tissue's morphology. Whole slide spatial staining and imaging was conducted on the Orion™ spatial biology platform, and H&E staining was performed after immunofluorescence (IF) imaging on the same section and imaged by brightfield microscopy. The full protocol is fairly quick and simple, using standard histology tools: - Mount sections on glass slides- De-paraffinize and perform antigen retrieval- Quench autofluorescence- Stain slides with a panel of ArgoFluor™ conjugated antibodies- Coverslip with ArgoFluor Mounting Medium and cure overnight- Image whole slides at 20X magnification using the Orion instrument- Process to ome.TIFF and analyze- De-coverslip in aqueous solution- Perform H&E staining and scanning on same section.
Results: Imaging data within each tissue type presented here reveals important biological insights which can then be used for quantitative analysis. The little to no tissue degradation due to the one round staining and imaging process also enables H&E capabilities after IF, further enhancing biomarker quantitation. The combination of speed and resolution proved effective for comprehensive phenotypic profiling and characterization of tissue architecture, tumor heterogeneity, and the immune response.
Conclusions: There is a need to show tissue biology in a high quality, high resolution, subcellular fashion as it provides a more in-depth understanding of each biological sample and thus can lead to improved spatial research of various human diseases. The single-stain and scan method described here improves the acquisition of subcellular spatial context and greatly reduces/removes errors in multiplex image data compared to cyclic methods. A single stain and image cycle across a 12-18 plex sample provides accurate downstream biomarker quantitation, offering better prediction of patient outcomes.

#5503 Ultrahigh-plex spatial phenotyping of head and neck cancer tissue uncovers multiomic signatures of immunotherapy response.

A. Pratapa[1], L. Hernandez[1], B. Ben Cheikh[1], N. Jhaveri[1], A. Kulasinghe[2];
[1]Akoya Biosciences, Marlborough, MA, [2]The University of Queensland, Brisbane, Australia

Background Targeted immune checkpoint inhibitors (ICI) with anti-PD-1/PD-L1 therapy offer durable treatment of mucosal head and neck squamous cell cancer (HNSCC), in both human papillomavirus-positive (HPV+) and negative (HPV-) patients. However, currently available biomarker signatures for targeted ICI therapies have limited predictive value. Our recent ultrahigh-plex profiling of HNSCC tissue with 100+ cancer hallmarks of tumor and immunobiology uncovered distinct spatial domains that serve as defining factors for clinical response and resistance.
Methods Our unbiased analysis of whole-slide metastatic HNSCC tumors is from a clinical cohort of patients treated with Pembrolizumab/Nivolumab. The cohort consisted of patients with a range of outcomes from complete vs partial vs progressive disease responses to ICI therapy. We first characterized the tumor microenvironment using our ultrahigh-plex protein panel with 100+ antibodies on the PhenoCycler®-Fusion platform. To expand upon our biomarker discovery, we included multiomic cancer hallmarks with a multimodal protein/RNA detection panel. Targeted spatial RNA detection was performed to complement and augment the microenvironment characterization achieved by our protein panel. To further consolidate the multiomic data, we leveraged MaxFuse, a state-of-the art computational framework that integrates multimodal spatial and single-cell expression data.
Results Our multiomic spatial phenotyping uncovered diverse tumor regions, each with distinct biomarker expression that is reflected across modalities including protein, RNA, and metabolic activity, indicating regions likely associated with resistance to immunotherapy. Our multiomic data integration also revealed spatial signatures associated with different tissue compartments, such as the tumor and non-tumor associated tertiary lymphoid structures.
Conclusions We demonstrate a multi-pronged approach that incorporated both novel experimental and computational techniques for elucidating tumor microenvironment in HNSCC tissue prior to ICI-based immunotherapy. Our multiomic approach provides deeper characterization of the HNSCC at the transcriptomic and proteomic level incorporating depth across the entire transcriptome and single-cell spatial resolution of key protein determinants for predicting and furthering our understanding of immunotherapy response to ICI therapy.

#5504 Integrating ultrahigh-plex spatial phenotyping: From discovery to clinical applications.

A. Pratapa, N. Ma, N. Jhaveri;
Akoya Biosciences, Marlborough, MA

Background The journey from discovering predictive spatial biomarkers (known as spatial signatures) for immunotherapy responses to their clinical application necessitates a cohesive approach bridging ultrahigh-plex discovery experiments with high-throughput translational studies. This study focuses on integrating Akoya Biosciences spatial multiplexed imaging technologies with advanced data analysis techniques for comprehensive spatial phenotyping across the discovery-to-clinical continuum.
Methods Human formalin-fixed, paraffin-embedded (FFPE) cancer tissues were profiled using ultrahigh-plex PhenoCode™ Discovery panels to examine cell lineage, immune activation, and checkpoint markers via the PhenoCycler®-Fusion spatial biology platform. The subsequent use of PhenoCode™ Signature panels targeted specific biomarkers of immune profile, immune contexture, tumor-infiltrating lymphocytes (TIL), macrophage polarization, and T cell status via the PhenoImager® HT platform. Open-source whole slide image analysis software QuPath was employed for precise image analysis, including ROI segmentation, cell detection, classification, exploration of spatial interactions, and identification of distinct spatial signatures.
Results Our analysis revealed distinct spatial relationships within various tumor types, quantifying immune cell distributions and their interactions. The ultrahigh-plex data correlated with high-throughput signature panel analyses, thus paving a new simplified way for targeted identification and development of predictive spatial signatures for immunotherapy outcomes.
Conclusions The combined use of ultrahigh-plex discovery panels, high-throughput signature panels, and deep-learning image analysis provides a comprehensive understanding of cellular interactions in the tumor microenvironment. This integrated approach, utilizing Akoya's end-to-end workflows, accelerates the identification of predictive spatial biomarker signatures across various human tissue samples.

#5505 Automating a spatial profiling workflow to explore the effects of hypoxia in the tumor microenvironment in head and neck cancer.

D. Mason[1], K. Teplitz[2], **J. R. Mansfield**[1], K. Hunter[3], J. Campos[3], J. Brooks[4];
[1]Visiopharm, Horsholm, Denmark, [2]NanoString Technologies, Seattle, WA, [3]Propath UK, Hereford, United Kingdom, [4]University of Birmingham, Birmingham, United Kingdom

Head and neck cancer (HNC) is a heterogeneous group of malignancies that arise from the mucosal surfaces of the upper aerodigestive tract. The tumor microenvironment (TME) of HNC is characterized by the presence of immune cells, stromal cells, and extracellular matrix components. A key feature of the TME is hypoxia, which promotes tumor growth, invasion, and metastasis by altering the expression of genes involved in angiogenesis, cell survival, and metabolism. Understanding the complex interplay between hypoxia and immune infiltrates in the TME of HNC is crucial for the development of novel therapeutic strategies for the treatment of this disease. Whole transcriptome analysis by digital spatial profiling is an excellent method of probing the TME, but assessing large cohorts can be time consuming. Automating a profiling workflow to reduce hands-on time and region of interest (ROI) selection bias will enable exploration of large cohorts to identify mechanisms of action, potential drug targets, and biomarkers.

We developed an optimized spatial multi-omic workflow to enable high-throughput spatial analysis on GeoMx® Digital Spatial Profiler (DSP) using the Whole Transcriptome Atlas (WTA) and immuno-fluorescent morphology markers: SYTO82 (nuclei), CAIX (hypoxia), pan-cytokeratin (epithelium), CD3 (T-cells). A.I.-based analysis (Oncotopix® Discovery) of serial section H&E images and GeoMx IF images was developed to identify ROIs for GeoMx collection. Immune hot and cold selection used leukocyte density; tumor/stromal interface selection used epithelial areas. Areas of illumination (AOI) were chosen using concentric CAIX expression gradients. Integrated analysis of digital images using Oncotopix Discovery and the whole transcriptome was done to assess the above TME compartments.

Automated ROI placement based on tumor/stroma, hypoxia and immune infiltration and AI /Deep Learning based AOI segmentation reduced AOI selection time and improved accuracy of tissue compartment enrichment, especially between samples and tissue types. Automated development of hypoxia gradient-based AOI enabled a selection strategy not possible in the standard DSP software. Cell phenotyping using IF morphology scan was used to supervise cell deconvolution. DSP results correlated well with patient outcomes.

This work shows that ROI-based spatial analyses can be used to explore the effects of hypoxia levels on immune infiltration in HNC. Automated AI-based ROI selection provides a means of sampling relevant tumor subtypes based on hypoxia and immune infiltrate criteria in an unbiased, reproducible manner, and can provide a standardized, automated method for selecting ROIs and segmenting AOIs across a cohort of mixed tissue types and pathological subtype, improving throughput.

#5506 HOST-Factor: A comprehensive platform for single-cell highplex immunofluorescence staining, digital imaging, spatial mapping, and quantitative analysis of the tumor microenvironment.

J. Franco-Barraza[1], F. Schneider[2], R. Norre-Sorensen[2], R. Ahrenkiel-Lyngby[2], C. Brown[1], D. Winkowski[2], **J. R. Mansfield**[2], E. Cukierman[1];
[1]Fox Chase Cancer Center/Lewis Katz School of Medicine, Philadelphia, PA, [2]Visiopharm, Horsholm, Denmark

Solid tumor complexity extends beyond the genetic and functional landscapes of heterogenous cancer cells, encompassing the tumor microenvironment (TME). Elucidating the TME's complexity requires a comprehensive assessment of its cellular composition, functional states, and spatial distributions. We developed the Harmonic Output of Stromal Traits (HOST) to identify TME cells, and the HOST-Factor to quantify their functional states. The HOST-Factor is a numerical value that reflects the relative contribution of cancer-associated fibroblasts (CAFs) to tumor-suppressive or tumor-promoting functions.
Our workflow combines automated cycling highplex immunofluorescent microscopy with artificial intelligence (AI)-guided image analysis. This generates HOST-Factor values for each identified TME cell within selected regions of interest, providing spatial distribution data. The TME signature encompasses 15 immune cells and 14 CAF antibody-detected biomarkers.
We applied our workflow to ten human pancreatic cancer specimens, generating OME-TIFF output images. This cancer model was used due to its significant TME makeup. The 29 highplex AI-based digital image analysis was conducted using the Phenoplex™ workflow from Visiopharm. The workflow included deep-learning-based tissue morphologic and cellular segmentations, cellular phenotyping, and integration of spatial/location data. Biomarker subsets were visualized, and a user-trained algorithm was used for tissue segmentation. Nuclear segmentation was done using a pre-trained algorithm on a DAPI-labeled DNA channel. Cellular phenotyping was performed using thresholds based on visual assessment and confirmation of positivity. Spatial neighborhood plots and metrics, heatmaps and partitioned t-SNE plots were generated for the dataset for downstream analysis. Importantly, the workflow's visualization templates, pre-trained nuclear/cytoplasm segmentation tools, and neighborhood plots and metrics, are reusable and fully customizable for new datasets.
Using HOST-Factor values, we successfully classified cancer and TME cells, along with their functional states, and spatial distributions.
This AI-based computational approach and user-friendly workflow provides a simple and effective way to obtain single-cell information from multiplex immunofluorescence images, making spatial phenotyping of several cell populations in tissues more accessible to researchers, providing a fully amendable means for future clinical translation.

#5507 High-resolution spatial atlas reveals insight into spatial landscape of lung cancer and chronic lung diseases.

R. Nandigama[1], B. Cheikh[2], J. Nabhanizadeh[1], F. Grimminger[1], W. Seeger[1], N. Jhaveri[2], S. Savai Pullamsetti[1], **R. Savai**[1];
[1]Justus Liebig University, Giessen, Giessen, Germany, [2]Akoya Biosciences, Massachusetts, MA

Background: Patients with lung cancer often have a high prevalence of severe comorbidities, primarily due to the significant correlation with cigarette smoking and the aging process. Dysregulations of the immune response are the cause of chronic inflammatory diseases such as chronic obstructive pulmonary disease (COPD), pulmonary arterial hypertension (PAH), pulmonary fibrosis (PF) and lung cancer. In addition, the lung microenvironment in these chronic inflammatory diseases has not yet been sufficiently investigated. Therefore, we aimed to investigate the spatio-temporal localization and cellular distribution in the lung microenvironment and to compare lung cancer with the concomitant diseases of lung cancer.
Methods: FFPE lung sections, each 3µm in thickness, were collected from patients with diagnoses of lung cancer, COPD, PAH, PF, and from healthy donors, with three samples taken for each category. These sections were subsequently imaged using the PhenoCycler®-Fusion system, utilizing a comprehensive panel of 45 antibodies, including immune, epithelial, vascular, proliferation and apoptosis markers. The first step of the analysis workflow consists of cell segmentation using a fine-tuned deep learning model leading to a total of 5.2 million cells across the whole dataset. Protein expressions were then calculated from the segmented cells, and unsupervised clustering was performed based on the normalized expression values. The resulting clusters were manually annotated into 16 cell phenotypes based on their protein expression patterns as displayed on a hierarchical clustering heatmap. The percentages of cell phenotypes were then calculated for each sample and compared between disease groups. Furthermore, the spatial proximity and cellular neighborhood analyses were performed to study the spatial organization of the different cell phenotypes in the tissues.
Results: Quantitative assessment revealed unique characteristics specific to each disease, identified by the varying abundance of different immune cell subtypes. Additionally, when comparing lungs from healthy donors with those affected by lung diseases, notable differences were observed in the spatial arrangement of immune cells and their proximity to lung blood vessels.
Conclusions: This study presents the first architectural map of lung cancer, COPD, PAH, and PF linking various immune cell types to their spatial location within the tissue. Such in-depth spatial analyses will aid in comprehending the spatial and temporal interplay within the lung's microenvironment in diverse lung conditions, as well as in developing targeted therapies for specific cell types.

#5508 Single-cell spatial landscape of the mutation-specific human lung tumor immune microenvironment.

R. Nandigama[1], B. Cheikh[2], N. Ma[2], J. Wilhelm[3], L. Klotz[4], F. Eichhorn[4], M. Kriegsmann[4], M. Bartkuhn[1], J. Nabhanizadeh[1], S. Seidel[1], T. Stiewe[5], A. Stenzinger[6], A. Weigert[7], M. Looso[8], F. Grimminger[1], W. Seeger[1], S. Savai Pullamsetti[1], N. Jhaveri[9], H. Winter[4], **R. Savai**[1];
[1]Justus Liebig University, Giessen, Giessen, Germany, [2]Akoya Biosciences, Massachusetts, MA, [3]Justus Liebig University Giessen, Giessen, Germany, [4]Thoraxklinik at the University Hospital, Heidelberg, Germany, [5]Philipps-Universitat, Marburg, Marburg, Germany, [6]Universitatsklinikum, Heidelberg, Heidelberg, Germany, [7]Goethe-University, Frankfurt, Frankfurt, Germany, [8]Max Planck Institute for Heart and Lung Research, Bad Nauheim, Germany, [9]Akoya Biosciences, Massachusetts, Germany

Background: Therapies targeting immune checkpoint have significantly transformed the treatment of several cancers, including lung cancer. However, only 20% of lung cancer patients show a response to immunotherapies. KRAS and EGFR mutations are significant factors in the development and progression of lung cancer and its response to immunotherapy. Hence, it's vital to understand intra-tumoral heterogeneity, the makeup of the Tumor Microenvironment (TME), and the cellular interactions in tumors with KRAS and EGFR mutations to uncover new insights.
Methods: Lung cancer tissues from 200 patients were collected, focusing on KRAS and EGFR mutation statuses, specifically KRAS+/EGFR-, KRAS-/EGFR+, and KRAS-/EGFR-. For each patient, two samples were taken, resulting in a total of 400 tissue microarray (TMA) cores. These samples were imaged at single-cell resolution using the PhenoCycler®-Fusion system, which employed a 42-plex antibody panel targeting immune, tumor, proliferation, and apoptosis markers. The first step in the analysis was cell segmentation, performed using a fine-tuned deep learning model. This process successfully segmented a total of 2.16 million cells across the entire collection of samples. Following this, the protein expressions for each cell were calculated, and unsupervised clustering was performed, resulting in 36 distinct clusters, that were manually annotated into 14 cell phenotypes. The proportions of these cell phenotypes were then quantified for each of the 400 TMA cores and compared across the three mutation groups. The analysis also included the spatial proximity and cellular neighborhoods in relation to these mutation groups.
Results: Quantitative analysis focusing on the relative abundance of cell types revealed that the ratio of tumor cells to immune cells was significantly lower in KRAS-/EGFR- tumors compared to those with KRAS+/EGFR- and KRAS-/EGFR+ mutations. Furthermore, the percentages of Regulatory T cells (Tregs) and M1 Macrophages were significantly higher in the KRAS+/EGFR- group compared to the KRAS-/EGFR+ group. Spatial proximity analysis indicated that in the KRAS-/EGFR+ group, M2 Macrophages were significantly closer to Cytotoxic T cells and Helper T cells compared to the distances observed in the other two groups. Moreover, neighborhood analysis identified 20 distinct cellular neighborhoods, each defined by specific cell-cell interactions. COX hazard analysis based on these cellular neighborhoods demonstrated notable variations among the three mutation groups, which are linked to differences in patient outcomes.
Conclusions: Through single-cell spatial phenotyping, this work has shown that the spatial immune landscape of lung tumors is influenced by KRAS and EGFR mutation statuses. This presents a novel opportunity to enhance our understanding of the spatial structure of lung cancer and to identify more effective therapeutic targets.

TUMOR BIOLOGY: Tumor Microenvironment of Metastasis
Poster Session

#5512 Cerebral endothelial FAK paradoxically inhibits brain metastasis *in vivo*.

S. Noda-Narita, A. Aiba;
The University of Tokyo, Tokyo, Japan

Introduction: In cancer metastasis in the trunk, the secreted proteins from tumors, such as VEGFs and TNF-α, activate focal adhesion kinase (FAK) in vascular endothelial cells (VECs). The activated FAK promotes VE-cadherin phosphorylation and the expression of cell adhesion molecules, and it facilitates the extravasation of cancer cells. In the cerebral blood vessels, the VECs maintain very strong cell adhesion supported by the surrounding pericytes and astrocytes. The strong barrier of cerebral VECs is called the blood-brain barrier (BBB) and is regulated differently from trunk VECs. Although the role of FAK in trunk metastasis is shown in many studies, its importance in brain metastasis is not verified. In this study, we focused on the role of the cerebral endothelial FAK and compared the role of FAK in brain metastasis with that in trunk metastasis.

Methods: We generated tamoxifen-inducible VEC-specific FAK knockout (FAK-cKO) mice (*VEcad-Cre*^{ERT2}*; Ptk2-flox/flox*) and brain metastatic (BrM) cell lines of Ex3LL (murine lung cancer cell line). We intracardially injected BrM cells of Ex3LL into the FAK-cKO mice and analyzed the tumor development using *in vivo* bioluminescence imaging and a CUBIC tissue clearing system. We also analyzed the intracranially injected mice of the parental and BrM cell lines to evaluate the tumor angiogenesis, which is reported to be promoted by the endothelial FAK.

Results: Although FAK-cKO in VECs has been reported to inhibit lung metastasis, brain metastasis was accelerated in FAK-cKO mice compared with control mice. The number of brain metastatic sites increased in FAK-cKO mice, but there was no difference in the individual tumor size. It suggests that the brain metastasis was promoted by FAK-cKO, but that the proliferation of brain metastasis was not promoted by FAK-cKO. Blood vessel density was decreased with irregular shape in the brain tumors of FAK-cKO mice, suggesting that the angiogenesis was inhibited by FAK-cKO. It indicates that the angiogenic function of endothelial FAK in the brain vasculature was not different from that in the trunk.

Conclusion: FAK-cKO in VECs exacerbated the brain metastasis of the BrM cells although it has been reported to inhibit the metastasis in the trunk. FAK-cKO in VECs decreased tumor angiogenesis both in the brain and the trunk. It suggests that the regulatory mechanism of cell adhesion and the FAK function in the brain vasculature is partly different from that in the other organs in the body trunk. We need further investigation to elucidate the function of endothelial FAK in brain metastasis.

#5513 Sexual differences in the aged melanoma tumor microenvironment dictates metastasis and therapeutic responses.

Y. Chhabra[1], M. Fane[2], S. Pramod[1], L. Hueser[1], D. Zabransky[3], V. Wang[1], E. Kumah[1], A. Carey[1], E. Harper[1], M. Ramos Rocha[1], A. Weeraratna[1];
[1]Johns Hopkins Bloomberg Sch. of Public Health, Baltimore, MD, [2]FoxChase Cancer Center, Philadelphia, PA, [3]Johns Hopkins University, Baltimore, MD

There is documented sex disparity in cutaneous melanoma incidence and mortality, increasing disproportionately with age and in the male sex. However, the underlying mechanisms remain unclear; while biological sex differences and inherent immune response variability have been assessed in tumor cells, the role of the microenvironment surrounding the tumor, contextually in aging, has been overlooked. We find that skin fibroblasts undergo age-mediated changes in their proliferation, senescence, ROS levels and stress response that vary with sex. We find that aged male fibroblasts selectively drive an invasive and slow-cycling phenotype in melanoma cells in vitro by increasing AXL expression. This is also evident in syngeneic mouse models where metastasis is increased in aged male mice. Mechanistically, intrinsic aging in male fibroblasts coupled with elevated ROS promotes EZH2 decline thereby increasing BMP2 secretion, which in turn drives the slower-cycling, highly invasive, and therapy-resistant melanoma cell phenotype, characteristic of the aged male TME. Inhibition of BMP2 activity blocks the emergence of the invasive phenotype and sensitizes melanoma cells to BRAF/MEK inhibition. Our data provides an integrated view of how age and sex of the host contributes to melanoma progression and therapy responses. Bridging this knowledge gap will improve patient stratification and assist in tailoring the therapy to the individual.

#5514 Crosstalk between prostatic epithelial cells and the tumor microenvironment drives cancer progression and metastasis.

D. Yanushko[1], B. German Falcon[2], C. Keime[1], T. Ye[1], C. Thibault-Carpentier[1], D. Metzger[1], G. Laverny[1];
[1]IGBMC - Univ. of Strasbourg, Illkirch, France, [2]Center of Prostate Disease Research, Bethesda, MD

Prostate cancer is a heterogeneous disease with a slow progression and a highly variable clinical outcome. Recent advances in the clinical handling of localized prostate cancers resulted in an almost 100% 10-year survival, but no curative treatment is currently available for metastatic disease. Thus, understanding the molecular mechanisms of progression of primary tumors to metastasis is crucial to develop new therapeutic strategies. While tumorigenesis initiates in prostatic epithelial cells, various cell types, including cancer associated fibroblasts (CAFs), immune and endothelial cells produce extra-cellular matrix and secrete signaling molecules that might contribute to tumor progression. However, the complex communication network driving tumor progression is poorly characterized. As the tumor suppressors *PTEN* and *TP53* are among the most frequently altered genes in prostate cancer, we generated genetically engineered mice with *Pten and Trp53* selective inactivation in prostatic epithelial cells at adulthood. Their analysis revealed that they develop precancerous lesions that progress to invasive and metastatic tumors. Spatial transcriptomic and single-cell analyses of *Pten*- and *Trp53*-deficient prostatic tumors identified the presence of a cancer cell population exhibiting cell plasticity driven by Jak/Stat3 signaling and induced by CAF-produced IL6. In addition, these tumors exhibit a hypoxic core and an immune infiltrate dominated by neutrophils. Inhibition of the hypoxic signaling reduced immune infiltration in primary tumors and their metastatic potential, but did not induce apoptosis of *Pten*- and *Trp53*- deficient epithelial cells, in contrast to those of *Pten*-deficient tumors. These results underline the importance of the tumor genomic background for therapeutic intervention. Taken together, our work highlights the key role of the tumor microenvironment in driving prostate cancer progression and uncovers new vulnerabilities of this disease.

#5515 Low body mass index (BMI) induces neuronal NPY and promotes brain metastasis of lung cancer.

A. Tyagi, S.-Y. Wu, R. Deshpande, K. Wu, L. Liu, K. Watabe;
Wake Forest Baptist Comprehensive Cancer Ctr., Winston-Salem, NC

Brain metastases (BrMs) are a common occurrence in lung cancer with a dismal outcome. To develop a more effective therapeutic strategy, it is crucial to understand the underlying pathological mechanism of brain metastasis. Recent clinical data has unveiled a significant association between low body mass index (BMI) and an increased risk of brain metastasis in lung cancer patients, leading to reduced survival rates compared to other primary tumors. However, the molecular mechanism underlying this paradoxical relationship, often referred to as the "obesity paradox," in the context of lung cancer mortality presents a complex and intriguing puzzle and warrants in-depth investigation. Here, we examined biological mechanism of how low BMI promotes lung cancer brain metastasis. In this study, we conducted a retrospective pan-analysis of 5,516 patient cohorts with brain metastasis originating from lung, breast, melanoma, and renal cancers with their BMI status. We found that lung cancer patients with low BMI have significantly higher brain metastatic incidence compared to the high BMI patients, in contrast to breast, melanoma, and renal cancers. Furthermore, we found that low BMI plays a pivotal role in mediating neuron activation within the brain and that the secretion of neuronal neuropeptide Y (NPY), a protein involved in appetite and energy homeostasis via GHSR-receptor manner, promotes metabolic switching through NPY/NPY5R axis in the tumor cells in the brain thereby enabling metastasis. Elevated levels of neuronal NPY in the brains of cancer-free subjects with low BMI suggest its potential utility as a promising prognostic biomarker for identifying the increased risk of metastatic disease in lung cancer patients with low BMI. We also demonstrated that reversing low BMI or blocking the NPY/Y5R interactions effectively abrogated brain metastasis in our animal model. Our findings suggest a novel pro-metastatic role of low BMI-induced NPY in the progression of brain metastasis. We emphasize the importance of elucidating the clinical implications of this relationship to develop an updated intervention strategy for the clinical care of patients with lung cancer and low BMI.

#5516 Aberrant activation and perpetuation of lung wound response facilitates osteosarcoma metastasis.

J. B. Reinecke, A. C. Gross, M. Cam, L. Jimenez Garcia, M. V. Cannon, R. D. Roberts;
Nationwide Children's Hospital, Columbus, OH

Introduction: The mechanisms that allow tumor cells to integrate with unfamiliar parenchymal cells within hostile distant tissues during metastatic colonization remain poorly defined. Nowhere are these mechanisms more important than in osteosarcoma-a pediatric bone tumor where metastases cause nearly all osteosarcoma related deaths and occur almost exclusively in the lung. The purpose of this study was to define the cellular and molecular events that facilitate osteosarcoma lung colonization to devise novel therapeutic strategies that prevent and treat metastasis.
Experimental Approach: We generated experimental lung metastases using a panel of immunocompetent murine and human xenograft osteosarcoma models. A combination of immunohistochemistry, single cell RNA sequencing, and spatial transcriptomics were used to define the metastatic niche. Relevant findings were validated in human primary tumor, lung metastasis, and normal lung tissue specimens.
Results: Disseminated osteosarcoma cells physically associate with alveolar epithelial cells and trigger changes in surrounding epithelial cells that are characteristic of the aberrant, non-resolving wound response seen in non-malignant lung diseases such as idiopathic pulmonary fibrosis (IPF). This process drives the accumulation of fibrotic epithelial cells and scar-associated macrophages confined within a dense fibronectin-based matrix. Anti-fibrotic tyrosine kinase inhibitors used to treat patients with IPF (nintedanib) prevent the observed fibrogenic changes and inhibit metastatic colonization. Epithelial-osteosarcoma paracrine signaling is dominated by an inflammatory cytokine milieu that facilitates this transition towards fibrosis. Blocking one of the dominant paracrine signals with a recombinant IL1 receptor antagonist (anakinra) has similar effects on both fibrosis and metastatic colonization.
Conclusions: Our study demonstrates that tumor interactions with host stromal cells are critical for metastasis. Metastatic colonization requires transformation of the local lung microenvironment into a fibrotic, non-resolving, cytokine-rich, wound-like state that is both provoked and sustained by tumor-epithelial interactions. These insights have identified several potential therapeutic approaches to prevent metastatic colonization and treat established metastases.

#5517 Chronic stress causes metastasis via neutrophil-mediated changes to the microenvironment.

X.-Y. He[1], Y. Gao[2], D. Ng[2], E. Michalopoulou[2], S. George[2], J. M. Adrover[2], L. Sun[2], J. Albrengues[2], J. Da?ler-Plenker[2], X. Han[2], L. Wan[2], X. S. Wu[2], L. S. Shui[2], Y.-H. Huang[2], B. Liu[2], C. Su[3], D. L. Spector[2], C. R. Vakoc[2], L. VanAelst[2], M. Egeblad[4];

[1]Washington University School of Medicine in St. Louis, St. Louis, MO, [2]Cold Spring Harbor Laboratory, Cold Spring Harbor, NY, [3]Weill Cornell Medicine, New York, NY, [4]Johns Hopkins University School of Medicine, Baltimore, MD

Chronic stress is associated with increased risk of metastasis and poor survival in cancer patients, yet the reasons are unclear. We show that chronic stress increased lung metastasis from disseminated cancer cells 2- to 4-fold in mice. Chronic stress significantly altered the lung microenvironment, with fibronectin accumulation, reduced T cell infiltration, and increased neutrophil infiltration. Depleting neutrophils abolished stress-induced metastasis, indicating their critical role. Chronic stress shifted neutrophils' normal circadian rhythm, and, via glucocorticoid release, caused increased neutrophil extracellular trap (NET) formation. Importantly, in mice with neutrophil-specific glucocorticoid receptor deletion, chronic stress failed to increase NETs and metastasis. Furthermore, digesting NETs with deoxyribonuclease (DNase) I prevented chronic stress-induced metastasis. Together, our data show that glucocorticoids released during chronic stress cause NET formation and establish a metastasis-promoting microenvironment. Therefore, NETs could be targets for preventing metastatic recurrence in cancer patients, many of whom will experience chronic stress due to their disease.

#5518 Tumor immune microenvironment of bone marrow metastasis in patients with solid tumor.

A. Saijo[1], K. Kinowaki[1], K. Yamamoto[1], S. Watanabe[1], K. Takemura[1], T. Yamaguchi[1], Y. Tanabe[1], K. Suyama[1], H. Yano[2], Y. Komohara[2], Y. Miura[1];
[1]Toranomon Hospital, Tokyo, Japan, [2]Graduate School of Medical Sciences, Kumamoto University, Kumamoto, Japan

Background: The tumor immune microenvironment plays a crucial role in tumor progression and treatment outcomes, both at the primary tumor site and metastatic sites. Metastatic growth within the bone marrow (BM) is relatively infrequent. Despite its unique immunological characteristics, there is a paucity of research on tumor immune microenvironment in the context of BM metastasis, particularly in patients with solid cancer. This study aims to elucidate the dominant immune cell populations within the BM of patients with solid cancer BM metastasis.
Materials and Methods: Patients with solid tumors, who underwent BM examinations (aspiration and/or biopsy) for suspected BM metastasis at our institution between 2016 and 2023 were extracted from the database of pathology. To evaluate BM immune microenvironment in patients with BM metastasis originating from solid tumor, we performed flow cytometry analysis of myeloid and lymphoid subsets using bone marrow aspiration. Myeloid-derived suppressor cells (MDSCs) were defined as $CD33^{+}CD14^{+}HLA\text{-}DR^{-/low}$. Additionally, a control group was established, consisting of patients in whom BM metastasis were pathologically ruled out.
Results: The study involved the BM examinations in 39 patients, 22 of whom were pathologically diagnosed with BM metastasis. No substantial difference in age or gender were observed between patients with or without BM metastasis. However, the incidence of bone metastasis was significantly higher in the BM metastasis group compared to the non-BM metastasis group (90.9 vs. 47.1%, P=0.004). The median duration from the initial diagnosis of metastatic state to the occurrence of BM metastasis was 14.5 days (range 0 - 2194 days) for patients with BM metastasis, whereas it was 170 days (range 0 - 1304 days) for those without BM metastasis. Among the patients who underwent BM examinations, flow cytometry analysis was available in 13 patients with BM metastasis and 11 patients without BM metastasis. Our analysis revealed that a substantial increase in the mean percentage of MDSCs ($CD14^{+}HLA\text{-}DR^{-/low}$) in $CD14^{+}$ monocytes of BM aspirates from patients with BM metastasis compared to those without (28.06 vs. 8.09%, P=0.0005). Additionally, while not statistically significant, the mean percentage of $CD3^{+}$ T cells in the total live cell population appeared to be higher in patients with BM metastasis compared to those without (10.26 vs. 6.67%, P=0.0622). In terms of lymphoid subsets, CD4/8 ratio was significantly elevated in patients with BM metastasis as opposed to those without BM metastasis (1.57 vs. 0.76%, P=0.0472).
Conclusion: The tumor immune microenvironment in BM metastasis was skewed toward immunosuppressive state. Further investigations are warranted to understand the involvement of other immune cells that also suppress immune system, such as regulatory T cells and M2 macrophages.

#5519 Enlarged metastasis-free tumor-draining lymph node is a marker of tumor invasion in local tissues with an active NK cell-mediated immunity.

Z. Wan, **H. Yu**;
The Sixth Affiliated Hospital of Sun Yat-sen University, Guangzhou, China

Background: Colorectal cancer (CRC) is the third most common cancer worldwide, accounting for about 10% of all new cancer cases. The tumor-draining lymph node (TDLN) is a key site for the development of anti-tumor immunity that has been reported to be involved in both CD8+ T and NK cells. As a major role of innate immunity, NK cells can produce IFN-γ, perforin and granzyme to eliminate tumor cells in the early stages of cancer development. This study aimed to investigate the difference of clinicopathological and immunological profiles in local tissues between CRC patients with enlarged and non-enlarged metastasis-free TDLNs.
Methods: The patient cohort was obtained from the NEPDC cohort (No. 2015CB554000). A total of 45 patients with pathologically confirmed stage I-II colorectal cancer were included in this study. Based on the MRI, these patients were divided into enlarged and non-enlarged TDLN groups (lymph nodes >/= 5mm and lymph nodes < 5mm). We collected the tumor tissue and tumor-adjacent normal tissue that was 2 cm away from the tumor lesion. The genomic DNA of the tumor and tumor-adjacent normal tissues was treated with bisulfite and analyzed with the EPIC methylation array. The MeTMEC algorithm based on the methylation profile estimated subsequent cell abundance in these patient tissues.
Results: The study sample was comprised of 22 enlarged TDLN and 23 non-enlarged TDLN patients. There were 4 T1-T2 and 18 T3-T4 patients in the enlarged TDLN group, with 12 T1-T2 and 11 T3-T4 patients in the non-enlarged TDLN group. The proportion of T3-T4 patients in the enlarged TDLN group was higher than that in the non-enlarged TDLN group (p=0.017, Chi-squared test), suggesting an advanced invasion in the local tissue of patients with enlarged TDLN. Then, the abundance of monocytes, dendritic cells, macrophages, neutrophils, eosinophils, Treg cells, naive T cells, memory T cells, CD8+ T cells, NK cells, and B cells in the tumor and tumor-adjacent normal tissues were inferred with the MeTMEC algorithm by using DNA methylation profile. In the T1-T2 subset, we found that the infiltration of NK cells in the tumor-adjacent normal tissues was significantly more abundant in the enlarged TDLN group compared with the non-enlarged TDLN group (p=0.021, t-test), suggesting an active immune response of NK cells for potential local tumor control. No significant difference in other immune cells was observed between the two groups.
Conclusion: Enlarged TDLN indicates an advanced invasion of tumors in local tissues with an active NK cell-mediated immunity. Our findings suggest that enlarged metastasis-free TDLN might be a promising marker for NK cell-based cancer immunotherapy.
Key words: Colorectal Cancer, Lymph Nodes, Natural Killer Cells

#5520 β2 adrenergic receptor signaling promotes colorectal cancer liver metastasis.

Y. Zhang, J. Chen, T. Chan, H. Wang, J. Lu, J. Li, J. Zhou;
The Chinese University of Hong Kong, Hong Kong, Hong Kong

Liver is the most common site for cancer metastases, which may be attributed to the hepatic immunosuppressive microenvironment. Recent studies have highlighted the immunomodulatory and tumor-supportive roles of neurotransmitter-receptor signals in various cancers. Given that various neurotransmitter receptors are expressed in the liver, we aimed to investigate their possible involvement in the metastatic-prone liver microenvironment. Single-cell RNA sequencing analysis identified *ADRB2*, which encodes β2-adrenergic receptor (β2-AR), as the top-upregulated neurotransmitter receptor gene in colorectal cancer (CRC) and liver metastasis in patients with CRC liver metastasis (CRLM). Co-immunofluorescence (co-IF) staining confirmed the colocalization of β2-AR with myeloid cell marker CD11b instead of T cell marker CD3 and NK cell marker CD56 in patients with CRLM. Consistently, we observed the upregulation of CD11b/β2-AR double-positive cells in the liver tissues from mice bearing CRC or CRLM compared to naïve mice through co-IF staining. High-dimensional flow cytometry analysis further revealed that β2-AR was mainly expressed in macrophages and myeloid-derived suppressor cells (MDSCs). Treatment of CRC-tumor bearing mice with pan β-AR inhibitor propranolol and β2-AR specific inhibitor showed a potential to reduce liver metastatic incidence without suppressing primary CRC. Mechanistically, β2-AR activation may upregulate the expression of *S100a8/9* to enhance the immunosuppressive activity of macrophages and MDSCs, thereby promoting CRC liver metastasis. Taken together, our findings reveal the potential of targeting β2-AR signaling for the prevention and treatment of liver metastasis.

This project is supported by the Hong Kong University Grants Committee through the General Research Fund (14104820, 14107622, 24110323) and the Strategic Seed Funding for Collaborative Research Scheme (SSFCRS) from the Chinese University of Hong Kong.
Conflict of interest: The authors declare no conflict of interest.

#5521 Nicotine promotes perineural brain metastasis of lung cancer by activating GABAergic neurons.

S.-Y. Wu[1], A. Tyagi[1], R. P. Deshpande[1], K. Wu[2], E. C. Smith[1], K. Watabe[1];
[1]Wake Forest University School of Medicine, Winston-Salem, NC, [2]University of North Carolina Greensboro, Greensboro, NC

Tobacco smoking significantly increases the incidence of brain metastasis. However, the pathological mechanism by which smoking promotes brain metastasis through modulating brain microenvironment is yet poorly understood. We previously showed that the incidence of brain metastasis is associated with nicotine intake. Nicotine enhanced polarization of M2 pro-tumor microglia, which promoted brain metastasis. In addition to the immune surveillance role, microglial cells also control neuronal synapse formation. Microglial cells promote neuron synapse formation in the developing brain, whereas microglia depletion suppresses synapse density. Furthermore, microglia-secreted microRNAs (miRNAs) have been shown to promote synaptic formation by targeting synapse-related genes of the DKK-Wnt family. Neurons are one of the most abundant cell types in the brain, and they are highly specialized for cell-to-cell signal activation. However, little is known about the roles of neurons in brain metastasis of lung cancer. We hypothesize that nicotine stimulates microglia to secrete exosomal miR-32-3p, which promotes brain metastasis by augmenting GABAergic synaptic formation and hence releasing GABA that serves as a metabolic substrate to fuel tumor cell growth. We also hypothesize that inhibiting the GABA transporter of tumor cells suppresses brain metastasis by blocking the GABA shunt. We found that lung cancer patients with a smoking history had significantly higher synaptic formation and the expression of GABA transporter in brain metastasis. To investigate the effect of smoking and nicotine intake on brain metastasis *in vivo*, mice were intracardially transplanted with lung cancer brain metastasis cells (H2030BrM and PC9BrM) followed by administration of nicotine or cigarette smoke exposure in a smoking chamber. We found that smoking and nicotine increased M2 microglia polarization, synaptic formation, and the expression of GABA in mouse brain metastasis. Furthermore, nicotine increased the secretion of miR-32-3p from nicotine-pretreated microglia, which promoted GABA release from GABAergic neurons. Treating H2030BrM and PC9BrM cells with conditioned medium (CM) obtained from neurons exposed to CM derived from nicotine-treated microglia exosomes resulted in increased tumor growth through the activation of the GABA shunt pathway. Blocking GABA transporter 1 (GAT1) by CRISPR/Cas9 or a small molecule of GAT1 inhibitor suppressed the GABAergic neuron-induced tumor progression. Our results indicate that nicotine-activated microglia enhanced GABA release from neurons followed by the promotion of GABA shunt in tumor cells and that a GAT inhibitor serves as a promising therapeutic tool for the treatment of lung cancer patients with brain metastasis.

#5522 Elucidating the role of P-selectin/P-selectin ligand-1 axis in lung cancer brain metastasis.

K. Salomon[1], E. Yeini[1], N. Frommer[1], I. Kamer[2], J. Bar[2], I. Barshack[2], R. Satchi-Fainaro[1];
[1]Sackler Faculty of Medicine Tel Aviv Univ., Tel-Aviv, Israel, [2]Sheba Medical Center, Tel-Aviv, Israel

Lung cancer (LC) stands as a prominent cause of cancer-related mortality. Brain metastasis (BM) is a common occurrence in LC, constituting nearly 50% of all BM cases with the brain emerging as the preferred site for LC metastasis. Unfortunately, current LCBM treatment options yield limited success, as reflected in the median survival of BM patients at 7.8 months. Consequently, there is an imperative need for novel and more efficacious therapeutic approaches targeting LCBM. Evidence suggests that brain microenvironment cells, particularly microglia and tumor-associated macrophages (TAMs), play a pivotal role in facilitating the colonization and growth of LCBM. Previous investigations from our lab have identified the involvement of the P-selectin/P-selectin glycoprotein ligand-1 (SELP/PSGL-1) axis in microglia/TAMs immunophenotypes, promoting pro-tumorigenic activity. This led us to explore the role of the SELP/PSGL-1 axis in the interactions between LCBM cells and the brain microenvironment[1]. Thus, we conducted Immunostaining on human tissue samples, revealing increased expression of SELP, PSGL-1, PD-1, PD-L1, IBA-1, and CD68 in LCBM tissues. Simultaneously, we employed advanced 3D models to investigate the intricate interactions between cancer cells and microglia/TAMs. Actively inhibiting the SELP/PSGL-1 axis with pharmacological agents led to a significant decrease in migration and invasion when LC cells were co-cultured with microglia and TAMs. Moreover, SELP inhibition prompted a shift in microglia/TAMs state towards an M1-like phenotype, enhancing the ability of CD4/CD8 cells to target cancer cells in our unique 3D LCBM models. This effect was further enhanced when co-treated with a PD-1 inhibitor, demonstrating a potential synergistic impact in targeting both pathways for therapeutic intervention. Our results suggest that combining SELP inhibition with other immunomodulators, including a small molecule PD-L1 inhibitor developed in our lab[2], could synergistically enhance both innate and adaptive anti-tumor immune responses. Taken together, this study may enhance our understanding of LCBM immunogenicity and contribute to the development of novel immunotherapeutic approaches that can improve patient outcomes.1.Yeini, E., *et al.* P-selectin axis plays a key role in microglia immunophenotype and glioblastoma progression. *Nat Commun* 12, 1912 (2021). 2. Acúrcio, R.C., *et al.* Therapeutic targeting of PD-1/PD-L1 blockade by novel small-molecule inhibitors recruits cytotoxic T cells into solid tumor microenvironment. *J Immunother Cancer* 10(2022).

#5523 granulocyte-colony stimulating factor secreted from cancer associated fibroblasts initiates tumorigenesis and metastasis in triple negative breast cancer.

N. Gotoh[1], Y. Tacheuchi[1], T. Murayama[1], R. Kashimura[1], K. Ikeda[2], K. Horie[2], S. Inoue[2], K. Okamoto[3];
[1]Kanazawa University Cancer Research Institute, Kanazawa, Japan, [2]Research Center for Genomic Medicine, Saitama Medical University, Saitama, Japan, [3]Teikyo University Advanced Comprehensive Research Organization, Itabashi-ku, Japan

Although cancer stem-like cells (CSCs) interact with cancer-associated fibroblasts (CAFs), it remains obscure how it occurs and what are the functional roles of this interaction. When patient-derived breast cancer cells (BCCs) were co-cultured with CAFs, significantly more spheroids were formed compared to those cells cultured alone. This suggests that CAFs produce soluble factors that increase the tumor-initiating ability of CSCs. Transcriptome analysis revealed that the expression of granulocyte colony stimulating factor (G-CSF) was highly upregulated in the conditioned medium of CAFs co-cultured with BCCs. Tumor-initiating ability was increased in the presence of G-CSF. Furthermore, G-CSF neutralizing antibody treatment suppressed tumorigenesis and bone metastasis in the patient-derived xenograft (PDX) model. These findings indicate that G-CSF secreted by CAFs induces CSCs to initiate tumors and metastasis. Inhibition of G-CSF would be a novel therapeutic target for breast cancer.

#5524 Identification of PAEP as an immune activity modulator to mediate the immune resistance in tumor metastasis.

Rand Gabriel M. Buenaventura[1], Weiping Chen[2], Shuling Zhang[1], Beverly Mock[1], Glenn Merlino[1], Yanlin Yu[1]

[1]Laboratory of Cancer Biology and Genetics, Center for Cancer Research, National Cancer Institute, National Institutes of Health, Bethesda, MD, [2]The National Institute of Diabetes and Digestive Kidney Diseases, National Institutes of Health, Bethesda, MD

Most cancer-related deaths are associated with the complex phenotypic behavior of metastasis, a process in which tumor cells spread from their initial site to distant sites. To successfully metastasize, the tumor cell will be required to make numerous adjustments and survive a series of stages involving intravasation, circulation in the blood or lymph system, extravasation, and growth at distant organs, and overcome the challenges of immunosurveillance. The tumor microenvironment is the ecosystem that surrounds and feeds the tumor. The molecular mechanism by which the metastatic tumors survive and escape from immune attack in the tumor microenvironment remains unclear. To study the molecular mechanism of interaction between metastatic tumors and the immune system in metastasis, we established immune-resistant metastatic models. We identified that PAEP, a progestogen-associated endometrial protein, is significantly upregulated in immune-resistant metastatic tumors compared with non-immune-resistant tumors. PAEP is a glycoprotein that inhibits cell immune function and plays an essential role in the pregnancy process. To examine the function of PAEP in tumor metastasis, we first introduced PAEP into non-immune resistant and poorly metastatic melanoma and rhabdomyosarcoma (RMS) cells. We found that overexpression of PAEP significantly promotes tumor metastatic potential of both melanoma and RMS cells in immunocompetent mice. Interestingly, there was no difference in metastasis between the control and overexpression groups in immunodeficient mice. These data suggest that PAEP may mediate tumor metastasis relating to host immunity. To further confirm the function of PAEP in tumor metastasis, we use CRISPR/Cas9 technology to knockout endogenous PAEP and will test the metastatic potential in different hosts. We will also investigate the molecular mechanisms using RNA sequencing and Digital Spatial Profiling (DSP) to analyze the metastatic samples. Our study will uncover a new mechanism for how tumors survive in the microenvironment and identify a novel target for the treatment of metastatic diseases.

#5525 Tissue-resident cytotoxic T cell infiltration predicts metachronous colorectal cancer metastasis.

R. Cohen[1], T. Lee-Pullen[1], T. Miller[1], S. Pirasteh[2], C. Platell[1], K. Meehan[1], K. Fuller[1], M. McCoy[1];
[1]University of Western Australia, Perth, Australia, [2]Western Diagnostic Pathology, Perth, Australia

Background: Identifying patients at high risk for metachronous colorectal cancer metastasis is essential for improving prognosis. The balance between host immune regulation and tumor immune evasion ultimately permits or prevents cancer progression. Lymphocytic infiltration in colorectal cancer can predict long-term clinical outcomes. However, these lymphocytes' origin, subtype and function have yet to be adequately explored. We investigated the association between the development of metastasis and $CD8^{\pm}$T cells expressing the integrin protein CD103, a marker of tissue-resident memory T cells.

Methods: In this retrospective, case-control matched study, we conducted multiplex immunofluorescence staining of tumor samples from 124 patients with colorectal cancer. Tissue microarrays containing representative cores of the central tumor, invasive margin, and adjacent normal tissue were immunostained for CD3, CD8, CD103, pSMAD3, and cytokeratin, using tyramide signal amplification. Cells were quantified using StrataQuest digital image analysis software, with intratumoral and stromal regions analyzed separately. Kruskal-Wallis one-way analysis of variance with subsequent Dunn's test for pair-wise comparisons was performed using the Bonferroni method of multiple-comparison correction.

Results: Central tumor and invasive margin $CD3^{\pm}$ densities were associated with synchronous metastasis. Compared to non-metastatic patients, those who went on to develop metachronous metastasis (n=42) had a low proportion of intra-epithelial $CD8^{\pm}CD103^{\pm}$ T cells at the central tumor (non-metastatic: 32.8%, IQR 15.0-42.7%; metachronous metastasis: 12.9%, IQR 2.08-28.4%; P = 0.013). Similarly, patients with metachronous metastasis had a low proportion of stromal $CD8^{\pm}CD103^{\pm}$ T cells at the invasive margin (non-metastatic: 3.51%, IQR 1.83-6.55%; metachronous metastasis: 1.75%, IQR 0.62-3.72%; P = 0.019). On multivariate Cox regression of histological features, amongst patients with metastasis, significant overall survival prognostic markers included a low proportional $CD8^{\pm}CD103^{\pm}$ T cell infiltration (HR 2.41, 95%CI 1.16-5.01, P = 0.019), mucinous features (HR 4.28, 95%CI 1.98-9.24, P < 0.001), and the presence of perineural invasion (HR 2.75, 95%CI 1.28-5.89, P < 0.001).

Conclusion: $CD8^{\pm}CD103^{\pm}$ lymphocytes may protect from the development of colorectal metastasis. Proportional $CD8^{\pm}CD103^{\pm}$ T cell infiltration is a promising prognostic marker in colorectal adenocarcinoma for the development of metachronous metastasis, and, amongst patients with metastasis, it is a prognostic marker of overall survival.

#5526 Activation of platelet-activating factor (PAF) in high-risk melanoma patients with nodal metastasis.

A. McMasters, J. Chariker, J. Y. Hwang, X. Yin, X. Ma, R. Xu, X. Zhang, J. W. Park, K. M. McMasters, **H. Hao**;
University of Louisville, Louisville, KY

Background: Platelet-activating factor (PAF) is one of the lipid mediators in ultraviolet-induced immunosuppression signaling. Sentinel lymph nodes (SLNs) are the first organs to receive lymphatic drainage via afferent lymphatic channels leading directly from the primary melanoma. In patients with nodal metastasis, it has been shown that the SLN has a profoundly immunotolerant microenvironment. We sought to determine whether lymphatic fluid signals, including PAF, may be involved in modulating the SLN immune microenvironment to favor melanoma metastasis.
Hypothesis: Upregulation of PAF can bind to its receptor on monocytes and activate downstream immunosuppressive chemokines, resulting in an immunosuppressed environment in SLNs that permits nodal metastasis and melanoma progression.
Methods: Lymphatic fluids, plasma samples, and SLN samples were collected from patients undergoing surgical excision of melanoma with SLN biopsy under an IRB-approved protocol. Metabolic analyses were performed on lymphatic fluids from high- versus low-risk patients by two-dimensional liquid chromatography system coupled with mass spectrometry (2D LC-MS). Single cell sequencing was done on single cell suspensions from SLN samples. Protein array was used to compare the cytokine and chemokine levels in plasma samples from high- versus low-risk melanoma patients. We compared two groups: low-risk (no SLN metastasis) and high-risk (with SLN metastasis).
Results: Lymphatic fluid PAF levels were 3-fold greater in high-risk melanoma patients compared with low-risk patients (p=0.0039). Macrophages were identified as the cell type with greatest PTAFR (platelet-activating factor receptor) expression by single cell sequencing. CCL17 levels in plasma samples from high-risk patients were significantly lower than in low-risk patients (p<0.05). These results suggest that increased PAF in lymphatic fluid may bind to PTAFR in SLN macrophages, inhibit chemokines (such as CCL17), and result in an immunosuppressive SLN environment to favor nodal metastasis and melanoma progression.
Conclusion: Lymphatic fluid PAF signaling may contribute to an immunotolerant microenvironment in the SLN that allows nodal metastasis and melanoma progression through downregulation of CCL17. Further studies will investigate whether this pathway can be exploited to therapeutic advantage.

#5527 Spatiotemporal analysis of growth factor regulation of osteosarcoma AKT and ERK signaling dynamics in an *ex vivo* lung metastasis model.

R. Makkawi[1], R. D. Roberts[2], J. Copperman[1], A. E. Davies[1];

[1]Knight Cancer Institute, Oregon Health & Science University, Portland, OR, [2]Abigail Wexner Research Institute at Nationwide Children's Hospital, Columbus, OH

In the present study, we investigated the relationships between spatiotemporal distribution of growth factors in the lung microenvironment, metastatic osteosarcoma cell signaling, and intratumoral gene expression heterogeneity. Osteosarcoma is an aggressive bone malignancy that commonly metastasizes to the lungs, resulting in significant patient mortality. During metastasis, disseminated cancer cells are exposed to microenvironment-derived growth factors that result in signaling pathway activation. Two such pathways are MAPK/ERK and PI3K/AKT, which regulate complex transcriptional programs underlying cell proliferation and survival decisions. In this study, we utilized precision cut lung slices (PCLS) obtained from mice with established osteosarcoma metastases to ex vivo model associations between the spatiotemporal distributions of growth factors in the lung, osteosarcoma signaling dynamics, and intratumoral gene expression heterogeneity, with single cell precision. To accomplish this, we engineered osteosarcoma cells that co-expressed genetically-encoded ERK and AKT sensors, engrafted them into PCLS tissues, then recorded sensor dynamics via live-cell microscopy. These tissues were subsequently fixed and immuno-stained for measurement of growth factor expression in resident lung cells and spatial correlation with observed tumor cell ERK-AKT signaling dynamics. Using this approach, we found that growth factor expression was diffusely increased within areas bordering osteosarcoma metastases. FGF2 and IGF1, which we have previously demonstrated to potently induce ERK signaling in osteosarcoma cells, were both significantly upregulated in these regions. However, despite relatively uniform overexpression of growth factors adjacent to tumors, individual osteosarcoma cells displayed stochastics patterns of ERK and AKT signaling, and downstream gene targets. These findings revealed that upregulation of lung growth factors, and the inherent systems-level properties of osteosarcoma signaling networks, can converge to promote intratumoral signaling and gene expression heterogeneity. Together, our results, using a novel PCLS and live-cell biosensor imaging approach, provide new insight into how spatial and temporal changes in microenvironmental signaling composition are integrated by metastatic osteosarcoma cells to promote heterogeneity.

#5528 Adaptive immune cells in colorectal cancer between normal mucosa, primary tumor and liver metastasis.

A. Trailin, W. Ye, E. Ali, S. Pavlov, L. Cervenkova, F. Ambrozkiewicz, O. Vycital, O. Daum, V. Liska, K. Hemminki;
Charles University in Prague, Medical faculty in Pilsen, Pilsen, Czech Republic

Introduction: We aimed to assess the role of local adaptive immunity in the metastatic process by comparing densities of adaptive immune cells between normal colorectal mucosa (NM), primary colorectal cancer (pCRC) and liver metastases (LM) in patients with synchronous and metachronous disease.
Patients and Methods: We enrolled patients, who underwent resection of pCRC and LM in Pilsen University Hospital between 1999 and 2022. 56 patients presented with LM (stage IV, synchronous) and 43 patients (stage II/III) developed LM later (metachronous). After immunohistochemical staining and whole slide scanning densities of CD3+ and CD8+ T cells and CD20+ B cells were quantified in NM, pCRC and LM using QuPath software. In pCRC and LM cell densities were measured in tumor center (TC), inner margin (IM), outer margin (OM) and peritumor (PT) region. IM and OM were defined as 500 µm on each side of the invasive tumor border.
Results: For all examined cells in both groups we found smaller densities in TC of pCRC and LM compared to NM (Table). In pCRC of synchronous group compared to LM densities of all cells were smaller in IM and OM and densities of CD3+ and CD8+ cells were smaller in PT region. In pCRC of metachronous group compared to LM densities of all cells were greater in TC, densities of CD3+ were smaller in OM and PT region, whereas densities of CD20+ cells were smaller only in OM. Compared to metachronous group patients with synchronous metastases had smaller densities of CD3+ T cells in IM and CD8+ T cells in TC and IM of pCRC.
Conclusion: Development of pCRC is accompanied by decreased densities of T and B cells in TC compared to NM, which further decrease in metachronous LM. Lower densities of T and B cells in IM and OM and T cells in PT region of pCRC compared to LM is a hallmark of synchronous group. TC of pCRC harbors larger numbers of T and B cells compared to LM in metachronous group. Low numbers of CD3+ and CD8+ T cells in IM and CD8+ T cells in TC of primary CRC may contribute to development of synchronous metastases.

Densities of CD3+, CD8+ and CD20+ cells per mm2 of the tissue (median)

	Patients witn liver metastases					
	Synchronous			Metachronous		
	NM	pCRC	LM	NM	pCRC	LM
CD3 NM	1014			1042		
CD3 TC		313 $p<0.05$ to NM	249 $p<0.05$ to NM		338 $p<0.05$ to NM	199 $p<0.05$ to NM and pCRC
CD3 IM		252	431 $p<0.05$ to pCRC		393 $p<0.05$ to pCRC in synchronous group	483
CD3 OM		521	1437 $p<0.05$ to pCRC		649	1953 $p<0.05$ to pCRC
CD3 PT		479	873 $p<0.05$ to pCRC		447	987 $p<0.05$ to pCRC
CD8 NM	319			390		
CD8 TC		58 $p<0.05$ to NM	52 $p<0.05$ to NM		102 $p<0.05$ to NM and to pCRC in synchronous group	52 $p<0.05$ to NM and pCRC
CD8 IM		65	96 $p<0.05$ to pCRC		102 $p<0.05$ to pCRC in synchronous group	120
CD8 OM		206	559 $p<0.05$ to pCRC		310	363
CD8 PT		177	369 $p<0.05$ to pCRC		218	291
CD20 NM	331			215		
CD20 TC		32 $p<0.05$ to NM	11 $p<0.05$ to NM		27 $p<0.05$ to NM	12 $p<0.05$ to NM and pCRC
CD20 IM		20	39 $p<0.05$ to pCRC		20	33
CD20 OM		137	327 $p<0.05$ to pCRC		134	303 $p<0.05$ to pCRC
CD20 PT		153	224		196	213

#5529 Mimicking CAFs, pial cells support leptomeningeal metastasis.

J. Snyder, J. Remsik, A. Boire;
Memorial Sloan Kettering Cancer Center, New York, NY

Leptomeningeal metastasis (LM), the spread of cancer into cerebrospinal fluid (CSF)-filled coverings of the brain and spinal cord, is a dismal complication of cancer leading to rapid neurologic disability and death. While a diverse array of primary tumors may result in LM, recent work from our laboratory (Chi Y et al 2020 Science) demonstrates a conserved transcriptional signature, independent of primary tumor, suggesting that tumor-microenvironmental interactions play a dominant role in this pathology. We have proteomically interrogated CSF collected from breast (n = 45), lung (n = 30), and melanoma (n = 27) patients with and without LM. We detect robust expression of inflammatory cytokines in all LM+ samples, 15 of these cytokines including IL8, IL6, and CXCL1 are conserved across tumor types in the presence of LM. Because cancer cells in the CSF do not express mRNA associated with these cytokines, we hypothesized that these inflammatory cytokines may originate from the microenvironment. Within the leptomeninges, LM cells adhere to and interact with the innermost layer of the meninges, the pia mater, which contains fibroblast-like cells. Co-culture of cancer cells with pial cells induced changes in the pial cell transcriptome and secretome, leading to increased IL8, IL6, and CXCL1 production. This communication between cancer cells and pial cells is preserved in the absence of direct cell-cell contact. These pial cells support cancer cell growth *in vivo*, as measured by co-implantation experiments. In addition, bulk RNA sequencing of mouse pial cells shows an inflammatory signature upregulated in the presence of LM. Taken together, these observations support a cancer-associated-fibroblast like role for pial cells in the setting of LM. Our work extends the CAF phenotype beyond classical fibroblasts to include pial cells, suggesting novel therapeutic opportunities within CNS malignancies.

#5530 Metastasis founder cells activate immunsuppression early in human metastatic colonization.

S. Guetter[1], C. Koenig[1], H. Koerkel-Qu[1], A. Markiewicz[1], S. Scheitler[1], M. Katzer[2], M. Berneburg[2], P. Renner[2], B. Cucuruz[2], L. Guttenberger[1], V. Naimer[1], K. Weidele[3], S. Treitschke[3], C. Werno[3], H. Jaser[1], T. Bargmann[4], A. Braun[4], F. Weber[1], K. Limm[1], R. Rachel[1], F. Baumann[1], L. Schmidleithner[5], K. Schambeck[5], A. Ulmer[6], S. Haferkamp[2], C. Klein[1], **M. Werner-Klein[1]**,

[1]University of Regensburg, Regensburg, Germany, [2]University Medical Center Regensburg, Regensburg, Germany, [3]Fraunhofer-Institute for Toxicology and Experimental Medicine, Regensburg, Germany, [4]Fraunhofer Institute for Toxicology and Experimental Medicine ITEM, Hannover, Germany, [5]Leibniz Institute for Immunotherapy, Regensburg, Germany, [6]University of Tubingen, Tubingen, Germany

Metastatic dissemination occurs very early in melanoma, often before diagnosis, rendering prevention of metastasis formation an important therapeutic goal. However, the earliest steps of lethal metastasis in patients are incompletely understood. Therefore, in this study we searched for the earliest detectable disseminated cancer cells (DCC) in sentinel lymph node biopsies of 492 stage I-III melanoma patients. We used micromanipulator-assisted isolation and single-cell transcriptome analysis of these extremely rare DCC and identified melanoma -associated chondroitin sulfate proteoglycan (MCSP) expressing melanoma cells as strong candidates for metastasis founder cells in lymph nodes. Based on a median follow-up time of 6 years, their detection was the strongest predictor of systemic metastasis and death upon multivariable analysis. Single-cell transcriptome analysis revealed that melanoma DCC were exposed to CD8 T cell attack during the transition from single cells to metastasis-initiating clusters, activated the extracellular vesicular exosomal pathway, and expressed the immunomodulatory proteins CD155 and CD276, but rarely PD-L1. CD155- and CD276-positive extracellular vesicles from patient-derived DCC models showed an immunosuppressive activity on CD8 T cells. In conclusion, our data suggest that either direct targeting of metastasis-founder cell with MCSP or their immune escape mechanisms may be key to curing early-stage melanoma.

#5531 Loss of csf2(gm-csf) with cisplatin treatment decreases metastasis and improves survival in a hpv positive head and neck cancer murine model.

P. Ghosh, C. Welbon, W. C. Spanos;
Sanford Research, Sioux Falls, SD

Granulocyte macrophages colony stimulating factor (GM-CSF) also known as CSF2 is a popular cytokine responsible for homeostasis. According to TCGA databank CSF2 expression upregulated in human HPV+ (Human Papilloma Virus) Head and Neck Small Cell Carcinoma (HNSCC) compared to normal tissue. The mechanism of CSF2 in tumor progression and chemo resistance has not been well studied. Previously, our lab generated a murine model of HPV+ HNSCC that is partially responsive to cisplatin and radiation (like human disease). The role of our study is to evaluate the importance of Csf2 with cisplatin treatment (CT) in HPV + HNSCC in the murine model. Using CRISPR-Cas9 technology we knocked out the expression of the Csf2 ligand in our parental mEERL (murine E6 E7 Ras Luciferase) tumor cell line and implanted both the parental mEERL tumor and the Csf2 KO mEERL tumor in the oral cavity of C57BL6/J mice. When tumors reached a palpable size, we administered Cisplatin (20mg/m^2, 3 doses total). We observed slow tumor growth in absence of Csf2 without treatment. On the other hand, we observed tumor regression in both tumor models with cisplatin treatment. Post treatment, mice with Csf2 KO tumors had a significantly prolonged rate of survival. To evaluate the role of Csf2 in the Tumor Microenvironment (TME), we collected the tumors 96 hours post CT and characterized the TME using multicolored flow cytometry. The results showed that post treatment mice with Csf2 KO tumors increased the number of the Natural Killer cell population and a surge of M-MDSC (Ly6Chi) population. The synergistic effect of knocking out Csf2 and cisplatin treatment in our tumor model appears to be driven by chemokine and cytokine changes in the TME. Simultaneously, we observed significantly lower levels of lung metastasis in Csf2 KO tumor bearing mice compared to those with parental mEERL tumors. Whereas we have seen increased metastasis in ipsilateral lymph node of Csf2 KO mice. This metastasis data mimics human disease where many patients have regional lymph node involvement, but few develop distant metastasis. These results indicate that GM-CSF (CSF2) in the TME could be an excellent target that would cause less metastasis and improved overall survival. Further investigations are needed to understand the underlying mechanism of immune response in the absence of CSF2 in the TME.

#5532 Differences in immune contexture across metastatic sites and tissue compartments in ovarian cancer.

B. Tate[1], E. Pavlatos[1], T. Kim[2], K. Wilson[1], E. Cid[1], J. Rao[2], G. Konecny[2], J. Pucilowska[1];
[1]Oregon Health & Science University, Portland, OR, [2]University of California, Los Angeles, Los Angeles, CA

Introduction: Characterizing the immune contexture within the tumor microenvironment (TME) can provide valuable biological insights that may impact treatment regimens and improve clinical outcomes. The advent of neoadjuvant chemotherapy has provided a unique opportunity to study matched, pre- and post-treatment sample pairs, but these samples are often obtained from different metastatic sites. Innate differences in the immune profiles across metastatic sites could therefore be a confounding factor when attempting to determine treatment-related effects. Furthermore, immune contexture can also vary by region within the TME, so results could vary depending on the regions of interest (ROIs) selected for analysis.

Methods: 36 matched, advanced primary ovarian cancer samples were obtained pre- and post- treatment with neoadjuvant chemotherapy aimed at reducing tumor burden. The first biopsy was taken at the time of initial diagnosis, whereas the second biopsy was collected after 3-4 rounds of carboplatin paclitaxel chemotherapy. Each slide was processed using a 26-plex multiplex immunohistochemistry (mIHC) assay, which interrogates immune cell densities and functional states for a broad range of immune cell populations, including CD8+ T cells, Tregs, TH1s, B cells, dendritic cells (DCs), granulocytes, macrophages, and monocytes. Tumor and stroma ROIs were selected by a board-certified pathologist using H&E slides immediately adjacent to the mIHC samples, and cell densities were calculated separately for each of the two tissue compartments.

Results: When comparing pre-treatment samples from the omentum (n = 8) with post-treatment samples from the omentum (n = 14), all of the statistically significant changes were found within the tumor compartment, with higher densities in the post-treatment samples for CD8+ T cells ($p = 0.009$), Tregs ($p = 0.012$), DCs ($p = 0.04$), and monocytes ($p = 0.027$). In contrast, when comparing post-treatment samples from the omentum (n = 14) and the ovary (n = 14), all of the significant differences were found within the stroma compartment, with higher densities in the omentum for CD8+ T cells ($p = 0.002$), Tregs ($p = 0.043$), TH1s ($p = 0.003$), and macrophages ($p = 0.048$).

Conclusions: These results demonstrate that the site of metastasis can be a significant confounding factor when making statistical comparisons between variables such as timepoint and that differences in immune cell density before and after treatment may be more apparent in the tumor, while differences between tissue types may be more apparent in the stroma. Further research into the immune profiles of different metastatic sites is warranted, but our findings demonstrate the importance of considering both tissue type and ROI selection strategy when designing a study with the intent to detect differences between longitudinal patient samples.

#5533 The difference of immune microenvironment between*de novo*metastatic and non-metastatic microsatellite instability-high colorectal cancer.

K.-H. Chen[1], C.-L. Hs[2], Y.-L. Su[3], C.-T. Yuan[1], J.-H. Tsai[2], Y.-H. Liang[2], A.-L. Cheng[1], K.-H. Yeh[2];
[1]National Taiwan University Cancer Center, Taipei, Taiwan, [2]National Taiwan University Hospital, Taipei, Taiwan, [3]Kaohsiung Chang Gung Memorial Hospital, Kaohsiung, Taiwan

Introduction: Microsatellite instability-high (MSI-H) colorectal cancer (CRC) consists of 15% of all CRC but only 2-4% of metastatic CRC. The favorable prognosis of non-metastatic (early-stage) MSI-H CRC may be related to vigorous immune reaction in tumor microenvironment. However, the mechanisms of immune evasion in metastatic (late stage) MSI-H CRC are largely unknown.
Materials and Methods: We retrospectively collected patients with MSI-H CRC from National Taiwan University Hospital and Kaohsiung Chang Gung Memorial Hospital. The archival tumor specimens were used for immune cells analysis by Nanostring PanCancer Immune Panel, and spatial immune characterization by multiplex immunofluorescence stains. Only surgical resected primary tumors and metastatic tumors were included. Gene expression and immune cells composition were compared between non-metastatic and *de novo* metastatic tumors.
Results: We enrolled 59 and 27 patients with early-stage and late-stage MSI-H CRC, respectively. Twelve metastatic site tumors were also collected. The clinicopathologic characteristics between patients who have early- and late-stage MSI-H CRC were not significantly different. There are heterogeneous immune cell compositions in these 98 MSI-H tumors. Compared to early-stage MSI-H tumors, there are significantly fewer cytotoxic (difference -0.497, p = 0.001) and dendritic cells (difference -0.528, p = 0.021) in late-stage MSI-H tumors. Gene set enrichment analysis disclosed significantly decrease in the expression of *JAK-STAT-IFN-γ-* and antigen processing-related pathways in late-stage MSI-H tumors. The top 5 genes with significantly differential expression between late-stage and early-stage tumors are *C7, TNFRSF12A, MFGE8*(up-regulated) and *CXCL5, IFNL1, GZMH, HMGB1* and *CXCR1* (down-regulated).
Conclusions: There are significantly fewer cytotoxic and dendritic cells in late-stage MSI-H CRC, compared to early-stage MSI-H CRC, which is associated with decrease expression in *JAK-STAT-IFN-γ-* and antigen processing-related pathways.

#5534 Needle biopsy induces pro-metastatic progression and systemic dissemination of estrogen receptor-positive breast cancer cells through the COX-2/PGE_2 cascade.

H. Kameyama[1], M. Leslie[1], R. Simmons[1], Y. Sun[2], M. Yi[3], P. Dondapati[1], J. F. Langenheim[3], K.-M. Fung[1], I. Chervoneva[3], H. Rui[3], T. Tanaka[1]; [1]University of Oklahoma Health Sciences Center, Oklahoma City, OK, [2]Medical College of Wisconsin, Milwaukee, WI, [3]Thomas Jefferson University, Philadelphia, PA

Breast cancer is the most commonly diagnosed malignancy in the U.S. and over two-thirds of invasive breast cancer cases are diagnosed early stage. However, 15-year survival rates for early-stage breast cancer remain in the range of 70-77%. Mounting evidence showed an increased risk of disease progression and mortality among early-stage breast cancer patients whose surgery was delayed over 60 days after the diagnostic biopsy. Yet, the mechanism(s) underlying the rapidly increased mortality due to delay of surgery after diagnosis remains unknown.

Our cohort analyses of early-stage breast cancer patients reveal the emergence of a significantly rising mortality risk when the biopsy-to-surgery interval was extended beyond 53 days. Additionally, histology of post-biopsy tumors shows prolonged retention of a metastasis-permissive wound stroma dominated by M2-like macrophages capable of promoting cancer cell epithelial-to-mesenchymal transition and angiogenesis by secretion of transforming growth factor beta 1 (TGF-β1) and vascular endothelial growth factor (VEGF). We show that needle biopsy promotes systemic dissemination of cancer cells through a mechanism of sustained activation of the cyclooxygenase-2 (COX-2)/prostaglandin E2 (PGE_2) cascade, which favors M2-polarization and its associated pro-metastatic changes, but are abrogated by oral treatment with COX-2 inhibitors in estrogen receptor-positive (ER+) syngeneic mouse tumor models.

Therefore, we conclude that needle biopsy of ER+ breast cancer provokes progressive pro-metastatic changes, which may explain the mortality risk posed by surgery delay after diagnosis. Also, our data may provide a rationale for a pharmacologic strategy to inhibit the COX-2/PGE_2 cascade in cases when delay of surgery is unavoidable.

#5535 Intracellular negative regulators of RTK-Ras-ERK signaling alter breast cancer perception of metastatic niche-derived growth factors.

V. Murthy[1], C. Erdem[2], J. Copperman[1], M. Birtwistle[2], A. Davies[1];
[1]Knight Cancer Institute, Oregon Health & Science University, Portland, OR, [2]Clemson University, Clemson, SC

Triple negative breast cancer (TNBC) is an aggressive breast cancer subtype that commonly metastasizes to distant organs, such as the lung, resulting in the poor clinical outcomes. TNBC cells commonly overexpress epidermal growth factor receptor (EGFR), a receptor tyrosine kinase (RTK) which when bound by microenvironmental growth factors, results in the activation of downstream effector kinases ERK-AKT and initiates transcriptional programs that control cell fate. Tumor cells, however, simultaneously receive many growth factor inputs from their respective microenvironments, many of which stimulate RTKs other than EGFR, that converge at ERK and AKT resulting in different transcriptional and cell fate outputs. This raises questions as to how tumor cells perceive, decode, and respond to a complex set of microenvironmental signals and what the relevance of this process may be for disease pathogenesis and treatment. To this end, our study aimed to determine how disseminated breast cancer cells perceive and respond to a complex growth factor milieu upon seeding and engraftment in the lung. Using live-cell microscopy techniques and TNBC cells carrying biosensors for ERK and Akt signaling pathways, we monitored the dynamic signaling behaviors of single tumor cells, in real-time, as they adapted to the environment in living human lung tissue. Strikingly, we found that individual disseminated tumor cells are *less* responsive to growth factors once seeded in the lung, as compared to outside this tissue, despite the presence of RTK stimulating ligands. We showed that partial activation of EGFR is necessary for complete activation of ERK signaling by other growth factor-RTK pairs, and expression of downstream ERK target genes, whereas AKT signaling was unaffected. Using quantitative modeling and experimentation, we showed that reshaping of ERK signaling response dynamics occurred via dysregulation of negative regulators that are dominantly controlled by EGFR signaling. Together, these results provide novel insight into how tumor cells perceive and respond to complex microenvironmental signals, which has important implications for drug targeting strategies.

#5536 The role of p38 MAPK in the tumor-induced immune suppressive microenvironment in metastatic breast cancer.

P. Rajan, R. Zollo, M. Lieberman, Y. Guo, M. Alruwaili, M. Alqarni, B. Morreale, S. Olejniczak, J. Barbi, S. Abrams, A. Bakin;
Roswell Park Comprehensive Cancer Center, Buffalo, NY

The tumor microenvironment (TME) in Metastatic Breast Cancer (MBC) is a major factor contributing to therapy resistance and suppression of antitumor immune response. Tumors promote expansion and recruitment of immune suppressive cells such as myeloid-derived suppressor cells (MDSCs) contributing to tumor invasion and suppressing anti-tumor T cells. Our prior work suggested a critical role of p38 MAPK in tumor-induced expansion and mobilization of myeloid cell populations thereby facilitating metastasis. The current study examined the role of p38 MAPK in tumor-induced changes in immune landscape and explored the mechanisms by which p38 mediates tumor-immune interactions. First, the contribution of T cells to anti-metastatic activity of p38 inhibitor (p38i) was addressed by depletion of CD8 T cells. Depletion of $CD8^+$ T cells negated the effects of p38i on tumor growth and metastasis in the syngeneic 4T1 model. Next, we examined whether p38i exhibits a direct effect on T cells *in vitro* or *in vivo*. The *in vitro* assays showed that p38 blockade increased levels of $CD44^+$ $CD62L^+$ $CD8^+$ T cells indicating enhancement of T cell differentiation. To determine the effects of p38 blockade on the immune landscape *in vivo*, single-cell RNA-seq and flow cytometry studies were performed in the 4T1 model with p38i or p38-deficient cells in which p38α/Mapk14 was inactivated by CRISPR/Cas9 (p38KO). The scRNA-seq data showed that p38 blockade increased the expression of T cell differentiation markers in the TME. Furthermore, p38 blockade significant decreased IL-6 signaling in myeloid cells, an important mediator of MDSC function. Assessment of myeloid cell populations showed a decreased expression of the immune suppressive signature. This observation was further validated in MDSCs isolated from the spleens of 4T1 tumor-bearing mice treated with p38i and in p38KO cohorts. Our prior work showed that p38i does not affect the generation of MDSCs *in vitro*. Therefore, we examined whether blockade of p38 affects the chemotactic capacity of conditioned media from MBC cells using mouse monocytes. The chemotaxis assays showed that p38i and p38KO largely reduced the ability of conditioned media to stimulate transwell migration of mouse monocytes. Notably, p38i and p38KO largely reduced expression of chemotactic cytokines in MBC cell models. Furthermore, p38i and p38KO reduced production and chemotactic ability of exosomes isolated from tumor cells. Together, these observations suggest that tumor p38 MAPK signaling promotes immune-suppressive TME and metastasis by facilitating expansion and mobilization of myeloid cell populations through the mechanisms involving production of exosomes and pro-myeloid chemokines/cytokines. This work highlights that p38 blockade can be utilized in combination with immune therapy or chemotherapy to enhance clinical benefits of immune therapy and reduce promyeloid effects of chemotherapy.

#5537 How aging promotes immune mediated reactivation from metastatic melanoma dormancy.

P. Datt[1], J. Passamonte[1], C. Price[1], D. Zabransky[2], Y. Chhabra[1], A. Weeraratna[3], **M. E. Fane**[1];
[1]Fox Chase Cancer Center, Philadelphia, PA, [2]Johns Hopkins School of Medicine, Baltimore, MD, [3]Johns Hopkins School of Public Health, Baltimore, MD

Disseminated cancer cells that escape the primary tumor can seed distal tissues but may take several years to grow into clinically detectable metastases, a phenomenon termed tumor dormancy. Despite its importance in metastasis and residual disease, few studies have been able to successfully model melanoma dormancy. We have previously shown that while tumors grow more slowly in aged mouse skin, they form more lung metastases in aged mice compared to young mice. We queried whether the lung microenvironment undergoes age-related changes that establish a permissive niche for metastatic outgrowth. We identified that Wnt5A and AXL are not only required for efficient dissemination away from the primary tumor but also activate dormancy of melanoma cells within the lung. The young lung microenvironment maintains melanoma cells in a dormant state; however, age-associated reprograming of lung fibroblasts increases secretion of the soluble Wnt antagonist sFRP1, which inhibits both Wnt5A and AXL to enable reactivation from dormancy and the formation of larger metastatic colonies in the aged lung. We found that downregulation of AXL in melanoma cells leads to an increase in the related TAM family receptor MERTK, which promotes a proliferative melanoma phenotype and enables reactivation from dormancy. We have now found that both the aged-pre and post metastatic niche regulate immune cells in the lung to create a permissive niche for reactivation of metastatic melanoma. NK cells are significantly decreased in the healthy lungs of aged mice, are significantly less active, and have increased exhaustion markers. NK cell infiltration remains low in early and late-stage metastasis in aged mice. Depletion of NK cells in young mice is sufficient to induce reactivation from dormancy. Further, MERTK induced reactivation of melanoma cells results in paracrine secretion of its own ligand PROS1 to facilitate a growth permissive lung microenvironment. Melanoma-secreted PROS1 increases infiltration of PMN-MDSCs and decreases macrophage infiltration to maintain an immunosuppressive lung niche for efficient outgrowth. Selective inhibition of PMN-MDSCs using a TRIAL-R2 agonistic antibody significantly decreases metastatic outgrowth and promotes smaller, non-proliferative dormant colonies. Our findings indicate a significant role that aging plays in altering NK-cell infiltration and function to create a growth permissive pre-metastatic niche and how reactivation from dormancy can further contribute to create an immunosuppressive microenvironment for efficient outgrowth via PROS1 induced infiltration of PMN-MDSCs. Importantly, the clear differences found in our young and aged mouse modelling systems for outgrowth in metastatic tissues necessitates the need for age-appropriate pre-clinical modelling for better patient and disease representation.

#5538 Efferocytosis-induced HIF-1α enhances tumor vascularization and promotes osteoblastic bone remodeling in metastatic prostate cancer.

G. G. Kleer, M. Molina Sanchez, V. Mendoza-Reinoso, A. J. Koh, J. Rubin, L. K. McCauley, H. Roca;
University of Michigan, Ann Arbor, MI

Metastatic prostate cancer (PCA) exhibits a predilection for bone metastasis, initiating a complex interplay with bone cells, leading to dysregulated remodeling and mixed-pathological bone alterations. Human PCA primarily yields osteoblastic bone lesions, linked to bone pain and an adverse prognosis. In this study, we explored the activation of HIF-1α in myeloid phagocytic cells by apoptotic cancer cells in the context of bone metastatic PCA. Our previous findings demonstrated HIF-1α stabilization in bone macrophages engulfing apoptotic PCA cells in vitro. This study extends our understanding to an in vivo setting using mouse prostate cancer cells designed to express inducible caspase 9, triggering apoptosis (and subsequent efferocytosis) when exposed to the dimerizer molecule AP20187 (AP). Our assessment of PCA tumor growth in bone utilized a syngeneic mouse model, introducing a loss-of-function Hif1a mutation into myeloid lineage cells using LysM-Cre mice crossed with Hif1a-floxed mice ($Hif1a^{mut}$ ($LysM\text{-}Cre^{+/-}$ $Hif1a^{flox}$)), compared with the $LysM\text{-}Cre^{-/-}$ $Hif1a^{flox}$ (WT). In the first model, cancer cells were inoculated into the tibiae of these mice and apoptosis was induced with AP on days 3 and 5 post-inoculation (AP model). Results were compared to a model where apoptosis was not induced after inoculation (No-AP). In the AP model, fractional bone volume (BV/TV) in the medullae was significantly higher in tumor-inoculated tibiae than in non-inoculated (No-tumor) contralateral bone, highlighting the predominance of osteoblastic lesions. Conversely, in the No-AP model, increased BV/TV significance was achieved in WT mice (tumor vs. No-tumor), but not in mutant mice. Trabecular thickness (Tb.Th) was increased in both models in the presence of tumor, regardless of the Hif1a phenotype. Importantly, significant differences in BV/TV and Tb.Th between WT and $Hif1a^{mut}$ tumor tibiae were exclusively noted in the context of induced apoptosis. Histological differences between tumors in the AP model were observed by immunofluorescence (IF) staining, which revealed a reduced fractional $F4/80^{\pm}$ area in $Hif1a^{mut}$ vs. WT tumors, with no differences in $TRAP^{\pm}$ (osteoclasts) lining bone surfaces. RNAseq analysis of $HIF1a^{mut}$ vs. WT macrophages efferocytosing apoptotic cancer cells showed downregulated processes related to vasculature development and blood vessel morphogenesis ($p< 10^{-5}$). In correlation, IF analysis with endomucin (EMCN) demonstrated a reduction in stained area ($EMCN^{\pm}$) relative to tumor area in $Hif1a^{mut}$ tibiae vs. WT, suggesting a role of efferocytosis-induced HIF-1α in tumor vascularization. This study unveils intricacies of metastatic tumor growth in bone and proposes a connection between efferocytosis-induced HIF-1α in myeloid phagocytic cells and the promotion of tumor vascularization, alongside the enhancement of osteoblastic bone remodeling.

#5539 PRDM16 is an intrinsic regulator of dormancy in bone disseminated prostate cancer cells.

M. M. Nasr, T. Li, R. T. Bishop, J. S. Frieling, C. C. Lynch;
H.Lee Moffitt Cancer Center, Tampa, FL

Metastatic prostate cancer (PCa) frequently occurs in the bone and can remain inactive for extended periods after primary tumor treatment. Understanding the intricate molecular mechanisms that govern this phenomenon could open the door to novel therapies, potentially reducing mortality rates. To address this, we developed a novel protocol to induce cellular dormancy in PCa cell lines (RM1, 22Rv1, LAPC4) *in vitro*. We noted that dormant cells exhibited distinctive clustering and could be reactivated when exposed to serum even after 21 days of stasis. The dormancy program was validated by multiple assays including cell cycle analysis, membrane dye retention, and $Edu^{\pm}$ incorporation. RNASeq analysis showed significant transcriptional changes during dormancy induction, with 8 genes commonly upregulated across multiple human and mouse PCa cell lines, of which the transcription factor, PRDM16. We focused on PRDM16 since, 1) it is a known regulator of hematopoietic stem cell quiescence, 2) our emerging data points to bone morphogenetic protein-7 (BMP7), a well-known exogenous mediator of dormancy as an inducer of PRDM16 expression and 3) clinically, PRDM16 is suppressed in primary PCa and active metastases. First, we validated the upregulation of PRDM16 during dormancy *in vitro*. Silencing PRDM16 led to impaired dormancy phenotype and cell death, while its overexpression significantly mitigated proliferation rates and promoted survival. *In vivo,* we employed an intra-iliac immunocompetent model (RM1 & C57BL6J) and demonstrated that overexpressing PRDM16 in active RM1 cells resulted in significant reduction of metastasis formation and Ki67 expression concurrent with extended survival when injected *in vivo* compared to control cells. Prostate cancer cells with PRDM16 over-expression were detected in bone sections as solitary or small clusters (<20 cells) demonstrating an inverse relationship between PRDM16 expression and metastatic outbreak. In defining the targets via which PRDM16 controls dormancy entry, we focused on RAR related orphan receptor C (RORC) based on bioinformatic analysis and publicly available PRDM16 ChIP-Seq. Our data demonstrate that pharmacological inhibition of RORC using GSK805 promoted the apoptosis of dormant PCa cells specifically when compared to their actively growing counterparts. In conclusion, our studies have revealed the critical role of PRDM16 in promoting PCa cell dormancy, in part via upregulating RORC. Translationally, clinically approved RORC inhibitors for non-cancerous conditions (psoriasis) have been developed. We expect, based on our results, that these inhibitors could be repurposed for the eradication of dormant PCa cells in patients with advanced disease.

#5540 Single cell multiomic analysis of human brain metastasis reveals conserved dormancy population.

R. Klotz[1], **Y. Wang**[1], A. Sunkara[1], F. Attenelo[2], M. Yu[1];
[1]University of Maryland, Baltimore, Baltimore, MD, [2]University of Southern California, Los Angeles, CA

This study explores the complex realm of brain metastasis, pivotal in crafting effective anti-tumor strategies. Leveraging single-cell multi-omics sequencing, we profiled the transcriptomes and chromatin accessibility landscapes of tumor cells and their surrounding microenvironment in human brain metastases that originated from across a spectrum of primary cancers. Our investigations have identified distinct, yet uniformly present, tumor cell subpopulations, each defined by unique gene expression patterns, chromatin accessibility, and the interactions between tumor and stromal cells. Notably, one such subpopulation exhibits a dormancy signature, characterized by enhanced interferon response, oxidative phosphorylation, and upregulated HLA class molecules, alongside alterations in circadian rhythms. Our trajectory analysis charts a course from these dormant cells to rapidly proliferating ones, with notable shifts in circadian rhythm genes, underscoring their potential role in brain metastasis. This aligns with recent findings that disruptions in circadian rhythms can modify stem cell characteristics in glioblastomas. This insight led us to focus on a specific circadian rhythm gene, highly active in the dormant cells and located on the HER2 amplicon—an area linked to high brain metastasis relapse rates in patients. We've developed inducible models for both overexpression and knockdown to scrutinize this gene's impact in her2 positive breast cancer cell lines, examining gene expression and proliferation in vitro. Complementing this, we are conducting spatial transcriptomic analysis to evaluate the microenvironmental regulation of tumor dormancy in human brain metastases. This multi-omics approach reveals a nuanced regulatory landscape of brain metastasis, highlighting a novel and often overlooked factor in metastasis progression and brain tumor relapse: the interplay between circadian rhythms and tumor dormancy. This discovery not only deepens our understanding of brain metastases but also opens potential new avenues for therapeutic interventions.

#5541 The unique metabolite landscape of the aged microenvironment dictates melanoma migratory and invasive capacity.

G. M. Alicea, P. Patel, M. Wei, V. Rebecca, D. Wirtz;
Johns Hopkins, Baltimore, MD

Metastatic burden and organ failure are the root causes of mortality in patients with advanced melanoma; however, little is known of the metabolic drivers that enable organ colonization and the formation of overt metastases. Recent studies have drawn attention to the importance of metabolism in the survival and colonization of cancer cells. In melanoma, there have been studies focusing on the invasive capabilities of cells; however, not much is known regarding metabolic plasticity in melanoma migratory, invasive and ultimately metastatic capabilities.We have previously shown changes in the lipid landscape of the aged microenvironment promotes melanoma resistance to targeted therapy. Here, we find a distinct metabolite landscape in the aged microenvironment elevates melanoma metastatic capacity. We utilized a panel of well characterized melanoma models and tested their invasiveness and motility under different metabolite levels modeled after the aged microenvironment. Transcriptomic and proteomic analysis identifies distinct signatures that explain the migratory and invasive differences in cells cultured in varying metabolic environments. We hypothesize that different nutrient availabilities melanoma cells are exposed to during the metastatic phase affect the migratory and invasive capacity of the cell. We tested this by performing 3D migration assays, organoids and transwell assays of cells grown in media with varying nutrient levels. Further analysis is currently underway to better understand the mechanisms in which these metabolic differences facilitate cell migration, invasion and eventually colonization. This work has important implications for our understanding of the metabolic determinants of melanoma migration and metastatic colonization, and we hypothesize restraining tumor metabolic plasticity is vital to prevent and treat metastases in melanoma.

TUMOR BIOLOGY: Tumor-Immune System Cross-Talk
Poster Session

#5545 FADD activation renders hepatocellular carcinoma sensitive to immune checkpoint blockade by turning cold tumors hot.
J. Zhou, J. Lu;
Chinese University of Hong Kong (CUHK), Hong Kong, Hong Kong

The heterogenicity of hepatocellular carcinoma (HCC) remains a key obstacle in turning the majority of 'immune-cold' tumors 'hot' for effective immune checkpoint blockade (ICB) therapy. Through studying the naturally-existed 'hot' HCC variant lymphoepithelioma-like (LEL)-HCC by RNA and whole exome sequencing analysis, we identified fas-associated death domain (FADD) as one of the top differentially expressed genes that associated with high tumoral $CD8^{\pm}$T cell abundance. Of note, FADD upregulation was also observed in HCC patients with better ICB responsiveness. As FADD was mainly expressed in tumor cells from HCC by scRNAseq analysis, we constructed *Fadd* knockout stable cells using murine HCC cell lines. Interestingly, CRISPR knockout of tumoral *Fadd* led to increased tumor weights in immunocompetent but not immunodeficient mice, accompanied with decreased tumoral $CD8^{\pm}$T cells. Mechanistically, FADD phosphorylation promoted NF-κB transcriptional activity to increase CCL5 secretion from HCC cells via interacting with its nuclear binding partners Src-associated-substrate-during-mitosis-of-68kDa/KH domain containing, RNA binding, signal transduction associated 1 (Sam68/KHDRBS1) and lysine (K)-specific methyltransferase 2D (KMT2D), thus directing $CD8^{\pm}$T cell tumor infiltration. In addition, anti-PD1 triggered FADD phosphorylation via IFN-γ and TNF-α release from $CD8^{\pm}$T cells in ICB-sensitive but not resistant tumors. Most importantly, sequential FADD activation via genetic and pharmacologic approaches could re-sensitize the therapeutic efficacy of anti-programmed death 1 (PD1) antibody in ICB-resistant orthotopic and spontaneous HCC models by turning cold tumors hot. Taken together, our findings reveal a key molecular feature of ICB-responsive hot tumors that may guide the development of sequential combinatory immunotherapies for the majority of HCC patients with low responsiveness to ICB monotherapy. This project is supported by the University Grants Committee through General Research Fund (24110323, 14107622, 14104820) and the Health and Medical Research Fund (07180556).

#5546 CRISPR-based kinome screen identifies *Ikbkb* as a regulator of phagocytic evasion in hepatocellular carcinoma.

S. Chan, T. Lee;
The Hong Kong Polytechnic University, Hong Kong, Hong Kong

Hepatocellular carcinoma (HCC) is one of the most lethal and prevalent malignancies worldwide and is associated with poor prognosis. Recently, immune checkpoint inhibitors (ICIs) have revolutionized the oncology landscape by targeting genes critical for immune checkpoint pathways, leading to the immune evasion of cancer cells. Phagocytosis checkpoints have emerged as essential checkpoints for cancer immunotherapy by functioning as “don’t eat me” signal to suppress immune response. Given the druggable properties of protein kinases, together with recent reports showing the antitumor immunity of kinase inhibitors, we aimed to identify protein kinases critical for phagocytic evasion in HCC by transducing a lentiviral sgRNA expression plasmid containing 2,852 unique single-guide RNAs (sgRNAs) targeting the 713 mouse kinase gene in mouse HCC cells, RIL-175, and subsequently co-incubated with RAW 264.7 macrophages. Based on the deep sequencing analysis comparing the sgRNA distribution in RIL-175 with or without co-incubation, we identified the *Ikbkb* gene as top-sensitizing hit on this screen, with at least two-fold sgRNA reduction upon incubation with macrophages.

To verify the phagocytic evasive role of *Ikbkb* in HCC, we have employed CRISPR/Cas9 knockout approach to delete *Ikbkb in mouse HCC cell line,* RIL-175 cells. The results showed that upon co-incubation with RAW 264.7 cells, the *Ikbkb* knockout cells exhibited increased phagocytosis, as confirmed by both flow cytometry analysis and microscopy observation. The analysis of the TCGA-LIHC cohort revealed that the expression level of *Ikbkb* was elevated and associated with unfavorable clinical outcomes. Notably, Ikbkb expression was found to be significantly correlated with established anti-phagocytic markers, including CD24, CD47, and CD274, further supporting their roles in the anti-phagocytic activities of HCC cells.

In summary, we have uncovered IKBKB as a cancer-intrinsic regulator of phagocytosis, which has the potential to target IKBKB as a novel therapeutic strategy to enhance the efficacy of current ICI treatments for HCC patients.

#5547 Non-invasive monitoring of tumor biomechanics and implications for immunotherapy in HCC.

A. C. Cortes, K. Minamiguchi,, H. Kostan, M. S. Stenkamp, S. Anfossi, N. Fowlkes, R. Avritcsher;
The University of Texas MD Anderson Cancer Center, Houston, TX

Shear-wave elastography (SWE) is a novel non-invasive technique used to quantify tissue stiffness. This approach can be used to longitudinally monitor tumor biomechanics and holds promise for guiding informed clinical decision-making. This study aims to explore the impact of tumor stiffness, as evaluated by SWE, on the proliferative potential of endothelial, tumor, and immune cells in a preclinical model of hepatocellular carcinoma. Tumor tissue sections from a Buffalo-McA-RH7777 rat HCC tumor model, utilizing a rat hepatoma cell line stably expressing green fluorescent protein genes (fluc/GFP) were selected based on the degree of tumor stiffness assessed by SWE. Nodules were separated based on mean shear wave values (3.05 versus 2.26 m/s) and categorized as stiff or soft, respectively. A 6-color panel was used to assess the percentages of different tumor, immune, and endothelial phenotypes in different areas of the tumor including immune cells (CD45+), endothelial cells (CD34+), green fluorescent protein (GFP), Ki67 (cell proliferation), and class-III intermediate filaments - vimentin. Our findings demonstrated increased expression of vimentin on immune cells (CD45+) within the tumor margin interphase. Stiffer tumors exhibited a higher percentage of CD45 cells co-expressing vimentin compared to softer tumors (P=0.01), whereas softer tumors showed an increased prevalence of CD34+ cells concurrently expressing Ki67 (P=0.01). Same pattern persisted in the tumor margin interphase regarding the proliferation of tumor cells identified by the expression of GFP co-expressing Ki67 (P<0.01). These findings highlight a significant association between tumor mechanical properties and the proliferative activity of endothelial and tumor cells, suggesting a link between tissue stiffness and the regulatory mechanisms associated with cellular proliferation and aggressiveness in HCC. Additionally, the presence of vimentin in immune cells may suggest that stiffer tumors may require enhanced migratory and invasive properties to compensate for changes in tumor mechanics thus potentially influencing immune function.

#5548 Cannabidiol enhances efficacy of atezolizumab via upregulation of PD-L1 expression by cGAS-STING pathway in triple negative breast cancer cells.

Bu Gyeom Kim[1], Bo Ram Kim[1], Dae Yeong Kim[1], Hyemi Yun[2], Dayoung Kim[2], Woo Young Kim[3], Sanghee Kang[3], Sun Il Lee[3], Sang Cheul Oh[1]

[1]Oncology, Korea University College of Medicine, Seoul, Korea, Republic of,[2]Biomedical Sciences, Korea University College of Medicine, Seoul, Korea, Republic of,[3]Surgery, Korea University Guro Hospital, Seoul, Korea, Republic of

The current treatment for patients with triple negative breast cancer (TNBC) relies on cytotoxic therapy. Currently, atezolizumab and chemotherapy can be combined in patients with TNBC, but this approach is not effective for all patients with low reactivity to atezolizumab. As there is a lack of alternative treatment options, new anti-cancer drugs are urgently needed to enhance atezolizumab reactivity against TNBC. Recent strategies have focused on regulating the expression of programmed death-ligand 1 (PD-L1) or enhancing immune response activation by combining anti-cancer drugs with immune checkpoint inhibitors (ICIs). Cannabidiol (CBD), a cannabinoid component derived from the cannabis plant, has been reported to have anti-cancer therapeutic potential because of its capacity to induce apoptotic cell death in tumor cells while avoiding cytotoxicity in normal cells. Previous studies have demonstrated the effects of CBD on apoptosis in various types of cancer cells. However, the potential role of CBD as an immune modulator in the regulation of PD-L1 expression and the anti-cancer immune response remains to be explored. In this study, we found that CBD stimulated PD-L1 expression in TNBC cells, which significantly induced CBD-mediated cGAS-STING pathway activation. Taken together, we demonstrated that the combination of CBD and anti-PD-L1 antibody enhances the anti-cancer immune response *in vitro* and *in vivo* experiments. Our findings identified the mechanism of PD-L1 regulation by CBD in TNBC cells and suggested that CBD could be a potential candidate for the development of new combinatorial strategies with ICIs in TNBC patients.

#5549 Multicellular spheroid structural and metabolic characterization through radial line profiling.

S. N. Bess, M. J. Igoe, G. K. Smart, T. J. Muldoon;
University of Arkansas, Fayetteville, AR

Three-dimensional multicellular tumor spheroids have emerged as a step between *in vitro* and *in vivo* models that can offer biological insight in fields such as tumor biology. Spheroids closely resemble *in vivo* solid tumors regarding their heterogeneous architecture and gradients of nutrients and oxygenation. These characteristics give the spheroid model great potential for studying basic tumor biology. However, traditional characterization methods investigate changes in the discrete regions within the spheroid, limiting the amount of spatial information regarding cellular metabolism. In this study, multicellular spheroids were created through a combination of hanging drops and gentle agitation using murine RAW 264.7 macrophages and colorectal adenocarcinoma CT26 cells. Hanging drops were maintained for three days then transferred to 6-well plates and placed on an orbital shaker set to 70 RPM for seven days. Prior to metabolic imaging, spheroids were moved to a microincubator with controllable temperature and humidified gas delivery (5% CO_2). A custom inverted multiphoton imaging system (Bruker) equipped with an Ultrafast Ti:Sapphire via a 60x/1.2NA water immersion objective (Olympus) and four close-proximity, high-efficiency GaAsP detectors. NADH fluorescence was captured with a 460 (± 20) nm band pass filter at 755 nm excitation and FAD fluorescence with a 525 (± 25) nm band pass filter at 855 nm excitation. NADH and FAD fluorescence were normalized by PMT gain and laser power. An integrated fluorescence lifetime imaging microscopy (FLIM) module was used to measure mitochondrial function regarding the different components contributing to NADH autofluorescence. Immunofluorescence was used to characterize macrophage populations (M1 vs M2) and cellular proliferation (Ki67) and apoptosis (CC3). CD206, a M2 marker, showed a lower normalized fluorescent intensity at the spheroid core (0.429) compared to the proliferative edge (0.570). Similar trends are also observed for CD80, a M1 marker and Ki67. CC3 showed a higher normalized fluorescent intensity at the spheroid core (0.823) compared to the proliferative edge (0.004). The optical redox ratio displays a slightly lower value at the core (0.429) compared to the proliferative edge (0.570). Overall, these results indicate that the proliferative edge shows higher numbers of immune cells and more oxidative metabolism compared to the core. Future work includes exposing this spheroid model to low levels of oxygen to investigate how environmental changes in oxygen can affect spheroid structure and metabolism.

#5550 Crosstalk of estrogen receptor B with tumor microenvironment signaling explains tumor suppressor actions in TNBC.

Kristina Diana A. Zambo[1], Harika Nagandla[1], Kim Cuong Cap[1], Aireana Phillips[1], Fotis Nikolos[2], Wei Qian[1], Jianying Zhou[1], Jenny Chang[1], Christoforos Thomas[1]

[1]Cancer Center, Houston Methodist, Houston, TX,[2]Urology, Houston Methodist, Houston, TX

Triple Negative Breast Cancer (TNBC) is a subtype of breast cancer lacking molecular targets, possessing one of the poorest prognoses of all breast cancers. Recent studies using breast tumor samples show an association between the expression of estrogen receptor β (ERβ) and improved survival of patients with TNBC. ERβ - whose function largely opposes that of oncogenic ERα - is involved in the regulation of many tumor repressive pathways and has lately been observed to partake in immune modulation, thus presenting a promising target for TNBC. Discovering selective ERβ agonists is critical to understanding the potential of activating the receptor as a therapy approach for TNBC. It enables us to elicit estrogen signaling response specific to the tumor suppressive function of the β receptor subtype. We have set out a screening process to test and identify ligands that display the greatest activation and specificity for ERβ as determined by reporter assays and changes in downstream target gene expression. We selected to study *in vitro* and *in vivo* the compounds with optimal biological activity to delineate tumor-intrinsic and -extrinsic effects and validate the mechanism of action employing human and mouse cell models that reflect the heterogeneity of the disease. We propose that activation of ERβ decreases the proliferative and metastatic ability of breast cancer cells by altering cellular pathways and crosstalk with immune cells. The results of these studies help lay the groundwork for further research on the clinical potential of ERβ especially in the realm of immunotherapy and treatment of TNBC.

#5551 Targeted nanoparticles co-delivering PARP inhibitor and other immune modulators overcome the immunosuppressive tumor microenvironment.

R. Khoury[1], R. Kleiner[1], E. Yeini[1], D. Rodriguez Ajamil[1], S. Israeli Dangoor[1], T. Sanalla[2], I. Barshack[2], R. Satchi-Fainaro[1];
[1]Tel Aviv University, Tel Aviv, Israel, [2]Sheba Medical Center, Ramat Gan, Israel

Several mutations have been identified that are associated with an increased risk of triple-negative breast cancer (TNBC), including those that are deleterious in the BRCA gene. TNBC is associated with the worst prognosis and the highest incidence of brain metastasis (30%) among all subtypes of BC. Despite objective responses to poly (ADP-ribose) polymerase (PARP) inhibition and improvements in progression-free survival (PFS) compared to standard chemotherapy in patients with BRCA-mutated TNBC, benefits are transitory. Furthermore, our understanding of the effect of PARP inhibitors (PARPi) in treating breast cancer brain metastasis (BCBM) and modulating its tumor microenvironment (TME) is still lacking. To this end, we analyzed the brain TME of BRCA-mutated BCBM in the absence or presence of treatment with PARPi. Interestingly, we found that the immune TME of the brain hinder the antitumor activity of PARPi by upregulating multiple immunosuppressive molecules, including PD-L1. Furthermore, we found that BCBM overexpress P-selectin through its interaction with the tumor-associated microglia, bone marrow-derived macrophages and endothelial cells in the TME. Thus, we designed a novel nanoparticle (NP) targeting P-selectin to serve as a brain-penetrant delivery system for the treatment of BCBM. In order to target BRCA-mutated BCBM, we harnessed our novel P-selectin-targeted NPs to entrap PARPi and other immune modulators that we found to exert synergistic activity when combined. To evaluate the antitumor activity of our P-selectin-targeted NPs, we established 3-dimensional (3D) *ex vivo* and *in vivo* BRCA-mutated BCBM models. Importantly, we saw favorable effects of the P-selectin-targeted NPs in comparison to the combination of the free drugs, suggesting that out targeted-NPs overcome the TME-mediated resistance to PARPi through the modulation of the immunosuppressive microenvironment of the brain.

#5552 Uncovering clinically significant tumor microenvironment interaction programs across diverse cancers.

Ido Nofech-Mozes, Vivian Wang, Philip Awadalla, Sagi Abelson

Ontario Institute for Cancer Research, Toronto, ON, Canada

Background: Cell-cell interactions (CCI) within the tumor microenvironment (TME) play pivotal roles in various tumor behaviors, including cancer growth, metastasis, immune evasion, and resistance to therapy. Compared to front-line treatments, targeting specific CCIs marks a paradigm shift in cancer therapy, aiming for enhanced response rates with reduced side effects. Although current approaches targeting immune regulation pathways exhibit effective anti-tumor responses, substantial variability in response rates across patients and cancer types persists. Consequently, a critical imperative emerges to discover novel interaction programs (IPs) across diverse TMEs, demonstrating clear clinical impact across a broad spectrum of patients.
Methods: *Characterization of pan cancer IPs.* We compiled a pan cancer single-cell RNA-seq (scRNA-seq) atlas, including 4 million cells from 890 tumors across 14 cancer types. In each sample, CCIs were inferred using a ligand-receptor (LR) analysis framework, generating ranked CCI scores based on consensus from various LR inference methods. To find IPs enriched across TMEs, we applied an unsupervised factorization approach. The outcome represents CCIs as factors, where sample loading indicates factors' strength, and feature loading highlights the cells and LR pairs constituting each IP.
Evaluating IPs in clinical RNA-seq cohorts. Given the more immediate translational potential of bulk cancer sequencing for patient stratification, we devised an approach to predict IPs' strengths in bulk RNA-seq. Random Forest regression models using pseudo-bulk expression of cancer genes were trained to predict the loading (strength) of factors (IPs) in each sample in the scRNA-seq pan-cancer atlas. These models were subsequently applied to cancer samples in The Cancer Genome Atlas (TCGA) cohort to assess the clinical impact of various IPs on patient mortality.
Results: We assessed the impact of IPs on 5-year overall survival using Cox proportional hazard models. We identified multiple factors significantly associated with survival in at least 4 cancer types. Notably, a robust prognostic factor linked to the inclusion of anti-tumor natural killer cell interactions and exclusion of pro-tumor macrophage interactions was found in MESO, LGG, ACC, and UVM (HR 1.6-6.6, $p < 0.05$). The validation of IPs using spatial transcriptomics and evaluation of IP prediction's utility in targeted treatment cohorts are currently underway.
Conclusion: We highlight a potent method for detecting clinically significant IPs involving cells in TME communicating through LR pairs. The ability to assess these scRNA-seq-derived IPs in clinical bulk RNA-seq cohorts signifies a valuable advancement. Our approach holds promise for expanding the repertoire of cell therapies, identifying new treatment targets, and improving our predictive capabilities for responses to existing therapies.

#5553 Glycan CA19-9 mediated immune modulation in the pancreatic tumor microenvironment.

J. Hsu, T. Oh, K. L. Peck, A. E. Rock, G. Bishop, S. R. Okhovat, S. M. Kaech, D. D. Engle;
Salk Institute, La Jolla, CA

Pancreatic ductal adenocarcinoma (PDA) is an intractable common malignancy with a pro-tumorigenic and immunosuppressive microenvironment (ME) that often limits treatment efficacy. Only 10-15% of patients are eligible for surgical resection, which is the only cure for PDA. The glycan CA19-9 is used to follow treatment response in PDA patients, but its functional role in PDA remained unknown until recently because rodents lack the ability to produce this carbohydrate. CA19-9 elevation in a KRAS-mutant background results in increased tumor proliferation and ME remodeling in mice. The tumor ME is encompassed by hypovascularized stroma consisting of cancer associated fibroblasts (CAFs) and tumor associated macrophages (TAMs) that contribute to desmoplasia and immunosuppression. All prior work investigating the tumor ME in PDA mouse models was performed in CA19-9 negative context, potentially missing a key element of PDA biology. Elevation of CA19-9 in mice caused expansion of both antigen-presenting (ap)CAFs and TAMs. CA19-9 induction in KRAS-mutant organoids increased gene expression of M-CSF, IL1a, and TGFb and led to increased apCAF and TAM differentiation. This project aims to uncover the mediators of CA19-9-mediated ME remodeling. CA19-9-modified macrophage colony-stimulating factor (M-CSF) was identified via immunoprecipitation and mass spectrometry from KRAS-mutant CA19-9-inducible pancreatic organoids. CA19-9-M-CSF induced increased immunosuppressive TAM differentiation *in vivo* and *in vitro* using a novel Macrophage, Organoid, and Fibroblast (MOrF) co-culture platform. This project will identify the mechanisms by which CA19-9 directly contributes to PDA ME immune modulation and unveil essential molecular underpinnings of PDA biology that will inform effective therapies in the future.

#5554 Breast cancer with different chemosensitivity has distinct influence on the immune microenvironment.

E. Skourti, K. Seip, E. V. Egeland, S. Jabeen, N. Mensali, I. Oynebraten, S. Juell, E. M. Inderberg, O. Engebraten, A. B. Corthay, G. M. Malandsmo, L. Prasmickaite;
Oslo University Hospital, Oslo, Norway

Triple Negative Breast Cancer (TNBC) is a BC subgroup with the least favorable outcome and limited therapeutic options. Chemotherapy has long been the standard treatment, but resistance often develops. In recent years, various immunotherapy approaches have diversified, including combinations of chemo and immunotherapies. Increased understanding on how the difference in chemosensitivity affects the immune cells is of importance for further development of chemo-immunotherapies for TNBC. In this project we investigate how TNBC with distinct chemosensitivity modulate the immune microenvironment. Specifically, we explore the influence of the secretome, derived from the chemoresistant versus the sensitive BC cells, on macrophages (MØs) and T-cells. We have disclosed the chemosensitivity-dependent differences in the secretome, which were associated with diverse effects on MØ recruitment, polarization, and activation. Currently we investigate the secretome influence on interferon (IFN)-activated MØ. IFN stimuli is known to trigger tumoricidal activities in MØ, and we are setting up a co-culture assay, where such MØ functions could be explored in vitro. To study the secretome influence on T-cells, we employ T cell receptor (TCR)-engineered T cells that become activated in the presence of target cells. The preliminary results indicate that activation of the TCR T-cells was reduced in the presence of the “chemoresistant” secretome, suggesting its immunosuppressive influence. Work is in progress to validate this observation using other TCR T cells and functional markers of active T cells.

#5555 Lung squamous cancer cell mTORC2 signaling suppresses antitumor immunity by up-regulation of PSGL-1, a ligand of VISTA/ PD-1H checkpoint receptor.

V. M. Ngwa, Y. Hwang, D. N. Edwards, W. Song, J. Chen;
Vanderbilt University Medical Center, Nashville, TN

Lung squamous cell carcinoma (LUSC) represents 30% of non-small cell lung cancer (NSCLC) cases and has a high mortality rate with limited targeted therapies. Unlike lung adenocarcinoma (LUAD), which has seen advancements in targeted therapies, LUSC has not benefited from similar breakthroughs despite having similar genetic abnormalities. While immune checkpoint inhibitor therapies have shown promise in some LUSC patients, a significant portion does not respond effectively, leaving limited treatment options. In this study, we investigated vulnerabilities in NSCLC and found that a substantial number of LUSC patients have genetic alterations in the PI3K-mTORC2-AKT signaling pathway. By using CRISPR/CAS-9, we showed that disrupting mTORC2 function in LUSC cells reduced glycolysis and lactate secretion, which in turn reduced tumor growth in vivo. Remarkably, the loss of mTORC2 also enhanced the activity of CD4+ and CD8+ T cells within the tumors. To further understand the metabolic and immune changes associated with mTORC2 loss of function, we performed RNA sequencing comparing wild-type (WT) and mTORC2-deficient cells. Our results confirmed a link between mTORC2 and HIF-2α, while regulating PSGL-1, a ligand of the VISTA/PD-1H checkpoint receptor. Furthermore, introducing a stable, non-degradable form of HIF-2α in mTORC2-deficient tumor cells restored PSGL-1 expression in vitro and in vivo. These results suggest that the interaction between PSGL-1 and VISTA plays a role in suppressing the anti-tumor immune response in LUSC tumors. Indeed, anti-VISTA treatment inhibited the growth of LUSC WT tumors in vivo, suggesting that mTORC2 plays a role in regulating PSGL-1 expression in the tumor microenvironment. Together, these data demonstrate that targeting mTORC2 or inhibiting VISTA checkpoint receptor may serve as a potential therapeutic strategy for improving immunotherapy in LUSC.

#5556 An vascularized melanoma model for with unidirectional perfusion of circulating immune cells for advancing immune-oncology research.

M. C. Torregrosa, S. de Ruiter, T. Burton, K. Queiroz, **W. Allen**, J. Komen, S. Trietsch, L. van den Broek;
MIMETAS, Oegstgeest, Netherlands

Understanding the interactions between the tumor the vascular systems and circulating immune cells is crucial for elucidating mechanisms of immune cell recruitment in cancer and in exploring potential immunotherapeutic approaches. However, current in vitro models often lack the fidelity to replicate these intricate dynamics observed in vivo. The OrganoPlate Graft has been developed for perfusion of peripheral blood mononuclear cells (PBMCs) through a vascular bed with a melanoma monolayer (A375) to study aspects such as immune cell adhesion, extravasation and interaction with the tumor. The OrganoPlate Graft comprises 48 chips per plate, each designed to simulate the conditions of vascular beds. The device achieves flow through passive leveling, utilizing gravity to induce a pressure drop and unidirectional flow across the vascular bed in both positive and negative inclines. This approach avoids the complications and potential artifacts introduced by external pump, reduces complexity, and increases the throughput with up to 16 plates (768 chips) served by each OrganoFlow rocker. In experimental settings, formation of the vascular bed was seen to be consistent in plates and the introduction of the chemokine CXCL-12 led to the establishment of a gradient. Subsequently, PBMCs were observed to localize in clusters as a result of extravasation towards this gradient and the A375 monolayer. This behavior is consistent with known chemotactic responses in more complex in vivo environments. A notable observation was the sustained activity of PBMCs within the system. Cells continued to perfuse through the vascular bed for up to three days after seeding. In summary, the OrganoPlate Graft provides a platform for studying immune interactions in an immunocompetent vascular bed model. Its design and functionality allow for the exploration of immune cell behaviors in proximity to tumor cells, offering potential insights for immune-oncology research. The system's ability to mimic immune cell migration and extravasation in a controlled environment, and future potential to observe tumour killing makes it a valuable tool for advancing our understanding of immune-tumor interactions and may contribute to the development of novel immune-oncology therapeutic strategies.

#5557 Stem-like T cells maintain latent anticancer activity and underly therapy resistance.

F. Tao, S. McElroy, J. Nemechek, I. Pushel, J. Szarejko, S. Khanal, T. Bradley, D. Myers, J. M. Perry;
Children's Mercy Research Institute, Kansas City, MO

Pre-cancerous cells are normally recognized and eliminated by immune cells. Cancer progresses only when this immunosurveillance system fails. Although immunotherapy has driven the most significant and exciting advances in cancer treatment in modern times, current approaches are running into barriers. An emerging area of interest includes evidence for rare but highly potent stem cell-like T cells. Stem-like T cells combine long-term persistence and high potency with immunological memory. Our recent findings reveal insights into the nature and regulation of stem-like T cells and their potential anticancer activity. Minimal residual disease (MRD) underlies therapeutic resistance, dictates treatment escalation, and predicts patient outcomes. We have shown that the Wnt and PI3K pathways promote the transformation of hematopoietic stem cells (HSCs) into chemoresistant leukemia stem cells (LSCs), which form the root of leukemia initiation and post-treatment recurrence. High-throughput screening revealed that LSCs could be targeted by low dose anthracycline treatment. Mechanistically, low dose, but not high dose anthracyclines indirectly target LSCs by inhibiting their unique properties of immune escape, allowing for their elimination by CD8+ T cells. We employed single-cell genomic and proteomic analysis to investigate immunological changes during development of HSCs, LSCs, and their progeny in response to low dose anthracycline treatment. While leukemia progression results in exhaustion of differentiated CD8+ T cells, stem-like T cells accumulate. However, low dose anthracycline treatment reverses this imbalance. Comparing MRD+ and MRD- patient samples, we found that differential proportions of stem-like T cells persist in the bone marrow of leukemia patients. While T cells of MRD- patients recover following chemotherapy induction, T cell recovery is severely attenuated in MRD+ patients. Furthermore, failure of immunological recovery is driven at least partially by a lack of stem-like T cells in MRD+ leukemia patients. Overall, our studies have revealed that low dose anthracyclines, in contrast to high dose, induce opposing, dichotomous effects on LSCs vs. HSCs and stem-like vs. differentiated T cells.

#5558 Whole-slide multiplexed tissue imaging of prostate adenocarcinoma reveals distinct immune niches in high- versus low-grade tumors.

J. Wala[1], J.-R. Lin[2], B. Labadie[3], D. Peiffer[4], A. Gagne[1], K. Chaudagar[4], Y.-A. Chen[2], E. Van Allen[1], P. Sorger[2], **A. Patnaik**[4];
[1]Dana-Farber Cancer Institute, Boston, MA, [2]Harvard Medical School, Boston, MA, [3]Columbia University Medical Center, New York, NY, [4]University of Chicago, Chicago, IL

Objectives
Tumor-immune interactions are a critical determinant of tumor evolution and are increasingly targeted by novel therapeutics (e.g. immune checkpoint blockade). However, their significance in treatment-naive localized prostate cancer remains largely unknown. Here, we employ multiplexed tissue imaging on radical prostatectomy specimens across Gleason grades to create a single-cell spatial atlas of primary prostate tumors and characterize their innate and adaptive immune landscape.

Methods
Whole-slide radical prostatectomy (RP) specimens were obtained from 28 patients: 14 with Gleason Grade Group ≤ 3 (Low-grade; LG) and 14 with Gleason Grade Group ≥ 4 (High-grade; HG). Tumors were imaged with our cyclic immunofluorescence (CyCIF) platform using a 27-marker panel encompassing epithelial, T-cell, innate immune and stromal markers. Tumor and stromal compartments were manually annotated by a pathologist. Cell densities were compared between tumor and stromal compartments of LG and HG tumors.

Results
Across the 28 RP specimens, we identified and spatially resolved over 27 million individual cells. Overall, higher Gleason grade was associated with a significantly increased innate and adaptive immune reaction. CD8+ cytotoxic T-cell density was significantly higher in HG vs LG ($p = 0.003$) specimens, although this effect was largely due to enrichment in adjacent stroma rather than direct tumor infiltration. By contrast, FOXP3+ T-cells were significantly increased throughout the tumor and stromal compartments of HG compared with LG tumors ($p = 0.001$). Tertiary lymphoid structures (TLS) and CD163+ myeloid cells were also significantly enriched in HG tumors relative to LG tumors ($p = 0.029$ and 0.039, respectively). PD-1+ cells were specifically enriched in TLS structures in HG tumors ($p < 0.001$). There were no significant differences in CD11c+ and CD103+ cell densities between LG and HG tumors.

Conclusions
This spatially resolved single-cell atlas of localized prostate cancer reveals that high-grade tumors exhibit significant inflammation, particularly of TLSs and stromal CD8+, and are enriched in markers of T-cell anergy and myeloid-derived suppression. These findings raise the hypothesis that immunotherapy may have activity in treatment-naïve high-grade prostate cancer, despite the failure of immune checkpoint blockade in mCRPC.

#5559 The anti-tumor efficacy and immune effects of combining of ceralasertib, an oral ATR kinase inhibitor, with imipridones, in prostate cancer treatment *in vitro* and *in vivo*.

Y. Xia[1], L. Zhang[2], M. Ghandali[1], M. P. Schwermann[1], W. El-Deiry[1];
[1]Legorreta Cancer Center at Brown University, Providence, RI, [2]Brown University, Providence, RI

Prostate cancer is the most common cancer and the second leading cause of cancer death among men in the United States. There is an estimated 10% to 50% of cases progress to metastatic castration resistant prostate cancer (mCRPC) state within 3 years of diagnosis. mCPRC remains lethal despite therapeutic advances. There is approximately 20% of mCRPC patients present somatic DNA damage repair (DDR) gene mutations. Ceralasertib, formerly known as AZD6738, is a potent and selective orally bioavailable inhibitor of the ataxia tenlangiectasia and Rad3-related (ATR) kinase, which is involved in DNA repair in response to DNA damage and replication stress. Preclinical studies have demonstrated ATRi sensitizing alterations in DNA damage response (DDR) genes. Ceralasertib's antitumor activity as a monotherapy in treating prostate cancer is moderate. Thus, we combined ceralasertib with imipridones (ONC201 and ONC206), which target mitochondrial caseinolytic protease P (ClpP) and the integrated stress response, resulting in enhanced antitumor efficacy in vitro. Prior data have demonstrated sensitivity of 4 prostate cancer lines to ceralasertib and imipridones monotherapies, synergistic activities with the combination treatments, and immune enhancement effects with the combination treatments when co-cultured with NK92MI cell line. We proceeded to a short term in-vivo study validating the combination treatment efficacy. Preliminary results include cytokine profiling using the Luminex 200 technology to understand treatment induced changes in the tumor microenvironment (TME) from both in vitro and in vivo studies. Our results guide novel clinical trials for effective clinical responses in mCPRC patients.

#5560 Role of SPARC and collagen in immunogenicity of cancer: A theoretical approach.

R. P. Are, A. Babu;
National Inst. of Technology Rourkela, Rourkela, India

Secreted protein acidic and rich in cysteine (SPARC), is a multifunction protein that interacts with extracellular matrix (ECM), cell surface receptors, and signaling molecules. These interactions in cancer cells result in less susceptible of cells to the immune system, leading to poor prognosis. SPARC plays a crucial role in transporting collagen, a significant component of the ECM, from the site of synthesis to the basement membrane of the cells. Collagen mediated rigidity enhancement of cell microenvironment promotes cancer cell growth, proliferation, and angiogenesis. Collagen remodeling plays a complex and multifaceted role in cancer immunomodulation. Our current research focuses on exploring the cancer treatment mechanism by immunomodulation based on SPARC and collagen through theoretical and computational approaches. Our previous investigations identified SPARC and collagen as potential biomarkers for targeting cancer cells. Our current theoretical research identifies the role of SPARC and collagen in tuning the tumor microenvironment and altering the immune system cell surface receptors. This theoretical investigation is followed by computational study to formulate the pathway from secretions of both SPARC and collagen to reprogramming of tumor microenvironment. SPARC and collagen's effects on the cell immune system are analyzed by performing molecular interaction and molecular dynamics studies for SPARC and collagen with the cell surface receptors. From our study, we identify the cellular mechanisms involved either actively or passively in the progression and prognosis of the cancer. Our study will provide insight into a novel pathway for targeting the cancer microenvironment, which will be helpful in the formation of low-dosage cancer drugs, resulting in the decreased adverse effects of drugs and increased patient quality of life.

#5561 Whole slide Imaging Mass Cytometry allows the rapid profiling of the immune landscape of histopathologically aggressive prostate tumors.

J. L. Gorman[1], L. Y. Liu[2], J. P. Hartig[3], N. Parsotam[4], A. Khoo[2], V. Ignatchenko[2], S. Asbury[1], S. Afiuni[1], R. Gonzalez[1], M. J. Geuenich[1], C. F. Harrigan[1], Y. Lee[1], J. Chen[5], L. Lim[4], Q. Raza[4], P. M. Angel[3], K. Campbell[1], S. K. Liu[5], M. R. Downes[6], R. R. Drake[3], T. Kislinger[2], D. King[4], H. W. Jackson[1];
[1]Lunenfeld-Tanenbaum Research Institute, Toronto, ON, Canada, [2]Princess Margaret Cancer Centre, Toronto, ON, Canada, [3]Medical University of South Carolina, Charleston, SC, [4]Standard BioTools Canada Inc., Markham, ON, Canada, [5]Sunnybrook Research Institute, Toronto, ON, Canada, [6]Sunnybrook Health Sciences Centre, Toronto, ON, Canada

Patients with Gleason pattern 4 or 5 prostate tumors have a high risk of biochemical recurrence and worse survival. Affected by their local environment, dynamic immune cell phenotypes can both hinder or drive cancer progression. To understand the proteomic environments that facilitate specific immune cell responses and interactions in advanced prostate cancer, we have spatially resolved the immune cell content and metabolic features of Gleason pattern 4 and 5 and subpatterns of prostate tumors. To scale quantitative multiplexed histopathology measurements to human disease, we have applied a new high-throughput whole slide modality of high-plex Imaging Mass Cytometry™ to simultaneously quantify immune cells, metabolic states, prostate specific pathways, and biomarkers in 125 whole slide sections from 42 patients over 100 cm^2 of tissue. It is essential to image whole slide sections in order to fully evaluate the complete heterogeneity of these cancer samples. In parallel, multi-region macrodissection shotgun proteomics and both glycan and extracellular matrix MALDI imaging mass spectrometry have quantified the proteome associated with specific immune cell environments. Together, we identify localized proteomic microenvironments associated with specific tumor supportive or inhibitory immune cell content in human tumors that may help differentiate which high-risk patients will have a rapid biochemical recurrence following radical prostatectomy.

#5562 Altered tumor microenvironment in animal model of concomitant GBM and Alzheimer's pathology.

D. Nascari, R. Eghlimi, A. Beniwal, D. Alton, J. Fryer, N. L. Tran;
Mayo Clinic Arizona, Scottsdale, AZ

Glioblastoma (GBM) and Alzheimer's disease (AD) are two devastating central nervous system diagnoses with no known cure. Both diseases are associated with advanced age. The majority of GBM tumors form in the frontal and temporal lobes, two of the brain regions most impacted by amyloid and tau pathology in AD. Females have a higher risk of AD, while males have a higher risk of GBM. Several large case series have established epidemiological evidence that the two diseases are inversely correlated. Nevertheless, it remains unknown whether presence of subclinical amyloid or tau pathology antagonizes the establishment or progression of GBM. The present study sought to characterize GBM growth, progression, and immune response in the setting of concomitant AD pathology using the syngeneic murine GL261 tumor model. To further understand the tumor cell changes that occur in the presence or absence of AD pathology, we engineered GL261 with a dual-tagged vector consisting of RiboTag (to allow for full-length mRNA profiling) and TurboID (to allow for proteomic profiling). GL261 cells were injected intracranially into $APP^{NL\text{-}G\text{-}F/NL\text{-}G\text{-}F}$ - $MAPT^{human/human}$, $APP^{NL\text{-}G\text{-}F/+}$ - $MAPT^{human/+}$, and wildtype C57BL/6J mice. Tumors in both wildtype and AD conditions contained ~50% intratumoral myeloid cells (Iba+, P2RY12-). Differential activation of intratumoral myeloid cells will be assessed with immunohistochemistry. Microgliosis (IBA1, P2RY12) and astrogliosis (GFAP) around the tumor in the setting of Alzheimer's pathology versus normal conditions will be compared. Invasiveness, proliferation, DNA damage (pH2AX), and apoptosis (cleaved PARP, cleaved Caspase 3) will be compared. Tumor cell-specific changes unique to tumors in the AD microenvironment will be assessed transcriptionally with RiboTag profiling as well as proteomically with TurboID purifications. Our preliminary data suggests that the presence of concomitant AD pathology affects GBM growth and progression as well as the immune response to the tumor, and warrants further investigation.

#5563 Novel approaches to measuring tumor-mutational burden provide insights into tumor-immune interaction in primary melanoma.

E. R. Shteinman[1], N. Maher[1], J. W. Conway[1], G. H. Attrill[1], F. Newell[2], N. Waddell[2], N. Hayward[2], J. V. Pearson[2], G. V. Long[1], R. A. Scolyer[1], J. S. Wilmott[1], I. A. Vergara[1];

[1]Melanoma Institute Australia, The University of Sydney, Sydney, NSW, Australia, [2]Cancer Program, QIMR Berghofer Medical Research Institute, Brisbane, Queensland, Australia

Background: Tumor mutation burden (TMB) has been widely explored in metastatic melanoma as a proxy of neoantigenic load. In contrast, the role of TMB on the biology of primary melanoma disease progression is less understood. In this study, we explored the associations between the immune context of melanoma subtypes and TMB as measured by several standard and novel criteria.

Methods: Whole-genome-sequencing and multiplex immunohistochemistry (mIHC) were used to characterize the genomic and immune landscape of a cohort of 116 primary melanomas, including cutaneous non-acral (n=59), acral (n=39) and mucosal (n=18) subtypes, as well as 5 mucosal metastases. mIHC was used to identify intratumoral CD8+ T-cells, memory T-cells, macrophages, dendritic cells, B-cells and PD-L1 expression. Standard measures of TMB -total mutational burden (tTMB) and non-synonymous (ns) mutational burden (nsTMB)- as well as novel measures that incorporate multiplicity and clonality -ns persistent mutation burden (ns-pTMB), and ns mutation dosage (ns-dosTMB) were calculated, and their association with immune profiles and clinical-pathological factors established.

Results: In cutaneous non-acral melanomas, ns-pTMB and ns-dosTMB were positively associated with CD8+ T cell proportions (p=0.02 for both comparisons). Clonal, but not subclonal ns-pTMB from mutations present in single-copy regions of the genome were positively associated with higher tumor-resident CD103+CD8 T-cell (p=0.01) and B-cell proportions (p=0.02). Higher single-copy ns-pTMB was also associated with tumors presenting early/intermediate regression compared to late regression. In mucosal melanomas, clonal ns-dosTMB had the strongest positive association with the presence of macrophages (CD68, p=0.005). Additionally, macrophages (p=0.01), tissue resident memory T-cells (p=0.02), PDL1+ cells (p=0.03) and B-cells (p=0.048) were found to be positively associated with clonal ns-pTMB from mutations present in multiple copies, which was also positively associated with the presence of lymphatic invasion (p=0.03). Mucosal patients who recurred had lower levels of single-copy ns-pTMB (p=0.03). In acral melanomas, all measures of TMB were positively associated with the presence of dendritic cells (CD11c), with no particular role for clonality observed. In both cutaneous non-acral (p=0.046) and acral melanomas (p=0.03), but not mucosal (p=0.4), clonal ns-dosTMB was found positively associated with tumor mitotic rate.

Conclusion: Novel TMB measures reveal associations between tumor and immune context that are not captured by standard TMB measures alone in primary melanomas. Different TMB measures are linked to distinct immune populations across melanoma subtypes that harbor unique genomic and immune landscapes. Clonal mutations play a dominant role in the associations of TMB with immune cell populations.

#5564 The regulation of PD-L1 in glioblastoma cells involves Pyk2 signaling.

T. Porter, L. Kucheryavykh;
Universidad Central del Caribe, Bayamon, PR

Glioblastoma (GBM), the most aggressive brain cancer which is usually fatal within a year after diagnosis, poses a significant therapeutic challenge with conventional treatments providing limited success. Despite advancements in immune checkpoint blockade, PD-L1 inhibitors exhibit suboptimal efficacy in recurrent GBMs with recent clinical trials demonstrating only 8% objective responses in patients. Utilizing the R2 Genomic Analysis Visualization Platform, we identified a positive 8-18% correlation between Pyk2 and PD-L1 gene expression in human GBM specimens. We hypothesize that Pyk2 signaling is involved in the regulation of PD-L1 expression in GBM cells. In this study, primary human glioblastoma cell lines and GL261 mouse glioma cells were assessed employing CRISPR/Cas9 Pyk2 knockout (Pyk2KO) combined with pharmacological Pyk2 inhibition. Flow cytometric analysis revealed a 35% decrease in PD-L1 expression in Pyk2KO GL261 cells compared to wild-type cells. SiRNA knockdown against Pyk2 in primary human GBM cells demonstrated a similar response, with a 50% decrease in PD-L1 expression compared to MOCK control cells. Additionally, the application of the Pyk2/FAK inhibitor defactinib at a concentration of 0.2 μM reduced PD-L1 expression by 32% in both GL261 and primary human GBM cells. These findings highlight Pyk2 as a potential therapeutic target for modulating the immunosuppressive microenvironment in GBM and enhancing the effectiveness of immune checkpoint blockade therapies.
This study was supported by: NIH Grant 1SC1GM122691 and PRSTRT2022.

#5565 Multiomic characterization of colorectal cancer using MICS technology reveals interaction of antigen presenting cancer associated fibroblasts and T cells.

Emily Neil[1], Rebecca C. Hennessey[1], David Agorku[2], Dongju Park[1], Julia Femel[2], Michael DiBuono[1], Hanna Lafayette[1], Erica Lloyd[1], Hsinyi Lo[1], Alex Makrigiorgos[1], Shaina Lu[1], John Lee[1], Sameh Soliman[1], Dominic Mangiardi[1], Paurush Praveen[2], Philip Strobel[3], Silvia Ruberg[2], Fabian Staubach[2], Ryan Hindman[1], Thomas Rothmann[2], Olaf Hardt[2], Hansueli Meyer[1], Tanya Wantenaar[2], Jinling Wang[1], Werner Muller[2], Robert Pinard[1], Andreas Bosio[2]

[1]Miltenyi Biotec, Waltham, MA,[2]Miltenyi Biotec, Bergisch Gladbach, Germany,[3]University Medical Center Gottingen, Gottingen, Germany

In solid tumors, the tumor microenvironment (TME) is composed of diverse cell types including cancer cells, immune cells, stromal cells, and other tissue specific cell types. The complex intercellular interactions that occur between these various cell populations determine cancer development and progression. Cancer-associated fibroblasts (CAFs) have been identified as key players in the TME, capable of promoting tumor cell growth and invasion, as well as manipulating immune responses. To better resolve potential subpopulations, spatial relationships, and signaling occurring between cell types within the TME, we performed same-section multiomic profiling of colorectal cancer (CRC) using the MACSima™ Imaging Cyclic Staining (MICS) technology. We combined a custom 40plex RNA panel with a panel of antibodies to characterize the drivers of tumorigenesis and the activation state of immune cells. FFPE CRC specimens were reviewed by a pathologist for clinical assessment and region of interest selection. Then, gene expression profiles were generated using RNAsky™ technology with each gene being detected via cyclic rounds of detection probe hybridization, image acquisition, and signal erasure. Subsequently, fluorescently labeled antibodies were applied to the same section following an equivalent acquisition process. Finally, multiomic clustering and cell population analyses were performed using MACS® iQ View software. The analysis revealed spatially separated subpopulations of CAFs. Functional characterization of cellular neighborhoods and the cell-to-cell interactions occurring within the TME showed that one of the CAF populations potentially promoted cancer cell growth while another subpopulation, resembling antigen-presenting CAFs (apCAFs), closely interacted with T cells in the TME. These findings will deepen our understanding of tumor progression in colorectal cancer and potentially other solid tumors.

#5566 Streamlining tissue sample preparation: A comparative study on the efficiency and reproducibility of the Omni-Stainer™ dewaxing and HIER protocol.

N. Samusik[1], Y. Goltsev[1], **N. Kedei**[2];
[1]Parhelia Biosciences, Austin, TX, [2]National Cancer Institute, Bethesda, MD

The evolution of life sciences research has entailed a shift toward understanding cellular functions within tissue microenvironments, with an emphasis on cell- and tissue-specific relationships. A key challenge in these endeavors is the need for accurate data acquisition, which can be impeded by variability in the multistep manual assay preparations. In the quest for developing reliable and efficient tissue sample preparation workflows, two protocols using multiple dewaxing agents have been compared: the Omni-Stainer™ Dewaxing and HIER antigen retrieval protocol from Parhelia Biosciences, Inc. and the analogous one on Leica BOND Rx. The objective of this research was to assess the efficiency and reproducibility of these methods in the context of a four-color morphology immunostaining used for GeoMx DSP RNA and protein detection assays (Nanostring). We examined the efficiency of automated dewaxing using various non-toxic xylene alternatives, including C12-15 alkyl Benzoate, diethylene glycol, methyl octanoate or methyl decanoate, and compared them to the proprietary Leica Bond Dewaxing solution. Then, we compared the quality of post-HIER immunostaining using two different four-antibody panels on human jejunum samples. After several rounds of optimization, we found that the V4 of the open-source Omni-Stainer™ dewax-HIER protocol resulted in identical quality of morphology immunostaining compared to proprietary Leica Bond protocol. This study validates the Omni-Stainer™ Dewaxing and HIER protocol as a viable and efficient approach for automation of sample prep for GeoMx DSP studies.

#5567 Breast cancer cell alteration of immune cell transcriptome through indirect communication.

J. Kennard, K. Norek, K. Fuh, R. D. Shepherd, K. D. Rinker, **O. A. Kharenko**;
Syantra Inc, Calgary, AB, Canada

Crosstalk between tumor and non-tumor cells plays an important role in cancer progression and metastasis often leading to a modification of non-malignant cells into pro-oncogenic phenotypes. Understanding this process is important for diagnostic and therapeutic advances. We previously reported clinical validation results for a new way to detect early-stage breast cancer using a panel of RNA biomarkers from whole blood and a machine learning software-powered testing system. Recently, we showed that immune cells undergo transcriptomic and functional changes upon direct contact with breast cancer cells. Here, we report results from investigation of indirect communication between breast cancer and immune cells leading to cancer-driven immune cell transformation and activation of multiple oncogenic pathways. To characterize these modifications, we performed RNAseq and pathway analysis on a human monocytic cell line, THP1, exposed to media from triple negative breast cancer (TNBC) cells (MDA-MB-231) in culture. Our results demonstrate that 24 hours of THP1 cell exposure to soluble factors secreted by tumor cells leads to significant gene modulation, with over 1,100 differentially expressed genes (|Fold Change|>2; $p<0.05$). KEGG and Reactome enrichment analysis revealed overlap of multiple pathways between THP1 cells exposed to direct and indirect cancer cell contact conditions, such as cytokine-cytokine receptor interaction, JAK-STAT signaling pathways and others. TNF, NMP1, STING1 and TGM2 were identified as key upstream regulators potentially driving this transformation in both direct and indirect contact conditions. The S100 pathway, which we previously found to be activated by fluid shear stress in MDA-MB-231 cells was also activated in THP1 cells upon both direct and indirect contact. The observed gene expression changes in THP1 cells exposed to media from MDA-MB-231 suggests that indirect intercellular communication alone can transmit an oncogenic signal. These results support a role for secreted factors from breast cancer cells in transforming immune cells and modulating the gene expression markers detected by our blood test, expanding the potential for leveraging this type of tumor education response in advancing cancer detection and treatment.

#5568 Understanding the role of immune exclusion in mammary tumor growth.

P. Mitra, J. Azpurua, H.-C. Chiang, R. Li;
The George Washington University, Washington, DC

Multiple solid tumor types, including triple-negative breast cancer (TNBC), respond poorly to immunotherapy due to low infiltration of CD8+ T cells into the tumor core. The extracellular matrix (ECM) and its components such as collagen have been found to contribute to immune cell exclusion. Discoidin domain receptor 1 (DDR1) is a collagen receptor known to be aberrantly expressed in TNBC among multiple solid tumor types. We have uncovered a previously unappreciated function of DDR1 in immune exclusion through shaping a collagen fiber-based tumor defense against anti-tumor immunity (Sun et al, ***Nature*** 599, 673-678 (2021)). Our study showed that deletion of DDR1 in mouse mammary carcinoma cell lines such as E0771 and M-Wnt (syngeneic with C57BL/6 strain background) promotes infiltration of CD8+ T cells and reduces tumor growth in an immunocompetent mouse model. Extending the published study to other immunocompetent mouse strain backgrounds, we observed that deletion of DDR1 in EMT6 cells, another immune excluded TNBC mouse model in the BALB/c strain, increased the infiltration of CD8+ T cells to the tumor core and reduced tumor growth. Data concerning the DDR1-dependent spatial architecture of the mammary tumor microenvironment will be presented. Identifying specific immune and stromal cell populations and proteins spatially modified in the presence or absence of DDR1 may aid in development of new stand-alone or combination anti-cancer treatments with anti DDR1 antibody.

#5569 Mechano-chemical control of secretory cues regulating immune tolerance, survival and invasion in oral squamous cell carcinomas.

B. R. Bareham, M. Dibble, L. Mouhib, A. Bermejo Arteagabeitia, S. Mukhopadhyay, M. Parsons;
King's College London, London, United Kingdom

Tissue fibrosis and extracellular matrix (ECM) stiffening have been shown to promote tumor cell proliferation, metastasis, and chemoresistance in a range of cancers. Stiffness of the ECM can lead to changes in cancer cell behavior, including enhanced proliferation, activation of mechano-sensitive signaling pathways, and potential genomic damage, with implications for cancer progression and immune responses. Recent research suggests stiff matrix may also induce the release of tumor-derived small extracellular vesicles (sEVs) that promote tumor growth. Tumor-derived sEVs carry bioactive cargo, such as micro-RNAs (miRNAs) and DNA fragments, and function as a unique form of intracellular communication promoting cell survival, growth, and metastasis. Understanding these mechano-sensing mechanisms is essential for identifying potential targets in precision medicine for solid tumor treatment. However, the influence of tumor stiffness on secretory cues, and their subsequent role in immunomodulation and/or chemo-resistance has not been extensively studied.
This project aims to explore how tumor stiffness can alter cell responses to genotoxic stress and how these responses can perpetuate feedback to the immune system through the release of secretory cues such as sEVs. Here, we outline the isolation and characterization of tumor-derived sEVs obtained from culture media of oral squamous cell carcinoma (OSCC) spheroids, cultured at varying stiffness (0.2kPa-1.5kPa). In this project, we use OSCC lines that are either sensitive or resistant to cisplatin (HSC-3 and HN-5, respectively). To explore the immunomodulatory effects of these tumor-derived sEVs, we first established a consistent supply of $CD206^{+ve}$ macrophages differentiated from human induced pluripotent stem cells (iMacs), following the established protocol of Douthwaite et al (2021). iMacs were then treated with sEVs with their resulting immunophenotype, and activation assessed. These preliminary experiments provide a step towards understanding how the biophysical environment influences tumor cell resistance to therapy and how sEVs can modulate the relationship between cancer cells and macrophages.

#5571 Collagen stabilization directs immune suppression in the head and neck squamous cell carcinoma hypoxic subtype.

S. Srivastava, J. Powers, R. Chaudhary, S. Marzban, R. J. C. Slebos, J. West, X. Song, J. A. Guevara-Patino, C. H. Chung, A. L. Amelio;
H. Lee Moffitt Cancer Center, Tampa, FL

Head & neck squamous cell carcinoma (HNSCC) show limited clinical benefit to immune checkpoint inhibitors (ICI). Interactions between extracellular matrix (ECM), tumor, and immune cells underly the mechanisms leading to immunosuppression and resistance to ICIs. Collagen matrix remodeling within tumor stroma can influence accessibility and function of immune cells. Specifically, telopeptidyl lysine residues in fibrillar collagen can be hydroxylated by Lysyl hydroxylase 2 (LH2) prior to cross-linking which leads to stiffened, stable collagen. We previously showed that this LH2-modified tumor microenvironment (TME) drives HNSCC invasion and metastasis. Here, we elucidate the interplay between LH2-modified collagen and the immune landscape within TME of hypoxic and immunosuppressive HNSCC.

Bioinformatics analyses of RNAseq datasets were performed to assess pathways regulating collagen deposition and stabilization. Tissue microarray having 81 primary, 28 recurrent primary, and 3 lymph node metastases tumor cores was analyzed. Cores were classified according to our published Hypoxia-Immune signature (Chaudhary R. et al. 2023, *Can Res Comm*). We performed Second Harmonic Generation imaging of H&E stained TMA section to analyze the orientation and length of collagen fibrils. Picrosirius red (PSR) staining allowed quantification of total collagen and collagen maturation was assessed by polarized light imaging of birefringence. Further, we performed multiplex immunofluorescence staining for CD3+ (T-cell); CD14+ (Monocyte & Macrophage); CD11c+ (Dendritic); Pax5+ (B-cell); Pan-Cytokeratin+ (tumor), and LH2.

Low (0-1) LH2 expression was seen in 29.5% of analyzed cores whereas 70.5% of cores scored high (2-3) for LH2 expression. Cores classified under the hypoxia subtype exhibit high LH2 and enrichment of collagen stability signature. Late-stage tumors have highly oriented collagen fibers compared to normal tissue or early-stage tumors which have randomly distributed fibers. CT-Fire-based measurements revealed that $LH2^{hi}$ cores have significantly increased fiber length and lower coefficient of variance for fiber angles. The area of collagen measured by PSR staining had no correlation with tumor stage or subtype indicating that collagen deposition is similarly high in HNSCCs. However, birefringence measurements showed that a higher fraction of mature fibrillar collagen is associated with late-stage $LH2^{hi}$ tumors. Interestingly, LH2 expression positively correlated with increased CD3+ T cells in stroma suggesting that anti-tumor T cells are physically obstructed by the presence of LH2-stabilized and stiffened collagen fibers.

LH2 expression influences the quality of collagen but not the quantity. Understanding the effect of LH2-mediated collagen modifications on the TIME may have implications for therapeutic strategies to enhance anti-tumor immune response in HNSCC.

#5572 Microneedle-guided lymphatic delivery of a natural immune modulator toxin for enhanced cancer immunotherapy.

S. Lim, B. Kim, P. LIU, J. Shin, J. Jeong;
Sungkyunkwan University School of Pharmacy, Suwon-si, Korea, Republic of

Cancer immunotherapy has demonstrated significant potential as a cancer treatment by enhancing the immune system's ability to recognize and eliminate cancer cells. However, its efficacy can be limited by factors such as tumor heterogeneity, immunosuppressive tumor microenvironments, and systemic toxicities. Recent advances in drug delivery systems have facilitated the development of more targeted and personalized cancer therapies. Microneedles have emerged as a promising platform for non-invasive and highly localized drug delivery, directly administering drugs, vaccines, and other therapeutic agents to the skin. In this study, we designed dissolving microneedles (dMN) based on a biocompatible amphiphilic tri-block copolymer, which enables the self-assembly of nano-micelles containing hydrophobic drugs when applied to the skin. We used the dMN technology to formulate SKKU-06, a hydrophobic natural immune modulator toxin derived from fungi, which exhibits anti-cancer and immunomodulatory properties in melanoma (SKKU-06@dMN). After intratumoral application of SSKU-06@dMN to skin tumors, the drug-loaded nano-micelles can migrate to tumor-draining lymph nodes (TDLN). The dMN-guided delivery of SKKU-06 to skin tumors and TDLN induced immunogenic cell death and stimulated the activation and maturation of antigen-presenting cells (APCs), promoting the development of humoral and cellular anti-tumor immunity. Furthermore, the immunomodulatory effects of SSKU-06@dMN were enhanced when combined with anti-PD-1 treatment, impacting the tumor microenvironment through increased intratumoral $CD8^{+}$ T cell infiltration and reduced T_{reg} populations. This resulted in efficient growth inhibition of established skin cancer and metastatic cancer, as well as prolonged survival. The dMN-guided lymphatic delivery of SKKU-06 demonstrates the potential for treating metastatic solid tumors and improving cancer immunotherapy efficacy by modulating the tumor microenvironment.

#5573 Loss of glutathione S-transferase omega 2 promotes immunosuppressive tumor microenvironment by the induction of PD-L1 expression in lung adenocarcinoma.

R. Sumiya[1], H. Hatano[2], T. Hagiwara[2], S. Nagasaka[2], K. Yamada[2], N. Kokudo[2], H. Suzuki[3], Y. I. Kawamura[2];
[1]Juntendo Univ. School of Medicine, Tokyo, Japan, [2]National Center for Global Health and Medicine, Tokyo, Japan, [3]Sapporo Medical University School of Medicine, Hokkaido, Japan

Glutathione S-transferase omega 2 (GSTO2) is known as one of important regulators for the glutathione redox balance. We recently reported that GSTO2 is exclusively expressed in airway basal cells, Clara cells, and type II alveolar cells, which have self-renewal capacity in the lungs; however, its expression was completely lost in lung squamous cell carcinoma (LSCC) (*Cancer Science*, 2022). In this study, we examined the expression of GSTO2 in lung adenocarcinoma (LAC), another type of lung cancer, and analyzed the relationship between GSTO2 expression and clinicopathological features. We enrolled 139 patients who were diagnosed with LAC and underwent surgery, and immunohistochemically evaluated the expression of GSTO2 using formalin-fixed, paraffin-embedded sections of surgical specimens. Fifty eight of 139 lung adenocarcinoma samples exhibited GSTO2 expression, while remaining 81 cases did not. The expression of GSTO2 in LAC samples was significantly associated with never or light (Brinkman Index < 400) smoking history (P=0.0027) and histological subtypes (lepidic 77%; acinar 44%; papillary 22%; micropapillary 16.7%; solid 9.6%; P<0.0001). There were no significant differences between the groups with respect to pN, pM, EGFR mutation, ALK fusion, and ROS-1 fusion. However, GSTO2 expression in LAC significantly associated with pT1 (P<0.0001), early stage (P<0.0001), and absence of PD-L1 expression (P=0.0027). Moreover, patients with GSTO2-negative LAC had a significantly lower disease-free survival rate than those with GSTO2-positve LAC (P=0.028). To examine whether GSTO2 expression affects PD-L1 expression, we prepared GSTO2-transfected and mock-transfected lung adenocarcinoma cell lines (A549 and PC-9). In both cell lines, mRNA level of PD-L1 was significantly reduced in GSTO2-transfectants. Because Jang RH et al reported that vimentin, reflecting to acquire mesenchymal traits in epithelial-mesenchymal transition (EMT), regulates the PD-L1 expression, we next examined whether GSTO2 overexpression affects the expression of EMT related molecules. There was no difference in a mRNA level of E-cadherin, while the mRNA expression of vimentin and SLUG, a transcriptional inducer of EMT, were significantly suppressed in GSTO2-transfected PC-9. In both cell lines, protein expression of vimentin was also significantly reduced in GSTO2-transfectants. The present study shed light on a novel function of GSTO2 as a PD-L1 regulator, which may contribute to prevention of tumor immune escape.

#5574 Degradation of PIP4K2C by novel bivalent functional degrader LRK-A induces tumor regression in CRC.

E. Corse, K. Goodman, M. O'Shea, G. Ye, M. Chow, J. Arnold, V. Giacalone, S. Hayes, E. Dube, S. Alnemy, O. Akinrinmade Adigun, K. Brown, **E. d'Hennezel**, C. Sabatos-Peyton;
Larkspur Biosciences, Inc., Watertown, MA

Phosphatidylinositol 5-phosphate 4-kinase, type II, gamma (PIP4K2C) is a lipid kinase with critical roles in vesicular trafficking, autophagy-dependent catabolism, and modulation of the immune system. Family members PIP4K2A and PIP4K2B are implicated in regulation of autophagy, cancer cell proliferation, and response to insulin, whereas PIP4K2C has a unique function in the immune response to cancer. Beyond the ability to convert PI5P to PI45P2, PIP4K2 kinases regulate membrane localization and clustering of PI45P2 and thus govern multiple aspects of membrane trafficking. These activities are likely to be independent of catalytic function[1]. The involvement of PIP4K2C in membrane lipid dynamics has the potential to broadly impact pro-tumor and immune-suppressive biology in cancer, including uptake of cancer cells by immune cells, and subsequently increase antigen processing, presentation, and T cell activation. Mice deficient in PIP4K2C develop immune cell infiltrates in tissues and increased proinflammatory cytokines in plasma[2], suggesting that modulation of PIP4K2C could enhance anti-tumor immunity in cancer patients.

Achieving potent targeting of PIP4K2C while sparing other family members or other lipid kinases has so far precluded the exploration of its potential as a therapeutic target. Here, we report the discovery of the highly potent and specific PIP4K2C bifunctional degrader LRK-A, which shows rapid and exclusive degradation of PIP4K2C. We show that LRK-A can rapidly and deeply degrade PIP4K2C in primary human PBMCs and cancer cells in vitro, and with broad species cross-reactivity. The specificity of LRK-A for PIP4K2C was established using whole-cell proteomic analyses, without co-degradation of off-target proteins including SALL4 and GSPT1. In mice treated with LRK-A, we observed a dose-dependent, profound, and sustained degradation of PIP4K2C. We further demonstrate that dosing of LRK-A as a single agent significantly reduced tumor growth, including full regressions, at low doses in a mouse syngeneic model of colorectal cancer.

Collectively, our results show that PIP4K2C can be specifically and effectively targeted in vivo using a bifunctional degrader. The reduced tumor growth we observed upon targeting PIP4K2C alone suggests that PIP4K2C is a highly promising target for therapeutic intervention. Further explorations are ongoing to enable the development of PIP4K2C-targeted therapeutic strategies.

References

1. Wang DG, Paddock MN, Lundquist MR, et al. PIP4Ks Suppress Insulin Signaling through a Catalytic-Independent Mechanism. *Cell Rep*. 2019;27(7):1991-2001. doi:10.1016/j.celrep.2019.04.0702. Shim H, Wu C, Ramsamooj S, et al. Deletion of the gene Pip4k2c, a novel phosphatidylinositol kinase, results in hyperactivation of the immune system. *Proc Natl Acad Sci U S A*. 2016;113(27):7596-7601. doi:10.1073/pnas.1600934113

MOLECULAR/CELLULAR BIOLOGY AND GENETICS: Advances in Cancer Prognostication, Therapeutic Response, and Immune Biology
Poster Session

#5577 TRPM8 mediated Ca2+ signaling as a therapeutic target in prostate cancer.

S. Asuthkar[1], K. Velpula[1], V. D. Griend[2];
[1]University of Illinois College of Medicine (Peoria), Peoria, IL, [2]University of Illinois College of Medicine (Peoria), Chicago, IL

Prostate cancer (PC) is a prevalent and deadly malignancy, necessitating the development of innovative therapeutic strategies. Transient receptor potential melastatin 8 (TRPM8), an ion channel highly expressed in prostate epithelium, has emerged as a potential target. Our preliminary studies demonstrate that TRPM8 plays a crucial role in PC progression. We observed an initial increase in TRPM8 mRNA expression during early-stage PC, followed by a decline in advanced and androgen-independent prostate cancer (AIPC) stages. Additionally, TRPM8 knockout mice exhibited elevated serum testosterone levels, heightened androgen receptor (AR) activity, and increased cell cycle, invasion, and adhesion-related effects. In xenograft models, TRPM8 demonstrated potent antitumor properties in both AR+ and AR- contexts. Our research suggests that TRPM8 activation on the plasma membrane promotes calcium influx and induces apoptosis in PC cells. Conversely, TRPM8 internalization correlates with PC pathogenesis. By exploring the effects of TRPM8 on PTEN-mediated cellular signaling, we aim to uncover novel insights into the molecular mechanisms underlying TRPM8's role in PC. This abstract underscores the potential of targeting TRPM8-mediated Ca2+ signaling as a promising therapeutic approach to combat PC progression, offering hope for improved patient outcomes.

#5578 Multi-omics approach reveals a SMAD4-deficiency signature, translational reprogramming and synthetic lethality in esophageal adenocarcinoma.

J. V. Milne, K. Fujihara, E. Kusnadi, M. Pechlivanis, N. Thio, C. Cabalag, T. Gulati, J. Gotovac, K. Simpson, C. Duong, L. Furic, W. Phillips, N. Clemons; Peter MacCallum Cancer Centre, Melbourne, Australia

Esophageal adenocarcinoma (EAC) is a cancer of high mutation burden with negligible recurrent and druggable driver genes and, therefore, a paucity of options for targeted therapy. Mutation or loss of the tumor suppressor gene *SMAD4* occurs in up to 20% of EAC cases, and we have previously shown that loss of SMAD4 is sufficient to promote EAC tumorigenesis in an *in vivo* xenograft model. The present study aimed to delineate the role of SMAD4 in EAC tumorigenesis and identify synthetic lethal interactions in SMAD4-deficient cancers as a novel approach for treating EAC.

Our multi-omics methodology integrated RNA-sequencing, proteomics, polysome-sequencing, reverse-phase protein arrays, and genome-wide CRISPR-Cas9 screening to unveil a SMAD4-deficiency signature and new therapeutic avenues for EAC. These data reveal a complex interplay between SMAD4 loss and regulation of mTOR signaling, with specific downstream effects to reprogram translation. SMAD4-deficient cells express decreased levels of 4E-BP1, the inhibitory binding partner of EIF4E, which is the rate-limiting component of the cap-dependent translation initiation complex. This was accompanied by increased mTOR activity, including phosphorylation and inactivation of 4E-BP1. We found that SMAD4-deficient cells exhibit vastly different polysome traces compared to their wildtype counterparts and preferentially upregulate cap-dependent translation, acquiring an addiction to translation of oncogenic mRNAs. Furthermore, perturbation of additional negative regulators of mTOR signaling in combination with *SMAD4* knockout exacerbated these effects and accelerated tumorigenesis *in vivo* and growth of patient-derived organoids *in vitro.*

This work advances our knowledge of EAC tumorigenesis, provides new mechanistic insights into SMAD4-driven transformation as well as novel potential therapeutic avenues for SMAD4-deficient EAC.

#5579 *MGA*loss-of-function regulates mitochondrial oxidative metabolism-induced cancer stem cell phenotype during lymphomagenesis with therapeutic potential.

J. Xiong, W.-F. Wang, W.-L. Zhao;
Shanghai Institute of Hematology, Shanghai, China

As an antagonist of *MYC* oncogene, *Max* gene associated (*MGA*) gene are implicated in multiple cancers, proposing the potential role of tumor suppressor. Using multi-omics data of The Cancer Genome Atlas (TCGA, n=10,295) and lymphoma datasets from our group (n=702), we defined genetic features associated with *MGA* and its related MYC/MAX/MXD network members across 36 cancers. Pan-cancer, *MGA* mutation, predominant as nonsense or frameshift, was observed in 4.39% of all samples. *MGA* expression was significantly downregulated in mutated samples than that of wild type samples. Moreover, *MGA* mutation was positively associated with inferior clinical outcomes in diffuse large B-cell lymphoma (P=0.001 and P<0.001 in 2 independent datasets), peripheral T-cell lymphoma (P=0.044) and natural killer/T-cell lymphoma (P=0.012), encouraging in-depth study on the important role of *MGA* in lymphomagenesis. Conditional knockout of *MGA* in hematopoietic system using Vav-iCre (*Mga*$^{fl/fl}$*, Vav-iCre* mice) led to reduction in the numbers of peripheral blood lymphocyte due to blockade differentiation and enhanced stemness as evidenced by flowcytometry and RNA-sequencing (RNA-seq). To investigate the molecular mechanism, we performed pulldown assay in NK-92 cells molecular silencing of *MGA* or scramble control, and subsequently subjected for mass spectrum analysis. A total of 97 proteins were identified to interaction with MGA and mainly enriched to nucleosome (26), cytosolic ribosome (16), immune response (13), and glycolysis (6). Molecular silencing of *MGA*, localizing in the nucleolus, interfered with ribosomal RNA processing, enhanced “onco-ribosome” biogenesis, and contributed to aberrant translational program characterized by mitochondrial oxidative metabolism. Changes in mitochondrial respiration and membrane potential are key to maintaining stemness in cancer cells. Considering that stemness is important for tumorigenesis, recurrence, metastasis, and drug resistance, we exploited high-throughput drug screening platform and found that targeted inhibition of Exportin 1 (XPO1) significantly suppressed the viability of tumor cells molecular silencing *MGA*, which were resistant to chemotherapeutic agents such as gemcitabine, etoposide, etc. Mechanically, molecular silencing *MGA* induced abnormalities of nucleocytoplasmic localization in 739 proteins involving in mitochondrial respiratory chain complex I assembly, oxidative phosphorylation, and mitochondrial translation, 50% (332/739) of which were rescued by treatment with XPO1 inhibitor Selinexor. In summary, MGA initiated lymphoma cell stemness via onco-ribosome mediated activation of mitochondrial oxidative metabolism. Selinexor targeted the aberrant nucleocytoplasmic localization and served as a promising therapeutic agent.

#5581 The DACH1 gene, frequently co-deleted with BRCA2 in prostate cancer, governs PARP inhibitor resistance.

Z. Li[1], X. Jiao[1], T. Khan[1], D. Li[1], S. Zha[2], L. Phoon[3], L. Lan[3], A. Robertson[4], A. W. Ashton[5], K. A. Iczkowski[6], A. D. Borowsky[6], A. Ashworth[7], **R. G. Pestell**[1]; [1]Baruch S. Blumberg Institute, Doylestown, PA, [2]Columbia University, New York, NY, [3]Duke University, Durham, NC, [4]Dxige Research Inc., Courtenay, BC, Canada, [5]Lankenau Institute for Medical Research, Wynnewood, PA, [6]UC Davis Health, Sacramento, CA, [7]University of California San Francisco, San Francisco, CA

Background: Prostate cancer (PCa), the second leading cause of death in American men, includes distinct genetic subtypes with distinct therapeutic vulnerabilities (1,2). The *DACH1* gene, in the 13q21.31-q21.33 region, encodes a winged helix/Forkhead DNA-binding protein that governs cell-fate determination that is deleted in ~ 18% of human PCa, where it is associated with poor prognosis (3). Prostate-specific deletion of the *Dach1* gene enhanced prostatic intraepithelial neoplasia (PIN).

Methods: Analysis of *DACH1* gene deletion and expression was conducted from public data bases and human prostate cancer samples. Cells derived from *Dach1* gene deletion mice and human prostate cancer cell lines with DACH1 overexpression were analyzed for PARP inhibitor responses and mechanisms of PARPi resistance. Transgenic prostate Oncomice were generated in which the *Dach1* gene was deleted in the prostate.

Results: Herein, *DACH1* was shown to be co-deleted with *BRCA2* in each of 8 separate cohorts (N=2,186 patients), in ~3-12% of patients. *Dach1* gene deletion or knockdown conferred PARP inhibitor resistance (talazoparib > niraparib > olaparib > rucaparib > veliparib). DACH1 enhanced PARP sensitivity through several mechanisms affecting replication stress, PARP1 binding, inhibiting G9a (reducing H3K9me2), inhibiting $CHK1^{p}$ and $CDK1^{p}$ and inducing expression of snoRNA, specifically the snoRNA known to bind PARP. PARP1 has a BRCT (BRCA1 C-terminus 1) homology domain governing PARP1 dimerization and binding to intact DNA in a complex within a nucleosome. DACH1 binding to PARP1 requires the BRCT domain.

Conclusions: There is a correlation between *DACH1a*$^{-/-}$ and PARPi resistance, correlating with PARPi trapping ability. As reduced *Dach1a* expression may define a subclass of PCa that warrants specific therapies, testing for DACH1a may be warranted.

References: 1. Sanchez-Vega F, Mina M, Armenia J, Chatila WK, Luna A, La KC, *et al.* Oncogenic Signaling Pathways in The Cancer Genome Atlas. Cell 2018;173:321-37 e102. Bailey MH, Tokheim C, Porta-Pardo E, Sengupta S, Bertrand D, Weerasinghe A, *et al.* Comprehensive Characterization of Cancer Driver Genes and Mutations. Cell **2018**;174:1034-53. Li Z, Jiao X, Robertson AG, Di Sante G, Ashton AW, DiRocco A, *et al.* The DACH1 gene is frequently deleted in prostate cancer, restrains prostatic intraepithelial neoplasia, decreases DNA damage repair, and predicts therapy responses. Oncogene **2023**;42:1857-73

#5582 Discovery and preclinical characterization of ISM8001, a covalent and selective FGFR2/FGFR3 dual inhibitor with strong monotherapy anti-tumor activity against advanced solid tumors.

Y. Zhang[1], Y. Wang[1], X. Cai[1], J. Liu[1], H. Cui[1], J. Qiao[1], X. Lin[1], X. Ding[1], S. Bavadekar[1], **S. Rao**[2], M. Zhang[1], F. Ren[1], A. Zhavoronkov[1];
[1]Insilico Medicine, Pu Dong Xin Qu, China, [2]Insilico Medicine, New York, NY

Oncogenic alterations in fibroblast growth factor receptors 2 and 3 (FGFR2 and FGFR3) are key drivers in intrahepatic cholangiocarcinoma, urothelial carcinoma and multiple other solid tumors. Currently approved pan-FGFR inhibitor therapy is limited by off-isoform toxicity (FGFR1-mediated hyperphosphatemia and FGFR4-mediated diarrhea) and acquired FGFR2 or FGFR3 kinase domain resistance mutations. The second generation of FGFR inhibitors currently undergoing clinical evaluation such as RLY-4008 and LOXO-435 are primarily focused on achieving selectivity against either the FGFR2 or FGFR3 isoform, which may narrow their clinical potential. To overcome this limitation and to allow a favorable toxicity profile, we designed and evaluated the anti-cancer effects of a novel and selective FGFR2/FGFR3 dual inhibitor, ISM8001. Biochemically, ISM8001 showed superior inhibition against FGFR2 and FGFR3 with >90-fold and >800-fold selectivity of FGFR2 over FGFR1 and FGFR4, respectively. As an irreversible inhibitor, ISM8001 displayed strong affinity and high efficiency of covalent bond formation with FGFR2/3. Additionally, ISM8001 showed broad inhibition against multiple FGFR2/3 mutant isoforms, especially gatekeeper mutation (FGFR2-V564F and FGFR3-V555M). ISM8001 inhibited cell proliferation of multiple human cancer cell lines with FGFR2/3 aberration with IC_{50} <10 nM while IC_{50} >1 μM was observed in cell lines without FGFR2/3 alterations. Furthermore, ISM8001 demonstrated robust *in vivo* anti-tumor efficacy in multiple cell line-derived xenograft mouse models including the SNU-16 gastric cancer model (FGFR2-amplification), the AN3CA endometrial cancer model (FGFR2 N549K mutation) and the RT4 bladder cancer model (FGFR3-fusion), with tumor growth inhibition varying from 80%~120% while no significant serum phosphate increase or body weight loss. ISM8001 also displayed strong anti-tumor effects in xenograft models of Ba/F3-FGFR2/3 engineered cell lines with different gatekeeper mutations. ISM8001 is classified as a BCS II compound with favorable DMPK properties and druggability, high permeability, low efflux ratio and low DDI risk. *In vivo* PK profiles showed moderate to low clearance and high oral bioavailability across preclinical species. In addition, ISM8001 showed a promising *in vitro* safety profile with favorable selectivity in 468-kinase and Cerep-44 panel studies, and no hERG concerns. Results of 28-day non-clinical toxicology studies in rat and dog showed a safety window of approximately 2-5 fold based on efficacious exposure in different models. Taken together, these data support the clinical development of ISM8001 as a novel, selective FGFR2/FGFR3 dual inhibitor for the potential tissue-agnostic therapy of advanced solid tumors with FGFR2/3 aberrations.

#5583 *Helicobacter pylori* induces the wee1, promoting immune suppressive in human gastric adenocarcinoma.

Md Obaidul Islam, Krishnapriya Thangaretnam, Heng Lu, Dunfa Peng, Nadeem Sidiq Bhat, Mohammed Soutto, Wael El-Rifai, Zheng Chen

University of Miami Miller School of Medicine, Miami, FL

Background: Gastric cancer (GC) is the fourth most common cause of cancer-related death worldwide. GC has a dismal 5-year survival rate of about 32%. *Helicobacter pylori* (*H. pylori*) infection is the strongest risk factor for gastric carcinogenesis. 75-90% of gastric cancer patients exhibit positive *H. pylori* serology. WEE1 is a nuclear kinase that regulates cell cycle progression by inhibiting cyclin-dependent kinases.

Methods & Results: Analysis of non-cancer normal stomach tissue (n=360) and human GC samples (n=1221) identified that WEE1 mRNA was significantly overexpressed in GC. Using immunohistochemistry (IHC) staining in 41 normal and 44 GC human samples, the data indicated that WEE1 protein was significantly overexpressed in GC. Western blot and immunofluorescence (IF) staining confirmed that *H. pylori* infection induces WEE1 overexpression in GC cells with an unexpected cytosolic localization of WEE1 in GC cells. *Tff1* knockout GC mouse model (*Tff1*$^{-/-}$) was infected with mouse-adapted *H. pylori* strain PMSS1. Western blot and immunohistochemistry data demonstrated that *H. pylori* infection induced WEE1 expression in *Tff1* $^{-/-}$ HGD/cancer mouse gastric tissues compared to control *Tff1* $^{-/-}$ mouse stomach. To study how *H. pylori* infection induces WEE1 in GC, analysis from miRTAR, Target Scan, and miRDB demonstrated that WEE1 is predicted to be targeted by miR-497-5p. Using qRT-PCR analysis, we assessed 30 normal and 30 GC human tissue samples, revealing a pronounced downregulation of miR-497-5p in GC specimens. Western blot analysis confirmed that the restoration of miR-497-5p in GC cells markedly reduced WEE1 protein expression. Interestingly, *H. pylori* infection further decreased miR-497-5p levels in GC cells, upregulating WEE1 protein expression. Since the miR-497-5P host gene promoter region contains CpG islands, we confirmed that treatment with 5 Azacytidine (demethylating agent) or DNMT1 knockdown induced expression of miR-497-5p with decreased WEE1 level in GC cells. Furthermore, our preliminary results indicate that aberrant WEE1 overexpression in GC demonstrates a significant positive correlation with immune-suppression gene signatures, underscoring its predictive value for unfavorable patient survival outcomes in GC. Using the *TFF1* knockout mouse GC model, we found that WEE1 inhibition notably decreases the number and activation of CD4+ and CD8+ T cells in neoplastic gastric tissues. These findings also indicate a crucial relationship between WEE1 and the immunosuppressive microenvironment in GC, establishing WEE1 as a promising therapeutic target to enhance therapeutic efficacy and overcome immunotherapy resistance in GC.

Conclusions: Our findings demonstrated a novel mechanism in which *H. pylori* activates the WEE1 in GC, promoting an immune suppressive microenvironment. WEE1 inhibition with immunotherapy could be a promising therapeutic method for GC patients.

#5584 Experimental 'loss-of function' annotation of STK11 mutations with prognostic and therapeutic implications (TNG260mutationfinder.com).

Leanne G. Ahronian, Preksha Shahagadkar, Lauren Flynn, Lauren Grove, Shangtao Liu, Samuel R. Meier, Binzheng Shen, Hannah Stowe, Hsin-Jung Wu, Yi Yu, Andre Mignault, Iga Sienczylo, Heather DiBenedetto, **Silvia Fenoglio**, Teng Teng

Tango Therapeutics, Boston, MA

Loss of function mutations in Serine Threonine Kinase 11 (STK11) occur in 15% of lung adenocarcinoma and have been shown to drive resistance to immune checkpoint blockade clinically, as well as in preclinical models. Though STK11 is commonly inactivated in human cancer with strong implications for treatment outcomes, few STK11 mutations identified from tumor samples have been functionally characterized.

TNG260 is an inhibitor of CoREST that is currently being investigated in combination with pembrolizumab for the treatment of STK11-mutant cancer (NCT05887492). Patients are eligible for enrollment in the TNG260 phase 1/2 trial if their tumor contains a deleterious STK11 mutation. To begin classifying non-annotated variants, over 2,000 distinct mutations in the STK11 gene were identified from STK11 literature or public repositories of tumor sequencing data such as AACR Project GENIE and ClinVar. Where possible, loss-of-function annotations were captured from literature or predictive tools such as PolyPhen-2. However, many STK11 variants, particularly missense mutations, have never been functionally characterized.

We developed a functional screening approach to characterize STK11 alterations using the lung adenocarcinoma cell line A549. A549 cells contain homozygous loss of STK11 via a truncation mutation at Q37, and re-expression of wild-type STK11 in these cells strongly impairs their growth in vitro and in vivo. We created a library of STK11 variant cDNAs, each containing a unique barcode. This library was expressed in A549, and cells were maintained in vitro or in vivo to allow for positive selection of STK11 loss-of-function variants and depletion of variants that behave like wild-type STK11. At the end of the screen, variants were quantified by NGS using each mutant cDNA's unique barcode and compared to well-annotated controls.

These data were assembled to generate TNG260mutationfinder.com -- the first website to curate STK11 variants with functional annotations.

#5585 Genetic variants of IDH and EGFR as diagnostic and prognostic biomarkers in glioblastoma multiforme: A case-control study in the Jordanian Arab population.

A. N. Al-Bzour, S. M. Al-Khatib, **M. N. Almajali**, T. A. Jarrad;
Jordan University of Science & Technology, Irbid, Jordan

Background: Glioblastoma multiforme (GBM) represents a highly aggressive primary brain tumor with poor prognosis. Mutation in the Isocitrate dehydrogenase (IDH1) gene and epidermal growth factor (EGFR) amplification are key diagnostic markers for GBM. However, the prognostic role of genetic variants of these genes remains unclear. Therefore, we aimed to investigate the association between specific single nucleotide polymorphisms (SNPs) for IDH and EGFR genes, and their impact on the risk and prognosis of GBM patients within the Jordanian Arab population.
Methods: We carried out a case-control study involving 63 GBM patients and 226 healthy controls at King Abdullah University Hospital in Jordan. Genomic DNA was extracted from formalin-fixed and paraffin-embedded tissue for GBM patients and blood samples for controls. IDH1 (rs121913500C>T), IDH2 (rs11540478G>A), EGFR (rs231677G>A), and EGFR (rs1468727C>T) SNPs were genotyped and analyzed using the Sequenom iPLEX assay sequencing technique. Overall survival (OS) was analyzed between SNPs using the univariable Cox proportional hazard model. The Cancer Genome Atlas (TCGA-GBM) cohort of 585 patients were analyzed for IDH1, IDH2, and EGFR alterations with OS, disease-free survival (DFS), and progression-free survival (PFS). Single-cell RNA analysis was performed on the following scRNA datasets from the Gene Expression Omnibus (GEO): GSE163108 (n=25,013 cells), and GSE102130 (n=3,321 cells) .
Results: Our study revealed a significant difference in genotype frequency between GBM cases and controls for IDH1 rs121913500C>T, and EGFR rs1468727C>T SNPs. Univariable Cox model showed that the G/G genotype of rs231677G>A (EGFR) SNP was associated with better OS in the codominant model (HR: 0.24, 95% CI: 0.08-0.73, p-value=0.012), and rs11540478G>A (IDH2) SNP (HR: 0.02, 95% CI: 0.0-0.29, p-value=0.005) showing significantly better prognosis compared to the A/G genotype. In the TCGA validation cohort, the altered group of IDH1 were significantly associated with better OS (HR: 0.35, 95% CI: 0.24-0.50, p-value<0.001), DFS (HR: 0.34, 95% CI: 0.23-0.50, p-value<0.001) , and PFS (HR: 0.43, 95% CI: 0.30-0.62, p-value<0.001). The scRNA analysis showed predominant expression of IDH1, IDH2, and EGFR by malignant cells, oligodendrocyte precursor cells, and macrophages.
Conclusion: Our investigation into the genetic landscape of GBM within the Jordanian population suggest that specific genetic variants, particularly in IDH1 genes and EGFR, may serve as diagnostic and prognostic biomarkers for GBM. Additionally, IDH1 alterations were associated with better prognostic outcomes. Single-cell RNA analysis further illuminates the predominant expression of IDH1, IDH2, and EGFR by malignant cells which can be used as potential avenues for targeted therapies based on genetic profiles.

#5586 Hijacking mutant E3 ligase for targeted protein degradation: Discovery of cancer-specific PROTACs for the treatment of FBXW7 R465C driven cancers.

H. Zhang;
Blueray Biopharma, Shanghai, Shanghai, China

Many cancers carry LOF mutations of tumor suppressor genes and drug discovery against these cancers are challenging. Fbxw7 is a major tumor suppressor E3 ligase and is frequently mutated (LOF) in cancer. Fbxw7 R465C mutation correlates with worse survival and resistance to both chemo- and targeted therapies. Blueray have discovered Fbxw7 R465C-selective ligands and developed PROTAC molecules selectively targeting cancers carrying Fbxw7 R465C mutation. The Fbxw7 R465C-based PROTACs show superior degradation activity for several target proteins and inhibit proliferation of cancer cells carrying Fbxw7 R465C mutations. These PROTACs show tumor growth inhibition in Fbxw7 R465C mutant cell derived xenograft models with clear PK/PD correlations. Development of bi-functional molecules such as PROTACs bring new options to target cancers with LOF mutations.

#5587 Regulator of chromosome condensation 1 (RCC1) as a novel therapeutic target in pancreatic ductal adenocarcinoma.

S. F. Bannoura[1], H. Y. Khan[1], A. Aboukameel[1], M. Uddin[1], R. Nimri[2], E. Beal[1], S. Kim[1], M. Al Hallak[1], B. El-Rayes[3], P. A. Philip[2], B. Pasche[1], R. Mohammad[1], A. S. Azmi[1];

[1]Wayne State University School of Medicine, Detroit, MI, [2]Henry Ford Cancer Institute, Henry Ford Health, Detroit, MI, [3]O'Neal Comprehensive Cancer Center, University of Alabama, Birmingham, AL

Background and Introduction: Pancreatic ductal adenocarcinoma (PDAC) is a highly lethal disease with limited treatment options. There is an urgent need for the identification of novel therapeutic targets for PDAC. The transport of molecular cargo between the nucleus and cytoplasm, facilitated by Ran-GTPase, is a critical process that dividing cells rely on to maintain their growth. Elevated nuclear Ran-GTP levels are produced by the activity of the Ran guanine nucleotide exchange factor (GEF) known as Regulator of Chromosome Condensation 1 (RCC1), which is found in the nucleus bound to chromatin. This creates a Ran-GTP gradient across the nuclear membrane, which maintains proper directional transport of proteins and RNA. To sustain proliferative signaling, cancer cells become reliant on high rates of nucleocytoplasmic transport through dysregulation of transport machinery.

Methods: We examined the role of RCC1 in the biology of PDAC. The impact of RCC1 modulation on PDAC growth was evaluated using RNA interference and CRISPR-Cas9 *in vitro* and *in vivo* using PDAC cell lines and LSL-$Kras^{G12D/+}$; LSL-$Trp53^{R172H/+}$; Pdx1-Cre (KPC) tumor-derived cells. The broader impact of RCC1 silencing on PDAC-sustaining signaling was evaluated through RNA-sequencing and proteomics.

Results: Transcriptomic sequencing of PDAC tissue (n=5,071) as well as analysis of publicly available data from the TCGA, CPTAC and GTEx revealed that RCC1 expression is higher in PDAC tissues compared to normal pancreas. Moreover, PDAC patients with higher RCC1 expression were more likely to have poorer outcomes. RCC1 silencing by RNAi and CRISPR-Cas9 resulted in reduced proliferation in 2D and 3D cultures and attenuated tumor growth *in vivo*. RCC1 KD decreased migration and colony formation, enhanced apoptosis, and altered the cell cycle in human and KPC mouse PDAC cells. Subcutaneous RCC1 KO cell line-derived xenografts show arrested growth. Subcellular Ran distribution was disrupted upon RCC1 KO, suggesting that nuclear Ran concentration is important for PDAC proliferation. Nuclear and cytosolic proteomic analysis revealed altered subcellular proteome in RCC1 KD KPC tumor-derived cells. Altered cytoplasmic protein pathways include several metabolic pathways, PI3K-AKT, and Hedgehog signaling. Nuclear enriched pathways include cell cycle, mitosis, metabolic processes, and RNA processing. RNA-seq of RCC1 KO cells showed widespread transcriptional alterations. Upstream of RCC1, c-MYC activates the RCC1-RAN axis, and RCC1 KO cells show differential sensitivity to c-MYC inhibitors. Finally, RCC1 KD resulted in the sensitization of PDAC cells to Gemcitabine. Molecular characterization of conditional $Rcc1^{fl/fl}$ KO transgenic model to study the role of RCC1 in PDAC *in vivo* is ongoing.

Conclusions: Overall, our results show that RCC1 is involved in the regulation of PDAC growth and is a potential target for therapy.

#5588 Protein Arginine Methyltransferase 2 is involved in the control of inflammatory processes in acute myeloid leukemia.

C. Sauter[1], T. Morin[1], F. Guidez[1], J. Simonet[1], C. Fournier[1], C. Row[2], D. Masnikov[1], B. Pernon[1], A. Largeot[3], A. Aznague[1], Y. Herault[4], G. Sauvageau[5], M. Maynadie[1], M. Callanan[1], J.-N. Bastie[1], R. Aucagne[1], **L. Levadny Delva**[1];

[1]Inserm U1231, Dijon, France, [2]Inserm U1231, Dijon Hospital, Dijon, France, [3]Luxembourg Institute of Health, Dijon, Luxembourg, [4]IGBMC, Illkirch, France, [5]IRIC, Montreal, QC, Canada

A direct link between chronic inflammation and development of Acute Myeloid Leukemia (AML) has been highlighted in the past few years, demonstrating an interconnection between marked inflammatory phenotype and aberrant myeloproliferation in AML patients. Treating AML patients exhibiting a higher inflammatory signature with anti-inflammatory molecules resulted in significant increase of overall survival. Protein Arginine Methyltransferases (PRMTs) are epigenetic factors known to regulate gene expression through methylation of histone tails. It has been previously reported that PRMT1, 4, and 5 inhibition exhibit anti-proliferative effects on AML models. In this study, we investigated the role of another PRMT, called PRMT2, in the development of AML through its regulatory roles in inflammatory pathways. We first determined from an AML cohort (The Leucegene project, IRIC, Montréal, QC, Canada) that patients with a low PRMT2 expression display an enrichment of proinflammatory pathways compared to patients with a high PRMT2 expression. Therefore, we hypothesized that PRMT2 could be a key regulator of inflammatory processes in AML. We thus used a PRMT2 knockout mouse model (Prmt2 KO) and a PRMT2 knockout human AML cell line to validate our hypothesis. Although we demonstrated no difference in the bone marrow progenitors or mature cell populations of Prmt2 KO mice compared to control, we observed that Prmt2 KO Bone-Marrow Derived Macrophages (BMDMs) are more sensitive to LPS stimulation and express higher levels of pro-inflammatory cytokines, supporting our previous findings for a role of PRMT2 in the negative regulation of inflammatory processes. PRMT2 depleted human AML cells displayed an increased pro-inflammatory signature due to overactivation of STAT3, which is caused by an enhanced activation of the NFkB signaling pathway, leading to an overproduction of IL6. Together, these findings demonstrate that PRMT2 is a key regulator of the control of inflammation in AML. Recognition of PRMT2 as a biomarker of inflammation in AML would help to adapt treatment possibly through the synergistic use of anti-inflammatory molecules with other cytotoxic drugs.

#5589 *CBFB::MYH11* expression activates *Trp53* in myeloid cells, which inhibits cell growth and sensitizes cells to cytarabine.

R. B. Day, J. A. Hickman, C. D. S. Katerndahl, S. Mukund Ramakrishnan, C. A. Miller, T. J. Ley;
Washington University In St. Louis, St. Louis, MO

CBFB::MYH11 acute myeloid leukemia (AML) is a subset of Core Binding Factor AML initiated by an oncofusion in which Core Binding Factor Beta (CBFB) is fused to the C-terminus of smooth muscle myosin heavy chain 11 (MYH11). *CBFB::MYH11* AML has a high cure rate with conventional anthracycline/cytarabine induction and high-dose cytarabine consolidation in patients under the age of 60, and remains chemosensitive after multiple relapses; the mechanisms underlying chemosensitivity are unknown. *TP53* is a key regulator of DNA damage response and apoptosis, and *TP53*-mutated AML is often chemoresistant. Large sequencing studies have revealed only rare co-occurrence of *TP53* mutations with *CBFB::MYH11*. We initially used *CBFB::MYH11* as a negative control for an unrelated study of *TP53* function and unexpectedly found striking synergy. While expression of *CBFB::MYH11* in WT murine hematopoietic stem and progenitor cells (HSPCs) induced a low-penetrance (~20%), long latency (~6 months) myelomonocytic AML, expression of *CBFB::MYH11* in *Trp53*$^{-/-}$ HSPCs induced AML with 100% penetrance and a median latency of 8 weeks. *CBFB::MYH11*-induced AMLs arising in *Trp53*$^{-/-}$ cells were similar by morphology and flow cytometry phenotype. We validated these findings in a second model, using a conditional *Trp53*$^{flox/flox}$ *x Vav1-Cre* model in which *Trp53* is inactivated in HSPCs, with nearly identical results. *Trp53*$^{-/-}$ cells transduced with Empty Vector did not develop AML, but did develop T cell lymphoma with a median latency of 16 weeks, similar to prior studies. *Trp53* deficiency also cooperated with *RUNX1::RUNX1T1*, the other Core Binding Factor oncofusion, to induce a high-penetrance (100%) and short latency AML (median latency 10 weeks); consistent with prior data, *RUNX1::RUNX1T1* expression alone in *Trp53* WT cells was insufficient to induce AML.

To determine whether *Trp53* influences the chemosensitivity of *CBFB::MYH11* expressing cells, we performed cytarabine dose-response experiments. While *CBFB::MYH11*-transduced WT HSPCs were very sensitive to cytarabine (relative to EV), sensitivity was reduced in *CBFB::MYH11*-transduced *Trp53*$^{-/-}$ cells, suggesting that *CBFB::MYH11*-induced chemosensitivity is, at least in part, mediated by the TP53 pathway. To determine whether *CBFB::MYH11* expression results in upregulation of key TP53 pathway genes, we transduced WT HSPCs with EV or *CBFB::MYH11*, transplanted cells into WT mice, harvested bone marrow at 3 months, and performed RNA-Seq. Key TP53 pathway genes were upregulated, including *Bbc3/Puma*, *Bax*, *Cdkn1a/p21*, and *Trp53* (all 2.6-4.6-fold, $p \leq 0.05$). These data suggest that the chemosensitivity and the favorable prognosis of *CBFB::MYH11* AML may be due to the direct activation of the TP53 pathway by *CBFB::MYH11*. Similar studies are underway with *RUNX1::RUNX1T1*-transduced cells to determine whether TP53 is relevant for the chemosensitivity of that CBF AML as well.

#5590 Engineered destabilized 3'UTR of TEAD1 therapeutically inhibits and degrades TEAD1 mRNA and YAP1 interactors across multiple cancers.

C. U. Awah;
UTR Therapeutics Inc, New York, NY

The hippo pathway mediated by TEAD1 is overexpressed and oncogenic in multiple cancers. We report here the development of engineered destabilized 3'UTR of TEAD1 which overwrote and degraded oncogenic TEAD1 in ethnically diverse breast cancers, prostate cancers, ovarian cancers, and pancreatic cancer. We validated the destabilization and degradation of TEAD1 on the transcript and protein levels. This led to the loss of cancer cell size causing severe shrinkage as hippo pathway controls cells size , impaired cancer cell migration abilities and loss of cancer cell viability. These properties are titratable and specific demonstrating the specific engagement of the engineered destabilized 3'UTR of TEAD1 with oncogenic TEAD1 mRNA in destabilizing and degrading it. In a dose dependent titration analysis, we determined the IC50 of the engineered destabilized 3'UTR of TEAD1 across many cancers. IC50 dose dependent titration comparison with the engineered destabilized 3'UTR of TEAD1 constructs and chemotherapies (DNA damaging agents, microtubules inhibiting drugs, alkylating agents) as well as immune checkpoint inhibitor. We found evidence that suggests that the engineered destabilized 3'UTR of TEAD1 is superior. Mechanistically, the loss of TEAD1 led to the loss of TEAD2,3 and YAP1 and FOSL1 , JUN and c-MYC.

#5591 ARID domain containing BAF subunits exhibit neomorphism: Have we identified the new Achilles heel in cancer?.

S. Sarkar, **M. D. Bashyam**;
Ctr. for DNA Fingerprinting & Diagnostics (CDFD), Hyderabad, India

The SWI/SNF chromatin remodeler utilizes energy of ATP hydrolysis to slide or evict nucleosomes or histones, respectively, thus enabling nuclear processes by driving an 'open' chromatin architecture. The mammalian SWI/SNF, also termed the BrG1/Brm associated factor (BAF) complex, is the major chromatin remodeler in ontogeny and adult life. Three major BAF complexes namely canonical (cBAF), polybromo (pBAF), and non-canonical (ncBAF) have been studied. BAF components, classified as a tumor suppressors, exhibit frequent mutations in cancers. Though, studies have evaluated functional roles of BAF subunits, very few attempted to study BAF mutations identified across cancer types. In our previous studies, we identified tumor specific mutations in the gene encoding 'A-T rich interaction domain containing 1B' (ARID1B), within its nuclear localization signal (NLS). NLS-inactivated ARID1B exhibited cytoplasmic localization and promoted tumorigenesis by activating the ERK and Wnt/β-catenin pathways. More recently, we detected inactivating mutations in the gene encoding ARID2, a component of the pBAF complex and an ARID1B paralogue. We now present detailed characterization of tumor-specific ARID2 truncations that were presumed to be inactivating in nature. One such truncation mutation viz. p.Ser989fsArg21*, identified in our previous study, is expected to yield an ARID2 protein truncating at amino acid position 1010 (as against the full length of 1835 amino acids). Scrutiny of The Cancer Genome Atlas cBioPortal and Cancer Cell Line Encyclopedia mutation data bases revealed several ARID2 mutations expected to truncate the protein around the 1010 position. Surprisingly, ectopic expression of truncated ARID2 forms promoted oncogenic function in both ARID2 proficient and deficient backgrounds, thus validating a neomorphic gain of function for the truncated protein. Fluorescence based intracellular localization assays revealed a surprising cytoplasmic localization of truncated ARID2. Further, we mapped the ARID2 NLS by *in silico* analysis followed by evaluation of several deletion constructs, to be located at 1488-1518 position; thus, explaining the cytoplasmic localization of ARID2 forms truncating around 1010 position. Further, truncated ARID2 was unable to bind other pBAF components and did not sequester other pBAF components to the cytoplasm, in both ARID2 proficient and deficient cells. Tandem Affinity Purification Mass-spectrometry revealed putative interaction partners for truncated ARID2; analysis is currently underway to reveal the mechanism of tumorigenic induction exhibited by truncated ARID2. Immunohistochemistry on colorectal and breast cancer tissue microarrays revealed ARID2 cytoplasmic localization in a significant fraction of samples. We have discovered a novel YIN-YANG function of BAF components expected to yield efficient therapeutic options in cancer.

#5592 HMGA1 modulates chromatin state and transcriptional networks involved in plasticity in refractory myeloid leukemia.

B. E. West[1], J.-H. Kim[1], A.-A. Supreme[1], I. Herrera[1], Z. Thompson[1], L. Z. Luo[1], F. Shaik[1], J. Kim[1], H. Woo[1], S. Meshinchi[2], R. E. Ries[2], L. M. S. Resar[1]; [1]Johns Hopkins University, Baltimore, MD, [2]Fred Hutchinson Cancer Research Center, Seattle, WA

Although High Mobility Group A1 (HMGA1) chromatin regulators are overexpressed in refractory acute myeloid leukemia (AML) and diverse solid tumors, targetable mechanisms underlying HMGA1 remain elusive. *HMGA1* is highly expressed in stem cells and poorly differentiated cancers where it modulates chromatin structure to activate developmental gene networks. In AML arising from *JAK2*^{V617F} myeloproliferative neoplasms (MPN), HMGA1 is required for leukemogenesis by inducing transcriptional networks that drive aberrant proliferation and cell fate. Like MPN AML, KMT2A-rearranged (KMT2A-r) AML is refractory to therapy and highly lethal. KMT2A-r AML is caused by rearrangements of the *KMT2A* gene, which encode abnormal fusion proteins that induce pro-leukemogenic genes, including *HOX* genes. While prior work identified KMT2A fusion partners and protein complexes, this has not led to better therapies for most patients. We therefore sought to examine HMGA1 function in KMT2A-r AML. We hypothesized that: 1) HMGA1 drives plasticity in KMT2A-r AML by altering chromatin state and transcriptional networks, and, 2) Targeting HMGA1 will enhance sensitivity to therapy. In two KMT2A-r AML patient cohorts, *HMGA1* is highly overexpressed compared to CD34^{+} stem and progenitors from healthy controls, suggesting it drives leukemogenesis. To define HMGA1 function, we silenced *HMGA1* using CRISPR or short hairpin RNA in KMT2A-r cell lines (MOLM-14, THP-1, MV4-11). Strikingly, silencing *HMGA1* disrupts proliferation and clonogenicity *in vitro*, while prolonging survival in immunosuppressed mice transplanted with KMT2A-r AML cells. Intriguingly, leukemic cells that engraft in the bone marrow from the pool of cells with *HMGA1* silencing express higher levels of *HMGA1*, suggesting that escape from gene silencing and a specific level of HMGA1 is required for leukemic engraftment and expansion. *HMGA1* also increases in KMT2A-r AML cells that become resistant to cytarabine (AraC), suggesting that HMGA1 endows AML cells with the capacity to survive and expand after AraC. Because repression of tumor suppressors was recently defined as a mechanism of therapy resistance in AML, we also examined tumor suppressor pathways in both *JAK2*^{V617F} and KMT2A-r AML. Intriguingly, HMGA1 occupies the promoter region of the *CDKN1A* locus by chromatin immunoprecipitation and represses its expression in KMT2A-r and *JAK2*^{V617F} AML cells. To define additional mechanisms underlying HMGA1 in KMT2A-r AML, multi-omics studies are underway. In preliminary work thus far, we also found that HMGA1 induces *HOX* genes. Together, these findings implicate HMGA1 as a promising therapeutic target and novel epigenetic regulator in KMT2A-r AML by altering chromatin state and downstream gene expression.

#5593 METTL3-NUP93 axis as a novel therapeutic target in castration-resistant prostate cancer (CRPC).

J. Lee, Z. Zhang, J. Hong, K. Xu;
UT Health Science Center at San Antonio, San Antonio, TX

Androgens and androgen receptor (AR) are the key factors driving the development and progression of prostate cancer. Extensive studies confirm both androgens and AR are required for normal growth and development of the prostate gland, and also in prostate cancer pathogenesis and androgen-independent cancer progression. Therefore, androgen deprivation therapies or targeting AR function have always been the mainstay of therapeutic strategy against advanced prostate cancers. However, the current therapeutic strategies are temporally effective in suppressing prostate tumors, and eventually develop metastatic disease. Nuclear pore complex (NPC) is a large complex composed of approximately 30 different proteins termed nucleoporins (NUPs), which serve as the structural and functional units for macromolecules shuttling including proteins and messenger RNAs (mRNAs) between nucleus and cytoplasm. Abnormal expression or genetic alterations of NUP genes has been indicated to involve in the progression of prostate cancer, but the underlying molecular mechanisms are poorly understood. We recently found that the m^6A methyltransferase METTL3 directly interacts with nucleoporin 93 (NUP93), one of the NPC components in multiple prostate cancer cells, which seems to be more robust in the castration-resistant prostate cancer (CRPC) cell lines. Disruption of METTL3-NUP93 axis abrogated proliferation and oncogenic phenotypes of CRPC cells, suggesting that the METTL3-NUP93 axis may play an important role in prostate cancer progression to castration resistance. Most importantly, a subgroup of mRNAs regulated through METTL3-NUP93 axis encode cholesterol biosynthesis enzymes that trigger the activation of persistent AR signaling in CRPC. Therefore, Our current findings suggest that inhibition of METTL3-NUP93 axis may represent a promising therapeutic strategy for CRPC, the lethal form of the disease.

#5594 Exploring genetic determinants: A comprehensive analysis of SERPINB family variants and prognosis in Jordanian glioblastoma multiforme patients.

S. Al-Khatib, **M. N. Almajali**, A. Al-Bzour, J. Al-Ramadneh, L. Sa'd, N. Othman;
Jordan University of Science & Technology, Irbid, Jordan

Background: Glioblastoma multiforme (GBM) is a major concern with high fatality rate. In Jordan, the incidence of GBM has notably increased, emphasizing the urgency for population-specific research. Serpins are serine proteinase inhibitors, with several Serpins being overexpressed in cancer cells however the exact mechanism by which they affect GBM progression remains unclear. Thus, we aim to analyze the single-nucleotide polymorphism (SNP) of SERPINB11 and its association with GBM survival.

Methods: A cohort of 63 GBM patients recruited from King Abdullah University Hospital (KAUH) in Jordan, underwent genomic DNA extraction, polymorphism analysis, and overall survival (OS) assessments. The Serpin B family were validated using The Cancer Genome Atlas (TCGA-GBM) cohort of 160 patients. We constructed a risk-score using the principal component analysis for the following Serpin genes: Serpinb3, Serpinb5, Serpinb6, Serpinb11, and Serpinb12, and patients were grouped into high- vs. low-risk based on median cutoff. Univariable Cox models were used to study the survival outcomes, differential expression analysis between the high- and low-risk groups was carried out to identify the differentially expressed genes (DEGs), gene ontology (GO and tumor microenvironment analyses were carried out.

Results: In our primary cohort, we identified a significant association between rs4940595 (*SERPINB11*) SNP and survival, with the G/T- genotype showing worse prognosis compared to the G/G-T/T genotype in the over dominant model (HR: 2.75, 95% CI: 1.29-5.88, p-value=0.009). In the TCGA validation-cohort, alterations in the *SERPINB3*gene showed significantly worse OS (Median: 9.53 vs. 14.3, p-value=0.044) compared to the no alteration group. Univariable Cox showed worse PFS outcomes with higher SERPINB5 (HR: 1.67, 95% CI: 1.15-2.43, p-value=0.007) and SERPINB6 expression (HR: 1.44, 95% CI: 1.06-1.96, p-value=0.021). A Serpin B 5-gene risk score was constructed revealing significant association with IDH mutation status and a trend towards worse PFS in the high-risk group. Upregulated DEGs showed GO enrichment in cytokine regulation and production, positive regulation of leukocyte activation and MAPK cascade. While the downregulated DEGs were enriched in forebrain development, and negative regulation of neuron differentiation. The high-risk group showed a significantly higher infiltration of M2 macrophages and activated mast cells.

Conclusion: Our findings showed a significant role of the Serpin B family with GBM survival in the Jordanian population. Molecular analyses showed potential mechanisms underlying these associations. Our exploration of SERPINB family and associated SNPs provides valuable insights into the molecular landscape of GBM, paving the way for potential targeted interventions and personalized treatment strategies.

#5595 Multifaceted role Cornulin in head and neck squamous cell carcinoma: From tumor suppressor pathophysiology to prognosticating biomarker.

R. Kaur, A. Chauhan, S. Ghoshal, J. Bakshi, R. Srinivasan, **A. Pal**;
Postgraduate Institute of Medical Education & Research (PGIMER), Chandigarh, India

Background: In our previous study, based on LC-MS/MS analysis, the salivary Cornulin, a relatively less explored protein, was found to be ~10-fold downregulated in Head and Neck Squamous Cell Carcinoma (HNSCC) patients. However, the exact role of Cornulin in the pathophysiology of HNSCC is not reported. Here, we investigated its role in the pathophysiology of HNSCC and elucidated its potential as a prognostic marker as well as its antitumour effect.
Methods: Sandwich ELISA and immunohistochemistry were performed to estimate the salivary and tissue levels of Cornulin, respectively, in HNSCC patients, along with an analysis of the effects of Cornulin levels on disease outcome. To investigate the antitumor effects ,its levels were upregulated through lentiviral transduction in low expressing Cal27, FaDu cell lines. Subsequently, various assays were conducted to examine the antitumor effects of Cornulin upregulation. The molecular signalling pathway was elucidated by analysing transcriptome. Additionally, the effects of increased Cornulin expression were also evaluated in an *in vivo* nude mice model.
Results: The pre-treatment salivary Cornulin levels were significantly low ($p=0.0001$) in HNSCC patients (n=128,146.4±5.589pg/mL) and in oral premalignant disease patients (n=25, 174.6 + 9.924 pg/mL) with respect to healthy controls (n=84,185.2±7.170pg/mL). Also, the tumor tissue expression of Cornulin (n=113,H-score=12.70±2.396) was significantly downregulated ($p<0.0001$) compared to the tumor-free margin (n=72,H-score=139.6±10.34). The patients showing complete clinical response regained normal salivary levels within 6 months of completion of treatment ($p<0.0001$). More importantly, low salivary Cornulin level at diagnosis was associated with poor overall survival ($p=0.0282$), indicating it to be a potential prognostic marker. On upregulation of Cornulin in low-expressing HNSCC cell lines (Cal27 and FaDu), the cellular viability, migration, and invasion showed a significant decrease. These indicate its potential as a tumor suppressor. RNAseq data of Cornulin overexpressed cell lines and further Gene set enrichment analysis, the G2/M checkpoint pathway was found to be positively enriched. Cornulin overexpression also arrests the G1/S phase of the cell cycle. GSEA and in vitro experiments revealed Cornulin to be involved in the PI3K/Akt/mTOR signalling pathway. In the nude mice xenograft model, decreased tumor progression, and tumor volume, was documented after Cornulin overexpression. There was an increase in differentiation in the xenograft tumors formed by Cornulin overexpressed cells.
Conclusion: Here, we report for the first time that intrinsic Cornulin has a role as a potent antitumor and has potential as a prognostic marker. However the exact molecular mechanism needs to be further evaluated.

#5596 Exploring BRCA1-Y1853ter and potential therapeutic targets in BRCA1-BRCT mutated cancers.

J. Chen;
The University of Kansas Medical Center, Kansas City, KS

The breast cancer gene BRCA1 plays a pivotal role as a tumor suppressor gene. Despite the use of poly (ADP-ribose) polymerase inhibitors (PARPi) in treating BRCA1 mutation carriers, the lack of response or the development of acquired drug resistance underscores the pressing need for new therapeutic targets. One intriguing BRCA1 mutation, BRCA1-Y1853ter, characterized by a minimal truncation, has been identified in multiple individuals with Hereditary Breast and Ovarian Cancer (HBOC) syndrome. We have developed a Halo Tag and adenovirus-based system where wild-type BRCA1 (WT BRCA1) and mutant BRCA1 protein complexes can be studied in multiple cell types. Here, we used this system to affinity purify BRCA1 wild-type and mutant complexes, followed by label-free quantitative proteomics to investigate the dynamic interactome variations between WT BRCA1 and BRCA1 mutant. Contrary to the assumed loss of function, our preliminary findings suggest a potential gain of function, as a significant number of candidate proteins exhibit enhanced binding affinity with the mutant BRCA1. We are currently exploring whether these distinct binding characteristics are shared among various BRCA1-BRCT mutants, which may hint at a common tumorigenesis mechanism. Our overarching hypothesis is that identifying a specific binding partner, shared among various BRCA-BRCT mutants, could unveil a novel therapeutic target with broader applicability in treating BRCA1-related malignancies.

#5597 Clinical significance of RNA polymerase I inhibitor in pancreatic cancer therapy.

M. Ahmad;
University of Texas Rio Grande Valley, McAllen, TX

Pancreatic cancer (PanCa) is the third leading cause of cancer-related deaths in the United States with limited therapeutic options available. Gemcitabine (GEM), a deoxycytidine nucleoside analog is currently considered the most effective therapy for PanCa. However, it shows only a marginal survival benefit of six months. Aberrant ribosome biogenesis occurs in most tumor types. We observed that PanCa cells are addicted to ribosome biogenesis (RiBi), which supports their highly aggressive metastatic phenotypes. Thus, strategically targeting RiBi process could be one of the ideal strategies for the prevention and treatment of PanCa. In this study, we elucidated the molecular mechanisms of POLR1A (RPA194) overexpression and how its targeting along with p53 status impacts RNA polymerase I inhibitor therapy against PanCa. The expression level of RPA194 was significantly elevated in pancreatic tumor tissues when compared with adjacent normal pancreatic tissues. BMH-21 is a potent pharmacological inhibitor of RNA Pol I, which is known to degrade RPA194 protein. Our results demonstrated that BMH-21 can selectively induce apoptosis in various PanCa cells but not in HPNE cells. We also found that the cytotoxic effect of BMH-21 was dependent on the expression pattern of RPA-194 and p53 status. We further examined the therapeutic efficacy of BMH-21 in orthotopic xenograft mouse models by using two different PanCa cells, AsPC1 which contains non-functional p53 and MIA PaCa-2 which contains functional mutant p53. We observed that BMH-21 significantly inhibited the growth of tumors derived from both cancer cell lines. Interestingly, BMH-21-mediated inhibition of tumor growth was more significant in tumors derived from MIA PaCa-2 cells compared to AsPC1 cells. Further examination revealed that the inhibition of tumor growth was correlated with RPA194 degradation followed by inhibition of cell proliferation. Overall, our results strongly suggest that BMH-21 is a promising non-toxic agent for the treatment of advanced PanCa and its therapeutic potential depends on RPA194 expression and p53 status in PanCa cells.

#5598 Combined loss of the chromosome 7 genes *CUX1* and *EZH2* promotes chemotherapy resistance.

M. R. M. Jotte, A. Stoddart, T. C. Martinez, Y. Xue, M. K. Imgruet, M. E. McNerney;
University of Chicago, Chicago, IL

Monosomy 7 (-7) or del(7q) are recurrent in high-risk myeloid neoplasms, including up to 50% of myeloid neoplasms arising after prior exposure to chemotherapy and/or radiation. Although putative chromosome 7 tumor suppressor genes have been identified, the effects of combinatorial 7q gene loss remain unclear. A barrier to understanding the pathogenesis of -7/del(7q) is the challenge of modeling aneuploidy in animal models. To address this knowledge gap, we established an *in vivo* model of del(7q) clonal hematopoiesis and drug resistance using multiplex CRISPR-Cas9 to simultaneously target four 7q genes (*Cux1, Ezh2, Kmt2c,* and *Kmt2e*) in murine hematopoietic stem cells. After chemotherapy exposure, we observe significant myeloid expansion of clones edited for both *Cux1* and *Ezh2*. Compared to the transcriptomes of control or single gene edited cells, *Cux1;Ezh2*-deficient cells fail to induce DNA damage response pathways after genotoxic stress. *Cux1*;*Ezh2*-deficient cells also display reduced deposition of γH2AX after DNA damage, as well as persistent, unrepaired DNA breaks, indicating perturbations to DNA damage recognition and repair. Collectively, our data support the concept of 7q as a contiguous gene syndrome region, in which combined loss of multiple genes drives drug resistance and disease development. This work reveals a genetic interaction between *CUX1* and *EZH2*, and sheds light on how -7/del(7q) contributes to the development and inherent drug resistance characteristic of high-risk myeloid disease. Further, our CRISPR-based approach may serve as a framework for interrogating other recurrent aneuploid events in cancer.

#5599 Role of HOX gene expression in differentiation of colon cancer stem cells.

B. T. Osmond[1], C. O. B. Facey[2], L. O. Opdenaker[2], C. Zhang[1], B. M. Boman[1];
[1]University of Delaware, Newark, DE, [2]Christiana Care Christiana Hospital, Newark, DE

HOX genes encode a highly conserved set of transcription factors critical for stem cell (SC) function and embryonic development. Several HOX genes have also been implicated in a myriad of cancers, including colorectal cancer (CRC). However, how HOX genes play a role in SC regulation and contributes to cancer development is unclear. HOX expression is regulated by WNT, FGF, and retinoic acid (RA) signaling - pathways which also become dysregulated in cancer. *Goal*: To determine how regulation of HOX genes specifies differentiation of colonic SCs into specialized cell lineages and how dysregulation of HOX genes contributes to CRC development. *Hypotheses*: *i*) Each of the different cell types within human colonic epithelium has a distinct HOX gene expression signature; *ii*) All-trans retinoic acid (ATRA) induced differentiation of CRC cells changes HOX expression that correlates with specific HOX expression signatures in normal colon and CRC cells. *Results*: Immunostaining shows that specific HOX proteins (e.g., HOXA9 & HOXC9) are selectively expressed in ALDH-positive SCs and expression of these HOX genes is increased in CRC tissues compared to normal epithelium. Bioinformatics analysis predicted that these HOX genes (plus HOXA4, HOXA10, HOXC8) are regulated by RA signaling. Accordingly, we studied how ATRA influences HOX expression in CRC cells (HT29 & SW480). We found ATRA treatment: 1) Decreases proliferation and increases neuroendocrine cell (NEC) differentiation; and 2). Leads to specific changes in HOX gene expression patterns. Using NanoString profiling, we also discovered that LGR5+ SCs, ALDH+ SCs and GLP2R+ NECs have unique HOX signatures. By defining how these HOX gene expression changes in response to ATRA treatment in comparison to the HOX gene signatures of different colonic cell lineages will help us understand the role that HOX genes play in SC differentiation and how dysregulation of HOX gene expression contributes to CRC development.

MOLECULAR/CELLULAR BIOLOGY AND GENETICS: DNA Damage and Repair 2
Poster Session

#5603 Defining the functions of the BRCA2 BRC repeats in modulating RAD51 binding and activity.
J. R. Jensen, R. B. Jensen;
Yale University, New Haven, CT

The BRCA2 (Breast Cancer Susceptibility 2) gene is critical for preserving genome integrity by regulating homology-directed repair (HDR) of DNA double-strand breaks (DSBs). Germline mutations in BRCA2 predispose individuals to a high risk for ovarian, breast, prostate, and pancreatic cancer. BRCA2 contains eight BRC repeats that mediate binding to RAD51. It remains unclear how exactly the different BRC repeats regulate RAD51 functions. In our study, we explore the importance of each BRC repeat, their interconnections, and their impact on RAD51 binding and filament stability. We engineered amino acid substitutions into the BRC FxTAS motif required for specific contacts within a hydrophobic binding pocket of RAD51 to disrupt BRC binding to RAD51. We further created mutations in RAD51 (F86E/A89E) that either prevent self-association but retain binding to the BRC repeats or a mutation (K133R) that results in a hyper-stable RAD51 nucleoprotein filament. Using both cell-based models and biochemical analyses, we have begun studies to parse out the specific functions of each BRC repeat. Our ultimate goal is to incorporate single amino acid changes into each BRC repeat within the context of the full-length BRCA2 protein to comprehensively characterize the contribution of each BRC repeat to HDR and response to chemotherapeutics such as PARP inhibitors.

#5604 Modulating DNA repair through endo-exonuclease inhibition: a new therapeutic paradigm in oncology.

T. Chow, J. Duan, P. Colin, C. Bier;
Montdorex Inc., Montreal, QC, Canada

DNA damage repair (DDR) mechanisms are crucial for the maintenance of genomic stability and are emerging as potential therapeutic targets for cancer. Endo-exonuclease (EE)[1] plays a key role in this process and increase EE expression has been observed in the cancer cells examined. In this context, we identified a dicationic diarylfuran, pentamidine, which is an antiparasitic drug that has been used clinically to treat opportunistic infections such as *Pneumocystis carinii*. Pentamidine is an inhibitor of the endo-exonuclease as determined by enzyme kinetic assay and is known to be active on cancer cells. In a proof of concept study[2], tumor with increased EE expression (determined by IHC) showed the best response to this drug.

We have now identified novel mono- and di-amidine analogs of pentamidine that are more effective than the parent drug in both *in vitro* and *in vivo* studies. Furthermore, pre-clinical animal studies of our lead candidate, MTDX203, showed an increased anti-cancer activity with a higher safety index than pentamidine. Based on a predictive PK/PD model, a human iv infusion dose administered twice weekly at ~0.4 mpk (i.e. 28 mg/day, ~10% of pentamidine effective iv dose) is expected to be clinically effective. Our work establishes the EE as a therapeutic target for cancer and identifies a new First in Class of novel anti-cancer agents.

[1]Chow et al. (2004) MCT 3:911-918[2] NCT01378143: Pentamidine (OCZ103-OS) in Patients With Unresectable and Locally Recurrent or Metastatic Colorectal Cancer Undergoing Standard Chemotherap

#5605 *Cutibacterium acnes* invades prostate epithelial cells to induce BRCAness as a possible pathogen of prostate cancer.

S. Ashida[1], C. Kawada[1], H. Tanaka[2], A. Kurabayashi[1], K.-i. Yagyu[1], S. Sakamoto[1], K. Maejima[3], S. Miyano[2], M. Daibata[1], H. Nakagawa[3], K. Inoue[1];
[1]Kochi Medical School, Nankoku, Japan, [2]Tokyo Medical and Dental University, Tokyo, Japan, [3]RIKEN Center for Integrative Medical Sciences, Yokohama, Japan

Abundant evidence suggests that chronic inflammation is linked to prostate cancer and that infection is a possible cause of prostate cancer. However, pathogen of prostate cancer remains to be found. To identify microbiota or pathogens associated with prostate cancer, we investigated the transcriptomes of 20 human prostate cancer tissues. We performed *de novo* assembly of non-human sequences from RNA-seq data and identified four bacteria as candidate microbiota in the prostate, including *Moraxella osloensis*, *Uncultured chroococcidiopsis*, *Cutibacterium acnes*, and *Micrococcus luteus*. Among these, *C. acnes* was detected in 19 of 20 prostate cancer tissue samples by immunohistochemistry. We then analyzed the gene expression profiles of prostate epithelial cells infected *in vitro* with *C. acnes* and found significant alterations in homologous recombination (HR) and Fanconi anemia pathway. Notably, electron microscopy showed that *C. acnes* invaded prostate epithelial cells and localized in perinuclear vesicles, whereas analysis of γH2AX foci and HR assay demonstrated impaired HR repair. In particular, *BRCA2* was significantly down-regulated in *C. acnes*-infected cells. These findings suggest that *C. acnes* infection in the prostate could lead to HR deficiency and BRCAness which promotes DNA double-strand breaks, thereby increasing the risk of cancer development.

#5606 The role of KMT2C in the homologous recombination repair in epithelial ovarian cancer.

M. C. Ma, **Z. Lin**, E. S. Ratner;
Yale University School of Medicine, New Haven, CT

Background: Epithelial ovarian cancer (EOC) with homologous recombination (HR) deficiency is susceptible to PARP inhibitor therapy due to synthetic lethality. Identification of the patient population for PARP inhibitor therapy is imperative to reduce recurrence of EOC and improve the survival outcomes of patients. Current biomarkers for PARP inhibitor therapy consist of an array of genes involved in the HR repair pathway in EOC, including BRCA1, BRCA2 and PALB2. Through TCGA analysis, we found that the lysine (K)-specific methyltransferase 2C (KMT2C) gene is mutated in 10.3% of all EOC patients and considerably enriched in BRCA1 mutated EOC patients. However, the role of KMT2C in HR repair and PARP inhibitor sensitivity of EOC remains largely undefined.
Methods: BRCA2-mutated PEO1 and BRCA2-wild type PEO1-NR cells were transfected with KMT2C siRNA and assayed for KMT2C protein expression by western blotting. DR-GFP (HR) and EJ5-GFP (NHEJ)-SKOV3 cell lines were co-transfected with the ISceI-expressing plasmid pCBA-ISceI and KMT2C siRNA. GFP-positive cells were analyzed by flow cytometry. SKOV3 cells were transfected with KMT2C siRNA and the expression of BRCA2 and Rad51 mRNA was determined using quantitative RT-PCR analysis.
Results: siRNA-mediated knockdown of KMT2C resulted in marked down-regulation of KMT2C protein in PEO1 and PEO1-NR cells. KMT2C knockdown caused a significant decrease in ISceI-induced HR activity in DR-GFP-SKOV3 cells ($p < 0.05$). In contrast, KMT2C knockdown had no effects on ISceI-induced NHEJ activity in EJ5-GFP-SKOV3 cells. As a control, Rad51 knockdown caused complete suppression of HR activity and had no effects on NHEJ activity. Furthermore, quantitative RT-PCR analysis of key HR genes showed that KMT2C knockdown resulted in a moderate but significant down-regulation of BRCA2 ($p < 0.05$) and Rad51 ($p < 0.01$) expression in SKOV3 cells.
Conclusion: Our results suggest that KMT2C partakes in the HR repair pathway in EOC. However, the contribution of KMT2C to HR activity is not rate-limiting. Based on the known function of KMT2C in histone modification, we speculate that KMT2C serves to positively regulate the transcription of HR genes and therefore promote HR activity. Future investigation into the exact roles of KMT2C in HR repair, etiology of EOC, and diagnostic biomarkers for the PARP inhibitor sensitivity of EOC is warranted.

#5607 A highly efficient donor system for CRISPR knock-in editing.

L. Wu, D. Yin, H. Su, J. Fellows, M. Fu, J. Heller, B. Park, A. Juminaga;
OriGene Technologies, Inc., Rockville, MD

CRISPR is a potent tool widely used for genome editing. While CRISPR knock-out, achieved through in-del mutations via cellular repair mechanisms, has proven remarkably effective, the knock-in system for exogenous fragment insertion encounters challenges due to limited specificity and efficiency. Two primary methods for exogenous fragment insertion, namely NHEJ (Non-Homologous End Joining) and HR (Homologous Recombination), exist. HR allows for the construction of DNA insertions with precise junctions but is comparatively less efficient than NHEJ. To address these limitations, our system focuses on enhancing the efficiency of HR-based genome editing. Primarily, we have optimized the Lenti All-in-one CRISPR system to augment the delivery and targeting efficiency of the Cas9-gRNA complex. The system has been successfully employed to knock out Glutamine Synthetase (GLUL) in HEK293T cells, exhibiting superior efficiency compared to commercially available tools. Secondly, we have implemented a pseudo-lenti system to amplify the entry capacity of donor DNA with homology arms into target cells. This technique has shown an improved HR effect in the experiment to tag a GFP at the C terminals of CDC25A. Lastly, we leverage proximity effects by fusing Cas9 with a capture protein that can grasp a bait sequence attached to the donor DNA, thereby facilitating its transfer to the target sites. Our system has demonstrated exceptional efficacy as a CRISPR knock-out platform and a powerful tool for DNA tagging functionality on target genes.

#5608 The BRCA1-associated role of CDK9 in response to DNA damage is independent of its canonical role in transcription.

T. C. Nepomuceno[1], M. A. Carvalho[2], A. N. Monteiro[1];
[1]Moffitt Cancer Center, Tampa, FL, [2]Instituto Federal do Rio de Janeiro, Rio de Janeiro, Brazil

The understanding of the biological role of BRCA1 in maintaining genomic integrity through homologous recombination (HR) repair has driven the development of targeted treatments with PARP inhibitors (PARPi) in *BRCA1*-linked tumors with promising results. Recently, cyclin-dependent kinase 9 (CDK9) inhibitors have emerged as therapeutic options to treat cancer. We have previously implicated CDK9 in genome integrity maintenance through HR repair by modulating BRCA1 recruitment to double-stranded break sites. CDK9 is a component of the positive transcription elongation (PTEF-b) complex and more recently was proposed by the hereditary breast case-control (BEACCON) study as a putative breast cancer (BC) predisposition gene in non-*BRCA* families. Differently from *BRCA1*-linked BCs, loss-of-function mutations in *CDK9* were significantly correlated with ER-positive and Lobular BCs. CDK9 expression is also elevated in metastatic and recurrent ovarian cancer (OC) tissue and correlates with poor prognosis in OC patients. Here we characterize the BRCA1/BARD1/CDK9 complex using protein-protein interaction assays. Our data indicate that the CDK9/BARD1 interaction occurs indirectly through BRCA1. We also generated a separation-of-function mutation in CDK9 (mutCDK9) that disrupts its interaction with BRCA1 but retains its kinase activity and preserves its role in transcription. We rescued the mutCDK9/BRCA1 interaction using a complementary mutation in BRCA1 (cmutBRCA1), that retains BRCA1 role in cell viability. Further, we employed CRISPR-based genome editing to generate genetically defined haploid HAP1 cell lines that express mutCDK9 in various *TP53BP1* and *BRCA1* backgrounds. The mutCDK9 cells preserve global RNA transcription and the phosphorylation status of the RNA polymerase II. We observed that mutCDK9 cells are more sensitive to the PARPi, rucaparib when compared to wild-type cells in proficient and deficient *TP53BP1* backgrounds. However, mutCDK9 expression did not affect the sensitivity of HAP1 cells expressing cmutBRCA1. Collectively, our data suggest that CDK9 acts in genome integrity maintenance by HR through its interaction with BRCA1 independently of its canonical role in transcription.

#5609 A WRN screening cascade to facilitate novel drug discovery.

Aicheng Wang, Kejun Mao, Tao Li, Lizhao Guan, Yuhong Chen, Haiting Dai, Xian Wu, Jiabao Lv, Xu Wang, Cong Huang, **Tiejun Bing**

ICE Bioscience, Inc., Beijing, China

Human RecQ deconjugating enzyme WRN is involved in DNA replication, DNA repair, recombination, transcription and telomere stabilization[1]. It plays a key role in nucleic acid metabolism as well. WRN defects lead to premature aging, type II diabetes, osteoporosis, atherosclerosis and cancer[2]. Hence it is of great interest of both pharmaceutical and academic field to develop the WRN inhibitors. Here we constructed an integrated experimental cascade, which contains both in vitro and in vivo assays, to conduct the high throughput hit-to-lead compound screen. WRN proteins of different length have been successfully purified and utilized to develop multiple biochemical assays such as unwinding assay and ATPase assay. We have also validated different cellular assays, including proliferation and immunofluorescence, to assess the cytotoxicity and the influence of downstream biomarkers of WRN inhibitors. A WRN knock-out cell line has been generated to better appreciate the inhibition mechanism. In addition, we have generated a WRN-HiBiT knock-in cell line to evaluate WRN degraders or target-compound interactions. Lastly, multiple CDX models utilizing different MSI or MSS cell lines have been validated to help determine the efficacy of WRN inhibitors thus shed light on the drug indications. Together our WRN screening cascade can provide comprehensive compound evaluation across in vitro and in vivo platforms, thus serve as an efficient screening platform for new drug discovery.

[1] Kitano K. Structural mechanisms of human RecQ helicases WRN and BLM. Front Genet. 2014 Oct 29;5:366.

[2]Hussain M, Krishnamurthy S, Patel J, Kim E, Baptiste BA, Croteau DL, Bohr VA. Skin Abnormalities in Disorders with DNA Repair Defects, Premature Aging, and Mitochondrial Dysfunction. J Invest Dermatol. 2021 Apr;141(4S):968-975.

#5610 Investigating the role of *BRCA2* in the development of pediatric rhabdomyosarcoma.

P. Weinstein[1], R. Zabriskie[1], C. Ozdemir[2], K. M. Miller[2], O. Medina-Martinez[1], J. D. Heaney[1], A. Sabo[1], P. J. Lupo[1], S. E. Plon[1];
[1]Baylor College of Medicine, Houston, TX, [2]The University of Texas at Austin, Austin, TX

Introduction: In a large-scale exome sequencing study of pediatric rhabdomyosarcoma (RMS) patients, we identified a statistical enrichment of patients with germline variants in *BRCA2* (Li, et al. *JNCI*, 2020), which prompted this study to assess the role of heterozygous *BRCA2* variants in the development of pediatric RMS in both precursor cell and mouse models. **Methods:** We engineered *BRCA2* loss of function (LoF) variants in lines of immortalized mesenchymal stem cells, a potential precursor cell to RMS, using CRISPR and Prime Editing (PE). CRISPR was used to induce frameshift alleles in Exons 10 and 11 and with PE, we created two RMS patient specific LOF variants in Exons 5 and 17. We generated a genetically engineered mouse model (GEMM) with heterozygous excision of Exon 11 of *Brca2*. This allele is now being crossed into two different previously established GEMMs of RMS: a myoblast-specific (MyoD1-Cre) conditional loss of *p53,* and a gain-of-function mutant *p53,* LSL-p53^{R172H} (Nakahata, et al. *Dis. Model. Mech.,* 2022), to assess changes in the pace of tumorigenesis and metastatic potential. Through an X01 agreement with the Gabriella Miller Kids First Program, we have submitted paired tumor-normal samples for additional whole-genome sequencing and RNA sequencing (tumor only) on >500 patients with RMS, including those with germline variants in *BRCA2*. **Results:** Using CRISPR, we generated cell lines heterozygous for the frameshift variants c.1345dup, c.5680del, and c.5680dup. With Prime Editing, we created heterozygous lines mimicking two specific variants detected in the RMS cohort, c.462_463del and c.7857G>A. Generation of a C57BL6 GEMM with a heterozygous removal of Exon 11 in *Brca2* has been successful. No homozygous mice were obtained following 7 heterozygous crosses (50 pups), a departure from Mendelian ratios (p=0.0001) consistent with embryonic lethality. Heterozygous *Brca2* mice derived from crosses into two RMS models are being monitored for tumor development. We have completed tumor-normal whole-genome and tumor RNA sequencing for 609 RMS patients, including 228 subjects not previously analyzed. We will directly assess whether there is evidence for mutation or loss of expression of the remaining *BRCA2* allele in tumors and whether these tumor genomes exhibit signatures of DNA repair deficiency. **Conclusions:** The goal of this project is to determine the molecular basis for the enrichment in germline *BRCA2* LOF variants in pediatric malignancies, including RMS. Ongoing experiments using the engineered heterozygous *BRCA2 in vitro* cell line models will assess genomic stability, homologous recombination proficiency, and DNA replication fork stability. Assessment of the effect of heterozygous *Brca2* variants in GEMMs of RMS, and subsequent analysis of additional sequencing data, will further elucidate what role this gene may play in increasing risk or progression of pediatric cancers.

#5611 Unraveling the role of F-actin in resistant GBM: Insights into DNA repair, GSC phenotype, and therapeutic implications.

Y. T. Magalhaes, F. L. Forti;
IQ USP, Sao Paulo, Brazil

Glioblastoma (GBM), a highly aggressive brain cancer, poses a formidable challenge marked by its resistance to conventional therapies. F-actin, a crucial cytoskeletal protein, influences DNA repair and impacts genomic stability. F-actin dynamics also shape the glioma stem cell (GSC) phenotype, affecting self-renewal and migration. Altered F-actin organization contributes to GBM resistance to conventional therapies. Understanding F-actin's multifaceted role is vital for developing targeted strategies to overcome treatment resistance and enhance outcomes for GBM patients. This study goes deeper into the intricate interplay between the F-actin cytoskeleton and the acquisition of resistance in GBM cells. Our primary goal was to explore the effects of pharmacological or genetic F-actin depolymerization on the reversal of acquired resistance to ionizing radiation (IR) and temozolomide (TMZ) in GBM cells, particularly focusing on the underlying mechanisms involving DNA repair, the glioma stem cell (GSC) phenotype, and therapeutic implications. To establish resistant sublines, GBM U87-MG cells underwent cycles of IR and TMZ exposure, revealing a significant increase in IC_{50} values for TMZ and ID_{50} values for IR through viability assays. Subsequent characterization of these sublines growth was in both adherent and spheroid cultures uncovering a distinct sphere-forming capacity. Notably, alterations in DNA repair and the Rho GTPase pathway were observed, with evident disorganized F-actin polymerization in resistant cells, especially at the periphery of spheroids. Elevated expression of stemness markers (Nestin, CD133, and CD44) highlighted a GSC-like profile in the resistant cells, a characteristic further accentuated in spheroid cultures. To assess the relevance of the actin cytoskeleton in maintaining the resistant phenotype, cells were treated with Rho-GTPase inhibitor (C3) or actin polymerization inhibitor (Cytochalasin D). Both treatments resulted in reduced TMZ IC_{50} and IR ID_{50} values, partially attributed to the negative modulation of DNA repair capacity - observed by alkaline comet and host-cell reactivation assays. Additionally, F-actin disassembly was found to impact the expression of stemness markers, further reinforcing the connection between cytoskeletal dynamics and the GSC phenotype. Overall, our data strongly suggest that F-actin cytoskeleton dynamics plays a pivotal role in the development and maintenance of resistance in GBM. Targeting these cytoskeletal components sees a promising pharmacological strategy for resensitizing recurrent and resistant GBM tumors, not only by diminishing DNA repair capabilities but also by influencing the GSC-like phenotype, thus opening new avenues for therapeutic interventions.

#5612 MRE11 function in DNA damage response is regulated by SIRT2 deacetylation.

M. Essien, F. Sesay, H. Zhang, A. Jung, D. Yu;
Emory University, Atlanta, GA

MRE11 is known to play a role in DNA damage repair through the MRE11-RAD50-NBS1 (MRN) complex and homologous recombination. However, the upstream signaling mechanisms regulating MRE11 in DNA repair are unclear. Here, we aimed to determine the extent to which MRE11 is regulated by deacetylation by the SIRT2 sirtuin deacetylase and tumor suppressor protein. We overexpressed MRE11 in HEK293T cells, induced DNA damage through radiation treatment, and performed a series of co-immunoprecipitation (co-IP) studies with and without ionizing radiation (IR). Additionally, we evaluated the acetylation of MRE11 with and without the presence of SIRT2. In a series of functional experiments, immunofluorescence staining assays were performed in U2OS-265 Fok1 cells with SIRT2 knockdown to determine the effect of on MRE11 recruitment to DNA damage sites. Co-IP studies and in vitro DNA pulldown assays were performed to determine the role of SIRT2 in impacting MRE11 interaction with RAD50 and NBS1 and binding to DNA damage. We also examined for IR-induced RPA70 foci formation and downstream ATM-dependent signaling. We found that SIRT2 interacts with and deacetylates MRE11. Furthermore, SIRT2 deacetylation facilitated MRE11 binding to DNA but not interaction with RAD50 and NBS1. Finally, SIRT2 deacetylation facilitated DNA end resection and ATM-dependent phosphorylation of KAP1. In conclusion, our results define a role for SIRT2 in directing MRE11 localization and binding to DNA to promote DNA end resection and ATM-dependent signaling through deacetylation.

#5613 Study of long non-coding RNA TUG1 kinetics under replication stress conditions in cancer cell.

T. Fujita[1], M. Suzuki[1], O. Masui[2], K. Shinjo[1], Y. Kondo[1];

[1]Nagoya University, Nagoya, Japan, [2]RIKEN Center for Integrative Medical Sciences, Yokohama, Japan

Long non-coding RNAs (lncRNAs) are transcripts longer than 200 nucleotides that are not translated into proteins. In contrast to protein-coding mRNAs, certain lncRNAs carry out their functions within the nucleus. A detailed elucidation of the kinetics of lncRNAs contributes to a comprehensive understanding of their bona fide biological characteristics. Consequently, advancements in the in vivo visualization of lncRNAs have continued. Currently, various techniques, including RNA imaging technologies, have been employed to facilitate real-time tracking and visualization of RNA molecules within living cells. Taurine upregulated gene 1 (TUG1) is an oncogenic lncRNA, playing a pivotal role in cancer cells by resolving R-loops formed at stalled replication forks, particularly under replication stress conditions such as Hydroxyurea (HU) treatment. Despite its significance, the dynamic regulation of TUG1 under replication stress conditions remains largely unknown. In this study, we developed a stem loop-based live imaging system enabling real-time visualization of TUG1, providing insights into its subcellular localization and dynamic roles in physiological contexts. Upon treatment with HU, a chemical that interferes with replication, TUG1 expression was rapidly upregulated in the nucleus within 20 minutes. Additionally, we observed TUG1 molecules relocating close to the nuclear membrane. Considering the reported relocation of collapsed forks to the nuclear pore complex, this suggests that TUG1 may be involved in this relocation structure. These data indicate that TUG1 is associated with the fork restore mechanism occurring at the relocated collapsed forks, and the current live-cell imaging system holds potential for further uncovering the critical roles of TUG1 in cancer cells. Our stem loop-based imaging may contribute to a more precise understanding of RNA dynamics in live cells.

#5614 Mechanical regulation of cisplatin-DNA adduct repair in mesenchymal stem cells.

A. G. Zavala, N. Nikitina, C. Cantu, D. DeLaCruz, G. Uzer;
Boise State University, Boise, ID

This study examined whether loss of mechanotransduction in pluripotent mesenchymal stem cells (MSCs) disrupted repair of bulky DNA adducts, such as those induced by ultraviolet light or cisplatin. MSCs are important for the maintenance and responsiveness of skeletal tissues to environmental mechanical challenges. Beyond regulating proliferative and differentiative capacity of MSCs, emerging evidence suggests that physical activity is associated with improved recovery from DNA damage caused by environmental genotoxic stressors associated with stress and aging. Highlighting the possible crosstalk between DNA repair and bone health, defects in nucleotide excision repair (NER), which removes bulky DNA adducts, are associated with myelosuppression and progeroid aging phenotypes that result in bone defects and lipidodystrophies in mice. Cancer, early aging syndromes, and certain musculoskeletal diseases are associated with disruption of the Linker of Nucleoskeleton and Cytoskeleton (LINC) complex that transduces environmental mechanical signals from the extracellular matrix into the nucleus of a cell. Loss of LINC complex elements is associated with breast cancer progression and poorer prognosis. We hypothesize that LINC-mediated mechanical stimulation into the nucleus is critical for repair of bulky DNA adducts. Our pilot project showed that mechanical stimulation applied in the form of low intensity vibration (LIV) improved NER of cisplatin-induced DNA adducts in cultured MSCs. Our findings show a 20% increase in repair of cisplatin-induced DNA adducts in LIV treated samples compared to non-vibrated samples at 24 hours ($P<0.005$). We also quantified the effect of LINC complex disruption on cisplatin-induced DNA damage removal. Intact MSCs showed significant adduct removal after 24 hours, while LINC disruption significantly reduced DNA repair ($P<0.001$). Furthermore, initial experiments suggest that LINC disrupted cells do not arrest at DNA repair checkpoints, therefore, loss of LINC complex may reduce entry into senescence increasing DNA mutagenesis. In conclusion, these findings suggest a novel interaction between mechanical stimulation, the DNA damage response, and LINC complex in DNA repair in multipotent mesenchymal stem cells. Furthermore, we suggest that LINC-mediated mechanical changes associated with LIV treatment may lead to novel therapeutic approaches to combat deleterious musculoskeletal conditions associated with anti-cancer treatments.

#5615 Functional analysis of variants of uncertain significance in the *MSH6* mismatch repair gene.

E. Szabo, E. Blackburn, A. Radecki, A. Rath, C. Heinen;
University of Connecticut Health Center, Farmington, CT

Lynch syndrome (LS) is a hereditary condition that increases patients' lifetime risk of cancer, primarily colorectal cancer. LS is caused by germline mutations in mismatch repair (MMR) genes, *MLH1, MSH2, MSH6*, and *PMS2*. Identification and classification of these mutations is important in LS diagnosis for guiding treatment plans and preventative care for patients' and their families. However, the consequences of some variants in these genes are not immediately obvious, granting them classification as variants of uncertain significance (VUS). Laboratory functional analysis to determine whether these variants disrupt MMR function in human cells can provide important evidence for understanding the pathogenicity of VUS and reclassifying them. Half of known variants in the MMR gene *MSH6* are VUS and, thus, the goal of my project is to provide evidence for a subset of these variants to help provide evidence for reclassification for these variants. We are calibrating and validating functional assays for *MSH6* variants, using known *MSH6* pathogenic and benign controls. We will then test *MSH6* VUS identified in patients as reported in the InSiGHT database, ClinVar database, and current literature. We are using CRISPR gene editing to recreate these variants in the endogenous *MSH6* loci in human embryonic stem cells (hESC). Using these edited hESC lines we are examining the impact of the variants on RNA and protein stability, repair of DNA microsatellites, which is a hallmark of normal MMR function, and induction of the MMR-dependent DNA damage response. With this compilation of data, we will convert the results into a quantitative Odds of Pathogenicity value. This Odds of Pathogenicity score can be used by expert variant interpretation committees to help readily reclassify these variants and provide a clearer diagnosis for these suspected Lynch syndrome patients.

#5616 Targeting the DNA damage response sensor replication protein A for first in class cancer therapy.

K. Pawelczak[1], P. VanderVere-Carozza[2], M. Jordan[2], J. Turchi[2];

[1]NERx Biosciences, Inc., Indianapolis, IN, [2]Indiana University School of Medicine, Indianapolis, IN

The DNA Damage Response (DDR) is an integrated network of DNA repair and cell signaling pathways that are critical towards maintaining genomic stability. The most successful DDR targeted therapies inhibit the DNA damage sensor, PARP, a protein that recognizes single strand DNA (ssDNA) breaks as well as other DNA secondary structures induced by single strand gaps that can initiate chromosome instability and cell death. Building on the initial clinical success of PARP inhibitors, development of DDR targeted therapeutics has become increasingly popular, however, the clinical outcomes with these therapeutics have not met expectations and thus a new approach to targeting the DDR pathway is needed. NERx Biosciences has developed a novel strategy of targeting the DDR by intervening upstream of the DDR kinases and targeting specific DDR sensors. The human ssDNA binding protein, replication protein A (RPA), is a critical sensor for the DDR, serving to sense the ssDNA at replication forks that arise from replication stress (RS) and is a novel target for cancer therapy. We have discovered, developed, and characterized a novel small molecule RPA inhibitor (RPAi) NERx-329 that blocks the RPA-DNA interaction and elicits a state of chemical RPA exhaustion that results in *in vivo* anticancer activity. Extensive chemical optimization enabled in vitro and in vivo analyses to elucidate mechanism of action, cellular engagement, and therapeutic activity of RPA-targeted agents. Biochemical reconstitution of the ATR signaling pathway shows that NERx-329 disrupts ATR kinase activity, further suggesting a novel mechanism of action driven by RPA inhibition induced replication catastrophe. In vivo analysis reveals activity in a series of lung and ovarian patient derived xenograft models of human cancer. Single agent activity results in a tumor growth delay, which can be enhanced in combination therapy with DDR inhibitors as well as traditional DNA damaging cancer therapeutics. Data demonstrate that tumor growth observed in vivo is a function of NERx329 bioavailability and not development of a specific resistance mechanism. In an effort to identify formulations effective in enhancing oral bioavailability, we have pursued the development of Spray-dried dispersions (SDD). PK analysis reveal a dose-dependent substantial increase in C_{MAX} and AUC, allowing for optimal dosing regimens for efficacy and safety studies. In addition, specific genetic predictors of RPAi sensitivity have been identified and results demonstrate specific genetic alterations increase RPAi activity in vitro and in vivo. NERx-329 represents the first clinically viable agent to target the DDR pathway by disrupting the RPA-DNA interaction and holds the potential for significant impact in cancer treatment.

#5617 Combined inhibition of ATR and ATM with tuvusertib and lartesertib (M4076) impacts the tumor microenvironment.

K. Laaber[1], A. Turchick[2], J. Jabs[1], B. Elenbaas[2], L. T. Vassilev[2], A. Zimmermann[1];
[1]The Healthcare Business of Merck KGaA, Darmstadt, Germany, [2]EMD Serono, Billerica, MA

Ataxia telangiectasia and Rad3-related protein (ATR) and ataxia telangiectasia mutated (ATM) are two of the main kinases of the DNA damage response (DDR). Recent work has demonstrated that the addition of ATM inhibitors enhances the cytotoxicity and *in vivo* anti-tumor efficacy of ATR inhibitors by abrogating the ATR inhibitor mediated G_1 cell cycle arrest and enhancing chromosomal damage.[1] Prior to causing cell death, damaged chromosome fragments can end up in the cytosol where they are detected by cytosolic nucleic acid sensors such as cGAS, resulting in the induction of inflammatory signaling pathways and an anti-tumor immune response. This suggests that the mode of action of DDR inhibitors may involve the tumor microenvironment (TME). We therefore aimed to assess the influence of combined pharmacological ATR and ATM inhibition on the TME to better understand how this could be exploited therapeutically.

In line with published results in human tumor models, the treatment of murine colon cancer MC-38 cells *in vitro* with a combination of ATR inhibitor tuvusertib and ATM inhibitor lartesertib led to cell death. Further analysis revealed an activation of the cGAS-STING signaling pathway, an upregulation of PD-L1 and the release of inflammatory cytokines. These results confirmed the activation of immune signaling pathways upon combined inhibition of ATR and ATM.

To analyze the stimulation of an anti-tumor immune response upon tuvusertib + lartesertib treatment *in vivo*, MC-38 cells were transplanted into immunocompetent C57BL/6J mice. Immunoprofiling by flow cytometry and immunohistochemistry staining confirmed that treatment with tuvusertib + lartesertib indeed altered the TME in this setting. In line with the *in vitro* findings, a significant upregulation of PD-L1 on immune and tumor cells could be observed after 24, 48, and 72 h of treatment even though MC-38 cells expressed high levels of PD-L1 already. Immunoprofiling did not reveal any changes in the TME immune cell content at these early time points. Interestingly, PD-L1 expression as well as tumor immune population changed after prolonged (23 days) treatment. PD-L1 was still expressed on tumor cells but to a significantly lesser extent and a depletion of CD8+ T-cells was observed. However, a significant increase in NK cells could be detected.

In summary, we show that inhibition of the DDR through a combination of ATR and ATM inhibitors influences the TME in the MC-38 tumor model. These findings suggest an additional mode of action beyond direct cancer cell cytotoxicity. Further studies on how this may be leveraged therapeutically, for example through a combination with immune checkpoint inhibitors, are warranted.

1. Turchick A, Zimmermann A, et al. *Mol Cancer Ther* 2023;22(7):859-872.

#5618 Evaluating the combination of datopotamab deruxtecan (Dato-DXd) with AZD5305, a highly potent, PARP1-selective inhibitor, -in preclinical models.

G. Patel, J. Owusu, C. Rane, A. Rosen, M. Griffin, M. Sung;
AstraZeneca US, Waltham, MA

Background: Dato-DXd is a TROP2-directed antibody drug conjugate comprised of a topoisomerase I inhibitor (an exatecan derivative, DXd) conjugated to datopotamab, a humanized anti-TROP2 IgG1 antibody, via a cleavable plasma-stable tetrapeptide-based linker. Topoisomerase I inhibitors stabilize DNA-topoisomerase cleavage complexes (Topo1cc) that lead to double-strand breaks and activation of DNA damage response (DDR). Poly(ADP-ribose) polymerase 1 (PARP1) mediates signal transduction in the DDR as an important regulator. AZD5305 is a highly potent and selective inhibitor of PARP1. Since PARP1 is a key component driving the repair of trapped Topo1cc, we aimed to investigate if combinations of Dato-DXd with AZ5305 lead to synergistic anti-tumor effects in preclinical models.

Methods: We evaluated the cytotoxic effect of the combination of Dato-DXd with AZD5305 in a panel of six non-small cell lung cancer (NSCLC) and five triple negative breast cancer (TNBC) cell lines in a 7-day viability assay. We evaluated PARylation inhibition and gH2AX response by Western blotting. Topo1cc accumulation in response to combination treatment was evaluated by immunofluorescence. This combination was evaluated *in vivo* in TROP2+, HRD-negative gastric cancer (GC) N87 cell line xenograft at varying concentrations of AZD5305 and in a TROP2+, PARPi-resistant Ovarian cancer patient derived xenograft (PDX) model (CTG-3718).

Results: The *in vitro* combination screen demonstrated enhanced cell killing by the Dato-DXd and AZD5305 combination over either single agent in both NSCLC and TNBC cell lines. Combination benefit was observed at all doses regardless of homologous recombination deficiency (HRD) status. We observed dose-dependent increase in PARylation inhibition and enhanced induction of gH2AX in the combination treatment. In a N87 tumor model, while Dato-DXd and AZD5305 provided 84% and 31% tumor growth inhibition (TGI) as monotherapies respectively, the addition of AZD5305 to Dato-DXd resulted in 95% TGI. This effect was observed with multiple dose levels of AZD5305. In a TROP2+, ovarian cancer PDX model, AZD5305 demonstrated limited monotherapy activity (<10% TGI) and Dato-DXd demonstrated robust monotherapy activity with 72% TGI. Additional anti-tumor activity was observed for the combination treatment compared to either monotherapy with 88% TGI. All treatment groups were well tolerated *in vivo.*

Conclusion: Dato-DXd combination with AZD5305 increased cytotoxic activity and pharmacodynamic response *in vitro*. This combination led to superior tumor growth inhibition in a GC xenograft model and a PARP1i-resistant Ovarian PDX model *in vivo.* These pre-clinical findings support the ongoing clinical evaluation of Dato-DXd as a monotherapy and in combination with AZD5305 in patients with various advanced solid tumor types (NCT05489211, NCT04644068).

MOLECULAR/CELLULAR BIOLOGY AND GENETICS: Gene Regulation and Transcriptional Profiles
Poster Session

#5622 Uncovering the transcriptional regulation of TPPP3.
J. W. Lord, D. Leshchiner, S. Horibata;
Michigan State University, East Lansing, MI

Tubulin Polymerization Promoting Protein 3 (TPPP3) is a protein coding gene primarily associated with microtubule bundling. However more recent research is beginning to reveal more diverse roles it may play in the cell, including B-catenin signaling and endothelial injury. TPPP3 has also been associated with increased cancer growth and proliferation as well epithelial to mesenchymal transition. However, it is unknown how TPPP3 is regulated. We used high grade serous ovarian cancer (HGSOC) as a model to uncover the regulation of TPPP3 as it is highly expressed in many HGSOC cases. To start, we downloaded ~500 HGSOC RNA-seq datasets from The Cancer Genome Atlas (TCGA) and, using python, created a co-expression network to identify a subset of genes exhibiting expression patterns correlated with TPPP3 across all datasets, resulting in the identification of 222 genes. Dynein arm assembly, cilia movement and assembly, and microtubule movement and structure were among the top GO-terms after gene ontology analysis. The genes associated with these processes are typically upregulated in the fallopian tube tissue which aligns with the fact that a majority of HGSOCs originate in the fallopian tube. Fork-head box J1 (FOXJ1) is a transcription factor associated with ciliogenesis and was among the top 222 genes from the co-expression network. It has not been confirmed to transcriptionally regulate TPPP3, but their expression patterns line up across many tissue types. In addition, the TPPP3 promoter contains an RFX2 binding site. RFX2 is DNA binding protein that FOXJ1 uses as a scaffold to bind to proximal promoters due to it binding at to DNA at a distal location. As a result of this evidence, we hypothesize that FOXJ1 transcriptionally regulates TPPP3 via RFX2. To test this hypothesis, we inhibited FOXJ1 and identified TPPP3 downregulation. We are further investigating the regulatory function of how TPPP3 is regulated.

#5624 Dec2, a circadian rhythm gene facilitates pancreatic cancer dormancy through evasion of antitumor immunity.

L. Wang, C. Harris, O. Prela, W. C. Narrow, D. R. Carpizo;
University of Rochester Medical Center, Rochester, NY

Metastatic recurrence following curative intent oncologic surgery is a major clinical problem in patients with pancreatic ductal adenocarcinoma (PDAC). These recurrences are from disseminated tumor cells (DTCs) and can sometimes occur years after surgery indicating that DTCs undergo a period of dormancy. The mechanisms that drive cancer dormancy and its awakening are poorly understood in part due to a lack of animal models that recapitulate dormant tumor cell biology. We created a novel model of PDAC dormancy where mice undergo surgery to remove the primary tumor and are followed for evidence of metastatic recurrence. Dormant DTCs can be isolated from mice without clinical evidence of recurrence for molecular studies. Single cell RNAseq of dormant DTCs detected that the circadian rhythm gene, Dec2 is upregulated. We knocked out (KO) Dec2 from murine pancreatic cancer cells and when implanted into the model we found almost no mice developed metastatic recurrence. When immunodeficient or immunocompetent mice depleted of CD4 and CD8 T cells were used as hosts, we observed no difference in survival in mice engrafted with Dec WT vs. KO cells indicating the survival benefit in the Dec KO group was due to an immune mediated mechanism. We performed a differential expression analysis on bulk RNAseq data comparing the Dec2 WT vs. KO cells and found antigen presentation a top upregulated pathway. We then observed that surface MHC-I was significantly upregulated in Dec2 KO cells as compared to wild type cells. Further mechanistic studies revealed that proteosome activity was significantly higher in Dec2 KO cells and treatment with proteosome inhibitors decreased surface MHCI levels in Dec2 KO cells. Cut and tag experiments revealed that Dec2 binds the promoter of a number of genes that regulate the proteosome. In conclusion, Dec2 promotes cancer dormancy by down regulating cell surface MHCI which facilitates immune evasion.

#5625 Targeting the nonsense mediated mRNA decay pathway to prevent the degradation of highly immunogenic frameshift mutated transcripts.

S. Fernandez Patel[1], R. Vendramin[1], D. Qian[1], Y. Zhao[1], L. Ligammari[1], K. Thakkar[1], J. Murai[1], E. Gronroos[2], J. Carlton[3], K. Litchfield[1];
[1]University College London, London, United Kingdom, [2]The Francis Crick Institute, London, United Kingdom, [3]King's College London, London, United Kingdom

Introduction: Frameshift insertions/deletions (fs-indels) can lead to the generation of immunogenic non-self-peptides which contribute to anti-tumor immune responses. However, fs-indels often generate premature termination codons (PTCs), leading to mRNA degradation by the nonsense mediated mRNA decay (NMD) pathway. Importantly, some PTC-containing transcripts naturally escape NMD degradation and produce highly immunogenic neoantigens. Therefore, we hypothesize that NMD inhibition could be used to increase the cellular pool of fs-indels derived neoantigens in cancer cells, and enhance anti-tumor immunogenicity. NMD also regulates other cellular processes by degrading a subset of non-PTC-containing self-transcripts. Therefore, by focusing NMD inhibition towards the degradation of PTC-transcripts only, toxicity may be limited in a clinical setting. We investigate how targeting different NMD proteins affects the degradation of fs-transcripts across several cancers types. To assess the clinical relevance of NMD inhibition, we study how it specifically affects p53 fs-transcripts, since p53 is the most mutated gene in cancer and fs-mutant p53 has been shown to be highly immunogenic.
Methods: Core NMD proteins were depleted across a panel of cell lines from different cancer types and transcriptomics, flow cytometry, qPCR and western blot were used to evaluate changes in the expression of NMD-targeted transcripts and NMD members. Proteomics and immunopeptidomics were used to study protein expression and HLA-peptide presentation arising from fs-transcripts. A Translating RNA Imaging by Coat protein Knock-off (TRICK) assay was developed to study the translation of NMD-targeted p53 mutants upon NMD inhibition. This assay can precisely quantify the translation of p53 mutant RNA upon different treatments and cellular stresses at single-molecule resolution.
Results: We found an increase in expression of PTC-transcripts upon silencing of multiple NMD members. Our data suggests that some NMD members are better targets for inhibition of NMD PTC-surveillance, whilst others are more appropriate for inhibition of NMD-mediated gene expression regulation. These data support the recently proposed hypothesis that NMD is a branched pathway, where each branch targets specific subsets of transcripts depending on the cell type. These results are clinically relevant as the method by which NMD is inhibited could help optimize the generation of immunogenic neoantigens whilst minimizing toxicity. The TRICK assay has shown that inhibiting NMD surveillance reduces the degradation of p53 fs-transcripts and increases their protein expression.
Conclusion: We have identified NMD pathway members that can be targeted to efficiently inhibit the surveillance role of NMD and prevent the degradation of fs-transcripts that could generate highly immunogenic neoantigens.

#5626 Essential role of Slug during the evolution of drug-tolerance in lung adenocarcinoma.

J. Ostendorp[1], H. Tumbrink[1], P. Hunold[1], M. Hoehne[1], P. Jurmeister[2], A. Dekker[1], F. Heisel[1], J. Bragelmann[1], F. Klauschen[2], R. Haensel-Hertsch[1], M. Sos[3]; [1]Faculty of Medicine and University Hospital Cologne, Cologne, Germany, [2]Ludwig-Maximilians-University Munchen, Munich, Germany, [3]German Cancer Research Center (DKFZ), The German Consortium for Translational Cancer Research (DKTK), Ludwig-Maximilians Univeristy Munchen, Munich, Germany

A major obstacle in the efficacy of targeted therapies of oncogene-driven tumors are drug-tolerant persister cells (DTPs) that build the basis for the outgrowth of drug-resistant clones and ultimately limit patient survival. During treatment, DTPs enter a reversible senescent state to survive therapy while cell death is induced in non-DTPs. Here, using RNA-Seq and proteomic analyses, we identified drug-induced TGFβ2 secretion in DTPs derived from different oncogene-driven lung cancer cell lines. As expected, TGFβ2 induces epithelial-to-mesenchymal transition (EMT) that over time promotes the ability of cells to survive targeted therapy. Using CRISPR/Cas9-mediated loss-of-function and reconstitution experiments we show that downstream of TGFβ2, expression of the transcription factor *SNAI2* (SLUG) is essential for the outgrowth of DTPs during targeted treatment. Unsupervised RNA-Seq data analyses in combination with Cut&Tag profiling revealed that EMT signaling is in part a SLUG regulated process but that is also independent of direct SLUG binding at the transcription start sites (TSS) of EMT signature genes. In contrast, we observed high occupancy of SLUG at TSS of genes involved in the regulation of cell cycle, being repressed in DTPs and at TSS of genes that regulate sphingolipid metabolism and MAPK signaling, being induced in DTPs. In line with our previous findings, a motif-based analysis of the Cut&Tag data (TOBIAS) furthermore uncovered a tight connection between DTP outgrowth and inflammatory signaling induced through IRF7, IRF4 or STAT1 activation. *In vivo, EGFR*-mutant SLUG deficient cells showed a significantly prolonged tumor onset and a higher response rate to osimertinib treatment. Overall, we uncover a major role of TGFβ2/SLUG-mediated EMT signaling that may be induced indirectly through SLUG-dependent reprogramming of cell cycle directed and metabolic processes in drug tolerant cells. These insights may offer unique therapeutic opportunities to limit the outgrowth of drug resistant tumors in cancer patients.

#5627 PPARG-high circulating monocytes exhibit an immunosuppressive phenotype in urothelial cancer patients treated with anti-PD1.

P. A. Nguyen, G. Zhang, B. Kakrecha, R. Marable, S. Kirov, M. Bowden, E. Gjini;
Flare Therapeutics, Cambridge, MA

Background:
PPARG is expressed in a variety of immune cells such as monocytes, macrophages, and lymphocytes, where it plays a role in their maturation and function. PPARG has been implicated in immune mediated resistance but to date, a comprehensive analysis of PPARG expression in peripheral blood mononuclear cells (PBMCs) in urothelial cancer (UC) patients is lacking. In this study, we identified the immunophenotypes associated with PPARG expression in UC patients treated with anti-PD1 therapy.

Methods:
We performed single-cell RNA sequencing of PBMCs from 5 UC patients and 3 normal healthy volunteers (NHV). Real-world samples (Discovery Life Sciences) were collected from patients who received prior Pembrolizumab. Time post-treatment to collection ranged from 46 to 307 days. An average of 9,500 cells were recovered per donor reflecting an ~80% QC pass rate. Count matrices were generated using 10x Genomics Cell Ranger pipeline (v7.0.0; GRCh38 reference). Downstream data processing, analysis and visualization were done on Cellenics software.

Results:
We evaluated 75,725 cells and identified 9 distinct cell populations. The proportion of T-cells was significantly decreased in UC samples compared to NHVs (40% vs 60%, p=0.03). Highest PPARG expression was observed on Classical Monocytes (CMs) cell population. PPARG expression was higher on CMs in UC compared to NHV samples (1.74 vs 0.11 logcounts; padj<0.001). Unsupervised clustering of all monocytes revealed two distinct CM clusters. In cluster A, 95% of the cells originated from UC samples, while most cells in cluster B (81%) originated from NHV samples. PPARG was the top differentially expressed gene upregulated in cluster A (PPARG-high) vs cluster B (PPARG-low) (1.89 vs 0.23 logcounts; padj<0.001). PPARG-high CMs are characterized by a gene signature inclusive of GPRIN3, RGCC, MAFB and IRF2BP, which have been shown to be upregulated in M2 polarized macrophages [1]. Moreover, pathway analysis using GSEA highlighted that PPARG-high CMs are enriched for TREM1 signaling genes (padj<0.001), whose high expression has been associated with immunosuppressive phenotypes in myeloid cells [2] and shorter survival of patients across other cancers [3].

Conclusion:
PPARG-high circulating CMs in UC patients exhibit a transcriptomic profile associated with immunosuppression and M2 macrophage polarization. FX-909, a first-in-class PPARG inverse agonist, is being evaluated in the clinic and the study includes an exploratory biomarker approach to assess the potential effect of PPARG inhibition on the CM immune-profile of advanced UC patients enrolled in the Ph1 study [4].

References:
1. Court et al, *Mol. Cell. Proteom.* **16**, 2153-2168 (2017)
2. Liao et al, *Cancer Sci.* **103**, 984-992 (2012)
3. Pullikuth et al, *Front. Oncol.* **11**, 734959 (2021)
4. Sims et al, *Cancer Res.* **83**(7_Suppl), Abstract ND08 (2023)

#5628 Aberrant 3'UTR processing regulates a tumor suppressor network in AML..

E. Wang[1], C. Han[1], A. Calderon[1], A. Lawal[1], S. H. Rajendran[1], S. Karma[1], N. Hariramani[1], I. Aifantis[2], A. Tsirigos[2];
[1]The Jackson Laboratory for Genomic Medicine, Farmington, CT, [2]NYU School of Medicine, New York, NY

Differentiation blockade is a hallmark of acute myeloid leukemia (AML). While inactivating mutations in tumor suppressor genes (TSGs) have been well-studied, non-genetic mechanisms that impair TSGs to promote myeloid differentiation and influence drug response remain poorly understood. In this study, we performed genome-wide *loss-of-function* CRISPR/Cas9 screens to identify suppressors of myeloid differentiation. These screens converged on the zinc finger transcriptional repressor, ZBTB7A whose ablation restricted myeloid maturation and promoted a dysregulated inflammatory state to protect leukemic cells from undergoing differentiation. Moreover, genetic deletion of ZBTB7A or its paralog, ZBTB7B impeded leukemia differentiation and conferred resistance to differentiation-inducing agents. Mechanistically, we found that leukemia cells hijack 3'UTR processes to reduce mRNA expression of the tumor suppressor gene paralogs *ZBTB7A* and *ZBTB7B*. These findings provide a molecular framework of altered 3'UTR regulation that orchestrate a tumor suppressive function and promote resistance to AML differentiation-based therapies.

#5629 MEF2D regulates T cell function via the CD70-CD27 signaling axis and promotes immune escape in hepatocellular carcinomas.

F. Kong[1], L. Wang[2], Q. Ye[3], Y. Xiong[1], **W. W. Hancock[4]**;

[1]Zhongnan Hospital of Wuhan University, Hubei, China, [2]Children's Hospital of Philadelphia, Philadelphia, PA, [3]Zhongnan Hospital of Wuhan University and The 3rd Xiangya Hospital of Central South University, Hubei and Changsha, China, [4]University of Pennsylvania, Philadelphia, PA

Background: Immune escape remains a challenge in the treatment of hepatocellular carcinoma (HCC), one of the most common and deadly cancers in the world. The transcription factor, myocyte enhancer factor 2D (MEF2D), is important in the regulation of differentiation and adaptive responses in many cancers, such that we tested its role in HCC.

Methods: We knocked down MEF2D in HCC cell lines and analyzed HCC tissues and cell lines by RNA sequencing, Western blot and immunohistochemistry. MEF2D protein acetylation and proteins that interact with MEF2D were identified by coimmunoprecipitation assay. Chromatin immunoprecipitation was used to analyze the regulation of CD70 transcription by MEF2D. H22 cells, with MEF2D knockout or without (controls), were injected into the livers of syngeneic BALB/c mice. Flow cytometry was used to analyze the function of T cells in tumors, spleens, and lymph nodes.

Results: Through database searches, we noted that MEF2D and CD70 were upregulated in HCC and associated with shorter patient survival times. Compared to WT tumors, injection of MEF2D-knockdown HCC cells into immunocompetent mice led to smaller tumors with increased T cell infiltration, activation, and impaired T-regulatory (Treg) cell suppressive function. Mechanistically, we found that MEF2D binds to the promoter region of CD70 gene and activates its transcription. Moreover, acetylation of MEF2D enhances the binding of MEF2D to the CD70 promoter and further promotes its transcription. CD70 blocking antibody inhibited activation of the CD70-CD27 signaling axis in murine HCC tumors, leading to impaired immunosuppressive function of Tregs and enhanced T cell-mediated anti-tumor immune responses. Thus, regulation of the CD70-CD27 signaling axis by MEF2D affects the numbers and functions of Treg cells and thereby controls T cell infiltration.

Conclusions: MEF2D in HCC cells increases the expression of CD70 and blocks T cell-mediated anti-tumor immunity via the CD70-CD27 signaling axis. Strategies to manipulate this pathway might increase the efficacy of immune therapies for HCC.

#5630 Targeting the LSD1/ADNP axis as an effective pro-differentiating strategy against acute myeloid leukemia AML.

M. Lone, M. Sayeed, A. Habieb, P. Kumar, M. E. Engel;
University of Virginia, Charlottesville, VA

Acute Myeloid Leukemia (AML) represents a diverse category of blood cancers marked by the clonal proliferation of atypical myeloid precursor cells within the bone marrow. Lysine Specific Demethylase 1 (LSD1), an epigenetic regulator, exhibits elevated expression in AML. Consequently, inhibiting LSD1 has emerged as a promising therapeutic approach for addressing blood and bone marrow cancers. While initial emphasis centered on LSD1's enzymatic inhibition, compelling evidence highlights its pivotal role as a scaffolding protein, orchestrating transcriptional and chromatin remodeling complexes that control cellular differentiation and proliferation. However, our understanding of the precise mechanisms governing these complexes remains limited, necessitating further investigation. The K562 erythroleukemia cell line has served as a prominent model for investigating the molecular factors influencing cell fate determination. In response to specific cues, these cells exhibit a bi-potential capacity, mirroring the behavior of normal hematopoietic megakaryocyte/erythrocyte progenitors (MEP). Notably, when LSD1 is either depleted or inhibited, the erythroid differentiation of K562 cells is hindered, even when exposed to various pro-differentiating triggers, including the BCR-ABL inhibitor Imatinib. In order to gain deeper insights and identify potential new protein partners involved in the K562 differentiation process that interact with LSD1, we employed the erythroleukemic K562 cell model. Using unbiased, proteome-wide proximity labeling we discovered that LSD1 serves as a scaffold for recruitment of the ChAHP complex, comprised of ADNP, CBX3, and CHD4. The ChAHP complex serves fundamental roles in chromatin remodeling, RNA splicing, and transcriptional control. We confirmed these proximity relationships by immunoblotting biotinylated proteins generated in situ by the promiscuous biotin ligase, (BirA*) when anchored to LSD1. We show that depleting ADNP induces spontaneous erythroid differentiation in K562 erythroleukemia cells, which is augmented by BCR-ABL inhibitor Imatinib treatment. ADNP-deficient K562 cells exhibited accelerated erythroid differentiation, as evidenced by a four-fold increase in the surface expression of erythroid markers (CD71, CD235a) and a significant upregulation of beta-globin gene cluster markers. These findings collectively suggest an antagonistic functional relationship between ADNP and LSD1, potentially counterbalancing LSD1's role in lineage allocation. Furthermore, we demonstrate that the loss of the key ChAHP component, ADNP, substantially hampers proliferation and increases apoptosis in K562 cells. These results underscore the potential of ADNP/ChAHP as an appealing target to modulate the choice between erythroid and megakaryocytic fates and offer promise as a target for pro-differentiation therapies in AML

#5631 YAP1 is a critical factor for FUS::DDIT3/BAF/c-Jun complex assembly in myxoid liposarcoma.

R. Berthold[1], I. Isfort[1], L. Heinst[1], E. Wardelmann[1], P. Aman[2], C. Scholl[3], M. Trautmann[1], S. Frohling[4], W. Hartmann[1];

[1]Gerhard-Domagk-Institute of Pathology, Munster University Hospital, Munster, Germany, [2]Sahlgrenska Center for Cancer Research, Institute of Biomedicine, Department of Laboratory Medicine, Sahlgrenska Academy, University of Gothenburg, Gothenburg, Sweden, [3]Division of Applied Functional Genomics, German Cancer Research Center (DKFZ) and National Center for Tumor Diseases (NCT) Heidelberg, Heidelberg, Germany, [4]Division of Translational Medical Oncology, National Center for Tumor Diseases (NCT) Heidelberg and German Cancer Research Center (DKFZ), German Cancer Consortium (DKTK), Heidelberg, Germany

Introduction: FUS::DDIT3 is the dominant fusion protein in myxoid liposarcoma (MLS), resulting from a disease-defining chromosomal translocation. Acting as an aberrant transcription factor, FUS::DDIT3 disturbs gene regulatory networks interfering with adipogenic differentiation, while driving oncogenic gene expression and proliferation. Functionally, FUS::DDIT3 has been shown to cooperate with the transcriptional coregulator YAP1 and to interact with the BAF chromatin remodeling complex. However, mechanistic details on FUS::DDIT3's function in transcriptional dysregulation leading to proliferative effects and the required interactome are incompletely understood. This study was performed to investigate transcriptional and epigenetic players recruited by FUS::DDIT3 to drive MLS proliferation and tumorigenesis.

Experimental Procedures: To study protein-protein interactions between FUS::DDIT3 and its interacting partners, co-immunoprecipitation experiments of nuclear extracts and proximity ligation assays were performed using human MLS cell lines. To further investigate dependencies of nuclear complex assembly, combined RNA interference (RNAi) experiments were conducted. MLS cell viability and proliferation were assessed using MTT assays and xCELLigence real-time analysis, respectively. RT-qPCRs were performed to analyze the expression of FUS::DDIT3 target genes. The expression of FUS::DDIT3's interacting proteins was evaluated by immunohistochemistry in primary human MLS specimens.

Results: Co-immunoprecipitation and proximity ligation assays demonstrated nuclear interactions between FUS::DDIT3, YAP1, and the canonical BAF (cBAF) complex in MLS cell lines. In addition, a novel interaction of FUS::DDIT3 with the AP-1 transcription factor c-Jun was identified. Knockdown of the cBAF-specific subunits ARID1A and ARID1B resulted in reduced MLS cell viability and proliferation. Similarly, RNAi-mediated silencing of c-Jun impaired MLS cell viability and led to decreased expression of FUS::DDIT3 target genes. Strikingly, RNAi-mediated silencing of YAP1 resulted in decreased interaction of FUS::DDIT3 with cBAF components and c-Jun in MLS cells.

Conclusions: Our results identify YAP1 as a key factor mediating the nuclear interaction of FUS::DDIT3 with the cBAF complex and the AP-1 transcription factor c-Jun, both shown to be essential for MLS cell proliferation.

#5632 Advancing transcriptome insights during RNA-Seq library construction of FFPE samples in a novel workflow.

C. Jiang, E. Jordan Dreskin, A. Olcott, L. Lingelbach, S. Perike;
Bio-Rad Laboratories, HERCULES, CA

Formalin-fixed, paraffin-embedded (FFPE) tumor tissue has significant clinical benefits in oncology research and is considered vital for studying tumor gene expression through RNA sequencing (RNA-Seq). However, RNA extracted from FFPE samples tends to be severely degraded, making it suboptimal for constructing high-quality RNA-Seq libraries. The RNA-Seq workflow can further impair data quality, as traditional library preparation and pre-library ribodepletion workflows may result in the loss of valuable information due to rare transcripts being not captured or washed away. Moreover, small, degraded fragments are a challenging template for ligases, and the resulting adapter addition may be inadequate. Here we assessed a novel workflow employing a proprietary enzyme to overcome the limitations and biases of cDNA synthesis using reverse transcriptase (RT) and ligases. This innovative RNA-Seq library preparation approach, coupled with a post-library ribodepletion strategy, aims to capture a more complete transcriptome profile from RNA extracted from FFPE breast cancer samples, and can also be used for evaluation of gene regulation through intronic and intergenic bases. The study also compared two commercially available kits, RecoverAll and PureLink, for FFPE RNA extraction, evaluating quality metrics such as RNA integrity number (RIN), DV200, recovery of small RNAs during NGS library construction, and transcriptome coverage. A parallel fresh frozen RNA sample, extracted using a phenol-based reagent, served as a benchmark. Our findings demonstrate that the novel workflow yields a richer dataset, encompassing a wider range of transcriptomic elements, including both small and long RNAs from FFPE samples. Performing ribodepletion after the library preparation procedure led to increased detection of small RNAs compared to pre-library ribodepletion. The robust analytical performance of this streamlined library preparation protocol enables its suitability for RNA-Seq analysis of archived FFPE specimens, offering substantial utility for oncology research.

#5633 Unravelling the pleiotropic role of HNF4α in invasive mucinous adenocarcinoma of the lung (IMA).

H. Essel Dadzie, G. Fort, K. Gillis, P. Fang, W. Orellana, E. L. Snyder;
University of Utah Huntsman Cancer Institute, Salt Lake City, UT

IMA is a distinct subtype of lung adenocarcinoma (LUAD), marked by a cellular identity shift from a pulmonary to a gastric lineage with the loss of the pulmonary lineage specifier NKX2-1. This distinctive transformation underscores the complexity of lung cancer heterogeneity and highlights the critical role of lineage-specifying transcription factors in dictating tumor behavior. Notably, both human and murine models of IMA overexpress HNF4α, a known lineage specifier for gastric differentiation in the adult mouse mucosa. Also, concomitant deletion of *Hnf4a* and *Nkx2-1* at tumor initiation impairs tumor growth and the extent of HNF4α in regulating IMA tumor growth, cellular identity and drug response remains unknown at large. Here, we utilized genetically engineered mouse models (GEMM) that relies on a sequential recombination strategy to delete *Hnf4a* in established tumors. We induce tumor formation through intratracheal delivery of Flp-O virus, activating the expression of mutant $KRAS^{G12D}$ and Cre in lung epithelial cells. Tamoxifen administration recombines either *Nkx2-1* alone (KN) or in combination with *Hnf4a* (KNH). We have extensively studied the phenotypic role of HNF4α in GEMM and organoids and identified gene sets regulated by HNF4α in IMA at the bulk level. To complement our findings, we profiled both the tumor and stromal compartments via scRNAseq analysis on our GEMM to gain insights into the cellular diversity within the tumor microenvironment (TME) and the role HNF4α plays. Additionally, we performed ChIPSeq in organoids to elucidate the genome occupancy of HNF4α and determine the mechanisms of gene regulation in IMA. We find that deletion of *Hnf4a* impairs tumor growth in GEMM and this is phenocopied in organoids. We identified numerous differentially expressed genes (DEGs) in KNH compared to KN and validated several DEGs in vivo. GSEA analysis reveals a significant involvement in regulating cellular identity and suggests a potential impact on anti-tumor immune responses. To this, our scRNAseq data revealed an enrichment of N2-TAN (tumor associated neutrophils) associated genes in KNH compared to KN, suggesting a nuanced interplay between HNF4α and the TME. Additionally, HNF4α exhibited dual functionality, acting as an activator and indirectly as a repressor by modulating the activity of other transcription factors like FOXA1. FOXA1 was found to bind de novo target genes following the loss of HNF4α. These findings so far collectively illuminate the multifaceted role of HNF4α in IMA, primarily driving tumorigenesis in a cell autonomous manner and secondarily skewing the TME towards a protumor via N2-TAN following loss of HNF4α in tumors.

#5634 Tristetraprolin induces an antitumorigenic phenotype in triple negative breast cancer via a novel non-canonical mechanism.

J. L. Rutherford, M. B. Stemberger, R. Mahmud, C. R. Ross, E. J. F. White, G. M. Wilson;
University of Maryland, Baltimore, Baltimore, MD

The ultimate cause of death for most triple negative breast cancer (TNBC) patients is metastatic disease, which has a five-year survival rate of 12.8%. This low survival rate is partly due to the lack of targeted treatments for metastatic TNBC, resulting from the heterogeneity of the disease. As such, further research is needed to identify novel molecular mechanisms that can be targeted to suppress TNBC malignancy. Tristetraprolin (TTP) is an RNA-binding protein that binds to AU-rich elements (AREs) in the 3' UTRs of select mRNAs, including many that encode proteins involved in cancer-related processes, and targets these mRNAs for degradation. Loss of TTP in tumors correlates with increased disease severity and decreased survival, suggesting a role as a tumor suppressor in multiple cancers, including breast cancer. While previous research has shown that TTP can suppress proliferation in breast cancer, the mechanism remains weakly defined. To elucidate how TTP impacts tumorigenic phenotypes in advanced breast cancer, we stably transfected a FLAG-TTP-expressing construct into three aggressive and metastatic TNBC cell lines. We analyzed TTP-induced changes in gene expression patterns among these cell lines using RNA-sequencing and observed that TTP alters the expression levels of many genes. Gene Set Enrichment Analysis (GSEA) of our datasets revealed that TTP affects multiple pathways, including significant suppression of pathways that promote cell growth, various metabolic processes contributing to tumor growth, and the response to hypoxia. As these pathways highly associated with tumorigenesis, we hypothesized that TTP would attenuate multiple tumor phenotypes. Our subsequent functional analyses revealed that TTP potently suppressed four tumor phenotypes in these cell models: cell proliferation, stem cell frequency, migration, and invasiveness. We hypothesized that inhibition of proliferation was mediated by cell cycle alterations, however, flow cytometry analysis revealed no substantial cell cycle perturbations between TTP-expressing cells and controls. Further analysis of cell cycle regulators revealed minimal changes in expression of proteins encoded by known or suspected TTP target mRNAs. Actinomycin D assays surprisingly revealed that TTP had no effect on the decay kinetics of several known TTP targets, suggesting that TTP's antitumorigenic properties observed in TNBC cells are independent of its RNA-destabilizing function. To confirm this finding, we constructed cell models expressing an RNA-binding defective mutant of TTP, C147R, which recapitulated suppression of the four tumorigenic phenotypes seen with the wild-type protein. Collectively, these findings reveal that expression of TTP can potently suppress several oncogenic phenotypes in TNBC cells via a mechanism independent of its canonical RNA-binding/destabilizing functions.

#5635 TPM4 overexpression promotes colon epithelial cell tumorigenesis *in vitro* and correlates with human colon tumor progression *in vivo*.

G. Ferrero[1], B. Pardini[2], A. Naccarati[2], **M. Papetti**[3];
[1]University of Turin, Turin, Italy, [2]Italian Institute for Genomic Medicine, Turin, Italy, [3]Touro University, New York, NY

Because colon cancer still exerts a heavy burden on human health, we are interested in identifying very early events in colon epithelial cell tumorigenesis in order to develop strategies to treat and possibly prevent colon carcinogenesis. We hypothesize that aberrant expression of genes involved in crypt-luminal colon epithelial cell migration, needed for proliferative, undifferentiated stem cells at the crypt bottom to mature into growth arrested, mature effector cells near the lumen, may disrupt normal differentiation and initiate events that can trigger the transition from a normal to premalignant state in colon epithelial cells. Forced upregulation of tropomyosin 4 (TPM4), an actin-binding protein that exerts many effects on contractility and migration, prevents certain aspects of Caco2 maturation induced by contact inhibition of growth, including increased expression of the digestive enzyme sucrose isomaltase and glutathione S-transferase alpha 1. Furthermore, TPM4.2-overexpressing cells exhibit numerous morphological abnormalities. Compared to untransfected Caco2 cells and empty-vector stable transfectant controls, TPM4.2-overexpressing Caco2 cell clones elaborate aberrant thin membrane protrusions and expanded membrane ruffles. Particularly striking are defective maintenance of dome structures at middle (day 14) and late (day 21) time points of induced differentiation in TPM4.2-overeexpressing clones. We further hypothesize that TPM4 is overexpressed in human colon tumors, particularly at early stages of tumorigenesis. In order to test this hypothesis, we examined TPM4 RNA expression in datasets obtained from human colon tissue at premalignant as well as tumorigenic stages. TPM4 trends toward overexpression in premalignant, relative to normal, human colon tissue (uninvolved mucosa from patients with familial adenomatous polyposis, or FAP) and is significantly overexpressed in adenocarcinoma tissue relative to normal controls. Interestingly, TPM4 overexpression may be more pronounced at earlier, rather than later, stages of adenocarcinoma. Our results suggest that aberrant TPM4 overexpression in colon epithelial cells can promote adoption of a tumorigenic state. Certain aspects of Caco2 cell maturation are disrupted by forced TPM4 overexpression during induced differentiation, and TPM4 overexpression correlates with early stages of colon tumorigenesis. Misregulation of TPM4 gene expression may therefore represent a critical molecular event that can block normal differentiation and induce early events in colon epithelial cell tumorigenesis. TPM4 expression level may therefore prove to be a useful biomarker that can, along with other diagnostics, help to determine tumorigenic progression in human colon tissue and to develop novel strategies to prevent colon cancer and treat it at early stages.

#5636 CUX1 transcriptionally regulates intestinal epithelial homeostasis.

K. Zawieracz, N. An, M. McNerney;
The University of Chicago, Chicago, IL

The small intestine digests and absorbs nutrients, a role made possible by specialized secretory and absorptive cells that constantly replenish from the intestinal stem cell niche. Disruption in intestinal epithelium homeostasis has been linked to pathologies including inflammatory bowel disease (IBD) and cancer. However, the processes regulating differentiation in healthy and disease setting are incompletely understood. CUX1 is a highly conserved homeodomain-containing transcription factor that is expressed in small intestinal crypts and has been previously shown to be essential in mice and *Drosophila*. CUX1 is upregulated upon inflammatory stress conditions, including intestinal damage and in IBD. In addition, CUX1 is predicted to be protective against IBD from genome-wide association studies. The aim of the current work is to determine the mechanistic role of CUX1 in secretory intestinal cells differentiation and epithelial homeostasis. To this end, we have generated transgenic mouse models that modulate CUX1 levels in an inducible manner. Mice with near-null CUX1 levels exhibit rapid weight loss requiring euthanasia while mice with ~50% residual CUX1 halt normal weight gain. Histologic examination of tissues from mice with CUX1 knock-down reveals a lack of mature secretory cells, including goblet and Paneth cells, the latter playing a supportive role to intestinal stem cells. Moreover, mouse intestinal tissues from our knock-down models demonstrated decreased proliferation with increased apoptosis. In transcriptome profiling, we observed downregulation of proliferation, intestinal stem cell, and digestive system developmental gene signatures and decreased levels of key secretory cell regulators, pointing towards a role for CUX1 in stem cell maintenance and differentiation. Indeed, reducing CUX1 levels decreased β-catenin protein levels, while Wnt/β-catenin signaling is required for the organization of the crypt-villus axis. Finally, CUX1 knock-down compromises the ability to form budding organoids, demonstrating the cell intrinsic role for CUX1 in stem cell differentiation. In ongoing studies, we are identifying CUX1 genome-wide binding targets and the epigenetic impact of CUX1 in intestinal epithelium cells. Our findings indicate that CUX1 is a critical regulator of intestinal epithelium homeostasis that has a role in differentiation and potential role in injury-induced de-differentiation in healthy as well as IBD patients. We propose that CUX1 regulates stem cell maintenance and crypt composition by regulating Wnt/β-catenin signaling and inducing fetal-like transcriptomic repair program shown to be coopted by colon cancers. Resolving an intricate network of transcriptional regulation of differentiation in the intestinal crypt holds the potential to successfully target inflammation-related damage in human intestines.

#5638 The BAF complex mediates intertwined activity of YAP1 and β-catenin in synovial sarcoma.

I. Isfort, R. Berthold, L. Heinst, A. Kuntze, E. Wardelmann, M. Trautmann, W. Hartmann;
Gerhard-Domagk-Institute of Pathology, Munster University Hospital, Munster, Germany

Introduction: Synovial sarcoma (SySa) is a rare malignant soft tissue tumor characterized by a specific reciprocal translocation t(X;18). The resulting chimeric SS18::SSX fusion protein drives SySa tumorigenesis by integrating into BAF chromatin remodeling complexes, changing their composition and dysregulating gene transcription. The role of BAF complexes in cancer steadily increases with ~20% of all malignancies having alterations in BAF complex subunits. BAF complexes are multiprotein complexes with several interaction partners determining their localization and functionality. Since previous analyses revealed an induced activation of the transcriptional coregulators YAP1 and β-catenin in SySa, the aim of this study was to analyze if nuclear YAP1 and β-catenin are interacting with BAF complexes and if this has an impact on their transcriptional activity.
Experimental procedures: Co-immunoprecipitation experiments on nuclear protein extracts and proximity ligation assays were performed to investigate interactions between YAP1, β-catenin, and BAF complex subunits in SySa cells. Knockdown of common and specific BAF complex subunits was conducted employing RNA interference. To assess changes in YAP1 and β-catenin transcriptional activities, TEAD and TOPFlash luciferase reporter assays were performed, respectively, and protein expression levels were detected by immunoblotting.
Results: In SySa, protein-protein interaction experiments revealed nuclear interactions between β-catenin, YAP1, the SS18::SSX fusion protein and various BAF subunits. YAP1 and β-catenin's transcriptional activities were found to be interdependent as they mutually enhanced each other's activation. Knockdown of SS18::SSX as well as specific BAF complex subunits was associated with diminished transcriptional activities of these coregulators and, interestingly, substantially affected their mutual activation. This indicates that SS18::SSX-containing BAF complex assembly is crucial for interdependent YAP1 and β-catenin activation in SySa cells.
Conclusions: This study reveals a significant role of the SySa-specific fusion protein and BAF chromatin remodeling complexes in mediating intertwined activation of YAP1 and β-catenin.

#5639 TIP60-independent mechanism of BRD8 is involved in colorectal tumorigenesis.

K. Yamaguchi[1], S. Nakagawa[1], R. Yamaguchi[2], P. Sheridan[1], K. Takane[1], T. Ikenoue[1], S. Nagatoishi[1], H. Kozuka-Hata[1], M. Oyama[1], S. Aikou[1], Y. Ahiko[1], D. Shida[1], K. Tsumoto[1], S. Miyano[1], S. Imoto[1], Y. Furukawa[1];

[1]University of Tokyo, Tokyo, Japan, [2]Aichi Cancer Center Research Institute, Nagoya, Japan

Modifications of histone tails control chromatin structure, and the acetylation is generally associated with euchromatin and transcriptional activation. Acetylated lysine residues are recognized by bromodomains, which serve as acetyl-lysine binding modules and participate in transcriptional regulation. Bromodomain-containing protein 8 (BRD8) is a subunit of the NuA4/TIP60-histone acetyltransferase complex. Although BRD8 has been considered to act as a co-activator of the complex, its biological role remains to be unclear. In this study, we revealed that BRD8 accumulates in colorectal cancer cells through the inhibition of ubiquitin-dependent protein degradation by the interaction with MRG domain binding protein (MRGBP). RNA-seq analysis coupled with genome-wide mapping of BRD8-binding sites disclosed that BRD8 transactivates a set of genes independently of TIP60, a catalytic subunit of NuA4 complex, and that BRD8 regulates the expression of multiple subunits of the pre-replicative complex (pre-RC) in concert with the activator protein-1 (AP-1) transcription factor. Depletion of BRD8 induced cell-cycle arrest at the G1 phase and suppressed proliferation of colorectal cancer cells. We have also shown that the bromodomain of BRD8 is indispensable for not only the interaction with histone H4 or transcriptional regulation but also its own protein stability. These findings provide a new insight into the roles played by BRD8 in human colorectal carcinogenesis and will contribute to the development of new chemotherapeutic agents targeting the bromodomain of BRD8.

#5640 Unlocking the therapeutic potential of SF3B1 inhibitors for bladder cancer treatment.

R. Columbres, A. Chakraborty, A. Apolo, R. Banday;
NIH-NCI, Bethesda, MD

RNA splicing dysregulation is a hallmark of cancer, occurring in multiple solid and hematological malignancies. Splicing factor 3 subunit B1 (SF3B1), a key component of the U2 small nuclear ribonucleoprotein (snRNP) complex that regulates RNA splicing, is frequently altered in a variety of cancer types, including non-muscle-invasive and muscle-invasive bladder cancer, where the E902K mutation is common. In this study, we investigated the therapeutic potential of the SF3B1 inhibitor, pladienolide B, in bladder cancer using *in vitro* models. We used a recombinant plasmid containing the SF3B1^{E902K} mutation and established an UMUC3^{E902K} mutant urothelial cell line. Both UMUC3^{WT} and UMUC3^{E902K} cells were treated with pladienolide B alone or in combination with cisplatin to evaluate differences in cell viability. Flow cytometry using annexin V staining and propidium iodide exclusion was utilized to assess the cell death mechanism. RNAseq was performed after RNA extraction from UMUC3^{WT}, UMUC3^{E902K}, RT4, and HT1376 bladder cancer cell lines were treated with pladienolide alone or combined with cisplatin. We determined that the IC50 for pladienolide B is 5nM for UMUC3 cells observed 72 hours post-treatment. Treatment with pladienolide B halted the cell cycle and caused cell death by apoptosis for both UMUC3^{WT} and UMUC3^{E902K} cell lines. We also observed that UMUC3^{E902K} cells were significantly more sensitive to pladienolide B compared to UMUC3^{WT} cells ($p \leq 0.05$). Furthermore, there was a synergistic effect observed after co-treatment with low-dose pladienolide B (2 nM) and cisplatin (3 µM) for both UMUC3^{WT} and UMUC3^{E902K} cell lines, with UMUC3^{E902K} cells showing greater sensitivity to combination treatment. Our results provide insights into the potential use of splicing inhibitors, alone or in combination with chemotherapy, for treating bladder cancer, specifically for tumors that bear driver mutations in splicing factors. Currently, we are evaluating the mechanism by which SF3B1 mutations make cells sensitive to pladienolide B *in vitro* and *in vivo,* with the goal of identifying specific mRNA splicing vulnerabilities that can be targeted by anti-sense or splice-switching oligonucleotides to achieve anti-tumor outcomes. Additional differential splicing patterns and preliminary *in vivo* results will be presented.

#5641 Transcriptional regulation by nuclear deformation.

A. Cook[1], R. Stephens[1], N. Fursova[2], C. C. Chow[1], D. Larson[2], Y. Miroshnikova[1];
[1]National Institute of Diabetes and Digestive and Kidney Diseases (NIDDK), Bethesda, MD, [2]National Cancer Institute (NCI), Bethesda, MD

Establishment and maintenance of cell identities requires transcriptional rewiring and modulation of three-dimensional genome organization. The nucleus is subject to constant mechanical forces, both intrinsic from the cytoskeleton and extrinsic, such as compression, confinement, and stretch. Recently, work from us and others implicate mechanical force, through activating biochemical signaling pathways as well as direct nuclear deformation, in remodeling nuclear architecture, chromatin state and global gene expression patterns. Thus, we hypothesize that mechanical force plays an important role in coordinating and thresholding transcriptional responses. Here, we challenge this hypothesis by quantifying the effect of nuclear deformation on transcription in real time at single cell resolution quasi genome wide. Further, recent work elucidated that the MYC oncogene exerts global effects on transcriptional output by altering the binding dynamics of transcription factors involved in the activation and productive elongation of RNA Polymerase II. This contrasts with mechanical stress which reduces global levels of RNA Polymerase II. Here we interrogate how transcriptional output is tuned for specific genetic programs/loci by mechanical force using MYC as a paradigm.

#5643 Targeted RNA-seq of dried blood microsamples for convenient RNA biomarker monitoring.

L. Kobzik, T. Liu, M. Makhanov, D. Hu, K. Ghias, P. Diehl, **A. Chenchik**;
Cellecta, Inc., Mountain View, CA

Microsampling lancet-induced blood drops enables frequent and comprehensive analysis of various metabolites, lipids, cytokines, and proteins. This approach holds promise for monitoring immunotherapy patients using RNA biomarkers, but a suitable method for processing RNA has been lacking.
In this study, we employed a targeted RNA-sequencing protocol, the DriverMap™ EXP assay, to process 30 ul of dried blood. We compared the gene expression profile in traditionally collected blood samples with that of blood absorbed onto a Mitra® microsampling device containing an RNA-stabilization reagent. Following endotoxin incubation, RNA was extracted from stimulated and unstimulated blood samples. Targeted PCR amplification of 274 immune/inflammatory genes using the DriverMap targeted RNA-Seq protocol demonstrated robust detection and high correlation (r = 0.94) between the two methods in both unstimulated and endotoxin-stimulated blood. Moreover, differentially expressed genes (DEGs) identified in standard and microsampling methods exhibited substantial overlap with publicly available datasets from similar experiments. Furthermore, we compared whole blood extracted from Tempus™ blood RNA tubes to Mitra microsamples pre- and post-immunization with the Pneumovax® vaccine using the DriverMap EXP genome-wide 19K panel for targeted RNA-sequencing. We observed approximately 90% overlap in the top 10K genes between Tempus and Mitra microsamples. Notably, microsamples stored at 4ºC for over a year exhibited similar expression profiles to more recently drawn whole blood samples.

#5644 The impact of ATF3, JDP2, FOXR2, NAA10, FOXL2, DDX20, and p14ARF on the transactivation of p53.

W. H. Yang, W.-H. Yang;
Mercer University School of Medicine, Savannah, GA

Cancer stands as a formidable health challenge in the 21st century, evoking widespread fear. Presently, the mortality rate associated with cancer in humans ranges from approximately 11% to 25%. Numerous nuclear and cytoplasmic proteins have demonstrated interactions with p53, influencing both its activity and abundance. In our prior, unpublished findings, we established that JDP2 interacts with p53, modulating its activity. Consequently, in the present investigation, we broaden our exploration to identify novel proteins capable of regulating p53 transactivation. First, we found a synergistic effect of ATF3 and JDP2 on p53 transactivation. Moreover, deSUMOylation of ATF3 and dephosphorylation of JDP2 further enhance p53 transactivation. Secondly, FOXR2 (an epigenetically regulated pan-cancer oncogene) and NAA10 (an acetyltransferase) also remarkably increase p53 transactivation in H1299 (p53 null) cells. Thirdly, in addition to MDM2 and MDM4 (MDMX) as p53 negative regulators, we further found that FOXL2 (a transcription factor in steroidogenesis regulation), DDX20 (a transcription factor for embryonic development and ovarian function), and p14ARF (for cell cycle regulation) significantly down-regulate p53 transactivation. Taken together, our preliminary results demonstrate that several transcription factors regulate p53 transactivation and possible p53 stability and/or degradation. This data is presented to substantiate the idea that numerous newly discovered proteins may engage with p53 and control its transactivation.

#5645 HuR regulates aerobic glycolysis in triple negative breast cancer (TNBC).

A. Dev J R, A. Gogia, S. R. Mathur, S. Deo, C. Prasad;
All India Institute of Medical Sciences (AIIMS) New Delhi, New Delhi, India

Introduction: The RNA-binding protein Human Antigen R (HuR/ELAVL1) is ubiquitously expressed and exerts post-transcriptional regulation on mRNAs characterized by U/AU-rich sequences in their 3' UTR. Elevated cytoplasmic expression of HuR has been associated with various malignancies, influencing key cellular processes such as proliferation, apoptosis, angiogenesis, and metastasis. The involvement of HuR influences prognostic outcomes and hence is a potential biomarker and therapeutic target in cancer research. The present study investigates the oncogenic role of HuR in TNBCs, an aggressive subtype of breast cancer.

Methods: Immunohistochemistry was performed on TNBC patient tumor tissue (n=40) to asses the expressions of HuR and MMP9. Human TNBC cell lines MDA-MB-231 and MDA-MB-468 were used for *in vitro* studies after confirming cytoplasmic HuR accumulation in these cells via Immunofluorescence. The RNA binding activity of HuR was disrupted using CMLD2, a specific inhibitor of HuR, and subsequent physiological changes were assessed through functional assays. An exploratory investigation of HuR-moderated metabolic changes was performed employing NANOSTRING nCounter XT gene expression assay using metabolic pathways panel. Investigation and/or validation of molecular changes were done via immunoblotting.

Results: Meta-analysis using Liu-2014 TNBC dataset correlated high HuR protein expression with reduced patient survival (p=0.028). HuR (77%) and MMP9(55%) were found to be overexpressed in TNBC tissues. Inhibiting HuR with CMLD2 resulted in the downregulation of the protein and its downstream targets CDK2, MMP9, and β catenin. HuR inhibition compromised proliferation, migration, Matrigel invasion and EMT (downregulated E-Cadherin, N-Cadherin, and Vimentin) in TNBC cell lines. Further, HuR inhibition resulted in decreased clonogenicity in 2D and 3D TNBC cultures. Transcriptomics studies showed that HuR inhibition in MDA-MB-231 altered the profile of glycolytic genes in addition to other pathways such as cell cycle and DNA damage repair. In accordance, the expression of glycolytic proteins was reduced upon CMLD2 treatment. Similar results were obtained on HuR knockdown by siRNA suggesting that HuR-mediated effects on TNBC progression might be in part through its modulation of aerobic glycolysis.

Conclusion: Overall, our results demonstrate HuR as a positive regulator of aerobic glycolysis in TNBCs and the ability of CMLD2 to inhibit HuR provides a rationale to consider it as a potential anticancer agent for TNBCs.

#5646 Altered intronic polyadenylation by mutant p53 impairs transcription of DNA repair genes in lung cancer.

Liang Liu, Elizabeth Forbes, Wei Zhang

Wake Forest School of Medicine, Winston Salem, NC

Introduction: Changes in alternative pre-mRNA processing have been found in many cancers. Aberrant intronic polyadenylation (IPA) causes a stop of normal transcription resulting in the production of truncated mRNA isoform or lncRNA. We sought to examine the role of mutant p53 in pre-mRNA processing, especially in IPA regulation in lung cancer.

Methods: We established stable cell lines transfected with mutant p53 (R273H, R175H, H179Q, C238Y, and C242F) or vector control using the NSCLC cell line H1299 with a homozygous deletion of the endogenous p53. Total RNA was used to build libraries enriched in sequences near polyadenylation sites (PASs) using the 3'mRNA-Seq REV library kit (Lexogen; Greenland, NH). Sequencing reads were mapped to the human genome (GRCh37), and PASs with ≥2 supporting reads and ≥0.05 usage in any experiment were identified. Counts for each Intronic Polyadenylation (IPA) and total reads in the terminal exon were compiled into matrices for each condition. DEXseq was applied to detect changes in the relative abundance of each exon part normalized to all exons within the gene. Gene Ontology (GO) analysis was implemented using the enrichR package.

Results: We identified 32,752 IPA sites in 5,718 genes, and 26,416 distal PASs (dPASs) in the 3'UTRs of 10,298 genes. Across all five cell lines, when compared individually to the vector control, a comprehensive shift in IPA events was observed, with a concurrent decrease in dPASs. Many of IPA isoforms exhibited consistent patterns of increased or decreased abundance changes. Upon closer examination of each individual cell line, such as the p53-R273H cell line (vs. vector), significant usage changes were identified for 2,389 IPA sites, of which 1,210 were increased and 1,128 terminal exons were altered, with 650 being suppressed. At the gene level, a total of 1,183 genes had at least one significantly increased IPA isoform, a significantly decreased distal isoform, or both. GO analysis showed that these genes were highly enriched in DNA repair-related functional terms such as DNA repair, double-strand break repair, and nucleotide excision repair. The observed IPA changes in DNA-repair genes were consistently observed across the other 4 mutant lines (vs. vector). This observation was further supported by analyzing data from patients with lung adenocarcinoma (LUAD) in the TCGA cohort, where we selected samples carrying nonsense/ frameshift mutations, and/or a deep deletion as the p53-null control group, and those carrying missense mutations as the p53-mutant group.

Conclusions: Our study illustrated a novel role of p53 mutants in the regulation of intronic polyadenylation processing that contributes to deficient DNA repair. These observations offer a fresh perspective on the multifaceted roles of p53 in cellular homeostasis.

Acknowledgment: This work was supported by NCI Cancer Center Support Grant P30CA012197 and NIH/NCI grant R03CA256100.

#5647 Investigating the role of AP-2α in melanomagenesis.

N. Bartschat, J. Chang, M. Suraju, R. Nagel, Z. Li, J. White, C. Kenny, R. Weigel;
University of Iowa, Iowa City, IA

Introduction: Transcription factor AP-2α (encoded by the *TFAP2A* gene) is a protein involved in the early development of multiple tissues, particularly the neural crest. Melanocytes are derived from the neural crest and their development appears to rely on AP-2α and its paralogues, along with master regulator MITF. Prior studies have indicated that AP-2α is a crucial regulator of melanoma metastasis. However, it is unclear if AP-2α plays a role in melanomagenesis. We sought to understand the role of AP-2α in melanomagenesis, hypothesizing that knock out (KO) of *TFAP2A* would suppress malignant potential *in vitro* and downregulate genetic pathways linked to malignant transformation.

Methods: *TFAP2A* KO was generated with a single-guide RNA CRISPR/Cas9 system targeting exon 3 of the gene in the human melanoma cell line A375. Tumorigenesis phenotype was assessed by evaluating contact-independent colony formation with the *in vitro* soft agar assay. To identify downstream regulatory programs controlled by *TFAP2A*, we then utilized RNA-seq and Gene Set Enrichment Analysis (GSEA, San Diego). RNA-seq was performed on four clones each for wildtype and *TFAP2A* KO samples and the resulting data was processed using GSEA to identify gene sets modified after *TFAP2A* KO.

Results: Targeting of *TFAP2A* with CRISPR/Cas9 effectively knocked out AP-2α protein expression in the A375 melanoma cell line. Colony formation on soft agar assay was significantly decreased after *TFAP2A* KO ($P < 0.01$). RNA-seq revealed significant differential expression of 11,195 genes after *TFAP2A* KO. Gene sets with negative enrichment after *TFAP2A* KO included those overall higher in tumors versus normal tissue (FWER $P = 0.003$) and multiple signaling pathways related to malignant transformation such as TGF-β (FWER $P = 0.003$), MYC (FWER $P = 0.009$), KRAS (FWER $P = 0.03$), and Notch (FWER $P = 0.043$).

Conclusions: Our data suggests that *TFAP2A* plays a role in cutaneous melanomagenesis. *TFAP2A* may represent a therapeutic target for melanoma, though further pre-clinical studies are needed. We plan to further test this hypothesis in a melanoma mouse model with conditional *TFAP2A* KO under the control of inducible Cre recombinase driven by the mouse tyrosinase gene promoter.

#5648 Decoding the non-canonical functions of HO-1 in prostate cancer: A nuclear perspective and its association with a neuroendocrine signature.

Seniuk A. Rocio[1], Agustina Sabater[2], Pablo Sanchis[2], Juan Bizzotto[1], Gaston Pascual[1], Estefania Labanca[3], Nicolas Anselmino[3], Nora Navone[3], Elba Vazquez[1], Pia Valacco[1], Javier Cotignola[1], Ayelen Toro[1], Geraldine Gueron[1]

[1]CONICET - IQUIBICEN, Ciudad Autonoma de Buenos Aires (CABA), Argentina, [2]1-CONICET - IQUIBICEN. 2-Universidad Argentina de la Empresa (UADE), Instituto de Tecnologia (INTEC), Ciudad Autonoma de Buenos Aires (CABA), Argentina, [3]Department of Genitourinary Medical Oncology and The David H. Koch Center for Applied Research of Genitourinary Cancers, The University of Texas MD Anderson Cancer Center, Houston, TX 77030, USA., Houston, TX, United States, Houston, TX

Previous studies have demonstrated the non-canonical anti-tumor effect of heme-oxygenase 1 (HO-1) in prostate cancer (PCa). Although HO-1 is crucial for free heme degradation, its nuclear expression unveils non-canonical functions beyond its enzymatic function. Understanding the specifics of its non-canonical role remains a critical unmet need. In this study, we identified nuclear interactors of HO-1 and assessed their association with PCa.PCa cells were treated with hemin (80 µM, 24 h), a specific pharmacological inducer of HO-1. Nuclear HO-1 immunoprecipitation and LC-ESI MS/MS analysis identified 11 differential nuclear associated-HO-1 proteins between control and hemin-treated PCa cells (ILF3, ILF2, BCLAF1, SAFB, DDX17, SLC25A5, CASP14, PRDX1, BRIX1, CCDC175, and GPATCH1). Next, we performed an Ingenuity Pathway Analysis (QIAGEN) showing that ILF3 appears as a master regulator of this signature. To assess the clinical relevance of these factors in PCa, we analyzed overall survival (OS), progression-free survival (PFS), relapse free survival (RFS) in multiple PCa datasets (GSE34312, GSE35988, GSE3933, GSE46602, GSE6956, GSE70768, TCGA-PRAD, GSE70770, GSE16560, GSE24136; n=1064). We performed univariable and multivariable analyses for these factors and identified the ones that significantly and independently affected the OS, RFS, PFS. Next, a risk score model was built based on the expression of 9 genes ($\sum n_i=1(Coef_i \times Expr_i)$) for the GSE70770 dataset using these factors identifying a subpopulation of PCa patients with high-risk of RFS (HR: 7.39 High vs Low score, $p<0.0001$); ascertaining the critical role of this signature in PCa. To elucidate the association of these factors with the aggressive phenotype of PCa, we analyzed RNA-seq expression data from the MDA-PCa-PDXs series (PCa Patient Derived Xenografts Program; MD Anderson Cancer Center), capturing PCa heterogeneity. Unsupervised clustering analysis revealed that samples with high expression of HO-1 nuclear interactors corresponded to neuroendocrine tumors, negative for androgen receptor staining. Principal Component Analysis identified ILF3 as the most relevant HO-1 interactor driving PDXs' samples variance, correlating with a significant decrease in relapse-free survival of PCa patients. Further, we used ChIP-Atlas to assess the epigenomic landscapes for these nuclear HO-1 interactors. Results indicated that 40% of HO-1 nuclear interactors were potential transcription regulators. Strikingly, KEGG pathways analyses revealed that their regulomes were significantly associated with neurodegenerative disorders, highlighting their relevance in neural processes. In conclusion, our findings suggest that HO-1 and its nuclear interactors may play a pivotal role in neuroendocrine PCa, shedding light on potential therapeutic targets for this aggressive form of the disease.

#5649 PRRX1-TOP2A interaction is a malignancy-promoting factor in human malignant peripheral nerve sheath tumors.

S. Takihira, E. Nakata, D. Yamada, T. Osone, T. Takao, T. Takarada, A. Hirasawa, T. Itano, T. Fujiwara, T. Kunisada, T. Ozaki;
Okayama Univ. Graduate School of Med., Dentistry & Pharm. Sci., Okayama, Japan

Background: Paired related-homeobox 1 (PRRX1) is a transcription factor in the regulation of developmental morphogenetic processes. There is growing evidence that PRRX1 is highly expressed in certain cancers and is critically involved in human survival prognosis. However, the molecular mechanism of PRRX1 in cancer malignancy remains to be elucidated.
Methods: PRRX1 expression in human Malignant peripheral nerve sheath tumors (MPNSTs) samples was detected immunohistochemically to evaluate survival prognosis. MPNST models with PRRX1 gene knockdown or overexpression were constructed in vitro, and the phenotype of MPNST cells was evaluated. Bioinformatics analysis combined with co-immunoprecipitation, mass spectrometry, RNA seq, and structural prediction were used to identify proteins interacting with PRRX1.
Results: High expression of PRRX1 was associated with a poor prognosis for MPNST. PRRX1 knockdown suppressed the tumorigenic potential. PRRX1 overexpressed in MPNSTs directly interacts with topoisomerase 2A (TOP2A) to cooperatively promote epithelial-mesenchymal transition and increase expression of tumor malignancy-related gene sets including mTORC1, KRAS, and SRC signaling pathways. Etoposide, a TOP2A inhibitor used in the treatment of MPNST, may exhibit one of its anticancer effects by inhibiting the PRRX1-TOP2A interaction.
Conclusion: Targeting the PRRX1-TOP2A interaction in malignant tumors with high PRRX1 expression might provide a novel tumor-selective therapeutic strategy.
Significance: MPNST is a malignant tumor with a poor prognosis and still lacks definitive treatment. Our results could hold promise as an alternative therapeutic strategy to inhibit the interaction between PRRX1 and TOP2A, and may improve the prognosis for malignant tumor patients with high expression of PRRX1 and TOP2A such as MPNSTs.

#5650 RNA regulatory disruption by 3'-dATP: A novel approach to inhibit ribosome biogenesis in cancer.

M. Elshani[1], Y. Zhang[1], I. Um[1], R. Plummer[2], S. P. Blagden[3], S. N. Symeonides[4], N. Cook[5], T. Evans[6], A. L. Dickson[1], D. J. Harrison[1];
[1]University of St. Andrews, St. Andrews, United Kingdom, [2]Newcastle University, Newcastle Upon Tyne, United Kingdom, [3]University of Oxford, Oxford, United Kingdom, [4]The University of Edinburgh, St. Andrews, United Kingdom, [5]The University of Manchester, Manchester, United Kingdom, [6]University of Glasgow, Glasgow, United Kingdom

Background: Ribosomes are a complex ensemble of ribosomal RNA and proteins. As the site where genetic information is translated to protein, they have a key role in cell survival, growth and proliferation. Ribosome biogenesis (RiBi), the process of creating ribosomes, is a complex function governed by precise checkpoints and surveillance mechanisms which may become dysregulated in cancer leading to tumor growth and therapeutic resistance. Ribosome-targeted therapy could provide a promising treatment for cancer. NUC-7738 (3'-deoxyadenosine [3'-dA] which is phosphorylated and protected with a phosphoramidate moiety attached at the 5'-position) generates sustained intracellular levels of 3'-dATP, a molecule that profoundly influences RNA regulatory processes, including poly(A) tail length, leading to alternative polyadenylation (APA) and splicing, resulting in impaired cellular responses. NUC-7738 is currently being investigated in combination with pembrolizumab in patients with advanced melanoma in the Phase 2 part of the clinical study (NCT03829254). Here, we investigate the impact of 3'-dATP on RNA regulation and RiBi utilizing a novel bioinformatic pipeline.
Material and Methods: RNA was extracted from melanoma and renal carcinoma cell lines treated with NUC-7738 for 24h and paired biopsies (pre and post treatment) from patients treated with NUC-7738 + pembrolizumab. Sequencing libraries used for long-read PCR-cDNA sequencing were generated. Gene-level expression was quantified using Salmon DeSeq2. In addition to gene expression, poly(A) tail length, APA and isoform switch were analyzed. Protein expression was determined using JESS Western analysis. Multiplexed analysis of protein localization and expression in tissue was carried out using an in-house immunofluorescence protocol.
Results: NUC-7738 caused a global reduction in poly(A) tail length in cell lines and patient biopsies that was most pronounced in the poly(A) tail exosome targeting (PAXT) long non-coding RNA (lncRNA) transcripts, including SNHG19, 5'TOP and YAE1, all of which play a role in RiBi. PAXT lncRNAs such as SNHG3 and SNHG19 increased in abundance. Ribosomal subunit proteins such as RPS3, RPS6, RPL17 decreased in expression. Expression of YAE1, a regulator of RiBi, also decreased. Distinct APA usage of various transcripts was observed in cell lines and patient biopsies.
Conclusion: Through the development of a novel bioinformatic pipeline we have been able to demonstrate that NUC-7738 disrupts RNA regulation, leading to perturbed RiBi. Targeting RiBi provides a promising approach to treating cancers

#5651 Personalized transcriptomic profiling for advanced prostate cancer: Guiding second-generation hormonal drug selection.

L.-H. Chang[1], H.-H. Chang[1], X.-Y. Lin[1], S.-C. Wang[1], C.-P. Chuu[2], D.-N. Chen[3], S.-P. Huang[1], C.-Y. Li[1];
[1]Kaohsiung Medical University, Kaohsiung City, Taiwan, [2]National Health Research Institutes, Miaoli City, Taiwan, [3]National Pingtung University of Science and Technology, Pingtung City, Taiwan

Introduction: Second-generation hormonal drugs have demonstrated significant efficacy in extending the survival of patients with advanced prostate cancer. These drugs operate through two distinct molecular mechanisms: inhibition of androgen biosynthesis and blockade of the androgen receptor. However, due to concerns of side effects, concurrent usage of multiple drugs is not recommended. A notable challenge is the eventual development of drug resistance, rendering all second-generation hormonal therapies ineffective. Currently, there is a lack of guidelines for helping patients choose the most suitable drug. In the context of pharmacogenomics, genetic differences can influence drug susceptibility and efficacy, with variations in genomic sequences and regulatory mechanisms impacting drug response at the transcriptional and translational levels. Considered the rapid processing capabilities of Affymetrix transcriptomic microarrays, we hypothesized that distinct gene signatures in patients who respond well or poorly to second-generation hormonal drugs could be identified and could act as a companion diagnostic tool.
Methods: We enrolled 180 advanced prostate cancer patients, who fulfilled Taiwan national health insurance criteria of using second-generation hormonal drugs, from seven medical centers or regional hospitals in Taiwan at 3 time points: prior to drug administration, 3 months after treatment started and drug resistance developed. The RNA expression data and clinical parameters were analyzed, and classification models were built using IPA and R. Good or poor responders were defined by 3-month prostate-specific antigen (PSA) lowered by 90 percent.
Results:: Differential expression and enrichment analyses post-treatment highlighted the activation of NF-kappa B signaling and various immune cell pathways. Notably, pathways related to primary immunodeficiency and IL-17 became prominent following the development of drug resistance. At the initial stages, distinct alterations in cell cycle pathways, particularly G1/S and G2/M, were observed between good and poor responders. This was elucidated through principal component analysis and subsequent dbscan clustering. To further distinguish between these responder groups, we utilized an integrative approach for feature selection, combining support vector machine, random forest classifier, and lasso regression. Despite the innovative approach, the model's error rate stood at approximately 15%, attributed mainly to the limited number of cases.
Conclusion: Our study highlights the potential of using transcriptomic analysis to predict responses to second-generation hormonal drugs in advanced prostate cancer, paving the way for personalized treatment strategies. However, the need for larger cohort studies is evident to refine these predictive models and enhance their accuracy.

MOLECULAR/CELLULAR BIOLOGY AND GENETICS: Genomic Changes and Intratumoral Heterogeneity as Predictive Biomarkers for Clinical Outcome
Poster Session

#5655 Association between tumor genomic variants and the long term post surgical recurrence as detected by a tumor informed ctDNA assay.
N. Friedman, M. Richters, J. Ortiz, R. Burns, S. L. Bristow, M. C. Liu, A. Aleshin, A. Jurdi, H. A. Costa;
Natera, Inc., Austin, TX

Background: While surgical resection of early stage cancers is often curative, a number of patients will experience disease recurrence. Given the genomic heterogeneity of cancer, we hypothesized that different driver mutations present in a patient's tumor may influence whether and when recurrence occurs. To investigate this, the association between the presence of driver mutations and rates of molecular residual disease (MRD) detection by circulating tumor DNA (ctDNA) was evaluated in patients with stage I-III colorectal cancer (CRC).
Methods: This was a retrospective evaluation of patients who underwent commercial ctDNA testing (Signatera™) following curative surgical resection for stage I-III CRC from 2019 to February 2023. For this analysis, patients who were ctDNA-negative post-surgery (2-12 weeks) and had ctDNA testing performed between 6-24 months after surgery were included. Patients were stratified based on the presence or absence of mutations in driver genes and the associated percentage of patients with ctDNA-positivity over time was calculated.
Results: Of 11,436 patients with stage I-III CRC, 45.7% (5,230) had ctDNA testing performed between 2-12 weeks post-surgery. During this window, 81% (4,239/5,230) had a negative post-surgical ctDNA test result available. For this analysis, 78.4% (3,323/4,239), 46.7% (1,979/4,239), 24% (1,017/4,239) and 8.2% (348/4,239) had follow-up ctDNA testing performed for at least 6, 12, 18, and 24 months post-surgery, respectively. Certain driver mutations were associated with increased risk of post-surgical ctDNA-positivity rate. In patients with stage I CRC, *APC* mutations were associated with elevated rates of ctDNA positivity at 12 months [(*APC*-mutated: 13% (11/85) vs. *APC*-wildtype 3% (1/31); p=0.06)] and 18 months [(*APC*-mutated: 38% (12/32) vs. *APC*-wildtype: 6% (1/18); p=0.02)]. Interestingly, similar findings were not observed in stage II or stage III CRC. Similarly in patients with stage III CRC, *SMAD4* mutations exhibited a substantially increased probability of ctDNA-positivity at 6 months [(*SMAD4*-mutated: 8% (15/194) vs. wildtype: 4% (54/1267) p=0.09)], 12 months [(*SMAD4*-mutated: 25% (32/129) vs. wildtype: 12.4% (102/817); p=0.0005)], and 24 months [(*SMAD4*-mutated: 69% (41/59) vs. wildtype: 53% (149/279); p=0.02)].
Conclusions: These findings point to several genomic alterations that may underlie cancer recurrence after a long period of undetectable disease with a differential impact across different stages. This may allow, in the future, for a personalized surveillance strategy based on driver mutations and stage of the disease. Correlation of ctDNA positivity with clinical outcomes based on driver mutational status may inform to what extent tumor-specific characteristics drive patient outcomes following a successful surgery.

#5656 Longitudinal spatial profiling reveals chemoresistance mechanisms and characteristics of minimal residual disease in high-grade serous ovarian cancer.

Y. Dai, A. Knisely, B. Lawson, S. Lee, K. M. Wani, R. N. Lazcano Segura, B. Melendez, J. Chen, Y. Liu, M. Chelvanambi, L. A. Gibson, S. B. Johnson, C.-C. Yeh, D. R. Ingram, C. W. Hudgens, K. Cho, G. Pei, J. Jiang, Y. Chu, A. J. Lazar, J. Gao, J. Wargo, L. Wang, A. A. Jazaeri;
The University of Texas MD Anderson Cancer Center, Houston, TX

High-grade serous ovarian cancer (HGSOC) is the most lethal gynecologic malignancy globally. Despite an initial response to upfront surgery and platinum-based chemotherapy in most cases, over 70% will relapse. A critical source of recurrence is minimal residual disease (MRD), which persists after upfront treatment yet is clinically undetectable. In this study, we performed second look laparoscopy (SLL) on advanced stage HGSOC patients who had received neoadjuvant chemotherapy (NACT) followed by interval debulking surgery and adjuvant chemotherapy and were in complete clinical remission by imaging and CA-125 tumor marker. Surgical MRD status was determined by pathological review of SLL biopsies. Matched samples from pre-treatment biopsy, interval debulking surgery and SLL in 4 MRD+ and 3 MRD- cases were analyzed using GeoMx Digital Spatial Profiling. Among them, samples from 1 MRD+ and 1 MRD- case were also profiled with Visium. The tumor cells of MRD+ cases exhibited stronger signaling related to hypoxia, angiogenesis, and epithelial-mesenchymal transition at baseline as well as diminished apoptosis signaling after NACT. In addition, progressively upregulated expressions of ATP binding cassette transporters were also observed over time in the tumor compartment of MRD+ cases, potentially contributing to chemoresistance. In the tumor microenvironment, MRD- cases displayed increased abundance of plasma cells, conventional dendritic cells and lymphocytes in both pre-treatment and interval debulking samples compared to MRD+ cases. Notably, Visium data of the MRD- case revealed tertiary lymphoid structures (TLS) in the pre-treatment sample, which became better organized following NACT, with plasma cells disseminating into adjacent tumor areas. Conversely, TLS were fewer and poorly organized in the MRD+ case. Longitudinal comparison of the 3 timepoints in MRD+ cases revealed more regulatory T cells in the stromal compartments of the MRD lesions. Furthermore, from Visium data, exclusion of CD8 T and plasma cells from the tumor core was evident in the MRD lesion. In line with this, strong TGF-β, IL-1β, IL6 and FGF2 signaling surrounding the tumor were noted, likely contributing to immune exclusion. The spatial distribution of multiple immune checkpoint molecules highly overlapped with that of CD8 T cells, indicating T cell exhaustion in the MRD lesion. In summary, these data suggested distinct cancer phenotypic states and immune features in surgically detected MRD+ HGSOC, shedding light on potential chemoresistance and immune evasion mechanisms that contribute to the MRD phase of disease. This study represents the first systemic characterization of ovarian cancer MRD by leveraging SLL, providing insights for designing personalized therapies aimed at eradicating these chemoresistant lesions and ultimately preventing disease recurrence.

#5657 The intricate relationship between genomic damage and epidemiological lung cancer risk in ever-smokers.

M. J. Przybilla[1], A. Ammar[2], H. Selway-Clarke[2], A. R. J. Lawson[1], H. Jung[1], A. Pennycuick[2], K. Gowers[2], R. C. Khaw[2], Z. Frazer[2], K. Davies[2], I. Martincorena[1], S. Janes[2], P. J. Campbell[1];

[1]Wellcome Sanger Institute, Cambridge, United Kingdom, [2]University College London, London, United Kingdom

Extensive epidemiological studies have illuminated the intricate relationship between tobacco smoking and lung cancer. Squamous cell carcinoma (LUSC), which is clinically tied to smoking, is formed in the proximal airway of the lung, whereas adenocarcinoma (LUAD), arising in the distal airway, has a weaker connection to tobacco and often occurs in never-smokers. The cessation of smoking promotes lung health and gradually lowers cancer risk. Dissecting the impact of smoking cessation on different lung cancer types in >650,000 individuals from UK Biobank and PLCO, we confirmed previous findings of LUSC risk diminishing more rapidly after quitting smoking, while LUAD risk endures over time. We previously found that normal bronchial epithelium in the proximal airway accumulates DNA damage proportionally to an individual's smoking habits. However, our analysis identified a population of cells with near-normal mutation burden, evading tobacco-induced damage. We hypothesized that the reduction in LUSC risk with smoking cessation could be explained by the repopulation of the proximal airway by these cells. Here, we followed up on this finding by exploring the genomics of alveolar stem cells (ASCs), which are believed to be the origin of LUAD. Analyzing WGS data of >800 single-cell-derived organoids from 9 patients, we found that tobacco smoking is the major driver of increased mutation burden in ever- compared to never-smokers. More importantly, our results demonstrated no significant difference in the burden of tobacco-induced genomic damage between ex- and current-smokers, suggesting that DNA damage in the distal airway is both persistent and long-lasting. Using single-molecule sequencing in a cohort of 43 individuals with heterogeneous smoking histories confirmed this observation. Overall, contrasting this finding with the results from bronchial epithelium and the epidemiological lung cancer risk brings forth a genomic explanation for the differences in long-term cancer risk, ingrained in the abundance of near-normal mutation burden cells. By contextualizing our results within the carcinogenic process in the lung, we suggest that persistent genomic alterations are the major driver in the long-standing discussion about the reason for an epidemiological shift from LUSC to LUAD in the last 30 years. As the largest proportion of lung cancers occurs within ex-smokers, the persistent genomic damage in the distal airway will result in a relative increase in LUAD incidence compared to LUSC, likely explaining this clinical phenomenon.

#5658 Genome-scale CRISPR screen in 3D tumor models identifies EGFR-TKI resistance mechanisms in human NSCLC.

Pranay Agarwal, Soon Youn Choi, Xin Liu, Jina Song, Maya Tureez, Aashka Mehta, Un Jae Baek, Kyuho Han, **Hong-Pyo Lee**

MEDiC Life Sciences Inc., Mountain View, CA

INTRODUCTION: Epidermal growth factor receptor (EGFR) tyrosine kinase inhibitors (TKIs) are the primary treatment for EGFR-mutated non-small-cell lung cancer (NSCLC). Despite Osimertinib, an FDA-approved EGFR-TKI, showing high selectivity for EGFR-activating mutations, resistance inevitably arises, leading to disease progression. The influence of genes within cancer on Osimertinib response remains unclear. To tackle this challenge, CRISPR screens have been extensively used. However, current CRISPR screens investigating EGFR TKI resistance heavily rely on 2D monolayer cell models, lacking the ability to replicate in vivo tumors accurately. In response, we conducted a genome-scale loss-of-function CRISPR screening employing 3D tumor models embedded in an extracellular matrix across various NSCLC cell lines. Utilizing a comprehensive panel of CRISPR screens in both 3D tumor models and 2D monolayer models, we systematically assessed how genetic alterations impact cell resistance and transformation against treatment with Osimertinib, in diverse cellular contexts.
METHOD: Genome-scale CRISPR-Cas9 screens in 10 NSCLC cell lines used 3D tumor models and 2D cells to pinpoint genes pivotal for EGFR TKI resistance. Cas9-expressing cell lines were transduced with a lentivirus carrying 60,000 sgRNAs targeting ~20,000 human genes. Cells were cultured in both models and treated with optimized Osimertinib or DMSO, inducing 20-30% cell growth inhibition for 3 days. Post-treatment, cells were recovered for 4 days. This treatment cycle was repeated 3-4 times in 3D models and 2-3 times in 2D cells. The sgRNA composition in each pool was analyzed using Next Generation Sequencing after treatment cycles in both models.
RESULTS: Upon analyzing CRISPR screening data across 10 distinct cell lines to assess drug phenotypes, we confirmed the enrichment of established resistance pathways like PI3K/AKT/mTOR, Hippo, and MAPK signaling pathways in both 2D monolayer cells and 3D tumor models. However, notable discrepancies in EGFR TKI resistance mechanisms were evident between these two models. Specifically, CRISPR screens conducted with 3D tumor models unveiled unique resistance mechanisms, notably the LKB1/AMPK/mTOR pathway (STK11, GSK3B), Ubiquitination (RNF7, ARIH2), and stabilization of E-cadherin adherens junction (NCKAP1, EXOC4) differing from those identified in conventional 2D monolayer model. Furthermore, the 3D tumor models exhibited significantly heightened enrichment of the MAPK and Hippo signaling pathways compared to their drug phenotype score in 2D monolayer cells.
CONCLUSION: This study underscores the significance of employing the 3D tumor model in drug phenotype CRISPR screen. This approach recapitulates unique gene dependency patterns and interactions linked to EGFR-TKI resistance in a 3D tumor context, revealing potential targetable vulnerabilities context-dependent.

#5659 Origin of synchronous or metachronous multiple pancreatic cancers.

T. Hirano[1], N. Kakiuchi[1], Y. Takeuchi[1], T. Anazawa[1], K. Nagai[1], T. Masui[2], S. Minamiguchi[1], H. Haga[1], T. Tanaka[3], A. Masuda[3], Y. Kodama[3], N. Uza[1], H. Seno[1], S. Miyano[4], H. Tanaka[4], S. Ogawa[1];

[1]Kyoto Univ. Graduate School of Medicine, Kyoto, Japan, [2]Kurashiki Central Hospital, Okayama, Japan, [3]Kobe Univ. Graduate School of Medicine, Hyogo, Japan, [4]Tokyo Medical and Dental University, Tokyo, Japan

[Introduction] The majority of patients with pancreatic cancer are inoperable at the time of diagnosis and even those cases with successful tumor resection for early-stage tumors frequently had second tumors within the remaining pancreas shortly after the surgery, contributing to a poor clinical outcome. Additionally, synchronous multiple pancreatic cancers have been frequently documented. One of the long-standing issues about such synchronous and/or metachronous multiple pancreatic cancers is their clonal origins. This study is designed to elucidate the origin of multiple pancreatic cancers through an unbiased detection of somatic mutations in primary and metachronous cancers, along with adjacent precursor lesions.

[Methods] Serially obtained formalin-fixed paraffin-embedded surgical specimens from 20 patients who had undergone curative surgery for an early-stage pancreatic cancer were subjected to laser microdissection for the enrichment of tumor and precancerous lesions, from which DNA was extracted and analyzed for somatic mutations using whole-exome sequencing (WES) with matched normal DNA. The investigation into the shared and private mutations across different samples aimed to unveil the clonal evolution history of these lesions.

[Results] We analyzed 20 patients with multiple pancreatic cancers of 2 metachronous and synchronous, 16 metachronous, and 2 synchronous tumors. In metachronous cases, all patients exhibited margin-negative pathology for the primary cancer, with a median interval of 38.9 months (ranging from 7 to 85 months) between the initial and second surgery. In addition, a total of 20 pancreatic intraepithelial neoplasia (PanIN) from 5 of these cases were analyzed. We identified a median of 66 (range: 31-232) and 20 (14-42) somatic mutations in cancer and PanIN lesions, respectively. None of the patients have known pathogenic germline variants. All samples had one or more driver mutations. In most cases (N=19), sharing many somatic mutations, multiple tumors had a common clonal origin. In another synchronous case, the synchronous tumors shared only one mutation, suggesting that they were clonally independent tumors. By contrast, none of the mutations other than hotspot KRAS mutations were shared between precursor and cancer lesions. While multiple independent clones were observed in precancerous lesions, most of multiple cancers originated from a common ancestor. Moreover, negative pathology of the margins at the initial surgery suggested that those multiple lesions arose from distant dissemination or metastasis, rather than contiguous, intraductal invasion.

[Conclusions] In conclusion, our study suggests that even in early pancreatic cancer, dissemination within the pancreas may occur, contributing to the development of synchronous and metachronous cancers.

#5660 Gene expression signatures from FFPE to predict recurrent metastatic nasopharyngeal cancer.

J. K. Tay[1], W. K. Teo[1], J. W. Foley[1], L. Suryani[1], B. C. Wu[2], C. H. Siow[1], K. S. Loh[1];

[1]National University of Singapore, Singapore, Singapore, [2]National University Hospital, Singapore, Singapore

Nasopharyngeal cancer (NPC) is an EBV-driven epithelial cancer endemic to Southeast Asia, Southern China and the Middle East. Accurate profiling of the gene expression of NPC has been challenging because of its intense inflammatory infiltrate, as well as the 3 - 4mm size of biopsies limiting the amount of available material. Here we present a large cohort of 339 micro-dissected gene expression libraries from formalin-fixed paraffin-embedded (FFPE) biopsies from NPC patients treated at the National University Health System, Singapore, as well as healthy controls. NPC tumors from patients who subsequently developed recurrent or metastatic disease (Group A), and patients who did not develop recurrent or metastatic disease (Group B) were profiled. Tumor epithelial and microenvironment compartments were separately obtained using laser-capture microdissection, followed by library preparation performed for RNA-Seq using an in-house specialised technique. Gene signatures for NPC tumor epithelial and microenvironment content were used to validate the purity of gene expression libraries. Our preliminary analysis revealed that primary, pre-treatment tumors from patients who subsequently developed recurrence (Group A) showed downregulation of processes related to interferon gamma and interferon alpha response (p-adj <0.001 for both), while processes related to epithelial-mesenchymal transition (p-adj < 0.05) were enriched compared to patients who remained healthy (Group B). In contrast to primary tumors, recurrent tumors in Group A were enriched for cellular respiration including oxidative phosphorylation (p-adj < 0.0001). Our approach highlights the utility of whole transcriptome profiling from small quantities of archival FFPE material. The gene signatures identified from the primary tumors of high-risk patients are biologically relevant and have the potential to be used in precision medicine to guide additional targeted intervention.

#5661 Identifying and intervening rare resistant subclones to BRAF/MEK inhibitors in metastatic melanoma.

H. Wang[1], M. Nakazawa[2], O. Veiseh[1], L. Kwong[2], D. Zhang[3];
[1]Rice University, Houston, TX, [2]MD Anderson, Houston, TX, [3]NuProbe, Houston, TX

Acquired drug resistance poses a significant challenge in the treatment of cancer. This study focuses on melanoma as a model system to understand and address pre-existing subclonal resistance. The use of BRAF and MEK inhibitors (BRAFi/MEKi) in patients with metastatic melanoma harboring BRAF activating mutations has resulted in remarkable responses in the majority of cases. However, most patients have disease relapse after one year, and there are limited subsequent treatment options. One possible cause of relapse is the existence of a subpopulation of cells resistant to BRAFi/MEKi prior to treatment, raising the possibility that commencing counter-resistance treatment earlier may delay or abolish resistance to BRAFi/MEKi. We aim to enhance the detection and treatment of low-frequency resistant mutations, addressing the current oversight by existing technologies. This research is crucial due to a lack of consensus on the clinical management of these mutations. By using quantitative blocker displacement amplification (qBDA) technology and integrating patient samples with cell line models, our project seeks to determine 1) the prevalence of low-frequency resistant subclones by measuring the Variant Allele Frequency (VAF) of known resistance mutations along the MAPK/PI3K pathways in FFPE biopsies from 149 metastatic melanoma patients and 2) determine the functional impact of different VAF levels on the outgrowth of resistant subclones. We assessed 14 loci in 6 known resistance genes: NRAS, KRAS, PIK3CA, AKT1, MAP2K1, and MAP2K2, as well as BRAF itself as a positive control. As expected, all 55 patients analyzed harbored BRAF activating mutations, while 17 patients had at least one resistant subclone above our preliminary cutoff of 60% VAF. To simulate the behavior of low-VAF resistance mutations, we conducted in vitro experiments by spiking in labeled BRAF/MEK inhibitor-resistant melanoma cells into their isogenic sensitive parental cell line. Our initial data demonstrated that, at least in this model system, a 10% VAF spike-in leads to the eventual outgrowth of resistant cells, but not in a 1% VAF spike-in, suggesting that either the density or the absolute number of the pre-existing resistant cells can dictate resistance evolution. In future experiments, we will assess multiple VAFs in an independent cell line as well as *in vivo* to identify the nature of its correlation with resistance outcomes and expand to additional models. In summary, our data suggest that a substantial proportion of metastatic melanoma patients with BRAF mutations have pre-existing resistant cell subclones, and that accurately assessing its VAF could provide clinically-relevant information. Ultimately, results from this work would be the basis for future personalized counter-resistance therapies, potentially extending treatment effectiveness for patients with pre-existing resistant mutations.

#5662 *PDCD1* and *CD48* significantly impact cancer recurrence and survival in pediatric acute lymphoblastic leukemia.

S. F. N. Alotaibi[1], L. Abuhadi[2], N. Alolyani[1], M. R. Alotaibi[1], A. R. Alhoshani[1], H. As Sobeai[1];
[1]King Saud University, College of Pharmacy, Riyadh, Saudi Arabia, [2]Minstry of Health, Riyadh, Saudi Arabia

Introduction: Immune checkpoints (ICPs) play a critical role in modulating the immune response, maintaining self-tolerance, and preventing excessive immune system activation. Dysregulation of immune checkpoints has been implicated in cancer progression and treatment resistance. In this study, we aimed to screen for dysregulated immune checkpoint genes that might be associated with cancer recurrence in pediatric acute lymphoblastic leukemia (ALL) following a course of cancer treatment. We hypothesized that certain ICPs would be significantly dysregulated in relapsed ALL patients, potentially providing insights into the underlying mechanisms driving therapy resistance and disease recurrence.

Methods: 51 ICP genomic data (gene expression, copy number alterations (CNAs), and mutation) of133 patients with relapse information [relapse-free (n=29) and relapsed (n=104)] extracted from the Therapeutically Applicable Research to Generate Effective Treatments (TARGET) were examined in the study. Patient's t-test (p-value < 0.05) was used to identify significant genetic factors between relapse-free and relapsed patients. Free and overall survival analyses were performed using log-rank test (p-value < 0.05) based on patient gene expression profiles.

Results: Among the 51 genes examined, *PDCD1, PVR*, *CD70,* and *CD48* were significantly upregulated in relapsed patients compared with relapse-free patients ($P < 0.05$). No significant CNAs nor mutations were detected in these four genes. Patients with high expression profiles of *PDCD1* and *CD48* at diagnosis were 1.71 and 1.47 more likely to relapse compared to patients with low expression profiles, respectively ($P < 0.05$). Furthermore, the upregulation of *PDCD1* (P= 0.0004, HR= 1.972) and *CD48* (P= 0.0344, HR= 1.533) demonstrated significantly increased mortality rates in patients following treatment, as indicated by overall survival analyses.

Conclusion: The upregulation of *PDCD1 and CD48* was significantly associated with relapse and survival of ALL patients. Promisingly, these two ICPs can potentially be used as prognostic biomarkers for relapse risk and rationale for alternative therapeutic strategies. Our study suggests that targeting *PDCD1* and *CD48* might be beneficial in enhancing the treatment efficiency and thereby reducing the recurrence risk. The study was funded by the Deputyship for Research and Innovation, Ministry of Education, Saudi Arabia (DRI-KSU-1273).

#5663 Collagen COL26A1 correlates with poor papillary thyroid cancer prognosis and *in vitro* characteristics of metastasis indicating a potential role as a biomarker or therapeutic target.

M. Carnazza, D. Quaranto, N. DeSouza, S. Dadafarin, A. Moscatello, H. K. Islam, J. S. Di Martino, R. K. Tiwari, J. Geliebter;
New York Medical College, Valhalla, NY

Papillary thyroid cancer (PTC) is the most common cancer in young women and is increasing 3% annually in incidence. While PTC is often slow-growing and surgically resectable, recurrence years to decades later occurs in 20% of patients (now only in their 40s/50s), decreasing survival by ~60%. The identification of prognostic biomarkers and actionable therapeutic targets for high-risk PTC is critically important and an unmet need. RNASeq analysis of our repository of PTC and matched normal tissues identified collagen 26A1 (COL26A1) as significantly upregulated in patients with extrathyroidal extension (ETE), lymph node metastasis, and multifocal tumors, indicative of high-risk for recurrence. Correspondingly, survival curves of The Cancer Genome Atlas (TCGA) demonstrated increased COL26A1 expression decreases survival probability by 25% (p=0.0086) and correlated with MACIS score (q=0.001), differentiation score (q=0.025), tumor stage (q=0.025), and ETE (p=0.0038). COL26A1 expression was increased in PTC cell lines K1 (3-fold) and TPC1 (5-fold) compared to “normal” thyroid epithelial cells, NThy-ori-3-1. CRISPR knockdown of COL26A1 repressed RNA (50%) and protein (70%) expression. COL26A1 repression decreased known cancer-promoting activities of collagens, including proliferation (30%), clonogenicity (33%), anchorage-independent growth (37%), cell motility (43%), Matrigel invasion (30%), in situ gelatin degradation (70%), and migration (33%). Cell-to-cell adhesion and cell-matrix adhesion also decreased (36% and 25%, respectively). This coincided with reduced anoikis resistance (31%), increased MMP expression (50%), and reductions in mesenchymal markers (30%) and increases in epithelial markers (3-fold). Evidence that COL26A1 is a secreted protein was validated by conditioned media isolations whereby expression was decreased in knockdowns compared to control cells (70%). Preliminary data indicate the control cells’ conditioned media can restore the aggressive phenotypes, including cell motility (51%). Qiagen Ingenuity Pathway Analysis (IPA) elucidated the potential role of androgen receptor (AR) in linking COL26A1 with PTC, coinciding with the known effects of sex hormones on collagen expression and organization, and the sex disparity in PTC. Preliminary data indicate that physiologic levels of androgen decrease COL26A1 RNA (46%) and protein (45%) expression in K1 cells expressing the androgen receptor. Thus, COL26A1 may serve as a prognostic marker and actionable target for small molecule inhibitors in high-risk PTC.

#5664 Genetic alterations and pharmacological response profiles from 10 cervical cancer cell lines.

S. Scholl[1], P. Gestraud[2], E. Girard[2], L. Lecompte[2], M. Halladjian[1], L. de Koning[3], N. Servant[2], M. Kamal[1], E. Del Nery[4];
[1]Department of Drug Development and Innovation (D3i), Institut Curie, Paris, France, [2]Bioinformatics and Computational Systems Biology of Cancer, PSL Research University, Mines Paris Tech, INSERM U900, Paris, France, [3]Translational Research Department, Institut Curie, PSL University Paris, Paris, France, [4]Biophenics, Institut Curie, PSL Research University, Department of Translational Research, Cell and Tissue Imaging Facility (PICT-IBiSA), Paris, France

Background: There are significant parallels between CC cell lines (CCCL) and newly diagnosed tumors, the most prominent being HPV infection/integrations and PI3K as well as epigenetic pathway alterations. Objectives: Identify genomic alterations associated with resistance to specific drug families in pharmacological profiles in Cell Lines (CL) and in Primary Tumors.
Material and Methods: 16 public and 4 newly patient-derived CL have been extensively characterized by HPV type, genetic (WES) and protein (RPPA) profiles. Pharmacological profiling against 32 drugs was carried out in triplicate samples and repeated on 10 selected CL. Variant calling of small-scale alterations (SNVs, InDels) was performed using GATK HaplotypeCaller (v4.0.2.1). Variants annotation was performed with Annovar (v 2017/07/06) using respectively gene (refGene), known polymorphims (avsnp v147, 1000G v2015/08, ESP6500v2, ExAC) and cancer databases (COSMIC v70, ICGC v21) as well as deleterious impact predictors (dbNSFP v33). Copy number alterations were assessed using Facets (v0.5.11) with 4 blood samples from the RAIDs tumor project used to generate a “baseline” copy number profiles for CLs.
Results: All 10 cell lines had strikingly similar DSS (drug sensitivity scores) to a family of four different microtubule targeting agents (MTAs). Bioinformatics subtraction of genetic alterations present in resistant (CRL 10302, CRL 7920, CRL 1550) and absent in sensitive CLs: (IC1, IC3, IC5), revealed a consistent LoF (loss of function) alteration in one single gene: *PABPC3* ‘Poly A tail binding protein, cytoplasmic C3’, a gene involved in messenger RNA stability and translational initiation. Additionally, 50 gene alterations from the pathway “POST TRANSLATIONAL MODIFICATIONS OF TUBULIN” were variably detected in resistant CLs. In primary tumors from the RAIDS database, alterations in *PABPC3* were present in 10/301 (3%), half of which documented by at least one database: (Cosmic, ICGC, Cancer Hotspot). *All* CLs were sensitive to Bortezomib, Omipalisib and Palbociclib. A *large spectrum* activity to Vorinostat, (HDAC inhibitor) in line with frequent (sensitizing) LoF alterations in epigenetic suppressor genes, contrasted with a *selective response* to other well-known CC drugs: Methotrexate, Gemcitabine, Sorafenib. Three out of CL were highly sensitive to APR246 (Eprenetapopt) as single agent. Bioinformatics gene subtraction identified *OSBPL1A*, a marker of synthetic lethality in the ferroptosis pathway, in all three CLs.
Discussion and Conclusion: A string of LoF alterations (*CSMD2/CSMD3, ZNF717, CDC27*) had been previously associated with poor response to radiation or to chemo-radiation, in tumors and are present in most CLs which are derived from resistant tumors. Future objectives are to validate the present biomarker findings in the context of a clinical platform trial.

#5665 Native nanopore sequencing of multiple tumor sites reveals genetic and epigenetic intra-tumor heterogeneity in canine osteosarcoma.

A. Keskus[1], **S. Aganezov**[2], T. Ahmad[1], X. Dai[2], R. Walker[3], J. Beaulaurier[2], S. Hickey[2], S. Juul[2], A. K. LeBlanc[1], P. S. Meltzer[3], M. Kolmogorov[1];

[1]Center for Cancer Research, National Cancer Institute, National Institutes of Health, Bethesda, MD, [2]Oxford Nanopore Technologies, New York, NY, [3]National Cancer Institute, Bethesda, MD

Osteosarcoma (OS) is an aggressive bone malignancy affecting children and young adults. Implementation and optimization of neoadjuvant chemotherapy led to significant improvements in outcome, but patients with recurrence or metastases at diagnosis continue to have poor prognosis. Whole genome sequencing (WGS) revealed that a hallmark of OS is a highly rearranged genome with complex copy number aberrations rather than point mutations. A better understanding of the key genomic and epigenetic factors driving clonal evolution may provide insights into the tumor progression and the therapy response.

Canine OS recapitulates the majority of the hallmark genetic and molecular factors of human OS and is recognized as an informative model. A significant difference is that initial surgery in canine OS allows us to explore tumor evolution unperturbed by treatment, providing invaluable resources to study the genetic and molecular landscape of tumor evolution.

Here, we present the first study to date in which we performed bulk WGS of multiple tumor sites and distal normal tissue in two dogs using nanopore long-read sequencing to analyze the genetic and epigenetic evolution of OS.

In both subjects, somatic structural variation detection using Severus revealed chromothripsis-like rearrangements in chr11, leading to the deletion of Cdkn2a, a known cell cycle regulator and tumor suppressor. Interestingly, in one of the subjects, the majority of the SVs (n = 131) shared across all the samples were localized on chr5, coinciding with perturbed copy number profiles and bi-allelic frequency of the SNVs, with all mutations identified using complementary bioinformatics analysis of the same native nanopore reads. The multi-site sample analysis identified subclonal structural alterations in TP53 and ATRX genes.

With phased nanopore reads, we observed subject-specific copy-neutral loss-of-heterozygosity events and long identical-by-descent blocks. Haplotype-specific copy-number analysis of tumors showed different aneuploidy patterns in both subjects, highlighted clonal compositions of samples from distinct sites, and identified regions of copy-number heterogeneity.

Furthermore, phased nanopore reads also revealed haplotype-specific 5mC and 5hmC methylation differences across tumor samples, where samples from different sites of the same tumor demonstrate distinct methylation patterns that overlap DLG2, RUNX2, KDR, and other genes known as mutational hotspots in canine/human OS.

Overall, we showcase how a single sequencing assay allows for a joint analysis of genetic and epigenetic tumor alterations, thus providing a richer understanding of the drivers of somatic evolution and their association with the molecular landscape in the canine OS. These findings can be translated into human disease and shed light on tumor progression and therapy response.

#5666 Exploring spatially resolved intra-tumoral heterogeneity of glioblastoma and neuronal mechanisms facilitating brain invasion.

F. Gaiti[1], Y. Wu[2], S. Mansouri[1], B. Wu[2], Y. Ellenbogen[2], X. Li[1], P. Habibi[1], J. Kant[1], P. Kossinna[1], S. Lau Rodriguez[1], G. Zadeh[1];
[1]UHN Princess Margaret Cancer Centre, Toronto, ON, Canada, [2]University of Toronto, Toronto, ON, Canada

Glioblastoma (GBM) is a highly lethal brain cancer, comprising about half of all central nervous system malignancies. Its recurrence and resistance to aggressive treatments, such as surgery, radiation, and chemotherapy, underscore its biological complexity. A key feature of GBM is intra-tumoral heterogeneity (ITH), stemming from a diversity of transcriptional cell states within the tumor. While genetic contributions to ITH are well-researched, the role of non-genetic factors, especially in promoting transitions between the various transcriptional cell states (referred to as plasticity), is less understood. This plasticity enables GBM cells to survive treatment pressures, necessitating a deeper dive into the epigenetic underpinnings that govern it and the role of the tumor microenvironment (TME) in influencing it. We proposed that the TME significantly impacts the epigenetic landscape of both malignant and surrounding non-malignant cells, thereby promoting ITH and cell state plasticity. To assess this, we analyzed samples from different anatomical areas of GBM tumors collected using MRI-guided selection. Utilizing advanced multimodal single-cell sequencing technologies, we profiled the transcriptomes and epigenomes of individual cells, revealing their spatially dependent phenotypic and epigenetic diversity. Our results indicated a higher enrichment of progenitor-like malignant cells, resembling neural or oligodendrocyte progenitors, around the tumor margins. In contrast, the core mainly contained differentiated cells with mesenchymal-like characteristics. Intriguingly, progenitor-like cells in the peri-tumoral zone expressed a unique neuronal activity program, including elevated levels of PRC2 complex targets, which are critical for maintaining the pluripotency and self-renewal capabilities of neural stem cells. Additionally, our analysis of cell-cell interactions between neurons and malignant cells identified ligand-receptor pairs crucial for axon guidance, neurogenesis, and tumor invasion. Proneural factors, critical for neural differentiation, were more accessible in peri-tumoral progenitor-like cells, suggesting that malignant cells might exploit neurodevelopmental routes for growth and invasion. This work underscores the significant spatial cellular heterogeneity of GBM and the variation in epigenetic states across the tumor, demonstrating how GBM cells can hijack neurodevelopmental pathways to foster invasion. Although surgical resection can target the tumor core, our insights into the invasive mechanisms of malignant cells provide a foundation for developing targeted therapies to combat the highly invasive cells persisting in regions adjacent to the tumor.

#5667 Intratumoral heterogeneity in gastric cancer related with survival and tumor microenvironment.

D.-e. Gu[1], W. Kwon[2], S. Rha[3], W.-Y. Park[4];

[1]Department of Health Sciences and Technology, Samsung Advanced Institute for Health Sciences and Technology, Sungkyunkwan University, Seoul, Korea, Republic of, [2]Song-Dang Institute for Cancer Research, Yonsei University College of Medicine, Seoul, Korea, Republic of, [3]Division of Medical Oncology, Department of Internal Medicine, Yonsei Cancer Center, Yonsei University Health System, Seoul, Korea, Republic of, [4]Samsung Genome Institute, Samsung Medical Center, Seoul, Korea, Republic of

Gastric cancer (GC), often diagnosed at an advanced stage, poses a significant therapeutic challenge due to its resistance to treatment. The understanding of intratumoral heterogeneity, crucial for tumor cell survival, remains limited in GC. We conducted a comprehensive analysis of three patient groups (intraperitoneal metastasis [IM], hematogenous metastasis [HM], and both metastasis [HIM]) undergoing immunotherapy (IO) and chemotherapy. Utilizing single-cell RNA sequencing and TCR sequencing, we examined 11 adjacent normal, 10 HM, 8 IM, and 5 HIM primary GC samples. In epithelial cells, three distinct tumor clusters (Tumor_1, Tumor_2, and Tumor_3) were identified. Trajectory analysis revealed the differentiation of chief cells into Tumor_1, subsequently dividing into more malignant cell types, Tumor_2 and Tumor_3. Tumor_2 was enriched in IM, while Tumor_1 was enriched in HM and HIM. Patients grouped by Tumor_1, 2, 3 levels showed varying survival outcomes. Surprisingly, high Tumor_2 levels correlated with increased survival, attributed to elevated HLA and PDL1 expression, promoting immune cell recruitment and robust response to IO therapy. Conversely, Tumor_3 high patients exhibited worse survival, with enrichment in metabolic pathways associated with glycolysis and hypoxia, linking to metastasis. We observed the proportion of T cells that increased presence of CD8 effector cells among patients exhibiting high levels of Tumor_1 and Tumor_2. Through TCR analysis, we found heightened clonality in both CD8 effector cells and exhausted T cells in patients with elevated Tumor_1 and Tumor_2 levels. This suggests that the activated CD8 effector T cells in these patients may enhance their ability to effectively target and attack cancer cells. In summary, this study provides a comprehensive picture of intratumoral heterogeneity in GC can impact the survival and tumor microenvironment. The unexpected high survival in Tumor_2 patients emphasizes the potential of targeting specific pathways for improved therapeutic outcomes. Additionally, the observed T cell dynamics and clonality in Tumor_1 and 2 underscore the importance of understanding the immune microenvironment for effective cancer attack.

#5668 Long non-coding RNA LINC01614 knockdown decreases carcinogenic behavior of papillary thyroid cancer *in vitro*.

D. Quaranto, M. Carnazza, N. R. DeSouza, S. Dadafarin, A. Moscatello, H. K. Islam, R. K. Tiwari, J. Geliebter;
New York Medical College, Valhalla, NY

Papillary thyroid cancer (PTC) accounts for the vast majority of thyroid cancer cases with increasing incidence over the past few decades. PTC has a significantly higher prevalence in females in their childbearing years. Despite high survival rates, disease recurrence and metastasis remain prominent issues, thus highlighting the critical need for molecular biomarker detection. A newer class of molecular regulators, known as long non-coding RNAs (lncRNAs), have demonstrated differential expression patterns in a multitude of cancers. The largest subclass of these RNA molecules in the human genome consists of long intergenic non-coding RNAs (lincRNAs) with many of their functions yet to be identified. Known functional roles of lncRNAs center on their ability to modulate gene expression and drive carcinogenic behavior, deeming them attractive biomarkers and/or therapeutic targets for study. Bioinformatic analysis of RNA sequencing data from our patient sample biobank identified LINC01614 as being significantly upregulated (~12 fold increase) in PTC, when compared to normal, matched thyroid tissue. Further, it was also upregulated ~30-fold in male PTC compared to ~5.5 fold increase in female PTC, highlighting a potential sex correlation for study. Thus, we are studying LINC01614 as a potential PTC biomarker. Gene expression analysis of LINC01614 in vitro was found to be upregulated in various thyroid cancer cell lines, specifically two PTC cell lines: TPC1 (~5 fold; RET/PTC rearrangement; female) and K1 (~2 fold; BRAFV600E; male) when compared to the immortalized “normal” thyroid cell line (Nthy-ori-3-1). For phenotypic evaluation, we utilized the CRISPRi technique to employ transcriptional repression of LINC01614 in both TPC1 and K1. LINC01614 knockdown in TPC1 and K1 resulted in decreased healing capacity (~20%), clonogenicity (~50% and ~34%, respectively), and proliferation (~55% and ~45%, respectively). Studies are currently underway to further assess invasion, morphology, and RNA localization within the cell in vitro, as well as the identification of potential protein interactions and mechanisms of action of LINC01614 in PTC. Studying lncRNAs and their regulatory roles in cancer cell function is critical in the identification of various diagnostic and prognostic biomarkers for therapeutic intervention. Our data support the potential biological role of LINC01614 in driving PTC growth and metastatic potential. Further elucidation of how LINC01614 impacts PTC development and progression is a promising avenue of exploration.

#5669 Rare germline variants on SI gene and the possibility of colorectal cancer development.

S. Kim[1], J. Bae[2], Y. Koh[2], S.-S. Yoon[2];

[1]Seoul National University, Seoul, Korea, Republic of, [2]Seoul National University Hospital, Seoul, Korea, Republic of

Research on cancer and germline variants has been ongoing. The germline variant in CPGs has been linked to cancer development. BRCA 1/2 is a typical case and oncometabolite production due to germline variants of the FH gene can affect the cancer progression. Among the genes related to IEMs, SI (Sucrase-isomaltase) is an enzyme that converts sucrose into glucose and fructose to allow normal metabolism in the small intestine. In addition, SI is highly specifically expressed in the gastrointestinal tract (nTPM = 435.9). So, we focused on and hypothesized the biological traits of the SI gene and alteration caused by germline variants could affect colorectal cancer progression. We used the public cancer databases PCAWG and TCGA and the healthy cohorts 1000G. We confirmed carriers with SI germline variants are the top gene with a high prevalence of IEM-related genes. We also established the hypothesis the SI gene may match “Knudson’s Two-hit hypothesis”. Depending on whether germline variants in IEM-related genes or not, we performed regression and utilized LOH (Loss of heterozygosity) information for each cancer sample from the public database. In COAD and STAD which are in the gastrointestinal tract, SI was confirmed to have a high tendency for LOH according to germline prevalence. Next, we performed DEG analysis and found SI germline carriers had upregulated genes related to the IFIT (Interferon-induced proteins with tetratricopeptide repeats) family. STRING network analysis also showed significance in pathways associated with “Interferon alpha/beta signaling (FDR = 0.00058)”, “Antiviral defense (FDR = 0.0016)”, “Innate immunity (FDR = 0.0317)”, and “Tetratricopeptide repeats (FDR = 0.0413)”. The following GSEA revealed that “KEGG_CYTOSOLIC DNA-SENSING PATHWAY” and “HALLMARK_INTERFERON_ALPHA_RESPONSE” were enriched in the SI germline carriers. In summary, it can be suggested immune regulation caused by SI germline variants may lead to cancer progression. We executed a follow-up analysis using the genes with low expression levels to the SI germline carriers. Among the down-regulated genes in the DEG, REG4 (Regenerating Family Member 4) and RELMβ (Resistin-Like Molecule Beta) genes were confirmed to express and function specifically only in the gastrointestinal tract. RELMβ is essential for preserving energy balance and glucose metabolism. As a validation at the protein level, we conducted IHC (Immunohistochemistry) on tissues from Korean colorectal cancer patients and confirmed lower REG4 and RELMβ expression were associated with poor prognosis. Our results suggest that SI germline carriers may cause colorectal cancer by affecting the immune system due to decreased SI enzyme function. Additionally, the decreased REG4 and RELMβ expression levels are associated with the SI germline variant and may affect cancer progression. Further analyses and experimental validations are still required.

#5670 CRISPR-Mediated knockout of Ceruloplasmin (CP) and UCHL1 reveals angiogenic role in renal cell carcinoma (RCC) cell survival and proliferation.

W. Caravan, Y. Wu, P. Lal, K. Sato, Y. Li, N. Naser Al Deen, S. Chen, A. Abedin, F. Chen, L. Ding;
Washington University In St. Louis, Saint Louis, MO

Clear cell renal cell carcinoma (ccRCC) is the most prevalent subtype of renal cell carcinoma, accounting for approximately 70% of all cases. Therapeutic treatment for metastatic ccRCC involve tyrosine kinase inhibitors or mTOR inhibiters. While these drugs extend patient survival, it also introduces a range of adverse side effects. Utilizing snRNA sequencing, snATACseq, and spatial transcriptomics, two potential ccRCC tumor specific markers have been identified: ceruloplasmin (CP) and UCHL1. These markers are notably overexpressed in a majority of ccRCC tumor cells and elevated CP levels have been correlated with reduced patient survival. To investigate the roles of CP and UCHL1 in ccRCC, CRISPR-based knockout experiments were conducted on two RCC cell lines, namely RCC4-VHL- and Caki-1. Through cell line characterization assays, we find that the absence of CP and UCHL1 impairs the cells' capabilities to migrate, proliferate, and adhere. Additionally, Cell-Derived Xenografts (CDX) of the knockout cell lines in nude mice revealed that cells lacking UCHL1 exhibited slower tumor growth compared to their parental lines. Bulk RNA sequencing further suggested a potential interrelationship between CP and UCHL1, as CP knockout cells showed increased UCHL1 expression relative to the parental line. These findings open new avenues for potential therapeutic strategies and biomarkers in the treatment and screening of ccRCC and further elevates our understandings of the roles of CP and UCHL1 in RCC tumor progression.

#5671 Profiling intra-tumor heterogeneity and chromosomal instability in malignant peripheral nerve sheath tumors.

Y. Cheng[1], H. Yan[2], M. Tarabichi[1], Z. Zhang[1], C. Gao[1], T. Lesluyes[3], A. Flanagan[4], P. Van Loo[1];

[1]UT MD Anderson Cancer Center, Houston, TX, [2]The Francis Crick Institute, London, United Kingdom, [3]IUCT Oncopole, Toulouse, France, [4]University College London, London, United Kingdom

Malignant peripheral nerve sheath tumors (MPNSTs) are rare soft-tissue sarcomas that manifest on peripheral nerves, constituting 2% of all sarcomas. While previous genomic analyses of MPNSTs have been conducted on small cohorts, often limited to single samples per patient and lacking comprehensive resolution, the extent of intra-tumor heterogeneity and the contribution of chromosomal instability to MPNST development remains unclear. To address these limitations, we developed a multi-omics integration pipeline and applied it to bulk Whole Genome Sequencing (WGS), single-cell RNA sequencing(scRNA-seq), single-cell DNA sequencing (scDNA-seq), spatial transcriptomics (ST), and Laser Capture Microsection (LCM) sequencing data. 60 tumor samples were collected from 17 patients with MPNST, and the above five techniques were applied to each sample. Overall, tumors harbor a high degree of chromosomal instability and evidence of whole-genome doubling (WGD). We reconstructed tumor phylogenetic trees from WGS data using Dirichlet Process-based methods. Intriguingly, our findings indicated that for patient 2.3, primary tumor samples PT_1 and PT_2 displayed a close phylogenetic relationship, while local recurrences LR_2 and LR_3 represented a different branch of the phylogenetic tree. Moreover, scRNA-seq analysis of patient 2.16 highlighted an enrichment of immune cells, including macrophages, B cells, and T cells. To infer copy number alterations (CNA) of tumor cells from scRNA-seq data, we leveraged inferCNV, with normal cells identified within the same sample as controls. Significant copy number gains were identified on chromosomes 5, 7, 8, and 15 in patient 2.16. The inferred copy number changes derived from scRNA-seq were validated against copy number profiles obtained through WGS using Battenberg, revealing a remarkable congruence. In the scDNA analysis of patient 2.12, we observed that all tumor cells exhibited biallelic loss of CDKN2A, with a majority showcasing WGD and chromosome 7 amplification. This finding underscored the potential significance of CDKN2A in the pathogenesis of this tumor, in keeping with the observation that CDKN2A is recurrently mutated and lost in MPNSTs. Our research profiled the tumors' evolutionary histories and intra-tumor heterogeneity down to single-cell resolution, highlighting the genotype and phenotype differences between tumor subclones. By shedding light on the genomic landscape of MPNSTs, we aspire to make profound contributions to the field of sarcoma research, ultimately improving patient outcomes.

#5672 Transcriptomic profiling of lung adenocarcinoma from never-smokers reveals molecular subtypes with clinical implications.

W. Zhao, T. Zhang, P. H. Hoang, J. Sang, M. Landi;
National Cancer Inst. - Bethesda Campus, Rockville, MD

Lung cancer is the leading cause of cancer mortality worldwide and about 10-25% of lung cancers are from never-smokers (LCINS). Previous genomic studies of LCINS identified multiple genomic subtypes with different genetic drivers and evolutionary processes. To dissect the profile of LCINS cell states and tumor microenvironment, and their relationship with genomic lesions, we sequenced and assembled a large RNA-seq data set of 685 samples of lung adenocarcinoma from never-smokers and integrated them with whole genome sequencing data, pathological features and clinical outcomes from the same subjects. We identified three transcriptomic subtypes defined by distinct gene expression patterns. The three subtypes were associated with different pathway activities and showed remarkable heterogeneity in cell composition, lineage fidelity and pathological features. The genomic driver events and mutational signatures were significantly enriched in specific subtypes. Clinical outcomes also differed across the subtypes. For example, one subtype had prolonged overall survival and was associated with predicted response to immune checkpoint blockade. This study emphasizes the importance of transcriptome-based classification of LCINS, which has profound clinical implications beyond those provided by genomic and pathological assessment.

#5673 Transposable element expression patterns in epigenetic mutational subtypes of clear cell renal cell carcinoma.

Kevin Meli[1], Cora A. Ricker[2], Sabrina Y. Camp[2], Christof C. Smith[3], Chris Labaki[2], Eddy Saad[2], Hanna Soulati[4], Brendan Reardon[2], Jihye Park[2], Natalie I. Vokes[5], Benjamin G. Vincent[6], Toni K. Choueiri[2], David A. Braun[4], Eliezer M. Van Allen[2]

[1]Harvard Medical School, Boston, MA,[2]Medical Oncology, Dana-Farber Cancer Institute, Boston, MA,[3]Department of Medicine, Brigham and Women's Hospital, Boston, MA,[4]Yale Cancer Center, Yale School of Medicine, New Haven, CT,[5]Thoracic Head and Neck Medical Oncology, MD Anderson Cancer Center, Houston, TX,[6]Lineberger Comprehensive Cancer Center, University of North Carolina at Chapel Hill, Chapel Hill, NC

Background: Clear cell renal cell carcinoma (ccRCC) is characterized by mutations in epigenetic modulators and by aberrant transposable element (TE) expression, each of which have been separately associated with immunotherapy (IO) benefit in specific clinical contexts. However, the relationship between mutations in epigenetic regulators and TE expression, and the potential effect of both somatic mutations and TE expression on clinical outcomes, has not been fully investigated.

Methods: We utilized RNA sequencing from ccRCC patients' tumors and cell lines to quantify TE subfamily expression with *TEtranscripts* (n=123 metastatic IO-treated; CheckMate-009, 010, 025, n=355 all stage TCGA untreated, n=8 CCLE). Locus-specific endogenous retrovirus (ERV) expression was quantified using *hervQuant*. Differential TE and ERV expression was determined using *DESeq2*. Samples were stratified by mutations in *PBRM1*, *SETD2*, *BAP1* and *KDM5C*, four of the top five mutated genes in ccRCC. Multivariable CoxPH models and the log-rank test were used to compare overall (OS) and progression-free survival (PFS). Two validation metastatic ccRCC cohorts were employed: the everolimus arm of CheckMate-025 (n=78, CM025e) and IMmotion150 (n=146, IM150).

Results: Global TE expression (LTR, LINE, SINE and DNA transposons) did not differ significantly across mutational and clinical subtypes. However, 29 of 795 TE subfamilies were differentially expressed in >1 mutational subtype across datasets, and 22 of 29 were ERVs. At locus-specific resolution, 52 of 3173 ERVs were differentially expressed in >1 mutational subtype across datasets. Additionally, 6 of the 52 ERVs nominally associated with PFS, and 4 nominally associated with OS, in the IO cohort. Among them, only ERVs 544 and 2014 associated with improved PFS (multivariable CoxPH p = 0.03 and 0.02, respectively) and were expressed across all datasets. Both ERVs also exhibited increased expression in *PBRM1* mutant and decreased expression in *BAP1* mutant vs. wildtype samples, in discovery (IO, TCGA, CCLE) and validation (CM025e, IM150) cohorts. Lastly, *PBRM1* mutant patients with high ERV 544 or 2014 expression had improved PFS in the IO (log-rank p = 0.04 and 0.03, multivariable CoxPH p = 0.008 and 0.009, respectively, HR = 0.43 both), but not in the CM025e cohort, compared to other patients regardless of *PBRM1* mutations.

Conclusion: ERVs 544 and 2014 were upregulated in *PBRM1* mutant and downregulated in *BAP1* mutant samples. Coupled with *PBRM1* inactivation, their expression served as a candidate biomarker of improved PFS in IO-treated ccRCC that may have additional biological relevance. Expanded functional and clinicogenomic studies of epigenetic mutational subtype-specific patterns of TE expression, and their relation to selective IO response, may guide additional discovery and therapeutic development strategies in ccRCC.

#5674 Characterizing Cellular Heterogeneity and Identifying Potential Biomarkers in Esophageal Squamous Cell Carcinoma (ESCC) Using Single-Cell RNA Sequencing.

T.-H. Hsiao[1], C.-H. Lin[1], T.-S. Wu[1], L.-W. Lee[1], C.-P. Hsu[2];

[1]Taichung Veterans General Hospital, Taichung, Taiwan, [2]Buddhist Tzu Chi General Hospital, Hualien, Taiwan

Esophageal squamous cell carcinoma (ESCC) exhibits significant cellular heterogeneity, rendering it susceptible to developing radioresistance and recurring tumors. Single-cell RNA sequencing (scRNA-seq) is an advanced technique that allows for the exploration of distinct gene expression profiles in individual cells. To investigate cellular heterogeneity in ESCC, scRNA-seq analysis was performed on tumor tissues from ten ESCC patients, as well as adjacent non-malignant esophageal tissues. The cellular composition revealed 19 distinct cell clusters, further categorized into seven cell populations: 69.31% Fibroblast, 15.36% T cell, 5.30% Monocytes, 5.26% Endothelial cells, 2.68% plasma cell, 1.91% Epithelial cells, and 0.18% ambiguous. Notably, Fibroblast and Endothelial cells were more prevalent in non-malignant tissues, while the remaining cell types were enriched in tumor tissues. Differential gene expression analysis identified 49 genes with higher expression in tumor cells and 37 genes with lower expression. Gene Set Enrichment Analysis (GSEA) revealed the top three most relevant GO Biological Processes pathways: positive regulation of immune response, regulation of T cell activation, and positive regulation of cell migration. Furthermore, in post-treatment follow-up, four patients were observed to develop metastasis within one year. Comparative analysis between metastatic and non-metastatic patients unveiled 9 Differentially Expressed Genes (DEGs), including KRT6A and AKR1B10, which exhibited specific expression in Epithelial cells and were highly expressed in tumor tissues. Additionally, IGLC2, IGHG4, and IGHG1 demonstrated specific expression in plasma cells, with elevated expression in tumor tissues. These findings suggest that KRT6A, AKR1B10, IGLC2, IGHG4, and IGHG1 may serve as potential biomarkers for predicting post-chemotherapy metastasis in ESCC patients.

#5675 An intronic SINE-VNTR-*Alu* element insertion in *CASP8* alters gene expression and confers resistance to induction of cell death in gastrointestinal cancer.

E. W. Lin[1], J. R. Kocher[1], C. Chu[2], P. J. Park[2], D. T. Ting[1];
[1]Massachusetts General Cancer Center, Boston, MA, [2]Harvard Medical School, Boston, MA

Transposable elements are a major source of variation in the human genome. SINE-VNTR-*Alu*s (SVAs), the hominid-specific and youngest active retrotransposon family, are highly polymorphic within the human germline and can contribute to disease risk and progression. In fact, polymorphic SVAs have previously been linked to several human diseases, including rare cases of hereditary cancer syndromes such as neurofibromatosis type I and Lynch syndrome. These examples illustrate that the mobility of SVAs in the genome can significantly impact gene function. Here, we sought to evaluate the potential of SVAs inserting into known tumor suppressors and oncogenes. To this end, we surveyed genomic data from Pan-Cancer Analysis of Whole Genomes (PCAWG) and identified 1956 unique germline SVA insertions in the introns of 1933 genes. Among these, we discovered a highly prevalent polymorphic SVA_E (subfamily) in an intronic region of *CASP8*. Given caspase-8's canonical role in apoptosis, we hypothesized that this SVA may impact both caspase-8 expression as well as cell death in cancer.

We first created a panel of colon and gastric cancer cell lines genotyped by PCR for the presence or absence of the *CASP8*-SVA (SVA+/+: RKO, NCI-N87, HT29, NCI-H747, OCUM-1; SVA-/-: HCT116, LoVo, SNU-407, 23132/87, KM12). RT-qPCR analysis showed significantly higher *CASP8* expression in SVA+/+ cell lines, which was concordant with caspase-8 protein expression by immunoblot. Treatment of these cell lines with cytotoxic chemotherapy (FOLFOXIRI) *in vitro* demonstrated increased resistance to cell death in SVA+/+ cell lines. Direct induction of caspase-8-mediated apoptosis via TRAIL (TNF-related apoptosis-inducing ligand) revealed decreased TRAIL-mediated cell death in SVA+/+ cell lines; interestingly, caspase-8 enzymatic activity was also decreased in SVA+/+ cell lines upon TRAIL stimulation despite increased pro-caspase-8 expression. To further isolate the effects of the *CASP8*-SVA, we generated an isogenic cell line (RKO *CASP8*-SVA knockout) model via CRISPR-Cas9. Deletion of the *CASP8*-SVA redemonstrated decreased *CASP8* expression at the mRNA and protein levels. Treatment with FOLFOXIRI in the *CASP8*-SVA KO cell line exhibited increased sensitivity compared to empty vector control.

In summary, our findings indicate that an intronic SVA insertion in *CASP8* increases gene and protein expression but decreases canonical caspase-8 activity, which was associated with increased resistance to FOLFIRINOX or TRAIL induced cell death. Additional interrogation of SVA-induced effects on transcriptional regulation (e.g., epigenetic effects) as well as non-canonical functions of caspase-8 (e.g., activation of NF-κB) is ongoing. To our knowledge this is the first report describing the mechanistic effects of a germline SVA insertion in the context of cancer and therapeutic resistance.

#5676 Spatial 3D genome organization reveals intratumor heterogeneity in primary glioblastoma samples.

Q. Wang[1], J. Wang[1], R. Mathur[2], M. W. Youngblood[1], Q. Jin[1], Y. Hou[1], L. A. Stasiak[1], Y. Luan[1], J. F. Costello[2], F. Yue[1];
[1]Northwestern University - Chicago, Chicago, IL, [2]University of California San Francisco, San Francisco, CA

Glioblastoma (GBM) represents the most prevalent malignant primary brain tumor with highly unfavorable prognosis. Currently, most genomic studies are conducted at a single site of a tumor, which do not reflect the complete genetic or epigenetic information across the whole tumor. Furthermore, the intra-tumoral heterogeneity (ITH) of 3D genome organization has also not been studied yet. To address these gaps, we performed Hi-C experiments in 21 samples obtained from 9 GBM patients, with 15 of them being spatially mapped based on their 3D coordinates from the same patients. We identified extensive inter-tumoral and intra-tumoral heterogeneity in genome compartmentalization and chromatin interactions. Notably, in a patient with 9 spatially mapped samples from both temporal and frontal regions, we accumulated over 6 billion reads and defined high-resolution region-specific chromatin interactions, regulatory networks, and key regulators within the same patient. We detected structural variation (SV) and enhancer hijacking across all the samples, and identified recurrent events that affect known cancer-related genes such as CDKN2A/B. Finally, we introduce the concept of 'enhancer amputation', defined as the loss of enhancers due to SVs which lead to decreased expression of their original target genes. To our knowledge, this study represents the first large-scale exploration of the 3D genome in primary GBM patients and the first investigation of 3D genome organization in multiple regions of the same tumor. Our findings provide unprecedented insights into the ITH of GBM at the 3D genomic level, opening new avenues for understanding and potentially targeting this devastating disease.

MOLECULAR/CELLULAR BIOLOGY AND GENETICS: microRNAs and Other Non-coding RNAs as Cancer Genes 2
Poster Session

#5680 Circular *MALAT1* - the new kid on the block in breast-to-brain metastatic cancer.
A. Szczepaniak, A. Bronisz, J. Godlewski;
Mossakowski Medical Research Institute Polish Academy of Sciences, Warsaw, Poland

Introduction: Breast-to-brain metastatic (BTB met) cancer constitutes a great challenge for modern medicine and science. As the research on protein-coding genes brought only incremental progress in developing anticancer therapy, much attention is devoted to understanding the role of non-coding RNAs, including a relatively recently discovered group - of circular RNAs. This project aimed to determine the relationship between BTB met cancer cells and cells derived from a deadly brain tumor - glioblastoma stem-like cells (GSCs), considering the circular RNA signatures and selecting a reliable candidate for mechanistic study - a circular form of non-coding oncogene *MALAT1* (circ*MALAT1*).
Methods: The circular RNA expression profile in patient-derived BTB met cancer cells (n=4), GSCs (n=8), and neural progenitor cells (NPC) as a non-malignant control (n=3) was evaluated by the microarray approach. Expression of circ*MALAT1* was also validated in non-malignant breast epithelial cells by digital PCR and data mining in the GEO database. Circ*MALAT1* knockdown by antisense oligonucleotides was followed by functional analysis.
Results: 12,660 circular RNAs were detected using the Arraystar platform, and upon applying the cutoff of FC ≥2 and p-value <0.05, 547 circular RNAs were selected as significantly deregulated in all cancer groups compared to NPC. Circ*MALAT1* was elevated in BTB met compared to NPC and normal breast epithelial cells. Knockdown of circ*MALAT1* affected cancer cell viability and proliferation while promoting p21 expression, thus decelerating the cell cycle manifested by a reduction in 3D spheroids volume.
Conclusions: The analysis of the circular RNA landscape showed for the first time some striking similarities between BTB mets and GSCs despite different tissue-of-origin. Of note, the circRNAome of BTB mets clustered especially closely with mesenchymal GSC - the most aggressive and therapy-resistant subtype of GSCs. These results also demonstrated the role of circ*MALAT1* in shaping the oncogenic traits of these cells. Therefore, circular RNAs can serve as valuable biomarkers and promising novel mechanistic candidates whose modulation may become a paradigm-shifting therapeutic approach.

#5681 Identification of dysregulated miRNAs involved in TNBC progression.

M. Lee, Y. Kim, D. Son, S. Lim, J. Park;
Sookmyung Women's University, Seoul, Korea, Republic of

Triple negative breast cancer (TNBC) is the most aggressive type of all breast cancer subtypes. Although various studies have been performed to identify prognostic and therapeutic targets for TNBC, the TNBC specific biomarkers have not yet been elucidated. Herein, we identified dysregulated miRNAs in TNBC via analysis of miRNA microarray in breast cancer tissues and found the oncogenic RNA (miR-374a-5p) and tumor suppressive miRNAs (miR-320c, miR-371b-5p). These miRNAs were closely related to overall survival of TNBC patients and status and involved in TNBC progression or drug responsiveness. Collectively, these results suggest that dysregulated miRNAs might serve as potential prognostic marker or therapeutic target for TNBC.

#5682 Micro RNA level changes in prostate cancer cells treated with MDMX and MDM2 inhibitors.

Rojin Fatirkhorani[1], Ahmed Saleh M. Alsarrani[2], Shyam Sundar Jaganathan[2], Umamaheswari Natarajan[2], Appu Rathinavelu[2]

[1]Kiran C. Patel College of Osteopathic Medicine, Nova Southeastern University, Fort Lauderdale, FL,[2]Rumbaugh-Goodwin Institute for Cancer Research, Barry and Judy Silverman College of Pharmacy, Nova Southeastern University, Fort Lauderdale, FL

INTRODUCTION: Prostate Cancer (PCa) is the most common non-cutaneous cancer and the second leading cause of cancer death among men in the United States. Most of the PCa cases are diagnosed in men between the ages of 65-74. Due to the recent push for frequent prostate screenings, these cancers are being detected early and treated much faster, leading to a 5-year survival of a localized or regional PCa to >99%. However, the 5-year survival of PCa with distant metastasis is significantly reduced to 32%, especially with involvement of osteoblastic bone lesions, lung lesions, and brain lesions. Therefore, there is a clinical need to identify prognostic markers and new targets for developing therapies and effectively treating advanced PCa. Previous studies have shown that levels of MDMX and MDM2, oncogenic inhibitors of p53 tumor suppressor protein, are significantly elevated in PCa cells. Inhibition of MDM2 and MDMX using specific inhibitors has been shown to elevate the levels of p21, p27, and p53 in LNCaP (Lymph Node Carcinoma of the Prostate) cells leading to cell death. Recent studies have demonstrated that micro RNAs (miRNAs) play an important role in supporting the tumor suppressor function of p53 through regulating the balance between p53 and MDM2. In this regard, several miRNAs were found to be significantly altered to modulate the level and intracellular mechanisms of p53 and MDM2 in various cancers.

OBJECTIVES: To determine the relative levels of miRNA31, miRNA-34a and miRNA-128 in LNCaP cells that were treated with NSC-207895 (MDMX inhibitor), SJ-172550 (MDMX inhibitor), and RG-7388 (MDM2 inhibitor).

METHODS: LNCaP cells were treated with NSC-207895 (20 uM), SJ-172550 (20 uM) or RG-7388 (2 uM) for 24 hrs. After completing the treatments, the miRNAs were extracted from the LNCaP cells using the miRNeasy Tissue/Cells Advanced Kit from Qiagen. We analyzed the levels of miRNA-31, miRNA-34a, and miRNA-128 in the treated samples using qRT-PCR analysis method and compared the levels to the control. During the qRT-PCR analysis the cDNA was amplified using Meridian Biosciences qPCR Master Mix and specific primers for miRNAs from Origene were used according to the manufacturer's protocol.

RESULTS: Our experimental results indicate that inhibition of MDMX using NSC-207895 and SJ-172550 can elevate the levels of p21, p27, and p53 leading to cell death. Determination of cell death markers in the past revealed induction of necroptosis following drug treatments. Our current results indicate measurable changes in the levels of miRNA-31 and miRNA-34a following inhibition of MDMX using SJ-172550. We are in the process of determining the possible link between the changes in the levels of miRNAs and cell death.

ACKNOWLEDGEMENT: This research was supported by the Royal Dames of Cancer Research, Ft. Lauderdale, Florida.

#5683 lncRNA-protein interactions that predict response to endocrine therapy in HR+ breast cancer.

K. D. Waiters, M. Quttina, A. F. Khan, S. Karami, A. S. Peidl, F. Babajide, T. Bawa-Khalfe;
University of Houston, Houston, TX

Hormone receptor positive (HR+) breast cancer (BCa) is the most frequently diagnosed BCa type accounting for 70% of all breast cancer cases. A large population of HR+ BCa patients (30-40%) are resistant to mainstay endocrine therapy and develop incurable metastatic disease. Hence, it is imperative to identify viable biomarkers that stratify patients as drug responders or non-responders.

Emerging scientific literature highlights the essential role of long non-coding RNAs (lncRNA) in cancer drug resistance and metastatic transformation; lncRNA include RNAs over 200 nucleotides in length that do not encode protein. Major biological functions of lncRNA rely on association with select protein interactors. As lncRNA equally bind proteins with and without canonical RNA-binding motifs, it is unclear what facilitates this lncRNA-protein interaction. Our recent studies show that SUMO post-translational modification (or SUMOylation) of target proteins potentiates binding with lncRNA, particularly at the chromatin. Using a small-scale screening, we see that SUMO-modification works to enhance association with lncRNAs for proteins with and without a canonical RNA binding domain (RBD). SUMOylation of RBD-expressing heterochromatin protein 1 α (HP1α) drives interaction with multiple chromatin-associated lncRNA both within and outside canonical heterochromatin foci. Interaction with lncRNA supports SUMOylated HP1α's unconventional function as a transcriptional repressor at select euchromatic loci. We now report an inverse relationship in which SUMOylated HP1α directs the stability of its lncRNA binding partner. Specifically, SUMO-modified HP1α directs cell-cycle dependent recruitment of the RNA degradation machinery to the chromatin and facilitates clearance of chromatin-bound lncRNA. This dynamic lncRNA degradation process is disturbed with cancer onset and instead favors aberrant cancer cell transformation. Consistently, restoring lncRNA degradation homeostasis decreases metastatic properties of HR+ BCa cells and increases sensitivity to targeted therapeutics currently in clinical trials. Our studies define a fundamental mechanism that dictates lncRNA stability and/or degradation in BCa cells. In addition, we present viable biomarkers that predict sensitivity to ET and alternative targeted therapies.

#5684 The role of the lncRNA *Slamon* and *Slc25a13* neighbor gene in melanoma aggressiveness.

B. C. B. Tonin[1], A. L. P. Ayub[1], A. H. Lengert[1], S. W. Han[1], E. M. R. Reis[2], F. J. Slack[3], **M. G. Jasiulionis**[1];
[1]Universidade Federal de Sao Paulo (UNIFESP), Sao Paulo, Brazil, [2]Universidade de Sao Paulo (USP), Sao Paulo, Brazil, [3]Harvard Medical School, Boston, MA

Melanomas are responsible for about 80% of all deaths related to skin cancers. This is due to its high potential of metastasizing and developing resistance to treatments. Novel therapeutic modalities and the identification of biomarkers able to predict the prognosis are necessary. Studies have revealed the central role of long non-coding RNAs (lncRNAs) in regulatory networks controlling cell behavior. The disruption of these regulatory networks as a consequence of altered expression of lncRNAs can contribute to cancer development and progression. Our laboratory has developed a linear cellular model of melanoma progression consisting of distinct cell lines: melan-a (melanocytes), 4C (pre-malignant melanocytes), 4C11- (undifferentiated, slow-growing and non-metastatic melanoma cells) and 4C11+ (differentiated, highly proliferative and metastatic melanoma cells), which were analyzed for their lncRNA expression profile. Differentially expressed lncRNAs identified by RNAseq were selected by *in silico* analyses based on their proximity to differentially expressed coding-genes in the same melanoma model. Correlation analyses were performed between the expression of differentially expressed lncRNA neighboring genes and their melanoma patient survival, using two independent melanoma cohorts (TCGA and Leeds). Among those lncRNA located near genes presenting prognostic value is the lncRNA Gm20619, here named *Slamon*, neighbor to *Slc25a13* gene (mitochondrial aspartate/glutamate carrier gene), which high expression correlates with poor prognosis. Both *Slamon* lncRNA and *Slc25a13* are highly expressed in the metastatic melanoma cells 4C11+ compared to melan-a, 4C and 4C11- cell lines. The knocking down of *Slamon* or *Slc25a13* were performed in 4C11+ melanoma cells, followed by analyses of collective migration, clonogenicity, proliferation, *anoikis* resistance, and dacarbazine and MEK inhibitor treatment. By knocking down *Slamon* lead 4C11+ cells significantly less migratory and less resistant to dacarbazine, and resulted in increased expression of *Slc25a13* gene. 4C11+ melanoma cells knocked down for *Slc25a13* also presented reduced migratory, clonogenicity, proliferation and *anoikis* resistance capability, diminished sensitivity to dacarbazine and MEK inhibitor treatment, and increased expression of *Slamon* lncRNA. The analysis of genes coexpressed with *Slc25a13* revealed genes related to tumor progression, as *Cdk15*, *Lsp1* and *Pdgfrb*. Our results suggest a crucial role of the lncRNA *Slamon* and *Slc25a13* coding gene in melanoma progression which has never been described before. *Slamon* regulates tumor aggressiveness associated with *Slc25a13*, forming a regulatory network. These findings reveal the importance of lncRNAs in melanoma biology, potentially indicating transcripts that can serve as prognostic biomarkers and therapeutic targets in melanoma.

#5685 MiR-345-5p attenuates pancreatic cancer metastasis through KLK7/E-Cad/ β-Catenin/Rap1 axis.

N. Sirpu Natesh[1], S. Nethi[2], B. White[2], J. Kaifi[3], S. Batra[4], S. Mallapragada[2], S. Rachagani[1];
[1]University of Missouri - Columbia, Columbia, MO, [2]Iowa State University, Ames, IA, [3]University of Missouri, Columbia, Columbia, MO, [4]University of Nebraska Medical Center, Omaha, NE

Background: Pancreatic cancer (PC) is a highly lethal malignancy with a 5-year survival rate of 10.8%, primarily attributed to early invasion and metastasis. Epithelial-to-mesenchymal transition (EMT) plays a crucial role in the metastatic progression of PC. Existing therapies, such as Gemcitabine, Abraxane, and FOLFIRINOX, have limited efficacy, emphasizing the need for identifying molecular targets to enhance PC patient survival. Recent advancements in miRNA therapies show promise, but a detailed understanding of miRNAs regulating PC growth and metastasis remains elusive. This study aims to uncover the role of miR-345-5p in regulating PC metastasis.
Methods: A miRNA microarray analysis of KC mouse data identified miR-345-5P as one of the significantly down-regulated miRNA, targeting multiple metastasis-related genes. Expression of miR-345-5p in PC was assessed using published databases, validated through qPCR and ISH in PC cell lines, serum samples, and patient tissue. *In vitro* overexpression and *in vivo* assays elucidated the functional roles of miR-345-5p in PC metastasis. A computational approach and dual-luciferase assays were used to identify the target of miR-345-5p. Western blots, immunohistochemistry, and immunofluorescence were utilized to decipher miR-345-5p mediated molecular mechanisms.
Results: MiR-345-5p expression was downregulated in PC tissue, serum, and cell lines compared to non-tumor tissues. Restoring miR-345-5p reduced PC cell proliferation, migration, and invasion *in vitro* and *in vivo*. KLK 7 was confirmed as a direct target, and functional experiments revealed miR-345-5p's acting as a tumor-suppressor by inhibiting the E-Cad/B-catenin/Rap1 axis signaling pathway. MiR-345-5p overexpression stabilized the E-Cadherin-β-catenin complex, leading to reduced β-catenin accumulation in the nucleus and thus leading to declined transcription of crucial genes (C-myc, cyclin D1 & MMP7) responsible for PC progression. Given the pivotal role of the c-myc gene in metabolism, we performed a metabolomic analysis. The findings unveiled significant metabolic rewiring, marked by reductions in glucose and amino acid metabolism, attributable to decreased C-myc expression due to restoration of miR-345 in PC cells.
Conclusion: MiR-345-5p overexpression negatively regulates PC proliferation and EMT by directly targeting KLK7/E-Cad/β-catenin/Rap1 axis. Restoring miR-345-5p with standard care therapies could be a promising strategy for improving survival in metastatic PC patients.

#5686 Identifying rare microRNA risk variants for hereditary breast cancer in African American individuals.

S. R. Glover, T. LoBue, N. D. Merner;
Auburn University College of Veterinary Medicine, Auburn, AL

Background: In the United States, breast cancer is the most frequently diagnosed cancer in women. However, African American women tend to have a higher incidence of triple negative breast cancer cases, and an earlier age of disease onset, which are hallmark characteristics of heredity disease. Even with current breakthroughs in breast cancer research, limited research participation from women of African descent has led to a gap in our knowledge of heredity factors that are involved in disease in this population. Furthermore, most breast cancer research has focused on protein coding genes being the culprit of tumorigenesis; however, within the last three decades, research efforts have begun to focus on noncoding RNAs, like microRNAs (miRNAs), as potential factors to promote carcinogenesis. miRNAs are short, noncoding RNA molecules that control gene expression at the post-translational level. miRNAs have several mechanisms to affect gene expression of cellular processes like cell proliferation, apoptosis, invasion, and metastasis. However, the identification and functional role miRNA risk variants play in African American breast cancer is still not fully understood.
Methods: 30X whole genome sequencing (WGS) was carried out on an Illumina platform on blood- or saliva-derived DNA from 120 African American breast cancer cases from the Alabama Hereditary Cancer Cohort. The WGS data was analyzed using our established bioinformatics pipeline, which has been adapted from the Genome Analysis Toolkit (GATK) Best Practice Pipeline. Focusing on miRNA variants as risk factors, a miRNA BED file was used to extract regions harboring miRNA genes. The resulting file was then filtered for rare miRNA variants (minor allele frequency <1%) in the African American population based on the Genome Aggregation Database (gnomAD) allele frequency. P-values for variants of interest were calculated using Fisher's Exact tests.
Results: Sequencing data have revealed three rare miRNA variants from our African American cohort that can be potentially associated with breast cancer risk. Upon statistical analysis comparing allele frequencies between the African American general population and the Alabama Hereditary Cancer Cohort, *miR7850, miR3145, and miR8074* had p-values 5.21E-05, 3.58E-05, and 2.19E-04, respectively.
Conclusions: We have identified three rare miRNA variants that were not previously known to be associated with breast cancer risk. Interestingly, both *miR7850* and *miR8074* target *TP53* and *miR3145* targets *GREM1* and *PALB2*, which these targets are known breast cancer susceptibility genes. Understanding the consequence of these variants is important to add to our knowledge of miRNAs that play critical roles in carcinogenesis leading to better treatment strategies.

#5687 Downregulation of DAX-1 expression by miRNA overexpression as a mechanism to potentiate breast cancer.

N. C. DeVito, C. Tzagarakis-Foster;
University of San Francisco, San Francisco, CA

The orphan nuclear receptor DAX-1 (Dosage Sensitive Sex Reversal, Adrenal Hypoplasia Congenita, critical region on the X chromosome, gene 1) plays a key role in sex determination and the synthesis of steroid hormones. In addition to these canonical examples, DAX-1 has been shown to play a contradictory role in cancer development. While DAX-1 is overexpressed in some types of cancer, it is completely absent or downregulated in several other cancers such as prostate and breast. One of the explanations for the paradoxical role of DAX-1 in cancer development could be microRNAs (miRNAs). Recent research has demonstrated that the dysregulated expression of these short non-coding RNAs increases the proliferative and anti-apoptotic capabilities of cancer cells. After broadly surveying over 180 miRNAs historically upregulated in MCF7 cells, we compared the activity of DAX-1 in MCF7 breast cancer cells and MCF10a normal breast epithelial cells with the presence of specific miRNA inhibitors. Our primary hypothesis remains that multiple miRNAs negatively regulate the expression of DAX-1 in human breast cancer cells and are not overexpressed in normal breast cells, providing another mechanism of lifting the repression of DAX-1 expression. Quantitative PCR and western blot analysis was performed indicating that inhibiting miRNAs 29c, 199a, and 424 significantly upregulate DAX-1 expression in MCF10a cells. We examined the invasive and metastatic properties of MCF7 cells following inhibition of these specific miRNAs. This research will allow clinicians to screen for additional miRNAs that could be elevated in breast cancer patients substantially increasing the number of people diagnosed with breast cancer early on. In addition, elucidating the pathways of how more and more miRNAs influence downstream targets will offer drug designers novel targets to improve treatment for breast cancer and other cancer patients.

#5689 miR-21: A therapeutic target that delays severe liver disease and hepatocellular carcinoma under high-fat-diet conditions.

U. Jagtap[1], A. Quan[1], Y. Ono[1], J. Lee[1], K. A. Shen[2], S. Manakov[2], G. Szabo[1], I. Nasser[1], F. J. Slack[1];
[1]Beth Israel Deaconess Medical Center, Boston, MA, [2]Eclipse BioInnovations, San Diego, CA

Liver disease is a major global health concern, claiming approximately 2 million lives worldwide annually, yet curative treatments remain elusive. In our study, we aimed to investigate the role of microRNA-21-5p (miR-21) in metabolic dysfunction-associated steatotic liver disease (previously NAFLD), metabolic-associated steatohepatitis (previously NASH), and hepatocellular carcinoma (HCC) within the context of a Western high-fat diet (HFD) and offering potential therapeutic insights. We found that reduced miR-21 levels correlated with liver disease progression in WT mice fed on HFD, while miR-21 knockout mice showed exacerbated metabolic dysfunction, including obesity, hepatomegaly, hyperglycemia, insulin resistance, steatosis, fibrosis, and HCC. Our study reveals that miR-21 plays a protective role in metabolic syndrome and in the progression of liver disease to cancer. miR-21 directly targets *Transforming growth factor beta-induced* (*Tgfbi*), a gene also known to be significantly upregulated and a potential oncogene in HCC. Further, our study showed that intervention with the administration of a miR-21 mimic in WT livers in HFD conditions effectively improves insulin sensitivity, steatosis, fibrosis, tumor burden, as well as *Tgfbi* expression. These findings indicate that miR-21 could serve as an effective strategy to delay or prevent liver disease in high-fat-diet environments.

#5690 Urinary microRNA expression in pancreatic cancer with cachexia.

M. Okada[1], S. Kondo[1], Y. Igawa[1], T. Yoshida[1], M. Havelka[2], M. Mizunuma[2], Y. Ichikawa[2], N. Yamamoto[1];
[1]National Cancer Center Hospital - Japan, Tokyo, Japan, [2]Craif Inc., Tokyo, Japan

Background: Cancer cachexia (CC) is a multifactorial syndrome characterized by appetite loss, weight loss and skeletal muscle wasting. It increases functional impairment, treatment-related toxicity, and a lower quality of life. Importantly, CC is one of the leading causes of cancer-related deaths, and its occurrence is particularly prevalent in advanced stages of pancreatic cancer (PC). The syndrome is thought to be associated with systemic inflammation and increased energy expenditure, yet the specific mechanisms remain to be fully understood. Although timely detection and intervention might be crucial in preventing CC's progression, early diagnosis of this syndrome remains challenging due to the absence of suitable biomarkers. Here, we analyzed urinary microRNAs (miRNAs) as a potential noninvasive biomarkers for detecting CC in patients (pts) with PC.

Methods: Clinical information including presence or absence of CC and urine samples were collected from pts with PC treated at National Cancer Center Hospital, Tokyo, Japan from March to October 2022. The diagnosis of CC was made according to the following definitions by Fearon. K et al. (1) weight loss of ≥5% within 6 months; (2) weight loss of ≥2% in pts with a BMI of <20 kg/m^2; or (3) weight loss of ≥2% in pts with sarcopenia. In this study, pts who met the definition of CC within 6 months of enrollment were considered to have CC.Urinary miRNA profiles from pts with PC were sequenced by NGS and analyzed using DESeq2 to identify differentially expressed miRNAs (DEMs) between pts with CC and those without. DEMs were further explored for associated pathways and target genes using miRPathDB v.2.0.

Results: Of the 64 subjects, 52 pts were included in the analysis after excluding three pts with low urine sample read coverage and nine pts with no information on CC status. Among those, 38 pts were classified as having CC. Patients' background was as follows (CC/no CC); median age 70 [range: 44-80]/ 67 [57-74], male and female 19/7 pts, respectively, cStage {I (6/0), II (1/0), III (17/4), IV (14/10)} pts, median BMI (male 22.1 [17.7-27.2]/21.7 [18.2-28.2], female 21.7 [14.6-25.2]/21.9 [16.6-27.4]) kg/m^2. Among 307 miRNAs detected in the urine of pts with PC, 49 miRNAs had previously been reported in CC research. The miR-141-5p was differentially expressed between pts with CC and those without CC (Wald test p_{BH} = 0.079). It was down-regulated in pts with CC (Mann-Whitney U test p = 6.4e-4) and most significantly associated with the FoxO signaling pathway (ORA p_{BH} = 1.84e-4), followed by the mTOR signaling pathway (ORA p_{BH} = 0.008).

Conclusions: Our study indicates that miR-141-5p holds potential as a noninvasive biomarker for the detection of CC in pts with PC. Although miR-141-5p has not been previously reported in CC, its significant association with the FoxO signaling pathway, which is one of the major pathways regulating skeletal muscle atrophy, underscores the relevance of miR-141-5p in the context of CC.

#5691 Identification of miRNA related to triple-negative breast cancer in African and European American women with obesity.

F. Hossain[1], **M. I. Gonzalez-Ramirez**[2], J. Garai[1], X.-C. Wu[1], C. Hicks[1], L. Del Valle[1], A. Ochoa[1], D. Danos[1], L. Miele[1], J. Zabaleta[1];
[1]Louisiana State University Health Sciences Center, New Orleans, LA, [2]Tulane University School of Medicine, New Orleans, LA

Triple-negative breast cancer (TNBC) represents 10-20% of all invasive breast cancers and is characterized by a lack of expression of estrogen receptor, progesterone receptor, and human epidermal growth factor receptor 2. TNBC typically manifests as high-grade tumors often diagnosed at advanced stages, and affects younger patients, especially African American (AA) women. Dysregulation of miRNA expression levels contributes to TNBC pathogenesis and prognosis. Dysregulated miRNAs in advanced-stage cancers alter tumor progression, migration, and metastasis. Obesity is associated with miRNA dysregulation in adipose tissue, which is a driver of BC development and growth. This study aimed at identifying differentially expressed (DE) miRNA in TNBC patients of European American (EA) and AA women with obesity, compared to adjacent non-tumor tissues. miRNAseq data from 48 tissue samples (TNBC tumor and adjacent non-tumor) were analyzed for differential expression. Samples were from 12 EA and 12 AA patients, with 6 patients in each ethnic group having obesity and 6 normal weight, based on BMI estimates. Stringent comparisons, with and without obesity, were conducted to identify TNBC and obesity-associated miRNAs within each ethnic group. Prediction of miRNA-target genes was performed in miRWalk and Key Pathway Advisor (KPA) was employed for pathway enrichment analysis. Differential expression analysis between obese and normal-weight patients in each ethnic group revealed 79 DE miRNAs in EA and 40 in AA. We identified 55 miRNAs associated exclusively with tumors in obese patients within the EA group and 33 miRNAs within the AA group. Target gene analysis showed that in EA, 9 out of the 55 miRNAs interacted with 68 mRNAs, with miR-204-5p and miR-181b-5p accounting for 75% of interactions. In AA, 20 out of the 33 miRNAs interacted with 284 mRNAs with miR-20a-5p, -195-5p, -34a-5p, and -130a-3p with 65% of the interactions. KPA identified 84 and 330 pathways for EA and AA, respectively, with 43 common pathways,15 of them related to cancer processes sharing the gene targets *GSKIP, TLBR1, TCF4, and TCF.* Our study outlined unique miRNA profiles in TNBC among AA and EA women with obesity. Although common mRNAs were identified between ethnic groups, leading to the identification of common pathways on KPA, more than 50% of the identified pathways are related to unique biological processes associated with TNBC and obesity for each ethnic group. These findings underscore the importance of considering ethnic-specific miRNA signatures for understanding TNBC in the context of obesity, offering insights for targeted therapeutic strategies.

#5692 Posttranscriptional molecular network facilitates KRAS-linked tumorigenesis via XRN1-miR-21 signaling in pancreatic cancers.

Y. Seo, **S. Oh**, J. Kim;
National Cancer Center, Ilsanro, Goyang, Korea, Republic of

Aberrant expression of mutant KRAS and miRNA-21 (miR-21) are commonly attribute to malignancy and tumorigenic progression of pancreatic cancers. However, few studies have explored the molecular mechanism linking these two prognostic factors. In this study, we explored the underlying molecular bridge between KRAS and miR-21 regulation in pancreatic cancer. Functional integrative analysis of KRAS, an essential oncogenic driver in pancreatic cancer progression, and together with miR-21 revealed XRN1, a 5′-3′ exoribonuclease, as RNA-linked top-scored molecule with a strong survival correlation and malignancy in pancreatic cancer patients. Depletion of XRN1 led to severe reduction in mature miR-21 expression, while unaltered precursor miR-21 levels; indicating that the XRN1 is critical in miR-21 maturation at post-Drosha step in conjunction with Dicer. Moreover, miR-21 sensor-based experiment also confirmed the critical role of XRN1 on miR-21 biogenesis. Depletion experiments showed that XRN1 positively regulates proliferation and self-renewal capacity of pancreatic cancer cells via its 5′-3′ exoribonuclease activity and concomitantly elevated the expression of PTEN and PDCD4 which are the key miR-21 cellular downstream targets. shRNA-mediated XRN1 depletion also yielded smaller tumor volume and longer survival in pancreatic cancer xenografts and syngeneic model demonstrating the therapeutic potential of targeting XRN1. Subsequent silencing of KRAS reduced XRN1 expression in pancreatic cancer cells, suggesting that KRAS plays a key role in this XRN1-miR-21 axis. Furthermore, drug-resistant pancreatic cells showed elevated expression of both KRAS and XRN1-miR-21 indicating that this axis is also associated with drug sensitivity. In sum, these results suggest that a novel KRAS-XRN1 posttranscriptional regulatory axis plays a pivotal role in tumor progression by mediating miR-21-directed signaling, and thus may suggest a novel targeting strategy for pancreatic cancer therapeutics.
Significance: This study identifies molecular regulatory interplay between KRAS and XRN1-miR-21 signaling in pancreatic cancers, elucidates how KRAS-XRN1 modulates tumorigenesis via miR-21, and demonstrates that targeting this signaling can contribute to therapeutic strategies for pancreatic cancers. [Y. Seo and S. E. Oh contributed equally to this work.]

#5694 Elucidating areca nut-induced miRNA-mRNA regulatory networks in head and neck cancer pathogenesis.

Hung-Han Huang[1], Guo-Rung You[2], Kai-Hsin Lin[2], Yin-Ju Chen[3], Ann-Joy Cheng[2]

[1]Graduate Institute of Biomedical Sciences, Chang Gung University, Taoyuan city, Taiwan,[2]Department of Medical Biotechnology and Laboratory Science, Chang Gung University, Taoyuan city, Taiwan,[3]Department of Biomedical Sciences, Chang Gung University, Taoyuan city, Taiwan

Areca nut has been considered a high-risk carcinogen for head and neck cancer (HNC) in Southeast Asia, while its molecular effects, especially on the miRNA regulatory roles, remain elusive. This study characterized miRNA-mRNA networks associated with areca nut-related HNC. We integratively analyzed the areca nut-induced mRNA profile and TCGA-HNSC gene set. A total of 2575 genes were identified, with 1971 upregulated and 604 downregulated in cancers. The KEGG pathway analysis revealed that these genes were enriched in the cellular functions related to motility and stress response. Experimental studies confirmed that arecoline promoted cell migration, invasion, and chemo-radioresistance. We further cross-analyzed the miRNAs induced by areca nut and dysregulated in TCGA-HNSC data and defined 71 molecules affected, with 35 upregulation and 36 downregulation. Using the multimiR tool to map potential mRNA-miRNA interactions, we uncovered that these miRNAs were connected to 2173 genes. These molecules participated in several oncogenic mechanisms, such as ErbB and PI3K-Akt signaling, cell adhesion, and DNA damage response. We endeavored to establish miRNA-mRNA interaction networks with the functions of cellular motility and stress response via the Cytoscape analytical method. Our data revealed nexus comprising 41 miRNAs with 83 mRNAs, and 38 miRNAs with 66 mRNAs, respectively, co-regulate these two malignant functions. A key miRNA, miR-410-3p, downregulated in HNC and decreased following areca nut treatment, was studied. Ectopic expression of miR-410-3p attenuated areca nut-induced cell invasion and exerted modulatory effects on its target oncogenes, CRK. Thus, our study delineates a comprehensive view of the miRNA-mRNA interplay altered by areca nut, illustrating a sophisticated mechanism of carcinogenesis and suggesting new avenues for diagnostic and therapeutic strategies in HNC.

#5695 miR-5787 suppresses cancer cell growth as a Fe_3O_4-nanoparticles induced pivotal miRNA.

M. Watanabe[1], H. Nakano[2], C. Matsuda[2], E. Usugi[2], H. Imai[2], Y. Hirokawa[1], K. Iijima[3];
[1]Mie University, Tsu, Japan, [2]Mie University Hospital, Tsu, Japan, [3]Yokohama National University, Tsu, Japan

Nanotechnology offers great potential for cancer diagnosis and treatments. Especially, nanoparticles (NPs) have been examined and utilized as drug delivery systems, hyperthermia and combination therapy. We have examined and reported the combined effects of Fe_3O_4-nanoparticles (Fe_3O_4-NPs) with chemotherapeutic agents on prostate cancer cell in vitro. miRNAs are an important factor in cancer progression, and elucidating the miRNA-mediated intracellular network of cancer cells could suggest new cancer treatment strategies. In this study, to identify microRNAs (miRNAs) associated with anticancer effects of Fe_3O_4-NPs, the comprehensive expression of miRNAs by Microarray (Agilent G4780A SuperPrint G3 Human v16 miRNA 8x60K Microarray kit) in A549 (lung cancer cell line), LNCaP (androgen-dependent prostate cancer cell line) and DU145 (androgen-independent prostate cancer cell line) under Fe_3O_4-NPs exposure was performed. miR-5787 was one of the increased miRNAs in three cancer cell lines under Fe_3O_4-NPs, and its increase in miR-5787 was due to the reactive oxygen species (ROS) production by Fe_3O_4-NPs. The additional analysis suggested that miR-5787 might suppressed the cancer cell growth by targeting the eIF5. In this study, we identified miR5787 as a Fe_3O_4-NPs induced pivotal miRNA in cancer cells, and can be used as a therapeutic target.

#5696 Exploring the association between miR-9-5p levels and the mTORC1/mTORC2 pathway in laryngeal cancer cell lines.

C. Gobin, M. Chang, C. C. Lattimore, K. M. Fredenburg;
University of Florida, Gainesville, FL

Background: We previously demonstrated that differing levels of miR-9-5p could predict chemosensitivity to cisplatin, and that miR-9-5p is a regulator of potential chemotherapeutic target MAP1B. As the mTOR/PIK3CA pathway has been implicated in the pathogenesis of laryngeal squamous cell carcinoma (LSCC), we sought to determine an association between differing miR-9-5p levels, mTOR pathway mediators including MAP1B, and methylation.
Methods: UM-SCC-98, UM-SCC-12, UM-SCC-11A, UM-SCC-10A (obtained from the University of Michigan) laryngeal cancer cell lines were used in this study. We previously showed UM-SCC-98 and UM-SCC-12 to have significantly lower miR-9-5p levels as compared to UM-SCC-11A and UM-SCC-10A (Northern blot analysis). The IC50 of an mTORC1 inhibitor (Rapamycin) and an mTORC1/C2 inhibitor (AZD-8055) were evaluated using the Cell Titer Blue Viability assay. Cells were treated with the de-methylating agent, 5-Azacytidine (1μM). Gene expression of mTOR pathway mediators- miR-9-5p, PTEN, EGFR, PIK3CA, and MAP1B- were determined in each cell line pre-and post-treatment via qPCR.
Results: All cell lines were resistant to treatment with Rapamycin (IC50 > 60μM) with the UM-SCC-12 cell line yielding the highest IC50 (> 150μM). Conversely, decreased cell proliferation was detected with AZD-8055. This was significantly associated with their miR-9-5p levels-- a higher AZD-8055 IC50 was associated with cell lines UM-SCC-98 (~40μM) and UM-SCC-12 (~23μM) compared to UM-SCC-10A (~16μM) and UM-SCC-11A (~8μM). Following demethylation treatment, miR-9-5p levels were significantly increased in UM-SCC-12 only (2-fold), and this corresponded to a significant decrease in MAP1B gene expression (2-fold) but not with EGFR, PIK3CA, and PTEN gene expression.
Conclusion: In conclusion, our study suggests that miR-9-5p may regulate MAP1B gene expression via the mTORC2 pathway. In addition, methylation may play a role in the regulation of the miR-9-5p gene and its downstream targets in laryngeal cancer tumorigenesis. Future studies will involve exploring epigenetic mechanisms of miR-9-5p inhibition and defining the role of key mediators of the mTOR pathway in LSCC.

#5697 MILIP drives triple-negative breast cancer through complexing with transfer RNAs to promote protein production.

Y. Feng[1], S. Zheng[2], X. Zhao[1], Y. Zhang[1], R. Xu[1], L. Xu[1], T. Preiss[3], L. Jin[1], J. Gao[2], X. Zhang[1];
[1]University of Newcastle, Callaghan, Australia, [2]Shanxi Bethune Hospital, Taiyuan, China, [3]Australian National University, Canberra, Australia

Despite the progress in endocrine therapy, targeted therapy and immunotherapy, the treatment of triple-negative breast cancer (TNBC), one of the most aggressive types of breast cancer, is challenging. This is closely associated with the lack of effective molecular targets in TNBC cells for therapeutic intervention. Here we report that the long noncoding RNA (lncRNA) MILIP drives TNBC cell survival, proliferation and tumorigenicity through complexing with transfer RNAs (tRNAs) to promote protein production, and thus represents a potential therapeutic target in TNBC.

MILIP was expressed at high levels in TNBC cells that commonly harbor loss-of-function mutations of the tumor suppressor p53, yet MILIP silencing diminished TNBC cell viability and retarded TNBC xenograft growth, indicating that MILIP functions distinctively in TNBC beyond its well-established role in repressing p53 in other types of cancers. Mechanistical investigations revealed that MILIP interacted with eukaryotic translation elongation factor 1 alpha 1 (eEF1α1) and formed an RNA-RNA duplex with $tRNA^{Leu}$ and $tRNA^{Ser}$, type II tRNAs, through their variable loops, thus facilitating the binding of eEF1α1 to these tRNAs. Disrupting the interaction between MILIP and eEF1α1 or tRNAs diminished protein production and cell viability, with therapeutic potential revealed where targeting MILIP using Gapmers inhibited TNBC growth and cooperated with the clinically available protein synthesis inhibitor omacetaxine mepesuccinate *in vivo*.

Collectively, these results identified MILIP as an RNA translation elongation factor to promote protein production in TNBC cells and demonstrated that experimental therapy with MILIP Gapmers inhibits TNBC growth, indicating MILIP targeting is a potential avenue for developing improved TNBC treatment through blocking protein synthesis.

MOLECULAR/CELLULAR BIOLOGY AND GENETICS: Pharmacologic Targeting of Cell Cycle Proteins
Poster Session

#5701 AU2-94: A CDK4-specific inhibitor with the marked anti-tumor efficacy.

L. Bantie, J. Likisa, M. Rahaman, T. Teo, A. Safaroghliazar, S. K. Basnet, R. Hassankhani, B. Noll, R. Milne, **S. Wang**;
University of South Australia, Adelaide, Australia

Cyclin-dependent kinases (CDKs) are a vital family of proteins in the cell development. Several CDK4/6 inhibitor drugs significantly extended the lives of subtypes breast cancer patients. However, they have some shortcomings. Many patients do not respond to them well mainly due to off-target toxicity requiring dose reductions and treatment interruptions, and thus building resistance, which limit their effectiveness. Here, we describe AU2-94, a highly selective CDK4 inhibitor, for the treatment of CDK4-dependent tumours including breast cancer (ER+ and TNBC), colorectal cancer and glioblastoma (GBM). AU2-94 exhibits high selectivity for CDK4 (K_i = 2 nM) over CDK6 (K_i = 279 nM). Consistent with the CDK4-targeted mechanism, AU2-94 arrested the G1 cells and inhibited cancer cell proliferation. Interestingly, AU2-94 reduced cellular CDK2, Cyclin E2, Cyclin A2, Cyclin B1, and induced apoptosis via reduction of Bcl-2, FOXM1 etc. In contrast to cancer cells, AU2-94 has little impact on the cell cycle, senescence, or apoptosis of human bone marrow cells, whereas the known CDK4/6 inhibitors increased the G1 cells. AU2-94 showed little or no effect on lymphocyte and neutrophil counts whilst the clinical CDK4/6 inhibitors reduced them. This lower effect of AU2-94 on the bone marrow, neutrophils and lymphocytes might be due to its lesser effect on CDK6 compared to the clinical CDK4/6 inhibitors. AU2-94 was highly efficacious against multiple *in vivo* tumour models. In the ER+ breast cancer T47D xenografts, AU2-94 caused tumour regression. In the model of MDA-MB-453 AR+ luminal breast cancer (CDK4, $KRAS^{mut}$, $PI3KCA^{mut}$), AU2-94 demonstrated remarkable efficacy, resulting in the 6 out of 7 (86%) mice tumour-free. In the colorectal cancer HCT116 (CDK4/6, $KRAS^{mut}$) xenografts, AU2-94 inhibited tumour growth markedly in a dose-dependent manner from 25 to 200 mg/kg without any overt toxicity. The pharmacokinetic and pharmacodynamic study revealed up to 500-fold higher concentration of AU2-94 in the tumours than in the plasma, suggesting its tumour targeting specificity. Several robust biomarkers/PD markers were identified. The Rb-CDK4-Cyclin D pathway is altered in the majority of GBM due to homozygous deletion of CDKN2A/B. AU2-94 has an excellent therapeutic potential as it crossed the blood-brain-barrier effectively. In the both U87 subcutaneous and orthotopic models, AU2-94 reduced the tumour burden and increased the survival of GBM bearing mice significantly compared to vehicle. Moreover, AU2-94 synergised the anti-cancer efficacy of PI3K/Akt/mTOR and HER2 inhibitors in combination. In summary, AU2-94 is a CDK4 inhibitor with high selectivity against a panel of 360 human kinases. This selectivity can be a reason for the better safety of AU2-94 compared to the clinical CDK4/6 inhibitors. The high oral bioavailability, robust antitumor efficacy and excellent safety profiles make AU2-94 a highly attractive candidate for clinical development.

#5702 BTX-9341, a bifunctional degrader of CDK4 and CDK6 for glioblastoma multiforme.

H. Majeski, K. Chahal, A. Okano, A. Pasis, C. Carlson, A. Shakya, Q. Liu, S. Huang, A. Hoskote Chourasia, L. Fung;
Biotheryx, Inc., San Diego, CA

Glioblastoma multiforme (GBM) is an aggressive form of brain cancer with limited treatment options. GBM has a high frequency of dysregulation of the CDKN2A-cyclin D-CDK4/CDK6 signaling node and should subsequently be sensitive to CDK4/6 inhibition. Despite this, the CDK4/6 inhibitors that are approved for HR+/HER2- breast cancer have shown limited efficacy in GBM due to poor blood brain barrier (BBB) penetration. BTX-9341 is a Cereblon (CRBN) mediated CDK4/6 bifunctional degrader that we have developed for HR+/HER2- breast cancer. This degrader shows good exposure in brain tissues with a high brain to plasma ratio. Given the exposure in the brain, we explored the *in vitro* and *in vivo* efficacy of BTX-9341 in GBM cell line and xenograft models. GBM cell lines treated with BTX-9341 showed up to 86% degradation of CDK4 and CDK6 with DC_{50}s <1nM. CDK4/6 phosphorylates the protein RB which releases the transcription factor E2F, inducing the expression of genes which promote cell cycle progression. We examined RB phosphorylation by immunoblot and cell cycle progression by propidium iodide staining followed by flow cytometry. BTX-9341 was potent in all downstream assays, with phospho-RB IC_{50}s <10nM, and G0/G1 cell cycle arrest at concentrations as low as 10nM. We used a 2D colony formation assay (CFA) to assess inhibition of proliferation by cell cycle arrest. BTX-9341 potently inhibited cell proliferation with CFA IC_{50}s of 13-100nM in GBM cell lines. BTX-9341 displays excellent pharmacokinetic properties with good oral bioavailability and high brain to plasma ratios which allowed for oral dosing in both subcutaneous and orthotopic xenograft studies. We examined tumor growth inhibition efficacy in two GBM xenograft models: an intracranial U87 model and a subcutaneous U118 model and saw robust tumor growth inhibition in both models with BTX-9341 treatment. The U118 cells have partially unmethylated MGMT, which lead to a loss of efficacy of temozolomide over time, while BTX-9341 maintained inhibition of tumor growth. This indicates that BTX-9341 may be effective in patient populations for which temozolomide is ineffective. The U87 intracranial xenograft model also showed dose-dependent tumor growth inhibition upon treatment with BTX-9341, indicating that BTX-9341 can cross the BBB and reach concentrations high enough to execute cell proliferation inhibition effects. BTX-9341 treated mice also had much better survival than abemaciclib treated mice, the only CDK4/6i which has BBB penetration. These results show that BTX-9341 displays excellent single agent activity *in vitro* and *in vivo* in GBM models. The xenograft data indicates that BTX-9341 can inhibit growth of MGMT methylated and unmethylated GBM cell lines, and that BTX-9341 can inhibit tumor growth in the brain more effectively than BBB penetrant CDK4/6i. Together this data shows that BTX-9341 may be a promising candidate for treating GBM.

#5703 Development of RVL-101, a CDK4/6-selective, small molecule inhibitor with superior CNS penetration and combinability potential for the effective treatment of primary and metastatic brain tumors.

J. E. Campbell, B.-S. Pan, M. Bower, P. Bertinato, N. Perez, V. Gras Andreu, N. Rana, S. Tabchouri, A. Gupta, J. Kallenbach;
Reverie Labs, Cambridge, MA

Cyclin-dependent kinases 4 and 6 (CDK4/6) are key regulators of the cell cycle that are frequently dysregulated in cancer, leading to unchecked cell growth. CDK4/6 inhibitors have emerged as a promising class of anticancer agents that selectively target this pathway. The primary mode of action of CDK4/6 inhibitors relies on the disruption of retinoblastoma (Rb) protein phosphorylation, which thereby blocks cell cycle progression from G1 to S phase and reduces proliferation of cancer cells by a cytostatic mechanism. However, despite their efficacy, approved and clinical-stage CDK4/6 inhibitors have modest penetration of unbound drug into the brain, limiting their utility in the treatment of brain metastases and primary brain tumors. Additionally, despite the potential benefits of CDK4/6 inhibitors as combination therapies with cytotoxic agents, adjunctive treatment options remain underexplored due to the poor safety profiles of existing therapies. RVL-101 is a preclinical, investigational drug with a novel pharmacophore that has a low nanomolar activity against CDK4, is CDK2,6,7,9-sparing, and maintains >500-fold selectivity over CDK1. To maximize the potential of RVL-101 as a preferred combination partner, this novel agent has been engineered to have exquisite kinome- and safety-panel selectivity with no measured CYP inhibition or induction liabilities. RVL-101 is differentiated from approved and clinical stage CDK4/6 inhibitors having both high partitioning into the brain (Kp) and high free-brain ($Kp_{u,u}$ = 0.7) levels resulting in equal levels of unbound drug in all relevant compartments at steady state. Like other CDK4/6 agents, RVL-101 is broadly efficacious in vivo in ER+/HER2- xenograft models at well-tolerated doses. However, RVL-101 has also demonstrated robust activity in HR-/HER2+ xenograft models as a single-agent and has uniquely shown improved tumor inhibition effect in combination with approved HER2 cytotoxic therapeutics tucatinib and fam-trastuzumab-deruxtecan. RVL-101 was also tested in a GBM model as a monotherapy and in conjunction with the cytotoxic agent temozolomide (TMZ). Remarkably, QD dosing of the cytostatic agent, RVL-101, after pulsatile pretreatment with TMZ led to dramatic synergistic efficacy compared to either agent alone, leading to 100% survival of all animals on the dual therapy arm for more than 3 weeks post discontinuation of dosing. RVL-101 offers the combination of substantial therapeutic benefit and consistent free-drug levels in plasma and CNS that could lead to safe and effective treatment for a broader patient population.

#5705 Discovery of a selective slow-off CDK2 inhibitor NKT3447 with distinct features of suppressing pCDK2, downregulating cyclin E, and achieving prolonged pathway inhibition.

J. Geng[1], **K. Liu**[1], Z. Yu[1], W. Sun[1], H. Wei[1], W. Li[1], J. Lu[1], J. Deng[2], L. Geng[2], Z. Liu[1], Z. Gao[1], Y. Lou[1];
[1]NiKang Therapeutics Inc., Wilmington, DE, [2]NiKang Therapeutics Inc., Shanghai, China

CDK2 is a cell cycle kinase that plays a critical role in controlling the G1 to S-phase transition and its abnormal activation through cyclin E1(CCNE1) amplification has been indicated as the primary oncogenic driver in advanced cancers including ovarian, endometrial, and gastric cancers. In addition, cyclin E1 overexpression has emerged as a key resistance mechanism to CDK4/6 inhibitors in hormone receptor-positive breast cancer patients. Therefore, CDK2 represents a promising novel oncology target. However, development of a potent and selective CDK2 inhibitor has been challenging due to the high homology of CDK2 with other CDKs, particularly CDK1, which is essential in normal cell cycle progression. NKT3447 is a novel, orally bioavailable small molecule CDK2 inhibitor with slow-off kinetics and is highly selective against CDK1 and other CDKs. In addition, NKT3447 exhibits a distinct mechanism of action, including suppression of the Thr160 activating phosphorylation on CDK2 and downregulation of cyclin E1. In biochemical assays, NKT3447 drives a concentration dependent disruption of the CDK2/cyclin E1 and CDK2/cyclin A2 complexes, but not the CDK1/cyclin B1 complex. Consequently, NKT3447 potently inhibits the phosphorylation of Rb (pRb) and induces G1 cell cycle arrest in CCNE1 amplified OVCAR3 cells, while showing minimal or no effect on G2/M phase distribution in all the cell lines tested, including OVCAR3 and KYSE520 (CDK1-dependent) cells. Importantly, NKT3447 has a slow-off kinetics, as demonstrated by NanoBRET target engagement assay, which leads to sustained pRb inhibition after treatment withdrawal. In addition, NKT3447 treatment reduces cyclin E1 protein levels and suppresses phospho-CDK2 (Thr160), which further represses CDK2 activity and prolongs the inhibition of CDK2 signaling. NKT3447 also demonstrates a selective anti-proliferation effect in a panel of human cancer cell lines with elevated cyclin E1 expression and/or dependency on CDK2 or cyclin E1 (DepMap). In line with cellular studies, pharmacodynamic study of NKT3447 in mouse tumor models recapitulates a significant repression of pRb, pCDK2 and cyclin E1. Furthermore, NKT3447 treatment results in a dose-dependent tumor growth inhibition or tumor regression in CCNE1 amplified OVCAR3 and MKN1 tumor models. In addition, the combination of NKT3447 with carboplatin exhibits enhanced anticancer effects in OVCAR3 and MFE-280 models. These results demonstrate that NKT3447 is a potent, selective CDK2 inhibitor with distinct properties and mechanism of action, which holds great potential to effectively treat patients with aberrant CDK2/Cyclin E activation in a variety of cancer types. NKT3447 is currently being investigated in a Phase 1 clinical trial in patients with advanced solid tumors.

#5707 Preclinical evaluation of KRLS-017, a potent, highly selective and reversible CDK7 inhibitor with broad antitumor effect in preclinical models, in preparation for a Phase 1 clinical trial in advanced solid tumor malignancies.

A. L. Hannah[1], S. Ritland[2], T. Steele[3], S. Smith[4], A. Ram[5], B. Slingsby[6], K. Dhingra[7], J. Chrisman[8], R. Dua[8], Y. Tokunaga[9], S. Kono[9], Y. Aga[9]; [1]Independent Consultant, Sebastopol, CA, [2]Independent Consultant, Midway, UT, [3]Independent Consultant, Amesbury, MA, [4]Independent Consultant, San Jose, CA, [5]Independent Consultant, San Francisco, CA, [6]Co-Founder, Seattle, WA, [7]Co-Founder, Sparta, NJ, [8]Independent Consultant, Seattle, WA, [9]Employee Ube Corporation, Minato City, Japan

KRLS-017 is a potent, selective, and reversible inhibitor of Cyclin Dependent Kinase 7 (CDK7). Its molecular formula is $C_{24}H_{35}N_5O_2Si$ and its molecular weight is 453.65 Daltons. KRLS-017 is being developed for the treatment of patients with advanced solid tumor malignancies.

To differentiate KRLS-017 from other CDK7 inhibitors, we created a reversible inhibitor to allow for treatment schedule optimization and maximization of therapeutic index in clinic. High selectivity of KRLS-017 for CDK7 was confirmed using a panel of 313 recombinant human kinases. The IC50 of KRLS-017 against recombinant human CDK7 was determined to be 16 nM, and no other kinases in the panel showed IC50 values less than 300 nM. Antiproliferative activity of KRLS-017 was investigated in vitro using a broad panel of human tumor cell lines. KRLS-017 showed potent antiproliferative effect across a wide variety of both solid and hematologic tumor types, producing GI50 values <200 nM in 258/302 human tumorcell lines tested.

Antitumor activity of KRLS-017 was investigated in vivo using multiple mouse xenograft tumormodels at dose levels ranging from 25 mg/kg to 200 mg/kg using both continuous (daily) andintermittent dosing schedules. Statistically significant tumor growth inhibition was seen at doselevels of 50 mg/kg and higher, with tumor regression observed at 100 mg/kg and 200 mg/kg. Better in vivo tolerability at efficacious doses was observed using intermittent dosing schedules in mouse xenograft models, which led to adoption of an intermittent schedule in the proposed first-in-human phase 1 trial.

KRLS-017 is orally bioavailable in mice, rats, and dogs and plasma drug exposure increased in a proportional manner with dose. Comparing first dose and 28th dose in the dog, minimal plasma accumulation was observed, suggesting once daily dosing in humans would be initially tested. Repeat dose 28 day GLP toxicology studies in rat and dog showed adverse effects in highly proliferative bone marrow and gastrointestinal tissues which is consistent with the known mechanism of action for CDK7 and is considered to be monitorable and manageable in the setting of oncology.

The clinical development plan for KRLS-017 includes an initial Phase 1 dose escalation study (KRLS-017-101) in patients with refractory solid tumor malignancies to assess pharmacokinetics / pharmacodynamics and to determine an optimal dose level and treatment schedule to test in expansion cohorts. Given the potential of CDK7 inhibitors in the treatment of hormone receptor positive breast cancer, combination work with other agents (such as selective estrogen receptor degraders) is on-going.

#5708 Silence exportin 7 sensitizes esophageal squamous cell cancer to CDK4/6 inhibition through block the cell cycle coresectory.

Z. Wu[1], L. Xu[1], C. Jiang[1], A. Bass[2], **J. Zhou**[1];

[1]West China Hospital of Sichuan University, Chengdu City, China, [2]Novartis Institutes of Biomedical Research, Cambridge, MA

Introduction: There is a lack of effective target therapies for esophageal squamous cell cancer. Our previous studies have demonstrated that CDK4/6 is a potency target for ESCC and combination with ERBB inhibitors is sufficient to achieve durable response. The aim of the current study is to prospectively map the landscape of sensitivity and resistance to CDK4/6 inhibition and develop novel combination therapies in ESCC.
Experimental Procedures: We performed a genome-wide functional genetic screening and mini-pool designed CRISPR screen approaches to identify the modulators whose depletion sensitize CDK4/6 inhibition or confer resistance to the CDK4/6 inhibitor Palbociclib and elucidate new therapeutic strategies.
Results: Our screen identified RB as the most enriched sgRNA, while guides targeting CCNE1 and CDK2 as the most depletion sgRNAs after CDK4/6 inhibition. These results validates our experimental approach as RB loss and CCNE1/CDK2 reactivation is the main mechanisms of CDK4/6 resistance. After gathering potential candidates from both screens, we found that genetically ablation of Exportin 7, a nuclear export factor, strongly sensitize CDK4/6 inhibition both in vitro and in vivo. RNAseq revealed a further repression of transcriptional activity of E2F and G2M by addition of XPO7depletion under CDK4/6 inhibitor treatment. To increase our insight in the molecular mechanism that could explain the synergy between XPO7 and CDK4/6, we further performed proteomics of nuclear and cytoplasm in ESCC lines with or without CDK4/6 inhibition. We found that silence XPO7 result in nuclear accumulation of mitosis-regulated genes such as CENPM, KIF4A and WEE1. Combined CDK4/6 inhibition with XPO7 depletion results in further downregulate of CENPM and KIF4A expression in nucleus, abrogating compensatory activation of cell cycle regulation and promote the cytostatic effect in ESCC. We further validated that CENPM and KIF4A depletion also sensitize CDK4/6 inhibition, and consequentially use WEE1 inhibitor after CDK4/6 inhibitor also effectively block the growth of ESCC lines.
Conclusion: Overall, our comprehensive functional genetic screening approach revealed modulation of sensitive and resistance to the inhibition of CDK4/6 in ESCC. XPO7 was identified as a driver to change cell cycle landscape and merits as a therapeutic target combined with CDK4/6 inhibition in ESCC, which is beneficial to provide a novel treatment strategy.

#5709 PF-07104091, a first-in-class CDK2-selective inhibitor for the treatment of HR+/HER2- breast cancer and CCNE1^{high} ovarian cancer.

C. Shen, M. Qiu, N. Huser, B. Pascual, Q. Zhang, T. VanArsdale, A. Murtaza, J. Almaden, K. Kim, L. Anders, K. Eisele;
Pfizer, Inc., San Diego, CA

The selective inhibition of Cyclin\CDK complexes controlling cell cycle progression has been established as cancer therapy by selective CDK4/6 inhibitors in HR+/HER2- breast cancer. Expanding control of the cell cycle through selective inhibition of CDK2 offers novel therapeutic opportunities in cancer, including targeting CCNE1 amplified tumors and countering resistance to CDK4\6 inhibitors in ER+ breast cancer. PF-07104091 is a first-in-class CDK2-selective inhibitor under clinical investigation in patients with HR+/HER2- breast cancer and ovarian cancer. Preclinical studies using PF-07104091 establish the therapeutic impact of CDK2 inhibition in both diseases and highlight distinct mechanistic roles for CDK2 in control of cancer cell proliferation. In models of CCNE1 amplified ovarian cancer, CDK2 plays the dominant role in control of RB1 phosphorylation and the G1 checkpoint. CDK2 inhibition with PF-07104091 induces G1 growth arrest and controls tumor xenograft growth as single agent therapy. In ER+ breast models CDK2 plays a supportive role in the control of RB1 phosphorylation cooperating with CDK4\6. Whole genome CRISPR KO and CRISPR activation screens in conjunction with CDK4\6 inhibition establish CDK2 KO as a primary sensitizer to CDK4\6 inhibition, and support Cyclin E\CDK2 complexes as the driver of resistance to CDK4\6 inhibitors in ER+ breast models. PF-07104091 combined with CDK4\6 inhibitor Palbociclib or CDK4-selective inhibitor PF-0060 synergistically controls proliferation of ER+ BC cells in vitro and induces tumor regression in ER+ BC xenograft models, including PDX models with acquired resistance to CDK4\6 inhibitors and endocrine therapy.

#5710 The brain penetrant CDK4/6 inhibitor, PRT3645, is highly effective in combination with other targeted therapies in preclinical models of breast cancer, CRC and NSCLC.

Y. Zou, K. Gallagher, S. Dhar, A. Busking, S. Pawley, R. Holmes, X. Wu, M. Wang, J. Rager, T. Emm, S. Ruepp, M. Cowart, A. Combs, K. Vaddi, S. Geeganage, P. Scherle, S. Lee;
Prelude Therapeutics, Wilmington, DE

Cell cycle deregulation is a hallmark of cancer and the hyperactivation and overexpression of cyclin-dependent kinase (CDK)s are often drivers of cancer pathogenesis. CDK4/6 are critical mediators of cellular transition into S phase and important for cancer initiation, growth, and survival. Previously we reported a novel brain penetrant CDK4/6 inhibitor, PRT3645, that exhibits single digit nanomolar biochemical potency against CDK4/6 and >2000-fold selectivity against other CDKs. PRT3645 inhibits cellular phosphorylation of Rb with nanomolar potency. Furthermore, PRT3645 exhibits favorable in-vivo safety pharmacology and ADME properties, including increased brain penetration, and demonstrates oral bioavailability across rodents, dog and non-human primates. Here, we explored the therapeutic potential of PRT3645 in tumor models harboring actionable genomic alterations but lacking effective targeted treatments. Specifically, we explored the combination of PRT3645 with a selective estrogen receptor degrader (SERD), an approved treatment for patients with HR+/HER2-, ESR1-mutated advanced or metastatic breast cancer. In an ESR1 mutated breast cancer PDX model, PRT3645 not only exhibited monotherapy activity but also induced significant tumor regression in combination with a SERD through inhibiting ER-mediated signaling. We also investigated PRT3645 single agent activity and combination with a clinically validated MEK inhibitor in a BRAF class III mutant colorectal CDX model. PRT3645 was well-tolerated and demonstrated significant anti-tumor efficacy, which was further enhanced by combination therapy. To further explore comprehensive inhibition of cell cycle progression and overcome potential resistance to CDK4/6 inhibition, we investigated dual inhibition of CDK4/6 and CDK2. CDK2 is a crucial player in regulating the cell cycle by controlling the late G1/S transition, promoting DNA replication, and contributing to the DNA repair processes. Additionally, CDK2 activation has been identified as a potential mechanism of resistance to CDK4/6 inhibition. We evaluated CDK2 and CDK4/6 dual inhibition in CDKN2A loss or CCNE amplified cancer cell lines and observed enhanced proliferation suppression, cell cycle arrest and senescence induction, underscoring the potential of this combination for improved therapeutic efficacy across various cancer types. In summary, PRT3645 displays an excellent balance of potency, selectivity, pharmacokinetic parameters across species as well as brain penetrance. In preclinical studies, PRT3645 was highly efficacious when combined with other targeted therapies, offering potential benefits across a wide spectrum of cancer types. In addition, the concept of dual inhibition of CDK4/6 and CDK2 presents a rational and promising approach to enhance the efficacy of cancer therapy.

#5711 Anti-tumor effects of fadraciclib, CDK2/9 inhibitor, in biliary tract cancer.

J.-M. Kim, A.-R. Nam, K.-S. Oh, J.-H. Bang, Y. Jeong, S. Choo, S. Lee, H. Kim, J. Yoon, T.-Y. Kim, D.-Y. Oh;
Seoul National University Cancer Research Institute, Seoul, Korea, Republic of

Background: Targeting CDKs has emerged as a significant strategy in the development of new drugs. The CDK4/6 inhibitors have proven their efficacy in several tumor types, while the CDK2 and CDK9 inhibitors are currently undergoing clinical trials. In biliary tract cancer (BTC), gene expressions of CDK2 and CDK9 are elevated compared to normal tissue. CDK9, a transcriptional CDK, regulates RNA polymerase II (RNAP II), leading to enhanced transcription of oncogenes, such as MCL1. Aberrant activation of these CDKs is associated with cancer progression and evading apoptosis in BTC. Notably, MCL1 is frequently amplified in intrahepatic cholangiocarcinoma (16-21%). This finding underscores the potential significance of CDK2 and CDK9 as therapeutic targets in BTC. However, in BTC, targeting CDK2 or CDK9 has not yet been studied. In this study, we aimed to test CDK2/9 targeting and develop possible biomarker strategies in BTC.

Method: A total 9 BTC cell lines (SNU245, SNU308, SNU478, SNU869, SNU1196, SNU2670, SNU2773, TFK1, and HUCCT1) were used. Fadraciclib (CDK2/9 dual inhibitor), Olaparib (PARP inhibitor), JQ1 (BRD4 inhibitor) was used. MTT assay, Colony formation assay, Annexin-V assay, and Cell cycle analysis were performed for evaluation of anti-cancer effects. The effect of Fadraciclib on homologous recombination (HR)-mediated DNA damage repair was assessed using focus formation assay and DRGFP assay. Combination of Fadraciclib with Olaparib or JQ1 was evaluated *in vitro* and *in vivo*.

Result: The anti-tumor effect of Fadraciclib monotherapy was relatively higher in MCL1-High BTC cells (SNU869, SNU2773) compared to MCL-Low cells (SNU245, SNU2670). In MCL1-High cells, Fadraciclib inhibited CDK9, leading to downregulation of RNAP II phosphorylation at Serine 2 and MCL1. Fadraciclib also interfered with HR-mediated DNA damage response by inhibiting transcription of HR-related genes. The combination of Fadraciclib and Olaparib exhibited synergistic anti-tumor effects *in vitro* in MCL1-High cells and *in vivo* xenograft model. Conversely, in MCL1-Low cells, Fadraciclib increased BRD4 mRNA expression, leading to the restoration of CDK9-RNAP II activity. This reactivation of RNAP II restored cellular transcription homeostasis, thereby reactivating the transcription of oncogenes such as MCL1. Combination of Fadraciclib and JQ1 showed synergistic effects *in vitro* in MCL1-Low cells and *in vivo* xenograft model by inhibiting restored CDK9-RNAP II activity.

Conclusion: MCL1-High BTC cells are sensitive to CDK2/9 inhibitor and show synergism between CDK2/9 inhibitor and PARP inhibitor. In MCL1-Low BTC, a combination of a CDK2/9 inhibitor and a BRD4 inhibitor might represent an optimal strategy for new drug development.

#5712 Functional dissection of CDK7 in transcription using a highly selective CDK7 inhibitor Q901.

H. Jung[1], D. Um[1], Y. Lee[2], D. Yu[2], D. Lee[2], J. Ahn[2], J. Kim[2], S.-J. Lee[2], J. Kim[2], K. Nam[2], T.-K. Kim[1];
[1]Pohang University of Science and Technology, Pohangsi, Korea, Republic of, [2]Qurient, Seongnamsi, Korea, Republic of

CDK7 is a well-known regulator of both the cell cycle and transcription and plays a crucial role in cell cycle progression by catalyzing T-loop phosphorylation of other CDKs. CDK7 is also an integral subunit of the general transcription factor, TFIIH and regulates transcription through phosphorylation of RNA Polymerase II (Pol II) at CTD Ser5 and CDK9. We used Q901, a highly selective CDK7 inhibitor to further investigate the molecular function of CDK7 in the transcriptional process. Q901 is currently being evaluated in a phase 1 clinical study for selected advanced solid tumors. Compared to previously reported CDK7 inhibitors, Q901 has increased specificity and efficacy, but the impact on transcription have not been studied in detail. In our study, we combined RNA Pol II (pan, Ser5P, Ser2P) ChIP-seq and PRO-seq techniques in the MCF7 breast cancer cell line. The findings demonstrated that the Q901 effectively altered transcription and the RNA Pol II profile in a subset of genes, leading to a significant reduction in Ser5 phosphorylation levels in RNA Pol II. The downregulated genes were associated with critical pathways including downstream of oncogenic genes (MYC and E2F), DNA damage repair, cell cycle checkpoint, and gene expression. To verify whether these genes were the direct targets of CDK7, we performed CDK7 ChIP-seq analysis. CDK7 binding exclusively to the genes that were downregulated by Q901, without any detectable binding to upregulated genes. Despite the universal role of general transcription machinery in transcription, the data demonstrated that the highly selective inhibition of CDK7 in transcription of various oncogenic pathways underlies the potent *in vitro and in vivo* anti-cancer efficacy of this specific CDK7 inhibitor.

#5714 Synergistic effect of the CDC7 inhibitor, monzosertib (AS-0141) with current therapies in AML models.

H. Endo[1], H. Furuichi[1], A. Arimura[2], Y. Nishioka[1], M. Sawa[1];
[1]Carna Biosciences, Inc., Kobe, Japan, [2]CarnaBio USA, Inc., South San Francisco, CA

Introduction: Cell division cycle 7 (CDC7) is a highly conserved serine-threonine kinase that plays an important role in the initiation of DNA replication and cell cycle progression. Aberrant expression of CDC7 have been reported to cause uncontrolled proliferation of many cancer types, suggesting that CDC7 inhibitors may provide a great potential for the development of novel therapy for cancers. Monzosertib (AS-0141) is a potent, selective, orally bioavailable small molecule inhibitor of CDC7, and is currently being evaluated in Phase I study for the treatment of solid tumors. In a preclinical cancer cell panel study, monzosertib showed strong antiproliferative activities against a variety of cancer types, and acute myeloid lymphoma (AML) cell lines were found to be the most sensitive to monzosertib. As a single agent, treatment with monzosertib accumulates DNA damage in cancer cells and induces cell death. In this study, we aimed to investigate the antitumor effects of monzosertib alone and in combination with other anticancer drugs in AML models.
Method: Antiproliferative activity of monzosertib was examined against a panel of 35 human cancer cell lines of various cancer types. DNA metyltransferase (DNMT) inhibitors (azacitidine or decitabine) and BCL2 inhibitor (venetoclax) were evaluated for their synergistic/antagonistic effects in combination with monzosertib against human AML cell lines (THP-1, HL-60, MV4-11, MOLM-14, TF-1, U-937 and NOMO-1). The combination index (CI) was calculated using the Chou-Talalay method. Flow cytometry assay was used to analyze apoptosis. To evaluate the in vivo efficacy, tumor-bearing mice were treated with monzosertib alone or in combination with venetoclax.
Results: The combination of monzosertib with azacitidine, decitabine, or venetoclax resulted in a significant synergistic antiproliferative effects against AML cell lines in vitro. The flow cytometry assay indicated that azacitidine combination induced apoptosis and increased cell death in THP-1 cells. In vivo, oral administration of monzosertib demonstrated robust in vivo antitumor efficacy in a MV4-11 tumor bearing xenograft mouse model, both as a single agent and in combination with venetoclax.
Conclusions: Monzosertib, a selective CDC7 inhibitor, demonstrated strong antiproliferative activity against human AML cell lines, both as a single agent and in combination with standard therapies. Monzosertib exerts synergistic antitumor effect with venetoclax in a human AML xenograft mouse model. These results suggest that monzosertib has a potential to enhance the antitumor efficacy of standard of care agents for AML patients.

#5715 CDK7 modulation of Hippo-YAP activity by RNAPII phosphorylation regulates CDK4/6 inhibitor resistance in hormone positive breast cancer.

C.-J. Yu[1], Y.-J. Zhuang[1], C.-Y. Lin[1], Y.-R. Tseng[1], T.-Y. Lin[1], H.-M. Shih[2], C.-Y. Liu[3], T.-C. Chao[3], L.-M. Tseng[3], C.-C. Huang[3], Y.-F. Tsai[3], F. Tsai[2], **J.-I. Lai[1]**;
[1]National Yang Ming Chiao Tung University, Taipei, Taiwan, [2]National Taiwan University, Taipei, Taiwan, [3]Taipei Veterans General Hospital, Taipei, Taiwan

Breast cancer is the leading cause of cancer in women and poses a massive social economic burden worldwide. CDK4/6 inhibitors have roles as standard of care in advanced and adjuvant setting for hormone positive (HR (+)), HER2 negative breast cancer. CDK6 amplification has been proposed to confer resistance to CDK4/6 inhibitors. By a small molecule screen, we discovered a multi-kinase inhibitor PIK-75 that suppressed the Hippo-YAP pathway and significantly downregulated CDK6, resulting in reversal of CDK6 amplification mediated CDK4/6 inhibitor resistance. To further probe the mechanism, we discovered that PIK-75 suppressed phosphorylation of the C-terminal domain (CTD) of RNA polymerase II (RNAPII) which then resulted in downregulation of YAP expression and the Hippo pathway. Chromatin immunoprecipitation (ChIP) confirmed suppression of RNAPII Ser5 occupancy at YAP promoter after PIK-75 or shCDK7 treatment. Integrating results from RNA sequencing and proteomic analysis in breast cancer cells treated with PIK-75 revealed widespread transcription suppression and substantial spliceosome defect. Alternative splicing analysis by PIK-75 treated cells revealed a widespread splicing defect affecting multiple genes, including YAP, providing an alternative pathway for PIK-75-CDK7 mediated transcriptional regulation. We then investigated the phenotypic impact mediated by PIK-75 and CDK7 inhibition. We discovered that CDK7 silenced cells showed downregulation of YAP intranuclear translocation, impairment of cell migration, and cell cycle progression. ChiP-sequencing of RNAPII was also performed to investigate changes in global RNAPII occupancy and impact on promoter proximal pausing. In vivo studies confirmed that PIK-75 treatment demonstrated tumoricidal efficacy in CDK6 amplified HR (+) breast cancer cells, while the CDK4/6 inhibitor abemaciclib showed minimal cytotoxicity. In conclusion, we discovered a novel CDK7-RNAPII phosphorylation-Hippo/YAP-CDK6 regulation axis that when perturbed, could regulate CDK4/6 inhibitor resistance in HR (+) breast cancer. Molecular studies and multi-omic profiling elucidated the role of CDK7 in hippo pathway and characterizes multiple roles of PIK-75. Our study provides intriguing novel insights into the link between "transcriptional CDKs" and the hippo pathway that could potentially be further probed for therapeutics in HR (+) breast cancer.

#5716 CDK7 as a drug target in advanced stage uveal melanoma.

F. J. Waltrich, Jr.;
Thomas Jefferson University, Philadelphia, PA

Uveal melanoma (UM) metastasizes predominantly to the liver, and most metastatic UM are BAP1-deficient. Targeted therapies, such as MEK inhibitors, have failed clinically. There are few FDA-approved therapies for metastatic UM, but these therapies are limited to only a subset of patients and have modest survival benefits. Hence, there is a need to identify novel and effective treatment strategies. Due to the low mutational burden in UM, targeting transcriptional may be an effective strategy. Here, we identified Cyclin Dependent Kinase 7 (CDK7), a key regulator of transcription, as an essential and druggable target in UM. CDK7 directly phosphorylates RNA polymerase II and is expressed in all UMs. siRNA-mediated knockdown of CDK7 decreased the growth of three BAP1-deficient UM cell lines. We tested a clinically relevant, highly specific CDK7 inhibitor, SY-5609, developed by Syros Pharmaceuticals and similarly showed that the cell lines were sensitive to the growth inhibitory effects of SY-5609. Furthermore, we observed synergistic effects on cell growth inhibition when combined with a MEK inhibitor (Trametinib). We performed RNA sequencing and identified several Hallmark Genesets to be positively enriched, including interferon-gamma response, TGF-beta signaling, and NFκB signaling after treatment with SY-5609. These results are validated using a multi-omic approach, utilizing Reverse Phase Protein Array (RPPA) data to validate transcriptome to proteome expression of these enriched pathways. Overall, our studies indicate that targeting CDK7 in uveal melanoma is a potential treatment strategy for BAP1-deficient UM and enhances MEK inhibitor efficacy.

#5717 CDK4 inhibition suppresses Rab11 mediated collective cell migration in colon cancer cells.

Chun Pu Cheng, Chia-En Ku, Shin-Ru Lee, Yu-Chun Wang, Yu-Chien Ching, Hui-Chun Chen, Wei-Ting Chao

Tunghai University, Taichung, Taiwan

In tumor progression, cell proliferation and cell adhesion are critical for tumor growth and metastasis. It has been demonstrated cell division which associated with microtubule organization also has impact on tubulin mediated focal adhesion turnover, however, the mechanism is not clear in the cell cohort migration which is accompanied with both cell proliferation and cell migration. This study is to investigate the effect of cell cycle inhibition in the collective cell migration. HT-29 colon cancer cells were treated with CDK4 inhibitor CINK4, paclitaxel and focal adhesion inhibitor PF573228. The cell proliferation rate was determined by MTT assay, cell migration ability was analyzed by wound healing assay. Rab11, E-cadherin and focal adhesion kinase were revealed by immuno-confocal microscopy. When HT-29 cells were treated with lower dose of CDK4 inhibitor CINK4, cell migration was suppressed. Meanwhile, in the result of immunostaining, the recycling endosomal protein Rab11which is involved in E-cadherin turnover in collective cell migration was not distributed in the cell membrane after CINK4 treatment. Furthermore, when cellular FAK activity were inhibited by PF573228 and tubulin disassembly was inhibited by paclitaxel, the cell area was increased with stable attachment, however, the membrane translocation of Rab11 was not affected. This study demonstrated cell cycle inhibition in G1 phase affected Rab11 mediated collective cell migration through tubulin regulated focal adhesion turnover for cell attachment. Keywords: CDK4, cell cycle, focal adhesion kinase, paclitaxel, colon cancer

#5718 TGN-1062, a dual CDK7 and FLT3 Inhibitor, shows potent anti-AML activity and synergizes with Venetoclax.

T. Thode[1], L. Nguyen[1], B. Durbin[1], A. Weston[1], S. Ng[1], T. Ghosh Halder[1], T. Bargenquast[1], R. Soldi[1], S. Kasibhatla[1], V. Chung[2], V. Villaflor[2], M. Kaadige[1], G. Marcucci[2], S. Sharma[1];

[1]TGen (The Translational Genomics Research Institute), Phoenix, AZ, [2]City of Hope, Duarte, CA

Purpose: Acute Myeloid leukemia (AML) is an aggressive malignancy of the hematopoietic system with poor survival rates. The best responses to treatment are achieved for young and fit patients who can tolerate chemotherapy followed by stem cell transplantation compared to older patients unfit to take intense chemotherapy. Since its approval venetoclax, a BCL2 inhibitor, has been the standard treatment for older patients in combination with a hypomethylating agent (HMA), such as azacitidine or decitabine, with a 76% complete response (CR). Despite this success as a frontline treatment, there is limited response for patients with relapse and refractory (r/r) and development of novel agents is required to improve overall therapeutic response. MYC has been shown to be frequently activated in AML and plays an important role in the induction of leukemogenesis and leukemic progression. While BCL2 inhibition via venetoclax has, in part, been shown to control c-MYC activation, the addition of another inhibitor which controls MYC may prove beneficial. CDK7 plays a dual role in tumor progression by regulating the cell cycle and transcription. CDK7 has also been shown to be associated with the overexpression of oncogenic driver genes such as BCL2 and MYC. Previously, we have presented the development of a potent and reversible CDK7 inhibitor, TGN-1062. Here, we have generated data supporting the potential benefit of CDK7 inhibition in combination with standard of care therapy for AML.

Methods: AML lines were co-treated with TGN-1062, venetoclax, and/or an HMA, assessed for viabilities with CellTiter-Glo, and analyzed with the Bliss synergy model. AML CDX or PDX cells were implanted subcutaneously or transplanted via tail vein, respectively, and treated with TGN-1062 and/or venetoclax. Subcutaneous tumors were measured to determine tumor growth inhibition (TGI) and correlating drug accumulation levels were measured in tumors and plasma using mass spectrometry. Leukemic burden and survival were evaluated at the end of treatment for transplanted models. Immunohistochemistry (IHC), Western blotting, and RT-PCR were performed to determine changes in relevant biomarkers in tumors and/or AML cell lines.

Results: Previously we have reported that TGN-1062 was effective in suppressing the growth of MV4-11 AML model. We extend these studies and show that TGN-1062 has activity at lower doses in both in vitro and in vivo AML models. In addition, we show synergy between TGN-1062 and other agents for AML treatment, including venetoclax or an HMA. Western blotting demonstrated significant changes in apoptotic markers. Survival of mice bearing AML was significantly increased with TGN-1062 treatment and combination treatment with venetoclax produced the longest survival.

Conclusion: Targeting CDK7 with TGN-1062 in combination with venetoclax or an HMA is a promising therapeutic approach for treatment of AML and needs further investigation.

#5719 Targeting CDK4/6 and BET proteins for the treatment of RB+ and RB- osteosarcoma.

R. Malko, P. H. Pandya, H. E. Shannon, B. J. Bailey, E. A. Dobrota, C. Young, F. Barghi, N. Riyahi, R. Justice, M. A. Trowbridge, K. L. Coy, A. L. Sinn, K. Bijangi-Vishehsaraei, M. J. Ferguson, M. Saadatzadeh, K. E. Pollok;
Indiana University School of Medicine, Indianapolis, IN

Osteosarcoma (OS) is the most common malignant bone cancer characterized by heterogeneity and genomic instability. Treatment and survival of patients have not improved in several decades, making it urgent to develop safe and effective therapies. Dysregulation of cell cycle regulators *CDKN2A*, cyclins, and CDK4/6 represent high-risk signatures in aggressive OS and can be targeted via CDK4/6 inhibitors (CDK4/6i). However, monotherapy often fails due to resistance from speculated RB loss as well as hyperactivation of compensatory signaling pathways in RB proficient cancers. In addition, >70% of OS patients have RB loss which is viewed as a biomarker of therapeutic response that negates the use of CDK4/6i. However, more research is needed in RB-deficient preclinical models to clearly define and validate the utility of RB as a biomarker for patient stratification. Based on our screening data, we hypothesize that combining CDK4/6i with bromodomain and extraterminal domain inhibitors (BETi) will potentiate anti-tumorigenic effects regardless of RB status in OS. BETi creates imbalances between transcription and replication which worsens oncogenic stress. In OS cell lines, combination index and Bliss analysis indicated additive-to-synergistic growth inhibition using CDK4/6i (abemaciclib or palbociclib) and BETi (AZD5153). Dual therapy also resulted in increased apoptosis at clinically relevant concentrations in an OS xenoline (TT2) compared to monotherapy. To determine potential for emergence of therapeutic resistance, an in-vitro longitudinal growth delay assay was established. While single agent therapies resulted in transient decreases in cell numbers over time, combination CDK4/6i+BETi resulted in cell death ($p<0.05$). To determine the effect of RB loss on therapeutic response to CDK4/6i, CRISPR mediated RB-knockout (KO) clones were developed in 143B human and K7M2 murine OS cell lines. RB KO cells exhibited sensitivity to CDK4/6i irrespective of RB status. However, levels of CDK4/6i required for 50% growth inhibition in RB KO were 1-3-fold higher using palbociclib, with negligible differences observed with abemaciclib in RB KO vs WT clones. To determine if therapeutic response is achievable in-vivo, a single-agent dosing study was conducted using palbociclib (40mg/kg, SID) and AZD5153 (1mg/kg, BID) in patient-derived xenograft (PDX) model derived from a metastatic lesion in the pelvis (TT2 PDX) harboring a CDK4/6 hyperactivation signature and monoallelic RB loss. Tumor growth reduction and survival was significantly higher in monotherapy groups compared to vehicle. However, one week after dosing was stopped, survival rates based on tumor volume endpoint were 40% and 100% for palbociclib and AZD5153 respectively. In-vivo efficacy of dual CDK46i+BETi is underway. This data provides rationale for further study of novel therapeutic options which may expand the clinical utility of CDK4/6i regardless of RB status.

#5720 Targeting CDK9 in cutaneous T-cell lymphoma using patient-derived xenograft models.

Y.-J. Liu, C.-H. Wu, L. Pincus, W. Z. Ai;
UCSF, San Francisco, CA

Cutaneous T-cell lymphoma (CTCL) is a rare form of non-Hodgkin lymphoma. Mycosis fungoides and Sézary syndrome (MF/SS) are the most common subtypes in CTCL. Early-stage MF/SS has a favorable prognosis. The advanced-stage CTCL has limited treatment options and a median survival of <5 years, highlighting the urgent need to develop targeted therapies in CTCL. Preclinical studies of CDK9 inhibitors have shown anti-tumor activity in various subtypes of hematologic malignancies. Several CDK9 inhibitors have entered clinical trials for lymphomas and leukemias. However, whether targeting CDK9 in CTCL is a therapeutic option is little known and has resulted in CTCL not being included in ongoing clinical investigations of CDK9 inhibitors. AZD4573 is a highly selective and potent CDK9 inhibitor currently under clinical investigation for Hodgkin and non-Hodgkin lymphomas. It was shown that AZD4573 induces tumor cell death through depletion of MCL-1. Overexpression of MCL-1 has been shown in CTCL cell lines and skin biopsy specimens of CTCL patients. MCL-1 expression appears to be particularly elevated in patients with advanced stage disease. Here, we investigated the ex vivo anti-tumor activity of AZD4573 using patient-derived CTCL xenograft models (PDXs).

Primary tumor cells harvested from CTCL PDX mice were activated with CD2/CD3/CD28 beads and incubated in hIL-2 and hIL-7 at an optimal cell density. Subsequently, cells were exposed to AZD4573 at various concentrations for 8 hr, then treated cells were harvested, washed, and placed in fresh media for another 48 hr. Growth inhibition was measured by the Real-Time Glo cell viability assay, and apoptotic activity was assessed by flow cytometry analysis of Caspase 3/7 activity and Annexin V + propidium iodide (PI) double staining. Additionally, we conducted RNA-seq analysis for MCL-1 expression in CTCL PDX primary tumor cells.

AZD4573 inhibited cell proliferation in a dose-dependent manner in primary tumor cells from three CTCL PDX mice (PRS-1, PRS-2 PRS-3), with GI_{50} of 43.5 nM, 175.4 nM, and 113.5 nM, respectively. Furthermore, AZD4573 significantly increased caspase 3/7 activity and apoptosis in PRS-1 and PRS-3, but not PRS-2 primary tumor cells. In addition, our RNA-seq analysis showed that compared with normal controls (normal PBMC from healthy donors), the MCL-1 gene expression is increased 10-fold (P-value <0.0001) in PRS1 cells. The MCL-1 gene expression in PRS2 and PRS3 cells is the same as normal control. Furthermore, PRS-1, which has the highest MCL-1 expression level, is most sensitive to AZD4573.

In conclusion, AZD4573 demonstrated dose-dependent growth inhibition and apoptosis induction in primary CTCL tumor cells. In addition, the expression level of MCL-1 appeared to be correlated with the ex vivo anti-tumor activity of AZD4573. Our findings provide a rationale for clinical investigation of targeting CDK9 in CTCL.

#5721 Dual targeting of CDK4/6 and CDK7 pathways augments tumor response in breast cancer.

E. Son, **S. Kim**, H. Park, M. Kim, H. Yang;
Columbia University Irving Medical Center, New York, NY

CDK7 plays a pivotal role in cell proliferation, serving as both a cell-cycle CDK regulator and a transcription machinery component. Clinical trials are currently exploring CDK7 inhibitors (CDK7i) as a second-line treatment for hormone receptor-positive (HR+) breast cancer post-CDK4/6 inhibitor (CDK4/6i) therapy progression and as a first-line treatment in triple-negative breast cancer (TNBC). This study evaluates the impact of CDK7i on transcription and CDKs activities and the synergistic potential of CDK7i in combination with CDK4/6i. Kinetic analyses indicate that CDK7i preferentially target global transcription over CDKs activities. Furthermore, a combination of CDK7i and CDK4/6i effectively suppresses cell proliferation in drug-naïve cells, albeit without the same efficacy in CDK4/6i-resistant cells. Our findings provide valuable insights into the evolving field of CDK inhibition strategies and provide critical guidance on the potential therapeutic application of CDK7i in breast cancer treatment.

#5722 Preclinical activity of CDK4/6 inhibitor alone or in sequential combination with chemotherapy using breast cancer cell line-derived organoid culture.

M. Kamita, H. Ali, E. Jiagge, J. Bensenhaver, E. Walker;
Henry Ford Health System, Detroit, MI

Breast cancer ranks as the most prevalent cancer globally, with lung and colorectal cancers following closely. Dysregulation of the cyclinD:CDK4/6:Rb axis has been shown to be a common feature in a number of human malignancies, including breast cancer. Targeting this pathway has emerged as a promising strategy for breast cancer treatment. Currently, the U.S. Food and Drug Administration has approved three CDK4/6 inhibitors for advanced hormone receptor-positive, HER2-negative breast cancer, when used in combination with endocrine therapy. However, there are still many breast cancer cases that do not qualify for these criteria and, therefore, do not benefit from CDK4/6 inhibitors prompting investigations into their potential synergy between CDK4/6 inhibitors with chemotherapy. Efforts are currently being made to test the application of these drugs in combination with chemotherapy. Previous studies have demonstrated a synergetic effect of combining CDK4/6 inhibitors and other therapies to treat breast and prostate cancers. While many studies administer these drugs concurrently, our hypothesis proposes a sequential combination approach. This method involves arresting cell cycle at the G0G1 phase using CDK 4/6 inhibitors and then releasing the drug when the cells are more vulnerable to chemotherapy treatment. Such an approach has the potential to expand the application of CDK4/6 inhibitors beyond ER+/HER2- breast cancer. The primary objective of this study is to evaluate the effectiveness of CDK4/6 inhibitors, both alone and in sequential combination with chemotherapy, across a range of breast cancer subtypes. Breast cancer cell lines (MDA-MB-231, HCC70 and T47D) were used in the study. For each cell line, a total of $3x10^5$ cells were seeded in a 6-well plate, and after an overnight incubation, the media was changed with or without a CDK4/6 inhibitor (abemaciclib) and cultured for up to 72 hours. We monitored the drug's efficacy through flow cytometry and cell counting. Abemaciclib suppressed cell proliferation and cell cycle in G0G1 phase in the treated cells compared with the control. The results were similar in both receptor-positive and triple-negative breast cancer cell lines. The effect of abemaciclib was dose-dependent, and reversible at least 48 hours after drug withdrawal, suggesting an opportune time for administering chemotherapy. Future research will delve into investigating the efficacy of sequential treatment with chemotherapy after CDK 4/6 inhibitor withdrawal, utilizing 2D and 3D culture systems.

#5723 Selectivity profiling of small molecule kinesin inhibitors using microplate-based ATPase activity assay.

B. P. Lee, S. Oh, K. Y. Horiuchi, **S. F. AbdulSalam**;
Reaction Biology Corporation, Malvern, PA

Kinesin superfamily proteins (KIFs) are a large family of molecular motor proteins, that share a highly conserved motor domain. KIFs play an important role in cell division and transport of vesicles and organelles within cells. Mitotic kinesins hydrolyze ATP through its ATPase activity to move along the spindle microtubules and carry out several functions during mitosis to facilitate precise chromosome segregation. Altered expressions of several kinesins are shown in various cancers, fueling the aggressive nature of cancers leading to genomic instability. KIF11/Eg5 overexpression is shown in various cancers including hepatic carcinoma, lung, prostate, colorectal, gastric, and pancreatic cancers. Small molecule inhibitors of KIF11/Eg5 and CENP-E are shown to result in mitotic arrest leading to apoptosis in tumor cell lines. Despite the poor clinical outcome of several Eg5 and CENP-E inhibitors entered in clinical trials, targeting kinesins remains an attractive anti-cancer therapeutic approach. Recently, an inhibitor of KIF18A has entered clinical trial for treatment of solid tumors with high chromosomal instability. Here we show development of a microplate based biochemical screening assays for a panel of kinesin motor domain proteins. We summarize kinetic characterization of kinesin proteins and study the selectivity of various previously reported KIF18A, Eg5, CENP-E inhibitors across a kinesin selectivity panel.

#5724 Preclinical evaluation of a novel CHK1 inhibitor encapsulated within the liposome, SMP-3124, for the treatment of solid cancer.

Yuka Kumagai[1], Ryosaku Inagaki[1], Kana Shimizu[1], Wataru Hirose[2], Naoaki Shimada[2], Kento Hayashi[2], Yoshiko Fukuoka[2], Makoto Matsuoka[2], Seiji Kamioka[2], Hitoshi Ban[2], Hiroki Umehara[1], Yusuke Sawayama[2]

[1]Cancer Reseach Unit, Sumitomo Pharma Co., Ltd, Osaka, Japan, [2]Sumitomo Pharma Co., Ltd, Osaka, Japan

Checkpoint kinase 1 (CHK1) is a serine/threonine kinase which plays a critical role for DNA damage responses (DDR) throughout the cell cycle in human cells. CHK1 is mainly activated by replication stress resulting in single-stranded DNA breaks induced by chemotherapeutic agents or mutations in DNA repair related genes. These kinds of stresses are reported to increase the dependency on DDR pathway molecule including CHK1. Therefore, targeting CHK1 is promising strategy for drug discovery. In fact, CHK1 inhibition induces S phase arrest and inhibits cell growth in wide range of cancer cell lines. Recently, a number of drugs in this pathway are tested in clinical trials. Although some of them showed obvious clinical responses in both monotherapy and combination therapy, their efficacies are limited because of their toxicities. To maximize the efficacy, we utilized CHK1 inhibitor with liposomal formulation which changes drug distribution to achieve longer drug retention in plasma and accumulation in tumor. Here, we generated SMP-3124, a novel and selective CHK1 inhibitor encapsulated within the liposome. SMP-3124 showed durable pharmacodynamic response due to the liposomal accumulation in the tumor in xenograft model. We confirmed potent anti-tumor activities of SMP-3124 in multiple subcutaneous xenografted models without severe side effects. In addition, SMP-3124 showed prolonged overall survival in both peritoneal dissemination and orthotopic model using human ovarian cancer cells. SMP-3124 synergistically inhibited tumor growth in combination with gemcitabine without additional hematological toxicities induced by gemcitabine. We are planning to an investigational new drug application in 2024.

#5725 Aurkin-A, a TPX2-Aurora A inhibitor disrupts alisertib-induced polyploidy in HG-diffuse large B cell lymphoma.

P. J. Conway III, B. De la Pena Avalos, J. Dao, S. Montagnino, D. Kovalskyy, E. Dray, D. Mahadevan;
UT Health Science Center at San Antonio, San Antonio, TX

Chemotherapy induced polyploidy (CIP) is a mechanism of inherited drug resistance resulting in an aggressive disease course in cancer patients. Alisertib, an Aurora Kinase A (AK-A) ATP site inhibitor, induces cell cycle disruption resulting in polyaneuploidy in high-grade (MYC and BCL2 amplified or expressed) Diffuse Large B Cell Lymphoma (HG-DLBCL). Propidium Iodide cycle flow cytometry was utilized to quantify alisertib induced polyploidy in U2932 and VAL cell lines. In U2932 cells, 1μM alisertib generated 8n+ polyploidy in 48% of the total cell population after five days of treatment. Addition of Aurkin A an AK-A/TPX2 site inhibitor, disrupted alisertib induced polyploidy in a dose-dependent manner with associated increased apoptosis in DLBCL cells. Combination of Aurkin A plus alisertib significantly reduced polyploidy and sensitized DLBCL cells to alisertib. The sensitization of alisertib with Aurkin A through complete AK-A inhibition is of high clinical importance as the alisertib dose can be significantly reduced while preventing polyploidy, enhancing efficacy, and significantly reducing toxicity to normal tissue. In clinical trials of alisertib in lymphoma, a maximum tolerated dose of 1.5μM was achieved. In U2932 cells, we found the addition of 100μM Aurkin A reduced the alisertib IC_{50} from 983nM to 34nM. We generated a stable FUCCI U2932 cell line expressing Geminin-clover (S/G2/M) and cdt1-mKO (G1), to help monitor cell cycle progression in live cells. Using this system, we identified alisertib-induced polyploidy through endomitosis, which was eliminated with Aurkin A treatment. In a VAL cell line mouse xenograft model, we show polyploidy generation in alisertib treated mice versus vehicle control or Aurkin A. Aurkin A plus alisertib significantly reduced polyploidy and tumor growth compared to vehicle control or Aurkin A levels. Finally, we performed Data-Independent Acquisition Mass Spectrometry on alisertib, Aurkin A, and combination alisertib/Aurkin A treated U2932 cells to identify therapy induced proteomic changes. This proteomic analysis has provided insight into the mechanism of alisertib polyploidy induction and the protective mechanism of within the combination therapy. Our in vitro and in vivo studies show that Aurkin A synergizes with alisertib and significantly decreases the alisertib dose needed to disrupt polyploidy while increasing apoptosis in HG-DLBCL cells.

#5726 The potential anti-cancer activity of dual TTK/PLK1 inhibitor, BAL0891, in bladder cancer.

J. Park[1], J.-e. Lee[1], M. Lee[1], J. Kim[1], W. Jang[1], J. Lee[2], J. Lee[2], M. Kang[2], W. Ham[1];

[1]Yonsei University College of Medicine, Seoul, Korea, Republic of, [2]SillaJen Inc., Seoul, Korea, Republic of

Background: BAL0891 is a novel dual inhibitor of threonine tyrosine kinase (TTK) and polo-like kinase 1 (PLK1) which affects mitotic spindle assembly checkpoint integrity resulting in aberrant mitotic progression of cancer cells. Since unlike other organs, bladder urothelium is highly regenerative in certain circumstances, there are high chances of cell cycle inhibitors to have anti-cancer activity over bladder cancer. In this study, we investigated the therapeutic potential of BAL0891 in bladder cancer compared to single TTK or PLK1 inhibitor and discovered the best therapeutic combination partner for BAL0891.
Methods: We performed meta-analysis of the mRNA expression levels of bladder cancer using Gene Expression Profiling Interactive Analysis 2 (GEPIA2). Representative bladder cancer cell lines (253J, 253J-BV, J82, RT4, T24, J82, HT1197, and HT1376) were treated with the dual protein kinase inhibitors, BAL0891, in comparison with TTK inhibitor (BAY1217389) or PLK1 inhibitor (onvansertib). BAL0891 was combined with CDK4/6 inhibitor, another cell cycle inhibitor working at different point from BAL0891. Cell viability was assessed using CCK-8 assay during 72 hours after treatment. Expression levels of TTK and PLK1 were measured by immunoblotting. Cell cycle analysis and cell apoptosis detection were performed on T24 cell.
Results: The mRNA expression levels of both TTK (16.7 times) and PLK1 (10.0 times) were significantly upregulated only in bladder cancers compared to normal bladder tissues (P<0.05). Compared to TTK or PLK1 inhibitor, BAL0891 was sensitive in 75% of bladder cancer cell lines (IC50 <0.1 uM) and significantly reduced proliferation of bladder cancer cell lines depending on the dosage. TTK and PLK1 expression levels of cancer cells were associated with the sensitivity to BAL0891. BAL0891 significantly induced necrosis and increased in polyploidy and G2/M arrest in T24 cell. The anti-cancer activity of BAL0891 was further enhanced in certain cell lines (RT4, and J82) by combination of CDK4/6 inhibitor.
Conclusion: This is the first study to suggest the potent anti-cancer activity of BAL0891 in bladder cancer. BAL0891 effectively worked on bladder cancer by two tracks which not only induced G2/M arrest but also increased in polyploidy. Furthermore, BAL0891 in combination with CDK4/6 inhibitor promoted anti-cancer effects. Lastly, this study suggests the use of TTK and PLK1 as the predictive biomarker for BAL0891. These data support further investigation of BAL0891 for the treatment of bladder cancer patients.

#5727 ISM9682A, a novel and potent KIF18A inhibitor, shows robust antitumor effects against chromosomally unstable cancers.

J. Zhang[1], F. Gao[1], W. Zhu[1], C. Xu[1], X. Ding[1], J. Shang[1], J. Qiao[1], S. Chen[1], X. Cai[1], X. Ding[1], S. Bavadekar[1], **S. Rao**[2], M. Zhang[1], F. Ren[1], A. Zhavoronkov[1]; [1]Insilico Medicine, Pu Dong Xin Qu, China, [2]Insilico Medicine, New York, NY

KIF18A belongs to the kinesin-8 subfamily and is a plus-end-directed motor, which regulates kinetochore microtubules dynamics to control mitotic chromosome alignment and spindle tension. Studies have shown that genetic depletion or pharmacological inhibition of KIF18A is a promising therapeutic approach for cancers, exhibiting high chromosomal instability (CIN-high), without having a significant impact on the normal division of euploid cells. Here, we report the discovery and preclinical evaluation of ISM9682A, a novel KIF18A inhibitor with excellent potency and high selectivity. ISM9682A is a potent KIF18A inhibitor with a single-digit nanomolar IC_{50} value and exhibits high selectivity over other kinesin family members. In addition, ISM9682A demonstrated excellent monotherapy anti-proliferative activity, with single-digit nanomolar IC_{50} values, in high-grade serous ovarian carcinoma (HGSOC) as well as in triple-negative breast cancer (TNBC) aneuploid cell lines with p53 mutation. Notably, ISM9682A exhibited a prolonged drug-target residence time indicated by both enzymatic and cellular assays. Consistent with the *in vitro* findings, ISM9682A displayed significant anti-tumor efficacy with a robust pharmacodynamic response (pH3, mitotic marker; γH2AX, DNA damage marker) in OVCAR3 and HCC1806 CDX models in a dose-dependent manner. In addition to its robust biological potency and high selectivity, ISM9682A exhibits favorable drug-like properties, including desirable *in vitro* ADMET characteristics and excellent *in vivo* exposure, clearance, as well as good oral bioavailability across multiple preclinical species. Collectively, these findings highlight the potential of ISM9682A as a novel and highly potent KIF18A inhibitor for the treatment of CIN-high cancers.

#5728 YB1 is a novel therapeutic for the treatment of triple negative breast cancer tumors.

W. Wang[1], L. Khalki[1], N. Zai[1], J. Szpendyk[2], A. Alkrekshi[2], B. Su[3], K. Sossey-Alaoui[1];
[1]Case Western Reserve University School of Medicine, Cleveland, OH, [2]MetroHealth System, Cleveland, OH, [3]Cleveland State University, Cleveland, OH

Metastatic breast cancer (BC) is the 2nd leading cause of death in women in the US, annually accounting for more than 43,000 deaths and 281,000 new cases of invasive BC. Amongst genetically distinct BC subtypes, those classified as being “triple-negative” (TNBC) are especially devastating due to their highly metastatic behavior, their propensity to recur rapidly, and their low response to standard-of-care therapies. In fact, the acquisition of chemoresistant phenotypes represents the main cause of disease recurrence, metastasis, and death in TNBC patients. Currently, the molecular mechanisms that regulate TNBC progression and metastasis remain unknown, as does the way these metastatic tumors acquire resistance to standard-of-care therapies. We recently established YB1 as a novel driver of these deadly TNBC activities, doing so by stimulating the cancer stem cell phenotype, and by disrupting normal cell cycle progression, therefore promoting therapy resistance and metastasis of TNBC tumors. YB1 is a multifunctional protein that acts as a transcription factor of cancer stem cell genes Nanog, Oct and Sox. Moreover, aberrant activation of YB1 contributes to the metastatic progression of several cancers, including TNBC. Our investigations revealed a major role of YB1 in the regulation of several hallmarks of cancer that drive TNBC tumors progression and metastasis, both in vitro and in preclinical mouse models of TNBC tumors. In extending these discoveries, we now show that aberrant YB1 expression activates oncogenic signaling leading to the dysregulation of cell cycle progression through the regulation of the Cyclin D/CDK4/6 complex signaling and the RB pathway. We also report the identification of a novel small molecule inhibitor, SU056, that specifically targets YB1 and inhibits its oncogenic activity in TNBC cell lines. We further show that the SU056-mediated inhibition of YB1, either as monotherapy or in combination with the CDK4/6 inhibitors, has a significant impact on inhibiting TNBC tumor progression and metastasis. In fact, the SU056-CDK4/6 inhibitors combination showed a synergistic effect when compared to monotherapy, at the same time reducing the toxicity associated with CDK4/6 inhibitors. Mechanistically, our studies revealed that genetic or pharmacologic targeting of YB1 inhibits TNBC tumor progression and metastasis through the regulation cyclin D-CDK4/6-RB pathway and blockade of cell cycle progression. Together, our data support the notion that targeting YB1 represents a potential therapeutic option for the treatment of TNBC, which could be enhanced when combined with standard of care treatment modalities.

#5729 ADCK1 inhibition alters cell proliferation and cell cycle progression in liver cancer cells.

N. A. Jacquet, Y. Zhao;
LSU Health Sciences Center - Shreveport, Shreveport, LA

In 2020, there were over 830,000 reported liver cancer deaths. Incidence rates of liver cancer have tripled, and death rates have doubled since the 1980s; giving this disease one of the highest mortality rates when compared to its incidence rate. Hepatocellular carcinoma (HCC) is derived from hepatocytes and is the main type of liver cancer in adults, accounting for 75-85% of all primary liver cancers. Current treatment options for HCC like radiation therapy and chemotherapy are imperfect and cause significant side effects. Tumorigenesis is dependent on an organism's cellular metabolism. Metabolic reprogramming is a promising area of focus for cancer therapeutics. Cancer cells thrive in nutrient-deficient environments by hijacking and reprogramming the cells existing cellular metabolism. Metabolic reprogramming is driven by genetic alterations and environmental cues. AarF Domain Containing Kinase 1 (ADCK1) is a protein-coding gene that acts as a mitochondrial protein with putative kinase activity. The role of ADCK1 has not been well studied, particularly in liver cancer. Our group has sought to study how ADCK1 impacts the metabolism and cellular environment of HCC cells to help establish a more effective drug target. Bioinformatics performed by our lab report that ADCK1 was highly expressed in HCC tumor cells. The expression levels of ADCK1 were also correlated with a decrease in patient survival. ADCK1 knockout clones were generated; these knockout cells showed decreased proliferation and altered cell cycle progression. Proteomics analysis demonstrated that loss of ADCK1 was also seen to alter the expression of proteins involved in several cellular processes related to the cell cycle and cellular metabolism. How ADCK1 regulates these processes will be studied in the future.

#5730 Targeting the cell cycle with AZD8421, a potent and highly selective CDK2 inhibitor.

C. R. Denz[1], M. Grondine[1], J. Fan[1], J.-R. Hsu[1], A. Jackson[2], J. Robinson[2], G. Guo[1], W. Li[1], Y. Wang[1], M. San Martin[1], L. Prickett[1], J. Johannes[1], A. Ghosh[1], D. Sudhan[1], C. Vasalou[1], R. Richards[1], K. Beaumont[1], M. Peters[1], L. Drew[1], S. Fawell[1], **F. W. Goldberg**[1];

[1]AstraZeneca Pharmaceuticals LP, Waltham, MA, [2]AstraZeneca Pharmaceuticals LP, Cambridge, United Kingdom

Cyclin-dependent Kinase 2 (CDK2) is a Ser/Thr kinase activated via interaction with its cyclin partners CCNE and CCNA, driving G1/S progression of the cell cycle. CDK2 inhibition has the potential to address multiple resistance mechanisms to CDK4/6 inhibitors in breast cancer. In addition, CCNE1 is frequently amplified and over-expressed in cancers including ovarian, uterine, breast, gastric and others, with pre-clinical data linking CDK2 inhibition sensitivity to high CCNE1. The CDK2 inhibitor field has historically suffered from high attrition in Phase I due to off-target toxicity. AZD8421 is a uniquely selective CDK2 inhibitor, that offers potential to show improved therapeutic index and combinability. As well as achieving CDK family selectivity in cells versus key off-targets (CDK1, CDK4/6, CDK9), AZD8421 had no significant kinase inhibition outside the CDK family. Only 7 distinct targets showed greater than 50% inhibition in a panel of 403 kinases when screened with 1µM of AZD8421. In nanoBRET assays measuring cellular target engagement, AZD8421 had an IC50 against CDK2 of 9nM with selectivity over CDK1, CDK4 and CDK6. In vitro cellular assays demonstrated that AZD8421 inhibits endogenous phospho-substrate at 58nM with >327-fold selectivity over CDK9 phospho-substrate pSer2 of RNAPII (>19.2 µM). In a CCNE1 amplified cell line, AZD8421 potently inhibited cell proliferation (69nM, OVCAR3), correlated with inhibition of pRB, arrest in G1/S phase of the cell cycle and induction of senescence, compared to a CCNE1 non-amplified cell line (SKOV3) with IC50 of 2.05 µM. In vitro combination assays in CDK4/6 inhibitor resistant breast cancer cell lines showed combination benefit with AZD8421 plus approved CDK4/6 inhibitors. In vivo, AZD8421 potently suppressed phosphorylation of Rb, and demonstrated robust monotherapy and CDK4/6i combination activity in breast and ovarian in vivo models. In vivo PD marker suppression and efficacy was demonstrated in CDK4/6 inhibitor resistant breast PDXs in combination with palbociclib (CDK4/6i). AZD8421 showed robust monotherapy activity in a CCNE1 amplified ovarian model OVCAR3 with regressions seen with monotherapy and in combination with palbociclib. Monotherapy activity and combination benefit in vivo with standard of care agents was also observed in ovarian PDX models with elevated levels of CCNE1. AZD8421 is a potent and highly selective CDK2 inhibitor, with double digit nM potency in cells, as well as suitable physical and pharmacokinetic properties for progression into the clinic.

CHEMISTRY: Drug Delivery
Poster Session

#5733 Development of a topoisomerase 1 inhibitor platform technology for efficacious and well tolerated ADCs.
R. Lyski, L. Bou, J. Sigurjonsson, D. Meyer, C. Neace, D. Ortiz, K. Snead, K. Smith, S. Jin, N. Stevens, J. Cochran, K. Alizadeh, N. Yeddula, E. McKinney, A. Peterson, L. Dotloe, J. Simmons, C. Carosino, K. Emmerton, N. Everds, S. Jeffrey, P. Senter;
Seagen Inc., Bothell, WA

Topoisomerase 1 (TOP1) inhibitors are a class of cytotoxic small molecules that have demonstrated effectiveness as therapeutic agents in cancer. However, the broad clinical application has been hindered by poor pharmacokinetic profiles and off-target toxicities. Antibody-drug conjugates (ADCs) enable the targeted delivery of cytotoxic payloads by specifically targeting cell-surface antigens expressed on cancers reducing systemic exposure and toxicity. TOP1-ADCs have received FDA approval for HER2- (trastuzumab-deruxtecan) and Trop2- (sacituzumab-govitecan) expressing solid tumors, demonstrating the promise for this drug class to improve the lives of patients. We have developed a novel drug-linker using a potent TOP1 inhibitor with desirable ADME properties, and a hydrophilic glycoside linker as a platform technology enabling ADCs with favorable physicochemical and biological properties. The TOP1 inhibitor payload was optimized for potency, with reduced P-glycoprotein efflux and enhanced permeability. The hydrophilicity of the linker facilitates the development of highly loaded ADCs (8 drugs/mAb) with high plasma stability, low aggregation, and pharmacokinetics similar to parental antibody. The resultant ADCs are potent and immunologically specific with activity in multidrug-resistant tumor models and bystander activity in heterogenous antigen models. Human cancer cell derived xenograft models demonstrated potent and specific ADC anti-tumor activity with several targets and indications. Improved activity was observed compared to corresponding govitecan- and deruxtecan-based ADCs. ADCs prepared from this drug-linker technology were well tolerated in rats after repeat administration of 60 mg/kg every 4 days for 4 doses. The excellent anti-tumor activity in several models and favorable safety profile demonstrates this platform TOP1 drug-linker technology has the potential for development as ADCs against many cancer targets.

#5734 Polymeric delivery with dual drug payloads for hepatocellular carcinoma (HCC) therapy.

L. Dai[1], G. Zhang[2], F. Dagher[1], A. Li[1], A. Gholizadeh[1], C. Li[2], D.-. Chow[1];

[1]University of Houston, Houston, TX, [2]University of Texas MD Anderson Cancer Center, Houston, TX

Background: The long-term survival of hepatocellular carcinoma (HCC) patients is hampered by high recurrence and drug resistance. Targeting sonic hedgehog (SHH) pathways can overcome drug resistance in HCC. In this study, we co-loaded SHH inhibitor, cyclopamine (CPA) and paclitaxel (PTX) in a novel polymeric nanomicellar drug delivery system (M-CPA/PTX), to overcome the drug resistance in HCC tumor models.

Method: The combinational effect *in vitro* was studied by treating HCC with CPA and PTX. The combinational index was calculated using CalcuSyn Biosoft software to determine the additive or synergistic effect of the combination. Three formulations (F0, F5, and F16) were selected for further testing based on formulation optimization using central composition design (CCD). The storage stability of M-CPA/PTXs at room temperature and 4 °C was evaluated by measuring the changes in micelle size, PDI, and encapsulation efficiency (EE) over pre-determined periods. In the pharmacokinetics (PK) study, nude mice were IP-injected with 5 mg/kg of PTX equivalent F0 and F16. Additionally, the toxicity of F0 was investigated using healthy Sprague Dawley rats, in which rats were intravenously injected with a single F0 dose of 1, 2, and 4 mg/kg/drug of M-CPA/PTX.

Results: Combinational effect study suggested that CPA and PTX, demonstrated synergistic effect in Hep3B and HepG2 cells compared to the mono-treatment, thus overcoming resistance. F0, F5, and F16 exhibited particle sizes of 75.27 ± 1.06, 54.63 ± 0.85, and 70.63 ± 3.39 nm, respectively. The release kinetics of both drugs from these micelles displayed significantly slow-release profiles from the micelles, with less than 10% cumulative release within 24 hours in plasma. The stability study indicated that both drugs' micelle size and EE were not appreciably changed over 6 weeks at room temperature and 4 °C. Notably, the biodistribution studies showed that F16 achieved significantly greater accumulations of CPA in the liver, kidney, and spleen compared to F0 ($P < 0.05$). Additionally, the maximal tolerable dose of F0 in rats was 4 mg/kg/drug for the M-CPA/PTX combination, which did not result in treatment-related mortality.

Conclusion: The combination of CPA and PTX offered promising synergistic effects on HCC treatment. F0, F5, and F16 were developed and characterized with the desired physicochemical properties and demonstrated controlled release characteristics for both payloads, suggesting their potential for sustained drug delivery in HCC therapy. Enhanced liver accumulation of F16 suggested favorable biodistribution for the site of action. Lastly, the safe toxicity profile supports the first choice of F0 among other lead candidates for further pre-clinical efficacy studies.

#5735 Efficient and safe delivery of doxorubicin by DNA fragments: A full preclinical study.

M. Park[1], Y. Kim[1], H. Cho[1], S. Mohammad[2], Y. Choi[2], H. Lee[1], S. Lee[1], E. Cedrone[3], B. Neun[3], M. Dobrovolskaia[3], D. Fruman[2], J. Kim[1], Y. Kwon[2]; [1]Pharma Research.Co., Ltd., Seongnam-si, Korea, Republic of, [2]University of California, Irvine, Irvine, CA, [3]National Cancer Institute, Frederick, MD

The clinical uses of anthracyclines (e.g., doxorubicin) are hampered especially by dose-dependent cardiac toxicity, resulting in a narrow therapeutic window. Doxorubicin formulations have marginally improved its therapeutic efficacy while suffering from difficult and costly manufacturing, poor characterization and quality control, limited scalability in production, and disappointingly low drug loading. This study employs DNA fragments extracted from the salmon sperm cells, which is known for high biocompatibility in various biomedical application, to self-assemble via intercalation by doxorubicin. DNA/DOX nanocomplexes are easy in manufacturing, high scalability, straightforward characterization and quantification, and efficiency in drug loading. Doxorubicin and DNA fragments were dissolved in water and mixed at the optimized 1:6 weight ratio, followed by stirring and incubation for 30 min. DNA/DOX nanocomplexes were characterized for doxorubicin loading and release, size, surface charge, and morphology by UV/fluorescence spectroscopy, stable isotope tracer ultrafiltration assay (SITUA), dynamic light scattering particle analysis, and transmission electron microscopy. The anticancer efficacy of the DNA/DOX nanocomplexes were tested in vitro and in vivo using syngeneic and PDX tumor models. Along with PD/PK studies, DNA/DOX nanocomplexes were also evaluated for their systemic and cardiac toxicity. Characterization and quantification studies revealed DNA/DOX nanocomplexes to be relatively monodisperse with a size of 40 nm in diameter, efficient for drug encapsulation (~100%) and drug loading (14.3%, w/w), and stable for storage while readily releasing doxorubicin in a cell. The self-assembled nanocomplexes were formed when doxorubicin inter- and intra-molecularly chelated DNA fragments. DNA/DOX nanocomplexes were more efficient in killing cancer cells in vitro than both doxorubicin and the liposomal doxorubicin Doxil. PD/PK studies demonstrated that DNA/DOX nanocomplexes circulated longer with less accumulation in the heart than doxorubicin, which altogether lower toxicity. A repeated administration of the DNA/DOX nanocomplexes to Sprague-Dawley rats exhibited a substantially lower cardiotoxicity score than that of doxorubicin. The improved anti-tumor efficacy of the DNA/DOX nanocomplexes were finally confirmed using a syngeneic lymphoma mouse model and PDX mouse models of triple-negative breast and ovarian cancers. Complexing doxorubicin with DNA fragments addresses the current technological challenges in achieving an efficient and safe therapy for a broad range of cancers. DNA/DOX nanocomplexes are amenable to rigorous chemistry, manufacturing, and controls (CMC) evaluation with proven anti-cancer efficacy and improved safety profiles. Clinical trials on DNA/DOX nanocomplexes for cancer chemotherapy are warranted to fully validate their clinical utilities.

#5736 Sonochemical preparation of SP94 peptide-decorated pH-responsive biodegradable biopolyester nanoparticles for targeted therapy in hepatocellular carcinoma.

M. Wu[1], Q. Wang[1], Z. Gong[1], Z. Liu[1], H. Zheng[1], X. Chen[1], **C. Zhong**[2];
[1]Zhejiang University of Science and Technology, Hangzhou, China, [2]Westlake University, Hangzhou, China

Stimulation in response to nanoparticles responding to endogenous stimuli in the tumor microenvironment has been extensively studied for the release of chemotherapeutic drug. Therefore, we aimed to develop a biocompatible delivery of taxol (TAX) delivery vector system for the treatment of hepatocellular carcinoma (HCC). A basic backbone, TAX loaded poly (3-hydroxybutyrate-co-3-hydroxyvalerate) PHBV nanoparticle (PHBV-TAX-NPs), were designed and prepared via sonochemical method. The pH-responsive shell of PHBV-TAX-NPs was formed by oxidative self-polymerization of dopamine (PDA) in an alkaline environment. The HCC-targeted peptide SP94 binds to PDA-coated nanoparticles (NPs) through the Michael reaction. Moreover, the nanoparticle surface-grafted SP94 peptide serve as a specific ligand for targeting HCC. The chemical structures and properties of these nanoparticles were characterized by transmission electron microscope, dynamic light scattering-autosizer, differential scanning calorimetry, fourier transform infrared spectroscopy, X-ray photoelectron spectroscopy and thermogravimetry. As expected, excellent targeting of these SP94-PDA-PHBV-TAX-NPs was demonstrated by cellular uptake and cytotoxicity experiments in HCC cells. Compared with that of free TAX, the SP94-PDA-PHBV-TAX-NPs showed more superior antitumor efficacy in the xenograft mouse model. Notably, the SP94-PDA-PHBV-TAX-NPs were except for their potent anticancer activity, it was less toxic *in vitro* and *in vivo* compared to TAX in mice. These studies suggest the potential beneficial use of SP94-PDA-PHBV-TAX-NPs in future HCC-targeted therapy with drug-loaded nanocarriers.

#5737 Enhancing cancer treatment Via a nanostructured chemoimmunotherapy gel facilitating interleukin-2 delivery and immunogenic cell death induction.

H. Mu[1], Y.-N. Ta[1], J. M. Tham[2], F.-F. Hsu[3], Y.-C. Lin[1], H.-C. Huang[1], Y.-C. Sung[1], C.-I. Huang[1], C.-L. Wu[1], C.-H. Chang[1], S. Yang[1], T.-Y. Lee[1], J. Wang[1], D. Duda[4], Y. Boucher[4], J.-H. Huang[1], W. Ang[2], Y. Chen[1];

[1]National Tsing Hua University, Hsinchu City, Taiwan, [2]National University of Singapore, Singapore, Singapore, [3]Academia Sinica, Taipei, Taiwan, [4]Massachusetts General Hospital and Harvard Medical School, Boston, MA

Background: The landscape of immunotherapy, employing recombinant cytokines like interleukin-2 (IL-2), confronts challenges marked by its short half-life, systemic toxicity, and constrained tumor accumulation. These hurdles are particularly evident in the context of the immunosuppressive milieu characterizing pancreatic ductal adenocarcinoma (PDAC). Chemo-immuno-therapeutic synergies, notably those provoking immunogenic cell death (ICD), have demonstrated superior efficacy. This investigation delves into Pt-NHC as a type II ICD inducer to surmount immunosuppression and amplify antitumor immunity within a highly tumor-accumulated liposomal drug delivery system. Additionally, the co-administration of the angiotensin receptor blocker, losartan, mitigates desmoplasia in PDAC, further augmenting the efficacy of immunotherapy.

Methods: To address the constraints of IL-2, a lipid-coated nanogel, IL2-Pt@Nanogel, was innovated, amalgamating silk fibroin-loaded IL-2 with Pt-NHC. The nanogel aimed to enhance IL-2 pharmacokinetics and optimize tumor targeting. Concurrently, losartan was employed to alleviate desmoplasia within the tumor microenvironment.

Result: The chemoimmunotherapy nanogel, when coupled with losartan, showcased therapeutic potential in murine models of desmoplastic PDAC. Pt-NHC induced ER-localized reactive oxygen species (ROS) and DAMP release, reshaping the immunosuppressive microenvironment by repolarizing M2-type macrophages to M1 and diminishing the regulatory T-cell population. Co-delivery of IL-2 and Pt-NHC in the nanogel enhanced T-cell infiltration and activation, curbing tumor progression in primary and liver metastasized PDAC models. Importantly, the addition of losartan reduced collagen accumulation within tumors, resulting in heightened infiltration of effector T cells and more pronounced suppression of tumor growth in PDAC and metastasized liver.

Conclusion: This study introduces an innovative nanogel delivery system (IL2-Pt@Nanogel) for chemoimmunotherapy, effectively addressing the challenges associated with IL-2 therapy. Leveraging the enhanced permeability and retention (EPR) effect, the nanogel improves IL-2 stability and tumor delivery. Pt-NHC incorporation induces ICD, reshaping the tumor microenvironment, and in synergy with losartan, elicits robust anticancer immunity. This strategy holds promise for clinical translation as a secure and efficient treatment for immunosuppressive and desmoplastic cancers, such as PDAC, presenting a distinctive therapeutic avenue.

#5738 Repurposing disulfiram for cancer: A drug delivery and population-based approach.

D. Heroux, A. W. Y. Leung, R. Gilabert-Oriol, M. B. Bally;
BC Cancer Research Institute, Vancouver, BC, Canada

Purpose: Disulfiram was approved by the FDA for treatment of alcohol abuse in 1951, although for over 40 years there has been evidence supporting disulfiram's use as an anti-cancer drug. Upon administration, disulfiram is hydrolyzed to form two molecules of DDC, which upon binding Cu forms $Cu(DDC)_2$, the proposed active form against cancer. It was our goal to formulate the water-insoluble $Cu(DDC)_2$ in liposomes to facilitate its repurposing for breast and colon cancers. In addition, we also initiated an ongoing population-based study assessing the protective and treatment effects of disulfiram with cancer.
Methods: $Cu(DDC)_2$ liposomes were generated by the thin-film hydration method followed by extrusion, using DSPC and cholesterol (55:45 molar ratio). DDC and $CuSO_4$ were added to the liposomes forming $Cu(DDC)_2$, which was transported inside the liposomes. Anti-tumor activity was evaluated in tumor-bearing mice with or without competent immune systems, and immune system activation was assessed via a cancer vaccination model and the expression of markers of immunogenic cell death (ICD). A study was also initiated for cancer cases and controls in British Columbia (BC Cancer) with at least one prescription of disulfiram from 1996-2022 (PharmaNET), patients treated with immune-modulating therapies (BC Cancer), and outcome of death (Vital Statistics).
Results: Liposomes encapsulating $Cu(DDC)_2$ had a size of 100 nm and polydispersity of 0.1, and caused a 40% reduction in tumor burden in a MDA-MB-231 xenograft model. In a syngeneic tumor model of breast cancer the response with immune-competent mice was greater than mice lacking immune function, and a cancer vaccination model and the presence of ATP, HMBG1 and surface-exposed calreticulin indicated the presence of ICD.
Conclusions: $Cu(DDC)_2$ was formulated in liposomes facilitating its parenteral administration, and its anti-cancer activity was found to be due in part to activation of the adaptive immune system through ICD. A case-control study is currently being employed to examine the clinical potential of disulfiram, as a protectant and as an adjuvant with immune-activating therapies such as checkpoint inhibitors and anthracyclines to potentially improve efficacy through induction of ICD.

#5740 Peptide-functionalized dendrimers for enhanced binding to immune checkpoint proteins.

P. A. Rawding[1], F. Coppola[2], D. Kim[1], M. Poellmann[1], D. Wheeler[1], P. Kral[2], S. Hong[1];
[1]University of Wisconsin-Madison, Madison, WI, [2]University of Illinois at Chicago, Chicago, IL

The human immune system has complex and dynamic mechanisms to distinguish and eliminate malignant cells and defend the body against cancer. Various therapeutic approaches to stimulate the immune system have thus been investigated, demonstrating strong anti-tumor immune responses capable of controlling metastasis and preventing recurrence. Nevertheless, existing cancer immunotherapies suffer from several limitations, including inconsistent benefits across cancer types and patients. In recent years, the utilization of peptides for immunotherapy has attracted a great deal of interest due to their ability to mimic protein functionalities while maintaining a high degree of modularity and synthetic reproducibility in their molecular design. However, the clinical translation of otherwise promising peptide-based immunotherapeutics has been hindered due to their significantly weaker binding to target proteins and short half-life in plasma circulation in comparison to their monoclonal antibody counterparts. Nevertheless, these issues can potentially be addressed by conjugation to nanoparticles, which enhances cell binding/uptake and prolongs circulation. To this end, our group has extensively investigated the use of poly(amidoamine) (PAMAM) dendrimers to improve the therapeutic utility of peptides. These dendrimers can facilitate the simultaneous binding of conjugated peptides to multiple cell receptors, resulting in a significantly enhanced binding interaction through the multivalent binding effect. Here, we report an efficient de novo nanoparticle design strategy that combines organic synthesis, phage display, and molecular dynamics to identify a novel immuno-oncology therapeutic modality. We first employed phage display to identify several highly selective sequences that bind to the mouse ortholog of TIGIT—an inhibitory receptor expressed on lymphocytes that has been identified as a potential therapeutic target to enhance anti-tumor immune responses. Subsequent computational modeling (NAMD with CHARMM force field) revealed several conserved regions of interaction that we hypothesize drive favorable binding interactions and enhance the binding affinity of the peptide inhibitors. We next incorporated experimental kinetic measurements of the identified sequences with adaptive evolution computational modeling to identify optimized mutant analogs for dendrimer conjugation. It was found that the TIGIT targeting DPCs (dendrimer-peptide conjugates) demonstrated increased binding avidity *in vitro* and anti-tumor efficacy *in vivo*, most notably when administered in combination with PD-L1 targeting DPCs to a syngeneic mouse model bearing mouse oral carcinoma (MOC1) tumors. Overall, this work demonstrates the potential of rational peptide design and our multi-functional DPC platform for the development of both effective and novel immuno-oncology therapeutics.

#5741 siteDAR, complete antibody drug conjugate, ADC characterization.

W. L. Martin, M. Senseney, B. Kusuma, J. Dugal-Tessier, **N. Jain**;
NJ Bio, Inc., Princeton, NJ

Antibody drug conjugate characterization currently extends to the global determination of the drug -to- antibody ratio (DAR). However, there can be confounding batch variability in pharmacological outcome from ADCs of the same drug, antibody, and DAR. Previously, DAR was obtained by quantifying the extent of modification of the intact antibody or its protein subunits. The coupling chemistry is used to infer which type of amino acids were modified but generally no specific sites of modification are identified and if identification is obtained, it is not quantitative. Borrowing the rigorously reproducible proteolytic digestion methods from multi-atribute mapping (MAM) used in monoclonal antibody manufacture, and compiling a comprehensive quantitative assignment of every abundant peptide in the ADC digest we can both calculate a DAR from the ion volume ratios and a quantitative map of the specific modified sites. This method, termed “siteDAR”, is applied here to both commercial Kadcyla® (ado-trastuzumab emtansine) and in-house preparations of ado-trastuzumab emtansine. We show that preparations of Kadcyla® with the same DAR can have significantly different quantitative maps of modification sites. We use siteDAR analysis in our ADC design cycle to characterize an ADC, and have developed an ADC synthesis method that was quantitatively verified, and had increased biosimilarity with commercially available Kadcyla®. siteDAR for commercial Kadcyla siteDAR for initial in-house Kadcyla Initial biosimilarity

#5742 Therapeutic efficacy of CA102N in pancreatic cancer.

L. Lin, S. Tu, **E. Tchaparian**;
Holy Stone Healthcare, Taipei, Taiwan

Pancreatic ductal adenocarcinoma (PDAC) is a challenging cancer to treat due to its aggressive nature and late-stage diagnosis. Considering the lack of effective therapies, there is an urgent need to develop new and effective therapeutics to improve the prognosis of patients. CA102N is a carrier-mediated novel anticancer product where hyaluronic acid is conjugated to Nimesulide-NH2. CA102N is currently under development for the treatment of solid tumors, including colorectal cancer. CA102N was safe and well tolerated in the first-in-human trial in patients with locally advanced or metastatic solid tumors. In the present study, the *in vitro* anticancer activity of CA102N was investigated in K-ras mutant PANC-1 pancreatic cancer cells. The antitumor efficacy was also tested *in vivo* in the PANC-1 mice model. Results demonstrated that CA102N inhibits cell growth, cell migration, angiogenesis, and cell proliferation in both K-ras mutant PANC-1 pancreatic cancer cells or tumors. Administration of CA102N in PANC-1 xenografts resulted in a dose-dependent and statistically significant decrease in tumor growth at 9.8 mg/kg and 14.7 mg/kg Nim equivalents, respectively, compared to the vehicle control group. A significant decrease (80%) in liver metastasis was also noted in the PANC-1 orthotopic mice model at 19.6 mg/kg Nim equivalents dose level. Mechanistically, CA102N was found to suppress the PI3k/Akt/mTOR and Raf/MEK/ERK signaling pathways, in addition to reducing the expressions of the N6-methyladenosine (m6A) reader and writer proteins, OCT3/4 transcription factor and RAS levels *in vivo*. CA102N also modified the tumor stroma and improved drug permeability *in vivo.* Based on this compelling data, CA102N shows promise as a potential treatment for pancreatic cancer. Combination therapies and regimens are currently being explored in *in vivo* models as a strategy for clinical development.

#5743 Liposome platform enables X-ray induced photodynamic therapy treatment against human triple negative breast cancer cells.

B. Yang[1], R. Sang[1], Y. Li[1], E. Goldys[1], **W. Deng**[2];
[1]University of New South Wales, Kensington, Australia, [2]University of Technology Sydney, Sydney, Australia

In this study, we employed X-ray induced photodynamic therapy (X-PDT) for the treatment on triple negative breast cancer (TNBC) cells. To do this, we rationally developed a liposome delivery system co-loaded with protoporphyrin IX (PPIX) and perfluorooctyl bromide (PFOB). Low-dose X-ray at 2Gy was employed to activate PPIX for reactive oxygen species (ROS) generation, and the co-loading of PFOB provided additional oxygen to augment ROS production. The highly toxic ROS triggered TNBC cell death. *In vitro* X-PDT effects including intracellular ROS generation, cytotoxicity, cell viability and apoptosis/necrosis assay in TNBC cells were studied. Our results indicate that the nanocarriers effectively induced X-PDT effect with very low dose radiation, which makes it possible to damage cancer cells. Our strategy may offer a paradigm-shifting treatment alternative for TNBC patients who need neoadjuvant radiotherapy but wish to avoid long term detrimental effect on functional outcome by undergoing X-PDT using only a fraction of the conventional radiotherapy.

#5745 Electrosprayed minocycline and temozolomide-loaded PLGA microparticles for the treatment of glioblastoma.

A. Rodriguez, J. Quintanilla, J. Amieva, M. A. Arriaga, S. Nievera, I. Davila, K. S. Martirosyan, S. Chew;
The University of Texas Rio Grande Valley, Brownsville, TX

Glioblastoma multiforme (GBM), the most common and aggressive form of malignant brain tumor, leads to poor prognoses with high rates of reoccurrence and low survival rates, therefore, it is vital to explore alternative treatments for GBM. Minocycline, a commonly used antibiotic and tetracycline derivative, has proven anti-angiogenic effects and the ability to inhibit tumor growth, making it an effective GBM treatment. Temozolomide is an alkylating antineoplastic agent and the current first-choice chemotherapy agent for GBM. Poly(lactic-co-glycolic acid) (PLGA) is widely used as a biomaterial for drug delivery due to its inert properties, great biocompatibility and versatility and has been approved by the FDA. Therefore, the objective of this project is to fabricate electrosprayed minocycline- and temozolomide-loaded PLGA microparticles with optimal morphology, drug loading, loading efficiency, and drug release kinetics for the treatment of GBM. The microparticles were fabricated by electrospraying vertically with a 2ml/hr flow rate, 14kV voltage, 20 cm distance for minocycline and a 10ml/hr flow rate, 10kV voltage, 10 cm distance for temozolomide with both collected on a copper/glass plate. The parameters that were investigated were the chamber humidity, duration of spraying, and the addition of polyethylene glycol (PEG), a hydrophilic polymer. To determine the microparticles' morphology, bright-field microscopy and scanning electron microscopy (SEM) were used. The absorbance measurements at 350 and 327 nm were used to determine drug loading, loading efficiency, and release kinetics for minocycline and temozolomide, respectively. Microparticles with low chamber humidity and duration of spraying were more spherical, less aggregated and easier to collect for both drugs. The addition of PEG to minocycline-loaded microparticles led to higher drug loading and loading efficiency (4.02% ± 0.34, 64.30% ± 5.47 vs. 3.23% ± 0.29, 49.40% ± 4.49) as the PEG helps the solubilization of minocycline. Using acetonitrile instead of dichloromethane as the solvent, increased drug loading and loading efficiency (4.72% ± 0.76, 70.77 ± 11.43 vs. 2.37% ± 0.27, 35.62% ± 4.09) for temozolomide-loaded microparticles as more temozolomide can be solubilized in acetonitrile. Drug release kinetics demonstrated a burst release of minocycline in the first hour (65.46%). To decrease the burst release, the microparticles can be incorporated into a scaffold or depot. Overall, electrospraying is a promising method to fabricate drug loaded PLGA microparticles with high drug loading, loading efficiency, and right morphology and we determined optimal parameters to successfully fabricate electrosprayed drug loaded PLGA microparticles in the micron size range with high drug loading and loading efficiency compared to the often-used emulsion solvent extraction/evaporation for microparticle fabrication.

#5746 Tris(4-methoxyphenyl) methanol conjugates of triptorelin as cell-penetrating anti-cancer prodrugs.

Ryan Beni, William Boadi, Jawzah Alnakhli, Samiyah Alhamed

Tennessee State University, Nashville, TN

Triptorelin® (TRP) is an anti-cancer drug used for the treatment of a wide range of hormone-responsive cancers, including prostate cancer. The increase in testosterone levels, known as the flare effect, is a major side effect of cancer chemotherapy when TRP is used in a combination regimen. Reports indicate that enhancing the cellular uptake and retention of TRP can improve its biological activity. In this study, TRP conjugates of tris(4-methoxyphenyl) methanol derivatives (TPMs) with optimized hydrophobicity were synthesized by reacting 2-substituted methoxybenzenes with 1,3,5-trioxane, followed by conjugation with TRP and sebacic acid to produce TRP-TPMs derivatives. The hydrophobicity of TRP was optimized by using the appropriate hydrophobic linker attached to the respective TPM to improve cellular uptake. The aim of the current studies was to evaluate the respective antiproliferative effects of the newly synthesized TRP-TPMs, physical mixtures of TPMs and TRP using different cell lines. Our hypothesis was that exposure of cells to TRP-TPMs derivatives can enhance the antiproliferative activities in cells in comparison to respective the physical mixtures and TRP. Antiproliferative studies in human acute lymphoblastic leukemia (CCRF-CEM), human ovarian adenocarcinoma (SK-OV-3), and mouse preadipocytes (3T3-L1) were carried out following exposure to the respective compounds. Our findings indicate that TRP-TPMs conjugates, at a concentration of 50 µM, significantly inhibited cell proliferation in CCRF-CEM, SK-OV-3, and 3T3-L1 cells by 21-37%, 24-73%, and 37-56%, respectively, following 72-hour incubation in comparison to the respective physical mixtures and TRP. Conjugation of TRP with the respective derivative of TPMs enhanced antiproliferative activities in all the cells (with no significant differences in cytotoxicity) compared to the physical mixtures of TPMs and TRP. The findings in the current studies suggest that TRP-TPMs can be used as potential prodrugs, to enhance the cells biological activity, and cellular uptake of TRP.

#5747 Microwave responsive thermosensitive lipid nanoparticles for spatiotemporal delivery of chemotherapeutics.

C. B. Aparicio-Lopez;
Kansas State University, Manhattan, KS

Pancreatic cancer is a highly lethal malignancy with an urge for the exploration of novel treatments. One promising approach is microwaved-induced hyperthermia, which has shown great antitumor and synergistic effects when combined with other therapies. The application of microwaves produces heat by dielectric hysteresis which depends on the dielectric properties of molecules. Ionic liquids (ILs) are compounds composed of ions with <100 °C melting point and have strong dielectric properties. In short, *we propose* the creation of microwave-sensitive nanoparticles using IL, enabling precise hyperthermia induction with low-powered microwaves in localized areas. To achieve this, we stabilize a core composed of 1-butyl-methylimidazolium bromide or 1-butyl-3-methylimidazolium hexafluorophosphate using Span 80, Tween 20, and Triton-X as surfactants, along with phosphatidylcholine lipids as “cosurfactants”. Employing a double emulsion procedure for fabrication, nanoparticles are characterized using dynamic light scattering, Fourier-transform infrared spectroscopy, and transmission electron microscopy. Furthermore, we assess microwave sensitivity by comparing thermal changes between liposomes loaded with 120 mM and 250 mM NaCl solutions. Subsequently, we evaluate biocompatibility and heat effects by incubating IL nanoparticles with BXPC3 and KPC cells, monitoring cell viability through MTT assays. We aim to confine the ILs within the nanoparticle core rather than incorporating them into the membrane. We anticipate increased microwave sensitivity, translating to reduced off-target effects and enhanced precision in hyperthermia treatment. This research holds promise for improving the therapeutic outcomes of pancreatic cancer treatment.

#5748 Inhibition of tumor growth using exosomes loaded with KRAS siRNA and surface-modified with tumor-targeted proapoptotic peptide.

L. Kang, S. Jeon, S. M. P. Vadevoo, S.-H. Kim, B. Lee;
Kyungpook National Univ. School of Med, Daegu, Korea, Republic of

Exosomes are extracellular vesicles naturally secreted by cells and serve as carriers of RNAs and proteins for cell-to-cell communications. KRAS is frequently mutated and plays a vital role in many tumors. Receptor expressed in lymphoid tissue (RELT), also known as tumor necrosis factor receptor superfamily 19-like, is upregulated in certain tumors such as lung and pancreatic tumors and is a potential tumor target. To selectively deliver cytotoxic agents to tumor, we loaded mesenchymal stem cell (MSC)-derived exosomes with a siRNA against KRAS and surface-modified them with the RELTpep-KLA peptide comprising a RELT-binding peptide (CRQTKN, named RELTpep) and proapoptotic peptide (KLAKLAKKLAKLAK, named KLA). Exosomes were isolated from cell culture medium using ultracentrifugation and transfected with the KRAS siRNA using a lipid-based reagent and then surfaced-modified with the RELTpep-KLA using a phospholipid-based membrane anchor. Compared with control peptide-KLA, RELTpep-KLA-targeted MSC-exosomes were more efficiently internalized into A549 lung tumor and Panc-1 pancreatic tumor cells expressing RELT on their surface and exhibited cytotoxicity to these tumor cells. RELTpep-KLA-targeted and KRAS siRNA-loaded MSC-exosomes reduced the phosphorylation of Erk and exhibited an enhanced cytotoxicity in A549 and Panc-1 tumor cells. Moreover, when intravenously injected, they inhibited tumor growth in Balb/c nude mice bearing subcutaneous Panc-1 human tumor xenografts more efficiently than those loaded with control siRNA or modified with control peptide-KLA. These results demonstrate that RELTpep-KLA-targeted MSC-exosomes carrying KRAS siRNA hold a potential for exosome-based targeted therapy against cancer.

#5750 Development of prostate specific membrane antigen-targeted liposomal zinc for the treatment of prostate cancer.

S. K. Mondal[1], A. L. Klibanov[2], A. Moore[1];
[1]Michigan State University, East lansing, MI, [2]University of Virginia, Charlottesville, VA

Introduction: Treatment choices for early-stage prostate cancer include mostly watchful waiting, radical prostatectomy, or radiation therapy, whereas for advanced cases hormone therapy followed by chemo/radiotherapy are the preferred options, despite their notable side effects. There is a need for more effective therapy with lower side effects, especially for advanced scenarios. Unlike normal epithelial prostate cells, cancerous ones show reduced zinc (Zn) levels due to ZIP1 zinc transporter downregulation. Zn deficiency allows m-aconitase to remain active, making prostate cancer cells energy efficient and grow. High levels of Zn are needed to inhibit m-aconitase, the enzyme responsible for the first reaction in the Krebs cycle. This study aims to induce energy starvation and cell death of prostate cancer cells by inhibiting m-aconitase using the prostate-specific membrane antigen (PSMA)-targeting liposomal zinc.
Methods: Liposomes were prepared by standard reverse phase evaporation method with DSPC, Cholesterol and DSPE-mPEG(2000) lipids. Zinc chloride was used to load Zn^{+2} into liposome following passive loading method. PSMA-expressing (PC3-PIP) and PSMA-null (PC3-LUC) human prostate cancer cells were used for in vitro studies. In the cell uptake study, cells were incubated with DiI-dye labeled liposomes for 2 hours before analyzing them by microscopy and flow cytometry. For the uptake inhibition study, cells were pre-incubated with PSMA-specific peptide for 2 hours before incubation with liposomes. Cytotoxicity studies were performed with PSMA-targeting Zn-loaded liposomes in PC3-PIP cells.
Results: We conjugated the PSMA-specific peptide and control peptide (ASP3) with DSPE-PEG(3400)-NHS, and used them at various amounts (1 to 4 mol% of total lipid) to prepare Zn-loaded PSMA-targeting liposomes (TL) and control liposomes (CL), respectively. The average hydrodynamic diameter of all the liposomes was 120 to 130 nm, and zeta potential ranged from -16 to -12 mV. The encapsulation efficiency and loading capacity of Zn^{+2} were 0.6% and 8.5%, respectively. Cellular uptake studies showed a higher accumulation of PSMA-targeting liposome (TL) compared to non-targeting liposome (CL) in PSMA-expressing PC3 cells, whereas both liposomes showed low uptake in PSMA non-expressing cell. Furthermore, pre-treatment of PSMA-expressing cells with PSMA-specific peptide reduced the uptake of TL, indicating that the uptake of TL liposome is PSMA dependent. Finally, cytotoxicity studies showed that Zn-loaded TL, induces cell death in the PSMA-expressing cells. Overall, we developed PSMA-targeting Zn-containing liposomes that selectively target and kill PSMA-expressing prostate cancer cells. Future work includes testing the effect of Zn-loaded TL on m-aconitase activity and testing of in vivo efficacy of the formulation in prostate cancer models.

#5751 Ultrasound responsive injectable hydrogels for on-demand drug delivery.

L. Xiang, G. Sener, A. Yildirim;
OHSU Knight Cancer Institute, Portland, OR

In this work, we developed ultrasound-responsive and injectable hydrogels for local and on-demand release of chemotherapeutics to solid tumors. Injectable hydrogels were prepared by using a zwitterionic monomer, sulfobetaine methacrylate (SBMA), without using any crosslinker. Gelation was performed at -20 ^{o}C using APS/TEMED as initiator, allowing the formation of strong electrostatic interactions between poly(SBMA) chains to physically crosslink the hydrogels. Monomer and initiator concentrations were carefully optimized to achieve injectable hydrogels with mechanical and thermal stability. To render ultrasound responsivity to the hydrogels, we loaded the hydrogels with hydrophobically (dodecyl) modified mesoporous silica nanoparticles (hMSNs) with sizes around 50 nm. When insonated with low-intensity focused ultrasound (LIUS), the hMSNs incept acoustic cavitation (i.e., growth and collapse of microsized bubbles), which in turn generates mechanical effects in the hydrogels such as shock waves or water jets. We found that loading the hydrogels with hMSN did not affect their injectability, and they remained mechanically stable at 37 °C for more than a week. hMSN-loaded hydrogels demonstrated strong ultrasound responsivity even at low particle concentrations (0.1 mg/mL) and ultrasound powers (25 W, 0.02% duty cycle). Finally, we loaded the hydrogels with a chemotherapy drug, doxorubicin (DOX, 0.2 mg/mL). DOX-loaded hydrogels demonstrated minimal release without LIUS treatment (<20% in a day). Application of LIUS (150 W, 1% duty cycle) for 5 min resulted in almost complete mechanical disintegration of the hydrogels, resulting in a burst DOX release. We also showed that the amount of released DOX could be controlled by tuning the LUIS power and its duration. In summary, we developed injectable hydrogels with strong ultrasound responsivity. These hydrogels hold great promise for local and on-demand drug delivery to solid tumors, which is currently under investigation in our laboratory.

#5752 Enhanced cancer therapy strategies utilizing gelatin-lipidoid hybrid nanoparticles for RNA delivery.

A. Gangula, D. Suresh, A. Suresh Babu, Z. Li, A. Upendran, R. Kannan;
University of Missouri - Columbia, Columbia, MO

Nanoparticle delivery platforms have provided impetus for the emergence of novel RNA-based cancer therapeutics due to their ability to circumvent the physiological and cellular barriers in the delivery. The clinical success of these strategies hinges primarily on the safety and efficacy of the delivery vehicle. Here, we have developed a gelatin-lipidoid hybrid nanoparticle (GLNP) that utilizes gelatin's biocompatibility, biodegradability, and lipidoids' high transfection efficiency. With GLNP, we have demonstrated the efficacy of delivering siRNA and silencing AXL, a receptor tyrosine kinase commonly associated with cancer progression, metastasis, and drug resistance. siRNA is attached to the surface of GLNP through covalent conjugation with gelatin, while the lipidoid on the system's interior electrostatically complexes with the siRNA. siRNAs are well protected by the GLNP when exposed to serum for at least 48 hours. The GLNP's bivalency significantly enhanced the downregulation of target genes *in vitro* and *in vivo*. Furthermore, the bivalent GLNP can simultaneously target and downregulate two oncogenes. Apart from siRNA, GLNP was also able to encapsulate and deliver mRNA, thereby suggesting the potential to simultaneously deliver RNA therapeutics to effect knockdown and expression of target proteins and maximize therapeutic effect. The length of the carbon chain of the lipidoid can be manipulated to influence the physico-chemical properties of the GLNP and its efficiency in encapsulating and delivering RNA drugs. Importantly, gelatin was found to effectively shield the cationic lipidoid and negate its toxicity. Toxicity studies indicate that high doses of GLNPs (up to 48 mg/kg BW) are well-tolerated with no significant changes in body weight, hematology, or serum chemistry. The co-administration of GLNP-siAXL and TKI in PDX models has shown notable control of tumor growth. It is important to note that immune checkpoint blockade (ICB) therapy has shown significant survival benefits in NSCLC patients. However, the therapeutic effect is limited to only 20% of patients due to several resistance mechanisms, such as increased expression of oncogenic proteins. Therefore, our future study will explore GLNP's ability to sensitize NSCLC tumors to immune therapy.

#5753 Milk-derived extracellular nanovesicles: A novel delivery strategy for transcriptome targeting therapies in cholangiocarcinoma.

Jack W. Sample[1], Mincheng Yu[2], Hendrien Kuipers[3], Danielle M. Carlson[2], Nathan W. Werneberg[2], Jennifer L. Tomlinson[1], Gregory J. Gores[2], Rory L. Smoot[4]

[1]Department of Surgery, Mayo Clinic, Rochester, MN,[2]Division of Gastroenterology and Hepatology, Mayo Clinic, Rochester, MN,[3]Department of Biochemistry and Molecular Biology, Mayo Clinic, Rochester, MN,[4]Department of Hepatobiliary and Pancreas Surgery, Mayo Clinic, Rochester, MN

Introduction: Cholangiocarcinoma (CCA) is an aggressive and heterogenous biliary malignancy. Previous therapeutic shortcomings have encouraged the investigation of new strategies, such as targeted therapeutics. YAP/TAZ, transcriptional coactivators of the hippo pathway, have been implicated in the tumorigenesis of CCA along with the Src familiar kinase, LCK. Milk-derived nanovesicles (MNVs) have emerged as a promising biologic delivery apparatus for hepatobiliary malignancy due to their predilection for hepatic uptake. We sought to investigate the utility of aptamer guided MNVs loaded with short interfering RNA (siRNA) targeting YAP, TAZ, and LCK.

Methods: MNVs were prepared and loaded with species-specific siRNA prior to decoration with an epithelial cellular adhesion molecule (EpCAM) targeting aptamer. In vitro studies were performed using murine and human CCA cell lines, SB1 and HuCCT-1, respectively. In vivo studies were carried out using C57BL/6 mice following Institutional Animal Care and Use Committee protocols.

Results: We previously validated EpCAM as an effective aptamer demonstrated by increased levels of expression in CCA cell lines using immunoblot, RT-PCR and immunofluorescence. Additionally, in vivo experiments demonstrated excellent biodistribution and affinity for tumor-selective uptake. To evaluate knockdown efficacy, CCA cell lines were incubated with EpCAM aptamer guided MNVs individually targeting YAP, TAZ, and LCK which resulted in downregulation of these targets on immunoblot and RT-PCR. MNVs were then loaded with equal concentrations of siRNA targeting YAP, TAZ, and LCK in combination which resulted in similar degrees of gene downregulation compared with single transcriptome targeting MNVs. Due to the role of YAP/TAZ activation in CCA systemic therapy resistance, we investigated the effect of MNVs loaded with either single target or combinatory target siRNA alongside and in combination with gemcitabine and cisplatin (GemCis). Incubation with both combinatory siRNA and GemCis significantly intensified cell death on Pi/Hoechst staining compared with single target knockdown alone. Similar findings were found using separate assays of cell viability, including ATP luminescent quantitation and caspase 3/7 activity. These data suggest MNV transcriptome targeting may induce a state of cell stress which allows for amplification of chemotherapy treatment effect.

Conclusion: Aptamer guided, nanovesicle mediated transcriptome targeting is a promising therapeutic strategy in preclinical CCA models that may potentiate chemotherapy response. Our future direction involves further investigating the role of CCA target downregulation and its effect on the tumor immune microenvironment utilizing aptamer guided nanovesicle delivery and inducible knockdown cell lines.

#5754 Targeting miR-92b with peptide-modified liposomes for glioblastoma treatment.

Annelis Odette Sanchez-Alvarez[1], Fatima Valiyeva[1], Pablo E. Vivas-Mejia[2]

[1]Cell Biology, University of Puerto Rico Comprehensive Cancer Center, San Juan, PR, [2]Biochemistry, University of Puerto Rico, Medical Sciences Campus, San Juan, PR

Focusing on enhancing drug delivery to the brain, we aim to optimize a nanocarrier system with a specific focus on glioblastoma (GBM). This involves the utilization of spherical nucleic acids (SNAs) enclosed in peptide-modified liposomes, a configuration previously proven to effectively penetrate the blood-brain barrier (BBB) in a GBM mouse model. Our objective is to enhance the nanocarrier's treatment load by optimizing the attachment of oligonucleotide-modified gold nanoparticles (OMI) to the SNAs. MicroRNAs (miRNAs) play crucial roles in GBM pathogenesis, with miR-92b identified as overexpressed in various cancers, including GBM. Previous research from our lab implicated miR-92b in targeting proteins (FBXW7 & SKP2) in the ubiquitination pathway. RNA sequencing confirmed the significance of these pathways. RNA sequencing of miR-92b inhibition in the U87 GBM cell line revealed impacts on cell cycle, apoptosis, DNA repair, and multiple cancer-related pathways. We successfully modified the gold nanoparticle size from 15 nm to 5 nm, increasing the surface area and improving OMI attachment efficiency from less than 5% to 50%. This alteration significantly enhances drug loading in the nanocarrier, providing a promising platform for clinical applications. Characterization of the optimized peptide-modified liposomes reassured the retention and potential improvement of original features related to nanoparticle size and internalization in cell cultures. Future in vivo experiments, utilizing a GBM mouse model, will assess the therapeutic effect of inhibiting miR-92b using peptide-modified liposomes as a drug delivery system. Our multifaceted approach, involving nanocarrier optimization and miR-92b inhibition, holds promise for developing an effective treatment strategy against GBM. The presented results highlight the potential translational impact of our research in addressing the challenges associated with GBM therapy.

#5755 Development of paclitaxel-loaded nanoparticles with high charge density.

Katherine Y. Bang, Preshita P. Desai

Department of Biotechnology and Pharmaceutical Sciences, Western University of Health Sciences, Pomona, CA

Paclitaxel (PTX) is a potent anticancer agent with desirable efficacy against pancreatic cancer when used in conjunction with gemcitabine. The current formulation of nab-paclitaxel shows an improved safety profile compared to the conventional PTX, but the highly potent nature of paclitaxel still poses a problem as it leads to severe side effects, such as neutropenia and neuropathy, calling for the development of carriers with better targeting ability. Tumor treating fields (TTFields) is a new noninvasive treatment modality which disrupts the mitosis of a cell with alternating electric fields with low and intermediate frequency (100 - 500 kHz). Highly polar or charged macromolecules are impacted by the presence of TTFields as they lose random motions essential for mitosis. In previous work on the formulation of self-assembling cationic-anionic nanoparticles (S-CAP NPs), gemcitabine was successfully loaded into the nanoparticles with optimal particle size, stability, and release profile responsive to TTFields. In this study, S-CAP NPs were developed with biocompatible polymers, DEAE-dextran (Ddex) and bovine serum albumin (BSA), via a relatively green method to load paclitaxel with minimal use of organic solvents. Based on the previous study and the proof of concept, it can be hypothesized that the S-CAP NPs can successfully carry PTX and release it in the presence of TTFields. Various parameters, such as temperature, rpm, and concentration, were tested to optimize the size, PDI, zeta potential, and stability of the particles. The HPLC method was developed for PTX and used to analyze drug loading. Numerous compositions of BSA and Ddex were tested, and the ratio of 10:1 (BSA:Ddex) developed the best parameters of the S-CAP NPs. At 50 °C, the zeta potential of the particle was -3.55 ± 0.23 mV for the NPs, but the particles agglomerated over time as BSA precipitates were formed. At -15°C, the particle size was 302.9 ± 2.0 nm (PDI = 0.307 ± 0.038). Varying concentrations of BSA and Ddex showed the formation of S-CAP NPs at lower concentration. The optimal particle was formed at room temperature (RT) with BSA 0.1% and Ddex 0.01% with a size of 264.6 ± 19.7 nm (PDI = 0.079 ± 0.028) and a zeta potential of -14.67 ± 0.07 mV. The particles showed desirable stability for 48 hours. The HPLC analysis (Agilent, Phenomenex C18, 150 x 4.6 mm, 5 micron) was tested for validity and robustness (r^2 = 0.9996). Currently, the drug loading was achieved at 1.9% and the optimization studies are ongoing. *In vitro* cell viability assay (MTS) with and without TTFields is under exploration. With the successful formulation of PTX-loaded S-CAP NPs, co-loading PTX and gemcitabine can be explored to reduce the treatment burden of the patients.

#5756 Silver graphene quantum dots as drug delivery platforms for anti-cancer application.

R. A. Villanueva[1], T. Cole[2], N. Medina[3], D. Morell[3], B. Weiner[3];
[1]University of Puerto Rico - Rio Piedras, San Juan, Puerto Rico, [2]University of Tulsa, Oklahoma, OK, [3]University of Puerto Rico - Rio Piedras, San Juan, PR

Prostate cancer (PCa) stands as the most frequently diagnosed cancer and the third leading cause of cancer-related deaths among men in the United States (2019). Various cancer treatments, including Rehabilitation therapy, Immunotherapy, Hormone therapy, Stem Cell Therapy, and Chemotherapy, are available. However, chemotherapy has notable limitations due to its tendency to harm healthy cells, resulting in side effects such as nausea, vomiting, alopecia, diarrhea, anemia, bleeding, and sterility. In response to these challenges, we developed nanoparticle (NP) drug delivery platforms for cancer treatment. These platforms utilize silver graphene quantum dots nanocomposites (AgGQD), known for their ability to enhance drug therapies. Silver nanoparticles (AgNPs) exhibit toxicity towards both normal and cancer cells by impacting mitochondrial function, reactive oxygen species (ROS) production, lactate dehydrogenase (LDH) release, cell cycle dysregulation, induction of apoptotic genes like Bax, micronucleus formation, chromosome aberration, and DNA damage. Additionally, AgNPs demonstrate antiangiogenic and antiproliferative properties by inhibiting PI3K phosphorylation of Akt, disrupting the signaling pathway, ultimately halting angiogenesis, depriving cells of oxygen, and causing tumor cell death. To mitigate the toxicity of AgNPs in healthy cells and enhance their performance as drug delivery platforms, graphene quantum dots (GQDs) were introduced in this study. Moreover, GQDs may contribute to improving the solubility of drugs with low water solubility. The NPs were synthesized using graphene quantum dots as reducing agents. The study involved identifying the IC50 value, conducting validation tests on AgGQD and AgGQD doped, and comparing their toxicity on cells. Confocal microscopy was employed to identify the intracellular location of the drug.

#5757 Graphene quantum dots-covered AuAg alloy nanoparticles as drug delivery platforms for anticancer applications.

A. D. Veloz Bonilla, B. Weiner, G. Morell, N. Medina-Berrios;
University of Puerto Rico, San Juan, Puerto Rico

Cancer continues to be a global health challenge, with millions suffering from its various forms. Prostate cancer, in particular, emerges as a significant health risk for men. Originating in the prostate gland—a small organ nestled in the male pelvis—this type of cancer the second most common cause of cancer-related deaths among men in the U.S. Despite numerous medical breakthroughs over the years, finding an effective treatment for prostate cancer remains a challenge. Our research is venturing into a new frontier in the fight against prostate cancer, focusing on an innovative method, it explores the potential of nanoparticles for targeted drug delivery. This targeted approach promises to not only intensify the therapeutic effect, but also minimize adverse side effects on healthy cells, ensuring a more balanced and effective treatment regimen. A key in this study is the drug Andrographolide (ADG), which has been previously recognized for its robust anti-cancer properties. However, one of its limitations is its hydrophobicity, which makes it challenging to administer due to solubility concerns. To navigate this challenge, we are pioneering the synthesis of AuAg (gold and silver) graphene quantum dots (GQDs) alloy nanoparticles. AuAg particles, in have been the subject of numerous studies due to their profound impact on cellular processes. By integrating a protective layer of GQDs, we aim to boost the nanoparticles' stability, all while preventing any potential release of harmful metallic ions. The primary objective of this advanced approach is to augment the solubility of andrographolide, paving the way for its targeted and efficient delivery to PC-3 cells. An integral part of our research involves determining the IC50 value, which is pivotal in indicating the concentration at which the drug can inhibit the growth of 50% of prostate cancer cells. Once the IC50 value for the AuAgGQDs is firmly established, our focus will shift to evaluating its effects on the morphology of Red Blood Cells (RBCs). By encapsulating andrographolide within the designed nanoparticles, such as AuAgGQDs and their derivatives, we aim to observe changes in morphology. If there is a change in morphology, it indicates successful drug encapsulation. Through this research, we are not just seeking a viable treatment method, but also aiming to expand the horizons of drug delivery systems. The insights gained from this study could very well revolutionize our understanding of therapeutic potential and underscore the importance of nanoparticles in the realm of biomedical applications.

#5758 Gold nanoparticles with graphene quantum dots as drug delivery platforms for anticancer applications.

F. M. Rosa Suarez[1], G. Morell[2], B. Weiner[1], N. Medina[2], W. Pantoja[1];
[1]Universidad de Puerto Recinto de Rio Piedras, San Juan, Puerto Rico, [2]Universidad de Puerto Rico Recinto de Rio Piedras, San Juan, Puerto Rico

Cancer is a global health challenge that has a profound impact on the lives of people worldwide, either directly affecting individuals or their loved ones. Among the various types of cancer, prostate cancer stands out as one of the most prevalent in men. Prostate cancer is primarily identified by symptoms related to urinary health. Conventional medical approaches often rely on drug-based treatments to address this form of cancer. However, like many treatments, drug therapy comes with its own set of challenges. In our research project, we propose an alternative approach for managing prostate cancer. Our innovative idea centers around utilizing nanoparticles as a means of drug delivery. Specifically, we are investigating the use of Taxol, also known as Paclitaxel, as the drug of interest. Taxol possesses a significant challenge due to its hydrophobic nature, which hinders its circulation within the bloodstream. Its solubility is extremely low, at 0.00025 mg per milliliter. To overcome this limitation, we have undertaken the synthesis and integration of AuNPs (gold nanoparticles) with GQDs (graphene quantum dots). This combination enhances the drug's hydrophilic properties, making it more effective in transportation. Our research has led us to conduct experiments on prostate cancer cells (specifically the PC3 cell line). We aim to compare the IC50 value, which represents the drug concentration required to kill 50% of the cancer cells, when using the drug alone versus when using the drug in conjunction with the nanoparticles. Taxol's IC50 value is determined to be 5.73nM. In addition to assessing the impact on cancer cells, we have also examined how the nanoparticles interact with blood, and how this interaction influences the morphology of red blood cells. Furthermore, we have characterized the system using various analytical techniques, including FTIR, NMR, Fluorescence, and UV-Vis spectroscopy. To pinpoint the accumulation sites of the drug and delivery agents, we have employed confocal microscopy on the cancer cells. Our ultimate objective is to equip the drug with the necessary components to facilitate its entry into prostate cancer cells effectively.

#5759 Design of Au-graphene quantum dot nanocomposite as a potential drug delivery system to solubilize Tetrandrine.

M. Perez Salva[1], N. Medina-Berrios[2], B. Weiner[1], G. Morell Marrero[1];
[1]University of Puerto Rico - Rio Piedras, San Juan, Puerto Rico, [2]University of Puerto Rico - Rio Piedras, San Juan, PR

Prostate cancer, along with various other types of cancer, has been a prominent focus in medical and clinical discussions for many years due to its high fatality rates and significant health risks. To enhance oncological healthcare, various methods and technologies, such as drug delivery systems (DDS), have been extensively studied. Developing an effective DDS offers distinct advantages compared to other approaches to anticancer drug treatment. Some anticancer drug molecules possess unfavorable properties that directly impact metabolism and solubility, issues that DDS aims to address. Recent progress in nanomaterial synthesis has introduced innovative and efficient drug systems, providing a new perspective on cancer treatments. Gold nanoparticles, particularly in conjunction with semiconductor graphene quantum dots (GQDs), play a role in creating a unified carrier system applicable to multiple therapeutic methods. The choice of graphene quantum dots is based on their widespread applications and diverse benefits, ranging from compatible size and core-shell chemistry richness to substantial progress in achieving signal homogeneity by reducing the distance between molecules and substrate. The selected model for the DDS is the hydrophobic alkaloid Tetrandrine. Despite its use in treating conditions such as hypertension, and arthritis, and exhibiting anti-cancer activities, Tetrandrine is highly insoluble as an anti-cancer drug, with a solubility of 24.1 µmol/L [15 µg/mL] in water and only 5mM in ethanol and DMSO. This research aims to enhance the solubility of hydrophobic Tetrandrine by incorporating it into gold graphene quantum dot nanocomposites, serving as a potential drug delivery system for combating prostate cancer. The synthesis of nanocomposites (Au-GQD, Au-NGQD, Au-SGQD) and Tetrandrine-loaded products (AuGQD-T, AuNGQD-T, AuSGQD-T) will be examined. Additionally, the properties of Tetrandrine loaded onto the nanoparticles will be scrutinized and characterized using NMR spectroscopy, UV-Vis, and fluorescence spectrum analyses.

#5760 Intra-tissue quantitative analysis using LC/MS will determine the mechanisms of interstitial pneumonia induced by antibody-drug conjugates.

S. Koganemaru[1], H. Fuchigami[2], C. Morizono[1], H. Shinohara[1], Y. Kuboki[1], K. Furuuchi[3], T. Uenaka[3], T. Doi[1], M. Yasunaga[2];
[1]National Cancer Center Hospital East, Kashiwa, Japan, [2]National Cancer Center, Kashiwa, Japan, [3]Eisai Inc., Exton, PA

Background: Antibody-drug conjugates (ADCs) are a new class of therapeutics that combine a monoclonal antibody with a cytotoxic agent (known as their payloads) via a synthetic linker. While ADCs are one of game changer and are the fastest growing classes with novel clinical benefits recently, interstitial pneumonia (ILD) is a clinical problem as a fatal adverse event. However, the mechanism of ADC-induced ILD is under investigation. Purpose: We clarify ADC-ILD mechanism by analyzing released payload distribution in the lung using a novel Trophoblast cell surface antigen 2 (TROP2)-targeting ADC.
Material and Methods: TROP2-eribulin is a novel TROP2-targeting ADC composed of the TROP2 antibody and cytotoxic payload eribulin conjugated by a cleavable linker. Four human cancer cell lines (A549, HeLa, NCI-H2110 and SKOV3) and one human- leukemia monocytic cell line (THP-1) were used in this study. Cell surface TROP2 antigen expression was evaluated by flow cytometry. We investigated the concentration and distribution of the TROP2-eribulin and the payload released from the TROP2-eribulin in tumor and lung tissue, using TROP2 low and high expression human cancer xenograft model that were treated with various doses of TROP2-eribulin. The concentration of erbulin was analyzed by liquid chromatograph mass spectrometry, and tissue distribution of ADCs was assessed by immunofluorescence (IF) assay.
Results: In vitro analysis showed that the concentration of intracellularly released eribulin was significantly higher in NCI-H2110 with high TROP2 expression compared to A549 with low TROP2 expression ($P < 0.05$). In vivo analysis, the concentration of released eribulin in tumor tissue was approximately 10-fold higher in the NIC-H2110 xenograft model than the A549 xenograft model, while analysis of lung tissue showed that TROP2-eribulin was distributed in lung tissue in a dose-dependent manner of TROP2-eribulin regardless of TROP2 expression, with significantly more eribulin released in the high-dose group of TROP2-eribulin than in the other dose groups ($P < 0.05$). IF assay showed that TROP2-eribuilin localized to alveolar macrophages. In the analysis using THP-1 cell, which mimic macrophage function, the concentration of eribulin released from TROP2-eribuilin was significantly reduced by the use of an Fc receptor inhibitor ($P < 0.05$).
Conclusions: Nonspecific uptake of ADC by alveolar macrophages via Fcγ receptors releases cytotoxic payload into lung tissue, regardless of tumor antigen expression levels. This understanding can help elucidate the pathogenesis of ADC-induced ILD.

#5761 A nanoplatform based on an *in situ* tumor vaccine and activation of STING and TLR7/8 pathways for enhanced NSCLC immunotherapy.

H. Zhou[1], H. Hou[2], B. Xu[3], Y. Huang[2], H. Qiu[4], **Z. Jiang**[5];

[1]Guangdong Provincial People's Hospital Guangdong Academy of Medical, Guangzhou, China, [2]South China University of Technology, Guangzhou, China, [3]School of Biomedical Sciences and Engineering, South China University of Technology, Guangzhou International Campus, Guangzhou, China, [4]Guangzhou University of Chinese Medicine, Guangzhou, China, [5]University of California, Berkeley, Berkeley, CA

Background: Immunotherapy has emerged as a promising treatment for tumors following surgical, radiotherapy, and chemotherapy interventions. Therapeutic tumor vaccines are considered highly effective in eliminating tumors and preventing their recurrence and metastasis due to their ability to induce or enhance T cell-mediated immune responses. However, the therapeutic efficacy of these vaccines is impeded by the heterogeneity present both between and within tumors. In contrast, in situ tumor vaccines, prepared from autologous antigens in tumor patients, present another promising strategy for generating comprehensive immune responses.

Methods: In this study, we designed a multifunctional nanopolymer, the transformable nanoassembly PEG-Ce6@PAEMA/R848. This assembly includes the photosensitizer polyethylene glycol-chlorin-e6 (PEG-Ce6), the tumor pH-sensitive polymer poly(2-azepane ethyl methacrylate) (PAEMA), and the immune adjuvant Resiquimod (R-848). The objective is to confirm the activation of bone marrow-derived dendritic cells (DCs) at the cellular level. Subsequently, we investigated the maturation of DCs in lymph nodes and tumor sites in vivo.

Results: In the particle characterization process, successful synthesis of nanoparticles was achieved, along with the verification of their acid-responsive function and toxic effects. Furthermore, in vitro experiments demonstrated the activation of bone marrow-derived dendritic cells (DCs) (Figure 1).To further investigate the in vivo vaccine effects, C57BL/6 mice were euthanized, and lymph nodes were extracted to examine the accumulation of FITC-PAEMA. It can be observed that, due to the reduction in size of the particles in the tumor acidic environment, the immune adjuvant can easily enter the lymph nodes. Activation of the STING pathway in dendritic cells within the lymph nodes was detected through qPCR. The maturation of dendritic cells (DCs) in the lymph nodes was determined using flow cytometry (Figure 2).

Conclusions: In this study, we developed a straightforward yet potent strategy focused on in situ tumor targeting. This approach effectively inhibits tumor growth while inducing immunogenic cell death and eliciting a systemic anti-tumor immune response against cancer cells. Additionally, we intend to validate the therapeutic efficacy of this strategy on metastatic and distal tumors in subsequent investigations.

#5762 Engineering cell membrane nanoparticlesenhance immunotherapy and radiodynamic therapy for lung adenocarcinoma by promoting cGAS-STING and ferroptosis.

Haiyu Zhou[1], Hongrui Qiu[1], Shiying Li[2], Bin Xu[3], Shengbo Liu[1], Huili Wang[1], Hengliang Hou[4], **Zhengyang Jiang**[5]

[1]Department of Thoracic Surgery, Guangdong Provincial People's Hospital (Guangdong Academy of Medical Sciences), Southern Medical University, Guangzhou, China,[2]Guangdong Provincial People's Hospital (Guangdong Academy of Medical Sciences), Southern Medical University, Guangzhou, China,[3]School of Biomedical Sciences and Engineering, South China University of Technology, Guangzhou International Campus, Guangzhou, China,[4]School of Medicine, South China University of Technology, Guangzhou, China,[5]University of California, Berkeley, Berkeley, CA

Background: Immunotherapy is a promising approach for lung cancer, but its effectiveness is limited by tumor heterogeneity. Nanoparticle-based targeted drug delivery systems offer advantages such as targeted drug-loading capacity, and hypotoxicity, showing great potential in improving therapeutic efficacy. This study introduces a targeted drug delivery strategy based on immune-activating nanoparticles that achieves precise drugs delivery in tumor areas. Consequently, this approach remodels the microenvironment and induces tumor cytotoxicity.

Method: In this study, we first constructed a targeted nanoparticle delivery system FP@CC. The vehicle utilized lung adenocarcinoma cell membranes as the outer shell and encapsulated iron-platinum nanoparticles and STING agonist Vadimezan. Then, TREM2 antibodies were conjugated on the outer layer. The structure of FP@CC-aT2 was characterized by HADDF-STEM and its safety was evaluated by hemolysis test. In vitro, its ability to induce death was verified by AM/PI staining, and to induce ferroptosis was detected by C11 assay. Furthermore, we evaluated its antitumor effects in subcutaneous tumor models. The composition of immune cells within the tumor microenvironment was analyzed using flow cytometry.

Results: We initially performed HADDF-STEM analysis on the nanoparticle precursor FP/Vad@CC, revealing its uniform sphericity. For security, no significant hemolysis was observed at different concentrations of FP/Vad@CC. Then, the structures of FP/Vad@CC-aT2 and FP/Vad@CC are relatively stable (Fig 1).The number of dead cells significantly increased after deal with FP@CC, and the effect was significantly enhanced when combined with X-ray. Moreover, C11, utilizing to assess the changes in intracellular reactive oxygen species (ROS), found that FP@CC led to a significant increase in ROS, comparable to induction by H2O2. Both could be effectively prevented by ferroptosis inhibitor(Fig 2).In vivo, FP/Vad@CC-aT2 was applied to a subcutaneous tumor model in C57. It exhibited excellent therapeutic efficacy and biocompatibility. Flow cytometry revealed that FP/Vad@CC-aT2 had the anticipated impact on macrophages within the tumor: a significant reduction in CD11high/CD206high cells and opposite in the ratio of M1/M2-like macrophages (Fig 3).

Conclusion: This study developed a targeted drug delivery strategy, FP/Vad@CC-aT2, to improve the tumor microenvironment (TME). We conducted preliminary experiments in vitro and in vivo to validate its physicochemical properties and tumor inhibitory effects, including the induction of ferroptosis. We assessed its safety in mouse and obtained initial evidence of FP/Vad@CC-aT2's ability to remodel the subtypes of macrophage.Moving forward, we will validate its therapeutic and impact on the TME after surgical procedures.

CHEMISTRY: Structural and Chemical Biology
Poster Session

#5766 Fungal genomes in drug discovery: Application of CETSA to study the mechanism of action of brefeldin A.

T. Friman[1], B. M. Fontaine[2], A. Chernobrovkin[1], D. Martinez Molina[1], V. Brehmer[1], S. Lundgren[1], P. M. Castaldi[2], G. L. Verdine[2];
[1]Pelago Bioscience, Stockholm, Sweden, [2]LifeMine Therapeutics, Cambridge, MA

Fungal genomes encode a vast collection of chemical diversity that has evolved over millions of years to engage specific targets and modulate diverse biological processes. These Genetically Encoded small Molecules (GEMs) constitute a largely untapped source of potential therapeutics. Although fungal GEMs such as cyclosporine, lovastatin, and penicillin have revolutionized modern medicine, these GEMs were discovered serendipitously through bioactivity-guided fractionation of fungal extracts. LifeMine is redefining GEM discovery through the deployment of proprietary genomic search algorithms that enable GEM target prediction a priori. Our strategy facilitates focused search-and-retrieval campaigns to rationally discover molecules selected by Nature to modulate the desired target protein. These GEM drug leads often exhibit unique structural and mechanistic features, necessitating comprehensive deconvolution of the human target profile and mechanism of action during the development process from GEM to clinical candidate. As a proof-of-concept study, we leveraged CETSA Explore to study the biological mechanism of the fungal polyketide lactone Brefeldin A (BFA) in human THP-1 cells. This GEM, originally isolated from the filamentous fungus Penicillium brefeldianis, inhibits protein trafficking between the endoplasmic reticulum and the Golgi complex, eliciting antiviral, antifungal, and anticancer activity. Our CETSA profiling study confirmed the Golgi-associated guanine nucleotide exchange factor GBF1 as the primary target of BFA, validating the established mechanism of this GEM as an inhibitor of GBF1-mediated activation of the small GTPase ARF1. These results demonstrate the utility of integrating the LifeMine GEM discovery engine with downstream proteomic profiling technologies to facilitate the mechanistic characterization of fungal GEMs en route to novel therapeutics.

#5767 DNA binding mechanism of prostate cancer target ONECUT2.

A. Chatterjee, B. Gallent, M. Katiki, C. Qian, M. Harter, M. Freeman, R. Murali;
Cedars-Sinai Medical Center, Los Angeles, CA

Transcription factors (TF) are essential determinants of gene regulation and their aberrant expression frequently drive cancers. The binding of TFs to cognate DNA is central to their role in gene regulation. An understanding of their DNA binding mechanism is, therefore, of fundamental and therapeutic relevance. Generally, TFs bind DNA through defined DNA binding domains. The CUT and homeodomain are two such evolutionarily conserved elements found paired in multiple transcription factor families including ONECUT (OC), POU, CUX and SATB. However, the mechanism of cross-talk between the CUT and homeodomain to coordinatedly bind DNA remains unknown. Here, we report an integrative DNA binding analyses of the transcription factor OC2, a promising target for treatment of aggressive prostate cancer. We demonstrate that the homeodomain of OC2 thermodynamically stabilizes the DNA binding through allosteric modulation of CUT. The binding energetics is further dependent on base interactions by evolutionarily conserved amino acids in both CUT and homeodomain. In addition, we have discovered a unique arginine pair in the homeodomain, conserved within the ONECUT family, but not across POU and SATB families. We show that one arginine of this pair binds distinctly to DNA in respective complexes formed by OC2 and OC1. Notably, the above base-interactions are crucial for OC2-driven disease progression in a prostate cancer cell-line model. Taken together, our studies show that base-interactions by the evolutionarily conserved residues determine the basic DNA binding functionality through establishing favorable thermodynamics, while interactions by the arginine motif impart family-specific attributes. These findings also establish the homeodomain as a key regulator of DNA binding by OC2 and provide a mechanism for cooperative DNA binding by the CUT-homeodomain module in general. Importantly, these insights reveal vulnerabilities for therapeutic targeting of OC2.

#5768 Proximity labeling with molecular signal sensing of oncogenic *PIK3CA*.

Rong Li, Donghee Lee, Md Abdullah, Jong Hyuk Kim

Department of Small Animal Clinical Sciences, University of Florida, Gainesville, FL

PIK3CA mutations are major oncogenic drivers for oncogenesis. Mutant *PIK3CA* continuously activates the PI3K pathway, transmitting oncogenic signals within the transformed cells. Despite decades of efforts focused on targeting oncogenic *PIK3CA* for cancer therapy, the precise molecular and functional machinery remains incomplete due to the molecular complexity of the PI3K pathway. Mapping of proximity proteins in the oncogenic PI3K pathway and identifying mutant signals will signify a deep understanding of oncogenesis and a broad range of therapeutic applications. In this study, we hypothesize that *PIK3CA* mutant cancer cells establish a unique molecular program networking with distinct proteins, which differs from that of cancer cells with wild-type (WT) *PIK3CA*. To test this hypothesis, we have developed a novel bioengineering approach to decode protein-protein interactions of oncogenic *PIK3CA* and identify key molecular partners, potentially providing therapeutic vulnerabilities in cancer cells. First, we applied the proximity labeling technique, based on the fusion of a promiscuous protein ligase to a targeting protein of interest (POI), featuring proximity-dependent biotinylation of interacting and neighboring proteins. The promiscuous biotin ligases, BioID and BioID2, were utilized to integrate WT *PIK3CA* or gain-of-function hotspot mutations in at E545K or H1047R residues. To optimize the labeling protocol and biotinylation conditions, the BioID and BioID2 plasmids were fused with each POI, incorporating multiple combinations of protein tags, including myc, HA, and red fluorescence protein. Lamin A was used as the positive control, and a total of 15 plasmids were constructed in pcDNA3.1 mammalian expression vector. The sizes of the plasmids and the gene sequences were validated by PCR amplification and Sanger sequencing. Next, we employed a programmable nuclease, the prokaryotic Argonaute (pAgo), assisted by fluorescence resonance energy transfer technology, to detect oncogenic signals derived from mutant *PIK3CA* in cell-free conditions. To test our methods, we engineered two cancer cell lines (DHSA-1426 and COSB) derived from naturally occurring hemangiosarcoma in dogs, to induce *PIK3CA* H1047R mutations using CRISPR/Cas9. Our technical approach enables temporal and spatial molecular sensing of oncogenic *PIK3CA* and its functional interactome in living cancer cells by integrating high-resolution molecular mapping with a pAgo-based detection system. Our ongoing work involves the standardization and optimization of proximity labeling for oncogenic *PIK3CA* across ontogenetically distinct cancer cells. Furthermore, we will determine the sensitivity and specificity of the integrated approach to achieve proximity labeling with programmable detection of molecular signals from oncogenic *PIK3CA*.

#5769 Target identification of T-cell activating immunomodulatory tetrahydrothiazepines: DGKα and DGKζ inhibitors.

T. Luebbers[1], A. Britschgi[1], V. Costa[1], T. Friess[2], J.-C. Hau[1], G. Heidkamp[2], H. Kuehne[1], L. J. Martin[1], F. Roudnicky[1], M. Tzouros[1], A. Vandemeulebroucke[1]; [1]F. Hoffmann-La Roche Ltd., Basel, Switzerland, [2]Roche Diagnostics GmbH, Penzberg, Germany

We became interested in bicyclic tetrahydrothiazepine derivatives described in a Patent (WO 2016/139181) having immunomodulatory activities on CD3-activated T cells (CD4+ & CD8+) and NK cell increasing the secretion of several cytokines such as, e.g., IL-2, IFN-γ and/or TNF-α whereas corresponding unstimulated immune cells do not respond. Surprisingly - in contrast to what has been described in the patent - the N-H of the Amides 1 and 2 described in the patent was not required for potency and the oxadiazoles 1 and 2 were significantly more potent in T-cell proliferation and IL-2 release. Compound 1 was *in vivo* active in a single dose PD study in mice after CD3 activation and in a MC38 xenograft mice model showing single agent activity. Amide 1 and Amide 2 were identified in a phenotypic screen and the mode of action was unknown. Because of the promising pharmacological profile and *in vivo* activity, we were interested in the target. Here we describe how we identified the potential targets DGKα and DGKζ.

#5770 Inhibition of KRAS G12D mutant with small molecules.

D.-H. Lee, J. Lee;
Gangneung-Wonju National University, Gangneung, Korea, Republic of

Background: RAS mutations are occurring at a high rate in colorectal cancer, lung cancer, and pancreatic cancer. RAS is family of small GTPase proteins with important roles in cell growth, differentiation, proliferation, and survival. There are three types of RAS genes: HRAS, KRAS, and NRAS. The The RAS gene is the most commonly found oncogene in human cancer. KRAS exhibits a highest mutation rate compared to those of HRAS and NRAS in various cancer types.
Methods: Colorectal cell line LIM1215, SW48 and NSCLC cell line NCI-H1975, NCI-H838 were used for MTT assays. Apoptosis assay was performed using the annexin V-FITC apoptosis detection kit (BioBud, Cat. LS-02-100). Colony forming assay was performed with 6-well culture plates by seeding 500 cells/well. The expression levels of proteins involved in Q2a-induced signaling pathway were determined by Western blot. In vivo study was performed with tumor xenografts. HT-29 cells were implanted into the right flank of 5-week-old BALB/c nude mice. Tumor size was determined by measuring the diameter (width, length) of the tumor every two days with a digital caliper. All group mice sacrificed at day 19.
Results: Patients with cancer involving KRAS mutations are resistant to therapeutics that target epidermal growth factor receptor and show poor outcomes. In addition, effective treatments that target G12D in KRAS have not been developed. Thus, therapeutic agents targeting the G12D mutation in KRAS are needed. In this study, we identified the Q2a compound, a quinazoline-based derivative that specifically acts on the KRAS G12D mutation. This compound induced cell apoptosis by reducing phosphorylation of AKT in the PI3K pathway downstream of KRAS. Q2a compound specifically inhibited the growth of KRAS G12D mutant cells. In addition, cells with the KRAS G12D mutation were more sensitive to Q2a compound compared to the sensitivity of wild-type cells and those with other KRAS mutations, resulting in apoptosis. Treatment with the Q2a compound also decreased C-RAF phosphorylation in the MAPK pathway, which is downstream of KRAS. In KRAS G12D-mutated colorectal cancer xenografts, Q2a compound inhibited tumor production without significant liver toxicity.
Conclusion: Q2a compounds show potential as therapeutic agents that target KRAS G12D mutations in colorectal and pancreatic cancers.
Kyewords: Anti-Cancer Drug, KRAS G12D Mutant, apoptosis, colon cancerJi Yoon Lee, Dae-Hee Lee*Department of Marine Bio Food Science, Gangneung-Wonju national University

#5771 Utilizing a photoreactive chloroalkane capture tag for target deconvolution.

T. Uyeda[1], R. Hurst[2], S. Levin[2], M. Rosenblatt[2], K. Zimmermann[2], R. F. Ohana[2];
[1]Promega Corporation, San Luis Obispo, CA, [2]Promega Corporation, Madison, WI

Identifying the physiologically relevant targets of bioactive compounds is often the rate limiting step toward understanding their mechanism of action. To this end, we developed a streamlined chemical proteomic strategy that utilizes a novel photoreactive cleavable chloroalkane tag, which can be attached to bioactive compounds to isolate their respective cellular targets for identification by mass spectrometry. The tag does not significantly affect compounds potency and membrane permeability, allowing for binding interactions to be established within intact cells under appropriate physiological conditions. UV-induced covalent photo-crosslinking “freezes” the cellular interactions and prevents their dissociation upon cell lysis. Effective enrichment of the cellular targets is achieved through their selective covalent capture onto HaloTag coated particles and subsequent selective release by tag cleavage. Putative targets identified by mass spectrometry can be readily verified using resonance energy transfer. By exchanging the chloroalkane tag for a fluorophore, direct binding to the targets can be revealed through proximity of the fluorophore to a small NanoLuc luciferase genetically fused to the putative target. This approach was used to identify physiologically relevant targets for bioactive compounds including those with low affinity and/or low abundance as well as insoluble targets with multiple trans membrane domains.

#5772 Structural insights and rational design, optimization of highly potent and selective novel GRK5/6 inhibitors for cancer therapy.

Yueyi Chen, Amol D. Sonawane, Rajesh Manda, Ranjith K. Gadi, Arun K. Ghosh, John J. G. Tesmer

Purdue University, West Lafayette, IN

G protein-coupled receptor kinases (GRKs) regulate cell signaling by triggering receptor desensitization via phosphorylation on G protein-coupled receptors (GPCRs). There are seven human GRKs (GRK1−GRK7) where GRK5 and GRK6 are structurally similar. GRK5 is ubiquitous and required for cancer progression in various cancer types. Knock-down of GRK5 has been shown to suppress prostate cancer and non-small-cell lung cancer growth. GRK6 is highly abundant in immune cells and is overexpressed in multiple myeloma (MM). Knocking down GRK6 has been shown to cause apoptosis of MM cells. Therefore, targeting GRK5 or 6 is a potential chemotherapeutic strategy. Currently, we are developing a series of inhibitors for GRK5/6 based on a lead compound derived from sunitinib and utilizing Cys474 residue unique in GRK5/6 to enhance selectivity by covalent capture. We tested a series of novel inhibitor warheads to improve potency and selectivity without potentially toxic functional groups. So far, we have identified several inhibitors with low nanomolar IC_{50} for GRK5 and more than 100,000-fold selectivity over GRK2, another closely related member expressed in the heart. I have developed a pipeline of X-ray crystallography of GRK5 available for soaking various ligands and have solved several structures of novel inhibitor-bound GRK5. The structure elucidated the binding mode of this new class of GRK5 inhibitors, where the core interacts with the adenine site, a fluorophenyl group stabilizes the P loop and density suggests in some cases covalent bond forming between the reversible covalent warhead and Cys474. Our ongoing studies focus on further compound optimizations based on SAR. Overall, the discovery of the inhibitors can significantly facilitate understanding and treatment and cancers.

#5773 Multi-omics profiling of chemotactic characteristics of brain microglia and astrocytoma.

Chih-Yi Chen[1], **Yu-Ching Huang**[1], Wen-Hsiu Su[1], Yi-Ting Liu[1], Chi-Sheng Chen[1], Chia-Yang Li[2], Kun-Che Chang[3], Chia-Yen Dai[4], Shu-Chi Wang[5]

[1]Kaohsiung Medical University, Kaohsiung, Taiwan,[2]Department of Biological Science and Technology / Department of Medicine, Graduate Institute of Medicine, College of Medicine, Kaohsiung Medical University / National Pingtung University of Science and Technology, Kaohsiung, Taiwan,[3]Department of Ophthalmology, Louis J. Fox Center for Vision Restoration, University of Pittsburgh School of Medicine, Pittsburgh, PA,[4]Hepatobiliary Division, Department of Internal Medicine, Kaohsiung Medical University Hospital / College of Medicine and Center of Excellence for Metabolic Associated Fatty Liver Disease, National Sun Yat-sen University, Kaohsiung, Taiwan,[5]Medical Laboratory Science and Biotechnology, Graduate Institute of Medicine, College of Medicine, Kaohsiung Medical University, Kaohsiung, Taiwan

Brain cancer is a deadly disease with low survival rates for over 70 % of patients. Therefore, there is a critical need to develop better treatment methods and strategies to improve patient outcomes. In this study, we explored the tumor microenvironment and discovered unique characteristics of microglia to interact with astrocytoma cells and promote proliferation and migration of collisions. The conditioned medium from the collisions expressed cell chemoattraction and anti-inflammatory responses. To further understand the interactions between microglia and astrocytoma cells, we used flow sorting and protein analysis found that the protein alterations were related to biogenesis in the astrocytoma cells and metabolic processes in the microglia. Both types of cells were involved in binding and activity in cell-cell interactions. Using STRING to demonstrate the protein cross-interaction between the cells. Furthermore, PHB and RDX interact with oncogenic proteins, which were significantly expressed in patients with Glioblastoma Multiforme (GBM) and low-grade glioma (LGG) according to GEPIA. To study the role of RDX in chemoattraction, the inhibitor-NSC668394 suppressed collision formation and migration in BV2 cells in vitro by down-regulating F-actin. Additionally, it suppressed macrophage infiltration in infiltrating islands in vivo of intracranial tumor-bearing mice. These findings provide evidence for the role of resident cells in mediating tumor development and invasiveness and suggest that potential interacting molecules may be a strategy for controlling tumor growth by regulating the infiltration of tumor-associated microglia in the brain tumor microenvironment.

#5774 Are 19del and L858R really not the same disease entities?.

Y. Heo[1], J. Kim[2], Y. Sung[3], **S. Kim**[2], C. Jung[3], J.-O. Kim[2], J.-y. Shin[2], G. Lee[4], S. Chun[4], S. Bu[5], Y. Lee[6], J. Kang[2];

[1]Research Center for Bioconvergence Analysis, Korea Basic Science Institute (KBSI), Chungcheongbuk-do,, Seoul, Korea, Republic of, [2]Seoul St. Mary's Hospital, Seoul, Korea, Republic of, [3]Department of Hospital Pathology, College of Medicine, The Catholic University of Korea,, Seoul, Korea, Republic of, [4]Division of Oncology, Department of Internal Medicine, College of Medicine, The Catholic University of Korea,, Seoul, Korea, Republic of, [5]Division of Cardiology, Department of Internal Medicine, Uijeongbu St. Mary's Hospital, College of Medicine, The Catholic University of Korea,, Seoul, Korea, Republic of, [6]Research Center for Bioconvergence Analysis, Korea Basic Science Institute (KBSI), Chungcheongbuk-do, Korea,, Seoul, Korea, Republic of

IntroductionThe similarities and differences between the two subtypes of common epidermal growth factor receptor (EGFR) mutations have been recognized by clinicians, but actual treatment strategies remain unchanged. The L858R mutation can be explained by the pharmacological conformational plasticity of the receptor protein and other co-occurring mutations, which may be subtypes of EGFR mutations or non-EGFR mutations, and differences in downstream signaling pathways. As long as we know that molecular differences lead to biological differences, it is a challenge for all of us that our treatment strategies must changeWe investigated the RWD, conformational structure and RNA expression profile about two types of common mutations in the mEGFR+ NSCLC patients.MethodWe collected the medical information for stage I-IIIA mEGFR+ NSCLC patients and explored the conformational structure by crystalized radiologic technique. And we performed RNA expression assay using multiplex IF and High-through-output Profiling. ResultOverall, the static structures of wild type (WT), L858R, and 19del (ΔL747-E749) EGFR did not show any significant differences. However, the difference in the static structure between WT-19del and L858R-19del was subtly greater than that of WT-L858R. In addition, further analyses demonstrated no significant structural differences in the phosphorylation sites. However, it should be noted that proteins do not exist as static structures in vivo, and they have a dynamic, flexible structure that changes over time, i.e., plasticity of proteins. Therefore, we investigated the X-ray B-factor value, which is an indicator of flexibility, dynamics, and plasticity of proteins. As expected, the loop or disordered regions mainly shows higher B-factor values, which indicates an active structure, highly changeable and dynamic. Together, the three types of the EGFR protein manifest wholly similar B-factor values, while several local regions present appreciably distinct B-factors. Physical properties such as the dynamic structure may affect intermolecular recognition of EGFR proteins and their function Recent biochemical and biophysical evidence suggests that oncogenic mutations have an impact on the conformational dynamics of enzymesConclusionIn conclusion, our results suggest that Patients with 19del and L858R mutations demonstrated a different clinical course.
It is necessary to consider the dynamic structural characteristics and functional differences of EGFR membrane proteins.

#5775 Structure and dynamics of the major *PDGFR*-β oncogene promoter G-quadruplex and insights into its cellular regulation.

Y. Han, J. Dickerhoff, D. Yang;
Purdue University, West Lafayette, IN

Overexpression of the receptor tyrosine kinase PDGFR-β promotes cancer growth and metastasis. PDGFR-β is a validated cancer target but PDGFR-β kinase inhibitors suffer from lack of selectivity and side effects. G-quadruplexes are an exciting class of non-B DNA secondary structures with functional importance. The G-quadruplex formed in the *PDGFR-β* promoter is a transcription repressor and targetable by small molecules. Therefore, the *PDGFR-β* promoter G-quadruplex is an attractive molecular target for anticancer drugs. Structural information of the *PDGFR-β* promoter G-quadruplex is crucial for understanding its cellular function and rational drug design. Herein, we used nuclear magnetic resonance (NMR) spectroscopy and biophysical methods to determine the structure and dynamics of the major G-quadruplex formed in the human *PDGFR-β* promoter. Unlike canonical G-quadruplexes formed by four runs of three continuous guanines (G), the major *PDGFR-β* G-quadruplex adopts a novel broken-strand structure where a two-G segment is continued by a non-adjacent guanine. The broken-strand G-quadruplex has a vacancy-G-tetrad (vG4) which is filled-in intramolecularly by a distal guanine. Interestingly, we discovered that the major *PDGFR-β* G-quadruplex is a novel mixture of two equilibrating broken-strand G-quadruplexes. Both structures adopt overall parallel-stranded folding with all 1-nt chain-reversal loops. However, a different 3'-filled-in guanine is delivered by a lateral loop, which forms structurally similar hairpin with a unique capping G-G base-pair. The formation of the equilibrating broken-strand G-quadruplexes and unique capping structures are both specific to the *PDGFR-β* promoter sequence. Intriguingly, the observed dynamic equilibrium between the two co-existing structures with different intramolecular fill-in guanines indicates a novel vG4 intermediate, which could be filled-in by cellular guanine metabolites such as cGMP. Therefore, our study provides critical insights into how the dynamics of the major *PDGFR-β* G-quadruplex lead to vG4 formation and potential regulation of gene transcription by cellular guanine metabolites. The determined molecular structures of the novel broken-strand G-quadruplexes provide a structural basis for rational design of small molecules to specifically target the major *PDGFR-β* promoter G-quadruplex for cancer therapeutics.

#5776 Target identification, selectivity profiling and binding site mapping of small molecule and peptide drugs by LiP-MS.

F. Sabino[1], M. Soste[1], D. Kamber[1], M. Ritorto[2], K. Hoeflich[2], M. Hale[2], B. Quade[2], X. Huang[2], N. Beaton[3], R. Bruderer[1], **Y. Feng**[1], L. Reiter[1];
[1]Biognosys AG, Schlieren, Switzerland, [2]Nested Therapeutics, Inc., Cambridge, MA, [3]Biognosys Inc., Newton, MA

Target identification in the cellular context is a critical step for both target-based and phenotypic drug discovery. Limited proteolysis coupled with mass spectrometry (LiP-MS) has emerged as a powerful technique for target deconvolution of small molecules or peptides in cell lysate without compound modification or genetic manipulation of cell lines [1,2,3,4]. Utilizing a non-specific protease under well-controlled conditions, LiP-MS exploits drug-induced structural alteration or steric hindrance on protein targets and utilizes quantitative mass spectrometry to probe over 250'000 peptides covering more than 9000 proteins in the proteome. To aid target ID, this workflow incorporates a 7-concentration dose response experiment and a machine-learning framework [1] to compute a LiP-score to rank identified target proteins, as well as predict potential binding site. In this study, we present target deconvolution results on four small molecule compounds and one peptide compound with very distinct pharmacological profile: 1) staurosporine, a broad-specific kinase inhibitor; 2) roniciclib, a failed clinical-stage pan-CDK inhibitor; 3) selumetinib, an allosteric, non-ATP-competitive MEK 1 and 2 inhibitor; 4) NST-628, a newly developed non-degradating molecular glue inhibiting the RAS/MAPK pathway; and 5) Acetyl-calpastatin, a 24 amino-acid polypeptide inhibitor of calpain 1 and 2. Target ID experiment with staurosporine and roniciclib yielded > 150 and 68 kinase targets were identified respectively. For the pan-kinase inhibitor roniciclib, both cell-cycle CDKs (CDK1/cyclin B, CDK2/cyclin E, CDK4 cyclin D) and transcriptional CDK9 were among the targets. For Selumetinib, LiP-score ranking identified MEK1 and MEK2 as the top two targets, and only kinases among a total of 23 targets. Furthermore, mapping the LiP-peptides from this experiment onto MEK1 showed that they are in close proximity to the selumetinib allosteric binding site on co-crystal structure. Last but not least, we assessed the target landscape of NST-628, a novel non-degrading molecular glue and identified MEK1 and MEK2 clearly as the primary targets. This finding is in line with orthogonal data obtained from X-ray crystallography [5]. Collectively, this data demonstrates that LiP-MS can be deployed to effectively identify protein drug targets and predict binding sites in complex cellular millieu independent of the compound's mechanism of action and without compound modification or labeling. These capabilities make LiP-MS a powerful addition to the target deconvolution toolbox.

[1] Piazza and Beaton et al. Nature Comm 2020 [2] Hendricks and Beaton et al. ACS Chem Bio 2021 [3] AACR 2022 [4] AACR 2023 [5] AACR-NCI-EORTC 2023

#5777 Rewiring EWS/FLI1 with transcriptional chemical inducers of proximity (TCIPs).

M. J. Bond[1], R. P. Golden[2], R. C. Sarott[2], G. DiGiovanni[1], B. A. Karim[2], B. Howard[1], K. Ross[1], N. S. Gray[2], K. Stegmaier[1];
[1]Dana-Farber Cancer Institute, Boston, MA, [2]Stanford University, Stanford, CA

The purpose of this study was to determine if EWS/FLI1 (E/F), the oncogenic fusion protein that drives Ewing Sarcoma (ES), can be rewired to enhance expression of BCL6-controlled genes using Transcriptional Chemical Inducers of Proximity (TCIPs), a novel bivalent small molecule platform.
TCIP molecules recruit a transcriptional regulator, such as BRD4, to the transcriptional repressor BCL6. Upon binding, a ternary complex is formed on chromatin at BCL6-bound loci, causing transcriptional upregulation of BCL6 target genes. Since E/F does not have a *bona fide* ligand, we have used an exogenously expressed N terminal $FKBP^{F36V}$-EWS/FLI1 (N-FK-E/F) fusion system to study how modulation of E/F by TCIPs impacts the transcriptome of ES cells. To eliminate background signal from endogenous E/F, we used CRISPR/Cas9 to knockout (KO) endogenous E/F. Our exogenously expressed N-FK-E/F has mutated PAM motifs and is resistant to KO. In our proof-of-concept study we used TCIP1 consisting of *ortho*-AP1867 (oAP), a synthetic ligand for $FKBP^{F36V}$, linked to the BCL6 inhibitor BI3812 (BI) to rewire N-FK-E/F. We have also tested a negative control TCIP (TCIP NEG) that links oAP to a BI derivative that abolishes BCL6 binding. TCIP NEG has similar physiochemical properties to our active TCIP1; however, it cannot bind BCL6, serving as a negative control for ternary complex formation.
TCIP1 rapidly and dose-dependently increases the RNA and protein expression of several BCL6 target genes, like p21, in multiple ES models that stably express N-FK-E/F. TCIP NEG does not increase the expression of BCL6 target genes in ES cells. TCIP1 induces ternary complex formation in ES cell lysates, and ternary complex formation is necessary for activity in ES cells. TCIP1 is specific and does not increase BCL6 target gene levels to the same extent in ES cells expressing a FKBP-GFP construct or in parental ES cells lacking N-FK-E/F. RNA sequencing of EWS502 N-FK-E/F expressing cells shows that TCIP1 treatment induces a larger increase in expression of BCL6 target gene RNA than BCL6 inhibition. Moreover, CUT&RUN experiments in EWS502 N-FK-E/F expressing cells suggest TCIP1 leads to an accumulation of N-FK-E/F at the promoters of BCL6 target genes. Motif analysis showed that TCIP1 increases the likelihood of N-FK-E/F binding to BCL6 consensus sequences as wells as increases the likelihood of BCL6 binding to E/F recognition sequences. In future studies we will conduct RNA sequencing, CUT&RUN, and other ‘omics’ approaches (e.g. DisP-seq) to compare TCIP1 to TCIP NEG in multiple cell lines at multiple concentrations and time points.
Our data suggests that N-FK-E/F can be rewired to induce the expression of BCL6 target genes in ES. Since ES is driven solely by E/F, TCIPs may be promising next generation therapeutics. Our study provides a proof-of-concept that will be the foundation for the development of future TCIP molecules that recruit endogenous E/F once suitable ligands are developed.

#5778 Determining the structure and function relationship of the oxysterol-binding protein (OSBP) to guide drug development.

R. Bayimenye[1], J. L. Berrios-Rivera[1], S. Nimmo[1], C. R. Bourne[2], A. W. G. Burgett[1];

[1]University of Oklahoma Health Sciences Center, Oklahoma City, OK, [2]University of Oklahoma, Norman, OK

The human Oxysterol Binding Protein Structure and function relationship remains elusive, yet the anti-cancer and antiviral molecules library targeting OSBP and OSBP-Related proteins (ORPs) continues to grow. OSBP is a ubiquitously expressed protein in most eukaryotes, functioning as a master lipid sensor and cholesterol regulator in cells. OSBP and its closely related protein ORP4 are also reported to be essential in several human diseases, including viral infection and cancer cell proliferation. Our lab has shown that the natural product OSW-1 has potential anti-viral and anti-cancer activity through targeting OSBP and ORP4, as confirmed with protein-ligand interactions that showed binding with high affinity. Moreover, several anti-cancer molecules targeting the ORPs provoke different protein conformation changes and, therefore, lead to varying OSBP functions. However, the structure of full-length OSBP is still unknown, which leaves a gap in knowledge regarding the compounds' mechanism of action or how OSBP could be established as a molecular anti-cancer target. Our goal is to determine the structure and function relationship of OSBP with emphasis on the effect of small molecule ligands on cellular OSBP levels and function. In pursuit of this research goal, we aim to determine the in vitro activity of OSW-1 analogs (OA) isolated in our lab, as well as determine their interaction with OSBP and ORP4 proteins in multiple cancer cell lines. We mainly seek to determine the structure and ligand interaction with the OSBP-ligand binding domain (LBD) and full-length OSBP to shed light on the conformation changes that occur upon ligand binding. Preliminary data indicate that the tested OA compounds are active in multiple cancer cell lines with reduced OSBP levels effect, suggesting a similar mechanism of action to OSW-1. A transient expression of full-length OSBP and LBD showed that the truncated OSBP (LBD) was mostly found in the pellet, which could imply low solubility, while the full-length OSBP showed sufficient solubility. Our efforts are currently focused on purifying full-length OSBP. We are also working towards purifying full-length OSBP with a cleavage site that allows cutting out the LBD, thus solving the insolubility issue. Once obtained, the full-length OSBP and the ligand binding domain will be used for both binding and structure determination studies.

#5779 Enhancing selectivity and overcoming tissue-specific toxicity in drug discovery: A novel BET inhibitor with targeted delivery for prostate cancer treatment.

C. Tang[1], R. Traquete[1], E. Henderson[2], J. Conde[1], S. Picaud[3], P. Filippakopoulos[2], G. Bernardes[4];
[1]Instituto de Medicina Molecular, Lisbon, Portugal, [2]Ludwic Cancer Institute, Oxford, United Kingdom, [3]Nuffield Department of Medicine, Oxford, United Kingdom, [4]Yusuf Hamied Department of Chemistry, Cambridge, United Kingdom

Improving selectivity and circumventing tissue-specific toxicity remain significant challenges in the realm of contemporary drug discovery. Despite the advanced development of highly selective inhibitors, their systemic distribution often stimulates off-tissue unwanted side-toxicity. To address this, we engineered a highly selective inhibitor that specifically targets and releases a small molecule drug payload to a desired cell type.
As a proof of concept, we apply this method to epigenetic inhibitors of BET proteins, which are crucial regulators of gene transcription implicated in the progression and survival of cancer. We engineered a novel BET-selective chemotype conjugated to a Prostate-Cancer specific targeting component in order to overcome the off-tissue effects of state-of-the-art BET inhibitors.
To achieve delivery of the compound, we modified the benzodiazepine (BzD) scaffold of the well-established BET inhibitor I-BET762, conjugating the tertiary amine with a self-immolating motif, allowing for intracellular compound release upon an enzymatic trigger. This new chemotype, RT53, maintains the biochemical properties of I-BET762, showing potent and selective binding to BET bromodomains in a range of established biophysical assays.
In cells, RT53 phenocopied I-BET762 on cancer cell lines, including prostate cancer. We validated the established strong anti-proliferative effect following BET inhibition using clonogenic assays, flow cytometry, and monitored the suppression of MYC expression. Moreover, we established the transcriptional rationale for loss of cellular fitness using RNA sequencing, discovering strong down-regulation of solute carriers, depriving cells of nutrient flux and disrupting normal processes.
Furthermore, RT53 exhibits antitumor activity *in vivo*, in localized models of prostate cancer established in male athymic nude mice. The targeted delivery of RT53 demonstrated superior efficacy *in vivo* ameliorating on-target, off-tissue toxicity, as low-dose treatment led to almost complete elimination of grafted tumor sites, significant extension of survival, and no signs of toxicity on non-targeted tissues.
Taken together, our data establish a novel class of BET-specific inhibitors offering a handle for selective delivery *in vivo*, enhancing the therapeutic index while avoiding on-target off-tissue toxicity.

#5780 Simultaneous targeting existing proteins and nascent proteins for synergistic anticancer activity.

B. X. Li[1], J. Wang[1], B. Chao[1], J. Piesner[1], F. Kelly[2], S. Kaech Petrie[1], **X. Xiao**[1];
[1]OHSU Knight Cancer Institute, Portland, OR, [2]Oregon health & Science University, Portland, OR

Protein synthesis and subsequent delivery to the target locations in cells are essential for their proper functions. Newly synthesized proteins and existing protein have differential properties that can potentially be exploited for targeting to maximize therapeutic potentials. Methods to label and distinguish newly synthesized proteins from existing ones are critical to assess their differential properties, but such methods are lacking. We describe the first chemical genetics-based approach for selective labeling of existing and newly synthesized proteins that we termed as $_{CG}$-SLENP. Using HaloTag in-frame fusion with lamin A (LA), we demonstrate that the two pools of proteins can be selectively labeled using $_{CG}$-SLENP in living cells (https://doi.org/10.1101/2023.11.02.565346). We further employ our recently developed selective small molecule ligand LBL1 for LA to probe the potential differences between newly synthesized and existing LA. Our results show that LBL1 can differentially modulate these two pools of LA. We further extend our $_{CG}$-SLENP strategy to evaluate the differences of the two pools for BRD4 (bromodomain containing 4). These observed differences motivated us to investigate the synergistic anticancer properties of BRD4 degraders and inhibitors in triple negative breast cancer. Our results show that simultaneous targeting newly synthesized proteins and existing proteins display strong synergistic anticancer activities.

#5781 Development of RNA-Seq library preparation method for highly degraded FFPE RNA and ultra-low RNA input.

E. Star[1], N. Karim[1], B. DeGroen[1], M. Salgado[1], D. Wang[1], J. Li[1], K. Ilic[1], S. Beaudoin[2], C. Vakulskas[2], B. Min[1], P. Chen[1];
[1]Integrated DNA Technologies, Inc., Redwood City, CA, [2]Integrated DNA Technologies, Inc., Coralville, IA

RNA sequencing (RNA-Seq) has been widely used for investigating genetic variations, splicing, and gene expression in cancer research. However, RNA-Seq library preparation from archived formalin fixed paraffin embedded (FFPE) samples tends to fail due to both limited quantity and high degradation. We aimed to overcome the sample quality and quantity limitations by leveraging both in-house cDNA synthesis modules and the unique, single-stranded ligation strategy of the IDT xGen cfDNA & FFPE DNA Library Prep chemistry and workflow. This approach delivers high library conversion of input molecules and maximizes high quality data from sequencing. To represent the types of challenging cancer samples that may be lost during traditional RNA-Seq analyses, we collected thirty-seven low quality RNA FFPE samples (RIN <3) from lung, breast, colorectal, thyroid tumors and more. In addition, twenty-one frozen tissue RNA samples and Nine RNA reference materials were used as controls. Regardless of sample origin, 25 ng of total RNA were taken for RNA-Seq library preparation. In-house cDNA synthesis modules were used for the 1st and 2nd strand cDNA synthesis followed by Illumina library generation using IDT's xGen™ cfDNA & FFPE DNA Library Prep Kit. All sample types generated sufficient high-quality libraries (>1 ug) for hybridization capture enrichment. The RNA-seq libraries were captured using IDT's custom designed panel with 56 known fusion targets. We detected all expected fusion targets from the tested samples. No correlation was observed between sample quality and the number of genes detected between the different types of samples including the low quality FFPE. To test the lower limits of the workflow, a degraded FFPE sample and a Universal Human Reference RNA (UHR) were used to construct libraries with inputs from 1ng to 10pg. High quality libraries were successfully constructed with as low as 10pg of UHR and 50pg of the FFPE RNA sample. We demonstrated the flexibility of our current cfDNA & FFPE DNA Library Prep whose high conversion rate could be used for constructing libraries from low quality and degraded FFPE RNA in conjunction with our in-house cDNA synthesis modules. Libraries were successfully constructed from ultralow RNA input which could be leveraged for cfRNA applications. The high RT efficiency enables processing FFPE samples with very low-quality scores and provides users with an effective solution for their degraded RNA samples challenges.

#5782 Probing monomer - dimer and conformational transitions of PLK1 using catalytic and polo-box domain inhibitors.

M. Sanhaji[1], M. Raab[1], G. Merhej[2], C. Nageswara Rao[2], I. Babic[3], E. Nurmemmedov[3], K. Strebhardt[1], M. Wyatt[2], **C. McInnes**[2];
[1]Goethe University, Frankfurt, Germany, [2]University of South Carolina, College of Pharmacy, Columbia, SC, [3]Nerd Bio, San Diego, CA

Polo Like Kinase 1 (PLK1), a sought-after target for drug discovery, is an essential mitotic kinase consisting of a catalytic domain (KD) and a polobox domain (PBD), the latter of which plays roles in substrate recognition, subcellular localization and further acting as an autoinhibitory regulatory domain. PLK1 can exist either in an inhibited closed conformation or an open active state allowing interaction with and phosphorylation of substrates. PLK1 has also been shown to be regulated by interchange between monomeric and dimeric forms through binding to the Bora protein and by activation loop phosphorylation. We have described PBD-binding molecules termed abbapolins that inhibit cellular phosphorylation of a PLK1 substrate and induce loss of intracellular PLK1. In addition, due to their engagement of the cryptic pocket (ligand induced) of the PBD, we proposed that abbapolins would interfere with formation of PLK1 dimers. Here we provide evidence further supporting the ability of abbapolins to block PLK1 cellular dimerization and that this is related to their mechanism of anti-proliferative activity. In a separate study, using a cellular thermal shift assay, KD inhibitors were shown to decrease soluble PLK1, indicating that catalytic-site binding results in less stable PLK1 suggestive of an open conformation. We have extended these observations using a sensitive readout of cellular target engagement employing a Microtag overexpressed PLK1. In this format, we observe heat-induced destabilization of PLK1 upon nanomolar engagement by two lead KD inhibitors, BI2536 and onvansertib, currently being clinically evaluated. Furthermore, cyclapolin 9, a low molecular weight kinase inhibitor that, unlike the other two KD inhibitors does not protrude from the active site, did not induce significant destabilization. We have also carried out experiments using a fluorescently labeled version of BI2536 to probe the conformational effects of PBD binding upon the KD. These data solidify the observations that relief of autoinhibited PLK1 is induced by certain KD binders and highlight the conformational perturbations from KD versus PBD binding. These observations have implications for the development of ATP-competitive PLK1 inhibitors because catalytic inhibitors may conversely promote PLK1 non-catalytic functions, which may explain their lack of clinical efficacy to date. Furthermore, the demonstration that the abbapolins are mechanistically unique in terms of blocking the dimerization of PLK through the PBD provides impetus for their development as next generation PLK1 inhibitors.

#5783 Receptor tyrosine kinase Tyro3 interaction with ligands and inhibitors.

K. N. Hardeman, C. Starbird;
University of North Carolina, Chapel Hill, NC

TAM receptors (Tyro3, Axl, Mer) are a sub-family of receptor tyrosine kinases that regulate cell survival and homeostasis primarily through their role in clearance of apoptotic cells. While several receptor tyrosine kinases (RTKs) are targeted in various types of cancer therapies, interest in Tyro3 as a potential target in breast cancers has only recently grown. Determining the structure of Tyro3 with and without tyrosine kinase inhibitors (TKIs) bound will provide important missing information to aid in the design of treatments that can be combined with existing cancer treatments, as dual treatment is often necessary. I have designed constructs that will be used for crystallization of the Tyro3 kinase domains. I mapped the full portion of the kinase (called "Small"), an extended kinase ("Big"), and a smaller catalytic domain ("Cat"). The kinases were made through a molecular cloning method (Gibson Assembly), sequence verified, and expressed in insect cells for large scale purification. Ni-NTA and gel filtration will be used, followed by crystallization and soaking with inhibitors.

#5784 Structure-based drug design against caPCNA for selective cancer chemotherapy development.

J. Jossart, P. Haratipour, L. Gu, C. M. Li, R. Lingeman, Y. Liu, R. J. Hickey, L. H. Malkas, J. J. P. Perry;
Beckman Research Institute of The City of Hope, Duarte, CA

Proliferating cell nuclear antigen (PCNA) is critical to DNA replication and repair processes, and it is also a proliferation biomarker in a variety of human tumors. A unique cancer-associated isoform of the protein, caPCNA, has been previously identified, allowing for rational-based drug discovery studies to develop leads with the potential for selective therapeutic targeting of cancer cells. Several strategies have been employed to develop agents targeting caPCNA, including peptide and small molecule-based inhibitors, but the success in developing therapeutically tractable compounds has been limited so far. Here, we present the crystal structures and corresponding biochemical characterizations of our novel small molecule-based caPCNA inhibitors, which bind into the PIP-box binding pocket of PCNA. One of our lead compounds is now an investigational new drug that we observed selectively kills cancer cells, and it appears to induce replication stress, apoptosis and increase cancer cell sensitivity to genotoxic agents, while these effects are not observed in non-malignant cell controls. This caPCNA inhibitor is orally administrable, metabolic stable and it suppresses tumor growth as a monotherapy or as a combination treatment, and it has entered clinical trials in the United States. PCNA plays a critical role in temporarily dislodging RNA polymerase II from transcription replication conflict sites, to enable the replication fork to proceed. Thus, structure-based drug discovery approaches to target transcription replication conflict resolution machinery, such as PCNA protein, may open a novel therapeutic avenue for exploiting this cancer-selective vulnerability.

#5785 Shedding light on PARP1-E2F1 interaction by Cryo-EM.

P. Iglesias[1], E. Casajus-Pelegay[2], M. Moreno-Morcillo[2], L. Gonzalez-Rendo[1], L. Porres-Ventin[1], V. Arce[1], R. Fernandez-Leiro[2], **J. Costoya**[1];
[1]Universidade de Santiago de Compostela, Santiago de Compostela, Spain, [2]Spanish National Cancer Research Centre (CNIO), Madrid, Spain

Cell division is orchestrated by a complex network of interactions between proteins involved in numerous signaling pathways that control cell proliferation. One of these main players is the E2F family of transcription factors. The role of these key players is to regulate the expression of several genes important in cell proliferation, particularly those involved in progression through G1 and into the S-phase of the cell cycle. In fact, cell cycle deregulation is a hallmark of cancer, and multiple studies have highlighted the critical role of E2F hyperactivation in tumor progression, angiogenesis, and metastasis. However, targeting a master regulator of cell growth will also have a pernicious effect on non-cancerous cells, thus limiting its applications. In order to overwhelm these restrictions, we propose a therapeutic approach in which E2F transcriptional activity is specifically reduced in cells with hyperactivation of the pathway, such as cancer cells.We and others have shown that poly (ADP-ribose) polymerase 1 (PARP1) is a transcriptional co-activator of E2F1 and, owing to this, loss of PARP results in cell cycle re-regulation and reduction of tumor growth. Interestingly, this effect of PARP1 does not depend on its enzymatic activity, thus opening a completely new strategic approach. Furthermore, considering that most oncogenic processes are associated with cell cycle deregulation, disruption of PARP1-E2F1 interaction could provide a new therapeutic target with a wide spectrum of indications in cancer. Currently, we lack comprehensive structural details regarding the PARP-1/E2F1 protein-protein interaction. To address this, we used cryo-EM to investigate both the standalone structure of PARP1 (full length) and its interaction with E2F1. This approach yielded high-resolution structural insights into the PARP1-E2F1 complex, enabling precise identification of the protein-protein interaction interface (PPI). Through this exploration of structural and molecular determinants governing this interaction, we aim to develop innovative strategies for designing drugs targeted at disrupting this complex. This work was supported by Agencia Estatal de Investigación (AEI/10.13039/501100011033), Xunta de Galicia (GPC GI-1862, ED431B 2020/26; ED431G 2019/02) and European Regional Development Fund-ERDF.

#5786 Epstein-Barr virus nuclear antigen 1 (EBNA1)-targeting probes stimulate interferon-β production by nasopharyngeal carcinoma (NPC) cells to enhance the natural killer cell-mediated cytotoxicity against NPC.

L. Chen[1], X. H. Liu[1], H. T. Yuen[1], **W. C. Cho**[2], K.-L. Wong[3], H. L. Lung[1];
[1]Hong Kong Baptist University, Hong Kong SAR, China, [2]Queen Elizabeth Hospital, Hong Kong SAR, China, [3]The Hong Kong Polytechnic University, Hong Kong SAR, China

Introduction: The prevailing histologic subtype of nasopharyngeal carcinoma (NPC) in the endemic regions is non-keratinizing carcinoma which shows almost consistent association with latent infection by Epstein-Barr virus (EBV). Previously our group developed a series of Epstein-Barr virus nuclear antigen 1 (EBNA1)-targeting probes, which can disrupt the EBV latency maintained by EBNA1, and such lytic induction could alert the immune cells.
Methods: Natural killer (NK) cells of the innate immunity play a significant role in controlling EBV infection. In this study, we investigated whether our EBNA1 probes (ZRL5P4 & L2P4) could activate NK cells to eliminate NPC.
Results: Studies of clinical specimens indicated that tumor infiltration of the cytotoxic NK cell subset is a favorable prognostic marker for NPC patients. Furthermore, the cytotoxicity of circulating NK cells derived from NPC patients is equally well the cells from healthy individuals. If those patients' NK cells can be attracted to infiltrate into the tumors, the tumor burden should be relieved. Indeed, the NPC xenograft with the ZRL5P4 treatment showed heavy mouse NK cell infiltration and tumor size reduction. The essential role of those mouse NK cells was demonstrated. Next, we showed that ZRL5P4 could induce the production of a soluble factor by NPC cells to stimulate the NK cell cytotoxicity. Such NK cell activity was verified in a metastasis NPC model. Mechanistically, the EBNA1 probe treatment could induce the expression of EBV early lytic gene Rta and EBNA1 itself. Both Rta and EBNA1 are known transcription factors to drive the expression of LMP1, the NF-κB signaling was then activated, which turned on the production of the well-known NK cell activation cytokine IFN-β.
Conclusion: Taken together, our results demonstrated that our EBNA1 probes can mobilize NK cells to the tumor sites and activate their anti-tumor activity via the EBV reactivation and stimulation of IFN-β production.

#5787 Structure-function mapping of DHODH shows deviations in protein structure.

Ruchika Pokhriyal[1], Laura Evans[1], Hyuk-Soo Seo[1], Jillian K. O'Neil[1], Betty Rouaisnel[1], Atanas Kamburov[2], Judith Guenther[2], Stefan Gradl[2], Haribabu Arthanari[1], Sven Christian[2], Xiaoping Yang[3], Sirano Dhe-Paganon[1], Julie-Aurore Losman[1]

[1]Dana-Farber Cancer Institute, Boston, MA,[2]Bayer AG, Berlin, Germany,[3]Broad Institute of Harvard and MIT, Cambridge, MA

Dihydroorotate dehydrogenase (DHODH) is a CoQ-dependent enzyme that converts dihydroorotate to orotate in the *de novo* pyrimidine biosynthesis pathway. Multiple structures of DHODH in complex with various small molecule inhibitors have been solved that indicate that DHODH inhibitors bind in the CoQ binding tunnel of DHODH and act as competitive inhibitors of CoQ. We performed saturating mutagenesis screens to identify mutations in DHODH that confer resistance to brequinar and BAY2402234, two highly potent DHODH inhibitors. As expected, many of the resistance mutations localized to the drug/CoQ-binding tunnel of the enzyme. Among the top-scoring drug-binding-domain mutants in both the brequinar and BAY2402234 screens were substitutions A58H and A58T. *In silico* analysis predicted that A58H should impair DHODH binding to both brequinar and BAY2402234. However, A58T was predicted to only impair binding of DHODH to brequinar. We expressed the mutants in a DHODH inhibitor sensitive cell line and confirmed that they both confer resistance to brequinar and BAY2402234, and we then assessed the ability of the mutants to bind drug by cellular thermal shift assay (CETSA). We found that, as predicted, DHODH A58H did not bind brequinar or BAY2402234. However, to our surprise, we detected binding of both brequinar and BAY2402234 to DHODH A58T. We generated recombinant DHODH A58T and confirmed that the purified protein was enzymatically active and strongly drug-resistant by DCIP assay and then assessed binding of the mutant protein to brequinar and BAY2402234 by thermal shift assay (TSA). Consistent with our CETSA results, recombinant DHODH A58T bound both brequinar and BAY2402234 *in vitro*. These results suggested that DHODH A58T can simultaneously bind drug and CoQ. However, previously reported DHODH structures indicated that the drug/CoQ binding tunnel is quite narrow and rigid. To determine whether the structure of catalytically-active DHODH is more flexible than inhibitor-bound catalytically-inactive DHODH, we co-crystallized wild-type DHODH with decylubiquinone (DCU), a CoQ analog that can act as a DHODH co-substrate *in vitro*. We found that the structure of DCU-bound DHODH differs from previously published DHODH structures in two important ways: (1) there appears to be a second point of ingress into the active site of DHODH next to the CoQ tunnel that may be able to accommodate a highly non-polar molecule such as CoQ/DCU and (2) the ‘flap’ covering the DHO/orotate ingress/egress region of DHODH, which is ‘closed’ in inhibitor-bound DHODH, is ‘open’ in DCU-bound DHODH. We are currently working to solve the crystal structure of DHODH A58T bound to inhibitor and DCU to ask if DCU can access the active site of DHODH through an alternative hydrophobic tunnel and if DHODH A58T remains in the ‘open’ configuration when bound to drug.

#5788 Targeting p97-NPL4 pathway by copper chelators.

M. Mistrik, Z. Skrott, M. Loffelmann;
Palacky University in Olomouc, Olomouc, Czech Republic

Copper chelators forming stable complexes, such as the bis(diethyldithiocarbamate)-copper complex (CuET), derived from Antabuse (disulfiram, DSF), have shown pronounced anticancer activity. CuET induces aggregation of NPL4, a crucial cofactor of the p97 segregase in the ubiquitin-proteasome system, leading to proteotoxic stress and subsequent cancer cell death. Our study investigates whether NPL4 inhibition is unique to CuET or extends to other dithiocarbamate-copper complexes and distinct copper chelators. Utilizing a cellular NPL4 aggregation screening assay, we examined various chelators for their ability to induce NPL4 aggregation. Our findings reveal that this capacity is relatively common among structurally diverse DTCs-copper complexes and other unrelated copper chelators. Compounds that caused NPL4 aggregation also triggered NPL4-p97 complex immobilization, polyubiquitinated protein accumulation, and unfolded protein and heat shock responses. These responses correlated strongly with cancer cell cytotoxicity, particularly potent at nanomolar concentrations, underscoring NPL4 as a critical target. Our results demonstrate the broad potential of copper chelators in targeting NPL4, inducing lethal proteotoxic stress in cancer cells, and offering significant implications for drug development.

EXPERIMENTAL AND MOLECULAR THERAPEUTICS: Cancer Treatment: New Technologies
Poster Session

#5792 Rapid and efficient generation of panels of T cell engaging (TCE) multispecific antibodies via complementary technologies.

Cory Ahonen, Nathan Sharkey, Melissa Durkin, Andrew Avery, Michael Battles, Beth Sharkey, Kyle Barlow, Arvind Sivasubramanian, Caitlin Stein, Bradley Lunde, **Kevin Schutz**, Bianka Prinz, Rob Pejchal, Paul Widboom, Eric Krauland

Adimab LLC, Lebanon, NH

A goal of immunotherapy is to induce an anti-tumor response that is potent and specific. However, there is increasing understanding that currently approved monospecific checkpoint inhibitors are not effective for all patients and/or indications. Thus, investigators are increasingly pursuing multispecific antibody treatments in an attempt to enhance clinical outcomes. These treatments may either take the form of mixtures (administered simultaneously or in series) of multiple monospecific antibodies, or as single entity, multispecific antibodies ('multispecifics'). In the case of multispecifics, the large number of possible topologies and complexity of manufacture necessitate the development and application of a robust set of complementary technologies. We have developed an exemplary set of such technologies. Herein, we demonstrate the ability to direct desired antibody chain pairing (HC-HC and HC-LC), isolate and engineer single-domain antibodies, as well as generate large (≥100) panels of multispecific antibodies with diverse topologies from a limited number of input molecules. These technologies can be leveraged in combination with our affinity and developability-optimized TCE αCD3 and αCD28 antibody panels to achieve desired potency without the need for additional discovery or engineering.

#5793 Functional DKK1 antibodies binding to cysteine-rich domain 1 or 2 of hDKK1 demonstrate antagonistic activities on tumor suppression or TCF/LEF signaling.

L. Wang, Z. Han, M. Yang, A. G. Lujan Hernandez, V. Prabhu, C. F. Hu, T. Htoy, M. Villalta, T. Z. Yuan, H. Giang, A. Sato;
Twist Bioscience, South San Francisco, CA

Wnt signaling plays an important role in embryonic development and tumorigenesis. These biological effects are exerted by activation of the β-catenin/TCF transcription complex and consequent regulation of a set of downstream genes. DKK1 has been shown to be a potent inhibitor of Wnt signaling via competing Wnt binding to LRP5/6. DKK1 is tumorigenic in multiple cancer types and also immunosuppressive via MDSCs and NK cells. Emerging evidence indicates that DKK1 has been involved in T cell differentiation and induction of cancer evasion of immune surveillance by accumulating MDSCs. Consequently, DKK1 has become a promising target for cancer immunotherapy, and the mechanisms of DKK1 affecting cancers and immune cells have received great attention. With Twist's precision DNA writing technologies, we have created phage display libraries with diversity greater than 1×10^{10}, and utilized machine learning model for optimal discovery. In this study, we discovered anti-DKK1 antibodies bind to different cysteine-rich domain (CRD) of hDKK1 by epitope binning and mapping, and block the binding of DKK1 to the receptor. Binding of the antibodies to different CRDs of hDKK1 lead to different activation effect. The *in vitro* functional assays showed that the interaction of Wnt to its receptor was restored in the presence of anti-DKK1 antibodies binding to DKK1 CRD2, resulting in TCF/LEF signaling upregulation. Moreover, anti-DKK1 antibodies binding to DKK1 CRD1 induced immune cell activation and led to tumor cell cytotoxicity. *In vivo* study indicated anti-DKK1 antibody lead is potent in tumor regression. Our anti-DKK1 lead shows promising efficacy in cancer immunotherapy without influencing Wnt canonical pathway.

#5794 DX2206, a humanized monoclonal antibody that targets IL1RAP, exhibits potent inhibition of IL-1 pathways and activities against tumors *in vitro* and *in vivo*.

Q. Liu, Y. Ru, Y. Jiang, H. Li, W. Li, L. Yang, **Q. Shi**;
Singlomics (Beijing DanXu) Biopharmaceuticals Co., Ltd., Beijing, China

Background: The Interleukin-1 Receptor Accessory Protein (IL1RAP) is found on cancer cells, stromal cells, and infiltrating immune cells within the tumor microenvironment (TME) of various cancers. It plays an important role in tumor development at various stages by activating IL-1 superfamily pathway, thus become an interesting target in cancer treatment.
Methods: We investigated the correlation between IL1RAP and tumor prognosis through the analysis of the public dataset. An antibody discovery campaign was performed and DX2206 was identified as the top clone against IL1RAP. Epitope of DX2206 was determined by examining the binding of DX2206 with different IL1RAP structural domains and in silico analysis. The activities of DX2206 against IL-1, IL-33, and IL-36 were examined using multiple assays with HEK293-Luc reporter cells, primary HUVEC cells, and A431 human skin squamous carcinoma cells. In vivo efficacy was evaluated in a CDX model.
Results: Based on public data, IL1RAP is overexpressed in various types of cancer patients compared to healthy individuals, and high expression of IL1RAP is associated with poor prognosis in multiple cancer types. Furthermore, high expression of the members of the IL-1 superfamily, such as IL1RAP, IL-1, and IL-36, are negatively correlated with pan-Cancer OS. Our epitope analysis indicated that DX2206 binds to a unique epitope within IL1RAP domain 2. In vitro assays demonstrated that DX2206 inhibited the activities of all three pathways, IL-1, IL-33, and IL-36, with sub-nanomolar IC50s. Simultaneously, it induced a potent ADCC effect in the tumor killing assay. Finally, in a CDX model, DX2206 significantly inhibited tumor growth in vivo.
Conclusions: We discovered a potent antagonist antibody, DX2206, that binds to a unique epitope of IL1RAP, inhibits all three pathways of signaling, and demonstrates in vitro and in vivo activities against tumors. Considering these characteristics, DX2206 emerges as an outstanding preclinical candidate for cancer therapy. IND enabling study was ongoing to expedite the candidate into clinic.

#5795 Potent and selective degradation of KAT2A and KAT2B induces profound cell state changes and inhibits growth of AML, SCLC and NEPC model systems.

K. S. Straley[1], J. Neef[1], I. Antony-Debre[2], M. Bhatta[1], S. Sharma[1], S. Sinicropi-Yao[1], J. DeBartolo[1], A. McRiner[1], B. Chan[1], H. Wilson[1], C. S. Lee[1], Z. Boudhraa[3], M. El Ezzy[3], U. Sharif[4], M. Bittinger[1], L. Antipov[1], T. G. Graeber[5], S. de Botton[2], K. E. Yen[1], D. S. Millan[1];
[1]Auron Therapeutics, Newton, MA, [2]Gustave Roussy Cancer Center, Villejuif, France, [3]Paraza Pharma, Inc., Laval, QC, Canada, [4]Sygnature Discovery, Alderley Park, United Kingdom, [5]UCLA, Los Angeles, CA

Phenotypic plasticity, or the ability of cancer cells to switch between cell states, has recently been recognized as a key hallmark of cancer. Cancer cells can hijack normal developmental pathways, preventing terminal differentiation or causing de-differentiation or transdifferentiation to a more proliferative, plastic cell state similar to those found in early development. Using our proprietary AI/ML platform AURIGIN, we created a high-resolution atlas to define the drivers of normal cell states during human development. After mapping primary human tumors to the atlas, we identified the histone acetyltransferase KAT2A as a key driver of tumor cell plasticity in a subset of acute myeloid leukemias (AML), small cell lung cancer (SCLC) and neuroendocrine prostate cancer (NEPC). Targeting KAT2A was genetically validated in MOLM-13 (AML) cells, where knockdown resulted in significant cell growth inhibition and induction of cell state changes consistent with a more mature differentiation phenotype. Similarly, an early tool heterobifunctional degrader of KAT2A and KAT2B (AUR101) resulted in potent growth inhibition and granulocytic differentiation in MOLM-13 cells and in 5/12 primary AML patient samples grown ex vivo. Treatment of NCI-H1048 SCLC cells with AUR101 potently degraded KAT2A/B, induced a significant shift from a dedifferentiated cell state to a more differentiated epithelial cell state and potently inhibited cell growth both in vitro and in vivo.

The strong biological validation of KAT2A/B in SCLC and AML tumors, led us to develop AUR1545, a novel sub-nanomolar degrader of KAT2A and KAT2B. AUR1545, with its improved drug like properties, was tested across representative models of AML, SCLC and NEPC. In vitro, treatment with AUR1545 inhibited proliferation and promoted profound cell state changes in MOLM-13 (AML) cells. In NCI-H1048 (SCLC), LASPC-01 (NEPC) cell lines as well as a primary NEPC organoid model, AUR1545 demonstrated potent antiproliferative effects. In vivo, AUR1545 significantly inhibited tumor growth in an NCI-H1048 xenograft model. Taken together, these data genetically and pharmacologically validate KAT2A and KAT2B as key drivers of cell state plasticity in SCLC, NEPC and AML tumors and point to their utility as novel targets in these aggressive, metastatic and drug resistant cancers.

#5796 A HER3 antibody that uniquely blocks the HER3 heterodimerization interface effectively inhibits tumor growth in pre-clinical models with potentially oncogenic HER3 mutations.

W. Toy[1], D. Thakkar[1], R. Magallanes[1], S. Wu[2], M. Poi[2], A. Mas[1], K. Paszkiewicz[1], P. Ingram[1], J. Boyd-Kirkup[1];
[1]Hummingbird Bioscience, Singapore, Singapore, [2]Caris Life Sciences, Phoenix, AZ

HER3 activation, via NRG1 ligand-dependent and -independent heterodimerization with HER2 or EGFR, has been associated with tumor progression and acquired resistance to therapies in multiple indications. HER3 mutations, detected in around 3% of cancer cases, may drive oncogenic signaling, leading to rapid tumor growth. Currently, there are no approved targeted therapies for HER3 mutations. Through analysis of real-world data and structural modelling of HER3 heterodimers, we identified four common HER3 mutations located within or close to the dimerization interface of HER3, suggesting a potential impact on HER3 heterodimerization. Immunoprecipitation assays confirmed that all four mutations increased the heterodimerization of HER3 with both HER2 and EGFR. Further, conversion of an endogenous HER3 mutation to wild type via CRISPR editing significantly reduced the growth of KYSE-150, a HER3 mutant cell line. HMBD-001 is a clinical-stage anti-HER3 antibody rationally developed to uniquely block the HER3 dimerization interface to potently inhibit HER3 heterodimerization. Through structural analysis and FACS binding on HER3 mutation cell lines, we confirmed that the binding epitope of HMBD-001 does not overlap with the selected HER3 mutations and therefore may be a good therapeutic option for patients with HER3 mutations. In vitro, HMBD-001 suppressed HER3 mutation-driven PI3K/AKT signaling, as demonstrated by the reduction of phosphorylated HER3 and AKT levels. In multiple cell- and patient-derived xenograft models with HER3 mutations HMBD-001 response achieved >80% tumor growth inhibition. Based on this encouraging preclinical data, a Phase Ib clinical trial (NCT05919537) has been initiated, evaluating HMBD-001 in patients with aberrant HER3 signaling, including HER3 mutations.

#5797 Next generation antibody drug conjugates: Multi-payload conjugates targeting multiple mechanisms of cell killing.

R. L. Kendall[1], M. Lobba[1], S. Johri[1], C. Symister[1], D. Trinter[1], M. Nguyen[1], D. Gutierrez[1], S. Brady[1], A. Lau[1], M. B. Francis[2];
[1]Catena Biosciences, Inc., Berkeley, CA, [2]University of California, Berkeley, Berkeley, CA

Introduction: ADCs have had tremendous impact on patient outcomes in breast cancer and are now second line therapy for stage IV HER2 positive metastatic breast cancer. However, many patients fail to respond or relapse after treatment with ADC therapies due to tumor heterogeneity and resistance to ADC payloads. We are developing next generation ADCs that deliver targeted combination chemotherapies with a single molecule.
Method: CatenaBio has developed a novel system capable of attaching distinct payloads at different sites to the same antibody, enabling the production of highly stable single-molecule targeted combination therapies, Multi-Payload-Conjugates (MPCs), with a well-defined drug-antibody ratio (DAR).
Results: We screened combinations of different payloads targeting several different mechanisms of cell division attached to trastuzumab at different DARs to optimize tumor cell killing. These targeted combination ADCs demonstrated robust killing in both HER2 high and low tumor cell lines. Additionally, these novel MPCs show potent inhibition of tumor growth in a HER2+ xenograft model of cancer.
Conclusion: Antibody Drug Conjugates have revolutionized the treatment of high HER2 positive breast cancer. More recently advances have been made in the design of ADCs to expand indications to include HER2 low as well as HER2 negative patients. Multi-payload Conjugates® offer the next step in ADC design and allow for the combination of multiple mechanisms of action in a single MPC that are highly effective across multiple breast cancer cell lines and HER2 expression levels. These molecules offer the potential to circumvent tumor resistance pathways and deliver deeper and more durable responses.

#5798 Preclinical safety assessment for specificity of biotherapeutics using the membrane proteome array.

K. S. Raghavan, J. T. Sullivan, C. Navia, R. H. Fong, B. J. Doranz;
Integral Molecular, Philadelphia, PA

Rigorous specificity analysis is critical for the development of antibody-based therapies, as even minimal off-target binding can lead to toxicity and clinical failures. Long believed to be exquisitely specific, recent preclinical data and our own work indicate that monoclonal antibodies (MAbs) frequently (~25%) display cross-reactivity. In many cases, off-target interactions occur with unrelated proteins that cannot be predicted by protein sequence homology. Cross-reactivity can lead to serious or even life-threatening consequences especially when MAbs are configured as bispecifics, antibody-drug conjugates (ADC) or CAR-T cell therapies, and IND applications for biotherapeutics require cross-reactivity assessment to prevent adverse events. Tissue cross-reactivity (TCR) studies have traditionally been used to screen for off-target binding, however, with poor predictive value for in vivo safety and toxicity. We developed the Membrane Proteome Array (MPA) platform to de-risk MAb-based therapeutics by testing for specificity across 6,000 human membrane proteins expressed in unfixed cells. The MPA assesses binding interactions by high-throughput flow cytometry allowing for high sensitivity detection and rapid analysis. All targets identified on the MPA screen are validated by secondary titration analysis. In contrast to TCR studies, proteins in the MPA exist in their native conformations and are not altered by fixation. Recently, we used the MPA to select a lead antibody candidate targeting the oncotherapeutic target Claudin 6 (CLDN6). Through MPA screening, we successfully identified a lead candidate devoid of cross-reactivity against other CLDN family members or any other membrane protein across the human genome. The MPA has also been used to rapidly evaluate the specificity of novel CAR-T cell therapies for cancer and autoimmunity. The MPA has been used for lead selection and data from the MPA has been accepted by the FDA as a part of IND applications for antibody-based therapies. The MPA is currently under consideration for being developed as an FDA-qualified Drug Development Tool.

#5800 Ultrasound-mediated nano-drug delivery system to enhance cancer treatment efficacy: An *in vitro* study.

Farshad Moradi Kashkooli, **Anshuman Jakhmola**, Tyler K. Hornsby, Graham A. Ferrier, Jahangir (Jahan) Tavakkoli, Michael C. Kolios

Toronto Metropolitan University, Toronto, ON, Canada

Conventional non-targeted nano-sized drug delivery systems face limitations such as restricted drug penetration depth and treatment efficacy in solid tumors. External stimulus such as ultrasound waves can trigger targeted, on-demand drug release from the nanocarriers. We demonstrate a first-of-its-kind use of low-intensity pulsed ultrasound (LIPUS) to induce Doxorubicin release from the surface of gold nanoparticle drug carriers. Our 1-MHz LIPUS beam is capable of penetrating tissue to sufficient depths with the required power/intensity for drug release applications with a nominal intensity of around 3 W/cm^2 in the region of interest (ROI). This level of intensity is necessary to elevate the tissue temperature to the mild hyperthermia range of 41 to 45 °C. Our *in vitro* experiments demonstrate a remarkable 22% enhancement in drug release with the addition of LIPUS. Measurements of drug release kinetics, with and without LIPUS, suggest that LIPUS shifts the drug release mechanisms from static (Fickian) to dynamic (non-Fickian) release *in vitro*. Thus, revealing the intricate interactions between ultrasound and drug release from gold nanoparticle drug carriers. To assess the efficacy of the delivery system, we developed an *in vitro* cell culture model with a customized ultrasound exposure setup. The LIPUS device was situated at the bottom base of a water tank, directing ultrasound beam upward toward a region of interest where the MDA-MB-231 breast cancer cells were located 35 mm away from the LIPUS element. We found that the LIPUS device operating at an acoustic power of around 4 W increased cell killing efficacy by approximately 15% ± 2% when compared to conventional nano-drug delivery, highlighting a significant improvement attributed to ultrasound-induced mechanical effects. At the cellular level, these results underscore the potential advantages of ultrasound-mediated nano-drug delivery over conventional chemotherapy and non-targeted nano-drug delivery.

#5801 Targeted delivery of Exatecan to tumors via a novel cell-penetrating, anti-DNA antibody.

Zaira Ianniello[1], Elias Quijano[2], Denise Hegan[1], Venu Bommireddy[3], Dale Ludwig[3], Peter M. Glazer[1]

[1]Therapeutic Radiology, Yale University School of Medicine, New Haven, CT,[2]Genetics, Yale University School of Medicine, New Haven, CT,[3]Gennao Bio, Pennington, NJ

The formulation of novel chemotherapeutics capable of precisely targeting and damaging tumor cells, while preserving the integrity of healthy tissues, represents a principal challenge and is recognized as one of the biggest achievements in cancer treatment in the last few decades. Antibody-drug conjugates (ADCs) hold significant potential as an effective cancer treatment, by targeting and delivering cytotoxic drugs exclusively to tumor cells that express distinct antigens associated with malignancy. Due to the necessity for specific surface antigens, therapies with ADCs are limited to specific tumor subtypes. In this study, we show the potential of a lupus-derived, cell-penetrating, anti-DNA antibody for delivering of cytotoxic payload to tumors *in vivo*. We utilized a fully humanized variant, named as V66, which was chemically linked to the Topoisomerase I inhibitor, Exatecan. The primary mechanism involved in V66 cellular penetration is mediated by the Equilibrative Nucleoside Transporter ENT2. The latter shows elevated expression in a substantial subset of cancer types in comparison to healthy tissues, broadening the range of applications for ADCs in tumor therapy. Using labeled V66, we demonstrated specific tumor delivery *in vivo*, with minimal impact on healthy tissues. *In vitro* experiments validated the nuclear localization of V66-Exatecan, where it triggers the activation of the DNA damage repair pathway (DDR). As a consequence of the profound DNA damage, exposure to V66-Exatecan leads to cell death, exhibiting low nanomolar EC_{50} values across a diverse range of cell lines. Furthermore, V66-Exatecan treatment presents synthetic lethality with BRCA2 deficiency, evidenced by a substantial increase in sensitivity. *In vivo* efficacy studies conducted in BRCA2 deficient tumors revealed a remarkable effectiveness of V66-Exatecan, leading to almost complete tumor regression and substantial improvement in the probability of survival. In addition to the lack of significant weight changes observed throughout the treatment, further toxicological studies conducted in serum and tissues demonstrated the absence of short- and long-term toxicity, with optimal liver and kidney function and the absence of damage to other tissues. Likewise, bone marrow cellularity remained unaffected. Collectively, these studies indicate that V66-Exatecan achieves targeted treatment of tumor cells, where it induces DNA damage leading to cell death. The *in vivo* application of V66-Exatecan leads to tumor regression without triggering general toxicity that is otherwise associated with Topoisomerase I inhibitors. This work provides the basis to advance a novel nuclear-penetrating ADC for delivering cytotoxic payloads.

#5802 An orally available small molecule JMBI-001 elicits MYC-synthetic lethality and anti-tumor immunity by disabling MKLP2-mediated cellular processes.

T. Zhang[1], Q. Shi[1], J. Kalashova[1], X. Liu[2], X. Zhou[2], C. Yang[1], Y. Long[1], H. Li[1], J. Li[1], G. Lv[1], D. Yu[1], X. Jiang[2], S. Zhang[2], J. Zhang[2], H. Liu[1], **D. Yang**[2]; [1]Chengdu Anticancer Bioscience, Chengdu, China, [2]J. Michael Bishop Institute of Cancer Research, Chengdu, China

The MYC oncogene, a pivotal regulator of various cellular processes, is deregulated in approximately 70 % of human malignancies. Mitotic Kinesin-like Protein 2 (MKLP2) plays a versatile role in both interphase and mitosis and has emerged as a significant prognostic indicator and therapeutic target in cancer. The undruggability of MYC and the scarcity of MKLP2 inhibitors, however, have impeded clinical translation. Our development of JMBI-001, a potent and orally bioavailable small-molecule compound, overcomes these barriers. JMBI-001 elicits loss of function phenotypes in MKLP2 and a synthetic lethal interaction with MYC overexpression. Extensive kinome and safety profiling have revealed no significant off-target effects, and the compound is well-tolerated in long-term animal studies. In preclinical models, JMBI-001 has demonstrated an average tumor growth inhibition rate of 75 % across more than 20 MYC-overexpressing tumor models, including those in the stomach, lung, colon, liver, breast, kidney, skin, and hematopoietic system. Its anti-tumor activity positively correlates with high MYC abundance, aligning with the selective eradication of cells with abundant MYC both *in vitro* and *in vivo*. Notably, JMBI-001 also robustly stimulates systemic anti-tumor immunity, enhancing NK and $CD3^{\pm}$ T cell infiltration in tumors of syngeneic cancer models. Moreover, additive or synergistic effects have been observed when combined with anti-PD1 therapy even in tumors refractory to the immune checkpoint blockade (ICB) therapy. The dual therapeutic actions of JMBI-001 stem from its disruption of MKLP2 functionalities, leading to anomalies, such as Golgi fragmentation in interphase and multipolarity in pro-metaphase. These disruptions lead to two key outcomes: apoptosis and immunogenic cell death, marked by secreted ATP, released high mobility group protein B1 (HMGB1), and surface-exposed calreticulin. These abnormalities, primed and amplified by deregulated MYC, are not observed in non-transformed cells, suggesting their potential as pharmacodynamic markers for monitoring JMBI-001's activity *in vivo*. In conclusion, JMBI-001 represents a novel class of anticancer agents that simultaneously triggers MYC synthetic lethality and anticancer immunity by targeting MKLP2-mediated cellular processes. Its unique mechanisms of action, exceptional bioavailability, potency at low nanomolar concentrations, wide-spectrum efficacy, and favorable safety profile establish JMBI-001 as a promising clinical study-ready drug candidate for treating MYC-driven cancers.

#5803 Tumor treating fields alter PDGFR-β localization in immortalized human pericytes in an *in vitro* model of the blood-brain barrier.

E. Salvador, T. Koeppl, A. F. Kessler, M. Burek, R.-I. Ernestus, M. Lohr, **C. Hagemann**;
University Hospital Wurzburg, Wuerzburg, Germany

Background: Tumor Treating Fields (TTFields) are alternating electric fields of intermediate frequency (100-500 kHz) and low intensity (1-3 V/cm). TTFields at 200 kHz, together with adjuvant chemotherapy, increased progression-free and overall survival of newly diagnosed Isocitrate dehydrogenase (IDH) wildtype and IDH mutant glioblastoma (GBM, WHO CNS 2016) patients in a randomized controlled trial and were therefore approved for the treatment of these patients. We recently demonstrated that TTFields at lower frequencies transiently increase the permeability of blood-brain barrier (BBB) models of murine and human origin by delocalizing junctional proteins such as claudin-5, ZO-1, and occludin in endothelial cells. The interaction between pericytes and endothelial cells contributes to the rigorous integrity of the BBB and is driven by endothelial cells releasing the platelet-derived growth factor β-subunit (PDGF-β), which binds to the receptor PDGFR-β on the surface of pericytes. Here, we investigated the effects of TTFields on pericytes in a human cell-based *in vitro* BBB model in order to gain a better understanding of the effects of TTFields on BBB integrity.
Methods: We prepared an in vitro BBB model composed of human brain microvascular endothelial cells and human pericytes. The model was subjected to TTFields at 100-300 kHz for 24 to 72 h. Afterwards, pericytes were incubated with Alexa Fluor 488-labeled anti-PDGFR-β antibody in order to visualize PDGFR-β localization and cell morphology under the microscope. To make sure that no cell loss occurred due to TTFields treatment, the nuclei of pericytes were counted.
Results: TTFields treatment altered the distribution of PDGFR-β staining after treatment, with fewer, less distinct and more punctate PDGFR-β foci. These changes were most prominent after 72 h of TTFields treatment at 300 kHz. We also observed larger nuclei in the pericytes after treatment but no significant loss of cells could be observed as per the nuclei count.
Conclusion: Together with the previously observed delocalization of tight junctional proteins in endothelial cells, the altered distribution of PDGFR-β pericytes could reveal new mechanistic insights into the effects of TTFields on BBB integrity.

#5804 Preclinical evaluation of LCB84, a novel next-generation TROP2 directed ADC utilizing a cancer selective linker and an MMAE payload.

S. Slocum, H. Kim, C.-W. Chung, C. Park;
LegoChem Biosciences, Inc, Daejeon, Korea, Republic of

LCB84 is an antibody-drug conjugate (ADC) that consists of an antibody targeting human trophoblast cell-surface antigen-2 (TROP2) linked to monomethyl auristatin E (MMAE) via a beta-glucuronidase cleavable linker with a drug-to-antibody ratio (DAR) of 4. LCB84 demonstrates tumor selective killing by multiple mechanisms, increasing both safety and efficacy in parallel. Firstly, the over-expression of TROP2 in many solid tumors allows for targeted delivery of MMAE by LCB84 to Trop2-positive tumor tissues. Secondly, the overexpression of beta-glucuronidase in the lysosome of most tumors facilitates the selective release of active payload within tumor cells compared to normal healthy tissues. Thirdly, the intrinsic selectivity of tubulin inhibitor payloads, such as MMAE, for proliferating cells provides additional protection for non-proliferating normal cells. MMAE is also cell-permeable in its free drug form and can lead to increased efficacy of LCB84 via a bystander effect, enabling activity in heterogenous tumors. LCB84 demonstrates superior efficacy in mouse tumor xenograft studies when compared to benchmark TROP2-targeting ADCs, including sacituzumab govitecan and datopotamab deruxtecan. LCB84 also shows an improved safety profile compared to these clinical benchmarks, as well as compared to traditional MMAE-bearing ADCs, in both *in vitro* and *in vivo* toxicity assessments. Additionally, LCB84 shows a stable preclinical pharmacokinetic profile with minimal loss of payload over time. The utilization of an ADC for target-mediated delivery, in combination with a stable beta-glucuronide trigger for selective payload release in tumors, allows for a superior preclinical therapeutic index which is expected to translate to a best-in-class ADC in the clinic.

#5805 A novel platform of diversified payloads to drive ADC innovation.

P. Orsini, M. Salsa, S. Rizzi, U. Cucchi, D. Faiardi, A. Burocchi, A. Ciavolella, R. Lupi, F. Gasparri, **B. Valsasina**;
Nerviano Medical Sciences, Nerviano, Italy

First generation of antibody drug conjugates (ADCs) for anticancer therapy has been described more than two decades ago with gemtuzumab-ozogamicin receiving the first approval in 2000. Over the last 4 years, 8 new ADCs got FDA approval essentially due to the innovation on the linker improving the disposition in patients and the manufacturability together with the technical advantages in the engineering of biologics and the introduction of new cytotoxic payloads such as deruxtecan. In the future, next generation ADCs will be developed exploring payloads beyond the currently used cytotoxins to improve safety, efficacy and durability of responses and therefore the short- and long-term therapeutic benefit to patients. Nerviano Medical Sciences (NMS) generated a portfolio of novel and diversified payload linkers leveraging on its proprietary chemical collection that includes cytotoxic and targeted payloads. A rigorous screening funnel has been applied considering diversification in terms of MoAs, pharmacokinetic properties, mechanism of resistance and combinability with other therapies to identify the optimal match with specific tumor types and targets, generating a new class of ADCs with improved selectivity and efficacy for hard-to-treat cancers even in chemoresistant settings. NMS ADC platform incorporates 1) our patent protected payload linker NMS-P945, a duocarmycin like DNA minor groove binder and alkylating agent inducing DNA damage, acting in chemoresistant cells with bystander effect and immunogenic cell death properties and generating ADCs highly efficacious in mouse xenograft models and safe when administered in NHP, 2) novel anthracyclines (PNU-682 derivatives) with an improved stability and safety profile and 3) targeted molecules with different mechanism of action including payloads active in synthetic lethality contexts. Payload linkers with different functionalization generated from each payload have been evaluated for chemical stability, sensitivity to lysosomal protease cleavage, and conjugability to monoclonal antibodies. The ADCs, generated with proof-of-concept antibodies (e.g. Trastuzumab), were characterized in terms of Drug to Antibody Ratio (DAR), aggregation level, plasma stability, antigen binding and differential antiproliferative activity in target positive vs target negative tumor cells. The best products resulting from the screening funnel have been subjected to a multidimensional analysis taking into consideration payload properties, tumor features and antigen expression in selected populations with the aim of identifying tumor types particularly sensitive to the payload. Our multidimensional approach coupling new payload linker with innovative MoA to careful selection of patients will allow to reach unprecedented efficacy and safety profile.

#5806 Discovery of a long half-life AURKA inhibitor to treat MYC-amplified solid tumors as a monotherapy and in combination with everolimus.

Y.-H. Chi, C.-P. Chang, T.-K. Yeh, C.-T. Chen, W.-P. Wang, Y.-T. Chen, C.-H. Tsai, Y.-F. Chen, Y.-Y. Ke, J.-Y. Wang, C.-P. Chen, T.-C. Hsieh, M.-H. Wu, C.-L. Huang, Y.-P. Chen, H. Zhuang;
National Health Research Insts., Miaoli County, Taiwan

Aurora kinase inhibitors such as alisertib can destabilize MYC-family oncoproteins and have demonstrated compelling anti-tumor efficacy. In this study, we report 6K465, a novel pyrimidine-based Aurora A (AURKA) inhibitor that reduces levels of c-MYC and N-MYC oncoproteins more potently than alisertib. In an analysis of the antiproliferative effect of 6K465, the sensitivities of small cell lung cancer (SCLC) and breast cancer (BC) cell lines to 6K465 were strongly associated with the protein levels of c-MYC and/or N-MYC. We also report DBPR728, an acyl-based prodrug of 6K465 bearing fewer hydrogen-bond donors that exhibited 10-fold improved oral bioavailability. DBPR728 induced durable tumor regression of c-MYC- and/or N-MYC- overexpressing xenografts including SCLC, triple-negative breast cancer (TNBC), hepatocellular carcinoma and medulloblastoma using a 5-on-2-off or once-a-week dosing regimen on a 21-day cycle. A single oral dose of DBPR728 at 300 mg/kg induced c-MYC reduction and cell apoptosis in the tumor xenografts for more than 7 days. The inhibitory effect of DBPR728 at a reduced dosing frequency was attributed to its uniquely high tumor/plasma ratio (3.6-fold within 7 days) and the long tumor half-life of active moiety 6K465. Furthermore, DBPR728 was found to synergize with the mTOR inhibitor everolimus to suppress c-MYC- or N-MYC- driven SCLC. Collectively, these results suggest DBPR728 has the potential to treat cancers overexpressing c-MYC- and/or N-MYC.

#5807 Bicycle Toxin Conjugates®for the treatment of solid tumors.

S. J. Walsh[1], J. Lahdenranta[2], P. Huxley[1], G. Mudd[1], G. Bennett[1], A. Brown[1], K. van Rietschoten[1], L. Chen[1], H. Scott[1], G. Ivanova-Berndt[1], K. Dzionek[1], M. Rigby[1], O. Burenkova[2], P. Jeffrey[1], P. Beswick[1], M. Skynner[1], N. Keen[2],

[1]Bicycle Therapeutics, Cambridge, United Kingdom, [2]Bicycle Therapeutics, Cambridge, MA

Bicycle Therapeutics is developing a unique class of chemically synthesized medicines. Based on its proprietary bicycle peptide (*Bicycle*®) phage display platform, Bicycles are a unique class of highly constrained peptides, which have demonstrated utility in the targeted delivery of different classes of payloads (for example cytotoxic agents, radioisotopes, immune modulators) into tumors. Bicycles are currently being explored in the clinic as Bicycle Toxin Conjugates® (BTCs) for targeted delivery of cytotoxic payloads into tumors. BTCs consist of a bicyclic peptide that is conjugated to a cytotoxic payload via a cleavable linker, which allows payload release in the tumor microenvironment or within the tumor cell. BTCs were developed to address the shortcomings of antibody drug conjugates (ADCs) in several ways. First, the small size of BTCs (~4 kDa) compared to large biologic entities such as monoclonal antibody (mAb)-based conjugates (~150 kDa) allows rapid distribution to tissues and extensive tumor penetration, which enables rapid delivery of payload into the tumor. Second, the peptidic nature of BTCs results in relatively short, yet tunable, duration of systemic exposure and liver-sparing renal elimination. These properties limit the body's exposure to payload and should therefore minimize damage to normal tissue. In this body of work, we used in vitro cytotoxicity and cell uptake assays and mouse and rat cell line derived xenograft models for 1) cytotoxicity and anti-tumor activity evaluation, and 2) Bicycle and toxin uptake and biodistribution evaluation. Here, we show that BTCs targeting a number of different tumor antigens can deliver toxins to tumor tissue producing durable responses in a range of preclinical in vivo models, spanning several solid tumor indications.

#5808 Designing arrays for delivering tumor treating fields (TTFields) to the mouse head.

S. Zbidat, R. Blatt, M. Sellevoll, M. Gabay, I. Schlachet, S. Cahal, S. Davidi, **I. Tzchori**, A. Haber, M. Giladi, Y. Palti;
Novocure Ltd, Haifa, Israel

Introduction: Tumor Treating Fields (TTFields) therapy is an approved treatment for glioblastoma (GBM), the most abundant malignant brain tumor. TTFields therapy is delivered to patients suffering from GBM continuously by two array pairs placed on their scalp. Since arrays for TTFields application to the mouse head are lacking, and as most GBM animal models are based on mice, in vivo studies of GBM treatment with TTFields are limited. The development of such arrays is challenging due to the small dimensions and specific geometries of the mouse head, but is needed to allow continued preclinical studies to broaden the understanding of the effects of TTFields on GBM.

Methods: We tested various array layouts to identify one that will be suited to the specific geometries of the mouse head. For animal well-being, the selected array was required to minimally restrict head movement. Additionally, we investigated adhesive tapes to allow on one hand good adherence of the arrays to the skin, and on the other hand easy array removal. To examine the feasibility of treating mice with these arrays, they were applied to mice for 11 days, while recording the electric currents and the actual treatment time (from which the percent usage could be calculated). To validate that the selected array layout delivers meaningful field intensity to the desired region, we performed field measurements using a floating scope.

Results: To tackle the limitation of the small head size, we developed an array layout in which only two arrays were situated on the head, while the opposing arrays were located on the mouse torso. Additionally, the arrays on the head were divided into two smaller disks. We also identified a thin and transparent adhesive tape (facilitating correct arrays positioning), that offered good tackiness and allowed easy removal without leaving residual adhesive on the skin. The arrays met the minimum treatment requirements: current ≥50 mA, usage ≥75%, field intensity ≥1 V/cm RMS. At the posterior side of the mouse head, at a location more directly underneath the arrays, field intensity was higher than at the anterior position.

Conclusion: TTFields could be delivered at sufficient intensities to mice heads by utilizing specifically engineered arrays. Our newly developed arrays are flexible and strongly adhering to enable efficient electric field delivery. By allowing TTFields delivery to mice heads, we will facilitate further advancing this research field.

#5810 The impact of scaffold, linker, homogeneity and payload selection on the efficacy and tolerability of anti-tubulin ADCs.

S. D. Collins, N. Keirstead, M. Damelin, D. Toader, K. Ishida, N. N. Kumar, K. L. Lancaster, K. C. Catcott, A. Yau, M. Bala, T. B. Lowinger; Mersana Therapeutics, Inc., Cambridge, MA

Antibody-drug conjugates (ADCs) achieve targeted drug delivery to a tumor and have demonstrated clinical success in many tumor types. The properties of an ADC, including its activity and safety profile, can be highly influenced by its characteristics and individual components, commonly viewed as the antibody, payload, linker, and drug-to-antibody ratio (DAR). However, multiple other characteristics can also significantly influence an ADC's overall drug-like properties, including DAR homogeneity, method of bioconjugation, hydrophilicity, and charge balance. Due to the multiparametric nature of ADC platform optimization, there are few examples in preclinical research, and even fewer in the clinical realm, where comparisons across platforms have been investigated for the same target, both preclinically and clinically, to elucidate how deliberate modifications in molecular design can improve drug-like properties and clinical outcomes. To that end, here we describe the improvements observed in preclinical characteristics, as well as their translational relevance to corresponding clinical characteristics. Two anti-NaPi2b ADCs were produced using two different platforms, XMT-1536 (Dolaflexin platform) and XMT-1592 (Dolasynthen platform), conjugated to the same antibody and employing the same payload. The Dolasynthen platform was deliberately designed, taking into account preclinical and clinical learnings from earlier ADC platforms, to improve both safety and efficacy. In addition, comparisons to clinically approved anti-tubulin ADC platforms are made to provide further context.

#5811 Ultralong CDR3 engineered interleukin-15 antibody fusion for T and NK cell expansion.

R. Huang, D. McGregor, V. Smider;
Applied Biomedical Science Institute, San Diego, CA

Interleukin (IL)-15 is a promising immunotherapeutic cytokine for cancer treatment because it can stimulate the proliferation and cytotoxicity of CD8+ T lymphocytes and nature killer (NK) cells, similar to the action of IL-2, which has been used to treat metastatic melanoma and renal cancer. IL-15 may have improved pharmacologic properties over IL-2 because it doesn't cause vascular leak syndrome or stimulate regulatory T cells. However, IL-15 is difficult to express as a stable soluble protein and has a short half-life *in vitro* and *in vivo*. To solve the problem, we designed an IL-15 ultralong CDR3 humanized bovine antibody fusion. Bovine ultralong CDR3 antibodies have a unique "stalk and knob" structure in which two antiparallel β-strands support a disulfide bonded knob protruding out of the antibody surface and forms a mini antigen binding domain. By replacing the knob domain with IL-15, we have created a chimeric CDR3-IL-15 IgG which functions as IL-15 *in vitro* and *in vivo* but can be easily produced in mammalian cells with increased stability. Thus, the CDR3 can stabilize IL-15 in the absence of its high affinity receptor α (Rα) chain. Furthermore, as IL-15 utilizes Rα for increased *trans* signaling to the receptor β and γ subunits, one variant candidate (CDR3-IL-15_Rα) was produced by co-expressing Rα sushi domain with the chimeric IgG. Both constructs have been demonstrated to be highly active in stimulating proliferation of NK cells and CD8+ T cells *in vitro* as well as in stimulating proliferation of NK cells and CD8+ T cells in rats and non-human primates (NHP). Although the CDR3-IL-15_Rα exhibited higher *in vitro* signaling activity than CDR3-IL-15, both were equally potent in stimulating the proliferation of NK cells and CD4+ and CD8+ T cells in NHP without any immunogenicity detected. Moreover, *in vivo* studies in NHP indicated that CDR3-IL-15 acted faster than CDR3-IL-15_Rα in stimulating the proliferation of these lymphocytes. CDR3-IL-15 is the first thermodynamically stabilized variant of IL-15 produced in the absence of its Rα chain, is highly active *in vivo*, and has multiple potential cancer applications as an T and NK cell stimulating agent.

#5812 Development of $\alpha_V\beta_5^+$ exosomes for liver-targeted therapy.

P. Acosta Montano, E. Olvera Felix, V. Castro Flores, P. Juarez, P. G. Fournier;
Centro de Investigacion Cientifica y de Educacion Superior de Ensenada, Ensenada, Mexico

Liver metastases are common in pancreatic and colorectal cancer. Their development is promoted by tumor-secreted exosomes that, thanks to the presence of the integrin $\alpha_V\beta_5$ on their membrane, home to the liver where they increase TGF-ß production by Kupffer cells, liver-resident macrophages, initiating the formation of the pre-metastatic niche. Considering that anti-TGF-β therapies have not been efficient in clinical trials or cause side-effects, our aim is to develop a liver-targeted anti-TGF-ß treatment using functionalized $\alpha_V\beta_5^+$ exosomes. We selected 293T cells as a human, non-cancerous cell line to obtain exosomes. 293T have an endogenous expression of $\alpha_V\beta_5$, and exosomes were isolated using differential centrifugation of conditioned media. The vesicles obtained had a diameter of 20 to 120nm according to dynamic light scattering and electron microscopy, as expected for exosomes, and Western blot confirmed the presence of the exosome marker CD81. When fluorescently labeled exosomes (SP-DiIC$_{18}$) were inoculated in the tail vein of Balb/C mice, they were detected in the liver 24 hours later. To increase the homing of 293T cell exosomes to the liver, we decided to overexpress $\alpha_V\beta_5$. 293T cells were co-transfected with plasmids coding the α_V and β_5 subunits. After antibiotic and clonal selections, we obtained 293T cells stably overexpressing $\alpha_V\beta_5$ (8.9x vs. parental), and isolated exosomes contained the exogenous integrin. *In vitro*, the internalization of $\alpha_V\beta_5^+$ exosomes was increased in RAW264.7 macrophages compared to exosomes from parental 293T cells. In mice, we confirmed that the overexpression of $\alpha_V\beta_5$ increases the homing of the exosomes to the liver (4.9x vs. parental) and that $\alpha_V\beta_5^+$ exosomes preferentially home to the liver when compared to lungs, kidneys, and brain. To functionalize the exosomes, we chose to express, in 293T cells, anti-TGF-ß factors that could be directly loaded into their exosomes before their isolation. First, we transduced 293T cells to express the mRNA of a soluble form of betaglycan (sBG) that can neutralize TGF-ß. sBG mRNA was detected in 293T cells, their exosomes, and in RAW264.7 cells treated with these exosomes. Low levels of sBG protein could be detected in the conditioned media of treated RAW264.7, but it did not prevent SMAD2/3 phosphorylation in HepG2 hepatocarcinoma cells, which could be due to the low levels of sBG mRNA in the exosomes. Since larger RNAs have been reported to be less transferred into exosomes, we used 2 shRNA to knock down *Tgfb1*. Although both shTgfb1 could efficiently knock down *Tgfb1* in transduced cells, the exosomes of 293T cells expressing these shTgfb1 did not decrease *Tgfb1* levels in treated RAW264.7 cells. Overall, although the functionalization of exosomes to target TGF-ß remains to be achieved, our results show that $\alpha_V\beta_5^+$ exosomes are nanocarriers that could be used for liver-targeted therapies.

#5813 AI-driven identification and validation of novel synthetic lethal gene pairs through deep mining of cancer dependency data.

D. S. Miller, O. Vipond, A. Brennan, A. Hercot;
Evariste Ltd, London, United Kingdom

The targeting of synthetic lethal (SL) gene pairs is emerging as a new paradigm in precision oncology, with the potential to deliver treatments with higher efficacy and fewer side-effects. However, existing approaches have focused on a few well-validated pairs, and there is a clear need to expand the toolbox of potential SL targets. We have performed deep mining of cancer dependency data using a suite of machine learning tools and AI algorithms underpinned by robust statistical analysis to identify the next generation of SL gene pairs.

To ensure robust, high confidence validation of multiple SL pairs simultaneously, we have used three cell lines and orthogonal assay formats. This has led to the confirmation of new druggable SL genes suitable for clinical development. We have identified the cancer subtypes with the strongest evidence of SL vulnerabilities and quantified patient populations who would most benefit from novel therapeutic agents. For one gene pair, we have generated novel best-in-class inhibitors of the target of interest, with exceptional selectivity over the SL partner, and used these chemical tools to validate the SL relationship in 2D and 3D models.

#5814 EPriL macrocycles as a platform for the rapid generation of effective kinase degrader antibody conjugates (DACs).

J. C. M. Uitdehaag, J. de Man, M. Muller, F. van Cauter, S. van Gemert, M. Hoffmann, Y. G. T. van Mil, W. R. Mulder, M. B. W. Prinsen, J. Sterrenburg, D. Vu, J. de Wit, E. Ensing, R. C. Buijsman;
Crossfire Oncology B.V., Oss, Netherlands

The therapeutic success of antibody drug conjugates (ADCs) drives a continuous search for novel payloads that can increase therapeutic window and thereby widen the applications for ADCs. Recently, heterobifunctional degraders have gained great interest as payloads, and degrader antibody conjugates (DACs) are seen as a novel therapeutic modality. Heterobifunctional degraders consist of a small molecule ligand that binds a target (protein of interest or POI), a spacer and an E3 ligase ligand, which can catalyze target degradation. Owing to their catalytic activity, degraders can have better potency than the equivalent inhibitors, making them suitable as ADC payload [1]. Degrader payloads can target a wider variety of mechanisms than classic payloads, which use the same antitumor strategies as chemotherapy, such as tubulin binding or topoisomerase inhibition.

Since many FDA-approved targeted therapies are based on the inhibition of protein kinases, we investigated degraders of these kinases as DAC payloads. Kinase DACs could bring enhanced targeting and therefore better therapeutic window to a field where classic ADC payloads have often shown substantial toxicities. As many heterobifunctional degraders show poor cell membrane penetration, their inhibitory potential could be increased as part of a DAC, where endocytic uptake is followed by intracellular release of the degrader payload.

To identify kinase degrader payloads, we present a workflow based on a platform called Energetically Privileged Ligands (EPriLs). EPriLs are macrocycle scaffolds that bind non-covalently in the kinase ATP pocket. Their unique binding mode avoids contacts with amino acid positions where resistance to kinase inhibitors frequently occurs. EPriL macrocycles can be decorated appropriately to rationally design specific inhibitors for many therapeutically relevant kinases, and provide synthetic handles to couple them to VHL or CRBN ligands to generate effective kinase degraders.

Here we describe how EPriL kinase degraders can be developed into effective DACs, using consecutive libraries of EPriL ligands, spacers, E3 ligase ligands and linkers. First, suitable degraders are identified, based on rapid and deep target degradation and potent antiproliferative activity on target cell lines. Degraders are then transformed into maleimide-linked degraders using convenient attachment of enzymatically cleavable linkers. In a medium throughput fashion, these maleimides are coupled to antibodies to generate DACs, which are tested for stability and biological potency. Applying this workflow to various well-validated kinase targets in oncology resulted in a promising kinase targeting DAC with favorable ADME properties, clear potentiation compared to the parent degrader, and increased selectivity for tumor cell lines.

1] Dragovich *et al.*, Chem. Soc. Rev. (2022) 51, 3886-3897.

#5815 Next-generation RNAi therapeutics: siRNA-loaded exosomes targeting KRAS G12C in non-small cell lung cancer (NSCLC).

H. Kim[1], Y. Choi[1], K. Kim[1], Y. Byun[1], T. Kim[1], J. Kim[1], S. An[1], D. Bae[1], M. Choi[1], J. Chung[1], K. Kwon[2];
[1]Exollence Biotechnology Co. Ltd, Seoul, Korea, Republic of, [2]Ewha Womans University School of Medicine and Ewha Medical Research Institute, Seoul, Korea, Republic of

Background: NSCLC represents the predominant subtype of lung cancer, boasting an overall 5-year survival rate of 26%, a figure that fluctuates based on the disease stage. Within NSCLC, certain cancer gene mutations, notably KRAS G12C, are currently classified as 'undruggable targets,' creating hurdles in achieving effective treatment. The development of innovative anticancer drugs aimed at these challenging targets is expected to present a viable solution to these difficulties.
Methods: Exosomes have garnered attention as an inventive drug delivery system for in vivo gene delivery through systemic injection. We used a new post-loading approach by actively loading KRAS G12C siRNA into exosomes using the shock waves (SWEET: shock wave exosome engineering technology) in this study. The effect of *in vitro* and *in vivo* were tested in NCI-H358 (KRAS G12C mt NSCLC) cells and its xenograft mouse model. The tumor size and weight were measured twice a week.
Results: We developed an exosome-based therapeutic using siRNA to effectively inhibit KRAS G12C, targeting NSCLC. The SWEET platform's post-loading method showed a high efficiency in loading KRAS G12C siRNA into exosomes. The KRAS G12C siRNA-loaded exosomes effectively silenced oncogenic KRAS G12C expression in cancer cells; they inhibited tumor growth when administered intravenously in a NSCLC xenograft mouse model. Remarkably, the anticancer effect of KRAS G12C-loaded exosome was similar to that of Sotorasib, a KRAS G12C mutation targeting anti-cancer drug.
Conclusion: Our study showed KRAS G12C siRNA loaded exosomes were effectively delivered to NSCLC tumor tissue via intravenous (IV) administration. And its anti-cancer effects were very similar to sotorasib, showing potential as a treatment for KRAS G12C mutation-expressing cancer. The effective delivery of siRNA to tumor tissues through exosomes highlights the potential of this technology as a promising approach for developing new RNAi therapeutics for cancer.

#5816 An effective delivery platform for nucleic acid therapeutics: Enhanced cancer cell internalization and endosomal escape.

S. Li[1], O. Tietz[2], A. H. El-Sagheer[3], T. Brown[1], K. A. Vallis[1];

[1]University of Oxford, Oxford, United Kingdom, [2]Macquarie University, Sydney, Australia, [3]University of Southampton, Southampton, United Kingdom

Nucleic acid therapeutics (NATs), such as siRNA and mRNA, show great potential as cancer medicines. However, translation of these compounds has been held back by their limited bioavailability in target tissues. The aim of this study was to test the use of a novel cell-penetrating peptide (CPP)-based delivery platform to enhance uptake of NAT into cancer cells. This platform consists of a highly efficient CPP that combines the advantages of multimerization and cyclization of the archetypal CPP, TAT peptide[1], plus a photochemical (PC) strategy to promote endosomal release of NAT into the cytoplasm[2]. Negatively charged NATs form complexes with cationic CPPs through charge:charge interaction. NATs (siRNA or mRNA) were incubated with CPP at different molar ratios and assessed in gel retardation assays. Efficiency of internalization of Cy3-NAT:CPP complexes was evaluated using live cell confocal imaging with quantification of intracellular fluorescence. The mechanism of cellular uptake of NAT:CPP was investigated using inhibitors of endocytosis (chlorpromazine, NaN3, amiloride and methyl-β-cyclodextrin). To trigger NAT release from intracellular vesicles, 420 nm/50 mA LED light irradiation was applied following pre-treatment of cells with a photosensitizer, fimaprofin. CPP-PC mediated internalization and endosomal release was used for delivery of glyceraldehyde 3-phosphate dehydrogenase (GAPDH) siRNA. GAPDH enzymatic activity assays (Sigma, USA) were conducted to confirm inhibition of GAPDH in HeLa, HEK293T and MDA-MB-231 cells. Transfection efficiency of mRNA encoding enhanced green fluorescence protein (eGFP) was evaluated by flow cytometry in HeLa cells. NAT:CPP complexes were found to be maximally efficient at a 10:1 molar ratio. Analysis of live cell confocal images indicated that GAPDH Cy3-siRNA:CPP complexes were more efficiently internalized compared to Cy3-siRNA + monomeric TAT or Cy3-siRNA + lipofectamine (****$p<0.0001$, one-way ANOVA). The combined CPP-PC platform delivers NAT via a clathrin-mediated endocytosis pathway. CPP-PC delivery of GAPDH siRNA caused marked GAPDH enzyme activity downregulation in HeLa (91%), MDA-MB-231 (51%) and HEK293T (44%) cells. These results were similar to the level of downregulation achieved with lipofectamine + GAPDH siRNA. Flow cytometric analysis revealed that 52.4% of HeLa cells expressed eGFP at 1 h following delivery of mRNA-eGFP by CPP-PC. Functional siRNA and mRNA were efficiently delivered into the cytoplasm of cancer cells through combined use of a multimeric/cyclized CPP plus photochemical-mediated endosomal release. This approach holds promise for clinical application, particularly in the treatment of intraluminal tumors. 1. Tietz, O. *et al.* Nat Chem. *14:* 284-93, 2022. 2. Selbo, P. K. *et al.* J Control Release. 148, 2-12, 2010.

#5817 pH responsive delivery of gemcitabine/pirarubicin co-loaded biodegradable polymeric nanoparticles for synergistic anti-cancer therapy.

P. Gupta[1], S. M. Kharbanda[2], H. Singh[1];

[1]Indian Institute of Technology Delhi (IIT Delhi), New Delhi, India, [2]Dana Farber Cancer Institute, Boston, MA

Gemcitabine, a nucleoside antimetabolite, is a widely known chemotherapeutic agent being used as a first line treatment alone or in combination with other chemo drugs for different types of cancer. However, due to its extremely short half-life in the body caused by enzymatic degradation and poor pharmacokinetics, the I.V. dosage of administration is quite high i.e., >1000 mg/m^2 for metastatic breast cancer treatment. Moreover, gemcitabine in combination with anthracyclines imparts synergy but free anthracyclines are reported to be associated with long term cardiac toxicity. Nanoparticle-based drug delivery systems have provided a befitted solution for improving the poor pharmacokinetic properties and systemic toxicity caused by the chemo drugs because of their ability to improve bioavailability of the drugs at the desired site as well as overcoming multi-drug resistance (MDR).In the present work, PLA-based biodegradable block copolymeric nanoparticles have been employed to co-load Gemcitabine and Pirarubicin for improved anti-cancer activity. Gemcitabine and Pirarubicin have been chemically conjugated to the amphiphilic block copolymer mPEG PLA via a pH responsive Schiff's Base linkage using a linker molecule Levulinic acid. The prepared PIRA/GEM co-loaded nanoparticles exhibited an optimum size, zeta potential and polydispersity index i.e., 187 ± 3.5 nm, -10 ± 2.0 and < 0.1 PDI respectively. Further, in the drug release experiments, these Nps displayed sustained and higher drug release in lysosomal pH (pH 5.0) than in the physiological buffer environment (pH 7.4) attributed to the pH sensitive bonding. The co-loaded Nps were prepared in multiple ratios (Pira: Gem - 1:1, 1:3, and 3:1) and investigated for *in-vitro* cellular inhibition studies in comparison to singly loaded drug Nps and corresponding free drug formulations in various breast cancer cell lines. Additionally, apoptotic studies revealed significant enhancement in synergistic activity in the case of PIRA/GEM co-loaded Nps in comparison to conventional free drug formulations. In conclusion, this nano-formulation demonstrated excellent anti-cancer activity against breast cancer cells therefore it may be used as a potential candidate for therapeutic use.

#5818 Differentiation of human papillomavirus-positive head and neck squamous cell carcinoma cells.

S. Gendreizig[1], L. Martinez-Ruiz[2], J. Florido[2], A. Lopez-Rodriguez[2], H. Pabla[1], F. Brasch[1], G. Escames[2], T. Busche[1], H. Sudhoff[1], L. U. Scholtz[1], I. Todt[1], F. Oppel[1];

[1]University Hospital OWL of Bielefeld University, Bielefeld, Germany, [2]University of Granada, Granada, Spain

Head and neck squamous cell carcinoma (HNSCC) represents a highly malignant disease and death rates remain at approximately 50% for decades. Thus, new tumor-targeting treatment strategies are desperately needed. In a previous study, we dissected human papillomavirus (HPV)-negative HNSCC cell differentiation via cornification and detected an epigenetically determined loss of cell malignancy. Analyzing the mechanisms underlying the differentiation of HNSCC cells may identify targets for anti-tumor therapy. Using patient-derived tumor cells, we created an HNSCC differentiation model in HPV+ tumor cells. Similar to HPV- cells, we observed a loss of malignant characteristics in HPV+ cell cultures in differentiating cell culture conditions including irregular enlarged cell morphology, cell cycle arrest with downregulation of Ki67, and reduced cell viability. Even though cornification was detected in HPV+ tumor cell cultures and HPV+ FFPE tumor tissue sections, cornification was not induced during HPV+ cell differentiation. Instead, RNA-seq and subsequent Gene Ontology analysis showed myocyte-like differentiation with upregulation of markers of myofibril assembly including TPM1, TAGLN, and ACTA1. Immunofluorescence staining of differentiated and undifferentiated primary HPV+ HNSCC cells confirmed an upregulation of these markers and the formation of parallel actin fibers, reminiscent of myoblast-lineage cells. Moreover, multi-marker immunofluorescence analysis of HPV+ tumor tissue sections revealed areas of cells co-expressing the identified markers of myofibril assembly, HPV surrogate marker p16, and stress-associated basal keratinocyte marker KRT17, indicating that the observed myocyte-like differentiation observed in vitro also occurred in human tissue. Normal tissue displayed a co-expression of TPM1, TAGLN, and ACTA1 in differentiating keratinocytes between the basal cell layer and the fully differentiated corneocytes. This shows that the expression of myocyte-lineage markers is reflected in differentiating non-malignant mucosal tissue. Our study suggests that the targeted differentiation of tumor cells might be therapeutically valuable in HPV+ HNSCCs as well.

#5819 An anti-TROP2-CPT113 ADC, exhibits potent targeted antitumor activity and favorable pharmacokinetic properties.

Huihui Guo, Xiangfei Kong, Yong Du, Zhicang Ye, Yongxiang Chen, Zhixiang Guo, Lingli Zhang, Lu Bai, Junxiang Jia, Yunxia Zheng, Wei Zheng, Jun Zheng, Wenjun Li, Yuanyuan Huang, Zhongliang Fan, Mengmeng Liu, Binbin Chen, Meng Dai, Juan Wang, Miaomiao Chen, Qingliang Yang, **Robert Y. Zhao**

Hangzhou DAC Biotechnology Co., Ltd., Hangzhou City, China

Trophoblast cell surface antigen 2 (TROP2) is highly expressed in a number of epithelial cancer types and is considered to be a poor prognostic marker. We have developed an anti-TROP2 antibody-drug conjugate, DXC1002, that contains a potent inhibitor of DNA topoisomerase I payload (CPT113) attached to the antibody mainly in the Fab region via a unique hydrophilic CrossConju™ linker. The anti-tumor activities of DXC1002 were studied in various human cancer cell lines and xenograft mouse models and pharmacokinetic profile of DXC1002 were evaluated in cynomolgus monkeys and rats. DXC1002 demonstrated potent anti-tumor activity in TROP2 tumor cells of various expression levels in vitro, and at low dose of 1 mg/kg for one injection, in both high and moderate Trop2 expression xenograft models. In plasma stability studies, wherein DXC1002 was incubated in the plasma of five different species for 168 hours (7 days) at 37 oC, over 90% ADC was intact, exhibiting good stability of the CrossConju™ linker. Pharmacokinetic studies of DXC1002 in monkeys (TROP2 cross-species) and rats (non-TROP2 cross-species) showed half-lives of about 61.27 and 236.77 hours, respectively. Systemic clearance in monkey and rat was 0.41-0.67 and 0.279-0.309 mL/h/kg, respectively. The longer half-lives and slower clearance observed in rats the results offered a more direct assessment of the linker stability as target-mediated clearance played no role in rats. In summary, with the conjugation of a DNA topoisomerase I inhibitor payload to Trop2 antibody via the CrossConju™ linker, DXC1002 demonstrates remarkable anti-tumor properties and pharmacokinetic profile, with a potential to be further validated in clinical applications.

#5820 An antibody drug conjugate platform based on novel camptothecin payloads with branch hydrophilic linkers and site-specific conjugation.

Yuanyuan Huang, Hangbo Ye, Qingliang Yang, Lingli Zhang, Huihui Guo, Xiaolei Liu, Wenjun Li, Lu Bai, Junxiang Jia, Juan Wang, Xiangfei Kong, Jun Zheng, Yifang Xu, Gengxiang Zhao, Linyao Zhao, Xiang Cai, Ziyu Zhao, Hui Xia, Xia Zhou, You Zhou, **Robert Y. Zhao**

Hangzhou DAC Biotechnology Co., Ltd., Hangzhou City, China

Antibody-drug conjugates (ADCs) have recently gained momentum as a therapeutic modality for the cell-specific delivery of small molecules beyond their originally-intended purpose of treating cancer. However, the selection of combinations of an optimum target, antibody, payload, linker as well conjugation, to achieve maximal therapeutic efficacy without excessive toxicity, still presents a significant challenge. Topoisomerase I (Topo I) inhibitors such as camptothecin (CPT) analogs represent the much success in ADC payload applications as two CPT analog-ADCs, trastuzumab deruxtecan (DS-8201a—Enhertu®) with Dxd payload and sacituzumab govitecan (Trodelvy™) with SN38 payload have been approved and over 20 CPT analog-ADCs are in the clinical trials now. Topo I inhibitors trigger cell apoptosis through their specific binding at the DNA-topoisomerase interface, leading to the inhibition of DNA supercoiling and entanglement, resulting in DNA damage and cell death. This class of payloads in ADCs has demonstrated more wider therapeutic windows in clinical trials than regular antitubulin payloads, such as maytansine and MMAE, based ADCs. Here, we detail the discovery of CPT analogs, as payloads with a branch hydrophilic linker and site-specific conjugation for ADCs designed to have a widened therapeutic window compared with Dxd-GGFG linked ADCs. The CPT analogs based on the core structure of SN-38, wherein the hydrogen of C-11 was replaced with fluorine, and the hydroxyl group of C-10 was optionally replaced with an amino or a ether group. Many of the novel CPT analogs were at single to tens of pM of IC_{50} potency in vitro against several tested tumor cell lines, and some were more potent than Exatecan in the comparison tests. The ADCs constructed with branch hydrophilic linkers and the CrossConju™ technology of chemically site-specific conjugation at Fab region of an antibody through C-10 position of the CPT payloads either with amide bond, either bond or carbamide bonds, or through C-20 position of the CPT payloads with carbamide or carbonate bonds, exhibited much better antitumor efficacy in vivo CDX tumor models, while having higher or similar MTDs in mice toxicity study in comparison with the ADC constructed with GGFG-Dxd, demonstrated wider therapeutic widows than that conjugated with GGFG-Dxd. Moreover, some of the constructed ADCs can overcomes *in vitro*- and *in vivo*-acquired resistance of commercial therapeutic drugs. Herein, we showcase our platform approach in CPT-ADC designs and constructions and can be thereby broadly applicable to construction of various CPT-ADCs for targeted treatment of cancers.

#5821 DXC008, a novel STEAP1 antibody-tubulysin analog conjugate with a function linker, demonstrates a potential to broaden therapeutic opportunities for prostate tumors.

Q. Yang, Y. Huang, J. Jia, H. Guo, L. Zhang, Y. Zhou, Z. Ye, H. Ye, Y. Xu, W. Li, Z. Zhao, L. Zhao, L. Bai, J. Zheng, **R. Y. Zhao**;
Hangzhou DAC Biotechnology Co., Ltd., Hangzhou, China

Six-transmembrane epithelial antigen of the prostate 1 (STEAP1), is a cell surface protein frequently expressed in prostate cancer, with limited expression in non-prostate tissues. A Steap1 antibody called Vandortuzumab conjugated with MMAE (DSTP3086S) was in the clinical phase I trial for treating STEAP1-expressing metastatic castration-resistant prostate cancer and showed acceptable safety at 2.4 mg/kg once every 3 weeks. However, many patients are nonresponsive to DSTP3086S due to low target expression levels and common treatment-related AEs which were caused by MMAE payloads. DXC008 was generated through screening the therapeutical index in vitro of conjugates of an anti-Steap1 antibody with varieties of payloads of tubulysin B analogs through function peptide spacer linkers. The generated DXC008 exhibited not only good affinity for Steap1 but also moderate affinity for Prostate-specific membrane antigen (PSMA) which is as well specifically overexpressed in most prostate cancer with limited expression in normal tissue. DXC008 demonstrated couple tens to a hundred of picomolar concentration (pM) of potency against several prostate tumor cells and over 60% internalization rate within 90 min in vitro. And in vivo it showed very good durable antitumor response as low dose as 1 mg/kg one injection in both high and moderate of both Steap1 and PSMA expression xenograft models. Pharmacokinetic profiles of DXC008 were favorable and the safety of Maximal Tolerable Dose (MTD) was over 120 mg/kg in single injection in mice. DXC008 has been forward to NHP toxicity study and it has potential to be a good STEAP1/PSMA-targeting ADC with a wide therapeutic window for prostate cancers.

EXPERIMENTAL AND MOLECULAR THERAPEUTICS: Drug Resistance 3: Regulation of Gene Expression
Poster Session

#5825 Non-genetic determinants driving the evolutional trajectories of drug-tolerant-persisters in KRAS Non-small cell lung cancer.

C. Li[1], C. J. Graser[2], Q. Qin[1], A. Nimbalkar[1], U. Syed[1], B. Karakyriakou[1], S. Clark[1], A. Y. Saiki[3], P. E. Hughes[3], C. Ott[1], L. Pinello[1], F. Michor[2], A. Hata[1];
[1]Harvard Medical School/Massachusetts General Hospital, Boston, MA, [2]Dana-Farber Cancer Institute, Boston, MA, [3]Amgen Inc., Thousand Oaks, CA

Rare cell populations manage to evade the effects of cancer therapies, ultimately leading to drug resistance and subsequent cancer relapse. These resilient populations, often referred to as "persisters," exhibit distinct molecular characteristics when compared to the broader tumor population. In the current standard of clinical care for non-small cell lung cancer (NSCLC), patients typically undergo a series of standard treatments, such as surgery followed by chemotherapy/immunotherapy, and then targeted therapy, based on the disease stages. This continues until drug resistance emerges, with little attention given to the state of these persister cells in response to these treatments. In the case of drug resistance in KRAS-mutated NSCLC, ongoing clinical investigations are exploring the combined efficacy of KRAS G12Ci inhibitors with drugs that target mitogen-activated protein kinase (MAPK) feedback reactivation, immunotherapy, and chemotherapy. Despite the myriad of combination therapies, persister populations invariably emerge. The manner in which these persisters evolve to withstand therapies remains elusive. We employed a DNA barcode lineage tracing analysis coupled with mathematical modeling to decode persister evolution to therapies targeting different pathways, e.g., KRAS+ SHP2, KRAS+CDK4/6, and KRAS+MCL-1. Our model reveals that rapidly emerging persister populations are predetermined and do not exhibit clear genetic alterations. In some cells, common persisters exist in response to different therapies. Single-cell ATAC-RNA sequencing showed that these persisters are enriched in chromatin-binding of transcription factors that regulate classic non-homologous end-joining (cNHEJ) DNA repair (ZNF384), interferon response (IRF1), and stem-like characteristics (FOXP1), along with the activation of an IFN-γ transcriptional signature. These findings underscore the connection between specific DNA repair processes, chromosomal instability, and resistance to KRAS G12Ci. In other cells, however, distinct persister populations exist to different therapies, leading to the hypothesis that these diverse persister populations can be targeted orthogonally or sequentially to achieve tumor regression. In summary, our study unveils the heterogeneity in persister evolution trajectories in KRAS NSCLC. Our platform identifies targetable persister populations in NSCLC models and offers a proof-of-concept for non-standard strategies to combat drug resistance based on persister cell states.

#5826 Comprehensive analysis with single-cell RNA sequence and spatial transcriptomics unravels distinctive expression profile of apoptotic-related genes in EGFR-mutated lung cancer.

M. Izumi, M. Fujii, V. Ho, I. S. Kobayashi, S. S. Kobayashi;
Beth Israel Deaconess Medical Center, Boston, MA

Despite an initial marked response to targeted therapy with tyrosine kinase inhibitors (TKIs) in EGFR-mutated lung cancer, the duration of response is limited due to the inevitable development of acquired resistance. Anti- and pro-apoptotic genes play an important role in the survival of tumor cells. Currently, variations in these gene expression levels are not well characterized due to the complex interplay between the inducement of expression changes by EGFR-TKIs and the presence of inter- and intra-tumor heterogeneity. Here, a comprehensive analysis of apoptosis-related genes, including BCL-2 family members and the IAP family members, was conducted via single-cell RNA sequence (scRNA-seq) and spatial transcriptomics. scRNA-seq captured changes in apoptosis-related gene expression after EGFR-TKI treatment using different EGFR-mutated lung cancer cell lines. Notably, *BCL2L1* expression increased, whereas *MCL1* expression decreased after EGFR-TKI treatment. Other anti- and pro-apoptotic genes did not display consistent trends in the cell lines used. Additionally, scRNA-seq was carried out on samples collected from patients with EGFR-mutated lung cancer after the development of resistance to EGFR-TKIs in order to validate the results obtained from cell line data and to compare gene expression levels between tumor and non-tumor cells. *BCL2L1* exhibited high expression specifically in tumor cells; in contrast, *MCL1* expression was lower in tumor cells compared to non-tumor cells. Moreover, *BAD* and *XIAP* were highly expressed in a tumor-specific manner. To further corroborate the scRNA-seq findings and delineate the spatial heterogeneity in tumors, spatial transcriptomics was performed using EGFR-driven lung cancer transgenic mouse specimens in three conditions: prior to treatment, during therapeutic response after short-term treatment, and following acquired resistance to EGFR-TKIs. Spatial transcriptomics data demonstrated that an increased *BCL2L1* expression was observed in tumor tissues and that *MCL1* expression was significantly higher in tissue adjacent to tumors than in tumors. Finally, we demonstrated that genetic ablation of *BCL2L1* and pharmacological inhibition of *BCL2L1* overcame or delayed resistance to EGFR-TKIs *in vitro* and *in vivo*. Overall, *BCL2L1* is particularly important for tumor cell survival during the emergence of drug tolerance and the development of acquired resistance to EGFR-TKIs.

#5827 Identification of potential novel drivers and biomarkers of CDK4/6 inhibitor resistance in metastatic breast cancer.

L. F. Ott, M. Alawi, M. Stoupiec, E. Laakmann, M. Kriegs, V. Muller, K. Pantel, S. Riethdorf;
University Medical Center Hamburg-Eppendorf, Hamburg, Germany

Background: Inhibitors of the cyclin-dependent kinases 4 and 6 (CDK4/6i) have become part of the standard of care for patients with hormone receptor-positive metastatic breast cancer. Despite their initial benefit for most patients, the development of resistance to this treatment is almost inevitable. However, there is a lack of predictive or clinical markers that can be utilized to monitor resistance development, and their definition remains an unmet challenge.
Methods: We aimed to identify novel drivers and potential biomarkers of CDK4/6i resistance by creating and characterizing two ribociclib-resistant breast cancer cell lines. Ribociclib-resistant derivatives of MCF7 cells and the CTC (circulating tumor cell)-derived cell line CTC-ITB-01 were created by long-term exposure to the inhibitor for a minimum of 6 months and potential novel resistance drivers were identified by transcriptome analysis using RNA-sequencing. In addition to mRNAs encoding proteins that may contribute to resistance, we also investigated microRNAs as they are poorly characterized in the context of CDK4/6i resistance. Additionally, changes in the kinome activity were assessed by using PamGene technology.
Results: The RNA-sequencing analysis identified ≥ 2000 genes with differential expression in both resistant cell lines compared to their respective parental counterparts. Over Representation Analysis revealed that a high number of these genes encode proteins associated with the cell cycle, proliferation, epithelial-to-mesenchymal transition, various signaling pathways like Wnt, and the complement system. Evaluation of kinase activity using functional kinome profiling in the resistant versus parental CTC-ITB-01 cell line showed increased activity of the CDK and MAPK kinase subgroups, indicating a multifactorial resistance mechanism. Furthermore, the analysis of deregulated ncRNAs demonstrated increased expression of miR-146a-5p in both resistant cell lines and interestingly, a significant decrease of miR-205-5p levels in the resistant CTC-ITB-01 cell line. MiR-205-5p is described as a negative regulator of EMT and progression in breast cancer but has not been linked to CDK4/6i resistance yet. This result was validated by qPCR and miRNA *in situ*-hybridization.
Conclusion: Through our comprehensive transcriptome analysis of two ribociclib-resistant cell lines, we were able to identify several novel potential resistance drivers. Their utility as predictive or monitoring biomarkers
requires further investigation. Furthermore, discovering new resistance mechanisms could also help find new therapeutic strategies after CDK4/6i resistance development.
Acknowledgment: This project received funding from the Deutsche Krebshilfe DETECT high project (Nr.: 70114705) and the Horizon 2020 program RNADiagon (Nr.: 824036).

#5828 The genomic architecture of ibrutinib resistance in CLL: Oligoclonal progression with variable anatomical distribution.

C. Underbayev, J. Chen, H. M. Harris, L. T. Vaughn, A. Itsara, A. Wiestner;
National Heart, Lung & Blood Institute, Hematology Branch, National Institutes of Health, Bethesda, MD

Progressive disease (PD) in patients with chronic lymphocytic leukemia (CLL) on ibrutinib often presents with acquired mutations in *BTK* and/or *PLCG2*. Reported variant allele frequencies (VAF) are often low, leading some to question the role of these mutations. Further, several co-existing mutations are often identified. Here we investigated the clonal composition of PD on single cell level, across time, and different anatomic compartments. 84 CLL patients (52 treatment-naïve; 32 relapsed/refractory) with either a *TP53* aberration or age ≥65 years received single-agent ibrutinib 420 mg once daily until PD or limiting side effects on a phase 2 study (NCT01500733). The median progression-free survival was 86.6 months. 39 (46.4%) patients progressed, 31 with CLL (PD-CLL), and 8 with Richter's transformation. Median time to PD-CLL was 57.2 months. In PD-CLL patients, peripheral blood (PB) was sent for genotyping of known hotspot mutations in *BTK*/*PLCG2* (Neogenomics). We then designed digital droplet PCR probes to test for *BTK* C481S/R/Y and *PLCG2* R665W/L845/S707F mutations in samples collected at baseline, during response to ibrutinib and at PD in 29 patients. 26 (89.7%) patients had detectable *BTK/PLCG2* mutations (VAF range 0.04 - 0.96). 12 (41%) patients carried multiple *BTK/PLCG2* mutations. In 11 evaluable cases single-cell DNA sequencing (Mission Bio) showed individual mutations present in separate cells consistent with branching evolution. Having confirmed oligoclonality, we calculated the cumulative cell fraction (cCF) of *BTK/PLCG2* mutations in the 29 PD-CLL patients. 16 (55%) patients had cCF >0.5 (range 0.59-0.96), 10 patients (35%) had cCF < 0.5 (range 0.04-0.43) and 3 patients (10%) had no detectable mutations. *BTK/PLCG2* mutations were detected in samples collected at median 21.6 months (range 0 - 75) prior to PD. In 11 cases, we tested lymph node (LN) biopsies at PD. In 6 cases with cCF <0.5 in PB, 4 corresponding LN samples had higher cCF (0.01/0.92; 0/0.85; 0.06/0.69; 0.46/0.99 for PB/LN, respectively). In 5 cases, PB contained 2-6 distinct subclones with cCF >0.5, in 3 cases the corresponding LN harbored fewer subclones than PB (6/3; 3/2; 3/0 for PB/LN, respectively). To characterize the genomic background of PD-CLL, we performed whole-exome sequencing of longitudinal samples from 26 patients. In addition to *BTK/PLCG2*, the most frequently mutated genes were *TP53*, *SF3B1*, *NOTCH1*, and *POT1*. Furthermore, copy number variations (CNA), such as del17p, del13q, del14q, del3p, and del8p, were common. In summary, in our cohort *BTK*/*PLCG2* mutations were identified in 89.7% of PD-CLL patients. These mutations arise in oligoclonal populations with variable distribution across anatomical sites. In rare patients without *BTK/PLCG2* mutations, the co-evolution of putative driver mutations and multiple CNAs generated genomic complexity reminiscent of lymphoma transformation.

#5829 Elucidating the significance of amphiregulin and its implications for EGFR inhibition strategies in LKB1-mutant NSCLC.

X. K. Solone[1], X. Zhou[1], M. Yu[1], J. W. Li[2], F. Rimay[1], F. Kaye[1], L. Wu[1];
[1]University of Florida College of Medicine, Gainesville, FL, [2]Brown University, Providen, RI

LKB1-mutant non-small cell lung cancer (NSCLC) is aggressive and treatment-refractory, underscoring the need for new therapeutic strategies. Our comparative study involving mouse lung tumors driven by oncogenic $Kras^{G12D}$ and LKB1 loss as well as tumors driven solely by $Kras^{G12D}$, revealed that LKB1 loss upregulated amphiregulin (Areg), a pro-growth EGFR ligand. Therefore, this study investigates how the inactivation of LKB1 enhances AREG expression, the significance of elevated AREG in sustaining lung cancer growth, and the responses of AREG-high lung cancer to EGFR inhibitors. We first evaluated the potential clinical significance of AREG using The Cancer Genome Atlas (TCGA) lung adenocarcinoma dataset and the Cancer Cell Line Encyclopedia (CCLE) database. We observed that LKB1-null tumors with high AREG levels were associated with shorter patient survival and exhibited transcriptional signatures similar to EGFR-mutant tumors. High AREG expression also correlated positively in NSCLC cell lines with LKB1 mutations and Western blot analysis confirmed that elevated AREG levels in lung cancer cells were associated with constitutive EGFR signaling. We next explored the impact of LKB1 loss on AREG expression in lung cancer. Our prior RNA-seq and ChIP-seq investigations demonstrated CRTC2 and CREB enrichment on the AREG promoter in LKB1-null lung cancer cells. Upon LKB1 reintroduction, the enrichment diminished, indicating that CRTC-CREB transcriptionally induces AREG in LKB1-null lung cancer. To corroborate, reintroducing LKB1 or expressing a dominant-negative construct (dnCRTC), disrupting CREB/CRTC interaction, decreased AREG levels, as confirmed by RT-qPCR in LKB1-null lung cancer cells. This supports that AREG is a direct target of CRTC-CREB activation induced by LKB1 loss. To assess the impact of elevated AREG in LKB1-mutant lung cancer growth, we used RNA interference and antibodies to inhibit AREG. Both interventions decreased cell growth and colony formation, underscoring AREG is critical for LKB1-mutant lung cancer growth. Moreover, we investigated the potential correlation between AREG and the response to the EGFR tyrosine-kinase inhibitor Erlotinib in NSCLC cell lines, utilizing AREG expression data from CCLE and Erlotinib response data from the Genomics of Drug Sensitivity in Cancer (CDSC) databases. Stratifying NSCLC cell lines into sensitive, intermediate, and resistant categories revealed a potential positive association between AREG expression and Erlotinib sensitivity. Notably, LKB1-null lung cell lines with high AREG expression demonstrated heightened sensitivity compared to those with low AREG expression. Our study revealed that LKB1 loss increases AREG, triggering aberrant EGFR signaling critical for lung cancer growth, and AREG expression might impact the Erlotinib response in LKB1-inactive cells.

#5830 A first-of-its-kind model that reconstitutes targeted drug-induced cellular transdifferentiation.

P. Gopal, M. Abazeed;
Northwestern Univ. Feinberg School of Medicine, Chicago, IL

Introduction: Lung tumors treated with targeted therapies ultimately relapse due to intra-genic resistance mutations, bypass pathway activation, or cellular lineage changes. Newer precision therapies have higher selectivity and potency against both resistant and activating gene mutations, resulting in a significant increase in incidence of cellular transdifferentiation. The most common form of transdifferentiation is the change from lung adenocarcinomas (LUADs) to small cell lung cancer (t-SCLC) upon drug treatment which remains very poorly understood.

Methods: We have combined patient derived xenografts (PDX) and *ex vivo* lines with multi-omic characterization, high-content image-based morphometry and fluorescence tracking, and single-cell barcode tracing to better understand the process of lung tumor transdifferentiation.

Results: We have developed a first-of-its-kind t-SCLC model that reconstitutes *ex vivo* LUAD to SCLC transdifferentiation. Genomic and transcriptomic analyses of our NSCLC PDX collection identified tumors with mutation in *TP53* and *RB1*, two genes that are altered in virtually all *de novo* SCLCs. PDX sample CBX336 was identified as having mutations in both *TP53* and *RB1*, in addition to expressing the $KRAS^{G12C}$ oncogene. Upon treatment with Sotorasib, CBX336 tumors initially demonstrated slow tumor growth, followed by a dramatic increase in the growth after prolonged drug exposure. Our experimental and computational data suggest a highly coordinated procession toward transdifferentiation with the parallel upregulation of the neuroendocrine transcription factor *NEUROD1* across numerous epithelial cellular clones.

Conclusions: Our new experimental system allows characterization at the single-cell level. Ongoing work includes the integration of new resources to study lineage reprogramming, and advancing new therapeutic strategies.

#5831 The TLE1 transcriptional and epigenetic machinery contributes to EGFR targeted therapy resistance in human lung adenocarcinoma.

Hector Ramos Biliran[1], Xin Yao[1], **Nasir Roberts**[1], Prince Iheukwumere[1], Renwei Chen[2], Ma. Carmela Dela Cruz[3]

[1]Biology, Xavier University of Louisiana, New Orleans, LA,[2]Marine Science Institute, University of California, Santa Barbara, Santa Barbara, CA,[3]Molecular Medicine, MD-PHD program, University of the Philippines Manila, Manila, Philippines

In human lung adenocarcinoma that carry Epidermal Growth Factor Receptor (EGFR) sensitizing mutations, targeting the EGFR pathway with the use of EGFR tyrosine kinase inhibitors (EGFR-TKIs) has emerged as a promising therapeutic strategy providing initial clinical benefit to many patients. Unfortunately, resistance to EGFR-TKIs eventually develops leading to disease progression. In addition to genetic mutations, transcriptional and epigenetic mediated changes in gene expression remain an important mechanism contributing to EGFR-TKI resistance. Here, we report a novel function of the transcriptional corepressor Transducin-Like Enhancer of Split-1 (TLE1) in mediating EGFR-TKI resistance in EGFR mutant LUAD cells through its survival promoting gene transcriptional program. In EGFR mutant, EGFR TKI sensitive LUAD cells, sole activation of the TLE1 nuclear function attenuates EGFR TKI sensitivity with concomittant reduction of EGFR-TKI-mediated apoptosis. Conversely, downregulation of endogenous TLE1 expression via siRNAs/shRNAs and deletion of TLE1 gene via CRISPR-Cas9 in EGFR-mutant, EGFR-TKI resistant cells partially restore EGFR-TKI sensitivity via induction of EGFR-TKI apoptosis. Mechanistically, the anti-apoptosis promoting gene transcriptional program of TLE1 is dependent on its functional interaction with the transcriptional repressor HES-1, a downstream Notch target which has been associated with relapse in LUAD patients following EGFR-TKI treatment. Collectively, these studies indicate the TLE1 corepressor as a determinant of resistance to EGFR targeted therapy and raise the possibility that inhibiting TLE1 nuclear function may serve as an adjuct therapy to circumvent EGFR-TKI resistance.

#5833 Genomic mechanisms of RET inhibitor resistance in RET-fusion positive NSCLC.

X. Liu[1], M. Nilsson[1], T. Takehara[1], J. He[1], X. Huo[2], A. Kumar[2], J. Heymach[1], R. Kittler[2];
[1]UT MD Anderson Cancer Center, Houston, TX, [2]UT Southwestern Medical Center, Dallas, TX

RET fusions are a driver oncogene detected in 1-2% of non-small cell lung cancer (NSCLC) cases. Currently, two selective RET inhibitors (RETi), selpercatinib and pralsetinib have received FDA approval for *RET* fusion-positive NSCLC. However, *RET* fusions are highly heterogeneous and the impact of specific fusion partners and breakpoints on RETi sensitivity is not well understood. Moreover, most patients eventually develop resistance to RETi, and secondary *RET* mutations are thought to be a key mechanism of acquired resistance. Thus, we aimed to identify *RET*-dependent mechanism of RETi resistance in effort to improve treatment options and clinical outcomes. We engineered a panel of Ba/F3 cells expressing various RET fusion partners and breakpoints observed in clinical cases of NSCLC and evaluated their drug sensitivity profile against a panel of RETi including selpercatinib, pralsetinib, TPX-0046, lovatinib, zeteletinib and ponatinib. We determined that individual RET fusions impart distinct sensitivities to RETi. For example, cells expressing KIF-RET (K22, R12) were sensitive to selpercatinib and pralsetinib but less sensitive to ponatinib, whereas cells expressing KIF-RET (K15, R12) were highly sensitive to selpercatinib, pralsetinib, and ponatinib. Moreover, using *RET*-fusion positive NSCLCs, we observed that the RETi sensitivity profile of human cell lines was similar to that observed using Ba/F3 models. To identify potential resistance mutations, we utilized the LentiMutate approach. In KIF5B-RET (K15, R12) expressing cells, we identified G810S as being associated with resistance to both selpercatinib and pralsetinib, a finding consistent with previous reports and clinical observations. In addition, we identified Y806H/N, V804M/E, and M918T as being associtated with selpercatinib-resistance and L730I/V, E732K, and Y806H/N as being associated with pralsetinib-resistance. We next constructed Ba/F3 cells expressing KIF5B-RET in combination with each secondary mutation and evaluated RETi sensitivity. G810S and Y806N conferred resistance to selpercatinib and pralsetinib, as well as to RET-targeting multi-kinase inhibitors. V804M/E mutations conferred resistance to selpercatinib but not pralsetinib, whereas L730I/V and E732K mutations conferred resistance to pralsetinib but not selpercatinib, demonstrating RETi-specific resistance mutations. Cells expressing G810S secondary mutations were resistant to selpercatinib and pralsetinib, but sensitive to zeteletinib. Collectively, we show that individual *RET* fusion variants have distinct drug sensitivity profiles and that secondary resistance mutations are non-overlapping between RETi. The comprehensive characterization of *RET*-dependent mechanisms of resistance to RETi may provide therapeutic guidance for treating *RET*-fusion driven NSCLC and provide structural insights that can guide the development of new therapeutic regimens.

#5834 The GR-LEDGF/p75 transcriptional network promotes therapy cross-resistance in prostate cancer cells.

P. T. Ochoa[1], E. S. Sanchez-Hernandez[2], K. Cheng[1], I. Kremsky[1], C. Wang[1], C. A. Casiano[1];
[1]Loma Linda University, Loma Linda, CA, [2]Sanford Burnham Prebys Medical Discovery Institute, San Diego, CA

Prostate cancer (PCa) is the second leading cause of cancer mortality for men in the U.S. Patients who develop advanced PCa ultimately acquire therapy resistance and succumb to the disease. An emerging challenge in the treatment of advanced PCa is the development of therapy cross-resistance, in which molecular pathways promoting resistance to a particular drug or treatment also promote resistance to subsequent treatments. Although the mechanisms driving PCa therapy cross-resistance are not clearly understood, recent studies from our group and others implicate the glucocorticoid receptor (GR), a transcription factor, in resistance to both androgen receptor signaling inhibitors such enzalutamide (ENZ), and taxane drugs such as docetaxel (DTX). Our studies also showed that GR upregulates and interacts with the lens epithelium derived growth factor of 75 kD (LEDGF/p75) in a large panel of PCa cell lines. LEDGF/p75 is a stress transcription co-activator and oncoprotein that promotes cancer cell resistance to DTX and DNA-damaging drugs. GR and LEDGF/p75 are part of a large transcriptional network that include other oncogenic transcription factors linked to cancer chemoresistance such as β-catenin, Menin, MLL, JPO2, and c-Myc. We hypothesized that this transcriptional network plays a role in PCa therapy cross-resistance and could be a promising therapeutic target. We observed by Western blotting (WB) that both GR and LEDGF/p75 proteins are upregulated in ENZ-resistant and DTX-resistant PCa cell lines, and that GR silencing in both contexts abrogated LEDGF/p75 expression. MTT viability assays showed that ENZ-resistant PCa cells also exhibited cross-resistance to DTX. Bioinformatics studies, using publicly available RNA-seq datasets, identified overlapping differentially expressed genes (DEGs) between ENZ-resistant and DTX-resistant PCa cells. Individual silencing of GR and LEDGF/p75 in two DTX-resistant PCa cell lines followed by RNA-seq analysis also identified an overlap between DEGs regulated by GR and LEDGF/p75 with DEGs associated with both ENZ and DTX resistance in PCa. GSEA analysis of DEGs targeted by both GR and LEDGF/p75 in DTX-resistant PCa cells revealed enriched pathways associated with stress responses, androgen responses, and regulation of cell death and cell cycle. Further, we initiated studies to evaluate the efficacy of small molecule inhibitors targeting multiple components of the GR-LEDGF/p75 transcriptional network in sensitizing therapy-resistant PCa cells to DTX and ENZ. In conclusion, our results implicate the GR-LEDGF/p75 axis in promoting resistance to both ENZ and DTX in PCa cells. Further mining of RNA-seq data will identify potential molecular targets associated with PCa therapy cross-resistance, leading to the design of novel therapeutic strategies to attenuate this resistance.

#5835 Genome-Wide CRISPR gene knockout screens combined with selpercatinib identifies potent combination therapies for RET driven medullary thyroid carcinoma.

A. Rahmy[1], A. Fallatah[2], D. Milewski[2], M. Tian[2], Y. Song[2], Y. Kim[2], H.-C. Chou[2], X. Wen[2], C. Wang[2], J. Wei[2], R. Hawley[3], J. Glod[2], J. Khan[2];
[1]Case Western Reserve University School of Medicine, Cleveland, OH, [2]National Institute of Health, Bethesda, MD, [3]The George Washington University School of Medicine and Health Sciences, Washington, DC

Background: Medullary thyroid carcinoma (MTC) is a rare neuroendocrine tumor driven primarily by activating mutations in the RET proto-oncogene. It accounts for approximately 13% of thyroid cancer-related deaths. Total thyroidectomy is the main treatment option for MTC patients; however, its efficacy is limited due to the high prevalence of metastatic disease at diagnosis. Vandetanib, cabozantinib, and selpercatinib are RET signaling inhibitors (RETi), that have been approved for treating advanced MTC. Despite their effectiveness, many patients relapse or have refractory disease due to eventual resistance to these RETis.
Methods: In our study, we employed genome-wide clustered regularly interspaced short palindromic repeats (CRISPR) gene knockout (KO) in MTC cell lines treated with selpercatinib or vehicle to investigate the genetic mechanisms of resistance or sensitivity to RETi. Our overarching goal was to identify potential synergistic or additive drug combinations that may prevent or treat resistant disease.
Results: Our research identified key genes and pathways confirming the sensitivity or resistance of MTC cells to RETi. Notably, apoptotic genes along with RAS and mTOR signaling pathways were found to play a significant role in resistance development. Knocking out negative regulators of these pathways (such as NF1 and TSC2) conferred growth advantages to cells treated with RETi. Alternatively, knocking out BCL2, an antiapoptotic protein, led to increased lethality. These findings suggested that targeting RAS, mTOR, or antiapoptotic pathways in conjunction with RETi may be synergistic or have additive activity. To validate the CRISPR screening, we selectively knocked down NF1 in MTC cells and found it led to a nearly two-fold increase in IC50 for selpercatinib. Furthermore, in-vitro and in-vivo testing confirmed significant synergistic activity when using the combination of trametinib, an MEK inhibitor (MEKi; downstream of the RAS pathway), with selpercatinib.
Conclusions and Future Directions: We have identified a potent synergistic combination of MEKi with RETi as a novel synergistic drug combination to treat MTC, which may also prevent resistance to RETi. These results will be translated to patients through clinical trials conduced at the NCI.

#5836 CRISPR/Cas9 screening identifies genes affecting the sensitivity to the copanlisib/venetoclax combination in lymphoma cells.

S. Napoli[1], A. J. Arribas[1], E. Cannas[1], F. Fuzio[1], L. Cascione[1], A. Rinaldi[1], E. Zucca[2], A. Alimonti[1], A. Stathis[2], **F. Bertoni**[1];
[1]IOR - Institute of Oncology Research, Bellinzona, Switzerland, [2]Oncology Institute of Southern Switzerland, Bellinzona, Switzerland

Background: Copanlisib, a PI3K inhibitor with a higher selectivity on PI3Kα and PI3Kδ, is currently being evaluated as a single agent and in combination for lymphoma and solid tumor patients. We and others reported the synergism achieved by adding the BCL2 inhibitor venetoclax, and the combination is in its early clinical assessment (NCT04939272, NCT04572763, NCT03886649). To explore genes affecting the response to the combination, we performed a genome-wide CRISPR Cas9 screen in a marginal zone B cell lymphoma (MZL) cell line under drug exposure.
Methods: We generated, via lentiviral infection, a stable Cas9-expressing VL51 line, which was then infected (MOI 0.3) with the genome-wide Brunello guide RNA library, interrogating 19114 genes. After puromycin selection, 40M cells underwent DNA extraction (T0), 40M were exposed to DMSO (control arm), 40M to copanlisib (0.5nM) + venetoclax (25nM) (experimental arm) for 2 weeks. DNA at T0 and extracted at 2 weeks underwent Illumina sequencing according to the Broad Institute Genetic Perturbation Platform protocol. MAGeCK-MLE was used to model sgRNA read counts and assess the sgRNAs statistical enrichment ($P<0.05$ FDR< 0.15), GSEA for genesets enrichments.
Results: In the DMSO-treated cells, 160 genes had a positive β value (i.e., the sgRNAs knocking down the genes were positively enriched after 2 weeks), while 1152 had a negative β value (i.e., the sgRNAs knocking down the genes were negatively enriched after two weeks), for a total of 1152 differential enriched targets. In the cells exposed to the drug combination, 207 genes had positive and 1324 negative β, for a total of 1531 differentially enriched targets. Genes defined as essential, according to DepMap, represented 768/1152 (67%) and 843/1531 (55%) in control and experimental arms, respectively. The experimental arm did not massively differ from the control arm as shown by 815 genes (615, 74%, defined as essential by DepMap) overlapping between the 2 conditions and by highly significant enrichments at GSEA. A few genes were relevant only in VL51 exposed to copanlisib/venetoclax and not to DMSO. Selected hits were individually validated. Knocking down VKORC1L1, XCL1, RFK, MAP2K6, POC1A, and WTN5A improved the activity of the combination. WTN5A was also validated using recombinant protein (10 ng/mL), which reduced the effect of copanlisib/venetoclax. SPARCL1, MAPK4, ID2, and MSTN silencing reduced the activity of the combination. MSTN, coding for myostatin, was also validated by adding the recombinant protein (10 ng/mL), which increased the drugs anti-tumor activity.
Conclusions: A genome-wide genetic screening identified genes modulating the lymphoma cells response to the copanlisib/venetoclax combination, providing novel therapeutic targets or biomarkers.

#5837 Aryl hydrocarbon receptor is critical for enzalutamide-resistant prostate cancer growth.

C.-H. Chen, B. Wu;
Washington State Univ. College of Pharmacy, Spokane, WA

Therapy resistance is a ubiquitous and major challenge for curing cancer including prostate cancer. As the most prevalent non-skin cancer for men, prostate cancer is responsible for more than 30,000 deaths annually in the U.S. Despite a favorable prognosis at early stages, prostate cancer progressively develop into an incurable castration-resistant stage (CRPC) where prostate cancer grows in a low-androgen environment. Enzalutamide (ENZ) is the first drug approved by FDA for treating CRPC by inhibiting the residual androgen signaling. While ENZ significantly improves overall survival and quality of life, resistance inevitably develops and greatly limits its benefit. To understand ENZ resistance and identify novel therapeutic targets with the hope of overcoming resistance, we performed RNA-seq to analyze mRNA expression profiles from three ENZ-resistant human CRPC cell lines (C4-2B^{ENZR}, CWR-R1^{ENZR} and VCaP^{ENZR}) and identified the aryl hydrocarbon receptor (AHR) among the 114 commonly upregulated genes. AHR is a ligand-dependent transcription factor that has been shown to drive disease progression in multiple types of cancer. Stable shRNA-mediated knockdown of AHR substantially decreased growth of ENZ-resistant CRPC cells. Our pilot study also showed that AHR knockdown resulted in fewer and smaller CWR-R1^{ENZR} tumors in a xenograft mouse model. To elucidate the underlying mechanism of AHR-mediated cancer growth, gene set enrichment analysis (GSEA) revealed a declining trend of enrichment of the 114 commonly ENZ-upregulated genes among differentially altered genes upon AHR knockdown in ENZ-resistant cells, suggesting that AHR may act as a master regulator of ENZ resistance. Moreover, we found that the Hallmark androgen response gene set is downregulated in AHR-silenced ENZ-resistant cells, implying a role of AHR in sustaining androgen response for ENZ-resistance. Consistently, we performed AHR ChIP-seq and confirmed that AHR bound to promoter regions of several androgen-regulated genes in CWR-R1^{ENZR} cells. In addition, three peroxisome-related Hallmark gene sets are also negatively enriched in AHR-knockdown cells, which provides a rationale for further exploring a potential AHR-dependent connection of peroxisomal function to ferroptosis as a newly emerging mechanism of action for ENZ. In summary, our study suggests that AHR plays a critical role in maintaining ENZ-resistant CRPC growth with the likely involvement of modulating androgen signaling and ferroptosis susceptibility.

#5838 Un-methylation of NUDT21 promotes the development of enzalutamide resistance in prostate cancer by regulation of 3'UTR usage switch.

S.-C. Lin, S.-C. Lin;
National Cheng Kung University, Tainan, Taiwan

Enzalutamide, a second-generation anti-androgen drug, is a new treatment option for castration resistant prostate cancer (CRPC) patient. However, almost all CRPC patients develop drug resistance for enzalutamide after six to twelve months of treatment. According to our current findings, 3'UTR usage switches of RNA transcripts were observed in the prostate cancer specimen after acquiring enzalutamide resistance and nudix hydrolase 21 (NUDT21), an alternative polyadenylation (APA) regulator, was overexpressed in the enzalutamide resistant (EnzaR) cells, suggesting its potential role involved in regulation of 3'UTR usage switch. However, the underlying mechanism of how NUDT21 regulates 3'UTR usage switch during the development of enzalutamide resistance is still unclear. Interestingly, a potential mono-methylation (MME) is identified in NUDT21 protein by us, and it has never been examined before. Thus, we hypothesize that MME of NUDT21 may regulate the specificity of 3'UTR usage switch and involve in the development of EnzaR. To test the idea, a monoclonal antibody recognized NUDT21 MME was generated by us. Moreover, protein arginine methyltransferase 7 (PRMT7) was identified to be responsible for adding MME to NUDT21. In addition, androgen treatment increased both expression levels of NUDT21 MME and PRMT7 while decreased the expression level of NUDT21 total form in LNCaP cells via androgen receptor (AR) dependent manner. Next, co-treatment of enzalutamide and PRMT7 inhibitor leaded to increase of un-MME form of NUDT21 and it greatly enhanced the enzalutamide resistance in LNCaP cells. Importantly, binding profile of NUDT21 total form indeed had 3'UTR usage switch from distal to proximal APA site in COUP-TFII transcript after acquiring enzalutamide resistance, while its MME form attenuated this phenomenon. In addition, expression levels of NUDT21 MME and its total form were shown to conversely express in prostate cancer specimens. Finally, un-MME form of NUDT21 promoted the cancer growth in vitro and in vivo while its MME form did not. Taken together, our results suggest that down-regulation of PRMT7 by enzalutamide may lead to decrease of NUDT21 MME level and contribute to develop enzalutamide resistance by causing the 3'UTR usage switch of NUDT21 downstream transcript.

#5839 Identification of low-dose ligand dependent drug-resistance in ALK/ROS1 positive NSCLC via CRISPR library screening.

N. Kondo[1], T. Utsumi[1], K. Uchibori[1], Y. Miyazaki[2], R. Katayama[1];

[1]Japanese Foundation for Cancer Research, Tokyo, Japan, [2]Tokyo Medical and Dental University, Tokyo, Japan

Tyrosine kinase inhibitor (TKI) therapy has displayed significant effectiveness in treating patients with anaplastic lymphoma kinase (ALK) and ROS proto-oncogene 1 (ROS1)-positive non-small cell lung cancer (NSCLC). Nonetheless, the emergence of acquired resistance in most patients presents a major challenge. Drug-tolerant persister (DTP) cells have recently gained attention as potential sources of resistance, highlighting the need for a deeper understanding of drug resistance mechanisms. To address this issue, a comprehensive genome-wide CRISPR-Cas9 knockout screening was conducted using an ALK-positive NSCLC cell line derived from pleural effusion in a patient who had not been exposed to ALK-TKI treatment. Following a 9-day ALK-TKI treatment, sequencing analysis was performed to identify sgRNAs in DTP cells. Notably, this analysis detected the involvement of tumor suppressor genes, including NF2, BAX, and ERRFI1.NF2 depletion was found to induce a substantial resistance to ALK-TKIs, and a combination therapy involving mTOR inhibitors showed promise in partially overcoming this resistance. Moreover, knockout of ERRFI1 or BAX led to an increase in DTP cells, drawing particular attention to ERRFI1, also known as MIG6, which is known for negatively regulating EGFR signaling. One intriguing discovery was that the loss of MIG6 induced resistance to ALK-TKIs when exposed to a relatively low dose of EGF, comparable to concentrations in plasma of healthy adults. This resistance was attributed to the upregulation of the MAPK and PI3K/Akt/mTOR pathways. Similar to ALK-rearranged NSCLC, ROS1 fusion-positive NSCLC cell lines also showed resistance by MIG6 knockout. Interestingly, some cell lines with reduced MIG6 expression tended to develop resistance with low-dose EGF, even without prior treatment, and overexpression of MIG6 restored sensitivity to TKIs. We further explored the potential of combination therapy, combining ALK-TKIs with anti-EGFR antibodies, and this approach effectively addressed acquired resistance in both in vivo and in vitro models. Furthermore, an analysis of clinical samples revealed that individuals resistant to ALK-TKIs displayed decreased mRNA MIG6 levels in comparison to their sensitive counterparts. Investigating the mechanisms behind MIG6 expression, we confirmed that ALK-TKI therapy suppressed MIG6 expression levels, while factors such as corticosteroid usage or exposure to hypoxia induced the upregulation of MIG6, potentially influencing the formation of DTP cells. In conclusion, this research has unveiled a novel factor contributing to resistance in ALK and ROS1-TKI therapies by activating the EGFR pathway through exposure to low-dose ligands, shedding light on potential therapeutic strategies to combat acquired resistance.

#5840 Identifying drug tolerant persister to neoadjuvant osimertinib in resectable non-small cell lung cancer harbouring EGFR mutations (NORA) via single-cell RNA sequencing.

J. Lee[1], S.-J. Choi[1], Y. Park[1], K.-H. Park[1], S. Yong[1], H. Shim[2], B. Park[1], C. Lee[1], M. Hong[1], B. Cho[1], S. Lim[1];

[1]Yonsei University College of Medicine, Seoul City, Korea, Republic of, [2]Yonsei University, Seoul City, Korea, Republic of

Introduction: Adjuvant osimertinib is the standard of care for resected, stage IB-IIIA non-small cell lung cancer (NSCLC) harboring activating epidermal growth factor receptor (*EGFR)* mutation. Yet, the role of neoadjuvant osimertinib is not clear. In the NORA trial (NCT04816838), we aimed to identify the drug tolerant persister (DTP) after neoadjuvant osimertinib for surgically resectable, *EGFR*-mutated stage IA-IIIA NSCLC.

Methods: Patients harboring EGFR Exon 19 deletion or L858R at clinical stage IA-IIIA were given 80 mg of neoadjuvant osimertinib daily for two 28-day cycles followed by surgical resection and adjuvant osimertinib for 3 years. The key exploratory endpoint was to characterize the DTP via single-cell RNA sequencing (scRNA-seq) with pre and post-osimertinib samples.

Results: We performed scRNA-seq on twenty-five patients enrolled at Yonsei Cancer Center from June 2021 to March 2022. Patients with stage IA (n=8, 32%), IB (n=7, 28%), IIA (n=4, 16%), IIB (n=4, 16%), and IIIA (n=2, 8%) were included. For *EGFR* mutation, exon 19 del and L858R accounted for 10 (40%) patients and 15 (60%) patients, respectively. The ORR (all partial response) was 44% (n=11), major pathologic response (MPR) rate was 24% (n=6), and pathologic complete response rate was 0%. ScRNA-seq revealed a total of 252,339 cells (60 clusters) annotated as epithelial cells (10 clusters), fibroblasts (7 clusters), immune cells (17 clusters), myeloid (15 clusters), endothelial cells (11 clusters) that showed distinct enrichment in post-osimertinib samples, non-MPR, and L858R subset. We found that a distint epithelial subset, namely EP8-AGER, identified as alveolar type 1 (AT1) cells was enriched in the non-MPR subset showing activation of *Wnt*, *Hippo*, and *YAP/TAZ* pathway. Pseudotemporal ordering of this cluster showed activation of signaling pathway for *COL4A2/COL4A3* related to structural consistuent of extracellular matrix, and *RTKN2* associated with NF-κB. In the fibroblast subset, the proportion of FB6-CD74 associated with chemokine activity and NF-κB was higher in the non-MPR and L858R group. In the myeloid subset, CD8-C1-GZMK identified as $CD8^{\pm}$ T cells with activation/effector and cytotoxic signatures was also enriched in the post-osimertinib samples. Among macrophages, 3 clusters (annotated as SELENOP+, SPP1+, PLXDC2+) showed enrichment of cholesterol metabolism with activation of apolipoprotein E that promotes conversion of proinflammatory macrophages into anti-inflammatory phenotypes. Lastly, the proportion of EC9-LYZ, annotated as scavenging endothelial cells was higher in the non-MPR and L858R group.

Conclusion: Neoadjuvant osimertinib resulted in the cellular reprogramming in the tumor microenvironment, notably AT1 epithelial cell which may lead to a loop between cancer cells and fibroblasts for the generation of DTP cells.

#5841 A genome wide CRISPR-Cas9 screen identifies mediators of resistance to dual PI3K/mTOR inhibition in glioblastoma multiforme.

A. V. Ferrotta[1], A. Izawa-Ishiguro[1], M. Grogan[2], I. K. Mellinghoff[2];

[1]Weill Cornell Graduate School of Medical Sciences, New York, NY, [2]Memorial Sloan Kettering Cancer Center, New York, NY

Glioblastoma multiforme (GBM) is a highly aggressive primary brain tumor with a devastating 5-year survival rate of 6.8%. The current standard of care, consisting of surgery, radiation, and temozolomide (TMZ), has remained unchanged for over the past 15 years despite its limited efficacy and the serious therapy-related adverse events associated to this regimen. Although some frequent genetic alterations have been identified in GBM, no targeted therapies have shown efficacy in these patients to date. Among these, the phosphoinositide 3-kinase (PI3K) pathway is a signaling network that regulates cell growth, proliferation, migration, and invasion. Extensive molecular characterization of GBM has identified alterations in the components of the PI3K pathway in 80% of primary GBMs, including amplification of receptor tyrosine kinases (RTKs), activating mutations in the PI3K catalytic subunit (PIK3CA), loss-of-function mutations in the PI3K regulatory subunit (PIK3R1), and loss of the major tumor suppressor of the pathway, phosphatase and tensin homologue (PTEN). Despite the universal upregulation of PI3K pathway signaling associated with these genetic alterations, clinical trials investigating PI3K inhibitors in GBM have failed due to insufficient antitumor activity and dose-limiting toxicities. To elucidate mechanisms of resistance to PI3K inhibition in GBM, we used a genome-wide functional CRISPR-Cas9 knockout screen to identify genes that mediate resistance to the dual PI3K/mTOR inhibitor XL765 in PTEN-null SF295 GBM cells. We identified reactivation of the PI3K pathway and inhibition of autophagy as potential resistance mechanisms to dual PI3K/mTOR inhibition. Using orthogonal approaches, we will functionally validate our candidate hits through mechanistic studies, with patient-derived models, and with *in vivo* orthotopic xenografts. Our findings will elucidate novel mechanisms of resistance to PI3K/mTOR inhibition in GBM and will streamline rational drug combinations aimed to overcome resistance, thus eventually maximizing therapeutic responses to PI3K inhibitors in GBM.

#5842 An epigenetic program that links oncogenic signaling to mitochondrial biogenesis supports leukemic cell survival in chronic lymphocytic leukemia.

O. M. Depies, S. Sinha, S. Parikh, N. Kay, **Z. Wang**;
Mayo Clinic, Rochester, MN

Therapeutic inhibition of BCR signaling using Bruton tyrosine kinase inhibitors (BTKis) has remarkable efficacy in the treatment of chronic lymphocytic leukemia (CLL). However, the efficacy of BTKis is limited by the development of drug resistance, which can be mediated through mutations in genes encoding proteins of BCR signaling pathways. Approaches targeting the BCR mutant proteins have been limited by the large heterogeneity of these mutations. In addition, BCR signaling mutations are only detected in up to two-thirds of the CLL patients who progressed with BTKi treatment, suggesting mechanisms beyond genetic mutations. We previously showed that the BCR signaling pathway impacts the chromatin landscapes of CLL B cells (Wang et al., Blood Cancer J. 2022), suggesting that epigenetic mechanisms are exploited by CLL B cells to support their survival. To gain insights into the epigenetic regulation of BTKi treatment in CLL B cells, we analyzed the genome-wide chromatin accessibility (ATAC-seq) and histone modification (H3K4me1, H3K4me3, H3K27ac, H3K27me3) profiles (CUT&Tag) of leukemic cells from 4 CLL patients on BTKi ibrutinib treatment in a sequential fashion (i.e., baseline, on ibrutinib treatment, and at relapse). We also performed the same analysis in a CLL cohort at two stages of ibrutinib treatment (baseline and while on treatment, n=20). Our studies showed that suppressing BCR signaling by BTKi leads to the downregulation of genes associated with mitochondrial translation, a key process of mitochondrial biogenesis. We also found decreased chromatin accessibility and H3K27ac deposition at the promoters of these MT genes. Interestingly, in patients who experienced disease progression on ibrutinib, there was a restoration of MT gene expression, chromatin accessibility, and H3K27ac levels at the MT gene promoters similar to baseline samples, suggesting an epigenetic-regulated MT both in BTKi treatment naïve and relapsed CLL patients. Importantly, MT inhibition led to a decreased survival of primary CLL B cells. These findings point toward an epigenetic mechanism utilized by BCR signaling to promote MT and leukemic cell survival. We then observed that the transcription factor NRF1 is enriched at the MT promoter in CLL B cells. CRISPR-mediated depletion of NRF1 led to reduced mitochondrial translation and cell survival in BCR signaling active malignant B cell lines and primary CLL B cells. These results suggest that NRF1 controls an epigenetic program linking BCR signaling to control MT, which in turn supports BCR signaling-dependent CLL B cell survival. Our findings demonstrated that BCR signaling utilizes epigenetic mechanisms that regulate mitochondrial metabolism to enhance cell survival in both treatment naïve and BTKi-relapsed CLL. These findings may provide new therapeutic directions for untreated and BTKi-relapsed CLL patients.

#5843 Exploring the implications of LPAR-1 expression in TKI-resistant NSCLC.

V. Srinivasan, Z. Li, R. Kannan, A. Upendran;
University of Missouri - Columbia, Columbia, MO

Introduction: Non-small cell lung cancer (NSCLC) is the most common type of lung cancer in the United States with a 5-year survival rate hovering between 20-30%. Mutations in EGFR can initially cause the tumors to respond to tyrosine kinase inhibitors (TKI). Osimertinib, a third generation TKI, is the preferred first or second line of treatment and despite being effective, recent reports indicate that patients develop resistance within 10-18 months of treatment. TKI resistance limits therapeutic options for patients and therefore, alternative strategies are being explored. In this context, Lysophosphatidic acid receptors (LPARs), a family of G-protein coupled receptors consisting of LPARs 1-6 expressed differentially in prostate, breast, ovarian, pancreatic, and brain cancers are being explored as potential targets for drug resistant cancers. Specifically, LPAR-1 has been shown to play a role in tumor cell clonogenicity, migration, and response to therapy in EGFR mutant NSCLC cells. Pharmacological inhibition or CRIPSR based deletion of LPAR-1 in EGFR mutant NSCLC cell lines HCC827 and NCI-H3255, increased TKI sensitivity by reducing clonogenic potential. Further, detailed pathway analysis in TKI sensitive and resistant EGFR mutant cell lines suggests that LPAR-1 expression influences drug sensitivity. Surprisingly, the role of LPAR-1 in TKI sensitivity is not well understood. In the present study, we have performed detailed investigation on the implications of LPAR-1 expression in the development of Osimertinib resistance.

Methods: Osimertinib resistant EGFR mutant cell lines (OR) were generated using dose-escalation method and drug-tolerant persisters (DTPs) were generated using a short-term high exposure method. Gene and protein expressions were examined using qPCR and western blotting. Subcutaneous tumor cell derived xenografts were generated for *in vivo* studies.

Results: LPAR-1 is downregulated in Osimertinib resistant NSCLC cells. Further, we also observe that LPAR-1 levels are lower in DTP cells, confirming a progressive loss of LPAR-1 with Osimertinib treatment. *In vivo* studies in cell derived xenografts correlated with the *in vitro* studies.

Conclusion: Our studies indicate LPAR-1 downregulation correlates to Osimertinib resistance in EGFR mutant NSCLC cell lines. LPAR-1 downregulation has a key role in development of Osimertinib resistance. Future studies will focus on delineating LPAR-1 signaling pathways related to TKI resistance and investigating the effect of LPAR-1 overexpression using CRISPR technology.

#5844 Landscapes of acquired EGFR and VEGF resistance alterations in colorectal cancer: findings from the PARADIGM biomarker study.

K. Tsuchihara[1], R. Yamashita[1], T. Yoshino[2], K. Shitara[2], J. Watanabe[3], H. Yasui[4], H. Ohori[5], M. Shiozawa[6], K. Muro[7], K. Yamazaki[4], E. Oki[8], T. Sato[9], T. Naitoh[10], Y. Komatsu[11], T. Kato[12], K. Yamanaka[13], I. Mori[13], M. Hihara[13], J. Soeda[13], K. Yamamoto[14], K. Akagi[15], A. Ochiai[16], V. E. Velculescu[17], H. Uetake[18];

[1]Exploratory Oncology Research and Clinical Trial Center, National Cancer Center, Chiba, Japan, [2]National Cancer Center Hospital East, Chiba, Japan, [3]Yokohama City University Medical Center, Yokohama, Japan, [4]Shizuoka Cancer Center, Shizuoka, Japan, [5]Japanese Red Cross Ishinomaki Hospital, Miyagi, Japan, [6]Kanagawa Cancer Center, Kanagawa, Japan, [7]Aichi Cancer Center Hospital, Nagoya, Japan, [8]Graduate School of Medical Sciences, Kyushu University, Fukuoka, Japan, [9]Kitasato University School of Medicine, Sagamihara, Kanagawa, Japan, [10]Kitasato University School of Medicine, Sagamihara, Japan, [11]Hokkaido University Hospital Cancer Center, Sapporo, Japan, [12]National Hospital Organization Osaka National Hospital, Osaka, Japan, [13]Takeda Pharmaceutical Company Ltd., Tokyo, Japan, [14]Yokohama City University School of Medicine, Yokohama, Japan, [15]Saitama Cancer Center, Saitama, Japan, [16]Tokyo University of Science, Tokyo, Japan, [17]Sidney Kimmel Comprehensive Cancer Center, Johns Hopkins University School of Medicine, Baltimore, MD, [18]Tokyo Medical and Dental University Graduate School of Medicine, Tokyo, Japan

Introduction: Resistance mechanisms to anti-epidermal growth factor receptor (EGFR) treatment, such as panitumumab (PAN), in patients (pts) with metastatic colorectal cancer (mCRC) depend on the diversity of acquired gene alterations and clonal variation. To explore resistance mechanisms and emerging genomic alterations during PAN treatment, we analyzed the circulating cell-free DNA (cfDNA) samples from the PARADIGM trial (NCT02394795), which demonstrated survival benefits of PAN over bevacizumab (BEV), an anti-vascular endothelial growth factor (VEGF) antibody, in combination with first-line chemotherapy in pts with *RAS* wild-type (WT) mCRC.

Methods: cfDNA from blood samples were obtained pre- and post-treatment and analyzed for gene alterations using the custom PlasmaSELECT-R 91 PGDx panel (NCT02394834). We analyzed the landscapes of acquired alterations and their association with functional pathways in mCRC according to The Cancer Genome Atlas signaling classification.

Result: Among the enrolled 802 pts, 390 discontinued treatment due to progressive disease, of which 276 (70.8%) had evaluable pre- and post-treatment cfDNA samples (PAN, n=126; BEV, n=150). Though the proportion of pts with acquired alterations in any of 30 *RTK-RAS*-related genes was similar in PAN vs BEV (44.4% vs 42.7%), known *EGFR* resistance-related genes were observed more frequently in PAN compared with BEV: *KRAS* (19.1 vs 2.7%), *NRAS* (9.5 vs 2.7%), *BRAF* (11.1 vs 0.7%), *MAP2K1* (5.6 vs 0.7%), and *EGFR* (5.6 vs 3.3%). These acquired mutations clustered at hotspots within those genes in the PAN group, unlike in the BEV group. Furthermore, the co-occurrence rates of acquired alterations among the *RTK-RAS* pathway of the individual cases were higher in PAN (25.4%) vs BEV (9.3%), suggesting an increased subclonal complexity in PAN. There were few acquired alterations predominantly observed in BEV, and their biological significance remains unclear.

Conclusion: These results suggest that PAN treatment, compared with BEV, more commonly induces multiple resistant subclones in specific pathways under selective treatment pressure. Our findings provide valuable insight for further investigations into the mechanisms of acquired and resistance associated with PAN and BEV.

#5845 Cytarabine resistance leads to a unique mutational signature.

D. Cao[1], M. Yin[1], Z. Zhang[1], T. Baslan[2], J. Zhu[1], R. Bertoli[1], P. Meltzer[1], P. Aplan[1];
[1]National Cancer Institute, Bethesda, MD, [2]Memorial Sloan Kettering Cancer Center, New York, NY

The prognosis of recurrent T-cell acute lymphoblastic leukemia (T-ALL) is poor, mainly due to chemotherapy resistance. The mechanism(s) leading to chemoresistance at relapse are incompletely understood. We previously characterized a mouse strain that is hypomorphic for the DNA replication factor Mcm2. $Mcm2^{hypo}$ mice develop T-ALL due to acquired DNA copy number variations (CNV) involving tumor suppressor or oncogenes. We hypothesize that treatment of $Mcm2^{hypo}$ cells with specific chemotherapy agents may reveal CNV that lead to chemoresistance. We treated two $Mcm2^{hypo}$ T-ALL cell lines (designated 2883 and 2869) and an Mcm2 WT T-ALL cell line (designated 7298) with cytarabine (ARAC), an active agent often incorporated in T-ALL treatment regimens. After one year of treatment with gradually increasing ARAC concentrations, we obtained ARAC resistant cell lines (designated with the suffix CR) that tolerate drug concentrations up to 10,000X that of parental cell lines. These samples were characterized by sparse WGS (for CNV assessment), RNA-Seq and WES. Both the 2883CR and 2869CR cell lines had bi-allelic mutations involving Dck, which is the rate-limiting enzyme in the cytidine salvage pathway, and is thought to be required for metabolism of ARAC. In both cases, one allele was deleted while the second allele had a splice site/region mutation leading to partial intron retention and resultant frameshift. The 7298CR cell line had homozygous deletion of Dck. Western blotting showed absence of WT Dck protein in all three cell lines. Further analysis of WES data revealed thousands of acquired single nucleotide variants (SNV) in both Dck mutant $Mcm2^{hypo}$ cell lines. These mutations occurred in a specific trinucleotide context (C>T in a GCG context, T>C in a GTC context, T>G mutations in GTC and GTT context, and C>G in a GCC context) generating a mutational signature that is not present in the COSMIC database. In addition, the parental 2883 and 2869 cell lines showed fewer mutations (ie, hundreds vs thousands) in a similar context (C>T in a GCG context, T>C in a GTC context, T>G mutations in GTC and GTT context, but not the C>G in GCC context). A GEMINI (Genotoxic Mutational Signature Identified After Clonal Expansion In Vitro) assay of untreated 2883CR and 2869CR cells demonstrated that ongoing ARAC exposure was not required for the mutational signature. We hypothesize that the basic signature (C>T in a GCG context, T>C in a GTC context, T>G mutations in GTC and GTT context) can be produced by Mcm2 deficiency, and this signature is amplified and modified (to include a C>G in GCC context) by Dck inactivation. In summary, we identified three mechanisms responsible for Dck inactivation associated with ARAC resistance: copy number loss, splice site mutations, and splice region mutations. Moreover, Dck inactivation leads to a specific mutation signature. These findings add to emerging data that exposure to specific chemotherapy agents can lead to specific mutational signatures.

#5846 Inhibiting elements of the proteasome recovery pathway sensitizes glioblastoma to proteasome inhibitors.

A. Anand, M. Shaikh, C. Chokshi, B. Brakel, W. Maich, S. Grewal, C. Venugopal, S. Singh;
McMaster University, Hamilton, ON, Canada

Bacground: Glioblastoma (GBM) is the most common primary brain tumor, accounting for 15% of all central nervous system related tumors. Despite the aggressive standard of care treatment including chemotherapy, radiotherapy, and maximally safe surgical resection, patient outcomes are abysmal: with 95% of patients relapsing and a median overall survival of 15 months. Thus, this necessitates the rapid query for personalized therapeutics and agents that can potentiate the clinical effects of currently approved treatments. One such pathway that demonstrates aberrant functioning in cancer and is a targetable mechanism is the ubiquitin-proteosome pathway (UPP). Studies have shown that UPP related proteolysis remains constitutively active in cancer cells leading to the rapid degradation of proteins that regulate tumor suppressor genes and oncogenes. Despite robust preclinical evaluations for the usage of proteosome inhibitors against GBM, most tested proteosome inhibitors failed in phase II and III trials, indicating resistance.
Methods: We conducted an unbiased genome wide CRISPR-Cas9 screen in human HAP1 cells treated with the proteosome inhibitor, Bortezomib (BTZ), to identify genes that may lead to a BTZ-resistant phenotype. We identified several genes that when perturbed, sensitized cells to BTZ including N-glycanase-1 (NGLY-1), Nuclear factor Erythroid 2-Like-1 (NFE2L1), and DNA damage inducible 1 homolog 2 (DDI2). Herein we sought to evaluate the effects of perturbing components of the proteosome rescue pathway in our Singh lab patient derived GBM cell lines by utilizing CRISPR/Cas9 knockout technology *in vitro* and *in vivo*.
Results: The generation of NGLY-1, DDI2, and NFE2L1 KO cell lines demonstrated functional sensitivity to the proteosome inhibitor Marizomib (MZB) as observed through a significant reduction of the IC50 in the KO cell lines compared to a control. Functional evaluation also revealed a reduction in proliferation capacity as well as sphere formation in these genetically modified GBM lines. Ongoing *in vivo* work will aim to evaluate the mitigation of this resistant pathway in our NSG mouse models orthotopically transplanted with these patient derived KO cell lines. In an ongoing collaborative effort, we are working to identify and functionally assess a novel small molecule NGLY-1 inhibitor to evaluate preclinical sensitivity to MZB in our *in vitro* and *in vivo* models.

#5847 Characterizing mechanisms of BRAF/MEK inhibitor resistance in BRAF V600 mutant colorectal cancer vs. melanoma.

J. Maxwell, E. Rousselle, L. An, A. Rose;
McGill University, Montreal, QC, Canada

Background: BRAF V600 mutations comprise ~80% of all oncogenic BRAF mutations in metastatic colorectal cancer (mCRC). While most cancers with BRAF V600 mutations can be effectively treated with combined BRAF and MEK inhibition, BRAF V600 mutant mCRC acquire resistance through EGFR-mediated signaling. The profound difference in response rates to BRAF/MEK inhibitors in BRAF V600 mutant mCRC (12%) vs. melanoma (63-68%) is not sufficiently explained by increased EGFR signaling in CRC. Therefore, we sought to characterize the differences that exist between BRAF V600 mutant CRC and melanomas that could explain the differential sensitivity to BRAF/MEK inhibition and identify more effective treatments for BRAF V600 mutant CRC.
Methods: We assessed cell survival by clonogenic assay in the presence of small molecule inhibitors. In parallel, we mined TCGA RNAseq data to calculate the MAPK Pathway Activity Score (MPAS). RTK expression was assessed in TCGA data from patients with BRAF V600 mutant CRC vs. melanoma. We developed cells with acquired resistance to BRAF+MEK inhibitors (Encorafenib+Binimetinib; E+B) by culturing cells in increasing concentrations of drug over several months. RNA-sequencing and analysis was performed on parental and resistant cells treated with vehicle control or BRAF+MEK inhibitors.
Results: When comparing the efficacy of BRAF+MEK inhibitors across BRAF V600 mutant cells, we found that BRAF V600 mutant CRC cell lines (n=2) were less sensitive than melanoma cell lines (n=2). MPAS scores were significantly lower in BRAF V600 mutant CRC (n=46) vs. melanoma (n=188) tumors. We interrogated protein array data from the DepMap and identified increased activation of several RTKs (EGFR, HER2, HER3) in BRAF V600 CRC (n=8) vs. melanoma (n=39) cell lines. Similarly, we established resistant HT29 (BRAF V600 CRC) cells and observed sustained MAPK pathway activity despite a lack of difference in EGFR activity in the presence of BRAF+MEK inhibitor treatment. Both HT29 parental and resistant cells showed re-establishment of MAPK signaling after 72 hours. Resistant SkMel28 (BRAF V600 melanoma) cells showed increased pERK levels compared to resistant HT29 cells. RNAseq revealed increased expression of multiple RTKs (PDGFRB, ERBB2, ERBB3) and ligands/growth factors for multiple RTKs (FGF3, PDGFA, HB-EGF) in resistant HT29 cells. Shp2 is a protein tyrosine phosphatase that regulates signaling of multiple RTKs to activate the MAPK pathway. Accordingly, we assessed the efficacy of an inhibitor of Shp2 (TNO155) overcoming MAPKi resistance in BRAF V600 CRC cells. We confirmed that E+B+TNO155 more effectively inhibited cell growth and MAPK pathway activity in BRAF V600 CRC cell lines (n=2) *in vitro*.
Conclusion: Together, these data identify key, actionable drivers of MAPK inhibitor resistance in CRC and highlight Shp2 as a potential therapeutic target for BRAF V600 CRC.

#5848 Unraveling c-MET targeting resistance mechanisms in gastric cancer via single-cell transcriptome analysis; Novel therapeutic target discovery of ERO1A and VEGFA.

H. Kim[1], J. Kim[1], S.-J. Myung[1], C. Park[2], S. Kim[1];

[1]Asan Medical Center (AMC), Seoul, Korea, Republic of, [2]National Cancer Center, Goyang, Korea, Republic of

Background: Gastric cancer (GC) is the fifth most prevalent malignant tumor worldwide, and the fourth most common cause of mortality. c-MET has been reported to be associated with poor prognosis in GC. Over the decades, treatment approaches targeting HGF/c-MET have been developed including small molecule tyrosine kinase inhibitors, anti-c-MET and anti-HGF monoclonal antibodies. Unfortunately, the results of previous study support the development of acquired resistance to HGF/c-Met inhibitors. They suggest a possible resistance mechanism involving poor MET-status detection, crosstalk between c-MET and compensatory signaling pathways, the occurrence of acquired a new mutation, however, knowledge regarding the mechanism of c-MET inhibitor is limited.2.
Purpose: We identify new markers and mechanisms that induce drug resistance when c-MET-targeted inhibitors are treated in c-MET-amplified GC cell lines in 3D culture, and discover new therapeutic targets for GC via single cell-RNA sequencing analysis.3.
Material and Methods: Single cell-RNA sequencing is performed on c-MET amplified GC cell line in the 2D and 3D culture methods according to the presence or absence of c-MET inhibitor treatment. Through DEG and clustering analysis, the candidate genes estimated to impart resistance are selected and verified by qPCR. Through over-expression, induction of resistance for c-MET inhibitor treatment with target gene is evaluated in c-MET amplified GC cell line. c-MET inhibitor selected gene is constructed as a xenograft model to reveal the mechanism of drug resistance. Retrospective analysis confirms the relationship between target gene expression level and the resistance for c-MET inhibitor or other TKI treated patients with GC. 4.
Results: Treatment of c-MET-amplified GC cell lines with c-MET inhibitors under the conditions of 2D and 3D cultures confirmed that resistance was induced only in the 3D. We performed a high-precision single cell RNA-Seq analysis of 18056 single cells in total from c-MET amplified GC cell line MKN-45 in 2D/3D culture control as well as corresponding samples with volitinib treatment investigate their gene expression signatures. Fifteen selected candidate genes presumed to induce drug resistance were screened and validated by qPCR, with a total of six genes consistent with the sequencing results. After over-expression of six genes to the c-MET amplified gastric cancer cell line, c-MET inhibitors were treated and cell viability was performed to check for resistance to cell viability. Finally, ERO1A and VEGFA were over-expressed to confirm the resistant for the c-MET inhibitor treatment in vitro and in vivo.5.
Discussion: We plan to build a xenograft mouse model with candidate genes such as ERO1a and VEGFA to prove whether the candidate gene overcomes drug resistance when they are on or off.

#5849 Integrated multi-omics of hydroxychloroquine evolved cancer cells reveal survival requires transcriptional upregulation of glycolysis, exocytosis, and chromosome fidelity, but not autophagy.

M. Clark, S. G. Vaena, J. R. Delaney;
The Medical University of South Carolina (MUSC), Charleston, SC

Repurposed drugs are undergoing a renaissance in the era of genomics, particularly in oncology. Over 2,300 FDA-approved and natural product small molecules now exist, but challenges remain in identifying which cancer patients may best benefit from such drugs. To best position repurposed drugs, mechanisms of action and resistance to the drug in a cancer cell setting must be determined. Hydroxychloroquine (HCQ) and chloroquine are repurposed drugs reported to disrupt autophagy, a molecular recycling pathway which is essential for tumor cell survival, chemotherapeutic resistance, and stem cell phenotypes. However, oncology trials with chloroquine have no biomarker or other genetic test to categorize patients who may best respond to HCQ therapy. It is unclear how tumors mechanistically evolve resistance to HCQ. We pursued a multi-omic strategy in OVCAR3 ovarian cancer and CCL218 colorectal cancer cells. Two genome-scale screens were performed. In the forward genetic screen, cell populations were passaged in 93-independent cultures for 15 drug pulse-chases with HCQ or vehicle control. Evolved cells were collected and processed for bulk RNA-seq, exome-seq, and single cell RNA-seq (scRNA-seq). In the reverse genetic screen, a pooled Brunello CRISPR-Cas9 library of 19,114 genes targeted by multiple sgRNAs was used in cells over three pulse-chases of HCQ or vehicle control treatments. HCQ evolved cells displayed remarkably few mutational differences, but substantial transcriptional differences. Bulk transcriptomes revealed multiple broad-spectrum pathways associated with resistance to HCQ, including upregulation of glycolysis, exocytosis, and chromosome condensation/segregation, as well as downregulation of translation and apoptosis. Analysis of scRNA-seq data indicated cell clusters were differentially reliant on cytoskeletal regulation, DNA repair, and metabolism. The genome-scale Cas9 screen identified remarkably few autophagy genes. However, an integrated analysis of Cas9 hits with RNA-seq upregulated genes confirmed glycolytic genes KDM3A, ENO2, and PDK3 were essential for HCQ resistance. Additional integrated hits were NEK2, involved in exocytosis, and chromosome condensation/segregation genes CDK1 and CENPA. Transcriptional plasticity was the primary mechanism by which cells evolved resistance to HCQ. Contrary to the widely presumed autophagy-related mode of cell death, the multi-omic analysis instead prioritized glycolytic metabolism, exocytosis, and chromosome condensation/segregation as most involved in cancer cell survival with HCQ. Integrated multi-omic analysis defined high-value biomarkers of HCQ sensitivity and resistance. Our analysis may serve as a model for how to better define the effects and positioning of repurposed drugs in oncology.

#5850 Multiomics analysis unravels tumor metabolic reprogramming and potential resistance mechanism(s) to curative therapy in TNBC.

Z. Ren[1], K. Kurmi[2], R. Morris[1], S. Joshi[2], E. Zaniewski[1], J. Kreuzer[1], G. Elena Gioia[1], V. I. Bossuyt[1], B. N. Dontchos[1], G. X. Wang[1], S.-H. S. Chou[1], L. M. Spring[1], W. Haas[1], M. C. Haigis[2], L. W. Ellisen[1];

[1]Massachusetts General Hospital/Harvard Medical School, Boston, MA, [2]Harvard Medical School, Boston, MA

Drug resistance is the leading cause of treatment failure to completely eliminate viable tumor cells in ~40% of patients with triple negative breast cancer (TNBC). Making a major impact on the treatment and prognosis for TNBC patients requires a better understanding of drug resistance mechanism(s). Combining clinical data with high-throughput metabolomic and proteomic analyses, we probed the molecular basis for chemotherapy resistance in treatment-naive TNBC primary tumors, reflected by pathological complete response (pCR) and non-pCR after neoadjuvant chemotherapy (NAC). Metabolic profiling uncovered that glycolysis and oxidative phosphorylation (OXPHOS) co-exist in TNBC primary tumors compared to benign lesions regardless of pCR status, indicating metabolic reprogramming. However, non-pCR tumors were more enriched in OXPHOS and less in glycolysis relative to pCR tumors, pointing to the potential importance of OXPHOS in drug resistance. Moreover, parallel proteomic profiling of these same TNBC tumors supported the results from metabolic profiling, showing that OXPHOS was indeed highly enriched at the protein level, and may be regulated by SIRT5-mediated sirtuin signaling. In alignment with these findings, non-pCR tumors were abundantly enriched in immune-inhibitory metabolites that may be due to the products of SIRT5-mediated mitochondrial metabolism. Thus, these findings led me to hypothesize that SIRT5 may play an important role in chemoresistance through regulation of mitochondrial metabolism and ROS detoxification. Together, the metabolite resulted from SIRT5-mediated mitochondrial metabolism led to the suppression of immune cell infiltration in non-pCR tumors. Understanding SIRT5-mediated chemoresistance mechanism may uncover a metabolic and therapeutic vulnerability to resistant TNBCs.

#5851 Dysregulated RNA splicing promotes AML quiescence and chemoresistance.

E. Wang[1], C. Han[1], A. Calderon[1], A. Lawal[1], N. Hariramani[1], E. Crosse[2], R. Bradley[2];

[1]The Jackson Laboratory for Genomic Medicine, Farmington, CT, [2]Fred Hutchinson Cancer Research Center, Seattle, WA

Chemotherapy is the first-line treatment for patients with acute myeloid leukemia (AML). Although most achieve initial remission, an estimated 50% of patients will relapse with poor clinical outcome. The paucity of genetic lesions in AML patients that relapse from chemotherapy implicate non-genetic alterations that mediate chemoresistance. In this study, we conducted a longitudinal analysis of alternative splicing changes in a cohort of 19 AML patients at diagnosis and relapse post-chemotherapy treatment. We found that the long isoform of the transcription factor-encoding gene *RUNX1* (also known as RUNX1C) is upregulated in AML relapse cohorts and conferred chemotherapy resistance. Mechanistically, we show that B cell translocation gene 2 (*BTG2*) is an RUNX1C isoform-specific transcriptional target that promote transition into a quiescent and treatment-resistant state. Direct targeting of *RUNX1C* mRNA augments chemotherapy response in AML patient-derived xenograft (PDX) models *in vivo*. These findings uncover an isoform-specific functionality that influences chemotherapy responsiveness and offers a therapeutic strategy to sensitize leukemic cells to conventional chemotherapy treatments.

#5852 Tumor gene expression patterns affecting response to BCl-2 inhibitor venetoclax in acute myeloid leukemia.

J. Raygoza Garay[1], S. Yun[2], A. Osman[3], R. Ramlal[4], D. Feith[5], M. Churchman[6], P. Dhakal[1];

[1]University of Iowa Holden Comprehensive Cancer Center, Iowa City, IA, [2]H. Lee Moffitt Cancer Center & Research Institute, Tampa, FL, [3]Huntsman Cancer Institute, Salt Lake City, UT, [4]University of Kentucky, Lexington, KY, [5]University of Virginia, Charlotesville, VA, [6]Aster Insights, Tampa, FL

Background: Venetoclax (VEN), a B-cell lymphoma-2 (BCL-2) inhibitor, is an important drug in acute myeloid leukemia (AML) treatment regimens. However, resistance to VEN-based therapy is a common challenge in AML management. Some factors contributing to resistance include dysregulation of BCL-2 family proteins, mutations in the TP53 gene, activating kinase mutations, and oxidative phosphorylation activity. Despite these insights, other mechanisms of resistance remain elusive. We aim to analyze tumor gene expression patterns associated with treatment response in patients who received VEN-based therapy.

Methods: Molecular and clinical data of the patients were obtained as part of the Oncology Research Information Exchange Network (ORIEN) Avatar dataset. RNA-Seq data from diagnostic Bone Marrow were processed to remove batch effects, and differential expression analysis was performed using DESeq2, while correcting for age at sample collection and sex of patients.

Results: We included 16 individuals treated with VEN-based therapy. Median age at the time of specimen collection was 65 years (interquartile range, 58-69), 9 (56%) male, 11 (69%) had active disease despite treatment with VEN. VEN-based therapy was used as 1st line, 2nd line, 3rd line, 4th line or more in 3, 4, 4, 2, and 3 patients, respectively. We found a total of 332 genes differentially expressed (fdr<0.05 and abs(log2FoldChange)>2.0) among patients having no evidence of active disease and those with no active disease at the time of last contact. Among those genes, we found HOXA7 and PRAME of particular interest. HOXA7 has been previously implicated in Bromodomain and Extraterminal Domain Inhibitors (BETi) inhibitor resistance in AML. This makes HOXA7 a potentially universal mechanism of chemotherapy resistance in AML. PRAME has been associated with leukemia cell survival, and its knockdown has been shown to induce apoptosis in K562 cells, which is only expressed in AML cells but not in normal hematopoietic cells. Pathway analysis found that the top two enriched pathways for the differentially expressed genes were *MET activates PTK2 signaling* (R-HSA-8874081) and *Metabolism of Angiotensinogen to Angiotensins*(R-HSA-2022377).

Conclusions: This study highlights some molecular mechanisms that give rise to AML resistance to VEN. Our results indicate that HOXA7 may potentially be a universal mechanism of chemotherapy resistance not limited to VEN-based therapy. Similarly, pathways enriched in resistant cells could be targeted to prevent or treat resistance to VEN-based therapy. These and other findings may help us identify resistance mechanisms in all AML cases vs those specific to VEN-based therapy, allowing the development of treatment strategies based on treatment mechanism. Also, analysis of these mechanisms can aid therapeutic decision-making and the development of effective treatment strategies to improve outcomes in AML.

#5853 Regulatory network inference of lung adenocarcinoma drug-tolerant persister cells.

L. Chabrier[1], C. Leonce[2], R. Schneider[2], C. Degletagne[2], P. Saintigny[2], A. Crombach[1], **S. Ortiz-Cuaran**[2];
[1]Inria Antenne Lyon La Doua. Universite de Lyon, INSA-Lyon, LIRIS, UMR 5205., Villeurbanne, France, [2]Univ Lyon, Claude Bernard Lyon 1 University, INSERM 1052, CNRS 5286, Centre Leon Berard, Cancer Research Center of Lyon, Lyon, France

Despite the effectiveness of the latest generation of cancer drugs, partial tumor response and subsequent disease relapse is commonly observed in patients. Recent evidence suggests that treatment resistance emerges from drug-tolerant persister cells (DTPC) that survive through non-genetic tumor cell adaptation. Although DTPC are mostly slow-cycling, a rare subset can re-enter the cell cycle under constitutive presence of treatment. Understanding how DTPC dynamically remodel their molecular portraits at the single-cell level may provide high-resolution insights into the molecular circuits associated with adaptive survival to therapy.Here, we use single-cell RNA sequencing (scRNA-seq) to identify potential mechanisms that promote survival of DTPC and decipher their underlying gene regulatory networks (GRNs), in a model of EGFR-mutant lung adenocarcinoma treated with osimertinib (EGFR inhibitor).
Gene expression analysis revealed fewer cell states in DTP compared to treatment-naïve cells (TN). We confirmed the acquisition of DTPC hallmarks (e.g., high epithelial-mesenchymal transition, slow-cycling phenotype, deficient DNA repair). We also identified subpopulations of cells that display intermediate transcriptional states: a pre-existing DTP-like state in a bulk of TN cells, and DTPC with enriched cell cycle signatures, evoking a phenotype of cycling DTPC. To characterize the GRN that govern TN cells, DTPC and the intermediate cell states, we applied the network inference tool PYSCENIC, which associates transcription factors (TFs) to their candidate target genes (TGs) on the basis of the scRNA-seq data and enrichment of TF binding motifs in the genomic regions around TGs. The resulting (GRN) consisted of 5 TF modules clustered on the basis of correlated TF activity.This analysis revealed that, compared to TN cells, DTPC and the intermediate cell states display a marked decreased expression of TFs and TGs involved in mRNA splicing, and more specifically in the initiation of spliceosome assembly through E-complex and A-complex formation. Interestingly, the splicing-related TFs all appear to have affinity for binding to a GCCxC consensus motif or close variant in genes (i.e., SNRPB and SNRPE) that code for key effectors of these initiation complexes. This pilot study highlights that scRNA-seq analyses coupled with inference of regulatory networks might enable the identification of molecular mechanisms that potentially trigger cell state transitions during drug-tolerance. The role of altered mRNA splicing in persistence to EGFR-targeted therapies will be explored experimentally in patient-derived cell lines and 3D organoid cultures.

EXPERIMENTAL AND MOLECULAR THERAPEUTICS: Mechanisms of Drug Resistance 3
Poster Session

#5857 Trastuzumab deruxtecan resistance can be mediated by payload resistance or secondary extracellular ERBB2 mutations but sensitivity to HER2 tyrosine kinase inhibitors is maintained.

M. B. Nilsson[1], X. Le[1], J. He[1], X. Yu[1], X. Huo[2], A. Kumar[2], A. Poteete[1], Q. Huang[1], R. Kittler[2], J. Heymach[1];
[1]UT MD Anderson Cancer Center, Houston, TX, [2]UT Southwestern Medical Center, Dallas, TX

Among NSCLC patients, the most common HER2 mutation is the exon 20 insertion mutation, Y772dupYVMA, which accounts for over 40% of all HER2 mutations in lung cancer. Trastuzumab deruxtecan (T-DXd), a HER2 antibody-drug conjugate (ADC), received FDA approval for the treatment of HER2 mutant NSCLC yielding a confirmed objective response of 52% and a median duration of response of greater than 9 months. Unfortunately, patients that initially respond to T-DXd will eventually acquire resistance, and the mechanisms of resistance as well as effective targeting strategies to overcome resistance are not yet elucidated. We generated Ba/F3 cells expressing the HER2 YVMA insertion mutation with acquired resistance to T-DXd by culturing cells in T-DXd until resistance occurred. T-DXd resistant cells retained expression of HER2, but were resistant to the payload, deruxtecan, as well as other topoisomerase inhibitors. T-DXd resistant cells exhibited loss of topoisomerase I, a previously reported mechanism of topoisomerase inhibitor resistance. In parallel, we generated a PDX model of acquired T-DXd resistance and observed sustained expression of HER2 but loss of TOP1 in resistant tumors. T-DXd resistant cell lines were sensitive to payloads with alternate mechanisms of action including maytansine and likewise retained sensitivity to the HER2 ADC trastuzumab emtansine (T-DM1) which utilizes DM1 as a payload. Given that T-DXd resistant cells retained HER2 expression, we assessed whether they were sensitive to HER2 tyrosine kinase inhibitors (TKI). T-DXd resistant cells remained highly sensitive to HER2 TKIs including poziotinib, afatinib, BI-4142, and BI-1622. To investigate whether genomic alterations of HER2 could facilitate HER2 ADC resistance, we utilized the LentiMutate approach which employs an error-prone HIV-1 reverse transcriptase to produce a high frequency of mutations to identify resistance-associated mutations in cells treated with a HER2 ADC. Sequencing analysis revealed that resistant cells had an enrichment in point mutations within HER2 domain IV (D582N, F595C/S, E580K, C623Y), which includes the binding site of trastuzumab. To validate the impact of these mutations on HER2 ADC resistance, we generated cells expressing a HER2 exon 20 insertion in combination with the observed domain IV mutations. D582N and F695C/S co-mutations conferred resistance to T-DXd and T-DM1 but not to HER2 TKIs. These data demonstrate that resistance to T-DXd can be mediated by loss of sensitivity to the ADC payload in which case ADCs bearing payloads with alternate mechanisms of action as well as HER2 TKIs retain anti-tumor cell activity. Moreover, resistance to trastuzumab-based ADCs can also be mediated by secondary mutations within domain IV of HER2. However, these resistance mutations do not diminish HER2 TKI activity.

#5858 Systematic identification of pathways associated with antibody drug conjugate sensitivity in breast cancer.

B. Wu[1], S. Sun[1], N. Thimmiah[1], A. Nagayama[1], J. T. Coates[1], T. Liu[1], W. Thant[1], E. Bitman[1], D. Li[1], J. Doench[2], A. Bardia[1], L. W. Ellisen[3]; [1]Harvard Medical School/Massachusetts General Hospital, Boston, MA, [2]Broad Institute of MIT and Harvard, Cambridge, MA, [3]Harvard Medical School/Massachusetts General Hospital, Ludwig Center at Harvard, Boston, MA

Antibody drug conjugates (ADCs) are revolutionizing precision therapeutics in oncology. Sacituzumab Govitecan (SG), combining a Topoisomerase I (TOP1) inhibitor payload (SN38) and the tumor-selective antigen TROP2-targeting antibody hRS7, has demonstrated efficacy in challenging cancers including triple negative breast cancer (TNBC). Despite its promising clinical efficacy, the intricacies of sensitivity and resistance mechanisms to SG remain elusive.
To systematically interrogate ADC sensitivity mechanisms, we employed genome-wide CRISPR-Cas9 knockout screening to discover novel regulators influencing SG sensitivity in human TNBC cells. Interactome analysis of top SG sensitizing hits showed clustered pathways of interest, including DNA repair/replication, mTORC1/metabolism, ubiquitin/proteolysis and endosome trafficking/sorting. A top druggable hit sensitizing to SG was PARP1, encoding the poly (ADP-ribose) polymerase 1 that is a key enzyme required for single-strand break repair pathways and for DNA replication fork stability. Furthermore, the synergistic lethality between SG and PARP1 was confirmed in experiments combining SG with PARP inhibitor treatment of TNBC cell lines. To selectively identify SG/ADC-specific genes and pathways, we performed a secondary round of CRISPR knockout and activation screens using a custom library comprising top hits discovered in the primary screen, treating cells in parallel with either SG or cytotoxic payload SN38 alone. Pathway analysis of genes selectively modulating sensitivity to SG but not SN38 revealed novel mediators involved in TROP2 turnover and recycling. We then performed validation and mechanistic studies to elucidate how specific genetic permutations regulate antibody delivery and sensitivity to SG.
In summary, employing a systematic CRISPR screening method, we uncovered numerous novel pathways associated with both resistance and sensitization, playing a role in ADC delivery and target protein turnover. Our current focus involves prioritizing druggable genes and pathways, laying the foundation for proof-of-concept studies that will combine ADCs with specific targeted therapeutics, aiming to enhance tumor-killing efficacy.

#5859 PLK1 predicts aggressive behavior in CRC patients and its inhibition reverse chemoresistance in CRC cells.

D. Padmaja, M. Al-Rasheed, P. Poyil, A. K. Siraj, S. K. Parvathareddy, W. Haqawi, F. Al-Dayel, K. S. Al-Kuraya;
King Faisal Specialist Hospital & Research Centre, Riyadh, Saudi Arabia

Polo-like kinase 1 (PLK1) is a serine/threonine-protein kinase, that is involved in multiple stages of cell cycle progression in mammals. Dysregulation of PLK1 has been found in a variety of human cancers and was associated with poor prognoses in various cancers. However, its role in the pathogenesis of CRC from Middle Eastern ethnicity has not yet been explored. Therefore, we examined the expression of PLK1 protein in a large cohort of over 1000 Middle Eastern CRC cases by immunohistochemistry. Correlation with clinico-pathological parameters were performed. PLK1 overexpression was noted in 60.3% (693/1149) CRC cases and was significantly associated with larger tumor size (T3/T4 tumors), lymphnode metastasis, Stage III tumors, MSI-H status and p-ERK1/2 over-expression. Interestingly, on multivariate logistic regression analysis, we found that PLK1 was an independent predictor of lymphnode metastasis. However, no association was noted between PLK1 expression and clinical outcomes (DFS, RFS, OS, CSS). Our in vitro experimentation revealed that CRC cells expressing high levels of PLK1 exhibited resistance to 5-Fu treatment, whereas cells with low PLK1 expression demonstrated sensitivity to the treatment. To explore the role of PLK1 on chemoresistance, we inhibited PLK1 using specific inhibitor, volasertib and we showed that volasertib effectively reversed 5-Fu resistance in these cells. Furthermore, knockdown of PLK1 reduced the progression of epithelial-to-mesenchymal transition (EMT) and the stem cell-like properties in 5-Fu resistant cells, showing the role of PLK1 on inducing EMT and stemness in CRC. Interestingly, the forced expression of PLK1 triggered the activation of the CRAF-MEK-ERK-ZEB1 signaling cascade, whereas its inhibition led to the suppression of this cascade. In addition, we showed that silencing of ERK1/2 reversed the chemoresistance, EMT and stemness of PLK1 expressing CRC cell lines. Our findings underscore the significant role of PLK1 in conferring chemoresistance, and targeting PLK1 could represent a viable therapeutic approach for the treatment of patients with an aggressive subtype of CRC.

#5860 Understanding the biological role of MMP16 in cisplatin resistance in ovarian cancer.

J. Bonilla-Liriano[1], M. Rivera-Serrano[2], V. Reyes-Burgos[3], J. Rolon-Perez[3], F. Valiyeva[4], P. Vivas-Mejia[3];
[1]Interamerican University of Puerto Rico-Fajardo Campus, Fajardo, PR, [2]University of Puerto Rico-Rio Piedras Campus, Rio Piedras, PR, [3]University of Puerto Rico Medical Sciences Campus, San Juan, PR, [4]University of Puerto Rico Comprehensive Cancer Center, San Juan, PR

High-Grade Serous Ovarian Cancer (HGSOC) is the most common and lethal of Ovarian Cancer (OC) types, which accounts for eighty percent of deaths. Treatment for OC includes surgery and platinum-based therapy. However, around 70% of women with HGSOC become resistant to chemotherapy. Therefore, new therapeutic agents with higher specificity and efficacy are needed for women with advanced and drug-resistant OC. Matrix metalloproteases (MMPs) are a group of enzymes involved in the degradation of the extracellular matrix (ECM). Deregulation of MMPs contributes to tumor growth and metastasis in several cancer types. Preliminary studies of our research team found that MMP16 is higher in cisplatin-resistant as compared with cisplatin-sensitive OC cells. The aim of this project is to understand the role of MMP16 in the cisplatin resistance of OC cells. We hypothesize that MMP16 increased expression may contribute to cancer progression and drug-resistance. We performed experiments in A2780/A2780CP20 and OVCAR3/OVCAR3CIS human OC cells. To assess the MMP16 protein levels we used western blot analysis. To measure the mRNA levels, we used qRT-PCR. Kaplan-Meier survival curves were generated by interrogation of the KM Plotter patient database. The MMP16 protein and qRT-PCR experiments confirmed that protein and mRNA levels are more abundant in cisplatin-resistant as compared with cisplatin-sensitive cells. Interrogation of the KM plotter database showed that OC patients with higher MMP16 mRNA levels live less as compared with OC patients with lower MMP16 levels. Ongoing experiments are testing the biological effect of small interference RNA (siRNA) targeting MMP16 in cisplatin-resistant OC cells.

#5861 CDK4/6 therapy-induced senescence as a resistance mechanism-MiDAS touch.

Y. Gokmen-Polar, Y. Gu, L. Ruan, S. S. Badve;
Emory University School of Medicine, Atlanta, GA

Background: Cyclin-dependent kinase inhibitors (CDK4/6i) have revolutionized the therapy for estrogen receptor positive (ER+) breast cancer. Despite the response to CDK4/6i, resistance and recurrence are still a clinical reality, resulting in death due to breast cancer. G1 cell cycle arrest has been considered as the main mechanism of action of CDK4/6i in luminal breast cancer. However, the response to therapy does not correlate with the expression of CDK4/6 or key cell cycle proteins. It is also unclear whether CDK4/6i-induced senescence enhances the therapeutic response or mediates development of resistance.
Experimental Procedures: We have developed drug-tolerant persisters resistant to CDK4/6 inhibitors (CDK4/6i-DTPs) in a panel of estrogen receptor positive (ER+) cells to explore the molecular mechanisms associated with resistance. Using different cell phenotype assays (i.e., cell viability/cell cycle, senescence/senescence reversibility and wound healing) as well as senescence-associated secretory phenotype (SASP) human cytokine array of 105 markers, we characterized the phenotype and secretome of these CDK4/6i DTPs.
Summary: CDK4/6i-DTPs induced by abemaciclib, palbociclib and ribociclib (all from Selleckchem) demonstrated resistance to these drugs and dramatically slowed growth. The percentage of senescent cells reached 30-89% of the total population for all cell lines in all three drugs, whereas control parental cells exhibited around 10%. CDK4/6i DTPs also exhibited significant cell migration, and increased lysosomal phenotype compared to their parental sensitive cells. Further analysis with human cytokine array revealed that protein levels of growth differentiation factor 15 (GDF-15) are elevated in both cell lysates and conditioned-media of CDK4/6i DTPs, whereas Serpin E1 (Plasminogen Activator Inhibitor, Type I, PAI-1) was unique to secreted CDK4/6i DTPs. Interestingly, we did not observe changes in pro-inflammatory senescence-associated secretory phenotype (SASP) markers such as interleukins. Apart from being a SASP protein, GDF-15 is a mitochondrial cytokine (mitokine), suggesting a role in mitochondrial dysfunction-associated senescence (MiDAS). HMGB1, and LMNB1 are also down-regulated in CDK4/6-DTPs supporting the MiDAS phenotype. CDK4/6i-induced MiDAS appears to be transient, as CDK4/6i-DTPs reverted to the parental phenotype in drug-free culture media 20 days after the removal of CDK4/6i's. This included growth characteristics and sensitivity to CDK4/6i. This reversion of phenotype was observed in all five cell line models tested with all three drugs.
Conclusions: CDK4/6-induces a mitochondrial dysfunction-associated senescence (MiDAS). This appears to be transient in nature as withdrawal of the drug results reacquisition of parental cell phenotype and drug-sensitivity. Targeting MiDAS pathway might be critical to improve efficacy of CDK4/6 inhibitors.

#5862 Retrotransposable elements mediate the drug-tolerant persistence in claudin-low breast cancer chemo-treatment.

Z. Zhang[1], Y. Wang[2], X. Luo[1], X. Zhan[1], J. Ding[2], **T. P. Wu[1]**;
[1]Baylor College of Medicine, Houston, TX, [2]McGill University, Montreal, QC, Canada

The emergence of acquired drug resistance through treatment remains a critical threat to efficient cancer therapies, which most often lead to relapse and metastasis. The development of resistance is an evolutionary adaptation process that heavily depends on tumor heterogeneity (underpinned by cellular plasticity). Therefore, a longitudinal deconvolution of treatment adaptation is critical to uncover the driving-force mechanisms underpinning resistance adaptation. In the clinic, chemotherapy remains the mainstream treatment for TNBC, and one of the primary chemo-agents is doxorubicin. Although the initial responsive rate of doxorubicin-based chemotherapies is up to 70%, it is well recognized that TNBC cells usually generate an adaptive response and result in acquired drug-resistance and multi-drug resistant phenotypes. Although numerous mechanisms of chemo-resistance evolution have been proposed, most of these studies focused on the initial and terminal states, from which we could not deconvolute the adaptation routes and might miss the transient fate-switching events. We hypothesize that the claudin-low TNBC chemo-resistant cells may derive from the early-stage reversible chemo-tolerant persistent state, and early-stage state-switching mediated by epigenetic landscape reprogramming might determine the adaptation through treatment. We developed an in vitro “pulsing-treatment” model to test the hypothesis, which could mimic the clinical treatment and provide therapeutically relevant insights into the acute drug-induced stress response and regrowth. Unexpectedly, we found that the human endogenous retrovirus-like elements (HERVs) show an aberrant bursting in the adaptation. To further interrogate the adaptation, we did the longitudinal single-cell multi-omics sequencing. With a novel bioinformatic workflow, we integrated the HERV’s expression information with protein-coding genes profiling and chromatin accessibility. The preliminary result indicated that a subpopulation of HERV-high cells might transiently mediate the persistence of cancer cells at the early stage of the treatment, which coupled with whole transcriptomic and chromatin landscape reprogramming, and molecular subtype switching. In this study, we employed a new strategy to investigate the longitudinal adaptation route through treatment and uncover a non-canonical element, which shed new light on drug resistance research and novel target screening.

#5863 Double-negative prostate cancer emerges through a mixed basal, club, and hillock cell identity driven by KLF5.

S. Pitzen, Y. Qiu, S. Munro, S. Dehm;
University of Minnesota, Minneapolis, MN

The purpose of this study was to characterize the phenotypes and drivers of therapy-induced lineage plasticity during the development of castration resistant prostate cancer (CRPC). While the majority of localized prostate cancer can be cured with surgery or radiation, metastatic disease is lethal. Therapies targeting the androgen receptor (AR) are initially effective, but eventually men will develop CRPC. About 70-75% of CRPC displays restored AR signaling (ARPC), while the remaining 25-30% display lineage plasticity evidenced by the emergence of AR-negative subtypes including those that display neuroendocrine (NE) markers, or double negative CRPC (DNPC) lacking both AR and NE markers. AR independent manifestations of CRPC represent a clinical challenge because no effective therapies are available and therapeutic targets are largely unknown. We analyzed publicly available bulk and single-cell RNA-seq datasets derived from clinical CRPC specimens to characterize the cellular identity of AR-negative tumors. Using a database of all known transcriptional regulators, we identified potential drivers of these phenotypes. We performed siRNA-mediated knockdown experiments in a model of DNPC to explore the extent to which the candidate regulators maintain AR-negative cell identity and sustain growth of DNPC prostate cancer cells. We identified a subset of CRPC tumors that co-express gene sets defining basal, club, and hillock cells in the benign prostate. This data supports the existence of epithelial cell lineage plasticity manifesting within CRPC tumors, as well as individual CRPC tumor cells, wherein AR-positive tumor cells transform to a phenotype encompassing basal, club, and hillock cell identities. We nominated the stem cell transcription factor KLF5 as a regulator of basal, club, and hillock cell identities in CRPC. In cell line models of DNPC, knock down of KLF5 inhibited cell growth and reduced the expression of genes defining basal, club, and hillock cell identities. This work links a prevalent and poorly-defined subtype of AR-negative CRPC to AR-negative epithelial cell types in benign prostate tissue. Inhibition of KLF5 and its downstream effectors could represent a therapeutic strategy to prevent or delay lineage plasticity and thereby extend patient response to AR-targeted therapies.

#5864 YAP1 defines a highly plastic, persister cell population in small cell lung cancer (SCLC) following relapse.

C. Stewart[1], S. M. Groves[2], R. Wang[1], K. Ramkumar[1], Y. Xi[1], L. Diao[1], A. G. Serrano[1], A. Tanimoto[1], A. M. Victorian[1], S. Bhattacharyya[1], A. J. Halliday[1], N. Kalhor[1], L. M. S. Soto[1], P. F. S. Da Rocha[3], N. Vokes[1], L. G. Karacosta[1], J. Wang[1], J. V. Heymach[1], V. Quaranta[4], B. Glisson[1], L. A. Byers[1], C. M. Gay[1]; [1]UT MD Anderson Cancer Center, Houston, TX, [2]University of Virginia, Charlottesville, VA, [3]Hospital del Mar, Barcelona, Spain, [4]Vanderbilt University, Nashville, TN

SCLC is an aggressive, neuroendocrine malignancy notable for rapid, albeit transient, responses to therapy. We have previously shown that transcriptional heterogeneity among treatment-naïve SCLC tumors underlies four distinct transcriptional subtypes, each with distinct clinical vulnerabilities. Though previously hypothesized to delineate a distinct subtype, expression of YAP1 is largely absent from treatment-naïve SCLC. Less clearly defined is the transcriptional landscape of relapsed SCLC, the evolution of which may underlie SCLC's capacity for insurmountable resistance. To better define the biology of relapsed SCLC, we performed mass cytometry analysis of patient circulating tumor cells (CTCs), immunohistochemistry for ASCL1, NEUROD1, POU2F3, MYC and YAP1, and single-cell (sc)RNAseq of core needle biopsies from SCLC patients and preclinical models following resistance to standard-of-care therapies. In contrast to treatment-naïve SCLC, YAP1 mRNA and protein are detectable in patient CTC populations and tumors from relapsed patients and PDXs, albeit at levels lower than subtype-defining transcription factors (e.g. ASCL1, NEUROD1, or POU2F3). Notably, however, scRNAseq reveals these *YAP1* expressing cells to be mutually exclusive with *ASCL1* and *NEUROD1*, though not necessarily *POU2F3. YAP1*-expressing cells possess unique mesenchymal, inflamed features and exhibit high levels of transcriptional plasticity. Consistent with the upregulation of YAP1 following chemotherapy, *YAP1*-positive cell populations express senescence associated secretory phenotype genes and cancer stem cell genes, suggesting that these populations represent drug tolerant persister cells that may serve as a source for renewal of classical neuroendocrine populations within the tumor. Targeting these resistant populations may be critical to re-establish response in relapsed SCLC, and these analyses identified high expression of several surface proteins that are currently under investigation as targets for antibody-drug conjugates in SCLC clinical trials, including B7H3, TROP2 and HER2 antibody drug conjugates. These data suggest that the acquisition of YAP1 expression delineates a particularly recalcitrant tumor cell population observed almost exclusively in relapsed SCLC that is capable of driving tumor persistence and treatment resistance. Clinically, these data underscore the importance of constraining transcriptional plasticity in the frontline management of SCLC, but also of developing therapies aimed specifically at emergent populations capable of driving resistance, as with the YAP1-high cells identified here. The emergence of YAP1 following resistance in SCLC and the observation of YAP1 as a common feature of other high-grade neuroendocrine carcinomas exclusive of SCLC, likely explains the initial mischaracterization of YAP1 as a subtype-defining feature of SCLC.

#5865 Characterization and resistance mechanisms of PNP inhibitor forodesin-resistant cell lines..

N. Hosono[1], K. Oiwa[2], T. Tasaki[3], R. Nishi[1], L. Scott[4], O. A. O'Connor[4], T. Yamauchi[1];

[1]University of Fukui, Eiheiji, Japan, [2]Osu Hospital, Nagoya, Japan, [3]Japanese Red Cross Fukui Hospital, Fukui, Japan, [4]Columbia University, New York, NY

Background: The enzyme purine nucleoside phosphorylase (PNP) is involved in the purine salvage pathway and is present at high levels in lymphoid tissues. Children born with PNP deficiency are known to have significantly reduced T-cell counts but relatively normal B-cell immunity, suggesting PNP as one of the most promising therapeutic targets for T-cell malignancies. Forodesine (For, BCX-1777), a novel PNP inhibitor, was approved in Japan for the treatment of relapsed/refractory PTCL. To understand the cytotoxic effect of For and its mechanism of action, we established a For-resistant (For-R) leukemia cell line and explored the mechanism of resistance.

Methods: We established two For-R T-lymphoblastic leukemia cell lines (CCRF-CEM and MOLT4) through repeated escalating exposure to For and 2'-deoxyguanosined(dGuo). Gene expression analysis was performed to identify the mechanisms of resistance.

Results: For-R cells showed very high resistance compared to parental cells (IC_{50} value, CEM/CEM-R 4.2nM/>5x10^{5}nM, MOLT4/MOLT4-R 8nM/>5x10^{5}nM). When cross-resistance was examined in these For-R cells showed mild resistance to cytarabine. The expression of hENT1, a nucleoside transporter, was examined and found to be upregulated in both CEM-R and MOLT4-R cells, while the expression level of deoxycytidine kinase (dCK) was unchanged in both cells. Next, high performance liquid chromatography was used to assess the intracellular dGTP in each parental and its For-R cells. In the parental cells, intracellular dGTP levels increased promptly 4-6 hours after fosteredin administration, whereas in resistant cells, intracellular dGTP levels were higher than before fosteredin administration, and there was little change in dGTP levels after administration.

Conclusion: The established For-R cell line acquired a high resistance to For and showed high intracellular dGTP levels. Imbalance in intracellular GTP levels may be involved in the induction of cell death by For.

IC50 value of each cell lines

#5866 TESC mediates resistance to lenvatinib in hepatocellular carcinoma by regulating cell autophagy.

H. Zhuang, T. Zhang, J. Chen;
The Affiliated Cancer Hospital of Zhengzhou University and Henan Cancer Hospital, Zhengzhou, China

Objective: To investigate the mechanism by which TESC (Tescalcin) induces lenvatinib resistance in hepatocellular carcinoma (HCC) through autophagy mediation.
Methods:1) Utilized established liver cancer organoids from over 70 patients for lenvatinib drug sensitivity screening and transcriptome sequencing to identify lenvatinib-resistant genes. 2) Constructed stable TESC overexpression and downregulation liver cancer cell lines. Employed CCK8 assays to plot IC50 drug sensitivity curves, elucidating changes in lenvatinib sensitivity in liver cancer cells after TESC overexpression or downregulation. 3) Used TESC-stable cells to establish subcutaneous tumor models and intrahepatic tumor models in nude mice. After tumor formation, administered lenvatinib orally to observe whether TESC affects liver cancer sensitivity to lenvatinib in vivo. 4) Conducted Western blot (WB) analysis to assess the expression of autophagy-related molecules (LC3B II/I, P62, and Beclin1 proteins) in TESC downregulated or overexpressed stable cell lines and their control cell lines. Utilized the LC3-GFP-mRFP fluorescence dual-labeling lentivirus system and laser confocal microscopy to examine autophagic flux. 5)Treated TESC downregulated cells with the autophagy inhibitor 3-MA. Conducted WB to assess the expression levels of autophagy-related proteins and plotted drug sensitivity curves using IC50 experiments to evaluate the impact of 3-MA on reversing liver cancer cell sensitivity to lenvatinib.
Results: Compared to the control group, HCC cells overexpressing TESC showed an increased IC50 value and reduced sensitivity to lenvatinib, while TESC downregulation resulted in a decreased IC50 value and decreased sensitivity to lenvatinib. Subcutaneous tumor experiments in nude mice indicated that, compared to the control group, tumors with reduced TESC expression were more sensitive to lenvatinib. Additionally, in HCC cells overexpressing TESC, protein expression levels of LC3B II/I and Beclin1 significantly decreased, while P62 expression increased. Conversely, TESC downregulation significantly increased protein expression levels of LC3B II/I and Beclin1, while P62 expression decreased. Furthermore, results from the LC3-GFP-mRFP autophagy dual-labeling lentivirus system showed a significant reduction in fluorescence spots in the TESC overexpression group compared to the control group, indicating weakened autophagic flux. Treatment of TESC downregulated liver cancer cells with 3-MA resulted in an increased IC50 value compared to the control group.
Conclusion: TESC expression levels are associated with the sensitivity of liver cancer cells to lenvatinib, possibly by inhibiting autophagy and affecting the sensitivity of liver cancer cells to lenvatinib.

#5867 Early activation of HGF-cMET serves as a bypass pathway to ALK and RET tyrosine kinase inhibitors in non-small cell lung cancer.

T. Patil, T. Hinz, S. Pine, H. Saabawy, P. Bunn, E. L. Schenk, R. Camidge, L. Heasley;
University of Colorado Anschutz Medical Campus, Aurora, CO

Introduction: Alterations of the HGF-cMET axis, often through *MET* gene amplification, can act as resistance mechanism to tyrosine kinase inhibitors (TKIs) in patients with ALK and RET rearranged non-small cell lung cancer (NSCLC). The efficacy of targeting the cMET pathway through use of MET tyrosine kinase inhibitors continues to evolve. An unresolved question is whether the HGF-cMET pathway is activated early in cancer cells after ALK and RET TKI exposure. Here, we evaluate novel pre-clinical models to better characterize the onset of MET pathway-mediated resistance using murine cell lines and orthotopic murine models.

Methods: Murine *Eml4-Alk* (EA1 and EA3) and *Trim24-Ret* (TR.1) cell lines were cultured with increasing doses of alectinib (EA1 and EA3) or pralestinib or selpercatinib (TR.1) until resistance was acquired. A cell line was established from an orthotopic TR.1 tumor that progressed on selpercatinib (TR.1-1092). Passage control cells and the TKI-resistant cultures were submitted to clonogenic growth assays in targeting TKI or crizotinib (MET TKI). Control and TKI-resistant cell lines were submitted to HGF ELISA, MET immunoblotting and RNAseq. Orthotopic TR.1 tumors were established in C57BL/6 mice and after ~2 weeks, daily treatment with selpercatinib was performed for 21 days with weekly mCT to monitor tumor size. At 21 days when the tumors were beginning to progress, half the mice were treated with selpercatinib and crizotinib (a MET TKI) while the other half continued on selpercatinib alone.

Results: HGF levels (pg/µg) were significantly higher in alectinib-resistant EA1 cells vs. EA3 cells and was associated with retained sensitivity to crizotinib in alectinib-resistant EA1, but not EA3 cells. MET mRNA (but not gene copy number) and HGF mRNA/ protein levels in pralsetinib and selpercatinib resistant TR.1 lines were significantly higher than controls and accompanied by acquired sensitivity to crizotinib. In C57BL/6 mice bearing orthotopic TR.1 tumors, the progression on selpercatinib occurring after 2-3 weeks of treatment was reversed in a durable manner by co-treatment with crizotinib.

Conclusions: The HGF-cMET axis is activated early in response to ALK and RET TKI exposure through transcriptional mechanisms without evidence of *MET* gene amplification. These findings unveil a potential therapeutic window to disrupt the MET bypass pathway in ALK and RET rearranged NSCLC prior to overt clinical progression.

#5868 Upregulation of HER3 and MET in non-small cell lung cancer cells resistant to EGFR tyrosine kinase inhibitor.

M. Larsen, H. Lyu, C. Tan, Y. Wu, B. Liu;
LSU Health Sciences Center New Orleans, New Orleans, LA

Introduction: Prior research demonstrates the importance of studying epidermal growth factor receptor (EGFR) activating mutations for better understanding the biology of non-small cell lung cancer (NSCLC), which comprises the majority (~80%) of lung cancers. EGFR-targeted tyrosine kinase inhibitors (TKIs) have been used in the clinic to treat NSCLC with EGFR activating mutations. First and second-generation EGFR-TKIs are effective in NSCLC patients with the most common EGFR mutations (exon 19 deletion (Del19) and exon 21-point mutation (L858R)). A third generation EGFR-TKI, osimertinib (AZD9291), has been developed to target the T790M resistance mutation, but patients are starting to show resistance to this line of therapy as well. Our study aims to elucidate the underlying mechanism(s) of EGFR-TKI resistance in NSCLC cells.
Methods: NSCLC cell lines, including PC-9 and HCC827, which have the Del19 EGFR activating mutation, were utilized for experiments. From the parental cell lines, several cell lines resistant to the EGFR-TKIs were previously established. Cell proliferation (MTS) assays were used to confirm the resistance phenotype of the established cell lines. Western blot assays and RT-qPCR were utilized to determine changes in the expression level of several membrane receptors and their downstream effectors.
Results: Our preliminary analysis showed that both human epidermal growth factor 3 (HER3) and mesenchymal-epithelial transition factor (MET) were upregulated in the EGFR-TKI-resistant cell lines as compared to their parental counterparts. Further studies revealed an increased level of phosphorylated STAT3 (p-STAT3) and ERK1/2 (p-ERK1/2) in the resistant cell lines when compared to the parental cell lines, suggesting the possible involvement of HER3 and/or MET in the activation of downstream signaling pathways. Upregulation of HER3 and MET was found at both the protein and mRNA level.
Conclusion: Based on our initial findings, membrane receptors, including HER3 and MET, could be working together to continue activating downstream signaling pathways to evade the effects of osimertinib, resulting in resistance. Additional work is underway to define the role of HER3 and MET in the NSCLC cells resistant to EGFR-TKIs.

#5869 Investigation of molecular alterations associated with double resistance to BRAF and MEK inhibition in melanoma.

A. J. Isaak[1], G. R. Clements[1], L. Huang[1], Y. Qin[1], Q. Zho[2], G. Merlino[1], Y. Yu[1];
[1]National Institutes of Health, Bethesda, MD, [2]Southern Medical University, Guangzhou, China

More than 50% of melanomas harbor activating BRAF kinase mutations, with BRAFV600E representing more than 90% of BRAF mutations. Inhibition of mutant BRAF by BRAF inhibitors (BRAFi) in patients with advanced melanoma yields a remarkable initial clinical response. Limited duration response and disease recurrence of inhibitors occurs due to acquired drug resistance. Recently identified mechanisms of MAPK hyperactivation in acquired resistance to BRAFi have encouraged clinicians to employ a combination of BRAF and MAPK inhibitors to block the MAPK signaling pathway more effectively. However, most patients treated with this combination therapy still relapse due to de novo drug resistance. Therefore, innovative strategies are still necessary to improve the precision and durability of anti-melanoma therapies. To investigate the mechanism of both BRAFi and MEKi resistance (double resistance, DR) in mutant BRAF melanomas, we have developed models from four human melanoma cell lines to explore the hypothesis that molecular alterations are related to double resistance to BRAFi and MEKi in melanoma. We have found that BRAFi-MEKi double-resistant models exhibit distinct differences in morphology and growth kinetics. Specifically, BRAFi-MEKi double-resistant human melanomas express a higher level of FGFb and PAI-1 expression. We confirmed that overexpression of FGFb and PAI-1 in parental cells could increase the ability to resist BRAF and MEK inhibition. Additionally, we discovered that decreased expression of FGFb and PAI-1, via knock-down, inhibition, or CRISPR in double resistant cells, can restore cell sensitivity to treatments of BRAFi and MEKi. To further elucidate the role of FGFb and PAI-1 on resistant melanoma, we have extended our scope to *in vivo* mouse xenograft models. Our findings uncovered the mechanism of how melanoma cells can escape BRAFi and MEKi attacks and offer a rational strategy to guide future clinical treatments.

#5870 ecDNA-based amplification of multi-drug resistance genes leads to acquired resistance to taxane-based chemotherapy.

Kristen Holmes, Dean Perusse, Cory DuPai, Homa Hemmati, Julie Weiss, Claire Kuelbs, John Bibay, Joan Chen, Debbie Liao, Christian Hassig, Shailaja Kasibhatla

Boundless Bio, Inc., San Diego, CA

Focal amplification on extrachromosomal DNA (ecDNA) drives high gene copy number and intercellular genomic heterogeneity, which can fuel tumor adaptation and drug resistance. Targeted therapies have largely failed in patients with oncogene amplification, and patients whose tumors harbor ecDNA-based gene amplification have particularly worse survival compared to patients whose cancers harbor other genetic drivers. Due to the lack of approved therapies for patients with oncogene amplified cancers, many patients receive chemotherapy; however, resistance often develops through mechanisms such as ATP-binding cassette (ABC) transporter overexpression, rendering cross-resistance to other forms of chemotherapy. We examined whether ecDNA amplification in tumor cell lines drives ABC transporter overexpression to mediate resistance to paclitaxel, a commonly prescribed taxane chemotherapy for cancer patients.

We selected non-amplified (DLD1 and SW48) and amplified cell lines, including COLO320DM and COLO320HSR (*MYC* amplified on ecDNA or chromosomal loci, respectively); SNU16 and H716, (*FGFR2* and *MYC* amplified ecDNA); and H2170 (*ERBB2* and *MYC* amplified on ecDNA). All cell lines developed paclitaxel resistance, with the majority (5/7) gaining focal amplification of *ABCB1*, which encodes P-glycoprotein (P-gp), a common multi-drug resistance transporter. Four models--COLO320DM, COLO320HSR, SNU16, and H2170—developed *ABCB1* amplification on ecDNA; one non-amplified cell line (DLD1) acquired focal *ABCB1* amplification via a breakage-fusion-bridge (BFB) mechanism, a distinct form of amplification from ecDNA. ecDNA-based *ABCB1* amplifications exhibited hallmarks of ecDNA, including intercellular copy number heterogeneity and paclitaxel dose-dependent rapid evolution of *ABCB1* copy number.

We next assessed whether drug resistance was reversible in *ABCB1* amplified cell lines following removal of paclitaxel. Reversal of resistance was observed in COLO320DM and COLO320HSR via loss of *ABCB1* ecDNA within 4-6 weeks. However, in SNU16 and H2170 resistant cells, *ABCB1* amplification was retained up to 12 weeks of drug removal, with apparent integration into *MYC* ecDNA, demonstrating that ecDNA-enabled plasticity can result in both short- and long-term paclitaxel resistance.

Although targeted therapies have revolutionized treatment approaches for patients with actionable oncodriver alterations, most cancer patients do not have actionable drivers and most patients still receive chemotherapy at some point in their course of treatment. We demonstrated that ecDNA-based resistance to paclitaxel is common in cancer cell lines and may also drive resistance to chemotherapy in patients. Thus, ecDNA-directed therapies (ecDTx) may be an important treatment option for chemo-resistant patients, who currently do not have many effective therapeutic options.

#5871 Unveiling mechanisms of CDK4/6 inhibitor resistance in ER+ breast cancer models with acquired resistance.

B. Li, G. Liu, T. Ni, W. Shi, Q. Gu;
WuXi AppTec, Suzhou, China

Introduction: Cyclin-dependent kinase 4 and 6 (CDK4/6) inhibitors, including palbociclib, ribociclib, and abemaciclib, have revolutionized the treatment of estrogen receptor-positive (ER+) breast cancer. However, the development of resistance to these inhibitors poses a formidable challenge in the clinical management of ER+ breast cancer. This study aims to explore the common resistance mechanisms in three CDK4/6 inhibitor-resistant models induced by chronic exposure to these agents.
Methods: We developed models of resistance to palbociclib, ribociclib, and abemaciclib by repeatedly exposing murine xenografts to these CDK4/6 inhibitors. Resistance was confirmed through cell viability assays and in vivo tumorigenesis studies. The tumors were sequenced using NGS analyses, and genes of interest were validated through Western blotting and qPCR.
Results: In all resistant models, we identified a common resistant mechanism via NGS analyses, which was characterized by the overexpression of the FAT1, CCNE1, and AR genes. The upregulation of these genes at mRNA and protein levels was confirmed by qPCR analyses and western blotting, respectively. Our data indicate that upregulation of FAT1, CCNE1, and AR genes may play a critical role in mediating resistance to CDK4/6 inhibitors, namely palbociclib, ribociclib, and abemaciclib.
Conclusion: Our investigation uncovered a shared mechanism, characterized by the overexpression of FAT1, CCNE1, and AR genes, that underlay CDK4/6 inhibitors-induced drug resistance in ER+ breast cancer. These findings shed light on the shared pathways that drive CDK4/6 inhibitor resistance and provide insights into potential therapeutic targets for overcoming this resistance in breast cancer patients. Understanding these mechanisms is crucial for the development of more effective treatment strategies for CDK4/6 inhibitor-resistant cancers.

#5872 CDK1-SOX9 axis contributes to chemotherapy resistance in gastric cancer.

M. M. Al-Mathkour, S. Zhu, M. Genoula, W. El-Rifai;
University of Miami Miller School of Medicine, Miami, FL

Gastric carcinoma (GC) is the third most prevalent cause of cancer-related mortality worldwide, presenting a formidable challenge with the rise of resistance to chemotherapeutic agents, leading to treatment failures. Cyclin-dependent kinase 1 (CDK1) has garnered attention due to its substantial overexpression in various tumors, including GC, and its association with poor overall survival and relapse-free survival. This study aimed to understand the molecular and functional mechanisms underlying the CDK1-SOX9 axis in GC chemotherapy resistance. Through a comprehensive analysis of data from The Cancer Genome Atlas (TCGA) and our own integrated gene expression study, we found a positive correlation between CDK1 and SOX9 in both human and mouse GC tissues ($p<0.001$). Additionally, conserved alterations in miRNAs have been identified in the context of gastric carcinogenesis, evident in our local cohort and the TCGA dataset. Our in-depth investigation of premiR-145 has shed light on the existence of several CpG nucleotides. Notably, treatment with a DNMT inhibitor (5-Aza) has triggered the upregulation of miR-145 expression. Furthermore, the ectopic expression of CDK1 has been associated with increased DNMT1 phosphorylation and enhanced enzymatic activity. Conversely, silencing CDK1 reversed this effect, and the inhibition of DNMT1 reduced SOX9 protein expression. Using cisplatin-resistant cell lines revealed a significant increase in CDK1 and SOX9 expression where silencing CDK1 and SOX9 sensitized these cells to chemotherapy. This study provides valuable insights into the intricate mechanisms governing the CDK1-SOX9 axis in GC chemotherapy resistance, providing potential avenues for therapeutic interventions in this challenging malignancy.

#5873 ERα coordinates with squalene synthase to confer statin resistance in lung cancer.

Y.-F. Yang;
Kaohsiung Veterans General Hospital, Kaohsiung, Taiwan

Statins are widely used to treat hypercholesterolemia by inhibiting hydroxymethylglutaryl coenzyme A reductase (HMGCR). Accumulating evidence suggests that statins also have protective effects against cancer recurrence. However, the role of statins in preventing lung cancer and biomarkers for predicting statin treatment response remains lacking. This study analyzes molecular features that dictate statin sensitivity in lung cancer by correlating large-scale statin sensitivity data and basal gene expression in a collection of 125 lung cancer patients. We identified a gene signature associated with lovastatin sensitivity and showed that gene expression in mesenchymal molecular features, the cholesterol biosynthesis pathway, and estrogen receptor alpha (ERα) signaling were key determinants of lovastatin sensitivity in lung cancer cells. To this end, we further discovered that overexpression of a committed step enzyme in cholesterol biosynthesis farnesyl-diphosphate farnesyltransferase 1 (FDFT1), also known as squalene synthase (SQS), is capable of activating ERα and is associated with increased statin tolerance. In clinical specimens, overexpression of SQS positively correlated with nuclear expression of ERα in lung cancer patients, and the combination of SQS and ERα is a powerful prognostic predictor for lung cancer.
Activation of the SQS-ERα signaling axis and epithelial-to-mesenchymal transition (EMT) status represents two important features in determining statin sensitivity in lung cancer.

Keywords: Statin, cholesterol biosynthesis, squalene synthase, estrogen receptor α, Epithelial-mesenchymal transition

#5874 Phenotypic plasticity of TKI resistance reprograms cytoskeleton organization through cadherin-catenin and integrin pathways.

Chun Ma[1], Chia-Mei Young[2], Jerry Chieh-Yu Chen[3], Mong-Lien Wang[4]

[1]National Taiwan University College of Medicine, Taipei City, Taiwan,[2]Institute of Pharmacology, College of Medicine, National Yang Ming Chiao Tung University, Taipei City, Taiwan,[3]Taiwan International Graduate Program in Molecular Medicine, National Yang Ming Chiao Tung University and Academia Sinica, Taipei City, Taiwan,[4]Department of Medical Research, Taipei Veterans General Hospital, Taipei City, Taiwan

The acquired resistance to EGFR tyrosine kinase inhibitors (TKIs) restricts its clinical utility. Clinically, acquired resistance has been highly associated with epithelial-mesenchymal transition (EMT) traits. In this study, we characterized shared phenotypic plasticity features of TKI-resistant cells and aimed to find its key driver in three different cell lines harboring mutant EGFR. In vitro resistance cell lines were generated by dose-escalation exposure to osimertinib, a 3rd generation TKI, for more than 2 months. We employed canonical markers (E-cadherin, vimentin, pan-cytokeratin, and N-cadherin) along with additional markers (EpCAM and fibronectin) to define the EMT status of resistant cells. Moreover, cytoskeleton architecture (F-actin and Vimentin) was utilized to clarify the types of cell motility. Transcriptomics analysis illustrated enriched pathways at focal adhesion and adherens junction. Loss of adherens junction-related catenin (α-E-catenin, β-catenin, γ-catenin, p120 catenin) and aberrant activation of focal adhesion-related protein (p-FAK Y397 and Y576/57, p-Src Y416) confirmed the transcriptomics analysis of reduced contact inhibition and cell polarity. The resulting migration mode of resistant cells highly resembles ameboid movement. Mechanistically, we identified that YTHDF3, a metastasis-promoting regulator of mRNA methylation, destabilizes the mRNA of E-cadherin. Depletion of YTHDF3 in resistant cells reversed the cadherin-catenin pathway and distribution of vimentin and f-actin. In conclusion, resistant cells display ameboid-like movement resulting from loss of contact inhibition and aberrant activation of focal adhesion. Mechanistically, we identified that YTHDF3, a metastasis-promoting regulator of mRNA methylation, destabilizes the mRNA of E-cadherin. Depletion of YTHDF3 in resistant cells reversed the cadherin-catenin pathway and distribution of vimentin and f-actin. YTHDF3 serves as an RNA epitranscriptomic regulator that destabilizes CDH1 mRNA, thereby disrupting adherens junction formation and reducing integrin-mediated focal adhesion stabilization.

#5875 Upregulation of the RNA binding protein HuR by cancer-secreted exosome to mediate multidrug resistance.

K. K. To;
Chinese University of Hong Kong (CUHK), Hong Kong, Hong Kong

Background and Aim: Multidrug resistance (MDR) is an unresolved obstacle to cancer chemotherapy. It is usually caused by overexpression of drug efflux transporters including ABCG2. Exosomes are extracellular lipid vesicles released from all cells upon the fusion of multivesicular bodies with plasma membrane. Tumor-derived exosomes have been shown to mediate cell-to-cell transfer of oncogenic materials to promote drug resistance. Human antigen R (HuR) is an extensively studied RNA binding protein that regulates the stability, translation, and nucleus-to-cytoplasm shuttling of mRNAs. Numerous HuR-targeting mRNAs play crucial roles in tumorigenesis, invasion and metastasis. We have previously reported the induction of ABCG2 and MDR phenotype by HuR overexpression in colon cancer. HuR overexpression is linked with high-grade malignancy and poor prognosis in cancer patients. This study investigated the enrichment of HuR inducing microRNAs (miRNAs) in exosomes secreted from MDR colon cancer and its intracellular transfer to drive MDR.
Method: Cancer exosome-mediated transfer of miRNAs from ABCG2-overexpressing resistant colon cancer cells S1M1-80 to a few sensitive colon cell lines was evaluated. Exosomes were isolated from S1M1-80 conditioned medium by differential centrifugation method. The uptake of fluorescence-labeled exosome from donor MDR cancer cells by recipient sensitive cells was visualized by fluorescence microscopy. MiRNA microarray was conducted to identify differentially expressed miRNAs in drug sensitive cells after incubation with S1M1-80-secreted exosomes. Western blot and qPCR analysis were conducted to measure HuR and ABCG2 expression.
Result: Exosomes were isolated from resistant S1M1-80 cells, whose purity was confirmed by the presence of exosomal markers (Tsg101 and Alix) but absence of cellular marker (GRP78) by Western blot analysis. These exosomes reduced the apoptotic effect of SN-38 or 5-fluorouracil in sensitive colon cancer cell lines (HCT116, S1, and SW480) by inducing both HuR and ABCG2. A common upregulated miRNA (miR-155-5p) was identified by miRNA microarray in the sensitive cell lines after incubation with S1M1-80-derived exosomes. MiR-155-5p was found to induce HuR expression by promoting its translation. MiR-155-5p inhibitor was shown to reverse the upregulation of HuR in HCT116 cells after exosome incubation, which subsequently suppressed ABCG2 expression and the MDR phenotype. Furthermore, inhibition of exosome uptake by dynasore was found to prevent the induction of HuR/ABCG2, and re-sensitize the exosome-treated sensitive cells to SN38.
Conclusion: MDR cells-derived exosomes may spread the drug resistance phenotype by transferring a miR-155-5p/HuR/ABCG2 regulatory machinery to sensitive cells. Inhibition of this exosomal transfer of regulatory materials may prevent the spread of MDR and sensitize cancer cells to chemotherapy.

#5876 ALDH3A1 as a predictive marker for gemcitabine treatment in pancreatic cancer.

J. kim, J. Keum, C. Park, S. Bang;
Yonsei University College of Medicine, Seoul, Korea, Republic of

Background: Pancreatic cancer is one of the incurable cancer. The currently preferred chemotherapy regimens, including gemcitabine, do not extend patient survival by more than a year, and studies on drug resistance mechanisms or biomarkers for the drug sensitivity are very limited. Aldehyde dehydrogenase (ALDH) is a family of enzymes that play an essential role in cell survival and protection. In cancer cells, it is thought that overexpression of the ALDHs confers a survival advantage to the cells, which is associated with a poor prognosis. In this study, we analyzed the drug sensitivity between ALDH3A1 expression and gemcitabine in PDAC cells.

Method: In this study, we investigated the relationship between ALDH3A1 expression and gemcitabine sensitivity using 8 pancreatic cancer cell line. We observed changes in the pattern of ALDH3A1 expression in established gemcitabine resistance pancreatic cancer cell line. Following this, we functionally inhibited ALDH3A1 to determine its impact on gemcitabine sensitivity using shRNA method. To elucidate the molecular mechanisms related with ALDH3A1, we performed multi-omics analysis such as transcriptomics and proteomics.

Results: As a results, there was a negative correlation between ALDH3A1 expression (Protein & mRNA) and gemcitabine resistance 8 pancreatic cancer cell lines. However, in established gemcitabine resistance BxPC3 cells compared to control cells, gemcitabine resistance increased more than 1000 fold while the protein expression was decreased. In these results correlated with inhibition of ALDH3A1 expression using shALDH3A1 experiments both change ALDH3A1 expression and gemcitabine resistance. In biological phenotype experiments, cell proliferation and migration increased in the ALDH3A1 inhibition groups. When using combination treatment of gemcitabine and CB29, a known ALDH3A1 inhibitor, drug resistance increased by more than 2,000 fold in the combination treatment groups. In RNAseq analysis, Adherens junction, Ras signaling, Axon guidance, and JAK-STAT signaling pathway related genes were up regulated in shALDH3A1 treatment group compared control.

Conclusion: In this study, we demonstrated the negative correlation between ALDH3A1 and gemcitabine resistant in pancreatic cancer cell lines and suggesting that it may serves as a predictive marker for gemcitabine treatment in pancreatic cancer patients.

Keywords: Pancreatic ductal adenocarcinoma (PDAC), Aldehyde dehydrogenase 3 family member A1 (ALDH3A1), Gemcitabine sensitivity.

#5877 Disulfiram and its metal complexes reversed hypoxia induced stemness and synergized with first line drugs in primary patient derived pancreatic ductal adenocarcinoma cells.

Benjamin J. Small[1], Ogechi Nkeonye[1], Vinodh Kannappan[2], Shalini Kumarasamy[1], Kate Butcher[2], Karim Azar[1], Gowtham Rajendran[1], Yoshitha Lakshmanan Lakshmanan[1], Mark Morris[1], Christopher Heeschen[3], Yaohe Wang[4], Weiguang Wang[1]

[1]University of Wolverhampton, Wolverhampton, United Kingdom,[2]Disulfican Ltd, Wolverhampton, United Kingdom,[3]School of Medicine, Center for Single-Cell Omics, Shanghai Jiao Tong University, China,[4]Centre for Biomarkers and Biotherapeutics, Barts Cancer Institute, Queen Mary University, London, United Kingdom

Pancreatic ductal adenocarcinoma (PDAC) has a dismal 5-year survival rate (12%) and is predicted to become the second leading cause of cancer related deaths by 2030. The main treatment option for advanced PDAC, gemcitabine (GEM) and nab-paclitaxel (PAC) chemotherapy, has limited efficacy due to adverse toxicities and chemoresistance. Extensive desmoplasia in the PDAC microenvironment induces hypoxia that drives epithelial to mesenchymal transition (EMT) and promotes cancer stem cells (CSCs) leading to metastasis and acquired resistance. Drugs that target CSCs and EMT to overcome chemoresistance could improve patient outcome. Disulfiram (DSF), an FDA approved anti alcoholism drug, has excellent anticancer activity on chelation with Cu^{2+}/ Zn^{2+} ions to form the anticancer metabolites, Copper or Zinc Diethyldithiocarbamate (CuDDC or ZnDDC). The anticancer application of the current oral version of DSF is prevented by its short plasma half-life (< 4 minutes) and separate administration of oral Cu/Zn supplement leading to bioavailability issues. A stable, long circulating, injectable formulation of DSF, CuDDC or ZnDDC may overcome these pharmacokinetic issues. In this study albumin was used to develop soluble, stable and homogenous CuDDC and ZnDDC nanoparticles (Alb-CuDDC, Alb-ZnDDC) and their efficacy was compared with free DSF-Cu in a panel of normoxic, hypoxic and spheroid cultures of patient PDAC cells derived from primary, circulating and metastatic sites. Hypoxia and spheroid cultures of PDAC cells were highly resistant to GEM and PAC and had increased expression of CSC markers such as ALDH, CD133, ABCG2 and CA9. Alb-CuDDC and Alb-ZnDDC were cytotoxic to all PDAC cells (IC_{50s} ~300 nM and ~7000 nM, respectively) in normoxia and hypoxia and synergized with GEM and PAC. While DSF-Cu and Alb-CuDDC significantly reduced the expression of CSC markers and inhibited sphere reformation and migration of PDAC cells, Alb-ZnDDC was less effective in inhibiting these features. Therefore, the ability of PDAC cells to acquire resistance to Alb-ZnDDC was investigated. After long term exposure (> 4 months) to increasing doses of each drug (DSF-Cu, Alb-CuDDC and Alb-ZnDDC), PANC1 and BXPC3 PDAC cells acquired resistance only to Alb-ZnDDC. $PANC1_{ZR6}$ and $BXPC3_{ZR5}$ resistant cells showed increased expression of CSC markers and significant cross-resistance to PAC and GEM suggesting multidrug resistance. Importantly, no cross-resistance to Alb-CuDDC or DSF-Cu was observed, suggesting alternative mechanisms for Alb-ZnDDC. RNA sequencing is underway to identify potential mechanisms involved. To conclude, albumin formulation improved the solubility and stability of DSF-metal complexes. Alb-CuDDC targets CSCs and overcomes resistance in PDAC, similar to free DSF-Cu. Alb-ZnDDC may have alternative mechanisms which are yet to be elucidated.

#5878 ZNF397 loss triggers TET2-driven epigenetic rewiring, lineage plasticity, and AR-targeted therapy resistance.

P. Mu, Y. Xu, S. Deng;
UT Southwestern Medical Center, Dallas, TX

Cancer cells exhibit phenotypical plasticity and epigenetic reprogramming, which allows them to evade lineage-dependent targeted treatments by adopting lineage plasticity. The underlying mechanisms by which cancer cells exploit the epigenetic regulatory machinery to acquire lineage plasticity and therapy resistance remain poorly understood. We identified Zinc Finger Protein 397 (ZNF397) as a *bona fide* co-activator of the androgen receptor (AR), essential for the transcriptional program governing AR-driven luminal lineage. ZNF397 deficiency facilitates the transition of cancer cell from an AR-driven luminal lineage to a Ten-Eleven Translocation 2 (TET2)-driven lineage plastic state, ultimately promoting resistance to therapies inhibiting AR signaling. Intriguingly, our findings indicate that TET2 inhibitor can eliminate the AR targeted therapies resistance in ZNF397-deficient tumors. These insights uncover a novel mechanism through which prostate and breast cancers acquire lineage plasticity via epigenetic rewiring and offer promising implications for clinical interventions designed to overcome therapy resistance dictated by lineage plasticity.

#5879 Role of the inner mitochondrial membrane protein (Mic60) in MAPKi-resistant melanoma.

J. C. Ghosh, S. Del Aguila, H. Li, J. Villanueva, D. C. Altieri;
The Wistar Institute, Philadelphia, PA

Introduction: Metastatic melanoma is one of the most aggressive cancers, despite recent improvements in therapy. The rising melanoma incidence and mortality, along with its high propensity for metastasis highlights the urgency to find more effective therapeutic targets. The efficacy of targeted MAPK signaling pathway inhibitors (MAPKi) in metastatic melanoma therapy is limited by the development of resistance mechanisms that result in disease relapse. This situation necessitates alternative treatments for melanoma patients who develop resistance to targeted therapy. We have recently found out that there exists a group of human tumors that express lower levels of Mic60, a mitochondrial structural protein also known as mitofilin or inner membrane mitochondrial protein (IMMT). In a model of prostate cancer, we showed that Mic60-low tumors have lower mitochondrial fitness, but increased cell motility, invasion, and propensity to metastasize. However, a potential differential expression of Mic60 in melanoma has not been investigated and whether reduced mitochondrial fitness in Mic60-low tumors can expose new therapeutic vulnerabilities in combination with targeted therapies has not been determined.
Experimental Procedures: We analyzed melanoma-specific TMA for differential expression of Mic60 in tumor vs. adjacent normal tissue by IHC. Differential mRNA expression levels were examined by single-cell RNA-Seq and quantified by bioinformatics analysis. Differential therapeutic vulnerabilities of Mic60-low melanoma cell lines to mitochondrial-targeted small molecule Hsp90 inhibitor, Gamitrinib, were assessed for cell death induction and mitochondrial dysfunction.
Results: We identified subsets of melanoma patients with constitutively reduced or outright undetectable expression of Mic60, in vivo. By single-cell RNA-Seq, Mic60-low melanomas were characterized by reduced oxidative phosphorylation and decreased ATP production, slower cell cycle progression but paradoxically increased cell motility and invasion. Loss of Mic60 exposed new, actionable therapeutic vulnerabilities, and the combination of Gamitrinib plus MAPKi potently induced mitochondrial cell death in MAPKi-resistant melanoma cell lines.
Conclusion: Mic60 is heterogeneously expressed and often reduced in melanoma. Although this is associated with increased cell invasion and metastatic propensity, the combination of Gamitrinib plus MAPKi restored mitochondrial cell death in therapy-resistant, Mic60-low melanoma cells.

#5880 Induction of the p-glycoprotein with atorvastatin using colorectal cancer cells.

C. L. Farrell[1], A. Messersmith[2], W. Lei[3], B. Dyer[1];
[1]Clemson University, Clinton, SC, [2]Presbyterian College, Clinton, SC, [3]Manchester University, Fort Wayne, IN

Chemotherapy resistance is responsible for a majority of the cancer-associated mortalities. Efflux of the P-glycoprotein (P-gp) transporter is one of the many causes for chemotherapy resistance. The increased activity of the P-gp on the surface of the tumor cells leads to the removal chemotherapy drugs and allows a cancer to survive. The purpose of this study was to evaluate how atorvastatin impacts the P-gp expression in colorectal cancer cells. The colorectal cells, CACO2 cell line, were separated into drug treatment groups. The experimental groups were treated with the statin drug, atorvastatin, at different concentrations and doxorubicin as the positive control, for 3-4 months. Atorvastatin was selected for the study since it is a P-gp substrate and a potential inducer. Exon-spanning primers for the *ABCB1* gene were used to monitor changes in mRNA expression of the P-gp. Once overexpression of the *ABCB1* gene was achieved, the cells were tested for protein expression through western blots and flow cytometry. The P-pg-induced cells, which consisted of the atorvastatin-treated and doxorubicin-treated cells, and the untreated cells were then tested for chemotherapy-resistance using the PrestoBlue proliferation assay. The atorvastatin treatments were repeated for reproducibility by using two other colorectal cancer cell lines. The P-pg-induced cells, which consisted of the atorvastatin-treated and doxorubicin-treated cells, and the untreated cells were also studied for stability by removing the treatments of the atorvastatin for three months and monitoring for changes in expression of the *ABCB1* gene with rt-qPCR. Drug pathways of the treated cells were also studied for expression changes using RNA Sequencing (RNA-Seq). For the results, the overexpression of the *ABCB1* gene occurred in the 4th month of the study of the bi-weekly atorvastatin and doxorubicin treatments using the CACO2 cells. Protein assays were able to confirm the P-gp overexpression in the atorvastatin-treated and doxorubicin-treated cells. The chemotherapy-resistant assay revealed that the atorvastatin-treated cells were just as drug resistant to the chemotherapy as the doxorubicin-treated cells. Through the reproducibility experiment, the overexpression of the ABCB1 gene was observed in two other cell lines after long-term treatment of the drug therapy. Removal of the atorvastatin for three months revealed that the P-gp overexpression was not reversible. The RNA-Seq analysis identified other possible drug resistant markers in the atorvastatin pathway. This study implicates that late-stage cancer patients, who are treated for hypercholesterolemia, may be at higher risk for developing chemotherapy-resistant tumor cells. With the identification of chemotherapy-resistant tumors in chemotherapy-naïve cancer patients, doctors will be able to provide more precise approaches to treating patients through effective drug therapies.

#5881 Upregulation of TET2 expression by DNA methyltransferase (DNMT) inhibitors is associated with resistance in DNMT1 knockout colorectal cancer cells.

A. B. A. Laranjeira, D. Nguyen, L. C. Pelosof, J. H. Doroshow, **S. X. Yang**;
National Cancer Institute, Rockville, MD

Ten-eleven-translocation 2 (TET2) is a member of the TET family proteins (TET1-3) that convert 5-methylcytosine to 5-hydroxymethylcytosine (5-hmC) in DNA and causes site-specific DNA demethylation. The effects of DNMT1 on TET2 phenotype following DNMT inhibitor treatment is unclear in human cancer. In colorectal cancer HCT116 cells with *DNMT1* gene intact (*DNMT1*$^{+/+}$) and deletion (DNMT1$^{-/-}$) status, we found that TET2 expression was robustly increased in *DNMT1*$^{-/-}$ cells after treatment with 0.5 μM and 5 μM decitabine for 72 h, 96 h, and 120 h. The augmentation in TET2 expression was accompanied by a dose-dependent re-expression of p16^{ink4A} in *DNMT1*$^{-/-}$ cells. Particularly, TET2 upregulation was associated with resistance to DNMT inhibitors, showing a lack of induction of DNA damage, cell-cycle arrest and apoptosis after drug exposure in *DNMT1*$^{-/-}$ compared to *DNMT1*$^{+/+}$ cells. The treatment with 4'-thio-5-aza-2'-deoxycytidine (aza-T-dCyd) only up-regulated TET2 and re-expressed p16^{ink4A} at the lower dose of 0.5 μM, which was consistent with our previous findings that high dose of aza-T-dCyd at 5 μM predominantly eliminates the cancer cells with severe DNA damage by undergoing apoptosis and cell death (Scientific Reports, 13:5964, 2023). Moreover, both decitabine and aza-T-dCyd had minimal effects on TET2 upregulation and p16^{ink4A} re-expression in cells with intact *DNMT1* gene. The data suggest that the absence of *DNMT1* gene made the cells prone to TET2 upregulation upon DNMT inhibitor challenges. Future study is needed to investigate the interactive relationship between DNMT1 and TET2 as well as demethylation, and its impact on cancer treatment with DNMT inhibitors.

#5882 Targeting vulnerabilities of drug-tolerant persister cells in gastric cancer.

E. Puliga[1], L. Negro[2], M. Olivero[3], C. Orru[2], F. Maina[4], D. Conticelli[2], S. Corso[2], S. Giordano[2];
[1]Candiolo Cancer Institute - IRCCS-FPO, Candiolo, Italy, [2]University of Turin; Candiolo Cancer Institute - IRCCS-FPO, Turin, Italy, [3]University of Turin, Turin, Italy, [4]Candiolo Cancer Institute- IRCCS-FPO, Candiolo, Italy

Cytotoxic drugs often fail to eradicate cancers due to the presence of treatment-persistent tumor cells that represent a reservoir for relapse. These “residual” cancer cells escape from chemotherapy- induced death by entering a reversible slow proliferation state, known as drug tolerant persister (DTP) state. Although improvement of treatment options achieved a survival benefit, Gastric Cancer (GC) is still endowed with poor prognosis. Surgery and neo/adjuvant chemotherapy remain the keystone of treatment. However, most patients with advanced cancer relapse even after complete surgical resection, suggesting a critical role for DTP cells. We obtained GC DTP cells from primary cells upon first- and second-line chemotherapy regimens (FLOT and FOLFIRI). Cells were treated with doses corresponding to the drug maximal plasmatic concentration. At the end of the treatment, cells were left without drugs (washout). During this window of time, when cells had regrown, they were re-challenged with chemotherapy and resulted still sensitive to the treatments, thus fulfilling the criteria for bona fide DTP cells. GC DTPs showed increased expression of markers associated with gastric stem cells (i.e. LGR5), downregulation of proliferative markers (i.e. Ki67) and decreased levels of PS6, evaluated as a readout of mTOR activation. Interestingly, DTPs resulted positive to X-gal-based β-galactosidase staining, suggesting a chemotherapy-induced senescence-like status. RNA-seq analysis and gene expression arrays allowed the identification of genes specifically down/upregulated in DTP cells. Using the intuitive enrichment analysis web-based tool Enrichr, we discovered that 54/173 of the downregulated genes characterizing the persister state were targets of a single miRNA. By quantitative real-time PCR, we validated the expression of this miR in all the models of FOLFIRI- and FLOT-obtained persister cells and we found it strongly upregulated (up to 8-fold), highlighting its possible contribute in the establishment of the persister state. Since among the target genes of this miR there are genes involved in the Homolougus Recombination (HR) system, we performed TaqMan™ Array assay for Human DNA repair gene expression on FOLFIRI-obtained DTPs. We identified a significant downregulation of genes strictly correlated to the HR machinery, suggesting that the FOLFIRI-induced persister cells can temporarily enter in a “BRCAness” status that may be used for a synthetic lethality approach using PARP inhibitors. Targeting the drug tolerant persister state is an essential approach to diminish cancer cells when they are potentially in their most vulnerable state.

#5883 Role of major facilitative folate transporters SLC19A1 and SLC46A1 in cyclic dinucleotide transport and STING signaling.

H. McQuithey[1], M. Brzezinski[1], C. O'Connor[1], L. Matherly[2], **Z. Hou**[2];
[1]Wayne State University, Detroit, MI, [2]Barbara Ann Karmanos Cancer Institute, Detroit, MI

Activation of stimulator of interferon genes (STING) activates the transcription factor pIRF3, promoting gene transcription encoding type I interferons including IFNβ that stimulate broader immune responses. Targeting the STING pathway for cancer is especially compelling given its importance to the malignant phenotype. Cyclic dinucleotides (CDNs) function as STING agonists. Inspired by preclinical studies, two phase I clinical trials with CDNs including ADU-S100 were initiated but concluded early due to lack of anti-tumor efficacy. The reduced folate carrier (RFC; SLC19A1) has been identified as one of the primary means to transport CDNs through the cell membrane, although a study suggested that CDN and folate binding to RFC was as least partly distinct. While depletion of the proton-coupled folate transporter (PCFT; SLC46A1) in THP-1 cells had nominal effects on CDN stimulation, overexpressing PCFT increased STING signaling. Limited clinical responses may reflect the impact of physiologic variables governing RFC and PCFT not previously considered. Understanding the mechanisms of CDN uptake by RFC and PCFT under physiologic conditions may elucidate the role of CDNs on STING signaling. To study the impact of RFC levels on CDN transport and STING signaling, we used an engineered R1-11/Tet-on-RFC HeLa cell model induced with doxycycline. In R1-11/Tet-on-RFC cells, ADU-S100 showed a low affinity for binding to RFC, as measured by direct competition for transport with [^{3}H]methotrexate. RFC dose-dependence of ADU-S100 uptake and STING activation was confirmed by monitoring IFN-β (qPCR) and pIRF3 (Westerns). Maximum induction of pIRF3/IFNβ was seen in THP-1 and R1-11/Tet-on-RFC cells by ADU-S100 treatment at pH 7.2 (RFC pH optimum) in the presence of 25 nM leucovorin. Induction of pIRF3/IFNβ by ADU-S100 in THP-1 and R1-11/Tet-on-RFC cells were partially abolished by treatment with 200 μM of leucovorin or 10 μM of PT523 (RFC-specific inhibitor), suggesting the transport of folates and CDNs may share common albeit distinct mechanisms. ADU-S100 treatment showed no pIRF3 or IFN-β production in an engineered R1-11/Tet-on-PCFT HeLa model expressing high levels of PCFT, suggesting no direct transport by PCFT, even under optimal pH conditions. Interestingly, pIRF3/IFN-β induction was enhanced in R1-11/Tet-on-RFC/PCFT cells expressing constitutive PCFT in addition to RFC, compared to R1-11/Tet-on-RFC cells that express comparable RFC without PCFT. This may reflect previously unrecognized functional interactions between RFC and PCFT. In conclusion, RFC mediates ADU-S100 uptake and STING activation under physiologic conditions and this process is enhanced by concomitant expression of PCFT. Additional characterization of key molecular and biochemical determinants of CDN-based cancer therapeutics may lead to improved approaches for CDN therapy based on enhanced cellular uptake.

EXPERIMENTAL AND MOLECULAR THERAPEUTICS: New Targets
Poster Session

#5887 Identifying new immunotherapy targets using machine learning and ex vivo validation.

M. Augustine[1], N. Rocha Nene[1], K. Thakkar[1], D. Qian[1], E. Fitzsimons[1], B. S. Simpson[1], C. Watkins[2], C. Swanton[3], K. Litchfield[1];
[1]University College London (UCL), London, United Kingdom, [2]Royal Holloway University of London, London, United Kingdom, [3]The Francis Crick Institute, London, United Kingdom

Overview: Immunotherapy has revolutionized cancer treatment. However, existing immune checkpoint inhibitors (CPI) yield low response rates in most cancers, highlighting the need for new therapeutic options. Traditional immune-oncology (IO) target discovery relies on preclinical models, which struggle to recapitulate human tumor complexity, limiting translation potential. Attention is thus directed at harnessing multimodal patient molecular data with modern machine learning (ML) techniques to identify new IO targets which may have higher clinical viability.
Approach: We posed IO target discovery as a binary classification task, training ML systems on known candidate drug targets that have progressed to stage I or higher clinical trials. We constructed a rich knowledge graph database to support model development. Graph nodes (n=11,919) comprised genes with edges linking genes involved in n=99,275 protein-protein interactions (PPIs; PMID: 28936969). Genes were labelled with n=6,387 gene-disease associations alongside bulk exome and transcriptome (RNAseq) features from n=1,317 CPI-treated patients (PMID: 33508232). We considered the role of different immune subsets by incorporating cell type-specific PPIs from single cell RNAseq atlases of n=350 samples (PMID: 31786210). To capture how antigen processing affects immunotherapy response, we also examined the immunopeptidome of n=60 patients (PMID: 30556813). Causal data on immune responses to genetic perturbation stemmed from n=7 publicly available CRISPR tumor-T cell co-cultures and n=15,442 SNP-phenotype links. Lastly, we used interpretability analysis to understand drivers of model predictions and elucidate critical genes that influence multiple IO target pathways.
Results: Firstly, we developed an ensemble ML approach which achieved test ROC-AUC>0.75. Next, we used a graph-based ML framework which yielded superior performance (test ROC-AUC>0.90). Orthogonal validation confirmed these models can discriminate known targets by trial phase ($p<0.001$), predict patient response in new CPI trials ($p<0.05$), and identify genes that rank highly in unseen genome-wide CRISPR screens. Targets from both methods have entered experimental validation in patient-derived explants and organoid-immune co-cultures. Already, we have identified 2 novel targets predicted to relate to macrophage activity. Early data suggest that perturbing them leads to macrophage repolarization. Further validation experiments are ongoing.
Conclusions: We will reveal candidate targets, showing that our method is effective at uncovering new IO targets and can identify critical nodes in biological networks that might be attractive hits. In addition, deciphering data types that drive model predictions provides a broader immunobiological understanding of anti-tumor immune responses. Thus, our results endorse using ML and multimodal data for novel IO target discovery.

#5888 Novel immune-therapeutic target for lung cancer uncovered by SpliceIO™, an innovative platform that identifies disease-specific alternative splicing.

M. A. Manzanares, K. Anderson, H. Zumrut, S. Gera, N. Habib, N. Williams, S. Stanton, T. Floyd, S. Shah, D. Trahan, M. Akerman, G. Arun; Envisagenics Inc., Long Island City, NY

Alternative splicing (AS) plays a critical role in generating tumor-specific neoantigens targetable through an arsenal of immunotherapeutic modalities. Previous studies have demonstrated tumor-promoting activity of deregulated AS isoforms and mutated splicing factors, both of which increase the yield of neoantigen-encoding AS isoforms. Therefore, the identification of AS isoforms has the potential to produce novel therapeutic targets, especially in lung tumors where splicing deregulation is frequent. Envisagenics has developed SpliceIO, a proprietary software platform for AS-derived neoantigen discovery. SpliceIO uses RNA-seq data to uncover extracellular neoantigens encoded by transmembrane proteins. This predictive ensemble maximizes the value of RNA-seq data to predict fundamental aspects of neoantigen activity, such as protein localization, epitope accessibility, and cancer pathway relevance. Here, we summarize the discovery and validation of novel AS-derived neoantigens identified using SpliceIO in non-small cell lung cancer (NSCLC). Our novel SpliceIO-identified neoantigens in NSCLC were validated following our well-established experimental pipeline. We have confirmed RNA expression of the neoantigen-expressing transcripts in lung cancer cell lines and patient samples using a combination of RT-PCR as well as RNA-ISH. Further, we have validated the membrane-bound extracellular localization of neoantigen-containing isoforms at the protein level using Western blotting, GFP and c-Myc tagged isoform generation, eukaryotic cells transfection, and microscopy. Our top target showed high tumor specificity, heterogeneous distribution in tumor samples, high prevalence, confirmed novel extracellular N-terminal domain, and strong biological relevance in lung cancer. This demonstrates the potential of utilizing RNA splicing for identifying many more membrane associated proteins for tumor specific immunotherapeutic targeting. The combination of computational and experimental approaches to neoantigen identification using SpliceIO allows for novel target discovery amenable for targeted immunotherapeutic development for lung cancer treatment and other indications driven by deregulated AS.

#5889 An immunoproteasome activator that expands the MHC-class I immunopeptidome, unmasks neoantigens and enhances antimyeloma T-cell activity.

P. S. Rana, J. J. Ignatz-Hoover, J. J. Driscoll;
UH Cleveland Medical Center, Cleveland, OH

A hallmark of cancer is the ability to evade immunosurveillance mechanisms and thwart the efficacy of immunotherapeutic agents. The proteasome functions as an essential component of immunosurveillance by generating peptides from intracellular proteins that are then presented to T-cells. Antigens generated by the proteasome promote the infiltration of immune cells into tumors and improve tumor regression in response to immunotherapy. Cancer cells can evade elimination by the immune system by deregulating the antigen presentation machinery to downregulate the expression of proteins recognized by immune cells as antigens, creating an immunosuppressive microenvironment. In contrast to constitutive proteasomes, immunoproteasomes are a highly specialized proteasome variant that are highly expressed in antigen-presenting cells. Immunoproteasomes contain distinct catalytic subunits with active site substrate specificities distinct from constitutive proteasomes. Immunoproteasome degrade intracellular proteins to generate antigenic peptides that are the presented by MHC-class I (MHC-I) molecules on tumor cells for recognition by cytotoxic T-cells. We hypothesized that immunoproteasome activation could concomitantly increase the relative abundance and diversity of MHC-I antigens presented on multiple myeloma (MM) cells. High-throughput screening identified a novel small molecule (Compound A) that selectively increased immunoproteasome catalytic activity. Global proteomic integral stability assays determined that Compound A binds the proteasome structural subunit PSMA1 and that treatment with Compound A increased association of the proteasome activator PA28α/β (PSME1/2) activator with immunoproteasomes. The effect of Compound A on immunoproteasomes was abolished after the ablation of *PSMA1*, *PSME1*, or *PSME2* or by the treatment of cells with suicide inhibitors that target immunoproteasome-specific catalytic sites. Treatment of MM cells with Compound A doubled the total number of MHC-I-bound peptides and increased the level of specific MHC-bound peptides up to 200-fold. Interestingly, a number of tumor-associated antigens and neoantigens were dramatically unmasked following treatment of MM cells with the immunoproteasome activator. Importantly, the treatment of patient $CD138^{+}$ cells with Compound A promoted the antimyeloma activity of allogenic and autologous patient-derived $CD8^{+}$ T-cells. Taken together, our results demonstrate the paradigm-shifting translational impact of immunoproteasome activators to expand the myeloma immunopeptidome and have revealed novel, actionable antigenic targets to personalize T-cell-directed immunotherapy.

#5890 ZNF451 and doxorubicin resistance.

A. Rees, A. Blackman, D. Evans, J. Delaney;
The Medical University of South Carolina (MUSC), Charleston, SC

Precision medicine most often utilizes mutations in patient selection, however targetable mutations are exceedingly rare in high-grade serous ovarian cancer (OV). Aneuploidy and chromosome instability are major contributors to such genomic changes in OV. Genes are pervasively disrupted by copy-number alterations: 39% of all genes in the median solid tumor of all cancer types, and 67% in OV. A common second-line OV chemotherapeutic is peggylated-liposomal doxorubicin, a topoisomerase-II poison. To address which genes in OV contribute to doxorubicin sensitivity and resistance, we performed a CRISPR-Cas9 screen on 19,114 human genes in the presence or absence of doxorubicin. Positive control genes involved in drug-efflux and DNA repair were significant hits. The gene with both the highest significance and greatest magnitude of doxorubicin sensitization upon knockout was the E3 SUMO2/3 ligase ZNF451. ZNF451 exhibits a copy-number loss in 14% of patients and corresponds to ZNF451 protein reduction. ZNF451 is an attractive target for future combination therapies with doxorubicin to induce conditional lethality. ZNF451 may be valuable to study as a prognostic biomarker for topoisomerase-II inhibitor chemotherapy.

#5891 An image-based phenotypic screen identified CBP/p300 as new cancer drug resistance target and enabled the development of the clinical candidate TT125-802.

D. Gruber, C.-H. Fabritius, T. Bohnacker, M. Schwill, S. Laudato, R. Herrador, K. Westritschnig, T. Pattupara, S. Fluckiger-Mangual;
TOLREMO therapeutics AG, Basel, Switzerland

Resistance to targeted therapies is a major challenge in oncology. Genetic mechanisms of resistance such as gatekeeper mutations in the primary drug target can be readily identified. However, drug targets responsible for non-genetic resistance mechanisms such as transcriptional reprogramming remain elusive. Here we describe an innovative phenotypic screening approach that led to the development of the clinical candidate TT125-802 and identification of its target CBP/p300 which we discovered as a novel regulator of transcriptional resistance to a range of targeted therapies. Targeted cancer therapies have been reported to induce profound transcriptional reprogramming leading to drug resistance. For instance, inhibition of oncogenic MAPK signaling using a BRAF/MEK inhibitor combination in BRAF-V600E mutated melanoma, triggers expression of the pluripotency transcription factor SOX2 along with broader expression of associated stemness and EMT genes. We used this system as a model to screen for small molecules that prevent transcriptional escape mechanisms to targeted cancer therapies. For this, we developed an automated high-throughput immunofluorescence staining and analysis method of SOX2 as a surrogate marker for resistance-conferring transcriptional reprogramming. A hit-like high diversity library of 16'000 small molecules was screened using an image-based multi-parameter readout with an integrated counter-screen for general cell toxicity. A battery of downstream assessments including patentability, synthetic tractability, physico-chemical properties, and dose-dependent modulation of transcriptional resistance signatures was used to select the chemical scaffold TT125 for further hit to lead optimization. Hit to lead optimization was initially target agnostic. To de-orphan the scaffold, a chemical probe of TT125 was developed in house and used in a chemoproteomics assay. The transcriptional co-activators CBP/p300 were identified as the target of TT125. Biochemical assays revealed that the TT125 scaffold binds specifically to the bromodomain of CBP/p300 but not the histone acetyl transferase domain. Moreover, TT125 was confirmed to bind highly selectively to the bromodomain of CBP/p300 but not other bromodomain-containing proteins such as BRD2 or BRD4. Structure-based drug design along with in vivo PD models using transcriptional short-term readouts were used for lead optimization that resulted in the development of the potent and highly selective clinical candidate TT125-802. Validating our phenotypic approach to drug discovery and development, TT125-802 is currently being evaluated in a phase I oncology trial. The modular setup of our phenotypic screening system has the potential to power the discovery of additional novel modulators of transcriptional drug resistance.

#5892 SCUBE3 promotes therapy resistance in triple negative breast cancer.

D. Singh[1], D. Medina[1], B. Onyeagucha[2], R. Mojidra[3], P. Subbarayallu[1], A. Taylor[3], D. Lyu[4], S. Timilsina[1], P. P. Venkata[1], S. S. Nirzhor[1], S. M. Abdulsahib[1], T. Do[1], Y. Chen[1], R. Vadlamudi[3], M. K. Rao[1];

[1]UT Health San Antonio Greehey Children's Cancer Res. Inst., San Antonio, TX, [2]Mississippi university of women, Columbus, MS, [3]UT Health Science Center at San Antonio, San Antonio, TX, [4]UT Health San Antonio Barshop institute, San Antonio, TX

Introduction: The development of novel targeted therapies is urgently required for improving the outcome of triple negative breast cancer (TNBC) patients. Chemotherapy is the common treatment option for TNBC. However, resistance and tumor relapse remain the major obstacles hindering the effectiveness of chemotherapeutic agents in cancer patients. Therefore, identifying genes/factors that sensitize breast cancer cells to chemotherapeutic agents could improve treatment outcome in patients. Here we report Signal peptide CUB domain EGF-like 3 (SCUBE3) genes as a novel therapeutic adjuvant that can improve the efficacy of doxorubicin, a chemotherapeutic agent commonly used in treating breast cancer patients.

Methods: Unbiased high-throughput loss of function genomic screen was performed on breast cancer cells in the presence or absence of doxorubicin. Breast cancer cells lines (MDA-MB-231 and MDA-MB-468) were purchased from the American Type Culture Collection and cultured in standard medium. Breast cancer cells were transfected either with SCUBE3 overexpression plasmid or shRNA specific to SCUBE3. These overexpression/knockdown breast cancer cells were analyzed for cell viability, migration, invasion, colony formation, cell cycle, apoptosis assays, western blotting, and in vivo tumor xenograft study.

Results: Our finding demonstrated that SCUBE3 promotes breast cancer cell progression as knockdown of SCUBE3 inhibited the ability of breast cancer cells to form colony, migrate, and invade, while overexpression of SCUBE3 promoted tumor growth in preclinical mouse models. Our results revealed that SCUBE3 mediates its protumor effects by regulating genes involved in growth and survival in the MAPK pathway, DNA damage surveillance pathway including RAD51 and FOXM1, and apoptotic pathway including Mcl-1. We demonstrated that SCUBE3 promotes tumor growth and progression by interacting with and activating several oncoproteins.

Conclusions: Overall, our data suggests that SCUBE3 can be a potent therapeutic target for treating TNBC patients.

#5893 Crosstalk between sensory innervation and pancreatic ductal adenocarcinoma.

K. Wang, B. Ni, X. Wang, J. Hao;
Tianjin Medical Univ. Cancer Inst. & Hospital, Tianjin, China

In recent years, a growing body of research has illuminated the integral role of the nervous system in the initiation and progression of cancer, giving rise to the establishment of an emergent field known as cancer neuroscience. Pancreatic ductal adenocarcinoma (PDAC), constituting 90% of pancreatic cancers, manifests as a highly malignant solid tumor characterized by insidious onset, strong invasiveness, and a notable propensity for recurrence or metastasis. Consequently, the 5-year survival rate for PDAC remained dismally low at approximately 10% in 2021. Notably, PDAC is distinguished by perineural invasion (PNI), a phenomenon linked to postoperative recurrence and metastasis. A thorough exploration of the interplay between peripheral innervation and PDAC holds promise for identifying novel targets and therapies to enhance outcomes in PDAC. This study unveils a correlation between PDAC patients exhibiting high calcitonin gene-related peptide-positive (CGRP+) sensory innervation in the tumor microenvironment (TME) and diminished overall survival (OS) and disease-free survival (DFS) compared to those with lower CGRP+ nociceptive innervation. Concurrently, heightened CGRP+ sensory innervation corresponds to increased cancer pain, as assessed by Visual Analog Scale (VAS) scores. Further analysis reveals a negative association between CGRP+ nociceptive nerves and lymphatic metastasis, as well as tumor size in PDAC patients. In a murine PDAC model, the genetic or chemical ablation of CGRP+ sensory neurons significantly impedes disease progression. Additionally, sensory neuron ablation attenuates cancer-induced vesical pain and enhances the locomotor function of mice, suggesting an improvement in overall quality of life. Mechanically, within the TME of PDAC, the secretion of neuropeptides substance P (SP) and CGRP from sensory neurons is elevated, with CGRP exhibiting a more pronounced increase. Furthermore, the expression of the CGRP receptor—receptor activity modifying protein 1 (RAMP1)—surpasses that of the SP receptor in the TME. Subsequent blockade of the CGRP pathway using the RAMP1 antagonist Rimegepant significantly suppresses PDAC progression and alleviates cancer pain, accompanied by improved locomotor function. In summary, sensory innervation actively participates in the progression of PDAC through the secretion of CGRP. Consequently, the inhibition of the CGRP pathway emerges as a potential therapeutic strategy for both PDAC and cancer-induced pain.

#5894 Novel splicing-derived neoantigen in triple negative breast cancer uncovered by SpliceIO™ a robust platform for the discovery and validation of disease-specific immunotherapies.

N. Williams, M. A. Manzanares, K. Anderson, H. Zunrut, S. Gera, N. Habib, S. Stanton, T. Floyd, S. Shah, D. Trahan, M. Akerman, G. Arun; Envisagenics Inc., Long Island City, NY

Splicing dysregulation is a major hallmark of cancer, affecting tumor progression, metastasis, and therapy resistance. Aberrant alternative splicing (AS) plays a critical role in generating tumor-specific neoantigens targetable through an arsenal of immunotherapeutic modalities. Such neoantigens cannot be discovered using conventional DNA-based tools; they require specialized software for AS analysis using RNA-seq data. SpliceIO is Envisagenics' AI platform for AS-derived neoantigen discovery. SpliceIO uses a "predictive ensemble" approach to uncover neoantigens that are both stably expressed and located on the extracellular membrane of cancer cells. Using SpliceIO, we have analyzed more than 10,000 RNA-seq samples from 5 patient cohorts covering 5 breast cancer subtypes as well as 2,647 normal RNA-seq samples from GTEx. Our analysis has identified tumor-specific neoantigens present in AS transmembrane proteins specific for Triple Negative Breast Cancer. SpliceIO target candidates were validated experimentally using our well-established pipeline in which isoform specific transcripts are tested in cancer cell lines by PCR and primary tumor tissues by qPCR to confirm RNA expression. Tumor heterogeneity and prevalence is confirmed by RNA in-situ hybridization in Tissue Microarrays. Extracellular localization of the novel epitope is confirmed by clone generation with GFP and c-Myc tagging followed by microscopy, Western blotting, and proteomic analysis. Our top validated target presents high TNBC tumor specificity and heterogeneous distribution, and contains a novel extracellular N-terminal domain. These results strongly support the role of aberrant AS as a major source of tumor-specific neoantigens. Our combined computational and experimental approach promotes novel target discovery, enabling the development of novel immunotherapeutic for TNBC patients who are in critical need of better treatment options.

#5895 N17350 kills cancer cells, spares immune cells, and regresses CDX tumors from chemotherapy naive and experienced patients.

C. Cui[1], R. Gujar[1], C. Lee[1], M. Fumagalli[1], N. Martinez[1], H. Liu[1], N. Grigaitis[1], S. Feau[1], A. Bahador[2], A. P. Algazi[3], L. Becker[1];
[1]Onchilles Pharma, Inc., San Diego, CA, [2]South Coast Gynecologic Oncology, Inc, San Diego, CA, [3]University of California San Francisco, San Francisco, CA

Background. While multiple studies have demonstrated improved clinical outcomes in patients receiving concurrent chemotherapy and immunotherapy, clinical synergy may be limited by the destructive effects of DNA-damaging chemotherapy on non-cancer cells, including key constituents of anti-tumor immunity (e.g. mature T cells). Furthermore, when first-line chemotherapy fails, subsequent lines of chemotherapy produce lower response rates. Thus, new approaches that eradicate cancer cells while preserving immune cells may be required to more efficiently induce anti-tumor immunity as monotherapy or in combination with immunotherapy. Neutrophil elastase (ELANE), a neutrophil-derived serine protease, kills a wide range of cancer cells without harming immune cells through a unique mechanism involving histone H1 and the death domain of CD95. Here, we compared N17350, an optimized biologic leveraging the ELANE pathway, and chemotherapies for their ability to kill cancer cells and preserve immune cells from primary tumors of ovarian cancer (OvCa) patients and evaluated efficacy in OvCa patient cell-derived xenografts (CDXs) and a 4T1 model of metastatic breast cancer.

Methods. For in vitro studies, cancer cells and CD45+ immune cells were isolated from primary tumors of chemotherapy naïve and experienced OvCa patients. Cells were treated with N17350, oxaliplatin, or doxorubicin 24h post-isolation, and viability was quantified by calcein-AM. For in vivo studies, primary OvCa cells were injected into nude mice to create CDX models. Mice were treated with 2 doses of N17350 (400µg/100mm3, intratumoral) or carboplatin (100mg/kg, intraperitoneal), and effects on tumor growth were quantified. In 4T1 model, N17350 was compared to oxaliplatin, alone or in combination with anti-CTLA4, and effects on tumor growth and immune profile were assessed.

Results. N17350 killed primary cancer cells from all OvCa patients tested but was well tolerated by CD45+ tumor immune cells from the same patients. In contrast, doxorubicin and oxaliplatin showed similar toxicity to both cell types. N17350 killed cancer cells from chemotherapy naïve and experienced patients with equal efficacy, while doxorubicin and oxaliplatin showed less efficacy in patients previously treated with chemotherapy. N17350 rapidly regressed tumors in all OvCa CDX models and exhibited markedly improved efficacy over carboplatin. In the 4T1 model, N17350 outperformed oxaliplatin in terms of regressing tumors, elevating tumor immune cells, and combining with anti-CTLA4.

Conclusions. Our data demonstrate that N17350 kills OvCa tumors in vitro and in vivo while sparing CD45+ immune cells in both chemotherapy naïve and experienced patients. Together with previous data showing that N17350 induces immunogenic tumor cell death, these findings suggest that N17350 could improve clinical outcomes compared to chemoimmunotherapy.

#5896 Platform approach to develop antibodies specifically recognizing cancer-associated glycoforms.

P. Kehler, J. Gellert, L. Kalfhues, S. Marinoff, M. Weis, A. Franz, N. Kast, S. Gurka, M. Morche, E. Hartung, T. Lischke, S. Mayer-Hain, A. Danielczyk; Glycotope GmbH, Berlin, Germany

Introduction: Recent advances in antibody engineering have created a portfolio of highly potent therapeutic approaches like antibody-drug conjugates (ADCs), radioimmunoconjugates (RITs), chimeric antigen receptors (CARs) or bi-specifics. Due to the increased potency, these drugs are more than ever dependent on very clean targets to prevent side effects. We aim to address this major problem through our approach to develop antibodies with improved tumor specificity and reduced on-target/off-tumor binding utilizing the aberrant O-glycosylation on tumor cells. Altered glycosylation of proteins and lipids is one of the most drastic changes in cancer, giving rise to truncated or highly fucosylated and highly sialylated glycans which are almost absent on normal cells. Thus, developing antibodies against protein/carbohydrate combined epitopes (GlycoTargets) comprising these tumor-specific glycans enables highly potent therapies with reduced off-tumor toxicity.

Experimental procedures: A workflow and corresponding database was established to evaluate the O-glycosylation of proteins. The first and most basic criterion is the presence of suitable O-glycosylated peptide stretches in the extracellular domain of a protein based on predictions. For proteins fulfilling this criterion cancer-relevant expression is analyzed in a second step. This is done either using publicly available data or experimentally (immunohistochemistry or protein expression data). During the final major step, the theoretical existence of suitable O-glycosylation is confirmed by our own experimental data. This includes analysis of cellularly expressed proteins by anti-glycan antibodies and mass spectrometric studies.

Results summary: Case studies will be presented that highlight our workflow to identify suitable GlycoTargets based on publicly available data analysis and experimental confirmation. Additionally, the subsequent development of antibodies against the identified GlycoTargets will be shown.

Conclusion: A standardized process was developed for the data collection and prioritization of potential GlycoTargets. The obtained information is subsequently used for targeted discovery of antibodies that bind to protein/carbohydrate combined glycoepitopes (GlycoTargets) offering increased tumor-specificity compared to simple protein targets.

#5897 Understanding and targeting fatty acid CoA ligase ACSL4 in human prostate cancer.

J. Wu[1], M.-E. Wang[1], M. Chen[1], P. Jeong[2], J. Hong[2], L. Wan[3];

[1]Duke University School of Medicine, Durham, NC, [2]Duke University, Durham, NC, [3]Moffitt Cancer Center, Tampa, FL

Prostate cancer (PCa) is the most common non-cutaneous malignancy among men. Although localized prostate cancer is curable, recurrence of metastatic castration-resistant prostate cancer (mCRPC) is almost inevitable and is the major cause of death in human PCa. Recent findings from our lab and others demonstrate that RB1 loss drives lineage plasticity, metastasis, and lethality of prostate tumors initiated by PTEN loss. A downstream target upregulated by RB1 loss is acyl CoA synthetase long chain family member 4 (ACSL4), a fatty acid ligase with an essential role in utilization of long chain fatty acids. ACSL4 has been reported to be upregulated in cancers of various histological origins, including prostate cancer, and its high expression is correlated with aggressiveness of cancer. We hypothesize that ACSL4 is a critical downstream effector of RB1 loss-driven prostate tumorigenesis and pharmacological inhibition of ACSL4 could represent a novel therapeutic approach to the treatment of lethal RB1 deficient or ACSL4 overexpressing prostate cancer. Here we aim to develop novel ACSL4 inhibitors for preclinical studies. Through a structure based virtual screening that targeted ATP binding domains of ACSL4, we successfully identified 15 potential ACSL4 inhibitors. To validate the result, we performed an in vitro screening using various parental and isogenic human PCa cell lines, and found that 4 out of 15 compounds effectively inhibited PCa cell proliferation in a dose-response manner and their inhibitory effects positively correlated with cellular levels of ACSL4. Next, we will perform isotope-labeling enzyme activity assays to determine the specificity of the 4 candidate drugs, and PDPK analyses followed by characterizing their in vivo efficacies in preclinical studies, with a final goal to develop a well-validated ACSL4 inhibitor. Successful completion of this work will provide great insights into contributions of ACSL4 to prostate tumorigenesis as well as preclinical data of ACSL4 inhibitors to treat lethal prostate cancer.

#5898 Inhibition of the LONP1 ATPase domain induces mitochondrial proteotoxic stress and is cytotoxic to acute myeloid leukemia cells.

M. Tcheng, M. Gronda, R. Hurren, L. Zhang, C. Sarathy, Y. Yan, A. Arruda, M. D. Minden, A. D. Schimmer;
Princess Margaret Cancer Centre, Toronto, ON, Canada

Compared to normal hematopoietic cells, AML cells exhibit a heightened reliance on mitochondrial metabolism for survival and proliferation. To support this unique phenotype, AML cells increase import of nuclear-encoded mitochondrial proteins which must be properly folded by mitochondrial chaperones, proteases, and heat shock proteins. Failure to properly fold these precursors leads to protein aggregation, mitochondrial dysfunction, and cell death. To evaluate the reliance of AML cells on maintaining mitochondrial proteostasis, we assessed gene dependency datasets (eg: depmap.org) and identified the mitochondrial protease LONP1, as the top essential gene. LONP1 is a matrix-localized nuclear-encoded AAA+ protease. Proteins are unfolded by its ATPase domain and degraded by its serine-catalyzed proteolytic domain. Compared to hematopoietic cells, LONP1 mRNA was overexpressed in AML across three publicly available datasets. By immunoblotting, LONP1 protein was increased in 16/30 primary AML samples compared to bulk (n=8) and CD34+ blood cells (n=3). LONP1 genetic depletion reduced the growth and viability of OCI-AML2, OCI-M2, NB4, and TEX leukemia cells as well as primary AML cells. LONP1 depletion increased aggregated mitochondrial proteins and reactive oxygen species (ROS) production while reducing mitochondrial respiration and membrane potential. To determine the domain of LONP1 that was necessary for mitochondrial protein solubility, mitochondrial function, and AML survival, we over-expressed wild type, ATPase dead (E591A), or proteolytically dead (S855A) LONP1 cDNA in OCI-AML2 cells and knocked down endogenous LONP1 with shRNA targeting the 3'UTR of the endogenous gene. Wild type or proteolytically dead (S855A) but not the ATPase mutant (E591A) rescued mitochondrial protein solubility, mitochondrial respiration, ROS generation, membrane potential, and cell viability. Thus, the ATPase domain but not the proteolytic activity of LONP1 is necessary for mitochondrial proteostasis. Bardoxolone methyl (CDDO-Me) is a synthetic triterpenoid that allosterically inhibits the LONP1 ATPase site. CDDO-Me killed OCI-AML2 and NB4 cells with IC50 values of 178.5±29.7 and 156.5±39.7 nM, respectively. CDDO-Me (200 nM) killed 3 out of 4 primary AML samples with high LONP1 expression but none of the 10 primary AML samples with low LONP1. Likewise, CDDO-Me induced mitochondrial protein aggregation in AML cell lines and primary AML patient samples with high LONP1 expression but not AML cells or primary AML patient samples with low LONP1. In summary, LONP1 is over-expressed in a subset of AML cells and primary samples where it maintains mitochondrial protein solubility. Selective inhibition of the LONP1 ATPase domain leads to mitochondrial protein aggregation and AML cell death, representing a novel therapeutic strategy for AML.

#5899 Evaluation of Up284 as a selective proteasome inhibitor for prostate cancer therapy.

B. Karanam[1], R. Anchoori[2], Y. Chang[2];
[1]Tuskegee University, Tuskegee, AL, [2]Up Therapeutics, Frederick, MD

Recent research into prostate cancer treatment has unveiled a promising contender known as Up284. In laboratory experiments, this compound has exhibited a remarkable preference for targeting prostate cancer cells as opposed to normal cells. Specifically, in vitro cell viability assays using MTT have shown that prostate cancer cells display high sensitivity to Up284 at low nanomolar IC50 values, while primary human prostate epithelial cells and mouse keratinocytes exhibit minimal sensitivity. This establishes a notable therapeutic window between cancerous and non-cancerous cells, with Up284 significantly inhibiting colony formation in PC3 cells. Additional functional assays have confirmed Up284's potential, including the 4UbFL Reporter Gene assay, which has revealed robust, dose-dependent proteasome inhibition. This effect is supported by the accumulation of polyubiquitinated proteins in various prostate cancer cell lines following Up284 treatment, suggesting a distinct mechanism of toxicity compared to bortezomib. Furthermore, Up284 has been found to induce apoptosis in PC3 cells, surpassing the efficacy of bortezomib. Competitive binding assays have shown that Up284 exhibits a stronger binding affinity to the proteasomal receptor RPN13 than the prototype inhibitor RA190B. This is further supported by a Cellular Thermo Stabilization Assay (CETSA), which indicates that Up284 stabilizes RPN13 in cells.

A preliminary in vivo study utilizing the bone metastatic prostate cancer genetically engineered mouse model(BMPC GEMM) model for metastatic prostate adenocarcinoma has demonstrated that Up284 leads to significant tumor regression and increased levels of poly-ubiquitinated proteins in residual tumor tissues. Moreover, when Up284 is conjugated with an E3 ligase ligand, it successfully degrades RPN13, resulting in the death of PC3 cells. Up284 has also shown favorable pharmacokinetics/pharmacodynamics (PK/PD) profiles and safety in animal models. It is well-tolerated in mice and holds promise for oral administration, demonstrating a proteasome-dependent reporter protein stabilization effect superior to ixazomib. Importantly, Up284 has induced tumor regression and improved survival rates in various cancer models, including ovarian and breast cancers.

In conclusion, Up284 emerges as a lead candidate for targeted prostate cancer therapy due to its high specificity, substantial therapeutic index, and potent anti-cancer activity both in vitro and in vivo. Further development and clinical investigation of Up284 are warranted to fully explore its therapeutic potential.

#5900 INCB161734: A novel, potent, and orally bioavailable KRAS G12D selective inhibitor demonstrates antitumor activity in *KRAS G12D* mutant tumors.

M. R. Farren, V. Roman, A. Gallion, A. Allali-Hassani, A. Sokolsky, W. Kong, A. Smith, H. Wang, G. Correa, M. Deller, L. B. Epling, J. Procak, G. Zhang, K. Pecko, K. Kennedy, J. Boer, K. Kurzeja-Lipinski, M. Covington, K.-J. Chen, R. Wallower, J. Rocha, R. Pan, A. Perry, B. Yuska, X. Wang, R. Macarron, S. Kim; Incyte Research Institute, Wilmington, DE

KRAS G12D (G12D) is one of the most frequent oncogenic driver mutations, and is especially common in pancreatic (PDAC) and colorectal (CRC) cancers. Patients with *G12D*-mutated disease experience poor treatment outcomes, representing a significant unmet medical need. *G12D* mutation results in constitutively active signaling, including hyperactivation of the ERK and PI3K pathways, which drive cell proliferation and survival. Here we describe INCB161734, a novel, potent, selective, and orally bioavailable small molecule G12D inhibitor that demonstrates *in vivo* efficacy in *G12D*-bearing tumor models.

INCB161734 binds to both the GDP and GTP forms of the G12D mutant at the switch II pocket with picomolar affinity (K_D), and exhibits >80-fold selectivity over wildtype (WT) KRAS. INCB161734 potently inhibits SOS1-dependent GDP/GTP exchange activity in cell-free assays (IC_{50} <3 nM), and exhibits >40-fold selectivity for G12D versus WT KRAS. Additionally, INCB161734 demonstrates high selectivity for G12D over WT in various cellular assays using *G12D* mutant versus WT cancer derived cell lines. INCB161734 potently inhibits ERK phosphorylation (a correlate for KRAS activity), with a mean IC_{50} of 14.3 nM (range: 1.9-45.2 nM) across 7 human and 3 mouse *G12D* cell lines; mean 21.5% inhibition was observed at 1 µM (maximum tested concentration) across 14 WT cell lines. Likewise, INCB161734 inhibits proliferation of *G12D* mutant cell lines, with a mean IC_{50} of 154 nM (range: 8.3-318 nM) across the same 7 human *G12D* cell lines; <30% inhibition (mean 13%) was observed at 1 µM across the same 14 WT cell lines. Treatment with INCB161734 induces caspase 3/7 cleavage in a PDAC cell line (*G12D* HPAC), with EC_{50} <100 nM; caspase 3/7 cleavage in a WT cell line (NCI-H838) was not induced at doses as high as 5 µM. In addition, INCB161734 induced cell cycle arrest (S-phase inhibition) in the *G12D* HPAC cell line, with IC_{50} 12.8 nM; S-phase inhibition in the WT NCI-H838 cell line only occurred at much higher doses (IC_{50} >3.3 µM).

INCB161734 demonstrates excellent oral bioavailability with good absorption, low clearance, and low metabolic turnover. Orally dosed INCB161734 clearly shows target engagement, generating continuous near-maximal KRAS inhibition in *G12D* HPAC mouse xenograft tumors for almost the entire dosing interval. INCB161734 is efficacious against multiple types of *G12D*-mutated tumors and xenografts, resulting in significant tumor growth inhibition, growth arrest and/or regression in multiple PDAC (HPAC, Panc0403, and 2838c3) and CRC (CT26, GP2D, and LS513) mouse tumor models.

These preclinical results demonstrate that INCB161734 is a potent, selective, and orally bioavailable KRAS G12D inhibitor, strongly efficacious against *KRAS G12D* mutant tumors. The potential benefit of INCB161734 for patients with *KRAS G12D* mutant disease is under investigation in ongoing clinical trials.

#5901 A targetable secreted protein drives pancreatic cancer metastatic colonization and HIF1a nuclear retention.

N. Yamaguchi[1], G. Wu[2], E. Ravetch[2], M. Takahashi[2], A. G. Khan[3], A. Hayashi[4], W. Mei[2], D. Hsu[2], E. d. Stanchina[5], I. C. Lorenz[6], C. Iacobuzio-Donahue[5], S. F. Tavazoie[2];

[1]National Cancer Institute, Bethesda, MD, [2]The Rockefeller University, New York, NY, [3]Tri Institutional Therapeutics Discovery Institute, New York, NY, [4]Memorial Sloan Keterring Cancer Center, New York, NY, [5]Memorial Sloan Kettering Cancer Center, New York, NY, [6]Tri-Institutional Therapeutics Discovery Institute, New York, NY

Pancreatic ductal adenocarcinoma (PDAC) is an increasingly diagnosed cancer that kills 90% of afflicted patients. Thus, effective systemic therapy to PDAC remains a significant unmet medical need. **NPTX1 is over-expressed in *in vivo*selected highly metastatic pancreatic cancer cells and promotes liver metastasis:** *Ex vivo* mRNAseq of highly metastatic human and murine PDAC liver metastatic tumors identified neuronal pentraxin 1 (NPTX1) as a cancer secreted protein that becomes over-expressed during PDAC metastatic progression. CRISPRi-based silencing of NPTX1 reduced liver metastatic tumor burden by 15-fold in the highly metastatic clones. **NPTX1 is over-expressed in PDAC liver metastases and predicts survival of PDAC patients:** To assess NPTX1 protein expression *in situ*, two independent board-certified pathologists developed an immunohistochemical (IHC) scoring system and blindly scored NPTX1 expression in a large cohort of 125 primary and 47 liver metastatic PDAC tumors obtained through the rapid-autopsy program at MSKCC. Liver metastatic samples exhibited significantly higher IHC scores than primary PDAC samples (>2-fold increase). **NPTX1 upregulation promotes cell growth under hypoxia:** NPTX1 depletion suppressed growth of PDAC cells under hypoxia but not normoxia. Extracellular supplementation of recombinant NPTX1 was sufficient to rescue cell growth of NPTX1 depleted cells supporting the critical role of secreted NPTX1 in promoting cell growth under hypoxia. **AMIGO2 is a cell surface NPTX1 receptor and mediates HIF1a nuclear retention via specific HIF1a residues:** We next sought to identify the cell surface receptor for NPTX1. We reasoned that a receptor for NPTX1 may become upregulated as a feedback response to depletion of its ligand. mRNA sequencing of *ex vivo* NPTX1-depleted tumors identified AMIGO2. AMIGO2 promoted nuclear retention of HIF1a and conversely, its depletion drove the degradation of HIF1a. HIF1a/hypoxia reporter assay revealed that AMIGO2 depletion led to 300-fold reduction of HIF1a activity. Overexpression of a phosphomimetic construct at HIF1a serine 641 and 643, not a full length HIF1a ORF rescued AMIGO2 mediated HIF1a reporter signal reduction. **Therapeutic targeting of NPTX1-AMIGO2 axis in primary and metastatic PDAC:** Through phage display and mouse immunization campaigns, we identified 6 human IgG1 and 1 murine IgG1 antibodies that exhibited high affinity binding to human NPTX1. We identified anti- NPTX1 murine IgG1 antibody 31B01(31B01) as a lead antibody that substantially and significantly suppressed liver metastatic colonization by >80% outperforming gemcitabine. We also tested the impact of 31B01 on the pancreas orthotopic tumor growth. 31B01 suppressed orthotopic patient derived organoid (PDO) growth (>70% reduction), caused a regression response and dramatically extended the overall survival of treated mice harboring PDAC PDO.

#5902 Targeting MAPK-driven tumors via inhibition of MAP2K4.

M. Wade, E. Tamanini, M. Unbekandt, N. Wallis, J. Lyons, J. Munck, A. Woodhead, P. Schopf, J. Stow, C. East, M. Clark, J. St. Denis, P. Pathuri; Astex Pharmaceuticals, Inc., Cambridge, United Kingdom

MAPK pathway activation is a feature of multiple tumor types. Drugging KRAS and BRAF, the two main oncogenic drivers in the MAPK pathway, has proven successful in the clinic. Inhibition of the downstream effectors, MEK and ERK, can also induce tumor regression. Despite this, many tumors are intrinsically resistant to MAPK pathway inhibitors, or acquire resistance under selective pressure to drug treatment. This creates a need for combination treatments to improve clinical responses. A synthetic lethal (SL) interaction between inhibition of the MAPK pathway and blockade of JNK-JUN signaling has recently been described[1]. Specifically, data from yeast genetics and CRISPR knockout experiments in human cells have identified MAP2K4 as a potential therapeutic target that could be combined with MAPK inhibitors. To date, however, no potent MAP2K4 inhibitors with in vitro and cellular selectivity against key anti-targets have been reported. Here, we describe the development of potent covalent inhibitors of MAP2K4 kinase activity. Biochemical and cell-based assays show that the compound(s) are selective for MAP2K4 versus anti-targets including MAP2K7 and ERK kinases. The combination of MAP2K4 and MEK/ERK inhibitors was effective in cell lines driven by MAPK signaling. These data provide the rationale for further development of MAP2K4 inhibitors to advance our understanding of this novel drug combination.

References: 1. Xue Z, Vis DJ, Bruna A, Sustic T, van Wageningen S, Batra AS, et al. MAP3K1 and MAP2K4 mutations are associated with sensitivity to MEK inhibitors in multiple cancer models. Cell Res. 2018; 28:719-29.

#5903 MASTL small-molecule inhibition to target mitosis for cancer therapy.

Chad M. Toledo, Koleen J. Eisele, Dong Hyun Kim, Xinmeng Mu, Sonja Brun, Carl Davis, Eric C. Greenwald, Fion Hui, Meilan He, Yanling Yang, Ana Flores-Bojorquez, Yuxin Li, Penney L. Khamphavong, Joseph H. Lee, Jian Li, Dana J. Ramms, Greg Jones, Marin Auth, Cory L. Painter, Andrew Nager, Jon Oyer, Sergei L. Timofeevski, William E. Pierceall, Anwar Murtaza, Jonathan R. Heyen, Rebecca Gallego, Casey Quinlan, Indrawan McAlpine, Todd L. VanArsdale

Pfizer, San Diego, CA

Cell cycle/tumor repressors can be pharmacologically activated to repress uncontrollable proliferation of cancer cells. However, targeting cell cycle regulators of G2/M and mitotic checkpoints to achieve maximum therapeutic benefit remains a challenge due to a limited therapeutic index. Here, we identified highly potent and selective oral bioavailable clinical candidate inhibitors to the first-in-class oncology target Microtubule Associated Serine/Threonine Kinase-Like (MASTL) aimed at expanding therapeutic control of the cell cycle for cancer therapy. Breath of efficacy screening in multiple tumor indications in vitro followed by computational analyses identified the regulatory subunit PPP2R2A as a potential patient selection biomarker that strongly correlates to MASTL inhibitor response irrespective of cancer genetic alterations. Functional genetics studies confirmed that sensitivity to MASTL inhibition is defined by PPP2R2A expression. To identify genetic mediators of MASTL inhibitor resistance, a whole genome CRISPR knockout screen with the MASTL inhibitor was performed and further established that the MASTL inhibitor response is dependent on PPP2R2A containing PP2A complexes. Mechanistic studies (proteomics, resistance, functional genetics, and time-lapse microscopy) demonstrated that MASTL inhibition disrupts mitosis by activating the tumor suppressor PP2A, leading to a switch from CDK1 activity to CDK1 inactivity, mitotic defects, and cancer cell death. MASTL inhibition treatment in tumor models *in vivo* and in patient-derived organoid models results in potent tumor growth inhibition. Our results demonstrate that the first identified highly selective MASTL clinical candidate inhibitors represent a potential new cancer therapeutic strategy to target mitosis and mitotic exit by activating the tumor repressor PP2A to counter CDK1 activity.
All procedures performed on animals were in accordance with regulations and established guidelines and were reviewed and approved by an Institutional Animal Care and Use Committee or through an ethical review process.

#5904 Targeting NaV1.7 channels in pancreatic cancer: Implications for EF2K and P-Src/P-Fak/integrin β1 signaling pathways.

M. A. Erdogan[1], A. Caner[2];
[1]Izmir Katip Celebi University, Faculty of Medicine, Izmir, Turkey, [2]Ege University, Izmir, Turkey

Pancreatic cancer (PaCa) ranks as the fourth leading cause of cancer-related deaths in the United States and is among the top five worldwide. Its hallmark characteristics include early invasion, metastasis, resistance to chemotherapy and radiotherapy, and aggressive tumor progression. Evaluating new generation treatments with significant potential in this ongoing battle against cancer is crucial. Voltage-gated sodium channels (VGSC), long detected in various metastatic cell lines and tissue samples beyond breast, lung, and prostate cancer, are of particular interest. This study aimed to explore the therapeutic effects of inhibiting NaV1.7 and its neonatal variant, nNaV1.7, in pancreatic cancer cells. The study utilized human normal keratinocyte cell line HaCaT and pancreatic cancer cell lines PANC-1 and MiaPaCa-2. It investigated the roles and effects of adult and neonatal isoforms of the NaV1.7 channel in pancreatic cancer proliferation, invasion, and metastasis. The findings revealed significantly higher adult and neonatal NaV1.7 mRNA expressions in PANC-1 and MiaPaCa-2 cell lines compared to HaCaT cells. Specific siRNAs effectively downregulated channel mRNA and protein expressions. Notably, NaV1.7 siRNA treatments significantly inhibited cell proliferation and colony-forming capacity in PANC-1 and MiaPaCa-2 cells, without cytotoxic effects on HaCaT cells. Combining gemcitabine with specific NaV1.7 siRNAs enhanced drug efficacy in the PANC-1 cell line. Furthermore, NaV1.7 siRNAs significantly reduced cell invasion, migration, and wound healing in both cell lines. These siRNAs also induced apoptosis and G1 arrest in the cell cycle. They inhibited protein expressions involved in key signaling pathways, including P-Src/P-Fak/Integrin β1, EF2K, P-Akt, P-mTOR, PARP, Caspase-3/9, Cyclin D1/E1. This study is pioneering, as literature lacks research on the expression and function of NaV1.7 and nNaV1.7 in pancreatic cancer cells or tissue samples. In conclusion, NaV1.7 channel isoforms play a significant role in the development, progression, and metastasis of pancreatic cancer and present as a potential therapeutic target in PaCa.

#5905 Propentofylline enhances GBM sensitivity to temozolomide via targeting TROY signaling.

R. Eghlimi[1], D. Nascari[1], A. Beniwal[1], D. Alton[1], D. Grief[2], J. Loftus[2], M. Haluska[3], D. Coleman[3], N. Tran[2];
[1]Mayo Clinic Alix School of Medicine, Scottsdale, AZ, [2]Mayo Clinic Department of Cancer Biology, Scottsdale, AZ, [3]Oleolive, Shreveport, LA

Glioblastoma (GBM) is a high grade glioma that accounts for the majority of primary malignant brain tumors. The standard of care for GBM consists of maximal surgical resection, concurrent radiation and temozolomide (TMZ), and adjuvant TMZ. However, this has only led to a modest increase in median patient survival. TROY (TNFRSF19) is an orphan member of the TNF receptor superfamily that is differentially upregulated in GBM with low expression in normal brain tissue. Previously, we have reported that TROY is overexpressed in GBM and signals to mediate cell invasion and therapeutic resistance. Propentofylline (PPF) is a well-studied synthetic methylxanthine derivative that has strong BBB penetrance. We have shown that PPF decreases TROY expression in gliomas, inhibits invasion, and sensitizes GBM to TMZ in vitro. Here we examined the efficacy of PPF in combination with TMZ using in vivo studies of intracranial models of GBM patient-derived xenograft (PDX) models in murine. We tested 3 models of GBM PDX cells with various TROY expression levels (GBM8-high TROY; GBM43-moderate TROY; GBM22-low/no TROY). Our intracranial PDX experiments showed that PPF treatment alone did not increase survival in all PDX cells. The combination of PPF and TMZ treatment did provide a survival benefit ($p < 0.039$) relative to TMZ alone (only in GBM8-high TROY and GBM43-moderate TROY) that was partially lost when treatment was discontinued. However, continuous PPF administration following a concomitant PPF and TMZ treatment course led to extended survival ($p < 0.0015$) compared to TMZ alone resulting in increased DNA damage (γH2AX) and apoptotic markers (Cleaved Caspase-3). Immunohistochemical analyses showed that TROY expression was decreased in tumors treated with PPF. In addition, PPF-treated tumors showed a differential myeloid population with well circumscribed tumors as compared to control-treated or TMZ-treated tumors. Thus, our data demonstrates that PPF may provide a pharmacological approach to targeting TROY concomitant with standard-of-care to increase patient survival.

#5906 A new combinatorial therapy that synergistically targets the NuRD complex and proteostasis to eradicate quiescent ovarian cancer cells.

Qi Jiang[1], Michelle Ertel[2], Santiago Panesso- Gomez[1], Sara Sannino[3], April Sagan[4], Alexander J. Cole[1], Stacy C. McGonigal[1], Betsy Ann Varghese[5], Wayne Stallaert[5], Jeffrey L. Brodsky[3], Hatice U. Osmanbeyoglu[4], Ronald J. Buckanovich[6]

[1]Department of Internal Medicine, Magee-Womens Research Inst. & Foundation, Pittsburgh, PA,[2]UPMC Magee Women's Hospital, Pittsburgh, PA,[3]Department of Biological Sciences, University of Pittsburgh, Pittsburgh, PA,[4]Department of Biomedical Informatics, University of Pittsburgh, Pittsburgh, PA,[5]Department of Computational and Systems Biology, UPMC Hillman Cancer Center, University of Pittsburgh, Pittsburgh, PA,[6]Department of Internal Medicine, Division of Gynecologic Oncology, Department of Obstetrics and Gyne, Magee-Womens Research Inst. & Foundation, UPMC Hillman Cancer Center, Pittsburgh, PA

Despite advances in immune and targeted therapies, chemotherapy remains the primary treatment for ovarian cancer (OvCa) patients. Unfortunately, most OvCa patients develop chemotherapy-resistant disease that is inevitably fatal. Quiescence is an important yet poorly understood mechanism underlying chemotherapy resistance. Therefore, we aimed to characterize quiescent ovarian cancer (qOvCa) cells to identify novel therapeutic targets to improve OvCa patient outcomes. Primary patient-derived qOvCa cells and proliferating cells were isolated using a single-cell microfluidics culture device and collected for single-cell RNA-seq. scRNA-seq of qOvCa cells identified (i) downregulation of MBD3 and CHD4, which are components of the Nucleosome Remodeling and Deacetylase (NuRD) complex, and (ii) upregulation of proteasome-associated genes. Knockdown of either MBD3 or CHD4 by shRNA, or NuRD complex pharmacologic inhibition with the HDAC inhibitors such as Vorinostat resulted in significant cell growth arrest without cell death. Standard and Fucci reporter-based cell cycle analysis further confirmed that inhibition of the NuRD complex with Vorinostat induced 94.47% cells in the G0 phase ($p<0.0001$), suggesting a dense quiescent state. Through cell cycle phase maps produced by iterative immunofluorescence of 30 core cell cycle regulators and manifold learning, we found Vorinostat-treated OvCa cells demonstrated a completely different cell cycle structure from control cells, with most of the cells in an extreme G0 phase. Bulk RNA-seq of Vorinostat-treated cells in three OvCa cell lines validated the downregulation of pathways relating to cell cycle, cell division, and DNA replication (LFC<-1, $p<0.05$), which is consistent with stem cells. Upregulation of several pathways involved in proteostasis were also noted. We therefore performed a targeted drug screen for combinatorial therapy approaches to eradicate qOvCa. We found that Vorinostat combined with the proteasome inhibitor Carfilzomib demonstrated the most profound synergistic cell death (Loewe index synergy score 23-73). Increased proteasome activity was also found in both primary and Vorinostat-induced qOvCa, suggesting the essential role of the proteasome in qOvCa. Tumor xenograft studies confirmed that Vorinostat alone can delay tumor growth ($p<0.05$) and combinatorial therapy of Vorinostat and Carfilzomib is more efficacious ($p=0.0049$). Taken together, NuRD complex inhibition induces quiescence. Combination therapy with Vorinostat to induce quiescence combined with proteasome inhibitors resulted in the profound death of therapy-resistant quiescent cells. Our work suggests this is a novel therapeutic approach to eradicate chemoresistant qOvCa cells and increase cure rates.

#5907 Pre-clinical evaluation of a novel antibody drug conjugate (ADC) LM-317 targeting NaPi2b.

W. Huang, Z. Liu, Y. Li, H. Pan, X. Qin, D. Fei, **R. Li**;
LaNova Medicines Limited, Shanghai, China

Introduction: NaPi2b is a multi-transmembrane type II sodium-dependent phosphate transporters that regulates phosphate homeostasis in normal physiological condition [1]. It is highly expressed in ovarian cancer (OC), non-small-cell lung cancer (NSCLC), and papillary thyroid cancer, with limited expression in normal tissue, making it a promising target for antibody-drug conjugates (ADCs) [2,3]. LM-317 is a novel NaPi2b targeted humanized monoclonal antibody LM-117 conjugated to the next-generation topoisomerase I inhibitor LDX2 via a cleavable linker, with antibody-drug ratio of 8. Here, we present the preclinical *in vivo and in vitro* results of LM-317.

Results: LM-317 is highly specific cross-reactive with rhesus monkeys, cynomolgus monkeys, mouse, and rat NaPi2b. Concentration-dependent cell binding and internalization effects of LM-317 were observed in human NaPi2b-expressing cells, and OC and NSCLC cells expressing NaPi2b, with EC-50 of 0.92 - 9.7 nM and 1.51 - 4.76 nM, respectively. The cytotoxicity effect of LM-317 in NaPi2b -positive tumor cells was superior to LM-117-DXD, with IC-50 of 0.002 - 0.52nM. The *in vivo* studies showed that 1 mg/kg of LM-317 almost completely eradicated tumors in the OVCAR-3 xenograft mice model of OC, and similar antitumor activity was observed in the NCI-H175-xenograft mice model of NSCLC at the dose of 3 mg/kg. Single dose of 6 mg/kg of LM-317 showed sustained tumor eradication in the NSCLC xenograft -mouse model. LM-317 also exhibited potent tumor regression in the PDX model of OC and NSCLC. The tumor growth inhibition (TGI) value was 80%-100% in OC and NSCLC PDX models with different expression degree of NaPi2b after treatment with LM-317. The antitumor activity of LM-317 in cell line- and PDX models of OC and NSLCL was comparable to those of LM-117-DXD.

Conclusion: The novel ADC LM-317 targeting NaPi2b showed robust antitumor activity *in vitro*, and in the OC and NSCLC cell line derived models and PDX models. LM-317 could potentially provide therapeutic benefit to treat NaPi2b-positive tumors including OC and NSCLC in the future.

Reference: 1.S. Banerjee et al. Cancer Treatment Reviews 112 (2023) 1024892.Finstad CL, Lloyd KO, Federici MG, et al. Clin. Cancer Res. 1997;3(8):1433-14423.Zhang et al. Tumor Biology July 2017: 1-7.

#5908 Angiosarcoma growth inhibition by targeting Doppel, a specific endothelial marker, with an antibody drug conjugate.

B. Kim[1], H. Lee[1], Y. Byun[1], Y. Ko[2], S. Kim[3];

[1]Seoul National University College of Pharmacy, Seoul, Korea, Republic of, [2]Pharosgen, Seoul, Korea, Republic of, [3]Asan Medical Center, University of Ulsan, Seoul, Korea, Republic of

Rare cancers are defined as cancers with an annual incidence rate lower than 15/100,000 by the National Cancer Institute. Despite what the terminology may suggest, rare cancers collectively are neither very rare, accounting for about a quarter of all cancers, nor less deadly than other forms of cancer. In fact, the comparative lack of research and case studies of rare cancers compared to other forms of cancer provides both an obstacle and a unique opportunity when it comes to drug development. While finding adequate animal models and cell lines to study the disease may be more difficult, the development of innovative treatment options for rare cancers is often incentivized by the Orphan Drug Act, accelerating approval from the FDA and acting as a gateway to approval for other indications. One such rare cancer is angiosarcoma, a rare cancer that originates from the endothelium. Angiosarcoma represents about 1% of total sarcomas and can develop anywhere in the body but occurs mainly in the breast, liver, or skin of the head and neck area. Angiosarcoma is characterized by a high metastasis rate of 16% to 44%, which results in a dismal prognosis, with overall survival ranging from 6 to 16 months. Considering the high reoccurrence rate and high metastatic potential of angiosarcoma, chemotherapeutic options seem to be the obvious choice. However, mainstream chemotherapies have failed to have long-term therapeutic effects. Another approach is the use of anti-angiogenic therapy, which proved effective but was unable to lead to a complete response. Herein, we describe a novel endothelial cell-targeting therapy option for the treatment of angiosarcoma. Previously, we have discovered Doppel, a 23 kDa GPI-anchored protein that is expressed specifically in the endothelium of tumor-associated blood vessels, except for the testis. Considering the fact that angiosarcoma is a rapidly growing tumor of endothelial origin, we hypothesized that Doppel might be a viable target for both the detection and treatment of angiosarcoma. We subsequently developed an antibody-drug conjugate to Doppel by conjugating a human antibody to MMAE using a unique linker, KGDEVD. When tested on xenografts of the angiosarcoma cell lines KU-CAS3 and KU-CAS5, the tumors responded extremely well to anti-Doppel ADC treatment. Most surprisingly, even tumors exceeding 1 cm^3 went into complete remission after 6 doses of the ADC. Thus, we delved deeper into the mechanism of action behind the ADC. ADC internalization was demonstrated using confocal microscopy. Apoptosis assays show that the ADC is capable of inducing apoptosis and caspase 3 expression in angiosarcoma cells, a crucial step in the activation of the KGDEVD linker. In-vitro toxicity assays of the ADC against KU-CAS3 show an IC50 value of 7.94 nM, much lower compared to normal endothelial cell lines.

#5909 Sulindac exhibits anti-proliferative effects in pre-clinical models of ovarian cancer.

N. Sinha, S. Chen, J. Haag, X. Shen, B. Deng, Z. Zhao, C. Zhou, V. Bae-Jump;
UNC Chapel Hill, Chapel Hill, NC

Objectives: Given the intricate relationship between inflammation and ovarian cancer (OC) development and progression, anti-inflammatory drugs may have potential in the prevention and treatment of OC. Sulindac exhibits potent anti-inflammatory effects through inhibition of COX1/COX2 pathways and promising anti-tumor activity in pre-clinical models of colorectal and endometrial cancer. Thus, we investigated the efficacy of sulindac as an anti-tumorigenic agent in OC pre-clinical cell and mouse models.

Methods: The human OC cell lines, MES and OVCAR5, and the K18-gT121$^{+/-}$;p53$^{fl/fl}$;Brca1$^{fl/fl}$ (KpB) mouse model of high-grade serous OC were used. Cellular proliferation was assessed by MTT and colony count assays. Apoptosis was assessed using cleaved caspase 3, 8, and 9 assays. To measure cellular stress, production of reactive oxygen species was measured by DCFH-DA assay, and the JC1 assay was used to assess changes in mitochondrial membrane potential. Cellular adhesion was evaluated by laminin assay, and cellular migration was determined by wound healing assay. Western immunoblotting was used to assess the effects of sulindac on downstream targets related to cellular stress, apoptosis, cellular invasion potential, cell cycle control, and inflammation. The KpB mice were treated with sulindac (7.5 mg/kg, oral gavage, daily) or placebo for four weeks.

Results: Sulindac inhibited cellular proliferation in a dose-dependent manner in the MES and OVCAR5 cells, with IC50s of 75.3 and 75.69 μM, respectively. Sulindac (100 μM) reduced colony formation by 81% in the MES cells and by 49% in the OVCAR5 cells ($p<0.01$). Treatment of MES and OVCAR5 cells with sulindac increased ROS production and decreased mitochondrial membrane potential, in a dose-dependent manner ($p<0.01$). Sulindac induced activity of cleaved caspase 3, 8, and 9, in MES and OVCAR5 cells ($p<0.01$). In addition, sulindac (100 μM) effectively decreased cellular adhesion by 31% in MES cells and by 23% in OVCAR5 cells ($p<0.01$). These results were confirmed by Western immunoblotting demonstrating that sulindac downregulated the anti-apoptotic proteins Bcl-xl and Mcl-1 and upregulated the pro-apoptotic proteins Bax and cellular stress proteins Bip, ATF-4, and PDI, in both cell lines. Sulindac downregulated expression of several epithelial-mesenchymal transition proteins in both cell lines, including beta-catenin, snail, and slug. Sulindac also downregulated expression of cell cycle proteins CDK4, CDK5, and Cyclin D1 and inflammatory protein COX-2 in both cell lines. After 4 wks of treatment, sulindac significantly inhibited tumor growth by 71% (1.89 g vs 0.54 g, $p<0.01$) in KpB mice.

Conclusions: Our results find that sulindac exhibited anti-tumorigenic effects in OC cell lines and the KpB OC mouse model. Given these promising pre-clinical results, further studies on the repurposing of sulindac for the prevention and treatment of OC is warranted.

#5910 Developing a novel humanized anti-FABP4 antibody for breast cancer treatment.

J. Hao, M. Yorek, J. Yu, A. Avellino, B. Li;
University of Iowa, Iowa City, IA

Circulating levels of adipocyte fatty acid binding protein (A-FABP, also known as FABP4) are linked with metabolic dysregulation. Our previous study demonstrated that high serum levels of FABP4 increased the risk of breast cancer, indicating that circulating FABP4 could be a potential therapeutic target for this disease. In this study, we generated mouse monoclonal antibodies (mAb) against FABP4 by immunizing C57BL/6 mice with recombinant human FABP4. After screening over 1300 hybridoma clones, we identified an FABP4 neutralizing mAb, named 12G2, which inhibited breast cancer growth in various mouse models. To facilitate clinical application, we engineered chimeric and humanized variants of the 12G2 mAb. Notably, the humanized variant, 12G2-variant 9 (12G2-vt9), effectively inhibited mammary tumor growth and progression by reducing the activity of FABP4/ALDH1 in different breast cancer mouse models. Our findings suggest that 12G2-Vt9 is a promising neutralizing mAb targeting FABP4-mediated cancer stemness through ALDH1 signaling, offering potential as a targeted therapeutic antibody for the clinical treatment of breast cancer.

#5911 *In vivo* efficacy of a novel peptide-conjugated drug in patient-derived xenograft models of breast cancer.

M. J. Elliott[1], M. Mcguire[1], J. Silvester[1], C. Tobin[1], S. El Ghamrasni[1], F. Lui[2], A. Zhai[2], O. Yoluk[2], A. Broom[2], T. Stone[2], G. Butterfoss[2], S. Popa[2], T. Lu[2], C. Ing[2], D. White[2], D. W. Cescon[1];

[1]UHN Princess Margaret Cancer Centre, Toronto, ON, Canada, [2]ProteinQure, Toronto, ON, Canada

Introduction: Antibody and peptide-conjugated drugs are rapidly entering the clinic for the treatment of patients with early and advanced breast cancer. These drugs are designed to achieve more targeted delivery of cytotoxic agents to tumor cells with robust clinical activity. ARB-1-6, a sortilin (*SORT1*) targeted peptide conjugated to the cytotoxic agent MMAE, has demonstrated pre-clinical activity and tolerability in cell line xenografts of breast cancer. To further characterize its spectrum of antitumor activity and biomarker correlates we evaluated ARB-1-6 in a collection of clinically and genomically annotated breast cancer patient-derived xenografts (PDX).

Methods: Breast cancer PDX models were generated and propagated under IRB approved protocols [14-8358]. ARB-1-6 was dosed in tumor-bearing SCID mice by tail vein injection at 3 mg/kg weekly x 4 doses. Tumor volume was measured twice weekly until day 35 or until models reached humane endpoints, after which tumors were collected. Animals were weighed regularly and assessed for treatment-related toxicity.

Results: 7 models (5 TN and 2 HR) have completed efficacy assessment to date. 3/7 models were derived from treatment naïve patients while 4/7 were derived from pre-treated patients (Table 1). Complete response (mRECIST) was seen in 5/7 (71.4%) models with stable disease occurring in 2/7 (28.6%). ARB-1-6 was well tolerated with no weight loss observed. Complete tumor regression was seen in a PDX derived from a patient with clinical resistance to a TROP2 antibody drug conjugate (ADC). Antitumor activity was observed in models with low *SORT1* RNA expression; SORT1 IHC and other correlatives studies are underway.

Conclusion: ARB-1-6 demonstrates substantial preclinical activity in PDX models at doses that are well tolerated in mice. Treatment of additional models is ongoing. Full results and correlative analyses including relationships between antitumor activity and target protein expression will be presented.

PDX Model Characteristics and Patient Treatment

PDX	Subtype	Pt. Treatment
1	TN	AC-T
2	TN	FEC-D, Gem+Carbo
3	TN	AC-T
4	TN	No
5	TN	No
6	HR	No
7	HR	TC, ET, Cape, Gem+Cis, TROP2-ADC

#5912 Rational design of a small-molecule inhibitor targeting the allosteric site of sos1 in oncogenic k-ras pancreatic cancer.

X. Duan, C. Evelyn, J. Biesiada, J. Johnson, W. Seibel, J. Meller, Y. Zheng;
Cincinnati Children's Hospital Medical Center, Cincinnati, OH

Oncogenic Kras signaling is a key therapeutic target in human cancers. Ras activation is catalyzed by guanine nucleotide exchange factors (GEFs), of which SOS1 is a major player that transduces receptor tyrosine kinase signaling to Ras. In addition to recently devised oncogenic Kras targeting small molecule inhibitors, disrupting the catalytic interaction between Ras and SOS1 has emerged as an attractive therapeutic strategy in working synergistically with Kras inhibitors and overcoming resistance. Previous studies have demonstrated an active “feed forward” loop of active Kras binding to the allosteric site of SOS1 that further stimulates SOS1 catalytic activation of wild type H/N/Kras, which is required for oncogenic Kras driven tumorigenesis. Here we have developed a rational approach that combines virtual screening with experimental screening to identify small molecule inhibitors that target the allosteric site of SOS1 to suppress oncogenic Kras mediated SOS1-regulated wild-type Ras activities. Unlike SOS1 catalytic site inhibitors which can have significant toxicity due to their ability to inhibit normal Ras signaling function, the lead SOS1 allosteric inhibitors developed in our laboratory binds to the allosteric site of SOS1 and blocks active Ras interaction with SOS1: we found these inhibitors can competitively suppresses SOS1-Ras interaction at the SOS1 allosteric site and dose-dependently inhibits the feed-forward SOS1 GEF activity. Mutagenesis and structure-activity relationship studies mapped the site of action to the SOS1 allosteric site, and preliminarily defined the chemical moieties in the inhibitor essential for the activity. The inhibitor showed dose-dependent and selective efficacy in inhibiting WT Ras activity, downstream signaling activities, and associated cell proliferation in KRAS mutation cells but not KRAS wild-type cells. Compared to the SOS1 catalytic inhibitor, BI3406, our inhibitors showed better selectivity for KRAS mutant pancreatic cancer cells vs. WT KRAS cells. These studies establish a proof of principle for the rational design of small molecule inhibitors targeting an oncogenic Kras specific allosteric site of SOS1 and provide a novel therapeutic concept to target KRAS-driven tumors more effectively.

#5913 TEAD1/4 inhibitors exhibit deeper biological impact and broader activity compared to TEAD1-only inhibitors in both monotherapy and combination without additional kidney toxicity.

F. Muller, S. Kunnimalaiyaan, P. Mangrolia, J. Olson;
Sporos Bioventures, LLC, Houston, TX

The TEAD transcription factors in association with the YAP/TAZ co-activators drive the expression of pro-proliferative and pro-oncogenic genes that underlies the transformed phenotype of many carcinomas. In addition, YAP-TEAD transcriptional activity is emerging as a major resistance mechanism for diverse precision oncology drugs, with the most extensive data for resistance to drugs targeting the MAPK pathway. There is a strong interest in generating inhibitors of YAP/TEAD transcriptional activity with TEAD palmitic acid site inhibitors having demonstrated encouraging pre-clinical activity and now clinical activity with confirmed objective responses with the TEAD1/2/3 inhibitor VT3989. However, the TEAD1-preferential inhibitor IK930 did not yield any objective responses but also showed a more favorable safety profile especially with respect to proteinuria. These contrasting clinical read-outs provide a good lead-in to a critical design challenge/question of TEAD palmitic acid site inhibitors: the optimization of inhibitory profile against the respective four TEAD paralogs (TEAD1-4). In depth bioinformatic analyses led Sporos investigators to conclude that while TEAD1 inhibition was a minimum requirement for anti-neoplastic activity, inhibition of other paralogs would be necessary for maximizing biological impact and a TEAD1/4 inhibitor would provide the best balance of anti-neoplastic activity and toxicity. Activity against TEAD2 was identified as counter-productive associated with a context-specific paradoxical stimulation of cell proliferation and tumor growth while activity against TEAD3 was flagged as a major driver of podocyte effacement and kidney toxicity. Here, we provide novel corroborating data supporting this selection of inhibitory profile. We provide an update on the pre-clinical efficacy and toxicology of SPR1, Sporos's TEAD1/4 preferential inhibitor which favorably contrasts with other TEAD inhibitors such as the TEAD1/3/4 inhibitor VT3989 and the TEAD1 inhibitor VT103 and IK930 in both the monotherapy and combination setting. We show that 1) SPR1 displays broader and deeper cell-based activity and extends the utility of TEAD inhibitors outside of mesothelioma and NF2 mutants 2) SPR1 shows stronger activity than TEAD1-only inhibitors in combination with MAPK and EGFR inhibitors in vitro and in vivo 3) SPR1 does not cause proteinuria in mice; dogs or rats even above therapeutic doses 4) SPR1 does not show the context-specific stimulation of tumor growth in Lung PDX previously observed with VT3989 and other inhibitors that include TEAD2 in their profile. Taken together - the data suggests SPR1 is positioned to become a best-in-class TEAD palmitic acid site inhibitor with broad utility in both monotherapy and combination setting.

#5914 Non-muscle myosin IIA as a promising therapeutic target in breast cancer.

Wasim Feroz, Rosalin Mishra, Mary Kate Kilroy, Joan T. Garrett

Pharmaceutical Sciences, University of Cincinnati, Cincinnati, OH

We aimed to determine the role of non-muscle myosin IIA (NMIIA) in breast cancer using various cancer cell lines including estrogen receptor (ER)+, HER2+ and triple negative breast cancers (TNBC). Myosin heavy chain 9 (*MYH9*) gene encodes for the heavy chain of the hexameric protein NMIIA. We have recently identified that NMIIA serves as a binding partner for HER3 following the inhibition of the HER family member compared to the vehicle control treatment, as observed in HER3 immunoprecipitates. We checked the basal protein and mRNA levels of NMIIA in different breast cancer cell lines and found higher levels of NMIIA in both HER2+ and TNBC cell lines compared to ER+ cell lines. These data correlate with clinical data of primary breast cancer patients with high *MYH9* being less likely in ER+ breast cancer patients and more likely in the PAM50 subtypes basal and HER2 enriched breast cancer patients. By employing a pool of four siRNA targeting *MYH9*, our data indicated a reduction in proliferation of HER2+ and TNBC cell lines when compared to the control siRNA. We have previously found that loss of *MYH9* sensitizes to the HER family inhibitor neratinib treatment as assessed by cell proliferation, colony formation on matrigel, cell migration and invasion. We aimed to determine if pharmacological inhibition of the NMIIA pathway would sensitize to neratinib. RhoA-associated kinase (ROCK) serves as a master regulator of NMIIA activity as it directly phosphorylates the regulatory light chain (RLC) of NMIIA. Pharmacological inhibition of ROCK-NMIIA pathway using the ROCK inhibitor GSK269962A alone or in combination with neratinib reduced the cell proliferation in HER2+ cell lines BT474 and MDA-MB-453 as indicated by MTT and cell proliferation assay. It is well known that HER2-targeted therapies cause the upregulation of HER3. Given our identification of NMIIA as one of the interacting partners of HER3, our focus will be on investigating the NMIIA-HER3 signaling axis to elucidate its contribution to an adaptive response to HER2 inhibition and potential treatment resistance. Furthermore, we will explore strategies to target NMIIA in breast cancer.

#5915 ADT-1004: A promising pan-RAS inhibitor for targeting KRAS mutations in pancreatic ductal adenocarcinoma.

D. Bandi[1], P. Ganji[1], S. Sarvesh[1], Y. Maxuitenko[2], J. Foote[1], A. Keeton[2], X. Chen[2], D. Buchsbaum[1], G. Piazza[2], B. El-Rayes[1];
[1]University of Alabama at Birmingham, Birmingham, AL, [2]Auburn University, Auburn, AL

Background/Objective: Pancreatic ductal adenocarcinoma (PDAC) is a highly challenging cancer with a dismal 5-year survival rate of under 12%. More than 90% of PDAC cases involve mutations in the GTPase KRAS. Unfortunately, existing drugs targeting the RAS family, like sotorasib, exclusively address the KRAS-G12C mutation, mainly found in NSCLC. In PDAC, most patients are diagnosed at advanced stages with unresectable tumors that exhibit various genetic mutations. Approximately 70% of these cases have KRAS-G12D mutations, often co-occurring with KRAS-G12V, KRAS-G12C, and KRAS-G12R mutations. This highlights the urgent need for innovative treatments that effectively address the complex mutation landscape in PDAC and avoid resistance mechanisms associated with mutant-specific or pan-KRAS inhibitors.

Methods: KPC-Luc (1×10^5) and 2838C3-Luc (1.5×10^5) PDAC cells carrying the KRAS-G12D mutation were injected into the pancreas of C57BL/6J mice. After one week, the mice were randomly divided into treatment groups (n = 7 per group) and received oral ADT-1004 at a dose of 40mg/kg body weight five times a week for four weeks. Tumor burden was assessed by bioluminescence signals using the IVIS Xenogen imaging system for patient-derived xenografts from PDAC patients with the KRAS-G12V mutation who were subcutaneously implanted in NSG mice. A week later, mice were randomized (n=7 per group) and treated orally with 40mg/kg of ADT-1004 five times a week for six weeks. Body weight and tumor size were measured twice weekly.

Results: ADT-1004, a prodrug of ADT-007 that exhibits potent inhibitory effects on the proliferation of both human and murine RAS mutant PDAC cell lines with single-digit nM IC_{50} values, compared with μM IC_{50} in PDAC cells with WT RAS, was well tolerated in mice at a dose up to 175 mg/kg bid orally with sustained plasma levels of ADT-007 that exceeded IC_{50} values by 50-fold and even higher concentrations in pancreatic tumors. When administered orally at 40mg/kg body weight, ADT-1004 resulted in substantial growth inhibition of the KRAS-G12D and KRAS-G12V tumors, leading to profound tumor regression without any accompanying loss in body weight. ADT-1004 also displayed a significant inhibitory effect on ERK phosphorylation. Notably, this inhibition is effective regardless of the specific RAS mutational codon or isozyme, as it specifically targets activated RAS and disrupts downstream KRAS signaling pathways.

Conclusion: These results highlight the promise of ADT-1004 as a potential breakthrough for treating PDAC. This novel pan-RAS inhibitor demonstrates potent inhibition of PDAC growth, irrespective of the specific KRAS mutation. Furthermore, it shows an excellent safety profile, with profound tumor regression and no impact on body weight in animal models. These findings open new possibilities for addressing the complex genetic landscape of PDAC.

EXPERIMENTAL AND MOLECULAR THERAPEUTICS: Novel Antitumor Agents 4
Poster Session

#5920 Inhibition of TBL1 and β-catenin interaction sensitizes acute lymphoblastic leukemia to chemotherapy.

S. Hurwitz[1], R. Friedmann[1], T. Fourfouris[1], K. Lee[1], Z. Wan[1], C. Parekh[1], F. Navid[1], D. Bhojwani[1], K. Holloway[2], Y.-M. Kim[1];
[1]Children's Hospital Los Angeles, Los Angeles, CA, [2]Iterion Therapeutic, Houston, TX

BACKGROUND: Relapse of T-cell acute lymphoblastic leukemia (T-ALL) and B-cell acute lymphoblastic leukemia (B-ALL) post-chemotherapy or post-immunotherapy remains a therapeutic problem warranting novel therapeutic approaches. Aberrant Wnt pathway activation is a common feature in ALL as Wnt activation through β-catenin is involved in self- renewal of drug resistant leukemia cells. A therapeutical approach to target Wnt signaling in T-ALL and B-ALL remains elusive. Here, we focus on the effect of transducin β-like protein 1 (TBL1) inhibitor tegavivint in combination with chemotherapy in T-ALL and B-ALL. We hypothesize that interrupting the binding of TBL1 to β-catenin abrogates leukemia cell survival and test if tegavivint sensitizes these cells to chemotherapeutic agents such as VDL (Vincristine, Dexamethasone, L-asparaginase) as part of preclinical evaluation of tegavivint in T- and B-cell ALL.
METHODS: Four T-ALL cell lines one patient-derived T-ALL case, B-ALL cell lines and eight patient-derived B-ALL cases were used in vitro. We performed cytotoxicity studies using Annexin V/7AAD stainings and flow cytometry or Trypanblue counts to exclude dead cells, western blots, and co-immunoprecipitation assays to investigate effects of TBL-1 inhibition using tegavivint on β-catenin-mediated signaling. Tegavivint was injected intraperitoneally along with chemotherapeutic drugs.
RESULTS: β-catenin and TBL1 were uniformly expressed in all T-ALL and B-ALL cells as determined by western blotting, albeit at different levels. Tegavivint decreases β-catenin protein expression as seen through western blot as well as decreases the binding of TBL1 to β-catenin as seen through co-immunoprecipitation (co-IP) in both the T-ALL and B-ALL samples. We also determined that tegavivint as a monotherapy induced apoptosis in both cell lines and patient samples at as little of a dose of 5nM after 24 hours of incubation using Annexin-V/DAPI staining by flow cytometry. We observed that tegavivint can sensitize all cases to chemotherapy (V: Vincristine, D: Dexamethasone, L:L-Asparaginase or Peg-Asparaginase) within 24 hours of incubation. Lastly, in vivo evaluation of tegavivint showed that tegavivint alone and in combination with VD chemotherapy significantly extends survival of NSG mice engrafted with patient-derived T-ALL and B-ALL compared to control treated mice.
CONCLUSION: Our preliminary data shows that T-ALL and B-ALL are sensitive to TBL1-β-catenin inhibition using tegavivint as a monotherapy. Tegavivint can also sensitize T-ALL and B-ALL to chemotherapy (VDL). As our data supports our hypothesis that TBL-1-β-catenin inhibition is a new target in ALL therapy, further studies are in progress to preclinically evaluate this approach for clinical care.

#5921 PH027-1, a potent and selective small-molecule WRN inhibitor that targets MSI-H tumors.

F. Gao[1], B. Liu[1], L. Jing[2], J. Wang[1], Y. Wu[2], J. Wan[1], P. Zhang[1], Y. Gao[1], Z. Li[3], Y. Guo[1];
[1]Puhe Biopharma, Beijing, China, [2]Gongkang Bio, Suzhou, China, [3]Shiyu Children Foundation, Beijing, China

Background: High microsatellite instability (MSI-H) is highly prevalent across many cancer types including endometrium, gastric, ovary and colorectal cancer. It is well known that there is a clear synthetic lethality (SL) interaction between MSI-H and Werner syndrome protein (WRN) inhibition. WRN is a member of RecQ helicase family and involved in the maintenance of genome integrity. Different from other RecQ family members, WRN has two activity centers responsible for helicase and exonuclease activity, respectively. Further studies confirmed that an inhibition on helicase activity, but not exonuclease activity, is responsible for SL interaction with MSI-H. Also, Recent clinical observations supported that though loss-of-function of WRN could cause an early-aged disease Werner syndrome, selective loss of helicase but not exonuclease leads to only mild to moderate symptoms, suggesting a selective inhibitor of helicase activity has the potential to induce the SL interaction with MSI-H and keep patients safe.
Methods: Biochemical assays and cell-based assays were performed to evaluate *in vitro* activity and selectivity of PH027-1. The *in vivo* anti-tumor efficacy was tested in two cell-derived xenograft (CDX) mouse models with tumors harboring MSI-H. The *in vivo* pharmacokinetics (PK) properties were evaluated in mice, rats and dogs, and other *in vitro* and *in vivo* PK and safety properties were assessed with corresponding assay methods.
Results: Biochemical assays showed that PH027-1 potently inhibited helicase activity of WRN (IC50, 0.8 nM), but had no effect on other RecQ family members even at the highest tested concentration of 10 μM (IC50, all≥10 μM for BLM, RecQ4 and RecQ5). At the same time, PH027-1 did not affect the exonuclease activity of WRN at all tested concentrations. In cell-based assays, PH027-1 potently inhibited cell viability of MSI-H cancer cells SW48 and HCT116 at tens of nM, but had no effect on MSS cells (HT29 cancer cells and CD34+ hematopoietic stem cells) even at 10 μM. The tests were further expanded to 18 cancer cell lines covering uterus, gastric, ovary and colorectal cancer. Nine of twelve MSI-H cell lines were very sensitive to WRN inhibition, and all six MSS cell lines were totally resistant to the treatment. PH027-1 possessed excellent PK profiles as shown by *in vivo* PK studies, with absolute bioavailability of 58%~102% in mice, rats and dogs. In two CDX models (SW48 and HCT116), oral administration of PH027-1 dose-dependently inhibited tumor growth, and a nearly complete inhibition was observed at a dose of 20 mg/kg QD. Tumor regression was clearly shown at higher doses. All other *in vitro* and *in vivo* PK and safety tests showed favorable results and supported for preclinical development of PH027-1.
Conclusion: As a highly selective and potent inhibitor on helicase activity of WRN, PH027-1 has the potential to become a novel and safe approach for treatment of MSI-H tumors.

#5922 Characterization of the biological effects of a quadruplex-interacting molecule in dedifferentiated liposarcoma cells.

Eisa Naghshineh[1], Beatrice Tosoni[2], Lorenzo Di Pietro[1], Sandro Pasquali[1], Nadia Zaffaroni[1], Stephen Neidle[3], Sara N. Richter[2], Marco Folini[1]

[1]Department of Experimental Oncology, Fondazione IRCCS Istituto Nazionale dei Tumori, Milan, Italy, [2]Department of Molecular Medicine, University of Padova, Padova, Italy, [3]UCL School of Pharmacy, University College London, London, United Kingdom

G-rich nucleic acid sequences can assume, under physiologic conditions, non-B secondary structures called G-quadruplexes (G4). The human genome contains thousands of putative quadruplex forming sequences (PQS), of which telomeres are the most extensively studied. PQS are frequently found in the promoters of oncogenes and transcription factors rather than in tumor suppressor or housekeeping genes, indicating an evolutionary selection of these elements based on gene function and suggesting a pivotal role of G4 in the regulation of gene expression. These observations have provided the rationale to explore G4 targeting as a therapeutic approach in cancer. Several small molecules have been indeed designed and characterized as G4-ligands (G4-L), most of them showing a "multiple-target" binding modality. Dedifferentiated liposarcoma (DDLPS) is a non-lipogenic disease characterized by aggressive local growth and multifocal local recurrences and the ability to elicit distant metastases. At the molecular level, DDLPS is marked by the amplification of the 12q13-q15 chromosomal region, leading to the abnormal expression of the *MDM2* oncogene. The gene has emerged as an actionable therapeutic target and, recently, PQS within its promoter have been reported to fold into G4 structures. In addition, in our previous study, we observed that pathways related to telomere maintenance are remarkably up-modulated in DDLPS. These findings open a new avenue to explore the therapeutic potential of G4-L in this malignancy. In the present study, the biological activity of a tetra-substituted naphthalene diimide (NDI) G4-L derivative (SOP1812/QN-302) has been characterized in two patient-derived DDLPS cell lines. In particular, the exposure of DDLPS cells to increasing concentrations of SOP1812 resulted in a marked cytotoxic activity *in vitro*, with IC50 values within the sub-micromolar range (~0.3 μM). Moreover, DDLPS cells treated with equitoxic amounts of the compound were characterized by an 80-90% inhibition of telomerase activity and a remarkable perturbation in the MDM2-p53 feedback loop, leading to a pronounced accumulation of basal and phosphorylated (S15/S46/S392) p53 protein. These effects were paralleled by a 3-4 time increase in the number of γ-H2AX foci, the appearance of the cleaved form of PARP-1 and a pronounced inhibition of cell growth over time. Altogether, our findings indicate that targeting G4 structures by quadruplex-interacting molecules may represent a potential novel and effective therapeutic strategy in DDLPS.

#5923 Innovative cyclic peptide disrupts IL-17RB/MLK4 Interaction for targeted pancreatic cancer therapy.

Y.-C. Lo, Y. Ko, C. Huang, J. Lee, D. Wu, Y. Wu, H. Yu, **C.-M. Hu**;
Academia Sinica - Genomics Research Center, Taipei, Taiwan

Interleukin-17B (IL-17B) and its receptor IL-17RB drive oncogenic signaling in pancreatic cancer by interacting with mixed-lineage kinase 4 (MLK4) and phosphorylating IL-17RB's tyrosine-447 site. Our study highlights a therapeutic peptide (amino acids 403-416 of IL-17RB) that disrupts MLK4 binding. Improving its efficacy, we transformed the linear peptide into a disulfide-bonded cyclic form, exhibiting enhanced uptake and stability. The modified cyclic peptide outperformed the linear counterpart, effectively inhibiting the growth and metastasis of PDAC tumor cells in vitro and in a mouse model. Molecularly, we identified the critical role of cysteine (C) residue C408 in IL-17RB, mediating interaction with arginine (R)216 in MLK4's kinase domain. This interaction is pivotal for the cyclic peptide's efficacy. Additionally, lysine (K) residue K410 in IL-17RB maintains the cyclic peptide's structural integrity. These findings provide a comprehensive molecular understanding of IL-17RB and MLK4 interaction, offering innovative strategies for designing therapeutic molecules against pancreatic cancer.

#5924 RNAi mediated inhibition of beta-catenin demonstrates anti-tumor efficacy and immune microenvironment modulation in preclinical hepatocellular carcinoma models.

T. Dadali[1], S. Miller[1], G. Saawant[1], S. Abbott[1], M. Yu[1], S. Morskaya[1], B. Lehrich[2], S. Monga[2], G. Lau[1], M. Maier[1], W. Broom[1];
[1]Alnylam Pharmaceuticals, Inc., Cambridge, MA, [2]University of Pittsburgh, Pittsburgh, PA

Hepatocellular carcinoma (HCC) is the fifth most common solid tumor worldwide, and the third most common cause of cancer-related deaths. For the 40% to 50% of HCC patients who are candidates for systemic therapies, the landscape has evolved significantly in the last 10 years, with most recently, immunotherapies such as combination of atezolizumab and bevacizumab emerging as the current first-line systemic therapy for patients with intermediate or advanced disease. However, there are no predictive biomarkers for patients with HCC to enable selection of those most likely to benefit from these therapies and this remains a disease with high unmet medical need. Activation of the WNT pathway via mutational events or indirect pathway activation is implicated in many cancers including up to 50% of HCC patient tumors. High expression of beta-catenin, encoded by the CTNNB1 gene, has been shown to correlate with decreased survival and more rapid disease progression in HCC patients. In addition, WNT/beta-catenin pathway activation has been shown to result in immune exclusion and resistance to immunotherapy in HCC. ALN-BCAT comprises a chemically modified siRNA encapsulated in a lipid nanoparticle formulation which generates robust and highly specific reductions of *CTNNB1* mRNA, downstream biomarkers and tumor cell proliferation in *in vitro* model systems. Anti-tumor activity has been demonstrated in multiple *in vivo* orthotopic HCC mouse models, in both early and late treatment settings as measured by liver to body weight ratio. Reductions in tumor burden were orthogonally confirmed by histology analysis and shown to be associated with changes in CTNNB1-related biomarkers. Finally, ALN-BCAT treatment results in changes in the tumor microenvironment in a mouse syngeneic HCC model, with increases in CD4+ and CD8+ T cells and reductions in M2 macrophages, consistent with a shift to a more immune stimulatory anti-tumor microenvironment. Here, we demonstrate that ALN-BCAT provides a novel approach to the inhibition of the WNT pathway as a therapeutic approach for treatment of HCC patients and WNT pathway activated tumors.

#5925 Safety, efficacy, pharmacokinetics, and pharmacodynamics of a second generation Irofulven analog CAP-0121 in preclinical cancer models.

R. T. Suhandynata[1], T. K. Nguyen[1], V. R. Kotamraju[2], J. D. Momper[1], M. J. Kelner[1];
[1]UC San Diego, La Jolla, CA, [2]Califia Pharma, San Diego, CA

Background: Irofulven is a semisynthetic sesquiterpene anticancer agent initially investigated for its unique mechanism of action and potential to overcome resistance observed in other chemotherapeutics. This study investigates the pharmacokinetics and pharmacodynamics of a second generation irofulven analog, CAP-121 (Califia Pharma), and its efficacy and safety in preclinical cancer models relative to irofulven.
Methods: 24-hour comprehensive PK was performed at two different intravenous (IV) doses in canines for irofulven (0.2 mg/kg and 1 mg/kg; MTD) and CAP-121 (1 mg/kg and 3 mg/kg). Plasma concentrations were measured by ultra-high performance liquid chromatography multiple reaction monitoring mass spectrometry. PK parameters were determined for both compounds using noncompartmental methods (Phoenix WinNonlin, version 8.4). PK parameters included area under the concentration vs time curve (AUC), maximum observed concentration (C_{max}), clearance (CL), volume of distribution (Vd), and elimination half-life ($t_{1/2}$). Canine platelet and neutrophil counts were measured across 28 days to ascertain the maximum tolerated dose (MTD); platelet count reversibility was also assessed. Mice xenograft models implanted with a drug resistant human ovarian cancer (A2870), or a drug-resistant human metastatic lung cancer (MV522), were dosed with irofulven (9 mg/kg; MTD) and CAP-121 (15, 20, and 25 mg/kg) and resulting tumor mass, % change in body weight, and platelet counts were compared relative to vehicle only.
Results: Systemic exposure, CL, Vd, and $t_{1/2}$ were similar between irofulven and CAP-121 at a 1 mg/kg IV dose. For irofulven, exposure increased approximately proportionally at doses of 0.2 mg/kg and 1 mg/kg. For CAP-121, exposure increased less than proportionally at doses of 1 mg/kg and 3 mg/kg. MTD of CAP-121 was found to be 3-fold higher in canines compared to irofulven as 3-fold more CAP-121 was required to match the platelet reduction with irofulven; platelet nadir was rapidly reversible for CAP-121. Canine nadir platelets were 3-fold higher for CAP-121 vs irofulven at the same dose (1 mg/kg). CAP-121 was superior to irofulven ($p < 0.02$) with regards to final tumor weights in mice xenograft models, even though MTD was not reached for CAP-121; a change in body weight and platelet loss was not observed for CAP-121 at up 25 mg/kg in mice.
Conclusion: The canine PK/PD study of CAP-121 demonstrates that CAP-121 has favorable PK parameters. With regards to *in vivo* anticancer cytotoxic activity, the two drug-resistant xenograft models confirm the superiority of CAP-121 over irofulven. Together, these findings indicate a wider therapeutic window in humans is expected for CAP-121 compared to irofulven, emphasizing the potential anticancer utility of CAP-121 for solid cancers without prolonged thrombocytopenia. Further investigation in clinical trials is warranted

#5926 YB-1 inhibition as an effective approach for the treatment of osteosarcoma.

K. Stefan[1], A. Dheeraj[1], D. Tailor[1], L. E. Davis[2], S. V. Malhotra[1];
[1]Knight Cancer Institute, Oregon Health & Science University, Portland, OR, [2]School of Medicine, Oregon Health & Science University, Portland, OR

Background: Osteosarcoma (OS) is a bone cancer primarily affecting adolescents and young adults, with about 20% of patients having detectable metastatic disease at the time of diagnosis. Despite a large number of clinical trial efforts, metastatic sarcoma remains a lethal disease, and there have been no meaningful advances in therapy or improvements in patient outcomes for decades. Y-box binding protein 1 (YB-1) is a multifunctional cold-shock protein that translationally activates diverse stress response factors with pro-metastatic activities in many cancer types. Importantly, YB-1 is strongly associated with poor outcomes in sarcoma patients and is a major metastatic driver in high-risk sarcomas.
Methods: We recently described a novel compound, CET056, that inhibits cancer progression via YB-1 inhibition. We hypothesized that CET056 had the potential to suppress the progression of OS and could provide a new treatment for this disease. We screened osteosarcoma human and mouse cell lines for YB-1 protein expression. OS cells were functionally characterized for responses to CET056 *in vitro* and *in vivo*.
Results: YB-1 expression was seen in nearly all cell lines tested. CET056 treatment of OS cells resulted in reduced cell viability and YB-1 protein expression in a dose- and time- dependent manner, as well as reduced formation of colonies and spheroids. *In vivo* efficacy studies, which employed a syngeneic subcutaneous tumor model, revealed that CET056 effectively inhibited tumor progression and enhanced overall survival in contrast to vehicle treated control mice.
Conclusion: These results support our hypothesis and illustrate that YB-1 inhibition by CET056 is a promising candidate for further development as a therapy for OS.

#5927 ACBP/DBI inhibition suppresses NASH-induced hepatocarcinogenesis.

S. Li[1], O. Motino[2], F. Lambertucci[2], M. C. Maiuri[2], I. Martins[2], G. Kroemer[2];

[1]Faculte de Medecine, Universite de Paris Saclay, Kremlin Bicetre, Centre de Recherche des Cordeliers UMRS1138, Inserm, Universite Paris Cite, Sorbonne Universite, Paris, France, [2]Centre de Recherche des Cordeliers UMRS1138, Inserm, Universite Paris Cite, Sorbonne Universite, Paris, France

Background: Non-alcoholic fatty liver disease (NAFLD) or its severe form non-alcoholic steatohepatitis (NASH) is becoming an ever more prevalent risk factor of hepatocellular carcinoma (HCC). Currently, there are no approved drugs for the treatment of NASH. Extracellular ACBP/DBI (Acyl coenzyme A binding protein, also called diazepam-binding inhibitor) acts as an autophagy checkpoint and neutralization of ACBP/DBI prevents NASH. Therefore, we investigated the functional roles, mechanisms, and clinical relevance of ACBP/DBI in HCC.

Methods: ACBP/DBI was blocked by four strategies: an inducible Acbp/Dbi knockout ($Acbp^{-/-}$, control: $Acbp^{+/+}$), a constitutive $Gabrg2^{F77I}$ mutation that prevents binding of ACBP/DBI to the receptor (control: WT), induction of ACBP/DBI-specific autoantibodies (induced by KLH-DBI, control: KLH), and monoclonal anti-DBI antibody (control: isotype). Three different types of HCC mouse models, including toxins/diet-based NASH-induced models (western diet plus CCl_4), hydrodynamic transfection of oncogenes (Myc+Ctnnb1), and orthotopic transplantation (Hep55.1C) were used in combination with the aforementioned ACBP/DBI inhibition strategies to determine the association of ACBP/DBI and HCC.

Results: ACBP/DBI inhibition attenuates tumorigenesis in mice with NASH, blunts oncogene induced HCC, and reduces the growth of orthotopically transplanted cancers. Mechanistically, ACBP/DBI inhibition retards cell cycle, suppresses cell proliferation, and favors ferroptosis, as determined by RNA-seq data and mass spectrometric metabolomics. CCK-8 proliferation, colony formation, and cell cycle assays performed on Huh-7, HepG2 and Hep55.1C cells demonstrated that ACBP/DBI knockdown reduced cell proliferation and induced G0/G1 arrest. IHC detection of Ki67 and PCNA in liver sections revealed antiproliferative effects of ACBP/DBI inhibition. qRT-PCR demonstrated the ACBP/DBI inhibition-induced upregulation of cell cycle inhibitor genes and downregulation of genes invoded in G0/G1 phase in liver tissues. qRT-PCR and immunoblot confirmed the upregulation of pro-ferroptotic and the downregulation of anti-ferroptotic genes and proteins in liver tissues upon ACBP/DBI inhibition. Primary HCC cell lines from $Acbp^{+/+}$ and $Acbp^{-/-}$ mice further confirmed the pro-ferroptotic effects of ACBP/DBI inhibition obtained in liver tissues. $Acbp^{-/-}$ cell lines were more sensitivity to RSL3-induced ferroptosis.

Conclusion: ACBP/DBI inhibition constitutes a potential strategy for treating NASH and NASH-induced HCC.

#5928 Structure-activity relationships for the pan-quadruplex experimental drug QN-302 and two analogs probed with comparative transcriptome profiling and molecular modeling.

Ahmed A. Ahmed[1], Shozeb Haider[1], Tariq Arshad[2], **Stephen Neidle**[1]

[1]School of Pharmacy, University College London (UCL), London, United Kingdom,[2]Qualigen Therapeutics Inc, Carlsbad, CA

The tetrasubstituted naphthalene diimide compound QN-302 binds to G-quadruplex DNA structures. It inhibits the transcription of cancer-related genes in pancreatic ductal adenocarcinoma (PDAC) cells, shows high potency in PDAC cells in vitro and in PDAC animal models. It is currently in Phase 1 clinical evaluation as an anticancer drug for advanced, metastatic solid tumors. A study of structure-activity relationships of QN-302 and two related analogs (CM03 and SOP1247) is reported here. These have been probed using comparisons of transcriptional profiles from whole-genome RNA-seq analyses, together with qualitative molecular modelling. Compounds CM03 and SOP1247 differ by the presence of a methoxy substituent in the former: these two have closely similar transcriptional profiles, whereas that of QN-302, although showing effects in the same cancer-related pathways, highlights the down regulation of distinct genes, for example in the hedgehog pathway. The distinct pattern of genes affected by QN-302 is hypothesized to contribute to its superior potency compared to CM03 and SOP1247. Its superior ability to stabilize quadruplex structures has been attributed to its benzyl-pyrrolidine substituent fitting into and filling most of the space in a quadruplex groove compared to the hydrogen atom in CM03 or the methoxy group in SOP1247.

#5929 HuR-targeted therapy promotes the adaptive immune response in medulloblastoma through the cGAS-Sting pathway.

M. Mehta, R. Raguraman, A. Munshi, R. Ramesh;
University of Oklahoma Health Sciences Center, Oklahoma City, OK

HuR is an RNA binding protein overexpressed in multiple human cancers and is involved in tumorigenesis, invasion, and metastasis. Genetic and pharmacologic inhibition of HuR demonstrated antitumor activity establishing HuR as a molecular target for cancer therapy. However, little is known about HuR's role in medulloblastoma (MB). In the present study, we investigated the effect of CMLD2, a small molecule inhibitor of HuR, on MB cell growth and on the adaptive immune response by assessing the cyclic GMP-AMP synthase (cGAS) - stimulator of interferon genes (STING) pathway. The cytoplasmic double-stranded DNA (dsDNA) sensing cGAS-STING signaling pathway plays pivotal role in host defense against cancers. Activation of the cGAS-STING signaling cascade induces the expression of pro-inflammatory cytokines and type I interferons promoting anti-tumor immunity. Human MB Daoy cells were treated with DMSO (control) or CMLD2 (20uM and 30uM). At 48 and 72 h after treatment, cells were collected and cell viability was determined using Trypan blue assay. A time and dose-dependent cytotoxicity was observed with 22.5% and 32.5% reduction in cell number with 20uM treatment ($p<0.01$) and 38.3% and 50.2% reduction with 30uM treatment ($p<0.001$) at 48 h and 72 h respectively compared to DMSO-treated control. Western blot analysis showed CMLD2 treatment inhibited HuR and markedly increased the expression of cGAS-STING pathway proteins (p-STING ^{Ser366}, p-TBK1 ^{Ser172}, p-IRF3^{Ser396} and pNF-KB^{Ser536}) at the two drug concentrations tested albeit greater increase in cGAS-STING protein expression was observed with 20uM treatment. Analysis for chemokines (CXCL10 and CCL5) and cytokine (IL-6) associated with the cGAS-STING pathway in cell culture supernatant collected from 20uM CMLD2 treatment showed significant increase in CXCL10 (1.96 ± 0.12 and 2.12 ± 0.06 fold increase at 48 h and 72 h; $p<0.01$) and CCL5 (1.21 ± 0.09 and 1.86 ± 0.05 fold increase at 48 h and 72 h; p=ns at 48 h; $p<0.01$ at 72 h) over DMSO-treated control. IL-6 expression significantly increased at 72h (1.98± 0.24 fold, $p<0.001$) but not at 48h after 20uM CMLD2 treatment compared to DMSO treated control. Our study results demonstrate CMLD2 mediated HuR targeting induces MB cell cytotoxicity and concurrently activates the cGAS-STING pathway. Testing of CMLD2 treatment in additional MB cell models and studying the impact of the cGAS-STING activation on immune cells (T cells, NK cells and macrophages) will aid in developing novel HuR-targeted treatment strategies in MB. Funding: The study was supported in part by a grant received from the National Cancer Institute of the National Institutes of Health (R01 CA 282735-01) and funds from the Jim and Christy Everest Endowed Chair in Cancer Developmental Therapeutics.

#5930 Measuring apoptotic effects of EP4A1 and EP4A2 on Kuramochi with a high-throughput multiplex image cytometric method.

J. McDonald[1], L. L. Chan[1], J. Reader[2], S. Mojica[1], M. Pierce[1];
[1]Revvity Health Sciences, Inc., Lawrence, MA, [2]University of Maryland, Princess Anne, MD

Ovarian cancer accounts for approximately 6% of all cancer death in women and has one of the highest mortality rates out of all gynecologic malignancies in the United States. Ovarian cancer can exhibit innate or acquired chemoresistance behavior, thus it is critical to identify novel therapeutic drug candidates. One of important characteristics of identifying potential chemotherapy drug candidate is the ability to induce apoptosis or programmed cell death in the target cancer cells. In order to measure apoptosis, various biomarkers are commonly employed such as Caspase 3, 7, 8 or 9, as well as Annexin V, which are all part of the cascade in apoptotic intrinsic pathway. However, typical fluorescent staining for image cytometry is not multiplexed that required multiple steps in order to determine the different type of apoptotic populations. In this work, we demonstrate a multiplexing apoptosis detection method to investigate the apoptotic effects of EP4A1, EP4A2, Paclitaxel, and Carboplatin on Kuramochi ovarian cancer cells. We employed the use of a high-throughput plate-based image cytometer (Celigo, Revvity Health Sciences Inc.) to image and analyze drug-treated Kuramochi cells stained with Annexin V-APC, Caspase 3/7 (488), and propidium iodide (PI) to assess the early- and late-stage apoptosis, as well as necrosis. We expected to see an increase in dual staining with the addition of EP4A to paclitaxel and carboplatin; however, the more interesting data was observed by separating single positive cell populations (Caspase, Annexin or PI only) from dual positive cell populations (Annexin + PI, Caspase + PI, Annexin +PI). The results show that treatment with EP4A lead to a time dependent increase in Caspase 3 cleavage but only in the single positive cell population. This trend was also observed in Annexin V single positive cell populations which is an indication of early apoptosis. The additive effect observed with the addition of EP4A was not seen in the dual positive cell populations. The high throughput nature of the image cytometry also allowed us to easily and quickly determine the optimal treatment conditions for this experiment. We were able to record multiple time points and not only capture proliferation, but also simultaneously collect data on caspase cleavage, Annexin-V staining and PI staining on multiple concentrations of compounds in monotherapy, dual therapy, and triple therapy combinations. Typically, it may be difficult to test multiple conditions in duplicate and triplicate using flow cytometry, while Celigo Image Cytometry may be used to obtain more robust data, and simultaneously acquire data of proliferation and multiplex staining with Annexin-V, PI and Caspase 3/7.

#5931 Investigating the therapeutic potential of STK17A inhibition in GBM.

J. R. Castro;
University of Miami Miller School of Medicine, Miami, FL

For decades, the survival rate for glioblastoma (GBM) has remained nearly stagnant, and currently the 5-year survival rate is only 5%. There is an unmet medical need for therapeutic development, as GBM is the most common primary brain tumor, yet only four FDA approved drugs have been developed for GBM over the last century. GBM is notoriously heterogeneous, and this has posed a challenge for researchers seeking to find therapeutic targets. However, by taking advantage of RNA sequencing, a potential biomarker and target for GBM has been identified: the kinase STK17A (Serine/Threonine Kinase 17A), also known as DRAK1. We confirmed that STK17A is overexpressed in brain cancers by analyzing public databases and single-cell RNA sequencing data from GBM patients, and further associated it with poor patient outcome. Little is known about STK17A, but it has been found to be involved with cell proliferation, tumorigenesis, and tumor metastasis. The role of STK17A in GBM pathophysiology and its therapeutic potential as a drug target remains a critical knowledge gap.In order to better understand STK17A's role in GBM pathophysiology, we first knocked down STK17A in GBM cell lines and determined that STK17A had functional roles in proliferation and morphology. Similar conclusions were drawn after knocking down STK17A *in vivo* in GBM xenograft mouse models. These findings supported STK17A as a viable therapeutic target. We then designed and optimized novel brain-penetrant STK17A inhibitors with IC50 values of <20nM in enzyme assays and <1μM in cell-based targeting engagement and proliferative assays. The designed and prepared novel STK17A inhibitors were further evaluated through kinase enzymatic assays and biological assays as well as *in vitro* proliferation and toxicity assays. We further characterized the inhibitors by showing Drug Metabolism and Pharmacokinetics (DMPK) properties *in vivo* in mouse models at 10 mg/kg via oral administration. We then used these potent, selective, and highly brain penetrant STK17A inhibitors to investigate the anti-tumor effects of STK17A inhibition in GBM *in vivo* and demonstrate the efficacy of our novel STK17A inhibitors.In conclusion, this work seeks to contribute to the field of targeted therapies for GBM by optimizing and examining the first iterations of novel brain penetrant STK17A inhibitors, initiating studies for the treatment of GBM *in vitro* and *in vivo*, and providing proof of efficacy for further studies in GBM patients. Ultimately, the results from our findings will lead to novel strategies for targeted drug development and more robust therapeutic options for GBM patients.

#5932 Immunomodulatory and anticancer effects of cyclical gemcitabine/nab-paclitaxel with continuous dosing of tinodasertib (AUM001) in preclinical KPC model.

W. Leong[1], S. Lee[2], J. Lim[1], S. Chen[2], F. Regis[2], R. Vidergar[1], S. K. Biswas[1], **B. Chowbay**[2];
[1]A*STAR - Singapore Immunology Network (SIgN), Singapore, Singapore, [2]National Cancer Centre Singapore, Singapore, Singapore

Background: PDAC has a poor 5-year survival outcome, and its aggressiveness limits the treatment efficacy. This is often driven by dysregulated mRNA translation of pro-tumorigenic genes that contribute to the proliferative and metastatic nature of PDAC. Synergizing chemotherapy with inhibition of oncogenic mRNA translation via MNK-coupled phosphorylation of eIF4E could potentially be viable. To support this hypothesis, we combined AUM001, a MNK inhibitor, with gemcitabine (GEM)-nab-paclitaxel (nPTX) with the aim of modulating tumor growth kinetics and maintaining it in a stable state.
Methods: PDAC KPC cells were subcutaneously inoculated into BL6 mice and randomized to five treatment groups. Chemotherapy involved administering GEM-nPTX intraperitoneally on days 1, 4, and 8. AUM001 was given orally daily for 8 days for both mono- and combination therapies and was further administered for an additional 3 weeks in continuous dosing group. IHC staining for Ki67, MVD, and stromal markers was conducted on FFPE sections as well as Western blot analysis of tumor tissues. Apoptosis was assessed using Annexin V. Immune profiling were evaluated by flow cytometric assay and GeoMx spatial transcriptomics analysis.
Results: The administration of GEM-nPTX and AUM001 (GPA) or GEM-nPTX alone (GP) led to an average 38% reduction in net tumor growth with no observed toxicity. Notably, continuous dosing of AUM001 (GPAc) following the cessation of chemotherapy exhibited a 45% decrease in net tumor growth (P=0.056) when compared to GPA. EIF4E phosphorylation and Myc expression were markedly inhibited in GPAc with lower recovery rate for MVD as compared to the GPA group at EOO ($P < 0.05$). A higher fraction of apoptotic cells was detected in the GPAc group at EOO than GPA group in reference to GP group (P=NS). GPA also resulted in a lower frequency of NK cells which was partially lifted in GPAc during observation phase. Macrophages which are known to have a pro-tumor role initially increased in frequency upon addition of AUM during chemotherapy, but subsequently decreased during observation. These modulations in infiltrating immune cells correlated with the differential expression of several immune related genes in the tumor associated CD45+ immune cells, revealed by the GeoMx analysis.
Conclusions: This study showed that sustained administration of AUM001 alongside cyclical GEM-nPTX is well-tolerated with good anti-tumor outcomes. Additionally, the maintenance of AUM001 may enhance the decrease in pro-oncogenic protein expression and remodel the tumor immune microenvironment. In conclusion, continuous dosing of AUM001 following the cessation of chemotherapy could stabilize the tumor state, potentiating its application in clinical settings as maintenance therapy for PDAC.

#5933 Identifying MC4R-targeted small molecule to investigate MC4R impact on cachexia progression.

J. Stokes, D. Taylor, M. Foss, B. Grau, S. Malhotra;
Oregon Health & Science University, Portland, OR

Background: The melanocortin system participates in energy homeostasis and appetiteregulation. This metabolic system is primarily located in the central nervous system,specifically in the hypothalamus and brainstem region. Within the melanocortin system,there are five established melanocortin receptors (MCR). MCRs are g-protein-coupledreceptors (GPCRs) and when these receptors are activated, they can increase neuronexcitation, regulate neurotransmitter release, regulate synaptic input, and alterconnection and strength. When Melanocortin-4 Receptor (MC4R) plays a critical role inthe progression of multiple metabolic diseases including cachexia. Cachexia is definedas the reduction of fat and lean mass, which is caused not just by lack of appetite, but byinflammatory impact. Cachexia is a symptom seen in numerous chronic diseases fromcancer to mitochondrial dysfunction to autoimmune inflictions. This makes MC4R apotentially strong therapeutic target.
Method: *In-silico* and high-throughput methods were used to identify small moleculesthat target and inhibit MC4R. For high-throughput screen, Hek293 cells withconstitutively active MC4R tagged with a nanoluciferase were used to identify molecules,specifically with inhibitory qualities. cAMP accumulation and β-arrestin recruitmentassay were used to determine the impact on MC4R functionality.
Results: 4738 small molecules were screened using high-throughput methods. Using a60% cutoff, 21 small molecules were identified as potential MC4R inhibitors. 17 arecurrently under investigation to confirm high-throughput results and identify functionalimpact. Several of these molecules have shown promising potential *in vitro* and will likelymove forward into *in vivo* studies.
Conclusion: This study identifies prospective small molecule inhibitors that targetMC4R and may be used as a probe to explore MC4R biology.

#5934 Ferroptosis induction therapy for castration resistant prostate cancer.

M. Awolowo, P. E. Dike, V. Odero-Marah;
Morgan State University, Baltimore, MD

Prostate cancer (PCa) is the most common non-skin cancer in men, and second leading cause of death. The fundamental treatment for treating PCa is androgen deprivation therapy which is an effective form of treatment initially. Nevertheless, the disease reoccurs in most men; this is referred to as castration-resistant PCa (CRPC), for which the standard treatment is enzalutamide. However, some develop resistance to this enzalutamide anti-androgen agent. Ferroptosis is an iron-dependent lipid peroxidation form of regulated cell death being investigated as a novel potential therapy for PCa using ferroptosis inducers such as RSL3; they have shown promise in selectively triggering cell death in cancer cells while sparing healthy tissues. We hypothesize that RSL3- induced ferroptosis will overcome enzalutamide resistance in PCa cells. To test this, we utilized C4-2B MDVR cells which represents a cell model for aggressive PCa that metastasized to the bone and is resistant to both castration therapy and the enzalutamide drug treatment. C42B-MDVR cells were treated with increasing concentrations of RSL3 followed by analysis of cell viability with MTS assay. A dose dependent reduction in cell viability was observed which was reversed by ferroptosis inhibitor, ferrostatin-1. Western blot analysis revealed a decreased expression of the antioxidant enzyme glutathione peroxidase 4 (GPX4) with ferroptosis induction indicating a mechanism of the RSL3-induced cell death. The limitations to our research are that the research was performed *in vitro* and have not been tested on mouse models to visualize the effects of the treatments in animals. In conclusion, ferroptosis inducer RSL3 decreases GPX4 expression and decreases proliferation of PCa cells while ferrostatin-1 reverses the effects of the RSL3 treatment. Thus, ferroptosis inducers present a potential novel therapeutic approach for CRPC patients who have developed resistance to conventional androgen therapies. NIH NIGMS RISE 5R25GM058904, NIH/NIMHD U54MD007590; U54MD013376

#5935 Non-allosteric inhibition of enolase 1 sensitizes triple-negative breast cancer for checkpoint inhibitors.

D. Tailor[1], F. J. Garcia-Marques[2], A. Bermudez[2], W. Li[1], A. Dheeraj[1], S. J. Pitteri[2], S. V. Malhotra[1];

[1]Knight Cancer Institute, Oregon Health & Science University, Portland, OR, [2]Stanford University School of Medicine, Palo Alto, CA

Background: Triple-negative breast cancer (TNBC) is an aggressive type of breast cancer that commonly returns and spreads. Currently, very few options are available for TNBC treatment. Cancer cells exploit glycolytic machinery for the Warburg effect and aerobic glycolysis. Enolase 1 (ENO1) is the glycolytic enzyme expressed in most tissues, and many cancer cells have higher expression. Apart from the glycolytic role in the cytosol, ENO1 also plays different roles in cancer cells, including as a surface receptor.

Method: non-allosteric chemical inhibition was developed and tested *in vitro* for its efficacy and target validation. Subsequently, *in vivo* examinations were conducted on emerging small molecules in syngeneic and patient-derived murine models of breast cancer to unveil their anti-tumor efficacy.

Results: Our non-allosteric small molecule inhibitor, SU212, binds to ENO1 and restricts its movement within cells. SU212 treatment leads to the accumulation of ENO1 in the nucleus where it restrains the activity of c-Myc. The treatment causes the production of truncated ENO1 called myc promoter-binding protein 1 (MBP-1), which limits the activity of c-Myc. Stand-alone treatment of SU212 restrains the tumor progression and metastasis in orthotopic syngeneic and PDX mouse models. Combining SU212 and Anti-PD1 significantly inhibits tumor growth and metastasis in mouse models. C-Myc is linked to protein transcription that aids immune resistance and tumor evasion of immune surveillance. Suppression of c-Myc activity *via* SU212 treatment sensitizes the TNBC tumors for anti-PD1 therapy.

Conclusions: This study provides compelling preclinical data for further development of SU0212 as an immune therapy sensitizer for the treatment of TNBC.

#5936 A novel class of orally bioavailable small molecules induces potent and sustained tumor growth inhibition and T cell infiltration in various solid tumor mouse models.

B. Gapp[1], G. Zischinsky[2], M. Urban[1], N. Birnbacher[1], A. Schwarzbock[1], S. Grunaug[1], T. Gastaldi[1], A. Stutz[3], P. Nussbaumer[2], S. Stranner[1], J. Buchberger[1], A. Birbach[1], D. Schogl[1], M. Kuttke[1], A. Dohnal[1], R. Gugenberger[1];

[1]invIOs GmbH, Vienna, Austria, [2]Lead Discovery Center GmbH, Dortmund, Germany, [3]Pharma R&D Consulting Stuetz GmbH, Altmunster, Austria

The introduction of targeted immunomodulating agents has transformed cancer treatment over the last decade by demonstrating unprecedented efficacy in patients who respond. However, limited clinical response rates as well as adverse events underline the need to identify additional novel modalities in cancer immunotherapy. Here we report on the discovery of a novel class of low molecular weight compounds for oral application that selectively enhance tumor-reactive T cell cytotoxicity. Hit-to-lead development of compound hit series A was performed based on medicinal chemistry to investigate structure-activity-relations. A-306, a representative of the A compound class, induced increased T cell proliferation, elevated levels of the activation markers CD25 and CD69 as well as enhanced secretion of IFN-γ, IL-2 and TNF-α upon anti-CD3/CD28 stimulation. A-306 treatment without T cell receptor ligation had no effect on T cell activation, suggesting selective activation potential only in the context of antigen encounter. Furthermore, A-306 strengthened T-cell mediated killing of M21 melanoma cells and enhanced T cell function in response to viral antigens by showing a Th1 signature. Medicinal chemistry efforts resulted in front runner compounds A-481 and A-687 that show a similar profile and potencies down to nanomolar level. In a murine B16-SIY melanoma and EO771 breast cancer model oral single-agent administration with front runner compounds was well tolerated, showed good bioavailability in lymphoid organs and plasma and resulted in significant tumor growth inhibition beyond the end of treatment (D21). T cells from tumor draining lymph nodes of long-term surviving mice in both cancer models showed a distinct activation pattern indicative of anti-tumor immunity. Furthermore, oral application of A-481 in combination with intra peritoneal administration of anti-PD1 antibodies eradicated B16-SIY melanoma cells in a synergistic manner. Taken together, we report on the identification of a novel class of small molecules possessing high potential for selective anti-tumor activation of the immune system upon oral administration. Front runner compounds A-481 and A-687, which significantly inhibit tumor growth in a B16-SIY melanoma and EO771 breast cancer mouse model, lead to prolonged survival beyond the end of treatment and display a good safety profile. The final candidate compound will undergo testing in toxicity studies and enter a first-in-human trial in selected solid tumors in 2025.

#5937 KS20226, a first-in-class IRP2 inhibitor, preferentially induces reprogramming of iron metabolism and suppresses tumor growth in colorectal cancer.

J. Hwang[1], A. Park[2], C. Kim[1], C. Kim[1], J. Kwak[2], B. Kim[2], H. Shin[2], M. Ku[1], J. Yang[1], A. Baek[3], J. Choi[4], H. Lim[3], K. No[3], X. Zhao[1], U. Choi[1], T. Kim[1], K.-S. Jeong[5], H. Lee[2], S. Shin[1];

[1]Yonsei University College of Medicine, Seoul, Korea, Republic of, [2]Korea Research Institute of Chemical Technology, Daejeon, Korea, Republic of, [3]Yonsei University, Incheon, Korea, Republic of, [4]Dongduk Women's University, Seoul, Korea, Republic of, [5]Yonsei University, Seoul, Korea, Republic of

Background: Iron homeostasis plays a role in redox activity, mitochondrial function, and cell cycle regulation. Specifically, the dysregulation of iron metabolism is implicated in malignant transformation and cancer progression. Iron regulatory protein 2 (IRP2) is crucial for maintaining balance within iron levels and primarily controls genes associated with iron utilization. Our discovery of KS20226, a first-in-class IRP2 inhibitor, reveals remarkable potential as an effective anti-cancer drug candidate. We have elucidated the mechanisms underlying the therapeutic effects of KS20226, thereby highlighting the feasibility of targeting IRP2 in colorectal cancer (CRC).

Methods: The proliferation inhibitory activity of KS20226 was assessed the CCK-8 and 3D Spheroid models. To investigate mitochondrial function, we conducted measurement of oxidative phosphorylation (OCR) and glycoPER. Furthermore, gene expression analysis was performed through RNA sequencing (RNA-seq) using the Illumina HiSeq 2500 system platform (Macrogen Inc.). Differential expressed gene (DEG) analysis was carried out using the R package DESeq2, and pathway enrichment analysis was analyzed using GSEA (v_4.2.3.). For the observation of autophagic morphology, we utilized transmission electron microscopy (TEM), immunofluorescence staining targeting the autophagy marker LC3B, and immunoblotting.

Results: KS20226 exhibited a remarkable growth inhibitory effect in 10 different CRC cell lines, with GI_{50} values ranging from 1 to 10 μM. KS20226 suppressed IRP2 expression and the corresponding occupancy of the iron-responsive elements of ferritin H and transferrin receptor 1, resulting in iron deprivation, and efficiently controlled CRC growth. Pharmacologic inhibition of IRP2 induced reprogramming of mitochondrial respiration, reducing reliance on oxidative phosphorylation. The observed mitochondrial dysfunction induced by KS20226 was correlated with pathway analysis, revealing a decrease in the gene-set for HALLMARK_OXIDATIVE_PHOSPHORYLATION (NES = -1.38, p-value = 0.008) and an increase in the gene-set for POSITIVE_REGULATION_OF_AUTOPHAGY (NES=1.43, p-value=0.016). Immunoblotting demonstrated that KS20226 activated the phosphorylation of AMPK, ULK, and Beclin1 cascade, leading to the autophagic cell death of the CRC cells.

Conclusions: The reliance of cancer cells on iron metabolism to drive proliferation has led to the development of therapeutic strategies targeting the inhibition of IRP2. KS20226, a first-in-class IPR2 inhibitor, exhibits distinct therapeutic properties, such as perturbation of mitochondrial iron metabolism and induction of autophagic cell death. Our findings represent important progress toward exploiting IRP2-mediated abnormal iron metabolism in cancer, an unexplored area of research with substantial unmet needs.

#5938 Development of HH044, an orally bioavailable nNOS inhibitor, for the treatment of cutaneous melanoma.

A. Patel[1], S. Tong[1], R. B. Silverman[2], S. Yang[1];
[1]Chapman University, Irvine, CA, [2]Northwestern University, Evanston, IL

Background: Human cutaneous melanoma is one of the few cancers in which the incidence rate continues to increase, and despite recent advances in immune and targeted therapies, the 5-year survival rate of metastatic disease remains low. Neuronal nitric oxide synthase (nNOS) has been identified to contribute to melanoma development, stimulating disease progression, and facilitating escape of melanoma cells from the immune response. We developed a novel small molecule, HH044, which specifically inhibits nNOS activity and reduced nitric oxide production in melanoma cells. We aim to conduct a proof-of-concept study using our nNOS inhibitor administered orally for anti-melanoma treatment.

Methods: Human melanoma cell lines (A375, Sk-Mel-28, wm3211) were employed to analyze the anti-cancer activities of HH044 *in vitro*. An immune-competent syngeneic melanoma mouse model was used to determine the anti-tumor activity of HH044 when administered orally (50 mg/kg/day) or intraperitoneally (10 mg/kg/day) for 21 days. A pharmacokinetic study of drug levels in serum and tumor samples was conducted after a single dose given intraperitoneally or orally using LC-MS/MS analysis at different time points.

Results: HH044 has high selectivity of nNOS over iNOS (340-fold) and eNOS (540-fold). The IC_{50} of HH044 in melanoma cell lines was 5.27 ± 3.3 μM, while iNOS inhibitor 1200W did not exhibit any cytotoxicity up to 100 μM concentration. Of note, nNOS blockade by HH044 did not result in reactivation of iNOS, and expression levels of iNOS were not changed after HH044 treatment. I*n vivo* studies demonstrated that HH044 treatment given intraperitoneally exhibited potent anti-tumor activity and reduced tumor weight to 45% of control. When administered orally, HH044 at 50 mg/kg significantly reduced tumor growth to 61% of control and extended mice median survival from 32 days to 53 days. Pharmacokinetic analysis showed that oral administration achieved sufficient drug levels in xenograft tumors, which were well above the K_i value (0.005 μM) despite a wide range of bioavailability. The drug level peaked at 2 hours after a single dose (2.27 ± 0.666 μM in the tumor and 23.68 ± 17.43 μM in the serum). Intraperitoneal injection achieved much higher levels in serum and tumor samples, which also declined slower compared to oral gavage administration. By 24 hours, the drug levels in serum and xenograft tumors remained at 1.55 ± 0.12 μM and 1.77 ± 0.24 μM concentration, respectively. No significant systemic toxicities were observed with HH044 treatments either given via *i.p.* injection or orally. Further *in vivo* studies combining nNOS inhibitors with immune checkpoint blockade are currently underway.

Conclusions: HH044, as the first-in-class nNOS inhibitor, exhibits potent anti-melanoma activity by oral administration. Developing selective nNOS inhibitors has shown to be a novel therapeutic strategy to improve melanoma treatment.

#5939 Enhancing nab-paclitaxel chemotherapy response in gastric cancer preclinical models through Inhibition of the HGF/c-Met pathway with merestinib.

Q. Kaurich, J. Huang, S. Hassan, U. Holzen, **N. Awasthi**;
Indiana University School of Medicine, South Bend, IN

Background: Current treatments for primary metastatic or recurrent gastric adenocarcinoma (GAC) primarily involve combination chemotherapy, but the median survival time remains under a year. Nab-paclitaxel has displayed significant antitumor activity in preclinical GAC studies. GAC often exhibits overexpression of various growth factors and their receptors, which play a critical role in its pathophysiology. Aberrant activation of the HGF/c-Met pathway has been reported in up to 50% of GAC patients. We investigated the therapeutic potential of merestinib, a novel inhibitor targeting c-Met, along with Axl and DDR1/2 pathways, in combination with nab-paclitaxel in GAC preclinical models.
Methods: Animal survival studies were conducted using peritoneal dissemination xenografts in NOD/SCID mice implanted with MKN-45 cells. Tumor growth was assessed in subcutaneous xenografts using MKN-45 and SNU-1 cells in NOD/SCID mice. IHC analyses were performed to evaluate tumor cell proliferation and microvessel density. *In vitro* cell proliferation and protein expression were assessed using the WST-1 assay and Western blot analysis, respectively.
Results: Animal survival significantly improved with nab-paclitaxel (118%) and merestinib (41%) individually. The combination of merestinib with nab-paclitaxel (153%) resulted in further increased animal survival. In MKN-45 xenografts with high c-Met expression, a substantial reduction in tumor growth was observed with nab-paclitaxel and merestinib, showing a synergistic response. The net change in tumor size in the control, nab-paclitaxel, merestinib, and combination groups was 503 mm^3, 115 mm^3, 91 mm^3, and -9.7 mm^3 (tumor regression). In low c-Met expressing SNU-1 xenografts, the effect of merestinib and nab-paclitaxel was less pronounced compared to MKN-45 xenografts. The net change in tumor size in the control, nab-paclitaxel, merestinib, and combination groups was 219 mm^3, 105 mm^3, 131 mm^3, and 57 mm^3. Tumor cell proliferation and microvessel density corroborated the tumor growth study results. Nab-paclitaxel and merestinib reduced *in vitro* cell proliferation, with an additive effect in combination. The reduction in cell proliferation by nab-paclitaxel (10 nM), merestinib (100 nM), and their combination was 87%, 82%, and 94% in MKN-45, 59%, 50%, and 82% in SNU-1, and 53%, 19%, and 66% in gastric fibroblasts. In MKN-45 cells, merestinib increased the expression of pro-apoptotic proteins and decreased the expression of phospho-c-Met, phospho-EGFR, phospho-IGF-1R, phospho-ERK, and phospho-AKT.
Conclusion: Merestinib has strong antitumor activity in GAC, especially when administered with nab-paclitaxel, demonstrating a synergistic effect. These results provide compelling evidence for the potential clinical relevance of this combination therapy in improving the survival of GAC patients.

#5940 JAB-30355: A highly potent, orally bioavailable p53-Y220C reactivator.

Q. Zheng, P. Wang, C. Liang, Y. Li, X. Sun, A. Li, W. Zhang, W. Long, Y. Wang;
Jacobio Pharmaceuticals Co., Ltd, BeiJing, China

Background: As a key tumor suppressor, p53 precisely regulates cellular events such as cell cycle arrest, apoptosis, senescence, and DNA repair under physiological conditions. In 50-60% of human cancers, *TP53* gene is mutated. The *TP53* Y220C is a hotspot loss-of-function mutation occurring in around 1% of solid tumors. Application of p53-Y220C reactivator for restoration of p53 function represents a promising treatment strategy for patients with this mutation.
Methods: The Induced Allosteric Drug Discovery Platform (IADDP), which integrates medicinal chemistry, biochemical and biophysical studies, and computational techniques, was applied for the development of JAB-30355. The proportion of p53-Y220C with wild-type protein-like structure after JAB-30355 treatment was determined by immunoprecipitation. Thermal shift assay was applied to assess the thermal stability of JAB-30355-reactivated p53-Y220C protein. DNA binding assay was developed to evaluate the *in vitro* DNA binding activity. p53-luciferase reporter system was developed to evaluate the cellular transcriptional activity. qPCR and Western blotting were performed to evaluate the transcriptional and translational levels of p53 downstream targets, respectively. CellTiter-Glo assay was performed to evaluate the inhibitory activity of JAB-30355 on the viability of tumor cell lines harboring wild-type or Y220C mutated *TP53*. *In vivo* PK-PD study was conducted to evaluate the relationship between JAB-30355 concentration and expression of p53 target genes. Multiple CDX and PDX mouse models harboring *TP53* Y220C were used to evaluate the antitumor activity of JAB-30355.
Results: Immunoprecipitation assay and thermal shift assay results demonstrated that JAB-30355 efficiently restored the wild-type p53-like structure and enhanced protein stability of p53-Y220C in a dose-dependent manner. In addition, JAB-30355 significantly enhanced the DNA binding activity of p53-Y220C and subsequently increased the expression of p53 target genes, such as *CDKN1A*, *MDM2* and *PUMA*. JAB-30355 inhibited cell viability of multiple *TP53* Y220C-mutated cancer cell lines with IC_{50}s ranging from 0.2 to 0.7 μM, and exhibited good selectivity against *TP53* wild-type cells. Overall, the *in vitro* data demonstrated that JAB-30355 is a potent and selective p53-Y220C reactivator. *In vivo* PK-PD study showed good correlation between JAB-30355 exposure and activation of p53 target genes. Furthermore, JAB-30355 exhibited dose-dependent anti-tumor activity, inducing tumor stasis or regression in multiple CDX and PDX models of ovarian cancer, pancreatic cancer, gastric cancer, and small cell lung cancer, with overall good tolerability.
Conclusions: JAB-30355 is a highly potent, selective, and orally bioavailable p53-Y220C reactivator that will be tested in clinical space soon.

#5941 Small molecule NSC59984 synergizes with PARP inhibitors in BRCA1 wild type ovarian cancer.

S. Zhang, L. Zhou, L. Zhang, M. Pinho-Schwermann, B. Carneiro, J. Sedivy, W. S. El-Deiry;
Brown University, Providence, RI

PARP inhibitors (PARPi) targeting poly (ADP-ribose) polymerase are the first clinically approved drugs designed to apply synthetic lethality in BRCA1 mutant/deficient cancer. However, the treatment can cause reversion of BRCA mutation which results in drug resistance. To explore new strategies to improve antitumor efficacy of PARPi, we applied PARPi in combination with a small molecule NSC59984 for cancer therapy. NSC59984 is a small molecular targeting mutant p53 degradation and activating p73 via ROS-ERK2-MDM2 pathway. The treatments with radiation or hydrogen peroxide showed that NSC59984 enhanced DNA comet tails and gamma-H2AX, correlated to reduction of rad51 foci in cancer cells. These results suggest that NSC59984 impairs DNA damage repair via abrogation of homologous recombination (HR). We further applied the combinational treatment of NSC59984 and PARPi in BRCA1 wild-type ovarian cancer cells and found that NSC59984 synergized with PARPi to reduce cell viability, inhibit colony formation, and increase cell death. The combination treatment enhanced DNA damage and correlated with reduction of BRCA1 at the protein level. These results, taken together, suggest that the induction of BRCAness causes a synthetical lethality with PARPi in BRCA1 wild-type cancer cells. Cell cycle profiling showed that the cells were arrested at the G2/M phase in response to combinational treatment. At the G2 phase arrest, the high doses of the combinational drugs led to cell death via mitotic catastrophe, and the intermediate doses induced cellular senescence defined by senescence phenotypic hallmarks including senescence-associated beta-gal staining and a secretome consistent with senescence-associated secretory phenotype (SASP). Therapy-induced senescence (TIS) in cancer cells is considered as one of the mechanisms of tumor recurrence and drug resistance. To reduce the risk of TIS in treatment, we applied senolytic treatment to target senescent cells in the combinational treatment. The senolytic drug ABT263 treatment eliminated the senescent cancer cells from the combinational treatment. ABT263, NSC59984 + PARPi combinational treatment further reduced cell viability. Our study provides a rationale for small molecular compounds targeting HR deficiency in combination with PARPi to treat BRCA1wild-type ovarian cancer cells, and additional senolytic treatment may be required to limit resistance by removal of the TIS.

#5942 Discovery of WRN inhibitors as targeted therapy in the treatment of microsatellite unstable (MSI-H) tumors.

W. Schonemann, A. Ludwig-Słomczyńska, &. Dudek, M. Krol, M. Farinone, U. Kulesza, W. Jasnosz, I. Mac, K. Zuchowicz, K. Wierzbicka, A. Buchcic-Szychowska, A. Gondela, A. Zagorska, O. Matuszewska, M. Sowińska, M. Nowogrodzki, M. Girardi, S. Paluch, S. Sukhomlinova, A. Chłopek, I. Levenets, K. Kozłowska-Tomczyk, K. Łagosz-Ćwik, M. Stoszko, S. Woroszyło, M. Mikulski, J. Jabłońska, M. Wiśniewska, K. Palus-Chramiec, P. Podkalicka-Gołda, A. Janiga, S. Sudoł-Tałaj, M. Sieprawska-Lupa, M. Miodek, J. Faber, R. Starczak, B. Winnik, A. Świrska, A. Kowal-Chwast, D. Gogola, S. Novak Ratajczak, A. Dudek, N. Gaud, G. Satała, A. Stachowicz, M. Swarbrick, K. Brzozka, **M. I. Zawadzka**;
Ryvu Therapeutics, Krakow, Poland

The synthetic lethality resulting from the inhibition of the WRN helicase protein has been observed in tumors characterized by high levels of microsatellite instability (MSI-H). This instability stems from a deficiency in the DNA mismatch repair (MMR) mechanisms, leading to the accumulation of DNA damage. This phenomenon is notably prevalent in 10-30% of colorectal, gastric, endometrial, and ovarian cancers. Specifically, the inhibition of WRN helicase activity induces DNA damage leading to cell cycle arrest and apoptosis exclusively in MSI-H cell lines. This selectivity underscores the therapeutic potential of WRN inhibitors, as they demonstrate efficacy against MSI-H cells while remaining non-toxic to microsatellite stable (MSS) cell lines. Ryvu is developing a chemical series of potent, selective WRN helicase inhibitors. Structure-based optimization facilitated the rapid expansion and delivery of a compound library with novel intellectual property (IP), demonstrating target engagement in cells and selective potency over other RecQ family members. The correlation between the cellular effect and selectivity upon treatment with these ligands was confirmed in the clonogenic assay, specifically in responder, microsatellite instable cell lines only, thereby leaving a substantial safety margin (>100x) relative to non-responder, microsatellite stable lines. Target engagement has been confirmed by dose dependent DNA damage pathway activation concomitant with WRN degradation in in vitro assays. The pharmacokinetic properties of these compounds are favorable for progressing to in vivo studies. The correlation between compound exposure and on-target effect was confirmed in PK/PD and efficacy studies in xenograft MSI-H cancer models. These data provide pharmacological proof-of-concept for the synthetic lethal effect of our inhibitors and support WRN inhibition as a new oncological therapy.

#5943 Development of a *SMART* theranostic agent for precision pancreatic cancer therapeutics.

E. A. Motea, J. J. Smith, O. Ketiku;
Indiana University School of Medicine, Indianapolis, IN

Pancreatic cancer is predicted to emerge as the second leading cause of cancer-related deaths in the United States by 2030. Pancreatic ductal adenocarcinoma (PDAC) - the most common form of pancreatic cancer - is often diagnosed as metastatic disease and has demonstrated the least improvement in overall survival over the last three decades with incidence rising by 0.5% to 1.0% per year due in part to lack of effective and tumor-selective treatment strategies. One approach to reduce host toxicity is the development of novel molecules and innovative therapeutic approaches that are nontoxic to normal cells but can be activated only under tumor-specific conditions for lethality, which we coined as SMART (Selective Method of Activation for Response in Tumors) therapeutic agents. We utilized explicit properties and biomarkers present in PDAC tumors but not in normal tissues to develop a SMART DNA-damaging anti-cancer agent with both therapeutic and diagnostic (theranostic) activities. We evaluated the tumoricidal effect of our SMART agent using long-term survival assays in PDAC cell lines and 3D co-culture spheroids, as well as in tumor xenograft model studies in mice. We also tested the ability of our SMART agent to treat, detect/diagnose (via click chemistry), and identify critical resistance mechanisms (via proteomics) as a single agent or as a chemosensitizer with predictive tumor biomarkers for tumor-selective therapeutic response. We found that our SMART small molecule induces tumor-selective lethal effects as a monotherapy or in combination with DNA repair inhibitors or small molecules known to generate hydrogen peroxide (H_2O_2) in a tumor-selective manner for activation. Using "click" chemistry, we detected and quantified the incorporation of our SMART small molecule as a DNA-damaging agent via flow cytometry that correlated with therapeutic response, which is a feature that could facilitate the stratification, treatment monitoring, and management of patients with pancreatic cancers. We also found that our SMART agent is less toxic and more effective as a monotherapy than cisplatin in PDAC cell line-derived xenograft studies in mice. Overall, our novel SMART theranostic agent could provide a significant advancement as they are preferentially activated under tumor-specific conditions to induce tumor-selective therapeutic response. Furthermore, the diagnostic component our SMART agent could provide oncologists with essential information to make rapid clinical decisions on treatment strategies. Our SMART agent is also remarkably versatile as it can be utilized as a chemosensitizer or as a chemical probe to identify targetable vulnerabilities to potentiate its therapeutic effects at lower doses.

#5944 Discovery of BH-30236: A novel macrocyclic CLK inhibitor targeting alternative splicing in cancers.

J. Cui, P. Jiang, W. Deng, D. Zhai, N. Ling, D. Li, Z. Wang, Y. Hu, L. Darjania, J. Whitten, E. Rogers, E. Rui;
BlossomHill Therapeutics, Inc., San Diego, CA

Aberrant alternative splicing is a newly recognized hallmark of cancer, that has been shown to play a critical role in tumorigenesis, cancer progression, and therapeutic resistance *via* multiple mechanisms, including increased proliferation, decreased apoptosis, promoted migration, enhanced metastatic potential, and induced evasion of immune surveillance. Serine and arginine-rich splicing factors (SRSFs) are RNA-binding proteins (RBPs) that regulate constitutive and alternative splicing. SRSFs are often mutated or overexpressed in cancers, resulting in widespread alterations in splicing patterns. The Cdc2-like kinase (CLK) family and dual-specificity tyrosine-regulated kinase (DYRK) phosphorylate SRSFs, influencing the assembly of spliceosome machinery, exon recognition, and splicing. Therefore, targeting CLK/DYRK kinases can modulate cancer specific splicing isoforms, opening avenues for new therapeutic interventions. BH-30236 was designed as a novel orally bioavailable, ATP-competitive, macrocyclic inhibitor of CLK with IC_{50}s of 0.134, 0.165, and 0.446 nM against CLK1, CLK2, and CLK4, respectively in enzymatic kinase assays. At clinically relevant concentrations, BH-30236 also inhibited DYRK1A/1B/2, proviral insertion site of moloney murine leukemia virus kinase 3 (PIM3), and FMS-like tyrosine kinase 3 (FLT3) with IC_{50}s of 0.111, 0.148, 0.562, 0.115 and 0.248 nM, respectively. In cancer cells, BH-30236 impaired the phosphorylation of SRSFs, Tau and 4EBP1, the direct downstream substrates of CLK, DYRK, and PIM kinases with IC_{50}s of 40-60 nM, ~50 nM, and ~80 nM, respectively. Furthermore, BH-30236 potently inhibited the FLT3 phosphorylation with an IC_{50} of 0.16 nM. Overall, BH-30236 regulated alternative splicing by primarily inducing skipped exons in favor of anti-tumor isoforms, leading to cancer cell death and growth suppression in a broad panel of cancer cell lines and *in vivo* efficacy studies. For example, BH-30236 potently inhibited cell proliferation with an IC_{50} of 0.62 nM in *FLT3-ITD* positive MV-4-11 cells and achieved complete tumor regression in the MV-4-11 cell-derived xenograft tumor model, even after dose cessation for 4 weeks. In MV-4-11 cells, BH-30236 increased pro-apoptosis splicing variant BCLxS, downregulated RNA expression of BCL2, MCL1, and AML stem cell markers CD33 and CD123. In addition, BH-30236 has demonstrated good human ADME and preclinical safety profiles. Collectively, the preclinical study results strongly support the clinical applications of the novel multikinase CLK inhibitor BH-30236 in hematological malignancies and solid tumors, as a single agent or in combination with other therapies.

#5945 Exploring the antiproliferative potential of KHS101 on triple negative breast cancer cell lines.

R. Gurung[1], A. W. Yirsaw[1], M. G. Khodary[1], T. Samuel[1], M. Sandey[2], C. C. Yates[3], D. Bedi[1];
[1]Tuskegee University, Tuskegee, AL, [2]Auburn University, Auburn, AL, [3]Johns Hopkins University, Baltimore, MD

Breast cancer is the second leading cause of cancer deaths in the world. Among its subtypes, triple-negative breast cancer (TNBC) is highly aggressive, particularly affecting African American (AA) women, with limited treatment choices. HSP60 protein promotes tumorigenesis and is being studied as a possible biomarker to treat cancers such as TNBC. The small molecule KHS101 specifically binds and inhibits the mitochondrial chaperone HSP60. In this study, we hypothesized that KHS101 would inhibit the proliferation of TNBC cells and therefore may have a therapeutic potential.We studied the antiproliferative effects of KHS101 on TNBC cell lines (MDA-MB-231, MDA-MB-468, HCC1806) through MTT cell proliferation and colony forming assays at varying doses and time points (24, 48, 72, and 96 hours). We performed cell cycle analysis to understand the cell cycle response and apoptotic events in treated or control cells. Additionally, the gene expression and frequently altered pathways resulting from KHS101 treatment were analyzed by RNA sequencing of cells treated with vehicle (DMSO) or with various concentrations of KHS101(1, 2.5, 5, and 7.5 uM) for 72 hours. We analyzed the data using GraphPad Prism and Microsoft Excel, with statistical significance set at $p \leq 0.05$.

TNBC cell lines exhibited significant dose-response and antiproliferative effects with increased KHS101 doses and treatment durations. Notably, AA breast cancer cells (MDA-MB-468) displayed heightened cytotoxicity and reduced proliferation compared to Caucasian American (CA) breast cancer cells (MDA-MB-231 and HCC1806). Cell cycle analysis revealed G2/M phase arrest, consistent with RNA sequencing data showing downregulation of the activation of ATM/ATR response in KHS101-treated cell lines compared to the controls. Gene set enrichment analysis indicated downregulation of the cell cycle control genes in MDA-MB-231 cells after 72 hours of KHS101 treatment (7.5 μM). Reactome pathway analysis in KHS101-treated MDA-MB-231 cells showed upregulation of IFN-gamma signaling and degradation of extracellular matrix. Similarly, Kegg pathway analysis showed upregulation in cell adhesion molecules, cytokine-cytokine receptor interaction, antigen processing and presentation, and Natural Killer cell-mediated cytotoxicity in KHS101-treated cancer cells compared to the controls. KHS101 demonstrates varying cytotoxic effects on TNBC cells, with potential implications for antitumor immune responses. Our findings highlight the distinct susceptibility of AA breast cancer cells and suggest KHS101 as a promising avenue for further research in understanding its mechanism of action and validating therapeutic potential in TNBC.

#5946 ZM-412, a potent and selective KIF18A inhibitor with robust efficacy as monotherapy in CIN-positive tumors and in combination with MMAE-conjugated ADC in CIN-negative tumors.

Feng Zhou[1], Lei Zhou[2], Ruina Wang[2], Liting Xue[1], Xiaokang Qin[2], Zhengtao Li[1], Jian Yu[2], Renhong Tang[1]

[1]State Key Laboratory of Neurology and Oncology Drug Development, Simcere Zaiming Pharmaceutical Co, Ltd., Shanghai, China, [2]Simcere Zaiming Pharmaceutical Co, Ltd., Shanghai, China

Chromosomal instability (CIN), a hallmark of human cancer, is defined as the perpetual missegregation of whole chromosomes during mitosis. KIF18A has emerged as a potential therapeutic target of synthetic lethality to induce CIN tumor cell death because it is more required for the proliferation of CIN tumor cells than normal diploidy cells. Here, we identified a potent and selective KIF18A inhibitor ZM-412. *In vitro*, ZM-412 inhibited the kinesin motor enzymatic activity with an IC_{50} less than 30 nM, and arrested OVCAR3 cells in the G2/M phase with an EC_{50} around 2.0 nM. ZM-412 also selectively inhibited the proliferation of a panel of CIN-positive tumor cell lines with IC_{50} values less than 50 nM, whereas it didn't affect the proliferation of CIN-negative cells such as PBMC and near-diploidy HCT116 as indicated by IC_{50} values over than 5 μM. A CIN-positive $HCT116^{CIN}$ model was established by cytochalasin D induction. Compared to parent HCT116 cells, it was sensitive to ZM-412 treatment, suggesting the high selectivity of ZM-412 to CIN tumors as monotherapy. Both KIF18A inhibitors and monomethyl auristatin E (MMAE) regulate microtubule dynamics, which provides a potential combination strategy. ZM-412 showed a significantly synergic effect with free MMAE or MMAE-conjugated ADC on the inhibition of proliferation in multiple kinds of cancer cell lines, including CIN-positive/negative tumor cell lines. *In vivo*, ZM-412 potently inhibited tumor growth in a dose-dependent manner in OVCAR3 and HT29 xenograft models. Moreover, ZM-412 showed a remarkable synergic effect on tumor growth inhibition with MMAE-conjugated LIV-1 ADC in OVCAR3 xenograft model. In conclusion, we discovered ZM-412 as a novel potent and selective KIF18A inhibitor, which has potential for the treatment of CIN cancers as monotherapy and for combination therapies for extended cancer types with MMAE-ADC.

#5947 Discovery of ACE-47228211, a highly potent and selective SOS1 inhibitor.

J. Wang, W. Li, S. Kumar, W. Pan, Z. Wen, T. Yin, G. Zhao, **K.-L. Yu**;
Acerand Therapeutics US, Carmel, IN

Dysregulation of receptor tyrosine kinase (RTKs) and KRAS signaling is the most frequent causes of cancer development and progression. SOS1 is one of the major guanine nucleotide exchange factors (GEFs) that facilitates the conversion of the inactive GDP-bound KRAS “off” state to the activated GTP-bound KRAS “on” state. SOS1 is therefore required for dysregulated RTKs, and wildtype and mutant KRAS proteins to drive cancer cells. In addition, SOS1 plays a crucial role in modulating the reactivation of the RAS/MAPK signaling upon the treatment of RAS/MEK/ERK inhibitors. Thus, blocking SOS1 and KRAS protein-protein interactions could be an effective strategy for targeting KRAS-MAPK driven cancers. Here, we report the discovery of a highly potent and orally bioavailable small molecule SOS1 inhibitor, ACE-47228211. This molecule has a unique novel scaffold. It exhibits an IC_{50} of 8.5 nM in the SOS1-KrasG12D (GDP) exchange assay and 5.0 nM in cellular ERK phosphorylation assay in H1957 cells. ACE-47228211 at 3 mg/kg (BID) demonstrated significant tumor growth inhibition in MiaPaca-2 KRAS G12C tumor model than MRTX0920 at 50 mg/kg (BID). When combined with Sotorasib (5 mg/kg QD), a Kras G12C inhibitor, ACE-47228211 at 3 mg/kg exhibited synergistic effect similar to MRTX0920 at 50 mg/kg. Further, ACE-47228211 demonstrated synergistic effects with EGFR and FGFR2 inhibitors in RTK mutant tumor models. ACE-47228211 has excellent ADME and physical properties with low risks of hERG, CYP inhibition and drug-drug interactions. The evaluation of ACE-47228211 in a safety panel of 87 targets and a kinase panel of >500 targets shows that this molecule has favorable selectivity and safety profiles. The molecule is currently in IND enabling stage of development.

#5948 FMC-376 a dual inhibitor of ON and OFF states of KRAS^{G12C} is broadly active in PDX models of resistance.

Y. Wang[1], R. M. Neve[2], J. Staunton[2], **K. R. Webster**[1];
[1]Frontier Medicines, Boston, MA, [2]Frontier Medicines, South San Francisco, CA

KRAS^{G12C} is a frequent activating mutation occurring in NSCLC, CRC, PDAC and other tumors that shifts KRAS into the active, GTP-bound (ON) state. KRAS was long considered undruggable until the recent discovery of single acting inhibitors, including those that bind the GDP-bound, inactive (OFF), state of KRAS^{G12C}. The most clinically advanced of these first-generation molecules have demonstrated clinical response rates of 37-43% and 6 to 7-month progression-free survival in lung cancer patients. While an important advance, a majority of cancers do not respond, and acquired resistance is common. FMC-376 is a next-generation dual inhibitor of both the ON and OFF states of KRAS^{G12C} with the potential to overcome resistance and deliver best-in-class durability of response. FMC-376 was discovered through the application of the Frontier^{TM} platform, which integrates chemoproteomics, machine-learning, and covalent fragment-based drug discovery. FMC-376 is a highly selective, irreversible inhibitor of KRAS^{G12C} that covalently binds to the mutant cysteine in KRAS^{G12C} and directly blocks the ON and OFF states of the mutant KRAS protein leading to a complete, durable blockade of downstream signaling. This further translates into more durable tumor regressions *in vivo* in comparison to OFF state inhibitors like sotorasib. Clinical resistance to first-generation inhibitors that can only bind the OFF state of KRAS^{G12C} has been associated with multiple mechanisms that drive upregulation of ON state KRAS^{G12C}. These known drivers of resistance include activating co-mutation/amplification/fusions of receptor tyrosine kinases, amplification of KRAS^{G12C} and non-mutational mechanisms that lead to paradoxical activation of KRAS^{G12C} due to release of negative feedback control upon KRAS inhibition, often referred to as adaptive resistance. In addition, multiple mutations that may act independently of KRAS are also associated with resistance. These include mutation of KEAP1, CDKN2A, SMARCA4, PI3K, PTEN, MTOR, HRAS, NRAS, RAF, and MAPK. *In vivo* profiling of FMC-376 against a panel KRAS^{G12C} mutant patient derived xenograft (PDX) models of NSCLC, CRC and PDAC, has demonstrated that dual inhibition of both ON and OFF KRAS^{G12C} leads to complete suppression and regression of tumors carrying a broad spectrum of known genomic and non-genomic (adaptive) drivers of clinical resistance to OFF state KRAS^{G12C} inhibitors. FMC-376 a clinical stage dual inhibitor of ON and OFF state KRAS^{G12C} has the potential to overcome limitations of single acting and OFF state KRAS^{G12C} inhibitors.

#5949 The clinical dual KRAS^{G12C} inhibitor FMC-376 has demonstrated potential as both a monotherapy and in combination for the treatment of patients with KRAS^{G12C} mutation positive NSCLC.

Y. Wang[1], A. Roberts[2], P. Calses[2], R. M. Neve[2], J. Staunton[2], **K. R. Webster[1]**;
[1]Frontier Medicines, Boston, MA, [2]Frontier Medicines, South San Francisco, CA

KRAS, a membrane-associated guanosine triphosphatase (GTPase), is the most frequently mutated oncogene in cancer with activating mutations occurring in approximately 25% of NSCLC. Of these, KRAS^{G12C} occurs in approximately 14% of adenocarcinomas and in 0.5 to 4% of squamous NSCLCs. This mutation impairs GTPase activity and GTP-hydrolysis leading to an increase in the active, GTP-bound (ON), state. KRAS was long considered undruggable until the recent discovery of inhibitors that bind the GDP-bound, inactive (OFF) state of KRAS^{G12C}. The most clinically advanced of these first-generation molecules have demonstrated clinical response rates of 37-43% and 6 to 7-month progression-free survival in patients with KRAS^{G12C} positive NSCLC. While significant, a majority of cancers do not respond, and acquired resistance is common. FMC-376 is a next-generation dual inhibitor of both the ON and OFF states of KRAS^{G12C}with the potential to deliver improved outcomes as both a monotherapy and in combination, for patients with KRAS^{G12C} positive NSCLC. FMC-376 was discovered through the Frontier^{TM} platform, which integrates chemoproteomics, machine-learning, and covalent fragment-based drug discovery. The potential for FMC-376 in the treatment of patients with KRAS^{G12C} mutant NSCLC has been assessed in a broad panel of NSCLC PDX models representing settings of sotorasib/adagrasib resistance, in a model of NSCLC CNS-metastasis and in combination with an immune checkpoint inhibitor. The dual ON + OFF state mechanism of action of FMC-376 is highly active across a panel of NSCLC CDX and PDX models, including those that carry co-mutations that are associated with both primary and acquired resistance to the OFF-state inhibitors adagrasib and sotorasib in NSCLC. These drivers of resistance include activating mutations of receptor tyrosine kinases (e.g. EGFR, MET, etc.), co-mutations including KEAP1 and adaptive resistance due to release of negative feedback control. Evaluation of FMC-376 in models where EGFR signaling is induced by EGF demonstrated rapid and durable target engagement in contrast to both sotorasib and adagrasib which show decreased effectiveness after EGF stimulation. As a result, FMC-376 is highly effective in NSCLC PDX models that have EGFR and MET upregulation. In addition, 27-42% of patients with KRAS^{G12C} positive NSCLC present with CNS metastasis. FMC-376 is highly active in an intracranial NSCLC model of CNS-metastasis, resulting in tumor regression. Furthermore, FMC-376 has demonstrated activity in combination with an anti-PD-1 mAb in a KRAS^{G12C} mutant mouse syngeneic tumor model. Together, these data demonstrate the potential of FMC-376, a next-generation clinical stage dual inhibitor of ON and OFF state KRAS^{G12C}, for the treatment of patients with KRAS^{G12C} mutant NSCLC as well as other KRAS^{G12C} positive tumors.

EXPERIMENTAL AND MOLECULAR THERAPEUTICS: Novel Biologic Therapies and Therapeutic Targets
Poster Session

#5953 DUSP6 is a novel target in neuroendocrine tumors.

Majid Momeny[1], Vahid Khalaj[1], Solmaz AghaAmiri[1], Po Hien Ear[2], Servando Hernandez Vargas[1], Sukhen Ghosh[1], Ali Azhdarinia[1]

[1]The Univeristy of Texas Health Science Center Houston, Houston, TX,[2]Department of Surgery, University of Iowa, Iowa city, IA

Background: Neuroendocrine tumors (NETs) are rare malignancies derived from enterochromaffin cells of the diffuse neuroendocrine system and most frequently observed in the gastrointestinal tract and bronchopulmonary system. Surgery is the major treatment for localized NETs. In high-grade NETs, treatment opportunities include chemotherapeutic drugs such as temozolomide (TEM), and capecitabine and small-molecule targeted therapies such as everolimus or sunitinib. Despite promising initial responses, most patients develop therapy resistance by unknown mechanisms. Therefore, there is a pressing need to apprehend the mechanisms of resistance to improve the therapeutic efficacy of the current treatments. Phosphatases are emerging and novel targets in human malignancies and their modulation yields significant anti-tumor activities. Dual specificity phosphatase 6 (DUSP6) is a MAPK phosphatase and mainly binds to and dephosphorylates extracellular signal-regulated kinase (ERK)1/2. DUSP6 expression is increased in several malignancies, correlating with distant metastases and a worse clinical outcome. Moreover, DUSP6 mediates resistance to certain chemotherapeutics and small molecular tyrosine kinase inhibitors and its blockade increases therapeutic sensitivity. The current study aimed to investigate the contribution of DUSP6 to therapy resistance in the NET models.
Material and Methods: Using Western blot analysis, the expression of DUSP6 was measured in 8 clinical samples of small bowel neuroendocrine tumors, the NET cell lines BON-1, H69, IMR-32, QGP and H524 and two PDX models, 1452 (rectal neuroendocrine) and 913 (pancreatic neuroendocrine). The effects of DUSP6 depletion on cell viability were explored using a pharmacological inhibitor, BCI, and its siRNA-mediated knockdown. Moreover, BCI-mediated apoptotic cell death was measured by an annexin V/PI staining assay.
Results: DUSP6 expression was positive in 5 out of 8 clinical samples, 4 NET cell lines and both the PDX models. BCI treatment induced an apoptotic response in the NET models and synergistically increased sensitivity to TMZ and cisplatin in 1452 cells., RNAi-mediated depletion of *DUSP6* also increased sensitivity to sunitinib and triggered TMZ-induced apoptotic cell death in 1452 cells, which was associated with changes in (O^6-Methylguanine-DNA-methyltransferase) MGMT expression. These findings suggest that DUSP6 is an important therapeutic target in neuroendocrine tumors and its blockade is a promising therapeutic approach to enhance the therapeutic index of current treatments.

#5954 Big data-driven discovery of novel oncogenic fusion genes for anticancer therapy.

D. Kim[1], J. Park[2], J.-A. Kim[3], J.-H. Kim[4], T. Park[1], J. Park[1];

[1]Seoul National University, Pyeongchang, Korea, Republic of, [2]Hyundai Pharm Co., Gyeonggi-do, Korea, Republic of, [3]Korea Research Institute of Bioscience and Biotechnology, Daejeon, Korea, Republic of, [4]Korea Research Institute of Bioscience and Biotechnology, Deojeon, Korea, Republic of

The integration of big data analytics with cancer research is catalyzing a transformative approach in cancer treatment, primarily focusing on the discovery of novel and efficacious anticancer targets. Our study presents an advanced algorithm, specifically crafted to exploit the extensive data available in the field of oncology. We started with the genomic and clinical information of 8,864 patients with 33 different cancers (TCGA). Then we implemented the following algorithm to discover anti-cancer targets by analyzing the clinical significance (cBioPortal), drug development status (Cortellis), and oncogenicity (DepMap) of candidate genes: Candidate genes = {gene | gene ∈ Genes, [Frequency(gene) > 50, Drug(gene) ∈ {'biological testing', 'preclinical stage'}, Association(gene) ≥ 0.4, Publication(gene) ≤ 200] ∨ [Publication(gene) ≥ 200 ∧ Boolean(gene)]}. We employed this algorithm to analyze fusion genes, which represent promising anti-cancer targets known for their potential to elicit substantial clinical responses, but there is a high demand for new ones. We identified four druggable therapeutic targets out of a total of 15,291 fusion genes through the algorithm: frame-shifted FGFR3-TACC3, in-framed DLK1-RPS11, frame-shifted CHP1-RAD51B, and in-framed TBC1D22A-SMYD3. We conducted in vitro validation studies of these fusion genes in NIH3T3 cell lines, and it confirmed that all of the fusion genes not only produce mRNA and protein levels but also induce oncogenic effects on cellular behavior. In the case of FGFR3-TACC3, the introduced fusion gene induced mRNA ($p < 0.05$) and protein expression ($p < 0.05$) even when frame-shifted. In addition, the proliferation rate of transformed cells increased more than 4-fold on day 10 ($p < 0.0001$) and colony formation increased more than 5-fold on day 21 ($p < 0.01$) compared to wild-type cells. These results demonstrate the tumorigenicity of the fusion genes. Taken together, this study emphasizes the crucial role of big data in propelling oncology research forward. The algorithm we developed can offer a new pathway for creating innovative cancer treatment, marking a significant advancement in the realm of personalized cancer therapy.

#5955 *In vivo* precision therapy for glioblastoma using a nanodrug targeting microRNA-10b.

Bryan Doyun Kim[1], Elizabeth Kenyon[2], Ming Chen[2], Sujan Mondal[2], Ana deCarvalho[3], Anna Moore[2]

[1]Biomedical Engineering, Michigan State University, East Lansing, MI,[2]Radiology, Michigan State University, East Lansing, MI,[3]Henry Ford Health, Detroit, MI

Glioblastoma multiforme (GBM) is the most common and aggressive primary brain malignancy, which accounts for about half of all brain tumors. Notably, GBM has been shown to express high levels of microRNA-10b (miR-10b) compared to normal brain tissue, which expresses virtually no miR-10b. Importantly, the mounting body of evidence suggests that suppressing miR-10b in glioblastoma cells disrupts various pathways involved in tumor formation, ultimately leading to the suppression of tumor growth and an increase in apoptosis. We have recently reported that our experimental nanodrug targeting miR-10b (MN-anti-miR10b) effectively suppresses miR-10b expression, inhibits tumor cell migration and invasion, and decreases GBM cell viability *in vitro*. MN-anti-miR10b consists of an iron oxide core with cross-linked dextran, which acts as the delivery vehicle, and is further conjugated with Cy5.5 fluorophores and therapeutic anti-miR-10b locked-nucleic acid antagomirs. The iron oxide core provides MR imaging contrast while Cy5.5 enables optical imaging modalities *in vivo*. In this study, U251, human GBM cells, were orthotopically implanted in nude, athymic mice and injected via tail vein with PBS, scrambled antagomir vehicle control (MN-Scr), or MN-anti-miR10b (10 and 20 mg Fe/kg), beginning on day 7 post-implantation. Mice were injected with respective treatments once a week for 6 weeks before assessing changes in survival and expression of miR-10b. In one trial, we assessed the differences in survival between treatment groups after completion of the injection regimen and found that MN-anti-miR10b can increase survival compared to control groups. In another trial, mice were euthanized one week after the last injection and GBM tissues were assessed for miR-10b expression by qRT-PCR. RNA samples extracted from this trial have been submitted for RNA sequencing and differential gene expression analysis will be performed. Here, we demonstrated *in vivo* that MN-anti-miR10b can efficiently decrease miR-10b expression (57%) and increase median survival (MN-anti-miR10b: 54.5 days vs MN-Scr: 44 days vs PBS: 44 days) compared to PBS and MN-Scr treatment groups. These studies suggest the use of MN-anti-miR10b can be effective in the treatment of GBM *in vivo*.

#5956 *FLT3* alterations and inhibition in triple negative B-cell adult acute lymphoblastic leukemia patients.

A. Ferrari[1], A. Ghelli Luserna di Rora[2], F. Lo Schiavo[1], E. Fonzi[1], G. Capirossi[1], C. Salvesi[1], M. Bochicchio[1], L. Ledda[1], C. Servilli[1], M. Paganelli[1], G. Marconi[1], C. Papayannidis[3], C. Sartor[3], M. Rondoni[4], A. Mianulli[5], B. Giannini[6], C. Pasciolla[7], F. Giglio[8], S. Galimberti[9], M. Fumagalli[10], P. Salutari[11], V. Gaidano[12], G. Martinelli[1], G. Simonetti[1];

[1]IRCCS Istituto Romagnolo per lo Studio dei Tumori (IRST) "Dino Amadori", Meldola, Italy, [2]Fondazione Pisana per la Scienza ONLUS, San Giuliano Terme,Pisa, Italy, [3]IRCCS Azienda Ospedaliero-Universitaria di Bologna, Istituto di Ematologia "Seragnoli", Bologna, Italy, [4]Hematology Unit & Romagna Transplant Network, Ravenna Hospital, Ravenna, Italy, [5]Hematology, Infermi Hospital, Rimini, Italy, [6]Laboratorio Unico- AUSL della Romagna Pievesestina, Cesena, Italy, [7]Hematology and Bone Marrow Transplantation Unit, Istituto Oncologico IRCCS "Giovanni Paolo II", Bari, Italy, [8]Hematology and Bone Marrow Transplantation Unit, IRCCS San Raffaele Scientific Institute, Milan, Italy, [9]Hematology Unit, AOUP Santa Chiara, Pisa, Italy, [10]Hematology Unit, Ospedale San Gerardo, Monza, Italy, [11]Dipartimento Oncologia Ematologia, Ospedale Civile Santo Spirito, Pescara, Italy, [12]SCDU Ematologia e Terapie cellulari, A.O. Ordine Mauriziano, Torino, Italy

Backgroud: The prognosis of B cell ALL patients (pts) relapsing after Hematopoietic Transplant is poor and new drugs are needed. In acute myeloid leukemia, FLT3-inhibitors (FLT3i) are showing promising results in *FLT3*-mutated (mut) cases. Their potential use in *FLT3*-mut B-ALL has been poorly investigated.
Aim: To assess if *FLT3* could be a valid targetable marker in B-ALL.
Methods: We sequenced with a capture based large RNA-seq panel (1385genes) 183 adult B-ALL [n=52 Pos for Ph or t(4;11) or t(1;19) and n=131 Triple-Negative (TN) pts that are negative for Ph (n=43), t(4;11) and t(1;19) translocations] and 15 donors. To confirm *FLT3* muts, 13 available samples were further sequenced with Extended Myeloid Solution (98 genes; SOPHiA) where *FLT3* gene is fully covered. *In vitro* studies using 5 FLT3i [Gilteritinib (Gil), Midostaurin, Crenolanib, Sorafenib and Quizartibin] and Venetoclax (Ven) were conducted on pt primary cells and on TN and other B-ALL cell lines (MUTZ5, MHH-CALL4 Ph-like; NALM6;RS4;11, 697, REH) and 2 AML cell lines (OCI-AML3 FLT3;MV-4-11 FLT3-ITD).
Results: We found 15 *FLT3* mut in 14/131 TN B-ALL and in 1/43 Ph+ cases: 43.8% were TKD mut, 3 ITD mut, 3 splicing site mut,1 N-terminal, 1 juxta-membrane domain and 1 Ig-like site (Fig. 1A). After pathogenicity interpretation we excluded 3 variants and one mutation was not confirmed at DNA level. Overall 7.6% of TN were mut (Ph+ 2.3%). 81.8% of *FLT3*mut pts potentially druggable with FLT3i, mainly TKD (63.3%). Targeted NGS revealed the co-occurrence with other mutations (range 2-15), and in particular with *CSMD1* (n=4), *KDM6A, KMT2D* and *CREBBP* (n=3) alterations. Moreover, 11/13 samples carried copy number alteration (mean 12), mostly amplifications. *CDKN2A & IKZF1* were the most frequently altered genes (n=5;4 CN-loss). *FLT3* expression was increased in 11/15 cases compared to donors and wt pts. As reported, the expression was higher in *ZNF384* or *MLLr* B-ALL subtypes.To evaluate the effect of FLT3is in ALL, we treated *ex vivo* primary leukemic cells of 6 adult ALL patients (*FLT3*-mut n=4; *FLT3*-wt n=2) with increasing concentrations of 5 FLT3i for 24, 48 and 72h. We observed a trend towards greater response of *FLT3*-mut ALL cells compared to wt ones. The average IC50 values in response to the five FLT3i was 1.6 uM and 24.5 uM after 72h of treatment in *FLT3*-mut and *FLT3*-wt B-ALL, respectively (Fig. 1B). We than evaluated the sensitivity to the 5 Inhs in all cell lines. Interestingly MHH-CALL4 wt were more sensitive to Gil compared to OCI AML3 wt, and showed the same effect compare to MV-4-11 AML mut (F.1C). Given the effect of Gil in single agent, we combined it with Ven in wt B-ALL cells at increasing concentrations. Interestingly We noticed a strong additive effect with the higher Gil concentration and all Ven doses(F.1D).
Conclusions: *FLT3* alterations identify a novel subgroup of TN B-ALL with therapeutic potential also in combination regimens. Ricerca Corrente Italian MoH L3P1946.

#5957 Development of a selective, oral ATP-competitive CDK9 inhibitor, BLX-3030, for treatment of pancreatic cancer.

Y. Barrera-Millan[1], Z. Li[2], H. Vankayalapati[2], D. J. Bearss[2], D. D. Von Hoff[1], H. Han[1];
[1]TGen (The Translational Genomics Research Institute), Phoenix, AZ, [2]Biolexis Therapeutics, American Fork, UT

Introduction Transcription regulators, such as cyclin-dependent kinase 9 (CDK9), have been implicated in the super-enhancer driven transcriptional control of oncogenes in multiple cancers including pancreatic cancer. CDK9 has been shown to be employed by cancer cells for the constant production of short-lived oncoproteins such as c-Myc to maintain their survival. Due to its critical role in regulating transcription in cancer cells, CDK9 has emerged as a potential therapeutic target. Here, we report the antitumor activity of a selective, oral ATP-competitive CDK9 inhibitor, BLX-3030, in preclinical models for pancreatic cancer.

Experimental Procedures Fragment-based MolecuLern driven AI workflow methods were used to design a series of ATP-competitive CDK9 specific kinase inhibitors. BLX-3030 was selected as one of the most potent leads with an IC_{50} of 1.1 nM in a cell-free CDK9 kinase assay. A Sulforhodamine B (SRB) assay was used to evaluate the cell growth inhibitory activity of BLX-3030 in a panel of 10 pancreatic ductal adenocarcinoma (PDAC) and 2 pancreatic neuroendocrine tumor (pNET) cell lines. Western blotting was used to determine the effects of BLX-3030 treatment on c-Myc expression in cancer cells. The combination effects between BLX-3030 and standard of care regimen, gemcitabine (GEM) and nab-paclitaxel (NP), was assessed using the SRB assay. Finally, the *in vivo* antitumor activity of BLX-3030 alone or in combination with GEM and NP was evaluated in a mouse cell line xenograft model for pancreatic cancer.

Results BLX-3030 exhibited potent cell growth inhibitory activity in the panel of pancreatic cancer cell lines with IC_{50} values ranging from 133.5 nM to 508.1 nM. The potency of BLX-3030 in the cell lines appears to correlate with the expression level of c-Myc in the cell lines. BLX-3030 showed similar activities in PDAC and pNET cell lines with mean IC_{50} values of 244.5 nM and 194.6 nM, respectively. However, treatment with BLX-3030 for 48 hours did not seem to significantly reduce c-Myc expression in PSN-1 PDAC cells. When combined with GEM and NP, BLX-3030 demonstrated mostly additive effects in PSN-1 cells. Preliminary data from the *in vivo* study show that BLX-3030 improves the antitumor activity of GEM and NP.

Conclusion In summary, BLX-3030 potently inhibited the growth of both PDAC and pNET cells *in vitro*. The growth inhibitory activity of BLX-3030 in PDAC cell lines correlates with their c-Myc expression levels. BLX-3030 showed an additive effect when combined with standard of care drugs (GEM and NP) in PDAC cell lines. Overall, the novel CDK9 inhibitor, BLX-3030, demonstrated potent activity in pancreatic cancer cell line models and presents a promising preclinical lead for pancreatic cancer. (This work was supported in part by Biolexis Therapeutics and the Seena Magowitz Foundation).

#5958 Exploring AKR1C3 as a therapeutic target to overcome erlotinib resistance in lung adenocarcinoma.

W. C. Cho, K. P. Li, C. F. Wong, K. Y. Fung, J. C. H. Chow, K. M. Cheung, J. C. H. Chan, E. Y. T. Lau;
Queen Elizabeth Hospital, Hong Kong SAR, China

Introduction: Erlotinib has demonstrated promising efficacy in lung adenocarcinoma (LUAD) patients with epidermal growth factor receptor mutation. However, the development of resistance to erlotinib poses a significant challenge in achieving long-lasting treatment responses. Aldo-keto reductase family 1 member C3 (AKR1C3) is associated with tumor progression, drug resistance, and unfavorable prognosis. This study aims to assess the potential of AKR1C3 as a therapeutic target for overcoming erlotinib resistance in LUAD.

Methods: AKR1C3 expression was assessed in paired tumor tissues from 100 LUAD patients using reverse transcription quantitative polymerase chain reaction. Both in vitro and in vivo experiments were categorized into four treatment groups: a saline control (CTR), erlotinib (ER), an AKR1C3 inhibitor 3-(4-trifluoromethyl)phenylamino)benzoic acid (BA), and the combination of erlotinib with the AKR1C3 inhibitor (COM). An erlotinib-resistant cell line was established from the LUAD cell line HCC4006. The MTS assay was used to evaluate cell proliferation and viability. The combined effect of erlotinib and the AKR1C3 inhibitor was assessed using Synergyfinder and CompuSyn calculation software. Both cell line-derived xenograft (CDX) and patient-derived xenograft (PDX) models of erlotinib resistance to LUAD were established in NSG mice. The mice received daily oral gavage administration of the drugs for 31 days, while tumor volume was monitored biweekly.

Results: AKR1C3 expression was significantly upregulated by more than three-fold in LUAD tumor samples compared to normal counterparts ($p < 0.0001$). After 24 hours of treatment in erlotinib-resistant cells, the ER and BA groups exhibited inhibition rates of 7% and 9%, respectively, while the COM group demonstrated a substantially higher inhibition rate of 45%. Synergyfinder and CompuSyn analysis revealed a synergy score of 12 and a combination index of 0.5 for the COM group, indicating a robust synergistic effect between the two drugs. In the CDX model, the COM group exhibited a tumor volume reduction of 25% in erlotinib-resistant cells and 64% in parental cells compared to the CTR group. In the PDX model, the COM group displayed a significant reduction of 50.4% in tumor volume compared to the CTR group. There was no significant difference in the weight of body and internal organs among the four treatment groups in both xenograft models.

Conclusions: AKR1C3 overexpression was observed in the tumor tissues of LUAD patients. The combination of erlotinib and AKR1C3 inhibitor showed promising efficacy in overcoming erlotinib resistance in both *in vitro* and *in vivo* experiments. These findings highlight AKR1C3 as a potential therapeutic target for managing erlotinib resistance in LUAD patients. Targeting AKR1C3 represents a novel approach to overcome resistance and enhance treatment outcomes in LUAD patients undergoing erlotinib therapy.

#5959 Targeting TRIM11 is a potential therapeutic strategy for malignant gliomas.

K. Di[1], B. C. Das[2], D. A. Abrams[3], D. A. Bota[1];

[1]University of California, Irvine, Irvine, CA, [2]Arnold & Marie Schwartz College of Pharmacy & Health Sciences, Long Island University, Brooklyn, NY, [3]Mercy Medical Center, Cedar Rapids, IA

Background: TRIM11 (tripartite motif-containing protein 11) belongs to the TRIM/RBCC (the RING B-box coiled-coil) family of E3 ubiquitin ligases. Emerging evidence has demonstrated that TRIM11 is a novel target against cancer and neurodegenerative diseases as it plays vital role in cellular proliferation, differentiation, tumor progression, and apoptosis. Our previous work demonstrated that TRIM11 is over-expressed in high-grade gliomas and promotes proliferation, invasion, migration and tumor growth, suggesting that TRIM11 may be used as a target for malignant glioma treatment. The tumor suppressor p53 plays critical roles in tumor prevention, and deregulated p53 pathway has been found in a majority of glioblastomas (GBMs). Recent studies have shown that TRIM proteins are involved in the regulation of p53, and TRIM proteins are also regulated by p53.

Methods: To evaluate the effect of TRIM11 on GBM progression *in vivo*, we intracranially implanted GBM cells over-expressing TRIM11 in immunocompromised mice, and the animal survival was monitored. We have synthesized a series of TRIM11 inhibitors and evaluated their anti-GBM potential *in vitro*. Furthermore, we tested the crosstalk between TRIM11 and p53 by knocking down TP53 through RNA interference.

Results: Our *in vivo* data showed that the control group mice (GL261 parent line) survived longer than the mice bearing TRIM11 over-expressing GL261 tumors ($p<0.05$), suggesting TRIM11 enhances tumor progression *in vivo*. *In vitro* data showed that the oncogenic effect of TRIM11 may be related to its influence on the apoptosis pathway since a robust induction of poly (ADP-ribose) polymerase (PARP) was observed in TRIM11 over-expressing GBM cells. When treated with Temozolomide (TMZ), TRIM11 over-expressing cells were more resistant and showed a higher survival rate compared to parental cells. We screened a small library of TRIM11 inhibitors (~ 25 compounds), and identified several compounds which significantly inhibited the growth of both established and primary GBM cells in a dose-dependent manner, implicating that TRIM11 inhibitors may serve as novel agents for GBM treatment. We found that inactivation of p53 by siRNA increased the expression of TRIM11 and modulated the sensitivities of GBM cells to chemotherapy drugs.

Conclusion: Despite remarkable advances in the prognosis and multidisciplinary treatment strategies, GBM is still the most lethal primary brain tumor, and there is a pressing need for newer anti-GBM agents with novel targets and mode of action. Our preclinical studies demonstrate a significant anti-tumor effect of TRIM11 inhibitors on malignant glioma cells. Our finding that TRIM11 may be modulated by p53 adds a new layer of regulation to this complicated signaling pathway. A better understanding of the crosstalk between p53 and TRIM11 will benefit the clinical application of targeting p53 and TRIM11 signaling pathways for therapeutical indications in GBM.

#5960 Targeting CDK8: A translatable therapeutic approach for fusion-positive aRMS.

S. Zhang[1], C. Malone[1], B. Guedes[2], K. Engel[1], M. Just[2], K. Ross[1], A. Fahs[2], G. Digiovanni[1], D. Granum[2], R. Bentley[2], L. Barbar[2], C. Cerda-Smith[2], E. mendes[2], O. Erdogan[2], A. Kovach[2], K. Oristian[2], S. Zimmerman[2], J. F. Shern[3], K. Wood[2], C. Counter[2], C. M. Linardic[2], K. Stegmaier[1];
[1]DFCI/Harvard Medical School, Boston, MA, [2]Duke University School of Medicine, Durham, NC, [3]National Institute of Health, Bethesda, MD

Alveolar rhabdomyosarcoma (aRMS), characterized by poor overall survival and limited advancements in therapy over the past four decades, poses a great challenge in childhood cancer treatment. More than 60% of high-risk aRMS is driven by the oncofusion protein PAX3-FOXO1. The direct targeting of transcription factor fusions, however, is quite difficult. Given that PAX3-FOXO1 is reported to drive disease by controlling transcriptional programs to maintain an undifferentiated myoblastic state, an alternative approach would be to target the transcriptional machinery recruited by the fusion. To identify potential novel targets in aRMS, we utilized the Broad Institute's Cancer Dependency Map dataset, a collection of genome-wide CRISPR-Cas9 screens performed in over 1000 cancer cell line models. We focused on druggable dependencies that are selective to fusion-positive aRMS and intersected this data with PAX3-FOXO1-associated transcriptional complexes. Among these candidates, we identified CDK8 as a top selective dependency. Importantly, other components of the CDK8 kinase module in the mediator complex, such as CCNC, also scored as a strong selective dependency in fusion-positive aRMS. CDK8 expression is notably elevated in aRMS tumors compared to other pediatric tumors, and aRMS cell lines exhibit significantly higher CDK8 protein levels than non-transformed primary skeletal muscle cells.

We next validated these in silico results through the application of shRNA knockdown, CRISPR knockout, and the use of CDK8 kinase inhibitory small molecules, including BI-1347, SEL-120-34A, and JH-XII-178, which demonstrated on-target activity as assessed by STAT1^{Ser727} phosphorylation. Both genetic loss of CDK8 function and kinase inhibition impaired aRMS cell line growth *in vitro*. *In vivo* studies demonstrated a significant inhibition of xenograft tumor growth with both doxycycline inducible CDK8-directed shRNAs and with pharmacologic inhibition of CDK8 with SEL120-34A treatment. To understand the mechanisms by which CDK8 inhibition impairs aRMS growth, we evaluated the transcriptional consequences of CDK8 inhibition by RNA-sequencing in aRMS, as well as the chromatin accessibility by ATAC-sequencing. We discovered that loss of CDK8 led to gain of chromatin accessibility and the upregulation of hallmark genes involved in myogenesis, such as *MYH3*, *MYOG*, *MEF2C*, and *MYBPH*, as well as alteration of PAX3-FOXO1 gene expression programs. We next validated this differentiation phenotype both *in vitro* through detection of increased myogenin staining by immunofluorescence and *in vivo* by visualization of myofibrils in the xenograft tumors and increased myoglobin quantified by qRT-PCR after CDK8 inhibition.

In conclusion, this work identifies CDK8 as a novel and readily translatable therapeutic target in fusion-positive aRMS laying a robust foundation for further mechanistic and preclinical studies.

#5961 NRF2-responsive kinases in esophageal squamous cell carcinoma.

B. Subramaniyan[1], Z. Xiong[2], C. Paiboonrungruang[2], Y. Li[1], M. Ben Major[3], X. Chen[1];
[1]Cooper University Health Care, Camden, NJ, [2]Coriell Institute for Medical Research, Camden, NJ, [3]Washington University in St. Louis, St. Louis, MO

Esophageal squamous cell carcinoma (ESCC) ranks as the 7th most frequently diagnosed cancer and the 6th leading cause of cancer-related death worldwide. NRF2 is identified as a therapeutic target for human ESCC, with a mutation rate of approximately 10-22%. Hyperactive NRF2 promotes proliferation, metastasis, and resistance to radiation and chemotherapy in ESCC. Although some evidence suggest NRF2 regulates kinases which contribute to these phenotypes, it remains unclear which kinases are responsive to hyperactive NRF2. Using NRF2 ChIP-seq analysis, we have enrichment of 42 kinases including *Akt2* and *Pkm* and 31 phosphatases including *Pten* and *Dusp16* enriched in the *Keap1*$^{-/-}$ mouse esophagus in comparison with the wild-type esophagus. We further confirmed the binding of NRF2 to the promoter regions of mouse *Akt2* and *Pten*. mRNA expression profiling revealed enrichement of the PI3K/AKT, RAS, ERK, and GSK3 pathways in the *Keap1*$^{-/-}$ esophagus as compared to the *Nrf2*$^{-/-}$;*Keap1*$^{-/-}$ esophagus. Immunohistochemical staining showed that pAKT, p-mTOR, pS6, PKM2 were overexpressed in the *Keap1*$^{-/-}$ esophagus, as well as in the adult NRF2-hyperactive esophagus (*Sox2CreER;LSL-Nrf2*$^{E79Q/+}$). Using PhosphoExplorer array and PamChip array to analyze *NRF2*^{W24C}-KYSE70 cells (in comparison with *NRF2*^{null}-KYSE70 cells) and *Sox2CreER;LSL-Nrf2*$^{E79Q/+}$ mouse esophageal epithelium in comparison with wild-type mouse tissue, we further identified multiple kinases including PI3K as potential NRF2-responsive kinases. These findings suggest a potential role for kinases such as PI3K in NRF2-driven ESCC, and support the idea of targeting both NRF2 and NRF2-responsive kinases as a therapeutic strategy for ESCC.

#5962 Novel xCT-targeted biologics significantly suppress metastasis, improve survival, and sensitize primary tumors to chemotherapy in TNBC xenograft models.

H. Gong[1], J. Li[1], C. Becker[1], L. Timmerman[2], S. Sikandar[3], **Y. Huang**[1];
[1]Xomics Biopharma, Inc., Redwood City, CA, [2]University of California, San Francisco, CA, [3]University of California, Santa Cruz, CA

Background: Triple negative breast cancer (TNBC) is a highly heterogeneous subset of breast cancer, which has the worst prognosis and lacks specifically targeted therapeutic options. The TNBC subtype termed M/MSL is enriched with cells of high mesenchymal state and increased stemness, and is particularly resistant to current therapies[1,2]. But this cancer cell phenotype is susceptible to ferroptosis, hence targeting these aggressive tumors with ferroptosis inducers such as xCT inhibitors (xCTi) is an attractive alternative. The cystine/glutamate exchanger xCT/*SLC7A11* plays a key role in maintaining redox homeostasis in cancer cells. xCT is expressed on subsets of most solid tumors, including stem/progenitor and metastatic tumor cells. xCT inhibition yields a variety of anti-proliferative phenotypes including death by ferroptosis[3]. xCT knockout mice exhibit normal development and lifespan. Altogether, targeting xCT outside of CNS may potentially have widespread clinical utility in cancer treatment.
Results: We present preclinical data demonstrating development of novel, first-in-class xCT-targeted biotherapeutics (AX68c, AX76c) using studies in TNBC cell lines *in vitro* and in xenograft. We find that these agents have highly favorable pharmacokinetics, with FcRn-dependent serum half-lives greatly exceeding those of known small molecule xCTi. *In vitro*, AX68c or AX76c reduces glutathione levels in TNBC cells in accord with inhibition of xCT function. Analysis of anti-proliferative effects in a panel of TNBC cell lines revealed particular potency against those of M/MSL phenotype (IC50s 0.3-1uM). We further tested the susceptibility of the mesenchymal phenotype to AX68c and found that EMT induction in epithelial cancer cells significantly increased sensitivity in a ferroptosis-dependent manner. In wildtype and immunodeficient mice, AX68c is well tolerated at steady-state serum concentrations that are 15-300 fold of its *in vitro* IC50s in tested TNBC cells. In orthotopic MDA-MB-231 xenografts, AX68c treatment significantly reduced tumor metastasis and sensitized primary tumors to cisplatin and paclitaxel. Bulk RNAseq and GSEA analysis on primary tumors revealed treatment associated alterations in key cancer signaling pathways such as TGFβ, INFγ and TNFα/NFκB. In MDA-MB-436 orthotopic xenografts, AX68c alone led to significantly improved survival primarily through abrogating metastasis. Combining AX68c and cisplatin further prolonged survival through concurrent suppression of metastasis and primary tumor growth.
Conclusions: We conclude that our anti-xCT biologics may provide novel targeted therapies for M/MSL-subtype TNBC and metastatic tumors with a large mesenchymal component.

1. Viswanathan, et al., Nature, 2017; 2. Wang, et al., npj Precision Oncology, 2021; 3. Koppula, et al., Protein and Cell, 2021 (review).

#5963 VGLL1-derived peptides demonstrated anticancer effect by inhibiting VGLL1-TEAD4 interaction.

S. Ock[1], C. Lee[1], W. Jung[1], I. Whang[2], K.-S. Kim[1], J. Han[1], S. Yim[1], B.-K. Kim[3], H.-S. Lee[1], K.-Y. Chang[1], **M. Won**[3];
[1]OneCureGEN Co., Ltd, Daejeon, Korea, Republic of, [2]Ewha Womans University, Seoul, Korea, Republic of, [3]Korea Research Institute of Bioscience & Biotechnology (KRIBB), Daejeon, Korea, Republic of

YAP/TAZ, cofactors of TEA domain-containing transcription factor TEADs (TEAD1-4), play a key role in the HIPPO pathway, which is involved in various function including embryonic development, organ size, cell proliferation, tissue regeneration, and the development and progression of several cancers. YAP/TAZ is therefore considered as master regulators of various cancers. However, we are interested in VGLL1, a cofactor of TEAD4, because it is mainly involved in the proliferation and metastasis of various cancers, including gastric, breast, pancreatic, and ovarian cancers. In gastric cancer, VGLL1 expression is regulated by the PI3K/AKT/β-catenin pathway. VGLL1 is then phosphorylated at S84 by TGF-β/ribosomal S6 kinase 2 (RSK2) and interacts with TEAD4 to express target genes such as MMP9, cyclin D1, IGFBP3, IGFBP5 and ITGαV. which are involved in cancer malignancy. We designed S84-containing VGLL1-derived peptides (VGLL1S84 peptides, SCVP), which consist of 7 to 15 amino acids linked to CPP, a cell-penetration peptide. We evaluated SCVP to inhibit the VGLL1-TEAD4 interaction and their therapeutic potential as anticancer agents. SCVP suppressed the growth of gastric and breast cancer cells expressing high levels of VGLL1, EGFR, and/or HER2. In the RNA-seq analysis of NUGC3 to elucidate the molecular mechanisms of SCVP induced cell death, SCVP-treated cells showed gene expression changes in metabolic pathway, RAS signaling, PI3K-AKT signaling, Wnt signaling, TNF signaling, and mTOR signaling. However, RNA-seq analysis of breast cancer cells treated with SCVP showed changes in the expression of genes involved in cell cycle, DNA replication, DNA repair, and apoptosis. Then, we performed CRISPR/Cas9 screening using SCVP and sgRNA library to explore companion biomarkers and genetic interactors of VGLL1 for targeted cancer therapy. As a result, we identified several candidate genes, including ZNF292 and PLK1, as synthetic lethal genes of VGLL1. As expected, HCC70 cells with ZNF292 mutation showed increased sensitivity to SCVP. We also found that SCVP in combination and the PLK inhibitor volasertib resulted in a synergistic effect on the growth inhibition of breast cancer cells. In conclusion, we demonstrated VGLL1 as a novel target for anticancer drug development, and elucidated the molecular mechanism and therapeutic potential of the SCVP in gastric and breast cancers.

#5964 Design and anticancer biological evaluation of novel 7-aza-8,9-methylenedioxyindenoisoquinoline derivatives that inhibit MYC and topoisomerase I.

Y. Han[1], **L. Chen**[1], A. Buric[1], V. Chintareddy[2], P. Chand[2], R. Riggs[3], M. Cushman[1], D. Yang[1];
[1]Purdue University, West Lafayette, IN, [2]Therachem Research Medilab LLC, Chelsea, AL, [3]Gibson Oncology LLC, Miami, FL

MYC is one of the most validated driver oncogenes and is overexpressed in most human cancers. However, the MYC protein is considered “undruggable” due to its disordered structure and difficulties associated with targeting transcription factors. The *MYC* gene promoter forms G- quadruplex, a four-stranded non-canonical DNA secondary structure. The *MYC* G-quadruplex functions as a transcription silencer and further inhibits *MYC* expression upon drug binding, representing an exciting approach for MYC-targeting cancer therapy. Indenoisoquinolines are topoisomerase I inhibitors with better physicochemical and biological properties than the clinical camptothecin drugs. We previously revealed a novel mechanism of action for active anticancer indenoisoquinolines by dual inhibition of MYC and topoisomerase I, where potent MYC inhibition was achieved through targeting its promoter G-quadruplex. Herein, we report the design, cellular activity, and in vivo efficacy of novel anticancer 7-aza-8,9-methylenedioxyindenoisoquinoline derivatives based on optimized substituents and π-π stacking interactions. Using biophysical, biochemical, and cellular assays, we demonstrated that the new indenoisoquinoline derivatives greatly stabilized the *MYC* promoter G-quadruplex, significantly lowered MYC protein and mRNA levels in cancer cells, and inhibited topoisomerase I activity. A *MYC* G-quadruplex mediated mechanism of action was evident by differential activities in Raji vs CA-46 cells. The importance of MYC targeting was corroborated by potent cytotoxicity against a panel of MYC-dependent cancer cell lines as well as the NCI-60 panel of human cancer cell lines. The top three candidates were evaluated for pharmacokinetics and in vivo anticancer properties. Excellent metabolic stability, bioavailability, and tumor accumulation were observed in xenograft mouse models. Potent and significant tumor growth inhibition was demonstrated in the aggressive RD-ES Ewing Sarcoma xenograft mouse model while the drugs were well-tolerated. In addition, favorable brain penetration and pharmacokinetics were established, which encourage future evaluations in difficult-to-treat brain tumors. In conclusion, we designed and developed 7-aza-8,9-methylenedioxyindenoisoquinoline derivatives that are dual inhibitors of MYC and topoisomerase I. Our drug candidates demonstrated excellent pharmacokinetics and in vivo anticancer activities with promising indications in MYC-dependent cancers.

#5965 First-in-class chemical induced proximity system achieves dose-dependent control of *TP53* activation in gastric cancer.

R. M. Kemper, T. J. Nelson, N. A. Hathaway, D. J. Crona;
UNC Eshelman School of Pharmacy, Chapel Hill, NC

Background: Gastric cancer (GC) remains a common and deadly disease, and inactivating *TP53* mutations occur in up to 68% of GC tumors. p53 is a master regulator of multiple cellular pathways, such as the cell cycle, apoptosis, and senescence. Previously, we demonstrated the ability to activate endogenous target gene expression using a novel chemical induced proximity system comprised of deactivated Cas9 (dCas9) and "chemical epigenetic modifiers" or "CEMs" (PMID: 31712774). In this study, we applied our dCas9-CEM system for the first time in oncology to activate *TP53* gene expression and selectively kill targeted cells in a preclinical model of GC.

Methods: AGS cells were derived from a gastric adenocarcinoma, and harbor wild-type *TP53*. They were transduced with our dCas9 system and either sgRNAs targeting *TP53 or a* non-targeting (NT) sgRNA. After 48 h CEM87 incubation (1-25 nM), expression of *TP53* and downstream targets (*CDKN1A and BBC3)* were evaluated by RT-qPCR. After 48 h CEM87 incubation (0.1-25 nM), colony-forming potential was assessed by crystal violet staining after 10 days. After 24 h incubation (5-25 nM), cells were fixed and stained with propidium iodide (PI), and DNA content was assessed by flow cytometry to determine cell cycle fractions. After 48 h incubation (50-200 nM), cells were fixed and stained with Annexin V and PI, and apoptosis was assessed by flow cytometry. Last, cells were treated with nine ascending concentrations (10 pM-100 μM) for 48 h, and cell viability was measured using CellTiter-Glo™. IC_{50} values were calculated using four-parameter non-linear regression.

Results: AGS-*TP53* cells show significantly increased expression of *TP53* and downstream target genes *CDKN1A* and *BBC3* versus AGS-NT cells after 10 nM CEM87 (105%, 99%, and 43% increase, *P*=0.004, 0.002, and 0.03, respectively; n=3). Colony formation was significantly reduced in AGS-*TP53* versus AGS-NT cells after 10 nM CEM87 (60.2% reduction, *P*=0.003; n=3). Treatment with 10 nM CEM87 also led to a G2/M stall after significantly reducing cells in both G1 (47.4% vs 38.9%, *P*<0.0001; n=3) and S-phase (25.1% vs 20.3%%, *P*<0.0001; n=3) in AGS-*TP53* versus AGS-NT cells. Treatment with 200 nM CEM87 significantly increased early apoptosis in AGS-*TP53* versus AGS-NT cells (28.7% vs 6.6%, respectively, *P*<0.0001; n=3). Last, CEM87 was 50 times more potent in AGS-*TP53* cells than AGS-NT cells (IC_{50}: 3 vs 146 nM; n=8).

Conclusions: These data highlight how our innovative system upregulates *TP53* expression and impacts downstream phenotypic effects of *TP53* activation in a preclinical model of GC.

#5966 PRT2527, a novel highly selective cyclin-dependent kinase 9 (CDK9) inhibitor, has potent antitumor activity in combination with BTK and BCL2 inhibition in various lymphoid malignancies.

N. Fultang, A. M. Schwab, S. McAneny-Droz, D. Heiser, P. Scherle, N. Bhagwat;
Prelude Therapeutics, Wilmington, DE

CDK9 is a master regulator of transcription that modulates transcription elongation via phosphorylation of RNA polymerase II. Short-term inhibition of CDK9 depletes short-lived transcripts and labile proteins such as MCL1, BFL1 and MYC to promote cancer cell death. We previously described PRT2527, a novel, potent, highly selective CDK9 inhibitor with anti-leukemic activity in various preclinical models. PRT2527 is currently under evaluation in a Phase I clinical trial in patients with relapsed/refractory hematologic malignancies (NCT05159518). Here we demonstrate PRT2527 potently inhibits cancer cell growth and induces cell death in various models of Diffuse Large B Cell Lymphoma (DLBCL), Mantle Cell Lymphoma (MCL) and Chronic Lymphocytic Leukemia (CLL), through depletion of MCL1, BFL1 and MYC. Specifically, we show that brief treatment with PRT2527 (6h) potently induces apoptosis and inhibits proliferation in DLBCL, MCL and CLL cell lines. We also show that the addition of BTK inhibitors (BTKi) or BCL2 inhibitors (BCL2i) potentiates the apoptosis response induced by PRT2527 *in vitro* and leads to more robust and durable responses including complete tumor regressions in DLBCL CDX and PDX models *in vivo*. In all studies, the combination of PRT2527 with BTKi or BCL2i is well tolerated. Mechanistically, we show that BTK inhibition upregulates BMF, an endogenous inhibitor of BCL2 and BCL-xL, driving cells towards MCL1 and BFL1 dependency in TMD-8 cells. Concurrent depletion of MCL1 and BFL1 with PRT2527 leads to complete inhibition of Bcl-2- family mediated survival signaling, potently inducing cell death. In similar fashion, Venetoclax-driven BCL2 inhibition also potentiates the anti-tumor activity of PRT2527. Consistent with these findings *in vitro*, we observe reduced BFL1 and MCL1 as well as increased BMF in tumors of mice treated with BTKi and PRT2527 suggesting complete Bcl-2 family inhibition. We also demonstrate potent induction of apoptosis in peripheral blood mononuclear cells isolated from patients with both treatment-naïve and relapse/refractory CLL following brief treatment with PRT2527 (6h). Co-treatment with BTKi or BCL2i further enhances the apoptotic effect of PRT2527, similarly suggesting combinatorial benefit. Additionally, we characterize the activity of PRT2527 in models of BTKi relapsed/refractory MCL where increased CDK9 dependency has previously been described. In an Ibrutinib-resistant Mino CDX model, we observe increased tumor growth inhibition following treatment with PRT2527 compared to tumors derived from parental Mino cells, suggesting PRT2527 is efficacious in BTKi-resistant MCL. Altogether these data provide a rationale for evaluating PRT2527 in combination with BTK and BCL2 inhibitors for the treatment of patients with relapsed/refractory lymphoid malignancies.

#5967 Blockade of Wnt5A/ROR1 signaling as cancer stem cell targeting therapy for metastatic prostate cancer.

C. A. Jamieson[1], J. Murtadha[1], C. S. Oh[1], M. T. Muldong[1], N. Etemadfard[1], E. Koutouan[1], Y. E. Yoon[2], S. Lee[1], O. S. Kwon[3], J. J. Oh[4], M. S. Kim[5], K. Willert[1], N. A. Cacalano[6], C. H. Jamieson[1], T. Gaasterland[1], R. R. Mckay[1], C. J. Kane[1], A. A. Kulidjian[7], C. E. Prussak[1];
[1]UC San Diego, La Jolla, CA, [2]Hanyang University College of Medicine, Seoul, Gyeonggi-do, Korea, Republic of, [3]Hallym University College of Medicine, Seoul, Youngdeungpo-gu, Korea, Republic of, [4]Seoul National University Bundang Hospital, Bundang-gu, Seongnam-si, Gyeonggi, Korea, Republic of, [5]Seoul Medical Center, Jungnang-gu, Seoul, Korea, Republic of, [6]UC Los Angeles, Los Angeles, CA, [7]Scripps Health MD Anderson, La Jolla, CA

BACKGROUND-- Wnt5A and its non-canonical Wnt receptor, ROR1, have emerged as a promising new signaling pathway target for lethal, metastatic prostate cancer. Wnt5A has emerged as a significant marker of poor prognosis in circulating tumor cells (CTCs) of metastatic castration resistant prostate cancer (mCRPC) patients. ROR1 is expressed in lethal types of mCRPC, especially neuroendocrine prostate cancer (NEPC). A therapeutic ROR1 antibody, Zilovertamab, has been clinically tested in chronic lymphocytic leukemia (CLL) and metastatic breast cancer and shown to be safe. We sought to investigate Zilovertamab-based therapies for metastatic prostate cancer in pre-clinical model systems.
HYPOTHESIS -- Wnt5A/ROR1 signaling may mediate a cancer stem cell program which makes cells resistant to therapies which target the cell cycle and proliferation. Blocking ROR1 may reveal vulnerabilities which sensitize cancer cells to chemotherapies like docetaxel.
METHODS-- ROR1 expression was determined using RNASeq, qRT-PCR, FACS, IHC and Western blotting. ROR1 signaling was blocked using the anti-ROR1 therapeutic antibody, Zilovertamab, or CRISPRCas9 ROR1 knock out. Cell growth was measured using an Incucyte real time imaging system. Stem cell activity was assessed in 3D organoids. Cell cycle analysis was performed in live cells in 2D cultures and 3D organoids using the *Fucci2BL* bicistronic Fluorescent, Ubiquitination-based Cell Cycle Indicator reporter system. PDX PCSD13 tumor growth was measured via calipers and IVIS. RNASeq was performed on tumors.
RESULTS-- We showed that ROR1 was expressed at high levels in mCRPC cell lines: PC3, DU145, and in the bone metastatic prostate cancer PDX: PCSD13. CRISPR/Cas9 Knock out of ROR1 in PC3 and DU145 cells showed increased sensitivity to docetaxel inhibition of proliferation in vitro in 2D real time Incucyte proliferation assays and in 3D organoids. Organoid formation was significantly reduced in ROR1 KO cells. Cells expressing the FUCCI live cell cycle tracker showed docetaxel led to G2 arrest and ROR1 signaling inhibition increased efficacy of docetaxel induced cell cycle arrest. Treatment of PCSD13 PDX in vivo with Zilovertamab plus docetaxel synergistically increased tumor growth inhibition in vivo and modulated cancer stem cell and cell cycle expression profiles.
CONCLUSIONS-- Cancer stem cells represent the fundamental precursors from which all diverse tumor subpopulations evolve. Thus, therapeutic targeting of these tumor initiating stem/progenitor cells may prevent the evolutionary diversification of a tumor and overcome a critical clinical barrier to cancer treatment. We showed synergistic response in our PDX and PCs cell line models to Zilovertamab plus docetaxel. We are now conducting a phase 1b clinical trial with zilovertamab plus docetaxel in patients with metastatic CRPC (CirmD, NCT05156905, PI R Mckay).

#5968 CDC7 is a targetable regulator of advanced prostate cancer.

A. B. Hartono[1], S. Paparaju[1], C. Lee[1], S. Liu[1], B. R. Alabi[2], E.-C. Hsu[2], J. D. Brooks[2], E. Corey[3], T. Stoyanova[1];

[1]UCLA - University of California Los Angeles, Los Angeles, CA, [2]Stanford University, Palo Alto, CA, [3]University of Washington, Seattle, WA

Prostate cancer is estimated to contribute to over 34,000 deaths in men residing in the United States, with the majority fatality due to metastatic disease. CDC7 is a kinase that regulates DNA replication and is an emerging cancer biomarker for poor prognosis in carcinomas such as Wilms tumor and hepatocellular carcinomas. In this study, we demonstrated that high level of CDC7 is associated with metastatic prostate cancer when compared to benign prostate tissues or localized prostate cancer. Furthermore, we found that CDC7 expression is highest in prostate cancer patient-derived xenografts (PDX) models of adenocarcinomas with neuroendocrine features. *In vitro*, we showed that inhibition of CDC7 with TAK-931, a CDC7 specific inhibitor, reduced the ability of aggressive prostate cancer cells to proliferate, migrate, and invade. Similarly, knock-down of CDC7 in prostate cancer cell lines inhibited cell growth in a colony formation assay. TAK-931 treated prostate cancer cell lines also showed an abnormal cell cycle profile, indicating that inhibiting CDC7 in aggressive prostate cancer could contribute to replication stress and promote apoptosis. Overall, this study demonstrates that CDC7 is a targetable protein that regulates advanced and aggressive prostate cancer growth.

#5969 VRK1 can be a therapeutic target in small cell neuroendocrine carcinoma of the uterine cervix.

Mariya Kobayashi[1], Satoshi Nakagawa[1], Mizuki Kanda[1], Yuji Kamei[1], Masuda Tatsuo[2], Mamoru Kakuda[1], Kosuke Hiramatsu[1], Toshihiro Kimura[1], Yutaka Ueda[1], Takayuki Enomoto[1], Masahiro Inoue[3], Tadashi Kimura[1]

[1]Department of Obstetrics and Gynecology, Osaka University, Suita, Japan,[2]StemRIM Institute of Regeneration-Inducing Medicine, Osaka University, Suita, Japan,[3]Department of Clinical Bio-Resource Research and Development, Graduate School of Medicine, Kyoto University, Kyoto, Japan

Objective: Small cell neuroendocrine carcinoma of the uterine cervix (SCNEC) is extremely rare but highly aggressive and its prognosis is usually poor. Vaccinia-related kinase (VRK)1 is a serine/threonine protein kinase that is involved in cell proliferation by regulating cell-cycle progression and inducing cell-cycle arrest in response to stress signals. VRK2 belongs to the same family as VRK1, and they are paralogs. VRK1 has been reported as a potential therapeutic target in nervous system tumors with low VRK2 expression. Previously, we identified high expression of VRK1 in SCNEC through proteomic analysis of isolated organoids. The objective of the present study is to investigate the effect of VRK1 on the proliferation of SCNEC and its potential as a therapeutic target.

Methods: The mRNA and protein expression of VRK1 and VRK2 in ten organoids and two cell lines derived from SCNEC were examined and compared with cervical cancer of other histological subtypes by RNA microarray and western blot analysis. The effect of VRK1 on tumor growth in vitro and in vivo (xenograft model) were evaluated by shRNA-mediated knockdown of VRK1 (shVRK1). RNA-seq was performed from the xenograft tumors. The effects of shVRK1 on cell proliferation were evaluated under various levels of oxidative stress induced by H_2O_2.

Results: VRK1 expression was higher in organoids and cell lines derived from SCNEC than those derived from squamous cell carcinoma and adenocarcinoma, while VRK2 expression was lower in SCNEC. Tumor growth was suppressed significantly by shVRK1 in vivo (mean weight: cell line 1: 0.62 vs 0.06g, $p<0.05$, 2: 1.79 vs 0.58g, $p<0.01$). Gene ontology analysis of RNA-seq data suggested that VRK1 is related to cellular responses to stress. Proliferation was slightly suppressed by shVRK1 under normal conditions; however, it was significantly enhanced under oxidative stress (Cell line 1: in shVRK1, -14.0% without oxidative stress vs -54.9% under H_2O_2 750μM, $p<0.01$, Cell line 2: similar to Cell line 1).

Conclusion: SCNEC exhibited high VRK1 and low VRK2 expression, and the tumor suppressive effect of shVRK1 was more significant in vivo than in vitro. VRK1 may play a role in the tumor microenvironment, including oxidative stress, and is a potential therapeutic target for SCNEC.

#5970 Carbamazepine mediated *SMARCA4* inhibition as a therapeutic target for *KRAS*-mutated CRC.

Aaron Shaykevich[1], Danbee Chae[1], Isaac Silverman[1], Jeremy Bassali[1], Netanel Louloueian[1], Alexander Siegman[1], Gargi Bandyopadhyaya[1], Sanjay Goel[2], Radhashree Maitra[1]

[1]Biology, Yeshiva University, New York, NY, [2]Oncology, Rutgers Cancer Institute of New Jersey, New Brunswik, NJ

Introduction: Carbamazepine (CBZ) is an autophagy inducer along with its other therapeutic properties. *KRAS*-mutated CRC has a worse prognosis and limited treatment options when compared to *KRAS* wild-type CRC. In this study, we followed the effects of CBZ treatment in the mutant and wild-type CRC cells. We herein report that CBZ exhibits mutant selectivity in efficacy and significantly modulates *SMARCA4* levels, a protein heavily implicated in both tumor suppression and proliferation, presenting a promising method for *KRAS*-mutated CRC treatment.

Methodology: 2 cell lines, HCT116 (*KRAS* mutant) and Hke3 (*KRAS* wild-type), were used in this study. These cells were treated with Carbamazepine (CBZ) for either 6 or 24 hours. Subsequently, RNA and protein extractions were performed to assess the expression levels of *SMARCA4* through quantitative polymerase chain reaction (qPCR) and Western blot analysis, respectively. Furthermore, the TCGA COAD-READ patient dataset was accessed using Xena. The data is used to assess the correlation of *KRAS* and *SMARCA4* wt-tumor vs. mutant-tumor. The dataset was also used to visualize the effect of high *SMARCA4* mRNA on the different patient cohorts.

Results: Basal levels of *SMARCA4* are higher in CRC patients than control ($p = 1.81e-16$). Patients with a *KRAS* mutation has higher levels than *KRAS*-wt ($p = 0.000005$). *KRAS* mutated cells treated with CBZ expressed less BRG1 (*SMARCA4* protein) at 24 hours (Fold Change = 0.68, $p= 0.041$). *KRAS* wildtype cells treated with CBZ expressed more BRG1 at 6 hours (Fold Change = 1.23, $p= 0.006$). The fold change of BRG1 in *KRAS*-mutant was significantly lower than in *KRAS*-wildtype at both 6 and 24 hours ($p= 0.013$ and $p= 0.002$). *KRAS* mutated cells treated with CBZ expressed less *SMARCA4* mRNA at 24 hours (Fold Change = 0.69, $p= 0.008$). *KRAS* wildtype cells treated with CBZ expressed more *SMARCA4* at 6 hours (Fold Change = 1.62, $p= 0.006$) and 24 hours (Fold Change = 1.31, $p= 0.06$). The fold change of *SMARCA4* in *KRAS*-mutant was significantly lower than in *KRAS*-wildtype at both 6 and 24 hours ($p= 0.0032$ and $p= 0.00009$). BRG1 expression affected overall survival for the first 1500 days - only in patients with a *KRAS*-mutant ($p= 0.015$).

Conclusion: This study sheds light on the potential therapeutic role of CBZ in colorectal cancer, particularly in the context of *KRAS*-mutated CRC. Our findings indicate that CBZ treatment has distinct effects on *SMARCA4* expression in CRC depending on *KRAS* mutation status. In *KRAS*-mutated cells, CBZ reduced *SMARCA4* protein and mRNA levels. Conversely, in *KRAS* wild-type cells, CBZ resulted in an increase in *SMARCA4* expression. Furthermore, our analysis of patient datasets reaffirmed the association between elevated *SMARCA4* and *KRAS*, since high *SMARCA4* expression led to worse overall survival rates, specifically in *KRAS*-mutant CRC patients. These findings emphasize the need for further exploration of CBZ as a potential treatment strategy for CRC.

#5971 F3 targeted near-infrared photoimmunotherapy: The ideal therapeutic approach for numerous malignancies.

S. Takao, A. Furusawa, H. Fukushima, S. Okuyama, M. Kano, H. Yamamoto, P. L. Choyke, H. Kobayashi;
National Cancer Institute, Bethesda, MD

Introduction: F3 is a cell surface protein that plays a role in blood clotting, but recent research has revealed its implication in cancer proliferation, metastasis, angiogenesis, and immune escape. TCGA cohort analysis has shown that elevated F3 is a common feature of many cancers, and generally correlates with poor patient survival. Therefore, the potential of F3 as a therapeutic target in cancer is worth exploring. Tisotsumab-vedotin, an antibody-drug conjugate (ADC) that targets F3, was approved by the FDA for cervical cancer and is undergoing clinical trials in some solid cancers. However, ADCs may give rise to concerns about drag resistance following cellular internalization. Herein, we developed and tested an F3 targeted near-infrared photoimmunotherapy (NIR-PIT) to overcome some of these resistance mechanisms.
Methods: We created a conjugate of tisotumab as an F3 antibody and IR700. The efficacy of F3-targeted NIR-PIT was investigated using multiple cancer cell lines (A431; epidermoid carcinoma, HPAF-II; pancreatic adenocarcinoma, HSC-2; oral carcinoma, HT-1376luc; bladder carcinoma, MDAMB231; breast adenocarcinoma, and SKOV-3; ovarian serous cystadenocarcinoma) in vitro. In vivo, the efficacy of F3-targeted NIR-PIT was evaluated in HPAF-II tumor using xenograft mouse models. In addition, the pathological change after NIR-PIT was also evaluated in A431, HPAF-II, HSC-2, HT-1376luc, MDAMB231, and SKOV-3 tumors.
Results: These cell lines showed F3 expression in vitro and in vivo. Additionally, F3 expression was specific to cancer cells in HPAF-II tumor model. In vitro, F3-targeted NIR-PIT damaged the multiple cell lines in an NIR light dose-dependent manner. In vivo, F3-targeted NIR-PIT suppressed tumor growth and improved survival rates compared to the untreated group. Pathologically, A431, HPAF-II, HSC-2, HT1376-luc, MDAMB231 and SKOV-3 tumors after NIR-PIT contain large numbers of necrotic cells that are shown typically less dark nuclei and eosinophilic cytoplasm with some vacuolar degeneration than untreated tumors.
Conclusions: F3-targeted NIR-PIT holds the efficacy against multiple cancers expressing F3, regardless of the specific cancer type. Therefore, this modality exhibits significant promise as a potential NIR-PIT option.

#5972 Therapeutic modulation of rock overcomes metabolic adaption to oxphos inhibition and suppresses tumor growth.

N. Blazanin, X. Liang, I. Mahmud, E. Kim, L. Tan, N. Esmaeili Anvar, W. Chan, M. Ha, R. Minelli, M. Peoples, P. Lorenzi, T. Hart, Y. Lissanu, N. Blazanin; UT MD Anderson Cancer Ctr., Houston, TX

Lung cancer is the top cause of cancer mortality. Despite recent advances, the majority of patients with lung cancer still lack effective therapeutic options, underscoring the dire need for additional treatment approaches. Genomic studies have identified frequent mutations in subunits of the SWI/SNF chromatin remodeling complex including *SMARCA4* and *ARID1A* in non-small cell lung cancer with a frequency of up to 33% in advanced stage disease, making it the most frequently mutated complex in lung cancer. Previous work in our lab, as well as others, have identified a metabolic vulnerability in targeting oxidative phosphorylation (OXPHOS) in SMARCA4-mutant lung cancer. However, OXPHOS inhibitors are still not approved to treat cancer due to modest efficacy and adverse effects. This strongly suggests that novel, efficacious and tolerated agents that synergize with OXPHOS inhibition are urgently needed. To this end, we undertook a functional genomics screen by utilizing a focused CRISPR-Cas9 library targeting genes with available FDA approved therapeutics in genetically defined lung cancer cell lines. Importantly, we utilized low doses of the OXPHOS inhibitor IACS-10759 that are known to be well tolerated in patients. Among our top validated hits was ROCK1/2 kinases and we demonstrate that Belumasudil, a clinically approved ROCK inhibitor with a robust safety and tolerability profile, displays a synergistic combination with IACS-10759. Furthermore, low doses of IACS-10759 synergized with ROCK inhibition in vivo eliciting marked tumor growth inhibition. Mechanistically, we showed that the combination of Belumasudil and IACS-10759 induced a profound energetic stress. This was primarily due to ROCK inhibition-mediated suppression of the normally observed adaptive increase in glycolysis upon OXPHOS inhibition. Steady-state metabolomics and C^{13}-glucose isotope tracing confirmed downregulation of multiple glycolytic metabolites and reduced glycolytic flux by the combination of ROCK inhibition and IACS-10759 and was associated with severe reduction in glucose uptake. In summary, our study identified a key role of ROCK kinases in metabolic adaptation of cancer cells and provides a strong rationale for pursuing ROCK inhibitors as novel combination agents with OXPHOS inhibition and lay the foundation for future clinical investigation in genetically defined subtypes of lung cancer.

#5973 Targeting prolyl 4-hydroxylase subunit alpha 1 with a small molecule inhibitor, diethyl-pythiDC, reduces pancreatic ductal adenocarcinoma growth and metastasis.

F. Afaq[1], M. Khushman[2], P. Bajpai[1], S. Al Diffalha[1], D. Otali[1], S. Varambally[1], U. Manne[1];

[1]University of Alabama at Birmingham, Birmingham, AL, [2]Washington University in St. Louis, St. Louis, MO

Background: Pancreatic ductal adenocarcinoma (PDAC) is a lethal disease that has a 5-yearrelative survival rate of less than 9%. It is the fourth leading cause of cancer-associated mortality,and is projected to become the second leading cause of cancer-related deaths by 2030. Since most(~80%) PDACs are diagnosed at late stages (metastasized), there is an urgent need to identifymolecular determinants that regulate PDAC progression and serve as candidates for therapeutictargeting. Prolyl 4-hydroxylase subunit alpha 1 (P4HA1) is the major isoform overexpressed inmost cancers, including PDAC. In PDAC, high expression of P4HA1 is associated with tumorprogression and poor clinical outcomes. Thus, we investigated if targeting P4HA1 in PDAC witha small molecule inhibitor; diethyl-pythiDC, had an inhibitory effect on cell proliferation, tumorprogression/growth, and metastasis.
Methods: To demonstrate the therapeutic efficacy of diethyl-pythiDC, we performed MTT, colonyformation, wound healing, Transwell, and western blot assays in various PDAC cell lines. Tumorgrowth and metastasis was evaluated with xenografts in NOD/SCID/IL2γ receptor-null (NSG)mice. Additionally, expression of P4HA1 in human PDAC and in adjacent normal pancreatictissues was assessed.
Results: In human PDACs, there was elevated expression of P4HA1 protein relative to adjacentnormal pancreatic tissues. Treatment of various PDAC cells (S2VP10, MIA PaCa2, BxPC-3, andPANC-1) with diethyl-pythiDC reduced cell proliferation and colony formation, and inducedG2/M cell cycle arrest. Diethyl-pythiDC reduced migration and invasion of PDAC cells bymodulating epithelial-mesenchymal transition (EMT) markers (N-cadherin, E-cadherin, andvimentin). In addition, diethyl-pythiDC reduced the expression of argonaute-2 (AGO2), acomponent of microRNA biogenesis implicated in tumorigenesis, and its downstream target,matrix metalloproteinase (MMP1). In preclinical animal models of PDAC, diethyl-pythiDCreduced tumor growth and metastasis. Furthermore, in xenograft tumors, diethyl-pythiDCtreatment reduced the expression of AGO2, MMP1, and the proliferative marker, PCNA, andmodulated proteins of the EMT.
Conclusions: Treatment with diethyl-pythiDC reduces PDAC progression by decreasing cellproliferation, arresting cells in the G2/M phase, downregulating AGO2/MMP1 expression, andmodulating the EMT. These findings suggest that targeting P4HA1 by diethyl-pythiDC could be aviable strategy to improve treatment for PDACs, particularly those expressing high levels ofP4HA1. They also provide a basis to conduct clinical trials to assess the utility of targeting P4HA1by diethyl-pythiDC.

#5974 Targeting VEGFR on tumor cells and activated vasculature through delivery of granzyme B.

K. A. Mohamedali, L. H. Cheung, A. Alvarez-Cienfuegos, W. N. Hittelman, M. G. Rosenblum;
UT MD Anderson Cancer Center, Houston, TX

Anti-VEGF therapy is a key therapeutic in several cancer treatment regimens. However, none of the current therapeutics are directly cytotoxic against tumor cells. $VEGF_{121}$ is the smallest isoform in the VEGF-A family of cytokines that binds to VEGF receptors R-1 and R-2. Both receptors are over-expressed on several tumor cells and the endothelium of tumor vasculature but not normal vasculature. We hypothesized that delivery of a cytotoxic payload through VEGFR-2 into tumor cells and tumor neovasculature would significantly enhance cancer therapy. Granzyme B is a key effector in immune-mediated cell killing through both caspase-dependent and -independent mechanisms. We previously reported the development of a fusion protein composed of granzyme B (GrB) and $VEGF_{121}$ (GrB/$VEGF_{121}$). Here, we report on GrB-Fc-$VEGF_{121}$, a fusion protein incorporating a human IgG heavy chain Fc fragment for dimerization to increase the molecular weight and improve *in vivo* circulation and targeting potential. We expressed and purified GrB-Fc-$VEGF_{121}$ from HEK-293E cells under serum-free conditions with a final yield of approximately 40 mg/L. The enzymatic activity of GrB in GrB-Fc-$VEGF_{121}$ was comparable to that of commercially available human GrB. We characterized this construct against both human and mouse VEGFR+ cell lines as this ligand cross-reacts to both species. GrB-Fc-$VEGF_{121}$ showed *in vitro* cytotoxicity in the nanomolar range against tumor and endothelial cell lines expressing high levels of VEGFR-1 or VEGFR-2, while receptor-negative cells demonstrated IC_{50} levels in the high micromolar range. GrB-Fc-$VEGF_{121}$ internalized into VEGFR-2+ tumor and endothelial cells within 2 hours of treatment while untargeted GrB did not internalize, suggesting internalization was receptor-mediated. Treatment of VEGFR2+ cells at the respective IC_{50} dose resulted in >50% cell death via apoptosis and/or necrosis within 48 h. *Ex vivo* serum stability studies indicated a gradual protein loss of GrB-Fc-$VEGF_{121}$ with an overall stability of about 50% over 96 hours. No toxicity was observed in mice treated with a total dose of 475 mg/kg (IP, QOD x 5), indicating that the maximum tolerated dose of GrB-Fc-$VEGF_{121}$ exceeds this dose level. *In vivo* efficacy studies in an OVCAR8 tumor xenograft model (20 mg/kg GrB-Fc-$VEGF_{121}$ x 5) resulted in significant growth inhibition of established tumors compared to vehicle controls. The number of CD31+ blood vessels and Ki-67+ proliferating tumor cells decreased significantly in treated tumors compared to controls. Pharmacokinetic studies are underway and will be reported. Thus, GrB-Fc-$VEGF_{121}$ significantly reduces tumor growth *in vivo* with no observed toxicity against normal tissues. This tumor- and vascular-targeting agent appears to have significant potential as a new class of targeted therapeutic agents with a unique mechanism of action. Research conducted, in part, by the Clayton Foundation for Research.

#5975 Characterization and pharmacokinetics of ligand traps targeting the human epidermal growth factor receptor (HER) family.

D. C. Maneval[1], C. Yang[2], C. Trevisiol[2], H. Shepard[2], P. Jin[2];

[1]Independent Consultant, Del Mar, CA, [2]Enosi Therapeutics, Eugene, OR

Antibodies targeting HER receptors have led to successful therapeutics for multiple human malignancies. Targeting the family of HER ligands provides an alternative strategy to inhibit signaling and subsequent proliferation of cancer cells. We have engineered ligand traps that bind the growth factors activating the HER family and have characterized a series of molecules (EN2000-Fc) using Surface Plasmon Resonance (SPR). Five distinct molecules were further evaluated for improved in vivo pharmacokinetics in mice that express human neonatal Fc receptor (FcRn). Mutations in the IgG Fc known to extend the *in-vivo* half-life of monoclonal antibodies were incorporated into the parental EN2000-Fc to generate 3 more distinct pan HER ligand traps. In addition, an EN2000-Fc variant with a full-length hinge was engineered, which is 5-amino-acid longer N-terminally than the parental molecule. These five molecules were synthesized (> 300 mg of each), purified (>98%), and characterized for *in vitro* and *in vivo* testing. Two variants were compared by evaluating the ligand binding affinity to 11 HER ligands using SPR. Both molecules showed comparable affinity against all ligands tested, confirming reproducibility of the pan HER ligand trap engineering technology. Among the ligands, HB-EGF had the highest affinity. High binding affinities to EGF, NRG1, NRG2, betacellulin and TGFα were also measured. The serum pharmacokinetics of the different ligand traps were compared in 6- to 8-week-old female C57BL/6 mice engineered to express human FcRn. Ligand traps were administered by single tail vein injection, and serum samples collected over a 28-day interval were analyzed by ELISA. Ligand traps with engineered Fc-mutations had 3- to 4-fold greater systemic exposure (area-under-the-curve) compared to ligand traps with the parental sequence, demonstrating improved *in vivo* characteristics of selected engineered fusion proteins. These results provide useful information for product candidate selection and for further preclinical development of a ligand trap targeting HER family receptors.

#5976 R9: A novel NuRD complex inhibitor for targeted therapy in triple negative breast cancer (TNBC).

k. zhang[1], S. Jacob[1], M. Dozmorov[1], I. Babic[2], E. Nurmemmedov[2], A. C. Faber[1];

[1]Virginia Commonwealth University - VCU, Richmond, VA, [2]Nerd bio, San Diego, CA

Triple Negative Breast Cancer (TNBC) is a highly aggressive breast cancer subtype, disproportionately affecting young and African American populations. TNBC constitutes up to 15% of breast cancers that lack effective targeted therapy. The Nucleosome Remodeling and Deacetylase (NuRD) complex, a pivotal chromatin remodeling entity, plays a crucial role in cancer development and progression. Specifically, the NuRD complex associates with SALL4 in cancer cells, contributing to the silencing of tumor-suppressor genes like PTEN. In this study, we discover R9, a novel small-molecule nucleotide analog, a first-in-class NuRD inhibitor. Utilizing computational and cellular methods, R9 demonstrated selective engagement with RBBP4, a key NuRD complex subunit. Cellular target engagement technology has been utilized to verify direct interaction of R9 with NuRD complex as well as to guide medicinal chemistry efforts. Mass spectrometry thermal proteome profiling (TPP) affirmed RBBP4 as the primary target of R9 with minimal off-target effects. In vitro studies reveal R9 displaying robust toxicity in TNBC cells, while sparing normal tissue derived cells. Encouragingly, R9 effectively impeded TNBC tumors growth in mice without inducing toxicity. Mechanistically, we demonstrate R9 induces DNA damage in sensitive TNBC cells, and the sensitivity correlates to DNA damage-vulnerable cancer cells, indicating DNA damage is a major effector of NuRD complex inhibition in TNBCs. We further demonstrate that R9 induces DNA damage through a c-MYC dependent manner. Ongoing studies aim to elucidate key transcription factors involved in NuRD complex inhibition and the role of MYC and DNA damage in response to NuRD complex inhibition. This research positions R9 as a promising candidate for targeted therapy in TNBC, offering potential insights into the intricate molecular pathways involved in TNBC tumor progression.

#5977 A first-in-human, open-label, multi-center phase 1 study of TST003, a GREM 1 inhibitor, in subjects with locally advanced or metastatic solid tumors.

Ismael Rodriguez Rivera[1], Lin Shen[2], Shivaani Kummar[3], Minal Barve[4], Caroline Germa[5], Chuan Qi[6], Lei chen[6], Jenny Milata[5], Jenny Yao[5], Li Shen[6], Xuelian Zhu[6]

[1]NEXT Oncology, San Antonio, TX,[2]Beijing Cancer Hospital, Beijing, China,[3]Division of Hematology and Medical Oncology, Oregon Health & Science University, Portland, OR,[4]Mary Crowley Cancer Research Centers, Dallas, TX,[5]Transcenta Therapeutics Inc., Princeton, NJ,[6]Suzhou Transcenta Therapeutics Co., Ltd, Shanghai, China

Background: Gremlin-1 (GREM1), a member of the TGF-β superfamily, plays a key role in EMT, and cancer cell proliferation by binding to BMPs. GREM1 is widely expressed in various human cancers and TME stromal cells. Overexpression of GREM1 is correlated with poor prognosis. TST003 is a novel humanized IgG1 monoclonal antibody targeting GREM1 with high affinity and selectivity, and it blocks GREM1 binding to BMP2/4 resulting in enhanced BMP signaling. This study will investigate TST003's safety, tolerability, and preliminary anti-tumor activity in patients with advanced solid tumors.
Objectives: The primary objectives are to evaluate the safety and tolerability and determine the maximum tolerated dose and/or optimal biologic dose(s) of TST003. Secondary objectives include pharmacokinetic, pharmacodynamic and preliminary anti-tumor activity of TST003. A comprehensive biomarker plan will be implemented to analyze GREM1 expression, BMP signaling pathway, and tumor microenvironment with tumor tissues (including tumor cells, CAFs, T_{eff}, T_{reg}, MDSCs and TAMs), as well as circulating tumor DNA to explore the correlation among drug exposure, pharmacodynamic markers and clinical outcomes.
Method: This is a first in human Phase 1 study in locally advanced or metastatic solid tumor subjects having tumor progression during or after prior therapies and have no standard therapy that could confer clinical benefit. It comprises of the Part 1 Dose Escalation and the Part 2 Pharmacodynamic Cohorts. Part 1 will evaluate sequential dose levels of 1, 3, 10, 20 and 30 mg/kg TST003 iv., every three weeks as a single agent. The traditional "3+3" design were used for dose escalation of the first two cohorts (1 and 3 mg/kg), and Bayesian Optimal Interval (BOIN) Design with prespecified cohort size of 3 is used in the following cohorts. Part 2 will include 2 pharmacodynamic cohorts to evaluate the pharmacokinetic (PK) profile, pharmacodynamic (PD) markers, preliminary tumor response, as well as safety of TST003 as monotherapy in locally advanced or metastatic colorectal adenocarcinoma (CRC) subjects. The 2 doses used in the pharmacodynamic cohorts will be chosen from Part 1 and are expected to be within the pharmacologically active range based on nonclinical PK/PD modeling and available clinical PK/PD data from the ongoing study. Baseline GREM1 expression will be analyzed by immunohistochemistry. In each pharmacodynamic cohort, around 13-18 subjects will be enrolled to ensure at least 7 GREM1 positive subjects. Eligible subjects will receive TST003 until unacceptable toxicity or disease progression by RECIST v1.1. The enrollment is ongoing in clinical centers in the US and China. No significant safety signals were reported in the first few patients treated with TST003.
Clinical Trial Information: NCT05731271.
Study Sponsor: Suzhou Transcenta Therapeutics Co., Ltd.

#5978 Therapeutic targeting of MELK using a drug repurposing approach to combat TNBC cells.

A. Arora, S. Sarkar, S. S. Ghosh;
Indian Institute of Technology Guwahati, Guwahati, India

Background: Triple-negative breast cancer (TNBC) is the most aggressive subtype of breast cancer linked to high chemo-resistant metastatic cases and limited therapeutic options due to the absence of conventional bioreceptors. Therefore, to treat TNBC, it is imperative to identify promising druggable biological targets.
Experimental Procedures: An integrated bioinformatic analysis of microarray datasets was performed to identify significantly differentially expressed genes (DEGs) in TNBC. For selecting a potent therapeutic target, the function and significance of the upregulated DEGs in TNBC was investigated by an *in silico* study employing the UALCAN portal, String database, KM plotter, and Enrichr tools. This analysis included gene expression validation, insights into protein-protein interactions, survival analysis, and pathway mapping of the genes. To obtain potent drugs binding to the selected target MELK (maternal embryonic leucine zipper kinase), a drug repurposing approach was employed starting with virtual screening followed by molecular dynamic simulation (MDS) using GROMACS. Further, the anti-cancer activity of the top two drugs was validated by live-dead imaging, gene expression analyses, MTT-based cell viability and ROS detection assays.
Results: Based on a stringent criterion for significant DEG identification ($log_2|FC|>1$ & adjust P-value < 0.05), 25 overlapping upregulated genes were obtained from three selected datasets. Further, *in silico* analysis revealed that MELK is significantly upregulated across the four stages and subtypes of breast cancer, including TNBC. Higher MELK expression and its oncogenic interactions correlated with poor overall survival of TNBC patients. Evidence suggests that the existing inhibitor for MELK (OTSSP167) has shown poor specificity. Therefore, to block its activity, a library of 1293 FDA-approved drugs was screened against the kinase domain of MELK. MDS study and analysis using parameters like RMSD, RMSF and pair distance revealed that the top 10 drugs were strongly stabilized by H-bonds in the binding pocket of MELK, with minimal deviation and reduced fluctuations of MELK upon drug binding. Binding free energy calculation of drug-MELK interaction using the MM-PBSA method revealed that nine drugs possessed higher binding energy than the inhibitor. The top two drugs obtained from the study (originally kinase and reductase inhibitors respectively) were further validated for their *in vitro* anti-cancer efficacy in MDA-MB-231 and MDA-MB-468 cells. Treatment with these drugs exhibited (a) a dose-dependent decrease in proliferation, (b) significant cell death, (c) a marked increase in the cellular ROS levels, and (d) a decrease in the expression of MELK and its downstream targets in TNBC cell lines.
Conclusion: The present study opens the avenue for using repurposed drugs as potential therapeutic molecules against MELK activity to combat TNBC progression.

#5979 Recombinant N-acetylgalactosamine-4-sulfatase (arylsulfatase B; ARSB) inhibits lung metastases in murine B16F10 syngeneic tumor model.

J. K. Tobacman[1], S. Bhattacharyya[2], I. O-Sullivan[1];
[1]University of Illinois at Chicago and Jesse Brown VAMC, Chicago, IL, [2]Jesse Brown VAMC, Chicago, IL

Activity of the enzyme N-acetylgalactosamine-4-sulfatase (Arylsulfatase B: ARSB), which removes the 4-sulfate group at the non-reducing end of chondroitin 4-sulfate (C4S) and dermatan sulfate, is reduced in several malignant cell lines and human tissues, including melanomas, mammary, prostate, and colon. Following tail vein injection of B16F10 melanoma cells in 12-week-old female C57BL/6J mice (n=11) and subsequent treatment by tail vein injection of bioactive, recombinant human ARSB (0.2 mg/kg), on days 2 and 7, development of metastatic lung lesions was markedly reduced. The average number of lesions declined from mean value of 114 (range: 10-278; n=5) to mean value of 2.5 (range: 0-9; n=6). These findings are consistent with our previous report of significant increase in survival and decrease in size of B16F10 subcutaneous melanomas in C57BL/6J mice treated with exogenous ARSB. The underlying mechanisms leading to inhibition of melanoma proliferation have profound impact on vital signaling pathways and transcriptional events. These pathways involve more or less binding with C4S when ARSB activity is modified. Notably, galectin-3 binding with C4S increases following exogenous ARSB, leading to decline in free nuclear galectin-3. This leads to reduced expression of the melanoma biomarker chondroitin sulfate proteoglycan CSPG)-4; also known as melanoma-associated chondroitin sulfate proteoglycan (MCSP). Expression of Programmed Death-Ligand 1 (PD-L1) is also reduced, declining from 1.34 ± 0.23 ng/mg protein (n=5) to 0.50 ± 0.05 ng/mg protein (n=6) following ARSB treatment. Inverse to the effect on galectin-3, SHP2, the ubiquitous non-receptor tyrosine phosphatase (PTPN11), binds less to C4S following treatment with exogenous ARSB. The resulting activation of SHP2 impacts on MAPK signaling, reducing phospho-ERK1/2 and phospho(T180/Y182)-p38-MAPK. These effects contribute to decline in matrix metalloproteinases MMP2 and MMP9 and thereby restrain invasiveness and metastasis. Following treatment with exogenous ARSB, the serum MMP2 declined from 267 ± 38 (ng/ml; n=5) to 121 ± 16 ng/ml (n=6), consistent with the observed decline in melanoma lesions. The impact of ARSB on signaling pathways and transcriptional events demonstrates how modification of a critical sulfation and the resulting impact on binding with C4S influences vital cell processes and can suppress tumor development. Recombinant human ARSB is an approved agent for the treatment of Mucopolysaccharidosis VI and is used safely and effectively for this congenital deficiency of ARSB. Exogenous ARSB may become an effective treatment for acquired deficiency of ARSB in melanoma.

#5980 Cancer therapeutic and prevention strategy targeting mutated mitochondria DNA.

H. Nagase;
Shin Nippon Biomedical Laboratories, Tokyo, Japan

As the energy factory for the cell, the mitochondrion, through its role of ATP production by oxidative phosphorylation, can be regarded as the guardian of well regulated cellular metabolism; the integrity of mitochondrial functions, however, is particularly vulnerable in cancer due to the lack of superstructures such as histone and lamina folds to protect the mitochondrial genome from unintended exposure, which consequently elevates risks of mutation. In cancer, mechanisms responsible for enforcing quality control surveillance for identifying and eliminating defective mitochondria are often poorly regulated, and certain uneliminated mitochondrial DNA (mtDNA) mutations and polymorphisms can be advantageous for the proliferation, progression, and metastasis of tumor cells and disseminated into microenvironment cells through extracellular vesicle and tunnel nano tube. Such pathogenic mtDNA aberrations are likely to increase and frequently be homoplasmic in metastatic cancer cells and, intriguingly, in normal cells in the tumor microenvironments as well. Distinct characteristics of these abnormalities in mtDNA may provide a new path for cancer therapy. We recently tested this hypothesis with a few PIP-TPP conjugates targeting mtDNA mutations to induce mutants reduction in heteoplasmic cells or apoptosis in homoplasmic or near homoplasmic cells in vivo model without major adverse effects. This finding reaffirms the feasibility of such a PIP-TPP-based mtDNA-targeting approach for anticancer therapy as well as perhaps cancer risk prevention. However, the absence of known mtDNA mutation hotspots limits the clinical application of somatic mutation-targeted PIP-TPPs. Thus, we designed CCCh-1005-TPP to selectively target a frequent ATP6 gene variant and often oncogenically homoplasmic in the associated with hypertrophic cardiomyopathy, colon, breast and ovarian cancer risk and found its anticancer effect in mouse xenograft models. Here we study preclinical trial of CCCh-1005-TPP, a promising novel anti-cancer agent for clearing abnormal mtDNA by reactivating mitochondrial quality control surveillance of mitophagy. Given those mechanistic insights may provide a promising therapeutic or maybe preventive approach of the pathogenic mtDNA removal in homoplasmic or heteroplasmic cells. Additional caveat is that this strategy may also use not only for cancer but also many other mitochondria related diseases, such as neurodegenerative, diabetic, renal, muscle and hearing loss diseases as well as aging.

#5981 Treatment of cholangiocarcinoma using humanized monoclonal antibodies targeting claudin-1.

Z. Nehme[1], M. Muller[1], E. Crouchet[1], F. Juehling[1], J. Moehlin[1], R. Desert[1], J. Brochon[1], F. Del Zompo[1], N. Roehlen[1], C. Thumann[1], P. Pessaux[1], E. Felli[1], A. Venkatasamy[2], P. Marchand[3], M. Onea[4], R. Iacone[5], M. Meyer[5], A. Toso[5], N. Bardeesy[6], L. Goyal[7], V. Ranvir[8], M. Fernandez-Vaquero[8], M. Heikenwalder[8], T. Ostyn[9], T. Roskams[9], P. Laquerriere[3], C. Schuster[1], L. Mailly[1], T. Baumert[1];

[1]University of Strasbourg, Inserm, Institut de Recherche sur les Maladies Virales et Hepatiques UMR_S1110, Strasbourg, France, [2]IHU Strasbourg, Institute of Image-Guided Surgery, Strasbourg, France, [3]CNRS, Institut Pluridisciplinaire Hubert Curien UMR 7178, Strasbourg, France, [4]Department of Pathology, Strasbourg University Hospital, Strasbourg, France, [5]Alentis Therapeutics, Allschwil, Switzerland, [6]Center for Cancer Research, Massachusetts General Hospital, Department of Medicine, Harvard Medical School, Boston, MA, [7]Division of Oncology, Stanford School of Medicine, Palo Alto, CA, [8]Division of Chronic Inflammation and Cancer, German Cancer Research Center, Heidelberg, Germany, [9]Department of Imaging and Pathology, University of Leuven, Leuven, Belgium

Introduction: Cholangiocarcinoma (CCA) is a highly aggressive adenocarcinoma of the hepatobiliary system showing an alarming rise in incidence and mortality with unsatisfactory treatment options. Claudin-1 (CLDN1) is a transmembrane protein expressed in tight junctions, but exposed at the cell surface on cancer epithelial cells. Using highly specific monoclonal antibodies (mAbs) targeting the extracellular loop 1 of exposed CLDN1 with an excellent safety profile (Roehlen, Saviano et al. Science Transl Med 2022), we aimed to investigate the role of CLDN1 as therapeutic target for CCA.

Methods: Integrative CCA patient CLDN1 expression analyses, spatial transcriptomics and mouse models were used to evaluate the role of CLDN1 as an oncogenic driver for CCA. Proof-of-concept studies were performed in cell line-derived xenograft (CDX) and patient-derived xenograft (PDX) mouse as well as patient CCA organoid models using humanized CLDN1 mAbs.

Results: Integrative expression analyses of CLDN1 in CCA patient tissues revealed robust CLDN1 upregulation across several cohorts and patients with well-characterized driver mutations. scRNASeq and spatial transcriptomics of patient CCA showed that CLDN1 expression in cancer cells is associated with stemness, oncogenic signaling and EMT. Gain-of-function studies using an orthotopic HDTVi and syngeneic mouse model revealed a decrease in survival and an enhanced tumor growth, unraveling a functional role of CLDN1 as an oncogenic driver in CCA. Targeting exposed CLDN1 using highly CLDN1-specific mAb demonstrated a robust anti-tumoral effect across intra- and extra-hepatic CCA mouse models, with a significant inhibition of metastatic disease including models with medium or low CLDN1 expression. Functional studies in patient-derived CCA organoids demonstrated that CLDN1 mAb decreased cellular viability and altered cancer cell plasticity and fate. Mechanistically, CLDN1 mAb treatment suppressed gene expression of pathways mediating proliferation, stemness and EMT by inhibition of Notch1, SRC-FAK, and Hippo-YAP signaling.

Conclusion: These results demonstrate that CLDN1 is a CCA driver and therapeutic target. The proof-of-concept studies in patient-derived models pave the way for the clinical development of CLDN1 mAbs to improve the outcomes of patients with advanced CCA.

#5982 Cannabinoid derived product is a potential novel therapeutic for papillary thyroid carcinoma.

C. Taico[1], I. Musa[1], F. Ardalani[1], A. Maskey[1], N. Yang[2], J. Breslin[3], R. Tiwari[1], J. Geliebter[1], X. Li[1];
[1]New York Medical College, Valhalla, NY, [2]General Nutraceutical Technology LLC, Elmsford, NY, [3]Breslin Research Institute, Taos, NM

Papillary thyroid carcinoma (PTC) is the most common thyroid cancer that usually affects women ages 20-50, presenting as an asymptomatic neck mass. Total or partial thyroidectomy shows an excellent prognosis; however, investigation into non-invasive therapeutics with minimal adverse effects is ongoing. In addition to driver mutations such as BRAF, RAS, and RET-PTC, p53 mutations have also been identified. The loss of function of p53 is linked to cancer progression from PTC to poorly differentiated thyroid cancer and possibly anaplastic thyroid cancer. The disruption of the Wnt cell pathway is documented to be related to malignant cell transformation in thyroid cancer, leading to remarkable upregulation of c-myc, resulting in enhancement of tumor growth and drug resistance. Previous studies revealed that upregulation of BCL-2 occurs at later stages of tumorigenesis and is involved in chemotherapy resistance in some forms of cancer. In PTC, the downregulation of BCL-2 is linked to its favorable prognosis. Cannabinoid Derived Products (CDPs) have shown effectiveness in inhibiting different types of cancer, with research dating back to the 1970s. Ongoing in-vitro and in-vivo studies show that CDPs can effectively modulate tumor growth. However, the apoptotic properties of CDPs are largely dependent on the cancer type and drug dose/concentration. Our investigation focuses on CDPs and its potential anti-cancer effects by modulation of gene expression. We investigated its effects on gene expression of p53, c-Myc, and BCL-2 in K1 cell line which consists of PTC cells obtained from metastasis of well-differentiated PTC. K1 PTC cells (1×10^6 cells/mL) were cultured with CDPs and incubated at 37°C under 5% CO_2 for 24 and 48 hours. Cells were harvested, and cell viability was determined via trypan blue exclusion assay. Using qRT-PCR, we determined the effects of CDPs on the expression of TP53, c-Myc, and BCL-2. Results show that the CDPs decreased the viability ($p < 0.001$) of K1 PTC cells in a dose and time-dependent manner. Within 24 hours, the cannabinoid-containing product increased the gene expression of TP53 ($p < 0.01$) and decreased the gene expression of BCL-2 ($p < 0.01$) and c-Myc ($p < 0.05$) in K1 PTC cells. The results suggest that CDPs interact as a potential regulator in cancer with the upregulation of p53 and downregulation of BCL-2 and c-Myc. Further in-vitro and in-vivo studies are needed to understand the mechanism and therapeutic potential of cannabinoid-containing products in papillary thyroid cancer.

EXPERIMENTAL AND MOLECULAR THERAPEUTICS: Novel Therapeutics and Preclinical Models
Poster Session

#5986 Significance of LIF/LIFR axis in the progression of inflammatory breast cancer.

Bianca Romo[1], Zenaida Fuentes[1], Lois Randolph[1], Bindu Santhamma[2], Hareesh Nair[2], Christoforos Thomas[3], Ratna Vadlamudi[1], Suryavathi Viswanadhapalli[1]

[1]The University of Texas Health Science Center At San Antonio, San Antonio, TX,[2]Evestra Inc., Schertz, TX,[3]Houston Methodist, Houston, TX

Background: Inflammatory breast cancer (IBC) is a rare form of locally progressed breast cancer. Even though it is uncommon, IBC accounts for 7% of breast cancer deaths. There is a critical need for novel therapeutic targets to develop new therapeutics. IBC is more common in young women. Altered levels of growth factors, and cytokine signaling are suspected to play a role in the progression of IBC. *Leukemia* inhibitory factor (*LIF*) is the most pleiotropic member of the *interleukin*-6 family of *cytokines*. LIF and its receptor LIFR have been linked to the progression of many cancers including triple negative breast cancer. We recently developed a first-in-class inhibitor targeting LIFR named EC359. However, the role of the LIF/LIFR axis in IBC progression remains unknown. In this study, we examined the significance of LIFR and the effectiveness of LIFR inhibitor EC359 in treating IBC.
Methods: The effect of LIFR inhibitor EC359 on cell survival, colony formation, and apoptosis was evaluated using three well-established IBC model cells (SUM149, SUM190PT, and KPL4). Mechanistic studies were conducted using Western blotting, CRISPR KO, reporter assays, and RT-qPCR. KPL4 cell-based xenografts were used to test the efficacy of EC359 *in vivo*.
Results: Our results using Western blotting confirmed increased expression of LIF and LIFR in IBC cells compared to normal and $ER^{\pm}$ breast cancer cells. Treatment with EC359 significantly decreased IBC cell viability, long term colony formation ability with an IC_{50} of ~10-20 nM. Similarly, knock out of LIFR significantly reduced the progression of IBC model cells in cell viability and colony formation assays. Further EC359 treatment promoted apoptosis of IBC cells. Mechanistic studies confirmed that EC359 treatment substantially reduced LIF/LIFR downstream signaling including STAT3, AKT, and mTOR signaling. We also tested the utility of EC359 in treating IBC in vivo using KPL4 xenografts. EC359 (5mg/kg/day) is highly efficacious in reducing IBC xenograft tumor growth *in vivo*. IHC analyses of tumors confirmed decreased cell proliferation as measured by Ki67 staining.
Conclusion: Collectively, these studies demonstrated the therapeutic benefit of using EC359 to target the LIF/LIFR axis and opened the door for the development of new treatment approaches.

#5987 Targeting the spliceosome in high-risk B-cell acute lymphoblastic leukemia.

Y. Murakami, H. Konishi, C. Tepper, J. McPherson, N. Satake;
University of California Davis, Sacramento, CA

The outcome for children with high-risk B-cell acute lymphoblastic leukemia (B-ALL) is poor. Disease relapse is speculated to be due to leukemia cells escaping treatment. Our group discovered a unique cell subpopulation in B-ALL that has the capacity to initiate leukemia and is resistant to treatment. Transcriptome studies of this cell population highlight a unique RNA regulation process, specifically RNA splicing. In B-ALL, dysregulated splicing is reported to be associated with drug resistance and disease relapse. SF3B1 is a core component of the spliceosome and an essential protein in the RNA splicing process. SF3B1 inhibition is therapeutic in many cancers. In our current studies, we investigated the therapeutic potential of pladienolide B (Plad-B), an SF3B1 inhibitor, in B-ALL. SF3B1 protein expression was significantly higher in cell lines (Reh and JM1) and 28 primary B-ALL samples (14 each for standard-risk and high-risk), regardless of the risk group, than in normal B-cells (NBs) and hematopoietic stem cells (HSCs). Plad-B showed significant dose-dependent cytotoxicity in the cell lines with IC50 of 1.2nM and 0.6nM, respectively, and three harvested high-risk patient-derived xenograft (PDX) samples with almost the same IC50 as the cell lines. Plad-B did not show cytotoxicity in NBs and HSCs at the same tested concentrations. *In vivo* efficacy of Plad-B was tested using an Reh xenograft mouse model and a high-risk PDX model. Plad-B, as a single drug treatment, significantly prolonged survival in both models ($p<0.01$). G2/M cell cycle arrest and apoptosis induction were observed at 24 hours after Plad-B treatment in Reh and JM1. Splicing events were examined by RNA-seq in the treated cells at different time points (15 min, 30 min, and 60 min). Plad B demonstrated rapid splicing inhibition as early as 15 min post-treatment and, at 60 min, splicing was inhibited in 1,669 genes, including apoptosis-associated genes. 2,625 differential splicing events were observed in these genes with ~96% from intron retention and exon skipping. Furthermore, 202 genes showed significant changes in their expression over this time frame. Most of the genes were rapidly downregulated in the treatment group compared to the control, and some were slowly downregulated. There were also some genes which were upregulated, either rapidly or slowly, compared to the control. We demonstrated that Plad-B induced short pro-apoptotic spliced isoforms, instead of anti-apoptotic forms, in *BCL2L1* and *MCL-1*, as early as 60 min after treatment. In conclusion, these data demonstrated the therapeutic potential of SF3B1 inhibition in high-risk B-ALL. Plad-B rapidly inhibited splicing in many genes and downregulated the anti-apoptotic forms of apoptosis-associated genes, leading to cell apoptosis. In future studies, we will identify the downstream targets of Plad-B and further investigate the mechanism of rapid apoptosis induction by SF3B1 inhibition.

#5988 The role of the deubiquitinase USP7 and the E3/E4 ubiquitin ligase complex ITCH/UBE4B in the regulation of cell death in neuroblastoma.

C. Le Clorennec, C. SAMPAIO, P. E. ZAGE;
UCSD Moores Cancer Center, La Jolla, CA

Dysregulation of the Ubiquitin Proteasome System has been linked to many human diseases, including cancer. Expression of UBE4B ubiquitin ligase is associated with neuroblastoma patient outcomes and its functional roles in neuroblastoma pathogenesis are not known. We have recently identified a ubiquitin complex ITCH /UBE4B which mediates ubiquitination of Ku70 and c-FLIPL proteins for proteasomal degradation allowing HDAC inhibitor-mediated caspase-8 dependent apoptosis. We also confirmed that the deubiquitinase USP7, critical player in tumor suppression and DNA repair, can be a potential therapeutic target for neuroblastoma. Highly selective USP7 inhibitors have demonstrated significant antitumor activity in preclinical models of adult cancer, and we reported that these inhibitors alone can be more effective against neuroblastoma tumor growth. Our hypothesis is that USP7 inhibition will be more effective against neuroblastoma tumors through destabilization of ITCH/UBE4B complex protein targets allowing a stronger induction of cell death in response to treatment for the children. To evaluate efficacy of USP7 inhibitors in combination with HDAC inhibitors or chemotherapy against neuroblastoma tumor growth, neuroblastoma cell lines depleted for UBE4B or USP7 were treated with increasing concentrations of USP7 inhibitors alone or in combination with chemotherapy or with HDAC inhibitors. Cell proliferation was measured using continuous live cell imaging and apoptosis by caspase cleavage and PARP cleavage detection by western blot. We have evaluated also, whether ubiquitination/deubiquitination and degradation rates of p53, Ku70 and c-FLIPL proteins could modulate induction of apoptosis and necroptosis. USP7 inhibition resulted in decreases in cell viability in p53 wild-type neuroblastoma cell lines. USP7 inhibition induced apoptosis and necroptosis by increasing phosphorylation of MLKL, RIPK3 and RIPK1. In UBE4B or USP7 depleted cells, a huge induction of necroptosis and a small rate of apoptosis were observed. We also identified USP7 as a deubiquitinase of Ku70, stabilizing Ku70 at the basal level, leading to stabilization of Ku70/c-FLIPL/Bax complex. USP7 inhibition destabilizes ku70 and c-FLIPL for protein degradation leading to induction of apoptosis as well as necroptosis. UBE4B depletion in neuroblastoma inhibits HDAC inhibitors mediated caspase-8 mediated apoptosis but enhances necroptosis, due to the inhibition of Ku70 and c-FLIPL proteins degradation leading to the blockade of caspase-8 activation and the activation of the necroptosome. Our data suggests that USP7 and ITCH/UBE4B can control the switch between apoptosis and necroptosis in response to USP7 and HDAC inhibitors. USP7 inhibition and ITCH/UBE4B activation by HDAC inhibitors could be a promising therapeutic strategy for children with high-risk and relapsed neuroblastoma.

#5990 Microtubule-associated serine/threonine kinase-likeinhibitor, AD1208, as a novel cancer therapeutics.

S. CHOI, J. Ahn, K. Baek, Y. Choi, M. Im, J. Kim, J. Kim, J. Khoo, S. Lee, W. Yao, Y.-W. Park;
Avelos Therapeutics, Inc., Seoul, Korea, Republic of

Microtubule-associated serine/threonine kinase-like is an essential regulator of mitosis and emerged as a novel oncogenic kinase. It is upregulated in several cancer types, correlating with chromosome instability and poor patient survival. Here, we are reporting a MASTL inhibitor, AD1208, as a new cancer therapeutics.AD1208 inhibits kinase activity of MASTL with IC50 value of 7nM in competitive manner against ATP and induces apoptosis of colorectal cancer cells with IC50 of 150nM. Selectivity index is higher than 100 folds when the cytotoxicity was measured in normal colon cells. Synthetic lethality with BRCA was observed in knock out studies. Cell panel analysis, consist of 300 cell lines, indicated that the AD1208 is effective in cancers originated from stomach, colon, leukemia, lymphoma, and soft tissue. *In vivo* efficacy was confirmed in mouse xenograft model in dose dependent manner and synergistic effect with PARP inhibitor was observed. Kinase Assay Panel screening revealed that AD1208 is highly selective against 468 kinases. Inhibition of MASTL resulted in decreasing phosphorylated ENSA, inactivating CDK1 and arresting cell cycle progression at G2/M phase. Clinical adverse drug reactions of AD1208 were predicted by *in vitro* Safety Functional Panel screening to exhibit no meaningful safety-related issues. Currently, AD1208 is being conducted in IND enabling GLP-Tox studies, including genotoxicity, mutagenicity, safety pharmacology as well as *in vivo* safety studies. Taken together, AD1208 is identified as a novel and selective MASTL inhibitor exhibiting significant therapeutic potential to be a development candidate.

#5991 Improved venetoclax therapy by a novel conjugate with artemisinin by NOXA-mediated reduction of Mcl-1 and cyclin D1 protein in myeloid leukemia cells.

J. Zhang[1], Z. Zhang[1], S. Waxman[2], L. Zhao[1], Y. Jing[1];

[1]Shenyang Pharmaceutical University, Shenyang, China, [2]Icahn School of Medicine at Mount Sinai, New York, NY

Evasion of apoptosis is crucial for the growth, survival and chemoresistance of myeloid leukemia. The Bcl-2 selective inhibitor venetoclax is the only apoptosis inducer approved for clinical use. Venetoclax in combination with hypomethylating agents or low-dose cytarabine has now become the standard care for elderly AML patients. However, a sizeable fraction of patients are either refractory to venetoclax combination therapy or ultimately relapse. High or induced expression of Mcl-1 and Bcl-xL mediates venetoclax resistance. Previously we reported that artemisinin enhances venetoclax apoptosis induction by degrading Mcl-1 through NOXA induction. We designed a novel conjugate A1 of venetoclax with dihydroartemisinin. A1 shows dual functions of inhibiting Bcl-2 and inducing NOXA. A1 treatment releases Bim from both Bcl-2 and Mcl-1, further degrades Mcl-1 protein, and presents ten-fold stronger apoptotic induction ability in venetoclax insensitive cells. Acquired increase of Mcl-1 protein was observed in venetoclax resistant MOLM-13/VEN cells, which are sensitive to A1-induced apoptosis. In Bcl-xL expressing venetoclax refractory leukemia cells A1 obtains a new mechanism of inhibiting cell cycling by downregulating cyclin D1 through a new NOXA/cyclin D1 cascade, mediated through the endoperoxide moiety of artemisinin and intracellular iron, independent of Bcl-2 inhibition. We reveal a new compound A1 overcoming venetoclax resistance by NOXA-mediated degradation of Mcl-1 and cyclin D1 protein.

#5992 Expression of oncogenic ASSP2k in acute myeloid leukemia directly contributes to resistance to therapy and aggressiveness of the disease.

Alessia Ruiba, Marcus Schittenhelm, Anna Lena Ahrens, Vanessa Aellig, Kerstin Kampa-Schittenhelm

Klinik fur medizinische Onkologie und Hamatologie, Kantonsspital St. Gallen, St. Gallen, Switzerland

Background ASPP2 is a critical p53 activator initiating apoptotic cascades in the presence of cell stress. ASPP2k is a novel, dominant-negative, oncogenic splicing isoform of the tumor suppressor ASPP2, discovered in the context of a mutational screening of AML/ALL patient biopsies (expressed in >40% of the samples) (Schittenhelm MM et atl, EBioMed 2019). ASPP2k results from an aberrant exon 17 skipping: a premature STOP codon at the new exon16-exon18 junction site leads to the translation of a truncated protein. Indeed, ASPP2k lacks the ASPP2 C-terminus, containing the important p53 binding sites. Thus, ASPP2k impairs p53-dependent apoptosis activation, resulting in accelerated proliferation and attenuated chemotherapy-induced apoptosis in cancer cells.
Results ASPP2k silencing (KD) and overexpression (KI) functional consequences were evaluated in vitro and in vivo. ASPP2k was silenced in MOLM-14 cells and primary AML blasts. We found proliferation to be attenuated in ASPP2k KD cells compared to EV cells in both models ($p<0.0001$). Silencing of ASPP2k rendered cells more susceptible towards standard chemotherapy compared to controls (+30% Daunorubicin 10 nM, +20% Venetoclax 15 nM, $p<0.01$, Annexin/PI). Both cell models were subsequently injected intravenously into NSG mice: ASPP2k KD lead to a less aggressive disease development, resulting in a longer lifespan (30 and 42 days for EV and KD, respectively). Significant splenomegaly was noted for all control mice, while spleens from mice injected with ASPP2k KD cells were on average half in size and weight, arguing for a less aggressive biology of KD leukemia cells. Vice versa, ASPP2k up-regulation resulted in opposite results. IL-3 dependent Ba/F3 cells are a standard model to evaluate the oncogenic capacities of potential tumor drivers. Upon ASPP2k KI, Ba/F3 cells lost their IL-3 dependency. In line, overexpression of ASPP2k resulted in accelerated proliferation (+9.32 and +127.75 fold-change at 96h for EV and KI cells respectively, compared to 24h). When injected into NSG mice, ASPP2k KI Luc+ cells spread rapidly and invaded spleen, liver and brain, while no disease dissemination was noticeable control mice. Data from regular blood counts confirmed this notion. Animals injected with ASPP2k KI cells showed a rapid disease progression, while EV mice showed no signs of the illness. Further an increase of +122.5% in spleen weight was assessed in mice injected with ASPP2k KI cells compared to control animals at termination day, further underlining oncogenic potential of ASPP2k.
Conclusions In summary, we here show that ASPP2k directly contributes to resistance towards therapy in AML as well as aggressiveness of disease in vivo in all the investigated models, arguing for an oncogenic potential of the variant. Future studies evaluating ASPP2k as a prognostic/predictive model and potential target for therapy are warranted.

#5993 Temporal dynamics of ferroptosis vulnerability in a resistant cancer cell state.

L. Loftus, K. Pienta, S. Amend;
Johns Hopkins University School of Medicine, Baltimore, MD

Once cancer has metastasized it remains incurable as a result of evolved resistance to nearly all systemic therapies. Our group has demonstrated that an endocycling cancer cell state is an underappreciated mechanism of therapeutic resistance in many cancer settings. Cells in this state uncouple DNA replication from cell division to obtain abnormally high genomic content and cell size (over 40x volume). Resulting polyploidy and cellular hypertrophy provide survival advantages such as elevated genomic content, higher oxidative buffer capacity, increased autophagy, and heightened resistance to chemotherapy. Endocycling cancer cells are induced by multiple different classes of chemotherapy and present in vivo at increased frequencies both in metastatic sites and following chemotherapy. We hypothesize elimination of this overlooked resistant cancer cell state is critical for sustained anticancer therapies. Cancer cells, including those in the endocycling cancer cell state, leverage canonical cell cycle and cell death programs to evade apoptosis from external stressors including all classes of chemotherapy. Engaging cell cycle-independent death pathways is an alternative therapeutic strategy that circumvents cancer's trademark manipulation of the cell cycle[1]. Ferroptosis is a cell cycle agnostic form of cell death that occurs due to dysregulation of cellular iron and subsequent lipid peroxidation. While ferroptosis is emerging as a vulnerability in resistant cancers, efficacy of ferroptosis induction is highly heterogeneous depending on tissue type, cellular metabolism, and many other factors. We characterized oxidative damage, labile iron, lipid content, and signaling pathways in cells pre- and post-chemotherapy to assess vulnerability to ferroptosis. By inhibiting GPX4, the sole lipophilic antioxidant enzyme, we show induction of ferroptotic cell death across multiple cell lines and chemotherapies with cells in the endocycling state being more susceptible. Importantly, targeting cells in the endocycling cancer cell state (as opposed to untreated cell lines), also affords a more uniform elimination by ferroptosis. Ferroptosis also has a capacity to be immunogenic that may direct anti-cancer immune licensing in addition to direct cytotoxicity. These studies will directly contribute to development of ferroptosis engaging therapeutic strategies for resistant cancer cell states, particularly concerning the timing of intervention.

[1]Loftus, L.V.; Amend, S.R.; Pienta, K.J. Interplay between Cell Death and Cell Proliferation Reveals New Strategies for Cancer Therapy. *Int. J. Mol. Sci.* **2022**, *23*, 4723. https://doi.org/10.3390/ijms23094723

#5994 Neutrophils internalized through LC3-associated phagocytosis trigger tumor ferroptotic cell death in glioblastoma.

T. Y. Lu, P. P. Yee, S. Y. Chih, D. G. Aregawi, M. J. Glantz, B. E. Zacharia, H.-G. Wang, W. Li;
Penn State Health Milton S. Hershey Med. Ctr., Hershey, PA

Necrosis is commonly found in various solid tumors and predicts worse outcome. Chronic ischemia can initiate tumor necrosis, however, how the damaged tissue further expands is unclear. Previous studies found that neutrophils associate with necrosis and could contribute the necrosis development in glioblastoma (GBM) through transferring myeloperoxidase-containing granules into tumor cells and inducing tumor cell ferroptosis. How the neutrophilic granule transfer occurs is unknown. Here, through an unbiased small molecule screen, we found that statins can inhibit the neutrophil-induced tumor cell death through blocking the neutrophilic content transfer into tumor cells. Surprisingly, we found that neutrophils are engulfed by tumor cells before they are fragmented and release the MPO-containing contents in tumor cells. This process is through LC3-associated phagocytosis (LAP) and can be blocked by inhibiting the Vps34-UVRAG-containing PI3K complex. Inhibition of MPO or depletion of Vps34 in an orthotopic xenograft GBM mouse model showed that necrosis formation is reduced, and the tumor-bearing mice can survive longer. Therefore, this study revealed that the neutrophilic granule transfer is through LAP-mediated neutrophil internalization, which then trigger tumor ferroptotic cell death in glioblastoma. Blocking this process may improve prognosis of GBM.

#5995 How FDA-approved drug, Aprepitant, induces immunogenic death of cancer cells.

X. Dai, J. Zhu, S. Perry, Q. Jiang, D. J. Shapiro;
University of Illinois at Urbana-Champaign, Champaign, IL

Aprepitant is a long-standing FDA approved anti-nausea drug, recently re-purposed as an early-stage anticancer agent; how aprepitant kills cancer cells was not well studied. We find that aprepitant kills human and mouse cancer cells by hyperactivating the stress response pathway, the anticipatory unfolded protein response (a-UPR), thereby inducing immune cell activating necrotic cell death. Aprepitant is a small molecule neurokinin-1 receptor (NK-1R) antagonist widely used to prevent nausea and vomiting in cancer patients undergoing chemotherapy. Recently aprepitant has shown promise in mouse xenograft studies of colon, lung and pancreatic cancer and melanoma. Since aprepitant was thought to trigger release of calcium stored in the lumen of the endoplasmic reticulum, the step that we showed triggers hyperactivation of the a-UPR by ErSO family anticancer agents, we explored the role of the a-UPR in aprepitant action. Aprepitatnt robustly activates the PERK arm of the UPR increasing p-PERK and peIF2α, inhibiting protein synthesis. Notably, aprepitant treatment results in ATP depletion and activation of AMPK. Aprepitant induced rapid cell death was not blocked by apoptosis inhibitors or necroptosis inhibitors. In both standard 2-dimensional cell culture and 3-dimensional organoid culture aprepitant-treated breast cancer cells displayed typical features of necrotic cell death, including cell swelling, membrane rupture, and cytoplasmic vacuolization. Cell death by necrosis and membrane rupture leads to release of immune cell activating cell contents termed damage-associated molecular patterns (DAMPs). Aprepitant treatment induces release of the classic DAMPs, HMGB1 and ATP and medium from aprepitant-treated breast cancer cells enhances migration of differentiated human THP-1 macrophage. Thus aprepitant and other necrosis inducing therapies elicit immunogenic cell death (ICD) and may have the potential to enhance adjuvant immunotherapy. Genome-wide CRISPR screens with negative selection against aprepitant and other studies are being used to explore the pathways of aprepitant induced cell death and evaluate its therapeutic efficacy. Since FDA-approved aprepitant has been widely used for many years, identifying its pathway of action will both accelerate its clinical transition as an anticancer agent and help identify patients whose genetic profiles make them most likely to benefit from aprepitant therapy.

#5996 Genome-wide CRISPR screening reveals a central role for ferroptotic cell death in the anti-tumor response to mTOR inhibitors in HNSCC.

K. Koshizuka[1], X. Wu[1], K. Sato[1], P. T. T. Vo[1], G. M. Murawska[1], T. Ishikawa[1], Z. Wang[2], A. A. Molinolo[1], E. A. Dennis[1], P. Mali[1], J. Gutkind[1];
[1]University of California, San Diego, La Jolla, CA, [2]Zhejiang University School of Medicine, Zhejiang, China

Head and neck squamous cell carcinoma (HNSCC) is the sixth most common cancer globally, resulting in more than 300,000 deaths each year worldwide. Treatment options for HNSCC patients include surgery, radiation, chemotherapy and molecularly targeted therapies, and although immunotherapies have recently revolutionized the treatment landscape, <20% of HNSCC patients respond to immune check point blockade (ICB) therapies. The survival rate of HNSCC patients has changed only modestly over the past decades, and therefore HNSCC is a significant global health problem with high mortality and morbidity. Genomic alterations converging in the persistent activation of the PI3K/mTOR pathway (>80% cases) represent one of the most frequently altered signaling circuitries in HNSCC. This overreliance on PI3K/mTOR signaling for tumor growth may expose a cancer vulnerability that can be exploited therapeutically, as revealed in recent clinical trials using mTOR inhibitors (mTORi) in HNSCC in the adjuvant and neoadjuvant setting. Here, we took advantage of a whole-genome CRISPR screening approach to identify mechanisms of sensitivity and resistance to mTORi, aimed at increasing their clinical activity. We found that the activation of autophagy, a biological process that plays a paradoxical pro-survival or antitumoral role in a cancer specific fashion, is strictly required for mTORi cell growth inhibition in HNSCC. In depth analysis of our CRISPR screening also revealed multiple hits suggestive of a novel role for iron metabolism and ferroptosis downstream from mTORi. Ferroptosis is iron-dependent regulated cell death process caused by the peroxidation of polyunsaturated fatty acids. Indeed, we found that mTORi induces ferroptosis in HNSCC cells, and that inhibition of ferroptosis reduces the effect of mTORi. Evidence will be presented supporting a novel mechanism linking mTORi-triggered autophagy and the activation of ferroptotic death programs, as well as new synergistic combinations with mTORi by repurposing approved drugs that disable cellular ferroptotic defense mechanisms. Our studies uncovered how mTORi act in HNSCC, thereby revealing new multimodal precision therapies for HNSCC and many human malignancies displaying overactive PI3K/mTOR signaling.

#5998 Pharmacological inhibition of the LIF-LIFR autocrine loop reveals vulnerability of ovarian cancer to ferroptosis.

B. Ebrahimi[1], S. Viswanadhapalli[1], U. P. Pratap[1], R. Gopalam[1], X. Yang[1], P. P. Venkata[1], V. Drel[1], B. Santhamma[2], S. Konda[2], X. Li[1], A. L. Rodriguez Sanchez[1], H. Yan[1], G. R. Sareddy[1], Z. Xu[1], B. B. Singh[1], P. T. Valente[1], Y. Chen[1], Z. Lai[1], M. Rao[1], E. R. Kost[1], T. Curiel[3], R. R. Tekmal[1], H. B. Nair[2], R. K. Vadlamudi[1];

[1]University of Texas Health San Antonio, San Antonio, TX, [2]Evestra Inc, San Antonio, TX, [3]Dartmouth College, Hanover, NH

Introduction: Of all gynecologic cancers, epithelial ovarian cancer (OCa) stands out with the highest mortality rates. Despite all efforts, 90% of individuals who receive standard surgical and cytotoxic therapy experience disease recurrence. The potential involvement of leukemia inhibitory factor (LIF) and its receptor (LIFR) in the progression of OCa is still obscure. In this study, we examined the mechanisms by which disruption of LIF/LIFR autocrine loops contributes to the cell death of ovarian cancer cells.

Methods: The expression profiles of LIF and LIFR were obtained using 24 distinct OCa model cells, comprising both primary and established cell lines. The effects of EC359 on OCa cells were evaluated using reporter assays, colony formation, cell death, and cell viability. Flow cytometry was utilized to analyze lipid peroxidation. The Agilent Seahorse XF Pro Analyzer was used to calculate the extracellular acidification rate (ECAR) and oxygen consumption rate (OCR). Furthermore, flow cytometry was used for the preparation and analysis of lymphocytes. Mechanistic investigations were performed with RT-qPCR and RNA-seq analysis. The efficacy of the LIFR inhibitor EC359 as a targeted therapy was investigated using cell-based xenografts, syngeneic xenografts, patient-derived organoids (PDO), and patient-derived xenograft (PDX) models.

Results: Analysis of cancer databases revealed that elevated expression of LIF or LIFR was associated with poor progression-free survival of OCa patients and a predictor of poor response to chemotherapy. Using 24 different primary and established OCa cell lines that represent four subtypes of epithelial OCa, we demonstrated that LIF/LIFR autocrine signaling is active in OCa. Moreover, treatment with EC359, a novel LIFR inhibitor, significantly reduced OCa cell viability and cell survival with an IC_{50} ranging from 5 to 50 nM. Furthermore, EC359 diminished the stemness of OCa cells. Mechanistic studies using RNA-seq and rescue experiments unveiled that EC359 primarily induced ferroptosis by suppressing the glutathione antioxidant defense system. Using multiple in vitro, ex vivo, and in vivo models including organoids, cell-based xenografts, patient-derived explants, and xenograft tumors, we demonstrated that EC359 dramatically reduced the growth and progression of OCa. Additionally, EC359 therapy considerably improved tumor immunogenicity by robust $CD45^{+}$ leukocyte tumor infiltration and polarizing tumor-associated macrophages (TAMs) toward M1 phenotype while showing no impact on normal T-, B-, and other immune cells.

Conclusions: Collectively, our findings indicate that the LIF/LIFR autocrine loop plays an essential role in OCa progression and that EC359 could be a promising therapeutic agent for OCa.

#5999 Bitter taste receptors trigger pyroptosis and apoptosis through NLRP3 activation in oral cancer cells in response to a dysbiotic bacterial molecule: A possible role as pattern recognition receptors.

S. Yu, H. Lee, J. Shin, N.-Y. Song;
Yonsei University, Seoul, Korea, Republic of

Oral squamous cell carcinoma (OSCC) is the most common type of head and neck cancers. It has been reported that the composition of the oral microbiome was shifted in OSCC patients compared to healthy subjects. In particular, *Pseudomonas aeruginosa* is one of the most abundant oral microbes in OSCC patients. Bitter taste receptors (taste 2 receptors, TAS2Rs), known as G protein-coupled receptors (GPCRs), can recognize *P. aeruginosa*-derived quorum sensing molecules, such as N-(3-oxododecanoyl)-L-homoserine lactone (oxo-C12). Therefore, we explored the role of TAS2Rs in oral dysbiosis and cancers. Herein, we observed that TAS2Rs, such as TAS2R4, TAS2R14, and TAS2R38, mediated both pyroptosis and apoptosis, two distinct types of programmed cell death, in human OSCC HSC3 cells exposed to oxo-C12. Unexpectedly, TAS2Rs provoked pyroptosis and apoptosis in a GPCR-independent manner. Instead, TAS2Rs seemed to recruit NLRP3 inflammasome and subsequently activate caspase-8 in response to oxo-C12, implying the TAS2Rs-NLRP3-caspase-8 axis. Notably, the immunofluorescence staining showed considerable expression of TAS2Rs and NLRP3 in oxo-C12-treated HSC3 cells as well as human OSCC tissues, further supporting the presence of the alternative activation pathway of TAS2Rs. Moreover, siRNA knockdown of *MyD88* diminished oxo-C12-induced NLRP3 activation, caspase-8 cleavage and cell death marker expression, which implies that MyD88 is involved in activation of the TAS2Rs-NLRP3-caspase-8 axis. This also suggests that TAS2Rs might function as potential pattern recognition receptors, similar to toll-like receptors responsible for recognition of pathogen and their molecules. Based on The Cancer Genome Atlas analysis, downregulation of TAS2Rs was correlated with poor prognosis in OSCC patients. Taken together, TAS2Rs might trigger the host defense mechanism against microbial dysbiosis-induced cancer development. Thus, TAS2Rs could be promising chemotherapeutic targets for OSCC treatment, particularly via disconnecting interkingdom molecular links between microbial alterations and carcinogenesis.

#6000 A novel pathway controlling anticancer drug induced immunogenic cell death.

J. Zhu[1], S. Ghosh[1], D. Duraki[1], M. Boudreau[1], M. Jabeen[1], C. Mao[1], B. H. Park[2], G. Cheng[3], E. R. Nelson[1], P. J. Hergenrother[1], D. J. Shapiro[1];
[1]University of Illinois at Urbana-Champaign, Urbana, IL, [2]Vanderbilt Ingram Cancer Center, Nashville, TN, [3]Carle Illinois College of Medicine, Urbana, IL

Acting through estrogen receptor alpha (ERα), in orthotopic mouse xenograft models and a PDX, our non-competitive anticancer drug ErSO induces complete or near complete regression of primary and metastatic therapy-resistant ERα-positive breast, ovarian and endometrial tumors. ErSO is also highly effective in ovarian cancer PDOs from patient ascites. Unlike most anticancer agents which inhibit cancer cell proliferation or induce apoptosis, ErSO induces immune-cell-activating necrosis through sustained hyperactivation of the anticipatory unfolded protein response (a-UPR) pathway resulting in ATP depletion and cell swelling followed by membrane rupture. The medium from cancer cells killed by ErSO not only robustly activates mouse and human macrophages, but also dramatically increases monocyte migration. ErSO therefore has the potential to help extend the reach of immunotherapy to many solid tumors that do not express neoantigens. However, unlike apoptosis which has an established signaling pathway, how ErSO induces necrosis was unknown. From a genome-wide CRISPR-Cas9 screen in MCF-7 cells with negative selection against ErSO, we identified FGD3, a guanine exchange factor (GEF) of Rho GTPase Cdc42 as the top target. Consistent with the screen, through subsequent knockout and overexpression of FGD3 in human breast cancer cells, we found that the knockout cells have significant resistance to ErSO while the overexpressing cells exhibit increased sensitivity to killing by ErSO in both 2D cell culture and a 3D organoid model. Our data indicates that this protein is not an upstream regulator of the ErSO-induced necrosis pathway. Instead, it is a regulator of the last stage of necrosis - cell membrane rupture. Thus, we identified an actin reorganization signaling pathway with multiple components that plays a pivotal role in whether the breast cancer cell responds to a-UPR activation and swelling by membrane rupture and necrotic cell death or reorganizes its actin enabling the cancer cell to survive. RNA-seq and other studies indicate that by regulating actin reorganization, this axis is important in ErSO-persister breast cancer cells exhibiting long-term survival in ErSO. This work enables identification of breast cancer patients whose elevated levels of components of this signaling pathway make them most likely to benefit from this novel therapy. Notably, FGD3 knockout cells also show considerable resistance to necrosis or necroptosis induced by other anticancer drugs. Here, we describe a therapy that induces immunogenic cell death in ERα-positive breast, ovarian and endometrial cancer cells. We also show that, as cancer cells respond to agents that induce immunogenic cell death through membrane rupture, an actin regulating pathway plays a critical role in life-death decisions.

#6001 Repurposing dihydroergotamine mesylate as a potential MCL-1 inhibitor and its antitumor effect in pancreatic cancer cells.

P. Mittal[1], J. H. Lo[1], S. Soni[1], F. Battaglin[1], S. R. Gupta[2], L. Torres-Gonzalez[1], Y. Yang[1], S. Algaze[1], P. Jayachandran[1], K. Ashouri[1], A. Wong[1], W. Zhang[1], J. Yu[1], L. Zhang[1], J. Millstein[1], I. K. Singh[2], H. J. Lenz[1];

[1]USC - University of Southern California, Los Angeles, CA, [2]Deshbandhu College, University of Delhi, New Delhi, India

Background: Myeloid cell leukemia 1 (MCL-1) is an anti-apoptotic member of the BCL-2 protein family which is involved in intrinsic (mitochondrial) pathway of apoptosis and is deregulated in several cancers. Current MCL-1 specific inhibitors have limitations in terms of efficiency, tolerability, and off-target effects and challenges associated with shallow binding groove of MCL-1. In this study, dihydroergotamine mesylate (DHE), an approved anti-migraine drug, was found as a potential ligand of the MCL-1 BH3-binding pocket and was further evaluated for its potential MCL-1 inhibition and effect on pancreatic cancer cells.

Methods: PubChem Database was used for library preparation and virtual screening (OpenBabel and AutoDock Vina). The 55 crystal structures available for MCL-1 in Protein Data Bank (PDB) were clustered using principal component analysis with Bio3D R-package to select representative PDBs for further screening. Consensus voting and *k-means* clustering was used to shortlist compounds for Molecular dynamics (MD) simulations. MD simulations (100 nanoseconds) by GROMACS were employed to measure stability of ligands in MCL-1 binding pocket. DHE efficacy on cell proliferation was evaluated with MTS and clonogenic assays and on apoptosis using the FITC/Annexin V flow cytometry assay in MiaPaCa-2 and PANC-1 pancreatic cancer cell lines. Effect of DHE treatment on *MCL-1* gene and protein expression was analyzed using qRT-PCR and western blotting, respectively.

Results: Computational screening identified DHE (PubChem ID: 12308974) as a top hit exhibiting consistent interactions within the MCL-1 BH3-binding pocket. Notably, DHE displayed stable RMSD and formed four hydrogen bonds throughout MD simulations. *In vitro* results showed that DHE significantly reduced viability of MiaPaCa-2 and PANC-1 pancreatic cancer cells with IC50 values of 31 μM and 47 μM, respectively. DHE significantly (P<0.001) suppressed colony formation by pancreatic cancer cells in a dose-dependent (10μM, 20μM, and 40μM) manner. The percentage of Annexin V-positive and Propidium iodide-negative fraction in MiaPaCa-2 cells treated with DHE also increased in a dose-dependent manner. DHE did not have significant effect on *MCL-1* mRNA expression. However, western blotting demonstrated MCL-1 protein levels were significantly reduced in both pancreatic cancer cell lines upon DHE treatment.

Conclusion: Our findings showed DHE suppresses the pancreatic cancer cells viability and proliferation, and significantly increased early apoptotic cells. DHE treatment had no effect on *MCL-1* at the transcription level but significantly reduced the protein, suggesting posttranslational modifications, and thus future mechanism of action studies is required. The present study reports that the anti-migraine drug DHE might be a novel therapeutic agent for pancreatic cancer and needs to be explored further.

#6002 Increased ferroptosis sensitivity and epithelial to mesenchymal transition of breast cancer cells overcoming chemotherapeutic mediated apoptotic caspase activation.

R. Hausman[1], W. Brown[2], P. McDonald[2], S. Awrey[2], G. Sun[3], D. Montell[4], S. Dedhar[1];
[1]University of British Columbia, Vancouver, BC, Canada, [2]BC Cancer Research Institute, Vancouver, BC, Canada, [3]Cheeloo College of Medicine, Shandong University, Jinan, China, [4]University of California Santa Barbara, Santa Barbara, CA

The survival of cancer cells post chemotherapeutic treatment can lead to the presence of recurrent tumors and continues to be a barrier to effective cancer treatment. The majority of chemotherapeutics kill cells through the induction of executioner caspases and subsequent apoptotic death, and resistance to apoptosis can lead to the presence of anastatic cancer cells. Executioner caspase release was previously thought to be the point of no return from apoptotic cell death, however, it has been shown that removal of the reagent causing caspase release can lead to recovery of cells from apoptotic signaling, a phenomenon which has been termed ``Anastasis``. This presents a need for a better understanding of the underlying mechanisms behind cancer cell survival and the mechanisms that lead to cell recovery and recurrent tumors. We have hypothesized that when treated with chemotherapeutics, some cells will evade cell death even when executioner caspases have been activated. By identifying surviving anastatic cells and the pathways involved in their evasion of cell death, we hope to propose novel therapeutic strategies to prevent their survival. The novel CasExpress system, developed by the Denise Montell lab group, was used to identify and isolate a population of cells surviving caspase-3 activation as a result of chemotherapeutic treatment in Triple Negative Breast Cancer (TNBC) cell lines. The CasExpress system permanently labels these cells with GFP post caspase-3 activation. Analysis of this population of SUM159 anastatic cells, identified by their GFP expression, demonstrates that these cells have an increased resistance to further chemotherapeutic treatment, a decrease in levels of active caspase-3, an up-regulation of Cancer Stem Cell marker CD44, and a more mesenchymal phenotype. Furthermore, these “anastatic cells” express decreased levels of GPX-4, an enzyme that mitigates ferroptosis via lipid peroxide reduction, and are more sensitive to GPX-4 and xCT inhibitor mediated ferroptosis cell death.To investigate the link between Epithelial to Mesenchymal Transition (EMT) and ferroptosis mediated cell death, we used TGF-b to stimulate EMT in NMe mouse epithelial cells. We found that TGF-b induced EMT is associated with increased sensitivity to ferroptosis mediated by GPX-4 inhibition. Furthermore, the TGF-b induced EMT cells have a marked decrease in the expression of GPX4, similar to what was observed in the TNBC anastatic cells. These results indicate a potential link between EMT and an increased sensitivity to ferroptosis, and provide novel strategies for identifying and targeting chemotherapeutic resistant tumor cells.

#6003 The TNF-α-induced protein 3-interacting protein1 (TNIP1) suppresses HGF mediated NF-kB pathway activation and growth in gastric cancer cells.

J. Jung, s. koh, k. lee;
Yeungnam Univ., Daegu, Korea, Republic of

Background: TNF-α-induced protein 3-interacting protein 1 (TNIP1), an integral component in the regulation of immune responses and cellular pathways, is gaining increased attention in the scientific community. Its ability to interact with A20, a crucial ubiquitin-editing enzyme, forms a significant part of the body's mechanism to control inflammation and prevent unregulated immune responses, which are pivotal in the pathogenesis of autoimmune diseases. TNIP1's role extends beyond autoimmunity; it is also implicated in the regulation of cancer cell proliferation and survival, making it a potential target in cancer therapy. However, TNIP1 has not yet been elucidated on the tumorigenesis, proliferation, and invasion of human gastric cancer, and needs to be researched and discovered. In this study, the HGF-mediated association of TNIP1, nuclear factor kappa-B (NF-κB), and matrix metalloproteinase 9 (MMP9) and cancer cell proliferation and invasion were investigated in two types of human gastric cancer cell lines.
Methods: In this study, cell culture, cDNA microarray analysis, western blotting, Real-Time Polymerase chain reaction, Zymography, 3-(4,5-dimethylthiazol-2-yl)-2,5-diphenyltetrazolium bromide (MTT) assay, TNIP1 knock-down with short hairpin RNA (shRNA), apoptosis, reagents and antibodies, standard two chamber invasion assay.
Results: In our study on gastric cancer cells, we found that hepatocyte growth factor (HGF) stimulation altered TNIP1 expression at both mRNA and protein levels, indicating a dynamic interaction between HGF and TNIP1. The use of LY294002, a PI3K/AKT pathway inhibitor, revealed TNIP1's involvement in the NF-kB pathway, showing changes in NFkB and TNIP1 expression post-HGF stimulation. TNIP1-shRNA expressing cells exhibited altered expression of p53, BCL-2, NFkB, and MMP9, markers crucial for tumor progression and metastasis. Notably, TNIP1 knockdown led to increased cell proliferation and enhanced invasion capabilities in gastric cancer cells. Furthermore, TNIP1 knockdown cells showed a significant decrease in apoptosis rates upon HGF treatment, as confirmed by propidium iodide staining and FACS analysis.
Conclusions: In conclusion, our results demonstrate that TNIP1 is closely associated with the NF-kB pathway and plays a critical role in modulating tumor invasion and apoptosis in gastric cancer cells. These findings suggest that TNIP1 could be a potential therapeutic target for the treatment of gastric cancer, providing new insights into the mechanisms of tumor progression and the development of targeted therapies.

#6004 HOXC8 epigenetically controls caspse-1 expression and pyroptosis in lung cancer cells.

L. Sun[1], R. Padia[1], O. Calbay[1], C. Chi[1], M. Akter[1], L. Jin[2], S. Huang[1];
[1]University of Florida, Gainesville, FL, [2]UT Health San Antonio, San Antonio, TX

Homeobox C8 (HOXC8) is a transcription factor preferentially overexpressed in a large percentage of lung adenocarcinoma (LUAD). To investigate the function of HOXC8 in LUAD, we showed that knockdown of HOXC8 led to massive LUAD cell death in a mechanism of pyroptosis because both YVAD, a caspase-1 (CASP1) inhibitor, and disulfiram, which prevents gasdemin D (GSDMD) pore formation, blocked cell death caused by HOXC8 depletion. Intriguingly, ASC and NLRP3, components of canonic inflammasome, were not involved in pyroptosis occurring in HOXC8-depleted cells. Instead, we found that silencing HOXC8 led to a marked increase in CASP1 abundance. As forced expression of CASP1 is sufficient to induce CASP1 activation and pyroptosis, we reason that HOXC8 deters pyroptosis by suppressing the level of CASP1. Moreover, we revealed that knockdown of HOXC8 augmented CASP1 transcription involving in HDAC1/2. In fact, HOXC8 and HDAC1 were in the same immunocomplex and the presence of HOXC8 is required for the recruitment of HDAC1 to CASP1 promoter. Since HOXC8 also binds CASP1 promoter, we conclude that HOXC8 negatively regulates CASP1 expression by drafting HDAC1/2 to CASP1. This study suggests that HOXC8 participates LUAD development by controlling CASP1 expression and pyroptosis.

#6005 Generation of new oncology cell models through long-term acclimation under hypoxic and hyperbaric culture conditions.

Y. Xing[1], A. Czachorowski[1], J. Lim[2], S. Wise[1];
[1]Labcorp, Ann Arbor, MI, [2]Xcell Biosciences, San Francisco, CA

Traditional cancer cell lines used as surrogate models *in vitro* and *in vivo* have made significant contributions to cancer research and drug discovery. While cell culture and animal studies are critical steps in determining the efficacy, pharmacodynamics, and mechanism of action of novel anti-cancer drugs, it is well-known that cells grown in 2D culture systems have modified growth characteristics and different responses to chemotherapeutic drugs compared to tumors *in vivo* as a result of differing structural and environmental conditions that fail to replicate *in vivo* tumor microenvironments. AVATAR bioreactors (Xcell Biosciences, San Francisco, CA) were invented to address these limitations by providing discrete control over oxygen and hyperbaric pressure levels to better mimic the *in vivo* environment and allow cultured cells to be grown in conditions which mimic the human body. To better serve preclinical research needs, we generated new tumor cell models by long-term acclimating (LTA) existing cancer cells in the AVATAR incubator system using 1% O_2 and 2 PSI conditions similar to the conditions expected in the tumor microenvironment (TME). Six different cancer cell lines of diverse origins including pancreas (MIA PaCa-2), breast (BT-474), colon (HCT116), prostate (LNCaP, PC-3) and melanoma (A-375) were adapted for 2-3 months with phenotypic changes recorded. Key marker changes were commonly observed in LTA cells compared to parental lines. For example, in HCT116 colorectal cancer cells, TME culture conditions induced a higher expression level of E-cadherin in both protein and mRNA levels (2.2-fold change), indicating a mesenchymal-epithelial transition of the cell after adaptation. This coincides with the observation that LTA adapted HCT116 cell bodies had a more angular cell morphology as compared to parental cells grown under conventional normoxic culture conditions. In-depth gene-expression analysis using a Nanostring tumor signaling pathway panel identified several common and tissue-specific gene and pathway changes. These included VEGFA, EGF receptor signaling pathway (EGFR, E-Cadherin, GRB7, c-Fos), TGF pathway (IGFBP3, TGFB1, TGFB2, SMAD7), and extracellular matrix signaling (LAMB3, ITGA5, ITGB3, ITGB8, PDGFA, CCND2). Current studies are focusing on drug response testing in 2D and 3D cultures based on above-mentioned gene and signaling pathway changes. Cell proliferation and migration capacity of xenograft LTA cells will be evaluated for the purposes of creating novel murine models for drug screening applications.

#6006 Modeling antibody drug conjugate sensitivity using urothelial carcinoma patient-derived models.

X. Tang[1], Z. Chen[1], J. Thomas[1], K. Nagar[1], J. Christin[2], N. Rustgi[2], S. Gao[1], E. de Stanchina[1], J. Coleman[1], M. Shen[2], H. Al-Ahmadie[1], G. Iyer[1], K. Kim[1], D. Solit[1];

[1]Memorial Sloan Kettering Cancer Center, New York, NY, [2]Columbia University, New York, NY

Introduction: Enfortumab Vedotin (EV), an antibody-drug conjugate (ADC) targeting Nectin-4, has emerged as a new standard-of-care for patients with metastatic urothelial cancer (UC). Promising results have also been observed in bladder cancer (BLCA) patients with ADCs targeting HER2. To identify predictive biomarkers of ADC sensitivity, we characterized a large and expanding biobank of patient-derived organoid (PDO) and xenograft (PDX) models for Nectin-4 and HER2 expression, and Nectin-4 and HER2-targeted ADC sensitivity.

Methods: We generated 19 PDOs and 34 PDXs that reflect the genomic and biologic heterogeneity of human UC. A subset of these models was further characterized using a multiplatform approach, including bulk and single-cell DNA and RNA sequencing and immunoblot for Nectin-4 and HER2 expression. We leveraged these models to study the biologic determinants of sensitivity to EV and the HER2-targeted ADC trastuzumab deruxtecan (T-DXd). PDX models were treated with EV (5 mg/kg IV on day 1, 3, 6) or T-DXd (10 mg/kg IV on day 1, 21, 42) or vehicle only as control. We also studied sensitivity to T-DXd and EV, as well as to their cytotoxic payloads (exatecan and vedotin) *in vitro* using paired PDO models.

Results: We observed high degree of variability of HER2 and Nectin-4 expression across UC PDOs and PDXs. In PDO models, sensitivity to EV correlated strongly with Nectin-4 expression, whereas HER2 expression was not strongly correlated with sensitivity to T-DXd. We also noted a poor correlation between Nectin-4 expression in PDOs and PDXs derived from the same patient. A subset of models, for example, SMBO-104 (*ERBB2* wildtype with low HER2 expression), exhibited significantly greater sensitivity to EV than to T-DXd. Conversely, T-DXd was significantly more active than EV in SMBO-170, a model with *ERBB2* amplification (~40 copies) and HER2 3+ expression. Sensitivity to exatecan, an analogue of the T-DXd payload deruxtecan, as measured by inhibition of cell proliferation and induction of apoptosis, was more predictive of T-DXd sensitivity than HER2 expression level.

Conclusion: In this study, we generated and biologically characterized UC patient-derived models with the goal of identifying predictive biomarkers of sensitivity to Nectin-4 and HER2-targeted ADCs. We observed significant heterogeneity of HER2 and Nectin-4 expression across models. Models were identified in which T-DXd was superior to EV, and vice versa. Sensitivity to the T-DXd cytotoxic payload was more predictive of PDX response than HER2 expression levels, with significant tumor regression observed with T-DXd in BLCA models with low HER2 expression. Our data suggest that clinical trials of HER2-targeted ADCs such as T-DXd should not be restricted to patients with HER2 overexpression and that novel biomarkers will be needed to identify those UC patients most likely to benefit from FDA-approved and investigational ADCs.

#6010 BRCA2 reversion alleles confer PARPi resistance via homology-directed repair, not fork protection.

R. Jensen, G. Moore, S. Lahiri;
Yale University School of Medicine, New Haven, CT

BRCA2 reversion alleles have been identified in relapsed, treatment resistant cancer patients. The reversions restore the open reading frame of the BRCA2 protein often resulting in significant sequence deletions with unknown functional consequences. No reports to date have introduced patient reversion mutations into a BRCA2 null cell model to analyze which BRCA2 functions are re-established and whether all or a subset of activities are required for PARPi resistance. Our study utilized BRCA2 reversion alleles identified through sequencing of circulating tumor DNA (ctDNA) from PARPi resistant ovarian cancer patients. We rigorously evaluated whether altered BRCA2 reversion proteins restore homology-directed repair (HDR), fork protection, or gap suppression to determine the specific activities required for PARPi resistance. We found that reverted BRCA2 proteins are functional for HDR by assessing survival response to PARPi, analyzing RAD51 foci at DSBs, DR-GFP reporter assays, RAD51 binding, and CRISPR/Cas9 gene targeting assays. Surprisingly, using the DNA fibercombing approach to assess replication fork dynamics, we identify two separation-of-function mutants, T1974 and C1654_M1890, which are deficient in fork protection, yet confer PARPi resistance. The mutations are located within the BRC 5-8 domain of BRCA2 proposed to play an important role in RAD51 nucleoprotein filament stability. Biochemical analyses of the purified proteins using single molecule FRET (smFRET) indicate reduced filament stability potentially explaining the deficit in fork protection. In conclusion, these separation-of-function BRCA2 mutations provide new mechanistic insight into the underlying biology of BRCA2 and reveal the specific functions needed to overcome PARPi-mediated cell death.

#6011 Pharmacological inhibition of PMS2 increases tumor mutational burden, induces microsatellite instability and elicits immune mediated rejection *in vivo*.

Eleonora Piumatti[1], Alexia Hervieu[2], Philippe Riou[2], Julian Blagg[2], Adam Peall[3], Sam Weeks[2], Maria T. Rodriguez-Plata[2], Giuseppe Rospo[1], Sasi Arunachalam[4], Bettina Meier[5], Paige Tongue[3], Tessa McLaren[3], Kalpesh Parmar[6], Pradip Patel[6], David Clark[7], Gareth Langley[7], Charles Nichols[7], Benoit Rousseau[8], Paul Winship[7], Matthew Baker[2], Martin Drysdale[2], Giovanni Germano[1], Alberto Bardelli[1]

[1]Department of Oncology, University of Turin, Turin, Italy,[2]NeoPhore Ltd, Altrincham, Cheshire, United Kingdom,[3]Charnwood Discovery, Loughborough, United Kingdom,[4]BCRO, Sanford, FL,[5]Fios Genomics, Edinburgh, United Kingdom,[6]O2h Discovery Pvt Ltd, Ahmedabad, India,[7]Charles River Laboratories, Saffron Walden, United Kingdom,[8]Memorial Sloan Kettering Cancer Center, New York, NY

Tumors carrying defects in DNA mismatch repair (MMR-d) display high tumor mutational burden (TMB) and increased tumor neoantigen levels. MMR-d leads to accumulation of single nucleotide variants (SNVs) and insertions or deletions (indels) amongst repetitive DNA sequences generating microsatellite instability (MSI). Cancers that harbor >40% microsatellite variations are described as MSI-high (MSI-H). These tumors display unique clinical features including better prognosis, increased immune infiltration and remarkable response to immune checkpoint blockade (ICB) therapy. Colorectal cancer (CRC) patients with MMR-d often respond to therapies based on immune checkpoint blockade, whilst those with mismatch repair proficient (MMR-p) tumors do not. Therefore, identifying strategies to enhance the efficacy of immunotherapeutic treatments and transform this prevalent subgroup of CRCs from immunologically cold to hot remains an urgent and an unmet clinical need. We discovered NP1867 a first-in-class, potent, selective, covalent small molecule inhibitor of the DNA Mismatch Repair protein PMS2. We show by biochemical, biophysical, and protein-ligand X-ray crystallographic methods that NP1867 binds irreversibly to the ATP binding site of the *N*-terminal ATPase domain of PMS2. NP1867 displays potent binding to PMS2 in a NanoBRET cellular target engagement assay and inhibits MMR activity in mechanistic and functional cell-based assays of MMR-dependent DNA repair. Continuous treatment of murine CRC cell line CT26 (MMR-p) with NP1867 increases TMB, specifically enriches gained mutations with typical MMR-d related COSMIC mutational signatures, and elicits MSI-H status in a time-dependent manner, demonstrating for the first time that inhibition of PMS2 with a small molecule phenocopies the inactivation of MMR observed in patients. Remarkably, inoculation of immune-competent mice with CT26 cells pre-treated with NP1867 elicits tumor regressions in anti-PD1-treated animals, recapitulating the unique clinical features of MMR-d/MSI-H tumors. Conversely, no response is observed in immune-competent animals inoculated with control-treated cells. The extent of *in vivo* response correlates with the duration of *in vitro* NP1867 treatment and with the MSI-H status of treated CT26 cells. In conclusion, small molecule NP1867 functionally inhibits DNA MMR by targeting PMS2, enriches gained mutations with MMR-d COSMIC signatures, elicits MSI-H status, and enhances immune surveillance in preclinical models. These findings pave the way for the development of orally bioavailable compounds suitable for long-term dosing in animal models.

#6013 VIO-01, a pan-DDR DNA decoy mediating DNA repair abrogation and unleashing the anti-tumor immune response.

V. Zakharova, C. Doizelet, N. Babault, M.-C. Lienafa, F. Mazed, M. Debiais, P. Vilela, E. Perroud, W. Jdey;
Valerio Therapeutics, Paris, France

Background: Targeting specific DNA Damage Response (DDR) proteins has been worldwide studied and developed, with the example of PARP inhibitors being the only approved treatments in this field. Here, we describe the antineoplastic and immunomodulatory effects of VIO-01, a first-in-class DNA decoy-cholesterol conjugate, that operates as a pan repair proteins decoy, resulting in constitutive exhaustion of the DNA damage response.
Methods: VIO-01-induced DDR proteins trapping and cell cytotoxicity were examined in both homologous recombination proficient (HRP) and deficient (HRD) cancer cells. DNA repair efficacy was monitored by analyzing repair protein recruitment to damage sites. RNAseq analysis in HRP/HRD ovarian cancer cells was employed to uncover the molecular mechanisms underlying VIO-01 effects. Effects on the innate and adaptive immune responses were assessed by following T-cell mediated anti-tumor cytotoxicity. VIO-01 antitumor efficacy and biodistribution were also assessed. Additionally, the interest of cholesterol as a vector for VIO-01 was analyzed compared to other ligands like the folate receptor ligand.
Results: VIO-01 bounds to several DDR proteins, such as PARP1, KU70/80, MRN complex and MSH2/MSH3 with high affinity, resulting in an abrogation of single- and double-strand break repair. In line with this, and through global transcriptome analysis, VIO-01 treatment resulted in notable downregulation of Base Excision Repair, NHEJ and Nucleotide Excision Repair pathways in both HRP/HRD cell lines. Additionally, VIO-01 elicited the activation of the immune system and inflammatory responses in ovarian cancer cells. Conjointly, VIO-01 treatment induced a significant differentiation of monocytes into non-classical monocytes, leading to a shaping of the tumor microenvironment via CD8+ T cell recruitment in early stage of activation. The activity of VIO-01 was specific to tumor cells, while sparing healthy and immune cells, at odds with PARP inhibitors. In line with *in vitro* results, VIO-01 mediated antitumor efficacy *in vivo* coupled to tumor-targeting T-cell responses. These interesting effects were driven by a favorable ADME/PK profile, showing a long-lasting VIO-01 residence time VIO-01 into tumors (at least 3 days post treatment), coupled to a clear hijacking from the liver and a rapid blood clearance, ensuring a minimal toxicity. Moreover, regulatory toxicology studies demonstrated a favorable safety profile of VIO-01 in non-human primate with the major findings being a transient increase in complement factors induced by the binding of VIO-01 to factor H, which was not observed in human serum, predicting favorable safety profile in humans.
Conclusions: Our results provide a preclinical rationale for using VIO-01 to trigger DNA damage exhaustion and an antitumor immune response, paving the way for rapid clinical application in patients bearing HRD or HRP tumors.

#6014 PLK1-dependent phosphorylation of PRMT5 promotes DNA damage response in prostate cancer.

J. Peng[1], **Y. Zhang**[1], J. Wang[1], Q. Li[2], D. He[1], X. Wang[1], X. Rao[1], M. Wu[1], P. Mo[1], L. Wang[1], S. Wu[1], R. Wang[1], J. Liu[1], M. Nouri[1], I. Tadahide[1], X. Liu[1]; [1]University of Kentucky, Lexington, KY, [2]Emory University, Atlanta, GA

Prostate cancer stands out as the most frequently diagnosed cancer in men and is projected to be the second leading cause of cancer-related deaths among men in the US. Consequently, there is an urgent need for studies focusing on innovative therapeutic approaches. DNA Damage Response (DDR) is critical for cell survival, as it promotes genomic stability and reduces the risk of inheriting damage. DDR also promotes cancer cells' survival, making it a therapeutic target in cancer. PRMT5, an enzyme in the methyltransferase family, is frequently activated and overexpressed in various cancers, including prostate cancer. Furthermore, research has revealed that PRMT5 has been implicated in DDR in prostate cancer, and the regulation of PRMT5-dependent DDR is influenced by its phosphorylation. Polo-like kinase 1 (PLK1) is a serine/threonine kinase also reportedly involved in DDR in prostate cancer. Our preliminary study found that PRMT5 is positively correlated with PLK1 in prostate cancer based on the TCGA database. Nonetheless, the mechanism through which PRMT5 is regulated needs to be clarified. Here, we found that PLK1 phosphorylates PRMT5 at the S470 site, and this specific phosphorylation is required for maintaining the enzymatic activity of PRMT5. Moreover, Plk1-associated phosphorylation of PRMT5 subsequently promotes DNA damage repair, indicated by the decreasing level of γH2AX after DNA double-strand breaks (DSB). Our RNA-seq analyses of prostate cancer cells with wild-type or mutant S470 sites indicate that Plk1-associated phosphorylation on the S470 site exerts an influence on DNA replication and DDR pathways. These findings shed light on a novel perspective regarding the roles of PLK1-mediated PRMT5 phosphorylation in DDR, offering potential therapeutic strategies in prostate cancer.

#6015 Effect of antineoplastic drugs on cell-to-cell communication in the progression of colorectal cancer.

T. Lugo, A. Nguyen;
Texas Tech University, Amarilo, TX

Background: In the past few years, there has been notable progress in colorectal cancer research, resulting in novel development and delivery of drugs specifically designed for individual patient requirements. However, one of the major roadblocks in designing and treating colorectal cancer is the drug resistance found in advanced stages. Thus, there is a profound need to establish new methods to overcome this barrier. Previous work illustrated that cell-to-cell communications are dysfunctional for multitude of reasons in colorectal cancer cells. Restoration of cell-to-cell communication is a mean to deliver antineoplastic drugs via bystanding effect. Prior research has demonstrated that restoring gap junctions of cell-to-cell communication in breast cancer cells enhances the efficacy of cisplatin, a drug previously deemed resistant. Hence, this study seeks to assess the potency and efficacy of antineoplastic agents known to show resistance in colorectal cancer, with the intention to investigate how gap junctions can increase the efficacy of antineoplastic agents via restoration of cell-to-cell communication.
Method: We assessed cell viability utilizing the RealTime Glo MT Cell Viability assay (Promega, Inc.). Four specific colorectal cancer cell lines, Caco2, HT-29, SW620, and SW480, were used. Four antineoplastic agents, doxorubicin, cediranib, nilotinib, and erlotinib, were selected for the study and subsequently in the combination study of gap junction enhancer. The lethal dose at 50% (LD50) was calculated for each antineoplastic agent in each cell line.
Results: The results show significant variation of LD50. HT-29 cells dosed with doxorubicin showed LD50 of 8.9 µM, 1.6 µM, and 0.5 µM at 24 hours, 36 hours, and 48 hours of exposure, respectively. HT-29 cells dosed with erlotinib showed LD50 of 15.8 µM and 8.9 µM at 48 hours and 60 hours of exposure, respectively. SW620 dosed with doxorubicin showed LD50 is 0.5 µM at 36 hours of exposure. SW620 dosed with erlotinib showed LD50 of 15.8 µM and 0.5 µM at 48 hours and 60 hours of exposure, respectively. Caco2 cells dosed with cediranib showed LD50 of 2.8 µM and 1.6 µM at 36 hours and 48 hours of exposure, respectively.
Conclusion: The findings from this study revealed varying LD50 values for these cell lines when treated with the four distinct drugs. This enabled us to determine a foundational effect of these drugs on these cell lines, which had not been previously identified. Discovering this foundational effect will allow us to investigate the synergy effect when combined with gap junction enhancer by setting a baseline effect using these results.

EXPERIMENTAL AND MOLECULAR THERAPEUTICS: Radiation, Theranostics, Radiotheranostics, Normal Tissue, and Cellular Stress
Poster Session

#6019 Biodistribution, molecular imaging and efficacy evaluation of a novel GPC3-targeted radiopharmaceutical therapy for hepatocellular carcinoma.

F. Lin[1], R. Clift[1], S. Horton[1], M. Guest[1], A. Noncovich[1], A. Bhat[1], S. Ballal[2], C. Bal[2], K. Shah[1], A. Karmann[1], **G. Li**[1];
[1]RayzeBio, San Diego, CA, [2]All India Institute of Medical Sciences, New Delhi, India

Introduction: Glypican-3 (GPC3) is a membrane-anchored oncofetal protein with minimal expression in normal tissues. Significant upregulation of GPC3 protein has been observed in the majority of hepatocellular carcinomas (HCC), and is associated with poor prognosis. The differential expression of GPC3 between tumor and normal tissues provides an opportunity for targeted radiopharmaceutical therapy (RPT) to treat HCC, a leading cause for cancer-related deaths worldwide.
Methods: The novel RPT agent RYZ-GPC3 comprises a small macrocyclic peptide binder with high affinity to GPC3 linked with a tetraxetan moiety capable of chelating a variety of radioisotopes. The affinity of peptide binders to GPC3 was determined by surface plasma resonance (SPR) and radioligand binding assays. Cellular internalization was radiometrically measured at multiple time points. Non-human primate (NHP) PET imaging was performed with ^{64}Cu. In vivo biodistribution, monotherapy and combination treatments with ^{177}Lu or ^{225}Ac were performed in HCC xenografts. Human imaging was conducted in HCC patients with ^{68}Ga PET/CT.
Results: The novel agent is a highly potent (K_D=0.7 nM) and selective peptide binder to GPC3 of human, mouse, canine and NHP origins, and is compatible with multiple radiometal isotopes. In vivo biodistribution study of [^{177}Lu]Lu-RYZ-GPC3 in HCC xenografts showed sustained tumor uptake of 16.6, 16.4, and 8.8 %ID/g at 24, 48, and 96 hours with fast renal clearance, resulting in favorable tumor/kidney ratios of 3.6, 10.2, and 13.0, respectively. Minimal or no uptake was observed in other normal tissues. PET imaging in NHP confirmed absence of on-target uptake by liver or other organs, and fast renal clearance. As monotherapy, durable (>60 days) tumor regression (TGI>100%) was achieved with ^{177}Lu (111 MBq)- and ^{225}Ac (0.111 MBq)-labeled RYZ-GPC3. At 10x lower injected activity, ^{177}Lu- and ^{225}Ac-labeled RYZ-GPC3 significantly improved anti-tumor effect of lenvatinib in multiple HCC models. Furthermore, PET/CT imaging in a 70-year-old patient with histologically proven HCC demonstrated distinct and avid [^{68}Ga]Ga-RYZ-GPC3 tumor uptake.
Conclusion: Preclinical data and preliminary human imaging demonstrate the potential of the novel binder as a theranostic agent for the treatment of patients with GPC3+ HCC.

#6020 GPC3-targeted radiopharmaceutical therapy for neuroendocrine prostate cancer.

R. Clift, F. Lin, K. Salvador, M. Guest, D. Kim, G. Han, **G. Li**;
RayzeBio, San Diego, CA

Introduction: Glypican-3 (GPC3) is a membrane-anchored oncofetal protein with minimal expression in normal tissues. Besides hepatocellular carcinoma, upregulation of GPC3 protein has been observed in a significant subset of treatment-emergent neuroendocrine prostate cancer (NEPC), which accounts for to 30% of prostate cancer cases refractory to anti-androgen and other therapies. The differential expression of GPC3 between NEPC cells and normal tissues provides a theranostic opportunity for targeted radiopharmaceutical therapy (RPT).

Methods: The novel RPT agent RYZ-GPC3 comprises a small macrocyclic peptide binder with high affinity to GPC3 linked with a tetraxetan moiety capable of chelating a variety of radioisotopes. The expression of GPC3 in NEPC cells was assessed by flow cytometry and immunohistochemistry (IHC). The affinity of peptide binders to GPC3 was determined by surface plasma resonance (SPR) and radioligand binding assays. In vivo biodistribution of [^{177}Lu]Lu-RYZ-GPC3 and anti-tumor therapy with [^{177}Lu]Lu-RYZ-GPC3 or [^{225}Ac]Ac-RYZ-GPC3 were performed in NEPC xenografts.

Results: The novel agent is a highly potent and selective peptide binder to GPC3 of human, mouse and NHP origins, and is compatible with multiple radiometal isotopes. In vivo biodistribution study of [^{177}Lu]Lu-RYZ-GPC3 in GPC3-positive NEPC xenografts showed sustained tumor uptake of 10.8, 12.6, 5.1, and 2.2 %ID/g at 2, 24, 72 and 168 hours post dose, respectively, with fast renal clearance. Minimal or no uptake was observed in other normal tissues. A single injection of [^{225}Ac]Ac-RYZ-GPC3 (11.1 kBq) resulted in significant tumor growth inhibition (TGI 109%) with durable regression and prolonged survival. All treatments were well tolerated.

Conclusion: Preclinical in vitro and in vivo data demonstrated the potential of the novel binder as a theranostic agent for the treatment of patients with GPC3+ NEPC.

#6021 Lutetium-177 (^{177}Lu) radiolabeled engineered antibody fragment against human prostate stem cell antigen (hPSCA) demonstrates targeting and antitumor effects in a syngeneic mouse model of pancreatic ductal adenocarcinoma (PDAC).

B. Chen, M. Farshbaf, F. B. Salazar, S. N. Ahmed, S. Jaiswal, J. Chean, A. Sherman, T. Hong, P. J. Yazaki, T. Olafsen, K. A. Zettlitz, A. M. Wu;
City of Hope, Duarte, CA

Introduction: hPSCA is a cell surface protein overexpressed in PDAC but minimally expressed in normal tissues, making it a promising therapeutic marker for targeted radiopharmaceutical therapy (TRT). Anti-hPSCA A2 scFv-Fc2DM antibody (A2DM) was engineered with a double mutation in the FcRn binding site for rapid blood clearance to the liver, reducing bone marrow and kidney radiotoxicity. The potential of using ^{177}Lu radiolabeled A2DM antibody for targeted anti-hPSCA imaging and TRT was investigated in a syngeneic mouse model of PDAC.

Methods: hPSCA knock-in mice were engrafted subcutaneously with KPC cells overexpressing hPSCA (KPC-hPSCA). ImmunoPET with zirconium-89 (^{89}Zr) radiolabeled with A2DM was conducted to confirm *in vivo* targeting. For imaging, A2DM and an isotype control (anti-CD20) antibody were radiolabeled with ^{89}Zr. Mice (n = 5; tumor sizes: 150 mm^3 - 180 mm^3) were i.v. injected with ^{89}Zr-A2DM or ^{89}Zr-isotype control (administered activity: 1.5 MBq/10 µg) or co-injected with excess cold antibody. ImmunoPET was acquired at 21 h post-injection. *Ex vivo* biodistribution was conducted and %ID/g was calculated based on decay-corrected standards. For therapy, KPC-hPSCA tumor bearing mice (n = 8 - 9, average tumor sizes: 20.1 ± 5.1 mm^3) was i.v. injected with ^{177}Lu-A2DM (administered activity: 17.8 MBq/10 µg or 9.25 MBq/10 µg) or saline. Tumor sizes and body weights measured every 2-3 days.

Results: ^{89}Zr immunoPET and biodistribution of A2DM demonstrated significantly higher tumor uptake (15.6 ± 0.6 %ID/g) than theisotype control (10.7 ± 1.0 %ID/g, p= 0.0001) or blocked control with 70-fold excess cold antibody (8.6 ± 1.3 %ID/g, p< 0.0001), suggesting A2DM binds to hPSCA-positive tumors in an antigen-specific manner. Therapy studies show tumor growth inhibition in a dose-dependent manner when treated with 17.8 MBq of ^{177}Lu-A2DM (tumor size at day 25: 178 ± 119 mm^3) or 9.25 MBq of ^{177}Lu-A2DM (tumor size at day 25: 309 ± 182 mm^3) (tumor size at day 25: 740 ± 317 mm^3, p= 0.006, 0.04 respectively, compared to saline). Median survival was significantly improved in mice treated with high dose of 17.8 MBq ^{177}Lu-A2DM compared to saline-treated group (48 vs. 25 days, p= 0.002). Median survival of mice treated with low dose 9.25 MBq of ^{177}Lu-A2DM showed a trend towards improved survival but results were not significant (48 vs. 34 days, p= 0.25). Minimal weight loss observed in the ^{177}Lu-A2DM and saline groups, suggesting the ^{177}Lu therapy was well tolerated.

Conclusions: ^{89}Zr immunoPET studies confirmed specific targeting of A2DM to KPC-hPSCA tumors *in vivo*. ^{177}Lu-A2DM therapeutic studies demonstrated significant tumor growth delay in a dose-dependent manner. Future studies will explore dose fractionation strategies, with the aim to enhance tumor growth control for PDAC.

#6022 Investigating the mechanisms behind salivary gland tissue sparing in response to ultra-high dose-rate FLASH proton radiotherapy.

G. S. Morcos, P. Chowdhury, M. M. Kim, K. Shoniyozov, J. Metz, L. Dong, C. Koumenis;
University of Pennsylvania, Philadelphia, NY

Background: Radiotherapy (RT) is a primary treatment for cancers of the head and neck. However, although highly efficacious in eliminating tumors, incidental damage to underlying tissue remains a major limitation of RT. In the case of head and neck cancer, damage to the otherwise healthy salivary glands is often unavoidable even at low dosages, leaving patients with lifelong xerostomia and other comorbidities. FLASH Proton RT (F-PRT) is a form of ultra-high dose RT and has been reported to spare healthy tissues while retaining its tumor-controlling efficacy. The first system to deliver dosimetrically identical FLASH Proton RT (F-PRT; 60- 110 Gy/sec) or Standard Proton RT (S-PRT; 0.5-1 Gy/sec) using double-scattered protons was designed by our group.
Aim: In this study, we aimed to investigate the effect of F-PRT on radiation-induced salivary gland dysfunction and the potential mechanism of this sparing effect by analyzing the effects of FLASH on two distinct salivary gland cell types: acinar and ductal cells.
Methods: The head and neck area of C57BL/6 mice were irradiated with a single dose of 16 Gy of F-PRT (128Gy/s) or S-PRT (0.95 Gy/s). Radiation-induced xerostomia was studied by measuring the saliva flow rate of mice at 5, 10, 14, and 28 days post-PRT. Expression of AQP5, SOX9, and Keratin- 18, 19 was studied at 2, 5, 10, 14, and 28 days post irradiation by both immunofluorescence and protein immunoblotting.
Results: Following irradiation with a single dose of 16 Gy, saliva flow was reduced by both treatments. However, the F-PRT-treated mice showed a significant improvement in salivary flow at 14 and 28 days post-irradiation, compared to those treated with S-PRT. Expression of AQP5 was significantly downregulated at 2, 5, 10 and 14 days post irradiation with S-PRT while F-PRT-treated mice showed a significant restoration of the AQP5 expression during the same time points. Expression of SOX9 showed no significant differences between S-PRT and F-PRT treated mice at earlier time points (2, 14 days), however, there was a significant difference in expression of SOX9 between the irradiated and unirradiated group. The difference in expression of SOX9 was visible from day 28 post-irradiation, where the F-PRT treated group showed increased expression compared to S-PRT.
Conclusion: Our findings demonstrate that F-PRT reduces radiation-induced hyposalivation and reinstates the expression of AQP5 in the acinar cells of the submandibular gland of mice. Furthermore, it demonstrates that on day 28 post-irradiation, F-PRT-treated mice displayed more SOX9-expressing progenitor cells in the submandibular salivary glands compared to S-PRT.
Acknowledgements: This work was supported by a Sponsored Research Agreement from IBA to Drs. C. Koumenis and L. Dong.

#6023 ^{225}Ac-FL-020 is a novel PSMA-targeting radionuclide drug conjugate (RDC) with superior in vivo anti-tumor activity.

F. Liu[1], J. Zhang[1], J. Yang[1], K. T. Thrane[2], M. W. Hallund[2], R. V. Gronlund[2], N. C. L. Wong[1];
[1]Full-Life Technologies Limited, Shanghai, China, [2]Minerva Imaging ApS, Olstykke, Denmark

Despite significant developments over the last few decades, metastatic castration-resistant prostate cancer (mCRPC) remains incurable. Prostate specific membrane antigen (PSMA), a prostate cancer-specific membrane marker which directly correlates with androgen independence, metastasis, and disease progression, has been well-established as a radioligand target for the diagnosis and treatment of mCRPC. Lutetium-177 (^{177}Lu)-PSMA-617 (PLUVICTO^{TM}) was approved in 2022 for the treatment of progressive PSMA-positive mCRPC. However, only 30% of patients showed a radiological response in the registrational trial. Meanwhile, recent clinical experience has shown very limited efficacy in low PSMA expressing patients. These data collectively request for further improvement in the clinical benefit of PSMA-targeted radiotherapy. Actinium-225 (^{225}Ac), an alpha emitter, is significantly more potent on cancer cell killing and has a shorter range in tissue penetration when compared to the beta emitter ^{177}Lu. Such a profile supports the development of ^{225}Ac based radiotherapies. Using our proprietary Clear-X^{TM} technology platform, we developed ^{225}Ac-FL-020, a novel ^{225}Ac-based PSMA radioligand therapy candidate which has demonstrated prominent pre-clinical properties. We have assessed the binding affinity against PSMA of the non-labeled vector FL-020 *in vitro*. The *in vivo* biodistribution profile of FL-020 was characterized by SPECT/CT imaging and biodistribution using Indium-111 (^{111}In)-FL-020 in PSMA high LNCaP tumor-bearing nude mice. In addition, anti-tumor activities of ^{225}Ac-FL-020 were evaluated in the LNCaP xenograft model and directly compared to ^{225}Ac-PSMA-617. FL-020 was found bound to LNCaP cells with an IC_{50} value of 51.55 nM. Meanwhile, the off-target screening showed that less than 50% inhibition of binding or activity was observed by FL-020 at 10 μM against 85 targets including receptors, ion channels, enzymes, and transporters, indicating the high selectivity of FL-020. Moreover, ^{111}In-FL-020 displayed a very promising *in vivo* distribution profile with high and sustained tumor uptake and fast systemic clearance. Furthermore, ^{225}Ac-FL-020 exhibited superior anti-tumor activity compared to ^{225}Ac-PSMA-617 at the same dose level (10 KBq/mouse) in the LNCaP xenograft model with a favorable safety profile as indicated by body weight and hematological parameters. A mechanistic study was also conducted in ^{225}Ac-FL-020-treated LNCaP tumor samples where DNA double-strand breaks and tumor cell apoptosis were observed, confirming the MOA of alpha emitters. Taken together, these results collectively demonstrate that ^{225}Ac-FL-020 is a potent and selective PSMA-targeting radioligand therapy candidate with superior anti-tumor activity and a favorable safety profile warranting further clinical development.

#6024 A novel carbonic anhydrase IX targeting radiopeptide, ^{64}Cu-PD-32766 and ^{177}Lu-PD-32766, exhibit promising theranostic potential in ccRCC tumors.

Yoshihide Mizukoshi[1], Shota Tsuchida[1], Hiroko Inaba[1], Tatsuro Kotake[1], Takanori Aoki[1], Kai Orihara[2], Yuichi Funase[2], Naoki Kanazawa[2], Hikaru Shimizu[1], Kaita Sawano[2], Kentaro Suzuki[2], Hayato Yanagida[1], Takeru Ehara[1], Hidetomo Kitamura[1], Satoshi Matsushima[2], Masato Murakami[1]

[1]PeptiDream Inc., Kawasaki, Japan,[2]PDRadiopharma Inc., Sammu, Japan

Introduction: Carbonic Anhydrase IX (CA9) is a zinc metalloenzyme that regulates the pH for cell growth. CA9 is considered an attractive target and is upregulated in a variety of cancers, especially, in 95% of clear cell renal cell carcinoma (ccRCC) where there remains a large clinical unmet need despite the availability of several newly approved medicines. PeptiDream has identified PD-32766, a novel macrocyclic peptide, targeting CA9 and can be labeled with radionuclides such as copper (^{64}Cu) and lutetium (^{177}Lu), which enables tumor-specific PET bioimaging and radiotherapy. Here we report the theranostic translational feasibility of PD-32766 for ccRCC.

Materials and Methods: PD-32766 was discovered using Peptide Discovery Platform System (PDPS), a proprietary screening system of PeptiDream. Binding affinity of PD-32766, ^{63}Cu-PD-32766 and ^{175}Lu-PD-32766 to CA9 was measured by SPR. For *in vivo* evaluation, we used a xenograft model in which VMRC-RCW (ccRCC cell line with similar CA9 expression level to clinical samples) was subcutaneously transplanted into nude mice. To assess biodistribution, ^{64}Cu-PD-32766 or ^{177}Lu-PD-32766 was dosed to VMRC-RCW xenograft mice, and the percentage of injected dose in tumors and major organs was quantified by cut and count method. To evaluate whether PET imaging can detect tumors, ^{64}Cu-PD-32766 was dosed to VMRC-RCW xenograft mice and after dosing, PET scanning was performed. For therapeutic experiments, ^{177}Lu-PD-32766 was dosed to VMRC-RCW xenograft mice and tumor volume was measured for 45 days after dosing.

Results: SPR analysis revealed that PD-32766, ^{63}Cu-PD-32766 and ^{175}Lu-PD-32766 exhibits an affinity of less than 0.2 nM for CA9. In *in vivo* biodistribution experiment, ^{64}Cu-PD-32766 and ^{177}Lu-PD-32766 showed specific and strong accumulation in tumors 4 hours after dosing (88 and 107% ID/g, for ^{64}Cu-PD-32766 and ^{177}Lu-PD-32766, respectively) and were highly retained in the tumors at 48 hours after dosing (37 and 51% ID/g, for ^{64}Cu-PD-32766 and ^{177}Lu-PD-32766, respectively). Maximal intensity in other normal tissues were 23 and 9 %ID/g (tumor/kidney=3.8 and 11.9 for ^{64}Cu-PD-32766 and ^{177}Lu-PD-32766, respectively at 4 hrs.). PET bioimaging of ^{64}Cu-PD-32766 clearly detected only tumors, consistent with the biodistribution data. In therapeutic experiments, ^{177}Lu-PD-32766 (30 MBq/mouse single or QW x3) was well tolerated and strikingly improved mouse survival compared with control animals for 45 days after transplantation, which suggests a robust tumor growth inhibition of ^{177}Lu-PD-32766 dosing. Taken together, PD-32766 showed specific tumor accumulation and strong therapeutic effect in a clinically relevant xenograft model of ccRCC.

Conclusion: PD-32766 has preferable properties for imaging and therapy with radionuclides and a great potential for theranostic use in ccRCC.

#6025 Discovery of novel macrocyclic peptide radioligands for tumor therapy by mRNA display.

A. Jaekel[1], K. Sherry[2], P. Desai[1], D. Fox III[2], T. Guo-Qing[2], M. Sturzbecher-Hoehne[1], D. Mewis[1], K. Noridomi[2], L. Rayman[1], P. Ye[2];
[1]Ariceum Therapeutics GmbH, Berlin, Germany, [2]UCB, Cambridge, MA

Radioligand therapeutics (RLT) aim to selectively deliver radioisotopes to cancer tissues to eradicate tumor cells while limiting the damage to surrounding tissues. They are composed of a tumor-targeting ligand and a radioactive payload. The therapeutic potential of RLT strongly depends on their biostability and residence time in tumor and healthy tissue after injection. Macrocyclic peptides are effective tumor-targeting ligands because their size and molecular characteristics confer optimal pharmacologic properties that can be fine-tuned during the development process. mRNA display is a powerful platform for macrocyclic peptide drug discovery that identifies high affinity peptide ligands through *in vitro* selection. Here, we describe the selection and initial characterization of macrocyclic peptides discovered by mRNA display that bind to the extracellular domain of a tumor target. Enrichment of the library for peptides that bound to the recombinant target protein was observed after four rounds of selection with no further enrichment in round five. The library of round 5 was sequenced by Illumina sequencing and the top 1,000 sequences (highest counts) were used to perform cluster analysis. We tested the top sequences of 43 different clusters in *in vitro* translation binding assays to validate the selection output and identify sequences for hit confirmation. Most of the sequences tested showed clear binding to the target protein and only a few peptides showed binding to a closely related protein from the same protein family. No non-specific binding of the discovered peptides to an irrelevant protein was observed showing the high specificity of the generated library. From this confirmatory selection data, we chose a subset of peptides for chemical synthesis. Binding affinity measurements were determined by surface plasmon resonance (SPR) and cellular binding of selected candidates to target-positive and -negative tumor cells was analyzed by flow cytometry. From this hit confirmation data, *in vitro* internalization and *in vitro* anti-tumor efficacy of radiolabeled peptide candidates for RLT are assessed. Our data highlights the potential of mRNA display platforms for fast and efficient discovery of highly specific macrocyclic peptides with optimal binding properties suitable for RLT.

#6026 A novel lutetium-177 radioligand therapy targeting FAP has potent antitumor activity in xenograft cancer model.

S. Lindeman, J. Higgins;
Immunome, Bothell, WA

Fibroblast Activation Protein (FAP) is an attractive target for cancer therapy due to its overexpression in most solid tumors, predominantly localized on cancer associated fibroblasts. Unfortunately, trials with first generation FAP-targeted radioligand therapies (RLTs) have produced only modest clinical responses, indicating the need for improvements. We developed a library of over 40 fully synthetic, novel FAP-targeted RLTs comprising a FAP inhibitor with a stable linker to an albumin binding domain and a DOTA-lutetium-177 payload. Screening this library for binding, biodistribution and pharmacology properties identified a ^{177}Lu-FAP RLT lead molecule. The novel ^{177}Lu-FAP RLT demonstrates high selectivity and binds to FAP with a sub-nanomolar binding affinity. Biodistribution of the ^{177}Lu-FAP RLT was evaluated in mice bearing U87MG tumors, demonstrating delivery and retention of a high tumor absorbed dose. In vivo efficacy of the ^{177}Lu-FAP RLT at 150 µCi or 500 µCi was evaluated in mice bearing U87MG tumors. The ^{177}Lu-FAP RLT elicits potent and dose-dependent antitumor activity with >80% reduction in tumor volume of 8/10 mice following a single 500 µCi dose. The treatment was well-tolerated, with no significant weight loss or deaths. The outstanding antitumor activity and high selectivity for FAP support further evaluation of this investigational RLT in patients with solid tumors.

#6027 ^{89}Zr-matuzumab and ^{225}Ac-matuzumab as a theranostic for epidermal growth factor receptor-positive KRAS wild-type colorectal and breast cancer xenografts.

F. Tikum, H. Fonge, F. Njotu, H. Babeker, J. K. Pougoue, N. Henning, A. Doroudi;
University of Saskatchewan, Saskatoon, SK, Canada

Background: About 80% of colorectal cancer (CRC) and 50 % of Triple-Negative breast cancer (TNBC) patients overexpress epidermal growth factor receptor (EGFR). Mutations in the KRAS oncogene (present in 40% of mCRC) lead to constitutive over-activation of EGFR and drive *de novo* resistance to anti-EGFR drugs. Here, we propose to target KRAS-mutant/BRAF mutant EGFR positive mCRC and TNBC using ^{225}Ac-labeled matuzumab, a humanized anti-EGFR monoclonal antibody.

Methods: *p*- -SCN-macropa was used to conjugate matuzumab for radiolabeling with ^{225}Ac and SCN-deferoxamine was used to conjugate matuzumab for labelling with ^{89}Zr. The radioimmunoconjugates were characterized by flow cytometry, HPLC and iTLC. *in vitro* cytotoxicity was evaluated in EGFR-positive mCRC, TNBC cell lines and 3D spheroids with different levels of EGFR density. Tumor growth was monitored using digital caliper. Mice were treated with either 10 MBq of ^{89}Zr-matuzumab for imaging or three doses of 13 KBq/dose administered of ^{225}Ac-matuzumab 10 days apart. *In vivo* study endpoint was tumor volume greater than or equal to 1500 mm^3.

Results: Flow cytometry showed about 95% binding to the cells in all EGFR-positive colorectal cell lines (DLD-1, SW620, SNU-C2B, HT-29) and breast cancer cell lines (MDA-MB-468, MDA-MB-231). *in vitro* studies showed enhanced cytotoxicity of ^{225}Ac-matuzumab compared with matuzumab. IC_{50} in the MDA-MB-468 cell line for ^{225}Ac-matuzumab (1.86 ± nM) was 35 times more effective than matuzumab (65.25± 7 nM). Similar trends were observed in the other KRAS-mutant mCRC cell lines and breast cancer cell lines. In 3D spheroid models, the IC_{50} of ^{225}Ac-matuzumab (3.0 ± 2 nM) in MDA-MB-468, was 20.79 times more effective than matuzumab (62.3 ± 1.38 nM). Similar trends were observed for all the other spheroid models as well. High uptake of ^{89}Zr-matuzumab was observed in both mCRC and TNBC xenografts. ^{225}Ac-matuzumab slowed tumor growth rate in MDA-MB-468 and MDA-MB-231 tumors models compared with control antibody or non-treated controls for 30 days. This study is still ongoing and will last for 2 more months.

Conclusion: ^{225}Ac-matuzumab shows very promising outcomes in KRAS-mutant mCRC models and breast cancer models and warrants further investigation.

#6028 Preferential tumor-to-normal tissue biodistribution and single-dose efficacy with ABD147, a DLL3-targeted engineered antibody-based radiotherapeutic, in preclinical small cell lung cancer models.

I. Kulic, **E. S. Melese**, E. Cummins, A. Mandel, R. Viswas, M. Abrams, A. Judge;
Abdera Therapeutics Inc., Vancouver, BC, Canada

Targeted radiotherapies represent an emerging treatment modality for aggressive cancers with limited treatment options, such as small cell lung cancer (SCLC). ABD147 is a Delta Ligand 3 (DLL3)-targeted antibody conjugate designed to carry and deliver cytotoxic radioactive isotopes to DLL3-expressing tumor cells. DLL3 is commonly expressed on the cell surface of neuroendocrine cancer cells, including SCLC, but has limited and predominantly intracellular expression in non-malignant tissues. The ABD147 antibody specifically binds human DLL3 with high affinity and is internalized by DLL3-expressing cancer cells. To minimize radiation exposure to normal tissue, ABD147 has been engineered to clear quickly from the blood compartment. Using indium-111 to determine ABD147 pharmacokinetics and biodistribution in mice, we demonstrate rapid blood and normal tissue clearance of ^{111}In-ABD147, as designed, following a single intravenous dose administration. However, ^{111}In-ABD147 retains high tumor accumulation (activity concentration of up to 30% ID/g) in xenograft mouse models of SCLC despite low DLL3 surface antigen expression on tumor cells (≤ 3000 copies). ^{111}In-ABD147 shows a favorable tumor-to-normal tissue distribution with predominant liver clearance. Following ABD147 therapeutic radioisotope delivery of actinium-225 or lutetium-177 (^{225}Ac-ABD147, ^{177}Lu-ABD147), we demonstrate single-dose tumor regression and dose-dependent sustained anti-tumor efficacy, corresponding to an extension of survival out to 84 days in multiple SCLC xenograft models. In summary, ABD147 can preferentially deliver radionuclides to DLL3-expressing tumor tissue while substantially reducing the systemic radioactive exposure typical of conventional IgG radioconjugates. Following promising results in preclinical models, including potent anti-tumor activity, ^{225}Ac-ABD147 is now progressing into clinical development.

#6029 ^{225}Ac/^{89}Zr labeled anti nectin 4 radioimmunoconjugates as theranostics against nectin 4 positive triple negative breast cancer.

H. Babeker, F. Njotu, J. Ketchmen, F. Tikum, A. Doroudi, E. Nwangele, M. Uppalapati, H. Fonge;
University of Saskatchewan, Saskatoon, SK, Canada

Nectin4 (N4) is a biomarker that is overexpressed in ~62% of triple negative breast cancer (TNBC) and its lack of expression in normal tissues makes it an ideal target for the therapy and PET imaging of TNBC. Methods: We developed a fully human antibody against nectin 4 (anti N4) using phage display. Anti N4 was radiolabeled with ^{89}Zr & ^{225}Ac, respectively, for imaging & radiotherapy using TNBC xenograft & syngeneic mouse models. TNBC murine 4T1 cells were transduced with human N4 and N4 expression was confirmed by FACS. Biodistribution & PET imaging of ^{89}Zr anti N4 radioimmunoconjugate (RIC) was studied in mice bearing N4 positive xenografts. Dosimetry of ^{225}Ac anti N4 was studied in healthy mice & the therapeutic efficacy was evaluated for 90 days in mice bearing MDA MB 468 xenograft & transduced 4T1 syngeneic models. Mice were treated with 2 doses of 350 nCi administered at 10 days apart. Tumor growth was monitored by a digital caliper. Results: The pharmacokinetic profile of ^{89}Zr-anti-N4 RIC showed biphasic distribution with a moderate elimination of 63 h. PET imaging & biodistribution of ^{89}Zr anti N4 in mice bearing MDA MB 468 xenograft showed high tumor uptake of 13.2 ± 1.12 %IA/g at 120 h. ^{225}Ac anti N4 was effectively internalized in MDA MB 468 and was cytotoxic to the cells with IC50 of 1.2 kBq/mL. Treatment with ^{225}Ac anti N4 led to complete tumor remission in all mice bearing MDA MB 468 xenografts and 4T1 syngeneic model by day 20 and 28, respectively. Conclusions: ^{89}Zr anti N4 was an effective PET imaging probe with specific uptake in tumor. ^{225}Ac anti N4 was effective as a therapeutic agent resulting in complete remission of tumors in both mouse xenograft & syngeneic models. These results are promising for the development of anti-N4 RICs as theranostics for TNBC.

#6030 Optimizing the therapeutic index of targeted α-particle radioimmuotherapy (TART) of HER2-positive breast cancer tumors in NRG mice with ^{225}Ac-labeled trastuzumab.

M. Kondo, Z. Cai, C. Chan, R. M. Reilly;
University of Toronto, Toronto, ON, Canada

Introduction: Our aim was to optimize the therapeutic index of TART of HER2-positive BC in NRG mice by studying the effectiveness and normal tissue toxicity of trastuzumab IgG, F(ab')$_2$ or Fab modified with DOTA for complexing the α-particle emitter, ^{225}Ac.

Methods: The toxicity of [^{225}Ac]Ac-DOTA-trastuzumab IgG, F(ab')$_2$ and Fab were assessed in NRG mice (n=5) injected i.v. with 2 and 4 kBq (total 80 μg) separated by 8 d. Body weight was monitored and complete blood cell (CBC) counts and alanine aminotransferase (ALT) and creatinine (CRE) were measured at 14 d post-injection (p.i.). TART was performed in NRG mice (n=7) with s.c. HER2-positive 164/8-1B/H2N.luc+ xenografts injected i.v. with 2 and 4 kBq (total 80 μg) separated by 8 d of [^{225}Ac]Ac-DOTA-trastuzumab IgG, F(ab')$_2$ or Fab. Control mice received irrelevant [^{225}Ac]Ac-DOTA-IgG, trastuzumab or saline. The tumor growth index (TGI=tumor volume/initial tumor volume) was measured and Kaplan-Meier median survival estimated. Tumor and normal tissue uptake (%ID/g) of [^{225}Ac]Ac-DOTA-trastuzumab IgG, F(ab')$_2$ and Fab (4 kBq) in tumor-bearing NRG mice were measured up to 14 d p.i..

Results: [^{225}Ac]Ac-DOTA-trastuzumab F(ab')$_2$ and Fab caused no decrease in CBC, while [^{225}Ac]Ac-DOTA-trastuzumab IgG decreased white blood cells by 4.5-fold, platelets by 7.5-fold, red blood cells by 1.2-fold and hematocrit by 1.2-fold compared to saline-treated mice. [^{225}Ac]Ac-trastuzumab F(ab')$_2$ or Fab caused no increase in ALT or CRE. Body weight was not decreased in all groups of mice. [^{225}Ac]Ac-DOTA-trastuzumab IgG, F(ab')$_2$ or Fab inhibited tumor growth (TGI at 15 d = 2.5, 1.8, and 1.9, respectively) vs. saline or trastuzumab (TGI= 6.3 and 5.2; P=0.0047 and 0.0028). Median survival was increased to 46 d for mice treated with [^{225}Ac]Ac-DOTA-trastuzumab F(ab')$_2$ vs. 29 d for Fab (P=0.008), 22 d for IgG (P=0.0005) and 15 d for saline (P=0.0005). Median survival for mice treated with [^{225}Ac]Ac-DOTA-IgG was 20 d and for trastuzumab was 22 d. Tumor uptake of [^{225}Ac]Ac-DOTA-trastuzumab IgG and F(ab')$_2$ at 48 h p.i. were 10.6 ± 0.6 and 8.7 ± 0.8, respectively, while uptake of [^{225}Ac]Ac-DOTA-trastuzumab Fab at 18 h p.i. was 3.1 ± 0.5 %ID/g. Elimination from the blood was slowest for [^{225}Ac]Ac-DOTA-trastuzumab IgG followed by F(ab')$_2$ then Fab. Spleen and liver uptake were greatest for [^{225}Ac]Ac-DOTA-trastuzumab IgG but much lower for F(ab')$_2$ and Fab. Kidney uptake was highest for [^{225}Ac]Ac-DOTA-trastuzumab Fab.

Conclusion: [^{225}Ac]Ac-DOTA-trastuzumab F(ab')$_2$ provided the highest therapeutic index, inhibiting tumor growth and improving survival while minimizing toxicity. TART with [^{225}Ac]Ac-DOTA-trastuzumab F(ab')$_2$ is a promising new treatment for HER2-positive BC that could be more effective than trastuzumab.

#6031 Fasting associated microbiota contributes to small intestinal radioprotection by modulating the epigenome.

P. Barrodia, E. Arslan, S. Jeter-Jones, R. R. Jeng, K. Rai, H. Piwnica-Worms;
UT MD Anderson Cancer Center, Houston, TX

Normal tissue toxicity often restricts the administration of effective radiation doses for optimal tumor cell elimination. We identified a novel host-protective effect conferred by short-term fasting when treating mice with high dose radiation. We showed that fasting mice for 24h induces epigenetic and transcriptional changes in small intestinal epithelial cells (siECs) and confers protection to small intestinal stem cells from high dose radiation. Here we report that fasting induces changes in the gut microbiome favoring bacteria producing metabolites, specifically short-chain fatty acids, that induce epigenetic changes in siECs. 16S rRNA sequencing of feces isolated from the small intestines of fed and fasted mice revealed a marked enrichment of *Akkermansia muciniphila* (*AKK*) in fasted relative to fed mice. Specific depletion of *AKK* through antibiotic treatment impaired the ability of fasting to provide organismal radioprotection whereas both organismal and OLFM4+ stem cell protection was restored in fasted animals upon reintroduction of *AKK*. *AKK* produces short chain fatty acids (SCFAs) including propionate which is able to induce histone modifications and our metabolomic analysis of feces isolated from the ileums of mice demonstrated a significant increase in propionic acid levels in fasted mice compared to fed mice. Importantly, we showed that *AKK* conditioned medium as well as its metabolite (propionate) are able to induce histone acetylation in Lgr5+ stem cell enriched epithelial spheroids cultured in vitro. We are currently employing high-dimensional analysis techniques, including single cell analysis, Cut&Tag and RNAseq to determine how the epigenetic and transcriptional changes induced by fasting provide organismal and SI radioprotection.

#6032 A novel “add-on” nanobody with an albumin-binding moiety based on the intelligent ligase-dependent conjugation (iLDC) technology: An innovative and versatile approach for next-generation radionuclide drug conjugates (RDCs) with enhanced pharmacokinetics and druggability.

C. Liu, K. Li, J. Li, J. Wang, X. Gao, Z. Mu, L. Shi, P. H. Song, G. Qin;
GeneQuantum Healthcare (Suzhou) Co., Ltd., Suzhou, China

Background: Radionuclide Drug Conjugates (RDCs) have become an attractive strategy in cancer treatment, but still faces significant drawbacks due to poor tumor penetration and undesirable pharmacokinetics of the targeting vehicles. Nanobodies, the smallest natural antigen-binding fragments, have been developed as targeting vehicles for RDCs owing to their outstanding tumor penetration, high affinity, high stability and low immunogenicity. However, the limitation of radiolabeling methods, the short blood circulation half-life and tumor retention time of nanobody hamper their application in targeted radionuclide therapy. To address those problems, this study explores a ^{177}Lu labeled anti-PSMA nanobody site-specifically conjugated with an albumin binding moiety, which improves PK profiles and radiotherapeutic efficacy by increasing circulation half-life and tumor uptake.

Results: A molecule with an albumin-binding moiety and a DOTA chelator fused in one molecular entity, utilizing a highly hydrophilic and stable branch linker, was efficiently and site-specifically conjugated to an anti-PSMA nanobody in a one-step manner based on GQ’s iLDC technology, which allows for more flexibilities in ^{177}Lu-labeling. The albumin-binding RDC maintained comparable antigen binding affinity and internalization compared to the parental nanobody, exhibiting medium affinity to albumin. Biodistribution and SPECT imaging studies performed in PSMA positive tumor-bearing mice showed enhanced blood circulation half-life of the albumin-binding RDC and, thereby, prolonged the time window for binding to PSMA, which resulted in a significantly higher accumulation and retention over time in PSMA positive tumor with higher tumor-to-blood and tumor-to-liver ratios compared to ^{177}Lu-PSMA-617. Remarkably, the albumin-binding RDC demonstrated superior antitumor efficacy with significant regression of tumor growth and no apparent toxicity or body weight loss was observed in all treated mice.

Conclusion: The introduction of an albumin-binding moiety enhanced blood circulation of the novel RDC developed by GQ’s iLDC, resulting in unprecedentedly high tumor uptake and retention over time, which conferred superior anti-tumor therapeutic efficacy. The applied strategy provides one promising novel paradigm for future RDC discovery and development which requires nanobody or other antibody fragments as targeting moiety, hence significantly expanding promise beyond current format.

#6033 Preclinical evaluation of an actinium-225 labeled PSMA-targeting small molecule (^{225}Ac-PSMA-Trillium (BAY 3563254)) for the treatment of metastatic castration resistant prostate cancer (mCRPC).

S. Zitzmann-Kolbe[1], A. Papple[2], T. Poethko[3], I. Moen[2], C. Schatz[1], S. Hillier[4], J. W. Babich[4], A. Cuthbertson[2], U. B. Hagemann[1];
[1]Bayer AG, Berlin, Germany, [2]Bayer AS, Oslo, Norway, [3]Bayer AG, Wuppertal, Germany, [4]Ratio Therapeutics, Inc., Boston, MA

PSMA is a clinically validated target for the treatment of mCRPC. Since the linear energy transfer and degree of induced DNA damage of alpha particles far exceeds that of beta particles, several investigational PSMA-targeted small molecules labeled with the alpha-emitter actinium-225 (^{225}Ac) have shown encouraging clinical signs of efficacy. However, xerostomia is often found as a dose-limiting side effect, presumably due to low levels of PSMA expression and efficient uptake of small molecules in salivary glands. To reduce these unwanted side effects a PSMA-targeted radioligand comprising a triad of important features was investigated. It consists of a high-affinity PSMA binder for specific tumor-targeting; a customized albumin-binding moiety designed to prolong plasma residence time and increase the therapeutic index by improving tumor uptake while reducing salivary gland uptake; and a chelator for efficient complexation of ^{225}Ac. From a series of compounds containing the same high-affinity PSMA-targeting moiety, but different chain lengths and albumin-binding domains, compound RPS-072 containing a PEG-3 and PEG-8 chain and an iodobenzyl moiety as albumin-binder was selected for further evaluation (J Nucl Med 2019; 60:656-663). This compound was the basis for the PSMA-Trillium with a DOTA chelator for imaging applications in humans (NCT05773703) or a macropa chelator for ^{225}Ac labeling resulting in ^{225}Ac-PSMA-Trillium. *In vitro* preclinical characterization of ^{225}Ac-PSMA-Trillium was performed to test affinities for PSMA and albumin. In a SPR assay, K_d was measured as 4.88×10^{11} M, K_{on} as 1.4×10^{7} 1/Ms and K_{off} as 6.6×10^{-4} 1/Ms. ^{225}Ac-PSMA-Trillium demonstrated good stability up to 48 h and induced potent in vitro cytotoxicity in the LNCaP subclone C4-2 (0.114 kBq/ml). *In vivo* biodistribution of ^{225}Ac-PSMA-Trillium showed consistent with the albumin binding property a relatively slow pharmacokinetics profile with 5 % ID/g still in the blood after 24 h and tumor accumulation peaking at ~ 20 % ID/g after 5-7 days. Tumor penetration was investigated using autoradiography which demonstrated fast, homogeneous, and even distribution across the tumor within 15 mins after injection. This property was also reflected by strong therapeutic efficacy in several PrCa models. In the LNCaP model a tumor growth inhibition was observed at a single dose dependent efficacy at 150 kBq/kg and 300 kBq/kg and increased the time to reach 400 mm^3 by 35 days for the 300 kBq/kg group. In the androgen independent PDX KuCaP-1 model, a single dose of 250 kBq/kg ^{225}Ac-PSMA-Trillium induced strong tumor growth inhibition over the course of 35 days. A first-in-human trial with ^{225}Ac-PSMA-Trillium is anticipated to start in the first half of 2024.

#6034 PSMA targeted alpha radiopharmaceutical [^{211}At]PSAt-3 inhibits tumor growth in a preclinical model of prostate cancer.

Lars Hvass[1], Marius Muller[2], Anne Clausen[1], Matthias Herth[2], Andreas Kjaer[1]

[1]Department of Biomedical Sciences, University of Copenhagen, Copenhagen, Denmark,[2]Department of Drug Design and Pharmacology, University of Copenhagen, Copenhagen, Denmark

Introduction: Prostate cancer continues to be a highly prevalent cancer diagnosis among men and a leading cause of cancer related deaths worldwide. With the introduction[^{177}Lu]Lu-PSMA-617, targeted radionuclide therapy has proven successful in increasing survival time for patients with metastasized castration resistant prostate cancer. However, despite encouraging results, such patients tend to develop progressive disease, and thus, enhanced efficacy is warranted. To this end, the use of radiopharmaceuticals harnessing alpha-emitters is a promising venue due to the potent energy deposition and short range of alpha particles in tissue. Here, we employ the PSMA targeting vector, [^{211}At]PSAt-3, for targeted alpha radionuclide therapy in a preclinical prostate cancer model.

Methods: [^{211}At]PSAt-3, a structural derivative of PSMA-617, in which the L-2-naphtylalanine was replaced by L-3-[^{211}At]astato-phenylalanine, was obtained by electrophilic [^{211}At]astatodesilylation. Evaluation of [^{211}At]PSAt-3 was conducted in male inbred nude mice of Balb/c background xenografted subcutaneously with human prostate cancer cells (LNCaP). Prior biodistribution studies were carried out with approximately 100 kBq intravenous injections, and subsequent biodistribution 2, 6 and 24h post injection (P.I.). For establishment of therapeutic effect, a single intravenous dose of [^{211}At]PSAt-3 was administered. To asses hematological toxicity, blood cell composition was assessed weekly.

Results: Favorable tumor uptake of 15.2±6 %ID/g was observed 2h after injection of [^{211}At]PSAt-3 in LNCaP xenografted nude mice, with subsequent 9±5.1% ID/g and 6.4±2.4% ID/g 6 and 24h P.I., respectively. [^{211}At]PSAt-3 cleared mainly by the kidneys, in which uptake was 72, 38 and 6% ID/g at 2, 6 and 24h P.I., respectively. Thyroid/throat uptake remained low at ~0.1% ID for all timepoints investigated, indicating a low degree of de-astatination. Initial efficacy studies using a single intravenous dose of 0.5 MBq (~20 MBq/kg) demonstrated significant growth delay and tumor volume reduction compared with control mice (saline). Blood platelet count was reduced after administration of [^{211}At]PSAt-3 and subsequently recovered. No signs of severe toxicity, and no significant weight loss between control and treated mice was observed, suggesting that the treatment is well tolerated.

Conclusion: 0.5 MBq [^{211}At]PSAt-3 was well tolerated in mice and demonstrated tumor volume reduction and significant delay of tumor growth. These findings suggest [^{211}At]PSAt-3 as a promising candidate for clinical translation.

#6035 Fluoride effects on thermal properties of irradiated dentin and enamel.

R. J. Kulchar[1], Y. Kakiuchi[1], V. Sanchez-Gamarra[1], J. Deng[2], F. Mante[1];
[1]University of Pennsylvania School of Dental Medicine, Philadelphia, PA, [2]University of Pennsylvania School of Nursing, Philadelphia, PA

Aim: Radiation therapy to treat oral cancer introduces various harms, including decreased hardness of dentin and enamel. Fluoride treatments, including silver diamine fluoride (SDF), have been used as a tool to combat these harms, but its influences on the thermal properties of dentin and enamel prior to and after radiation therapy are not well understood. Thus, this study analyzed how SDF influences the thermal stability of dentin and enamel that has been exposed to radiation therapy intended for head and neck cancer patients.
Methods: Forty human posterior teeth were collected, cleaned of debris and soft tissue, and then mounted into acrylic resin molds. The teeth were divided into two equal groups, with one group being the control (no treatment) and the other group receiving SDF treatment. Using an X-Rad 320ix biological irradiator, all teeth were subjected to two grays of radiation therapy every day for six weeks. Afterwards, the dentin and enamel were pulverized a SPEX freezer mill. Samples were heated in a NETZSCH Thermal Analysis instrument, and the amount of carbon dioxide and water released was determined. All teeth were heated to 1429 °C from room temperature.
Results: The SDF-treated dentin released the most carbon dioxide (49,611.82 ppm/mg), followed by irradiated dentin (47,672.76 ppm/mg) and untreated dentin (45,249.66 ppm/mg). In contrast, the SDF-treated enamel released less carbon dioxide (7,367.62 ppm/mg) than the control enamel (8,172.01 ppm/mg). The pattern of release of water was different from that of carbon dioxide. The control dentin group released the most water (45.56 ppt/mg), followed by the SDF-treated (39.72 ppt/mg) and irradiated dentin (23.51 ppt/mg). Similarly, the control enamel also released the highest amount of water (0.83 ppt/mg), as well as the highest amount of carbon dioxide. The SDF-treated enamel released around 65% of the water compared to the control enamel group (0.54 ppt/mg). Furthermore, the irradiated dentin had the largest heat reversal temperatures for carbon dioxide (85.19 °C) and water (86.57 °C).
Conclusions: The impacts of SDF treatment and radiation vary between dentin and enamel. Comparatively, dentin has a higher content of combustible material than enamel. Radiation treatment reduces the water content of both enamel and dentin, which may make teeth more susceptible to fracture. Therefore, regular dental check-ups and frequent fluoride treatment to increase the strength of the teeth are recommended for patients undergoing radiation therapy.

#6036 Flash proton radiotherapy mitigates radiation-induced salivary gland dysfunction and oral mucositis in mice.

P. Chowdhury, A. Velalopoulou, I. Verginadis, G. Morcos, M. Kim, J. Metz, L. Dong, A. Lin, C. Koumenis;
University of Pennsylvania, Philadelphia, PA

Background- Recent studies have reported that ultra-high dose rate "FLASH" Proton radiation therapy (F-PRT) decreases normal tissue toxicity while maintaining tumor-controlling efficacy compared to Standard Proton RT (S-PRT), that are used for patient treatments. However, although highly efficacious in eliminating tumors, damage to the otherwise healthy salivary glands and oral mucosa is often unavoidable in patients with head and neck cancer, leaving patients with lifelong xerostomia and other comorbidities.
Aim- In this study, we aimed to investigate the effect of F-PRT on radiation-induced oral mucositis and salivary gland dysfunction and in controlling orthotopic tumor growth.
Methods- The head and neck area of C57Bl/6 mice was irradiated with a single dose of 16 Gy or a fractionated dose of 8 Gy x 3 of F-PRT (128Gy/s) or S-PRT (0.95 Gy/s). Oral mucositis was analyzed by histopathological examination. Radiation-induced xerostomia was studied by measuring the saliva flow rate of mice. To examine the ability of F-PRT to control orthotopic head and neck tumors, tongue tumors were generated in mice and then irradiated with F-PRT/S-PRT.
Results- Following irradiation with a single dose or a fractionated dose, saliva flow was reduced by both treatments. However, the F-PRT-treated mice showed a significant improvement in salivary flow at 14 days ($p<0.05$) and 28 days ($p<0.005$) post irradiation. Expression of AQP5 was found to be significantly down-regulated at 2, 5, 10, and 14 days post irradiation with S-PRT. However, mice irradiated with F-PRT showed a significant restoration of the AQP5 expression post-RT. Oral mucositis started to appear on day 14, which showed more severity on day 28 post-irradiation with S-PRT. Histopathological analysis showed the presence of lingual gland atrophy only in the tongue of mice treated with S-PRT 28 and 60 days post-irradiation. F-PRT ameliorates radiation-induced jawbone loss compared to S-PRT as observed in mice irradiated either with a single dose or in a fractionated regime. The surviving fraction of F-PRT-treated mice with orthotopic tongue tumors was significantly ameliorated compared to S-PRT-treated mice.
Conclusion- This study demonstrates that F-PRT minimizes radiation-induced normal tissue toxicity after irradiation in mice's head and neck region. Moreover, the ability of F-PRT to control orthotopic head and neck tumors further determines the efficacy of this modality for clinical applications.

#6037 Copper-67 as a next-generation radioconjugate warhead for cancer therapy.

M. Harris[1], K. Gehlsen[1], L. McInnes[1], J. Lewis[2];

[1]Clarity Pharmaceuticals, Sydney, Australia, [2]Memorial Sloan Kettering Cancer Center, New York City, NY

Background and Purpose: Antibody drug conjugates (ADCs) have shown promise as cancer treatments. However, the efficacy of ADCs has been limited in solid tumors and can come with significant toxicities. Radioconjugates utilize various radionuclides that are chelated and can be conjugated to small molecules, peptides and antibodies. We propose Targeted Copper Theranostics (TCTs) which use copper-64 to image tumors and beta-emitting copper-67 to irradiate and kill cancer cells using various molecular targets of oncological relevance. We have evaluated the efficacy of copper-67 based therapy in three formats; peptides, antibodies, and pre-targeting of antibody conjugates in relevant tumor mouse models. Benefits of copper-67 [half-life, 61.8 h; 100% β^- energy in the range of 0.18-0.56 MeV] include high purity, high specific activity, manufacturing in a centralized distribution model at high yields on electron accelerators, and half-life suitable to various targeting formats. Copper-64 and copper-67 provide multiple logistical benefits relative to other radionuclides including Ga-68, F-18 and Lu-177.

Methods: We evaluated three tumor-targeting moieties conjugated to a sarcophagine bifunctional chelator (SAR), including: a peptide dimer targeting prostate specific membrane antigen (SAR-bisPSMA); an antibody 5B1, targeting the PDAC-specific biomarker carbohydrate antigen-19-9 (CA19-9); and a Tz-TCO IDEEA huA33 antibody/sarcophagine tetrazine conjugate targeting transmembrane glycoprotein A33. Various doses were administered of [^{67}Cu]Cu-SAR-bisPSMA in LNCAP xenografts; [^{67}Cu]Cu-SAR-5B1 (~10 µg) in FC1245 Ft2Ab PDAC tumor-bearing C57BL/6 mice; and [^{67}Cu]Cu-MeCOSAR-Tz in athymic nude mice bearing A33 antigen-expressing SW1222 human colorectal carcinoma xenografts 72 hours after administration of huA33-TCO.

Results: Administration of either 7.5, 15 or 30 MBq of [^{67}Cu]Cu-SAR-bisPSMA increased overall survival relative to the control group. Similarly, after administration of 4, 11, 18 MBq of [^{67}Cu]Cu-5B1, treated groups enhanced overall survival to 32 days compared to control (14 days). Pre-targeting using ~18.5, 37.0 or 55.5 MBq or fractionated dosing of two 27.8 MBq doses of [^{67}Cu]Cu-MeCOSAR-Tz showed efficient tumor growth reduction with enhanced overall survival for treated mice pre-administered huA33-TCO, from 68 days to >200 days (dose dependent) compared to control (21 days).

Conclusion: We report the inhibition of tumor growth with minimal radiotoxicity and each format demonstrated significantly improved overall survival compared to controls. Collectively our results demonstrated that TCTs using the sarcophagine chelator with copper-67 are effective radioconjugates across multiple formats with an acceptable safety profile. Copper-67-based TCTs are being translated in multiple theranostic clinical trials in the USA and Australia.

#6038 Copper-67 based targeted radiotherapy primes immunologically cold PDAC for immunotherapy.

Y. Rao[1], T. Viray[1], K. Gehlsen[2], **M. Harris**[2], L. McInnes[2], O. Majekodunmi[1], J. Lewis[1];
[1]Memorial Sloan Kettering Cancer Center, New York City, NY, [2]Clarity Pharmaceuticals, Sydney, Australia

Background and Purpose: Immune checkpoint therapy (ICT) has revolutionized cancer treatment however efficacy remains dismal for some cancers, including pancreatic cancers. Strategies to enhance immune responses include combining ICT with other existing cancer therapies. Targeted radiotherapy (TRT) uses a radiolabeled cancer-targeting vector, allowing for systematic delivery of specific radiation to all tumor sites while minimizing radiation exposure to healthy tissues. We propose Targeted Copper Theranostics (TCTs) as a TRT, utilizing copper-67 to irradiate and prime immunologically “cold” pancreatic adenocarcinoma (PDAC) and evaluate the efficacy of copper-67-based TRT-ICT combination therapy.
Methods: We evaluated two tumor-targeting vectors conjugated to a sarcophagine macrobicyclic chelator (SAR), an antibody—5B1, targeting the PDAC-specific biomarker carbohydrate antigen-19-9 (CA19-9), and a peptide RGD, targeting the αvβ3 integrin receptor, which is highly expressed in some PDAC tumors. We administrated ~1.1 MBq of [64Cu]Cu-SAR-bisRGD (~0.1 μg) or [64Cu]Cu-SAR-5B1 (~10 μg) to FC1245 Ft2Ab PDAC (a murine PDAC cell line expressing CA19-9) tumor-bearing C57BL/6 mice and performed biodistribution studies at 1 and 4 h for [64Cu]Cu-SAR-bisRGD-injected mice and at 24 and 48 h for [64Cu]Cu-5B1-injected mice. [67Cu]Cu-SAR-bisRGD- and [67Cu]Cu-SAR-5B1-based dose escalation studies and the combination of a copper-67-based TRT and ICT were performed to evaluate therapeutic efficacy of copper-67-based TRT and potential synergistic effects of combination therapy.
Results: Tumor uptake of [64Cu]Cu-SAR-bisRGD is ~5 %ID/g at 4h-post injection, and tumor uptake of [64Cu]Cu-SAR-5B1 is ~55 %ID/g 24h-post injection. In dose escalation studies, administration of ~11, 22, and 37 MBq of [67Cu]Cu-SAR-bisRGD (~1 μg) or administration of ~4, 11, 18 MBq of [67Cu]Cu-5B1(~150 μg) improved overall survival to 25 or 32 days respectively, compared to the control cohort (14 days). Based on weekly whole-blood analyses, no significant radiotoxicity was observed in mice receiving various doses of TRTs. The combination of 11 MBq of either [67Cu]Cu-SAR-bisRGD or [67Cu]Cu-SAR-5B1 in combination with either antiPD-L1/PD1 or antiCTLA4, improved overall survival by ~7 days compared to ICT-treated control groups.
Conclusion: Biodistribution studies demonstrated relatively high tumor specific uptake for [64Cu]Cu-SAR-bisRGD and [64Cu]Cu-SAR-5B1. Dose escalation study results suggest copper-67-based TRT could effectively inhibit tumor growth with minimal radiotoxicity. The combination of TRT with ICTs improved overall survival compared to single-ICT-treated control groups. Collectively, our results strongly support the hypothesis that TRT with [67Cu]Cu-SAR-bisRGD or [67Cu]Cu-SAR-5B1 could prime immunologically “cold” pancreatic adenocarcinoma (PDAC) to be responsive to ICTs.

EXPERIMENTAL AND MOLECULAR THERAPEUTICS: Targeted Protein Degraders
Poster Session

#6042 CBP-8008: A first-in-class targeted pan-Bet protein degradation therapy using bi-specific XDC (Bi-XDC) technology for TNBC and mCRPC.

T. Wang, Z. Zhang, G. Wang, F. Pan, **R. Huang**;
Coherent biopharma (Suzhou) Co., Ltd., Suzhou, China

Bi-XDC is a breakthrough cellular targeting technology using multi-targeting ligands to effectively deliver the payload to and into specific cells. Several anticancer Bi-ligand drug conjugates including CBP-1008, CBP-1018, and CBP-1019 have been brought into various clinical stages in China and US. Targeted protein degradation molecules can degrade previously “undruggable” target proteins through their catalytic mechanism of action. The field target protein degradation has evolved since 2001, and more than 20 PROTACs are under clinical trials at different stages.

To increase the efficacy vs. tolerability window, we combine Bi-XDC technology and the catalytic approach of targeted protein degradation, to form C-PROTAC, by taking advantage of our privileged Bi-XDC technology and PROTAC’s degradation property. Further medicinal chemistry optimization, spacer optimization, and evaluation of many linker payloads led to the identification of our preclinical candidate CBP-8008, a highly potent pan-Bet protein degrader conjugated to bi-ligand via a cleavable linker.

A small panel of cell lines was screened to identify which tumors were sensitive to the pan-Bet protein degradation. All the tested breast cancer and prostate cell lines were the most sensitive to the payload. CBP-8008 had a high affinity to the Prostate Specific Membrane Antigen (PSMA) and the folate receptor alpha (FRα). Much more CBP-8008 were binding the 293T-FP which overexpress both FR-α and PSMA than the cell lines which only express one target (293T-F or 293T-P) or negative cell line (293T). CBP-8008 can quickly enter cells through endocytosis after treatment for 15 min, and degradation of BRD2, BRD3, and BRD4 was observed in MDA-MB-231 after 6 h, which was similar to its payload. The compound was very stable in mouse and human plasma in vitro, and limited free payload was detected which potentially avoids hematotoxicity in clinical. In the tumor-beaning mice DMPK study, fewer free payload was detected in 6 hours while much more free payload was detected in the tumor than in the blood and the time was extended to 72 hours after a single dose treatment. We evaluated CBP-8008 in TNBC and mCRPC xenograft model and robust efficacy was observed as lower as 3 MPK, significantly better than BMS-986158, a potent Bet inhibitor in clinical.

In conclusion: CBP-8008 is currently in preclinical development as a potential first-in-class pan-Bet protein degradation therapy using Bi-XDC technology for TNBC and mCRPC

#6043 Discovery and characterization of a p300-selective degrader with potent anti-tumor activity in CBP mutant cancers.

M. R. Russell, C. L. Lowenstein, X. Zhang, J. Roach, J. Song, R. Nagilla, N. Kendsersky, S. Joshi, P. Orth, M. Tudor, Q. Deng, C. Aguilar-Bonavides, E. Behshad, S. Banjade, Z. Sui, C. Strickland, L. Jolivette, H. P. Mohammad;
SK Life Science Labs, King of Prussia, PA

Although precision medicine strategies for the treatment of human cancers are clinically successful, they have also revealed that only a small fraction of cancers carry actionable alterations in oncogenic drivers. To expand the druggable genome while maintaining an emphasis on genetically targeted therapies, recent efforts have focused on exploiting synthetic lethal relationships. Paralogous protein pairs are particularly compelling targets in this context due to the clear mechanistic basis for the synthetic lethality. As such, functional genomics screens as well as work from Ogiwara et al. have shown compelling rationale for targeting the histone acetylase transferase p300 in the context of CBP-deficient cancer types. We discovered potent heterobifunctional degraders with demonstrated selectivity for p300 over CBP. Our compound exhibits degradation of p300 within 2 hours (DC_{50} < 10nM, D_{max} > 90%) with minimal impact on CBP through 48 h (DC_{50} >1uM, D_{max} = 30%). Utilizing CRISPR-generated isogenic cell lines depleted for either CBP or p300, we observed significant growth inhibition in CBP knockout (KO) cells (gIC_{50} = 17nM) with minimal impact on growth of p300 KO (gIC_{50} = >10uM) or parental wild-type cells (gIC_{50} > 10uM). This translated to downstream pharmacology, where we observed a rapid and potent inhibition of global H3K27 acetylation in the CBP deficient context but a significantly attenuated response in p300 deleted or parental cells. We subsequently employed computational methods to identify and characterize CBP alterations, defining a putative loss-of-function (LoF) phenotype and confirming this sensitivity pharmacologically in cancer cell types harboring these endogenous mutations. Results mirrored what we observed with CBP depletion in these endogenous CBP LoF cell lines, with potent growth inhibition seen in multiple cell lines including LK-2 (gIC_{50} = 8nM), H1703 (gIC_{50} = 9nM), and TE-8 cells (gIC_{50} = 23nM). To confirm the *in vitro* results in an *in vivo* setting, we evaluated the response in mice harboring H1703 xenografts. Once daily oral administration of our compound led to almost complete degradation of p300 within H1703 xenograft tumors, resulting in a pronounced inhibition of tumor growth. Lastly, we profiled p300 degradation in human bone marrow derived myeloid progenitor colony-forming assays where we observed a significant reduction in toxicity (IC_{50} = 3.9uM) compared to a dual CBP/p300 inhibitor (IC_{50} = 121nM) or degrader (IC_{50} = 16nM), supporting the hypothesis that a p300-specific mechanism will offer an improved therapeutic index while maintaining anti-tumor efficacy in a biomarker population Taken together, our results suggest that a p300-selective degrader has the potential to serve as an effective therapeutic modality in CBP-mutated cancers.

#6044 EPriL: A platform for the rapid identification of degraders of inhibitor-resistant kinases.

M. Muller, J. de Man, J. C. M. Uitdehaag, F. van Cauter, S. van Gemert, M. Hoffmann, Y. G. T. van Mil, W. R. Mulder, M. B. W. Prinsen, J. Sterrenburg, D. Vu, J. de Wit, E. Ensing, R. C. Buijsman;
Crossfire Oncology B.V., Oss, Netherlands

Heterobifunctional kinase degraders (HKDs) are an important new class of therapeutic modalities, of which the first have recently entered clinical trials. HKDs are small molecules that comprise a kinase-of-interest binding moiety and an E3 ligase binding moiety connected via a spacer. HKDs are excellently suited to target kinases that have a scaffolding function, or that are resistant against conventional inhibitors. A HKD brings a kinase and an E3 ligase in proximity forming a ternary complex leading to ubiquitin-dependent catalytic degradation of the kinase of interest. This ternary complex formation is unique for each kinase which can make HKDs highly specific.

To discover novel HKDs, we have developed a platform called Energetically Privileged Ligands (EPriLs), which is based on a macrocycle scaffold that binds non-covalently in the kinase ATP pocket with near-covalent affinity, and allows binding to kinases that have acquired known inhibitor resistance mutations. The macrocyclic structure allows attachment of E3 ligase ligands with multiple exit vectors. With the EPriL platform, we have developed novel HKDs for various clinically relevant kinase targets, including Bruton's Tyrosine Kinase (BTK).

BTK inhibitor drugs are used as first line treatment for chronic lymphocytic leukemia (CLL), Waldenström macroglobulinemia (WM) and as second line treatment for mantle cell lymphoma (MCL). Despite their great success in the clinic, many patients on BTK inhibitors relapse eventually, mostly because of the emergence of resistance mutations in the BTK protein. These include BTK^{C481S}, which abrogates binding of covalent drugs, and BTK^{T474I}, BTK^{L528W} and BTK^{V416L} which preclude binding of non-covalent inhibitors like pirtobrutinib. HKDs can combat resistance by degrading such BTK variants, and by removing the scaffold function of BTK. BTK degraders such as NX-5948 and NX-2127 are currently in clinical Phase 1.

To show the applicability of the EPriL platform for the discovery of novel BTK degraders, we screened a library of more than 100 EPriL HKDs for biochemical binding to BTK, and tested their propensity to induce degradation of HiBiT-tagged BTK^{WT}, BTK^{C481S} and BTK^{T474I} in HEK293 cell lines. The degrading activity of hits was verified through western blot on the BTK-dependent DLBCL cell line TMD8. The best degraders - based on potency and efficacy - were tested in cell proliferation assays on a panel of TMD8 BTK mutant cell lines. In these lines, endogenous BTK was mutated by CRISPR to BTK^{C481S}, BTK^{T474I}, BTK^{L528W} or BTK^{V416L}. Several BTK degraders had potent (< 20 nM IC_{50}) antiproliferative activity on most TMD8 lines, including difficult-to-target variants such as BTK^{V416L} and BTK^{L528W}.

The unique binding mode of the EPriL scaffold thus translates to broad activity on resistance variants, while its selectivity ensures minimal degradation of off-target tyrosine kinases as observed for other degraders.

#6045 Development and characterization of ATC-324: An AUTOTAC-based androgen receptor degrader for prostate cancer treatment.

T. Pham[1], T. Bae[2], K. Sung[2], A. Najy[1], A. Zamiri[1], H. Jang[1], S. Mun[2], S. Kim[1], D. Shi[3], S. Kregel[4], E. Heath[1], M. Cher[1], Y. Kwon[2], H.-R. Kim[1];
[1]Wayne State University School of Medicine, Detroit, MI, [2]Seoul National University, Seoul, Korea, Republic of, [3]Wayne State University College of Pharmacy and Health Sciences, Detroit, MI, [4]Loyola University, Chicago, IL

Prostate cancer (PCa) progression is largely driven by the androgen receptor (AR), making it a prime target for therapy. However, therapy resistance often arises due to AR mutations and splice variants, such as AR-v7. AUTOTAC (AUTOphagy-TArgeting Chimera) is a novel protein degradation platform that utilizes the autophagy-lysosomal pathway to selectively degrade disease-causing proteins. In this study, we characterize ATC-324, an AUTOTAC-based AR degrader designed for the treatment of PCa. ATC-324 comprises enzalutamide linked to YT 6-2, a small molecule activator of the autophagy receptor p62/SQSTM1. ATC-324 induces the formation of the AR/p62 complex while activating autophagic flux, leading to the autophagy-lysosomal degradation of AR. To characterize ATC-324, we employed various AR-dependent, AR-null, and enzalutamide-resistant PCa cell lines. Given that bone metastasis is a major clinical complication of castrate-resistant PCa associated with greater morbidity and mortality, we utilized the bone-in-culture array (BICA) assay, an *ex vivo* bones culture model, to investigate the impact of ATC-324 on PCa cell survival and growth in the bone microenvironment. We demonstrated that ATC-324 effectively degrades wild-type, mutant, and splice variants of AR. In addition, ATC-324 induces AR-dependent apoptosis and cytotoxicity. Importantly, ATC-324 maintains its potency in enzalutamide-resistant PCa cells. Utilizing the BICA assay, we showed that ATC-324 exhibits cytotoxicity against 22Rv1 bone micrometastases at even lower concentrations than in 2D cell culture. In conclusion, our study demonstrates the successful development and characterization of ATC-324 as a potent and selective degrader of various forms of AR. Furthermore, its effectiveness against enzalutamide-resistant cells indicates its capability to overcome therapy resistance. The observed cytotoxicity against bone micrometastases suggests a therapeutic potential for combating bone metastasis, a major complication of castration-resistant PCa. Our study underscores the potential of the AUTOTAC platform to selectively degrade disease-causing proteins

#6046 CFT8634, a BRD9 BiDAC™ degrader, is active in a subset of multiple myeloma cell line models and synergistic when combined with pomalidomide or dexamethasone.

L. L. Poling, D. Cocozziello, M. He, E. Hurh, R. Lobbardi, K. L. Jackson, S. L. Fisher, R. M. Pollock;
C4 Therapeutics, Inc., Watertown, MA

Recent literature has shown that loss-of-function of BRD9, a component of the noncanonical SWI/SNF (ncSWI/SNF) complex, mediated by RNA interference or by BRD9 degrader compounds can inhibit multiple myeloma (MM) cell lines and primary MM cell proliferation *in vitro*, as well as inhibit mouse MM xenograft tumor growth *in vivo*. Additionally, *in vitro* synergy was observed when a BRD9 degrader was combined with either dexamethasone or pomalidomide. CFT8634 is a potent and selective oral BiDAC™ degrader of BRD9 that entered a clinical trial for the treatment of SMARCB1-perturbed cancers, including synovial sarcoma and SMARCB1-null tumors. Pharmacokinetic and pharmacodynamic data from this trial demonstrated dose-proportional human plasma exposure and robust BRD9 degradation in patients.

Here we show that CFT8634 has anti-proliferative activity in a subset of MM cell lines that translates into tumor growth inhibition in MM xenograft models at clinically relevant CFT8634 exposures. We observe that cell lines less sensitive to pomalidomide tend to be significantly more sensitive to CFT8634 treatment. As pomalidomide is a SoC treatment in MM, we interrogated the ability to combine CFT8634 and pomalidomide. CFT8634 demonstrates synergy with pomalidomide in MM cell lines where CFT8634 is anti-proliferative as a single agent. We further show that clinically relevant exposures of CFT8634 demonstrate synergy with pomalidomide *in vivo* in the NCI-H929 mouse xenograft model. This model is relatively unresponsive to pomalidomide alone, suggesting that CFT8634 can render otherwise recalcitrant MM tumors sensitive to the effects of pomalidomide in combination. Pharmacokinetic and pharmacodynamic analyses show that in combination, CFT8634 and pomalidomide do not interfere with the ability to degrade each other's targets (BRD9 and IKZF1/3, respectively) despite both utilizing the E3 ligase cereblon.

As the corticosteroid dexamethasone is another SoC treatment given in combination with pomalidomide, we explored the ability to combine dexamethasone with CFT8634. CFT8634 demonstrates synergy with dexamethasone in the RPMI-8226 *in vivo* xenograft model. This combination leads to tumor regressions at clinically relevant doses and outperforms the current combination of pomalidomide with dexamethasone.

In conclusion, we demonstrate *in vitro* and *in vivo* activity in an expanded set of MM models using the clinical oral BRD9 degrader CFT8634 as a single agent and show *in vivo* synergy between CFT8634 and SoC agents pomalidomide and dexamethasone at clinically relevant doses.

#6047 Discovery and characterization of PVTX-321, an estrogen receptor heterobifunctional degrader .

C. G. Havens, G. Xu, C. Lowenstein, D. Samanta, B. Vidal, E. Behshad, R. Nagilla, M. Russell, P. Orth, W. Wu, L. Jolivette, S. Priestley, H. Mohammad, Z. Sui; SK Life Science Labs, King of Prussia, PA

The estrogen receptor α (ERα) is a clinically validated target for the treatment of estrogen receptor-positive and human epidermal growth factor receptor 2-negative (ER+/HER2-) breast cancer. However, resistance to early line endocrine treatments due to mutations of the ESR1 gene encoding ERα is associated with poor prognosis and remains an area of unmet clinical need. ERα degradation using heterobifunctional degraders has emerged as a promising approach to tackle endocrine resistance through proteasome mediated degradation of the receptor. Here, we present the preclinical results for the development candidate, PVTX-321, an ERα heterobifunctional degrader. PVTX-321 is a rapid and potent ER heterobifunctional degrader as well as a full ERα antagonist. Both properties translate into potent antiproliferative activity across multiple ER+ breast cancer cell lines bearing either wild-type or clinically relevant ERα mutations (E380Q, Y537S and D538G). PVTX-321 demonstrates favorable oral bioavailability across different species and effectively induces dose-dependent degradation of ERα *in vivo*. Moreover, PVTX-321 achieves tumor regression as an oral agent at 10 mg/kg in MCF-7 mouse xenograft model. Furthermore, PVTX-321 possesses excellent *in vitro* and *in vivo* safety profiles and warrants further development for the treatment of ER+/HER2- breast cancer.

#6048 Targeting AR positive prostate cancer cells by the novel P300/CBP oral available PROTAC degrader.

j. luo, A. Prolia, Y. Qiao, j. tian, R. Mannan, S. Mahapatra, z. chen, R. Seri, S. Wang, A. Chinnaiyan;
University of Michigan, Ann ARBOR, MI

Background The Androgen Receptor (AR) serves as the core lineage-specific transcription factor for prostatic epithelial cells. Targeting AR is currently the most promising therapeutic strategy. However, the inevitable development of acquired resistance to anti-androgen treatments underscores the urgent need to devise new therapeutic strategies. Recent studies have revealed that in prostate cancer cells, AR is hijacked by oncogenic transcription factors, such as FOXA1 and HOXB13, which promiscuously bind to distinct enhancer sites, driving the progression of prostate cancer. This process leads to the formation of a substantially rewired AR cancer specific enhanceosome, requiring a variety of coregulators to exhibit oncogenic driver characteristics, which can be potential therapeutic targets for prostate cancer. Histone acetyltransferases (HATs) P300 and CBP are paralogs which play dominant roles in orchestrating high-order chromatin structures and transcription factor complexes by acetylating histone proteins at multiple residuals. Although accumulating evidence suggests that P300/CBP function as AR coregulator and targeting P300/CBP can markedly suppress AR-positive prostate cancer cell growth, including growth of castration-resistant prostate cancer (CRPC), most of the P300/CBP inhibitors have performed poorly in clinical trials.
Methods We developed a novel P300/CBP dual oral available PROTAC degrader, namely CBPD-409. The on-target effects of CBPD-409 were assessed by quantitative proteomics (TMT-mass spectrometry) in prostate cancer cell lines. The RNA-seq analysis was conducted to investigate CBPD-409 effects on global transcriptome in prostate cancer cells. The cytotoxicity of CBPD-409 in multiple prostate cancer cell lines was examined by cell-titer-glo and incucyte assays.
Conclusion In multiple cell lines, CBPD-409 exhibits remarked potency to degrade both P300 and CBP proteins in time and does dependent manner, without evident off-target effects. By employing CBPD-409, we demonstrate that degrading P300/CBP preferentially suppress AR+ prostate cancer cell growth. The global transcriptomic profiling in CBPD-409 treated prostate cancer cells revealed that loss of P300/CBP results in remarkedly downregulation of AR, Myc, FOXA1 and ERG signaling. Assessment of CBPD-409 cytotoxicity in a panel prostate cancer cell lines suggests that AR positive prostate cancer cells display highest sensitivity to CBPD-409.

#6049 Cell-based PROTAC screening for cancer drug discovery.

Y. Wan, H. Ma, J. Wu;
Reaction Biology, Malvern, PA

Proteolysis-Targeting Chimeras (PROTACs) have emerged as a promising strategy for selectively degrading specific target proteins, thereby offering a novel approach to precision cancer therapy. Among the most notable oncogenes, KRAS with the G12C mutation is responsible for 45%-50% of KRAS mutations in non-small cell lung carcinomas. Additionally, BRD4, a well-studied member of the Bromo- and Extra-Terminal (BET) protein family, is implicated in various hematological and solid tumors. The implementation of cell-based screening for PROTACs targeting either KRAS(G12C) or BRD4 represents a highly valuable platform for advancing cancer drug discovery. We utilized the NanoBRET™ Ternary Complex Assay, NanoBiT™ Assay, and Western Blot assay to evaluate the efficacy of PROTACs. The NanoBRET™ Ternary Complex Assay revealed that KRAS G12C degrader-1 and LC-2 effectively degrade KRAS(G12C), while dBET6 and MZ-1 demonstrated the ability to degrade BRD4. Notably, the NanoBiT™ assay showed that LC-2 dose-dependently degrades KRAS(G12C) in HEK293 cells co-transfected with KRAS(G12C)-LgBiT and KRAS(G12C)-SmBiT. Moreover, BET6 exhibited a dose-dependent degradation of endogenous BRD4 in HepG2 cells, and LC-2 demonstrated the degradation of endogenous KRAS(G12C) in MiaPaCa2 cells. In summary, the development of a robust cell-based assay platform for high-throughput screening of PROTACs marks a substantial advancement in cancer drug discovery. This approach not only enables the identification of promising PROTACs but also holds the potential for more effective and targeted interventions in the ongoing battle against cancer.

#6050 Targeting KRAS G12D mutant tumors with the PROTAC degrader RP03707.

X. Ji[1], H. Li[1], G. Wu[1], Q. Zhang[1], X. He[1], Y. Wu[1], B. Zong[1], X. Xu[1], C. Liang[1], B. Wang[1], Y. Zhang[1], Q. Hu[1], J. Zhou[2], W. Guo[1], B. Bai[1], L. Wang[1], J. Ai[1], L. Zhang[1], H. Zhou[1], S. Sun[1], Y. Wang[1], Y. Wang[1], Q. Fan[1], D. Chen[1], **T. Zhou**[1], J. Lu[1];

[1]Risen Pharmaceuticals Private Ltd., Shanghai, China, [2]University of California San Diego, San Diego, CA

RAS oncogene mutations are prevalent in approximately 19% of cancer patients, with the most frequent alteration occurring in codon 12 of the KRAS gene, resulting in a variety of G12X oncoproteins. Recent advances in drug discovery have yielded several KRAS G12C inhibitors currently in clinical use, benefiting a subset of patients. However, addressing the high-prevalence G12D mutation remains a substantial unmet medical need. Targeted protein degradation using PROTAC molecules offers a promising approach for treating KRAS G12D-associated tumors, potentially providing superior efficacy and mitigating the development of resistance, a challenge frequently observed with KRAS G12C inhibitors in clinical settings. In the present study, we report a PROTAC compound RP03707 that efficiently induces the degradation of the KRAS G12D mutant protein and inhibits tumor growth. Treatment of AsPc-1 cells with RP03707 results in significant degradation of the KRAS G12D protein, with a DC50 value in the sub-nanomolar range. Within 24 hours, the compound eliminates over 90% of G12D proteins and effectively suppresses downstream cellular MAPK signaling. Additional *in vitro* experiments demonstrate that RP03707 inhibits cell proliferation in multiple KRAS G12D mutant cell lines, surpassing the anti-tumor efficacy of enzyme inhibitors. In a mouse GP2d xenograft tumor model, a single intravenous administration of RP03707 at 10 mpk results in excellent compound penetration and retention in tumor tissues, followed by 90% reduction of G12D protein levels for 7 days. Profound inhibition of tumor growth is observed not only in mouse GP2d xenograft but also in other mouse KRAS G12D tumor models, even when the compound is administered in low and infrequent doses. Moreover, RP03707 exhibits high selectivity for degrading the KRAS G12D protein and possesses favorable drug-like properties. RP03707, therefore, meets the criteria for advancing into drug development and represents a valuable therapeutic option for treating KRAS G12D-associated tumors.

#6051 Discovery of oral SMARCA2 degraders for the treatment of SMARCA4 mutant tumors.

J. C. Clemente, L. Harikrishnan, S. Knight, D. Samanta, Z. Li, R. Nagilla, N. Kendsersky, S. Joshi, P. Orth, M. Tudor, Q. Deng, C. Aguilar-Bonavides, E. Behshad, Z. Sui, C. Strickland, L. Jolivette, H. P. Mohammad;
SK life science labs, King of Prussia, PA

The paralog enzymes SMARCA2 and SMARCA4 are mutually exclusive members within the SWI/SNF chromatin remodeling complex. This complex plays a crucial role in governing gene expression by altering the chromatin and rendering it accessible to transcription machinery. The process of chromatin remodeling by the SWI/SNF complex is dependent on ATP hydrolysis. Within the complex, either SMARCA2 or SMARCA4 serves as the sole component capable of catalyzing ATP hydrolysis and are thereby essential to the activity of the complex. SMARCA4 has been found to be mutated in various cancer types, including non-small cell lung carcinoma, colon adenocarcinoma, bladder, and endometrial cancer. In cancer cells where SMARCA4 is deleted, the functionality of the SWI/SNF complex and cell survival is dependent on the presence of SMARCA2, thereby resulting in synthetic lethality if SMARCA2 is depleted. Utilizing in vitro and in vivo model systems we have discovered potent, selective, and orally bioavailable heterobifunctional degraders targeting SMARCA2. Our lead molecules exhibit potent and selective degradation of SMARCA2 (DC_{50} < 10 nM) with no impact on SMARCA4 (DC_{50} > 1000 nM). Furthermore, a striking selective activity in proliferation assays was observed with SMARCA4 deleted cells exhibiting gIC50 ranging from 1 -10 nM and SMARCA4 WT cells > 1000 nM. Oral administration in mice harboring human cancer cell line xenografts revealed dose-dependent and selective *in vivo* degradation of SMARCA2. Degradation of SMARCA2 led to significant anti-tumor activity in SMARCA4 mutant NSCLC xenograft models. Together, these data demonstrate a foundation for the development of a best-in-class degrader for the treatment of SMARCA4 deleted cancers.

#6052 Systematic identification of novel targeted protein degradation mechanisms using SITESEEKER® technology.

C. Dillon;
PhoreMost Limited, Pampisford, United Kingdom

The rise of Targeted Protein Degradation (TPD) is rapidly changing perceptions about therapeutic target druggability and is rewriting many preconceived notions on drug design. However, the majority of monovalent molecular glue and heterobifunctional degraders in clinical and preclinical development rely predominantly on the recruitment of a single E3 ligase, Cereblon. Arising resistance, toxicities and restricted Protein-of-Interest scope may limit clinical potential, highlighting the need to uncover novel TPD mechanisms. To expand the potential of this modality, we have developed SITESEEKER®, a screening technology operating at substantially greater magnitude of complexity than extant target discovery platforms. SITESEEKER® utilizes computationally-derived encoded mini-protein fragments with huge shape diversity to systematically identify novel degrader mechanisms and define functionally-active binding sites on targets. SITSEEKER® allows for the discovery of targets that may be missed through traditional gene editing or knockdown approaches and can additionally provide valuable mechanistic insights that help to inform, unlock and truncate the path from target ID to drug discovery. We describe the identification of a cache of degrader motifs which showcase the breadth of proteome space yet to be explored within TPD. Moreover, we identify peptide motifs capable of driving degradation in a selective manner with potential to be translated into tissue- or cancer-selective degraders. The functional dependencies of prioritized degraders have been mapped to their cognate E3 ligase using combinatorial screening, giving rise to a number of E3 ligases with potential to be hijacked for TPD. PhoreMost is progressing a pipeline of monovalent and heterobifunctional oncology degrader programs arising from its platform. We demonstrate the effective hijacking of selected E3 ligases, identified by SITESEEKER®, through the discovery of high affinity small molecule binders and subsequent discovery of efficient heterobifunctional degraders against selected Proteins-of-Interest.

#6053 Mechanism of action of tumor-selective, chaperone-mediated protein degraders (CHAMPs).

X. Yang[1], Y. Dai[1], Q. Ding[1], F. Du[1], J. Li[1], C. Liu[1], C. Lv[1], L. Ma[1], T. L. Prince[2], Y. Sun[1], M. Wang[1], R. Wang[1], Y. Wang[1], Z. Wang[1], M. Wu[1], M. Xu[1], Z. Yang[1], L. Ye[1], W. Yin[1], C. Ying[1], H. Zhou[1], G. Wang[1], W. Ying[1], K. P. Foley[2];

[1]Ranok Therapeutics, Hangzhou, China, [2]Ranok Therapeutics, Waltham, MA

HSP90 mediates the folding of many important cancer-associated proteins, but it can also direct its substrates towards degradation via the ubiquitin-proteasome system. Furthermore, in tumor tissues, HSP90 complexes are in an activated state relative to normal tissues, and small molecule HSP90 inhibitors display unique tumor-selective pharmacokinetics. To take advantage of these attributes, we have developed a novel targeted protein degradation technology, termed Chaperone-Mediated Protein Degradation (CHAMP), and present here an in-depth characterization of the CHAMP mechanism of action. Initially, from a chemical library of greater than 1000 linkered HSP90 binders, hetero-bifunctional CHAMPs were synthesized in which target protein binders and HSP90 binders were covalently coupled together by short linkers. The resulting compounds were screened for target protein degradation and cancer cell cytotoxicity to identify promising leads for further optimization. We found that CHAMPs can degrade a wide variety of target proteins. This included proteins that are known to be regulated by HSP90, such as transcription factor BRD4 or ERK5 kinase. However, proteins that are normally independent of HSP90 function can also be degraded, including mutated KRAS and SHP2 phosphatase. In vitro, CHAMP treatment of cells resulted in formation of a ternary complex between the target protein, CHAMP compound and HSP90. Moreover, an X-ray crystal structure was solved for a mKRAS-CHAMP-HSP90 ternary complex. CHAMP-mediated degradation required both the target- and HSP90-binding moieties to be covalently coupled and involved ubiquitination of the target protein. Multiple ubiquitin E3 ligases were present in ternary complexes, and depending on the target protein, NEDD8 inhibition or CRISPR knockouts of individual E3 ligases could suppress proteasome-dependent target degradation. In vivo, irrespective of target, CHAMPs displayed prolonged exposure in tumors relative to plasma and normal tissues, resulting in prolonged target degradation in tumors and strong tumor growth inhibition at well-tolerated doses. CHAMP technology can be applied to a diversity of cancer-associated targets and has potential advantages relative to other protein degradation approaches, including an improved safety margin due to preferential accumulation in tumor tissues.

#6054 UPPGRADER: a bioinformatics-based novel E3 ligase discovery platform.

K. Ha[1], W. Song[2], W. Choi[1], G. Lee[1], S. Ryu[1], J. Lee[1], **H. Lee**[2];
[1]UPPTHERA, Incheon, Korea, Republic of, [2]Kyunghee University, Seoul, Korea, Republic of

In Target Protein Degradation (TPD) field, conventional E3 ligases utilized in the clinic are limited to CRBN and VHL, which opens the need for exploration of novel E3 ligases for the advancement of TPD. To address this, we have developed a proprietary platform, UPPGRADER, for systematic discovery of novel E3 ligases based on -omics data including single cell RNA sequencing (scRNA-seq) and whole genome sequencing (WGS), in conjunction with proteomics data and bioinformatics tools.UPPGRADER enables systematic analyses on alterations occurred in all genomic areas including E3 ligase genes and potential target genes. For example, analyzing Pan-Cancer Analysis of Whole Genomes (PCAWG) data identified amino acid changes into Cysteine or Lysine, which can be targeted by covalent binders with cancer specificity. Through such analysis, we discovered several novel E3 ligases, including but not limited to FBXW7, with the categorization of the findings based on specific cancer types.At the single cell expression level, UPPGRADER provides the capability to assess gene expression levels of E3 ligases and target proteins by proprietary measurements based on gene detection rate. This system also allows assessment of E3 ligase-Target gene co-expression per single cell. In colorectal cancer, UPPGRADER has shown that the co-expression of E3 ligase FBXW7 and well-known colorectal cancer target (KRAS) increases from 1% (4 out of 334) in normal epithelial cells to 17% (2,967 out of 17,458) in cancerous epithelial cells, highlighting a significant change in their simultaneous expression patterns during cancer progression.UPPGRADER also identified E3 ligase X which showed high co-expression level with KRAS gene alongside universal expression properties and high cancer cell dependencies. For E3 ligase X, we developed novel small molecule binders (nM binding affinity) with bioavailability > 20% in animal pharmacokinetics. Bifunctional degraders utilizing these binders displayed BRD4 degradation in more than 20 cell lines with double to triple digit nM DC50 and DC90 values. Other targets (AURKA, CRBN and others) were potently degraded with anticipated mechanism of action (assessed by E3 ligase KO cell line and proteasomal inhibitors).To conclude, UPPGRADER is a comprehensive bioinformatics tool for discovering novel E3 ligases with biological validations. Through recent explosion of scRNA-seq and WGS datasets in different diseases and mechanism-based identification of additional molecular targets, UPPGRADER is poised to advance the field of TPD.

#6055 COOTO-Me (10e) acts as a molecular glue to target NCOR/HDAC3 degradation.

P. Gong[1], M. Huang[1], X. Li[1], H. Wang[1], S. Waxman[2], L. Zhao[1], Y. Jing[1];

[1]Shenyang Pharmaceutical University, Shenyang, China, [2]Icahn School of Medicine at Mount Sinai, New York, NY

Histone deacetylase 3 (HDAC3) is overexpressed in cancer cells and functions as transcription repression complex with nuclear receptor corepressor (NCOR) to inhibit gene transcription. The pan-HDAC inhibitors have been approved for T-cell lymphoma with evident side effects. The selective HDAC3 inhibitors needs to be developed. Proteolysis-targeting chimera (PROTAC) approach is taken to design HDAC3 degraders with unsolved bioavailability obstacle. We screened small molecules with HDAC3 degradation ability and found two small molecules derived from glycyrrhetinic acid, methyl 2-cyano-3-oxo-18β-olean-1,9(11), 12-trien-30-oate (COOTO, 10e) and methyl 2-cyano-3,12-dioxo-18β-olean-1,9(11)-dien-30-oate (CDODO-Me, 10d), selectively decreased HDAC3 protein with increased acetylation of Histone 3. We explored the mechanism of HDAC3 degradation and found that 10e interrupted the interaction of HDAC3 with NCOR and induced degradation of both HDAC3 and NCOR protein. Biotin labeled 10e shows binding to both HDAC3 and NCOR directly as well as to E3 ligases SIAH2 and ITCH. Mass spectrometry analysis profiling reveals covalent interactions of 10e with multiple cysteine sites of SIAH2 in the binding regions for NCOR and HDAC3. Silencing SIAH2 blocks degradation of HDAC3. *N*-Acetylcysteine and GSH block the binding of 10e to HDAC3, NCOR and SIAH2. In addition, 10e decreased the levels of c-FLIP protein and increased the levels of NOXA protein leading to apoptosis induction. These data suggest that 10e functions as a molecular glue to attract SIAH2 to HDAC3 and NCOR to cause degradation through covalent binding.

#6056 Identification of first-in-class, orally bioavailable SOS1 bifunctional degraders for the treatment of KRAS- and RTK-driven cancers.

K. Begovich, A. Schoolmeesters, N. Rajapakse, E. Martinez, Q. Liu, A. Shakya, A. Okano, V. Mali, S. Huang, A. Chourasia, L. Fung;
BioTheryX, Inc., San Diego, CA

Monotherapies which target nodes within the RTK-RAS-MAPK pathway often display early potency in the clinic, but their preliminary response is limited as tumors begin to regrow due to adaptive and acquired resistance mechanisms. Disrupting proteins that mitigate either type of resistance mechanism in combination with oncogene-targeted agents could help extend and enhance the clinical potential of these drugs. Son of Sevenless 1 (SOS1), a RAS guanine nucleotide exchange factor, is a highly attractable protein to target given its role in transducing inputs from upstream receptor tyrosine kinases (RTKs) to downstream RAS proteins to regulate signaling pathways involved in cell proliferation and survival. Additionally, SOS1 is subject to MAPK-mediated negative feedback inhibition and drugs targeting upstream and downstream nodes relieves SOS1 from this inhibition resulting in pathway reactivation. To address this need, we have developed orally bioavailable SOS1 bifunctional degraders for cancers driven by KRAS and RTKs. Our top two lead molecules demonstrate CRBN- and proteasomal-mediated SOS1 degradation with DC_{50}s < 10nM and maximum degradation > 90%. Consistent with this notion, SOS1 degradation inhibited downstream signaling marker phopshoERK with IC_{50}s < 5nM and were 26- or 53-fold more potent when compared to the clinical SOS1 inhibitor. Notably, the SOS1 degraders exhibited weaker SOS1 binding compared to other SOS1 inhibitors highlighting that the potency is heavily driven by the catalytic nature of degradation rather than occupancy-driven events. Both SOS1 degraders displayed CRBN- and SOS1-dependent antiproliferative activity in KRAS- and EGFR- mutant, solid tumor cell lines as well as in BCR-ABL driven, CML cells with IC_{50} values ranging from 0.5-10nM. Consistent with our *in vitro* data, oral administration of our SOS1 degraders in mice harboring H358 (KRAS G12C) and H441 (KRAS G12V) xenografts resulted in SOS1 degradation, phosphoERK reduction and significant tumor growth inhibition. While SOS1 degrader monotherapy demonstrated *in vitro* and *in vivo* potency, combination of mutant or allele specific EGFR and KRAS inhibitors and ABL inhibitors with our proof-of-concept degraders prevented pathway reactivation associated with these inhibitors and lead to a more durable response. These combinations also yielded synergistic effects in *in vitro* proliferation assays as well as enhanced tumor growth inhibition in KRAS-mutant xenograft models. Together, our SOS1 degraders alone and in combination with other targeted agents demonstrated anti-tumor activity in a variety of KRAS- and RTK-driven cancer cell lines and xenograft models. These results support the potential of orally bioavailable SOS1 degraders to help mitigate pathway reactivation for enhanced efficacy and prolonged response duration.

#6057 Evaluation of a highly potent and selective STAT3 degrader as a new class of immunotherapy.

L. Bai, H. Zhou, J. Zhou, D. Wu, R. Acharyya, H. Metwally, D. McEachern, B. Wen, D. Sun, W. Zou, S. Wang;
University of Michigan, Ann Arbor, MI

STAT3 (signal transducer and activator of transcription 3) is a transcription factor and a promising therapeutic target for cancer and other human diseases. In addition to its role in regulation of tumor cells, STAT3 also plays a key role in regulation of immunity and is a promising therapeutic target for the development of new immuno-oncology drugs. Our laboratory has previously reported the development of potent and highly selective STAT3 degraders, including SD-36 and SD-91. Extensive optimization of SD-36 and SD-91 yielded new, highly potent, selective and efficacious STAT3 degraders. In direct comparison, our most potent, new STAT3 degrader (compound 1) is >50-times more potent than SD-36 in inducing STAT3 degradation in cells and demonstrates >500-fold degradation selectivity over other STAT members. A single intravenous administration of compound 1 in mice is highly effective in inducing complete depletion of STAT3 protein in tissues for 48-96 h without reducing the levels of other STAT proteins. Compound 1 is very effective in inhibition of tumor growth not only in tumor models responsive to immune checkpoint blockade (ICB) but also in tumor models resistant to ICB. Furthermore, combination of compound 1 with PD-1/PD-L1 antibodies greatly enhances the antitumor activity as compared to SD-1218 or ICB. Of significance, compound 1 is well tolerated in mice without any signs of toxicity in mice at highly efficacious doses. Our mechanistic studies show that STAT3 depletion has a major effect in modulation of the immune cells in mice. Collectively, our data suggest that selective STAT3 degradation hold great promise for new cancer immunotherapy.

#6059 Discovery of ETS-007, a first-in-class degrader targeting N-terminal domain of androgen receptor derived from AR liquid-liquid phase separation inhibitor.

Y. Li, M. Fei, Y. Miao, L. Feng, X. Fan, J. Li, Y. Chen, M. Xu, W. Cui, Q. Zheng, **J. Zhu**;
ETERN Therapeutics Co., Ltd., WuXi, China

Patients with advanced prostate cancer inevitably acquire resistance to anti-androgen therapies, and progress to lethal castration-resistant prostate cancer (CRPC). The resistance mechanisms involve AR gene amplification and overexpression, constitutively active ligand-independent splice variants such as AR-V7, and the mutations in the AR ligand-binding domain (LBD). Our previous study has shown that the AR N-terminal domain (NTD) is responsible for AR liquid-liquid phase separation (LLPS) capability, which is essential for AR/AR-V7 transcriptional activity. We conducted a compound library screening using an AR LLPS phenotypic assay and identified ET0516 as a hit to specifically inhibit AR LLPS and its downstream gene expression, indicating that inhibition of AR. LLPS through targeting its NTD is a feasible approach to overcome the resistance to current anti-androgens therapy. Here we report the identification of a novel AR degrader, ETS-007 which is originated and evolved from internal LLPS phenotypic screening, that effectively degrades both AR and AR-V7 proteins with DC_{50} of single-digit nM by inducing a protein-protein interaction between AR NTD and an E3 ligase complex. ETS-007 induced AR and AR-V7 polyubiquitination, followed by degradation which could be blocked by the protease inhibitor MG132. ETS-007 significantly inhibited cell proliferation in AR and/or AR-V7 positive cell lines, e.g. LNCaP and 22RV1, and downregulated the androgen responsive genes such as PSA and TMPRSS2. Compared with enzalutamide and ARV-110, ETS-007 could block transcriptional activities of AR-V7, and AR mutants in luciferase report assay. Oral administration of ETS-007 in an enzalutamide-resistant 22RV1 xenograft model led to intratumoral AR-V7 degradation and concomitant decrease in PSA protein levels, resulting in a remarkable tumor regression. Taken together, our findings provide preclinical evidence that ETS-007 as a potent AR-NTD degrader derived from our LLPS platform can effectively block the transcriptional activities of both AR and AR-V7 for the treatment of metastatic CRPC.

#6060 Discovery of potent SHP2 protein degraders with strong anti-tumor activities in KRAS mutant cancers.

S. Kim[1], J. Lee[2], J. Song[1], G.-T. Park[1], J. Jung[1], J. Na[1], D. Lee[1], S. Lee[2], J. Park[2], J. Kim[2], O. Bae[2], J. Han[2], J. Kang[2], M. Moon[1], Y. Shin[1], J. Ryu[2], S. Lee[2], S.-K. Park[1];

[1]SK Biopharmaceuticals Co., Ltd., Seongnam-si, Korea, Republic of, [2]Ubix Therapeutics, Seoul, Korea, Republic of

Background: SHP2 plays a pivotal role in modulating the RTK/RAS/MAPK signaling pathway, which is frequently dysregulated in various cancers. Multiple allosteric SHP2 inhibitors have been under active development for the treatment of RTK/RAS/MAPK-dependent cancers, while certain limitations have come to light, such as their inability to target the active form of SHP2 and narrow therapeutic index necessitating intermittent dosing to mitigate toxicity. To overcome these challenges, we have discovered SHP2 protein degraders as next generation SHP2 targeting agents. Here, we present compelling profiles of our SHP2 degraders.

Methods: We employed a variety of cancer cell lines harboring mutations in RTK, KRAS, or SHP2 for assessing *in vitro* activity of SHP2 degraders. For *in vivo* assessment of pharmacological profile, we utilized an NCI-H358 KRAS G12C mutant NSCLC xenograft. SHP2 protein levels in cell lysates and tumors were analyzed to assess SHP2 degradation efficiency. Simultaneously, ERK phosphorylation and DUSP6 mRNA levels were analyzed to evaluate downstream effects. Immunoprecipitation assays were used to assess the impact on SHP2's scaffolding roles.

Results: A series of SHP2 degraders have been identified, demonstrating highly efficient SHP2 degradation activity with DC_{50} values in subnanomolar ranges. Robust inhibition of ERK phosphorylation, followed by remarkable anti-cancer effects in multiple KRAS mutant cancer cell lines were observed. Interestingly, *in vitro* cell growth inhibition by SHP2 degraders are 10 times more potent than SHP2 inhibitors currently under clinical development. Further characterization reveals several advantages of SHP2 degraders compared to SHP2 inhibitors. First, we observed a more efficient disruption of SHP2 scaffolding function, such as the formation of the SHP2-GRB2-GAB1 complex. Second, we detected effective degradation of activating mutants of SHP2, such as E76K and T507K, which are typically not targeted by SHP2 inhibitors. Experiments using a KRAS mutant CDX model demonstrate compelling *in vivo* profiles. A single administration of lead compounds resulted in D_{max} values exceeding 95% in tumors, accompanied by the significant reduction of downstream signaling markers, such as p-ERK and DUSP6 mRNA. Notably, the reduced levels of SHP2 and downstream markers persist for several days. This suggests that utilizing intermittent dosing could be a viable approach with SHP2 degraders. Once-weekly intravenous administration achieved strong tumor growth inhibition without causing significant body weight loss.

Conclusion: We have successfully discovered novel SHP2 degraders exhibiting remarkable activities. We demonstrate that SHP2 degraders have potential to overcome the limitations associated with allosteric SHP2 inhibitors and provide a promising therapeutic option for RTK/RAS/MAPK-dependent cancer patients.

#6061 Development of target cell-penetrating scFv conjugate degrader for the selective inhibition of mutant, resistant KRAS cancer.

G. Yoon[1], B. Jo[1], D. Lee[1], J. Yang[2], M.-H. Park[2], S. Seok[2], J. Lee[2], C. Chung[2], Y. Park[1];

[1]Seoul National University, Seoul, Korea, Republic of, [2]Nano Intelligent Biomedical Engineering Corporation (NIBEC), Seoul, Korea, Republic of

The activation of mutations in the RAS gene, which is frequently observed in human cancers, induces downstream critical effectors, contributing to tumorigenesis. While attempts to directly target the GTP-bound, activated RAS have shown some success in certain cancer treatments, resistance remains a challenge. Our objective is to develop a cell-penetrating single-chain fragment variable (scFv) degrader that targets mutant KRAS for degradation. The scFv, binding specifically to antigens, can mitigate the side effects of non-specific binding seen with chemical drugs. However, due to the limited cell-penetrating capability of scFv, a delivery carrier is often necessary. In this study, a cancer targeting, and cell-penetrating synthetic peptide (CPP) was developed as a drug delivery carrier and added to the sequence of scFv. To this conjugate, a von Hippel-Lindau (VHL) expressing sequence was added to enable the scFv binding to mutant KRAS, enabling its proteasomal degradation. These conjugates were engineered as a plasmid DNA to be expressed as a protein conjugate in CHO cells. The purity of the scFv-VHL-CPP degrader was confirmed by SDS PAGE. In SPR results, the degrader not only exhibited high binding ability to mutant KRAS but also influenced the proliferation of KRAS mutant cells in cell viability tests. Mutant GTP-bound KRAS was reduced by the KRAS degrader in KRAS mutant cancer cells. The in vivo study further confirmed the degradation of the KRAS, as reflected by the significantly reduced tumor growth. In conclusion, a degrader protein binding to mutant KRAS that consists of cell penetrating peptide, scFv, and VHL is expected to become a new protein anticancer drug especially effective against mutant, resistant KRAS-mediated cancer cells. Especially, the design of the target cell penetrating peptide-scFv-VHL would be served as a platform for the target protein degrader development.

#6062 Potent and orally bioavailable BCL6 protein degraders demonstrate efficacy in pre-clinical models of diffuse large B-cell lymphoma (DLBCL).

J. Xu[1], Y. Li[1], **J. Wang**[1], P. Tang[2], Y. Liao[2], C. Zhang[2], P. Yan[2];
[1]Haisco Pharmaceutical Group Co., Ltd., Shanghai, China, [2]Haisco Pharmaceutical Group Co., Ltd., Chengdu, China

The B-cell lymphoma 6 (BCL6) transcription repressor protein is a protooncogene especially in diffuse large B-cell lymphoma (DLBCL), conferring survival, protection, and maintenance of lymphoma cells. BCL6 expression in normal B cells contributes to initiation and maintenance of the germinal centers (GC). Somatic mutations of the BCL6 gene including chromosome translocations have been shown to result in the deregulation of BCL6 expression and contributes to a subgroup of poor prognostic double- and triple-hit lymphomas. To solve this unmet clinical need, we have developed highly specific, potent, and orally bioavailable BCL6 protein degrader HSK43608 that demonstrates potent in vitro and in vivo efficacy in multiple pre-clinical DLBCL models. HSK43608 achieves >90% BCL6 degradation at 10 nM and DC_{50} of <1 nM in the OCI-Ly1 model following 24 hr treatment. Time-course studies showed >90% BCL6 degradation within 1 hr which could be maintained at 24 hrs. Importantly, medicinal chemistry efforts have resulted in the successful development of new-generation IMIDs to improve the oral bioavailability of BCL6 degrader for in vivo treatment. As expected, concentration of HSK43608 in tumor tissue was much higher than that in plasma in the DLBCL xenograft models. This tumor tissue enrichment of HSK43608 achieved >95% BCL6 degradation 48 hr after last dosing and convincing tumor growth inhibition. It is worth noting that BCL6 knockout mice suffer from myocarditis with eosinophils infiltration in heart muscle. The tissue distribution study demonstrated less HSK43608 in heart than in plasma, partially explained why there was no sign of myocarditis with eosinophils infiltration in the heart of the HSK43608 treated mice. Taking advantage of the new IMIDs structure, HSK43608 barely induce the degradation of the first generation IMIDs targets including GSPT1, SALL4, CK1α, Aiolos and Ikaros, indicating its safety. In summary, these results indicate HSK43608 as a potent and orally bioavailable BCL6 degrader and support further development.

#6064 Discovery of potent and selective EP300 degraders with anti-cancer activity.

M. Zimmerman, A. Adam, H. Ahmad, B. Adams, K. Adhikari, W. Austin, B. Bullock, J. Di Bernardo, T. Dixon, D. Daniels, C. Dominici, G. Elliot, B. Ethell, A. Gervais, M. Hossain, D. Huang, D. Lahr, M. Lin, D. Mayhew, K. Mizeracka, S. Negretti, T. Nguyen, O. Prifti, D. Sappal, S. Schiller, B. Sherbanee, D. Terry, N. Ucisik, E. Wittenborn, Q. Zhou, L. La Bonte;
Foghorn Therapeutics, Cambridge, MA

E1A binding protein (EP300) and CREB binding protein (CBP) are paralog histone acetyltransferases involved in many cellular processes via their activity as transcriptional co-activators. Dysregulation of one or both proteins has been implicated in various cancers, and functional genomic screens have demonstrated a bidirectional synthetic lethal relationship between the two genes in tumor cells. Due to the high homology between EP300 and CBP, identifying chemical matter that selectively targets EP300 or CBP has proven challenging. Here, we describe a potent, highly selective heterobifunctional degrader of EP300 with biological activity in CBP-deficient and EP300-dependent tumor cells. Targeted degradation of EP300 protein resulted in a stronger suppression of cell growth and survival than targeting the bromodomain or HAT activity of EP300/CBP with small molecule inhibitors. Anti-proliferative effects have been demonstrated in multiple cancer types, including malignant lymphomas and castration-resistant prostate tumors, highlighting the essential role of EP300 in mediating oncogenic transcription required for tumor cell growth and survival. Degradation of EP300 *in vivo* attenuated androgen-driven transcription and inhibited tumor growth in VCAP (AR+) prostate tumor xenografts. Importantly, no evidence of overt toxicity or thrombocytopenia was observed at therapeutically efficacious doses. These findings indicate that selective targeting of EP300 with targeted protein degradation is a safe and effective treatment strategy for advanced tumors.

#6065 Identification and characterization of paralogue selective CBP degraders for potential use in cancer therapy.

S. Thiyagarajan, C. Abbineni, K. Chaitanya T, A. Apte, I. Khan Iqbal, N. Kumar R, A. A B, A. Kumar, G. A R, A. B Kamath, D. Dattatray Mane, G. Raj A, R. Reghu, S. Mohapatra, S. Marappan, S. T Gore, S. Mukherjee, G. Daginakatte, K. Nellore, S. Chelur, M. Ramachandra, **S. Samajdar**;
Aurigene Oncology Limited, Bangalore, India

CBP and p300 are closely related epigenetic modulators that participate in chromatin remodeling and transcription and play an oncogenic role in a variety of cancers. Studies have indicated that the selective targeting of CBP is a highly attractive therapeutic strategy for cancers with p300 mutations because of synthetic lethality, those that are dependent on Wnt/β-catenin signaling and ERα and HER2-positive breast cancers. Prevalence of high mutation frequency of p300 in several cancers including skin cancers (27%), small cell lung cancers (8%), lymphoma (8-13%) and bladder cancer (9%) further highlight an opportunity for selective inactivation of CBP in cancer therapy. However, it has not been possible to identify selective inhibitors of p300 or CBP because of the conserved sequence and structure of functional domains such as HAT domain or bromodomain. We sought to achieve selective CBP targeting by utilizing the degrader approach, which in the recent time has proven to be useful in achieving paralog selectivity due to differentiated ternary complex formation. Additionally, the degrader approach offers several inherent advantages including stronger phenotype due to greater potency, sustained action due to catalytic mode of action, overcoming resistance and greater selectivity. Utilizing a combination of structure-guided modelling and iterative medicinal chemistry strategies, we identified first-in-class selective degraders targeting CBP with varying linker lengths and compositions. Our lead compounds exhibit remarkable bias in degrading CBP in cell lines harboring loss-of-function mutations in p300, while sparing wild-type cells. Selective CBP degraders disrupted β-catenin transactivation function in a dose-dependent manner and demonstrated good oral bioavailability and PK profile in preclinical species. Further optimization of potency, selectivity, ADME properties while evaluating *in vivo* efficacy in appropriate models and tolerability in higher species is ongoing towards identifying a development candidate.

#6066 An inhibitor of deubiquitinating enzyme UCHL5/USP14, VLX1570, enhances the cytotoxic effects of temsirolimus by suppressing PCNA in uuman renal cell carcinoma.

K.-L. Kuo[1], P.-M. Chow[2], C.-H. Hsu[2], S.-M. Liao[3], Y.-L. Chiu[4], J.-R. Dong[2], T.-Y. Ke[1], K.-H. Huang[1];
[1]National Taiwan University College of Medicine and Hospital, Taipei, Taiwan, [2]National Taiwan University Hospital, Taipei, Taiwan, [3]National Taiwan University College of Medicine, Taipei, Taiwan, [4]Far Eastern Memorial Hospital, New Taipei City, Taiwan

Renal cell carcinoma (RCC) is a common type of kidney cancer. The overall 5-year survival rate is 74%, but it drops to only 8% for Stage 4 cancers. Several treatments are available for metastatic RCC, including tyrosine kinase inhibitors, mTOR inhibitors, and immune checkpoint inhibitors. However, these treatments have limited success. VLX1570 is an inhibitor of deubiquitylating enzymes UCHL5/USP14 that is currently in Phase I clinical trials. It has shown promise in various cancer models, but its effects on RCC have not been reported. This study investigated the impact of UCHL5/USP14 expression on tumor progression and patient survival in a clinical cohort. The results showed that VLX1570 induced apoptosis and cell cycle arrest in RCC cells, leading to reduced cell viability. Additionally, VLX1570 synergized with temsirolimus in vitro, likely by inhibiting PCNA. Moreover, the combination treatment suppressed tumor growth in vivo more effectively than either VLX1570 or temsirolimus alone. These findings suggest that UCHL5/USP14 plays a role in RCC progression and prognosis, making it a promising therapeutic target for overcoming drug resistance in this cancer.

#6067 Identification of selective CBP degraders with robust preclinical PK, PD, efficacy and safety across solid tumor indications.

D. Sappal, A. Adam, H. Ahmad, B. Adams, K. Adhikari, W. Austin, B. Bullock, J. Di Bernardo, T. Dixon, D. Daniels, C. Dominici, G. Elliot, B. Ethell, A. Gervais, M. Hossain, D. Huang, D. Lahr, M. Lin, D. Mayhew, K. Mizeracka, S. Negretti, T. Nguyen, O. Prifti, S. Schiller, B. Sherbanee, D. Terry, N. Ucisik, E. Wittenborn, Q. Zhou, M. Zimmerman, L. La Bonte;
Foghorn Therapeutics, Cambridge, MA

CREB binding protein (CBP) and E1A binding protein (EP300) are paralog histone acetyltransferases involved in many cellular processes via their activity as transcription factor co-activators. Dysregulation of one or both proteins has been implicated in various cancer types, and functional genomic screens have revealed a bidirectional synthetic lethal relationship between these two paralogs in tumor cells. Due to the high homology between CBP and EP300, identifying selective chemical matter that selectively disrupts the activity of CBP has proven challenging. Small molecule inhibitors targeting the HAT or bromodomain of CBP/EP300 have been developed, however these agents exhibit hematopoietic toxicity resulting from dual inhibition, which limits their therapeutic window. Herein, we describe the PK, PD, and efficacy of selective, potent CBP degraders across various EP300-mutant cancer xenograft models. Our results show deep and sustained CBP degradation, leading to significant tumor growth inhibition in solid tumors. This anti-tumor activity was not associated with significant body weight loss or hematopoietic toxicity. Our CBP-selective protein degraders have the potential to be a first-in-class therapeutic option for patients with tumors harboring EP300 mutations.

#6068 Discovery of BTX-9341, a bifunctional degrader of CDK4 and CDK6 for HR+/HER2- breast cancer.

H. Majeski, A. Okano, K. Chahal, A. Pasis, C. Carlson, A. Shakya, Q. Liu, S. Huang, A. Hoskote Chourasia, L. Fung;
BioTheryX, Inc., San Diego, CA

CDK4/6 inhibitors (CDK4/6i) such as palbociclib, abemaciclib and ribociclib are used to treat HR+/HER2- breast cancer, but patients can develop resistance via many mechanisms, several of which converge on the upregulation of the cyclin D-CDK4/6 signaling node. This has been shown to limit the effectiveness of CDK4/6i in ER+ breast cancer with up to 20% patients exhibiting innate resistance and up to 70% patients developing acquired resistance after 3 years on therapy (Scheidemann, 2021). To address acquired resistance, we sought a degrader approach. We utilized our PRODEGY platform of Cereblon (CRBN) binders to synthesize CRBN mediated CDK4/6 bifunctional degraders and identified BTX-9341 as a development candidate. Breast cancer cell lines treated with BTX-9341 showed up to 85% degradation of CDK4 and CDK6 with DC_{50}s <1nM. CDK4/6 phosphorylates the protein RB which releases the transcription factor E2F, inducing the expression of genes which promote cell cycle progression. We examined RB phosphorylation by in-cell western, E2F target gene expression by qPCR and cell cycle progression by propidium iodide staining followed by flow cytometry. BTX-9341 was potent in all downstream assays, with phospho-RB IC_{50}s <30nM, E2F target gene downregulation and G0/G1 cell cycle arrest at concentrations as low as 10nM. These downstream effects were sustained throughout 72 hours with BTX-9341 treatment but recovered more rapidly with Palbociclib treatment. We used a 2D colony formation assay (CFA) to assess inhibition of proliferation by cell cycle arrest. BTX-9341 potently inhibited cell proliferation with CFA IC_{50}s of 20-50nM while CDK4/6i had CFA IC_{50}s of 50-1000nM. This increased activity was due to CRBN mediated target degradation, as demonstrated by a shift in CFA IC_{50} values in a CRBN knockout cell line towards the values seen with the inhibitors. In palbociclib-resistant HR+/HER2- cell line models BTX-9341 maintained a low CFA IC_{50} (<150nM) while CDK4/6i displayed micromolar CFA IC_{50}s. BTX-9341 displays excellent pharmacokinetic properties which allowed for oral dosing in xenograft studies. In several breast cancer xenograft models, BTX-9341 showed dose-dependent tumor growth inhibition, tumor regression at higher dose levels, and was effective with multiple alternate dosing regimens. These results show that BTX-9341 displays excellent single agent activity *in vitro* and *in vivo* and that this activity is maintained in CDK4/6i resistant models. This indicates that a degrader approach to targeting this pathway may be more effective than current therapies, and that using this modality in a post CDK4/6i setting may be more effective than switching CDK4/6 inhibitors.

Reference: Scheidemann, Erin R, and Ayesha N Shajahan-Haq. “Resistance to CDK4/6 Inhibitors in Estrogen Receptor-Positive Breast Cancer.” *International journal of molecular sciences* vol. 22,22 12292. 14 Nov. 2021, doi:10.3390/ijms222212292

#6069 Discovery and preclinical development of orally bioavailable potent BTK degrader, and its early clinical development for the treatment of relapsed and refractory B-cell malignancies.

S. Lee, S.-M. Yoo, Y. Lim, H. Kim, J. Ryu, J. Lim;
Ubix Therapeutics Co., Ltd., Seoul, Korea, Republic of

Background : Bruton tyrosine kinase (BTK) is an important signaling hub that activates the B-cell receptor (BCR) signaling cascade, which is critical for growth and survival of B-cell lymphoma or leukemia. BTK inhibitors have shown anti-tumor activity in patients with B-NHL. However, nearly half of the patients on current BTK inhibitors discontinue the treatment due to adverse effects and/or mutation-induced drug resistance. A degrader is a heterobifunctional chemical compound aimed at eliminating disease-causing proteins, rather than simply inhibiting proteins' enzymatic function, through the ubiquitin-proteasome system (UPS)-mediated protein degradation. This approach offers a unique solution for addressing relapse or refractory disease by removing overexpressed and mutated proteins, unlike traditional inhibitors. We thus designed UBX-382, a degrader targeting BTK.

Results : UBX-382 showed superior degradation activity for both wild-type (WT) and mutant BTK proteins in a single-digit nanomolar range of half-maximal degradation concentration when compared to the competing degrader programs in diffuse large B-cell lymphoma cell line. UBX-382 effectively addressed 7 out of 8 previously reported resistant BTK mutants in *in vitro* experiments and outperformed ibrutinib, ARQ-531, and MT-802 in inhibiting tumor growth in murine xenograft models harboring WT or C481S mutant BTK-expressing TMD-8 cells. Remarkably, oral dosing of UBX-382 for <2 weeks led to complete tumor regression in 3 and 10 mg/kg groups in murine xenograft models. Following this, further optimization was carried out for potency and PK profile. We nominated the candidate for IND filing and are planning a phase 1 clinical trial. For the first-in-human, open-label, multicenter, phase 1 study, patients in part 1 (dose escalation with BOIN design) had R/R B-cell malignancies and had received at least 2 prior therapies. The candidate will be administered orally at 5 mg once daily followed by 2 days, for a 7-day schedule over 28-day cycles. Part 2 (dose expansion) consisted of disease-specific cohorts, including CLL/SLL, DLBCL, MCL, FL, MZL, and WM. The primary endpoints were safety and tolerability, along with the definition of the maximum tolerated dose. Secondary endpoints included pharmacokinetics/pharmacodynamics and preliminary efficacy.

Conclusions : We have discovered potent BTK degrader exhibiting excellent anti-tumor activity in vitro and in vivo. In pre-clinical safety studies, the candidate of UBX demonstrated an acceptable safety profile. The candidate of UBX is currently preparing phase 1 clinical trials for hematological malignancies.

#6070 Identification of a molecular glue degrader that engages a cancer-specific E3 ligase.

Y. Liu, M. Larsen, B. Lin, I. A. Cardenal, J. R. Kennerdell, T. Finkel, **B. B. Chen**;
University of Pittsburgh School of Medicine, Pittsburgh, PA

To date, most successful molecular glues have leveraged ubiquitously expressed E3 ligases, most notably Cereblon in the case of the thalidomide derivatives. However, a number of specific E3 ligases are highly over-expressed in certain tumors. Compounds that engage such tumor-specific E3 ligases might provide a unique opportunity to develop molecular glues with higher therapeutic indexes. One such tumor-specific E3 ligase is FBXO5, a member of the F-box family of E3 ligases. Expression analysis suggests this E3 ligase is highly expressed in a wide array of tumor tissues when compared to the corresponding normal tissue, and that within a given tumor type, higher FBXO5 expression correlates with advanced tumor stage and worse disease-free survival. Here, we describe a small molecule (MW~400 Daltons) that uses FBXO5 to function as a molecular glue degrader. This compound, CL-200, exerts cytotoxicity in the nanomolar range across a number of diverse tumor types. The cytotoxicity of CL-200 is abrogated when FBXO5 is knockdown using siRNA. We have further determined that CL-200 induces the FBXO5-dependent proteasomal degradation of at least two critical neosubstrates. One identified neosubstrate is the p150 isoform of ADAR1, an enzyme that catalyzes the posttranscriptional conversion of adenosine to inosine in double-stranded RNA (dsRNA). Evidence suggests that ADAR1p150 is the isoform that confers oncogenic and immune modulating effects in many tumors. Another neosubstrate targeted by CL-200 is c-myc, a critical transcription factor linked to a wide array of tumors. Of note, both p150 ADAR1 or c-myc have been viewed as difficult-to-drug if not undruggable targets. As such, these data suggests that CL-200 functions as a novel molecular glue degrader that engages the cancer-specific E3 ligase FBXO5 to degrade both p150 ADAR1 and c-myc. Structural alteration of CL-200 suggest that chemical modifications can be made that retain the engagement with FBXO5 while altering the neosubstrate profile. Together, these results demonstrate the possibility of leveraging cancer-specific E3 ligases to develop novel molecular glues.

#6071 Identification of a molecular glue degrader targeting the full-length AR and AR-V7 splice variant.

Y. Liu, M. B. Larsen, B. Lin, I. A. Cardenal, J. Kennerdell, T. Finkel, **B. B. Chen**;
University of Pittsburgh School of Medicine, Pittsburgh, PA

Prostate cancer is the most common cancer in males and the fifth leading cause of cancer mortality worldwide. A variety of therapeutic approaches exist including steroid synthesis inhibitors and next-generation ligand binding domain (LBD) antagonists [e.g., enzalutamide (Enza)]. However, these approaches are only effective against tumors bearing the full-length androgen receptor (AR-FL). In the course of their disease, many patients acquire androgen receptor splice variant 7 (AR-V7), a mutant form of the receptor which lacks the LBD and is constitutively activated. To date, no effective therapy has been demonstrated for patients with metastatic prostate cancer bearing the AR-V7 signature. We have recently developed a high throughput platform that allows for the identification of ligands that can bind to a wide variety of protein targets. Using this approach, we screened a diverse chemical library of 100,000 small molecules to identify compounds that are bound to AR-V7. One such molecule, AR-600, directly bound to AR-V7 and moreover, induced proteasomal-mediated targeted protein degradation of both AR-V7 and AR-FL. In prostate cancer cell lines expressing AR-FL, AR-600 induced a gene expression profile similar to cells treated with Enza including a marked reduction in KLK3 (PSA) expression. Moreover, AR-600 inhibited the growth of 22RV1 cells (IC50=23 nM), a cell line that predominantly expresses AR-V7, as well as C4-2 cells that express predominantly full-length AR (IC50=51 nM). In contrast, the compound did not affect the growth of a wide variety of non-tumorigenic cells, non-prostate tumor cell lines or PC3 cells, a prostate cell line that exhibits AR-independent cell growth (IC50>100uM). Preliminary exploration of the mechanism of action of AR-600 (M.W. ~300 Daltons) demonstrates the compound works as a molecular glue. These results thereby identify a small molecule glue degrader that can specifically induce the targeted protein degradation of the AR-V7 splice variant. Given the strong association of this isoform with treatment resistance, this approach would appear to provide an attractive strategy for patients with metastatic castration resistant prostate cancer.

PREVENTION / EARLY DETECTION / INTERCEPTION: Biomarker-Based Screening
Poster Session

#6075 Most cancer deaths are unaddressed by current screening paradigms.

E. T. Chang[1], A. Kansal[1], **E. A. Hubbell**[1], G. A. Colditz[2], A. W. Kurian[3], C. A. Clarke[1];
[1]GRAIL, LLC, Menlo Park, CA, [2]Washington University School of Medicine, St. Louis, MO, [3]Stanford University, Stanford, CA

Cancer is the leading cause of death at ages ≤80 in the US. To understand the burden of cancer death potentially addressable by new or improved screening approaches, we estimated the proportion of US cancer deaths without recommended guideline-based screening, especially after accounting for lung cancer screening eligibility and adherence. Using 2018-2019 mortality data from the National Center for Health Statistics and published estimates of the proportion of screening-eligible lung cancer patients, we estimated that 31.4% of nearly 600,000 annual cancer deaths were from colorectal, female breast, cervical, and smoking-eligible lung cancers (Table). Further accounting for adherence to lung cancer screening guidelines reduced the estimated proportion of screened cancer deaths to 17.4%; thus, 82.6% of cancer deaths may not be addressed by current guideline-based screening. Among the cancers not covered by guideline-based screening are uncommon cancer types, which (as defined by the National Cancer Institute) comprised 30.4% of cancer deaths. According to incidence-based mortality data from Surveillance, Epidemiology, and End Results registries, 24.7% of all cancer deaths were from stage 4 cancer types without guideline-based screening. These estimates, based on population data without patient-level information on mode of diagnosis, almost certainly underestimate the percentage of cancer deaths missed by currently available screening efforts. The large proportion of cancer deaths unaddressed by guideline-based screening represents a vast opportunity for new cancer screening technologies that are safe, effective, accessible, and affordable to enable earlier detection and successful treatment of the full spectrum of cancer types that contribute to the overall cancer burden.

Table. Deaths from cancer by primary type in 2018-2019, US National Center for Health Statistics, with eligibility for and adherence to guideline-based low-dose computed tomography screening for lung cancer

	All cancer types	Lung	Colon/rectum	Breast (female)	Uterine cervix	**Total screened**	**% of all**
All cancer deaths	1,198,854	281,681	104,059	84,745	8,290	478,775	**39.9%**
Eligible for screening based on smoking (63.7% of lung)*		179,431	104,059	84,745	8,290	376,525	**31.4%**
Adherent to smoking-guideline-based screening (6.6% of lung)†		11,842	104,059	84,745	8,290	208,936	**17.4%**
*Modeled estimate of proportion of lung cancer patients eligible for screening (Landy et al. 2023). †Lung cancer screening receipt from 2019 American College of Radiology Lung Cancer Screening Registry (Fedewa et al. 2022).							

#6076 Mathematical oncology in the context of early breast cancer detection.

J. Mason, S. N. Shishido, G. Courcoubetis, D. Tessone, E. Liljegren, A. Naghdloo, J. Hicks, J. J. Nieva, P. Kuhn;
USC - University of Southern California, Los Angeles, CA

Breast cancer (BC) is the most common cancer in women globally, with approximately 94% of patients initially diagnosed with early-stage disease. However, despite the initial lack of detectable metastases and administration of subsequent treatments, 40% of these patients will develop recurrence over their lifetime. The standard screening method for BC is mammography, with a tissue biopsy to confirm diagnosis. However, only ~60% of all cases are currently diagnosed via this pathway, primarily due to the limited (86.9%) sensitivity. To demonstrate the feasibility of a liquid biopsy (LBx) test for early BC detection and assessment, we employed the third-generation, High Definition Single Cell Assay (HDSCA3.0) to detect and characterize rare cells (e.g., circulating tumor cells [CTCs]) and acellular structures (e.g., oncosomes) in patient peripheral blood samples using immunofluorescent (IF) imaging. We have previously investigated this signal in a cohort of early-stage BC patients (n = 74), late-stage BC patients (n = 26), and age- and gender-matched controls (n = 30) and observed statistically significant differences in levels of total rare cells, CTCs, and oncosomes via a manual approach. For this study, we employed a hybrid methodology, that utilizes both automatic and manual techniques, to investigate the reproducibility of the signal in an expanded validation set. Within this modified approach, we employ an outlier detection algorithm to accelerate the rare event identification and curation process (minimizing the manual portion), a separate machine learning model to classify the events based on their IF expressions, and a suite of applications to enumerate and quantify the result. After implementation, we quantified the results of the fully manual and hybrid approaches to determine the signal loss associated with scale up. Utilizing the hybrid approach, we observed similar results as with the fully manual and were able to stratify the three cohorts with high accuracy. Namely, there was an increase in the total rare cell and CTC populations in late-stage BC patients, and an increase in the oncosome population for the early-stage BC patients. To note, these patients included a subset with invasive lobular carcinoma (ILC; n = 19), which manifests in ~5-15% of BC cases and is considered “mammogram silent” due to the biological development of the disease. Additionally, employing the hybrid approach allowed for analyzing patient samples in less time while minimizing overall signal loss. In summary, we have been able to detect reproducible patterns in the enumeration of rare cells and oncosomes with high accuracy. When utilized at the patient-level, these analytes can power prediction models that are capable of stratifying disease from non-disease. The results presented here demonstrate the utility of a LBx test as a companion to screening mammography in the detection of early-stage BC across various histologies.

#6077 Chimeric RNAs are abundantly expressed in precancerous breast tissue of sporadic breast cancer patients.

A. Bhardwaj[1], S. Thevasagayampillai[2], S. Rankothgedera[2], P. Verma[1], M. B. Castillo[2], A. C. Koh[1], C. Albarracin[1], P. H. Gunaratne[2], I. Bedrosian[1];
[1]UT MD Anderson Cancer Center, Houston, TX, [2]University of Houston, Houston, TX

Background: Immuno-prevention efforts in breast cancer (BC) have been hampered by the lack of known neoantigenic targets that can be used for a cancer prevention vaccine. RNA fusions represent attractive candidates as these are more immunogenic than insertion / deletion mutations and are substantial source of neoantigens. The objective of this study was to characterize chimeric RNAs in precancerous breast tissue. **Methodology:** Novel RNA fusions were identified by mining the sequence reads from RNA sequencing of 25 Her2 positive, 25 hormone receptor positive (HR) and 25 triple negative (TN) breast tumors and paired histologically normal tissues by Qiagen's CLC pipeline. Breast samples from women undergoing breast reduction surgery were used as controls to exclude normal tissue associated chimeric mRNAs from analysis. Neoantigen prediction was performed by MHCnuggets. Chimeric mRNAs were validated by PCR. Ribosomal profiling was performed to assess if fusion transcripts are engaged with ribosomes. **Results:** A median of 36 novel RNA fusions (range 7-877) were identified in the tumor samples. In line with high genomic instability of TNBC subtype of BC, about 1/3 of the TN tumors expressed greater than 300 RNA fusions. In order to identify RNA fusions that are relevant for BC prevention, we investigated the presence of RNA fusions in the paired histologically normal samples as compared to the index tumor. We restricted these analyses to top 20 fusion transcripts that were present across the set of 75 tumor samples and also detected in 1 or more of the TCGA samples. Interestingly, we found that more than 1/3 of the histologically normal samples express at least 1 of the top 20 RNA fusions. When compared to the corresponding tumor, we found up to 50% of the paired normal tissue expressed RNA fusions identified in the tumor, supporting a role for these chimeric mRNA as an early molecular change during breast tumorigenesis. To validate the robustness of the prediction pipeline, PCR validation was performed for the chimeric mRNA with highest prevalence, NSFP1- LRRC37A2 which confirmed the presence of the transcript in 72% (13/18) of the predicted positive patient samples. MHCnuggets pipeline predicted 15 neopeptides from intergenically spliced chimeric NSFP1 [Exon 1-13] - LRRC37A2 [Exon 2-14], ¼ of which we validated to be immunogenic by ELISA. In order to confirm that the translation of the chimeric NSFP1- LRRC37A2 transcript, we investigated their enrichment in polysome enriched fraction obtained from a BC cell line confirmed to express the fusion transcript by PCR. Enrichment of transcripts in the polysomal fraction confirmed that these transcripts are likely to be translated. **Conclusions:** RNA fusions are frequently present in at risk breast tissue and are the source of substantial number of neoantigens. These RNA fusion- derived neoantigens may provide novel opportunities for developing vaccines for BC prevention.

#6078 Circulating tumor cell-based early detection of breast cancer.

J. M. Drake[1], K. J. Kamalanathan[2], C. Galeano-Garces[2], N. Bristow[2], N. Heller[2], M. Ahmadi[2], O. Hedeen[2], A. Hesch[2], G. Schaap[2], J. Hapke[2], J. Miller[2], I. Babris[2], T. Le[2], T. Clacko[2], J. Hong[1], B. Konety[3], J. Parthasarathy[2];

[1]University of Minnesota, Minneapolis, MN, [2]Astrin Biosciences, Inc., Saint Paul, MN, [3]Allina Health, Minneapolis, MN

Although mammograms have been a useful tool since the first half of the 20th century and have an acceptable sensitivity (87%) in the general population, that drops to <50% in women with dense breasts making it an ineffective screening tool in this population. Cell free DNA (cfDNA) has proven to be an inadequate alternative in this population, and while MRI is acceptable, it is expensive. Astrin Biosciences has developed a blood-based assay that detects circulating tumor cells (CTCs) at a high sensitivity to serve as an alternative screening method to mammography in breast cancer early detection, specifically in women with high-density breasts.

Astrin's technology integrates holographic imaging, machine learning, and microfluidics to identify CTCs in the blood stream. Omics analysis can then be performed on the collected cells to further differentiate patients with cancer from matched healthy controls. Astrin has initiated a small cohort study to investigate the sensitivity and specificity of CTC detection in women with early-stage breast cancer. Astrin's small cohort study, including patients with ductal carcinoma in situ, stage 1, and stage 2 breast cancer patients, demonstrated > 85% sensitivity and specificity. A large cohort study is being conducted to validate these preliminary results.

The small cohort study demonstrates the ability of Astrin Bioscience's platform to detect cancer cells at an early stage, particularly in breast cancer. This technology will drastically increase the effectiveness of breast cancer screening modalities available to patients. Additionally, since it is a blood-based assay, it can be performed at shorter intervals in high-risk populations than mammograms which require a full patient appointment.

#6079 Comparison of FIT and cell-free DNA analyses for detection of individuals with colorectal cancer in population based screening.

P. H. Wisse[1], C. Rubio-Alarcon[1], S. J. Schraa[2], A. C. Mosquera[1], M. Sausen[3], R. J. A. Fijneman[1], G. R. Vink[2], M. de Wit[1], J. Phallen[4], V. E. Velculescu[4], B. Carvalho[1], G. A. Meijer[1];

[1]Netherlands Cancer Institute, Amsterdam, Netherlands, [2]University Medical Center Utrecht, Utrecht, Netherlands, [3]Personal Genome Diagnostics, Baltimore, MD, [4]Johns Hopkins University School of Medicine, Baltimore, MD

Background The fecal immunochemical test (FIT) is widely used in population based colorectal cancer (CRC) screening programs. Recently, circulating cell-free DNA (cfDNA) analyses have emerged as a new avenue for early cancer detection. The performance of cfDNA methods in comparison with FIT is currently unknown. The present study compared pre-operative cfDNA analyses to FIT for detection of patients with CRC who participated in a population-based screening program. **Methods** In the Dutch national CRC screening program, individuals aged 55-75 years are biennially invited to perform a single FIT. The database of the Dutch CRC screening program was queried to identify individuals with FIT data who also participated in two cfDNA studies, PLCRC-MEDOCC and PLCRC-PROVENC3 (AACR abstract C. Rubio Alarcón). Sensitivities with 95% confidence intervals (CI) for detecting individuals with CRC were determined for FIT, tumor-informed cfDNA analyses, as well as both tests combined. For FIT, sensitivities were determined at 20 µg and 47 µg hemoglobin (Hb)/g feces positivity cut-offs as these represent the most commonly used international and Dutch cut-offs, respectively. Liquid biopsy analyses were performed using next generation sequencing of cfDNA. Tumor-specific alterations were identified through parallel next generation sequence analysis of resected tumor tissues. **Results** The query identified 120 individuals with stage I (n=3, 2.5%), stage II (n= 57, 47.5%) and stage III (n=60, 50.0%) CRC who had participated in the Dutch CRC screening program and either PLCRC-MEDOCC or PLCRC-PROVENC3. All FIT samples were collected at a median time of 38 days before diagnosis (IQR 27-112 days). FIT sensitivity for detection of individuals with CRC was 83.3% (100/120 CRCs, 95% CI 75.4-89.5%) at a 20 µg Hb/g feces cut-off and 80.0% (96/120, 95% CI 71.7-86.7%) at a 47 µg Hb/g feces cut-off. Tumor-informed cfDNA analyses detected 75.8% (91/120, 95% CI 67.2-83.2%) of individuals with CRC in this population. The combination of cfDNA analyses and and FIT (20 µg Hb/g feces cut-off) identified almost all individuals with CRCs (119/120, sensitivity 99.2%, 95% CI 97.0-100%). The individual who was missed had a cancer that was a T3N0 microsatellite stable moderately differentiated adenocarcinoma in the ascending colon. **Discussion** While both FIT and cfDNA analyses identified most CRC cases (75-83%) in this series, both tests also demonstrated a substantial level of complementarity, indicating that in principle combining FIT with cell-free DNA testing would allow to increase sensitivity of CRC screening. Since the cell-free DNA tests used here are tumor-informed, which in real life screening practice is not feasible, it remains to be determined to what extent this result can be reached using non-tumor-informed approaches.

#6081 DNA integrity and preanalytical handling of endocervical samples for use in liquid biopsy-based diagnostics and monitoring of gynecological cancer.

J. M. Lauesgaard, T. Carlsson, A. Linder, S. Schumacher, K. Sundfeldt;
University of Gothenburg, Gothenburg, Sweden

Background: Liquid biopsies from the gynecological tract can be useful for analysis of cell free DNA (cfDNA) (1, 2, 3). Sampling procedure and optimal preanalytical handling are poorly investigated. In this study, we aimed to evaluate how the profile and integrity of DNA, sampled from the female genital tract, were affected by preanalytical handling.

Methods: Biobanked/archival (stored at -80℃ after 48h at room temperature (RT)) and freshly obtained clinical samples were analyzed together with standardized *in vitro* samples. Archival and *in vitro* samples were preserved in methanol-based solution, imitating clinical handling of endocervical samples which are initially stored at RT for 48h before further handling. The fragmentation profile of archival and *in vitro* samples was analyzed. Time series of *in vitro* samples at RT and 4℃, with extraction at 6-hour intervals from 0 to 96h, were performed. The fresh clinical samples were collected from the endocervix in methanol-based solution and from the vagina in a solution designed to preserve DNA and placed at 4℃ resp RT. Extraction was performed within 4h and at 48h.

Results: Accumulation of short DNA fragments were observed in the archival samples and in the in *vitro* samples, indicating that fragmentation was initiated prior to 48h. Time series showed that the quantity of short DNA fragments gradually increased with time at both RT and 4℃ but at a slower rate in 4℃. At RT the percentage of fragments between 100-350bp increased 12-fold (0.39% vs 4.75%, p=0.002). The freshly obtained endocervical samples showed a similar significant increase in short fragments in samples stored at RT compared with samples stored at 4℃ (p= 0.02 for 100-230bp; p= 0.007 for 230-350bp; p= 0.03 for 100-2500bp) at 4h-48h.

Conclusion: Pre-analytical handling of endocervical samples can be optimized. Lowering temperature from RT to 4℃ immediately haltered DNA fragmentation.

#6082 Rapid on-site nucleic acid detection using CRISPR and digital signal processing for portable and integrated cervical cancer screening in low resource settings.

C. Lee, H. Kim, H. Lee, T. Randall, A. Ly, H. Lee, **C. M. Castro**;
Massachusetts General Hospital, Boston, MA

Addressing the global disparity in cancer care necessitates the development of rapid and affordable nucleic acid (NA) testing technologies. This need is particularly critical for cervical cancer. Molecular detection of human papillomavirus (HPV) has emerged as a highly accurate screening method, surpassing traditional Pap smears. However, implementing this transition in low- and middle-income countries has been challenging due to the high costs and centralized facilities required for current NA tests. Here, we present CreDiT (CRISPR Enhanced Digital Testing), an advanced diagnostic system for rapid, on-site NA detection. CreDiT integrates two major technical breakthroughs: i) a one-pot CRISPR strategy that simultaneously amplifies both target NAs and analytical signals, and ii) a robust fluorescent detection method based on digital communication (encoding/decoding) technology. These innovations enhance CreDiT's practical utility, offering a rapid assay (<35 minutes) that integrates NA extraction and detection in a single streamlined workflow. Furthermore, CreDiT's straightforward probe design enables easy incorporation of new NA targets, while its compact device provides robust signal detection. We adapted CreDiT for point-of-care HPV screening by designing probes for high-risk HPV genes (HPV16, HPV18, HPV45, HPV31, HPV33, HPV58) and oncoprotein mRNAs (*E6*, *E7*, $p16^{INK4a}$) and developing a portable CreDiT device capable of processing 12 samples. CreDiT demonstrated sensitive detection of cell-derived HPV DNA targets down to single copies and accurately identified HPV types in every clinical cervical brushing specimen (n = 121) we tested. This technology has the potential to facilitate prompt and reliable triaging of high-risk HPV, overcoming pathology bottlenecks and circumventing geographical and socioeconomic barriers to effective cervical cancer screening in resource-limited regions. This work has spearheaded recent screening research efforts in Uganda and Ghana.

#6083 Inter-observer agreement in ultrasound-detected steatotic liver in the Chile Biliary Longitudinal Study (BiLS).

Maria Spencer Sandino[1], Vanessa Van De Wyngard[1], David Wynne[2], Maya Balakrishnan[3], Noldy Mardones[4], Ruth Pfeiffer[5], Allan Hildesheim[5], Catterina Ferreccio[1], Jill Koshiol[5]

[1]Public Health, Pontificia Universidad Catolica de Chile, Santiago, Chile,[2]Interventional Radiology, Baylor College of Medicine, Houston, TX,[3]Gastroenterology, Baylor College of Medicine, Houston, TX,[4]Hospital Dr. Hernan Henriquez Aravena, Temuco, Chile,[5]Infections and Immunoepidemiology Branch, Nacional Cancer Institute, Rockville, MD

Background: Metabolic-associated steatotic liver disease (MASLD) is a prevalent chronic liver condition with an increased risk of cancer-related mortality. In Latin America, MASLD prevalence is estimated at 40%, with Chile reporting rates of 47.5% in 2019. Early detection is crucial for MASLD control and management. Liver biopsy, the gold standard for diagnosis, is invasive and costly. Ultrasound (US) is a preferred alternative, yet its precision varies depending on the observer interpretation.

Methods: We conducted a cross-sectional analysis of a subset of baseline US images from the Chile Biliary Longitudinal Study (Chile BiLS), a cohort of women aged 50-74 with gallstones in Chile. Of the 4,032 participants recruited from Cautín Province in the Araucanía region, a random sample of 10% of the images were selected for review by a radiologist from Baylor College of Medicine (Observer 1) and compared to the original readings generated at the baseline exam by a team of Chile BiLS ultrasound technicians. To assess reproducibility, 33 blinded duplicate images from the 10% sample were reanalyzed by Observer 1 and an additional Chile BiLS technician who was not part of the original baseline team (Observer 2). Inter- and intra-observer agreement was assessed using weighted kappa values. Images were categorized as none, mild, moderate/severe.

Results: Of the 409 images reviewed, agreement between Observer 1 and original readings across all categories of steatosis was poor (kappa: 0.09; CI 95% 0.06;0.11, p <0.001). The 33 duplicates compared to the original readings showed slight agreement for Observer 1 (kappa: 0.11 CI 95% 0.02;0.20, p <0.05) and fair for Observer 2 (kappa: 0.28 (CI 95% 0.07 - 0.49, p <0.001). The intra-observer agreement for Observer 1 was moderate, with a kappa of 0.41 (CI 95% 0.09 - 0.74, p <0.05), and for Observer 2, it was substantial with a weighted kappa of 0.69 (CI 95% 0.5 - 0.9, p <0.001).

Conclusion: The study highlights the variability in US interpretation of hepatic steatosis, emphasizing the importance of standardized training and methodology. US's sensitivity and specificity is operator dependence, which impacts the diagnostic interpretation. Our findings underscore the significance of inter and intra-observer comparisons for optimal diagnosis, especially when US is the primary diagnostic tool in MASLD assessment. Finally, our results emphasize the importance of group training. Observer 2, who underwent the same training as the original Chile BiLS ultrasound technicians and was consistently exposed to this technique as a diagnostic method, exhibited more consistent results. This reinforces the importance of collective training initiatives to enhance the reliability and accuracy of US in MASLD diagnosis.

#6084 Identification of plasma proteins for early detection of cancer, including lung, in the Atherosclerosis Risk in Communities (ARIC) study.

M. Ru[1], C. Douville[1], K. R. Butler[2], C. E. Joshu[1], J. Lu[1], A. Prizment[3], J. Coresh[1], E. A. Platz[1];

[1]Johns Hopkins University, Baltimore, MD, [2]University of Mississippi Medical Center, Jackson, MS, [3]University of Minnesota, Minneapolis, MN

Background: Plasma proteins, directly secreted from tumor cells or a result of the body's response to a tumor, may have utility for early detection. We aimed to identify plasma protein combinations that predict prediagnostic cancers in a prospective study.

Methods: We sampled from 8,186 ARIC study participants without a cancer diagnosis at blood draw and with 4,877 log2-transformed proteins measured by SomaScan. We selected as cases those diagnosed within 5 years after blood draw and were registry/medical record confirmed. We selected as controls those who never had a cancer history by 2015 and did not die of cancer. Participants with possible liver, kidney, or inflammatory conditions were excluded (eGFR-cr<30, top 1% of plasma AST, ALT, CRP). Highly correlated proteins (r>±0.75), abundant or known markers (albumin, CRP, PSA), and proteins with wide log2-transformed distributions (SD>1 and >10% outliers-1.5 IQR away from 25th or 75th percentile) among controls were excluded. Recursive feature elimination (RFE) with random forest (RF) was used to select the top 10 informative proteins based on accuracy. Non-protein features included demographic, lifestyle (e.g., smoking), and medical factors. We next divided participants into train and test sets in 7:3 ratio stratified by case status. RF including top 10 proteins from the RFE and non-protein features trained in the train set were used to predict near-term cancer status in the test set and to calculate prediction performance. Random Over-Sampling Examples were used to balance between rare cases (<3%) and controls in the dataset.

Results: We included 210 cases (98 diagnosed within 2 years) and 7,042 controls with 3,476 proteins. 58% were female, 24% were Black, and median age was 57 years (IQR: 52-62). The most common cancer was lung (27%). In the test set, sensitivity and specificity of the model for total cases diagnosed within 2 years were 0.19 and 0.91. Results for cases diagnosed within 3 (0.24, 0.88) and 5 (0.29, 0.87) years were similar. Using the top 10 informative proteins for total cancer, sensitivity was 0.68 and specificity was 0.56 for lung cancers diagnosed within 2 years; for lung cancers diagnosed within 3 (0.55, 0.77) or 5 (0.53, 0.79) years, sensitivity decreased but specificity increased. Using the top 10 informative proteins specific for lung cancer, which did not overlap with the top 10 for total cancer, sensitivity and specificity were 0.69 and 0.67 for lung cancers diagnosed within 2 years.

Conclusions: In this study, in which blood draw preceded diagnosis, top informative proteins did not provide sufficient sensitivity for all-cancer near-term prediction. For lung cancer, further optimization may improve the sensitivity and specificity to achieve the range required for population implementation for screening. Validation with more cases, and on other proteomic platforms are needed. Funding NHLBI, NCI, NPCR

#6085 Leveraging targeted epigenetic and genetic detection for cost-effective cancer classification.

R. Crawford[1], B. Krajacich[2], E. Lleshi[1], A. Negrea[1], L. Andreasen[1], J. Fullgrabe[1], J. Monahan[1], D. Morley[1], F. Puddu[1], D. McDade Walker[1], S. Kruglyak[3], P. Creed[1];

[1]biomodal, Cambridge, United Kingdom, [2]Element Biosciences, San Diego, CA, [3]Element Biosciences, San Diego, United Kingdom

The combinatorial power of genetics and epigenetics is vital to understanding biology in healthy and cancerous states. Utilizing a recent novel approach, we enable the simultaneous identification of modified cytosine and the canonical bases A, C, T & G in an enzymatic single-workflow solution. Generating this information across the whole genome provides a much-improved understanding of genetic and epigenetic changes, but can require a large amount of sequencing, particularly when exploring at depth. Enrichment protocols such as target enrichment enable deep interrogation of target areas whilst maintaining cost effectiveness.

Target enrichment panels enable the selective isolation of sequences of interest through target hybridization. Using commercially available panels combined with the novel enzymatic single-workflow solution we show uniform performance across a range of input amounts with reduced sequencing requirements. Samples used were cell free DNA (cfDNA) from patient samples with either Stage I or IV Colorectal Cancer and reportedly healthy controls and were targeted using pan-cancer and methylome panels. Widespread differences such as hypermethylation are clearly observed in late-stage cancer vs early-stage or healthy controls demonstrating utility of the approach for applications such as liquid biopsy.

Refining genetic and epigenetic investigations to a narrower region of interest can improve detection of low prevalence disease associated biomarkers at significant sequencing depth and lower sequencing costs.

#6087 Cytomics-on-chip and AI-driven predictive analysis platform for early detection of epithelial cancers.

K. Srinivasan Rajsri[1], M. P. McRae[1], N. J. Christodoulides[1], K. Algashaamy[2], M. T. Garcia-Buitrago[3], F. Chen[4], F.-M. Deng[4], J. S. Smith[5], J. T. McDevitt[1]; [1]NYU, New York, NY, [2]Jupiter Medical Center, Jupiter, FL, [3]University of Miami, Miller School of Medicine, Miami, FL, [4]NYU Langone Health, New York, NY, [5]University of North Carolina, Gillings School of Global Public Health, Chapel Hill, NC

Cancer is the 2nd leading cause of death (over 605,000 people) in the US, at an expense of over $200B, with 1 in 3 people projected to have cancer during their lifetime per CDC. Despite the significant impact of early detection and screening on prognosis, only some cancers are diagnosed at an early stage. Carcinomas, comprising >80% of cancer incidence, allow ease in cytology sample access chairside, due to the lesions' epithelial presentation. This presents a unique opportunity for early detection and screening in epithelial cancers. In low-resource healthcare settings, from clinical examination to the long, tedious and expensive diagnostic journey for cancers & pre-cancerous lesions, can lead to missed, delayed or over diagnosis scenarios. This affects treatment initiation and potentially outcome. To facilitate early intervention, there is compelling need to develop accurate and effective minimally invasive screening platforms. Recent advances in the -omics disciplines, microfluidics and AI tools are starting to reveal promising signatures of early disease detection, with potential to drastically improve screening and diagnostic systems. We are developing a novel application of the cytomics-on-chip platform, for enabling chairside, quantitative screening of suspicious epithelial lesions. The biosensor module involves 1. a single use, cytomics platform employing a cartridge with cellular array and high specificity biomarker reagents, that allows single cell molecular imaging to be completed in a portable analyzer. 2. a microfluidics module that allows cytomorphometric measurements to be completed. 3. The results generated are utilized to train machine learning algorithms to detect cyto-signatures and provide an intuitive result that may be utilized by health care practitioners in clinical-decision making. The first cell-based point-of-care oncology tool has recently been validated with high accuracy (99.3%), sensitivity and specificity, in a multi-site prospective clinical study. Here we demonstrate a pilot study towards development of a smart single cell cytomics-on-chip platform for prompt cytomorphometric and biomarker characterization towards diagnosis of urothelial, anal and cervical cancers, and dysplasia lesions, utilizing brush/pap and fresh urine samples. This has potential for continuous quantitative indexing, for disease categorization. As cancers become more pervasive, improved early detection/screening methods that are accurate, cost effective, easy to implement during routine clinical practice, and providing minimal discomfort to the patient, are urgently needed, improving confidence in clinicians' decisions.

#6088 Predicting the risk of any-type cancer in asymptomatic adults using noninvasive glycosaminoglycan profiling.

F. Gatto;
Karolinska Institutet, Stockholm, Sweden

Background: Early detection of cancers through screening can reduce mortality. However, screening excludes individuals not considered at an increased risk of developing cancer, as determined by age, sex, or tobacco use. No molecular biomarker is routinely used to predict risk. Here, we investigated urine glycosaminoglycan profiles (GAGomes) as noninvasive biomarkers for any-cancer risk prediction.
Methods: In this population-based case-control study, we included adults aged over 18 years from the Lifelines Cohort Study, Netherlands who were presumed healthy at baseline. All cases who self-reported any-type cancer or died by the 5-year study visit were confirmed in the Dutch Cancer Registry and matched 1:3 to randomly selected controls (1:1 for the interim analysis). We first developed a logistic regression reference model, including age, sex, and clinical variables to predict any-type cancer. Next, we added urine GAGomes (as a single aggregate score) to the model and assessed model improvement using the likelihood ratio test. We categorized the output of the saturated model (clinical variables plus urine GAGome score) into four groups based on bespoke specificity cut-offs: low-, moderate-, intermediate-, and high-risk. We estimated odds-ratios (ORs) for their association with any-type cancer compared to the moderate-risk group, as well as their sensitivity across subsets. Using the so-estimated OR in the high-risk group, we calculated the minimum pre-test 5-year absolute risk needed to reclassify an adult into a post-test 5-year absolute risk >3.00%.
Results: In the interim analysis, we included 2054 adults (median age = 51 years, 57% females). Of them, 924 were diagnosed with any-type cancer over a 6 year-follow-up period (median time to diagnosis = 1.4 years). Urine GAGomes were found to be independent risk factors when added to the reference model, explaining 27% of the variance (Nagelkerke R^2 = 0.26 vs. 0.21, $p < 0.0001$). The ORs in the low-, intermediate-, and high-risk groups were 0.05 (95% CI: 0.02-0.13 p < 0.0001), 5.31 (95% CI: 3.84-7.48, p < 0.0001) and 27.6 (95% CI: 14.3 - 51.6, p < 0.0001), respectively. The high-risk group detected +80% more cancers than the reference model at the same specificity (99.29%), particularly *in situ* and stage I (+204% and +64%) and among those aged 50-69 (+247%). Adults with a pre-test 5-year absolute risk > 0.25% returning a high-risk group would be reclassified to a post-test 5-year absolute risk > 3.00% for any-type cancer.
Conclusion: Implementing urine GAGomes as a strategy for risk-stratified targeted screening could identify adults with increased risk of any-type cancer who are currently excluded from screening.

#6090 Integration of innate and adaptive immune signatures for early detection of cancer.

E. Fitzsimons[1], A. Coulton[1], H. Fu[1], M. Augustine[1], R. Lee[2], J. Reading[1], K. Litchfield[1];

[1]University College of London (Incorporated in England and Wales), London, United Kingdom, [2]The Royal Marsden NHS Foundation Trust, London, United Kingdom

Up to 50% of cancer patients are diagnosed at a late stage with tumors that are often unresectable, leading to intensive treatments and a preventable loss of life. Whilst multiple assays have been developed to tackle the issue of disease mortality, these approaches have serious limitations. For example, circulating tumor DNA (ctDNA) preferentially detects hard-to-treat tumors and micrometastatic disease, with limited sensitivity and specificity for early-stage malignancy, underscoring an urgent need for novel early detection strategies.

Substantial evidence exists to demonstrate that signals related to innate (e.g. pro-inflammatory cytokines) and adaptive (e.g. antibodies and T cell receptors [TCRs]) immune engagement arise early in the development of cancer. The immune system therefore offers potential as an exquisitely sensitive and highly specific intrinsic early detection system for cancer. Here we propose the development of a pan-cancer novel early detection assay, using peripheral blood to measure three key cancer-specific components of the anti-tumor immune response: i) T cell receptor (TCR) sequences, ii) antibody signatures, iii) cytokine markers.

Our preliminary data demonstrates that an age and smoking-matched cohort of lung cancer patients can be distinguished from healthy donors using TCR sequencing data processed through a published machine learning approach ($p<0.01$). In support of this, a pilot study on a custom peptide microarray comprised of lung cancer associated antigens and recurrent neoantigens demonstrated that lung cancer patient samples show significantly higher antibody intensities than healthy donors. Thirdly, using data from a prospective cohort study, we have demonstrated that inflammatory markers can be leveraged to predict future cancer diagnosis, and identified key protein markers for future work. These data provide proof-of-principle for the use of these analytes as a tool for early detection.

We are actively curating a unique cohort of samples for this work from a prospective study, Nodule Immunophenotyping Biomarker for Lung Cancer Early Diagnosis (NIMBLE) (NCT05432739), which recruits patients with indeterminate lung nodules that may represent early cancers (>280 patients to date). This malignancy has high mortality rates and a significant need for early detection strategies. Through this, we aim to understand the early immunobiological response to cancer and leverage this information to design a novel multi-parametric immunopredictor assay for early detection of cancer.

#6091 Multi-cancer early cancer detection and cancer-type identification with high sensitivity non-invasive using urine: Pancreatic lung cancer early detection.

E. Di Luccio[1], T. Hirotsu[2];

[1]HIROTSU BIO SCIENCE INC., Fujisawa city, Japan, [2]HIROTSU BIO SCIENCE INC., Tokyo, Japan

N-NOSE, a breakthrough cancer detection test from HIROTSU BIO SCIENCE, utilizes the unique chemotactic behavior of the nematode *C. elegans*. This nematode is drawn to the urine of individuals with 15 different types of cancers (including stomach, colon-rectum, lung, breast, pancreas, liver, prostate, uterus, esophagus, gallbladder, bile duct, kidney, urinary bladder, ovary, oropharynx) while avoiding urine from healthy persons, making N-NOSE a comprehensive primary screening tool. It has a high accuracy rate, with 87.5% sensitivity and 90.2% specificity for early-stage cancers. Being non-invasive and reasonably priced, N-NOSE has been a significant success in Japan since its 2020 launch, with over 500,000 screenings.This presentation delves into the technology aspect of N-NOSE in Japan, comparing its clinical research and key findings with competitors to underscore its effectiveness in early cancer detection. Furthermore, N-NOSE now advances to not only detect cancer but also identify its type in a noninvasive way, using urine and with high PPV.With pancreatic cancer being particularly lethal, we outline “N-NOSE plus pancreas,” the world’s first pancreatic cancer detection test at an early stage. This involves genetically modifying *C. elegans* to react specifically to early-stage pancreatic cancer urine samples, a development centered on the newly identified cr-4 GPCR in AWC neurons. Next, we profile our newest liver-cancer-specific test, “N-NOSE plus liver,” which offers early liver cancer detection with high sensitivity and specificity using urine.Finally, we highlight how N-NOSE bridges the gap in cancer screening and type identification, offering a complete, non-invasive solution.

#6092 Three-dimensional multi-omic analysis of early invasion of human pancreatic ductal adenocarcinoma from IPMN.

S. Datta, S. M. Shin, J. Kanacharoen, M. J. Pfluger, K. Hirose, A. Forjaz, S. Graham, P.-H. Wu, R. H. Hruban, D. Wirtz, W. J. Ho, A. L. Kiemen, L. D. Wood; Johns Hopkins University School of Medicine, Baltimore, MD

Background: Pancreatic ductal adenocarcinoma (PDAC) is a deadly cancer, with only 11% of patients surviving beyond 5 years. Intraductal papillary mucinous neoplasm (IPMN), a precancerous lesion and the most common type of neoplastic pancreatic cyst, presents a critical opportunity for cancer interception, but the drivers of malignant progression in IPMN are still largely unknown. Although the immunosuppressive microenvironment of PDAC has been well characterized, the timing of the development of these immune alterations in IPMNs is not well studied and could provide a rational foundation for cancer immuno-prevention. Moreover, the inception of invasive PDAC and its spread into the microenvironment from IPMN is complex, multifactorial, and, due to its unique anatomy, challenging to analyze with traditional 2-dimensional visualization. We sought to capture the precise point of transition from IPMN to invasive carcinoma utilizing CODA, a supervised deep learning tool for three-dimensional (3D) reconstruction of serially sectioned human tissue, in order to quantitatively assess the molecular and cellular alterations associated with malignant progression.

Method: Formalin-fixed paraffin-embedded (FFPE) tissue blocks with PDAC arising from IPMN were serially sectioned, every third slide was stained with H&E, and digitized at 20x magnification. Following pathologist-guided annotations on a subset of H&E slides, CODA generated 3D models of each tissue block, including automated annotation of 9 pancreatic tissue components. Using these annotations, we identified the transition from IPMN to invasive carcinoma in each sample and selected regions for multi-omic profiling based on quantitative features of the cellular microenvironment. Multi-omic profiling of IPMN, transition zone, and PDAC included laser capture microdissection followed by whole exome sequencing to identify somatic DNA alterations, as well as spatial transcriptomics to identify alterations in gene expression in neoplastic cells and spatial proteomics to identify cellular alterations in the surrounding microenvironment.

Results: CODA generated accurate annotation on all the H&E slides from each case and robustly identified regions of interest for multi-omic profiling. Spatial proteomic profiling using imaging mass cytometry revealed a decrease in T cell density as IPMNs transition into PDAC. Sub-clustering of the T cell compartment identified decreases in multiple T cell subsets, including activated cytotoxic T cells and helper T cells, in the transition zone compared to IPMN.

Conclusion: In this study, we integrated multi-omic profiling with CODA-generated high-resolution 3D tissue maps to identify molecular and cellular drivers of malignant progression in human PDAC.

#6093 Evaluation of preanalytical and physiological variables affecting cfDNA-based multi-cancer early detection test.

H. Bao, X. Chen, X. Wu, W. Tang, M. Wu, S. Tang, X. Wu, Y. Shao;
Nanjing Geneseeq Technology Inc., Nanjing, China

Background: The multi-cancer early detection (MCED) tests utilizing blood-based circulating cell-free DNA (cfDNA) have gained significant attention in the market as a promising approach for early cancer detection. However, potential effects of preanalytical and physiological variables, including extraction methods, preservation techniques, and physiological factors such as diet, on the accuracy and reliability of MCED results remains poorly investigated. In this study, we aimed to evaluate the impact of physiological variables during blood collection and preanalytical procedures on the outcomes of a MCED test.
Methods: A total of 105 plasma samples from 19 healthy donors was collected and analyzed using a MCED test (MERCURY) which leverages the low-coverage whole-genome sequencing and a set of genome-wide features based on cfDNA fragmentomics. Samples were controlled for preanalytical procedures, including transportation condition and preservation time or physiological conditions (before/after meal or exercise) at blood collection.
Results: Repeat blood collection (N=4) from the 5 healthy participants consistently yielded negative results for cancer (PPA: 100.0%; 95% CI [56.6%,100.0%]). Among the 5 healthy participants, plasma samples frozen within 1 year (7 days, 3 months, 9 months) showed the same agreement with the reference condition as non-frozen samples (PPA: 100.0%; 95% CI [56.6%,100.0%]), except for one sample frozen for 1 year, which showed a higher risk score and became a positive signal (PPA:80.0%; 95% CI [37.6%,96.4%]). Transportation conditions within 2 hours, 24 hours, 48 hours, and 96 hours at room temperature or 4℃ did not affect the test outcomes, as all samples remained in agreement with the reference condition as of 2 hours at 4℃ (PPA:100.0%; 95% CI [61.0%,100.0%]). Physiological conditions, including pre- and post-meal as well as pre- and post-exercise states, did not exert any influence on the test results, as all samples exhibited agreement with the reference condition (PPA:100.0%; 95% CI [43.9%,100.0%]).
Conclusions: The results of this study suggest that variables such as time of blood collection and plasma freezing time may not significantly affect the accuracy of the MCED test in healthy participants. Transportation conditions and physiological conditions evaluated in this study did not have a notable influence on the test outcomes. Nevertheless, it is advised that the freezing duration of plasma samples should not exceed one year.

#6094 Detection of MRD assessment with the Personalis NeXT Personal assay using MATRIX plasma-in-plasma contrived samples.

P. Labrousse[1], H. Russell[1], S. Hamid[2], G. Bartha[3], J. Lyle[3], D. Norton[3], J. Northcott[3], **S. M. Boyle**[3], R. Chen[3], D. Stetson[1], J. Hadfield[2];
[1]AstraZeneca, Waltham, MA, [2]AstraZeneca, Cambridge, United Kingdom, [3]Personalis, Inc., Fremont, CA

Detection of circulating tumor DNA (ctDNA) has been shown to correlate with clinical outcome of oncology patients. Molecular residual disease (MRD) profiling by ctDNA is being rapidly deployed. Current tumor-informed MRD tests assess a relatively small number of personalized variants, placing limits on their detection sensitivity and ultimately leading to false-negative results due to insufficient assay limit of detection (LOD). Here we report a performance evaluation of the Personalis NeXT Personal tumor-informed MRD assay, using a novel design for contrived samples that are highly commutable to clinical samples, enabling robust assessment of these emerging MRD assays.

Novel samples were built from commercially acquired matched tumor and plasma samples, across different indications. The cancer patient plasma was diluted into a background of healthy donor plasma to create the 72 plasma-in-plasma samples in each study (total of 144). Personalis performed WGS on the matched solid tumor and normal samples from each patient. ~1800 somatic variants were selected for each patient. A personalized panel was designed and used to enrich for the selected targets in the individual plasma samples. An aggregated signal across MRD targets was evaluated to determine the presence of ctDNA in each plasma sample.

MATRIX 1 panels averaged 1863 variants (range: 1818 to 1888) selected for MRD tracking. With 152 clinically relevant variants and additional assay components, an average of 2206 variants were assessed per patient. MATRIX 2 panels averaged 1836 variants (range: 1819 to 1867) selected for MRD tracking. In the MATRIX 1 study, tumor signal was detected in all analyzed samples, including 9 samples at 0.002% tumor plasma dilution, with an assay sensitivity of 100%. The MATRIX 2 study showed tumor signal detected in 14 of 16 samples at 0.001% tumor plasma dilution. The 2 false negatives were reported at the 0.001% tumor plasma dilution. Thus, the assay sensitivity was 87.5% at the lowest dilution (0.001%) and 96.8% overall.

The MATRIX plasma-in-plasma approach is a robust option for assessing the analytical sensitivity of MRD assays to low levels of ctDNA. This approach addresses all parts of an MRD assay for both the plasma and tumor/normal tissues, utilizing real clinical samples while allowing direct interrogation of sensitivity. The Personalis NeXT Personal assay shows ultra-high sensitivity with reproducible data down to the 1-3 PPM range.

#6095 Lung cancer risk assessment with the INTEGRAL protein panel: Preliminary results from development and validation in the Lung Cancer Cohort Consortium.

H. Zahed[1], K. Alcala[1], D. C. Muller[2], R. Hung[3], M. Johansson[1], **H. A. Robbins**[1], The Lung Cancer Cohort Consortium;
[1]International Agency for Research on Cancer, Lyon, France, [2]Imperial College London, London, United Kingdom, [3]Lunenfeld-Tanenbaum Research Institute, Sinai Health, Toronto, ON, Canada

Background: In the NCI-funded Integrative Analysis of Lung Cancer Etiology and Risk (INTEGRAL) program, the Lung Cancer Cohort Consortium (LC3) recently identified 36 proteins associated with lung cancer risk in pre-diagnostic blood samples after evaluating 1,161 proteins in 731 case-control pairs (Nature Communications, 2023). Based on these data, we designed the INTEGRAL panel, which measures absolute concentrations of 21 proteins, to optimize lung cancer risk assessment for screening beyond prediction models (e.g. PLCOm2012) or categorical screening criteria (e.g. USPSTF-2021).
Methods: To evaluate the performance of the INTEGRAL panel, we assayed blood from participants selected as a representative case-cohort sample from 14 LC3 cohorts, divided into development and validation sets (Annals of Epidemiology, 2023). Here, we present preliminary results from the 7 cohorts in the development set, including 807 lung cancer cases diagnosed within 3 years of blood draw and 1,144 sub-cohort representatives, who were weighted to represent all current and former smokers in their corresponding cohorts. We first fit a flexible parametric survival model in 4 cohorts (n=478 cases) including a subset of proteins and age, smoking duration, and smoking intensity. The model was subsequently evaluated in the remaining 3 cohorts (n=329 cases) and benchmarked against the PLCOm2012 risk score and USPSTF2021 screening criteria.
Results: The preliminary model includes 4 proteins (CEACAM5, MMP12, SCF, LPL). Compared with the PLCOm2012 score, the model improved discrimination of future lung cancer for cases occurring over 3 years (AUC=0.81 vs. 0.76, p<0.0001) and over 1 year (AUC=0.86 vs. 0.78, p<0.0001). At the USPSTF-2021 specificity of 76%, the protein model increased sensitivity by an absolute difference of 14% over 3 years and 25% over 1 year compared to USPSTF-2021, and by 9% over 3 years and 17% over 1 year compared to the PLCOm2012 model. When screening the same number of participants as PLCOm2012, the protein model identified more future cases (223 vs 193), and the cases identified only by the protein model were predicted to gain more life-years from 3 LDCT screens compared with the PLCOm2012-identified cases (4.2 vs. 3.6 life-years).
Conclusions: Preliminary results suggest that the INTEGRAL protein panel can improve risk discrimination beyond questionnaire-based risk prediction models, as well as identify future cases who have more life-years to gain from screening. Final validation is planned for completion in early 2024, by analysis of fully independent data from 7 additional LC3 cohorts (n=560 cases and 1,126 sub-cohort representatives).

#6096 Targeting premalignant lung cancer to intercept progression to invasive disease.

M. Martin, Y. He, B. Bhinder, L. Yoffe, S. L. Zhong, A. Singh, O. Elemento, S. Jiang, N. Altorki, **V. Mittal**;
Weill Cornell Medicine, New York, NY

Increased implementation of low dose CT-guided screens in the clinic has led to the identification of premalignant lung nodules (ground glass opacity, GGO) which progress to invasive adenocarcinoma[1,2]. Using integrated genomic analysis of a cohort of >300 patients with premalignant lesions, we constructed the first high-resolution landscape of composition, lineage/functional states, developmental trajectories, and multicellular crosstalk networks, which revealed potential targets for therapeutic intervention. We uncovered that early lesions exhibit marked immune-suppressive phenotypes characterized by increased T lymphocyte exhaustion to cytotoxic scores, decrease in NKT cells, elevated Tregs, increased myeloid suppressor activity, accumulation of immunosuppressive myeloid cells activation of unfolded protein response (UPR) sensor IRE1α that activates the multitasking transcription factor XBP1 known to drive malignant progression. Targeting IRE1α endoribouclease with a small molecule drug limited disease progression with marked immunomodulation in our newly developed Kras and EGFR driven mouse models, which mirror progression of human precursor lesions to invasive disease. As an immunoprevention approach, we have generated LNP-mRNA vaccines targeting top two shared neoantigens in premalignant lesions, which have shown marked immunogenicity and efficacy in early disease. Our work provides the molecular foundation for precision oncology strategies to intercept transition of preinvasive to invasive adenocarcinoma. 1. Altorki, N.K.*, et al. Nat Rev Cancer*, 2019. *2*. Altorki, N.K.*, et al. Cell Rep,* 2022.

#6097 The role of B-cell receptor repertoire in lung squamous premalignant lesions.

D. J. Chiu, C. Merenstein, M. Lenburg, S. Mazzilli, J. Beane;
Boston Univ. School of Medicine, Boston, MA

Objective: B cells and plasma cells (PCs) play a vital role in the pathogenesis of lung cancer and provide prognostic predictive value. However, the role of B cells in the bronchial premalignant lesions (PMLs), the precursor of lung squamous cell carcinoma, is poorly understood. Prior work has shown that progression of proliferative subtype, a PML molecular subtype enriched with bronchial dysplasia, to a higher histology grade is associated with downregulation of antigen processing and presentation. In this study, we seek to understand the role of B cells, PCs, and the B-cell receptor (BCR) repertoire in progression of the bronchial PML.

Methods: We performed bulk targeted BCR sequencing on 69 endobronchial biopsies obtained from 29 subjects at high-risk for developing lung cancer. The Immcantation pipeline were applied to obtain the V(D)J germline segment assignment using the human reference from IMGT, clonal cluster assignment, and mutational load quantification for each BCR sequences by pooling all the BCR sequences from the same subjects. The clones with frequency less than 10^{-4} were filtered out. We then performed the repertoire analysis, such as clonality diversity, isotype switching frequency, and somatic hypermutation rate (SHM) rate at sample levels and investigated the association with transcriptional signature derived from bulk RNA-seq and the clinical progression of PMLs.

Results: The B cell and PC transcriptional signatures and B cell chemoattractants gene expression are associated with progression in proliferative subtype PMLs. The number of BCR clones, the class switch from IgG3 to IgG1, and the mutational rates of total and CDR3 regions were positively correlated with the B cells and PCs transcriptional signatures. Among the 31 PMLs of proliferative subtype, regressive lesions showed higher proportions of IgG heavy chain usage, higher SHM rate in CDR3 and total BCR regions, and higher frequency of class switch from IgD/M to IgG and from IgG3 to IgG1. Biopsies within the same patient had a higher proportion of shared BCR clones when they were sampled at the same timepoint than when they were sampled from the same anatomic location at different timepoints. The preserved clones of BCRs at the same anatomic location over different times had higher clonality, more class switch from IgD/M to IgG or IgA and from IgG3 to IgG1, and increased SHM rates than the non-preserved clones.

Conclusions: These results suggest B and plasma cells exert anti-tumor effects that prevent bronchial PMLs from progressing to higher grade lesions by switching to IgG1 BCRs and increasing SHM rates.

#6098 Spatial single-cell immune microenvironment analysis reveals the transition from innate to adaptive immune response during early lung adenocarcinoma carcinogenesis.

B. Zhu[1], P. Chen[1], M. Aminu[1], J. Fujimoto[1], L. Hong[1], A. L. Moreira[2], J.-R. Li[3], Y. Tian[1], L. M. Solis Soto[1], P. Edwin Roger[1], O. Shi[1], H. Chen[1], F. R. Rojas[1], E. Vilar[1], A. Maitra[1], K. Chen[1], N. Navin[1], C. L. Haymacker[1], V. Velcheti[4], D. H. Sterman[4], P. Andrew Futreal[1], D. L. Gibbons[1], I. I. Wistuba[1], J. V. Heymach[1], C. Cheng[3], H. I. Pass[2], J. Wu[1], J. Zhang[1];

[1]UT MD Anderson Cancer Center, Houston, TX, [2]NYU Langone Health, New York, NY, [3]Baylor College of Medicine, Houston, TX, [4]NYU Grossman School of Medicine, New York, NY

Introduction: Lung cancer remains the leading cause of cancer death worldwide. Although prevention holds the promise to reduce lung cancer mortality, the results from randomized trials have been disappointing, likely due to our rudimentary knowledge of early lung cancer carcinogenesis. Cancer initiation and progression involve complex processes dependent on the dynamic interplay of individual cells within the tumor microenvironment (TME). Our understanding of the multicellular composition, interaction, spatial distribution, and functional dynamics during the early evolution from precancer to invasive LUAD is limited.

Methods: We performed spatial single cell immune microenvironment analysis of 10 normal, 40 AAH, 22 AIS, 18 MIA, and 34 IAC by Imaging Mass Cytometry (IMC) and analyzed high-dimensional images of 1,618 regions-of-interest (ROIs) using a 34-plex marker. Using machine learning approaches, we classified 4,828,879 cells into 14 major cell types, which were subjected to further analysis for multicellular composition, interaction, spatial distribution, and functional dynamics in LUAD precursors of different stages.

Results: From AAH to AIS, MIA, and IAC, we observed a gradual escalation in the density (number of cells/mm2) of all immune subsets. Proportionally, adaptive immune cells exhibited a progressive increase, whereas innate immune cells demonstrated a concurrent decrease with the neoplastic progression from normal lung to AAH, AIS, MIA, and ADC. Notably, macrophages emerged as the predominant immune cells within the immune microenvironment of these LUAD precursors. Upon closer examination of subtypes, protumor M2 macrophages showed a gradual increase from AAH to AIS, MIA, and IAC, whereas anti-tumor M1 macrophages increased from normal to AIH, AIS and subsequently decreased in AIS, MIA, and IAC stages. These alterations resulted in a progressive increase in M2/M1 ratios from AAH to IAC stages. Furthermore, M2 macrophages exhibited higher heterotypic interactions with epithelial cells than M1 across LUAD precursors of different stages, especially in the later stages. Co-expression analysis revealed 5 modules that distinguishes each histological stage. Tim-3 module was significantly enriched in AAH lesions, while NK cell-related features were enriched at AIS stage, B cell-related features enriched at MIA stage and Ki-67-related adaptive immune features enriched in IAC stage.

Conclusion: The spatial single cell immune microenvironment analysis revealed a transition from innate to adaptive immunity during initiation and early progression of LUAD progression and innate immunity may play critical roles during early LUAD development. Therefore, reprograming innate immunity such as repolarization of M2/M1 may provide avenues to intercept LUAD precursors to prevent invasive LUAD.

#6099 Identification of intrinsic precursors of Barrett's and gastric intestinal metaplasia.

Wa Xian[1], Frank McKeon[1], Yusuke Yamamoto[2], Melika Khorrami[1], Melina Khorrami[1], zaal Mory[1], Jeremy Siegelman[1], Amber Su[1], Raul Caballero Montes[1], Ashley Hoffman[1], Jaffer Ajani[1], Christopher Crum[3], William Bachovchin[4], Shan Wang[1], Matthew Vincent[1], Crystal Nguyen[1]

[1]University of Houston, Houston, TX,[2]National Cancer Institute, Tokyo, Japan,[3]Harvard University, Boston, MA,[4]Tufts University, Boston, MA

The origin of Barrett's esophagus (BE) and gastric intestinal metaplasia (GIM), obligate precursors of esophageal adenocarcinoma (EAC) and intestinal gastric cancer (iGC), has intrigued investigators for decades and would likely guide preemptive strategies. From endoscopic biopsies of clinically confirmed BE and GIM, we have cloned stem cells committed to intestinal metaplasia in vitro. Remarkably, the gene expression profiles of BE and GIM stem cells are highly related down to broad arrays of transcription factors compared with stem cells of the normal gastric mucosa. Using cell surface markers in common between BE and GIM stem cells, we have identified clusters of cells at the squamocolumnar junction and the distal stomach in mice and have used Fluorescence-activated cell sorting (FACS) to clone these cells from both sites. These murine clones can be differentiated in air-liquid interface cultures, and both are committed to intestinal metaplasia marked by goblet cells and Alcian blue staining. To ask whether similar cells exist in humans, we generated stem cell libraries from endoscopic biopsies taken from the gastroesophageal junction (GEJ) and the antrum-body junction (ABJ) in patients without BE or GIM. FACS sorting of these stem cell libraries using the same cell surface markers common to BE and GIM stem cells and the murine precursors, we have identified stem cells from the GEJ and ABJ that show similar gene expression profiles and share a commitment to intestinal metaplasia upon in vitro differentiation. Using identical transformation protocols involving retrovirally transduced protooncogenes, we find that these transformed intrinsic cells give rise to tumors with expression profiles similar to EAC and iGC in TCGA datasets, whereas transformed gastric mucosal stem cells yield tumors marked by signet ring cells typical of diffuse gastric cancer. Lastly, we find that drugs we have developed that target the stem cells of BE and GIM also eliminate the putative precursor cells of BE and GIM, suggesting the potential of therapeutics that might eliminate the emergence of intestinal metaplasia and the cancers derived from them.

#6101 PLASMUT: An R Package for estimating the probability of tumor-specific mutations in cell-free DNA.

A. S. Arun[1], J. E. Medina[2], S. Cristiano[2], D. C. Bruhm[2], R. J. A. Fijneman[3], G. A. Meijer[3], A. Leal[2], V. E. Velculescu[2], R. B. Scharpf[2];
[1]Yale University School of Medicine, New Haven, CT, [2]Sidney Kimmel Comprehensive Cancer Center, Johns Hopkins University School of Medicine, Baltimore, MD, [3]Department of Pathology, Netherlands Cancer Institute, Amsterdam, Netherlands

Noninvasive approaches for detection of tumor-specific mutations in cell-free DNA (cfDNA) have the potential to track a patient's response to treatment, enabling effective and timely decisions on therapy. However, mutations in cfDNA arising from clonal hematopoeisis (CH) are common and tumor biopsies for definitive identification of the origin of these mutations are not always available. Sequencing of matched cells from buffy coat and the absence of mutations in these cells has been used to rule-out white blood cell (WBC) mutations, but uneven sequencing depths between matched cfDNA and buffy coat and the fraction of mutant alleles are generally ignored by rule-based tests. A probabilistic approach that quantifies the evidence of tumor-derived mutations in cfDNA is needed.
We developed a Bayesian framework to estimate the probability that a mutation identified in cfDNA is tumor specific. Our approach requires the number of reads with a mutant allele in plasma (y_p) and WBCs (y_w) and the corresponding number of total distinct reads at these locations. The posterior odds that a mutation is tumor-derived (S) versus CH or germline (H) is given by the ratio of the probabilities of observing the distinct reads given each model times the prior odds. Estimation of the Bayes factor is obtained by integrating over the unobserved mutant allele fractions in plasma and WBCs using Monte Carlo importance sampling. We applied this approach to 52 patients with initially unresectable colorectal cancer (CRC) liver metastases in the CAIRO5 clinical trial (NCT02162563), using ultra-deep targeted sequencing of cfDNA from plasma and matched WBCs.
Among the CAIRO5 patients analyzed, we identified 95 mutations with moderate evidence of tumor-derived cfDNA mutations (Bayes factor > 10) and 19 mutations that were CH-derived (Bayes factor < 0.1). For a subset of 47 cfDNA mutations with no corresponding mutation identified by WBC sequencing, the evidence of tumor origin was highly variable (Bayes factor range: 0.03 to 5.6). While the standard rule-based approach identifies all of these mutations as tumor-derived, none of these mutations reach a moderate evidence cutpoint (all Bayes factors < 6). As a false positive would lead to identification of cfDNA mutations that do not track tumor burden, requiring even higher levels of evidence (Bayes factor > 99) for the selection of cfDNA mutations could be warranted, and still identifies one or more cfDNA mutations in 43 of the patients. This approach is implemented in the R package PLASMUT available from Bioconductor (doi:10.18129/B9.bioc.plasmut).
We developed an approach that quantifies the evidence between two competing models for the origin of mutations in cfDNA. A cutpoint for determination of the probability of tumor-derived cfDNA mutations can be tailored to the disease application, balancing the potential benefits of noninvasive testing with the harms of false positives and negatives.

#6102 Clinicopathological and genetics features of endometrial cancer in Algerian women: The first nation-wide study.

F. Cherbal[1], C. Mehemmai[1], M. Saidi[1], Y. Santoudji[1], D.-E. Seddik[1], A.-L. Boumehdi[1], F. Gouaref[2], K. Bentabak[2], H. Mahfouf[3], M. Oukkal[4]; [1]Molecular Genetics Team, LBCM, Faculty of Biological Sci., USTHB, Algiers, Algeria, [2]Oncological Surgery and LiverTransplantation services, EHS Pierre and Marie Curie, Univ. of Algiers 1, Algiers, Algeria, [3]Mohamed El Kolli Publ. Hosp., Academic Med. Oncology Services,Rouiba, Sch. of Med., Univ. of Algiers1, Algiers, Algeria, [4]Clinic of Med. Oncology Amine Zirout, Univ. Hosp. of Beni-Messous, Sch. of Med., Univ. of Algiers-1, Algiers, Algeria

Background: Endometrial cancer represents the fourth common cancer in women in Algeria and the fifth cause of cancer mortality. In the present study, we aimed to determine, clinical, tumor and genetics characteristics associated with endometrial cancer in Algerian women. In addition, we screened for germline pathogenic variants in MMR genes in endometrial cancer patients with strong family history of Lynch syndrome (LS).

Materials and Methods: Our study population included 273 patients diagnosed with endometrial cancer between 2010 and 2021. Data were collected from three public hospitals that covered 29 provinces among 48 in Algeria. Patient and tumor information included: age at diagnosis, menopausal status, histological type, histological grade, TNM stage, FIGO stage, tumor markers CA125, ACE, CA19-9, family history with cancer and age at menarche . *MLH1* (exons 1, 9, 10, 13, 16), *MSH2* (exons 5, 6, 7, 12), *MSH6* (exons 4 and 8) and *PMS 2*(exons 6 and 10) were screened by PCR-Sanger direct sequencing in 14 LS families .

Results: The mean age at diagnosis was 58.88 years. The mean age at menarche was 13.5 years. The proportion of endometrial cancer patients with premenopausal status was 21.62%. The commonest histological type was endometrioid adenocarcinoma (66.79%) followed by clear cell carcinoma (8.10%), carcinosarcomas (3.86%), serous carcinoma (3.47%) and mucinous carcinoma (2.7%). We found that the proportion of tumors with histological grade I (34.74%), grade II (27.41%) and grade IV (21.40%) was commonest in 83.55% of the patients. Our results showed that 73.74% of the patients were diagnosed at stage I (50.19%), stage II (12.74%) and stage III (10.81%), respectively. For the FIGO staging, our results showed that 74.12% of the patients were diagnosed at stage I (52.89%), stage III (10.81%) and stage I (10.42%), respectively. 16.21%, 3.08%, 6.94% of the patients were positive for CA125, ACE and CA19-9, respectively. We noticed that 56 patients (20.43%) had a positive family history with HBOC syndrome (17), Lynch syndrome (26) and Cowden syndrome (13), respectively. We identified two distinct germline pathogenic variants in *MLH1* gene in two LS families. We detected the new germline pathogenic variant *MLH1* c.53_63delinsT in young patient diagnosed with endometrial cancer and colorectal cancer (CRC) at age 43y and 44 y, respectively. The rare pathogenic germline variant *MLH1* c.1546C>T has been detected in young woman diagnosed with CRC at age 41y and endometrial and ovarian cancers at age 52y, respectively.

Conclusions : In this first study, we reported some clinical, biological, tumor and genetics features of endometrial cancer in Algerian women. Interestingly, we noticed that the median age of diagnosis was younger that the average age in Europe and America. Genetic counseling and testing is recommended for endometrial cancer patients diagnosed before age 50 with a family history of Lynch syndrome.

#6103 The association of genetic polymorphisms in DNA repair genes XRCC1 and 3 with cervical cancer risk among Bangladeshi females.

M. Rahman[1], L. Das[1], S. Rahman[1], A. Hossain[2], R. Sultana[3];

[1]Khulna University, Bangladesh, Khulna, Bangladesh, [2]Dhaka International University, Bangladesh, Dhaka, Bangladesh, [3]Decent Spacialized Dental Care, Khulna, Bangladesh

Introduction and Objective: Worldwide, cervical cancer ranks the second most common cancer in women. Sequence variations in DNA repair genes X-ray repair cross complementing (XRCC) 1 and 3 genes can lead to can result cellular function aberration leading to cancers. Single nucleotide polymorphisms (SNPs) in XRCC1 (Arg399Gln) and XRCC3 (Thr241Met) genes have been shown to cause individual variation in their DNA repair capacity. The aim of this study was to investigate the association of XRCC1 Arg399Gln and XRCC3 Thr241Met SNPs with susceptibility to cervical cancer among Bangladeshi populations.
Methods: In the current case-control study 124 cervical cancer patients and 148 age matched healthy controls were recruited. Genomic DNAs were isolated from peripheral blood collected from the participants and genotyped for candidate SNPs using polymerase chain reaction-restriction fragment length polymorphism (PCR-RFLP) method.
Results: For XRCC1, heterozygous Arg/Gln and combined heterozygous plus variant homozygous Gln/Gln genotypes showed 1.78-fold (95% CI 1.0037 to 2.8771, p=0.0484) and 1.8627-fold (95% CI 1.1470 to 3.0250, p = 0.0119) increased risk of cervical cancer, respectively, when compared with normal homozygous Arg/Arg genotype. The variant Gln allele was positively associated with cervical cancer by 1.68-fold increase (95% CI 1.1732 to 2.3980, p = 0.0046). Similarly, for XRCC3, Thr/Met heterozygous and combined Thr/Met + Met/Met genotypes were found to be associated with 1.6993-fold (95% CI 1.0398 to 3.0166, p=0.0354) and 1.8312-fold (95% CI 1.0890 to 3.0791, p = 0.0225) higher risk, respectively, when compared with normal homozygous Thr/Thr genotypes. The variant Met allele showed significant association with 1.71-fold increased risk.
Conclusion: XRCC1 (Arg399Gln) and XRCC3 (Thr241Met) SNPs may be positively associated with increased cervical cancer risk in Bangladeshi females.

#6104 EDRN Lung Team Project #2 validation of molecular biomarkers for the early detection of lung cancer in the setting of indeterminate pulmonary nodules.

J. C. Willey[1], E. L. Grogan[2], S. A. Deppen[2], J. G. Herman[3], M. N. Kammer[2], M. B. Schabath[4], L. Sorbara[5], H. I. Pass[6], J.-C. J. Tsay[7], Z. Feng[8], A. Spira[9], E. L. Crawford[1], J. Dahlgren[10], S. M. Dubinett[11], K. R. Rieger-Christ[12], M. E. Lenburg[9].

[1]University of Toledo, Toledo, OH, [2]Vanderbilt University Medical Center, Nashville, TN, [3]University of Toledo, Pittsburg, PA, [4]Moffitt Cancer Center, Tampa, FL, [5]National Cancer Institute, Bethesda, MD, [6]NYU Langone Health, New York, NY, [7]New York University School of Medicine, New York, NY, [8]Fred Hutchinson Cancer Center, Seattle, WA, [9]Boston University, Boston, MA, [10]Fred Hutchinson Cancer Center, Toledo, OH, [11]University of California Los Angeles, Los Angeles, CA, [12]Lahey Hospital and Medical Center, Burlington, MA

Background: The goal of the Early Detection Research Network (EDRN) Lung Team Project #2 (LTP-2) is to establish a cohort (n= 300) of high-risk people with indeterminate pulmonary nodules (6mm-30mm) to clinically validate the diagnostic accuracy of existing molecular and imaging biomarkers discovered and analytically validated through the EDRN program. These biomarkers comprise signals measured in serum (glycan or cytokine), plasma (protein, miRNA, RNA, or methylated circulating tumor DNA), airway epithelial cells (RNA or DNA), nasal brush cells (RNA or DNA), and/or chest CT images.

Methods: Eligible participants had an indeterminate nodule discovered incidentally or through low-dose CT screening within 14 months prior to enrollment and were aged 45-90 years, with 20 pack-years or more cigarette smoking history, free of lung cancer, and willing to provide blood, nasal brushing, and optionally bronchoscopic brush biopsy specimens. Baseline medical and demographic data were collected from each subject. Baseline and years 1 and 2 follow-up CT images were obtained. Each specimen at each respective site was labeled with a 2-D barcode provided by the DMCC and specimen information was entered into the Validation Study Information Management System (VSIMS) developed by the EDRN Data Management and Coordinating Center (DMCC). Aliquots of blinded specimens from selected cases and controls will be dispensed to each EDRN site for biomarker analysis. Analysis plan: Primary endpoint: The positive diagnostic likelihood ratio (DLR+) will be used to measure biomarker performance within values of DLR+ >= 2 or DLR- <= 0.5, a range considered clinically useful for any patients with indeterminate lung nodules. The sample size calculation targeted >80% power to test the null hypotheses that a) a positive biomarker does not alter risk across a range of specificities, and b) a negative biomarker does not alter risk across a range of sensitivities. The EDRN Data Management and Coordinating Center (DMCC) will unblind and complete analysis and report results. Exploratory endpoint: The diagnostic accuracy of combined biomarkers will be calculated using a logistic regression model with flexible functional forms.

Results and Discussion: More than 300 subjects were enrolled into the LTP2 cohort including a sufficient number of cases and controls (cohort size n>300) to reach power according to calculated estimates. Chest CT images were collected and are in the process of transfer to a central database. Plasma specimens have been distributed to test sites. RNA and DNA extraction from NBC and AEC is in process and based on results thus far the specimen quality and quantity is more than sufficient from the number of subjects needed to reach power for the primary endpoint and to conduct the planned exploratory analyses.

POPULATION SCIENCES: Cancer Disparities 3: Using Molecular Epidemiological Approaches to Decipher Cancer Disparities
Poster Session

#6107 Survival differences by socioeconomic status in Merkel cell carcinoma: A retrospective analysis using the National Cancer Database.
R. C. Chang, E. K. Brunsgaard, D. Reid;
Rush University Medical Center, Chicago, IL

Introduction: Merkel cell carcinoma (MCC) is a rare and aggressive skin cancer whose incidence and survival outcomes demonstrate disparities based on patients' socioeconomic status (SES). This study aims to evaluate the impact of SES on MCC diagnosis age, comorbidity burden, treatment modalities, and survival outcomes using the National Cancer Database.
Methods: We conducted a retrospective analysis of 9742 patients diagnosed with MCC from 2016 to 2020 in the United States. To assess how socioeconomic status influences outcomes, a composite score was created by adding income and education quartile assignments (1, 2, 3, 4), to create new composite SES quartiles of 2-3, 4-5, 6-7, and 8. Patients were stratified into quartiles based on their SES (lowest Q1 to highest Q4). Binomial test was performed for categorical variables and ANOVA was performed for continuous. Survival differences were examined with Cox proportional hazards models and Kaplan-Meier curves.
Results: Patients with lower SES presented with MCC at younger ages, with the average age of patients in the lowest SES Q1 being 73.8 years (95% CI 73.15-74.35) and the highest SES Q4 being 75.0 years (95% CI 74.48-75.46). Patients in SES Q1 also had higher Charson-Deyo scores, indicating more comorbidities than patients in SES Q4 (8.41% vs 5.8%, $p < 0.001$). They were also more likely to have advanced stage 4 MCC (9.67% vs 7.79%, $p < 0.01$) compared to patients in SES Q4. When treated with surgery, patients in SES Q1 were more likely to be treated with local tumor excision (14.39% vs 10.83%, $p < 0.001$) whereas patients in SES Q4 were more likely treated with Mohs surgery (5.02% vs 3.56%, $p < 0.01$). Survival probabilities for patients SES Q1 were worse at 1 year (82.99% vs 85.81%, $p<0.001$), 3 years (61.18% vs 68.49%, $p < 0.001$) and 5 years (45.99% vs 55.09%, $p < 0.001$) compared to patients in SES Q4.
Conclusion: This study highlights disparities in age at diagnosis, comorbidities, treatment, and survival outcomes in MCC patients based on SES. Patients in lower SES quartiles are diagnosed younger, bear higher comorbidity burdens, and have worse rates of survival.

#6108 Investigation of breast tumor biology and microenvironment in women of African descent using a single cell multiomic approach.

A. R. Harris[1], H. Liu[2], B. Jenkins-Lord[3], T. H. Dorsey[2], F. Makokha[4], S. Sayed[5], G. Gierach[1], S. Ambs[2];
[1]National Cancer Institute, Rockville, MD, [2]National Cancer Institute, Bethesda, MD, [3]Johns Hopkins Bloomberg School of Public Health, Baltimore, MD, [4]Mount Kenya University, Thika, Kenya, [5]Aga Khan University Medical Center, Nairobi, Kenya

Women of African descent are at an increased risk of developing and dying from aggressive subtypes of breast cancer. A connection between aggressive disease and Western Sub-Saharan African ancestry has been postulated, but it remains largely unknown to what extent breast cancer in Africa is reminiscent of breast cancer in U.S. African American (AA) women who experience disproportionately high mortality rates. We performed ATAC- and RNA-sequencing on 9 human triple-negative breast cancer cell lines of U.S. origin and discovered that African ancestry influences the chromatin landscape, leading to disparate transcription factor (TF) activity and downstream gene expression patterns indicative of an aggressive tumor biology. Here, we describe an ambitious study that employs single-nucleus (sn) ATAC- and RNA-sequencing (snMultiome) of frozen breast tumors to characterize chromatin accessibility and gene expression patterns with single-cell resolution in AA (n=33), Kenyan (n=25), and European American (EA, n=24) women in relation to genetic ancestry, risk factor exposures, clinical characteristics, and 5-year survival. To achieve this, we successfully isolated intact, high-quality single nuclei from archival frozen breast tumor tissue through an optimized combination of enzymatic digestion and automated tissue homogenization. We performed snMultiome sequencing of 82 tumors using the 10x Genomics platform. Following filtering, normalization (SCT for snRNA; LSI for snATAC), peak calling (MACS2), and integration (Harmony), our dataset includes a total of 296,557 nuclei. Cancerous (163,419 nuclei) and non-cancerous (133,138 nuclei) cells were distinguished based on DNA copy number (CopyKat). Within the microenvironment, 11 major immune, epithelial, and stromal cell types were successfully annotated, exhibiting distinct patterns by population group (e.g. AA tumors showed markedly increased abundance of myeloid and T-cells, while Kenyan tumors showed increased abundance of pericytes and fibroblasts). A large number of enriched TFs within each cell type varied significantly by population group, suggesting distinct chromatin accessibility patterns related to genetic ancestry. Within cancerous cells, striking intra- and inter-tumoral heterogeneity was observed by genetic ancestry even within molecular subtype groups. Current efforts focus on in-depth molecular characterization of ancestry- and risk factor-related differences in the tumor epithelium and microenvironment and distinct signatures present in lethal disease. This project holds the potential to yield crucial insights into how ancestry or other factors may influence the etiology of different breast cancer subtypes, as well as produce clinically actionable biomarkers and therapeutic targets to enhance precision medicine within patient populations at high risk for aggressive disease.

#6109 Determinants of generalized self-efficacy and genetic knowledge among Hispanic/Latino colorectal cancer patients participating in ENLACE: A Cancer Moonshot Study.

J. Sanchez Mendez[1], J. O. Culver[1], C. N. Ricker[1], N. Gutierrez[1], S. Algaze[1], J. D. Carpten[2], H.-J. Lenz[1], M. C. Stern[1];
[1]USC - University of Southern California, Los Angeles, CA, [2]City of Hope, Duarte, CA

Background: Colorectal cancer (CRC) is the third most common cancer, and second cause of cancer death in the United States (US). Among US Hispanic/Latino/a/x (H/L) individuals, CRC represents the second and the third most common cancer and the most common cause of cancer death for men and women, respectively. Despite this, the tumor landscape, and key determinants of outcomes in CRC H/L patients are understudied.
Methods: To address this need, we launched the ENLACE study, to engage H/L CRC patients in germline and somatic sequencing and identify the optimal approaches for patient participation. Through the Center for Patient Engagement in Cancer Characterization Studies (COPECC) patients were recruited from two healthcare facilities: a safety-net hospital (Los Angeles General Medical Center, LA Gen) and the USC Norris Comprehensive Cancer Center (Norris) a university medical center. Surveys to assess demographics, acculturation, Latino values, health literacy, discrimination, health system distrust, numeracy, and generalized self-efficacy (GSE) were evaluated upon recruitment, and after return-of-results (ROR) for somatic and germline testing.
Results: After the first year of the project, a total of 100 H/L CRC patients >18 years of age were included in the ENLACE study, 89 participants completed baseline surveys (49 female, median age 53 (IQR = 16) and 21 completed questionnaires after ROR. A majority self-identified as White (61%), Mexico born (51%), catholic (74%), only spoke Spanish at home (35%) and married (49%). Higher levels of GSE were reported in patients with higher scores for numeracy ($p = 0.005$) and in males when compared to females ($p = 0.016$). This association was driven by participants from Norris (n=33) as reported by stratified analyses. In contrast, among participants from LA Gen (n=66) we observed an association with higher median values for the Mexican American acculturation scale and mainstream values and a marginally significant increase in the GSE ($p = 0.072$ & 0.083, respectively). Additionally, LA Gen participants with a greater than the median score for GSE had a marginally significant higher mean score in the KnowGene scale ($p = 0.056$) with a reduction in the number of times the “Don’t Know” option was selected ($p = 0.045$). No statistically significant difference in the generalized self-efficacy score and KnowGene scale were reported after reception of results ($p = 0.2386$ & 0.1337, respectively)
Conclusion: We report differences in GSE and cancer genetic knowledge amongst CRC H/L patients in the ENLACE study that may inform understanding of disparities and social determinants in the populations treated at two different healthcare facilities.

#6110 Computational exploration of genomic differences in Black patients treated with chemoradiation for head and neck squamous cell carcinoma (HNSCC).

C. C. Lattimore, C. J. Washington, D. Braithwaite, S. D. Karanth, K. M. Fredenburg;
University of Florida, Gainesville, FL

Background: Black patients treated with chemoradiation for head and neck squamous cell carcinoma (HNSCC) experience significantly worse survival outcomes than White patients treated with the same modality. Our group aims to explore potential sociodemographic and biological factors undermining this differing response to therapy. Here, we present our computational findings of genomic differences in Black compared with White HNSCC patients receiving chemoradiation.

Methods: We obtained gene expression, phenotype, and clinical datasets for the Cancer Genome Atlas (TCGA) HNSCC cohort from the UCSC Xena web browser. Of the 528 HNSCC patients, 131 (Black=13, White=118) of those receiving chemoradiation had gene expression, phenotype, and clinical data available. Our analysis included anatomic sites involving the oral cavity, hypopharynx, and larynx, and excluded the oropharynx. We performed differential gene expression analysis in Black compared with White (reference population) patients via edgeR in R studio (-log2FC < -1 or log2FC >1; p value < 0.05; FDR < 0.05). The Database for Annotation, Visualization, and Integrated Discovery (DAVID) webtool was used to identify significantly enriched molecular processes and pathways.

Results: 462 genes were found to be significantly differentially expressed between Black and White HNSCC patients receiving chemoradiation. Of these genes, 198 were found to be higher in Black patients, and the most significant included *JPH3, PCSK1N, DCUN1D5, CRYGS*, and *CCL7* ($p < 0.005$, FDR < 0.005). 264 were found to be lower in Black patients, with the most significant being *KBTBD12*, *CMYA5*, *NEFH*, *LDB3*, *PYGM* ($p < 0.005$, FDR < 0.005). Genes found to be higher in Black patients showed enrichment for processes such as EGFR tyrosine kinase inhibitor resistance ($p < 0.005$), drug metabolism ($p < 0.005$), and chemical carcinogenesis ($p < 0.005$). Genes found to be lower in Black patients showed enrichment for muscle-related processes such as myogenesis ($p < 0.005$), actin-binding ($p < 0.005$), muscle protein ($p < 0.005$), and hypertrophic cardiomyopathy ($p < 0.005$).

Conclusion: In conclusion, using TCGA, we identified differentially expressed genes between Black and White HNSCC patients receiving chemoradiation. Moreover, these findings suggest that biological processes may differ in Black compared with White patients receiving chemoradiation, and this may dictate differing response to therapy. Additional studies will involve further computational analysis using other datasets for validation.

#6111 Real world incidence of ALK alterations in Hispanic NSCLC patients in Los Angeles.

R. C. Hsu, D. Poei, J. S. Thomas, J. J. Nieva;
USC - University of Southern California, Los Angeles, CA

Introduction: Race and ethnicity affect the distribution of molecular alterations seen in populations of lung cancer patients. ALK fusions occur in 4-5% of non-small cell lung cancer (NSCLC) patients overall. We characterized ALK alteration presence in NSCLC Hispanics treated at a large academic institution in Los Angeles. Methods: 607 NSCLC patients treated at Los Angeles General Medical Center (LAGMC) (n=174) and Norris Comprehensive Cancer Center (NCCC) (n=433) who received comprehensive genomic profiling (CGP) were evaluated from July 2017 to June 2023. Fisher's exact test was done to compare differences in prevalence between Hispanics and non-Hispanics. Multivariate logistic regression was performed to evaluate the role of Hispanic ethnicity controlling for site of treatment, age at initial diagnosis, sex, and smoking history. Results: Hispanics represented 23% (n=141) and 7.2% of patients (n=44) had ALK alterations (Table 1). Hispanics (12.76%, n = 18/141) were more likely to have ALK alterations than Non-Hispanics (5.58%, n = 26/466) (p=0.0083). In 18 Hispanic ALK patients, the median age was 53 years, 50% female (n=9), and 61.11% never smokers (n=11) versus a median age of 62.1 years, 46.80% female (n=66), and 53.19% never smokers (n=75) in all Hispanics (n=141). 94.44% of ALK Hispanics (n=17) were diagnosed as Stage IV versus 72.34% (n=102) in all Hispanics. Brain metastasis was seen in 61.11% (n=11) of Hispanic ALK patients versus 33.33% (n=47) in all Hispanics. Multivariate logistic regression showed Hispanic ethnicity HR 2.338 (95% CI 1.105-4.907) and age at diagnosis HR 0.9275 (95% CI 0.9025-0.9519) were significant variables in ALK alteration incidence. Conclusions: Hispanics represented 23% of the NSCLC population tested for CGP but 41% of the ALK altered patients. This highlights the need to study Hispanic ethnicity in the biology of ALK alterations, ensure Hispanics have equal access to CGP, and greater Hispanic representation in ALK inhibitor clinical trials.

Clinical Characteristics of NSCLC patients at LAGMC and NCCC receiving CGP

	Hispanic	**Asian**	**Non-Hispanic Black**	**Non-Hispanic White**	**Other/Unknown**	**Total**
Number of ALK alterations (%)	18 (12.76%)	9 (4.41%)	0 (0.00%)	15 (8.24%)	2 (4.44%)	44 (7.2%)
Total Population	141	204	35	182	45	607
Median Age of Diagnosis						
ALK population	53	52	-	55	51.5	53
Total population	62.1	66.1	63.6	68.4	65.6	65.7
Sex						
Females in ALK population (%)	9 (50.00%)	5 (55.56%)	-	8 (53.33%)	1 (50.00%)	23 (52.27%)
Females in total population (%)	66 (46.80%)	105 (51.47%)	14 (40.00%)	89 (48.90%)	20 (44.44%)	294 (48.43%)
Smoking History						
Never smoker in ALK population (%)	11 (61.11%)	7 (77.78%)	-	10 (66.67%)	1 (50.00%)	29 (65.90%)
Never smoker in total population (%)	75 (53.19%)	122 (59.80%)	8 (22.86%)	55 (30.22%)	18 (40.00%)	278 (45.80%)
Histology						
Adenocarcinoma in ALK population (%)	17 (94.44%)	7 (77.78%)	-	14 (93.33%)	0 (0.00%)	38 (86.36%)
	114 (80.85%)	161 (78.92%)	25 (71.43%)	121 (66.48%)	30 (66.67%)	451 (74.30%)
Stage						
Stage IV at diagnosis in ALK population (%)	17 (94.44%)	7 (77.78%)	-	13 (86.67%)	2 (100.00%)	39 (88.64%)
Stage IV at diagnosis in total population (%)	102 (72.34%)	113 (55.39%)	16 (45.71%)	95 (52.20%)	22 (48.89%)	348 (57.33%)
Brain Metastasis						
Brain metastasis in ALK population (%)	11 (61.11%)	2 (22.22%)	-	8 (53.33%)	2 (100.00%)	23 (52.28%)
Brain metastasis in total population (%)	47 (33.33%)	57 (27.94%)	10 (28.57%)	38 (20.88%)	6 (13.33%)	158 (26.0%)

#6112 Uncovering clinicopathological factors contributing to racial inequities in pancreatic cancer in Hampton Roads, Virginia.

F. W. Chaudhry, Z. L. Kolkey, A. E. Hannah, R. A. Hoefer, A. Tang;
Eastern Virginia Medical School, Norfolk, VA

Introduction: Pancreatic Ductal Adenocarcinoma (PDAC) is the 3rd leading cause of cancer-related deaths, with 12% surviving 5 years post-diagnosis. The delayed symptom onset, lack of effective screening, and advanced presentation render most patients ineligible for surgery. For inoperable PDAC, treatment offers only palliative support, resulting in a 1-year median survival, in contrast to 3 years for operable cases. Black patients face a 30-70% higher PDAC mortality rate than other racial groups in the United States. In Hampton Roads, Virginia, from 2015-2019, the black PDAC population had a mortality rate of 17.3%, notably surpassing the 10.8% rate among white PDAC patients. Consequently, this project aims to address the disparate disease burden of PDAC in the black Hampton Roads community.

Methods: Chart review of 427 inoperable PDAC patients from the Sentara Cancer Network and Virginia Oncology Associates was conducted. Age at diagnosis, treatment date, treatment type, and death date of the black and white inoperable cohorts were extracted. Average length of disease, age of onset, and time from diagnosis to treatment were calculated. KM survival analysis compared the cohorts' survival rates.

Results: From 2008 to 2016, the white cohort had shorter survival rates than the black cohort. The black population averaged a disease length of 249 days, while the white population faced 190 days. The average age at diagnosis was 67 in the black cohort and 70 in the white cohort. 42.1% of white PDAC patients did not receive treatment, while 29.9% of black PDAC patients went untreated.

Discussion: While the black population faces higher mortality, the white PDAC inoperable cohort had shorter disease duration and lower survival. A higher number of white patients also did not receive therapy, likely due to their older age, leading to added comorbidities and advanced stages of disease. Elder patients often decline treatment due to its limited impact on lifespan and quality of life. Further, the longer survival found in black patients may paradoxically contribute to a high mortality rate in Black patients. 21% of the black cohort survived over a year, prompting questions about their classification as inoperable and their access to the only curative treatment. This discovery motivates examination of the decisions behind labeling these patients as inoperable. The ongoing investigation into factors, such as stage at diagnosis and standard of care adherence, strives to continue to uncover the reasons for the high mortality rate in the Black PDAC Hampton Roads population.

#6113 Racial disparity in HER2-positive breast cancer: A single cancer center registry review.

A. Hodges[1], C. Rosenbaum[2], C. Santana[3], P. A. Niravath[3], H. Mai[3], D. Jain[3], J. C. Chang[3], J. Xu[2], **K. Sun**[3];
[1]Houston Methodist Research Institute, Houston, TX, [2]Houston Methodist Center for Health Data Science & Analytics, Houston, TX, [3]Houston Methodist Neal Cancer Center, Houston, TX

Background: Racial disparity outcomes in HER2-positive breast cancer have been previously described but the literature is limited. We examined data from our cancer center registry to investigate racial disparity in HER2-positive breast cancer.
Method: We retrospectively queried patients diagnosed with HER2-positive breast cancer from Houston Methodist Cancer Center registry from 2016 to 2022. Patients' demographics, cancer staging, treatment and outcomes including recurrence and survival were recorded and analyzed. We used the distressed communities index (DCI), a composite metric of multiple socioeconomic factors based on the patient's zip code at diagnosis, as a surrogate of socioeconomic status. Multivariable logistic regression and Cox proportional hazards analysis were used. A p value <0.05 is considered statistically significant.
Results: From 2016 to 2022, 992 patients were retrieved. 58.4% (579/992) patients were White, 17.3% (172/992) black, 16.2% (161/992) Hispanic and 8.1% (80/992) Asian. Although Black and Hispanic patients lived in more distressed communities, Black and Asian patients were diagnosed with more advanced disease. There were no statistically significant differences in neoadjuvant treatment received and pathologic complete response (pCR) rate among racial groups (table 1). Patients with higher stages are more likely to receive neoadjuvant treatment (OR: 5.49 [CI: 3.61-8.49] and 5.59 [CI: 3.15-10.2] for Stage 2 and 3 respectively). ER-HER2+ subtype was the only predictor of achieving pCR (OR: 0.47, CI: 0.29-0.79). Younger age, receiving neoadjuvant treatment and earlier stages were associated with improved all-cause mortality. There were no differences in receiving neoadjuvant treatment between racial groups, DCI; race and DCI are not associated with pCR or all-cause mortality.
Conclusion: Our retrospective study from a single institution revealed no significant racial disparities in the treatment and outcome of HER2-positive breast cancers.

Table 1 Characteristics of HER2-positive breast cancer in different racial groups

Variables	**Asian**, N = 80	**Black**, N = 172	**Spanish**, N = 161	**White**, N = 579	**p-value**
Age (at diagnosis), mean (SD)	54 (13)	54 (12)	53 (13)	57 (13)	<0.001
Distressed communities index, mean (SD)	28 (28)	49 (31)	49 (31)	35 (29)	<0.001
HER2 subtype					0.7
ER-HER2+	33/80 (41%)	64/169 (38%)	55/161 (34%)	204/576 (35%)	
ER+HER2+	47/80 (59%)	105/169 (62%)	106/161 (66%)	372/576 (65%)	
Cancer stage					0.010
0	4/80 (5.0%)	4/172 (2.3%)	8/161 (5.0%)	31/579 (5.4%)	
1	34/80 (43%)	51/172 (30%)	52/161 (32%)	227/579 (39%)	
2	14/80 (18%)	44/172 (26%)	49/161 (30%)	172/579 (30%)	
3	12/80 (15%)	30/172 (17%)	23/161 (14%)	52/579 (9.0%)	
4	13/80 (16%)	30/172 (17%)	16/161 (9.9%)	63/579 (11%)	
Unknown	3/80 (3.8%)	13/172 (7.6%)	13/161 (8.1%)	34/579 (5.9%)	
Received neoadjuvant					0.074
No	31/66 (47%)	68/136 (50%)	54/134 (40%)	263/497 (53%)	
Yes	35/66 (53%)	68/136 (50%)	80/134 (60%)	234/497 (47%)	
Complete pathological response					0.9
No	17/35 (49%)	34/70 (49%)	40/75 (53%)	111/230 (48%)	
Yes	18/35 (51%)	36/70 (51%)	35/75 (47%)	119/230 (52%)	
Mortality (all cause)					0.052
Alive	76/80 (95%)	150/172 (87%)	147/161 (91%)	540/579 (93%)	
Dead	4/80 (5.0%)	22/172 (13%)	14/161 (8.7%)	39/579 (6.7%)	

#6114 Trends in hematological cancer subtype mortality by educational attainment and sex in the United States, 2000-2020.

E. C. Marlow, F. Islami, A. Jemal;
American Cancer Society, Atlanta, GA

Objective: To examine mortality trends for hematological cancer subtypes (leukemia, Hodgkin's lymphoma, non-Hodgkin's lymphoma, and myeloma) by educational attainment and sex in the United States.
Methods: Using data on 1,082,234 U.S. deaths from 2000-2020, age-standardized death rates were calculated by sex and educational attainment (high school/GED or less, some college, and 4 years of college or more). Annual percentage change (APC) and 95% confidence intervals (CI) for mortality rates were generated using Joinpoint regression.
Results: For all hematological cancer subtypes, mortality rates were largest among males and those with the least education for all study years. In general, decreasing trends were observed in recent years for non-Hodgkin's lymphoma, myeloma, and leukemia mortality rates. Non-Hodgkin's lymphoma mortality rates, for example, decreased among males and females in 2009-2020 (APC: -2.0%; 95%CI: -2.4%, -1.5% and APC: -2.8%; 95%CI -3.2%, -2.3%). As another example, non-Hodgkin's lymphoma mortality rates among most educated males decreased in 2000-2012 (APC: -1.8%; 95%CI: -2.2%, -1.3%) followed by a steeper decline in 2012-2020 (APC: -3.7%; 95%CI: -4.4%, -2.9%); a similar pattern was observed among most educated females (APC: -1.6%; 95%CI: -2.2%, -1.0% in 2000-2011 and APC: -4.1%; 95%CI: -4.9%, -3.4% in 2011-2020). Trends in Hodgkin's lymphoma death rates however differed by educational attainment. For example, mortality rates among least educated males increased in 2000-2009 (APC: 1.7%; 95%CI: 0.8%, 2.5%) and remained unchanged in 2009-2020 (APC: -0.3%; 95%CI: -0.9%, 0.3%). Rates among least educated females also increased in 2000-2020 (APC: 0.4%; 95%CI: 0.1%, 0.7%). In contrast, mortality rates declined for most educated males from 2010-2020 (APC: -1.9%; 95%CI: -2.6%, -1.2%) and most educated females from 2011-2020 (APC: -3.5%; 95%CI: -4.8%, -2.2%).
Conclusion: Hematological cancer mortality rates were highest among males and those with least education. In general, mortality rates have declined in recent years for non-Hodgkin's lymphoma, myeloma, and leukemia for males and females among all educational attainment groups, while Hodgkin's lymphoma has shown a slight increasing trend among least educated males and females.

#6115 Genetic ancestry specific meQTLs control immune function regulation in a breast cancer cohort of African and European patients.

K. Founta[1], N. Chambwe[2];
[1]Zucker School of Med. at Hofstra/Northwell, Hempstead, NY, [2]The Feinstein Institutes for Medical Research, Manhasset, NY

Black women with significant African ancestry experience a disproportionately higher incidence of the most aggressive and invasive breast cancer subtypes, along with worse clinical outcomes across all demographic groups within the United States. These health disparities arise from complex interactions between genetic, sociocultural, and environmental factors. Epigenetic mechanisms, such as DNA methylation (DNAm), which regulate gene expression have been proposed as a means to capture the molecular impact of adverse environments on tumor biology. While DNAm levels can be influenced by environmental stimuli, they are also regulated by individual genotypes at methylation quantitative trait loci (meQTLs), posing a challenge to modeling the impact of the environment on cancer molecular characteristics. We hypothesized that ancestry differential DNAm in breast cancer is a result of differential genotype frequencies of SNPs due to ancestry at meQTL loci that can result in phenotypic differences between breast cancer patients of African and European ancestry through differential gene expression regulation. To investigate this hypothesis, we leveraged multi-omic data from The Cancer Genome Atlas (TCGA) breast cancer cohort to perform integrative analysis in patients of European and African ancestry (n=578). 804 CpGs were significantly differentially methylated between European and African ancestry breast cancer patients. meQTL analysis at these sites identified 37 cis-meQTLs and 748 trans-meQTLs, regulating methylation at CpG sites enriched in CpG Islands, enhancers, and other open chromatin regions. 54% of the cis- and 69% of the trans-meQTLs show evidence of differential genotype frequencies by ancestry. Association analysis between methylation and local gene expression revealed that 683 of the 804 ancestry differentially methylated sites regulate the expression of 5,774 genes. We found a statistically significant enrichment for genes involved in immune-related functions such as MHC class II protein complex assembly and the regulation of leukocyte cell-cell adhesion. Intriguingly, 10.5% of these genes encode transcription factors (TFs), and out of these ~23% are linked to African-ancestry specific open chromatin regions in breast cancer cell lines derived from African-ancestry donors. Our findings show that ancestry specific DNAm differences display strong genetic associations via ancestry associated meQTLs, affecting fundamental immunological processes in breast cancer. Our findings suggest that the effects of ancestry-specific genetic regulation may be more profound than previously appreciated, while pointing to the potential for confounding due to genetic ancestry when using DNA methylation as a molecular readout of environmental exposures.

#6116 Rs2363956, a coding variant of ANKLE1, drives triple-negative breast cancer disparity by altering DNA damage response.

Y. Guerra[1], R. Martini[1], O. Elemento[1], M. B. Davis[2];

[1]Weill Cornell Medicine, New York, NY, [2]Morehouse School of Medicine, Atlanta, GA

African American women have a 42% higher breast cancer mortality rate than European American women and are over twice as likely to develop triple-negative breast cancer (TNBC). We have previously demonstrated that this higher incidence of TNBC is tied to ancestry-related biological determinants of TNBC tumor biology, including possible novel genetic drivers that may result in reduced treatment efficacy.

Within the TCGA BRCA cohort, we have previously found that high ANKLE1 gene expression significantly improves survival in European Americans but not in African Americans. This difference may be attributed to the presence of a polymorphic variant of ANKLE1, rs2363956. The minor G allele of rs2363956 leads to a structural alteration in ANKLE1, potentially changing its functionality. Interestingly, among our International Center for the Study of Breast Cancer Subtypes (ICSBCS) patient cohort, we observed that 41-53% of European Americans with TNBC were homozygous for the G allele as compared to only ~14% of African American patients. These observations suggest that the presence of the rs2363956 polymorphic variant may drive differences between European American and African American patients.

ANKLE1 is a conserved gene among eukaryotic organisms and has been reported as an endonuclease implicated in DNA damage repair. Among our patient cohort (n=62) we have observed that patients homozygous for the G allele (n=13) are enriched for COSMIC mutational signatures 2 and 13 ($P \leq .05$ and $P \leq .001$, respectively), that denote overactivity of APOBEC deaminases, as compared to patients homozygous for the T allele (n=19). Therefore, the increased mutational burden present in those patients caused by APOBEC overactivity may sensitize those cancer cells to chemotherapeutics or other therapies.

Alternatively, the patients homozygous for the T allele may have an increased capacity for DNA damage repair that does not involve APOBEC activity. Using the MDA-MB-231 cell line, which is homozygous for the T allele, we performed an ANKLE1 knockdown with siRNA in order to examine the impact of ANKLE1 loss on DNA damage repair. Upon treatment with 25 µM, 10 µM, and 5 µM of Cisplatin we observe increased γ-H2AX and cell shrinkage in the ANKLE1 knockdowns as compared to cells treated with control siRNA, denoting increased DNA damage and apoptosis. Additionally, after knocking down ANKLE1 we observed decreased proliferation.

Based on these observations, ANKLE1 is critical for DNA damage response in TNBC cells and may be implicated in the genomic stability of TNBC. The polymorphic variants observed may impact this function and in part explain why European American patients have improved survival, as compared to African American patients.

#6117 Characterizing cancer patterns in Okinawan vs. mainland Japanese Americans: The Multiethnic Cohort.

S. A. Streicher[1], S.-Y. Park[1], C. W. K. Chiang[2], X. Sheng[2], D. Bogumil[2], D. V. Conti[2], C. A. Haiman[2], L. R. Wilkens[1], L. Le Marchand[1];
[1]University of Hawai'i Cancer Center, Honolulu, HI, [2]University of Southern California, Los Angeles, CA

Differences in chronic disease rates have been documented in Japan between Okinawa and mainland Japan. Limited data exist on whether these differences are also present in Okinawans and mainland Japanese who have migrated to the US. We used genotyped genome-wide association study data from the Multiethnic Cohort Study (MEC) to identify Japanese Americans of Okinawan or mainland ancestral similarity, and to investigate these two groups for differences in baseline chronic disease risk factors and for incidence of the four most common cancers during follow-up after blood draw. Cancer cases were identified via linkage to state cancer registries. Principal component analysis followed by uniform manifold approximation and projection (UMAP) was run using 15,678 single nucleotide polymorphisms among the 24,484 MEC Japanese Americans with blood samples. The Okinawan cluster was confirmed by labeling male MEC participants with Okinawan surnames on UMAP plots. Hazard ratios (HR), 95% confidence intervals (CI), and two-sided p-values were reported for Cox proportional hazards models, comparing cancer incidence between Okinawan and mainland Japanese individuals. The Okinawan cluster included 3,649 individuals (15% of the MEC Japanese Americans) and the mainland Japanese cluster included 19,611 individuals (80% of the MEC Japanese Americans). Small clusters of part-Okinawan and/or part-mainland Japanese (5% of the MEC Japanese Americans) were not included in the analysis. Ninety-six percent of Okinawan Americans and 94% of mainland Japanese Americans in MEC were born in the US. Okinawans were more likely to have a higher body mass index and daily alcohol intake, and less likely to be a current or former smoker, compared to mainland Japanese (all p-values<0.05). Post-menopausal Okinawan women were significantly more likely to be diagnosed with breast cancer (age-adjusted HR=1.39, 95% CI=1.10-1.75) compared to post-menopausal mainland Japanese women. This association was not modified by adjusting for additional known breast cancer risk factors (HR=1.36, 95% CI=1.07-1.73). Okinawans were also less likely to be diagnosed with lung cancer (HR=0.75, 95% CI=0.58-0.98); however, this association was no longer significant when adjusting for known risk factors, including smoking history (HR=0.82, 95% CI=0.62-1.07). There were no significant differences in risk of colorectal or prostate cancer between Okinawan and mainland Japanese individuals. Our results in this US-based sample are consistent with recent trends of higher breast cancer and lower lung cancer age-adjusted incidence rates reported from Japan for the Okinawan prefecture compared to mainland prefectures. Investigating reasons for the observed breast cancer risk difference may identify new risk factors for this disease in the Okinawan and other populations.

#6118 Sex-related disparity in immune checkpoint inhibitor benefit for patients with esophageal squamous cell carcinoma: A systematic review and meta-analysis.

C. Zhang, P. Wu, J. Liu, D. Li, N. Sun, J. He;
National Cancer Center/National Clinical Research Center for Cancer/Cancer Hospital, Chinese Academy of Medical Sciences and Peking Union Medical College, Beijing, China

Sex-related dimorphism in cancer incidence and immune response is widely recognized, yet the impact of an individual's sex on the effectiveness of Immune Checkpoint Inhibitors (ICIs) for patients with advanced esophageal squamous cell carcinoma (ESCC) remains poorly understood. In this study, we conducted a comprehensive meta-analysis to evaluate the heterogeneity of ICIs in patients with advanced ESCC. We collected studies from PubMed, MEDLINE, Embase, and Scopus, spanning from the inception of the databases to September 30, 2023. These studies focused on phase III randomized trials comparing first-line ICIs (PD-1/PD-L1) plus chemotherapy with chemotherapy alone for advanced or metastatic ESCC. Additionally, we reviewed abstracts and presentations from AACR, ASCO, ESMO, and WCLC. Inclusion criteria mandated the reporting of overall survival (OS) data stratified by sex and nonselective baseline PD-L1 expression. The study adhered to Preferred Reporting Items for Systematic Reviews and Meta-analyses (PRISMA) guidelines. The analysis included 6 randomized clinical trials comprising 3603 ESCC patients, of whom 3090 (85.8%) were male and 513 (14.2%) were female. A significant OS benefit was observed for ICIs plus chemotherapy in all patients (HR, 0.68; 95% CI, 0.62-0.74; P < 0.001). Similarly, ICIs plus chemotherapy correlated with a significantly prolonged OS in males (HR, 0.67; 95% CI, 0.61-0.74, P < 0.001). However, there was no significant OS benefit observed in females with ICIs plus chemotherapy (HR, 0.79; 95% CI, 0.58-1.09; P = 0.148). Females had a tendency toward less benefit than males (pooled HR, 1.18; 95% CI, 0.89-1.57; P = 0.245). Our findings suggest that there is no statistically significant association between patient sex and the efficacy of ICIs for ESCC patients. Importantly, we report, for the first time, a lack of survival benefit with the ICI plus chemotherapy regimen in the first-line setting compared to chemotherapy alone in female ESCC patients.

#6119 Association of genetic African ancestry and triple-negative breast cancer risk: Findings from the African-ancestry breast cancer genetics consortium.

G. Jia[1], L. Liu[1], J. R. Palmer[2], C. A. Haiman[3], W. Zheng[1];

[1]Division of Epidemiology, Department of Medicine, Vanderbilt Epidemiology Center, Vanderbilt-Ingram Cancer Center, Vanderbilt University Medical Center, Nashville, TN, [2]Slone Epidemiology Center at Boston University, Boston, MA, [3]Department of Preventive Medicine, Keck School of Medicine, University of Southern California, Los Angeles, CA

Triple-negative breast cancer (TNBC) is an aggressive breast cancer subtype that lacks target treatments. It has been reported that African-American women have a higher incidence of TNBC and are diagnosed at an earlier age than women of European ancestry. This disparity may be attributed to both genetic and non-genetic risk factors that are associated with the African ancestry. In this study, we investigated whether genotype-derived African ancestry might be related to an elevated risk of TNBC, with adjustments for several known genetic and non-genetic risk factors. Included in the study are self-reported Black breast cancer patients diagnosed with TNBC (n =2,292) or estrogen receptor (ER)-positive cancer (n =7,863) and 9,324 controls included in the African-ancestry Breast Cancer Genetics (AABCG) Consortium. We estimated the global ancestry by Admixture and the local ancestry by FLARE, using reference of the European- and African-ancestry samples from the 1000 Genome Project. Odds ratios (OR) and 95% confidence interval (CI) per ten percent increase of the global African ancestry proportion were estimated using logistic regressions comparing TNBC with controls (case-control analyses) or with ER-positive cases (case-case analyses), adjusted for age. Similar analyses were conducted for the local African ancestry proportion at each of the 12 genomic regions that were identified in AABCG in relation to TNBC risk. Results for each participating study were meta-analyzed using fixed or random effect models. We further adjusted for non-genetic risk factors including body mass index (BMI), number of live births, breastfeeding, and menopausal status. A polygenic risk score (PRS) was constructed using 13 independent risk variants at the 12 TNBC risk loci. The PRS was additionally adjusted to investigate whether these risk variants mediated the association of African ancestry with TNBC risk. No significant association was observed between TNBC risk and global African ancestry proportion (OR: 1.03, 95% CI: 0.98-1.08) in case-control comparisons. Compared with ER-positive cases, however, TNBC cases had a higher global African ancestry, resulted in an OR of 1.09 (95% CI: 1.04, 1.13, P =5.35×10^{-5}). A similar association was observed with additional adjustment for non-genetic risk factors, with an OR of 1.08 (95% CI: 1.03, 1.12, P =0.003). Similar patterns were also found for local ancestry proportion at six of the 12 TNBC risk loci (P <0.05). Further adjustment for the PRS attenuated the association between global ancestry and a TNBC diagnosis in case-case comparisons (OR: 1.05, 95% CI: 1.01, 1.10, P =0.013). Our study suggests that women with a higher African ancestry are more likely to be diagnosed with a TNBC than ER-positive breast cancer and genetic factors identified to date partially explain this association.

#6120 Genomic profiling of *KRAS* and *EGFR*-altered non-squamous non-small cell lung cancer reveal ancestry-specific co-alterations with therapeutic implications.

S. D. Sisoudiya[1], A. A. Houle[2], T. M. Fernando[2], T. R. Wilson[2], J. L. Schutzman[2], J. K. Lee[1], A. B. Schrock[1], E. S. Sokol[1], S. Sivakumar[1], Z. Shi[2], G. Pathria[2]; [1]Foundation Medicine, Inc., Cambridge, MA, [2]Genentech, Inc., South San Francisco, CA

Background: Racial and ethnic disparities are highly prevalent in cancer care and impact treatment outcomes, with an underrepresentation of minority populations in clinical studies. The impact of genetic ancestry on the genomic landscape of tumors remains understudied. To address this, we sought to comprehensively characterize the ancestry-based genomic co-alteration landscape and immunotherapy-related biomarkers in *KRAS* and *EGFR*-altered tumors, two major driver populations in non-squamous non-small cell lung cancer (non-Sq NSCLC).

Methods: Our study consisted of 68,197 adult patients with non-Sq NSCLC who underwent comprehensive genomic profiling using FoundationOne® or FoundationOne®CDx during routine clinical care in the United States. Genetic ancestry was inferred using a SNP-based approach. Tumor mutational burden (TMB) was calculated across 0.8-1.2 megabases. PD-L1 expression was determined by immunohistochemistry using the Dako 22C3 PD-L1 antibody.

Results: Overall, 81% of the patients were of European (EUR; n= 55,430), 10% of African (AFR; n=7,062), 5% of East Asian (EAS; n=3,297), 3% of Admixed American (AMR; n=2,011) and less than 1% of South Asian ancestry (SAS; n=497). *KRAS* was the most frequently altered oncogene in EUR (39%) and AFR (33%), whereas *EGFR* was most frequently altered in EAS (53%), SAS (36%), and AMR (30%) ancestry groups. While *STK11* and *KEAP1* alterations co-occurred with *KRAS* across all ancestry groups, they were significantly (FDR p <= 0.05) less frequent in EAS (16%) and AMR (15%) compared to EUR (28%). Additional ancestry-specific co-alteration patterns in *KRAS*-altered tumors included co-occurrence with *GNAS* alterations in AMR (Odds ratio, OR: 3.5, $p < 10^{-5}$), co-occurrence with *ARID1A* alterations in SAS (OR: 4.7, p = 0.02), and mutual exclusivity with *NF1* alterations in EUR (OR: 0.4, $p < 10^{-5}$) and AFR (OR: 0.4, $p < 10^{-5}$). In contrast, *EGFR*-altered tumors had a more conserved co-alteration landscape across all ancestry groups. Despite the known mutual exclusivity of *KRAS* and *EGFR* alterations, 13% of patients of EAS ancestry (compared to 2-4% of other ancestry groups) with *KRAS* alterations had co-occurring *EGFR* alterations; notably, a majority of these patients had an amplification in *KRAS* and/or *EGFR*, potentially representing treatment resistance mechanisms. Among immunotherapy-associated biomarkers, PD-L1 expression was similar across ancestries. Of note, patients of AFR ancestry with *KRAS* or *EGFR* alterations had higher TMB and the SAS ancestry group had the lowest TMB.

Conclusion: Our study provides a comprehensive landscape of ancestry-specific patterns in *KRAS* and *EGFR*-altered non-Sq NSCLC. These findings can help better understand cancer disparities, aid in the development of new therapeutic strategies and inform more inclusive clinical trials and treatment decisions.

#6121 Racial differences in the intratumoral immune cell infiltrate in luminal breast cancer.

N. Hippalgaonkar[1], G. Chlipala[1], D. Huo[2], G. Rauscher[1], N. Adler[1], J. Kitajewski[1], K. Hoskins[1];
[1]University of Illinois at Chicago, Chicago, IL, [2]University of Chicago, Chicago, IL

Background: Black women have a higher rate of breast cancer mortality compared with their non-Hispanic White (NHW) counterparts, with an 80% higher likelihood of breast cancer death from axillary node-negative, ER-positive (a.k.a. luminal) tumors (Hoskins et al, JAMA Oncol 2021). Black women are 30% more likely to have ER-positive tumors with a high-risk gene expression profile, indicating a role for tumor biology in this disparity (Hoskins et al, JAMA Oncol 2023). The underlying biological mechanisms responsible are unknown. The aim of this study was to investigate the immune cell infiltrate in ER-positive breast tumors as a potential driver of disproportionately aggressive luminal tumor biology among Black women.

Methods: Gene expression data from ER-positive tumors diagnosed in women identified as Black or NHW in The Cancer Genome Atlas (TCGA) were deconvoluted with the CIBERSORT tool to estimate the relative intratumoral proportion of 22 immune cell types within each tumor. Differential analysis of imputed immune cell fractions comparing race was conducted with the Mann-Whitney test. P-values were adjusted for multiple comparisons with the false discovery rate (FDR) method. Linear regression of previously reported ancestry estimates for breast cancer patients in TCGA (Huo, et al, JAMA Oncol 2017) was used to test for association between African ancestry and proportion of regulatory T cells (Tregs) in tumors from Black women.

Results: CIBERSORT analysis of tumors found a significantly increased proportion of Tregs in tumors from Black (n=86) than NHW (n=534) patients, with $\log_2$ fold-change= 0.74 (FDR-corrected p-value= 0.01). Plasma cells, T follicular helper cells and M_0 macrophages were increased in tumors from Black women with uncorrected p-values < 0.05, but racial differences in these cell types were not significant after FDR correction (p >0.1). Ancestry analysis among Black women indicated that African ancestry was not associated with the intratumoral proportion of Tregs (1 SD change in proportion African ancestry was associated with 0.06 standard deviation increase in Tregs, p > 0.3). Confirmation of findings with a racially diverse breast tumor TMA from an independent cohort is ongoing and results will be presented.

Conclusions: Increased pro-tumorigenic Treg infiltrate in ER-positive breast tumors from Black women may contribute to a disproportionately aggressive tumor phenotype and racial survival disparity. The findings could have therapeutic implications and suggest that immune checkpoint inhibitors may have increased activity against luminal breast cancer in Black patients. Although this study did not show a statistically significant effect for genetic admixture within African Americans, larger studies are needed to distinguish the contribution of ancestry vs. social context, environmental, and behavioral factors as the driver of this racial difference in tumor biology.

#6122 Disparities in biomarker testing practices in patients with metastatic non-small cell lung cancer (NSCLC) in the United States (US).

M. J. Dennis[1], D. Abrahami[2], M. Vieira[2], D. Benjumea[3], M. Boyd[3], A. Shao[3], K. Duncan[2], J. Kelton[2], **S. P. Patel**[4];
[1]Dana-Farber Cancer Institute, Boston, MA, [2]Pfizer, Inc., New York, NY, [3]Genesis Research Group, Hoboken, NJ, [4]University of California - San Diego, San Diego, CA

Background: Molecular testing is recommended in National Comprehensive Cancer Network guidelines for nonsquamous mNSCLC patients. While testing rates have been increasing, data from other tumor types suggest possible disparities in access to and use of biomarker testing. This study investigated real-world biomarker testing characteristics stratified by demographics for the EGFR, ALK, ROS-1, BRAF, MET, RET, and PD-L1 biomarkers in US patients diagnosed with mNSCLC.
Methods: This study of adults ≥18 years old with stage IV mNSCLC used the nationwide Flatiron Health electronic health record (EHR)-derived de-identified database (01/2011-04/2023). Biomarker testing rate (i.e., proportion of patients with mNSCLC with at least one biomarker test) was quantified. Unadjusted biomarker testing rates were assessed in groups of patients stratified by demographic and clinical characteristics, including age group, sex, race, insurance type, Eastern Cooperative Oncology Group (ECOG) performance status (PS), smoking status, histology, and US region.
Results: In 42,037 patients with mNSCLC, 34,510 (82.1%) received at least one test. The rates for each test were: ALK: 71.6%, BRAF: 48.8%, EGFR: 74.9%, MET: 41.4%, PD-L1: 49.3%, RET: 42.3%, and ROS1: 54.2%. Yearly testing rates increased, with the most recent year suggesting that anywhere from 78.7% of patients to 88.7% of patients received a test for at least one biomarker, with PD-L1 and EGFR being the least and most frequently tested, respectively. Rates of testing varied by age group, with 87.2% of younger patients (ages 18 to <50) receiving a test compared to 80.8% of older patients (ages ≥80). Asian patients had the highest testing rate (91.5%) whereas Black and Hispanic/Latino patients had the lowest (80.8% and 80.6% respectively). 82.2% of White patients, the largest racial demographic in this dataset, received at least one test. Commercial health plans had a slightly higher testing rate compared to Medicare or Medicaid (87.1%, 81.6% and 81.2%, respectively). Rates decreased as ECOG PS increased; in patients with ECOG PS=0, 89.6% received a biomarker test, whereas in patients with ECOG PS=3 and ECOG PS=4, 81.1% and 76.3% received a test, respectively. Smoking status (current or former) was associated with less testing (80.7%) compared to patients with no history of smoking (91.1%), and patients with non-squamous histology were more frequently tested (88.0%) compared to squamous histology (61.2%). The differences by sex and region were marginal.
Conclusion: This study provides contemporary data on real-world biomarker testing and disparities in mNSCLC in the US. Results suggest that more work can be done to evaluate and address disparity gaps in specific subsets, including Black and Hispanic patients and those with a current or former history of smoking.

#6123 Validating cancer modulated allostatic load as a composite biomarker for mortality in patients with cancer.

Christopher J. Fong[1], Kaicheng U[2], Cheryl Phua[1], Xuechun Bai[1], Michele Waters[1], Tom Fu[1], Kanika Arora[1], Tomin Perea-Chamblee[1], Devika Jutagir[1], Michael Berger[1], Nikolaus Schultz[1], Adam Schoenfeld[1], Francesca Gany[1], Justin Jee[1], Jian Carrot-Zhang[1]

[1]Memorial Sloan Kettering Cancer Center, New York, NY, [2]Cornell University, Ithica, NY

Allostatic load (AL) is the cumulative burden of chronic stress and life events typically measured by lab and vital values routinely collected during standard care. AL has been associated with adverse socioenvironmental stressors and increased mortality rates including risk of cancer death. Despite modifications of AL as a result of progressing cancer and anti-cancer treatments, AL may serve as a valuable biomarker for cancer outcomes, and highlight similar disparities across sociodemographic groups agnostic of a history of cancer diagnosis. Recent investigations have shown associations of AL with overall mortality rates in patients with non-small cell lung cancer (NSCLC) and breast cancer, as well as various social determinants of health. The impact of AL on different malignancies, particularly in the context of genetic variations identified through genomic profiling, is yet to be thoroughly investigated.

We identified a pan-cancer cohort of 29,433 patients sequenced with the MSK-IMPACT targeted panel sequencing assay, and collected clinical, genomic, and lab data. We first studied the association of AL with patient and tumor characteristics such as tumor type, stage, cancer genomics, comorbidities, social deprivation defined by the Yost index, and genetic ancestry. We derived AL using 10 standard biomarkers across cardiovascular, metabolic, renal, and immune systems, and created a composite AL summary score with a range between 0 and 10. Composite AL summary score into quartiles for comparisons. We found that AL was increased with higher cancer stage, older age, smoking, multiple comorbidities, African ancestry, and Yost index. Multivariate logistic regression analysis showed that AL was correlated with mutations e in KRAS and anti-correlated with EGFR mutations (FDR<0.02).

Next, we investigated AL as a biomarker for mortality in patients with cancer and compared its prognostic value to other biomarkers. Using a Cox proportional hazard model we found that AL was significantly associated with shorter overall survival, controlling for stage and socioeconomic variables (HR=1.7, 2.2, 2.7 in AL Quartiles 2-4 respectively). Finally, we decomposed AL into its individual markers to quantify the most important features driving outcomes. Using a Random Survival Forest model with a focus on NSCLC patients, we found that albumin and alkaline phosphatase were the strongest features of shorter survival in our AL composite model.

Our findings suggest that elevated AL is associated with a poorer prognosis across multiple cancer types, a trend observable across different stages of cancer. The association between AL and clinically actionable mutations highlights the importance of understanding the relationship between somatic alterations and social/environmental factors. The study underscores the utility of AL as a powerful prognostic tool that can be routinely collected in a clinical setting.

#6124 A comprehensive pan-cancer study nominating NF-κB-mediated TNFA signaling-induced hypoxia as a risk factor in Hispanic cancer progression.

T. Samanta, J. Park, B. Kaipparettu;
Baylor College of Medicine, Houston, TX

The Hispanic (HA) population is the second largest racial/ethnic group in the United States after non-Hispanic White (NHW). Though the HA population usually has a lower reported incidence of cancers compared to NHW, there are racial disparities exist in the mortality rate of some of the cancers. Factors related to the Social Determinants of Health (SDOH), such as higher poverty rates, less education, and reduced access to health care, are known to increase the risk of diagnosing advanced-stage cancer in HA compared to the NHW population. The contribution of such SDOH in the HA cancer population has been studied in the past years. However, the contribution of biological and genetic mechanisms to HA cancer disparity has not been well understood. Thus, in this study, we performed a comprehensive analysis of different databanks to understand the common genetic and biological factors that contribute to the pan-cancer disparity in the HA population. To identify HA and NHW populations, we used self-reported racial/ethnic information. Analysis of the "*All of Us*" database suggested a high prevalence of infection-related cancers such as Liver, Stomach, and Cervix Uteri in the HA population compared to the NHW population. SEER database also showed an increased percentage of diagnoses with infection-related cancers and poor survival of the HA population with these cancers compared to the NHW. We then analyzed the TCGA transcriptome data from primary tumors from HA and NHW patients. We only selected cancers with data from at least ten patients in each group. TCGA data confirmed that the tumors from HA cancer patients primarily express high inflammatory and immune-responsive signatures. Specifically, we found a high enrichment of NF-κB induced TNFA signaling in HA tumors. We also observed a significant correlation between TNFA and Hypoxia signature in many HA cancers. Since hypoxia is known to be associated with resistance to radiation and chemotherapy, targeting the increased hypoxia signature in HA tumors may be critical for sensitizing HA patients to cancer therapy. Overall, our pan-cancer analyses suggest an increased prevalence of many infection-related cancers in the HA population. HA tumors are enriched with TNFA, NF-κB, and hypoxic signatures. Specific targeting of these signatures may be critical in managing the HA patients who currently suffer from racial disparity in cancer incidence and survival.

#6125 Differential expression of chemokine genes by race and Breast Cancer Consensus Subtypes in hormone receptor positive breast cancer.

A. M. Fielder, M. Ratnam, G. Dyson, K. Purrington;
Wayne State University School of Medicine, Detroit, MI

Hormone receptor positive (HR+) breast cancer is a heterogeneous subtype and African American women (AAW) are twice as likely to have HR+ tumors with lower levels of HR staining (1-10%) compared to European American women (EAW). These tumors are associated with substantially worse survival compared to strongly HR+ tumors. We further hypothesized that HR+ tumors from AAW would be more likely to have molecular features typically associated with HR-negative breast cancer and poor prognosis. To test this, we used the Breast Cancer Consensus Subtyping (BCCS) method and evaluated expression of chemokine receptors known to be differentially expressed by race, PAM50 subtypes, and survival. We downloaded The Cancer Genome Atlas (TCGA) expression data for 394 female EA and AA HR+/HER2- breast cancer patients using the cBio Cancer Genomics Portal. Breast Cancer Consensus Subtypes (BCCS) were determined using the R program BCCSclassifier. BCCS classification results in five subtypes: ER-negative non-basal-like (BCS1), ER-negative basal-like (BCS2), ER+ highly proliferative with poor prognosis (BCS3), ER+ stromal infiltration with good prognosis (BCS4), and ER+ hormone response genes highly expressed with good prognosis (BCS5). High and low expression of chemokines (*ACKR1*, *ACKR4*, *CCR3*, *CCR6*, *CCRL2*, *CXCR1*, *CXCR2*, *CXCR4*, *CXCR6*, *CX3CR1*) was dichotomized based on median expression of each gene within our study cohort. Distribution of BCCS by race was assessed with multinomial logistic regression. Associations between chemokine gene expression, BCC subtype and race were evaluated using logistic regression. An alpha value of 0.05 was set to determine statistical significance. From the TCGA cohort, AAW were more likely to have the BCS2 ER-negative basal-like phenotype (OR=7.17, p<0.001) as well as the poor prognosis highly proliferative ER+ BCS3 phenotype (OR=2.83, p=0.036) versus the high hormone expression BCS5 subtype. In multivariable models evaluating both race and BCCS subtype, AAW were 6.17 times more likely to have lower than median expression of *CX3CR1* (p<0.001) and *CXCR2* (OR=2.23, p=0.0096) compared to EAW. Notably, all chemokine receptors consistently showed significantly lower expression in BCS1-4 subtypes compared to BCS5. For *CCRL2*, the effect estimates for BCS4 vs. BCS5 significantly differed by race (p=0.039). In AAW, BCS4 was associated with higher than median expression (OR=1.99, p=0.49), although not statistically significant. In EAW, BCS4 was associated with lower than median expression (0.23, p<0.001). Our findings show that AAW with HR+ breast cancer have tumors with more inherently aggressive molecular subtypes associated with poor prognosis compared to EAW. These results also further support the premise that HR+/HER2- tumors are highly heterogeneous and strongly suggest that chemokine gene expression is associated with breast cancer subtype.

#6126 Understanding disparities in lung cancer using single cell RNA sequencing data transformed by the Gerchberg Saxton algorithm.

S. Ay[1], L. Liu[1], E. Forbes[1], U. Topaloglu[2], W. Zhang[1];

[1]Wake Forest University School of Medicine, Winston Salem, NC, [2]National Cancer Institue, Rockville, MD

Purpose An overarching goal of this study is to reduce disparities in lung cancer research commonly manifested by racial and/or gender under-representations. By employing the Gerchberg-Saxton (GS) algorithm, we aim to diminish data noise/bias in single-cell RNA sequencing (scRNA-seq) gene expression data, thereby enabling more equitable research outcomes. An immediate goal is to remove extensive data bias associated with scRNA-seq data thus enhancing downstream Machine Learning analyses.

Background: We have successfully applied the GS algorithm for fairer mortality rate predictions across different racial groups [1]. In this study, we seek to apply the GS algorithm to the scRNA-seq data that interrogate the cellular landscapes of lung cancer and the tumor microenvironment.

Methodology: The application of the GS algorithm to single cell RNA data involved a series of steps. Initially, all data frames were transposed, switching columns and rows to represent gene expressions and single cells, respectively. The algorithm was then meticulously applied to each column, allowing for the uniform distribution of certain specific gene expression information across all single cells within the data frame. This column-wise application was crucial to maintain the integrity of individual cell characteristics while ensuring a fair structural distribution of gene expression data. The process aimed to balance the representation of genes across all cells, addressing inherent biases and noises in the original data structure.

Data: The study utilizes a previously unpublished scRNA-seq dataset comprising 14 lung cancer patients from Wake Forest Baptist Comprehensive Cancer Center, including 6 African American and 8 Caucasian patients.

Results: One out of 14 preliminary clustering results are presented in Figure 2 using ScanPy [2]. The initial findings are based on a restricted set of cell marker genes, which will be further developed with additional markers in subsequent analyses. With the application of the Gerchberg-Saxton algorithm, the Shannon Entropy [3] analysis revealed a more uniform randomness across gene expressions (Figure 1), and the unsupervised clustering indicated a clearer separation of cell types, significantly enhancing the ability for downstream analyses. The data transformation will be applied to the whole dataset for comparative analyses of cellular landscapes between lung cancer from different races and genders, to be reported at the AACR 2024 Annual Meeting.

Conclusions: Our preliminary studies showed that the Gerchberg-Saxton algorithm is effectiveness in normalizing data distribution for scRNA-seq data, which has led to enhanced resolution of cell type differentiations in clustering analysis. With this refined methodology, we are better poised to better address lung cancer health disparities revealed by single cell sequencing analysis.

#6127 Characterization of germline and somatic homologous recombination deficiency features in high-grade serous ovarian cancer among Black individuals.

K. Lawson-Michod[1], M. E. Barnard[2], N. Davidson[3], L. J. Collin[1], C. Johnson[4], L. A. Salas[5], C. Greene[3], J. R. Marks[6], L. Peres[7], J. M. Schildkraut[8], J. A. Doherty[1];

[1]University of Utah Huntsman Cancer Institute, Salt Lake City, UT, [2]Boston University Chobanian & Avedisian School of Medicine, Boston, MA, [3]University of Colorado Anschutz Medical Campus, Denver, CO, [4]Rollins School of Public Health, Emory University, Atlanta, GA, [5]Geisel School of Medicine at Dartmouth, Dartmouth Cancer Center, Hanover, NH, [6]Duke University School of Medicine, Durham, NC, [7]Moffitt Cancer Center, Tampa, FL, [8]Rollins School of Public Health Emory University, Atlanta, GA

Background: Approximately 50% of high-grade serous ovarian carcinomas (HGSOC) are homologous recombination deficient (HRD). HRD is associated with increased T-cell infiltration and improved survival. This study aimed to describe the distribution of HRD features and cytotoxic T-cell infiltration by gene expression subtype among Black HGSOC cases.

Methods: We included Black HGSOC cases from the African American Cancer Epidemiology Study and the North Carolina Ovarian Cancer Study. We used RNASeq data to assign gene expression subtypes (n=160), and whole exome sequencing data from matched blood and tumor formalin-fixed paraffin-embedded specimens (n=206) to characterize HRD features. We defined HRD features as (1) germline variants and somatic mutations in HRD genes, and (2) HRD-associated signatures (SBS3 and ID6) that we obtained from de novo mutational signature analysis for single-base pair substitution, insertion, and deletion. We estimated the proportion of intratumoral cytotoxic T cells using multiplex immunofluorescence (n=125).

Results: The subtype distribution in our study was 39% immunoreactive, 29% mesenchymal 27% proliferative, and 4% differentiated. Germline variants and somatic mutations in any HRD gene were observed in 27% and 23% of cases, respectively, and at least one of these was observed in 42% of cases. Pathogenic germline variants and somatic mutations were observed in 7% and 3% of cases, respectively. The prevalence of germline or somatic variants by gene was 16% for *BRCA1*, 14% for *BRCA2*, 11% for *ATM*, 5% for *RAD51*, and 2% each for *BRIP1*, *PALB2*, and *BARD1*. We observed a COSMIC HRD signature in 43% of cases, with 25% SBS3 only, 5% ID6 only, and 13% with both signatures. The prevalence of any HRD gene variant or signature was higher in immunoreactive cases (52% and 59%, respectively) than in mesenchymal (28% and 43%) or proliferative (44% and 28%) cases. Germline HRD variants were more common in the proliferative subtype (44%) compared with immunoreactive (25%) and mesenchymal (17%). In contrast, somatic HRD mutations were more common in the immunoreactive subtype (33%), compared with proliferative (16%) and mesenchymal (15%). This was due to a higher occurrence of *BRCA1* somatic mutations in the immunoreactive subtype (25%) compared with proliferative (9%) and mesenchymal (8%). A higher proportion of cytotoxic T-cells (≥1% vs <1%) was also observed in the immunoreactive subtype (44%) compared with mesenchymal (31%) and proliferative (11%).

Conclusion: We observed differences in the distribution of HRD features and cytotoxic T-cells by gene expression subtype. In particular, in the immunoreactive subtype, the most common gene expression subtype in Black HGSOC cases, we observed a higher occurrence of any HRD feature, somatic *BRCA1* mutations, and cytotoxic T cell infiltration than in any of the other gene expression subtypes.

#6128 Association between neighborhood disinvestment and all-cause survival moderated by epigenetic age among women with breast cancer.

J. J. Plascak[1], K. Archer[2], A. A. M. Llanos[3], S. J. Mooney[4], C. Y. Xing[5], A. G. Rundle[3], H. Zarbl[6], B. Qin[7], N. Zeinomar[7], M. Schootman[8], S. Yao[9], C. Ambrosone[9], K. Pawlish[10], K. Demissie[11], E. V. Bandera[7], C.-C. Hong[9];

[1]The Ohio State University College of Medicine, Columbus, OH, [2]The Ohio State University College of Public Health, Columbus, OH, [3]Columbia University Mailman School of Public Health, New York, NY, [4]University of Washington School of Public Health, Seattle, WA, [5]San Francisco Department of Public Health, San Francisco, CA, [6]Rutgers University School of Public Health, Piscataway, NJ, [7]Rutgers Cancer Institute of New Jersey, New Brunswick, NJ, [8]University of Arkansas for Medical Sciences College of Medicine, Fayetteville, AR, [9]Roswell Park Comprehensive Cancer Center, Buffalo, NY, [10]New Jersey Department of Health, Trenton, NJ, [11]SUNY Downstate Health Sciences University School of Public Health, Brooklyn, NY

Background: DNA methylation is hypothesized to mediate relationships between chronic social disadvantage and cancer outcomes. We investigated whether epigenetic age acceleration mediates the association between modifiable neighborhood disinvestment and survival within a cohort of women with breast cancer.
Methods: Individual-level data were from the Women's Circle of Health Follow-up Study, a breast cancer cohort comprising women self-identifying as African American or Black, diagnosed 2013-2019 in New Jersey residents. Demographic, socioeconomic, health behavior, and dietary characteristics were self-reported. Peripheral blood samples from 312 participants collected 18-24 months after diagnosis were profiled for DNA methylation using Illumina's MethylationEPIC array. After pre-processing, pace of biological aging was estimated using DunedinPACE. Neighborhood disinvestment was assessed using a previously validated virtual audit of 6 disinvestment indicators - garbage, graffiti, dumpsters, poor building conditions, poor yard conditions, abandoned buildings - in 14,671 Google Streetview streetscapes. Accelerated failure time models of all-cause mortality as functions of neighborhood disinvestment and pace of biologic aging were fit to estimate survival time ratios (TR), adjusted for stage at diagnosis and neighborhood socioeconomic composition using causal mediation analyses. End of follow-up was August 13, 2023.
Results: There were 46 all-cause deaths through follow-up (median=6.9 years), and 5-year overall survival probability was 0.90 (95% CI: 0.86, 0.93). Minimum, median, and maximum pace of biologic aging was 0.87, 1.26, and 1.72 indicating accelerated aging (> 1.0) among most participants. There was no evidence for mediation of the neighborhood disinvestment - survival effect by pace of biologic aging (indirect effect p-value=0.33). There was evidence of an interaction between pace of biologic aging and neighborhood disinvestment in the adjusted model: survival time decreased 37% (95% CI: 4% - 59%, p=0.03) per 1 standard deviation (SD) increase in neighborhood disinvestment at pace of biologic aging values 1 SD below the average (< 1.13). There was no evidence of such association at pace of biologic aging values 1 SD above the average (p=0.86).
Conclusion: Greater neighborhood disinvestment may be associated with shorter survival following a breast cancer diagnosis among those with slower than average epigenetic age acceleration, due to the cumulative nature of neighborhood disinvestment as a chronic indicator of social disadvantage.

#6129 Emerging disparities in the clinical actionability landscape for patients with inferred African ancestry.

K. Arora, S. P. Suehnholz, H. Zhang, R. Kundra, S. Nandakumar, M. Nissan, A. Brannon, C. Bandlamudi, M. Ladanyi, A. Drilon, D. B. Solit, N. Schultz, M. F. Berger, D. Chakravarty;
Memorial Sloan Kettering Cancer Center, New York, NY

The past decade has seen a surge in the approval and availability of precision oncology therapies targeting distinct genomic alterations. We sought to determine whether these advances have benefitted patients with cancer from various ancestral backgrounds equally over time. We therefore annotated all genomic alterations identified in a pan-cancer cohort of 55,970 solid tumor samples sequenced with the MSK-IMPACT clinical assay using incremental versions of the precision oncology knowledge base OncoKB and computed the fraction of samples with OncoKB Level 1 alterations (biomarkers included in the FDA drug label) per year based on the annual cumulative FDA-approved targeted therapies. In 2010, 4.4% of patients with inferred African ancestry (AFR), and 2.4% of patients with inferred non-Ashkenazi Jewish European ancestry (EUR) had Level 1 alterations, largely explained by differences in cancer type prevalence between these groups. However, by mid-2023, AFR had a significantly lower percent of Level 1 alterations (25.3%) compared to EUR (31.2%), and this difference remained significant after adjusting for cancer type and disease status (q-value = 2.6e-08).

Next, we compared AFR versus EUR percentages of Level 1 alterations over time in breast and colorectal (CRC) patient samples, two cancers in which racial disparities of cancer incidence and outcomes are well-documented. We observed that prior to 2019, the fraction of breast cancer patient samples with a Level 1 alteration was similar among AFR (13%) and EUR (12.2%), primarily due to comparable rates of *ERBB2* amplifications (12.4% in AFR, 11.7% in EUR). However, following the breast cancer-specific FDA approvals of alpelisib+fulvestrant for *PIK3CA*-mutant disease in 2019 and elacestrant for *ESR1*-mutant disease in 2023, a significant shift in Level 1 actionability was observed between EUR (45%) and AFR (34%) attributed in part to the paucity of *PIK3CA* (26.3% vs. 36.2% in EUR) and *ESR1* (4.1% vs. 7.5% in EUR) oncogenic alterations in AFR.

We further observed AFR with CRC to have lower prevalence of MSI-H (5.8% vs.10.7% in EUR), TMB (12.5% vs. 18.8% in EUR) and *BRAF* V600E (5.1% vs. 9% in EUR). Correspondingly, in 2023, 16.4% of AFR with CRC have Level 1 alterations compared to 25.4% of EUR. Moreover, while AFR have higher rates of *KRAS* mutations (57.2% vs. 42.6% in EUR), they have a lower prevalence of the standard care biomarker KRAS G12C (3.4% vs. 7% of *KRAS*-mutant CRC in EUR) further exacerbating the disparities in CRC clinical actionability.

Taken together, here we demonstrate that a significant disparity exists in the clinical actionability landscape of AFR with cancer compared to EUR, largely due to differences in relative mutational frequencies of Level 1 genomic alterations.

#6130 Association of vitamin D-related genetic variants and prostate cancer risk in Black men.

T. M. Layne[1], J. H. Rothstein[1], X. Song[1], W. Sieh[2], R. J. Klein[1];
[1]Icahn School of Medicine at Mount Sinai, New York, NY, [2]MD Anderson Cancer Center, Houston, TX

Background: What we know of the relationship between vitamin D status and prostate cancer has largely been characterized among men of European ancestry, hereafter referred to as “White”. Research among White men indicate positive associations between circulating vitamin D status, as measured by concentrations of 25-hydroxyvitamin D (25(OH)D), with prostate cancer risk, and that genetic scores based on genome-wide associated single nucleotide polymorphisms (SNPs) reflecting high vs. low 25(OHD) is positively associated with aggressive disease. Limited research exists elucidating this relationship among men of African ancestry, hereafter referred to as “Black”. This is despite the fact that Black populations experience chronically lower circulating 25(OH)D, and ancestry-specific differences in genetic variants in some vitamin D-related genes. Given the paucity of research in this area, we examined the role of genetic variants in six commonly studied genes in the vitamin D pathway involved in synthesis (*CYP27A1* and *CYP27B1)*, transport (*GC)*, activity (*VDR* and *RXR*), and metabolism (*CYP24A1*) in relation to prostate cancer among Black men.
Methods: We assessed a total of 78 candidate SNPs in six vitamin D pathway genes that were either previously associated with circulating 25(OHD) and/or associated with prostate cancer risk in studies of White men. We compared vitamin D gene SNP associations with prostate cancer in Black and White men using summary statistics from a large GWAS of over 10,000 prostate cancer cases and 10,000 controls among Black men and over 85,000 cases and 91,000 controls among White men. A statistical significance threshold of 0.00064 (0.05/78 candidate SNPs) was used to adjust for multiple comparisons.
Results: None of the examined SNPs were significantly associated with prostate cancer risk among Black men after adjustment for multiple comparisons. However, four SNPs were nominally significant in Black men, including two in *RXR* [rs41400444 OR=1.09, 95% CI: 1.01-1.17, *P* = 0.024 and rs10881574 OR = 0.93, 0.867-0.999, *P* = 0.04556] and two in *VDR* [rs2853563 OR = 1.07, 1.012-1.13, *P* = 0.0173 and rs1156882 OR = 1.06, 1.00-1.12, *P* = 0.0495]. The latter SNP rs1156882 was also positively associated with prostate cancer risk in White men (OR = 1.035, 1.02-1.06, *P* = 0.00024), along with VDR SNP rs4516035 (OR = 1.027, 1.012-1.042, *P* = 0.00055), both after correction for multiple comparisons.
Conclusions: We observed non-significant, though suggestive, associations between genetic variants in vitamin D pathway genes previously associated with prostate cancer or vitamin D levels in White populations and prostate cancer risk in Black men. Future research exploring the potential role of vitamin D pathway genes and prostate cancer in Black men -- a population at high risk both for low circulating vitamin D and prostate cancer - will need to identify vitamin D-related genetic variants specific to carcinogenesis in Black men.

#6131 Increasing self efficacy, self confidence, and genetic knowledge via the Community Genetic Navigation Engagement Specialist Train-the-Trainer program.

Janet Rodriguez[1], Joel Sanchez Mendez[2], Yaneth L. Rodriguez[2], Lourdes Baezconde-Garbanati[2], Charite Ricker[3], Rosa Barahona[2], Bianca Rosales[2], Daisy Hernandez[3], Natalia Gutierrez[3], Julie Culver[3], Mariana Stern[1]

[1]USC Norris Comprehensive Cancer Center, Los Angeles, CA,[2]Department of Population and Public Health Sciences, Keck School of Medicine of USC, University of Southern California, Los Angeles, CA,[3]Department of Medicine, Division of Medical Oncology, USC Norris Comprehensive Cancer Center, Los Angeles, CA

Background: Colorectal cancer (CRC) is the second and third leading cause of cancer deaths in US Hispanic/Latino (H/L) men and women, respectively. The Community Genetic Navigation Specialists (CoGENES) train-the-trainer program created a workforce of community health workers (CHWs) to educate H/L individuals about genetic testing, counseling, and research.

Methods: The CoGENES three-week program, consisted of six in-person sessions, with a curriculum in both Spanish/English developed and delivered by experts, in Spanish, using presentations and hands-on activities. Acculturation, Latino values, self-efficacy, genetics and tumor testing knowledge, and self-confidence were assessed via pre- and post-training. Differences in scores were analyzed via Wilcoxon matched-pairs signed-rank tests with exact p-values.

Results: Median age of the 12 participants was 50 (IQR = 12), 9 were female, 92% were Mexican-born, half completed 1-2 years of college, and 67% were very hispanic oriented. Self-efficacy increased after training, with pre- training median-score = 38.5 (IQR = 3) and post-training score = 39.5 (IQR =2.5) ($p = 0.0547$). Certainty about understanding tumor testing increased after training ($p = 0.0039$). The median number of correct answers on the 16-item genetic knowledge scale increased from 6.5 to 9.5 and the median number of “don’t know” responses decreased from 5 to 0 after training. Finally, self-confidence to train future CoGENES was significantly higher ($p = 0.0098$) at post-test.

Conclusion: The CoGENES culturally tailored program led to improved self-efficacy, increased genetic knowledge, and self-confidence in a cohort of Hispanic community health educators. Findings will be shared within COPECC, and other NCI funded programs.

#6132 Exploring genomic complexity in lung cancer at the Tijuana/California border: A real-world perspective through liquid biopsy comprehensive genomic profiling.

Jorge Alberto Guadarrama-Orozco[1], Jennifer Ramirez-Puente[2], Elizabeth Dominguez-Gonzalez[3]

[1]Hospital General Tijuana, Tijuana, Mexico,[2]ISSSTE Tijuana, Tijuana, Mexico,[3]Universidad Autonoma de Baja California, Tijuana, Mexico

Objective: This study explores the application of liquid biopsy with next-generation sequencing (NGS) in profiling the genomic landscape of lung cancer patients from the Tijuana/California Border region. Specifically, we employ blood-based comprehensive genomic profiling (CGP) to assess the complexity of the genomic profile in these patients.

Materials and Methods: From April 2019 to November 2023, 37 lung cancer patients from Tijuana underwent profiling using the FoundationOne®Liquid CDx (F1LCDx®) assay, focusing on circulating tumor DNA (ctDNA). The assay, which spans 324 cancer-related genes and genomic signatures, provides insights into tumor fraction (TF) and blood-based tumor mutational burden (bTMB). Variants were classified based on the ESMO Scale of Clinical Actionability for molecular Targets (ESCAT).

Results: A notable 88.6% of patients exhibited at least one detectable alteration in plasma. The most frequently mutated genes were TP53 (51.3%), EGFR (16.2%), DNMT3A (13.5%), and KRAS (10.8%). Tumor mutational burden (TMB) was assessable in 9 out of 37 patients, with values ranging from 0 to 10 mut/Mb. According to ESCAT classification, 63.1% of samples revealed potentially actionable alterations (Tier I-II), while an additional 24.1% harbored alterations for which approved drugs are available in other cancer types (Tier III).

Conclusion: Liquid biopsy NGS emerges as a viable and valuable strategy for guiding personalized therapy. Given restricted accessibility to new drugs or clinical trials in Mexico, the use of blood-based CGP may enhance the identification of druggable alterations, thereby increasing the likelihood of accessing targeted drugs or enrolling in clinical trials.

#6133 Genetic profiling landscape among gynecological and breast cancer patients in the borde city of Tijuana, Mexico: A comprehensive study.

Jorge Alberto Guadarrama-Orozco[1], Paula Leal-Anaya[2], Eva Guerrero-Santillan[3]

[1]Medical Oncology, Hospital General Tijuana, Tijuana, Mexico,[2]Medical Genetics, Hospital General Tijuana, Tijuana, Mexico,[3]Prevencion y Control del Cancer de la Jurisdiccion de Servicios de Salud No. 2, Tijuana, Mexico

Background: Individuals in Tijuana have been identified as having multicultural and racial diversity. In Baja, California, Mexico, the prevalence and composition of cancer-predisposing germline variants in gynecologic cancers in Tijuana patients have not been evaluated.
Aim and Methods: We aimed to evaluate the prevalence of pathogenic variants (PV) using a panel of 84 cancer-predisposing genes in breast, endometrial, and ovarian cancer from the General Hospital of Tijuana during the period of October 2021-October 2023, who were contacted and invited to participate in the evaluation. Pre- and post-test genetic counseling was given, and a questionnaire on personal, gyneco-obstetric, demographic, and lifestyle variables was conducted. Peripheral blood samples were obtained from all patients, and Next-generation sequencing (NGS) was performed on the Illumina commercial platform (Illumina, SD, USA). Variants were classified according to the American College of Medical Genetics and Genomics (ACMG). Data was collected and descriptive statistics was applied to describe the characteristics of the population.
Results: A total of 51 patients were included in our cohort; 98.0% (50/51) were females and 2% (1/51) were males. Among study participants (mean age ±standard deviation: 46.1 ± 10.9), 49% reported a personal history of cancer (25/51). Diagnosis of breast cancer was present in 80.3% of the patients (41/51), 9% (5/51) with ovarian cancer, and 3.9% (2/51) with endometrial cancer. Twenty-five percent of participants (13/51) harbor a PV or likely pathogenic (LP) variant distributed among four cancer-risk genes (BRCA1, BRCA2, ATM, and TP53). The distribution by gene in the patients with a PV was: BRCA1 in 61% (8/13), BRCA2 in 23% (3/13), TP53 in 8% (1/13), and ATM in 8% (1/13). Whereas 39.2% (20/51) had variants of uncertain clinical significance in genes with ambiguous or non-well-established risk association for cancer (BARD1, AXIN2, GPC3, NF2, CEBPA, MSH3, ALK, DIS3L2, CDC73, BAP1, RAD51D, NF1, MSH2, BLM, NBN, BRCA2, BARD1, RUNX1, RECQL4, EGFR, PALB2, CASR, and POLD1), and 35.2% (18/51) had negative results for both; PV and VUS.
Conclusion: Our findings show a diverse pathogenic variant composition among the recruited individuals of the gynecological cancer population in Tijuana, Mexico, consistent with being a high-risk population for genetic diseases, which warrants further investigation to adequately assess the burden of hereditary cancer and implement appropriate preventative programs. Disparities in access to testing have a significant impact on affected populations, due in part to underrepresentation in surveys of regional cancer etiology and in genomic variant databases.

#6134 The Latino Colorectal Cancer Consortium: A resource for colorectal cancer disparities research.

N. C. Lorona[1], M. Matejcic[2], D. Sobieski[3], N. T. Nguyen[1], H. J. Hoehn[4], D. B. Diaz[5], K. Shankar[3], E. Jean-Baptiste[4], D. Coppola[6], C. Fulmer[7], O. Saglam[6], K. Jiang[6], T. Munoz-Antonia[8], I. Flores[8], E. Gordian[9], J. A. Oliveras Torres[8], S. I. Felder[10], J. A. Sanchez[10], J. Fleming[10], E. M. Siegel[4], D. Cress[9], M. C. Stern[11], J. K. Teer[12], S. L. Schmit[3], J. C. Figueiredo[1];

[1]Samuel Oschin Comprehensive Cancer Institute, Cedars Sinai Medical Center, Los Angeles, CA, [2]H. Lee Moffitt Cancer Center & Research Institute, Tampa, FL, [3]Genomic Medicine Institute, Lerner Research Institute, Cleveland Clinic, Cleveland, OH, [4]Department of Cancer Epidemiology, H. Lee Moffitt Cancer Center & Research Institute, Tampa, FL, [5]Non-Therapeutic Research Office, H. Lee Moffitt Cancer Center & Research Institute, Tampa, FL, [6]Department of Anatomic Pathology, H. Lee Moffitt Cancer Center & Research Institute, Tampa, FL, [7]Department of Pathology, Robert J. Tomsich Pathology and Laboratory Medicine Institute, Cleveland Clinic Foundation, Cleveland, OH, [8]Puerto Rico Biobank, Ponce Health Sciences University, Ponce, PR, [9]Department of Molecular Oncology, H. Lee Moffitt Cancer Center & Research Institute, Tampa, FL, [10]Department of Gastrointestinal Oncology, H. Lee Moffitt Cancer Center & Research Institute, Tampa, FL, [11]Department of Preventive Medicine, Keck School of Medicine, University of Southern California/Norris Comprehensive Cancer Center, Los Angeles, CA, [12]Department of Biostatistics and Bioinformatics, H. Lee Moffitt Cancer Center & Research Institute, Tampa, FL

Purpose: The Latino Colorectal Cancer Consortium (LC3) was established to fill a gap in representation of the diverse Hispanic/Latino/a/x community in cancer genomic research and to enhance understanding of determinants of disparities in the burden of colorectal cancer (CRC).

Methods: The LC3 joins together three established studies with deeply-annotated clinical, epidemiologic, and biologic data available for a heterogenous group of Hispanic/Latino/a/x men and women diagnosed with primary colorectal adenocarcinoma: the Hispanic Colorectal Cancer Study (California), the Total Cancer Care Protocol at Moffitt Cancer Center (Florida), and the Puerto Rico Biobank (southern Puerto Rico). Each contributing study collected data on demographics, medical history, family history, and lifestyle factors. Vital status, cause of death, treatment, and clinical characteristics were obtained through medical chart abstraction and/or linkage to cancer registries. Blood, saliva, or normal colonic tissues were used to extract and genotype germline DNA for a subset of participants. Tumor tissues (snap frozen or formalin-fixed paraffin-embedded) were evaluated by pathologists for diagnosis, tissue content, tumor cellularity, necrosis, immune infiltration, and additional histopathologic characteristics.

Results: The LC3 has assembled 2,041 participants across the three studies to date, with recruitment ongoing. Median age at diagnosis is 57 (range: 19-93), 54% of participants are male, and 63% are colon cancer cases (vs. rectal cancer). Participants were diagnosed between 1999 and 2022. The target is to generate comprehensive multi-omic data on 600 LC3 participants. To date, 243 have genome-wide germline genotyping, 323 have paired tumor/normal whole exome sequencing, and 257 have T cell receptor immunosequencing (immunoSEQ, Adaptive Biotechnologies). Further, 206 cases are represented on a set of tissue microarray blocks (target N=281). Bulk RNA-seq data are to be generated on 250 tumors.

Conclusions: The LC3 fills an important gap in research infrastructure for the scientific community. Key strengths of this unique consortium are its ability to capture a diversity of Latino CRC patients with respect to nativity and cultural heritage and to represent the spectrum of stages from early to metastatic. Ultimately, research from the LC3 will inform development of equitable precision medicine approaches and predictive models to improve the health of the rapidly-growing, heterogeneous Hispanic/Latino/a population.

#6135 Racial and ethnic differences in site of *de novo* metastases in patients with colorectal cancer: A SEER analysis.

N. C. Lorona[1], M. C. Stern[2], S. L. Schmit[3], J. C. Figueiredo[1];

[1]Samuel Oschin Comprehensive Cancer Institute, Cedars Sinai Medical Center, Los Angeles, CA, [2]University of Southern California/Norris Comprehensive Cancer Center, Los Angeles, CA, [3]Cleveland Clinic, Cleveland, OH

Purpose: Disparities in colorectal cancer (CRC) mortality may be driven by differences in access to care, tumor biology, and propensity to spread to distant sites. We examine differences in patterns of de novo metastases by race/ethnicity and age.

Methods: We identified 248,732 CRC patients listed in the Surveillance, Epidemiology, and End Results (SEER) database diagnosed with a first primary invasive CRC from 2010-2020, aged 20+ years at diagnosis, with complete data on SEER summary stage, and not diagnosed only by autopsy/death certificate. Outcomes included de novo metastatic site (no metastasis, liver, lung, brain, bone) and pattern (no metastasis, liver only, lung only, liver and lung, other). We used logistic regression to calculate odds ratios (OR) and 95% confidence intervals (95% CI) for the associations between 1) demographic and tumor characteristics (site, side, T stage, N stage) and site of de novo metastases , and 2) race/ethnicity and site of de novo metastases stratified by age (20-49, 50-74, 75+). We used multinomial logistic regression to assess the association between demographic and tumor characteristics and pattern of metastasis. Models adjusted for age, race/ethnicity, sex, site (colon, rectum), side (left, right), T stage, and N stage.

Results: 62,844 stage IV CRC cases were diagnosed from 2010-2020, and liver was the most common metastatic site (72%). Relative to age 50-74, age 20-49 at diagnosis was more strongly associated with de novo liver metastases (OR: 1.07; 95% CI: 1.02-1.11) and less with lung (OR: 0.86; 95% CI: 0.80-0.92) or brain (OR: 0.69; 95% CI: 0.52-0.93) metastases. Relative to Non-Hispanic White (NHW) patients, Non-Hispanic American Indian/Alaskan Native (AI/AN) patients had a higher risk of lung metastases (OR: 1.33; 95% CI: 1.07-1.65), Non-Hispanic Asian/Pacific Islander (API) patients had lower risks of liver (OR: 0.87; 95% CI: 0.83-0.92) and brain (OR: 0.67; 95% CI: 0.48-0.95) metastases, and Non-Hispanic Black (NHB) patients had higher risks of liver (OR: 1.35; 95% CI: 1.29-1.41), lung (OR: 1.36; 95% CI: 1.27-1.45), and bone (OR: 1.23; 95% CI: 1.08-1.41) metastases. In age-stratified analyses, the risks for NHB patients persisted across groups, while lower risks for API patients were not observed in the 20-49 group. API patients aged 20-49 had a higher risk of de novo lung (OR: 1.31; 95% CI: 1.06-1.61) and bone (OR: 1.63; 95% CI: 1.13-2.37) metastases, and the increased risk of lung metastases for AI/AN patients was larger in magnitude (OR: 2.26; 95% CI: 1.39-3.68). Age 20-49 was more strongly associated with a liver-only pattern (OR: 1.14; 95% CI: 1.09-1.19) and with less common distant sites (OR: 1.33; 95% CI: 1.25-1.41).

Conclusions: Racial/ethnic differences in de novo metastatic CRC patterns exist overall and across age groups. These findings are consistent with disparities in risk of stage IV CRC and can inform surveillance priorities in CRC survivors.

POPULATION SCIENCES: Genetic Epidemiology 1: GxE, GWAS, and Next-Generation Sequencing
Poster Session

#6139 Genetic modifiers of KRAS-mutant colorectal cancer.

N. P. Tjader[1], J. Ramroop[2], T. Gandhi[1], P. T. Campbell[3], A. T. Chan[4], S. Gallinger[5], G. G. Giles[6], M. J. Gunter[7], T. A. Harrison[8], M. Hoffmeister[9], P. A. Newcomb[8], S. Ogino[10], A. I. Phipps[8], C. Qu[8], R. E. Schoen[11], A. Pellatt[12], M. O. Woods[13], B. Van Guelpen[14], P. Stevens[1], H. Hampel[15], U. Peters[8], J. P. McElroy[1], A. E. Toland[1];

[1]The Ohio State University, Columbus, OH, [2]The City College of the City, University of New York, New York, NY, [3]Albert Einstein College of Medicine, Bronx, NY, [4]Harvard Medical School, Boston, MA, [5]University of Toronto, Toronto, ON, Canada, [6]Cancer Council Victoria, East Melbourne, Australia, [7]Imperial College London, London, United Kingdom, [8]Fred Hutchinson Cancer Center, Seattle, WA, [9]German Cancer Research Center (DKFZ), Heidelberg, Germany, [10]Harvard T.H. Chan School of Public Health, Boston, MA, [11]University of Pittsburgh, Pittsburgh, PA, [12]MD Anderson Cancer Center, Houston, TX, [13]Memorial University of Newfoundland, St. John's, NL, Canada, [14]Umea University, Umea, Sweden, [15]City of Hope National Medical Center, Duarte, CA

Somatic driver mutations in *KRAS* are found in ~40% of colorectal cancers (CRCs) and are associated with worse outcomes. In the US, individuals of African ancestry with CRC are more likely to have tumors with *KRAS* mutations than individuals of European ancestry, even after considering differences in socioeconomic status and other risk factors. Germline variants can influence somatic mutation events and may provide a selective advantage such that a mutated cell is more likely to progress to a cancer. Germline variants have been found to associate with somatic mutations in a variety of tumors. Based on ancestry differences in *KRAS* tumor mutation frequency, we hypothesized that germline variants altering molecular pathways that support *KRAS* tumorigenesis will associate with *KRAS*-mutant status. To test this, we performed a two-step association study using *KRAS* mutation status as our phenotype in individuals with microsatellite stable CRC. First, we conducted a discovery analysis using genome-wide germline genotypes and somatic mutation data from 6,386 non-Hispanic White CRC patients from the Cancer Genome Atlas and the GECCO consortium, considering sex and tumor location as covariates. To select variants for additional study, we used *in-silico* tools, such as expression quantitative trait loci (eQTL), to predict how associated variants may alter gene expression and chromatin. After reviewing relevant genomic features, excluding SNVs with minor allele frequency <10% and pruning SNVs in linkage disequilibrium (r^2>0.75), we identified candidate loci for a multi-ancestry independent validation analysis. In the discovery analysis, no variants met genome-wide significance thresholds (*p*-value <$5x10^{-8}$), though 3 SNVs associated with *KRAS* mutation status with *p*-values <$1x10^{-6}$ and 50 with *p*-values <$1x10^{-5}$. Of these 50 SNVs, 21 met criteria for validation. We chose 80 additional SNVs (*p*-value <$1x10^{-4}$) with predicted functional effect, for a total of 101 SNVs for analyses. In our preliminary validation analysis of 1,487 individuals grouped by self-reported race, no variants had a significant association in all populations. The rs726800 variant showed nominal association with *KRAS* mutation status (*p*-value=0.028) in self-reported non-Hispanic White individuals. This variant is within potential cis-regulatory distance of *HS3ST3A1* and *COX10-DT*, both of which have been reported as cancer biomarkers. Nominal associations were identified in self-reported Black (n=7 SNVs) and Hispanic or Latino (n=3 SNVs) individuals, though both groups had limited sample sizes. Additional validation samples are being analyzed, as well as analysis with adjustment for genetic ancestry. Future functional studies of top candidate variants will add mechanistic insight. In summary, we identified germline SNVs that associate with *KRAS* somatic mutations in CRC and may inform the cellular context that supports development of colorectal tumors with *KRAS* mutations.

#6140 Gene-environment interactions for lifetime water arsenic exposure and bladder cancer risk in the New England Bladder Cancer study.

H. Pomares-Millan[1], S. Koutros[2], N. Rothman[2], D. Baris[2], M. Schwenn[3], A. Johnson[4], D. T. Silverman[2], M. R. Karagas[1], M. N. Passarelli[1];
[1]Dartmouth Geisel School of Medicine, Hanover, NH, [2]National Cancer Institute, Bethesda, MD, [3]Formerly Maine Cancer Registry, Augusta, ME, [4]Formerly Vermont Department of Health, Burlington, VT

Environmental arsenic and genetic susceptibility have both been shown to increase bladder cancer risk, yet little is known about their respective interaction. We conducted a gene-environment interaction (GxE) study to characterize lifetime arsenic exposure from drinking water, inherited susceptibility, and bladder cancer risk in the New England Bladder Cancer Study. Exposures were estimated from arsenic measured in water samples collected at home and workplace. We evaluated common single-nucleotide polymorphisms (SNPs) i) from the latest bladder cancer genome-wide association study (n= 28), ii) from candidate gene studies of arsenic or bladder cancer (n= 16 SNPs), and iii) SNPs from a large genome-wide association study of arsenic metabolism (n = 4 SNPs) as potential effect modifiers of the arsenic-bladder cancer relationship. We coded SNPs as the absence or presence of a risk/effect allele for bladder cancer or arsenic metabolism in 2,019 adults (928 bladder cancer cases and 1,091 controls) and arsenic exposures as tertiles. Odds ratios (OR) with 95% confidence intervals (CI) adjusted for age, sex, smoking status, high-risk occupation, and principal components of genetic ancestry were estimated using logistic regression models. P-values for multiplicative interaction were calculated. Out of 48 SNPs, we found evidence of interaction for 7 SNPs at the statistical significance level of $P<0.05$. Most SNPs involved in GxE interactions are mapped to genomic regions known or suspected to function in arsenic metabolism. For the association between cumulative lifetime water arsenic (mg) and bladder cancer, the strongest evidence of an interaction was with rs1046428 (near *GSTZ1* on 14q23); among those with one or two copies of the T risk allele, OR_{T2vsT1}: 1.52, CI: 1.11 - 2.07; $OR_{T3\ vsT1}$: 1.44, CI: 1.05 - 1.98, $P_{interaction}$ = 0.01; among those with no risk allele copy, OR_{T2vsT1}: 0.91, CI: 0.62 - 1.35; $OR_{T3\ vsT1}$: 0.97, CI: 0.65 - 1.44. For average daily water arsenic (µg/day), we found evidence of interaction among those with risk allele for rs1801133 (A/A, A/G; *MTHFR* on 1p36) $OR_{T2\ vsT1}$: 1.70, CI: 1.18 - 2.44; $OR_{T3\ vsT1}$: 1.53, CI: 1.06 - 2.23, $P_{interaction}$ = 0.02, in those with no copies of risk allele OR_{T2vsT1}: 0.85, CI: 0.61 - 1.17; $OR_{T3\ vsT1}$: 1.11, CI: 0.79 - 1.54; and rs1801131 (G/G; G/T; *MTHFR*) $OR_{T2\ vsT1}$: 1.59, CI: 1.14 - 2.22; $OR_{T3\ vsT1}$: 1.63, CI: 1.16 - 2.29, $P_{interaction}$ = 0.01, whereas in those with no risk allele OR_{T2vsT1}: 0.84, CI: 0.59 - 1.19; $OR_{T3\ vsT1}$: 1, CI: 0.69 - 1.44. For 40-year lagged cumulative lifetime water arsenic (mg) and average daily water arsenic (µg/day), we found suggestive interactions with rs2234636 (*SLC39A2* on 14q11), and rs1495741 (*NAT2* on 8p22). Our study provides evidence of interactions between lifetime arsenic exposure and genetic variants that function in xenobiotic metabolism on bladder cancer occurrence.

#6141 Genetic risk, health-associated lifestyle, and risk of early-onset total cancer and breast cancer: A prospective cohort study.

Y. Zhang[1], Y. Liu[1], K. L. Penney[1], S. Lindstrom[2], P. Kraft[3];

[1]Harvard T.H. Chan School of Public Health, Boston, MA, [2]University of Washington, Seattle, WA, [3]National Cancer Institute, Rockville, MD

Background Early-onset cancer (diagnosed under 50 years of age) is generally more aggressive. Its rising incidence is a global concern. The associations between genetic risk, lifestyle, and the risk of early-onset cancer may inform preventive strategies.

Methods We studied the association between genetic risk, lifestyle and early-onset cancers among 66308 white British participants enrolled in the UK Biobank before age 50. Genetic risk was assessed using sex-specific composite total cancer polygenic risk scores (PRSs). We calculated composite PRSs as weighted sums of previously-developed cancer site-specific PRSs using weights obtained from lasso regression. We considered a breast cancer-specific PRS for analyses on breast cancer among women. A health-associated lifestyle score (HLS) was calculated based on baseline smoking, BMI (men only), physical activity, alcohol intake, and diet. Cox models were used to estimate hazard ratios (HRs) and 95% confidence intervals (CIs) of early-onset total cancer and breast cancer across genetic risk and HLS groups in women and men.

Results A total of 1247 incident invasive early-onset cancer cases (820 in women, 427 in men) were documented, including 386 cases of early-onset breast cancer. In multivariable-adjusted analyses with 2-year latency, higher genetic risk (highest vs. lowest tertile of PRS) was associated with significantly increased risks of early-onset total cancer in women (composite PRS HR=1.85; 95% CI, 1.50-2.29), early onset total cancer in men (composite PRS HR=1.94; 95% CI, 1.45-2.59), and early-onset breast cancer in women (breast-cancer PRS HR=3.06; 95% CI, 2.20-4.25). The HRs (95% CI) of early-onset total cancer in women and men, and early-onset breast cancer in women associated with adopting an unfavorable lifestyle (highest vs. lowest tertile of HLS) were 1.49 (0.99, 2.25), 1.14 (0.67, 1.95), and 1.78 (0.97, 3.24), respectively, in the total study population; 1.85 (1.02, 3.36), 3.27 (0.78, 13.72), and 1.67 (0.71, 3.90), respectively, in those with high genetic risk; 1.25 (0.60, 2.57), 1.11 (0.42, 2.89), and 1.66 (0.54, 5.11), respectively, in those with intermediate genetic risk; and 1.15 (0.44, 2.98), 1.16 (0.39, 3.40), and 2.10 (0.57, 7.75), respectively, in those with low genetic risk. Compared to individuals with both low genetic risk and a favorable lifestyle, those with high genetic risk and an unfavorable lifestyle had substantially increased risks of early-onset total cancer in women (3.07; 1.64-5.78) and men (2.18; 0.78-6.11), and significantly higher early-onset breast cancer risk in women (4.11; 1.56-10.85).

Conclusion Genetic and lifestyle factors were independently associated with risks of early-onset total cancer and breast cancer. Compared to those with low genetic risk, individuals with a high genetic risk may benefit more from adopting a healthy lifestyle in preventing early-onset cancer.

#6142 Interactions of processed meat and red meat intake with pathway-based polygenic risk scores for colorectal cancer: A novel approach for PRSs construction.

J. Sanchez Mendez[1], M. C. Stern[1], Y. Fu[1], J. Morrison[1], J. P. Lewinger[1], E. Kawaguchi[1], B. Queme[1], H. Mi[1], F. Qu[2], U. Peters[2], L. Hsu[2], S. B. Gruber[3], L. Li[4], M. Cotterchio[5], L. Le Marchand[6], A. J. Pellat[7], E. A. Platz[8], W. J. Gauderman[1];

[1]USC - University of Southern California, Los Angeles, CA, [2]Fred Hutchinson Cancer Research Center, Seattle, WA, [3]CIty of Hope National Medical Center, Duarte, CA, [4]Univesity of Virginia, Charlottesville, VA, [5]Cancer Care Ontario, Ontario, ON, Canada, [6]University of Hawaii Cancer Center, Honolulu, HI, [7]University of Utah, Salt Lake City, UT, [8]Johns Hopkins Bloomberg School of Public Health, Baltimore, MD

Introduction: Colorectal cancer (CRC) is the third most common cancer, and second cause of cancer death worldwide. Established CRC risk factors (E) include high red meat and processed meat intake. Genome-wide association studies (GWAS) have reported over 200 genetic variants associated with CRC risk. We used functional annotation data to identify subsets of GWAS variants within known pathways and constructed corresponding pathway Polygenic Risk Scores (pPRS). We evaluated pPRS by E interactions to determine whether genes within specific pathways interacted with meat intake to impact CRC risk.
Methods: A pooled sample of 54,531 CRC controls and 48,260 cases of European ancestry from 27 studies were analyzed. Study-specific quartiles for red and processed meat intake were generated through in-person interviews and structured self-administered questionnaires. Variants were imported to AnnoQ for annotation (n=203) and analyzed for overrepresentation in PANTHER-reported pathways with Fisher's exact test. Standard approaches were used to compute polygenic risk score weights relating the 203 variants to CRC. The subset of weights corresponding to each of five pathways were then used to compute the corresponding pPRS. Covariate-adjusted logistic regression models evaluated pPRSxE interactions with red meat and processed meat intake.
Results: A total of 34 unique variants were overrepresented in five pathways: Apoptosis signaling, Alzheimer disease-presenilin, Wnt-signaling, Gonadotropin-releasing hormone receptor, and TGF-beta signaling. We found a statistically significant interaction between TGF-beta-pPRS and red meat intake ($p = 0.0012$). Stratified analyses reported a dose-response trend in the red meat and CRC risk association, with decreasing estimates of red meat and CRC risk association, comparing first to fourth quartiles of meat intake, with increasing quartiles of TGF-beta-pPRS: 13% (Q1), 12% (Q2), 7% (Q3), and 6% (Q4). This association remained significant after adjustment for all other variants ($p = 0.0013$), and all other pPRS with variants that did not overlap with the TGF-beta-pPRS ($p = 0.0012$). Independent GxE interaction models for individual variants that were included in the TGF-beta pathway showed significant interactions with red meat for rs2337113 (intron *SMAD7* gene, Chr18), and rs2208603 (intergenic region *BMP5*, Chr6) ($p = 0.013$ & 0.0108, respectively). We did not find significant pPRS x red meat interactions for the other four pathways or with any pPRS x processed meat.
Conclusion: This pathway-based interaction analysis revealed a statistical interaction between SNPs in the TGF-beta pathway and red meat consumption that impacts CRC risk. These findings shed light into the possible mechanistic link between CRC risk and red meat consumption.

#6143 Association of polygenic risk score and prostate tumor biomarkers with lethal prostate cancer.

A. Wang[1], A. Plym[2], K. H. Stopsack[1], L. A. Mucci[1], K. L. Penney[1];
[1]Harvard T.H. Chan School of Public Health, Boston, MA, [2]Karolinska Institutet, Stockholm, Sweden

Prostate cancer (PCa) is a highly heritable cancer. While polygenic risk scores (PRS) stratify overall PCa risk among cancer-free men, they have not been reported to predict lethal outcomes in PCa patients. We aimed to examine to what extent PRS modifies associations between tumor biomarkers with cancer prognosis after diagnosis.

We included men with primary, non-metastatic PCa in the Health Professionals Follow-up Study (HPFS) and Physicians' Health Study (PHS). The PRS was constructed with 451 risk variants identified from prior PCa GWAS, measured on DNA from blood or buccal, standardized by adjusting for mean and standard deviation (SD) based on men without PCa with array-based genotyping data in HPFS/PHS. Prostate tumor biomarkers of molecular subtypes (*TMPRSS2:ERG* fusion, PTEN loss, and *TP53* missense mutations from validated immunohistochemistry assays), insulin/lipid signaling pathways (FASN, IR, and IGF1-R), and cellular proliferation and tumor microenvironment (Ki-67, apoptosis rates, and angiogenesis) were measured on tumor tissue from radical prostatectomy or TURMP. Sample sizes varied by tumor biomarkers, ranging from 214 for angiogenesis markers to 598 for ERG protein expression. We first used either logistic or negative binomial regression to evaluate the association between the PRS and the protein expression (levels) of each individual biomarker, and then evaluated the addition of multiplicative interaction terms between PRS and biomarkers to logistic regression models for lethal PCa, defined as metastases or death from PCa. Lastly, we evaluated the predictive performance for lethal PCa by area under the curve (AUC). All models adjusted for age at diagnosis and Gleason score.

Among all patients included in the analysis, the median age at diagnosis was 66 (interquartile range: 62-70) years, with 20% having a Gleason score≥8 and 10% having lethal PCa. PRS showed no association with lethal PCa (OR per SD increase PRS=0.95, 95%CI 0.85-1.06) or most tumor biomarkers, except for the apoptosis index (per SD in PRS corresponding to 0.22 units increase, 95%CI 0.02-0.42). Statistically significant interactions were found between PRS and p53 overexpression (p interaction = $1.6x10^{-5}$), PTEN loss ($p=3.7x10^{-3}$), FASN (p=0.03), and Ki-67 ($p=1.6x10^{-3}$), suggesting that compared to men with a PRS higher than the median, *TP53* missense mutation, PTEN loss, higher FASN intensity, and higher Ki-67 indices were more strongly associated with lethal PCa in patients with lower PRS. Incorporating PRS with tumor biomarkers into predictive models enhanced the AUC beyond a model with tumor biomarker and age. The largest improvements were observed when combining the PRS with Ki-67 and apoptosis, showing absolute increases of 5% and 7% respectively.

In conclusion, PRS integration with tumor biomarkers at diagnosis potentially improves the prediction of lethal PCa, thereby informing more targeted management strategies.

#6144 A polymorphic *TERT* tandem repeat creating an expandable intronic G4 quadruplex is associated with *TERT* expression, relative leukocyte telomere length and cancer risk.

O. Florez-Vargas[1], M. Ho[1], M. Hogshead[1], C.-H. Lee[1], K. Forsythe[1], B. Papenberg[1], K. Jones[1], W. Luo[1], K. Teshome[1], C. Blauwendraat[2], M. Kolmogorov[3], S. J. Chanock[1], M. J. Machiela[1], J. Schneekloth[3], S. Gadalla[1], S. A. Savage[1], S. M. Mbulaiteye[1], L. Prokunina-Olsson[1];

[1]National Cancer Institute, Rockville, MD, [2]National Institute on Aging, Bethesda, MD, [3]National Cancer Institute, Bethesda, MD

A multi-cancer GWAS region at human chromosome 5p15 encodes telomerase reverse transcriptase (TERT). One of the GWAS signals is rs10069690-T, which creates an alternative intron 4 splicing site, co-producing full-length (FL) and truncated *INS1b* transcript for dominant-negative telomerase-nonfunctional TERT. A variable number tandem repeat (VNTR6-1, 38 bp repeat unit) within intron 6 remains uncharacterized in relation to GWAS signals and cancer risk. We hypothesized that VNTR6-1 might contribute to GWAS signals represented by rs10069690.

We scored VNTR6-1 and rs10069690 in short-read WGS data (n=3,202) from the 1000 Genomes Project with a machine learning model using the GLMnet engine, and in phased long-read assemblies (n=544). We defined two VNTR6-1 groups: Short (24-27 copies) and Long (40.5-66.5 copies); the VNTR6-1-Long group was preferentially linked with rs10069690-T compared to C allele (p=2.53E-13). We show that haplotypes of rs56345976 and rs33961405 alleles can predict VNTR6-1 groups. We imputed VNTR6-1 in UK Biobank controls (n=351,634), PLCO cancer cases and controls (n=100,445), and African Burkitt lymphoma cases (aBL, n=79).

Functional studies in aBL tumors revealed a suggestive association between reduced total *TERT* expression, rs10096690-T (p=0.035) and VNTR6-1-Long (p=0.053). VNTR6-1 forms a G4 quadruplex structure sensitive to G4 stabilizing ligands, altering the ratio between *FL-TERT* and a dominant-negative *TERT-β* isoform in isogenic cell lines with/without VNTR6-1. In GTEx and TCGA, several metrics related to cell proliferation and telomerase activity correlated positively with *FL-TERT* expression and negatively with *TERT-β* expression.

We created a composite marker with 0, 1 or 2 copies of the *FL-TERT*-associated haplotype (VNTR6-1-Short/rs10069690-C) to capture the effects of these variants that negatively affect *TERT* expression and telomerase activity. The number of copies of the VNTR6-1/rs10069690 haplotype was associated with relative leukocyte telomere length in UK Biobank controlling for sex and age (β=0.049, p=8.75E-78). This marker was also associated with a reduced risk of bladder and prostate cancer but an increased risk of breast, endometrial, ovarian, thyroid cancer, and glioma in PLCO.

Our findings reveal that germline variants VNTR6-1-Long/rs10069690-T underlie the multi-cancer GWAS signal and jointly decrease *TERT* expression and telomerase activity, potentially reducing the risk of some cancers by limiting cell growth. However, decreased telomerase activity could deregulate stem cell-driven tissue regeneration and genome integrity, increasing the risk of other cancers. Our findings unveil novel mechanisms of cancer susceptibility and propose therapeutic avenues for targeting *TERT* isoform ratios to modulate telomerase activity and its cellular effects.

#6145 A trans-ethnic meta-analysis identified additional novel genomic loci associated with cervical cancer.

A. B. Kamiza, J.-T. Brandenburg, M. Ramsay, C. Mathew;
University of the Witwatersrand, Johannesburg, South Africa

Introduction: Cervical cancer is the second most common cause of cancer-related deaths among women worldwide. Genome-wide association studies (GWAS) have identified genetic variants associated with cervical cancer. However, these discoveries have been limited by the small sample sizes of the individual cohorts. To identify additional novel loci associated with cervical cancer, we performed a trans-ethnic meta-analysis.
Methods: GWAS summary data for trans-ethic meta-analysis were identified in women of European ancestry from the UK Biobank, East Asian ancestry from Biobank Japan, and African ancestries from the pan-UK Biobank and Johannesburg cancer study. Meta-analyses were performed using fixed effect inverse variance weighted method implemented in GWAMA. To localize putative genomic loci associated with cervical cancer, we performed fine mapping using the Bayesian approach by calculating the marginal posterior probability of causality for each single nucleotide polymorphisms (SNPs) and 99% credible set size.
Results: Our meta-analysis identified four additional novel genomic loci associated with cervical cancer. These loci include: rs147778467 (odds ratio [OR] = 1.12, 95% confidence interval [CI] = 1.08-1.16, P-value = 3.12×10^{-08}) in *RGS21*, rs53150478 (OR =1.03, 95%CI = 1.01-1.05, P-value = 4.48×10^{-08}) in *MAN1C1*, rs113842373 (OR = 0.68, 95%CI = 0.56-0.81, P-value = 2.31×10^{-09}) in *LINCO1850* and rs75372437 (OR = 0.80, 95%CI = 0.72-0.88, P-value = 3.32×10^{-08}) in *RNU6-356P*. These loci are implicated in carcinogenic pathways. Moreover, our Bayesian fine mapping identified five loci with a marginal posterior probability of causality > 1 and reduced the 99% credible set sizes.
Conclusion: We identified additional novel loci associated with cervical cancer and our fine mapping identified loci with a high posterior probability of being causal.

#6146 Characterizing underlying molecular mechanisms of prostate cancer risk variants identified from multi-ethnic GWAS.

Z. Wu, A. Vu, E. S. Nelson-Moore, H. Cao, S. K. Rhie;
USC - University of Southern California, Los Angeles, CA

Prostate cancer (PCa) is a complex disease with the second leading cause of cancer death in US males. Multi-ethnic genome-wide association studies (GWAS) identified a thousand genetic variants associated with PCa risk in different races. However, the majority of risk variants are located in non-coding regions, making it challenging to understand their contribution to PCa risk. Non-coding regions include functional regulatory elements (REs) such as promoters and enhancers, whose activity can be evaluated by histone modification H3K4me3 and H3K27ac, respectively. In this study, we integrated PCa risk variants with hundreds of H3K4me3 and H3K27ac ChIP-seq data from normal and cancer prostate cell lines and tissues, finding 122 variants in promoters and 301 variants in enhancers. Enhancers are distal to promoters, and they form loops to regulate gene expression, mediated by transcription factors (TFs). Enhancer activities are tightly associated with cell fate. Genetic variants can affect the activity of enhancers by changing the binding preference of TFs and such changes can affect chromatin interactions and dysregulate gene expression. We hypothesize that allele changes of enhancer variants contribute to PCa risk differently among individuals from different ancestries, leading to the development of heterogeneous PCa molecular subgroups, characterized by genetic alterations including TMPRSS2-ERG fusion. By integrating H3K27ac ChIP-seq data from prostate cell lines derived from European (EUR) and African (AFR) ancestries, we found 185 risk variants in enhancers in EUR cell lines and 69 risk variants in enhancers in AFR cell lines. Next, we integrated patient tissue-derived H3K27ac ChIP-seq data and performed chromatin quantitative trait loci (cQTL) and allelic imbalance (AI) analyses to determine risk variants associated with enhancer activity. Among the 185 risk enhancer variants in EUR and 69 in AFR cell lines, we found 130 and 46 with significant association, respectively. To determine TFs that change binding upon allele change of enhancer risk variants, we integrated hundreds of TF ChIP-seq data from prostate cell lines and tissues. Among the 185 risk enhancer variants in EUR and 69 in AFR cell lines, we found 142 and 44 variants bound by TFs, respectively. When we further performed cQTL and AI analyses for FOXA1, HOXB13, and AR, we found 87 and 29 variants significantly associated with TF binding affinity, respectively. Moreover, we found that these associations differ between TMPRSS2-ERG fusion positive and negative tumors. To identify the target genes of enhancer risk variants, we are currently integrating chromatin interaction data including Hi-C and Micro-C. Overall, this study provides valuable insights into the underlying molecular mechanisms of risk variants in various populations and individuals which lead to the development of heterogeneous PCa subgroups.

#6147 Genome-wide association study identifies new genetic susceptibility loci for multiple primary cancers.

S. He[1], J. Perry[2], S. Li[1], B. D. Mitchell[3], Y. Zhang[2], S. Chen[2], L. Beane-Freeman[1], K. H. Barry[3], S. I. Berndt[1];

[1]National Cancer Institute, Shady Grove, MD, [2]University of Maryland Baltimore, Baltimore, MD, [3]University of Maryland School of Medicine, Baltimore, MD

Objectives: Genetic susceptibility is thought to contribute to the development of multiple primary cancers (MPC), often called secondary cancers. Although rare variants contribute to risk, these only account for a small fraction of MPC cases. The contribution of common variants to risk is unknown.

Methods: To identify common genetic variants associated with the risk of MPC, we conducted a trans-ancestry meta-analysis of genome-wide association studies (GWAS), including 7,360 MPC cases and 138,684 controls from the Prostate, Lung, Colorectal and Ovarian (PLCO) Cancer Screening Trial and UK Biobank (UKBB). Association analyses were performed separately by genetic ancestry, genotype platform, and study, adjusting for age, sex, and principal components, and the results were meta-analyzed together using a fixed effects model. Genome-wide SNP heritability was estimated using GCTA. Pathway and functional enrichment analyses were conducted to gain insights into potential biological mechanisms underlying discovered loci.

Results: We identified one novel locus at chromosome 3q26.2 (LRRC34, rs7621631) that was associated with MPC risk ($P=1.16x10^{-8}$). Variants in this region have been previously associated with telomere length, suggesting a possible underlying mechanism. In sex-stratified analyses, we identified an additional locus at chromosome 12q24.33 (intergenic, rs10466868) associated with MPC in men ($P= 7.76x10^{-8}$), but not women. Although the risk associated with these two discovered loci was small, the genome-wide SNP heritability was estimated to be 12%, suggesting that there are likely more common variants to be discovered for MPC risk.

Conclusions: Our study demonstrates that common genetic variation contributes to the risk of multiple primary cancers and suggests additional loci are likely to be identified with larger studies.

#6148 Multiple new Ewing sarcoma susceptibility loci expand knowledge of germline genetic etiology and nominate mechanisms of risk.

A. K. Hubbard[1], W. Zhou[1], C. Boyce[2], J. Khan[3], M. M. Hudson[4], K. K. Ness[4], Z. Wang[5], K. A. Janeway[6], P. J. Lupo[7], L. M. Morton[1], S. J. Chanock[1], T. G. P. Grunewald[8], O. Delattre[9], M. J. Machiela[1], Ewing Sarcoma Germline Genetics Group;

[1]National Cancer Institute, Rockville, MD, [2]Westat, Rockville, MD, [3]National Cancer Institute, Bethesda, MD, [4]St. Jude's Children's Hospital, Memphis, TN, [5]St. Jude's Children's Research Hospital, Memphis, TN, [6]Dana-Farber, Boston, MA, [7]Baylor College of Medicine, Houston, TX, [8]German Cancer Research Center, Heidelberg, Germany, [9]Institut Curie Research Center, Paris, France

Ewing sarcoma (EwS) is a rare and aggressive pediatric cancer with peak incidence in the second decade of life. EwS occurs primarily in children of European ancestry suggesting a genetic component to susceptibility. Prior investigations identified six susceptibility loci associated with EwS, with evidence for additional signals not reaching the commonly accepted threshold for genome-wide significance (i.e., $p<5\times10^{-8}$). At least two of these loci demonstrate evidence of tagging variation in length of nearby GGAA microsatellites, which alter binding of the pathognomonic *EWSR1::FLI1* fusion resulting in downstream dysregulation of target genes promoting sarcomagenesis. To identify additional susceptibility loci, we performed the largest genome-wide association study (GWAS) to date consisting of 1,640 EwS cases and 8,457 cancer-free individuals of European ancestry from 8 studies and matched by principal components. Genotype imputation was carried out by study/array using TOPMed data as the reference and each set was analyzed using PLINK 1.9 adjusting for significant principal components. Variants were included in each study if minor allele count was greater than five in each set of cases. Individual study results were combined using fixed effects meta-analysis in Metasoft with variants demonstrating evidence for heterogeneity excluded.For previously reported EwS loci (i.e., 1p36.22, 6p25.1, 10q21.3, 15q15.1, 20p11.22 and 20p11.23), odds ratios (OR) remained high for GWAS (OR=1.5-2.4) and the $-\log_{10}$ p-values grew by several orders of magnitude, providing strong evidence for replication in the additional 907 EwS cases and 7,111 cancer-free controls. Our analysis identified five novel loci reaching genome-wide significance ($P\text{-value}_{meta}< 5\times10^{-8}$) at 5q32, 7q32.3, 8q24.2, 13q32.3, and 17q23.2. Risk allele frequency of newly identified loci ranged from 0.001 to 0.75with estimated ORs ranging from 1.31-4.30. eQTL analyses nominated nearby biologically plausible candidate genes for future functional investigation including *LARS1*, a gene implicated in osteosarcoma and skeletal muscle dysgenesis, at the 5q32 locus and *COX5BP6*, a gene implicated in age at menarche and testosterone levels, at 13q32.3.Our results add to evidence supporting a strong inherited genetic component to EwS risk and particularly a genetic architecture harboring a substantial number of common variants with moderate effect. Ongoing work is focusing on enrichment analyses of GGAA microsatellite repeat sequences in identified risk loci to search for evidence for germline-somatic interactions with *EWSR1::FLI1*.

#6149 Polygenic risk score and lung adenocarcinoma risk among never-smokers by *EGFR* mutation status.

B. Blechter[1], C. Hsiung[2], K. Matsuo[3], K. Shiraishi[4], K. Wang[1], H. Zhang[1], W. Seow[5], J. Shi[1], N. Chatterjee[6], J. Y. Wong[7], J. Dai[8], H. Hosgood[9], I.-S. Chang[2], J. Choi[1], W. Hu[1], W. Zheng[10], Y. Kim[11], X.-O. Shu[10], Q. Cai[10], P.-C. Yang[12], D. Lin[13], K. Chen[14], Y.-L. Wu[15], H. Shen[16], T. Kohno[4], S. J. Chanock[1], N. Rothman[1], Q. Lan[1];

[1]National Cancer Institute, Rockville, MD, [2]National Health Research Institutes, Zhunan, Taiwan, [3]Aichi Cancer Center Research Institute, Nagoya, Japan, [4]National Cancer Research Institute, Tokyo, Japan, [5]National University of Singapore and National University Health System, Singapre, Singapore, [6]Johns Hopkins Bloomberg School of Public Health, Baltimore, MD, [7]National Heart Lung and Blood Institute, Bethesda, MD, [8]School of Public Health, Nanjing Medical University, Nanjin, China, [9]Albert Einstein College of Medicine, Bronx, NY, [10]Vanderbilt University, Nashville, TN, [11]Seoul National University College of Medicine, Seul, Korea, Republic of, [12]National Taiwan University Hospital, Taipei, Taiwan, [13]Chinese Academy of Medical Sciences and Peking Union Medical College, Beijing, China, [14]Tianjin Medical University Cancer Institute and Hospital, Tianjin, China, [15]Guangdong Academy of Medical Sciences, Guangzhou, China, [16]Nanjing Medical University, Nanjing, China

Background: Lung cancer is the leading cause of cancer mortality worldwide, and incidence rates for the disease in never-smokers is among the highest in East Asian (EAS) women. Epidermal growth factor receptor (EGFR) is a transmembrane protein that regulates cellular proliferation and apoptosis, and mutations in the EGFR gene have been found to be a defining hallmark of lung adenocarcinoma (LUAD). We investigated if overall genetic susceptibility to LUAD, defined as a polygenic risk score (PRS), is differentially associated with LUAD by EGFR mutation status.

Methods: The study consists of 998 female never-smoking histologically confirmed LUAD cases with data on EGFR mutation status and 4,544 female never-smoking controls from the Female Lung Cancer Consortium in Asia. Germline DNA samples were genotyped using the 370K, 610Q, or 660W microarrays. Genomic DNA extracted from fresh, frozen or formalin-fixed paraffin-embedded tumor tissue samples of LUAD cases were genotyped for EGFR mutations on exons 19 and 21. We defined cases with EGFR mutation on either exon as EGFR+ (n=518) and cases without such EGFR mutation as EGFR- (n=480). Weights from 942,592 single nucleotide variants derived from a previously conducted genome-wide association study were used in a Bayesian-based approach, LDpred2, to derive a PRS for all participants. We estimated the odds ratios (OR) and 95% confidence intervals (CI) for the association between continuous PRS, PRS quartiles and tumor EGFR mutation status using logistic regression models in a case-case analysis, as well as using a multinomial logistic regression treating controls as the reference. All models were adjusted for age, study and the top 10 principal components.

Results: In case-case comparisons, compared to EGFR- LUAD, we found a positive association between continuous PRS and risk of EGFR+ LUAD (OR=1.17, 95% CI: 1.02, 1.34), as well as a dose-response relationship between quartiles of the PRS and EGFR+ LUAD (p-trend=0.003). We further found that the association between the fourth quartile of the PRS with EGFR+ LUAD (OR=8.63, 95% CI: 5.67, 13.14) was significantly higher than the association between the fourth quartile of the PRS with EGFR- LUAD (OR=3.50, 95% CI: 2.44, 5.00) compared to controls (p-heterogeneity=0.004).

Conclusions: We found that the PRS developed for LUAD in EAS individuals was more strongly associated with EGFR+ LUAD compared to EGFR- LUAD, suggesting that germline genetic susceptibility may be differentially associated with LUAD in never-smoking female EAS patients depending on the cancer's mutation status. Given that patients with LUAD respond differently to treatments that are used as targeted therapy depending on their EGFR mutation status, our findings may have important public health and clinical implications, which may guide risk stratification, screening, and treatment.

#6150 *MMP14* and *MKLN1* as colorectal cancer susceptibility genes and a drug repurposing candidate from genome-wide association study in South Korea.

D. Yun[1], J.-H. Yang[2], S.-S. Kweon[2], J.-a. Sim[3], M. Kim[4], J. Park[4], S. Jeong[4], A. Shin[4], N. Song[1];
[1]Chungbuk National University, Cheongju, Korea, Republic of, [2]Chonnam National University, Hwasun, Korea, Republic of, [3]Hallym University, Chuncheon, Korea, Republic of, [4]Seoul National University, Seoul, Korea, Republic of

Background: One of the major topics about colorectal cancer (CRC) is to find susceptible genes. Furthermore, functional interpretation of post-GWAS analysis gains attention and various approaches to find drug-repurposing candidates are used in cancer research. Our study aims to identify susceptible genes for CRC and provide drug-repurposing candidates.
Methods: CRC patients in Seoul National University Hospital with prospective follow-up were recruited. From blood-derived DNA, genome-wide SNPs were genotyped using the Korea Biobank Array and 409,063 SNPs were extracted. SNP-based logistic regression model was fit for the event of CRC estimating beta values. Furthermore, post-GWAS analysis was conducted using regulatory function, multiple annotation and gene expression database. Drug-repurposing candidate was identified through the pre-trained deep neural network with susceptible genes.
Results: We used 500 participants of CRC cases and 1,500 participants of healthy controls. For GWAS, statistically significant associations were mapped to *MKLN1*, *MMP14*, *PTPN14* and *MKL2* genes. For post-GWAS analysis, strong associations were found for *MKLN1* (rs75170436, 7q32.3, Beta=-0.90, *P*-value=5.90×10^{-13}) and *MMP14* (rs3751489, 14q11.2, Beta=-1.91, *P*-value=2.31×10^{-12}). From the drug-repurposing analysis, PPARδ/β agonist (GW0742; Binding score=3.79(*MKLN1*), 12.06(*MMP14*)) was identified for both genes with the highest score.
Conclusions: We revealed *MKLN1* and *MMP14* genes as susceptible genes associated with CRC development. Additionally, we identified PPARδ/β agonist (GW0742) as a drug-repurposing candidate for the treatment of CRC. These findings can promote the understanding of CRC development and provide a novel therapeutic candidate for CRC patients in the future.

#6151 Relationship between polygenic risk score, lifestyle factors, and colorectal cancer risk.

W.-Y. Huang, E. Loftfield, R. Landy, D. Wang, H. A. Katki, J. Shi, L. Wang, M. J. Machiela, N. D. Freedman, S. I. Berndt;
NCI Div. of Cancer Epidemiology & Genetics, Bethesda, MD

Although heritable factors are estimated to explain up to 35% of colorectal cancers (CRC), most are diagnosed in people without a family history of CRC suggesting that inherited genetic variants, environmental factors, or a combination of both, contribute to CRC risk. We explored the relationship between a polygenic risk score (PRS) for CRC risk and lifestyle risk factors to understand whether individuals with higher genetic risk, who do not develop CRC, engage in healthier lifestyle behaviors, or conversely, whether those with lower genetic risk, who do develop CRC, engage in riskier behaviors in the Prostate, Lung, Colorectal, and Ovarian (PLCO) Cancer Screening Trial.

Using summary statistics obtained from a large independent GWAS meta-analysis of CRC by the GECCO consortium, we developed a genome-wide PRS for CRC using SBayesR and applied it to participants of European ancestry genotyped in the PLCO Trial (n=74,396). For all subjects, we computed an environmental (E) score based on 19 lifestyle risk factors for CRC, a WCRF/AICR score that measured adherence to the 2018 Cancer Prevention recommendations, and a 2015 healthy eating index (HEI) with higher values indicating healthier lifestyle profiles. We used t-tests to evaluate differences in lifestyle scores between CRC-free participants in the highest quartile of PRS and incident CRC cases in the lowest quartile of PRS. To examine the correlations between the PRS and lifestyle scores, we performed multivariable linear regression models regressing PRS on each lifestyle score. We used multivariable Cox hazards regression models to compute hazard ratios and 95% confidence intervals for CRC risk; multiplicative interactions between PRS and lifestyle scores were evaluated using the Wald test for the interaction terms.

During the 15 years follow-up period, a total of 1,052 CRC cases were diagnosed. Individuals in the highest quartile of PRS who remained cancer-free were more likely to engage in healthier behaviors than those in the lowest quartile of PRS who were diagnosed with incident CRC (E-score: -0.01 vs. -0.18, WCRF/AICR score: -0.05 vs. -0.32, HEI score: 0.06 vs. -0.13); however, differences were not statistically significant (*P* value: 0.1 to 0.4). PRS and lifestyle scores were significantly (all *P* <0.0001), albeit weakly (β: -0.02 to -0.03), associated among participants who remained CRC-free but not among CRC cases (*P*: 0.1 to 0.3). PRS-lifestyle score interactions were not statistically significant (*P*: 0.2 to 0.4).

Although the differences and multiplicative interaction models were not statistically significant, we found that individuals with a higher PRS who remained CRC-free were slightly more likely to engage in healthier behaviors than those at a lower genetic score who developed CRC. Additional studies with larger sample size are warranted to further explore the interplay between genetic risk and lifestyle factors related to CRC risk.

#6152 Genetic associations with hematologic malignancies: An evaluation of CLL polygenic risk score and MBL status in the Mayo Clinic Biobank Cohort.

R. Mwangi[1], D. P. Robinson[1], S. J. Achenbach[1], G. Kleinstern[2], A. D. Norman[1], K. G. Rabe[1], J. E. Olson[1], N. E. Kay[1], R. Griffin[1], N. J. Boddicker[1], E. Braggio[3], S. A. Parikh[1], C. A. Hanson[1], C. M. Vachon[1], J. R. Cerhan[1], T. D. Shanafelt[4], S. L. Slager[1];

[1]Mayo Clinic, Rochester, MN, [2]University of Haifa, Haifa, Israel, [3]Mayo Clinic, Phoenix, AZ, [4]Stanford University, Stanford, CA

Chronic Lymphocytic Leukemia (CLL) exhibits a substantial familial risk that extends beyond CLL to other B-cell lymphomas (including follicular lymphoma and diffuse large B-cell lymphoma). Monoclonal B-cell Lymphocytosis (MBL), a precursor to CLL, is also associated with a significant risk for hematologic malignancies overall and for lymphoid malignancies, specifically. Moreover, previous research has shown an association between the CLL polygenic risk score (CLL-PRS) and common lymphoma subtypes. This study aims to further evaluate CLL-PRS associations with hematological cancer overall and by lineage while also considering MBL status a strong risk factor for lymphoid malignancies.

Utilizing the Mayo Clinic Biobank, we selected individuals aged 40 years or older, residing in proximal counties, who had no prior hematologic malignancies, and with available biospecimens. MBL screening was done using 8-color flow cytometry, and MBL with CLL (CD5+/CD20dim) or atypical CLL (CD5+/CD20+) immunophenotype were included. CLL-PRS was calculated from 41 known susceptibility variants, with weights being the log of the odds ratios from the largest CLL genome-wide association study. Incident hematologic malignancies were ascertained through ICD codes and confirmed via medical record review. Hazard ratios (HR) and 95% confidence intervals (CIs) for associations with hematologic malignancies were estimated through Cox regression.

Of 7,332 participants, 1,150 (16%) screened positive for MBL; median age was 67 years (range 40-101), and 37% male. Median follow-up was 2.9 years (range 0-13), and 56 hematologic cancers were identified. After adjusting for age and sex, the CLL-PRS was associated with increased risk of developing hematologic (HR=1.49, 95%CI=1.12-1.98, P=0.006) which was all attributable to lymphoid cancers (HR=1.79, 95%CI=1.26-2.56, P=0.001). When adjusting for baseline MBL status in the models, the CLL-PRS associations remained significant but were attenuated for hematological (HR=1.33, 95%CI=0.99-1.79, P=0.058) and lymphoid (HR=1.56, 95%CI=1.07-2.26, P=0.020) malignancies, while MBL status was also significantly associated with risk of hematologic (HR=2.76, 95%CI=1.55-4.91, P=0.001) and lymphoid (HR=3.61, 95%CI=1.78-3.32, P<0.001) malignancies.

In this prospective cohort study of individuals screened for MBL, CLL-PRS was associated with an elevated risk of hematologic malignancies overall and within the lymphoid lineage, underscoring a shared genetic etiology across many B-cell lymphomas. However, the associations between CLL-PRS and hematologic malignancies were attenuated when accounting for MBL status or when analyzing among MBL-positive individuals, highlighting the role of MBL status in these associations. Further research with expanded cohorts is needed to unravel these complex genetic and clinical interactions.

#6153 Proteome-wide association study and functional validation identify novel protein markers for pancreatic ductal adenocarcinoma.

J. Zhu[1], K. Wu[2], S. Liu[1], A. Masca[1], H. Zhong[1], T. Yang[3], D. H. Ghoneim[1], P. Surendran[4], T. Liu[5], Q. Yao[6], T. Liu[7], S. Fahle[4], A. Butterworth[4], M. A. Alam[8], J. V. Vadgama[2], Y. Deng[1], H.-W. Deng[9], C. Wu[10], Y. Wu[2], **L. Wu**[1];

[1]University of Hawaii at Manoa, Honolulu, HI, [2]Charles R Drew University of Medicine and Science, Los Angeles, CA, [3]University of Michigan School of Public Health, Ann Arbor, MI, [4]University of Cambridge, Cambridge, United Kingdom, [5]Johns Hopkins University, Baltimore, MD, [6]Baylor College of Medicine, Houston, TX, [7]Pacific Northwest National Laboratory, Richland, WA, [8]Tulane University, New Orleans, LA, [9]Tulane University, New Orlean, LA, [10]The University of Texas MD Anderson Cancer Center, Houston, TX

Pancreatic ductal adenocarcinoma (PDAC) remains a lethal malignancy, largely due to the paucity of reliable biomarkers for early detection and therapeutic targeting. Existing blood protein biomarkers for PDAC often suffer from replicability issues, arising from inherent limitations such as unmeasured confounding factors in conventional epidemiologic study designs. To circumvent these limitations, we use genetic instruments to identify proteins with genetically predicted levels to be associated with PDAC risk. Leveraging genome and plasma proteome data from the INTERVAL study, we established and validated models to predict protein levels using genetic variants. By examining 8,275 PDAC cases and 6,723 controls, we identified 40 associated proteins, of which 16 are novel. Functionally validating these candidates by focusing on two selected novel protein-encoding genes, *GOLM1* and *B4GALT1*, we demonstrated their pivotal roles in driving PDAC cell proliferation, migration, and invasion. Furthermore, we also identified potential drug repurposing opportunities for treating PDAC. Our dual approach enhances our understanding of PDAC etiology and potentially opens new avenues for therapeutic interventions.

#6154 Targeted CRISPRi screen identifies functional variants and novel target genes at multiple renal cell carcinoma (RCC) susceptibility loci.

Timothy Winter[1], Timothy Myers[1], Leandro Colli[2], Lea Jessop[1], Jiyeon Choi[1], Mitchell J. Machiela[1], Mark P. Purdue[1], Kevin Brown[1], Stephen Chanock[1]

[1]National Cancer Institute Center for Cancer Research, Rockville, MD, [2]Universidade de Sao Paulo (USP), Faculdade de Medicina de Ribeirao Preto (FMRP), Sao Paulo, Brazil

Genome-wide association studies (GWAS) have identified 13 renal cell carcinoma (RCC) risk regions, as well as 7 regions with nominal significance, but detailed investigation of how these regions function is required to reveal the underlying biological bases of disease susceptibility. While detailed study of four loci have implicated critical pathways in RCC, causal genes and pathways for most loci remain unidentified. To identify such causative variants and target genes, we evaluated a set of variants based on Massively Parallel Reporter Assays (MPRA), eQTL analysis, capture Hi-C, and an arrayed CRISPR inhibition (CRISPRi) screen. The MPRA identified 196 variants across 19 regions with significant allele-specific effects, indicating cis-regulatory activity. Of these, 39 variants across 10 RCC loci displayed chromatin loops allowing physical interaction with the promoter of 24 nearby putative gene targets, as well as a significant cis-eQTL with the same gene. To confirm the presence of a cis-regulatory relationship between these 39 candidate variants and 24 putative target genes, we performed an arrayed CRISPRi screen in ACHN (RCC) and HEK293T (embryonic renal) cells covering each of the 10 nominated regions. Cells were stably transduced with inactive Cas9 fused to the ZIM3 transcriptional repressor domain and cis-regulatory relationships were assessed by TaqMan qPCR for the target genes. The screen identified multiple novel relevant target genes of RCC predisposition variants, including *UCK2* at 1q24, *ABL2 and TDRD5* at 1q25, *GTDC1* at 2q22, *GPR37* at 7q31, *AGBL3* and *CALD1* at 7q33, and *MAP2K1* at 15q22. At some regions, evidence indicates cis-regulatory relationships occur between a target gene and all variants predicted to be 'causative' at the region (e.g., *UCK2* at 1q24 and *ABL2* at 1q25). For other regions, cis-regulatory relationships occur between a gene and only one variant tested (e.g., *GPR37* at 7q31 and *TDRD5* at 1q25).Previously, target genes of only four RCC susceptibility regions had been identified and published. This study identifies eight novel target genes across six additional RCC susceptibility regions, representing a significant advance in understanding of the underlying biology of RCC susceptibility variants. Furthermore, ongoing screening using the orthologous method, CRISPR activation (CRISPRa), and integration of both normoxic and hypoxic conditions continues to provide further insight into the underlying biology at these regions.

#6155 Germline variants in cancer susceptibility genes and subsequent neoplasm risks after childhood cancer: A pooled analysis of two large-scale cohorts.

S. A. Zamani[1], D. M. Karyadi[1], S. W. Hartley[1], J. N. Sampson[2], T. Gibson[1], P. Kraft[1], S. J. Chanock[1], L. M. Morton[1];
[1]National Cancer Institute, Rockville, MD, [2]Food and Drug Administration, Silver Spring, MD

Background: Increasing evidence suggests germline genetic susceptibility influences the risk of developing subsequent neoplasms (SNs)—a major cause of morbidity and mortality—among childhood cancer survivors, but studies have been hampered by sample size and limited gene sets. We pooled two large-scale cohorts of childhood cancer survivors to characterize overall and specific SN risks among individuals carrying germline variants in 88 known cancer susceptibility genes with an autosomal dominant inheritance pattern.
Methods: Using whole-genome or whole-exome sequencing data from the Childhood Cancer Survivor Study and St. Jude Lifetime Cohort (median [interquartile range] follow-up, 29.7 [13.8] years), we identified rare, potentially protein-damaging germline variants with SnpEff/ClinVar. Conditional logistic regression evaluated overall SN and SN-specific risk, with up to 100 SN-free controls matched to cases by age, sex, primary childhood cancer type, SN type, radiation dose, chemotherapy, study, and follow-up time.
Results: Among 11840 individuals (50.6% female) who survived childhood cancer, 2162 (18.3%) developed at least one SN. The risk of developing any SN was elevated among 288 survivors carrying rare, potentially protein-damaging germline variants in an autosomal dominant cancer susceptibility gene (cases=13.3%; controls=9.6%; odds ratio [OR], 1.48; 95% confidence interval [CI], 1.30-1.70; P=5.12x10^{-5}). A similar proportion of carriers was observed among those who developed common SNs such as basal cell carcinoma (N=107/882, 12.1%), meningioma (N=52/373, 13.9%), breast cancer (N=49/353, 13.9%), and thyroid cancer (N=32/243, 13.2%). Higher frequencies of carriers were observed in less common SNs, specifically sarcoma (N=24/151, 15.9%), colorectal cancer (N=15/72, 20.8%), and glioma (N=16/64, 25.0%). The observed associations were generally consistent regardless of treatment type for first primary childhood cancer. Gene-specific analyses revealed that the risk of developing any SN was most pronounced among individuals carrying variants in *TP53* (cases=0.6%; controls=0.04%; OR, 9.93; 95% CI, 4.62-21.34; P=0.001) and *FANCM* (cases=0.9%; controls=0.5%; OR, 2.45; 95% CI, 1.48-4.03; P=0.018).
Conclusion: In large-scale cohorts of childhood cancer survivors with long-term follow-up, individuals carrying potentially protein-damaging germline variants in known autosomal dominant cancer susceptibility genes have substantially increased SN risk, emphasizing the importance of genetic testing and consideration of genetic risk in follow-up guidelines. However, these individuals account for a small fraction of all SN cases, warranting future research on underlying risk factors in this population.

#6156 Deciphering the genomic landscape of Chilean cancer: Unveiling driver pathway divergence, and novel germline and actionable somatic variants.

E. Gonzalez[1], J. Toro[2], A. Blanco[1], C. Tapia[2], S. Rivas[1], J. Erices[2], F. Osorio[2], G. Sepulveda-Hermosilla[3], M. Freire[3], V. Garate[3], J. Caceres-Molina[3], I. Gallegos[2], O. Barajas[2], M. Ahumada[2], E. Bustamante[2], J. Gonzalez[2], C. Ibanez[4], A. Corvalan[4], G. Owen[4], M. Garrido[5], R. Armisen[1], **K. Marcelain**[2]; [1]Universidad del Desarrollo, Santiago, Chile, [2]Universidad de Chile, Santiago, Chile, [3]CORFO Center of Excellence in Precision Medicine, Pfizer Chile, Santiago, Chile, [4]Pontificia Universidad Catolica de Chile, Santiago, Chile, [5]Universidad Mayor, Santiago, Chile

Advances in understanding the genetic landscape of cancer have paved the way for more precise molecular profiling and the development of more efficacious therapeutic options. However, underrepresentation in clinical research endeavors has left the Latin American population uncharacterized, which may prevent them from reaping the benefits of these advancements. This study sought to identify the genetic drivers and actionable mutations in solid tumors from Chilean patients, enhancing our understanding of the mutational landscape in a population with a genetically diverse background shaped by admixture.Methods: 468 biopsy tissues from gastric (171), gallbladder (91), breast (72), Ovarian (69), and colorectal (65) Chilean cancer patients were collected in several pathology services and biobank at Universidad de Chile. Target-sequencing was performed using Oncomine Comprehensive Assay v.1 and v.3; and TumorSec cancer panel. Data from TCGA, MSK-IMPACT, and ACCR GENIE cohorts was accessed through cBioportal and used for comparison with non-Hispanic populations. Variants were annotated with CGI, CancerVar, OncoKB, and ClinVar tools.Results: Overall, tumors have mutations mainly in TP53 (42.4%), PIK3CA (12.5%), KRAS (9.6%), PTEN (4.7%), BRCA1/2 (9%). Driver mutations were present in TP53 (42%), PIK3CA (16%), KRAS (10%), ERBB2 (7%), PTEN (7%), BRCA1/2 (8%), ATM (7%), among others. Accionable mutations were found primarily in PIK3CA (17%), KRAS (10%), ERBB2 (9%), and NTRK1/2/3 (4.8%). Besides already-known mutations, many “novel” mutations were also found in all tumor types. About 5-15% of novel variants were predicted drivers, including variants in CDH1, NOTCH1, BRCA1/2, MTOR, TSC2, and MSH2 genes. Significantly, key driver mutations identified in non-Hispanic patients from international cohorts are also prevalent in admixed Chilean patients. However, variations at the driver pathway level were also observed. Notably, the PI3K and MTOR pathways were more frequently affected in Chilean CRC and GBC, respectively. Furthermore, mutations in specific genes, such as TP53 in GBC, were associated with Amerindian genetic ancestry.The observed differences could be attributed to the abundance of newly identified driver-predicted variants, though the possibility of the admixed genetic background influencing the oncogenic process in various tissue types cannot be excluded.

#6157 Population-specific 5-hydroxymethylcytosine signatures in circulating cell-free DNA and overall survival among Blacks and Whites with multiple myeloma.

B. Wang[1], Z. Zhang[2], B. Derman[1], K. Kowitwanich[1], J. Cheung[1], A. Jakubowiak[1], C. He[1], W. Zhang[2], B. Chiu[1];
[1]University of Chicago, Chicago, IL, [2]Northwestern University Feinberg School of Medicine, Chicago, IL

Background: Epigenetic modifications play important roles in the prognosis of multiple myeloma (MM). To date, DNA methylation (i.e., 5-methylcytosine) is the most extensively studied cytosine modification. Emerging evidence suggests that 5-hydroxymethylcytosine (5hmC), a product of 5mC through demethylation, in circulating cell-free DNA (cfDNA) is associated with the overall survival (OS) of MM. We also showed that African Americans (AAs) and European Americans (EAs) with MM have distinct genome-wide 5hmC profiles. However, no study has evaluated whether the association between 5hmC profiles and OS in MM differs between EAs and AAs.
Methods: A total of 586 newly diagnosed patients with MM at the University of Chicago Medical Center were prospectively enrolled between 2010-2019. The current study profiled genome-wide 5hmC in plasma-derived cfDNA for 303 patients using the 5hmC-Seal and next-generation sequencing. Data cutoff was February 28, 2022. Vital status was ascertained using the National Death Index. OS was defined as the time from diagnosis until death from any cause. The 5hmC-Seal data were mapped to the human genome reference (hg19) and annotated to gene bodies. In each population, patients were randomly divided into a training set (EAs, n=147; AAs, n=64) and a testing set (EAs, n=64; AAs, n=28). After selecting the top 10% candidate genes associated with OS in age-adjusted univariate Cox proportional hazards model, we applied multivariable Cox models with elastic net regularization for feature selection through leave-one-out cross-validation. The optimal "*alpha*" and "*lambda*" were evaluated to maximize model performance measured by the Harrell's Concordance Index. The differential 5hmC enrichment levels of selected genes were used to compute a weighted prognostic score (wp-score). The associations between the wp-scores and OS were evaluated in the testing sets, adjusting for established prognostic factors (e.g., age, stage).
Results: Of the 303 MM patients, 94 (30.92%) were AA and 210 (69.08%) were EA. The median follow-up was 108 months. Our preliminary analyses identified 26 and 10 5hmC marker genes associated with OS in EAs and AAs, respectively. Importantly, none of these genes overlap between the two groups. We used these genes to compute wp-scores in EAs and AAs. In the training sets, patients with a higher wp-score had worse OS. The same trend was observed in the testing sets: hazard ratios (HR) in EAs: 1.31, 95% CI: (0.83, 2.06) and HR in AA: 11.94, 95% CI: (1.88, 75.68) after controlling for established prognostic factors.
Conclusions: Our findings suggest that different epigenetic modifications in cfDNA might be associated with OS between EAs and AAs with MM and the 5hmC marker gene-based wp-scores are independent prognostic factors for MM.

#6158 Tumor genomic heterogeneity in non-small cell lung cancer (NSCLC) patients from Latin America.

Javiera Garrido[1], Evelin Gonzalez[1], Gonzalo Sepulveda-Hermosilla[1], Matias Freire[2], Alejandro Blanco[1], Solange Rivas[1], Katherine Marcelain[3], Gareth I. Owen[4], Carolina Ibañez[4], Alejandro Corvalan[4], Marcelo Garrido[5], Rodrigo Assar[2], Rodrigo Lizana[2], Javier Caceres-Molina[2], Diego Ampuero[2], Liliana Ramos[2], Paola Perez[6], Osvaldo Aren[7], Sara Chernilo[8], Cristina Fernandez[8], Maria Loreto Spencer[9], Jacqueline Flores[10], Giuliano Bernal[11], Monica Ahumada[3], German Rasse[12], Carolina Sanchez[13], Maria Galli de Amorim[14], Gabriela Branco[14], Diana Noronha Nunes[14], Emmanuel Dias-Neto[14], Helano C. Freitas[14], NIRVANA team, Ricardo Armisen[1]

[1]Centro Genetica y Genomica, Instituto de Ciencias e Innovacion en Medicina, Facultad de Medicina, Universidad del Desarrollo, Santiago, Chile,[2]Center of Excellence in Precision Medicine, Pfizer, CORFO, Santiago, Chile,[3]Departamento de Oncologia Basico Clinica, Facultad de Medicina, Universidad de Chile, Santiago, Chile,[4]Advanced Center for Chronic Diseases and Department of Hematology and Oncology, Pontificia Universidad Catolica de Chile, Santiago, Chile,[5]Centro de Oncologia de Precision, Universidad Mayor, Santiago, Chile,[6]National Institute of Health, National Institute of Dental and Craniofacial Research, Bethesda, MD,[7]Centro de Investigacion Clinica Bradford Hill, Santiago, Chile,[8]Instituto Nacional del Torax, Santiago, Chile,[9]Department of Pathology, Hospital Clinico Regional de Concepcion Dr. Guillermo Grant Benavente, Concepcion, Chile,[10]Departamento de Salud Publica, Facultad de Medicina, Universidad Catolica del Norte, Coquimbo, Chile,[11]Departamento de Ciencias Biomedicas, Facultad de Medicina, Universidad Catolica del Norte, Coquimbo, Chile,[12]Hospital de Puerto Montt, Puerto Montt, Chile,[13]Centro de Genomica y Bioinformatica, Universidad Mayor, Santiago, Chile,[14]Laboratory of Medical Genomics, A. C. Camargo Cancer Center, Sao Paulo, Brazil

Motivation: Life prospects of non-small cell lung cancer (NSCLC) patients have greatly improved over the last decades with the adoption of tumor genomic profiling. A better understanding of the mutational landscape has allowed for a more precise molecular characterization and the development of more effective treatment alternatives. However, tumors present a widespread heterogeneity, and many challenges remain to fully comprehend the influencing factors. Of particular importance is the Latin America population which i) is commonly underrepresented in clinical trials and large-scale epidemiological studies, ii) presents higher incidence and mortality rates in comparison to the developed world, and iii) is constituted by a genetically admixed population. Our research attempts to close this gap by investigating the interplay between sociodemographic, clinical, and lifestyle factors, and the effect these exert on the mutational profiles of Latin-American NSCLC patients.

Methodology: The study population is derived from the NIRVANA study, a cross-sectional multicenter observational study aiming to characterize and validate molecular diagnostic technologies for NSCLC patients in Chile, Brazil, and Peru. Between July 2015 to October 2018, 5030 NSCLC patients were recruited from 37 centers, meeting inclusion criteria of age ≥18, histologically or cytological proven NSCLC diagnostic, and naïve treatment. Exclusion criteria included prior chemotherapy treatment and refusal to give informed consent. Primary or metastatic NSCLC samples were collected during standard of care biopsy and processed for the DNA and RNA isolation. Next Generation Sequencing (NSG) genomics profiles were obtained using the Oncomine Focus Assay (OFA). Covariates of interest, including sociodemographic, clinical, and lifestyle factors, were assessed at enrollment. QC-approved genomic profiles were obtained for 1864 participants.

Results and Conclusions: The prevalence of mutations and fusions in the eight most relevant NSCLC genes (*EGFR*, *KRAS*, *ALK*, *MET*, *RET*, *BRAF*, *ROS1* and *ERBB2*) varies based on sociodemographic, clinical and lifestyle characteristics. Clear distinctions emerged in the prevalence of *EGFR*, *KRAS* and *ERBB2* mutations among the three countries (*EGFR*: 20.9%, 17.6%, 35.3%; *KRAS*: 21.8%, 15.6%, 10.3%; *ERBB2*: 2.8%, 3.3%, 4.4% for Brazil, Chile, and Peru, respectively). Furthermore, distinct association patterns were identified between the prevalence of genetic alterations and the studied factors, with attributes such as sex, tobacco use and ethnicity mostly influencing the occurrence of *EGFR*, *ALK* and *ROS1* alterations. These findings provide novel insights into NSCLC studies among Latin-American patients, potentially serving as guidelines for more tailored strategies in the overall management of this underrepresented population.

#6159 Single cell analysis of circulating peripheral blood mononuclear cells in African American men with prostate cancer and their association with lethal disease.

M. U. Ahmed, T. Dorsey, S. Ambs;
National Cancer Institute, Bethesda, MD

Prostate cancer is a leading cause of cancer-related deaths among men in the United States and affects African American (AA) men more so than other men. We and others previously described a distinct tumor immunobiology in AA prostate cancer patients. Furthermore, we discovered a serum proteome-defined suppression of tumor immunity signature that is prevalent among these patients and associated with lethal prostate cancer. In the current study, we sought to investigate the composition of circulating peripheral blood mononuclear cells (PBMCs) in AA and European American (EA) prostate cancer patients and their association with patient group and lethal prostate cancer. We obtained high-quality RNA-sequencing data for 277336 single cells representing circulating PBMCs from 59 AA and EA men. In the analysis, being an AA patients associated with an increased abundance of exhausted T cells, higher numbers of plasma B cells and CD16+ monocytes. Gene signatures indicative of T cell exhaustion and Treg activity were generally elevated in AA PBMCs while T cell effector function features were decreased. Within the overall cell population, interferon gene signatures were robustly elevated in AA than EA patients. This gene signature pattern that we observed in AA patients also associated with lethal prostate cancer, namely the T cell exhaustion, Treg activity and elevated interferon signaling gene signatures, may contribute to immune dysfunction and immune injury; pointing to potential clinical implications. Lastly, the interferon-induced transmembrane protein (IFITM3), interferon alpha inducible protein (IFI6), cysteine rich protein-1 (CRIP1), and the RAC family small GTPase2 (RAC2) were notably upregulated in AA patient-derived immune cells. In summary, we show that circulating immune cell populations and the associated gene signatures differ between men of African and European descent. Those elevated in AA patients correlated with lethal prostate cancer.

#6160 Mutational signatures and their associations with social determinants of health.

P. Swaminathan, M. Deaton, C. Hattum, B. Solomon, W. Spanos, D. Starks, R. Elsey, C. Williams, T. Meissner;
Avera Cancer Institute, Sioux Falls, SD

Introduction: Mutational signatures, or unique patterns of genetic mutations due to exogenous and endogenous mutational processes, are being continuously identified through the analysis of cancer patients' genomes. While cancer research has developed and mortality rates have declined, disparities in cancer outcomes have widened. Social determinants of health (SDOH), such as access to health care, education, and economic stability are essential to addressing health equity. While much research is ongoing regarding the identification and etiology of mutational signatures, little work has been published regarding the associations of these signatures with SDOH. Therefore, this study proposes an exploration into the relationships between the presence of mutational signatures and SDOH within an adult pan-cancer patient population.

Methods: Variant calls from whole exome sequencing for each patient was used to infer the presence of 58 single base substitution (SBS) mutational signatures. Descriptive statistics were calculated for 455 unique patients. Previously documented associations between primary diagnosis site and distinct signatures were used to validate the predicted signatures in the patient population. Signature profiles were then linked to 208 patient health records with complete SDOH. Logistic regression predicting the presence of each signature was modeled for these patients. Full models for each signature included age, gender, Rural-Urban Commuting Area (RUCA) code, tobacco and alcohol usage, education, income, housing condition, and access to healthcare. Stepwise selection was used to determine significant variables.

Results: The most common signatures in the complete population (n = 455) were SBS1 (clock-like; 98%) and SBS39 (95%), followed by SBS5 (clock-like; 38%) and SBS22 (aristolochic acid exposure; 36%). However, SBS24 (aflatoxin exposure; p = .019) and SBS7a (UV exposure; p = .002) were significantly more common in lung and skin cancer patients respectively. Each patient had 4.1 signatures on average, with a range of 2-7. The average number of signatures per patient varied significantly by primary diagnosis (ANOVA p = .014). Patients with a vulva/vagina (4.8) or bladder/urinary tract (4.9) diagnosis had the highest number of signatures while those with a liver (3.3) or kidney (3.6) diagnosis had the lowest. Logistic regression models for the population with SDOH (n = 208) showed poor housing condition was associated with SBS4 (tobacco smoking; p = 0.091). Any issue in accessing healthcare was associated with SBS13 (AID/APOBEC; p = 0.114) and SBS21 (MMR; p = 0.076). Greater rurality was associated with SBS16 (p = .144) and SBS21 (p = .107). The relationship was inverse for SBS1 (p = .121).

Conclusion: Multiple significant relationships between different SDOH and mutational signatures was revealed, pointing the need to extend this research to larger patient populations with diverse SDOH.

#6161 Investigating the relationships between race and socioeconomic status on the biology of ER+ breast cancer.

J. T. DeWitt, E. Oropeza, S. Haricharan;
Sanford Burnham Prebys Med. Discovery Inst., San Diego, CA

Black women in the US have worse health care options, poorer educational opportunities, and decreased income quality which collectively contribute to an overall lower socioeconomic status (SES) compared to white women. Furthermore, although the incidence of estrogen receptor positive (ER+) breast cancer is similar for Black and white women in the US, Black patients have significantly worse outcomes. The field has traditionally focused on systemic factors such as SES to explain outcome disparities. Consequently, differences in the molecular biology between tumors from Black and White women remains a gap in knowledge in the field. Recent studies have found that Black cancer patients have a unique gene expression profile that may modulate treatment response. However, how SES contributes to these differences in molecular biology and whether these differences in SES alter treatment response remain unknown. One challenge to addressing these questions is that existing datasets significantly underrepresent Black women and are not sufficiently annotated to understand the complex interplay between molecular biology and SES. Here, we present analysis of RNA expression datasets from 60 ER+ patient tumors (38 Black, 22 White), with corresponding SES and patient outcome annotations which suggest that the ECM and TIME of ER+ breast cancer are influenced by race and factors of SES including BMI and community poverty burden. We further provide evidence that these alterations in the TME may also associate with worse patient outcomes.

BIOINFORMATICS / COMPUTATIONAL BIOLOGY / SYSTEMS BIOLOGY / CONVERGENT SCIENCE: Detection, Imaging, and Pathology
Poster Session

#6165 Early detection of pancreatic cancer by hyperpolarized magnetic resonance.

P. L. Smith, J. S. Enriquez, R. Howell, O. L. Roux, S. Pudakalakatti, P. Dutta, F. Mcallister, P. Bhattacharya;
UT MD Anderson Cancer Center, Houston, TX

Introduction: Pancreatic cancer is difficult to diagnose due to its asymptomatic presentation at early stages. Therefore, there is an unmet need for non-invasive imaging markers that can help identify the aggressive pancreatic lesions at an early time point. One of the most promising imaging biomarkers is the conversion of hyperpolarized (HP) pyruvate to lactate[1-3]. With HP metabolic imaging, the conversion will be monitored among different premalignant models at different timepoints as well as tested against pancreatitis, a known confounder of pancreatic cancer in the clinic.

Methods: HP [1-^{13}C]pyruvate Magnetic Resonance Spectroscopy (MRS) was employed to study the metabolic processes in tamoxifen inducible genetically engineered mouse models (P48CreERT2;LSL-K*ras*^{G12D}(iKC)) with pre-invasive pancreatic intraepithelial neoplasia (PanIN) precursor lesions, invasive pancreatic cancer model (P48CreERT2;LSL-K*ras*^{G12D}; LSL-*p53*^{R172H} (iKPC)) and control animals (P48CreERT2 (iC)) at 7T Bruker MRI scanner. These mice were imaged before tamoxifen induction at 10-, 20-, and 30-weeks post induction. For the pancreatitis model, iC and iKC mice they were treated with caerulein for three weeks, 7 weeks after tamoxifen induction. The pancreatitis mice were imaged 24 hours after the last caerulein injection.

Results/Discussion: HP lactate-to-pyruvate ratio is increased in the cancer models compared to the control model. In the iKPC mouse model, at the 20-week post induction imaging there was a significant increase of the lactate-to-pyruvate ratio compared to the 10-weektime point after induction. The 20-week iKPC time point ratio compared to the iKC and control mouse models was significantly higher, indicating the aggressive nature of the disease. Even in the iKC model there is a slight increase
of the lactate-to-pyruvate ratio at 20-weeks post induction compared to both previous time points, pre-induction and 10-week. No change in the lactate-to-pyruvate ratio was not observed with the pancreatitis phenotype. In the future, we plan on imaging at earlier timepoints or at smaller intervals in the iKPC model, to observe the exact moment the metabolism switches to lactate.

Conclusion: Our data demonstrates that the metabolic flux to lactate is only increasing in the premalignant models of pancreatic cancer but not in the pancreatitis model, suggesting that the differentiation between early pancreatic cancer and pancreatitis can be achieved by hyperpolarized metabolic imaging. We are currently in the process of translating this in a clinical trial at MD Anderson Cancer Center.

#6166 A whole-organ *ex vivo* optical imaging technique for non-destructive, more precise identification of serous tubal intraepithelial carcinoma (STIC) in fallopian tubes.

N. M. Bardhan[1], V. Rastogi[1], R. L. Stone[2], A. M. Belcher[1];

[1]Massachusetts Institute of Technology (MIT), Cambridge, MA, [2]Johns Hopkins University School of Medicine, Baltimore, MD

Objective

With the recent discovery of the fallopian tube (FT) origin of the most common and lethal type of ovarian cancer, high grade serous cancer (HGSC), engineering solutions to overcome the limitations of standard histopathology to more reliably identify incipient HGSCs and their serous tubal intraepithelial carcinoma (STIC) precursors are much needed. This investigation tests the potential of whole-organ *ex vivo* optical imaging of freshly excised FTs to label and sample abnormal tubal epithelium prior to formalin fixation and paraffin embedding for standard histopathology.

Methods

This investigation prototyped “OVASEEK”, a whole-organ, near-infrared optical imaging platform for identification of STICs. This prospective biospecimen protocol with annotated clinical data was approved by the IRB. Following salpingectomy at the time of hysterectomy for benign indications, FTs from study participants are longitudinally bivalved. Half of the FT is retained for routine evaluation using the Sectioning and Extensively Examining the Fimbriated end (SEE-FIM) protocol by Johns Hopkins gynecologic pathologists (Gyn Path), while the other half is sent overnight in organ transplant media to MIT for imaging on OVASEEK. Hyperspectral “label free” first pass imaging is performed using a series of band-pass filters. Second pass fluorescence imaging is then performed using nanoparticles tagged with anti-LAMC1 antibodies targeting laminin γ1, a known STIC surface marker. Abnormal signal(s) on OVASEEK imaging of the FT epithelium are tattooed with black ink, the tissue is formalin fixed and returned to Gyn Path for serial sectioning. Research findings are reported in an addendum to the formal pathology report in the electronic medical record and discussed with the patient by the gynecologic oncologist co-investigator.

Results

OVASEEK enabled non-destructive imaging over a wide field-of-view ~ 12×12 cm, with features of interest in the 1,050-1,550 nm range. In this pilot study, OVASEEK identified histopathologic abnormalities missed by standard SEE-FIM in 20% of FTs (n=2 out of 10). In each case, OVASEEK found microscopic (~200 µm) foci of salpingitis, a lymphoplasmacytic infiltrate consistent with inflammation. Performance of serial sectioning and histopathologic examination of the tattooed epithelium yielded this diagnosis.

Conclusion

Work is ongoing to improve the resolution, speed and sensitivity of OVASEEK for STIC detection. Identification of µm-sized foci of inflammation using OVASEEK is proof-of-principle that whole-organ *ex vivo* imaging of freshly excised FTs may be an innovation that improves the diagnostic performance of routine histopathology. Accurate and reproducible diagnosis of STIC and concurrent microscopic HGSC is imperative to the understanding of the early pathogenesis of HGSC in clinically actionable ways.

#6167 Spatial transcriptomic analysis identifies pancreatic cancer cell surface markers for imaging and therapy.

J. Wang, A. J. Kare, M. K. Schneider, J. Seo, A. Iagaru, G. W. Charville, W. G. Park, K. W. Ferrara;
Stanford University, Palo Alto, CA

Pancreatic cysts and precancer lesions have been reported in up to 50% of adults; however, few of the precancer lesions develop into aggressive pancreatic ductal adenocarcinoma (PDAC). Strategies for the differentiation of precancers and PDAC are needed. Recently proposed molecular imaging targets to accomplish this goal include integrin $\alpha_v\beta_6$ and fibroblast activation protein (FAP). To discover and quantitatively evaluate potential imaging and therapeutic targets, we performed Visium spatial transcriptomic (ST) sequencing on human surgical sections of normal tissue adjacent to precancers, intraductal papillary mucinous neoplasms and PDAC. All human tissues were collected in accordance with the Stanford Institutional Review Board. The resulting data were correlated with immunohistochemistry (IHC) and combined with analysis with publicly available spatial and single cell PDAC datasets to create a quantitative PDAC cancer surfaceome score. Pseudotime and receiver operating characteristic (ROC) analyses were also performed. We found that clusters with high cancer surfacesome scores were spatially correlated with a cellular morphology consistent with cancer. In the cancer cluster, the expression of surface markers *CLDN4*, *GPRC5A*, *TSPAN8*, and *CEACAM5* was enhanced more than 13-fold compared with the normal pancreas, while *FAP* and *ITGB6* were differentially expressed by less than 4-fold. Within cancer clusters, the fraction of spots overexpressing *CLDN4*, *S100P*, *ITGB6*, *MUC5AC*, *TFF1*, *CEACAM5*, and *FAP* was 88%, 87%, 78%, 66%, 59%, 47%, and 38%, respectively. The Pearson's correlation across space and expression intensity between *CLDN4*, *S100P*, *GPRC5A*, *TSPAN8*, *MUC1* and *TFF1* was greater than 0.6 for all combinations. The correlation of mRNA encoding *ITGB6* and *FAP* with cancer surfaceome markers was smaller, e.g. 0.37 and 0.01 versus *S100P*, respectively. The area under the curve (AUC) for the differentiation of PDAC from normal or precancerous tissue for *CLDN4*, *S100P*, *MUC5AC*, *TFF1*, *CEACAM5*, and *TSPAN8* was 0.9, 0.5, 0.3, 0.5, 0.8, and 0.4, respectively. From pseudotime trajectory analysis, we found that *MUC5AC* and *TFF1* increased at a precancerous pseudotime whereas *CLDN4* increased in time and space in spots corresponding to a PDAC-specific surfaceome score. This work demonstrates the feasibility of using spatial transcriptomics and IHC in human pancreatic cancer samples to discover and compare the expression of cell surface markers that can be employed in imaging and therapeutic protocols.

#6168 Sex-distinct patterns of molecular pathways associated with brain tumor edema.

P. R. Jackson[1], L. Curtin[1], S. Ranjbar[1], K. W. Singleton[1], M. M. Mrugala[1], R. S. Zimmerman[1], B. R. Bendok[1], P. Canoll[2], K. R. Swanson[1];
[1]Mayo Clinic, Phoenix, AZ, [2]Columbia University Irving Medical Center, New York, NY

Magnetic resonance imaging (MRI) is a centerpiece of clinical management of brain tumor patients, yet the biology underlying even commonly interpreted imaging changes is unclear. The purpose of this project was to understand what biology is associated with brain tumor edema abundance and if that association was sex distinct. We have developed a two-compartment model of MRI signal intensity to quantitatively estimate relative edema abundance from T2-weighted MRIs. Multiparametric MRIs were preprocessed with bias field correction and intensity normalization. The images were co-registered and segmented for abnormal regions and normal tissue. The segmentations and preprocessed images were utilized in the edema mathematical model to estimate the fraction of extracellular space (Fecs) and fraction of intracellular space (Fics). Through an ongoing image-localized biopsy collection protocol, we analyzed 179 samples (Female: 75; Male: 104) from 55 patients (Female: 21; Male: 34) for bulk RNA-Seq. Samples were characterized by their edema Fecs scores and underwent differential expression, gene set enrichment analysis using MSigDB hallmarks and cellular deconvolution using CIBERSORTx. Through differential expression and gene set enrichment analyses of these spatial biopsies, we have identified sex-distinct gene expression and pathways corresponding to regions of high vs low edema. Within highly edematous regions, male samples were amplified for respiratory pathways, while female samples were suppressed. Connecting changes on MRIs with molecular markers from image-localized biopsies provides an opportunity to identify the biological drivers of brain tumor associated imageable edema. Specifically, elucidating the sex-distinct patterns connecting changes on MRI with cellular populations and molecular pathways could be used to better interpret imaging of patients and interpreting treatment response.

#6169 High throughput *in-situ* spatial sequencing of proteins and RNA in FFPE tissue.

Michael Lawson, Yuji Ishitsuka, Andrew Pawlowski, Zhenmin Hong, Jake Koh, Kenneth Gouin, Nathan Ing, Richard Que, Yeoan Youn, Sara Ding, Tony Facchini, Ryan Costello, Katelyn Nelson, Jamie Stover, Howon Lee, Sarthak Duggal, Taylor Plaziak, Kaitlin Cameron, Mimi Abdu, Daan Witters, Martin Fabani, Eli Glezer

Singular Genomics, San Diego, CA

We have developed an high throughput high resolution in situ multi-omic platform to enable studies in the rapidly evolving landscape of oncology and immunology research.

Despite the potential of existing tools, the speed and throughput of current methodologies pose significant limitations. Here, we introduce a novel spatial sequencing platform employing a rapid 4-color SBS chemistry with sub-micron resolution imaging and an ultra-high throughput capacity. The platform simultaneously profiles RNA transcripts and proteins within formalin-fixed paraffin-embedded (FFPE) tissues. With up to 40 cm^2 of tissue area imaging within a 24-hour timeframe, the platform can power extensive, multi-omic studies in cancer research.

To evaluate the performance of the platform, we prepared 5 um serial sections from healthy and tumor kidney FFPE block and used a novel tool to precisely position multiple tissue sections on a slide. Following probe binding and amplification, we used SBS readout to profile 105 transcripts and 6 proteins (via DNA-conjugated antibodies). Images were analyzed using a custom pipeline for feature detection and decoding, and cell segmentation using Cellpose. Results showed strong correlation to single-cell transcription profiles and cell type signatures defined by scRNA-Seq. Additionally, we see good agreement between single cell transcript and protein profiles. Existing spatial biology platforms are known to struggle with degraded and challenging clinical sample types (e.g. decalcified bone marrow), due to RNA fragmentation. We successfully profiled immune cells in FFPE-embedded bone marrow biopsies, measuring 143 transcript targets and 8 proteins. We believe this represents a significant step forward for in-situ analysis of bone marrow samples, and could be valuable for studying the pathology and response to treatment in blood cancers such as AML and CML.

In-situ sequencing of antibody genes and T-cell receptors provides a deeper view of cellular immune response. As a step towards this goal, we demonstrated in-situ sequencing of antibody heavy and light chains within a B cell line, resulting in accurate readout of 28 bases within the CDR3 regions.

In conclusion, we present an SBS-based approach for in-situ detection of targeted gene transcripts and proteins at an unprecedented throughput, and its application to the analysis of human kidney and bone marrow FFPE tissue samples. The capability to deeply profile tissues at high throughput could enable larger translational studies, and assembly of 3D maps of gene and protein expression at sub-cellular resolution.

#6170 Risk stratification of smoldering multiple myeloma using fourier transform infrared spectroscopy of serum.

D. Dingli[1], D. Khonkhammy[2], C. Gunnarson[2], G. Schlauderaff[2], D. Q. Pham[2], A. Khammanivong[2];
[1]Mayo Clinic, Rochester, MN, [2]Oncodea Corporation, St Paul, MN

Background: Smoldering multiple myeloma (SMM) is a state where patients have more than 10% clonal plasma cells or a serum monoclonal protein > 3g/dl but no evidence of end organ damage. Patients with SMM are at risk of developing active multiple myeloma (defined by the CRAB criteria). The best stratification system with respect to the risk of progression to active myeloma is the 20/2/20 (20% plasma cells, M protein >2.0 g/dl, and involved to uninvolved immunoglobulin free light chain ratio >20). The presence of ≥2 criteria predicts a 50 - 60% risk of progression within 2 years. Thus, many patients considered 'high-risk' may *not* progress in this time frame, and patients with ≤1 risk factor *can* progress to active myeloma. Therefore, improved risk stratification methods are needed to correctly identify patients at high risk of progression. We hypothesized that Fourier Transform InfraRed (FTIR) spectroscopic analysis of serum combined with artificial intelligence (AI) can correctly risk stratify patients with SMM.

Methods: We identified 192 SMM patients: 96 who progressed and 96 who did not progress within 2 years of diagnosis. We used stored sera from the time of diagnosis to perform FTIR to determine differences in the spectra of patients who did/did not progress and train an AI algorithm. A randomized 10-fold cross-validation analysis was performed using 172 samples (86 from each group) for training and the remaining 20 for testing to assess the model across 10 independent iterations. Subsequently, we blindly tested the trained model against an independent set of serum samples (N=24) from patients who progressed ≤3 years of diagnosis. Receiver operator characteristic (ROC) analysis was used to assess the FTIR AI algorithm output compared to the clinical outcome data.

Results: From the 96 patients who *progressed*, 48 had complete data for the 20/2/20 risk stratification. 11 patients (23%) had ≤1 of the criteria and so would have been considered at low likelihood to progress. Of the 96 who did *not progress* within 2 years, 49 had complete data for risk stratification. Of these, 27 (55.1%) met the high-risk criteria of the 20/2/20 classification and would have been predicted to progress within 2 years. FTIR/AI model correctly identified the patients at risk of progression (95% accuracy) with AUC of 0.96. Similarly, it was able to classify patients who did not progress within 2 years of diagnosis (94% accuracy) with an AUC of 0.96. FTIR/AI correctly predicted the patients at risk of progression within 2 years (90%) and 3 years (87.5%) in the blinded validation group with an AUC of 0.89 and 0.82, respectively.

Conclusion: Analysis of serum in patients with newly diagnosed SMM with FTIR is able to correctly identify those at risk of progression within 2 or 3 years of diagnosis with an accuracy of ~90% in a blinded external validation study. FTIR may, therefore, be used to assess SMM patient risk before committing to potentially toxic therapy.

#6171 Evolution of the spatial myeloid-lymphoid engagement in glioblastoma under temozolomide treatment.

S. P. Castillo, A. Jahedi, P. Gupta, J. T. Huse, K. Kannan, Y. Yuan, K. P. L. Bhat;
The University of Texas MD Anderson Cancer Center, Houston, TX

The current standard of care for glioblastoma (GBM), encompassing surgery, chemotherapy, and radiation, fails to extend patient survival beyond ~12-15 months. Even advanced immunotherapies, such as checkpoint blockade and chimeric antigen receptor-armored T-cell therapies, are ineffective in GBM due to tissue-specific niche-dependent escape strategies employed by glioma cells. Immune effectiveness, a finely regulated spatial and context-dependent process, underpins such a dismal state of the present therapeutic options. Herein, we applied CO-Detection by indEXing (CODEX), a state-of-the-art multiplex imaging platform, to elucidate the immune cell networks of the tumor microenvironment. By harnessing computational tools on multiplexed regions of interest across whole-slide images, we characterize the immune repertoire of GBMs by studying intratumor heterogeneity across space-histological territories- and time, matching pre- and post-treatment tissue sections of GBMs from seven patients under treatment (Stupp protocol). We aimed to assess changes in the interactions between the two main compartments of the immune system, myeloid and lymphoid, pre- and post-treatment using spatial statistics. We designed a computational workflow for the georeferencing, classification, and phenotyping individual cells of CODEX images across 105 regions of interest, representative of a mosaic of histologically defined cellular tumor (CT) or infiltrating tumor. We defined six major immune phenotypes and evaluated their spatial association with $Cd45^{-}Nestin^{\pm}Olig2^{\pm}$ glioma cells. We modeled the GBM ecosystem and the cells' spatial coexistence as spatial point processes that allowed the projection of coexistence networks. After stringent quality control, we detected and phenotyped 2.3M cells. Despite interpatient heterogeneity, some patients maintained an even immune composition, while others showed an enrichment in microglia, particularly in CT. Spatial network analyses revealed an increased coexistence between myeloid and lymphoid cells after treatments despite T cells being canonically considered moderately abundant. Quantitatively, the immune meta-network displayed higher edge density and lower modularity post-treatment compared with pre-treatment, reflecting increased lymphoid-myeloid engagement. In summary, we detected an increased spatial myeloid-lymphoid engagement in GBM undergoing chemo-radiation treatments. Spatiotemporal rearrangement of tumor-immune interactions indicates mechanisms implicated in disease recurrence and resistance to standard treatment, opening the frontiers for developing new targeted immunotherapies.

#6172 Accurate PD-L1 IHC assessment in urothelial carcinoma by an AI algorithm robust across multiple sites, antibody clones, and scanners.

N. Abele[1], D. Calvopina[2], D. Mulder[2], P. Frey[2], E. Karakok[3], F. G. Salman[3], M. Oktay[3], M. Eckstein[1], S. Springenberg[2], A. Hartmann[1], T. Lang[2];

[1]Institute of Pathology, University Hospital Erlangen, Friedrich-Alexander-Universitat Erlangen-Nurnberg, Comprehensive Cancer Center Erlangen-EMN (CCC ER-EMN), Erlangen, Germany, [2]Mindpeak GmbH, Hamburg, Germany, [3]Memorial Hospitals Group, Istanbul, Turkey

Background: Immunotherapy against PD-L1 is used for treatment of several indications of Urothelial Carcinoma (UC). Recent results indicate that it is likely to become part of the standard first-line treatment regimen for advanced UC in the near future. Accurate readout of Immunohistochemical (IHC) PD-L1 expression is therefore essential to inform UC treatment decisions. However, manual PD-L1-scoring is prone to high inter- and intra-observer variability. Artificial intelligence (AI) may help to improve standardization, accuracy and efficiency of PD-L1 IHC scoring. Yet, previous AI-based approaches struggled to show consistency across images that are diverse with regards to the source institutions, antibody clones, and scanning hardware used. Methods: We developed an AI software for PD-L1 tumor proportion scoring (TPS/TC) on whole-slide images (WSIs) of UC without human supervision. PD-L1 analysis by the software is fully-automated, does not require any adaptation steps, and is concordant with current clinical guidelines. The performance of the software was evaluated on two cohorts of PD-L1 stained UC samples against ground-truth (GT) TPS/TC scores given by human pathologists in clinical routine. The first cohort (n = 53) consisted of samples stained with the 22C3 antibody clone (Agilent) derived from four institutions and three scanner models. It contained both tissue microarray samples and scans of UC resectates. A second validation cohort consisted of n = 83 WSIs stained with the SP263 clone (Ventana), collected from two institutions. Results: For the threshold of TPS≥1% (cut-off established for adjuvant therapy with Nivolumab), agreement rates of AI scores with human GT scores were 92.5% for cohort 1 (22C3) and 96.4% for cohort 2 (SP263). Sensitivity/specificity values were 92.3%/92.9% for cohort 1 and 100%/93.6% for cohort 2. Across both cohorts (n = 136) the agreement rate between AI and human was 94.9%. Conclusions: Across 136 UC samples stained with two PD-L1 antibody clones, and derived from a total of four institutions and three scanner models, the fully automatic AI system showed excellent agreement with human pathologist scores. These results on challenging validation data show the potential of AI applications to standardize and optimize PD-L1 scoring and demonstrate consistency and safety of suitable AI-based systems for application in clinical routine.

#6173 The development and evaluation of a convolutional neural network for melanoma detection in whole slide images.

E. L. Clarke[1], D. Magee[1], J. Newton-Bishop[1], W. Merchant[2], M. Hall[1], R. Insall[3], N. Maher[4], R. Scolyer[4], G. Farnworth[1], A. Ali[1], S. O'Shea[5], D. Treanor[1]; [1]University of Leeds, Leeds, United Kingdom, [2]Leeds Teaching Hospitals NHS Trust, Leeds, United Kingdom, [3]University College London, London, United Kingdom, [4]Melanoma Institute Australia, Sydney, Australia, [5]South Infirmary Victoria University Hospital, Cork, Ireland

The current melanoma staging system is predictive of 74% of the variance in survival, with prognostic biomarkers subject to high levels of inter-observer variation. The application of convolutional neural networks (CNNs) to whole slide images (WSIs), may reveal new insights into tumor morphology and therefore patient prognosis.

Melanoma morphology appears to be of greater significance than in other solid tumors, with Breslow thickness remaining the strongest prognostic indicator. Other biomarkers based on tumor morphology have been generated and although some have been found to be prognostically superior to Breslow thickness, none have been integrated into clinical workflows. This may in part be explained by their demands on pathologist time. Therefore, this work outlines the development and evaluation of a CNN for invasive cutaneous melanoma detection in WSIs, which may be used for prognostic biomarker generation.

1,157 WSIs containing cutaneous melanoma from five datasets (three from the University of Leeds, one from the Melanoma Institute Australia, as well as The Cancer Genome Atlas) have been used in the initial development and evaluation of the CNN. A custom-designed 2-class tumor segmentation network with a fully convolutional architecture was trained using annotations. The CNN was evaluated using various methodologies, including comparison at per-pixel and per-tumor levels as compared to manual annotation, as well as variation across 3 scanning platforms (Leica Aperio AT2 (Milton Keynes, UK), Roche Ventana DP600 (Arizona, US) and Hamamatsu NanoZoomer S360 (Hamamatsu City, Japan).

The CNN detected and located invasive melanoma tissue of no specific type with an average per-pixel sensitivity and specificity of 97.6% and 99.9% respectively across the 5 test sets. There were no statistical differences between tumor dimensions generated by the CNN as compared to manual annotation. Similarly, there were no statistically significant differences between CNN generated tumor dimensions across three scanning platforms.

We have developed and performed initial evaluation of a CNN which appears to accurately detect invasive cutaneous melanoma of no specific type in WSIs for objective evaluation of tumor morphology. Future work should interrogate these data further for its propensity to predict survival outcomes.

#6175 Deep learning-based survival prediction for hepatocellular carcinoma using whole slide images.

S. Lee[1], H.-J. Jang[2];

[1]Seoul St. Mary's Hospital, The Catholic University of Korea, Seoul, Korea, Republic of, [2]College of Medicine, The Catholic University of Korea, Seoul, Korea, Republic of

There is an increasing need for classifiers to effectively stratify prognosis in patients with hepatocellular carcinoma (HCC). Deriving interpretable prognostic features using deep-learning (DL)-based prognostic models from pathology images remains a challenge. In this study, we developed a computational approach based on DL to predict the overall survival (OS) of HCC patients from formalin-fixed paraffin-embedded histopathology whole slide images. A DL model for classifying good and poor prognosis was developed on a total of 460 patients with 2 independent cohorts from Seoul St. Mary's Hospital. The primary outcome was OS. The training set (SSM1, n = 292) included HCC patients that had undergone surgical resection. The classifier was then independently tested on the second HCC dataset (SSM2, n = 168). The area under the curve (AUC) for the receiver operating characteristic (ROC) curves was 0.850 and 0.781 for SSM1 and SSM2 datasets, respectively. In addition, we have tried to establish DL model for prediction of OS based on clinicopathological features, including Edmondson-Steiner grade, pT stage, vascular invasion, Ki-67 index, and cytokeratin 19 immunohistochemical expression. Random forest model was applied to classify the good and poor prognosis groups and The AUROCs for the random forest was 0.705 for the SSM1 dataset, which are inferior to that of DL prediction. These findings suggest that the DL techniques can be applied to refine the prognostic prediction of HCC patients.

#6176 Identifying poor prognosis stage I lung adenocarcinoma patients through novel morphological biomarker based on computational pathology.

F. J. Song[1], A. Andoni[1], M. Kordahi[2], S. Batelli[1], A. Meier[1], M. Schick[1], E. Mahieu[1], G. Schmidt[1], C. E. Myers[3], M. Abadier[4], A. Dasgupta[3], C. Abbosh[5], D. Hodgson[5], M. Orain[2], F. C. Lamaze[2], Y. Bosse[2], P. Joubert[2];

[1]AstraZeneca, Munich, Germany, [2]Institut universitaire de cardiologie et de pneumologie de Quebec - Universite Laval, Quebec City, QC, Canada, [3]AstraZeneca, Gaithersburg, MD, [4]AstraZeneca, Waltham, MA, [5]AstraZeneca, Cambridge, United Kingdom

Current practice for evaluating prognosis of resectable lung adenocarcinoma (LUAD) patients relies on the Tumor, Node, Metastasis staging system. Despite low relapse risk, post-recurrence survival in a stage I population is poor with a median post relapse survival of around 25 months. There is a need for a biomarker that can enrich for stage I patients with relapse risk to identify a population likely to benefit from adjuvant therapy. In this study, we aim to identify a predictive biomarker of relapse in early-stage lung cancer following surgical resection using AI-based computational pathology.

The retrospective patient cohort analyzed in this study consisted of a total of 166 patients that underwent surgical resection for a clinical stage I LUAD. Out of these, 54 patients experienced disease recurrence within 5 years, and 112 patients had a confirmed disease-free period of at least 5 years post-surgery. For each patient, at least one digitized slide (average = 2.46) stained with haematoxylin and eosin (H&E) was available for analysis. The project was accepted by the IUCPQ ethics committee (2022-3751, 22138).

Manual annotations delineating the tumor core (TC) were drawn by pathologists. We then applied several proprietary image analysis models capable of distinguishing epithelium, stroma, and necrosis within the tumor tissue as well as detecting tumor infiltrating lymphocytes (TILs) and cell nuclei. In this project, we additionally introduce a novel approach rooted in mathematical graph theory to encoding topological aspects of the tissue morphology. A cell-graph constructed from the positions of cell nuclei was used to calculate cell-level graph-theoretic measures which were then aggregated to the slide-level by computing the median. In total, 23 data readouts were obtained of which 14 were based on the standard image analysis pipeline alone, and a further 9 originated from our newly developed graph-based approach.

We identified promising biomarkers using the Wilcoxon rank-sum test and the area under the ROC curve (AUROC); robustness of this evaluation was investigating using resampling methods, using 100 bootstrap samples and 100 repeats of 3-fold cross-validation, respectively. This allowed us to evaluate the prognostic value of the biomarkers with respect to 5-year relapse or death.

We were able to identify the best prognostic biomarker for relapse to be the median weighted clustering coefficient (CC) across all cells in the TC area, which is derived from the graph-based analyses. The median CC was able to achieve a whole-cohort AUROC of 0.695 (average cross-validated AUROC = 0.675, 95% interval 61.7%-70.4%) as well as a relapse vs relapse-free Wilcoxon test p-value of 4.65x10-5 (bootstrapped average = 0.0002). In addition, we were also able to demonstrate that the biomarker shows some relation to the architecture patterns.

#6177 Machine learning enables prediction of ADC targets from whole slide H&E images.

Z. R. McCaw, A. Shcherbina, Y. Shah, insitro Research Team, P. Tagari, D. Koller, C. Probert;
Insitro, South San Francisco, CA

Background: The efficacy of antibody-drug conjugates (ADCs) depends on the expression and specificity of the target antigen by tumor cells. Although H&E-stained slides are routinely collected during cancer care, specialized IHC staining is typically required to ascertain antigen expression. Such stains are not always available or readily deployed. The need to perform separate IHC tests for each candidate ADC may burden clinical labs and can hinder access to care in resource-limited settings. Here we develop an ensemble of machine learning models to accurately predict the expression of 166 distinct ADC targets directly from H&E images.

Methods: For each ADC-targeted gene, patients with copy-number amplifications (CNAs) were identified from somatic whole exome sequencing. Genes differentially expressed in patients with CNAs were identified from bulk transcriptomics. For each gene, an expression signature was developed based on the expression levels of differentially upregulated genes. Next, whole-slide, H&E-stained histopathology images were embedded into a lower-dimensional representation via a transformer model trained with self-supervised learning. Neural networks were developed to predict a patient's probability of having a CNA in an ADC-targeted gene, as indicated by an expression signature exceeding the p90. All evaluation metrics were ascertained by 5-fold cross-validation, with training and evaluation on independent patients.

Results: For each of the 166 ADC-targeted genes, a median of 154 patients were found to harbor a CNA, and the expression signature included a median of 180 genes. In all cases, patients with CNAs had significantly higher expression signatures than those without. For predicting likely CNA status directly from H&E histopathology images, the mean AUROC was 0.888 (95% CI, 0.876-0.900) and the mean AUPRC was 0.571 (95% CI, 0.531-0.611). Among the 166 ADC-targeted genes, the AUROC exceeded 0.95 for 31.3%, 0.8 for 80.7%, and 0.725 for 100%. The best-predicted ADC target was SLC7A5 (AUROC: 0.995 [95% CI, 0.994-0.998]; AUPRC: 0.967 [95% CI, 0.963-0.976]).

Conclusion: We have developed models that accurately predict the likely expression of ADC targets based solely on H&E images. The ability to accurately discern the presence of ADC antigens from H&E images has numerous potential applications, including cohort refinement, computer-aided diagnosis, and personalized treatment planning.

#6178 Automating tumor purity assessment: Advanced AI-driven segmentation and classification of nuclei in H&E stained slides.

N. R. Wagner, K. Kikuchi, K. Fukuda, N. Spasic, S. Littlechild, S. Todorovic, D. Stojnev, M. Jovanovic, C. Weston;
Reveal Biosciences Inc., San Diego, CA

Background
Tumor purity, the proportion of cancerous cells within a tumor mass, is a pivotal factor in oncological research and clinical practice and plays a significant role in the molecular testing workflow, particularly when selecting samples for genomic analysis. Accurate assessment of tumor purity is crucial for understanding tumor behavior, guiding treatment decisions, and predicting patient outcomes. Traditional methods of analyzing hematoxylin and eosin (H&E) stained slides for tumor purity are predominantly pathologist manual readouts. This process is both time-consuming and prone to inter- and intra-observer variability, leading to inconsistencies in diagnosis and treatment planning. Here, we introduce an automated AI-based product designed to streamline tumor purity analysis. The RevealAI-HE digital assay leverages state-of-the-art AI algorithms to automate the segmentation and classification of nuclei in H&E slides, enhancing the accuracy, consistency, and speed of tumor purity assessment. RevealAI-HE aims to assist pathologists in decision-making, support oncology research, streamline molecular testing workflows, and improve personalized care.
Methods
H&E stained solid tumor slides were imaged using 3D-Histech Pannoramic 1000 and 250 scanners. From this dataset, 104 regions of interest (ROIs) were manually selected to cover a wide range of H&E stain intensities in 14 different indications. A nuclear segmentation model based on StarDist-H&E was deployed on these ROIs, and a pathology expert manually assigned one of three classifications to each nuclei: tumor, immune, and stroma. The resulting ground-truth dataset of over 26,000 classified nuclei was used for training a classifier model based on a ResNet architecture. For model evaluation, the nuclei dataset was randomly split into training (80%) and testing (20%) the model, and the training data was batched and randomized for each training epoch to ensure robustness and generalizability. The nuclear segmentation, nucleus classifier, and tumor purity statistics models were integrated into an end-to-end digital assay (RevealAI-HE) using Reveal Biosciences' proprietary digital assay development pipeline. RevealAI-HE is integrated into Reveal Biosciences' flagship whole slide image management system, ImageDx.
Results
The RevealAI-HE digital assay's nucleus classification model achieved a high accuracy across all 14 indications. Compared to manual methods, the AI system significantly reduced the time required for tumor purity analysis. Furthermore, the AI model exhibited excellent consistency in its analyses, addressing the issue of variability seen in manual assessments. These results indicate that our AI product, in many aspects, surpasses the current gold standard of tumor purity analysis (pathologist readout), offering a more efficient, accurate, and reproducible approach.

#6179 Machine learning (ML)-spatial quantification of the tumor microenvironment (TME) identifies differences associated with response to bintrafusp alfa (BA) *vs* pembrolizumab (PEM) treatment in the Phase 3 INTR@PID Lung 037 study.

J. Abel[1], A. Machl[2], A. Gerhold-Ay[3], L. Yu[1], D. Sanghavi[1], B. Trotter[1], N. Patel[1], Y. Gerardin[1], R. Srinivasan[4], S. Brutus[5], T. Mrowiec[3]; [1]PathAI, Boston, MA, [2]EMD Serono, Billerica, MA, [3]The Healthcare Business of Merck KGaA, Darmstadt, Germany, [4]Calico Life Sciences, South San Francisco, CA, [5]Mass General Brigham Ventures, Cambridge, MA

Background: ML digital pathology models can accurately quantify predictive biomarkers like PD-L1.[1] We combined tissue conserving ML assessment of the TME in hematoxylin and eosin (H&E)-stained whole slide images (WSI) with RNAseq for high-dimensional TME quantification for biomarker discovery. The orthogonal methods were applied to a retrospective analysis of a Phase 3 trial directly comparing BA, a first-in-class bifunctional fusion protein composed of the extracellular domain of TGF-βRII (a TGF-β “trap”) fused to a human IgG1 monoclonal antibody blocking PD-L1, and the anti-PD-1 PEM.

Methods: Non-small cell lung cancer ML models previously trained to exhaustively quantify cell types and tissue regions in H&E-stained tissue were refined and deployed on 273 WSI from the INTR@PID Lung 037 study/NCT03631706. Human interpretable features (HIFs) describing the complex spatial organization of the TME were extracted from model predictions. HIFs were selected for analysis using K-means consensus clustering and describe the frequency of lymphocytes in cancer epithelium (cTILs); macrophages, fibroblasts, and granulocytes in stroma; and the abundance of cancer cells relative to all other cells in tumor. Bulk RNAseq was performed for 186 samples yielding 177 WSI-RNAseq pairs. Spearman correlation between HIFs and gene expression or signature was computed. Top gene associations were analyzed via gene-set enrichment analysis. HIFs were used for immunophenotyping (immune excluded, inflamed, and desert) via prespecified cutoffs on tumor-infiltrating lymphocyte abundance, and for biomarker discovery via Cox modeling of PFS and OS.

Results: Gene expression and signatures were associated with HIFs quantifying immune spatial abundance in TME (e.g., cTILs vs. immune checkpoint signature[2]). Improved PFS and OS were associated with an immune-inflamed phenotype for PEM (PFS, HR=0.36, p=0.007, 95% CI 0.17-0.75; OS, HR=0.37, p=0.065, 95% CI 0.13-1.06). In interaction with BA, stromal macrophages were associated with improved survival (PFS, HR=0.72, p=0.062, 95% CI 0.53-1.02; OS, HR=0.62, p=0.058, 95% CI 0.38-1.02) and an increased likelihood of treatment response (odds ratio=1.61, p=0.015). PFS and OS were nearly identical between arms in immune-excluded cases (PEM vs. BA PFS, HR=0.93, p=0.73, 95% CI 0.63-1.39; OS, HR=1.09, p=0.77, 95% CI 0.62-1.92.

Conclusion: Together HIFs and immunophenotyping enabled response prediction to BA and PEM. PEM response was greater for immune-inflamed tumors, while BA response was associated with macrophage infiltration of stroma. ML-based spatial analysis of the TME shows promise for immunotherapy biomarker discovery and validation. [1]V Baxi, et al. *Modern Pathology*. 2022; 35(1):23-32. [2]S Mariathasan, et al. *Nature*. 2018; 554(7693):544-548.

#6180 Tumor microenvironment phenotypes predict recurrence in African Americans diagnosed with colorectal cancer: A comparative study of manual grading with digital pathology.

D. Wu[1], R. Xia[1], M. Alawad[1], L. Lee[2], T. Gonda[1], W. Cao[1], S. Hacking[1];

[1]NYU Grossman School of Medicine, New York, NY, [2]NYU Long Island School of Medicine, New York, NY

African Americans face a higher rate of colorectal cancer (CRC) incidence and mortality compared to other ethnicities. Identifying key prognostic factors is essential for better outcomes in this group. This study focused on the prognostic value of stromal grading in the tumor microenvironment (TME) of African American CRC patients, using both manual grading and digital pathology. A retrospective analysis of CRC cases in African Americans was conducted. Two cohorts were established: a control cohort (patients without recurrence) and a recurrence cohort (patients with recurrence). Stromal grading was performed manually, categorizing tumors into Grade 1 (low risk), Grade 2 (moderate risk), and Grade 3 (high risk), and we also quantified the TME percentages by digital pathology: myxoid, collagen, immune and tumor. In the control cohort (N=40), stromal grading identified 30 Grade 1, 7 Grade 2, and 3 Grade 3 cases. Conversely, the recurrence cohort (N=17) demonstrated a starkly different distribution, with 1 Grade 1, 3 Grade 2, and 13 Grade 3 cases. The Chi-square statistic was notably significant ($p<0.0001$), indicating a strong association between higher stromal grades and the likelihood of recurrence. By unpaired t-test, high myxoid stroma ($p<0.0001$), low collagen ($p<0.0001$), and low tumor ($p=0.0002$) by digital pathology were associated with recurrence. TME phenotypes are a significant prognostic and recurrence indicator in African American patients with CRC. The marked difference in stromal grades and digital pathology features between the control and recurrence cohorts suggests that higher stromal grades, along with higher myxoid, lower collagen and lower tumor percentages are associated with an increased risk of recurrence. These findings underscore the need for tailored therapeutic strategies and more vigilant surveillance in African American patients exhibiting high-risk TME phenotypes. The efficacy of manual and digital pathology evaluation of the TME also warrants further exploration to enhance prognostic accuracy and treatment personalization.

#6181 Digital pathology workflow: Building a bridge for translational biomarker development in humanized mice.

M. Hakkarainen[1], T. Bragge[1], J. Rytkonen[1], E. Oswald[2], **J. B. Schueler**[2];
[1]Charles River Laboratories, Inc., Kuopio, Finland, [2]Charles River Laboratories, Inc., Freiburg, Germany

The introduction of immune checkpoint inhibitors (ICIs) directed against programmed death protein 1 (PD-1), as well as cytotoxic T lymphocyte antigen 4 (CTLA-4), has revolutionized the treatment of non-small cell lung cancer (NSCLC) in the last decade. These therapies have shown significant success in a subset of NSCLC patients, leading to durable response and improved overall survival. However, clear predictive biomarkers for response are still yet to be defined. Tumor-infiltrating lymphocytes (TILs) as one important part of the tumor microenvironment (TME) have proven to be predictive biomarkers in other tumor types such as melanoma, whereas not fully understood in NSCLC. The assessment of TILs typically involves techniques such as flow cytometry (FC) or immunohistochemistry (IHC). While the former has the advantage of being quantitative and relatively easy to standardize it lacks translational value as most clinical samples will be examined using IHC. The current study aims to compare both methods at terminal end point and for treatment outcome, using a panel of 14 NSCLC PDX models, implanted in humanized NSG mice and treated with anti-CTLA4, anti-PD1 and the combination thereof. Based on FC analyses of the untreated tumor tissue the PDX models were stratified into seven hot (>5% TILs) and seven cold (<5% TILs) tumors. The IHC samples were analyzed by digital pathology for TIL infiltration by making use of automated segmentation of the three main tissue classes: tumor, stroma and necrosis. Small number of IHC slides were manually annotated to form a training set, which were then used to train a deep learning model using Visiopharm, a commercial AI platform for image analysis. By quantification of TILs in a spatial context of the tumor tissue, across all models, tumor was the most prominent tissue class. The tissue class distribution as well as the TIL rate (FC or IHC measure) is a model immanent feature. Under treatment, the ratio was stable in case of the cold tumors. In the hot tumors the stroma compartment increased while tumor tissue decreased. Treatment sensitive models displayed an increase of TILs confirmed by FC and IHC. The latter revealed that the TILs specifically increased in the tumor tissue whereas decreased or was stable in the stroma. This observation was significantly more pronounced in cold tumors compared to hot tumors (Oneway ANOVA, $p < 0.001$). Furthermore, a positive correlation between FC and IHC results on CD45 positive cells in the tumors ($p< 0.002$) could be confirmed. In this study, we proofed the feasibility of software-based image analysis as translational relevant read-out in preclinical animal experiments. The possibility to reproducibly quantify tissue classes, immune cell markers and including spatial information paves the way towards discovery of novel features predicting response in translational immuno-oncology research.

#6182 Artificial intelligence (AI)-powered quantification of glypican-3 (GPC3) expression facilitates patient selection for GPC3-targeted therapy in solid tumors.

E. Meng[1], R. Meng[2], Y. Tong[3], Y. Li[3], H. Wang[2], P. Fiorentini[4], E. Attieh[5], Q. Tang[2], A. Kefsi[4], S. Masciari[2], G. Abbadessa[2], C. Combeau[5], L. Tang[1], B. Pasquier[5], **R. Wang**[2];

[1]Sanofi, Jiangsu, China, [2]Sanofi, Newton, MA, [3]WuXi AppTec Co., Ltd., Shanghai, China, [4]Sanofi, Vitry-sur-Seine, France, [5]Sanofi, Chilly-Mazarin, France

Introduction: GPC3 is a glycosyl-phosphatidylinositol-anchored cell surface glycoprotein that functions to control cell growth and differentiation in early development. Membrane GPC3 is highly expressed in hepatocellular carcinoma (HCC) and moderately in squamous non-small cell lung cancer (SQ-NSCLC) with limited expression in normal tissues which makes it an attractive target for immune cell engagers. This study aims to develop an AI-powered algorithm to evaluate GPC3 expression and compare it with manual immunohistochemistry (IHC) scoring in HCC, adeno-NSCLC and SQ-NSCLC.

Methods: 147 NSCLC (94 SQ-NSCLC and 53 adeno-NSCLC) and 113 HCC FFPE tumor blocks were obtained from commercial sources. GPC3 protein level was quantified by a qualified IHC assay for tumor cell membrane and cytoplasm individually. PD-L1 expression is reported as tumor cell proportion score (TPS), combined positive score (CPS) and immune cell proportion score (IPS/IC) TPS, regardless of staining pattern and intensity. FFPE slides were stained for GPC3+ (GC33, Ventana), PD-L1+ (22C3, Dako) cells and then scanned at 20x using the Aperio Versa8 scanner. Machine learning (ML) models were developed using the digitized whole slide images to identify GPC3+ tumor area. Data-driven cutoffs were applied to model-generated human-interpretable features of GPC3+ percentage of tumor area to classify samples as positive and negative. As an orthogonal approach to the GPC3+ percentage cutoff method, tissue and cell annotations were used to train a convolutional neural network (CNN) to classify GPC3 positivity.

Results: The epidemiology profiling results revealed that GPC3 protein is highly expressed in HCC (57.5% cases with > 1% positive cells), followed by SQ-NSCLC (52.1%) and adeno-NSCLC (5.7%). GPC3 expression was only detected in tumor cells with two staining patterns observed: membrane + cytoplasm and cytoplasm-only. There was no significant correlation between GPC3 and PD-L1 expression across tumor types, although a trend of lower level of PD-L1 was observed in the samples with GPC3 ≥50%. ML model quantification of GPC3+ and GPC3- showed high concordance with the consensus score of 2 independent pathologists on a test set of held-out samples not used in training. This concordance was comparable to that of individual annotators to consensus. Instead, GPC3 positivity results using both cutoff and CNN methods showed moderate concordance with 2-way pathologist consensus.

Conclusions: Here we profiled GPC3 expression across tumor types and showed high level of expression in HCC followed by SQ-NSCLC. We have established an AI-powered digital pathology platform that can provide a standardized, scalable, and reproducible method of characterizing GPC3 positivity to support further patient selection in clinical study.

#6183 Exploring the role of microenvironment context on diagnostic accuracy in tissue microarray core selection.

A. Woicik[1], Z. R. McCaw[1], B. Dulken[2], insitro Research Team, C. Probert[1];
[1]Insitro, South San Francisco, CA, [2]Stanford School of Medicine, Stanford, CA

Background: Tissue Microarrays (TMAs) stand to significantly improve the efficiency of multiplex spatial studies by including core samples taken from many tumor blocks in a single slide. However, as TMAs become increasingly prevalent, the implication of core selection within the tumor microenvironment (TME) on downstream discoveries is not well understood. This raises the question of which TME contexts are most predictive for scientific analyses.
Methods: We segment whole tissue section (WTS) slides with a U-Net trained on pathologist annotations of tumor, DCIS, LCIS, normal, stromal, immune, and necrotic microenvironment contexts in 100 TCGA BRCA slides. We focus on 5-way PAM50 subtype prediction in breast cancer. We produce image embeddings for each core using a vision transformer pre-trained on histopathology images and use an attention-based aggregation model to predict PAM50 subtype. To evaluate the impact of core TME contexts in a held-out test set, we sample 0.6mm radius circular sections from 281 WTS images from 54 patients to produce one dataset of “majority non-cancerous” cores that the TME annotation model predicts as majority normal breast epithelial or necrotic tissue and one “majority cancerous” TMA dataset for the remaining cores.
Results: We find that core microenvironment context directly influences diagnostic accuracy. Maximizing tumor content improves diagnostic accuracy on the PAM50 task, with the majority cancerous TMAs obtaining an AUROC of 0.80 (95% confidence interval 0.75-0.85), relative to 0.72 (95% CI 0.66-0.78) for majority non-cancerous TMAs and 0.82 (95% CI 0.80-0.84) for WTS images.
Notably, our context-aware TMA sampling achieves accuracy within 2% of the WTS images, while poorly selected TMA cores underperform the WTS baseline by 10% on average. While TCGA is curated to contain patients with a very high tumor burden, and consequently random TMA selection performs well on this cohort (AUROC 0.77; 95% CI 0.74-0.79), our study indicates that tissue context is an important consideration when selecting cores from real donor tissue blocks.
Our results demonstrate that TMA core sampling protocols should be informed by TME context to maximize analysis accuracy, and that intelligent core sampling can largely close the gap to WTS image accuracies on clinically-relevant tasks like PAM50 subtype prediction. These findings highlight the need for thoughtful TMA dataset construction and usage, especially as core selection becomes increasingly automated. We argue both for more targeted core selection from donor tissue blocks and for filtering of existing datasets. To avoid performance degradation, pipelines should identify and exclude these less task-relevant TMEs, where simulation serves as an efficient and task-specific approximation of TME context relevance.

#6184 A novel approach to Barrett's esophagus risk stratification: Whole-slide image analysis for aneuploidy detection.

C. Ercan[1], X. Pan[1], T. G. Paulson[2], M. D. Stachler[3], C. C. Maley[4], Y. Yuan[1];

[1]The University of Texas MD Anderson Cancer Center, Houston, TX, [2]Fred Hutchinson Cancer, Seattle, WA, [3]University of California San Francisco, San Francisco, CA, [4]Arizona State University, Tempe, AZ

Background

Barrett's esophagus (BE) is the only known precursor of esophageal adenocarcinoma (EAC) and there is a need for biomarkers in BE for risk stratification for cancer progression. Aneuploidy has been suggested as a factor in the development, initiation or progression of EAC in patients with BE, and it has been found predictive for EAC progression (Hadjinicolaou, et al. 2020, Sikkema, et al. 2009). However, current assays for detecting aneuploidy require valuable tissue, hence validation studies are limited. We hypothesise that routine histology images can be used to detect ploidy status. We aim to develop a sensitive, accurate, and easy-to-use deep learning tool for this purpose.

Methods

We used a weakly supervised deep learning-based approach called clustering-constrained-attention multiple-instance learning (CLAM) (Lu et al., 2021) to detect aneuploidy on hematoxylin and eosin-stained whole slide images of endoscopical biopsies from BE, for which the ploidy status had been determined by flow cytometry. To benchmark the model's performance, we also trained a traditional fully supervised algorithm, ResNet50 (He et al., 2016), with the same dataset. The models were trained on 388 slides (51 aneuploid) from the Seattle Barrett's Esophagus Annotated Resource (BEAR) and then applied to an independent test cohort of BEAR patients, consisting of 279 slides (36 aneuploid).

Results

The multi-attention-branch CLAM model achieved AUC of 0.82 and 76.4% balanced accuracy for aneuploidy on the internal test subset (10% of the cohort). On the independent test dataset, the model achieved AUC of 0.85 and 79.3% balanced accuracy, while performance of the fully supervised model was AUC of 0.65 and 33.1 balanced accuracy. In a challenging subset for image-based diagnosis, including 253 samples (29 aneuploid) without dysplasia or atypical mitosis (a major feature of aneuploidy samples) the model achieved a 67.6% accuracy and an AUC of 0.83. Both the flow results (p=2.84e-7) and the model's predictions (p=2.18e-3) revealed a correlation between progression to EAC and ploidy status.

Conclusion

We developed a deep learning model for predicting aneuploidy in BE biopsies. The weakly-supervised approach can perform much better compared to the traditional fully-supervised model. Aneuploidy is correlated with cancer progression and stands as a promising candidate for the prediction of cancer progression in BE patients. Although atypical mitosis is the primary histological indicator of aneuploidy, our model can still make aneuploid predictions in the absence of atypical mitosis, as it doesn't rely solely on a single parameter. Our model is efficient, capable of processing hundreds of samples resource-effectively, and thus an ideal adjunct to standard histologic evaluation. This classifier may facilitate molecular-based improvements in identifying individuals at high risk of progression.

#6185 Generative AI for virtual HE-staining of whole slide images of unstained breast cancer tissue.

L. Latonen[1], U. Khan[2], S. Koivukoski[1], J. Hartman[3], **P. Ruusuvuori**[2];
[1]University of Eastern Finland, Kuopio, Finland, [2]University of Turku, Turku, Finland, [3]Karolinska Institutet, Stockholm, Sweden

Introduction Hematoxylin and eosin (HE) is the standard stain used in histology to make tissue visible to the human eye by highlighting certain cellular and tissue structures, and it is a technique that is widely used in the diagnosis of cancer and other pathologies. Chemical staining, however, is irreversible, making the tissue unusable for subsequent measurements, such as spatial transcriptomics. Here we utilize generative AI method based on pix2pix image-to-image translation to generate virtual HE-staining for whole slide images (WSIs) acquired of unstained tissue with brightfield microscopy and perform a thorough histological evaluation for the feasibility in breast cancer diagnostics.

Materials and Methods We optimized sample preparation and imaging setup for virtual staining purposes, and developed a custom generative adversarial network architecture for learning the virtual staining from paires samples of unstained and H&E stained tissue. Here, we focus on the utility of virtual staining in breast cancer diagnostics, using a set of breast cancer samples for acquiring whole slide images from unstained tissue before H&E staining and from reference H&E stained tissue after chemical staining. Hold-out set of sample pairs are left for validation, allowing us to evaluate the virtual staining performance for a vast array of tissue components and to examine the potential shortcomings in staining reproduction. We use a comprehensive set of quantitative metrics both on pixel and object level to evaluate virtual staining quality. In addition, we perform thorough visual evaluation of histological feasibility by histology experts to examine the computational staining.

Results We demonstrate that by careful optimization of both sample preparation and imaging workflow, as well as the computational methods, generative adversarial networks can be used for virtual staining of whole slide images of breast cancer tissue acquired from unstained tissue using regular bright field microscopy. We analyzed the virtual staining performance quantitatively and visually, and highlight the potential of the method through successful cases and demonstrate the applicability in breast cancer diagnostics, as well as discuss the challenges and shortcomings of virtual staining for clinical samples.

Conclusions We demonstrate the potential of virtual HE staining for clinical histopathology of breast cancer tissue. Notably, our virtual staining based on generative AI shows promise towards more sustainable and streamlined sample processing and staining process in digital pathology.

#6186 Histopathology-derived molecular portrait of serous ovarian cancer.

Yajas Shah, Zachary R. McCaw, Anna Shcherbina, Christopher Probert

insitro, South San Francisco, CA

Background: The progression of ovarian cancer (OV) is often evaluated through clinical staging and molecular profiling of genomic alterations and subtypes, with the molecular profiling of tumors playing a crucial role in cancer management by informing therapeutic decisions. However, collecting molecular data is expensive, time-consuming, and can be sensitive to sample handling protocols. These factors prevent routine implementation at many care centers, thereby limiting benefit to patients. This work examines the viability of an image-centric method for inferring molecular endophenotypes and predicting overall survival in OV, leveraging commonly gathered histopathology scans.

Methods: Embedding representations of digitized Hematoxylin and Eosin slides were produced using a self-supervised histology model. First, we assessed the ability of the embeddings to predict overall survival using Cox proportional hazards models by calculating the concordance index. Next, these embeddings served as input features to machine learning models trained to predict genomic patterns within tumors, including molecular subtypes, driver gene alterations, and mutational processes, leading to a more comprehensive analysis of the prognostic potential of our approach.

Results: Histopathological embeddings were found to be more predictive of patient survival than traditional factors such as age, histological grade, and clinical stage. Embedding risk combined with clinicopathological risk had a higher predictive value than clinicopathological risk alone (0.578 vs 0.569, p = 0.025). Moreover, embedding risk alone was more predictive of survival (0.577 vs 0.569, p = 0.038). Risk scores derived from embeddings and all clinicopathological features were uncorrelated (R = 0.03), indicating that embeddings provide unique prognostic information. Motivated by these findings, we investigated the reasons behind the enhanced accuracy in survival prediction. We found that models trained on embeddings predicted previously defined molecular subtypes (TCGA, 2011), achieving area under the receiver operating characteristic curve (AUROC) scores as follows: Differentiated (0.86), Immunoreactive (0.85), Mesenchymal (0.9), and Proliferative (0.89). Similarly, our models identified crucial oncogenic events, including the loss of TP53 and CDKN2A, and instances of whole genome duplication (AUROCs of 0.85, 0.99 and 0.8).

Conclusions: Taken together, this work showcases the potential utility of standard of care digitized histopathology scans for imputing genomic patterns and predicting overall survival in OV. Our results suggest that imputation could provide a fast and scalable solution for deploying patient screening biomarkers, thereby playing a pivotal role in shaping the future of precision medicine.

#6187 Multimodal characterization of tertiary lymphoid structures identified via deep learning on digitized H&E images in NSCLC.

N. Beig, E. Liu, G. Schau, A. Amitai, B. Nabet, R. Jesudason, E. Fuentes, H. Koeppen, S. Kaya, N. S. Patil, M. K. Srivastava, R. Johnston, C. Kozlowski, J. Giltnane, D. Ruderman;
Genentech, Inc., South San Francisco, CA

Background: Tertiary lymphoid structures (TLS) have recently shown association with improved outcomes for patients treated with immunotherapy across several cancer types. But pathologist-led identification of TLS on routine hematoxylin and eosin (H&E) stained images is time-consuming & lacks standardization. We developed a deep learning (DL) approach to identify TLS on digitized H&E whole slide images (WSI) of non-small cell lung cancer (NSCLC). We also elucidate underlying identified TLS biology by investigating corresponding transcriptomic profiles & multiplex immunofluorescence (mIF) images.
Methods: DL model was trained using mature TLS (mTLS) annotated by 5 board-certified pathologists following standardized definitions across WSI of NSCLC, breast & bladder cancers. Model was validated using blinded, exhaustive annotations on 60 WSI by the same pathologists in consensus. To identify underlying biology associated with model-identified TLS presence, phase 3 clinical trial of advanced NSCLC with H&E and corresponding bulk RNA-Seq was analyzed using differentially expressed genes(DEG). Cellular phenotypes of model-identified TLS were elucidated in procured NSCLC WSI labeled with mIF panel & then H&E stained.
Results: DL model achieved a validation F1-score of 0.56 (precision=0.52). DEG analyses resulted in significant association of TLS related gene signatures with model-identified TLS presence ($q<0.05$). Immuno-histopathological evaluation of model-identified mTLS revealed concordance with central clusters of CD20+ B cells surrounded by a mix of CD20+ B & CD3+ T cells.
Conclusions: We developed a DL model to detect TLS in H&E WSI & demonstrated their concordance in transcriptomics and mIF. With further validation, DL identified TLS could potentially serve as an imaging-based biomarker in clinical outcome datasets.

A. **Model development**

Cancer type	***Training***		***Validation***		
	Digitized H&E Slides with mTLS by Pathologists	mTLS countby Pathologists	Digitized H&E Slides tested	mTLS count by Pathologists (in consensus)	True positive mTLS count(Model identified)
NSCLC	98	283	20	99	57
Breast	107	315	20	48	35
Bladder	103	262	20	65	48

B. Model deployment in independent cohorts

NSCLC Dataset	***H&E images***			***Other corresponding modality***	***Samples***
	Total Digitized Slides	Digitized H&E Slides with mTLS by Pathologists	Digitized H&E Slides with model identified TLS		
OAK (clinical trial, NCT02008227)	320	68	55	**Matched patients with RNA seq**	282
Procured	23	6	4	**Matched slides with mIF panel** (pan-cytokeratin, CD3, CD8, CD163/68, CD20, CD138, BCMA, DC-LAMP)	23

Table 1: Data distribution for instance-based deep learning model training, validation and independent deployment

#6188 Pathomics of prostate cancer incorporating histology and mass spectrometry imaging.

J. M. Luna[1], H. Nakhoul[1], C. Weimholt[1], E. H. Kim[1], S.-K. Song[1], P. M. Angel[2], R. R. Drake[2], J. E. Ippolito[1];

[1]Washington University School of Medicine in St. Louis, St. Louis, MO, [2]Medical University of South Carolina, Charleston, SC

Background: Recent evidence shows that interactions between tumor cells, immune cells, and extracellular matrix (ECM) proteins in the stroma play an important role in prostate cancer (PCa) progression. However, to date these factors are not accounted for in clinical evaluation of PCa patients. Our team has developed methods based on matrix-assisted laser desorption/ionization (MALDI) imaging to identify sets of ECM glycan and collagen molecules associated with PCa. In this study, we leverage computational imaging methods and pathomic textural features to assess the potential of MALDI imaging to guide the identification of regions in PCa hematoxylin and eosin stain (H&E) images as tumor or non-tumor.

Methods: We used a cohort of PCa patients (n=10), who have undergone radical prostatectomy, with grade groups GG3−GG5, and with available H&E and N-glycan MALDI images. We used five MALDI images per patient representing the distribution of N-glycan species at 1419, 2539, 2686, 1663, and 1809 m/z. For each MALDI image, an N-glycan mask was generated and co-registered with the corresponding H&E image via computational imaging methods (i.e., Otsu thresholding, largest connected components labeling, sequential affine and B-spline registration using mutual information). To quantify the overlap of each mask with tumor regions, we calculated Dice scores between the masks and the pathology annotation in H&E. To assess differences in imaging patterns of regions indicated by the different masks, we extracted a set of pathomic textural features (n=70) from the H&E image within each mask using PyRadiomics, and we performed Wilcoxon signed rank tests across all pathomic textural features for all paired combinations of the five masks.

Results: The mean Dice scores between the pathology tumor annotation and the N-glycan masks from 1419 (0.56 [0.44–0.65]) and 2539 m/z (0.64 [0.59–0.82]) was significantly higher ($p<0.008$) than the Dice score of 1663 (0.24 [0.17–0.36]), 1809 (0.31 [0.13–0.45]), and 2686 m/z (0.32 [0.19–0.37]). This suggests a large overlap between 1419 and 2539 m/z and tumor, and large overlap between 1663 and 1809 m/z and non-tumor regions. Consistent with these results, our pathomic textural analysis showed that 50 out of 70 features were significantly different ($p<0.05$) between the masks derived from 1419 and 1663 m/z, 52 between 1419 and 1809 m/z, 62 between 2539 and 1663 m/z, and 57 between 2539 and 1809 m/z ($p<0.05$). Moreover, there were only 23 significantly different features between 1419 and 2539 m/z ($p<0.05$), and 0 features between 1663 and 1809 m/z. Further evaluation is needed for 2686 m/z for which a mean of 54 [45–64] significantly different features ($p<0.05$) from all other masks were found.

Conclusions: We provide preliminary evidence that MALDI imaging can elucidate tissue properties and guide pathomic textural analysis in H&E images, with potential applications in treatment guidance and prognostication of PCa.

#6189 Deep-learning model trained on multiplex immunofluorescence-stained tissue samples predicts the survival of patients with non-small cell lung cancer better than PD-L1 TPS alone.

K. V. Hoebel, J. R. Lindsay, J. V. M. Alessi, J. L. Weirather, I. D. Dryg, J. Altreuter, M. M. Awad, S. J. Rodig, W. E. Lotter;
Dana-Farber Cancer Institute, Boston, MA

In non-small cell lung cancer (NSCLC), the composition and structure of the tumor immune microenvironment (TME) critically impact patient outcomes, necessitating improved computational approaches to characterize the TME beyond traditional metrics like the PD-L1 tumor proportion score (TPS). Here, we developed an interpretable deep-learning model that robustly predicts patient overall survival (OS) and identifies unique PD-L1 enriched neighborhoods linked to patient prognosis.

We utilized a dataset of 507 NSCLC patient biopsy samples prospectively acquired as part of the DFCI ImmunoPROFILE project. Each sample was stained for Cytokeratin as tumor marker, PD-L1, PD-1, CD8, and FOXP3 using a targeted multiplex immunofluorescence assay. Inner tumor regions of interest were automatically processed for spatially resolved identification and quantification of marker expression at the single-cell level.

The dataset was divided into 380 patients for model development and 127 for testing. The deep-learning model, a graph neural network (GNN), was trained to predict OS based on local cell neighborhoods using a weakly supervised training paradigm. The GNN models neighborhoods as a graph, with cells and their corresponding marker expression representing nodes and edges connecting adjacent cells, for an average of 42 cells per neighborhood. Survival predictions were obtained by averaging predictions over all neighborhoods from one sample.

The GNN model demonstrated robust performance with a concordance index (c-index) of 0.79 on the test data, surpassing traditional metrics such as TPS and immune marker density-based models (c-index: 0.50 and 0.74, respectively).

Beyond assessing performance, we investigated the features learned by the GNN using k-means clustering in the model's feature space. We identified three clusters that were notably enriched in PD-L1 positive tumor cells. The first cluster shows an especially "high TPS" phenotype, where the GNN predicted such neighborhoods to be generally poor for survival. The other two clusters were additionally enriched with PD-L1 positive immune cells (ICs) and associated with favorable survival predictions. Notably, one cluster was also enriched with other types of ICs ("PD-L1 IC mixed"), which the GNN predicted as especially favorable for survival compared to exclusive enrichment of PD-L1 ICs ("PD-L1 IC dominant"). A score summarizing these three PD-L1 expression patterns was significantly associated with OS (p-value: 0.01; HR: 0.72, 95% CI: 0.16-1.27), validating the features learned by the GNN.

In sum, we developed a highly interpretable deep-learning model leveraging cellular neighborhood graphs, which effectively identifies expression patterns correlating with NSCLC prognosis, offering promise for developing personalized treatment strategies.

#6190 Patterns of EGFR and HER3 co-expression in solid tumors.

M. Wood, C. Morrison, J. S. Khalili, Y. Zhu;
SystImmune Inc., Redmond, WA

EGFR and HER3 are members of the ERBB receptor family and transmit growth and survival signals to cancer cells upon ligand binding. While both receptors are well established targets for cancer therapy, greater understanding of the relationship of their expression patterns in human cancer is needed to establish the scope of therapeutic potential. To evaluate the co-expression pattern of EGFR and HER3, cancer FFPE tissue microarrays from several cancer types were evaluated by immunofluorescence imaging and digital pathology, including cell-by-cell marker intensity and spatial analyses within the tumor and stromal compartments. Tissue cores were assigned H-scores, and individual cells were binned into 0, 1+, 2+, 3+ scoring based on established digital pathology methods using QuPath software. Spatial cytometry was used to further evaluate single-cell expression intensity. Analysis was conducted widely on multiple normal human tissues as well as cases of NSCLC adenocarcinoma n=86, NSCLC squamous cell carcinoma n=84, SCLC n=43, TNBC n=45, Biliary tract cancers n=80, Nasopharyngeal carcinomas n=60. Overall, the results of this analysis show the intermediate to high prevalence of EGFR and HER3 co-expression within each indication, as well as the frequency of EGFR and HER3 expressing cells. Furthermore, EGFR and HER3 heterodimers were confirmed by proximity ligation assay in certain index cases. Notably, of several observations, we observe NSCLC cases show a profound absence of EGFR- HER3+ tumor cells. Additionally, we observe that co-expression of EGFR and HER3 in normal human tissues is rare and of low signal intensity.

#6191 Simultaneous prediction of tumor microenvironment biomarkers from pathology slides using multi-task deep regression.

Omar S. M. El Nahhas, Marta Ligero, Jakob N. Kather

EKFZ for Digital Health, UK Carl Gustav Carus der TU Dresden, Dresden, Germany

Understanding the Tumor Microenvironment (TME) is crucial for tailoring personalized cancer treatments and improving patient outcomes. Using deep learning, we can predict properties of the TME from standard Hematoxylin and Eosin (H&E) stained slides, including specific gene expression signatures. While past models were limited to single signature predictions, we explore the potential of multi-task deep learning to identify multiple biomarkers at once, allowing more complex relationships and interactions to be modeled simultaneously. Our study focuses on the prediction of expression patterns of tumor, stromal, and immune cells in breast cancer (BC).

We developed a multi-task transformer-based deep regression model, trained in a weakly-supervised setting, to predict biomarkers in the TME from routine H&E-stained pathology slides of a BC cohort (n=876). The performance was evaluated using Pearson's correlation coefficient (r) and spatial heatmaps generated via gradient-weighted class activation mapping.

Our model achieved a significant correlation coefficient above 0.40 ($p<0.0001$) for all predicted TME biomarkers in the holdout test set (n=176). This includes the biomarkers lymphocyte infiltrating signature score ($r=0.46$, $p<0.0001$), tumor infiltrating lymphocyte regional fraction ($r=0.48$, $p<0.0001$), leukocyte fraction ($r=0.43$, $p<0.0001$), stromal fraction ($r=0.42$, $p<0.0001$), and tumor cell proliferation ($r=0.47$, $p<0.0001$). Notably, the model's heatmaps highlighted the pertinent cells and histological characteristics for its predictions.

These data show that our deep learning model accurately predicts multiple TME biomarkers concurrently from routine pathology slides. This approach offers a promising avenue for cost-effective and efficient biomarker quantification in the TME, with potential applicability across various cancer types.

#6193 Exploring interplay between tumor intrinsic features and immune cell phenotypes in multi-tumor tissue microarrays by a single step 15-plex fluorescence immunohistochemistry and imaging on the Orion platform.

R. Van Krieken, J. O. Bender, S. Kekchidou, M. Burgin, K. Ruma, N. Dakappagari, J. Bordeaux;
Navigate BioPharma, Carlsbad, CA

Purpose: Deeper understanding of the intricacies between tumor microenvironments and immune cell infiltrates is critical for creation of next generation therapies. However, current immunohistochemistry protocols in clinical practice are restricted to one to six markers (cell types) and rely on multiple rounds of antigen retrieval and sequential staining over two days. This current workflow has high risk for tissue and signal loss. Hence, we explored utility of a single step staining workflow using 15 distinct antibodies conjugated novel flours (Argo Dye System) of formalin fixed paraffin embedded (FFPE) tumor microarrays and imaged on the Orion microscope (Rarecyte). Fidelity of the staining was assessed by comparing data from the Orion platform to internally developed clinical grade assays. The implementation of higher plex imaging will enable greater insight into immune surveillance, mechanisms of resistance and patient stratification while minimizing patient tissue required for analysis.

Study Design: We utilized a custom panel developed by RareCyte (Hoescht, CD3e, CD4, CD8a, CD20, CD68, CD163, FOXP3, Ki67, Pan-CK, PD1, PDL1, CD45, Granzyme B, LAG3) to evaluate expression of immune markers on a pan-tumor and melanoma TMA including Hodgkin's lymphoma, ovarian cancer, esophageal carcinoma, hepatic cell carcinoma, head and neck cancer. Serial sections were stained with 6-plex clinical grade assays, and correlation scores were determined between the 15-plex Orion and 6-plex assays utilizing TSA-based amplification.

Results: In this study, the performance of Orion platform was assessed by quantitative and qualitative measures. Linear regression between the 6-plex clinical grade assays and 15-plex Orion workflow were calculated for a panel of biomarkers including CD3, CD4, CD8, CD68, CD163, CK, FOXP3, GZMB, Ki67, and PD1. Our results demonstrated that the Orion performed similarly to clinical grade assays both in terms of proportion of cells and fluorescence intensity (R^2 ~ 0.7-0.98, Slope ~ 0.7-1.1).

Conclusion: Our results suggest that the Orion platform offers a reliable and efficient solution for comprehensive biomarker analysis. Our results demonstrate that this platform can successfully capture the expression of 15 biomarkers on a single FFPE slide which offers workflow advantages over traditional TSA-based fIHC multiplexing that is limited to detection of 6 biomarkers on a single slide. The ability to analyze a wider range of biomarkers through a single platform has the potential to enhance the efficiency of biomarker analysis, leading to improved diagnostic and therapeutic outcomes in clinical practice.

BIOINFORMATICS / COMPUTATIONAL BIOLOGY / SYSTEMS BIOLOGY / CONVERGENT SCIENCE: Integrative Cancer Science Poster Session

#6198 *TP53* mutational clusters stratify the Li-Fraumeni syndrome spectrum.

N. W. Fischer[1], B. Laverty[2], R. Kafri[3], K. N. Maxwell[4], E. R. Woodward[5], C. Kratz[6], D. Malkin[1];
[1]The Hospital for Sick Children, Toronto, ON, Canada, [2]The University of Toronto, Toronto, ON, Canada, [3]University of Toronto, Toronto, ON, Canada, [4]University of Pennsylvania, Pennsylvania, PA, [5]University of Manchester, Manchester, United Kingdom, [6]Hannover Medical School, Hannover, Germany

Li-Fraumeni syndrome (LFS) is a highly penetrant cancer predisposition disorder caused by germline variants in the *TP53* tumor suppressor gene. LFS has recently been redefined as a 'spectrum' disorder to reflect the highly variable cancer types with largely unpredictable ages-of-onset and disease severity. The broad functional gradient associated with different *TP53* variants is thought to contribute to LFS heterogeneity, although it is still poorly understood and there is an unmet clinical need for risk stratification strategies to improve variant interpretation and patient care. Here, we performed an unsupervised cluster analysis leveraging p53 mutagenesis datasets (Kato et al., 2003 & Giacomelli et al., 2018) that revealed five *TP53* mutational clusters with unique mutation patterns, structural features, and functional consequences. Stratifying germline carriers based on the five clusters exposed important clinical characteristics to consider for patient management, such as ages-of-onset, tumor type development, and survival outcomes. In particular, we discovered an osteosarcoma-prone subgroup comprised of monomeric mutant p53 carriers with aggressive cancer phenotypes. We also identified a cluster of *TP53* variants found more often in non-cancer and healthy older populations, and carriers of these variants that developed cancer had less "LFS-like" phenotypes including an older age-of-onset and a significantly higher frequency of colorectal cancers. Remarkably, our *TP53* variant clustering strategy could also stratify breast cancer survival among germline carriers. This work provides a new framework to delineate the LFS spectrum toward the development of machine learning-based approaches for personalized cancer surveillance plans.

#6199 Defining and capturing progression in glioma by harnessing NLP in unstructured electronic health records.

S. Chappidi[1], H. Lee[2], **S. Jagasia**[3], C. Syal[4], G. Zaki[3], D. Junkin[4], N. Golightly[4], P. Chitwood[4], K. Camphausen[3], A. Krauze[3];
[1]National Cancer Institute / University of Cambridge, Bethesda, MD / Cambridge, United Kingdom, [2]National Cancer Institute / Johns Hopkins University, Bethesda / Baltimore, MD, [3]National Cancer Institute, Bethesda, MD, [4]NIH Integrated Data Analysis Platform, National Institutes of Health, Bethesda, MD

Gliomas exhibit nearly uniform recurrence and poor prognosis. Management of high-grade tumors is surgery followed by chemoirradiation (CRT). Radiographic progression is assessed using contrast-enhanced MRI with reporting captured in Electronic Health Records (EHR). The ability to harness large scale EHR data is limited by the Response Assessment in Neuro-Oncology (RANO) tumor progression criteria, which defines progression as an aggregate of clinical and/or radiographic parameters requiring clinician judgement. As a result, glioma progression is not captured systematically in large data sets, limiting Progression Free Survival (PFS) as an outcome endpoint in data analysis. We developed an AI-based method using natural language processing to capture PFS parameters for analysis of MRI radiology reports. 1088 available brain MRI radiology reports for 81 patients with a pathologically confirmed diagnosis of glioblastoma (GBM) were aggregated in the NIH Integrated Data Analysis Platform. MRI reports were systematically analyzed and PFS manually captured using RANO criteria as ground truth. Common report terms indicating progression were compiled and included in task prompts applied to Large Language Model (LLM) Extraction Tools. The words *progression* (n=1047) and *stable* (n=1133) did not necessarily indicate either overall progression or stability in a report. Yet, in the 24 (30%) patients who progressed within 3 months of CRT, *recurrence* and *mass effect* occurred in 3.7% and 53% of reports, respectively, which was comparable to the term frequencies of 5.8% and 54% in patients with stable disease. Thus, *mass effect* and *recurrence* could not necessarily be used alone as terms to signal overall progression. The analysis identified other commonly employed radiology report terms relevant to determining tumor progression including *enhancement* (n=2445), *perfusion* (n=2085), *enhancing* (n=1785), *resection* (n=1576), and *increased* (n=1331), which allowed for experimentation with more detailed LLM extraction task prompts. Our method flagged radiographic progression prior to clinician-coded progression in 43 (53%) patients. Future directions include handling further clinical context such as surgical features, radiation therapy dates, progress notes, and the coadministration of agents such as bevacizumab and steroids. These results indicate the feasibility of LLMs to identify tumor progression dates using EHR text with potential transferability to large glioma data sets pending further optimization and validation.

#6200 Single-cell analyses unravel novel immune and tumor cell characteristics linked to the response to neoadjuvant immune checkpoint blockade in patients with gastric cancer.

E. Dai[1], J.-J. Qin[2], C. Hu[2], Z. Xu[2], G. Han[1], Y. Chu[1], R. Wang[1], M. Dang[1], Y. Liu[1], G. Pei[1], J. Jiang[1], F. Peng[1], Y. Zhang[1], A. L. Faustino[1], J. A. Ajani[1], L. Wang[1], X. Cheng[2];

[1]The University of Texas MD Anderson Cancer Center, Houston, TX, [2]The Cancer Hospital of the University of Chinese Academy of Sciences, Hangzhou, China

Background: Gastric cancer remains the leading cause of cancer-related deaths worldwide, ranking fifth for incidence and fourth for mortality. Combining neoadjuvant therapy with immune checkpoint inhibitors has demonstrated improved outcomes for patients with gastric cancer. However, responses exhibit heterogeneity, and the understanding of the mediators influencing therapy response is limited.

Methods: In this study, we collected 80 blood and tumor samples from 22 gastric cancer patients treated with XELOX/SOX alone or its combination with Nivolumab (anti-PD-1). Paired single-cell RNA-, TCR-, and BCR-sequencing were performed on pre- and post-treatment samples to investigate the dynamics of immune and tumor cells during the development of response/resistance to therapy.

Results: Our findings revealed that elevated levels of baseline CD4 and $CD8^{+}$ tissue-resident memory T (T_{RM}) cells, in activated and stressed states, are associated with a superior response to combined therapy, and treatment further amplifies this cell population in responsive patients. Tracking T cell receptor clones across pre-/post-treated blood and tumor samples disclosed that the expanded clonotypes of T_{RM} cells are exclusively detected in tumors, and considerable preexisting clones contribute to the expansion of these T cell populations following treatment. The simultaneous presence of T_{RM}, B, and dendritic cells in pre-treated tumors predicted a favorable response, and they concertedly expanded in tumors responsive to anti-PD-1 therapy.

Conclusions: Our findings highlight the significance of T_{RM} cells in effective responses to anti-PD-1 therapies and indicate that their cellular communication with B and dendritic cells play a pivotal role in shaping the antitumor immunity elicited by combination therapy. Together, this study illuminates vital immune cell subsets during immune checkpoint blockade treatment, provides biological insights into the mechanism of successful combination therapy, and unravels potential targets for improving treatment efficacy in gastric cancer.

#6201 Early-onset CRC, vitamin A deficiency, and stem cell origin of cancer.

B. M. Boman, V. O. Hunsu, C. O. B. Facey;
Helen F. Graham Cancer Center & Research Institute, Newark, DE

The recent surge in early-onset CRC (EOCRC) has been attributed to a Westernized lifestyle, but the underlying molecular mechanism is largely unknown. In our cancer genetics clinic, we provide care for 10-20 young (<50 age) CRC patients per year. But, only a fraction (~15%) of these young CRC patients are found to have CRC-predisposing germline mutations which doesn't provide a hereditary factor that can explain EOCRC. Other genetic studies have found that the spectrum of somatic alterations was largely comparable between EOCRC and adult-onset CRC, particularly common are mutations occurring in *APC* and other members of the WNT pathway. Since a genetic etiology has not turned-up, we are exploring possible lifestyle factors. We hypothesize that vitamin A (retinol) deficiency is a likely etiologic factor because vitamin A is an essential nutrient that is not made by the human body. Thus, young individuals might be prone to any cancer-initiating effects of a vitamin A deficient diet. Indeed, many population-based studies (including ones on well-nourished populations) have reported a high prevalence of vitamin A deficiency in pre-school-aged children. Since *APC* mutation commonly occurs in early-onset CRCs, we conjecture that vitamin A (retinol) metabolism and *APC* mutation-induced activation of WNT signaling may be co-factors in promoting EOCRC. Accordingly, we have been investigating whether there is a functional connection between WNT and vitamin A/retinoic acid (RA) signaling, and if *APC* mutation generates an imbalance in a WNT:RA-linked mechanism that contributes to CRC development by impeding retinoid-induced colonic stem cell (SC) differentiation. We previously reported that RA signaling mainly occurs in aldehyde dehydrogenase-positive (ALDH+) SCs and that *APC* mutation leads to overpopulation of ALDH+ SCs and incomplete differentiation during CRC development. Thus, our findings suggest that *APC* mutation attenuates RA signaling in ALDH+ SCs, which might explain how vitamin A deficiency contributes to EOCRC development.

#6202 Integrating public single-cell transcriptomics and patient profiles to guide clinical development.

J. Russella-Pollard, J. Whitener, J. Byck, M. Manne, H. Alostaz, M. Elia, K. Krukowski, G. Wong, F. Adrian, L. Schweizer, R. H. I. Andtbacka, **C. Hatzis**; HiFiBiO Therapeutics, Cambridge, MA

Background: Single-cell technologies provide invaluable insights into disease biology and drug development by revealing complex interactions among different cell types within patients. However, harnessing the potential of publicly available single-cell data remains challenging due to the lack of integrated data across diverse single cell platforms.

Methods: To maximize the potential of single cell insights, we have created an AI/ML powered curation and data integration process within our Drug Intelligence Science (DIS®) platform. This automated process integrates single cell transcriptomic data from publicly available sources with our in-house generated datasets from ex vivo translational efforts and clinical programs. Relevant public datasets are identified and retrieved using an automated Python-based GEO dataset crawler tool, and standardized metadata are curated. A reference atlas of 31 immune and 4 non-immune cell types is generated from the database and is used to consistently label cells across datasets. Additionally, cell-level gene expression integration and normalization across datasets is achieved using generative modeling techniques. To facilitate multiuser visualization and interrogation of the curated and integrated datasets, we have developed Cellect, a customized version of CellxGene Gateway.

Results: The current single-cell database comprises 15 million cells analyzed in >5,000 samples collected from >2,500 patients across 160 curated unique human studies, spanning oncology (56%), autoimmune disease (AID, 21%), and viral infection (15%), with the remaining being from reference healthy tissues (8%). We focused dataset curation on indications of interest for our internal clinical development efforts. Uniquely, data from approximately 300 patients who received standard of care (SOC) treatment including immune checkpoint inhibitor (IO) therapy were integrated to delineate mechanisms of drug response and resistance. The post-SOC resource was used to identify (1) treatment settings where these mechanisms are enriched and (2) markers co-expressed with targets of interest (e.g., PD1, CTLA4, OX40, TNFR2, etc.) in specific cell populations to inform combination strategies.

Conclusions: We have presented an AI/ML guided approach to address the key challenge of integrating single-cell data across platforms and demonstrated that relevant disease biology is retained upon integration. We outline a path for deploying this solution at scale for bench and computational scientists to guide target as well as indication selection, as was done for our ongoing clinical programs, including our first-in-class TNFR2 agonist (HFB200301, NCT05238883) and second-generation OX40 agonist (HFB301001, NCT05229601).

#6203 An altered profile of ribosomal proteins and ERK-eIF4E translational control in an inflammatory breast cancer model of acquired resistance and reversal is associated with pathological complete response in patients.

G. R. Devi[1], P. PAI[1], M. W. Foster[1], D. S. Sannareddy[1], S. Lee[1], S. V. Laere[2];
[1]Duke University School of Medicine, Durham, NC, [2]University of Antwerp, Antwerp, Belgium

Background: Drug resistance is a major challenge in inflammatory breast cancer (IBC), a hyperproliferative subtype characterized by the presence of diffuse tumor cell clusters that show high level of heterogeneity. As the degree of tumor heterogeneity during cancer progression can cause evolution of cell states that can either compete or co-operate resulting in therapeutic failure, the study objective was to identify drug resistance networks that can serve as biomarkers or therapeutic targets.
Methods: Integrated transcriptomic and proteomic profiling approach was conducted in a progression model of acquired drug resistance and its reversal comprised of a treatment-naïve patient-derived SUM149 cell line, along with two isogenic derivatives and representing drug-resistant (rSUM149) and resistance-reversal states (rrSUM149). Global gene expression analysis in IBC patients (n=87) recorded responses to neoadjuvant chemotherapy. Based on the data, targeted multikinase inhibitors were evaluated in viability and signaling assays.
Results: We identified specific ribosomal proteins associated with resistance acquisition, which correlated with high levels of pERK, CDK1, XIAP, and SOD2. Conversely, the resistance reversal in rrSUM149 showed almost complete normalization to the profile of SUM149. However, VIPER analysis revealed proteins related to ribosomal processes (AGO2, Exportin 1, RPL5) that did not revert in rrSUM149, suggesting this pathway may have pleiotropic effects in governing drug resistance. Notably, genes linked to ribosomal processes were significantly enriched ($P<0.001$) among the overexpressed genes in IBC patients (n=87) who exhibited pCR to neoadjuvant chemotherapy. This is crucial as IBC tumors, including rSUM149, exhibit MAPK hyperactivation including in the presence of EGFR tyrosine kinase inhibitors. Treatment with Merestinib, a multikinase inhibitor, suppressed pERK, peIF4E, downstream targets like CDK1, and ribosomal protein IMP3 underscoring the impact on protein synthesis signaling crucial for countering translational dependence in cancer cells. Additionally, Merestinib synergized with EGFR-TKI (lapatinib) in increasing cell death in all three states.
Conclusion: Overall, our study describes adaptive changes in response to both therapeutic stress and therapy break that have the potential to serve as biomarkers or extended for pharmacological interrogation toward precision medicine for this rare, understudied cancer. Furthermore, the ability of Merestinib, in clinical trials, to target translational dependence is attractive as cancer cells often appropriate these signaling pathways to gain tolerance to various stress stimuli. Support: NIH-R01CA264529; DoD Breast Cancer Breakthrough level 2 Award W81XWH2010153

#6204 Differential gut microbiome alpha diversity in endometrial and ovarian carcinoma patients.

C. T. Finnicum[1], T. Meissner[2], C. Davis[1], S. Viet[1], J. L. Petersen[1], M. Deaton[2], B. Solomon[2], W. Spanos[2], D. Starks[2], R. Elsey[2], E. A. Ehli[1], C. Williams[2]; [1]Avera Genetics, Sioux Falls, SD, [2]Avera Cancer Institute, Sioux Falls, SD

Background: Emerging research underscores the gut microbiome's critical role in cancer development, progression, and response to treatment. As a part of the “ASAP” study, which focuses on the implementation of comprehensive molecular profiling and deep clinical annotation of electronic health records in participants diagnosed with or at risk of developing cancer, we have established a microbiome-associated biobank and corresponding clinical dataset to systematically explore the dynamics of the gut microbiome as patients progress through cancer treatment. We describe a pilot project where we explore the baseline microbiome samples collected from ASAP participants, particularly from those with endometrial and ovarian carcinomas.

Methods: Stool samples from patients were collected at the time of enrollment in the ASAP study and sampling is repeated every three months to align with the additional biosampling procedures. Microbial DNA was extracted from the baseline stool samples and subjected to sequencing of the V4 region of the 16S rRNA gene. After generating species level operational taxonomic units (OTUs), alpha diversity measures were generated in the form of the inverse Simpson index. In order to determine whether there was a difference in alpha diversity between individuals with ovarian (N = 37) and endometrial (N = 35) carcinomas, we employed a t-test with 100,000 permutations to derive an empirical p-value.

Results: We present sequencing results from the initial n=297 samples. Our comparison of the alpha diversity between ASAP study participants with ovarian and endometrial carcinomas showed a significant difference between the two groups, with the ovarian cancer patients having a lower alpha diversity (empirical p-value = 0.03915). Due to the uniform sampling, biobanking, and analytical procedures, our study allows the ability to explore microbiome features amongst various cancer diagnoses while minimizing laboratory and analytical differences that plague microbiome reproducibility.

Conclusions: We observed a significant difference in alpha diversity between patients with endometrial and ovarian carcinomas. Although the current results are preliminary, the wealth of information available in the ASAP protocol will allow us to continue exploring the association of the gut microbiome with cancer and the associated treatment.

#6205 Identify drugs for metastatic castration-resistance prostate cancer (mCRPC) patients with high glycolytic activity through *in silico* approach.

M.-C. Su, A. Lee, R. Huang;
University of Minnesota, Minneapolis, MN

Prostate cancer (PC) remains a prominent cause of cancer-related mortality among men in the United States. A significant factor contributing to the mortality of PC patients is the development of resistance to second-generation antiandrogen therapies, particularly androgen receptor-signaling inhibitors (ARSI), which is pronounced in patients with late-stage PC, metastatic castration-resistance prostate cancer (mCRPC). Therefore, there is an urgent need for novel therapeutics beyond AR signaling inhibition for patients with mCRPC. One of the key drivers of resistance to ARSI and a critical feature of CRPC is cancer metabolism reprogramming to elevated glycolysis. However, the current research on finding drugs to impede high-glycolytic tumor growth is hurdled by a resistance raised from metabolic plasticity. The aim of this research is to quickly repurpose existing drugs for inhibiting high-glycolytic mCRPC growth while proactively circumstancing resistance from metabolic plasticity through computational approaches. To do this, we imputed a large number of drug responses in patients with mCRPC using a computational algorithm (OncoPredict), identified drugs that were projected to show higher sensitivity in high-glycolytic tumors, and performed in vitro validation. Furthermore, to maximize drug efficacy, we identified biomarkers for drug candidates. By implementing this computational pipeline, we identified a number of drugs with various mechanisms of action that show higher efficacy in mCRPC with high glycolysis. Furthermore, we successfully validated the efficacy of these nominated drug candidates including an anti-parasitic agent, an HSP90 inhibitor, and a CDK inhibitor. These drug candidates exhibited superior tumor growth inhibition in *in vitro* models of high glycolysis-induced advanced PC. In conclusion, this study introduces an innovative *in silico* approach to unveil the existing drugs' unknown potential for the treatment of patients with mCRPC. Our findings hold promise for development of effective therapeutics for combating this challenging disease.

#6206 Molecular stratification of AML: Integrative genomic and immune profiling points to high risk subgroup and targetable molecular drivers.

K. Karagoz, L. Brady, B. Higgs, H. Si;
Genmab, Plainsboro, NJ

Background: Acute Myeloid Leukemia (AML) is a complex hematological malignancy characterized by clinical diversity. The ability to accurately subtype patients can inform prognosis and guide therapeutic approaches. With the integration of multi-omics data, it is possible to elucidate the molecular mechanisms underpinning unique AML subtypes, with intent to identify potential drug targeting pathways in a precision medicine strategy.
Method: RNAseq datasets from Beat-AML (discovery, N=462), TCGA-AML (validation, N=173), and Leucegene (validation, N=452) were analyzed through non-negative matrix factorization to delineate distinct transcriptomic-driven molecular subtypes within AML. A curated set of the top 1,000 most variable genes was utilized to minimize analytical noise. GSVA was used for pathway analyses across Hallmark, KEGG, Reactome, and the immune microenvironment was characterized via xCell. Recurring DNA variants were examined in each subtype. Clinical outcomes of each subtype were analyzed using the Kaplan-Meier method and assessed by a log-rank test. These insights were subsequently validated in two independent cohorts - TCGA AML and Leucegene. The most influential components of immunological effector mechanisms, which characterize poor prognostic subpopulation, were assessed using bootstrap forest partitioning as a feature selection technique.
Results: Our Beat-AML analysis identified 5 distinct clusters. Cluster 3 consisted of 20% of AML cases (n=86), and displayed a worse overall survival with a HR (95% CI) of 1.41 (1.03, 1.92, P=0.03). This cluster was characterized by three co-mutations: FLT3, NPM1, and DNMT3A. Pathway analysis highlighted biological processes key to antibody therapy intervention, specifically complement pathways, NK cell cytotoxicity, and FCGR-mediated phagocytosis as enriched within this subpopulation. Concurrently, oncogenic (PI3K/AKT/MTOR, TGFB, NOTCH) and metabolic pathways (fatty acid and oxidative phosphorylation) were activated. Immune profiling indicated increased levels of M2 macrophages. Using bootstrap forest partitioning, C2 and ITGAM were identified as key genes defining cluster 3. These observations were confirmed in TCGA AML and Leucegene cohorts.
Conclusion: Our comprehensive analysis identified a distinct high-risk AML subgroup characterized by unique genomic, transcriptomic, and immunological patterns. The combined presence of NPM1/FLT3-ITD and DNMT3A mutations in cluster 3—each previously attributed with varied prognostic outcomes—warrants in-depth biological investigation. With these consistent AML subgroup results identified across three independent cohorts (total of 1,087 patients), we highlight the complexities within the molecular landscape of AML and emphasize the need for tailored therapeutic approaches - a transformative shift in AML treatment.

#6207 Exploring colorectal cancer with ARIA: Biomedical insights.

N. Nikolic[1], S. Kleinstein[2], J. Radenkovic[1], M. Kovacevic[1];
[1]Velsera, Belgrade, Serbia, [2]Velsera, Charlestown, MA

Gaining the promised benefits from the population-scale datasets, both clinical and genomic, is often hindered by the inability to easily access, explore and manipulate such complex data - a difficulty that ARIA was designed to overcome.
In the field of biomedicine, organizations harness extensive datasets, gaining profound insights into patients and participants, thereby unleashing possibilities for accelerating research, especially in the realms of drug development and precision medicine. To facilitate navigation through the intricate landscape of biomedical data, Velsera has innovated ARIA to catalyse efficient and insightful analysis, with a keen emphasis on user-friendliness to ensure accessibility across a diverse professional audience. To demonstrate the practical application of ARIA, we explore genomic and clinical datasets to identify key differences in colorectal cancer progression. CRC, the third most common cancer globally, has unique characteristics in origination and progression from benign to pathogenic. Here we investigate differences between patients with polyps that do and do not progress to CRC, including key environmental factors such as smoking history, inactive lifestyle and obesity in conjunction with their known clinical and genetic risk factors. This exploration into the abilities of ARIA demonstrate the ability to analyse complex datasets combining both clinical and genomics data at a large scale.
For the purpose of this demonstration, a Synthea Dataset, encompassing synthetic clinical and genomic data for 122,011 patients across various age groups, was utilized. This dataset was generated by Velsera specifically for testing ARIA functionalities.
In conclusion, ARIA empowers efficient analysis of complex biomedical datasets, providing a comprehensive understanding of disease mechanisms and facilitating valuable insights.

#6208 Characterization of molecular evolution in myelodysplastic neoplasms.

Ivan Civettini[1], Valentina Crippa[1], Federica Malighetti[1], Matteo Villa[1], Andrea Aroldi[2], Fabrizio Cavalca[2], Alex Graudenzi[3], Lorenza Maria Borin[2], Luca Mologni[1], Rocco Piazza[1], Carlo Gambacorti-Passerini[1], Daniele Ramazzotti[1]

[1]Medicine and Surgery, University of Milano-Bicocca, Milan, Italy,[2]Hematology, Fondazione IRCCS San Gerardo dei Tintori, Monza, Italy,[3]Department of Informatics, University of Milano-Bicocca, Milan, Italy

Myelodysplastic neoplasms (MDS) are hematopoietic stem cell disorders. The IPSS-Mol model, a scoring system that combines molecular and clinical features to stratify MDS patients, can identify individuals at high-risk of developing Acute Myeloid Leukemia (AML), enabling the targeted application of disease-modifying therapies. However, the molecular evolutionary patterns in MDS and their impact on Overall Survival (OS) and Leukemia-Free Survival (LFS) remain unexplored. Shifting from conventional static mutational analyses used by IPSS-Mol to a dynamic evolutionary approach, we employed the ASCETIC framework to analyze data from the IPSS-Mol Database (3,323 patients, 152 genes) and understand the dynamics of MDS progression. According to ASCETIC, genes related to DNA methylation displayed low ranks, indicating their tendency to manifest early in the progression of the disease. In contrast, genes associated with cellular signaling typically appeared in the later stages of tumor progression, while genes involved in RNA splicing exhibited intermediate ranks.Regarding molecular evolution in MDS, ASCETIC identified five clusters, each characterized by distinct evolutionary signatures and significantly different OS and LFS rates ($p < 0.001$). The median OS for the C1, C2, C3, C4, and C5 clusters were 79.3, 64.1, 28.9, 16.2, and 14.8 months, respectively. Subsequently, we compared ASCETIC's clusters with the different risk groups defined by the IPSS-Mol score. Among the 1158 patients initially classified as V-Low/M-Low risk by IPSS-Mol, ASCETIC identified 55 patients placed in C4 and C5. These patients exhibited lower OS ($p = 0.005$) and LFS ($p = 0.02$). Conversely, among the 905 IPSS-Mol M-High/V-High risk patients, ASCETIC identified 468 patients (51.7%) classified as low risk (C1-C2-C3), who were associated with longer median OS and LFS ($p < 0.001$). The differences between conventional mutational analyses and our evolutionary approach primarily, but not exclusively, arise from the evaluation of TP53 mutations and ASXL1. In the IPSS-Mol model, a higher risk is conferred if multi-hit TP53 alterations occur or in the presence of ASXL1 mutations.Conversely, ASCETIC assesses the impact of mutations differently. It considers not only the Variant Allele Frequencies of individual- and/or co-mutations but also the evolutionary trajectories that lead to TP53 and/or ASXL1. This approach results in different risk weights assigned to each evolutionary trajectory.Lastly, we identified patients with NPM1 mutations, classified as MDS patients in the original dataset but now categorized as AML according to 2022-WHO. Within this high-risk context, ASCETIC differentiated between patients with shorter and longer Overall Survival (OS) ($p < 0.001$).Our study reveals the influence of evolution on MDS prognosis, offering insights into the integration of the ASCETIC framework with the IPSS-Mol. Validation on external cohort is ongoing.

#6209 From data disparity to data harmony: A comprehensive pan-cancer omics data collection.

L. Meunier, G. Appe, A. Behdenna, V. Bernu, H. Brull Corretger, P. Dhillon, E. Fox, J. Haziza, C. Lescure, C. Marijon, C. Petit, S. Weill, A. Nordor;
Epigene Labs, Paris, France

In cancer research, the exponential growth of omics datasets offers a significant opportunity for scientific advancement. However, challenges such as the lack of uniform standards, in both clinical and omic data, hinder the effective utilization of these datasets, thus impeding our understanding of cancer biology and the development of innovative therapeutic approaches.Addressing these challenges, we have created a novel collection of pan-cancer omics datasets with extensive clinical data harmonization and consistent omic data normalization.Here, we focused on patient-derived gene expression microarray datasets from the Gene Expression Omnibus database. To navigate the complexities presented by the diverse clinical descriptions inherent in these datasets, we leveraged our proprietary ontology, machine learning models, and domain expert quality control processes to homogenize the clinical data elements.Datasets were then selected based on sample composition, molecular data compatibility, and clinical data availability, then passed through a uniform preprocessing and normalization pipeline to maximize data quality. Finally, gene names were aligned on a single annotation reference, and potential batch effects were adjusted before expression data were merged together.We obtained a total of 32,825 transcriptomic sample profiles from 470 datasets, covering 13,435 genes and 45 clinical data elements, across 30 cancer types. Healthy tissue was favored over adjacent tissue, to minimize the risk of introducing biases related to cancer patient background genomic profiles into downstream analyses. We compared our collection with The Cancer Genome Atlas (TCGA), the most commonly used RNA-seq transcriptomic dataset in cancer research. It covers 30 out of the 33 TCGA cancer types, with on average 4.2 times more samples per cancer type ([0.3; 45.5], median 3.4). Despite the two data collections being based on distinct technologies, we observed a Pearson correlation of 0.69 over the 11,753 genes in common, and a 100% overlap of the differentially expressed genes between genders. This consistency highlights cross-technology reliability and complementarity.We have built and continuously enriched a comprehensive dataset collection enabling the secondary analysis of high-quality omic data. This initial work - focused on microarray datasets - allows us to streamline design, exploration and validation of various omics data-driven studies in cancer research.Our ongoing efforts involve not only the continued integration of microarray datasets but also the integration of pan-cancer RNA-seq and single-cell data. This initiative is set to expand further, encompassing a broader range of omics datasets in the future.

#6210 The cancer omics and drug experimental response dataset (CODERData): A harmonized benchmark dataset for machine learning models of drug response prediction.

J. Jacobson[1], S. Schwartz[2], M. Weil[3], N. Kumar[2], S. Gosline[1];

[1]Pacific Northwest National Laboratory, Seattle, WA, [2]Pacific Northwest National Laboratory, Richland, WA, [3]Frederick National Laboratory for Cancer Research, Frederick, MD

Background: Determining a patient's response to a specific therapy is a vital step in developing personalized cancer treatment. Personalized treatment relies on two key technological advancements: algorithms tailored to each patient's molecular profiles, and comprehensive datasets detailing the effects of patient diversity on drug response. Despite recent advancements in machine learning-based models, each new algorithm requires curation of numerous datasets, which poses a significant burden to researchers who need to evaluate and compare various algorithms. Currently, datasets include extensive genomics, transcriptomics, proteomics and metabolomics measurements along with drug response data (i.e., cell viability) for each cell line, collected through the Cancer Cell Line Encyclopedia (CCLE) and other initiatives. Additional omics data is available for tumor organoids and patient samples generated by consortia such as Human Cancer Model Initiative (HCMI) and the Clinical Proteomic Tumor Analysis Consortium (CPTAC). However, to date there has been little public effort to annotate and harmonize these data across repositories.

Methods: To address this need, we developed the Python package *coderdata* that collates the most up-to-date cancer omics and drug response data. We curated four public cancer datasets, establishing reproducible pipelines that standardize data retrieval, formatting, and integration so the datasets can be built on a cluster if needed. The datasets undergo bi-monthly synchronization with FigShare, ensuring the data is up to date and available. Scientists can use *coderdata* to retrieve and format data on the command line interface as well as within Python scripts.

Results: *Coderdata* is a straightforward Python package that will enable the development and benchmarking of diverse machine learning applications in cancer research. At its core, it represents reproducible data harmonization that enables heterogeneous datasets to be analyzed in bulk. This Python package downloads and standardizes data from multiple consortia-related resources including HCMI, CPTAC, CCLE, and BeatAML, together representing 4931 multi-omics samples from across 250+ cancer types. These datasets include cancer data metrics such as copy number, mutation, transcriptomics, proteomics, miRNA, methylation, and drug response data.

Conclusions: The applications of machine learning in cancer biology are hampered by the distributed nature of existing datasets. As such, the collection and standardization of data by *coderdata* substantially reduces the time investment required for data curation in cancer research. Direct access to benchmark multi-omics and drug response datasets enables scientists to focus on algorithm development for tumor drug response prediction, potentially accelerating the discovery of therapeutic strategies.

#6211 Clinical and prognostic assessment of the lncRNA ZFAS1-related gene signature in colorectal cancer.

P. Ahluwalia, T. Leeman, A. Mondal, A. Vashisht, H. Singh, N. Omar, K. Jones, R. Kolhe;
Augusta University, Augusta, GA

Colorectal cancer (CRC) is one of the leading causes of cancer death with a rapidly rising incidence rate in younger adults. It is projected to be the leading cause of death in adults under 50 years old by 2030. Although progress over the last couple of decades has improved the clinical management of patients affected by CRC, there is a lack of accurate biomarkers to stratify CRC patients. Among several other biomolecules, lncRNAs (long non-coding RNAs) are non-coding transcripts under 200 nucleotides that can regulate gene expression. Furthermore, lncRNAs are important players in oncogenesis and cancer progression and have the potential to be used as reliable biomarkers. Through this study, we explored the clinical relevance of lncRNAs in colorectal cancer. To analyze the distribution of lncRNAs, we utilized de-identified FFPE (formalin-fixed paraffin-embedded) blocks from Augusta University (n = 88). FFPE blocks were sectioned to extract tissue segments and were subsequently stained using H&E (hematoxylin and eosin dyes) to identify the tumor and adjacent normal regions. The quantification of the gene expression was performed using a medium-throughput NanoString platform. Further analyses were performed using clinicopathological features of the institutional cohort and an independent Cancer Genome Atlas (TCGA) dataset. TCGA contains genomic data along with clinical and molecular characterization of over 11,000 samples of various lineages. In the institutional cohort, *ZFAS1* showed higher gene expression in the low survival group for stage II and III colorectal cancer patients, while no significant difference was observed in stage I and IV patients. *ZFAS1* expression did not significantly correlate with other clinicopathological parameters, including race, alcohol consumption, tobacco consumption, age, grade, and family history of cancer. In an orthogonal TCGA analysis, higher *ZFAS1* expression was associated with genomic perturbations, including significantly altered tumor mutational burden (TMB), aneuploidy, fractional genome alteration, and microsatellite instability. Further, a 21-gene signature was developed for prognostication using gene co-expression network analysis. The gene signature was significantly associated with overall and disease-free survival in the TCGA-CRC cohort. Immune deconvolution analysis of the RNA sequencing data revealed that higher expression of the 21-gene signature was associated with increased infiltration of regulatory T cells while being inversely correlated with the overall level of T cells. In conclusion, our study identified the clinicopathological role of *ZFAS1* lncRNA and its interaction genes with prognostic significance in colorectal cancer. Further investigation into the therapeutic relevance of the *ZFAS1*-related gene signature may prove invaluable in improving the clinical outcomes of colorectal cancer patients.

#6212 A differential ligand-receptor network inference method to identify alterations in communication between myeloid cells and CD8 T cells in response to PancVAX neo-epitope peptide vaccine, anti-CTLA-4 and anti-PD-1 antibodies in a murine model of pancreatic ductal adenocarcinoma.

J. T. Mitchell, A. Deshpande, A. L. Huff, C. Cherry, S. Nagaraj, K. Krishnan, D. Lvovs, J. H. Elisseeff, E. M. Jaffee, N. Zaidi, E. J. Fertig;
Johns Hopkins University School of Medicine, Baltimore, MD

Pancreatic Ductal Adenocarcinoma (PDAC) is a deadly cancer with a low tumor mutational burden that leads to the generation of few neo-epitopes derived from mutated genes that can be recognized by cytotoxic T cells. The immunosuppressive microenvironment of PDAC comprises suppressive cell populations that include myeloid cells, cancer associated fibroblast subpopulations, and regulatory T cells that reduce T cell infiltration and cytotoxic function. We have developed a murine personalized cancer vaccine to enhance cytotoxic T cell function against PDAC, PancVAX (Kinkead et al, *JCI Insight* 2018). Survival benefit with PancVAX was dependent on the addition of immune checkpoint inhibitor (ICI) therapy to increase the number of cytotoxic CD8 T cells infiltrating tumors and maintain their cytotoxic function (Huff et al, *JCI Insight* 2023). Yet, the impact of cell-cell communication on effector T cell function arising from the immunosuppressive microenvironment of PDAC remains unknown. We previously developed a ligand-receptor inference method called Domino that infers inter- and intra-cellular signaling networks in single-cell RNA-seq data (Cherry et al, *Nat Biomed Eng* 2021). However, this technique is limited to data from single conditions. Understanding how this combination immunotherapy alters cellular signaling networks requires new computational tools that identify changes in regulatory networks between treatment conditions. We developed capabilities for assessment of differential signaling with Domino founded on a basis of differential signal receipt. Active receptors are identified by receptor expression in recipient cells that is correlated with downstream transcription factors in the intracellular signaling cascade. Identification of causative ligands for receptor activation is assessed by a probability of interaction for ligand-receptor interactions between cell types. This probability metric considers mean expression of ligand and receptor genes as well as the number of sender cells for comparison across treatment groups. Comparing communication networks in PancVAX alone to PancVAX with ICI, PancVAX with ICI enhances cell-cell adhesion and interferon gamma signaling in cytotoxic CD8 T cells towards exhausted CD8 T cells. Macrophages in PancVAX with ICI enhance expression of immune checkpoint ligands towards CD8 T cells, despite the presence of blocking ICI antibodies. Intracellular signaling downstream of PD-1 in exhausted T cells shows diminished numbers of transcription factors linked to PD-1 signaling. This software informs prioritization of inhibitory signals for modulation in future immunotherapy regimens and can be applied generally to other tumor subtypes and treatment contexts.

#6213 *De*termination of permissive and restraining *c*ancer-*a*ssociated *f*ibroblast (DeCAF) subtypes.

Xianlu Laura Peng[1], Elena Kharitonova[2], Joseph Kearney[3], Yi Xu[1], Priscilla Chan[4], Changfei Luan[4], Brian Belt[5], Roheena Panni[6], Arthi Hariharan[4], Ian McCabe[1], Ashley Morrison[4], Ashley Cliff[4], David C. Linehan[5], Alina Iuga[7], Naim U. Rashid[2], Jen Jen Yeh[3]

[1]Department of Pharmacology, The University of North Carolina at Chapel Hill, Chapel Hill, NC,[2]Department of Biostatistics, The University of North Carolina at Chapel Hill, Chapel Hill, NC,[3]Department of Surgery, The University of North Carolina at Chapel Hill, Chapel Hill, NC,[4]Lineberger Comprehensive Cancer Center, The University of North Carolina at Chapel Hill, Chapel Hill, NC,[5]The Center for Tumor Immunology Research, University of Rochester Medical Center, Rochester, NY,[6]Department of Surgery, Washington University at St. Louis Hill, St. Louis, MO,[7]Department of Pathology and Laboratory Medicine, The University of North Carolina at Chapel Hill, Chapel Hill, NC

Cancer-associated fibroblasts (CAFs) in pancreatic adenocarcinoma (PDAC) are known to play a significant role in regulating tumor progression, invasion, and metastasis. Multiple studies using experimental strategies, as well as single-cell RNA-sequencing (scRNAseq) technology, have shown the existence of subpopulations of PDAC CAFs, with divergent physical and biological characteristics. However, how these CAF subpopulations translate to clinical practice remains unclear. Using a combination of sc- and bulk RNAseq data, we present two CAF subtypes with permissive (permCAF) and restraining (restCAF) characteristics in patients, and developed a clinically usable single-sample classifier (DeCAF) using using 11 independent datasets with high reproducibility (AUC = 0.961). We found that the permCAF patients tend to be associated with a “myxoid” histological features, while restCAF samples were more “collagenized” ($p = 0.018$). Patients with permCAF tumors had a median overall survival (OS) of 18.5 m compared to 30.2 m for restCAF tumors, with a stratified HR = 1.66 ($p < 0.001$) for patients with permCAF tumors. Basal-like tumors were found to be associated permCAF subtype ($p < 0.001$). DeCAF and PurIST (basal-like/classical) subtypes were independently associated with OS ($p < 0.001$). Analysis of a phase Ib trial FOLFIRINOX in combination with a CCR2 inhibitor (PF-04136309; NCT01413022) , we found that in patients with classical tumors, increasing permCAF probability was associated with response ($r = -0.688$, $p<0.001$). Tumors with permCAF subtype are enriched in neutrophils using CIBERSORT and may explain the positive response to CCR2 inhibition. More intriguingly, we found similar associations with OS in kidney renal clear cell carcinoma (KIRC, $p = 0.001$) and mesothelioma (MESO, $p = 0.019$). DeCAF subtypes are associated with histological subtype in MESO ($p = 0.021$) and grade in KIRC ($p = 0.056$). Taken together, DeCAF subtypes explain the role of CAF subtypes in patients, provide a foundation for the translation of preclinical studies, and facilitate the design of future therapeutic approaches and clinical trials.

#6214 OncodynamiX as an artificial intelligence (AI) based platform for precision medicine.

D. Sivanandhan[1], P. R. Bhargav[2], S. M. Vasista[2], S. Narayanbhatla[2], S. Kamath[2], O. Sailaja[2], D. Chakraborty[2], S. Babu[1];
[1]TheraIndx Lifesciences, Bangalore, India, [2]OncoDynamiX Lifesciences, Bangalore, India

Introduction: In spite of the recent advances in cancer research, cancer incidence and mortality rate still remain high. Although genomic based approaches are used more extensively for identifying the right treatment approach, only a few patients benefit from this because a) only a limited number of mutations have been classified as driver mutations that are of 'significance' and b) in case of multiple mutations, the approach to identify right drug or drug combinations is not well understood. In this regard, there is a need for approaches that use artificial intelligence where exhaustive omics data is effectively processed, mined and utilized to device personalized therapy. Therefore, we used OncodynamiX an AI driven Cancer Biology platform to identify the right drug(s) for patients that had limited or no treatment options. We present here 2 case studies, one patient with stage 4 uterine serous adenocarcinoma and another one with endometrial adenocarcinoma.

Methods: OncodynamiX platform has over 15 million data points, including mutation, CNA, mRNA and protein data for 1500 cell lines as well as potency, efficacy, target, phenotype and network information on more than 250 drugs. Based NGS data from the patients, OncodynamiX platform identified direct or indirect targetable alterations and then picked drugs or compounds shown to be active in the altered pathways. Based on this, a drug-gene alteration matrix was created which formed the basis for identification of appropriate drug(s).

Results: The first patient with uterine serous adenocarcinoma had the following mutations: PIK3CA (Gain of function, GoF), TP53 (Loss of Function, LoF), PPP2R1A (LoF), APC (Conservation of function); Copy number amplification or high expression was reported for the following genes: BRD4, MYC, NOTCH3, CCNE1 and MUC16. Based on the drug-gene alteration matrix and all available drug data, WEE1 inhibitor was suggested to be the best therapy option for this patient. Accordingly, the patient was treated with WEE1 inhibitor in a then ongoing clinical trial. The second patient with endometrial adenocarcinoma had FBXW7, BRCA1, and PIK3R1 LoF, PIK3CA GoF and TP53 switch of function mutations, amplifications in CCNE1, FGFR1, NSD3, ZNF217 and ZNF70033 and loss of PTEN and FAS. For this patient, Pazopanib and Evrolimus combination was recommended and the patient was treated accordingly. Both patients responded well for the treatment as measured by RECIST response and continued with the treatment for over a year.

Conclusion: The studies presented above highlight the promise of this AI-based approach in personalized medicine. In multiple cases we have used OncodynamiX approach where clear clinical benefit was demonstrated. To further validate this approach, we are initiating a clinical trial with 250 patients. Such approaches should be adopted more widely for significant improvement in life expectancy as well as in quality of life of patients.

#6215 Systematic identification and clinical implications of glycogenes in cancer research: An integrative omics approach.

Y.-H. Chen, Y.-S. Jou;
Academia Sinica - Institute of Biomedical Sciences (IBMS), Taipei, Taiwan

Glycosylation and its products are crucial in clinical routines but are overshadowed by a framework embedding genomic participants in cancer development. The glycosylation scheme varies between research groups, presenting clinical concerns that demand understanding in cancer research beyond the glycome. Our work aims (a) to enhance the canonical framework by identifying potential glycosylation-associated genes (glycogenes) and (b) to advance translational cancer study, offering a unified perspective on integrative omics and explainable machine learning with glycogene integration.

The expansion of the glycosylation framework involved initial text mining from curated databases like OMIM, InterPro, and Reactome. Dysregulation of identified genes was affirmed across 29 TCGA solid cancers, encompassing over 7,000 patients with primary tumors. And healthy tissue data from GTEx facilitated tumor-normal comparisons. Subsequently, integrative omic analysis, involving transcriptome and methylome, was applied to confirm the stratification feasibility of glycogenes and to revealed cancer clusters within the UMAP space. After cluster discovery, profiling from survival analysis and drug response prediction highlighted clinical differences between clusters. Employing a survival forest model and explainable artificial intelligence (XAI), personalized assessments, including a 5-year survival predictor and risk factors for individuals, were developed.

Our study verified over 3,000 glycogenes, expanding the conventional configuration of glycosylation and constituting 10-30% of differentially expressed genes between tumors and healthy tissues. Whether transcriptome or methylome alone, glycogenes demonstrated stratification ability. Advanced omic integration further discovered 16 cancer clusters out of 29 TCGA cancers, associated with anatomical source, morphology, and genomic similarity. Utilizing drug resources from GDSC, this specialized geneset exhibited drug predicting ability, displaying a distinct drug response profile among the 16 clusters. To finalize the clinical potential, a survival forest for 5-year survival model construction concluded forecasters with a time-dependent AUC (0.77 to 0.92 on average) for each cancer cluster. With XAI implementation, survival risk factors were developed and assessed for each individual locally.

Here we identified over 3,000 glycogenes, elaborating the classic glycosylation structure and emphasizing genomic importance in cancer research. Glycogenes demonstrated translational potential, supported by diverse survival distributions and drug responses across cancer clusters discovered by the integrative omic approach. The integration of XAI provided a tailored perspective for implementing glycogenes in clinical cancer research.

#6216 Single cell DNA sequencing of BRAF treatment resistant anaplastic thyroid cancer.

A. Thennavan, M. Tarabichi, P. Wu, M. Martin, R. Dadu, M. Cabanillas, N. Busaidy, Y. C. Henderson, M. Zafereo, M. D. Williams, S. Lai, N. Navin, J. R. Wang; UT MD Anderson Cancer Center, Houston, TX

Anaplastic thyroid cancer (ATC) is one of the most lethal cancers. Although dramatic responses to *BRAFV600E*-mutated ATC are seen with BRAF/MEK inhibition, treatment resistance inevitably develops, limiting survival. In this study we sequentially profiled *BRAFV600E*-mutated ATC at diagnosis, after BRAF/MEK targeted therapy and at the time of disease recurrence using both bulk and single-cell DNA/RNA sequencing. We profiled (~400-800 single cells) for each patient - Patient 1 (n = 704 cells); Patient 2 (n = 817 cells) and Patient 3 (n = 407 cells). At diagnosis, we show that tumor cell populations were characterized by a predominance of arm-level aneuploidies. Across all patients, there is a sharp decline in tumor cells post BRAF-targeted treatment. Interestingly, we observe at least 2 distinct tumor subclones present in the pre-treatment tumor and subsequently there was an expansion event that occurred in each patient after BRAF treatment. This was associated with acquiring unique copy number aberrations (CNA)events and the dominance of these subclones in the recurrent disease. For Patient 2, we also performed single-cell RNA sequencing and show that the recurrent tumor cells have high proliferation and stem-cell like cell states even though they had higher differentiation scores. Importantly, correlating the scDNAseq identified CNA with the inferred CNA from scRNAseq, we show proof of concept that copy number aberrations can be directly correlated with gene expression changes and gene dosage effects. Collectively our data reveal an early polyclonal dissemination model of clones in BRAF-mutated ATCs and suggests that treatment resistance to BRAF inhibition develops as a results of incomplete elimination of viable tumor cell reservoirs in ATC.

#6217 Differential genome-wide gene regulatory networks for lung cancer.

M. Zhang[1], Z. Jiang[2], D. Zhang[1];

[1]University of California, Irvine, Irvine, CA, [2]Purdue University, West Lafayette, IN

Background: Lung cancer remains the leading cause of cancer death worldwide due to the fact that most cases are diagnosed at distant stages, and treatment is less effective. During the past two decades, much effort has been devoted to understanding tumor biology and developing targeted therapeutics, which have significantly improved patient survival. With the increasingly available multi-omics data from healthy controls and lung cancer patients, we constructed gene regulatory networks for the two main subtypes of non-small-cell lung cancer (NSCLC), the most common type of lung cancer. In addition, differential networks were constructed by integrative analysis of data from lung cancer tissue and tissues from healthy lungs.

Methods: Transcriptomics and genomic data were obtained from the patients with lung adenocarcinoma (LUAD) and lung squamous cell carcinoma (LUSC) tissue available in The Cancer Genome Atlas (TCGA) project, and both types of omics data of normal lung tissue were downloaded from The Genotype-Tissue Expression (GTEx) consortium. The networks for each subtype and the differential networks were constructed by utilizing our newly developed machine learning tools, two-stage penalized least square (2SPLS) approach, and analysis of variance of directed networks (NetANOVA), respectively.

Results: For the top three identified subnetworks of LUAD, we identified some well-known genes associated with lung cancer, such as EGFR, IRF1, KRAS, ERBB2, PIK3CA, MYC, at bootstrap frequency >90%. Based on the top three subnetworks with a bootstrap frequency of 100%, results from the Ingenuity Pathway Analysis (IPA) indicated several significant pathways, primary immunodeficiency signaling and communication between innate and adaptive immune cells. GO enrichment analysis showed statistically significant biological processes, including immune response, extracellular matrix organization, and significant KEGG pathways such as Hematopoietic cell lineage. The differential networks between LUAD, LUSC, and healthy lungs showed the same regulations across all three groups, such as the regulation between EEF2 and RACK1, the perturbations between LUAD and healthy (two-way regulations between HIGD2A and ARL10), and LUSC and healthy (GRB14 regulates EIF3E) respectively. In addition, we identified the differences between LUAD and LUSC, such as bi-directional regulations between CLTB and ARL10.

Conclusion: Although all groups share most regulations, we identified differential gene regulations between healthy lung tissue and lung cancer tissue and between LUAD and LUSC of NSCLC. Using multi-omics data generated from lung tissues, coupled with advanced machine learning methods, the causal relationships between genome-wide genes from the analysis will help us understand the molecular mechanism of lung cancer and facilitate the development of personalized treatment strategies.

#6218 Haplotype-resolved analysis of cancer genomes and epigenomes using Oxford Nanopore sequencing.

P. Reschenederr[1], P. James[1], S. McKenzie[2], A. Talenti[1], S. Aganezov[2], D. Turner[1], S. Juul[2];
[1]Oxford Nanopore Technologies plc, Oxford, United Kingdom, [2]Oxford Nanopore Technologies Inc, New York, NY

Cancer is a complex and dynamic disease driven by somatic genomic and epigenomic alterations that accumulate over time. These changes give rise to heterogeneous collections of cells or clones, each with distinct (epi)genomic profiles within a single tumour. Accurate characterisation of these changes is crucial for understanding the mechanisms driving the disease, identifying potential therapeutic targets, and personalising treatment strategies. Due to the technological constraints of short-read and array-based approaches, cancer research has historically had a strong focus on detecting small genomic changes like SNPs and small indels (SNVs) as well as the broad characterisation of large-scale copy number changes (CNVs), mostly ignoring other important variant classes and epigenetic modifications. Here we demonstrate how Oxford Nanopore native long-read sequencing enables the direct detection of not only SNVs, but also break point-resolved simple and complex structural variants (SVs and CNVs), haplotype phasing of all variant types, and identification of DNA modifications like 5-methylcytosine (5mC) and 5-hydroxy-methylcytosine (5hmC) from a single tumour-normal dataset. We illustrate how our end-to-end somatic workflow streamlines analysis for the different variant classes and benchmark somatic SNV and SV calling performance using well characterised cancer cell lines and in-silico benchmarking datasets at different sequencing depths. Finally, we use real-world tumour-normal pairs to showcase a comprehensive sample to answer tumour-normal analysis using Nanopore sequencing. This includes the characterisation of complex patterns of somatic SVs in the different cancer samples, the identification of unique 5mC methylation patterns, exploring characteristic differences in 5hmC levels between tumour and normal samples as well as showing how Nanopore long reads enable haplotype and clone specific CNV calling as well as phasing of genetic and epigenetic variation.

#6219 Type V collagen promotes lung adenocarcinoma metastasis by regulating tumor mechanical stress and the implication for prognosis and therapeutic strategies.

G. Zhu, Y. Wang, Y. Wang, C. Chen, Y. Li, H. Liu, **J. Chen**;
Tianjin Medical University, Tianjin, China

Introduction: The mechanical environment of the human body influences physiological and pathological processes, and understanding these biomechanical aspects holds promise for medical research. Tumor microenvironment changes, including extracellular matrix (ECM) alterations, result the changing of mechanical characteristics of the tissue, play a crucial role in cancer progression and metastasis, including lung adenocarcinoma (LUAD), one of a major histology type of lung cancer. This study focuses on elucidating how mechanical characteristics, especially those related to the ECM, influence LUAD and the signaling pathways involved.
Methods: Cell culture, transfection, Western blot, immunofluorescence, immunohistochemistry, Transwell assay, scratch wound-healing assay were used to investigate the behavior changes of LUAD cells under different treatment. Bioinformatics analyses, and machine learning-based integrative approaches were employed to build the SVM_Score, which was built with relevant base membrane (BM) genes. Patient-derived tumor organoids, myofibroblasts, and co-culture systems were established. Sorafenib, which can inhibited collagen and fibronectin synthesis, was used to explore the proliferation and migration changing of lung cancer cells co-cultured with myofibroblasts.
Results: Mechanical stress, simulated by matrix application, enhanced LUAD cell migration and invasion, correlating with ECM alterations and EMT pathway activation. SVM_Score predicted LUAD patient prognosis and EMT propensity across multiple datasets, revealing its robust prognostic capabilities. Lower SVM_Scores were associated with worse survival outcomes, increased cancer-related pathways, higher Tumor Mutation Burden and altered immune microenvironment characteristics. SVM_Score was also linked to myofibroblast-secreted COL5A1, a key marker for mechanical stress. Patient tissues with low SVM_Scores exhibited higher COL5A1 expression, enhanced EMT propensity, and increased internal mechanical stress. Sorafenib, by inhibiting COL5A1 secretion, attenuated the pro-tumor effects of myofibroblasts, inhibiting proliferation and migration of LUAD cells, and rendering LUAD cells more sensitive to chemotherapy.
Conclusion: This comprehensive study unveils the intricate relationship between mechanical stress, ECM alterations, and LUAD progression. SVM_Score emerges as a potent prognostic tool, reflects tumor mechanical characteristics. Sorafenib intervention targeting COL5A1 secretion provides a potential therapeutic strategy to mitigate LUAD aggressiveness. These findings contribute to a deeper understanding of the biomechanical aspects of LUAD, offering insights for future research and clinical applications.

#6220 TRIP13 augments pancreatic cancer progression- An integrated systems biology study.

S. Dhasmana[1], A. Dhasmana[1], S. Rios[1], I. A. E. Perez[1], S. Khan[1], F. Afaq[2], U. Manne[2], M. M. Yallapu[1], S. C. Chauhan[1];
[1]University of Texas Rio Grande Valley, McAllen, TX, [2]University of Alabama at Birmingham, Birmingham, AL

Background- Pancreatic cancer (PanCa) is one of the most aggressive forms of cancer and its incidence rate is continuously increasing every year. It is expected that by 2030, PanCa will become the 2nd leading cause of cancer related deaths in the United States due to the lack of understanding of the complexity of disease, early diagnostic methods, and extremely poor survival. Despite great advancements in biomedical research, there are very limited modalities available for the early detection of PanCa and its treatment. Thus, understanding of disease biology and identification of newer diagnostic and therapeutic modalities are high priority research in the field. Our group has identified Thyroid Receptor Interacting Protein -13 (TRIP13) as an oncogenic protein which contributes to early events of PanCa.

Methodology- High dimensional omics and structural elucidation of TRIP13 was conducted using publicly available databases like Consurf, Phosphosite, GTEx and GEPIA2. Molecular biology techniques were applied to cross validate all our bioinformatics data. qPCR, immunoblotting and IHC analysis was performed in progressive PDAC cell lines and human tissues to decipher the expression level of TRIP13 in various pathological staging including functional enrichment analysis using Linkdomics.

Results- The structural elucidation analysis revealed that most of the functionally exposed residues, phosphorylation and ubiquitylation sites situated at AAA domain of TRIP13. As compared to normal, TRIP13 is significantly over expressed in pancreatic tumor samples. Pathological staging 2 and 1 (early stages) showed relatively higher expression of TRIP13 as compared advanced stage. Of the total 7 isoforms of TRIP13, only one isoform (TRIP13-001) has shown the over expression in pancreatic tumor samples and shown association with poor survival. In correlation studies, TRIP13 has shown positive association with other pancreatic cancer biomarkers (CEACAM5, S100A4, MUC1, MSLN, CA125). The functional enrichment analyses suggest that TRIP13 is involved in important patho-physiological pathways like DNA repair, viral carcinogenesis, cellular senescence, and cell cycle. Our wet lab experiments also support our computational biology observation.

Conclusion- This integrated computational biology study suggests a potential role of TRIP13 in pancreatic cancer progression *via* modulation of important oncological pathways. Wet lab experimentations also validated the involvement of TRIP13 in pancreatic cancer progression. TRIP13 expression may be associated with patient prognosis. Thus, its inhibitory small molecules can be useful for boosting pancreatic cancer therapies in clinical settings.

Key words- TRIP13, Pancreatic cancer, Early events of cancer, Integrative Biology, Transcriptomics, Computational biology

#6221 First-in-human study of acoustic cluster therapy consisting of PS101 combined with chemotherapy and insonation in patients with liver metastases of colorectal cancer origin.

U. Banerji[1], W. Yau[2], M. T. O'Leary[1], N. Bush[3], S. Gurung[2], A. Snapir[4], J. C. Bamber[1], N. Tunariu[1];

[1]The Institute of Cancer Research and The Royal Marsden Hospital NHS Foundation Trust, London, United Kingdom, [2]The Royal Marsden Hospital NHS Foundation Trust, London, United Kingdom, [3]The Institute of Cancer Research, Sutton, United Kingdom, [4]EXACT Therapeutics AS, Oslo, Norway

Background: Suboptimal delivery of anti-cancer agents to cancer tissue compromises the effectiveness of therapeutics. PS101 consists of microclusters of perfluorobutane microbubbles and perfluoromethylcyclopentane (PFMCP) microdroplets. Acoustic cluster therapy (ACT) consists of PS101 administered intravenously and insonated over a tumour with diagnostic ultrasound (2 MHz or above), which fuses the components of PS101 to form larger ACT bubbles that are temporarily trapped in capillaries, followed by low frequency (0.5 MHz) insonation, which induces oscillation of the ACT bubbles, stretching capillaries. Given concurrently with chemotherapy, this enhances delivery of chemotherapy to target tissues.

Methods: We describe a first-in-human phase1 study to evaluate the safety and tolerability, pharmacokinetics, and preliminary anti-cancer activity of ACT treatment and the chemotherapy regimens FOLFOX or FOLFIRI in patients with liver metastases of colorectal origin (NCT04021277). The dose escalation cohorts evaluated safety of 20 µL/kg and 40 µL/kg dose levels of PS101 combined with chemotherapy. The primary assessment of anti-tumor activity consisted of within-patient comparison of radiographic responses between ACT-treated lesions (insonated) and control lesions (non-insonated).

Results: We had previously treated mice bearing SW620 xenografts treated with a control arm of Irinotecan at 60 mg/kg IP or Irinotecan plus PS101 at 2ml/kg and insonation in the experimental arm and showed a difference in survival in the experimental arm 34 days Vs 54 days p <0.01 (1). In the first in human clinical trial 8 patients were enrolled into the dose escalation part of the study, of which 2 subjects were not evaluable for dose escalation decision. There were no CTCAE grade 3, or above AEs or SAEs related to PS101 or the ultrasound. 4/8 patients discontinued treatment due to AEs - all related to chemotherapy. Median plasma concentration of PFMPC 5 minutes after the injection was 117 ng/ml (n=3, range 82 to 158) in the 20 µl/kg cohort and 233 ng/ml (n=4, range 217 to 275) in the 40 µl/kg cohort. 5 out of 6 patients had greater shrinkage of the insonated lesion compared with control lesions. The median percentage difference in maximum diameter of lesions between baseline and week 8 assessments, for insonated and non-insonated lesions, was -16% (range 25 to -42) and -3% (range 12 to -19), respectively. The dose expansion part of the study is ongoing, randomizing patients receiving FOLFIRI chemotherapy up to 10 patients each between 20 µl/kg and 40 µl/kg dose levels.

Conclusions: Following preclinical activity in xenograft models, the ongoing first in human study of ACT in patients with colorectal cancer has shown clinical translation of differential activity in insonated metastasis. Reference:

Reference: 1.Bush N et al Front Pharmacol 2019, 10:1299

#6222 Exposing the heterogeneity of the lipidome in the TME of cutaneous melanoma following treatment with NUC-7738 in combination with anti-PD-1 therapy.

A. L. Dickson[1], G. M. Zickuhr[1], I. Um[1], Y. Zhang[1], R. Plummer[2], S. P. Blagden[3], S. N. Symeonides[4], N. Cook[5], T. Evans[6], M. Elshani[1], D. J. Harrison[1]; [1]University of St. Andrews, St. Andrews, United Kingdom, [2]Freeman Hospital, Newcastle Upon Tyne, United Kingdom, [3]Churchill Hospital, Oxford, United Kingdom, [4]Western General Hospital, Edinburgh, United Kingdom, [5]University of Manchester, Manchester, United Kingdom, [6]The University of Glasgow, Glasgow, United Kingdom

Background. Malignant melanoma exhibits distinct lipid profiles compared to normal tissue and changes in the lipidome influence multiple aspects of tumor biology. Lipidomic alterations within the tumor microenvironment (TME) may influence the efficacy of anti-PD-1 therapy. In combination with anti-PD-1 agent pembrolizumab, NUC-7738 (3'-deoxyadenosine [3'-dA] which is phosphorylated and protected with a phosphoramidate moiety attached at the 5'-position) has shown promising activity in anti-PD-1 refractory melanoma (Phase 2; NCT03829254). NUC-7738 generates sustained intracellular levels of 3'-dATP, which profoundly alters RNA regulatory processes in tumor cells, resulting in impaired cellular responses and changes in expression of proteins related to lipid biosynthesis. To interrogate components of the TME before and after NUC-7738 + pembrolizumab treatment, we developed a novel workflow incorporating Mass Spectrometry Imaging (MSI) to co-register lipidomic changes with molecular markers. Machine learning accelerated the interpretation of complex data obtained from paired patient biopsies.

Methods. Snap frozen paired biopsies from patients with advanced cutaneous melanoma treated with NUC-7738 ±pembrolizumab were analyzed by desorption electrospray ionization (DESI)-MSI. Specific metabolic (e.g., ASAH1) and immune (e.g., CD8, CD20) markers were investigated by multiplex immunofluorescence (mIF) post DESI-MSI. Target selection was guided by bulk RNA-seq data. Raw MSI data was visualized using Waters HDI® software. Data extracted from selected regions of interest was exported into MetaboAnalyst 5.0 for statistical analysis. LIPID MAPS® Structure Database was used to assign lipid species. mIF/mIHC images were analyzed by HALO® AI.

Results. Single 10 µm tissue sections allowed co-registered DESI-MSI and mIF, suitable for further informatic and AI-enabled image analysis. This facilitated direct comparison of lipids, cells, and protein expression in the TME, before and after treatment with NUC-7738, a compound known to cause profound changes in poly(A) tail regulation. MSI data analyses of the TME uncovered intra-tumoral heterogeneity of the lipidome and demonstrated changes following treatment.

Conclusion. This platform provides a powerful investigative tool to simultaneously explore the myriad of factors in the TME that contribute to tumorigenesis and therapeutic response. Further analyses of the role of the lipidome in the TME and intra-tumoral heterogeneity will be explored in paired biopsies from patients with PD-1 inhibitor refractory melanoma.

#6223 Personalized MRI-informed forecasting of prostate cancer progression during active surveillance.

G. Lorenzo Gomez[1], C. Wu[2], J. P. Yung[2], J. F. Ward[2], H. Gomez[3], A. Reali[4], T. E. Yankeelov[5], A. M. Venkatesan[2], T. J. R. Hughes[5];
[1]Fundacion Instituto de Investigacion Sanitaria de Santiago de Compostela, Santiago de Compostela, Spain, [2]The University of Texas MD Anderson Cancer Center, Houston, TX, [3]Purdue University, West Lafayette, IN, [4]University of Pavia, Pavia, Italy, [5]The University of Texas at Austin, Austin, TX

Low and intermediate-risk prostate cancer (PCa) patients are eligible for active surveillance (AS), whereby treatment is delayed until progression to higher-risk disease is detected via longitudinal multiparametric magnetic resonance imaging (mpMRI) scans, biopsies, and prostate specific antigen (PSA) tests. However, AS relies on a population-based observational paradigm in which standard testing frequencies may not match the patient's tumor dynamics, resulting in a delayed diagnosis of progressive disease. To address these issues, we propose to advance AS towards a patient-specific predictive paradigm by leveraging computational tumor forecasts obtained with a biomechanistic model informed by mpMRI and clinical data collected during standard AS.

Here, we present a retrospective study with n = 16 PCa cases. All patients had three mpMRI scans obtained over 2.6 to 5.6 years during AS. Our biomechanistic model describes PCa growth in terms of the dynamics of tumor cell density as a combination of tumor cell mobility and net proliferation. The model is defined on the patient's prostate geometry, which is segmented on T2-weighted MRI data. Tumor cell density estimates are derived from apparent diffusion coefficient (ADC) maps obtained from diffusion-weighted MRI data. To facilitate modeling, the longitudinal imaging datasets are non-rigidly co-registered for each patient. We initialize the model with the tumor cell density map obtained from the ADC map of the first scan. The model is parameterized by minimizing the model-data mismatch in tumor cell density at the second scan date, and then we perform a tumor forecast up to the third scan date. Finally, we build a logistic classifier from a panel of model-based biomarkers calculated from the personalized model forecasts (e.g., tumor volume, total proliferation activity) at the times of histopathological assessment (i.e., biopsy, surgery) to classify tumors as low risk (Gleason score 3+3, n = 16) or intermediate-high risk (Gleason score ≥ 3+4, n = 15).

We obtained a concordance correlation coefficient (CCC) for tumor volume of 0.89 at both model calibration and forecasting horizon. The spatial fit of tumor cell density yielded a median Dice score and CCC of 0.80 and 0.59 at the second mpMRI date, and of 0.76 and 0.60 at the third mpMRI date, respectively. The logistic classifier of PCa risk yielded an area under the ROC curve of 0.90 and operates at optimal sensitivity, specificity, and accuracy of 86.7%, 93.8%, and 90.3%, respectively. The time trajectories of PCa risk obtained from the temporal predictions of the model-based biomarkers enabled identification of PCa progression by more than 1 year. Thus, while further development and validation over larger cohorts are required, these results suggest that our forecasting technology is a promising tool to predict PCa progression in AS and, hence, optimally guide monitoring and treatment decisions during AS.

#6224 Drop-like deformation of nuclei in cancer patient tissue.

C. R. Dubell[1], T.-C. Wang[1], I. Singh[1], D. G. Rosen[2], S. Chakraborty[3], T. P. Lele[1];
[1]Texas A&M University, College Station, TX, [2]Michael E. Debackey Veterans Affairs Medical Center, Houston, TX, [3]University at Buffalo, Buffalo, NY

In this study, we investigated nuclear deformations in cancer tissues and their clinical relevance to diagnostics.
Introduction: Cancers are graded by pathologists examining biopsy slides stained with hematoxylin and eosin for factors including nuclear atypia, which can include features like lobules, invaginations, large nuclear size, and prominent nucleoli. While the importance of nuclear atypia has been known for centuries, its cause remains unclear. Nuclear shaping has been studied extensively in vitro, leading to the liquid drop model of nuclear shaping, which states that nuclear shape changes can occur due to excess area in the form of wrinkles or folds in the lamina. When the lamina becomes fully taut, the nucleus reaches a limiting steady shape. Wrinkles allow the nuclear shape to mirror the cell shape such as in invading cancer cells. The applicability of this model to nuclei in cancer tissues from human patients is untested. Here, tissues were stained for nuclear lamina proteins to test for the presence of excess area in the lamina. Diagnostic relevance of the drop model was assessed by quantitative Fourier analysis of high-resolution images of lamin-stained nuclei.
Methods: Deidentified patient tissues from breast, colon, head and neck, and skin were immunostained for lamin B1 and imaged at high resolution (60X, 1.5 NA). Nuclei were then roughly segmented by the deep learning program Cellpose, followed by segmentation with a custom approach that sensitively detects micron-scale variations in the laminar contour. An Elliptical Fourier Analysis was performed to quantify nuclear irregularity by describing nuclear shape with a series of elliptical harmonics. More irregular nuclei are described by larger Fourier coefficients at higher frequencies.
Results: Folds and wrinkles in the nuclear lamina were observed in healthy tissue from all four tissue types studied, indicating the presence of excess area in the lamina. The presence of irregular nuclear shape including wrinkling/folds in the lamina was quantified with the Elliptical Fourier Coefficient (EFC) ratio. Posterior probability analysis related EFC ratio to tumor grade to assess the clinical value of the excess area found in the nuclear lamina. This revealed cancer-type dependent trends between EFC ratio and tumor grade.
Conclusions: Observations of wrinkling/folds in the nuclear lamina in healthy and cancerous tissue are consistent with the liquid drop model of nuclear deformation. Quantification of nuclear lamina wrinkling with the EFC ratio, along with other nuclear shape parameters, can be a powerful approach for computer-based, explainable, clinical grading. Our findings reveal a fundamental principle of nuclear deformation in cancer tissues and suggest a new approach for improving the accuracy in cancer grading.

#6225 Tumor evolution through selection by ECM stiffness.

T.-C. Wang[1], S. Sawhney[1], D. Morgan[2], R. Rashmi[3], M. R. Estecio[4], A. Brock[2], I. Singh[3], R. L. Bennett[5], C. F. Baer[5], J. D. Licht[5], T. P. Lele[1]; [1]Texas A&M University, College Station, TX, [2]The University of Texas at Austin, Austin, TX, [3]Texas A&M University, Bryan, TX, [4]University of Texas MD Cancer Center, Houston, TX, [5]University of Florida, Gainesville, FL

In this study, we used experimental evolution to investigate the extent to which the mechanical stiffness of the tumor extracellular matrix (ECM) exerts selection pressure on a genetically diverse population of breast cancer cells. Polyacrylamide hydrogels were fabricated and conjugated with collagen type I to create the ECM with different stiffness. MDA-MB-231 cells were continuously cultured on the hydrogels of the same corresponding stiffness. Growth rate was determined at certain time points by harvesting and counting the cells. Abundance of clonal MDA-MB-231 cells labeled with heritable DNA barcodes underwent the same selection was identified with sequencing of DNA barcode tags. Cellular phenotypes were characterized through immunofluorescence staining and confocal microscopy. 3D migration of the cancer cells was examined using Boyden chamber assay. Cellular contractility was measured through traction force microscopy. Whole genome transcriptome sequencing (RNA-seq), assay for transposase-accessible chromatin with sequencing, and reduced representation bisulfite sequencing were performed for transcriptomic and epigenetic analysis. Sustained culture of MDA-MB-231 breast cancer cells overall three months on soft ECM resulted in an increased proliferation rate and beta1 integrin-dependent spreading area of the cells. Such changes did not occur in clonal cells with low genetic variation and did not occur in ancestral cells on stiff substrates. Barcode analysis revealed two distinct surviving populations post-genetic selection, with one demonstrating robust proliferation on both soft and stiff ECM, and the other exhibiting preferential adaptation to the soft matrix. The soft-selected populations exhibited nuclear localization of the transcriptional regulator yes-associated protein and less wrinkled nuclei compared with ancestral populations when both populations were grown on soft ECM. Aggressive migration was observed in the soft-selected populations, indicating a more malignant selected phenotype. The soft-selected cells showed increased RhoA activity and contractile tension on a soft substrate compared to the ancestral cells. RNA-seq analysis revealed systematic differences between ancestral, stiff-selected, and soft-selected populations corresponding to enriched biological processes related to cell adhesion and ECM organization. Significant differences in DNA methylation and chromatin accessibility were observed in soft selected populations which were correlated with changes in RNA expression. ECM stiffness exerts selection pressure on genetically variable cancer cell populations, selecting specific genetic variants in a cell population optimally adapted for that stiffness. Selected variants on soft ECM tend to be highly migratory, proliferative and generate high traction even on soft ECM. Our results highlight the importance of ECM stiffness-driven evolution in cancer development.

#6226 Identifying nested spatial units as a conserved organizing principle of the spatial tumor microenvironment.

V. Behera, H. Giba, B. A. Doran, J. P. Kline, A. S. Raman;
University of Chicago, Chicago, IL

Heterogeneity of therapeutic response amongst cancer patients has a profound impact on cancer-related mortality. It has been widely hypothesized that diversity in clinical outcomes is driven by variability in tumor biology at scales ranging from inter-patient to inter-cellular. Indeed, the advent of technologies describing the tumor microenvironment (TME) at cellular resolution has demonstrated that TME organization is heterogeneous with respect to intra-tumor spatial location, body tumor location (primary vs metastatic), patient, and tumor type. However, the organizing principles that govern TME heterogeneity remain unclear. Without such organizing principles, it remains an arduous task to link descriptions of tumor biology heterogeneity to clinical outcomes in a mechanistically explainable manner. Through the application of network statistical inference models to spatial transcriptomic data, we have identified that nested spatial units (NSUs) are a core organizing principle of the TME. We find that NSUs are widely conserved across 96 patient biopsies of 14 distinct tumor types and 3 body locations (primary, abdominal metastases, brain metastases). Moreover, NSUs represent a transferrable organizing blueprint that allows for the spatial location of individual spots (5-50 cells) in a tumor biopsy to be predicted by the NSUs of a secondary, unrelated biopsy (Pearson correlation of spot-spot distance: 0.04 - 0.71, median 0.25). By using NSUs as the organizing unit of comparison, we identify variation in gene expression, biological pathways, and multicellular structures occurring across tumors in a distance-dependent manner. In summary, NSUs provide a foundation for the comparative analysis of tumor spatial biology and a path by which spatial biology can be mechanistically linked to patient outcomes.

#6227 A systems biology approach for identifying targetable vulnerabilities in Ewing sarcoma.

F. S. Dela Cruz[1], P. S. Mundi[2], A. Siddiquee[1], K. Guillan[1], D. You[1], G. Ibanez Sanchez[1], A. Ndengu[1], A. Califano[3], A. L. Kung[1],
[1]Memorial Sloan Kettering Cancer Center, New York, NY, [2]Columbia University Irving Medical Center:, New York, NY, [3]Columbia University Irving Medical Center, New York, NY

Background: Targeting fusion oncoproteins like the canonical EWS/ETS fusions in Ewing sarcoma remain an elusive challenge. To circumvent these challenges, we have utilized transcriptome-based systems biology approaches that identify targetable Master Regulator proteins (MRs) critical to maintaining the cancer cell state. OncoTarget analysis generates a rank order list of targetable MRs while OncoTreat analysis uses cognate cell lines matched to patient tumors to identify drugs that invert the MR signature. We used OncoTarget and OncoTreat analyses to identify existing drugs which could be repurposed to target MRs active in Ewing sarcoma.
Methods: A gene regulatory interactome was developed from 122 pediatric sarcoma samples to enable identification of MR targets using OncoTarget. To enable OncoTreat analysis, 2 cognate cell lines were subjected to high-throughput drug perturbational screens. Cells were treated with sub-lethal concentrations of 335 compounds (FDA approved or investigational drugs). Ex vivo drug screens using PDX-derived cells were performed as a complementary assay to validate predictions. In vivo validation was performed in Ewing sarcoma PDXs.
Results: The MR architecture of 3 Ewing sarcoma PDX models was evaluated using OncoTarget. OncoTreat analysis identified 43 drugs predicted to be active in at least 1 Ewing sarcoma PDX while OncoTarget analysis identified 20 MR targets predicted in at least 1 Ewing sarcoma PDX. DOT1L and AURKB were predicted targets across multiple Ewing sarcoma PDXs. Ex vivo screening of dissociated cells from 2 Ewing sarcoma PDXs was performed to select the most potent agents for in vivo validation. Three OncoTreat (clarithromycin, tivozanib and obataclax) and two OncoTarget (DOT1L targeted with EPZ-5676 and AURKB targeted with baracertib) predicted drugs were evaluated in a STAG2 mutant Ewing sarcoma PDX and all demonstrated significant abrogation of tumor growth including complete regression in baracertib-treated animals ($p<0.01$).
Conclusion: These systems biology approaches can identify non-oncogene encoded vulnerabilities in Ewing sarcoma and hold the potential for expanding the number of therapeutic options for tumors driven by untargetable oncoproteins.

BIOINFORMATICS / COMPUTATIONAL BIOLOGY / SYSTEMS BIOLOGY / CONVERGENT SCIENCE: Integrative Computational Approaches 2 / Sequence Analysis / Systems Engineering
Poster Session

#6231 Multi-omic characterisation of clear cell renal carcinoma reveals endogenous and exogenous processes related to its aetiology.

R. Cortez Cardoso Penha II[1], A. Sexton Oates[1], S. Senkin[1], H. Park[1], N. Alcala[1], M. Foll[1], K. Smith-Byrne[2], P. Brennan[1], J. Mckay[1];
[1]International Agency for Research on Cancer, Lyon, France, [2]Oxford University, Oxford, United Kingdom

Endogenous and exogenous exposures are associated with distinctive molecular marks in somatic tissues, including human tumours. Integrative multi-omic approaches could help improving the resolution to detect the molecular marks associated with disease aetiology. Here, we leveraged the overlapping molecular information of clear cell renal cell carcinomas (ccRCC) tumours from Mutographs cohort by integrating DNA methylation, transcriptome, and whole-genome sequencing-based somatic mutation data to explore and gain new insights into exposures linked to ccRCC aetiology. Our novel framework identified important sources of biological variance across ccRCC tumours that were summarized as molecular components. We inferred these molecular ccRCC components into independent datasets to further explore their relationship with molecular and epidemiological features of ccRCC, normal adjacent kidney tissues, and other cancer types. Our results revealed a major ccRCC molecular component correlating with cellular mitotic age-related features, particularly the mitotic epigenetic clock (age-adjusted epiTOC2), clock-like DNA mutational signatures (SBS1/ID1), and telomere attrition. This molecular component was overrepresented in ccRCC tumours in comparison with normal paired kidney tissues, associating with *PBRM1* and *SETD2* somatic cancer driver mutations, genome stability, tumor stage, grade and ccRCC patient survival, independently to chronological age. Pan-cancer analysis supported the mitotic-age effect, represented by this molecular component, in other cancer types. Another ccRCC component was associated with tobacco usage, the presence of tobacco related DNA mutational and methylation signatures, increased total mutation burden, and sex. This component was also related to the epigenetic regulation of xenobiotic metabolism-related genes (e.g., *GSTP1*), further suggesting a relationship with genotoxic compounds. We further identified molecular components related to the ccRCC tumour microenvironment and cell proliferation, including one component related to *BAP1* cancer driver mutations, pro-inflammatory immune cells, and ccRCC patient survival. In conclusion, our study reports a novel framework to molecular characterize ccRCC tumours using an integrative multi-omic approach, providing additional insights into the molecular footprints of endogenous and exogenous exposures in ccRCC tumours, including molecular components with prognostic value for patients.

#6233 Characterizing variants of uncertain significance in the tumor suppressor gene known as phosphatase and tensin homolog (PTEN).

Ajay P. Singh, Jasmine Wen, David Nguyen, Vedanta Khan, Kiran Dhami, Kaitlynn Meier-Ross, Benjamin Martin, Jesse T. Chao

Medical Biophysics, University of Toronto, Toronto, ON, Canada

PTEN is an important tumor suppressor that plays an essential role in regulating cell proliferation. Loss of PTEN function is implicated in approximately 50% of metastatic cancers. Individuals with pathogenic *PTEN* variants are at significantly elevated risk of developing hereditary cancer syndromes such as PTEN hamartoma tumor syndrome. While genetic testing for *PTEN* is valuable for identifying individuals at risk, 47% of 3065 publicly reported *PTEN* variants are not conclusively classified; they either have conflicting interpretations of pathogenicity or are labeled as “Variants of Uncertain Significance (VUS)” and are not clinically actionable. The lack of a clear interpretation for these *PTEN* variants hinders the targeted care and surveillance of patients and places a strain on the healthcare system. To overcome this issue, our aim is to develop a clinically relevant tool for assessing the pathogenic effects of *PTEN* variants.We hypothesize that loss of function (LoF) PTEN variants will lead to changes in cellular phenotypic profiles that can be measured through single-cell phenotypic profiling. Thus, our goal is to investigate the functional status of exogenously expressed *PTEN* variants in *PTEN*-/- HEK 293 cells. We developed a multiplexed high content imaging assay to characterize PTEN and its key signaling partners such as phospho-Akt. Additionally, we developed a deep learning based single-cell phenotypic profiling pipeline named Paracell that uses subcellular segmentation to extract 540 phenotypic features. Cells that exhibit abnormal phenotypic profiles are indicative of loss of PTEN function. Preliminary results from testing 73 missense variants of *PTEN* showed that functional and LoF PTEN variants form distinctive clusters in a two-dimensional UMAP plot based on Paracell outputs, suggesting that our approach can identify potentially pathogenic variants of PTEN.Through characterizing novel VUS, we can elucidate structural domains involved in PTEN’s tumor suppressing activity. The result of these classifications will enable more optimized detection, diagnosis, and surveillance strategies for *PTEN*-related cancers. Ultimately, we aim to contribute to improving the genetic testing of PTEN and the development of targeted therapies.

#6234 Single-cell analysis of state-transition from health to leukemia and the leukemic cell heterogeneities in inv(16) acute myeloid leukemia (AML).

Y.-H. Fu, L. Zhang, Y.-C. Chen, D. E. Frankhouser, L. Uechi, D. O'Meally, S. Branciamore, G. Marcucci, R. Rockne, Y.-H. Kuo;
City of Hope National Medical Center, Duarte, CA

AML is an aggressive hematological malignancy with heterogeneous genetic abnormalities. Using a conditional knock-in mouse model (*Cbfb*$^{56M/+}$*/Mx1-Cre*) to mimic the somatic acquisition of fusion gene *CBFB-MYH11* (CM), created in the recurrent chromosome translocation inv(16)(p13q22) of AML, we previously reported that the blood transcriptome undergoes state-transition from health to leukemia. In this study, we analyze the transcriptomic alterations and leukemic cell heterogeneities in a leukemia state-space using single-cell RNA sequencing (scRNA-seq). CM expression was induced in *Cbfb*$^{56M/+}$*/Mx1-Cre* mice by poly (I:C) injection, and scRNA-seq analysis was performed on peripheral blood mononuclear cells (PBMC) and bone marrow (BM) cells from leukemic mice and age-matched wild-type (WT) controls. More than 105,000 cells were subjected to the following dimensionality reduction and cell type annotation. By performing principal component analysis (PCA), we observed a Y-shape cell distribution with emergence of a divergent branch occupied by leukemic cells which can be mapped to a leukemic state. The principal components 1 and 2 (PC1 and PC2) clearly distinguish the leukemic cells from normal cell types such as myeloid cells and lymphocytes. By accessing the eigenvalue of genes for PC1 and PC2, we quantified the crucial genes and pathways related to leukemia progression at a single-cell level. We characterized cKit+ leukemic cell clusters by transcriptome-based correlation and gene expression pattern and found that they resembled stem cells and megakaryocytic-erythroid progenitors (MEP) with dysregulated pathways, including upregulated "inflammatory response" and downregulated pathways related to Myc targets, oxidative phosphorylation, mitochondrial protein translation, and ribosomal biogenesis/assembly. Examining the 31 clusters (C0-C30) seen in cKit+ BM cells, we identified 9 leukemic clusters exhibiting distinct features, including high heme-metabolism (C0, C1, and C2), high proliferation (C1, C8), S phase (C4, C10), low oxidative phosphorylation (C2, C5, C17), high Cd9 (C10), high Egfl7 (C7, C8). In conclusion, our study unveils state-transition from health to leukemia at single-cell resolution, and uncovers diverse biological heterogeneities associated with the inv(16) AML state. Further refinement of transcriptome state-transition and single-cell analysis will provide an analytical framework for modeling the dynamic changes during disease evolution at the single-cell level.

#6235 Clinical and phenotypic consequences of HLA mediated antigen presentation deficiency in pancreatic adenocarcinoma at bulk and single-cell resolution.

M. J. Geuenich[1], B. Gruenwald[2], G. O'Kane[2], C. Yu[1], T. Ju[1], A. Zhang[3], O. Hamza[3], G. Jang[3], F. Notta[3], S. Gallinger[3], K. R. Campbell[1];
[1]Lunenfeld-Tanenbaum Research Institute, Toronto, ON, Canada, [2]Princess Margaret Cancer Centre, Toronto, ON, Canada, [3]Ontario Institute of Cancer Research, Toronto, ON, Canada

Introduction:
Pancreatic ductal adenocarcinoma (PDAC) is a highly lethal neoplasm of the pancreas characterized by a low survival rate and limited treatment options. Despite the success of immunotherapy in various cancer types, its efficacy in PDAC remains low. The underlying reasons for this discrepancy are not fully understood, despite PDAC exhibiting a moderate mutation burden. One possible determinant could be the loss of heterozygosity (LOH) at the human leukocyte antigen (HLA) loci, resulting in compromised antigen presentation. In this work, we aim to identify and validate HLA LOH events in two independent cohorts to gain insights into both their prevalence and clinical and phenotypic impact on PDAC.
Methods:
We applied LOHHLA, a specialized pipeline to identify HLA LOH events from paired whole genome sequencing to two independent cohorts comprising over 650 patients. We contextualized these results with the paired transcriptome-wide gene expression data and immunohistochemistry stains. In addition, we developed a machine learning classifier to predict HLA LOH from transcriptomic data. We transfer this classifier to single cell RNA sequencing data to identify the impact of (subclonal) HLA LOH on the tumor microenvironment.
Results:
HLA LOH events occur in approximately 30% of PDAC patients, with about 50% of these deletions being focal deletions. We find evidence that focal but not non-focal LOH is a driver of immune escape. Overall, we find that HLA LOH events are early genetic alterations and observe a significant association between HLA LOH and the Basal PDAC expression subtype. In addition, we find that HLA expression is the most important determinant of lymphocyte infiltration followed by an intact HLA locus. Moreover, our transcriptomic classifier allowed us to accurately identify HLA LOH events from RNA sequencing data, which we successfully validated in an independent cohort. Finally, we applied this classifier to single cell sequencing data and identified phenotypic differences in multiple compartments of the tumor microenvironment between samples with intact HLA and HLA LOH.
Conclusions:
In conclusion, our study provides the most in depth characterization of the consequences of altered antigen presentation in PDAC to date. We have demonstrated that HLA LOH occurs in a substantial proportion of patients. Overall, these findings contribute to a better understanding of the immune landscape in PDAC and may have implications for the development of immunotherapeutic strategies tailored to this challenging cancer type.

#6236 Systems biology modeling identifies SMARCD3 as a master regulator facilitating everolimus resistance in ER+ breast cancer.

E. F. Medina, P. A. Cosgrove, E. Farmaki, V. K. Grolmusz, F. Chi, J. I. Griffiths, A. H. Bild, A. Nath;
Beckman Research Institute of The City of Hope, Duarte, CA

Breast cancer is the most common malignancy in women and estrogen receptor positive (ER+) breast cancers represent nearly 75% of all breast tumors. Everolimus, an mTORC1 inhibitor, in combination with exemestane has been approved for patients with metastatic ER+ breast cancer. However, many patients eventually develop resistance to everolimus and leads to poor survival outcomes. Characterizing everolimus-resistant cells can reveal targetable molecular phenotypes that can eventually lead to new therapeutic targets. In this study, we elucidate systems-level phenotypic distinctions between everolimus sensitive and refractory cells. We generated several isogenic ER+ breast cancer cell lines resistant or sensitive to everolimus. We then leveraged transcriptomic profiles from sensitive and resistant cells before or after everolimus treatment to decipher the underlying mechanisms essential to the resistant state. Using linear mixed effect models, we identified several meta-phenotypes that were distinct between sensitive and resistant cell states. These included growth-factor signaling, cell cycle, metabolism, stemness, and apoptosis meta-phenotypes. Our analyses also identified strong activation of growth-factor receptors including IGF1R/INSR and ESR1 in the resistant cells, which were maintained despite everolimus treatment. Next, we adopted a transcriptional regulatory network reconstruction framework to identify the master regulators responsible for the activation of resistance meta-phenotypes. We identified SMARCD3 as the key master regulator controlling expression of genes across diverse resistance meta-phenotypes, including growth-factor signaling. Further, using transcriptomic profiles from a neoadjuvant trial of 23 post-menopausal ER+ breast cancers treated with everolimus, we found that SMARCD3 expression was elevated in resistant tumors. To confirm the role of SMARCD3 in everolimus resistance, we repressed transcription of the SMARCD3 gene using CRISPR interference to re-sensitize resistant cells to everolimus treatment. In conclusion, we used context-specific cell transcriptomic profiles and integrative systems-biology approaches to elucidate mechanisms of resistance in response to everolimus treatment in ER+ breast cancer. Our findings suggest SMARCD3 upregulation promotes resistance to everolimus treatment and may serve as a novel therapeutic target in ER+ breast cancer.

#6237 Large-scale imputation models for multi-ancestry proteome-wide association analysis.

C. Wu[1], Z. Zhang[1], X. Yang[2], B. Zhao[3];

[1]UT MD Anderson Cancer Center, Houston, TX, [2]Purdue University, West Lafayette, IN, [3]University of Pennsylvania, Philadelphia, PA

Proteome-wide association studies (PWAS) decode the intricate proteomic landscape of biological mechanisms for complex diseases. Traditional PWAS model training relies heavily on individual-level reference proteomes, thereby restricting its capacity to harness the emerging summary-level protein quantitative trait loci (pQTL) data in the public domain. Here we introduced a novel framework to train PWAS models directly from pQTL summary statistics. By leveraging extensive pQTL data from the UK Biobank, deCODE, and ARIC studies, we applied our approach to train large-scale European PWAS models (total n = 88,838 subjects). Furthermore, we developed PWAS models tailored for Asian and African ancestries by integrating multi-ancestry summary and individual-level data resources (total n = 914 for Asian and 3,042 for African ancestries). We validated the performance of our PWAS models through a systematic multi-ancestry analysis of over 700 phenotypes across five major genetic data resources. Specifically, we identified several novel and well-known genes for various cancers; we highlighted eight genes associated with six cancer traits across all three PWAS model cohorts, including CTSF, RSPO3, CRTAM, LAYN, CHRDL2, DPEP1, NFASC, and NAAA. Our results bridge the gap between genomics and proteomics for drug discovery, highlighting novel protein-phenotype links and their transferability across diverse ancestries. The developed PWAS models and data resources are freely available at www.gcbhub.org.

#6238 Integrated multi-omic/modal profiling enables improved characterization of oncogenic processes, with impact to clinical actionability in the GenMineTOP tested population.

B. Losic[1], K. Tatsuno[2], V. R. Singan[1], H. Ueda[2], A. Ushiku[3], V. Jayakumar[4], E. Hattori[4], T. Ichijo[4], T. Sasa[4], M. Akahori[4], S. Hayashi[4], E. Hsiao[1], S. Feupe[1], D. Vo[1], T. Geier[1], S. Tsutsumi[2], T. Ushiku[3], K. Watanabe[3], K. Oda[3], H. Kage[3], J. Radecki-Crandall[1], D. T. Cheng[1], H. Aburatani[2];
[1]Realm IDx, Aliso Viejo, CA, [2]Research Center for Advanced Science and Technology, The University of Tokyo, Tokyo, Japan, [3]The University of Tokyo Hospital, Tokyo, Japan, [4]Konica Minolta, Tokyo, Japan

Introduction: It is becoming increasingly apparent that tumor gene expression and spatial H&E profiling can be used to improve the accuracy of DNA-only tumor profiling for clinically relevant use-cases. Future development and deployment of integrative (multi-omic (DNA+RNA) and/or multi-modality (omics + imaging)) tests for treatment and clinical trial profiling hinges on the demonstration of clear robustness and performance gains of prognostic and predictive integrative predictors in a clinical setting. In this work we present several analyses quantifying the utility of integrative testing. We show that a multi-omic test combining tumor expression signatures with DNA profiles substantially improves tumor-of-origin prediction for cancers of unknown primary and also significantly improves MSI detection and resolution. We also show that a simple multi-modality model combining spatial features of tumor infiltrating lymphocytes of tumors with tumor expression is prognostic for MSI-positive patients.

Methods: *Multi-omic*Tumor-of-origin: 163 patient sample expression profiles were profiled using the GenMineTOP test. GenMineTOP is a tumor-normal, joint DNA+RNA capture PMDA-approved test in current clinical service in Japan. The samples were clustered using DNA-only, RNA-only, and joint DNA+RNA profiling signatures. MSI prediction: 940 samples from the TCGA COAD, UCEC, and READ cohorts with matched MMR IHC MSI-calling, DNA-NGS-based MSI calling, and RNA-seq data were utilized to train, test and validate an expression-based pan-cancer MSI caller. Additional orthogonal validation was carried out using GenMineTOP multi-omic profiles. *Multi-modality* Spatial context of TIL and tumor-expression: 158 MSI+ samples from the TCGA-UCEC cohort with matched fresh-frozen H&E 20X images and RNA-seq data were utilized to mine spatial features of tumor-infiltrating lymphocytes and derive gene expression signatures, respectively. A Cox-proportional hazard model for patient survival using gene expression and spatial TIL features was constructed while regressing out tumor stage, gender, age, and ethnicity.

Results & Conclusions: Our multi-omic results quantify the benefit of combining DNA and RNA profiles from GenMineTOP to classify tumor-of-origin from unknown primaries reduces classification error by approximately 50%. Additionally, our expression-based MSI status prediction model not only significantly improves NGS DNA (MSI-sensor) based MSI prediction (log-ratio test, pval < 1e-7) but also strongly suggests that nonlinear differential expression drives the improvement in MSI prediction. Our multi-modality results demonstrate that mining the spatial context of endogenous tumor immune response has nontrivial prognostic utility ($p < .05$).

#6239 Human computer interface guided approach to accelerate anticancer drug discovery: Application to human estrogen receptor interactome.

R. V. Rajnarayanan, A. Alsabagh;
NYITCOM at Arkansas State, Jonesboro, AR

Structure-based drug discovery of target specific drugs greatly rely on the existence of high resolution X-ray crystal structure of the target proteins. Flexible and dynamic regions including hinges and loops which constitute major protein-protein interaction sites as well as allosteric sites are often beyond the scope of current tools and techniques available for protein folding and modeling. Human ability in recognizing patterns and to solve complex puzzles are far superior to any existing computer program at folding these atypical regions of proteins. We have utilized an unconventional combination of using dynamic three-dimensional protein models as physical human computer interface (HCI) devices and integrated proteomics data to predict flexible and dynamic protein-protein interfaces and allosteric pockets of key regulatory proteins to accelerate compound discovery. To this end, we have successfully utilized 1) Flexible HCI devices to generate an ensemble of dynamic three dimensional structures which includes a subset of biologically active conformations among others (thereby exploring the viable chemical space) and 2) Structure refinement and efficient filtering of biologically active conformations can be accomplished by integrating protein-protein interface and fold proteomics data. Here we present AI ready, HCI guided exploration of human estrogen receptor interactome and early in vitro confirmatory analyses. AI approachs to predict 3D protein structures from amino acid sequences like AlphaFold are often on par with experimentally generated structures and AI-guided structure prediction or docking approaches have been reported to significantly reduce computer time utilization. Streamlining of HCIguided tools to enable access to dynamic druggable pockets in protein targets will accelerate drug discovery.

#6240 Mutation impact on mRNA versus protein expression across human cancers.

Y. Liu, A. Elmas, **K.-l. Huang**;
Icahn School of Medicine at Mount Sinai, New York, NY

Cancer mutations are often assumed to alter proteins, thus promoting tumorigenesis. However, how mutations affect protein expression has rarely been systematically investigated. We conduct a comprehensive analysis of mutation impacts on mRNA- and protein-level expressions of 953 cancer cases with paired genomics and global proteomic profiling across six cancer types. Protein-level impacts are validated for 47.2% of the somatic expression quantitative trait loci (seQTLs), including mutations from likely “long-tail” driver genes. Devising a statistical pipeline for identifying somatic protein-specific QTLs (spsQTLs), we reveal several gene mutations, including *NF1* and *MAP2K4* truncations and *TP53* missenses showing disproportional influence on protein abundance not readily explained by transcriptomics. Cross-validating with data from massively parallel assays of variant effects (MAVE), *TP53* missenses associated with high tumor TP53 proteins were experimentally confirmed as functional. Our study demonstrates the importance of considering protein-level expression to validate mutation impacts and identify functional genes and mutations.

#6241 A large scale proteogenomic atlas for precision oncology research.

N. Simchi, O. Givton, D. Daitchman, E. Seger, K. Pevzner;
Protai, TEL AVIV, Israel

Recent advances in the field of mass spectrometry proteomics have led to growth in proteomics research resulting in a massive and rapid increase in the volume of high-quality publicly available proteomics datasets. This growth creates an underutilized resource with potential for new discoveries. Effectively utilizing this vast resource of preclinical and clinical samples is a major challenge.

We utilize the growing availability of proteomics and post-translational modifications (PTMs) data for drug and biomarker discovery. This innovative computational approach enables the integration of preclinical and clinical data, both public and proprietary, with a specific emphasis on extracting valuable biological insights that are only observable at the protein level or through PTMs.

We developed a platform that combines multi-omic data curated from the public domain, together with internally generated high quality proteomic and phosphoproteomic data. The platform incorporates diverse clinical annotations, tumor and normal samples, drug sensitivity, patient outcomes and relevant bioinformatic knowledge bases.

The platform can be leveraged to generate insights addressing diverse clinical needs. For example, we demonstrate how our platform can be utilized to estimate the clinical prevalence of a certain protein or protein signature, in order to identify novel response biomarkers with the highest likelihood of success by confirming its presence and variance in clinical datasets. In addition, these insights enable novel understanding of response and resistance mechanisms, thus establishing a framework that expedites the generation of hypotheses for subsequent investigation and experimental validation.

#6242 A workflow execution system in a data fabric for integrative cancer analyses.

A. Venkat, P. Ribeyre, J. Qureshi, S. S. Narumanchi, J. M. Maxwell, B. Winslow, S. V. d. Garcia, C. Meyer, T. Garcia, P. Vassilatos, C. Malson, **Z. Zhang**, R. Grossman;
University of Chicago, Chicago, IL

Cancer researchers are increasingly conducting multi-omic research and performing integrative analyses on combinations of genomic, proteomic, transcriptomic, imaging, single cell and other data modalities. However, it is quite challenging for a researcher to effectively access, aggregate and analyze data and metadata from different data sources in a scalable and reproducible manner, as the individual datasets may be disconnected from each other, and have separate authentication and authorization requirements. We developed a workflow execution system in a data fabric called the Biomedical Research Hub (BRH) to overcome these challenges for academic researchers. The BRH is powered by the Gen3 technology, an open-source Kubernetes based software stack that allows cancer researchers to create their own data fabric and interoperate with data from multiple data sources. The workflow execution system utilizes nextflow and allows researchers to run containerized applications in the cloud in a secure and isolated environment. Data from multiple resources can be combined for analysis using convenient pay models including NIH STRIDES. We plan to demonstrate the application of our system on a scientific use case involving Clonal Hematopoiesis of Indeterminate potential (CHIP), a phenomenon that has been associated with aging, cancer, cardiovascular diseases, infection and all-cause mortality. We run containerized CHIP workflows on the cloud, utilizing two datasets accessible through BRH: i) The Genomic Data Commons, the world's largest source of harmonized cancer data and ii) BioDataCatalyst, an NHLBI ecosystem that drives discovery and innovation for heart, lung, blood and sleep disorders. Our system is ideally suited for machine learning on large aggregated cancer datasets and federated learning tasks.

#6243 Rapid autopsy reveals the interplay of tumor heterogeneity at genomic, transcriptomic, and spatial dimensions.

N. Yao[1], R. Vanguri[2], J. Patel[1], J. Lihm[1], A. Fisher[3], I. Jarchum[3], S. Umeda[1], H. Li[1], S. Ely[3], T. Hollmann[3], C. Iacobuzio-Donahue[1], B. Greenbaum[1];
[1]Memorial Sloan Kettering Cancer Center, New York, NY, [2]Children's Hospital of Philadelphia, Philadelphia, PA, [3]Bristol Myers Squibb, New York, NY

Incomplete understanding of tumor heterogeneity across primary and metastatic sites often lead to ineffective cancer treatments. To comprehensively interrogate tumor heterogeneity at genomic, transcriptomic, and spatial levels, we established a novel rapid autopsy protocol to obtain multiregional tri-omic data consisted of whole exome sequencing, mRNA-sequencing, and multiplexed immunohistochemistry on primary and metastatic tumors and associated microenvironments (TMEs). We applied this protocol to six patients with various primary tumor types: non-small cell lung cancer (NSCLC), small cell lung cancer (SCLC), urothelial cancer, and one mixed case with both NSCLC and SCLC. A total of 50 tumor samples with paired tri-omic data were obtained across 16 different primary and metastatic organs to interrogate heterogeneities underlying tumor evolution and treatment resistance mechanisms.

We constructed mutation-based phylogeny trees to reveal structural differences in tumor evolution trajectories across patients and infer heterogeneous tumor antigen landscape. We uncovered highly entropic phylogenetic structures having unique variants gained at each metastasis as well as low entropic structures with high sharing across sites. The mixed case had a clonal sweep structure with two metastases developed prior to the rest of the metastasis. In this case, older clones were shown to have strong association with APOBEC mutation signatures, enhanced subclonal mutation burden and loss of human leukocyte antigen heterozygosity as mechanisms of immune evasion.

Integrating transcriptome and spatial profiles, we revealed that tumor intrinsic expressions and extrinsic immune infiltration levels covary with tissue types rather than with mutation-based phylogenetic clusters. Across patients, samples that had high similarities in mutational landscape varied in their pro-tumor expression programs and the cellular composition of TMEs. In particular, lung samples across patients had the highest effector T cell population and major histocompatibility complex (MHC) class I, II presentations compared to other tissue types. Contrasting small cell carcinoma (SCC) and adenocarcinoma (Adeno) samples from lung tissues further revealed that SCC had more immunosuppressive TMEs with downregulation of MHC class II. Liver metastasis samples were further characterized to have the most aggressive phenotypes enriched in genomic instability measured by aneuploidy compared to other metastatic sites.

In sum, we present a novel technology and computational framework that enables a three-dimensional profiling of tumor heterogeneity. This work suggests that single-site biopsies are insufficient to capture tumor heterogeneity and calls for multi-modal integrations to design treatments that can overcome tumor-specific resistance mechanisms.

#6244 MultiTME: A Bayesian method for integration and analysis of multimodal, multi-patient spatial profiling data.

Haoran Zhang[1], Jeff Quinn[2], Liron Yoffe[3], Vivek Mittal[3], Wesley Tansey[2]

[1]Department of Computer Science, The University of Texas At Austin, Austin, TX,[2]Computational Oncology, Memorial Sloan Kettering Cancer Center, New York, NY,[3]Weill Cornell Medicine, New York, NY

The role of the tumor microenvironment (TME) in cancer evolution and progression is complex and multi-faceted. Multiple cellular phenotypes and patterns of cell-cell communication have been implicated as drivers of drug resistance and metastasis. The spatial architecture of the TME is emerging as particularly important in characterizing the trajectory of tumor growth and response to therapy. Accordingly, there has been a rapid rise in technologies to spatially profile the TME. Each technology focuses on a different modality (e.g. transcriptomics, proteomics, metabolomics) and operates at a different granularity, from coarse-grained tissue spots aggregating dozens of cells to fine-grained subcellular resolution. There is currently no computational method capable of drawing unified inferences across modalities. We introduce MultiTME, a single, holistic generative model for jointly modeling multimodal data across multiple samples in a cohort. MultiTME addresses these challenges through a two-dimensional integration of both samples and multimodal data. MultiTME incorporates a cohort of tissue samples, enabling the joint modeling of different samples within a single analytical framework. This integration allows for a comprehensive analysis of the spatial distribution of cell types across multiple samples, enhancing the understanding of TME variability and the identification of robust biomarkers. MultiTME also integrates multimodal data with varying resolutions, such as Spatial Transcriptomics (ST), single-cell RNA sequencing (scRNA-seq), and Imaging Mass Cytometry (IMC), and provides a multi-layered understanding of the TME. This integration enables the modeling of TME at a finer scale and the discovery of cell types and subtypes that are not distinguishable using single-modal approaches. It also provides concurrent expression profiles across different modalities, leading to the identification of novel biomarkers. We demonstrate MultiTME's efficiency and scalability with a dataset of coupled ST, scRNA-seq, and IMC from a cohort of 8 lung cancer patients. MultiTME's capability to handle both intra-cohort and inter-modality variability offers a panoramic view of TME and helps identify biomarkers and therapeutic targets for cancer screening and treatment. MultiTME is open source.

#6245 Missed opportunity at the subcellular level: Enhancing the utility of cellular imaging modality in spatial transcriptomic profiling of tumor tissues.

X. Song, X. Yu, C. M. Moran-Segura, G. D. Grass, R. Li, **X. Wang**;
Moffitt Cancer Center, Tampa, FL

Mini-bulk or single-spot spatial transcriptomic technologies, such as GeoMX Digital Spatial Profiler (DSP), have revolutionized our ability to probe spatial heterogeneity and examine transcripts at a subcellular level. In cancer research, this level of granularity is crucial for uncovering the distinct gene expression signatures within specific compartments or structures of interest such as tumor, immune, stroma, and tertiary lymphoid structures. However, in most GeoMX DSP studies, the spatial information obtained from multiplex immunofluorescence imaging has been primarily used for identifying the regions of interest (ROI), rather than as an integral part of the downstream transcriptomic data interpretation. To fix this missed opportunity, we developed a machine learning based analytical framework to fully leverage the rich spatial context provided by the in situ imaging modality. The framework has two main functionalities. (1) ROI cropping and cell segmentation: our framework enables the automated cropping of ROI images, followed by a cell segmentation process utilizing a multi-color-optimized deep learning model pre-trained based on the TissueNet. (2) Cell typing and integrative spatial analysis: the pipeline extracts cell-level morphological features (e.g. cell size and circularity), and AI-driven characteristics. These features are subsequently employed for cell typing and the quantification of cell mixture. The framework is equipped to perform a series of advanced spatial analyses, such as spatial metrics calculation and consensus clustering analysis with the matched gene expression data. To validate the framework, we conducted GeoMX DSP analyses on samples obtained from bladder cancer and upper tract urothelial carcinoma, encompassing 56 ROIs annotated by pathologists. Our results demonstrated high accuracy, with the calculated tumor-immune proportions aligning precisely with the original annotations. We further compared the cell deconvolution results of our framework with those obtained using SpatialDecon. Consistency was noted across both methods, with a high correlation reaching 0.90. However, we observed that SpatialDecon tends to underestimate tumor purity in tumor core regions, with discrepancies as large as 0.30, and overestimating tumor purity in stromal regions. Additionally, analysis of ROIs in tumor margins revealed that SpatialDecon consistently overestimates the overall proportions of immune cells. In conclusion, our results underscore the importance of integrating in situ imaging with subcellular-level spatial transcriptomics for a more accurate and reliable analysis of tumor tissues. Our approach provides critical insights into the tumor microenvironment and cellular interactions, with significant implications for both research and clinical applications in oncology.

#6246 De novo mutation discovery in a mouse model and a human patient sample of non-Hodgkin's lymphoma.

D. K. Sullivan[1], E. Albinali[2], M. Boffelli[3], L. Pachter[3];
[1]David Geffen School of Medicine, University of California, Los Angeles, Los Angeles, CA, [2]Gretchen Whitney High School, Cerritos, CA, [3]California Institute of Technology, Pasadena, CA

Cancer encompasses many different diseases, all typically involving an accumulation of genetic alterations. However, despite the genomic complexity of this group of diseases, cancer genomic studies typically rely on sequence alignment to a "reference genome" prior to analysis. Such approaches can provide gene expression quantification of known, annotated genes. However, they miss the detection of fusion genes, novel transcripts, virus insertions, and other genetic insults that may be present in cancer beyond an altered gene expression profile. Here, we develop a workflow for de novo identification and quantification of "outside of reference genome" genetic aberrations. This workflow leverages klue, a method we developed that is based on the compact de Bruijn graph, which can extract sequences uniquely found in a "tumor" sample but not in a "normal" control sample from genomic sequencing data. We first applied this method to an RNA-seq experiment from the EμSRα-tTA/TetO-MYC mouse model, which is a MYC-driven autochthonous transgenic mouse model of T-cell acute lymphoblastic lymphoma (T-ALL). We extracted k-mer contigs present in the mouse tumor samples but are present neither in the spleens of wild-type mice of the same genetic background nor in the standard mouse reference genome assembly. We then mapped RNA-seq reads from the T-ALL mouse tumor samples to these contigs. The contigs with the highest number of mapped reads (i.e. the highest counts) were run through BLAST to determine their identities. The mapped contigs with the highest counts were the tTA transgenic element sequence and the human MYC transgene. This result showcases this workflow's success in isolating and quantifying "reference-absent" tumor-unique sequences. Next, we applied klue to whole genome sequencing (WGS), whole exome sequencing (WES), and RNA-seq data from a patient with B-cell follicular lymphoma (with matched normal specimen) from the Texas Cancer Research Biobank, as this data is unrestricted open access. Tumor-unique contigs in sequencing reads were extracted and analyzed with BLAST and BLAT. In one case, a nonsynonymous point mutation in the SPI1 (also known as PU.1) oncogene was found. The sequencing reads from the tumor sample showed both the "normal variant" of SPI1 as well as the mutant SPI1:H268P, suggesting a heterozygous mutation. Altogether, these results suggest that the idea of first identifying tumor-unique sequences then doing post hoc analysis of those sequences is a viable approach for de novo mutation discovery in cancer genomics.

#6247 Comprehensive characterization of cancers with epithelial mesenchymal transition phenotype through long-read sequencing.

Y. Tanaka, H. Mano;
National Cancer Center Japan, Tokyo, Japan

Introduction: Pancreatic ductal adenocarcinoma (PDAC) and linitis-plastica type gastric cancer (STAD) are the most representative refractory cancers even in the era of molecularly targeted therapy and immunotherapy. Extensive characterization of these tumors, especially regarding the genomic and epigenomic characteristics of pure cancer cells, has been hampered by the high stromal content in the primary tumor samples. Here we took advantage of cancer cells purified from malignant ascites and established corresponding cell lines to overcome the limitations associated with the analysis and to discover their vulnerabilities.

Methods: We developed cell lines from malignant ascitic fluid samples obtained from 60 patients with PDAC and 59 patients with linitis-plastica type STAD. We performed comprehensive multi-omic analyses of these cell lines using long-read whole-genome sequencing (WGS) for complex somatic genomic alterations and for methylation aberration. We also conducted long-read RNA sequencing (iso-seq) for full-length isoform exploration, and chromatin immunoprecipitation coupled with sequencing (ChIP-seq) for enhancer analysis. Complementary short-read whole-genome sequencing and RNA sequencing were also performed.

Results: Comprehensive transcriptome analyses identified a cluster with high epithelial-mesenchymal transition (EMT) characteristics, consisting of the majority of the PDAC cell lines and a half of the STAD cell lines. ChIP-seq analysis against H3K27ac revealed the distinct transcriptional circuit that generated EMT cluster-specific super-enhancers governed by SMAD3, independent of cancer type. Most of the transcriptional activity was controlled by the gene methylation. We also identified the differential expression levels of the splicing factors between the EMT-activated and the non-activated groups. Comprehensive isoform analysis by iso-seq revealed that the isoform usage was completely different between the EMT group and the other, especially in genes of the actomyosin pathway which confer characteristic features of the EMT cluster in the cell morphology and cell motility. Using the CHM13 reference genome, long-read WGS analyses revealed the recurrent structural alterations specific to the EMT group such as those involving *CDKN2A*. We also identified PDAC-specific structural alterations.

Conclusion: We identified the distinct molecular characteristics of the EMT-activated group in PDAC and linitis-plastica type STAD which may confer the therapeutic resistance. Our findings provide an interesting insight for the further innovation of the treatment strategy for these intractable cancers.

#6248 Multilayered molecular interactions underlying glioblastoma pathogenesis through multi-omics analysis.

T. Nakashima[1], Y. Funakoshi[1], R. Yamamoto[1], Y. Sugihara[1], S. Nambu[2], Y. Arakawa[3], S. Tanaka[2], J. Ishida[4], R. Saito[5], R. Hanaya[6], K. Yoshimoto[7], Y. Narita[1], H. Suzuki[1];

[1]National Cancer Center Japan, Tokyo, Japan, [2]The University of Tokyo, Tokyo, Japan, [3]Kyoto University Graduate School of Medicine, Kyoto, Japan, [4]Okayama University Graduate School of Medicine, Okayama, Japan, [5]Nagoya University Graduate School of Medicine, Aichi, Japan, [6]Graduate School of Medical and Dental Sciences, Kagoshima University, Kagoshima, Japan, [7]Graduate School of Medical Science, Kyushu University, Fukuoka, Japan

Glioblastoma, IDH-wild type (GBM) is the most common malignant and treatment-refractory brain tumor with a dismal prognosis. Despite the identification of various driver genes in previous large-scale genomic analyses, there has been limited progress in the development of novel treatments. Acquiring an extensive understanding of the molecular mechanisms underlying GBM pathogenesis is crucial to improve prognostic outcomes. We analyzed 289 whole-genome sequencing data (WGS) including 159 unpublished deep WGS (≥ ×120 coverage) along with RNA-seq, DNA methylation array, and assay for transposase-accessible chromatin with sequencing (ATAC-seq) to uncover the molecular mechanisms regulating development and progression of GBM. Our deep WGS enables us to delineate a fine view of clonal architecture, where mutational signature varies between clonal and subclonal mutations, suggesting that different mutational processes contribute to GBM pathogenesis depending on its developmental stage. The differentiation status of tumor cells detected by transcriptional deconvolution analysis is associated with multi-layer profiles including genomic alterations, expression subtypes, DNA methylation, and open chromatin status. Tumors predominantly comprised of differentiated cells display genetic and epigenetic profiles that align with the classical subtype, whereas tumors predominantly composed of stem-like cells exhibit profiles consistent with the proneural subtype. ATAC-seq unveils genome-wide chromatin accessibility features associated with gene expression subtypes. Motif enrichment analysis of differentially accessible sites among the subtypes identified specific transcription factors. The proneural subtype is enriched for the SOX10 binding motif, which is associated with regulating cell states, and exhibits higher expression of SOX10 compared to other subtypes. Conversely, the mesenchymal and classical subtypes are enriched for the CREB1 binding motif, which promotes cell proliferation and angiogenesis through TGFβ2 upregulation, wherein TGFβ2 expression is significantly elevated. These findings support a model in which the difference in chromatin structure also regulates the progression of GBM.Our analysis reveals the multi-layer molecular interactions underlying the progression of GBM enhancing our understanding of the pathogenesis.

#6249 Single-cell RNA sequencing investigation of multi-stage NASH-related HCC mouse model.

T. Suoangbaji, V. X. Zhang, D. W. Ho, I. O. Ng;
The University of Hong Kong, Pokfulam, Hong Kong

Hepatocellular carcinoma (HCC) is one of the most frequent malignancies and a leading cause of cancer-related death worldwide. Its incidence is also one of the most rapidly increasing in the West. Most (>80%) of HCCs are diagnosed at advanced stage and therefore not operable. Even after surgical resection, the long-term prognosis of HCC remains unsatisfactory due to high recurrence rates. It is also an extremely difficult-to-treat cancer. Most HCC patients have a background of chronic liver disease, including chronic viral infection, excessive alcohol consumption or non-alcoholic fatty liver disease NAFLD)/steatohepatitis (NASH). In June 2023, new nomenclature of NAFLD and NASH have been internationally announced as metabolic dysfunction-associated steatotic liver disease (MASLD) and metabolic dysfunction-associated steatohepatitis, respectively. Due to the enforcement of neonatal HBV vaccination program and the availability of effective antiviral treatments on HBV and HCV, the global incidence of viral hepatitis-related HCC has been declining, whereas NAFLD/NASH-related incidence of HCC has been increasing. We established NASH-related HCC mouse model using Western diet (WD) plus carbon tetrachloride (CCl_4) method. This model demonstrated steatosis, fibrosis, obesity and HCC with high incidence. It has also been reported to accurately portrait the key pathological features of the patients. Next, we collected liver tissue samples at different timepoints (normal; Week 12: NAFLD/NASH; Week 18: fibrosis/cirrhosis; Week 32: HCC) and analyzed them using single-cell RNA sequencing (scRNA-seq). Single-cell sequencing offers an unprecedented platform to perform systematic and in-depth investigation of the admixed tumor microenvironment (TME) in HCC tumor. We have taken advantage of the unique multi-dimensional capacity of scRNA-seq to delineate multifaceted landscapes and cell-cell communication in multi-stage NASH-related HCC mouse model. After removing the low-quality cells, our multi-stage dataset consisted of >130,000 cells. Using typical cell type markers, we identified major cell types, namely T cells, B cells, myeloid cells, liver sinusoidal endothelial cells, hepatic stellate cells, hepatocytes and HCC tumor cells. We observed a change in the cell type composition during disease progression. Throughout our study, we closely examined the communication level between different cell types to identify any irregularities or disturbances that could lead to NASH-related HCC. Our findings concluded that hepatic stellate cells, despite existing in low proportion at all stages, exhibited the strongest level of interaction with other cell types. Moreover, our data also established the comprehensive multi-stage cellular landscape of NASH-relative HCC.

#6250 The RNA editing landscape of lung cancer in never smokers.

J. Sang, W. Zhao, T. Zhang, M. Landi;
National Cancer Institute, Rockville, MD

Adenosine-to-Inosine (A-to-I) editing represents a crucial RNA modification mechanism, holding the potential to drive carcinogenesis. This sophisticated post-transcriptional process is catalyzed by a series of ADAR (adenosine deaminase acting on RNA) family members, which can profoundly reshape the cellular epitranscriptomic landscape. While previous explorations have illuminated the important role of A-to-I editing in lung cancer tumorigenesis and prognosis, most studies have focused on lung cancer from smokers. To investigate the contribution on RNA-editing in lung cancers in never smokers (LCINS) , we embarked on a rigorous dissection of A-to-I RNA editing events in 603 LCINS. Harnessing transcriptome and whole-genome sequencing technologies, we identified 15,880 A-to-I sites, of which 75% were positively linked to the enzymatic activity of *ADAR1*. 92.80% of detected editing sites were located at Alu repetitive regions, with the remainder in non_Alu repeat (4.1%) and non-repeat regions (3.1%). The global RNA editing levels, measured as Alu Editing Index (AEI), were found to be significantly associated with *ADAR1* expression, Tumor Mutational Burden, and Neoantigens Burden. A subtle correlation between global RNA editing levels and tumor stage was also noted. Delving into cancer-associated editing events, we identified 5,539 differentially edited sites in tumors compared with normal tissues, which were located at 823 genes, including several key tumor suppressors and oncogenes, like *MDM2*, *BRAF*, *TP53*, *BRCA2*, *ATM*, and *VHL*. Subsequent pathway analysis identified TGF-beta, Notch Signaling, and DNA Damage Response as the key pathways for cancer progression. Using the characterized A-to-I editing profiles, we built a prognostic risk stratification model, with high risk scores significantly linked to poor survival outcomes, even after adjusting for other clinical factors. Our study provides a comprehensive A-to-I editing landscape of lung cancer in never smokers, highlighting the potential roles of RNA modifications in the pathogenesis of this lethal disease.

#6251 Validation and implementation of whole-transcriptome sequencing assay into cancer care: An experience from a cancer center.

Jillian A. Moran[1], Edward G. Hughes[2], Donald C. Green[2], Shrey Sukhadia[2], Gregory J. Tsongalis[2], Samantha F. Allen[2], Laura Tafe[2], Brianna Houde[2], Nevena B. Ognjenovic[3], Jennifer N. Barbuto[2], Ivy Riano[4], Parth Shah[5]

[1]Geisel School of Medicine at Dartmouth College, Hanover, NH,[2]Department of Pathology and Laboratory Medicine, Dartmouth-Hitchcock Medical Center, Lebanon, NH,[3]Department of Molecular and Systems Biology, Geisel School of Medicine, Hanover, NH,[4]Hematology/Oncology, Dartmouth Cancer Center, Lebanon, NH,[5]Dartmouth Cancer Center, Lebanon, NH

Introduction Transcriptome sequencing is a well-established diagnostic tool to characterize and quantify gene expression profiles and to detect fusion transcripts. The utilization of whole-transcriptome sequencing (WTS), in clinical workflows can tremendously help improve diagnosis, risk stratification, and therapy selection. However, there are multiple challenges to widespread clinical implementation of WTS including nucleic acid input, defining appropriate quality control (QC) criteria, tumor specific baseline controls and depth of sequencing. Here, we present a validation study to deploy routine whole transcriptome sequencing with automated analysis in a mid-size academic center. **Methods** Nucleic acid material was obtained through clinical residual samples in the Center for Genomics and Advanced Technology. RNA samples were extracted using the Purigen Ionic® FFPE to Pure RNA Kit. RNA input sample quantities ranged from 34-100ng. WTS libraries were prepared using the Illumina® RNA Prep with Enrichment (L) Tagmentation kit with the Illumina Exome Panel for FFPE tumor samples. The validation was performed on a set of patient samples with known clinically reported variants from the Illumina TruSight® Tumor 170 assay. A total of 84 true positives with reportable fusions, 5 splicing events, 16 negative samples, and 15 limit of detection (LOD) samples were used. Libraries were prepared in a three-plex format. Sequencing was performed on the Novaseq-6000 system using S2 and S4 flow cells with a target read count of 100 million. All data was processed through the AUGMET informatics platform for demultiplexing, quality control, fusion detection, transcript quantification and determination of alternatively spliced transcript. **Results** The WTS validation assay demonstrated 98% (n=49/50) sensitivity, with only one false negative, and 100% (n=68/68) specificity. A final review of our data was determined to develop stable QC standards for RNA sequenced libraries to be > 60M reads and > 130bp read length. When analyzing (LOD) for WTS, interestingly, read length was inversely proportional to input and as a result detection of the clinically relevant fusion. Based on our LOD experiments, a minimum input threshold of 20ng of RNA was determined to maintain the sensitivity and specificity. An LOD study for tumor purity was not performed due to the known lack of correlation between tumor purity and fusion transcript quantity. **Discussion** WTS can detect all clinically reported fusions and splicing events with comparable sensitivity to panel assays. Moreover, simultaneously available transcript quantification and variant calling provide the ability to implement several disease classifiers. This work lays the foundation for integration with our clinically available tumor exome sequencing assay to allow joint exome transcriptome analysis in a single informatics platform.

#6252 Driver indel discovery and allelic imbalance in >9,000 tumor RNA-Seq samples from the Cancer Genome Atlas (TCGA).

K. Hagiwara, A. Thrasher, J. Zhang;
St. Jude Children's Research Hospital, Memphis, TN

High-throughput DNA sequencing technologies have enabled unbiased screening of genomic alterations such as single nucleotide variants (SNVs) and small insertions/deletions (indels). However, variant analysis using transcriptomic sequencing (RNA-seq) data has not become standard due to challenges in distinguishing true variants, in particular indels, from artifacts that can arise from RNA-seq mapping and library preparation. We have previously developed a tool, RNAIndel, which classifies indels as somatic, germline, or artifacts using a machine learning-based model. Here, we present enhanced somatic indel discovery by incorporating tumor RNA-Seq data with conventional paired tumor-normal DNA-Seq by re-analyzing the Cancer Genome Atlas (TCGA) data using RNAIndel. Our analytic process involves running RNAIndel on 9,101 TCGA tumor RNA-Seq samples across 33 cancer types hosted on Cancer Genomics Cloud by Seven Bridges Genomics (https://www.cancergenomicscloud.org) and comparing the result with the reference somatic indel set generated from paired tumor/normal whole-exome sequencing (WES) data using an ensemble caller developed by NCI Genomic Data Commons (GDC). The comparison validates the RNAIndel variants by matching to the corresponding WES dataset. We also use the GDC indel set to test their expression in RNA-Seq. Indel alignments across sequencing platforms were compared by indelPost, an algorithm that we developed, to perform indel realignment to overcome the differences in mapping algorithms (BWA vs. STAR) and read lengths (100-bp vs. 50-bp) in WES versus RNA-Seq data.The joint DNA/RNA indel analysis provides important insights into the expression profile of indels in known cancer driver genes versus non-drivers. First, indels in driver genes are more likely expressed than those in non-drivers (79% vs. 50%, $p < 2.2 \times 10^{-16}$). Second, mutant allele expression is frequently upregulated for truncating indels in tumor-suppressor genes (TSG) as allelic imbalance was detected in 6% of such variants in TSGs vs. 2% non-drivers. This may indicate a potential second hit leading to loss of the wild-type allele of in the TSGs. Third, allelic imbalance for in-frame indels was also frequent for oncogenes (20%) compared with the non-drivers (7%). The high expression likelihood of driver genes and the enriched indel allele expression for TSGs and oncogenes both support the use of RNA-Seq to enhance driver indel discovery. Indeed, our analysis reveals ~10% additional driver indels by RNA-Seq analysis which are absent from the GDC reference indel set. These indels affect prominent driver genes, most frequently *CDKN2A*, *TP53* and *ARID1A*. Our experience argues for incorporating de novo indel analysis in RNA-Seq as a standard approach for future cancer genomic analysis.

#6253 Single-cell RNA sequencing reveals metastatic site-specific biomarkers for predicting response to CDK4/6 inhibition in advanced HR+/HER2- breast cancer.

L. Luo[1], P. Yang[2], S. Mastoraki[1], Y. Wang[1], N. M. Kettner[1], A. Singareeka Raghavendra[1], D. Tripathy[1], S. Damodaran[1], K. K. Hunt[1], Z. Li[1], K. Keyomarsi[1]; [1]UT MD Anderson Cancer Center, Houston, TX, [2]Rice University, Houston, TX

Background: Cyclin-dependent kinase 4/6 inhibitors (CDK4/6i), in combination with endocrine therapy, are established as standard treatment for advanced HR+/HER2- breast cancer (BC). However, response heterogeneity is observed, with approximately one-third of patients exhibiting intrinsic resistance. This study investigates the mechanisms of variable responses to CDK4/6i through single-cell RNA sequencing of metastatic site biopsies, revealing distinct biomarkers for predicting CDK4/6i response.

Methods: Single-cell RNA sequencing analyzed metastatic tumors from advanced HR+/HER2- BC patients pre-CDK4/6i treatment at baseline (BL) and/or at disease progression. BL samples were from CDK4/6i responders (n = 8, median progression-free survival [mPFS] = 17 months), while progressors were categorized as early-progressors (EP, n = 3, mPFS = 3 months) and late-progressors (LP, n = 8, mPFS = 10 months). Metastatic sites included liver (10), pleural effusions (6), ascites (2), and bone (1). InferCNV distinguished tumor cells, and functional analysis utilized the Molecular Signatures Database.

Results: Both EP and LP tumor cells exhibited reduced estrogen response and increased IFN-γ pathways compared to BL tumors. LP tumors displayed enhanced Myc targets, EMT, TNF-α, and inflammatory pathways compared to EP tumors, revealing differential mechanisms of early versus late progression. Predictive signatures, including *TFF3* and *MGP*, were significantly upregulated in BL tumor cells across different metastatic sites. Metastasis-specific markers included *APOA* and *SERPINA1* (liver), and *AGR2* (pleural effusion). BL and LP responders showed increased tumor infiltrating CD8+ T cell and NK cells compared to EP non-responders. Notably, despite a high CD8+ T frequency in responder tumors, functional analysis revealed a significant upregulation of genes associated with stress/apoptosis and exhaustion in proliferative CD4+ and CD8+ T cells from BL compared to LP tumors, including *HSP90* and *HSPA8*, associated with poor response to immune checkpoint inhibitors. These findings suggest potential benefits of immunotherapy for CDK4/6i late progressors. Longitudinal biopsies further revealed dynamic NK cell expansion and enhanced cytotoxic T cell activity alongside the downregulation of stress/apoptosis gene expression at progression compared to BL tumors.

Conclusion: This study underscores the significance of metastatic site-specific biomarkers in predicting outcomes to CDK4/6i. Tumor-infiltration lymphocytes may also serve as baseline predictors, while stress/apoptosis gene signatures suggest checkpoint inhibitor usage in CDK4/6i late progressors. These potentially actionable findings emphasize the need to optimize therapeutic approaches based on microenvironment-specific changes following disease progression.

#6254 Casein kinase II (CK2) expression in pediatric solid tumors.

A. Beeravally Nagulapally, C. Behura, D. Gandra, G. Sholler;
Penn State Health Milton S. Hershey Med. Ctr., Hershey, PA

Despite recent advances, high-risk neuroblastoma (NB) and sarcomas account for 15% and 5% of all pediatric cancer deaths, respectively. Many patients attain remission, but approximately half of patients relapse. Genomic alterations such as MYCN amplification and ALK mutations have been shown to be important in prognosis and treatment. Despite improvements, approximately 20% of patients have refractory or recurrent disease after therapy, underscoring the need for further genomic understanding and new approaches to treatment.CK2 is a serine/threonine kinase that regulates numerous cellular processes such as cell growth, proliferation, and survival. Overexpression of CK2 is associated with a poor prognosis in several adult solid tumors, making it a potential target of interest in pediatric solid tumors. This study aims to investigate CK2 expression among patients with NB, Ewing sarcoma (EWS), and rhabdomyosarcoma (RMS) and its correlation with patient survival. MethodsPatients were enrolled in NMTRC008/009: “Feasibility Trial Using Molecular Guided Therapy for Patients with Relapsed/ Refractory Childhood Cancer” and BCC-001. WES and RNA-Seq were performed at the Translational Genomics Research Institute and Sema4 or Caris respectively. RNA expression levels were compared to a normal whole-body reference and a pediatric cancer reference. Differential expression data were interpreted in the context of systems biology.ResultsTumor WES was performed on 297 patients (212 NB, 50 EWS, 35 RMS) and RNA-Seq on 284 patients (210 NB, 39 EWS, 35 RMS). The most common mutations or copy number alterations were seen in MYCN, ATRX, ALK, CDKN2A, and chr17q+ in NB; EWSR1-FLI1 fusion in EWS; PAX3-FOXO1 fusion in RMS. RNA expression analysis was performed to understand MYCN-driver status by covariance and interactions and to identify subsets of patients with high/low expression of CK2 in different tumors. CK2 bimodal expression is seen across various cancers and normal tissues, implying distinct sub-groups exist in the data. In NB, overexpression of the CK2 gene with statistical significance was found in MYCN-amplified and chr17q+ tumors. A positive and negative correlation of the CK2 gene is seen with several target genes like MYCN, TRIM71, LIN28B, and HMGA2, JAK2, AR, STAT3, EGFR, LEF1, and NFKB2, respectively. In EWS and RMS, subgroups are identified with high and low expression of the CK2 gene.ConclusionGenomic sequencing of pediatric solid tumors showed a low mutation burden. RNA analysis resulted in the identification of potential novel therapeutic targets involving CK2 pathways. High expression of CK2 correlates with MYCN status. Further analysis of patient molecular subgroups is ongoing.

#6255 Personalized medicine for DCIS.

A. Hazra;
Brigham and Women's Hospital, Harvard Medical School, Boston, MA

Background: In 2023, 55,720 women will be diagnosed with non-invasive ductal carcinoma in situ (DCIS) in the United States. We evaluated RNA sequencing (RNA-Seq), clinical and social factors that drive subsequent breast events in a DCIS study population enriched for Black women (30%).
Methods: RNA was extracted from macrosections of archival formalin-fixed paraffin-embedded (FFPE) DCIS tissue from Resource Archival Human Breast Tissue (RAHBT) from the St. Louis Breast Tissue Registry at Washington University School of Medicine and the Dana Farber Cancer Institute patient cohorts. Tissues were prepared by microsection of 5 uM whole section from unstained slides (Fisher). RNA was extracted using Qiagen RNeasy FFPE Kits from macrosectioned DCIS specimens. Purified total RNA was evaluated for quality and quantity using the Agilent Fragment Analyzer RNA assay. Bulk RNA sequencing was piloted in DCIS case-control samples using the SMART-seq and Hybrid Capture platforms at the DFCI Molecular Biology Core Facilities. Raw reads were aligned to the GRCh38/hg38 reference genome using STAR. Preliminary quality control analysis of a curated gene list showed higher quality data using the Hybrid Capture technology. Libraries for Hybrid Capture were pooled in 8plex reactions and hybridized to Twist Exome 2.0 probes for target enrichment. The final library pools were sequenced on an Illumina NovaSeq. Cases were defined as women diagnosed with DCIS in 1999 or later with subsequent invasive breast cancer, local DCIS recurrence, or lobular CIS recurrence. Controls were defined as women diagnosed with DCIS in 1999 or later without subsequent breast events during a similar follow-up time. The R package DESeq2 was used for data analysis.
Results: The mean age at DCIS diagnosis was 56.3 (Std Dev 10.23). The mean follow-up time was 147.8 months. Hybrid Capture RNA-Seq files are stored and analyzed from the Harvard Medical School O2 Cluster using R programming (version 4.2.2, DEGreport). Quality control analyses demonstrated that the majority of the samples sequenced by Hybrid Capture had over 20 million total reads. Principal Component Analyses (PCA) and hierarchical clustering analyses of 19,821 protein-coding genes were conducted on the 143 DCIS samples sequenced using Hybrid Capture. PC1 was race (9%). A significant association was observed for follow-up time (PC3, 4.03%).
First, we explored the association of the candidate gene ERBB2. The mean transcript abundance for ERBB2 was 11784.37 (case-control p-value=0.08). Preliminary analysis of selected genes of interest did not show statistically significant differences between cases and controls after FDR p-value adjustment. Differential gene expression analyses are ongoing.
Conclusion: This study demonstrates the feasibility of generating high-quality RNA-seq data from diverse, archival DCIS samples.

#6256 Prevalence of BRCA1 and BRCA2 proteins in breast cancer in a nigerian population and their relationship with different breast cancer morphological variants.

S. Raphael, A. Oluwasesan;
University of Abuja, Abuja, Nigeria

Background: Breast cancer is the commonest site specific cancer in women and a leading cause of cancer death among women in Nigeria and globally. The trend in Nigeria and Africa is that breast cancers are seen in younger age groups, are of higher grades and follow an aggressive course. It has been suggested that this may largely be due to mutation in BRCA genes with the attendant alteration in function of its proteins. This study aimed at determining the prevalence of BRCA1 and BRCA2 proteins in breast cancers seen in our environment as well as to see any association between these proteins and different morphological variants.

Materials and Methods: A descriptive study using tissue blocks of all histologically diagnosed breast cancer in our department between 2013 and 2017. Fresh sections were recut for histological grading and immunohistochemistry. Proteintech BRCA1 and BRCA2 polyclonal antibodies and detection kit were used.

Results: One hundred and thirty (130) cases met the inclusion criteria for this study. The mean (SD) age of the patients was 44.8 (10.3) years with ages ranging from 26 to 79 years. There were more cases of breast cancer (73.1%) seen before 50 years. Two (2) Male Breast Cancer (MBC) cases were seen, giving the female to male ratio of 64:1. The commonest morphological variant encountered was Invasive Carcinoma, No Special Type at 84.6% of cases. This was followed by invasive medullary (7.8%). The least common variant was papillary cancer at 0.8%. The tumors seen were mostly grade 3 (71.2%), followed by grade 2 at 22.7% and the least was grade 1 at 6.1%. Positivity for BRCA1 and BRCA2 proteins was seen in 27.7% and 30.0% of cases respectively. One of the MBC showed reactivity for BRCA1 protein. No significant relationship was seen between BRCA 1/2 proteins expression and age or breast cancer histotypes.

Conclusion: BRCA 1 and 2 proteins are an important risk factor for breast cancers seen in this environment. However, there is no association with age distribution and morphological variants of the breast cancer in our population.

#6257 Genome wide, high-throughput, high-resolution structural variation detection at low variant allele fraction for oncology samples.

A. R. Hastie, P. Lynch;
Bionano, San Diego, CA

Structural variation detection remains an elusive undertaking. For decades, G-banded karyotyping has remained the standard practice for nearly all hematological malignancy samples. Cancers are diseases of the genome and structural variants (SVs) are a hallmark of nearly all cancers, are often drivers of oncogenicity, and can sometimes be targeted for treatment, as highlighted by the discovery of the Philadelphia chromosome and later the development of targeted kinase inhibitors. One of the most important limitations of karyotyping, its requirement for cells to divide in culture, has prevented its application for most solid tumors and therefore, there is considerably less understanding of the impact of SVs in solid tumors. Optical genome mapping is a technique that is revolutionizing cytogenomics and unlocking the understanding of SVs in the genome at a level never seen before. It not only can detect nearly all variants that a karyotype can, but it can provide 10,000x higher resolution and does not require cell culture. Because of this, it is being adopted for oncology studies across hematological malignancies and solid tumors. This study demonstrates the performance of a new high throughput Stratys instrument for generation of optical genome map data at extraordinarily high coverage depth. With this instrument, 12 samples can be loaded at once, each loaded onto its own cartridge and the instrument can collect 400x genome coverage for each of these samples in 24 hours. The instrument has random access to the cartridges so that completed samples can be swapped out to facilitate optimal instrument run efficiency. To date, this system has been demonstrated to run 60 samples in a week, each at 400x coverage. Data from the instrument can be processed by Bionano Access™ and VIA™ software to call SVs, copy number variants (CNVs), regions of loss of heterozygosity (LOH), on a genome wide basis, and to classify those variants automatically according to guidelines such as the National Comprehensive Cancer Network (NCCN), World Health Organization (WHO), and National Health Services (NHS, United Kingdom). This new high throughput system with advanced bioinformatic data analysis has the potential to further transform structural variation analysis in cancer research.

#6258 Inference of gene expression using fragmentation patterns from targeted high-depth sequencing of cell-free DNA.

Emily Leff, **Alexander Tseng**, Victoria Cheung, Ehsan Tabari, Kimberly Walter, Alex Lovejoy, Cheng-Ho J. Lin

Freenome, South San Francisco, CA

Cell-free DNA (cfDNA) circulating in blood plasma arises primarily from cellular chromatin fragmentation and release due to cell death. Studies have demonstrated that the assessment of fragmentomic features of cfDNA enables gene expression inference and tissue-of-origin classification with potential applications for noninvasive cancer detection. However, due to low depth of coverage of sites of interest, current whole genome sequencing (WGS) methods have not been able to infer expression of individual genes or limited gene sets. Therefore, we developed a targeted sequencing approach that enables individual gene expression inference from cfDNA fragmentation patterns based on transcriptional start-site gene activation probability (TSS-GAP).

To assess the sensitivity of this method for cfDNA-inferred gene expression profiling, we applied TSS-GAP to blends of micrococcal nuclease (MNase)-digested DNA from a cancer cell line (LS180) and sorted peripheral blood mononuclear cells (PBMC), with LS180 DNA at varying concentrations (0.1-10%). This enabled the determination of the limit of detection (LoD), relative to healthy donor background levels, on the basis of the genes' activation probabilities (TSS-GAP scores).

We found 936 genes with high inferred expression in the LS180 cancer cell line and low inferred expression in non-cancer samples (i.e. CD4, CD14, and plasma cfDNA from 4 healthy donors) and used those for healthy donor background and LoD assessment. Using these gene-level background values as cutoffs, blends were assessed to determine the lowest blend level at which expression of the gene was able to be differentiated from background. Out of the 936 genes, 326 (34.8%) were detectable at a blend level of 0.1%, 59 (6.3%) at 0.3%, 31 (3.3%) at 1%, 19 (2.0%) at 3%, and 39 (4.2%) at 10%. In total, 416 genes could be detected by TSS-GAP at levels 1% of or lower above background, highlighting the potential of our method for detecting expression of certain genes even from a small fraction of cells contributing cfDNA to liquid biopsy samples. Further expansion of this work could consider the utility of such a method for circulating tumor DNA (ctDNA) detection, cfDNA tissue-of-origin classification, and deconvolution of cell types contributing to cfDNA found in blood.

[EL and AT contributed equally to this work]

ENDOCRINOLOGY: Molecular, Preclinical, and Clinical Endocrinology 2
Poster Session

#6262 Optimal cut-off age for AJCC staging system in Middle Eastern patients with differentiated thyroid cancer.
S. K. Parvathareddy, A. K. Siraj, P. Annaiyappanaidu, S. O. Ahmed, N. Siraj, Z. Qadri, S. Azam, K. S. Al-Kuraya;
King Faisal Specialist Hospital & Research Centre, Riyadh, Saudi Arabia

Background: Differentiated Thyroid Cancer (DTC) has an indolent nature and generally has favorable prognosis. AJCC TNM classification is the most adopted system to evaluate the biological behavior of DTC. Age cut-off of 55 years has been included in the eighth edition of TNM staging system since it led to better prediction of disease specific survival (DSS) of patients with DTC. However, optimal age cut-off in DTC patients from Middle Eastern ethnicity has not been fully explored. We evaluated the optimal age cut-off for the TNM staging system to predict DSS in Middle Eastern patients with DTC.
Methods: We retrospectively analyzed a large cohort of 1721 adult DTC patients who underwent surgery between 1990 to 2018. The optimal age cut-off value was determined using several age cut-offs (between 20 and 85 years) to assess DSS. Harrel's C-Index, Akaike information criterion (AIC) and Bayesian Information Criterion (BIC) were used to assess the statistical model performance of the TNM staging system (eighth edition), with different age cut-offs for prediction of DSS. The proportion of variation explained (PVE) was also calculated to compare predictability of DSS in patients with DTC.
Results: The median age of patients at diagnosis was 39.9 years (IQR 31.0 - 51.7 years) and 75.5% (1299/1721) were female. Median follow up was 9.3 years and 10 years DSS was 97.1%. For DTC overall, an age cut-off of 50 years had the best statistical model performance. On receiver operating characteristic curve analysis, the optimal age cut-off for prediction of DSS was 50.5 years (area under the curve = 0.872, $p < 0.0001$).
Conclusion: In this large cohort of Middle Eastern DTC patients, an age cut-off of 50 years was more appropriate for TNM staging to achieve better predictability for DSS. Therefore, implementation of different age cut-off for DTC in Middle Eastern patients could improve the predictive value for TNM staging system, and allow for better therapeutic and surveillance approach for these patients.

#6264 Role of Nuclear ErbB3 localization in regulating ligand-dependent ErbB2-ErbB3 heterodimer activation and downstream targets in prostate cancer.

M. K. Jathal, M. M. Mudryj, P. M. Ghosh;
UC Davis, Sacramento, CA

Objective: Prostate cancer (PCa)-specific nuclear expression of ErbB3, a receptor tyrosine kinase of the epidermal growth factor receptor (EGFR) family, has long been recognized. While an 80kDa nuclear variant of ErbB3 has been identified, full-length 185 kDa ErbB3 also translocates to the nucleus in PCa in a bone microenvironment and androgen status-dependent manner. Here, we studied potential mechanisms by which nuclear ErbB3 may regulate PCa progression.
Methods: ErbB3 localization was investigated *in vitro* (human prostate cancer cell lines, LNCaP, C4-2, 22Rv1) using amiloride or heregulin-1β (ErbB3-specific ligand). ErbB3 expression and subcellular localization were analyzed using immunofluorescent microscopy and subcellular fractionation followed by immunoblot. Physiological readouts included viability, migration and reporter gene assays.
Results: Here we show that ErbB3 can occupy a nuclear/perinuclear location in prostate cancer cells. The hormone sensitive PCa line LNCaP expressed higher levels of nuclear ErbB3 compared to castration resistant lines C4-2 and 22Rv1. The diuretic amiloride was previously shown to inhibit ErbB3 internalization by macropinocytosis thus we investigated whether it could also modulate ErbB3 nuclear localization in PCa cells. In LNCaP cells, amiloride dose dependently prevented ErbB3 nuclear transport, whereas in C4-2 and 22Rv1, no such effect was observed. Further analysis revealed that amiloride promoted ErbB3 expression in the membrane, where ErbB3 underwent ligand-dependent phosphorylation, formed ErbB2/ErbB3 dimers, and in turn phosphorylated the downstream targets AKT and ERK1/2 (p42/p44MAPK). On the other hand, EGFR phosphorylation and dimerization were unaffected by amiloride. Our results suggest that ErbB3 is stored in the nuclear region in an inactive form, whereas upon stress induction, including androgen deprivation, ErbB3 is translocated to the plasma membrane, where it is activated by ligand binding, and causes downstream signaling.
Conclusion: We previously showed that the EGFR/ErbB2 dual inhibitor lapatinib failed to affect PCa - we now show that this may be due to modulation of nuclear and cytoplasmic ErbB3 expression. Amiloride prevented translocation (and thus expression of) ErbB3 to the nucleus and retained this RTK in the membrane, resulting in the formation of active ErbB2/ErbB3 dimers. Lapatinib was then able to inhibit and inactivate its specific target, ErbB2, thereby inducing significant apoptosis. The above indicates a novel role for nuclear ErbB3 in PCa that can be regulated by the combination of amiloride and lapatinib.

#6265 FLCN variants and their role in parathyroid cancer and atypical parathyroid tumors.

C. Burke, J. Bellizzi, J. Costa-Guda, A. Arnold;
UConn Health, Farmington, CT

Parathyroid carcinoma (PC) is rare, poses challenges in definitive diagnosis and treatment, and carries a high rate of recurrence and mortality. Atypical parathyroid tumors (APT) have histopathologic features of malignancy but lack unequivocal evidence of invasion and are of uncertain malignant potential. Analysis of genetic alterations that may play a role in PC development, particularly those that might serve as markers of malignant potential, is important for further understanding this disease. *FLCN* is a gene found on chromosome 17 that encodes folliculin, a ubiquitously expressed protein with roles in multiple cellular processes such as apoptosis and cell signaling. Inactivating *FLCN* mutations cause Birt-Hogg-Dubé syndrome (BHD), an autosomal dominant condition characterized by benign fibrofolliculomas, pulmonary cysts and spontaneous pneumothorax, and increased risk of renal cancer. Benign parathyroid tumors had previously been reported in a few BHD patients and recently one study has reported a link between *FLCN* mutations and parathyroid carcinoma. Germline frameshift mutations in *FLCN*, accompanied by somatic loss of the normal allele, were reported in two unrelated PC patients, both with clinical features suggestive of BHD, but no established diagnosis of BHD. An identical somatic frameshift *FLCN* mutation was reported in one PC and one APT. Interestingly, the authors noted low coverage of *FLCN* on whole exome sequencing, resulting in the failure to detect variants identified by Sanger sequencing, thus raising the possibility that prior studies may have missed *FLCN* variants. To better understand the frequency of germline or somatic *FLCN* mutations in PC and APT, we performed Sanger sequence analysis of the entire coding region of the *FLCN* gene on available tumor DNA from 11 PCs and 15 APTs. We identified no inactivating *FLCN* mutations in any of the PC or APT samples examined. A germline missense variant, resulting in a p.Gly325Val change, predicted to be benign/tolerated by *in silico* analyses, was seen in one PC and a synonymous variant (c.1233G>A) was seen in one APT. The absence of pathogenic mutations in our series parathyroid carcinoma and atypical parathyroid tumors suggests that *FLCN* mutations are rare in these parathyroid tumors. Nevertheless, germline *FLCN* testing and/or additional screening for BHD-related lesions in parathyroid carcinoma patients merits further consideration and study.

#6266 Neurotensin receptor 1 regulates dimerization of HER2-HER4 and proliferation of non-small cell lung cancer cells.

T. W. Moody[1], I. Ramos-Alvarez[2], R. T. Jensen[2];

[1]National Cancer Institute, Rockville, MD, [2]NIDDK, Bethesda, MD

The neurotensin receptor 1 (NTSR1) is a 418 amino acid type A G protein-coupled receptor which causes phosphatidylinositol turnover and proliferation of non-small cell lung cancer (NSCLC) cells (Moody et al., Peptides 2021; 137: 710480). Adding the agonist NTS to NSCLC cells increases transactivation of the receptor tyrosine kinases (RTK) EGFR, HER2 and HER3 (Moody et al., Biology 2023 12: 957). The RTK tyrosine phosphorylation and growth caused by NTS is impaired by SR48692, a small molecule NTSR1 antagonist. The effects of NTS were investigated on HER4 using NSCLC cells. By Western blot, cell lines NCI-H522 and H661 had high levels of NTSR1, HER 4 and neuregulin 1 (NRG1), a ligand for HER4 but not NTSR2, HER3 or NRG2. By RT-PCT, high levels of HER4 and its isoforms JM-a, CYT1 and CYT2 were present in NCI-H522 and H661 cells. Adding NTS (0.1 μM) or NRG1 (0.01 μg/ml) to NCI-H522 or H661 cells increased P-Tyr^{1284}-HER4 and P-ERK 3-fold. Using immunoprecipitation techniques, adding NTS to NSCLC cells increased formation of HER4-HER2 heterodimers which leads to cancer proliferation (Lucas et al., Pharmacol Rev 2022; 74:18). The increase in PY1284-HER4 caused by NTS was impaired by SR48692, HER4 siRNA, NRG1 siRNA or ibrutinib (TKI). The NTSR1 regulation of HER4 transactivation is impaired by GM6001 (MMP inhibitor]), PP2 (Src inhibitor) or N-acetylcysteine (antioxidant). The clonal growth of NSCLC cells is increased by NTS or NRG1 but decreased by SR48692 or ibrutinib. The results indicate that NTS increases the formation of HER2/HER4 heterodimers leading to the proliferation of NSCLC cells.

#6267 Evaluating estrogen receptor signaling modifications at bone marrow related stiffnesses in metastatic breast cancer.

L. A. Northcutt, M. Rafat, J. Rhoades;
Vanderbilt University, Nashville, TN

Bone metastasis is highly prevalent in breast cancer (BC) patients with metastatic disease and can increase the risk of hypercalcemia and pathological fractures. Several studies have evaluated the mechanisms of metastasized BC cells' involvement in bone destruction, but how the bone marrow (BM) microenvironment contributes to this process remains ambiguous. Recent studies have shown that as BC cells experience increased stiffnesses outside of the primary microenvironment, there is higher expression of epithelial-to-mesenchymal transition (EMT) markers, increased expression of osteolytic proteins, and decreased drug responses. However, these changes have not been evaluated at stiffnesses relative to the BM. Estrogen receptor (ER) status also plays a pivotal role in BC patient survival. Clinical studies have indicated that the majority of ER+ patients with metastatic disease have more incidences of bone metastases compared to ER- patients. There is some evidence that suggests that the physical properties can also affect estrogen receptor signaling at the primary site, however, there is minimal work to establish how the physical factors of the BM can affect ER sensitivity after metastasis. We hypothesize that higher stiffness ranges of the BM can alter the estrogen receptor sensitivity of metastasized tumor cells and increase osteolysis. To analyze this question, we seeded ER+ BC cell lines (MCF7s and T47Ds) on CytoSoft® Rigidity Plates that mimicked the stiffness of the BM (0.5 - 32 kPa). After 2 days in culture, we probed the expression of downstream estrogen signaling factors, GREB1, PGR, and TIFF1, to evaluate estrogen activity using western blot. Our results show an increase in downstream estrogen signaling at higher stiffnesses (32 kPa) compared to lower stiffnesses (0.5 kPa) at the protein level but not at the transcriptional level. In the future, we will analyze factors associated with osteolysis (*ITGB3*, *TGFB-RII*, and *PTHLH*). Additionally, we plan to conduct RNA sequencing to analyze any larger transcriptional changes at different stiffnesses. Overall, this work gives insight into how estrogen signaling changes in the BM compared to the primary site. It will also give us insight into potential therapeutic targets for ER+ BC after metastasis to the bone.

#6268 A study of orphan nuclear receptor SHP (NR0B2) in prostate cancer progression.

H. Lam, F. Chan;
The Chinese University of Hong Kong, NA, Hong Kong

Prostate cancer (PCa) is a significant male cancer in many countries accounting for around 14% of new cancer cases globally in 2020 and ranked as 3rd common cancer in males in Hong Kong. The major risk factors include old age, high-fat diet, and genetics. Compared to other cancers, PCa is unique as its initial and advanced growth is androgen dependent. As tumor progresses, it accumulates numerous genetic alterations. Main therapeutic options include surgery, radiotherapy and or active surveillance. Upon treatment failure or when metastasis develops, androgen-deprivation therapy (ADT) with the use of potent androgen receptor (AR) antagonists and androgen biosynthesis inhibitors (e.g. Enzalutamide and abiraterone acetate) aiming to suppress AR signaling axis are the standard treatment options. However, the effect of these treatments is short-lived, in which nearly all patients will inevitably relapse to a hormone-independent and metastatic stage known as metastatic castration-resistant prostate cancer (mCRPC) within few years and further drive progression to a more lethal subtype, described as treatment-induced neuroendocrine prostate cancer (NEPC). The treatment options are limited and therefore resulted in high mortality, representing an emerging clinical problem. Recent studies have illustrated that NEPC progression follows a lineage plasticity model with a phenotypic transition to AR loss and neuroendocrine transdifferentiation. Our preliminary study has identified a nuclear receptor NR0B2 (SHP, small heterodimer partner SHP), which is a unique ligand-independent orphan nuclear receptor without a DNA-binding domain, that displays a significant up-regulation in clinical NEPC and prostate cancer cells with NEPC phenotype. Mechanistic studies revealed that SHP could directly interact with AR utilizing its NR Box1 motif while inducing repression on the AR transactivation via its another NR Box2 motif. Based on this, we conducted *in vitro* growth studies and revealed that NR0B2 overexpression could promote growth differentially in AR-negative PCa cells. However, AR-positive PCa cells were insensitive to AR blockade, providing supporting evidence that NR0B2 may be involved in repressing AR activity in prostate cancer cells. Multiple key NEPC and oncogenic TGFβ signaling markers showed significant upregulation in gene expression. Based on this, we hypothesize that upregulation of NR0B2 could play an important role in driving the advanced progression of CRPC via its direct interference of AR signaling axis and through other AR-independent signaling pathways, including activation of TGFβ signaling. (Study supported by a CUHK Direct Grant for Research 2022-2023, Project No. 2022.081)

#6269 Assessment of new generation endocrine therapies for the treatment of breast to bone metastasis.

E. K. Zboril, J. E. Altman, N. S. Hairr, R. K. Myrick, A. L. Olex, M. G. Dozmorov, J. Harrell;
Virginia Commonwealth University - VCU, Richmond, VA

Estrogen receptor (ER) signaling is the main driver of tumorigenesis in ER+ breast cancers by inducing proliferation and survival through genomic and non-genomic means, therefore inhibition of ER signaling has been a mainstay of treatment for decades. Roughly 30 percent of patients will develop treatment-refractory recurrence or metastasis within their lifetime, which may include metastasis to the bone, lung, liver, and brain. Although advances in treatment approaches have prolonged average progression free survival, metastatic breast cancer remains incurable. A new endocrine therapy, Elacestrant, has been approved by the FDA for the treatment of ER+, ESR1-mutant advanced or metastatic breast cancer. The mechanism of action of Elacestrant involves both degradation of ER and modulation of ER signaling through non-degradative means. The central hypothesis of this study was that Elacestrant may prolong progression free survival in animal models of breast to bone metastasis, because modulation of ER in the bone would decrease the incidence of osteoporosis which is induced by other endocrine therapies. However, we discovered that prolonged Elacestrant treatment induces destruction of the trabecular bone structure and increased adipocyte mass within the bone, consistent with an osteoporotic phenotype. Ongoing studies will seek to determine if other endocrine therapies will provide better protection to the bone architecture while reducing metastatic burden in animal models. Additionally, we will evaluate organotropic efficacy of new endocrine therapies on multi-organ metastasis to determine if utility is contingent upon the metastatic site.

#6270 Anti-metastatic effects of estrogen receptor β in inflammatory breast cancer.

H. Nagandla[1], S. Tastsoglou[2], K. Cuong Cap[1], A. Phillips[1], W. Qian[1], J. Zhou[1], J. Chang[1], S. Krishnamurthy[3], N. Ueno[4], A. Hatzigeorgiou[2], C. Thomas[1]; [1]Houston Methodist Research Institute, Houston, TX, [2]University of Thessaly, Lamia, Greece, [3]University of Texas, Houston, TX, [4]University of Hawaii, Honolulu, HI

Inflammatory breast cancer (IBC) is a rare but highly aggressive form of breast cancer with a 5-year survival rate of less than 50%. Although 20-30% of women with IBC have distant metastasis at the time of diagnosis, the biology underlying the aggressive behavior of the disease is poorly understood and molecular markers that distinguish IBC from non-IBC have not yet been identified. In response to the urgent need of discovering new targeted therapies in IBC, we have studied the second estrogen receptor (ERβ) since prior work from our lab correlated higher tumor expression of ERβ in samples from IBC patients with longer metastasis free survival. We showed that ERβ exerted anti-metastatic activity in IBC by inhibiting actin-based cell migration through the suppression of RhoC GTPase signaling. However, since estrogen receptors elicit their effects by inducing global cellular alterations, we have now adopted an integrated genomic approach to fully understand the anti-metastatic effects of ERβ in IBC and delineate the underlying transcriptional regulatory circuits. We found ERβ binding sites in IBC cells and combined this information with gene expression data to identify downstream direct target genes and associated pathways. Our findings suggest the regulation of tumor micro-environment and metabolism as the primary targets of ERβ and we are currently working to pinpoint the crucial regulatory components in these functions. Our findings thus offer an opportunity to better understand the mechanism of ERβ action in aggressive breast cancer, serving as a critical step in validating its tumor repressive role.

#6271 Novel insights into androgen receptor-variant 7 subnuclear localization and function in castration resistant prostate cancer.

M. K. Naidoo, P. Giannakakou;
Weill Cornell Medicine, New York, NY

Prostate cancer (PC) stands as the most frequently diagnosed and second leading cause of cancer death among American men. PC mortality is predominantly attributed to castration-resistant prostate cancer (CRPC), often emerging within 2-3 years following the initiation of androgen deprivation therapy. This resistance primarily arises from sustained androgen receptor (AR) signaling, ultimately resulting in a compromised response to AR-directed therapies. AR splice variant expression is a key contributor to the persistent AR signaling in CRPC. AR-variant 7 (AR-V7) is the most clinically prevalent variant, expressed in about 75% of patients with CRPC and confers resistance to standard of care (SoC) treatments. AR-V7 differs from the full-length AR (AR-fl) because it lacks the ligand binding and hinge domains, rendering it resistant to SoC treatments. Currently, there are no selective inhibitors for AR-V7. Therefore, we sought to identify unique biological features of AR-V7, distinct from AR-fl, to exploit therapeutic options for targeting AR-V7. Previous studies have demonstrated high sequence homology, largely overlapping cistromes, and gene transactivation profiles between AR-V7 and AR-FL. Our published mechanistic studies revealed that AR-V7 utilizes a unique nuclear import pathway, not shared by AR-fl, allowing for constitutive import and activation of target genes in the nucleus. Herein, we report an additional novel subnuclear phenotype of AR-V7 in LNCAP95 and 22RV1 cells modeling CRPC. Staining with AR-V7- and AR-fl- specific antibodies revealed that unlike AR-fl, AR-V7 exhibited prominent nucleolar localization. To validate AR-V7 nucleolar localization, CRPC cells stained with fibrillarin (nucleolar marker), and subsequent fluorescence intensity analysis revealed that AR-V7 was predominantly localized in fibrillarin positive nucleoli, whereas AR-fl protein was solely localized in the nucleoplasm. This suggests a novel functional role of AR-V7 in the nucleus. To further confirm AR-V7 nucleolar localization, Actinomycin D (ActD) was used as a tool compound to disrupt nucleolar integrity. Treatment with ActD for 4 hours in CRPC cells significantly reduced the area of fibrillarin positive nucleoli and prompted AR-V7 re-distribution out of the nucleoli and into the nucleoplasm. Ongoing efforts to further investigate AR-V7 nucleolar function in CRPC cells include mutating the predicted nucleolar localization signal located in AR-V7 and identifying nucleolar-interacting proteins through proximity-labeling assays. In conclusion, we unveiled a novel nuclear compartmentalization of AR-V7 within the nucleolus, the primary hub for ribosomal biogenesis. These observations suggest that AR-V7 could regulate the high levels of protein synthesis occurring in CRPC cells, creating a window of a potential therapeutic opportunity for selective inhibition.

#6272 Loss of SIRT6 diverts TGF-β signaling to promote liver cancer.

K. Ohshiro[1], X. Xiang[2], X. Yang[2], K. Bhowmick[2], M. I. Hassan[3], T. Mohammad[3], **L. Mishra**[2];
[1]Feinstein Institutes for Medical Research, New York, NY, [2]Feinstein Institutes for Medical Research & Cold Spring Harbor Laboratory, New York, NY, [3]Jamia Millia Islamia, New Delhi, India

Background: In the US, ~35% of individuals on the waitlist for a liver transplant who had hepatocellular cancer (HCC) also had metabolic dysfunction-associated steatohepatitis (MASH). Yet, key signaling mechanisms controlling cellular transformation in this obesity-driven HCC remain only partially understood. SIRT6 is NAD^+-dependent protein deacetylases that limits the activity of the lipogenic transcription factors SREBP1/2. Reduced SIRT6 is associated with human fatty liver and cancer. However, SIRT6 also limits liver fibrosis by inhibiting TGF-β signaling through the deacetylation of SMAD2 and SMAD3. We found that Smad3 driven TGF-β signaling is modulated by βII-Spectrin (encoded by *SPTBN1*), and that a hot mutation in HCC- D1089Y encompasses the SPTBN1-SMAD3 binding site (*Gastro 2018; 154:195-210*). In stressed hepatocytes, βII-Spectrin promotes lipogenesis through interactions between caspase-cleaved forms of both SREBP1 and βII-Spectrin *(Sci Transl Med 2021;13:624)*. Liver-specific knockout of βII-Spectrin (LSKO) blocks fatty liver and HCC. Here we explored the extent of βII-spectrin-D1089Y regulation of SIRT6 expression through SMAD3, and the combined roles of SIRT6 and SPTBN1 in human HCC.
Methods: We generated a SPTBN1-D1089Y mutant mouse and examined SIRT6 in the SPTBN1-D1089Y mutant mouse liver tissues and MEFs. TGF-β/Smad3 pathway activity was analyzed in SPTBN1-D1089Y mutant MEFs via western blot and RNA-seq. SIRT6 expression was examined in mouse MAFLD/MASH (GSE156059). Structure-based molecular docking simulations using three-dimensional structural coordinates of human SIRT6 (ID: Q8N6T7) and β2SP (ID: Q01082) from the AlphaFold database, followed by interactions between SIRT6 and SPTBN1.
Results: SIRT6 levels are decreased in SPTBN1-D1089Y mutant liver cancer cell line and mouse liver tissues. TGF-β/SMAD3 pathway activity was altered in SPTBN1-D1089Y mutant MEF cells with decreased phospho-SMAD3 levels. The structural model predicted specific interactions between human SPTBN1 and SIRT6. Overexpression of Flag-SIRT6 reduced βII-Spectrin acetylation in HepG2 cells. TGF-β induced SMAD3, βII-Spectrin coimmunoprecipitation with SIRT6. SIRT6 knockdown increases nSREBP1, SCD1 (encoded by a nSREBP1 target gene), and βII-Spectrin in HepG2 cells. SIRT6 RNA expression is significantly decreased in liver macrophages from mice with NAFLD/NASH.
Conclusions: Our data indicated a SMAD dependent as well as a SMAD3 independent role of SPTBN1 in regulating SIRT6. βII-spectrin-D1089Y together with SIRT6 deficiency may increase the susceptibility to MASH/HCC via regulating the crosstalk between macrophage and hepatocytes or regulating MASH and HCC.

#6273 GGCT expression is a useful marker for the diagnosis of follicular thyroid carcinoma.

T. Mitsuhashi[1], S. Ogasawara[1], M. Nakayama[1], R. Kondo[1], J. Akiba[1], K. Murotani[2], T. Ono[1], F. Sato[1], H. Umeno[1], H. Yano[1];
[1]Kurume Univ. School of Medicine, Kurume, Japan, [2]Kurume Univ., Kurume, Japan

Background: Follicular thyroid carcinoma (FTC) and follicular adenoma (FA) have similar histological findings. FTC is distinct from FA based on the presence of capsular or vascular invasion in the tissues, but it is difficult to confirm the diagnosis in some cases. In this study, we aimed to establish useful molecular maker for differential diagnosis between FTC and FA.
Methods: This study included FTC (n = 32), FA (n = 64), and follicular tumors of uncertain malignant potential (FT-UMP, n = 5). Invasive front tissue and tumor center tissue from 3 cases of FTC were collected using a laser microdissection system; RNA was extracted, followed by microarray analysis to examine molecules that were commonly highly expressed in the invasive front. Subsequently, immunohistochemical staining of gamma-glutamyl cyclotransferase (GGCT) was performed. For assessment of GGCT expression, the intensity of the nuclear staining was stratified using a four-tiered scale (0 to 3) and percentage of positive cells (0-100%) in the hotspot. Multiplying intensity score and percent of positive cells, an expression score ranging from 0 to 300 was calculated. The Ki-67 labeling index was examined in 20 cases of FTC, 25 cases of FA, and 4 cases of FT-UMP from the same cohort. We counted at least 2,000 tumor cells in the hot spot for the assessment of Ki-67 labeling index.
Results: Microarray analysis revealed GGCT exhibited high expression levels at the invasive front of FTC. In immunohistochemical assessment, GGCT expression scores were significantly higher in FTC than in FA (118.5 ± 51.4 vs. 57.3 ± 34.7, $p < 0.0001$). The median Ki-67 labeling index were 3.9% (range 0.2 - 16.1) for FTC and 2.4% (range 0.3 - 7.0) for FA. FTC showed a higher Ki-67 index than FA (Wilcoxon rank sum test, $p = 0.0444$). With GGCT expression score, applying a cutoff value of 101.1, the distinction between FTC and FA resulted in a sensitivity of 68.8% and a specificity of 87.5% (AUC: 0.832). With Ki-67 labeling index, applying a cutoff value of 4.0%, the distinction between FTC and FA resulted in a sensitivity of 50.0% and a specificity of 80.0% (AUC: 0.677). The GGCT expression score was positively related with the Ki-67 labeling index in the FTC cases. (Spearman's $\rho = 0.5293$, $p = 0.0164$). There were no significant associations between GGCT expression scores and clinicopathological parameters, including age, gender, tumor diameter, pT stage, pN stage, pattern of capsular invasion, number of foci of vascular invasion, and the presence of distant metastasis.
Conclusions: GGCT is a potential marker for differentiating FTC from FA. The GGCT expression of FTC may contribute to estimating the invasive activity and proliferative activity.

#6274 Integrated multi-omics revealed the involvement of MYC and mTOR pathways in radiation resistance of adrenocortical cancer.

B. Ramamoorthy[1], P. Mishra[1], M. Boufraqech[1], N. Michael[1], M. Cam[1], R. Finney[1], T. Meyer[2], R. Holewinski[2], T. Andresson[2], M. Wong[1], S. Shema[1], D. Tillo[1], N. Nilubol[1];

[1]National Cancer Institute, Bethesda, MD, [2]Leidos Biomedical Research, Inc., Frederick, MD

The morbidity and mortality of patients with adrenocortical cancer (ACC) are commonly due to locoregional postoperative recurrence and progressive systemic metastasis. Surgical resection remains the only curative treatment option, but even with complete resection, locoregional recurrence rates remain high. Adjuvant radiation therapy (RT) has been shown to reduce recurrence rates and may improve overall survival in selected patients. However, half of the patients receiving postoperative RT still develop locoregional recurrence, clearly demonstrating the heterogeneous nature of ACC. Minimal investigation into the mechanisms underlying radiation response and resistance in ACC has been performed, but elucidating this information is critical to improving outcomes. To address this knowledge gap, NCI-H295R cells were treated with fractionated radiation at 1 Gray (Gy) per day for 5 consecutive days for two consecutive weeks, cumulating in a total radiation dose of 10 Gy. Treated and control ACC cells were harvested on days 7 and 14 for bulk RNA-sequencing (RNA-Seq) and total proteomics by liquid chromatography and tandem mass spectrometry. Significantly differentially expressed genes (DEGs) and proteomes (adj. p. value <0.05) that overlapped between day 7 and day 14 were selected for further analysis and comparison with publicly available gene expression data sets in ACC (The Cancer Genome Atlas (TCGA); Gene Expression Omnibus: GSE12368, GSE33371, GSE75415, GSE90713).

There were 3993 DEGs and 423 proteomes identified, respectively. Of these, there were 139 overlapping DEGs with respective proteomes found, 72 of which were differentially expressed in the 4 GEO data sets comparing normal adrenal cortex to ACC. RNA-Seq pathway analysis demonstrated enrichment of E2F targets, G2M checkpoint, mTORC1 signaling, and MYC targets v1, while total proteomics pathway analysis revealed enrichment of cell cycle, transcriptional regulation, cellular stress and injury, alterations of RNA metabolism, and metabolism proteomes. Given that *MYC* and *mTOR* are both involved in transcriptional regulation and cell cycle regulation, and mTORC1 in particular is associated with cellular metabolism, the RNA-Seq and proteomics pathway analyses show general consistency with each other.

TCGA gene expression analysis showed that overexpression of *MYC* or *mTOR* was correlated with shorter overall survival (OS) and disease-free survival (DFS) in the entire ACC cohort ($p<0.05$). Together, the combination of *in vitro* pathway analysis and TCGA analysis suggests a potential involvement of the MYC and mTOR pathways in radiation resistance in ACC. Further *in vitro* and *in vivo* studies are warranted to identify specific molecular compounds that target MYC and mTOR pathways and improve radiation response in ACC.

#6275 Exposure to neighborhood violence rewires glucocorticoid receptor binding and drives proliferation and invasiveness in lung tumor samples.

H. Heath[1], J. Yoo[1], V. Sharma[1], H. McGee[1], A. Soliman[1], A. Mohamed[2], A. K. Matthews[3], R. Winn[4], Z. Madak-Erdogan[1], S. Kim[5];
[1]University of Illinois at Urbana-Champaign, Champaign, IL, [2]University of Illinois at Chicago, Chicago, IL, [3]Columbia University, New York, NY, [4]Virginia Commonwealth University, Richmond, VA, [5]University of Illinois at Chicago, Champaign, IL

Background: Despite smoking less, Black men experience higher incidence of lung cancer compared to white men. This health disparity is even more prevalent in Black men from Chicago, suggesting local neighborhood factors impacting tumorigenesis. Preliminary data indicate that, compared to white men, Black men are more likely to reside in neighborhoods with high levels of violence and have elevated levels of hair cortisol.
Objective: To understand the link between lung tumorigenesis and exposure to neighborhood violence, our objective is to investigate the chromatin recruitment of the receptor for cortisol, called the glucocorticoid receptor (GR), and to correlate this recruitment with target gene expression levels.
Methods: Utilizing CUT & RUN, we identified the gene binding sites of GR using 15 lung tumor and corresponding healthy tissue samples from lung cancer patients living in Chicago. GR recruitment to chromatin was correlated with the neighborhood homicide rate obtained using patients' zip codes. Spatial transcriptome profiles for these 15 lung tumor samples were obtained from the Space Ranger pipeline and gene expression hot spots of GR target genes were visualized using Loupe Browser (10x Genomics).
Results: GR recruitment to regulatory regions of chromatin increases with greater zip code level violence rates. In patients from high violence neighborhoods, tumor samples had higher magnitude of binding compared to normal neighboring tissue. In tumor samples from patients living in high violence compared to low violence neighborhoods, GR binding is seen in genes that are associated with increased tumor aggressiveness. Hot-spot analysis of these genes found strong co-expression of genes associated with proliferation and invasion in samples from high violence but not low violence neighborhoods.
Conclusion: Exposure to neighborhood violence may impact tumor biology via increased GR recruitment to genes associated with proliferation and invasion.

#6276 In vitro neuroendocrine differentiation of BPH-1 cells under beta-adrenergic stimulation.

N. Pigat, L. N. Garrido, C. Lefevre, M. Baures, V. Goffin, A.-S. Armand, **T. Capiod**;
Institut Necker-Enfants Malades (INEM), Paris, France

Recent studies have shown that adrenergic fibers from the sympathetic nervous system (SNS), acting through stromal β2-adrenergic receptors, play an important role in the initial phases of cancer development by promoting tumor cell survival. Recent epidemiological data suggest that β-blocker intake is associated with improved survival of prostate cancer patients. Hypertension and high blood pressure have been suggested to increase prostate cancer development suggesting that the use of β-blockers in these patients could also reduce prostate cancer risk. β-adrenoceptors signal through the cAMP/PKA pathway that is known to promote neuroendocrine differentiation (NED) in LNCaP prostate cancer cell line. While neuroendocrine (NE) cells expressing synaptophysin (SYN) represent a minor cell population in the epithelial compartment of normal prostate glands, the population of NE-like cells, exhibiting NE phenotypes and expressing NE markers, is increased in, and correlates with, cancer progression, androgen-independent state and poor prognosis. Expression of the routine tissue biomarker of *prostate cancer* AMACR in NE-like cells discriminates them from NE cells. Our aim was to investigate whether NED could also be associated with benign prostatic hyperplasia (BPH) as recent studies showed that an increase in neuroendocrine cell density occurred before development of BPH in hypertensive rats. Our results showed that a 10-day treatment with 100µM IBMX (blocking cAMP degradation) and 10µM forskolin (FSK, adenylate cyclase activator) to trigger sustained activation of the cAMP/PKA pathway led to an increase in SYN and AMACR expression in BPH-1 cells (qPCR and WB). Similar results were observed by combining the effect of the β-adrenoceptor agonist isoproterenol (1µM) and FSK. The same treatments reduced BPH-1 cell proliferation rates by 40% and 60%, respectively, as expected for NED. Effects on AMACR and SYN expression and cell proliferation were fully reversed by the β-blocker carvedilol (5µM). This data suggests that β-adrenoceptors could be linked to the development of NE-like cells in BPH, a non-lethal disease affecting the transition zone (TZ). As 20% of the prostate cancer occur in this TZ, this observation may need further investigation.

#6277 Tall cell variant papillary thyroid carcinoma from Middle Eastern patients have worse outcome than classical papillary thyroid carcinoma using propensity score matching.

K. S. Al-Kuraya, S. K. Parvathareddy, A. K. Siraj, S. O. Ahmed, N. Siraj, M. Manakhan, H. Aldossari;
King Faisal Specialist Hospital & Research Centre, Riyadh, Saudi Arabia

The tall cell variant of Papillary Thyroid Carcinoma (TCV-PTC) is the most common aggressive variant of PTC. The impact of TCV-PTC on patients' prognosis still remains controversial. Moreover, the clinico-pathological and prognostic effect of TCV-PTC from Middle Eastern ethnicity remains unexplored. We aimed to study TCV-PTC in comparison to classical PTC in Middle Eastern patients and their impact on prognosis. We performed a retrospective cohort study of tall cell variant (TCV-PTC) and classic variant of papillary thyroid carcinoma (CV-PTC) after post-surgical radioactive iodine therapy. We used the propensity score matching (1:3 matching ratio) to account for differences between recipients of TCV-PTC vs CV-PTC. Univariate and multivariate analysis were performed to assess the independent factors for persistent/recurrent disease. Kaplan-Meier curve analyses were used to compare disease-free survival (DFS). In total, 174 (16.3%) patients with TCV-PTC and 891 (83.7%) patients with CV-PTC were included. After propensity score matching, 174 pairs of patients were selected (TCV-PTC, n = 174; CV-PTC, n = 522). In the matched analysis, higher proportions of TCV-PTC experienced persistent/recurrent disease compared with CV-PTC (25.7% vs 31.4%; p = 0.0119). In multivariate analyses of clinical and tumor characteristics, histological type of TCV-PTC (odds ratio, 2.09; 95% confidence interval, 1.28-3.40; p = 0.0031) was associated with increased risk of persistent/recurrent disease. The five-year DFS rates for the TCV-PTC and CV-PTC groups were 48.5% and 73.1%, respectively. The Kaplan- Meier analysis indicated that the TCV-PTC group (p < 0.0001) had shorter DFS. In conclusion, when other clinico-pathological factors were similar, this propensity score matched analysis showed that histological subtype TCV-PTC is by itself an independent predictive marker of persistent/recurrent disease in Middle Eastern patients. Therefore, individualized therapeutic approaches might be needed for this aggressive PTC subtype.

#6278 Effect of tumor size and BRAF mutational status in Middle Eastern differentiated thyroid cancer.

R. Bu, A. K. Siraj, S. K. Parvathareddy, K. Iqbal, S. Azam, Z. Qadri, M. Al-Rasheed, W. Haqawi, A. D. Benito, K. S. Al-Kuraya;
King Faisal Specialist Hospital & Research Centre, Riyadh, Saudi Arabia

Background: Risk stratified treatment strategies have become a focus in the treatment of Differentiated Thyroid Cancer (DTC). Tumor size at diagnosis has been widely used as a major mortality risk factor in risk stratification of DTC, but whether this is generally applicable, particularly in patient with different *BRAF* genetic backgrounds, is unclear. The current study was designed to analyze whether tumor size at diagnosis is a major prognostic factor in Middle Eastern DTC.
Methods: We conducted a comparative study of the relationship between tumor size at diagnosis and event free survival with respect to *BRAF* status in 1709 consecutive patients treated surgically for Middle Eastern DTC. Patients were divided into four groups according to the size of tumor (≤4 cm vs. >4 cm) and BRAF mutation status: Group 1 (≤4 cm without BRAF mutation, n = 587), Group 2 (≤4 cm with BRAF mutation, n = 765), Group 3 (>4 cm without BRAF mutation, n = 198) and Group 4 (>4 cm with BRAF mutation, n = 159). Predictors of event-free survival (EFS) were compared using the Log-rank test and Cox proportional hazards models.
Results: Following multivariate analysis, patients with tumors >4cm did worse than patients with tumors <4cm with respect to EFS (Group 3 vs Group1 HRadjusted=1.38, 95% CI=1.02-1.86, p = 0.0359; Group 4 vs Group 2 HRadjusted=1.61, 95% CI=1.20-2.16, p = 0.0017). However, patients did not differ according to EFS, regardless of the presence of *BRAF* mutation within each size category (Group 2 vs Group 1 HRadjusted=0.98 CI=.78-1.23, p=0.8415 ; Group 4 vs Group 3 HRadjusted=1.17, 95% CI=0.84-1.62, p=0.3523]
Conclusion: Tumor size is an independent predictor of EFS in Middle Eastern DTC patients, regardless of *BRAF* mutational status.

#6279 Estrogen signaling in low-grade serous ovarian carcinoma.

Y. T. Tsang, C. O. Ng, D. Gershenson, **K.-K. Wong**;
UT MD Anderson Cancer Center, Houston, TX

High level of estrogen in the blood of women has been linked to the progression and possibly development of ovarian cancer. Almost all low-grade serous ovarian cancer (LGSOC) expresses estrogen receptor alpha (ERα protein encoded by the gene *ESR1*) and develops during reproductive age of women. However, recent studies suggested that a higher expression of ERα correlates with better survival. In a phase II clinical trial, hormonal therapies have been shown to be associated with a clinical benefit rate of 61% for recurrent ER-positive LGSOC patients. The study also indicated that women with recurrent LGSOC who received hormonal therapies had a significantly longer progression-free survival but not overall survival. Endocrine therapies have proven to be effective in treating breast cancer. Unfortunately, in ovarian cancer clinical trials (GOG0281 and PARAGON), these treatments have not achieved comparable results, with an objective response rate of only approximately 14%. To understand the ESR1 regulation in LGSOC, we have performed RNAseq and ChIPseq analyses of LGSOC tumor tissues. We also forced over-expression of ESR1 in LGSOC cell lines. Using RNAseq data, we aligned the sequencing reads to all the known ESR1 transcript variants. We found that ESR1 transcript variant 1, 2, 3 and X11 were the major transcripts expressed. Variants 1, 2 and 3 encode the regular 66 kDa ESR1 protein, while the X11 variant encodes a 52 kDa ESR1 protein. Both 66 kDa and 52 kDa ESR1 proteins were also detected in LGSOC tumor tissues by western blots. To further explore the function of ESR1 66kDa in LGSOC, we over-expressed ESR1 variant 1 in two LGSOC cell lines (HOC-7 and HCC5075) by transfecting with an expression plasmid. Total proteins were extracted from the mock control and transfected cells for functional proteomic analysis by reverse phase protein arrays (RPPA). From the RPPA data, overexpressing ESR1 in LGSOC cell lines suppressed DNA repair pathways but activated cell cycle and mitosis pathways. To further delineate the ESR1 DNA binding sites in LGSOC, we performed ChIPseq analysis of these tumor samples as well as two ovarian cancer cell lines that express ESR1 protein. Our results demonstrated that ESR1 regulated “cistromes” in ER positive ovarian carcinoma is very different from that in ER positive breast cancer as much less ESR1 binding sites were found in LGSOC. There are ESR1 binding sites common to both types of cancers, but we found quite a few unique ESR1 binding sites. We are trying to integrate the ChIPseq and RNAseq data and hopefully identify, for the first time, an ovarian cancer specific ERα cistrome. ER expression may not always correlate with activation of ESR1 signaling pathways, which may be one of the reasons underlying endocrine therapy resistance in ovarian cancer. The results of an integrated analyses will also give us insight on the management of ER positive LGSOC by identifying new genetic targets that may be used in combination with endocrine therapy.

#6280 Vitamin D enhances luminal differentiation of prostate organoids more than androgens.

O. F. Cerna, Jr., L. Nonn, M. Schlicht, K. Krieger;
University of Illinois at Chicago, Chicago, IL

Background: Prostate Cancer (PCa) is a prevalent disease affecting over two million men worldwide. Vitamin D is a fat-soluble hormone that is well-known for its role in the maintenance of strong bones and has anti-cancer effects in prostate cancer. Vitamin D is synthesized in the skin in response to sun exposure and may be supplemented with diet. However, since melanin hinders this synthesis many African Americans are deficient in vitamin D. Vitamin D circulates as 25-hydroxyvitamin D3 (25D) and 25-dihydroxyvitamin D3 (1,25D). Hydroxylation of 25D by the kidney or within tissues forms the active hormone 1,25D. 1,25D binds the vitamin D receptor (VDR), a steroid transcription factor. Androgens are the main regulatory hormones involved in prostate growth and differentiation. Epithelial differentiation is the process in which progenitor or stem cells become specialized cells, such as basal or luminal. In the prostate, luminal epithelial cells are the most differentiated and are the origin of PCa. We used mouse prostate organoids to replicate the differentiation process in vitro and to help identify the role of 1,25D on epithelial differentiation in the presence and absence of other androgens.
Methods: Primary mouse prostate cells were isolated from dorsal lateral lobes and grown as organoids. Over two weeks, we treated these organoids with concentrations of 1,25D and androgen (dihydrotestosterone, DHT). The four treatment groups were control, 1,25D only, DHT only and 1,25D+DHT. Organoids were imaged and analyzed for number, size and phenotype. Phenotypes were identified as luminal, acinar, or solid.
Results: Luminal phenotypes were more prevalent in 1,25D conditions compared to control or DHT alone. The number, size and percent of luminal organoids was highest in 1,25D + DHT compared to all other groups. Ongoing studies include examination of prostate organoids from mice with a vitamin D-deficient diet and staining of the organoids for differentiation markers.
Conclusions/Significance: We observed that 1,25D enhanced luminal epithelial differentiation in mouse prostate organoids. These findings suggest that chronic vitamin D deficiency may increase risk of aggressive prostate cancer, due to decreased epithelial differentiation. This has implications for the disparity of aggressive PCa observed in African American men who have lower vitamin D levels compared to their white counterparts.

#6281 Context dependent role of glucocorticoids in breast cancer..

W. Effah, S. Ponnusamy, S. Asemota, Y. Khosrosereski, R. Narayanan;
University of Tennessee Health Science Center, Memphis, TN

Glucocorticoids bind to the transcription factor glucocorticoid receptor (GR) and regulate genes in response to cellular metabolism, inflammation, and stress. Although GR has been extensively evaluated in inflammation and metabolic diseases, its role as a therapeutic target in cancer has not been thoroughly studied. Results from studies with another member of the steroid receptor family, androgen receptor (AR), demonstrated that the AR is an oncogene in estrogen receptor (ER)-negative breast cancer, but a tumor suppressor in ER-positive breast cancer. We expected a comparable mechanism with GR in different breast cancer subtypes. In this study, we evaluated the role of GR in various breast cancer subtypes and discerned the mechanism of action. Six breast cancer cell lines and seven patient-derived xenografts (PDXs) were characterized by Western blot for their expression of GR, ER and AR. Proliferation assays were performed in cell lines with a dose-response of a synthetic glucocorticoid, dexamethasone. Subsequently, we performed xenograft studies in cell line xenografts (CDXs) and PDXs. GR was ubiquitously expressed in various cell lines and PDX models. Dexamethasone reduced cell proliferation in ER-positive models, while it increased the proliferation in ER-negative cell lines, suggesting that the GR might have a mechanism of action that is similar to AR. GR antagonist, mifepristone, reversed the effects of dexamethasone. CDX studies in an ER-positive cell line, MCF7 suggested that dexamethasone (10 mpk) inhibited the tumor growth significantly that was better than the standard of care fulvestrant. This result was confirmed in an ER positive PDX model HCI013. Study by Obradović et al, indicates that glucocorticoids have an oncogenic role and furthermore promote breast cancer metastasis in TNBC model thereby validating the subtype and context dependent role of the glucocorticoid receptor. We are currently exploring the mechanism of GR's context-dependent tumor suppressor and oncogenic role in distinct breast cancer subtypes.

#6282 Novel androgen related gene network in prostate cancer cell model.

Alex L. McDonald, Spencer Snow, Shuk-mei Ho, Yuet-kin Leung

Pharmacology and Toxicology, University of Arkansas for Medical Sciences, Little Rock, AR

Prostate cancer stands as the foremost cause of cancer-related deaths among men in the United States, with the primary treatment being androgen receptor (AR) antagonists relying on current androgen signaling knowledge. Most of this knowledge is derived from next-generation sequencing experiments, but the oversight of splice variants and highly similar sequences in multiple loci can hinder a comprehensive understanding. In an effort to unveil the complete androgen receptor transcriptional program, we employed a novel sequencing analysis protocol. Using a R1881-LNCaP model, we identified 212 upregulated and 92 downregulated genes, of which a notable one-third (68 upregulated and 39 downregulated) had not been previously associated with androgen. Among these novel transcripts, 5.6% lacked splice variants, while 16.3% exhibited one or more splice variants, including 3.8% from seven unique gene families. Recognized androgen-regulated genes, such as ORM1, STEAP4, NPPC, ORM2, and KLK3, were validated as upregulated, while GRB10, FN1, PPFIA2, and PLA2G2A were confirmed as downregulated in this in-vitro model. Utilizing chromatin immunoprecipitation-sequencing (ChIP-seq) data, we found that 13% of the genes contained at least one androgen response element within 5 kb upstream or downstream. Further validation through real-time PCR confirmed the expression levels of 90% of the selected genes (18). Ingenuity Pathway Analysis revealed two major regulators (ESRRA and ARFGEF2) in causal networks likely interacting with the novel genes. Intriguingly, 57.1% of ESRRA-involved genes contained at least one ESRRA binding site in a ChIP-seq dataset. Although ESRRA is known to activate androgen biosynthesis in castration-resistant prostate cancer, its interaction with AR and co-regulation of androgen signaling remain unknown. Ongoing studies involve the characterization of these networks in prostate cancer cell lines, examining anchorage-independent capacity, invasion, migration, proliferation, and progression. Data collection and comparison will ascertain whether the signaling is driven by mutated AR, and the role of ARv7 will be elucidated through gene lockdown experiments.

#6283 Tumor repressive effects of estrogen receptor β mRNA-based therapy in aggressive breast cancers.

K. Cap, A. Phillips, K. A. Court Pinto, K. D. Zambo, W. Qian, J. Zhou, J. Chang, B. Godin, **C. Thomas**;
Houston Methodist Research Institute, Houston, TX

Inflammatory breast cancer (IBC) and triple-negative breast cancer (TNBC) are the most aggressive forms of breast cancer due to their high propensity to develop distant metastases and the lack of specific effective targeted therapies. The failure of previous research to produce viable therapeutic targets combined with the absence of estrogen receptor α (ERα) in TNBC and the majority of IBC led us to explore the second ER (ERβ) as a molecule with targeting potential. We previously reported the anti-metastatic effects of ERβ in both TNBC and IBC. Considering the anti-tumor activity together with the decreased expression of ERβ in IBC and TNBC tumors, we employed an mRNA-based approach to induce tumor-specific upregulation of the receptor and restore its anti-metastatic activity. Our findings show that complexes of ERβ mRNA with lipid nanoparticles (LNPs) enable *in vitro* translation of a functional protein with strong anti-invasive activity. More importantly, direct administration of ERβ mRNA-LNPs in orthotopically grown IBC and TNBC tumors results in high tumor levels of the receptor and an evident inhibition of metastasis demonstrating for the first time the ability of ERβ mRNA to prevent progression of the disease. Our study may have important clinical implications by establishing ERβ mRNA as a novel and specific therapy intervention that either alone or in combination with existing treatments can substantially repress metastasis, eliminate associated mortality and benefit patients with aggressive breast cancer.

#6284 Multimoics reveal aberrant pathways and regulation of castration resistant and metastatic prostate cancer.

A. M. Horning, C.-N. Hung, B. Liebermann, C.-W. Chou, C.-K. Lin, Y. V. Wang, V. X. Jin, M. A. Liss, C.-M. Wang, C.-L. Lin, M. Chen, T. H. Huang, **C.-L. Chen**; UT Health Science Center at San Antonio, San Antonio, TX

Prostate cancer is a highly heterogeneous disease and in the end, 30% of patients will experience metastatic and fatal castration resistant prostate cancer (mCRPC). In spite of the vigorous efforts to search the causes of metastatic CRPC (mCRPC), the mechanisms are still largely unresolved. To understand the progression of mCRPC, we utilized scRNA-seq to profile global expression patterns in LNCaP, LNCaP-Abl and PC3 representing castration sensitive and resistant states. ScRNA-seq revealed 335 and 2393 differentially expressed (DE) genes in early and advanced castration resistant states enriched in 43 and 163 aberrant pathways. These included focal adhesion, adherens junction, leukocyte transendothelial migration, ECM-receptor interaction, regulation of actins, gap junction, TGFb, WNT, Hippo, Ephrin and other pathways. Upregulation of these pathways predicted worst disease free/overall survival of The Cancer Genomes Atlas (TCGA) PC cohort using Kaplan-Meir estimation. Further scRNA-seq also indicated most of the pathways were also enriched in *ex vivo* circulating tumor cells derived from biochemical recurrent or mCRPC patients. Small molecule perturbation verified function of 9 pathways involved in cell proliferation, migration, invasion, and organoid formation of mCRPC cell lines and CTCs. We then delved into how these genes are regulated by the global chromatin landscape through Assay for Transposase-Accessible Chromatin and high throughput DNA-seq (ATAC-seq). In castration sensitive LNCaP, active chromatins are associated with genes but most of them are located in distal intergenic regions. Conversely, the majority (51.9-57.6%) of open chromatins in castration resistant PC cells are situated in promoters that lie within 1kb of transcription start sites. KEGG pathway enrichment analysis uncovered Hippo, Wnt, tight junction, adherens junction, circadian and other pathways that corroborate the scRNA-seq findings. GRO-seq data indicated that nascent transcription supports gene body transcription in castration resistant cells but leads to massive pausing in castration sensitive cells.

#6285 Defining androgen receptor function and the effects of PARP inhibition in BRCA1/2-deficient vs. proficient prostate cancer.

N. A. Traphagen, E. Wheeler, R. Li, X. Qiu, M. Brown;
Dana-Farber Cancer Institute, Boston, MA

Mutation or loss of the tumor suppressor genes *BRCA1* and *BRCA2* promotes the development of aggressive prostate cancer with poor outcomes and a high risk of metastatic relapse. Approximately 15% of metastatic prostate tumors are BRCA1/2-deficient. These tumors are frequently resistant to standard-of-care treatments that block androgen receptor (AR) function, although the mechanisms underlying this effect remain unclear. PARP inhibitors are synthetically lethal with BRCA1/2-deficiency and are commonly used as a late-line treatment in metastatic prostate cancer; however, both preclinical and clinical data have provided conflicting results on whether PARP inhibitors can be effective in BRCA1/2-proficient prostate tumors. BRCA1, BRCA2, PARP-1, and PARP-2 all have proposed roles in regulating transcription and the chromatin landscape. We therefore hypothesized that loss of BRCA1, BRCA2, and/or inhibition of PARP modulates AR function through changes in global chromatin structure and transcriptional pathways. We used patient-derived xenograft models and next-generation sequencing techniques to profile AR function in BRCA1/2-deficient vs. proficient prostate tumors. We found that loss of BRCA1 and BRCA2 is associated with chromatin accessibility changes, and differentially accessible regions correlate with DNA binding motifs for AR and AR cofactors. ChIP-seq for AR in these tumors demonstrated that BRCA1/2-deficiency is associated with an altered AR cistrome and a global decrease in AR genomic binding. Corresponding RNA-seq data confirmed a downregulated androgen response in BRCA1/2-deficient tumors. In cell line models, inhibition of PARP1 and PARP1/2 inhibited AR-driven transcription. Combining PARP inhibition with either androgen deprivation or the AR antagonist enzalutamide dampened the growth-inhibitory effects of PARP inhibitor treatment. Together, these results indicate that BRCA1/2-deficiency and PARP inhibition modulate AR function in prostate cancer.

#6286 Metabolic abnormalities are early predictors of liver metastasis in patients with ER+ breast tumors.

A. N. Mogol[1], M. Goel[1], A. Lam[1], D. Dutta[2], B. Barnick[2], M. Grosse Perdekamp[2], Z. Madak Erdogan[1];
[1]University of Illinois at Urbana-Champaign, Urbana, IL, [2]Carle Cancer Institute, Urbana, IL

Approximately 70% of human breast cancers express estrogen receptor alpha (ERα), providing a potential for targeted endocrine therapy for patients. Unfortunately, 30-40% of ER+ patients still experience recurrence and metastasis, with a 5-year relative overall survival rate of just 24% for patients with metastatic disease. In our preliminary analysis of the data from a large cohort of ER+ MBC patients, liver metastases were associated with reduced overall survival compared to other sites, while on the standard of care estrogen receptor antagonist, Fulvestrant (Fulv). This supports data from previous clinical trials showing that patients with liver metastases are less responsive to estrogen receptor alpha (ERα) targeting endocrine therapies compared to patients with bone or lung metastases. However, the factors underlying site-specific responses of MBC to ER antagonists are unknown.

In this study, we investigated the concept that response of liver metastatic tumors is impacted by systemic glucose metabolism and the presence of liver metastatic tumors in turn will affect glucose homeostasis in the body. In our preliminary studies, metastatic liver tumors upregulated expression of enzymes that increased glycogen deposition in tumor cells in response to Fulv. Further analysis showed that a ketogenic diet restored Fulv response of metastatic liver tumors. Based on these results, we investigated if there was a relationship between metastatic site and response to endocrine therapy and if the metabolic status related to glucose homeostasis impacts metastatic disease response. We also searched if glucose homeostasis abnormalities can be indicators of liver metastasis.

We obtained electronic health records from 192 patients with stage IV estrogen receptor positive breast cancer and analyzed glucose metabolism and liver panel markers including ALT, AST and ALP. Our results showed that more than 85% of patients with liver metastases have another accompanying metastasis and these patients are at a higher risk of diabetes diagnosis compared to other metastatic site patients. A higher % of patients with liver metastasis were deceased. We also observed increased levels of ALT, AST and ALP with liver metastasis and our preliminary analysis indicates that these blood biomarkers along with metabolic disease status (diabetes, hypertension, lipidemia) are good predictors of liver metastasis. Detecting early changes in markers of glucose metabolism may provide an easy diagnostic tool for early detection of liver metastases as well as assessment of treatment response. This may lead to accurate adjustment of treatment choices with improved outcome of patients with liver metastases from breast cancer.

CLINICAL RESEARCH: Addressing Physical and Psychological Effects of Cancer Survivorship
Poster Session

#6290 Effects of a circuit, interval-based exercise program on vascular function among cancer survivors.
C. N. Christopher, D.-W. Kang, P. Gonzalo-Encabo, R. L. Wilson, A. J. Normann, M. K. Norris, C. M. Dieli-Conwright;
Dana-Farber Cancer Institute, Boston, MA

Background: Cancer survivors are at an increased risk of cardiovascular comorbidity, including atherosclerosis, hypertension, and heart failure, due to negative impacts of cancer treatments on vascular function. Exercise is recommended in recent cardio-oncology rehabilitation guidelines and has been shown to improve vascular function in clinical populations; however, its effects on vascular function are understudied in clinical oncology settings.
Purpose: This pilot study examined whether a circuit, interval-based exercise intervention can improve vascular function, assessed by brachial artery flow-mediated dilation (baFMD) and carotid intima media thickness (cIMT) in breast, prostate, and colorectal cancer survivors.
Methods: Overweight or obese (BMI>25.0 kg/m^2), sedentary breast, prostate or colorectal cancer survivors were randomized to exercise (n=60) or usual care (n=30). Survivors in the 4-month exercise intervention trained three times/week, in a circuit, interval-based supervised moderate-vigorous aerobic (65-85% of VO_2max) and resistance (65-85% of 1-repetition maximum) program. cIMT and baFMD were measured at baseline and post-intervention via an ultrasound. Paired t-tests and repeated-measures analysis of variance were run to assess within- and between-group differences.
Results: The study sample included breast (n=38), prostate (n=24), colorectal (n=28) cancer survivors who were 63.2 ± 10.8 years old, completed chemotherapy and/or radiation (75%) and were obese (87%). Post-intervention, baFMD significantly increased in the exercise group compared to the control group (between-group mean difference: 6.3%; 95% CI: [1.9 to 9.3], p=0.001). There was also a significant reduction in cIMT in the exercise group compared to the control group (between-group mean difference: -0.039mm, 95% CI: [-0.080 to -0.009], p=0.002).
Conclusions: Our findings in this pilot study support that a circuit, interval-based aerobic and resistance exercise intervention may improve vascular function in breast, prostate, and colorectal cancer survivors. Future studies are recommended to understand how exercise interventions can be utilized clinically to improve cardiovascular disease risk and co-morbidity among cancer survivors.

#6291 Changes in physical activity and ischemic stroke risk after cancer diagnosis: A nationwide cohort study.

D. Shin[1], W. Jung[2], I. Cho[1], J. Jung[3], M. Cho[4], H. Koo[5], B.-L. Cho[6], J. Park[6], H. Kwon[6], K. Han[7], Y.-M. M. Park[8];
[1]Samsung Medical Center, Seoul, Korea, Republic of, [2]Kangdong Sacred Hospital, Seoul, Korea, Republic of, [3]The Catholic University of Korea, Seoul, Korea, Republic of, [4]Kangbuk Samsung Hospital, Seoul, Korea, Republic of, [5]Seoul National University Bundang Hospital, Seongnam, Korea, Republic of, [6]Seoul National University Hospital, Seoul, Korea, Republic of, [7]Soongsil University, Seoul, Korea, Republic of, [8]University of Arkansas for Medical Sciences, Little Rock, AR

Background: Physical inactivity is prevalent after cancer treatment, which may pose a greater risk of ischemic stroke in cancer survivors.
Objective: To investigate the association between physical activity change from pre- to post-diagnosis and ischemic stroke risk among cancer survivors.
Methods: Cancer survivors without prior history of cardiovascular disease were identified. Pre- and Post-adherence to physical activity was determined within two years from cancer diagnosis. The primary outcome was incident ischemic stroke. Using the Fine-Gray model, sub-distribution hazard ratios (sHRs) and 95% confidence intervals (CIs) for ischemic stroke risk were calculated, considering death as a competing risk.
Results: Among 269,943 cancer survivors (mean [SD] age 56.3 [12.1] years, 45.7% male), 10.1% remained active, 11.4% became inactive, and 16.6% became active post-diagnosis. During 1,109,566.68 person-years[YMP1] , remaining active both pre- and post-diagnosis was associated with 15% decreased risk of ischemic stroke (sHR 0.85, 95% CI 0.75-0.96), compared to those who remained inactive. Cancer survivors who became active, and inactive post-diagnosis showed a 16%, and 11% lower risk of ischemic stroke (sHR 0.84, 95% CI 0.75-0.93; sHR 0.89, 95% CI 0.79-0.99) than those who remained inactive.
Conclusions: Our findings suggest that staying physically active is associated with a reduced risk of ischemic stroke among cancer survivors. Notably, these advantages are not limited to individuals who were physically active before their diagnosis, and it is not too late to start post-diagnosis. Preventive strategies against ischemic stroke in cancer survivors should emphasize the incorporation of regular physical activity at any stage of their cancer journey.

#6293 Influence of prescription opioids and recreational cannabis use on efficacy outcomes and adverse events related to immune checkpoint inhibitors.

H. Mahadevia, B. Eidenschink, A.-L. Cheng, A. Desai, S. Harry, L. Kujtan;
University of Missouri - Kansas City School of Medicine, Kansas City, MO

Introduction: Opioids and cannabis possess immunomodulatory properties. However, the effect of opioid receptor activity on immune function is complicated, facilitated by several mechanisms and can lead to enhancement or inhibition. Similarly, the relation between cannabinoid ligands of diverse types and endocannabinoid receptors on various immune cells is complex. We hereby delineate the effect of prescription opioids and recreational cannabis use on immune-related adverse events (IRAEs) during immune checkpoint inhibitor (ICI) therapy in various cancers, as well as efficacy outcomes in advanced non-small cell lung cancer (aNSCLC).

Methods: This is a retrospective cohort study of adult patients with advanced cancers who received ICI with or without chemotherapy for at least two months at an urban safety net hospital from January 2016 to June 2022. All patients, as well as a subset of patients with aNSCLC, were divided into two arms based on whether they were prescribed opioids during ICI therapy or not (OP vs. NO). Similarly, they were grouped based on whether they reported recreational cannabis use during ICI therapy (since initiation of therapy) or not (CA vs. NC). Incidence of IRAEs, median overall survival (mOS) and median progression-free survival (mPFS) calculated per RECIST 1.1 were the outcome variables. Multivariate logistic regression and alternative log-rank test were utilized for analysis with adjustments for demographics, insurance status, BMI, ECOG, PD-L1, TMB, smoking and concurrent chemotherapy.

Results: 230 patients received ICI-based therapy; 47% were female, 34% were African American and 6.5% were Hispanic. There was no significant difference in the incidence of IRAEs between OP (n=144) and NO (n=86; p=0.225). However, CA (n=44) had higher IRAEs than NC (n=186) with an odds ratio estimate of 2.023 (X^2=4.18, CI 1.03-3.97, p=0.04). Among 110 patients with aNSCLC, 46% were female. Patients with aNSCLC in the OP arm (n=69) had no significant difference in mOS (HR=1.34, CI 0.8-2.25, p=0.26) or mPFS (HR=1.21, CI 0.69-2.1, p=0.51) compared to patients in the NO arm (n=51). Similarly, the two arms CA (n=21) and NC (n=89) had no difference in mOS (HR:0.96, CI 0.5-1.83, p=0.89) or mPFS (HR:1.18, CI 0.61-2.29, p=0.63) for aNSCLC.

Conclusion: Recreational cannabis use during ICI therapy increased the incidence of IRAEs. Prescription opioids and recreational cannabis use did not significantly affect survival outcomes for ICI in aNSCLC. Prescription opioid use also did not significantly influence the occurrence of IRAEs. This study suggests that recreational cannabis may need to be used with caution in this patient population due to its influence on IRAEs. On the other hand, opioids appear to be a safe option for pain management in these patients. Larger studies are warranted to shed more insight into the effect of these substances on ICI therapy.

#6294 Subclinical atherosclerosis in newly diagnosed colorectal cancer patients.

Julia A. Levy[1], Maimoona Nadri[1], Elham Kazemian[1], Katelyn M. Atkins[2], Jordan O. Gasho[2], Katrina D. Silos[2], Cody Ramin[3], Andriana P. Nikolova[4], Erin M. Siegel[5], Biljana Gigic[6], Adetunji T. Toriola[7], Jennifer Ose[8], Christopher I. Li[9], David Shibata[10], Cornelia M. Ulrich[8], Jane C. Figueiredo[1]

[1]Department of Medicine, Samuel Oschin Comprehensive Cancer Institute, Cedars-Sinai Medical Center, Los Angeles, CA,[2]Department of Radiation Oncology, Samuel Oschin Comprehensive Cancer Institute, Cedars-Sinai Medical Center, Los Angeles, CA,[3]Department of Biomedical Sciences, Samuel Oschin Comprehensive Cancer Institute, Cedars-Sinai Medical Center, Los Angeles, CA,[4]Department of Cardiology, Cedars-Sinai Medical Center, Los Angeles, CA,[5]Department of Cancer Epidemiology, Moffitt Cancer Center, Tampa, FL,[6]Department of General, Visceral and Transplantation Surgery, Heidelberg University Hospital, Heidelberg, Germany,[7]Division of Public Health Sciences, Department of Surgery, Washington University School of Medicine, St. Louis, MO,[8]Department of Population Health Sciences, Huntsman Cancer Institute, University of Utah, Salt Lake City, UT,[9]Division of Public Health Sciences, Fred Hutchinson Cancer Research Cente, Seattle, WA,[10]Department of Surgery, Washington University, St. Louis, MO

Introduction: Recent advances in early detection and treatment have improved survival rates for patients with colorectal cancer (CRC), and emerging data suggests patients may be at elevated risk of cardiovascular disease (CVD). However, there are no standard recommendations for assessing CVD risk in patients with CRC. Coronary artery calcium (CAC) is a measure of the quantity of coronary artery calcification using noninvasive scanning and has been shown to be predictive of CVD risk. This prospective cohort study utilizes CAC to evaluate the occurrence of subclinical atherosclerosis at the time of CRC diagnosis and the risk of major adverse cardiovascular events (MACE). **Methods:** The ColoCare Study is a prospective cohort study across six U.S. and European sites. Data from one of the ColoCare consortium sites in Los Angeles, California was analyzed. Adults with newly diagnosed stage I- IV colorectal cancer and available non-contrast CT scans were included. Electronic medical records were reviewed for assessment of baseline cardiovascular risk factors and adverse events. Subclinical atherosclerosis was defined as the presence of CAC (CAC>0). CAC was manually measured from routine oncologic diagnostic CT and PET-CT scans at the time of cancer diagnosis using the Agatston method. MACE was defined as hospitalization due to heart failure, cardiomyopathy, ischemic heart disease, or ischemic stroke after the diagnosis of CRC cancer. Multivariable-adjusted Cox regression was used to evaluate the association between CAC at diagnosis and the risk of MACE. **Results:** Among 109 individuals with CAC measured at the time of CRC diagnosis, 41 (37.6%) had subclinical atherosclerosis (CAC=1-399 [n=29], CAC>400 [n=12]). Individuals with CAC>0 were older (67.0 vs. 51.9 years, p<0.01), more likely to be former or current smokers (48.0 vs. 29.0 years, p=0.04), and to have hypertension (61% vs. 23%, p<0.01) compared to those without CAC (CAC=0). Among individuals with CAC (n=41), 51.2% had scores >100, and 29.2% had scores >400, indicating moderate and severe atherosclerosis respectively. Among patients with moderate or greater CAC burden (>100; statin therapy indicated), 28.6% were not on statin therapy. CAC>0 was associated with an increased incidence of MACE (13% vs. 53%, p<0.01). **Discussion:** Subclinical atherosclerosis was observed in nearly 40% of patients with CRC at diagnosis and MACE occurred in 38.2% of patients. Most patients were under-optimized for CVD risk, with nearly 30% of statin-eligible patients with at least moderate CAC burden not prescribed statin therapy. These findings highlight an opportunity for improved CVD risk mitigation in patients with CRC, including guidelines-based CVD risk factor modification.

#6295 Role of MAPK11 in the protective mechanisms against toxicity of tyrosine kinase inhibitors.

Anna Pavlovna Hnatiuk, David Staudt, Mark Mercola

Cardiovascular Institute, Stanford University, Stanford, CA

Introduction and purpose of the study: Targeted therapies with Tyrosine Kinase Inhibitors (TKIs) have drastically improved the survival of cancer patients. However, long term exposure to TKIs has been associated with severe adverse events such as heart failure, impairing patient survival and life quality, and limiting treatment options. Cardioprotective effect of MAPK11 has been described against cardiac ischemic disease. In addition, MAPK11 has also been reported as an important mediator in cancer development and progression. Therefore the aim of this study is to evaluate the potential therapeutic and dual anti-cancer and cardio-protective effect of MAPK11 inhibition during TKI treatment.

Experimental procedures: For this study we used the TKI ponatinib as a paradigm of cardiac toxicity. Ponatinib has been used as a gold standard therapy for the drug resistant type of Chronic Myeloid Leukemia (CML) due to T315I-ABL1 mutation, and has been associated with high risk of cardiac toxicity. We performed *in vitro* functional assays to evaluate the cardiotoxicity and cardiac protection using human iPSC-cardiomyocytes (hiPSC-CMs), and anti-cancer effect in T315I mutated KCL-22 CML cells. The cardiotoxicity was evaluated by impairment of cardiomyocytes contractile function during TKI (ponatinib) treatment, the cardiac-protection was evaluated by restoration of contractile function post-inhibition of MAPK11 with RNA silencing (siRNA) technique. The anti-cancer effect was evaluated using a cell viability and proliferation assay during inhibition of MAPK11 by siRNA and ABL1 inhibition as a positive control.

Summary of unpublished data: Pretreatment with siRNA MAPK11 inhibition significantly improved the contractile function of the cardiomyocytes during treatment with ponatinib when compared to those that did not receive MAPK11 inhibition. Moreover, when compared to the positive control of siRNA ABL1 inhibition, the MAPK11 inhibition showed similar anti-cancer effect in the T315I mutated KCL-22 CML cells proliferation and survival assay.

Conclusions: Our study suggests that the inhibition of MAPK11 is a potential druggable therapeutic target with dual action of anti-cancer effect for the mutant form of CML, as well as a substantial protective effect against the cardiac toxicity associated with the TKI ponatinib that could bring insights in the development of safer oncological drugs.

#6296 Biomarkers associated with atherosclerosis-related cardiovascular dysfunction in cancer survivors treated with anthracyclines.

K. W. Reding[1], A. Vasbinder[1], N. O'Connell[2], B. Demissei[3], W. Szewczyk[1], R. Cheng[1], A. Ladd[4], A. Lucas[4], J. Meyer[1], S. Bowen[1], F. Salloum[4], R. D'Agostino, Jr.[2], G. Lesser[2], K. Weaver[2], B. Ky[3], W. Tang[5], W. Hundley[4];

[1]University of Washington, Seattle, WA, [2]Wake Forest University, WInston-Salem, NC, [3]University of Pennsylvania, Philadelphia, PA, [4]Virginia Commonwealth University, Richmond, VA, [5]Cleveland Clinic, Cleveland, OH

Introduction: Cancer survival has increased in part due to treatment advances. However, anthracycline chemotherapy increases cardiovascular (CV) morbidity risk, including atherosclerotic CV disease (ASCVD). Among those receiving anthracyclines, it is yet unclear who is at greatest risk of ASCVD, a major cause of CV mortality. Elucidating pathophysiologic processes involved in the development ASCVD could shed light on strategies to identify those at risk.
Methods: Analyses were performed on 279 lymphoma and breast cancer survivors enrolled in the PREVENT study [clinical trial WF-98213) through Wake Forest NCI Community Oncology Research Base (NCORP) and Alliance (A221501)]. CV dysfunction was measured via cardiac MRI (cMRI) at baseline (pre-treatment) and 6-months post-diagnosis to ascertain aortic distensibility and wall thickness in the descending aorta. Biomarkers were measured at baseline and 6-months and were log-transformed to base 2. Multiple linear regression was used to determine associations between biomarker and outcome at 6 months, adjusted for baseline biomarker and cMRI outcome, age, race, sex, body mass index, and smoking history.
Results: The mean age (SD) of cancer survivors 49 (12) years; 92% were women. The mean aortic distensibility and mean wall thickness at baseline was 0.002 (0.0014) and 2.99 (0.41), respectively. Table 1 shows the associations between biomarkers and aortic distensibility and wall thickness of the descending aorta. After adjustment for confounders, Arginine, CRP, MPO, and ornithine were associated with 6-month aortic distensibility, and the HDL and SDMA were associated with aortic wall thickness.
Conclusions: The findings of this study suggest that biomarkers in oxidative stress and inflammatory pathways may be involved in pathophysiology of ASCVD among cancer survivors receiving anthracyclines. These results require further study in larger cohorts to better define mechanistic pathways involved.

Association of Biomarkers with Atherosclerosis-Related Cardiovascular Dysfunction

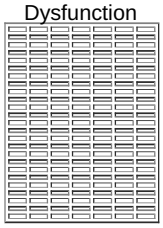

#6297 “They should get a cardiologist to be a part of the team when you first go”: A qualitative analysis of racial differences in the cancer care experience amongst breast cancer patients receiving cardiotoxic therapy.

A. Turner[1], A. Vijil[1], S. Gomez-Trillos[2], V. Williams[1], P. Omeaku[3], S. Hong[4], A. L. Sutton[1];
[1]Virginia Commonwealth University, Richmond, VA, [2]Lombardi Comprehensive Cancer Center, Washington D.C., DC, [3]Virginia Commonwealth University School of Population Health, Richmond, VA, [4]Massey Comprehensive Cancer Center, Richmond, VA

Background: Black breast cancer survivors are up to three times more likely to develop cancer therapy-related cardiac dysfunction (CTRCD) when compared to White survivors. Reasons behind this disparity are not fully understood, and studies examining these disparities have been limited. One contributor may be variations in communications about CTRCD risk and risk prevention strategies between providers and patients by race and ethnicity. This study assessed racial differences in Black versus White breast cancer patients with provider communication regarding cardiotoxic treatments.
Methods: Study participants were recruited from a comprehensive cancer center. Eligibility included identifying as a Black/African American or White woman, a diagnosis of stage I-III breast cancer, and receipt of anthracyclines and/or trastuzumab. Semi-structured interviews were conducted with survivors. Interviews were audio-recorded, transcribed, and were reconciled using Dedoose.
Results: Interviews were conducted with 16 survivors (8 Black, 8 White) with a median age at diagnosis of 53 years. Prior to starting treatment, 100% of white survivors reported that a provider discussed CTRCD risk, however only 75% black survivors reported CTRCD discussion. Although all women received information on prevention strategies including exercise and nutrition, there were differences in timing of information delivered. Black women desired to have information at the beginning of treatment, but no White women mentioned a desire to receive information earlier. A greater proportion of White women reported engaging in prevention strategies such as exercising and eating healthy during treatment. In terms of knowledge gained, 75% of White Women reported being satisfied with the information given regarding cardiotoxic risk and prevention whereas only 45% of Black women reported being satisfied.As 65% of Black women (vs. White) reported being less than satisfied with the information given, Black women were also more likely to recommend access to additional resources. For example, one Black woman suggested that “they [care team] should get a cardiologist to be a part of the team when they first go.
Conclusion & Implications: Fewer Black women reported being satisfied with their medical visits regarding CTRCD risk and prevention strategies. Racial differences in assessments of these experiences highlight opportunities to develop culturally-tailored communication interventions to reduce racial disparities in CTRCD; however, future research is needed to assess interpersonal aspects of care during the receipt of cardiotoxic treatment.

#6298 The value of routine trastuzumab-related cardiac toxicity monitoring in gastrointestinal cancers.

S. R. Kosydar, M. Castrichini, M. Zhu, H. Xie;
Mayo Clinic, Rochester, MN

Background: It is a common practice to monitor trastuzumab-related cardiac toxicity (TRCT) using left ventricular ejection fraction (LVEF) in patients who receive trastuzumab-containing therapy for human epidermal growth factor receptor 2 (HER2)-positive cancers. However, this monitoring approach does not appear cost effective in patients with HER2-positive gastrointestinal (GI) cancers given poor overall survival (OS). Here, we aim to examine the incidence of clinically significant TRCT in this target population.

Methods: This is a retrospective cohort study of patients with advanced HER2-positive GI cancers who received trastuzumab-containing therapies (trastuzumab +/- pertuzumab, chemotherapy +/- immunotherapy + trastuzumab, trastuzumab deruxtecan) between 2011 and 2023. HER2 status was determined by immunohistochemistry, fluorescent in situ hybridization, and/or next generation sequencing. LVEF was estimated by serial transthoracic echocardiograms (TTE). Continuous variables were summarized as median and interquartile range (IQR). Paired Wilcoxon signed rank test was used to compare serial LVEF. OS was estimated using Kaplan-Meier method.

Results: A total of 243 patients were included in this study with a median age of 64 (IQR: 55-70) years. 139 (57%) patients had esophageal or GEJ adenocarcinoma; 45 (19%) patients had gastric cancer; 37 (15%) patients had colorectal cancer; and the rest had other GI cancers. Median follow-up time was 18.6 (IQR: 9.2-36) months. Median OS from cancer diagnosis and the first dose of trastuzumab-containing therapy were 24.1 (95%CI: 20.2-30.2) and 11.7 (95%CI: 10.4-15.6) months, respectively. Patients received a median of 13 cycles of trastuzumab-containing therapy for a median duration of 4.1 (IQR: 1.4-10.1) months. The median number of TTE each patient had throughout therapy was 2 (IQR: 1-4). Median baseline LVEF was 61% (IQR: 56-65%) which was significantly higher ($p<0.001$) than the median lowest LVEF of 58% (IQR: 53-62%) during therapy, but not different ($p=0.14$) from the most recent median LVEF of 60% (IQR: 56-64%) after discontinuation of trastuzumab. Among 176 patients with serial LVEF data, 16 (9%) had > 10% LVEF drop; 7 (44%) of these 16 patients had LVEF recovery. None of the cardiovascular risk factors prior to trastuzumab treatment including hypertension, diabetes, hyperlipidemia, peripheral arterial disease, coronary artery disease, and stroke were significantly associated with the development of TRCT.

Conclusion: The incidence of clinically significant LVEF drop appears low in patients with advanced GI cancers as post-treatment LVEF recovery to baseline was observed at the population level. The value of using TTE to monitor TRCT in these patients with short OS should be further assessed in the perspective of cost effectiveness.

#6299 Psychometric evaluation of the FACIT-SP 12 in a primary brain tumor patient population.

E. Vera, B. Ozer, A. Acquaye-Mallory, V. Pillai, A. Choi, E. Grajkowska, T. Kunst, H. Miller, K. Reinhart, T. S. Armstrong, M. Stockdill;
National Cancer Institute, Bethesda, MD

Spirituality is a social determinant of health associated with psychosocial adjustment to serious illnesses including cancer but is not often assessed in clinical care. Here we perform psychometric evaluation of a tool developed to report spiritual well-being in chronic illness in a cohort of 248 patients with primary brain tumors (PBT) enrolled in a natural history study (NCT02851706, PI: T. Armstrong). Participants completed the Functional Assessment of Chronic Illness Therapy-Spiritual Well-Being 12 (FACIT-SP 12) as part of yearly clinical outcome assessments. Total score, Meaning/Peace and Faith scores were calculated. Internal consistency (Cronbach's alpha) and construct validity (principal components analysis with varimax rotation) evaluated psychometric properties of the FACIT-SP 12; one-way ANOVAs, one-sample t-test and Wilcoxon signed rank tests evaluated group differences (sig. $p<0.05$) on patient report of spirituality/beliefs including belief in god(s)/higher power, being religious, and prayer and in comparison to scores of previously reported studies. Participants were majority male (57%), white (79%) with high grade tumor (59%) and a median age of 48 (range: 20-82). Seven different religions were reported (majority Christianity [55%]) but also spiritual non-religious (9%), no beliefs (13%), and 6% preferring not to answer. The principal components analysis confirmed the original 2 factor solution (Meaning/Peace and Faith) and explained 66.8% of the variance (KMO =0.87, 43% of residuals < 0.05), with one item not loading cleanly on either factor ("I know that whatever happens with my illness, things will be okay"). Cronbach's alphas were 0.90, 0.90, and 0.89, for the total, Meaning/Peace, and Faith scales, respectively. For all three spiritual/belief questions, patients who responded "yes" had higher total and faith scores than those who responded "no"; but not in the Meaning/Peace score when reporting religion ($p=0.108$). This cohort reported lower total scores (mean=32.5), Meaning/Peace scores (mean=23.4, median=24.0) and Faith scores (mean=9.2, median=10.0) compared to the initial validation in other solid tumors and HIV/AIDs (means=38.5, 25.2, 13.6, respectively) and to a smaller, less diverse PBT sample (medians: Meaning/Peace=25.8, Faith=14.0). The FACIT-SP 12 demonstrated internal consistency and construct validity, with lower scores in comparison to populations in prior studies. More diverse belief systems than previously reported may contribute to differences among studies. Future analysis should explore the increased percentage of "prefer not to answer" respondents compared to earlier reports, associations with clinical and self-reported outcomes including symptoms and quality of life, evaluation of illness-related factors that contribute to poor spiritual well-being, and a longitudinal look at spiritual well-being.

#6300 Associations of biological aging with perceived stress in patients with head and neck cancer: A longitudinal study.

Y. Lin, T. Spikes, D. Bruner, S. Paul, A. Miller, K. Conneely, N. Saba, C. Xiao;
Emory University, Atlanta, GA

Introduction: Biological aging leads to an increased risk of morbidity and mortality in patients with head and neck cancer (HNC) undergoing intensity-modulated radiotherapy (IMRT). This progression can be exacerbated by the burden of stress arising from HNC and IMRT. While stress has been linked to inflammation, the associations of biological aging measures including inflammatory markers and epigenetic age acceleration (EAA) with stress over cancer treatment remain underexplored. The purpose of this study was to examine the associations between biological aging and stress in patients with HNC receiving IMRT across four time points (i.e., pre- (T1), end of (T2), 3 months (T3), and 12 months (T4) post-IMRT).

Methods: We conducted a prospective longitudinal study. Stress was assessed using the Perceived Stress Scale (PSS) across four time points along with the assessment of biological aging markers: peripheral inflammatory markers (i.e., interleukin [IL-6], IL-1β, IL-10, IL-1ra, C-reactive protein [CRP], soluble tumor necrosis factor receptor 2 [sTNFR2], and TNF-α) and EAA. EAA was calculated using DNAmPhenoAge, adjusted for chronological age. Liner mixed effects models were used to examine the associations between biological aging measures and stress across time.

Results: A total of 176 patients with HNC were enrolled in the study with a mean age of 59.9±10.0 years, 72.7% male, and 77.3% non-Hispanic White. Stress scores increased from T1 to T2 (p<0.001), decreased significantly at T3 (p<0.001) which were lower than the baseline scores (T1), and then gradually decreased at T4 (p=0.029). Significant associations of CRP, IL- 1ra, and TNFR-2 with stress were identified across time (all p values <0.05), controlling for covariates (i.e., age, human papillomavirus status, chemotherapy, and surgery): elevated inflammatory markers were associated with higher levels of stress. In a separate model, higher stress scores were also associated with increased EAA controlling for the same covariates (p=0.015): an increment of 10 units in stress scores was associated with an age acceleration of 7.2 months across time.

Conclusions: Findings from our study suggest that biological aging measures (inflammatory markers and EAA) are associated with stress across time in patients with HNC receiving IMRT. Clinicians and researchers may use the findings to develop personalized psychosocial interventions that reduce stress so as to deaccelerate biological aging for patients with HNC during their treatment and survivorship.

#6301 Mapping survivor-specific supportive care resources: A digital landscape analysis of NCI-designated cancer centers.

A. Taylor, K. Sterba, E. Graboyes;
The Medical University of South Carolina (MUSC), Charleston, SC

Background: Optimal care for cancer survivors requires a comprehensive array of supportive care services to address the multitude of physical, psychological, social, financial, and health promotion needs of this population. To understand options to address their unique needs, survivors and their caregivers may seek information from online sources. Although National Cancer Institute-Designated Cancer Centers (NCIDCCs) serve as leaders in cancer treatment and care delivery, as well as credible sources for survivors to receive information on their recovery, no study has characterized the digital landscape of survivorship offerings on their website. This study aims to characterize the supportive care services offered to cancer survivors on NCIDCCs.
Methods: Of the 72 NCIDCCs, 65 provide clinical care. We reviewed the webpage of each to identify supportive care offerings. Services were categorized based on the four domains of the quality-of-life model: (1) physical well-being, (2) psychological well-being, (3) social well-being, and (4) spiritual well-being. Supportive care services were classified as survivor-specific if the online description included information that specifically catered to cancer survivors.
Results: Of the 65 clinical NCIDCC websites, 100% offer supportive care services and 54% offer supportive care services specific to survivors (**Table**). The most common supportive care service offered was nutrition (90.6%) and the least commonly offered was caregiver support (7.9%). Behavioral medicine was offered most frequently for survivors (28.3%) and caregiver support was offered the least (0%). Out of the four domains of the quality-of-life model, spiritual well-being services were offered the least at NCIDCCs.
Conclusion: More than half of the NCIDCC websites provided survivor-specific supportive care services.

Supportive care services on websites of NCI-Designated or Comprehensive Cancer Centers (N = 65)

	Supportive Care Service (*n*)	**%**	**Supportive Care Service Specific to Cancer Survivors (*n*)**	**%**
Physical Well Being Services				
Nutrition	58	90.6	14	24.1
Genetics	53	82.8	5	9.4
Pain and Palliative Care	52	81.3	8	15.4
Complementary and Alternative Medicine	49	75.4	6	12.2
Integrative Medicine	47	73.4	9	19.1
Occupational Therapy	45	70.3	6	13.3
Fertility Preservation	43	66.2	6	14
Tobacco Cessation	38	58.5	6	15.8
Speech	36	56.3	3	8.3
Exercise	29	45.3	5	17.2
Primary Care	6	9.2	3	50
Psychological Well-Being Services				
Behavioral Medicine	53	81.5	15	28.3
Recreational Therapy	36	58.1	5	13.9
Social Well-Being Services				
Oncology Social Work	56	87.5	5	8.9
Patient Navigation	33	51.6	3	9.1
Financial Counseling	32	50	4	12.5
Self-Image	27	41.5	3	11.1
Reproductive and Sexual Health	22	33.8	5	22.7
Caregiver Support	5	7.9	0	0
Spiritual Well-Being Services				
Pastoral Services	49	75.4	5	10.2

#6303 Innovative strategies for managing chemotherapy-induced alopecia: Scalp cooling.

S. I. Gaumond[1], R. Abdin[2], R. O. McPhillips[1], L. M. Ferrari[1], S. Mufarrej[1], J. J. Jimenez[1];
[1]University of Miami Miller School of Medicine, Miami, FL, [2]Florida Atlantic University, Boca Raton, FL

Chemotherapy-Induced Alopecia (CIA) is a visibly distressing consequence of chemotherapy. Although it does not pose a life-threatening risk, CIA can significantly affect patient's self-esteem. Regarding the mechanism of action, stress induced by chemotherapy treatment can lead to the shedding of hair follicles, generating varying degrees of hair loss. In recent years, scalp cooling has emerged as a beneficial preventative agent for CIA due to its ability to induce vasoconstriction in the scalp and reduce follicular metabolic rate. To assess the efficacy of scalp cooling in preventing CIA, we conducted a review of randomized control trials published on PubMed in the last 10 years. Five studies met our inclusion criteria, in which three examined hair preservation and two evaluated treatment duration efficacy. All studies investigating hair preservation with scalp cooling reported highly significant results from the cooling device when compared to a placebo (56.3% vs. 0%, 39.3% vs. 0%, and 50.5% vs. 0%, respectively). Additionally, one of these studies also assessed hair regrowth, revealing higher rates in the scalp cooling group compared to the control at 6 weeks (89% vs. 12%) and at 12 weeks (100% vs. 59%). Both studies evaluating the effectiveness of scalp cooling based on treatment duration concluded that 20 minutes of cooling was as effective as 45 and 90 minutes in preventing CIA. Collectively, these findings add to the mounting evidence endorsing scalp cooling as a powerful management strategy in averting CIA.

#6304 Seizure self-report and monitoring: Agreement between patient and clinician report and implications for care in patients with IDH-mutant and IDH-wild type gliomas.

H. Miller[1], E. Grajkowska[1], A. Acquaye-Mallory[1], A. Choi[1], J. Reyes[1], M. R. Gilbert[1], E. K. Avila[2], T. S. Armstrong[1], E. Vera[1];
[1]National Cancer Institute, Bethesda, MD, [2]Memorial Sloan Kettering Cancer Center, New York, NY

Primary brain tumor (PBT) patients commonly experience seizures, which can be measured and monitored by a variety of tools. Here, we explore the concordance between 2 tools and their use in reporting seizures over time among PBT patients enrolled in a natural history study (NCT02851706, PI: T. Armstrong). Patients complete the M.D. Anderson Symptom Inventory - Brain Tumor (MDASI-BT), which measures symptom severity (including seizure) within the last 24 hours from 0-10; and, as part of the same visit, pairs of clinicians and patients complete the Seizure Control Composite Index (RANO-SCCI), which includes the questions 'Have you ever had a seizure' (RANO-SCCIQ1) and 'Have you had a seizure since your last clinic visit' (RANO-SCCIQ2). Responses to each measure are reported in aggregate and by IDH status. Participants included 89 patients with gliomas who were primarily white (84%) males (62%) with a median age of 48 years (range: 27-78) and KPS ≥ 90 (85%). Based on patient reports, 65% endorsed ever having a seizure (RANO-SCCIQ1), 17% had a recent seizure (RANO-SCCIQ2), and 12% had a seizure within the last 24 hours (MDASI-BT). For the RANO-SCCIQ1 data, patients and clinicians generally agreed except for 6 pairs (7%) where clinicians indicated a seizure but patients did not. Of the 59 who reported recent seizures (RANO-SCCIQ2), two pairs (3%) disagreed, with patients indicating a recent seizure but clinicians not endorsing a seizure had occurred. Good overall agreement (86%) was observed between the RANO-SCCIQ2 and MDASI-BT for both clinician and patient responses, with 3 and 2 paired disagreements respectively, in which seizures were indicated in the last 24 hours but not recorded as a recent seizure on the (RANO-SCCIQ2). Comparing clinician report of seizures in those with IDH-mutated (n=39) to IDH-wildtype (n=15) tumors, 85% (33/39) versus 47% (7/15) reported ever having a seizure and 7 of 33 (21%) with IDH-mutant and 1 of 7 (14%) with IDH-wild type (IDH-WT) tumors respectively reported a seizure since the last visit. Disparities in recognition of seizures between patient and clinician highlights a need for patient education to increase awareness of events and recognition of ongoing risk. Although those with IDH-mutated tumors are at higher risk of having seizures, nearly half of those with IDH-WT reported ever having seizures, underscoring the need for all patients to be educated on recognizing and assessing seizure symptoms.

#6305 Evaluating clinical and sociodemographic risk for symptom-related functional interference in the primary brain tumor population.

B. A. McIver, T. S. Davis, K. Reinhart, E. Vera, A. Choi, T. Kunst, M. Johnson, E. Grajkowska, H. Miller, T. S. Armstrong, M. L. Wright;
National Cancer Inst. - Bethesda Campus, Bethesda, MD

Purpose: Primary brain tumors have a high propensity for causing physical and activity-related disabilities due to the location within the brain and use of targeted treatments resulting in significant symptom burden. In other cancers, physical function impacts mood, quality of life, and even mortality. This exploratory study aims to identify factors associated with activity-related functional interference in a cross-sectional cohort of 584 primary brain tumor patients enrolled in a natural history study (NCT03251989, PI: T.S. Armstrong).

Methods: Sociodemographic (age, race, ethnicity, income, education, employment, body mass index [BMI]) and disease-related clinical data were collected at study entry. Activity-related interference (work, walking, and general activity) and health status were reported via the MD Anderson Symptom Inventory-Brain Tumor. Activity-related interference means ≥ 2 were categorized as moderate/severe. Logistic regression assessed univariate associations with moderate/severe interference, with sig. <0.05.

Results: This sample had a median age of 49 years (range 18-85), and was mostly male (57%), with a high-grade tumor (grade 3/4) (74%), glioblastoma (39%), on active treatment (21%) and prior tumor recurrence (49%). Risk factors for moderate/severe activity-related interference included: ≥ 2 surgeries (OR = 1.55, 95% CI [1.11, 2.18], $P = 0.011$), ≥ 2 radiation treatments (OR = 2.87, 95% CI [1.59, 5.17], $P < 0.001$), currently on active treatment (OR = 1.47, 95% CI [0.97, 2.22], $P = 0.066$), disease progression (OR = 1.87, 95% CI [1.24, 2.84], $P = 0.003$), prior recurrence (OR = 1.57, 95% CI [1.13, 2.19], $P = 0.007$), and poor KPS (OR = 3.61, 95% CI [2.55, 5.12], $P < 0.001$), but not tumor grade (OR = 1.05, 95% CI [0.72, 1.54], $P = 0.790$). Sociodemographic risk factors for moderate/severe activity-related interference included: less than a high school education (OR = 2.03, 95% CI [1.18, 3.51], $P = 0.011$), on disability (OR = 3.20, 95% CI [1.79, 5.71], $P < 0.001$), or unemployed (OR = 3.81, 95% CI [2.34, 6.19], $P < 0.001$), an annual income less than $49,999 (OR = 2.62, 95% CI [1.28, 5.35], $P = 0.008$), or childhood in a rural area (OR = 1.87, 95% CI [1.24, 2.84], $P = 0.003$), but not BMI, smoking status, or past physical activity in the 10 years prior to report.

Conclusion: As expected, activity-related interference is associated with disease and treatment associated clinical characteristics, with significant risk derived from sociodemographic factors such as education, childhood environment, employment, and household income. Future studies should further explore these associations longitudinally to identify individuals at the highest risk of activity-related interference due to their brain tumor as well as interventions designed for those who may be socioeconomically disadvantaged.

CLINICAL RESEARCH: Adoptive Cellular Therapy 2
Poster Session

#6311 From bench to bedside: GMP manufacturing and testing of an LGR5-targeting CAR-T against colorectal cancer.

V. Bandara[1], B. Gundsambuu[1], S. Napoli[1], J. Foeng[1], D. McPeake[1], T. Tylis[1], E. Thompson[2], S. Mills[3], A. Cowin[3], C. Bonder[2], T. Sadlon[1], S. McColl[4], S. Barry[1];

[1]University of Adelaide, North Adelaide, Australia, [2]University of South Australia, Adelaide, Australia, [3]University of South Australia, Mawson Lakes, Australia, [4]Carina Biotech, Mawson Lakes, Australia

Colorectal cancer is the third most diagnosed cancer worldwide, and is responsible for the second largest number of cancer related deaths, warranting the need for new treatments. The successful use of chimeric antigen receptor T (CAR-T) cells against B-cell malignancies has inspired the search for CAR-T cell therapies against solid tumours such as colorectal cancer. Cancer stem cells (CSC) are a small population of cells within a tumour with the capacity to self-renew, differentiate, and initiate new tumours. CSC are resistant to chemotherapy and radiotherapy and are enriched in residual disease. Targeting CSC is a strategy to reduce the tumours' ability to generate new cells. Leucine-rich G protein-coupled receptor 5 (LGR5) is a marker of CSC and LGR5^{+} cancer cells are implicated in tumour progression and metastasis in colorectal cancer. We designed and tested a chimeric antigen receptor (CAR) targeting the extracellular domain of LGR5. LGR5-targeting CAR-T cells showed significant antigen-specific cytotoxicity and IFNγ release against colorectal cancer (CRC) cell lines *in vitro,* and *in vivo* efficacy in a CRC xenograft mouse model. We confirmed the specificity and safety of the LGR5 targeting CAR-T cells by testing against normal human tissues. A GMP ready protocol for clinical scale manufacture of LGR5-targeting CAR-T cells have been developed using CD3+ T-cells from healthy donors. We have successfully tested this protocol using CRC patient-derived CD3+ T-cells and were able to generate clinically relevant cell numbers (80-fold expansion) with high CAR expression. Cells manufactured using this GMP protocol expressed markers of self-renewing naïve-like and central memory phenotype and showed very low percentage of cells that were triple-positive for PD1, TIM3 and LAG3. This protocol has been successfully tested and validated in a GMP manufacturing facility for the production of LGR5 targeting CAR-T cells, in preparation for an FDA approved first in man clinical trial against metastatic colorectal cancer, starting in 2023 (NCT05759728).

#6312 Orthogonal IL-2/IL-2Rβ signaling selectively enhances and sustains a synthetic effector state via a novel mechanism and outperforms constitutive armoring approaches.

Ethan Jung, Helena Silva, Marie Semana, Ivan Cheng, Somya Singh, Michele Bauer, Mohammed Ali, Henry Rosas, Ryan Burgess, George Zeng, Woei Chang, Navneet Ratti, Deepti Rokkam, Patrick J. Lupardus, Martin Oft, **Paul-Joseph Aspuria**

Synthekine, Menlo Park, CA

CAR T cell therapy has demonstrated remarkable clinical efficacy against blood malignancies. However, prominent barriers, including limited proliferation, CAR T cell persistence, and poor T cell effector function, hinder its potential, especially in solid tumors. Various engineering approaches attempt to address these issues by armoring CAR T cells with factors that enhance the function and maintenance of T cells in the anti-tumor response. We previously described a human orthogonal IL-2/IL-2R system consisting of a pegylated, IL-2 mutein (STK- 009) that does not significantly activate the wild type receptor and a mutated IL-2 Receptor Beta (oRβ) that does not significantly respond to its native ligand, wild type IL-2. This system provides a “private IL-2 signal” in engineered oRβ-expressing cells while avoiding signaling in bystander immune cells, reducing toxicities. We have demonstrated STK-009/oRβ’s ability to selectively expand oRβ-expressing CAR T cells (SYNCAR T cells) targeting heme (SYNCAR-001, CD19) and solid tumor (SYNCAR-002, GPC3) targets at will. Importantly, the system enhanced anti-tumor control driving deep and durable responses in both bulky lymphoma and hepatocellular carcinoma (HCC) tumor models. Additionally, in a non-human primate model, STK-009 did not potentiate wild type T or NK cells and exhibited no evidence of toxicity. Currently, the combination of STK-009 + SYNCAR-001 is undergoing Phase I clinical trials (NCT05665062).

Here, we conducted a direct comparison of several armoring approaches including the SYNCAR platform, the overexpression of c-Jun, an IL-15/IL-15Rα fusion, and IL-18 in human CAR T cells targeting GPC3. To assess their effects in overcoming CAR T cell dysfunction, cells were subjected to continuous antigen exposure *in vitro*. STK-009 treated SYNCAR-002 T cells displayed an enhanced proliferative capacity, sustained effector cytokine secretion, and an increased activation state when compared to other armoring technologies and PBS treatment. In a HCC tumor model, treatment with STK-009/SYNCAR-002 demonstrated superior tumor control with minimal toxicities. Interestingly, IL-18 overexpression also controlled tumors, but was accompanied by uncontrolled CAR T cell expansion and toxicity resembling severe GVHD.

scRNAseq analyses revealed STK-009-treated SYNCAR-002 T cells simultaneously activated effector genes and repressed an exhaustion gene signature. This analysis also identified a novel mechanism by which STK-009/oRβ signaling induces a superior synthetic effector state via transcriptional repression of the stress response/proteosome.

These findings support the advantages of an orthogonal platform that selectively drives and sustains potent T cell effector function without safety concerns associated with constitutively expressed armored approaches.

#6313 Enhancing CAR T cell-based immunotherapy outcomes in PDAC: Evaluating iC9.B7-H3 CAR T cells in adjuvant, neoadjuvant, and monotherapy settings.

S. Arya[1], S. Sanatkar[1], M. Ventin[1], G. Cattaneo[1], C. Martin[1], G. Lionetto[1], J. Jia[1], F. Chen[1], D. Ting[1], X. Wang[1], S. Ryeom[2], C. Ferrone[3], S. Ferrone[1];
[1]Massachusetts General Hospital, Boston, MA, [2]Columbia University Irving Medical Center, New York, NY, [3]Cedars-Sinai Medical Center, Los Angeles, CA

Background: Pancreatic ductal adenocarcinoma (PDAC) is among the most aggressive and lethal cancers worldwide. Despite negative margin resections and subsequent systemic therapy, PDAC often recurs. Additionally, most patients present with locally advanced and unresectable tumors at the time of diagnosis. Cancer-associated fibroblasts (CAFs) contribute to the highly desmoplastic tumor microenvironment (TME) and form a biophysical barrier, limiting immune cell infiltration. Moreover, CAF-secreted factors suppress the anti-tumor activity of T cells and shift cancer cells toward invasive proliferative and mesenchymal phenotypes. Therefore, targeting CAFs can enhance T-cell infiltration and improve the efficacy of T-cell based immunotherapeutic strategies. B7-H3 is an immune checkpoint molecule highly expressed on PDAC cells and CAFs. In this study, we investigate the use of Chimeric Antigen Receptor (CAR) T cells targeting B7-H3 to eliminate metastatic PDAC in a preclinical mouse model in three different settings: I. Adjuvant II. Neoadjuvant III. CAR T cell monotherapy. Our CART-B7-H3 construct includes an inducible caspase 9 (iC9) suicide gene, which allows for the controlled elimination of the CAR T cells in the event of overwhelming cytokine release syndrome.

Methods: To validate the therapeutic potential of iC9.B7-H3 CAR T cells *in vivo*, NSG mice were orthotopically engrafted with $1x10^5$ patient-derived PDAC6 cells and $9x10^5$ hCAF1 cells at a ratio of 1:9, reflecting a clinically relevant model. In the adjuvant group, mice underwent surgical resection of the primary tumor (distal pancreatectomy and splenectomy) after 25 days. On days 30 and 60, they received systemic iC9.B7-H3 CAR T cell treatment ($5x10^6$). In the neoadjuvant group, mice were systemically treated with iC9.B7-H3 CAR T cells on day 19 and underwent surgical resection of the primary tumor on day 25, following another systemic CAR T cell dose on day 60. In the CAR T monotherapy group, mice received systemic iC9.B7-H3 CAR T cells on days 19 and 60.

Results: *In vivo*, iC9.B7-H3 CAR T cells in the neoadjuvant group effectively eradicated both local and distant PDAC metastases for the length of the experiment (180 days) and significantly increased the survival ($P=0.0018$), indicating long-term efficacy in the treatment of PDAC metastases with no adverse side effects. In the adjuvant and CAR T monotherapy groups, iC9.B7-H3 CAR T cells effectively control tumor growth, eliminate metastases, and significantly increase survival ($P<0.0001$ and $P=0.0007$, respectively).

Conclusion: These data suggest that the neoadjuvant application of iC9.B7-H3 CAR T cells may demonstrate persistent efficacy in eradicating both local and distant PDAC metastases. iC9.B7-H3 CAR T cells adjuvantly and as monotherapy achieved significant tumor control.

#6314 Potent inhibition of tumor relapse after anti-HER2 affibody tagged with cotinine (switch) plus anti-cotinine switchable CAR T cell therapy by repeated re-injection of the switch.

K. Kim[1], S. Kim[1], E.-H. Lee[1], S.-Y. Lim[1], S. Kim[1], E.-Y. Kim[1], H.-J. Lee[1], S. Kim[1], M. Yoon[1], Y.-H. Lee[1], I.-S. Hwang[1], Y. Lee[1], J.-H. Kim[1], J.-S. Lee[1], **J. Chung**[2];

[1]AbClon, Inc., Seoul, Korea, Republic of, [2]Cancer Research Institute, Seoul National University College of Medicine, Seoul, Korea, Republic of

Chimeric antigen receptor (CAR) T cells targeting CD19 or the B cell maturation antigen (BCMA) have demonstrated impressive initial clinical responses. However, on follow-up assessment, a notable fraction of the patients with significant initial clinical response eventually experienced relapse. CAR T cell therapies targeting solid tumors have shown an even lower rate of clinical response as well as shorter remission periods. A prior study has shown that re-injection of the anti-HER2 CAR T cells was effective in a rhabdomyosarcoma relapse patient (Cancer Res 79, LB147 (2019)), but the repeated production of CAR T cells is costly, thus raising questions about its feasibility in practice. Previously, we developed a cotinine-based CAR T cell system (zCART) comprised of a tumor antigen-specific affibody conjugated with cotinine and an anti-cotinine scFv CAR, and demonstrated the anti-tumor activity of an anti-HER2 zCART treatment in both *in vitro* and *in vivo* settings. In this study, we tested the efficacy of anti-HER2 zCART treatment *in vivo* using an intraperitoneal (IP) tumor model with a single infusion of zCART cells. The anti-HER2 switch was injected daily for 7 days. When the HER2 positive tumor relapsed, the mice were re-treated with the same dose of anti-HER2 switch treatment for an additional 7 days. We observed that re-injection of only the anti-HER2 switch and not combined with zCART cells effectively and potently inhibited relapse of HER2 positive tumors. Furthermore, the efficacy of the anti-HER2 switch re-injection treatment was maintained in one additional relapse. In summary, the zCART system has potential to treat cancer relapse following CAR T cell therapy without the need for an additional production round of CAR T cells.

#6316 Exploring the resistant mechanism of CAR T cell therapy targeting CLDN18.2 by single-cell sequencing.

Mingyang Ma[1], Changsong Qi[1], Chang Liu[1], Lei Jiang[1], Min Tao[1], Dan Liu[1], Panpan Zhang[1], Zhi Peng[1], Xiaotian Zhang[1], Jifang Gong[1], Yang Chen[1], Chunhong Zheng[2], Mi Deng[2], Lin Shen[1]

[1]Peking University Cancer Hospital, Bei Jing, China,[2]Peking University International Cancer Institute, Bei Jing, China

Chimeric antigen receptor T cell (CAR T) therapy has achieved remarkable success in treating hematological malignancies but still faces overwhelming challenges for solid tumors. Our previous clinical trial (NCT03874897) has demonstrated promising results in patients with advanced CLDN18.2-positive gastric after receiving CT041 CAR T cell product. Though the disease control rate (DCR) reached 73% in 37 patients, it was unclear who would benefit from this therapy. Here in this study, we dynamically collected peripheral blood and ascites samples from 5 patients in this clinical trial before and at 3 and 7 days after the infusion of CT041, respectively. Utilizing single-cell sequencing analysis, we found that patients with a high proportion of naive-like T cells were more likely to benefit from CT041. Furthermore, we discovered that the high expression of CLDN18 in the ascites epithelial cells was correlated with a favorable prognosis, while ascites epithelial cells showing high MYC expression and the strong interaction between tumor cells and T cells were identified as adverse prognostic factors for CT041 treatment. These findings may provide theoretical evidence for subsequent screening of CAR T cell therapy benefitable population and improving the efficacy of CAR T cell therapy.

#6317 Developing a fully human heavy chain only Claudin-18.2-specific CAR-T cell therapy.

Jason Noon, Yao Lu, Itishree Kaushik, Oyku Ay, Adam Luk, Bradley Delaney, David DeMeritt, **Musheng Bao**

NONA BIOSCIENCES, Natick, MA

Camelid VHH/nanobodies have been widely applied as the antigen binding domain of CAR-T cell therapies due to a smaller size and simpler structure compared to the traditionally used single chain variable fragment (scFv). Additionally, camelid VHH/nanobodies provide greater flexibility for dual-targeting CAR-T cell therapies. However, camelid VHH/nanobodies require laborious and costly humanization and still have a significant risk of inducing anti-drug antibodies when administered to patients. Transgenic mice exclusively harboring the most stable human VH genes (HCAb Harbour Mice®) provide one of the best solutions to get fully human heavy chain only antibodies (HCAbs). To efficiently identify lead HCAb VHs for Claudin-18.2-targeting CAR-T cells, we developed an innovative direct CAR-function based HCAb library screening platform. From Claudin-18.2-immunized HCAb Harbour Mice®, we constructed a total VH library in a CAR lentiviral vector that we developed in-house. After producing the lentiviral particle library, we transduced a Jurkat-NFAT-GFP reporter cell line and stimulated with Claudin-18.2 overexpression cell line. Subsequently, GFP positive reporter cells, representing Claudin-18.2-specific CARs, were isolated through FACS sorting, expanded, and further stimulated with Claudin-18.2-positive NUGC-4 tumor cells. Then, Next Generation Sequencing and abundance ranking was performed on VHs recovered from sorted CAR-reporter cells. Lead VH candidates were cloned into the CAR-P2A-RFP lentiviral vector, and many of these VH clones exhibited superior Claudin-18.2-specific functionality compared to a clinically-validated reference scFv in both reporter and primary CAR-T cells. Many lead VH clones also exhibited excellent developability as soluble HCAbs. These data suggest that this innovative method of combining our fully human HCAb and CAR-based library screening platform will provide new avenues for CAR-T cell therapies.

#6318 Development of an anti-PD-L1 CAR T therapeutic treating advanced gastric cancer with enhanced efficacy and lower off-tumor activities.

M. Baek[1], J.-I. Yu[1], E.-J. Choi[1], Y. Lim[1], J. Yang[1], S.-R. Choi[1], Y. Choi[2], M. Kim[1], J. H. Rhee[1], J.-J. Lee[1];

[1]Vaxcell-Bio Therapeutics, Hwasun-eup, Jeollanamdo, Korea, Republic of, [2]Chonnam National University Medical School, Hwasun-eup, Jeollanamdo, Korea, Republic of

Purpose: Driven by a relentless unmet need with unsatisfied cancer therapy, we aimed to develop chimeric antigen receptor T-cell (CAR-T) therapy for targeting advanced gastric cancer (AGC) expressing PD-L1. We constructed a 2nd generation CAR lentiviral vector expressing a unique anti-PD-L1 scFv with moderate affinity (VaxCAR001) in order to compare scFvs derived from Avelumab or Atezolizumab. This project focused on the efficacy and safety of PD-L1 CAR-Ts, which are affected by their binding affinity and dissociation with the target protein, PD-L1 during the treatment period.

Methods and Results: The findings of this study revealed significant differences among PD-L1-targeting CAR-T cells with different affinities and dissociations. VaxCAR001 cells, showing intermediate affinity, demonstrated a higher CD8 ratio (up to 78% compared to 58% in Avelumab-derived and 45% in Atezolizumab-derived CAR-T), reduced expression of inhibitory markers including Tim-3, LAG-3, and TIGIT, (8%, 39% and 13% in VaxCAR001 vs 35%, 55% and 42 % in Avelumab, 19%, 51% and 34% in Atezolizumab scFv-derived CAR-T, respectively) and more sustained cytotoxicity. Notably, it maintained strong cytotoxicity even one month after production, while the Avelumab or Atezolizumab ScFv-derived CAR-T cells did not. In multicellular spheroid 3D co-culture with CAR T cells, VaxCAR001 exhibited superior infiltration into the core of spheroid and induced higher CAR-T-mediated killing for 3D tumor spheroids as indicated by LDH assay (68%, 800% increased than Avelumab or Atezolizumab scFv-derived CAR-T). Moreover, in an MSI-high AGC mouse model, treatment with VaxCAR001 cells resulted in a significant reduction in tumor size and prolonged survival until the end of the study period. On the other hand, treatment with the Avelumab or Atezolizumab scFv-derived CAR-T cells led to high mortality, with most mice succumbing within three weeks after CAR-T cell injection, suggesting an on-target off-tumor effect.

Conclusion: This study demonstrates that VaxCAR001 cells bearing intermediate affinity and high dissociation rate for target PD-L1 showed the superior killing of PD-L expressing tumor cells in vitro and in vivo and manifested better safety profiles, as compared to CAR-T cells bearing scFv derived from commercial anti-PD-L1 targeting monoclonal antibodies such as avelumab and atezolizumab. VaxCAR001 revealed extended cytotoxicity, enhanced infiltration into tumor spheroids, and greater tumor size reduction in *in vivo* models. Importantly, it also demonstrated superior safety profiles, as evidenced by reduced expression of inhibitory markers and fewer off-tumor adverse effects. These findings would accelerate the clinical stage developments as an effective and safer treatment strategy against AGC.

#6319 Characterization of AB-1015 logic-gated CAR induction (ON kinetics), receptor turnover (OFF kinetics), and logic gate sensitivity to ALPG/P and MSLN.

X. Tang, M. Chew, R. Sudhakar, H. Yun, D. Sakamoto, V. Sail, A. Fearon, J. Williams, J. Feng, S. Santoro;
Arsenal Biosciences, South San Francisco, CA

CAR T cell activity in solid tumors is limited, in part, by off-tumor toxicity. To address this obstacle, AB-1015 contains an “AND” logic gate, consisting of a priming receptor (PrimeR) and an inducible chimeric antigen receptor (CAR) that is upregulated by PrimeR activation. The AB-1015 logic gate targets ALPG/P and MSLN, which are coexpressed in ovarian tumors but not normal tissues. AB-1015 CAR induction within the tumor is expected to be a dynamic process influenced by multiple factors, including antigen density, target cell abundance, as well as tumor microenvironmental factors. To characterize CAR induction and receptor turnover, we developed an in vitro assay with plate-bound ALPG to induce CAR. CAR induction occurred quickly in response to ALPG priming, with most ICT cells expressing CAR within 24 hrs, and plateaued by 72 hrs. Once removed from ALPG, CAR expression returned to baseline within 96 hrs. Similar to conventional CAR T cells, the presence of the cytolytic target antigen (MSLN) was expected to increase the rate of CAR turnover on AB-1015. To assess this, we measured the CAR functional half-life of AB-1015 cells once removed from ALPG priming. The cytotoxic activity of AB-1015 cells rapidly decreased in the absence of ALPG, reaching baseline within 24 hrs. Of note, our in vitro assay did not result in 100% CAR induction from all PrimeR+ AB-1015 cells. To understand whether this reflected biology versus a limitation of our in vitro assay, we conducted a CAR induction, sorted the CAR- cells, then performed a second induction. ICT cells that did not express CAR after the first induction were shown to be able to induce CAR during the second induction assay, thereby demonstrating that all PrimeR+ ICT cells have the potential to induce CAR. To assess the sensitivity of AB-1015 for low density ALPG/P and MSLN, isogenic cell lines were engineered to express each antigen at variable levels. In co-culture, AB-1015 was able to prime and kill targets expressing ALPG and MSLN at or below the limit of detection using immunohistochemistry. In light of these observations, the specificity of AB-1015 was verified using a dual flank in vivo model where one tumor expressed both ALPG and MSLN, and the contralateral tumor expressed MSLN alone. While robust anti-tumor activity was observed against the ALPG+/MSLN+ tumor, no activity was detected against the MSLN+ tumor. In summary, AB-1015 CAR induction and receptor turnover kinetics is a dynamic process. A reductionist in vitro model system was developed, enabling analysis of CAR induction and receptor turnover. Importantly, we demonstrated that all PrimeR+ ICT cells have the potential to induce CAR. Finally, the in vivo specificity of AB-1015 for ALPG+/MSLN+ tumors was established using a dual flank specificity model. Together, these data support the continued development of AB-1015 in a phase I clinical trial (NCT05617755).

#6320 CAR-T cells targeting LGR5: An effective treatment for chemotherapy resistant ovarian cancer.

W. Wang[1], V. Bandara[2], N. A. Lokman[1], Z. K. Price[1], T. M. Noye[1], S. Napoli[2], B. Gundsambuu[2], M. K. Oehler[1], S. C. Barry[2], **C. Ricciardelli**[1];
[1]University of Adelaide, Adelaide, Australia, [2]University of Adelaide, North Adelaide, Australia

Ovarian cancer is the second leading cause of cancer-related mortality among gynaecological cancers in the Western world. CAR-T cell therapy is an adoptive immunotherapy used to treat some blood cancers. This study has investigated whether leucine-rich repeat-containing G protein-coupled receptor 5 (LGR5) is a suitable target for CAR-T cell therapy for ovarian cancer. We assessed the cytotoxic effects of LGR5-targeting CAR-T cells on a range of ovarian cancer cell lines and primary serous ovarian cancer cells derived from patient ascites (at diagnosis and following relapse with chemotherapy resistant disease) in monolayer culture, 3D spheroid assays and patient-derived explant assays. OVCAR3 and a chemoresistant patient-derived xenograft (PDX) models have been used to assess whether LGR5-targeting CAR-T cells can inhibit growth and metastasis *in vivo*. We found that LGR5 is highly expressed in high-grade serous ovarian carcinoma (HGSOC) cancer cell lines and LGR5 expression was increased in chemotherapy resistant primary ovarian cancer cells. We demonstrated that LGR5-targeting CAR-T cells were cytotoxic and significantly inhibited the survival of ovarian cancer cell lines and chemotherapy-resistant primary ovarian cancer cells with high LGR5 expression levels in both monolayer culture and 3D spheroids compared to un-transduced CD3+ T cells. In patient-derived explant assays, we observed increased apoptosis in HGSOC tissues expressing high LGR5 following treatment with LGR5-targeting CAR-T cells. *In vivo,* LGR5-targeting CAR-T cell treatment decreased the tumour burden in mice with OVCAR3 xenografts and a chemotherapy-resistant PDX model with high LGR5 expression, compared to CD3+ T cells. In summary, LGR5-targeting CAR-T cells have great potential to be developed as a novel immunotherapy for ovarian cancer.

#6321 Developing a lenalidomide-inducible safety switch for CAR T cell therapy.

D. Sarkar[1], W. Lin[1], J. Y. Kim[1], N. H. Knudsen[2], I. C. Lane[1], T. Kienka[1], M. C. Kann[1], A. A. Bouffard[1], A. Cheng[2], M. V. Maus[1], R. T. Manguso[2], M. Jan[1]; [1]Massachusetts General Hospital, Boston, MA, [2]Broad Institute of MIT and Harvard, Boston, MA

While CAR T cell therapy is a medical breakthrough against various hematological malignancies, yet treatment failures often occur at least in part due to excessive engineered T cell activity leading to severe toxicities. To combat this, strategies pairing CAR T cells with safety systems, for example, suicide switches engineered to induce cell death are being actively pursued. However, existing designs have limited performance characteristics and generally use unapproved small molecule controllers or non-human sequences. To overcome these issues, we have developed a novel suicide switch leveraging the well-tolerated, FDA-approved anti-cancer drug lenalidomide, as a controller of the stability of fusion proteins tagged with a “degron” sequence. Specifically, we engineered a stoichiometric pair of transgenes using the apoptotic DNase pair, caspase activating DNase (CAD) and its degron tagged inhibitor (ICAD-degron). We hypothesized that the overexpressed ICAD-degron could restrain CAD, until lenalidomide treatment degrades ICAD to unleash CAD for apoptosis. We found that our system was stably overexpressed and rapidly induced cell death even at sub-nanomolar concentrations of lenalidomide. A comparison of our design with the frontline safety switch, inducible Caspase 9 in primary human T cells revealed that the lenalidomide-induced suicide switch enabled more complete depletion of engineered cells. We tested the effects of our suicide switch on CAR T cell function and found comparable proliferation and tumor cell cytolysis with fast depletion upon lenalidomide addition. In vivo, lenalidomide suicide switch CAR T cells exhibited similar anti-tumor function as control CAR T cells and were rapidly depleted after drug treatment. In summary, utilizing all human sequences and a clinically approved drug controller, we developed a suicide switch that is well tolerated and can rapidly induce cell death even at sub-therapeutic concentrations of lenalidomide. More broadly, chemogenetic regulation of stoichiometric protein pairs is a generalizable strategy for post-translational control of highly active transgenic elements.

#6322 CCTx-001 CAR T-cells targeting the AML specific antigen IL-1RAP show robust pre-clinical anti-tumor efficacy.

E. De Dreuzy, S. Reda El Sayed, D. Genin, C. Primus, L. Bouquet, A. Collette, O. Favre-Bulle, E. Rutjens, J. Hasskarl, K. Pavletic, M. Deschamps, C. Ferrand, R. C. Sainson;
Advesya, Besancon, France

Despite significant advancements in acute myeloid leukemia (AML) treatment, patients with relapsed/refractory (r/r) AML have limited therapeutic options. Novel approaches are urgently needed. CAR T-cell therapy has shown remarkable success in hematological malignancies. However, its application in AML has been hampered by the absence of highly AML-specific antigens, making current CAR T-cell AML therapies under development poorly tolerated and effective. This pre-clinical study introduces a novel CAR T-cell therapy, CCTx-001, specifically designed to target IL-1RAP, a 78-kDa transmembrane glycoprotein. IL-1RAP, is highly expressed on AML cells but not on healthy hematopoietic stem and progenitor cells (CD34+ HSPC). Additionally, transcriptomic analyses reveal a correlation between high IL-1RAP expression and poor prognosis in AML patients. IL-1RAP's predominant presence on myeloid leukemia cells, coupled with their dependence to IL-1RAP-related pathways for their survival, presents a promising avenue for CAR T-cell therapy without the risk of treatment-induced antigen loss. CCTx-001, an autologous CAR T-cell therapy, was developed to target IL-1RAP on AML cells. It comprises CD8+ and CD4+ T-cells transduced with a highly specific anti-IL-1RAP Single-Chain Variable Fragment (scFv), an IgG1 hinge region, CD28, 4-1BB co-stimulatory domains, and a CD3ζ activation domain. In vitro experiments confirmed CCTx-001's efficacy in killing AML cell lines and primary AML cells of varying IL-1RAP expression levels, also demonstrating cytotoxicity and cytokine release that was dependent on the (E:T) ratio and target expression. Furthermore, in vivo studies using immunocompromised NCG mice confirmed CCTx-001's ability to target IL-1RAP and inhibit the growth of IL-1RAP-positive human AML tumor xenografts, leading to increased survival time. Biodistribution analyses confirmed the successful adoptive transfer, expansion and persistence of CCTx-001 CAR T-cells in vivo, only when injected into IL-1RAP-expressing tumor-bearing mice, which correlated with reduced levels of circulating AML cells. The promising preclinical data presented herein warrant the evaluation of CCTx-001 CAR T-cell therapy in clinical trials for r/r AML patients. CCTx-001 CAR T-cell therapy offers a potential breakthrough in addressing the unmet medical needs of AML patients with resistant or refractory disease.

#6323 Preclinical evaluation of CB-012, an allogeneic anti-CLL-1 CAR-T cell therapy, that exhibits specific and potent cytotoxicity in acute myeloid leukemia (AML) xenograft models.

B. Francica, E. Garner, S. Namburi, C. Colgan, T. Fowler, D. Mutha, A. Aviles, M. Stanaway, R. Guo, Z. An, E. Kelly, E. Degagne, G. Kwong, L. Edwards, E. Jakes, M. Shaw, B. Schilling, J. Huynh, R. Luu, M. Sidorov, R. Mousali, M. Otsmaa, P. Lauer, J. Skoble, S. Kanner;
Caribou Biosciences, Berkeley, CA

Background: CLL-1 is a compelling therapeutic target for AML as it is highly expressed on AML tumor cells and leukemic stem cells but is not expressed on hematopoietic stem cells. CB-012 was engineered with a next-generation Cas12a CRISPR hybrid RNA-DNA (chRDNA) genome-editing technology and leverages both checkpoint disruption and immune cloaking armoring strategies to potentially improve antitumor activity. The CB-012 anti-CLL-1 CAR was developed with a fully human scFv and the CD28 costimulatory domain and is currently in development for the treatment of relapsed or refractory AML (r/r AML). Here we describe preclinical studies that supported the CB-012 IND clearance by the FDA in October 2023.

Methods: Cas12a chRDNA guides were implemented to generate five genome edits in the manufacture of CB-012. A multiplex genome-editing strategy was designed to enhance the antitumor activity of CB-012 through prevention of GvHD, PD-1 checkpoint disruption, and suppression of allograft rejection. *In vitro* and *in vivo* studies evaluated the specificity of antigen binding, antigen-dependent activity, and toxicologic potential.

Results: CB-012 demonstrated potent antigen-dependent expansion and cytotoxic activity against CLL-1^{+} human AML cell lines and patient-derived cells in co-cultures. In AML xenograft models, a single dose of CB-012 CAR-T cells resulted in robust tumor control, leading to significant prolongation of survival. CB-012 co-culture with multiple CLL-1-negative cell types representing vital tissues demonstrated that the anti-CLL-1 scFv does not exhibit tissue cross-reactivity. In an unbiased cell surface protein microarray, the anti-CLL-1 scFv demonstrated highly specific interaction with human CLL-1, with no detectable non-specific interactions. CB-012 CAR-T cells exhibited limited tissue infiltration and expansion in treatment naïve, immunocompromised murine models.

Conclusion: CB-012, the first allogeneic anti-CLL-1 CAR-T cell therapy using both checkpoint disruption and immune cloaking armoring, demonstrated specific and potent CLL-1-targeted cytolytic activity *in vitro* and *in vivo*. Specificity of the anti-CLL-1 scFv was demonstrated in an unbiased protein-binding study and no adverse safety signals were observed from CB-012 in murine toxicology models. These preclinical studies supported the IND clearance of CB-012, which is being evaluated in the AMpLify trial, a Phase 1, first-in-human clinical trial for patients with r/r AML (NCT06128044).

#6324 Antagonism-enforced braking system to enhance CAR T cell therapeutic specificity.

T. Kondo[1], F. X. P. Bourassa[2], S. Achar[1], J. DuSold[1], P. Cespedes[3], M. Wahlsten[1], A. Kvalvaag[3], G. Gaud[4], P. Love[4], M. Dustin[3], G. Altan-Bonnet[1], P. Francois[2], N. Taylor[1];

[1]National Cancer Institute, Bethesda, MD, [2]McGill University, Montreal, MD, [3]University of Oxford, Oxford, United Kingdom, [4]Eunice Kennedy Shriver National Institute of Child Health and Human Development, Bethesda, MD

Chimeric Antigen Receptor (CAR) T cell immunotherapy represents a breakthrough in the treatment of hematological malignancies. However, the rarity of cell surface protein targets that are specific to cancerous but not vital healthy tissue has hindered its broad application to solid tumor treatment. While new logic-gated CAR designs have shown reduced toxicity against healthy tissues, the generalizability of such approaches across tumors remains unclear. Here, we harness a universal characteristic of endogenous T cell receptors (TCRs), their ability to discriminate between self and non-self ligands through inhibition of response against self (weak) antigens, to develop a broadly applicable method of enhancing immunotherapeutic precision. We hypothesized that this discriminatory mechanism, known as antagonism, would apply across receptors, allowing for a transfer of specificity from TCRs onto CARs. We therefore systematically mapped out the responses of CAR T cells to joint TCR and CAR stimulations. We first engineered murine T cells with an ovalbumin-specific TCR to express a CAR targeting murine CD19 and discovered that the expression of a strong TCR antigen on $CD19^{\pm}$ leukemia enhanced CAR T killing. Importantly though, the presence of a weak TCR antigen antagonized CAR T responses, assessed by *in vitro* multiplexed dynamic profiling as well as *in vivo* cytotoxicity. We developed a mathematical model based on cross-receptor inhibitory coupling that accurately predicted the extent of TCR/CAR antagonism across a wide range of immunological settings. This model was validated in a $CD19^{\pm}$ B16 mouse melanoma model showing that TCR/CAR antagonism decreased the infiltration of a tumor-reactive T cell cluster, while TCR/CAR agonism enhanced infiltration of this T cell cluster. We then applied our quantitative knowledge of TCR/CAR crosstalk to design an Antagonism-Enforced Braking System (AEBS) for CAR T cell therapy. This was assessed in a model system using a CAR targeting the tyrosine-protein kinase erbB-2 (HER2) together with a hedgehog acyltransferase (HHAT) peptide-specific TCR that binds strongly to mutated tumor neoantigen while retaining weak affinity for the wild-type self-antigen on healthy tissue. We established a humanized *in vivo* model of CAR T function and found that AEBS CAR T cells maintained high anti-tumor activity against a human lung adenocarcinoma (PC9) but notably, their anti-tissue cytotoxicity against human bronchial epithelial cells (BEAS-2B) was minimized. AEBS CAR T cells therefore sharpen the discriminatory power of synthetic anti-tumor lymphocytes. Our work highlights a novel mechanism by which TCRs can enforce CAR T cell specificity, with practical implications for the rational design of future anti-leukemia immunotherapies.

#6325 Lineage tracing defines responding CAR T cells in patients with B cell malignancies.

Z. Good[1], M. P. Hamilton[1], J. Y. Spiegel[2], M. H. Desai[1], Z. J. Ehlinger[1], P. J. Quinn[1], Y. Chen[1], S. Prabhu[1], S.-H. Chiou[3], S. Kurra[1], E. Yang[1], M. G. Ozawa[1], M. J. Frank[1], L. Muffly[1], G. K. Claire[1], S. Bharadwaj[1], S. Dahiya[1], K. A. Kong[1], M. M. Davis[1], S. K. Plevritis[1], E. Sotillo[1], B. Sahaf[1], D. B. Miklos[1], C. L. Mackall[1]; [1]Stanford University, Stanford, CA, [2]University of Miami, Miami, FL, [3]Rutgers University - New Brunswick, New Brunswick, NJ

Autologous T cells engineered to express a chimeric antigen receptor (CAR) have transformed the standard of care for patients with B cell malignancies, but >50% of patients progress following therapy. Here, we sought to understand key T cell intrinsic factors impacting efficacy: CAR T cell expansion, persistence, and homing to the tumor. Using an endogenous T cell receptor (TCR) sequence as a 'barcode', we followed individual T cell clonotypes at the single-cell level from pre-manufacture apheresis and infusion products to tumor-involved lymph nodes and blood at peak and late expansion in 22 adult patients with relapsed or refractory large B cell lymphoma (LBCL) or acute lymphoblastic leukemia (ALL) treated with axicabtagene ciloleucel, an FDA-approved CD19-CAR T cell therapy, or bispecific CD19/CD22-CAR T cells on an investigator-initiated trial (NCT03233854). The resulting CAR T cell atlas comprises matched transcriptome (scRNA-seq) and surface protein expression (CITE-seq) for 846,344 cells from 97 samples, with 251,175 unique TCR clonotypes identified, including 17,479 clonotypes that could be traced across ≥2 timepoints in $CAR^{\pm}$ cells, enabling lineage tracing at scale for the first time. We found that T cells present in apheresis that preferentially expand during manufacturing primarily comprise T central memory (T_{cm}) cells and are enriched for predicted specificity to common viruses, including influenza, but also include a subset of T regulatory (T_{reg}) cells. In infusion products, CAR T conventional (non-T_{reg}) cells with superior abilities to home to the tumor, expand, and persist post-infusion share features of activated T effector memory (T_{em}) phenotype enriched for expression of BATF3 and high TCF4 transcription factor activity. Baseline apheresis and infusion products were enriched for cells classified as T_{regs} in patients with poor response. This observation aligned with our recent work linking post-infusion CAR T_{regs} to progression following CD19-CAR T cell therapy. We therefore performed lineage tracing and methylation analysis of the T_{reg}-specific demethylated region (TSDR) in the *FOXP3* gene and found that post-infusion CAR T_{regs} are primarily derived from pre-existing T_{regs}. Of interest, flow cytometry analysis of baseline blood from a cohort of 53 patients treated with CD19-CAR for LBCL showed that T_{regs} are elevated in baseline blood relative to healthy donors. Removing T_{regs} from healthy donor T cells prior to manufacturing enhanced CAR T cell expansion and anti-tumor activity against JeKo-1 human lymphoma cell line, whereas adding 5% T_{regs} to mimic patient T cells rendered the resulting CAR T cells less active. These analyses pinpoint the identities of apheresis T cells and infusion CAR T cells with properties impacting efficacy, and also identify pre-existing T_{regs} as limiting efficacy of CAR T cell immunotherapies.

#6326 Targeting *PRDM1* to enhance CAR T cell efficacy against diffuse large B cell lymphoma (DLBCL).

S. Wang, L. Xie, X. Chen, A. Cooper, J. Chorazeczewski, J. Kline;
University of Chicago, Chicago, IL

CAR T cell therapy has shown remarkable success in treating patients with relapsed or refractory (r/r) DLBCL, but a majority (>60%) will experience disease progression. A key failure mechanism is the rapid terminal differentiation and exhaustion of CAR T cells, driven by persistent antigen exposure *in vitro* during manufacturing and *in vivo* in the DLBCL environment, which culminates in poor persistence and short-term effector functions. Recent studies have identified the transcriptional repressor PR/SET domain 1 (*PRDM1*) as a key regulator that drives differentiation of T cells toward these unwanted fates. Further, single cell transcriptomic profiling of r/r DLBCL biopsies has revealed *PRDM1* enrichment in a cluster of exhausted-like $CD8^{\pm}$ CAR T cells. These observations indicate that targeting *PRDM1* could prevent or delay terminal differentiation/exhaustion in CAR T cells, thereby enhancing their persistence for lasting anti-tumor activity. Using CRISPR/Cas9 targeting, we have demonstrated that *PRDM1*-deficient CAR T cells exhibit enhanced proliferative capacity, memory characteristics, and resilience against exhaustion upon repeated stimulation. Moreover, genetic ablation of *PRDM1* also promoted the *in vivo* expansion and persistence of CAR T cells, which led to significantly improved survival of lymphoma-bearing mice. Mechanistically, loss of *PRDM1* leads to de-repression of PPARGC1A (PGC1α), a master regulator of mitochondrial biogenesis and antioxidant activity. This confers elevated tolerance to oxidative damage in CAR T cells lacking *PRDM1*, which showed increased capacity to buffer oxidative stress induced by mitochondrial uncouplers and constant stimulation. These findings suggest that *PRDM1* loss may improve CAR T cell fitness through PGC1α upregulation and mitochondrial activation. From a translational perspective, we assessed the potential synergistic effects of PGC1α agonist, bezafibrate, with CAR T cells. Dual therapy with bezafibrate and CAR T cells mediated more robust expansion and anti-tumor immunity of CAR T cells without causing discernible adverse events. Importantly, bezafibrate alone had no direct tumoricidal effects, which indicates that bezafibrate suppressed tumor growth through modulating CAR T cell functions. Moving forward, we will uncover the previously uncharted role of *PRDM1* in orchestrating the mitochondrial and metabolic activity of CAR T cells. Building upon a correlation between *PRDM1* expression and CAR T cell dysfunction, we aim to pioneer the use of *PRDM1* and/or its target genes as novel biomarkers for predicting clinical responses of r/r DLBCL patients to CAR T cell therapy. Our endeavors will shed light on the long-standing conundrum of CAR T cell dysfunction and offer solutions that may be applicable for improving T cell-based therapy against cancer in general.

#6327 Impact of G-CSF on safety and efficacy of CAR T-cell therapy in non-Hodgkin lymphoma.

Lay She Ng[1], Claire I. Yee[2], Radhika Bansal[1], Mohamed A. Kharfan-Dabaja[3], Grzegorz S. Nowakowski[1], Allison C. Rosenthal[2], Javier Munoz[2], Januario Castro[2], Wern Lynn Ng[4], Hemant S. Murthy[3], Yi Lin[1], Matthew R. Buras[2], Madiha Iqbal[3], Yucai Wang[1], Talal Hilal[2]

[1]Mayo Clinic Minnesota, Rochester, MN,[2]Mayo Clinic Arizona, Phoenix, AZ,[3]Mayo Clinic Florida, Jacksonville, FL,[4]UPMC Harrisburg, Harrisburg, PA

Introduction: Chimeric antigen receptor T-cell (CAR-T) therapy is an established treatment modality for the management of refractory and/or relapsed non-Hodgkin lymphoma (NHL). Despite restrictions on granulocyte colony-stimulating factor (G-CSF) use in registration clinical trials due to potential worsening of cytokine release syndrome (CRS), G-CSF is often prescribed for neutrophil recovery post-CAR-T in clinical practice. We conducted a retrospective study to assess the association between G-CSF use and the safety and efficacy of CAR-T.

Methods: Following Institutional Review Board approval, we retrospectively analyzed NHL patients receiving commercial CD19-targeted CAR-T across Mayo Clinic sites (Arizona, Florida, and Minnesota) between October 2017 and May 2023. Demographics, labs, and post CAR-T events were collected. Electronic medical records were reviewed for G-CSF exposure within Day 1 - 100 post-CAR T. Differences by G-CSF status were examined using a Chi-square test and Kruskal Wallis tests. Hazard ratios (HR) and 95% confidence intervals (CI) for overall survival (OS) were calculated using Cox model.

Results: Among 270 CAR-T patients; 106 received G-CSF within 30 days and 164 did not. Median age was 56.9 with G-CSF and 58.3 without G-CSF. Most were male (75.2% G-CSF, 62.6% no G-CSF). Diffuse large B cell lymphoma was the predominant NHL subtype (67.0% G-CSF, 65.2% no G-CSF).

G-CSF within 30 days was not associated with reduced incidence of neutropenic fever (11.7% G-CSF vs 9.9% no G-CSF, p = 0.6593) or documented infection (22.1% vs 18.3%, p = 0.4439). G-CSF correlated with decreased profound neutropenia duration (ANC < 100 µL, 0 vs 2 days, p < 0.0001) and incidence within 30 days (31.7% vs 60.4%, p < 0.0001) as well as incidence of protracted profound neutropenia (> 7 days, 3.8% vs 22.8%, p < 0.0001). G-CSF was associated with a higher incidence of cytopenias between days 30 -100: severe neutropenia (ANC < 500/uL, 28.8% vs 15.2%, p = 0.0075), severe anemia (Hb < 8 g/dL, 21% vs 9.7%, p = 0.0114), and severe thrombocytopenia (Plt < 50 g/L, 35.2% vs 20.9%, p = 0.0099). Logistic regression analysis showed that none of the examined covariates, including prior autologous stem cell transplant, ECOG PS score, and receipt of bridging therapy, were associated with severe neutropenia likelihood.

G-CSF was associated with a higher CRS incidence (89.6% vs 79.9%, p = 0.0343), but grade 3 CRS or higher (4.7% vs 3.7%, p = 0.6675) was no different. No difference in complete response rates (66% vs 61.1%, p = 0.4707) or 2-year OS (p = 0.523) was observed between the 2 groups.

Conclusion: G-CSF within 30 days was associated with reduced duration and incidence of profound neutropenia without a significant impact on incidence of neutropenic fever or documented infections. There was a signal of association between G-CSF and increased incidence of low-grade CRS and delayed cytopenias (day 30-100) that warrants confirmation in larger studies.

#6328 Preclinical development of CAR T cells with antigen-inducible IL-18 enforcement to treat G_{D2}-positive solid cancers.

L. Fischer-Riepe[1], S. Kailayangiri[1], K. Zimmermann[2], R. Pfeifer[3], M. Aigner[4], B. Altvater[1], S. Kretschmann[4], S. Voelkl[4], J. Hartley[5], C. Dreger[5], K. Petry[3], A. Bosio[3], A. von Doellen[6], W. Hartmann[7], H. Lode[8], D. Goerlich[9], A. Mackensen[4], M. Jungblut[3], A. Schambach[2], H. Abken[5], **C. Rossig**[1];
[1]University Children's Hospital Munster, Muenster, Germany, [2]Institute of Experimental Hematology, Hannover Medical School, Hannover, Germany, [3]Miltenyi Biotec B.V. & Co. KG, Bergisch Gladbach, Germany, [4]Friedrich Alexander University Erlangen-Nuremberg (FAU) and Universitatsklinikum Erlangen, Erlangen, Germany, [5]Leibniz Institute for Immunotherapy (LIT) and University of Regensburg, Regensburg, Germany, [6]Institute of Transfusion Medicine and Cell Therapy, University Hospital Muenster, Muenster, Germany, [7]Gerhard-Domagk-Institute of Pathology, University of Muenster, Muenster, Germany, [8]University Medicine Greifswald, Greifswald, Germany, [9]Institute of Biostatistics and Clinical Research, University of Muenster, Muenster, Germany

Cytokine-engineering is a promising strategy to overcome limitations of CAR T cell therapy in solid tumors. We have developed a novel investigational medicinal product, consisting of CAR T cells directed against ganglioside GD2 along with CAR-inducible secretion of IL-18, to enforce their activation response and effector functions in the microenvironment of solid cancers. Our lentiviral all-in-one vector combines constitutive expression of a 14.G2a antibody-derived GD2-specific, 4-1BB-costimulated CAR with inducible nuclear factor of activated T cells (NFAT)-driven expression of the human IL-18 transgene. A control construct contains EGFP in the place of IL-18 (GD2EGFPCART). Lentiviral transduction of T cells from various individual donors with both preclinical and clinical batches of virus resulted in CAR surface expression in >40% of T cells. GD2IL18CART contained effector memory and central memory T cell phenotypes at similar frequencies as the control. CAR engagement by immobilized anti-idiotype antibody or by GD2-positive tumor cells selectively induced IL-18 release, with production of IL-18 strictly depending on GD2 antigen engagement. GD2IL18CART responded to interaction with GD2-positive tumor cells with superior IFN-γ, TNF-α and IL-2 cytokine release and superior target cytolysis compared to the control CAR T cells without inducible IL-18, whereas IL-6 was secreted at similar concentrations. In an NSG xenograft model of disseminated GD2-positive tumors, GD2IL18CART had superior *in vivo* anti-tumor activity than GD2EGFPCART, with eradication of GD2-positive tumor xenografts as detected by bioluminescence imaging while the control achieved only limited extension of progression-free survival. Finally, we established GMP-compliant manufacturing of GD2IL18CART that is feasible and efficient at clinical scale, using an automated protocol and device. Three validation runs confirmed robust expansion of CAR+ T cells to final cell numbers of $3.5x10^9$ CAR+ cells (median; range 3.4 to $3.7x10^9$), with consistent transduction efficiencies of >54% at the in-process control time-point and at harvest. GD2IL18CART from clinical-scale manufacturing runs responded to interaction with GD2 with strictly antigen-dependent secretion of both IL-18 and IFN-γ and efficiently lysed various GD2-positive tumor targets. In conclusion, we assembled all prerequisites for clinical evaluation of an IL-18 cytokine enhanced, GD2-specific CAR T cell product for the treatment of patients with a variety of solid tumors, recruited on the basis of GD2 immunofluorescence pre-screening (EU CT 2022-501725-21-00). Besides addressing the safety of GD2IL18CART therapy in pediatric and adult patients as the primary endpoint, the study will allow to gain substantial knowledge on the biological effects of IL-18 in the TME of the individual solid tumors.

#6329 Pooled *in vivo* screening of hundreds of T cell therapy designs using spatial multi-omics identifies novel designs with superior TME performance.

C. Kontur, G. Povysil, M. Sah, M. London, N. Chen, A. Dyatel, S. Pu, D. V. Phizicky, **X. Wang**;
Waypoint Bio, Inc., New York, NY

Background: Adoptive cell therapies such as CAR T have been curative for many liquid tumors, yet this success has struggled to translate to solid tumors due to the challenges posed by the solid tumor microenvironment (TME). Pooled CAR screens (e.g. CAR-POOLING) have recently emerged as a powerful approach for testing many designs for improving CAR T cell performance. However, these screens are typically restricted to univariate readouts (e.g. abundance) and cannot measure the cell-cell and cell-TME interactions that are critical for CAR T success in solid tumors. Here, we present a platform for performing pooled screens *in vivo* using spatial biology, facilitating simultaneous measurement of cell autonomous phenotypes, cell-cell interactions, and cell-environment interactions for hundreds of distinct cell therapy designs in a single mouse.

Methods: We developed a custom spatial biology workflow to determine the identity of specific CAR constructs, armorings, or combinations in specific individual cells from a microscope image ("design deconvolution"). We combined this design deconvolution with simultaneous multiplexed spatial biology phenotyping in the same cells & samples, followed by computer vision interpretation to quantify each design's performance across functional categories important for efficacy in solid tumors such as: tumor infiltration, tumor cell killing, proliferation, response to antigen heterogeneity & escape, exhaustion, persistence, and activity in immunosuppressive tumor microenvironments. In multiple mouse cancer models, we quantified the performance of hundreds of different cell therapy designs.

Results: Using our pooled screens, we identified designs with superior performance in solid tumors across one or more key functional categories (e.g. infiltration, activity in immunosuppressive TMEs, etc.). We also mapped the landscape of cell therapy design principles by comparing dozens of existing designs derived from the literature head-to-head in the same animal, and we compared these benchmarked designs to novel cell therapies designed to improve CAR T function. We used these data to identify common rules that govern the design-phenotype relationship for CAR Ts in solid tumors and to identify CAR T designs with desired properties in solid tumors.

Conclusions: Using a pooled *in vivo* screening platform, we discovered cell therapies that outperform existing designs across a variety of clinically-relevant metrics. Our spatial multi-omics measurements are critical for identifying designs that can effectively traffic to, infiltrate, and function in the solid tumor microenvironment. We are now using our pooled *in vivo* screens to identify highly efficacious designs in multiple solid tumor models.

#6330 A novel monoclonal antibody for the detection, enrichment and activation of cells expressing scFv-based chimeric antigen receptors.

A. Singh, S. L'Heureux, J. Fisher;
Cell Signaling Technology, Inc., Danvers, MA

Introduction: Chimeric Antigen Receptor (CAR)-T cell therapy is a highly innovative form of immunotherapy that has proven to be successful in the treatment of B cell malignancies and multiple myeloma. As this treatment modality continues to evolve toward the targeting of novel tumor antigens and engineering of CAR constructs that enhance cell persistence, there is a need for reagents that can be leveraged to selectively interrogate multiple aspects of CAR-T cell biology. Here, we report on a novel and highly versatile recombinant rabbit monoclonal antibody raised against the Gly4Ser peptide linker, which is commonly integrated into single-chain variable fragment (scFv)-based CARs. This antibody can be leveraged for flow cytometry-based CAR detection, bead-based CAR-T cell enrichment, and selective activation of CAR transduced cells.

Methods: The recombinant monoclonal antibody, E7O2V, was generated by immunizing rabbits with a synthetic peptide containing multiple repeats of the Gly4Ser core pentapeptide. E7O2V was directly conjugated to a panel of fluorophores and validated for specificity in a live cell flow cytometry assay using non-transduced and CAR-transduced primary human T cells. To assess its utility in cell enrichment using bead-based sorting, a biotinylated conjugate of E7O2V was used in combination with streptavidin releasable magnetic meads to immunoaffinity purify CAR transduced cells from a mixed population. Finally, a plate-bound antibody stimulation assay was leveraged to assess the ability of E7O2V to selectively activate CAR transduced cells.

Results: Live cell flow cytometric analysis of CAR-transduced primary human T cells revealed that E7O2V could detect surface expressed CARs, independent of scFv specificity. No specific staining was observed on non-transduced cells. Furthermore, flow cytometric analysis of bead-free, purified cells revealed that biotinylated E7O2V could enrich CAR transduced cells to a high degree of purity and viability. E7O2V was found to selectively activate CAR transduced cells, but not non-transduced cells, as demonstrated by upregulation of cell surface activation markers, including CD69 and CD25.

Conclusions: Exploiting the commonly used Gly4Ser linker of scFv-based CARs for antibody discovery, we identified a novel and highly versatile monoclonal antibody, E7O2V. This antibody binds to CARs of varying antigen specificity and can be leveraged in multiple assay formats to interrogate various attributes of CAR transduced cells, including CAR expression, CAR signaling, and transcriptome profiling enabled by bead-based enrichment.

#6331 A novel automated platform for rapid manufacturing of CAR T cells.

S. sa, E. Nguyen, J. Pan, **L. Yu**;
Applied Cells, Santa Clara, CA

Autologous cell therapy using genetically modified T cells to express chimeric antigen receptor (CAR) has yielded durable responses in cancers patients. However, currently only a small portion of patients are privileged to receive the treatment. High cost and long manufacturing time contribute to the key limitations prohibiting cell therapy broad adoption. Researchers discovered that reducing ex vivo culture improves anti-tumor activity of CAR T cells[1] and recently demonstrated the process of generating functional CAR T cells within 24 hours[2]. This rapid process provides great promise in cost reduction of CAR T therapy and opportunity to have cells manufactured in close-to-patient settings. CART cell manufacturing process involves: (1) collection of peripheral blood; (2) isolation of T cells; (3) performing transduction via viral vector; (4) washing CAR T cells to remove viral vector, and (5) harvesting CAR T cells in IV fluid. Conventional process uses magnetic separation and serial centrifugation technologies on multiple platforms with manual operations. Here we demonstrate the feasibility of rapid manufacturing CAR T cells on an automated platform with closed fluidics without centrifugation steps. The platform, MARS® Atlas, is built with innovative technologies in immune-magnetic cell isolation and acoustic cell washing and implemented as a modular system. In this feasibility test, T cells were isolated from peripheral blood from a healthy donoron MARS® magnetic module. eGFP expressing lentivirus were added to the enriched T cells. After short incubation, cells and virus were washed with fresh medium on the MARS® acoustic module and cells were incubated with virus overnight without activation. Infected cells were washed on the acoustic module to remove free virus. Product CAR T cells were harvested in saline solution and ready for QC analysis. Starting from 20mL of peripheral blood, magnetic T cell separation was done 2mL/min achieving 90% T cell purity, 90% recovery. In the first acoustic wash, medium exchange of the mixture of cells and virus took place at 0.9mL/min flow rate. As a result, 90% removal of contaminating molecule and 99.6% recovery of T cells were achieved. The second acoustic wash completed medium exchange of transfected cells at 0.9mL/min with 96.7% removal of virus and 90% CAR T cell recovery. As a result, 18 million GFP expressing T cells were produced.

In this study we have demonstrated the feasibility of rapidly manufacturing CAR-T cells on an automated platform MARS® Atlas. This result indicates the MARS® Atlas being a potential CAR T manufacturing platform to be used in close-to-patient settings to enable low-cost cell therapy.

[1] Saba Ghassemi, Reducing Ex Vivo Culture Improves the Antileukemic Activity of Chimeric Antigen Receptor (CAR) T Cells, Cancer Immunol Res; 6(9) September 2018

[2] Saba Ghassemi, Rapid manufacturing of non-activated potent CAR T cells, Nature Biomedical Engineering | VOL 6 | February 2022 | 118-128

#6332 Evaluating the relationship of affinity, functional avidity, and *in vivo* potency in KIR-CAR T cells.

J. Xu[1], S. Nunez-Cruz[2], J. M. Leferovich[2], G. Gulendran[2], C. Zhang[2], N. D. Yucel[1], M. C. Blair[1], W. S. Stanley[1], L. A. Johnson[1], D. L. Siegel[2], M. C. Milone[2]; [1]Verismo Therapeutics, Philadelphia, PA, [2]University of Pennsylvania, Philadelphia, PA

Chimeric antigen receptors (CARs) targeting CD19 demonstrate remarkable clinical outcomes in patients (pts) with B-cell malignancies. Importantly, all four FDA-approved CD3ζ-based CAR T cell therapies use the same FMC63-derived single-chain variable fragment (scFv) to target CD19+ tumors. Although response rates are high in diffuse large B cell lymphoma, only ~40% of pts achieve durable, long-term remissions. Improved CAR T cell therapies are therefore needed. We have previously shown that a novel killer immunoglobulin receptor (KIR)-based CAR expressed in T cells as a multichain receptor with DAP12 (KIR-CAR T) has enhanced anti-tumor activity in several preclinical solid tumor models suggesting that this platform may show better activity in lymphoma. Some recent studies report that lower-affinity CD19 binders compared to the benchmark FMC63-scFv yield equivalent or increased anti-tumor activity of CAR T in pts, raising the question of optimal affinity for a KIR-based CAR. In this study, we aimed to evaluate the relationship of affinity, functional avidity, and in vivo potency of CD19 binders in a KIR-based CAR T cell. Using a highly-diverse 40-billion member canine scFv phage display library, we generated 19 unique human CD19-specific binders that compete with FMC63 binder supporting a similar binding epitope. Different KIR-CAR T cells were generated, and relative affinities were compared via binding to a recombinant (rec) CD19 protein. We found that although CAR receptor expression was similarly expressed, the concentration of soluble rec CD19 protein required to saturate the surface CAR varied more than 2-log among the different scFv binders suggesting a range of affinities relative to FMC63. We selected several scFvs with lower, and equivalent CD19 binding MFI compared to the FMC63-scFv and found that all scFvs could mediate similarly robust in vitro potency. In vivo anti-tumor efficacy was next assessed using the NSG xenograft mouse model of B-cell leukemia NALM6 cells. Interestingly, despite their comparable in vitro functions, some binders with relatively similar binding MFI failed to control the tumors. In contrast, two binders with an ~30-fold apparent affinity relative to FMC63 exhibited robust anti-tumor activity comparable to the benchmark scFv. These preliminary data suggest that the in vivo functional activity of chimeric KIR-based immunoreceptors is insensitive to binder affinity over a wide range of affinities. The failure of some scFvs with comparable affinity and binding epitope suggest that other, yet to be characterized attributes of the binder may be critical for optimal function. Further characterization of these binders is being conducted to understand the relationship between affinity, functional avidity, antigen density, and in vivo potency. This study paves the way for developing an improved CD19-specific KIR-CAR T cell therapy for treating pts with B-cell malignancies.

#6333 A high-parameter mass cytometry panel for the functional characterization of CAR T cells.

D. Mahamed, G. Awong, T. Selvanatham;
Standard BioTools, Markham, ON, Canada

High-parameter flow cytometry provides a powerful tool for in-depth analysis of CAR T cell therapy, from characterizing CAR T cell populations to understanding their interactions within the tumor microenvironment. This information is crucial for advancing CAR T cell therapies and improving their effectiveness in treating cancer.

To address the need for deep immunoprofiling at all stages of CAR T cell therapy, we created a robust and comprehensive mass cytometry panel of antibodies against 44 cell surface and intracellular markers. This assay allows for comprehensive characterization of CAR T cell features including surface marker expression, activation state, cytokine production, and differentiation status. These data will provide researchers with a better understanding of the phenotype of the CAR T cells used in therapy and can guide optimization efforts to enhance expansion, persistence, and self-renewal. For example, newer-generation CAR T cells (T cells redirected for antigen-unrestricted cytokine-initiated killing, or TRUCKs) that are engineered to produce cytokines such as IL-2 to enhance their own survival can be evaluated *in vitro* to select CAR constructs with the most potent anti-tumor activity.

The lyophilized and validated 30-marker Maxpar® Direct™ Immune Profiling Assay™ enables comprehensive characterization of immune cell populations in both whole blood and PBMC. The 7-marker Maxpar Direct T Cell Expansion Panel 3 (OX40, TIGIT, CD69, PD-1, Tim-3, ICOS, and 4-1BB) and the Maxpar Direct Basic Activation Expansion Panel (CD107a, IL-2, TNFα, IFNγ, perforin, and granzyme B) are add-on modules that can further characterize CAR T cell exhaustion, degranulation, cytokine production, and cytotoxicity against target cells. We also compared CAR T detection options for sensitivity and specificity using a CD19 CAR-transduced cell line spiked into healthy donor PBMC. Indirect staining with Miltenyi Biotec biotinylated CD19 CAR Detection Reagent followed by anti-biotin- or streptavidin-conjugated metal tags was compared against a directly conjugated or biotinylated anti-G4S linker antibody. We included sample multiplexing using 6 metal-tagged CD45 antibodies to address the need to minimize batch effects, crucial to multi-site and longitudinal studies. Samples were acquired on a CyTOF® XT™ instrument, and preliminary data analysis was performed using Maxpar Pathsetter™ for automated enumeration of immune cells.

By combining the lyophilized single-tube Maxpar Immune Profiling Assay and Expansion Panels with specific detection of CAR T cells, this assay enables researchers to analyze multiple key parameters simultaneously at the single-cell level at all stages of CAR T therapy development.

For Research Use Only. Not for use in diagnostic procedures.

#6334 Metabolic reprogramming enhances expansion and potency of CAR T cells.

Y. Xing[1], S. Eaker[2], Y. Bronevetsky[2], C. Garcia[2], H. Lemar[2], E. Massi[2], A. Wong[2], S. Barnes[1], D. Germain[1], S. Wise[1], **J. Lim**[2];
[1]Labcorp Early Development Laboratories, Ann Arbor, MI, [2]Xcellbio, San Francisco, CA

Cell therapies, such as Chimeric Antigen Receptor (CAR) T cell therapy, have revolutionized the treatment of hematological malignancies, but their use in solid tumors remains a significant challenge for the field. This is due, in part, to immunosuppressive mechanisms in the tumor microenvironment (TME), which include reduced oxygen tension, high interstitial pressure, and an abundance of immunosuppressive proteins, resulting in mitochondrial dysfunction, exhaustion, and depletion of adoptively transferred cells. Metabolic manipulation of therapeutic cells could overcome these barriers to enable cell therapy success in solid tumors. To this end, we have employed AVATAR technology (Xcellbio, San Francisco, CA), an incubation system that enables precise control of oxygen tension and hyperbaric pressure on cells in culture to improve the manufacture of adoptive T cell therapies. Using a CD19 CAR T model system, we have shown that transduction and expansion of CAR T cells under reduced oxygen and hyperbaric pressure conditions yield greater percentages and total numbers of lentiviral-transduced cells. While cells transduced in a standard CO_2 incubator yielded 10-20% CD19 CAR+ cells, transduction in the AVATAR system with increased pressure yielded 15-40% CD19 CAR+ cells. Similarly, T cell cultures performed under pressurized AVATAR conditions generated ~2X more viable cells after 10 days. Furthermore, these metabolically reprogrammed cells exhibit enhanced potency, with improved anti-tumor cytotoxic activity in vitro. We have extended these studies to measure the ability of AVATAR-expanded CD19 CAR T cells to control the growth of CD19-expressing NALM6-Luc tumor cells in vivo compared to CAR T cells grown in a conventional CO_2 incubator. Mice (female NOD.Cg-*Prkdc*^{scid} *Il2rg*^{tm1Wjl}/SzJ, Jackson Laboratories, Bar Harbor, ME) dosed with the AVATAR-expanded cells exhibited good tumor control and increased persistence of CAR T cells in relevant organs, along with alterations in cell trafficking to the bone marrow and spleen. The transferred cells maintained a less differentiated phenotype, with central memory and effector memory populations, as measured by expression of the markers CD45RA and CD62L, dominating the T cell compartment. This work showcases the benefits of metabolic reprogramming to improve the yield and functional potency of CAR T cells, which has direct applications to reducing the cost and improving the efficacy of these lifesaving treatments. The AVATAR technology is currently being translated into a closed system bioreactor for use in GMP cell therapy manufacturing.

#6335 Armoring CAR-T therapy with PD-1 blockade: a powerful strategy for enhancing anti-tumor effects in pancreatic cancer.

Z. Zhang, J. Huang, Z. Zhao, X. Wang, C. He, S. Yang, Q. Gu;
WuXi AppTec, Shanghai, China

Chimeric antigen receptor-modified T cells (CAR-T) have been widely applied in the treatment of hematological malignancies and are currently under investigation for their potential effectiveness against solid tumors. Nevertheless, the effectiveness of CAR-T in treating solid tumors remains unsatisfactory due to a range of factors, including CAR-T cell infiltration and heterogeneity. The efficacy of CAR-T therapy is substantially influenced by the tumor microenvironment. This is particularly evident when PD-L1 is activated through CAR-T, leading to the inhibition of CAR-T cell activity via the PD-1 pathway. In this study, we engineered a CAR-T therapy that targets mesothelin and concurrently expresses a membrane-bound PD-1 receptor. This design blocks the PD-1 on CAR-T cells, effectively counteracting the suppression of CAR-T function mediated by PD-L1. We observed a substantial upregulation of PD-L1 on AsPC-1 tumor cells after 4 hours of IFN-γ stimulation in vitro. CAR-T cells engineered to co-express PD-1 antibody (aMSLN-28BBZ-mPD-1) exhibited similar short-term cytotoxicity and cytokine secretion profiles to those of the traditional third-generation CAR-T (aMSLN-28BBZ). Notably, aMSLN-28BBZ-mPD-1 displayed significantly improved long-term target cell killing. Furthermore, in an *in vivo* model of pancreatic cancer, aMSLN-28BBZ-mPD-1 demonstrated enhanced anti-tumor activity when compared to the traditional aMSLN-28BBZ, as supported by RNAscope analysis and immunofluorescence assays of tumor tissues. These analyses revealed a marked upregulation of PD-L1 expression and enhanced CAR-T cell infiltration in the aMSLN-28BBZ-mPD-1 treatment group. In summary, our study demonstrates that co-expression of a membrane-bound PD-1 antibody overcomes PD-L1 mediated CAR-T suppression, as observed in both *in vitro* and *in vivo*. This innovative strategy underscores its therapeutic potential and value in treating solid tumors. Keywords: CAR-T, PD-1, Tumor Microenvironment, Pancreatic Cancer

#6336 Unleashing CAR T cell activity against osteosarcoma using tumor specific RNA-based vaccination.

A. Barpujari, R. Liu, E. Ogando-Rivas, X. Ma, H. Taoa, H. Gomez, D. Mitchell, J. Huang, E. Sayour, P. Castillo;
University of Florida, Gainesville, FL

Background: Metastatic osteosarcoma (OSA) has a dismal prognosis despite novel targeted therapies, including CAR T cells. Unleashing CAR T cell therapy against poorly immunogenic cancers requires new technologies that activate the tumor microenvironment (TME), while inducing CAR T cell migration, proliferation, and persistence into tumor to sustain tumor-specific immunity. We have developed tumor RNA-loaded nanoparticle (CD70-encoding RNA-NP) vaccines to overcome CD70-specific CAR T cell limitations in OSA.

Methods: Using two murine solid tumor models (K7M2 osteosarcoma and B16F0 melanoma, in Balb/c and C57Bl/6 background) highly metastatic to lungs, we implant K7M2 and B16F0 intravenously (i.v.). We subsequently generated NPs complexed with RNA encoding for CD70 antigen and control vaccine (GFP RNA). RNA-NPs are administered intravenously beginning on day 5 post-tumor implantation and day 7, 14 & 21. Mouse CD70-specific CAR T cells are manufactured after activation of T cells with CD3 and CD28 antibodies for 2 days. CAR T cells are ready for use in downstream experiments 2 days after pMSGV8-mCAR transduction and cells were injected (i.v.) on day 6.

Results: In preliminary data, we show that intravenous administration of CD70-encoding RNA-NPs rapidly recruit CD70-directed CAR T cells into tumor stroma unlocking their activity in two immunocompetent aggressive lung metastatic tumor models. Interestingly, regression of CD70-expressing tumors associates with CAR T cell mobilization out of peripheral blood and into reticuloendothelial (RES) tissues (i.e., lung, and spleen), a phenomenon that correlates with upregulation of vaccine-induced type I interferon (IFN) and activation of CCR2 pathway. In addition to the CAR T-mediated antitumor killing, an antigen spreading phenomenon was observed. The long-term survival benefit (150 days) provided by this approach reached 70-80% in both models compared with 0-10% of control groups.

Conclusions: Based on these findings, we hypothesize that tumor trafficking and persistence of CD70 CAR T cells depend on coordinated cytokine/chemokine signaling that can be ignited through intravenous RNA-NP vaccination. RNA-NPs in combination with CAR T cells prolong long-term survival of mice bearing these aggressive tumor models which was not only mediated by CAR T cells but also by activation of endogenous adaptive immunity. Future studies include the evaluation of this approach in large animal models prior to translation into first-in-human clinical trials.

CLINICAL RESEARCH: Antibodies 2
Poster Session

#6340 Novel conditionally active tetravalent B7-H3 x CD3 T-cell engagers targeting solid tumors.
A. Cugnetti, PhD, H. Liu, P. McNeeley, K. Woodard, C. Chang, G. Frey, W. J. Boyle, J. M. Short;
BioAtla, San Diego, CA

B7-H3, also known as CD276, is an immune-checkpoint molecule and a type 1 transmembrane protein that exerts a variety of biological functions. In cancer biology, the overexpression of B7-H3 is correlated with tumor cell invasion and metastasis, decreased T-cell infiltration and function, poor prognosis, and resistance to therapy. As B7-H3 is expressed in multiple solid tumors and plays an important role in modulating anti-tumor immune response as well as promoting cancer cell formation, it became an important target for the development of antibody-based immunotherapy. Many forms of bispecific antibodies targeting B7-H3 have shown antitumor response in preclinical studies. However, bispecific T-cell engagers (TCE) targeting B7H3 and CD3 have been correlated with cytokine release syndrome and hepatic adverse events, a common toxicity observed using TCEs which has limited the development of this immunotherapeutic in clinic. We leveraged BioAtla's Conditionally Active Biologic (CAB) platform (1) to develop a DualCAB T-cell engager targeting B7-H3 and CD3. This DualCAB-TCE molecule, BA3142, was engineered to bind with high affinity to both recombinant B7-H3 and CD3 receptor/antigens under conditions that mimic the acidic tumor microenvironment, but with low affinity in alkaline physiological conditions. *In vitro* and *in vivo* efficacy and toxicity data for the clone BA3142 will be presented. Our data demonstrated that BA3142 promotes cytotoxicity of B7-H3-expressing cancer cells *in vitro* and induces significant tumor regression *in vivo*. In Non-Human Primates BA3142 bispecific antibody was tolerated up to 25 mg/kg with minimal cytokine release and no clinical and histopathological signs of toxicities. The CAB technology offers the opportunity to expand the number of targets suitable for drug development in a new class of DualCAB TCEs with superior safety margin and potency in the clinic.
(1) Chang HW, Frey G, Liu H, Xing C, Steinman L, Boyle WJ, and Short, J.M. Generating tumor-selective conditionally active biologic anti-CTLA4 antibodies via protein-associated chemical switches. Proc Natl Acad Sci U S A 2021;118.

#6341 Targeting myeloid epithelial tyrosine kinase (MERTK) receptor in acute myeloid leukemia using a novel antibody-drug conjugate, RGX-019-MMAE.

A. Tyagi[1], M. Siddiqui[1], I. Kurth[2], S. Takeda[2], A. Eckstrom[1], J. Borgman[1], A. Maiti[1], V. Battula[1];
[1]UT MD Anderson Cancer Center, Houston, TX, [2]Inspirna, Inc., New York, NY

Background: Myeloid epithelial reproductive tyrosine kinase (MERTK), a transmembrane protein receptor from the TAM (Tyro3, Axl, Mertk) family, is overexpressed in cancer and associated with reduced apoptosis and chemoresistance, making it an attractive therapeutic target. RGX-019-MMAE, a novel humanized IgG1-MMAE antibody-drug conjugate (ADC) (Inspirna, Inc), selectively binds to MERTK with high affinity on tumor cells, resulting in internalization and degradation of the receptor. It then induces cytotoxicity through the release of the payload, MMAE (monomethyl auristatin E), which disrupts mitosis. We hypothesize that targeting MERTK via RGX-019-MMAE exerts an antileukemic effect.

Methods: First, to determine the clinical relevance of MERTK, using the Oregon Health and Science University (OHSU) acute myeloid leukemia (AML) dataset, we divided patients into low and high MERTK mRNA expression based on mean expression and compared their overall survival. To identify the AML subtypes with the highest MERTK expression, we analyzed samples from 810 AML patients at MD Anderson using reverse phase protein arrays (RPPA), as well as 8 AML cell lines and the peripheral blood of 9 AML patients using flow cytometry. Then, the cell lines with the highest MERTK expression were treated with varying doses of RGX-019-MMAE or isotype control for 120 hours and assessed for viability with CellTiter-Glo 2.0. Likewise, we administered RGX-019-MMAE to primary cells from AML patients and determined the anti-leukemic effect. Finally, we investigated the synergistic effect of RGX-019-MMAE with venetoclax, a BCL2 inhibitor, or cytarabine, a chemotherapy agent, *in vitro*.

Results: In the AML OHSU dataset, patients with high MERTK mRNA expression had significantly worse overall survival (p=0.02). RPPA revealed that patients with PTPN11 mutation, t (9;11), and monocytic AML subtypes had significantly higher MERTK protein expression. MERTK protein expression varied in AML cell lines and was highest in Kasumi-1 and OCI-AML3. Treatment of these two cell lines with RGX-019-MMAE resulted in significantly more killing of leukemic cells than the isotype control ADC in a dose-dependent manner (p<0.01). Similarly, in primary AML cells with high MERTK expression, RGX-019-MMAE treatment induced significant cell death compared to the control ADC. In addition, Kasumi-1 and OCI-AML3 cells treated with RGX-019-MMAE combined with venetoclax or cytarabine showed a synergistic cytotoxic effect in a dose-dependent manner.

Conclusion: High MERTK expression in monocytic AML suggested that MERTK is a promising therapeutic target in this subtype. RGX-019-MMAE significantly induced AML cell death and produced a synergistic anti-leukemic effect in combination with chemotherapeutic agents and targeted therapy *in vitro*, suggesting its potential for targeting patients with high-risk AML.

#6342 Anti-tumor in vivo efficacy of different classes of anti-CLEC-1 myeloid checkpoint antibodies in monotherapy and in combination with chemotherapeutic agents.

A. Morello[1], M. Derame[1], M. Drouin[1], E. Wilhelm[1], S. Neyton[1], I. Baccelli[1], C. Mary[1], V. Gauttier[1], I. Girault[1], K. Biteau[1], C. Batty[1], G. Teppaz[1], A. Desselle[1], M. Colonello[1], M. Malloci[1], E. Chiffoleau[2], N. poirier[1];

[1]OSE Immunotherapeutics, Nantes, France, [2]Nantes Universite, Inserm, Centre de Recherche en Transplantation et Immunologie Translationnelle, UMR 1064, ITUN, Nantes, France

The c-type lectin receptor CLEC-1 is a pattern recognition receptor [1] expressed by endothelial and myeloid cells in mice, non-human primates, and humans. While genetic deletion of CLEC-1 in mice does not lead to any developmental defect, CLEC-1 deletion or CLEC-1 targeting promotes anti-tumor response by increasing cross-presentation of necrotic or damaged cells by cDC1 dendritic cells and by enhancing T-cell activation [2]. To date, the identification of CLEC-1 endogenous ligand(s) and their biological activity into myeloid or endothelial cells remained to be fully investigated. We aimed to further characterize ligands that are involved into CLEC-1 activation and develop monoclonal antagonist anti CLEC-1 antibody anti-tumor therapy that are able fully counteract inhibitory signaling induced into myeloid cells. Using LC/MS campaign, we confirmed CLEC-1 specific binding to the E3 ubiquitin ligase TRIM21and to the secreted histidine rich glycoprotein (HRG) as previously described [2] and also identify several novel intra-cellular and cell surface proteins that bind to CLEC-1 receptor in protein specific-manner. To block interaction of CLEC-1 ligands, we developed different class of antagonist monoclonal antibodies and evaluated their anti-tumor efficacy in humanized CLEC-1 KI orthotopic and ectopic tumor mouse models fully resistant or partially resistant to ICI therapy. While blocking of CLEC-1 binding to its secreted ligand HRG moderately increases anti-tumor responses, inhibition of CLEC-1 binding to its cytoplasmic and membrane ligands significantly impairs MC38 tumor growth (n=12, p=0.04). Importantly, high anti-tumor efficacy was observed in combination therapy with cyclophosphamide in MC38 mouse model. Additionally, antagonist anti-CLEC-1 antibodies significantly increase overall survival of Hepa1.6-bearing mice (n=32 for each treatment, $p<0.002$), as compared to corresponding isotype control treatment in 3 independent experiments. Altogether, our results further dissect the mechanism of action of the myeloid checkpoint CLEC-1 in its ability to impair anti-tumor immunity and support its use as a novel and highly promising anti-CLEC antagonist antibody for cancer immunotherapy.

#6343 AnTenGager™, a novel "2+1" T cell engager platform, enables conditional T cell activation with reduced risk of CRS.

Bing Hou[1], Hui Yuwen[2], Tengteng Li[2], Yijing Ren[2], Ao Sun[2], Zaoshun Hu[3], Jay Mei[1], Bo Shan[1]

[1]Antengene Corporation, Shaoxing, China,[2]Antengene Corporation, Shanghai, China,[3]Antengene Biologics, Hangzhou, China

Background: CD3+ T cell engaging bispecific antibodies (TCE) redirect T cells to attack targeted tumor cells by simultaneously binding TAA on cancer cells and CD3 complex on a T cell to form a TCR-independent immune synapse. Multiple TCEs have demonstrated promising therapeutic efficacy in the treatment of hematological malignancies. In contrast, suboptimal efficacy in the treatment of solid tumors and the risk of inducing cytokine release syndrome (CRS) continue to be major challenges. Several factors, such as format, affinity, and valency of the antibody, TAA copy number, and antigen size and epitope, can impact the therapeutic efficacy and safety of a TCE. In this study, we developed a novel "2+1" TCE platform, AnTenGager™, which enables conditional T cell binding and activation upon TAA-crosslinking, potent anti-tumor activity, and reduced risk of CRS.

Methods: Humanized CD3 antibodies were derived from mouse hybridoma, followed by affinity optimization utilizing Computer Aided Drug Design. The Fab-scFv-Fab format was used as the backbone structure of AnTenGagers. The anti-CD3 scFv sequences and the length of peptide linkers between VH/VL, scFv/CH1, and scFv/CH2 were screened and compared in different preclinical assays. LALA mutations (L234A, L235A) were introduced to abolish the Fc receptor binding capability. In a series of *in vitro* and/or *in vivo* models, the efficacy, safety and developability of AnTenGagers targeting multiple TAAs, such as Her2, GD2, CDH6, LILRB4, FLT3 and GPRC5D, were evaluated.

Results: A library of humanized parental CD3 antibodies with a broad spectrum of affinities were generated, some of which cross react with monkey CD3. AnTenGagers exhibited limited binding to CD3-positive cells before TAA-crosslinking, suggesting a reduced risk of CRS that is caused by systemic CD3+T cell activation. Four CD3 sequences with varying affinities were utilized to construct AnTenGagers with identical TAA-targeting arm. Compared to clinical benchmarks targeting the same TAA, all AnTenGagers demonstrated substantially lower binding capacity to CD3+ cells in the absence of TAA-crosslinking, while inducing increased cytotoxicity against target-positive tumor cells. In addition, they induced significantly less ex-vivo cytokine release by human PBMC than benchmarks. Notably, all AnTenGagers demonstrated enhanced in vivo efficacy compared to the benchmark, exhibiting complete response (CR) in PBMC humanized MM1S mouse CDX model while the serum concentration of proinflammatory cytokines was substantially lower in groups treated with AnTenGagers. AnTenGagers also demonstrated good developability with high expression yield, good thermostability and high stability under different stress conditions.

Conclusions: These results suggested that AnTenGager™ is a promising platform for developing the next generation of TCEs with enhanced efficacy and safety.

#6344 Engineering of ICAM-1 refractory antibodies for the development of therapeutic antibodies and antibody drug conjugates (ADCs) in ICAM-1 over-expressing cancers.

B. Kline, L. Grasso, N. Nicolaides;
Navrogen Inc., Cheyney, PA

Human cancers employ a number of mechanisms to evade host immune responses against novel antigens generated from aberrant over-expression, mutations and/or epigenetic alterations. Humoral immunity utilizes antibodies and immune-effector cells as well as molecular immune complexes involving the complement system to mediate the killing of dysregulated cancer cells. We refer to these anti-cancer mechanisms as Humoral Immuno-Oncology (HIO). HIO suppression is mediated by tumor-produced proteins called HIO factors. One such factor is CA125, which was previously shown to bind IgG-type antibodies and inhibit their immune-effector activities, including antibody dependent (ADCC) and complement dependent (CDC) cellular cytotoxicity. Using a combination of experimental screening and literature searches, a second protein produced by tumors and associated with a variety of cancer indications was discovered and found to be soluble ICAM-1 (sICAM-1). Through various functional studies we reported that sICAM-1 and membrane ICAM-1 (mICAM-1) are capable of binding IgG1-type antibodies that in turn inhibits their immune-effector activity. Through a combination of truncation and substitution mutagenesis, we identified a four amino acid motif within the CH3 domain of IgG1 essential for ICAM-1 binding, resulting in the inhibition of ADCC activity. While traditional glycine and alanine substitutions in this region abrogated ICAM-1 binding, these modifications caused tertiary structural changes in the Fc domain that resulted in loss of ADCC activity. Through a combinatorial amino acid substitution approach, we identified a four amino acid combination within the $_{407}$YSKL$_{410}$ to $_{407}$FARV$_{410}$ motif that resulted in antibodies refractory to sICAM-1 binding with robust ADCC activity. Additionally, isogenic wildtype and ICAM-1 knockdown target cell lines showed mICAM-1 inhibited target cell killing of a saporin antibody drug conjugate (ADC) and this was the direct result of mICAM-1 reducing antibody internalization, a requisite for maximal ADC target cell killing. The inhibitory activity of mICAM-1 could be overcome employing antibodies containing the $_{407}$FARV$_{410}$ substitution. These findings highlight yet another mechanism by which tumors can suppress the host's immune system for survival and offer new concepts for developing antibody-based therapies that can aid in the treatment of various cancer indications, especially those over-expressing ICAM-1. Moreover, the findings here offer diagnostic and therapeutic clinical design opportunities to improve upon existing approved immune-mediated therapies for which this factor is present.

#6345 In vitro characterization of a dual antagonistic anti-LILRB2/LILRB4 monoclonal antibody.

B. L. Daugherty[1], X. Ge[2], C. L. Hsieh[2], B. A. Zabel[2], S. Lederman[1];

[1]Tonix Pharmaceuticals, Inc, Chatham, NJ, [2]Curia Global, Inc, San Carlos, CA

Introduction: Myeloid-derived suppressor cells (MDSCs) in the tumor microenvironment are a potential therapeutic target in immune checkpoint cancer therapy, but MDSC-targeted therapies have yet been shown to improve survival. The leukocyte immunoglobulin (Ig)-like receptor B2 is a member of the leukocyte Ig-like receptor (LILR) family and is predominantly expressed on the surface of cells of the myelomonocytic lineage (monocytes, macrophages and dendritic cells). LILRB2 is a negative regulator of myeloid cells and is an immune checkpoint receptor. We chose to generate mAbs against LILRB2 as a potential immunotherapeutic for cancer.

Methods: PentaMice® strains (5 WT mouse strains comprising 9 MHC class II haplotypes to maximize Ab diversity) were immunized with human LILRB2. Lymphocytes were fused with a myeloma partner to generate lead monoclonal hybridomas. 24 purified anti-LILRB2 mAbs were generated and evaluated by arrayed surface plasma resonance (SPR, Carterra® LSA® instrument) to assign epitope bins. mAb humanization was performed in silico to maximize T20 “humanness” scores (algorithm developed by Curia). Humanized mAbs were transiently expressed using Curia’s TunaCHO™ platform and tested in in vitro MDSC assays. Autologous co-cultures of magnetic bead enriched-human blood-derived MDSC (HLA-DR-CD14+) model cells and T cells (CD3+) were stimulated with plate-bound anti-CD3/CD28 to induce T cell activation. Cytokine secretion was assessed 4 days later.

Results: A total of 384 hybridoma supernatants were selected from the primary screen. 245 were confirmed by ELISA and 178 stained HEK293 cells expressing LILRB2 cells by flow cytometry (FACS). 24 hybridomas were further selected, cloned and sequenced. Five epitope bins were identified via Carterra® LSA® instrument. Two clones were chosen for humanization, designated 6-I11A and 4-O19A and were recombinantly expressed with the human IgG4 isotype. FACS analysis on HEK293 cells expressing either huLILRB2 or huLILRB4 revealed that clone hu4-O19A-IgG4 was specific for huLILRB2. Surprisingly, clone hu6-I11A-IgG4 stained both huLILRB2 and huLILRB4. FACS analysis with hu4-O19A-IgG4 on human MDSCs exhibited an EC50 of 11.9 nM and a KD of 1.5 nM in binding to recombinant huLILRB2 antigen, while hu6-I11A-IgG4 had an EC50 of 3.2 nM and a KD of 0.6 nM. In co-cultures with human MDSCs and T cells, both hu6-I11A-IgG4 and hu4-O19A-IgG4 reversed cytokine suppression by the MDSCs by increasing GM-CSF, IL-10, TNFα, and IL-6, while suppressing IL-13, and had little effect on IL-17A, MIP-3α, IL-4, IL-2 and IFNγ compared to treatment with the isotype control, with hu6-I11A-IgG4 having a greater effect as an antagonist than hu4-O19A-IgG4.

Conclusions: We have identified a dual anti-LILRB2/LILRB4 antagonist. Targeting MDSCs with this antibody offers great promise for immunotherapy for cancer as well as its immense potential for synergy with PD-1 blockade.

#6346 IgG engineered to target PIGR-mediated transcytosis specifically targets intracellular oncoproteins and abrogated tumor growth.

C. Anadon Galindo, L. Lopez-Bailon, R. A. Chaurio, J. A. Mine, N. E. Plappert, J. R. Conejo-Garcia;
Duke University School of Medicine, Durham, NC

Despite their long half-life, therapeutic antibodies are considered ineffective against intracellular antigens due to their perceived inability to penetrate epithelial cells. Using recombinant antibodies targeting common mutations in oncogenes, we have demonstrated that dimeric IgA, but not the same antibody on an IgG backbone, penetrates human epithelial cancer cells through PIGR-dependent directional transcytosis, specifically neutralizing mutated oncodrivers and expelling antigens outside the cell, bound to secretory IgA. Accordingly, targeting of KRASG12D abrogated tumor cell proliferation in cell culture assays. In vivo, $KRAS^{G12D}$-specific dIgA1 limited the growth of RAS^{G12D}-mutated ovarian and lung carcinomas, including in syngeneic tumor-bearing immunocompetent mice. Moreover, dIgA targeting of $KRAS^{G12D}$ restricted tumor growth more effectively than small-molecule $KRAS^{G12D}$ inhibitors, supporting the potential of this approach for the treatment of human cancers. Since producing dimeric IgA is more challenging than producing monomeric IgG, and because the half-life of IgA is shorter (4-7 days) than IgG (21 days), we have developed a new approach combining $KRAS^{G12D}$ specific IgG with a peptide that could join PIGR and penetrates tumor cells through transcytosis, that showed the same effect than IgA controlling tumor growth. Our results provide a rationale for developing modified IgG cell-penetrating antibodies to effectively target common mutations in intracellular oncogenes that drive many aggressive and frequent human cancers. In addition, further experiments suggest that these antibodies could be effectively used to target tumors that have become resistant to existing KRAS inhibitors.

#6347 To develop a tumor selective INF-γ-Yervoy fusion antibody to increase the therapeutic effect and safety of current Yervoy therapy in cancer.

C.-H. Chuang;
Department of Medical Laboratory Science and Biotechnology, Kaohsiung Medical University, Kaohsiung, Taiwan

Introduction: Immune checkpoint inhibitor therapy is a highly promising strategy for clinical treatment of cancer. Among these inhibitors, yervoy stands out for its ability to induce cytotoxic T cell proliferation and activation by binding to CTLA-4. However, FDA has reported that yervoy would induce the over-activation of immune cells and cause the serious side effects. In additional, the therapeutic efficacy and application of Yervoy were still limited by the MHC expression of patient's tumor.
Strategy: Therefore, we have developed a protease specific pro INF-γ-Yervoy to increase the therapeutic effect and safety of current immune checkpoint blockade therapy in cancer. We used the MMP-2/9 protease substrate as a linker between INF-γ and Yervoy. Using the concept of spatial shielding, IFNγ and Yervoy can block their functions from each other. Once the INF-γ-Yervoy arrives to the tumoral region, the INF-γ-Yervoy will be removed from Hinge Yervoy by the over-expressed MMPs protease locally so that the Yervoy will recruit its binding ability in order to increase the drug selectivity and improve the side effects. The INF-γ also can increase the MHC I expression in tumor to overcome the MHC-limitation of Yervoy.
Result: On activation by MMP, IFNγ-yervoy not only restored yervoy's binding ability but also released biologically active IFNγ. This finding confirms the reliability of IFNγ-yervoy's functionality. In vivo studies demonstrated that IFNγ-yervoy enhances the therapeutic effect of yervoy against colorectal cancer by increasing CD8+ and CD4+ lymphocyte infiltration into the tumor area and inducing MHC-I expression in tumor cells. Mice treated with IFNγ-yervoy showed higher survival rates and body weight, as well as lower CD4+ and CD8+ lymphocyte activation rates in the blood and reduced organ damage.
Conclusion: These results provide strong evidence that tumor-selective IFNγ-yervoy can improve the effectiveness of yervoy while reducing its side effects. It is likely that future immunotherapies would rely on such antibodies to activate local cancer cells or immune cells, thereby increasing the therapeutic effectiveness of cancer treatments and ensuring their safety. Keyword: Immune checkpoint inhibitor therapy, IFNγ, yervoy, rectal cancer, CTLA4

#6348 Unveiling diverse trimeric forms of STEAP1 in human prostate cancer cells: Exploring STEAP1-STEAP2 interdependence for expression and plasma membrane localization.

C. Li[1], L. Liang[1], J. Park[1], O. Pryshchep[1], B. Staley[1], P. Li[1], B. Alba[1], X. Liu[1], F. Li[1], G. L. Moore[2], M. J. Bernett[2], U. Muchhal[2], J. Desjarlais[2], A. Coxon[3], J. M. Bailis[1];

[1]Amgen, South San Francisco, CA, [2]Xencor, Inc, Pasadena, CA, [3]Amgen, Thousand Oaks, CA

Six-Transmembrane Epithelial Antigen of the Prostate 1 (STEAP1) is an emerging therapeutic target that is a member of the STEAP1-4 family of metalloreductases. We recently reported the preclinical characterization of xaluritamig (AMG 509), a STEAP1 XmAb® 2+1 T-cell engager molecule that is being developed for the treatment of prostate cancer (Nolan-Stevaux et al, 2023). Xaluritamig is designed to preferentially target tumor cells that express high levels of STEAP1. However, prostate tumor cells also express high levels of STEAP2. Here, we characterize the interactions between STEAP1 and STEAP2 in prostate cancer cell lines and the impact to xaluritamig activity. Bulk mRNA as well as single-cell gene expression data (scRNAseq) reveal a strong correlation between STEAP1 and STEAP2 expression in human prostate cancer, suggesting that the STEAP proteins may form both homotrimers and heterotrimers in prostate tumors. To test this idea, we investigated the structural behavior of STEAP1/2 trimers in human prostate cancer cell lines that endogenously express STEAP1 and STEAP2. Using xaluritamig and the parental anti-STEAP1 antibody, we show that STEAP1 primarily forms heterotrimers with STEAP2 in prostate cancer cells but can also assemble as homotrimers in the absence of STEAP2. Both STEAP1/2 heterotrimers and STEAP1 homotrimers can be targeted by xaluritamig, leading to T cell-dependent cellular cytotoxicity. Similarly, we found that anti-STEAP2 antibodies detected STEAP2 homotrimers when STEAP1 expression was ablated in cells, and that both STEAP1/2 heterotrimers and STEAP2 homotrimers were targeted by a STEAP2-specific T-cell engager molecule. We also demonstrate that neither STEAP1 nor STEAP2 significantly influences the mRNA or protein expression of the other. Our data elucidates the versatility of STEAP family members in forming both homotrimers and heterotrimers on the plasma membrane of human prostate cancer cells and the potential for therapeutic targeting with STEAP1/2-directed therapies. Characterizing the capability of existing STEAP1 or STEAP2 targeting therapeutics to bind their respective targets, whether within a homotrimer or heterotrimer, is crucial for a comprehensive understanding of the therapeutic potential of these drugs. Further research will help delineate the mechanism underlying the formation of STEAP1/2 trimers in cancer cells and continue advancing our understanding of this intriguing biological relationship.

#6349 2MW4991, a novel ADCC-enhanced integrin αvβ8 blocker, exhibits high anti-tumor potency and was well tolerated in cynomolgus monkeys.

C. Guo, Z. Han, X. Cen, Sr., H. Wu, J. Zhang, X. Gui;
Mabwell (Shanghai) Bioscience Co., Ltd., Shanghai, China

Background: The three highly structurally related TGF-β isoforms (TGF-β1, TGF-β2, and TGF-β3) exert greatly different effects on cancer and immune cells under various physiological conditions. Efforts to target the TGF-β pathway have been hampered by systemic toxicity or limited efficacy due to challenges associated with the global inhibition of TGF-βs. Recently, TGF-β1 was proven to be a critical player in generating an immunosuppressive tumor microenvironment (TME). TGF-β1 is expressed as an inactive latent form (L-TGF-β1) and activated upon binding to integrins, and integrin αvβ8 is a key activator of TGF-β1 in TME. Here, an ADCC-enhanced αvβ8 blocking antibody, 2MW4991, was developed to specifically inhibit TGF-β1-mediated signaling for the treatment of αvβ8-expressing cancers.

Methods: Binding ability, specificity, and affinity of antibodies were measured by Flow cytometry and Biacore T200. A blocking assay was performed using U251MG cells and TGF-β signaling reporter cells. Jurkat/h FcγRIIIa reporter system was used to assess the ADCC activity of 2MW4991. Mouse syngeneic tumor models were used to characterize the *in vivo* anti-tumor efficacy. A repeat dose administration study was performed in cynomolgus monkeys to evaluate the pharmacokinetic and toxicity profiles of 2MW4991.

Results: ScRNA-seq analysis of kidney renal clear cell carcinoma (KIRC) and head and neck squamous cell carcinoma (HNSCC) clinical samples revealed that αvβ8 highly expresses in tumor and some myeloid-derived cells, suggesting the development of ADCC-enhanced αvβ8 blocking antibodies for the treatment of αvβ8-expressing cancers. 2MW4991 showed sub-nanomolar binding affinity and high specificity to αvβ8, with no cross-reactivity to other integrins. 2MW4991 could effectively block TGF-β1 release in a GARP/L-TGF-β1/αvβ8 reporter system. In an immune-excluded EMT6 syngeneic model, 2MW4991 promoted substantial tumor regression and reversed immune suppressive TME by significantly increasing tumor infiltration of CD8+ T and innate immune cells. As expected, TGF-β1 blockade significantly increased the sensitivity of anti-PD-1 therapy in a combination study. Furthermore, 2MW4991 displayed potent anti-tumor efficacy in the human αvβ8 knock-in syngeneic model mimicking αvβ8 expression in human cancers. In a repeat dose administration NHP study, 2MW4991 showed a good pharmacokinetic profile and was well tolerated at a high dose of 100 mg/kg, accompanied by significantly declined pharmacodynamic biomarker TGF-β1 in peripheral blood.

Conclusion: Integrin αvβ8 is a main activator of TGF-β1 in the TME and overexpressed in some cancer types. 2MW4991 demonstrated potent anti-tumor activity by unleashing the immune cells suppressed by TGF-β1 in TME and Fc-mediated immune functions. These compelling preclinical results support further evaluation of 2MW4991 in clinical trials.

#6350 2MW4691, a novel CCR8/CTLA-4 bispecific antibody, displays potent anti-tumor efficacy by specifically depeleting tumor-infiltrating Tregs and blocking CTLA-4 signaling on CD8+ T cells.

C. Guo, Jr.[1], X. Dai[1], X. Xiong[1], H. Liu[2], X. Cen, Sr.[1], H. Wu[1], J. Zhang[1], X. Gui[1];

[1]Mabwell (Shanghai) Bioscience Co., Ltd., Shanghai, China, [2]Institution: ShanghaiTech University, Shanghai, China

Background: Regulatory T cells (Tregs) are one of the representative immunosuppressive cells playing a critical role in tumor microenvironment by suppressing anti-tumor immune responses. A great many Treg-depleting therapeutics targeting CTLA-4, CCR8, and CD25 are currently being investigated in clinical trials, and the overwhelming majority of these studies showed systemic toxicity or limited efficacy. Novel modalities favoring tumor-infiltrating Tregs depletion are urgently needed. Here, a CCR8/CTLA-4 bispecific antibody 2MW4691 with inequivalent target arm affinities was developed to specifically deplete tumor-infiltrating Tregs and block CTLA-4 signaling on CD8+ T cells.

Methods: Single-cell RNA sequencing data collection and computational analysis were applied to investigate CCR8 and CTLA-4 gene expression profiles in tumor-infiltrating Tregs. 2MW4691 was generated by combining parental bivalent anti-CCR8 and anti-CTLA-4 antibodies with different target arm affinities. CCR8 and CTLA-4 single and double-positive cells were used to evaluate the binding and blocking abilities of 2MW4691. Human FcγRIIIa receptor system, NK cells, and hPBMCs were used to assess the ADCC activity of 2MW4691. hCCR8/hCTLA-4 double transgenic mouse syngeneic models were used to evaluate the anti-tumor efficacy of 2MW4691 *in vivo*. A repeat dose administration study was performed in cynomolgus monkeys to evaluate the pharmacokinetic and toxicity profiles of 2MW6471.

Results: Single-cell RNA sequencing analysis confirmed the co-expression of CCR8 and CTLA-4 in tumor-infiltrating Tregs of NSCLC patients. 2MW4691 was designed as a tetravalency symmetric structure with high binding affinity to CCR8 and low binding affinity to CTLA-4, which resulted in strong ADCC activity towards CCR8 single and CCR8/CTLA4 double-positive cells, but limited ADCC activity towards CTLA-4 single positive cells in cell-based assays. In the staphylococcal enterotoxin B stimulation assay, 2MW4691 promoted T-cell activation, suggesting that it maintained the ability to block CTLA-4-mediated downstream signaling from its parental anti-CTLA-4 antibody. *In vivo*, 2MW4691 exhibited potent anti-tumor efficacy in hCCR8 or hCTLA4 humanized mice bearing MC38 tumors. Further, the advantage in tumor inhibition of 2MW4691 compared with its parental antibodies was proved in the hCCR8/hCTLA-4 double knock-in mouse model. In the NHP study, 2MW4691 exhibited good pharmacokinetic and safety profiles with negligible impact on peripheral T cells.

Conclusion: 2MW4691 demonstrated superior anti-tumor efficacy compared with its parental antibodies in CDX models and favorable tolerability in NHPs. The encouraging preclinical results support further evaluation of 2MW4691 in clinical trials.

#6351 MUC1*-ADCs are effective against heterogeneous solid tumor cancers.

C. C. Bamdad, B. S. Smagghe, S. T. Moe, M. G. Carter, T. J. Grant, K. R. Yi, M. J. Nash, J. P. Marquez, N. K. Miller, J.-L. S. Nash, D. S. Miller, D. M. Walkley, A. K. Stewart;
Minerva Biotechnologies, Waltham, MA

Purpose: To develop a MUC1*-ADC for the treatment of over 75% of solid tumor cancers.
Methods: MUC1* (muk 1 star) is a growth factor receptor created after cleavage and release of the N-terminal portion of MUC1. The targeting antibody, huMNC2, has already demonstrated safety and cancer selectivity in a 1st-in-human CAR-T clinical trial for treatment of metastatic breast cancers. MNC2 is an IgG1 antibody that only recognizes the conformational epitope created when MUC1 is cleaved by specific tumor-associated enzymes. Confocal microscopy and pHlourin2 were employed to measure antibody internalization as a function of time. We conjugated MNC2 to MMAE, MMAF, Dxd and exatecan via several different linkers. MUC1*-ADCs with DARs ranging from 4-8 were tested in vitro and in vivo for efficacy against a panel of solid tumor cancers. Heterogenous MUC1* tumors were made by mixing different ratios of mCherry wild-type cancer cells with GFP MUC1* overexpressed cancer cells. Resulting H scores ranged from 10-280 (max 300).
Results: Cancer cells internalized the MUC1* MNC2 antibody within 2 hours. In vitro, MUC1*-ADC IC50s ranged from 1.3nM to 20.0nM, depending on the linker-payload and cancer subtype, wherein the majority had an IC50 of about 10nM. In general, efficacy in animals was seen across multiple cancer sub-types treated with multiple MUC1*-ADCs. Efficacy in animals xenografted with heterogeneous MUC1* tumors showed a dependence on antigen density. Greatest efficacy was observed for breast cancer xenografts with an H Score >10 treated with MNC2-Deruxtecan. However, only pancreatic tumors with higher H Scores were completely eliminated by MNC2-MMAE, MNC2-Deruxtecan and MNC2-exatecan. MNC2-ADC and MNC2-CAR share the same antibody. No off-tumor toxicity was observed in animals treated with MNC2-ADC, which mimicked lack of off-target toxicities for MNC2-CAR T cells in humans.
Conclusions: These data, combined with MNC2-CAR T data from our 1st-in-human trial for metastatic breast cancer, supports a conclusion that the MUC1* antibody MNC2 is safe and could have high therapeutic value as a MUC1*-ADC for multiple solid tumors with both high and low antigen density.

#6352 Preclinical discovery of ARX622: A site-specific, TLR7 agonist, HER2-targeted immune-stimulatory antibody drug conjugate for treatment of multiple solid tumor types.

D. Mills, J. Kim, E. Wood, K. Tatsukawa, N. Knudsen, J. Nelson, L. Skidmore, K. GC, H. Tran, M. Pal, H. Hashemi, Y. Buechler, S. Zhang, D. O'Connor; Ambrx, San Diego, CA

Traditional antibody-drug conjugates leverage the specificity of antibodies to deliver cytotoxic payloads to tumor microenvironments (TMEs), thereby reducing systemic toxicities associated with non-targeted chemotherapeutics. Analogously, a novel class of immune-stimulating antibody conjugates (ISACs) has recently emerged to selectively deliver synthetic immune agonists to the TME without systemic immune activation. The first generation of ISACs and the majority of approved and investigational ADCs contain payloads linked to native lysine or cysteine residues, which can lead to heterogenous drug-antibody ratios (DARs), reduced antibody stability, and labile conjugation, all of which limit therapeutic index. Here we describe the generation and preclinical characterization of ARX622, a site-specific TLR7-selective agonist ISAC targeting HER2. To avoid the instability issues of previous generation ADCs and ISACs, ARX622 has a homogenous and stable DAR via oxime bond-mediated payload conjugation to a synthetic amino acid, para-acetyl phenylalanine (pAF), which is recombinantly incorporated at defined heavy chain positions. Similar to cytotoxic ADCs built on this site-specific conjugation platform, ARX622 ISAC and total mAb pharmacokinetic (PK) profiles in non-human primates (NHPs) are indistinguishable, demonstrating in vivo stability and minimal payload deconjugation. Accordingly, ARX622 displays an extended PK profile in mice compared to a DAR-matched random cysteine ISAC containing the same antibody and payload. In the presence of HER2-expressing cells, ARX622 selectively induces proinflammatory cytokine production, type I and III IFN secretion, and APC maturation. In a syngeneic tumor model, ARX622 promotes complete tumor regressions, immunologic memory, and epitope spreading. In xenograft systems, single doses of ARX622 induce complete regression of large, established tumors (>1000mm3), and robustly inhibit tumor growth in mice that have progressed through prior treatment with HER2-targeted mAbs or ADCs. In HER2-low xenografts, ARX622 monotherapy inhibits tumor growth, and promotes complete regression of late-stage (800mm3) tumors when sequentially combined with a HER2-ADC. Based on PK data at efficacious doses in mice and tolerated exposures in NHP toxicity studies, ARX622 has an estimated therapeutic index of ~60x. Taken together, ARX622's mAb-like properties, high stability, broad immune mechanism induction, strong anti-tumor activity alone or in combination with ADCs, and wide therapeutic index make it a strong candidate for further development toward treating patients with a variety of HER2-expressing solid tumors.

#6353 AM105: A novel bispecific antibody with Anti 4-1BB affibodies and EGFR antibody.

D.-W. Kim, H.-J. Lee, S. Kim, M. Yoon, Y. Lee, I.-S. Hwang, Y. Lee, J.-H. Kim, J.-S. Lee;
AbClon, Inc., Seoul, Korea, Republic of

T cell engaging bispecific antibodies have emerged as promising treatments for hematologic malignancies. While most antibodies are CD3-based, offering therapeutic benefits, they are often associated with severe side effects and limited efficacy in solid tumors. To address these challenges, we present AM105, a groundbreaking anti 4-1BB affibodies based bispecific antibody designed to target EGFR. We carefully engineered AM105 with distinct binding affinities for EGFR (KD = 1.8 nM) and 4-1BB (KD = 60 nM), favoring EGFR binding. Affibody specificity was confirmed through a cross-reactivity test with proteins of TNF-receptor superfamily and 21 cell lines expressing 4-1BB or not. In cytotoxicity assays, AM105 exhibited superior tumor cell killing compared to cetuximab, particularly in EGFR-expressing cell lines. Notably, AM105 displayed remarkable efficacy in cell lines harboring RAS and/or BRAF mutations, traditionally unresponsive to EGFR-targeting treatments. In vivo experiments utilizing humanized 4-1BB mice demonstrated AM105's exceptional tumor cell elimination compared to cetuximab. The anti-tumor effects persisted even in the face of new tumor cell introductions, suggesting the induction of T cell memory function. Our findings collectively establish AM105 as a potent therapeutic agent with strong anti-tumor T cell activity. The unique 4-1BB based Affibodies (AffiMab format) of AM105 holds promise for addressing the limitations of current bispecific antibodies, positioning it as a potential breakthrough in cancer immunotherapy.

#6354 The HER2/4-1BB bispecific antibody, YH32367 (ABL105) demonstrates optimal efficacy and safety for HER2-expressing tumors and exhibits synergistic efficacy when combined with anti-PD-L1.

E. Lee[1], Y. Park[1], M. Choi[1], J. Shin[1], K. Kim[1], J. Park[1], J. Kim[1], K. Ahn[1], Y. Lee[2], K. Park[2], W. Son[2], D. Yeom[2], J. Eon[2], H. Lee[2], H. Jung[2], J. Won[2], S.-W. Oh[1], Y. Kim[1],

[1]Yuhan Co, Ltd., Seoul, Korea, Republic of, [2]ABL Bio Inc., Seongnam-Si, Korea, Republic of

Overexpression/amplification of the human epidermal growth factor receptor 2 (HER2) is associated with clinically aggressive subtypes in various cancers. Currently, new HER2-targeted therapy like trastuzumab deruxtecan have improved outcomes not only for HER2-positive tumors but also for HER2-low tumors. However, curing cancer patients who develop resistance to current HER2-targeted therapies or experience unwanted side effects remains a significant challenge. Therefore, there is a pressing need for more advanced treatments, and one promising approach involves combination with immunotherapy. 4-1BB (CD137) is a key costimulatory receptor expressed on activated T-cells and natural killer cells, making it a promising therapeutic target in cancer. This study presents the anti-tumor efficacy of the HER2/4-1BB bispecific antibody, YH32367 (ABL105), against both HER2-positive and HER2-low tumors. Additionally, the study suggests that YH32367 could be a viable treatment option for combination with anti-PD-1 antibody (Ab). YH32367 has been designed to overcome the challenges with HER2 resistance via tumor-directed 4-1BB agonism. YH32367 induced IFN-γ secretion and thereby eliciting tumor cell death in co-culture condition with hPBMC and HER2-expressing tumor cells. YH32367 showed superior efficacy in eradicating tumors and triggered long-term anti-tumor immunity in MC38/hHER2-bearing h4-1BB KI mouse models, compared to benchmark 4-1BB/HER2-bispecific molecule and anti-HER2 Ab. Even in HER2-low tumor, YH32367 was more effective than benchmark 4-1BB/HER2-bispecific molecule. Additionally, when YH32367 was administered in combination with anti-PD-1 Ab to h4-1BB KI mice bearing HER2-low tumors, a synergistic effect was observed, surpassing the effects of anti-PD-1 Ab alone or anti-HER2 Ab-drug conjugate. The potent anti-tumor efficacy of YH32367 was also verified in HER2 expressing tumor-bearing hPBMC humanized mice. In terms of toxicity, YH32367 demonstrates a favorable safety profile, which was confirmed through a 4-week GLP toxicity study using cynomolgus monkeys at doses of 10, 30, and 100 mg/kg. In summary, YH32367 has demonstrated significant anti-tumor effects, impacting tumor immunity in h4-1BB KI mice with HER2-low and HER2-positive tumors. Furthermore, its combination with anti-PD-1 Ab has shown synergistic efficacy, indicating that YH32367 may offer treatment options not only as a monotherapy but also in combination therapy for HER2 expressing tumors. The phase 1 dose escalation study is currently underway (NCT05523947), and a dose optimization study to determine the recommended phase 2 dose (RP2D) is scheduled for the second half of 2024.

#6355 Urokinase plasminogen activator receptor-associated protein (uPARAP) is overexpressed in human glioblastomas and is a therapeutic target for antibody-drug conjugates (ADC).

I. Gregersen[1], C. R. Lokke[1], J. B. Lange[1], P. Barkholt[1], C. Come[1], T. Broberg[1], M. M. Petersen[1], C. M. Lynch[1], D. Mumberg[1], N. Behrendt[2], L. H. Engelholm[2]; [1]Adcendo ApS, Copenhagen, Denmark, [2]The Finsen Laboratory, Copenhagen, Denmark

Background: Glioblastoma Multiforme (GBM), primarily arising in the brain's frontal and temporal lobes, is a devastating malignancy originating from astrocytes. Despite treatment advancements, the prognosis remains bleak, with a median survival of 15-18 months and a 10% five-year survival rate.Our study explored a novel targeted approach to combat this challenge. uPARAP is an endocytic receptor expressed at low levels on selected mesenchymal cell types but highly overexpressed on the majority of Soft-Tissue- and Bone Sarcomas. It internalizes fragments of collagen and transfers them to the lysosome for degradation.
Methods & Results: First, we analyzed formalin-fixed paraffin-embedded (FFPE) tumors from GBM patients through immunohistochemistry (IHC) staining. Interestingly, a majority of the samples showed strong but varying uPARAP expression. In parallel, we detected and quantified uPARAP receptor expression in GBM cell lines by flow cytometry, underscoring its potential as a therapeutic target.Next, we generated an antibody-drug conjugate (ADC) linked to monomethyl auristatin E (MMAE), a potent antimitotic agent. Confocal microscopy showed rapid internalization of the ADC in several GBM cell lines *in vitro*. Cellular cytotoxicity was demonstrated in Incucyte and Alamar Blue *in vitro* assays. Finally, anti-tumor activity of the uPARAP-ADC was studied in a GBM patient-derived xenograft (PDX) model *in vivo*, where it resulted in significant tumor regression with a tumor growth inhibition (TGI) of 92 and 97% at 3 and 6 mg/kg, respectively.
Conclusions: Our findings show that uPARAP is overexpressed on GBM tumors and that a uPARAP-targeted ADC has anti-tumor activity in a PDX model of GBM. This research provides initial evidence that uPARAP-ADCs could become a novel treatment option for this highly aggressive disease.

#6356 Novel antibody targeting tumor NKG2D ligand MIC: Preclinical studies and clinical development plan for mCRPC.

J. D. Wu[1], J. Sosman[1], M. Kocherginsky[2], A. Serritella[1], M. Hussian[1], D. J. Vanderweele[1];
[1]Northwestern University - Evanston, Chicago, IL, [2]Northwestern University, Chicago, IL

In response to genomic insults and DNA double-strand breaks, the stressed epithelial cells express the MHC I-chain related molecule (MIC) on the surface as a byproduct of activating the ATM pathway. The MIC molecule itself has no known impact on tumor survival or growth. In the context of immune microenvironment, tumor cell surface MIC can activate NK cells and co-stimulate CD8 T cells by engaging in the activating receptor NKG2D to hinder the early tumorigenesis. However, in established malignancies, in particular metastatic diseases, tumor cells shed surface MIC to release the soluble form MIC (sMIC). It has been well demonstrated that, in contrary to cell surface MIC, sMIC is highly immune suppressive by disturbing NK cell homeostasis and repolarizing NK cells function, impairing antigen-specific CD8 T cell function by downmodulating NKG2D expression and CD3z expression, and facilitating immune suppression of MDSCs and TAMs in tumor microenvironment. We have demonstrated that MIC is prevalently expressed by prostate tumor cells and significantly upregulated in mCRPC tumors. We have shown significantly elevated levels of serum sMIC in prostate cancer patients with metastatic diseases. We have developed a novel class of clinical candidate monoclonal antibody huB10G5 that can target both sMIC and surface MIC to re-invigorate both NK and CD8 T cell function and inhibit MDSCs and TAMs in preclinical models. The huB10G5 has an acceptable safety profile and is currently completing CMC for IND enabling. We hypothesize that huB10G5 is a novel immune therapeutic reagent for mCRPC patients. To test our hypothesis, we first conducted serial studies of the clinical candidate huB10G5 in pre-clinical models of prostate cancers. We found that huB10G5 can effectively induce 100% long-term tumor complete regression (CR) as low as 1.0 mg/KG. These animals are fully protected from tumor re-challenge. The anti-tumor effect is mediated by the combined action of NK and CD8 T cells. With the support of our pre-clinical efficacy and safety data, we have planned to initiate Phase I clinical trial with huB10G5 for mCRPC patients in 2024.

#6358 Arming tumor-associated macrophages to inhibit cancer progression.

J. P. Reddy[1], Z. Yu[1], R. M. Shepard[1], T. Von Schalscha[1], S. J. McCormack[2], S. M. Weis[1], D. A. Cheresh[1], H. I. Wettersten[1];
[1]University of California San Diego - UCSD, La Jolla, CA, [2]Alpha Beta Therapeutics, Camden, DE

Integrin αvβ3 is a marker of cancer progression in a range of epithelial cancers. In the 1990s, a humanized anti-αvβ3 antibody (Etaracizumab) was developed to target αvβ3+ cancer cells via NK cell-mediated cytotoxicity. While it demonstrated safety and some efficacy in clinical trials, our recent study of the immune microenvironment in αvβ3+ human epithelial tumors revealed increased tumor-associated macrophages (TAMs) but minimal NK cell accumulation. Accordingly, we re-engineered Etaracizumab to favor TAM engagement over NK cells and compared the efficacy of this antibody (ABT101) to that of Etaracizumab in various αvβ3+ epithelial cancer models. While ABT101 and Etaracizumab exhibited identical affinity for αvβ3, ABT 101 showed superior anti-tumor activity in vivo. Notably, depleting NK cells in mice had no impact on ABT101's effectiveness, while macrophage depletion completely abolished its anti-tumor activity. Interestingly, tumors in mice treated with ABT101 displayed a significant increase in TAMs. Here we define an "antigen-effector cell matching" strategy that allows for maximal anti-tumor activity for various drug resistant epithelial cancers. ABT101 will enter clinical trials for patients with drug resistant lung cancer in the first quarter of 2024.

#6359 Development of PSMA x CD3 T-cell engagers using an integrated, functional approach.

V. de Puyraimond, M. Mai, A. Amash, N. Blamey, G. Conaghan, J. Fernandes Scortecci, A. Goodman, A. Lee, I. Yu, F. von Bank, K. Caldwell, L. Clifford, I. Knarston, K. Bullock, M. Cid, C.-L. Crichlow, L. Devorkin, F. Dickson, P. Farber, S. Hannie, C. Lai, V. Li, S. K. Masterman, I. Niemietz, P. Pouliot, P. Xiang, B. C. Barnhart, **R. Tonikian**;
AbCellera, Vancouver, BC, Canada

In this study, we used a functional approach to generate CD3 T-cell engager (TCE) molecules targeting prostate-specific membrane antigen (PSMA). We present data on the robust *in vitro* characterization of T-cell activity and selection of molecules for further assessment. TCE function is dictated by the interplay between multiple factors that form the immune synapse, including binding kinetics, binding geometry, and epitopes of the CD3- and tumor-binding arms. To diversify immune synapse parameters, we engineer hundreds of bispecific molecules from highly diverse parental antibodies, and employ a high-throughput process to select molecules with desired functional properties. We applied this approach to engineer CD3 TCEs targeting PSMA. PSMA is an attractive target for the treatment of castration-resistant prostate cancer due to its high expression in prostate cancer cells and low relative expression in other tissues. We discovered hundreds of diverse, fully human PSMA-binding antibodies using high-throughput single B-cell screening and selected human/cynomolgus cross-reactive binders with a broad range of affinities and epitopes. We paired these with human/cynomolgus cross-reactive CD3-binding antibodies from our TCE platform to generate 180 bispecific PSMA x CD3 TCEs. CD3-binding antibodies covered several orders of magnitude of affinity (nanomolar to micromolar) and included binders specific for different CD3 subunits. We used high-throughput T-cell dependent cellular cytotoxicity (TDCC) and cytokine release assays to identify molecules with desired functional profiles. Bispecifics selected for further assessment had functional profiles spanning a range of properties that have been observed in clinical molecules, including potent killing and low cytokine release. To profile T-cell properties that are associated with anti-tumor immune responses, we subjected selected molecules to a battery of additional *in vitro* functional assessments, including proliferation, cytokine and chemokine production, and TDCC using cynomolgus T cells. Results demonstrate that a functional approach that begins with highly diverse CD3- and tumor-binding antibodies can generate promising TCEs with minimal need for protein engineering and optimization.

#6360 A novel CAR-NK cell therapy to target lung adenocarcinoma cells.

S. Zolov, **S. Chuikov**, S. Katkam, D. Shield, V. G. Keshamouni;
University Of Michigan, Ann Arbor, MI

Cell Adhesion Molecule (CADM1) is a Bonafede tumor suppressor with 40% of NSCLC tumors lose CADM1 expression either by loss of heterozygosity or promoter hypermethylation. The tumor suppressive ability of CADM1 is attributed to its cell adhesion function. However, we previously demonstrated that CADM1 also mediates its tumor suppression through regulation of NK-mediated immunosurveillance. In tumors that do not lose CADM1, it is expressed on cell surface and up regulated during TGF-β-induced EMT making it a biomarker for potential therapeutic targeting. Here we report the design and development of T and NK specific CAR that would specifically target lung cancer cells in CADM1 dependent manner. Anti-CADM1 single chain variable fragment (CADM1-scFv) was fused to NK or T cell specific transmembrane and co-stimulatory domains. The resulting CAR constructs were cloned into a retroviral vector, from which viral stocks were generated to transduce human and mouse cells. Next, we introduced anti-CADM1-CAR-NK construct into NK92 cell line and tested it in a cytotoxicity assay using A549-GFP-ffluc cell line as a target. We observed a significant increase in the killing of target cells with anti-CADM1-CAR-NK cells compared with non-transduced NK92 cells. This effect was significantly reduced when A549- GFP-ffluc-CADM1 KO cells were used as target. Next, we generated anti-CADM1-CAR-T cells by transducing human $CD3^{\pm}$ T-cells purified from human PBMCs. Similar to anti -CADM1-CAR-NK, anti-CADM1-CAR-T cells showed increased T-cell specific cytotoxicity in a CADM1-dependent manner. Next, we evaluated the efficacy of anti-CADM1-CAR-T cells through adoptive transfer into NSG mice xenografted with human lung adenocarcinoma cells into mouse lungs. The administration of anti-CADM1-CAR-T cells markedly reduced tumor size and enhanced the survival rate of the mice. Importantly this effect was dependent on CADM1 expression, as mice xenografted with human CADM1 KO cells showed neither tumor size reduction nor increased survival. Finally, using IHC staining, we demonstrated that anti-CADM1-CAR-T cells directly target xenografted tumors in the mouse lungs. In conclusion, our findings indicate that CAR-NK and CAR-T cells targeting CADM1-expressing lung tumors have a significant therapeutic potential for the treatment of NSCLC.

#6361 KY-HC-mouse: A low-cost and rapid nanobody discovery platform.

G. Wu, F. Hao, F. He, H. Peng, Y. Gu, J. Ning;
Kyinno Biotechnology Co., Ltd, Beijing, China

Nanobodies, primarily derived from camelid animals, have gained prominence in antibody-drug development due to their small molecular weight and ease of modification. However, the high cost associated with camelid animals for nanobody discovery led us to develop a strain of heavy-chain mice known as KY-HC-mouse. This genetically modified mouse expresses IgG without the CH1 domain, resulting in the production of nanobodies in IgG format. Utilizing hybridoma techniques, we developed a variety of nanobodies against multiple targets, such as PSMA, CD38, PD-L1, CD28, and 4-1BB, from KY-HC-mouse. These nanobodies all demonstrate high affinity, with KD ranging from 0.01 nM to 10 nM. We also selected antagonist nanobodies that block the interaction of PD1 and PDL1, as well as agonist nanobodies that stimulate 4-1BB signaling in T cells. After humanization, most nanobodies have a half-life of more than five days in the blood of both mice and monkeys. Subjected to various treatments, such as high concentration, low pH, repeated freezing and thawing, and high temperature, most humanized nanobodies show neither aggregation nor degradation, suggesting good developability of these nanobodies. Finally, we have developed multiple bispecific antibodies (BsAbs) targeting both PDL1 and 4-1BB, PSMA and 4-1BB, or B7H3 and 4-1BB. These BsAbs exhibit good developability and efficacy. In conclusion, our KY-HC-mouse is a powerful nanobody discovery platform.

#6362 The bispecific antibody KA-3002, targeting PSMA and 4-1BB, specifically enhances T cell activity within prostate tumors.

G. Wu, J. Liang, H. Peng, F. Hao, T. Liu, J. Ning;
Kyinno Biotechnology Co., Ltd, Beijing, China

Cancer immunotherapy with 4-1BB agonists has faced limitations in further clinical development due to dose-limiting toxicity. PSMA, highly expressed in normal prostate tissue and prostate cancer, is a clinically validated target for prostate cancer treatment. In this study, we developed a bispecific antibody (BsAb), KA-3002, targeting PSMA and human 4-1BB, with the aim of restricting 4-1BB stimulation to the interior of tumors. KA-3002 was developed based on our nanobody antibody discovery platform. KA-3002, in IgG1 format, features mutations in the Fc domain to eliminate ADCC, ADCP, and CDC activity. It contains two identical nanobodies at the C-terminal against 4-1BB to stimulate 4-1BB signaling in T cells and binds to PSMA with two Fabs at the N-terminal. KA-3002 exhibits high avidity binding to prostate tumor cells expressing PSMA (EC50<1nM) and also binds to 4-1BB expressed on 293T cells and activated human T cells. In the presence of a low concentration of CD3 antibody to stimulate T cell activation, co-culture of tumor cells expressing PSMA with primary T cells isolated from human PBMC enhances T cell activation and proliferation. In PBMC humanized immunodeficient mouse tumor models, KA-3002 effectively suppresses the growth of 22Rv1 tumors, which highly express PSMA. The antibody also demonstrates a half-life of more than five days in the blood of Balb/c mice. Finally, we assessed the developability of this antibody with different treatments such as high concentration, low pH, repeated freezing and thawing, and high temperature. KA-3002 shows neither aggregation nor degradation. In conclusion, the BsAb KA-3002, developed with our nanobody antibody discovery platform, emerges as a promising pre-clinical candidate drug for the treatment of prostate cancer.

#6363 The biparatopic antibody KA-3005 against MET is suitable for developing antibody-drug conjugates (ADCs) to treat MET-expressing cancers.

G. Wu, J. Liang, H. Peng, F. Hao, T. Liu, J. Ning;
Kyinno Biotechnology Co., Ltd, Beijing, China

MET is overexpressed in a significant fraction of lung (25%-50%) and gastroesophageal cancers, making the targeting of MET with an antibody-drug conjugate (ADC) an attractive approach. Here, we developed a bispecific antibody (BsAb) named KA-3005, targeting two different epitopes within the extracellular domain of MET using our common light chain antibody discovery platform. KA-3005 has a regular antibody structure with an identical light chain, developed using knob-into-hole technology. This antibody exhibits significantly higher avidity to MET expressed on tumor cells, with an EC50 of less than 0.1nM compared to its parent antibodies. It also completely blocks the binding of HGF to MET and the MET downstream pathway at a concentration as low as 1nM. This biparatopic antibody demonstrates a faster internalization rate upon binding to the surface of tumor cells expressing MET than its parent antibodies. KA-3005 effectively suppressed the growth of HCC827-HGF tumors in a xenograft mouse model. Additionally, it has a half-life of more than five days in the blood of Balb/c mice. Finally, we assessed the developability of KA-3005 under different treatments such as high concentration, low pH, repeated freezing and thawing, and high temperature, and it showed neither aggregation nor degradation. In conclusion, this biparatopic antibody, KA-3005, developed with our common light chain antibody discovery platform, is stable and holds potential for the development of ADCs targeting MET.

#6364 The bispecific antibody KA-3006 against both EGFR and MET surpasses amivantamab in efficacy.

G. Wu, J. Liang, H. Peng, F. Hao, T. Liu, J. Ning;
Kyinno Biotechnology Co., Ltd, Beijing, China

A bispecific antibody (BsAb) like amivantamab, which targets both the epidermal growth factor receptor (EGFR) and mesenchymal-epithelial transition factor (MET) by blocking downstream pathways, has been proven to overcome resistance to targeted therapies, including EGFR inhibitors, in patients with various cancers. In this study, we developed a bispecific antibody, KA-3006, targeting both EGFR and MET using our common light chain antibody discovery platform. KA-3006 has a regular antibody structure with an identical light chain, developed through knob-into-hole technology. It exhibits high affinity for MET and relatively low affinity for EGFR. KA-3006 specifically blocks both the binding of EGF to EGFR and HGF to MET with higher efficiency than amivantamab, resulting in the blockade of downstream signaling from EGFR and MET. In comparison to amivantamab, KA-3006 demonstrates a faster internalization rate when binding to the surface of tumor cells expressing both EGFR and MET. KA-3006 showed superior antitumor activity over amivantamab in the HCC827-HGF in vivo model. Additionally, KA-3006 has a half-life of more than five days in the blood of Balb/c mice. Finally, we assessed the developability of this BsAb with different treatments such as high concentration, low pH, repeated freezing and thawing, and high temperature, and KA-3006 showed neither aggregation nor degradation. In conclusion, the BsAb KA-3006, developed with our common light chain antibody discovery platform, is a promising pre-clinical candidate drug for the treatment of various solid cancers with overactivated EGFR and MET signaling, and it holds potential for developing ADCs targeting both EGFR and MET.

#6365 The bispecific antibody KA-3008, targeting both EGFR and B7H3, increases internalization and minimizes on-target, off-tumor toxicity.

G. Wu, L. Ding, H. Peng, F. Hao, F. He, J. Ning;
Kyinno Biotechnology Co., Ltd, Beijing, China

EGFR and B7H3 are highly expressed in various solid tumors, as well as in different normal tissues. Targeting EGFR or B7H3 alone with inhibitory monoclonal antibodies or antibody-drug conjugates (ADCs) may result in on-target, off-tumor toxicity. In this study, we developed a bispecific antibody (BsAb) named KA-3008, targeting both EGFR and B7H3 using our common light chain antibody discovery platform. KA-3008, in IgG1 format, features a regular antibody structure with an identical light chain, developed through knob-into-hole technology. Compared to its parent antibodies, its affinities for both EGFR and B7H3 decrease by more than ten times. It binds to cell lines expressing EGFR or B7H3 alone with an EC50 of more than 10nM, while it binds to cell lines expressing both EGFR and B7H3 with an EC50 of less than 1nM. KA-3008 also blocks the binding of EGF to EGFR and increases internalization when binding to both EGFR and B7H3 compared to binding to EGFR or B7H3 alone. In human tumor mouse models, KA-3008 effectively suppresses the growth of NCI-H1568 tumors expressing both EGFR and B7H3, but does not affect the growth of MS751 tumors that only highly express EGFR with low expression of B7H3. Additionally, KA-3008 has a half-life of more than five days in the blood of Balb/c mice. Finally, we assessed the developability of this BsAb with different treatments such as high concentration, low pH, repeated freezing and thawing, and high temperature, and KA-3008 shows neither aggregation nor degradation. In conclusion, the BsAb KA-3008, developed with our common light chain antibody discovery platform, is stable and holds potential for the development of ADCs targeting both EGFR and B7H3.

#6366 The triple-specific antibody KA-3009 against EGFR, B7H3, and 4-1BB specifically enhances T cell activity within the tumor.

G. Wu, T. Liu, J. Liang, H. Peng, F. Hao, J. Ning;
Kyinno Biotechnology Co., Ltd, Beijing, China

Cancer immunotherapy with 4-1BB agonists faces limited further clinical development due to dose-limiting toxicity. Moreover, EGFR and B7H3 are highly expressed in various solid tumors, as well as in different normal tissues. In this study, we developed a trispecific antibody, KA-3009, targeting EGFR, B7-H3, and human 4-1BB, with the aim of restricting 4-1BB stimulation within tumors. KA-3009 was developed based on our common light chain bispecific antibody discovery platform and nanobody antibody discovery platform using knob-into-hole technology. It is in IgG1 format with mutations in the Fc domain to eliminate ADCC, ADCP, and CDC activity. Featuring two identical nanobodies at the C-terminal against 4-1BB, KA-3009 binds to EGFR and B7H3 respectively with two Fabs at the N-terminal, sharing an identical light chain. KA-3009 exhibits low avidity binding to tumor cells expressing only EGFR or B7H3, while binding to tumor cells co-overexpressing EGFR and B7H3 with increased avidity by more than ten times. Additionally, KA-3009 binds to 4-1BB expressed on 293T cells and activated human T cells. In the presence of a low concentration of CD3 antibody to stimulate T cell activation, co-culture of tumor cells co-expressing EGFR and B7H3 with primary T cells isolated from human PBMC enhances T cell activation and proliferation. In PBMC humanized immunodeficient mouse tumor models, KA-3009 effectively suppresses the growth of NCI-H1568 tumors expressing both EGFR and B7H3 but does not affect the growth of MS751 and NCI-H661 tumors, which only express EGFR or B7H3, respectively. Moreover, KA-3009 has a half-life of more than five days in the blood of Balb/c mice. Finally, we assessed the developability of this antibody with different treatments such as high concentration, low pH, repeated freezing and thawing, and high temperature, and KA-3009 shows neither aggregation nor degradation. In conclusion, the triple-specific antibody KA-3009, developed with our common light chain antibody discovery platform and nanobody antibody discovery platform, is a promising pre-clinical candidate drug for the treatment of different solid cancers that co-overexpress EGFR and B7H3.

CLINICAL RESEARCH: Pediatric Clinical Research and Late Effects
Poster Session

#6370 Evaluating the risk of carcinomas among children with congenital anomalies: A population-based study of 21 million births.

J. M. Schraw[1], T. A. Desrosiers[2], T. M. Chambers[1], M. E. Scheurer[1], C. J. Shumate[3], W. N. Nembhard[4], M. M. Yazdy[5], E. Nestoridi[5], A. E. Janitz[6], J. Tanner[7], R. S. Kirby[7], J. L. Salemi[7], C. D. Huff[8], S. E. Plon[1], P. J. Lupo[1];
[1]Baylor College of Medicine, Houston, TX, [2]University of North Carolina at Chapel Hill, Chapel Hill, NC, [3]Texas Department of State Health Services, Austin, TX, [4]University of Arkansas for Medical Sciences, Little Rock, AR, [5]Massachusetts Department of Public Health, Boston, MA, [6]University of Oklahoma Health Sciences Center, Oklahoma City, OK, [7]University of South Florida, Tampa, FL, [8]University of Texas MD Anderson Cancer Center, Houston, TX

Background: Carcinomas in childhood are rare, limiting our understanding of their epidemiology. While congenital anomalies are one of the strongest risk factors for childhood cancer overall, their association with carcinomas is understudied. We evaluated the associations between chromosomal and non-chromosomal congenital anomalies and risk of carcinoma through age 18 years.
Methods: We leveraged the Genetic Overlap Between Anomalies and Cancer in Kids (GOBACK) Cohort, which includes linked data from population-based birth defects and cancer registries for 21 million births between 1990-2018 in nine U.S. states. We used Cox regression to estimate the hazard ratio (HR) and 95% confidence interval (CI) for the hazard of carcinomas among children with major congenital anomalies relative to children without these conditions, adjusting for sex, state of birth, and maternal age. We performed sensitivity analyses excluding cases diagnosed with carcinomas during the first 2 years of life to assess the potential impact of incidental discovery of anomalies during cancer diagnosis or treatment on our findings.
Results: Our study population numbered 21,829,628 children, including 635,632 with major anomalies and 879 with carcinomas (incidence rate: 4.2 per million person-years). Mean follow-up time was 9.6 years. The most common diagnoses were thyroid (N=600 cases) and hepatocellular carcinoma (HCC; N=68 cases). Prevalence of major anomalies was 4.0% in children with carcinomas and 2.9% in children without carcinomas. The hazard of carcinomas was increased for both children with chromosomal or genetic syndromes (HR 5.3, CI 2.6-10.6; N=8) and children with non-syndromic anomalies (HR 1.6, CI 1.2-2.4; N=31). When we evaluated carcinomas by type, we observed associations between 1) chromosomal or genetic syndromes and renal cell carcinoma (HR 57.8, CI 20.7-161.3; N<5), 2) non-syndromic congenital anomalies and HCC (HR 3.8, CI 1.6-8.8; N=6), and to a lesser degree, 3) non-syndromic congenital anomalies and thyroid carcinoma (HR 1.4, CI 0.9-2.2; N=17). Notably, sensitivity analyses suggested associations were not attributable to incidental discovery of anomalies during cancer diagnosis or treatment.
Discussion: In this comprehensive assessment of congenital anomalies and carcinomas in children, we report novel associations. The observed associations between congenital anomalies and carcinoma could be due to factors including: 1) common genetic pathways; 2) *in utero* exposures that lead to both conditions; or 3) postnatal exposures among children with congenital anomalies. Ultimately, our findings could yield new insights into the etiologies of carcinomas in childhood and inform clinical surveillance practices for children with congenital anomalies.

#6371 Prenatal exposure to medication and risk of childhood cancer - A systematic review and meta-analysis.

A. Lubtow, M. Marron, **R. Nagrani**, W. Ahrens, L. Brackmann;
Leibniz Institute for Prevention Research and Epidemiology - BIPS, Bremen, Germany

The use of medication during pregnancy carries a potential health risk for the unborn child. However, the majority of drugs examined in previous observational studies have shown inconsistent results with the risk of childhood cancer, and these findings have not been consolidated in drug-specific meta-analyses. To address this gap, a systematic search was conducted in the databases PubMed and Science Citation Index for studies on medication use during pregnancy and the risk of childhood cancer. Studies with exposure to diethylstilbestrol as a known teratogen were excluded. Meta-analyses with estimates for random effects models with 95% confidence intervals were conducted, if at least three studies on the same research question were available. The I^2 statistic was calculated to quantify between-study heterogeneity. Statistical significance of I^2 was analyzed with the Q statistic (*P* value for heterogeneity (*P*)). Study quality was summarized based on a self-developed scoring system with five items. The systematic literature search yielded 2,373 studies, of which 62 were included in the systematic review. We conducted a total of 37 analyses including exposure to 12 different types of medications during pregnancy and 13 different outcomes of childhood cancer. Pooled odds ratios (OR) showed an increased risk of acute leukemia (AL) and its subtype acute lymphoblastic leukemia (ALL) after prenatal exposure to antiemetics (AL: OR= 1.47 (95 % confidence interval 1.02; 2.14) I^2= 0.0 % *P*= 0.44; ALL: OR= 1.27 (1.01;1.59) I^2= 0.0 % *P*= 0.93) and any kind of antibiotics (AL: OR= 1.13 (1.01; 1.27) I^2= 0.0 % *P*= 0.53; ALL: OR= 1.12 (1.01; 1.24) I^2= 19.7 % *P*= 0.26). In addition, an increased risk of childhood cancer in general was observed when mothers took nitrosatable antibiotics (OR= 1.32 (1.14; 1.53) I^2= 0.0 % *P*= 0.97). Finally, the use of analgesics (OR= 1.40 (1.00; 1.95) I^2= 43.8 % *P*= 0.15) during pregnancy was associated with an increased risk of neuroblastoma in the offspring. All these analyses did not reveal any indications of heterogeneity between the analyzed studies. The remaining 31 analyses showed no association. Our results suggest that the use of nitrosatable antibiotics during pregnancy may be associated with an increased risk of childhood cancer. Maternal intake of antibiotics and antiemetics may increase the risk of AL and ALL in their children. An increased risk of childhood neuroblastoma could be associated with prenatal exposure to analgesics. However, the underlying disease of the mother, which is treated with the investigated medication, could be the actual reason for the development of childhood cancer in the offspring.

#6372 Germline pathogenic variants are enriched in pediatric central nervous system tumor patients and associate with somatic functional consequences.

R. J. Corbett[1], R. Kaufman[1], S. W. McQuaid[2], Z. Vaksman[1], S. Phul[1], M. A. Brown[1], J. L. Mason[1], H. Desai[3], R. Hausler[3], A. S. Naqvi[1], A. Chroni[1], Z. Geng[1], B. Zhang[1], C. Zhong[1], Y. Zhu[1], A. P. Heath[1], M. Li[1], Penn Medicine BioBank, P. B. Storm[1], A. C. Resnick[1], K. N. Maxwell[3], M. Bornhorst[4], K. A. Cole[1], A. J. Waanders[2], S. P. MacFarland[1], J. Rokita[1], S. J. Diskin[1];

[1]Children's Hospital of Philadelphia, Philadelphia, PA, [2]Ann & Robert H. Lurie Children's Hospital of Chicago, Chicago, IL, [3]University of Pennsylvania, Philadelphia, PA, [4]Children's National Hospital, Washington, DC, DC

The genetic contribution of rare pathogenic germline variation to central nervous system (CNS) tumor formation in pediatric patients without a family history of cancer remains unclear. We sought to characterize the prevalence, spectrum, and clinical significance of pathogenic germline variation in cancer predisposition genes (CPGs) in 838 patients profiled in the Pediatric Brain Tumor Atlas (PBTA) by whole genome sequencing (n=821) or whole exome sequencing (n=17). Rare variants in 214 CPGs were annotated as pathogenic (P) or likely pathogenic (LP) consistent with American College of Medical Genetics criteria using AutoGVP, our open-source automated pathogenicity assessment tool. To assess enrichment of P/LP variants in the PBTA, we compared the frequency of CPG P/LP variants in cases to a tumor-free control cohort from Penn Medicine BioBank (PMBB; n=6,295). Somatic alterations, mutational signatures, and gene set enrichment analyses from matched tumor sequencing were integrated to characterize functional consequences associated with germline pathogenic variation. We observed 215 germline P/LP variants within 76 distinct CPGs in 189 (22.6%) PBTA patients. CPG P/LP variants were most prevalent among patients with a plexiform neurofibroma diagnosis (9/14, 64.3%), and least prevalent among patients with craniopharyngioma (3/39, 7.8%). We detected syndrome-associated P/LP variants in 45/58 (77.6%) patients with a clinically reported cancer predisposition syndrome and incidentally in another 37 patients. CPG P/LP variants were significantly enriched in the PBTA cohort relative to the PMBB control cohort (OR=2.0, p=1.0E-12, CI=1.6-2.4), and *NF1* harbored the most significant excess P/LP variant burden (OR=30.7, p=4.57E-13, CI=11.2-105.1). We observed a significant enrichment of mismatch repair (MMR) gene P/LP variants in patients with high-grade gliomas (HGG) and tumors from MMR P/LP carriers exhibited significantly higher MMR-deficiency mutational signature exposures relative to tumors from non-carrier HGG patients (SBS14: W=478, p=1.71E-05). Overall, 90/215 (41.9%) of identified germline P/LP variants co-occurred with at least one corresponding somatic alteration in matched tumors, including oncogenic SNV (n=5), copy number variation (n=28), loss of heterozygosity (n=54), differential gene expression (n=23), and proximal alternative splicing (n=19). In summary, rare germline P/LP variants are enriched in PBTA patients and are associated with somatic events in the same gene, resulting in gene- and pathway-specific functional consequences. Our work emphasizes a role for pathogenic germline variation in pediatric CNS tumor development and frequent under-identification of cancer predisposition syndromes, underscoring the importance of germline sequencing in personalized patient care strategies.

#6373 Effectiveness of tumor surveillance across pediatric cancer predisposition syndromes.

M. R. Perrino[1], A. Blake[1], C. E. Morin[2], L. Taylor[1], R. B. McGee[1], S. Lewis[1], S. Hines-Dowell[1], A. Pandey[1], P. Turner[1], M. Kubal[1], Y. Su[1], L. Tang[1], L. Howell[1], L. W. Harrison[1], Z. Abramson[1], A. Schechter[1], N. D. Sabin[1], K. E. Nichols[1];

[1]St. Jude Children's Research Hospital, Memphis, TN, [2]Cincinnati Children's Hospital Medical Center, Cincinnati, OH

Background: Pediatric oncology patients are increasingly recognized as having an underlying cancer predisposing syndrome (CPS). For individuals diagnosed with a CPS, surveillance is often recommended to detect new tumors at their earliest and most curable stages. Screening is heavily based on radiologic imaging, however data on the effectiveness and outcomes of surveillance are limited.

Methods: Patients with a clinical and/or molecular CPS diagnosis, including 274 children and young adults with 35 CPS at a single specialty pediatric oncology center, were monitored using standardized surveillance protocols over an average of 3 years (range 1 month - 12 years). Patients with hereditary retinoblastoma were excluded as surveillance was completed by a separate team. The cohort included 139 patients (50.7%) with a prior tumor history while 135 (49.3%) had no prior cancer. This study reviewed tumors diagnosed, method of detection, clinical course, and patient outcomes. Individual reports from 1,533 surveillance tests including diagnostic imaging, colonoscopy, and upper endoscopy, were assessed and classified for accuracy. Sensitivity, specificity, positive predictive value (PPV), and negative predictive values (NPV) were calculated for selected surveillance methods, and themes of common strengths or weaknesses of specific imaging modalities were identified.

Results: During the study period from January 1, 2009 - September 31, 2021**,** 35 asymptomatic tumors were detected in 27 patients through surveillance (9.9% of the cohort), while five symptomatic tumors were detected in five patients (1.8%) outside of surveillance. Ten tumors (28.6%) discovered through surveillance were identified on first surveillance imaging. Among these 35 new tumors, 19 (54.3%) were diagnosed in children with a previously treated cancer, six (17.1%) were diagnosed in patients still being treated for cancer, and 10 (28.6%) were diagnosed in those with no prior cancer history. Malignant solid and brain tumors identified through surveillance were more often localized (20 of 24; 83.3%) than similar tumors detected before CPS diagnosis (71 of 125; 56.8%, $p \leq 0.0001$). Of the 24 tumors identified through surveillance and surgically resected, 17 (70.8%) had completely negative margins. When analyzed across all CPS, the sensitivity (96.4%), specificity (99.6%), PPV (95.7%), and NPV (99.6%) of surveillance testing was high, with few false positive (n=6/1,533, 0.4%) or false negative (n=5/1,533, 0.3%) reports. No invasive interventions were performed due to false positive results.

Conclusion: Patients with CPS are at increased risk of primary and secondary tumor development with 10% of our cohort developing a tumor in a short time span. Surveillance effectively enabled early detection of new brain and solid tumors across a wide spectrum of CPS which allowed for complete surgical resection and successful treatment in most cases.

#6374 Socio-demographic predictors of recruitment in neuroblastoma therapeutic clinical trials.

D. Hunter-Schlichting, J. Sample, K. Knowles, D. Van Riper, L. Spector, E. Marcotte;
University of Minnesota, Minneapolis, MN

The generalizability of clinical trial outcomes hinges upon the equitable access and enrollment of diverse patient populations. Yet, disparities persist that may influence enrollment patterns. In neuroblastoma, the impact of ethnicity, socioeconomic status (SES), distance to care, and age at diagnosis on enrollment in therapeutic trials remains underexplored. We aimed to investigate these factors in neuroblastoma patients to identify potential disparities in clinical trial participation. We utilized the Childhood Cancer Research Network data, selecting neuroblastoma cases from 2008-2015, excluding those >21 years old or with incomplete data. We focused on factors influencing enrollment in therapeutic trials (ANBL0032, ANBL0421, ANBL0531, ANBL0532, ANBL0621, ANBL0931, ANBL1021, ANBL1221, ANBL1232). Key predictors examined were ethnicity, age at diagnosis, SES (via Yost Index), and distance to care from home to treatment hospital. We employed Poisson regression to calculate adjusted risk ratios (aRR) and 95% confidence intervals for trial participation. Analyzing 3,148 neuroblastoma cases from the CCRN registry, the ethnic composition was as follows: 68% were non-Hispanic White, 14% Hispanic, and 10% NH Black and SES distribution was even across quintiles. Age at diagnosis was a significant factor in trial enrollment: children >2 years were 94% more likely to enroll than those under 2 years ($p < 0.001$). Race, ethnicity, SES, and distance to care showed no significant effect on enrollment, all with non-significant p-values. In CCRN, neuroblastoma patient's age at diagnosis was a determinant in therapeutic trial enrollment, providing insight into design strategies to encourage trial participation. While common barriers like race, ethnicity, SES, and distance to care did not impact enrollment in our cohort, the significant role of age highlights an area where focused efforts can ensure that all age groups have equitable access to the potential benefits of therapeutic trials.

Category		**N**	**aRR (95% CI)**	**p-value**
Race and Ethnicity	Non-Hispanic (NH) White	2139	ref	
	Hispanic (All races)	436	0.93 (0.81, 1.08)	0.36
	NH Black	320	1.07 (0.93, 1.23)	0.33
	NH Asian/Pacific Islander	98	1.14 (0.89, 1.47)	0.30
	NH American Indian/Alaska Native	17	0.95 (0.48, 1.88)	0.89
	Other	138	0.94 (0.75, 1.17)	0.55
SES (Yost Index)	Quintile 1	493	0.88 (0.75, 1.02)	0.09
	Quintile 2	524	0.95 (0.83, 1.10)	0.53
	Quintile 3	606	0.98 (0.86, 1.11)	0.71
	Quintile 4	554	0.92 (0.80, 1.06)	0.24
	Quintile 5	563	ref	
Age at Diagnosis	<2 year	1790	ref	
	>2 years	1354	**1.94 (1.76, 2.12)**	**<0.001**
Distance to Care	0-25 miles	1520	ref	
	>25-50 miles	535	1.05 (0.93, 1.18)	0.36
	>50-100 miles	412	0.97 (0.85, 1.11)	0.91
	>100-250 miles	239	0.99 (0.87, 1.13)	0.60
	>250 miles	82	0.99 (0.77, 1.28)	0.97

#6375 Genetic testing station increases access to germline genetic testing.

C. Hamilton[1], M. Niell Swiller[1], F. Bhansali[2], A. Hoover[1], S. Bottomley[1], M. Lewis[1], B. Russell[1], J. A. Martinez[1], B. Karlan[1], N. Federman[1], V. Y. Chang[1]; [1]University of California, Los Angeles, Los Angeles, CA, [2]Kaiser Pernanente Northwest, Vancouver, WA

Despite evidence of clear benefit, genetic testing of pediatric oncology patients for germline variants remains rare due to a variety of factors, including insurance/financial barriers, limited knowledge about genetic testing, and competing interests for time and resources. Limited access to genetic testing, pre-test counseling and multidisciplinary care have been shown to disproportionately affect patients with limited resources. This represents a critical unmet need in pediatric oncology. Genetic testing station (GTS) is a pre-test counseling video tool that reviews what genetic testing is, why it might be indicated, and explains potential results. Similar video tools have been successfully used in other settings to increase rates of genetic testing, but there are no published reports on the effectiveness of a video education intervention to increase genetic testing in pediatric oncology patients. To test the effectiveness of GTS on genetic testing knowledge and feelings about genetic testing compared to in-person counseling, we use 5 previously validated tools pre- and post-intervention. The initial surveys measure genetic testing knowledge, decisional conflict, healthy literacy, evaluation of GTS and demographics. If participants complete genetic testing, we use the MICRA to assess the impact on their cancer risk assessment. Our GTS arm is recruited from UCLA Pediatric Sarcoma patients, and the in-person counseling arm is recruited from the UCLA Cancer Predisposition clinic. We have recruited 28 participants in the GTS arm and seven in the in-person counseling arm, of which 10 are patients over 18 years old, two are patients between 12-17 years old, and 23 are parents. In our GTS arm, there are 20 female and eight male participants. A majority identify as white or Latino. For the in-person counseling arm, there are four male and three female participants who identify as white, Middle Eastern, or Latino. A similar percentage score with high health literacy, 68% in the GTS arm and 71% for the in-person counseling arm. The majority of patients have no decisional conflict pre- or post-intervention for the GTS group, while the in-person counseling arm shows high initial decision conflict that is fully resolved with counseling. There is a statistically significant increase in genetic testing knowledge for five out of 10 questions comparing pre- and post-GTS. For GTS participants who have completed genetic testing and the MICRA, there is overall low distress and uncertainty, but higher scores for parents than adult or minor patients. In conclusion, there has been high interest in germline genetic testing in pediatric oncology patients with all families deciding to pursue genetic testing after viewing GTS. GTS is an effective tool in increasing genetic testing knowledge in participants. Therefore, GTS is a promising approach to increase access to genetic testing, while providing adequate pre-test counseling and no decisional conflict.

#6376 Establishment of the Consortium for Childhood Cancer Predisposition and the Childhood Cancer Predisposition Study.

A. Villani[1], G. M. Brodeur[2], L. R. Diller[3], C. Edgerton[4], J. Kamihara[3], W. Kohlmann[5], S. P. MacFarland[2], L. Maese[5], D. Malkin[1], K. E. Nichols[6], M. R. Perrino[6], S. E. Plon[7], S. Rednam[7], **C. C. Porter**[4];

[1]The Hospital for Sick Children, University of Toronto, Toronto, ON, Canada, [2]Children's Hospital of Philadelphia, University of Pennsylvania, Philadelphia, PA, [3]Dana-Farber/Boston Children's Cancer and Blood Disorders Center, Harvard Medical School, Boston, MA, [4]Children's Healthcare of Atlanta & Emory University, Atlanta, GA, [5]Huntsman Cancer Institute, University of Utah, Salt Lake City, UT, [6]St. Jude Children's Research Hospital, Memphis, TN, [7]Texas Children's Hospital, Baylor College of Medicine, Houston, TX

Background: Genetic predisposition contributes to a much higher proportion of cancer in children than previously appreciated. This creates a unique opportunity to develop improved methods to identify children at increased risk for cancer, enable early detection or prevention of tumors, and improve cure rates with decreased morbidity. However, several challenges have impeded successful research and systematic approaches to the care of children with cancer predisposition.

Methods: We established the Consortium for Childhood Cancer Predisposition (C^3P), currently comprised of seven large pediatric institutions in North America. The long-term goal of C^3P is to improve outcomes for children with genetic susceptibility to cancer through collaborative research and data sharing. To this end, we have developed the Childhood Cancer Predisposition Study (CCPS), a multicenter registry and biorepository, to achieve three main aims: 1) Establish and maintain the infrastructure for recruitment, participation, collection and sharing of clinical data and biological samples for children with cancer predisposition syndromes (CPS); 2) Define the spectrum of disease in children with CPS and explore the unique characteristics and management approaches of CPS-related tumors compared to their sporadic counterparts; and 3) Evaluate the clinical impact and effectiveness of standard and emerging tumor surveillance strategies.

Results: The CCPS opened to enrollment in May, 2021 and is currently recruiting at 3 member sites. To date, 276 primary subjects and 44 family members have been enrolled, 211 in the last year. In total, 37 different cancer predisposition diagnoses are represented among participants, including those that are more prevalent, e.g., Li-Fraumeni syndrome (n=42), DICER1 syndrome (n=27), and PTEN Hamartoma Syndrome (n=21), and those which are very rare, e.g., Rothmund-Thomson syndrome (n=2). There is excellent uptake on obtaining samples, with the CCPS Biorepository at Emory University receiving biospecimens from 261 subjects to date, including constitutional DNA (n=261), frozen peripheral blood mononuclear cells (n=32), and plasma samples for ctDNA analysis (n=26).

Conclusions: C^3P has established the infrastructure to facilitate comprehensive collaborative work to improve outcomes for children with cancer predisposition, which represent a wide variety of disorders. Future efforts will include the development of innovative strategies to promote recruitment beyond the primary C^3P sites and the support of additional clinical and biological studies of specific CPS.

#6377 UNC AYA Cancer Program: Reach and influence on cancer care delivery.

J. N. Stein[1], D. M. Ritzwoller[1], A. C. Wardell[1], E. R. Haines[2], B. Thom[1], L. Lux[1], A. B. Smitherman[1];

[1]University of North Carolina Chapel Hill, Chapel Hill, NC, [2]Wake Forest University School of Medicine, Wake Forest, NC

Category:

Cancer Disparities and Inequities Research

Purpose of the study

Adolescent and young adults (AYAs, aged 13-39) with cancer face barriers to care and stagnant outcomes. National groups have called for the development of AYA-specific programs, yet how these programs influence outcomes remains largely unexplored. With a dedicated AYA Cancer Program at the University of North Carolina (UNC) since 2015, we conducted a retrospective study to describe the AYA population and compare outcomes between those receiving program support and those who did not.

Methods

Linking electronic health records and NC Cancer Registry data, we defined a cohort of AYA patients who received cancer treatment at UNC from 2014-2022. We compared sociodemographic, clinical, utilization, and supportive care measures for those who received AYA Program contact and those who did not. Chi-square and two-group t-tests were used for comparison.

Results

Of 4044 AYAs receiving care at UNC, 670 engaged with our AYA Program (**Table 1**). Program-contacted patients were younger at diagnosis, more likely to be Black, have metastatic disease or hematologic malignancies, and more likely to receive systemic therapy. Program patients had increased clinical trial enrollment, more palliative care and fertility counseling.

Conclusions

Our findings suggest AYAs contacted by our program represent a distinct population with higher clinical and social needs. Despite higher rates of acute care events and no-shows, they were more likely to receive guideline-recommended care - clinical trial enrollment, fertility counseling, and palliative care. Future analyses will compare outcomes using adjusted modeling, and track trends over time. Results will inform next steps for the UNC AYA Cancer Program and other centers aiming to improve care delivery for AYAs.

Table 1. Notable results for AYAs with and without program contact

		AYA Program Contact (n=670)	No AYA Program Contact (n=3374)	P value
Age at diagnosis	Mean years	27	31	<0.01
Sex	Female	55%	61%	0.02
	Male	45%	39%	
Race	White	56%	61%	<0.01
	Black	26%	20%	
	Other	18%	16%	
Ethnicity	Hispanic	13%	12%	0.29
	Non-Hispanic	86%	84%	
Marital Status	Married/Partnered	34%	42%	<0.01
	Not Married	65%	51%	
Cancer Type	Solid	54%	87%	<0.01
	Hematologic	46%	13%	
Stage	Metastatic	52%	18%	<0.01
Treatment	Chemotherapy	85%	37%	<0.01
	Radiotherapy	6%	12%	
	Immunotherapy	18%	9%	
Clinical Trial Enrollment		45%	26%	<0.01
No-Shows	Mean	7	4	<0.01
Supportive Care	Palliative care visits	19%	3%	<0.01
	Advance Care Planning	14%	5%	
	Fertility visit	18%	2%	
	Hospice enrollment	3%	0.7%	
Complications	ED visit	68%	48%	<0.01
	Unplanned hospitalization	63%	29%	

#6378 Systems-level immunomonitoring in children with solid tumors.

Q. Chen[1], **B. Zhao**[1], Z. Tan[1], G. Hedberg[1], J. Wang[1], L. Gonzalez[1], C. Mugabo[1], A. Johnsson[1], L. Paez[1], L. Rodriguez[1], A. James[1], Y. Chen[1], J. Mikes[1], H. Barcenilla[1], C. Wang[2], M. M. Davis[2], L.-M. Carlson[1], N. Pal[1], N. Herold[1], K. Blomgren[1], D. Repsilber[3], T. Lakshmikanth[1], P. Kogner[1], L. Ljungblad[1], P. Brodin[1]; [1]Karolinska Institutet, Stockholm, Sweden, [2]Stanford University School of Medicine, Stanford, CA, [3]Orebro University, Orebro, Sweden

Background: Cancer is the leading cause of death from disease in children. Curing cancer requires cytostatic drugs and radiation, as well as systemic immune responses to clear malignant cells. Determinants of such responses in children of different ages and with different tumors are unknown. Novel immunotherapies can potentiate anti-tumor immune responses, but so far, very few children with solid tumors have benefitted and markers of productive anti-tumor immune responses in children are lacking.

Methods: 119 children at the Section for Pediatric Oncology, Astrid Lindgren Children's Hospital, Karolinska University Hospital in Stockholm, Sweden, diagnosed with solid tumors were recruited to Immune Systems Against Cancer in Children (ISAC) cohort from March 2018 to April 2021. Whole blood samples were collected for immune cell composition (Mass cytometry), plasma protein abundances (Olink assays), transcriptomics, and clonality analysis. Whole genome sequencing data from tumor tissue of children included in the ISAC cohort was obtained from the Swedish Childhood Tumor Biobank and was used for mutational load and signatures analysis.

Results: We find that the variation among systemic immune system states is determined predominantly by tumor type, and not age or sex as is the case among healthy children. We also show that specific groups of tumors elicit similar immune response states, which could inspire future updates to treatment protocols for such cancers. This illustrates the potential of this unbiased approach and inclusion of children with diverse solid tumors, whereby shared patterns can lead to novel hypotheses regarding underlying mechanisms among groups of patients, rarely considered together in more reductionist studies of individual tumor types. We also report that general, as well as specific, mutational profiles of neuroblastomas are associated with specific differences in immune responses and finally, we show that clonally expanded T cell responses are rarely observed at baseline in children but can be elicited by successful treatments and monitored as biosensors of therapeutic responses enabling precision oncology in the future. Such monitoring should be considered a complement to the already established precision medicine approaches based on tumor genetics.

Conclusions: Our findings suggest the importance of systemic immunity in coordinating and sustaining immune responses against tumors, but also that the developmental changes in human immune systems must be considered when developing and applying new immunotherapeutic interventions for children of different ages with various tumors. Our findings could also inspire the development of future strategies to trigger more productive immune responses against tumors in children.

#6379 Comparison of lipid profiles in children with solid tumors receiving chemotherapy and healthy children.

J. Bai[1], M. Houser[1], M. Martin[2], C. Powell[2], K. Maner-Smith[1], K. S. Sutton[1], T. Olson[1], D. W. Bruner[1];
[1]Emory University, Atlanta, GA, [2]Children's Healthcare of Atlanta, Atlanta, GA

Background: Lipid metabolism plays an important role in the regulation of synaptic function and plasticity.Cancer chemotherapy (chemo) can disturb the lipid profile, potentially linked with neuropsychological toxicities. This study aimed to compare the lipid profiles between children with cancer receiving chemo and healthy children.
Methods: A prospective, observational study was conducted in 21 children with solid tumors enrolled from Children's Healthcare of Atlanta (CHOA) and 16 controls. Children with solid tumors were consented precycle 2 chemo (T_1) and followed at the end of chemo (T_2). Controls completed one timepoint of data collection. At T_1 (n=21) and T_2 (n=13), fecal samples were collected for lipidomics analysis. Fecal lipids were processed using a high-resolution, untargeted lipidomics LC-MS approach. MetaboAnalyst and linear mixed models were used to analyze the data with false discovery rate correction (FDR 0.2).
Results: There were no significant differences in age, sex, race, and body mass index between the groups. In total 241 lipid features were identified with high confidence and analyzed. A comparison between children with solid tumors at T_2 (n=12) vs. controls (n=16) detected 8 differential lipids, which can be clustered into 4 classes, including 4 triglycerides (TG), 2 phosphatidylcholine (PC), 1 sphingomyelin (SM), and 1 lysophosphatidylcholine (LPC). Additionally, 24 differential lipids were detected for children with solid tumors from T_1 to T_2 (n=12), including 6 classes: 9 SM, 7 PC, 3 diacylglycerols (DG), 2 TG, 2 monoacylglycerols (MG), and 1 phosphatidylethanolamine (PE). Compared with controls, children with solid tumors at T_2 had higher levels of SM (e.g., SM(d36:1)) and lower levels of TG (e.g., TG(18:0/18:0/20:0)), LPC (e.g., LPC(20:4)), and PC (e.g., PC(33:4). Compared with children at T_1, those at T_2 had higher levels of SM (e.g., SM(d36:1)), PE (e.g., PE(16:0p/20:4), PC (e.g., PC(30:0), and PC(36:1)), and lower levels of TG (e.g., TG(18:0/18:0/20:0) and TG(18:0/16:0/18:0)), LPC (e.g., LPC(20:4)), DG (e.g., DG(18:0/16:0) and DG(18:0/18:0)), and MG (e.g., MG(18:0)).
Conclusion: Children with cancer chemo had alterations in fecal lipid profiles impacting the metabolism of PC, SM, TG, PE, MG, and DG. The increased PC and the dysregulation of LPC in comparison with controls suggest the decreased activity of phospholipase A2 (PLA2), primarily reported in inflammatory disease. Altered activity of lysophospholipid acyltransferase (LPCAT), diacylglyceride acyltransferase (DGAT), and phosphatidylethanolamine methyl transferase (PEMT) could also explain changes in PC and glycerolipids. Combined, these suggest dysregulation of the Kennedy or Lands pathways towards PC synthesis. Future work is needed to study whether the disturbed lipid metabolisms were associated with treatment toxicities and outcomes such as cognitive dysfunction based on literature.

#6380 Exploring immune checkpoint inhibitor-related adverse events in pediatric cancer patients: A pharmacovigilance analysis of VigiBase and the FDA adverse event reporting system (FAERS) database.

J. Shen[1], A. Lin[1], Q. Cheng[2], J. Zhang[1], P. Luo[1];

[1]Department of Oncology, Zhujiang Hospital, Southern Medical University, Guangzhou, China, [2]Xiangya Hospital, Central South University, Changsha, China

Background: With the widespread use of immune checkpoint inhibitors (ICIs) in the treatment of childhood cancers, their associated ICIs-related adverse events (irAEs) have become an important challenge. Our study was conducted to explore the pediatric high-risk ICIs-related AEs (pediatric irAEs) and explore the underlying mechanisms of pediatric irAEs.

Methods: We analyzed ICIs-related adverse reaction reports in VigiBase from 1967 to 2023 and the FDA Adverse Event Reporting System (FAERS) database from 2013 to 2022. Using three methods, the reporting odds ratio (ROR), the proportional reporting ratio (PRR), and the information component (IC), we conducted a disproportionality analysis between pediatric and adult cancer patients using ICIs to discover pediatric irAEs. Furthermore, we explored the impact of clinical factors on the occurrence of pediatric irAEs and their subsequent prognosis through univariate and multivariate logistic regression analyses. Finally, combining these data with pan-cancer transcriptome data from the Gene Expression Omnibus (GEO) database, we explored the potential biological mechanisms related to pediatric irAEs.

Results: We identified 4 categories of pediatric irAEs in the VigiBase and FAERS databases, including cytokine release syndrome ($ROR_{VigiBase}$ = 17.05; ROR_{FAERS} = 14.17), acute respiratory distress syndrome ($ROR_{VigiBase}$ = 10.26; ROR_{FAERS} = 12.39), seizure ($ROR_{VigiBase}$ = 7.18; ROR_{FAERS} = 10.63) and febrile neutropenia (FN) ($ROR_{VigiBase}$ = 3.01; ROR_{FAERS} = 4.84). The occurrence of pediatric irAEs may be related to mechanisms such as activation of immune cells, imbalance of inflammatory factors, activation of pathogen recognition, downregulation of inhibitory synapses, excitation/inhibition imbalance and central nervous system dysfunction.

Conclusion: This study systematically analyzed the high-risk irAEs that may occur after using ICIs in pediatric cancer patients. Next, we explored the possible biological mechanisms of these pediatric irAEs to provide certain theoretical guidance for the prevention and treatment of adverse reactions in pediatric cancer patients after treatment with ICIs.

#6381 Long-term kidney function after treatment for unilateral, non-metastatic, non-syndromic Wilms tumor. A report from the St. Jude Lifetime Cohort Study.

D. M. Green, M. Wang, M. J. Krasin, A. M. Davidoff, D. Srivastava, D. W. Jay, K. K. Ness, B. L. Shulkin, J. Q. Lanctot, K. C. Shelton, R. C. Brennan, M. J. Ehrhardt, S. Dixon, B. A. Kurt, L. L. Robison, M. M. Hudson, S. L. Spunt;
St. Jude Children's Research Hospital, Memphis, TN

Background: We previously reported that the estimated glomerular filtration rate (eGFR) was decreased among survivors of unilateral, non-metastatic, non-syndromic Wilms tumor (WT) treated with whole abdomen radiation therapy (WART) compared to controls, but not compared to unirradiated WT survivors (Pediatr Blood Cancer 2020;67:e28271). The impact of sex on estimates of kidney function among adult survivors of WT has not been well-documented.
Methods: We clinically evaluated male and female WT survivors with creatinine and cystatin C, calculated eGFR using the Chronic Kidney Disease - Epidemiology (CKD-EPI) equations with and without cystatin C and measured ^{99m}Tc diethylenetriamine pentaacetic acid (DTPA) plasma clearance. WT survivors consisted of 20 treated with unilateral nephrectomy (UN), non-nephrotoxic chemotherapy (NNC) and whole abdomen radiation therapy (WART) (mean - 20.2 Gray (Gy); standard deviation (SD) - 9.12 Gy), and 20 treated with UN, no radiation therapy, and NNC. Correlations between ^{99m}Tc DTPA clearance and eGFR were calculated.
Results: Among female WT survivors, none of the eGFR calculations was statistically significantly correlated with ^{99m}Tc DTPA clearance. Among male WT survivors, ^{99m}Tc DTPA clearance correlated well with eGFR calculations that included creatinine. Results are shown in the Table.
Conclusions: Among female survivors of unilateral, non-metastatic, non-syndromic WT who have undergone UN, eGFR is poorly correlated with ^{99m}Tc DTPA clearance. Evaluation of treatment-related changes in body composition may provide insight into these results.

Correlation between eGFR and 99mTc DTPA clearance

		Females		
eGFR(CKD-EPI)		^{99m}Tc DTPA clearance		
	No radiation therapy (n=13)		Whole abdomen radiation therapy(n=12)	
	Pearson correlation coefficient	p-value	Pearson correlation coefficient	p-value
Creatinine only	0.109	0.723	-0.295	0.352
Cystatin C only	0.311	0.301	0.094	0.782
Creatinine and cystatin C	0.348	0.244	-0.028	0.935
		Males		
	No radiation therapy (n=6)		Whole abdomen radiation therapy(n=6)	
	Pearson correlation coefficient	p-value	Pearson correlation coefficient	p-value
Creatinine only	0.827	0.043	0.859	0.028
Cystatin C only	0.811	0.050	0.592	0.216
Creatinine and cystatin C	0.878	0.021	0.866	0.026

#6382 Risk prediction of dyslipidemia in long-term survivors of childhood cancer: A report from the St. Jude Lifetime Cohort.

K. Petrykey[1], K. Li[1], L. Xie[1], A. Neupane[1], A. Delaney[1], C. Yu[1], S. Dixon[1], B. Ky[2], C. Im[3], I. B. Rhea[4], J. A. Towbin[1], J. N. Johnson[1], M. Bolier[5], V. G. Pluimakers[6], L. Broer[5], S. J. C. Neggers[5], M. M. van den Heuvel-Eibrink[6], R. M. Howell[7], K. K. Ness[1], M. M. Hudson[1], G. T. Armstrong[1], Y. Yasui[1], Y. Sapkota[1];

[1]St. Jude Children's Research Hospital, Memphis, TN, [2]University of Pennsylvania School of Medicine, Philadelphia, PA, [3]University of Minnesota, Minneapolis, MN, [4]University of Tennessee Health Science Center, Memphis, TN, [5]Erasmus Medical Center, Rotterdam, Netherlands, [6]Princess Maxima Center for Pediatric Oncology, Utrecht, Netherlands, [7]The University of Texas MD Anderson Cancer Center, Houston, TX

Background: Dyslipidemia is a significant contributor to the increased risk of cardiovascular morbidity and premature mortality in long-term survivors of childhood cancer. Identifying individuals at risk at an early stage provides an opportunity for tailored prevention approaches.
Methods: Long-term childhood cancer survivors from the St. Jude Lifetime Cohort, (SJLIFE, n=2,559; median age 41 years, range 20-77 years) were directly assessed for dyslipidemia. Risk factors under consideration included demographic characteristics, cancer treatment exposures (cumulative doses of anthracyclines, platinum agents, glucocorticoids, and radiation therapy), comorbid conditions at the time of assessment (hypertension, diabetes mellitus, growth hormone deficiency, hypogonadism, hypothyroidism, cardiomyopathy, and chronic kidney disease), and externally validated multi-ancestry general-population polygenic risk scores (PRSs) for lipid values (total cholesterol, LDL-C, HDL-C, and triglycerides). Multivariable logistic regression predicted a 15-year risk of dyslipidemia (CTCAE grade ≥2 hypercholesterolemia and/or hypertriglyceridemia) including variables selected by the stepwise approach. Performance of the model was assessed by the area under the receiver operating characteristic curve (AUC).
Results: Dyslipidemia was clinically identified in 543 (25.1%) SJLIFE survivors. AUC of a clinical model with sex, race, age at prediction, and comorbid conditions (diabetes, growth hormone deficiency, hypogonadism, hypothyroidism, and hypertension) was 0.80 (95% CI, 0.78-0.82). Inclusion of cancer treatment exposures (cumulative doses of anthracyclines, cisplatin, carboplatin, glucocorticoids, abdominal and cranial radiation therapy) significantly increased AUC to 0.82 (95% CI, 0.80-0.84; $P=2.1\times10^{-4}$). Addition of two PRSs for LDL-C (one included only genome-wide significant variants adjusted for statins and another consisted of all genome-wide variants) and the PRS for triglycerides provided further significant improvement in AUC to 0.86 (95% CI, 0.84-0.88; $P=4.2\times10^{-12}$).
Conclusions: We developed a prediction model with good performance for identifying the risk of dyslipidemia in childhood cancer survivors. In addition to demographics and comorbidities, cancer treatments and inherited genetic factors contributed significantly to improving the risk prediction of dyslipidemia. Results may refine risk stratification for dyslipidemia in survivors and present opportunities for more precise and personalized preventive strategies to address cardiovascular health. Independent validation in survivors from the Childhood Cancer Survivor Study and the Dutch Childhood Cancer Survivor Study (DCCSS)-LATER is currently underway.

#6383 Targeting radiation-induced fibrosis: Exploring promising therapeutic avenues and innovative assessment methods.

P.-A. Bissey[1], L. Massignan[2], R. Mancini[2], W. Shi[1], J. Williams[1], M. Reed[2], K. W. Yip[1], F.-F. Liu[1];

[1]Research, Princess Margaret Cancer Centre, University Health Network, Toronto, ON, Canada, [2]Centre for Medicinal Chemistry and Drug Discovery, Krembil Research Institute, University Health Network, Toronto, ON, Canada

Introduction: Radiation therapy is a vital cancer treatment for nearly 50% of patients, yet it poses a significant challenge in the form of radiation-induced fibrosis (RF). RF affects about 60% of those undergoing radiation, leading to painful scarring from excessive collagen accumulation. In head and neck cancer patients, as an example, RF reduces tissue flexibility, causing limited neck mobility and impaired swallowing. Furthermore, approximately 30% of patients also face disease recurrence post-radiation, with RF increasing surgical complications. Our laboratory previously identified the role of reduced fatty acid oxidation in RF (Zhao *et al; Nat Metab*;1(1):147 2019), offering a promising avenue for future drug development. We described the potential therapeutic benefit of caffeic acid phenethyl ester (CAPE) in countering pro-fibrotic metabolic changes. Our current objective is to develop more effective lead compounds to mitigate RF.
Methods: Collagen expression, utilized as a surrogate marker for fibrosis, was quantified using ELISA, Western blot analysis, and RT-qPCR. Metabolic changes were assessed by examining the expression levels of PPARG and CD36. CAPE-like analogs were derived from an in-house collection, a commercially available library, and structure-activity relationship (SAR) analyses. *In vivo*, RF was induced in the hindlimbs of mice through exposure to 40 Gy, followed by weekly X-ray evaluations of hindlimb angles for 16 weeks. During X-ray assessments, both hindlimbs were subjected to a 5 g weight to enable measurement of the joint angle between the femur and tibia (wherein higher acute angles were a measure of worsening fibrosis). Skin samples from irradiated and unirradiated limbs were collected for the evaluation of collagen deposition, utilizing Picro Sirius staining followed by polarized microscopy.
Results: Amongst 200 newly synthesized analogs, approximately one-third successfully reduced collagen secretion in human primary dermal fibroblasts. The most promising compounds exhibited a half-maximum inhibition concentration (IC50) for collagen secretion from 1 to 5µM. They also decreased intracellular collagen production and gene expression, associated with upregulation of PPARG and CD36 transcripts. The joint angle measurements *in vivo* revealed three distinct phases in the development of dermal fibrosis: 1) inflammatory; 2) recovery; and 3) fibrotic phases.
Conclusions: We have successfully synthesized novel and potent analogs of CAPE which were able to reduce secretion of collagen. Furthermore, a novel method for the *in vivo* assessment of fibrosis was also developed. This innovative approach will facilitate the detailed assessments of future compounds capable of reducing collagen deposition *in vivo*, thereby providing an innovative avenue to mitigate one of the most pressing late normal tissue toxicities of radiation therapy.

#6384 DNA methylation based aging biomarkers mediate the association between patient-reported symptoms and all-cause late-mortality: A report from the St. Jude Lifetime Cohort.

Q. Li, Y. Pan, X. Zhang, N.-M. Plonski, C. Chen, Q. Dong, K. Shelton, J. Easton, H. Mulder, J. Zhang, G. Neale, E. Walker, D. Srivastava, G. T. Armstrong, K. Ness, I.-C. Huang, Z. Wang;
St. Jude Children's Research Hospital, Memphis, TN

Background: Long-term survivors of childhood cancer experience high rates of patient-reported symptoms and evidence for accelerated molecular aging. Both are established to increase the risk for late-mortality (>5 years from cancer diagnosis). We aim to investigate if accelerated molecular aging mediates the association between symptoms and all-cause late-mortality.
Methods: DNA methylation (DNAm)-based aging biomarkers were derived from the DNAm Age Calculator, including epigenetic age acceleration (EAA) using multiple clocks (e.g., GrimAge and PhenoAge) and other DNAm-predicted biomarkers (e.g., DNAmB2M: beta-2-microglobulin, DNAmTL: telomere length) adjusted for age and standardized. Survivors self-reported the presence of 10 symptom domains (cardiac, pulmonary, sensory, motor/movement, nausea, pain, fatigue, memory, anxiety, and depression) that were aggregated into a total symptom burden score. Multiple linear regression tested the association between each aging biomarker and symptom prevalence, adjusting for the age of symptom survey, sex, and cancer treatment exposures. Cox regression tested the association of each aging biomarker or symptom domain with mortality. Aging biomarkers mediation for the symptom-mortality association was assessed by using the Accelerated Failure Time model and the mediation R package. False discovery rate was controlled for multiple testing.
Results: Among 2,206 survivors (47% males) who had DNAm measured on (52%) or after the survey, the median duration from the symptom survey to DNA sampling were 0.48 years (IQR: 0.09-4.27 years). EAA_GrimAge was the aging biomarker most closely associated with total symptom burden (beta [95%CI] = 0.576 [0.455, 0.697] years, $P=2.89\times10^{-18}$) and eight of ten domain-specific symptoms except for motor/movement and memory. Seven aging biomarkers (e.g., DNAmB2M: 1.91 [1.48, 2.48], $P=1.87\times10^{-5}$; EAA_GrimAge: HR [95%CI] = 1.17 [1.09, 1.26], $P=3.1\times10^{-4}$) and five symptom domains (e.g., pulmonary: 2.54 [1.44, 4.49], P=0.004; cardiac: 2.25[1.28, 3.97], P=0.01; total symptom burden: 1.47 [1.18, 1.82], P=0.0019) were associated with mortality risk. EAA (e.g., EAA_GrimAge) mediated the association between symptoms (cardiac: % mediation =0.13 [0.044, 0.379], P=0.008; pulmonary: 0.186 [0.075, 0.486], P=0.008; and total symptoms: 0.206 [0.078, 0.503], P=0.012) and late mortality. In addition, the association between symptoms and mortality was mediated by DNAmB2M and DNAmTL (e.g., pulmonary: 0.152 [0.046, 0.378], P=0.008; 0.12 [0.031, 0.373], P=0.021).
Conclusions: EAA, DNAmB2M and DNAmTL mediated the association between the presence of specific symptom domains and late-mortality, suggesting that accelerated molecular aging may be an underlying biological pathway explaining the associations between symptom burden and mortality.

#6385 St. Jude Survivorship Portal: Sharing and analyzing large clinical and genomic datasets from pediatric cancer survivors.

G. Matt[1], E. Sioson[1], J. Wang[1], C. Lu[1], A. Zaldivar Peraza[1], K. Gangwani[1], R. Paul[1], C. Reilly[1], A. Ać[1], K. Shelton[1], Q. Liu[2], S. Sandor[1], C. McLeod[1], W. Qiu[2], J. Patel[1], F. Wang[1], C. Im[3], Z. Wang[1], C. L. Wilson[1], N. Bhakta[1], K. Ness[1], G. T. Armstrong[1], M. M. Hudson[1], L. L. Robison[1], J. Zhang[1], Y. Yasui[1], X. Zhou[1];

[1]St. Jude Children's Research Hospital, Memphis, TN, [2]University of Alberta, Edmonton, AB, Canada, [3]University of Minnesota Medical School, Minneapolis, MN

Survivors of childhood cancer are at risk for developing various adverse health conditions as adults that are attributable to the cancer and treatments they were exposed to as children. Cancer survivorship research relies on large-scale, longitudinal studies that generate a wide range of demographic, clinical, and genetic data on cancer survivors. Nevertheless, the absence of cancer survivorship data portals has made it challenging to broadly share cancer survivorship data. We have created the St. Jude Survivorship Portal (https://survivorship.stjude.cloud), the first data portal for sharing, analyzing, and visualizing childhood cancer survivorship data. The portal hosts data from two large cohorts of pediatric cancer survivors: the St. Jude Lifetime Cohort Study (SJLIFE) and the Childhood Cancer Survivor Study (CCSS). Over 1,600 clinical variables and over 400 million genetic variants from over 7,700 childhood cancer survivors are stored on the portal. The data can be explored using an interactive data dictionary and a genome browser specialized for population genetics analysis. Summary statistics of variables and genetic variants are computed on-the-fly and visualized through interactive and customizable charts. Survivor cohorts can be filtered or customized and may also be divided into groups for comparative analysis. Tools for performing cumulative incidence and regression analyses have been integrated into portal environment, allowing users to perform real-time statistical analyses on the stored survivorship data. Finally, users may also download individual-level clinical and genotype data from the portal using the controlled-access data download feature. Through various use-cases of survivorship research, we used the portal to explore the ototoxic effects of platinum-based chemotherapy, uncover a novel association between limb amputation, age, and long-term mental health, and identify a novel haplotype in *MAGI3* strongly associated with cardiomyopathy specifically in survivors of African ancestry. The St. Jude Survivorship Portal provides a comprehensive, powerful, and easy-to-use interface for sharing and analyzing childhood cancer survivorship data that will serve as a valuable research tool for the broader survivorship research community.

CLINICAL RESEARCH: Predictive Biomarkers 5
Poster Session

#6389 An exosome-based liquid biopsy powered by machine learning predicts progression-free and overall survival before commencing first-line EGFR inhibitors for metastatic colorectal cancer: *The EXONERATE Study*.

X. Caiming[1], A. Mannucci[1], R. Souvick[1], E. Francis[2], O. Helena[2], A.-O. Vicente[3], E. Pilar[4], F.-M. Carlos[5], S. Antonieta[6], G. Javier[7], R. Jose Ramon[8], M.-R. M. Marta[9], F.-P. Julen[10], M. Hermini[11], A. Jorge[12], F. Jaime[13], M. Joan[2], A. Goel[1];

[1]Beckman Research Institute of The City of Hope, Duarte, CA, [2]IDIBAPS, University of Barcelona, Barcelona, Spain, [3]Hospital Universitario Miguel Servet, Zaragoza, Spain, [4]Hospital Universitario Lozano Blesa, Zaragoza, Spain, [5]Fundacion Instituto Valenciano de Oncologia, Valencia, Spain, [6]Hospital Universitari Arnau de Vilanova, Lleida, Spain, [7]Hospital General Universitario of Elche, Elche, Spain, [8]Hospital Infanta Cristina, Badajoz, Spain, [9]Hospital de la Santa Creu i Sant Pau, Barcelona, Spain, [10]Hospital Mutua de Terrasa, Barcelona, Spain, [11]Hospital Son Espases, Palma, Spain, [12]Hospital La Fe de Valencia, Valencia, Spain, [13]Hospital Universitario La Paz, CIBERONC, Madrid, Spain

Introduction: We developed a liquid biopsy assay based on **exo**somal and cell-free microR**N**A (exo- and cf-miRNA, respectively) for patients with chemotherapy-naïve, m**e**tastatic, unresectable, **RA**S and BRAF wild-type colorectal cancer (mCRC), to predict progression-free (PFS) and overall survival (OS) before the commencement of first-line **t**reatment with **E**GFR inhibitors (EXONERATE).
Methods: Patients with mCRC were consecutively enrolled in two open-label, nationwide clinical trials and received first-line cetuximab or panitumumab. Cf- and exo-miRNA expression was quantified using RT-qPCR in plasma samples obtained before exposure to EGFR inhibitors. The prespecified primary endpoint was 12-month PFS, hierarchically tested in left-sided mCRC, right-sided mCRC, and the entire cohort. As secondary endpoints, the EXONERATE status was correlated with PFS and OS hazard ratios (HR).
Results: After excluding those with RAS/BRAF mutations and unavailable samples, the complete analysis dataset comprised 120 patients (94 with left-sided and 26 with right-sided mCRC; 87 received cetuximab and 33 panitumumab). As expected, right-sided mCRC patients showed inferior PFS and OS outcomes (HR 1.80 [$CI_{95\%}$ = 1.13 - 2.80] and 1.80 [$CI_{95\%}$ = 1.00 - 3.27], respectively). Genome-wide small RNA sequencing on 20 patient samples identified 12 cf- and 14 exo-miRNA candidates, then narrowed to 8 and 9 based on best performance. We employed machine learning algorithms to develop two liquid biopsy assays, one based on cf- and the other on exo-miRNAs, predicting 12mPFS with AUC values of 0.84 and 0.81, respectively. These were then combined to establish the EXONERATE assay for left-sided mCRC (AUC = 0.89), successfully validated in right-sided mCRC patients (AUC= 0.84). Among left-sided mCRC patients, 35% were EXONERATE-high, exhibiting shorter median PFS (mPFS = 9.5 vs. 18.5 months, p<.001) and a higher mortality rate (HR 0.21 [$CI_{95\%}$ = 0.10 - 0.42]). In the right-sided mCRC cohort, the EXONERATE-high panel robustly identified patients with shorter mPFS (8.6 vs. 23.7 months, p=.0042) and predicted 12mPFS with high accuracy (sensitivity 100%, NPV 81%, PPV 100%). Although in univariate analysis both the EXONERATE panel and sidedness showed associations with PFS and OS, in multivariate analysis only the EXONERATE panel could fully account for the differences in PFS and OS (HR 0.22 and HR 0.19, respectively). Hence, we employed the EXONERATE panel agnostically of tumor sidedness and observed that EXONERATE-high patients demonstrated poorer survival outcomes in mPFS (8.9 vs. 19.6 months, HR 0.27 [$CI_{95\%}$ = 0.17 - 0.41]) and mOS (22.6 vs. >60 months, HR 0.18 [$CI_{95\%}$ = 0.09 - 0.37]).
Conclusion: The EXONERATE panel robustly predicted PFS and OS outcomes in both right- and left-sided mCRC patients before receiving either EGFR inhibitor.

#6390 Exploratory biomarker analysis of phase 3 ASTRUM-005 study: Serplulimab versus placebo plus chemotherapy for extensive-stage small cell lung cancer.

Y. Cheng[1], L. Han[2], L. Wu[3], J. Chen[4], H. Sun[5], G. Wen[6], Y. Ji[7], A. Zimina[8], J. Shi[9], Z. Pan[10], J. Shi[11], X. Wang[12], F. Yang[13], X. Yang[13], M. Chen[13], S. Zhong[13], Q. Wang[13], J. Li[13], J. Cheng[13], C. Ling[13], Y. Shan[13], J. Zhu[13], The ASTRUM-005 Study Group;

[1]Jilin Cancer Hospital, Changchun, China, [2]Xuzhou Central Hospital, Xuzhou, China, [3]Hunan Cancer Hospital/the Affiliated Cancer Hospital of Xiangya School of Medicine, Central South University, Changsha, China, [4]Tianjin Medical University General Hospital, Tianjin, China, [5]Jiamusi Cancer Hospital, Jiamusi, China, [6]The First Affiliated Hospital of Nanchang University, Nanchang, China, [7]The First Affiliated Hospital of Xinxiang Medical University, Xinxiang, China, [8]Budgetary Healthcare Institution of Omsk Region "Clinical Oncology Dispensary", Omsk, Russian Federation, [9]Linyi Cancer Hospital, Linyi, China, [10]The First Affiliated Hospital of Zhejiang University School of Medicine, Hangzhou, China, [11]Cangzhou People's Hospital, Cangzhou, China, [12]The First Affiliated Hospital of Guangdong Pharmaceutical University, Guangzhou, China, [13]Shanghai Henlius Biotech, Inc., Shanghai, China

Background First-line serplulimab plus chemotherapy (chemo) significantly improved OS compared with chemo alone for patients with extensive-stage small cell lung cancer (ES-SCLC) in the phase 3 ASTRUM-005 study. In this exploratory biomarker analysis, we retrospectively evaluated the association of proteome signature, genetic mutations, and hematological indices with efficacy.

Methods: Serum proteomics data were generated via Olink® Explore 3072 platform for 168 patients (training: 80; validation: 88). Genetic mutations were assessed by Med1CDx™ panel for 305 patients. Baseline neutrophil-to-lymphocyte ratio (NLR), platelet-to-lymphocyte ratio (PLR), and lactate dehydrogenase (LDH) levels were analyzed in all 585 patients. Clinical data cutoff date was June 13, 2022.

Results: From Olink data, we generated a 15-protein signature. Results in the validation cohort are shown in the table below. Patients with upper signature score derived higher PFS (7.89 vs 4.17 mo, HR 0.37) and OS (17.18 vs 9.74 mo, HR 0.27) benefit from adding serplulimab, than those with lower signature score (PFS: 4.40 vs 4.34 mo, HR 0.68; OS: 9.05 vs 9.22 mo, HR 0.76). Patients with mutations in RB1 or NOTCH pathway had better tumor responses to the treatment of serplulimab-chemo (ORR: 80% and 86%, respectively) when compared to patients without mutations in RB1 or NOTCH pathway (ORR: 58% and 68%). Patients with NLR ≤4.6, PLR ≤338.3, and LDH ≤ upper limit of normal tended to have longer PFS and OS in both treatment groups; NLR and LDH were further proven to be independent prognostic biomarkers in multivariate regression (P = 0.002 and P <0.001, respectively).

Conclusions: We found a 15-protein signature showing predictive power for serplulimab-chemo treatment; RB1 or NOTCH pathway mutations were enriched in serplulimab-chemo responders; baseline NLR and LDH were independent prognostic biomarkers for ES-SCLC. The above findings warrant further investigations.

	Serplulimab-chemo (n=48)	Placebo-chemo (n=40)	HR (95% CI)	P
Upper signature score, n	31	34		
Median PFS (95% CI), months	7.89 (1.27, 10.74)	4.17 (2.96, 4.34)	0.37 (0.21, 0.66)	<0.001
Median OS (95% CI), months	17.18 (11.01, NE)	9.74 (6.90, 12.65)	0.27 (0.15, 0.50)	<0.001
Lower signature score, n	17	6		
Median PFS (95% CI), months	4.40 (3.61, 5.75)	4.34 (2.66, NE)	0.68 (0.23, 2.02)	0.488
Median OS (95% CI), months	9.05 (6.67, 11.73)	9.22 (4.53, NE)	0.76 (0.29, 1.98)	0.570

#6391 Spatial proteomic profiling unveils pre-existing anti-tumor immunity as a hallmark of exceptional benefit from immunotherapy in NSCLC.

S. Hernandez[1], R. Bach[2], M. Giner[2], W. Lu[1], L. Kostousov[1], S. Barnes[1], K. Khan[1], L. Masfarre[2], X. Villanueva[2], I. Sanchez[2], N. Navarro[2], A. Taus[2], M. Galindo[2], M. Hardy[2], R. Del Rey-Vergara[3], A. Inanez[3], B. Sanchez-Espiridion[1], L. Moliner[4], S. Clave[2], B. Bellosillo[2], A. Rovira[3], J. Perera-Bel[3], I. Wistuba[1], E. Arriola[2], L. M. Solis[1], **P. Rocha**[2];

[1]MDAnderson Cancer Center, Houston, TX, [2]Hospital del Mar, Barcelona, Spain, [3]Hospital del Mar Research Institute, Barcelona, Spain, [4]Catalan Institute of Oncology, Barcelona, Spain

Background: Immunotherapy is firmly established as a treatment regimen in various solid tumors due to its exceptional benefits observed in a select group of patients. Despite widespread use of immune checkpoint blockade (ICB) across diverse solid tumors, including non-small cell lung cancer (NSCLC), the quest for a clinically informative biomarker for long-term benefit remains unmet. Here we investigate the potential utility of clinicopathological and spatial proteomic profiling of tumor specimens from NSCLC patients to identify predictive biomarkers of long-term benefit to ICB.

Methods: Forty-nine patients diagnosed with advanced NSCLC who received ICB at Hospital del Mar, Barcelona between 2017-2021 were included. Long-term responders (LTR, n=21) were defined as patients achieving a maintained radiologic response for more than 2 years, and short-term responders (STR, n=28) as patients presenting disease progression within the first six months of ICB initiation. Clinicopathological information, incidence of immune related adverse (irAES) and PD-L1 tumor proportion score assessed by IHC was available for all of them. DSP GeoMx was performed in subset of patients (LTR n=14 and STR n=14), to assess 49 immune biomarkers. Pancytokeratin (panCK; epithelial), CD3, CD20 and SYTO 13 (nuclear) were utilized as morphology biomarkers. Regions of interest were placed in tissue areas containing tumor and segmented in Tumor (PanCK+) and tumor microenvironment (TME) (PanCK-) that was used on downstream analysis. Digital counts were normalized using the protein expression of housekeeper proteins. Statistical analysis was performed using linear mixed models. A *P* value less than 0.05 was considered significant.

Results: Our analysis revealed specific characteristics of LTR patients compared with STR, namely LTR population was enriched for PD-L1 positive in tumors ($p=0.005$) and a higher incidence of immune-related adverse events (irAEs) ($p=0.001$). Within the Tumor compartment, LTR patients displayed significantly higher levels of IDO1, CD8, PD-L1, CD45, HLA-DR and STING, while STR patients exhibit higher levels of B7-H3, CD56 and OX40L ($p<0.05$ for all proteins). Comparison analysis of the TME compartment between LTR and STR revealed augmented levels of IDO1, CD8, CD45, CD11c, CD27 and CD3 in LTR patients, and lower levels of B7H3 and OX40L compared with STR patients ($p<0.05$ for all proteins).

Conclusions: Our comprehensive analysis of metastatic NSCLC patients treated with ICB has unveiled distinct clinicopathological and immunological features associated with long-term benefit of ICB, highlighting the presence of pre-existing antitumor immunity as a stronger predictor of long-term benefit. These findings offer insights into potential biomarkers and therapeutic strategies for enhancing ICB outcomes in metastatic NSCLC.

#6392 Activity of HER2-and TROP2- antibody drug conjugates (ADCs) in small cell lung cancer (SCLC) models with SLFN11 as a predictive biomarker.

B. Zhang, A. Ibrahim, C. Stewart, L. Diao, Q. Wang, L. Shen, Y. Xi, A. Serrano, L. M. Solis, W.-L. Wang, K. Ramkumar, R. J. Cardnell, R. Wang, A. Duarte, Jr., J. Wang, L. A. Byers, C. Gay;
UT MD Anderson Cancer Center, Houston, TX

Background: Small-cell lung cancer (SCLC) is a highly aggressive malignancy with its few treatment options devoid of biomarker selection, and a 5-year survival rate of less than 7%. Our group previously established four transcriptionally defined subtypes of SCLC, each with distinct cell surface targets (*Gay et al, Cancer Cell 2021).* Further, we identified SLFN11 (a putative DNA/RNA helicase) as a candidate biomarker of sensitivity to DNA-damaging agents, including topoisomerase inhibitors. Human epidermal growth factor receptor 2 (HER2/*ERBB2*) expression has been previously described in a subset of SCLCs and has been linked to poor prognosis. HER2 antibody-drug conjugates (ADCs) like trastuzumab deruxtecan (T-DXd) (where the payload is a topoisomerase I inhibitor) have received FDA approval for various solid tumors, highlighting their therapeutic potential. Similarly, TROP2 (*TACSTD2*) ADC sacituzumab govitecan has shown promising clinical efficacy in a SCLC (TROPiCS-03 basket trial). However, it is unclear what the predictive biomarkers are to these ADCs in SCLC.
Methods: Expression of *ERBB2 and TACSTD2* mRNA was analyzed using publicly available patient datasets. We also characterized surface expression of HER2 and TROP2 by flow cytometry in SCLC cell lines at baseline and after cisplatin/etoposide treatment. We then assessed the cytotoxicity of T-Dxd and sacituzumab govitecan in a panel of SCLC cell lines representative of each SCLC subtype, as well as SLFN11 status.
Results: Analyses of HER2/*ERBB2* and TROP2/*TACSTD2* in SCLC cell lines and patient datasets showed a range of *ERBB2* and *TACSTD2* expression with enrichment in the non-neuroendocrine subtypes (SCLC-P and SCLC- I subtypes). We further validated HER2 and TROP2 surface levels by flow cytometry in a subset of SCLC cell lines. Intriguingly, we observed that surface expression of both HER2 and TROP2 increase after frontline chemotherapy cisplatin/etoposide treatment. As expected, T-Dxd and sacituzumab govitecan exhibit cytotoxicity in a subset of SCLC cell lines. We found a strong correlation between the *in vitro* cytotoxicity (IC50) of sacituzumab govitecan with SLFN11 (rho= 0.74, p=0.015). Importantly, SLFN11 is bimodally distributed in SCLC and we found *ERBB2* and *TACSTD2* to be enriched in the SLFN11-high group of SCLC patients. We also found *ERBB2* and *TACSTD2* to be correlated with each other (rho = 0.53, p <0.001).
Conclusion: In this study, we demonstrate that HER2/*ERBB2* and TROP2/*TACSTD2* are enriched in a subset of SCLC. FDA-approved ADCs, T-DXd and sacituzumab govitecan each have preclinical activity in SCLC with SLFN11 as a predictive biomarker of payload cytotoxicity. We also found HER2 and TROP2 target levels increase after frontline chemotherapy (cisplatin/etoposide) in SCLC, which suggest their efficacy may be enhanced in relapsed SCLC where treatment options are extremely limited.

#6393 The predictive role of TNF-related genes in patients receiving immune checkpoint inhibitors.

O. E. Ababneh[1], S. Kato[2], D. Nishizaki[2], H. Miyashita[3], S. Lee[2], M. Nesline[4], S. Pabla[5], J. Conroy[5], P. DePietro[5], H. Ko[4], R. Kurzrock[6];
[1]Jordan University of Science & Technology, Irbid, Jordan, [2]University of California San Diego, San Diego, CA, [3]Dartmouth Cancer Center, Lebanon, NH, [4]Labcorp Oncology, Durham, NC, [5]OmniSeq Inc., Buffalo, NY, [6]Medical College of Wisconsin Cancer Center, Milwaukee, WI

Introduction: Not all patients respond to immune checkpoint inhibitors (ICI) even when they have favorable FDA-approved biomarkers. The tumor necrosis factor superfamily (TNFSF) and tumor necrosis factor receptor superfamily (TNFRSR) play critical roles in various biological processes, including inflammation, immune regulation, and cell death. In this study, we sought to investigate the predictive role of TNF-related genes in patients receiving ICI.
Methods: The RNA expression levels of 18 TNF-related genes were assessed in a pan-cancer cohort of 217 patients treated with immune checkpoint inhibitors (ICI) at the University of California San Diego (UCSD) Moores Cancer Center. Using a reference population of 735 tumors and 35 histologies, transcript abundance was adjusted to internal housekeeping gene profiles and rated (0-100th percentile). The patients were clustered into two groups based on the 18 TNF-related genes expression using Ward's hierarchical clustering. Associations between overall survival and previously demonstrated independent ICI predictive variables were assessed. Bonferroni correction for multiple comparisons was used and considered statistically significant when p-value ≤ 0.05.
Results: Four TNF-related genes (CD137, CD70, GITR, and TNFSF9) were associated with positive programmed death-ligand 1 (PD-L1) expression (PD-L1≥1% immunohistochemistry TPS), while TNFSF18 was associated with negative PD-L1 expression (corrected p-value<0.05). No gene was associated with microsatellite instability-high (MSI-H) or high tumor mutational burden (TMB-H) (TMB≥10 mutations/Mb) (corrected p-value>0.05). We clustered the patients based on their 18 TNF-related genes expression into two signature clusters, high (n=94) and low (n=123). Patients in the high expression signature cluster were more likely to have high PD-L1 compared to the low expression cluster (corrected p-value<0.05). The high expression signature cluster was associated with better survival compared with the low expression cluster (HR=1.49, 95%CI: 1.05-2.13 (p=0.026)). When adjusting for TMB, MSI, PD-L1, TP53 and KRAS status, the TNF high expression signature cluster was still associated with better overall survival (HR=1.71, 95%CI:1.11-2.66 (p=0.016)). Other than the TNF high expression signature cluster group, only the presence of KRAS mutation was a predictor of a longer survival (HR=2.09, 95%CI:1.28-3.42 (p=0.003)).
Conclusion: A high TNF-related gene expression profile may serve as an independent predictor for longer overall survival for patients treated with ICI.

#6394 Tissue nanomechanical signature predicts response to neoadjuvant chemotherapy in patients with breast cancer.

M. Gachechiladze[1], S. Nizzero[1], T. Appenzeller[1], L. Briner[2], R. Burian[1], S. Schadelin[2], S. Muenst-Soysal[2], T. Vlaijnic[2], E. Obermann[3], S. Dellas[2], S. Forte[4], Z. Marusić[5], A. Jizawi[1], P. Ndiaye[1], P. Oertle[1], G. Zaugg[1], M. Loparic[1], M. Plodinec[1];

[1]ARTIDIS AG, Basel, Switzerland, [2]University Hospital Basel, Basel, Switzerland, [3]Cantonal Hospital Luzern, Luzern, Switzerland, [4]Radiology Clinic Baden, Baden, Switzerland, [5]University Hospital Centre Zagreb, Zagreb, Croatia

Background: Neoadjuvant chemotherapy (NACT) is increasingly used in patients with breast cancer. However, predicting response to NACT remains a challenge in everyday clinical practice. Increasing (pre)- and clinical evidence demonstrate the importance of cancer biomechanics in mediating therapy response. We and others have previously demonstrated that complex biomechanical alterations in cancer tissues, can be measured by the Atomic Force Microscopy (AFM) at the nanoscale level. Incorporating AFM measurements of clinical biopsies within standard of care is thus a promising avenue to leverage tissue mechanics as prognostic and predictive biomarker for solid cancers.

Methods: Fresh clinical biopsy samples from 545 breast cancer patients were measured using the AFM-based Automated and Reliable Tissue Diagnostics (ARTIDIS) investigational device - ART-1. Measurements were performed on baseline biopsies within routine clinical workflow in the Breast Clinic, University Hospital Basel. This cohort comprises 30 patients who received NACT including: anthracycline and/or taxane based chemo (n=17), and anthracycline and/or taxane with platinum chemo (n=13). Study endpoints were radiological complete response (rCR) prior and pathological complete response (pCR) after surgery. Multiparametric nnanomechanical signature data has been analyzed in an automated manner using the proprietary ARTIDISNET software platform.

Results: From the 30 patients who received NACT, 12 patients presented with rCR, 17 patients presented with rPR, and 1 patient presented with rNR. pCR has been achieved only in 9 patients. In this study, he ARTIDIS nanomechanical signature of response to NACT in breast cancer showed 100% negative predictive value (NPV) and 89% positive predictive value (PPV), with 93% of accuracy for patients receiving chemotherapy, independent of molecular subtype or treatment regimen. Sensitivity was 100% and specificity was 85% (AUC=0.91).

Conclusion: ARTIDIS nanomechanical signature can be seamlessly integrated within clinical settings to predict response to standard of care NACT in patients with breast cancer in a prospective manner. These results are currently being validated in a global, multicentre prospective study in breast cancer (ANGEL, NCT06085833), enrolling in total 2706 patients, with the aim to support implementation of the ARTIDIS nanomechanical signature into routine clinical practice.

#6395 Metabolic dysregulation as a determinant of prognosis and response to sorafenib in liver cancer.

H. Park[1], S. Park[1], S.-H. Lee[2], Y. Jeong[1], B. Sohn[1], S. Yim[3], J.-S. Lee[1];

[1]UT MD Anderson Cancer Center, Houston, TX, [2]CHA Bundang Medical Center, Seoul, Korea, Republic of, [3]Korea University, Seoul, Korea, Republic of

Background & Aims: Elevated metabolic activity is a defining characteristic of liver cancer. Nevertheless, our understanding of the molecular underpinnings of high metabolic activity in liver cancer and its impact on clinical outcomes and treatment responses remains limited. We aimed to elucidate the metabolic features of liver cancer associated with clinical outcomes, particularly overall survival and responsiveness to sorafenib treatment.

Methods: Utilizing cross-species comparisons of genomic data, we integrated gene expression profiles from liver tissues in metabolically challenged mice and from patients with cirrhosis and liver cancer. To categorize patients, we developed a genomic predictor and applied it to gene expression data from a cirrhosis cohort (n=216) and large liver cancer cohorts (n=1390). Comprehensive statistical and informatics analyses were conducted to evaluate clinical significance, including overall survival and responses to standard treatments. Moreover, we integrated genomic data derived from patient-derived xenograft (PDX) models into our analytical framework.

Results: Our integrated data analysis unveiled three distinct metabolic subtypes of tissues: high, moderate, and low metabolic subtypes. In the cirrhosis cohort, the high metabolic subtype was significantly associated with early liver cancer development. Among liver cancer cohorts, the high metabolic subtype exhibited characteristics such as poor survival, heightened hepatic stem cell features, increased genomic instability, and elevated expression of AFP, KRT19, EPCAM, and SALL4. Notably, when liver cancer patients undergoing systemic sorafenib treatment were stratified using our genomic predictor, those with low and moderate metabolic activity derived significant benefits from sorafenib therapy. Conversely, the high metabolic subtype displayed substantial resistance to sorafenib, suggesting that metabolic activity may dictate the response of liver cancer cells to sorafenib treatment. Gene network analysis of the metabolic expression signature identified multiple signaling pathways that potentially contribute to sorafenib resistance in liver cancer cells. Our analysis predicted the activation of pathways such as the TGF-β pathway (TGFB1), consistent with previous findings of TGF-β pathway activation in highly metabolic cancer cells. Additionally, our analysis identified YAP1, HIF1A, and MAPK pathways as activated pathways in sorafenib-resistant liver cancer.

Conclusions: This study identifies clinically and metabolically distinct subtypes of liver cancer, biomarkers associated with these subtypes, and mechanisms underlying metabolic-mediated resistance of liver cancer cells to sorafenib. Furthermore, the metabolic subtypes observed in PDX models provide valuable tools for selecting appropriate preclinical models for future research endeavors.

#6396 Ex vivo 3D micro tumor testing to assess chemotherapy and immunotherapy responses for NSCLC patients.

E. Koedoot[1], T. J. P. Sijsenaar[1], L. J. Ceton[1], D. J. van der Meer[1], T. J. van Brakel[2], P. van Zwam[3], E. Geraedts[4], **W. Vader**[1], E. F. Smit[5], L. C. Steinbusch[5], C. M. J. Steendam[2];

[1]VitroScan B.V., Leiden, Netherlands, [2]Catharina Ziekenhuis, Eindhoven, Netherlands, [3]PAMM, Eindhoven, Netherlands, [4]Groene Hart Ziekenhuis, Gouda, Netherlands, [5]LUMC, Leiden, Netherlands

Background: Systemic treatment options for NSCLC patients consists of chemo-, targeted or immunotherapy. Although predictive biomarkers can guide treatment decisions, response prediction for chemo- and immunotherapy is still a challenge. Recent studies showed the potential of functional testing to assess patient sensitivity to drugs in various cancers, but NSCLC is lacking. This study reports the feasibility of ex vivo 3D micro lung tumor testing with native tumor microenvironment (TME) to enable treatment sensitivity profiling for all drug classes in parallel.

Methods: Fresh NSCLC tumor tissue was collected from pleural fluid stage IVa/b (N=24) or resected primary tumor for stage I-III disease (N=11). Tumor clusters were isolated and exposed to drugs, while preserving the TME. Thirteen therapies were included, including cisplatin, pembrolizumab, osimertinib, and positive control for immune sensitivity (SEA). Morphological features were extracted from high-throughput 3D imaging data. Chemo- and targeted therapy sensitivity was based on AUC comparison of fitted dose-response curves. Immunotherapy sensitivity was classified on percentage and statistical significance of tumor killing, immune cell proliferation and cytokine profiling.

Results: The overall assay success rate for solid samples was 64% (7/11), with 100% (4/4) success after protocol optimization. For pleural fluids, the overall success rate was 33% (8/24), caused by many samples arriving without tumor content (13/24, 54%). Excluding these samples, a technical success rate of 73% (8/11) was obtained. The assay was robust and reproducible (mean Z' = 0.38, CV = 16.1%). Results were delivered in two weeks and on average, eight treatments were tested in parallel per sample.

Patient-specific response profiles were observed for chemo-, targeted and immunotherapy. General immunotherapy sensitivity (SEA) was measured in 50% (6/12) of the tissues. Distinct responses were observed for the different immunotherapies: 33% (4/12), 17% (2/12) and 8% (1/12) of the patients responded to pembrolizumab, atezolizumab and/or ipilimumab, respectively. Strong response to osimertinib was observed in a patient with EGFR exon 19 mutation (AUC = 0.26) versus resistance in a WT patient (AUC=0.92).

Conclusion: Ex vivo 3D micro tumor testing using liquid and solid tissues is feasible for NSCLC patients with resected primary tumor or pleuritis carcinomatosa. Distinct patient sensitivity profiles for chemo-, targeted and immunotherapies were measured. A preliminary correlation of targeted therapy response with mutation status was found.

Discussion: The ex vivo 3D micro tumor testing platform is proven predictive for platinum-based therapy. The current study established the methods to accurately measure ex vivo NSCLC responses to all drug classes to correlate with clinical measures and further validate the platform for guiding treatment decisions.

#6397 Immune profiling for improving responsiveness to ipilimumab plus nivolumab checkpoint blockade treatment in patients with metastatic melanoma.

J. Baginska, **J. Chen**, G. Tarantino, A. Giobbie-Hurder, J. L. Weirather, M. Severgnini, M. Manos, K. Burke, J. D. Russell, M. Brainard, E. Gabriel, R. Brennick, M. Nazzaro, E. Hathaway, M. Holovatska, C. Manuszak, S. Ranashinge, D. Liu, F. Hodi;
Dana-Farber Cancer Institute, Boston, MA

Background:aCTLA-4 and aPD-1 combination therapy has significantly improved clinical outcomes in patients with metastatic melanoma, with 50%-60% of patients responding to treatment, but predictors of response and treatment induced immunological effects are poorly characterized. Identifying circulating immune populations as biomarkers could reveal crucial insights into the mechanisms driving treatment success.
Methods: Using unbiased single-cell profiling (with cytometry by Time-Of-Flight, CyTOF), we characterized the systemic immune compartments of over 250 peripheral blood mononuclear samples from 89 patients with advanced melanoma before and during combination therapy. We evaluated the association between circulating immune populations and clinical outcome using nonparametric Mann-Whitney tests, and investigated the prognostic values of these features using survival analysis. Additionally, we assessed treatment-induced immunological effects, providing insights into the dynamic changes within the immune system during therapy.
Results: We characterized circulating T cells, NK cells, B cells, and monocytes from peripheral blood. Following combination therapy, there was a shift from naïve and central memory T cells to effector populations in both CD4+ and CD8+ T cells compartments. There was also a broad activation observed in both adaptive and innate populations, characterized by an elevation of multiple co-stimulatory and co-inhibitory molecules. Lower CD8+ NK cell populations prior to combination therapy were predictive of durable clinical benefit (DCB). Pre-treatment measurements of Tregs were not predictive of outcome, but higher Tregs one month after starting therapy, as well as increases of Tregs from pre to post treatment, predicted better progression free survival (PFS) and overall survival (OS). Starting from early on treatment, higher “exhausted-like” CD8+ T cells, characterized by positive expression of at least two co-inhibitory markers, is associated with resistance.
Conclusions:aCTLA-4 and aPD-1 combination therapy led to a longitudinal shift from naïve and central memory to effector phenotypes in T cells, along with a broad activation in both adaptive and innate populations. Within innate immune compartment, favorable clinical outcome was associated with lower CD8+ NK cells, capable of regulating proliferation and activation of CD4+ T cells. Interestingly, one month after the start of the therapy, the increase in Tregs and a decrease in 'exhausted-like' CD8+ T populations are associated with a better response. Collectively, these analyses suggest potential treatment-specific correlates of efficacy and may enable biomarker-selected patient populations in future.

#6399 Real-world experience of an Asian pan-cancer combined DNA/RNA next generation sequencing (NGS) tissue biopsy assay.

J. Chan[1], J. Lee[1], Z. Wan[2], A. Lim[1], T. Ko[1], C.-Y. Ng[1], D. Poon[3], J. Samol[4], T. So[5], S. Choo[6], R. Kanesvaran[1], C.-V. Hui[7], J.-K. Au[8], A. Helali[9], T. Yip[2], V. Rajasegaran[1], S. Lim[10], R. Weng[10], P. Tan[11], B. Teh[1], M.-H. Tan[2], J. Poh[2];

[1]National Cancer Centre Singapore, Singapore, Singapore, [2]Lucence Diagnostics Pte Ltd, Singapore, Singapore, [3]Dr DYH Poon & Associates, Mt Elizabeth Novena Specialist Centre, Singapore, Singapore, [4]Department of Medical Oncology, Tan Tock Seng Hospital, Singapore, Singapore, [5]Hong Kong Integrative Oncology Centre, Hong Kong SAR, Hong Kong, [6]Curie Oncology, Singapore, Singapore, [7]Department of Oncology, Centro Hospitalar Conde de Sao Januario, MACAO SAR, Macao, [8]Hong Kong Precision Oncology Society, HONG KONG SAR, Hong Kong, [9]LKS Faculty of Medicine, The University of Hong Kong, HONG KONG SAR, Hong Kong, [10]Diagnostics Development Hub (DxD Hub), A National Platform Hosted by A*STAR, Singapore, Singapore, [11]Luma Medical Centre, Singapore, Singapore

Introduction: Comprehensive molecular profiling with combined DNA-RNA next-generation sequencing (NGS) on tumor tissue is now increasingly being used as standard-of-care for sequence therapy selection to improve cancer survival. Combined DNA-RNA NGS is also considered standard-of-care for central nervous system (CNS) tumor classification. Despite the genetic heterogeneity and diversity of cancers, most commercial combined DNA/RNA NGS assays are validated in Western populations, resulting in knowledge gaps in patient outcomes. We report here for the first time a range of actionable outcomes from a comprehensive DNA/RNA tissue NGS assay designed specifically to probe Asian-prevalent cancers and biomarkers in an international multicenter real-world study in Asia.

Methods: 1,002 formalin-fixed paraffin-embedded tissue samples from 995 Asian cancer patients across >70 centers in 7 countries and/or territories underwent real-world DNA/RNA NGS testing in a CAP-accredited CLIA-certified laboratory. Genomic alterations including SNVs, INDELS, gene fusions, CNVs, TMB, and MSI were analyzed using an Asian-centric pan-cancer hybrid-capture NGS panel that comprehensively profiles 572 cancer-related genes and 91 RNA fusion partners (UNITED). Biomarkers were considered actionable if the therapeutic indication in any solid tumor or hematological cancer was FDA-approved, guidelines-recommended, or supported by well-powered phase III clinical trials.

Results: 27 cancer types were represented in 1,002 tissue samples, with lung, breast, colorectal, and prostate cancers comprising 45.5% of clinical volume. 79.5% of samples harbored ≥1 actionable biomarker, with the most frequently altered genes being *TP53*, *KRAS*, *PIK3CA, EGFR,* and *NF1*. Overall, 42.6% of samples had ≥1 biomarker with an indication in the patient's cancer type, including 81.5% of lung, 59.0% of breast, 61.8% of colorectal, and 42.1% of prostate cancers. Across the pan-cancer cohort, 13.3% was TMB-high and 1.9% was MSI-high. 26.3% of samples were from cancer types outside the original assay design; the top 3 were pancreatic cancer (7.3%), sarcoma (3.3%), and CNS tumor (3.1%). Cancers of unknown primary (CUP) also constituted a significant proportion (3.8%). In CNS tumors, 38.7% harbored an actionable mutation in *IDH1*, *BRAF*, or *H3-3A*. In CUP, 78.8% harbored an actionable mutation; 50% of samples harbored biomarkers that additionally informed potential tumor origin, including mutations in *EGFR*, *MET*, *ALK*, *ROS1*, and *BRCA1*.

Conclusion: The use of an Asian-focused pan-cancer DNA/RNA NGS panel resulted in detection of actionable biomarkers in 79.5% of clinical cases. These findings support the utility of DNA/RNA NGS assays in informing standard-of-care therapeutic decisions in Asian cancer patients for maximizing cancer survival.

#6400 Tislelizumab combined with XELOX as a neoadjuvant therapy for locally advanced gastric and gastroesophageal junction adenocarcinomas: A prospective, phase II trial.

H. Zhou[1], T. Han[1], L. Tuo[1], Q. Yang[2], R. Gao[1], P. Yu[1], J. Wei[1], C. Zhu[3], J. Wang[3], P. Cheng[3], X. Kang[3], S. Pi[4], H. Liu[4], X. Pan[4], X. Li[1], G. Ji[1];
[1]Department of Gastrointestinal Surgery, Xijing Hospital of Digestive Diseases, Xijing Hospital, Fourth Military Medical University, Xi'an, Shaanxi, China, [2]State Key Laboratory of Cancer Biology, National Clinical Research Center for Digestive Diseases and Xijing Hospital of Digestive Diseases, The Fourth Military Medical University, Xi'an, China, [3]Department of Translational Medicine, Amoy Diagnostics Co., Ltd., Xiamen, China, [4]Medical Affairs Department of BeiGene (Beijing) Co., Ltd., Beijing, China

Background: Combing anti-PD-(L)1 antibody with chemotherapy in neoadjuvant therapy of gastric/gastroesophageal junction (G/GEJ) adenocarcinomas is a promising strategy, but clinical data are remain insufficient. Whether immunotherapy biomarkers in previous studies (TMB, MSI, PD-L1, etc.) have equivalent predictive value for G/GEJ remains to be verified. In this phase II clinical trial of tislelizumab in combination with chemotherapy, potential therapy-related biomarkers in tumor samples, and changes in the tumor microenvironment during treatment were analyzed, and a predictive model for efficacy was developed.
Methods: This was a prospective, single-center, single-arm, phase II trial. Patients with G/GEJ adenocarcinomas (stage cT3-4aN+M0) were treated with PD-1 inhibitor tislelizumab in combination with oxaliplatin plus capecitabine (XELOX) as neoadjuvant treatment for 2 or 3 cycles. The primary endpoint was the major pathological response (MPR). The secondary endpoints included pathological complete response (pCR) rate, R0 resection rate, and safety. Tumor samples underwent RNA-sequencing (Amoy Diagnostics Co Ltd, Xiamen, China), to identify potential biomarkers, and a predictive model was developed to explore factors influencing tumor response and survival.
Results: 28 patients were enrolled; mean age was 59.5 years (SD = 8.2), 19 (67.9%) patients were male; 14 (50.0%) patients with primary tumor location in the stomach, and 14 (50.0%) patients with primary tumor location in the GEJ. All patients were EB virus negative. Except one patient with PMS2 loss, 27 patients were pMMR. Nine (32.1%) patients achieved MPR after treatment, with four (14.3%) of them achieved pCR. The R0 resection rate was 96.4%, with 14 (50.0%) patients achieved objective response. No serious adverse events were reported. The most common grade 2 TRAEs during neoadjuvant treatment were anemia (5 of 28, 17.86%) and nausea (3 of 28, 10.71%). Analysis of differentially expressed genes revealed enrichment of the antigen processing and presentation pathway in the MPR group, while the TGF-β signaling pathway was enriched in the non-MPR group. Notably, the differential immune microenvironment analysis also uncovered significant differences in the TGF-β signature between the MPR and non-MPR groups. Additionally, a therapeutic response prediction model (HT score) was developed with an AUC of 0.98 (0.932-1) in the training set, and its performance was validated in publicly available datasets.
Conclusion: Tislelizumab combined with XELOX holds promise as a neoadjuvant therapy for resectable G/GEJ adenocarcinomas, especially for EBV- and pMMR population, offering a well-tolerated safety profile. Moreover, the HT score has the potential to predict treatment efficacy in this regimen.
Trial registration numbers: NCT05507658 and NCT05508399.

#6401 Predictive models for first-line immunotherapy based on spatial tumor immune microenvironment in patients with advanced non-small cell lung cancer (NSCLC).

C. Xiang[1], J. Zheng[2], S. Chen[2], Z. Shang[1], S. Yang[2], L. Guo[1], L. Jiao[3], Y. Wang[2], **Y. Han**[1];
[1]Shanghai Chest Hospital, Shanghai, China, [2]Virtue Diagnostics (Suzhou) Co., Ltd., Shanghai, China, [3]Panovue Biotechnology (Beijing) Co., Ltd, Beijing, China

Background: Anti-programmed cell death protein 1/programmed cell death ligand 1 (anti-PD1/PDL1) based immunotherapy is the standard first-line treatment for advanced NSCLC patients without targetable driver mutations, but PDL1 immunohistochemistry (IHC) shows limited predictive value as companion diagnostics. Recent studies have elucidated a strong relationship between immunotherapy efficacy and tumor immune microenvironment (TIME) using single-cell multi-omics technology. In this study, we aim to develop predictive models for both objective response rate (ORR) and progression-free survival (PFS) using TIME features with machine learning in advanced NSCLC patients treated with first-line immunotherapy.

Methods: A total of 210 patients with advanced NSCLC who received anti-PD-1/PDL-1 therapy at Shanghai Chest Hospital from Jan. 2020 to Jan. 2023 were included in this study. Among them, 110 cases who received pembrolizumab were randomly split into training set and validation set with a 2:1 ratio. The remaining patients were designated as independent validation cohort. Five multiplex immunohistochemistry (mIHC) panels were developed based on literature review and in-house dataset mining. mIHC tests were performed using baseline tumor samples. Immunotherapy efficacy was evaluated by ORR and PFS (RECIST v1.1). ORR and PFS models were developed using machine learning methods in training set with 5-fold cross-validation and further validated in validation set and independent validation cohort.

Results: After data cleaning, 68 cases in training set and 34 cases in validation set were further analyzed. In terms of single immune- or spatial- based biomarker, positive rate of PD1+ cells in stroma and spatial relationship of PD1+/PDL1+ cell pairs exhibited the highest correlation with ORR. In addition, positive rate of PDL1+ tumor cells and nearest distance between FOXP3+ cells and tumor cells were highly correlated with PFS. Our ORR model achieved an AUC of 0.82 in the training set and 0.82 in the validation set. When applying optimal cutoff in our PFS model to stratify patients into low- and high- risk groups, low-risk group showed prolonged PFS in both training set ($p < 0.0001$; HR: 0.25, 95% CI [0.13 - 0.51]) and validation set ($p = 0.00046$; HR: 0.22, 95% CI [0.09 - 0.55]). Moreover, our ORR model outperformed PDL1 IHC (AUC: 0.81 vs 0.60; DeLong's test $p = 0.005$) in these 102 patients. Independent validation of the models is still awaited.

Conclusion: Using machine learning methods, we developed and validated ORR and PFS predictive models for first-line immunotherapy in advanced NSCLC patients based on mIHC technology. Our models displayed superior diagnostic performance compared to PDL1 IHC results.

#6402 Treatment resistance and survival prediction using a machine learning gene expression signature in pancreatic adenocarcinoma.

J. Liu[1], X. Lin[1], C. D. Shriver[2], H. Hu[1];

[1]Chan Soon-Shiong Institute of Molecular Medicine at Windber, Windber, PA, [2]Uniformed Services University of the Health Sciences; Walter Reed National Military Medical Center, Bethesda, MD

Background: Pancreatic adenocarcinoma (PAAD) is highly aggressive and difficult to treat. The 5-year survival rate is only 12.5%. The Cancer Genome Atlas (TCGA) data has shown about 51% of PAAD patients didn't achieve complete response after first course of treatment (CRAFCT); this study is to use TCGA data to develop survival-treatment associated gene signature to screen the patients, and provide novel therapeutic strategies to customize patient treatment. **Methods:** RNAseq data of 177 PAAD patients and their clinical data were downloaded from TCGA data portal and processed. The dataset was randomly split into training and testing data. RNAseq data analysis and survival analyses were performed on the training data to identify the survival-treatment associated genes, and a survival-treatment gene signature was derived and independently tested on the test data using signature score by cutoff, logistic regression, and random forest. Furthermore, the signature was validated by an independent dataset of 96 cases. **Results:** Among the 177 patients, 137 patients had the information of CRAFCT, and 122 patients had specific treatment information. Among those 122 patients, 99% received chemotherapy, 36% received radiation therapy. About half of the PAAD patients (51%) didn't achieve CRAFCT. RNAseq data analysis identified 304 significantly expressed genes associated with the status of complete response Yes vs No, and survival analyses further selected 55 genes associated with both treatment and survival as a signature. This signature, using z-scaled scores and the cut-off of 0.3, was applied to the 99 patients of training data; the accuracy is 0.66, and the patients predicted to be Yes had a significantly better (p=0.005, HR=0.42) overall survival than those predicted No. To further test the signature, we applied it to the test data of 78 patients; the random forest model showed patients screened to be Yes had a significantly better (p=0.016, HR=0.43) overall survival than those screened No. The signature (using 40 of the 55 genes) was applied to an independent dataset of 96 cases to significantly screen the patients to be Yes vs No (resistance to treatment) with p=0.04 and HR=0.57, showing the 55-gene signature is valid and robust. **Conclusion:** A 55 survival-treatment associated gene signature was developed and validated robustly, and can potentially be applied as a novel strategy to screen patients for treatment response/resistance. These 55 genes could also be targeted to develop new drugs for those difficult to treat PAAD patients. **Disclaimer:** The contents of this publication are the sole responsibility of the author(s) and do not necessarily reflect the views, opinions or policies of USUHS, HJF, the DoD or the Departments of the Army, Navy or Air Force. Mention of trade names, commercial products, or organizations does not imply endorsement by the U.S. Government.

#6403 Presence of Stroma AReactive Invasion Front Areas (SARIFA) - a potential novel histopathological tool for therapy response prediction in colorectal cancer.

N. G. Reitsam[1], K. Offermanns[2], B. Grosser[1], J. Zimmermann[1], C. Simons[2], J. N. Kather[3], P. A. van den Brandt[4], B. Markl[1], H. I. Grabsch[2],
[1]University of Augsburg, Augsburg, Germany, [2]University Medical Center+, Maastricht, Netherlands, [3]Technical University Dresden, Dresden, Germany, [4]Department of Epidemiology, Maastricht, Netherlands

Background: Although many approaches based either on molecular investigations or on deep-learning algorithms applied to tissue sections have been proposed to stratify colorectal cancers (CRC) patients, clinical implementation of these novel cost-and time-consuming techniques is lacking, and conventional tumor-node-metastasis (TNM) staging remains one of the key factors to determine patient's treatment. Hence, we developed a novel and solely Haematoxylin and Eosin (H&E) based histopathologic prognostic biomarker, called SARIFA (Stroma AReactive Invasion Front Areas, i.e., direct contact between tumor cells and fat cells).

Materials/Methods: Based on a previous study, in which we could show that gene-expression based computational drug response prediction (*oncoPredict*) indicates a SARIFA-dependent differential drug sensitivity, we investigated whether SARIFA-status can predict which CRC patients might benefit from adjuvant therapy. SARIFA-status was established for 1,727 CRC patients from the prospective Netherlands Cohort Study. Multivariate-adjusted Cox regression analysis was performed (median follow-up: 4.79 years, with 1,463 deaths being observed in the first 10 years of follow-up [933, 63.8%, were CRC-related]). Only stages II to IV were included for further analysis regarding differential treatment response (n = 1,384).

Results: In Multivariate-adjusted Cox regression analysis including patient age, sex, tumor location, pTNM stage, grade of differentiation, and mismatch repair status, SARIFA-positive CRC patients (n=496) benefitted significantly from adjuvant therapy ($HR_{CRC\text{-}specific}$ 0.59; 95% CI 0.44-0.78) compared to SARIFA-positive patients treated with surgery alone, which was not significant for SARIFA-negative CRC patients ($HR_{CRC\text{-}specific}$ 0.88; 95% CI 0.68-1.15). Regarding overall survival (OS), adjuvant therapy led to better OS outcomes regardless of SARIFA-status ($HR_{overall\ all\ patients}$ 0.74; 95% CI 0.62-0.87).

Conclusion: Our results suggest that SARIFA-positivity predicts a CRC-specific survival benefit from adjuvant therapy. As SARIFA-positivity is closely linked to an upregulation of lipid metabolism and an altered immune response, further studies are warranted to explore the potential benefit of not only conventional chemotherapy but also immunotherapy, targeted therapy as well novel drugs targeting lipid-metabolism. As SARIFA-status can be assessed fast and easily on for every cancer patient available H&E slides, SARIFA-status could serve as an ideal biomarker for a more detailed patient stratification in prospective clinical trials, and should be implemented into clinical routine if further validated.

#6404 GRB2 stabilizes RAD51 at reversed replication forks restricting genomic instability and associated innate immune response.

Z. Ahmed, Z. Ye, S. Xu, Y. Shi, X. Cheng, Y. Zhang, S. Roy, S. Namjoshi, M. A. Longo, T. Link, K. Schlacher, G. Peng, D. Yu, B. Wang, J. Tainer;
The University of Texas MD Anderson Cancer Center, Houston, TX

Growth factor receptor-bound protein 2 (GRB2) is a cytoplasmic adapter for tyrosine kinase signaling and a nuclear adaptor for homology-directed-DNA repair. Here we find nuclear GRB2 protects DNA at stalled replication forks from MRE11-mediated degradation in the BRCA2 replication fork protection axis. Mechanistically, GRB2 binds and inhibits RAD51 ATPase activity to stabilize RAD51 on stalled replication forks. In GRB2-depleted cells, PARP inhibitor (PARPi) treatment releases DNA fragments from stalled forks into the cytoplasm that activate the cGAS-STING pathway to trigger pro-inflammatory cytokine production. Moreover in a syngeneic mouse metastatic ovarian cancer model, GRB2 depletion in the context of PARPi treatment reduced tumor burden and enabled high survival consistent with immune suppression of cancer growth. Collective findings unveil GRB2 function and mechanism for fork protection in the BRCA2-RAD51-MRE11 axis and suggest GRB2 as a potential therapeutic target and an enabling predictive biomarker for patient selection for PARPi and immunotherapy combination.

#6405 Identification of molecular targets in bladder cancer variants using single-cell analysis.

H. Yang[1], H. Song[1], P. Allegakoen[1], K. Lu[1], E. Yip[1], K. Hui[1], K. Chang[1], C. Kasap[1], J. Gayle[2], B. Stohr[1], A. Wiita[1], C.-K. C. Ding[1], M. V. Meng[1], J. Chou[1], S. P. Porten[1], F. W. Huang[1];

[1]University of California San Francisco, San Francisco, CA, [2]University of California Santa Barbara, Santa Barbara, CA

Introduction and objectives: Variant subtypes in bladder cancer, also known as histologic variants, are clinically aggressive tumors associated with poor prognosis. The rarity of these tumors has made molecular characterization elusive using bulk transcriptional profiling. The aim of this study was to use single cell RNA sequencing to identify molecular features associated with variant subtypes that could be potential targets for therapy.

Methods: Fresh tissue from bladder cancer patients undergoing surgery at our institution was sequenced using a bead-based single-cell RNA sequencing platform (Seq-Well) to generate an atlas of 9 tumors containing variants (micropapillary, nested, squamous differentiation, pleomorphic giant-cell like, plasmacytoid, small cell) and 3 tumors with pure urothelial carcinoma (UC) histology. Pathologic diagnoses were independently confirmed. Analysis was performed using the Seurat package in R Studio. Immunostaining validation was performed on a separately banked cohort. Bulk RNA sequencing data and clinical data were extracted and analyzed from The Cancer Genome Atlas (TCGA) database. Chimeric Antigen Receptor (CAR) T cells targeting TM4SF1 were generated by lentiviral transduction of primary human T cells and tested against publicly available bladder cancer cell lines.

Results: Variant tumors were enriched in TM4SF1, a surface molecule that we demonstrate to be susceptible to CAR T therapy in vitro. Variants also share a cell state characterized by highly specific expression of *MUC16* (CA125), which is enriched in metastatic sites, harbors transcriptional hallmarks of epithelial-mesenchymal transition and luminal-basal plasticity, and is associated with poor survival and resistance to chemotherapy. Finally, we find evidence of transcriptional mimicry between variants and similar appearing non-urothelial cells (e.g. plasmacytoid:plasma cell), suggesting common pathways between distinct cell types that could be exploited.

Conclusion: We have identified several targetable molecular features within variant bladder cancer subtypes. These findings set a critical starting point for future therapeutic investigation.

Funding**:** California Urology Foundation (HY)Conflicts of interest: noneKeywords: Single cell analysis, bladder cancer, variants, genomics, biomarkers

#6406 Clinical and translational results of the academic ARIANES Phase 2 basket study: Longitudinal single-cell analysis of patient tumors identifies biological correlates of response to PARP inhibitors and anti-PD-L1 therapy.

J. Vibert[1], C. Henon[1], L. Tselikas[1], B. Bonnet[1], A. Pages[1], A. Bernard-Tessier[1], L. Colmet-Daage[1], R. Chabanon[1], N. Dorvault[1], C. Astier[1], A. Gazzah[1], A. Jeanson[1], A. Parpaleix[1], R. Flippot[1], N. Naoun[1], A. Patrikidou[1], P. Lavaud[1], G. Baciarello[1], E. Colomba[1], A. Fuerea[1], L. Albiges[1], C. Massard[1], S. Ponce[1], Y. Loriot[1], S. Champiat[1], C. Baldini[1], F. Bouquet[2], N. Droin[1], K. Fizazi[1], D. Vasseur[1], P. Martin-Romano[1], E. Rouleau[1], K. Ouali[1], S. Postel-Vinay[1];
[1]Gustave Roussy, Villejuif, France, [2]F. Hoffmann-La Roche Ltd, Basel, Switzerland

Background: Poly (ADP-ribose) polymerase inhibitors (PARPi) have immunomodulatory properties that may potentiate anti-PD-L1 therapy. To explore this, we developed the academic ARIANES phase 2 basket trial, which evaluated the PARPi rucaparib (R) and the anti-PD-L1 atezolizumab (A) in selected patients (pts). We performed single-cell RNA + T cell receptor sequencing (scRNA+TCR-seq) on 3 sequential tumor biopsies in a pts subset.
Methods: ARIANES comprised 4 molecularly-selected DNA damage response deficient (DDRd), 3 platinum-sensitive, and 2 unselected cohorts of pts with non-small cell lung (NSCLC), prostate (CRPC), and other non-breast non-ovarian cancers. R was administered for 3 weeks, followed by R+A. Primary endpoint was overall response rate (ORR) at 12 weeks per cohort. scRNA+TCR-seq was performed on fresh biopsies collected at baseline, on R, and on R + A in the same lesion, with concomitant plasma collection. We tracked the evolution over time of tumor and microenvironment cells, differentially expressed genes and signatures within each cell population, and TCR clonal dynamics.
Results: ARIANES enrolled 130 pts, including 27 DDRd CRPC and 3 DDRd NSCLC pts, on which we focus here. Best ORR by RECIST v1.1 was 22% (6/27) in CRPC pts, and mPFS: 7.9 months (95% CI 4 - 11.1) at data cut-off. ORR was 0% in NSCLC pts. We successfully profiled 3 sequential fresh biopsies in 2 *BRCA2*-mutant CRPC, 1 *ATM*-mutant, and 1 *RAD54L*-mutant NSCLC pts. Tumor, T and B lymphoid, myeloid, plasma, dendritic, NK, endothelial, and stromal cells were identified in all samples. Differential expression testing unveiled *PARP1* upregulation in tumor cells on R. One CRPC pt with prolonged partial response displayed activation of innate immune sensing pathways (including cGAS-STING and IFN signaling) in tumor and immune cells, as well as JAK/STAT and *CCL5*, all increasing gradually on R and R + A; scTCR-seq revealed the expansion of specific T cell clonotypes on R + A. One *ATM*-mutant NSCLC pt with 6-month stable disease displayed increased cGAS/STING, JAK/STAT and *CCL5* activation on R in NK cells only, and no TCR expansion. None of the above was observed in the 2 pts who progressed. Complete clinical and translational study results will be presented at the congress.
Conclusion: Sequential scRNA+TCR-seq enables the dynamic assessment of tumor and immune cells on therapy. Our data confirms the potential of R to activate innate immune pathways in pt tumors, and R + A to induce T cell activation and clonal expansion. To our knowledge, this is the first study providing a longitudinal single-cell resolution analysis of the clonal evolution of tumor and immune cells in pts on PARPi + anti-PD-L1. We identify potential biological correlates of therapy response, including the activation of innate immune pathways and TCR expansion.

#6407 Identification of novel chemotherapy-related CHIP variations in patients with high-grade serous ovarian cancer.

S. Corvigno, A. Asare, J. Yao, L. Zhao, N. Fleming, J. Celestino, R. A. Hajek, E. A. Arboleda Goette, R. T. Rogers, T. V. Nguyen, R. N. Montoya, K. H. Lu, A. A. Jazaeri, S. N. Westin, A. K. Sood, S. Lee;
UT MD Anderson Cancer Center, Houston, TX

Background: Hematopoietic lineage differentiation is subjected to genetic mutations that, due to fitness advantages, might give rise to clonally expanded populations. Clonal hematopoiesis of indeterminate potential (CHIP) is defined as the outgrowth of a single clone driven by acquired somatic mutations in hematopoietic stem cells (HSCs), in the absence of hematological abnormalities. Previous studies have shown the association of CH with aging and a higher risk of developing secondary hematologic malignancies in cancer patients treated with chemotherapy agents. It is therefore of great interest to study CH incidence prior to and post chemotherapy exposure and its association with the evolution of hematologic malignancies. We aimed to characterize CHIP variants of a highly selected group of patients with high-grade serous ovarian cancer (HGSC) who underwent neoadjuvant chemotherapy (NACT).
Methods: Comprehensive ultra-high-depth whole exome sequencing, employing unique molecular barcode technologies, was performed using plasma-derived cell-free DNA (cfDNA) and matched white blood cells (WBC) DNA and tumor DNA from pre-NACT (n=10) and post-NACT (n=10) samples of patients with HGSC. CHIP variants were defined as heterozygous variants found in both the WBC and cfDNA samples from the same patients with variant allele frequency less than 5% in the WBC and higher than 0.5% in cfDNA samples.
Results: Our analysis identified 93,088 variants, impacting 13,780 genes. Among them, 463 variants were already known and published, and 5,548 variants were common to the COSMIC genes signature. The number of CHIP variants significantly decreased after chemotherapy ($p = 0.004$). We then focused on CHIP variants enriched after chemotherapy and identified 77 that showed higher VAF in post-NACT cfDNA samples, which may be associated with the development of therapy-related acute myeloid leukemia/myelodysplastic syndrome (t-AML/MDS). Among them, interestingly, we found a missense mutation with protein change in *CDK12* (chr17_39492765_G_T). We noticed that 38% of the CHIP variants found in cfDNA samples, were also found in matched tumor samples. Among these, another *CDK12* missense mutation (chr17_39492768_A_T) showed higher VAF in post-NACT tumors.
Conclusions: Our innovative approach detected a higher number of CHIP variants than currently characterized. Analysis of cfDNA from HGSC patients consistently demonstrated a reduction in CHIP mutations post-NACT. The subset of variants with increased VAF post-NACT may be associated with therapy-related t-AML/MDS. The detection of cfDNA CHIP variants in matched tumors highlights the potential predictive role of CHIP in t-AML/MDS development, emphasizing its consideration in therapeutic protocols.

#6408 Early carcinoembryonic antigen (CEA) dynamics to predict the efficacy of fruquintinib (F) + best supportive care (BSC) in patients with metastatic colorectal cancer (mCRC) enrolled in FRESCO-2.

Sara Lonardi[1], Arvind Dasari[2], Rocio Garcia-Carbonero[3], Takayuki Yoshino[4], Pilar Garcia-Alfonso[5], Judit Kocsis[6], Chiara Cremolini[7], Francois Ghiringhelli[8], **Ardaman Shergill**[9], Howard S Hochster[10], Michel Ducreux[11], Dirk Arnold[12], Varsha Sundaresan[13], Siddha Kasar[13], Adela Pina[13], Ziji Yu[13], William R Schelman[14], Lucy Chen[13], Josep Tabernero[15]

[1]Medical Oncology Unit 1, Veneto Institute of Oncology IOV-IRCCS Padua, Padua, Italy,[2]Department of Gastrointestinal Medical Oncology, University of Texas MD Anderson Cancer Center, Houston, TX,[3]Oncology Department, Hospital Universitario 12 de Octubre, Imas 12, UCM, Madrid, Spain,[4]Department of Gastroenterology and Gastrointestinal Oncology, National Cancer Center Hospital East, Kashiwa, Chiba, Japan,[5]Medical Oncology, Hospital Universitario Gregorio Maranon, Madrid, Spain,[6]Department of Oncoradiology, Bacs-Kiskun Megyei Oktatokorhaz, Kecskemet, Hungary,[7]Department of Translational Research and New Technologies in Medicine and Surgery, University of Pisa, Pisa, Italy,[8]Department of Medical Oncology, Centre Georges Francois Leclerc, Dijon, France,[9]University of Chicago, Biological Sciences Division, Chicago, IL,[10]Rutgers Cancer Institute of New Jersey, New Brunswick, NJ,[11]Gustave Roussy Cancer Center, Inserm U1279 Tumors Cell Dynamics, Universite Paris Saclay, Villejuif, France,[12]Asklepios Tumorzentrum Hamburg, Department of Oncology and Hematology, AK Altona, Hamburg, Germany,[13]Takeda Development Center Americas, Inc. (TDCA), Lexington, MA,[14]HUTCHMED, Florham Park, NJ,[15]Vall d'Hebron Barcelona Hospital Campus, Vall d'Hebron Institute of Oncology (VHIO), Barcelona, Spain

Background: The phase 3 FRESCO-2 trial (NCT04322539) demonstrated a significant survival benefit with fruquintinib (F) + BSC vs placebo (P) + BSC as third or later line of therapy for patients (pts) with mCRC. Based on the results of FRESCO-2, F was FDA-approved for adults with previously treated mCRC, irrespective of biomarker status. In mCRC, CEA levels and imaging are routinely used to monitor response to systemic therapy. We investigated early CEA changes during treatment in FRESCO-2 and possible relationships with efficacy.

Methods: Pts with abnormal baseline (BL) CEA were included based on local lab reference ranges. Serum CEA levels were measured at BL and Day 1 (D1) of each 28-day cycle (C) except C1. Changes in CEA levels were analyzed at C2D1 and C3D1. CEA response was defined as ≥50% decrease from BL, and CEA progression was defined as ≥100% increase from BL. Tumor evaluation was performed by CT or MRI scan every 2 cycles. Overall survival (OS) and progression-free survival (PFS) were evaluated by Kaplan-Meier method; hazard ratio (HR) was estimated via Cox proportional hazards model; p-value was generated from log rank test.

Results: Overall, 88.3% (407/461) vs 90.4% (208/230) of pts had abnormal BL CEA in F vs P arms; median BL CEA values were similar between treatment arms (Table). At C3D1, the proportion of pts who had a CEA response was significantly higher with F vs P (35.5% vs 3.8%, *P* <0.001) and the proportion who had CEA progression was significantly lower (5.7% vs 47.2%, *P* <0.001). Pts in the F arm with CEA response at C3D1 had improved OS and PFS vs pts without CEA response and pts with CEA progression (Table). These results were consistent for pts who had an early CEA response at C2D1 (Table).

Conclusion: CEA response at C2D1 and C3D1 could be considered an early predictor for improved OS and PFS. Pts with CEA response seem to benefit from F + BSC compared with pts without response or with CEA progression.

Table. CEA changes from baseline in pts in the F + BSC vs P + BSC arms, and OS and PFS based on CEA response in pts in the F + BSC arm

	CEA changes from baseline by treatment arm (ITT population)			
	F + BSC (N=461)		**P + BSC (N=230)**	
Baseline, n	407		208	
Median CEA (range), µg/L	132.4 (3.0-213000.0)		169.6 (3.2-90010.0)	
C2D1, n	340		151	
Median CEA (range), µg/L	93.3 (2.0-98660.0)		133.5 (2.7-255910.0)	
Median change from baseline (range), %	-19.2 (-90.5-467.8)		44.2 (-61.7-606.8)	
C3D1, n	245		53	
Median CEA (range), µg/L	78.3 (1.7-133390.0)		145.2 (3.9-17782.0)	
Median change from baseline (range), %	-31.0 (-91.4-2195.8)		90.5 (-68.9-3776.6)	
	OS and PFS for pts in the F + BSC arm with or without CEA response at C2D1 and C3D1			
	Pts with early CEA response at C2D1 (n=66)	**Pts without early CEA response at C2D1 (n=274)**	**Pts with CEA response at C3D1 (n=87)**	**Pts without CEA response at C3D1 (n=158)**
Median OS, months	10.0	7.4	11.1	8.5
HR (95% CI), *P* value	0.62 (0.44-0.89), *P* = 0.009		0.65 (0.46-0.92), *P* = 0.015	
Median PFS, months	5.6	3.7	5.8	4.2
HR (95% CI), *P* value	0.68 (0.51-0.92), *P* = 0.01		0.58 (0.44-0.78), *P* = 0.0003	
	OS and PFS for pts in the F + BSC arm with CEA response or CEA progression at C2D1 and C3D1			
	Pts with early CEA response at C2D1 (n=66)	**Pts with early CEA progression at C2D1 (n=15)**	**Pts with CEA response at C3D1 (n=87)**	**Pts with CEA progression at C3D1 (n=14)**
Median OS, months	10.0	4.3	11.1	5.6
HR (95% CI), *P* value	0.27 (0.14-0.51), *P* <0.0001		0.23 (0.12-0.45), *P* <0.0001	
Median PFS, months	5.6	1.9	5.8	3.4
HR (95% CI), *P* value	0.30 (0.16-0.56), *P* <0.0001		0.25 (0.13-0.48), *P* <0.0001	

#6409 A multiparametric flow cytometry assay to monitor regeneration of B-cells following anti B-cell therapy in cancer and autoimmune patients.

Amit Kumar Mehta, Ruby Tandon, Anil Pahuja, Jane Gao, Kevin Nguyen, Naveen Dakappagari, Zeni Alfonso

Navigate BioPharma, Carlsbad, CA

Purpose Functional dysregulation of B-cells leads to a variety of autoimmune disorders and blood cancers. Multiple B-cell depleting therapies (e.g., BTK inhibitors, antibodies or CAR-Ts) are currently in active clinical trial investigation. Following therapeutic elimination of pathogenic B-cells, it is critical to monitor the productive regeneration of fully functional B-cells as they mediate innate and adaptive immune responses. To this end, we developed a multiparametric flow cytometry assay for exquisite monitoring of early stages of B cell development, maturation, and antibody production to correlate it with treatment outcomes and determine if continuous depletion of B-cells is necessary to maintain clinical benefits for patients.

Study Design We designed a high throughput 12-parameter flow cytometry panel incorporating primary differentiation markers namely, CD45, CD3, CD38, CD10, CD27, CD19, CD20, IgD, Lambda & Kappa Light Chains required for identification of different developmental stages of B-cells in peripheral blood using an in vitro diagnostic grade flow cytometry system (BD FACSLyric). The optimized method underwent robust fit-for-purpose analytical validation per CLSI H62 guidelines with emphasis on establishing assay sensitivity, specificity, and reproducibility across experimental days, operators, and instruments.

Results We were able to reliably identify different stages of B-cell development, namely, Naïve (CD19+CD20+IgD+CD27-), Unswitched/Marginal (CD19+CD20+IgD+CD27+), Memory (CD19+CD20+IgD-CD27+), Transitional (CD19+CD20+IgD+CD27-CD10+), Antibody Secreting Cells (CD19+CD20-IgD-CD27+CD38^{hi}) as well as clonality (CD19+CD20+Lambda+ or Kappa+). The lower limit of quantitation was determined to be around 60 events, based upon analysis of 90 data points with good reproducibility (CV range: 0-11.7%) across experimental days, operators and instruments demonstrating sensitive detection and robust performance.

Conclusion In summary, we have developed and validated a 12-parameter flow cytometry assay focusing on monitoring the regeneration of different subsets of B-cells in various B-cell malignancies (Non-Hodgkin's Lymphoma, B CLL) and autoimmune disorders (Multiple Sclerosis, Rheumatoid Arthritis, Systemic Lupus Erythematosus). The high reproducibility/robustness of the assay demonstrates its suitability for use in clinical trials as a valuable tool for safety monitoring and disease evaluation enabling development of novel therapeutic agents.

#6410 An exosomal microRNA signature predicts the efficacy of ramucirumab plus paclitaxel in advanced gastric cancer: Findings from the prospective IVY trial.

K. Shoda[1], C. Xu[1], Y. Asahii[2], T. Nagasaka[3], D. Ichikawa[4], A. Goel[1];

[1]Beckman Research Institute of City of Hope, Monrovia, CA, [2]Biomedical Research Center of City of Hope, Monrovia, CA, [3]Kawasaki Medical School, Okayama, Japan, [4]University of Yamanashi, Yamanashi, Japan

Purpose: With rapid advances in the development of effective therapeutic regimens in patients with advanced gastric cancer, it is imperative to establish individualized treatment approaches that can help identify patient subsets that have the highest likelihood of response to a specific regimen. Although ramucirumab plus paclitaxel therapy is the standard second-line treatment for patients with advanced gastric cancer, biomarkers that can help predict therapeutic response are still lacking. This longitudinal study aimed to establish a liquid-biopsy assay that can predict response to ramucirumab plus paclitaxel therapy in patients with advanced gastric cancer.

Experimental Design: A prospective observational multicenter study (named the IVY study) enrolled 115 patients who received ramucirumab plus paclitaxel treatment. We collected serum specimens prior to the initiation of the treatment regimen. Patients were divided into responders and non-responders according to the response evaluation criteria in solid tumors (RECIST). We performed small RNA-sequencing (sRNA-Seq) in a subset of 28 patients with and without response to identify exosomal microRNA-based biomarkers that allowed risk stratification and response prediction in patients with advanced gastric cancer.

Results: The sRNA-Seq analysis and rigorous bioinformatic approaches using machine-learning algorithms allowed us to identify a panel of 10 exosomal microRNAs that robustly predicted resistance to ramucirumab plus paclitaxel treatment (AUC: 0.83). The panel of exosomal miRNAs was also shown to have a robust prognostic value for predicting survival outcomes in gastric cancer patients treated with ramucirumab plus paclitaxel, and Cox proportional hazards regression analysis showed that patients classified as high risk on the panel of exosomal miRNAs independent poor prognostic factor (OS: HR = 2.74, 95% CI = 1.56-4.81, P < 0.01, RFS: HR = 1.84, 95% CI = 1.16-2.92, P < 0.01). Following logistic regression and backward elimination, we trained a clinically feasible 5 exosomal miRNA signature by combining it with the Body Mass Index data, an independent clinical predictor (AUC: 0.84). We subsequently successfully validated the performance of this signature in the prospective clinical trial cohort (AUC: 0.87). Finally, we established a prognostic risk nomogram based on the circulating exosomal miRNA signature for a non-invasive and personalized pre-therapeutic selection approach.

Conclusions: We have developed a novel liquid biopsy-based assay that allows robust prediction of response to ramucirumab plus paclitaxel treatment in gastric cancer patients, and our assay provides a framework for a personalized medicine approach that can provide risk-based management and treatment for each patient prior to the initiation of therapy.

#6411 The gut microbiome is associated with recurrence free survival in patients with resected Stage III or Stage IV melanoma treated with immune checkpoint inhibitors.

M. Usyk[1], R. B. Hayes[1], R. Knight[2], A. Gonzalez[2], H. Li[1], I. Osman[1], J. S. Weber[1], J. Ahn[1];
[1]NYU Grossman School of Medicine, New York, NY, [2]University of California - San Diego, San Diego, CA

The gut microbiome (GMB) plays a crucial role in immune checkpoint blockade (ICB) therapy outcomes for metastatic melanoma patients, yet there remains a lack of consensus regarding the specific microbiota associated with clinical outcomes, particularly across different geographic regions. Furthermore, investigations into the relationship between GMB and melanoma outcomes in the adjuvant setting are notably absent. This highlights the pressing need for a comprehensive, large-scale study spanning diverse geographic locations within a well-controlled clinical trial environment. In this study, we conducted shotgun sequencing on pre-treatment stool samples collected from 674 melanoma patients participating in an international, randomized, double-blind, phase III adjuvant trial evaluating clinical outcomes following adjuvant nivolumab plus ipilimumab versus nivolumab. Our recruitment encompassed three continents and five geographically distinct regions. Given the significant influence of geographic region on GMB composition, we employed three analytical approaches: (a) region-specific analyses, (b) combined meta-analyses across regions, and (c) sub-set paired analyses involving subjects closely matched for overall GMB. Additionally, we assessed GMB stability by examining samples collected serially prior to therapy and at weeks 7 and 29 of ICB treatment. Through region-specific and meta-analyses, we identified ten pre-treatment gut bacterial markers, including Eubacterium, Ruminococcus, Clostridium, and Firmicutes, which exhibited associations with melanoma recurrence in the adjuvant setting. The predictive capacity of these microbial markers was directly proportion to GMB similarity (Spearman correlation = 0.86, $p<0.001$ for AUC vs. beta-diversity). Notably, for closely matched patients in terms of their GMB composition, the prediction of recurrence using the recurrence-associated markers, in conjunction with clinical characteristics, yielded an AUC of 0.917 (95% CI: 0.825-1.00). Furthermore, GMB remained largely stable across serial samples collected before and after treatment (PERMANOVA $R2 = 0.867$, $p\text{-val}<0.001$, at baseline, week 7, and week 29). This study underscores the remarkable stability of GMB during adjuvant ICB therapy for melanoma and identifies specific bacterial biomarkers that hold promise for predicting melanoma recurrence within the adjuvant treatment setting. The gut microbiome emerges as a potential source of microbial biomarkers for individualized prediction of melanoma recurrence in clinical practice.

#6412 Combination of liquid biopsy and PET/CT enhances prediction of pathological response to neoadjuvant immunochemotherapy in patients with esophageal squamous cell carcinoma.

Weixiong Yang[1], Zengli Fang[1], Xiaoyan Wang[2], Hui Luo[2], Shuishen Zhang[1], Bo Zeng[1], Zhenguo Liu[1], Chenxuan Wang[3], Qiuxiang Ou[3], Lingling Yang[3], **Haimeng Tang**[3], Sai-Ching J. Yeung[4], Chao Cheng[1]

[1]Department of Thoracic Surgery, The First Affiliated Hospital of Sun Yat-sen University, Guangzhou, China,[2]Department of Nuclear Medicine, The First Affiliated Hospital of Sun Yat-sen University, Guangzhou, China,[3]Nanjing Geneseeq Technology Inc, Nanjing, China,[4]Department of Emergency Medicine, The University of Texas MD Anderson Cancer Center, Houston, TX

Background: Neoadjuvant immunochemotherapy (NICT) demonstrated remarkable efficacy in esophageal squamous cell carcinoma (ESCC) patients. An accurate evaluation of treatment response is critical before surgery. Therefore, this study aimed to explore and evaluate the use of non-invasive and clinical assessments to predict pathological response to NICT prior to surgery in these patients.

Methods: A total of 71 ESCC patients who received NICT between March 2020 and February 2022 were recruited in this study. Clinicopathological characteristics and PET/CT assessment before and after NICT were evaluated. Peripheral blood mononuclear cells (PBMCs) were prospectively collected for genomic and T cell receptor (TCR) profiling using targeted next-generation sequencing and multiplex PCR, respectively. Univariate analysis was performed to identify features associated with pathological complete response (pCR) of primary tumor. Optimal predictive features were identified using the least absolute shrinkage and selection operator (LASSO) regression model. Subsequently, a prediction model was established using logistic regression, followed by receiver operating characteristic (ROC) analysis and internal validation.

Results: Univariate analyses revealed significant associations between pCR and post-NICT features, including ctDNA, PET/CT parameters, and TCR clonality and diversity. Optimal predictive features were identified as post-NICT SUVmax, ctDNA positivity, and TCR clonotype clonality, and their area under the ROC curve (AUC) was 0.784 (95%CI: 0.644-0.924), 0.739 (95%CI: 0.664-0.813), and 0.682 (95%CI: 0.535-0.829), respectively. The final prediction model integrating these three features achieved an AUC of 0.918 (95%CI: 0.849-0.986), an accuracy of 0.768 (95%CI: 0.661-0.875), a sensitivity of 1.000 (95%CI: 1.000-1.000), and a specificity of 0.705 (95%CI: 0.568-0.841), indicating excellent predictive performance.

Conclusion: The combination of post-therapy ctDNA status, TCR clonality, and PET/CT assessments showed robust predictive power for assessing pathological response to NICT in ESCC, suggesting the potential to inform clinical decision-making for these patients. Future large-scale studies are warranted to strengthen and verify the findings from our study.

#6413 Biomarkers of response and progression to Pembrolizumab and Vorinostat combination in late-stage squamous cell carcinoma patients of different locations included in the PEVOsq basket trial.

C. Le Tourneau[1], L. Mazzarella[2], B. Cabarrou[3], M. Francisco[4], C. Dupain[1], M. Halladjian[1], G. Frige[2], B. Duso[2], Y. Zhan[2], E. Guerini-Rocco[2], R. Noberini[2], T. Bonaldi[2], M. Tonini[5], G. Marret[1], C. Coutzac[6], E. Coquan[7], M. Saint-Ghislain[1], O. Le Saux[6], L. Chanas[1], F. Legrand[8], D. Filippini[1], E. Jeannot[1], S. Bernhart[9], G. Balogh[9], M. Jimenez[8], T. Filleron[3], N. Servant[4], M. Kamal[1];

[1]Institut Curie, Paris, France, [2]IEO - Istituto Europeo di Oncologia IRCCS, Milan, Italy, [3]Institut Claudius Regaud, IUCT-Oncopole, Toulouse, France, [4]INSERM U900, Paris, France, [5]Luxembourg Institute of Health, Luxembourg, Luxembourg, [6]Centre Leon Berard, Lyon, France, [7]Centre Francois Baclesse, Caen, France, [8]Unicancer, Paris, France, [9]Universitat Leipzig, Leipzig, Germany

Background: Epigenetic modulation plays a major role in escaping tumor immunosurveillance. PEVOsq (NCT04357873) was an open-label, non-randomized, multi-center, basket phase II trial evaluating the efficacy of pembrolizumab (P) and the vorinostat (V) HDAC inhibitor in 112 patients (pts) with recurrent and/or metastatic squamous cell carcinoma (SCC) of the cervix, head and neck, anus, vulva/vagina, penis, and lung. Results showed an objective response rate (ORR) of 25%, the highest being in anal (31%) and cervical (39%) (ASCO #397612). We report here early biomarkers of response and progression to P+V.

Patients and Methods: Pts had to undergo a tumor biopsy at baseline, and optional biopsies on-treatment (after cycle 2), and at progression for translational analyses. PD-L1 expression (n=102), tumor-infiltrating lymphocytes quantification (n=39), HPV typing (n=111), WES (n=83), RNAseq (n=82) and liquid chromatography-mass spectrometry (LC-MS) quantitative analysis of histone post-translational modifications (PTMs) (n=44) were performed on baseline samples.SNVs, CNVs, TMB, MSI status (by MSI sensor), aneuploidy score (AS), mutational signatures, immune signatures, and histone modifications were correlated with response and progression.

Results: Sixty-six pts were HPV+ (59%). Most frequently altered genes were *PIK3CA* (30%), *TP53* (30%), *KMT2D/C* (18 and 17%), and *FGF3/4* (17%). MSI was detected in 4 pts (5%), and TMB-high (>10mut/Mb) in 13 pts (16%). High AS (>10) was detected in 34 pts (40%), and was significantly associated with HPV- status (p=0.03). TMB high and MSI were associated with MMR mutational signatures (p<0.01). TMB high was also associated with APOBEC (p=0.02) and DNA polymerase (POL) signatures (p <0.01). Biomarkers associated with improved overall survival (OS) included HPV positivity (7.8 months versus 17.4 months, p<0.01), high TMB (not reached versus 10.3 months, p=0.01), and high PD-L1 CPS score (13.2 months versus 7.0 months, p=0.06).Deconvolution of immune cell infiltration showed an expected trend for increased CD8 and decreased neutrophil infiltration in non progressor pts.Interestingly, LC-MS histone PTMs profiling showed a significant decrease in H4K5K8K12K16-4ac (p=0.05) and increase in H3K27me2K36me1 in non progressor pts (p=0.03). At the transcriptomic level, although not statistically significant, we observed modulation in the expression of genes associated with H3K36me1 (KDM2A, SETD3, SMYD2), and H3K27me3 (KDM6A) regulation, as well as HDAC genes.

Conclusions: HPV+ status was associated with improved OS, together with a high TMB and PD-L1 expression. CD8, macrophages and neutrophil signatures at baseline were associated with response. Promising epigenetic biomarkers were identified using LC/MS and will be correlated to transcriptomic and genomic data.

#6414 Molecular differentiation between complete and incomplete responders to neoadjuvant therapy in rectal cancer.

F. Huang[1], M. McLeod[1], R. Irwin[1], M. Smithson[1], Z. Yue[2], M. Gao[1], K. Hardiman[1], Z. Chong[1];
[1]University of Alabama at Birmingham, Birmingham, AL, [2]Auburn University, Auburn, AL

Neoadjuvant chemoradiotherapy (nCRT) is the standard treatment for locally advanced rectal cancer, but only 20-40% of patients completely respond to this treatment. This study aims to identify the molecular features associated with a response to nCRT. We generated and collected genomic and transcriptomic data from 712 cancers prior to treatment from our own data and from publicly available data. A comprehensive integrated analysis was performed. We found that patients with a complete response have decreased risk of both local recurrence and future metastasis. We identified multiple molecular differences between complete and incomplete responders. Complete responders have a higher tumor mutation burden and more significant co-occurring mutations than the incomplete responders. In addition, mutations in DNA repair genes were enriched in complete responders and they also had lower expression of these genes indicating that defective DNA repair is associated with complete response to nCRT. Using logistic regression, we identified three significant predictors of complete response: tumor size, mutations within specific network genes, and the existence of three or more specific co-occurrent mutations. In incompletely responder tumors, abnormal cell-cell interaction and increased cancer associated fibroblasts were associated with recurrence. Additionally, gene expression analysis identified a subset of immune hot tumors with worse outcomes and upregulation of immune checkpoint proteins. Our study directly informs the clinical management of rectal cancer by elucidating the molecular differences between tumors with complete and incomplete responses to neoadjuvant chemoradiotherapy (nCRT), as well as the features of tumors prone to recurrence. We have pinpointed critical molecular markers and clinical indicators—such as tumor size, specific gene mutations, and particular mutation patterns—that are significant predictors of treatment response. These findings offer valuable biomarkers for personalizing treatment strategies. Additionally, the observed mutation enrichment in DNA repair genes among complete responders suggests new avenues for therapeutic innovation. By highlighting the distinct molecular and immune profiles of non-responder tumors at higher recurrence risk, our research supports the advancement of precision oncology approaches, enhancing prognosis and treatment customization in rectal cancer care, ultimately striving to bridge the gap between scientific discovery and clinical application.

#6415 Comparison the results from PD-L1 IHC and PD-L1 multiplex immunofluorescence for the prediction of anti-PD-1 immunotherapeutic response.

H. Sun[1], X. Liu[1], T. Jiao[2], Q. Guo[2], H. Du[2], S. Han[1], L. Zhu[1], Z. Zhang[1], Y. Kong[2], **N. Li**[1];

[1]Beijing PhenoVision Bio Co., ltd, Beijing, China, [2]Department of Renal Cancer and Melanoma, Peking University Cancer Hospital & Beijing Institute for Cancer Research, Beijing, China

PD-L1 immunohistochemistry (IHC) is a popular clinical test before anti PD-1/PD-L1 immunotherapy (IMT). Multiplex immunofluorescence (mIF) exhibits its advantage to evaluate more than one target on one FFPE section to provide the features of multiple target expression and co-expression signals. Here, based on our pathology controlled mIF detection system and AI based analysis data, we compared IHC PD-L1 TPS to mIF PD-L1 TPS, PD-L1 positive rate, and other target positive rates in one mIF panel, to evaluate their correlations. The correlations of IHC PD-L1 TPS, mIF PD-L1 TPS, mIF PD-L1 positive rate and other marker positive rate to anti PD-1 IMT response were further analyzed in this study. Thirty melanoma patient samples in this study have received PD-1 IMT. 13 cases exhibited partial response (PR) and 17 cases were progressive disease (PD). PFS of PR group and PD group was 27.3 and 4.8 months, respectively. Archived patient FFPE sections were examined utilizing mIF of PN 6-Plex Detection Kit (Beijing PhenoVision Bio Co., ltd) targeted CD68, CD3, CD20, S100, PD-L1 (CST, E1L3N) and PD-1. The staining images were scanned, tumor areas were labeled by pathologists and analyzed using PhenoVision mIF AI analysis system trained from Oncotopix Discovery system (Visopharm). Series sections were examined utilizing Dako PD-L1 IHC 22C3 pharmDx and TPS was scored by one clinical pathologist. mIF TPS was calculated after AI data analysis, using PD-L1/S100 co-positive cell number divided by S100 positive cell number. Data mining was performed using log-rank Mantel-Cox test, Cox regression analysis and binary logistic regression model in SPSS. In current study, the correlation between pathology scored TPS (pTPS) and mIF PD-L1 positive rate was observed (Pearson correlation coefficient (PCC)=0.447, $p<0.05$). The consistency rate between pTPS and mIF TPS was 70% with no statistical significance. Moreover, the correlation between pTPS and mIF PD1/CD3 copositive rate was detected (PCC=0.604, $p<0.01$). Interestingly, mIF PD-1/CD3 copositive rate predicted PR and PD groups (AUC=0.8, $p<0.01$). Not pTPS nor mIF PD-L1 rate showed predictions here. Current results indicate that pTPS exhibited correlation to mIF PD-L1 positive rate instead of mIF PD-L1 TPS. CD3/PD-1 copositive rate but not pTPS nor mIF PD-L1 positive rate, shows its potential to predict anti PD-1 IMT response through the pathology controlled mIF detection system and AI based analysis system.

#6416 Early stage endometrioid endometrial cancer recurrence risk stratification using a machine learning RNA-seq gene expression signature.

Rafi Pelossof[1], Talal Ahmed[1], Seung Won Hyun[1], Chithra Sangali[1], Ben Terdich[1], Calvin Chao[1], Michael Toboni[2], Casey Cosgrove[3], Elizabeth Kidd[4], Brook Howitt[5], **Timothy Taxter**[1]

[1]Tempus, Chicago, IL,[2]Obstetrics and Gynecology, University of Alabama Birmingham, Birmingham, AL,[3]Gynecologic Oncology, The Ohio State University, Columbus, OH,[4]Radiation Oncology, Stanford University, Palo Alto, CA,[5]Pathology, Stanford University , Palo Alto, CA

Endometrioid endometrial cancer (EEC) adjuvant therapy decisions rely on risk stratification using histology, grade, stage, and lymphovascular space invasion (LVSI). Recently, molecular classification systems originating from TCGA, evaluated in GOG-210 and PORTEC-3 defined four prognostic subtypes based on POLE, MSI-H/MMR-D, and p53 alterations. Although valuable, this molecular approach still has significant limitations such as applicability to the majority of EEC patients categorized as no-specific molecular profile (NSMP) and the potential need to resolve pathogenic and prognostic heterogeneity within MMR-D, and TP53 subtypes. These unmet needs were key motivators for Tempus to develop a molecular classifier predicting distant recurrence risk in early-stage EEC with a focus on high intermediate-risk (HIR) patients.

The RNA-seq-based gene expression profiler (GEP) was trained using a machine-learning pipeline with TCGA data which resulted in a 24 gene signature that classifies EEC patients as molecular risk (MR) high or low (MR-high, MR-low). The GEP MR test was then evaluated on a de-identified cohort of EEC patients (N=1037) from Tempus to test associations with known pathologic or molecular prognostic features. The GEP-MR risk predictor showed significant enrichment of MR high-risk in G3 versus G1/2 histology (p-value < 5e-8). A high correlation was found between the MR score and copy number alteration score (t-test p-value < 1e-5). Next, a clinical evaluation was performed in an early-stage EEC case-control cohort of patients with documented recurrence or no recurrence event at four years (N=109), from Stanford. In the entire cohort, the MR-high group had a significantly higher rate of distant recurrence in comparison to the MR-low group (HR=4.8, N=109). Next, we performed a subgroup analysis in the clinically important HIR patients. In this subgroup, the MR-high group had a significantly higher rate of distant recurrence in comparison to the MR-low group (HR=8.0, N=56). Lastly, given the significance of genomic biomarkers in the evolution of EEC FIGO staging, we stratified outcomes by the established TCGA subtypes as a reference standard and performed a subgroup analysis in patients classified as having no specific molecular profile (NSMP). Among patients who were NSMP, the MR-high group showed a significantly higher rate of distant recurrence in comparison to the MR-low group (HR=7.92, N=67).

These evaluation studies demonstrate the performance of the GEP MR test in early-stage EEC distant recurrence risk stratification, specifically HIR patients, necessitating further studies to validate the test for clinical use in informing adjuvant clinical management.

#6417 Urinary PKM2 in muscle invasive bladder cancer.

D. Matye, J. Leak, E. Abbott, B. Woolbright, J. Taylor III;
University of Kansas Medical Center, Kansas City, MO

Background & Aims: Biomarkers are commonly used for both detection of cancer and monitoring response to treatment. Although several biomarkers have demonstrated promise in patients with bladder cancer (BCa), only urine cytology is widely utilized. Increased availability of effective biomarkers may improve clinical decision making and reduce the need for more invasive imaging. The M2 isoform of pyruvate kinase (PKM2) is upregulated in a number of cancers, including BCa, and promotes metabolic changes, including a shift to aerobic glycolysis. The aim of this study was to determine whether urine PKM2 levels are useful for detection and monitoring response to cisplatin-based neoadjuvant chemotherapy in patients with muscle invasive BCa.
Methods: Urine samples from patients enrolled in the University of Kanas Medical Center Bladder Cancer Biorepository were analyzed for levels of PKM2. Patients were included if they had both T2 stage disease and had received cisplatin-based neoadjuvant chemotherapy and were compared to healthy controls. Patients were categorized based on their pathological response to treatment and recurrence of disease within two years of definitive surgery. Urinary PKM2 levels were measured and evaluated for their ability to predict response to treatment and two-year disease-free survival.
Results: Immunohistochemistry revealed high levels of PKM2 within muscle invasive tumors compared to adjacent tissue. Patients with BCa had 150-fold increase in levels of urinary PKM2 compared to controls. However, there were no differences in urine PKM2 levels in patients with complete pathological response compared to those with no response. Urine PKM2 showed limited predictive value for disease recurrence (area under receiver operating characteristic curve = 0.65).
Conclusion: Urine levels of PKM2 are significantly elevated in patients with muscle invasive BCa and may be useful for tumor detection. Urinary PKM2 is less effective at monitoring response to treatment and may instead represent a marker of urothelial susceptibility to tumor formation.

#6418 Single-cell double expression of MYC and BCL2 proteins by fluorescent multiplex IHC is mainly in lymphoma cells with significant prognostic impact in large B-cell lymphoma while suggesting high cutoffs for routine IHC.

Z. Y. Xu-Monette[1], Y. Li[2], Q. Au[3], H. Nunns[3], W. Shi[1], A. Tzankov[4], C. Visco[5], G. Bhagat[6], E. Hsi[7], X. X. Zhao[7], K. Dybkaer[8], A. Chiu[9], W. Tam[10], Y. Zu[11], F. B. Hagemeister[12], A. Song[13], M. Pellegrino[13], H. Go[14], M. Ponzoni[15], A. Ferreri[15], M. B. Moller[16], B. Parsons[17], J. van Krieken[18], M. A. Piris[19], J. N. Winter[20], M. Zhang[21], B. Xu[22], K. H. Young[1];

[1]Duke University Medical Center, Durham, NC, [2]Baylor College of Medicine, Houston, TX, [3]NeoGenomics Laboratories, Aliso Viejo, CA, [4]University Hospital Basel, Basel, Switzerland, [5]University of Verona, Verona, Italy, [6]Columbia University Irving Medical Center and New York Presbyterian Hospital, New York, NY, [7]Wake Forest University, Winston-Salem, NC, [8]Aalborg University Hospital, Aalborg, Denmark, [9]Mayo Clinic, Rochester, MN, [10]Weill Medical College of Cornell University, New York, NY, [11]The Methodist Hospital, Houston, TX, [12]The University of Texas MD Anderson Cancer Center, Houston, TX, [13]Dana-Farber Cancer Institute, Boston, MA, [14]Asan Medical Center, Seoul, Korea, Republic of, [15]San Raffaele H. Scientific Institute, Milan, Italy, [16]Odense University Hospital, Odense, Denmark, [17]Gundersen Lutheran Health System, La Crosse, WI, [18]Radboud University Nijmegen Medical Centre, Nijmegen, Netherlands, [19]Hospital Universitario Marques de Valdecilla, Santander, Spain, [20]Northwestern University, Chicago, IL, [21]The First Affiliated Hospital of Zhengzhou University, Zhengzhou, China, [22]The First Affiliated Hospital of Xiamen University, Xiamen, China

Introduction: MYC+BCL2+ double expression (DE) is a biomarker for poor prognosis in diffuse large B-cell lymphoma (DLBCL), likely due to the cooperation between MYC and BCL2 oncoproteins in tumor cells. However, as generally MYC and BCL2 are separately assessed on two different slides by immunohistochemistry (IHC), MYC+ and BCL2+ results are from different cells. With the WHO-recommended cutoffs, ≥40% for MYC and ≥50% for BCL2 (sum < 100%), there is chance that the so-called DE comes from non-overlapping regions of the tumor (not single-cell DE). Moreover, tumor expression scores based on morphology assessment often vary among pathologists. In this study, we performed fluorescent multiplex IHC (fmIHC) using a MultiOmyx™ immunofluorescence platform (NeoGenomics Laboratories, Inc.) to determine single-cell MYC and BCL2 co-expression for prognostic analysis in DLBCL.
Patients and Methods: Co-expression of MYC, BCL2, and 11 immunophenotypic markers by fmIHC was digitally quantified for 547 patients with DLBCL. Percentage of cells with MYC/BCL2 double or single expression was calculated for various cell types. Prognostic analysis was performed for de novo DLBCL cases, including 108 patients treated CHOP chemotherapy, and 356 patients treated with rituximab (R)-CHOP.
Results: First, although MYC and BCL2 were expressed in multiple cell types, the vast majority (>90%) of MYC+BCL2+ DE cells were lymphoma cells. Frequencies of MYC and BCL2 co-expression were consistent with random distribution of independent MYC/BCL2 expression in positive cases. The activated B-cell-like subtype compared with the germinal center B-cell-like subtype had a significantly higher mean percentage of MYC+BCL2+ DE, but not single BCL2 or MYC expression, in PAX5+ cells. Second, in both the R-CHOP and CHOP cohorts, high percentages of DE in PAX5+ cells and in all DAPI+ cells were associated with significantly poorer survival of DLBCL patients. Very high percentage of single BCL2 expression in PAX5+ cells was also associated with poorer survival, however, only in a small number of patients in both cohorts. Only in the R-CHOP cohort, high single MYC expression in PAX5+ cells (in a significant proportion of the cohort) was associated with significantly poorer overall survival. In the R-CHOP cohort, eight cases had *MYC*/*BCL2* double hit by FISH, including 3 cases with MYC/IGH fusions (DE) and 5 cases with MYC/non-IGH rearrangements (only one DE). The exclusion of these double hit cases did not impact the significance of DE and single MYC+ expression.
Summary: True MYC+BCL2+ double protein expression at the single cell level is predominantly in lymphoma cells, and associated with significantly poor survival of DLBCL patients. Our results suggest high cutoffs for common MYC/BCL2 IHC to identify true double expressor lymphoma.

CLINICAL RESEARCH: Predictive Biomarkers 6
Poster Session

#6422 Comprehensive proteogenomic profiling and biomarker analyses in resected extrahepatic cholangiocarcinoma: A prespecified exploratory analysis of the phase 2 STAMP trial.

H. Jeong[1], J.-H. Oh[1], H.-S. Ahn[1], B.-Y. Ryoo[1], K.-p. Kim[1], J. Jeong[1], I. Park[1], S.-M. Hong[1], J. Shin[1], C. Park[1], Y. Cho[2], K. Kim[1], C. Sung[1], C. Yoo[1]; [1]Asan Medical Center (AMC), Seoul, Korea, Republic of, [2]AMC Sciences, Seoul, Korea, Republic of

Background: Biliary tract cancer constitutes a heterogeneous group of diseases with a limited understanding of its molecular characteristics and prognostic/predictive biomarkers. We performed prespecified exploratory analyses of the STAMP trial, a multicenter randomized phase 2 trial of adjuvant capecitabine (CAP) or gemcitabine plus cisplatin (GemCis) for patients with resected extrahepatic cholangiocarcinoma (EH-CCA) with regional lymph node metastasis.
Methods: Among 101 patients included in the intention-to-treat population of the STAMP trial, a total of 89 patients (45 in the GemCis group and 44 in the CAP group) were included in the current biomarker analysis after excluding 12 patients without available tissue and blood samples. Whole exome sequencing and proteomics were performed using surgical specimens.
Results: *TP53* (63%), *SMAD4* (20%), and *KRAS* (18%) mutations were the most frequent in the pooled population. Somatic mutations in homologous recombination deficient (HRD) genes were present in 20% of patients, while one patient (1%) had a germline *ATM* mutation. The prevalence of microsatellite instability was 1%. Somatic mutations in known targetable genes were observed in 54 patients (60.7%) and proteogenomic integrative analysis revealed significant HER2 pathway alteration with *HER2* amplification in 4 patients (7%). The characteristics of prognostic biomarkers varied by the adjuvant regimen used. In the adjuvant GemCis group, somatic mutations were associated with poor disease-free survival (DFS) and overall survival (OS), including *KRAS* (log-rank p=0.004 for DFS and p=0.003 for OS), *FBXW7* (p=0.021 for DFS and p=0.011 for OS), and *PIK3CA* (p<0.001 for DFS and p=0.042 for OS) mutations. In the adjuvant CAP group, copy number alterations (CNAs) such as 8q24.21 amplification (p=0.006 for DFS and p=0.707 for OS) and 3q26.1 amplification (p=0.020 for DFS and p=0.026 for OS) were associated with poor survival, while 11q13.3 amplification (p=0.017 for DFS and p=0.099 for OS) was associated with improved survival. Additionally, a higher HRD score showed a tendency toward better DFS and OS in the GemCis group, but not in the CAP group, although it did not reach statistical significance in both groups (p>0.05). Non-negative matrix clustering of proteomics data classified patients into 4 clusters. Among those, cluster 2, which showed alterations in the metabolism pathway, was associated with higher CNA level, higher tendency of HRD scores, and favorable survival with GemCis (p=0.039 for DFS and p=0.100 for OS) but not with CAP.
Conclusions: Comprehensive proteogenomic analyses enable the identification of prognostic biomarkers and may guide the selection of adjuvant chemotherapy in resected EH-CCA.

#6423 KRAS mutation detection by Sanger sequencing using the SeqStudio Flex capillary electrophoresis instrument.

A. Karger[1], A. Patel[1], K. Tseng[1], C. Ornelas[1], M. Napier[1], R. Beck[2], K. Collwell[2], S. Fahl[2], C. Bornarth[1];
[1]Thermo Fisher Scientific, Pleasanton, CA, [2]Discovery Life Sciences, Huntsville, AL

The detection of mutations in the KRAS gene highly associated with cancer is one of the most widely used Sanger sequencing capillary electrophoresis (CE) applications in molecular diagnostics. In addition to their traditional role in cancer diagnostic, KRAS mutations have recently gained additional relevance as pharmacogenomics (PGx) markers for a significant number of new oncology therapeutics. KRAS mutation detection assays are used as companion diagnostics (CDx) for these cancer treatments. Analysis by Sanger Sequencing of KRAS mutations is cost effective and lends itself for use in resource limited healthcare settings. While there are currently no commercial kits for targeted sequencing of the KRAS mutation hotspots available, the online Applied Biosystems Primer Designer™ Tool (thermofisher.com) allows standardization of the PCR primer design between labs and repeat orders of the KRAS assays by using these commercially available assay ID numbers. Here we demonstrate the use of Primer Designer KRAS mutation detections assays for mutation in codon 12, 13 and 61 totaling to 8 allele variants. The data was generated on the SeqStudio Flex CE instrument using reference standard DNA as well as DNA extracted from FFPE solid tumor samples. We show accuracy of variant call (OPA 100% (64/64)) and concordance (OPA 98.3% (59/60)) in a side-by-side comparison of the SeqStudio Flex with the legacy Model 3500 Genetic Analyzer instrument using a set of commercially available (Horizon Discovery) KRAS reference DNA samples. Primary solid tumor samples are processed to Fresh Frozen Paraffin Embedded samples (FFPE) for further disease marker evaluation. These samples are stable for long term at ambient temperatures and provide the opportunity to evaluate prospective biomarkers at large scale to understand their potential utility. Discovery Life Sciences has generated a large-scale biorepository of human biospecimen, including FFPE, plasma/sera, buffy coat, and PBMCs. Archival FFPE samples from oncology indications associated with KRAS mutations, such as non-small cell lung cancer and colorectal cancer, were analyzed and identified samples with KRAS mutations, demonstrating the potential diagnostic utility of these assays. Finally, cell-free (cf) DNA from double spun plasma from relevant indications was also successfully evaluated for KRAS mutations, highlighting the potential for these assays in liquid biopsy studies. The study demonstrates the robustness of the Primer Designer KRAS mutation detection sequencing assays using reference standard DNA as well as DNA derived from FFPE DNA and cfDNA from patient derived tumor samples. For Research Use Only. Not for use in diagnostic procedures.

#6424 A patient centric full spectrum flow cytometry assay for comprehensive phenotyping of CAR T cells in clinical trials.

K. Vaughan, S. Muthusamy, C. Zhao, A. Carbajal, C. Fu, N. Dakappagari, Z. Alfonso;
Navigate BioPharma, Carlsbad, CA

Purpose While there is a strong desire to fully understand next generation CAR-T product characteristics in clinical trials, limited amounts of blood specimens are available as the enrolled patients are very sick and lymphodepleted. To address this high unmet need, we developed a single tube 20-color full spectrum flow cytometry assay for an in-depth characterization of CAR-T cells that support fulfilment of five key clinical trial endpoints, namely, manufacturing success (fitness and memory state), pharmacokinetics, response or resistance (ICIs), efficacy (gross tumor burden) and safety (B cell regeneration) for use across a broad range of CAR-T therapies and clinical indications.

Study Design: The single tube 20-parameter full spectrum flow cytometry (FC) assay was designed to include CD45, HLA-DR, CD3, CD4, CD8, CD56 as backbone markers, CD45RA, CCR7, CD95, CD25 and CD127 antibodies allowed for the identification of all major subsets of CD4 and CD8 T cells. CXCR3, CD38, PD1, LAG3, and TIM3 were used for identification of activation/exhaustion phenotypes, while CD20 and HLA-DR were useful for identification of B cells and monocytes respectively. Additionally, we left two parameters (PE and AF647) open for customized CAR-T detection reagents or other customized markers. This assay was developed using Cytek® Northern Lights™ and frozen PBMCs.

Results This robust 20-color full spectrum FC assay allowed a thorough analysis of the major T cell populations cells. FMO (Fluorescence-Minus-One) control studies confirmed the specificity of the antibodies and of the panel in identifying Naïve, EMRA, CM, EM, Th17, T stem cell memory and regulatory T cells with minimum background on all parameters. This method showed to be highly reproducible and can be adapted for use with many CAR-T detection reagents.

Conclusion In summary, we developed a robust 20-parameter multiparameter full spectrum flow cytometry assay focused on different populations of T cells in a single tube. The inclusion of drop ins for prospective CAR-T cell detection reagents allows for easy integration of future advances in CAR-T cell research. This universal panel shows great potential for usage across CAR-T clinical trials, as it serves as a valuable tool understand product fitness, PK, biomarker monitoring and disease burden simultaneously.

#6425 Harnessing big data from pan-cancer concerning more than 1300 patients with immune checkpoint inhibitors identifies novel predictive biomarkers.

P. Wu, C. Zhang, A. Shen, X. Gu, N. Sun, J. He;
National Cancer Center/National Clinical Research Center for Cancer/Cancer Hospital, Beijing, China

Immune-checkpoint inhibitors (ICIs) have revolutionized cancer therapy, yet many patients face the challenges of either not benefiting or developing resistance to ICIs. Advances in genome sequencing allow the exploitation of high-dimension oncological data in the research and development of precision immuno-oncology. We conducted a comprehensive literature review involving cancer patients treated with ICIs [anti-programmed cell death protein 1 (PD-1)/programmed death-ligand 1 (PD-L1), anti-cytotoxic T-lymphocyte antigen 4 (CTLA-4), or their combination] and collected available transcriptomic data from pretreatment biopsies along with corresponding clinical outcomes. Biomarkers for ICI response were independently investigated within each study using the logistic regression method and combined with the odds ratio (OR) for meta-analysis. A total of 210 formalin-fixed paraffin-embedded pan-cancer samples with pretreatment biopsies from the National Cancer Center retrospective cohort were collected for validation. Reverse transcription-quantitative polymerase chain reaction (RT-qPCR) and immunohistochemistry (IHC) were employed to validate the stable and clinically applicable utility of the genomic biomarker identified in our analysis. Across 18 studies, we identified 1106 cancer patients who received immunotherapy with pre-treatment transcriptomic data, including melanoma, non-small cell lung cancer (NSCLC), renal cell carcinoma (RCC), stomach adenocarcinoma (STAD), glioblastoma (GBM), and bladder urothelial carcinoma (BLCA), of which 8421 genes were available in all datasets. Meta-analysis based on a common effect model revealed that 332 genes were positively correlated with a favorable response to ICIs, and 404 genes were negatively associated with the therapeutic outcome, with all pooled OR being statistically significant (P <0.05). We identified a novel biomarker, ZBED2 (Zinc Finger BED-Type Containing 2), which demonstrated superior predictive value over other biomarkers for ICI efficacy (pooled OR, 0.596; 95% CI, 0.450-0.788, P =0.002). Similarly, RT-qPCR (AUC: 0.821) and IHC (AUC: 0.789) results further validated the predictive utility for ICI response in the real-world cohort of 210 cancer patients with pretreatment samples receiving ICIs. Additionally, we observed that the expression of ZBED2 was favorably associated with the overall survival of patients receiving immunotherapy (HR: 0.72). In summary, our study provides a in-depth analysis of potentially predictable biomarkers for ICIs in cancer and highlights the potential of large-scale meta-analyses in identifying stable biomarkers. ZBED2 emerges as a novel predictive biomarker for ICIs and may guide the implementation of risk-related therapeutic strategies.

#6426 Identification of potential immune biomarkers for GSK-3 inhibitor elraglusib (9-ING-41) in patients with relapsed/refractory metastatic cancer.

T. Weiskittel[1], K. Huntington[2], L. Zhang[3], A. Koukol[4], B. A. Carneiro[5], H. Li[1], A. Ugolkov[4], W. El-Deiry[3], A. Mazar[4];

[1]Mayo Clinic, Rochester, MN, [2]Genesis Drug Discovery & Development (GD3), Hamilton Township, NJ, [3]The Warren Alpert Medical School of Brown University, Providence, RI, [4]Actuate Therapeutics, Inc., Fort Worth, TX, [5]Brown University, Providence, RI

Cytokines mediate strong immunomodulatory effects in cancer. Elraglusib (9-ING-41), an inhibitor of GSK-3, is a potent antitumor and immune-modulatory agent in phase 2 clinical trials for the treatment of various cancers. Here, we examined the immune environment of elraglusib-treated cancer patients by measuring peripheral blood protein levels to explore whether the expression level of cytokines/chemokines/soluble cell receptors/growth factors (CCSG) is correlated with clinical outcome. Using a customized Luminex platform, the expression of forty CCSG hypothesized to be linked to GSK-3 activity was assessed in pre-dose plasma samples obtained from 45 cancer patients with relapsed/refractory metastatic disease (NCT03678883; the 1801 trial). All patients in the 1801 trial were treated with elraglusib (dose range: 1-15 mg/kg) either as a single agent (Part 1; n=21) or in combination with chemotherapy (Part 2; n=24). Pre-dose peripheral blood protein levels were examined as binary predictors of clinical outcome using optimal cutoff points determined by maximally selected rank statistics. In the aggregate Part 1 and 2 populations (n=45), we identified 13 CCSG that significantly stratified the cohort by overall survival (OS). High pre-dose levels of CD95 and TNFRSF10C were associated with better OS. CD95 was a better prognostic of OS than TNFRSF10C (HR: 2.27, 95% CI: 1.10-4.67, p-value: 0.023). Low pre-dose levels of 11 CCSG were also significantly associated with favorable OS, with IL-8 being the most predictive (HR: 0.137, 95% CI: 0.0545-0.346, p-value: <0.0001). Part 1 and 2 predose samples were also analyzed separately, and many of the biomarkers identified in the aggregate analysis retained significance in the separated analysis. In Part 1, CXCL5, IFN-alpha, and IL-18 emerged as unique markers, and in Part 2, CCL22 was the single unique marker.The results of our exploratory study identified several putative biomarkers of elraglusib clinical benefit and demonstrated potential immunomodulatory mechanisms of elraglusib that will be used to inform the further clinical development of elraglusib for the treatment of metastatic cancer.

#6427 Phase II study of trametinib alone and in combination with uprosertib in patients with metastatic triple negative breast cancer previously treated with chemotherapy: OSU 13317.

V. Prasath[1], H. Boutrid[2], E. Mrozek[2], M. Lustberg[3], R. Weslowski[1], R. Layman[4], M. Abdel-Rasoul[1], C. Timmers[5], E. MacRae[6], G. T. Budd[7], L. Harris[8], C. Isaacs[9], R. Ismail-Khan[10], E. C. Dees[11], A. S. Poklepovic[12], H. X. Chen[8], M. Villalona-Calero[13], W. Carson[1], G. L. Johnson[11], D. G. Stover[1], B. Ramaswamy[1]; [1]The Ohio State University College of Medicine, Columbus, OH, [2]The Ohio State University Medical Center, Columbus, OH, [3]Yale School of Medicine, New Haven, CT, [4]MD Anderson Cancer Center, Houston, TX, [5]Incyte, Wilmington, DE, [6]Columbus Oncology Associates, Columbus, OH, [7]Cleveland Clinic Foundation, Cleveland, OH, [8]National Cancer Institute, Bethesda, MD, [9]Georgetown University Medical Center, Washington, DC, [10]Moffitt Cancer Center, Tampa, FL, [11]UNC School of Medicine, Chapel Hill, NC, [12]Virginia Commonwealth University, Richmond, VA, [13]City of Hope, Duarte, CA

Introduction: Triple negative breast cancers (TNBCs) are a poor prognosis subset of breast cancer and preclinical data implicate activation of the RAS/MEK/ERK pathway in TNBC chemotherapy resistance. Preclinical data demonstrate that blockade of both RAS/MEK/ERK and PI3K/AKT pathways synergizes to overcome resistance to single agent MEK inhibitors. The purpose of this study was to determine the response rate for the selective allosteric MEK1/MEK2 inhibitor trametinib alone and in combination with AKT inhibitor uprosertib in patients with metastatic TNBC previously treated with chemotherapy.

Patients and Methods: This was an open-label, two-part, phase II, single-arm, multicenter study through the ETCTN. Eligibility criteria included patients with metastatic TNBC with measurable disease who had received between 1-3 prior chemotherapy regimens. All patients underwent a mandatory pretreament biopsy and received trametinib alone (2mg) as Part I of the study. At progression, patients underwent a second biopsy and moved to Part II with trametinib (1.5mg) and uprosertib (50mg). Available biopsies were profiled quantitative targeted absolute proteomics (QTAP) for kinome assay and whole transcriptome profiling via microarray. Blood samples were collected at baseline, at cycle 2 day 1 (C2D1), and at progression for circulating tumor DNA (ctDNA) analysis via ultra-low pass whole genome sequencing.

Results: Between October 2013 and January 2017, 37 patients were enrolled at 8 centers and, subsequently, 19 of these patients entered Part II. Adverse event data has been previously presented. On trametinib alone (Part I), 2 patients had a partial response (PR) and 6 patients had stable disease (SD) as best response. Of the 19 evaluable patients on trametinib + uprosertib (Part II), 3 patients had a PR and 3 patients had SD. Integrated analysis of matched samples with QTAP kinome and transcriptome data QTAP kinome assay in demonstrated MEK1/2 inhibition at progression on trametinib alone in 4/4 patients with evaluable tissue confirming target engagement and one patient with biopsy after trametinib+uprosertib demonstrated AKT1 inhibition. ctDNA was evaluable in 34 patients at C1D1 with tumor fraction (TFx) range 0-75.9%. 6/23 patients had ctDNA ‘clearance’ (tumor fraction of 0%) at C2D1. Of these 6, 3 (50%) had PR as best response, compared with only PR in only 1/17 patients without ctDNA clearance at C2D1.

Conclusions: Trametinib alone and in combination with uprosertib demonstrates anti-tumor activity in a subset of TNBC patients with kinome evidence of target engagment. ctDNA clearance at C2D1 may be useful as an early biomarker to identify patients most likely to respond. Understanding biomarkers of response and resistance may guide future opportunities for MEK/AKT inhibition in TNBC.

#6428 Transcriptome analysis of tissues and peripheral blood revealed potential biomarkers for chemo/radio-immunotherapy in non-small cell lung cancer.

J. Hu[1], J. Zhang[1], P. Cheng[2], Y. Chen[2], C. Zhu[2], F. Yi[2], C. Xie[1];
[1]Department of radiation and medical oncology, Zhongnan Hospital of Wuhan University, Wuhan, China, [2]Amoy Diagnostics Co., Ltd., Xiamen, China

Background: Combination of anti-PD-(L)1 antibody with chemotherapy has shown promising efficacy in advanced/metastatic non-small cell lung cancer (NSCLC). Dynamics of peripheral blood mononuclear cells (PBMC) might have impact on repertore of immune cells further resulting different immune infiltration in tumor microenvironment. Thus, monitoring changes in PBMC during therapy or measuring tumor microenvironment provides the possibility to predict the efficacy of tumor immunotherapy.
Methods: Patients diagnosed with NSCLC (Stage III-IV)were enrolled in this study. Anti-PD-L1 and chemo/radio combination therapy was performed as adjuvant therapy. Tumor samples were obtained prior to adjuvant therapy PBMC samples were obtaind at multiple time points, including prior adjuvant therapy, 3 months after adjuvant therapy, and 3 months after adjuvant therapy. Tumor and PBMC mRNA sequencing were performed by Amoy Diagnostics Co Ltd. (Xiamen, China). Patients who achieved CR/PR/SD and PFS > 6 months were defined as well responders. Pathway enrichment and GSEA analyses were performed by clusterProfiler (version 4.0.5) on GO, KEGG, and from six different gene sets. Correlations between immune cellular signature ES scores and gene expression were estimated using Pearson correlation.
Results: 28 patients were enrolled; mean age was 60.38±7.86 years, 27 (96.4%) patients were male. 21 (75.0%) patients were identified as responder and 7 (25.0%) were non-responder. In the baseline tumor samples, immune infiltration was more extensive in responders compared to non-responders. Cytotoxic lymphocytes, activated $CD8^{\pm}$ T cell, and NK cells were significantly enriched in responders. High expression of CCL17 and down regulation of CTSG/PLK1/PRTN3, a signaling axis that inhibits histone H3 hydrolysis and promotes monocyte to macrophage differentiation, was significant in responders. Dynamic monitoring of PBMC before and after treatment showed significant upregulation of immune infiltration-related pathways in responders, including effector cells, NK cells and $CD8^{\pm}$ T cells. In the non-responder group, the up-regulated pathways after treatment were mainly enriched in tumor growth rate, EMT, and matrix remodeling. Multi-time point analysis showed that CEACAM5/ MKI67 level and tumor proliferation rate in non-responders were higher than those in responders at each time point after treatment.
Conclusion: Baseline tumor transcripton signatures and dynamic changes in PBMC could be applied to develop novel biomarkers for immune-related therapy. Patients with stronger immune infiltration signals in baseline tumor samples and PBMC after treatment had better immune response. The upregulation of proliferation-related signals in PBMC predicts poor immune response.

#6429 Critical role of elevated TMEM176B gene expression in humanized patient-derived xenografts mouse models of triple negative breast cancer.

Y. Her, J. Yun, W. Heo, J.-I. Kim, H.-B. Lee, W. Han, H.-G. Moon;
Seoul National University, Seoul, Korea, Republic of

Objective: In the cancer research, a highly promising in vivo platform for personalized treatment involves the adoption of an advanced approach—specifically, the grafting of patient-derived xenografts (PDX) onto humanized mouse models. These models capture distinctive aspects of interaction with the human immune system and the tumor microenvironment (TME). In this study, we have engineered humanized triple-negative breast cancer (TNBC) PDX models to observe alterations in differentially expressed genes, thereby enhancing our understanding of the intricacies of personalized treatment in this context.
Method: We utilized two TNBC PDX models established for the humanized models, where CD34+ hematopoietic stem cells were transplanted into immunodeficient mice. RNA sequencing was performed to identify altered gene expression in humanized PDX models compared to NSG PDXs. Additionally, we generated stable cell lines overexpressing TMEM176B in MDAMB231 and Hs578T cells, and we knocked down TMEM176B in 4T1 cells using recombinant techniques
Results: In the humanized model, the growth of PDX tumors did not show a significantly faster or markedly different rate compared to previous studies. However, upon conducting RNA sequencing in the PDX model, the expression of the TMEM176B gene was consistently downregulated. Consequently, we transfected and observed that the increased expression of TMEM176B in MDAMB231 and Hs578T cell lines resulted in enhanced cell proliferation in vitro. Transplanting MDAMB231 cells overexpressing TMEM176B into athymic nude mice resulted in accelerated tumor growth. The study further investigates the expression of TMEM176B in an immune-competent environment by knocking down the gene in 4T1 cells or transplanting the control group into a balb/c mouse model. Tumors with TMEM176B knockdown exhibited inhibited growth, increased CD3+ T cell infiltration, and significant inhibition when treated with anti-PD-L1 compared to the control group.
Conclusion: This research demonstrates the utility of PDX models, particularly humanized PDX models, in studying the complexities of cancer biology and the tumor microenvironment. The findings regarding TMEM176B and its role in tumorigenesis and immune responses in triple-negative breast cancer provide valuable insights for further research and potential therapeutic interventions.

#6430 Gene expression signature quantifies the cellular contribution of the tumor *vs.* the microenvironment in determining colorectal cancer prognosis and therapeutic outcome.

M. Yang[1], T. J. Yeatman[1], M. V. Nebozhyn[2], M. J. Schell[3], L. Pflieger[4], A. Loboda[2], W. J. Pledger[5], R. Soundararajan[1], M. Maurin[1], H. Wang[1], J. Rodriguez Silva[1], A. Alden[1];

[1]University of South Florida, Tampa, FL, [2]Merck, Sharp and Dohme, West Point, PA, [3]Moffitt Cancer Center & Research Institute, Tampa, FL, [4]Phenome Health, Seattle, WA, [5]Tampa General Hospital Cancer Institute, Tampa, FL

Accumulating evidence has suggested that cancer progression and therapeutic response may depend on not only tumor cells but also their tumor microenvironment (TME). However, their contributory roles are complex and not well understood. Here we report an analysis of 2373 human colorectal cancer (CRC) tumors representing all stages, leading to identification of a 20-gene signature capable of quantifying the cellular contribution of the tumor vs. the TME in determining colorectal cancer prognosis and therapeutic outcome. We classified these tumors into the consensus molecular subtypes (CMS1-4) with distinct, variable TME cellular features defined by CIBERSORT deconvolution analysis of bulk gene expression data. Surprisingly, all the 10 positive signature genes (portending worse survival) were strongly correlated with the TME-rich CMS1 and CMS4 tumors. By contrast, all the 10 negative signature genes (portending better survival) were highly related to the TME-poor CMS2 and CMS3 tumors. A single cell expression analysis from an independent database further revealed that strikingly, all the 10 positive genes were principally expressed by the immune/stromal TME whereas all the 10 negative genes were predominantly expressed in epithelial tumor cells. These data suggest that the TME has an equally important role as do tumor cells in determining CRC prognosis and support targeting the TME to improve survival. Moreover, distinct gene expression from tumor cells versus the TME also showed a differential impact on therapeutic outcome. Retrospective analyses on two independent clinical trial datasets show that the 20-gene signature score significantly predicted progression free survival in metastatic CRC patients treated with cetuximab, an FDA-approved EGFR inhibitor therapy. These data suggest a potential for the 20-gene signature as a predictive biomarker to identify “sensitive” versus “resistant” subpopulations of CRC patients to improve outcome of EGFR-targeted therapy.

#6431 First NGS-based companion diagnostic to aid in the selection of targeted therapy for anaplastic thyroid cancer patients with *BRAF V600E* mutations.

T. Clark, T. Nater, J. Maxfield, J. Peterson, K. Hotchkiss, C. Russo, A. Velasco Roth;
Thermo Fisher Scientific, Carlsbad, CA

Introduction: While anaplastic thyroid cancer (ATC) is rare, it is the most aggressive form of thyroid cancer. All ATCs are considered stage IV at diagnosis and response rates to standard systemic therapies are poor with dismal long-term outcomes. As such, molecular profiling of ATCs has increasingly been used to identify therapeutic targets that may inform individualized therapy. Current clinical guidelines recommend molecular profiling, especially *BRAF V600E* mutation assessment, be performed at the time of ATC diagnosis to inform decisions related to the use of targeted therapies. On September 29, 2023, the FDA granted companion diagnostic approval to the Oncomine™ Dx Target Test (ODxT Test) as an aid in the selection of patients with *BRAF V600E*-mutated ATC who may be eligible for treatment with dabrafenib in combination with trametinib. Here we report the assay performance data which supports the clinical benefit of the ODxT Test as an aid in the selection of targeted therapy for ATC patients with *BRAF V600E* mutations.

Methods: The ODxT Test is a targeted next-generation sequencing (NGS) *in vitro* diagnostic assay used to detect somatic changes in human DNA and RNA isolated from FFPE tissue samples. To validate the clinical benefit of the ODxT Test for the selection of ATC patients with *BRAF V600E* mutations, a retrospective clinical concordance study was performed on 35 patients enrolled in the ATC cohort of the ROAR trial, a phase II study of dabrafenib in combination with trametinib in subjects with rare cancers with *BRAF V600E* mutations. The study evaluated the overall percent agreement (OPA), positive percent agreement (PPA), and negative percent agreement (NPA) for the detection of *BRAF V600E* mutations between the ROAR trial central confirmatory assay, bioMerieux THxID™ BRAF test (THxID), and the ODxT Test. Due to the small number of *BRAF V600E*-mutated ATC patients enrolled in the ROAR trial, 167 commercially-obtained thyroid cancer specimens were also included in the concordance analysis.

Results: Of the 202 specimens included in the study with a valid ThxID result, 199 had sufficient material for testing with the ODxT Test and were included in the clinical concordance analysis. The point estimates of PPA, NPA and OPA were 99.0%, 100%, and 99.4%, respectively, when excluding ODxT Test invalid results and the lower bounds of the 95% Wilson Score confidence intervals for PPA, NPA, and OPA were 94.4%, 93.7%, and 96.4% respectively.

Conclusion: The ODxT Test was shown to be effective in identifying *BRAF V600E* mutations in ATC patients through a clinical concordance study using specimens from patients enrolled in the ROAR trial and commercially-sourced samples. The results support the expanded indication to the ODxT Test and marks the first FDA-approved NGS-based companion diagnostic for patients with *BRAF V600E*-mutated ATC.

#6432 Co-expression of HERV-R, CCND1, BRAF, FOXA1, TMPRSS2, ATF4 and low expression of BAZ1B and KMT2D is associated with early detection and poor prognosis of prostate cancer in African Black men from Nigeria.

F. Mohammed[1], K. Stawiski[2], H. S. Musa[3], S. K. Owolabi[1], S. Abubakar[4], S. O. Rotimi[5], A. K. Umar[6], Y. Iliyasu[7], A. Bello[1], F. T. Odedina[8], C. C. Yates[9], K. Petrie[3], F. W. Huang[10], S. Ibrahim[1];

[1]Ahmadu Bello University, Zaria, Nigeria, [2]Medical University of Lodz, Lodz, Poland, [3]University of Sunderland, Sunderland, United Kingdom, [4]Aminu Kano Teaching Hospital, Kano, Nigeria, [5]Covenant University, Ota, Nigeria, [6]Federal Medical Centre, Birnin Kebbi, Nigeria, [7]Ahmadu Bello University Teaching Hospital, Zaria, Nigeria, [8]Mayo Clinic, Jacksonville, FL, [9]Johns Hopkins School of Medicine, Baltimore, MD, [10]University of California, San Francisco, San Francisco, CA

Prostate cancer (CaP) is a heterogeneous disease characterized by features of non-aggressive, slow-growing disorders to fast-growing disease. Men of African ancestry have disproportionately higher incidence and mortality rates for CaP than men of European ancestry. While there is evidence for a higher genetic predisposition for incidence of CaP in men of African ancestry compared to men of European ancestry, there is paucity of molecular biology and transcriptomic studies on the role of Human endogenous retroviruses (HERVs) in relation to CaP-associated genes in CaP pathogenesis and prognosis. In this study, we performed bulk RNA sequencing (RNA-seq) on formalin-fixed paraffin-embeded (FFPE) CaP samples from Nigerian CaP patients to investigate the expression significance of HERV-R in relation to FOXA1, TMPRSS2, BAZ1B, KMT2D, ATF4 and BRAF genes. Based on this findings, we used immunohistochemistry (IHC), enzyme-linked immunosorbent assay (ELISA) and immunofluorescence (IF) to confirm the expression pattern of the HERV-R and FOXA1, TMPRSS2, BAZ1B, KMT2D, ATF4 and BRAF proteins on 45 FFPE CaP and blood plasma samples, and 5 CaP-free samples from patients in Zaria, Nigeria. Most of these patients were longitudinally followed from 2017 to date. The DESeq2 procedure was used for data processing, analysis, and differential expression analysis of the aforementioned genes. We found a significant expression of HERV-R in relation with FOXA1, TMPRSS2, BAZ1B, KMT2D, ATF4, CCND1 and BRAF in the CaP from rural Africans in Nigeria. HERV-R expression was found to be associated with increased PSA level, higher Gleason grade and poor prognosis of CaP. A CaP sample from an 80-year-old patient that was histologically diagnosed to have no malignancy seen despite high PSA level of >100 and poor disease outcomes shows a significant cytoplasmic expression of HERV-R, indicating that HERV-R may serve as an important biomarker for early detection. Unfortunately, we lost the 80-year-old patient to late detection before revisiting his case for proper histological diagnosis and management. In addition, some histologically diagnosed BPH samples that are apparently reported to be CaP-free show stromal cells expression of HERV-R and in some cases show expression of HERV-R in the prostatic glandular areas. In contrast, stromal cells of the CaP samples show no expression of HERV-R, but strong expression in the glandular areas. This may implicate a gradual transition from benign prostatic lesion to malignant prostatic disease. HERV-R expression in CaP may have a relationship with BRAF, CCND1, FOXA1, TMPRSS2 and ATF4 genes. These findings combined together, underscore the importance of the expanded concept of HERV-R expression and CaP associated genes in early detection of CaP and prognosis.

#6433 Anti-CD36 monoclonal antibody can sensitize the neoadjuvant chemotherapy response in PDAC by eliminating the senescent tertiary lymphatic structure.

J. Yan, T. Zhou, C. Yang, Y. Xie, J. Yu, J. Hao;
Pancreas Center, Tianjin Medical University Cancer Institute and Hospital, National Clinical Research Center for Cancer; Tianjin Key Laboratory of Digestive Cancer; Tianjin's Clinical Research Center for Cancer, Tianjin, China

Objective: Pancreatic ductal adenocarcinoma (PDAC) is deadly and aggressive. Neoadjuvant chemotherapy (NAC) may reduce tumor volume and alter the resectability of the tumor. The efficacy of neoadjuvant chemotherapy in patients is still limited. Tertiary lymphoid structures (TLSs) develop in peripheral non-lymphoid tissues and are essential for the immune response and correlate with chemotherapy in various tumor types. However, more research is needed to determine how TLSs affect neoadjuvant chemotherapy in PDAC. We aim to determine how neoadjuvant chemotherapy affects tumor-infiltrating lymphocytes (TLSs) in PDAC patients. We also want to find a biomarker to boost PDAC neoadjuvant chemotherapy response.
Methods: We retrospectively collected formalin-fixed paraffin embedded (FFPE) tissues from 115 PDAC patients without preoperative treatment and 72 patients pretreated with neoadjuvant chemotherapy. Multispectral images were processed using AI-powered image analysis software (Tissue Gnostics; Zeiss, Germany). The 10X Genomics platform was used to sequence single cells in tissue samples from five patients who received neoadjuvant chemotherapy (NAC) and five patients who had not received any treatment before analysis (pretreatment naïve, PN). TLS was separated using Laser Microdissection. The mouse model was created by orthotopically injecting tumor cells into the pancreas.
Results: Patients who received NAC have a senescent microenvironment. High-throughput single-cell sequencing showed that the senescent gene signature score was enriched in the NAC group, especially in immune cells. The percentage of $p16^{\pm}$ $CD20^{\pm}$ B cells and $P16^{\pm}$ $CD3^{\pm}$ T cells in TLSs also increased in the NAC group. Spatial transcriptomics analysis exhibited that CD36 is highly expressed in senescent TLSs, which suggested that CD36 may be a marker for senescent TLSs. Moreover, CD36+ TLSs induced the infiltration of MDSCs and regulatory T cells. CD36+ TLSs were an independent prognostic factor for poor overall survival (OS) (HR=0.67, p=0.002) and progression-free survival (PFS) (HR=0.71, p=0.003). A mice orthotopic xenograft model showed that an anti-CD36 monoclonal antibody eliminated senescent TLSs in pancreatic tissue. MDSCs and Tregs in the surrounding tissue also decreased. Additionally, in vivo KPC mice model showed that the combination of an anti-CD36 and chemotherapy reduced tumor volume and increased survival compared to chemotherapy alone.
Conclusion: NAC has the potential to induce the senescence of tumor-associated TLSs, a phenomenon that has been linked to unfavorable prognosis in PDAC. CD36 serves as a viable marker for senescent TLSs that can be targeted. The administration of an anti-CD36 monoclonal antibody can potentially enhance the efficacy of chemotherapy in PDAC by selectively eliminating CD36+ senescent TLSs in mouse models.

#6434 Microenvironment of adjacent non-neoplastic regions determines prognostic outcomes in locally advanced colorectal cancer after surgical resection: A multi-center & multi-omics study.

Y. Bang[1], J. Choi[1], K. Park[1], J. Lim[1], D. Pyo[1], Y. Cho[1], T.-Y. Kim[2], K. Park[2], S.-B. Ryoo[2], S.-B. Kang[3], C. Yu[4], K.-y. Lee[5], J. Lee[5], J.-Y. Lee[6], Y.-J. Kim[6], W.-Y. Park[1];

[1]Samsung Medical Center, Sungkyunkwan University School of Medicine, Seoul, Korea, Republic of, [2]Seoul National University Hospital, Seoul National University College of Medicine, Seoul, Korea, Republic of, [3]Seoul National University College of Medicine, Seoul National University Bundang Hospital, Seongnam, Korea, Republic of, [4]Asan Medical Center, University of Ulsan College of Medicine, Seoul, Korea, Republic of, [5]Uijeongbu St. Mary's Hospital, College of Medicine, The Catholic University, Uijeongbu, Korea, Republic of, [6]College of Life Science and Biotechnology, Yonsei University, Seoul, Korea, Republic of

Background: There is an unmet need for additive predictive biomarkers for the recurrence of stage II/III colorectal cancer (CRC) after surgery. We hypothesized that the heterogeneities of tumors present a substantial impediment to finding agnostic biomarkers. To avoid this, we focused on the normal tissue from the margins of resected specimens.

Methods: We divide the groups using RNA sequencing derived from 273 tumors and 273 paired normal tissues from 5 Korean cancer centers. Groups were defined as follows: tumor-like microenvironment in normal mucosa (tNME): high level of tumor signature in normal mucosa; healthy normal microenvironment (hNME): low tumor signature in normal tissue. The impact of this classification was further evaluated in TCGA cohort. For the mechanistic explanation, we conducted 16s rRNA metagenomics and single-cell RNA sequencing from 47 patients and validated by spatial transcriptomics.

Results: There were no significant differences between subgroups in baseline characteristics, including age, sex, medical centers, sidedness, stage and the distance between tumor and paired normal tissue. With a median follow-up of 58.2 months, the tNME group showed poor 5-year recurrence-free survival (54.7 vs. 73.0%, HR=1.94, *P*=0.002) and 5-year overall survival (OS; 78.2 vs. 83.0%, HR=1.76, *P*=0.033). In addition, tNME showed a trend toward poorer 5-year OS (34.5% vs. 68.8%, HR=3.76, *P*=0.071) in TCGA. The pathway analysis exhibited tNME had decreased maintenance of membrane while increased expression of humoral reaction to bacteria. Only the tNME group showed similar microbiome diversity between tumor and normal tissues, consisting of more proportion of carcinogenic genera, including fusobacterium and bacteroides than hNME. scRNA-seq revealed a positive co-occurrence of Th17, *GZMK*^{high}CD8+T cells, and *IL1B*^{high} neutrophils in the tumor and normal tissues of tNME. A high proportion of *EMP1*^{high} epithelial cells, were observed in the tNME group, with upregulated epithelial-mesenchymal transition (EMT), bacterial-cellular-invasion and leukocyte signaling pathways. The cell-cell interaction analysis suggest Th17 cells promote *IL1B*^{high} neutrophil retention, increasing crosstalk with CD8+ T cells, and inducing the production of high levels of *GZMK*, which in turn decreases E-cadherin in the intestinal epithelium. A weak intestinal barrier may provoke more bacteria-infected cancer cells, promoting cancer cell progression via EMT and recruiting *IL1B*^{high} neutrophils and *GZMK*^{high}CD8+T cells, resulting in a vicious cycle.

Conclusions: The microenvironmental status of normal tissues offers a promising biomarker for stage II/III CRC. Microbiota dysbiosis-induced organized microniches with immune and epithelial cells was related to metachronous recurrence after surgical resection.

#6436 Tumor-educated platelets for therapy stratification of metastasized castration resistant prostate cancer (CRPC).

J. A. Nilsson, M. Lundholm, L.-A. Tjon-Kon-Fat, L. Kohn, C. Thellenberg-Karlsson, A. Josefsson, P. Wikstrom;
Umea University, Umea, Sweden

One in ten men diagnosed with prostate cancer will have metastases. At some point the metastases becomes castration therapy resistant, contributing leading to the high mortality of prostate cancer. Novel androgen directed treatments, like abiraterone and enzalutamide, have made substantial difference to therapy response, yet only within subgroups of CRPC patients. Correct therapy stratification may prolong the life of the patients, possibly turning a deadly disease into a more chronic disease. For this to happen we need predictive biomarkers that can be used to longitudinally follow the disease in order to identify vulnerabilities and to monitor acquired resistance, e.g. we need to develop personalized liquid biopsy platforms. Using the platelet enriched fraction of a blood sample we here show that we can use the platelets ability to sequester material during circulation to provide information derived from the tumor, a.k.a. tumor-educated platelets. This information could be used as a companion diagnostic to identify patients that will respond to therapy, and to longitudinally monitor tumor progression. In this study, a previously published three gene profile, plt3G profile, was validated in a larger cohort (n=97) and showed that combined analysis of the three genes transcripts (*KLK3, FOLH1, NPY*) could be used to identify long-term responders regarding progression-free survival after enzalutamide (n=47; PFS; LR p<0,001, HR 0,32, p<0,001) or abiraterone (n=50; PFS; LR p=0.007, HR 0,45, p=0,009) -treatment. Furthermore, progression and resistance development could be accurately longitudinal followed. The plt3G profile showed a significant overlap with circulating tumor DNA (ctDNA) biomarkers, but in addition also provided predictive information around treatment response. Tumor-educated platelets provide therapy-predictive biomarkers as well as biomarkers for longitudinal monitoring of disease progression and resistance development, which ultimately could provide information for therapy switching. Their easy accessibility makes tumor-educated platelets an attractive biosource to be used alone or in combination others, to enable a fluid biomarker platform with the aim to turn a lethal cancer disease into a more chronic disease.

#6438 Subcutaneous fat mass predicts progression-free survival in patients treated with antibody-drug-conjugates in early-phase clinical trials.

M. Delaye[1], L. Lawrance[2], Y. Belkouchi[2], F. Wirth[2], P. Decazes[3], A. Bone[4], K. Ouali[1], A. Hollebecque[1], C. Smolenschi[1], R. Bahleda[1], A. Gazzah[1], S. Champiat[1], F.-X. Danlos[1], C. Henon[1], K. Beshiri[1], M. Sakkal[1], A. Marabelle[1], J.-M. Michot[1], V. Ribrag[1], C. Parisi[1], C. Massard[1], V. Goldschmidt[1], P. Vera[3], S. Ponce-Aix[1], N. Lassau[5], S. Ammari[5], C. Baldini[1];

[1]Gustave Roussy, Villejuif, France, [2]Biomaps, UMR1281 INSERM, CEA, CNRS, University of Paris-Saclay, Villejuif, France, [3]Henri Becquerel Cancer Center, Rouen, France, [4]Guerbet Research, Villepinte, France, [5]Gustave Roussy Cancer Campus, Villejuif, France

Background: Antibody drug conjugates (ADCs) have revolutionized the treatment of many solid tumours and hematological diseases. Little is known about the influence of body composition on efficacy and safety of ADCs.

Methods: All patients treated with ADCs in early phase clinical trials between 03/2015 and 03/2023 at the Drug Development Department at Gustave Roussy were retrospectively included in the analysis. A deep learning software (Anthropometer3DNet) automatically measured anthropometric parameters in 3D on pretreatment scans, allowing multi-slice measurements of muscle body mass (MBM), fat body mass (FBM), subcutaneous fat mass (SFM) and visceral fat mass (VFM). Other clinical and biological parameters were also retrieved and evaluated. Primary endpoints were progression-free survival (PFS) and overall survival (OS). Survival analysis was performed using Cox regression models and Kaplan-Meier (KM) estimator. Cut-offs were determined using the maxstat method. Anthropometric parameters' effect on toxicity was also evaluated using a ROC analysis.

Results: A total of 136 patients were treated with ADCs. The most frequent tumor types were non-small cell lung cancer (56 patients, 41%) and colorectal cancer (31 patients, 23%). Median age, ECOG PS, albumin and number of previous lines of treatment were 60.8 years (30 to 85), 1, 42 g/L and 3 respectively. In the overall cohort, median PFS and OS were 2.8 and 8.6 months respectively, 90 (66%) patients had experienced toxicity, of which 46 were grade 3-4. The Royal Marsden Hospital (RMH) prognostic score of 2 or more was significantly associated with worse PFS (HR=2.13, p=0.007) and OS (HR=2.12, p=0.008). The number of treatment lines was significantly associated with worse OS (HR=1.21, p<0.001). For the anthropometric parameters, SFM (HR=0.89, p=0.013) and FBM (HR=0.89, p=0.02) were significantly associated to PFS. Higher SFM (cutoff: 3.3 kg/m2) and FBM (cutoff: 3.6 kg/m2) were significantly associated with longer PFS (mPFS=3.8 vs 2.3 months and 3.7 vs 1.9 respectively). Patients with higher SFM and FBM had numerically but non-significantly longer (mOS=8.5 vs 7.7 months and 8.6 vs 6.4 months respectively). All anthropometric parameters were significantly associated with all-grade toxicity in the univariate but not in the multivariate analysis. None of the parameters were associated with grade 3-4 toxicity.

Conclusions: In this large monocenter cohort, 3D measured high SFM and FBM were significantly associated with PFS. Automatic extraction of body composition parameters using AI may help in anticipating the benefits of ADCs in patients included in early-phase clinical trials.

#6439 Next-generation sequencing based detection of HER2 copy number predicts pathological response to neoadjuvant therapy in HER2 positive breast cancer.

H. Dai, D. Jiao, X. Guo, J. Qiao, L. Li, Z. Lu, X. Chen, C. Wang, M. Yan, Z. Liu;
The Affiliated Cancer Hospital of Zhengzhou University, Zheng Zhou, China

Purpose: Achieving pathologic complete response (pCR) following neoadjuvant chemotherapy is associated with better prognosis for HER2 positive breast cancer. However, clinical and biological heterogeneity of HER2 positive disease significantly affect prognosis and treatment response. Early prediction of treatment benefit could enable tailored anti-HER2 therapy. Next-generation sequencing (NGS) based genomic tests including copy number (CN) detection are widely used in breast cancer patients. We aim to evaluate the association of HER2 copy number detected by NGS with pCR rate of HER2 positive breast cancer after neoadjuvant chemotherapy.

Methods: HER2 positive breast cancer patients underwent neoajuvant chemotherapy in Henan Cancer Hospital From January 2022 to March 2023 were included in the study. Pretreatment tumour specimens were subjected to pan-cancer 1021-gene panel genomic sequencing. Copy number of HER2 was obtained from the panel. Copy number of >=4 was classified as HER2 amplified and HER2 copy number <4 was classified as HER2 non-amplified. All patients underwnt definitive surgery after receieveing neoadjuvant chemotherapy containing taxanes, trastuzumab and pertuzumab. pCR was defined as pathological stage ypT0/Tis ypN0.

Results: In total, 299 HER2 positive breast cancer patients were eligible for the analysis. 87 were classified as HER2 non-amplified (29.1%) by copy number and 212 patients were classified as amplified group (70.9%). The HER2 non-amplified group tends to have a higher proportion of hormone receptor positive (HR+) patients (71.3% vs. 50.5%, p=0.002). Other clinicopathological parameters were well distributed between the groups. 91.3% of patients in HER2 amplified group had strong positive HER2 expression (IHC 3+), while only 10.5% of patients in HER2 non-amplified group had HER2 expression of IHC 3+. Patients with HER2 IHC 3+ had a PCR rate of 75.8% and Patients with HER2 IHC 2+ had a pCR rate of 20.0% (20.0% vs. 75.8% p<0.001). Patients in the amplified group had a pCR rate of 76.9% and pCR rate of the non-amplified group was12.6% (12.6% vs. 76.9% p<0.001). In a multivariable logistic regression with HER2 copy number by NGS, HR status and HER2 IHC, the HER2 copy number predicted pCR rate independently of HER2 IHC and HR status.

Conclusions: NGS based detection of HER2 copy number could predict response to neoadjuvant therapy in HER2 positive patients. The discordance between IHC/FISH and NGS based detection of HER2 amplification may reflect HER2 heterogeneity. HER2 heterogeneity promotes resistance to anti-HER2 therapy. Noval antibody-drug conjugates (ADC) with bystander effect, such as Trastuzumab deruxtecan, have shown anti-tumor effect even in HER2 low expression tumors. Thus, prospective study is needed to optimize anti-HER2 therapy for patients with HER2 heterogeneity.

#6440 Novel N-myristoyltransferase immunohistochemistry-based predictive and prognostic tests for breast cancer.

A. Shrivastav[1], D. Reddick[1], A. Meher[1], S. Varma Shrivastav[2], S. Mittal[1], V. K. Gadi[3], L. Murphy[4];

[1]The University of Winnipeg, Winnipeg, MB, Canada, [2]Oncodrex Inc., Winnipeg, MB, Canada, [3]University of Illinois Cancer Center, Chicago, IL, [4]CancerCare Manitoba, Winnipeg, MB, Canada

Breast cancer (BC) is the most common cancer worldwide, surpassing lung cancer incidence for the first time in 2020, and is the most common cancer diagnosed in American women. Despite the relative success of endocrine therapies in treating hormone receptor-positive (HR+) BC, de novo and developed resistances to these therapies (endocrine resistance) are still significant concerns. Furthermore, triple-negative breast cancer has a poor prognosis and remains one of the most challenging cancers to treat. We have discovered that the expression and localization of N-myristoyltransferase 2 (NMT2) could be prognostic and predictive markers for metastatic BC. We determined the expression patterns of NMT2 by immunohistochemical (IHC) analyses on primary tumor samples from treatment naïve BC patients. This retrospective study was blinded, and the tumor tissues in duplicate were stained with NMT2 monoclonal/polyclonal antibodies on an autostainer (Leica Bond). Stained slides were scored, and an "H" score representing the intensity and percent positive cells was given to each sample. In a combined cohort of BC represented by ER+, Triple Positive, and Triple Negative (n= 598) cases, we determined the expression and localization of NMT2. The localization pattern of NMT2 turned out to be a significant prognostic and predictive molecular signature. The nuclear localization serves as both prognostic and predictive markers. In a cohort of 447 ER+ BC cases that included 18 triple positive cases, the majority of the cases showed negative staining for nuclear NMT2 (n=394) and positive nuclear staining with differential expression in 53 cases. Whereas, in a cohort of 151 TNBC cases, nuclear NMT2 staining was positive in most cases (n= 116) and negative in 20 cases (undetermined; n= 15). The most important finding was the dichotomy of the nuclear NMT2 staining in predicting treatment response and prognosis. Both high cytoplasmic H score (>180) and positive nuclear staining (>0) predicted significant association with worse clinical outcomes for OS (HR = 1.72, *P* = .0284, 95% CI 1.06 to 2.81 for cytoplasmic NMT2 and HR = 1.74, *P* = 0.0006, CI 1.27 to 2.39 for the nuclear NMT2). Nuclear NMT2 status alone predicted a significant association with worse clinical outcomes to RFS (HR = 1.56, *P* = 0.0027, CI 1.17 to 2.09). The data from our study indicate that NMT2 could be a potential marker for predicting the likelihood of recurrence of BC and become part of routine first-line prognostic and predictive tests.

#6441 Discovery of ARID1A loss as a patient biomarker for NXP800 - A developmental activator of the integrated stress response (ISR) and inhibitor of the HSF1 pathway in ovarian cancer.

Robert H. te Poele, Marissa Powers, Swee Sharp, Emmanuel de Billy, Maria Taskinen, Loredana Pellegrino, Sharon Gowan, Asadh Miah, Angela Hayes, Matthew Cheeseman, Keith Jones, Suzanne Eccles, Florence Raynaud, Paul Clarke, Paul Workman

Centre for Cancer Drug Discovery, The Institute of Cancer Research, Sutton, United Kingdom

Background. HSF1 helps cancer cells cope with multiple stresses caused by oncogene activation.
Methods. See details below.
Results. We discovered the bisamide NXP800 as an inhibitor of HSF1-mediated transcription through phenotypic screening and med chem optimization. Gene expression microarray analysis of human cancer cell lines and tumor xenografts treated with bisamide inhibitors indicated activation of the ATF4 axis of the ISR as a key mechanism of action. In SK-OV-3 ovarian cancer xenografts, NXP800 showed clear PK/PD relationships with increased expression of ATF4 transcriptional target genes alongside decreased expression of HSF1 transcriptional targets. NXP800 also caused tumor regressions in this model. Expanding in additional human ovarian cancer xenograft models, we observed efficacy in five and a complete lack of response in three others. The sensitive models all had homozygous deleterious mutations in the ARID1A gene, whereas the non-responding xenografts were all wild type (WT). ARID1A is a component of the SWI/SNF chromatin remodelling complex involved in repression and activation of target genes. Subsequent screening of the large Sanger human cancer cell line panel confirmed ARID1A as the most significant common disease-related alteration predicting sensitivity to NXP800 in ovarian cancer cell lines. This predictive relationship was confirmed in an ARID1A isogenic HCT-116 cell line pair; sensitivity was greater in the homozygous ARID1A mutant cells compared to WT, resulting in PARP cleavage in the mutant cells only. In vivo there was no effect in WT HCT-116 xenografts whereas growth inhibition was observed in the homozygous mutant cells, resulting in significantly smaller tumors. In addition, the induction of ATF4 target genes was stronger and more prolonged in the mutant cells. It is known that whereas short term ATF4 activation is adaptive, persistent activation can promote the induction of apoptosis. CHIP-seq analysis confirmed clear relationships between ARID1A status, ATF4 and HSF1 promoter occupancy, and the distribution of BRG1 and RNA pol II at target sites, although these were often gene-specific and complex. A relatively simple example is the regulation of the INHBE gene (expression of which is a PD biomarker). In untreated samples there is no binding of ATF4, BRG1 and RNA pol II at the INHBE promoter. NXP800 treatment results in the recruitment of BRG1, ATF4 and RNA pol II in ARID1A mutant TOV-21G cells but not in the RMGI WT cells, leading to increased expression in the mutant cells only.
Conclusions. We propose that ARID1A loss alters the binding and recruitment of ATF4 and HSF1 leading to the altered and prolonged expression of ATF4 target genes and increased sensitivity to NXP800. NXP800 is currently in phase Ib for the treatment of ARID1A mutant platinum resistant ovarian cancer (NCT05226507).

#6442 Evaluation of drug target engagement on pharmacodynamic biomarkers in human plucked scalp hair.

G. Tudor, F. Ponthan, A. Boanas, M. Brown, C. Booth;
Epistem Ltd., Manchester, United Kingdom

Plucked hair is a valuable surrogate tissue to monitor pharmacodynamic (PD) responses in a clinical trial. Hair collection is a minimally invasive, simple technique amenable to frequent sampling and hence patient compliance. We have developed a method to assess target expression changes following exposure of plucked hairs to chemotherapeutic agents and other potential therapeutics. Successful *ex vivo* responses provide proof of concept data prior to clinical studies. Since hairs are epithelial appendages, many signaling pathways active in other epithelial tissues, including cancers, are also present in hairs. Highly proliferative scalp hair can be utilized as a surrogate tissue to measure proliferation, phosphorylation and DNA damage responses after treatment. Furthermore, hairs are highly vascularized, suggesting administered Test Articles may be delivered efficiently to the hair in a similar manner to other highly vascularized tissues, including many tumor types. Human plucked scalp hair was placed in maintenance media in the presence of chemotherapeutic agents that have different mechanisms of action (e.g. Gemcitabine, Epirubicin, Erlotinib) for a range of timepoints. Hairs were fixed post-exposure and longitudinal sections were immunohistochemically labelled for markers relating to DNA damage/repair or signaling pathways directly relating to target engagement. Examples include p-Chk1, g-H2AX, p-ERK1/2, and p-AKT. Quantitative image analysis to measure the level of labelling was performed using an Aperio ScanScope®. The relative number of positively labelled cell nuclei or relative labelled tissue area (depending on the labelling pattern of the target), of the hair outer root sheath was analyzed, along with label intensity. In subsequent clinical trials, formaldehyde fixed hairs from patients were returned to the lab, sectioned, labelled and quantified. If antibody labelling is not possible or more detailed information on pathway modulation may be useful, drug treated plucked hairs can be subjected to Next Generation Sequencing (NGS) gene expression analysis. The expected changes in labelling were observed, reflecting known tumor responses. For example, Gemcitabine (linked to DNA polymerase inhibition) increased p-Chk1 labelling after 4 hours and strongly induced p53 by 24 hours. Epirubicin (anthracycline topoisomerase II inhibitor) increased g-H2AX labelling up to 24 hours. Erlotinib (EGFr pathway inhibitor) decreased levels of both p-ERK1/2 and p-AKT after only 10 minutes. We have demonstrated that plucked hair is a valuable PD biomarker tissue for various chemotherapy agents. Proof of concept studies performed *ex vivo* can inform the design of clinical studies by indicating optimum biomarkers and timepoints. Further, each hair is an independent unit thereby allowing replicate tissues (hairs) to be sampled, improving statistical confidence compared to single readout markers.

#6443 Enhanced detection of ctDNA molecular response for immunotherapy treated non-small cell lung cancer through analyses of cell-free and matched white blood cell DNA.

J. B. Jackson[1], P. Rocha[2], J. R. White[1], A. P. Georgiadis[1], E. L. Verner[1], A. Greer[1], R. B. Mora[3], L. M. Pinto[3], N. Navarro[3], A. Taus[3], B. B. Paricio[3], S. Clave[3], M. T. Sausen[1], E. Arriola[2],

[1]Personal Genome Diagnostics (PGDx)/Labcorp, Baltimore, MD, [2]Hospital del Mar Medical Research Institute, Barcelona, Spain, [3]Hospital del Mar, Barcelona, Spain

Introduction: Immune checkpoint inhibitors (ICIs) have greatly improved clinical outcomes for patients with non-small cell lung cancer (NSCLC), however, programmed death-ligand 1 (PD-L1) and tumor mutation burden (TMB) have failed to consistently predict therapeutic response and outcomes in this population. There remains a critical unmet need to identify patients who are likely to experience clinical benefit from treatment, particularly as additional treatment regimens become available. Longitudinal cell-free tumor DNA (ctDNA) assessments have recently been applied as a strategy to identify molecular response (mR) and better predict long term clinical response. Through this real-world analysis of NSCLC, we explore the technical and biological considerations associated with determination of ctDNA mR through matched cell-free and white blood cell (WBC) DNA analyses and apply this optimized approach to assess therapeutic response to ICIs.

Methods: Plasma from 50 patients with advanced or metastatic NSCLC who received ICIs from 2017-2019 at Hospital del Mar had detectable pre-treatment ctDNA and underwent analysis using the 521 gene PGDx elio plasma complete liquid biopsy assay. Patient blood was collected prior to the start of ICI therapy, early on-treatment (median 4 weeks; range 2.4-9 weeks) and longitudinally throughout clinical follow-up and disease progression. Matched WBCs were also analyzed for each patient to identify alterations arising from germline polymorphisms and clonal hematopoiesis (CH). mR was calculated as the percent change in mean variant allele frequency of the tumor-specific alterations assessed at the early on-treatment timepoint compared to the pre-treatment timepoint, and compared to radiographic response, progression-free, and overall survival (OS).

Results: Best overall response for patients within the cohort was 4% complete response, 26% partial response, 34% stable disease, and 36% progressive disease. The removal of germline or CH variants allowed for improved characterization of tumor-specific somatic alterations and associations with radiographic and survival-based endpoints. With the integrated ctDNA and matched WBC approach, we observed a mR rate of 34% (17/50) with a median OS of 36.8 months compared to 9.2 months for patients experiencing molecular progression at the early on-treatment timepoint (HR 5.6, 95% CI 2.4-12.7, p<0.001, log-rank test). Specifically, of all patients that survived ≤12 months after initiation of treatment, 84% (21/25) were categorized as experiencing molecular progression through early on-treatment ctDNA analyses.

Conclusions: This real-world study of ICI treated, advanced NSCLC highlights the opportunity afforded through integrated analyses of ctDNA and matched WBCs to accurately determine mR and the associations with radiographic response and OS.

#6444 Assessing cytotoxic T cell responses to immune checkpoint inhibitors in murine and human tumor samples using metabolic imaging.

J. Ouellette[1], J. Degnan[1], A. Kellner[1], E. Flietner[1], L. Doebert[1], Z. Swider[1], E. Wait[1], V. Pope[1], L. Hrycyniak[1], S. Caenepeel[1], K. Eliceiri[2], T. S. Ramasubramanian[1], **M. J. Korrer**[1];

[1]Elephas Bio, Madison, WI, [2]University of Wisconsin, Madison, WI

Background Immune checkpoint inhibitors (ICI) have revolutionized cancer treatment. Unfortunately, existing FDA approved biomarkers do not accurately predict which patients will respond. The Elephas Cybrid™ platform aims to improve ICI response prediction by imaging a patient's biopsy treated with ICI ex vivo. Multiphoton microscopy (MPM) is a powerful imaging technique to interrogate the biological changes in live tumor fragments (LTFs) following ICI treatment. MPM allows rapid visualization of biological processes in 3D living tissues in a non-destructive fashion allowing for longitudinal assessment of a sample. We and others have used label-free metabolic imaging to demonstrate that changes in T cell metabolism and activation status are correlated. Using MPM imaging we successfully demonstrated T cell activation and T cell mediated cytotoxicity in response to ICI in LTFs and tumor biopsies.

Methods Tumors were cut into LTFs, sorted, and cultured using the Cybrid platform. LTF structure and metabolic status were assessed using intrinsically fluorescent NAD(P)H and FAD. Anti-CD8 nanobodies and cleaved caspase 3/7 dye were used to characterize T cell cytotoxicity. Multi-channel fluorescence intensity and lifetime were obtained over 48 hours using MPM.

Results Murine CT26 LTFs generated with the Cybrid platform were treated with ICI and cytotoxicity was assessed in the intact LTFs by monitoring caspase 3/7 activity using MPM over 48 hours. We found that ICI treatment resulted in a significant increase in caspase 3/7 activity compared to control treated LTFs. By blocking the interaction of T cells with tumor cells through antibody blockade, we demonstrated that the cytotoxicity observed was T cell mediated. As additional confirmation, we measured changes in cytotoxicity in the ICI resistant LLC1 tumor model. As expected, we did not observe an increase in cytotoxicity in LLC1 LTFs treated with ICI. MPM allows for the tracking of labeled T cells and characterization of their metabolism as a means of assessing changes in their activation state. We used a CD8 nanobody to label T cells in CT26 LTFs and then characterized the shift in metabolism following ICI treatment. Finally, we applied the Cybrid platform to human biopsies treated with ICI and characterized the cytotoxicity and shifts in T cell metabolism in living tissue. These data show that the Cybrid platform can measure changes in T cell metabolism and T cell cytotoxicity in response to ICI in 3D living tissue.

Conclusions The methods presented herein will advance the field of cancer diagnostics by progressing from fixed tissue imaging and genetic characterization to the assessment of clinically relevant ICI-treated biopsies. Understanding the response of biopsies to immunotherapies will allow clinicians to make more informed treatment decisions and improve the lives of those with cancer.

#6445 Exploring the relationship between PSCA and PD-L1 by a comprehensive tumor immunohistochemical analysis.

Y. Guo[1], R. Gonzalez[1], J. Yom[1], B. Gilmore[1], T. Qu[1], X. Hu[2], A. Han[1], Z. Guo[1], E. Zewdu[1], X. Liu[1], W. Fu[1];

[1]Origene Technologies Inc, Rockville, MD, [2]OriGene Wuxi Biotechnology Co., Ltd, Wuxi, China

Prostate Stem Cell Antigen (PSCA) is a well-established diagnostic marker in various cancers and a promising target for immunotherapy. Programmed Death-Ligand 1 (PD-L1) plays a crucial role in cancer immune regulation and is known to influence patient response to checkpoint inhibitors. The objective of this study is to elucidate the relationship between PSCA and PD-L1 in diverse cancer types and to provide valuable insights for the development of an effective immunotherapy strategy.

To accomplish this, immunohistochemical (IHC) analysis was conducted on paraffin-embedded Cytosections obtained from 20 lung cancers, 20 prostate cancers, 32 bladder cancers, and 20 normal tissues for each respective cancer type. Antibodies generated by Origene were utilized to detect the expression of PSCA and PD-L1 on the cell surface. The IHC results of tumor tissue were standardized against corresponding normal samples, and the correlation between these two genes was statistically analyzed using analysis of variance (ANOVA). The findings reveal a significant positive correlation between the expression of PSCA and PD-L1 ($r=+0.78$, $P=0.016$), suggesting an underlying mechanism driving their co-expression in the studied cancers.

Understanding PSCA and PD-L1 coexpression in bladder, lung, and prostate cancers has great potential for informing tailored immunotherapies. Future research should explore functional consequences within the tumor microenvironment, advancing precision immunotherapy for improved outcomes in these challenging malignancies.

#6446 Genialis™ krasID: Biology-Driven Machine Learning to Personalize KRAS Inhibitor Therapeutics.

J. Wheeler, A. Lovse, K. Ziberna, M. Stajdohar, L. Ausec, J. Kokosar, D. Pointing, A. Pai, R. Rosengarten, M. Uhlik;
Genialis, Inc, Boston, MA

Breakthroughs in targeted KRAS therapeutics (KRASi) have the potential to transform the treatment landscape for several of the most common cancers including lung, colorectal, and pancreatic. Despite the recent approvals of KRASi and the anticipation of more to come, both the rate of patient response and the durability of these responses remain significant areas requiring improvement. Biomarkers that can predict response to KRASi and guide effective patient selection and drug combination strategies will be key to realizing the full potential of this emerging therapeutic field. While most biomarkers predominantly rely on a single analyte (e.g. KRAS mutation status), Genialis' biomarkers are constructed using high-dimensional and/or multimodal data that capture the underlying biological complexity unique to each individual patient. Genialis' ResponderID™ is a machine learning-based biomarker discovery framework that models fundamental aspects of cancer biology to predict the clinical benefit based on the patient's own biology. Here we report progress towards the development of a first-in-class, RNA-based biomarker, ResponderID™ KRAS, capable of stratifying KRAS G12C inhibitor response in lung cancer patients using RNA sequencing data. Trained on thousands of lung cancer samples, our biomarker models therapeutic response by unifying two core KRAS biologic axes, dependency and activation, to identify those patients most likely to respond. The performance characteristics of ResponderID™ KRAS thus far has been evaluated on a real world dataset of lung cancer patients treated with Sotorasib. ResponderID™ KRAS serves as an independent biomarker designed to inform clinical trial design, select for therapeutic efficacy, identify rational combination strategies, and expedite approvals across various therapeutic contexts.

#6447 Development of a fully automated immunoassay system of serum pembrolizumab to forecast therapeutic effectiveness.

N. Noda[1], T. Takahashi[1], S. Yagishita[2], M. Miura[1], Y. Takahashi[1], Y. Irino[1], M. Yanagida[1], A. Hamada[2];
[1]Sysmex Corporation, Kobe, Japan, [2]National Cancer Center Research Institute, Tokyo, Japan

Recently, immuno-oncology treatments utilizing immune checkpoint inhibitors including pembrolizumab have attracted attention. Such treatments demonstrate potential effectiveness against cancers resistant to existing drugs, while offering the benefit of reduced side effects. Nonetheless, there is a specific group of patients who do not experience adequate therapeutic benefits from pembrolizumab. Despite the issue, the development of a comprehensive evaluation system to forecast therapeutic effectiveness is still in development. A strategy to predict therapeutic effectiveness involves evaluating the trough level or the steady state plasma-concentration of a drug in the blood. Ohuchi, M. *et al.* (Lung Cancer, 2022) demonstrated that patients with lower trough levels have shorter overall survival and progression-free survival durations, according to LC-MS/MS measurement of pembrolizumab. Furthermore, Wang, N. *et al* (Lung Cancer, 2023) demonstrated that the optimization of the dosage interval, grounded on the steady state plasma-concentration (target concentration, 15 µg/mL) of pembrolizumab, extended the duration of progression-free survival. Despite the potential of LC-MS/MS measurements in predicting patient prognosis and the benefits of PK-guided therapy, their implementation in clinical settings is hindered by the complex and time-consuming pre-treatment process for samples. Consequently, there is a growing need for a practical and clinically feasible drug concentration measurement system. Aiming to construct a clinically applicable pembrolizumab measurement system, we have been dedicated to developing a fully automated immunoassay system using anti-pembrolizumab antibodies. We developed two measurement systems of pembrolizumab in serum using two different antibodies targeting pembrolizumab. Using less than 10 µl serum, these systems can quantify the concentration of pembrolizumab ranging from 0.125 to 500 µg/mL within an hour, thereby enabling PK-guided therapy in clinical settings. After developing the measurement systems, we performed a correlation analysis with the LC-MS/MS system, using 70 samples with varying pembrolizumab concentrations ranging from 1.80 to 85.0 µg/mL. The results demonstrated that our measurement systems have a good correlation with LC-MS/MS measurement. Furthermore, the two immunometric measurement systems demonstrated a significant correlation with each other, substantiating the accuracy of the newly developed measurement system in determining the levels of pembrolizumab in the serum. The fully automated immunoassay systems we developed can measure pembrolizumab in serum within an hour, potentially paving the way for personalized treatment based on the serum concentration of pembrolizumab in clinical practice.

#6448 Prevalence and spectrum of *PIK3CA* mutations in Indian breast cancer patients.

R. Katara, T. Bhardwaj, M. Rawat, D. K. Sharma, V. Kumar, S. Sharma, V. Dagar, P. Kumar, S. K. Mohanty;
CORE Diagnostics India, Gurgaon, India

Introduction: Breast carcinomas are the most commonly encountered cancers in women globally. Due to advancements in cancer research the death rate in breast cancer has reduced by 41% since 1989; however, the downward trend has recently slowed emphasizing on new breast carcinomas treatment discovery. Breast carcinomas are molecularly categorized by the expression of specific hormone receptors, as well as the overexpression of human epidermal growth factor receptor 2 (HER2). Approximately 80% of breast cancers have been termed HER2-negative, but researchers now recognize that 55% of all breast cancers may actually contain low levels of HER2, levels that are still targetable by HER2-directed therapies such as Trastuzumab Deruxtecan. The phosphoinositide 3-kinase (PI3K) pathway is the most frequently altered pathway in HR+/HER2- breast carcinomas and is associated with tumor development, disease progression, and endocrine resistance.

Methodology: The study entailed histological verification of breast cancer, and thence the extraction of DNA from formalin fixed, paraffin embedded (FFPE) tissue samples. A tumor content of 20% was the cut-off for performing the *PIK3CA* mutation analysis. The DNA was subjected to mutation analysis using a FDA-approved *PIK3CA* RGQ Real Time PCR based assay that has ability to detect 11 mutations in the *PIK3CA* gene encompasses exons 7, 9, and 20.

Results: A total of 696 breast cancer patient samples (with more than 20% neoplastic tissue content) were screened for *PIK3CA* mutations. Of these, 275 (39.5%) (Male: Female ratio = 1:26.5; Age range = 30-80 years) harbored a mutation of the *PIK3CA* gene. Females were commonly affected; however, the males were also found to have *PIK3CA* mutation. The most common affected age group is from 41 to50 years. The positivity rate exon wise were as follows: Exon 7 (1.45%), Exon 9 (39.27%), and Exon 20 (44.27%). There was presence of co-mutations amongst different exons, which comprised of 4%. HR+/HER2- (50%) followed by HR-/Her2- (3.27%) and HR+/HER2+ (1.82%). The HER2- cases (Score 1 and Score 2) by IHC were considered as low positive cases (14%).

Conclusion: This is one of the largest study to report frequency of *PIK3CA* mutations in the Indian population. *PIK3CA* mutations are commonly encountered in hormone receptor positive and HER2 Negative metastatic breast cancer and have shown promising clinical outcome leading to better prognosis. It provides insights into genotyping each breast cancer and exploits the usage of PI3K/AKT inhibitors together with other combination of drugs for effective target treatment strategies.

Keywords: Breast carcinomas, *PIK3CA*, HR/HER2, Targeted Therapeutic

#6449 KDM6A expression loss is a common feature in low grade non-invasive urothelial carcinomas of the urinary bladder.

F. Viehweger[1], N. Gorbokon[1], H. Plage[2], S. Hofbauer[2], K. Furlano[2], S. Weinberger[2], B. Ralla[2], A. Franz[2], A. Fendler[2], M. de Martino[2], F. Ro?ner[2], S. Schallenberg[2], S. Elezkurtaj[2], **M. Lennartz**[1], T. Mandelkow[1], E. Bady[1], A. H. Marx[3], H. Samtleben[3], M. Fisch[1], M. Rink[4], M. Slojewski[5], K. Kaczmarek[5], T. Ecke[6], S. Koch[6], N. Adamini[7], R. Simon[1], G. Sauter[1], J. Weischenfeldt[8], T. Klatte[2], T. Schlomm[2], D. Horst[2], H. Zecha[7], M. Kluth[1], S. Minner[1];
[1]University Medical Center Hamburg-Eppendorf, Hamburg, Germany, [2]Charite - Universitatsmedizin Berlin, Corporate Member of Freie Universitat Berlin, Humboldt-Universitat zu Berlin and Berlin Institute of Health, Berlin, Germany, [3]Academic Hospital Fuerth, Fuerth, Germany, [4]Marienhospital Hamburg, Hamburg, Germany, [5]Pomeranian Medical University, Szczecin, Poland, [6]Helios Hospital Bad Saarow, Bad Saarow, Germany, [7]Albertinen Hospital, Hamburg, Germany, [8]University of Copenhagen, Copenhagen, Denmark

KDM6A, also known as UTX (ubiquitously transcribed X chromosome tetratricopeptide repeat protein) is an epigenetic regulator which is frequently mutated in urothelial carcinoma. Because KDM6A loss causes a dependency on EZH2, a potential therapeutic target, KDM6A analysis may have therapeutic importance. Most data on KDM6A mutations are derived from next generation sequencing (NGS). However, because of the combination of a high rate of truncating KDM6A mutations, the localization of KDM6A on chromosome Xp11.3, and the male predominance in bladder cancer, many KDM6A mutations should result in a complete loss of KDM6A protein expression and become detectable by immunohistochemistry (IHC). To study the prevalence and the potential diagnostic and clinical role of KDM6A expression loss, more than 2,100 tumors were analyzed by IHC in a tissue microarray format. The cohort included 1,128 patients who underwent radical cystectomy for muscle-invasive disease (pT2-4). A complete KDM6A expression loss occurred in 36% of 350 pTa G2 low-grade, 23% of 152 pTa G2 high-grade, and 18.5% of 92 pTa G3 tumors (p=0.0002). As compared to pTa G3 tumors, the frequency of KDM6A expression loss did not differ significantly in pT2 (17.2%), pT3 (21.9%), and pT4 (18.2%) cancers. Within pT2-4 carcinomas, KDM6A staining was unrelated to pT, pN, grade, L-status, V-status, overall survival, recurrence-free survival, and cancer-specific survival (p≥0.18 each). A KDM6A loss was more common in male (22.2%) than in female patients (15.4%; p<0.0001), and within male patients, a KDM6A loss was more frequent in tumors with Y-chromosome loss (36.1%) than in cancers without a Y-chromosome loss (16.3%; p<0.0001). KDM6A expression loss was significantly associated with increased p63 expression (p<0.0001) and high uroplakin 1b staining (p=0.0013) but unrelated to CK20, GATA3, UpK1b, and p53 staining. In summary, our data demonstrate that truncating KDM6A mutations occur in a significant subset of urothelial carcinomas which is linked to low-grade non-invasive cancer, male gender and loss of the Y chromosome. The predominance of KDM6A loss in low grade tumors makes KDM6A IHC a promising new tool for identification of low grade dysplasia in biopsies and early bladder cancer detection in cytology.

#6450 High mobility group protein 2 (HMGA2) is highly expressed in a broad range of human cancers.

K. Moller, F. Lutz, F. Viehweger, M. Kluth, C. Hube-Magg, C. Bernreuther, G. Sauter, A. H. Marx, R. Simon, T. Krech, S. Steurer, C. Fraune, S. Minner, N. Gorbokon, **M. Lennartz**, E. Burandt, A. Menz;
University Medical Center Hamburg-Eppendorf, Hamburg, Germany

The high mobility group protein 2 (HMGA2) is an essential component of the enhanceosome. It can attach to AT-rich binding sites in the DNA minor groove, affect the conformation of the DNA, and thereby modify the transcription of numerous genes. HMGA2 is preferentially expressed during organogenesis. Aberrant expression of HMGA2 in adult tissues is commonly associated with tumor formation and cancer aggressiveness. Accordingly, HMGA2 represents a potential drug target. To better comprehend the role of HMGA2 expression in cancer, a tissue microarray containing 8,344 samples from 115 different tumor entities and 608 samples of 76 different normal tissue types was analyzed. In normal tissues, a strong nuclear HMGA2 staining was limited to few cell types from the amnion, placenta, seminal vesicle, endocervix, fallopian tube, and respiratory epithelium. HMGA2 expression was generally markedly higher in cancer than in corresponding normal tissues. HMGA2 staining was found in 2,695 (42.7%) of the 6,313 interpretable tumor samples, including 701 (11.1%) with weak, 769 (12.2%) with moderate, and 1,225 (19.4%) with strong positivity. A total of 93 of 115 tumor categories showed HMGA2 expression in at least one case, and 69 tumor categories included at least one case with strong HMGA2 staining. The frequency of HMGA2 positivity was particularly high in cancers of the ovary and the endometrium (52.6-92.6%), pancreatico-biliary cancers (48.1-75.5%), thyroidal neoplasms (53.4-95%), salivary gland neoplasms (66.7-98%), nonseminomatous testicular germ cell tumors (73.5-93.5%), colorectal adenocarcinoma (81.6%), papillary renal cell carcinoma (68.2%), and in squamous cell carcinomas (36-81.5%). Tumor entities with a particularly low expression of HMGA2 included prostatic adenocarcinomas (1.3-4%), non-invasive urothelial carcinomas (1.8-4.3%), hepatocellular carcinoma (3.2%), and non-Hodgkin’s lymphomas (0%) It is concluded, that HMGA2 is highly expressed in a very broad range of tumor entities. These findings emphasize a potential role of HMGA2 as a drug target and demonstrate utility for HMGA2 IHC for the distinction of neoplastic from non-neoplastic tissues in several organs.

CLINICAL RESEARCH: Profiling Cancer with Real-World Evidence
Poster Session

#6454 Genomic characterization of vulvar squamous cell carcinoma.

S. R. Selitsky[1], T. Thong[1], K. Roche[1], J. Guinney[1], P. Sethupathy[2], C. Igartua[1];
[1]Tempus Labs, Chicago, IL, [2]Cornell University, Ithaca, NY

Introduction: Understanding the molecular underpinnings of vulvar squamous cell carcinoma (vSCC) has strong potential for clinical impact, given the unmet need for this rare cancer. vSCCs have two main etiologies, including human papillomavirus (HPV) infection or skin conditions such as lichen sclerosis. Clinically, few treatment options with limited efficacy are available for recurrent vSCCs and large whole transcriptome disease subtyping studies are limited due to the rarity of this cancer type. Here, we present a whole transcriptome subtyping study of 244 vSCC clinical samples with DNA genomic profiling. Furthermore, we compared vSCCs to other SCC disease subtypes (pan-SCC), including lung, esophageal, skin, urothelial, anal, and head and neck (HN). Our goal was to gain novel insights into the molecular landscape of vSCCs to inform new routes of therapy.
Methods: Deidentified records of SCC patients were selected from the Tempus clinico-genomic database. The vSCC cohort was predominantly composed of, but not exclusively, naive or pre-treatment primary tissue. The pan-SCC cohort was limited to randomly sampled primary pre-treatment female samples with paired RNA and DNA sequencing. To perform vSCC subtyping, we used bulk RNA-seq and clustered the samples using FastPG-CC, an internally developed consensus-clustering extension of FastPG, a graph-based parallelized clustering tool. We next performed differential expression, pathway analysis, and cell type abundance estimation.
Results: Unbiased gene expression clustering analysis identified three vSCCs clusters; an HPV+ cluster (HPV+, 32% of vSCC samples), HPV- cluster (HPV-, 33%), and an intermediate cluster which contained both HPV+ and HPV- samples (Mix, 35%). The HPV- cluster was enriched for TP53 and TERT promoter mutations, EMT and tumor microenvironment gene expression-derived pathways, and was most similar to HPV- oral HN tumors. The HPV+ cluster was enriched with PIK3CA mutations, cell cycle gene expression and was most similar to other HPV+ SCC samples, including cervical, anal, and HN. The Mix cluster was enriched for neutrophils, fatty acid metabolism and was most similar to skin SCC.
Conclusions: We performed a multi-modal molecular subtyping analysis on a large cohort of vSCCs and identified three molecular subtypes, which enabled us to identify heterogeneity within vSCC, and observe that a subset of vSCCs share features with SCC tumor types for which there are emerging therapy options. Thus, this approach identifies a subset vSCCs that may be responsive to existing SCC therapeutics.

#6455 Investigating clinical trial eligibility criteria to improve MatchMiner trial matching.

H. Klein, T. Mazor, M. Galvin, J. Hansel, E. Mallaber, P. Trukhanov, J. Provencher, J. Lindsay, M. Hassett, E. Cerami;
Dana-Farber Cancer Institute, Boston, MA

As the number of precision medicine (PM) trials and the volume of patient genomic data have grown, it has become challenging for clinicians and trial staff to identify PM trial options for patients. At Dana-Farber Cancer Institute (DFCI), we have addressed this challenge by developing our own open source institutional trial matching software called MatchMiner. MatchMiner algorithmically matches patient genomic and clinical data with PM trial eligibility data. PM trial eligibility data is manually curated into a human- and computer-readable structured format called clinical trial markup language (CTML), for trial matching with DFCI's institutional genomic assay OncoPanel. MatchMiner has 2 main modes of clinical use: (1) patient-centric, where clinicians can search for trial matches for individual patients and (2) trial-centric, where trial staff can identify patients that match their trial's genomic eligibility. Thus far, more than 300 DFCI patients have enrolled onto trials facilitated by MatchMiner.

In its current implementation, MatchMiner uses limited clinical data (gender, age, and cancer type) to match patients to trials. Although this limited data gives clinicians a head start on assessing available trial options, incorporating more clinical data into MatchMiner would provide more precise trials options and reduce additional work to assess patient eligibility. Here, we investigated clinical trial eligibility criteria that were available for trials at DFCI with the goal of improving specificity of trial matching for MatchMiner. We attempted to answer 2 main research questions 1) what categories of clinical data comprise the eligibility criteria for precision medicine trials at DFCI and 2) which categories are most relevant for trial matching?

We first investigated the clinical eligibility criteria across several PM lung cancer trials. After extracting the inclusion and exclusion criteria from the protocol documents, we found criteria could be classified into 10 distinct categories. The most common categories making up almost half of the eligibility criteria were "Prior Therapy" and "Prior or Concurrent Non-Cancerous Disease". Within some categories, we found it appropriate to also make subcategories to make our analysis more informative such as "Prior Therapy, Surgery" or "Disease Status, CNS". We next broadened our search to non-lung trials to see if criteria was consistent across other cancer types. We found similar proportions of clinical criteria for the non-lung trials compared to the lung trials, but did find some additional subcategories. Overall, having similar categories of criteria across trials suggests that common clinical data could be used for many different PM trials. Currently, we are investigating which categories are most relevant for trial matching and the use of AI for structuring unstructured clinical data.

#6456 The utility of clinical sequencing in the diagnosis and treatment of soft tissue sarcomas; Real world data based on nation-wide database.

E. Nakada, T. Fujiwara, T. Kunisada, S. Takihira, D. Ennishi, H. Yamamoto, K. Ninomiya, S. Tomida, M. Futagawa, A. Hirasawa, S. Toyooka, T. Ozaki; Okayama University Hospital, Okayama City, Japan

Purpose: Soft tissue sarcomas (STS) are rare and heterogeneous tumors arising from mesenchymal connective tissue, accounting for approximately 1%-2% of all malignancies. Due to their rarity and heterogeneity, it is challenging for accurate diagnosis, prognosis, and treatment of sarcoma. Recently, next-generation sequencing (NGS)-based comprehensive cancer genome profiling (CGP) has increasingly become a routine practice for patients with solid cancers worldwide. To collect genomic information and clinical characteristics of patients who underwent CGP, the Center for Cancer Genomics and Advanced Therapeutics (C-CAT) has also been established since 2018 in Japan. Almost all the clinical and genomic data of patients who received CGP tests the had been collected in C-CAT. Here, we examined the utility of CGP test in the diagnosis and treatment of STS using this nation-wide database.

Patients and Methods: We retrospectively evaluated the records of patients with STS who received F1CDx between 2019 and 2022 and registered in C-CAT. This assay carries 324 genes and determines nucleotide substitutions, insertions/deletions, and copy number (CN) alterations of 309 genes, fusions of 36 genes, tumor mutation burden (TMB) and microsatellite instability (MSI). High TMB (TMB-H) was defined as a TMB value >10 muts/Mb. Ranges of the MSI score were assigned MSI-High (MSI-H) or microsatellite stable (MSS).

Results: From 2019 to 2022, 1387 patients with STS were registered in C-CAT. The histological types included leiomyosarcoma in 357 patients, dedifferentiated liposarcoma in 178 patients, and undifferentiated pleomorphic sarcoma in 82 patients, and the others. The most commonly altered genes included TP53, CDKN2A, Rb1, and CDKN2B. Among the 1387 cases, we observed 110 fusion events in 108 cases (7.7%), and 2 cases showed 2 types of fusion transcripts. Fifteen (2.8%) patients were re-classified based on the detection of highly histology-specific translocations. Among them, an initial diagnosis of sarcoma NOS was classified as Ewing Sarcoma (*EWSR1-FLI1* in 2 patients), *NTRK*-rearranged spindle cell neoplasm (NTRK fusion in 3 patients), *CIC*-rearranged sarcoma (*CIC-DUX4* in 3 patients), and sarcoma with *BCOR* genetic alterations (*BCOR-ZC3H7B* in 1 patient) as these gene fusions were identified. Druggable gene alterations was detected in 347 patients (25%) and 55 patients (4%) who received genotype-matched therapy. In 38 patients for whom the effect of treatment could be evaluated, complete response and partial response were achieved in 2 (5%) and 10 (26%) patients, respectively.

Discussion: In conclusion, the comprehensive genomic profiling test appears to be an important tool in the diagnosis and treatment of sarcomas.

#6457 The real-world data of comprehensive genomic profiling tests with tissue specimens from lung cancer patients in Japan.

K. Fujii, M. Morishita, M. Ueki, H. Ikushima, H. Isago, K. Watanabe, K. Oda, H. Kage;
The University of Tokyo Hospital, Tokyo, Japan

Introduction: Molecularly targeted therapy improves prognosis of lung cancer patients with specific genomic alterations, and thus it is important to identify actionable genomic alterations leading to appropriate therapy. In Japan, comprehensive genomic profiling (CGP) tests have been covered by insurance since June 2019. 99.7% of the CGP data under insurance coverage have been registered with the nationwide database: Center for Cancer Genomics and Advanced Therapeutics (C-CAT). C-CAT data include CGP test results and clinical information such as companion diagnostic results for *EGFR*, *ALK*, *ROS1*, and *BRAF* as well as therapeutic history. The aim of this study is to evaluate the usefulness of CGP tests for identifying actionable genomic alterations in real-world lung cancer patients.

Methods: Among the 3,240 lung cancer patients registered in the C-CAT database by September 2023, 2,076 non-small cell lung cancer cases were tested using tissue specimens and analyzed retrospectively. The analysis was based on the levels of evidence defined by C-CAT. Level A indicated approved drugs for the particular cancer type, while level C indicated approved drugs or presence of positive clinical trials regardless of cancer type. Level F indicated that the genomic alteration was an oncogenic marker.

Results: The cases were divided into two groups: 335 cases with known genomic alterations with positive results from companion diagnostic tests or use of specific inhibitors and 1,741 cases without. Genomic alterations with level A, A to C, and A to F were identified in 430 cases (24.7%), 1174 cases (67.4%), and 1718 cases (98.7%) with unknown genomic alterations, respectively. Genomic alterations with level A included rearrangement of *RET* (43 of 1741 cases, 2.5%), *ALK* (14 cases, 0.8%), *ROS1* (8 cases, 0.5%), and *NTRK1* (2 cases, 0.1%), and mutations of *EGFR* (124 cases, 7.1%), *MET* (38 cases, 2.2%), *ERBB2* (122 cases, 7.0%), *KRAS G12C* (66 cases, 3.8%), and *BRAF V600E* (15 cases, 0.9%). Genomic alterations with level C included mutations in *KRAS* (185 cases, 10.6%), *PIK3CA* (99 cases, 5.7%), *BRAF* (55 cases, 3.2%), and *PTEN* (32 cases, 1.8%) and amplifications in *ERBB2* (147 cases, 8.4%) and *MET* (68 cases, 3.9%). Among cases with known genomic alterations, *ALK* and *ROS1* fusion genes were not detected in 11 of 49 (22.4%) and 17 of 46 (37.0%), while *EGFR* and *BRAF* mutation was not detected in 11 of 218 (5.0%) and 3 of 4 cases (75.0%), respectively. The detection rate of fusion genes was lower than that of mutated genes (70.5% vs 93.7%, $p<0.001$).

Conclusion: In non-small cell lung cancer patients with unknown driver genes, driver oncogenes with corresponding approved therapy were found in a quarter of the patients. CGP tests offer the possibility of increasing the opportunities of receiving new therapies. CGP tests may have a lower detection rate for fusion genes compared with other mutations.

#6458 Clinical significance of cancer genome profiling tests for gastrointestinal cancer patients with liver metastasis.

T. Sakuma, M. Yashiro, Y. Fukui, K. Maruo, G. Tsujio, Y. Yamamoto, H. Kasashima, K. Maeda;
Osaka Metropolitan University, Osaka City, Japan

Introduction: Distant metastasis is one of critical prognostic factors for patients with gastrointestinal cancer. Especially, liver metastasis shows high effects on prognosis of patients with gastrointestinal cancer. In Japan, cancer genome profiling (CGP) testing have been available for patients who have no selective standard treatment options since 2019. Based on the genetic mutations by CGP test, therapeutic drugs with evidence have been discussed at expert panels. CGP data has been accumulated in around 60,000 cases. It is necessary to evaluate the clinical significance of CGP tests for gastrointestinal cancer patients with liver metastasis to receive high benefits of CGP testing through C-CAT. **Aims**: We aimed to analyze the clinical significance CGP tests for gastrointestinal cancer patients with liver metastasis. **Materials and methods**: A total of 3,738 patients of gastrointestinal cancer with liver metastases including 215 cases of esophageal cancer, 347 cases of gastric cancer, and 3,176 cases of colorectal cancer, was enrolled in this study. Three types of CGP tests, including NCC Oncopanel, FoundationOne CDx, and FoundationOne Liquid, were performed, and the CGP data was collected to Center for Cancer Genomics and Advanced Therapeutics in Japan (C-CAT) database. Adequate treatment for each patient was discussed at the expert panel meeting according to the results from the CGP tests. **Results**: A total of 2,882 cases (77.1%) in 3,176 cases have been revealed druggable. However, only 216 cases (13.3%) were medicated by anti-cancer treatments. In the 216 treated cases, disease control case, complete response (CR), partial response (PR), or stable disease (SD) was only 52 cases. In 52 cases, six cases (4 of SD cases and 2 of PR cases) was administered encorafenib-based chemotherapies based on *BRAF* gene mutation. Five genes, *ZNF217, SRC, ARFRP1, BARD1, FGF10*, were significantly more frequently expressed on liver metastasis cases, in compared to other metastasis cases in gastrointestinal cancer. **Conclusion**: Around 13% of gastrointestinal cancer patients with liver metastasis might have a druggable benefit by CGP testing. *BRAF* mutation might be promising target for patients with liver metastasis. *ZNF217, SRC, ARFRP1, BARD1, FGF10* might be associated with metastatic process to liver in gastrointestinal cancer.

#6459 Molecular profiling of advanced non-small cell lung cancer in response to first-line immune checkpoint inhibitors and/or chemotherapy using multimodal real-world data.

X. Fu, J. Kardos, P. Correa, M. Wang, L. Li, J. Egen, S. Iqbal;
Gilead Sciences, Foster City, CA

Background: Up to 85% of lung cancer patients have non-small cell lung cancer (NSCLC). Standard of care for NSCLC includes immune checkpoint inhibitors (ICI) and/or platinum-based chemotherapy (CT). However, therapy success is limited with up to 70% of patients not responding to ICI. Mechanisms of resistance across treatments are not fully understood. In this study, we explore real-world data to characterize molecular and genomic changes in advanced NSCLC treated with ICI, ICI+CT, or CT.

Methods: Stage III/IV NSCLC patients receiving first-line (1L) ICI, ICI+CT, or CT were identified from Tempus Labs, Inc.'s de-identified, multimodal real-world database. Patients' solid tissue biopsies taken pre- or post-1L underwent next generation sequencing with the Tempus xT assays (DNAseq of 648 genes at 500x coverage and whole transcriptome RNAseq). Patients' clinical and outcome data were abstracted from electronic health records. We analyzed changes in gene expression, pathway enrichment, estimated immune cell components, and somatic mutations in responders (complete/partial response) and non-responders (progression/stable disease) upon 1L treatment.

Results: 1L non-responders (70%, 51%, and 47%) were identified across cohorts (143 ICI, 764 ICI+CT, and 228 CT, respectively). 58% of pre-1L biopsies were taken from distal metastatic tissues. Distinct pathways altered post-1L include the downregulated E2F target pathway in CT cohort, and upregulated TNFα/NFκB signaling and the hypoxia and protein secretion pathways in ICI cohort. Significant (FDR < 0.05) augmented expression was observed for 90, 23, and 65 genes in non-responders vs. responders post ICI, ICI+CT, and CT, respectively. RNAseq deconvolution reveals decreased plasma and CD4+ activated T cell fraction in metastatic biopsies, whereas increased CD4+ activated T cell and monocyte fraction was seen after treatment only in ICI cohort. Genes with oncogenic driver mutations reported in NSCLC were detected including TP53 (68%), KRAS (30%), STK11 (13%), EGFR (11%), CDKN2A (10%), KEAP1 (9%), and NF1 (7%). Of the 250 mutated genes, 72 (29%) were commonly not detected post-1L, whereas 38, 3, and 8 unique genes with loss of detectable mutations were identified post-1L of ICI, ICI+CT, and CT, respectively. Since loss of detectable mutations is a sign of loss of subpopulations of cancer cells hosting such mutations that succumb to therapy, these genetic mutations could be used to select patients who can benefit from such therapy.

Conclusions: Distinct molecular characteristics including tumor immune components and genomic alterations are associated with 1L response in advanced NSCLC. Real-world data analyses provide opportunity to explore distinct mechanisms of therapy resistance and identify potential biomarkers of therapy response for further validation in clinical studies.

#6460 Incidence of pathogenic germline variants and presumed germline pathogenic variants in Japanese lung cancer patients using comprehensive genomic profiling tests.

M. Ueki, K. Watanabe, M. Morishita, K. Fujii, H. Ikushima, H. Isago, K. Oda, H. Kage;
The University of Tokyo Hospital, Tokyo, Japan

Introduction: Pathogenic germline variants (PGVs) and presumed germline pathogenic variants (PGPVs) are often detected with comprehensive genomic profiling (CGP) tests. Using the Center for Advanced Cancer Genomics and Therapeutics (C-CAT) database, we investigated the incidence of PGV and PGPV detected by CGP tests in Japanese lung cancer patients.
Methods: Among 3,240 lung cancer cases registered in C-CAT between June 2019 and August 2023, 321 were tumor/normal paired NCC Oncopanel (NOP), 773 were FoundationOne Liquid CDx (F1L), and 2,145 were tumor-only FoundationOne CDx (F1CDx). We analyzed cancer susceptibility genes in accordance with the national guideline. In F1L and F1CDx, PGPV was determined based on variant allele frequency (VAF) and medical history. Differences between groups in the detection of PGV and PGPV were tested using chi-squared test, and differences in age were tested using t-test.
Results: The incidence of PGV in NOP and PGPV in F1L and F1CDx were 4/321 (1.2%), 36/773 (4.7%), and 141/2145 (6.6%), respectively (NOP vs F1L vs F1CDx; p = 0.001 NOP vs F1L; p = 0.006, NOP vs F1CDx; p < 0.001, F1L vs F1CDx;p=0.190). The 4 PGVs detected by NOP were in the *ATM*, *BRCA2*, *MSH6*, and *TP53* genes. Notably, two out of four patients were in their 30s while the other two were in their 70s. In the F1L dataset, 36 patients (4.7%) had PGPV: 8 patients (1.0%) had *PALB2*, 6 patients (0.8%) had *BRCA2*, and 4 patients (0.5%) had *CHEK2* variants. In the F1CDx dataset, 141 had PGPV: 19 patients (0.9%) each had *BRCA1* or *BRCA2* variants and 18 patients (0.8%) had *PALB2* variant. There was no significant age difference between PGPV(-) and PGPV(+) patients (F1L:63.3 vs. 62.4 years; p = 0.938, F1CDx: 65.5 vs 65.0 years; p = 0.749). Most cases with PGV or PGPV were non-small cell lung cancer: 4/4 in NOP, 34/36 in F1L, and 110/141 in F1CDx.
Discussion: The incidence of PGV in lung cancer patients was at least 1% and found in both younger and older patients. A circulating tumor DNA panel and a tumor-only tissue panel detected PGPVs at a significantly higher rate than detection of true PGVs by tumor/normal paired tissue panel, suggesting the use of tumor/normal paired panels may mitigate the burden of both patients and clinicians with concerns from false positive PGPV. The majority of detected PGV/PGPV were in homologous recombination repair genes.

#6461 Prevalence and implications of potentially pathogenic germline variants among adult patients in the Philippines with solid malignancies who underwent tumor genomic profiling: A multi-institutional, cross-sectional study.

Paula Isabel Gimena Franco, Frances Victoria Que, Jose Jasper Andal, Daphne Ang

St. Luke's Medical Center, Quezon City, Philippines

Background: In high income countries, 2-10% of tumor genomic profiling reports reveal incidental pathogenic germline variants. A third of these patients would not qualify for genetic testing based on current guidelines. In South East Asia, despite increased use of outsourced genomic profiling platforms, there are no published studies exploring the prevalence of these potentially pathogenic germline variants (PPGV). Our study determined the prevalence of PPGVs among adult patients with solid malignancies who underwent liquid or tissue-based tumor genomic profiling in the Philippines.
Methods: Annotated reports of patients with solid cancers who underwent tumor genomic profiling using *FoundationOne* or *FoundationOne Heme*between January 2021 to July 2023 were reviewed (Ethical Board ID: SL-23143). PPGVs were identified according to recommendations from American Board of Medical Genetics and Genomics and expert review. PPGV criteria include having a variant allele frequency of >30% and were categorized as: 1) high penetrance gene (HP), founder variant (FV), or variant associated with clinical presentation (VA). Cross-checking the pathogenicity through *ClinVar* database was also done.
Results: Out of 446 patients, 13 PPGV variants were found in 50 (11.2%) patients at a median age of 60.5 years. Of these, 28 (54%) had high penetrance (*BRCA1, BRCA2, MSH2, MSH6, MLH1, RAD51C, RAD51D*), 24 (46%) patients had VA (*APC, SMAD4, CDH1, CDKN2A,PTEN*) and two patients with lung cancer had a founder variant (*EGFR p.Thr790Met*). PPGVs were primarily found in colorectal (42% of 50 patients with PPGVs), breast (16%), ovarian (6%) and lung (6%) cancer patients ($p<0.001$). HP genes were mostly found in females (71.4%, $p = 0.03$), driven by *BRCA1/2* variants (15 females and 2 males).
Conclusions: The presence of PPGVs warrants formal genetic counselling and germline testing. Given the similar prevalence of PPGVs in this study compared with data from other countries, and the diagnostic and therapeutic implications of detecting incidental PPGVs, we underscore the need for cancer genetics to be incorporated into standard oncologic care in the Philippines.

#6462 Somatic mutational profile in MUTYH- associated colorectal cancers (MUTYH-CRCs).

D. Kaldas[1], T. Biachi de Castria[2];

[1]University of South Florida, Tampa, FL, [2]Moffitt Cancer Center, Tampa, FL

Background: Biallelic inactivation of MUTYH leads to hereditary predisposition to colorectal polyposis and CRC. Herein we evaluated co-alterations in somatic next-generation sequencing (NGS) in patients with MUTYH-CRC, mainly KRAS G12C, high tumor mutational burden and microsatellite instability (MSI-H)/mismatch repair deficiency (dMMR).

Methods: Data was collected on patients with MUTYH-CRC in the period between 2015 and 2023 at Moffitt Cancer Center (Tampa, Florida, United States). All patients with MUTYH-CRC were included regardless disease stage. Different germline panels were used to detect MUTYH and Foundation One, Caris and Moffitt STAR (in house NGS) were used to detect somatic co-alterations.

Results: A total of 36 patients were identified with MUTYH- CRC, the median age at diagnosis was 44-year-old, 55% were men. All patients had a somatic NGS available, 18 patients (50%) had KRAS mutation, and specifically KRAS G12C was detected in 9 patients (24%), 6 patients (17%) had MSI-H/dMMR, 5 patients (14%) had BRAF mutation and 4 patients (11%) with BRCA2 mutation.

Conclusion: MUTYH-CRC is associated with a high incidence of targetable alterations including KRAS G12C and BRAF. Considering unique characteristics in MUTYH-CRC tumor microenvironment, including T cell infiltrate, trials combining KRAS G12C/ BRAF inhibitors and immune checkpoint inhibitors are warranted.

#6463 Highly frequent gene mutations and co-occurring genes analysis in colorectal cancer.

Q. Zha, F. Scarpa, M. Rengaraj, A. Juncker-Jensen;
NeoGenomics, Aliso Viejo, CA

Background: Colorectal cancer (CRC) is the second most leading cause of cancer-related deaths worldwide. Understanding the molecular alterations that drive CRC is critical for improving patient outcomes. Next-generation sequencing (NGS) has revolutionized CRC molecular profiling by simultaneous analysis of multiple genes with high accuracy and sensitivity. In this study, we analyzed a cohort of CRC formalin-fixed paraffin-embedded (FFPE) samples to identify highly frequent gene mutations and co-occurring genes in CRC.

Methods: FFPE samples from CRC patients tested from January 2020 to May 2023 were analyzed using NeoTYPE® Colorectal Tumor Profile. This profile analyzes 44 biomarkers through a combination of NGS focusing on a panel of 36 genes known to be frequently mutated in CRC, as well as 3 FISH and 3 IHC biomarkers. Gene mutation frequency, co-occurring mutation genes and clinical significance were explored and analyzed. In addition, immunotherapy markers, Microsatellite Instability (MSI) and Tumor Mutation Burden (TMB) were assessed.

Results: A total of 2,920 patients (1,577 men and 1,343 women) with CRC were included in this study. Average sequence coverage was 2386X with mean minor allelic frequency of 30%. A higher average number of variant allele frequency were observed in metastatic versus primary colorectal cancer ($P < .001$). We found that APC, TP53, KRAS, PIK3CA and ARID1A were the most frequently mutated genes. APC truncated mutation p. R1450* were the most common mutations. KRAS, PIK3CA and TP53 missense mutations are the prevalent consequence. Notably, a subset of patients exhibited high microsatellite instability (MSI-H) or TMB high, indicating potential eligibility for immune checkpoint inhibitor therapy. In addition, we found APC mutations co-occurring with TP53 or KRAS mutations ($p <.001$) in our cohort.

Conclusion: Our results provide insight into the genetic landscape of CRC and highlight the importance of understanding co-occurring mutations in this disease. Specifically, APC mutations frequently coincide with TP53 mutations, jointly contributing to the onset of CRC. TP53 often play a role in promoting genomic instability and evading mechanisms that regulate cell growth. The identification of highly frequent mutations and co-occurring genes may have important implications for the development of targeted therapies and personalized treatment approaches for CRC patients.

#6464 Real-world evidence (RWE) presented at AACR annual meetings: A 10-year trend analysis.

J. Zong[1], L. C. Bylsma[2], O. Lunacsek[1], X. Jiang[2], J. Fryzek[2];
[1]Bayer HealthCare Pharmaceuticals Inc., Whippany, NJ, [2]EpidStrategies, A Division of ToxStrategies, LLC, Rockville, MD

Introduction: RWE is increasingly used in the oncology community, particularly following the 2016 21st Century Cures Act. A recent analysis of RWE presented at ASCO reported a significant increase in relative frequency of RWE abstracts from 2011-2021[1]. We conducted a similar trend analysis of RWE presented at AACR and predictive factors associated with publication.
Methods: EMBASE was queried for abstracts presented at AACR 2013-2022, using terms related to study designs and methodologies that employ use of RWE. Details on study design, location, data source, patient number, cancer site, analytical approach, endpoints, and presentation type (oral vs. poster) were extracted and analyzed. Searches in Google Scholar identified published manuscripts associated with each abstract. The Cochran-Armitage trend test and Monte-Carlo estimation of the exact test were used to detect trends over time; p-values are provided for descriptive purposes. Relative risk ratios were calculated to determine statistically significant predictors of publication.
Results: Of 56,920 total abstracts presented at AACR from 2013-2022, 611 (1.1%) RWE abstracts were identified. The proportion of presented abstracts with RWE increased from 0.6% in 2013 to 2.0% in 2022 ($p<0.001$). Among the RWE abstracts, use of electronic medical record (2013: 0% vs. 2022: 9.3%; $p=0.002$) and genomics databases (i.e., GENIE) (2013: 0% vs. 2022: 8.3%; $p=0.006$) increased over time. While majority of RWE abstracts were presented as posters (95.9%), the proportion of oral presentations increased in the last decade (2013: 0.0% vs. 2022: 3.7%; $p=0.005$). Abstracts with sample sizes <500 decreased significantly over time ($p=0.002$); those with sample sizes 5,000-<50,000 increased significantly over time ($p=0.001$). The proportion of abstracts including multiple cancer sites (vs. single-site) increased from 5.1% in 2013 to 20.4% in 2022 ($p<0.001$). The most common cancer sites were lung, breast, and colorectal. Statistically significant factors associated with publishing an abstract into a manuscript included study sample size 500-<5,000 or ≥100,000, inferential statistics (vs. descriptive), propensity score matching, and effectiveness or disease burden endpoints.Conclusion: RWE studies presented at AACR increased in the recent decade, with more robust study designs, incorporation of novel clinico-genomic databases such as GENIE, and advanced analytical approaches. These findings suggest the value of RWE has been increasingly recognized by the oncology research community and that RWE is being used to provide critical insights and inform patient care. Given FDA's recent guidance on RWE to support regulatory decision-making, this trend will likely continue.
[1] Azad Fet al. Longitudinal trends of real-world evidence (RWE) reporting in oncology conferences: An 11-year ASCO Annual Meeting analysis.

#6465 A population-based analysis of brain metastasis burden and management in 8705 small cell lung cancer patients.

K. Gaebe[1], A. W. Erickson[1], S. Chen[2], A. Sahgal[3], B. H. Lok[4], K. K. W. Chan[3], S. Das[5];
[1]University of Toronto, Toronto, ON, Canada, [2]Queens University, Kingston, ON, Canada, [3]Sunnybrook Health Sciences Centre, Toronto, ON, Canada, [4]Princess Margaret Cancer Centre, Toronto, ON, Canada, [5]St. Michael's Hospital, Toronto, ON, Canada

Introduction: Patients with small cell lung cancer (SCLC) have historically been characterized by poor overall survival (OS) and high risk for brain metastases (BM), but large-scale real-world evidence on clinical presentation and treatment in this population is lacking.
Methods: The aim of this study was to describe the clinical characteristics and outcomes of patients with SCLC and BM in Ontario, Canada. This retrospective cohort study included all patients in Ontario, Canada, who were diagnosed with SCLC between April 2010 and March 2018. Data were analyzed between June 2022 and July 2023. Kaplan-Meier and multivariable Cox regression analyses were performed to compare overall survival (OS) between patient cohorts stratified by disease stage, BM diagnosis, or first-line intracranial treatment modality.
Results: 8705 patients were included. Median age at diagnosis was 68 years (range 18-103). Median OS of all patients was 7.46 months (95% confidence interval, CI, 7.23-7.69). 32% (n=2686) of patients developed BM (synchronous, 43.7%; asynchronous, 56.3%) and had median OS of 9.76 months (95% CI, 9.36-10.22). 102, 1654, and 880 patients received stereotactic radiosurgery (SRS), whole brain radiation therapy (WBRT), and no treatment, respectively, for their BM in the first-line setting or after prophylactic cranial irradiation (PCI). In propensity score-matched analyses, OS was equivocal between SRS- and WBRT-treated cohorts among patients who did not receive PCI (hazard ratio, HR, 1.18, 95% CI, 0.75-1.81) and those who received PCI prior to BM development (HR, 0.77, 95% CI, 0.53-1.13).
Conclusions: Survival for patients with SCLC remains poor, and many patients present with BMs. With careful selection, patients with SCLC may benefit from SRS treatment.

#6466 Multi-omics analysis of molecular characteristics and transformation mechanisms of stage I-III micropapillary lung adenocarcinoma.

K. Shao[1], S. Gao[1], F. Tan[1], A. Shao[2], X. Feng[1], Q. Xue[1], Y. Qu[1], B. Zheng[1], W. Zheng[1], H. Chen[3], Q. Ou[3], **H. Tang**[3];

[1]National Cancer Center/National Clinical Research Center for Cancer/Cancer Hospital, Chinese Academy of Medical Sciences and Peking Union Medical College, Beijing, China, [2]Columbia University Irving Medical Center, Vagelos College of Physicians and Surgeons, New York, NY, [3]Nanjing Geneseeq Technology Inc., Nanjing, China

Background: The micropapillary pattern (MIP) is recognized as a high-grade histological subtype in lung adenocarcinoma (LUAD), with its presence often indicative of a poorer prognosis. Despite distinctive molecular characteristics of MIP, there is a research gap regarding the molecular mechanisms underlying micropapillary transformation and prognosis factors for micropapillary LUAD.

Methods: Surgically resected tumor samples from 101 patients with stage I-III LUAD and MIP components exceeding 30% were collected. The tumor samples were microdissected to separate MIP components from non-MIP components, and both fractions underwent RNA and DNA whole-exome sequencing (WES). The molecular profiles between MIP and non-MIP components, along with MIP-naïve LUAD tissues from an external cohort, were compared. Associations between molecular characteristics and recurrence-free survival were also assessed.

Results: The genomic landscapes of MIP and non-MIP components within tumor tissues featuring MIP patterns exhibited remarkable similarity. At the transcriptomic level, MIP components displayed elevated PRB4 expression (FDR < 0.001), an up-regulated cell cycle pathway (P = 0.004), and reduced natural killer cell-mediated cytotoxicity (P = 0.066). Nevertheless, in comparison to MIP-naïve LUAD tissues, the MIP components showed higher chromosomal instability (P < 0.001) and revealed eighteen enriched somatic alterations, encompassing EGFR mutations, EGFR amplifications, and CDKN2A/CDKN2B deletions, all linked to up-regulations in cell proliferation pathways and down-regulated immune pathways. In the context of MIP transformation, shared mutations were observed in 97.8% (91/93) of patients between MIP and non-MIP components within the same tissues, suggesting a common origin. The subclonal fractions were comparable between paired MIP and non-MIP components, while a significant co-occurrence of EGFR amplification, CDKN2A deletion, and CDKN2B deletion was identified in MIP components. A comprehensive analysis combining differential gene expression and Cox analysis, employing a both-direction stepwise Akaike Information Criteria selection, identified the high expressions of five genes (*GALNT4, MIAT, FOSL1, LAT2, SMN2*) as adverse factors associated with the recurrence of micropapillary LUAD.

Conclusions: We conducted an in-depth analysis of the molecular characteristics and transformation mechanisms of micropapillary lung adenocarcinoma, employing microdissection techniques to investigate at both genomic and transcriptomic levels within a substantial cohort, providing insights for the precision medicine of this aggressive cancer subtype.

#6467 Causal personalized treatment estimation framework using real-world electronic health record (EHR) data to inform cancer care decisions.

Sumana Srivatsa[1], David Walsh[1], Mayada Aljehani[2], Jason Weinreb[1], Nathan Becker[1], Benjamin H. Ellis[1], Renee George[1], Xingyao Chen[2], Naim Matasci[2], Reva Basho[2], **Mitchell E. Gross**[3], Christine L. Swisher[4]

[1]The Ronin Project Inc, San Mateo, CA, [2]Ellison Institute of Technology, Los Angeles, CA, [3]Ellison Institute of Technology & University of Southern California, Los Angeles, CA, [4]The Ronin Project Inc & Ellison Institute of Technology, San Mateo & Los Angeles, CA

Background: The average treatment effects (ATEs) from randomized controlled trials often do not generalize across populations, or they are not sufficiently personalized to capture the benefits and risks to individual patients. Real-world data aids in validating and extending trial results, but can introduce biases that invalidate the causal interpretation. Here, we propose a robust statistical framework, which uses real-world EHR data to evaluate the efficacy of cancer treatments at both population and individual levels. We demonstrate the ability of our framework to deliver personalized insights in metastatic prostate cancer treatments.

Methods: We assembled a retrospective cohort of metastatic prostate cancer patients from a large academic medical center. We gathered demographic, comorbidity, cancer treatment, and outcome data from the EHR or natural language processing of clinician narratives, and social determinants of health from Census data. We used doubly robust machine learning with bootstrap standard errors to compute the ATE and personalized treatment estimates (PTEs), comparing the impact of ADT (androgen depravation therapy) + chemotherapy (ACT) and ADT + combination anti-androgen therapy (ACAT) on percentage reduction in PSA levels in metastatic prostate cancer.

Results: The baseline characteristics of our cohort are summarized in Table 1a. Our approach found that ACAT reduces PSA levels significantly more than ACT, and captured the heterogeneity in treatment effects across individuals (Table 1b). Through simulation studies, we demonstrated that any reasonable bias from unobserved confounding or missing information was small compared to the estimated treatment effects and their standard errors.

Conclusion: We presented a doubly robust framework and demonstrated its utility in analyzing real-world data, enabling us to uncover the diversity in treatment responses among individuals with metastatic prostate cancer.

Results summary

a. Baseline demographic characteristics.		
	ADT + chemotherapy N = 302	**ADT + combination therapy N = 114**
Treatments	Any ADT + Docetaxel or Cabazitaxel	Any ADT + Abiraterone or apalutamide or Enzalutamide
Age		
Mean (SD)	69.3 (8.76)	66.7 (8.17)
Median [Min, Max]	69.0 [47.0, 94.0]	66.5 [46.0, 86.0]
Race		
Asian	8 (2.6%)	2 (1.8%)
Black or African American	48 (15.9%)	7 (6.1%)
White or Caucasian	224 (74.2%)	99 (86.8%)
Other	22 (7.3%)	6 (5.3%)
Max PSA treatment start (ng/mL)		
Mean (SD)	34.9 (98.5)	83.3 (448)
b. Treatment effects estimation		
ATE (95% CI)	32.0% [24.6%, 40.8%]	
PTEs: 25th and 75th percentiles	29.0%, 34.3%	

#6468 Nodular lymphocyte predominant hodgkin lymphoma: A national cancer database analysis with focus on hispanics.

E. Toro Velez[1], D. Rosas[2], C. Velez-Mejia[1], Q. Liu[1], J. Michalek[1], A. Diaz Duque[3];
[1]UT Health Science Center at San Antonio, San Antonio, TX, [2]Memorial Healthcare System, Pembroke Pines, FL, [3]Mays Cancer Center, San Antonio, TX

Background: Nodular lymphocyte-predominant Hodgkin lymphoma (NLPHL) is a rare and distinct subtype of Hodgkin Lymphoma.(PMID 26149294) 80% manifest at early stages, with a male and black race predilection.(PMID 26149195) Previous analysis have shown similar survival of Hispanics (HI) compared to Non-Hispanics (NH).(J Clin Oncol 10.1200/JCO.2023.41.16_suppl.e19512) This National Cancer Database (NCDB) analysis aims to clarify how sociodemographic factors affect presentation and survival in HI vs NH patients with NLPHL. **Methods:**Data were analyzed on NLPHL patients in the United States reported to the NCDB 2004-2019. Demographic and treatment characteristics were compared between ethnic groups. Kaplan-Meier and Cox regression analyses were used to compare overall survival (OS) between HI and NH populations. Multivariate analysis and propensity score matching was performed. **Results:**Of 5517 of NLPHL patients, 379 were HI, and 4904 NH. Male gender and white race predominated for both. HI were diagnosed at a younger median age of 44 years (y) vs 48 y for NH, p=0.001. Most patients were diagnosed between years 2016-2019. Stage I predominated for both, p<0.001. As to Charlson-Deyo score ≥2, both HI and NH had 4%. Private insurance as primary payer was the most prevalent type for HI (53%) and NH (65%). HI had a higher percentage of unknown/uninsured, 12% vs 6% for NH, p<0.001. In relation to census median income (2008-2012), the most prevalent bracket for HI (27%) was $48,000-$62,000, and for NH (35%) was >$63,000. Regarding median income of <$38,000, HI were 29% vs 16% for NH, p<0.001. For median distance in miles (mi) between the patient's residence and the hospital that reported the case (great circle distance), HI lived at a median of 6.3mi, vs NH at median of 9.5mi. Majority of HI (56%) were treated at Academic/Research programs; while most of NH (39%) were treated at Comprehensive Community Cancer programs, p<0.001. On survival analysis, the survival probability at 2, 5 and 10 y for HI was 96%, 92%, 86%, vs for NH was 96%, 92%, 84%, respectively. The median survival time wasn't reached for both HI and NH, and no statically significant difference was seen, p=0.57. On multivariate analysis, HI was not associated with worse OS (HR 0.76, CI 0.44-1.31, p=0,33). The propensity matched analysis confirmed not reached OS on both cohorts. **Conclusion:**NLPHL is a disease that affects young males, at early stages, for both HI and NH. Unlike previous studies, in this analysis white race predominates; which could be explained by the increase in reported cases over years. Despite HI having more uninsured population with lower median income quartiles, this wasn't a barrier to access care at academic/research programs. Although no difference in OS was seen among ethnicities, there is a tendency that might favor HI. More studies are needed to determine if specific demographic factors truly influence survival in NLPHL.

#6469 The association of mismatch repair gene alterations with elevated tumor mutational burden in microsatellite stable gastrointestinal cancers.

C. D. O'Donnell, M. Zhu, H. Xie;
Mayo Clinic, Rochester, MN

Background: Benefit from single-agent immune checkpoint inhibitor has been observed in 5-10% of the patients with microsatellite stable (MSS) gastrointestinal (GI) cancers. However, a reliable predictive marker to immune checkpoint inhibitor has not been discovered in this patient population. We sought to assess the incidence of mismatch repair (MMR) gene alterations and their association with tumor mutational burden (TMB) in MSS GI cancers.
Methods: This is a retrospective cohort study of patients with advanced GI cancer who had molecular profiling of the tumor using either Guardant360 blood-based or Tempus tissue next generation sequencing (NGS) platforms between 2020 and 2023. We assessed four MMR genes including *MLH1*, *MSH2*, *MSH6* and *PMS2* for alterations. Continuous variables were summarized as median and interquartile range (IQR) and compared using Mann-Whitney test. Categorical variables were summarized as counts and proportions and compared using Fisher's exact test.
Results: A total of 2920 patients with Guardant360 were included with a median age of 65 (IQR: 56-73) years. 870 (30%) patients had pancreas cancer; 846 (29%) patients had colorectal cancer; 688 (24%) patients had biliary tract cancers; and the rest had other GI cancers. Among patients evaluable for microsatellite instability (MSI) status, 58 patients (2%) had MSI-high GI cancers, 31 (53%) of whom had MMR gene alterations. 2445 (98%) patients had MSS GI cancers, 130 (5.3%) of whom had MMR gene alterations. Patients with MSS GI cancers bearing MMR gene alterations had a median age of 70 (IQR: 62-75) years, significantly older than those without MMR gene alterations ($p<0.001$). In addition, patients with MMR gene alterations had significantly higher median blood TMB of 11 (IQR: 7.4-16) mut/Mb compared to 7.7 (IQR: 4.8-11) mut/Mb in patients without MMR gene alterations. In MSS GI cancers, MMR gene alterations are more commonly associated with the presence of alterations in *APC* ($p=0.03$), *TP53* ($p=0.01$), *CTNNB1* ($p<0.001$) and *SMAD4* ($p=0.01$). 1453 patients with GI cancer and Tempus tissue NGS data were included as a validation cohort. They had comparable demographics with the Guardant360 cohort. 14 (1.6%) of 896 patients with MSS GI cancers had MMR gene alterations, significantly fewer ($p<0.001$) than those found in the Guardant360 cohort. Patients with MMR gene alterations and wild type POLE had significantly higher ($p=0.001$) median TMB of 9.8 (IQR: 4.8-14) mut/Mb compared to 4.7 (IQR: 3.2-6.3) mut/Mb in patients without MMR gene alterations.
Conclusions: MMR gene alterations can be identified by clinical NGS platforms in a small proportion of patients with MSS GI cancers. They are associated with elevated TMB, which may suggest a hypermutated profile serving as a basis for potential role of immune checkpoint inhibitor in MSS GI cancers.

#6470 Real-world analysis of insurance status and survival in patients with selected GI cancers.

R. AbuAyed[1], J. Schwanke[1], B. Patterson[1], M. White[1], S. Marmor[1], E. Jensen[1], C. Tignanelli[1], E. Lou[2], A. Prakash[2];
[1]University of Minnesota Medical School, Minneapolis, MN, [2]University of Minnesota, Minneapolis, MN

Background: Health insurance is a critical determinant of healthcare access and outcomes in gastrointestinal (GI) cancers. Epidemiological data have shown that insurance-associated healthcare outcomes vary by diagnosis, geographic location, and demographics. Thus, it is critical for cancer providers to understand local impacts of insurance status on patient outcomes. Here, we present real-world outcomes for pancreatic, hepatobiliary, and colorectal cancer (CRC) patients in 11 Midwest hospitals based on insurance status.
Methods: We identified patients diagnosed with colorectal, pancreatic, and hepatobiliary cancers within 11 Midwest hospitals from 2011-2021 with North American Association of Central Cancer Registries data. Health insurance was defined as private, Medicaid, Medicare, and uninsured. Effect of insurance status at diagnosis on overall survival (OS) in selected cancers combined and by cancer type were calculated using a Cox proportional hazard (CoxPH) model controlling for age, sex, race, stage, time to treatment initiation (TTI), and Charlson Comorbidity Index (CCI). We evaluated differences in TTI by insurance status using t-tests. We analyzed stage and treatment modality by insurance status using chi-square tests. Post-hoc analysis of TTI by OS used CoxPH.
Results: Relative to private insurance, Medicaid and Medicare insurance status significantly reduced OS for all selected GI cancers combined (HR 1.38, 95% CI 1.17 - 1.62 and HR 1.25, 95% CI 1.11 - 1.40, respectively; $p<0.001$) and for CRC (HR 1.49, 95% CI 1.12 - 1.98 and HR 1.28, 95% CI 1.06 - 1.54, respectively; $p<0.01$). Uninsured patients had significantly reduced OS only for pancreas cancer (HR 6.36, 95% CI 2.56 - 15.8; $p<0.001$). No significant associations between insurance status and OS were noted in Hepatobiliary cancer. TTI was significantly associated with insurance status ($p<0.001$) and mean TTI for Medicaid (35.8 days) and Medicare (27.9 days) patients was longer than mean TTI for privately insured patients (23.3 days; $p<0.01$). TTI for uninsured patients was not significantly different than for privately insured. Analysis of TTI and OS showed no increased hazard for patients with TTI of 36 days versus 23 days (HR 0.87, 95% CI 0.75 - 1.02; $p=0.085$). Treatment modality and stage did not differ as a function of insurance status in this dataset.
Discussion: Our results expand previous work by demonstrating a survival impact for GI cancer patients with Medicaid or Medicare insurance. This disparity persists despite controlling for known prognostic factors such as age, stage, CCI, and TTI. Notably, TTI varied by insurance suggesting it may account for a portion of this disparity but did not independently drive survival. Further work is required to identify and develop targeted interventions to address other drivers of reduced survival in those without private insurance.

#6471 Trends in chemotherapy utilization in acute myeloid leukemia (AML) in last 15 years.

P. Dhakal[1], B. Loeffler[1], A. Ravindra[1], A. Pyakuryal[2], V. R. Bhatt[3];

[1]University of Iowa, Iowa City, IA, [2]Pokhara University, Pokhara, Nepal, [3]University of Nebraska Medical Center, Omaha, NE

Introduction: Chemotherapy (Chemo) can relieve symptoms and improve quality of life and survival in AML, including in many older and frail adults. However, in a prior study from the US, almost a quarter of patients (pts) with new diagnoses of AML between years (yrs) 2003 and 2011 did not receive chemo (Bhatt et al., Blood Advances, 2018). Our study examined trends in chemo utilization in the last 15 yrs to test the hypothesis that chemo use has increased in more recent yrs. We also examined any disparities in chemo use.

Methods: We utilized the National Cancer Database to identify 78,864 pts diagnosed with AML between 2004 and 2019 and divided them into 2 cohorts based on date of diagnosis, 2004-2010 and 2011-2019. We used logistic regression to estimate effect of demographic and disease characteristics on odds of receiving chemo and evaluate differences in these effects between the constructed patient cohorts.

Results: Seventy-seven percent of total pts received chemo. Compared to 73% in 2004, 81% of pts received chemo in 2019. The receipt of chemo declined with increasing age with higher use of chemo in all groups in 2011-2019 compared to 2004-2010: >80 (yrs)= 40 vs 33%, 71-80 yrs= 72 vs 63%, 60-70 yrs= 87 vs 84%, 41-59 yrs= 93 vs 92%, and 18-40 yrs = 95 vs 94%.The receipt of chemo was lowest in white pts overall; in black pts, receipt of chemo increased in 2011-2019

compared to 2004-2010: black= 83 vs 76%, white= 78 vs 75%, and others 83 vs 83%. The receipt of chemo was lowest in therapy-related (t)-AML in 2011-2019 and 2004-2010: t-AML 64 vs 60%, acute promyelocytic leukemia= 88 vs 87%, core binding factor AML 93 vs 88% and other 77 vs 74%. In multivariable analysis, the odds of receiving chemo increased in 2011-2019 compared to 2004-2010 in all pts, particularly in older adults. Compared to white, black pts had similar odds of receiving chemo in 2004-2010, but odds were higher in 2011-2019 (Odds ratio, 1.2, 95% confidence interval, 1.1-1.3. Pts with t-AML were less likely to receive chemo compared to all other subtypes in 2004-2010 and 2011-2019. Female sex, lower income, public insurance, higher comorbidity score, and shorter distance to treatment facility were associated with a lower likelihood of receiving chemo; however, chemo utilization did not differ over the two time periods based on these variables.

Conclusion: To our knowledge, this is the largest scale analysis of chemo utilization in AML in real-world practice. Chemo receipt increased significantly over the yrs, particularly among older adults, black pts, core binding factor, and t-AML. These recent trends are encouraging and represent novel findings. Despite these results, healthcare disparity based on sex, socioeconomic, and healthcare system factors continues to persist. In addition to developing safer and more effective chemo regimens, other innovative strategies to tackle these disparities are crucial to improve outcomes.

#6472 Response to PARP inhibitors in patients with breast cancer metastatic to the central nervous system.

S. Lee[1], R. Bansal[2], M. E. Hughes[3], A. E. D. Van Swearingen[2], H. N. Moore[2], D. O. Kamson[1], S. Sahebjam[1], G. Kirkner[3], A. Gorfinkel[3], S. Sammons[3], N. U. Lin[3], C. Anders[2], C. A. Santa-Maria[1];

[1]Johns Hopkins University, Baltimore, MD, [2]Duke Cancer Institute, Durham, NC, [3]Dana-Farber Cancer Institute, Boston, MA

Background: Central nervous system (CNS) metastasis from breast cancer can be challenging to treat due to the limited blood brain barrier penetration of many systemic therapies. PARP inhibitors (PARPi) block single-strand DNA break repairs and have activity in cancers with homologous recombination repair deficiency; they are FDA approved for patients with metastatic HER2 negative breast cancer with germline BRCA1/2 mutations. While preclinical studies suggest that PARPi have CNS penetration, clinical data is limited. The goal of our study is to describe the clinical benefit of PARPi in patients with breast cancer CNS metastasis.

Methods: This retrospective case series was conducted at three academic cancer centers (Johns Hopkins, Dana-Farber, and Duke) and included patients with the following criteria: (1) age≥18 years with a breast cancer diagnosis (any subtype); (2) diagnosis of parenchymal brain metastasis or leptomeningeal disease (LMD); and (3) received PARPi (olaparib, talazoparib) for CNS metastasis. Clinical and pathologic information were analyzed with descriptive statistics (median, range) and Kruskal-Wallis rank sum tests. Survival analysis was performed using Kaplan-Meier curves with log-rank p-values.

Results: Although this analysis includes one center's experience, we will present a combined dataset (N = 45) at the main conference. 11 patients were identified at Johns Hopkins. 4 (36.4%) were Black and 6 (54.5%) were White; 6 (54.5%) had ER+HER2- disease and 5 (45.5%) had TNBC at time of brain metastasis; 5 (45.5%) had BRCA1 mutations, 5 (45.5%) had a BRCA2 mutations, and 1 patient (9%) had a BARD1 mutation; 7 (63.6%) had brain metastasis and 4 (36.4%) had LMD. Median lines of therapy prior to PARPi was 6 [1 - 11]; 8 patients (72.7%) had previous CNS radiation (5 SRS and 3 WBRT) and 3 (27.3%) had previous CNS surgery. On average, patients remained on PARPi for 5 months [0.5 - 66], and overall survival (OS) time from PARPi to death was 16 months [2 - 66]. Time on PARPi was 5 months [2 - 66] for patients with brain metastasis and 3 months [0.5 - 10] for those with LMD (p=0.22). Duration of PARPi and OS did not differ significantly between ER+HER2- and TNBC (p=0.74 and 0.69, respectively), BRCA 1 and 2 (p=0.78 and 0.72, respectively), or brain and LMD metastasis (p=0.22 and 0.91, respectively). Black patients had significantly shorter PARPi duration and survival than White patients (PARPi 2 vs. 8 months, p=0.028 and OS 4 vs 18 months, p=0.028). Prior CNS radiation was significantly associated with longer PARPi duration and survival (PARPi 5 vs 1 month, p=0.02 and OS 17 vs. 3 months, p=0.032). Prior CNS surgery was significantly associated with longer PARPi duration, but not overall survival (PARPi 18 vs 3 months, p=0.05 and OS 28 vs. 7 months, p=0.14).

Conclusions: PARPi are associated with significant clinical benefit in patients with breast cancer CNS metastasis. Larger data series will help confirm these observations.

#6473 Evaluation of bladder cancer patients' utilization of urologic telehealth services.

S. Goldenthal, T. Posid, V. Heh, D. Denis-Diaz, H. Asif, C. Arnold, H. Gold, **T.-H. Kim**, A. Ndumele, S. Amin, M. Lierz, V. Xu, T. Cronin, A. Khuhro, C. Lee;
The Ohio State University Wexner Medical Center, Columbus, OH

Introduction: Infection control practices and public policy in response to the COVID-19 pandemic shifted healthcare practices towards a telemedicine format. Even two years after peak onset of the pandemic, many clinics, including our own institution, maintain a working telehealth option for patient visits. Our objective was to evaluate patient utilization of telehealth visits versus in-person visits at our institution and whether this was impacted by clinical stage, rural/urban status, distance from a large urban academic center, payor status, or comorbidities.

Methods: Medical Record Numbers for all patients with bladder cancer were pulled via the Qlik platform from the period 7/1/2019-2/28/2022. Chart review was conducted to pull clinical data on patients including telehealth versus in person visits, demographic data, clinical stage, comorbidities (diabetes, smoking status, BMI), rural/urban status by zip code (>50,000, <50,000 individuals) and income levels by zip code (25K-49.9K, 50K-99.9K, <100K), payor status (Medicare, Managed care, Medicaid, other government, ODRC, or self-pay), patient distance, and gas savings/carbon footprint.

Results: 430 patients completed in person visits while 268 completed telehealth visits. There was no statistically significant difference for in person visits vs. telehealth visits regarding patients' race (p=0.541), ethnicity (p=0.394) age (p=0.862), urban/rural status (p=0.507), payor status (p=0.127), mean zip code income (p=0.175), and comorbidities (p=0.626 for diabetes, p = 0.706 for smoking, p = 0.459 for BMI), and clinical stage (p=0.07). There was a statistically significant difference in mean distance (14.85 miles versus 26.86 miles, p<0.01).

Conclusion: Patients' with bladder cancer receive care from their urologist via in person visits versus telehealth at similar rates irrespective of their urban/rural status, demographics, payor status, relevant comorbidities, or relative income. Patients are more likely to engage in care with their urologist via telehealth if they live farther from a large urban academic center, which produces an economical and environmental impact via gas/time savings and reduced carbon footprint.

#6474 Real-world assessment of turn-around time for actionable variant testing in NSCLC in the community setting.

B. D'Alessio, A. Stephen, C. Cochran, C. Hager, Z. Velasco, A. Weaver, L. Jackson, J. Riley, A. Tubbs, **G. A. Pestano**;
Biodesix, Inc., Boulder, CO

Introduction: Rapid turnaround times (TAT) is a key parameter when evaluating the performance of cell free (cf) nucleic acid testing in clinical oncology practice. The purpose of this study was to evaluate the impact of the real-world factors on TAT for actionable variants in NSCLC, detected using commercially available molecular diagnostic tests. These test services are run in a single, centralized laboratory site and utilized primarily by practices in the community across the United States.

Methods: In this study, de-identified reference data was reviewed for a ddPCR test that evaluates hotspot mutations including Single Nucleotide Variants (SNV), Insertions and Deletions (INDEL), and gene fusions. The NGS panel additionally tests for Copy Number Amplification (CNA) mutations. Specimen processing was initiated when the specimen was entered into the Laboratory Information System (LIS) and ended when the test result was ready for release. The turnaround time evaluation excluded holidays, and weekends unless the start or end-point occurred on a non-business day.

Results: In total, 35,441 specimen results were analyzed. Specimens were typically received in the laboratory within 24 hours of being shipped (88% in 24 hours). Tests by ddPCR included 30,490 (86%) results, while NGS testing accounted for 4,951 (14%) of results. The average analytic lab processing TAT for the ddPCR and NGS test ranged between 2 and 3 days (ddPCR median = 24.5 hours; NGS panel median = 69.7 hours). When no information was missing on the specimen test request form, the turn-around time for the ddPCR tests averaged 30.2 hours and NGS panel averaged 66.2 hours. The percentage of missing or inaccurate information was similar when test requests were initially received. The largest impact factor impacting initiation of specimen processing was information related annotation of the stage of cancer, followed by demographic information related to patient and specimen identifiers.

Conclusion: The focus on rapid turnaround times from specimen collection to results released is critical in oncology. Site and patient information, shipping methods, technologies and workflows used in the laboratory are all part of the test process and impact the release of potentially actionable results. Our study has highlighted that rapid turnaround of results is highly feasible for molecular tests being sent out from community practices across the US to a centralized reference laboratory. Specifically, actionable variant results related to NSCLC were successfully detected in the laboratory and were ready for delivery in 2 to 3 days. Automated methods for parsing the information necessary for test requests and delivery will continue to be important in maintaining rapid test result turnaround times.

#6475 Leveraging real-world pancreatic cancer datasets to drive drug discovery and patient health.

K. Abdilleh[1], **Z. Worman**[2], R. Beck[2], C. Fisher[2], D. Sain[2], J. DiGiovanna[2], L. Matrisian[1], S. Doss[1], B. Davis-Dusenbery[2];
[1]Pancreatic Action Network, Manhattan Beach, CA, [2]Velsera, Cambridge, MA

Pancreatic cancer is the third leading cause of cancer-related death in the United States. Current therapeutic options offer a dismal overall survival with the 5-year survival at just ~12%. Analysis of the clinical and molecular underpinnings of pancreatic cancer is critical to developing both early detection methodologies as well as novel therapeutic options. The aggressiveness and deadly nature of this disease warranted the development of a data repository and analysis system dedicated to pancreatic cancer data. The Pancreatic Cancer Action Network's (PanCAN) SPARK platform is a cloud-based data and analytics platform, powered by Velsera, that integrates real-world patient health data from PanCAN research initiatives and accelerates research by making pancreatic cancer data easier to access and use. Encompassing clinical, imaging, and genomics data from over 600 patients with pancreatic cancer within PanCAN's Know Your Tumor ® (KYT) precision medicine service, the SPARK platform connects with petabytes of publicly available cancer data via the Cancer Genomics Cloud (CGC), also powered by Velsera. The CGC is part of NCI's Cancer Research Data Commons (CRDC), a cloud-based data science infrastructure that connects data with analytics tools to allow researchers to share, integrate, analyze, visualize, and drive scientific discovery.

Here, we demonstrate the application of these datasets by providing a case study demonstrating how to combine and enrich data to accelerate pancreatic cancer research. Currently, the genomic and proteomic data available on CRDC amounts to 402 and 304 cases of pancreatic tumor samples, respectively. We will use the capabilities of the SPARK and CGC platforms, which provide ready-to-use tools for multi-omics analysis that require no coding knowledge. Using the KYT and CRDC open-access pancreatic cancer data, we aim to demonstrate how to perform integrated analysis of data from diverse scientific domains, and share with collaborators all in one space, streamlining and increasing the potential for new scientific discoveries.

Further expansion of the PanCAN and CGC datasets will undoubtedly provide a more comprehensive understanding of pancreatic cancer tumor biology. SPARK and CGC's cloud based computation infrastructure, along with numerous available cancer datasets and easy-to-use multi-omics data processing workflows and data analytic tools will be instrumental in this process.

#6476 Solving the real-world data challenge: A hybrid resourcing model to curate RWD at scale.

J. Rudolph[1], K. L. Kehl[2], M. Bernstein[3];

[1]Memorial Sloan Kettering Cancer Center, New York, NY, [2]Dana-Farber Cancer Institute, Boston, MA, [3]Vasta Global (an Omega Healthcare company), Boca Raton, FL

Introduction: As cancer treatments become more complex, the need for structured real-world data (RWD) to support clinical research is critical. However, researchers often lack resources to curate data in-house. Organizations are challenged with timely data curation at the quality and scale needed for real world applications.

Methods: As members of the AACR Project GENIE (Genomics Evidence Neoplasia Information Exchange) Biopharma Collaborative (BPC), Memorial Sloan Kettering Cancer Center (MSK) and Dana-Farber Cancer Institute (DFCI) partnered with Vasta Global, an Omega Healthcare company, to build a model for curating RWD at scale, allowing for cost-effective RWD curation while leveraging expert resources and best practices. The approach includes managing a hybrid onshore and offshore team with clear communication and recurring check-ins, cross-training curators on different EHRs to reallocate Vasta Global resources and maintain project pace, building program-specific clinical data curation training, establishing QA and delivery methods, standardizing data curation, assigning productivity standards, aligning data quality practices and benchmarks, and developing data visualizations and analytics to show progress and insights.

Results: In Phase 1 of the AACR GENIE BPC, data was curated from four sites: MSK, DFCI, Vanderbilt Ingram Cancer Center (VICC) in Nashville, and Princess Margaret Cancer Centre, University Health Network (UHN) in Toronto. During Phase 1, MSK and DFCI, with Vasta Global's assistance, delivered high-quality RWD for 6,475 patients (NSCLC = 1,591; CRC = 1,264; Bladder = 639; Breast = 957; Pancreas 989; and Prostate = 1,035). All data for these cohorts will be publicly available by Spring 2024 in the AACR Project GENIE cBioPortal. MSK and DFCI generated usable and fit-for-purpose RWD to help advance oncology clinical decision-making and data sharing.

Conclusion: Accelerating RWD curation will empower the oncology community to leverage data-driven insights and advance treatment opportunities for cancer patients. Working alongside lead sites, a partner like Vasta Global enables researchers to leverage extensive expertise in the BPC data model, allowing for consistency and scalability of the BPC program. In this hybrid model, research partners can curate RWD in a cost-effective way, while remaining focused on core research responsibilities.

#6477 Modulators of hospital length of stay after intracranial neoplasm excision.

J. Hsiung[1], K. Taneja[2], L. Ladehoff[3], K. Patel[4], E. Toloza[5];
[1]Highland Park High School, Highland Park, NJ, [2]Stony Brook University, Stony Brook, NY, [3]University of Florida, Gainesville, FL, [4]Cooper Medical School, Camden, NJ, [5]Moffitt Cancer Center, Tampa, FL

Purpose: Intracranial neoplasms are the leading cause of cancer death among men under 40 years old. A major part of the standard of care is excision of the tumor, but there is a lack of robust large-patient studies of outcomes for these patients.
Methods: The Nationwide Inpatient Sample was queried from 2018 to 2020 to identify patients with an intracranial neoplasm. Multivariable linear regression with patient- and hospital-level characteristics as covariates was used to identify factors associated with long hospital stays.
Results: From 2018 to 2020, there were 97,795 hospital encounters with a primary diagnosis of an intracranial neoplasm. Of these patients, 64.6% underwent a tumor excision procedure during their hospital visit. The average age of these patients undergoing excision was 57.80.2 years. Most patients were male (58.6%), white (79.1%), private insurance beneficiaries (46.3%), and of the highest income quartile (26.8%). These patients most commonly presented to hospitals in the West (34.9%), with a medium number of beds (36.4%), and presented to rural hospitals (41.7%). The most common locations of these neoplasms were the frontal (29.1%), temporal (21.3%), and parietal (12.1%) lobes. Neoplasms in more than one location in the brain occurred in 4.5% of patients. Multivariable linear regression identified the following factors as significantly associated with longer hospital stays: identifying as Black (beta=2.08; p<0.001), identifying as an Asian or Pacific Islander (beta=1.22; p=0.017), being a Medicaid beneficiary (beta=2.25; p<0.001), and being uninsured (beta=1.63; p<0.001). Having a neoplasm in the cerebral ventricle (beta=4.93; p<0.001), cerebellum (beta=2.81; p<0.001), or brain stem (beta=3.45; p<0.001), and having multiple neoplasms (beta=1.85; p=0.008) were also associated with longer hospital stays. Interestingly, having a parietal (beta=-0.54; p=0.011) or occipital (b=-0.99; p<0.001) lobe neoplasm was associated with shorter hospital stays.
Conclusion: Intracranial neoplasms are deadly condition and excision of tumor is a important life-saving treatment option. In this study, we demonstrated that location of neoplasm, race, and insurance status are significant modulators of the length of a hospital stay after surgery.

#6478 Intracranial neoplasms: Disparities in access to care.

J. Hsiung[1], K. Taneja[2], L. Ladehoff[3], K. Patel[4], E. Toloza[5];
[1]Highland Park High School, Highland Park, NJ, [2]Stony Brook University, Stony Brook, NY, [3]University of Florida, Gainesville, FL, [4]Cooper Medical School, Camden, NJ, [5]Moffitt Cancer Center, Tampa, FL

Purpose: Excision of intracranial neoplasms is a life-saving procedure. However, there is not much research that has demonstrated how demographic variables interact with a patient's access to healthcare for intracranial neoplasms.
Methods: The Nationwide Inpatient Sample was queried from 2018 to 2020 to identify patients with an intracranial neoplasm. Multivariable logistic regression with patient- and hospital-level characteristics as covariates was used to identify factors associated with receiving an intracranial tumor excision.
Results: From 2018 to 2020, there were 97,795 hospital encounters with a primary diagnosis of an intracranial neoplasm. Of these patients, 64.6% underwent a tumor excision procedure during their hospital visit. The average age of all patients with intracranial neoplasm was 58.90.2 years. Most intracranial neoplasm patients were male (59.0%), White (73.8%), Medicare beneficiaries (45.1%), and of the highest income quartile (26.4%). These patients commonly presented to hospitals in the West (35.0%), with a medium number of beds (36.4%), and to rural hospitals (39.1%). The most common locations of these neoplasms were the frontal (18.9%), temporal (12.0%), and parietal (7.5%) lobes. Neoplasms in more than one location in the brain occurred in 5.8% of patients. Multivariable logistic regression identified the following factors as significantly associated with a decreased odds ratio (OR) of receiving an excision surgery: identifying as Black (OR=0.63; p<0.001), Hispanic (OR=0.82; p=0.001), or Asian or Pacific Islander (OR=0.78; p=0.009) and being a Medicaid Beneficiary (OR=0.84; p=0.008). Presenting to a hospital in the South (OR=1.30; p<0.001) or in the West (OR=1.38; p<0.001) were associated with higher chances of having a surgical excision.
Conclusion: There are very substantial differences in access to care for brain cancer patients. Race and insurance status are related to a patient's chance of receiving tumor excision therapy.

#6479 Metastases in uveal melanoma patients: Trends and risk factors.

A. A. Beneke[1], **K. Taneja**[2], L. Ladehoff[3], K. Root[1], E. Toloza[4];

[1]University of Florida, Gainesville, FL, [2]Stony Brook University, Stony Brook, NY, [3]University of South Florida, Tampa, FL, [4]Moffitt Cancer Center, Tampa, FL

Purpose: Uveal melanoma has a high tendency to metastasize. Due to its rarity, there has not been large population studies that have demonstrated the effect of demographic variables on a patient's risk to have metastases.

Methods: The Nationwide Emergency Department Sample was queried from the last quarter of 2015 to 2019 to identify patients with a diagnosis of uveal melanoma. Multivariable logistic regression, with patient- and hospital-level characteristics as covariates, was used to identify factors associated with a higher chance of developing a metastasis and specific metastasis locations.

Results: From the last quarter of 2015 to 2019, there were 7,561 ED encounters with a diagnosis of uveal melanoma. Of these patients, 5.8% had at least one metastasis. Most patients with a metastasis were at least 65 years of age (47.1%), male (54.4%), a Medicare beneficiary (45.2%), and belonged to a family in the highest income quartile (29.7%). The median age of these patients was 61 years (IQR: 32-74). Most patients presented to hospitals in the South (40.7%), with a Trauma Level I designation (56.1%), and to a metropolitan teaching hospital (72.9%). The most common sites of metastasis were liver (17.0%), brain (5.3%), and bone (2.0%). Multivariable logistic regression identified the following factors to be associated with increased risk of developing a metastasis: private insurance (odds ratio [OR]=1.62; p=0.012), highest income quartile (OR=2.30; p<0.001), and 2nd highest income quartile (OR=1.78; p=0.002). The following factors were associated with higher odds of developing a liver metastasis specifically: no-charge/charity work (OR=15.8; p=0.012), highest income quartile (OR=1.99; p=0.003), and second highest income quartile (OR=1.66; p=0.035). Presenting to a Trauma Level I hospital was associated with decreased risk of developing a liver metastasis (OR=0.57; p=0.016). Belonging to the highest income quartile was associated with a higher chance of developing a brain metastasis (OR=2.13; p=0.023) or a bone metastasis (OR=2.74; p=0.045). Among patients with a metastasis, the in-hospital mortality rate was 8.3%.

Conclusion: Metastasis is an important complication to monitor in uveal melanoma patients. In this study, we have demonstrated that income and insurance status are factors that are associated with higher rates of metastases. Physicians should place special attention to these groups to ensure that metastases are minimized.

#6480 In-hospital mortality risk factors for uveal melanoma patients in the emergency department.

A. A. Beneke[1], **K. Taneja**[2], L. Ladehoff[3], K. Root[1], E. Toloza[4];
[1]University of Florida, Gainesville, FL, [2]Stony Brook University, Renaissance School of Medicine, Stony Brook, FL, [3]University of South Florida, Tampa, FL, [4]Moffitt Cancer Center, Tampa, FL

Purpose: A considerable amount of uveal melanoma patients present to the emergency department (ED) for a complication related to their primary tumor. However, there is not much research into the primary reasons for these patients to present to the ED and their outcomes.
Methods: The Nationwide Emergency Department Sample was queried from the last quarter of 2015 to 2019 to identify patients with a diagnosis of uveal melanoma. Multivariable logistic regression, with patient- and hospital-level characteristics as covariates, was used to identify factors associated with increased risk of in-hospital death.
Results: From the last quarter of 2015 to 2019, there were 7,561 ED encounters with a secondary diagnosis of uveal melanoma. Most patients were at least 65 years of age (43.5%), male (52.5%), and a Medicare beneficiary (44.2%), or belong to a family in the 3rd income quartile (25.6%). The median age of these patients was 61 years (IQR: 32-74). Most patients presented to hospitals in the South (40.8%), with a Trauma Level I designation (47.2%), and to a metropolitan teaching hospital (72.6%). The most common diagnosis for presentation to the ED were the following general clinical categories: blood disorders (7.1%), genitourinary tract disorders (5.1%), infections (6.0%), respiratory diseases (9.0%), nervous system disorders (4.8%), endocrine/nutrition disorders (4.3%), and vascular disorders (8.3%). The rate of metastatic uveal melanoma was 5.8%. The rate of in-hospital mortality was 3.6%. In a multivariable logistic regression identified the following clinical categories as factors associated with a higher risk of in-hospital death: infections (odds ratio [OR]=10.22; p<0.001), metastases (OR=10.22; p<0.001), genitourinary tract disorders (OR=7.05; p<0.001), respiratory diseases (OR=3.31; p=0.031), and vascular disorders (OR=3.14; p=0.044). Nervous system, blood, and endocrine/nutrition disorders were not associated with a higher rate of in-hospital mortality. The only demographic variable associated with a higher risk of in-hospital death was being part of the top income quartile (OR=3.10; p=0.14).
Conclusion: Physicians have to be mindful of different complications associated with uveal melanoma that can lead to presentation to the ED and possible in-hospital death. Specifically, physicians need to be mindful of infections, metastases, genitourinary tract disorders, respiratory diseases, and vascular disorders in these patients.

CLINICAL RESEARCH: Targeting Kinase and ERK Pathways
Poster Session

#6484 Overcoming resistance to EGFR-TKI in NSCLC by simultaneously inhibition of anti-apoptotic proteins.

Sandra Weller[1], Tobias Beigl[1], Frank Essmann[1], Annika Harsch[1], Hans-Georg Kopp[2], Tom Ekstrom[1]

[1]Robert Bosch Center for Tumor Diseases (RBCT), Stuttgart, Germany,[2]Robert Bosch Center for Tumor Diseases, Stuttgart, Germany; Robert Bosch Hospital, Stuttgart, Germany

Lung cancer is the second most common cancer worldwide with 1.8 million deaths in 2020 being the leading cause of cancer related death. With 86% of cases, non-small cell lung cancer (NSCLC) is the most prominent subtype. The survival rate improved over the past 20 years by application of targeted therapies. Driver mutations in protein kinases such as the epidermal growth factor receptor (EGFR) are frequent and have evolved as therapeutic targets in anti-cancer therapy. Inhibitors of receptor tyrosine kinase (RTKIs), prominently EGFR-TKIs, are effective in anti-cancer therapy but tumor evolution inevitably generates resistance. Thus, strategies for the treatment of patients with acquired resistance to RTKIs remains an urgent need. Resistance in solid tumors is overcome by a combination of bortezomib with the BH3-mimetic ABT-199 (Muenchow et al. 2020). Also, overcoming ALK-TKI resistance in NSCLC was described by Tanimoto et al. (2021) by proteasome inhibiton that mediates induction of NOXA. Furthermore, the novel described BCL-2 independent activity of ABT-199 to transactivate NOXA expression (Weller et al. 2022) represents a generally active principle by combining drugs with independent mechanism of action. We hypothesize, that combined treatment of EGFR-TKI Osimertinib (OSI) with BH3-mimetics enhances sensitivity to apoptosis induction. To explore this hypothesis, we investigated cell death induction by combined administration of OSI and BH3-mimetics or PIs in NSCLC differing in their mutational status. In addition, we analyzed the expression of BCL-2 family proteins and their relevance and regulation during RTKI-induced cell death by RNA sequencing and Western Blot. These analyses will be performed in cellular model systems of NSCLC with specific resistance mediating mutations of EGFR or activated parallel survival pathways. We found that BCL-2 inhibitors enhance efficacy of OSI in NSCLC, resulting in synergistic cell death induction. Additionally, the sensitivity to BCL-2 inhibitors tends to increase in OSI-resistant NSCLC. Western Blot analysis and RNA sequencing data of OSI-resistant NSCLC identified BCL-2 overexpression and an EMT signature as resistance-mediating mechanisms, which can be overcome by combination of OSI with BCL-2 inhibitors. Indeed, our data suggest that combination of OSI with BCL-2 inhibitors disrupts resistance to OSI in NSCLC. We propose that BCL-2 inhibitors sensitize OSI-resistant NSCLC to effectively induce cell death. Thus, studying the molecular mechanism of synergistic efficacy of RTKI/BCL-2 inhibitor combination therapies, should prompt future efforts in the clinical evaluation of combinatorial regimens. We hypothesize that a general therapeutic concept which relies on simultaneous blocking of driver mutations and survival-promoting BCL-2 proteins represents a generally active principle of a tumor-agnostic mechanism of action.

#6485 Profile guided low dose drug combination strategies and kinase activities with prognostic and therapeutic avenues in pancreatic ductal adenocarcinoma.

A. Valles Marti[1], G. Mantini[2], C. Waasdorp[2], R. de Goeij- de Haas[2], A. Henneman[2], S. Piersma[2], T. Pham[2], J. Knol[2], J. Verheij[3], F. Dijk[3], H. Halfwerk[3], E. Giovannetti[2], C. Jimenez[2], M. F. Bijlsma[2],

[1]Leiden University Medical Center, Leiden, Netherlands, [2]Cancer Center Amsterdam, Amsterdam UMC, Amsterdam, Netherlands, [3]Amsterdam UMC, Amsterdam, Netherlands

Introduction: Pancreatic ductal adenocarcinoma (PDAC) is a devastating disease, commonly characterized by multiple aberrant signaling. Phosphoproteomics provides a direct read-out of these complex signaling networks and the resultant clinically relevant phenotype, as well as a functional scaffold to identify new targets. In the absence of an oncogenic driver, low dose (LD) kinase inhibitor (KI) combinations against multiple (parallel) activated kinases might provide higher efficacy and reduce toxicity as compared to single drug treatment. Aims: 1) To identify targets and test combinations of multiple KIs at LDs for potential synergism in preclinical models. 2) To chart the phosphoproteome of 42 PDAC tumors to reveal signalling pathways that may be involved in PDAC progression.
Methods: By using a two step phosphopeptide enrichment with phosphotyrosine immunoprecipitation and immobilized metal affinity chromatography, followed by label free MS analysis, we analyzed phosphoproteome data of 7 immortalized and 2 primary PDAC cell lines, and of 42 PDAC tumors. We used integrative inferred kinase activity (INKA) scoring of the maxquant output to identify hyperactive kinases. For the cell line panel, five KIs were selected based on targeting coverage of the INKA profiles. LD were set as IC20s for 2,3,4 drug combinations. Cell growth inhibition was assessed by SRB assay. Median-effect analysis was used to assess synergy. Functional testing was performed in immortalized 2D, xenoderived 2D and 3D cultures. Effective low dose 3 drug combinations were further validated using patient-derived xenografts.
Results: High INKA scoring of multiple activities per cell line without clear outliers of single kinases underscores the need for combination therapies. Multiple LD combinations showed effective growth inhibition (70 to 92%) and synergism, mostly 3 drug combinations, which required targeting of several RTKs and downstream signaling. Different responses were further observed between epithelial and mesenchymal cell lines. These top performing combinations were further validated in PDAC organoids and *in vivo*. Clinical utility of these kinase targets was then confirmed in 42 tumor phosphoprofiles, which were characterized in different subtypes with distinct therapeutic options. Phosphoproteome signals and kinases activities with potential prognostic value and mutational associations were further described.
Conclusion: Our INKA pipeline, which can rank kinase activities in individual tumors, is optimally suited to specifically prioritize actionable kinases with targeting purposes. Tailored LD combination strategies exhibited promising efficacy in preclinical models and may ultimately improve treatment outcomes.
Next Steps: Multicellular patient-derived models will be used to further study and target the TME in PDAC tumors.

#6486 Correlation of *nab*-sirolimus tumor drug levels and improved tumor suppression in *KRAS G12C* non-small cell lung cancer xenografts treated with *nab*-sirolimus in combination with *KRAS* inhibitors.

S. Hou[1], J. Nieva[2], M. Zalath[1], N. Desai[1];

[1]Aadi Bioscience, Inc., Pacific Palisades, CA, [2]University of Southern California, Los Angeles, CA

Background: *KRAS* mutations are found in a variety of tumor types, including non-small cell lung cancer (NSCLC), where *KRAS G12C* mutation is present in ~12% of NSCLC patients. *KRAS G12C* inhibitors (KRAS G12Cis), sotorasib and adagrasib, are approved for the treatment of *KRAS G12C*-mutated, locally advanced or metastatic NSCLC. The mTOR pathway is often activated in patients with *KRAS* mutations and may contribute to resistance to KRAS G12Cis. *nab*-Sirolimus is a nanoparticle albumin-bound intravenously (IV) administered form of the mTOR inhibitor (mTORi) sirolimus and is approved for the treatment of patients with advanced malignant perivascular epithelioid cell tumors. This study assessed tumor and blood drug level correlation with antitumor activity of *nab*-sirolimus or everolimus alone or in combination with KRAS G12Cis.

Methods: Athymic mice bearing subcutaneous *KRAS G12C*- and *STK11*-mutated NSCLC xenografts (NCI-H2122) were treated with saline, mTORis *nab*-sirolimus (IV) or everolimus (oral) at clinically relevant and equal weekly dose of 15 mg/kg/wk, or KRAS G12Cis sotorasib (oral) or adagrasib (oral) at 30 mg/kg/day alone or in combination. Tumor volume changes from baseline were assessed; tumor and blood samples were harvested at the end of study (6 wks) for analysis of trough drug levels by LC-MS/MS, and tumor lysates were analyzed for downstream markers for mTOR inhibition by Western blot.

Results: In *nab*-sirolimus plus KRAS G12Ci treated groups, significantly slower tumor growth was observed compared with single agent treated groups and everolimus plus KRAS G12Ci treated groups. Compared with single-agent *nab*-sirolimus (170.1 ng/g), treatment with *nab*-sirolimus plus sotorasib resulted in reduced tumor *nab*-sirolimus drug levels (73.6 ng/g, P=0.0040); while similar tumor *nab*-sirolimus drug levels were observed for *nab*-sirolimus plus adagrasib (121.6 ng/g, P=ns). Corresponding to greater antitumor activity, significantly greater tumor trough mTORi drug levels were observed in *nab*-sirolimus plus either sotorasib or adagrasib treated groups compared with similar everolimus combinations (85-fold, P<0.0001; and 91-fold, P=0.0050, respectively). Correspondingly, stronger mTOR downstream target inhibition of pS6 were observed for *nab*-sirolimus plus KRAS G12Ci treated groups compared with everolimus plus KRAS G12Ci treated groups.

Conclusions: The addition of a KRAS G12Ci to *nab*-sirolimus significantly reduced tumor volume and increased tumor drug levels, suggesting enhanced tumor targeting compared with everolimus plus KRAS G12Cis and correlating to improved antitumor activity and mTOR target suppression. Clinical dose-finding studies are needed to determine potential drug-drug interactions between *nab*-sirolimus and KRASis.

#6487 The selective WEE1 inhibitor azenosertib shows synergistic anti-tumor activity with KRAS^{G12C} inhibitors in multiple KRAS^{G12C} models.

Nathan M. Jameson, Gabriel Kim, Catherine Lee, Blake Skrable, Alexandra Shea, Monah Abed, Olivier Harismendy, Jianhui Ma, Doris Kim, Mark R. Lackner

Zentalis Pharmaceuticals, San Diego, CA

KRAS^{G12C} is a potent oncogenic driver which results in downstream hyperactivation of MAPK signaling and unchecked oncogenic growth, while simultaneously increasing replication stress (RS) and accumulation of DNA damage. KRAS^{G12C}-specific inhibitors are approved and/or recommended in metastatic non-small cell lung cancer (NSCLC) and colorectal cancer (CRC), and while responses are robust, some patients are inherently resistant, and most responders acquire resistance. Resistance mechanisms include reactivation of MAPK signaling, and cancer cells which escape MAPKi are reported to have high levels of genomic instability. WEE1 is a kinase involved in cell cycle progression, allowing cells to repair damaged DNA before entering the next cell cycle phase. Consequently, inhibition of WEE1 leads to premature cell cycle entry and RS, thereby driving cancer cells through the cell cycle with unchecked accumulation of DNA damage, ultimately resulting in mitotic catastrophe and cell death. We hypothesized that high levels of genomic instability and RS in *KRAS^{G12C}* mutant and KRAS^{G12C} inhibitor-resistant tumors present a vulnerability to WEE1 inhibition and provide rationale for combining azenosertib, a novel, selective, and orally bioavailable WEE1 inhibitor, with KRAS^{G12C} inhibitors.

Here, we report azenosertib in combination with KRAS^{G12C} inhibitors as an effective therapeutic strategy for *KRAS^{G12C}* tumors. *In vitro* combination of azenosertib with multiple KRAS^{G12C} inhibitors demonstrated synergistic cell growth inhibition across a panel of *KRAS^{G12C}* cell lines in both 2D and 3D assays. *In vivo* treatment with azenosertib in KRAS^{G12C} inhibitor-sensitive cell line-derived xenograft (CDX) models of NSCLC (NCI-H358, NCI-H2122, NCI-H1792), CRC (SW837, SW1463), and pancreatic cancer (MIA PaCa-2) demonstrated significant monotherapy activity as well as synergistic tumor growth inhibition (TGI) when combined with KRAS^{G12C} inhibitors, including tumor regression in some models. Importantly, the KRAS^{G12C} inhibitor-resistant SW1573 NSCLC CDX model demonstrated synergistic TGI in the combo arm (84%) when compared against monotherapy azenosertib (31%) or adagrasib (58%). Similarly, treatment of a KRAS^{G12C} inhibitor-resistant patient-derived xenograft (PDX) model of CRC resulted in synergistic TGI in the combination arm (61%) relative to monotherapy azenosertib (17%) or adagrasib (2%). Finally, analysis of biomarkers from both *in vitro* and *in vivo* tumor samples demonstrated synergistic increases in protein markers of RS, DNA damage, and apoptosis with combination therapy.

Taken together, our results suggest that the combination of azenosertib with KRAS^{G12C} inhibitors enhances tumor growth inhibition over single agent therapy and may be an effective treatment option for patients with *KRAS^{G12C}* tumors.

#6489 Paradoxical activation of kinases occurs directly with ATP-competitive kinase inhibitors and is observable biochemically at physiologically relevant drug concentrations.

C. M. Loch, M. Eason, S. Liang, A. Goupil, A. Acinapura, J. Purcell, M. Domiguez;
Reaction Biology Corporation, Malvern, PA

We sought to screen all FDA approved, cancer-indicated, kinase targeting drugs using the gold standard radiometric biochemical activity assay (HotSpot) against the largest collection of kinases in the world (>100 drugs against 735 total kinases including 395 wild type and 340 mutants). One of these drugs, mitapivat, is an activator of Pyruvate Kinase. Here, we show mitapivat-driven biochemical inhibition of several, but not all, mutants of c-KIT. We also observed the equal and opposite phenomenon whereby many ATP-competitive kinase inhibitors demonstrate biochemical activation of certain kinases, several of which seem particularly susceptible to the effect. Previous work by other investigators (at Genentech and the Rosen lab, MSKCC) demonstrated that PLX4720 (precursor to Vemurafenib) paradoxically activated wild type BRAF, but not BRAF mutants, by driving dimerization of the kinase in drug concentrations insufficient to inhibit both members of the dimerized pair. Our data suggests this phenomenon may be more widespread than previously appreciated and fully observable in vitro. Such paradoxical activation could be driving both toxicities and inefficacy against cancers expressing some of these activatable kinases. This information could suggest novel opportunities for combination therapy and improve outcomes by contraindicating certain medication from use based on tumor expression profile.

#6490 Pt1a and sorafenib combination treatment exerts synergistic anti-hepatocellular carcinoma effect through RNA m^{6}A methylation modification.

Y. Huang[1], Y. Cui[1], I. B. Huang[2], Y. Wang[1], Y. Xuan[1], P. Wan[3], C. Lok[2], C. Che[3], S. Ma[4];

[1]School of Biomedical Sciences, Li Ka Shing Faculty of Medicine, The University of Hong Kong, Hong Kong SAR, China, [2]Laboratory for Synthetic Chemistry and Chemical Biology, Health@InnoHK, Hong Kong SAR, China, [3]State Key Laboratory of Synthetic Chemistry, Department of Chemistry, The University of Hong Kong, Hong Kong SAR, China, [4]State Key Laboratory of Liver Research, The University of Hong Kong, Hong Kong SAR, China

Hepatocellular carcinoma (HCC) is the most common type of liver cancer and has a poor prognosis. The survival benefits of sorafenib in patients with advanced HCC are modest owing to acquired resistance. Accumulating evidence has demonstrated that cancer stemness is an important cause of drug resistance and the root cause of tumor recurrence. [PtII(C^N^N)(NHC2Bu)]PF6 (Pt1a) is a newly developed platinum-based drug containing N-heterocyclic carbene with proven anticancer properties against a range of tumor types. However, its role in targeting cancer stemness and its ability to sensitize cancer cells to overcome molecular-targeted therapy drug resistance in HCC remains elusive. Herein, we demonstrate the synergistic inhibitory effect of sorafenib and Pt1a combination treatment on HCC through RNA m^{6}A methylation modification. In cultured HCC cells and patient-derived organoids, the drug combination synergistically reduced the cell viability and promoted cell apoptosis compared to single-drug treatment. Combination treatment also attenuated self-renewal, as evidenced by a marked decrease in tumor-initiating cancer cell frequency, as measured by limiting dilution spheroid formation assay. These findings were further validated in HCC patient-derived xenograft mouse models and a mouse HCC model induced by hydrodynamic tail vein delivery of NRAS+AKT coactivation plasmids. Notably, the combination treatment with sorafenib and Pt1a, but not a single treatment, led to a significant reduction in tumor burden. The combination treatment was also effective in decreasing tumor-initiating cell frequency, as measured by subjecting the harvested tumor cells for limiting dilution spheroid formation assay *ex vivo*. Mechanistically, integrative RNA-sequencing and thermal proteome profiling analyses both indicated the enrichment of m^{6}A-related pathways in combination drug treatment. An increased global m^{6}A level upon combination treatment was validated using m^{6}A dot blotting, confirming that the synergistic effect may be mediated by the elevated global m^{6}A level in HCC cells. Collectively, our study demonstrated that Pt1a and sorafenib combination treatment synergistically inhibited the viability and stemness of HCC cells by increasing global RNA m^{6}A level. These findings supported the potential of Pt1a as a therapeutic option for HCC and overcoming sorafenib drug resistance. Ongoing studies are focused on identifying m^{6}A regulators and downstream targets involved in combination treatment.

#6491 Epigenetic-based combinatorial therapy is synergistic in KRAS/LKB1 mutant non-small cell lung cancers.

M. Zucker, K. Devore, L. Chesney, G. Hirschfeld, A. Reyna, B. Linnane, J. Mascarenhas, M. Murray, A. Miller, P. Gonzales, S. Gately;
Translational Drug Development, LLC (TD2), Scottsdale, AZ

KRAS and LKB1 mutations (KL) in non-small cell lung cancer (NSCLC) patients often results in poor prognosis, a high tumor mutational burden, and resistance to conventional therapy. The metabolic changes with these mutations can create unique vulnerabilities to be targeted therapeutically. HDAC inhibition has been reported as a promising approach to overcome MEK inhibitor resistance in animal models of melanoma, pancreatic cancer, and KL mutant NSCLC. Inhibition of HDAC3 and HDAC6 have independently been shown to have therapeutic activity in KL NSCLC. We now report on the activity of two novel HDAC3/6 inhibitors in cell culture and mouse models of human KL (A549) compared to KRAS/TP53-mutant NSCLC (KP) (CALU-6) alone and individually combined with the MEK inhibitor trametinib. GB-1101 inhibits HDAC3 and HDAC6 and GB-3103 inhibits HDAC1,3,6,10. SynergyFinder multi-dose combination data analytics showed synergistic interactions for both GB-1101 or GB-3103 when combined with trametinib in KL mutant A549 cells with maximum synergy scores of δ = 9.24 and 4.21, using zero interaction potency (ZIP) for synergy scoring. GB-1101 or GB-3103 when combined with trametinib in KP mutant CALU-6 cells did not demonstrate synergistic interaction with synergy scores of δ = -1.58 and -0.53, respectively. Mice were inoculated subcutaneously with $5.0x10^6$ A549 or CALU-6 cells and treatment with GB-1101 (75 mg/kg qd, oral), GB-3103 (5.0 mg/kg qd, subcutaneous), trametinib (1.0 mg/kg qd, oral) and each drug in combination with trametinib was initiated when tumors reached an average of $120mm^3$. Single agent and combination treatments were well tolerated. GB-1101 exhibited tumor growth inhibition (TGI) of 33.0% in the A549 (KL) compared to 8.5% in CALU-6 (KP). In combination with trametinib, GB-1101 showed increased activity (TGI=92.7%) compared to trametinib alone (TGI=69.5%) in KL mutant A549. In KP mutant CALU-6 tumors, combination benefit was not observed; combination of GB-1101 and trametinib yielded a TGI=93% equivalent to trametinib alone (TGI=91%). GB-3103 resulted in a TGI of 66.7% in the KL mutant A549 and TGI= 55.9% in KP mutant CALU-6. In KL mutant A549, GB-3103 in combination with trametinib, showed increased inhibition (TGI=94.3%) compared to trametinib alone (TGI=69.5%). No combination benefit was seen for GB-3103 in KP mutant CALU-6 with the combination treatment TGI of 93.1% compared to trametinib alone TGI=90.7%. These results confirm and extend the finding that for KL mutant NSCLC, HDAC3/6 inhibitors show therapeutic benefit in combination with trametinib that is not observed in KP tumors. These data reveal a promising epigenetic-based combinatorial strategy for treating lung cancers harboring concurrent KRAS/LKB1 mutations, a path for clinical translation, and the potential to improve treatments for KRAS/LKB1 mutant NSCLC patients where there are currently no robust therapeutic strategies.

#6492 KRAS inhibitor-based combinations in pancreatic cancer identified through Optim.AI.

J. Lim[1], E. K. Chow[2], M. Rashid[1];

[1]KYAN Technologies Pte Ltd, KYAN Technologies Pte Ltd, Singapore, [2]National University of Singapore, Singapore, Singapore

PURPOSE: KRAS is the most frequently mutated oncogene in almost all cancers, including pancreatic ductal carcinoma (PDAC) and colorectal cancer. Increased development efforts targeting KRAS mutations have yielded recent FDA approvals of two KRAS G12C inhibitors. However, this is beneficial for only a small proportion of patients especially with indications like PDAC, where G12C mutations are rare (1%) while G12D mutations account for approximately 45%. Hence, there is a need to develop methods to target a broader range of KRAS mutations. Beyond direct gene mutation, activation of oncogenic KRAS and downstream or parallel signaling through other genomic alterations may benefit from KRAS-specific therapeutic strategies, especially combination therapy. In this study, Optim.AI™, a hybrid computational-experimental platform is harnessed to identify mutation-specific optimal therapies and to stratify efficacious drug combinations containing KRAS inhibitors in pancreatic cancer.

METHODS: Optim.AI™ utilizes small datasets to rationally converge upon optimal drug combinations within a defined drug search space. By mapping experimental data points to a second-order quadratic function, Optim.AI™ predicts cell killing efficacies for all possible combinations, independent of the background of the models utilized. In this study, pancreatic cancer cell lines, with varying KRAS mutations, were tested with an array of 155 different combinations consisting of 12 drugs at varying concentrations. The drugs include KRAS G12C inhibitors, Sotorasib and Adagrasib, KRAS inhibitors in development, and approved therapies used clinically for PDAC. Post-drug treatment viability was measured and used for Optim.AI™ analysis, to rank and compare the top therapies across the different cell lines.

RESULTS: Through Optim.AI™ analysis, we observed a range of sensitivities towards KRAS inhibition, even for both Sotorasib and Adagrasib. Compared against HT-29 cell line, harboring wild type KRAS, we have identified distinct combinations of KRAS inhibitors with standard of care drugs on cell lines with G12D, G12V and G12C KRAS mutants. Subsequent validation of the top and bottom ranked combinations for the respective cell lines correspond to the predicted Optim.AI™ results.

CONCLUSIONS: This study has demonstrated the differential sensitivities of the KRAS inhibitors across several pancreatic cancer cell lines, with different KRAS mutational profiles. Notably, we have identified KRAS inhibitor-based combinations that are distinctly different from wild type KRAS cell line. These preliminary findings could be used to drive precision medicine by identifying suitable biomarkers to potentially stratify pancreatic cancer patients and improve treatment outcomes. Future work includes evaluating the clinical significance of these combinations by validating them on patient-derived organoids.

#6493 CRISPR-directed prime editing sensitizes EGFR inhibitor by correcting oncogenic KRAS mutants In NSCLC.

Q. Fang, C. Yang, C. Huang, H. Wang, j. Yu, J. Hao;
Tianjin Medical Univ. Cancer Inst. & Hospital, Tianjin, China

EGFR inhibitor has been demonstrated with huge therapeutic potential in advanced non-small cell lung cancer (NSCLC), while the patients carrying KRAS mutation had poor response to EGFR inhibitor. KRAS mutation is the most frequent molecular alteration found in advanced NSCLC, which is associated with a poor prognosis without available targeted therapy. Previous research showed that CRISPR-directed prime editor could induce unconstrained correction for KRAS mutants (*KRAS*^{G12D}, *KRAS*^{G12C}, *KRAS*^{G12V}). Accordingly, it would be a promising strategy to combine PE-based genetic therapy with EGFR inhibitor for enhanced therapy in NSCLC. Here,we selected several PE variants with reported highly efficient reverse transcriptase, among which eEc48-based PE6a showed the highest editing efficiency toward KRAS mutation. The lentivirus-mediated PE6a editing inhibited cell proliferation and invasion *in vitro* and *in vivo*. After that, EGFR inhibitor combined with PE6a was employed in patient-derived organoid (PDO) model carrying diverse KRAS mutants. We found that PE6a editing significantly inhibited PDO proliferation compared to EGFR inhibitor alone and control. Correspondingly, the transcriptome sequencing also showed that the cell apoptosis, cell growth and cell motility signaling were inhibited upon PE6a editing. Our findings demonstrated that the PE-directed genetic therapy could sensitize EGFR inhibitor in NSCLC, providing an alternative choice for NSCLC patients carrying KRAS mutant.

#6495 Lenvatinib as a potential treatment option for invasive mucinous lung adenocarcinoma.

Tarik Demir, Carolyn Moloney, Liam Il-Young Chung, Young Kwang Chae

Feinberg School of Medicine, Northwestern University, Chicago, IL

Introduction: Invasive mucinous adenocarcinoma (IMA) accounts for approximately 4-20% of non-small-cell lung carcinoma (NSCLC). Genetic alterations and RNA sequencing analysis of IMAs reveal a unique mucinous signature similar to gastrointestinal mucinous tumors. Due to its rarity, focused clinical trials for IMA patients are often not feasible. These patients respond poorly to platinum-based conventional chemotherapy, or immunotherapy. Lenvatinib is a multitargeted-TKI with demonstrated activity in patients with RET fusion-positive lung adenocarcinoma, thyroid, hepatocellular and gastric carcinoma.
Methods: Here, we present two RET fusion-negative mucinous lung adenocarcinoma cases that received a multitargeted TKI lenvatinib with a clinical and survival benefit.
Results: Case #1: An 81-year-old female initially diagnosed with cT4N0M0 IMA (TTF1 and CDX2 focally positive) was started on neoadjuvant treatment for a 12cm tumor. She underwent right thoracotomy/right lower lobectomy/mediastinal lymph node dissection, and pathology confirmed ypT4N1M0 mucinous adenocarcinoma. Three months post-operatively, the patient had disease progression in the lungs. She had no targetable mutations. She had four subsequent lines of treatment including nivolumab/nab-paclitaxel as the fourth-line treatment. After six months of nivolumab/nab-paclitaxel, lenvatinib was added to the combination due to clear disease progression evident on imaging. After twelve cycles of nivolumab/nab-paclitaxel/lenvatinib combination treatment, patient achieved a partial response per RECIST 1.1 (-35.7% change from baseline to current). The patient reported less dyspnea and increased activity tolerance. Approximately nine months after the start of the treatment, patient showed progressive lung disease. The patient died after one more line treatment with 41 months of total overall survival. **Case#2:** A 56-year-old male initially diagnosed with stage IVA IMA (TTF1 negative). After four lines of treatments, patient was started on lenvatinib alone. The patient reported marked improvement in dyspnea and pain and increased activity tolerance with lenvatinib. Imaging confirmed treatment response after three months of treatment. The patient was subsequently enrolled in the double lung transplant (DLT) registry aimed for lung-limited malignancies (D.R.E.A.M.) registry study (NCT05671887), and he is alive with 25 months follow-up since DLT.
Conclusion: We report two cases of metastatic RET fusion-negative mucinous lung adenocarcinoma, in which treatment with the multitargeted TKI Lenvatinib led to significant clinical improvement. Biological rationale to explain the effect of lenvatinib in invasive mucinous lung adenocarcinoma needs to be explored.

#6496 Assessment of tyrosine kinase inhibitor bypass mechanisms in lung cancer using single cell multiomics, patient derived organoids and rationally designed drug screens.

L. Liu, A. Strange, S. Lee, B. Gao, D. Merrick, T. Patil, J. DeGregori, D. Camidge, S. R. Pine, **H. E. Sabaawy**;
University of Colorado Anschutz Medical Campus, Aurora, CO

Lung cancer (LC) is the leading cause of cancer-induced mortality, with 350 patients in the US dying from LC daily, the majority from non-small cell lung cancer (NSCLC). Molecular-targeted therapy such as tyrosine kinase inhibitors (TKI) are effective in first and subsequent lines of therapy against oncogenic drivers (KRAS, EGFR, or ALK fusions, others); however, nearly all treated patients progress eventually and run out of therapeutic options. Key reasons are the lack of predictive biomarkers and LC models that reflect the underlying heterogeneity and different phenotypic cell states among subclones within and between patients. Here, we developed a novel platform for refining the resolution of molecular interrogation to the single cell level, using single cell spatial multiomic (scSpMO), coupled with rational designed drug screens in patient-derived organoids (PDOs) from LC biopsies obtained upon progression. By deriving LC PDOs in epithelial and tumor microenvironment (TME) conditions to faithfully maintain the histological and genetic features of their respective LC tissues, we identified enrichment conditions for LC PDOs guided by tumor mutation variants and activated pathways. PDOs are maintained under the same treatment condition in the clinic (e.g., Lorlatinib) and drug testing is tailored to identify next lines of combined therapy. With six patients enrolled and others in ongoing studies, single cell PDOs (at >80% establishment rate) were used to determine key molecular bypass mechanism for resistance to TKI, including on-target variants, driver bypass, lineage plasticity and acquired resistance. Functional assays for acquired resistance such as PI3K/AKT signaling, Src kinase, BRAF fusion and MET hyperactivity allow the identification of potential novel combined lines of therapy for each patient through the compassionate care program and/or trial participation. Our platform when empowered with datasets of bulk, scRNA-seq and scSpMO signatures of primary human NSCLC, together with PDOs offer the ability to perform analysis of LC phenotypes such as lineage transformation in high-content assays, predict and/or act on resistance to therapy and provides a path for precision medicine-guided immediate impact on patient care.

#6497 Molecular characterization and drug sensitivity of a gastric FGFR2-TACC2 and a pancreatic KRAS p.G12C primary culture.

S. Garcia-Roman[1], E. Meshoulam Nikolaeva[2], J. Garcia Mosquera[2], M. Garzon Ibanez[1], R. Roman[1], S. Rodriguez[1], C. Rodriguez[1], C. Mayo de las Casas[1], R. Rosell[2], M. A. Molina-Vila[1], C. Aguado Esteban[1];

[1]Pangaea Oncology, Barcelona, Spain, [2]Instituto Oncologico Dr. Rosell, Barcelona, Spain

Introduction and Objectives: Gastric and pancreatic cancers lack effective therapies, leading to low survival rates particularly in the metastatic setting. Fibroblast growth factor receptor 2 (*FGFR2*) amplification and fusions with *TACC2* appear in 5.5% and 2.1% of gastric tumors, respectively. In pancreatic cancers, the *KRAS* p.G12C mutation is limited to 1-2% of cases. FDA has recently approved drugs targeting both alterations, pemigatinib and infigratinib for cholangiocarcinoma with *FGFR2* fusions; sotorasib and adagrasib for *KRAS* p.G12C mutant lung cancers. Here, we report the initiation of primary cultures that can be used as preclinical models for testing antitumor agents in gastric and pancreatic tumor cells.

Materials and Methods: Pleural effusions were collected from a gastric and a pancreatic cancer patient, both metastatic. Cells were isolated by centrifugation, cultured for 2-3 months in complete medium and genotyped using next generation sequencing (NGS) and RNA nCounter hybridization. Primary cultures were treated with specific drugs depending on their molecular alterations and clinical guidelines. Cell viability was determined by MTT.

Results: Tumor cells from the pleural effusion of the gastric cancer patient were grown in suspension. NGS and nCounter revealed a *FGFR2-TACC2* fusion, a *FGFR2* amplification (160 copies) and a *TP53* p.G245S mutation (100% variant allele fraction, VAF). The fusion and the amplification were confirmed by FISH. Cells were sensitive to erdafitinib, with IC_{50}=40 nM in MTT assays. Irinotecan, 5-fluorouracil and cisplatin were also tested; IC_{50} were below the described plasma C_{max} in the first two cases. The patient was treated with first-line fluoropyrimidine and oxaliplatin with partial response and a 5-month progression-free survival. Due to rapid deterioration, 2nd line treatment was not administered. The tumor cells from the pancreatic cancer patient were adherent, NGS revealed a *KRAS* amplification (9 copies) accompanied by a *KRAS* p.G12C mutation (81% VAF) and a *TP53* p.R175H mutation (99% VAF). MTT assays were performed to determine the cells' response to oxaliplatin, 5-fluorouracil, irinotecan, gemcitabine, nab-paclitaxel, adagrasib and sotorasib. IC_{50}s below plasma C_{max} were found in the last three cases. Remarkably, the IC_{50} for sotorasib was 100 nM and for adagrasib was 300 nM. The patient was treated with first-line gemcitabine and nab-paclitaxel with partial response but discontinued after three months due to hematological toxicity.

Conclusions: Primary cultures can be initiated from malignant pleural effusions and used for genetic characterization and drug sensitivity profiling. Primaries with specific alterations can be employed as preclinical models to test targeted therapies.

#6498 MEK inhibitor mirdametinib suppresses MAP kinase pathway activity and inhibits tumor growth in atypical teratoid/rhabdoid tumors.

Y. Deng, K. Malebranche, T. Findlay, A. Geethadevi, C. Eberhart, J. Rubens, E. Raabe;
Johns Hopkins University School of Medicine, Baltimore, MD

Atypical teratoid/rhabdoid tumors (AT/RT) are deadly infantile brain tumors currently lacking effective treatments. Our prior studies examining AT/RT primary tissues have shown an elevated expression of phospho-ERK, a downstream effector of MEK in the mitogen-activated protein (MAP) kinase pathway. The increased activity of this pathway potentially leads to more aggressive cancer growth, emergence of drug resistance, and poor treatment outcomes in AT/RT patients. Mirdametinib is a novel, highly specific MEK1/2 inhibitor that has been reported to have superior blood-brain-barrier penetration compared to other MEK inhibitors. It is currently in development as a monotherapy for low-grade glioma as well as NF1-related plexiform neurofibromas. We hypothesized that mirdametinib can inhibit AT/RT tumor growth and improve overall survival. We examined the in vitro effect of mirdametinib treatment on five AT/RT cell lines (CHLA04, CHLA05, CHLA06, CHLA266, and BT37). Mirdametinib decreased MAP kinase pathway activity in the tested cell lines (western blot, phospho-ERK). Cell lines treated with mirdametinib exhibited decreased viability at 72hr (Muse Cell Viability Assay, CHLA05 t-test $p=0.011$, CHLA06 t-test $p<0.001$, BT37 t-test $p<0.01$ compared to DMSO control) and lower rates of proliferation (western blot, phospho-RB; BrdU immunofluorescence staining, CHLA05 t-test $p=0.015$, CHLA06 t-test $p<0.0001$, BT37 t-test $p<0.0001$ compared to DMSO control). Furthermore, mirdametinib induced apoptosis in AT/RT cells (western blot, cPARP; Muse Annexin V Assay, CHLA04, CHLA05, CHLA06, and BT37, t-test $p<0.0001$, CHLA266, t-test $p<0.01$ compared to DMSO control; cleaved caspase-3 immunofluorescence staining, CHLA05, CHLA06, and BT37, t-test $p<0.0001$ compared to DMSO control). We then tested the efficacy of mirdametinib in vivo. We treated mice bearing orthotopic CHLA06 tumors with a daily oral delivery of the drug. Mirdametinib treatment significantly extended the survival of treated mice in this very aggressive model (17 to 24 days, log-rank test $p=0.038$ compared to vehicle control) and decreased the expression of phospho-ERK (western blot, phospho-ERK), demonstrating that mirdametinib engaged its target in vivo. Testing against additional AT/RT orthotopic xenografts is currently underway. Our studies suggest that pharmacologically inhibiting the MAP kinase pathway may be an effective strategy to target AT/RT. Mirdametinib can potentially be an effective treatment to help extend survival in this deadly disease.

#6499 The landscape of MET exon 14 skipping mutations in non-small cell lung cancer patients identified by next-generation sequencing.

C. Shi[1], G. Ning[2], Z. Qinglan[2];

[1]Jiangsu Province Hospital of Chinese Medicine, Affiliated Hospital of Nanjing University of Chinese Medicine, Nanjing, China, [2]3D Medicines Inc., Shanghai, China

Background: MET exon 14 skipping mutations (METex14) account for approximately 0.9%-4% in patients with non-small cell lung cancer (NSCLC). The primary detection methods are DNA and RNA-based next-generation sequencing (NGS). However, the effect of amplicon-based library construction (ALC) and capture-based library construction (CLC) on the detection characteristics of METex14 during the NGS process is not yet fully understood. Here we described the landscape of METex14 in NSCLC patients, as identified by NGS using two different library construction methods.

Methods: A total of 6811 samples with NSCLC were enrolled in this study, including 3839 samples performed by DNA-based NGS with CLC, 64 samples performed by RNA-based NGS with CLC and 2908 samples performed by the synchronous DNA-based and RNA-based NGS with ALC. Only the pathogenic mutations and likely pathogenic mutations in clinical significance were rolled into our analysis.

Results: The ranking of different methods, as determined by the positive rates for METex14, was RNA-based NGS with ALC (71/2908, 2.44%), RNA-based NGS with CLC (1/64, 1.56%), DNA-based NGS with CLC (54/3839, 1.41%) and DNA-based NGS with ALC (14/2908, 0.48%). Out of 2908 samples performed by the synchronous DNA-based and RNA-based NGS with ALC, 73 samples (2.51%) had METex14 detected at either the DNA or RNA level. METex14 were only detected at the RNA level in 59 patients, while they were only detected at the DNA level in 2 patients. This might be due to the limited probe design at DNA level and the Y1003 site which could not be detected at RNA level. As revealed by DNA-based NGS, the mutation forms causing METex14 include point mutations, indels, and large segment duplications. And the highest mutation rate is in the splice donor site (30.9%), the lowest is observed at position Y1003 (2.9%). Additionally, METex14 is more prevalent in patients over 60 years of age in Chinese NSCLC, with a statistically significant difference (P=0.0043).

Conclusion: RNA-based detection of MET 14 skipping yielded a higher detection rate compared to DNA-based NGS, regardless of ALC or CLC. Combining DNA and RNA analysis is more suitable for detecting MET exon 14 skipping and increases the positive rate.

#6500 Dependence of EGFR-mutant NSCLC on MET as demonstrated by vebreltinib, a novel and selective brain-penetrating MET kinase inhibitor.

X. Zhang[1], E. Liu[2], Y. Song[1], P. Yu[1], S. Redkar[1], G.-L. Yu[1];

[1]Apollomics, Inc., Foster City, CA, [2]Zhejiang Apollomics Biotech Co., Ltd., Hangzhou, China

Background: Although EGFR inhibitors (EGFRi), preferably osimertinib, have offered substantial benefit for the classical plus T790M EGFR-mutant NSCLC patients, drug resistance develops and poses a critical challenge for long-term survival. The resistance is rooted to either on-target secondary EGFR mutations or compensatory oncogenic pathways bypassing EGFRi intervention, one of which appears to be treatment-acquired *MET* amplification (*MET*amp). In this study we set out to understand the conditions when the tumor cells become dependent on MET.

Methods: NSCLC patient-derived tumor models (PDX) carrying classical and T790M EGFR driver mutations were selected based on EGFRi history and concurrent *MET* gene copy numbers or RNA expression levels: Type 1) resistant to osimertinib with *MET*amp; Type 2) partially resistant to osimertinib with *MET*amp; and Type 3) sensitive to osimertinib with low *MET* expression, no *MET*amp. These PDX xenograft mice were treated with vebreltinib (APL-101) at clinically relevant doses as single agent or in combination with osimertinib. The pharmacodynamic effects on EGFR and MET phosphor (P)- and total proteins were analyzed from tumor samples harvested during and at the end of treatments.

Results: Vebreltinib single agent inhibited tumor growth of the type-1 PDX. One such PDX was resistant to chemotherapies, BRAF inhibitor and EGFRi including osimertinib, was inhibited by vebreltinib with ED50 of 3 mg/kg (p.o/q.d.). Another such PDX tumor appeared to be eradicated by vebreltinib treatment at 10 mg/kg (p.o/q.d.) and the mice became tumor-free on Day 18 and remained so after dosing stop on day 21 with last observation at study end (Day 70). In comparison, reference METi savolitinib showed only partial tumor size reduction against the same PDX tumor, not as durable as vebreltinib, and did not eradicate tumor growth at the same dose as vebreltinib or in combo with Osimertinib. Re-grown tumor after savolitinib osimertinib combo dosing stop was inhibited completely by vebreltinib follow-on treatment. In the type-2 PDX, tumor growth was partially inhibited by vebreltinib but was completely inhibited by combo of vebreltinib and osimertinib. The anti-tumor activity of vebreltinib in type-1 and type-2 PDX was associated with pharmacodynamic inhibition of P-MET and P-EGFR and MET protein degradation. In the type-3 PDX, tumor growth appeared to be eradicated by osimertinib and not inhibited by vebreltinib. However, addition of vebreltinib suppressed tumor re-growth after osimertinib dosing stop.

Conclusion: EGFR-mutant NSCLC resistance to EGFRi may be dependent on MET pathway regardless of acquired *MET*amp, whereas *MET*amp may dictate the degree of MET dependence. Our data supports the hypothesis that adding vebreltinib to EGFRi overcome MET dependent resistance with durable effect or preventing MET dependent resistance to maximize therapeutic benefits.

#6501 Development and characterization of covalent inhibitors of the RAS-PIK3CA interaction.

J. Klebba, J. Tamiya, J. Wang, H. Miao, K. Lamb, A. Snead, A. Esparza-Oros, R. Lin, C. Yue, S. Grabow, S. Bernard, Y. Liu, B. Horning, M. Hoffman, M. Pariollaud, T. Wyrick, H. Parker, J. Sigler, M. Pastuszka, D. Weinstein, T. Kinsella, M. Patricelli;
Vividion Therapeutics, San Diego, CA

RAS proteins are membrane bound GTPases that when hyperactivated, act as oncogenes through activation of the MAPK & PI3K pathways. Each of these pathways has oncogenic potential, as exemplified by the high frequency of BRAF mutations in melanoma and PIK3CA and PTEN mutations in breast and gynecological cancers. Simultaneous activation of these pathways, as occurs in RAS driven cancers, generates aggressive cancers that present a significant clinical challenge. KRAS, the most commonly mutated RAS isoform, is also the most frequently mutated oncogene in cancer. While treatment options have improved for a subset of these patients due to the accelerated approval of KRAS-G12C inhibitors, the rapid development of resistance highlights the continued need for effective treatments. In RAS driven cell and animal models, dual inhibition of the MAPK &PI3K pathways has shown superior efficacy relative to targeting the individual pathways, however dose limiting toxicities in humans have prevented this combination strategy from finding clinical success. While physiological activation of the MAPK pathway is RAS dependent, the interaction between RAS and the catalytic subunit of PI3Kα, PIK3CA, serves as an amplifier but not a primary activator of this pathway. This interaction is particularly important in cancerous cells as it serves to amplify basal PI3K activity and support tumor progression. Conversely, in healthy cells, RAS independent activation of PI3K by upstream signaling factors is sufficient for maintaining physiological homeostasis. Unfortunately, traditional strategies of targeting the PI3K pathway have been unable to capitalize on this therapeutic opportunity as they do not discriminate between RAS dependent and RAS independent signaling. This leads to on-target dose-limiting toxicities, most commonly hyperglycemia and rash. We have discovered small molecules that disrupt the RAS:PIK3CA interaction through covalent ligation of C242, in the RAS binding domain, adjacent to the RAS binding interface. Using a Nanobit system to measure the RAS:PIK3CA interaction and signaling assays in “RAS active” cells, we have optimized molecules that disrupt the RAS:PIK3CA interaction and inhibit RAS mediated activation of PIK3CA. These molecules show robust inhibition of PIK3CA signaling, and tumor growth inhibition in cancer models, but unlike PIK3CA active site inhibitors, they do not impact glucose handling. Profound efficacy is seen when these RAS:PIK3CA inhibitors are used in combination with an agent targeting the MAPK pathway or with a therapy directly targeting mutant KRAS. Finally, we found that ligation of C242 on PIK3CA blocks HER2/3 driven activation of PI3Kα in a RAS independent manner. Overall, our data supports the clinical investigation of these molecules, particularly in combination with rationally chosen therapies where they may provide a tolerable and efficacious means of blocking the PI3K pathway.

#6503 D3S-001, a second-generation GDP-bound KRAS G12C inhibitor, overcomes nucleotide cycling and demonstrates robust preclinical and clinical activities.

J. Zhang[1], S. Lim[2], M. Yu[3], C. Chen[1], J. Wang[1], W. Wang[1], H. Rui[1], J. Lu[1], S. Lu[4], T. Mok[5], Z. Chen[1], B. Cho[2];

[1]D3 Bio (Wuxi) Co., Ltd., Shanghai, China, [2]Yonsei Cancer Center, Yonsei University College of Medicine, Seoul, Korea, Republic of, [3]Yonsei University College of Medicine, Seoul, Korea, Republic of, [4]School of Medicine, Shanghai Jiaotong University, Shanghai, China, [5]Chinese University of Hong Kong, Hong Kong, Hong Kong, China

First-generation KRAS G12C inhibitors [G12Ci(s)], such as sotorasib and adagrasib, are limited by the depth and duration of clinical responses. One potential explanation for their modest clinical activity is the dynamic “cycling” of KRAS between its GDP- and GTP-bound states, raising controversy whether targeting the GDP-bound form can fully block this oncogenic driver. We herein report D3S-001, a second-generation GDP-bound G12Ci with faster target engagement (TE) kinetics, depletes cellular active KRAS G12C at sub-nanomolar concentrations, overcomes nucleotide cycling, and demonstrates durable anti-tumor activities preclinically and in a phase 1 clinical trial (NCT05410145).

Covalent efficiency and TE kinetics were measured by SPR, LC-MS and ELISA. Anti-tumor efficacy was assessed in cell line-derived xenograft (CDX) and patient-derived xenograft or organoid (PDX or PDO) models. Activity in brain metastatic tumors and tumors with acquired resistance to sotorasib was investigated.

Preclinically, D3S-001 exhibited exceptionally high covalent efficiency with a k_{inact}/K_I of 1.43×10^6 $M^{-1}s^{-1}$, the highest among all reported G12Ci(s) to date and a 20- to 70-fold improvement over adagrasib and sotorasib, respectively. In whole cells, D3S-001 depleted GTP-bound active KRAS G12C with an inactivation $t_{1/2}$ of 5.8 minutes, allowing >95% TE (5x $t_{1/2}$) in 30 minutes which is within the time required for epithelial growth factor (EGF) to induce KRAS GDP to GTP transition. By contrast, sotorasib and adagrasib required 3.7 and 2.8 hours, respectively, to reach 95% TE. In the presence of EGF, the ability of sotorasib and adagrasib to block KRAS was compromised by over 55%, whereas TE kinetics of D3S-001 was nearly unaffected, a unique feature differentiating D3S-001 from earlier GDP-bound G12Ci(s). The covalent efficiency of D3S-001 correlated with robust anti-tumor activity at sub-nanomolar concentrations and durable tumor regressions in CDX and PDX/PDO models of different cancer types. In a sotorasib-resistant PDX model, D3S-001 exhibited robust efficacy of tumor regression, while sotorasib and adagrasib showed no effect. Treatment with D3S-001 also resulted in sustained intracranial tumor remission in brain metastasis models.

In the first-in-human trial of D3S-001, durable RECIST responses in patients were observed across all dose cohorts from 50 mg to 900 mg QD. Durable intracranial activity was also observed. Response rate and duration are reported in a companion clinical trial abstract submitted to this AACR meeting.

In conclusion, D3S-001 is a second-generation GDP-bound KRAS G12Ci that overcomes GDP-to-GTP cycling. Its high covalent efficiency and rapid TE kinetics correlated with robust anti-tumor activity preclinically and translated into promising clinical activity with a high response rate and durable responses in a phase 1 trial.

#6504 Exploratory analysis using serial cell-free DNA in patients treated with amivantamab in non-small cell lung cancer with EGFR exon 20 insertion mutations.

Geun-Ho Park, Sehhoon Park, Hyen-Ae Jung, Jong-Mu Sun, Jin Seok Ahn, Myung-Ju Ahn, Se-Hoon Lee

Division of Hematology-Oncology, Department of Medicine, Sungkyunkwan University School of Medicine, Samsung Medical Center, Seoul, Korea, Republic of

Introduction: Epidermal growth factor receptor (EGFR) exon 20 insertion (ex20 ins) mutation showed limited clinical activity with conventional EGFR tyrosine kinase inhibitors (TKIs). Amivantamab is the first bispecific antibody to be approved for the treatment of metastatic non-small cell lung cancer (NSCLC) with EGFR ex20ins mutation. However, limited data is available in terms of predictive biomarkers and the resistance mechanism. In this study, we conducted an exploratory analysis to elucidate a genomic landscape using circulating tumor DNA (ctDNA) from plasma samples.

Patients and Methods: This study include result from 79 blood samples, which has been prospectively collected from 27 EGFR ex20ins mutated NSCLC patients (confirmed by either tissue or plasma-based test) who were treated with amivantamab. ctDNAs were obtained from plasma, which was serially collected at baseline, after 2 cycles of treatment, 2 cycles prior to the treatment discontinuation, and at the time point of disease progression. Guardant OMNI panel (Guardant Health, CA, USA) was used for the genomic profiling.

Results: The median follow-up duration was 5.8 months (range 2.7-12.7). The overall response rate was 40.7% (95% confidence interval [CI] 24.5-59.2, n=11), and median progression-free survival was 5.8 months (95% CI 3.9-15.9) with a median duration of response of 9.8 months (95% CI, 7.3-NA). Patients with EGFR ex20ins not detected from ctDNA at baseline (n=10) showed significantly longer PFS compared to patients with EGFR ex20ins identified at baseline plasma sample (n=17) (14.6 vs 3.9 months; hazard ratio [HR] 0.40, 95% CI 0.17-0.95, P<0.05).The most common concurrent somatic variations at baseline were *TP53* (62.9%), *TERT* (18.5%), *ATM* (18.5%). Longer median PFS was observed in patients without EGFR amplification (n=18) compared to patients with concurrent EGFR amplification (n=9) (11.1 vs. 2.5 months; HR 0.30, 95% CI 0.11-0.77, *P* <0.05).

The presence of plasma EGFR ex20ins at C2D15 predicted poor PFS (17.8 vs 2.7 months; HR 0.17, 95% CI 0.06-0.47, *P* <0.01), regardless of baseline its presence or absence. Based on the paired analysis using baseline and at the timepoint of disease progression, putative resistance mechanism to amivantamab was identified in 14 patients (60.8%), which were *PDGFRB* (28.5%), followed by *PTEN* (21.4%), *CHEK2* (21.4%).

Conclusions: This study provides a comprehensive longitudinal ctDNA analysis in patients with EGFR ex20ins mutant NSCLC who were treated with amivantamab. Our results suggested that the presence of ctDNA for EGFR ex20ins mutation and co-alteration with EGFR amplification at baseline might be related to the clinical outcomes of amivantamab.

#6505 Targeting *PINK1* reduces medulloblastoma progression in animal models.

R. N. Alsubaiee[1], A. Alghamdi[1], B. M. Alrfaei[2];
[1]King Saud University, Riyadh, Saudi Arabia, [2]King Abdullah Internation Medical Research Center, Riyadh, Saudi Arabia

Medulloblastoma is a brain cancer that mainly arises during infancy and childhood. Medulloblastoma is the most common pediatric malignant brain tumor worldwide. It comprises of approximately 20% of all childhood brain tumors and 63% of intracranial embryonic tumors. One of the major effects of proliferating cancer cells is altered mitochondrial metabolism, as well as aberrant metabolism. Medulloblastoma patients suffer severe complications due to intensive and long-term treatments. Thus, we aim to improve applications against medulloblastoma by targeting the *PINK1* gene. We hypothesize that *PINK1* inactivation slows down medulloblastoma progression. PINK1 is a mitochondrial serine/threonine protein kinase that protects cells by controlling mitochondria quality in response to cellular stress. PINK1 recruits parkin to target damaged mitochondria for degradation through autophagy. In this study, *PINK1* has been knocked-out using gene editing technology (CRISPR/Cas9) in two commercial medulloblastoma cell lines (DAOY, and D283 cell lines). We validated *PINK1* editing using RT-PCR and Western blot. Then, cell viability was studied in comparison to the control sample. The control sample contained scramble fragments with empty CRISPR/Cas9. We studied apoptosis and performed cell cycle analysis using flow cytometry. Next, orthotopic medulloblastoma mouse model was generated which showed differential survivals comparing the *PINK1* knockout group and control. The results showed a low expression of *PINK1* within the *PINK1* knockout group. In addition, the Western blot showed reductions in *PINK1* expression in the knockout group. The knockout group showed more apoptosis (cell death) 40% more than the control. The mouse model showed increased survival of the *PINK1* knockout group compared to the control with a p-value of 0.0288 (log-rank). Our analysis shows that survival differences approximately extend human life by one year. We conclude that inhibiting the *PINK1* gene in medulloblastoma decreases cell metabolic activities. *PINK1* Knockout in medulloblastoma enhances the apoptosis pathways. Engrafted medulloblastoma mouse model treated with *PINK1* inhibitor showed superior survival than the control. These results qualify PINK1 to be used as potential therapeutic target for medulloblastoma. The Future work needs additional preclinical studies to investigate the proper dose of *PINK1* inhibitor and measurement of toxicity index.

#6506 SOS1 inhibition in combination with HER2 inhibition in models of HER2-driven cancer.

R. L. Schenk[1], K. Kostyrko[1], J. Popow[1], C. Gewinner[2], A. Baum[1], C. Albrecht[1], M. Hinkel[1], R. Jacob[1], T. Madensky[1], R. Ruzicka[1], E. Strauss[1], H. Lyu[3], A. M. Lopez[3], N. Feng[3], C. P. Vellano[3], J. R. Marszalek[3], T. P. Heffernan[3], M. Pearson[1], M. H. Hofmann[1];

[1]Boehringer Ingelheim RCV GmbH & Co. KG, Vienna, Austria, [2]Boehringer Ingelheim Pharma GmbH & Co.KG, Biberach, Germany, [3]The University of Texas MD Anderson Cancer Center, Houston, TX

Cancers driven by amplifications or mutations of the gene *ERBB2* (coding for the receptor tyrosine kinase (RTK) HER2) have been the focus of HER2-targeting antibodies as well as small molecule inhibitors. Despite initial efficacy, resistance to these HER2-targeted therapies inevitably develops. One strategy to tackle this resistance is to identify rational combinations to address common pathways/factors that contribute to resistance. One such common mechanism of resistance is reactivation of the Mitogen-activated protein kinase (MAPK) pathway. SOS1 is a guanine nucleotide exchange factor (GEF) which regulates the MAPK pathway by catalyzing the exchange of RAS-GDP (inactive) to RAS-GTP (active). SOS1 is activated by multiple different RTKs - upon RTK-ligand binding, autophosphorylation of the RTK recruits the GRB2-SOS1 protein complex to the plasma membrane, enabling the complex to bind and activate RAS-GDP. Given SOS1's role downstream of RTKs and upstream of the MAPK pathway, we sought to investigate the potential of a SOS1 inhibitor (SOS1i) in combination with a HER2 inhibitor (HER2i) in preclinical models of cancer driven by HER2 mutation or gene amplification. Using in vitro and in vivo models we found evidence of added benefit of SOS1i in combination with HER2i, as well as enhanced inhibition of MAPK signaling, as seen by decrease in ERK activation and expression of MAPK effector genes such as DUSP6. Taken together, we propose that SOS1 inhibition combined with HER2 inhibition may be a rational strategy for deeper and more prolonged responses to HER2 inhibitor treatment by preventing resistance via the MAPK pathway.

#6507 Simulation driven identification of combinations for the WEE1 inhibitor Debio 0123 results in synergistic effect with cabozantinib validated *in vivo*.

B. Elek[1], A. V. Chessex[2], L. Piggott[2], O. Papp[1], I. Fekete[1], **D. Veres**[1];
[1]Turbine.AI, Budapest, Hungary, [2]Debiopharm International SA, Lausanne, Switzerland

Introduction: Debio 0123, a potential best-in-class, brain-penetrant, WEE1 inhibitor is being studied as monotherapy and in combination with standard of care therapies in patients with solid tumors in Phase I trials. The compound's mechanism of action enables a wide range of combination treatment options with the aim to increase therapeutic window, and improve treatment outcomes in cancer. WEE1 is a tyrosine kinase that is activated in response to DNA-damage acting at the G2/M and S-phase checkpoints, allowing DNA damage repair before entering mitosis. Inhibition of WEE1 increases cell sensitivity to DNA damaging agents leading to genomic instability and apoptosis. Debiopharm, in collaboration with Turbine set out to identify novel combination opportunities for Debio 0123.
Methods: Two approaches were used to identify synergistic combinations of Debio 0123. (1) an *in vitro* screening panel of 35 cancer cell lines and 70 compounds and (2) using Turbine's proprietary Simulated Cell™ solution. The *in silico* approach combines simulation with machine learning, modelling how thousands of signalling proteins interact thereby characterizing cellular level cancer behaviour and response or resistance to treatment. Millions of simulations can be carried out, identifying responder/resistant cell lines to single-or combined drug treatments, thus informing wet lab screening. Turbine built a comprehensive *in silico* model of WEE1 and associated mechanistic pathways based on scientific literature. Network-based *in silico* avatars of 116 cancer cell lines were established using public/proprietary genomic and transcriptomic data, and trained on *in vitro* dose-response to a representative set of reference compounds. High-resolution combination matrices of 59 compounds and Debio-0123 were tested *in silico*. Synergistic combinations were identified and taken forward to *in vitro* assays and *in vivo* studies.
Results: Sensitizing combinations, including DNA damaging agents as well as targeted therapies were identified using both the *in silico* and *in vitro* screens. Turbine predicted synergistic anti-tumour activity *in silico* between Debio 0123 and cabozantinib. Although previously tested using traditional screening methods, this combination had not been identified as a synergistic combination for Debio 0123. Further *in vitro* testing in multiple cell lines demonstrated synergy between these agents at all doses tested. *In vivo* testing in a CAKI-1 (renal cell carcinoma) model showed moderate monotherapy effects but significant synergy when Debio 0123 and cabozantinib were dosed in combination.
Conclusion: We demonstrated that an *in silico* computational approach to model cancer signalling pathways can complement conventional screening methodologies to identify novel, clinically actionable combination opportunities for Debio 0123.

#6509 GT0486, a novel mTORC1/2 dual inhibitor, exhibits synergistic antitumor efficacy in combination with BTK inhibitors.

X. Hou, H. Yan, X. Zhang, W. Qian, D. Chen, Z. Ren, Y. Tong;
Kintor Pharmaceutical Limited, Suzhou, China

Mammalian target of rapamycin (mTOR), a serine/threonine kinase, is the central signal molecule in regulating cell growth, metabolism, angiogenesis, and survival. The first generation of mTOR inhibitors specifically inhibit mTORC1 but are insensitive to mTORC2 and cannot eliminate the downstream signaling cascade in cancer. GT0486, a second-generation mTORC1/2 dual inhibitor, can selectively suppress mTOR kinase activity while has no inhibitory effect on other kinase receptors. We investigate the anti-tumor efficacy of GT0486 in a variety of tumor cells and xenograft animal models *in vitro* and *in vivo*. The combination effects of GT0486 and BTKi (BTK inhibitor) were also evaluated. Compared with other mTOR inhibitors (GDC-0349, AZD-2014, Rapamycin, GDC-0941, and CC-223), GT0486 exhibits the stronger inhibitory activity on human tumor cells, such as U87(glioma), PC-3(prostate cancer), MDA-MB-468(breast cancer) and Huh-7(liver cancer). In B-cell lymphoma, compared with the CC-223, GT0486 shows greater inhibitory potency against TMD8, DoHH2 and WSU-DLCL2, with IC50 values of 85nM, 96nM and 83nM, respectively. Moreover, in the U87 and the PC-3 xenograft animal models, GT0486 strongly reduced tumor growth in dose dependent manner. High synergistic effects were observed with GT0486 in combination with BTK inhibitors, including Acalabrutinib, Ibrutinib, Zanubrutinib and Orelabrutinib in the BTKi sensitive TMD8 cells. In BTKi resistant DoHH2 cells, GT0486 also enhanced the drug sensitivity of BTKi. The possible biomarkers on the synergistic mechanism were further studied. GT0486 improves the role of BTKi on cell cycle arrest in phase G1. At the same time, the phosphorylation levels of mTOR downstream effectors AKT, 4EBP1 and S6 were dose-dependently downregulated after GT0486 treatment, and a significant reduction were observed when combined with BTKi. These results demonstrate that GT0486 is a promising dual mTOR1/2 inhibitor, which is currently undergoing clinical phase I study in China for the treatment of solid tumors. Strong synergistic effects observed with GT0486 in combination with BTKi in this study might open a way for a novel treatment strategy in clinical trials.

#6510 BPI-511966,a potent and selective HPK1 inhibitor with robust single-agent efficacy for cancer immunotherapy.

Y. Zhang, X. Zhu, W. Wu, Z. Xia, Z. Zou, H. Han, C. Yang, H. Chen, T. Ma, X. Liu, J. Guo, H. Wu, **H. Lan**, L. Ding, J. Wang, Q. Zhou;
Betta Pharmaceuticals Co.,Ltd, Hangzhou, China

Although immune checkpoint inhibitors (ICIs) have become the standard treatment for many types of cancers, a large proportion of patients fail to respond to ICIs. Hematopoietic progenitor kinase 1 (HPK1) has been validated as a negative intracellular immune checkpoint that constrains T-cell activation. Genetic or pharmacological ablation of HPK1 induces a robust anti-cancer immune response *in vivo*, highlighting the potential of HPK1 as a next-generation target for cancer immunotherapy. Herein, we reported the discovery of BPI-511966, a highly potent ATP-competitive HPK1 inhibitor. The compound strongly inhibited HPK1 kinase with an IC_{50} of 2.3 nM at physiologically relevant ATP concentration (1 mM) and reduced phosphorylation of SLP-76, a substrate adaptor of HPK1, in Jurkat T cells *in vitro*, with an IC_{50} value of 11 nM. Development of an optimal HPK1 inhibitor requires not only high potency for target engagement but also high selectivity to spare other kinases that are essential for T cell activation. BPI-511966 showed >100-fold higher IC_{50} (364 nM) against MAP4K3/GLK, an HPK1 homology kinase promoting T-cell activation, and also demonstrated weak inhibition in a panel of other immune-related kinases. The remarkable potency and selectivity of BPI-511966 translate into robust T cell-enhancing efficacy *in vitro*. Treatment with BPI-511966 promoted both IL-2 and IFN-γ production by Jurkat T cell and human PBMC in a dose-dependent manner. The on-target action of BPI-511966 was validated in HPK1-KO Jurkat T cells, in which no significant impacts on SLP-76 phosphorylation and IL-2 secretion were observed. *In vivo*, single dose escalation of BPI-511966 in mice leads to dose-proportional increases in drug exposure, accompanied by inhibition of SLP-76 phosphorylation in peripheral $CD3^{\pm}$ T cells. Furthermore, repeated oral administration of BPI-511966 as a single agent significantly suppressed CT-26 tumor growth in immune-competent mice (92% TGI), correlating with increased infiltration of $CD45^{\pm}$ $CD8^{\pm}$ cells and enhanced cytokine production in tumor. Notably, the efficacy of BPI-511966 is abrogated in immune-compromised mice, suggesting its vital role in promoting anti-cancer immunity. In summary, this study presents a novel, highly potent, and selective HPK1 inhibitor BPI-511966. The robust single-agent activity of BPI-511966 makes it a promising small molecule I/O agent to address ICI resistance as monotherapy or in combination.

#6511 BPI-520105, a highly potent, CNS-penetrant 4th generation EGFR inhibitor overcoming major EGFR resistance mutations in NSCLC.

J. Guo, L. Liu, X. Liu, B. Fu, G. Bai, C. Qiu, W. Ren, X. Song, G. Du, X. Sun, Y. Zhang, W. Cai, P. Wang, H. Chen, X. Liu, Z. Zou, J. Zhao, X. Jv, H. Lan, L. Ding, J. Wang;

Betta Pharmaceuticals Co.,Ltd, Hangzhou, China

EGFR activating mutations are prevalent in 10-50% of NSCLC patients. The most common EGFR mutations, L858R (L) and Del19 (D), initially respond to first-, second-, or third-generation (1G, 2G and 3G) EGFR-TKIs. However, on-target resistance, primarily by T790M (T) and C797X(C), inevitably emerges post-treatment and leads to disease progression. Different treatment sequence give rise to different complex mutations. In patients resistant to the 3G TKI osimertinib, double mutations L858R/ C797X or Del19/C797X (LC or DC) were observed at a frequency of up to 12% after first-line osimertinib, and triple mutations L858R/T790M/C797S or Del19/T790M/C797S (LTC or DTC) were up to 20% after second-line osimertinib. There are no approved targeted therapy options for these complex resistant mutations. In this study, we developed BPI-520105, a 4th generation EGFR inhibitor capable of targeting all aforementioned major forms of EGFR activating and resistance mutations in NSCLC. It might be an optimal way to address this urgent medical need. *In vitro,* BPI-520105 potently inhibited the activity of a variety of EGFR kinases, as well as inhibited the proliferation and EGFR phosphorylation in cell lines bearing relative mutations, including single (D, L), double (DT, LT, and DC, LC) and triple (LTC, DTC) mutations. Meanwhile, BPI-520105 exhibited relative weakness towards wild type EGFR and IGF1R, demonstrating good selectivity in kinase and cell-based assays. Despite being a reversible EGFR inhibitor, BPI-520105 sustained the inhibition of pEGFR and pERK for up to 24 hours in the western blot assay. *In vivo*, oral administration of BPI-520105 displayed significant dose-dependent antitumor effect in multiple EGFR mutant xenograft models, including HCC827 (D), NCI-H1975 (LT), BaF3-EGFR-LC/DC, and BaF3-EGFR-LTC models. Remarkably, BPI-520105 significantly prolonged the lifespan of mice with brain orthotropic BaF3-EGFR-DTC-Luc2 allografts, demonstrating its activity towards brain metastasis. Additionally, BPI-520105 exhibited favorable ADME properties, with high oral exposure across various preclinical species. In summary, BPI-520105 is a highly potent, CNS-penetrant, wide type sparing, and orally bioavailable 4th generation EGFR inhibitor, holding promise for the treatment of NSCLC patients with resistance mutations post 3G progression or even at front line.

#6512 BPI-501836: A highly potent small molecule inhibitor targeting KRAS^{G12D} mutation.

X. Yang, Y. Lu, R. Xu, X. Kong, Y. Sun, X. Zhu, X. Liu, Z. Zou, H. Chen, Y. Liu, J. Sun, H. Han, C. Yang, J. Guo, H. Lan, Q. Zhou, L. Ding, H. Wu, **J. Wang**; Betta Pharmaceuticals Co.,Ltd, Beijing, China

As one of the most notorious un-druggable oncogenes, mutant KRAS impairs the transition of RAS from its active GTP-binding form to the inactive GDP-binding form, leading to sustained activation of downstream MAPK pathway and ultimately tumorigenesis. The recent approved KRAS^{G12C} inhibitors have demonstrated clinical benefits in KARS^{G12C} mutant patients. However, the other prevalent KRAS mutations, such as KRAS^{G12D}, remain a huge unmet medical challenge. There's no approved KRAS^{G12D} specific inhibitors yet. Here we present BPI-501836, a highly potent and selective small molecular inhibitor for KRAS^{G12D}. *In vitro,* BPI-501836 exhibited very high potency by disrupting the KRAS^{G12D} and cRAF interaction in a cell-free assay. In cell-based assays, BPI-501836 inhibited proliferation of KRAS^{G12D} mutant cell lines with sub-nanomolar IC_{50} values, without affecting wide type or non-G12D KRAS mutant cell lines. Moreover, it also attenuated ERK phosphorylation in KRAS^{G12D} mutant cells. *In vivo*, tumor regression was observed following the administration of 6 mg/kg (iv, QW) BPI-501836 in KRAS^{G12D} human pancreatic Panc04.03 xenograft mouse models, or in the KRAS^{G12D} human pancreatic PK-59 xenograft mouse models with an intraperitoneal injection of 20 mg/kg per week. Noteworthy was the prolonged half-life of BPI-501836 observed across various species, coupled with its high distribution in tumor tissues. Moreover, sustained suppression of ERK phosphorylation in tumor tissues persisted for up to 144 hours after the last dose of BPI-501836 in both xenograft mouse models. This extended pharmacodynamic effect supports the feasibility of a once-weekly dosing schedule in clinical applications. Safety assessments conducted through a 4-week repeated infusion (intravenous, twice weekly) of BPI-501836 in beagle dog demonstrated favorable safety profiles. In conclusion, BPI-501836 emerges as a highly potent and selective KRAS^{G12D} inhibitor, exhibiting promising pharmacokinetics, pharmacodynamics, and safety profiles in pre-clinicalstudies. BPI-501836 is currently in IND-enabling stage and holds potential for further development as a therapeutic agent.

#6513 Discovery and characterization of a KRAS$^{G12C/D/V}$ degrader with potent anti-tumor activity in KRAS^{mut}-driven preclinical models.

Z. Li, R. Xu, X. Yang, Z. Zou, X. Kong, H. Chen, Y. Sun, Y. Zhao, J. Guo, C. Yang, H. Han, X. Liu, H. Lan, L. Ding, Q. Zhou, H. Wu, **J. Wang**;
Betta Pharmaceuticals Co.,Ltd, Beijing, China

KRAS mutations are one of the most common oncogenic drivers for multiple cancers. KRAS^{G12X} mutations are identified in approximately 25% of lung cancer, 24% of colorectal (CRC), and 79% of pancreatic ductal adenocarcinoma (PDAC). Although the approval of Sotorasib in 2021 by the FDA partially addressed the needs of patients with KRAS^{G12C} mutant, other mutations, such as G12D and G12V, still lack effective target therapies. Here, we report RD0255359, a proteolysis targeting chimera (PROTAC) KRAS$^{G12C/D/V}$ degrader with highly potent cell viability and KRAS$^{G12C/D/V}$ degradation ability. *In vitro*, RD0255359 exhibited a remarkable KRAS degradation property in NCI-H358 (G12C), AGS (G12D), and SW620 (G12V) cell lines at concentrations below 10 nM. RD0255359 suppressed the proliferation of these cells with nanomolar IC_{50} without affecting the viability of KRAS^{WT} or KRAS-independent cell lines. Meanwhile, using protease inhibitor MG132 or corresponding ligand pretreatment and VHL^{KD}-AGS cell experiment confirmed that RD0255359-induced KRAS degradation was VHL and UPS dependent. *In vivo*, weekly IV injection of 1-10 mg/kg RD0255359 led to tumor growth suppression or tumor regression in PK-59 PDAC xenograft model. The *in vivo* PK/PD demonstrated that durable KRAS degradation could be achieved with once- weekly IV injection. Notably, after injection, the drug can distribute into tumor tissue rapidly and abundantly, and maintaining a high concentration till the next administration. Taken together, RD0255359 is a highly potent and selective KRAS$^{G12C/D/V}$ degrader with favorable PK properties. It exhibits a promising therapeutic index in preclinical studies.

CLINICAL RESEARCH: Tumor Microenvironment and Cancer Immunity
Poster Session

#6516 Single-cell protein activity inference reveals lymphocytic immune infiltration in diffuse intrinsic pontine glioma induced by focused ultrasound.

E. White[1], H.-J. Wei[2], E. Fernandez[2], H. Minns[2], J. Pavisic[2], R. Gartrell[2], C.-C. Wu[2], A. Califano[2], **A. Obradovic**[2];
[1]Columbia University, New York, NY, [2]Columbia University Irving Medical Center, New York, NY

Diffuse intrinsic pontine glioma (DIPG) is a highly aggressive pediatric brain tumor, located in the brainstem, and traditionally thought to be immune-excluded with no significant infiltration by cytotoxic T-cells, and therefore not amenable to immunotherapies. Focused ultrasound technology (FUS) for drug delivery is being investigated for DIPG in both preclinical and clinical trial settings. In this study, we sought to study the effects of FUS and radiation therapy (RT) on immune cell infiltration in DIPG tumors to assess their ability to alter the immune microenvironment and potentially enhance combination immunotherapies. Specifically, we generated single-cell RNAseq profiles for 27,780 cells from syngeneic orthotopic DIPG tumors (KPAP cell line containing H3K27M mutation, ATRX and P53 loss, and PDGFRA overexpression) after 14 days of tumor growth across the following treatment arms: vehicle control, FUS, and RT (n=2 each group). FUS was applied by 4-point sonication around the tumor with a pressure of 0.6 Mpa at days 8 and 11 post tumor implantation (PTI). RT was administered in fractions of 3 Gy daily from days 8 to 11 PTI (12Gy total). We leveraged a set of algorithms for network-based inference of regulatory protein activity to infer a set of context-matched gene regulatory networks from which protein activity can be inferred by expression of downstream targets. By this approach, we identified distinct clusters of immune cells segregating by cell type as inferred by singleR and activity of known lineage markers. Strikingly, we found that both RT and FUS significantly depleted a TGFb-expressing population of immune-suppressive macrophages as compared to vehicle controls. Importantly, FUS only additionally increased T-cell infiltration into the tumor micro-environment over three-fold as compared to vehicle controls, which was not observed in response to RT. Further protein validation is underway. This has significant implications for therapeutic combinations of FUS-mediated drug delivery with immune checkpoint inhibitors in DIPG, such that in addition to drug delivery, FUS-mediated immune modulatory effects may provide more proinflammatory response to enhance immunotherapy.

#6517 ALDOC as an indicator of HMGB1 blockade combined with checkpoint inhibitor based immunotherapy in GBM patients.

Y.-F. Yang[1], M.-H. Chan[2], C.-L. Chen[3], M. Hsiao[4], **Y.-C. Chang**[2];
[1]Kaohsiung Veterans General Hospital, Kaohsiung, Taiwan, [2]National Yang Ming Chiao Tung University, Taipei, Taiwan, [3]Taipei Medical University Hospital, Taipei, Taiwan, [4]Academia Sinica, Taipei, Taiwan

Aldolase is an enzyme that takes part in glycolysis by catalyzing a six-carbon intermediate to yield two three-carbon products, requiring ATP. The aldolase family comprises three members, namely ALDOA, ALDOB, and brain-specific ALDOC. Low-grade gliomas and glioblastoma (GBM) are characterized by shared genetic events, including chromosome 1p/19q codeletion, EGFR amplification, and ATRX loss of function, in which ALDOC plays a role. Additionally, ALDOC is responsive to IDH1 mutations. If patients display IDH1 mutations, it is expected that ALDOC performance will be relatively higher. This finding suggests a more favorable prognosis. The ALDOC promoter region's function is impeded by hypermethylation, which declines as glioma progresses. The regulatory mechanisms and implications remain unclear. We established a multi-omics profile and identified several crucial mechanisms activated upon the loss of ALDOC expression. Among these mechanisms, we found HMGB1 to have a key role in linking the immune response, tumor microenvironment, and epigenetic modifications. We compared the proteomic and secretomic platforms in an ALDOC overexpression/knockdown model, which showed abundant HMGB1 expression following ALDOC inhibition. Importantly, there is an inverse correlation between ALDOC expression and HMGB1 protein levels. Additionally, our findings reveal that upregulation of ALDOC promotes its translocation to the nucleus, thereby enhancing its binding affinity with HMGB1. This, in turn, enables extracellular release of HMGB1 in GBM, which triggers signaling via receptors for advanced glycation end-products (RAGE) and several cytokines. Moreover, HMGB1 remodels the immune microenvironment and upregulates multiple immune checkpoint molecules, including PD-L1, PD-L2, B7-H3, and MHCs. Not all GBM models exhibited significant effects when combined with immune checkpoint blockade using HMGB1 blockade. However, ALDOC knockout mice demonstrated poorer survival and treatment efficacy, suggesting that ALDOC may be crucial for a personalized immunotherapy strategy.

#6518 BPM 31510: Targeting the tumor microenvironment (TME) via mitochondrial-mediated ROS production.

S. Gesta[1], M. D. Nastke[1], S. Nagpal[2], L. Recht[2], M. A. Kiebish[1], N. R. Narain[1], V. R. Modur[1];

[1]BPGbio Inc., Framingham, MA, [2]Stanford University, Palo Alto, CA

The tumor microenvironment (TME) consists of an enriched population of immune cells and milieu of factors that modulate key cellular processes such as angiogenesis, metabolism, apoptosis, migration, and proliferation. Previous studies have suggested that BPM 31510 induces ROS through high intra-cellular levels of ubidecarenone in aggressive cancer phenotypes both *in vitro* and *in vivo* through induction of mitochondrial ROS. Furthermore, we have previously observed efficacy of BPM 31510 in a highly aggressive *in vivo* orthotopic rat C6 glioma model where BPM 31510 was administered in combination with radiotherapy. In a pancreatic xenograft mouse model, we previously reported that BPM 31510 impacted the immune cells in the TME by increasing absolute number of infiltrated CD8+ T-cells and decreasing absolute number of infiltrated CD4+ T-cells. Moreover, an *ex vivo* study of PBMC's from healthy volunteers suggests that BPM 31510 increases T-cell viability and function while also decreasing T-cell exhaustion. Currently, an ongoing first-line phase 2b study of BPM 31510 in glioblastoma in combination with radiotherapy and temozolomide will assess the clinical efficacy and potential for mechanistic synergy of multiple ROS-inducing mitochondrial mediated regimens on this aggressive cancer phenotype. BPM 31510 will be assessed in this study to provide further evidence for the impact of ROS on immunomodulation. Taken together, BPM 31510 increases mitochondrial ROS/OXPHOS in cancer cells while impacting TME-related immune cell modulation.

#6519 Dendritic cell vaccine cell numbers and survival in patients with primary glioblastoma.

R. O. Dillman, G. I. Nistor, K. Godding, R. Robles, H. S. Keirstead;
AIVITA Biomedical, Inc., Irvine, CA

Standard glioblastoma (GBM) treatment is associated with poor survival. A promising novel immunotherapy consists of autologous dendritic cells (DC) pulsed with autologous tumor antigens (ATA) from a lysate of irradiated self-renewing autologous cancer cells. An open-label, phase 2 trial was conducted in 57 patients with primary GBM. Here we report correlations between survival and DC-ATA doses. Two autologous intermediate products were manufactured for each patient: a tumor cell line established from resected GBM, and DC differentiated from cryopreserved peripheral blood monocytes (MC). Patients were enrolled prior to standard radiation therapy (RT) and temozolomide (TMZ) chemotherapy. DC-ATA were manufactured during RT/TMZ, divided into individual doses, then cryopreserved in liquid nitrogen. For each patient-specific vaccine batch, cell numbers were calculated using a hemocytometer; viability was determined before cryopreservation (cryo) using trypan blue and post-cryo using 7ADD per flow cytometry. After RT/TMZ, up to 8 doses were injected s.c. concurrent with TMZ over 6 months. Patients were grouped into tertiles based on DC-ATA cell numbers and survival. Prism 10.03 was used to generate survival curves and calculate correlation coefficients and log-rank and T-Test comparisons. As previously reported, cell line success rate was 71/73, sufficient MC numbers were collected by leukapheresis for 63/65; DC-ATA was successfully manufactured for 60/60; 57 patients were treated; median progression free survival (PFS) and overall survival (OS) were 10.4 and 16.0 months respectively. Correlations were strong between total and viable DC-ATA pre-cryo (0.97, $p<0.0001$) and post-cryo (0.95, $p<0.0001$), but weaker between DC-ATA pre- and post-cryo (0.30, $p=0.02$), and between viable DC-ATA pre- and post-cryo (0.37, $p=0.004$). When patients were grouped by OS tertiles, medians were 9.8, 18.1, and more than 36 months. There were no differences in the average millions (M) of DC-ATA pre-cryo (10.0, 9.7, 9.6), viable DC-ATA pre-cryo (8.5, 7.8, 7.9), DC-ATA post-cryo (9.0, 10.3, 10.8) or viable DC-ATA post-cryo (6.0, 7.3, 7.4). Similarly, when patients were grouped into tertiles by DC-ATA numbers, there were no differences in OS curves associated with DC-ATA pre-cryo, viable DC-ATA pre-cryo, DC-ATA post-cryo, or viable DC-ATA post-cryo. Pre-cryo viable DC-ATA numbers ranged from 0.27 to 27.0 M. An ineffective dose was not identified; pre-cryo viable DC-ATA doses of less than 2M were associated with OS of 10.4, 13.0, 13.3, and 36.4+ months. Also, there was no OS difference by number of MC used to manufacture DC or by number of DC manufactured. In conclusion, there was no evidence for a dose/response relationship between DC-ATA dose and OS for any of the parameters tested. This data supports that pre-cryo cell counts can be used to establish treatment doses. Pre-cryo viable cell counts of 2M DC-ATA per dose seem sufficient.

#6520 Clinical verification oftherelationship betweenserum lipid metabolism andtumor immune microenvironment inpostmenopausal hormone receptor-positive/HER2-negative breast cancer patients.

W. Goto, H. Matsuda, S. Henmi, M. Nishikawa, A. Kouchi, R. Kouhashi, A. Yabumoto, K. Takada, Y. Tauchi, K. Ogisawa, T. Morisaki, S. Kashiwagi; Osaka Metropolitan University, Abenoku, Osaka, Japan

Background: Recently, some basic research has reported that the tumor immune microenvironment (TIME) is related to the therapeutic efficacy and prognosis of breast cancer patients, and that the regulation of metabolism can affect TIME and enhance antitumor immunity. Suppression of aromatase expression from adipose tissue is the standard adjuvant endocrine therapy for postmenopausal hormone receptor (HR)-positive/human epidermal growth factor receptor 2 (HER2)-negative breast cancer, but few studies have examined the impact of controlling lipid metabolism on TIME and cancer prognosis.
Materials and Methods: Except for patients with ductal carcinoma in situ, 531 postmenopausal HR-positive/HER2-negative breast cancer patients treated with curative surgery between 2011 and 2017 were examined. Serum lipid levels and systemic immune-related markers were evaluated by blood samples, and tumor-infiltrating lymphocytes (TILs) in cancer tissue samples were investigated by immunohistochemistry. We also examined the relationship between lipid metabolism, TIME, and prognosis, respectively.
Results: Good serum lipid control group was significantly correlated with low neutrophil- to-lymphocyte ratio (NLR) ($p = 0.024$) and high TILs ($p = 0.039$). The median follow-up time for the assessment of prognosis was 5.5 years, and 67 patients had recurrence. Only patients treated with aromatase inhibitor as adjuvant endocrine therapy showed significantly better recurrence-free survival (RFS) in the good lipid control group ($p = 0.025$, log-rank). Also, multivariate analyses showed that good serum lipid control was an independent prognostic factor for recurrence (HRs = 4.722, 95%CI: 1.006-22.161, $p = 0.049$). Patients with high CD8/FOXP3 ratio (CFR) had significantly better RFS ($p=0.027$, log-rank) and tended to have good lipid control.
Conclusions: Good control of serum lipid metabolism may inhibit the acquisition of resistance to endocrine therapy by improving TIME and induce favorable outcome in postmenopausal HR-positive/HER2-negative breast cancer patients.

#6521 Macrophage-targeting immunotherapy enhances chemotherapy response in primary and metastatic triple-negative breast cancer models.

M. E. Fernandez, Y. Alshehry, L. Graham, J. E. Koblinski, H. D. Bear, D. H. Sweet, S. R. P. da Rocha;
Virginia Commonwealth University - VCU, Richmond, VA

Triple-negative breast cancer (TNBC) is a highly aggressive breast cancer subtype that lacks targeted treatment options. While immune checkpoint blockade leads to significant benefits in the treatment of TNBC when in combination with chemotherapy, recurrence, metastasis, and chemoresistance still remain major challenges. The purpose of this study was to assess the ability of a colony-stimulating factor 1 receptor inhibitor (CSF-1Ri) to shift the phenotype of the tumor microenvironment (TME) in murine models of TNBC, and the potential benefit of such in enhancing standard of care chemotherapy. We focused on targeting tumor-associated macrophages (TAMs) as they are the most abundant immune infiltrate in the TNBC TME and are associated with worsening overall survival (OS) and metastasis free survival (MFS). Targeting TAMs, specifically M2-like TAMs, has been shown to inhibit tumor progression and improve OS in the clinic. We selected pexidartinib (PLX) as the CSF-1Ri of choice, given its translational potential (FDA approved) and gemcitabine (GEM) as chemotherapy, given its ability to target myeloid derived suppressor cells and M2-like TAMs. For primary TNBC we employed 4T1 mammary carcinoma cells transfected with luciferase reporter gene in BALB/c mice as an immunocompetent model. Mice were injected with 100,000 cells in the 4^{th} mammary fat pad, and tumors established over the course of fifteen days. Mice were then exposed to daily administrations of PLX (8 mg/kg), and weekly administrations of GEM (60 mg/kg). Tumor volumes were recorded every other day. The TME was analyzed with flow cytometry (FC), immunohistochemistry (IHC), and multiplex immunofluorescence (mIF). For the metastatic model, mice were inoculated with 100,000 4T1-luc cells in the flank. On day six, mice were exposed to treatments as outlined above. Mice underwent survival surgery to remove the primary tumor on day thirteen and were then treated with adjuvant therapy. Metastasis and OS were tracked. FC analysis indicated only combination therapy (11.8% ± 2.1) significantly decreased total TAMs compared to vehicle (22% ± 2) in the primary tumor. Combination therapy also showed the greatest depletion of M2-like TAMs (2.2% ± 0.6), with a significant decrease compared to both vehicle (15.6% ± 0.4) and GEM (6.6% ± 0.9). This TME modulation was confirmed using IHC and mIF. After four cycles of treatment, combination therapy (232.9 mm^3 ± 130.8) had a significant effect on tumor burden compared to GEM alone (369.7 mm^3 ± 165.8), indicating a correlation between tumor phenotype and therapeutic benefit. Furthermore, combination therapy led to the greatest prolongation of MFS and OS in the resection model, indicating that combination therapy has efficacy in the neoadjuvant and adjuvant setting. In conclusion, targeting TAMs in TNBC primes the tumor for combination with chemotherapy in TNBC.

#6522 Epigenetic modulation decreases myeloid suppression to improve response to immune checkpoint inhibition in breast cancer.

A. G. Baugh[1], E. Gonzalez[1], J. Kreger[2], Y. Liu[2], B. Al-Zubeidy[1], L. Danilova[3], S. M. Shin[3], V. H. Narumi[1], S. Castanon[1], J. Jang[1], E. J. Fertig[3], A. Cimino-Mathews[3], E. M. Jaffee[3], V. Stearns[3], R. M. Connolly[4], W. Ho[3], A. MacLean[2], **E. T. Roussos Torres**[1];

[1]Keck School of Medicine, University of Southern California, Los Angeles, CA, [2]University of Southern California, Los Angeles, CA, [3]Johns Hopkins University, Baltimore, MD, [4]University College Cork, Cork, Ireland

Immune checkpoint inhibitors (ICIs) promote a durable anti-tumor immune response. Unfortunately, many patients with breast cancer are thought to be intrinsically resistant. One potential mechanism of resistance is a myeloid suppressed tumor microenvironment (TME). Targeting myeloid suppression is under investigation as a therapeutic strategy to sensitize tumors to ICI. In our trial, NCI-9844, we demonstrated that the combination of the epigenetic modulator, entinostat with ICIs—nivolumab (anti-PD-1) + ipilimumab (anti-CTLA-4), leads to a 25% objective response rate in patients with advanced breast cancer. Work in our preclinical models showed entinostat decreases suppressive function by myeloid derived suppressor cells (MDSCs). We hypothesized that entinostat decreases intra-tumoral MDSC suppression via the STAT3/AP-1 axis and drives cellular shifts within the TME to improve response to ICI. Here, we examined expression of upstream, downstream, and interacting factors within the STAT3 pathway in MDSCs treated with entinostat. Macro-dissected lung metastases from entinostat treated NeuN mice revealed differential gene expression of AP-1 subunits JunB and FOSL1 in MDSCs identified by single cell RNA sequencing (scRNAseq). Western blot of isolated intratumoral MDSCs from lung metastases revealed decreased STAT3 phosphorylation upon entinostat treatment. In an entinostat treated MDSC-like cell line, J774M, JunB phosphorylation and FOSL1 were both decreased. scRNAseq also revealed decreased gene expression of STAT3 upstream receptors IL4RA and IFNGR1 and increased expression of STAT3 negative regulator SOCS3. Chromatin immunoprecipitation sequencing is planned to further narrow the molecular mechanism of action. Cell-cell communication analysis of scRNAseq data was performed to evaluate the contribution of entinostat treated macrophages, dendritic cells (DCs), and natural killer (NK) cells on MDSC function. We observed increased frequency of DC populations (classic DC2s and Ccr7 DCs). Following combined treatment with entinostat + ICIs, we also found increased DC to T cell signaling strength for receptor-ligand pairs involved in T cell activation, including Tnfsf9__Tnfrsf9, Cd70_Cd27, H2-dmb2_Cd4, and Cd80_Cd28. Analysis of macrophage-T cell interactions revealed a synergistic decrease in signaling associated with immunosuppression after combined treatment, such as Cd80_Ctla4, Tnf_Tnfrsf1b, and Entpd1_Adora2a. Suppressive function of treated sub-populations of macrophages is planned to determine functional effect of findings. Finally, we are using imaging mass cytometry and bulk RNA sequencing to evaluate proposed mechanisms in patient specimens (NCI-9844). The goal of this work is to identify the molecular and cellular mechanisms driving myeloid suppression of the TME thereby identifying potential therapeutic targets.

#6523 TOX upregulation promotes a GPX4-dependent CD8$^{\pm}$ T cell ferroptosis in tumor microenvironments.

J. Li, Q. Zhu, X. Liu;
Sun Yat-sen University Cancer Center (SYSUCC), Guangzhou, China

Frequency and function of CD8$^{\pm}$ tumor-infiltrating T cells (TILs) decide on clinical outcome of cancer immunotherapy; and TOX function as a crucial regulator of TIL dysfunction. In the present study, we found that multiplex factors, such as tumor cell, viral antigens and hypoxia, in tumor microenvironments (TME) induced CD8$^{\pm}$ TIL ferroptosis by upregulating TOX. Single cell RNA-sequencing revealed that TOX modulated *Havcr2, Pdcd1, Hmox1, Gpx4,* and *Ctsb* transcription in human and murine CD8+ TILs. We further generated TOX conditional knockout in CD8+ T cell ($Tox^{flox/flox}Cd8^{Cre}$, CKO) mice and the tumor-bearing CKO mice exhibited increased anti-tumor immunity and survival time. TOX upregulation increased reactive oxygen species (ROS), lipid peroxidation, and ferrous iron, leading to a GPX4-dependent CD8$^{\pm}$ T cell ferroptosis. Genetic or antibody ablation of TOX, TIM-3, or HO-1 indicated that these molecules orchestrated CD8$^{\pm}$ TIL ferroptosis by inducing iron overload and lipid peroxidation. Targeting TOX, PD-1, TIM-3, or ferroptosis boosted the anti-tumor suppression of tumor-specific T cell-based adoptive cell therapy (ACT) in murine tumor model. TOX, TIM-3 and GPX4 were prognostic predictors in human cervical cancer. This finding identifies a novel mechanism of tumor-induced CD8$^{\pm}$ T cell ferroptosis underwent by TOX that provides new insights in improving TIL-based ACT immunotherapy.

Key words: TOX, CD8$^{\pm}$ T cells, ferroptosis, tumor microenvironments, cancer immunotherapy

#6524 Single-cell landscape of cancer-associated fibroblasts in immunotherapy resistance of hepatocellular carcinoma.

P. P. Wong, J. Cao, Z. Xiong, H. Wu, Q. Cao, B. Chen, K.-F. To, S. L. Chan, W. Kang, A. S. Cheng;
Chinese University of Hong Kong (CUHK), Hong Kong, Hong Kong

Introduction: The advent of immune checkpoint blockade (ICB) therapy has revolutionized the treatment approach for hepatocellular carcinoma (HCC). However, the response rate to ICB therapy remains low (below 20%). This limited response rate can be attributed to the considerable heterogeneity observed in HCC cells and the tumor microenvironment (TME). Recent research has highlighted the pivotal role of cancer-associated fibroblasts (CAFs) in orchestrating various components within the TME of HCC. Although the significance of lipid metabolism-associated CAFs in the efficacy of ICB therapy has been demonstrated in HCC murine models [1], the functions and contributions of other CAF subtypes remain largely unknown. Therefore, identifying CAF heterogeneity could advance our comprehension of HCC TME and potentially augment ICB efficacy.

Methods: We performed single-cell RNA sequencing on tumor biopsy specimens obtained from patients with advanced HBV-related HCC who had participated in a pembrolizumab (anti-PD1) phase II clinical trial (NCT03419481). Our objective was to examine the dynamic alterations in the HCC TME before and during anti-PD1 treatment (upon 2-cycle). We utilized the Seurat and Cellchat packages for bioinformatics analysis which enabled us to investigate the associations between changes in the proportions of CAF subtypes and the patients' clinical responses, as well as the potential cell-cell interactions involving CAF and other TME components.

Results: We identified four CAF subtypes within the TME: cycling, inflammatory, matrix, and vascular CAFs in our anti-PD1 HCC patient cohort. Among the anti-PD1 non-responders, there was a significant increase in the proportions of cycling CAFs (cCAFs) and matrix CAFs (matCAFs) compared to the responders. Notably, matCAFs exhibited a high enrichment of Gene Ontology (GO) Terms related to the extracellular matrix (ECM), whose higher proportion correlated with poor prognosis of patients. Moreover, a distinct collagen pathway signal was found between matCAFs and two immunosuppressive cell types, namely regulatory T cells and M2 macrophages in the non-responders.

Discussion and Conclusion: The presence of matCAFs within the HCC tumor may associate with the development of an immunosuppressive TME and unfavorable prognosis for patients. Targeting this specific CAF subtype holds promise as a potential strategy to overcome resistance to ICB therapy.

Acknowledgments: The CUHK Strategic Seed Funding for Collaborative Research Scheme and The Li Ka Shing Foundation.

References: 1. Zhu, GQ., Tang, Z., Huang, R. et al. CD36^{+} cancer-associated fibroblasts provide immunosuppressive microenvironment for hepatocellular carcinoma via secretion of macrophage migration inhibitory factor. Cell Discov 9, 25 (2023).

#6525 Modulating the immune response in cholangiocarcinoma: Targeting sulfatase-2 for therapeutic intervention.

T. R. Brooks[1], N. Campbell[2], M. Keim[2], L. R. Roberts[2];

[1]Mayo Clinic Graduate School of Biomedical Sciences, Rochester, MN, [2]Mayo Clinic, Rochester, MN

Cholangiocarcinoma (CCA) is an aggressive epithelial malignancy of the bile ducts. Recent reports have suggested a rise in the incidence of CCA globally. Current treatments for CCA have limited effectiveness, with only 20-30% response rates in patients with advanced cancer. Thus, there is a growing need to investigate new therapeutic targets for CCA. The tumor microenvironment (TME) is a potential target for novel therapies. The TME plays an important role in progression and metastasis of cancer through facilitating immune escape. Recent studies have demonstrated potential roles for heparan sulfate proteoglycans (HSPGs) in tumorigenesis. Sulfatase 2 (SULF2) is a heparan sulfate editing sulfatase that removes the 6-O sulfate moiety within the heparan sulfate (HS) chains and alters the affinity of HS chains for growth factors and cytokines and their receptors, thus modulating HSPG function in cell signaling pathways. HSPG specific sulfatases have been recently identified as a potential therapeutic target in CCA. We aimed to assess the effects of anti-Sulfatase-2 antibody on immune cells in the tumor microenvironment of syngeneic CCA xenografts in C57BL6 mice. Mice bearing syngeneic CCA xenografts were treated with an anti-sulf2 antibody, and the tumors compared to untreated control xenografts. After treatment, the tumors were harvested and analyzed by Cytometry by time of flight (Cytof) to identify changes in the types and numbers of immune cells in the tumor xenografts. Treatment with anti-sulf2 antibody resulted in a decrease in immunosuppressive cells such as tumor associated macrophages (TAMs) and myeloid derived suppressor cells (MDSC) compared to the control. There was also an increase in anti-tumor cells such as T-cells and NK cells, suggesting that suppressing sulf-2 in the microenvironment can shift the TME toward an anti-tumorigenic rather than a pro-tumorigenic environment. In summary, our work demonstrates the potential to target Sulfatase 2 as a therapeutic mechanism for immunomodulation of the tumor microenvironment. Future experiments to determine the relationship between specific clinical phenotypes and the number, activities and types of immune cells seen in the TME, and experiments in other hepatobiliary cancers models, such as hepatocellular carcinoma and gallbladder cancer, will be conducted.

#6526 Spatial characterisation of the tumour immune microenvironment in ARID1A-deficient gastric cancer.

Norbert Sheng Cong Tay[1], Yan Fen Peng[1], Heike Grabsch[2], Anand D. Jeyasekharan[1]

[1]Cancer Science Institute of Singapore, Singapore, Singapore, [2]Pathology, Maastricht University Medical Center, Maastricht, Netherlands

AT-Rich Interacting Domain 1A (ARID1A) is an important component in SWI/SNF Complex, a chromatin remodeller and an established tumor suppressor gene that is mutated in a variety of cancer types. This includes endometrial (~45%), bladder (~20%), and gastric (~15%). ARID1A mutations usually lead to a loss of protein expression or function, which results in tumor progression. The loss of ARID1A has been linked to genomic instability, potentially making the tumor more immunogenic/ amenable to immune checkpoint inhibitor therapy. However, there is a discrepancy between clinical and mechanistic studies in determining the consequence of ARID1A-loss on the tumor immune microenvironment (TIME): clinical studies have shown that ARID1A mutation is a potential predictive biomarker for immunotherapy success, whereas another mechanistic study found that ARID1A-loss results in a cold TIME that is less amenable to immunotherapy. Considering this controversy, our overarching objective is to use multiple high-dimensional microscopy-based techniques to robustly and comprehensively characterize the TIME sculpted by ARID1A-loss. We study this in the context of gastric cancer, a disease which has heterogenous responses to PD-1 based immunotherapy and also shows frequent (10-25%) mutations in ARID1A. We looked at two retrospective cohorts with 250 patients each, one from UK (Leeds) and one from Japan (KCCH). To ascertain ARID1A-loss in these patients, we have set up an IHC-based assay comparing ARID1A expression between tumor and stroma regions. From this, we derive a ratio. In both studies, we were able to clearly stratify the cohort into ARID1A-loss and ARID1A-wildtype. Leeds had about 23 cases (10%) of ARID1A-loss, while KCCH had 39 cases (17.9%). Looking at the clinical parameters, we realized that ARID1A-loss does not stratify for survival nor staging of the tumor, which is also seen in ARID1A-mutation studies. Using multiplex immunohistochemistry (IHC), we saw differences in the immune cell population. ARID1A-loss patients seem to have a greater proportion of CD3+ cells in the Leeds (1423 vs 666 cells/mm^2, p = 0.0269) and KCCH cohorts (1457 vs 1268 cells/mm^2, p = 0.1745). Interestingly, CD68+ cells also show an increase in the ARID1A-loss population in the Leeds (802.1 cells/mm^2 vs 580.3 cells/mm^2, p = 0.0649) and KCCH cohorts (659 vs 623.2 cells/mm^2). However, CD20+ cells show no changes in abundance for either cohort (249.1 vs 193.2 cells/mm^2, p = 0.4985; and 361.6 vs 357.5 cells/mm^2, p = 0.9634) respectively. Overall, there seems to be an increase in the T-cell population in ARID1A-loss tumors and an increase in the macrophage population in stroma regions of ARID1A-loss tumors. The B-cell population remains unchanged. To complement our preliminary findings, we will leverage hyperplex and spatial transcriptome techniques to uncover the interactions between tumor cells and the TIME.

#6527 Fucosyltransferase 5 promotes immune evasion in ovarian cancer by suppressing double negative T cells.

S. Fung[1], S. To[1], A. Hassan[2], P. Ip[2], A. Wong[2];
[1]Laboratory for Synthetic Chemistry and Chemical Biology, Hong Kong, China, [2]The University of Hong Kong, Hong Kong, China

Emerging evidence suggests that aberrant glycosylation in cancer impact on various stages in the disease progression including immunomodulation, but the underlying mechanisms remain poorly understood. Our previous data demonstrated that fucosyltransferase 5 (FUT5), a glycosyltransferase responsible for the terminal step in synthesizing Lewis antigens, may contribute to peritoneal metastasis of ovarian cancer. In this study, using clinical samples of high grade serous ovarian cancer (HGSOC), the most common subtype, we found that high expression of FUT5 is associated with a worse outcome. By employing multiplex immunohistochemistry (IHC) to examine T cell subsets, we found a significant decrease in $CD3^{+}CD4^{-}CD8^{-}$ (double negative, DN) T cells in $FUT5^{high}$ (n=10) compared to $FUT5^{low}$ samples (n=10), while there is no difference in the abundance of $CD8^{+}$ cytotoxic T cells, $CD4^{+}$ helper T cells or $CD4^{+}Foxp3^{+}$ regulatory T cells. Tumor-infiltrating DN T cells has been shown to mediate potent anti-tumor response. In addition to their cytotoxic capabilities, DN T cells largely exhibit modulatory functions on other T cell subsets. To further investigate, we performed additional IHC staining and observed a significant increase in proliferating ($Ki67^{+}$) $CD8^{+}$ tissue resident memory cells, which are known to be important for cancer immunity. In addition, we observed a decrease in metastases in the FUT5 knockdown group, accompanied by an increase in DN T cells in ascites and omental metastatic tumors in humanised mice, as revealed by flow cytometry, confirming a direct immunomodulatory role of FUT5. Together, these findings reveal a novel role of FUT5 in promoting immune evasion by suppressing anti-tumor DN T cells, which could provide novel insights for immunotherapy in HGSOC, which has a low response rate to immune checkpoint inhibitors (This research is supported by RGC SRFS2223-7S05, HMRF 08192286 and LSCCB under the Health@InnoHK Program launched by ITC, HKSAR).

#6528 Integrin αvβ6 upregulation as a mechanism of T-cell evasion in head and neck squamous cell carcinoma.

W. J. MacDonald, P. R. Srinivasan, M. Pinho-Schwermann, S. Zhang, V. Tajiknia, C. Purcell, J. Strandberg, N. Stubbs, W. S. El-Deiry;
Legorreta Cancer Center at Brown University, Providence, RI

Head and neck squamous cell carcinoma (HNSCC) encompasses malignancies of the mucosal epithelium in the oral cavity, pharynx, and larynx. The lack of effective screening strategies and the typically late stage of detection are contributors to a considerable annual death toll of HNSCC. Additionally, the anatomical proximity of the malignancy to delicate structures of the head and neck leads to tremendous treatment-related morbidity. Therefore, there is great interest in developing life-saving therapies and strategies for treatment de-escalation. The immune checkpoint inhibitor pembrolizumab (αPD-1) has been approved for recurrent or metastatic HNSCC and as a frontline therapy for unresectable disease. However, only about a quarter of patients respond to αPD-1 therapy. The immunosuppressive effect of TGFβ has been widely described as relevant to the HNSCC tumor microenvironment. However, attempts to blockade TGFβ have failed mainly due to the widespread side effects of disrupting a highly promiscuous cytokine. Integrin αvβ6 is a major activator of the inert latent TGFβ into the active, immunosuppressive form. With its high relative specificity to HNSCC tissue, inhibition of αvβ6 could offer a safer approach for disrupting TGFβ to overcome resistance to immune checkpoint blockade. After screening αvβ6 expression levels of HNSCC cell lines via flow cytometry, cell lines FaDu and CAL27 were selected for further investigation due to high endogenous ITGB6 expression (FaDu 35.57% cells ITGB6+, CAL27 95.69% cells ITGB6+). The cell lines were transduced with a doxycycline-inducible short hairpin RNA (shRNA) knockdown of αvβ6 using a lentiviral system. Both knockdown and control shRNA cell lines were pretreated with 1 μg/mL of doxycycline for five days to induce the shRNA and subsequently co-cultured with TALL-104 T-cells. Quantitative fluorescence microscopy of the co-culture revealed that the knockdown of αvβ6 substantially increased T-cell killing over 24hrs (FaDu CTRL shRNA 6.72%±2.49 dead vs. FaDu ITGB6 shRNA 12.80%±3.16 dead, $p<0.001$). However, treatment of FaDu and CAL27 cell lines with active-TGFβ showed no change in PD-L1 expression via flow cytometric analysis. To determine whether the T cell evasive effect of αvβ6 is driven by other immune checkpoints on the cancer cells or by the direct effect that TGFβ has on immune cells, we show the generation of relevant mouse αvβ6 shRNA knockdown cells. These syngeneic in vivo studies will facilitate cytokine profiling to uncover the dynamics of tumor-immune cell interactions in response to αvβ6 inhibition.

#6529 Multi-lineage de-differentiation (MLDD) towards the TTF1-low phenotype is a major determinant of immune response within STK11-deficient non-small cell lung cancer.

R. Shivahare[1], N. J. Song[1], B. Nourmohammadi[1], J. Imam[1], O. Sanabria[1], J. M. Amann[1], Q. Ma[2], Z. Li[1], D. P. Carbone[1], J. Kaufman[1];
[1]The Ohio State University Comprehensive Cancer Center, Columbus, OH, [2]The Ohio State University College of Medicine, Columbus, OH

Background: The loss of serine/threonine kinase 11 (STK11) in non-small cell lung cancer (NSCLC) is associated with poor prognosis and resistance to immune checkpoint blockade (ICB) in 20-25% of cases. Experimental evidence from murine models suggests that STK11 loss contributes to lineage plasticity, while clinical observations indicate its impact on differentiation phenotypes in patients. However, the intricate interplay between differentiation states, the tumor microenvironment (TME), and clinical outcomes remains poorly elucidated. This study aims to comprehensively characterize these interactions to enhance our understanding of the complex dynamics underlying STK11-deficient NSCLC pathogenesis and therapeutic responses.
Methods: By leveraging large multi-omics datasets, we already demonstrated the low immune infiltration in TTF1-low and neuroendocrine MLDD subsets of LKB1-deficient tumors. In this study, we used GEMM-derived two KPL (Kras, TP53, and STK11 mutations) and one KPL-restored line to inject subcutaneously in F1 hybrid mice of B6 and Sv129 backgrounds. Tumor size was monitored at regular intervals, and upon reaching a sufficient size, tumors were harvested and partitioned for the characterization of immune cells (T-cells and NK cells) by flow cytometry and identification of the MLDD phenotypes through gene expression analysis using Nanostring technology.
Results: Mice injected with the STK11 WT line (2695L) exhibited smaller tumor volumes compared to those injected with STK11 mutant lines (2695X and 2381T4). Our comprehensive analysis, combining flow cytometry and Nanostring techniques, revealed that STK11 mutant lines displayed notably low infiltration of CD8+ T-cells, an elevated proportion of exhausted T-cells, and a manifestation of the TTF1-low immune phenotype characterized by high myeloid-derived suppressor cells (MDSCs) and increased KLRC1/KLRC2 expression. The presence of MDSCs in the STK11 mutant line correlated with pro-inflammatory cytokines but exhibited an inverse correlation with MHC-2 expression. MHC-2 expression was inversely correlated with CD8+ T-cell percentage and positively correlated with naïve T-cell percentage.
Conclusions: The data obtained from the study indicates that the MDSC phenotype seems to be important for immune evasion in STK11-loss tumors. Follow-up flow cytometry and gene expression experiments with combined T-cells and myeloid/PMN MDSC-related gene panels, along with further experiments involving cIAP1/PD1 inhibitors, are imperative to substantiate and expand upon our current findings.

#6530 TREM1 inhibition: A novel approach to suppress tumor growth and enhance immune checkpoint therapy.

A. Ajith, K. Moamouni, D. Horuzsko, A. Horuzsko;
Augusta University, Augusta, GA

In the context of cancer, inflammation is a multifaceted contributor to tumorigenesis. The Triggering Receptor Expressed on Myeloid Cells 1 (TREM1) is recognized for its role in amplifying inflammatory responses, yet its specific pro-tumorigenic mechanisms have remained elusive. This study employs Trem1-deficient mice and a novel inhibitor, VJDT, to explore the therapeutic potential of targeting TREM1 in cancer. Both genetic silencing and pharmacological inhibiton of Trem1 led to remarkable reductions in tumor growth in mouse models of melanoma (B16F10) and fibrosarcoma (MCA205). In-depth analysis using single-cell RNA sequencing unveiled that TREM1 deficiency resulted in a decrease in the frequency and suppressive capabilities of myeloid-derived suppressor cells (MDSCs) within the tumor microenvironment, concomitant with an increase in cytotoxic CD8+ T cells and enhanced T cell activation. Furthermore, TREM1 inhibition not only curtailed tumor growth but also potentiated the effectiveness of anti-PD-1 therapy, primarily by mitigating MDSC frequency and reversing T cell exhaustion. Notably, in melanoma xenografts from patient samples, pharmacological TREM1 inhibition via VJDT treatment significantly downregulated critical oncogenic pathways linked to cell proliferation, migration, and survival. This research underscores the pivotal role of TREM1, expressed both within cancer cells and the tumor microenvironment, in driving cancer progression. Consequently, targeting TREM1 for therapeutic intervention holds promise for reshaping the immunosuppressive tumor milieu and augmenting the success of immune checkpoint therapy.

#6531 Anti-tumor immune function of NR2F6, an orphan nuclear receptor, in stromal cells.

H. Kim[1], Y. Feng[1], M. Radaeva[2], E. Sergienko[1], A. Cherkasov[2], Z. A. Ronai[1];

[1]Sanford Burnham Prebys Med. Discovery Inst., La Jolla, CA, [2]Vancouver Prostate Centre, Vancouver, BC, Canada

Growing evidence points to the importance of the tumor microenvironment (TME) in tumor growth control, progression, and therapy response. Among those is the greater understanding of immune system components within the TME as mediators of tumor growth control. NR2F6 is an orphan nuclear receptor, which was shown to serve as an immune intrinsic checkpoint component and has been suggested to elicit tumor-intrinsic suppression of anti-tumor immunity. Correspondingly, genetic depletion of NR2F6 in CD8 T cells abrogates the immune-activating cytokines (e.g., IL-2, IFNg). In addition, genetic ablation of NR2F6 in melanoma cells activates CD8 T cell-mediated anti-tumor immunity partly by suppressing the expression of tumor-intrinsic immune repressors NACC1 and FKBP10. Notably, combined genetic ablation of tumor cells (NR2F6 KO melanoma) and stroma cells (NR2F6 KO mouse) resulted in a more pronounced inhibition of tumor growth compared with ablation of either tumor cells or TME. The latter provides the foundation for screening NR2F6 inhibitors, which are expected to have a strong systemic (tumor inhibition and immune cell activation) effect on tumor growth. Interestingly, single-cell transcriptomic data from human tumors identified high expression of NR2F6 in stroma cells, cancer-associated fibroblasts (CAFs), and tumor-associated endothelial cells (TAEs). Consistent with these, scRNAseq analysis of mouse melanoma revealed higher expression of NR2F6 in SMA+ immune suppressive myo-CAFs than in immune activating CAFs. Studies that directly reveal the role of stromal NR2F6 in anti-tumor immunity and tumor growth and the state of NR2F6 inhibitors will be discussed.

#6532 Blockade of CD24 sensitizes pancreatic cancer to Kras inhibitors.

Y. Wei[1], M. Liu[1], E.-Y. Yen[1], J. Yao[1], P. T. Nguyen[1], X. Wang[1], Z. Yang[1], A. Yousef[1], D. Pan[1], Y. Jin[1], M. S. Theady[1], J. Park[1], Y. Cai[1], M. Takeda[1], M. Vasquez[2], Y. Zhou[3], H. Zhao[2], A. Viale[1], H. Wang[1], D. Zhao[1], R. A. DePinho[1], W. Yao[1], H. Ying[1];

[1]UT MD Anderson Cancer Center, Houston, TX, [2]Houston Methodist Cancer Center, Houston, TX, [3]University of Texas Health Science Center at Houston, Houston, TX

Pancreatic ductal adenocarcinoma (PDAC) is predominantly driven by KRAS oncogene. KRAS, long considered an undruggable target, has been targeted by drugs including a $KRAS^{G12C}$ inhibitor (G12Ci), AMG 510, which is approved for the treatment of $KRAS^{G12C}$-mutant non-small cell lung cancer (NSCLC). AMG 510 also exhibited promising anticancer activity in human PDAC, with 21% response rate and over 70% patients experiencing certain level of tumor control. However, targeting KRAS oncogenes faces the major challenge of therapy resistance, which severely limited its survival benefit. While multiple studies have elucidated potential resistance mechanisms to G12Ci in lung cancer, the molecular mechanisms underlying resistance in PDAC remains elusive. Here, using $KRAS^{G12C}$-driven mouse PDAC model, we found that similar to the clinical observation, $KRAS^{G12C}$ tumors exhibit only partial response to AMG 510 treatment. CyTOF analysis indicates that such tumor persistence following G12Ci treatment occurs even in the presence of conversion from a ‘cold’ pro-tumor immune microenvironment to a ‘hot’ anti-tumor immune environment, as evidenced by the prominent increase in both cytotoxic T cells and M1-like macrophages. Interestingly, we discovered that the expression of CD24, which was recently identified as a new ‘do not eat me’ signal, is significantly upregulated on the surface of persist tumor cells after G12Ci treatment which suppresses the function of anti-tumor macrophages. Anti-CD24 blocking mAb enhanced macrophage-mediated phagocytosis in vitro and significantly sensitizes $KRAS^{G12C}$ tumors to AMG 510 treatment in vivo in a macrophage-dependent manner. Similar findings were observed in $KRAS^{G12D}$-driven PDAC model. Our findings identified a novel immune combination to improve the outcome of KRAS targeted therapy in PDAC.

#6533 Pivotal role of specific LYVE1^{+} tissue resident macrophages in PDAC progression & immunotherapy resistance.

H. Li, J. Yan;
University of Louisville, Louisville, KY

Pancreatic ductal adenocarcinoma (PDAC) is characterized by dense fibrotic stroma and abundant myeloid cell infiltration, which render it resistant to any therapeutic interventions, including immunocheckpoint blockade (ICB) therapy. Understanding the composition and function of myeloid cells within the PDAC microenvironment may help identify promising targets for PDAC immunotherapy. Tissue resident macrophages (TRMs) contribute to organogenesis and tissue regeneration and metabolism. In this study, we discovered a distinct population of pancreas TRMs that highly express lymphatic vessel hyaluronan receptor 1 (LYVE-1). Single cell RNAseq data reveal that LYVE-1+ TRM cluster in the pancreas expresses high levels of complement activation genes and transcription factors such as c-Maf and Stab1. RNAseq data also confirm that LYVE-1+ TRMs express enriched genes related to mannose binding, endocytosis, and glutathione metabolic process, while LYVE-1 negative macrophages express enriched genes related to antigen processing and presentation, T cell activation, and phagocytosis. Multiparameter flow cytometric analysis demonstrates that LYVE-1+ TRMs express M2-like markers, including increased CD163, CD206 and decreased MHC Class II molecule. During PDAC development and progression, LYVE-1+ TRMs expand and localize around the tumor border, promoting fibrotic stroma formation. Imaging mass cytometry (IMC) also reveals abundant infiltration of LYVE-1+CD14+CD68+ macrophages in human PDAC tumors and colocalized with collagen deposition. This subset of macrophages also highly express c-Maf. Through the use of Lys-Cre-c-Maf $^{f/f}$ mice, we demonstrate that depletion of c-Maf from myeloid cells significantly reduces LYVE-1+ TRMs and polarizes them to resemble an M1-like phenotype. In conclusion, our findings suggest that LYVE-1+ macrophages are a unique subset of myeloid cells within the pancreas and likely play a critical role in PDAC progression and immunotherapeutic resistance. Future work will focus on targeting LYVE1+ TRMs using various approaches, such as conditional knockout mice and small molecule inhibitors, to determine their therapeutic potential for PDAC treatment.

Presented by Dr. Hong Li

#6534 Overcoming B regulatory cell induced STING resistance by dual functional albumin nanomedicine to prolong survival of pancreatic cancer.

C. Li, S. Mao, H. Zhao, D. Mahamadou, Z. Liu, H. Wen, M. He, M. Wang, J. Tao, B. Wen, T. Hoang, B. Jacobovitz, F. Wen, W. Gao, D. Sun;
University of Michigan, Ann Arbor, MI

Pancreatic cancer is the most lethal form of cancer with a 5-year survival at 11% and lacks treatment options. Immunotherapy, specifically anti-PD-1/PD-L1 antibody, proves ineffective for pancreatic cancer patients due to the immunosuppressive tumor microenvironment (TME). STING agonist has emerged as the most effective immune modulator to regulate immunosuppressive TME to enhance the efficacy of immunotherapy across many different cancer types. However, two challenges hinder the use of STING agonist in pancreatic cancer: (A) STING agonist strongly stimulates induction of B regulatory cells (Bregs) in pancreatic tumor and lymph node, leading to an intrinsic resistance to STING agonist and a severe compromised efficacy. (B) Most STING agonists are used by local intra-tumor injection in clinical trials, which only shrinks the local tumors without inhibiting distal tumors or metastasis, whereas it is also not feasible for intra-tumor injection for pancreatic cancer in clinical trials. In response, we developed a first-in-class dual functional drug (SH-273) to overcome STING resistance by eliminating Bregs in both tumors and lymph nodes for long-term efficacy in pancreatic cancer. SH-273 has dual function to stimulates STING function (EC50 100 nM) and inhibits PI3Kγ (IC50 7 nM) that eliminate Bregs to overcome STING resistance. Interestingly, SH-273 achieved dual function with an opposite mechanism in regulating IRF3 phosphorylation in myeloid cells (increase) vs. in Bregs (decrease). In addition, we developed an albumin nanoparticle of SH-273 (Nano-273) for systemic delivery to enhance drug targeting to tumor and lymph node to activate systemic anticancer immunity. 3D imaging results indicated that albumin nano formulation greatly enhanced drug lymphoid draining and pancreatic tumor penetrating. Nano-273, combined with anti-PD-1, achieved long-term median survival of 200 days in LSL-KrasG12D; LSL-Trp53R172H/+; Pdx1cre/+ (KPC) mice (a substantial 67% increase from 120 days without treatment). The 80-day survival extension is significant as KPC mice mimic human pancreatic cancers with Kras/P53 mutations that are unresponsive to other available therapies. Single cell RNA-sequencing and flow cytometry revealed that Nano-273, combined with anti-PD-1, reduces Bregs by 5 to 7-fold while increasing other B cell subtypes by 4-fold in both pancreatic tumors and lymph nodes, compared to control group or group treated with STING agonist alone. These findings suggest that Nano-273 overcomes STING resistance by eliminating Bregs and induced systemic immunity to achieve long-term anti-tumor efficacy in pancreatic cancer.

#6535 Targeting estrogen receptor signaling in tumor associated myeloid cells to enhance anti-tumor immunity.

B. Chakraborty[1], M. Brown[1], P. Chakraborty[2], A. Goyal[3], C. Chang[1], D. McDonnell[1];
[1]Duke University, Durham, NC, [2]UNC Chapel Hill, Chapel Hill, NC, [3]U MASS Med School, Worcester, MA

Immune checkpoint inhibitors (ICB) have significantly improved outcomes across the spectrum of cancers, especially in patients with metastatic melanoma or non-small cell lung cancer (NSCLC). Despite encouraging efficacy in some patients, the development of primary and acquired resistance and severe toxicity associated with these treatment regimens, together with the overall low response rates, have limited their widespread use. Mining publicly available transcriptomic datasets, we have demonstrated that the response to ICB in patients with melanoma is influenced by the functionality of tumor associated macrophages (TAMs). Thus, it is of significance that we have demonstrated that 17-β estradiol (E2), working through myeloid cell intrinsic estrogen receptor alpha (ERα), promotes tumor growth in preclinical mouse models by polarizing tumor associated macrophages towards an immune-suppressive state in a manner that suppresses $CD8^{+}$T cell functionality and limits ICB efficacy independent of gender. Transcriptomic analysis of tumor infiltrating myeloid cells isolated from E2-treated syngeneic tumors revealed that the type I interferon (IFN) signaling pathway was suppressed and that this activity could be reversed by the addition of fulvestrant a Selective Estrogen Receptor Downregulator. The importance of type I IFN signaling in E2-regulated tumor growth was confirmed in syngeneic mouse tumor models (B16F10-melanoma and LLC1-NSCLC cells) by showing that inhibiting type I interferon receptor (IFNAR) activity using blocking antibodies reversed the protective effects of E2 deprivation (ovariectomy) on tumor growth. Further, using *in vitro* cultures of macrophages from mouse bone marrow or peripheral blood mononuclear cells from deidentified human donors, we demonstrated that E2-dependent inhibition of type I IFN signaling could be attributed to increased efferocytosis by myeloid cells. These findings were recapitulated *in vivo* using an IFN reporter mouse (*Mx1-egfp*) implanted with labelled tumor cells (mCherry-Spectrin labelled LLC1), where we demonstrated that E2 mediated-suppression of myeloid cell intrinsic interferon signaling within the tumor microenvironment is contingent upon their engulfment of apoptotic cancer cells. Mechanistically, this enhanced efferocytosis was attributed to increased expression of the fractalkine receptor (CX3CR1) in E2-treated myeloid cells- as either genetic or pharmacological depletion of CX3CR1 in mouse reversed E2-mediated tumor growth (B16F10 and LLC1), myeloid cell polarization (from immunosuppressive to proinflammatory), myeloid cell intrinsic type I IFN signaling and reinvigorated $CD8^{+}$T cell function. Taken together, our results highlight the potential clinical utility of targeting the E2/ER-CX3CR1 pathway as a means to enhance response to ICBs.

#6536 Enhanced membrane stability of mRNA nanoparticle derived TNFSF14 results in superior T-cell and NK cell stimulation.

A. Sallets[1], W. Liu[1], M. L. Leong[1], R. Prins[2], D. M. Da Silva[2], D. J. Fernandez[2], C. J. McKinlay[1], E. E. Lemmens[1], C. S. Rae[1], S. Adusumilli[1], R. Low[1], S. Bandi[1], G. Kannan[1], W. Kast[2], S. Deutsch[1], O. A. W. Haabeth[1];

[1]Nutcracker Therapeutics, Inc., Emeryville, CA, [2]University of Southern California, Los Angeles, CA

Resulting from intracellular translation of nanoparticle delivered mRNA, mRNA therapeutics offers an unparalleled opportunity to direct the expression of proteins to specific subcellular compartments. Many cytokines, especially the immunomodulatory Tumor Necrosis Factor (TNF) superfamily members, exist as both membrane and soluble proteins. Trimeric members of the TNF superfamily are known to be susceptible to protease cleavage resulting in their release from the membrane. Membrane and soluble versions of the immunomodulators may have different activity. Several studies have shown that membrane expressed TNFSF members more efficiently cross-link TNFSF receptors resulting in a stronger activation or inhibition signal. Moreover, the activity of membrane expressed proteins is confined to the cells that express the protein and the cells that interact with the protein expressing cell. Thus, directing the expression of immunostimulatory proteins to the membrane could be a transformative way to enhance the activity while mitigating the toxicity by limiting systemic exposure. In this study we utilized Nutcracker Therapeutics Inc. unique mRNA platform to develop a membrane stabilized version of tumor necrosis factor super family member 14, also known as LIGHT, with superior co-stimulatory activity and stability. LIGHT is an immunomodulatory cytokine that primarily acts on lymphocytes and innate immune cells through the cis or trans binding of HVEM or lymphotoxin beta receptor (LtbR). LIGHT has been implicated in multiple inflammatory diseases and is currently being evaluated in the development of immunotherapies against cancer. LIGHT stimulatory activity depends on the displacement of the inhibitory BTLA that is normally bound to HVEM and LtbR. Studies have shown that membrane bound LIGHT, but not soluble LIGHT, can effectively displace BTLA. In this study, we hypothesized that the advantageous activities of mRNA derived membrane expressed LIGHT could be further enhanced with an engineered LIGHT molecule that is less susceptible to membrane shedding. We made multiple variants of Engineered LIGHT where different regions of the putative protease sensitive sites were replaced with either a flexible or rigid linker. In short, we found that i) the soluble version of LIGHT can inhibit immune stimulatory capability of membrane expressed LIGHT; ii) membrane bound LIGHT enhances co-stimulation of antigen-specific T cells; iii) engineered LIGHT enhances membrane expression and increases stability; and iv) a design using a novel rigid linker to replace the putative protease sensitive region of LIGHT showed best overall activity. Here, we demonstrate the capability of our integrated platform to design and deliver an enhanced, membrane stabilized LIGHT molecule. This engineered transmembrane molecule represents a new class of drug uniquely enabled by nanoparticle delivered mRNA.

#6537 A novel CCR4 antagonist induces potent anti-tumor response through inhibition of Treg migration into the tumor microenvironment.

Rashmi Nair, Chandrasekhar Abbineni, Krishna Chaitanya Talluri, Amit A Dhudashiya, Aravind AB, Naveen Kumar R, Ramya R, D. Balasubramanyam, Pathur Obanna, Rabin Madhaiyan, DS Samiulla, Girish Daginakatte, Kishore Narayanan, Kavitha Nellore, Shekar Chelur, Susanta Samajdar, Murali Ramachandra

Aurigene Oncology Limited, Bangalore, India

Regulatory T cells (Tregs), an immunosuppressive subset of $CD4^{\pm}$ T cells, play a vital role in maintaining immune homeostasis by regulating response to self antigens and maintaining tolerance. On the contrary, Tregs infiltrating the tumor microenvironment (TME) impede effective anti-tumor immunity by inhibiting tumor-specific T cell responses and generating a suppressive TME, thus promoting tumor progression. Clinically, Tregs have been proven to play a significant role in resistance to immune checkpoint inhibitors (ICIs) leading to lower response rates. Hence, targeting Tregs would lead to activation of tumor-specific effector T cells and improved long-term anti-tumor immune responses with ICI treatment. CCR4, a chemokine receptor highly expressed on Tregs, spearhead the migration of Tregs and their accumulation in the TME, by responding to the chemokines CCL22 and CCL17 secreted by the inflamed cells in the tumor. CCR4 expression is associated with poor prognosis in various solid tumors. This warrants the therapeutic targeting of CCR4-expressing Tregs to enable effective and durable anti-tumor immune responses. We sought to discover and develop novel small molecule antagonists of CCR4 for use in cancer therapy. Multiple series of CCR4 antagonists were identified by iterative medicinal chemistry efforts and SAR based approach. These compounds were optimized towards attaining required potency, acceptable physicochemical properties, high selectivity and desirable pharmacokinetic profile to achieve anti-tumor activity. Aurigene's CCR4 antagonists exhibited potent inhibition of CCR4 activity in the reporter-based β-arrestin recruitment assay. This translated well into potent inhibition of CCL22-mediated chemotaxis of CCR4-expressing Tregs in an *in vitro* cell migration assay. Furthemore, the lead compounds showed desirable drug-like properties and excellent pharmacokinetic exposure in rodents. In an ongoing study in a syngeneic mice tumor model, one of the lead compounds is being evaluated for impact on Treg infiltration, CD8:Treg ratio in the tumor and efficacy. In summary, we have identified novel CCR4 antagonists with desirable drug-like properties that are being evaluated further to identify a clinical candidate.

#6538 Modulation of human macrophage differentiation, phenotype and function *in vitro* as a strategy to characterize novel tumor microenvironment modulators.

C. N. Castro, T. Sahner, C. Obodozie, P. Metzger, **H. Weber**;
Reaction Biology Europe GmbH, Freiburg, Germany

Macrophage infiltration of the tumor microenvironment is a key process that can determine the success or failure of anti-tumor therapies. Thus, many immunooncology therapies are being developed to modulate the macrophage differentiation program towards the anti-tumor M1 subset, while hindering the M2 subset associated with tumor progression. Monocyte-derived macrophages comprise a crucial in vitro cellular tool to evaluate the plasticity potential between the different polarization states. Several hurdles like their in vitro adherence, low cell number yield and the donor-to-donor variability pose technical challenges when using in vitro differentiated macrophages for compound screening and titration or functional assays.
At Reaction Biology we have established human macrophage assay pipelines to evaluate the novel macrophage polarization compounds in vitro. By isolating monocytes from frozen PBMC stocks it is possible to have access to the same donor or group of donors PBMC for repetitive analysis. We have developed a differentiation protocol that allows us to use different plate format from 6-well to 48 well plates, and thus increase and modulate the throughput according to the required readout.
The effect of therapeutic compounds can be analyzed by flow cytometry. Our data shows that human primary monocytes grown under M1 polarizing conditions express high levels of CD86 and CD80 in contrast to those cultivated under M2 polarizing conditions, with high expression of CD163, CD206, and CD209. Cell culture supernatant can be used to determine cytokine secretion. The functionality of the different macrophage subtypes can be further investigated using a pH-sensitive phagocytosis tracker, like pHRodo-Zymosan or pHRodo-Ecoli, which shows differential uptake according to differentiation profile. Moreover, treated macrophages can be used in coculture with T cells to investigate their capability to foster or inhibit an immune response.
Our data shows the value of monocyte-derived macrophage assays in the evaluation and efficacy assessment of TME modulators.

#6539 RNAi mediated silencing of *STAT3* in tumor-associated immune cells induces robust anti-tumor effects in immunotherapy resistant tumors.

S. Ganesh, M. Kim, J. Lee, X. Feng, H. Sivagurunatha Krishnan, R. Rijnbrand, A. Beaudry, J. A. Lockridge, V. Uttamsingh, J. Hanrahan;
Dicerna Pharmaceuticals, Inc., Lexington, MA

Malignant tumors are often associated with an immunosuppressive tumor microenvironment (TME), rendering most of them resistant to standard-of-care immune checkpoint inhibitors (CPIs). Signal transducer and activator of transcription 3 (STAT3), a ubiquitously expressed transcription factor, has well-defined immunosuppressive functions in several leukocyte populations within the TME. Since the STAT3 protein has been challenging to target using conventional pharmaceutical modalities, we investigated the feasibility of applying systemically delivered RNA interference (RNAi) agents to silence its mRNA directly in tumor-associated immune cells. In preclinical murine tumor models, chemically stabilized acetylated small-interfering RNAs (siRNAs) selectively silenced *Stat3* mRNA in multiple relevant cell types in TME and tumor-draining lymph nodes (TDLN), reduced STAT3 protein levels, and increased cytotoxic T-cell infiltration. In murine models of CPI-resistant tumors, RNAi-mediated *Stat3* silencing resulted in tumor growth inhibition, which was further enhanced and resulted in tumor regressions in combination with CPIs. Our findings suggest that targeting *STAT3* directly and reducing STAT3 protein in the suppressive immune cell populations in the TME and TDLN may overcome some of the current limitations of immunotherapy and be of therapeutic benefit especially for cancer patients who failed to respond to standard immunotherapy treatments alone. A human active STAT3 conjugate is currently in Phase 1 clinical trial for treatment of immunotherapy refractory cancer types (NCT06098651).

BIOINFORMATICS / COMPUTATIONAL BIOLOGY / SYSTEMS BIOLOGY / CONVERGENT SCIENCE: Computational Approaches to Precision Medicine Minisymposium

#6543 A map of osteosarcoma cell architecture reveals convergence of pediatric cancer mutations on protein assemblies.

M. Hu[1], L. V. Schaffer[1], E. L. Huttlin[2], G. Qian[1], A. Latham[3], A. Pal[3], L. Vaites[2], T. Le[4], Y. Qin[1], C. Churas[1], D. Pratt[1], R. Bachelder[1], P. Zage[1], I. Echeverria[3], A. Sali[3], J. Harper[2], S. P. Gygi[2], E. Lundberg[4], T. Ideker[1],

[1]University of California San Diego - UCSD, La Jolla, CA, [2]Harvard Medical School, Boston, MA, [3]University of California San Francisco - UCSF, San Francisco, CA, [4]Stanford University, Stanford, CA

Pediatric tumors are characterized by a low incidence of somatic mutations, which occur in different genomic patterns from adult cancers. For these reasons, interpreting the functional impact of mutations in pediatric cancer patients has remained difficult. One approach to interpreting rare coding mutations is to analyze the convergence of these mutations on larger structural and functional units, such as protein complexes, super assemblies, biomolecular condensates, and organelles. Towards this aim, we created a cancer cell map in the osteosarcoma cell line based on proteome-wide integration of protein interactions and immunofluorescent imaging in U-2 OS pediatric bone cancer cells. This multiscale integrated cell map of U-2 OS cell organizes 5,254 proteins into 270 protein assemblies. Using this multiscale cell map, we analyze 772 genomes from 18 cancer types reported in the DKFZ pan-pediatric cancer study to identify 25 protein assemblies in the map under mutational pressure. This analysis reveals mutated protein assemblies involved with chromatin maintenance and remodeling as well as cell integrity and mobility. For example, we identify a Collagen Biosynthesis and Remodeling Complex, as mutated in 9 cancer types and 15 patients in the dataset, indicating extracellular matrix remodeling is associated with pediatric cancer progression. We also identify a putative biological condensate, which we call the Nuclear Transcription Suppression Complex (NTSC). This protein assembly is found mutated in 20 patients across 10 cancer types, implicating intrinsically disordered proteins in development of pediatric cancer. Overall, this work illustrates how a global multiscale map of cell architecture enables a mechanistic understanding of clinical patient genomes.

#6544 Targeting resistance mechanisms to AR-targeted therapy in prostate cancer through inhibition of CREBBP/EP300.

B. V. Dougherty[1], B. C. Thomas[2], A. M. Walsh[1], V. Calvo[1], K. E. Ware[3], A. J. Armstrong[3], J. Renstrup[1], J. A. Somarelli[3], E. E. Schadt[1];
[1]Pathos, Chicago, IL, [2]Nova Southeastern University, Fort Lauderdale, FL, [3]Duke University, Duram, NC

Standard initial treatment for men with metastatic prostate cancer involves targeting the androgen receptor (AR) with androgen deprivation therapy or androgen-receptor signaling inhibitors. Resistance eventually develops, such as through AR-activating alterations, leaving few targeted options for patients. Here, we utilize data from 4,509 prostate cancer patients with longitudinal clinical and DNA/RNA sequencing data to elucidate mechanisms of resistance and identify potential therapeutic vulnerabilities in resistant disease. By constructing comprehensive regulatory networks, termed hybrid networks, built across different disease stages, combining features from WGCNA, causal mediation analysis, probabilistic causal network inference, and public knowledge graphs, we uncover subnetworks strongly associated with disease progression and resistance. These subnetworks reflect biological processes for cell cycle, E2F, DNA repair, MYC, and AR, comprehensively identifying broad transcriptional changes that drive disease progression and resistance.

Selected subnetwork scores, derived from RNA expression, were significantly associated with outcomes in both the hormone-sensitive and castration-resistant settings, demonstrating that the subnetworks capture early and late resistance. The hybrid networks identified the transcriptional co-activators CREBBP and EP300 as key modulators of these subnetworks, suggesting that targeting CREBBP/EP300 may be effective in treating both early and late-stage disease.

Prostate cancer cell lines were treated with FT-6876, a small molecule inhibitor of CREBBP/EP300, and growth inhibition was measured in both enzalutamide sensitive and resistant cell lines, covering a wide range of resistance mechanisms. The selected subnetworks were enriched for genes down-regulated following treatment with FT-6876, suggesting that targeting CREBBP/P300 addresses multiple resistance-related pathways. Differential changes in protein abundance and protein acetylation between enzalutamide sensitive and resistant cell lines identified changes in fatty acid metabolism as a common, downstream event in response to treatment with FT-6876, suggesting an additional mechanism for response to FT-6876.

Together, our integrated theoretical and experimental analyses support the hypothesis that targeting CREBBP/EP300 may provide therapeutic benefits to prostate cancer patients. Further, the subnetworks identified may serve as mechanistically-informed biomarkers for identifying patients who may benefit from inhibition of CREBBP/EP300.

#6545 Reversing lineage plasticity and drug resistance in lethal prostate cancer.

A. Vasciaveo, J. J. Li, D. Karagiannis, X. Chen, A. Califano, C. Lu, M. M. Shen;
Columbia University Irving Medical Center, New York, NY

Although major mechanisms of resistance to targeted therapies include mutation of the drug target, recent evidence suggests cell-adaptive mechanisms as alternative avenues for escaping treatment. In several cancers, tumor cells become plastic in response to target inhibition, changing their identity and molecular programs without acquiring further mutations. In the case of castration-resistant prostate cancer (CRPC) treated with standard-of-care, next-generation anti-androgens enzalutamide, tumor cells often switch lineage to survive drug pressure, acquiring neuroendocrine (NE) features and thereby transforming into neuroendocrine prostate cancer (CRPC-NE). Existing targeted therapies for CRPC and CRPC-NE provide limited benefit, representing an unmet clinical need. Hence, the elucidation of tumor plasticity and consequent heterogeneity that contribute to drug resistance is of paramount importance to identify novel therapeutic opportunities.

We have recently developed a network-based precision cancer medicine framework to characterize molecular and drug sensitivity profiles of ~100 Genetically-Engineered Mouse Models (GEMM)-derived tumors of prostate cancer (Vasciaveo, et al. 2023). This study revealed that tumors derived from GEMMs with the loss of function of both Pten and Trp53 (NPp53) align with CRPC patients and exhibit high heterogeneity in regulatory programs and histopathologic features, including NE differentiation. We then adopted the NPp53 model to generate several 3D organoid lines in order to study tumor plasticity and heterogeneity. To elucidate their tumors' regulatory programs, we reverse-engineered genome-wide regulatory networks using multimodal single-cell RNASeq and ATACSeq data to identify Master Regulator (MR) proteins implementing tumor cell identities and characterize their epigenetic landscape.

Our network-based regulatory analysis identified several distinct cell populations, including cells activating epithelial-to-mesenchymal (EMT) programs and NE differentiation, all resistant to enzalutamide treatment. Cross-species analysis aligned these cells to human CRPC and CRPC-NE tumors. In particular, our analyses have shed light into the roles of NSD2, a known MR of lethal prostate cancer, whose ablation restored sensitivity to enzalutamide.

In summary, we leveraged single-cell, multimodal data from CRPC and CRPC-NE 3D mouse organoids to elucidate regulatory programs of drug resistant, lethal prostate cancer and characterize its heterogeneity. Importantly, we also identified a mechanism that can be exploited for therapeutic intervention to restore tumor cells' sensitivity

#6546 Spatial immunology landscapes that correlate with survival in triple negative breast cancer.

A. Foroughi pour[1], J. Martinek[1], T.-C. Wu[1], S. Sivajothi[1], Z. Liu[1], J. Zhou[1], D. Rimm[2], P. Robson[1], K. Bates[2], K. Palucka[1], J. H. Chuang[1];
[1]The Jackson Laboratory for Genomic Medicine, Farmington, CT, [2]Yale University School of Medicine, New Haven, CT

Triple negative breast cancer (TNBC) is an aggressive subtype of breast cancer characterized by negative immunohistochemistry staining for estrogen receptor (ER), progesterone receptor (PR), and human epidermal growth factor receptor 2 (HER2). Treatment options for TNBCs are limited due to lack of tumor-specific targeted therapies, resulting in poor prognosis and patient survival. This is exacerbated by lack of prognostic markers of response. While current studies suggest tumor immune interactions are important, current immune activity quantifications, such as scores quantifying abundance of tumor-infiltrating lymphocytes (TILs), are not sufficient to define tumor immune status. We used imaging mass cytometry (IMC) to measure 33 markers on primary tumors of 100 patients undergone chemotherapy with long-term follow-up to explore the tumor immune microenvironment of TNBCs. Concordant with previous studies, a higher ratio of T-cells was associated with response to chemotherapy and longer overall survival (adjusted p-value<0.05). Moreover, using Kmeans clustering we identified 13 distinct cellular neighborhoods, reflective of the heterogenous nature of TNBCs. Among others, we identified a neighborhood, characterized by low CD14+ expression, low cytokeratin, high vimentin expression and high CD45RO, that contributes highest impact on correlation with overall survival (adjusted p-value<0.01). These results suggest an important role for memory T cells in the stroma. Thus, resolving spatial organization of the tissue is important to understanding patient response to therapy in TNBCs.

#6547 Dysregulated FGFR3 signaling alters immune landscape in bladder cancer and presents therapeutic possibilities.

D. R. Bergman[1], E. Trujillo[2], L. Li[3], A. T. Pearson[3], R. Sweis[3], T. L. Jackson[4];
[1]Johns Hopkins University, Baltimore, MD, [2]GemPharmatech, San Diego, CA, [3]University of Chicago, Chicago, IL, [4]University of Michigan, Ann Arbor, MI

Bladder cancer is an increasingly prevalent global disease that continues to cause morbidity and mortality despite recent advances in treatment. Immune checkpoint inhibitors (ICI) and FGFR-targeted therapeutics have had limited success in bladder cancer when used as monotherapy. Emerging data suggests that the combination of these two therapies could lead to improved clinical outcomes. The optimal strategy for combining these agents remains uncertain. Mathematical models, and more specifically agent-based models (ABMs), have shown recent successes in uncovering the multiscale dynamics that shape the trajectory of cancer. They have enabled the optimization of treatment methods and identification of novel therapeutic strategies. To assess the combined effects of anti-PD-1 antibodies and anti-FGFR3 small molecule inhibitors (SMI) on tumor growth and the immune response, we built an ABM that captures key facets of tumor heterogeneity and CD8+ T cell compartments, their spatial interactions, and their response to therapeutic pressures. With our model, we quantify how tumor antigenicity and FGFR3 activating mutations impact disease trajectory and response to anti-PD-1 antibodies and anti-FGFR3 SMI. We find that even a small population of weakly antigenic tumor cells bearing an FGFR3 mutation can render the tumor resistant to combination therapy. However, highly antigenic tumors can overcome therapeutic resistance mediated by FGFR3 mutation. The optimal therapy depends on the strength of the FGFR3 signaling pathway. Under certain conditions, ICI alone is optimal; in others, ICI followed by anti-FGFR3 therapy is best. These results point to the need to quantify FGFR3 signaling and the fitness advantage conferred on bladder cancer cells harboring this mutation. Employing this ABM modeling approach may enable rationally designed treatment plans to improve clinical outcomes.

#6548 Leveraging compact feature sets for TCGA-based molecular subtype classification on new samples.

K. Ellrott[1], C. K. Wong[2], C. Yau[3], M. A. A. Castro[4], J. Lee[1], B. Karlberg[1], J. K. Grewal[5], V. Lagani[6], B. Tercan[7], V. Friedl[2], T. Hinoue[8], V. Uzunangelov[2], L. Westlake[9], X. Loinaz[9], I. Felau[10], P. Wang[10], A. Kemal[10], S. J. Caesar-Johnson[10], I. Shmulevich[7], A. J. Lazar[11], I. Tsamardinos[6], K. A. Hoadley[12], The Cancer Genome Atlas Analysis Network, G. A. Robertson[5], T. A. Knijnenburg[7], C. C. Benz[13], J. M. Stuart[2], J. C. Zenklusen[10], A. D. Cherniack[9], P. W. Laird[8];
[1]OHSU, Portland, OR, [2]University of California Santa Cruz, Portland, OR, [3]University of California, San Francisco, San Fransico, CA, [4]Federal University of Parana, Curitiba, Brazil, [5]BC Cancer, Vancouver, BC, Canada, [6]JADBio Gnosis DA, Heraklion, Greece, [7]Institute for Systems Biology, Seattle, WA, [8]Van Andel Institute, Grand Rapids, MI, [9]Broad Institute, Cambridge, MA, [10]National Cancer Institute, Bethesda, MD, [11]The University of Texas MD Anderson Cancer Center, Houston, TX, [12]University of North Carolina at Chapel Hill, Chapel Hill, NC, [13]Buck Institute for Research on Aging, Novato, CA

The NCI's The Cancer Genome Atlas (TCGA) project profiled over 10,000 tumor samples over the course of 10 years. As different tissue-specific working groups reviewed all of the available data, these patient samples were separated into distinct molecular subtypes, and these clusters were reported in various marker papers. While these assignments provided invaluable information about the common patterns of molecular characteristics in different types of cancer there was no consistent methodology for assigning new samples to these defined molecular subtypes.The NCI's Tumor Molecular Pathology group was formulated to create machine learning-based models that could be applied to non-TCGA samples and determine their TCGA mapped subtypes. Five modeling systems, JADBio, SKGrid by the Oregon Health and Science University, CloudForest by the Institute of Systems Biology, AKLIMATE by University of California Santa Cruz and subSCOPE by BC Cancer's Genome Sciences Centre, were trained to recognize TCGA subtypes using multi-omic measurements from gene expression, DNA methylation, miRNA expression, copy number, and somatic mutation calls. While the TCGA samples were profiled using multi-omic technologies, single platform and/or compact feature set models also were assessed for their ability to assign these classifications. Each machine learning system created predictive models for 106 subtypes from 26 cancer types using as few features as possible, with a maximum of 100 features allowed for scored models. A set of 411,706 models was developed, composed of results of each of the learning methods across the various omic platforms. Top models, both multi-omic and single platform, were selected for each cancer type. On average, models were able to achieve an overall weighted F1 score of 0.895 with 42 features. While the top models for each cancer type had an overall weighted F1 mean performance of 0.936 with a mean of 29 features, in 20 of the 26 cancer types models using only gene expression provided the best performance. Analysis of features selected by the models showed some known onco-drivers were selected by many models, but many times different models would utilize features of different genes with similar levels of performance. Network-level analysis revealed that many genes of these selected features operated within the same pathways.Transferability of these models to external datasets was tested, taking TCGA breast cancer trained models and applying them to AURORA and METABRIC datasets. Interestingly, despite the data platform difference between TCGA (RNAseq) and METABRIC (microarray), model performance saw only minimal degradation of F1 values in transfer. This set of models and the training dataset will provide new opportunities for researchers and translational scientists to connect new tumors to the subtypes seen in the TCGA cohorts.

#6549 Mechanistic models of tumor and patient heterogeneity explain and predict clinical outcomes of large B-cell lymphoma (LBCL) treatment.

A. E. Pomeroy, A. C. Palmer;
University of North Carolina at Chapel Hill, Chapel Hill, NC

Introduction: Heterogeneity between patients and within tumors poses challenges to effective cancer treatment. Drug combinations can overcome heterogeneity by increasing the probability that a patient will have response to one or more drugs. This approach is successful in numerous disease settings, but technological advances have led to new approach to addressing heterogeneity: precision approaches to stratify patients into subpopulations with more uniform, stronger responses to specific drugs. These strategies can be implemented together to improve patient outcomes. We have developed computational mechanistic models of cancer treatment in the context of both sources of heterogeneity which explain and predict clinical outcomes of treatment of LBCL with combination therapy and CAR T-cell therapy.

Combination therapy: Our novel population tumor kinetics (pop-TK) model simulates clinical combination therapy outcomes by implementing multidrug dose response functions in heterogeneous populations of tumor cells, within heterogeneous cohorts of patients. Informed by the outcomes of novel drugs in phase 2 trials in relapsed/refractory (r/r) patients, the pop-TK model accurately predicted of outcomes of seven first-line phase 3 trials of novel combinations. Most notably, informed by treatment of r/r LBCL with polatuzumab-vedotin (pola), the pop-TK predicted the success of modifying the standard treatment regimen (RCHOP) with pola before the clinical trial results were published. The pola combination improves overall survival (OS) and PFS in Activated B-Cell (ABC) LBCL (hazard ratio (HR): OS 0.3, PFS 0.4), but reduces OS (HR: 1.6) and does not improve PFS (HR: 1.0) in Germinal Center B-Cell (GCB) LBCL. The subtype specific difference in PFS was also predictable based on subtype results of r/r trials (predicted HR: ABC 0.3, GCB 0.9).

CAR T-cell therapy: We used a population pharmacokinetic/pharmacodynamic (pop-PK/PD) model of CAR T-cell therapy to reproduce the PFS distribution and the distribution CAR T-cell abundance for CAR T therapy in r/r LBCL patients. The impact of tumor size on patient outcome in our model and in clinical studies led us to computationally explore the impact treating smaller tumors with CAR T-cell therapy on treatment outcomes. We found that using detectable circulating tumor DNA (ctDNA) as a biomarker for administering CAR T-cell therapy immediately after RCHOP increased the proportion of simulated patients without a second disease progression event by 30% (HR: 0.43 [0.34, 0.55]).

Conclusions: The pop-TK model supports LBCL subtype biomarker for pola performance, and the pop-PK/PD model demonstrates that detectable ctDNA is a potential biomarker for early CAR T-cell administration. These examples of model-driven precision trial design have the potential to improve outcomes using readily-available biomarkers and existing therapies.

CLINICAL RESEARCH: Immuno-oncology
Minisymposium

#6550 Biopsy analysis of trial S1616: Ipilimumab plus nivolumab versus ipilimumab alone in patients with anti-PD-1 refractory melanoma.

K. M. Campbell[1], Z. Bustami[1], D. G. Chen[1], E. Medina[1], C. R. Gonzalez[1], N. Naser Aldeen[1], I. Baselga-Carretero[1], A. Vega-Crespo[1], J. Maxey[2], J. M. Chen[1], L. F. Kuklinski[1], K. L. Kendra[3], B. Chmielowski[1], T.-G. Truong[4], N. I. Khushalani[5], F. Collichio[6], A. Ikeguchi[7], A. I. Victor[8], K. Margolin[9], J. A. Sosman[10], S. P. Patel[11], S. Hu-Lieskovan[12], J. Moon[13], S. Bellasea[13], D. K. Wells[2], C. N. Spencer[2], M. A. Thompson[2], M. Wu[13], P. O. Scumpia[1], A. VanderWalde[14], A. Ribas[1]; [1]UCLA - University of California Los Angeles, Los Angeles, CA, [2]Parker Institute for Cancer Immunotherapy, San Francisco, CA, [3]Ohio State University Wexner Medical Center, Columbus, OH, [4]Kaiser Permanente Northern California, Vallejo, CA, [5]Moffitt Cancer Center, Tampa, FL, [6]University of North Carolina Lineberger Comprehensive Cancer Center, Chapel Hill, NC, [7]University of Oklahoma Health Sciences Center, Oklahoma City, OK, [8]University of Rochester, Rochester, NY, [9]City of Hope Comprehensive Cancer Center, Duarte, CA, [10]Robert H. Lurie Comprehensive Cancer Center of Northwestern University, Chicago, IL, [11]The University of Texas MD Anderson Cancer Center, Houston, TX, [12]University of Utah, Huntsman Cancer Institute, Salt Lake City, UT, [13]SWOG Statistics and Data Management Center, Seattle, WA; Fred Hutchinson Cancer Center, Seattle, WA, [14]The West Clinic, Wolf River, Germantown, TN

Background: The phase II randomized trial S1616 (NCT03033576) showed that patients with melanoma refractory to anti-PD-1-based therapy had improved progression free survival (HR=0.63, p=0.037) and objective response (28% vs 9%) to the combination of ipilimumab with nivolumab compared to ipilimumab. Here, we report molecular and spatial proteomic features of biopsies collected from patients on S1616, both prior to and during therapy.
Methods: Biopsies collected from patients from both arms at baseline (N=68 patients total) and early on-therapy (N=51; 43 with paired timepoints) were analyzed by whole exome sequencing (n=185 samples), RNA sequencing (n=105), histopathologic staining (n=149), and multiplexed ion beam imaging (n=45). Multiple biopsies were available for some patients. Mutations, gene expression, and tumor microenvironment were compared across timepoints and response to combination (N=18 responders [CR/PR], N=44 nonresponders [SD/PD]).
Results: Baseline biopsies from patients responsive to combination had increased expression of genes (n=482, FDR<0.05) associated with coagulation and complement, fatty acid metabolism, oxidative phosphorylation, hypoxia, and interferon gamma response gene sets (FDR<0.05), compared to nonresponsive biopsies. Baseline biopsies from responders also had low levels of effector CD8 T cells (PD1+, TIM-3+, GZMB+, Ki67+) colocalized with tumor cells and myeloid populations expressing higher levels of MHC Class II.
On-therapy biopsies from responders showed decreased detection of driver mutations by genomics, reduced gene expression of pathways enriched at baseline (oxidative phosphorylation, complement) by transcriptomics, and increased CD8 T cell to tumor cell ratios by histopathology, supporting observations of tumor regression. On-therapy biopsies from responders also had increased gene expression of genes related to inflammatory cytokine signaling. This correlated with increased proportions of effector CD8 T cells, compared to paired baseline or nonresponding biopsies, and increased organization of nonactivated CD8 T cells near mature endothelial structures (SMA+, CD31+ regions) adjacent to tumor.
Biopsies from nonresponders did not demonstrate these dynamics and instead contained exhausted CD8 T cells (PD1+, TIM-3+, granzyme B-, Ki67-) colocalized with FOXP3+, CD4+ Tregs and CD163+, PD-L1+ M2 macrophages, both at baseline and on-therapy.
Conclusion: In patients with melanoma refractory to anti-PD-1, addition of anti-CTLA-4 facilitates tumor-reactive CD8 T-cell infiltration and decreased suppressor cell dynamics, resulting in regression of some tumors with distinct transcriptome features. Conversely, biopsies from patients whose tumors progress on combination therapy lack expression of metabolic pathways and show CD8 T-cells restricted in proximity to M2 macrophages and Tregs.

#6551 Comprehensive genomic and transcriptomic analyses capture the effects of epigenetic therapy priming on immune checkpoint blockade response in non-small cell lung cancer.

B. V. Landon[1], K. A. Marrone[1], M. J. Topper[1], A. Annapragada[1], H.-L. Tsai[1], A. Balan[1], N. Niknafs[1], C. Cherry[1], J. R. White[1], G. Pereira[1], V. Adleff[1], C. Hu[1], J. Riemer[1], M. Fitzpatrick[1], P. Forde[1], C. L. Hann[1], R. J. Kelly[2], D. S. Ettinger[1], B. Levy[1], J. Nieva[3], J. Herman[4], V. E. Velculescu[1], S. Baylin[1], J. Brahmer[1], V. Anagnostou[1];

[1]Johns Hopkins University School of Medicine, Baltimore, MD, [2]Baylor University Medical Center, Dallas, TX, [3]University of Southern California Keck School of Medicine, Los Angeles, CA, [4]University of Pittsburgh Medical Center, Pittsburgh, PA

Introduction: Emergence of resistance to immune checkpoint blockade (ICB) mandates the development of strategies for ICB sensitization. Here we employed a multi-omic approach to understand the effects of epigenetic priming in re-shaping the tumor microenvironment, together with genomic drivers of therapeutic response of epigenetic therapy followed by ICB in non-small cell lung cancer (NSCLC).

Methods: We performed whole exome sequencing (WES) on 39 baseline tumors and bulk RNA sequencing (RNAseq) on 18 serial tumors across 42 patients with metastatic immunotherapy-naïve NSCLC, who received azacitidine and entinostat followed by nivolumab (NCT01928576). WES was utilized to assess co-mutations, mutation signatures and genome-wide structural changes. RNAseq was utilized for gene and gene set enrichment analysis (GSEA) and repeat element analysis. Response after nivolumab initiation was assessed using RECIST 1.1 criteria. Patients who were progression-free at 6 months or alive at 2 years after initial treatment were defined as exceptional responders.

Results: We found an enrichment in inactivating mutations in homologous recombination genes in radiographic responders (Fisher's exact, p=0.0007). Higher germline and somatic HLA class II diversity (Mann-Whitney U-test, p=0.05 and p=0.03 respectively), and an enrichment of smoking and DNA damage mutational signatures were noted in radiographic responders (Mann-Whitney U-test, p=0.03 and p=0.15 respectively). Radiographically responding tumors harbored a higher number of mutations in genomic regions that were haploid or present in multiple copies (persistent tumor mutation burden; Mann-Whitney U-test, p=0.018). GSEA revealed an upregulation of inflammatory response gene sets post-epigenetic therapy in patients attaining an exceptional response. Antigen presentation, interferon-alpha, and interferon-gamma related gene sets were upregulated in exceptional responders post epigenetic priming (FDR-adjusted p=0.005, p=0.009, and p=0.011 respectively). Additionally, we observed an enrichment in interferon-alpha, cancer testis antigens, and interferon-gamma related gene sets in patients with a longer progression-free survival (FDR-adjusted p=0.007, p=0.011, and p=0.013 respectively). Repeat element analysis showed an increase in long terminal repeats on-therapy in exceptional responders, suggesting induction of repeat element expression with epigenetic therapy. A higher expression of MAGE family tumor associated antigens (MAGEA10, MAGEB1, MAGEB2) was noted post-epigenetic therapy in exceptional responders.

Conclusions: Genomic and transcriptomic analyses reveal the potential of epigenetic-priming to re-shape the tumor microenvironment and highlight patients that could benefit from combination epigenetic therapy with immunotherapy.

#6552 Intratumoral (ITu) delivery of mRNA-2752 encoding human OX40L/IL-23/IL-36γ in combination with durvalumab induces an immunostimulatory effect within the tumor microenvironment (TME) of patients with advanced solid tumors.

Michael Abadier[1], **Ryan J. Sullivan**[2], Jacky Chow[1], Vasudha Sehgal[1], Randy F. Sweis[3], Adil Daud[4], Ronnie Shapira-Frommer[5], Ruth Perets[6], Shivaani Kummar[7], Meredith McKean[8], Ravit Geva[9], Manish R. Patel[10], Adnan Khattak[11], Pablo Fernandez-Penas[12], Sima Zacharek[1], Natalia Wahl[1], Russell M. Walker[1], Linh Van[1], Praveen Aanur[1], Jim Ward[1], Khanh T. Do[1], Georgina V. Long[13]

[1]Moderna, Inc., Cambridge, MA,[2]Massachusetts General Hospital, Boston, MA,[3]The University of Chicago, Chicago, IL,[4]UCSF Helen Diller Family Comprehensive Cancer Center, San Francisco, CA,[5]Sheba Medical Center, Ramat Gan, Israel,[6]Rambam Medical Center and Technion - Israel Institute of Technology, Haifa, Israel,[7]Oregon Health and Science University, Portland, OR,[8]Sarah Cannon Research Institute / Tennessee Oncology, PLLC, Nashville, TN,[9]Sourasky Medical Center, Tel Aviv, Israel,[10]Sarah Cannon Research Institute / Florida Cancer Specialists, Sarasota, FL,[11]One Clinical Research and Edith Cowan University, Perth, Australia,[12]Westmead Hospital, Sydney, Australia,[13]Melanoma Institute Australia, The University of Sydney and Royal North Shore and Mater Hospitals, Sydney, Australia

Background mRNA-2752 is a first-in-class ITu therapy composed of mRNA encoding human OX40L/IL-23/IL-36γ in a lipid nanoparticle. The combination of T cell costimulation and proinflammatory cytokines were developed to modulate the TME and allow a more robust immune response. Here we show evidence of the pharmacodynamic effect of ITu administration of mRNA-2752 in combination with PD-L1 antibody.

Methods In this ongoing phase 1 study (NCT03739931), patients (pts) with advanced solid tumors received 0.25-8 mg mRNA-2752 alone (Arm A) or in combination with 1500 mg IV durvalumab (Arm B)[1,2]. Pre and on-treatment peripheral and tumor samples were collected to monitor changes in cytokines by ligand binding assays, gene signatures by RNA sequencing, and T cell infiltration by immunohistochemistry. Tumor biopsies were taken at baseline, 24h, 15 and 28 days post treatment.

Results mRNA-2752 administration in combination with durvalumab revealed ≥2-fold plasma level increases of IL-23 (34/40, 85%) and IFN-γ (50/65, 77%) at 24h after first injection; exposure was induced in a dose-dependent manner. We observed induction of CD8 T cell abundance (20/49, 41%) and proliferation (23/49, 47%), and OX40L protein expression (28/49, 57%) in pts with evaluable post-treatment injected lesion biopsies. CD8 T cell abundance increased in 2 pts with evaluable post-treatment un-injected lesion biopsies. A positive correlation was observed between T cell abundance and T cell effector genes. All three mRNA (IL-23, IL-36γ, and OX40L) encoded genes were detected post treatment in tumor samples from 43 evaluable patients. In 18 pts with injected lesion biopsy samples at baseline and day 28 samples, the genes related to cytotoxic function (*IFNG, GZMB, PRF1)*, T cell migration (*CCL21, CCR7, KLF2*), T cell activation/memory phenotype (*TCF7, CD69, ITGAE*), and conventional type 1 dendritic cells (*CLEC9A, XCR1*) were induced 28 days post-treatment in pts with complete/partial response or stable disease (CR/PR/SD, n=7) compared to progressive disease (PD, n=11) pts. RNA-Seq transcriptome analysis showed increases in the immune inflamed gene signatures related to antitumor activity in 24/43 (56%) pts post-treatment, and the pre-existing immune inflamed phenotype within the TME was associated with clinical benefit.

Conclusions mRNA-2752 ITu injection induced a systemic immunomodulatory effect by elevating effector cytokines. This was associated with pharmacodynamic changes within the TME, including increases in T cell abundance and proliferation, and upregulation of immune gene signatures that correlate with antitumor response.

References 1. Patel M. *J ImmunoTherap*. 2021;9:Abs569 2. Olson D, et al. *J ImmunoTherap*. 2022;10:Abs767

Study support: Moderna, Inc.

#6553 Targeting macrophages and regulatory T cells improves response to chemotherapy in high-grade serous ovarian cancer.

S. Elorbany[1], C. Berlato[1], L. Carnevalli[2], S. Barry[3], E. Maniati[1], J. Wang[1], R. Manchanda[1], J. Kzhyshkowska[4], F. Balkwill[1];
[1]Queen Mary University of London, London, United Kingdom, [2]Roche, London, United Kingdom, [3]AstraZeneca, Cambridge Biomedical campus, London, United Kingdom, [4]Institute of Transfusion Medicine and Immunology, Mannheim, Germany

Despite the initial response to chemotherapy, most high-grade serous ovarian cancer (HGSOC) patients will suffer disease relapse within two years of diagnosis with no currently successful immunotherapy options.We performed single-cell RNA sequencing (scRNAseq) on omental metastasis from HGSOC patients. Analysis of 64,097 immune cells showed that neoadjuvant chemotherapy (NACT) induced immunosuppressive mechanisms that counteracted its potentially positive effects. We showed that while NACT enhanced phagocytosis and antigen presentation, this was counterbalanced by upregulation of Stabilin1 (STAB1) in eight out of eleven macrophage subpopulations we identified. The NACT associated increase in macrophage STAB1 expression was validated in a separate cohort of eighty HGSOC patients at the protein level. STAB1 is a macrophage scavenger receptor that transports phagocytosed targets to undergo significant lysosomal degradation reducing the efficiency of antigen presentation. In vitro anti-stabilin1 antibody (anti-stab1 ab) -treated macrophages had significantly reduced antigen degradation and higher CD11C expression than isotype-treated ones. Furthermore, T cells co-cultured with anti-stab1 ab -treated macrophages had increased T cell proliferation and killing.We identified thirteen CD4 subpopulations by scRNAseq, five of which were Tregs. We showed that NACT significantly upregulated and activated Tregs. Tregs displayed a shared developmental trajectory with naïve and effector T cells suggesting that those are induced rather than natural Tregs. This was supported by TCR clonal sharing between Tregs and other effector cells. In vitro T cells treated with FOXP3 anti-sense oligonucleotide (ASO), AZD8701, had an anti-tumor cytokine profile and enhanced tumor cell killing. Analysis of 69,781 scRNAseq cells from control and chemotherapy-treated HGSOC syngeneic mouse model showed similar responses. In two HGSOC syngeneic mouse models (HGS2 and 30200), combinations of chemotherapy with anti-stab1 ab and/or Foxp3-ASO significantly increased median survival of mice with established peritoneal disease compared to chemotherapy alone. Bulk RNAseq of tumors treated with anti-stab1 ab were enriched with CXCL9 positive macrophages, while Foxp3-ASO treatment showed significant increase in T helper cell infiltration and activation. Potentially cured long-term survivors (300 days+) were resistant to tumor rechallenge.In a third HGSOC mouse model (60577), in which tumors relapsed after a good initial response to chemotherapy, combinations of chemotherapy with anti-stab1 ab and/or Foxp3-ASO significantly increased the post relapse survival compared to chemotherapy alone.We believe that modulating Tregs and STAB1 could improve response to chemotherapy and can have translational potential as each AZD8701 and a humanized anti-stab1 ab are in phase I clinical trials.

#6554 Lurbinectedin induces multimodal immune activation and augments the anti-tumor immune response in small-cell lung cancer.

S. Chakraborty[1], Y. Mahendravarman[1], U. Sen[1], A. Banerjee[1], C. Coleman[2], D. Demircioglu[2], D. Hasson[2], T. Sen[3];
[1]Icahn School of Medicine at Mount Sinai, New York, NY, [2]Tisch Cancer Institute and Icahn School of Medicine at Mount Sinai, New York, NY, [3]Tisch Cancer Institute at Mount Sinai, Icahn School of Medicine at Mount Sinai,, New York, NY

Background: Small cell lung cancer (SCLC) is the most aggressive subtype of lung cancer, with a very poor prognosis and limited therapeutic options. Repression of the MHC-I and reduced tumor infiltration of cytotoxic T-lymphocytes is often associated with immunotherapy resistance in SCLC. Lurbinectedin is FDA-approved as a second-line treatment for SCLC and we previously showed lurbinectedin as an effective therapeutic strategy in SCLC preclinical models. There are ongoing clinical trials combining immune checkpoint blockade with lurbinectedin in ES-SCLC. However, there is no insight into the effect of lurbinectedin on the immune microenvironment in SCLC. In this study, we evaluated the effect of lurbinectedin on the immune microenvironment and the anti-tumor effect with or without PD-L1 blockade.

Results: To determine the effect of lurbinectedin in SCLC models, we treated immunocompetent flank RPP (*Rb1, Trp53, and p130*) and RPM (*Rb1, Trp53*, and *MYCT58A*) tumor-bearing mice with lurbinectedin (0.2 mg/kg, 1/7days) and/or anti-PD-L1 (300µg, 1/7days) for 3 weeks. Mice treated with anti-PD-L1 alone showed no anti-tumor response, and single-agent lurbinectedin caused a delay in tumor growth. However, 6 of the 10 mice treated with the combination of lurbinectedin and anti-PD-L1, had a complete response (100% reduction) and the other 4 had 90% tumor regression. Tumors were resected and analyzed by multicolor flow cytometry for changes in tumor-infiltrating lymphocytes (TILs). Furthermore, analysis of immune cells infiltrating into the tumors post- treatment showed significant induction of cytotoxic T-cells and a reduction of exhausted and regulatory T cells in the combination treatment arm. Similarly, pro-inflammatory M1 type macrophages and dendritic cells were increased, while immunosuppressive M2 type macrophages and MDSC cells were decreased. These effects are consistent with data showing that lurbinectedin treatment leads to an activation of the cGAS/STING pathway, type I/II interferons (IFNα/β), and pro-inflammatory chemokines (CCL5, CXCL10) in tumors. Interestingly, lurbinectedin treatment led to significant upregulation of mRNA and surface expression of MHC class-I genes (HLA-A/B/C) *in vitro* and *in vivo.* Finally, bulk RNA sequencing as well as RT-PCR of pre- and post-lurbinectedin treatment demonstrated an increase in DAMPs associated with immunogenic cell death.

Conclusion: We provide the first mechanistic insight into the lurbinectedin-induced multimodal immune modulation in SCLC leading to a dramatic anti-tumor activity accompanied by the establishment of a strong anti-tumor immune microenvironment. Since lurbinectedin is already approved as a second-line agent in SCLC, our preclinical data provide a strong rationale for combining this regimen with inhibitors of the PD-L1 pathway and also highlight the immune subsets that the combination targets.

#6555 scRNAseq and TCR repertoire analysis identifies immune correlates of response to combined BRAF/MEK/PD1 inhibition in a phase 2 trial.

H. Yao[1], V. Jorgji[1], A. L. Tang[2], D. Lieb[2], S. X. Chao[2], D. J. Stein[1], M. Spurrell[3], L. Elmelech[2], J. Tian[1], M. Sade-Feldman[1], K. Pelka[4], R. B. Corcoran[1], N. Hacohen[1], I. Korsunsky[1], J. Chen[1];

[1]Harvard Medical School, Boston, MA, [2]Broad Institute of Massachusetts Institute of Technology (MIT) and Harvard, Cambridge, MA, [3]Yale University, New Haven, CT, [4]Gladstone Institutes, San Francisco, CA

Background

Our recent clinical trial of combined BRAF, MEK, and PD-1 inhibition showed a 24% response rate in BRAF V600E mutant colon cancer (PMID: 36702949). Analysis of epithelial single-cell RNA sequencing data showed an increase in interferon-stimulated genes (ISG) and inhibition of the MAPK pathway in responders. MAPK inhibition in organoids also induced ISGs. These data suggest a synergy between MAPK inhibition and induction of immune responses.

Methods

We analyzed over 100,000 immune and stromal cells from 23 paired scRNAseq profiles of pre- and day 15 on-treatment tumor biopsies. Progression free survival greater than 6 months was defined as a clinical response. We performed traditional differentially expressed gene and gene program analyses, and tracked TCR repertoire in tumor and blood. We developed a novel approach based on supervised clustering (PMID: 34675423) to identify fine-grained cell subtypes associated with response. We applied supervised clustering separately to T and myeloid cells, and tested the association of each cluster's abundance with response.

Results

We applied supervised clustering to T cells and identified a CD74+IFNG+ CD8 T cell cluster that increased in only responders (p=0.0078). In the myeloid compartment, we identified two populations of CXCL10+ macrophages: one whose abundance increased in all patients and a CCL3+CCL4+ activation state expanded (p=0.01) only in responders. Pathway analysis of the expanded populations suggests an enrichment of ISGs in both CD74+IFNG+ CD8 T cells and CXCL10+CCL3+CCL4+ macrophages, with specific enrichment of interferon-gamma responsive genes GBP1 and GBP4 in the macrophages.

T cell analysis yielded two responders with marked clonal expansion within the CXCL13+ population, which likely represent tumor-specific T cells. Within the blood, these CXCL13+ clonotypes underwent a short-lived burst at day 15, yet represented only a minor population. We saw concomitant expansion of both CXCL13+ CD4 and CD8 populations within patients, suggesting CXCL13+ CD4s might provide help to the CXCL13+ CD8 T cells. The same two responders had increased stem-like TCF7+PD1+ CD8 T cells previously implicated in immunotherapy response and an increase in CCL19+ fibroblasts associated with stem-immunity hubs.

Conclusions

Our analysis of pre- and on-therapy biopsy scRNAseq data from our clinical trial of MAPK and PD-1 inhibition found expansion of ISG enriched CD74+IFNG+ CD8 T cells and CXCL10+CCL3+CCL4+ macrophages in responders. Both populations are enriched in ISGs: this coordinated expansion may result from a shared, interferon-rich microenvironment. Ongoing work will explore this hypothesis using spatial transcriptomics to identify these activated cells and their microenvironments.

Ethics approval

"This study was approved by the DF/HCC IRB as protocol 18-144 (see also ClinicalTrials.gov NCT03668431).

#6556 Targeting mesenchymal tumor cell-intrinsic factors sensitizes refractory tumors to immune checkpoint blockade therapy.

K. M. Bakhle, C. H. Sams, A. Dongre;
Cornell Univ. College of Veterinary Med., Ithaca, NY

Immune checkpoint blockade (ICB) therapy has emerged as a promising approach for treating breast cancer, however, only a fraction of patients derives clinical benefit and the underlying reasons for heterogeneous responses remain elusive. The epithelial-to-mesenchymal transition (EMT) enables these carcinomas to metastasize and acquire resistance to chemotherapy. We have recently demonstrated that the EMT program also confers resistance to immunotherapies. Specifically, epithelial tumors recruit $CD8^{\pm}$ T-cells to the tumor microenvironment and are sensitive to anti-CTLA4 ICB. In contrast, mesenchymal tumors assemble an immunosuppressive tumor microenvironment and are resistant to the same treatment. Furthermore, mesenchymal tumors express multiple immunosuppressive paracrine factors relative to their epithelial counterparts. Of these, abrogation of CSF1 or SPP1 from mesenchymal cancer cells generates partial responses to ICB therapy. Strikingly, abrogation of CD73 from mesenchymal carcinoma cells completely sensitizes otherwise refractory tumors to immunotherapy. While targeting cancer cell-intrinsic factors can sensitize mesenchymal tumors to ICB, the mechanisms that dictate partial versus complete responses are unclear. Furthermore, whether abrogation of CD73 can also sensitize mesenchymal tumors to other forms of ICB remains unknown. By performing immunofluorescent analysis of tumor sections, we observed that knockout of CD73 promoted the greatest infiltration of both $CD4^{\pm}$ and $CD8^{\pm}$ T-cells in response to anti-CTLA4 ICB compared to tumors knocked out for CSF1 and SPP1, which showed only intermediate levels of infiltration. Moreover, treatment of mesenchymal tumor-bearing mice with anti-CD73 generated synergistic responses with anti-CTLA4 ICB, but not with anti-PD1, or combinations of anti-CTLA4 and anti-PD1. In conclusion, our results demonstrate that the EMT program in cancer cells is predictive of responses to ICB. Targeting CD73 in mesenchymal breast tumors promotes an influx of both $CD4^{\pm}$ and $CD8^{\pm}$ T-cells and potentiates the efficacy of anti-CTLA4 ICB. Through mining of canine mammary tumor RNA sequencing data, we have found that canine tumors associated with EMT have increased expression of CD73, which suggests that these mechanisms of immune evasion may translate across species. These findings could promote therapies for both animals and humans that sensitize highly refractory populations of more-mesenchymal cancer cells.

CLINICAL RESEARCH: Liquid Biopsy
Minisymposium

#6557 Longitudinal cell-free tumor load dynamics represent an early endpoint for immunotherapy response in non-small cell lung cancer.

Lavanya Sivapalan[1], Bahar Alipanahi[2], Archana Balan[1], Jamie E. Medina[2], Noushin Niknafs[1], Erica Peters[2], Jaime Wehr[1], Alissa Konicki[2], Mimi Najjar[1], Bryan Chesnick[2], Gavin Pereira[1], Sarah Rongione[2], Nisha Rao[1], Michael Rongione[2], Brittany Shavatt[2], Lorenzo Rinaldi[2], Benjamin Levy[1], Victor E. Velculescu[1], Patrick M. Forde[1], Valsamo Anagnostou[1]

[1]The Sidney Kimmel Comprehensive Cancer Center, Johns Hopkins University School of Medicine, Baltimore, MD, [2]Delfi Diagnostics, Inc., Baltimore, MD

Background: Liquid biopsies can inform treatment strategies by rapidly and accurately assessing tumor burden; with emerging data supporting the clinical utility of circulating cell-free tumor DNA (ctDNA) as an early endpoint of immunotherapy response.
Methods: We performed targeted error-correction sequencing of ctDNA (n=330) and matched white blood cell (WBC) DNA (n=109) from 109 patients with advanced non-small cell lung cancer (NSCLC) who received immune checkpoint inhibitor monotherapy (n=79) or immunotherapy-containing combination regimens (n=30). Variant cellular origin was determined using a tumor-independent WBC DNA-informed approach. The maximum mutant allele fraction (maxMAF) of tumor-derived mutations was tracked longitudinally to assess changes in total cell-free tumor load (cfTL).
Results: Among 3,418 variants with resolved cellular origin, 2,452 (72%) were tumor-derived, 125 (4%) were germline, while 841 (25%) were related to clonal haematopoiesis (CH). Cell-free DNA fragments harbouring tumor-derived mutations were significantly shorter than fragments containing wild-type alleles; however, fragment length alone was insufficient to distinguish CH variants from wild-type. Overall, 97 (89%) patients with >1 detectable tumor mutation were considered for cfTL tracking and molecular response assessment. Clearance of cfTL indicated molecular response (mR) whereas persistence indicated molecular progression (mPD). Time-course analyses, aiming to establish the optimal timing for molecular response assessment, revealed that early cfTL clearance within 3-9 weeks was significantly linked to improved survival outcomes. Notably, blood tumor mutation burden above or below 16 mutations/megabase showed no association with overall survival (OS; log rank p=0.98) or progression-free survival (PFS; log rank p=0.95). Of 81 patients evaluated for early on-therapy molecular responses, 28 (35%) were classified as having an mR, while 53 (65%) patients were classified in the mPD category. The median time to mR was 5 weeks in patients receiving immune checkpoint monotherapy and 6 weeks in patients receiving chemo-immunotherapy combination regimens. Patients in the mR group achieved longer OS (log rank p=0.001) and PFS (log rank p=0.0003) compared to those with mPD. Assessment of landmark PFS at 6 months demonstrated a significant association between ctDNA molecular response and durable clinical benefit (DCB) in patients receiving immune checkpoint monotherapy ($p < 0.001$, Fisher's exact test), and a numerical association with DCB in patients on chemo-immunotherapy (p=0.07, Fisher's exact test).
Conclusions: Longitudinal tracking of ctDNA provides a real-time and accurate approach for monitoring immunotherapy response. These findings underscore the clinical utility of employing ctDNA molecular response to inform clinical decision-making.

#6558 Ultra-sensitive ctDNA detection predicts response to immune checkpoint inhibition in advanced melanoma patients.

C. Gebhardt[1], L. Keller[1], I. Heidrich[1], J. Koett[1], G. Geidel[1], D. J. Smit[1], R. Simon[1], S. W. Schneider[1], J. Pugh[2], C. W. Abbott[2], S. Boyle[2], R. O. Chen[2], K. Pantel[1];

[1]University Medical Center Hamburg-Eppendorf, Hamburg, Germany, [2]Personalis Inc., Menlo Park, CA

Immune checkpoint inhibition (ICI) provides clinical benefit to a subset of cancer patients. Monitoring circulating tumor DNA (ctDNA) in peripheral blood may allow clinicians to predict ICI response or resistance earlier than imaging and track response more frequently. In this study, melanoma patients receiving ICI were profiled using an ultra-sensitive, tumor-informed ctDNA detection platform, and the findings were correlated with clinical outcome. In this retrospective study, 188 plasma samples were collected from 23 advanced melanoma patients receiving immune checkpoint inhibitor (ICI) treatment, spanning a period of up to 40 months. Levels of ctDNA were then profiled using the NeXT Personal® assay. NeXT Personal is a liquid biopsy platform that utilizes whole-genome sequencing of tumor and normal samples to create a customized panel for each patient, encompassing up to 1,800 genetic somatic variants. This enables the detection of molecular residual disease (MRD) down to a limit of detection (LOD) of 1-3 parts per million (PPM). We subsequently compared the results obtained through NeXT Personal with RECIST-defined measurements and clinical outcomes. Ultra-sensitive ctDNA detection was achieved across a wide dynamic range, spanning from 2.3 PPM to over 130,000 PPM (median LOD = 2 PPM). A significant number of detections were attained at low PPM levels, with 30% (31/105) occurring below 100 PPM and 25% (26/105) occurring below 50 PPM. 94% (17/18) of baseline samples were ctDNA+ among patients without recent second-line therapy, including all patients who progressed. All ctDNA+ detections aligned with imaging results that indicated the presence of tumor. Likewise, all plasma timepoints corresponding to complete responses (CR) assessed via RECIST were ctDNA-. Early increase in ctDNA from baseline to treatment cycle 3 significantly predicted PFS (log-rank 0.003; Wald p=0.01, HR=8.35, 95% CI 1.62-43.15). Survival was predicted by both imaging CR (log-rank p=0.018) and ctDNA clearance (log-rank p=0.003). Molecular progression, defined as a 20% increase in ctDNA, significantly predicted OS (log-rank p=0.023), whereas imaging PD status did not predict OS (log-rank p=0.09). We achieved detection of ctDNA with an LOD down to 1.3 PPM in this cohort, with nearly a third of detections occurring below 100 PPM, suggesting the importance of an ultra-sensitive ctDNA approach even in late stage patients. Our findings suggest that ctDNA changes arepredictive of ICI response in late stage melanoma. These results highlight the potential for patient-specific ctDNA monitoring to inform patient management and for clincal trial design.

#6559 Clinical validity of post-surgery circulating tumor DNA testing in stage III colon cancer patients treated with adjuvant chemotherapy: The PROVENC3 study.

C. Rubio Alarcon[1], A. Georgiadis[2], I. A. Franken[3], H. Wang[4], S. C. M. van Nassau[3], S. J. Schraa[3], D. E. W. van der Kruijssen[3], K. van Rooijen[3], T. C. Linders[1], P. Delis-van Diemen[1], M. Alkemade[1], A. Bolijn[1], M. Tijssen[1], M. Lemmens[1], L. Meiqari[1], S. L. C. Ketelaars[1], A. Closa Mosquera[1], M. M. W. van Dongen[1], M. Lanfermeijer[1], B. I. Lissenberg-Witte[4], L. J. W. Bosch[1], T. Bisschop-Snetselaar[3], B. Adriaans[3], A. Greer[2], D. Riley[2], J. R. White[2], C. Greco[2], L. Cox[2], J. Fox[2], K. Victor[2], C. Leech[2], S. V. Angiuoli[2], N. F. M. Kok[1], C. J. A. Punt[5], D. van den Broek[1], M. Koopman[3], G. A. Meijer[1], V. E. Velculescu[6], J. M. L. Roodhart[3], V. M. H. Coupe[4], M. Sausen[2], G. R. Vink[7], R. J. A. Fijneman[1];

[1]Netherlands Cancer Institute, Amsterdam, Netherlands, [2]Personal Genome Diagnostics, Labcorp, Baltimore, MD, [3]University Medical Center Utrecht, Utrecht, Netherlands, [4]Amsterdam University Medical Centres, Location VU Medical Center, Amsterdam, Netherlands, [5]Julius Center, University Medical Center Utrecht, Utrecht, Netherlands, [6]Johns Hopkins University School of Medicine, Baltimore, MD, [7]University Medical Center Utrecht, Netherlands Comprehensive Cancer Organisation, Utrecht, Netherlands

Introduction: Surgery followed by adjuvant chemotherapy (ACT) is standard of care in stage III colon cancer. However, only 15-20% of patients benefit from ACT, as half of patients are cured by surgery, and 25-30% still experience a recurrence. Detection of circulating tumor DNA (ctDNA) after resection of the primary tumor is a strong prognostic biomarker in non-metastatic colon cancer and offers a promising approach to better stratify stage III colon cancer patients for ACT treatment decisions.

Aim: The PROVENC3 study aims to determine the clinical validity of post-surgery ctDNA detection in patients with stage III colon cancer treated with ACT.

Methods: Blood was collected pre-surgery, post-surgery and post-ACT for stage III colon cancer patients treated with ACT. Tumor-informed detection of ctDNA was performed through integrated whole genome sequencing (WGS) analyses of formalin-fixed paraffin-embedded tumor tissue DNA (80x), germline DNA (40x), and plasma cell-free DNA (30x). The primary outcome was time to recurrence (TTR).

Results: Results from 209 patients (median follow up: 40 months) show that ctDNA-positive patients post-surgery (n=28) had a higher risk of developing a recurrence than ctDNA-negative patients (HR: 6.3, [95%CI: 3.5-11.3], $P<10^{-8}$). 38% of patients with a recurrence within 3 years were ctDNA-positive post-surgery. Combination of post-surgery ctDNA status with established clinicopathological risk classification of low-risk (T1-3 and N1) and high-risk (T4 and/or N2) resulted in a 3-year cumulative recurrence risk of 82% for clinical high-risk ctDNA-positive patients compared to 7% for clinical low-risk ctDNA-negative patients (HR 28.9 [95%CI: 10.6-78.2]; $P<10^{-10}$). Results from 170 patients with post-ACT blood available showed that post-ACT ctDNA-positive patients (n=24) were at a higher risk of developing a recurrence (HR 7.9 [95%CI: 3.5-15.9]; $P<10^{-8}$) than ctDNA-negative patients. The patients experiencing a recurrence had higher aggregate ctDNA variant allele frequencies than patients not experiencing a recurrence post-surgery or post-ACT (P<0.001 and P<0.001, respectively).

Conclusion: Post-surgery ctDNA detection by tumor-informed WGS is a strong prognostic biomarker in stage III colon cancer patients, and improves the current risk stratification. Importantly, the post-surgery ctDNA-positive patients who did not experience a recurrence were likely cured by ACT. These data enable the design of clinical practice-changing ctDNA-guided interventional trials in stage III colon cancer to personalize adjuvant treatment decisions.

#6560 Cell-free RNA analysis for non-invasive cancer detection and characterization.

M. C. Nesselbush[1], B. A. Luca[1], Y.-J. Jeon[2], I. Jabara[1], C. B. Meador[3], M. S. Binkley[1], N. Xu[1], A. B. Hui[1], A. Garofalo[1], W. Y. Shi[1], K. J. Liu[1], T. Sugio[1], N. Kastelowitz[1], E. G. Hamilton[1], R. F. Bonilla[1], Y. Wang[1], A. Jiang[1], B. Lau[1], J. Eichholz[4], M. Banwait[3], J. Schroers-Martin[1], J. Boegeholz[1], D. A. King[5], M. S. Esfahani[1], T. Raclin[1], R. Tibshirani[1], S. Srinivas[1], V. S. Nair[6], J. M. Isbell[4], B. T. Li[4], Z. Piotrowska[3], L. V. Sequist[3], A. N. Hata[7], J. W. Neal[1], H. A. Wakelee[1], A. J. Gentles[1], A. A. Alizadeh[1], M. Diehn[1];

[1]Stanford University, Stanford, CA, [2]Sungkyunkwan University, Suwon, Korea, Republic of, [3]Massachusetts General Hospital and Harvard Medical School, Boston, MA, [4]Memorial Sloan Kettering Cancer Center, New York, NY, [5]Northwell Health Cancer Institute, Donald and Barbara Zucker School of Medicine at Hofstra, Feinstein Institute for Medical Research, Lake Success, NY, [6]Fred Hutchinson Cancer Center, Seattle, WA, [7]Massachusetts General Hospital, Boston, MA

Blood-based liquid biopsies enable non-invasive characterization of cancers. Cell-free RNA (cfRNA) analysis could potentially complement circulating tumor DNA (ctDNA) analysis and allow broader molecular characterization of cancers but has not been extensively explored. Here, we describe RARE-Seq, a novel cfRNA sequencing method designed to maximize sensitivity by targeting rare, tissue-specific transcripts, and simultaneously detecting both tumor-derived expression signatures and somatic mutations in circulating tumor RNA (ctRNA).

To interrogate samples for specific gene expression signatures, we developed and optimized a framework to measure tumor- and tissue-specific enrichment scores (ES) within cfRNA. We then empirically determined the limit of detection (LOD95) of RARE-Seq using admixtures of tumor cell line RNA and control cfRNA across a wide range of fractions. We found RARE-Seq to have an estimated LOD95 of 0.05% for cancer-derived RNA, which was 52-fold better than whole transcriptome cfRNA profiling.

To explore its potential clinical utility, we profiled 192 samples from 170 subjects with various cancers and non-cancer controls using RARE-Seq. Non-small cell lung cancer (NSCLC) expression signatures were significantly detected in 40 out of 51 NSCLC samples (78% sensitivity at 90% specificity). Detection increased with stage, ranging from 40% in stage I to 87% in stage IV. In a subset of stage IV NSCLC patients with matching ctDNA data (n=16), ctRNA levels were significantly correlated with ctDNA allele frequencies (Pearson R=0.84, P=0.005). Intriguingly, 86% of samples with undetectable ctDNA contained detectable ctRNA, suggesting potential complementarity of ctRNA and ctDNA analysis for cancer detection. We also developed and benchmarked a direct ctRNA genotyping approach, allowing noninvasive detection of driver mutations in 42% of patients with advanced NSCLC. When applied to other tumors, RARE-Seq demonstrated 80-100% sensitivity at 90% specificity for detection of pancreatic adenocarcinomas (PAAD), prostate adenocarcinomas (PRAD), and hepatocellular carcinomas (LIHC). Furthermore, when evaluating tissue of origin (TOO) classification performance, RARE-Seq achieved 85% median accuracy for the top predicted tissue and 96% median accuracy for the top two tissues.

These results highlight the potential value of ultrasensitive cfRNA analysis, providing proof-of-principle for detection of multiple tumor types using RARE-Seq.

#6561 Phenotypic and genotypic characterization of single circulating tumor cells in the follow-up of high-grade serous ovarian cancer.

S. Kasimir-Bauer[1], N. H. Stoecklein[2], R. P. L. Neves[2], S. T. Liffers[1], J. D. Kuhlmann[3], P. Wimberger[3], P. Buderath[1], R. Kimmig[1], C. Salmon[1];
[1]University Hospital Essen, Essen, Germany, [2]University Hospital Duesseldorf, Duesseldorf, Germany, [3]Medical Faculty and University Hospital Carl Gustav Carus, Technische Universitat Dresden, Dresden, Germany

Background: Ovarian Cancer (OC) is one of the leading causes of death among gynecological tumors with an insufficient understanding of OC disease evolution. Since tumor tissue is not always available, blood allows the investigation of single circulating tumor cells (sCTC) over time. We combined immunomagnetic enrichment and image-based sCTC sorting for phenotypic and genotypic analysis of sCTCs in the follow-up of OC to provide insights into sCTC heterogeneity and their malignant character.

Patients and Methods: 10 ml blood of high-grade serous OC patients (pts) at the time of primary diagnosis (n=42), after chemotherapy (n=23) and after Avastin (n=11) was analyzed for sCTCs using density-gradient centrifugation to further apply MACS® using CD45 and CD235a antibodies coupled to MACS® MicroBeads. For image-based sCTC sorting (DEPArray®), an immunofluorescence protocol staining for Hoechst, cytokeratin (CK), the folate receptor alpha (FRa), Vimentin (Vim) and CD45 was applied. Whole genome amplification (WGA) was performed in recovered single cells, comprising cell lysis, DNA digestion, adaptor ligation and an amplification PCR for subsequent copy number alteration (CNA) analysis. Ampli1™ low-pass analysis was used to analyze single cell WGA products. 21 primary tumors (PT) were assessed for whole-genome CNA and the Ampli 1™ OncoSeek panel was used for deep sequencing of sCTCs.

Results: Phenotypic assessment revealed FRa-positive cells in 28/42 (67%) pts, CK-positive cells in 32/42 (76%) pts and CK-FRa-double-positive cells in 15/42 (36%) pts, respectively, with a significant (p= 0.0205) reduction of cells after chemotherapy only documented for FRa-positive cells. Interestingly, cells with a high nuclear staining but no expression of target antigens were found in 37/42 pts (88%) and significantly (p=0.002) expanded during treatment. Genotyping revealed that only 7% (19/289) of single cells deriving from 13 different pts were aberrant. Whole genome CNA analysis in all pre-treatment sCTCs revealed enriched CNAs in chromosomes 2, 7 and 12. In post-treatment sCTCs, CNA dynamics highlighted the adaptive potential of the homologous recombination pathway and suggested further investigation of MAPK signaling in resistant OC. Low-pass CNA comparison between sCTCs and the PT was feasible in nine pts, 2/9 with persistent PT characteristics in sCTCs at different sampling times. TP53 variants were the most frequently detected ones, persistent CNA in the *CDK4* oncogene and emerging CNA in the *ALK* oncogene were found in sCTCs from two pts.

Conclusion: We identified sCTCs in the follow-up of OC and demonstrated interpatient as well as intrapatient heterogeneity of sCTCs. Matched sCTCs and PT data showed similar CNAs to a certain amount. Our low percentage of aberrant cells suggests that higher patient numbers are needed to confirm our findings to understand disease progression.

#6562 Comprehensive liquid biopsy: Multi-analyte evaluation of cellular and plasma components of blood in prostate cancer from a single blood collection tube.

J. Ladd, E. Bayer, B. Bartels, A. Tischner, R. Ponting, E. Kaldjian, A. Ramirez;
RareCyte, Inc., Seattle, WA

Background Liquid biopsy samples offer a non-invasive method for investigating drug targets and biomarkers in solid tumors. In this study, we describe a comprehensive liquid biopsy analysis of whole blood to identify circulating tumor cells (CTCs), large extracellular vesicles and CTC fragments, and CTC-white blood cell hybrids; quantify protein biomarker expression on CTCs; perform targeted mutation profiling on CTCs and cell-free DNA (cfDNA) from plasma; and analyze protein expression on white blood cells (WBCs) from a single 7.5 mL blood sample. This array of tests was applied to blood samples from patients with Stage IV prostate cancer to demonstrate clinical feasibility.

Methods A novel dual biomarker CTC assay was developed to measure protein expression of PSMA and ARv7 on CTCs from stage IV prostate cancer patients. Nucleated cells from clinical samples were processed to microscope slides using AccuCyte®, an unbiased, density-based separation method that also allows for plasma collection for downstream analysis. Slides were fixed and stained with antibodies to cytokeratin, EpCAM, and CD45 to detect CTCs and exclude WBCs, and with PSMA and ARv7 to evaluate protein biomarker expression on identified CTCs. The slides were imaged with the CyteFinder® automated immunofluorescence scanning microscope that identifies CTCs for confirmation by trained reviewers and quantitatively measures protein mean fluorescence intensity (MFI) on any cells detected on the slides (CTCs, CTC-WBC hybrids, large extracellular vesicles and CTC fragments and WBCs). Individual CTCs and control pools of WBCs from clinical samples with at least 4 CTCs were picked using CytePicker®, a needle-based system used to isolate single cells. cfDNA was isolated from plasma removed during the AccuCyte® process using a QIAamp MinElute ccfDNA kit. Picked CTCs, WBC pools, and isolated ctDNA were sequenced using the OncoZoom Cancer HotSpot panel from Paragon Genomics.

Results Nine progressing Stage IV prostate cancer patient blood samples were stained with a novel PSMA/ARv7 dual biomarker assay. CTCs were identified in all clinical samples (median 4, range 1 - 384). PSMA positivity in clinical samples ranged from 0% to 75%, and ARv7 positivity ranged from 33% to 100%, and. Additional analysis using QuPath was performed to determine PSMA/ARv7 protein expression on WBCs and CTC fragments. ctDNA analysis from 5 individual samples was compared to sequencing results from individual CTCs from the same samples.

Conclusions Using a single 7.5 mL blood liquid biopsy, we can measure protein expression on enumerated CTCs and quantify these same protein biomarkers on WBCs and CTC fragments/oncosomes, determine the genetic makeup of the tumor through the sequencing of cfDNA, and monitor genetic mutations in intact CTCs in circulation.

#6563 PSMA-based detection and global proteome-based analysis of circulating tumor cells in castration resistant prostate cancer patients.

J. M. Drake[1], A. Arafa[1], A. Horrmann[2], K. J. Kamalanathan[2], C. Galeano-Garces[2], Z. Sychev[1], N. Heller[2], M. Ahmadi[2], M. Ludwig[1], O. Hedeen[2], A. Hesch[2], G. Schaap[2], J. Hapke[2], J. Miller[2], I. Babris[2], T. Lee[2], T. Clacko[2], J. Hwang[1], J. Hong[1], B. Konety[3], J. Parthasarathy[2], E. Antonarakis[1];

[1]University of Minnesota, Minneapolis, MN, [2]Astrin Biosciences, St. Paul, MN, [3]Allina Health, Minneapolis, MN

In recent years, many new targeted and immuno-therapies have entered the cancer treatment landscape with the potential to drastically improve patient outcomes; however, selecting the optimal drug target especially as the disease progresses becomes increasingly important. Liquid biopsies show great promise in providing insights on the current disease state, but generally rely on a small number of protein markers identified through immunofluorescence staining or genomic mutations determined from cell-free DNA which limits the amount of information available to make treatment decisions. One way to better select the optimal drug target is to generate unbiased mass-spectrometry based proteomic data from the circulating tumor cells (CTCs) isolated from blood. In this study, we collaborated with Astrin Biosciences using their patented isolation technology to enrich CTCs with high purity from the blood of 57 metastatic castration resistant prostate cancer (mCRPC) patients. The CTC-enriched sample (along with a patient-matched control sample consisting primarily of white blood cells) was analyzed in real time for either PSMA protein (Lutetium-PSMA-617 study, n=32) or via mass-spectrometry (CTC proteomics study, n=25). Over 1,500 peptides corresponding to greater than 600 proteins were identified from each patient's CTCs. These included increased epithelial cell markers in the CTC-enriched sample and increased WBC markers in the control sample. Specifically, detection of the androgen receptor protein was identified in the CTC-enriched sample which is of particular interest in mCRPC patients. Furthermore, this method is able to detect and quantify PSMA expression, which is of clear relevance in the context of PSMA-directed therapeutics. This study demonstrates the feasibility of obtaining large scale proteomic data from a liquid biopsy. Future studies will focus on cancer signaling mechanisms and biomarkers to elucidate the clinical utility of such data. As more patients are analyzed, we will compare proteomic data with known tissue proteome information when available and to correlate these with drug response to improve treatment selection and patient outcomes.

CLINICAL RESEARCH: Novel Approaches for Targeted Therapies
Minisymposium

#6564 SOS1 inhibitor treatment improves response to Venetoclax in acute myeloid leukemia.

K. Kostyrko[1], M. Hinkel[1], M. G. Rees[2], M. M. Ronan[2], J. A. Roth[2], D. Gerlach[1], I. Waizenegger[1];
[1]Boehringer Ingelheim RCV GmbH & Co. KG, Vienna, Austria, [2]Broad Institute of MIT and Harvard, Cambridge, MA

Acute myeloid leukemia (AML) is the most common type of acute leukemia in adults. First-line treatment of AML patients consists primarily of chemotherapy, sometimes combined with a targeted therapy. However, elderly patients unfit for chemotherapy receive venetoclax, a BCL2 inhibitor, combined with azacitadine or decitabine. While responses in these patients are high (50-70%, with median OS of 10-17 months), around 30-50% of them do not respond and most relapse within 1-10 years. Increased MAPK pathway activity or low frequency RAS pathway mutations have been identified as key mediators of resistance to standard-of-care targeted therapies for AML, including venetoclax. Here, we found that in DepMap whole-genome CRISPR screens, leukemia cell lines, including AML, show a particular dependency on SOS1. A subsequent PRISM screen with a selective inhibitor of SOS1 confirmed these results. To validate these results in vitro, we treated 7 AML cell lines showing strongest dependency on SOS1 based on DepMap and PRISM screens, with SOS1i or a SHP2 inhibitor. We found that in 4 of 7 cell lines treatment with SOS1i or SHP2i strongly impaired proliferation. In 3 of 4 responding cell lines, the anti-proliferative effect with either SOS1i or SHP2i was stronger than azacytidine single agent treatment. We next treated 29 primary ex vivo cultures of AML with SOS1i and found that the treatment induced strong or intermediate anti-proliferative effect in 21 of 29 models (72%). In two AML PDX models, treatment with SOS1i as a single agent resulted in approximately 25% reduction of human CD45+ AML blast cells in both models. Venetoclax treatment led to approximately 75% decrease in AML blasts, while the combined venetoclax and SOS1i treatment resulted in near complete eradication of the disease. Annexin V staining of AML monoblasts demonstrated that this decrease was due to an increase in apoptosis in the combination groups. In summary, we demonstrate that SOS1 inhibitor treatment may be used to improve responses to venetoclax in AML patients.

#6565 Improving survival of atypical teratoid/rhabdoid tumor orthotopic xenografts through the combination of PI3K inhibitor paxalisib and nucleoside analog gemcitabine.

T. Findlay, K. Malebranche, A. Geethadevi, C. Eberhart, J. Rubens, E. Raabe;
Johns Hopkins University School of Medicine, Baltimore, MD

Atypical teratoid/rhabdoid tumors (AT/RT) are an aggressive infantile brain tumor with a dismal four-year event-free survival of 37%. We have previously identified high activation of mTORC1 and mTORC2 within AT/RT and shown that the highly brain penetrant PI3K inhibitor paxalisib is capable of simultaneously inhibiting mTORC1/2 by acting upstream of both complexes. In two orthotopic xenograft models, paxalisib slowed tumor growth and significantly extended survival (CHLA-06: 40 to 54 days, p=0.001; BT-12: 21 to 35 days, p=0.02). RNAseq analysis following mTOR inhibition in AT/RT cell lines showed an upregulation of genes involved in the activation of the integrated stress response (ISR) (*ATF4*, *CHOP*, *PPP1R15A* *t*-test p<0.05). Analysis of primary pediatric brain tumors through the Children's Brain Tumor Network showed increased levels of *ATF4* mRNA and eIF2α protein and mRNA in AT/RT compared to other indolent pediatric brain tumors. Increased expression of ISR components suggests this pathway may be a dependency in AT/RT. Activation of this pathway is known to be cytoprotective, however persistent over-activation drives cell death through induction of pro-apoptotic factors. Gemcitabine is a pyrimidine analog functioning to inhibit DNA synthesis and induce DNA damage; notably, recent literature has correlated DNA damage to activation of the ISR with downstream phosphorylation of eIF2α. We hypothesize that due to high baseline activation of ISR for AT/RT, paxalisib combined with gemcitabine will result in an over-activation of the ISR leading to AT/RT cell death. Western blot analysis of combination therapy compared to DMSO control showed induction of phospho-eIF2α, ATF4, and CHOP, denoting an activation of the ISR. Combination therapy in AT/RT cells induces cell death (Western blot analysis cPARP, MUSE Annexin V assay, SynergyFinder BLISS score [viability] CHLA-06: 21.50, CHLA-266: 22.60) and synergizes to decrease cell growth (SynergyFinder BLISS score [inhibition] CHLA-06: 16.80, BT-12: 14.30, CHLA-266: 13.90, BT-37: 11.40, CHLA-05: 10.40). Paxalisib/gemcitabine combination therapy in murine orthotopic xenograft models of AT/RT has slowed tumor growth (bioluminescent imaging) and led to significant extension of survival. Mice bearing BT-37 orthotopic xenografts and treated with vehicle control had a median survival of 56 days, while all of the paxalisib/gemcitabine treated mice were alive at 100 days of treatment (p<0.0001). In CHLA-06 orthotopic tumors combination therapy extended median survival from 22 days for control to 82.5 days (p<0.0001). Based on these findings, the Pacific Pediatric Neuro-Oncology Consortium (PNOC) is planning to include paxalisib/gemcitabine combination therapy in the next international clinical trial for patients with relapsed/recurrent AT/RT.

#6566 Clinical evaluation of functional combinatorial precision medicine platform to predict treatment outcomes and enhance combination therapy design in soft tissue sarcomas.

E. K. Chow[1], S. P. Y. Chan[1], T. Toh[1], M. Rashid[2], V. S. Yang[3];

[1]National University of Singapore (NUS), Singapore, Singapore, [2]KYAN Technologies, Singapore, Singapore, [3]National Cancer Centre Singapore, Singapore, Singapore

Purpose: Soft tissue sarcomas (STS) are a collection of heterogenous cancers with limited range of treatment options and poor outcomes. First line treatment for most STS is anthracycline-based, with gemcitabine-based combinations, pazopanib or ifosfamide as treatment options in refractory/relapsed STS. There is a clinical unmet need to improve treatment options for STS as median time to progression following second- and third-line treatments is less than 4 months. We have previously demonstrated in a 71-patient relapsed/refractory non-Hodgkin's lymphoma clinical study that a functional precision medicine platform can effectively guide treatment, with several exceptional responders (Science Translational Medicine, 2022). This ex vivo drug sensitivity platform, quadratic phenotypic optimization platform (QPOP), analyses a predesigned array of 155 test combinations performed on a primary patient sample to rank and compare all possible therapeutic combinations from a 12-drug set. In this study, we evaluated clinical concordance of QPOP to predict treatment outcomes in an STS cohort. We also explored QPOP's combination therapy ranking function to identify novel combinations that may benefit larger groups of STS patients when appropriately guided.

Experimental Detail: A 12-drug set comprised of STS standard of care, FDA approved drugs and promising investigational drugs was evaluated in QPOP analysis of primary STS tumor samples. Ex vivo cultures of primary STS samples were treated with a predesigned array of 155 test combinations to provide a quantitative phenotypic output for each test combination. This dataset was analyzed by QPOP to rank all possible drug combinations towards a predicted treatment outcome. Concordance analysis was then performed comparing patient sample results with either parallel treatment initiated at time of sample collection or physician choice to use QPOP-guided treatment. Validation of QPOP-derived top-ranked drug combinations was also performed.

Results: 12-drug, 3-level QPOP was successfully performed on 45 of 51 primary patient samples. Clinical concordance analysis showed QPOP had a total predictive value (TPV) of 76.9% and an AUC_{ROC} of 85.7%. Exceptional responders to guided treatment with pazopanib or eribulin were observed. Additionally, top-ranked epigenetic-based combinations were identified as effective across multiple STS subtypes and validated preclinically.

Conclusion: The results show the potential for QPOP to predict clinical response in solid cancers, such as STS. Furthermore, QPOP can improve drug development pipelines through patient samples-based design of effective combinations with investigational drugs or underutilized drugs that may benefit larger populations of patients or specific subgroups of patients.

#6567 Affinity and cooperativity modulate ternary complex formation to drive degradation of SMARCA2.

I. Archibeque[1], K. Dellamaggiore[1], K. Rex[1], S. Ghimire-Rijal[2], K. Choi[2], S. Kate[2], A. Amegadzie[2], N. Chen[2], X. Li[2], R. Wurz[2], A. Vaish[2], P. Hughes[1], **D. Mohl**[1]; [1]Amgen Oncology, Thousand Oaks, CA, [2]Amgen, Therapeutic Discovery, Thousand Oaks, CA

Small molecules that hijack the ubiquitin-proteasome system to degrade target proteins have gained traction as tools for chemical biology and as promising clinical candidates. Targeted degradation strategies encompass relatively large hetero-bifunctional small molecules (hSMs) that are built from target and effector ligands joined by a linker to much smaller molecular glues that have limited affinity for the target or effector proteins outside of a ternary complex. There is good reason for medicinal chemists to move from linkered hSMs toward glue-like scaffolds. Molecular glues can be considerably smaller, e.g., the IMiDs, and thus are less likely to possess atoms and functional motifs that add up to poor permeability and higher protein binding.

Guided by the principle that hSMs with reduced molecular weight will have superior druglike properties, we have used SMARCA2, a potential therapeutic target in patients that have both copies of SMARCA4 inactivated, as a test of our own ability to drive rapid target degradation in relevant models. The hetero-bifunctional degraders that resulted from our work trade conventional linkers for chemical spacers that orient SMARCA2 and VHL to promote fortuitous protein-protein contacts in the ternary complex. Following in the footsteps of previously published works, we employed surface plasmon resonance (SPR), x-ray crystallography, and molecular modeling to understand the relationships between our cell-based metrics of degrader activity and the biophysical parameters that describe the ternary complex. Consequently, we found that cooperativity (α) and ternary complex affinity (K_{LPT}) correlated well with both DC50 and initial rate of degradation. Within our series of novel SMARCA2 degraders, compound 1 exhibited exceptional cooperativity and ternary complex affinity, α = 12.8 and K_{LPT} = 4.7 ± 1. The result of high cooperativity and enhanced affinity was rapid and near complete SMARCA2 degradation. Treatment of a cancer cell line with compound 1 resulted in 50% of SMARCA2 being degraded
in under 30 minutes, and greater than 90% degradation in 2 hours. Most importantly, the near complete degradation of SMARCA2 resulted in potent effects on SWI/SNF dependent transcription in vitro and in inhibition of tumor cell growth both in vitro and in vivo.

#6568 *PTCH1* loss-of-function alterations: Mutational landscape and therapeutic outcomes to hedgehog pathway inhibitors in non-canonical histologies.

Antoine Desilets, Matteo Repetto, Soo Ryum Yang, Monica Chen, Dazhi Liu, Nikhil Rizvi, Ezra Rosen, Alan L. Ho, Alexander Drilon, Yonina R. Murciano-Goroff

Memorial Sloan Kettering Cancer Center, New York, NY

Background: Loss-of-function (LOF) alterations of the *PTCH1* tumor suppressor gene represent canonical events involved in basal cell carcinoma (BCC) oncogenesis. Hedgehog pathway inhibitors (HPIs) are approved for the treatment of advanced BCC, but genomic characterization and therapeutic outcomes remain limited in tumor agnostic cohorts.

Methods: Using the MSK Clinical Sequencing Cohort, we performed a mutational landscape analysis of *PTCH1* LOF alterations in non-BCC histologies, including Fraction and Allele-Specific Copy Number Estimates from Tumor Sequencing (FACETS) annotation, and analyzed response and progression-free survival (PFS) with HPIs.

Results: Out of 115,619 samples, 1972 samples from advanced solid tumors with *PTCH1* LOF alterations were identified. Excluding 1306 variants of unknown significance (VUSs) using OncoKB knowledge base as well as 44 BCC samples, a total of 622 samples from 570 patients with oncogenic *PTCH1* alterations were identified across histologies. In addition, 124 patients received ≥1 line(s) of HPI at our institution between 2013 and 2023, including 16 patients with non-BCC histologies presenting *PTCH1* alterations. At the patient level (n=570), *PTCH1* LOF alterations were present across 33 primary sites, including colorectal cancer (CRC; 34%; n=192), endometrial cancer (17%; n=98), gastroesophageal adenocarcinomas (ADC) (8%; n=46), non-small cell lung cancer (NSCLC; 6%; n=34) and soft tissue sarcomas (STS; 4%; n=25). At the sample level (n=622), TMB ≥10 was seen in 83% (n=516), including 324 samples with MSI-high status. *PTCH1* alterations most frequently involved frameshift (fs) indels (69%; n=429), followed by nonsense mutations (18%; n=114), splice site mutations (8%; n=47) and fusions (5%; n=32). Recurrent fs events involved S1203Afs*52 (24%; n=150) and R1308Efs*64 (14%; n=89), among others. When comparing monoallelic (monoall) vs biallelic (biall) *PTCH1* alterations through FACETS annotation, monoall showed a strong association with higher TMB ($p<0.01$) whereas biall were associated with higher loss of heterozygosity (LOH; $p<0.01$). In the 16 non-BCC patients treated with HPIs, histologies included lung squamous cell cancer (SCC; n=4), cutaneous SCC (n=2), medulloblastoma (n=2), carcinosarcoma (n=2), osteosarcoma, chondrosarcoma, chordoma, sebaceous ADC, anal SCC and CRC (each n=1). TMB ≥10 was seen in 31% (n=5), all of which were MSI-low. Tumor regressions on HPI were seen in 50% (n=8), including lung SCC, cutaneous SCC, sebaceous ADC and medulloblastoma, with median time to response of 3.6 months (mo). Median PFS on HPI was 3.9 mo and median OS was 22.7 mo. Median PFS was higher in patients with TMB ≥10 vs TMB <10 (11.8 vs. 1.8 mo, $p=0.02$).

Conclusion: *PTCH1* LOF alterations appear actionable in non-BCC cutaneous/adnexal primaries, lung SCC and medulloblastoma, including TMB-high tumors.

#6569 KLIPP: Precision targeting of cancer with CRISPR.

M. Ljungman, H. Yang, R. Hulbatte, N. Gratsch, A. Kelher, J. Raupp, Y. Wang, K. Dorsey, T. Halseth, A. Schwendeman, P. Palmbos;
University of Michigan Medical School, Ann Arbor, MI

Current cancer therapeutic treatments are typically associated with significant collateral damage to normal tissues and the emergence of treatment resistance. Thus, there is an unmet need to develop therapies that are uniquely cancer specific and unhindered by the emergence of resistance. We have developed an RNA therapy approach based on CRISPR technology, known as “KLIPP”, that targets cancer-specific structural variant junctions (SVJs), a so far untapped cancer “Achilles heel”, that are highly abundant across cancer types. KLIPP uses a “split enzyme” system consisting of dCas9 conjugated to an endonuclease, Fok1, that requires dimerization for its activity. By designing sgRNAs that bind to sequences flanking the cancer-specific SVJs, Fok1-dCas9 dimers are formed, leading to the induction of DNA double strand breaks (DSBs) specifically at SVJs in cancer cells. We verify induction of DSBs by γH2AX foci staining in the nucleus of KLIPP-treated cells and resulting loss of clonogenic survival and induction of apoptosis, while cells lacking the targeted SVJs are unaffected. Importantly, we show elimination of orthotopic bladder cancer tumors *in vivo* after turning on expression of the KLIPP reagents by doxycycline in the drinking water. Finally, we show successful lipid nanoparticle delivery of KLIPP reagents to orthotopic bladder tumors *in vivo* using catheter-mediated delivery, leading to specific targeting of bladder cancer cells. Independently of the cancer-driving mutations, the omnipresence of cancer-specific SVJs is exploited by KLIPP to force cancer cells into apoptosis while leaving normal cells unperturbed. We believe that the successful implementation of precision KLIPP therapy could be transformative for the treatment of cancer patients.

#6570 *HLA* genotyping and HLA-based clinical trial matching using MSK-IMPACT, a targeted next-generation sequencing assay.

M. F. Chen, M. V. Gormally, A. Noronha, K. Panageas, M. Reynolds, K. Kohlasch, B. Novak, T. Kee-Velez, N. Clarke, C. Kyi, C. Friedman, S. D'Angelo, M. G. Kris, C. A. Klebanoff, R. Shah, M. Berger, C. Bandlamudi, A. Drilon, M. T. A. Donoghue;
Memorial Sloan Kettering Cancer Center, New York, NY

Purpose: Performing tumor next-generation sequencing (NGS) and human leukocyte antigen (*HLA*) typing in a single test can maximize the likelihood of matching patients with cancer to clinical trials. We investigated the utility of a clinical-grade NGS assay for this purpose.
Methods: HLA class I genotypes were determined on an investigational basis by MSK-IMPACT (FDA-authorized hybrid-capture, tumor and matched normal DNA-based NGS) using POLYSOLVER for patients with cancers of any histology between March 2014 and September 2023. Patient *HLA* genotype matches for phase I clinical trials were identified; for a subset of patients, concordance between *HLA* genotyping was compared to a CLIA-certified laboratory test.
Results: 60,565 patients successfully underwent complete class I *HLA* genotyping (two alleles each of *HLA-A, HLA-B,* and *HLA-C*). The median age at diagnosis was 64 years old and most patients were female (55%) and white (76%). The most common genotypes were *HLA-A*02:01* (42%, n=25,457), *HLA-C*04:01* (28%, n=17,274), *HLA-A*01:01* (25%, n=14,867), *HLA-C*07:01* (24%, n=14,538), *HLA-A*03:01* (21%, n=12,668), *HLA-C*07:02* (21%, n=12,493), and *HLA-B*07:02* (16%, n=9,787). Most patients (96%, n=58,287) were *HLA* genotype eligible [*HLA-A*02:01* (n=28), *HLA-A*11:01* (n=3), *HLA-A*01:01* (n=1), and *HLA-C*07:02* (n=1)] for ≥1 of 33 active early phase adoptive T cell therapy or T cell receptor bispecific trials on Clinicialtrials.gov. 280 patients with *HLA* class I matches were screened for phase I trial candidacy by the MSK phase I group. 117 were candidates for confirmatory *HLA* and neoantigen testing, of whom 43 patients were enrolled on a trial after additional screening. 72 patients had *HLA* genotyping both by MSK-IMPACT and an outside CLIA-certified laboratory; 100% (72/72) of these subjects had concordant genotypes.
Conclusions: MSK-IMPACT successfully determined class I *HLA* genotypes in a large, multi-ethnic population of patients. A substantial proportion of patients were identified as potential candidates for *HLA*-matched trials, supporting local trial enrollment.

ENDOCRINOLOGY: Molecular, Preclinical, and Clinical Endocrinology 3
Minisymposium

#6571 O-GlcNAc sites on progesterone receptor are critical for its ligand independent repression of interferon signaling in breast cancer.
H. I. Saunders, S. Holloran, E. Chowanec, J. Tinoco, C. Slawson, C. Hagan;
University of Kansas Medical Center, Kansas City, KS

The role of hormone receptors in breast cancer has been well established as a key contributor to breast cancer tumorigenesis. Estrogen receptor and progesterone receptors are present in nearly 70% of breast cancers. Estrogen receptor and estrogens in breast cancer has been extensively studied and targeted effectively through endocrine therapy, however the impact of progesterone and the progesterone receptor (PR) independent of estrogen is not well understood. We have previously demonstrated that PR promotes tumor growth and drives an immune suppressive environment, therefore understanding the biology of PR in breast cancer is critical. We demonstrated that PR attenuates type 1 interferon signaling via inhibition of STAT1 phosphorylation and increased degradation of STAT2. In this study we investigated the mechanism of PR regulation of IFN signaling. Post-translational modifications such as phosphorylation and SUMOylation can influence PR target gene promoter selectivity thereby altering its function. We have identified that PR is modified by O-GlcNAc, a single N-acetyl-glucosamine sugar that cycles on and off and serine or threonine amino acids in nuclear, cytoplasmic and mitochondrial proteins. Levels of total O-GlcNAc staining are higher in breast cancer tissue compared to adjacent normal tissue. Active O-GlcNAcylation, as evidenced by immunohistochemistry staining of O-GlcNAc-transferase (OGT), is elevated in patients with PR+ tumors compared to PR-. Using T47D breast cancer cells (an ER/PR-positive tumor line), mass spectrometry analysis revealed an O-GlcNAc site at S499, S733 and S735 on PR. Using a naturally occurring PR-negative variant of T47D cells, we introduced stable expression of a mutant PR with serine to alanine substitution at the O-GlcNAc sites (S499A, S733A, S75A), thereby blocking O-GlcNAc flux, in addition to wt PR as a control. RNA-Seq analysis of these cells following treatment with progesterone revealed ligand dependent PR gene regulation, however major differences were observed in gene expression of the two cell lines independent of ligand. These results indicate ligand independent PR suppression of IFN signaling requires O-GlcNAc at these three sites. Additionally, T47D-mutant PR cell lines implanted into immune deficient mice had significantly decreased growth compared to WT-PR control tumors. Together these findings indicate O-GlcNAcylation of PR contributes to PR driven breast cancer tumor growth and immune evasion via modulation of IFN signaling.

#6572 Screening of drug library targeting neural signaling identifies cholecystokinin B receptor as a potential therapeutic target in small cell lung cancer.

M. Tokunaga, N. Nakagawa, M. Ka, Y. Sugiura, T. Iida, T. Ando, K. Watanabe, H. Kage, M. Kawakami;
The University of Tokyo Hospital, Tokyo, Japan

Small cell lung cancer (SCLC) is characterized by poor prognosis with limited therapeutic agents. Development of a new therapeutic strategy is urgently needed. SCLC can be classified into subtypes based on the expression levels of four transcription factors: ASCL1, NEUROD1, POU2F3, and YAP1 (SCLC-A, SCLC-N, SCLC-P, and SCLC-Y, respectively). SCLC-A and SCLC-N are neuroendocrine (NE)-type tumors that secrete neurotransmitters and express their receptors. Recently, neural activity has been noted as a key regulator of cancer growth that affects cancer and other cells in the tumor microenvironment. We hypothesized that neurotransmitters that regulate the biology of NE-type SCLC (SCLC-A, SCLC-N) can be therapeutic targets. To explore this, we created a drug library consisting of 560 drugs known to target neural signaling including various G protein-coupled receptors and examined their growth-inhibitory effects in SCLC cell lines. When three NE-type SCLC cell lines (NCI-H146, SHP-77, and NCI-H446) were treated with 10 μM of the drugs as the first screening, 56 drugs in the library exhibited more than 50% inhibition of cell growth. After excluding drugs with possible nonspecific effects, the IC50 values of 24 drugs were examined in an expanded panel of 20 SCLC cell lines (7 of SCLC-A, 5 of SCLC-N, 3 of SCLC-P, and 5 of SCLC-Y cell lines) as the second screening. Sograzepide, a cholecystokinin B receptor (CCKBR) inhibitor exhibited distinctly lower IC50s in NE-type SCLC cells relative to non-NE-type cells, suggesting that CCKBR is potentially a specific therapeutic target for NE-type SCLC. CCK plays roles both as a neuropeptide in the central nervous system and as a peptide hormone in the gut. In our *in silico* analysis, CCKBR expression was high in the brain and the stomach, but not detectable in the lung when normal tissues were analyzed with NCBI database. Interestingly, when cancer cells were analyzed with CCLE database, CCKBR expression was substantially high in NE-type SCLC cells, compared with other cancer cells. Furthermore, we found that the growth-inhibitory effects of sograzepide examined in the drug screening were correlated with CCKBR expression levels. Then, we conducted functional analysis of CCKBR in NE-type SCLC cell lines with high CCKBR expression: NCI-H146 (SCLC-A), H209 (SCLC-A), and H524 (SCLC-N) cells. Knockdown of CCKBR by siRNAs inhibited cell proliferation and induced apoptosis. When treated with sograzepide, apoptosis was induced dose-dependently, and cell cycle assays showed increase in sub G1 phase in these cells. Collectively, we identified CCKBR as a potential therapeutic target in NE-type SCLC through screening of drug library targeting neural signaling. Further studies are warranted to reveal the mechanism for antineoplastic effects of antagonizing this neuropeptide receptor in SCLC.

#6573 Targeting DLK1, a Notch ligand, with an antibody-drug conjugate in adrenocortical carcinoma.

N.-Y. Sun[1], S. Kumar[1], A. Weiner[2], Y. Kim[1], A. Mendoza[1], R. Nguyen[1], R. Okada[1], Y. Pommier[1], D. Martinez[3], J. Pogoriler[3], S. Diskin[4], J. Maris[2], J. Del Rivero[1], N. Roper[1];

[1]National Cancer Institute Center for Cancer Research, Bethesda, MD, [2]Perelman School of Medicine, University of Pennsylvania, Philadelphia, PA, [3]Children's Hospital of Philadelphia, Philadelphia, PA, [4]Perelman School of Medicine, University of Pennsylvania,, Philadelphia, PA

Adrenocortical carcinoma (ACC) is an aggressive and rare endocrine malignancy with poor prognosis. First-line therapy (adrenolytic agent mitotane in combination with chemotherapy) for recurrent and metastatic ACC has limited efficacy and there are no approved second-line therapies. Antibody-drug conjugates (ADCs) are an emerging immunotherapeutic class in which a cytotoxic payload is directed to tumor cells via antibodies to cell surface proteins. As Notch ligands, such as DLL3, are ADC targets in neuroendocrine cancers, we screened for expression of Notch ligands in ACC. Among Notch ligands (DLL1, DLL3, DLK1, JAG1, JAG2), DLK1 (delta-like non-canonical Notch ligand 1) was the most highly expressed. Moreover, ACC had the near highest expression of DLK1 across all TCGA tumors likely because this ligand is of adrenal origin (with limited expression in other normal tissues apart from the pituitary gland and ovaries). By immunohistochemistry, we verified DLK1 to be expressed, at variable levels, in 97% of ACC tumors (n=30/31). We then tested a DLK1-directed antibody-drug conjugate (ADCT-701; DLK1-PBD), consisting of a humanized anti-DLK1 monoclonal antibody coupled to DNA damaging pyrrolobenzodiazepine (PBD) dimers (SG3199; drug-to-antibody ratio~1.8) via a cleavable linker in ACC pre-clinical models. ADCT-701 exhibited potent, nanomolar cytotoxicity in DLK1-expressing ACC cell lines and ACC patient-derived short-term organoid cultures. ADCT-701 cytotoxicity was dependent on *DLK1* expression as *DLK1* knockout and *DLK1* overexpression abrogated and facilitated cytotoxicity, respectively. Mechanistically, ADCT-701 induced cytotoxicity through DLK1 dependent receptor-mediated internalization and DNA damage (γH2AX) as well as apoptosis (annexin V/PI positive cells, cleaved PARP, and cleaved caspase-3). *In vivo* studies showed that ADCT-701 was highly effective against DLK1-positive ACC xenografts and PDX models with durable anti-tumor activity. Our pre-clinical data demonstrate DLK1 as an important therapeutic target in ACC and support an upcoming phase I clinical trial of ADCT-701 in patients with neuroendocrine tumors including ACC (NCT06041516).

#6574 UCHL1 is a molecular indicator and a therapeutic target for neuroendocrine carcinomas.

S. Liu[1], T. Chai[2], F. Marques[2], Q. Yin[2], E.-C. Hsu[2], M. Shen[1], A. Toland[2], A. Bermudez[2], A. B. Hartono[1], C. F. Massey[1], C. S. Lee[1], L. Zheng[2], M. Baron[2], C. J. Denning[2], M. Aslan[2], H. Nguyen[3], R. Nolley[2], A. Zoubeidi[4], M. Das[2], C. Kunder[2], B. Howitt[2], H. Soh[2], I. L. Weissman[2], M. A. Liss[5], A. I. Chin[1], J. D. Brooks[2], E. Corey[3], S. Pitteri[2], J. Huang[6], **T. I. Stoyanova**[1];

[1]University of California Los Angeles, Los Angeles, CA, [2]Stanford University, Palo Alto, CA, [3]University of Washington, seattle, WA, [4]University of British Columbia, Vancouver, BC, Canada, [5]UT Health San Antonio, San Antonio, TX, [6]Duke University, Durham, NC

Neuroendocrine carcinomas, such as neuroendocrine prostate cancer (NEPC), small cell lung cancer (SCLC), and neuroblastoma, share common histological features, including expression of neuroendocrine markers, rapid relapse after treatment, and poor prognosis. Due to the poor clinical outcome of patients with neuroendocrine carcinomas, there is a critical need to identify new drivers, therapeutic targets, and effective therapeutic strategies for these malignancies. Ubiquitin carboxy-terminal hydrolase L1 (UCHL1) is a protease that has a dual function in regulating protein stability. We demonstrated that UCHL1 is significantly elevated in tissues from patients with NEPC, SCLC, and neuroblastoma. Loss of UCHL1 decreases tumor growth and inhibits metastasis of these malignancies. UCHL1 maintains neuroendocrine differentiation and promotes cancer progression by regulating nucleoporin, POM121, and p53. UCHL1 binds, deubiquitinates, and stabilizes POM121 to regulate POM121-associated nuclear transport of key transcriptional factors, E2F1 and c-MYC. Conversely, UCHL1 binds p53 and promotes p53 degradation. Importantly, treatment with UCHL1 inhibitors significantly reduces tumor growth and metastasis of neuroendocrine carcinomas. The combination of UCHL1 inhibitors with cisplatin, the standard of care used for neuroendocrine carcinomas, halts tumor growth in pre-clinical settings. Our study reveals new mechanisms of UCHL1 function in neuroendocrine carcinomas tumorigenesis and identifies UCHL1 as a therapeutic target and potential molecular indicator for diagnosis and monitoring treatment responses in neuroendocrine carcinomas.

#6575 Selective targeting of integrins αVβ8 and αVβ1 within the dynamic ecosystem of pancreatic cancer to improve the overall anti-tumor response.

D. Upton[1], D. Chacon Fajardo[1], S. Omari[1], S. Porazinski[1], B. McLean[1], D. Schuhmacher[1], A. Istadi[1], Australian Pancreatic Cancer Genome Initiative, V. Kothari[2], D. Finkelstein[2], T. Machajewski[2], F. Rock[2], S. Turner[2], M. Pajic[3];

[1]Garvan Institute of Medical Research, University of New South Wales, Sydney, Australia, [2]Pliant Therapeutics, South San Francisco, CA, [3]Garvan Institute of Medical Research, Darlinghurst, Australia

Pancreatic ductal adenocarcinoma (PDA) has a 5-year survival of less than 10% and remains the 3rd leading cause of cancer-related death in Western societies. New treatment options are urgently needed. TGF-β promotes stromal cell reprogramming, immunosuppression, and fibrinogenesis in cancers, including PDA. Integrins αVβ8 and αVβ1 are important activators of TGF-β signalling. Selective integrin blockade has recently emerged as a promising therapeutic approach to address TGF-β-mediated immunotherapy resistance and improve anti-tumour response across cancer models. The purpose of this study was to assess the in vivo efficacy of small molecule inhibitor PLN-104, a selective inhibitor of αVβ1, and PLN-101095, a dual inhibitor of αVβ8 and αVβ1, in well-annotated models of advanced PDA.

We determined the preclinical efficacy and detailed anti-stromal effect of PLN-101095 inhibitor in genetically defined and patient-derived PDA models, including clinically relevant combinations with standard of care (SoC) chemotherapy and anti-programmed death receptor-1 antibody (anti-mPD-1). Mechanistic assessment of alterations in tumour cell-stromal cell crosstalk was performed using comprehensive transcriptomics and immunofluorescence approaches.

Dual targeting of αVβ8 and αVβ1 with PLN-101095 in the syngeneic LSL-KrasG12D/+;LSL-Trp53R172H/+;Pdx1-Cre (KPC) model effectively reduced tumour growth by 45% in comparison to the vehicle, and significantly delayed disease progression *in vivo*. Single-cell analysis of PLN-101095-treated KPC pancreatic tumours revealed a positive reprogramming of malignant cells from a mesenchymal to a more epithelial-like state. This effect was further associated with an upregulation of MHC type I/II markers and corresponding downregulation of pro-metastatic factors across diverse cancer sub-populations. Additionally, combining PLN-101095 with anti-mPD-1 antibody further improved survival in this aggressive model of metastatic PDA. In a second syngeneic model, Pan02, PLN-101095 in combination with anti-mPD-1 antibody significantly reduced tumour growth, while increasing CD8+ lymphocyte infiltration. The combination of PLN-101095 with Anti-PD1 increased MHC and IFN gene expression. Finally, utilizing patient-derived models of metastatic PDA revealed that both PLN-104 and PLN-101095 significantly blocked tumour growth, improved the response to SoC chemotherapy Gemcitabine/Abraxane, and reduced metastatic spread to distant sites. In conclusion, these data provide scientific rationale for the design of future PLN-101095 and SoC chemotherapy as well as immunotherapy combinations in pancreatic cancer, with Phase I first-in-human oncology studies with PLN-101095 plus ICB already underway.

#6576 Discovery of potent and selective novel small molecule drugs to target estrogen receptor mutants in endocrine-resistant breast cancer.

A. Devakrishnan, C. Madasu, S. A. Fuqua, M. M. Matzuk, **M. Palaniappan**;
Baylor College of Medicine, Houston, TX

Introduction: The acquisition of estrogen receptor alpha (ERα) gene (*ESR1*) mutations is a key driver for the development of resistance to current endocrine therapy in breast cancer. Clinical studies have shown that *ESR1* mutations are frequently observed in metastatic ER-positive breast cancer patients and are associated with poor survival. It is well appreciated that activating *ESR1* somatic mutations, especially Y537S and D538G, can drive estrogen-independent activities. In addition, these *ESR1* mutations diminish the potency of the current standard-of-care agents (tamoxifen and fulvestrant) that bind ERα directly. Therefore, it is an unmet need to develop next-generation antiestrogens that inhibit ERα mutant signaling in breast cancer to improve patient survival. Here, we search for small molecule inhibitors against ERα mutants Y537S and D538G using DNA-encoded chemical library (DEL).

Methods: ERα ligand binding domain (LBD) proteins corresponding to wild type (WT), Y537S and D538G mutants were expressed in *E. coli* and purified by Ni-NTA, anion exchange, and size exclusion chromatography. The ability of these purified proteins to bind ligands was tested in biochemical assays to validate their use in DEL selections. We conducted a DEL affinity selection using our in-house collection of 6 billion small molecule compounds against WT, Y537S and D538G mutants ER LBD proteins in the presence and absence of estradiol. Selection hits that enriched with these targets were resynthesized off-DNA and tested in biochemical and functional studies using CRISPR-Cas9 knock-in Y537S or D538G mutant breast cancer cells.

Results: We have successfully purified microgram amounts of ERα LBD for WT, Y537S, and D538G proteins. In our biochemical assay, the SRC3 peptide binds to the WT ERα LBD in the presence of estradiol, whereas Y537S and D538G LBDs bind the SRC3 peptide in the absence of estradiol, consistent with these mutants constitutively binding to SRC3. Our multibillion small molecule collections of DELs can screen and identify several hits in WT and mutant ERα LBDs. To confirm the selection output, we synthesized off-DNA compounds and validated these in biochemical and cell-based studies. Compounds CDD-1274 and CDD-1802 dramatically decrease the WT and mutant ERα protein levels in multiple ER+ breast cancer cells. These compounds greatly reduce protein levels for GREB1, TFF1, c-MYC, E2F1, and survivin in wildtype and mutant breast cancer cells, and they increase levels of cleaved PARP, a marker for apoptosis in wildtype and mutant ER+ breast cancer cells but not in ER-negative breast cancer cells.

Conclusion: Our study rapidly identified potent and novel small molecule drugs to target estrogen receptor mutants using our DNA-encoded chemical library platform.

Acknowledgments: Funding sources (NIH/NCI R03 CA259664 and CPRIT RP220524 to MP).

#6577 Chemoproteomic evaluation of PROTACs targeting estrogen receptor alpha for ER+ breast cancer.

Z. Sandusky, M. Brown;
Dana-Farber Cancer Institute, Boston, MA

In our investigation of estrogen receptor (ER) targeted protein degraders for advanced ER+ breast cancer, we assessed three proteolysis targeting chimeras (PROTACs), ARV471, ERD308, and ERD3111. Global proteomic analysis unveiled off-target protein degradation of progesterone receptor (PR) and phosphodiesterase 6D (PDE6D) by ER targeted PROTACs, but not selective ER degraders (SERDs). PR and PDE6D have previously been implicated as targets in cancer treatment. Protein degradation is rescued in CRBN- or VHL-knockout cells. Co-treating ER+ breast cancer cells with ligands for PR or PDE6D outcompeted PROTAC-mediated degradation and stabilized the respective protein, demonstrating the PROTACs are targeting the PR and PDE6D ligand-binding domains. Competition assays in ER-negative cell lines confirmed PR and PDE6D protein degradation is ER-independent. These findings underscore the importance of understanding off-target effects for developing more selective and effective therapeutics in ER+ breast cancer.

EXPERIMENTAL AND MOLECULAR THERAPEUTICS: Drug Discovery 2: New Therapies
Minisymposium

#6578 N17465, a systemically deliverable elastase, attenuates tumorigenesis and stimulates anti-tumor immunity.
R. Gujar, C. Cui, C. Lee, M. Fumagalli, N. Martinez, H. Liu, N. Grigaitis, S. Feau, L. Becker;
Onchilles Pharma, Inc., San Diego, CA

Background. Neutrophil elastase (ELANE) - a neutrophil-derived serine protease - kills a wide range of cancer cells without harming non-cancer cells through a unique killing program involving histone H1 and the death domain of CD95. Although ELANE attenuates tumor growth and induces anti-tumor immunity following intratumoral delivery (Cui et al., Cell, 2021), systemic delivery is stymied by the presence of serine protease inhibitors in blood (eg. alpha-1-antitrypsin (A1AT) which rapidly inhibit its enzymatic activity essential for its anti-cancer function. To overcome this challenge, we developed N17465, an enzyme that resists serine protease inhibitors in blood, and tested its effects on tumor growth, both as a monotherapy and in combination with checkpoint inhibitors.
Methods. Enzymatic properties: N17465 enzymatic activity was quantified in the +/- of A1AT or plasma in vitro, and in blood following intravenous (I.V) injection into tumor-bearing mice. Enzyme activity assays included a fluorogenic substrate AAPV-AMC and the C-terminal domain of CD95 (amino acids212-335). Anti-cancer properties: For in vitro studies, cells were treated with N17465 and viability was quantified by calcein-AM and immunogenic cell death (ICD) markers. Cancer/non-cancer cells included human/murine cell lines and primary cells from ovarian cancer (OvCa) patients. For in vivo studies, N17465 was injected I.V and effects on tumor growth, immunology and survival were assessed as monotherapy or in combination with a checkpoint inhibitor (anti-CTLA4) in pre-clinical models.
Results. N17465 maintained enzymatic activity following incubation with A1AT or mouse/human plasma in vitro, and following I.V injection into CT26 tumor-bearing mice in vivo. Importantly, protecting N17465 from serine protease inhibitors did not interfere with its ability to cleave CD95 (therapeutic target) or selectively kill cancer cells in vitro. Indeed, N17465 induced ICD markers, killed a wide range of murine/human cancer cells and also well tolerated by non-cancer cells. Systemically delivered N17465 produced durable tumor regression in a murine CT26 colon cancer model resulting in ~50% tumor-free mice, induced a favorable immune profile, and synergized with anti-CTLA4. N17465 also exhibited efficacy across a range of xenograft models spanning human colon, prostate, and lung cancer, as well as OvCa patient-derived CDX models.
Conclusions. Altogether, our data demonstrate that N17465 selectively kills cancer cells, produces durable responses in mice, induces favorable immunology and synergies with checkpoint inhibitors in pre-clinical models. Its ability to maintain enzymatic activity in blood following systemic delivery, selectively kill a wide range of cancer cells, and stimulate anti-tumor immunity warrants further investigation of this unique therapeutic modality across a wide range of solid tumors.

#6579 DS-3939a, a novel TA-MUC1-targeting antibody-drug conjugate (ADC) with a DNA topoisomerase I inhibitor DXd, exhibits potent antitumor activity in preclinical models.

M. Yukiura[1], **K. Takano**[1], K. Takahashi[1], A. Zembutsu[1], M. Kitamura[1], Y. Shiose[2], K. Honda[1], K. Oyama[1], W. Obuchi[1], M. Yamada[1], R. Goto[1], K. Sakurai[1], K. Kumagai[1], T. Kagari[1], Y. Abe[1], T. Agatsuma[1];

[1]Daiichi Sankyo Co., Ltd., Tokyo, Japan, [2]Daiichi Sankyo, Inc., Basking Ridge, NJ

Background: Tumor-associated mucin-1 (TA-MUC1) is a tumor-specific transmembrane glycoprotein with aberrant glycosylation. It is highly expressed in various human epithelial cancers, making it an attractive target for cancer therapy. DS-3939a is a TA-MUC1 targeting antibody-drug conjugate (ADC) structurally composed of a humanized anti-TA-MUC1 antibody, an enzymatically cleavable tetrapeptide-based linker, and a DNA topoisomerase I inhibitor (DXd) with a high drug-to-antibody ratio (DAR). In this study, the pharmacological activity of DS-3939a was evaluated using preclinical in vitro and in vivo models.
Methods: TA-MUC1 expression was assessed by immunohistochemistry and flow cytometry. Binding specificity of DS-3939a was confirmed by enzyme-linked immunosorbent assay. Induction of DNA damage and apoptosis to cancer cells by DS-3939a treatment were detected by Simple Western System. In vitro cell growth inhibitory and in vivo antitumor activities of DS-3939a were evaluated using various cancer cell lines and patient-derived xenograft (PDX) models.
Results: Many specimens across multiple cancer types showed positive staining for TA-MUC1, with a particularly high positive rate observed in bladder, lung, and breast cancers. DS-3939a specifically bound to aberrantly glycosylated MUC1 peptides by recognizing both the glycan and backbone peptide moiety of MUC1. In vitro, DS-3939a inhibited the growth of TA-MUC1-positive cancer cells but not of TA-MUC1-negative cancer cells. Neither a parental anti-TA-MUC1 antibody nor isotype control ADC inhibited the growth of these cells. In addition, treatment with DS-3939a and DXd alone induced DNA damage and apoptosis in cancer cells. These results demonstrate that DS-3939a exhibits TA-MUC1-dependent cell growth inhibition through DXd-mediated cytotoxic effect. Moreover, DS-3939a exhibited significant antitumor effects in the several TA-MUC1-positive cancer cell line-derived xenograft models and various PDX models. DS-3939a also induced strong tumor regression even after treatment of other cytotoxic ADCs in several xenograft models.
Conclusion: Based on these preclinical results, DS-3939a could provide valuable therapy with potential benefits for patients with TA-MUC1-expressing tumors. A first-in-human phase 1/2 study in patients with advanced solid tumors is currently in progress (NCT05875168).

#6580 A Novel EGFR x cMET bispecific ADC PRO1286 demonstrated broad antitumor activity and promising tolerability in preclinical models.

Y. Xiao[1], H. Huang[1], J. Yin[1], X. Qiu[1], L. Wang[1], H. Liu[1], B. Zhao[2], **Z. Chen**[2];
[1]ProfoundBio (Suzhou) Co., Ltd., Suzhou, China, [2]Profound Bio US Co., Seattle, WA

EGFR and cMET are frequently co-expressed on tumor cells, often upregulated as the escape mechanism for each other, and both well-validated targets in oncology. Small molecule TKIs and amivantamab have been approved for non-small cell lung cancer with relevant actionable genomic alterations (AGA), and monoclonal antibodies offer treatment options for EGFR-expressing head and neck and colorectal cancers without AGA. Yet high unmet need in these tumors still exists. We sought to develop an EGFR and cMET dual-targeting ADC using our proprietary technology platform with carefully chosen design features for the many tumors expressing EGFR and cMET with or without AGA. PRO1286 is comprised of a monovalent bispecific human IgG1 (dubbed as “Bsab”) with fine-tuned affinity on EGFR and cMET, and the proprietary topoisomerase 1 inhibitor-based linker-drug, sesutecan. Sesutecan previously demonstrated promising characteristics in preclinical studies with multiple targets and conferred an encouraging benefit:risk profile in the clinic with a FRα-directed ADC (rinatabart sesutecan). PRO1286 at DAR8 displays high hydrophilicity and excellent stability and developability in vitro. PRO1286 binds selectively and specifically to each target with a low nanomolar EC_{50} in the CHO-K1 cells overexpressing each target. PRO1286 exhibited efficient internalization (~50-80% internalized in 4 hrs) and strong cytotoxicity (sub-nanomolar IC_{50}) against a broad panel of tumor cell lines with higher potency than the parent mAbs. PRO1286 produced marked and dose dependent anti-tumor activity in mouse xenograft models encompassing a wide range of target expression levels, tumor types (head and neck, lung, esophageal, gastric, colorectal), and genomic landscape (with or without AGA in EGFR or cMET; with diverse additional co-mutations). Sustained tumor growth inhibition or complete remission was observed in several xenograft models after treatment with a single dose (2 mg/kg) of PRO1286. PRO1286 was more efficacious than benchmarking molecules in the mouse studies. In an exploratory toxicity study in cynomolgus monkeys, PRO1286 was well tolerated at 30 mg/kg with the main toxicity being payload-driven and residing in bone marrow. PRO1286 exhibited a stable PK profile that was similar to that of the Bsab in rats and favorable PK characteristics in monkeys. In summary, PRO1286 demonstrated promising physiochemical properties, PK/PD, antitumor activity, and tolerability in preclinical studies. It may carry an expanded therapeutic index compared to other EGFR- and/or cMET-directed ADCs. It may also differentiate from existing EGFR- and/or cMET-targeting agents on broad coverage of EGFR and cMET-expressing tumors with or without the respective AGAs. Effort is under way to advance a DAR optimized molecule to the clinic for the treatment of many EGFR- or cMET-expressing solid tumors.

#6581 DX126-262 combined with chemotherapy (Cisplatin and 5-Fu) demonstrates promising antitumor efficacy in HER2-positive gastric cancer.

X. Cai, M. Cao, H. Guo, Q. Yang, X. Kong, Y. Du, Z. Ye, Z. Guo, L. Zhang, L. Bai, J. Jia, Y. Zheng, Y. Chen, M. Chen, W. Zheng, J. Zheng, W. Li, Y. Huang, M. Liu, Z. Fan, H. Ye, Y. Xu, B. Chen, M. Dai, **R. Y. Zhao**;
Hangzhou DAC Biotechnology Co., Ltd., Hangzhou City, China

Gastric cancer is a common malignant tumor of the digestive system, and its morbidity and mortality rank among the top five in the world. Although significant progress has been made in cytotoxic chemotherapy, immunotherapy and targeted therapy in recent years, the long-term prognosis of patients with advanced or metastatic gastric cancer is still poor. Trastuzumab combined with chemotherapy is the first-line standard of care (SOC) for HER2-positive advanced or metastatic gastric cancer. Two ADC drugs targeting HER2, DS-8201 and RC-48, have also been approved for the treatment of gastric cancer. However, their limited clinical benefits and occurrence of adverse events still present a significant challenge. Therefore, minimizing the off-target toxicity and collateral damage while achieving significant chemotherapy efficacy has become the focus of gastric cancer treatment. DX126-262 is a novel HER2-targeting antibody-drug conjugate (ADC), generated by conjugating a Tubulysin B analogue to a recombinant humanized anti-HER2 monoclonal antibody through a linker containing branched hydrophilic polyethylene glycol, using thiol-maleimide chemistry to achieve drug antibody ratio (DAR) of 3.8. Previous studies have confirmed that DX126-262 monotherapy showed excellent efficacy in HER2-positive gastric cancer NCI-N87 cells in vitro and in vivo. And the efficacy has also been demonstrated in clinical trials (now in phase II, CTR20211871). Based on above results, we intended to further explore whether combination therapy of DX126-262 with Cisplatin and 5-FU can improve the anti-tumor efficacy compared with SOC (Herceptin plus Cisplatin and 5-FU) or DS-8201 monotherapy. The triple-drug combination therapy demonstrated much better therapeutic efficacy than single drug (DX126-262, Cisplatin, 5-FU, Herceptin, or DS-8201) or double-drug combination (Cisplatin plus 5-FU) or SOC (Herceptin plus Cisplatin and 5-FU) on human gastric cancer cells in vitro and in vivo. Meanwhile, triple-drug combination therapy did not exhibit superimposed toxicity, judging by the body weight of mice and hemal biochemistry assays. These results suggested that DX126-262 plus Cisplatin and 5-FU might be a promising strategy for treatment of HER2-positive advanced or metastatic gastric cancer in clinic.

#6582 Preclinical characterization of IPH45, a novel topoisomerase I inhibitor ADC targeting Nectin-4 for the treatment of Nectin-4 expressing tumors.

R. Remark, C. Bonnafous, L. Chiossone, C. Soulas, C. Perrier, G. Habif, S. Bokobza, A. Maguer, R. Courtois, J. Lopez, G. Fenaux, O. Benac, B. Carrette, R. Letay-Drouet, R. Bonifay, S. Augier, L. Simon, B. Rossi, A. Morel, A. Represa, N. Beltraminelli, Y. Morel, C. Paturel, E. Vivier;
Innate Pharma, Marseille, France

Background: Nectin-4 is a cell membrane adhesion protein overexpressed in several solid tumors, including urothelial, breast, lung, ovarian, and pancreatic cancers, with limited expression in normal tissues, making it an ideal target for antibody-drug conjugates (ADC). Enfortumab Vedotin (EV, PADCEV®) is an ADC targeting Nectin-4 with a monomethyl auristatin E (MMAE) payload approved for the treatment of patients with urothelial carcinoma (UC), but with limited clinical activity reported beyond UC. In addition, EV causes peripheral neuropathy and skin toxicity, leading to treatment discontinuation. To overcome these limitations and the mechanism of resistance to EV, IPH45, a novel topoisomerase I inhibitor ADC targeting Nectin-4 with an improved therapeutic index, was developed.
Methods: *In vitro* studies were performed to investigate internalization, tumor cell killing and bystander effect, antibody-dependent cellular cytotoxicity (ADCC) and complement activation. *In vivo* efficacy studies were performed on cell line-derived xenografts (CDX) of triple negative breast cancer, patient-derived xenografts (PDX) of urothelial carcinoma and syngeneic tumor models expressing human Nectin-4. IPH45 efficacy was compared to EV. Toxicology studies to determine the dose range were conducted in rat and non-human primates (NHP).
Results: IPH45 consists of a humanized IgG1 targeting a unique epitope in human Nectin-4, non-overlapping with EV, a cleavable linker, and a topoisomerase I inhibitor with a high drug-to-antibody ratio (DAR). *In vitro*, IPH45 is internalized upon binding to its target and induces direct killing of Nectin-4–expressing tumor cells as well as bystander killing of Nectin-4 non-expressing tumor cells in mixed culture. IPH45 mediates ADCC and complement-mediated killing. IPH45 demonstrates activity in CDX and PDX models with similar effective dose as EV. Moreover, IPH45 shows anti-tumor efficacy *in vitro* and *in vivo* in primary and secondary EV resistant models. In dose-range finding toxicology studies in rats and NHP, IPH45, unlike EV, does not elicit skin toxicity. IPH45 remains well tolerated up to the highest dose tested, suggesting a potentially larger therapeutic index than MMAE-based ADCs. Pharmacokinetic analyses in mice, rats, and NHP show minimal release of free toxin in the serum and half-life compatible with Q2W or less frequent dosing schedules in clinic.
Conclusion: IPH45 is a topoisomerase I ADC targeting Nectin-4 with the potential for larger therapeutic index than EV, improved safety and dosing regimen, and ability to overcome primary and secondary resistance to EV or other Nectin-4 ADC in development. IPH45 is progressing to the clinic where the translatability of this unique profile into improved patient outcomes will be assessed across indications.

#6583 Developing a selective cancer chemotherapy by small molecule-based targeting of PCNA protein.

J. Jossart, L. Gu, P. Haratipour, C. Li, R. Lingeman, R. Hickey, L. Malkas, **J. J. P. Perry**;
Beckman Research Institute of The City of Hope, Duarte, CA

Proliferating cell nuclear antigen (PCNA) is a proliferation biomarker in a variety of human tumors and has critical cellular functions in DNA replication and repair. We previously identified a unique cancer-associated isoform of the protein, termed caPCNA, which allows for structure-based drug discovery studies to develop inhibitors for selective therapeutic targeting of cancer cells. Distinct strategies have been used to develop caPCNA targeting agents, which includes peptide and small molecule-based compounds, although the success in developing therapeutically tractable compounds has been limited so far. Here, we present the crystal structures and corresponding biochemical characterizations of our novel small molecule-based caPCNA inhibitors, which bind into the PIP-box binding pocket of PCNA. Our lead compound selectively kills cancer cells, and it appears to induce replication stress, apoptosis and increase cancer cell sensitivity to genotoxic agents, while these effects are not observed in non-malignant cell controls. This caPCNA inhibitor is orally administrable, metabolic stable and it suppresses tumor growth as a monotherapy or as a combination treatment and is now an investigational new drug in Phase 1 clinical trials. PCNA plays a critical role enabling the replication fork to proceed from transcription replication conflict sites, by temporarily dislodging RNA polymerase II. Thus, structure-based drug discovery against caPCNA may open a novel therapeutic avenue for the development of selective chemotherapeutics, through targeting a cancer cell's vulnerability to unresolved transcription replication conflicts.

#6584 Aberrant TRIM7 expression potentiates RACO-1 mediated proliferation and dysregulated interferon responsiveness in the setting of anti-PD-1 acquired resistance in cancer.

T.-A. T. Nguyen[1], M. Morra[1], K. Li[2], U. Bhatt[2], J. Mwangi[1], Y. Rivera-Molina[1], N. Oien[1], J. Medina[2], T. H. Schreiber[1], **G. Fromm**[1];
[1]Shattuck Labs, Durham, NC, [2]R2M Pharma, Inc, San Francisco, CA

While checkpoint inhibitor treatment has extended the survival of many cancer patients, most initial responders will later develop disease progression through a variety of poorly understood acquired resistance mechanisms (CPI-AR). One such recently described mechanism involves the transcriptional hyperactivation of genes associated with interferon (IFN) signaling, JAK/STAT, and antigen processing/presentation pathways. Aberrant IFN regulation in the setting of AR suggests that tumor cell intrinsic mechanisms have conferred a growth advantage despite the presence of immune-mediated pressure unleashed by PD-1/L1 antibody blockade. Analysis of transcripts progressively upregulated during acquisition of AR *in vivo* and transcripts upregulated by IFN exposure of isolated AR cell lines *in vitro* identified the E3 ubiquitin ligase TRIM7 as a candidate mediator of the AR phenotype. A specific pocket on the PRY/SPRY domain of TRIM7 has been shown to bind viral peptides, resulting in ubiquitination and degradation as a mechanism to mitigate viral propagation. Here we describe the evaluation of small molecule inhibitors (SMI) designed to the TRIM7 PRY/SPRY viral-pocket domain, where binding specificity was confirmed using mass spec analysis. These SMI competitively inhibited TRIM7 mediated stabilization of RACO-1, resulting in decreased cancer cell proliferation which was associated with altered c-Jun/AP-1 transcription. TRIM7 SMI also disrupted STING and MAVS ubiquitination and restored IFN responsiveness and sensitivity to PD-1 inhibitor treatment. Finally, given the position of TRIM7 downstream of growth factor receptor and kras signaling, combination of TRIM7 inhibitors with kras, braf, and/or MEK inhibitors was shown to additively suppress proliferation of tumor cells with kras mutations. These results provide evidence that upregulation of TRIM7 mediates both a pro-proliferative and IFN resistant phenotype in the setting of CPI-AR, and that inhibition of TRIM7 with small molecule inhibitors may prevent or reverse AR to PD-1/L1 blockade.

EXPERIMENTAL AND MOLECULAR THERAPEUTICS: Novel Antitumor Agents 5
Minisymposium

#6585 Combination RAS^{G12C}(ON) and RAS^{MULTI}(ON) inhibition overcomes resistance and prolongs durability in preclinical models of mutant KRAS^{G12C}-driven cancers.

X. Wei, M. Holderfield, Y. Yang, K. Seamon, J. Dinglasan, N. Montazar, B. Lee, S. Cai, L. Lai, I. Aronchik, S. Chang, Z. Wang, P. Wildes, J. A. Smith, J. Jiang, M. Singh;
Revolution Medicines, Inc., Redwood City, CA

Inhibitors of the GDP-bound state of mutant KRAS^{G12C} protein (KRAS^{G12C}(OFF)), e.g., adagrasib and sotorasib, have shown clinical activity in patients with KRAS^{G12C}-driven NSCLC, CRC and PDAC. However, most patients exhibit progression on monotherapy treatment in months, underlining the need for combination therapeutic approaches that improve the durability of the anti-tumor activity seen with KRAS^{G12C} inhibitors.

RMC-6291 is a mutant-selective covalent inhibitor of the GTP-bound RAS(ON) form of RAS^{G12C}, while RMC-6236 is a non-covalent RAS^{MULTI}(ON) inhibitor of both mutant and wild-type variants of canonical RAS isoforms. In models harboring diverse alterations driving resistance mechanisms to KRAS^{G12C}(OFF) inhibitors -- including reactivation of KRAS^{G12C} and wild-type RAS by increased RTK signaling, acquired secondary oncogenic RAS mutations, and KRAS amplification -- both RMC-6291 and RMC-6236 exhibited superior anti-cancer activity as single agents when compared to KRAS^{G12C}(OFF) inhibitors. Thus, we hypothesized that a combination of RMC-6291 and RMC-6236 could address a broad spectrum of observed clinically relevant resistance mechanisms to KRAS^{G12C}(OFF) inhibitors that reactivate RAS signaling via mutant and wild-type RAS isoforms and compromise the depth and durability of anti-tumor response.

In a mouse clinical trial with KRAS^{G12C} xenograft models, daily oral administration of RMC-6291 induced objective responses in 18 out of 25 NSCLC PDX and CDX models as assessed by mRECIST. In a subpanel of 7 NSCLC models that are relatively refractory to KRAS^{G12C}(OFF) inhibitor monotherapy, RMC-6236 alone somewhat prolonged the durability of response, while the combination of RMC-6291 with RMC-6236 improved the depth of response and significantly extended the durability thereof. In contrast to NSCLC, in models of KRAS^{G12C} CRC tumors a more heterogeneous response to RMC-6291 monotherapy was observed with objective responses in 4 out of 15 CRC models. The addition of RMC-6236 to RMC-6291 substantially improved the depth and duration of anti-tumor response in the resistant models to KRAS^{G12C} inhibitor alone. The combination of RMC-6291 with RMC-6236 at preclinical target doses did not affect the systemic or tumor exposures of each compound and was well tolerated in tumor-bearing immune-deficient animals.

Both investigational agents RMC-6236 and RMC-6291 have shown promising anti-tumor activity as monotherapies in preclinical models and, more recently, showed preliminary clinical activity in patients with RAS-driven tumors at exposures that were well tolerated. The addition of RMC-6236 to RMC-6291 shows combinatorial activity in preclinical models that are relatively less responsive to either inhibitor alone. A clinical trial combining RMC-6291 with RMC-6236 in patients with mutant KRAS^{G12C} tumors is currently enrolling.

#6586 ORIC-944, a potent and selective allosteric PRC2 inhibitor with best-in-class properties, demonstrates combination synergy with AR pathway inhibitors in prostate cancer models.

A. Daemen[1], N. Yuen[1], A. Wang[1], A. Pankov[1], L. Ulicna[1], C. Chen[1], F. L. Duong[1], J. Long[1], M. A. Marx[2], J. G. Christensen[2], L. S. Friedman[1], M. R. Junttila[1]; [1]ORIC Pharmaceuticals, South San Francisco, CA, [2]Mirati Therapeutics, San Diego, CA

Polycomb repressive complex 2 (PRC2) dysregulation occurs in multiple tumor types and is associated with poor prognosis in patients with prostate cancer. In patients treated with androgen receptor pathway inhibitors (ARPI), emergence of tumor cell plasticity is associated with resistance to therapy. Dysregulation of epigenetic reprogramming factors, including PRC2, creates an environment that is permissive for such lineage plasticity. Inhibition of the PRC2 complex therefore may provide an opportunity to overcome or prevent the emergence of plasticity in prostate cancer. Notably, emerging clinical trial data has demonstrated the potential of ARPI and PRC2 inhibitor combination therapy to improve outcomes in patients with metastatic prostate cancer.

PRC2 tri-methylates histone H3 at lysine 27 (H3K27me3), leading to long-term transcriptional silencing, a key mechanism regulating cellular functions such as cell growth and differentiation. Three core subunits comprise PRC2: the catalytic subunit enhancer of zeste homolog 2 (EZH2), suppressor of zeste 12 (SUZ12) and embryonic ectoderm development (EED). EED is essential for the histone methyltransferase activity of PRC2. First-generation PRC2 inhibitors, which target EZH2, exhibit poor drug properties, drug-drug interaction liabilities and short half-life requiring twice daily dosing at high doses in patients.

We developed a second generation PRC2 inhibitor, ORIC-944, an allosteric inhibitor of PRC2 that binds the EED subunit. ORIC-944 is a potent, highly selective, orally bioavailable inhibitor with best-in-class properties. ORIC-944 demonstrated single agent tumor growth inhibition in a spectrum of in vivo prostate cancer models, including AR-positive, AR-mutant, ARv7, ARPI-responsive and ARPI-resistant models. In vitro analysis of the combination of ARPIs and ORIC-944 showed synergy in multiple prostate cancer cells, utilizing BLISS and other quantitative methods. In vivo studies revealed that ORIC-944 demonstrated increased efficacy in combination with ARPI, consistent with the in vitro synergy. RNA-seq analysis of transcriptional changes induced by ORIC-944 provided mechanistic insight into the role of PRC2 in prostate cancer lineage plasticity and combination response.

These results position ORIC-944 as a best-in-class PRC2 inhibitor for evaluation in combination with ARPI in patients with metastatic prostate cancer. A phase 1b trial of ORIC-944 is ongoing (NCT05413421).

#6587 Discovery of molecular glue of FBXW7:MYC interaction using small molecule microarray.

Shenghao Guo[1], Morgan Stilgenbauer[2], Bocheng Wu[2], Yatin Mankan[2], Angela N. Koehler[2]

[1]Biological Engineering, Massachusetts Institute of Technology (MIT), Cambridge, MA,[2]Koch Institute For Integrative Cancer Research at MIT, Cambridge, MA

MYC deregulation is a key driver and feature of many human cancers. Yet, despite its importance in cancer progression, MYC is considered “undruggable” by small molecules due to its disordered conformation. Therefore, interfering with its interactions with protein partners to modulate MYC activity appears viable. FBXW7 is an E3 ligase, which serves as a constituent of the SCF (Skp1-Cul1-F box) ubiquitin ligase complex. It mediates the degradation of both c-Myc and Cyclin E through ubiquitin-dependent proteolysis. FBXW7 mutations are found in various human tumor types, establishing its role as a general human tumor suppressor. Specifically, FBXW7 down-regulation increases MYC level, and its expression correlates to lethal outcomes of breast epithelial cells, poor prognosis in glioblastoma, and T cell acute lymphoblastic leukemia remission. Therefore, our project aims to discover potent small molecule glues that would enhance the interaction between FBXW7 and MYC, leading to MYC degradation through proteolysis and eventually suppression of various cancers. Taking advantage of our high throughput screening technology, Small Molecule Microarrays (SMMs), we successfully identified 29 compounds that potently bind to both c-Myc and FBXW7 after screening our 65,000 ‘drug-like’ small molecule library. We then performed secondary assays using a mCherry-GFP MYC reporter cell line to identify our lead compound, KI-FBX-001, which decreases MYC’s expression:transcription ratio by over 50% compared to control. Additionally, this down-regulation can be rescued by protease inhibitor MG132, indicating that the effect is achieved via proteolysis. *In vitro* dose-response and time-course treatment revealed an optimal drugging concentration at 15uM in K562 cells, with inhibition reaching its peak at the 4-hour time point at over 60%. Using the Qiagen MYC reporter assay, the in vitro IC50 of KI-FBX-001 is found at 7.42uM. Beyond the protein level, the qPCR result also reveals a decrease in MYC mRNA level at over 70%. Surface Plasmon Resonance (SPR) is used to confirm direct binding between FBXW7 and KI-FBX-001, which showed promising binding with kd=0.17μM. Proximity Ligation Assay further confirms KI-FBX-001’s effect in enhancing FBXW7:MYC interaction in the cell. In summary, our findings proved that KI-FBX-001 is a promising molecular glue in the FBXW7:MYC interaction, and can effectively modulate the MYC level for future therapeutic purposes.

#6588 Discovery of ASTX295, a potent, next-generation small molecule antagonist of MDM2 with differentiated pharmacokinetic profile.

M. Ahn[1], L. Bevan[1], I. Buck[1], C. Cano[2], J. Castro[1], B. Cons[1], J. Endicott[2], L. Fazal[1], N. Ferrari[1], I. Hardcastle[2], K. Hearn[1], R. Holvey[1], S. Howard[1], C. Johnson[1], C. Jennings[2], J. Kucia-Tran[1], S. Kyle[2], J. Lunec[3], J. Lyons[1], D. Miller[2], D. Rees[1], M. Noble[2], D. R. Newell[2], J. Reeks[1], H. Saini[1], J. St. Denis[1], E. Tamanini[1], H. Thomas[2], N. Thompson[1], M. Vinkovic[1], G. Ward[1], N. Wallis[1], H. Walton[1], S. Wedge[2], P. Williams[1], E. Willmore[2], N. Wilsher[1], Y. Zhao[2], G. Chessari[1],

[1]Astex Pharmaceuticals, Cambridge, United Kingdom, [2]Cancer Research Horizons Therapeutic Innovation, Newcastle Drug Discovery Group, Newcastle University, Newcastle upon Tyne, United Kingdom, [3]Biosciences Institute, Newcastle University, Newcastle upon Tyne, United Kingdom

In response to cellular stress, the tumor suppressor p53 is activated to modulate cell cycle progression, DNA repair, and apoptosis. Inhibition of the MDM2-p53 interaction in tumors carrying wild-type p53 prevents its degradation and can reactivate p53 to elicit an anti-cancer effect. Targeting the p53-MDM2 interaction therefore remains a promising strategy for cancer therapy. However, development of first generation MDM2 antagonists has been challenged by dose-limiting, on-target bone marrow toxicities. Understanding of differential effects of p53 pathway activation in normal hematopoietic versus cancer cells (to be presented in a separate abstract) together with our expertise in structure-based drug design have led to the discovery of ASTX295, a potent MDM2 antagonist with differentiated pharmacokinetic profile aimed at sparing bone marrow toxicities and increasing the therapeutic index. Here, we present the first disclosure of the structure and pre-clinical characterisation of ASTX295. ASTX295 exhibits potent activity (IC_{50}<1 nM) against MDM2 in an ELISA-based *in vitro* assay and induces significant growth reduction in p53 wild-type, MDM2-amplified SJSA-1 cells (GI_{50}=27 nM). Antiproliferative activity of ASTX295 was further demonstrated in a panel of 219 p53 wild-type cell lines, with 143 cell lines showing GI_{50} values less than 1 µM and 50 showing values less than 0.1 µM. Effects of ASTX295 are shown in cell lines carrying functional p53 as confirmed in three p53 wild-type and mutant cell line pairs (SJSA1 and SN40R2, A2780 and A2780CP, HCT116 and HCT116 $p53^{-/-}$). In addition to inhibiting cell cycle progression and cell proliferation, ASTX295 also potently induces apoptosis following 24-48 hour treatment. Further in vitro analyses of ASTX295 demonstrated an increase in the levels of p53 (EC_{50}=10 nM after 2 hours) and its transcriptional targets such as p21 and MDM2. In vivo, ASTX295 shows robust induction of p53 and its target genes at 3 and 6 hours after oral administration together with dose-dependent inhibition of tumour growth in the SJSA-1 xenograft model. Importantly, ASTX295 exhibits optimised pharmacokinetic and pharmacodynamic profiles with relatively short duration of pathway modulation and a desired predicted human half-life of 2-8 hours. Based on our pre-clinical hypothesis on differential time-dependent sensitivities of normal versus cancer cells to p53 activation, achieving such a profile while maintaining potency may increase the therapeutic index. These data highlight the therapeutic potential of ASTX295, which is currently being tested in a Phase 1/2 clinical trial in advanced solid tumors with wild-type p53 (NCT03975387). We plan to present preliminary clinical data in a separate abstract at this meeting.

#6589 Discovery of potent and selective pan-TEAD autopalmitoylation inhibitors for the treatment of Hippo-pathway altered cancers.

J. A. Gordon[1], J. Dubauskaite[1], M. DuPont[1], N. Guan[1], G. Holdgate[2], S. Mlynarski[1], N. Umbreit[1], D. Sanchez[1], A. Srivastava[2], J. Suski[1], N. Su[1], R. Richards[1], S. Cosulich[2], C. Reimer[1], J. Brownell[1];

[1]AstraZeneca, Boston, MA, [2]AstraZeneca, Cambridge, United Kingdom

TEAD1-4 are DNA bound transcription factors regulated by the Hippo tumor suppressor pathway that bind the coactivators YAP/TAZ to activate oncogenic gene expression programs involved in cell survival, proliferation, and drug resistance. TEAD-dependent transcription is activated in many tumor types through a variety of mechanisms including LOF Hippo pathway mutations (e.g. NF2, LATS) and YAP/TAZ amplification, and also as an adaptive resistance mechanism, for example in response to EGFR TKI and KRAS inhibition. Here, we report the initial characterization of a novel pan-TEAD inhibitor, AZ4331, which was identified following a structure-guided drug design campaign. AZ4331 disrupts the post-translational palmitoylation of TEAD proteins through covalent binding to a conserved cysteine residue resulting in inhibition of TEAD-dependent transcriptional output. AZ4331 inhibited the proliferation of NF2m NCI-H226 cells (GI50: 92 nM) while having no effect on Hippo-wild type NCI-H2452 (GI50: undetermined). Cell-based metabolic labeling studies demonstrated the ability of AZ4331 to inhibit palmitoylation of all four TEAD paralogs and led to disruption of the YAP/TEAD complex assessed by immunoprecipitation resulting in reduced TEAD transcriptional output as assessed by qPCR. Furthermore, in vivo profiling showed AZ4331 achieved sufficient exposures (plasma free Cmax: 2.7 µM) and robust target engagement as measured through reduction of multiple canonical TEAD target genes (CTGF [IC50: 0.127 µM] , ANKRD1, AMOTL2 and CYR61) in Hippo-altered mesothelioma xenograft tumors. This target engagement in turn drove inhibition of tumor proliferation in xenograft models representing common Hippo-alterations. AZ4331 treatment of NF2m NCI-H226 and LATS1/2 loss MSTO-211H mesothelioma xenografts drove 50% and 93% regression of tumors, respectively. While treatment of head and neck squamous cell carcinoma FAT1m FaDu and YAP1amp Detroit562 xenografts lead to 58% tumor growth inhibition and 35% tumor regression, respectively. These findings identify AZ4331 as a potent inhibitor of the TEAD transcription factor family and further validate the inhibition of TEAD in Hippo-altered cancers as a potential therapeutic strategy.

#6590 Novel WRN helicase inhibitors selectively target microsatellite unstable cancer cells.

G. Picco[1], Y. Rao[2], A. Al Saedi[1], S. F. Vieira[1], Y. Lee[2], R. Shenje[2], S. Bhosle[1], S. Walker[1], K. May[3], C. Herranz-Ors[1], C. Dicer[1], F. Gibson[1], R. Banerjee[1], T. Werner[4], J. Cottom[2], Y. Peng[2], N. Deng[5], P. Landis[2], T. Angel[2], J. Bush[6], M. G. Rees[7], M. M. Ronan[7], J. A. Roth[1], H. Lightfoot[1], F. Zappacosta[2], J. Pettinger[6], S. Barthorpe[1], C. Eberl[4], B. Jones[8], J. Schneck[2], D. Murphy[2], J. Taygerly[8], M. DeMartino[2], M. Coelho[1], J. Houseley[3], B. Schwartz[2], M. J. Garnett[1];
[1]Wellcome Sanger Institute, Hinxton, United Kingdom, [2]GSK, Upper Providence, PA, [3]Babraham Institute, Cambridge, United Kingdom, [4]GSK, Heidelberg, Germany, [5]GSK, Cambridge, MA, [6]GSK, Stevenage, United Kingdom, [7]Broad Institute of MIT and Harvard, Cambridge, MA, [8]IDEAYA, San Francisco, CA

Microsatellite-unstable (MSI) cancers depend on the WRN helicase to resolve replication stress from expanded (TA)-dinucleotide repeats. WRN is a promising synthetic lethal target for MSI tumours and WRN inhibitors are being developed. Here, we used CRISPR-Cas9 base editing to map WRN residues critical for MSI synthetic lethality, validating the helicase domain as the primary target and guiding inhibitor discovery. Fragment-based screening led to the discovery of potent and highly selective WRN helicase covalent inhibitors from the same chemical series. These compounds strikingly and selectively suppressed MSI model growth in vitro and in vivo by mimicking genetic WRN loss, inducing DNA double-strand breaks at expanded TA repeats and DNA damage response. We characterized WRN inhibition across cancer cell lines and patient-derived tumour organoids, enabling biomarker assessment of TA-repeat expansions and MMR status to refine patient selection, with compound efficacy correlating with TA-repeat expansions in MSI cells. Efficacy was also confirmed in patient-derived organoids and PDX models refractory to immunotherapy. The discovery of potent and selective covalent WRN inhibitors provides proof-of-concept for targeting MSI cancers and provides tools to unlock the molecular dissection of the WRN biology and MSI synthetic lethality.

IMMUNOLOGY: New Insights for Therapies Modulating Antitumor T-Cell Responses
Minisymposium

#6592 Deciphering the effects of age on T cell immunity and immunotherapy.

S. Han[1], P. Georgiev[1], J. Schneider[1], A. Huang[1], Z. Nugmanova[1], T. H. Nguyen[1], C. Yao[1], S. Johnson[1], S. Joshi[1], I. Dhiman[1], J. M. Drijvers[1], M. Fung[1], J. H. Rowe[1], B. C. Miller[2], G. J. Freeman[3], A. E. Ringel[4], M. C. Haigis[1], A. H. Sharpe[1];
[1]Harvard Medical School, Boston, MA, [2]University of North Carolina at Chapel Hill, Chapel Hill, NC, [3]Dana-Farber Cancer Institute and Harvard Medical School, Boston, MA, [4]Massachusetts Institute of Technology, Boston, MA

Aging induces profound alterations in host biology and correlates with unfavorable clinical outcomes in age-related diseases such as cancer. While the pivotal role of the immune system in regulating tumor progression is well-acknowledged, the precise mechanisms through which aging influences anti-tumor T cell immunity and responsiveness to immune checkpoint blockade (ICB) remain elusive. In this study, we employed syngeneic murine tumor models (B16, MC38, and E0771) in young (2-4 months) and aged (20-24 months) cohorts to elucidate the early impacts of aging on tumor development and T cell responses. Our findings demonstrate that aged mice exhibit accelerated tumor growth across various models. In-depth analysis of tumor-infiltrating lymphocytes (TILs) uncovered distinct alterations in the $CD8^{\pm}$ T cell population, characterized by decreased activation status and diminished tumor specificity in aged mice. Correspondingly, aged mice exhibited resistance to anti-PD-1 immunotherapy. To unravel the underlying environmental factors contributing to compromised anti-tumor T cell responses and ICB resistance, we characterized the immune and metabolic landscapes of the aged tumor-draining lymph nodes and tumors. Furthermore, we established a genetically engineered mouse model of lung adenocarcinoma in both young and aged mice, unveiling novel functions and mechanisms associated with age-related T cells actively impeding effective tumor control. In the context of increasing average life expectancy, comprehending the intricate interplay between age-related T cell dysfunction and cancer assumes paramount importance. Such insights hold the key to the development of innovative therapeutic strategies tailored for the growing population of older patients.

#6593 Rejuvenation of tumor-infiltrating lymphocytes (TIL): A novel strategy to revitalize TIL antitumor function for cell therapy.

R. Vizcardo, Y. Huang, J. Fioravanti, T. Maeda, N. Tamaoki, Y. Yamazaki, B. Kutlu, K. Bahl, B. Wang, Z. Zhong, S. Potluri, N. P. Restifo, G. Lee;
Lyell Immunopharma, South San Francisco, CA

TIL therapy is a promising approach for the treatment of metastatic solid tumors, but its efficacy is limited by T-cell exhaustion and terminal differentiation. In addition, recent studies have underscored the adverse effects of aging on T cells. Reprogramming T cells into induced pluripotent stem cells (iPSC) and differentiating them back to the T-cell lineage has proven to be complex and time-consuming. In particular for TIL applications, de novo T cell production via iPSCs requires each TCR in the final product to be derived from an independently established iPSC clone. To overcome these barriers, we developed a novel technology called Rejuvenation, which bypasses the need for reprogramming of T cells into iPSCs. Rejuvenated TIL products retain their TCR diversity while offering several significant advantages, including reduced T-cell epigenetic age, improved expansion capacity, stem cell-like phenotype, and enhanced secretion of cytokines upon activation by target antigens. In this study, we used TIL derived from patients with melanoma and NSCLC. Rejuvenated TIL were generated by the transient expression of transcription factors in a process called 'Partial Reprogramming' and returned back to a T-cell lineage phenotype by a process called 'Redirection'. Partially reprogrammed TIL showed an altered morphology resembling adherent stromal cells and down-regulated conventional T-cell markers including CD3, CD4, and CD8. Redirected T cells reacquired a conventional CD4/CD8 phenotype including morphology, surface markers and function, and demonstrated decreased epigenetic age (>7 years younger, N=3). We also observed a higher proliferative capacity, improved metabolic state, and increased expression of biomarkers associated with T-cell stemness, including CCR7 and CD62L, when compared with untreated TIL. Rejuvenated TIL demonstrated improved cytokine secretion, including IFNγ, TNFα and IL-2 in functional assays. Immune repertoire analysis revealed a significant polyclonal population of putative tumor-reactive TCRs. In vivo functionality was also evaluated using a xenograft model of engineered A375 melanoma cell line that agonizes T-cells in hIL2-NOG mice. Adoptive transfer of rejuvenated TIL resulted in significantly improved suppression of tumor growth and prolonged survival compared with TIL expanded by conventional methods. These results were also confirmed in other surrogate models, including rejuvenated PBMC, TCR and CAR T cells, demonstrating the broad applicability of Rejuvenation technology. Our results indicate TIL Rejuvenation enhances the functionality and antitumor characteristics of T cells, while preserving a broad TCR repertoire. This technology holds substantial promise and may pave the way for the development of the first rejuvenated autologous polyclonal TIL therapy for treatment of advanced solid tumors.

#6594 4-1BB: A double-edged sword for T cells.

L. Yang, T. P. Sheets, Y. Feng, K.-S. Hsu, G. Yu, S. Seaman, P. Bajgain, D. So, J. Lee, R. Chari, B. St. Croix;
National Institutes of Health (NIH), Frederick, MD

Background: The costimulatory receptor 4-1BB (CD137) is expressed on the surface of activated T cells, playing a pivotal role in enhancing T cell responses and emerging as a promising target for cancer immunotherapy. Its primary ligand, 4-1BBL (CD137L), is found on antigen-presenting cells and various immune cells. The interaction between 4-1BBL and 4-1BB provides crucial costimulatory signals to both CD4+ and CD8+ T cells, amplifying their activation and effector functions. However, recent studies have shed light on a distinct role of 4-1BB in T cells. Prior work has revealed that 4-1BB can distinguish intratumoral regulatory T cells (Tregs) from peripheral Tregs and other CD4 lineage T cells in cancer patients, and the overexpression of 4-1BB on Tregs has been associated with unfavorable survival outcomes. Additionally, targeting 4-1BB with IgG2a isotype antibodies has shown significant anti-tumor efficacy in preclinical models by depleting Tregs. Furthermore, agonist monoclonal antibodies targeting 4-1BB have not only shown promise in inducing tumor regressions but also demonstrated improved outcomes in mouse models of autoimmune diseases induced by autoreactive CD4+ T cells. These findings indicate the existence of specific ligands or factors that modulate 4-1BB function on T cells that can vary depending on the disease state.
Methods: To identify potential ligand(s) involved in the modulation of 4-1BB function, we developed an innovative CRISPR/Cas9-based transcriptional activation (CRISPRa) screening system that integrates CRISPR/Cas9-guide mediated gene activation, high avidity bead-based selection, serial enrichment, and flow cytometry-based monitoring. This screening platform provides enhanced sensitivity for identifying extracellular interactions between receptor-ligand partners that have not been fully characterized before, even with low-affinity.
Results: Through our unbiased CRISPRa screen, we discovered that Myelin-Associated Glycoprotein (MAG), also known as siglec-4, a member of the siglec (sialic acid-binding immunoglobulin-like lectins) family, interacts with 4-1BB *in trans*. Our study demonstrated that MAG binds to activated T cells via 4-1BB and inhibits their activation and proliferation, suggesting a potential role of the MAG-4-1BB interaction in modulating T cell function. Notably, our data revealed that trans-binding to MAG-positive cells inhibits c-Jun signaling in activated T cells. Furthermore, the presence of MAG on target cells can hinder Chimeric Antigen Receptor (CAR) T-cell activity.
Conclusion: Utilizing a highly efficient cell-based CRISPRa system, we discovered a novel interactor of 4-1BB capable of modulating T cell activation through its interaction with 4-1BB. This interaction suggests an immunosuppressive role of 4-1BB, explaining the paradoxical roles of 4-1BB in T cells. These findings provide crucial insights for the development of precise therapeutics targeting 4-1BB.

#6595 HDAC8 targeting impairs Foxp3+Treg cell function and promotes anti-tumor immunity.

F. Kong[1], L. Wang[2], A. Beeler[3], **W. W. Hancock**[4];

[1]Zhongnan Hospital of Wuhan University, Hubei, China, [2]Children's Hospital of Philadelphia, Philadelphia, PA, [3]Boston University, Boston, MA, [4]Children's Hospital of Philadelphia and University of Pennsylvania, Philadelphia, PA

HDAC8 is an evolutionarily distinct, X-linked, zinc-dependent class I histone/protein deacetylase implicated in developmental disorders, parasitic infections, myopathy, and cancers such as neuroblastoma, gastric cancer, hepatocellular carcinoma, oral squamous cell carcinoma, and childhood acute lymphoblastic leukemia. Here, we highlight a hitherto unknown role of HDAC8 in immune cells by presenting data on conditional targeting of HDAC8 in T cells and the effects of selective HDAC8 inhibitors (HDAC8i) on T cell-dependent immune responses. First, as a genetic approach, we produced C57BL/6 mice with floxed exon 3 of the HDAC8 gene suitable for targeted deletion of HDAC8 and, after crossing with syngeneic CD4cre mice, demonstrated conditional deletion of HDAC8 and enhanced acetylation of SMC3, a classic HDAC8 substrate, in their T-cells. Next, in a pharmacologic approach, we tested isoform-selective inhibitors of HDAC8 (OJ-1, PCI-34051) and assessed effects on Foxp3+ T-regulatory (Treg) cell suppressive function. Finally, we performed flow cytometry, RNAseq, CHIP-seq and mass spectrometry to investigate the underlying mechanisms by which HDAC8 knockout affected Treg function. Our data demonstrate that knocking down or inhibiting HDAC8: (i) impaired murine Treg suppressive function in vitro and in vivo, including inhibiting the ability of Tregs to promote mouse cardiac allograft survival ($p<0.01$); (ii) decreased Treg function in homeostatic proliferation assays ($p<0.01$), e.g., involving adoptive transfer of WT or HDAC8-/- Tregs plus WT conventional T cells into immunodeficient hosts; (iii) decreased intratumoral Tregs, increased CD4 and CD8 T cells, increased production of effectors such as IFN-g and granzyme-B, and limited growth of syngeneic mouse non-small cell lung cancer cell lines ($p<0.01$) (whereas no effect of Hdac8i on tumor growth was seen in immunodeficient hosts, indicating the key action was via immune cell targeting). Mechanistically, HDAC8 co-precipitated with Foxp3 and NFAT5 and promoted the deacetylation of Foxp3 and NFAT5, and knockout of HDAC8 enhanced the acetylation level of NFAT5 and promoted cytokine expression. Hence, our combined genetic and pharmacologic studies establish the importance of HDAC8 in Foxp3+ Treg cells and show that therapy with selective HDAC8 inhibitors can be a novel therapeutic approach in immuno-oncology.

#6596 BRMS1 downregulation alters the tumor microenvironment and induces immunotherapy resistance in lung adenocarcinoma.

M. B. Lankadasari[1], Y. Liu[1], B. Mastrogiacomo[1], Y. Zhu[1], E. G. Dunne[1], C. N. Fick[1], C. Harsha[1], J. S. Reis-Filho[2], D. R. Jones[1];

[1]Memorial Sloan Kettering Cancer Center, New York, NY, [2]AstraZeneca, Gaithersburg, MD

Background: Lung cancer is the leading cause of cancer-related deaths globally. During cancer progression, tumor cells interact with tumor-infiltrating immune cells (TIICs) creating an immunosuppressive microenvironment. Therefore, it is essential to delineate the communication dynamics between cancer cells and TIICs to identify novel pathways for therapeutic targeting. *BRMS1* is a metastasis suppressor gene that is frequently downregulated in lung adenocarcinoma (LUAD). We, and others, have shown that loss of BRMS1 results in increased distant metastatic disease. Given the strong correlation between immune suppression, metastasis, and immunotherapy resistance we sought to elucidate if BRMS1 contributes to these processes. Specifically, we hypothesized that loss of BRMS1 in LUAD cells influences the immune cell composition, shaping an immunosuppressive microenvironment and decreasing tumor response to immunotherapy.

Methods: To experimentally address our hypothesis, we generated *Kras*^{G12D} *P53*$^{fl/fl}$ *Brms1*$^{-/-}$ mice inducing spontaneous tumors with Ad-Cre intratracheal inoculation. RNA-seq scRNA-seq on *Brms1*$^{+/+}$ and *Brms1*$^{-/-}$ tumors, coupled with cell type annotations using mMCP-counter and DCATS were used to identify diverse TIIC subsets. To validate our observation, we performed immunofluorescence and flow cytometry to assess the number of TIICs. To explore the impact of *Brms1* loss on the efficacy of anti-PD1 immunotherapy, a syngeneic CMT167 mouse model with *BRMS1*^{KD} cells implanted in the flank was treated with an anti-PD1 antibody.

Results: Differential gene expression analysis of RNA-seq data revealed a reduction in CCL9, CCL24, CLEC1B, PYCARD and other proinflammatory molecules in *Brms1*$^{-/-}$ tumors. Gene ontology and GSEA highlighted a diminished immune response signature in *Brms1*$^{-/-}$ tumors. In contrast, hallmark gene sets like IFNγ response, IL6 signaling, and inflammation are highly enriched in *Brms1*$^{+/+}$ tumors. mMCP-counter suggested a decrease in CD8+ T cells in *Brms1*$^{-/-}$ tumors. Likewise, scRNA-seq data confirmed a significant decrease in cytotoxic CD8+ T cells in the *Brms1*$^{-/-}$ mice. Immunofluorescence and flow cytometric analysis showed a reduction in cytotoxic CD8+ T cells with low proliferative potential (Ki67+) in the *Brms1*$^{-/-}$ mice. Postmortem on our syngeneic mouse tumors after a 30-day anti-PD1 antibody treatment revealed a significantly larger mean tumor size in the *BRMS1*^{KD} group compared to the WT group (942.4 mm^3 vs. 184 mm^3; $p<0.023$). Immunophenotyping on these tumors using flow cytometry also demonstrated reduced cytotoxic CD8+ T cells in the KD group post-treatment.

Conclusion: Our data suggest that reduced BRMS1 expression in LUAD alters CD8+ T cell composition and primary tumor response to immunotherapy. Implications of our findings underscore the potential of BRMS1 as a therapeutic target in the context of immunotherapy-resistant LUAD.

#6597 CD40 agonism induces CD4 T cell mediated rejection of major histocompatibility complex class I deficient pancreatic tumors.

M. E. Haerr[1], S. I. Kim[2], C. Arora[2], K. P. Gribbin[1], R. H. Vonderheide[2], K. T. Byrne[1];

[1]Oregon Health & Science University, Portland, OR, [2]University of Pennsylvania, Philadelphia, PA

Cytotoxic CD8 T cells are the canonical mediators of tumor clearance by the adaptive immune system. As such, current immunotherapies, including immune checkpoint blockade (ICB), target exhausted CD8 T cells with the hope of reinvigorating the CD8 T cells to drive tumor clearance. However, many tumors, including pancreatic ductal adenocarcinoma (PDAC), can evade CD8 T cell detection via downregulation of the antigen presentation molecule, major histocompatibility complex I (MHC I) as either primary or acquired resistance to immunotherapy. We have previously reported that agonistic CD40 antibody (αCD40), which promotes the maturation and licensing of dendritic cells to drive T cell priming, synergizes with ICB to induce tumor rejection dependent on both CD4 and CD8 T cells in mouse models of PDAC. Given the potential mechanisms of resistance to CD8 T cell immunity, we hypothesized that interrogation of the mechanisms underlying αCD40-induced CD4 T cell rejection of PDAC will reveal targets for improving CD4 T cell-directed immunotherapies. Here, we show that implantation of an MHC I deficient PDAC cell line derived from the genetically engineered *Kras*^{G12D}*Trp53*^{R172H}*Pdx1-Cre* (KPC) mouse model results in normal tumor establishment and progression. Upon treatment with combined αCD40 and ICB, tumor growth was significantly decreased in a CD4, but not CD8, T cell-dependent manner. Using genetic knockout mice, we determined that tumor regression was perforin-independent and identified host expression of IFNγ as requisite for therapeutic efficacy. To identify the cellular subset mediating CD4 T cell-rejection of the tumor, we assessed the major histocompatibility complex II (MHC II) positive cells in the tumor microenvironment (TME), which possess the ability to directly synapse with CD4 T cells to drive anti-tumorigenic T cell programs. We determined that macrophage and myeloid cells were dispensable for treatment efficacy, however non-immune cells in the TME can also interact with CD4 T cells through expression of MHC II. Interrogation of stromal cells reveals an increase in the proportion of MHC II+ subsets after combined αCD40/ICB treatment, with a concomitant decrease in the proportion of MHC II+ tumor cells. These data support the notion that CD4 T cell control of tumors may be mediated by both direct and indirect mechanisms of tumor killing. Findings from this work will elucidate non-canonical mechanisms of CD4 T cell-mediated rejection of tumors and may be leveraged to discover novel translational targets for immunotherapy.

#6598 Inhibition of cGAS as a strategy to restore anti-tumor immunity response to STING agonist in chromosomally unstable tumors.

Christy Hong[1], Lindsay Caprio[2], Mercedes Duran[1], Meri Rogava[2], Hsiang-His Ling[2], Sreeharsha Gurrapu[2], Leon Ebel[2], Melody Di Bona[1], Benjamin Izar[2], Samuel F. Bakhoum[1]

[1]Human Oncology and Pathogenesis Program, Memorial Sloan Kettering Cancer Center, New York, NY, [2]Department of Medicine, Columbia University Irving Medical Center, New York, NY

The activation of STING (stimulator of interferon genes) has been widely shown to induce signaling pathways, triggering type I interferon and ultimately generating anti-tumor immunity. Whereas initial preclinical studies on STING agonists exhibited boost in anti-tumor response, clinical trials combining STING agonist and immune checkpoint blockade agent PD-1 reported that only small subset of patients benefited from the treatment. This study highlights a potential key mechanism underlying the lack of benefit from STING agonist observed in most clinical trial patients. We reveal a phenomenon known as chromosomal instability (CIN), characterized by persistent chromosome segregation errors over multiple rounds of mitosis, drives chronic activation of cGAS (cyclic GMP–AMP synthase) through continuously supplying its substrate in the form of micronuclei. Chronic activation of cGAS stimulates degradation of its downstream target STING in a feedback-loop manner. This consequently attenuates type I interferon signaling upon STING activation, blunting its anti-tumor response. Remarkably, we show suppression of CIN, achieved through introduction of mitotic centromere-associated kinesin (MCAK), or inhibition of cGAS activity, either by pharmacological agent or total genetic ablation of cGAS using CRISPR-Cas9, restores type I interferon production and anti-tumor immunity upon the administration of STING agonist, MSA-2 in four of the five advanced tumor models. Furthermore, we show this restoration of type I interferon signaling and anti-tumor immunity is cancer cell STING-dependent as genetic deletion of STING in the tumor cells nullifies this effect. In summary, we provide a mechanistic insight underlying the limited anti-tumor response observed in STING agonist trials and propose potential strategies, through finetuning of CIN level or inhibition of cGAS activity, to illicit stronger anti-tumor immunity in combination with STING agonist treatment.

MOLECULAR/CELLULAR BIOLOGY AND GENETICS: Chromatin and Transcriptional Regulatory Mechanisms in Cancer Minisymposium

#6599 3D genomic analysis reveals novel enhancer hijacking mechanisms caused by complex structural alterations that drive oncogene overexpression.

Katelyn L. Mortenson[1], Courtney Dawes[2], Emily R. Wilson[1], Nathan E. Patchen[2], Hailey Johnson[1], Jason Gertz[1], Swneke D. Bailey[3], Yan Liu[2], Katherine E. Varley[1], Xiaoyang Zhang[1]

[1]Oncological Sciences, University of Utah, Salt Lake City, UT,[2]Biochemistry, University of Utah, Salt Lake City, UT,[3]Surgery and Human Genetics, McGill University, Montreal, QC, Canada

Enhancer hijacking, caused by structural alterations on chromosomes as well as extrachromosomal DNA (ecDNA), is a common cancer driver event. The complexity and ubiquity of structural alterations in cancer genomes make it difficult to identify enhancer hijacking with genome sequencing alone. Here we describe a 3D genomics-based analysis called HAPI (Highly Active Promoter Interactions) to characterize enhancer hijacking caused by various types of structural alterations. Applying HAPI analysis to HiChIP data from 34 cancer cell lines, we identified novel enhancers hijacked through chromosomal rearrangements to activate both known and potentially novel oncogenes such as *MYC, CCND1*, *ETV1*, *CRKL*, and *ID4*, which we validated using CRISPRi assays and RNA-seq analysis. Furthermore, we found that ecDNAs often contain multiple oncogenes from different chromosomes, which cause nested enhancer hijacking among them. For instance, we found that *MYC* ecDNAs relocate additional oncogenes from other chromosomes such as *CDX2, ERBB2,* or *CD44* near the *MYC* locus, co-opting *MYC*'s enhancers for their overexpression, which we validated using dual-color DNA FISH and CRISPRi assays. This multiple oncogenes-involved enhancer hijacking mechanism may suggest novel therapeutic strategies such as targeting either the co-opting oncogenes or the hijacked enhancers for ecDNAs. Our study provides a robust strategy to detect enhancer hijacking events using our publicly available HAPI analysis tool and reveals novel mechanisms underlying oncogene activation caused by chromosomal and extrachromosomal structural alterations.

#6600 Investigating molecular regulators of a dual identity state in lung adenocarcinoma.

G. Fort[1], S. Camolotto[2], R. Tariq[1], P. Fang[1], K. L. Gillis[1], C. Stubben[1], E. L. Snyder[1];

[1]University of Utah Huntsman Cancer Institute, Salt Lake City, UT, [2]Recursion Pharmaceuticals, Salt Lake City, UT

Lung adenocarcinoma (LUAD) is the largest subtype of lung cancer and is the most common cause of cancer related death. LUAD progression is driven by both genetic alterations and epigenetic changes that confer increased lineage plasticity and heterogeneity, but underlying mechanisms dictating cell identity in LUAD remain incompletely understood. The lineage defining transcription factors, NKX2-1 and FoxA1/2, coordinately maintain a pulmonary identity in LUAD. Recent work suggests that NKX2-1-positive (NKX2-1+) LUAD evolves from an alveolar-like state and adopts various disparate cell fates that drive progression, including “dual-identity” states, characterized by acquisition of gastrointestinal (GI) and pulmonary-like states in the same cell. Using sophisticated genetically engineered mouse models and 3D organoid cultures, we demonstrated that the gastrointestinal transcription factor HNF4α, which robustly marks the dual-identity state, is critical for growth in NKX2-1+ LUAD. We performed bulk RNA-seq and single cell RNA-seq in vitro and in vivo, and we found that loss of HNF4α alters the differentiation state of NKX2-1+ LUAD, causing cells to shed elements of their gastric identity in favor of alternate differentiation states. Using paired chromatin immunoprecipitation sequencing and RNA-seq in dual-identity organoids, we found that HNF4α can access and activate many of its canonical gastrointestinal target genes despite being aberrantly expressed in the lung, where it is typically epigenetically silenced early in development. Surprisingly, HNF4α also colocalizes with NKX2-1 and FoxA1/2 and binds at novel sites, suggesting that HNF4α acquires expanded activity in this state beyond its canonical roles. Together, our work unveils key insights into the mechanisms by which lineage defining transcription factors regulate cellular identity and growth in LUAD.

#6601 Menin drives oncogenesis in Ewing sarcoma cells by activating transcription of key metastatic factors.

K. A. Braun[1], A. Miyaki[1], N. M. Garcia[1], D. Tu[1], F. Wu[2], J. F. Sarthy[1], E. R. Lawlor[1];

[1]Seattle Children's Research Institute, Seattle, WA, [2]Fred Hutchinson Cancer Research Center, Seattle, WA

Ewing sarcoma (EwS) is a bone and soft tissue tumor that is driven by the fusion of FET and ETS genes, most commonly resulting in creation of the EWS::FLI1 chimeric oncoprotein. The scaffolding protein Menin regulates transcription through interactions with transcription factors and chromatin modifying enzymes and has both oncogenic and tumor suppressive roles, depending on the cellular context. The half-life of Menin is prolonged in EwS cells leading to high levels of the protein that is dependent on EWS::FLI1 expression. To investigate tumorigenic functions of Menin in EwS, we used CRISPR/Cas9 to generate clonal A673 and TC32 Menin knockout cells. Consistent with our earlier studies using shRNA-mediated knockdown, loss of Menin had little effect on proliferation in 2-D culture but resulted in reduced anchorage-independent growth in soft agar assays. When MEN1-KO cells were injected into NSG mice, either subcutaneously or by tail vein, tumor formation was delayed. Injection of MEN1-KO cells into the renal subcapsule of NSG mice resulted in locally invasive tumors but their capacity to metastasize to the liver was reduced compared to control cells. To elucidate how loss of Menin led to diminished tumorigenic and metastatic potential, we performed RNA-seq of control and MEN1-KO cells. This analysis revealed significant and reproducible down-regulation of MYC target genes and up-regulation of the epithelial to mesenchymal transition pathway and extracellular matrix protein-encoding genes in MEN1-KO cells. To determine if genes altered in MEN1-KO cells were dependent on the role of Menin in Menin/MLL methyltransferase complexes, we analyzed transcriptomes of EwS cells that had been exposed to the Menin/MLL interaction inhibitor, VTP-50469. Only a subset of genes altered by the MEN1-KO were also altered by the Menin/MLL inhibitor, suggesting that Menin regulates gene expression in EwS cells by both MLL-dependent and MLL-independent mechanisms. To test this, we performed CUT&RUN to define Menin binding sites and discovered that Menin binds not only at H3K4me3-marked gene promoters but also at intragenic enhancers marked by H3K27Ac. Importantly, comparison of RNA-seq data revealed substantial overlap between Menin-regulated and established EWS::FLI1 target genes and we identified that a subset of EWS::FLI1-bound intragenic enhancers are also bound by Menin. Significantly, these co-bound, co-regulated loci encode for pro-metastatic genes, including *IL1RAP*, *STEAP1*, and *CAV1*. Finally, we found that Menin and EWS::FLI1 co-immunoprecipitate in EwS nuclear extracts suggesting that they may exist in complex with one another at sites of shared gene regulation. Taken together, these data indicate that Menin promotes EwS metastasis and that this is achieved by its function as a scaffolding protein that augments the transcriptional activity of EWS::FLI1 at intragenic enhancers of pro-metastasis genes.

#6602 Targeting the SWI/SNF complex in POU2F-POU2AF transcription factor-driven malignancies.

L. Xiao[1], T. He[1], O. Klingbeil[2], Y. Eleanor[1], X. Wu[2], Y. Qiao[1], A. Parolia[1], S. Eyunni[1], R. Mannan[1], S. Mahapatra[1], N. Kim[1], H. Zheng[1], F. Su[1], X. Cao[1], S. Samajdar[3], M. Ramachandra[3], C. R. Vakoc[2], A. M. Chinnaiyan[1];

[1]University of Michigan, Ann Arbor, MI, [2]Cold Spring Harbor Laboratory, Cold Spring Harbor, NY, [3]Aurigene Oncology, Bengaluru, India

Background: Small cell lung cancer (SCLC) is a rapidly progressing subtype of lung cancer with a high growth rate and early metastasis propensity, often resulting in a more advanced disease stage at diagnosis. A recent transcriptome analysis of human SCLC tumors revealed that SCLC could be characterized by the expression pattern of certain transcription factors (TFs), including ASCL1 (achaete-scute family bHLH transcription factor 1) and POU2F3 (POU domain class 2 transcription factor 3), exemplifying SCLC as a TF-driven malignancy. ASCL1-driven SCLC (SCLC-A) manifests a neuroendocrine phenotype, while POU2F3-driven SCLC (SCLC-P) is characterized as a tuft-cell-like variant. Recent studies revealed that POU domain class 2 transcription factors uniquely rely on coactivators to achieve their lineage-defining functions in the tuft cell and B cell lineages. In tuft-cell-like SCLC cells, the coactivators of POU2F3 (POU2AF2 and POU2AF3) endow POU2F3 with a critical transactivation domain by forming a master regulator complex, which supports enhancer-mediated cancer-promoting gene activation in SCLC-P cells. This indicates a potential therapeutic vulnerability of tuft-cell-like SCLC whereby strategies aimed at blocking POU2F3-POU2AF2/3 function may lead to clinical benefit.

Methods: We conducted a domain-targeted CRISPR screen to identify druggable targets for SCLC-P, followed by pharmacological validation in preclinical SCLC models. Multi-omics techniques, including ATAC-seq, ChIP-seq, RNA-seq, and RIME, were employed to elucidate the SWI/SNF complex's regulatory influence on the POU2F-POU2AF axis.

Results: Here we identified that the POU2F3 molecular subtype of SCLC (SCLC-P) exhibits an exquisite dependence on the activity of the SWI/SNF epigenetic complex. SCLC-P cell lines were sensitive to low nanomolar levels of a SWI/SNF ATPase degrader when compared to other molecular subtypes of SCLC. Co-factors of POU2F were found to interact with components of the SWI/SNF complex. The POU2F3 transcription factor complex is evicted from chromatin upon SWI/SNF ATPase degradation. A novel, orally bioavailable SWI/SNF ATPase PROTAC degrader demonstrated preferential efficacy in SCLC-P relative to the SCLC-A subtype. The SWI/SNF ATPase PROTAC degrader did not alter normal tuft cell numbers in lung or colon, nor did it exhibit toxicity in mice. B cell malignancies which displayed a dependency on the POU2F co-factor, POU2AF1, were also remarkably sensitive to SWI/SNF ATPase degradation. In a POU2AF1-dependent, disseminated murine model of multiple myeloma, AU-24118 had an enhanced survival benefit as compared to pomalidomide, an approved treatment for multiple myeloma.

Conclusions: Taken together, our studies suggest that POU2F-POU2AF driven malignancies have an intrinsic dependence on the SWI/SNF complex representing a striking therapeutic vulnerability.

#6603 A TBX2-driven signaling switch from androgen receptor to glucocorticoid receptor confers enzalutamide resistance in prostate cancer.

S. Dutta, G. K. Patel, H. Khedmatgozar, D. Latour, J. Welsh, M. Tripathi, S. Nandana;
Texas Tech University Health Sciences Center, Lubbock, TX

Background: Recent studies suggest that glucocorticoid receptor (GR) activation can cause enzalutamide resistance in advanced prostate cancer (PCa) via functional bypass of androgen receptor (AR) signaling. However, the specific molecular mechanism(s) driving this process remain unknown. In an effort to identify drivers of prostate cancer progression, in a previous study, we determined that TBX2, a developmental T-box transcription factor (TF) master regulator, is over-expressed in CRPC and drives bone metastatic progression. A recent report confirmed that TBX2 and GR are two of the four TFs that drive enzalutamide resistance in advanced PCa. Our current study demonstrates that TBX2 with known repressor and activator functions, is the molecular switch that represses AR levels while activating GR expression thereby resulting in the replacement of AR signaling to control tumor growth.
Methods: We genetically modulated TBX2 using multiple approaches: a) dominant negative, DN, to block TBX2 (TBX2DN), and b) overexpression, OE, to increase TBX2 expression (TBX2OE), c) shRNA mediated knockdown (shTBX2). RNA-seq was performed, and qRT-PCR, Western blot and immunohistochemical (IHC) analyses were used for validation. Further, we used chromatin immunoprecipitation (ChIP) and site directed mutagenesis (SDM) to confirm TBX2 binding on the AR promoter. We also used co-immunoprecipitation (Co-IP) to determine protein partners of TBX2.
Results: Mechanistically, our studies revealed that TBX2 bound to the promoters of both AR and GATA2, an AR coregulator, thereby resulting in a bimodal repression of AR expression. Conversely, TBX2 upregulated GR via direct GR promoter binding and TBX2-GR protein-protein interaction. Together, concurrent repression of the AR and activation of GR resulted in enzalutamide resistance. Importantly, we found that SP2509, an allosteric inhibitor of the demethylase-independent function of LSD1, a TBX2-interacting protein in the COREST complex, can disrupt both TBX2-LSD1 and TBX2-GR protein-protein interactions thereby uncovering a unique mode of SP2509 action in CRPC. Together, our study supports a molecular model of CRPC wherein: 1) TBX2, LSD1 and GR proteins interface with each other, and 2) pharmacological inhibition of LSD1 blocks the TBX2-driven AR-to-GR switch through disruption of TBX2-GR interaction.
Conclusions: In summary, our study identifies TBX2 as the molecular switch that drives the AR to GR signaling bypass thereby conferring enzalutamide resistance. Further, our study provides key insights into a potential therapeutic modality for targeting the AR to GR signaling switch via disruption of the TBX2-LSD1 and TBX2-GR protein-protein interactions

#6604 Spatial transcriptomics delineates tumor heterogeneity in NACT triple-negative breast cancer.

I. Wall[1], J. Quist[1], S. Pinder[1], K. Cancer Biobank[1], S. Irshad[1], C. Gillet[1], V. Seewaldt[2], K. Mukund[3], D. Frankhouser[2], S. Subramaniam[3], M. Parsons[1], A. Grigoriadis[1];

[1]King's College London, London, United Kingdom, [2]City of Hope, Duarte, CA, [3]University of California, San Diego, CA

BACKGROUND: Triple-Negative Breast Cancer (TNBC) is a highly aggressive subtype of breast cancer and only ~40% of TNBC patients achieve a pathological complete response (pCR) following neoadjuvant chemotherapy (NACT). Since molecular heterogeneity of TNBC may contribute to variable responses to NACT, we aimed to deconvolute TNBC's histological and spatial transcriptomics (ST) patterns.

METHODS: In total, 90 pre-treatment biopsies were collected from NACT-treated TNBC patients from archival samples and the ongoing FORCE (NCT03238144) clinical trial at Guy's Hospital, London, UK. Of these, 38 achieved pCR (Responder), 46 had residual disease (Non-Responder) whilst 6 are currently undergoing NACT; 46 post-treatment surgical resections were collected from Non-Responders.Each sample was H&E stained, imaged, and annotated by a pathologist. A 6-digit classifier was designed to capture the histology of each region of interest (ROI), characterizing the tumour region, epithelial type and immune cell localization, population, distribution, and abundance.H&Es were used to guide ST profiling of serial sections which was performed on the GeoMx Digital Spatial Profiler. Tissues were stained with fluorescent antibodies against PanCK and CD45 to visualize the tissue, select ROIs and illuminate spatially resolved tumor and immune-enriched compartments, defined as PanCK+/CD45- and PanCK-/CD45+, respectively.Data analysis was performed in R 4.3.1 using the limma, dplyr, EdgeR, GeoMx Tools, GeoMx Workflows, RUV4, Spatial Experiment, SpatialDecon and GSVA packages, facilitating quality control, batch correction, differential and topographical gene expression, immune cell deconvolution and gene set enrichment analysis (GSEA), respectively.

RESULTS: To date, we have performed ST profiling of 120 TNBC samples from 82 patients (46 Non-Responders; 36 Responders), totaling 3917 tumor or immune-cell enriched regions. Preliminary analyses revealed KEGG pathways involved in tissue adhesion are upregulated in tumor compartments of Non-Responders compared to Responders, whilst those involved in genomic integrity are suppressed. Unsupervised clustering of PanCK+CD45- regions in Non-Responders identified tumor clusters present in both pre- and post-NACT samples, suggesting potential chemo-resistant properties. Moreover, immune cell deconvolution of the PanCK-/CD45+ regions revealed spatially distinct patters of immune cell composition mapped to histological annotations identified by our ROI classifier.

CONCLUSION: (S)Large scale ST of TNBC before and after NACT reveals novel patterns associated with response to treatment. We have designed a novel ROI classifier to spatially resolved transcriptomes of histological features, as such provide an in-depth characterization of the histo-genomics of TNBC.

#6605 Understanding the role of sumoylated Etv1 in mammary oncogenesis.

Z. Li[1], K. E. Koch[2], D. T. Thompson[1], D. M. Van der Heide[1], J. Chang[1], C. M. Franke[1], M. O. Suraju[1], A. C. Beck[3], A. W. Lorenzen[1], J. R. White[1], M. V. Kulak[1], D. K. Meyerholz[1], C. Kenny[1], R. J. Weigel[1];

[1]University of Iowa Holden Comprehensive Cancer Center, Iowa City, IA, [2]Yale New Haven Hospital, New Haven, CT, [3]University of Wisconsin, Madison, WI

The Small Ubiquitin-like Modifier (SUMO) pathway is a major post-translational regulatory mechanism involved in a variety of cellular functions including the DNA damage response, transcriptional regulation, and carcinogenesis. Recent discoveries by our group demonstrated that inhibiting the SUMO pathway can repress the growth of breast cancer xenografts and Neu-driven mammary oncogenesis in a genetically engineered mouse model with conditional knockout (CKO) of the SUMOylation E2 conjugating enzyme, *Ube2i*. However, despite the consistency of the findings, there remains considerable debate concerning the mechanisms through which SUMO inhibition represses tumorigenesis. Our downstream analysis suggested ETS Translocation Variant 1, encoded by *ETV1* gene, acts as a SUMO-sensitive transcription factor that drives mammary oncogenesis and cancer growth. To examine oncogenic properties of SUMO-conjugated ETV1 in breast cancer, we cloned HA-tagged WT Etv1, SUMO-resistant Etv1^{5xKR}, or SUMO mimetic SUMO-1-Etv1^{5xKR} into a lentiviral vector with a GFP cassette. Proliferation, colony formation in soft agar, and *in vivo* xenograft assays were evaluated in the Ube2iF/F cell line derived from a tumor in a MMTV-*c-neu/Ube2i*$^{fl/fl}$ animal. We did ChIP-seq in Ube2iF/F cells using SUMO-1 and Etv1 antibodies to examine the effects of SUMO conjugation on Etv1 genomic occupancy. RNA-seq using siEtv1 or AdCre was also performed to compare changes in gene expression with SUMO-conjugated Etv1 genomic occupancy. Inhibition of SUMOylation via AdCre caused a significant reduction in proliferation and colony formation *in vitro* and completely block the formation of flank xenografts *in vivo*. Interestingly, expressing a SUMO-resistant ETV1^{5xKR} rescued *in vitro* growth effects, whereas a SUMO mimetic SUMO-1-ETV1^{5xKR} had no effect on restoring proliferation. On the contrary, *in vivo* xenograft assays demonstrated that the Etv1^{5xKR}-SUMO1 efficiently induced tumor formation despite the loss of Ube2i while the sumo-resistant Etv1^{5xKR} was unable to rescue tumorigenesis. Bulk RNA-seq and ChIP seq performed demonstrated different patterns of gene regulation between sumoylated and unsumoylated Etv1. Gene set enrichment analysis (GSEA) showed genes associated with cancer stemness were significantly enriched in cells expressing Etv1^{5xKR}-SUMO1. Collectively, these observations support Etv1 acting as a SUMO-sensitive transcription factor that drives a stem cell phenotype necessary for mammary oncogenesis and progression.

MOLECULAR/CELLULAR BIOLOGY AND GENETICS: Metabolism and Cancer Minisymposium

#6606 HK2 is conditionally essential for growth in human cancer cells.

Kimberly S. Huggler, Kyle M. Flickinger, Jason R. Cantor

Biochemistry, University of Wisconsin - Madison, Madison, WI

The genetic drivers of cell growth can depend on an interplay of intrinsic factors and environmental context. However, there is often little consideration into how nutrient availability affects the genetic dependencies of proliferating human cells. Moreover, efforts such as DepMap have catalogued cell fitness genes using *in vitro* CRISPR screens across hundreds of cancer cell lines cultured in traditional media, which poorly replicate nutrient conditions found in the body. We recently tested the hypothesis that the nutrient environment can affect gene essentiality in human cells. By performing CRISPR screens with blood cancer cell lines, we identified sets of genes differentially required for cells cultured in traditional (e.g., RPMI) versus Human Plasma-Like Medium (HPLM). Among the strongest HPLM-essential hits was *HK2*, which encodes for the glycolytic enzyme hexokinase 2. Notably, most cancer cell lines co-express two hexokinases (HK1; HK2) that can each catalyze the phosphorylation of glucose to glucose-6-phosphate. Interestingly, while these two HKs share high degrees of structural and biochemical similarity, only *HK2* deletion had differentially stronger effects in HPLM. Further, both HK1 and HK2 contain an N-terminal region that permits association with the outer mitochondrial membrane (OMM). To investigate the conditional phenotype for loss of *HK2*, we generated *HK2*-knockout K562 leukemia cells, which displayed *HK1* expression levels comparable to those measured in control cells. We also confirmed that our *HK2*-knockout cells showed a stronger relative growth defect in HPLM versus RPMI. Importantly, the expression of HK2 cDNA normalized this defect. By contrast, the expression of kinase-dead HK2 did not provide any rescue effects, suggesting that HK activity is required for the conditionally essential role of HK2. We also engineered a cytosol-restricted HK2 by truncating its N-terminal OMM binding region. When we expressed this cDNA in our *HK2*-knockout cells, we observed complete rescue of the relative growth defect, suggesting that subcellular HK2 activity contributes to conditional *HK2* essentiality. We are now purifying mitochondria to ask how the subcellular distributions of HK1 and HK2 vary with nutrient conditions. In addition, we are also comparing the tracing patterns of 13C glucose in *HK2*-knockout and control cells to ask how *HK2* deletion affects glucose utilization. Finally, given that we normalized glucose levels across our screening conditions, we are applying a systematic approach to determine the gene-nutrient interaction that underlies the conditional phenotype for *HK2* deletion. Collectively, our data suggest that HK2 serves a non-redundant and conditionally essential role. We expect to generate novel insights into how *HK2* supports human cell growth and why this role can further depend on nutrient availability.

#6607 Serine depletion promotes antitumor immunity throughmitochondrial DNA-mediated cGAS/STING1 activation.

S. Saha[1], M. Ghosh[1], L. Jinyu[1], A. Wen[1], L. Galluzzi[2], L. Martinez[1], **D. C. Montrose**[1];
[1]Stony Brook University Hospital, Stony Brook, NY, [2]Weill Cornell Medicine, New York, NY

Serine is critical for supporting cancer metabolism, and as such, depriving malignant cells of this non-essential amino acid exerts anticancer effects, in large part, through disrupting their metabolic pathways. However, the impact of these metabolic defects on tumor-targeting immunity remains poorly understood. Here, we show that restricting endogenous and exogenous serine in colorectal cancer (CRC) cells results in mitochondrial dysfunction coupled to cytosolic mitochondrial DNA accumulation and cGAS/STING1-dependent type I interferon secretion. Serine-deprived tumors have suppressed growth, accompanied by type I interferon signaling and tumor infiltration by immune effector cells. Blocking cGAS/STING1 signaling in tumor cells limits the immunostimulatory and anticancer effects of serine deprivation. Moreover, serine-depleted tumors exhibit increased sensitivity to a programmed cell death 1 blocker. Lastly, transcriptomic data from human CRCs suggest that malignant lesions with reduced serine abundance have higher immune infiltration. Taken together, our findings reveal a novel role for serine as a gatekeeper of mitochondrial integrity and hence a suppressor of anticancerimmunity.

#6608 Therapeutic enzyme depletion of L-serine for the treatment of serine auxotrophic tumors.

Vipin Rawat[1], Huiping Zhao[1], Ladan Mashouri[2], Prarthana Prasanth[1], Kelly Conger[1], Sarita Bhetawal[2], Alessandra Araujo[2], Everett Stone[2], Jonathan Coloff[1]

[1]Physiology and Biophysics, University of Illinois College of Med. at Chicago, Chicago, IL, [2]University of Texas at Austin, Austin, TX

The non-essential amino acid L-serine (serine) plays an important role in cancer cell growth due to its diverse biosynthetic functions. In many cancer cells, serine can be taken up from the circulation or can be synthesized through the serine synthesis pathway (SSP) . We have recently discovered that luminal breast tumors are auxotrophic for serine due to lineage-specific silencing of the SSP gene *PSAT1*, rendering luminal breast cancer cells sensitive to serine deprivation both *in vitro* and *in vivo*. At present the only way to reduce serine availability for tumors *in vivo* is through dietary serine starvation, which in mice reduces circulating serine levels by ~50% and has been shown to inhibit the growth of numerous mouse models of cancer. Importantly, dietary serine is achieved in mice using a synthetic protein-free diet that may be difficult for humans to sustain. Nevertheless, dietary serine starvation is currently being explored in a clinical trial for pancreatic cancer. To circumvent some of the challenges associated with dietary serine starvation, we have developed a therapeutic serine degrading enzyme that we are exploring as a potential treatment for serine auxotrophic tumors. Our enzyme, eSDH, is based on the human serine dehydratase enzyme that facilitates the pyridoxal phosphate-dependent irreversible deamination of serine to pyruvate and ammonia. Relative to wild-type serine dehydratase, eSDH has significantly improved stability in serum as well increased activity towards serine. Injection of eSDH into mice is well-tolerated and leads to long-term, near-complete (>95%) reduction in circulating serine levels without the need for dietary changes. Importantly, eSDH treatment inhibits the growth of serine auxotrophic cancer cells *in vitro* and *in vivo*. We are currently assessing the efficacy of eSDH treatment in advanced models of luminal/ER+ breast cancer and when utilized in combination with endocrine therapy and other standard-of-care treatments for luminal/ER+ cancer patients. In addition to the degradation of serine, eSDH also depletes circulating L-threonine (threonine), which could contribute to the *in vivo* activity of eSDH. However, we have recently developed new eSDH variants that are highly selective for serine over threonine and show enhanced specificity for serine auxotrophic cancer cells. In conclusion, we have developed a prototypical therapeutic serine degrading enzyme that may provide an opportunity to clinically achieve more complete serine starvation in patients without the need for restrictive dietary changes.

#6609 NRF2/ACSS2 axis regulates alcohol-induced metabolic reprogramming in esophageal squamous epithelial cells.

Z. Xiong[1], B. Subramaniyan[2], C. Paiboonrungruang[1], Y. Li[2], W. He[3], H. Yuan[4], G. Zhang[3], X. Chen[1];
[1]Coriell Institute for Medical Research, Camden, NJ, [2]Cooper University Health Care, Camden, NJ, [3]Duke University Medical Center, Durham, NC, [4]University of North Carolina at Chapel Hill, Chapel Hill, NC

Esophageal diseases such as gastroesophageal reflux disease (GERD) and esophageal cancer have a strong association with alcohol drinking. However, the molecular mechanisms of alcohol-induced esophageal pathology remain unclear. In our previous study, we identified acyl-CoA synthetase short-chain family member 2 (ACSS2) as a transcriptional target of nuclear factor erythroid 2-related factor 2 (NRF2) in the esophageal epithelial cells *in vitro* and *in vivo*. Ethanol exposure enhanced *de novo* lipogenesis in $NRF2^{high}$ cells and generated a more energetic and invasive phenotype. In this study, we aimed to investigate the role of the NRF2/ACSS2 axis in regulating alcohol-induced metabolic reprogramming in esophageal squamous epithelial cells. We first demonstrated that ethanol exposure activated NRF2 signaling and upregulated the expression of NRF2 and ACSS2 in human esophageal squamous epithelial cells. ^{13}C-ethanol/^{13}C-acetate metabolic flux assay showed a dramatic NRF2-dependent increase of labeling of the TCA cycle intermediates and *de novo* lipogenesis in $NRF2^{high}$ cells in comparison with $NRF2^{null}$ or $NRF2^{low}$ cells. Long-term ethanol exposure caused metabolic reprogramming, in particular induced *de novo* lipogenesis, in the mouse esophagus according to metabolomics profiling of 833 metabolites. PET/CT and autoradiography showed increased ^{11}C-acetate uptake in the $NRF2^{high}$ esophagus of a conditional tissue-specific mouse (*Sox2CreER;LSL-Nrf2*^{E79Q}) due to upregulation of transporters and metabolic enzymes. In summary, Our data demonstrated the functional role of the NRF2-ACSS2 axis in alcohol-induced metabolic reprogramming in esophageal squamous epithelial cells both *in vitro* and *in vivo*, suggesting NRF2/ACSS2 inhibition as a novel mechanism-based prevention for alcohol-associated esophageal pathology.

#6610 Metabolic patterns of pancreatic cancer cachexia: Cross-tissue lipid networks predict cachexia progression.

D. Mathur[1], B. Majem[1], C. Beaulieu[2], L. Dailey[2], S. Jeanfavre[2], J. Xavier[3], C. Clish[2], N. Kalaany[1];

[1]Boston Children's Hospital, Boston, MA, [2]The Broad Institute, Boston, MA, [3]Memorial Sloan Kettering Cancer Center, New York, NY

Pancreatic ductal adenocarcinoma (PDAC) is among the most lethal of all cancer types. A key — yet poorly understood — facet in the disease state is cachexia, a multi-organ pathological state characterized by physical wasting and tissue catabolism. It occurs in 80% of PDAC patients, and to date there are no preventative or early detection methods. Cachexia leads to limited tolerance to anti-cancer therapy and contributes to disease lethality. Here, we present the first-of-its-kind systemic metabolomic analysis across cachectic stages to better understand disease progression.

We used the well-established mutant $KRAS^{G12D}$(LSL/+) mutant p53 inducible mouse model of PDAC. Model physiology faithfully recaptures human cachexia: we observe progressive overall weight loss as well as loss of skeletal muscle and adipose tissue. As with human disease, weight loss occurs prior to loss of appetite in the animals, suggesting physiological changes independent of nutrition. Importantly, our model captures the period prior to weight loss (pre-CAC), as well as early-CAC (<10% weight loss) and late-CAC (>10% weight loss).

We profiled the metabolomes of the pancreas, interstitial fluid, plasma, liver, 3 different adipose tissues, and 3 skeletal muscles, from male and female mice, control and tumor-bearing, across all 3 stages of cachexia. Each tissue has a unique metabolic trajectory across cachexia stages; pathway and correlation analyses showed a particular emphasis on lipid alterations in peripheral tissues. Strikingly, we find systemic metabolic changes prior to tissue wasting, including rewiring in the liver before the presence of metastases. This indicates systemic alterations as early as pre-CAC.

We therefore used computational modeling to identify metabolites that may be participating in cross-tissue networks. A key finding, confirmed by ^{13}C tracing, was the circulation of lactate and glucose and their uptake by the liver and pancreas. Network maps also suggest lipid rewiring in distal tissues, changes in abundances of these same lipid species in plasma, and their consequent alterations in the tumor and liver.

A fundamental question remains: can we predict cachexia development before the manifestation of symptoms? We used feature selection algorithms based on statistical learning, training the models only on a subset of data. Specific sphingolipids and triglycerides were the key lipid species that distinguished control and pre-CAC. We find that the model — trained only on pre-CAC — is able to determine early-CAC with an 85% accuracy and late-CAC with a 90% accuracy. Thus, a limited set of metabolites that are altered in pre-CAC could have predictive value for future cachexia development.

Overall, our work provides a resource for the field and advances our understanding of systemic metabolism in PDAC cachexia. We hope this will lay the foundation for cachexia prevention and treatment.

#6611 Unbiased functional genetic screens reveal essential RNA modifications in human cancer and drug resistance.

C. Pauli[1], M. Kienhofer[1], C. Muller-Tidow[1], **M. Frye**[2];
[1]Heidelberg University Hospital, Heidelberg, Germany, [2]DKFZ German Cancer Research Center, Heidelberg, Germany

RNA modification pathways are mis-regulated in multiple types of human cancer. To comprehensively identify cancer-relevant RNA modifications and their regulators, we screened all 150 annotated human RNA modifying proteins across 18 different normal and cancer cell lines using a CRISPR-based genetic knockout system. Fifty RNA modifying proteins were essential for survival of at least one cell type. A third of these essential genes were amplified in 38 different human primary cancer types and potentially drive cancer growth. Unexpectedly, the number of essential genes per cell line varied considerably, and this variation was not due to tissue of origin. Instead, we found that cancer cell-specific mitochondrial metabolic plasticity was responsible for the unique requirement of certain RNA modifications. For example, leukemia cells with high intrinsic drug tolerance required mitochondrial flexibility to survive treatment with the anti-leukemic drugs cytarabine and venetoclax. Synthetic lethality screens revealed that drug-resistance is abolished by deleting the mitochondrial methyltransferase TRMT5, which is responsible for the formation of N1-methylguanosine (m1G) in the tRNA anticodon loop. In summary, our study identifies cancer-relevant RNA modifying enzymes, and reveals a novel promising drug target for therapy-resistant acute myeloid leukemia.

#6612 Therapy-resistant endocycling cancer cells alter mitochondrial structure and metabolism to survive therapeutic stress.

M. Li, S. R. Amend, K. J. Pienta;
Johns Hopkins University School of Medicine, Baltimore, MD

Therapy resistance is responsible for 90% of cancer-related deaths. We identified a novel mechanism of therapy resistance in which cancer cells enter an endocycling cell state, undergoing repeated S and G phases without dividing. As a result, resistant endocycling cells are 40 times larger than mitotic cancer cell controls. Interestingly, we observed that these non-proliferative endocycling cells can eventually give rise to proliferative progeny weeks after chemotherapy is removed, modeling cancer recurrence. We hypothesize that this endocycling cancer cell state is a critical driver of therapy resistance and cancer lethality.

We evaluated oxidative stress in endocycling cells that survived the days and weeks following chemotherapy treatment using DCF-DA staining. We found increased levels of reactive oxygen species (ROS) in endocycling prostate cancer cells compared to untreated mitotic cells when normalized to cell size. Given that mitochondria are major producers and regulators of ROS, we hypothesize that cells surviving in this resistant state alter mitochondrial structure and function in response to increased oxidative stress. We performed immunofluorescence and confocal microscopy on mitochondria in untreated cells and cells following chemotherapy treatment to observe their morphology. Surviving endocycling cells had increased mitochondrial fragmentation when compared to the untreated group, a result that was further supported by reduced expression of phospho-DRP1 Ser637 via western blot.

To assess changes in glucose metabolism, we then utilized isotope tracing-based metabolomics with [U-^{13}C]glucose on untreated and surviving endocycling cells following chemotherapy. Endocycling cells had decreased labeling of ^{13}C in TCA cycle metabolites, suggesting a decrease in mitochondrial function when compared to untreated cells. Ongoing work involves further studying metabolic reprogramming as cells enter this resistant state with parallel labeling experiments using [1,2-^{13}C]glucose and [U-^{13}C]glutamine to perform mathematical modeling-based ^{13}C-metabolic flux analysis. In addition, we engineered a cell line to track mitochondria in real-time to quantify mitochondrial dynamics underlying the morphology observed in untreated and surviving cells.

Our goal is to characterize how this therapy-resistant cell state alters its mitochondrial structure and function to survive therapeutic stress. Identifying vulnerabilities of this phenotype will enable new approaches for eliminating drug resistance in cancer.

POPULATION SCIENCES: Molecular Epidemiology
Minisymposium

#6613 Understanding the causes of head and neck cancer using mutational signature analysis.

L. Torrens[1], S. Moody[2], C. De Carvalho[1], S. Senkin[1], S. Cheema[2], M. Kazachkova[3], V. Gaborieau[1], B. Abedi-Ardekani[1], R. Cortez Cardoso Penha[1], J. Atkins[1], P. Chopard[1], J. Wang[2], S. Fitzgerald[2], C. Latimer[2], C. Carreira[1], T. Cattiaux[1], M. Diaz-Gay[3], L. Humphreys[2], L. B. Alexandrov[3], M. R. Stratton[2], S. Perdomo[1], P. Brennan[1], HEADSpAcE consortium;

[1]International Agency for Research on Cancer (IARC/WHO), Lyon, France, [2]Wellcome Sanger Institute, Cambridge, United Kingdom, [3]University of California San Diego, La Jolla, CA

The geographical incidence of head and neck cancer (HNC) is heterogeneous, reflecting the prevalence of its main risk factors. Tobacco, either alone or combined with alcohol, is the predominant cause of HNC, while the potential of alcohol as an independent carcinogen is uncertain. Moreover, the etiology remains unknown for ~28% of cases. In this study, we used mutational signature analysis to 1) track the exposure to known and putative risk factors for HNC across multiple geographical regions and subsites, 2) evaluate whether an alcohol signature is present in HNC, and 3) assess its interaction with tobacco or other risk factors.

Whole-genome sequencing data was generated from 265 HNC cases from retrospective HNC studies in Europe and South America with available lifestyle and environmental exposure data. Mutational and copy number (CN) signatures were extracted with SigProfilerExtractor and decomposed into COSMIC reference signatures. Associations between the mutational signatures and epidemiological or molecular data were assessed using multivariate regression analysis.

The analysis revealed known and previously unreported signatures of endogenous and exogenous exposures. APOBEC-driven signatures (SBS2, SBS13) were identified in 97% (258/265) of cases. We observed differences in tobacco-related mutagenesis across anatomical subsites. While known tobacco signatures (SBS4, SBS92, DBS2, and ID3) were found in larynx cases, the novel signature SBS1536I was enriched in oral cavity cases from ever-smokers, which suggests a site-specific mutagenic effect from different tobacco carcinogens. Furthermore, we demonstrate that signatures associated with alcohol consumption (SBS16, DBS4, and ID11) were enriched in cases exposed to both tobacco and alcohol, indicating an interaction between the two. We also extracted signatures indicative of ultraviolet (UV) light exposure (SBS7a-c, DBS1, and ID13) in cases from the inner lip, tongue, and floor of the mouth, implying a role of UV exposure in oral cavity carcinogenesis. Finally, hierarchical clustering analysis revealed three distinct CN profiles in HNC, each linked to different risk factors and driver mutations: 1) A CN-rich polyploid cluster associated with tobacco smoking and CN signatures of chromosomal instability, including one novel signature (CN48G) enriched in samples from South America, 2) a CN-rich diploid cluster comprising cases related to both tobacco and human papillomavirus infection; and 3) a CN-neutral cluster enriched in samples with unknown etiology.

This study uncovers APOBEC signaling, tobacco, alcohol, and potentially UV light exposure, as potent mutagenic agents in HNC. Our findings suggest that the mutational impact of tobacco in HNC is tissue-specific, and that tobacco may enhance the oncogenic effects of alcohol. Finally, the CN profile in HNC is strongly influenced by exposure to risk factors and driver mutations in the tumors.

#6614 Integrating single-cell RNA-seq and large genome-wide association study data to identify colorectal cancer cell-of-origin populations.

C. Li[1], Z. Chen[1], Q. Li[1], J. Choi[2], Q. Sheng[1], W. Wen[1], X. Shu[3], X.-o. Shu[1], J. Long[1], Q. Cai[1], B. Singh[1], M. J. Shrubsole[1], K. S. Lau[4], W. Zheng[1], **X. Guo**[1]; [1]Vanderbilt University Medical Center, Brentwood, TN, [2]Korea University College of Medicine, Ansan, Korea, Republic of, [3]Memorial Sloan Kettering Cancer Center, New York, NY, [4]Vanderbilt University School of Medicine, Brentwood, TN

Background: Single-cell RNA sequencing (scRNA-seq) enables the precise identification of distinct cell populations and the measurement of gene expression within each population. Recently, integrating scRNA-seq and genome-wide association study (GWAS) data has shown promise in identifying cell-of-origin populations in human diseases. Colorectal cancer (CRC) progresses through a phenotypic continuum from normal colon to adenoma, and ultimately CRC. However, the specific disease cell-of-origin populations underlying each stage of CRC development at a single-cell resolution have not been well studied. Additionally, while transcriptome-wide association studies (TWAS) have identified more than 200 putative risk genes in CRC, the precise disease cell-of-origin populations associated with these genes remain elusive.

Materials and methods: We analyzed scRNA-seq datasets from 31 normal colon, 8 colon serrated polyps, and 15 conventional adenoma tissues of individuals participated the Colorectal Molecular Atlas Project (COLON MAP). We next conducted an integrative analysis of the aforementioned scRNA-seq data, with extensive epigenomics data and summary statistics from a large CRC GWAS conducted among European ancestry populations (78,473 CRC cases and 107,143 controls) using single-cell disease relevance score (scDRS), to investigate cell-of-origin populations underlying the CRC development. We conducted correlation analysis between gene expression and individual cell risk scores derived from scDRS. Additionally, we performed differential expression analysis comparing disease cell-of-origin populations with other cell populations at each stage.

Results: We identified multiple cell-of-origin populations associated with CRC, including absorptive cells (ABS) ($P < 1 \times 10\text{-}4$) and goblet cells (GOB) ($P < 7 \times 10\text{-}3$) in the normal colon, ABS ($P < 2 \times 10\text{-}3$), enteroendocrine cells (EE) ($P < 0.04$), and serrated-specific cells (SSC) ($P < 1 \times 10\text{-}4$) in serrated polyps, and ABS ($P < 9 \times 10\text{-}3$) and SSC ($P < 6 \times 10\text{-}4$) in adenomas. Among the previously reported 205 risk genes from TWAS, a majority show high correlations of their expressions with the risk scores of the single cells (median value $R^2 = 0.07, 0.14, 0.137$ at normal colon, serrated polyps, adenoma, respectively). Moreover, 57 of these TWAS-reported genes (27.8% of 205 genes) exhibited evidence of differential expression in disease cell-of-origin populations compared to other cell populations at a nominal p-value < 0.05 in at least one stage (Binomial test, $P < 0.01$ for all).

Conclusion: This study reveals the cell-of-origin populations that influence the development of CRC, and provides evidence of the role of risk genes in these populations. These findings are crucial for identifying causal genes and understanding the cellular mechanisms that drive the biology and etiology of CRC.

#6615 Reduced penetrance *BRCA1* and *BRCA2* pathogenic variants in clinical germline genetic testing.

T. Pal[1], E. Mundt[2], M. Richardson[3], E. Chao[3], T. Pesaran[3], T. P. Slavin[2], F. Couch[4], **A. N. Monteiro[5]**;
[1]Vanderbilt-Ingram Cancer Center, University Medical Center, Vanderbilt University, Nashville, TN, [2]Myriad Genetics, Salt Lake City, UT, [3]Ambry Genetics, Aliso Viejo, CA, [4]Mayo Clinic, Rochester, MN, [5]Moffitt Cancer Center, Tampa, FL

Despite the current binary clinical classification of variants (pathogenic versus benign), it is widely recognized that risk is a continuum. Prior studies have suggested the existence of reduced penetrance pathogenic variants (RPPVs), which pose challenges for identification, reporting, patient counseling and care. Through the current study, we sought to establish RPPVs as a new category of variants, with efforts focused specifically on *BRCA1* and *BRCA2* (*BRCA*).
We compiled, compared, and assessed data for *BRCA* RPPVs from two large clinical diagnostic laboratories to establish an initial set of reduced penetrance pathogenic variants. Specifically, candidate *BRCA* RPPVs provided by clinical diagnostic laboratories were compiled to identify those with the highest prior likelihood of being a RPPV, based on concordant interpretations. Evidence of reduced penetrance included: 1) the identification of biallelic Fanconi Anemia-affected carriers; 2) splicing, missense, and nonsense-mediated RNA decay (NMD)-escaping variants; 3) laboratory-validated cancer history weighting models; 4) published variant-specific risk estimation data; 5) extrapolation of a reduced-risk interpretation onto close match variants that are expected to have the same effect; and 6) functional data.
Sixteen candidate *BRCA* RPPV present in both lists from both laboratories were systematically assessed. For *BRCA1,* variants included c.5096G>A p.(Arg1699Gln) and variants impacting the canonical c.671 splice acceptor site. For *BRCA2,* variants included three frameshift (c.658_658delGT, c.9672dupA, c.9699_9702delTATG), two spliceogenic (c.8488-1G>A and c.8488-1G>T), and three missense (c.7878G>C, T, p.(Trp2626Cys); and c.9302T>G p.(Leu3101Arg)) variants.
Our study is the first to clearly evaluate and establish *BRCA* RPPVs as a new class of variants, based on consistency in results across 16 variants using different interpretation strategies between laboratories. These variants impart a moderately increased risk of breast cancer, often considered to be between 2-4 fold, which should be considered when determining risk-informed cancer prevention strategies. Furthermore, our study establishes a framework to harmonize interpretation and standardize reporting of *BRCA* RPPV, by providing evidence to support this new classification for 16 variants. Further work to define clinically meaningful risk thresholds and categories for reporting *BRCA* RPPV are needed to personalize cancer risks in conjunction with other risk factors.

#6616 Polygenic risk score associated with risk of upgrading and tumor features in a prospective cohort of prostate cancer patients on active surveillance.

L. B. Goss[1], M. Liu[2], Y. Zheng[2], B. Guo[1], D. V. Conti[3], C. A. Haiman[3], W. J. Catalona[4], J. S. Witte[5], D. W. Lin[1], L. F. Newcomb[2], B. F. Darst[2]; [1]University of Washington, Seattle, WA, [2]Fred Hutchinson Cancer Center, Seattle, WA, [3]University of Southern California, Los Angeles, CA, [4]Northwestern University Feinberg School of Medicine, Chicago, IL, [5]Stanford University, Stanford, CA

BACKGROUND: Active surveillance (AS) is now the preferred treatment strategy for the >50% of prostate cancer (PCa) patients diagnosed with low-risk disease, where five-year survival rates are >99%. However, AS requires frequent and costly healthcare visits. In a case-only study of AS patients, we investigated whether polygenic risk scores (PRS) could identify patients who may benefit from intensive vs passive surveillance to reduce these burdens.

METHODS: This study included 1,220 PCa patients on AS in the Canary Prostate Active Surveillance Study (PASS). A previously developed multi-ancestry PRS of 451 PCa risk variants (PRS_{451}) was constructed in PASS, along with a PRS of 400 variants, excluding 51 PSA-associated variants (PRS_{400}). Outcomes included upgrading and extreme upgrading at follow up and prostate volume, PSA, percent of biopsy cores with cancer, and Gleason grade at diagnosis. We investigated PRS associations with risk of upgrading with Cox proportional hazards regression adjusting for age at diagnosis and 10 principal components (PCs) of ancestry. Associations with risk of extreme upgrading were performed similarly but with a competing risk analysis, where the competing event was treatment. Discriminative ability was evaluated with Harrell's C-index. To better account for population structure, we also fit mixed models with fixed effects for PRS, age at diagnosis, and 10 PCs, with a random effect for a genetic relationship matrix.

RESULTS: Of the 1,220 AS patients, 38.5% (n=470) upgraded during the median 4.2 years of follow up and 85% (n=1041) self-reported as non-Hispanic White. In time-to-event analyses, each SD unit increase in PRS_{451} was associated with a 23% increased risk of upgrading ($P=4.2x10^{-5}$), while PRS_{400} was associated with a 27% increased risk ($P=1.6x10^{-6}$). PRS were similarly associated with 21% (95% CI=1.02-1.44, P=0.03) and 27% (95% CI=1.06-1.52, P=0.01) increased risk of extreme upgrading, respectively. Compared to a model with age at diagnosis, PCs, and clinical risk factors (C-index=0.617, 95% CI=0.590-0.644), including PRS_{400} slightly improved the ability to detect risk of upgrading (C-index=0.632, 95% CI=0.604-0.659). Mixed model results were highly consistent. Each SD unit increase in PRS_{400} was associated with 1.38 higher percentage points of biopsy cores with cancer (95% CI=0.76-2.00, $P=1.1x10^{-5}$), 1.48 cc smaller prostate volume (95% CI=-2.82, -0.14, P=0.03), and 0.18 ng/mL higher PSA (95% CI=0.01-0.35, P=0.05) at diagnosis. Except for PSA, associations were similar or weaker for PRS_{451}.

CONCLUSION: In patients on AS, high PRS was associated with increased risk of upgrading, extreme upgrading, smaller prostate volume, and possibly tumor multifocality. As such, PRS could inform the intensity of surveillance for low-risk PCa patients, reducing the burden of AS for patients with low risk of disease progression.

#6617 Oral microbiome and subsequent risk for head and neck squamous cell cancer development.

S. Kwak[1], M. Usyk[1], F. Wu[1], N. D. Freedman[2], W.-Y. Huang[2], M. L. Mccullough[3], C. Y. Um[3], M. J. Shrubsole[4], Q. Cai[4], C. Wang[1], H. Li[1], J. Ahn[1], R. B. Hayes[1];

[1]NYU Grossman School of Medicine, New York, NY, [2]National Cancer Institute, Bethesda, MD, [3]American Cancer Society, Atlanta, GA, [4]Vanderbilt-Ingram Cancer Center, Nashville, TN

Background: The oral microbiota may be involved in head and neck squamous cell cancer (HNSCC) etiology, yet current evidence is largely limited to bacterial 16S amplicon sequencing or small retrospective case-control studies. We tested whether any oral bacteria and/or fungi influence the subsequent risk of HNSCC development.

Methods: We conducted a prospective case-control study nested within three epidemiological cohorts: the ACS-Cancer Prevention Study-II Nutrition Cohort (ACS-CPS-II), the Prostate, Lung, Colorectal, and Ovarian Cancer Screening Trial (PLCO), and the Southern Community Cohort Study (SCCS). Among 159,840 cohort participants, 236 individuals developed HNSCC during an average of 5.1 years of follow-up, and 485 controls who remained HNSCC-free were selected by 2:1 frequency matching, by cohort, age, sex, race/ethnicity, and time since mouthwash collection. All participants provided mouthwash samples and were cancer-free at baseline. We characterized the oral bacterial microbiome, using whole-genome shotgun sequencing, and the oral fungal microbiome, using ITS sequencing. We assessed relative abundance of microbiome-wide bacterial and fungal taxa for association with HNSCC by ANCOM-BC analysis. We also evaluated selected oral pathogen complexes for association with HNSCC by logistic regression. A microbial risk score (MRS) for HNSCC risk was calculated from all risk-associated microbes.

Results: Overall microbiome diversity at baseline was not related to the subsequent risk of HNSCC; however, we found that 13 oral bacterial species were differentially associated with development of this disease (P<0.05), including newly identified *Prevotella salivae*, *Streptococcus sanguinis*, *Leptotrichia sp*, and several species belonging to *Beta-* and *Gamma-proteobacteria*. Furthermore, *a priori* periodontal pathogen complexes were associated with a higher risk of HNSCC ("red/orange" complex, OR=1.06, 95% CI=1.00-1.12). We did not identify any fungal taxa associated with HNSCC risk. Together, an MRS constructed for risk-associated bacteria and bacterial periodontal complexes conferred a 50% increase in HNSCC risk, per standard deviation increase in the MRS (multivariate OR=1.50, 95% CI=1.21-1.85).

Conclusions: Our research yields compelling evidence that oral bacteria are a risk factor for the development of HNSCC. The identified bacteria and bacterial complexes hold promise for identifying high-risk individuals and may further lead to personalized prevention approaches for HNSCC.

#6618 Pleiotropic GATA3 locus is associated with multiple childhood cancers: harnessing the existing data from the St. Jude Lifetime Cohort and the Childhood Cancer Survivor Study for genetic etiology research.

C. Chen[1], X. Zhang[2], Q. Dong[2], H. L. Mulder[2], J. Easton[2], X. Ma[2], J. Zhang[2], J. Yang[2], K. E. Nichols[2], G. T. Armstong[2], K. K. Ness[2], M. M. Hudson[2], H. Wang[1], N. Chatterjee[3], C. Im[4], Z. Wang[2];

[1]Shanghai Jiao Tong Univ., School of Med., Shanghai, China, [2]St.Jude Children's Research Hospital, Memphis, TN, [3]Johns Hopkins University, Baltimore, MD, [4]University of Minnesota, Minneapolis, MN

Background: A genetic variant (rs3824662) at *GATA3* was previously associated with risk of Philadelphia chromosome-like acute lymphoblastic leukemia (Ph-like ALL) and relapse. Our recently published childhood Hodgkin lymphoma (HL) study identified a genome-wide significant association for another genetic variant (rs3781093) in high linkage disequilibrium (D'=1.0, R^2=0.91) with rs3824662. We hypothesize that *GATA3* is a pleiotropic locus associated with multiple childhood cancers.

Methods: The study was performed by combining 3 cohorts of childhood cancer survivors: the St Jude Lifetime Cohort Study (SJLIFE), the original and expansion cohorts of the Childhood Cancer Survivor Study (CCSS). The CCSS original cohort had SNP array genotyping and imputation, and the SJLIFE and CCSS expansion cohort underwent whole-genome sequencing. Associations between the variants mapped to *GATA3* and risks of different cancer types were analyzed (a specific cancer type was selected as the case group and all other unselected cancer types served as controls, then repeated for 13 cancer types). Summary statistics were subsequently analyzed with the ASSET (Association analysis for SubSETs) method which is powerful for pooling association signals across multiple cancer types when true effects may exist only in a subset and be in opposite directions across cancer types.

Results: Genotype data were available for 11623 childhood cancer survivors (5325 from the CCSS original cohort, 2428 from the CCSS expansion cohort, and 3870 from the SJLIFE, all European ancestry) were initially considered. After excluding individuals with dual enrollment or as outliers in the principal components analysis (n=667), a total of 10956 individuals remained for genetic association analysis. We identified a bi-directional association for a subset of childhood cancers with rs3781093 (2-sided P value of 6.22×10^{-19}): the same effect allele (C) was associated with increased risk of ALL or soft tissue sarcoma [STS] (OR=1.21; 95% CI=1.13-1.29; $P=7.4\times10^{-9}$), and was associated with decreased risk of HL (OR=0.66; 95% CI=0.59-074; $P=1.80\times10^{-12}$). The frequencies of the effect allele (C) for rs3781093 in ALL cases (17.9%), STS cases (17.8%) and HL cases (12.5%) relative to non-cancer community controls in the SJLIFE (15.6%) and non-cancer gnomAD samples (14.9%) corroborate this finding. In our combined dataset, there were 1380 Hodgkin lymphoma cases, 2961 ALL cases and 692 STS cases.

Conclusion: We discovered a novel variant in the *GATA3* locus exhibiting pleiotropy with both tumor-promoting and protective effects, suggesting a shared mechanistic pathway involving *GATA3* may underlie the carcinogenesis for ALL, STS and HL. Conducting systematic searches for childhood cancer pleiotropy represents an important research direction.

#6619 Dynamic prediction with repeated mammogram images improves 5-year breast cancer risk performance.

G. A. Colditz[1], R. M. Tamimi[2], B. Rosner[3], **S. Jiang**[1];

[1]Washington University School of Medicine in St. Louis, St. Louis, MO, [2]Weill Cornell Medical School, New York, NY, [3]Harvard medical school, Boston, MA

Background: Increasing use of digital screening mammography opens potential to add individualized dynamic measures of breast image history to predict future breast cancer risk. Current prediction models use a single mammogram measure, usually breast density, at one point in time, to add to prediction models based on established risk factors. Our previous work has shown that change in each breast over time is related to risk of diagnosis with breast cancer.

Methods: We apply a dynamic prediction model that includes full field digital mammogram in each breast to predict future 5-year risk. Data from Joanne Knight Breast Health Cohort (JKBHC) serve as training population with 290 pathology-confirmed breast cancer cases and 658 controls sampled with a total number of 8,712 craniocaudal (CC) view mammograms for analysis. Nurses' Health Study 2 (NHS2) serves as the external validation with 188 cases and 462 controls sampled with a total number of 3,712 CC-views. The dynamic risk prediction model aims to estimate the probability of future breast cancer risk conditional on the past history of the longitudinal mammograms. We train the model on the JKBH cohort, retaining 20% for testing and 15% for validation. We report a time dependent AUC when evaluating model performance.

Results: The mean age of women was 56.6 years at entry to cohort; 81.3% were white. Adding trajectory of mammogram images in each breast to a model improved performance. The mean number of mammograms conditional on 5 years of observation in JKBHC was 3.36 (1.49) and in NHS2 2.36 (1.53). We obtained a 5-year dynamic AUC of 0.81 (0.05) in the JKBHC internal validation and 0.77 (0.06) in the NHS2 external validation. Model performance was comparable in pre- and postmenopausal women. Because breasts with high mammographic density hinder detection of tumors we stratify analyses by dense and non-dense at baseline. Among women with dense breasts at baseline (BIRADS C and D), we observe a dynamic 5-year risk AUC = 0.77. In the subgroup with less dense breasts (BIRADS A and B) we observe AUC = 0.74.

Conclusions: With this approach we can accommodate the irregularly observed time-varying images and project only partial information prior to doing the prediction. Adding trajectory of mammogram history in each breast improves 5-year breast cancer risk prediction beyond models used in clinic today.

TUMOR BIOLOGY: Nonclinical Models of Cancer
Minisymposium

#6620 PDX models of TNBC established from pre- and post-therapy tumors identify vulnerabilities of resistant disease.

A. L. Rinkenbaugh[1], Y. Qi[1], R. T. Powell[2], S. Cai[1], J. Shao[1], F. Baameur Hancock[1], L. Guo[2], X. Zhang[1], S. Jeter-Jones[1], C. Fu[1], R. Gould[1], J. B. White[1], C. Stephan[2], G. V. Echeverria[1], P. J. Davies[2], S. Moulder[1], W. Symmans[1], J. T. Chang[3], H. Piwnica-Worms[1];
[1]UT MD Anderson Cancer Center, Houston, TX, [2]Texas A&M Health Science Center, Houston, TX, [3]University of Texas Health Science Center, Houston, TX

Chemotherapy, along with the PD1 inhibitor pembrolizumab, is the recommended standard of care for patients with primary triple negative breast cancer (TNBC). Nearly half of TNBC patients treated with standard neoadjuvant chemotherapy (NACT) have excellent responses. However, those patients with significant residual cancer burden (RCB) after NACT are at high risk of recurrence or metastatic relapse within two years. Due to the challenges posed by the inter- and intratumoral heterogeneity of TNBC, it is critical to develop appropriate models for predicting and overcoming therapy resistance. We established a collection of 92 orthotopic patient-derived xenograft (PDX) models of TNBC from 84 patients before, during, and after NACT while they were enrolled in the ARTEMIS trial (NCT02276443) at MD Anderson Cancer Center. Serial biopsies were obtained from patients prior to treatment (pre-NACT), from poorly responsive disease after four cycles of Adriamycin and cyclophosphamide (AC, mid-NACT), after a 3-month course of additional chemotherapy and/or different experimental therapies in cases of AC resistance (post-NACT), and from the metastatic lesions of two patients. The collection includes 12 longitudinal sets. Models were established from chemo-sensitive and -resistant tumors, but engraftment success was higher from those cancers that proved to be treatment resistant (RCB II/III). The PDX collection includes models encompassing a broad heterogeneity of chemotherapy responses, histologic features, and molecular TNBC subtypes. In addition, the majority of models develop spontaneous lung metastases. Whole exome sequencing demonstrated conservation of mutations between patient tumors and corresponding PDX models, with *TP53* being the most commonly mutated gene. A similar comparison of patient and PDX transcriptomes revealed conservation of signaling pathway signatures, with those related to immune and stromal interactions being the most variable, as anticipated when adapting human tumors to growth in mice. The subclonal architecture of the tumors exhibited little overall change throughout NACT, suggesting that selection for resistant subclones is not likely to be a significant contributor to resistance. Tumor cells from the longitudinal PDX collections were subjected to high throughput drug susceptibility profiling to identify targetable vulnerabilities associated with resistance to NACT. We found that post-NACT tumors exhibited enhanced sensitivity to drugs targeting protein homeostasis pathways. Preclinical studies with pevonedistat validated the neddylation pathway as an effective target in chemoresistant TNBC.

#6621 Development of a melanocyte lineage-specific knockout system in zebrafish.

S. Perlee[1], Y. Ma[1], J. Swanson[2], Z. Ming[3], J. Xia[1], T. Lionnet[2], M. McGrail[3], R. White[4];

[1]Memorial Sloan Kettering Cancer Center, New York, NY, [2]NYU Grossman School of Medicine, New York, NY, [3]Iowa State University, Ames, IA, [4]Ludwig Cancer Institute, Oxford, United Kingdom

Zebrafish have emerged as an ideal model organism for investigating melanocyte and melanoma biology. While CRISPR-Cas9 technology has significantly advanced our understanding of gene functions in zebrafish, two challenges remain: 1) how do we knock out embryonic lethal genes in adult melanocytes? and 2) how do we knock out tumor promoting genes (rather than tumor suppressors)? To address this, we have developed a new transgenic line in which Cas9 is knocked into the melanocyte-specific endogenous *mitfa* locus. To test this system in normal melanocytes, Tg(mitfa:Cas9) embryos were injected with a plasmid containing albino sgRNA. Cells with integration of this plasmid exhibited almost complete loss of pigmentation, demonstrating the high efficiency of our approach. This system can now be rapidly used to knock out embryonic essential genes specifically in melanocytes and evaluate the phenotype of adult fish. In melanoma, the commonly available zebrafish lines overexpress the oncogene BRAFV600E in melanocytes with germline knockout of tp53. This is not comparable to the situation in humans, where global p53 loss is rare. By utilizing our mitfa:Cas9 system, we have generated tumors with melanoma-specific loss of tp53 or ptena/b, thereby eliminating non-specific tumors that originate from knockout of tumor suppressors in other cell types. Using this system, we are now testing whether knockout of tumor promoting genes delays melanoma onset and progression, something that has previously been difficult to efficiently achieve in zebrafish. In addition to specificity, an additional advantage of our system is that we can create nearly complete knockout of genes in the melanocytes by the F1, rather than the F2 generation. This saves several months of time and reduces the number of uninformative animals without the relevant genotype. Collectively, our system provides a highly efficient mechanism to study essential genes in melanocytes and melanoma in the zebrafish system.

#6622 Identification of early oncogenic lesions following concomitant Vhl and Pbrm1 loss in the murine kidney.

Joanna Lima, Samvid Kurlekar, Norma Masson, Ayslan B. Barros, Maria Fernanda Soares, Christopher W. Pugh, Julie Adam, Peter J. Ratcliffe

University of Oxford, Oxford, United Kingdom

Characterizing the early events preceding tumorigenesis is a major challenge in understanding cancer. To address this, we are investigating the paradigm of clear cell renal cell carcinoma (ccRCC) that is driven by the biallelic loss of the von Hippel Lindau (*VHL*) tumor suppressor gene. Though VHL loss is required, additional mutations have been found in the evolution of the cancer, most commonly in Polybromo-1 (*PBRM1)*, a subunit of the PBAF SWI/SNF chromatin remodeling complex. Concomitant *Vhl* and *Pbrm1* deletion, but not *Vhl* deletion alone, in the renal tubular epithelium (RTE) has been reported to be sufficient to drive the formation of renal tumors in mice. However, the early *in vivo* consequences of *Vhl* loss, and the exact requirement for *Pbrm1* loss to tumorigenesis remain poorly studied. We have previously reported the development of a novel lineage-tracing model of *Vhl* deletion that directly couples loss of a conditional *Vhl* allele to the expression of a tdTomato reporter and allows accurate identification and retrieval of marked *Vhl*-null cells. In the work reported here, we have combined this system with conditional *Pbrm1* deletion using an RTE-restricted *Pax8-CreERT2* to precisely identify and assay *Vhl*/*Pbrm1*-null cells. We describe the histological abnormalities specifically comprising *Vhl*/*Pbrm1*-null cells observed at early (1-3 weeks), intermediate (10 months), and late (17 months) intervals post recombination. We found that *Vhl*/*Pbrm1*-null cells formed extensive 'tumorlets', disorganized, multilayered tubules, and cystic dilated tubules specifically in the renal cortex at 17 months post recombination. Immunohistochemistry confirmed that all epithelial cells in the lesions were *Vhl*/*Pbrm1* null and expressed HIF1 and HIF2. These lesions contained cycling cells as identified by dual tdTomato/Ki67 staining, foci of immune cells and were strikingly surrounded by cells expressing high levels of p-ERK. We then traced these lesions to earlier timepoints, and observed *Vhl*/*Pbrm1*-null lesions resembling 'tumorlet' precursors and disorganized tubules at 10 months post recombination specifically in the renal cortex. Interestingly, these precursors were encompassed by macrophages and could be discerned *in situ* by a ring of p-ERK-expressing cells surrounding these lesions. No similar lesions were detected at 3 weeks after recombination. Interestingly, the presence of cortical lesions was associated with a region-specific expansion of the total *Vhl*/*Pbrm1*-null population over time. Our data suggest that morphological abnormalities arise after a general proliferation of *Vhl*/*Pbrm1*-null cells in the renal cortex and from a subset of cells expressing specific markers. We are now comparing the differential gene expression patterns of *Vhl*-null cells and *Vhl*/*Pbrm1*-null normal and transformed cells at single cell resolution to expand on these observations.

#6623 Ala59 mutants of KRAS cooperate with Nf1 loss to enhance colon tumorigenesis.

C. W. Johnson[1], E. M. Terrell[2], J. Cook[1], B. Shui[1], E. O'Donoghue[1], S. Hull[1], M. Hee Yang[1], S. Sheth[1], R. Yaeger[3], S. Kopetz[4], D. K. Morrison[2], K. Haigis[1]; [1]Dana-Farber Cancer Institute, Boston, MA, [2]National Cancer Institute, Frederick, MD, [3]Memorial Sloan Kettering Cancer Center, New York, NY, [4]MD Anderson Cancer Center, Houston, TX

Understanding the role of KRAS allele heterogeneity in tumor development, and its influence on therapeutic efficacy, is critical for the improvement of cancer treatment. The Kirsten rat sarcoma (*KRAS*) gene is the most frequently mutated oncogene in colorectal cancer (CRC) and patients with CRC tumors positive for KRAS mutations have poorer outcomes and limited treatment options. Extensive work over the past four decades has shown that common oncogenic alleles of *KRAS* are associated with hyperactivation of the MAPK signaling pathway (i.e. RAF/MEK/ERK), and it is for this reason that patients with KRAS mutant tumors are excluded from targeted therapies against EGFR. Recently, we characterized two alleles of KRAS, $KRAS^{A59T}$ and $KRAS^{A59E}$, that paradoxically promote KRAS activation but are impaired in their ability to promote BRAF dimerization (*Johnson et al. Mol Cell. 2022. PMID: 35202574*). Consistent with these biochemical functions, $KRAS^{A59T}$ and $KRAS^{A59E}$ are enriched in CRC tumors that already have genetic alterations in genes that regulate MAPK signaling (e.g. EGFR, BRAF, NRAS, NF1). Further, unlike other described oncogenic alleles of KRAS, clinical data suggest that these $KRAS^{A59T}$ and $KRAS^{A59E}$ may not confer intrinsic resistance to anti-EGFR therapies at all. While $KRAS^{A59T}$ and $KRAS^{A59E}$ may not promote BRAF dimers, here we show that $KRAS^{A59T}$ and $KRAS^{A59E}$ does promote dimerization between ARAF and CRAF, and using an unpublished conditional mouse mode of K-Ras (i.e. LSL-K-Ras^{A59E}) we tested (1) whether Ala59 alleles are oncogenic or (2) require cooperation with additional MAPK pathway activating mutations, and (3) whether Ala59 alleles can promote intrinsic resistance to EGFR inhibition. Here, we show that endogenous K-Ras^{A59E} can disturb colon homeostasis and decrease mouse survival in an autochthonous colon tumor model, demonstrating that A59E alone is an oncogenic allele of KRAS in the colon. Breeding of LSL-K-Ras^{A59E} mice with mice harboring a conditional knockout of Nf1 (i.e. $Nf1^{fl/fl}$), a GTPase activating protein (GAP) that promotes activation of wildtype RAS, show that combined expression of K-Ras^{A59E} and wildtype RAS activation cooperatively perturb colon homeostasis and decrease mouse survival. Thus, while $KRAS^{A59E}$ may not require a second genetic alteration to activate the MAPK signaling pathway, it can cooperate with these alterations to increase the severity of disease. Finally, using mouse colon derived organoids, we show that endogenous K-Ras^{A59E} neither promotes EGF independence of organoid growth nor confers on these organoids a resistance to EGFR inhibition. Thus, our data support a unique role for RAF dimer function in in KRAS mutant tumors of the colon in both development and sensitivity to drugs, as well as argue for the inclusion of $KRAS^{A59T}$ and $KRAS^{A59E}$ bearing CRC tumors in anti-EGFR therapies.

#6624 MYC promotes lobuloalveologenesis and mammary tumorigenesis in male mice.

E. M. Pulver[1], E. van der Burg[1], A. Drenth[1], J. Yemelyanenko[1], N. Ravensbergen[1], R. de Bruijn[1], S. Klarenbeek[1], J.-Y. Song[1], M. Boeije[1], B. Siteur[1], N. Proost[1], C. Scheele[2], P. Bouwman[3], J. Jonkers[1];

[1]Netherlands Cancer Institute, Amsterdam, Netherlands, [2]KU Leuven, Leuven, Belgium, [3]Leiden University, Leiden, Netherlands

Male breast cancer is a rare disease that is largely overlooked and clinically regarded to recapitulate female breast cancer biology. The worse overall outcome for male patients compared to females, however, underscores inadequate disease management and a sex-based divergence in disease biology. To gain more insight into male breast biology and pathology, we used mouse models of triple-negative breast cancer and 3D whole-mount confocal imaging techniques to evaluate both *in vivo* and *ex vivo* mammary gland development, tumor formation, and hormone signaling dependence. Our results show that *Myc* overexpression in collaboration with *Trp53* deficiency drives mammary tumorigenesis in male mice. We show that MYC overexpression promotes estrogen-independent formation of lobuloalveolar structures, which progress into tumors with a similar histology and immune landscape as female mammary tumors but with significantly more genomic instability. In female mice, MYC overexpression bypasses the dependency on paracrine estrogen signaling in mammary tumorigenesis. These data provide robust evidence that MYC overrides mammary tumor estrogen dependence and abolishes the tumor-preventive effect of a low-estrogen environment. Supporting this notion, *in vitro* experiments in human female breast cancer cell lines indicate that MYC overexpression may functionally contribute to endocrine therapy resistance and therefore could possibly serve as a prognostic biomarker or clinically targetable pathway for treating both male and female breast cancers. Collectively, this preclinical work presents new insights into male mammary gland biology and mechanisms of cancer progression that might translate to a broader range of breast cancers in the clinic.

#6625 Development of novel mixed-cell models to capture heterogeneity in castration-resistant prostate cancer.

S. Jena[1], D. Kim[1], A. M. Lee[1], W. Zhang[1], S. Dehm[2], R. Huang[1];
[1]University of Minnesota, College of Pharmacy, Minneapolis, MN, [2]University of Minnesota, Medical School, Minneapolis, MN

Heterogeneity is ubiquitous in cancer and treatment responses among patient cohorts are highly variable, leading to drug resistance and disease relapse. Yet, preclinical drug screening is usually performed in cell lines or patient cells, one at a time, without consideration of cancer heterogeneity. Consequentially, positive outcomes obtained in the preclinical stage do not translate well into subsequent clinical successes. Castration-resistant prostate cancer (CRPC) is a highly lethal form of prostate cancer (PC) exhibiting a high degree of genetic and phenotypic heterogeneity with very few therapeutic options. Therefore, we created mixed-cell models depicting heterogeneity in various clinical contexts, where multiple PC cell lines representative of distinct CRPC tumor variants were labeled and combined in co-cultures to mimic the complex molecular landscape of CRPC patient cohorts. Specifically, transcriptomic profiles of PC cell lines were clustered with patient tumor specimens to identify cell lines that are genetically similar to distinct patient clusters representing CRPC tumor subtypes. Since heterogeneity has been linked to the clinical efficacy of combinatorial therapies, we applied these models to evaluate drug combinations. A combination of docetaxel and dasatinib that was previously assessed in a PC trial, was tested in the mixed-cell model and experimental findings concurred with the published clinical results, demonstrating the utility and accuracy of the model. Additionally, a computational model, IDACombo, was employed to nominate novel potentially efficacious drug combinations using monotherapy response data of cancer cell lines, a number of which were successfully validated in the mixed-cell model. More importantly, we demonstrated that while individual cell line screens may result in erroneous conclusions, combination efficacy can be accurately measured in a heterogeneous cell pool emulating a diverse patient cohort. We further explored phenotypic heterogeneity in advanced disease states, by mixing parent and standard-of-care (SOC)-resistant CRPC clonal variants. Drugs with selective potency in the resistant (vs. the parent) clone were computational prioritized and when combined with the SOC and tested in the mixed-cell models, outperformed either monotherapy. Additionally, we investigated the effects of altering the relative proportion of the constituent clones to mimic different stages of acquired therapy resistance. Furthermore, we generated mixed-cell xenograft models by subcutaneously injecting the labeled cell-line mixtures in mice and characterized the harvested tumors to detect and quantify the individual subpopulations. Development of these preclinical models holds enormous promise not only for advancing novel therapeutic strategies for cancer, but also for providing insights into the mechanisms of resistance and recurrence.

#6626 Functional and molecular interrogation of a high-plasticity cell state in lung cancer.

J. E. Chan[1], C.-H. Pan[1], C. Sussman[1], H. Styers[1], E. Brown[1], G. Hartmann[1], B. Meskauskaitė[1], M. Blum[1], S. Ding[1], S. Torborg[2], Z. Li[3], S. Joost[1], E. Rivas-Hernandez[1], T. Norman[1], R. Chaligne[1], Y. Yan[1], T. Tammela[1],

[1]Memorial Sloan Kettering Cancer Center, New York, NY, [2]Tri-Institutional MD-PhD Program, New York, NY, [3]Weill-Cornell Graduate School of Medical Sciences, New York, NY

Despite recent advancements in lung adenocarcinoma (LUAD) treatment, mortality remains high. Thus, a need exists for novel therapeutic concepts to enhance treatment efficacy and improve patient survival. Cancer cell plasticity, the capacity for cancer cells to differentiate and adapt to cell-extrinsic pressures, drives LUAD progression and enables treatment resistance. We discovered a molecularly distinct "high-plasticity cell state" (HPCS), which emerges during the initial stages of tumor development and is maintained in established tumors, comprising 10-15% of the cancer cell pool. We hypothesized that the HPCS is critical for tumor progression and drug resistance. To functionally interrogate this cell state, we engineered a novel genetic system that enables both *in situ* ablation (via a suicide gene) and longitudinal lineage tracing (via secreted luciferases) of the HPCS in an autochthonous genetically engineered mouse LUAD model. Lineage-tracing revealed the HPCS harbors high differentiation potential (plasticity) and growth potential *in situ*. Strikingly, ablation of the HPCS led to robust tumor regression and growth suppression. Motivated by these findings, we sought to identify molecular drivers of the HPCS using an *in vivo* multiplexed gene perturbation approach coupled to single-cell RNA sequencing. This effort led to the identification of central transcriptional plasticity drivers. This study motivates the therapeutic targeting of the HPCS in lung cancer and uncovers candidate targets.

TUMOR BIOLOGY: The Microenvironment: Beyond Surrounding the Tumor
Minisymposium

#6627 Boosting macrophage-specific BCAA oxidation enhances immune activation within the tumor microenvironment and diminishes tumor growth in pancreatic cancer.

G. Mirji[1], S. A. Bhat[1], Z. Schug[1], B. Z. Stanger[2], Z. Arany[2], R. S. Shinde[1];
[1]The Wistar Institute, Philadelphia, PA, [2]University of Pennsylvania, Philadelphia, PA

Treating pancreatic ductal adenocarcinoma (PDAC) poses a significant challenge, mainly due to therapy resistance linked to the immunosuppressive tumor microenvironment (TME) within PDAC tumors. This TME is characterized by a fibrotic stroma and an abundance of immunosuppressive cells, notably tumor-associated macrophages (TAMs). TAMs crucially hinder effector T cell activity and contribute to T cell exhaustion. Redirecting TAMs toward an immunostimulatory state has emerged as a promising approach in PDAC treatment. Recent investigations, including our own studies, reveal a profound influence of metabolic pathways on the immune phenotype of TAMs. Specifically, dysregulation in branched-chain amino acid (BCAA) metabolism has been observed in PDAC patients, manifesting as elevated circulating BCAA levels correlating with a doubled risk of PDAC development. However, the extent to which BCAA metabolism influences TAM phenotype and anti-tumor immune responses remains a largely unexplored territory, presenting a challenge for PDAC treatment. Our focus revolves around understanding how heightened BCAA levels in PDAC affect TAM phenotype, the immunosuppressive tumor environment, and tumor progression. Employing an orthotopic PDAC model and genetically modified mice, specifically BCKDKfl/fl BCKDK LysMcre/+ (mimicking increased BCAA oxidation), alongside a BCKDK-targeting pharmacological inhibitor (BT-2), multicolor flow cytometry, and in vitro models, our research has revealed crucial insights. We found a diminished expression of BCAA oxidation genes in TAMs compared to normal pancreatic macrophages. Interestingly, M1 and M2 macrophages seemed to utilize BCAAs differently, reflected in varying levels of TCA cycle intermediates derived from BCAA oxidation. Notably, boosting BCAA oxidation specifically in TAMs through genetic modifications resulted in reduced PDAC growth associated with an enhanced immunostimulatory TAM phenotype and activation of CD8+ T cells in the TME. Conversely, administering BCAAs induced an immunosuppressive TAM phenotype, fostering PDAC growth, suggesting a direct influence of BCAAs on TAM phenotype. Pharmacologically enhancing BCAA oxidation via BT-2 bolstered immune activation within the tumor environment and reduced PDAC growth. Intriguingly, our analysis of publicly available data unveiled a significant correlation between high BCAA oxidation and favorable responses to anti-PD1 therapy in cancer patients. Our findings emphasize the pivotal role of BCAA metabolism in shaping the immune landscape of PDAC, offering potential avenues for therapeutic interventions targeting TAMs and mitigating TME immunosuppression.

#6628 Mapping the spatial and molecular determinants of macrophage heterogeneity in breast cancer.

Nir Ben Chetrit[1], Xiang Niu[1], Jesus Sotelo[1], Ariel D. Swett[1], Vinagolu K. Rajasekhar[2], Maria S. Jiao[3], Caitlin M. Stewart[1], Priya Bhardwaj[1], Sanjay Kottapalli[1], Saravanan Ganesan[1], Pierre-Louis Loyher[4], Catherine Potenski[1], Kristy A. Brown[1], Neil M. Iyengar[5], Dilip D. Giri[6], Scott W. Lowe[7], John H. Healey[2], Frederic Geissmann[4], Irit Sagi[8], Johanna A. Joyce[9], Dan A. Landau[1]

[1]Medicine, Weill Cornell Medicine, New York, NY,[2]Department of Surgery, Memorial Sloan Kettering Cancer Center, New York, NY,[3]Center of Comparative Medicine and Pathology, Memorial Sloan Kettering Cancer Center, New York, NY,[4]Immunology Program, Memorial Sloan Kettering Cancer Center, New York, NY,[5]Department of Medicine, Memorial Sloan Kettering Cancer Center, New York, NY,[6]Department of Pathology, Memorial Sloan Kettering Cancer Center, New York, NY,[7]Cancer Biology and Genetics Program, Memorial Sloan Kettering Cancer Center, New York, NY,[8]Department of Biological Regulation, Weizmann Institute of Science, Rehovot, Israel,[9]Department of Oncology, University of Lausanne, Lausanne, Switzerland

Tumor-infiltrating macrophages support critical steps in tumor progression, and their accumulation in the tumor microenvironment (TME) is associated with adverse outcomes and therapeutic resistance across human cancers. In the TME, macrophages adopt diverse phenotypic alterations, giving rise to heterogeneous immune activation states and induction of cell cycle. While the transcriptional profiles of these activation states are well-annotated across human cancers, the underlying signals that regulate macrophage heterogeneity and accumulation remain incompletely understood. Here, we leveraged a novel ex vivo organotypic TME (oTME) model of breast cancer, in vivo murine models, and human samples to map the determinants of functional heterogeneity of TME macrophages. We identified a subset of F4/80high Sca-1+ self-renewing macrophages maintained by type-I interferon (IFN) signaling and requiring physical contact with cancer-associated fibroblasts. We discovered that the contact-dependent self-renewal of TME macrophages is mediated via Notch4, and its inhibition abrogated tumor growth of breast and ovarian carcinomas in vivo, as well as lung dissemination in a PDX model of triple-negative breast cancer (TNBC). Through spatial multi-omic profiling of protein markers and transcriptomes, we found that the localization of macrophages further dictates functionally distinct but reversible phenotypes, regardless of their ontogeny. Whereas immune-stimulatory macrophages (CD11C+CD86+) populated the tumor epithelial nests, the stroma-associated macrophages (SAMs) were proliferative, immunosuppressive (Sca-1+CD206+PD-L1+), resistant to CSF-1R depletion, and associated with worse patient outcomes. Notably, following cessation of CSF-1R depletion, macrophages rebounded primarily to the SAM phenotype, which was associated with accelerated growth of mammary tumors. Our work reveals the spatial determinants of macrophage heterogeneity in breast cancer and highlights the disruption of macrophage self-renewal as a potential new therapeutic strategy.

#6629 Cancer-associated nerves regulate anti-tumor immunity in pancreatic cancer.

Ruiyuan Xu, Jianlu Song, Yuan Chen, Xinpeng Yin, Chengcheng Wang, Yupei Zhao

Peking Union Medical College Hospital, Chinese Academy of Medical Sciences and Peking Union Medical College, Beijing, China

Nerves serve an emerging component of the tumor microenvironment (TME), contributing to tumorigenesis and cancer progression. Neural invasion (NI) is a common feature of pancreatic ductal adenocarcinoma (PDAC), accounting for distant metastasis and local recurrence. However, the mechanism by which tumor associated nerves (TANs) regulate anti-tumor immunity remains largely elusive. Here, we investigated the association between TANs and immunosuppressive TME to develop more effective therapeutic strategies for PDAC. Using tumor samples of PDAC patients, we identified that the nerves invaded by cancer cells showed increased adrenergic activation accompanied with no parasympathetic or sensory innervation changes. Patients with severe NI were associated with increased catecholamine levels. Additionally, single-cell RNA-sequencing and spatial transcriptome analysis of tumors from patients with PDAC revealed that peri-neural niches of severe NI patients were characterized by decreased $CD8^{\pm}$ T cells and increased activity of M2 polarization of tumor-associated macrophages (TAMs), and regulatory T (Treg) cells, which was validated by multiplexed immunofluorescence staining. We further identified that $CD8^{\pm}$ T cells expressing β-adrenaline receptors (β-ARs) reduced proliferation and cytokine production when exposure to catecholamines in a dose-dependent manner or co-cultured with dorsal root ganglia pretreated with cancer cells. $Kras^{LSL\text{-}G12D}$; $p53^{LoxP}$; Pdx1-CreER (KPC) mice treated with catecholamines accelerated tumor progression by inhibiting T cell-mediated antitumor responses, which was abrogated by surgical sympathectomy of KPC mice. Especially, in an orthotopic PDAC model, nonselective β-blocker propranolol in combination with immune checkpoint blockade (ICB) significantly enhanced active $CD8^{\pm}$ T cells with concurrent reduced tumor growth. We suggest a novel regulatory mechanism of inhibiting anti-tumor immunity that can promote cancer progression mediated by TANs invasion. These data establish a close connection between the nerves, cancer cells, and immune cells and provide the potential novel targets of therapeutic approaches in PDAC.

#6630 Non-cell-autonomous cancer progression from chromosomal instability.

J. Li[1], M. Hubisz[2], E. Earlie[2], M. Duran[1], C. Hong[1], A. Varela[2], E. Lettera[1], M. Deyell[2], B. Tavora[3], J. Havel[3], P. Su[3], A. Dipak Amin[4], K. Budre[2], E. Kamiya[2], J.-A. Cavallo[1], C. Garris[5], S. Powell[1], J. Reis-Filho[1], H. Wen[1], S. Bettigole[3], A. Khan[1], B. Izar[4], E. Parkes[6], A. Laughney[2], S. Bakhoum[1];
[1]Memorial Sloan Kettering Cancer Center, New York, NY, [2]Weill Cornell Medicine, New York, NY, [3]Volastra Therapeutics Inc, New York, NY, [4]Columbia University Medical Center, New York, NY, [5]Harvard Medical School, Boston, MA, [6]University of Oxford, Oxford, United Kingdom

Chromosomal instability (CIN) is a driver of cancer metastasis, yet the extent to which this effect depends on the immune system remains unknown. Using ContactTracing—a newly developed, validated and benchmarked tool to infer the nature and conditional dependence of cell-cell interactions from single-cell transcriptomic data—we show that CIN-induced chronic activation of the cGAS-STING pathway promotes downstream signal re-wiring in cancer cells, leading to a pro-metastatic tumor microenvironment. This re-wiring is manifested by type I interferon tachyphylaxis selectively downstream of STING and a corresponding increase in cancer cell-derived endoplasmic reticulum (ER) stress response. Reversal of CIN, depletion of cancer cell STING or inhibition of ER stress response signaling abrogates CIN-dependent effects on the tumor microenvironment and suppresses metastasis in immune competent, but not severely immune compromised, settings. Treatment with STING inhibitors reduces CIN-driven metastasis in melanoma, breast and colorectal cancers in a manner dependent on tumor cell-intrinsic STING. Finally, we show that CIN and pervasive cGAS activation in micronuclei are associated with ER stress signaling, immune suppression and metastasis in human triple-negative breast cancer, highlighting a viable strategy to identify and therapeutically intervene in tumors spurred by CIN-induced inflammation.

#6631 Aging influences the pancreatic ductal adenocarcinoma tumor immune microenvironment to promote features of immunosuppression.

E. Kartalia[1], J. M. Leatherman[1], J. W. Lee[1], E. M. Jaffee[1], A. T. Weeraratna[2], **D. J. Zabransky**[1];
[1]Johns Hopkins University, Baltimore, MD, [2]Johns Hopkins University School of Public Health, Baltimore, MD

Advancing age is the strongest independent risk factor for the development of pancreatic ductal adenocarcinoma (PDAC) and a negative prognostic factor. PDACs are typically immunologically “cold” tumors and do not often respond to currently approved immunotherapy treatment approaches. How aging may alter non-malignant cells, such as fibroblasts and immune cell populations, in the PDAC tumor microenvironment (TME) to decrease anti-tumor immune responses is not understood.

We identified that aged microenvironments significantly alter the growth and progression of PDAC tumors. Orthotopic KPC and Panc02 mouse PDAC cell line injections into the pancreata of aged (>64-week-old) compared to young (6-8-week-old) C57BL/6 mice result in more rapid tumor growth and increased frequency of liver metastases *in vivo*. Tumors from aged mice have high expression of the TGFβ family member GDF-15 and hyperactivation of AKT signaling driven by the release of secreted factors from aged pancreatic fibroblasts.

We found that in aged microenvironments there is a marked reduction in the number of CD8+ T cells and an increase in FoxP3+ regulatory T cells in primary orthotopic pancreatic tumors using the KPC and Panc02 models. In addition, we performed portal vein injections to establish liver metastases to study the differences in immune cell infiltration in metastases from young vs. aged microenvironments. Aged mice form more and larger liver metastases compared to young mice, and metastatic lesions in aged mice have decreased CD8+ T cell infiltration when compared to young mice.

Since tumors in aged microenvironments have increased AKT activation compared to young microenvironments, we next tested if AKT signaling was sufficient to alter immune cell infiltration in PDAC tumors. In young mice, treatment with recombinant GDF-15, which activates AKT signaling, reduced CD8+ T cell infiltration into tumors. Conversely, in KPC tumors grown in aged mice treated with the AKT inhibitor MK-2206, there was a trend toward increased CD8+ T cell infiltration and a significant reduction in immunosuppressive FoxP3+ Tregs.

Together, these data highlight age-dependent differences in the immune infiltration in PDAC tumors. They suggest that activation of AKT signaling can drive features of immunosuppression in PDAC, providing the rationale for targeting AKT signaling to improve antitumor immune responses in PDAC.

#6632 Adipocyte death drives dormant breast cancer cell reactivation.

X. Yuan, Q. Ren, S. A. Stewart;
Washington University In St. Louis, St. Louis, MO

Despite significant responses to initial treatments, upwards of 30% of breast cancer patients will experience a recurrence of their disease. Unfortunately, there are few clinical features that predict which patients will recur, relegating patients and their doctors to a wait-and-see approach where they must remain vigilant. Recent studies have reported that the presence of disseminated tumor cells (DTCs) in the bone marrow of early-stage breast cancer patients predicts a higher chance of recurrence and that obese patients experience 35%-40% higher rates of recurrence than lean patients. Interestingly, in addition to increased adipocyte size, obese patients experience higher rates of adipocyte apoptosis, macrophage recruitment to adipocyte tissue, and increased inflammation, shown as the formation of crown-like structures (CLSs). Given the rising prevalence of obesity, the need for mechanistic studies to elucidate its contribution to breast cancer dormancy and recurrence is urgent. To investigate how microenvironmental changes associated with obesity affect breast cancer dormancy, we utilized a well-established syngeneic mouse model of ER+ breast cancer dormancy (D2.0R). We found that D2.0R cells remained dormant in the visceral fat of wildtype mice but were reactivated upon adipocyte death due to obesity or genetic manipulation, and this reactivation required the recruitment of macrophages. To understand why macrophages were recruited to the adipose tissue and how they led to dormant tumor cell reactivation, we profiled the microenvironmental changes in visceral fat using single-cell RNA-sequencing and found that the infiltrating macrophages exhibited unique pro-inflammatory and lipid regulatory phenotypes. Further investigation revealed that macrophages activated the integrin-focal adhesion kinase (FAK) pathway in dormant D2.0R cells and the inhibition of integrin and FAK inhibited this activation. Given tumor cells can metastasize to visceral fat depots in breast cancer patients, our findings provide an important model to determine what drives dormant tumor cell growth in adipose tissue. Our study provides novel insights into how tumor microenvironment (TME) impacts breast cancer dormancy and also highlights the importance of adipose tissue as a unique reservoir that potentiates cancer relapse.

#6633 Tracking cell-cell interactions using intercellular barcode transfer.

N. Q. Tay, T. Juan, J. J. Muldoon, J. Eyquem, M. T. McManus;
University of California, San Francisco, San Francisco, CA

Cell-cell interaction is one of the fundamental biological mechanisms by which cells communicate and is a key modality by which cancer cells interact with other cells in their microenvironment. Current methods, such as enzymatic labeling and proximity-based tagging, allow the experimental tracking of these interactions but are not compatible with sequencing-based readouts, which are essential for high-throughput analyses. We have developed a highly scalable intercellular barcode transfer technology that bridges this gap. Our novel “Relay” technology offers a scalable solution to monitor cell-cell interactions with unprecedented single-cell resolution, seamlessly integrating with existing high-throughput and sequencing platforms. Relay employs RNA barcodes to mark and track cell interaction events, providing definitive quantitative data on cell interaction partners. We used Relay to track interactions between cancer cells and T cells, capturing both potent antigen-specific engagements and subtler contacts involved in antigen sampling. Additionally, by integrating CRISPR libraries with Relay, we pioneered a novel approach for pooled CRISPR screens, focusing on intercellular interactions across different cell types. In this context, the cell harboring genetic perturbation may differ from the cell under analysis. To demonstrate this, we are conducting genome-wide perturbations in cancer cells and interrogating cancer cell factors that affect antigen sampling and trogocytosis by T cells and macrophages. Beyond its application in CRISPR screening, Relay can also be used with single-cell RNA sequencing to directly track and measure immune-cancer and immune-immune cell interactions at the single cell level. We applied single-cell Relay to a dendritic cell-T cell system to link dendritic cell signatures to T cell signatures based on direct cell contact and regulatory signaling. The design of Relay as a highly modular system extends its utility beyond cancer research, making it broadly applicable across various biological models and systems where cell-cell communication is a fundamental property in complex multicellular settings. This tool promises to accelerate the transition from theoretical understanding to practical exploration of cell-cell interactions, with profound implications for immunology, oncology, and beyond.

Wednesday, April 10, 2024

IMMUNOLOGY: Immune Modulation by Viruses, Bacteria, Radiation, and Other Modalities
Poster Session

#6637 The Haemophilus influenzae vaccine mitigates pancreatic tumor progression and lowers immunoregulatory cell levels in the tumor microenvironment.

E. F. Giurini, S. G. Pappas, K. H. Gupta;
Rush University Medical Center, Chicago, IL

Pancreatic ductal adenocarcinoma (PDAC) is a devastating disease projected to become the second leading cause of cancer deaths by 2030. First-line chemotherapies gemcitabine and FOLFIRINOX provide little therapeutic benefit and are accompanied by severe adverse toxicities, precluding long-term treatment. In addition, PDAC is notoriously refractory to checkpoint inhibitor immunotherapies, due to poor immunogenicity and a tumor microenvironment dominated by suppressive cell types. Thus, there is an unmet need for innovative, immune-based strategies to combat PDAC. A previous study utilized engineered bacteria to effectively kill PDAC tumor cells by directly delivering immunogenic tetanus toxoid to the tumor. Given the potential toxicity in using live bacteria, our group utilized a less toxic alternative, an FDA-approved *Haemophilus influenzae* type b vaccine (HibVx) also containing a tetanus toxoid component. To determine the antitumor potential of HibVx, our group used a physiologically relevant murine model, low T cell clone murine PDAC tumor model 641c95 and clinically relevant KPC mice model for PDAC. After tumors were established, animals received three consecutive daily treatments of HibVx via intraperitoneal injection. HibVx-treated animals experienced a dramatic reduction in tumor growth compared to PBS-treated controls ($p<0.001$). Given that tetanus toxoid is highly immunogenic in nature, changes in intratumoral immune cell populations following HibVx treatments were of great interest. Using flow cytometry analysis, HibVx-treated tumors had a significant increase in natural killer cells compared to control tumors ($p\leq0.05$). In addition, HibVx affected myeloid-derived suppressor cell populations (MDSCs), which are heavily implicated in the suppressive nature of PDAC tumors. HibVx also significantly decreased MDSCs within the tumor ($p<0.05$). In all, these findings position HibVx as an effective immunostimulatory agent that can be used as an alternative to live bacteria-based therapy for the treatment of PDAC.

#6639 Mechanisms of action of a killed, bacteria-based, multiple immune receptor agonist in development for pulsed anti-tumor immunotherapy.

M. J. Newman, D. Singh;
Indaptus Therapeutics, Inc., New York, NY

Activation of immune receptors, such as Toll-like (TLR), NOD-like (NLR) and Stimulator of Interferon Genes (STING) is required for efficient innate and adaptive immunity. Gram-negative bacteria (G-NB) contain multiple TLR, NOD and STING agonists. Potential utility of G-NB for cancer immunotherapy is supported by observations of tumor regression in the setting of infection and Coley's Toxins. Coley reported that intravenous (i.v.) administration was likely most effective but produced toxicity. The discovery of TLRs and their agonists, particularly the potent/multi-functional TLR4 agonist lipopolysaccharide (LPS)-endotoxin, comprising ~75% of the outer membrane of G-NB, suggests that it may be both a critical active ingredient and responsible for dose-limiting toxicity of i.v. G-NB. We have produced killed, intact bacteria products from non-pathogenic G-NB with ~90% reduction of LPS activity. One product, Decoy10, contained TLR2,4,8,9, NOD2 and STING agonist activity and exhibited reduced i.v. toxicity in mice and rabbits relative to unprocessed cells. Decoy10 and closely related Decoy20 produced single agent activity or combination-mediated durable regressions, with immunological memory, in mice with syngeneic or human breast, colorectal, hepatocellular, pancreatic carcinomas or non-Hodgkin's lymphoma. Regressions were observed in combination with chemotherapy, a non-steroidal anti-inflammatory drug, anti-PD-1, or rituximab, were associated with induction of 18-26 plasma cytokines/chemokines, activation of innate and adaptive immune pathways in tumors, and were dependent on NK, CD4+ and CD8+ T cells (Newman, Cancer Res 2023;83(7 Suppl):Abstract nr 4165). These and preliminary clinical results demonstrating rapid clearance of Decoy20 with transient induction of >50 plasma cytokines/chemokines (Newman et al., J Immunother Cancer 2023;11(Suppl 2)782-E:A1770) are supportive of a "pulse-prime" mechanism, whereby Decoy bacteria produce transient, but broad innate and adaptive immune activation. We have now analyzed immune activation by Decoy bacteria *in vitro* using human peripheral blood mononuclear cells (PBMCs). Decoy10 enhanced polarization of CD14+ monocytes to M1 macrophages and inhibited Treg polarization. Decoy10 enhanced monocyte-derived dendritic cell maturation and enhanced Th1, Th2 and Th17 CD4+ polarization, with Th1 at 10-100-fold lower Decoy10 concentrations than Th2 or Th17. Decoy10 also activated NKT and T cells, and enhanced PBMC-mediated tumor cell killing. The results demonstrate that Decoy bacteria stimulate polarization, maturation, or activation of cellular mediators of innate and adaptive anti-tumor immune responses, inhibit an immune-suppressive mechanism, and enhance immune cell killing of tumor cells. The results are consistent with and significantly extend our previously reported *in vivo* data.

#6640 Zap! Irreversible electroporation in pancreatic cancer cells induces proinflammatory cell death and improves progression free survival.

M. Powar, K. Imran, I. Allen, R. Davalos, Z. Salamah, K. Aycock, R. Brock, S. Coutermarsh-Ott, K. Orr;
Virginia Tech, Blacksburg, VA

Pancreatic cancer is the third leading cause of cancer-related death due to its late diagnosis, few treatment options, and extremely low survival rates due to its immunosuppressive microenvironment. Irreversible electroporation (IRE),is a tumor non-thermal ablation technique that applies high-voltage electrical pulses to permeabilize the cell membrane that is irreversible and leads to necrotic cell death. IRE has had strong success in clinical trials nevertheless, little is known about the effect of IRE beyond the initiation of cell death in the tumor tissue. We hypothesize that IRE can not only induce cell death by membrane disruption to facilitate a proinflammatory microenvironment but also causes death via cell cycle arrest. We utilized in-vitro, and immunocompetent in-vivo murine models to investigate changes to pancreatic cancer and the tumor microenvironment. Our findings show that treating the cells with an increasing voltage of IRE induces more cell death. We observed cell cycle arrest in the G1 phase which may have been caused by DNA damage. There was upregulation of DNA damage repair machinery in the treated samples. Our histopathology data suggests increased necrosis on the tumor treated with IRE, as also PCR array analysis showed more proinflammatory cell death caused by pyroptosis. Finally, we demonstrated a reduction in the tumor size and a better survival rate aftertreatment. Our data suggest that Irreversible electroporation has a promising future in inducing proinflammatory type of cell death in the tumor and benefits increased patient survival. More investigation is needed to define ideal parameters for the electrical pulses and device development for tumor ablation in larger animals like porcine models.

#6641 Improving response to bladder-sparing therapies by combining radiotherapy to immuno-potentiating agents in immunologically cold models of bladder cancer.

E. Michaud[1], S. Fehric[1], G. Marcq[1], J. Huang[1], F. Cury[2], M. Koti[3], **J. Mansure**[1], C. Piccirillo[4], W. Kassouf[2];
[1]McGill University Health Centre Research Institute, Montreal, QC, Canada, [2]Division of Urology, Department of Surgery, McGill University Health Centre, Montreal, QC, Canada, [3]Dept. of Biomedical and Molecular Sciences, Queen's University, Kingston, ON, Canada, [4]4Dept. of Microbiology and Immunology, McGill University, Montreal, QC, Canada

INTRODUCTION: Radiation therapy (RT) is a promising approach for bladder-sparing in muscle-invasive bladder cancer (MIBC). Despite its efficacy, 30% of patients develop radioresistant tumors necessitating salvage surgery. Combining RT with immune checkpoint inhibitor was reported to have synergic effects on anti-tumor immunity. In addition, activation of the STING pathway induces cell death, cancer cell antigens release and presentation, and promote T cells trafficking into tumors. Previous *in vivo* results from our team using the immunologically 'hot' murine tumor model MB49 demonstrated significant improvement of survival and immune cell infiltration upon STING agonist treatment, when combined with RT and anti-PDL1 treatment. Oppositely, treating the 'cold' tumor model UPPL with a combination of RT and anti-PDL1 treatment did not improve survival compared to RT alone. Consistently, UPPL tumors present low T cell and high neutrophil infiltration *in vivo*. Thus, the main objective of the present study is to evaluate whether combining RT, anti-PDL-1 and STING agonist treatments can improve the immunogenicity of UPPL tumors.
METHODS: Male C57BL/6 mice were subcutaneously injected with 5.106 UPPL cells then randomized into various treatment combinations of RT, anti-PDL-1 and STING agonist. Midpoint and endpoint tumors were harvested for flow cytometry and IHC and stools for 16S-sequencing.
RESULTS: We report that RT-combined treatments delayed tumor growth and prolonged survival in vivo. Neighborhood analyses in tissue revealed that response to RT combinations associated with increased macrophages density in the vicinity of infiltrating CD8+ T cells and with gut enrichment in *Faecalibaculum*, *Bifidobacterium*, and *Candidatus arthomitus*. Network analyses showed strong positive correlations between pro-tumor neutrophil recruitment and beneficial gut microbes in non-responders. Network analyses revealed positive correlations between pro-tumor neutrophil recruitment and dysbiotic gut microbes in non-responders. Conversely, these same neutrophil populations were associated to families associated to gut health in responding mice.
CONCLUSIONS: Our results suggest combining RT in cold tumors enhances the TME, boosting T cell function *via* macrophage support. Furthermore, distal gut microbes may impact local anti-tumor immunity by influencing neutrophil polarization. This study contributes to the limited literature exploring immune modulation in a conventionally 'cold' bladder tumor cell lines, which has implications for treating human resistant tumors.

#6642 Exploring the x-ray psoralen activated cancer therapy mechanism of action in a genetically engineered mouse model of soft tissue sarcoma.

Beatrice Schleupner[1], Alexandra Hunter Aitchison[2], Elle MacAlpine[3], Nicole Cantor[4], Sorana Morrissy[5], Kiran Narta[5], Jason Somarelli[6], Brian Brigman[1], Julia Visgauss[1], Michael Monument[7], William Eward[1]

[1]Department of Orthopaedic Surgery, Duke University Medical Center, Durham, NC,[2]Duke University School of Medicine, Durham, NC,[3]Department of Orthopaedics, Washington University School of Medicine, St. Louis, MO,[4]Campbell University School of Osteopathic Medicine, Lillington, NC,[5]Department of Biochemistry & Molecular Biology, University of Calgary, Calgary, AB, Canada,[6]Department of Medicine, Duke University Cancer Institute, Durham, NC,[7]Department of Orthopaedic Surgery, University of Calgary, Calgary, AB, Canada

BACKGROUND: Psoralen is a natural ultraviolet activated compound that has been used for over 70 years to treat skin cancer, psoriasis, and vitiligo. Recently, to expand its use beyond external treatment, a novel therapeutic called X-PACT (X-ray psoralen activated cancer therapy) was created to treat internal tumors. A combination of 8-methoxypsoralen and phosphors that convert low doses of x-ray radiation to ultraviolet (UV) light are injected into solid tumors and subsequently activated by x-ray photons with considerable antineoplastic effect. Notably, canine clinical trials have observed significant abscopal effects of X-PACT therapy on metastatic lesions throughout patients, but the immunomodulatory mechanisms of action are unclear (Nolan *et al*, in submission). Here, we present preliminary data investigating the immune response to X-PACT therapy in a murine soft tissue sarcoma (STS) model.
METHODS: Six mice of the inducible KrasG12D/+; p53flox/flox (KP) murine STS model with palpable, gastrocnemius tumors were used in this initial study. Four mice underwent treatment with X-PACT. In this group, psoralen was mixed with energy converters and injected into the tumor. The mice then received low-level radiation to activate the drug. Treatment was performed five times over a 15-day period and the animals were sacrificed within 48 hours of final treatment. The other two mice with induced tumors received no treatment prior to sacrifice. For both groups, a cardiac blood draw was performed at the time of sacrifice to obtain plasma serum for analysis. Luminex xMAP technology was used for multiplexed quantification of 45 mouse cytokines, chemokines and growth factors.
RESULTS: There were five markers that showed significantly different levels between the treated and control groups. Results indicated significantly higher ($p = 0.006$) plasma concentrations of macrophage derived chemokine (MDC) following five rounds of treatment with X-PACT therapy. Additionally, the treated mice displayed significantly lower concentrations of granulocyte colony-stimulating factor (G-CSF, $p = 0.003$), eotaxin ($p = 0.016$), tissue inhibitor of matrix metalloproteinase 1 (TIMP1, $p = 0.024$), and interleukin-1β (IL-1β, $p = 0.033$) compared to untreated mice with STS.
CONCLUSION: In humans, MDC levels are associated with longer survival and lower cancer severity. G-CSF, eotaxin, TIMP1, and IL-1β are upregulated in cancer patients and correlate with disease severity. Together, the lower concentrations of G-CSF, Eotaxin, TIMP1, and IL-1β suggest a softening of cancer severity following X-PACT treatment. Further studies and larger sample sizes are necessary to confirm and expand upon these preliminary findings.

#6643 Hyperthermic induction of immunotherapeutic response in *in vitro* melanoma model.

T. Jarboe[1], D. Quaranto[1], N. R. DeSouza[1], K. Kopec[1], J. Geliebter[1], R. K. Tiwari[1], M. D. Hurwitz[2];
[1]New York Medical College, Valhalla, NY, [2]Westchester Medical Center, Valhalla, NY

Immunotherapy has revolutionized the treatment of advanced melanoma, yet challenges persist with non-responders, development of resistance, and dosage concerns. Our strategy to enhance checkpoint inhibitor efficacy is to combine it with hyperthermia. Moderate hyperthermia, 39-45°C, is an interesting anti-neoplastic therapy which induces production of tumor associated antigens rendering tumor sites more amenable to immunotherapy. To investigate temperature-induced alterations on carcinogenic phenotypes in vitro, B16-F10 melanoma cells were grown at 37°C under normal culture conditions, or incubated at 41°C for 2 hours for moderate, febrile hyperthermic induction. Hyperthermia-induced changes were analyzed by trypan blue exclusion assay, scratch wound assay, collection of conditioned media for cytokine array, and protein isolation for Western Blot. Conditioned media from the hyperthermia-treated group showed an inflammatory shift in cytokine and chemokine expression, with increased TNFa and decreased IL-4 expression. Prior studies found the hyperthermia-induced apoptotic effect is directly correlated to endogenous TNFa levels, elucidating a potential molecular mechanism. Treatment for two hours at 41°C decreased proliferation of B16-F10 cells by 62% after 48 hours and 94% after 72 hours. Additionally, hyperthermia decreased cellular migration by 70% after 24 hours. Further evaluation of cellular interactions in important pathways responsible for these hyperthermia-induced changes were investigated via Western blot. Expression of constitutively active MAPK signaling cascade effectors pERK and ERK was decreased by 86% and 50%, respectively, helping to regulate pro-tumorigenic proliferative signaling. Some cancer cells have been demonstrated to resist hyperthermia via mechanisms to inhibit induction of caspase-3, however, in our model caspase-3 expression increased by 31% following 41°C treatment, thus allowing for induction of apoptosis via caspase-3 in this model. Cellular stress may induce these cell death pathways, as well as heat shock responses. Following febrile hyperthermic induction, hsp70 expression increased by 188% compared to cells cultured at 37°C. Hsp70 has a well-established role in supporting tumor-specific immune responses. Induction of hyperthermia in combination with anti-PDL1, anti-PD-1, or IL-15 immunotherapy is currently being evaluated in a C57BL/6 mouse model by our group. These studies aim to assess if hyperthermia augments response to immunotherapies in vivo. Our current works suggests that moderate, non-ablative hyperthermia helps initiate anti-tumor immune responses, assisting in the induction of anti-tumorigenic cell programs and, potentially, the production of additional tumor associated antigens, thereby making it an interesting candidate for combination with immune checkpoint inhibition and other immunotherapeutic approaches.

#6644 aPD1 treatment of urothelial cancers is synergistically enhanced by activating anti tumor immunity using vascular targeted photodynamic therapy.

Lilach Agemy, Keren Sasson, Tamar Yechezkel, Rachel Hamri, Raz Robas, David Kain, Avigdor Scherz

Weizmann Institute of Science, Rehovot, Israel

Background: Recurrence and progression rate following surgical treatment of locally advanced urothelial cancer is high, underscoring the unmet need to develop an effective, well tolerated treatment strategies, particularly for high grade upper tract urothelial cancer (HG-UTUC). The treatment success of low grade UTUC by vascular targeted photodynamic therapy (VTP) with WST11 (Padeliporfin) in phase I clinical trials led the FDA to approve Phase 3 trial in a fast track, orphan drug designation for low grade UTUC (ENLIGHT). Recently, treatment with immune checkpoint inhibitor (ICIs) of the PD1/PD-L1 axis has been approved for treatment of HG-UTUC. Yet, the failure rate of aPD1 therapy in HG-UTUC is high.We hypothesized that immune checkpoint inhibition needs to be complemented by the massive priming and accrual of newly activated anti-tumor immune cells through tumor immunogenic cell death. Early evidence indicated that WST11 VTP promotes anti-tumor immunity suggesting that VTP/aPD1 combinations may significantly improve the treatment success of HG-UTUC.
Methods: Mice bearing s.c. MB49-Luc, were subjected to WST11 VTP at 14d post implantation at suboptimal dose of drug or partial area of illumination. 4 or 5 doses of aPD1 were intraperitonealy administrated every 3 days starting at 1d post VTP (aPD1+1), or every 3 days till 10 days post-treatment starting at 2 days before VTP (aPD1-2). Tumor progression was followed up to 90 days post treatment using IVIS. Hematoxylin-eosin staining, and multiplex immunohistochemistry (mIHC) were performed on controls and treated animals.
Results: WST11 VTP with suboptimal drug dose, aPD1+1, and aPD1-2 resulted in 17%, 23% and 43% cure at day 90 post VTP. VTP at suboptimal drug dose combined with aPD1+1 or aPD1-2, resulted in 50% and 77% cure rate at 90 days, respectively. VTP with optimal drug dose (5mg/kg) but partial illumination resulted in 20% cure rate while combining this treatment modality with aPD1-2 resulted in 90% animal cure rate at day 90.At 24h post VTP mIHC showed a 2-3 fold increase of cytotoxic T cells, dendritic and NK cells, and a ~4 folds overexpression of PD1 and PD-L1 in the treated tumor tissue. At 2 days post aPD1-2 initiation, PD1 and PD-L1 apparent expression dropped to 0 and 2 folds higher than control, respectively. Following the combined VTP and aPD1-2 treatment, both PD1 and PDL-1 contents dropped down to zero and the CD8 content reached 3 folds enhancement compared to control.
Conclusions: These observations indicate that elevating the content of anti-tumor immune cells in the tumor microenvironment by VTP in combination with ICI synergistically enhances the therapeutic effect providing a much higher complete cure compared with the individual therapies. The cure rate extent strongly depends on the synchronization of the two modalities providing guidelines for the clinical management of HG-UTUC treatment.

#6645 Temporal immune profiling reveals systemic anti tumor immunity in triple negative breast cancer(TNBC) patients treated with immunotherapy and radiation.

V. Devarakonda, J. Viramontes, S. Stevens, T. Dar, E. Ko, E. Canesco, K. Anderson, J. Guarnerio, S. Knott, S. Shiao;
Cedars-Sinai Medical Center, Los Angeles, CA

Combining pembrolizumab (anti-PD1) with radiation therapy (RT) has shown to enhance response rates in TNBC. We hypothesize that this improved efficacy is not just localized to the tumor bed, but also involves a broader systemic immune response, although the precise mechanisms are yet to be fully understood. Therefore, in this study, we aimed to investigate T cell clonal dynamics in Tumor and peripheral blood mononuclear cells (PBMCs) in 9 patients (6 responders(R) and 3 non-responders (NR)) from 3 different timepoints (before therapy (Baseline), after anti-PD1 alone and after anti-PD1+RT). CD45+ positive stained cells were sorted for subsequent single-cell RNA and T-cell receptor (TCR) sequencing analysis.Through single-cell analysis, we identified increased proportions of exhausted CD8+ and Treg cells from baseline to both treatment points, whereas exhaustedCD4+ T cells increased in proportions after PD1 alone in Responders. We aimed to then understand the origin of these cells, and how they might contribute to systemic immunity. Hence, by TCR overlap between Tumor and PBMC's we detected 590 overlapped clones in CD8 and 1000 overlapped clones in CD4 T cells. Neo-TCR score was higher in these overlapped clones, suggesting tumor reactive clones can be identified in PBMC's. Compared to exhausted CD4, exhausted CD8 T cell and Treg had higher overlapped clones between Tumor and PBMC. We also found that exhausted CD8+T cells clonal expansion after treatment was higher in pre-existing clones, compared to new clones in Responders. These pre-existing clones consisted of overlapped clones, suggesting tumor reactivity to be present in PBMC's before treatment. Further investigation suggested that exhausted CD8+ cells also showed increased transition to TEMRA (in PBMC) and a tissue-resident memory CD8 T cell subset, under combination therapy. This pattern was not seen in exhausted CD4+Tcells or Treg cells, indicating that CD8+ T cell subsets in the blood are crucial in driving systemic anti-tumor immunity. Overall, this study has identified the systemic immune response triggered by the combination of anti-PD1 and radiation therapy highlighting its potential to inform and refine future therapeutic strategies in TNBC treatment.

#6646 Investigating the combination of radiation and subsequent immune checkpoint inhibitor treatment in head and neck squamous cell carcinoma models.

H. Lind[1], A. A. Strait[2], S. Hall[2], J. B. Goon[1], J. D. Aleman[2], S. Chen[2], P. Owens[2], J. H. Wang[3], C. Young[2], X.-J. Wang[1];
[1]UC Davis Comprehensive Cancer Center, Sacramento, CA, [2]University of Colorado, Anschutz Medical Center, Aurora, CO, [3]University of Pittsburgh, Pittsburgh, PA

Purpose: Head and neck squamous cell carcinoma (HNSCC) is often marked by an immunosuppressive tumor microenvironment, which contributes to the dismal 10-20% response rate to immune checkpoint inhibitor (ICI) therapy in HNSCC patients. Radiotherapy (RT) is a currently standard of care and frontline therapy for HNSCC, yet resistance is common. We sought to examine the combination therapy of RT followed by ICI therapy to test if RT induces an *in situ vaccination* which enhances the efficacy of subsequent ICI.

Methods: We utilized SCC cell lines derived from K15.Kras^{G12D}/Smad4$^{-/-}$ SCCs, which mimic the progression of HPV-unrelated HNSCC, and transplanted SCC cells into immune-competent C57BL/6J mouse recipients. Mice were subjected to RT followed by anti-PD-L1/anti-TGFb therapy. CD8$^{\pm}$ splenic T cells of responder or non-responder mice were examined by paired single-cell VDJ sequencing and single cell RNA sequencing (TCR/sc-RNAseq) to look for adaptations of the cytotoxic T cell compartment following combination therapy. Responder and non-responder tumor lines or tumors were treated with RT alone *in vitro* and *in vivo*, respectively, to examine major histocompatibility complex I (MHC-I) levels on tumor cells.

Results: Responders to this combination therapy exhibited complete tumor eradication while non-responders displayed rapid tumor progression. When re-challenged with same HNSCCs cells, responders rejected implanted tumor cells while naïve recipients rapidly developed HNSCCs. Single-cell TCR sequencing of splenic CD8$^{\pm}$ T cells revealed that responders, but not naïve recipients exhibited multiclonal CD8$^{\pm}$ T cell expansion specifically of memory cell populations. Responder tumor cells exhibited greater levels of MHC-I protein level presentation than non-responders when stimulated with RT.

Conclusions: Our data suggest that 1) elevated MHC-I by SCC tumor cells presentation driven by RT and ICI combination therapy facilitate a systemic expansion of memory CD8$^{\pm}$ T cell clonotypes which drive anti-tumor immunity and 2) MHC-I expression at baseline or when induced by RT may serve as a predictive marker for therapeutic response to RT and ICI combination therapy in HNSCCs.

#6647 Established 3D tumor-spheroid co-culture models demonstrate macrophage plasticity and unveil potential supportive roles of macrophages in the T cell-tumor-macrophage crosstalk post radiation therapy.

Aanchal Preet Kaur, Alejandro F. Alice, Megan R. Potuznik, Gwen Kramer, Jason Baird, David J. Friedman, Marka R. Crittenden, Michael J. Gough

Earle A. Chiles Research Institute, Providence Cancer Institute, Portland, OR

Ionizing radiation therapy (RT) has been characterized as an immunogenic event that in some tumors results in cell-death mediated activation of innate inflammatory and immunostimulatory mediators. These inflammatory mediators in turn modulate lymphocyte effector function in the tumor environment that can contribute to radiation-mediated control of tumors. We aim to model these interactions ex vivo, to identify the critical signals regulating immune function. We demonstrate that it is necessary to establish a three-dimensional model for crosstalk between tumor cells and immune cells to recapitulate myeloid and T cell responses to radiation. We have established 3D tumor spheroid co-culture models using murine MC38 colon carcinoma and Panc02-SIY pancreatic carcinoma cell lines with bone-marrow derived macrophages (BMDM). The spheroid cultures were exposed to 12 Gy RT and maintained in culture over a period of 5 days. Analyses were done using live-cell imaging and flow cytometry. Our findings demonstrate a decrease in hypoxia post RT, and exposure to RT increased the phagocytosis of dying cancer cells by macrophages. This was followed by a significant increase in CD80 and CD86 expression on the surface of macrophages in co-cultures on day 3 and day 4 post RT. These data matched our analyses of tumors treated in vivo with radiation and analyzed on day 4 post RT. In addition to RT-mediated upregulation of costimulatory molecules on macrophages, we also observed an increase in PD-L1 expression that may also impact T cell responses. To test T cell function in the 3D model, antigen-specific T cells were added to the Panc-02-SIY and BMDM spheroid co-cultures, which resulted in enhanced T cell proliferation in RT-treated groups. To assess the mechanism of macrophage activation in co-cultures, we evaluated HMGB1 as an innate adjuvant that may cause TLR4-mediated macrophage activation; however, the pattern of activation did not match that of RT. The involvement of the nucleic acid sensing cGAS-STING pathway was assessed by using BMDM from STING knockout (KO) mice in the 3D co-cultures. Similar upregulation of CD80 and CD86 were observed on STING KO macrophages in 3D co-cultures on day 4 post RT, indicating the observed phenomena to be independent of STING signaling. Ongoing studies aim to decrypt the innate downstream signaling pathways involved in RT-mediated polarization of macrophages so as to identify potential targeted therapies for tumor-associated macrophages, and also translate this to patient tumors.

#6648 Low-intensity pulsed ultrasound enhances the presentation of brain-derived antigens by facilitating the migration of antigen-presenting cells from the brain to the periphery.

M. Gallus[1], V. Andres Arrieta[2], A. Saijo[1], P. Chuntova[1], A. Yamamichi[1], J. Haegelin[1], S. Phyu[1], L. Phung[1], S. Amir-Kabirian[1], S. Lakshmanachetty[1], L. Chen[2], K. Habashy[2], A. Gould[2], C. Amidei[2], C. Lee Chang[2], R. Stupp[2], M. Canney[3], H. Okada[1];

[1]University of California San Francisco, San Francisco, CA, [2]Northwestern University, Chicago, IL, [3]Carthera, Lyon, France

Gliomas, the most common primary brain tumors, remain largely incurable despite advancements in surgical and adjuvant therapies. While immunotherapies offer promising avenues, their efficacy has been limited by formidable anatomical barriers, such as the blood-brain barrier (BBB), which restricts the migration of immune cells into the brain and impedes the efficient drainage of brain-derived antigens, establishing an immune-privileged environment. Consequently, neoplastic formations within the brain often escape detection by the peripheral immune system, complicating therapeutic interventions. The application of low-intensity pulsed ultrasound with microbubbles (LIPU/MB) has emerged as a potential solution, enabling the transient opening of the BBB. This facilitates drug transport and immune cell trafficking, including Chimeric Antigen Receptor (CAR) T cells, into brain tumors. However, challenges such as antigen-loss escape persist with CAR T cells. One proposed solution involves promoting antigen/epitope spreading by inducing the presentation of brain (tumor) antigens to the systemic immune system. To investigate this, we conducted intravital imaging using Colony-stimulating factor receptor 1 (CSFR1) and CX3CR1 reporter mice, visualizing antigen-presenting cell locomotion in the brain before and after LIPU/MB treatment using two-photon microscopy. Within one hour after LIPU/MB, we observed the migration of CSFR1+ and CX3CR1+ immune cells from the brain parenchyma and perivascular space into the bloodstream, a phenomenon absent prior to LIPU/MB treatment. Beyond that, flow cytometry identified $CD45^{intermediate}CD11b^{\pm}$-$CX3CR1^{\pm}$-$TMEM119^{\pm}$-$P2RY12^{\pm}$microglia-like' cells in the blood. To further assess the immunological effects of LIPU/MB on brain antigen presentation, we utilized transgenic mice expressing a minigene encoding four immunogenic peptides under the glial fibrillary acidic protein (GFAP) promoter. LIPU/MB treatment was associated with increased proliferation and priming of adoptively transferred CNS antigen-specific naïve T cells in cervical lymph nodes, ultimately homing into the CNS, indicating enhanced antigen presentation. Furthermore, in a subset of glioblastoma (GBM) patients undergoing LIPU/MB combined with doxorubicin and anti-PD-1 blocking antibodies, CD11b+CD14+P2YR12+ microglia were detected in blood samples during cycles 3-6 of treatment. This increase was absent in blood samples from healthy donors.Collectively, our findings suggest that LIPU/MB represents a novel approach to augment brain-antigen presentation in the periphery, holding potential implications for improving the immunotherapeutic management of gliomas.[M.G., V.A.A., A.M.S., and H.O. contributed equally to this work.]

#6649 Tumor treating fields (TTFields) induce an anti-tumor immune response in a pancreatic cancer mouse model.

T. Kan, T. Haj Khalil, Y. Barsheshet, **T. Voloshin**, A. Vorontsov, B. Brant, L. Koren, R. Blatt, S. Cahal, E. Zemer-Tov, R. Paz, A. Klein-Goldberg, C. Tempel Brami, S. Jacobovitch, A. Volodin, B. Koltun, C. David, A. Haber, M. Giladi, U. Weinberg, Y. Palti;
Novocure, Haifa, Israel

Background: Pancreatic ductal adenocarcinoma (PDAC) is a deadly malignancy with few therapeutic options. Tumor Treating Fields (TTFields) are low-intensity electric fields that disrupt cellular processes critical for cancer cell division and tumor progression and are approved for the treatment of glioblastoma and pleural mesothelioma. A phase 3 clinical trial is in progress to test the efficacy and safety of TTFields concomitant with standard-of-care gemcitabine and nab-paclitaxel (GnP) as front-line treatment of locally advanced PDAC. TTFields have been shown to induce immunogenic cell death (ICD) in cancer cells and elicit a systemic anti-cancer immune response. Accordingly, the benefit of applying TTFields together with immune checkpoint inhibitors (ICI) was demonstrated in a phase 3 study in patients with non-small cell lung carcinoma. This preclinical study investigated TTFields-induced immune responses in PDAC.
Methods: An orthotopic PDAC tumor model was established by inoculating 4X105 Panc02 pancreatic cancer cells with stable luciferase expression into the pancreas tail of immune-competent C57BL/6 mice. The mice were randomized into four groups following bioluminescence detection of tumor volume: control, TTFields (150 kHz, 10 days), GnP (50 mg/kg for each drug, i.p. injected once a week for a total of two administrations), and GnP + TTFields. At the end of treatment, tumor volume was measured using caliper, and blood was collected for spectral flow cytometry-based immunophenotyping and ELISA testing for the ICD marker HMGB-1. In vitro, Panc02 cells were treated for 72h with TTFields (150 kHz, 1.62 V/cm RMS) and examined by flow cytometry for apoptosis and ATP secretion (using quinacrine staining) and surface exposure of calreticulin.
Results: TTFields markedly reduced the tumor size in Panc02 tumor-bearing mice compared to control mice. Analysis of peripheral blood effector (CD62L-CD44+) and central (CD62L+CD44+) memory T cells demonstrated the induction of circulating effector-memory cytotoxic CD8+ T cells. Additionally, serum HMGB-1 concentrations were significantly elevated in mice treated with TTFields compared to control mice, implying the involvement of ICD in the response to TTFields. In vitro, TTFields application induced apoptosis of Panc02 cells and increased ICD, as indicated by increased surface exposure of calreticulin and ATP depletion. When TTFields were used in Panc02 tumor bearing mice concomitantly with GnP, a substantial reduction in tumor size was detected, and a complete tumor regression was observed in a number of mice.
Conclusions: Our results suggest that TTFields may enhance the effects of standard-of-care chemotherapy for the treatment of PDAC. Furthermore, TTFields were shown to induce ICD and activate an antitumor immune response in PDAC, supporting future studies evaluating the efficacy of TTFields together with ICI in PDAC.

#6650 Macrophage pro-inflammatory phenotype skewing by the application of tumor treating fields (TTFields).

T. Kan, Y. Barsheshet, B. Brant, T. Haj Khalil, **T. Voloshin**, A. Volodin, L. Koren, B. Koltun, A. Klein-Goldberg, E. Zemer-Tov, R. Paz, A. Haber, M. Giladi, U. Weinberg, Y. Palti;
Novocure Ltd, Haifa, Israel

Introduction: Tumor Treating Fields (TTFields) are low intensity electric fields that disrupt cellular processes critical for cancer cell viability. TTFields have previously been shown to induce immunogenic cell death, promote dendritic cell maturation, and elicit a systemic anti-cancer immune response in preclinical models. The benefit of applying TTFields together with immune checkpoint inhibitors (ICI) was demonstrated in a phase 3 study in non-small cell lung carcinoma. In the current research, we investigated possible effects of TTFields on regulation of macrophage phenotype.
Methods: Bone marrow-derived macrophages (BMDMs) were generated from the femurs and tibias of 5-8-week-old Balb\C mice. LPS+IFN-γ or IL-4 were applied to the BMDMs to induce polarization (M1 and M2, respectively). The BMDMs were then treated with TTFields (150 kHz, 24 h), and then examined by flow cytometry for surface expression of the macrophage biomarker F4/80 and the activation markers CD80, major histocompatibility complex class II (MHC II), inducible nitric oxide synthase (iNOS), CD206, and ARG-1. Cell supernatants were collected and analyzed by multiplexed secretion assay for secretion levels of CXCL1 (KC), IL-18, IL-23, IL-12p70, IL6, TNF-α, IL-12p40, TGF-β1, CCL22 (MDC), IL-10, IL-6, G-CSF, CCL17 (TARC), and IL-1β. Cell lysates were examined using a RhoA activation kit and Western blot to determine GEF-H1, c-Jun, and p65 phosphorylation levels.
Results: BMDMs exposed to TTFields demonstrated elevated expression of the pro-inflammatory M1 markers $CD80^{+}$ and MHC II^{high}, and decreased expression of the M2 markers CD206 and ARG-1. A pro-inflammatory secretion pattern was detected, with increased levels of CXCL1, IL-18, IL-23, IL-12p70, TNF-α, IL-12p40, CCL22, G-CSF, CCL17 and IL-1β. The treated cells further demonstrated RhoA activation and GEF-H1 phosphorylation, with subsequent activation of the transcription factors c-Jun and p65.
Conclusions: This study reveals a novel immunomodulatory role for TTFields, promoting *in vitro* pro-inflammatory polarization of macrophage.

#6651 Compromised TGFβ signaling and DNA repair primes immune poor tumors response to immune checkpoint blockade by activating NK cells.

J. T. Moore, J. Gkantalis, I. Guix, M. Barcellos-Hoff;
UCSF - University of California San Francisco, San Francisco, CA

We investigated the interplay between transforming growth factor beta (TGFβ) regulation of immunosuppressive signaling and immunogenic DNA repair. Loss of TGFβ signaling by cancer cells is accompanied by increased use of error-prone repair. We described a transcriptomic score, βAlt, that reports the TGFβ/DNA repair functional relationship. Pan-cancer analysis showed that high βAlt cancers (i.e., low TGFβ and high error-prone DNA repair) are sensitive to chemoradiation and have a greater fraction of genome altered compared to low βAlt cancers. Defective mismatch repair is associated with T cell infiltration and response to immune checkpoint blockade (ICB), hence we investigated the immune context of bAlt. Unsupervised clustering of RNAseq profiles 12 independent immunocompetent mouse tumor derived transplant (mTDT) tumors based on βAlt score indicated that high βAlt was associated with immune poor phenotype and lack of type I interferon signatures. A similar relationship was evident in the bladder, breast, and lung TCGA data. A high βAlt, immune poor mTDT in which T cells were only 20% of 10% CD45 were treated with monotherapy consisting of single fraction 10 Gy radiation, anti-PD-L1 or TGFβ inhibition, dual or triple treatment. Only monotherapy or combinations with radiation significantly increased survival. However, these ICB resistant tumors responded to triple treatment. Response was accompanied by increased tumor infiltrating $CD45^{+}$ cells ($P=0.02$), circulating CD8 T cells ($P<0.001$) and natural killer (NK) cells ($P<0.001$). As NK cells tripled and TGFβ broadly impairs NK cell effector function, we depleted NK cells to test whether they were required for the response to triple treatment. NK depletion completely abrogated response ($P<0.00001$) indicating NK cells can provoke an ICB response in high βAlt immune poor tumors. Both mouse tumors and human cancers show that loss of TGFβ signaling resulting in error-prone DNA damage response is strongly associated with immune poor tumors and suggests that TGFβ inhibition can override NK cell dysfunction to create vulnerability to ICB.

#6652 Advanced glioblastoma immunotherapy: Attenuated herpes oncolytic virus armed with anti-PD-1 antibody and IL-12.

L. Wang, X. Zhou, **X. Chen**, Y. Liu, Y. Zheng, R. Yan, Y. Liu, J. Zhao, G. Zhou;
ImmVira Co.,Ltd., Shenzhen, China

Background: Glioblastoma (GBM), the most common and deadly primary brain tumor in adults, has limited treatment options with poor outcomes. The urgent need for innovative treatments has spurred research into immunotherapy and oncolytic virus therapy as promising alternatives. Herein, we have developed a new generation oncolytic herpes simplex virus (oHSV) armed with IL-12 and anti-PD-1 antibody to provide a synergistic anti-GBM efficacy for immune-oncolytic therapy.

Methods: MVR-C5252, a novel oHSV, was created by genetic engineering, which included the removal of a 15-kb internal repeat (IR) region and both copies of the γ34.5 genes, along with the insertion of two exogenous genes encoding the anti-PD-1 antibody and IL-12. MVR-C5252 was characterized and assessed for its anti-GBM activities through a series of experiments as follows: 1) Safety assessments, including evaluations of neurotoxicity and latency-reactivation characteristics, were conducted in Balb/C mice. 2) Anti-tumor activities were evaluated in cell cultures, subcutaneous and orthotopic xenograft mouse models, and immunocompetent mouse models. 3) Mechanistic studies were performed to uncover the mode of action of MVR-C5252, with a specific focus on its ability to induce cell death in GBM cells and activate the immune response *in vivo*.

Results: 1) *In vitro* studies showed that MVR-C5252 is highly replication attenuated but with higher cell-killing activity in GBM cells compared to the first generation oHSV, R3616, which has γ34.5 deletions only. 2) Mechanistic studies showed that MVR-C5252 infection increased cell death by reducing CNTNRα expression, which typically prevents caspase 3 activation and has an anti-apoptotic effect in glioma cells. 3) Intracranial injection of MVR-C5252 revealed a remarkable safety profile, with over an 800-fold reduction in virulence compared to wild-type HSV-1. Furthermore, the mouse trigeminal ganglion (TG) infection model suggested that MVR-C5252 was unable to establish latency or reactivate in the TG. 4) *In vivo* subcutaneous and orthotopic xenograft mouse models showed that compared to the R3616 group, enhanced anti-tumor activity and extended survival were observed in the MVR-C5252 group. Additionally, in the syngeneic mice model, MVR-C5252 exhibited superior anti-tumor activity and immune activation over the backbone virus.

Conclusions: With the unique combination of safety, potent anti-tumor activity, and immune-stimulatory properties, MVR-C5252 makes it a big potential candidate to address the pressing need for effective treatment strategies of GBM.

#6653 Oncolytic virotherapy induces a long-term immune antitumoral response leading to glioma eradication.

Francesca Piaggio[1], Francesco Alessandrini[2], Chiara Riviera[3], Irene Appolloni[3], Davide Ceresa[1], Daniela Marubbi[3], Tatiana Gianni[4], Gabriella Campadelli-Fiume[4], **Paolo Malatesta**[3]

[1]IRCCS Ospedale Policlinico San Martino, Genova, Italy,[2]Department of Neurology, Northwestern University , Feinberg School of Medicine, Chicago, IL,[3]Department of Experimental Medicine (DIMES), University of Genoa, Genova, Italy,[4]Department of Medical and Surgical Sciences, University of Bologna, Bologna, Italy

Oncolytic herpes simplex viruses (oHSVs) have shown promise as effective treatments against various cancers. Our study evaluated the efficacy of R-115, an oHSV retargeted to human Her2 (hHer2), fully virulent in its target cells and expressing murine interleukin 12 (mIL12), in a high-grade, immunocompetent murine glioma model. This model is based on orthotopically transplant of cells derived from PDGFB-induced primary gliomas in syngeneic mice, engineered to express hHer2. Our experimental design compared the impact of R-115 on gliomas where all cells expressed hHer2 against a setup where only about 50% of cells expressed hHer2. The latter aimed to replicate the heterogeneity of patient's high-grade gliomas, where not all cells express the target molecule. Strikingly, results in terms of overall survival and tumor eradication were similar in both setups, with about a quarter of animals showing complete glioma eradication. This suggests that mIL12-armed oHSV's impact is less about direct viral-induced cell death and more about the immune response elicited by the mIL12-expressing virus. This response effectively targets cells lacking the viral-targeted protein but likely sharing other neoantigens with hHer2-positive cells. Mice cured in both experimental setups were rechallenged with purely hHer2-negative cells. Almost all did not develop gliomas, indicating a strong immune response capable of rejecting the tumor. Plasma analysis revealed that R-115-treated mice from both setups were more immunoreactive against both hHer2-positive and negative cells compared to untreated mice. Further, co-culturing long-surviving mice's splenocytes with glioma cells showed increased cell division in CD8, CD4 and CD19 populations, and elevated IFN-γ, granzyme B, and TNF-α production. These findings underscore R-115's profound anti-cancer potential, especially its capacity to elicit an immune response effective against glioma cells, irrespective of their expression of the target molecule. This outcome, coupled with the results of the rechallenge experiments, is pivotal. It suggests that in a clinical context, an interleukin-12-expressing oHSV could effectively target not only residual cells post-surgical resection but also infiltrating cells that are distant from the site of virus administration. Encouraged by these promising findings, we are currently advancing our research with a novel oHSV that expresses mIL12 and targets EGFRvIII, a mutation found exclusively in tumor cells. This is aimed at enhancing the safety and translatability of this therapeutic approach.

#6654 Oncolytic virotherapy targeting high-grade glioma tumor antigens.

J. Hedberg, A. Martin, D. Kim, J. Navarro, A. Rivaldi, Y. Kim, I. Hernandez-Aguirre, E. Garfinkle, K. Miller, K. Cassady, E. Mardis;
Nationwide Children's Hospital, Columbus, OH

Glioblastoma, the most common primary brain malignancy in adults, is an aggressive cancer with five-year median survival of ~6.8%. New treatment options are urgently needed for glioblastoma and other high-grade gliomas (HGGs). Oncolytic viruses (OVs) are an emerging class of cancer therapy currently being evaluated as treatments for a variety of malignancies, including glioblastoma. Our labs developed OV C134, now under evaluation in a phase I clinical trial of recurrent glioblastoma (NCT03657576). In addition to directly infecting and lysing tumor cells, OVs are capable of stimulating anti-tumor immune responses. We previously showed in the CT2A syngeneic mouse model of HGG that treatment with a version of C134 engineered to express the shared tumor antigen Ephrin-A2 (EPHA2; commonly upregulated in glioblastoma) significantly increased survival and produced EPHA2-specific T cell responses. This finding led us to hypothesize that C134 could be further engineered to stimulate antigen-specific immune responses against tumor-specific neoantigens. We first assessed the impact of C134 treatment on immune cell dynamics in HGGs, by performing single cell RNA sequencing of CD45+ immune cell infiltrate from CT2A HGGs treated with C134 or saline (control). Clustering of these data identified 17 distinct immune cell types, and differential expression analyses revealed several C134-induced changes. These included increased expression of genes involved in antigen presentation and STAT signaling in microglia and macrophage subsets, the proliferation marker *Mki67* in germinal center B cells, the chemokine *Ccl12* from microglia, and tissue-resident memory marker genes *Fos* and *Jun* in T cells. These data suggest C134 treatment poises the tumor immune microenvironment for antigen presentation and antigen-specific immune responses. Next, we evaluated CT2A to identify candidate tumor neoantigens by isolating DNA and RNA from orthotopic tumors and DNA from tail snips of mice treated with saline or C134. We carried out RNA sequencing (tumors) and whole exome sequencing (tumor and normal), and employed the Personalized Variant Antigens by Cancer Sequencing (pVAC-Seq) computational pipeline. This pipeline takes somatic variant calls from the exome comparison of tumor to normal DNA, validates RNA expression of called variants, and feeds corresponding peptide sequences into algorithms that predict the binding of variant-containing peptides to major histocompatibility complex (MHC), thereby assessing for potential neoantigens. Our pVAC-Seq analysis revealed a conserved set of 1,264 tumor-exclusive variants expressed at the RNA level with high (ic50<500nm) predicted binding to mouse MHC. I will present details of C134-induced immune remodeling in syngeneic HGG models, and describe a plan to engineer C134 to express a prioritized set of neoantigens to evaluate how efficacy from OV therapy may be further enhanced in a patient-specific manner.

#6655 Oncolytic adenovirus dually expressing interferon beta and membrane-stable CD40 ligand increases polyfunctional $CD8^+$ T cells associated with antitumor activity.

M. J. Cantwell[1], A. N. Saltos[2], H. Zheng[2], D. Foresman[2], A. A. Beg[2];
[1]Memgen Inc., Houston, TX, [2]Moffitt Cancer Center, Tampa, FL

MEM-288 is a dual-transgene armed oncolytic adenovirus in phase 1 clinical development as a standalone agent and in combination with immune checkpoint inhibitors (ICI). It encodes two potent immune agonists: IFNβ and a recombinant membrane-stable chimeric form of CD40L (MEM40). We previously demonstrated this agonist combination is better than either agonist individually to activate conventional dendritic cells type 1 (cDC1) crucial for $CD8^+$ T cell cross-priming, and to increase tumor-antigen reactive $CD8^+$ T cells. Furthermore, first-in-human Phase 1 clinical trial (NCT05076760) results of MEM-288 for advanced non-small cell lung cancer (NSCLC) and other solid tumors showed MEM-288 tumor shrinkage was associated with systemic antitumor T cell immunity as demonstrated by cytokine, T cell clonotype, and tumor neoantigen analysis. Here, we investigated the precise nature of the localized and systemic T cell response induced by MEM40 + IFNβ in preclinical tumor models. Single-cell RNA sequencing of tumor infiltrating T lymphocytes (TILs) revealed that MEM40 + IFNβ elicited a strong increase in T cells expressing Granzyme B and PRF1, key effector cytokines and cytotoxicity mediators. We tracked the $CD8^+$ T cell response in CD45.1 C57BL/6 mice implanted with syngeneic B16 tumor expressing the model antigen OVA. Interestingly, intratumoral treatment with adenovirus encoding MEM40 + IFNβ did not cause an appreciable increase in absolute numbers of antigen-reactive $CD8^+$ T cells, despite tumor growth inhibition. However, MEM40 + IFNβ compared to control unarmed adenovirus induced a significant ($p < 0.005$) 5-fold increase in polyfunctional $IFNγ^+TNFα^+PRF1^+$ and $IFNγ^+TNFα^+$Granzyme B^+ $CD8^+$ T cells. Polyfunctional $CD8^+$ T cells have the capacity to simultaneously produce effector cytokines and cytotoxicity mediators and are known to be strongly associated with antitumor T cell activity. The robust polyfunctional $CD8^+$ T cell response in these studies is consistent with T cell-driven antitumor activity found in both our preclinical tumor experiments and our clinical studies in advanced NSCLC patients responding to MEM-288. Overall, our findings suggest MEM40 + IFNβ generates a strong polyfunctional $CD8^+$ T cell response in the TME that warrants continued evaluation to understand the pleiotropic mechanisms of this cancer immunotherapy.

#6656 Revolutionizing solid tumor treatment : Viral protein-targeted CAR-T with oncolytic virus.

S. Choi[1], K. Kim[1], S. Lee[1], J. Choi[1], S.-J. Lee[1], Y. Lee[2], J. Kim[3], H. Lee[3], K. Kim[3], M.-S. Park[3], S.-W. Song[1];

[1]R&D center, CellabMED Inc., Seoul, Korea, Republic of, [2]Hanyang University, Ansan, Korea, Republic of, [3]Vaccine Innovation Center, Institute for Viral Diseases, Korea University College of Medicine, Seoul, Korea, Republic of

Major challenges for CAR-T cell therapy in solid tumors include various limitations due to the issue of appropriate antigen selection, tumor heterogeneity, and the immune-suppressive tumor microenvironment (TME). To overcome these hurdles, we've developed a novel therapy, CLM-202 which is a combination therapy of oncolytic Newcastle disease virus (NDV) and NDV F protein-targeted CAR-T cell therapy (NDV F CAR-T). After NDV infects tumor cells, NDV envelope protein F is expressed on the tumor cell surface. NDV F CAR-T recognizes NDV F protein and kills the tumor cells. This approach can be applied to patients with various indications, regardless of the presence of the target protein. Using NDV to deliver antigens minimizes the risk of tumor recurrence due to tumor heterogeneity. Furthermore, it mitigates off-target toxicity by targeting oncolytic virus-derived proteins, not human proteins. Oncolytic NDV also triggers a potent immune response within the tumor microenvironment, thereby altering the immunosuppressive conditions of the tumor and improving CAR-T efficacy. Therefore, CLM-202 can be a multipurpose solution for solid tumors. We have developed a second-generation CAR-T cell therapy, NDV F CAR-T, which can be used in combination with an oncolytic virus known as NDV. NDV F CAR-T is designed to specifically target the F protein expressed when cells are infected by NDV. It incorporates a single-chain variable fragment (scFv) derived from an antibody that can bind specifically to the F protein of NDV-infected cells. To assess the activity of NDV F CAR-T in tumor cells against a variety of solid tumors as indications, we conducted several experiments. We initially confirmed the expression of the F protein in NDV-infected tumor cells. We also conducted cytotoxicity tests to confirm NDV F CAR-T's ability to induce death in NDV-infected tumor cell lines. Furthermore, to assess the efficacy of NDV F CAR-T in an in vivo model, we established an orthotopic mouse model. In this model, we administered NDV via intratumoral injection, followed by the single-dose administration of NDV F CAR-T to perform the efficacy test. We have confirmed that NDV infects all solid tumor cell lines representing different indications and induces the expression of the F protein in infected tumor cells. Furthermore, we have observed that NDV infection in these diverse tumor cells results in robust tumor cell-killing activity by NDV F CAR-T and the subsequent activation of CAR-T. Moreover, in an orthotopic mouse model, we have demonstrated that the administration of NDV followed by NDV F CAR-T induces potent tumor growth inhibition. In summary, our research proposes a novel therapeutic strategy, CLM-202 that utilizes NDV F CAR-T and NDV to overcome the limitations of CAR-T cell therapy in solid tumors, including tumor heterogeneity and immune-suppressive tumor microenvironments. This approach aims to effectively treat a wide range of indications.

#6657 Oncolytic Vaccinia Virus Carrying OPCML Tumor Suppressor is active in Epithelial Ovarian Cancer.

Y. Tang[1], Y. Liu[2], M. Deng[1], F. Huang[1], J. Wang[3], P. Blake[4], H. Gabra[4], **Q. Wang**[2];
[1]Guangxi Medical University, Nanning, China, [2]Guangxi Medical University Cancer Hospital (Guangxi Tumor Control Institute), Nanning, China, [3]Genvira Biosciences Inc., Ottawa, ON, Canada, [4]Papyrus Therapeutics Inc., West Chester, PA

Objective: Epithelial Ovarian cancer (EOC) has the highest mortality rate among gynecologic malignancies, necessitating novel therapeutic approaches. Viral oncolytic immunotherapy with recombinant oncolytic vaccinia virus (OVV) offers promise for advanced-stage cancer treatment. OPCML is a GPI-anchored 3 Ig-domain tumor suppressor inactivated by somatic methylation in 87% of EOC. OVV with OPCML (OVV-OPCML) gene insertion may have potential as a therapeutic agent. This study explores the oncolytic, signaling-inhibitory, anti-angiogenic and synergistic immunotherapeutic properties of OVV-OPCML in EOC treatment, evaluating its therapeutic potential.

Methods: To create OVV-OPCML, the virulent vaccinia virus Copenhagen strain F3L site was modified with OPCML cDNA, confirmed by qPCR and western blot. Oncolytic potential was assessed through in vitro and in vivo EOC cell infection with OVV-OPCML. Real-time cell analysis (RTCA) assessed cell proliferation. Xenograft tumor models in nude mice were used to evaluate in vivo oncolytic activity, while OVV-OPCML combined with anti-PD-1 treatment was tested using a syngeneic orthotopic EOC mouse model (ID8) in C57BL/6 immunocompetent mice. Serum IFN-γ and TNF-α were quantified via ELISA. Receptor Tyrosine Kinases, angiogenesis and phosphorylation together with immune markers were examined by western blotting and by multiplex immunohistochemistry (mIHC) analysis of tumor sections.

Results: OVV-OPCML selectively infected OC cells, leading to viral replication and tumor cell death, while sparing normal ovarian cells in-vitro. OPCML protein expression increased post-infection. OVV-OPCML reduced ERBB2, EGFR, and FGFR1 expression in SKVO3 OV cells. Intratumoral or intraperitoneal (IP) OVV-OPCML administration in human ovarian cancer nude mouse models reduced tumor growth and improved survival. IP in-vivo OVV-OPCML in combination with anti-PD-1 treatment in vivo, in the IP ID8 syngeneic model demonstrated synergy with survival improvement. H&E staining showed tumor cell damage without significant harm to normal tissues. Protein expression of ERBB2, EGFR, FGFR1, and their phosphorylated forms decreased. CD31, VEGFR2, p-VEGFR2 (Tyr1175), and p-VEGFR2 (Tyr1214) downregulation suggested tumor angiogenesis disruption. OVV-OPCML treatment elevated serum TNF-α and INF-γ levels and increased CD8+ T cells and PD-L1 expression in OVV-OPCML treated syngeneic tumors.

Conclusions: OPCML gene enhances OVV selectivity against OC cells through direct oncolysis and OPCML protein production, inhibiting specific RTKs, suppressing angiogenesis, and activating antitumor immune responses synergistically with anti-PD-1. OVV-OPCML therapy shows promise as a targeted strategy for ovarian cancer treatment.

#6658 TcE armed oncolytic virus VSV-GP combines oncolysis and T-cell retargeting for improved efficacy.

A. Ponnurangam[1], T. Schwaiger[1], S. Walter[2], S. Bartl[1], M. Mayr[1], M. Petersson[1], T. Schoenberger[3], F. Heinemann[3], P. Gross[3], W. Rist[3], S. Kasturirangan[4], C. Lempp[3], J. Petschenka[3], **K. Das**[1], N. Tobias[1];

[1]ViraTherapeutics GmbH, Rum, Austria, [2]Boehringer Ingelheim RCV GmbH & Co KG, Vienna, Austria, [3]Boehringer Ingelheim Pharma GmbH & Co. KG, Biberach a.d. Riss, Germany, [4]Boehringer Ingelheim Pharmaceutical, Inc., Ridgefield, CT

Background: Oncolytic viruses, such as the chimeric vesicular stomatitis virus variant VSV-GP have dual modes of action, direct tumor-cell killing, and activation of tumor-specific immunity. While tumor cells deficient in type I interferon (IFN) response are permissive to VSV-GP replication and killing, IFN competent tumor cells are protected from VSV-GP-mediated oncolysis. Our previous data demonstrated that VSV-GP therapy turns immunologically 'cold' tumors 'hot' by increasing infiltration of T cells into the tumor. The aim of this study was to use the VSV-GP platform to locally express a T cell engager (TcE) molecule to redirect these T cells to destroy non-permissive IFN competent tumor cells expressing the target of the TcE on their cell surface.

Methods: We selected EpCAM as the target antigen and used a bispecific EpCAM-TcE molecule consisting of two variable single chain fragments against EpCAM and CD3, respectively. VSV-GP encoding EpCAM-TcE (VSV-GP-EpCAM-TcE) or an invariant control TcE (VSV-GP-TNP-TcE) were generated as previously described. T cells were co-cultured with human target cells expressing EpCAM on their cell surface, either infected with the VSV-GP-EpCAM-TcE virus or with supernatant from VSV-GP-EpCAM-TcE infected cells. T cell activation, proliferation, degranulation and cytokine secretion were analyzed by flow cytometry and multiplex cytokine assays as a measure of TcE mediated cross-linking of T cells to their target on cancer cells. Patient-derived head and neck squamous cell carcinoma (HNSCC) tumors were sectioned into approximately 200 µM slices and infected with the virus. T cell activation was measured by cytokine secretion. The therapeutic potential of VSV-GP-EpCAM-TcE was tested *in vivo* in cell-line derived xenograft (CDX) models implanted in immunodeficient mice humanized with donor-derived PBMCs or CD34+ cells.

Results: Virus fitness was maintained for VSV-GP encoding the TcE molecule. Using co-culture assays, we demonstrated that EpCAM-TcE molecule is successfully expressed by VSV-GP and can activate both CD4+ and CD8+ T cells resulting in proliferation, degranulation, and cytokine secretion. Furthermore, we validated the concept using patient-derived HNSCC tumor slices which are representative of complex human tumor ecosystems. We could confirm that cancer cells infected by VSV-GP-EpCAM-TcE virus express functional TcE molecule and activates T cells to secrete IFNγ and TNFα. Finally, we tested the concept in two different CDX models where VSV-GP-EpCAM-TcE showed improved tumor growth inhibition due to a combined effect of oncolysis and T cell activation by EpCAM-CD3 TcE.

Summary: The oncolytic virus VSV-GP can be successfully armed with a TcE to redirect tumor-infiltrating T cells to destroy tumor cells which are not permissive to viral replication. This resulted in an enhanced therapeutic efficacy compared to just the oncolytic effect.

#6659 Oncolytic herpes simplex virus expressing XCL1 and FLT3L modulate the intratumoral immune response and improve the anti-tumor efficacy in a metastatic breast tumor model.

Himanshu Soni[1], Liqun Gu[2], Sylvie Roberge[2], Heena Kumra[2], Hiroshi Nakashima[1], E. Antonio Chiocca[1], Yves Boucher[2]

[1]Harvey W. Cushing Neuro-oncology Laboratories (HCNL), Department of Neurosurgery, Harvard Medical School and Brigham and Women's Hospital, Boston, MA,[2]Edwin L. Steele Laboratories, Radiation Oncology, Massachusetts General Hospital, Boston, MA

Patients with metastatic breast cancer (MBC) have a dismal prognosis, with a 5-year survival rate of only 26%. The inadequate infiltration of immune cells targeting the tumor microenvironment (TME) is a key factor contributing to this low survival rate. Immune effector cells, including CD8+ cytotoxic T cells, NKT cells, and NK cells, play a crucial role in targeting tumor cells. The activation of immune effector cells relies on the presence of conventional type I dendritic cells (cDC1), which present tumor-specific antigenic peptides on their surface. Recent studies have identified the chemokine XCL1 and growth factor FLT3L as critical factors involved in the intratumoral recruitment and expansion of dendritic cells. To enhance the activity of cDC1 in the TME we designed an oncolytic herpes simplex virus (oHSV) expressing XCL1 and FLT3L. The recombinant oHSV, rQ1-XF, was generated by incorporating LoxP sites into the viral genome through recombination with a carrier plasmid carrying the polycistronic cassette. To enhance the intratumoral penetration of oHSV injected intravenously in primary tumors and MBC lesions in the lung, we employed the cancer drug ganetespib, which can increase the permeability of tumor blood vessels. In comparison to untreated mice, ganetespib combined with rQ1-XF reduced the size of primary tumors and induced a short but significant increase in the survival of mice. Additionally, compared to the ganetespib alone treatment, ganetespib combined with rQ1-XF reduced MBC burden in the lung. The flow cytometry analysis of immune cells revealed an increased infiltration of CD11c+CD11b- dendritic cells in primary tumors treated with oHSV combination therapy compared to the ganetespib only control. A similar trend was also observed in CD4 T cells and CD8 T cells in primary tumors. As expected, there was a negative correlation between tumor burden and the infiltration of CD4+ T cells and CD8+ T cells in primary tumors. Ganetespib combined with oHSV also reduced the infiltration of CD4+ regulatory T cells (Tregs) in primary tumors, however the number of Tregs increased with primary tumor size as well as tumor burden in the lung. This could potentially lead to reduced efficacy of tumor-infiltrating dendritic cells in activating effector T cells in tumors treated with ganetespib and rQ1-XF. Moreover, the combination therapy did not yield significant alterations in the populations of DCs, CD4+ T cells, and CD8+ T cells in lungs with metastatic lesions. Further studies are underway to investigate whether the depletion of Treg cells in combination with rQ1-XF enhances effector T cell activation against metastatic breast tumor cells. The findings of this study will provide valuable insights into the effectiveness of using XCL1 and FLT3L-armed oncolytic viruses in patients with MBC.

#6660 The novel codon-modified Zika virus CDX-602 shows anti-tumor efficacy and remodels the tumor microenvironment in preclinical models.

N. Jahan[1], Y. Zhao[1], K. Blagovic[1], Y. Wang[2], J. Coleman[2], S. Mueller[2], **J. K. Kaufmann**[1];
[1]Codagenix, Inc., Cambridge, MA, [2]Codagenix, Inc., Farmingdale, NY

Multiple oncolytic viruses have been shown to induce multifaceted changes in the tumor microenvironment, that ultimately support induction of anti-tumor immune responses. We have previously demonstrated that CodaLytic, a codon-modified influenza virus, can kickstart the cancer immunity cycle at various steps in several mouse models with differing baseline immune contextures. Here, we are describing the activity of a new codon-modified virotherapeutic derived from the same synthetic viral engineering platform [Coleman *et al.*, Science 2008]. Zika virus strain MR766 was synthetically codon-modified at 664 positions in the envelop gene to yield CDX-602. Virus was originally passaged in Vero cells and working stocks were expanded in BSR-T7 cells for *in vivo* use after titration on MA104.1 cells. Efficacy after intratumoral injection of 10^7 PFU/dose CDX-602 alone or in combination with 200 µg/dose αPD-1 blockade (RMP1-14, i.p.) was determined in subcutaneous B16-F10 melanoma and orthotopic EMT6 breast cancer models (n = 10). Changes in the tumor immune infiltrate were characterized using flow cytometry 6 or 8 days after treatment initiation, respectively (n = 5). In the immunotherapy-resistant B16-F10 model, CDX-602 monotherapy led to highly reproducible tumor growth inhibition (TGI, 52%, $p < 0.0001$ vs vehicle control), resulting in modest, but significant prolongation of median survival (25%, $p < 0.01$). Anti-tumor efficacy correlated with increased tumor immune infiltration with $CD4^+$ and $CD8^+$ T cells ($R^2 = 0.68$ and 0.67, respectively, $p < 0.01$). Importantly, frequencies of cross-presenting dendritic cells (cDC) were increased 3.8-fold ($p < 0.0001$) after virus treatment, while no compensatory influx of $CD206^+$ macrophages was observed, suggesting immune contexture changes conducive to anti-tumor immune induction. Efficacy was confirmed in the EMT6 model, in which monotherapy TGI was 44% and thus on par with αPD-1 blockade (50%, both $p < 0.0001$ vs control). Combination viroimmunotherapy in this model further improved efficacy, leading to 71% TGI and a doubling in complete regressions to 40%. Inclusion of CDX-602 in the treatment regimen led to similar changes in immune infiltration, in particular recruitment of $CD8^+$ T cells and cDCs (9.7-fold and 6.9-fold increase after combination, respectively). Additional *ex vivo* analyses to confirm induction of anti-tumor immune responses are ongoing. Taken together, this preclinical data establishes CDX-602 as a novel virotherapeutic candidate that engages multiple mechanisms of action that contribute to anti-tumor activity. CDX-602 is the second virotherapeutic candidate derived from Codagenix's codon modification platform, further supporting the utility of this synthetic viral engineering technology for viroimmunotherapy of cancer and highlighting its potential across multiple viral species.

#6661 Profiling response to oncolytic adenovirus and immune checkpoint inhibitors by mass cytometry in a triple negative breast cancer mouse model.

W. Xu[1], Q. Lin[2], Y. Li[2], B. Filimon[1], S. Shin[1], M. Olson[2], M. Chen[2];

[1]NorthShore University HealthSystem, Chicago, IL, [2]The University of Chicago, Chicago, IL

Immune checkpoint inhibitors (ICIs) based immunotherapy has found success in treating breast cancers but for more immunosuppressive cancer types, especially most of triple negative breast cancers (TNBCs), response rates generally are low. Also, combination immunotherapy with oncolytic adenoviruses (OAVs) has been shown to induce a more immune inflamed phenotype in many pre-clinical studies. Here, by using a 40-antibody panel for mass cytometry, we profiled comprehensive changes of cell phenotypes in a TNBC mouse model both systemically and in the tumor microenvironment in response to the treatment of ICIs and/or a new systemically delivered, TGFβ signaling inhibiting OAV, mHAdLyp.sT. The samples in this study were collected on day 16 of tumor cell inoculation, while mHAdLyp.sT were applied by tail vein on day 7 and 9, and anti-PD-1 and anti-CTLA-4 antibodies were injected Intraperitoneally on day 8, 10, 12, 14. After sample processing and data acquisition on Helios system, a standard workflow was applied for data preprocessing including normalization, compensation, transformation, diagnostic analysis, marker ranking, cell population identification, visual representation, differential analysis, and statistical analysis. In blood samples, for T cell clusters, percentages of effector $CD8^{\pm}$ T cells, naïve $CD8^{\pm}$ T cells, and $CD44^{low}CD62L^{low}$ $CD8^{\pm}$ T cells among total cells were increased by mHAdLyp.sT, anti-PD-1, and anti-CTLA-4 combination when compared to the buffer group but none of these significant changes were observed in groups treated with mHAdLyp.sT or ICI antibodies alone. Combination treatment also increased percentages of clusters of $CD272^{high}CD44^{high}$ DCs, $CD44^{high}CD62L^{low}$ B cells, and $CD44^{high}$ macrophages significantly. In spleen, combination treatment significantly increased several T cell clusters, including $TCR\beta^{high}CD38^{high}ROR\gamma t^{high}$ T cells, $TCR\beta^{high}$ $CD4^{\pm}$ T cells, effector $CD8^{\pm}$ T cells, $TCR\beta^{high}CD44^{low}CD62L^{low}$ $CD8^{\pm}$ T cells, and $CD11b^{high}$ $CD8^{\pm}$ T cells when compared to the buffer group. Interestingly, while ICIs treatment increased several macrophage clusters, such as $CD44^{high}$Ly-6G/C^{high} macrophages, $CD11b^{low}$ macrophages, and $CD44^{high}CD11b^{high}$ macrophages, they are not significantly increased in the combination treatment group. In the tumor, we did not detect any significant changes by the combination treatment in the clusters we identified now although the average percentages of several clusters were either increased or decreased. We will refine these algorithm-generated clusters from tumors once we obtain our data from day 24 sample collection point for advanced analysis. In short, our current results suggested that the combination therapy is more potent in generating cytotoxic T cells and other anti-tumor immune cell populations systemically in the early stage of the treatment and tumor progression.

#6662 Modified oncolytic viruses with immunomodulatory genes enhance anti-tumor efficacy.

Z. Song, G. Ding, A. Xia, W. Ma, Q. Li, C. He, X. Chen, Z. Zhang, Q. Gu;
WuXi AppTec, Nantong, China

While chemotherapy and radiotherapy are considered first-line treatments for most cancers, their significant side effects have prompted ongoing innovation and the discovery of novel cancer treatment strategies. Oncolytic viruses (OV) as one of the most advanced cancer treatments have shown promising results in treating otherwise untreatable types of cancer in last two decades. After selectively targeting tumor cells, OVs could directly kill cancer cells, and induce a powerful anti-cancer immunity.

Recently, we evaluated the anti-tumor effect of a modified OV (mOV) *in vitro* and *in vivo*. Firstly, the expression of the transgenes were validated on different tumor cells by FCM and ELISA assay. The results showed that a susceptible cell line was identified which has high expression efficiency of transgenes. In order to evaluate the cytotoxicity of mOV, CCK-8 assay was performed on 30+ tumor cell lines. It indicated that mOV has stronger killing effect on susceptible cells through inducing cellular apoptosis. To further evaluate the biological activity of the transgenes on immune cells, mOV-infected tumor cells and supernatant were collected to treat T cell, NK cell or MoDC. The results demonstrated that mOV infection could significantly promote T cell and NK cell activation, and increase the maturation of moDC cells, resulting in the secretion of IFN-γ by CD8+ T cells. In the *in vivo* efficacy study, MC38 syngeneic model was used to test the anti-tumor effect of mOV. The result showed that mOV could significantly inhibit the growth of the treatment side tumor, and reduce the contralateral tumor to a certain extent. Blood FCM analysis revealed that the percentage of IFN-γ+CD3+, IFN-γ+CD4+ and IFN-γ+CD8+ T cells were markedly increased by mOV treatment compared with vehicle. In addition, IHC analysis of tumor showed that mOV treatment could promote the infiltration of CD4+, CD8+ and CD86+ positive cells. To study the safety or PK of the mOV, viral bio-distribution and shedding assay were performed to detect viral genome at different tissues or excreta. It indicated that mOV was almost undetectable or at very low levels for 14 days after administration. In conclusion, our study revealed that modified OVs with immunomodulatory genes have good anti-tumor efficacy both *in vitro* and *in vivo*, which could obviously induce the activation of several immune cells. Moreover, the mOV genome was almost undetectable or at very low levels in mouse tissues and excreta.

Keywords: Oncolytic virus, immunotherapy, immunomodulatory genes

#6663 Innovative CPMV immunotherapy: A canine model for poor-prognosis breast cancer treatment.

G. Valdivia[1], D. Perez-Alenza[1], L. Barreno[1], A. Alonso-Diez[1], J. Affonso de Oliveira[2], M. Suarez-Redondo[1], S. F. Fiering[3], N. F. Steinmetz[2], **L. Pena**[1];
[1]Complutense University of Madrid, Madrid, Spain, [2]University of California San Diego, San Diego, CA, [3]Geisel School of Medicine at Dartmouth, Madrid, NH

Cowpea Mosaic Virus (CPMV) is a plant comovirus non-infectious to humans or animals. In mice models, intratumor immunotherapy (ITI) with CPMV devoid of nucleic acids (empty CPMV, eCPMV) and full CPMV results in a highly potent, systemic, antitumor immune response, with full CPMV being much more effective. Dogs with spontaneous mammary (breast) cancer (MC) serve as a valuable model for studying breast cancer (BC), bridging the gap between studies in rodents and human clinical trials. Canine MC develops in the presence of an intact immune system and has a unique advantage of shorter endpoint periods compared to women BC clinical trials. New immunotherapeutic approaches are necessary for poor-prognosis BC, such as triple-negative BC, metastatic BC, and the very aggressive and lethal inflammatory BC (IBC). Previous studies by our group using eCPMV ITI in dogs with MC revealed a substantial reduction in tumor size in both injected and non-injected tumors (abscopal effect), extended survival, and improved quality of life without any adverse effects or toxicity. In this clinical trial, we employed full CPMV nanoparticles ITI in dogs with poor-prognosis (inoperable) MC, comparing them with untreated controls. Regular tumor volume assessments and clinical evaluations have been conducted. Histopathology and immunohistochemistry of immune cell populations were performed to study tumor microenvironment (TME) modifications. Thus far, 5 dogs have been treated: four cases of inflammatory mammary cancer (IMC) and one case of metastatic MC. After at least two weekly CPMV ITI sessions, a significant reduction in tumor volumes was observed. In IMC cases, marked clinical improvement of typical signs (warmth, edema, erythema, and cutaneous pain) was observed in 3 out of 4 cases, and tumor reduction was so remarkable in one dog that surgery was recommended and successfully carried out. In IMC CPMV ITI cases, the survival of 2 dogs exceeded historical IMC records; the dog with metastatic MC maintains stable disease after one year, which is also superior to controls. TME studies showed that eCPMV immunotherapy significantly increased intratumor inflammatory infiltrates, neutrophils, T lymphocytes, and macrophages. Additionally, Treg cells (FOXP3+)/T lymphocytes (CD3+) ratio was significantly reduced. Our results demonstrate that immunotherapy with eCPMV induces a potent immunostimulatory effect on dogs with poor-prognosis MC by recruiting and activating neutrophils as the main drivers of the inflammatory response. This process reduces the immunosuppressive action of regulatory T lymphocytes and produces a breakdown of tumor immune suppression. These findings underscore the therapeutic potential of CPMV nanoparticles ITI in the management of canine IMC and metastatic MC. From a translational point of view, this study lays the groundwork for advancing the treatment of human breast cancer.

#6664 In situ vaccination with hyper-interferon sensitive influenza induces adaptive immune response and sensitizes murine non-small cell lung cancer to PD-1 blockade.

R. Salehi-Rad, Y. Du, T. Zhang, Y. Shi, B. Liu, S. Ren;
UCLA - University of California Los Angeles, Los Angeles, CA

Despite recent advances in immunotherapy with immune checkpoint inhibitors (ICI), many patients with non-small cell lung cancer (NSCLC) fail to respond or develop resistance after an initial response. The exclusion of T cells from the tumor or the presence of a dysfunctional T cell compartment within the tumor microenvironment (TME) constitute two central hallmarks of resistance to ICI in patients with NSCLC. Seminal studies have identified that loss of LKB1 in *KRAS*-mutant NSCLC drives resistance to ICI, potentially by suppressing STING, thereby leading to dysregulation of the interferon (IFN) signaling. There is a pressing demand for the development of innovative immune therapies designed to bolster anti-tumor T cell responses to overcome resistance to ICI. *In situ* vaccination (ISV) with oncolytic viruses has emerged as a promising, antigen-agnostic strategy capable of conditioning the TME and amplifying anti-tumor T cell responses. We engineered a live attenuated viral vaccine, Hyper-Interferon Sensitive virus (HIS), by conducting a genome-wide functional screening and introducing eight interferon (IFN)-sensitive mutations in the influenza A genome. We utilized multiple syngeneic murine models of NSCLC with distinct driver mutations [$Kras^{G12D}/P53^{+/-}/Lkb1^{-/-}$ (KPL); $Kras^{G12D}/P53^{+/-}$ (KP); and $Kras^{G12D}$ (K)] and varying tumor mutational burden to assess the safety and efficacy of intratumoral HIS virotherapy. Compared to wild-type (WT) influenza, HIS replication was attenuated, enhancing its potential as a safe option for cancer therapy. HIS ISV elicited robust yet transient type I IFN responses in murine NSCLCs, leading an influx of polyfunctional effector Th1 CD4 and cytotoxic CD8 T cells into the tumor. HIS ISV demonstrated enhanced anti-tumor efficacy compared to WT in multiple syngeneic murine models of NSCLC. This efficacy was dependent on host type 1 IFN responses and T lymphocytes. HIS ISV synergized with anti-PD-1 to eradicate immune resistant LKB-1 deficient NSCLC in a subset of mice, resulting in improved overall survival and enduring systemic tumor-specific immunity. These studies provide compelling evidence to support further clinical evaluation of HIS as a novel ‘off-the-shelf’ ISV strategy for patients with NSCLC refractory to ICI.

#6666 Leveraging an obligate anaerobic salmonella strain for targeted cargo delivery in the tumor microenvironment to restore immunotherapy sensitivity.

Y. He, J. Huang;
University of Hong Kong, The - Li Ka Shing Faculty of Medicine, Pok Fu Lam, Hong Kong

Tumor immunotherapy is often hindered by unresponsive cold tumor microenvironments (TME). Although *Salmonella*-based immunotherapy has shown potential in overcoming these cold immune environments, safety concerns remain. Our study introduces a genetically reprogrammed *Salmonella typhimurium* strain (OASL) with a dual safety lock to enhance safety and modify immunosuppressive TME, sensitizing tumors to immunotherapies. We propose using OASL to alter the cold TME and locally release therapeutic cargos such as PDL1 nanobodies and tumor-specific neoantigen peptides identified through bioinformatic algorithms, activating immune cells within the tumor while minimizing side effects. We selected YB1, an obligate anaerobic Salmonella strain that thrives in hypoxic environments, as our base strain and incorporated a self-lysis genetic circuit for controlled bacterial growth and cargo release upon reaching a specific population density within the tumor core. We assembled and evaluated the self-lysis gene circuit in vitro, documenting the event using an optical density (OD) reader and confirming OASL's ability to express genetic cargos through western blot analysis. We then investigated OASL's therapeutic effect in vivo and characterized TME changes using flow cytometry and immunohistochemistry staining. Our results indicate that OASL undergoes lysis and releases cargos upon reaching a specific population density in vitro. Additionally, OASL-delivered neoantigen peptides elicited a tumor-specific immune response in vivo. OASL also demonstrated the capacity to modify the TME and restore sensitivity to PDL1 in previously unresponsive tumors, enhancing therapeutic effects.

IMMUNOLOGY: Microbiome, Inflammation, and Cancer
Poster Session

#6670 Could immunotherapy offer potential in managing bacterial dysbiosis in prostate cancer?.

T. Oliver[1], B. Nedjai[2], E. Lane[2], F. Chinegwundoh[3], P. Rajan[1], J. Cuzick[2];
[1]Barts Cancer Centre, London, United Kingdom, [2]Wolfson Institute, London, United Kingdom, [3]Barts Cancer Institute, London, United Kingdom

Background: Since 2006 three studies, involving 289,089 adolescents, demonstrated a significant association (1.67(0.79-3.55),1.7(1.03-2.70),2.37(1.19-4.73)) between pubertal acne and poor outcome prostate cancer(PC) 30+ years later. This suggested *Cutibacterium acnes*, amicroaerophylic bacterium, might be contributing to PC bacterial dysbiosis analogous to the role of *H. pylori* in stomach cancer and explain why circumcision reduces PC risk. Six years ago, using MALDI-TOF, we demonstrated that the presence of seven obligate anaerobe species in addition to *C. acnes* were increased in PC and linked to increased PSA. This presentation studies stored samples from the PROVENT chemoprevention randomised PC active surveillance phase 2 trial analysed using 16S rDNA sequencing, and comparing obligate anaerobe frequency with those detected by culture and MALDI-TOF identification and their influence on PSA expression.
Methods: 89 urines of PROVENT trial patients were studied using 16S rDNA sequencing and followed for 24 months. In addition, 39 previously reported MALDI-TOF screened cohort patients (21 PCs and 18 BPHs) followed for 43 months. The frequency of 7 obligate bacterial genera (Actinobaculum, Finegoldia, Prevotella, Peptoniphilus, Peptostreptococcus & Viellonella) was studied.
Results: Twenty six of 89 (29%) PROVENT urine samples had a majority of bacteria detected as obligate anaerobes (mean=68%), while it was 12 of the 39 (31%) in PC tested in MALDI-TOF. In the combined series, those patients (n=38) with obligate anaerobes had mean PSA of 9.59 ug/L, while those without obligate anaerobes had a mean PSA of 6.29 ug/L (n=90), (t=-2.925, p = 0.0058). In the MALDI-TOF series, statistically increased urological intervention rate was associated with the presence of anaerobes (p=0.045, Fisher's exact test).
Discussion: These findings suggest that obligate anaerobe bacterial dysbiosis could be contributing to raised PSA through prostate cell damage, and possibly participating in the chronic inflammation and hypervascular changes that are seen in precancerous lesions. Checkpoint inhibitors have shown little benefit in prostate cancer. Recent reports from animal model studies of BCG resistance have suggested a short course combination of anti PDLI and anti NKG2a could break immune tolerance associated with expression of HLA-E and this approach could be of use to break tolerance to bacterial dysbiosis in the future.

#6671 Harnessing radiation and microbiome modulation for enhanced antitumor immune response in early-stage NSCLC treatment.

S. J. Feigenberg, F. Costabile, S. Pierini, N. Kostopoulos, R. Perales-Linares, M. Uribe-Herranz, E. Ben-Josef, C. Koumeis, **A. Facciabene**;
Univ. of Pennsylvania, Philadelphia, PA

In recent years, research has highlighted radiotherapy's (RT) capacity to induce Immunogenic Cell Death (ICD), activating tumor-infiltrating Dendritic Cells (DCs) for cross-presenting tumor-associated antigens (TAAs), leading to robust systemic immune responses. Simultaneously, emerging studies underscore the gut microbiota's crucial role in modulating immunity across diverse human diseases. Our investigation focuses on gut microbiome modulation, specifically using oral Vancomycin, a locally acting antibiotic. This approach enhances the direct and abscopal antitumor effects of RT, evident across multiple cancer models. Findings demonstrate Vancomycin significantly increases CD8+ T cell infiltration, targeting TAAs in primary and abscopal tumors, leading to elevated IFN-β and IFN-γ expression in tumor-derived lymph nodes (TDLNs). Vancomycin's remarkable influence on RT effectiveness directly traces back to its impact on the gut microbiome composition, including a shift from gram-positive to gram-negative bacteria, enrichment of Vancomycin-resistant strains, reduced bacterial diversity, and decreased SCFA concentrations.. Building on these compelling outcomes, we initiated a randomized pilot study involving stage I non-small cell lung cancer (NSCLC) patients undergoing stereotactic body RT (SBRT). Patients were randomized to receive Vancomycin versus placebo, administered at 125 mg four times daily, commencing one week before SBRT and continuing during and after treatment for five total weeks. In an interim analysis, despite a small sample size, significant improvements in Progression-Free Survival (PFS) and Overall Survival (OS) were observed in those receiving the combination therapy. Additional investigations have reaffirmed our earlier findings in mice, emphasizing the depletion of specific bacterial populations, the rise in Vancomycin-resistant strains, and substantial reductions in SCFA concentrations in stool samples. Pathway analysis further underscores the impact of oral Vancomycin on gene expression related to the cross-presentation of TAAs. Together, these findings from both murine and human studies robustly affirm the concept that modulating the gut microbiome with Vancomycin can augment the ability of RT to trigger an anti-cancer immune response. We posit that this pioneering strategy is not only cost-effective but also holds the promise of substantially enhancing patient outcomes.

#6672 Unraveling the microbiome: antibiotic impact on CAR T therapy and the synergistic potential of vancomycin in enhancing antitumor immunity.

A. Facciabene, M. Uribe-Herranz, V. Bhoj;
Univ. of Pennsylvania, Philadelphia, PA

The landscape of treating hematologic malignancies has undergone a revolutionary transformation with the advent of Anti-CD19 chimeric antigen receptor T cell therapy (CART-19). Despite its success, persistent challenges like disease relapse and CAR-mediated toxicities remain. A comprehensive multicenter study involving 228 individuals revealed a significant association between antibiotic administration, particularly piperacillin/tazobactam, meropenem, and imipenem/cilastatin (P-I-M), targeting anaerobes within four weeks preceding CART-19 therapy, and adverse outcomes, including worsened survival and increased neurotoxicity. Intriguingly, another antibiotic, Cefepime, also used for neutropenic fever, displayed a positive trend when compared with P-I-M. This highlights the intricate relationship between the modulation of the intestinal microbiome and outcomes in CART-19 therapy for B cell malignancies. Building on these critical observations, our study delved into the impact of vancomycin-induced gut microbiota dysbiosis on chimeric antigen receptor (CAR) T immunotherapy. Utilizing preclinical models of CD19+ A20 lymphoma and CD19+ B16 melanoma, we discovered that mice receiving vancomycin alongside CART-19 therapy exhibited enhanced tumor control and increased cross-presentation of tumor-associated antigens (TAAs) compared to those receiving CART-19 alone. This effect was further validated through fecal microbiota transplants from healthy human donors to pre-conditioned mice, replicating the favorable findings. Importantly, our study extends to clinical correlates, as B cell acute lymphoblastic leukemia patients treated with CART-19 and oral vancomycin displayed elevated CART-19 peak expansion compared to unexposed patients. These compelling results underscore the profound influence of the gut microbiota on CAR T cell therapy and suggest that vancomycin-induced gut microbiota modulation may emerge as a potent strategy to enhance therapeutic outcomes across various tumor types.

#6673 Tumor microbial burden is regulated by mast cells and determines immunotherapy responses.

H. Rajaei[1], J.-H. Jang[1], H. Liu[1], E. Faraoni[1], O. Le Roux[1], V. Chandra[1], V. Tahan[1], L. Li[1], E. Riquelme[2], J. White[3], L. Diaz Jr.[4], F. McAllister[1];
[1]UT MD Anderson Cancer Center, Houston, TX, [2]Pontifical Catholic University of Chile, Santiago, Chile, [3]Resphera Biosciences, Baltimore, MD, [4]Memorial Sloan Kettering Cancer Center, New York, NY

Immune checkpoint inhibitors (ICI) have notably improved overall survival rates across various cancers, particularly in cases of mismatch repair deficient cancer (MMRd). However, numerous factors influence patient response following ICI treatment. Beyond genetic factors, mutations, and levels of immune cell infiltration, several studies highlight the correlation between the gut microbiome and treatment response rates. Furthermore, specific bacterial compositions have been observed to shift during therapeutic interventions. Notably, studies have demonstrated that patients who used antibiotics before and during ICI treatment exhibited lower progression-free survival and overall survival, serving as evidence for this association. Our previous investigations elucidated the impact of distinct tumor microbial burdens on modulating immune activation. Consequently, our hypothesis posits the substantive involvement of the interplay between tumor microbial burden and the immune system response to ICI treatment.

We evaluated the presence of intra-tumoral microbes within Colorectal cancers (CRC) by examining TCGA data. Patients with elevated microbial levels demonstrated heightened immune activity and better survival rates. Using cybersport analysis, we validated increased mast cell infiltration in CRC patients with abundant microbes. Quantification involved assessing bacterial burden through 16s rRNA via FISH staining and mast cell counts using tryptase via IHC staining. Reducing bacterial load in MC38 cancer model, achieved by locally administering antibiotics, led to a diminished immune response when PD-1 was introduced to these mice. Cross-referencing TCGA data, we identified upregulated genes in CRC patients with high microbial burden and downregulated genes in mice receiving local antibiotics after MC38 cell implantation. The common genes were associated with immune responses, suggesting a strong correlation between bacterial burden and immune activity in CRCs. In conclusion, the high burden of bacteria in CRC improves immune response to ICI and increases the infiltration of mast cells, which all contribute to better survival rates.

#6674 Fungi utilizes exocytosis pathway to facilitate the release of DAMPs from pancreatic cancer cells.

A. Alam, S. S. Mayengbam,, S. Senchanthisai, B. Irmak, P. Dey;
Roswell Park Comprehensive Cancer Center, Buffalo, NY

Recent studies overwhelmingly show that microbiome is pervasive to tumor and play key role in immunotherapy response and reprograming tumor immune microenvironment (TIME). However, it remains unknown how microbiome facilitates the host-immune cell crosstalk and promote tumorigenesis. Our recent study in pancreatic ductal adenocarcinoma (PDAC) show that intratumor fungal microbiome facilitate the release of a damage associated molecular pattern (DAMP) molecule IL-33 from cancer cells. The secreted IL33 from cancer cells in turns recruits ILC2 and T_H2 cells which promotes PDAC tumorigenesis. However, the mechanism of fungal mediated IL-33 release from PDAC cells remains unknown. Our follow up studies using high throughput integrated proteomic profiling and immunoprecipitation revealed a group of exocyst complex proteins interacting with IL-33 in the presence of fungus. The exocyst complex consists of eight sub-unit proteins that tethers the secretory vesicles to the plasma membrane and implicated in cellular exocytosis. We found EXOC6B a component of exocyst complex, modulates IL-33 release via exocytosis pathway from the PDAC cells. Genetic depletion of EXOC6B resulted in shunted IL-33 release and significantly abrogated PDAC tumor progression. Mechanistically, we found that mycobiome activates a non-canonical TLR2-CARD9 pathway, thereby driving IL-33 nucleocytoplasmic transport and exocytosis. This study identifies a unique mechanism of EXOC6B mediated release of IL-33 that expands our knowledge on how host-mycobiome interaction shapes PDAC tumor microenvironment by intricate molecular mechanism. Our study identifies EXOC6B as a new therapeutics target involved in the mycobiome driven IL-33 secretion in pancreatic cancer.

#6675 Dissecting the relationship between mucin 5AC and the lung/gut microbiome in the pathogenesis of K-ras mutant lung cancer.

M. T. Grimaldo[1], M. J. Clowers[1], A. Krishna[1], K. E. Larsen[2], N. Karimi[2], Y. H. Rezai[2], A. Gaitonde[2], F. Khalaj[2], H. Liu[1], F. McAllister[2], S. Moghaddam[2]; [1]The University of Texas MD Anderson Cancer Center UTHealth Houston Graduate School of Biomedical Sciences, Houston, TX, [2]The University of Texas MD Anderson Cancer Center, Houston, TX

Non-small cell lung cancer, including its most common subtype, lung adenocarcinoma (LUAD), is one of the most prevalent and lethal forms of cancer worldwide. This is largely due to patients having progressed to an advanced stage of disease by the time of diagnosis. Thus, better understanding the pathogenesis of early LUAD is paramount for the identification of key targets and development of preventive and therapeutic strategies for clinical management of the disease. *KRAS* mutations are the most common oncogenic driver alteration in human LUAD. Previously, we have found that *KRAS* mutant LUAD patients whose tumors harbor high expression of Mucin 5 AC (MUC5AC), a main airway secretory mucin, have significantly lower survival and poor prognosis. Mucins are membrane-bound and secreted hydrophilic proteins essential in clearance of allergens, pathogens, and debris in the lung airway. However, overproduction of mucins, such as MUC5AC, plays roles in the pathogenesis of airway diseases such as chronic obstructive pulmonary disease (COPD) and lung cancer. Given the known effect of mucin polymers on bacterial growth and the immune microenvironment in the context of other airway inflammatory diseases, in this study, our objective is to better understand the MUC5AC-to-microbiome relationship using a lung epithelial specific mouse model of KRAS-mutant LUAD (CC-LR) and test the combinatorial effects of genetic deletion of MUC5AC (CC-LR/Muc5ac$^{-/-}$) and the pan-microbiome depletion on tumor progression, the lung immune contexture, and microbiome (lung and gut). Thus far, we found that genetic deletion of MUC5AC or pan-microbiome depletion significantly decreases the tumor burden (66% vs 50%, respectively). Additionally, both groups show to have a significantly decreased percentage of tumor-specific Ki67+ cells, a cell proliferation marker, and ERG+ cells, an angiogenesis marker, in comparison to the CC-LR controls. The combination of the lack of MUC5AC with pan-microbiome depletion has also shown to reduce tumor development that needs further investigation. These findings highlight the need to better understand the mechanistic interaction between mucins and the lung/gut microbiome in the context of KRAS-mutant lung cancer which we are currently exploring. It also suggests that their relationship could be a key target for modulation, potentially leading to the development of a minimally invasive alternative preventive and/or treatment modality against *KRAS*-mutant LUAD.

#6676 Microbiome modification impacts PSCA directed chimeric antigen receptor (CAR) T cell therapy for prostate cancer.

J. P. Murad[1], L. Christian[1], Y. Yamaguchi[1], L. Lopez[1], C. Ouyang[1], H. Sato[2], B. Jarman[2], S. Stromberg[2], S. J. Forman[1], S. Van Dien[2], S. Culler[2], S. J. Priceman[1];

[1]City of Hope National Medical Center, Duarte, CA, [2]Persephone Biosciences, San Diego, CA

Background: There is growing evidence that responsiveness to immunotherapy is influenced by the composition of a patient's gut microbiota. Recent analysis identified strong correlations between abundance of gut microbial species and positive response to immune based therapies in cancer patients. Further, enrichment of commensal microbes can promote immunostimulatory effects, immune based anti-tumor responses, and increased cytotoxic T cell abundance within the TME. Conversely, the presence of gut microbes known to cause inflammatory states in gut tissues may be correlated to negative immunotherapy outcomes or toxicities. To this end, we aimed to evaluate the impact of microbiome manipulation on gut microbe diversity, systemic immunity, local TME, and PSCA-targeted chimeric antigen receptor (CAR) T cell therapy in our established syngeneic prostate cancer mouse model.

Methods: In an immune competent mouse model of PSCA+ prostate cancer developed in our lab, we sequentially modified the gut microbiome using antibiotic clearance followed by distinct human derived fecal matter transfers (CPI-FMT, HD-FMT, or No-FMT). Simultaneously, we treated microbiome modified tumor bearing mice with PSCA-targeting CAR T cells and measured differences in anti-tumor efficacy and survival. To provide mechanistic insight, we performed longitudinal whole genome sequencing (WGS) of fecal matter microbes and RNA sequencing on spleen and tissues following FMT administration.

Results: In our model, a unique checkpoint inhibitor (CPI) treated patient derived human FMT (CPI-FMT) improved PSCA-CAR anti-tumor responses relative to healthy donor (HD-FMT) or No-FMT treatment controls. CPI-FMT administration also significantly improved overall survival in CAR T cell and non-targeting T cell control treated mice. Temporal analysis of microbes present in the gut following CPI-FMT and HD-FMT treatment show CPI-FMT treated mice exhibit favorable maintenance of gut microbe species richness and significant increase in microbiota diversity. We identify CPI-FMT provides an enrichment of specific microbes associated with preservation of gut homeostasis and improved immune response. RNA sequencing analysis on tumor tissues show differential transcription of immune related pathways following FMT which may influence immune and CAR T cell function.

Conclusions: We show that our mouse prostate cancer model is sensitive microbiome modulation and can significantly impact PSCA-CAR T cell directed anti-tumor responses. Temporal WGS analysis of gut fecal matter reveal enrichment suggest specific species abundances which may promote gut homeostasis over dysbiosis or inflammatory states and may account for improved CAR T cell response. We aim to further develop this model to interrogate candidate targeted microbiome modifiers which may impact mechanisms which promote CAR T cell and immune function.

#6678 Microbial regulation of anti-tumor immunity in colorectal cancer.

C. Chung[1], E. Ozcelik[1], J. Habel[1], J. Zhang[1], Y. Qin[1], L. Garcia[1], J. Merrill[1], T. Chung[1], S. Lyons[1], Z. Shen[2], J. G. Fox[2], P. Westcott[1], S. Beyaz[1];
[1]Cold Spring Harbor Laboratory, Cold Spring Harbor, NY, [2]MIT, Cambridge, MA

Colorectal cancer (CRC) is the 3rd leading site of cancers and cause of cancer cell death. Although Immunotherapies revolutionized cancer therapy, the majority of CRC patients, particularly with metastatic disease, do not respond to the treatments. This necessitates a better mechanistic understanding of the tumor-immune cell interactions in the context of CRC. Microbiome influences multiple biological aspects of the host including immune responses against cancers. Here, we show that the gut microbiome influences cancer MHC-I and -II expression levels and restricts tumor progression and metastasis, resulting in longer survival in 3 different CRC models and two different mouse strains. We found that the anti-tumor effects are dependent on T cells and B cells. Interestingly, depletion of B cell negated anti-metastatic effects of gut microbiome. Mechanistically, MHC-II expression in cancer cells mediates the anti-tumor effects of the microbiome. MHC-II upregulation on human CRC organoids enhances cancer-immune cell interactions and associated apoptosis, demonstrating an anti-tumor role and significance of MHC-II in human CRC. Thus, gut microbes that enhance MHC-II antigen presentation promotes anti-tumor immunity and may be utilized to enhance efficacy of immunotherapy in metastatic CRC.

#6679 Deciphering the mechanism of action of a live biotherapeutic product for the treatment of cancer.

E. Katkeviciute, F. Ferraro, M. Schwill, P. Busenhart, A. Montalban-Arques;
University of Zurich, Zurich, Switzerland

Intestinal microbiota is essential in shaping the immune system and its functions. In our effort to harness the potential of beneficial gut microbiota, we identified specific bacterial species that are less abundant in colorectal cancer patients compared to healthy individuals. Oral supplementation of these bacteria causes an effective anti-tumor activity in various cancer models through specific activation of cytotoxic T-cells. Based on these results, we aimed to identify the mechanism of action of this bacterial treatment. In vivo studies were performed in C57BL/6 and BALB/c mice. MC-38, CT-26, B16, LLC1.1 and 4T1 cells were used for the heterotopic tumor injections. Immunophenotyping was performed using flow cytometry and immunohistochemistry. Metagenomics analysis and whole genome sequence were performed to identify the bacterial strains. Metabolomics analyses were conducted to analyze bacterial supernatant and serum compositions of mice and patients. Since we found that the bacterial treatment led to a systemic anti-tumor effect, we analyzed serum of the mice that received the bacteria and found that a specific metabolite was highly upregulated compared to untreated mice. Analysis of the medium supernatant from cultures of the bacterial strains led to the discovery that metabolite identified in the serum is being produced by our bacteria. Applying this bacterial metabolite alone in the mouse cancer models led to a similar immune activation and anti-tumor effect as the supplementation with our bacterial strains. Furthermore, we identified the receptor that is targeted by this molecule through experiments with known agonists and antagonists for the target. The anti-tumor effect of the bacteria as well as the bacterial metabolite was blocked through the application of a receptor antagonist, proving that activation of this receptor is the mechanism that drives the enhanced anti-tumor immune response. Activation of the receptor, which is mainly expressed on macrophages led to enhanced IL-12 production and recruitment of cytotoxic T-cells into the tumor. Together, we have fully characterized the mechanism of action of our bacterial treatment, including the secreted active metabolite, the target receptor, and the activated immune cells. We are developing a live biotherapeutic product for the treatment of cancer based on oral administration of lyophilized bacteria. The known mechanism of action of our bacteria helps us to optimize the efficacy of our product, define the right dosage and understand possible side effects. Additionally, it enables us to improve patient selection and prediction of treatment response. Since our product is based on commensal bacteria that are commonly present in healthy individuals, we expect a very good safety and tolerability profile. Therefore, our therapy aims to significantly improve the efficacy of cancer treatment as well as the quality of life of cancer patients.

#6680 High-fiber diet induces favorable gut microbiota, reduces immunosuppression, and inhibits lung cancer development.

Manvi Sharma[1], Yuejiang Liu[1], Hannah Moreno[2], Inti C. T. Reischle[1], Mohamed A. Jamal[3], Tieling Zhou[1], Zahraa Rahal[1], Chidera O. Chukwuocha[1], Ke Liang[1], Robert R. Jenq[3], Matthew C. Ross[2], Kristi L. Hoffman[2], Humam Kadara[1]

[1]Translational Molecular Pathology, UT MD Anderson Cancer Center, Houston, TX,[2]Molecular Virology and Microbiology, Baylor College of Medicine, Houston, TX,[3]Genomic Medicine, UT MD Anderson Cancer Center, Houston, TX

Emerging evidence suggests that resident microbial communities act as a central regulator of host homeostasis. The dynamic structure, composition, and function of gut microbiota can be influenced by numerous factors, among which nutritional profile act as most crucial determinant. Microbial consortia inhabiting the gut have been implicated in the etiology and pathogenesis of various cancers and are known to influence cancer immunosurveillance and response to immunotherapy. Despite these known associations, the underlying mechanisms by which dietary interventions such as those rich in fiber (high-fiber diet) regulate gut-immune axis in prevention of lung cancer are poorly defined. Here, we employed a human-relevant mouse model in which knockout of G-protein coupled receptor 5A (*Gprc5a*$^{-/-}$) and exposure to tobacco lead to development of preneoplasia and lung adenocarcinoma (LUAD). Mice were randomly grouped based on dietary treatment: no fiber (control), 10% cellulose, 10% pectin-inulin following weaning (early life) or after transplant of MDA-F471 NNK-induced LUAD cells (dietary intervention). Tumor growth and volumes were most significantly reduced in mice fed a high-fiber pectin-inulin diet. Notably, anti-tumor effects of the high-fiber diet were observed in both early life and later dietary intervention settings. 16S rRNA-Seq analysis of fecal pellets revealed significant differences in gut alpha as well as beta diversity, the latter indicating clear separation of community structure between fiber-deprived versus high-fiber diet groups. Evidently, gut microbiota of pectin-inulin fed mice displayed significantly elevated relative abundance of *Bacteroides sartorii*, *Bacteroides caecimuris*, *Akkermansia muciniphila* and *Bifidobacterium pseudolongum,* taxa that have been reported to be strongly associated with favorable responses to immunotherapy. High-fiber fed mice also showed significantly reduced fractions of tumor-promoting genera such as *Odoribacter* and *Alistipes.* These effects were accompanied by widespread changes in the tumor immune microenvironment between fiber-rich and fiber-poor groups. Pectin-inulin fed mice displayed enhanced antitumor immune responses evident by remarkably increased fractions of B lineage cells, cDC1s and M1-likemacrophages and, conversely, reduced levels of activated cDC2s, M2 macrophages and polymorphonuclear myeloid-derived suppressor cells. Our findings inform on novel mechanisms by which dietary fiber robustly impacts gut consortia and immune milieu in the inhibition of LUAD. Our findings also suggest that the incorporation of dietary fiber in cancer treatment (e.g., immunotherapy) could improve outcomes for patients with LUAD.

#6681 Altered microbial community stability and increases in circulating B cells are associated with the development of severe immune related adverse events during ICI-immunotherapy.

R. C. Simpson[1], E. R. Shanahan[2], I. P. Silva[1], I. L. Reijers[3], J. M. Versluis[3], A. M. Menzies[1], G. Maria[1], U. Palendira[2], J. S. Wilmott[1], C. Blank[3], R. A. Scolyer[1], G. V. Long[1];

[1]Melanoma Institute Australia, Sydney, Australia, [2]The University of Sydney, Sydney, Australia, [3]Netherlands Cancer Institute, Amsterdam, Netherlands

Background: Immune related adverse events (irAEs) are a major hurdle to the success of immune checkpoint inhibitor (ICI) immunotherapy. There is increasing evidence that the gut microbiota influences irAE development, however the microbe-immune crosstalk underpinning this remains cryptic.

Methods: Paired pre- & post-treatment (baseline/week 6) stool samples from 129 Australian and Dutch melanoma patients treated on trial with neo-adjuvant combination anti-PD1/anti-CTLA4 immunotherapy were analyzed with 16S rRNA gene sequencing. Matched PBMCs at both timepoints were analyzed using mass cytometry (n=71).

Results: ICI immunotherapy resulted in changes in the relative abundance of specific bacterial groups in the faecal microbiota, however the microbial community as a whole remained relatively stable. In particular enhanced oralization of the gut microbiome was observed with treatment, including a significant increase in the relative abundance of oral *Streptococcus* species in the gut (P=0.0004). These changes were particularly evident in patients whose microbial communities were *Bacteroidaceae* (Ba)-dominated at baseline, and those who developed severe (grade 3+) irAEs. Indeed, Ba-dominated microbiomes were linked with comparatively higher rates of severe irAEs compared to patients with *Ruminococcaceae* (Ru)-dominated gut microbiomes (P= 0.0440). Furthermore, Ba patients developed severe irAEs earlier during treatment, prior to week 6 (P=0.0016). A significant reduction in transitional B cells (CD24+ CD38hi CD27-) (P<0.0001) and an increase in activated B cells subsets (CD27- CD38- CD24- populations) (P=0.0022) were observed between baseline and week 6 across all patients who developed or went on to develop severe irAEs. Most notably, Ba patients who developed early, severe irAEs specifically had significantly higher frequencies of overall circulating B cells (P=0.0018) and lower frequencies of ICOS+ Tregs at week 6 post treatment (P=0.0005), which was not observed in Ru-dominated irAE patients.

Conclusions: Higher risk of early, severe irAEs were associated with *Bacteroidaceae*-dominated gut microbiomes, reduced microbial community stability, and increases in activated circulating B cells during treatment. We postulate that differing baseline microbial community assemblages are associated with altered pre-established intestinal homeostasis influencing the likelihood of irAE development. Together, the data highlights a potential relationship between B cells, the gut microbiota and irAE development which may point to early steps in the induction of irAEs during ICI immunotherapy.

#6682 Bile acid profiles and racial disparities in colorectal cancer: Exploring the protective role of secondary bile acid derivatives.

H. Dai[1], P. G. Wolf[2], L. Tussing-Humphreys[3], E. Mutlu[3], J. M. Ridlon[1], R. Gaskins[1];
[1]University of Illinois at Urbana-Champaign, Urbana, IL, [2]Purdue University, West Lafayette, IN, [3]University of Illinois at Chicago, Chicago, IL

Background: Colorectal cancer (CRC) is the third leading cause of cancer death in the United States, with diet and gut microbiota-derived bile acids implicated as long-term risk factors. The interplay between bile acids and immune cell differentiation, particularly of macrophages and T-cells, is a crucial aspect of the CRC microenvironment. Given the high-animal-fat diets' influence on the microbiome's production of hydrophobic secondary bile acids such as deoxycholic acid (DCA) and lithocholic acid (LCA), this study investigates the potential immunomodulatory effects of their lower concentrations and their isomers in possibly fostering M2-like macrophage expansion.
Methods: Clinical samples were obtained during colonoscopies with no tumor findings at Rush University Medical Center, Chicago. RNA was extracted from colonoscopy biopsies for NanoString RNA expression analysis, while bile acids were isolated from both lyophilized stool and frozen serum samples. To explore the immunological effects of secondary bile acids, the macrophage RAW 264.7 cell line, alongside peritoneal macrophages and bone marrow-derived macrophages (BMDMs) from C57BL/6J mice, were treated with LCA and LCA isomers. Following the bile acid treatment, LPS (100 ng/mL) or IL-4 (40 ng/ml) was added to elicit pro-inflammatory or anti-inflammatory states, respectively. After 48 hours, conditioned media were collected for enzyme-linked immunosorbent assay (ELISA), while cells were analyzed by flow cytometry and rt-qPCR.
Results: Contrary to initial hypotheses, the levels of DCA and LCA levels were not significantly different between African American and non-Hispanic White subjects. Notably, allo-isomers and oxo-derivatives of these bile acids, which may promote Treg and M2-like macrophage expansion, were substantially lower in African American subjects. Ex vivo treatments with isoalloLCA and IsoLCA led to notable changes in the M2 macrophage differentiation and shifts in PGE2 production upon exposure to inflammatory or anti-inflammatory stimuli, suggesting a nuanced alteration in the macrophage-mediated inflammatory response.
Conclusion: This study highlights a significant ethnic variation in bile acid profiles, with a potential impact on immune modulation and CRC risk. The reduced presence of certain bile acid isomers in African American subjects may influence the risk of CRC through altered macrophage differentiation and function. These findings emphasize the need for personalized dietary and therapeutic strategies to modulate the bile acid metabolome, potentially reducing CRC disparities.

#6683 The abundance of *Fusobacteria nucleatum* in tumor tissue is a prognostic factor in patients of right-sided colorectal cancer.

T. Miyasaka, T. Yamada, S. Kuriyama, A. Matsuda, K. Uehara, S. Shinji, Y. Yokoyama, G. Takahashi, T. Iwai, K. Takeda, S. Kanaka, H. Yoshida;
Nippon Medical School, Tokyo, Japan

Background: A significant association between the gut microbiome and colorectal carcinogenesis, as well as cancer progression. It has been reported that *Fusobacteria nucleatum* (*F. nucleatum*) is one of the most famous bacteria associated with colorectal cancer (CRC). It has been reported that the abundance of *F. nucleatum* is associated with colorectal cancer-specific survival (CSS), however it remains unclear for association with *F. nulceatum* and relapse-free survival (RFS). If *F. nucleatum* has a significant involvement in tumor progression of colorectal cancer, the abundance of *F. nucleatum* should be associated with not only CSS but also RFS in colorectal cancer. In this study, we measured the bacterial mass of F. nucleatum in tumor tissue of CRC patients in Stage II-III to explore the differences in prognosis. **Methods**: We included patients with CRC in stage II-III who underwent surgical treatment at Nippon Medical School Hospital between January 2017 and December 2020 except patients who received preoperative chemoradiotherapy and had multiple cancers. We measured the absolute of *F. nucleatum* copy number of the DNA exacted tumor tissues using droplet digital PCR. **Results**: 253 patients with CRC were included. 128 patients had pathological stage II and 125 patients had pathological stage III. Among 253 patients, 104 patients had right-sided CRC, 89 patients had left-sided, and 60 patients had rectal cancer. *F. nucleatum* was detected in 166 patients (65.6%), and the median of *F. nucleatum* copy number was 1.08 (range; 0.00 - 2791.3). *F. nucleatum* copy number was more abundant in right-sided CRC than in left-sided and rectal cancer (p= 0.02, p=0.01). There was no significant difference between stage II CRC and stage III. We categorized patients into two groups based on the median cut point of *F. nucleatum* copy number: the *F. nucleatum-high* group and the *F. nucleatum*-low group for comparison with clinicopathological features and prognosis. Patients with high abundance of *F. nucleatum* exhibited T4 of tumor depth (p=0.03), right-sided CRC (p=0.01), longer tumor circumference (p <0.001), longer tumor length (p <0.001), and no lymph node metastasis (p=0.024). There was no significant difference in relapse-free survival between the *F. nucleatum*-high group and *F. nucleatum*-low group among whole patients (p=0.53). Analyzing divided tumor location, in right-sided CRC high abundance of *F. nucleatum* was significantly associated with shorter relapse-free survival than low abundance (p=0.02), while in left-sided and rectal cancer there was no significant difference (p=0.61). **Conclusion**: *F. nucleatum* was more abundant in right-sided CRC and associated with relapse-free survival only in right-sided CRC. *F. nucleatum* may make a greater impact on right-sided CRC than on left-sided and rectal cancer.

#6684 Impact of fecal microbiome on the efficacy of neoadjuvant chemo-immunotherapy and colitis adverse events: Findings from the NADIM II Trial.

R. Serna-Blasco[1], A. Rodriguez Festa[1], S. Sanz-Moreno[1], L. Robado de Lope[1], P. Mediavilla Medel[1], E. Nadal[2], J. Gonzalez Larriba[3], A. Martinez-Marti[4], R. Bernabe[5], J. Bosch-Barrera[6], J. Casal-Rubio[7], V. Calvo[8], A. Insa[9], S. Ponce[10], N. Reguart[11], J. de Castro[12], J. Mosquera[13], M. Cobo[14], A. Aguilar[15], C. Camps[16], R. Lopez de Castro[17], T. Moran[18], I. Barneto[19], D. Rodriguez-Abreu[20], C. Aguado de la Rosa[3], R. Palmero[2], F. Hernando-Trancho[3], J. Martin-Lopez[8], A. Cruz-Bermudez[1], B. Massuti[21], M. Molina Vila[22], A. Romero[1], M. Provencio[8],

[1]Instituto de Investigacion Sanitaria Puerta de Hierro - Segovia de Arana, Majadahonda, Spain, [2]Institut Catala d'Oncologia, L'Hospitalet de Llobregat, Barcelona, Spain, [3]Hospital Universitario Clinico San Carlos, Madrid, Spain, [4]Vall d'Hebron Institute of Oncology, Hospital Universitari Vall d'Hebron, Barcelona, Spain, [5]Hospital Universitario Virgen del Rocio, Sevilla, Spain, [6]Institut Catala d'Oncologia, Hospital Universitari Dr. Josep Trueta, Girona, Spain, [7]Complejo Hospitalario Universitario de Vigo, Vigo, Spain, [8]Hospital Universitario Puerta de Hierro, Majadahonda, Spain, [9]Hospital Clinico Universitario de Valencia, Valencia, Spain, [10]Hospital Universitario 12 de Octubre, Madrid, Spain, [11]Hospital Clinic and Translational Genomics and Targeted Therapies in Solid Tumors, Institut de Investigacions Biomediques, Barcelona, Spain, [12]Hospital Universitario La Paz, Madrid, Spain, [13]Complejo Hospitalario Universitario A Coruna, A Coruna, Spain, [14]Instituto de Investigacion Biomedica de Malaga, Malaga, Spain, [15]Instituto Oncologico Dr. Rosell, Dexeus University Hospital, Barcelona, Spain, [16]Hospital General Universitario de Valencia, Valencia, Spain, [17]Hospital Clinico Universitario de Valladolid, Valladolid, Spain, [18]Catalan Institute of Oncology, Badalona-Germans Trias i Pujol Hospital, Badalona, Spain, [19]Hospital Universitario Reina Sofia de Cordoba, Cordoba, Spain, [20]Hospital Universitario Insular de Gran Canaria, Las Palmas de Gran Canaria, Spain, [21]Hospital Universitario Dr. Balmis Alicante, Alicante, Spain, [22]Instituto Oncologico Dr. Rosell, Barcelona, Spain

Introduction: The balance and composition of the gut microbiome play a pivotal role in modulating the host immune system, and they have been associated with survival outcomes in patients undergoing immunotherapy-based treatments and immune-related adverse events. In this study, our objective was to analyze the fecal microbiota of non-small-cell lung cancer (NSCLC) patients with locally advanced disease undergoing neoadjuvant chemo-immunotherapy (IO-CT).
Methods and patients: Baseline stool samples were collected from 86 resectable stage IIIA/B NSCLC patients enrolled in the NADIM II clinical trial (NCT03838159). The patients were randomly assigned to receive either neoadjuvant nivolumab plus chemotherapy (CT) or CT alone. DNA extraction was performed using the QIAamp PowerFecal DNA Kit (Qiagen), and the samples were analyzed using the Ion AmpliSeq Microbiome Health Research assay (ThermoFisher). The NGS analysis utilized the AmpliSeq Microbiome Health w1.3 workflow. Alpha diversity was assessed using the Simpson and Chao1 Index.
Results: Among the 86 collected stool samples, 77 were deemed valid for analysis. *Bacteroides* were the most common genus with a relative percentage (RP) of 18.9% ± 14.8 followed by *Faecalibacterium* (13.4% ± 7.8). The presence of bacteria from the genera *Bifidobacterium*, and *Faecalibacterium* was associated with improved progression-free survival (PFS) [HR = 0.4 (0.16-0.98), and HR = 0.08 (0.01-0.72), respectively] and overall survival (OS) [HR = 0.19 (0.06-0.62)], and HR = 0.04 [0.01-0.43], respectively), in the experimental arm. The detection of *Faecalibacterium prausnitzii* (validated by qPCR) was associated with improved PFS [HR = 0.17 (0.04-0.76)] and OS [HR = 0.05 (0.01-0.29)] in the experimental. On the other hand, detection of bacteria from the genera *Synergistes*, *Lactobacillus*, and *Anaerotruncus* was associated to higher risk of disease progression [HR = 9.9 (1.2-85), HR = 3.7 (1.5-9.1), and HR = 12 (1.4-110)] and death [HR = 51 (3.2-820), HR = 6.7 (2-23), and HR = 25 (2.3-280)] in this set of patients.In the entire cohort, patients whose samples were in the highest tertile of alpha diversity, had significantly prolonged PFS compared to those with intermediate or low diversity [HR = 0.39 (0.16-0.94)]. Finally, 25 colitis adverse events (CAE) occurred in 18 patients, including two Grade 3 (2.3%) and four Grade 2 (4.6%) events. A higher RP of *Bacteroides* were found in patients who did not suffer colitis events (P = 0.016), whereas higher RP of *Coriobacterium* were detected in patients who suffered CAE (P = 0.023).
Conclusions: Our findings suggest that composition of the gut microbiome may play a crucial role in the effectiveness of neoadjuvant IO-CT in NSCLC patients. Specifically, the presence of *F. prausnitzii* may enhance the antitumor activity of these treatments.

#6685 Control of melanoma development by *B. rodentium* in germ free mice.

X. Diaz Olea[1], K. Beede[2], A. Osterman[1], D. Scott[1], C. Petucci[3], D. Kelly[3], A. Ramer-Tait[2], Z. Ronai[1];
[1]Sanford Burnham Prebys Medical Discovery Institute, La Jolla, California, CA, [2]University of Nebraska-Lincoln, Lincoln, NE, [3]University of Pennsylvania, Philadelphia, PA

Growing evidence supports the importance of the gut microbiota in controlling tumor development, often via activation of anti-tumor immunity. Earlier studies from our laboratory identified 11 bacterial strains that were sufficient to inhibit melanoma development by inducing anti-tumor immunity in germ-free mice. Of these, three were predominant at the time of tumor collection. We thus set out to address whether fewer bacterial strains may be sufficient for melanoma growth inhibition. Here, we demonstrate that the administration of one bacterial strain, *B. rodentium*, was sufficient to attenuate melanoma growth in gnotobiotic mice. In all cases, gnotobiotic mice were also administered the altered Schadler flora (ASF), a mixture of 8 bacterial strains that are provided to establish minimal flora in these mice. RNAseq-based gene expression studies identified enrichment of immune-related genes, suggesting enhanced anti-tumor immunity. Metabolomic analysis identified reduced levels of tryptophane and isoleucine, which were implicated in control of immune system function. These findings point to a mechanism which may provide novel means to alter anti-tumor immunity and limit melanoma growth.

#6686 The mechanism of gut microbiome-mediated immune activation on the clinical efficacy of PD-1 blocking treatment in solid tumors.

N.-T. Lin[1], S. Fukuoka[1], D. Motooka[2], Y. Shigeno[3], T. Irie[1], D. M. Tourlousse[4], K. Murotomi[4], Y. Sekiguchi[4], H. Tamaki[5], M. Shindo[6], T. Tsuji[6], H. Wake[6], K. Goto[7], T. Doi[8], K. Shitara[8], K. Watanabe[9], Y. Maeda[9], S. Nakamura[2], Y. Benno[10], H. Nishikawa[1], S. Koyama[1];

[1]Research Institute/Exploratory Oncology Research & Clinical Trial Center (EPOC), National Cancer Center, Chiba, Japan, [2]Department of Infection Metagenomics, Genome Information Research Center, Research Institute for Microbial Diseases, Osaka University, Suita, Japan, [3]Benno Laboratory, RIKEN Baton Zone Program, RIKEN Cluster for Science Technology and Innovation Lab, Saitama, Japan, [4]Biomedical Research Institute, National Institute of Advanced Industrial Science and Technology (AIST), Ibaraki, Japan, [5]Bioproduction Research Institute, National Institute of Advanced Industrial Science and Technology (AIST), Ibaraki, Japan, [6]Department of Anatomy and Molecular Cell Biology, Nagoya University Graduate School of Medicine, Nagoya, Japan, [7]Department of Thoracic Oncology, National Cancer Center Hospital East, Chiba, Japan, [8]Department of Gastroenterology and Gastrointestinal Oncology, National Cancer Center Hospital East, Chiba, Japan, [9]National Cancer Center Japan Research Institute, Tokyo, Japan, [10]Benno Institute for Gut Microflora (BIGM), Saitama Industrial Technology Center, Saitama, Japan

Gut microbiota is associated with antitumor efficacy of immune checkpoint blockade therapies, yet the mechanism is not largely understood. Here, we show that a novel bacterial strain of *Ruminococcaceae* isolated from the feces of patients who respond to PD-1 (programmed cell death 1) blockade efficiently primes/activates tumor-specific $CD8^{\pm}$ T cells through effective stimulation/maturation of $CD103^{\pm}$ dendritic cells (DCs) during migration from the gut to the tumor microenvironment (TME). The administration of this bacteria strain with PD-1 blockade significantly inhibited tumor growth, even when adding them to fecal transplantation of non-responder patients in animal models. Mechanistically, the bacterial strain promoted the IRF8-driven differentiation of $CD103^{\pm}$ DCs by stimulating multiple Toll-like receptors and the accumulation of these DCs in tumors and tumor-draining lymph nodes. These $CD103^{\pm}$ DCs prolonged engagement with cognate antigen-specific $CD8^{\pm}$ T cells, which induced the activation of $CD8^{\pm}$ T cells specific for a wide variety of tumor antigens and fostered their PD-1 expression through enhanced T-cell activation signals with NFATc1 nuclear translocation, thereby leading to abundant $PD\text{-}1^{\pm}CD8^{\pm}$ T cells, a key effector cell population in PD-1 blockade, with a broader T-cell receptor repertoire in the TME. Our findings with novel single bacterium isolated from feces of responder patients demonstrate the mode of action by gut microbiota to augment antitumor immunity.

#6687 Evaluation of a new co-cultured microbiome ecosystem therapy candidate (MaaT034) for clinical testing as adjuvant/neoadjuvant to immune checkpoint inhibitors in solid tumors.

B. Laperrousaz, J. Reygner, C. Gasc, C. Petitjean, A. Duquenoy, L. Martin, V. Bonnaud, M. Robin, S. Declomesnil, C. Schwintner, N. Corvaia;
MaaT Pharma, Lyon, France

Background: Increasing evidence suggests that gut microbiome composition modulates tumor response to therapies, including immune checkpoint inhibitors (ICI). Clinical proofs of concept were obtained in pilot studies using healthy or ICI-responder donor-derived fecal matter transplants to modulate the gut microbiome of non-responding cancer patients and improve their response to ICI. These results support the development of Microbiome Ecosystem Therapies™ (MET) replicating at large industrial scale the effects of ICI-responders gut microbiome. MaaT Pharma, a clinical-stage biotech, has developed a unique, ground-breaking, patented co-culture process (MET-C). MaaT034, the first-in-class co-cultured microbiome product, has been selected for optimizing intestinal homeostasis and to activate immune functions alone and in combination with an ICI treatment.
Method: We combined metagenomic analysis, metabolite quantification by LC-MRM/MS, Caco-2/THP-1 leaky gut model, PBMC assay and mixed lymphocyte reaction (MLR) to assess the impact of MaaT034 on gut homeostasis and immune activation.
Results: Metagenomic analysis demonstrates that MaaT034 replicates the richness and diversity of native-based microbiome ecosystems. Metabolite quantification also revealed that MaaT034 microbes secrete anti-inflammatory metabolites such as short chain fatty acids and indoles, as well as metabolites associated with ICI response such as secondary biliary acids. Using a Caco-2/THP-1 leaky gut model, we then demonstrate that MaaT034 conditioned medium was able to restore the integrity of a THP-1-induced damaged gut barrier. This was associated with and a reduction of inflammatory signals. We further performed a human PBMC assay to evaluate the impact of MaaT034 on immune cell activation. We observed the secretion of immunostimulatory cytokines associated with myeloid cell activation in response to MaaT034 conditioned medium. Notably, anti-CD3 mediated T-cells activation was further increased in response to MaaT034 conditioned medium as evidenced by increased IFNγ release associated with increased Granzyme B and CD25. Finally, MLR was performed to determine the immunomodulatory potential of MaaT034 through the interaction between T-cells and monocytes-derived dendritic cells (moDC). Interestingly, MaaT034 conditioned medium improved moDC maturation as well as moDC-induced T-cell activation. MaaT034 conditioned medium further increased anti-PD-1 mediated T-cell activation, as evidenced by IFNγ release.
Conclusion: Altogether, these results highlight the potential of MaaT034 to produce metabolites involved in the restoration of gut barrier integrity and stimulation of immune cell response to ICI therapy, with potential benefit for solid tumors treatment.

#6688 Peripheral CCR6$^{\pm}$ T-cell profile in healthy volunteers after ingestion of *Lactobacillus*-derived exopolysaccharide which was reported as an ICI-efficacy enhancer *in vivo*.

H. Kawanabe-Matsuda[1], T. Yokoo[2], S. Tou[2], S. Ishii[2], M. Nakamura[1], R. Watanabe[2], M. Ogawa[2], K. Takeda[3], T. Sashihara[2], H. Shimizu[1];
[1]Meiji Holdings Co., Ltd., Hachioji, Japan, [2]Meiji Co., Ltd., Hachioji, Japan, [3]Juntendo University, Tokyo, Japan

Introduction: Exopolysaccharides (EPS) are high-molecular-weight polymers composed of sugar residues secreted by bacteria into the surrounding environment. We (Juntendo University and Meiji Holdings) recently reported that oral administration of EPS derived from *Lactobacillus delbrueckii* subsp. *bulgaricus* OLL1073R-1 (R-1EPS) enhanced therapeutic efficacies of immune-checkpoint inhibitors (ICIs) *in vivo* (Kawanabe-Matsuda *et al*. *Cancer Discov*. 2022.). Briefly, R-1EPS increased CCR6$^{\pm}$ CD8$^{\pm}$ T cells in the small intestine, and these T cells migrated into the tumor tissue to improve the immune microenvironment via a high IFN-γ productivity. As an early step for a medicine, we tested the R-1EPS on healthy volunteers, focusing on the peripheral immune profiling, especially for CCR6-expressing T cells.

Methods: This trial was randomized, placebo-controlled, double-blinded, and parallel-grouped. Japanese healthy adults were divided into R-1EPS and placebo groups and ingested daily test substance for four weeks. We collected PBMCs from all subjects before and after the ingestion to analyze by mass-cytometry based on Maxpar Direct^{TM} Immune Profiling Assay with T Cell Expansion Panel 2 [Standard BioTools, *N* = 44 (R-1EPS) and *N* = 43 (placebo)].

Results: By manual gating strategy, we found that MAIT/NKT cells (CD45$^{\pm}$CD66b^{-}CD19^{-}CD20^{-}CD14^{-}CD11c^{-}CD3$^{\pm}$TCRγδ^{-}CD4^{-}CD28$^{\pm}$CD161^{high}) were increased in the R-1EPS group. Most MAIT/NKT (about 60 - 90 %) were CCR6$^{\pm}$ CD8$^{\pm}$ cells. Moreover, we characterized three distinct CCR6$^{\pm}$ CD4$^{\pm}$ T-cell clusters by analyzing the CITRUS (cluster identification, characterization, and regression) algorithm, and found that CCR6$^{\pm}$ Th1-like CD4$^{\pm}$ T cells were also increased in the R-1EPS group. Notably, these CCR6$^{\pm}$ Th1-like CD4$^{\pm}$ T cells are phenotypically similar to Th7R cells, that was previously reported as a peripheral correlative biomarker of ICI response (Kagamu *et al. Cancer Immunol Res*. 2020., Kagamu *et al. Cancer Res*. 2022.).

Conclusion: These results suggested that oral administration of R-1EPS for humans specifically increased some CCR6$^{\pm}$ CD8$^{\pm}$ T cells, as previously reported *in vivo*, and CCR6$^{\pm}$ Th1-like CD4$^{\pm}$ T cells. Therefore, we (Meiji Holdings Co., Ltd.) consider a clinical trial for the drug development using R-1EPS to treat cancer patients with ICIs.

#6689 Modulation of MAITs by the tumor microbiome in anti-PD1 treated cancers.

P. Birla, L. Yang, C. Sears, F. Shaikh, D. Pardoll, F. Housseau;
Johns Hopkins University School of Medicine, Baltimore, MD

Mucosal associated invariant T (MAIT) cells are innate like T-cells that recognize non-peptide metabolite antigens presented on monomorphic MHC related-1 (MR1) making them an attractive off the shelf tool for cancer immunotherapy. In this study, we investigate the function of MAITs in the tumor microenvironment of neoadjuvant anti-PD1 treated lung cancer patients (NCT02259621)). Paired single cell RNA/TCR sequencing analysis revealed an oligoclonal expansion of MAITs comprising of canonical TRAV1-2+ and non-canonical MAITs TRAV1-2-. TCR capture from canonical MAIT clonotypes confirmed their *in vitro* recognition of 5-OP-RU, bacteria derived riboflavin derivative as well as MR1 dependent recognition of live bacteria present in the tumor. However, the nature of antigens recognized by non-canonical MAITs remains poorly understood. On mining transcriptional profiles of MAITs, we observed that canonical MAITs were characterized by high clonal amplification whereas the non-canonical clonotypes expressed a strong activation/exhaustion gene signature. This suggests that both these MAIT populations recognize different types of antigens, differentially activate, and respond to immune checkpoint blockade (ICB), the non-canonical MAITs being highly dysfunctional. Using bacterial 16S RNA amplicon and metagenomics sequencing, we seek to identify microbial and metabolomics signatures associated with MAIT activation and response to ICB. We identified MAITs to express a cytotoxic signature making them a potential target for cancer immunotherapy. Our findings will provide further insights into the nature of ligands recognized by MAITs and the mechanisms associated with MR1 dependent recognition and tumor killing. Investigating the role of unconventional T-cells in response to ICB has the potential to reveal new tumor-associated antigens which could open avenues into innovative combination immunotherapies.

#6690 Gut microbial metabolite butyrate facilitates antitumor efficacy of telomerase-specific oncolytic adenovirus via MHC-I and cGAS-STING pathway activation.

M. Sakamoto;
Okayama University Hospital, Okayama City, Japan

Introduction: Gut microbiota has been reported to have a potential to modulate tumor sensitivity to chemo- or immuno-therapies although the underlying mechanism is still unclear. Oncolytic virotherapy is a promising antitumor treatment that selectively induces oncolytic cell death in tumor cells. We have previously developed OBP-702, a telomerase-specific oncolytic adenovirus armed with the p53 tumor suppressor gene, highlighting potent antitumor effects across different cancer types. To explore the potential of gut microbial metabolites, particularly butyrate, in augmenting the antitumor efficacy of oncolytic virotherapy.
Materials and Methods: We assessed the synergistic antitumor effects of butyrate and OBP-702 in cytotoxic assay using two human (HCT116, SW48) and two murine (CT26, MC38) colorectal cancer cell lines in vitro, and the in vivo antitumor effects in subcutaneous tumor models using HCT116 and CT26. We explored underlying mechanisms of the synergistic effects, focusing on the influences of butylate on viral infectivity via Coxsackie-Adenovirus Receptor (CAR) and integrins, and antitumor immunity via tumor MHC-I expression and CD8-positive T cells.
Results: Butyrate and OBP-702 showed potent synergistic effects in all four cell lines in vitro, and the combination suppressed tumor growth significantly in HCT116 and CT26 subcutaneous tumors compared to each monotherapy. These synergistic effects were produced by butyrate increasing the potential of OBP-702 by enhancing viral infection efficiency via upregulating expressions of CAR and integrins on tumor cells. Butyrate also increased MHC-I expression on tumor cells by activating the cGAS-STING pathway, leading to increased CXCL10 expression, which led to activation of antitumor immunity through recruitment of CD8-positive T cells in tumor tissues. The synergistic effects of butyrate and OBP-702 were proved in an orthotopic colorectal tumor model with liver metastases using CT26 cells expressing luciferase, in which this combination not only reduced tumor growth, but also improved survival by activating antitumor immunity via CD8-positive T cells.
Conclusion: Butyrate and OBP-702 showed synergistic antitumor effects via activation of systemic antitumor immunity in addition to direct effects of butyrate on viral cytotoxic potential, which provides valuable insights into the development of innovative cancer treatment strategies.

#6691 Engraftment as a determinant of response in fecal microbiome transplantation interventions for immunotherapy in melanoma.

M. Chelvanambi[1], A. V. Damania[1], S. B. Johnson[1], G. Morad[1], R. N. Lazcano[1], B. A. Helmink[1], L. W. Fong[1], K. Wani[1], Y. D. Seo[1], E. M. Park[1], R. I. Ayabe[1], B. Singh[1], M. C. Wong[1], D. R. Ingram[1], M. G. White[1], A. J. Lazar[1], A. K. Mishra[2], N. J. Ajami[1], E. N. Baruch[1], J. A. Wargo[1];

[1]UT MD Anderson Cancer Center, Houston, TX, [2]University of Georgia, Athens, GA

Background: Distinct gut microbiome signatures are associated with response, resistance, and toxicity to immune checkpoint blockade (ICB). Fecal microbiome transplants (FMT) have validated the importance of the gut microbiome in enhancing response and overcoming resistance to immunotherapy. However, donor selection remains a key challenge for FMT. Heterogenous responses using Healthy Donors (HD) and ICB Complete Responders (CR) as FMT donors suggest donor characteristics alone do not determine response. Here, we posit that donor-recipient relationships are critical in determining clinical responses to FMT.

Methods: We studied a cohort of ICB-refractory, metastatic melanoma patients treated with combined FMT and ICB (10 recipients, 2 donors). Patient gut microbiomes were profiled using whole metagenomic sequencing (WMS) of longitudinal stool collections (baseline, day 7, day 31, and day 65 post-FMT). Immune infiltration of on-treatment tumor and colon biopsies was quantified with immunohistochemistry. mTraCX, an Earth Mover's Distance-based algorithm, was used to evaluate taxonomic engraftment between donors and recipients. Bray-Curtis distance was used to measure functional similarities between donor and recipient gut microbiome. Clinical findings were validated in pre-clinical FMT experiments performed on $Braf^{V600E}Pten^{-/-}$ melanoma-bearing mice.

Results: One-third of recipients (3/10) developed an objective response (R) to ICB following FMT. mTraCX demonstrated an association between clinical response to FMT and durable engraftment of donor microbiota at day 65 post-FMT (p=0.025). Taxonomic engraftment (mTraCX) correlated positively with functional engraftment (Bray-Curtis distance) (r=0.89, p<0.0001). Enhanced engraftment was associated with increased CD4 (r = -0.87, p=0.0045) and CD8 (r = -0.6, p=0.09) T-cell infiltration in the colon, and a trend towards increased CD8 T-cell infiltration (r = -0.5, p=0.2) in the tumor following treatment with FMT+ICB. Pre-clinical models paralleled our clinical findings as responding mice showed better donor engraftment than non-responding mice (p<0.0001 on day 4 and day 24 following FMT).

Conclusions: Our data shows that donor engraftment is a favorable prognostic factor for ICB treatments combined with FMT. Future investigations will aim to develop donor-recipient matching criteria to enhance the feasibility and integration of FMTs into clinical practice.

#6692 Intermittent fasting-remodeled gut microbiota improves anti-tumor immunity in pancreatic cancer.

L. Li[1], V. Chandra[1], O. L. Roux[1], R. M. Howell[1], V. Tahan[1], N. Putluri[2], J. Petrosino[2], A. Sreekumar[2], J. K. Kolls[3], J. White[4], F. McAllister[1];
[1]UT MD Anderson Cancer Center, Houston, TX, [2]Baylor College of Medicine, Houston, TX, [3]Tulane University School of Medicine, New Orleans, LA, [4]Resphera Biosciences, Baltimore, MD

Pancreatic ductal adenocarcinoma (PDAC) has become the third leading cause of cancer-related death in the United States with high resistance to therapies, presentation at late stages and aggressive biology. Immunotherapy has revolutionized cancer therapy by offering survival benefit in many solid malignancies, however, it is still not effective in pancreatic cancer. Host factors are crucial modulators of responses to immunotherapy. The roles of gut microbiome in modulating the immune system and determining cancer outcomes have been well established. Eating patterns can alter the gut microbiota and metabolic output, both of which affect anti-tumor immune responses. Intermittent fasting (IF), a form of dietary restriction which is characterized by limited feeding with unlimited calorie consumption during a certain time window. IF has been shown to affect gut microbiota composition, modulate immunity, and metabolic processes. Despite the well-known beneficial role of fasting in pancreatic conditions, including pancreatitis and diabetes, its effect in the treatment of pancreatic cancer has not been explored. Our study found that IF reverses immunotherapy resistance in PDAC. IF can reshape gut microbiota composition and reprogram the metabolism of host. We found that IF improves anti-tumor immunity through modulating gut microbiota. Depletion of gut microbiota can abrogate the beneficial effect of IF on anti-tumor response, while fecal microbiota transplantation from mice exposed to IF can sensitize the anti-tumor effects of immunotherapy. Using 16S rRNA sequencing, metabolic profiling and transcriptomic sequencing, our findings elucidate the mechanism of IF-remodeled gut bacteria influencing metabolic molecules which drive immune cells activation. Our study suggests that IF-based interventions have potential utility for the prevention and treatment of PDAC.

#6693 Deleted in malignant brain tumors 1 (DMBT1) glycoprotein is lost in colonic dysplasia.

Emily H. Green[1], Subhag R. Kotrannavar[1], Megan E. Rutherford[2], Harsimran Kaur[1], Hannah M. Lunnemann[2], Cody N. Heiser[1], Shaoguang Wu[3], Hua Ding[3], J. Alan Simmons[1], Xiao Liu[2], D. Borden Lacy[4], Martha J. Shrubsole[2], Qi Liu[2], Ken S. Lau[1], Cynthia L. Sears[3], Robert J. Coffey[2], Julia L. Drewes[3], Nicholas O. Markham[4]

[1]Vanderbilt University, Nashville, TN,[2]Vanderbilt University Medical Center, Nashville, TN,[3]Johns Hopkins University, Baltimore, MD,[4]Department of Veterans Affairs, Nashville, TN

Colorectal cancer (CRC) is the third most common cancer in the United States and is responsible for more than 50,000 deaths annually. Emerging evidence strongly supports a causal role for specific pro-carcinogenic driver bacteria within the colonic microbiota. Invasive bacterial biofilms may initiate or accelerate CRC through epithelium-autonomous or inflammation-dependent mechanisms. To better understand host-microbe interactions during colonic tumorigenesis, we combined single-cell RNA-sequencing (scRNA-seq), spatial transcriptomics, and immunofluorescence to define the molecular spatial organization of colonic tissue from germ-free *Apc*$^{Min/+}$ mice colonized with bacteria from human biofilm-associated CRC. In absorptive colonocytes, differential gene expression analysis showed the gastric metaplasia-associated glycoprotein *Deleted in Malignant Brain Tumors 1 (DMBT1)* is highly upregulated by *C. difficile*. Surprisingly, our spatial transcriptomic analysis showed *DMBT1* was dramatically downregulated in dysplastic foci compared with normal-appearing tissue. We show that DMBT1 protein is downregulated in 100% of dysplastic foci across 3 different mouse models of colonic tumorigenesis: *C. difficile*-associated tumorigenesis in *Apc*$^{Min/+}$, azoxymethane/dextran sodium sulfate, and *Lrig1*$^{CreER/+}$;*Apc*$^{fl/+}$ mice (n = 57 foci from 11 mice). Immunofluorescent staining of DMBT1 is markedly downregulated compared with normal adjacent crypts. Using scRNA-seq data and tissue microscopy in human CRC, we confirmed the same pattern of downregulated DMBT1 expression in dysplastic crypts compared with normal-appearing crypts. We present data from a human mucosal biofilm-associated colonic tumorigenesis murine model at single-cell resolution to reveal interesting cell type-specific transitions and generalizable mechanisms of tumorigenesis. We hypothesize that DMBT1 is a component of the gut epithelial response to pathogens and a critical regulator of proliferation and differentiation during post-injury restitution. We are now functionally testing how the loss of DMBT1 impacts tumorigenesis using human organoids. Ultimately, these studies aim to reveal novel biomarkers and/or targets for therapeutic intervention in CRC.

#6694 Gut microbial drivers of response to bladder-sparing therapy in human muscle-invasive bladder cancer enhance immunotherapy efficacy and limit immunosuppression following fecal microbiome transplantation *in vivo*.

E. Michaud[1], S. Fehric[1], C. Faubert[2], B. Routy[3], I. King[4], J. Mansure[1], W. Kassouf[5],

[1]McGill University Health Centre Research Institute, Montreal, QC, Canada, [2]McGill Interdisciplinary Initiative in Infection and Immunity, Montreal, QC, Canada, [3]Hematology-Oncology Division, Department of Medicine, Centre Hospitalier de l'Universite de Montreal, Montreal, QC, Canada, [4]Meakins-Christie Laboratories, Department of Medicine, McGill University Health Centre, Montreal, QC, Canada, [5]Division of Urology, Department of Surgery, McGill University Health Centre, Montreal, QC, Canada

BACKGROUND: Radiation therapy (RT) is a bladder-sparing option for Muscle-Invasive Bladder Cancer (MIBC), yet encounters a 30% non-response rate, with half of the patients succumbing to metastasis. Preclinical models demonstrate enhanced antitumor responses with RT combined with PD-1/PD-L1 blockade but give limited insight into the determinants of success for such combination therapies (CT). The gut microbiome, pivotal in conditioning local and peripheral immunity, influences PD-1-based immunotherapy efficacy in various cancers. Immune profiling indicates heightened systemic and antitumor immunity in responders with a favorable gut microbiome, enriched in *Akkermansia muciniphila, Bifidobacterium*, and *Faecalibacterium*. Oral gavage of immunogenic bacteria further enhances combined RT and anti-PD-L1 therapy. We thus aim to 1) elucidate the role of patients' microbiome in shaping anti-tumor immune responses to CT, and 2) use its composition as a predictive factor for CT success.

METHODS: We performed shotgun metagenomics on microbial DNA from fecal materials of MIBC RT responders (R, n=26) and non-responders (NR, n=11). Fecal homogenates from donors were gavaged into germ-free (GF) mice. Three weeks post-gavage, MB49 tumor cells were subcutaneously delivered to mice, randomized into four groups: control, anti-PD-L1, RT, and RT + anti-PD-L1. Tumors were harvested seven days post-treatment for single-cell RNA-seq and TCR sequencing (10X Genomics), while stool samples were collected weekly for 16S sequencing.

RESULTS: Significant gut microbial disparities were observed between R and NR MIBC patients, with particular enrichment in known promoters of anti-PD-L1 response, such as *Phocaeicola dorei* in R. Transplantation of R microbiome into GF mice resulted in significant increases in predicted survival, tumor growth delay, and counts of effector $CD4^{\pm}$ T cell infiltration in the RT+PD-L1 arm. Conversely, NR microbiome transplantation correlated with increased neutrophil and T_{reg} infiltration, abrogating the survival tumor growth delay benefits of the combination arm. Spatial tissue analyses revealed higher neutrophil densities around $CD8^{\pm}$ T cells in all NR arms. Single-cell RNA-seq of tumor-infiltrating immune cells unveiled skewed CD4 and CD8 polarization between R and NR *in vivo* batches.

SIGNIFICANCE: To our knowledge, this is the first study to use FMT as a modulator of response in the context of radiation therapy combinations in MIBC. Our results highlight that the gut microbiome alone may condition a favorable immune terrain for combinatorial therapies involving radiation. This offers strong predictive value for personalized therapeutic approaches in selecting patients who will benefit the most from bladder-sparing therapies.

#6696 Microbial signatures and serum markers in colon cancer of African American patients.

S. C. Tortora[1], E. Vogtmann[2], L. Martello-Rooney[1];
[1]SUNY Downstate Health Sciences University, New York, NY, [2]National Cancer Institute, Bethesda, MD

Among all the racial/ethnic groups, African American (AA) patients have the highest incidence of CRC and mortality rate. There is growing evidence indicating that the oral bacteria might translocate to the intestine, potentially causing disruptions in the balance of gut microbes. Our study delves into the complex interplay between oral pathogens, gut microbiota, and colon carcinogenesis in AA patients. Methods: 16S rRNA sequencing of tumor and non-tumor tissues, utilized qPCR for detection of oral bacteria *Fusobacterium nucleatum* (Fn) and *Porphyromonas gingivalis* (Pg) relative abundance, performed cytokine profiling via multiplex ELISA, and employed NAPPA for antibody response assessment. Results: Colon tumor tissues had lower microbial diversity, notably in right-sided tumors, with distinct biofilm-associated bacteria. Novel discoveries emerged from differential abundance testing, revealing *Prevotella intermedia* and *Treponema socranski to be* associated with early cancer stage and left-sided location, and *Fusobacterium necrophorum* with advanced cancer stage and right-sided location. qPCR demonstrated Fn and Pg elevation in right-sided tumors and late cancer stages. Both were detected in 45% of tumors versus 37% in non-tumor tissues and 19.15% of tumors and 25.53% in non-tumor tissues, respectively. Fn-positive groups exhibited distinct microbial signatures, with altered bacterial abundances and dysbiosis, including increased CRC-associated bacteria *Faecalibacterium and Helicobacter*, increased oral pathogen abundance (*Fusobacterium, Porphyromonas, Prevotella, Treponema*), and reduced beneficial bacteria. Serological analysis highlighted elevated levels of IL-2, IL-10, IFN-γ, and RANK in advanced cancer stages and increased CRP levels in right-sided tumors. By NAPPA analysis, 30 bacterial proteins (anti-IgG) showed a seroprevalence of more than 15% in the samples, with those being the most seroprevalent anti-HP131 and anti-HP-1564 (68% and 61% of all samples) of *Helicobacter pylori*, and anti-msnK (64%) of *Streptococcus gallolyticus*. Conclusions: Our study emphasized the reduced diversity in tumor tissues, particularly in right-sided tumors in AA colon cancer. Fn presence in colonic tumors correlated with CRC-associated bacteria and oral pathogen aggregation, suggesting its potential role in cancer pathogenesis. Combining the analysis of cytokines and pathogenic bacteria antibodies may serve as broader serological biomarkers for disease severity and location. These findings advance our comprehension of microbiota-cancer interactions, directing personalized diagnostics and treatments in this population.

#6697 The role of microbiomes in pediatric cancer prevention: A survey of population awareness.

A. Abd Elmoneim, M. A. Alshanqiti, Y. S. Aljohani, L. H. Alomari;
Taibah University, Madinah, Saudi Arabia

Background: Gut microbiome includes the genome of all gut microorganisms; it plays a crucial role in the body's nutritional, metabolic, physiological, and immunological processes. Persistent imbalance of the gut microbial community is associated with the onset of metabolic and inflammatory disorders, including cancer. The environment has a major role in the great variability of microbiome composition among different people. This high heterogeneity between individuals may be a source of differences in susceptibility to disease. Dietary and lifestyle choices as well as social interactions play a significant role in makeup and function of the gut microbiota, which may affect microbiome-associated diseases. Therefore, strategies that might favorably modulate the gut microbiota to reduce the risk of cancer through diet and lifestyle changes are of great interest.
Aim: To detect and increase self-awareness about gut microbiota and its relation to diet and lifestyle habits.
Methods: A survey questionnaire is provided asking for microbiome knowledge and lifestyle habits and distributed among the population in Madina city in Saudi Arabia. Study population are the children aged 2-18 years. Data gathered from older children or the parents/guardian of young children.
Results: A profile involving each participant' diet, physical activity, and sociodemographic characteristics through self- reporting questionnaire is obtained.
Discussion: Gut microbiota can regulate many functions of the tumor-bearing meta-organism, typically through immunomodulation. Known microbial mechanisms can alter non-hematopoietic and hematopoietic components of the gut epithelial barrier, modulate lymphoid organ activities, and regulate immune tone of the tumor microenvironment (TME).
Conclusion: Understanding information about microbiome and its role in causing diseases as well as each participant' diet, physical activity and other sociodemographic characteristics help to raise participants' awareness about the importance of taking care of their gut health.

#6698 Tumor microbiota associated with immune enrichment in breast tumor.

L.-F. Yeo[1], B. K. Lim[2], T. Islam[3], L.-Y. Teoh[3], S. Jamaris[3], M.-H. See[3], L.-M. Looi[3], N. Mohd Taib[3], C.-H. Yip[4], P. Rajadurai[4], S.-H. Teo[1], J. Pan[1];
[1]Cancer Research Malaysia, Subang Jaya, Malaysia, [2]Universiti Kebangsaan Malaysia, Selangor, Malaysia, [3]University Malaya, Kuala Lumpur, Malaysia, [4]Subang Jaya Medical Centre, Subang Jaya, Malaysia

Asian cancer patients have enriched immune profiles when compared to Caucasians. This is associated with improved overall survival and potentially better response to immunotherapy. Yet the reason behind enriched Asian immune profiles is unclear. This study investigated microbes found in Malaysian breast tumors in association with immune profiles. We used an existing dataset of RNA-seq data from fresh frozen breast tumor tissue (n=978). Sequencing reads were trimmed and filtered to remove human reads. Non-human reads were mapped to Kraken2 and relative abundance was estimated using Bracken. Microbiome analysis was conducted on R following Microbiome OMA guidebook. The top five genera found in the Malaysian Breast Cancer (MyBrCa) cohort were *Pseudomonas, Siphoviridae, Bacillus, Escherichia and Klebsiella*. Alpha diversity of basal subtype microbiota was significantly higher than Her2 subtype (Shannon index, p=0.027) whilst the other subtypes were more homogenous. MyBrCa patients with low immune scores were significantly different from high immune scores while controlling for age, stage, grade, ethnicity and PAM50 subtype (PERMANOVA, F-statistic = 1.656, p=0.05). Differential abundance analysis revealed *Sulfidibacter* and *Priestia* to be significantly different in abundance between high vs low IFNg groups (FDR-adjusted p-value < 0.05) using ALDEx2, ANCOM-BC2 and ZicoSeq and LinDA algorithms. *Sulfidibacter* was significantly different between high vs low immune group for Bindea combined immune score and ESTIMATE score groups (FDR-adjusted p-value <0.05). An independent breast cancer cohort (n=419) was used as validation where *Sulfidibacter* and *Priestia* were also significantly different in abundance for immune high vs low groups. Machine learning using Random Forest model predicted immune group with an AUC of 0.79 (CI = 0.74, 0.83; p-value < 0.01). The top five most important features contributing to the random forest model were *Sulfidibacter, Prestia, Cutibacterium, Acinetobacter* and *Rhizobium*. This study is the largest to date that characterize the tumor microbiota of an Asian cohort of breast cancers, where *Sulfidibacter* and *Priestia*, both relatively new and uncharacterized bacteria, were differentially abundant among patients with high vs low immune scores.

#6699 Delineating germline, tumor and extrinsic factors driving mucosal melanoma (MM) risk and response to immune checkpoint inhibitor (ICI) treatment.

F. Dimitriou, P. Nagarajan, S. Prabhakaran, N. Bota, M. Knafl, R. A. Chu, A. V. Damania, P. V. Sahasrabhojane, Y. Hoballah, J. S. Losh, N. J. Ajami, S. E. Woodman, J. A. Wargo, A. Futreal, J. L. McQuade;
UT MD Anderson Cancer Center, Houston, TX

Introduction MM is a rare melanoma subtype with distinct biology, low immunogenicity and tumor mutational burden, and subsequently lower response rates to ICIs. The biology of MM is poorly understood. We sought to prospectively, uniformly, and comprehensively profile a cohort of MM patients to determine the interplay of molecular variation, germline predisposition, immunity, gut, mucosal and tumor microbiome and modifiable risk factors on ICI response and resistance in advanced MM.

Methods Patients (pts) with MM treated with standard-of-care ICI as any treatment line presenting to MD Anderson are being prospectively enrolled for longitudinal collection for molecular, microbiome, and lifestyle factor profiling. Planned analyses include: whole genome sequencing of normal and tumor tissue, RNA sequencing, and T cell receptor sequencing from fresh tumor samples; germline sequencing and genotype analyses; NanoString Digital Spatial Profiling (DSP) from formalin-fixed paraffin embedded (FFPE) specimens; whole genome shotgun, microbiome profiling and 16S rRNA gene sequencing (16S) of fecal specimens and affected mucosal and tumor sites (swabs); participant lifestyle and patient reported outcomes (PROs) assessments. Fresh tissue is collected and used to develop PDX models and cell lines.

Results 98 pts have been enrolled to date; 83 (85%) Caucasians, 8 (8%) Hispanic, 4 (4%) Asians. 67 (68%) females. Median age at MM diagnosis is 64 years (range 32-91 years). MM primary sites include 24 (24%) naso-oral, 29 (30%) urogenital, 26 (27%) anorectal, 7 (7%) conjunctival and 12 (12%) other. Clinical somatic mutation testing was performed in 76 (76%) pts and common mutations were *KIT* (n = 12, 16%), *NRAS* (n = 8, 11%) and *BRAF* V600 or non-V600 (n = 9, 12%). At data cut-off (November 2023), 18 (18%) pts deceased. Median follow-up from first diagnosis to last visit/death was 16 months (range 1-178 months). Sample collections at data cut-off include: blood samples (n = 95; 219 samples); fecal specimens (n = 50; 97 samples); mucosal swabs (tumor/tumor adjacent/oral cavity; n = 38; 101 samples); fresh frozen tumor/normal (n = 38; 55 samples), fresh tumor/normal (n = 28; 36 samples) and FFPE tumor (n = 21; 37 samples) tissue. PROs and dietary assessments have been collected from 47 pts. Fresh tissue for PDX model and cell line development has been collected from 11 pts.

Conclusion This is an ongoing prospective study that is expected to drive insights into the tumor/microenvironment/host interactions and factors regulating immunogenicity to predict response and resistance to ICIs in a rare and understudied melanoma subtype. Interrogation of the role of the gut microbiome and its modifiable determinants will lead to the investigation of new therapeutic strategies to modulate the microbiome to improve treatment outcomes in MM. Data will be presented from initial cohort analyses.

IMMUNOLOGY: Targeted Immune Cell Engagers
Poster Session

#6703 Innovative mRNA strategies to encode CD19/CD3 T cell engagers in the treatment of B cell hematological malignancies.

Xia Zhong, Liang Du, Zhenxing Yang, Xiaoli Xu, **Jijun Yuan**, Bo Ying

Abogen Bioscience, Suzhou, China

The advent of T Cell Engager (TCE) immunotherapies marks a transformative shift in cancer treatment paradigms, introducing a novel action mechanism. Blinatumomab, a bispecific CD19/CD3 TCE, has shown remarkable efficacy in treating refractory or relapsed B-cell Acute Lymphoblastic Leukaemia (B-ALL), including cases resistant to conventional chemotherapy, leading to its global approval for B-ALL management. Despite its pronounced clinical success, Blinatumomab faces challenges with patient adherence, primarily due to the protein's short half-life. This necessitates continuous administration requested 24 hours injection throughout the treatment course. Additionally, the drug's association with the induction of cytokine release syndrome (CRS), presumably linked to the hyperactivation of the cytokine network, presents a significant concern.

To address these limitations, we leverage mRNA modality to develop innovative therapeutic mRNAs encoding CD19/CD3 TCE. These mRNA drugs hold the potential to improve protein exposure *in vivo* with a steady production of encoded protein in-situ. On the other hand, with the gradual expression of protein, mRNA shifted the transient, "pulse"-like pharmacokinetic (PK) feature of the protein drugs to a more "plateau"PK curve, which allows a natural priming of T cells to reduce the risk of CRS induction.

In this work, we developed a series of mRNAs encoding CD19/CD3 TCE through our mRNA technology platform and LNP delivery platform. Comparative analyses demonstrated that the TCEs produced *in vivo* by these mRNAs match the structure and function of recombinantly expressed proteins. PK studies in both mice and non-human primates confirmed a favorable PK profile with over 10-fold increase in TCE exposure compared to their protein counterparts. This increased exposure correlated with superior antitumor efficacy in both ALL and lymphoma models, evidenced by the potent effects of single mRNA doses compared to multiple doses of protein-based treatments. Meanwhile IL6 cytokines induced in mRNA treated mice were significantly alleviated than those in protein treated animals, indicating a reduced risk of induction of CRS. One candidate mRNA demonstrated an optimal "plateau" pharmacokinetic profile, achieving extensive target cell eradication over 20 days with a single low dose of 0.001 mpk in non-human primates.

An investigator-initiated clinical study with mRNA encoding CD19/CD3 TCE is underway in relapsed and/or refractory acute lymphoblastic leukemia patients. The preliminary data from the on-going study showed ABO2015 with an acceptable safety profile, and activation of peripheral T cells was observed in one patient with low dose.

These findings underscore the significant clinical potential of mRNA-encoded CD19/CD3 TCE in treating B-cell malignancies, heralding a paradigm shift in the clinical application of protein-based T cell engagers.

#6704 Development and characterization of a tri-specific selective CD8 T cell engager (CD8xCD3xCD19) for treatment of B cell lymphoma.

Zheng Yang[1], Wuzhong Shen[1], Guiyun Tu[1], Shenjie Xue[1], Ying Tan[1], Bingbin Xie[1], Jason Xu[2], Hanyang Chen[1], Shui Liu[1], **Xiaoqiang Yan**[1]

[1]ITabMed Ltd., Shanghai, China,[2]University of pennsylvania, Philadelphia, PA

The recent development of CD3 bi-specific antibodies (BsAbs) targeting CD20, BCMA, GPRC5D and CD19 to treat B cell malignancies have resulted in significant clinical benefit to patients. However, long-term remission rates and survival remain to be demonstrated. Current CD3 BsAbs preferentially bind to and activate CD4 T cells. However, CD8 cytotoxic T cells also play the key role in anti-tumor response and T cell exhaustion in cancer immunity. To potentially enhance anti-tumor efficacy by augmenting CD8 T-cell response, we developed a novel tri-specific T cell engager (TriTE) IM-8319, which simultaneously binds human CD3, CD8 and CD19 epitopes with K_D at 14.2 nM, 3.3 nM and 0.3 nM, respectively. The binding affinity to human CD8 T cells and CD4 T cells was measured with EC_{50} at 0.02 nM and 1.2 nM, respectively. In human PBMC-killing assays, IM-8319 was found to preferentially activate CD8 T cells with EC_{50} of 6.0 pM, compared to an EC_{50} of 94 pM for activating CD4 T cells. Unique cytokine release responses were seen with IM-8319 treatment. Compared to bi-specific TCE controls without CD8 binding domain, IM-8319 in human PBMC assays increased INFγ and TNFα in CD8 T cells and blunted IL-2 release in CD4 T cells. We observed robust cytotoxic killing of $CD19^{\pm}$ B cells with IM-8319. Compared the bi-specific TCE controls lacking CD8 binding domain, *in vitro* $CD19^{\pm}$ B-cell depletion was increased 6-fold with IM-8319. In addition, we observed notable structure activity relationships, with >100-fold increases in TriTE cytotoxicity with a weak CD3 binding domain. T-cell fratricide has hindered the development of antibodies containing 2+ T-cell epitopes. We observed correctable, dose-dependent CD8 T cell depletion at high concentrations of CD8xCD3xCD19 TriTEs *in vitro* and xenograft mouse models. This unwanted biological effect was not a surprise when the TriTE binds to CD8 T cells in *trans*. However, by structure engineering IM-8319 to allow for *cis* binding of CD3 and CD8, we effectively eliminated CD8 T cell fratricide at therapeutic doses. In a Raji-inoculated murine xenograft that was reconstituted with human PBMC, IM-8319 significantly inhibited tumor growth without obvious CD8 T cell depletion. In summary, we report a novel TriTE (IM-8319) that selectively binds to and activates CD8 T cells. IM-8319 results in robust on-target cytotoxicty with specific activation of CD8 T cells, suggesting potential to reduce systemic toxicities such as cytokine release syndrome (CRS) while augmenting direct antitumor efficacy. Further preclinical evaluation of IM-8319 is warranted in patients with B-cell leukemias and lymphomas.

#6705 A novel tri-specific T cell engager targeting the intracellular oncoprotein WT1.

S. Gao[1], L. Yang[1], J. Du[2], W. Jiang[1], **L. Fang**[1];

[1]Concept to Medicine Biotech Co., Ltd., Shanghai, China, [2]Biocytogen Pharmaceuticals (Beijing) Co., Ltd., Beijing, China

Background: Wilms' tumor gene 1 (WT1) is considered an oncogenic factor, with high expression observed in several hematological malignancies and solid tumors. However, its expression is rarely found in normal adult tissue. WT1 can be degraded by the proteasome, processed and presented on the cell surface as major histocompatibility complex (MHC) I epitopes and recognized by T cell receptors (TCR). Here, we described the development of WT1-TOPAbody, a novel tri-specific T cell engager (TCE), that activated T cells by both CD3 and 4-1BB signaling upon recognition of WT1 in the context of HLA-A02, leading to superior anti-tumor efficacy.

Materials and Methods: WT1-TOPAbody was evaluated for its antigen binding activity and target specificity by a series protein/peptide and cell-based assays. In vitro cytotoxicity and T cell activation mediated by WT1-TOPAbody was further assessed in a panel of WT1$^{\pm}$ tumor cell lines in coculture with effector cells. Anti-tumor activity was investigated in a humanized syngeneic mice model bearing WT1/HLA-A02 expressing tumors. Safety assessment including cytokine release assay (CRA) and preliminary CMC developability was also performed.

Results: WT1-TOPAbody exhibited superior binding affinity to the WT1/HLA-A02 complex while displaying lower binding to off-target peptides and CD34$^{\pm}$ HSC from healthy donor than clinical benchmark WT1-CD3 bispecific antibody, RG-6007. WT1-TOPAbody effectively induced tumor lysis in multiple WT1$^{\pm}$ tumors including leukemia, ovarian, breast, and colon cancer cells. Moreover, serial killing of tumor cells were observed in WT1-TOPAbody treated T cells, accompanied by lower exhaustion markers expressed, suggesting a prolonged anti-tumor inhibition effect of WT1-TOPAbody. In a humanized CD3e/4-1BB/HLA-A2.1 mouse model, WT1-TOPAbody significantly inhibited tumor growth in a dose-dependent manner and the efficacy was superior than that of the benchmark. Additionally, IL-6 release was minimal in PBMC upon treatment of the antibody, indicating a reduced risk of inducing cytokine release syndrome (CRS). Drug developability assessment indicated that the leading WT1-TOPAbody was a reasonably developable molecule to be taken forward.

Conclusion: WT1-TOPAbody is a differentiated WT1/HLA-A02 targeted T cell engagers that displayed potent and durable anti-tumor activity. These results collectively support the potential of WT1-TOPAbody as a novel therapeutic agent against WT1/HLA-A02$^{\pm}$ cancers and warrant its further development.

#6706 An anti-claudin 18.2/CD3 bispecific antibody for the treatment of claudin 18.2 positive gastric cancer.

L. Zhao[1], G. Zhang[2], Z. Liu[2], J. Xu[2], L. Zhao[2], G. Li[2], B. Li[2], Z. Zhu[2], W. Peng[2], Y. Zhu[2], Z. Chen[2], **Z. Li**[2];
[1]Lunan New Time Bio-tech Co., Ltd., Linyi, China, [2]Lunan Pharmaceutical Group Co. Ltd., Linyi, China

The claudin18.2 (CLDN18.2) protein shows four transmembrane domains (TMDs) with two extracellular loops (ECL), ECL-1 and ECL-2. It is a highly selective biomarker with limited expression in normal tissues and often exhibits abnormal expression during the occurrence and development of various primary malignant tumors. The specific expression pattern supports the notion that CLDN18.2 is a distinctive molecule for targeted therapy in various cancers, particularly gastric and pancreatic cancers. Various drugs targeting CLDN18.2, including monoclonal antibodies, ADCs, CAR-T, and bispecific antibodies, have also entered clinical trials. As of this writing, there are currently no commercially available products worldwide that specifically target CLDN18.2. However, Zolbetuximab (IMAB362) has successfully reached the Phase III end point, indicating positive clinical outcomes and establishing CLDN18.2 as a promising cellular and antibody therapeutic option. Here, we describe LNF2007, an anti-CLDN 18.2/CD3 bispecific antibody that can redirect CD3+ effector T cells to CLDN18.2+ tumor sites, resulting in the activation of T cells and subsequent killing of target cells. The design of LNF2007 focuses on selecting a relatively weak and reasonable affinity to CD3, accompanied by the suppression of Fc-mediated effector functions. This aim is to minimize off-target toxicity and maximize therapeutic efficacy. In vitro data demonstrate that LNF2007 binds more strongly to CLDN18.2+cells than to CD3+ cells. LNF2007 exhibited good dose-dependent activation and cytotoxicity against engineered cell lines BXPC3-hCLDN18.2-Luc and CHOK1-hCLDN18.2-Luc, which are positive for CLDN18.2 expression .In the in vivo pharmacodynamics assay, LNF2007 also demonstrated superior efficacy in the humanized NUGC4-CLDN18.2 model and BxPC3-CLDN18.2 model. Furthermore, a 4-week repeated dose (up to 1 mg/kg) toxicity study in cynomolgus monkeys showed that LNF2007 was safe and well tolerated. In vitro cytokine release was lower in the LNF2007 group than that in the AMG 910 and AZD5863 (two another anti-claudin18.2/CD3 bispecific antibody) groups. In conclusion, the novel anti-CLDN18.2 × anti-CD3 bispecific antibody LNF2007 demonstrates similar efficacy to AMG 910 and AZD5863 and is safer. LNF2007 provides a promising therapy for claudin 18.2-positive cancer patients.Taishan Industry Leading Talents Project of Shandong Province was a sponsor of this research.

#6707 IgG based B7-H3xCD3 bispecific antibody for treatment of gynecological tumors.

S. M. Greiner, J. Mauermann, M. Lutz, I. Hagelstein, E. Tobias, A. Koch, H. Andreas, B. Sara, L. Zekri, M. Marklin;
University Hospital and Medical Faculty Tubingen, Tubingen, Germany

Ovarian cancer is characterized by late stage disease and a poor prognosis. Endometrial cancer is a heterogeneous disease with different prognoses depending on the molecular subtype. Novel treatment strategies are needed to improve patient survival in both entities.
T cell-based immunotherapy has significantly improved the treatment options for many malignancies. B7-H3 (CD276) is an interesting target for immunotherapeutic approaches because it is overexpressed on a wide range of tumor entities and has characteristics of immune checkpoint molecules. Its expression not only on tumor cells but also on the tumor vasculature allows improved infiltration of immune effector cells into the tumor to overcome the major limitation of T cell-based therapy of solid tumors, which is the access of immune cells to the tumor site. A novel bispecific antibody in an IgG-based format called CC-3 with B7-H3xCD3 specificity has already been shown to efficiently induce T cell responses against gastrointestinal malignancies.
Here we show that B7-H3 is highly expressed on endometrial and ovarian cancer cell lines. Treatment with CC-3 induced T cell activation and degranulation as well as secretion of IL-2, IFNγ and perforin. These results demonstrate CC-3 induced T cell reactivity against ovarian and endometrial cancer cells. In addition, CC-3 induced efficient T cell proliferation and formation of T cell memory subsets. This resulted in potent target cell lysis.
Taken together, our results underscore the potential of CC-3, which is currently in GMP manufacturing, to enable clinical evaluation for the treatment of gynecologic malignancies.

#6708 MAIT engagers: Bispecific antibody-mediated redirection of mucosal associated invariant T cells to treat solid tumors.

S. E. Plyte[1], M. Fraudeau[1], D. Winterberg[2], C. Germain[1], C. Rousseau[1], G. Sodaro[1], L. Fenou[3], M. Audin[1], A. Ivagnes[1], H.-H. Oberg[2], P. Gerard[1], I. Navarro-Teulon[3], D. Wesch[2], M. Peipp[2], J. Prigent[1];

[1]Biomunex Pharmaceuticals, Paris, France, [2]Universitatsklinikum Schleswig-Holstein, Kiel, Germany, [3]IRCM, University of Montpellier, Montpellier, France

Background. Using bispecific antibodies (BiXAb) to redirect T cells to engage and kill cancer cells is an efficacious modality in the treatment of haematological cancers but has had limited success in the treatment of solid tumors. Mucosal-Associated Invariant T cells (MAITs) are an abundant subset of non-conventional T-cells with potent cytotoxic capacity (up to 20% of circulating T-cells) that are naturally resident in many tissues and solid tumors. MAIT cells utilize a semi-invariant TCR and recognize bacterial metabolites presented in the context of the MR1 protein. Biomunex has generated bispecific antibodies that bind the MAIT semi-invariant TCR (iTCR) and the HER2 receptor tyrosine kinase expressed on tumor cells. At difference to classical T-cell engagers that activate all T-cell subsets, MAIT engagers only modulate the activity of the cytotoxic MAIT cells leading to efficient tumor control and greater safety profile.

Methods. Using the Biomunex proprietary BiXAb platform, bispecific, tetravalent antibodies were generated that target the MAIT iTCR and the HER2. MAIT-cell activation, proliferation and degranulation were followed by gating on MAIT cells within a purified CD8 cell population. Tumor cell lines (varying in [HER2] expression) were co-cultured with MAIT cells and the BiXAbs in several cytotoxic assays (evaluated by Chromium release). Cytokine release was assessed by Legend Plex assays or ELISA. Cytotoxicity of tumor-resident MAITs, from fresh patient samples, was determined by impedence measurements and in patient-derived 3D organoids by The Hub organoids (imaging). For in vivo analysis, sub-cutaneous tumor growth was measured with callipers.

Results. MAIT engagers induce the rapid activation, proliferation and degranulation of MAIT cells leading to efficient killing of engaged HER2+ cancer cells with a potency similar to that of a classical HER2-directed TCE (in clinical development). The MAIT engager did not activate the regulatory T cells or other CD4/CD8 subsets. In addition, using PBMCs, total cytokine release was 1000-fold less with the MAIT engager compared to a classical TCE, opening up a large therapeutic window, which should permit effective treatment of solid tumors. *Ex vivo* cytotoxicity of tumor-resident MAIT cells using dissociated ovarian cancer samples at “real E:T ratios”, MAIT engager-mediated cytotoxicity of patient-derived organoids (CRC) and *in vivo* evaluation of tumor control will be shown.

Conclusions. MAIT cell redirection is a promising approach for the treatment of solid tumors that has the potency and efficacy of a classical TCE but with a significantly improved cytokine safety profile leading to a larger therapeutic window.

#6709 P329G-Engager: A novel universal antibody-based adaptor platform for cancer immunotherapy.

M. Surowka[1], I. Hutter-Karakoc[1], D. Darowski[1], C. Claus[1], C. Ferrara Koller[1], A. Freimoser-Grundschober[1], T. Hofer[1], A. Sobieniecki[1], D. Assisi[1], S. Leclair[2], E. Moessner[1], P. Umana[1], M. Amann[1], C. Klein[1];

[1]Roche Innovation Center Zurich, Schlieren, Switzerland, [2]Roche Innovation Center Munich, Penzberg, Germany

Bispecific immune cell engagers are showing promise in cancer immunotherapy. To achieve optimal efficacy, there is a growing need for patient personalization, tackling intra-tumor heterogeneity, and simplified combination therapies.

Here, we present a novel modular anti-P329G adaptor platform aiming to address these issues, which is based on the recognition of the P329G mutation in the Fc portion of a targeting adaptor antibody. This P329G mutation can serve to recruit different anti-P329G effector cell engagers, including innate cell engagers, T cell engagers, costimulators or immunocytokines. Specifically, upon identifying patient-specific tumor surface targets, the primary antigen-binding IgG1 antibodies bearing Fc-silencing P329G LALA mutations are applied. Subsequently, based on the tumor's immune profile, the best-suited anti-tumoral effector cell type is chosen for recruitment and activation. Based on this information, the secondary antibody recognizing the P329G mutation is chosen from an array of effector cell engagers with different modes of action: P329G-T cell bispecifics (P329G-TCB), ADCC-competent P329G innate cell engagers (P329G-ICE), P329G costimulatory molecules (P329G-CD28/4-1BBL) or P329G immunocytokines (P329G-IL2v).

In vitro assays showed all P329G modalities inducing anti-tumoral and/or immunomodulatory cell activity. Anti-tumoral efficacy of secondary antibodies was observed only in presence of tumor-targeted P329G adaptors, while no effect was observed in their absence. The readouts consisted of tumor killing quantification, CD4+ and CD8+ T cell activation, cytokine release and cytokine receptor signaling. As a proof of concept study *in vivo*, an experiment in MKN-45 (CEACAM5+)-bearing humanized mice was performed, using an anti-CEACAM5 P329G-IgG adaptor and a P329G-TCB. Both tumor volume shrinkage and T cell infiltration into the tumor confirmed anti-tumoral efficacy of the platform, as compared to a conventional CEACAM5-targeted TCB. Neither the individual P329G IgG nor the individual P329G-TCB induced anti-tumoral efficacy, validating the requirement for primary and secondary antibody binding for T cell engaging activity.

These results provide *in vitro* and *in vivo* evidence that the universal P329G engager platform can be used as an efficacious cancer treatment. Ultimately, this modular approach may enable off-the-shelf personalization *via* combination of patient-specific antibodies and universal effector cell engagers based on the patient's tumor target and immune profile.

#6712 LBL-043, a novel LILRB4xCD3 T cell engager, for the treatment of LILRB4 positive leukemia.

Yujia Dang, Xiao Huang, Yurong Qin, Xiaoya Liu, Min Chen, Duqing Jiang, Guojin Wu, Mi Ye, Jianming Sun, Baohui Wang, Jing Guan, Tingting Li, Jordan Zhu, Shoupeng Lai, Xiaoqiang Kang, **Hong Ling**

Nanjing Leads Biolabs Co., Ltd., Nanjing, China

Background: Acute myeloid leukemia (AML) is a malignant clonal disorder linked to a broad spectrum of molecular alterations. It is still an incurable cancer, the prognosis is even worse in elderly patients, where overall survival (OS) at 1 year is approximately 10-15%. Now, several CD3 bispecific immunotherapies that harness T cells against AML are at various stages of preclinical and clinical development, but most of them are hampered by the lack of specific targets to distinguish tumor cells from normal hematopoietic stem cells (HSC). Leukocyte immunoglobulin-like receptor B4 (LILRB4) is an immune checkpoint inhibitory receptor, which is highly expressed on FAB M4 and M5 AML cells with a lack of expression on normal HSC and progenitor cells. LILRB4 expression level inversely correlates with OS of patients with M4 and M5 AML. All of these indicate that LILRB4 represents a promising target for developing a T cell redirecting bispecific antibody to treat patients with AML, especially for more aggressive M4 and M5 subtype. Herein a novel bispecific antibody targeting LILRB4 and CD3, LBL-043, is developed to specifically kill LILRB4 positive tumor cells by engaging T cells.

Methods: LBL-043 was constructed using our proprietary LeadsBody^{TM} T cell engager platform, which is a 2:1 format bispecific antibody with two VHH arms targeting LILRB4 with high affinity and one scFv arm targeting CD3 with fine-tuned low affinity. The binding affinity of LBL-043 to LILRB4 and CD3 was determined with Fortebio, while the activity was measured using several cell based assays including reporter gene and TDCC assays. The anti-tumor activity of LBL-043 was investigated in B-NDG/hu-PBMC reconstructed mice implanted with MOLM-13 (human AML-M5a) tumor model.

Results: The binding affinity of LBL-043 to LILRB4 and CD3 protein was 0.724 nM and 35.7 nM, respectively. In CD3 reporter gene assays, LBL-043 could activate the NFAT reporter signaling through LILRB4 binding dependent CD3 cross-linking with an EC_{50} value of 2.459 nM. LBL-043 was shown a potent TDCC activity in different LILRB4 expression level MOLM-13 cells and HL-60 cells with T cell activation and cytokine release. In B-NDG/hu-PBMC reconstructed mice implanted with MOLM-13 tumor cells, LBL-043 was shown significant anti-tumor activity. Simultaneously, LBL-043 can effectively improve the survival rate and maintain relatively stable body weight in the study compared to the vehicle group.

Conclusion: LBL-043, a novel bispecific antibody targeting CD3 and LILRB4 with affinity differentiation, induces T cell killing of AML cells by simultaneously binding LILRB4 expressed on tumor cells and CD3 on T cells, redirecting T cells to efficiently killing of AML cells. It is also shown a great anti-tumor efficacy in CDX mouse models. These data support LBL-043 as a novel therapeutic bispecific antibody for the treatment of LILRB4 positive AML and CMML leukemia patients.

#6713 TICTE, A trispecific T-cell engager with immune checkpoint modulation for solid tumors.

X. Wu, X. Min, Y. Wu, L. Liu, J. Zhou, S. Hudson, S.-p. Chen, J. Li, W. Draper, S. Dash, S. Ma, H. Chen, **Z. Wang**;
RemeGen Biosciences, Inc., South San Francisco, CA

Background: Bispecific T-cell engager (BiTE) is a targeted cancer immunotherapy which bridges T-cells to cancer cells, leading to activation of T-cells and killing cancer cells. While BiTEs have shown promising therapeutic efficacy in the treatment of hematological malignancies, therapeutic benefit of T-cell engagers are still in exploration for the treatment of solid tumors. Upregulation of immune checkpoints presents one of the major resistant mechanisms of the BiTE therapy. Here, we report a Trispecific Immune Check-point T-Cell Engager (TICTE) platform that targets both CD3 and PD-L1 simultaneously, which activates the T-cells as well as modulates the immune checkpoint blockade through the PD/PD-L1 axis, respectively. Our *in vitro* and *in vivo* studies demonstrate that the TICTEs induce dramatic and superior antitumor activity compared to its counterpart BiTE alone and the BiTE with anti-PD-L1 combination. These studies suggest that the TICTE (CD3xTAAxPD-L1), a single-agent with dual function of T-cell activation and immune checkpoint modulation, may provide an efficacious therapy to patients with solid tumors.

Methods: Various TICTEs and BiTEs formats using the human IgG like architecture in three different TAA examples were generated. Their biophysical and biological activities were characterized. The cell binding activity and antigen density of cell lines were determined using flow cytometry. TDCC activity was measured using xCELLigence RTCA eSight system. In vitro efficacy was evaluated with multiple cancer cell lines and toxicity was evaluated with normal cell lines. The humanized xenograft models were utilized to investigate the TICTEs efficacy *in vivo*.

Results: All TICTEs adopted their intended forms and showed robust biophysical properties. The TICTEs demonstrated the blockade activity of PD1/PD-L1 axis, as well preferentially targeted tumor cells expressed both TAAs and PD-L1. Large therapeutic windows were observed in three TAA (cMET, Her2 and Trop2) TICTEs. TICTEs showed a superior efficacy compared to counterpart BiTEs and combination of BiTE with a PD-L1 inhibitor *in vitro* and *in vivo*. Low cytokine release was observed compared to combination of BiTEs with a PD-L1 inhibitor, signifying the reduced risk of cytokine release syndrome (CRS) often associated with BiTE therapy.

Conclusion: A single agent of the TICTE platform with unique biological property, superior efficacy and low cytokine release could represent an alternative combination immunotherapy for solid tumors.

#6714 AI-guided tailor-made anti-TROP2 T-cell engagers for T-cell mediated cancer immunotherapy with enhanced therapeutic index.

Chuan Chen, Liang Tian, Chenpeng Su, Dandan Liu, Xiaoqian Chen, Yifei Zhou, Suze Jiang, Guifang Wang, Jiyuan Tian, Yuan Yuan, Bing Yang, Jian Peng

Helixon, New York, NY

Bispecific T-cell engagers (TCEs) have shown significant therapeutic advances in the treatment of hematologic cancers. However, the clinical efficacy of TCEs in treating solid tumors remains to be demonstrated. Accumulating evidence suggests novel TCE modalities that simultaneously engage both CD3 (signal 1) and CD28 (signal 2) co-stimulatory signals may offer potential advantage to enhance clinical efficacy of TCEs with improved therapeutic index. To explore the full potential of TCEs as a powerful approach of immunotherapy for solid tumors, we developed an integrated AI-guided TCE platform to streamline the discovery, optimization and high-throughput function screening and characterization of TCE molecules. Here we report the construction and characterization of a novel panel of TROP2-targeting TCEs by leveraging our AI-guided optimization technology, plus a high-throughput in vitro screening platform. These tailor-made TCE molecules exhibit favorable developability and functional properties. Our data show that a novel TROP2 × CD3 x CD28 trispecific TCE that contains a CD3-targeting arm in concomitant with a CD28-targeting arm can induce potent T-cell co-stimulation and promising synergistic T cell-mediated tumor cell killing in vitro, compared to its counterparts with a single CD3-targeting arm. We further generate a trivalent TROP2 x CD3 bispecific TCE constructed as an asymmetric '2+1' format with bivalent binding to TROP2 but a monovalent CD3-targeting arm. This molecule stimulates very low levels of cytokine release, but drives robust antigen-specific killing in in vitro assessment. Anti-tumor activity of the various TROP2 x CD3 TCEs is currently being investigated in multiple tumor xenograft mouse models.

#6715 CLDN6: Biological insight into therapeutic potency of SAIL66, a next generation of T-cell engager targeting CLDN6.

N. Kimura[1], K. Taniguchi[1], T. Kamikawa[1], **M. Yoshimoto**[1], S. Ishii[1], M. Muraoka[1], M. Shimada[1], M. Kamata-Sakurai[1], T. Kitazawa[1], T. Igawa[2];
[1]Chugai Pharmaceutical Co., Ltd., Yokohama, Kanagawa, Japan, [2]Chugai Pharmaceutical Co., Ltd., Tokyo, Japan

Background: Because of high recurrence rate, ovarian cancer continues to demand new treatments. Recently, we have developed a next-generation T-cell engager SAIL66, which is a tri-specific monoclonal antibody designed to bind to CLDN6 on cancer cells with one Fab arm and to both CD3 and CD137 with the other Fab arm. By boosting T cell activation through both CD3 and CD137 binding, SAIL66 shows potent anti tumor efficacy against CLDN6-positive cancers and are currently being evaluated in patients with CLDN6-positive solid cancers including ovarian cancer (NCT05735366). CLDN6 is upregulated in many solid tumors but shows minimal or no expression in healthy adult tissues. Due to its cancer specific expression profile, CLDN6 has been utilized as a target for cancer immune therapies. Here, we demonstrate that CLDN6 is an attractive therapeutic target from its biological perspective in ovarian cancer.
Methods and Results: In a HuNOG tumor-bearing mouse model transplanted with CLDN6-positive ovarian cancer cells (OV90, OVCAR3), SAIL66 showed potent antitumor activity as a single agent. Surprisingly, CLDN6 expression in transplanted tumors was significantly lower compared to in vitro cultured cells, suggesting that CLDN6 expression is highly variable. In vitro, CLDN6 expression reversibly fluctuated depending on cell density, and its expression was consistent with the expression of epithelial-mesenchymal transition (EMT) and stemness-related genes. Furthermore, FACS and qPCR revealed that chemotherapeutic agents increased CLDN6-positive cells, and this fluctuation was accompanied by the expression of EMT and stemness-related genes. Based on this biology, we tested the combination effect of SAIL66 and chemotherapies in a non-clinical tumor-bearing mouse model. As a result, significant tumor regression was observed in mice treated with SAIL66 in combination with carboplatin.
Conclusion and Discussion: Ovarian cancer is characterized by significant tumor heterogeneity. The presence of cancer stem/stem-like cells or EMT has been proposed to elucidate the underlying mechanisms of the heterogeneity. Our study potentially could offer valuable insights into the biology of CLDN6-positive cells and the causes of ovarian cancer heterogeneity. Furthermore, it could help in patient selection, the development of combination strategies, and future clinical validation of SAIL66.

#6716 DLL3 TriTCE Co-Stim: A next generation trispecific T cell engager with integrated CD28 costimulation for the treatment of DLL3-expressing cancers.

P. Repenning, D. Lau, D. C. Hernaez, A. Robinson, D. P. Escanda, M. Rocha, B. S. Moreno, J. Zhang, P. Shao, N. Escalante, L. Newhook, P. Bhojane, C. L. Piscitelli, P. A. Moore, T. Spreter Von Kreudenstein, N. E. Weisser;
Zymeworks BC Inc., Vancouver, BC, Canada

Small cell lung cancer (SCLC) is an aggressive neuroendocrine cancer with a poor prognosis and high unmet medical need. Current standards of care, including chemotherapy, targeted therapy and immunotherapy, are associated with limited duration of response. Furthermore, SCLC is characterized by an immunosuppressive microenvironment and poor T cell infiltration which present additional treatment challenges. Delta-like ligand 3 (DLL3) is an inhibitory Notch ligand that is aberrantly overexpressed in SCLC and other neuroendocrine tumors, but minimally expressed in normal tissues, and is a new therapeutic target. Bispecific T cell engagers (TCE) targeting DLL3 have entered the clinic and demonstrated promising anti-tumor activity in SCLC patients; however, we believe there is room to improve on the rate and depth of response. To address treatment challenges and enhance the durability and sustainability of T cell activation, we have engineered a trispecific co-stimulatory T cell engager (TriTCE Co-stim) molecule that optimally engages CD3 and CD28 and redirects and enhances cytotoxic T cell responses to DLL3-expressing tumor cells while maintaining a desired safety profile. A panel of DLL3xCD3xCD28 trispecific antibodies (Abs) was engineered with a conventional anti-CD28 agonist paratope in a variety of Ab formats, geometries, paratope affinities and specificities. Geometry and design features of the tri-specific Abs were informed by prior TriTCE Co-stim molecule optimization[1]. Azymetric™ and EFECT™ platforms were used to facilitate heterodimeric multi-chain antibody assembly with silenced Fc gamma function. Lead TriTCE Co-stim Abs were selected for enhanced DLL3-dependent antitumor cytotoxic activity and increased T cell function including T cell activation, proliferation and cytokine production, compared to competitor bispecific TCEs. DLL3-independent activity and cytokine release were assessed with human PBMCs in solid and solution phase assays to evaluate the potential for cytokine release induction. In summary, we have identified multiple TriTCE Co-Stim Ab formats with improved DLL3-dependent cytotoxicity and T cell activation over competitor bispecific TCEs across multiple DLL3-expressing tumors. By screening various Ab formats, geometries and paratope affinities, we have selected lead DLL3 TriTCE Co-stim Abs displaying target-dependent activation of T cells with potent anti-tumor activity which may translate to improved and more durable antitumor responses in the treatment DLL3-expressing cancers.

#6717 Targeting mutant KRAS proteins with novel TCR-mimic fully human antibodies.

J. Du, W. Tang, X. Jiao, L. Zhao, P. Du, Y. Zhang, J. Bao, H. Chen, **C. Guo**, W. An;
Biocytogen Pharmaceuticals (Beijing) Co., Ltd., Beijing, China

Mutated KRAS proteins are ideal cancer targets, as they are expressed frequently and specifically in certain solid tumors. A large proportion of human colorectal cancer and pancreatic ductal adenocarcinoma express the tumor driver KRAS gene mutations G12V/G12D, but drugs targeting G12V/G12D are not available, revealing a huge unmet clinical need. While small molecules often fail to target the KRAS mutation G12V/G12D, T cell receptor-mimic (TCR-mimic) antibodies can specifically recognize KRAS mutations presented by human leukocyte antigen (HLA), opening up possibilities for targeting such intracellular antigens. Here, we discovered novel antibodies highly specific to G12V/HLA and G12D/HLA complexes by immunizing our proprietary RenTCR-mimic™ mice and using high-throughput Beacon-based screening. These TCR-mimic antibodies have higher affinities compared to endogenous TCRs, which may effectively reduce the possibility of tumor escape. Germline distribution analysis indicated their high sequence diversity, which suggests diverse epitope targeting. Although pancreatic cancer is extremely difficult to treat and has an extremely low KRAS mutant peptide-HLA complex density on the cell surface, our TCR-mimic antibodies exhibited potent in vitro tumor lysis activity when assembled into CD3 T cell engagers. Furthermore, these antibodies demonstrated convincing off-target safety. Together, our results indicate promising therapeutic potential of these KRAS mutation-targeted TCR-mimic antibodies for the treatment of solid tumors.

#6718 Evaluating toxicity and efficacy of bispecific EGFRXCD3 T cell engager in solid tumor-bearing humanized animal model.

G. Yang, L.-C. Yao, J. G. Keck, M. Cheng;
The Jackson Laboratory, Sacramento, CA

Background: Cancer immunotherapy has currently become a highly active research area of oncology and a common treatment strategy for several cancer types. One prominent reason is that the utilized animal models could not accurately predict the of toxic response of human immune system to anti-cancer drug. For improving the safety of immune drug development, it is urgent to establish a predictive nonclinical animal platform that can accurately predict human immune response to the drugs and detect potential unwanted toxicity to human patient will be critical. We have demonstrated a disseminated tumor-bearing humanized mouse model that can evaluate the toxicity and efficacy of bispecific T cell engager (BiTE). In this study, we co-engrafted disseminated and solid tumor cells to the same mice and compared with mice engrafted with disseminated tumor or solid tumor. The purpose is to develop a novel tumor-bearing mouse model that can simultaneously evaluate the long-term efficacy against solid tumors in addition to cytokine level assessment.
Method: Epidermal growth factor receptor (EGFR) expressing human triple negative breast cancer MDA-MB-231/Luciferase-2A-GFP (MDA) cell line was utilized to establish solid tumors in mice. The cells were implanted into PBMC humanized NSG-MHC class I/II double knock out (DKO) mice via orthotopic injection into mammary fat pad (MFP). Disseminated MDA cells were injected intravenously (IV) and tumor cells normally colonize in mouse lungs. Following EGFRxCD3 BiTE dosing initiation, tumor burden in MFP and lungs were evaluated via in vivo Xenogen imaging system, and solid tumor volume in MFP was measured 2 to 3 times a week by a digital caliper. To evaluate the toxicity in response to EGFRxCD3 BiTE treatment, human inflammatory cytokine levels was analyzed by BD cytometric bead. Clinical observations and body weight change, and human immune cell activation were evaluated.
Result: EGFRxCD3 BiTE treatments significantly inhibited MFP solid tumor growth regardless the presence of IV implanted with MDA cells. EGFRxCD3 BiTE treatment induced elevated human inflammatory cytokines from humanized mice implanted with combined MFP and IV tumors. By comparison, the serum cytokine levels were low in mice implanted with MDA cells via MFP alone, suggesting that disseminated tumor cells are required for cytokine production induced by EGFRxCD3 BiTE.
Conclusion: Without disseminated tumor, MFP solid tumor-bearing mice can be served as a model for drug efficacy but did not induce inflammatory cytokines by EGFRxCD3 BiTE treatment. Combination of solid and disseminated tumor models in the same mice provide a new approach for simultaneously evaluating the toxic cytokine release and efficacy of immunotherapy drugs.

#6719 TriTCE Co-Stim: A next generation trispecific T cell engager platform with integrated CD28 costimulation, engineered to improve responses in the treatment of solid tumors.

L. Newhook, P. Bhojane, K. Stahl, N. E. Escalante, P. Repenning, D. Perez Escanda, P. Shao, M. C. Poffenberger, A. Robinson, K. Patel, A. Livernois, C. L. Piscitelli, N. Afacan, P. A. Moore, N. E. Weisser, T. Spreter von Kreudenstein;
Zymeworks BC Inc., Vancouver, BC, Canada

Bispecific T cell engagers (TCEs) have exhibited clinical successes in the treatment of hematological cancers, while treatment of solid tumors remains a challenge. Treatment of solid tumors with conventional CD3-engaging TCEs can result in limited T cell proliferation and recruitment to the tumor site, and treatment related T cell anergy, thus restricting the ability of bispecific TCEs to inhibit growth of these poorly infiltrated tumors and rapidly growing tumors. Next generation tumor-targeting, trispecific T cell engagers with integrated costimulation (TriTCE Co-Stim) have the potential to provide more durable responses and re-invigorate T cell responses by mediating integrated signaling through CD3 (signal 1) and co-stimulation through CD28 (signal 2). Superagonist anti-CD28 antibodies activate T cells but resulted in clinical toxicities with severe cytokine release syndrome (CRS). Therefore, achieving a balance between signal 1 and 2 is critical for optimal T cell activation and proliferation. Using our Azymetric™ and EFECT™ platforms, we generated heterodimeric TriTCE Co-Stim antibody formats with various geometries and affinities to optimize T cell response and widen the therapeutic window for the treatment of solid tumors.

We have previously described screening and interrogation of different TriTCE Co-stim formats and paratope affinities, and the selection of a lead format with optimized CD3 and CD28 T cell activation. Here, we have further expanded our validation of the TriTCE Co-stim platform with our lead CLDN18.2 TriTCE co-stim format, to include a tolerability assessment in nonhuman primates.Our lead TriTCE Co-Stim format exhibited a favorable safety profile *in vitro* and mediated target-dependent induction of T cell activity, with enhanced proliferation, survival, and T cell-mediated cytotoxic potency compared to bispecific TCEs. In a predictive *in vivo* model of CRS, our lead TriTCE Co-Stim did not exhibit systemic toxicity or peripheral cytokine release. TriTCE Co-Stim mediated enhanced tumor growth regression *in* vivo with an increase of T cells within the tumor and no increase of T cells within the periphery.

Repeat doses of the lead TriTCE Co-Stim molecule at 3 mg/kg were well-tolerated in nonhuman primates with no abnormal clinical signs. Minor decreases in body weight and food consumption were observed. Clinical pathology changes were consistent with a mild systemic inflammatory response.

In summary, our lead TriTCE co-stim molecule has enhanced target-dependent antitumor activity vs. bispecific benchmarks and is tolerated a murine CRS model and repeat dose non-human primate study. These data suggest TriTCE Co-stim may provide tolerable and more durable antitumor responses and contribute to improved clinical outcomes.

#6720 HINT1 steric masked, protease-activatable bispecific protein nanorings direct human T and NK cells to eradicate EGFR+ solid tumors.

A. Kulkarni, D. Paul, D. Dahlberg, K. Ligori, F. Rodriguez, L. Rozumalski, B. Walcheck, C. R. Wagner;
University of Minnesota, Minneapolis, MN

Introduction/Purpose: The Wagner lab has developed a protein nanoring based platform to direct human immune cells to combat solid tumors. These nanorings are bispecific, comprised of tumor-targeting and immune cell-targeting dihydrofolate reductase ($DHFR^2$) fusion proteins. These protein nanorings direct immune cells to target and destroy cancer cells. For treating solid tumors, we aimed to target epidermal growth factor receptor (EGFR). However, targeting EGFR could lead to potential "*on-target, off-tumor*" effects due to expression of EGFR in healthy tissue. Matrix metalloproteinases are overexpressed in a variety of solid tumors. Therefore, to improve tumor specificity, we hypothesized that masking the immune cell targeting $DHFR^2$ protein through a matrix metalloproteinase-2 (MMP-2) sensitive linker will prevent engagement and activation of immune cells outside the tumor microenvironment (TME). Once these protease-activatable nanorings enter the TME and bind to EGFR, cleavage by MMP-2 will lead to unmasking of the immune cell binder, thereby crosslinking and activating immune cells, causing targeted cancer cell lysis.

Methods: We designed human histidine triad nucleotide binding protein-1 (HINT1) masked anti-immune cell targeting nanobody-$DHFR^2$ fusion proteins. HINT1 was hypothesized to sterically block the engagement of immune cells outside the tumor. HINT1-anti-TCR-$DHFR^2$ (TCR = T cell receptor) and HINT1-anti-CD16-$DHFR^2$ were cloned, expressed, purified, and characterized. Their apparent binding affinities were determined using flow cytometry. The anti-tumor efficacy of these nanorings was evaluated against EGFR overexpressing A431 (human epidermoid carcinoma) cells.

Results: HINT1-anti-TCR-$DHFR^2$ and HINT1-anti-CD16-$DHFR^2$ rings showed reduced binding to T and NK-92-CD16 cells, respectively. *In vitro* MMP-2 cleavage assay showed complete removal of the HINT1 mask within 2 hours. Western blot analysis showed that both proteins were stable in human serum up to 3 days. 2D cytotoxicity assays with protein nanorings assembled using anti-EGFR-$DHFR^2$ and anti-TCR-$DHFR^2$ or anti-CD16-$DHFR^2$ with T and NK-92-CD16 cells respectively, showed a potent lysis of A431 cells. The EGFR-targeted lysis was diminished in the presence of HINT1 mask, thereby providing proof-of-concept for the steric masking of the anti-immune cell targeting nanobodies.

Conclusion: Protease-activatable nanorings can selectively lyse EGFR+ tumor cells *in vitro*. Their antitumor efficacy and safety are currently being evaluated using a previously established *in vivo* mouse model. Therefore, HINT1-steric masking can serve as a simple and effective strategy to address off-tumor toxicities associated with bispecific immunotherapies.

#6721 AI-guided generation of novel GUCY2C-targeting T-cell engagers for the treatment of colorectal cancer.

Liang Tian, Jinxiu Hou, Chenpeng Su, Xiaoou Xu, Xiaoqian Chen, Dandan Liu, Jiyuan Tian, Rui Shen, Yi Pan, Yuan Yuan, Lisha Dong, Tingting Gu, Jian Peng

Helixon, New York, NY

Colorectal cancer (CRC) ranks as one of the most lethal cancers worldwide. Given the advances in immunotherapy and targeted therapy, the survival time in CRC has been improving recently. However, the development of novel and effective therapies for CRC still remains an unmet medical need. Guanylyl cyclase C (GUCY2C) is a transmembrane receptor expressed on the surface of intestinal epithelial cells. Recent studies have demonstrated that GUCY2C is causally linked to intestinal inflammation, dysbiosis, and tumorigenesis. To this end, GUCY2C has emerged as a promising target for immunotherapy and a diagnostic marker of primary and metastatic cancer. Here we describe the discovery and optimization of a novel panel of GUCY2C-targeting T cell engagers (TCEs) developed via our streamlined AI-guided TCE development platform. We have identified a number of anti-GUCY2C antibodies with various binding epitopes on GUCY2C, and subsequently generated a panel of novel GUCY2C-targeting multispecific antibodies with favorable developability and functionalities via our AI-driven engineering technology. Our data demonstrate that a biparatopic GUCY2C x CD3 TCE engineered as an asymmetric ‘1+2’ format can recognize two distinct epitopes on GUCY2C. This biparatopic GUCY2C x CD3 TCE shows enhanced tumor cell binding affinity and superior T cell-mediated cytotoxicity compared to the ‘1+1’ GUCY2C x CD3 TCE and ‘1+2’ bivalent GUCY2C x CD3 TCE where the two GUCY2C targeting arms can only bind to an identical epitope on GUCY2C. In addition, we have engineered a novel GUCY2C × CD3 x CD28 trispecific TCE, in which the CD3-targeting arm in tandem with the co-stimulating CD28-targeting arm mediate the interaction with T cells. This anti-GUCY2C trispecific TCE induces favorable synergistic T cell activation and tumor cell killing in vitro compared to the bispecific counterparts. In vivo anti-tumor activity assessments of these multispecific TCE molecules in various tumor xenograft mouse models are currently ongoing.

#6722 A CD33 antigen targeted Gamma Delta T-cell engager in combination with zoledronate promotes Vg9Vd2^{+} T cell proliferation and cytotoxicity against acute myeloid leukemia.

A. Y. Lai[1], C. Wang[2], D. C. Baiu[2], K. Smith[2], A. Patel[1], K. Evans[1], N. Murr[1], D. Franklin[1], M. Hussain[1], J. Pate[1], N. Oien[1], V. Makani[1], A. Shukla[1], K. Wilson[1], G. Fromm[1], T. H. Schreiber[1], J. E. Gumperz[2], S. De Silva[1];

[1]Shattuck Labs, Durham, NC, [2]University of Wisconsin School of Medicine and Public Health, Madison, WI

Vγ9Vδ2^{+} T cell (GDT) targeted immunotherapy is of interest to harness its MHC-independent cytotoxic potential to promote anti-tumor immunity. However, it remains unclear whether GDT (1-5% of total T cells) are present at sufficient numbers to be therapeutically relevant. Accumulation of intracellular phosphoantigens promotes heterodimerization of butyrophilin (BTN) 2A1 and BTN3A1 on the cell surface, leading to TCR-mediated activation of GDT. To date, clinical trials in cancer patients have failed to demonstrate monotherapy activity using a variety of GDT activating agents, including aminobisphosphonates such as zoledronic acid (ZA), Vδ2^{+} targeted T cell engagers and BTN3A1 targeted antibodies. These data leave fundamental questions regarding the therapeutic potential of GDT unanswered, including whether they are present in sufficient numbers, whether the agents in question are providing adequate GDT activation, and whether GDT are being directed to tumor cell targets. The studies herein were thus designed to further understand the role of phosphoantigens, butyrophilins and antigen presenting cells (APCs) in activating GDT. Specifically, APC mediated GDT activation was studied in an in vitro co-culture system in the presence and absence of ZA or a CD33-directed GDT engager incorporating a heterodimer of BTN2A1 and BTN3A1 to dissect the contribution of phosphoantigens, butyrophilins and other costimulatory molecules on GDT proliferation and activation. To this end, while BTN2A1/3A1-Fc-CD33scFv treatment alone in T and monocyte-derived dendritic cell (mDC) co-cultures or in unfractionated PBMCs increased the frequency of GDT by 2 to 10-fold after 7-12 days, the combination with low dose ZA (0.5 to 2 μM) synergistically increased GDT proliferation by 40 to 100-fold. These results indicate that GDT proliferation relies both on the abundance of BTN2A1/3A1 heterodimers and other costimulatory signals activated by ZA. Synergistic effects of ZA and BTN2A1/3A1-Fc-CD33scFv in GDT proliferation was similarly observed in human PBMC-engrafted NSG-IL-15tg mice 12 days after treatment. Importantly, the addition of BTN2A1/3A1-Fc-CD33scFv to T (or PBMC) and CD33^{+} AML co-cultures enhanced both GDT proliferation and anti-leukemic activity while sparing healthy CD33^{+} immune cells. Collectively, these results demonstrate that GDT proliferation and effector function is dependent both upon the abundance of butyrophilin heterodimers, and other cell surface molecules which are modulated by intracellular phosphoantigen accumulation.

#6724 Mechanistic validation of MAIT cell engagers in HUB patient-derived organoids (PDO) co-culture model.

Y. Abouleila[1], J. Prigent[2], M. Doorn[1], C. Germain[2], S. Boj[1], S. Plyte[2], C. Verissimo[1];
[1]HUB Organoids, Utrecht, Netherlands, [2]BIOMUNEX Pharmaceuticals, Paris, France

In the field of cancer immunotherapy, bispecific antibodies have emerged as a promising approach for redirecting T-cells to target and combat tumors. However, their efficacy is limited to only a subset of patients. A major challenge that hinders the development of bispecific antibody targets is the lack of preclinical models that preserve patient-specific tumor antigens and recapitulate the complex interaction between the human immune system and tumor cells. HUB Organoids technology presents a valuable platform for novel immunotherapies testing and validation as they are directly derived from patient tumor tissues, accurately reflecting patient-specific tumor antigens. BIOMUNEX Pharmaceuticals has developed the BiXAb® technology platform, a computational modeling approach that rapidly generates bispecific antibodies from various monospecific monoclonal antibodies, eliminating the need for extensive engineering. This platform includes a bivalent T cell engager specifically targeting MAIT cells and human epithelial growth factor receptor (HER2), a tumor antigen highly expressed in some colorectal cancer (CRC) patients. This innovative approach forms an efficient immunological synapse, allowing exclusive redirection of MAIT cells to directly eliminate cancer cells. In a collaborative research initiative between HUB Organoids® and BIOMUNEX Pharmaceuticals, the mechanisms by which BiXAb® induce tumor cell killing were confirmed using CRC patient-derived organoids (HUB Organoids® or PDOs) co-cultured with allogenic MAIT cells in an *in vitro* model. The study results depicted BiXAb® induced MAIT-cell activation in a dose-dependent manner, as detected by FACS and ELISA. Furthermore, BiXAb®-mediated MAIT-cell-specific killing of CRC PDOs was observed in a HER2-dependent manner, determined using an image-based viability assay. In conclusion, the co-culture platform of CRC PDOs-MAIT cells described here effectively captured the activation and targeted killing of MAIT cells mediated by BiXAb®, underscoring the added value of this PDO-based co-culture platform in developing novel immunotherapies.

#6725 NTX-470, a novel multispecific T cell engager expressed from mRNA targets PSMA and STEAP1 prostate cancer antigens to generate enhanced functional activity.

C. Rae[1], S. Adusumilli[1], S. Bandi[1], S. Lal[1], P. Dhungel[1], K. Ferry[1], S. Gholizadeh[1], A. Sharma[1], A. Sallets[1], W. Liu[1], E. McCartney-Melstad[1], P.-K. Hsu[1], R. Low[1], C. McKinlay[1], M. Leong[1], D. Y. Oh[2], L. Fong[2], G. Kannan[1], S. Deutsch[1], O. Haabeth[1];
[1]Nutcracker Therapeutics, Inc., Emeryville, CA, [2]University of California, San Francisco, San Francisco, CA

Prostate cancer is the most common cancer in American men and the second leading cause of cancer death in men in western countries. Most metastatic patients develop castration resistant prostate cancer, which despite advances in immunotherapy, is limited in treatment options and represents a critical unmet need. Bi-specific T cell engagers (TCEs) targeting prostate cancer antigens represent a modality that has demonstrated preliminary clinical activity. Clinically validated antigens that are highly expressed in prostate cancers include Prostate-Specific Membrane Antigen (PSMA) and Six Transmembrane Epithelial Antigen of the Prostate 1 (STEAP1). TCEs targeting either PSMA or STEAP1 individually have shown promising clinical activity, but challenges with durability and toxicity have been reported, potentially attributable to antigen escape, target-independent T cell activation (bystander activation) and specificity issues. Contrary to its name, PSMA expression is not exclusive to prostate cells and can be found in several other tissues and/or conditions, including normal nonprostatic epithelial cells, inflammation/infection, nonprostatic neoplastic cells and nonprostatic tumor-associated neovasculature. The widespread expression of PSMA may limit the therapeutic window of PSMA-specific TCEs and drive immunotoxicity by increased on-target, off-tumor binding. To address these issues, Nutcracker Therapeutics (NTX) has developed novel and highly complex multispecific TCE molecules that target both PSMA and STEAP1, which can be expressed using NTX's proprietary mRNA therapeutics platform. A wide library of molecules was designed with attenuated PSMA and CD3 binding to mitigate on-target, off-tumor binding and target-independent T cell activation. Molecules were screened and selected based on their propensity to cause bystander T cell activation and the strength of PSMA binding. We identified a small number of molecules that are capable of engaging CD3 T cells but display minimal activity in the absence of STEAP1 or PSMA expressing target cells, including molecules that retain low bystander activity and attenuated PSMA binding yet maintain robust target cell killing. These molecules include NTX-470, which targets both STEAP1 and PSMA on tumor cells with minimal bystander activity.

#6726 Costimulatory IgM T-cell engagers with enhanced and durable cytotoxicity.

J. Xue, K. Li, P. Yakkundi, P. Chadasama, T. Mao, Z. Malik, V. Rao, M. Joglekar, K. Mai, G. Li, D. Pandya, R. Rosete, Z. Ye, L. Tahrani, J. Wang, N. Hanna, E. Perez, Y. Wang, S. Ahmed, L. Widjaja, P. Hinton, K. Bzymek, B. Keyt, M. Oyasu, L. Liu, **A. Sinclair**, U. S. Muchhal;
IGM Biosciences, Inc., Mountain View, CA

T-cell engagers (TCEs) have established therapeutic effect in treatment of various cancers by harnessing the power of the immune system against tumors in a targeted manner. IgM-based TCEs may offer high avidity, specificity, and safety advantages over other modalities because of their multivalent architecture and unique positioning of the CD3 binding domain on the J-chain. We have built a costimulatory IgM TCE platform that engages both signal 1 and signal 2 on T-cells, with the goal of enabling their optimal activation and survival for more robust and durable cytotoxic activity.

Multiple antigen targeting costimulatory IgM TCEs were generated and activity was evaluated both in vitro and in vivo to assess the role of CD28 co-stimulation. Costimulatory IgM TCEs engaged both CD3 and CD28 on the T-cell surface, enhancing in vitro cytotoxicity and T-cell activation. Levels of IL-2 increased significantly with dual signal engagement promoting proliferation and survival of T-cells. In long-term culture assays, costimulatory IgM TCEs promoted better T-cell proliferation and survival compared to IgM TCEs with only a CD3 binder, and was even more pronounced at low E:T ratios. In the absence of CD3 engagement, CD28 binding alone did not induce any T-cell activation, cytotoxicity, or cytokines. Activation of T-cells was also fully dependent on the presence of target cells, underscoring the safety profile of the platform.

In Hu-PBMC xenograft tumor models, costimulatory IgM TCEs exhibited stronger in vivo anti-tumor activity compared to TCEs only engaging CD3. Tumor growth inhibition was maintained for longer after dosing was stopped with costimulatory IgM TCEs, indicating the durability of responses. Costimulatory IgM TCEs suppressed tumor growth in xenograft studies using cell lines that expressed both high and low target copy numbers suggestive of their broad utility against multiple tumor types. Enhanced in vivo anti-tumor activity of costimulatory IgM TCEs was associated with significant increases in intra-tumoral CD8/CD3^{+}T-cells.Both peripheral and intra-tumoral T-cells exhibited enhanced anti-apoptotic and cytotoxic phenotypes indicative of the costimulatory activation.

IgM-based costimulatory TCEs provide enhanced cytotoxicity through optimal T-cell activation and proliferation/survival. This dual engagement of T-cell activation signals, along with the high avidity target binding offered by IgM platform, could enable the creation of effective therapeutics targeting pathogenic cells in autoimmune diseases and solid tumors that will maintain activity even in conditions with low T-cell counts.

#6727 QL335, a novel T cell engager with enhanced safety profile targeting MSS colorectal cancer.

S. Gu[1], G. Guo[1], H. Yee[1], H. V. Tran[1], S. Chen[1], C. Cao[2], K. Liu[2], C. Jin[2], W. Lun[2], R. Ma[2], L. Ren[2];
[1]QLSF Biotherapeutics, South San Francisco, CA, [2]Qilu Pharmaceutical Co., Ltd., Jinan, China

Colorectal cancer (CRC) is the fourth leading cause of death in the world with a global mortality rate of over 700,000 annually. While recent advancement in diagnosis and prevention has reduced the overall number of deaths, the lack of effective and durable treatment has not significantly improved survival rate. Emerging modalities in immunotherapy such as T cell engagers have paved new ways for disease management. However, a common challenge to advancing T cell engagers in the clinic is poor target specificity and high toxicity associated with non-specific T cell activation and cytokine release. To overcome these shortcomings, we have developed QL335, a bispecific antibody bridging LY6G6D antigen on tumor cells and CD3 on T cells. LY6G6D or Lymphocyte Antigen 6 Family Member G6D, is a GPI-anchored membrane protein that, according to TCGA RNAseq data, is highly expressed in microsatellite stable (MSS) colorectal cancer but not in normal tissues. We analyzed LY6G6D expression by IHC in over 200 CRC patient tumors and 40+ normal tissue samples from different organs, confirming its highly restricted CRC expression pattern. We constructed our bispecific antibody in a 2+1 format, comprising two high affinity LY6G6D binding domains and one reduced affinity CD3 binding domain. Such format allows for higher tumor accumulation while mitigating non-specific T cell activation in the periphery. In vitro evaluation showed that QL335 induced potent yet highly specific T cell activation and killing of only target cells expressing LY6G6D. QL335 demonstrated robust anti-tumor efficacy in vivo against human colon cancer xenograft models with human PBMC reconstitution. Importantly, QL335 was well tolerated in cynomolgus monkeys dosed up to 50 mg/kg, supporting the enhanced safety profile by design of this therapeutic candidate. QL335 is currently being evaluated in a phase 1 clinical trial.

#6728 Preclinical development of QL325, a novel T cell engager targeting CLEC12A-positive AML.

S. Gu[1], H. V. Tran[1], S. Chen[1], K. Liu[2], X. Zhang[2], L. Jia[2], R. Ma[2], J. Fu[2];

[1]QLSF Biotherapeutics, South San Francisco, CA, [2]Qilu Pharmaceutical Co., Ltd., Jinan, China

Despite advancement in targeted therapies, treatment options for patients with acute myeloid leukemia (AML) that provide a tolerable and durable response remain elusive. We have developed a CD3 bispecific antibody, QL325, targeting CLEC12A, a c-type lectin protein that is highly expressed on AML blasts. Normally, CLEC12A expression is mostly confined to the CD34+CD38- progenitor population and largely absent on normal and regenerating bone marrow stem cells. Our bispecific antibody is configured in a 2 + 1 format, with bivalent avidity binding to CLEC12A, monovalent low affinity binding to CD3, and an effector-null Fc for extending half-life. In our preclinical studies, QL325 induced CLEC12A -dependent activation and proliferation of T cells. Redirected T cell-dependent cytotoxicity mediated by QL325 was restricted to AML cancer cells expressing CLEC12A. QL325 demonstrated dose dependent suppression of tumor growth in xenograft models of AML, significantly more potent than a clinical benchmark antibody. In non-human primates, QL325 was tolerated up to 0.03 mg/kg for IV dosing and under 0.1 mg/kg for SC dosing, well above the predicted effective therapeutic dose. A phase 1 clinical trial is currently ongoing to determine the safety and early efficacy in patients with refractory or relapsed AML.

IMMUNOLOGY: Vaccines, Antigens, and Antigen Presentation 2
Poster Session

#6732 Immunomodulatory and anti-tumor effect of a CCR2-targeted STING agonist iADC in human lung cancer.

A. Porciuncula[1], V. A. Appleman[2], A. Parent[2], J. Raizer[2], R. C. Gregory[2], N. Lineberry[2], A. O. Abu-Yousif[2], K. A. Schalper[1];
[1]Yale University School of Medicine, New Haven, CT, [2]Takeda Development Center Americas, Lexington, MA

Introduction: Antibody drug conjugates (ADCs) targeting cancer-cell antigens can improve therapeutic index and show prominent clinical impact. Limited studies have used ADCs to target antigens present in non-malignant cells in the tumor microenvironment or to deliver immunomodulatory agents. We developed an immune-cell directed antibody drug conjugate (iADC) TAK-500 that selectively activates STING in C-C chemokine receptor type 2 (CCR2) expressing cells to achieve enhanced efficacy over non-targeted STING agonists. Here, we spatially mapped CCR2 protein in human NSCLC and studied the immunomodulatory role and anti-tumor effect of the novel iADC TAK-500 on human lung cancer tumor explants *ex vivo*.
Methods: Using multiplexed quantitative immunofluorescence (mQIF) panels we measured the levels of CCR2 protein, myeloid cell populations and tumor infiltrating lymphocyte (TIL) subsets in 411 primary NSCLC carcinomas from treatment-naïve patients in 2 independent cohorts and determined their clinical significance. In addition, we longitudinally studied CCR2 levels, myeloid cells (DAPI/CCR2/CD68/CD11b), TILs (DAPI/CK/CD4/CD8/CD20), T-cell functional markers (DAPI/CK/CD3/Ki-67/GZMB [Granzyme B]) and cancer-cell death/proliferation markers (DAPI/CK/TFR1/Ki-67/CC3 [Cleaved Caspase 3]) in 314 primary cultured tissue fragments from paired tumor and non-tumor specimens resected from 11 lung cancer patients at Yale New Haven Hospital between 2021-2023 (8 adenocarcinomas, 2 small cell carcinomas, and 1 squamous cell carcinoma). Each biopsy was divided into 4-mm^2 fragments, cultured in extracellular matrix for 5 days with or without TAK-500 treatment. Samples were processed into FFPE tissue and stained with mQIF panels using a tissue microarray format.
Results: CCR2 protein was detected in 386 of 411 (94%) NSCLCs from 2 independent cohorts predominantly localized in CD11b+ intratumor myeloid cells and CD68+ tumor-associated macrophages (TAMs). Elevated CCR2 was associated with adenocarcinoma histology, increased PD-L1, activating KRAS mutations and longer survival. Treatment with TAK-500 for 5 days reduced CCR2 levels in myeloid cells and CD68+ TAMs, without significant changes in TIL or T-cell GZMB/Ki-67 levels. TAK-500 also significantly reduced tumor proliferation (Ki-67 expression) and increased tumor cell apoptosis (CC3 levels) after 5 days of treatment. Notably, these TAK-500-induced changes were observed only in tumor specimens with high baseline CCR2 levels above the median in retrospective NSCLC cohorts. No significant effect was observed in the paired non-tumor fragments.
Conclusion: Our results reveal prominent myeloid CCR2 expression in a subset of human NSCLCs with distinct clinicopathologic/molecular characteristics. Using a novel lung cancer explant *ex vivo* system, we demonstrate a CCR2-dependent immunomodulatory and anti-tumor effect of TAK-500 iADC.

#6733 Multiomics analysis of impact of CD8+ and other cell populations in STING agonist treated *ex vivo* mesothelioma samples.

E. Ivanova[1], S. R. Park[1], A. P. Zlota[1], N. Spicer[1], M. Ha[1], S. Kivlehan[1], I. Gjeci[1], S. Innocenti[2], L. Zasadil[1], P. Lizotte[1], M. Y. Tolstorukov[1], K. Ding[3], A. O. Abu-Yousif[3], J. Raizer[3], V. A. Appleman[3], R. Bueno[2], D. A. Barbie[1], C. P. Paweletz[1];

[1]Dana-Farber Cancer Institute, Boston, MA, [2]Brigham and Women's Hospital, Boston, MA, [3]Takeda, Lexington, MA

Background: Collective evidence highlights that agonism of the host STING pathway plays a critical role in eliciting robust and durable anti-tumor immunity. Dazostinag (TAK-676) is a novel systemically delivered STING agonist that ignites the innate immune system and mobilizes adaptive immunity. Preclinical studies with dazostinag demonstrated a strong, persistent CD8+ T cell anti-tumor response driven by innate immune derived type I IFN and pro-inflammatory cytokines. The role of CD8+ T cells in response to dazostinag was further supported by a previously demonstrated correlation between response and CD8+ T cell frequency in a patient-derived organotypic tumor spheroids (PDOTS) model of mesothelioma. Within the current work, we sought to determine the extent to which response to dazostinag in mesothelioma depends on CD8+ T cells versus the contribution of other immune cells.

Methods: Surgical mesothelioma cases were collected along with clinicopathological variables at Brigham and Women's Hospital under an IRB-approved protocol. PDOTS were generated as described previously. Ex vivo response was determined by fluorescent life/dead imaging, and orthogonally evaluated by multiplexed cytokine array, immunofluorescence, and flow cytometry; subset of tumors was studied using single cell RNA sequencing (scRNAseq).

Results: Dazostinag-driven tumor cell killing was evaluated in 20 mesothelioma PDOTS. 11 samples were characterized as responders (R) with a cut-off of ≥30% reduction in live cell area; 9 as non-responders (NR). In 12 out of 20 PDOTS, CD8 neutralization effect was assessed: four were TAK-676 NR, and out of 8 R 4 had at least 20% killing abrogated by aCD8. Effect did not depend on the baseline amount of CD8+ T cells in the sample. scRNAseq analysis showed that R and NR T cells have different activation/exhaustion phenotypes and varying levels of interferon stimulated genes (ISG) in response to STING agonism. Other cell populations emerged as candidates for dazostinag resistance: NR cases carried remodeled immunosuppressive myeloid cells or matrix metalloproteinases-expressing fibroblasts. In general, myeloid cell abundance at baseline characterized by flow had a trend in negatively correlating with dazostinag response. Intrinsic expression of type I interferons shown by multiplexed cytokine array was linked to dazostinag sensitivity (R vs. NR IFN-β p=0.028; IFNα2a p=0.016) and can potentially be used as a predictor for response.

Conclusion: We evaluated immune modulations in mesothelioma after treatment with a systemic STING agonist dazostinag using human tumor ex vivo culture. Innate interferon type I expression was higher in responding samples. TAK-676 efficacy was partially reduced in absence of effector lymphocytes, however other cells, such as immunosuppressive myeloid cells and fibroblasts, can have a negative impact on dazostinag response in mesothelioma.

#6734 Preclinical impact of pretreatment with CRS mitigation agents on pharmacodynamic response to TAK-500, a systemically delivered CCR2-targeted STING agonist iADC.

E. Rosentrater, M. Ganno, T. Hatten, H. Mack, A. Bollampalli, D. Zhang, A. Parent, J. Raizer, R. Gregory, N. Lineberry, V. Appleman;
Takeda Development Center Americas, Inc. (TDCA), Lexington, MA

Background: Stimulator of interferon genes (STING) agonists elicit potent innate immune enhancement and mobilize robust adaptive immune responses. Given the potential risk of immunotoxicity from associated cytokine release due to STING agonist treatment, there is a need to identify mitigation strategies that minimize immune-related toxicity while offering a therapeutic window for STING-mediated anti-tumor effects. This strategy is particularly relevant for myeloid-targeted immunotherapies, as cytokine release syndrome (CRS) can be myeloid cell-mediated. We utilized preclinical models to evaluate the pharmacological impact of pretreatment with agents routinely used for management of CRS in advance of delivering TAK-500, a novel, systemic, immune-cell directed STING agonist antibody drug conjugate (iADC) that selectively targets CCR2+ myeloid cells.

Methods: Dexamethasone and anti-IL-6R antibodies were tested at clinically relevant doses 1 hour prior to treatment with TAK-500 or mTAK-500, a murine surrogate, to study immunomodulatory and anti-tumor effects in preclinical models. Induction of innate and adaptive immune responses and cytokine release was evaluated in human, ex vivo, and in tumor-bearing mouse models to characterize potential impact of premedication strategies on drug pharmacology and anti-tumor efficacy.

Results: TAK-500 triggered dose-dependent monocyte activation and cytokine secretion ex vivo. Monocyte activation was minimally impacted by dexamethasone or anti-IL-6R pretreatment. Suppression of IL-6 and IFN-γ and increase in IL-10 were observed following dexamethasone pretreatment, whereas anti-IL-6R maintained a more proinflammatory milieu. In syngeneic mouse models, pretreatment with dexamethasone and anti-mouse IL-6R had minimal impact on mTAK-500 anti-tumor efficacy. Key pharmacodynamic effects, including innate immune cell activation in periphery and tumor-draining lymph node and intratumoral CD8+ T cell accumulation, were minimally impacted by either pretreatment agent. Serum cytokine analyses demonstrated suppression of IL-6, IFN-γ and increases in IL-10 with dexamethasone, but not with anti-IL-6R, similar to ex vivo findings.

Conclusion: Premedication of TAK-500 and mTAK-500 with dexamethasone or anti-IL-6R antibodies does not substantially impact STING-mediated innate immune activation, mobilization of adaptive immune responses or anti-tumor efficacy, despite altered cytokine profiles compared to (m)TAK-500 without premedication. Clinically, these premedication strategies have been effective in mitigating immunotherapy-associated CRS with T cell therapeutics, and here resulted in maintained anti-tumor activity when used in combination with TAK-500, suggesting a viable potential strategy for mitigation of STING-induced immunotoxicities in patients.

#6735 A systemically administered non-nucleotide STING agonist in albumin nanoformulation with potent antitumor activity and low toxicity.

JINSONG TAO, Hongyi Zhao, Zhongwei Liu, Hanning Wen, Chengyi Li, Qiuxia Li, Miao He, Bo Wen, Wei Gao, Duxin Sun

Department of Pharmaceutical Sciences, College of Pharmacy, Rogel Cancer Center, University of Michigan, Ann Arbor, MI

Background: Stimulator of interferon genes (STING), a dimeric transmembrane adapter protein, plays a pivotal role in regulating tumor immune microenvironment and has been explored as a therapeutic strategy against tumors. Most STING agonists were tested in clinical trials using intratumoral injection with limited systemic efficacy. Several systemically administered STING agonists have progressed to clinical trials, with their efficacy yet to be determined, while their systemic toxicity may limit their application. Our study aimed to develop a novel systemically administrated non-nucleotide STING agonist formulated within albumin nanoparticles, demonstrating potent antitumor activity and low systemic toxicity.

Methods & Results: We synthesized a novel non-nucleotide small molecule STING dimer ZSA-51D. The acid form of ZSA-51D exhibited a high binding affinity (EC 50: 1.3 nM) to human STING. ZSA-51D demonstrated potent STING activation in THP1-Blue™ ISG cells, with an EC50 of 5.1 nM. To enable systemic delivery, ZSA-51D was encapsulated in albumin nanoparticles (nano ZSA-51D) with a particle size of 115 nm. Surprisingly, nano ZSA-51D exhibited a tenfold increase in STING activation (EC50 of 0.44 nM) compared to free ZSA-51D. Furthermore, nano ZSA-51D demonstrated sevenfold greater activation of bone marrow-derived dendritic cells (EC 50 of 3.5 nM), and eightfold enhanced repolarization of bone marrow-derived macrophages (EC 50 of 4.2 nM) from M2 to M1 compared to free ZSA-51D. The *in-vivo* anticancer efficacy was evaluated on MC-38 and KPC 6620 xenograft in C57BL/6 mice using intravenous administration of ZSA-51D (1 mg/kg) or nano ZSA-51D, in combination with PD-1 antibody (α-PD1, 100 μg) for 5 dose every 3 days. The results revealed that nano ZSA-51D exhibited superior anticancer effects compared to free ZSA-51D. Remarkedly, nano ZSA-51D, in combination with α-PD1, completely eradicated cancer in the MC-38 xenograft model. These cured mice completely rejected the rechallenge with MC38 cells 120 days after the initial tumor inoculation, indicating potent and long-term anticancer immune memory for anticancer activity. In addition, we performed the toxicity evaluation of nano ZSA-51D and free ZSA-51D at the same dose regime as the efficacy study. Nano ZSA-51D shows no hematological and liver toxicity. However, free ZSA-51D has a sever local inflammation after injections, whereas nano ZSA-51D has no local toxicity.

Conclusion: In this study, we developed a novel systemically administered non-nucleotide sting agonist formulated within albumin nanoparticles. Nano ZSA-51, in combination with α-PD1, demonstrated superior anticancer efficacy and low toxicity, holding the potential for future clinical trials. The significantly enhanced STING activation and in vivo efficacy of nano ZSA-51D warrant further investigation into its underlying mechanisms.

#6736 Overcome the challenge for intratumoral injection of STING agonist for pancreatic cancer by systemic administration.

Keyu Li[1], Junke Wang[1], Birginia Espinoza[2], Yirui Xiong[3], Nan Niu[4], Jianxin Wang[5], Noelle Jurcak[2], Noah Rozich[2], Arsen Osipov[6], MacKenzie Henderson[2], Vanessa Funes[2], Melissa Lyman[2], Alex B. Blair[2], Brian Herbst[2], Mengni He[2], Jialong Yuan[2], Diego Trafton[2], Chunhui Yuan[7], Michael Wichroski[8], Xubao Liu[1], Yuquan Wei[3], Lei Zheng[2]

[1]Department of General Surgery, West China Hospital of Sichuan University, Chengdu, China,[2]Department of Oncology, Johns Hopkins University School of Medicine, Baltimore, MD,[3]State Key Laboratory of Biotherapy, West China Hospital of Sichuan University, Chengdu, China,[4]Zhejiang Provisional People's Hospital, Hangzhou, China,[5]The First-affiliated Hospital of Zhejiang University, Hangzhou, China,[6]Cedars-Sinai Medical Center, Los Angeles, CA,[7]Peking University Third Hospital, Beijing, China,[8]Bristol Myers Squibb Co, Princeton, NJ

Objective: Due to the challenge for intratumoral administration, innate agonists have not made it beyond preclinical studies for efficacy testing in most of tumor types. Pancreatic ductal adenocarcinoma (PDAC) has a T-cell excluded or deserted tumor microenvironment. Innate agonist treatments may serve as a T cell priming mechanism to sensitize PDACs to anti-PD-1 antibody (a-PD-1) treatment.
Design: Using a transplant murine model with spontaneously formed liver metastasis and also the genetically engineered KPC mouse model that spontaneously develops PDAC, we compared the antitumor efficacy between intrahepatic/intratumoral and intramuscular systemic administration of BMS-986301, a next-generation STING agonist. Flow cytometry, Nanostring, and cytokine assays were used to evaluate local and systemic immune responses.
Results: The study demonstrated that administration of STING agonist systemically via intramuscular injection is equivalent or potentially superior to its intratumoral injection in inducing both effector T cell response and antitumor efficacy. Compared to intratumoral administration, T cell exhaustion and immunosuppressive signals induced by systemic administration were attenuated. Nonetheless, either local or systemic treatment of STING agonist was associated with increased expression of CTLA-4 in the tumors. However, the combination of a-PD-1 and anti-CTLA-4 antibody with systemic STING agonist demonstrated the antitumor efficacy in the KPC mouse spontaneous PDAC model. Our study also demonstrated the feasibility and antitumor efficacy of systemic administration of BMS-986299, a new NLRP3 agonist.
Conclusion: For the first time, our study supports the clinical development of innate agonists via systemic administration, instead of local administration, for treating PDAC.

#6737 Pharmacologic modulation of nonsense-mediated decay induces anti-tumor immunogenicity in *ex vivo* patient tumors.

R. Vendramin[1], H. Fu[1], Y. Zhao[1], S. Fernandez-Patel[1], D. Qian[1], L. Ligammari[1], G. Beattie[1], R. Levy[2], P. Greenberg[2], O. Bartok[2], K. Thakkar[1], J. Murai[1], D. Karagianni[1], C. Sng[1], M. Shah[1], F. Galvez-Cancino[1], K. Djikstra[3], S. Quezada[1], Y. Samuels[2], TRACERx consortium, J. Reading[1], C. Swanton[3], K. Litchfield[1]; [1]University College London (UCL) Cancer Institute, London, United Kingdom, [2]Weizmann Institute of Science, Rehovot, Israel, [3]The Francis Crick Institute, London, United Kingdom

Introduction: Immunogenic neoantigens derived from somatic tumor mutations are essential to initiate and sustain robust anti-tumor immune responses. Frameshift insertion/deletions (fs-indels) are a key source of immunogenic neoantigens. However, fs-indels often result in the introduction of premature termination codons (PTCs), leading to mRNA degradation by the nonsense-mediated mRNA decay (NMD) pathway. In human malignancies, NMD activity is increased in response to the heightened burden of somatic fs-indel mutations and effectively prevents the generation of highly immunogenic tumor-specific neoantigens, thereby promoting immune evasion.

Approach: Here, we pharmacologically targeted SMG1, a core component of the NMD pathway, for the first time in patient tumor and normal samples as well as in a panel of human cancer cell lines and patient-derived organoids, to prevent the degradation of highly immunogenic frame-shifted transcripts. We analyzed the changes in transcriptome, proteome and immunopeptidome following SMG1 inhibition (SMG1i). We then made use of tumor-T cell co-cultures and Patient-Derived Tumor Fragments (PDTFs) to assess the effects of SMG1i on anti-tumor immunogenicity. Ex vivo immunological responses were measured by high-dimensional flow cytometry, cytometric bead array and single cell RNA and TCR sequencing.

Results: Our data demonstrates a significant increase in T cell activation, expansion of tumor-reactive intratumoural $CD8^{\pm}$ lymphocytes and cytokine secretion following SMG1 inhibition in ex vivo PTDFs (n=15) but not in matched normal-adjacent tissue (n=10). Mechanistically, SMG1 inhibition increased the abundance of frame-shifted mRNA transcripts, and aberrant HLA-presented peptides. Co-culture of tumor cells and patient-derived organoids with $CD8^{\pm}$ T cells upon SMG1 inhibition induced potent MHC class I antigen-dependent T cell activation and tumor cell killing.

Conclusion: Our findings, in a clinically relevant platform, highlight SMG1 inhibition as a novel cancer immunotherapy approach to promote neoantigen production and to induce anti-tumor immunogenicity irrespective of the tumor type or TMB status.

#6738 Overlapping and distinct mechanisms of effective neoantigen cancer vaccines and immune checkpoint therapy.

S. Keshari, A. S. Shavkunov, Q. Miao, A. Saha, C. D. Williams, J. E. Pineda, K. Hu, K. E. Pauken, K. Chen, M. M. Gubin;
UT MD Anderson Cancer Center, Houston, TX

The goal of cancer vaccines and immune checkpoint therapy (ICT) is to expand and sustain T cells with enhanced anti-tumor capabilities. Here, we asked whether these distinct immunotherapies utilize similar cellular and functional mechanisms. We used multiple approaches to compare effective therapeutic mutant neoantigen (NeoAg) cancer vaccines with αPD-1, αCTLA-4, or αPD-1 and αCTLA-4 ICT in preclinical *Braf*^{V600E}*Pten*$^{-/-}$*Cdkn2a*$^{-/-}$ melanoma models. Synthetic long peptide (SLP) MHC-I NeoAg vaccines induced a more than 3-fold expansion of proliferating intratumoral NeoAg-specific CD8 T cells that were functional despite high expression of PD-1 and TIM-3. NeoAg vaccines required not only CD8, but also CD4 T cells for efficacy. αCTLA-4 and/or αPD-1 ICT also increased the frequency and effector capabilities of CD8 T cells but to much less of an extent than NeoAg vaccines. These included NeoAg-specific CD8 T cells that displayed reduced expression of PD-1 and TIM-3. αCTLA-4 treated tumors displayed robust induction of ICOS^{+} Th1-like CD4 T cells expressing Bhlhe40 that resembled Th1-like CD4 T cells described in αCTLA-4-treated patients and when αCTLA-4 was combined with αPD-1, a small subset of Th2-like CD4 T cells was observed. Remarkably, we noted divergent effects on certain subsets of intratumoral macrophage populations induced by NeoAg vaccines as compared to ICT. Although effective NeoAg vaccines expanded M1-like iNOS^{+} macrophages with ICT also following this same pattern, NeoAg vaccines expanded rather than suppressed (as observed with ICT) distinct subpopulations of M2-like CX3CR1^{+} CD206^{+} macrophages. CODEX spatial imaging using a 46-marker panel revealed tumors from mice treated with NeoAg vaccines displayed concentrations of CD8 T cells expressing functional markers and the proliferation marker Ki67, with mice treated with αCTLA-4 or αPD-1 displaying both Ki67^{+} conventional CD4 and CD8 T cells within interior regions of tumor. Interestingly, these regions contained prominent blood vessels, along with MHC-II^{+} dendritic cells and iNOS^{+} macrophages. Our work shows that NeoAg vaccines lead to distinct, as well as overlapping alterations when compared to ICT. These distinct alterations provided a rationale for combination therapies that we validated in both our melanoma model, as well as the MC38 tumor model, where delayed treatment with NeoAg vaccines combined with αCTLA-4 or αPD-1 yielded anti-tumor immunity that was superior to combination αPD-1 and αCTLA-4. These findings suggest that NeoAg vaccines combined with single-agent ICT may be an effective therapy with potentially less toxicity than αPD-1/αCTLA-4 combination ICT. Further, we hypothesize that immunotherapies that deplete CX3CR1^{+} CD206^{+} macrophages may synergize with NeoAg cancer vaccines, which we are currently assessing.

#6739 Efficacy and toxicity of microbial mimetic mesoporous silica nanoparticles in a mouse model of ovarian cancer.

L. Y. Medina, R. E. Serda, B. Marwedel, M. S. Jun, J. Adogola;
University of New Mexico, Albuquerque, NM

Ovarian cancer is predominately left undetected and untreated until the later stages of the disease where it becomes incredibly difficult to treat. Preclinical studies demonstrate that immunotherapy can be highly effective. Our lab has been working on an immunotherapy approach to treat women with ovarian cancer that utilizes mesoporous silica nanoparticles(MSN). MSN that present pathogen-associated molecular patterns (PAMPS) are able to significantly reduce tumor burden in mouse models of serous epithelial ovarian cancer when administered by intraperitoneal injection. These microbial mimetic particles are decorated with polyethyleneimine (PEI), CpG oligonucleotide, and monophosphoryl lipid A (MPLA). When in the presence of antigen presenting cells, they bind to Toll-like receptors (TLR) present on the cell surface and within the endosome. To better understand mechanisms underlying their efficacy, we injected fluorescent MSN-PEI-CpG-MPLA (100 or 500 nm) or unmodified MSN into mice with advanced ovarian cancer. The particles, regardless of the presence of TLR-agonists, were rapidly internalized by myeloid cells, with trafficking almost exclusively to immune clusters located in tumor-burdened adipose tissues when administered by intraperitoneal injection. Conversely, intravenous injection of MSN-PEI-CpG-MPLA led to predominate accumulation in liver, with no particles found in tertiary lymphoid clusters 24 hours post injection. Furthermore, unlike intraperitoneal injection, intravenous injection of MSN-PEI-CpG-MPLA was without therapeutic effect. Currently we are studying MSN safety and the impact of administration route and dose on efficacy and cytotoxicity. In summary, MSN, with and without TLR agonists, are trafficked by myeloid cells to tumor-burdened fat-associated lymphoid clusters when administered by intraperitoneal injection. Intraperitoneal injection of TLR-agonist modified MSN effectively reduces tumor burden in mice with ovarian cancer.

#6740 Next-generation LNPs induce effective anti-tumor T cell responses.

D. G. Millar[1], **M. J. Gold**[2], K. Olsen[2], Y. Wu[2], Y. Karpov[2], R. Nechanitzky[2], H. Menon[2], R. Krishnan[2], R. Georgantas[2], P. Ohashi[1], N. Martin-Orozco[2];
[1]Princess Margaret Cancer Centre, Toronto, ON, Canada, [2]Providence Therapeutics Inc, Calgary, AB, Canada

mRNA immunotherapies have gained interest for the treatment of tumors from various origins, however, their ability to provide long -term durable tumor control has been underwhelming. Here we report that novel mRNA lipid nanoparticle (LNP) vaccinations induce robust expansion of antigen-specific T cells, although this does not always correlate with their ability to infiltrate and kill solid tumors. Using a portfolio of novel ionizable lipids and a robust *in vivo* model that reliably identifies LNPs with prominent anti-tissue T cell activity we have identified a putative LNP candidate that provides long term tumor control in a murine syngeneic tumor model.

We utilized the model antigen glycoprotein (Gp), from the lymphocytic choriomeningitis virus (LCMV), and produced mRNA encoding the immunodominant epitopes $gp33_{33-41}$, $gp61_{61-80}$ and $gp276_{276-286}$ (3GP-mRNA). This mRNA was encapsulated in various novel LNP formulations and administered i.m. into naïve C57Bl/6 mice to track the induction of a robust $CD8^{\pm}$ T cell response identified using tetramers to gp33 and gp276. Successful candidate LNPs were then tested in the RIPgp model of autoimmune diabetes. RIPgp transgenic mice express LCMV-Gp in the pancreatic β cells and offer a robust assay for the ability to induce antigen-specific T cells capable of breaking self-tolerance and infiltrating and killing target tissue. Utilizing the RIPgp model to screen LNP candidates we identified a lead candidate, C2-5A, that both induced a robust expansion of antigen-specific T cells and tissue destruction. When utilized in a colon adenocarcinoma model expressing the LCMV-Gp antigen (MC38-Gp), therapeutic dosing of LNP C2-5A as a monotherapy lead to long term tumor clearance in 40% of the treated animals. We believe this screening platform allows the selection of LNP candidates capable of breaking self-tolerance, and one such candidate C2-5A provides a potent vehicle and adjuvant for mRNA based cancer vaccines.

#6741 Targeting glutamine metabolism potentiates antigen presentation in colorectal cancer.

T. Yu, K. Van der Jeught, H. Zhu, Z. Zhou, S. Sharma, S. Liu, K. So, H. Eyvani, X. Wang, G. E. Sandusky, Y. Liu, M. Opyrchal, S. Cao, J. Wan, C. Zhang, X. Zhang;
Indiana University School of Medicine, Indianapolis, IN

Colorectal cancer (CRC) ranks among the most prevalent cancers worldwide, causing substantial mortality. The urgent need for effective treatments has driven research into immune checkpoint blockade (ICB) therapies, which have demonstrated significant clinical benefits across various cancer types. Despite the success of ICB therapies, a significant proportion of CRC patients exhibit resistance to treatment, prompting the identification of mechanisms that hinder therapy resistance or enhance treatment response. CRC cells display remarkable adaptability, orchestrating metabolic changes that confer growth advantages, pro-tumor microenvironment, and therapeutic resistance. One such metabolic change occurs in glutamine metabolism. In this study, we found that colorectal tumors with high glutaminase (GLS) expression exhibit reduced T-cell infiltration and cytotoxicity, leading to poor clinical outcomes. To validate these findings, we applied the ovalbumin (OVA)/OT-I T cell-based cytotoxicity assay and the CRC patient-derived organoids (PDOs)/autologous T cell killing assay. Our results indicated that inhibition of GLS significantly enhanced T-cell cytotoxicity in vitro and ex vivo. Mechanistically, we elucidated that inhibition of GLS activated reactive oxygen species-related signaling pathways in tumor cells, thereby potentially increasing tumor immunogenicity by promoting antigen presentation. The combinational therapy of GLS inhibitor and ICB exhibited a superior tumor growth inhibitory effect in comparison with either of the monotherapies. These findings shed new light on clinical therapeutic strategies for CRC patients, offering a promising approach to enhance the efficacy of ICB therapy.

#6742 PV 10 induces endoplasmic reticulum stress and autophagy, triggering immunogenic cell death and anti-tumor immunity in head and neck squamous cell carcinoma.

S. Thatikonda[1], R. Chaudhary[1], Y. Meshkovska[1], M. I. Biernacki[1], R. Slebos[1], S. P. Thomas[1], A. L. Antonio[1], E. A. Wachter[2], C. H. Chung[1];
[1]H. Lee Moffitt Cancer Center, Tampa, FL, [2]Provectus Biopharmaceuticals, Knoxville, TN

Introduction: Head and neck squamous cell carcinoma (HNSCC) are complex, diverse cancers affecting mucosal linings of the upper aerodigestive tract. Globally, HNSCC is the sixth most common cancer, leading to over 890,000 new cases and more than 450,000 deaths annually. Primary risk factors include human papillomavirus (HPV) infection (HPV-positive HNSCC) and exposure to tobacco and excessive alcohol (HPV-negative HNSCC). Despite multimodal treatments, survival rates remain low due to recurrence and metastasis (R/M HNSCC), creating a need for safe, innovative therapies to reduce tumor burden with minimal adverse events. PV-10 (10% rose bengal sodium) is a novel intratumoral immunotherapeutic agent that has demonstrated promising anti-tumor activity in multiple solid tumor cancer types with few adverse effects in pre-clinical research and clinical trials. However, the role of PV-10 in HNSCCs and its role in enhancing immune response warrants further investigation.

Methods: Cell viability was assessed using Alamar blue assay after PV-10 treatment of murine mEER and MTE-RAS HNSCC tumor cell lines. To evaluate the immunomodulatory properties of PV-10, we employed flow cytometry, confocal analysis, and luminescence-based assays. Additionally, we performed a DCFDA assay to measure the reactive oxygen species (ROS) and an Alexa Fluor 488 Annexin V/dead cell apoptosis assay to evaluate apoptosis. To gain insights into the mechanisms underlying PV-10's immunomodulatory effects in cancer cells and tumors from mice, western blotting and multiplex immunohistochemistry (mIHC) were used.

Results: Our *in vitro* findings reveal that PV-10 induces cytotoxicity in both mEER and MTE-RAS cells. Notably, PV-10 promotes a significant increase in ROS, leading to an elevation in late apoptotic cells. Markers of immunogenic cell death (ICD), including a statistically significant increase in the release of damage-associated molecular pattern molecules HMGB1 and ATP, as well as enhanced surface expression of calreticulin, HSP-70, and HSP-90, were observed. At the molecular level, a remarkable activation of endoplasmic reticulum (ER) stress, pro-apoptotic protein, and autophagy markers were observed. Intratumoral PV-10 injection *in vivo* has shown significant tumor regression in both mEER and MTE-RAS tumors, and a complete response was noticed in some mice, indicating that PV-10 induces potent ICD in both mEER and MTE-RAS tumors.

Conclusion: Our collated evidence strongly suggests that PV-10 induces ICD-associated immunogenicity in both mEER and MTE-RAS *in vitro* and *in vivo,* fostered by ROS-based ER stress and apoptosis. These findings hold promise for potential therapeutic avenues to manage HNSCC.

#6743 Identifying new cellular adjuvants for cancer vaccines and immunotherapies.

J. Rucker, N. Nwogu, N. M. Molino, A. Snyder, J. T. Sullivan, B. J. Doranz;
Integral Molecular, Philadelphia, PA

Background: Cancer vaccines represent a promising strategy for antitumor immunotherapy. Despite considerable research efforts and progress, the effectiveness of cancer vaccines remains a challenge. This is primarily due to relatively low immune responses against tumors, stemming from issues of poor immunogenicity and the immunosuppressive microenvironment commonly found in many solid tumors. Use of an optimal adjuvant can augment immune responses against tumor antigens and guide them towards a specific adaptive immune enhancement. Dendritic cells (DCs) play a primary role in initiating immunes response to vaccines, often through activation of toll-like receptors (TLRs). Identifying novel immunomodulatory proteins that regulate DCs or TLR activation can identify novel adjuvant candidates with applications for cancer immunotherapy.
Methods: We constructed a Membrane Proteome Array (MPA) encompassing ~6,000 structurally intact human membrane proteins in their native conformation (94% of the entire membrane proteome) and used it to screen for cellular proteins that can modulate response to vaccination through DCs and TLRs. To identify proteins that interact with TLRs, the library was expressed in live TLR reporter cells, and these cells were tested for response to known activators. In addition, cells expressing the MPA were presented to DCs to identify membrane proteins that modulate DC activity. TLR-expressing cell activation was measuring using an NF-kB-activated luciferase reporter, while DC assays used upregulation of cell surface markers (CD80, CD83, and MHCII) to measure the activation of immature monocyte-derived dendritic cells.
Results: Screening of TLR2, TLR3, and TLR5 reporter cell lines identified both known and novel regulators of TLR activation. Activators common to several TLRs were identified as well as activators unique to individual TLRs. Screening of primary human DCs likewise identified known regulators of activation (for example CD40L) and several novel targets. Putative novel regulators of DC activation are being further investigated to determine their biological significance.
Conclusion: Discovering novel immunomodulatory targets and proteins that regulate DCs and TLR activation can identify novel adjuvant candidates with targeted immune outcomes, such as immune stimulating and anti-cancer responses. This study identified novel regulators of immune activation which are being further investigated as adjuvant candidates for cancer vaccines.

#6744 Activating anti-MDS immunity with polarized dendritic cell vaccines.

D. Alvarado[1], J. Peresie[1], A. Brinkman[1], C. Allen[1], W. Jiang[1], P. Kalinski[1], **T. Tanaka**[2], E. Griffiths[1], M. Nemeth[1];
[1]Roswell Park Comprehensive Cancer Center, Buffalo, NY, [2]UC San Diego Moores Cancer Center, La Jolla, CA

Less than 50% of patients with higher-risk myelodysplastic syndromes (MDS) show clinical response to standard-of-care hypomethylating (HMA) therapy. Significant enthusiasm existed for immunotherapy/HMA combinations for these patients, but studies have failed to deliver on the initial promise. We have demonstrated that patients with MDS have a deficiency in antigen-presenting cells, called CD141^{Hi} dendritic cells (DC). DC-deficient MDS patients have reduced response to HMAs, worse overall survival, and show less response to cancer vaccination. We hypothesized that restoration of this population using a novel DC vaccination approach - alpha-type-1 polarized dendritic cells (αDC1) - might compensate for this deficiency and restore immunity. To generate αDC1s, we collected monocytes from MDS patients and healthy donors (HD) and cultured them for 6 days *in vitro* in the presence of recombinant human GM-CSF and IL-4 followed by an additional 18-24 hours in the presence of αDC1 maturation factors (poly-I:C/IFNα/IFNγ/TNFα/IL-1β). Overall, we attempted to generate αDC1s from 15 MDS samples; 13/15 exhibited intermediate to very high-risk disease and 10/15 are currently receiving HMA therapy. We successfully cultured cells from 8/15 samples (53%). Of the 8 MDS samples, 5 were collected from patients receiving HMA therapy (62.5%). We were unable to successfully culture αDC1s from the other 5 patients receiving HMA therapy, and thus the effect of HMA therapy on aDC1 generation remains unclear. To test the function of MDS αDC1s, we focused on two signals necessary to activate immune responses: 1) the expression of co-stimulatory molecules and 2) the production of IL-12p70. Flow cytometric analysis on αDC1s and immature DCs from MDS samples revealed intra-patient variation in the fold-change surface expression of CD40/80/83/86 and HLA-DR proteins. Additionally, there was a trend towards decreased up-regulation of CD80 and CD86 in MDS specimens compared to HD. To assess production of IL-12p70, we stimulated immature DCs and αDC1s with CD40L and performed ELISA analysis on the media supernatant. We found that 3 out of 4 samples could produce IL-12p70 (range 27 - 5,480 pg/ml). To date, our results suggest that generation of MDS patient-derived αDC1 cells is feasible and additional work is being performed to fully characterize their ability to activate anti-MDS immune responses. Since αDC1s have an established safety profile in patients with solid tumors, we anticipate that we will be able to rapidly translate our results to the clinic.

#6745 Crafting hyaluronic acid-based nanoparticles for enhanced LN targeting as a potent priming tool in immunotherapy.

T. Nakai[1], F. Momose[2], K. Yabuuchi[1], M. Yamane[2], T. Hayashi[2], L. Wang[2], Y. Nakagawa[1], S. Aso[1], T. Katsumata[1], T. Shimoboji[1], Y. Miyahara[2];
[1]Asahi Kasei, Fuji, Japan, [2]Mie University Graduate School of Medicine, Tsu, Japan

Background: Cholesterol-conjugated hyaluronic acid, synthesized by grafting cholesterol moieties onto hyaluronic acid, spontaneously formed nano-sized hydrogel of approximately 30-100nm in water. This hyaluronic acid derivative (HA nanogel) has demonstrated the ability to encapsulate various modalities, including low- and medium-sized molecules, peptides, and proteins. Previous reports have highlighted its efficacy in solubilizing poorly water-soluble drugs and serving as a sustained-release matrix. In this study, we explore the potential of HA nanogels encapsulating antigen peptides with adjuvant as a cancer vaccine and a priming tool for combinational immunotherapy.
Method: We prepared HA nanogels as a novel peptide carrier for cancer vaccines and attempted to encapsulate various peptides, including neoantigen (mERK2) peptides expressed in immune checkpoint inhibitor (ICI) therapy-resistant fibrosarcoma cell line CMS5a, gp-100 peptides expressed in metastatic melanoma cell line B16F10, and MAGEA4. Our experiments covered APC uptake, antigen-specific CTL induction, and anti-tumor studies to demonstrate the utility of HA nanogels in these applications.
Results: HA nanogel efficiently formed stable complexes with mERK2, gp-100 and MAGEA4 long peptides, each with diameters of 30-100nm. The facile and simple vaccine formulation processes with HA nanogel achieved high drug content and high encapsulation efficiency of 90% or higher. Fluorescently labeled mERK2 long peptide encapsulated in HA nanogel vaccines were subcutaneously administered to BALB/c mice, and uptake analysis of mERK2 long peptides in draining lymph nodes (dLN) was performed using flow cytometry. In comparison to the group receiving mERK2 long peptide without nanogel encapsulation, the HA nanogel group exhibited higher uptake by macrophages and dendritic cells in the dLN. Administering HA nanogel vaccines containing mERK2 long peptides with CpG oligoDNA resulted in higher antigen-specific $CD8^{+}$ T cells compared to the group receiving mERK2 long peptides without encapsulation. Strong anti-tumor effects were demonstrated in mice models with subcutaneously transplanted CMS5a and B16F10 cell lines. The enhanced efficacy through co-administration with ICI was also confirmed.
Conclusion: HA nanogel vaccines efficiently deliver antigen peptides to macrophages and dendritic cells, inducing antigen-specific CTL responses, thereby demonstrating anti-tumor effects against cold tumors such as CMS5a and B16F10. HA nanogels have the potential not only as carriers for cancer vaccines but also as priming tools for combinational immunotherapy.

#6746 A B-cell targeted TLR9 agonist antibody conjugate potentiates cancer vaccine efficacy and rejuvenates vaccine responses in the elderly.

M. Z. Bonacorsi, A. Chen, O. Harrabi, M. Li, E. R. B. Sangalang, D. Fontaine, J. Sim, P. Strop, H. I. Wan, M. Costa;
Tallac Therapeutics, Burlingame, CA

TLR9 agonists (unmethylated CpG oligodeoxynucleotides) are clinically validated as vaccine adjuvants and cancer therapeutics[1,2]. We developed a Toll-like Receptor Agonist Antibody Conjugate (TRAAC) comprised of a potent TLR9 agonist (T-CpG) conjugated to an antibody against CD22, a receptor restricted to B cells (TAC-001). Systemically administered TAC-001 delivers T-CpG to B cells, resulting in TLR9 activation, and innate and adaptive anti-tumor immunity[3]. TAC-001 is being evaluated as an immunotherapy in a Phase 1 clinical trial in patients with advanced solid tumors (NCT05399654)[4]. In this study, we investigated whether TAC-001 mouse surrogate, mCD22 TRAAC, can potentiate cancer vaccine efficacy using preclinical vaccination models. Human Nectin-4 ectodomain protein (N4, 94% homology to its mouse ortholog) was used as a neoantigen-like vaccine, alone and in combination with mCD22 TRAAC, MPLA (a TLR4 agonist), or unconjugated T-CpG. Mice were immunized, then challenged 2 months later with syngeneic CT26 tumors expressing N4. Mice in treatment combination cohorts that resisted tumor development were split into two groups and rechallenged 3.5 months later with a more aggressive tumor, syngeneic 4T1 or 4T1 expressing N4. The combination of vaccine with mCD22 TRAAC was the only treatment able to inhibit growth of the 4T1-N4 tumor. No efficacy was observed in mice inoculated with parental 4T1, thereby demonstrating neoantigen vaccine specific anti-tumor immunity. An MHCI restricted peptide of HER2/neu, GP2, fused to a B cell epitope peptide, P4, and conjugated to KLH, was used as another vaccine model[5]. GP2-P4-KLH was administered to mice alone or in combination with mCD22 TRAAC or unconjugated T-CpG. *Ex vivo* GP2/GP2-P4 stimulation of lymphoid organ immune cells from mice treated with vaccine plus mCD22 TRAAC resulted in elevated Granzyme B, IFNγ and IL17A levels, indicating that mCD22 TRAAC enhances T cell activation and cytotoxic activity. Lastly, to investigate the effect of mCD22 TRAAC in elderly mice, SARS-CoV-2 spike protein was used as a vaccine. Spike was administered alone or in combination with mCD22 TRAAC, MPLA or T-CpG. Combining mCD22 TRAAC with vaccine resulted in high levels of spike neutralizing IgG in both youth and elderly cohorts, showing that mCD22 TRAAC rejuvenates vaccine responses in elderly. In all studies, mCD22 TRAAC led to the most potent vaccine recall response, with high antigen specific IgG titers skewing towards a Th1 phenotype, as shown by elevated levels of effector function antibodies of IgG2a subclass and increased IFNγ production. These findings provide a strong rationale for combining TAC-001 with cancer vaccines. References[1]Hyer et al., *Vaccine* 2018; 36(19) [2]Long et al., *Annals of Oncology* 2018; 29(8) [3]Kuo et al., *Cancer Research* 2021; 81(13)[4]Perez et al., *JITC* 2023; 11(1) [5]Nordin et al., *Cancers* 2021; 13(19)

#6747 Engineering M13 filamentous phages to target dendritic cells and elicit anti-tumor immunity.

Y. Au-Yeung, Z. Zeng, J. Huang;
University of Hong Kong, The - Li Ka Shing Faculty of Medicine, Hong Kong, Hong Kong

Filamentous phage is a safe and effective vaccine vector that can elicit robust immune responses by activating Toll-like receptor pathways. However, engineering neoantigen-displaying phages for cancer vaccines using phage display technology has been challenging and yielded inconsistent results.
We developed a dendritic cell (DC)-targeting cancer vaccine platform with M13 filamentous phages using the phage display technology. The engineered phages express DC-targeting peptides (SLS) on p3 sites and spy-catcher proteins on p8 positions, allowing neoantigens and proteins of interest to be linked to the phage vector. We named our platform SCP (SLS-spy catcher phage). Imaging and western blot showed that spy-tagged proteins can be easily attached to SCP by simple mixing. Further studies demonstrated that targeting DCs can enhance antigen presentation and anti-cancer immunity.
We tested SCP in MB49 and B16 mouse models and the serum, spleen and tumor tissues were isolated for further investigation of immune response upon treatment. We found that SCP effectively suppressed tumor growth by inducing systemic anti-tumor humoral and cell-mediated immunity. SCP also showed efficacy in late-stage tumor models. SCP treatment triggered particularly robust local anti-tumor response. Histological and flow cytometry analysis revealed increased infiltration of innate and adaptive immune cells, reduced PDL1 expression, and restricted neovascularization in the tumor microenvironment after intratumoral administration of SCP.
Our study demonstrated that SCP can induce multifactorial modifications in the tumor microenvironment to impede tumor growth. SCP overcomes the limitations of traditional phage display technology, enabling a wide variety of peptides and proteins to be loaded onto the phage vectors. SCP is also cost-effective and scalable as phage production and purification processes are relatively mature. We propose that SCP can serve as a universal platform for cancer immunotherapy, and may offer novel treatment options for patients.

#6748 Intramuscular delivery of tumor associated antigen DNA vaccines elicits strong cellular immune response, delays tumor growth and prolongs survival.

K. Rayavara[1], J. Henderson[1], M. Kinsella[1], J. Kim[1], M. Matar[1], S. Sood[1], O. Signer[1], C. Bellmon[1], C. Le Goff[2], K. Anwer[1], J. Boyer[1];
[1]Imunon Inc, Huntsville, AL, [2]Imunon Inc, Lawrenceville, NJ

The development of effective cancer vaccines that can trigger strong and enduring memory T cell responses against specific tumor associated antigens (TAAs) is crucial for advancing immunotherapy. DNA-based cancer vaccines have shown promise in generating precise and long-lasting immune responses. In particular DNA vaccines are capable of inducing both humoral and cellular immune responses. In this study, we aimed to investigate the effectiveness of DNA vaccines targeting the mouse Tyrosine-related protein-2 (Trp2) and human New York esophageal squamous cell carcinoma 1 (NY-ESO-1) TAAs in mouse melanoma model. These DNA vaccines were formulated with a functionalized polymer designed to protect DNA from degradation and improve its bioavailability. DNA vaccines targeting both mouse Trp2 (pVACTR) and human NYESO-1 (pVACNY) were constructed. A mouse melanoma cell line (B16F10-NY) overexpressing human NYESO-1 was also generated and demonstrated to induce tumors in C57BL/6 mice. Female C57BL/6 mice received two doses of intramuscular (i.m.) injection of formulated pVACTR or pVACNY or a combination *thereof*, formulated with the synthetic functionalized polymer, with a 3-week interval. The DNA vaccination induced a potent T cell response, as evidenced by ELISPOT assays showing strong IFN-γ secreting T cells against NYESO-1 and Trp2. Flow cytometry analysis of spleenocytes showed strong IFN-γ and TNF-α secreting CD4 T cells against NYESO-1. We further evaluated the prophylactic and therapeutic efficacy of DNA vaccines targeting both Trp2 and NYESO-1 using a murine syngeneic model. Animals were challenged with a lethal dose of B16F10-NY two weeks after the second immunization exhibited a significant ($p<0.0001$) delay in tumor progression and a substantial increase in survival compared to the mock control group. In the therapeutic testing, animals challenged with B16F10-NY and subsequently vaccinated at 4, 11, and 25 days also demonstrated delayed tumor growth and prolonged survival. These findings indicate that formulated DNA vaccine delivered via i.m. triggers robust T cell responses and exhibit both prophylactic and therapeutic efficacy, leading to significantly prolonged survival and delayed tumor growth. A DNA-based vaccine independent of viral vector or device has potential to elicit potent anti-tumor responses with better safety and compliance.

#6749 A dendritic cell targeted nanosystem to overcome immune suppression and enhance the efficacy of the standard of care for pancreatic cancer.

R. Kleiner[1], D. Vaskovich-Koubi[1], R. Acurcio[2], B. Carreira[2], H. Florindo[3], R. Satchi-Fainaro[4];

[1]Sackler Faculty of Medicine Tel Aviv Univ., Tel Aviv, Israel, [2]Research Institute for Medicines (iMed.ULisboa), Faculty of Pharmacy, Universidade de Lisbon, Lisbon, Portugal, [3]Research Institute for Medicines (iMed.ULisboa), Faculty of Pharmacy, Lisbon, Portugal, [4]Sackler Faculty of Medicine Tel Aviv University, Tel Aviv, Israel

The development of novel therapies for pancreatic ductal adenocarcinoma (PDAC) remains an urgent unmet medical need, as it was proven to be refractory to most conventional anti-neoplastic therapies. PDAC is characterized by highly dense stroma, immunosuppressive tumor microenvironment (TME), high resistance to chemotherapy, and poor presentation of tumor-associated antigens (TAA) by dendritic cells (DC), which results in low immune cell infiltration to the tumor site. To that end, we designed a DC-targeted nanovaccine (NV) containing PDAC TAA and TLR agonists to modulate the PDAC immune-microenvironment. In recent years, the combination of immunotherapy with chemotherapy has been explored for PDAC therapy to improve efficacy. Therefore, we demonstrate the effect of our NV on the anti-tumor immune-mediated response in PDAC-bearing mice, alone and in combination with Gemcitabine and Nab-Paclitaxel (Gem/NabP). Our DC-targeted NV was formulated by the double emulsion method and loaded with PDAC's TAA and immune potentiators. We conjugated the NV to a mannose moiety as a targeting moiety for the mannose receptor expressed on DC to increase the NV uptake, which resulted in the enhanced presentation of the encapsulated TAA. Followed by physicochemical characterization and evaluation of preclinical safety of the NV, the stimulation of T cell-specific response against PDAC tumor was assessed *in vivo* and *ex vivo*. The NV induced significant changes in PDAC's TME, such as increased $CD8^{+}$ T cells, decreased $CD4^{+}$ T regulatory cells, and induced memory immunity in the tumor site. The combination of NV and Gem/NabP inhibited tumor growth and prolonged survival compared to mice treated with Gem/NabP alone. This could also be related to the immunogenic cell death effect caused by the chemotherapies. In addition to our mice model of PDAC, we also established a patient-derived model, in which we generate 3D-spheroids from the patient's tumor and activate PBMCs with our NV from the same patient. This unique 3D model enables us to evaluate *ex vivo* the NV effect in a more clinically relevant manner. The NV proposed herein could induce a strong antigen-specific immune response against PDAC with restricted tumor growth while re-shaping PDAC immunosuppressive TME. Furthermore, our 3D patient-derived PDAC model allows us to assess the ability of our NV to generate specific immune responses in patients and to test other possible drug combinations predicting the clinical outcome.

#6750 Validation of a platform to develop new dendritic cell vaccines for cancer immunotherapy.

V. Alonso-Camino, W. Mirsch;
Mill Creek Life Sciences, Rochester, MN

Osteosarcoma is the most common malignant form of bone cancer that generally causes patients to die of pulmonary metastasis. If detected before the tumor has metastasized, osteosarcoma has a 75% survival at 5 years after the conventional therapy with surgery and chemotherapy. However, most osteosarcomas are high-grade tumors that grow quickly and spread before being detected, lowering patient survival to 20%.

Our unique protocol using the human platelet lysate PLTMax® allows establishing tumor cell lines without genetically modifying cells and with minimal genetic drift. The use of PLTMax® and allogeneic tumor cell cultures has proven to be a major advantage for the generation of large amounts of rich tumor antigen libraries for dendritic cell (DC) vaccines. This protocol was used in an autologous dendritic cell / allogeneic tumor lysate vaccine developed at the Mayo Clinic and licensed to Mill Creek Life Sciences (MCLS) to treat newly diagnosed glioblastoma (GBM), which normally has a poor survival rate at only 2%. The technology was used in a phase I clinical trial (MC1272) performed at the Mayo Clinic. The clinical outcomes proved over a 10 time increase in survival rate of patients that received the DC vaccine after the conventional therapy, providing over 20% three-year survival rate.

Our technology differs from other clinically used DC vaccines in three primary ways:

a) Highly efficient cell line establishment: The unique method for generating tumor cell lines uses Mill Creek Life Sciences' PLTMax®, a media supplement derived from human platelets. PLTMax® more closely mimics the native microenvironment of tumors and is used to reduce genetic drift and senescence.

b) High genetic fidelity: GBM tumor cells expanded via PLTMax® maintain genetic fidelity and TAA expression—a feat that has not been previously achieved by any other GBM cell culture method.

c) Reduction of treatment delays and inclusion of all patients that qualify for treatment: Because we will use allogeneic tumor cell lines, we will be able to avoid delays in treatment caused by the time required to culture autologous tumor cell lines, and all patients may receive treatment without exclusion.

Through our preliminary work we transferred the technology from a labor-intensive, small-scale approach, to an automated scalable system. Our ultimate goal is to apply this strategy to not only osteosarcoma, but also several other tumor types to validate it as a platform. Like osteosarcoma, there are other therapy-refractory cancers that we believe can benefit from the use of our platform technology, through the use of DC vaccines that offer an immune response against a wider panel of tumor antigens.

#6751 *In situ* vaccination with *Flt3l* gene modified CD103+ type 1 conventional dendritic cells synergizes with anti-PD-1 checkpoint blockade in murine models of non-small cell lung cancer .

J. W. Abascal, R. J. Lim, R. Salehi-Rad, Z. Jing, M. S. Oh, W. P. Crosson, B. P. Kahangi, E. Perez Reyes, C. Dumitras, D. Reyimjan, J. Yhu, L. M. Tran, M. Paul, K. Krysan, B. Liu, S. M. Dubinett;
UCLA Jonsson Comprehensive Cancer Center, Los Angeles, CA

A major hurdle in treatment of Non-Small Cell Lung Cancer (NSCLC) with anti-PD-1 immune checkpoint blockade (ICB) therapy is a lack of response (primary resistance) and relapse after an initial response (acquired resistance). Recent studies reveal that responses to PD-1/PD-L1 blockade are associated with high tumor mutational burden (TMB), increased $CD8^+$ T cell infiltration and high baseline PD-L1 expression within the tumor microenvironment (TME), while impaired tumor antigen presentation and the immunosuppressive TME have been associated with resistance to ICB. One approach to overcome anti-PD-1 resistance is to intratumorally vaccinate NSCLC tumors with gene modified conventional dendritic cells (cDC), specifically the type I conventional DC (cDC1) lineage. Recent studies have established that generation of an anti-tumor immune response driven by $CD8^+$ T cells requires the cross presentation of tumor associated antigens and that cDC1s are the primary cross presenting APC subtype *in vivo,* which can license $CD8^+$ T cells to initiate an adaptive anti-tumor immune response. In addition, previous studies have shown that intratumoral administration of the FMS-like tyrosine kinase 3 ligand (FLT3L) protein can expand endogenous $CD103^+$ cDC1s in the TME and augment anti-tumor immune responses to ICB therapy. Here, we engineered murine $CD103^+$ cDC1s to constitutively secrete soluble FLT3L (FLT3L_cDC1) and performed *in situ* vaccination studies on anti-PD1 resistant murine models of NSCLC with LKB1-deficiency and elevated TMB that better represents human disease. *In situ* vaccination with FLT3L_cDC1 enhances anti-tumor efficacy compared to non-modified cDC1 vaccination and synergizes with anti-PD-1 ICB to inhibit tumor growth. FLT3L_cDC1 + anti-PD-1 combination therapy induces significant activation and expansion T cells and cDC1s within the TME. Furthermore, combination therapy significantly increases DC progenitor numbers within the tumor draining lymph node, including DC progenitors that are committed to the cDC1 lineage. Our data suggests *in situ* vaccination with FLT3L_cDC1 may represent a promising strategy to potentiate the efficacy of ICB and improve outcomes for patients with primary resistance PD-1/PD-L1 monotherapy.

#6752 Targeting of neoantigen cancer vaccines to antigen presenting cells results in faster and broader T cell responses whether encoded in DNA or mRNA.

B. T. Weinert[1], L. Skullerud[1], E. Solbakken[1], A. Textor[1], M. Durkoop[2], I. Winge[1], G. Norheim[1], E. Stubsrud[1], S. Granum[1], M. W. Pedersen[1], H. Norell[1];
[1]Nykode Therapeutics ASA, Oslo, Norway, [2]Oslo University Hospital, Oslo, Norway

Individualized cancer vaccines based on patient-specific neoantigens represent a groundbreaking approach in oncology, offering a highly individualized treatment option for cancer patients. Unlike traditional vaccines, which are designed to prevent diseases by stimulating an immune response against a specific pathogen, personalized cancer vaccines are therapeutic, aiming to treat cancer by training the immune system to recognize and attack the patient's own cancer cells. The key is to induce a fast, strong, broad, and persistent CD8+ T cell response.

Nykode Therapeutics has developed a platform that targets antigens directly to antigen presenting cells (APCs) using a modular dimeric protein format known as a Vaccibody™. Individualized neoantigen vaccines delivered in a DNA-encoded Vaccibody format have been shown to induce strong and broad T cell responses in pre-clinical and clinical settings.

Here, we wanted to determine if the APC-targeted approach leads to superior T cell responses if Vaccibody vaccines are encoded in mRNA and administered in a lipid nanoparticle (LNP) formulation. For this purpose, we designed and evaluated a model cancer vaccine composed of 20 unstructured 27 amino acid long neoantigens derived from the murine MC38 tumor model.

A DNA-encoded Vaccibody vaccine elicited faster T cell responses compared to an untargeted mRNA-LNP-encoded vaccine. DNA-encoded Vaccibody responses were also broader, targeting a substantially greater number of neoantigens.

Next, we compared the APC-targeting Vaccibody vaccine to an untargeted vaccine when both were formulated in an mRNA-LNP format. The APC-targeting Vaccibody vaccine elicited a greater breath and magnitude of T cell responses compared to the untargeted vaccine. Further studies to evaluate the functional differences associated with the various formats, in terms of T cell phenotype and response to tumor challenge, are ongoing.

In summary, the data demonstrate that an APC-targeted Vaccibody vaccine containing MC38 neoantigens can be encoded in both DNA and mRNA-LNP to induce faster, broader, and stronger T cell responses compared to a non-targeted neoantigen vaccine.

#6753 Bria-OTS immunotherapy platform: Harnessing gene-modified tumor cells to reinvigorate the cancer immunity cycle for precision anti-tumor responses.

M. A. Lopez-Lago, V. Bhardwaj, P. Kesarwani, X. Zheng, S. Pachhal, P. Cournoo, R. Cortez, C. L. Wiseman, W. V. Williams;
BriaCell, Philadelphia, PA

Background: For an immune response to lead to an effective anti-tumor response, a series of stepwise events involving a complex network of iterative cellular and molecular interactions must take place. Cancer, however, often derails this immune cycle, prompting contemporary cancer immunotherapy approaches to seek its reinstatement. Despite significant advances, the inherent disruption of the cancer immunity cycle at multiple junctures, coupled with current therapeutic strategies focusing on isolated stages within this intricate process, has left the attainment of curative therapies as an aspirational goal. We believe that targeting multiple immune processes can restore natural anti-cancer immunity and yield sustained responses. To this end, BriaCell is utilizing gene-modified tumor cells as an immunotherapeutic platform. Our initial version, SV-BR-1-GM, a breast cancer cell line expressing GM-CSF, demonstrates promising clinical outcomes by directly activating CD4+ T-cells in an antigen-specific, HLA-restricted manner. Building on our findings, we hypothesize that tumor cells not only supply antigens but also directly stimulate the immune system. Presenting our second-generation platform, we enhance antigen cross-presentation and direct immune activation through the expression of cytokines, co-stimulatory factors, and HLA alleles.

Methods: To achieve this objective, we have developed Bria-OTS cell lines derived from various cancer types with the following genetic modifications: 1) Expression of costimulatory molecules (CD80, CD86, 4-1BBL, CD40) and immunomodulatory cytokines (GM-CSF, IFNα, IL-12 and IL-7). This modification aims to improve the cell's ability to present antigens and activate the host immune system. 2) Expanding HLA alleles to create semi-allogeneic cell lines matching at least one HLA allele across the population aims to enhance the host immune response, enabling recognition of tumor-associated antigens in the context of syngeneic HLA molecules

Results: We generated four cell lines for each tumor type, and these cell lines secreted GM-CSF, IFNα, IL12 & IL7, while also expressing CD80, CD86, CD40, and different combinations of both Class I and Class II HLA alleles. In functional assays, our cell lines demonstrated potent antigen presentation, effectively triggering anti-tumor immune responses across diverse immune populations, including T-, NK, and NKT cells.

Conclusions: The Bria-OTS cell lines will offer the following key features: 1) multimodal mechanisms of action including thwarting some mechanisms of cancer immune escape. 2) Precision Therapy; Bria-OTS will be precisely matched to individual patients based on their HLA alleles, encompassing over 99% of the U.S. population. 3) rapid, cost-effective treatment as our 'off-the-shelf' cell lines eliminate the need for personalized manufacturing.

#6754 A microneedle array patch chemo-immunotherapy for cutaneous squamous cell carcinoma.

Y. Yang, H. Zhang, C. D. Carey, J. Zhang, S. C. Balmert, E. Korkmaz, L. D. Falo, Jr.;
University of Pittsburgh, Pittsburgh, PA

Cutaneous squamous cell carcinoma (cSCC) is the second most common human malignancy worldwide. Current therapies, including surgical excision, are associated with significant morbidities and considerable expense. Multiple efforts are now underway to develop novel therapies that are effective, durable, safe, cost-effective, and patient-friendly. Here, we report ongoing efforts to develop a localized dissolvable microneedle array patch (MAP) based therapy for cSCC. Our approach is based on the hypothesis that the delivery of an immunogenic cell death (ICD) inducing chemotherapeutic agent to the tumor microenvironment (TME) of accessible cSCCs could kill tumor cells as a source of antigen and induce a proinflammatory TME to generate a potent patient-specific anti-tumor immune response. Specifically, we evaluated MAP therapy using a UV-induced preclinical cSCC mouse model. We applied MAPs delivering the potent ICD-inducing chemotherapeutic agent, doxorubicin (DOX) to UV-induced tumors. MAPs efficiently delivered DOX to the tumor microenvironment. Compared to traditional needle injection, MAP delivery resulted in sustained high levels of DOX in the TME with minimally systemic exposure. Cell death was evident in MAP-DOX-treated tumors, and treatment resulted in tumor regression, increased survival, and long-term immune protection. Further, we found that tumor regression was associated with an early proinflammatory neutrophilic infiltrate. Taken together, our results suggest that MAP delivery of doxorubicin may be a promising approach to cSCC treatment, and that proinflammatory neutrophils are likely an important component of the early infiltrate that leads to tumor regression.

#6755 NKT activation enhanced the therapeutic efficacy of neoantigen vaccine in hepatocellular carcinoma.

R. Li, J.-C. Hu, L. Rong, Y. Wu, Y. He, J. Huang;
University of Hong Kong, The - Li Ka Shing Faculty of Medicine, Pok Fu Lam, Hong Kong, China

One sentence introduction: This study indicated the potential of combinational therapy of neoantigen vaccine and iNKT activator α-GalCer in Hepatocellular carcinoma. Hepatocellular carcinoma (HCC) is a leading cause of death around the world. Current immune checkpoint blockade therapies only show effectiveness in some cancer patients, so there is an urgent need for more effective immunotherapy strategies. One alternative is the use of neoantigen-based cancer vaccines, which target tumor-specific antigens (neoantigens) on cancer cells and induce strong T-cell responses. Advances in technology now allow for precise identification of tumor neoantigens using bioinformatic analysis or mass spectrometry. While cancer vaccines have demonstrated strong anti-tumor immune responses and therapeutic effectiveness in some cancer types, their success in HCC remains limited. A contributing factor is the suppressive tumor microenvironment (TME) found in advanced HCC. Some studies suggest that combining neoantigen vaccines with anti-PD1/PD-L1 therapies can significantly enhance HCC treatment outcomes. Overcoming the suppressive immune microenvironment is crucial in cancer treatment, and reactivating intratumoral immunity is essential. In our study, we developed an HCC cancer vaccine using transcriptome sequencing and bioinformatics analysis. Our ELISpot assay results showed that this vaccine induced strong tumor-specific immune responses and significantly inhibited tumor growth in early-stage orthotopic HCC mouse models when administered five days after tumor inoculation. However, the effectiveness decreased in advanced tumors when administered ten days after tumor inoculation. We also discovered a significant relationship between the therapeutic effectiveness of the neoantigen vaccine and the activation of intratumoral NKT cells in HCC. Our study suggested that the type-I NKT cell activator, α-Galactosylceramide (α-GalCer), significantly improved the therapeutic outcomes of the cancer neoantigen vaccine in advanced orthotopic HCC mouse models. In some cases, tumors were almost completely eliminated. This indicates the potential of combining iNKT activators with neoantigen vaccines for HCC treatment. To further understand the role of NKT cells in HCC's TME, we plan to investigate intratumoral NKT cell subtypes following neoantigen vaccine therapy. Additionally, we will develop a new delivery system to deliver type I NKT cell activators and type II NKT inhibitors to tumor sites, aiming to reactivate the suppressive TME in HCC after neoantigen vaccine therapy.

#6756 Our RNA production platform and the associated tools facilitate the development of RNA-based vaccine.

C. Bosso-Lefevre, E. Cirri, **E. Mennesson**, D. Szymczak, F. Carpentier, A. Foucher, A. Komarkova, M. Rochet, A. Vindrios, R. Goulay;
Tebubio, Le Perray-en-Yvelines, France

mRNA vaccines have shown their full potential in the Covid-19 pandemic. The application of these technologies for the treatment of cancers represents significant hope, but clinical effectiveness remains to be demonstrated. For this purpose, researchers require high quality production of vaccine mRNA and accurate and cost-saving test tools that are adapted to oncology research. Since 2021, Tebubio has developed a miniscale RNA production platform for providing RNAs (from 100 µg to 1 mg) to researchers around the world. This service is completed by offers on RNA delivery solutions using lipid nanoparticles (LNPs) and cellular tests with biomarker analysis. Through an ingenious design, our DNA matrix for mRNA is easily transferable for GMP production for clinical studies. Recently, Tebubio has developed DNA matrices for circular RNA production. Indeed, circular RNA has many advantages by being less immunogenic and more stable than linear RNA. We compared the quality and the quantity of CAP1 capped linear RNA and circular RNA produced from our DNA templates. We also assessed the stability of both RNAs expressing GFP and the typical tumor antigen, p53, and their relative expression into antigen-presenting cells (APCs). Finally, we quantified the response of the APCs expressing p53 by using our biomarker multiplex analysis system. This new type of RNA and its efficiency testing in APCs will constitute a new addition to our pipeline of RNA production and testing for preclinical studies.

#6757 The anti-tumor efficacy of Th1-specific TROP2 vaccine (AST-07X) in a triple-negative breast cancer murine model.

J. Kang[1], H.-H. Park[1], J. Choi[2], S.-Y. Jang[3], M.-A. Kim[3], M.-K. Park[3], A. Y. Kim[4], E. Joung[1], H. Jung[1];

[1]Aston Sci., Seoul, Korea, Republic of, [2]Jeonbuk National University Medical School, Jeonju, Korea, Republic of, [3]Korea testing & Research institute, Hwasun, Korea, Republic of, [4]Aston Sci. USA, Inc., Seattle, WA

Background: The trophoblast cell-surface antigen 2 (TROP2) is associated with enhanced tumor proliferation and poor prognosis in breast cancer. TROP2 overexpresses on various epithelial cancer cell surfaces, and is commonly found in prostate, colon, pancreas, lung, and breast cancer. Therefore, anticancer strategy targeting TROP2 may be a potential treatment option for patients with metastatic triple-negative breast cancer (TNBC). Sacituzumab govitecan, a Trop-2-directed antibody drug conjugate (ADC), has shown significant benefits associated with progression-free and overall survival compared to standard chemotherapy for treating metastatic TNBC; however, its toxic effects were more frequent than that of chemotherapy (NCT02574455). In this study, we discovered TROP2 target peptides with T-helper 1 (Th1) polarization and anticancer efficacy. We then evaluated the anti-tumor efficacy of these epitopes and possibility of co-administration with ADC in a TNBC murine model.

Materials and Methods: Th1 peptides were identified using the Th-Vac® platform and the predictive binding affinity ranking that indicates potential immunogenicity points of interest for HLA class II. Human peripheral blood mononuclear cell (PBMC) Th1-specific polarization-induced activity and in vivo immunogenicity (Module 2b) were evaluated using flow cytometry and ELISpot analysis. The anti-tumor efficacy of the selected Th1 peptide was evaluated against MDA-MB-23 inoculated athymic Balb/c mice. Each peptide was administered intradermally once weekly for a total of four times at a concentration of 100 μg/head. Sacituzumab govitecan (0.81 mg/kg) was administered intravenously once weekly, for a total of two times.

Results: Ten peptides with high affinity for HLA class II were selected, and three epitopes that induce differentiation of T cells secreting TROP2-specific IFN-γ were subsequently selected. These epitopes (p1, p3 and p6) showed tumor growth inhibition efficacy of 52.4%, 38.5%, and 57.2%, respectively, compared to the control (vehicle) group in the TNBC tumor-bearing mice. The cocktail vaccine (AST-07X), which combined these epitopes, was the most dominant at 65.4%. The anti-tumor efficacy of the combination group of the cocktail vaccine and ADC was 77.4% compared with the control group, showing a potent synergistic effect compared to the 46.1% anti-tumor efficacy of the ADC-mono group.

Conclusion: AST-07X that induce TROP2-specific Th1 anticancer immune responses, showed sufficient anti-tumor efficacy; these effects were evident under immunodeficient conditions, such as those of TNBC tumor-bearing athymic mice. Synergy effects were also induced via combined ADC administration. We are currently conducting further research on humanized mice to address the limitations of the immunodeficient murine model.

#6758 Eradication of tumors and development of immunity from pHLIP-targeted intracellular delivery of STINGa.

M. DuPont[1], A. Moshnikova[1], M. Iraca[1], C. Klumpp[1], H. Visca[1], D. Allababidi[1], P. Pelzer[1], D. Engelman[2], O. Andreev[1], Y. Reshetnyak[1];
[1]University of Rhode Island, Kingston, RI, [2]Yale, New Haven, CT

Activation of the stimulator of interferon genes (STING) pathway causes the release of factors that trigger the immune response in the tumor microenvironment (TME). Transient strong activation leads to immune activation and tumor suppression, while prolonged weak activation leads to immuno-suppression promoting tumor development. Reprogramming of M2-type tumor-associated macrophages (M2-TAMs) toward an M1 phenotype, suppression of cancer-associated fibroblasts (CAFs) and myeloid-derived suppressor cells (mMDSCs), as well as activation of dendritic cells (DCs) to train T-cells are advantageous, while the activation of STING pathway in T-cells is leads to their apoptosis. Thus, targeted delivery of STINGa to specific cells with TME to induce strong transient activation may be a key to therapy. We have developed a delivery approach that uses one or two pH Low Insertion Peptides (pHLIPs) that collaborate in the targeted intracellular delivery of a STINGa. STINGa were conjugated with pHLIPs via S-S cleavable self-immolating linkers. Biophysical studies were performed to ensure proper interactions of pHLIP-STINGa agents with membrane lipid bilayers. pHLIPs extend the lifetime of STINGa in the blood and target them to acidic cancer and stromal cells (CAFs), as well as M2-TAMs, mMDSCs and DCs within TME. The targeting results in selective cytokine activation in tumors with no systemic activation, which triggers the eradication of small (100 mm3) and large (400-700 mm3) CT26 tumors in mice after one or two doses of pHLIP-STINGa. The tumor stroma was destroyed, intratumoral hemorrhage developed, and the level of acidity within the TME was reduced. No tumors developed in mice re-challenged by an additional injection of cancer cells in a 90-day experiment. Thus, targeted delivery of STINGa to cancer cells, tumor stroma and TAMs induces activation of signaling, potentially resulting in the recruitment and infiltration of T- and NK-cells, which gain access to the tumor core. The cytotoxic activity of T- and NK-cells is not impaired by the acidic environment and immune memory is developed. The pHLIP technology may allow transformation of immuno-activating agents into more potent therapeutics, since pHLIP can target and deliver these agents to cancer cells, tumor stroma and myeloid cells.

#6759 Antigen-pHLIP for tumor treatment.

M. DuPont[1], H. Visca[1], A. Moshnikova[1], D. Engelman[2], Y. Reshetnyak[1], O. Andreev[1];
[1]University of Rhode Island, Kingston, RI, [2]Yale, New Haven, CT

Targeted antigen delivery allows activation of the immune system to kill tumor cells. Among the immunogenic epitopes widely investigated is α-Gal, since humans exhibit specific anti-Gal reactivity. However, the repertoire of immunogenic epitopes could be significantly enhanced if therapeutic efficacy did not rely on the presence of natural antibodies, but instead relied on the production of anti-epitope endogenous antibodies induced by immunization against the selected epitope. Therefore, we designed and tested several HA-pHLIP agents, where the HA peptide (YPYDVPDYA) from the influenza virus was selected as an exogenous highly immunogenic epitope, since it is absent in the human genome, and a pH Low Insertion Peptide (pHLIP) was selected as the tumor targeting agent. HA peptides were attached to the N-termini of pHLIPs either directly or via PEG polymers. To enhance the overall binding affinity of HA-pHLIP to anti-HA antibodies, double headed HA-pHLIP agents were introduced, where two HA epitopes were linked to a single pHLIP peptide via PEG12 polymers. The pHLIP sequence was modified to ensure proper pKs of insertion into cell membranes. HA epitopes were targeted to cancer cells in mouse tumors, and remained exposed to the extracelullar space within tumors for about 24 hours. Double-headed HA-pHLIP treatments of imunized mice (a high titer of anti-HA antibodies was developed in mice after immunization with KLH-HA), bearing 4T1 triple negative or B16F10 MHC-I negative melanoma tumors resulted in a 55% reduction of tumor growth. Further reduction of tumor growth was impossible to achive, since all of the anti-HA antibodies in the blood were captured after 3 injections of HA-pHLIP and additional boosts would be required to restore the level of free anti-HA antibodies to induce a more significant therapeutic efficacy.

TUMOR BIOLOGY: 3D and Tissue Recombinant Models of Cancer
Poster Session

#6763 A human-relevant vascularized organ-on-a chip platform for anti-tumor drug efficacy and liver injury assessment.
J. Navarro-Yepes, Q. Dasgupta, P. Purkayastha, K. Janson, C. Mello, A. Narkar, S. Ng, T. Pereira;
SYSTEMIC BIO, LLC, Houston, TX

Cancer global burden accounts for 19.3 million new cases and 10 million deaths in 2020. Despite advances on the understanding of disease progression and efforts to find successful therapeutic strategies, most drugs fail in clinical stages. Lack of models with clinical mimicry recapitulating the *in vivo* pathophysiology and the organ microenvironment where the tumor forms is a key driver reducing the success rate of anti-cancer drugs. Animal models remain the gold standard for preclinical research but fail to recapitulate the complex human tumor microenvironment, a critical component determining tumor development, progression, and response to treatments. Organ-on-a-chip models allow to control the environment and organization of cells in an *in vivo*-like arrangement by culturing multiple cell types to better replicate human conditions, and by implementing different biochemical and physical stimuli, such as fluid shear stress, chemical/nutrient gradients, and perfusion/flow to recapitulate the human vascular system physiology. We leverage our 3D bioprinting technologies to develop complex vascularized organ-on-a-chip models aimed to recapitulate the tumor and liver niche. Both organ-systems are interconnected by our h-VIOS™ platform, allowing dynamic perfusion for 21 days and enabling the simultaneous assessment of anti-tumor therapeutic efficacy and drug-induced liver injury. Our hydrogels feature a complex perfusable vasculature that interfaces with an interstitial chamber where tissues of interest are grown. The vasculature allows for continued and controlled delivery of nutrients, oxygen, and small molecule drugs. Dextran diffusion studies revealed diffusion coefficients ranging from 43.2 $\mu m^2/s$ (4kDa) to 8 $\mu m^2/s$ (70kDa). Vascular architectures are lined with endothelial cells forming a functional barrier expressing the junctional markers ZO-1 and PECAM-1. Moreover, we can modulate the permeability of our vasculature architecture, allowing the extravasation of immune and cancer cells. PBMC-derived T cells and Jurkat cells undergo transendothelial migration in response to a CXCL12 gradient, highlighting the applicability of our model for immunotherapeutic efficacy studies. The tumor interstitial chamber incorporates co-culture of cancer spheroids or tumoroids, fibroblasts, endothelial and immune cells. Colon carcinoma spheroids effectively integrate into the tumor niche with no growth arrest. The liver model consists of an interstitial chamber with a lobular microstructure supporting the monoculture of primary human hepatocytes, and sustaining their viability and function for 9 days as demonstrated by high albumin production, urea synthesis and CYP activity. Our organ-on-a-chip models are fully customizable and anticipated to contribute to advance personalized medicine and improve clinical translation rates.

#6764 Vascularized tumor-on-chip model for evaluating chemotherapeutic-mediated damage to adjacent healthy tissue.

D. Ramsey, J. Rosano, C. Gordon, G. Fewell;
SYNVIVO INC., Huntsville, AL

Introduction: Systemic chemotherapy is an effective anticancer treatment for all stages of breast cancer, with intravenous (IV) infusion being the principal method of administration. In addition to targeting cancer, systemic chemotherapy can impact the viability and function of surrounding normal tissues and vasculature. Early-discovery research tools comparing novel and existing systemic treatment strategies are urgently needed to support predictive efficacy and toxicity efforts. Microfluidic systems have the potential to fill this need while simultaneously reducing animal use. The overall goal of the study is to use an advanced microfluidic tumor-on-chip system to simultaneously evaluate the therapeutic and toxic effects of IV chemotherapy on normal and cancerous tissues.
Materials and Methods: Synthetic Tumor Networks, which are comprised of primary and secondary tissue sites separated by an interconnected vasculature, were developed using in vivo images and fabricated using soft lithography. Primary vascular endothelial cells were used to establish microvasculature. A normal breast cell line (MCF 10A), or a GFP-labeled metastatic human breast cancer cell line (MDA-MB-231/GFP), were cultured in the tissue sites in a three-dimensional (3D) environment using a human-derived hydrogel. The vascular networks were perfused with endothelial cell media under physiological fluid flow conditions to establish the model. An EZH2 methyltransferase inhibitor (EZH2 inhibitor III) was delivered by IV infusion to the model tissues. Real-time monitoring of cellular growth, tumor invasion and extravasation, and cellular viability were performed using fluorescence microscopy over a two-week period.
Results and Discussion: Metastatic MDA-MB-231/GFP breast cancer cells proliferated rapidly in the primary tumor site. Tumor intravasation into the vascular channels was observed in models that received no anticancer treatment, as well as extravasation into the secondary tissue site and invasion of the healthy breast tissue. Differences in tumor viability and migratory behavior were observed between untreated models or models receiving IV infusions of the EZH2 inhibitor through the vascular networks. Vascular barrier integrity and normal breast tissue viability were monitored at early (24-72 hr) and late (7-14 days) timepoints after anticancer treatment to measure short- and long-term adverse drug impacts. These results provide a unique perspective on the in vivo realism of an in vitro system for monitoring both therapeutic and toxic effects of systemic chemotherapies.
Conclusions: We have developed a 3D vascularized tumor-on-chip model for monitoring the impacts of systemic chemotherapeutic agents on tumor and healthy tissues. This model can be used to investigate therapeutic and toxic effects on multiple tissue types simultaneously using real-time imaging techniques.

#6765 A patient-derived hepatocellular carcinoma multicellular spheroid platform harnessing autologous patient serum to model the tumor microenvironment and treatment response.

E. Crouchet[1], N. Almeida[1], S. C. Durand[1], M. Parnot[1], M. A. Oudot[1], F. Giannone[2], C. Gadenne[1], S. Cherradi[1], N. Roehlen[1], A. Saviano[2], E. Emanuele Felli[2], P. Pessaux[2], K. Chayama[3], H. F. Duong[1], T. F. Baumert[1], C. Schuster[1],

[1]University of Strasbourg, Strasbourg, France, [2]Institut hospitalo-universitaire (IHU), University of Strasbourg, Strasbourg, France, [3]Institute of Biomedical & Health Sciences, Hiroshima University, Hiroshima, Japan

Hepatocellular carcinoma (HCC) is the third leading and fastest rising cause of cancer-related death worldwide. The discovery and preclinical development of compounds targeting HCC is hampered by the absence of authentic tractable systems recapitulating the heterogeneity of patient HCC tumors and the tumor microenvironment (TME). Here, we established a novel, simple and robust patient-derived multicellular tumorspheroid model based on clinical HCC tumor tissues combined with the autologous patient serum. The model was robust and reproducible independently from cancer etiology and grade recapitulating key functional features of original tissue. We show that the use of autologous patient serum was essential for the TME function. The tumorspheroids comprised the main cell compartments including epithelial cancer cells as well as all major cell populations of the TME (cancer-associated fibroblasts, macrophages and T cells). Cell type proportions were variable between tumorspheroids reflecting HCC heterogeneity. Moreover, we observed differential responses to FDA HCC approved drugs (including tyrosine kinase and checkpoint inhibitors as well as VEGF-targeting agents) between donors as in patients. This patient HCC serum-tumorspheroid model provides novel opportunities for drug discovery and development as well mechanism of action studies including compounds targeting the TME. In conclusion, this HCC serum-tumorspheroid platform will contribute to improve the dismal outcome of patients with HCC.

#6766 Assessing the impact of immunotherapies and cell therapies in 3D heterospheroid models mimicking tumor microenvironments.

N. H. Madsen[1], B. S. Nielsen[1], K. Holmstrom[1], G. H. Olofsson[2], P. t. Straten[3], S. Skov[4], C. Rodriguez-Pardo[5], M. Ormhoj[5], J. Larsen[1], M. Gad[1];
[1]Bioneer A/S, Horsholm, Denmark, [2]Copenhagen University Hospital Herlev and Gentofte, Herlev, Denmark, [3]Copenhagen University Hospital Herlev and Gentofte, University of Copenhagen, Copenhagen, Denmark, [4]University of Copenhagen, Copenhagen, Denmark, [5]Technical University of Denmark, Lyngby, Denmark

Immunotherapies and cell therapies show substantial potential in the treatment of cancer. However, their efficacy within the complex microenvironment of solid tumors remains a critical area of investigation. In this study, we employ physiologically relevant 3D multicellular heterospheroid models to quantitatively assess the impact of these therapies on immune and tumor cells residing in tumor-like microenvironments. The spheroids are composed of cancer cell lines, fibroblasts and various primary immune cell types matched to the specific target of immunotherapy.

We have previously reported that interactions between cancer cells and fibroblasts promote a tumor-like environment, recruiting and polarizing monocytes into M2 macrophages. Treatment of spheroids with immunomodulating compounds successfully reprogrammed the macrophages into M1-like macrophages with increased pro-inflammatory cytokine secretion.

To mimic tumor-specific T cell responses observed in cancer patients, we here educated T cells to recognize target cell antigens through a 14-day co-culture of PBMCs and PANC-1 tumor cells. Subsequent re-challenge with PANC-1 heterospheroids revealed 70% specific killing by educated T cells, whereas T cells educated with a breast cancer cell line did not exhibit this targeted cytotoxicity. FACS analysis demonstrated increased expression of activation markers and immune checkpoint molecules such as PD-1, LAG-3 and TIGIT on educated T cells. Furthermore, we observed infiltration of educated $CD4^{\pm}$ and $CD8^{\pm}$ T cells into heterospheroids by immunohistochemistry, indicating the replication of a tumor-specific response within solid tumors. We are currently investigating the enhancement of educated T cell killing using various immune checkpoint inhibitors including antibodies targeting PD-1, TIGIT and LAG-3. Another means of eliciting tumor-specific responses is by employing CAR T cells. Antigen-specific CAR-T cells or untransduced CAR-T cells derived from the same donor were added to HT-29 and HCT-116 heterospheroids at various target-to-effector ratios. By using cancer cells genetically engineered to express a luciferase enzyme, we assessed the specific killing of cancer cells within the heterospheroids. Analysis showed a clear dose-dependent increase in luminescence, indicating greater antigen-specific CAR-T cell killing potential (60-80% specific lysis) compared to the non-specific killing observed with untransduced CAR-T cells (<5% specific lysis). Additionally, preliminary data demonstrate the killing of heterospheroids by γδ T cells and that this killing is enhanced by immune checkpoint inhibitors.

In conclusion, we have developed 3D heterospheroids from various cancer types that faithfully mimic tumor-like microenvironments, enabling us to evaluate the effects of immunotherapies and cell therapies in physiologically relevant models.

#6767 Multivariate analysis of *ex vivo* kidney 3D immune-microtumors for functional precision medicine.

E. Peerani[1], K. Nan[1], D. A. Wiskerke[1], T. D. L. Richardson[1], P. Maximchick[1], J. Kearney[1], G. R. T. de Fraine[1], K. L. Loughrey[1], J. Ient[1], J. A. Hudson[1], A. Kaffa[1], A. M. Crawley[1], N. K. Bah[1], E. G. Lopez Molina[1], E. Tham[1], F. Iori[1], M. H. Williams[1], M. G. B. Tran[2], D. N. B. Ranatunga[1];
[1]Ourotech Ltd t/a Pear Bio, London, United Kingdom, [2]Royal Free London NHS Foundation Trust, London, United Kingdom

Immuno-oncology (IO) represents a significant paradigm shift in cancer treatment, focused on leveraging and mobilizing a patient's own immune response and anti-tumor capabilities. Despite accounting for the majority of available treatment options, there are currently no diagnostic tests capable of predicting combination immunotherapy response in kidney cancer. We have developed a fully human 3D IO model for clinical drug efficacy prediction through multivariate analysis of the tumor-immune microenvironment (TiME) combining functional assays, artificial intelligence and multi-omics. These immune-microtumors recapitulate a patient's unique pathophysiology and allow 3D spatio-temporal analyses of functional metrics at both bulk and single-cell resolutions.
Renal cell carcinoma (RCC) resections and matched blood were collected and processed for single cell isolation of tumor and PBMCs (N=20, ISRCTN10001405). Flow cytometry (FC) and immunofluorescence (IF) were used to characterize TiME cell subpopulations (cancer, immune, stromal etc.) in pellets and 3D cultures, and to deconvolute bulk RNAseq data. Target (tumor) and effector cells (PBMCs and CD8+) were stained with fluorescent probes, activated using αCD3 and encapsulated in TiME-mimicking 3D matrices. 3D immune-microtumors were treated with FDA-approved regimens including immunotherapies (ipilimumab, nivolumab, pembrolizumab) and receptor-tyrosine kinase inhibitors (TKIs)(cabozantinib, lenvatinib, axitinib) as monotherapies or combination therapies. Differential drug efficacies were functionally quantified over 4 days using 3D confocal microscopy and computer vision pipelines to extract cell behavior metrics such as immune cell infiltration, immune/tumor cell migration speed, and tumor killing/viability.
We devised a specialized RCC hydrogel formulation with superior viability compared to MatrigelTM alone (N=7). FC/IF/RNAseq were used to quantify relative cell subpopulations after isolation and show protein/transcriptional signature retention after 3D culture (N=7). The platform was conducive to the testing of various drugs with varying MoAs including immunotherapies, TKIs, targeted therapies and cell therapies. Treatment with pembrolizumab led to 26% higher PBMC infiltration, 14% higher CD8+ infiltration and 15% increased tumor cell death compared to control. When in combination, pembrolizumab reduced cell viability by 10% and 19% with lenvatinib and axitinib respectively (N=1). Population analyses revealed intra-patient response heterogeneity (N=7).
In conclusion, we showed MoA-agnostic, patient-dependent responses to FDA-approved clinical treatment regimens via molecular and functional spatio-temporal analyses. Clinical outcome correlation is currently underway in our advanced RCC study PEAR-TREE2 as well as in breast NCT05435352 and brain NCT06038760 tumors.

#6768 Matched XPDX™derivative models as a platform for continuity across preclinical drug development.

M. Millard[1], A. Carlson[1], D. Y. Nadeau[1], K. J. Burgess[1], A. Simonson[2], A. Diaz III[2], M. Wick[2], T. M. DesRochers[1];
[1]Kiyatec Inc., Greenville, SC, [2]XenoSTART, San Antonio, TX

Drug discovery is a reductive process in which druglike entities are carried through increasingly complex assay formats to tease out the compounds best suited for human studies. *In vivo* efficacy remains the benchmark for successful preclinical drug development. Cell-based models are a mainstay in early stages but translatability of different models across platforms remains a challenge. In oncology, patient-derived xenografts (PDX) are the gold standard for animal studies because they recapitulate key features of human tumors including the cellular heterogeneity, growth patterns, and drug response of the original patient tumor. *Ex vivo*, PDX derivatives have the potential to harness these same traits thereby extending the utility of PDX models to earlier stages of preclinical drug development. The KIYA-Predict™ platform is a clinically validated tool for the assessment of *ex vivo* drug responses across a broad range of drug classes that when applied to XPDX models shows good correlation to *in vivo* drug responses and excellent intra-sample reproducibility over time. Working with the well-characterized XenoSTART™ XPDX model repository, Kiyatec has derived 2D cell lines and organotypic 3D-expansion cultures to complement the *ex vivo* predictive value of our KIYA-PREDICT™ XPDX drug response profiling (DRP) platform. The development of syngeneic models applicable to simpler, high-throughput library screening (2D formats) and lower-throughput more complex mechanistic studies (3D organotypic models) could alleviate the burden and pitfalls of extrapolating data across unrelated models. Matched sets of 2D cell lines (2D-XPDX™) and 3D organotypic (XPDXO™) cultures were established from single cell suspensions of digested, mouse-cell depleted XPDX™ tissue samples. Drug response profiling of the XPDX™ in their various *ex vivo* culture formats showed relative similarities across platforms. Genomic profiling of the derivates confirmed shared tissue origin and retention of genomic and phenotypic signatures to varying degrees across models. Mechanistic evaluation of 3D organotypic culture demonstrated that disease-relevant biomarkers and processes are maintained. Together these results demonstrate the feasibility of this novel drug discovery platform that avoids ambiguity imparted by discordant models.

#6769 Applications of a novel fibrous extracellular matrix for advanced *in vitro* cancer models.

N. Kaur[1], D. Yang[2], J. Ali[1];
[1]FAMU-FSU College of Engineering, Tallahassee, FL, [2]Acrogenic Technologies Inc., Rockville, MD

Compared to traditional *in vitro* two-dimensional (2D) planar cell culture system, three-dimensional (3D) mammalian cell culture can better recapitulate physiological environments and the complexity of natural tissues, hence they are crucial in modern biomedical research. Extracellular matrices (ECM) play a key role in *in vitro* mammalian cell culture systems. The role of the ECM on *in vitro* 3D cell culture are: 1) to simulate an *in vivo*-like physiological environment, 2) support cell-cell and cell-ECM interactions, 3) promote cell adhesion, migration, and communication, 4) aid in tissue development, morphogenesis, differentiation, and functioning. Although basal membrane extracts (BME) are the most popular type of ECM supporting 3D modeling *in vitro*, they often have significant limitations including limited long-term stability, significant batch to batch heterogeneity, restricted cell movement, and relatively high cost for culturing many cancer cell lines. In this investigation, we employ a novel micro-fibrous scaffold that closely mimics natural ECM, providing porous and interconnected networks for 3D culturing of hepatic cells, lung cancer, breast cancer, pancreatic cancer. As revealed by optical and scanning electron microscopy, the scaffold promotes significant cell-to-cell and cell-to-matrix interactions. Moreover, we observed improved cell growth in 3D culture over longer periods than 2D culture systems for all cell types examined. We also evaluated the anticancer efficiency of different drugs including Lapatinib, Cisplatin, Docetaxel, Doxorubicin and observed that 2D cultured cells were more sensitive to drugs treatment in comparison to 3D. Furthermore, ECM was observed to support 3D growth and structure formation with cell pools of primary cells achieved from disassociated human tumors. Tumor organoids were able to form within seven days and ready for anticancer screening within 14 days. We achieved an 80% success rate in developing breast cancer organoids from patient tissues. Additionally, tissue granules were also able to be cultured under the same condition, which allowed us to investigate the invasion of cancer cells into tissue. The primary cells from human tumors formed cell clusters resembling the original tumor tissue's structure. In conclusion, the novel micro-fibrous scaffold, closely mimicking natural extracellular matrixes, promotes significant cell-to-cell and cell-to-matrix interactions, while also facilitating cell growth over extended periods providing a more physiologically relevant platform for evaluating drug responses for various cancer cell types, further showing the importance of 3D culture systems in cancer research.

#6770 Acquired temozolomide resistance instructs patterns of glioblastoma cell motility and proteome expression within gelatin hydrogels.

Viktoriia Kriuchkovskaia[1], Ela Eames[1], Rebecca Riggins[2], Brendan Harley[1]

[1]University of Illinois Urbana-Champaign, Champaign, IL,[2]Georgetown University, Washington, DC

Acquired drug resistance in glioblastoma (GBM) presents a major clinical challenge and is one of the key factors contributing to the abysmal prognosis with less than 15 months median overall survival. The aggressive chemotherapy with the frontline therapeutic, temozolomide (TMZ), ultimately fails to kill residual, highly invasive tumor cells after surgical resection and radiotherapy. Here, we present a robust three-dimensional (3D) *in vitro* hydrogel model of acquired temozolomide (TMZ) resistance using isogenically-matched glioblastoma (GBM) cell lines. We demonstrate distinct drug response patterns between TMZ-sensitive and TMZ-resistant GBM cells, emphasizing our model's promise for future pre-clinical investigations aimed at developing novel therapies targeting drug-resistant GBM. Importantly, our model detects apoptosis-related protein changes in response to TMZ, validating its ability to study drug-induced molecular changes. Furthermore, our study delves into the migratory potential of GBM cells within the 3D extracellular matrix environment. Additionally, we uncover significant alterations in cytokine expression associated with matrix remodeling and angiogenesis, providing new avenues for therapeutic investigation. Although our findings are derived from a specific set of isogenically-matched cell lines, this model highlights the potential to explore personalized treatment strategies. Ongoing research in our lab is dedicated to gaining a more profound understanding of matrix remodeling and the migratory potential of TMZ-resistant GBM cells. Moreover, our future work will aim to expand our study to include a wider range of cell lines and patient-derived xenografts within our advanced microphysiological systems that include key elements of GBM tumor microenvironment such as perivascular niche. This endeavor seeks to establish connections between observed therapeutic behaviors and clinical outcomes, ultimately contributing to the development of more effective treatments for GBM patients.

#6771 Tumor-microenvironment-on-chip: an *ex vivo* drug screening platform enabling real-time observation of regional tumor responses during drug development and clinical treatments.

Chiao-Min Lin[1], Hsaun-Yu Mu[1], Li-An Chu[1], Ya-Hui Lin[1], Ji Li[1], Chao-Yu Liu[1], Hsi-Chien Huang[1], Sheng-Liang Cheng[1], Tsung-Ying Lee[1], Hsin Mei Lee[1], Hsin-Min Chen[1], Yun-Jen Tsai[1], Tzu-Hung Hsiao[2], Kee-Ming Man[3], Yunching Chen[1], Jen-Huang Huang[1]

[1]National Tsing Hua University, Hsinchu, Taiwan,[2]Taichung Veterans General Hospital, Taichung, Taiwan,[3]China Medical University Hospital, Hsinchu, Taiwan

Background: Current tumor models face challenges in accurately replicating the intricate and dynamic conditions of the tumor microenvironment (TME), limiting predictions of drug efficacy in drug development and personalized treatment. Furthermore, the continuous and real-time observation of drug responses variations resulting from tumor heterogeneity poses challenges in existing models, including patient-derived organoids and animal models. To address these limitations, our study introduces a novel approach through a tumor-microenvironment-on-chip (TMoC) that combines 3D tissue cultivation and a circulation system, incorporating physiological gradients of oxygen and nutrients. Serving as a tool to faithfully replicate the intricate TME, TMoC facilitates highly accurate drug screening for enhanced therapeutic precision.

Method: Based on organ-on-chip and microfluidic systems, our platform reconstructs the cellular heterogeneity of the TME using tumor tissue-dissociated cells in collagen I or Matrigel within a strip-shaped 3D cultivation space, enabling simple analysis of regional responses. A circulation system, powered by a peristaltic pump, aids medication and immune cell entry for combination immunotherapy assessment. Real-time apoptosis analysis via fluorescence microscopy and sample retrieval for in-depth analysis are enabled. In drug screening, TMoC results are compared with mouse model outcomes and medication records for various cancers and treatments.

Result: TMoC reconstructed physiological-like gradients, including oxygen levels, and facilitated the infiltration of cytotoxic $CD8^+$ T cells, providing a distinctive model for assessing the synergistic impact of immune checkpoint inhibitors and chemotherapy drugs. Additionally, tissues cultured in TMoC retained their original cellular composition. TMoC demonstrated efficacy in drug screening across various cancer models, including breast, pancreatic, and colorectal cancers. In clinical studies, tumor tissue-derived cells from patients were cultivated on the TMoC, and the treating results are subsequently compared with clinical outcomes. Whether in animal models or clinical cases, the drug screening outcomes of TMoC consistently aligned with *in vivo* drug responses.

Conclusion: The TMoC offering a platform that modeling some complex characteristics of TME. With applications in drug screening and clinical studies, it shows promising correlations between TMoC and *in vivo* responses.

#6772 A 3D model of breast cancer-bone metastasis to mimic dysregulation of bone remodeling and drug response.

M. Tai, E. C. Gonzalez Diaz, C. E. Monette, J. Wu, F. Yang;
Stanford University, Stanford, CA

Introduction: Bone metastases are common among advanced stage breast cancer patients and induce dysregulation of bone remodeling. Crosstalk between cancer cells and the bone niche drives the vicious cycle of bone loss and breast cancer growth. To accelerate discovery of targeted therapies, there is a critical need for experimental models that can mimic breast cancer-induced dysregulation of bone remodeling in patients. Mouse models are the current gold standard, but are low throughput, costly, and cannot fully recapitulate human-human cell interactions. To address these limitations, our goal is to engineer a fully human 3D *in vitro* model of breast cancer-bone metastasis that can mimic dysregulation of bone remodeling and drug responses in patients, and enable screening of potential new drug candidates.

Methods: Two human breast cancer cell lines (MDA-MB-231, MCF-7) were chosen given their well characterized clinical features and tendency to invade bone. Our 3D model comprises an outer ring of tissue engineered (TE) bone and a center of breast cancer cells to mimic invasion through the bone marrow/long bone interface. Human mesenchymal stem cells were encapsulated in 3D gelatin microribbon scaffolds and cultured in osteogenic media for 28 days to form TE bone. Human monocyte-derived osteoclasts were seeded onto the bone, and the center was replaced with GFP-labeled breast cancer cells. Denosumab and zoledronic acid were selected as they are standard treatments for reducing bone loss in patients, and were used to treat the model at 30 µg/mL and 2 µg/mL, respectively. Intermittent parathyroid hormone (iPTH) treatment was selected as it showed efficacy in animal models, and was used to treat the model at 10 µg/mL for 6 hours daily. All groups were treated with drugs for 14 days. Bone volume was assessed using microCT. Cancer cell proliferation and invasion into bone was monitored with fluorescence confocal microscopy.

Results: MicroCT imaging showed both breast cancer cell lines induced bone loss in the triculture model, compared to the control with no breast cancer cells in the center. Consistent with known clinical features, the more aggressive cell line (MDA-MB-231) induced a greater amount of bone loss than the less aggressive breast cancer cell line (MCF-7). Consistent with clinical findings, both denosumab and zoledronic acid reduced bone loss in our 3D model, and zoledronic acid further reduced breast cancer cell invasion and proliferation. Finally, the 3D model recapitulated the *in vivo* drug response of iPTH treatment, reducing bone resorption and breast cancer invasion.

Conclusions: Here we report a fully human triculture model of breast cancer-bone metastasis that can mimic key clinical features of breast cancer-induced bone resorption and drug response in patients. Such a 3D model could enable screening of drug candidates with reduced time and cost and enable identification of novel druggable targets.

#6773 Tissue engineered colorectal cancer microspheres for drug screening.

Y. Tian[1], M. Hashemi[1], B. Anbiah[1], R. Zhang[2], I. Hassani[1], R. Boohaker[3], E. Lipke[1];
[1]Auburn University, Auburn, AL, [2]Biocytogen, Waltham, MA, [3]Southern Research, Birmingham, AL

Three-dimensional (3D) disease models have garnered widespread interest for use in later stages of the drug discovery process, such as preclinical efficacy and toxicology studies, due to their pathophysiologically relevant properties. However, there is a need and opportunity for 3D cancer models to be used earlier in the drug screening process. To meet this need, the 3D models must strike a balance between throughput, which includes scalability and uniformity, and physiological relevance, such as the ability to modulate key attribute of the tumor microenvironment.

Here we report the creation of 3D colorectal cancer (CRC) tissue models, referred to as VivoSpheres, and demonstrated their relevance to cancer drug screening. The VivoSphere production platform couples tissue engineering toolkits with microfluidics, enabling the scalable production of engineered cancer microspheres. The model supports the long-term maintenance of the cancer cell phenotype. In a preliminary study, we were able to generate more physiologically relevant drug responses.

We formed CRC VivoSpheres by encapsulating HT-29 CRC cells within poly(ethylene glycol)-fibrinogen hydrogel microspheres using our previously developed microfluidic platform. CRC VivoSpheres were rapidly produced with high cell densities (20×10^6 cells/ml) and high uniformity on day 0 with a coefficient of variation (COV) < 7%. This high uniformity was maintained for 15 days (COV ≤ 10%), which is critical for long-term dose studies. The cells maintained high viability and showed high proliferative capability with a significant increase in colony size and expression of Ki67 up to day 29. The encapsulated cells maintained the CRC phenotype over time with the expression of CD44 (cancer stem cell marker) and CK20 (CRC marker).

After establishing shipping conditions that maintained cell viability for remote use, the HT-29 VivoSpheres were shipped to the oncology team at Southern Research for drug testing. The CRC VivoSpheres were treated with DMSO, GANT61, and SRI-38832, the latter two of which are GLI1 inhibitors. Phase contrast images and western blot were used to assess the response of CRC VivoSpheres to the treatments. Oncogenic GLI1 transcription activity and NBS1 overexpression have been found to contribute to chemotherapeutic resistance, negating the anti-tumor effects of 5-fluorouracil. While 2D cultured HT-29s responded to treatment with GANT61, HT-29 VivoSpheres continued to express NBS1 following GANT1 treatment, but downregulated NBS1 in response to the GLI1 inhibitor SRI-38832, which is the same response Southern Research has seen in *in vivo* tumor models.

In conclusion, we have developed tissue-engineered 3D CRC models that hold promise for use in drug screening. These models have demonstrated an initial capability to reproduce the CRC phenotype and mimic *in vivo* drug response.

#6774 Establishment and optimization of an air liquid interface co-culture system to evaluate phenotypic changes in primary human Barrett's esophagus cells upon different environmental exposures.

A. Chatterjee[1], J. Azevedo-Martins[1], C. C. Tanyolac[1], Q.-U. Ain[1], H. Yu[1], S. Camilleri-Broet[2], L. Ferri[2], P. Gascard[1], T. D. Tlsty[1], M. D. Stachler[1];
[1]University of California, San Francisco, CA, [2]Montreal General Hospital, McGill University, Montreal, QC, Canada

Esophageal adenocarcinoma (EAC) is a deadly cancer with an increasing incidence which arises out of it's precancerous precursor, termed Barrett's esophagus (BE). A better understanding of the factors that influence BE progression is essential for early detection and novel therapeutics. 3D Air Liquid Interface (ALI) cultures provide an edge over traditional 2D cultures as they better mimic the in vivo conditions of the esophagus. The aim of the study was to establish conditions for a BE ALI model and to evaluate the phenotypic and molecular changes in primary human BE cells upon interaction with different types of esophageal fibroblasts (EF) and exposure to bile acids(BA) (a major component of gastroesophageal reflux). ALI conditions that allowed growth of both primary BE and fibroblast for at least 30 days were optimized. Non dysplastic BE cells from two patients were utilized with one having EAC (P) and the other with no history of progression (NP). The BE cells were cultured in our ALI model with 3 types of EFs: normal esophageal fibroblasts(NFs), BE associated fibroblasts(BFs) and EAC associated fibroblasts(CFs). To determine the effect of BA exposure, ALI cultures underwent daily 1 hour exposure to bile salts. To determine if BE cells that lacked p53 responded differently to BA exposure, CRISPR Cas9 was utilized to knockout *TP53*. ALI cultures were conducted for 28 days. Phenotypic differences were determined by H&E staining and immunofluorescence (IF). Changes in cell proliferation was evaluated by Ki67 IF. Successful ALI cultures were validated by positive expression of laminin, pan-cytokeratin, Muc2 and Muc5ac by IF. Upon co-culture, we observed opposing histologic changes in the BE cells from the P and NP patients. The NP BE cells had a less complex structure upon culture with the BFs and CFs compared to NFs. The P BE cells showed the development of a complex morphology upon culture with the CFs compared to the BFs and the NFs. In both patients, we observed an increase in Ki67 positivity with fibroblast co culture; NFs (NP: 6.91%, p=0.070, P: 10.6%, p=0.001), BFs (NP: 12.49%, p=0.0001, P: 11.196%, p=0.003) and CFs (NP: 19.88%, p<0.0001, P:14.63 %, p=0.0001) compared to no fibroblasts (NP = 5.32%, P= 7.25% Ki67+). Co-culture with CFs increased Ki67 staining compared to either NFs or BFs (p=0.007,0.014). Exposure to BA showed a thinning but intact BE epithelial surface in both patients with and without *TP53* knockout. Overall, primary BE cells and fibroblasts can be maintained long term in an ALI culture and co-culture with fibroblasts drive increased proliferation in BE cells. The histology changes observed in NP and P cell could be an indication of possible activation and interaction of differential signaling pathways. Ongoing studies aim to identify these pathways and determine transcriptional changes due to co-culture and BA exposure.

#6775 3D culture aggregation morphology depends on cell phenotype and gene expression profiles in lung cancer.

Naohiro Hayashi[1], Shimpei Tsudaka[1], Ken Suzawa[2], Tomoaki Higashihara[1], Yin Min Thu[1], Atsushi Matsuoka[1], Daisuke Mizuno[1], Ryo Yoshichika[1], Fumiaki Mukohara[1], Mao Yoshikawa[1], Kazuhiko Shien[2], Hiromasa Yamamoto[2], Shinichi Toyooka[1]

[1]Department of General Thoracic Surgery and Breast and Endocrinological Surgery, Okayama University Graduate School of Medicine, Dentistry and Pharmaceutical Sciences, Okayama, Japan,[2]Department of Thoracic Surgery, Okayama University Hospital, Okayama, Japan

Background: Three-dimensional (3D) cell culture allows for the reproduction of tissue structure and function in a state more akin to the in vivo environment compared to two-dimensional (2D) cell culture. It is established that 3D culture more faithfully replicates cell morphology, differentiation, proliferation, gene and protein expression, and responsiveness to stimulation, as well as drug metabolism. Focusing on the observation that lung cancer cell lines exhibit different clustering morphologies in 3D cell culture, we conducted a comparative study on the relationship between these clustering morphologies and the characteristics of the lung cancer cell lines.

Methods: We cultured 30 lung cancer cell lines using 3D culture plate, and classified the types of cell clustering morphologies formed. We evaluated the molecular and cellular biology characteristics of all cell lines. Additionally, comprehensive gene expression analysis using RNA sequencing was performed on the 30 3D-cultured cell samples, and the characteristics of gene expression between different clustering types were compared.

Results: The 3D culture aggregation morphology of 30 lung cancer cell lines were classified into three types (monolayer sheet, NOS, spheroid). Monolayer sheet-type cells exhibited higher proliferation, migration, and invasion capabilities compared to spheroid-type cells. In the transcriptomic bioinformatics analysis of the acquired gene expression data, GSEA analysis using Hallmark gene sets showed that the enrichment of epithelial-mesenchymal transition (EMT) and cancer metastasis-related genes in the monolayer type cells significantly compared to the spheroid type cells. Conversely, cell adhesion and intercellular binding-related gene sets were highly enriched in the spheroid type cells.

Conclusion: 3D culture aggregation morphology represents phenotypic properties and transcriptomic profiles in non-small cell lung cancer cells.

#6777 An *ex-vivo* organotypic culture platform of mucinous carcinomatosis peritonei identifies CDK4-6 inhibition as a novel treatment.

J. Weitz[1], D. Nishizaki[1], J. Patel[1], I. Ng[1], S. Sun[1], D. Ramms[1], J. Zou[2], J. Baumgartner[1], K. Kelly[3], H. Patel[1], R. White[1], J. Veerapong[1], P. Vu[1], S. Gutkind[1], H. Tiriac[1], S. Kato[1], A. Lowy[1];

[1]UCSD Moores Cancer Center, San Diego, CA, [2]UCSD, San Diego, CA, [3]University of Wisconsin, Madison, WI

Concomitant mutations in *KRAS* and *GNAS* have been linked to mucinous histology in gastrointestinal neoplasms of the appendix, colon, and pancreas (IPMN). Upon progression, these tumors are characterized by metastasis which favors the peritoneal surface, resulting in mucinous carcinomatosis peritonei (MCP). Recently we have described a novel technique which allows for long term culture and drug intervention of human MCP tumors *ex-vivo*. With evidence of durable clinical benefit of CDK4-6 inhibition in a single patient with chemo refractory MCP of appendiceal origin, we sought to further investigate anti-tumor responses using CDK4-6 inhibition in *ex-vivo* tumor slices, in order to identify candidates for a personalized clinical therapy trial. Here, in a comparison of *ex-vivo* patient tumor slices from 18 individual donors, treatment using CDK4-6 inhibitors revealed *a* significant reduction in cancer cell specific proliferation in mucinous *GNAS-mut* tumors compared to non-mucinous cancers. Anti-tumor responses of CDK4-6 were determined to be tumor-cell intrinsic, as CDK4-6 inhibition blocked proliferation of stromal cells in the TME independently of patient tumor mutational and mucin status. Based on these finding a personalized clinical trial was conducted where we report that 13 of 16 patients (81%) enrolled with MCP treated with palbociclib had at least a 10% decrease in CEA, as compared to historical chemotherapy responses rates reported from 14-30%. These results indicate that CDK4/6 inhibition is a novel and efficacious treatment for patients with MCP.

#6778 New microplate platform with cryopreserved 3D tumor spheroids for faster and convenient pre-clinical testing.

N. Goedecke[1], S. Stroebel[1], S. Hutter[1], T. Issa[1], I. Agarkova[1], L.-A. Ligeon[1], O. Frey[1], **M. Nag**[2];
[1]InSphero AG, Schlieren, Switzerland, [2]InSphero AG, Brunswick, ME

Drug discovery and safety testing depend on predictive *in vitro* models, including multicellular tissues with organotypic functions. While traditional 2D tumor cell cultures have been extensively used in early drug screening due to their user-friendly nature, automation compatibility, and high throughput, they fall short in representing the intricate 3-dimensional structure, physiology, and complex multicellular nature of actual tumors. However, generating such 3D tissues for each test campaign is labor intensive. In addition, not all researchers have the resources to establish these 3D models. To pave the way, we developed a new platform that offers a range of cryopreserved 3D tumor models in micro plate format allowing for high-content screening. It enables users to start testing compounds within a 3-to-5 days simply by thawing an ARCTis™ plate (Always Ready Cryo Tissues) and following clear instructions. Another advantage of these cryopreserved 3D models derives from the fact that they are made in larger batches which means the start point for compound testing is always the same. This improves data quality, maximizes the test window length, and makes the data comparable across work groups. Currently, our growing portfolio consists of 25 tumor cell lines from ATCC representing the most common solid tumors. Their functionality has been determined based on efficacy tests for each cell line with the apoptotic agent Staurosporine. Various cell lines exhibited compact spheroids with a round morphology, less compact aggregates with non-spherical morphology, or loose cell-cell interaction aggregates, which can correlate with their tumor site of origin. Upon treatment with Staurosporine the dose-response profiles indicated growth inhibition, tumor shrinkage, or tumor cell killing effects based on size assessment and cell metabolic analysis (ATP). Moreover, we demonstrated the robust performance of these assays from plates stored for up to 6 months at -80°C.In conclusion, this groundbreaking approach addresses the limitations of traditional 2D cell cultures by providing a high-throughput, in-plate frozen, 3D cell culture platform. By offering a combination of a more physiologically relevant representation of tumors with a robust frozen-storage and time flexible assay platform our method holds great promise for advancing cancer drug discovery by easing the exploration of complex drug testing screens *in vitro*.

#6779 Modality agnostic tumor models of cancer which can more accurately define drug efficacy and mechanism to help develop more effective therapeutics.

P. Samuel, D. O. Ochola, H. Del Mundo, **B. Dave**;
Spanios, Houston, TX

Introduction: In the path to clinic, researchers require robust tools to effectively evaluate the capacity of novel therapeutic modalities to generate anti-tumor responses. Using human-relevant, translational ex-vivo models is widely considered to reduce attrition during drug discovery and development for a more effective prediction of clinical outcomes during preclinical testing of drug candidates. **Methods:** The three levels of our patient derived tumoroid model platform, COMPASS (Custom Organoid Modeling Platform for Accurate SolutionS) was built to be versatile modality-agnostic human on human model system for pre-clinical testing. COMPASS 1 has stroma with epithelium; COMPASS 2 has stroma, epithelium, and immune components (from PBMCs) and COMPASS 3 has stroma, epithelium, immune components, and oxygenation. For widespread adaptation and utilization of our COMPASS platform we encourage extensive characterization by articulating the context of use to help build confidence in cases where limited knowledge and only few real-life cases exist. **Results:** Our proof-of-concept examples articulating the context of use demonstrate the modality-agnostic adaptability our COMPASS platform brings to the field of preclinical testing. We encourage a collaborative approach with researchers to support their testing needs to build confidence in our model to enable transition from existing screens, assays, and animal models. We envision preclinical use of COMPASS to help stratify patients for clinical trials, identify subpopulations that need dose modification and predict the response of patients and/or their risk of adverse effects. **Conclusion:** Due to its greater physiological relevance and ability to encompass downstream processes in a time and cost-efficient way, industry and academia should deliberate the impact platform such as COMPASS would have on their workflow and consider adapting to using these models routinely.

#6781 Maintaining the tumor microenvironment: Serum-free cell culture for an advanced 3D in vitro tissue model.

A. Siebenmorgen[1], C. Wohle[1], K. Lamfried[1], L. Martinez Carrera[1], B. Heller[2], K. Lupar[2], G. Bergamini[2], D. Poeckel[2], O. Hardt[1], **B. Theek**[1];
[1]Miltenyi Biotec B.V. & Co. KG, Bergisch Gladbach, Germany, [2]Cellzome GmbH, a GSK company, Heidelberg, Germany

Cancer research has made significant progress in recent years, especially in the field of immunotherapy that uses immune modulators. A significant portion of these novel therapeutic strategies focuses on manipulating the tumor microenvironment (TME). The TME is a complex structure that comprises various cellular elements, including cancer cells, immune cells, and structural components, such as secreted factors and extracellular matrix proteins. However, replicating the human TME in experimental murine models has proved challenging. Therefore, researchers have started to develop ex vivo cultivation protocols of tumor tissues, particularly precision-cut slices (PCS), that offer a three-dimensional representation of the TME. It is essential to select the best culture conditions to ensure the preservation of the TME that closely resembles the in vivo conditions. To further this research, a serum-free cell culture medium has been developed to propagate primary epithelial tumor cells originating from pancreatic, renal, and ovarian tissues. The optimized media formulation was successfully employed in the derivation and expansion of tumor cell lines, sourced from both primary and xenotransplanted tumors. An additional serum-free cell culture medium has been designed to cultivate primary lung cancer cells. Suitable culturing conditions have been introduced that maintain TME composition ex vivo cultured PCS prepared from fresh non-small cell lung carcinoma (NSCLC) tissue. Lung TumorMACS Medium and a serum-containing medium were compared, and it was found that the cellular composition of PCS cultivated in Lung TumorMACS was comparable to the original composition. At the same time, PCS cultivated in Lung TumorMACS showed a lower expression of stress genes, compared to the serum-containing alternative.

#6782 3D-EXpress - an *ex vivo* platform using viably cryopreserved tumoroids for rapid assessment of targeted therapeutic outcomes.

V. Garrido, M. Ataya, N. R. Dhanushkodi, S. Currlin, A. Humphrey, J. Ehrhart, R. Chakraborty;
Nilogen Oncosystems, Tampa, FL

Background: it has been a significant challenge to select, combine, and sequence the multiple FDA-approved IO therapies and pharmaceutical agents, highlighting the need to develop a precision oncology platform to explore novel combination treatments. 3D-EXpress is a unique *ex vivo* therapeutics testing platform using a biorepository of fresh patient tumoroids that were never dissociated, propagated, or reassembled to retain an intact microenvironment. Therefore, these specimens provide an excellent *ex vivo* platform to investigate the efficacy of therapeutics targeting the tumor microenvironment. Here, we employed the 3D-EXpress platform to compare the efficacy of different therapeutic modalities targeting tumor antigens and immune checkpoint *ex vivo*.
Methods: Tumoroids measuring 150 µm in size retaining tumor cell heterogeneity, tumor-resident immune cells, stromal components, and extracellular matrix interaction were prepared from human endometrial and colorectal tumors. Tumoroids were cryopreserved and were selected based on tumor antigen status. Samples were treated for 72 hours *ex vivo* with antibody-drug conjugates, chimeric antigen receptor (CAR)T cells, or bispecific antibodies alone and in combinations. Treatment-mediated changes in tumor cell killing and tumor immune microenvironment were investigated.
Results: 3D high throughput confocal imaging and Nilogen Oncosystem's proprietary algorithm were used to detect and analyze treatment-induced tumor cell killing activity in tumoroids. The impact of *ex vivo* treatment by different modalities in combination with chemotherapeutic agents upon tumor resident immune cell populations was monitored by deep immune phenotyping and multiplex cytokine release assay. Based on the *ex vivo* responses tumors were assigned to treatment sensitive and resistant groups. Correlative analysis was performed and compared with detailed clinicopathologic data that is readily available for Biorepository tumors.
Conclusions: The 3D-EXpress platform using cryopreserved 3D tumoroids with intact tumor microenvironment is an effective tool for the pre-clinical assessment of rational drug combinations for treatment of solid tumors. Furthermore, the 3D-EXpress platform provides unique insight into the microenvironment of both treatment responsive and non-responsive tumors and can aid in the development of patient-centered therapeutic regimens.

#6784 Cancer cell heterospheroids with stromal component used as drug testing and immune cell infiltration models.

B. S. Nielsen, N. H. Madsen, J. Larsen, M. Gad, K. Holmstrom;
Bioneer A/S, Horsholm, Denmark

3D cancer cell cultures have enabled new opportunities for replacing compound testing in experimental animals. However, driven by increased understanding of the need for more complex cancer cell models that consider drug resistance and penetration, hypoxia, and immuno-oncology applications, we have developed multicellular tumor heterospheroids composed of cancer cell lines, fibroblasts and immune cells. We have studied heterospheroids of cancer cell lines, HT29, MCF7, PANC1 and SW480 co-cultured with fibroblasts and 1) explored the architectural organization, 2) performed whole transcriptome analysis (WTA) of mono and co-cultures and 3) tested their capacity of immune cell infiltration. The architectural organization was studied in embedded heterospheroids. HT29 and MCF7 cells developed spheroids with the cancer cells surrounding the fibroblasts, whereas PANC1 cells mingled with the fibroblasts and SW480 cells were surrounded by fibroblasts. The fibroblasts expressed FAP-α mRNA as determined by ISH as well as collagen-1 as determined by immunohistochemistry. The hypoxia marker, Ca-IX, and the apoptosis marker, cleaved-Caspase-3, were dominating in the central core of the spheroids but the Ca-IX and Caspase-3 expression was not coordinated. In addition, WTA performed on day-7 heterospheroids, showed upregulated LOX, indicating that hypoxia-related markers known from genuine cancers are upregulated also in heterospheroids. WTA of day-7 mono-cell cultured and hetero-cultured spheroids, showed abundant ECM-, EMT-, and fibrosis-related expression in heterospheroids, thus reflecting a representative tumor-like microenvironment in heterospheroids compared to mono-culture spheroids. In particular, PANC1 spheroids showed a strong EMT profile with abundant FOXC2, TGF-β and TWIST expression. Genes related to Akt/mTOR and EGF pathways were consistently expressed in the tested heterospheroids. Evaluation of the cytotoxicity of anti-cancer compounds was performed using both cell viability and apoptosis assays. Exposure of the NCI drug library composed of 166 cytotoxic compounds to the heterospheroids, interestingly, revealed a complex output with limited correlation between cytotoxic and apoptotic effects. A subset of drug candidates is currently being further examined. PBMC-derived immune cells infiltrate heterospheroids and their infiltration is strongly enhanced after activation. The T cells' ability to infiltrate heterospheroids of different cancer types may serve as models of cold and hot tumors. We conclude that the cancer cell lines determine the architectural structure of heterospheroids, that ECM development is a prevalent part of the heterospheroids, and that the different heterospheroids possess varying ability of immune cell infiltration.

#6785 KIYA-PREDICT™ XPDX: An *ex vivo* 3D spheroid platform for modeling *in vivo* responses to multiple classes of oncology therapeutics.

A. L. Carlson[1], N. W. Dance[1], K. J. Burgess[1], D. Y. Nadeau[1], M. Millard[1], A. Simonson[2], A. Diaz III[2], M. Wick[2], T. M. DesRochers[1];
[1]Kiyatec, Greenville, SC, [2]XenoSTART, San Antonio, TX

Patient-derived xenografts (PDX) are a powerful and commonly used tool in preclinical drug development as they represent an *in vivo* platform for screening drug response in human tumors that recapitulate many molecular and histological features of the original patient tumor. However, these models are costly and time-intensive, necessitating the development of *ex vivo* platforms for assessing drug response to PDX-derived tumors to de-risk *in vivo* studies by aiding in model selection and reducing the number of animals and costs associated with *in vivo* experimentation. The KIYA-PREDICT™ platform is a clinically validated, *ex vivo* 3D cell culture platform with demonstrated ability to predict patient response to chemotherapy in high grade glioma and ovarian cancer. Here, we apply this platform to profiling XPDX from XenoSTART's comprehensive library of well-characterized models as a tool for assessing drug response and mechanism of action *ex vivo* while also aiding in model selection for *in vivo* studies. Over 100 XPDX models have been profiled *ex vivo* for response to several classes of cancer therapeutics, including chemotherapy, targeted therapy, and antibody-drug conjugates (ADCs), demonstrating robust concordance with *in vivo* drug response. CDK4/6 inhibitors palbociclib and ribociclib evaluated *ex vivo* in breast XPDX display strong correlation to *in vivo* response and recapitulate palbociclib resistance. Similarly, G12C inhibitors sotorasib (AMG-510) and adagrasib (MRTX849) screened against a panel of non-small cell lung cancer XPDX *ex vivo* match *in vivo* response and drug resistance. Finally, *ex vivo* and *in vivo* responses to FDA approved ADC enfortumab vedotin were evaluated in a panel of bladder cancer PDX, with *ex vivo* and *in vivo* responses showing good concordance and expected modulation based on Nectin-4 expression levels. The combination of the KIYA-PREDICT™ platform with XenoSTART's XPDX catalogue is a flexible and powerful tool that can be utilized for streamlining preclinical drug development for a wide range of therapeutic classes.

#6786 Assessment of immune cell infiltration and cancer metastatic potential in Akura™ Immune Flow Chip - A microfluidic 3D spheroid system.

T. Hafeli[1], S. Riss[1], C. Lohasz[2], D. Hasanova[2], S. Lutzow[2], L. Holting[1], M. Rudnik[1], F. Linke[3], W. M van Weerden[3], **L.-A. Ligeon**[1], A. Hierlemann[2], M. Modena[2], O. Frey[1];

[1]InSphero AG, Schlieren, Switzerland, [2]ETH Zurich, Department of Biosystems Science and Engineering, Basel, Switzerland, [3]Experimental Urology, Cancer Institute, Erasmus Medical Center, Rotterdam, Netherlands

Evaluation of novel therapeutics often fails to reliably predict severe complications in patients, especially when circulating cells are involved. The reasons may include inter-species differences upon using animal models or the lack of relevant *in vitro* systems. Moreover, existing *in vitro* systems mostly rely on static investigations of different cell types leading to overestimation of effects due to non-representative cell-tissue interactions. The incorporation of medium flow may facilitate to mimic physiological conditions more closely. To tackle current limitations of perfused organ-on-chip approaches, we developed a microfluidic chip and operation concept, which prevents undesired sedimentation and accumulation of cells in suspensions. The Akura™ Immune Flow platform was designed to study flow-dependent recruitment of circulating cells to different tissue spheroids via gravity-driven perfusion over several days. The Akura™ Immune Flow platform features standardized formats for co-culturing up to seven spheroids with suspended cells in each microfluidic channel. On-chip staining protocols enabled monitoring of the co-culture. The system allowed for application and extractions of cellular components and liquid for further off-chip analysis. Primary tissue and cell line spheroids (liver and tumor) could be retained in the respective chambers and remained viable over six to 14 days. Circulating cells were kept viable and in suspension for up to six days (PBMCs) and14 days (Prostate Cancer (PCa) cells) respectively. PBMCs were not activated by flow-induced shear forces. Unspecific stimulation of T-cells led to physiological expression of early and late activation markers (CD69 and CD25), which were detected by flow cytometry in periodically collected cells. Multi-photon microscopy imaging confirmed that PBMCs interacted with and infiltrated into 3D tumor spheroids. Application of PCa cells to primary liver spheroids, cultured in Akura™ Immune Flow chips allowed for assessment of their invasive potential. Confocal imaging revealed adhesion of cancer cells to the liver spheroids and offers the potential to study the ability of tissue invasion at later time points. The simple design of the chip facilitates user-friendly operation and high-throughput implementation in cancer research and drug testing. The selected applications support the relevance of using flow solutions for physiologically more complex processes. This work constitutes an important step towards device application as a tool for basic research as well as for efficacy studies of immunotherapeutic drug candidates

#6787 Evaluation of CAR-T cytotoxicity in solid tumors: A screening workflow using 3D patient-derived tumoroids.

X. Yang[1], M. Mafreshi[1], G. Wong[1], V. Chandra[1], C. Paul[2], C. Yankaskas[2], B. Balhouse[2], J. Sharp[1], M. Dallas[2], E. Willems[1], D. Kuninger[2];
[1]Thermo Fisher Scientific, Carlsbad, CA, [2]Thermo Fisher Scientific, Frederick, MD

Introduction: Over the last decade, chimeric antigen receptor T cell (CAR-T)-based immunotherapy has achieved unprecedented clinical benefits for the treatment of hematological malignancies. However, application of CAR-T therapy to solid tumors remains challenging, in part due to tumor antigen heterogeneity and microenvironmental complexity present in these tumors. Therefore, selecting physiologically-relevant models is critical for validation of the on-target efficacy and off-target effect of CAR-T therapy. Emerging 3D patient-derived tumoroid models better recapitulate the morphological organization, mutational status, and gene expression levels of patient tumors. Hereby, we propose a screening platform to evaluate mesothelin (MSLN)-targeted CAR-T therapy for solid tumors using patient-derived tumoroids.

Methods: T cells were isolated from peripheral blood mononuclear cells of healthy human donors. Meso3 (region III of MSLN) or CD19 CARs (served as control) were knocked-in (KI) to activated T cells using electroporation-based CRISPR/Cas9 system followed by CAR Cassette containing adeno-associated virus (AAV) transduction. T-cell receptor (TCR) knockout (KO) and CAR-KI efficiency were validated by flow cytometry. Patient-derived tumoroids with high and low MSLN expression were co-cultured with various effector-to-target ratios of Meso3 CAR, CD19 CAR and Control (TCR KO without CAR KI) T cells. Cytotoxicity was evaluated by caspase-based live cell imaging. Key cytokine secretion was measured using a multiplexing platform 2-3 days post co-culture.

Results: T-cell electroporation of CRISPR/Cas9 yielded a high KO efficiency (>90%) of TCR as well as high AAV-mediated CAR cassette-KI efficiency (>70%). The killing efficiency of Meso3 CAR-T cells with different effector to target ratios was successfully captured in a ratio-dependent manner via live cell imaging and analysis platform in the MSLN-high tumoroids, while minimum killing was observed in MSLN-low tumoroids. As expected, control and CD19 CAR-T cells showed no killing towards MSLN-high or -low tumoroids, which do not express CD19. Moreover, the observed killing ability correlated with secretion of cytokines associated with T cell-mediated cytotoxicity.

Conclusion: These findings demonstrated the ability of 3D patient-derived models as a screening platform for validations of CAR-T cell therapy in vitro. This platform has potential advantages over commonly used impedance-based and flow cytometry-based killing assay since it better captures the 3D architecture and microenvironment of the tumor origin and allows real-time quantification. With the ability of accurately detecting on and off-target killing, quick turn-around time, and cost-effectiveness compared to in vivo systems, this platform allows for high-throughput screening workflows for CAR-T cell therapies.

#6788 Comparative analysis of anti-HER2 antibody-drug conjugates in tumor spheroid models.

K. McBain, K. Barnes, N. Bevan;
Sartorius, Royston, United Kingdom

Robust techniques are needed to screen the anti-tumor activity of antibody-drug conjugates (ADCs) *in vitro*. Traditional monolayer models provide a cost-effective and scalable option but lack many features of the tumor microenvironment, such as complex cell-cell and cell-extracellular matrix interactions. Tumor spheroids afford a more translational model for quantification of ADCs. Here, spheroids are used to compare the mechanism of action (MoA) of anti-HER2 ADCs. Single spheroids were formed from mono- or co-cultures of HER2 over-expressing cancer cells and HER2 negative control cells. Incucyte® Nuclight Green Lentivirus was used to label HER2 positive BT474 cells, whilst HER2 negative MDA-MB-231 cells were left unlabeled. Antibodies were added after 72 hours of spheroid formation in 96-well ultra-low attachment plates. Brightfield and fluorescence images were captured every 3 hours using the Incucyte® Live-Cell Analysis System and quantified, for metrics such as spheroid size and fluorescence intensity, to give an indication of ADC cytotoxicity. Co-culture spheroids were dissociated at assay endpoint and the remaining proportion of green and unlabeled cells was measured using the iQue® Advanced Flow Cytometry Platform. The area of the BT474 mono-culture spheroids decreased in a concentration-dependent manner in the presence of both ADCs tested (trastuzumab emtansine and trastuzumab deruxtecan), indicating increased cytotoxicity. In contrast, only the highest concentration of trastuzumab, which is the monoclonal antibody backbone on which they are based, resulted in a reduction in spheroid size. This displays the increased anti-tumor activity due to the addition of the ADC payloads. In the co-culture model, only the trastuzumab deruxtecan induced a reduction in spheroid area, with the size of the spheroids in the presence of trastuzumab emtansine and trastuzumab remaining comparable to control levels. Analysis of the spheroid composition using flow cytometry showed that for the BT474 cells, again, percentage cell death compared to the IgG control was greater for the two ADCs, at 96.4% and 97.2%, respectively. This death was greater than with trastuzumab, which induced 46.4% cell death. Unlike in the mono-culture assays, a high level of death of the HER2 low expressing cells was also seen in the co-culture in the presence of trastuzumab deruxtecan (94.1% death compared to control). This displays the unique bystander activity of trastuzumab deruxtecan, which has led to its approval as a treatment for both HER2 high and HER2 low breast cancers. These data display how the Incucyte® Live-Cell Analysis System combined with iQue® Advanced Flow Cytometry can be leveraged to provide comprehensive assessment of the *in vitro* function of ADCs and how it can enable differences in their MoAs to be distinguished in 3D spheroid models.

#6789 Development of an *in vitro* gastric cancer 3D co-culture platform using a microphysiological system (MPS) to improve outcomes in oncology clinical trials.

Y. Choi[1], S. Kim[1], Y. Song[1], Y. Kim[1], J. Jang[1], S. Kim[1], J. Baek[1], D. Donnelly[1], B. Rajiput[1], B. Lee[1], W. Kwon[2], T.-L. Liu[1], K. Baek[1], S. Yoo[1], S. Rha[2]; [1]Qureator, Inc., San Diego, CA, [2]Yonsei University College of Medicine, Seoul, Korea, Republic of

Introduction: Despite significant advancements in scientific and diagnostic technologies, clinical trials for cancer often fail due to a lack of efficacy. Access to a platform that accurately predicts patient response is crucial to increase the success rate of clinical studies, and to minimize unnecessary exposure to ineffective and potentially harmful drug testing for patients. Because of the complexity of the disease, it would be beneficial to deploy patient samples for drug testing in a side-by-side comparison during the clinical trial. An accurate prediction of patient response earlier in the clinical study would aid decision making to determine the appropriate duration of treatment for each patient.

Methods: We developed a 3D human cell co-culture model using our proprietary MPS technology, the Curio-spheroid Curiochip. Using patient samples isolated and expanded from either ascites fluids or biopsies to recapitulate the clinical phenotypes of advanced gastric cancer, we quantified the migratory properties of the patient cancer cells (i.e., the unique metastatic potential), and measured the level of secretion of VEGF. Somatic mutational analyses using NGS and RNAseq were performed for subtyping and clustering the samples. The patient cancer cells were expanded within 2 weeks post-collection, and used to form a spheroid that was loaded into a hydrogel embedded within the Curio-Spheroid, enabling the patient spheroids to interact through the hydrogel with neighboring (healthy) human endothelial cells. The patient spheroids induced aggressive vasculogenesis in the co-culture model, which was subdued by the anti-VEGFR2 antibody Ramucirumab. The platform was retrospectively validated with the Standard-of-Care (SOC) treatments that the patients received.

Results: The patient cell testing took 3-4 weeks from sample collection to imaging. The patient cells preserved their migratory capacity, pro-angiogenic potential and drug responses in the vascularized model. The dose responses to SOC in the platform were consistent with the actual patient response assessments based on RECIST criteria, supporting the potential to use this platform to accurately predict patient clinical responses.

Conclusions: The Curio-spheroid 3D co-culture model of vascularized gastric cancer provides a dynamic microenvironment to preserve the phenotypes of the patient cells and cell-cell interactions that are known to influence drug responses. This platform is compatible with high-throughput screening (HTS) for target or drug discovery with a good assay window. The ability to accurately recapitulate patient responses to SOC in the clinic make the Curio-Spheroid platform a promising method to test patient samples and measure drug responses of patients in real time during ongoing clinical trials.

#6790 Breaking barriers: A high-throughput 3D drug discovery platform for ovarian cancer.

E. George[1], D. I. Pedro[1], A. Pepe[1], A. M. Rivera[1], R. A. Smolchek[2], J. E. Famiglietti[2], W. Sawyer[1];
[1]Moffitt Cancer Center, Tampa, FL, [2]Aurita Bioscience, Gainesville, FL

Background: Ovarian Cancer (OVCA) is a formidable challenge in oncology and remains the most lethal gynecologic malignancy with many cases (~80%) diagnosed at a late stage with an equally high rate of recurrence. Yet, no established OVCA models exist that faithfully recapitulate the biological complexity of metastatic OVCA. This multidisciplinary team developed a new in vitro high-throughput model that maintains the characteristics of the patient's tumor including resident immune cells. Key breakthroughs include long term (>21 day) culture of patient-derived microtumors, a functional and perfusable microgel medium (Liquid Like Solids - LLS™), microplates with controlled "pumpless" perfusion of culture media (Darcy Plates™), and integrated in situ imaging.
Methods: We designed, fabricated, and validated a new 3D culture device in the standard SBS microplate format (Darcy Plate) that integrates in situ microscopy and perfusion through a bio-conjugated microgel bed (LLS). Patient tumors were collected during debulking surgery, micronized into 1 µl microtumors, suspended in LLS, and plated into the 48-well Darcy Plate. Viability and proliferation were assessed over 21 days in situ using a standard LIVE/DEAD™ kit and EDU staining, respectively. Epithelial OVCA cells and immune cells were identified with immunofluorescence microscopy.
Results: Optimal media conditions (HPLM media with 10% FBS, 1% Pen/Strep, 2.5 mg L^{-1} Amphotericin B, 10 mM HEPES, 0.5 µM A83-01 -TGF-β inhibitor-, and ITS) and perfusion flow rates (100 µl/day per well) were identified that resulted in outstanding cell viability after 21 days (~100% - no detectable cell death using LIVE/DEAD™). PAX8 nuclear expression, a marker for epithelial metastatic OVCA, was retained. EDU staining confirmed cell proliferation and CD45 staining revealed retention of viable immune cells on and within the microtumor at 21 days. Drug testing to evaluate tumor response to chemotherapeutic agents, carboplatin, and emerging targeted therapies was performed by dosing the feed-wells at different concentrations and evaluating cell death through LIVE/DEAD imaging after 5 days of treatment.
Conclusions: OVCA is a challenging disease with understudied biological complexity and extensive metastatic involvement. This study demonstrates that drug screening with 3D microtumors has important clinical implications and provides a unique opportunity to evaluate drug responses and personalized treatment strategies. These patient-derived microtumors retain crosstalk between diverse cell populations and the tumor microenvironment, which increases the likelihood of identifying effective therapies and drug candidates. This system retains patient-specific tumor heterogeneity and microenvironmental complexity of OVCA, offering a promising platform for drug screening, high-throughput assays, biomarker discovery, and ultimately improving treatment outcomes.

#6791 Investigation of sex hormone effects in an organ chip model of endothelial barrier dysfunction in the triple negative breast cancer microenvironment.

D. Carlino, A. Martier, Y. Maurice, G. Kpeli, M. Burow, M. Mondrinos;
Tulane University, New Orleans, LA

Inflammation and pathological vasculature are common features of the tumor microenvironment (TME). Sex hormones potently modulate vascular physiology and immune cell functions, and there are established correlations with the outcomes of triple negative (TNBC) despite the defining feature of receptor negativity. Circulating estrogens and androgens have been hypothesized as drivers of TNBC through the actions exerted by receptor-positive cells in the TME. Here, we present an organ chip model of the TNBC microenvironment for quantifying the impact of configurable TME variables such as the ECM composition and the relative densities and phenotypes of tumor cells, cancer associated fibroblasts, and myeloid cells on endothelial barrier function. After establishing baselines of vascular permeability in the presence and absence of TNBC cells, we tested the effect of estradiol, estrone, and dihydrotestosterone on barrier permeability. Multilayer polydimethylsiloxane (PDMS) organ chips were fabricated using standard soft lithography. The layers of the device were separated with semi-permeable membranes that allow exchange of soluble factors. Once assembled, the upper channel was loaded with female (XX) human umbilical vein endothelial cells. Collagen hydrogels were injected into the tissue layer and the devices were cultured on a rocker to induce endothelial barrier alignment via application of an average shear stress of 5 dynes/cm^2. We optimized rocking conditions by assessing endothelial layer alignment, junctional organization, and permeability. TNBC cells and XX mammary carcinoma fibroblasts were added to the hydrogel to model the effects of TME-derived signals on endothelial barrier permeability. 40 kDa FITC- Dextran was chosen to assay permeability as it can show leakage due to active disruption of the barrier. Staining for F-actin and ZO-1 allowed for quantification of junctional organization. Sex hormone modulation of proinflammatory gene expression was assessed by RT-qPCR. The presence of TNBC cells significantly increased transport of 40kDa FITC-Dextran across the endothelial barrier, disrupted intercellular junction quality, and induced the expression of inflammatory adhesion molecules including ICAM-1. Our results demonstrate that sex hormones modulate TNBC-associated changes in endothelial cell bioenergetics, junctional organization, and macromolecular barrier permeability. Ongoing work will investigate the effects of age-matched XX monocyte derived macrophages on barrier function in the model. This organ chip platform provides an assay for measuring altered vascular inflammation and permeability in the TNBC microenvironment and may provide a venue for investigating vascular-normalizing effects of various candidate therapeutics.

#6792 Investigating differential expression of Palladin isoform 3 in 2D and 3D pancreatic cancer cell cultures.

S. Biswas, J. A. Bush;
California State University, Fresno, Fresno, CA

Palladin (*PALLD*) is an actin-binding protein widely expressed in mammalian tissues that modulates cytoskeletal dynamics. Palladin is linked to the progression of breast, pancreatic, and renal cancers. There are at least 9 known isoforms of PALLD but isoforms 3 (iso3) and 4 (iso4) appear most significant in cancer cells and associated fibroblasts. Our goal is to understand iso3 in pancreatic cancer (PC) cell lines grown in various culture environments to shed light on the intricate interplay between culture conditions and gene regulation. Cell models were developed as 3D spheroids from hanging drops after optimizing culture conditions by utilizing a combination of inexpensive methylcellulose (MC) and rat tail collagen viscosity ranges across cell seeding densities. The quality of the developed spheroids was assessed using multiple parameters, like diameter, integrity, and circularity to determine ideal spheroid characteristics. Spheroids that formed at a lower MC viscosity range (350-550 mPa·s) led to peripheral loose cells and a higher viscosity range (7,000-10,000 mPa·s) resulted in elongated shapes. Moderate viscosity ranges (1,000-1,800 mPa·s and 3,500-5,600 mPa·s) consistently produced circular and compact spheroids. Optimal incubation times varied from 72 to 96 hr depending on the cell line. Invasion dynamics within collagen-MC gels revealed that PANC-1 had significantly higher invasion potential compared to BxPC-3 and a control cell line C2C12. RT-qPCR results show that *PALLD* iso3 was particularly overexpressed in the 3D culture environment of PANC-1, suggesting that elevated *PALLD* isoform 3 expression may be a characteristic of 3D culture, particularly in invasive PC types. Taken together, the study validates the importance of extracellular viscosity for influencing spheroid characteristics toward generating reproducible 3D spheroids. The investigation also highlights *PALLD* iso3 as a potentially valuable biomarker for aggressive forms of pancreatic cancer.

TUMOR BIOLOGY: Chemokines and Cytokines in Cancer
Poster Session

#6797 CCR5/CCL4 axis in lung cancer clinicopathological significance and its therapeutic application.
S. K. Singh, R. Singh;
Morehouse School of Medicine, Atlanta, GA

Lung cancer (LC) is the most prevalent type of cancer globally and the leading cause of cancer-related deaths. Based on the histology and type of treatments, LC is divided into small-cells and non-small cell lung cancer (NSCLC) carcinomas, which are more aggressive and less responsive to chemotherapy. Since LC is known to be a highly heterogeneous cell population, treatment is challenging. It has been observed that chemokine receptor-ligand interaction is essential for cancer cells homing to distant sites. Most malignancies, including LC, have established disease status indicators concerning elevated levels of CCL4, a structurally unique chemokine, and its receptor (CCR5). Therefore, treatment strategies that inhibit the LC cell's tumor environment may improve patients' quality of life. However, the CCR5/CCL4 interface in LC invasion and metastasis is poorly understood. In this study, we examined the expression and function of the CCR5/CCL4 axis in the development and invasiveness of LC patient's clinical tissues and cell lines. We conducted immunohistochemistry (IHC) dual staining of CCR5/CCL4 antibodies in LC tissues. Our findings demonstrated significantly ($p < 0.001$) higher expression of CCR5 and CCL4 in advanced-stage malignant tissues than in normal tissues. The in-vitro analysis of the human LC cell lines NCI-H1437, NCI-H1573, and NCI-H1975 revealed CCL4 activation expressing higher CCR5, determined by immunofluorescence, western blots, flow cytometry, 3D-invasion assay, and RT-qPCR methods. Further, a calcium mobilization assay confirmed the direct interaction between CCR5 and CCL4. However, treating with Maraviroc, a small molecule inhibitor of CCR5, to LC cells blocks their ability to proliferate, demonstrating the crucial role that CCR5-CCL4 chemotaxis plays in LC metastasis. Our findings show both the biological and clinical significance of CCR5 and CCL4 expression, which may serve as potential indicators for metastatic LC. Therefore, inhibiting the CCR5/CCL4 interaction may offer a more effective therapeutic approach for managing the progression of LC.

#6799 The impact of targeting TRAF2 and NCK-interacting protein kinase on anti-tumor effect and tumor immune environment in cMYC-high small cell lung cancer.

A. Tanimoto, K. Ramkumar, A. Stewart, B. Zhang, R. Cardnell, S. Li, Q. Wang, J. Wang, C. Gay, L. A. Byers;
The University of Texas MD Anderson Cancer Center, Houston, TX

Background: Small cell lung cancer (SCLC) is a highly lethal malignancy with rapidly acquired chemotherapy resistance. While the inflamed SCLC subtype is associated with a significantly improved response to immunotherapy, the non-inflamed SCLC subtypes, encompassing most SCLC patients, experience only modest survival gains with chemo-immunotherapy. Wnt signaling pathway activation is associated with resistance to chemotherapy and an immune checkpoint inhibitor in several tumors. TRAF2 and NCK-interacting protein kinase (TNIK), which interacts with downstream effectors, TCF4/β-catenin transcriptional complex, is an essential activator of Wnt target genes. TNIK is highly expressed in several cancers, but the efficacy of TNIK inhibition in SCLC has not previously been researched. We previously demonstrated that single agent TNIK inhibitors are effective in a subset of SCLC. Here, we hypothesize that targeting TNIK will show an anti-tumor effect based on specific biomarkers and also modify the tumor immune environment in SCLC.

Methods: We evaluated susceptibility to a small molecule TNIK inhibitor, NCB-0846, in 29 human-derived SCLC cell lines using 96-hour proliferation assays. To investigate efficacy biomarkers, we correlated NCB-0846 IC50 values with proteomic expression (profiled using reverse phase protein array). cMYC and FOXK1 expression was reduced by siRNA. Chemokine concentrations were determined by ELISA.

Results: SCLC cell lines with high cMYC levels, were more sensitive to the TNIK inhibitor, NCB-0846 (F.C.=-2.07, p=0.01), while SCLC cell lines with high expression of TTF-1 were more resistant (F.C.=2.48, p<0.01). Knockdown of cMYC conferred resistance to NCB-0846 in cMYC-high cells, while NCB-0846 treatment resulted in decreased cMYC expression in a concentration-dependent manner. Additionally, NCB-0846 treatment decreased the immunosuppressive chemokine CCL2 levels in the supernatant of human-derived SCLC cell lines and GEMM-derived cell lines. The expression of FOXK1, a transcription factor of CCL2, was also reduced in cell lines treated with NCB-0846.

Conclusions: These findings show that TNIK inhibition is more effective in cMYC-high SCLC, acting through downregulating cMYC levels. TNIK inhibition also decreases the production of CCL2, an immunosuppressive chemokine implicated in resistance to anti-PD-L1 immunotherapy. Together, these findings highlight the promising potential of TNIK inhibitors in cMYC-high SCLC. Additionally, suppressing CCL2 by TNIK inhibition supports the rationale for combining the TNIK inhibitor and an anti-PD-L1 antibody in the non-inflamed SCLC subtypes.

#6800 The tumor progression mechanism of increasing CXCL16-CXCR6 pathway within the tumor microenvironment in TNBC.

Y. Lee, C. Lee, S. Ha, S. Lee, J. Yang, Y. Kim, S. Kim, S. Kim;
Cellus, Seoul, Korea, Republic of

Background: Triple negative breast cancer (TNBC) is characterized rapid progression, higher relapse, and poor prognosis, so the establishment of an effective therapeutic target is required. CXCL16, a chemokine abundantly present in the TNBC tumor microenvironment (TME), is secreted by tumor-associated macrophages (TAM) and is known to promote tumor growth and metastasis. However, the exact mechanism through which CXCL16 facilitates tumor growth and metastasis remains unclear. This study aims to study the role of CXCL16 in the tumor progression and confirm the anti-tumor effects of CXCL16 neutralization in TNBC model.

Method: MDA-MB-231 human TNBC cell lines were utilized for in vitro validation, and a syngeneic model involving 4T1 mouse TNBC cell lines and Balb/c mice was used for in vivo studies.

Results: Stimulation of TNBC cells with recombinant human CXCL16 protein (rhCXCL16) activates the tumor growth signaling pathways, including pAKT and STAT3, as well as EMT markers. These results shows that CXCL16 can promote tumor growth and metastasis. Treatment with CXCL16 neutralizing antibodies inhibited the promotion of cancer growth and metastasis by rhCXCL16. Additionally, combination treatment of CXCL16 antibodies with PD-1 antibodies in the 4T1 syngeneic model increased the proportion of $CD8^{+}$ T cells and $CD80^{+}$ M1 like macrophages. These results shows that neutralization of CXCL16 can regulate polarization of macrophage and proportion of T cells. These regulation and changes of immune cells allow neutralization of CXCL16 control the TME to resist tumor cells, suggesting that optimal condition can be constructed to maximize the effectiveness of anti-cancer drugs.

Conclusion: This study confirms that the CXCL16-CXCR6 pathway within the TME triggers tumor growth and metastasis, while neutralization of CXCL16 can inhibit tumor progression. This effect is attributed to the increase in $CD8^{+}$ T cell and M1 macrophage proportions within the TME. In conclusion, these research findings propose the potential of CXCL16 as a novel biomarker and therapeutic target for TNBC.

#6801 Cellular senescence involves spatial evolution in colorectal cancer.

T. Park, S. Kang, J. Kim, H. Lee, Y. Choi, S. Park, Y.-K. Lee;
Ajou University School of Medicine, Suwon, Korea, Republic of

Cancer evolution is a continuous process involving cellular changes that promote progression and metastasis. Recent studies demonstrate that cancer evolution is spatially associated: a phenomenon called “the spatial evolution of cancer.” In our data, colorectal cancer cells gradually evolve from an adenoid to a collective invasion morphology, ultimately developing a partial epithelial-mesenchymal transition phenotype as they form an invasive front. Trajectory analysis showed that cancer cells at the invasive front of a tumor exhibit a totally different gene expression pattern from those at the center, and that cellular senescence plays a crucial role in this transition. Epigenetic changes in the promoter/exon1 region of the *CDKN2A* gene caused by increased reactive oxygen species level are crucial for expression of $p16^{INK4A}$ and induction of senescence in the cancer cells. Two types of senescent tumor cells (type I and type II) were observed, and they played different roles in cancer progression due to different gene expression. Type II senescent tumor cells ($p16^{INK4A+}$/$LAMC2^{\pm}$/$MMP7^{\pm}$), a final evolved form of cancer cells, are strongly associated with local invasion and lymph node metastasis of colorectal cancer and worsen the prognosis for patients.

#6802 CXCR4 transgene improves in vivo migration and efficacy of engineered iPSC-derived natural killer cells.

H. J. Millar, D. Walker, L. R. Campion, C. Budd, A. Kolluri, H. Sharma, B. Gurung, J. M. Carton, D. J. Perry, N. Alexander, H. Levitsky, M. Naso, B. A. Morse; Century Therapeutics LLC, Philadelphia, PA

Chimeric antigen receptor (CAR)-engineered induced pluripotent stem cell (iPSC)-derived natural killer (iNK) cells have shown a favorable safety profile and early evidence of clinical efficacy in the treatment of patients with certain hematologic malignancies. CAR-iNK cells retain phenotypic and functional similarities to primary natural killer cells, with additional capabilities for recognition of tumors. For the treatment of cancers that are located in the bone marrow, it is critical that iNK cells are able to migrate efficiently to relevant sites of disease. CXCR4 (C-X-C chemokine receptor type 4) is a chemokine receptor specific for stromal-derived-factor-1 (SDF-1), and mediates the migration of hematopoietic cells to the bone marrow upon binding SDF-1. Here we describe novel engineering of iPSCs resulting in efficient migration and efficacy of iNK cells. iPSC were sequentially engineered at defined loci with Crispr/MAD7/HDR to incorporate Allo-Evasion^{TM} edits, a CAR targeting antigens expressed on different hematological malignancies, constitutive interleukin-15 (IL-15) cytokine support, with and without wild-type CXCR4. iPSCs were then differentiated into natural killer cells using a proprietary differentiation process. Cytolysis of a panel of target cells by iNK was evaluated using an Incucyte-based killing assay. Anti-tumor efficacy was tested in disseminated xenograft models of hematological malignancies following intravenous injection of engineered iNK cells. Additionally, in vivo migration was evaluated using immunohistochemistry (IHC) and flow cytometry (FACS) of blood, bone marrow, and other organs. Engineering with CXCR4 resulted in a bulk population of iNK with a heterogenous expression of CXCR4. No significant impact of CXCR4 engineering was detected on iPSC differentiation, phenotype, or iNK yield. iNK^{CXCR4+} and iNK^{CXCR4-} cells had equivalent target tumor cell cytolysis in vitro, indicating the CXCR4 transgene does not affect killing potential. In vivo, iNK^{CXCR4+} cells migrated to the bone marrow of both tumor-bearing and non-tumor-bearing animals, and the presence of these cells was enhanced in tumor-bearing mice, indicating CXCR4-mediated migration and possibly CAR-mediated expansion and/or retention of iNK. Migration to the bone marrow was not observed with iNK^{CXCR4-} cells. As a result, iNK^{CXCR4+} cells significantly impacted anti-tumor efficacy, effectively eliminating bone disease. We have demonstrated the CAR-specific killing and enhanced iNK migration and subsequent tumor killing in the bone marrow, with the addition of a CXCR4 transgene in iPSC-derived NK cells. The addition of the CXCR4 transgene in iPSC-derived effector cells may allow for a higher therapeutic response in axial-skeletal located tumors.

#6803 TRIM16 regulates IL-6 secretion in head and neck cancer-associated fibroblasts.

T. Ly[1], B. Pickard[1], A. Pandey[1], N. Martinez-Rivera[2], E. Rosa-Molinar[2], M. Washburn[1], W.-X. Ding[1], S. M. Thomas[1];
[1]University of Kansas Medical Center, Kansas City, KS, [2]University of Kansas, Lawrence, KS

Despite current therapy, head and neck squamous cell carcinoma (HNSCC), the 7th most common cancer worldwide, is associated with high morbidity and mortality. Response to current therapies could be improved with a better understanding of the tumor microenvironment of HNSCC. We previously reported that cancer-associated fibroblasts (CAFs), the most abundant stromal cell type in the HNSCC microenvironment, have elevated levels of basal autophagy than oral fibroblasts from cancer-free subjects (NF). Disrupting autophagy in CAFs with Beclin-1 siRNA reduced secretion of IL-6, IL-8, and other factors known to promote HNSCC progression. The recent emerging role of autophagy in secretion of tumor promoting factors has high impact because (i) the mechanism can provide a new target to block the secretion of protumor factors from CAFs that contribute to HNSCC progression, and (ii) these cytokines can serve as potential indicators for the efficacy of autophagy-targeted therapies. To this end, we carried out an unbiased assessment of the proteins associated with autophagosomes in primary CAFs from HNSCC samples using mass spectrometry. We performed immunoprecipitation of LC3B from the isolated small vesicles of the CAFs, identified and validated the association of several trafficking proteins in secretory autophagy including VAMP3 and SNAP23. Further, the tripartite motif (TRIM) proteins have been shown to mediate the fate of autophagosomes either for degradation or secretion. We hypothesized that TRIM proteins are involved in transport of secretory autophagosomes. Our data demonstrate CAFs express higher levels of TRIM16 mRNA than NF. We demonstrate immunogold labeling of TRIM16 or IL-6 localized to the autophagosomes using transmission electron microscopy. Further, using immunofluorescence, we demonstrated the colocalization of TRIM16 and IL-6, as well as IL-6 and LC3B in cytoplasmic puncta. In addition, we used proximity ligation assays to confirm the interaction of TRIM16 and IL-6, as well as IL-6 and LC3B. TRIM16 knockdown using siRNA in CAFs reduced the secretion of IL-6 as measured by ELISA. In conclusion, we demonstrate an important role of TRIM16 in secretory autophagy making it a potential therapeutic target to mitigate CAF-mediated HNSCC growth.

#6804 High IL12family levels are associated with pathologic complete response amongst HER2- patients in the neoadjuvant I-SPY2 TRIAL.

Kingsley V. Chow[1], Silver Al Khafaji[1], Denise Wolf[1], Christina Yau[1], Kailey Dubinsky[1], Elene Tsopurashvili[1], Kirthiga Ramalingam[1], Fluorentine van Nouhuijs[1], Zheyun Xun[1], Anna van Montfort[1], Diane Heditsian[2], Douglas Yee[3], Laura Esserman[1], Michael Campbell[1], Laura van't Veer[1], Rosalyn W. Sayaman[1]

[1]UCSF - University of California San Francisco, San Francisco, CA,[2]Breast Science Advocacy Core, UCSF - University of California San Francisco, San Francisco, CA,[3]University of Minnesota, Minneapolis, Minneapolis, MN

Background: Immune contexture of the tumor microenvironment (TME) is associated with response to therapy. We hypothesize that expression of interleukin (IL) family of cytokines which plays essential roles in the activation and differentiation of immune cells, shapes the landscape of therapeutic response in breast cancers. We leverage published gene expression, molecular and clinical data from the I-SPY2 Trial (PMID35623341) - a neoadjuvant trial for locally advanced breast cancers. We explored the contribution of expression-based signatures of IL signaling at pre-treatment in relation to pathological complete response (pCR).

Methods: We curated 32 IL gene sets from literature. Signatures scores characterizing IL signaling were calculated from gene expression profiles of pre-treatment tumor samples from 987 I-SPY2 patients in the first 10 treatment arms of the trial. Association of IL signatures with pCR in HR/HER2 receptor subtypes, and the five I-SPY response-predictive subtypes (RPS) were evaluated using non-parametric tests. Significance levels were defined at adj. $p < 0.05$. Correlations of IL signatures with multiplex immunofluorescence staining of immune infiltrates in the PD1-inhibitor (PD1i) arm were also assessed.

Results: High expression of IL signatures in HER2- patients, regardless of HR status, was associated with pCR especially in the Trebananib, Veliparib/Carboplatin (VC) and PD1i arms. In the PD1i arm, expression of almost all IL signatures was highly correlated with density of T, CD8+ cytotoxic T, CD8- T, and B cells and their colocalization with tumor cells; IL-6 signatures correlated with density of proliferating tumor cells.Within RPS subtypes, enrichment of IL signatures in HER2-/Immune+ such as pro-inflammatory IL-1 and IL-12 signaling was associated with pCR in the VC, PD1i, Ganetespib, and control arms. Furthermore, we identified an IL-12 signature in the HER2-/Immune-/DRD- subtype associated with pCR, with responders characterized by high IL-12 family signaling (Fisher adj. $p < 0.05$). IL-12 family signaling was positively associated with CD8+ cytotoxic T, Th1 and B cell enrichment, IFN-γ signaling, and inflammatory response overall and in HER2- breast cancers.

Conclusion: High pre-treatment expression of IL signatures was associated with HER2- receptor and RPS HER2-/Immune+ subtype-specific response to I-SPY2 agents, and the colocalization of immune and tumor cells in the tumor bed. In HER2- breast cancers, high levels of IL-12 family signaling were associated with response to therapy and enrichment of known IL-12-related pathways that stimulate effective anti-cancer response including CD8+ T cell expansion, Th1 cell differentiation, B cell activation, IFN-γ secretion, and inflammatory response. These findings suggest that IL signaling may serve as a valuable predictive biomarker in this patient population.

#6805 CD81 and CD82 in tumor infiltrating lymphocytes within the NSCLC tumor microenvironment play a crucial role in T cell activation and cytokine production.

K. Na[1], S. Lee[1], D. Kim[1], Y. Kim[1], J. Hwang[1], S.-s. Kang[2], S. Baek[1], C. Lee[1], S. Yang[1], Y. Han[1], M. Kim[1], H. Han[1], Y. Kim[1], J. Kim[1], S. Jeon[1], Y. Byeon[1], J. Lee[1], S. Lim[1], M. Hong[1], K.-H. Pyo[1], B. Cho[1];

[1]Yonsei University College of Medicine, Seoul, Korea, Republic of, [2]JEUK Co., Ltd., Seoul, Korea, Republic of

Background: The role of tetraspanins, particularly CD81 and CD82, in T cell activation, shedding light on their contribution to anti-tumor effects in the tumor microenvironment. The findings provide insights for potential applications of these tetraspanins in immunotherapy.

Method: The study employed 10x Genomics for single-cell RNA sequencing and processed the data using Seurat. It focused on the tumor microenvironment, categorizing cell types, especially TIL subsets. T cells were sorted based on CD81 and CD82 expression and activated, and their activation markers and cytokine production were analyzed. Bulk RNA sequencing was performed on both sorted T cells and tumor samples, and the TCR repertoire was examined. Cytotoxicity of CD81 and CD82 transduced cells was measured using the xCELLigence RTCA HT system.

Result: Tetraspanins have been linked to T cell co-stimulation and activation, with CD81 and CD82 playing a significant role in TCR signaling and activation. Single-cell and bulk RNA sequencing data from lung cancer patients reveal high expression of CD81 and CD82 in the tumor microenvironment, especially in T cells, correlating with T cell activation and cytokine production. In vitro experiments confirm the activation and effector cytokines, especially IFN-γ, TNF-α, and IL-2, producing potential of T cells expressing CD81 and CD82, suggesting their importance in anti-cancer immunity. Overexpression of CD81 and CD82 enhances T cell cytotoxicity against cancer cells, further supporting their role in T cell function. Despite some limitations, these findings shed light on the significant impact of tetraspanins in modulating immune responses, particularly in the context of cancer immunotherapy.

Conclusion: We report that CD81 and CD82 serve as specific markers for activated T cells within the TME. CD81 and CD82 are correlated with the activation and regulation of T cells, and they may also mediate the regulation of relevant cytokines. Overall, our findings provide better insights into the molecular mechanisms regulating TILs present in the TME of non-small cell carcinoma and propose CD81 and CD82 as associated markers. These discoveries could serve as a foundation for the development of new immunotherapies targeting the TME.

#6806 Single cell RNA sequencing of human and murine cancers demonstrates metastases-specific neutrophil phenotypes driven by the IL-1β/CXCR2 signaling axis - Disruption of this pathway abrogates neutrophil immunosuppressive effects and reduces tumor burden.

A. S. McLaren, R. Fetit, M. White, M. L. Mills, T. Lannagan, J. Falconer, X. Cortes-Lavaud, K. Gilroy, R. Ridgway, C. Nixon, V. Naiker, R. Njunge, C. J. Clarke, D. Whyte, K. Kirschner, R. Jackstadt, J. C. Norman, L. M. Carlin, A. D. Campbell, O. J. Sansom, C. W. Steele;
CRUK Scotland Institute, Glasgow, United Kingdom

Introduction: Neutrophils are a highly heterogenous, plastic cell population, known to play a vital role in the tumor microenvironment and progression of CMS4 colorectal cancer (CRC) metastases. We have performed a comprehensive examination of different neutrophil transcriptional states, through utilization of single-cell RNA sequencing of publicly available and independently generated data across health and malignancy in human and murine disease, and validated findings using in vivo and in vitro models of CMS4 subtype CRC.

Methods: Publicly available and independently generated breast, lung and CRC datasets from human disease mouse models were integrated to establish and validate reproducibility of neutrophil-gene signatures, and pseudo-time analysis was used to identify genes driving neutrophil development along a lineage from health to tumor using Seurat on R. Findings were validated in healthy and *Kras*$^{G12D/+}$, *Trp53*$^{fl/fl}$, *Rosa*$^{26N1CD/+}$ (KPN) tumor-bearing wild type or Mrp8CreCxcr2$^{fl/fl}$ genetically engineered mouse models with neutrophil-specific loss of Cxcr2.

Results: We have identified distinct neutrophil subtypes in health and primary tumors, preserved in murine and human cancer and across multiple tumor types. In CRC metastases, discrete neutrophil transcriptomic subtypes are identified, with phenotypes from health to those identified in metastases driven by the IL-1β/CXCL8/CXCR2 signalling axis. Assessment of global signalling of single-cell transcripts has identified CD4+ T cells and macrophages as dominant regulators of the metastatic niche. Neutrophils sorted from the metastatic niche strongly suppress T cell proliferation, identifying them as immunosuppressive. Loss of neutrophil-specific Cxcr2 attenuates suppression of T cell proliferation in co-culture with neutrophils from the metastatic niche of tumor-bearing mice. T cell proliferation is unaffected in co-culture with healthy wild type or Cxcr2$^{fl/fl}$ neutrophils. We currently are running orthotopic intrasplenic models to assess the importance of loss of neutrophil-specific Cxcr2 in generation of metastases *in vivo* in CMS4 CRC.

Conclusions: We speculate that ablation of metastasis specific neutrophil subsets in CMS4 CRC in combination with other therapies, may alter the immunosuppressive nature of the immune microenvironment and allow for reduction in tumor burden in metastatic disease.

#6807 Cancer suppressive mechanism of IL-6 secreted by cancer-related fibroblasts in biliary tract cancer.

K. Kimura, R. Tanaka, S. Eguchi, K. Hatta, M. Kinoshita, J. Tauchi, H. Shinkawa, K. Nishio, G. Ohira, T. Ishizawa;
Osaka Metropolitan University, Osaka, Japan

Background and aims: Cancer-associated fibroblasts (CAFs) are a major component of the tumor microenvironment and can exhibit cancer-promoting functions; however, recent studies indicate that CAFs can also inhibit cancer growth and progression. In this study, we identified CAFs that act in an inhibitory manner in biliary tract cancer and elucidated their mechanisms.
Methods: Three biliary tract cancer cell lines and CAFs isolated from resected specimens from four types of biliary tract cancer were used to evaluate the proliferative potential of cancer cells. Potential suppressors that inhibited the growth of cancer cells were identified using protein arrays from CAFs. We determined the effects of these suppressors on cancer cells.
Results: Among the biliary tract cancer CAFs, we identified CAFs that inhibited cancer growth. Protein arrays of conditioned medium from CAFs revealed that Interleukin-6 (IL-6) was one such growth inhibitor. Treatment of biliary tract cancer cell lines with IL-6 significantly reduced their proliferative potential. SOCS3 expression levels increased and STAT3 expression level decreased, suggesting that SOCS3, a downstream signal of IL-6, may be involved.
Conclusion: Inhibitory CAFs are present among biliary tract cancer CAFs and IL-6 production by CAFs may inhibit the growth of biliary tract cancer cells.

#6808 Investigating the role of CXCR3+ monocytes on CAR T cell function.

C. Ong[1], S. Kaczanowska[2], W. Ju[2], J. Cronk[2], S. Ramakrishna[3], R. Kaplan[2];
[1]Kirk Kerkorian School of Medicine at UNLV, Las Vegas, NV, [2]National Cancer Institute, Bethesda, MD, [3]Stanford Cancer Institute, Palo Alto, CA

Chimeric antigen receptor T cells (CAR-Ts) are an emerging immunotherapy that have remarkable efficacy against leukemias and lymphomas but limited success against solid tumors. We conducted a phase I clinical trial (NCT 02107963) of GD2 CAR-T (GD2-CAR.OX40.28.z.ICD9) administration to children and young adults with neuroblastoma and, for the first time, osteosarcoma. While all patients progressed and were switched to alternative therapy, we observed a significant association between good CAR-T expanders and expression of C-X-C Motif Chemokine receptor 3 (CXCR3) on monocytes detected in pretreatment apheresis. This study seeks to uncover the possible interactions between CXCR3 and CAR-Ts that may alter CAR-T function and ultimately lead to better CAR-T expansion. We hypothesize that CXCR3+ monocytes induce functional change in CAR-Ts resulting in improved expansion.

To recapitulate the interaction between tumor, CAR-Ts and monocytes, we took 143Bs (osteosarcoma cell line) and GD2 CAR-Ts and co cultured them with THP-1s (a monocytic leukemia cell line) that were either untransduced (UTD) or transduced via lentivirus to express CXCR3 (CXCR3+). The ratio of UTD or CXCR3+ THP-1s to CAR-Ts and 143Bs was varied between co cultures. Enzyme-linked immunoassay (ELISA) for interferon gamma (IFNγ) expression was run as a proxy measurement for CAR-T cell activity. Flow cytometry was used to assess for expression of activation and exhaustion markers. Differences between UTD and CXCR3+ co cultures were evaluated for statistical significance via unpaired t-test.

We observed that CXCR3 was elevated on GD2 CAR-Ts co cultured with CXCR3+ monocytes. This pattern was seen most prominently in CD4+ CAR-Ts, but also subtly in CD8+ T-cells. Exhaustion markers CD39 and LAG3 were elevated in CAR-Ts co cultured with CXCR3+ monocytes. Additionally, CAR-Ts co cultured with CXCR3+ monocytes displayed greater activity via elevated IFNγ expression.

We conclude that GD-2 CAR-T cells co cultured with CXCR3+ monocytes express elevated exhaustion markers due to possible increased activity when in the presence of CXCR3+ monocytes. Additionally, we suspect that elevated CXCR3 expression on CAR-Ts co cultured with CXCR3+ monocytes may be helping CAR-Ts better target tumor cells, thus leading to improved expansion. If CXCR3 can improve CAR-T cell function, this could lead to better optimization of CAR-Ts against solid tumors and create a viable treatment option for neuroblastoma and osteosarcoma patients.

#6809 Tumor-associated macrophages promote bladder cancer cell migration and invasion through activation of CCL20-CCR6 axis.

R. Nakagawa, I. Kouji, R. Toriumi, S. Aoyama, T. Kamjima, H. Kano, T. Makino, R. Naito, H. Yaegashi, T. Nohara, H. Nakata, A. Mizokami; Kanazawa University, Kanazawa, Japan

We focused on Tumor-Associated Macrophages (TAM) and explored its effects on bladder cancer (BC). Co-culturing PMA-treated THP-1 with BC cell lines (UMUC3 and T24) induced THP-1 to develop suppressed CD68 and increased CD206 expression which differentiated into M2-like macrophages. Co-culture of BC with TAM of this M2-like macrophage enhanced the migration and invasive activities of BC, as well as the expression of EMT marker. Human cytokine antibody array of conditioned medium from the co-culture of BC and TAM showed high CCL20, CCL2 and CXCL7. qPCR revealed that these chemokines were mainly derived from TAMs, not BC. Only CCL20 enhanced the migration and invasion of BC and the expression of EMT markers when each of these three recombinant chemokines was administered to BC. Furthermore, inhibiting CCR6, a receptor specific for CCL20, suppressed migration and invasion as expected. In BC, TAMs promote progression and metastasis by secreting CCL20, and inhibition of CCR6 may be one potential therapeutic approach to suppress BC activity.

#6810 Macrophage secreted CCL9/CCL5 induces CCR1-mediated ovarian cancer metastasis to the omentum in the absence of CCL6.

Supreeti Tallapragada, Justine Chan, Venkatesh Krishnan, Oliver Dorigo

Department of Obstetrics and Gynaecology, Stanford University, Stanford, CA

The tumor-microenvironment (TME) of the omentum plays an important role in providing a pre-metastatic niche for high-grade serous ovarian cancer (HGSC-OvCa) progression. Omentum, a layer of fatty adipose tissue within the peritoneal cavity, is the preferred primary metastatic site for OvCa. Omentum is a well-vascularized fatty tissue containing wide-spread immune clusters (milky spots). Milky spots in the omentum are primarily composed of B cells, T cells, macrophages, NK cells, and dendritic cells. Previous studies from our laboratory have highlighted the importance of CCL6 secreted by omental macrophages as a key chemokine in providing a pre-metastatic niche by activating the CCR1 axis on the cancer cells required for OvCa invasion. We engineered and characterized a CCL6-depleted *in vivo* mouse model using CRISPR/Cas9 to study the effect on OvCa progression and macrophage biology. We demonstrate that deletion of CCL6 in mice alters characteristics of omental tissue-resident (OM-Macφ) and bone marrow-derived macrophages (BMDM) derived from circulating monocytes. RNA sequencing of OM-Macφ and microarray study of BMDM revealed that CCL6 deletion produces enhanced TGFβ1$^{\pm}$CSF-1$^{\pm}$CCL5$^{\pm}$ expression in OM-Macφ and an increase in TGFβ1$^{\pm}$CSF-1$^{\pm}$CCL9$^{\pm}$ in BMDM. This acts as a rescue mechanism to maintain activation of their shared CCR1 receptor with a pro-M2 stimulation profile. Deep multiplexed imaging of the omentum tissue by CODEX showed that CCL6 deletion alters the architecture of milky spots, with enriched macrophage content and reduced B-cell and T-cell-rich neighborhoods. While our previous studies indicated that CCL6 deletion could potentially have an anti-tumoral effect, we found that it does not significantly affect murine ID8 ovarian cancer tumor burden in both short-term (7 days) and long-term *in vivo* studies and provides no added survival advantage. We report that CCL9$^{\pm}$F4/80$^{\pm}$ macrophages accumulate in the omentum post-tumor infiltration in the CCL6-KO model, and neutralizing CCL9 in the CCL6-KO BMDM macrophage-derived conditioned media significantly reduces migration of ID8 cancer cells *in vitro*. Furthermore, we demonstrate that murine CCL9 and its analog, human CCL15, promote the epithelial-mesenchymal transition (EMT) of mouse ID8 and human A2780 OvCa cells. Moreover, our findings indicate that human CCL15 is a prognostic biomarker for reduced survival in OvCa patient cohorts (Stages I&II and Stage III&IV). Further classification of HGSC-OV patients (n=375) from TCGA-OV based on CCL15 and CCR1-high expression correlated with a higher expression of TGFβ1, CCL5, and a T-cell exhaustion signature in the TME. Taken together, given the apparent redundancy of the chemokine network controlling CCR1 signaling, our findings support the strategy of therapeutically blocking the CCR1 receptor to potentially produce a favorable anti-tumor response in HGSC-OvCa patients.

#6811 IL-9 enhances lung tumor growth through intrinsic and ARG1-dependent transcriptomic changes in interstitial macrophages.

A. Cannon, M. H. Kaplan;
Indiana University School of Medicine, Indianapolis, IN

A defining characteristic of cancer is its ability to evade detection by immune cells through the generation of a myeloid cell-dependent immunosuppressive tumor microenvironment. Arginine is utilized by Arginase 1 (ARG1) or nitric oxide synthase in tumor-associated macrophages to respectively elicit pro-tumor or anti-tumor activity. The balance between these enzymes is regulated by extracellular cytokines including Interleukin 9 (IL-9), a pleiotropic cytokine that can be a positive or negative regulator of tumor growth. Our lab identified that IL-9 promotes tumor development in the lung by expanding interstitial macrophage populations and inducing ARG1. Lung tumor growth is attenuated in mice with myeloid cell deficiency of Arg1. Similarly, macrophage-targeting nanoparticles containing *Arg1* siRNA can therapeutically reduce tumor burden and alter macrophage populations in the lung toward an immunostimulatory phenotype. However, an understanding of the mechanism by which IL-9R/ARG1+ interstitial macrophages drive tumor progression remains incomplete. Here, using a B16F10 lung metastasis model in mixed-bone marrow chimeric mice, we demonstrate that IL-9-responsive interstitial macrophages are intrinsically altered at the transcriptomic level toward an ARG1-dependent immunosuppressive phenotype. Furthermore, our research shows that the absence of IL-9 signaling or ARG1 expression in macrophages has a notable impact on the levels of arginine and its metabolites in the lung tissue and bronchoalveolar lavage fluid of tumor-bearing mice. These alterations subsequently lead to an enhanced anti-tumoral immune response, reflected by changes in Interferon-gamma expression in both lung macrophages and T cells. Thus, our work suggests that the IL-9R/ARG1/interstitial macrophage axis promotes lung tumor development by altering intrinsic arginine metabolism and reprogramming immune cell populations toward an immunosuppressive phenotype.

#6812 Durable control of brain tumors by glioma inhibitory macrophages and IL33.

S. V. Menon[1], X. Lun[2], P. Zeng[1], J. Zhang[1], B. Ahn[2], H. Yu[1], A. Poole[2], N. Dang[2], K. Osz[2], J. A. Chan[2], D. F. Quail[3], S. M. Robbins[1], D. L. Senger[1];
[1]Lady Davis Institute at the Jewish General Hospital, Montreal, QC, Canada, [2]Arnie Charbonneau Cancer Institute, Calgary, AB, Canada, [3]Rosalind and Morris Goodman Cancer Institute, Montreal, QC, Canada

Glioblastoma is the most common and deadly form of brain cancer. Even with aggressive treatment including surgery, chemotherapy, and radiotherapy, survival outcomes for newly diagnosed glioblastoma patients remains less than two years. Novel high throughput omics technologies have expanded our understanding of the role of innate immune system in brain tumors, that are generally believed to drive glioma progression and enable evasion of the adaptive immune system. However, targeting of this axis in the clinic remains an unmet opportunity. Previously, we discovered that the dual-function (secreted and nuclear) cytokine IL-33 is a crucial regulator of the inflammatory microenvironment that promotes glioma tumorigenesis through phenotypic and functional changes in the innate immune cell repertoire. Strikingly, when IL-33 is prevented from entering the nucleus, by deletion of its nuclear localization sequence (ΔNLS IL-33), but is still secreted, *in vivo* tumor growth is dramatically inhibited resulting in prolonged long-term survival. Using multiplex immunohistochemistry and spatial transcriptomics with temporal resolution across different stages of tumor progression, we identified a population of glioma-inhibitory macrophages (GIMs) unique to this suppressive environment. Assessment of GIMs in xenografts generated from patient brain tumor initiating cells found an enriched presence of these cells in xenografts with long-term survival (greater than 300 days) versus short-term survival (less than 100 days). The ability of GIMs to inhibit glioma progression was demonstrated when tumors established using a combination of ΔNLS IL-33 expressing cancer cells together with highly tumorigenic cells resulted in a growth inhibitory environment that significantly extended survival. A deeper molecular characterization of this phenotype and development of clinical strategies are currently underway.

#6813 Immunosuppressive monocytes suppress CART19 functions through modulation of the IL-1 pathway.

K. Yun, R. Sakemura, T. Huynh, C. Manriquez Roman, O. Sirpilla, C. Stewart, J. Girsch, E. Ogbodo, I. Can, J. Feigin, L. Mai, H. Xia, B. Kimball, M. Rodriguez, L. Kankeu Fonkoua, M. Hefazi, M. Ruff, E. Siegler, S. Kenderian;
Mayo Clinic, Rochester, MN

CD19-directed chimeric antigen receptor T (CART19) cell therapy has shown remarkable outcomes in B cell malignancies and was FDA approved in multiple indications, but durable remissions are limited to ~40%. Inhibitory myeloid cells in the tumor microenvironment have been found to suppress T cell expansion and contribute to CART19 failure. Here, we studied interactions between monocytes, CART19, and tumor cells to understand the impact of monocytes on CART19 effector functions. First, CD28-costimulated CART19 (CART19-28ζ) generated in the lab from healthy donors were cocultured with JeKo-1, a $CD19^{\pm}$ mantle cell lymphoma cell line, and freshly isolated monocytes or *ex vivo* differentiated M2-like macrophages. M2-like macrophages were generated by incubating fresh monocytes with rhGM-CSF followed by coculturing with JeKo-1. CART19 antigen-specific proliferation was significantly inhibited by M2-like macrophages but not fresh monocytes (*JeKo-1+CART19 vs JeKo-1+M2+CART19, p=0.00503*). Transwell assays indicated that suppression from M2-like macrophages was not contact-dependent. IL-1 receptor antagonist (IL-1ra) was significantly elevated in M2-like macrophage coculture supernatant (*JeKo-1+Mono+CART19 vs JeKo-1+M2+CART19, p=0.0292*) and intracellularly in M2-like macrophages after coculture (*90%+)*. We therefore hypothesized that M2-like macrophages inhibit CART19 by secreting IL-1ra, which blocks IL-1 signaling in CART19. We interrogated the role of IL-1ra in CART19. JeKo-1 was cocultured with CART19, supplemented with rhIL-1β only, IL-1β + IL-1ra, or IL-1β +IL-1ra + IL-1ra neutralizing antibody (neuAb). CART19 antigen-specific proliferation was improved by IL-1β (*PBS vs IL-1β, p<0.0001*). IL-1ra inhibited IL-1β-dependent CART19 proliferation (*IL-1β vs IL-1β+IL1ra p=0.0006*), which was restored by IL-1ra neutralization (*IL-1β+IL-1ra vs IL-1β+IL-1ra+IL-1ra neuAb, p=0.0215*). Additionally, expression of IL-1RI, the receptor of IL-1β and IL-1ra, was measured on T cells after coculturing CART19, JeKo-1, and M2-like macrophages. M2-like macrophages downregulated IL-1RI expression on CART cells, which is a potential mechanism of blocking CART response to IL-1β, resulting in further suppression of CART proliferation (*JeKo-1+M2+CART19 vs JeKo-1+CART19, p=0.001*). Next, we assessed the impact of IL-1ra on CART cell functions in the presence of M2-like macrophage in a mantle cell lymphoma xenograft model. NOD-SCID-$\gamma^{-/-}$ (NSG) mice were subcutaneously injected with human macrophages and $luciferase^{\pm}$ JeKo-1 cells. Upon tumor engraftment by bioluminescent imaging, mice were randomized to treatment with CART19 + IL-1ra neuAb or control IgG for 3 weeks. CART19 + IL-1ra neuAb led to improved antitumor activity (*IL-1ra neuAb vs control IgG, p=0.0033*). Overall, our study revealed a role of IL-1ra in macrophage-induced CART inhibition mediated by blocking IL-1β signaling through IL-1RI.

#6814 E2F1-induced autocrine IL-6 inflammatory loop mediates cancer-immune cell crosstalk that regulates metastatic properties in melanoma.

P. Dhar[1], K. P. Singh[2], S. K. Gupta[2], D. Peringot[1], A. Spitschak[1], **B. M. Putzer**[1];
[1]Rostock University Medical Center, Rostock, Germany, [2]University of Rostock, Rostock, Germany

Melanoma is a cancer that is metastatic, drug-refractory and fatal if managed late or inadequately. The transcription factor E2F1 is a key player in melanoma pathology, promoting metastatic traits like EMT, neoangiogenesis, chemoresistance and evasion of immune surveillance. Particularly, high levels of E2F1 trigger tumor progression by developing protein-protein interactions (PPI) with coregulators that enhance its potential to activate a prometastatic gene regulatory network (GRN). We aimed to investigate the extent to which E2F1-expressing melanoma cells influence the immune response.
Methods: We combined transcriptomic approaches with bioinformatics and structural modeling to search for target genes involved in E2F1-activated immunomodulatory and prometastatic GRNs in aggressive melanoma. Immunoprecipitation and ChIP were performed to verify both PPI and protein-DNA interactions. Functional analyses, including qRT-PCR, immunoblotting and luciferase assays, were performed to verify expression and regulation of downstream targets. Additionally, we established a melanoma-immune cell coculture system with patient-derived CD4+ and CD8+ T cells. Cytokine arrays and ELISA were used for measurement of cytokine secretion to analyze the E2F1-induced tumor-immuno-crosstalk.
Results: We identified an E2F1-dependent GRN with IL-6 as a central factor mediating EMT and immune regulation. Mechanistically, E2F1-induced activation and secretion of IL-6 leads to an autocrine inflammatory forward-feedback loop, which in turn further promotes invasiveness and EMT marker expression in melanoma cells. Interestingly, IL6 activated STAT3 associates with E2F1 in a structure-dependent manner, forming a complex that enhances IL-6 expression by binding to a composite E2F1:STAT3-responsive promoter element. Moreover, we observed that the E2F1-IL6 axis dispenses immunomodulatory effects on surrounding CD4+ and CD8+ T cells, further stimulating IL-6 release, but also leading to secretion of IL-10 into the TME. Although IL-10 has an immunosuppressive function, it also showed anti-metastatic properties in melanoma cells. Thus, in contrast to IL-6, IL-10 decreased cell motility and reduced the expression of Vim, Slug, and Snai1, while simultaneous knockdown of E2F1 increased these effects. The findings are supported by clinical data sets showing that melanoma patients who have high levels of *E2F1* and *IL-6* and low *IL-10* exhibit poor survival.
Conclusion: Our results unveil a novel gene regulatory program by which E2F1-associated IL-6 release induces the formation of an E2F1:STAT3 complex, resulting in a forward-feedback loop that promotes cancer invasion and regulates T cells response through intercellular cytokine signaling in the tumor microenvironment.

#6816 Prevention of cancer cachexia by inhibition of soluble epoxide hydrolase.

R. L. Bayer[1], S. Virani[1], M. Gillespie[1], J. Capuano[1], K. Smith[1], K. Quinlivan[1], K. Vasquez[1], J. Yang[2], H. Yang[2], N. Mitsiades[3], B. D. Hammock[3], D. Panigrahy[1]; [1]Center for Vascular Biology Research, Beth Israel Deaconess Medical Center, Harvard Medical School, Boston, MA, [2]College of Food Science and Nutritional Engineering, China Agricultural University, Beijing, China, [3]Department of Hematology and Oncology, and UCD Comprehensive Cancer Center, University of California, Davis, CA

Background: Cancer cachexia is a devastating syndrome characterized by progressive muscle wasting and hyperinflammation. The underlying mechanisms remain poorly understood with no treatment options available. Cachexia is driven by systemic inflammation, pro-inflammatory cytokines, and apoptotic cell death (debris). The resolution of inflammation as an active biochemical process is regulated by novel pro-resolving lipid mediators. Arachidonic acid-derived epoxyeicosatrienoic acids (EETs) are lipid mediators stimulating inflammation resolution. EETs are rapidly metabolized by the enzyme soluble epoxide hydrolase (sEH). sEH is a critical cause of inflammation and a biomarker in several chronic inflammatory diseases. sEH inhibitors promote tissue regeneration and counter-regulate pro-inflammatory cytokines. We hypothesized that pharmacological inhibition of the sEH may prevent cachexia.
Methods: We investigated murine cancer cachexia models using genetically engineered pancreatic (KPC) and prostate (TRAMP C1) tumor cell lines, and “TRAMP” mice (transgenic adenocarcinoma of the mouse prostate). We performed LC-MS/MS-based profiling of bioactive lipids in plasma from KPC and colon cancer (CT26)-induced cachectic mice.
Results: KPC cells injected intraperitoneally induced 19.7% and 54.1% reduction in muscle weight in the tibialis anterior and soleus, respectively, in immunocompetent C57BL/6 mice compared to non-tumor bearing (NTB) mice. LC-MS/MS revealed KPC and CT26 cachexia induced a pro-inflammatory eicosanoid-driven cytokine storm. The human sEH inhibitor EC5026 delayed the onset of cachexia, leading to sustained survival over 250 days post-injection in the KPC model (n=15 mice/group). sEH expression was increased in the gastrocnemius of KPC mice by day 22 post-tumor cell injection vs. NTB. EC5026 counter-regulated sEH expression compared to vehicle-treated. In the TRAMP model, 5/5 of mice treated with EC5026 survived 230 days post-treatment compared to no survival of vehicle-treated mice (n=5). The transplanted KPC and TRAMP showed reduced CD4+ and CD8+ T lymphocytes and B lymphocytes in the tibialis anterior and gastrocnemius vs. NTB after flow cytometry analysis. EC5026 stimulated a general increase in CD3+ T lymphocytes and counter-regulated an eicosanoid-driven cytokine storm as shown by cytokine assays. EC5026 treatment increased tibialis anterior and gastrocnemius muscle weights and body weights compared to vehicle-treated KPC and TRAMP mice.
Conclusions: sEH inhibition may be a novel therapeutic approach to cachexia by targeting the immune response via stimulation of resolution of inflammation without toxicity or immunosuppression. Since sEH inhibitors have proven safe and effective in clinical trials for controlling multiple inflammatory diseases, this study provides a basis for the rapid clinical translation of sEH inhibitors to prevent/reverse cachexia in cancer patients.

#6817 Control of breast cancer via pro-resolving mediators.

S. A. Virani[1], M. Gillespie[1], H. Yang[2], D. R. Bielenberg[3], M. W. Kieran[4], S. Huang[5], C. N. Serhan[6], D. Panigrahy[1];

[1]Department of Pathology and Center for Vascular Biology Research, Beth Israel Deaconess Medical Center and Harvard Medical School, Boston, MA, [2]College of Food Science and Nutritional Engineering, China Agricultural University, Beijing, China, [3]Vascular Biology Program, Boston Children's Hospital, Boston, MA, [4]Division of Pediatric Oncology, Dana-Farber Cancer Institute, Harvard Medical School; Department of Pediatric Hematology/Oncology, Boston Children's Hospital, Harvard Medical School, Boston, MA, [5]Institute of Systems Biology, Seattle, WA, [6]Center for Experimental Therapeutics and Reperfusion Injury, Brigham and Women's Hospital and Harvard Medical School, Boston, MA

Tumor recurrence is the principal cause of mortality in breast cancer, yet the underlying mechanisms are not well understood. Anti-estrogen therapy, including tamoxifen, reduces tumor burden by inducing apoptosis and necrosis of cancerous tissue. The resulting cellular debris may stimulate tumor growth by disrupting inflammation resolution and creating pro-inflammatory and pro-tumorigenic microenvironments. Compared to estrogen receptor (ER)-positive breast cancer, ER-negative behaves aggressively, and patients have a poor prognosis due to the lack of treatment options. Here, we demonstrate that breast tumor cells killed by cytotoxic anti-estrogen therapy or chemotherapy ("tumor cell debris") stimulate primary tumor growth when co-injected with a subthreshold (nontumorigenic) inoculum of tumor cells by triggering a macrophage-derived pro-inflammatory and pro-angiogenic "cytokine storm." Thus, tumor cell debris is a critical risk factor for aggressive breast cancer growth. To assess whether stimulating the clearance of debris would impact breast cancer progression *in vivo*, we utilized maresin 1 (MaR1), maresin conjugates in tissue regeneration (MCTR1, MCTR2) and protectin conjugates in tissue regeneration (PCTRs), which are specialized pro-resolving lipid autacoid mediators (SPMs). We treated established models of ER-positive (EO771) and negative (4T1) breast cancer. Each maresin sharply reduced tumor growth in debris-stimulated and spontaneous (e.g. MMTV-PyMT) breast cancer models at nanogram concentrations without toxicity. Notably, PCTR1 inhibited orthotopic triple-negative (4T1) growth and proliferation compared to chemotherapy (paclitaxel) or immunotherapy (anti-cytotoxic T-lymphocyte-associated protein 4, CTLA4). Similarly, PCTR1 alone or in combination with chemotherapy (paclitaxel) reduced gene expression and protein levels of pro-angiogenic factor CXCL12/SDF1 in the ER-negative (4T1) tumor microenvironment. In ER-positive (EO771), a triple combination of PCTR1, chemotherapy (paclitaxel), and immunotherapy (anti-CTLA4) treatment potentiated the immune checkpoint blockade. Maresins also stimulated macrophage phagocytosis of therapy-generated breast tumor cell debris, inhibited tumor angiogenesis, and dampened a therapy-induced cytokine storm, including TNF-α, MIP-2/CXCL2, CCL2/MCP-1, IL- 1ra/IL-1F3, and G-CSF. Expression of SPM receptors (e.g. resolvin D1 (RvD1) receptor ALX/FPR2, resolvin D2 (RvD2) receptor GPR18, maresin 1 (MaR1) receptor LGR6, and resolvin E1 (RvE1) receptor ChemR23) were specifically identified in breast cancer tissue. Taken together, the maresin and protectin pathway mediators may represent a new therapeutic approach to stimulate the resolution of inflammation in breast cancer.

#6818 Obesity-mediated perineural invasion promotes PDAC tumorigenesis.

S. S. Mayengbam, A. Alam, S. Senchanthisai, I. Bektas, P. Dey;
Roswell Park Comprehensive Cancer Center, Buffalo, NY

Obesity is a modifiable host factor that has been reported to increase the risk of pancreatic ductal adenocarcinoma (PDAC) by ~60% and the mortality by two-fold, however, the exact mechanisms by which obesity enhances PDAC aggressiveness is incompletely understood. Given that nearly 74% of U.S. adults are overweight or obese (US Center for Disease Control), resolving the complex association between obesity and PDAC may unveil new targets for prevention and/or intervention to decrease incidence and improve outcomes. The prevailing notion is that obesity-induced tumor *in situ* factors (i.e., oxidative, hypoxic, nutrient, and biochemical) play crucial roles in enhancing cancer cell fitness and survival. However, these concepts have yet to lead to the identification of any actionable target in patients, with obesity-related cancer in general and PDAC in particular. Prior studies and our preliminary data show the presence of a distinctive tumor immune profile in PDAC models under conditions of obesity, which encompasses immune suppressive myeloid and type 2 immune cells, namely M2-like tumor-associated macrophages (TAMs), and myeloid-derived suppressor cells (MDSCs), that inhibit effector $CD8^{+}$ T cell expansion and function enabling PDAC progression. However, the genesis of this ‘type 2 immune cell’ dominant tumor-immune microenvironment (TIME) of obesity-driven PDAC remains to be fully understood. This led us to take a holistic approach utilizing multiple genetically engineered mouse models (GEMMs), pharmacological inhibitors, transcriptomic analysis (RNA-seq, spatial transcriptomic, and scRNA-seq), fresh PDAC patient samples, and imaging technologies (confocal microscopy) to understand the molecular mechanisms. Our novel mechanistic study using some of the above-mentioned tools shows that obesity-driven PDAC has significantly higher perineural invasion (PNI) that enhances PDAC progression. We found that sympathetic nerve terminals (of the PNI) via neurotransmitter release control the expression of integral cytokines that cause a dramatic remodeling of the TIME. Specifically, the PNI-mediated neuro-adrenergic signaling activates β2-adrenergic receptor (β2-AR) on PDAC cells, leading to increased tumor cell production/proliferation and secretion of the ‘alarmins’ IL-33 and IL-1β. Importantly, we showed that mitigation of adrenergic signaling using two separate approaches: (i) pharmacological antagonists of β2-ARs (β-blockers), and (ii) the use of a thermoneutral model leads to substantial abrogation of obesity-mediated tumor progression. These, and other key data raise the provocative question that reducing adrenergic signaling-dependent IL-33 expression and release favor a pro-inflammatory TIME and significantly increase patient survival in obesity-driven PDAC.

#6819 Exploring the impact of *IDH1*-mutations on antitumor immunity in intrahepatic cholangiocarcinoma.

E. Kartalia, J. M. Leatherman, J. W. Lee, K. Yoshima, **D. J. Zabransky**, M. Yarchoan;
Johns Hopkins University, Baltimore, MD

Intrahepatic cholangiocarcinoma (CCA) is an aggressive biliary tract cancer that carries unfavorable prognosis. 10-20% of intrahepatic CCAs harbor a mutation in *IDH1* that can be targeted with mutant IDH1-specific inhibitors. However, objective and durable responses to treatment with mutant IDH1 inhibitors are rare in CCA. Mutant IDH1 has neomorphic enzymatic activity that produces the oncometabolite D-2-hydroxyglutarate (D-2-HG). D-2-HG promotes biliary tumor formation through cancer cell-intrinsic mechanisms but is also a paracrine factor in the tumor microenvironment (TME). Our group and others have identified that *IDH1*-mutant CCAs are not responsive to immunotherapy treatment approaches in part due to decreased CD8+ T cell infiltration and an increase in immunosuppressive macrophage cells in the TME. To better understand the immunosuppressive features of the *IDH1*-mutant CCA TME, we generated an isogenic cell line panel of *IDH1*-mutant (MUT) and *IDH1*-wild type (WT) mouse cholangiocarcinoma cells in the SB1 cell line background through a CRISPR homology directed repair approach. Compared to *IDH1*-WT cells, *IDH1*-MUT cells produce high levels of D-2-HG and both cell line panels readily form tumors in immunocompetent C57BL/6 mice. Tumors formed from *IDH1*-mut cells have reduced CD8+ T cell infiltration compared to *IDH1*-WT tumors, a finding that correlates with analysis of human CCA samples. Using cytometry by time of flight (CyTOF), we identified that CD8+ T cells in *IDH1*-MUT tumors have decreased expression of key regulators of the antitumor immune response including EOMES, TBET, and GZMB compared to those isolated from *IDH1*-WT tumors. Analysis of secreted factors from these *IDH1*-MUT and *IDH1*-WT cells identified that *IDH1*-MUT cells release increased levels of CCL2, a chemokine shown to diminish the antitumor immune response across multiple cancer types, compared to *IDH1*-WT cells. Further, IDH*1*-MUT tumors grown in syngeneic, immunocompetent mice have increased CCL2 staining by IHC compared to *IDH1*-WT tumors. CCL2 expression is also increased in a preliminary analysis of *IDH1*-mutant human CCA primary tumors. Treatment of mice harboring orthotopic liver tumors formed from *IDH1*-MUT cells with a CCL2 neutralizing antibody resulted in decreased tumor size compared to isotype control. Together, our data suggest that CCL2 is a mediator of immunosuppression in the *IDH1*-mutant CCA TME and that modulation of CCL2 activity may improve outcomes in this rare disease subtype. Further work to understand the mechanisms through which *IDH1* mutations regulate CCL2 levels in these tumors is underway.

TUMOR BIOLOGY: Gene Expression Regulation in the Tumor Microenvironment
Poster Session

#6824 Secretion of MAGE-A3 and MAGE-A4 in cell lines and lung cancer.

Bailey Gilmore[1], Dehe Kong[1], Rachel Gonzalez[1], Jina Yom[1], Andy Han[1], Tianli Qu[1], Alex Strom[1], Xiaoxiao Zhao[1], Eden Zewdu[1], Hailey Guo[1], Zhaoying Guo[1], Ranran Zhang[2], Xiaomin Hu[3], Qi Ren[3], Xuan Liu[1], Wei Fu[1]

[1]OriGene Technologies, Inc., Rockville, MD,[2]Origene Wuxi Biotechnology Co., Wuxi, China,[3]OriGene Wuxi Biotechnology Co., Wuxi, China

Melanoma-associated antigen gene A (MAGE-A) family of proteins have previously been shown to express in a variety of tumors, having different roles in cancer pathogenesis. MAGE-A3 and MAGE-A4 have both been shown to inhibit the p53 pathway which leads increased cell growth by stopping apoptosis. Both of these proteins have been associated with cancer progression and poor prognosis. In our studies, we have evaluated multiple MAGE-A3 and MAGE-A4 antibodies using CytoSections. While previous research had only pointed to these proteins being intracellular, our overexpression studies in the development of CytoSections indicated that some MAGE-A proteins were secreted. In this study, ELISA binding assays corroborated that MAGE-A3 and MAGE-A4 were secreted from cells overexpressing these proteins, and serum MAGE-A4 was detected in 24% of lung cancer patients. Flow cytometry data was then collected to see that exogenous MAGE-A proteins were binding to cells in a pattern consistent with secretion data from IHC experiments. Variants of MAGE-A4, differing by only a handful of amino acids, showed very different levels of secretion from one another. MAGE-A3 and MAGE-A6 share 95% homology and were also extremely different in secretion shown between IHC, flow cytometry, and ELISA. This study validates that certain members of the MAGE-A family are secreted from cells.

#6825 Epigenetic dysregulation in well-differentiated pancreatic neuroendocrine tumor (PNET): An immunohistochemistry (IHC) analysis.

Z. Saleh, Y. Ghanem, H. Joshi, M. C. Moccia, H. Toma, Y. Li, U. Joneja, T. Gao, Y. Hong;
Cooper Univ. Hospital, Camden, NJ

Epigenetic dysregulation through DNA Methyltransferase 1 (DNMT1) is integral to pancreatic neuroendocrine tumorigenesis. We aim to investigate the interplay between epigenetic modifiers and pathogenetic markers in the PNET microenvironment. 12 paraffin-embedded PNET specimens and 12 benign adjacent tissue specimens, used as controls, were obtained from Cooper University Hospital Pathology Department (IRB 23-130). IHC was performed using epigenetic markers, including DNMT1, DNMT3A, DNMT3B, and 5-Hydroxymethylcytosine (5-HMC), and pathogenic markers, including Multiple Endocrine Neoplasia 1 (MEN1), Protein-Tyrosine Phosphatase (PTEN), and Ras Association Domain Family 1 (RASSF1). Image J software was utilized for IHC scoring under the guidance of a board-certified pathologist. DNMT1 was upregulated in PNET tumor specimens with a mean density score of 72.02 +/- 31 versus 16.02 +/- 17 in adjacent benign tissue ($p<.001$). Grade 2 tumors displayed increased DNMT1 expression compared to Grade 1 tumors with a mean score of 37 +/-21 versus 71 +/- 23 ($p<.05$). Decreased expression of 5-HMC was noted in tumor specimens in comparison to benign tissue with a mean score of 3.92 +/- 5.05 versus 19.37 +/- 5.05 ($p<.05$). Loss of 5-HMC was observed in higher tumor grades with a mean score of .79 +/- 2 versus 8.2+/-2 ($p<.01$). DNMT3B was upregulated in PNET tumor specimens with a mean score of 13.16 +/- 3.94 versus 7.02+/- 2.553 ($p<.01$) in adjacent benign tissue and was positively correlated to DNMT1 expression. DNMT3A was not found to have a difference in expression between tumor and benign tissue. MEN1 was downregulated in PNET, with 45% of tumor specimens displaying loss of MEN1 expression. Mean MEN1 density in tumor tissue was 4.47 +/- 5.95 versus 11.41 +/- 3.53 in adjacent benign ($p<.01$). Increased expression of DNMT1 found to negatively correlate with MEN1 expression ($R^2=.23$). Loss of RASSF1 expression was present in 70% of tumor specimens with a mean score of 1.32 +/- 1.99 versus 9.50+/- 6.89 ($p<.001$) in adjacent benign tissue. RASSF1 expression correlated negatively with DNMT1 ($R^2=.21$). PTEN expression showed intratumoral homogeneity to benign tissue, and its expression was not correlated with any epigenetic markers. Our work provides a framework of epigenetic regulators involved in the pathobiology of PNET, and can refine prognostic evaluation while providing therapeutic benefits for patients with PNET.

#6826 Comparative analysis of a predictive transcriptomic model and functional gene expression signatures (FGES) for tertiary lymphoid structure (TLS) detection in lung adenocarcinoma (LUAD).

N. Lukashevich, D. Dymov, A. Sarachakov, S. Kust, A. Love, I. Valiev, D. Ivchenkov, A. Bagaev, V. Svekolkin, N. Kotlov, V. Kushnarev; BostonGene, Waltham, MA

Background: TLS are recognized as significant biomarkers for patient prognosis and therapy selection. In current clinical practice, TLS are often detected by manual assessment of H&E slides, which has been associated with reproducibility issues. Here, we developed a transcriptomic model using TLS density to stratify LUAD patients into TLS-high and -low groups and compared it with 5 published TLS FGES to assess the predictive value for patient outcomes.

Design: A regression model to predict TLS density (units(u)/mm²) was created using RNA expression data and histological mapping of 415 TCGA-LUAD samples. Features were chosen based on differential gene expression analysis of sample groups with low (<Q1, 0.26 u/mm²) and high (>Q3, 2.04 u/mm²) TLS density. The model was trained on 269 samples and independently validated on 146 TCGA and 9 internal samples. The RNA model and five previously reported TLS FGES were compared by Wilcoxon paired test to Spearman's ρ and F1-scores from bootstrapped validation set. The resulting predictions stratified immunotherapy-treated samples from SU2C-MARK (n=58) and GSE182328 (n=28) into TLS-high and TLS-low groups by Q2 threshold for TLS density (0.78 u/mm²) for further univariate (Kaplan-Meier) and multivariate (Cox model, adjusted for age and sex) analyses for overall survival (OS) with log-rank tests. P-values were adjusted with Bonferroni correction, and 95% confidence intervals (CIs) were provided.

Results: Statistically significant upregulated genes in samples with high TLS density included FDCSP, MS4A1, and CXCL13 (logFC ≥ 0.95, FDR<0.01). The transcriptomic model showed confident superiority in correlation with TLS density compared to the best FGES in TCGA samples (ρ=0.53±0.03 vs 0.41±0.03, p<0.001). The TLS model also outperformed the highest performing FGES when stratifying TCGA samples into TLS-high and TLS-low groups (F1=0.73±0.02 vs 0.69±0.02, p<0.005). In the internal cohort, the model demonstrated robust performance (F1=0.76±0.05, ρ=0.81±0.04) and outperformed all FGES except one (FGES F1=0.78±0.05, ρ=0.86±0.05). The TLS-high group defined by the TLS RNA model had a significantly better prognosis on immunotherapy cohorts (p=0.01; 1 year OS 49% for TLS-low vs 70% for TLS-high), whereas no discernible difference in OS was identified for the 5 TLS FGES. The TLS model had a log hazard ratio (logHR) of -3.11 (CI:-5.31,-0.91; p<0.05, Harrell's C-index=0.64), indicative of a stronger association with OS than of the TLS FGES (logHR=-2.11; CI:-4.1,-0.08; p=ns; C-index=0.59).

Conclusions: Comparative analysis of the proposed transcriptomic model for TLS detection in LUAD samples demonstrated improved performance metrics and prognostic value compared to previously reported TLS FGES, affirming its potential for guiding therapeutic decision-making.

#6827 Myocardin and myocardin-related transcription factor as potential drivers of the myofibroblastic cancer-associated fibroblast phenotype in colorectal cancer.

A. B. Cornelio, K. A. Johnson, Y. Gadalla, S. Nath, C. A. Pasch, W. Zhang, K. A. Matkowskyj, D. A. Deming;
University of Wisconsin - Madison, Madison, WI

Background: Cancer-associated fibroblasts (CAFs) play a key role in modifying the tumor microenvironment (TME) and could be a future target for treatment. CAFs are typically categorized based on function: myofibroblastic CAFs (myCAFs) amplify extracellular matrix production that blocks therapy and immune cell infiltration while inflammatory CAFs (iCAFs) produce immuno-suppressive cytokines and chemokines. Here we sought to better understand the role and mechanisms of myCAFs in altering the TME by identifying their unique markers and potential drivers.
Methods: Z-scores of ACTA2/TAGLN or ICAM1/PDPN were used to create datasets high in myCAF and iCAF markers, respectively, from TCGA data. A gene set enrichment analysis (GSEA) was performed on the resulting differential expression. Samples of patients were collected to create a cohort of colorectal cancers that were stained via immunohistochemistry (IHC) for alpha-smooth muscle actin (αSMA), transgelin (TAGLN), myocardin (MYOCD) and myocardin-related transcription factor A (MRTFA). Slides were evaluated for collagen using Masson's trichrome stain. MYOCD and MRTFA nuclear expression was expressed as positively stained nuclei per high powered field (HPF; 400x). TAGLN, αSMA, and collagen were scored on a scale of 0-3+.
Results: Of the 592 TCGA patients compiled across all disease stages, 23 (median age 63) formed the myCAF-high group (7 males, 16 females). Within this group, GSEA indicated an upregulation of myogenesis ($q < 0.001$) with the following genes positively associated with myCAF markers: MYLK ($q < 0.001$, log2 fold change [FC] 1.52), DES ($q < 0.001$, 5.32), and MYH11 ($q < 0.001$, 3.57). The following were also upregulated in the myCAF high cohort: CNN1 ($q < 0.001$, 2.95) and MYOCD ($q < 0.001$, 2.27). These genes are targets of MYOCD and MRTFA transcription factors potentially driving the myCAF phenotype. To assess this potential relationship, we evaluated 306 tumor samples from 153 patients with CRC. The cohort consisted of 56 female patients and 97 male patients aged 13-90 years old across all disease stages. High amounts of nuclear MRTFA were associated with high scores for myCAF markers aSMA (average score 1.54 when MRTFA+ nuclei < 5 per HPF vs 2.06 when MRTFA + nuclei > 5 per HPF, $p<0.001$, Wilcoxon Rank Sum Test), TAGLN (1.37 vs 1.62, $p = 0.043$), and collagen (1.73 vs 2.10, $p = 0.009$). Likewise, for MYOCD, αSMA (1.79 vs 2.14, $p = 0.001$) and collagen (1.87 vs 2.15, $p = 0.017$) were positively correlated.
Conclusions: Increased nuclear expression of MYOCD and MRTFA in stromal cells of CRC are positively correlated with myCAF gene expression, supporting our initial hypothesis of these being drivers of the phenotype. Our findings now motivate further analysis as to whether the inhibition of these transcription factors could lead to a reduction in the immune regulatory myCAF phenotype.

#6829 Identification of immune suppressive features in tumor-associated endothelial cells (TECs) in EGFR-mutant non-small cell lung cancer via single-cell RNA sequencing.

S.-J. Choi[1], J. Lee[2], K.-H. Pyo[3], G.-T. Lee[1], Y. Park[3], Y. Lee[4], M. Yun[3], K. Lim[5], J. Lee[1], M. Hong[2], S. Lim[2], B. Cho[2];

[1]Dept. of Research Support, Yonsei Biomedical Research Institute, Yonsei University College of Medicine, Seoul, Korea, Republic of, [2]Division of Medical Oncology, Department of Internal Medicine and Yonsei Cancer Center, Severance Hospital, Yonsei University College of Medicine, Seoul, Korea, Republic of, [3]Severance Biomedical Science Institute, Yonsei University College of Medicine, Seoul, Korea, Republic of, [4]Yonsei New Il Han Institute for Integrative Lung Cancer Research, Yonsei University College of Medicine, Seoul, Korea, Republic of, [5]JEUK Institute for Cancer Research, JEUK Co., Ltd., Gumi, Korea, Republic of

Introduction: Within the tumor microenvironment (TME), tumor-associated endothelial cells (TECs) exhibit distinct features from normal cells, and diverse phenotypes of TECs result in intratumoral heterogeneity. Here, we aimed to characterize the phenotypes of the TECs of non-small cell lung cancer (NSCLC), identify distinct features that are pivotal in tumor progression, and discover potential therapeutic applications.

Methods: We performed single-cell RNA sequencing (scRNA-seq) from 128 NSCLC patients to include I (N=52), II (N=18), III (N=21), and IV (N=14), and compared them with normal cells (N=24). Epidermal growth factor receptor (*EGFR*)-mutant accounted for 69 samples. *EGFR*-wild (N=35) was further classified as programmed death-ligand 1 (PD-L1) high (N=14) and low (N=21) with PD-L1 high defined as tumor proportion score > 50%.

Results: Twelve distinct EC types were characterized based on clinical information, including *EGFR* mutations and PD-L1 expression. We classified our subset as normal cells and tumor-enriched ECs, which were further classified as *EGFR*-wild or mutant ECs. Compared to normal cells, phenotypes such as activated post-capillary veins (APCVs), tip ECs, and endothelial mesenchymal transition (endoMT) ECs were predominantly observed in all tumor-enriched ECs. In *EGFR*-mutant ECs, ribosomal ECs, and vascular mimicry (VM) ECs were primarily enriched. Trajectory analysis showed that endoMT and VM ECs had lineage tracing of fibroblasts and epithelial cells, respectively. By clinical stage, APCVs, tip ECs, endoMT, and VM ECs were more enriched at advanced stages. PD-L1-high subset had higher expression of adhesion molecules, APCVs, and median transmigration score than other phenotypes. Also, high endothelial venules (HEVs) mediating lymphocyte trafficking to lymphoid organs were enriched in high PD-L1 subset. In the APCVs of *EGFR*-mutant group, there were interactions related to immune cell suppression and interactions of chemokines/chemokine receptors involved in recruitment.

Conclusion: Our findings reveal distinct phenotypes of ECs, including the enrichment of APCVs, tip ECs, and endoMT ECs in all tumor-enriched EC populations, as well as VM ECs in *EGFR*-mutant ECs. APCVs, which is abundant high PD-L1 subset, play a crucial role in the transmigration progress of immune cells across vascular endothelium. In *EGFR*-mutant NSCLC, dysfunctional immune cells are recruited into the tumor, along with relatively low transmigration, resulting in poor tumor-killing effect.

#6830 Xenium *in situ* analysis and reproducibility study of multiple carcinomas for clinical studies.

E. Cheung, B. Zhang, L. Zhang, T. Lu, R. Gakhar, **V. Sundaram**;
BioChain Institute, Inc., Newark, CA

10x Genomics' Xenium is the newest in situ spatial transcriptomics platform offering sub-cellular resolution in frozen and FFPE tissue sections for a deeper study of cellular mechanisms and interactions. Mapping RNA targets at high specificity with fully customizable assays and quick workflow, it uses rolling circle amplification and interpretation-ready data is available immediately after the run. At BioChain Institute, Inc. (BioChain), we are conducting validation studies for reproducibility of results with the Xenium platform using BioChain's oncology biospecimen.FFPE tissues from BioChain's repository were screened by our pathologist for tumor content above 30%. Four carcinoma tissues from Breast, Colon, Lung, and Kidney with high DV200 scores were selected. An array was constructed with these tissues to fit the Xenium slide's imageable area. Two serial sections were used for the Xenium run per 10x Genomics' protocol. The Off-the-shelf Human Multi-Tissue and Cancer Panel was used for targeting 377 genes. H&E staining and imaging was performed, and the image was integrated with the data on the Xenium platform. The results were found to be reproducible between two different operators. For example, in the breast section, over 96,000 cells were detected and median transcripts per cell were 70 in both the runs. There were 20 clusters representing different cell types/ states, 99% transcripts were within cells, and ~85% of the transcripts were found to be high quality. Furthermore, we are analyzing the expression of unique tumor type and immune transcripts to map the heterogeneity of the tissues, as well as sensitivity, and standard deviation between the runs. The Xenium platform is a powerful tool for the sub-cellular spatial transcriptomics study of tissues with targeted gene panels. However, one of the four tissues used here failed to show enough transcripts. Further investigation is underway to examine the issue and conclude best practices thereafter. Our future studies will include accuracy and concordance validation with Xenium run on different days and Visium whole transcriptome assay post- Xenium.

#6831 Single-cell-based epigenetic and transcriptomic analysis in the KPC pancreatic cancer mouse model revealed dynamiccharacteristic subtypes of cancer-associated fibroblasts.

K. Sasaki[1], K. Shinjo[2], X. Wang[2], K. Kumegawa[3], R. Raruyama[3], S. Mii[2], Y. Murofushi[2], M. Suzuki[2], A. Enomoto[2], Y. Kondo[2];
[1]Nagoya University, Nagoya, Japan, [2]Nagoya University Graduate School of Medicine, Nagoya, Japan, [3]Japanese Foundation for Cancer Research, Tokyo, Japan

Pancreatic cancer features robust fibrosis, with 40-80% fibrotic tissue and a dense stroma, highlighting the crucial need to grasp cellular interactions in the cancer microenvironment.
In this study, we used single-cell RNA sequencing (scRNA-seq) to analyze pancreatic tissues from 60-day-old normal mouse (n=1) (GSE125588) and KPC (LSL-KrasG12D/+; LSL-Trp53R172H/+; Pdx-1-Cre) cancer model with tumor diameter of 1-2 cm (n=2) (GSE129455). By examining fibroblast clusters, we identified distinct subtypes of cancer-associated fibroblasts (CAFs), and revealed four clusters: normal fibroblasts cluster, inflammatory CAFs (iCAFs) cluster marked by increased expression of IL6 and other cytokines, myofibroblast CAFs (myCAFs) cluster solely in the KPC model, and antigen-presenting CAFs (apCAFs) cluster expressing Mesothelin. We found that expression pattern of iCAFs in the KPC appeared similar to normal cells than myCAFs, suggesting a potential role in inhibiting cancer. it is reported that mesothelial cells might transition to apCAFs under the influence of IL6 and TGFβ due to tissue damage and inflammatory effects. This transition was visualized in our apCAF cluster, suggesting a potential pathway for the transformation of mesothelial cells into apCAFs.
Next, in order to analyze epigenetic profiles of fibroblasts, we conducted single-cell Assay for Transposase-Accessible Chromatin with high-throughput sequencing (scATAC-seq) using 90-day-old KPC mice (n=2) and a wild-type mouse (n=1).scATAC-seq showed that there are mainly two clusters of fibroblasts, one cluster corresponded to myCAF, enriched with PDPN, while the other represented iCAF cluster, enriched with COL1A2. These data suggest that in terms of the epigenetic state, myCAF contain several different CAFs and have the potential to differentiate into either myCAFs or other type of based on certain stimulation. Ultimately, CAF differentiated into three distinct subtypes as revealed by scRNA-seq. This highlights that despite similar epigenetic states, various transcription factors characterize the functionality of these fibroblast subtypes. Further exploration of the underlying mechanism that lead to different CAF subtypes might help in controlling the microenvironment of pancreatic cancer.

#6832 Gender specific role of LMTK3 in neuronal-tumor microenvironment crosstalk in CRC.

L. Torres-Gonzalez[1], S. Soni[1], Y. Yang[2], G. Smbatyan[1], J. Lo[1], P. Mittal[1], F. Battaglin[1], I. K. Singh[3], P. Jayachandran[1], S. Algaze[1], A. Wong[1], K. Ashouri[1], W. Zhang[1], G. Giamas[4], J. Millstein[2], H.-J. Lenz[1];

[1]USC Norris Comprehensive Cancer Center, Los Angeles, CA, [2]University of Southern California, Los Angeles, CA, [3]Deshbandhu College & Delhi School of Public Health, Institute of Eminence, University of Delhi, New Delhi, India, [4]School of Life Sciences, University of Sussex, Falmer, Brighton, United Kingdom

Background: Lemur tail kinase 3 (LMTK3) is a serine/threonine protein kinase with roles in multiple cellular pathways, including Wnt signaling, KIT modulation, and the estrogen receptor pathway; identifying it as a potential target in various cancers. LMTK3 is highly expressed within the central nervous system (CNS) and has been demonstrated to influence neuronal signaling. This study aimed to investigate the potential connection between LMTK3 and neuronal signaling pathways in colorectal cancer (CRC).

Methods: Using the Cre/loxP system, we generated a C57BL/6 mouse strain that lacks the expression of LMTK3. $1x10^6$ MC38 cells were subcutaneously implanted into 8 weeks old male and female wildtype (WT) and knockout (KO) mice. Tumor growth was measured until endpoint was reached. Tumors were then processed for RNA sequencing. Differentially expressed genes (DEGs) for each comparison group: WT Female vs WT Male, WT Female vs KO Female, WT Male vs KO Male, and KO Female vs KO Male were analyzed. Ingenuity pathway analysis (IPA) was done for identification of upstream regulators involved and affected cellular pathways. Expression levels of DEGs for glutamate receptor subunits were validated using qRT-PCR.

Results: Both male and female LMTK3 KO mice showed highly significant ($p<0.01$) reduced tumor size when compared to WT mice of the same sex. Additionally, the KO female tumors were significantly ($p<0.05$) smaller when compared to the KO males. RNA sequencing revealed 761 DEGs in KO and WT female and 133 DEGs in KO female and male cohort comparisons ($q<0.05$). IPA results showed significant ($p<0.01$, Z-score<-2) alterations in pathways including glutaminergic receptor signaling, neurovascular coupling, CREB signaling in neurons, and synaptic long-term depression in the WT vs KO female tumor cohort comparison. Within these pathways DEGs: CACNA1E, CACNA2DA, CACNG2, GRIA1, GRIA2, GRIN1, and GRIN2B, were downregulated in KO females. Upstream regulator analysis identified transcription regulators such as OTX2 and NEUROD1 as well as beta-estradiol to be significantly inhibited ($p<0.01$, Z-score<-2) in KO females. qRT-PCR analysis showed significant ($p<0.05$) decreased expression in GRIA1, GRIN1, and GRIN2B as well as GRIN2A and GRIN2C in KO females when compared to WT females or KO males, validating RNA seq results.

Conclusions: These results showed the involvement of LMTK3 in the gut-brain axis and its effect on CRC tumor growth. Downregulation of multiple neuronal pathways and genes suggest that LMTK3 may influence neuron signaling and neurotransmitter release to produce stimulatory or inhibitory effects within the tumor environment. The concurrent inhibition of beta-estradiol in LMTK3 KO tumors allude to possible sex differences the kinase's effect on the observed tumor growth. Further studies are needed to confirm the mechanism of interaction of LMTK3 within these pathways.

#6833 Microenvironment-specific transcriptomic changes in osteosarcoma metastasis.

Shimara Gunawardana-Zeigler[1], Dan Peng[2], Patrick Cahan[2], David Loeb[1]

[1]Developmental and Molecular Biology/Pediatrics, Albert Einstein College of Medicine, Bronx, NY,[2]Biomedical Engineering, Johns Hopkins University School of Medicine, Baltimore, MD

Osteosarcoma (OS) is the most common primary malignancy of bone in children and adolescents. While conventional chemotherapy has improved 5-year survival rates for localized disease to 70%, metastatic disease remains at 20-30%. Failure of modern treatment options to improve survival reflects the failure of agents that appear promising in preclinical models to demonstrate clinical efficacy in human patients. We hypothesize that this is because most preclinical testing is performed on tumors implanted subcutaneously in immune deficient mice. Our previous work has shown that tumors implanted subcutaneously do not metastasize, whereas genetically identical tumors implanted orthotopically (in the tibia) metastasize to lungs and bones. Thus, to better understand non-genetic drivers of metastasis, we implanted patient-derived xenografts (PDXs) either orthotopically or subcutaneously into NSG mice. Once tumors reached 1.5cm, tumors were extracted along with distant metastases and analyzed by single-cell RNA sequencing. Transcriptomic analysis reveals 1) that fragments of the same tumor implanted subcutaneously have a vastly different transcriptome than fragments implanted orthotopically, 2) the transcriptome of distant metastases is dramatically different from the transcriptome of the primary tumor, and 3) the gene expression profile of metastases is different in different metastatic sites. In all 3 of these circumstances, these differences reflect differences in differentiation status, signaling pathway activation, and immune cell infiltrate. Thus, we conclude that the environment in which a tumor grows significantly alters its gene expression and phenotype. Our study highlights the need for careful consideration of the tumor microenvironment when designing pre-clinical studies to ensure accurate representation of human osteosarcoma and may help to explain the dismal record of translating novel agents from preclinical studies into standard therapy.

#6834 Periostin involvement in cellular senescence in ovarian cancer.

J. Feng, E. Nguyen, J. Reyes, Z. Huang;
Duke University Medical Center, Durham, NC

Purpose: Despite improvements in care and advancements in the understanding of ovarian cancer (OC) pathobiology and genetics, survival rates remain disappointingly low compared to other types of cancer. This is due to a lack of diagnosis strategies, high recurrence rates, and the development of chemo-resistant diseases, which require synergy between cancer cells and the tumor microenvironment (TME). We have demonstrated the functional importance of a TME gene, periostin (POSTN), in OC and recurrent OC, using in vitro and in vivo models. Our objectives were to identify differentially expressed genes by POSTN expression in the TME that contribute to the progression of ovarian cancers.

Procedures: Gene expression data was generated from an ovarian cancer cell line, HEYA8, cultured in a high POSTN conditioned 3D cell culture environment, using the NovaSeq 6000 system to generate RNA-seq data. The data was analyzed to determine the genes expressed at different levels between the HEYA8 cells grown with or without POSTN-high conditioned medium (CM). The gene functional annotation and KEGG pathway enrichment were further analyzed from 10,115 significant differentially expressed genes between the HEYA8 cells grown in high levels of POSTN ($CM^{POSTNhigh}$) or low levels of POSTN (CM^{CTL}) culture conditions, using DAVID bioinformatics.

Results: Using a cell culture and co-culture model, we found that OC cells cultured under conditioned media containing $CM^{POSTNhigh}$ exhibited faster cell migration, more invasiveness ($p=0.006$), more chemo-resistance ($p<0.05$), and increased resistance to paclitaxel-induced apoptosis, compared to OC cells cultured with control medium (CM^{CTL}). OC cell lines cultured with $CM^{POSTNhigh}$ showed increased side population cells relative to CM^{CTL} -cultured cells, suggesting POSTN plays important roles in cancer stem cell enrichment. POSTN-transfected 3T3-L1 cells exhibited more intracellular and extracellular lipids and were linked to increased cancer cell expression of the oncogene fatty acid synthetase. In correspondence to the functions of POSTN in OC cells, the pathways identified to be significantly impacted by POSTN expression included, but were not limited to, the cell cycle, apoptosis, p53 signaling, MAPK signaling, and PI3K-Akt signaling pathways. Interestingly, we also found cellular senescence pathways was one of the most significantly impacted by POSTN suggesting that POSTN may play roles in ovarian cancer via the regulation of cellular senescence, which has not yet been explored.

Conclusions: These data emphasize the importance of TME factors in tumor progression and prognosis via various ways in ovarian cancer, establishing promising potential therapeutic targets of OC.

#6835 Profiling of new prostate cancer vulnerabilities through single-nucleus RNAseq implicates the CAF-specific TGF-β pathway in tumor progression.

A. P. Alloy[1], S. Chamling Rai[2], B. O'Brien[2], A. Lyubetskaya[2], A. Amzallag[2], B. Chen[2], A. Lako[2];
[1]Bristol Myers Squibb, Summit, NJ, [2]Bristol Myers Squibb, Cambridge, MA

Background: Transcriptomic profiles of primary high grade prostate cancer (hgPCa) have been extensively studied and prognostic gene expression signatures to classify patients for risk have been identified. However, such studies have employed bulk genomic techniques that blur the contributions of the different cell types. Indeed, tumor microenvironment (TME) cells can significantly contribute to these transcriptomic signatures thereby confounding the lineage of potential therapeutic targets. These challenges underscore the potential of single-nucleus (sn)RNAseq to elucidate new PCa vulnerabilities. We set out to assess whether the TME, particularly cancer-associated fibroblasts (CAFs) drive poor outcome in PCa.
Methods: We obtained 15 treatment-naïve frozen primary high risk PCa tissue samples, mostly Gleason >=8. A PCa nuclei dissociation protocol was adapted for single nucleus snRNAseq (10X Genomics). Sample profiling included all cell populations in the tissue including tumor and TME. Output was analyzed using Seurat (v.4.1.1), corrected for ambient RNA expression with CellBender (v.0.3.1) and detected and removed doublets with Scds (v.3.9). Tumor cells were distinguished from normal epithelium cells by a combination of inferCNV (v.1.12.0) and supervised learning with random forests classification.
Results: Through snRNAseq, we show that CAFs, and not tumor cells, entirely drive the expression of previously validated poor prognostic signatures (Mortensen, 2015). Our analysis revealed that the TGFβ pathway expression, TGF-β1 in particular, is upregulated in CAFs rather than PCa cells. This pathway, along with poor prognosis signatures are selectively elevated in CAFs from patients with Gleason high compared to low, implicating the TGFb axis as a PCa vulnerability. We also derived a snRNAseq CAF signature that differentiates non-responders to immune checkpoint therapy in mCRPC (Nivolumab+Ipilimumab). Furthermore, cluster profiling of tumor nuclei revealed that hgPCa harbors high heterogeneity with distinct niches of hgPC, mCRPC or neuroendocrine phenotypes for each patient.
Conclusions: Through snRNAseq we show that CAFs are the main contributors to prior bulk RNAseq classifiers of poor response, resulting in a refined CAF signature that allows for direct investigation of the contribution of CAFs in other patient segments (mCRPC). Our findings point to a hgPCa patient segment with high CAF representation that may benefit from the addition of a CAF targeting agent (ie.TGFbi) to androgen deprivation therapy. This data has the potential to help refine our prognostic classifiers for patient selection and clinical applicability. Further study of the reported tumor heterogeneity will inform rational combination therapies to tackle resistance mechanisms.

#6836 Single-cell RNA sequencing of FUS::DDIT3 myxoid/round cell liposarcoma delineates mechanisms of oncogenic progression and immune escape.

R. Gularte-Merida, **E. Seffar**, G. Li, Y.-M. Kim, N. Agaram, N. Socci, F. Sanchez-Vega, N. Schultz, S. Singer;
Memorial Sloan Kettering Cancer Center, New York, NY

Myxoid/Round Cell Liposarcoma (MRCL) is an understudied soft tissue sarcoma that typically affects young adults and accounts for 30% of all liposarcomas. MRCL is characterized by oncogenic DDIT3 fusions, with FUS::DDIT3 being present in over 90% of cases. However, the cellular origins and oncogenic mechanisms of MRCL remain incompletely defined. Here we report oncogene transcription, and tumor-immune interactions in a cohort of 5 patient tumors with matched normal tissue for which we sequenced the transcriptomes of approximately 45,000 single cells using 10X Genomics, and full-length transcripts in approximately 20,000 single cells via Oxford Nanopore in 2 of these patients.

Our results reveal two distinct cancer cell populations: Early Cancer Cells (ECC) and Advanced Cancer Cells (ACC). These cells appear to derive from adipose stem progenitor cells (ASPC) and fall along an ASPC→ECC→ACC pseudo-time axis. Along this axis, a distinct pattern emerges where oncogenes tend to be upregulated and tumor suppressor genes (TSG) tend to be downregulated and these appear to be mutually exclusive. Comparing ECC to ASPC we see increased expression of HIPPO and PI3K pathway oncogenes, FGFR2 and IGF1R RTKs, and downregulation of the TSG CDKN2A and CDKN1A. ACC show upregulation of hedgehog, ErbB, WNT, HIPPO, PI3K, and MAPK signaling pathways compared to ECC. Full-length transcript sequencing at the single-cell level shows a consistent expression of the FUS::DDIT3 fusion transcript in both ECC and ACC populations, confirming that these populations are cancer cells. Furthermore, MRCL displays several immune escape mechanisms, including poor immune infiltration and a marked decline of HLA Class I expression along the pseudo-time axis from ECC to ACC, suggesting a complex interplay between oncogenic signaling and immune evasion.

These results suggest that MRCL likely originates from ASPC and expression of FUS:DDIT3 oncoprotein induces early HIPPO, PI3K, FGFR2, and insulin signaling pathway expression in ECC with further hedgehog, ErbB, MAPK, and WNT pathway activation in ACC. This progressive activation in oncogenic signaling is associated with immune evasion. This is the first single-cell RNA seq analysis to detect the presence of the FUS::DDIT3 fusion in ECC and ACC significantly advancing our understanding of the mechanisms of MRCL oncogenesis, immune escape, and identifies potential novel therapeutic targets.

#6837 Prolonged effects of hypoxia in luminal breast cancer cells.

A. Moriarty[1], O. Iriondo[2], Y. Amzaleg[2], R. Klotz[1], M. Yu[1];
[1]University of Maryland School of Medicine, Baltimore, MD, [2]USC Keck School of Medicine, Los Angeles, CA

Metastasis is the main cause of tumor-related mortality in breast cancer patients. Improving our understanding of the metastatic cascade is imperative to improve patient outcomes. Prior research indicates cancer cells with increased metastatic potential have acquired adaptive properties induced by factors in the tumor microenvironment (TME), including hypoxia. However, previous hypoxia research has primarily focused on signaling changes that occur when cancer cells are in the hypoxic TME and does not account for long-term changes that may occur once cancer cells re-enter normoxia, such as when they metastasize. Our research in patient-derived circulating tumor cell (CTCs) lines and breast cancer cell lines indicates that certain transcriptional changes are maintained after cells leave hypoxia, and that these post-hypoxic cells maintain a higher metastatic potential compared to cells not exposed to hypoxia. Taking an un-biased approach to define changes in hypoxia-exposed breast cancer cells upon reoxygenation, we performed bulk RNA-Seq on post-hypoxic luminal breast cancer cell lines compared to normoxic controls cultured either in adherent or suspension conditions, the latter to mimic the physiological context of CTCs. We found that a subset of genes that were differentially expressed in hypoxic conditions were maintained as up- or down-regulated after cells were reoxygenated, indicating a “hypoxic memory”. Additionally, a subset of differentially expressed genes were unique to the post-hypoxic cells, demonstrating both prolonged and novel gene expression changes induced by hypoxia exposure. We also performed functional assays and observed that this post-hypoxic state is associated with a more aggressive phenotype. Current research in our lab is on-going to understand the epigenetic changes that may be responsible for this hypoxic memory. Overall, this research will improve our understanding of the prolonged consequences of hypoxia on CTC biology and metastasis.

#6838 Adipose tissue features in breast cancer patients: Impact and modifications induced by tumor according to body mass index.

S. Romero-Cordoba[1], R. Agresti[2], V. Regondi[2], G. Trecate[2], F. Bianchi[3], L. Sfondrini[3], S. M. Pupa[2], E. Tagliabue[2], **T. Triulzi**[2];
[1]Instituto de Investigaciones Biomedicas, Universidad Nacional Autonoma de Mexico, Mexico city, Mexico, [2]Fondazione IRCCS Istituto Nazionale dei Tumori, Milano, Italy, [3]Universita degli Studi di Milano, Milano, Italy

Adipose tissue (AT) is emerging as a contributing factor to cancer development and progression, especially in obesity. However, the mechanisms underlying this association are not yet fully understood. Based on the described *in vitro* interplay between cancer cells and adipocytes that induces adipocyte dedifferentiation and the acquisition of an inflammatory phenotype, it is conceivable that tumor-adipocyte crosstalk promotes cancer progression even in normal weight patients (pts). To study tumor-induced AT alterations, we performed a transcriptomic analysis of matched adjacent and distant tumor AT samples from 41 breast cancer (BC) pts (78% Luminal B, 12% HER2+, 7% TNBC) undergoing mastectomy. Comparison of the gene expression landscape of BC-adjacent *vs* distant ATs derived from normal weight pts (BMI<25, n=28) identified 723 differentially expressed genes (FDR<10%). Metabolic signaling processes were over-represented in genes resulted downmodulated in the BC-adjacent AT, while those upmodulated were mainly classified into proliferation, migration and inflammatory response, cell programs associated with dedifferentiated adipocytes *in vitro*. Accordingly, BC-adjacent ATs were found to be enriched (NES=1.78, p<0.0001) in a set of genes unique of *in vitro* dedifferentiated adipocytes compared to mature adipocytes. In overweight/obese pts, no differentially expressed genes were found between BC-adjacent and -distant ATs, although gene sets composed of modulated genes in normal weight pts were found to be significantly enriched (NES=1.50, p<0.0001; NES=-1.52, p=0.0025). In addition, a significant enrichment of altered BC-adjacent AT genes and inflammatory response process was observed (NES=1.49, p=0.0029; NES=1.62, p=0.011) in the BC-distal AT of overweight/obese *vs* normal weight pts, indicating that AT is already altered and inflamed independently of the presence of the tumor in overweight/obese women. To further analyze AT heterogeneity, we performed an unsupervised clustering of all AT samples using the K-means algorithm. Five stable clusters were identified, which were independent of sampling site. Indeed, the matched AT samples derived from 70% of the pts were assigned to the same cluster, with a significant grouping of overweight/obese pts in clusters K1 and K2 (p=0.0217). BC-adjacent AT samples from the remaining pts clustered significantly (p=0.030) in the other 3 clusters, especially in K5, which had the highest CAA score, a signature reflecting adipocyte dedifferentiation. Consistent with the association with obesity, K1/K2 pts had significantly higher circulating PCR, cholesterol, triglycerides and insulin and recurrence rate. Overall these data suggest that BC cells induce adipocyte modifications in normal weight pts and that obesity-associated BC aggressiveness is related to intrinsic characteristics of adipose tissue.(Supported by AIRC)

#6839 Comprehensive transcriptomic analysis of acquired resistance after immune-checkpoint inhibitors in non-small cell lung cancer.

C. Joe, Y. Bang, S. Park, H. Jung, J.-M. Sun, Y.-L. Choi, J. Ahn, M.-J. Ahn, S.-H. Lee;
Samsung Medical Center, Seoul, Korea, Republic of

Background: Treatment of lung cancer has changed dramatically with the use of immune checkpoint inhibitors (ICI). Nevertheless, most patients underwent drug resistance even though they initially showed a response to ICI, and there is an unmet need to delineate the mechanism.
Method: We analyzed RNA sequencing data of paired pre- and post-ICI samples from 31 NSCLC patients. Among them, we identified 17 patients who underwent acquired resistance (AR) who initially showed partial or complete response or stable disease lasting more than six months, and the remaining 14 patients who showed primary resistance (PR) to ICI. The analysis was performed using a tumor microenvironment (TME) classifier, classifying immune-enriched [IE], immune-enriched and fibrotic [IE/F], fibrotic [F] and immune-desert [D] subtype, and CIBERSORTx, the immune cell deconvolutional analysis tool.
Results: Most patients with AR were initially classified as IE or IE/F subtypes (N=12, 70.6%), but six out of 14 with PR (42.8%) showed IE or IE/F subtypes. Among 12 patients with initial IE or IE/F subtypes, seven (58.3%) patients turned into the D subtype after AR to ICI. Most patients initially classified as D or F subtypes (N=5, 29.4%) maintained their subtypes (N=4, 80%) after AR.When assessing the pre-ICI samples, memory B cell was enriched, and M2 macrophage and regulatory T cell were depleted in AR patients compared to PR. The memory B cell and resting memory CD4+T cell decreased, and M2 macrophage increased after AR to ICI. These immune cell composition changes were not observed in PR patients.
Conclusions: We observed differences in TME phenotype and immune cell composition before ICI between AR & PR patients. The TME change from immune-enriched to desert and cell composition change of increased M2 macrophages and decreased memory B and resting CD4+ T cells after AR to ICI could be significant mechanisms of AR to ICI.

#6840 Automated preparation of single nuclei from FFPE samples for snRNA-Seq.

S. Jovanovich[1], N. Pereira[1], D. Meyer[1], C. Snopkowski[2], I. Masilionis[2], B. Meskauskaitė[2], M. Takizawa[2], Z. Abou-Mrad[2], K. Yu[2], V. Tabar[2], K. Luckett[2], K. Ganesh[2], N. Khan[1], R. Chaligne[2];

[1]S2 Genomics, inc., Livermore, CA, [2]Memorial Sloan Kettering Cancer Center, New York, NY

S2 Genomics developed the Singulator™ 100 and 200 Systems to automate the processing of fresh, frozen, or OCT tissues into single cell or single nuclei suspensions using disposable cartridges, reagents, and customizable protocols. The systems have been used to prepare cells or nuclei from a wide range of tissues and organisms, including human, mouse, chicken, insects, snails, zebrafish, and plants.

Formalin-fixed, paraffin-embedded (FFPE) tissues are the preferred format for pathologists and as many as one billion FFPE slides are in repositories. FFPE tissue samples have traditionally been difficult to study with molecular techniques due to the chemical modifications caused by the formalin fixation, which can lead to degradation and sequestration of RNA and DNA. Recent advances in single cell/nuclei RNA-Seq library preparation technology have made it possible to overcome these challenges and generate high-quality single cell or nuclei genomic data from FFPE samples. Protocols have been released for processing previously deparaffinized and rehydrated FFPE samples on the Singulator 100 or 200 into single nuclei.

We now report the development of a fully automated workflow for the deparaffinization and rehydration of FFPE tissues in about 40 min, with an optional enzymatic treatment of 45 min, and processing of FFPE tissues into singulated cells or nuclei on prototype Singulator 200 systems. Data will be presented for the optimization of process parameters for cell or nuclei recovery and RNA quality for six tissues. Finally, single nuclei sequencing data will be presented for snRNA-Seq libraries from healthy and cancerous human FFPE samples including glioblastomas and colorectal cancer. These data demonstrate the successful recovery of genomic materials from FFPE samples using an automated sample preparation system for single cell/nuclei transcriptomics.

#6841 Mutation specific mechanisms of resistance to oncogenic KRAS inhibition.

I. Barravecchia, E. Lasse-Opsahl, S. Cavanaugh, L. Rober, R. Baliira, M. Robotti, R. Hinshaw, J. M. Lee, Y. Zhang, M. Pasca di Magliano, S. Galban; University of Michigan, Ann Arbor, MI

Mechanisms of resistance to inhibitors against mutant KRAS are linked to the remodeling of the tumor microenvironment (TME). Understanding this remodeling process during intervention and tumor recurrence will likely guide the development of future therapeutic treatment paradigms with long-term responses. 56% of never-smokers with non-small cell lung cancer have $KRAS^{G12D}$ mutant cancer and respond little to immune checkpoint therapy (ICI) compared to smokers, who often have mutations in $KRAS^{G12C}$. Our analysis of the TME in a unique $Kras^{G12D}$ inducible and reversible mouse model of NSCLC using single cell RNA sequencing data shows $Kras^{G12D}$-dependent control of the TME, particularly of the expression of PDL1 in a subset of myeloid cells. PDL1 expression was found to be $Kras^{G12D}$ dependent as it was reduced significantly when $Kras^{G12D}$ was turned ON in mouse lungs. Interestingly, when $Kras^{G12D}$ was turned OFF, the expression of PDL1 increased, indicating mechanisms of resistance. Furthermore, the cytokine expression and secretion of IL6, a known regulator of PDL1 expression, increased in lung tissue and lung cancer cells derived from this model upon genetic and chemical (MRTX1133) Kras inhibition. Moreover, the mechanisms of resistance to oncogenic Kras inhibition appear to be mutant specific. Transcriptome and secretome analyses in human and murine $Kras^{G12D}$ or $Kras^{G12C}$ mutant lung cancer cells show distinct cytokine regulation upon KRAS inhibition. Identification of mechanisms of resistance like the induction of PDL1 expression upon KrasG12D inhibition may provide a strong rationale for co-treatment of KRAS inhibitors with ICI for KrasG12D never-smokers with NSCLC.

#6842 The effect of intra-tumoral *Candida albicans* on host gene expression.

A. Loncar[1], D. Grencewicz III[2], R. Hoyd[3], A. Pallerla[1], N. Williams[3], M. Benej[3], Y. Mehra[3], S. Jahanbakhshi[3], M. Anderson[4], N. Denko[3], D. Spakowicz[2]; [1]The Ohio State University, Columbus, OH, [2]The Ohio State University College Of Medicine, Columbus, OH, [3]The Ohio State University Comprehensive Cancer Center, Columbus, OH, [4]University Of Wisconsin - Madison, Madison, WI

The gut and tumor microbiome have been shown to affect tumorigenesis, tumor immune infiltration, and response to traditional cancer therapeutics such as radiation therapy. Further, specific microbe-cancer relationships have been established. One such microbe is *Candida albicans,* which has been identified within several gastrointestinal cancers and is associated with an increased risk of metastases and decreased overall survival. By completing RNA-sequencing on murine rectal tumors colonized with *C. albicans*, we can better understand whether intratumoral changes in gene expression exist based on colonization of specific microbes. This study utilizes gut-to-tumor translocation and whole transcriptome analysis for a discovery-based approach to identify the effects of *C. albicans* on the host tumor.

We established a rectal tumor model with C57BL/6 mice using MC38 rectal cancer cells subcutaneously injected on the right flank, local radiation to the tumor (standard-of-care for rectal cancer), and gavage with either *C. albicans* (*Ca*) or PBS. Fungal presence within tumors was validated by staining with calcofluor white and subsequently, tumors were sent for bulk RNA-sequencing to determine differences in gene expression using DeSeq2 and a gene set enrichment analysis (GSEA).

In unsupervised analysis of gene expression differences between PBS-gavaged and *Ca*-gavaged with bulk RNA sequencing, tumors gavaged with *C. albicans* possessed unique gene expression and pathway analysis when compared to PBS-gavaged mice. Global differential gene expression showed 1,947 genes upregulated in *Ca* gavage and 593 genes upregulated in the PBS gavage ($p < 0.05$). *C. albicans* colonized tumors showed decreased expression in gene pathways relating to immune activation (interferon alpha response, IL-6 and *STAT3* signaling), *p53* expression, DNA repair, oxidative phosphorylation, *NOTCH* signaling, and apoptosis. We subsequently used a network-based approach to identify the most important genes driving the differences in the tumors, calculating the degree, closeness, and betweenness centralities.

Several microbes have been regarded as potential contributors to decreased treatment response and survival in rectal cancer. In the case of tumors colonized with *C. albicans,* bulk RNA-sequencing indicates down regulation of gene pathways related to cell proliferation, immune activation, and DNA maintenance. Down regulation of gene pathways related to cell cycle control and arrest suggests that intratumoral colonization of *C. albicans* may causally affect tumorigenesis. Decreases in immune signaling in tumors suggest a potentially causal role of *C. albicans* immune suppression. These results highlight initial steps to understand how intratumoral *C. albicans* may be affecting rectal cancer progression and treatment response and serve as a technique to allow better insight to individual microbial impact on tumors.

#6843 Comprehensive multi-omics approaches for identification of genetic alterations in head and neck squamous cell carcinoma.

Kirsteen Maclean, Qinqin Zha, Lakshmi Chandramohan, Anna Juncker-Jensen

NeoGenomics, Aliso Viejo, CA

Background: Head and neck squamous cell carcinoma (HNSCC) is one of the most difficult and challenging malignancies, with a high level of heterogeneity and a wide range of treatment responses, regardless of the clinical stage. Oral squamous cell carcinoma (OSCC) is the most common head and neck cancer and accounts for over 90% of cancers that develop in the mucosal epithelium of the oral cavity. Additional carcinogenic risk factors, including tobacco, alcohol, and HPV infection are also associated with the pathogenesis of oral carcinogenesis. Unfortunately, today the failure of standard treatment modalities such as surgery, radiotherapy, and chemotherapy underscore the need for comprehensive genomic profiling to provide a better picture of the genetic alterations and gain an improved understanding of the complex signaling networks involved in the development of potential treatment resistance as well as the identification of novel biomarkers that discriminate between smokers and non-smokers.

Methods: A retrospective analysis was performed on biopsied Formalin-Fixed Paraffin-Embedded (FFPE) samples from OSCC patients with and without a history of smoking and treated +/- chemotherapy. Patient samples representing matched normal tissue to serve as controls were compared to tumor squamous cell carcinoma samples and profiled using a single assay panel that includes 517 genes by both DNA and RNA NGS, microsatellite instability (MSI), and tumor mutational burden (TMB). Further analysis was also performed using the NanoString nCounter® PanCancer Immune Profiling Panel (PCIP), 770-comprehensive gene expression panel

Results: The Neo Comprehensive™ Solid Tumor pan cancer assay enabled simultaneously analysis of both DNA and RNA in one integrated workflow with an accompanying Dragen™ bioinformatics analysis platform and provided comprehensive genomic profiling of sequence and structural variants, as well as genomic signatures such as TMB and MSI in OSCC patients. Utility of the NanoString PCIP highlighted immune-relevant gene expression changes within the different sample cohorts. The detailed molecular information highlighted by our study emphasizes the need for improved patient classification based on smoking status in the management of OSCC and also in establishing potential therapeutic options based on the many altered cell signaling pathways that we identified. By combining a multi-omics approach with expression data for immune-related genes and associated overall survival data, we provide an effective strategy and workflow for the identification of prognostic biomarkers in OSCC.

#6844 Discovery of a novel sialic acid O-acetyltransferase in colon tissue.

B. Lee[1], A. Cook[1], M. Zeineldin[1], S. Sur[1], L. Dobbyn[1], M. Popoli[1], S. Khalili[2], B. Vogelstein[1], N. Papadopoulos[1], S. Zhou[1], C. Bettegowda[1], P. Buckhaults[2], T. Larman[1], K. Gabrielson[1], K. W. Kinzler[1], N. Wyhs[1];

[1]Johns Hopkins University School of Medicine, Baltimore, MD, [2]University of South Carolina, Columbia, SC

Sialic acids have critical functions relating to host-pathogenic interactions and the immune microenvironment. Subsequent post-translational O-acetyl modifications add an extra layer of control by modulating many of these interactions in both normal and transformed colorectal cells. The processes through which this modification is added to sialic acids are not completely understood. To date only one gene, *CASD1*, has been identified to encode a sialic acid O-acetyltransferase in human cells. We used whole-genome sequencing on normal human colon tissue to identify a haplotype strongly associated with colorectal sialic acid O-acetylation, as determined by histopathological mPAS staining. Only SNP's of a single candidate gene within the haplotype correlated perfectly in a 91-sample validation set. CRISPR-Cas9 editing of this gene in 2D cell line and 3D normal colon organoid models yielded changes to modified sialic acid levels. These findings suggest that this candidate gene functions as a novel sialic acid O-acetyltransferase in colorectal tissue and could have implications as a diagnostic tool for patients with inflammatory diseases of the bowel or as an indicator for therapeutic targets in cancer.

#6845 MAGEA3 expression and secretion in MMR-MSH6 and MMR-PMS2 microsatellite-stable colorectal cancer.

J. Yom, R. Gonzalez, B. Gilmore, Z. Guo, A. Han, E. Zewdu, D. Kong, T. Qu, H. Guo, A. Strom, Z. Zhao, X. Hu, Q. Ren, Y. Ma, R. Zhang, Z. Wu, X. Liu, W. Fu; OriGene Technologies, Inc., Rockville, MD

Despite the breakthrough of PD-1/PD-L1 blockade therapy in the recent years, mixed responses have been shown across multiple tumor types, including in colorectal cancer (CRC), the second leading cause of death worldwide. This immunotherapy has proven to be successful for a subtype of CRC that carries mismatch repair deficiency (dMMR) and high microsatellite instability (MSI-H), despite a lack of response by microsatellite-stable CRC. For these types of non-responsive cancers, new immunotherapy targets are currently being investigated for alternative therapy such as the MAGE-A cancer testis antigen family whose expression is restricted to germline cells in normal tissue but is overexpressed in many cancer cells. In this study, we examine the relationship between MAGEA3 and MMR proteins MSH6 and PMS2. Immunohistochemical staining of CRC tissues demonstrated co-expression between MAGEA3 with both MSH6 and PMS2. Immune cells were observed to express MAGEA3 in CRC as well. To investigate the possibility of secreted MAGEA3 from tumor cells, we performed western blot analysis of CRC cell lines, ELISA, and binding assay on cell lines and the positive results suggest that MAGEA3 protein is secreted. The results suggest that MAGE-A3 may be a promising target for microsatellite-stable colorectal cancer immunotherapy.

#6846 Tumor cell metaplastic programs and failure of T cell remodeling drive resistance and progression to frontline chemoimmunotherapy in advanced gastric cancer.

Samuel J. Wright[1], Minae An[2], Byung Hoon Min[3], You Jeong Heo[4], Milan Parikh[1], Lynn Bi[1], Hyuk Lee[3], Taejun Kim[3], Song-Yi Lee[5], Jeonghyeon Moon[6], Ryan J. Park[1], Matthew R. Strickland[7], Woong Yang Park[8], Won Ki Kang[5], Kyoung-Mee Kim[9], Seung Tae Kim[5], Arnav Mehta[1], Samuel J. Klempner[7], Jeeyun Lee[5]

[1]Broad Institute of MIT and Harvard, Cambridge, MA,[2]Experimental Therapeutics Development Center, Samsung Medical Center, Seoul, Korea, Republic of,[3]Department of Gastroenterology, Samsung Medical Center, Sungkyunkwan University School of Medicine, Seoul, Korea, Republic of,[4]Neocella, Inc., Irvine, CA,[5]Division of Hematology-Oncology, Department of Medicine, Samsung Medical Center, Sungkyunkwan University School of Medicine, Seoul, Korea, Republic of,[6]Departments of Neurology and Immunology, Yale School of Medicine, New Haven, CT,[7]Department of Medicine, Division of Hematology-Oncology, Massachusetts General Hospital, Boston, MA,[8]Geninus Inc, Seoul, Korea, Republic of,[9]Department of Pathology and Translational Genomics, Samsung Medical Center, Sungkyunkwan University School of Medicine, Seoul, Korea, Republic of

Adding aPD1 to 5-FU/platinum in advanced gastroesophageal adenocarcinomas (GEA) has yielded modest and heterogeneous results. Understanding cooperativity between these two treatment modalities will inform novel combination treatments for GEA. Towards this end, we conducted a trial (n = 47) sequentially adding pembrolizumab to 5-FU/platinum in previously untreated advanced GEA. Using serial biopsy of the primary tumor at baseline, after one cycle of 5-FU/platinum, and after the addition of pembrolizumab we transcriptionally profiled 358,067 single cells and obtained TCR-sequences from single tumor-resident T cells. Stratifying patients into slow- (> 6 months) and fast-progressing (< 6 months) groups based on progression-free survival allowed us to quantify differences in immune, stromal and epithelial subpopulations across treatment time points. Using topic modeling with consensus non-negative matrix factorization (cNMF), we identified gene expression programs in each population at each time point and developed a methodology to verify the stability of those programs across the cohort using cross-validation. Faster clinical progression featured decreased M1-like macrophage repolarization and increased MUC5A and MSLN containing metaplasia programs in tumor cells. We next selected features from cell state gene programs and identified trajectories of tumor cells across a spectrum of treatment sensitive and resistant states. We identified several factors that correlated with these trajectories and regulons that may be influencing them. After pembrolizumab we observed slower progression was associated with further increased CD8 T cell infiltration with increased CXCL13+ T cells. We next calculated covarying programs between patient samples at each time point and performed permutation testing to identify which programs (and respective cell types they were expressed in) were significantly correlated to infer the presence of multicellular tumor communities. We found that the tumor cell interferon program co-varied with the CXCL13 T cell program, and the emergence of a covarying module with tumor-reactive CXCL13 program expression happens as early as after the first dose of chemotherapy. To better understand the behavior of tumor reactive T cells within the tumor microenvironment, we leveraged TCR-sequencing data to study T cell clonality and diversity across treatment time points and between fast and slow progressors. Our data provide an invaluable resource to dissect chemoimmunotherapy response in tumor cells, understand T cell behavior and propose strategies to drive anti-tumor immune hub formation to expand the portion of patients benefiting from immunotherapy approaches.

#6847 IGF2BP3 promotes esophageal squamous cell carcinoma progressions via Wnt/CTNNB1 pathway.

Z. Tian[1], Y. Zhou[1], Y. Ding[1], Z. Wu[2], **X. Zhao**[1];

[1]The Second Hospital of Shandong University, Jinhua Shi, China, [2]The Second Hospital of Shandong University, Jinan, China

The M6A RNA modification plays a crucial role in the progression of tumors. Simultaneously, IGF2BP3 is primarily expressed in the tumor cells of squamous cell carcinoma, rather than in stromal cells, including esophageal squamous cell carcinoma (ESCC), a subtype mainly prevalent in East Asia. However, the mechanism of IGF2BP3 in the progression of esophageal squamous cell carcinoma and its role in the tumor microenvironment (TME) remain unknown and require further exploration. Our research reveals that IGF2BP3 not only plays a significant oncogenic role in tumor cells, including the activation of the Wnt pathway, PI3K-AKT pathway, and MAPK pathway, but also, the high expression of IGF2BP3 is positively correlated with the enrichment of M2 macrophages in ESCC tissues, in the TME, IGF2BP3 promotes the infiltration of M2 macrophages, ultimately facilitating the progression of ESCC. Mechanistically, IGF2BP3 enhances the translation of USP36 mRNA by directly binding to its mRNA, rather than increasing the stability of mRNA. The IGF2BP3-mediated USP36 protein elevation enhances the binding capacity with CTNNB1 protein, reducing its degradation through the ubiquitin-proteasome pathway, and following improved the Wnt/CTNNB1 pathway activating. Ultimate, IGF2BP3 aggravated the malignancy of the tumor. Additionally, the activation of the Wnt pathway promotes TGFB1 transcription and secretion, subsequently activating the polarization of M2 macrophages, infuriating the formation of the tumor immune-suppressive microenvironment, ultimately promoting the progression of esophageal squamous cell carcinoma. Our findings strongly emphasize the oncogenic role of IGF2BP3 in the progression of ESCC both in vitro and in
vivo, providing new insights and perspectives for the treatment of esophageal squamous cell carcinoma.

#6848 Analysis of the bone microenvironment cells by single cell transcriptomics reveals altered features in multiple myeloma patients compared to pre-malignant monoclonal gammopathies.

P. Storti[1], T. Torelli[2], C. Manferdini[3], D. Toscani[1], A. Guidi[2], R. Vescovini[1], N. Iannozzi[1], B. Dalla Palma[4], M. Scita[4], F. Librale[4], S. Ricci[4], V. Raimondi[1], O. Lungu[1], G. Todaro[4], G. Sammarelli[4], E. Aleo[5], G. Lisignoli[3], L. Agnelli[2], N. Giuliani[1];

[1]University of Parma, Parma, Italy, [2]IRCCS Istituto Nazionale Tumori, Milano, Italy, [3]IRCCS Istituto Ortopedico Rizzoli, Bologna, Italy, [4]Azienda Ospedaliero-Universitaria di Parma, Parma, Italy, [5]IGA Technology Services, Udine, Italy

Multiple myeloma (MM) is a malignant plasma cell dyscrasia that can be preceded by monoclonal gammopathy of undetermined significance (MGUS) and smoldering MM (SMM). How the bone microenvironment (BME) changes and contributes to tumoral progression in MM remains unresolved. Published data on BME are mainly produced *in vitro* and few data are on MGUS/SMM patients. Up to date, no single-cell RNA sequencing database of the BME cells has been described in MM. The aim of this project was to characterize for the first time at single cell level, the BME in patients with newly diagnosed MM (MMD) and MGUS/SMM to identify alterations involved in tumoral progression. From 15 bone biopsies of MMD, MGUS and SMM patients, we depleted CD235a+, CD45+, CD31+, and CD138+ cells to enrich the rare BME non-hemopoietic cells. The CD45-CD31-CD235a-CD138- cells were analyzed by scRNAseq. Data were generated on Chromium 10X Genomics. Cellranger and Seurat pipeline in R software has been used. Cell identities were assigned by manual curation. The trajectory analysis has been made by Monocle3. Decouple R and FindMarkers were used to compare pathways, and differential gene expression (DGE) of the samples throughout the different conditions. A total of 35723 cells were profiled. We identified 13 BME cell type clusters: 7 mesenchymal stromal cells (MSCs) clusters (proliferating MSC, MSC DDK-OPG-, MSC DKK+, MSC RUNX2-, MSC OPG+, MSC Osteogenic, Perivascular MSC) and 6 osteoblasts (OBs) clusters (OB precursor, OB precursor LEPR+, OB BGLAP+, OB SPP1+, OB NFkB+, OB late). Psdeudotime analyses highlighted a complex trajectory of differentiation from more immature cell clusters (proliferating MSC) to late OB cluster, confirming the ability of the dataset to snapshot the *in vivo* complexity of BME and we highlighted an alteration of the MSCs clusters trajectories starting in SMM samples till a disruption in MM. Pathway analyses, in MMD compared to MGUS/SMM, revealed an upregulation of VEGF and PI3K activity in proliferating MSC, perivascular MSC and OB clusters. TRAIL pathway activity, known to suppress MM cell proliferation, was upregulated in MSC osteogenic and OB BGLAP+ in MGUS. Finally, DGE analyses revealed the modulation of different genes, many not yet described in MM. MGUS MSCs clusters showed an upregulation of *FBLN1, SERPNF1* and MMD MSCs clusters dramatically downregulated *WISP2* and upregulated *SRGN*, involved in MM cell proliferation. Interestingly, in SMM samples, we reported an upregulation of genes involved both in the promotion of osteoblastogenesis (*SCARA3, SPON2*) and inhibition (*GREM1*), likely underling the attempt to contrast the establishment of altered BME, characteristic of MM. Our approach is able to dissect the complex organization of the BME and to highlight at single cells level the alterations of the BME in patients with MM compared to MGUS and SMM.

#6849 Characterizing a discernible stromal fibroblastic gene signature in the shift from high-grade prostatic intraepithelial neoplasia to aggressive prostate cancer.

Mohammad K. Alexanderani, Lucio Queiroz, Mohamed Omar, Claudio Zanettini, Hubert Pakula, Luigi Marchionni, Massimo Loda

Weill Cornell Medicine, New York, NY

Background: High-grade prostatic intraepithelial neoplasia (HGPIN) is a preneoplastic lesion that precedes the development of both indolent and aggressive variants of prostate cancer (PCa). However, the specific stromal molecular mechanisms underlying the progression of HGPIN and their contribution to epithelial cancer cell motility and invasiveness remain poorly understood. This study aims to elucidate the driver genomic alterations involved in shaping the perineoplastic stroma of HGPIN, with the goal of unraveling their role in promoting cancer invasion, and metastasis.

Methods: We performed gene expression profiling on laser capture microdissected perineoplastic stroma of HGPIN and PCa in tissue samples from 25 PCa cases, including 12 low-grade (Gleason 6) and 13 high-grade (Gleason >/= 8) cases. We used the standard moderated t-test from the Bioconductor limma package to assess the statistical significance of differential gene expression between perineoplastic stroma high grade PCa and perineoplastic stroma HGPIN, as well as between perineoplastic stroma low grade PCa and HGPIN. The -log10 *p*-values represents the level of statistical significance for each gene, while the log2 fold change represents the magnitude of gene expression difference between the two comparison groups. Additionally, we computed Gene Set Enrichment Analysis (GSEA) scores using the Bioconductor package and discerned the leading-edge genes among the pathways. This study is supported by the NIH-NCI-T32 program for next-generation pathologists at our institution.

Results: In the gene expression analysis comparing High Grade PCa and HGPIN, several genes, including ***POSTN, BGN, GREM1****, C1QA, THBS4, COL1A1, COL1A2, SFRP4, RNU6-847P, FCGR2P, and TOMM22,* exhibited the highest level of both biological and statistical significance. GSEA revealed that the multi-invasive pathway had the highest enrichment score (>2). Notably, the top overexpressed genes in this pathway exhibited a fibroblastic signature (in bold), including ***POSTN, BGN,*** **GREM1**, **FBN1,** *COL1A2,* **COL3A1, COL5A2**, *ASPN,* **SPARC**, *VCAN, COMP,* **INHBA**, *THBS2, and SFRP4.* The presence of this signature indicates the invasiveness of the disease. Importantly, these genes were not associated with the progression to low grade PCa, indicating their exclusive association with the aggressive variant.

Conclusion: To our knowledge, this study is the first to explore the stroma's role in HGPIN-to-aggressive PCa progression. It highlights a key stromal pathway enriched with fibroblastic gene signature. These findings offer potential biomarkers for targeted therapies and improved care through HGPIN patient stratification.

#6850 Unraveling molecular factors contributing to metallomic dyshomeostasis induced by triple-negative breast cancer using single-cell RNA sequencing.

N. R. Hum[1], J. M. Rolison[1], N. F. Leon[1], A. Navid[1], A. Sebastian[1], J. Wimpenny[1], G. Loots[2];
[1]Lawrence Livermore National Laboratory, Livermore, CA, [2]University of California, Davis, Davis, CA

Triple-negative breast cancer (TNBC) comprises 20% of breast cancer cases and exhibits an aggressive phenotype with increased metastasis; these patients have limited treatment options, poorer prognosis and higher mortality than other breast cancers (BC). Metallomics is a relatively new discipline that studies the abundance of metal ions in biological samples. Metallomic analysis has identified differences in BC patients in elements such as iron (Fe) and zinc (Zn) but it is unclear if these reflect metabolic changes in the tumor. In this study, we conducted metallomic profiling to characterize 55 trace elements in the circulation and in the tumor microenvironment of orthotopic mammary fat pad tumors from two isogenic BC cell lines (highly metastatic 4T1; nonmetastatic 67NR). We complemented this analysis with single-cell RNA sequencing of the tumor to determine if complementary changes occur in molecules known to utilize metals as co-factors or transporters and identify drivers of metal metabolism in different tumors. We performed analysis on systemic metal elements by examining whole blood (including blood cells and platelets) and plasma separately. Tumor samples were assessed at the whole tissue level, and we also profiled separated immune or non-immune cells from the tumor. Li, Na, Mg, P, S, K, Ca, Fe, Cu, Zn, Rb were detectable within 100ul of input of whole blood or plasma. Metallomic analysis of the tumor and associated cell populations detected differential levels of Na, Mg, P, S, K Ca, Fe, Zn, and Rb from an average of 200mg of tissue or 2 million cells. Based on scRNAseq analysis, 67NR tumors were composed of greater proportions of cancer cells relative to the 4T1 tumors (79.1% vs 58.8% of tumor cells respectively) and endothelial cells (2.5% vs 1.8%). 4T1 tumors contained an increased abundance of cancer-associated fibroblasts (5.6% vs 2.1%) as well as immune infiltration (33.8% vs 16.3%). Fibroblasts and macrophage populations also showed elevated metal transporter expression levels based on gene expression relative to other tumor residing cell types yet minor differences induced by cancer type. Cancer cells express high levels of metal transport genes (Zn, Ca, Co, Na, Mg, Fe). 67NR cancer cells exhibited increased gene expression of many metal-transporting proteins including numerous solute carrier (*SLC*) group of membrane transport proteins such as *Slc41a2* when compared to the more aggressive 4T1 cells. This study underscores the potential of linking metallomic profiling to tumor composition and cancer behaviors, offering a pathway for identifying novel biomarkers to differentiate aggressive and non-aggressive forms of breast cancer.

This work was performed under the auspices of the U.S. Department of Energy by Lawrence Livermore National Laboratory under Contract DE-AC52-07NA27344.

#6851 The genomic, transcriptomic, and immunologic landscape of TEM8 (*ANTXR1*) in neuroendocrine neoplasms (NENs).

S. A. Kareff[1], H. Krause[2], A. Elliott[2], P. Hosein[1], E. Lou[3], H. Soares[4], M. Oberley[2], A. Chauhan[1];
[1]University of Miami, Miami, FL, [2]Caris Life Sciences, Phoenix, AZ, [3]University of Minnesota, Minneapolis, MN, [4]University of Utah, Salt Lake City, UT

Introduction: TEM8 (coded by *ANTXR1*) is overexpressed in malignant tissues, with oncolytic viruses such as SVV-01 uniquely binding to this receptor on tumor-associated angiogenic endothelial cells, pericytes, fibroblasts, and immune inflammatory cells. Recent pre-clinical data suggest that TEM8-targeting therapies may convert immunologically “cold” tumor microenvironments (TME) into “hot” milieu more amenable to treatment with immune checkpoint inhibitors (ICIs).
Methods: NextGen sequencing of DNA (592 genes or WES) and RNA (WTS) was performed on neuroendocrine neoplasms (NENs; *N* = 1724), excluding small-cell lung cancer, submitted to Caris Life Sciences (Phoenix, AZ). Mutations were defined as pathogenic SNVs/indels. *ANTXR1* expression was divided by *ANTXR1*-expression quartiles (transcripts per million [TPM];Q4:^{H};Q1:^{L}). PD-L1 expression (SP142; Positive (+): ≥2+,≥%5) was assessed by IHC. High tumor mutational burden (TMB-H) was defined as ≥10 mutations per MB. Cell infiltration in the TME was estimated by QuantiSEQ. Gene expression profiles were analyzed for transcriptional signatures predictive of response to immunotherapy (T cell-inflamed) and MAPK pathway activation score (MPAS). Overall survival (OS) data was obtained from insurance claims, and Kaplan-Meier estimates were calculated for molecularly defined subpopulations of patients. Mann-Whitney U and X^2/Fisher-Exact tests were applied where appropriate, with *p*-values adjusted for multiple comparisons ($p<0.05$).
Results: NENs from the adrenal gland had the highest median *ANTXR1* expression (50 TPM), followed by those from the colon and rectum (43.5), genitourinary organs (43.3), and small bowel (excluding appendix) (39.2). The lowest median *ANTXR1* expression was observed in NENs from the pancreas (31.5). No pathogenic mutations were significantly associated with *ANTXR1*^{H} vs ^{L} tumors ($p>0.05$ for all), along with no differences in the prevalence of TMB-H (8.6% vs 12.6%, $p=1$) or PD-L1+ (5.8%: vs 3.1%, $p=1$). A greater proportion of B cells (5.34 % vs 3.78%, $p<0.001$), M1 (1.46% vs 0.15%, $p<0.001$) and M2 macrophages (3.92% vs 2.67%, $p<0.001$), and T-regulatory cells (1.77% vs 1.08%, $p<0.001$) was observed in ANTXR1^{H} TMEs, which were more frequently classified as T cell-inflamed compared to *ANTXR1*^{L} (42% vs 8%, $p<0.001$). *ANTXR1*^{H} tumors also had higher MPAS compared to *ANTXR1*^{L} (1.16 vs -1.61 arbitrary units, $p<0.001$). There was no significant difference in median OS between *ANTXR1*^{H} vs ^{L} tumors (18.8 mo. vs 21.2 months, Hazard Ratio:1.18, $p=0.114$).
Conclusion: The increased immune cell infiltrate and prevalence of T-cell inflamed status among *ANTXR1*^{H} NENs suggests these tumors might be more responsive to treatment with ICIs. As trials incorporating intratumoral injections of SVV-01 in combination with ICIs are underway, further investigation of clinical and molecular associations with *ANTXR1* expression in NENs is warranted.

#6852 Immune microenvironment profiling of pregnancy associated breast cancer: A transcriptomic and multiplex immunohistochemical analyses.

I.-C. Chen[1], C.-H. Chen[2], C.-L. Hsu[3], T.-P. Lu[2], Y.-S. Lu[3], C.-H. Lin[1];

[1]National Taiwan University Cancer Center (NTUCC), Taipei, Taiwan, [2]National Taiwan University, Taipei, Taiwan, [3]National Taiwan University Hospital, Taipei, Taiwan

Background: Pregnancy-associated breast cancer (PABC) is BC diagnosed during pregnancy or within 2 years after pregnancy. Although PABC is a rare subgroup of BC, the outcome of PABC is worse than BC developed in the same age group unrelated to pregnancy. The proliferation and involution of mammary gland during and after pregnancy create a unique immune microenvironment in the breast. Comprehensive profiling of the tumor immune microenvironment in PABC is important but lacking.

Methods: We retrospectively identified PABC patients from electronic medical records and their tumor blocks from pathology department in our institution. Age- and stage-matched BC patients were selected as control group. NanoString Breast Cancer 360 Gene Expression panel and Opal Polaris 7 color immunohistochemical (IHC) were utilized to profile PABC from transcriptome and protein levels.

Result: PABC (N=26), BC developed 2 years (BC>2Y, N=54) after pregnancy, and matched non-pregnant BC patients (NPBC, N=27) were included in the final analysis respectively. Samples from BC>2Y (remote influence from pregnancy) and NPBC (pregnancy did not contribute to BC) both served as control groups for PABC patients in our study. PAM50 subtyping categorized patients into luminal A(N=42), luminal B(N=26), basal(N=12), and HER2 (N=25) enriched subgroups. In multiplex IHC analysis, CD4+ cells, CD8+ cells, CD20+ cells, and CD68+/CD163+ (M2) cells were all statistically higher in the tumor samples from PABC and BC>2Y than from NPBC. This suggests a potential contribution of pregnancy in the immune microenvironment. In the luminal A subgroup, CD8+ cells, CD20+ cells, and CD68+/CD163+ cells remain statistically higher in the PABC than in the NPBC samples. In NanoString BC360 transcriptomic profiling, immune cell abundance was evaluated from representative gene signatures. Mast cells were significantly lower in the PABC group than in the NPBC group. Cytotoxic T cells are significantly higher both in the PABC and BC>2Y groups than in the NPBC group.

Conclusion: We are the first study to profile immune microenvironment using both transcriptomic and IHC methods. Our study is also unique in using NPBC and BC>2Y patients as control groups for PABC patients. CD8+ T cells are statistically higher in PABC patients than in NPBC patients using either transcriptomic profiling or multiplex IHC analysis. M2 macrophages, which promote tumor growth, are abundant in all the PABC and the luminal A PABC samples.

#6853 Spatial proteomic and transcriptomic characterization of the inflammatory landscape of formalin fixed paraffin embedded Barrett's esophagus tissues.

Q. Ain[1], N. Frei[2], A. M. Khoshiwal[2], P. Stougie[2], R. Odze[3], S. Camilleri-Broet[4], L. Ferri[4], L. C. Duits[2], J. Bergman[2], M. D. Stachler[1];
[1]UCSF - University of California San Francisco, San Francisco, CA, [2]University of Amsterdam, Amsterdam, Netherlands, [3]Tufts University, Boston, MA, [4]McGill University, Montreal, QC, Canada

Esophageal adenocarcinoma (EAC), a significant cause of morbidity and mortality, develops from its metaplastic precursor lesion termed Barrett's esophagus (BE). BE progresses to EAC within an inflammation rich environment, however a detailed understanding of the types of inflammatory cells present, how that population changes over time or diagnosis, and the related immunomodulatory pathways that may mediate BEs progression is still understudied. Traditional immunohistochemistry is often inadequate to provide detailed information about a broad number of cells, local cellular proportions, and cellular heterogeneity; while bulk or single cell RNA sequencing lose the spatial context and relationships between the stroma and epithelium. Utilizing modern multiplex profiling technologies such as Nanostring's GeoMx digital Profiler (DSP) aid in identifying both cellular composition and distribution of cells within the epithelium and stroma. Therefore, our aim of this study was to determine the suitability of the DSP platform for analyzing formalin fixed paraffin embedded (FFPE) endoscopic samples of BE and determine any differences between non-dysplastic BE (NDBE) samples from patients who eventually progressed (progressors) compared to those who did not (non-progressors), with the goal to gain deeper insights about cellular composition and spatial distribution of immune cells that may dictate progression of BE. Our secondary goal was to investigate the relationship of these cells to the BE epithelial cells through understanding the immune signaling and regulatory pathways. Our pilot study utilizing a 49-plex antibody panel on 7 NDBE samples from progressors and 8 NDBE samples from non-progressors showed good quality metrics and deciphered an immune rich microenvironment in BE with several immune markers including CD66b (neutrophils), CD14 (monocytes), CD68 (macrophages) and CD56 (NK cells) being overexpressed in the stroma of progressors compared with non-progressors, corrected p value less than 0.05. The myeloid activation marker CD80 was overexpressed in the BE epithelial cells of progressors. To determine how spatial transcriptomic profiling performed in FFPE endoscopic samples, 1,812 transcripts within 48 regions of interest of four BE, HGD, and EAC samples was interrogated. Only 36 (2%) probes fell below the limit of detection quality threshold. Thus, our pilot results show that robust proteomic and transcriptomic profiling can be obtained from endoscopic BE biopsies using this system. Based on these results, we systematically interrogated the immune cell makeup and distribution as well as their related inflammatory and immunoregulatory pathways in 40 NDBE biopsies (20 progressors and 20 with stable non-progressing disease) within discrete compartments (stroma and epithelium) through spatial whole transcriptome profiling.

TUMOR BIOLOGY: Immune Cells in the Tumor Microenvironment 2
Poster Session

#6857 Evolution of myeloid-mediated mechanisms of immunotherapy resistance at single-cell resolution with prostate cancer progression.

A. Lyu[1], Z. Fan[1], D. Luong[1], A. Setayesh[1], A. Starzinski[1], L. Valderrabano[2], E. Van Allen[2], L. Fong[1];
[1]UCSF - University of California San Francisco, San Francisco, CA, [2]Dana-Farber Cancer Institute, Boston, MA

Background: Patients with metastatic castration-resistant prostate cancer (mCRPC) are largely refractory to immune checkpoint inhibitors (ICIs). This resistance is, in part, attributed to the presence of immunosuppressive myeloid cells in tumors. However, attempts to target these cells broadly, such as CSF1R antagonism, have thus far failed clinically primarily due to their heterogeneous nature. Thus, we hypothesized that a more comprehensive understanding of immunosuppressive myeloid subsets and their molecular mechanisms at the single-cell level is critical to enhance the effectiveness of immunotherapy.
Methods: We performed single-cell profiling of patient biopsies with either localized, metastatic hormone-sensitive prostate cancer, or mCRPC. We then reverse translated these findings in a syngeneic mouse model of CRPC, where we performed multi-omic single-cell assessment and conducted studies to assess tumor efficacy and gain mechanistic insights.

Results: We identified a specific subset of tumor-associated macrophages with elevated hypoxia signatures, including higher *SPP1* transcript levels (*SPP1*^{hi}-TAMs). These macrophages become significantly more abundant as the disease advances, expressing elevated immunosuppressive molecular programs. Notably, *CSF1R* transcripts were significantly reduced in *SPP1*^{hi}-TAMs, suggesting their potential role in the clinical ineffectiveness of CSF1R blockade. In a syngeneic mouse CRPC model, we identified an analogous macrophage subset through single-cell profiling and flow cytometry. These macrophages possess the ability to suppress T cell activity in co-culture. Consistent with these findings, adoptive transfer of *Spp1*^{hi}-TAMs into CRPC promoted ICI resistance and worsened survival in vivo. Importantly, these macrophages proved resistant to anti-CSF1R treatment, underscoring the need to target their immunosuppressive signals as a potential therapeutic approach. Pathway analysis revealed enrichment of gene signatures associated with adenosine signaling in *SPP1*^{hi}-TAMs both in patients and in mice, implicating this pathway as their immunosuppressive mechanism. Indeed, blocking adenosine signaling using antibodies or pharmacologic inhibitors resulted in a significant reduction in T cell suppression mediated by *Spp1*^{hi}-TAMs in culture. Furthermore, pharmacologic blockade of adenosine receptors in vivo significantly decreased tumor growth and enhanced the responsiveness of tumor cells to ICI therapies.

Conclusions: Our studies demonstrate that *SPP1*^{hi}-TAMs become prevalent as the disease progresses. They are resistant to CSF1R blockade and play a key role in mediating immunotherapeutic resistance in vivo by activating adenosine signaling pathways. These findings highlight the potential of the associated signals as promising targets for therapeutic intervention.

#6858 PPARδ and type 1 interferon collaboratively regulate CIITA-MHCII pathway: Unveiling novel mechanisms of tumor Tregs.

Q. Yang, Y. Liang, Y. Zheng;
Salk Institute For Biological Studies, San Diego, CA

Regulatory T cells (Tregs) play an essential role in suppressing anti-tumor immunity, often resulting in unfavorable clinical outcomes across numerous cancers. However, systemic Treg depletion, while augmenting anti-tumor responses, also triggers detrimental autoimmune disorders. Thus, dissecting the mechanisms by which Tregs navigate and exert their functions within the tumor microenvironment (TME) is pivotal for devising innovative Treg-centric cancer therapies. Our study highlights the role of peroxisome proliferator-activated receptor β/δ (PPARδ), a nuclear hormone receptor involved in fatty acid metabolism. Remarkably, PPARδ ablation in Tregs escalated tumor growth and augmented the immunosuppressive characteristics of the TME. This absence of PPARδ spurred an increased expression of genes central to antigen presentation, notably CIITA and MHCII. Our results showcase a novel association where the absence of CIITA in PPARδ-deficient Tregs bolsters anti-tumor responses, casting CIITA as a pivotal downstream regulator of PPARδ within Tregs. In vitro assays demonstrated that elevated CIITA levels enhance the suppressive capacity of Tregs, facilitated by an antigen-independent interaction between Treg-MHCII and Tconv-TCR/CD4/Lag3. A significant revelation was the role of type 1 interferon as a TME signal that promotes the genesis of MHCII^{+} Tregs; this process is accentuated by PPARδ deficiency. In conclusion, the co-regulation between TME cues and PPARδ signaling shapes the adaptive and suppressive roles of Treg cells through the CIITA-MHCII pathway. Strategically targeting the potent MHCII^{+} Treg population could open a new avenue for cancer therapies by boosting anti-tumor defenses while curbing autoimmune threats.

#6859 A novel immune checkpoint CD97/CD55 in the initiation and progression of papillary thyroid cancer by scRNA-seq.

Xuan Qin[1], Jia Li[2], Dapeng Li[1], Xing Wan[1], Xianhui Ruan[1], Yimeng Liu[1], Weijing Hao[1], Kejia Xu[2], Yi Shi[2], Yongjun Piao[2], Xiangqian Zheng[1]

[1]Department of Thyroid and Neck Oncology, Tianjin Medical Univ. Cancer Inst. & Hospital, Tianjin, China,[2]The School of Medicine, Nankai University, Tianjin, China

Thyroid cancer (TC), as the most common endocrine malignancy, has exhibited a significant increasing trend in incidence in China and globally, with papillary thyroid cancer (PTC) being the most common pathological type. However, the molecular mechanisms driving the initiation and progression of TC remains scarce, posing a bottleneck problem for the precise diagnosis and treatment. Tumors, as a complex heterogeneous composite consisting of tumor cells, immune cells, and stromal cells, have long been considered to play a key role in driving tumor occurrence and malignant progression through the proportion, spatial distribution, and interaction of tumor cells and immune cells in the tumor immune microenvironment(TIME).We performed single-cell RNA sequencing (scRNA-seq) on 16 clinical samples, including normal thyroid tissue, benign nodules, PTC, and PTC with cervical lymph node metastasis(LNM), delineating the cell atlas of the tumor microenvironment (TME) at various stages from normal thyroid to PTC development. Among these, we discovered a previously undefined $TNFSF9^{high}CD8^{\pm}$ T cell subset with a distinct transcriptional profile from classical exhausted T cells, which was highly enriched in PTC tumor tissues. Further cell interaction analysis revealed that the highly expressed CD97 receptor on these $CD8^{\pm}$ T cells binds to the highly expressed CD55 molecule on PTC tumor cells, promoting the exhaustion of $CD8^{\pm}$ T cells, suggesting that CD97/CD55 may be a key new immune checkpoint (IC) inducing $CD8^{\pm}$ T cell exhaustion and promoting immune escape of PTC tumor cells. We validated the co-localization of CD97/CD55-mediated $CD8^{\pm}$ T cell and tumor cell interactions in PTC patient specimens and spontaneous tumor samples from a mouse PTC model using multiplex immunofluorescence (mIHC). Flow cytometry analysis of the proportion of $CD97^{\pm}$ $CD8^{\pm}$ T cells in patient and mouse specimens revealed a significant increase in the proportion of $CD97^{\pm}$ $CD8^{\pm}$ T cells in PTC tumor tissues. Co-culture experiments of activated and expanded $CD8^{\pm}$ T cells from peripheral blood mononuclear cells(PBMC) of PTC patients with PTC tumor cells showed that CD55 overexpressing tumor cells inhibited the secretion of cytotoxic cytokines IFN-γ and IL-2 by activated $CD8^{\pm}$ T cells through the CD97/CD55 IC signal, thereby weakening the cytotoxity on PTC tumor cells. In summary, the IC regulatory signal formed by the highly expressed CD55 molecule on the surface of PTC tumors and the CD97 receptor on the surface of PTC-specific inhibitory $TNFSF9^{high}CD8^{\pm}$ T cells can reshape the TIME, promoting the formation of an immunosuppressive microenvironment, which may represent a novel molecular mechanism promoting immune escape of tumor cells during PTC initiation and progression.

#6860 Fluorescent tracking reveals that radiation therapy influences the migration and plasticity of Tregs within the tumor microenvironment.

D. J. Friedman[1], T. Blair[1], G. Kramer[1], A. Kaur[1], J. Baird[1], A. Alice[1], M. Potuznik[1], M. R. Crittenden[2], M. J. Gough[1];
[1]Earle A. Chiles Research Institute, Portland, OR, [2]The Oregon Clinic, Portland, OR

Radiation therapy (RT) has long been a cornerstone in cancer treatment, yet the mechanisms underlying its impact on the immune system remain incompletely understood. RT is recognized for its ability to induce DNA damage within cancer cells, leading to cancer cell death. For those cancer cells that do not die as a result of radiation, tumor infiltration by immune cells is closely associated with treatment outcomes. T cell infiltration is a dynamic process, with subsets taking up residence in the tumor while the majority recirculate through lymph nodes into the peripheral blood. T regulatory cells (Tregs) have been recognized as potent suppressors of anti-tumor immune responses, dampening immune-mediated clearance of cancer cells. While RT can initially contribute to an improved anti-tumor immune response, this beneficial effect is often counterbalanced by the presence of suppressive Tregs. Tregs can infiltrate the tumor microenvironment, ultimately impeding and overwhelming the immune response generated by RT. Our objective was to gain insights into the migratory patterns of Tregs to and from tumor sites and to elucidate how RT influences the dynamics of Treg recirculation. Utilizing the established photoconvertible Kaede mouse model we can track photoconverted cells following RT. Following photoconversion, photoconverted T cells were observable within the tumor and subsequently moved to the TdLN and on to other NdLN at later time points. In the TdLN of mice bearing MC38, Moc1, and Moc2 tumors, Tregs represented a significantly higher proportion of photoconverted cells compared to non-Treg CD4 or CD8 T cells. To validate their active departure from the tumor site, mice underwent FTY720 treatment, resulting in a reduction in both photoconverted Treg and non-Treg migration to the TdLN. When RT was administered to the tumor, there was a decrease in photoconverted Treg and non-Treg CD4 T cells within the TdLN, consistent with the expected cytotoxic effects on the irradiated tumor upstream. To focus on recruitment back from the TdLN, mice were analyzed after photoconversion of the TdLN. This revealed that a majority of TdLN Tregs exhibited a preference for relocating to the tumor, with only a minority migrating to the NdLN. The newly entered Tregs were analyzed in the tumor, at D1 and D3 post RT, and we found that these Tregs exhibited increased expression of CCR8, CD69, KLRG1 and Ly6C as compared to those in non-irradiated tumors, suggesting that these are recent entrants with limited suppressive capacity. These findings illuminate the intricate dynamics between RT, Tregs, and the use of site-specific photoconversion to track immune cell movement and changes over time to understand treatment responses. Our ongoing studies focus on the interplay between the Treg and the tumor environment that dictates the success of CD8 T cell mediated control of residual cancer cells following RT.

#6861 PIK3CA activating mutation promotes an immune suppressive microenvironment in squamous cell carcinoma.

B. T. Nicholson, W. Guo, Y. Miao;
University of Chicago, Chicago, IL

Head and neck squamous cell carcinoma (HNSCC) is a leader in cancer incidence worldwide. Recently, immunotherapies such as immune checkpoint blockade (ICB) have offered great promise in treating many solid tumors, including HNSCCs, that are refractory to chemotherapy and radiation. Challengingly, HNSCC patients often relapse following ICB treatment due to the lack of a thorough understanding of the mechanisms underlying cancer immune evasion. These disparities in patient outcomes strongly suggest the existence of genetic variations that underlie their distinct responses to ICB. Although the specific oncogenic mutations responsible for driving relapse in SCC patients remain unclear, it is imperative to grasp the mechanisms of cancer immune evasion in individuals with specific genetic profiles to enhance the precision of immunotherapy. Cancer immune evasion has emerged as a hallmark of cancer and is facilitated by a highly complex tumor microenvironment (TME). We aim to understand the genetic basis shaping the immune suppressive TME and hypothesize that oncogenic driver mutations play a dominant role in preventing the immune clearance of transformed cells by reprogramming the immune landscape in the tumors. To determine the critical genetic signatures enriched in SCC patients that can impact anti-tumor immunity, we analyzed TCGA data which revealed a strong negative correlation between *PIK3CA* level and CD8 T cell signatures. We have identified that activating mutations in the *PIK3CA* gene, found in 20% of HNSCCs, promote rapid tumor relapse after initial response to anti-PD-L1 and anti-CTLA-4 ICB treatments. Utilizing single-cell analysis, quantitative immune profiling, and multiplexed imaging, our lab showed that tumor-initiating cells (TICs) in SCCs can have an intricate dialogue with myeloid-derived suppressor cells (MDSCs) where TICs secrete factors to enhance MDSC recruitment and suppressive function on cytotoxic T cells. Additionally, our data supports that the tumor interstitial fluid (TIF) of *PIK3CA* mutant SCC tumors can enhance the suppressive activity of MDSCs on cytotoxic T cells. These results suggest that the acquisition of *PIK3CA* mutation may trigger TICs to release additional factors to further modify MDSC activities. A critical method by which MDSCs suppress T cells is through the production and respiratory burst of reactive oxygen species (ROS). RNA sequencing revealed that *PIK3CA* mutant SCCs have multiple mechanisms of increasing ROS in the TME and specifically in MDSCs, while simultaneously upregulating lipid metabolism genes, such as SCD1, to protect itself from MDSC-derived ROS. This study reveals a potential strategy for targeting *PIK3CA* mutant SCCs as a promising precision immunotherapy to enhance the efficacy of ICB treatments.

#6862 Loss of STAT1 promotes an immunosuppressive tumor microenvironment in KRAS-driven lung adenocarcinoma.

C. Trenk[1], M. Beres[1], K. Deszo[2], J. Horvath[1], M. Homolya[1], A. C. Luca[1], R. Eferl[1], H. P. Moll[1], E. Casanova[1];
[1]Medical University of Vienna, Wien, Austria, [2]Semmelweis University, Budapest, Hungary

Introduction: Lung cancer is the leading cause of death worldwide. One third of lung adenocarcinomas (LUADs), the most abundant form of lung cancer, harbors activating mutations in KRAS. Since human KRAS-mutant LUAD is correlated to an inflammatory phenotype, we hypothesized that the JAK-STAT pathway plays a crucial role in disease progression. Indeed, preliminary data demonstrated that human KRAS-mutant LUADs are associated with activation of the JAK-STAT signaling pathway, including upregulation of STAT1 expression. Therefore, we aimed to elucidate the tumorigenic functions of STAT1 in KRAS-mutant LUAD.
Methods: To analyze the functions of STAT1 in KRAS-driven LUAD, we used C57BL/6 mice, which were genetically engineered in order to develop KRAS-driven autochthonous LUAD deficient for P53. Tumors additionally expressed ovalbumin (OVA) which acts as a neoantigen to induce immune infiltration (KPO mice). In this immunogenic mouse model, STAT1 was deleted in the tumors (KPOS mice) and overall survival was assessed by Kaplan Meier analysis. Tumor burden and infiltration was analyzed in lungs via H&E, IHC, and IF staining 6 weeks after tumor induction. An inflammatory cytokine antibody array was performed with lung fluid and single cell sequencing with cells isolated from lungs at 10 weeks.
Results and discussion: Expression of OVA in tumor cells increased infiltration by T cells and prolonged survival suggesting neoantigen presentation in this mouse model. When STAT1 was deleted in OVA expressing tumors the survival was significantly decreased. Further, tumor burden as well as tumor size and grades were increased in KPOS lungs. Interestingly, infiltration of CD4 T cells was diminished upon loss of STAT1 while the percentage of CD8 T cells in tumors did not change suggesting an immunosuppressive tumor microenvironment. Indeed, M2 macrophages were increased in tumors lacking STAT1 and less proliferating immune cells were found indicating immune cell inhibition. This was further supported by the increase of CCL9 in KPOS lungs which might induce macrophage recruitment and further T cell inhibition. Finally, scRNAseq analysis revealed that KPOS lungs were composed of distinct immune cell populations as well as states.
Conclusion: This data suggests that loss of STAT1 in tumor cells promotes secretion of CCL9 that drives recruitment of immunosuppressive macrophages to the tumor microenvironment. As a result, T helper cells are excluded from tumors and cytotoxic T cells are inhibited or exhausted. Further experiments will delineate the immune cell states and the mechanisms leading to this interesting phenotype.

#6864 Tumor suppressor function of the ubiquitin ligase Siah1a in melanoma is mediated by myeloid derived suppressor cells.

M. Scortegagna, Y. Du, y. Feng, Z. Ronai;
Sanford Burnham Prebys Med. Discovery Inst., La Jolla, CA

Growing evidence supports the important role of myeloid-derived suppressor cells (MDSC) in melanoma progression and response to therapy. MDSC contributes to a pro-tumorigenic phenotype, yet the mechanistic basis for the immune suppressor properties acquired by MDSC remains largely unknown. Mammals have two homologous Siah genes, *Siah1 (Siah1a and Siah1b* in mice*)* and *Siah2*. In the context of melanoma, the ubiquitin ligases *Siah1a* and Siah2 have melanoma-intrinsic and -extrinsic (immune) functions. Correspondingly, ablation of Siah1a/2 in melanoma or its microenvironment attenuates melanoma development in a number of mouse melanoma models. Given that number of macrophage clusters infiltrated into melanoma when grown in Siah2 KO mice, we set to assess macrophage function in melanoma. Selective ablation of Siah1a or Siah2 in macrophages, using *Lyz2*^{Cre}, revealed that Siah1a but not Siah2 elicits a tumor suppressor function in melanoma. Inoculation of mouse melanoma Yummer1.7 cells (*Braf* mutated and *Pten* deleted) in mice lacking *Siah1a* in macrophages, resulted in bigger melanoma tumors compared to melanoma grown in either WT or mice in which macrophages were ablated of Siah2. FACS analysis of melanoma tumors grown in mice harboring Siah1a mutant macrophages revealed a significant increase in MDSC, which coincided with a decrease in CD4$^{\pm}$ and CD8$^{\pm}$ cells, compared with WT mice. These observations suggest that a lack of *Siah1a* in macrophages leads to an expansion of MDSC that affects surrounding immune cells, including T cells. RNA-seq analysis of MDSC that were differentiated *in vitro* from bone marrow cells of WT or Siah1a ablated macrophage mice revealed increased expression of genes involved in proliferation and alternative macrophage activation in MDSC lacking Siah1a when compared to the WT genotype. Mapping mechanisms underlying Siah1a tumor suppressor function is expected to reveal novel regulatory cues in melanoma control by the MDSC population while mapping novel means for stratifications of melanoma to therapy, and possibly new means for therapy of this tumor type.

#6865 Single cell analysis of melanoma reveals a prognostic myeloid cell associated with survival in melanoma with brain metastases.

M. Ahmad, L. Heo, R. V. Nair, S. Sharma, A. Kirane;
Stanford University School of Medicine, Stanford, CA

INTRODUCTION: The interface of the innate and adaptive immune system are a critical factor in tumor behavior and responses to immunotherapy with myeloid cell behavior varying widely between various biogeographies. We sought to elucidate myeloid sub-type differences to characterize biology and support therapeutic strategies.

METHODS: scRNA-seq of primary skin, acral, and metastatic melanoma were combined from 6 datasets with 126 patients for analysis. After integration, cells were analyzed with scCCESS, which uses an artificial neural network to reduce data and optimize k for k-means clusters. Myeloid clusters with analyzed with Recursive Partitioning Analysis (RPA), differential expressed gene (DEG) analysis, and pseudobulk comparison of RPA groups by gene expression.

RESULTS: 102,971 single cells from 126 patients were analyzed to generate a cluster of 15,303 myeloid cells further subjected to clustering generating 6 cell types. RPA analysis of 6 myeloid populations in 46 patients with melanoma brain metastases generated 3 nodes with differing median survival months (17 vs 41 vs 57, p=0.01). There was a trend towards more adjuvant immunotherapy (p=0.057) and targeted therapy (p=0.019) in the worst surviving group. Myeloid type 1 cells showed increased expression of CLEC10A and AXL genes compared to all other cells (adj p = 0.000). Pseudobulk comparison of patient groups of genes showed CLEC10A was significant between all groups (p<0.05).

CONCLUSIONS: Although there were no significant differences in neoadjuvant treatment, increased infiltration of CLEC10A myeloid cells showed improved survival in melanoma brain metastases. Targets of current therapies, such as AXL tyrosine kinase, have heterogenous presence across multiple cell types beyond tumors that may impact wide response variances, further study of these populations will have significant impact in both biomarker and therapeutics development.

#6866 Investigating the role of Epha2 in breast cancer-mediated myeloid cell expansion and function.

D. Parker, V. Ngwa, J. Chen, J. Rhoades;
Vanderbilt University, Nashville, TN

Bone metastases are present in over 70% of metastatic breast cancer patients, and current therapy reduces osteolysis in tumor-induced bone disease (TIBD) but does not improve overall survival. Frequently, TIBD is characterized by an increase in osteoclast proliferation and bone-resorbing activity, and patients often experience pain and pathologic fractures. Increased bone resorption releases growth factors that aid in the progression of tumor growth causing the 'vicious cycle'. Additionally, bone metastatic patients are often resistant to first- and second-line therapies highlighting an importance for research in this area. The receptor tyrosine kinase, Ephrin-type-A 2 receptor (EphA2), participates in both forward and reverse signaling during receptor/ligand engagement and participates in many physiological and pathological processes, including bone homeostasis, immunity, and cancer. Interestingly, EphA2 is highly expressed in bone metastases, and previous evidence suggests that EphA2 can promote TIBD and reduce anti-tumor immunity. We therefore hypothesize that *increased expression of EphA2 in breast cancer cells at the site of bone metastasis promotes expansion of myeloid cells, leading to TIBD*. Previous data shows a reduction in osteoclast number and bone lesions following EphA2 knockout. However, the mechanism by which EphA2 mediates the expansion of osteoclasts is not well understood. In agreement with previous work, our data shows that EphA2 deletion in murine breast cancer (BC) cell line, 4T1, reduces bone lesion area and number and the presence of bone metastasis-associated macrophages. Additionally, we observed a significant reduction in $Ly6C^{hi}$ cells. To assess the effects of EphA2 deletion on the behavior of 4T1 cells, we conducted a wound healing assay and observed a decrease in wound healing capacity in 4T1 cells following EphA2 deletion. This suggests that EphA2 expression in 4T1 cells may increase their metastatic potential. We will repeat these studies and incorporate factors from the bone marrow. Our future studies will investigate the role of EphA2 signaling and reverse signaling in BC cell lines, myeloid progenitor cells, osteoclasts, and bone metastasis-associated macrophages. We will utilize murine and human BC cell lines to elucidate the effects of EphA2 deletion in BC on immune cell populations, bone metastasis, and tumor progression. Additionally, we will investigate how EphA2 reverse signaling impacts osteoclasts' ability to modulate immune cells. We aim to reduce TIBD and tumor burden by reducing the expansion of osteoclasts and shifting the immune cells to an anti-tumorigenic phenotype. Our studies will provide additional insight into the underlying mechanisms of the vicious cycle which will offer new treatment strategies for patients with osteolytic breast cancer.

#6867 TWEAK-Fn14 signaling in glioblastoma-associated myeloid cells promotes tumor invasion via CCL5-CCR5 axis.

A. Beniwal[1], M. Dufault[2], P. Kanvinde[3], D. Nascari[1], R. Eghlimi[1], A. Malla[4], D. Hambardzumyan[5], H. Borges da Silva[6], G. Woodworth[3], J. Winkles[3], N. Tran[6]; [1]Mayo Clinic College of Medicine and Science, Scottsdale, AZ, [2]Midwestern University College of Osteopathic Medicine, Glendale, AZ, [3]University of Maryland School of Medicine, Baltimore, MD, [4]University of Maryland, Baltimore, MD, [5]Mount Sinai School of Medicine in New York City, New York, NY, [6]Mayo Clinic Arizona, Scottsdale, AZ

Glioblastoma remains difficult to treat with immunotherapy due to the immunosuppressive tumor microenvironment and the ability of glioma cells to invade diffusely into normal brain parenchyma. While it is known that glioblastoma-associated myeloid cells (GAMs) comprise a large proportion of the tumor microenvironment and can suppress adaptive and innate immune responses through various mechanisms, detailed mapping of myeloid lineages in glioblastoma is still missing. Further characterization of pro-tumoral myeloid-lineages in glioblastoma is important for identifying myeloid-based drug targets that may synergize with T cell-based therapies and produce a more meaningful anti-tumor immune response. Towards this end, we examined numerous scRNAseq datasets derived from glioblastoma patients and identified expression of TNFRSF12A, the gene encoding the TNF- family receptor, Fn14, in a subset of GAMs enriched for expression of cytokines such as CCL3, CCL5, IL-6, and IL-8. This result is intriguing since TWEAK (TNFSF12), the ligand for Fn14, is abundantly expressed within numerous patient-derived glioblastoma cell lines, namely GBM6, GBM8, GBM22, and GBM39. To validate Fn14 protein expression in GAMs, we isolated murine bone-marrow derived macrophages and treated them with glioma-conditioned media, which induced Fn14 gene expression. We then conducted *in vitro* experiments utilizing the human microglia line HMC3, the murine microglia line SIM-A9, and primary murine bone-marrow-derived macrophages to assess the effects of Fn14 activation in myeloid cells. We found that treatment of Fn14+ myeloid cells with TWEAK ligand upregulates CCL3, CCL5, IL-6, and IL-8 expression. We tested the conditioned media generated from TWEAK-treated Fn14+ myeloid cell lines and found that it promotes glioblastoma invasion in a CCL5-dependent manner. This aligns with previous reports demonstrating the CCL5-CCR5 signaling in glioma cells promotes invasion through calcium-dependent matrix metalloproteinase 2. To assess the spatial distribution of this myeloid subpopulation, we performed RNAscope hybridization against AIF1, TMEM119, CCR5, CCL5, and Fn14 transcripts on sections of murine gliomas generated using the RCAS/tv-a model of human glioblastoma. We found an abundance of Fn14+ plus AIF1+ as well as Fn14+plus TMEM119+ myeloid cells throughout the tumor core and rim of murine tumors and identified CCL5 expression in pseudo-palisades bordering necrotic regions. Our results to date suggest that Fn14 expression in GAMs can promote the invasion of tumor cells into normal brain parenchyma by release of CCL5. Currently, we are utilizing orthotopic patient-derived xenograft models co-implanted with Fn14+/- myeloid cells to test the hypothesis that TWEAK-Fn14 signaling in GAMs provides strong pro-tumoral signals in the glioblastoma microenvironment.

#6868 Exploring myeloid landscapes according to EGFR mutated NSCLC tumor microenvironment.

E. Lee[1], J. Ahn[1], Y. Lee[1], M. Kim[2], S. Oh[1], Y. Park[1], S.-J. Choi[1], J. Lee[1], K. Lim[2], K.-H. Pyo[1], J. Kim[3], J. Lee[1], M. Hong[1], S. Lim[1], M. Yun[3], B. Cho[1];
[1]Yonsei University College of Medicine, Seoul, Korea, Republic of, [2]JEUK Institute for Cancer Research, JEUK Co., Ltd.., Gumi, Korea, Republic of, [3]Severance Biomedical Science Institute, Yonsei University College of Medicine, Seoul, Korea, Republic of

Introduction: Although the use of immune checkpoint inhibitors (ICIs) has improved the survival rate of some patients, EGFR mutant (MT) NSCLC patients exhibit a poor response to ICIs compared to EGFR wild-type (WT) patients. It has been demonstrated that EGFR MT NSCLC cells contribute to immunosuppressive tumor microenvironments (TMEs) by secreting inhibitory cytokines and metabolites and recruiting pro-tumor immunogenic cells, thereby diminishing ICI efficacy. In particular, myeloid cells represent a major component of the TME and are involved in regulating tumor progression and metastasis, indicating anti- and pro-inflammatory heterogeneous functions. While single-cell based analyses have been conducted in various cell types, studies on the diversity of myeloid cells between EGFR WT and EGFR MT NSCLCs are insufficient. Therefore, we explored to reveal the presence of multifaceted myeloid cell populations and to modulate its functions to augment ICI response in NSCLC patients with EGFR MT using single-cell RNA analysis.
Methods: Using the 10x Genomics Chromium system, we have generated single-cell RNA expression of a total of 904,174 cells from primary lung tissues of 95 patients with EGFR-WT (n=35), EGFR-MT TKI naïve (n=55), TKI post (n=5) and matched normal (n=22). Nine distinct cell lineages were annotated with canonical marker gene expression, focusing particularly on the myeloid (n=212,673 cells).
Results: We characterized 22 transcriptional states of myeloid cells: 4 clusters of alveolar macrophages (AMs; *PPARG*$^{+}$), 4 clusters of interstitial macrophages (IMs; *SPP1*$^{+}$, *FOLR2*$^{+}$, *CCL2*$^{+}$), 4 clusters of conventional DCs (cDCs; *CLEC9A*$^{+}$, *CD1C*$^{+}$, *LAMP3*$^{+}$), 2 clusters of mast cells (*KIT*$^{+}$), 1 cluster of plasmacytoid DCs (pDCs; *LILRA4*$^{+}$), proliferating cells (*MKI67*$^{+}$), monocytes (*FCN1*$^{+}$), neutrophil like cells (*CSF3R*$^{+}$) and 4 other unidentified clusters. In tumor tissues, IMs constituted a significantly higher proportion compared to normal tissues ($p<0.001$), with EGFR-WT and EGFR-MT IMs exhibiting distinct characteristics. EGFR-WT IMs had a high proportion of cluster expressing *FOLR2*, a marker of tissue resident macrophages associated with CD8 T cell infiltration and activation. On the other hand, a major component of IMs from EGFR-MT was a cluster expressing *SPP1* and its regulator *MIF*. SPP1 is well known to be involved in cancer cell progression, epithelial-mesenchymal transition, autophagy, and epigenetic alterations. The abundance of SPP1 IMs in the EGFR-MT TME refers to the formation of an immunosuppressive TME, potentially compromising the effectiveness of ICIs.
Conclusions: We found that EGFR-MT TME comprised a high proportion of immunosuppressive IM cluster expressing SPP1, implying that it contributes to an immunosuppressive TME. Our findings suggest the possibility of developing strategies to enhance ICI responses by targeting SPP1-induced immunosuppressive TME in EGFR-mutant NSCLC patients.

#6870 Immunological aging in triple negative breast cancer leads to a chronic interferon phenotype and immune cell exhaustion that impedes response to therapy.

M. Spasic[1], A. Parsons[1], G. Goreczny[1], Q. Guo[1], A. Recko[2], E. Mittendorf[3], P. van Galen[1], S. McAllister[1];

[1]Harvard Medical School/Brigham and Women's Hospital, Boston, MA, [2]Dana Farber Cancer Institute, Boston, MA, [3]Brigham and Women's Hospital, Dana Farber Cancer Institute, Boston, MA

Age is the biggest risk factor for developing most forms of cancer, and understanding how age impacts cancer progression is critical to improving responses to therapy. As we age immune function declines suggesting that therapeutic responses, particularly to immunotherapies, will also change with age. Early clinical trial data suggests that there are age-associated responses to immunotherapies. Clinical trials, however, are not designed to reflect patient chronological and immunological ages - over 50% of breast cancer patients are over the age of 60, yet less than 25% of patients in clinical trials are in this age range. Here, we utilize a preclinical mouse model of immunological aging to understand how aging impacts immune responses to triple-negative breast cancer (TNBC). Immunologically young (8 weeks old) and aged (~12 months old) FVB mice were orthotopically injected with syngeneic Met1 TNBC cells. We previously established that this preclinical model mimics human immunological aging and enables us to better understand how age impacts disease progression and therapeutic responses. Once tumors became palpable, mice were treated with paclitaxel or vehicle control and/or anti-PDL1 to mimic first-line therapeutic strategies. Tumors grew significantly faster in young control mice compared to aged, but young mice had a more robust response to therapy. Notably, only young mice had a significant benefit of combo therapy (paclitaxel + anti-PDL1) over monotherapy alone. Tumors in aged mice had significantly more infiltration of CD8+ cytotoxic T cells and FOXP3+ inhibitory T-regulatory cells compared to young control mice, yet only tumors in young mice exhibited an increase in T cell infiltration with chemo or immunotherapy. Depletion of either CD8+ or CD4+ T cells in immune-competent FVB mice both led to a complete loss of age-associated differences in tumor growth. RNA sequencing analysis indicated that the infiltrating T cells in aged mice may be exhausted due to a chronic interferon phenotype, as indicated by enrichments of interferon alpha, interferon gamma, and IL2 signaling pathways, as well as expression of RIPK1, TNFa, and the immune exhaustion markers PD1, CTLA4, TIM3, and LAG3. Analysis of published single cell RNAseq data indicated the same interferon response pathways enriched with age in human TNBC, particularly in the T cell compartment.

Our findings show that the aging immune microenvironment significantly impacts tumor progression and that a chronic interferon phenotype with age may lead to T cell exhaustion and impaired therapeutic responses. This work suggests that targeting interferon signaling may lead to improved therapeutic responses. Together these findings demonstrate how immunological aging can impact disease progression and response to therapy and highlight the importance of developing age-stratified treatment strategies.

#6871 Tumor-infiltrating mregDC restrains anti-tumor immunity to promote cancer relapse in HCC.

Z. Zhang[1], J. Zhou[1], J. Fan[1], Y. Zhong[2], L. Wu[2], Y. Sun[1];
[1]Zhongshan Hospital Fudan University, Shanghai, China, [2]BGI Research, Shenzhen, China

Background and aims: Cancer relapse is one of the major causes of mortality in patients after curative resection of primary tumors. Furthermore, significant proportion of patients with recurrent tumor lack of effective treatments, thus novel therapeutic strategies are urgently needed. Although there have been several single-cell studies of primary tumor, functional roles and mechanism of tumor-infiltrating immune cells, especially those of myeloid cells in tumor relapse have remained to be elucidated.
Methods: We analyzed the RNA profile of 16498 cells from 12 primary and 6 early-relapse HCC cases. Digital pathology, multiplex immunofluorescent staining and digital spatial profiling (DSP) of paired primary and relapsed tumors from 41 HCC patients were also performed as our validation set. The molecular mechanisms associated with DCs was further tested through ex vivo and in vivo experiments.
Results: We performed single-cell clustering and visualized 3 DC clusters (cDC1, cDC2, and DC3). Compared with the other two subsets, the enrichment of DC3 in relapsed HCC was correlated with a higher second recurrence rate. Deeper inspections of the signature genes indicated this subset as 'mregDC', a DC subset enriched in maturation and regulatory molecules. Our results demonstrated that mregDC recruited $CD161^{\pm}CD8^{\pm}$ T cells that had an innate-like, low-cytotoxic, and low-clonal-expansion phenotype. $CD161^{\pm}CD8^{\pm}$ T cells secreted large amounts of TNF to activate non-canonical NF-κB pathway via tumor necrosis factor receptor 2 (TNFR2) and promoted the differentiation of immature DC into mregDC. This positive feedback loop between mregDC and $CD161^{\pm}CD8^{\pm}$ T cells shaped a dysfunctional anti-tumor immunity, facilitating cancer relapse in HCC. *In vivo* assay further indicated that therapy combining anti-TNFR2 and PD-L1 antibodies significantly inhibited HCC tumor growth via impeding the infiltration of mregDC compared with anti-PD-L1 monotherapy. We also found mregDC recruited $FCN1^{\pm}$ monocyte, a MDSC-like cell population to create an immunosuppressive niche of relapsed HCC.
Conclusions: We identified this population of mregDC with immunomodulatory function in recurrent HCC and demonstrated the role of these special DCs in shaping the immunosuppressive microenvironment of recurrent tumors. Our study suggests that mregDC may be a new target for the treatment of recurrent HCC in the future.

#6872 A spatio-temporal approach to mapping the dynamics of cutaneous squamous cell carcinoma progression and immunotherapy response: A journey through TiME.

N. Jhaveri[1], B. Ben Cheikh[1], D. Klymyshyn[1], N. Ma[1], A. Pratapa[1], J. Monkman[2], N. Nelson[3], A. Kulasinghe[2];
[1]Akoya Biosciences, Menlo Park, CA, [2]Frazer Institute, University of Queensland, Brisbane, Australia, [3]Abcam, Cambridge, United Kingdom

Background: Cutaneous squamous cell carcinoma (cSCC), arising from proliferation of malignant epidermal keratinocytes, is the second most common non-melanoma skin cancer. cSCC accounts for 75% of all skin cancer related deaths excluding melanoma, and metastatic and immunotherapy-resistant cases pose an emerging global threat. Tumor development is a gradual process characterized by high mutational burden and an immunosuppressive tumor immune microenvironment (TiME); therefore, identifying the underlying changes across the spatial and temporal landscape of these tumors will be crucial to understanding the key cellular and molecular drivers of disease progression and response.
Methods: In this longitudinal study, we used a single-cell, whole-slide approach to mapping key proteins of immune lineage, tissue architecture, cellular metabolism, and stress to study the spatial landscape of cSCC at baseline (pre-treatment) and multiple time points over the course of immunotherapy with the aim to develop a temporal atlas of the tumor. An ultra-high plex antibody panel encompassing over 50 major determinants in the tumor microenvironment was employed on the PhenoCycler®-Fusion spatial biology platform. Deep bioinformatic analyses was performed to identify cellular phenotypes, spatial neighborhoods, heterogenous functional states and cellular interactions by spatial proximity determinations.
Results: Previous studies in our laboratory have identified unique phenotypes correlating with response and resistance to immunotherapies in pre-treatment cSCC biopsies. Our results expand on these findings with temporal data tracking the dynamic changes in the TiME over the course of immune checkpoint inhibitor therapy. Apart from differences in immune cell composition and spatial localization patterns, we also saw differences in macrophage polarization and expression of metabolic markers in the responder and non-responder cohorts.
Conclusions: Overall, ultrahigh-plex spatio-temporal monitoring of cSCC revealed distinct signatures of response and resistance and identified key features in the TiME that reveal deeper insights into the pathobiology of the tumor. Our discovery-based approach identifies novel biomarkers for patient stratification and therapeutic modulation.

#6873 Prognostic impact of squamous cell carcinoma antigen as a mediator of anti-inflammatory macrophage polarization in tumor microenvironment.

L. Chen, V. Shi, E. Liu, J. Yang, A. Singh, M. Inkman, J. Zhang, J. Schwarz, S. Markovina;
Washington University School of Medicine in St. Louis, St. Louis, MO

Squamous cell carcinoma antigen 1 (SCCA1) is a potential biomarker and prognostic indicator for many epithelial cancers including cervix, head and neck, breast, and lung. Cancer patients with high serum levels of SCCA commonly experience treatment resistance and recurrence. We analyze SCCA expression in correlation with tumor microenvironment from 66 human cervical tumor biopsies and find that high serum SCCA is associated with increased macrophage infiltration in tumors and poor overall survival. In a single cell RNAseq analysis of 8 cervical tumors, patients with high SCCA1 show increased immunosuppressive genes (C1QA, C1QC, APOE) and reduced MHC molecules (HLA-DR, HLA-DQA1) in their tumor associated macrophages (TAMs), corresponding to decreased expression of T-cell cytotoxic-associated genes (IFNG, GZMB, PRF1). Thus, we aim to understand the impact of elevated SCCA1 on macrophages and its role in shaping the immune response. Co-culture of peritoneal macrophages isolated from SCCA1-treated mice with T cells from syngeneic wild-type mice, showed significant suppression in T cell proliferation. Downregulation of antigen presentation molecules was also observed SCCA1-treated macrophages and resulted in impaired ability to induce T cell activation by peptide-pulsed macrophages. Compared with treatment-naïve mice, SCCA1-treated macrophages showed increased anti-inflammatory cytokine CCL22, IL10 and immunosuppression regulators ARG1, PD-L1 expression. Moreover, human monocyte-derived M2 macrophages treated with SCCA1 during the differentiation process demonstrated inhibition toward CD3/28-induced T cell proliferation, accompanied by enhanced expression of cytokines, IL10 and CCL18. We further found that targeting SCCA1 by small interfering RNA knockdown significantly reduced tumor growth and macrophage infiltration, resulting in improved T-cell antitumor immunity. Lastly, analysis of cervical cancer patients with chemoradiation therapy showed that patients with high SCCA are associated with increased exhaustion (LAG3, CTLA4) and decreased antitumor gene signature (GZMB, IFNG) during treatment. In summary, SCCA expression promotes immunosuppressive macrophage polarization and function, contributing to T cell exhaustion phenotype and poor treatment response.

#6875 PIM kinases alter the prostate tumor immune microenvironment.

A. N. Clements[1], K. Sutterby[1], S. Kumar Deshmukh[2], S. Wu[2], J. Xiu[2], A. Farrell[2], M. Radovich[2], C. Nabhan[2], E. I. Heath[3], R. R. McKay[4], A. Recio-Boiles[1], N. A. Warfel[1];

[1]University of Arizona Cancer Center, Tucson, AZ, [2]Caris Life Sciences, Phoenix, AZ, [3]Wayne State University, Detroit, MI, [4]University of California, San Diego, CA

Prostate cancer is the second leading cause of cancer-related deaths in American men. While prostate cancer patients typically respond to androgen-deprivation therapy, androgen receptor signaling inhibitor (ARSI), and/or taxane chemotherapy, patients inevitably develop resistance, and the disease progresses to an untreatable and lethal form known as castrate resistant prostate cancer (CRPC). Immunotherapy has changed the treatment paradigm for many types of cancer; however, immune checkpoint inhibitors have not shown clinical benefits in CRPC. Clinical and preclinical evidence indicates that this lack of efficacy can largely be attributed to the immunosuppressive tumor microenvironment. Tumor associated macrophages (TAMs) secrete factors that promote tumor progression and suppress antitumor immunity, making them a promising therapeutic target. The Proviral Integration site for Moloney murine leukemia virus (PIM) kinases are serine/threonine kinases that are overexpressed in prostate cancer. PIM regulates many signaling pathways that promote cell proliferation and survival. However, how PIM kinase alters the prostate tumor immune microenvironment and impacts immunotherapy resistance is not well understood. We analyzed primary prostate and metastatic lymph node samples from treatment-naive metastatic hormone-sensitive prostate cancer patients. Prostate cancer samples with PIM1/PIM2/PIM3-high and -low expression were classified by top and bottom quartile, respectively. PIM high tumors had higher expression of immunostimulatory genes (*IL1β*, *TNF*, and *TNFSF13*), increased infiltration of M2 macrophages, B cells, and NK Cells, and a higher T cell inflamed score compared to PIM-low tumors. Our results demonstrate that PIM overexpressing prostate tumors display increased inflammation and infiltration of immunosuppressive immune cells, including M2 macrophages. Due to the changes observed in inflammation, we hypothesized that PIM kinase may regulate macrophage inflammatory signaling. We treated bone marrow derived macrophages with a PIM kinase inhibitor and showed that PIM inhibition suppresses inflammasome signaling and the release of the pro-inflammatory cytokine, IL-1β. Chronic inflammation can lead to the recruitment of TAMs, further promoting resistance to immune checkpoint inhibitors. Utilizing a syngeneic mouse model of prostate cancer, we demonstrated that PIM inhibition in combination with immune checkpoint blockade synergistically decreased tumor growth. Furthermore, immunoprofiling demonstrated that combination treatment enhances T cell activity. Overall, our results suggest that PIM kinase plays an important role in regulating the prostate tumor immune microenvironment and that PIM kinase may be a potential target to enhance the efficacy of immunotherapy for the treatment of prostate cancer.

#6876 Cyclic immunofluorescent analysis of the tumor microenvironment across human brain cancer subtypes.

D. Fails, M. Spencer;
Fortis Life Sciences, LLC, Montgomery, TX

Introduction: The tumor microenvironment (TME) has been the focus of a myriad of studies over the last decade and advancements in the field of cancer research have grown as a result. Improvements in the number of biomarkers that can be screened has increased across a variety of methods and the field of spatial profiling has largely adapted to keep pace with this. However, many challenges persist: 1) tissue microarrays can be limited by tumor heterogeneity and 2) newer technology can be cost-prohibitive. Brain tumors are of significant importance, especially those of glial origin, as they swiftly progress and result in a high fatality rate. As such, the need for more diverse therapeutic approaches is growing with many already pioneering new IHC-based strategies. The aim of this study was to address both challenges addressed above in the neurobiology space.

Methods: Biomarkers of importance in brain cancer tissues were identified and three distinct panels were designed. The first panel consisted of CD68, CTLA-4, p16ink4A, p14ARF, and p53. The second included PDPN, Calretinin, MAGE-D2, PTEN, and Vimentin. The third panel included IDH2, BRAF, GFAP, VEGF, and BOP1. Staining was achieved using Bethyl Laboratories IHC-validated primary and secondary antibodies and Akoya Opal™ Polaris 7-color IHC kit fluorophores (Akoya Biosciences [NEL861001KT]). Optimization was achieved using FFPE tissue microarrays containing normal neural tissue and brain cancer subtypes. The final optimized order was then tested on whole serial sections of meningioma, astrocytoma, and glioblastoma in six-color mIF. Images were generated using the PhenoImager HT® and subsequently merged and analyzed by Pathomics.

Results: Phenotyping and total cell counts for each marker were identified for each serially stained tissue set. Expression levels of MAGE-D2 and BRAF were high across malignant tissues of variable gradations. Conversely, in tissues with high expression of MAGE-D2, p53 levels in these samples were lower. This is consistent with findings that suggested that MAGE-D2 is a potential dissociator of p53 by impairing transcriptional activity. Macrophage expression appeared to correlate with CTLA4 and overall tumor infiltration.

Conclusions: Utilizing several unique biomarkers to understand the spatial relationships and phenotypes within the tumor microenvironment is becoming a more common practice among researchers. In using this method of serially staining tissue sections and merging the resulting images, more researchers will have access to spatial information which may have been cost-prohibitive otherwise. Additionally, in utilizing whole sections of difficult-to-treat cancerous tissue rather than microarrays, phenotypic information is available across the entire tumor microenvironment enabling a more comprehensive assessment of the TME.

#6877 Progesterone promotes immunosuppression in the murine mammary gland by causing T cell death.

A. Heard[1], L. R. Werner[1], E. I. Chowanec[1], H. Saunders[1], J. Tinoco[1], Z. C. Hartman[2], C. R. Hagan[1];
[1]University of Kansas Medical Center, Kansas City, KS, [2]Duke University, Durham, NC

Breast Cancer is the most common cancer diagnosed in women in the United States. Second only to lung cancer, breast cancer results in the greatest number of cancer deaths for women. Hormone receptor positive (HR+) breast cancers - cancers expressing the nuclear receptors for steroid hormones estrogen and progesterone, termed the estrogen receptor (ER) and progesterone receptor (PR) - make up the largest proportion of diagnosed breast cancers by a significant margin. So, although the HR+ subtype is less aggressive compared to others, it continues to be the largest contributor to breast cancer mortality. Treatment consists of anti-endocrine therapies, largely targeting ER/estrogen, the established drivers of breast cancer growth. Most women respond well to these therapies, but for women who do not, there are few alternative options. With the advent of immunotherapy and its successes in treating and controlling certain tumor types, many were hopeful that it could be employed for breast cancer as well. However, breast cancers, especially HR+ breast cancers, are considered “immune cold.” They lack high proportions of tumor-infiltrating lymphocytes (TILs), have low neoantigen production, and high percentages of immunosuppressive cells. A contributing factor could be the hormones present in the tumor microenvironment. The accepted paradigm is that lifetime exposure to estrogens drives the development of HR+ breast cancer, but both estrogen and progesterone are part of the normal menstrual cycle. Prior work from our lab has uncovered a novel immune-modulatory role for progesterone, pivotal to promoting the growth of PR-positive mammary tumors. Recent preliminary data from our lab show that progesterone treatment conveys immune protection against T cell killing in a co-culture with E0771 mammary gland tumor cells. However, when activated in monoculture, T cells exposed to increasing concentrations of progesterone have no differing expression of cell surface activation or exhaustion markers, implying that progesterone is not eliciting this effect by interfering with the T cell activation cascade nor is it inducing premature exhaustion. Interestingly, progesterone treatment instead leads to a concentration-dependent increase in T cell death compared to the untreated control. In vivo, these results are supported as progesterone treatment decreases the amount of total CD3+ T cells, and specifically the cytotoxic CD8+ subset, in the mammary glands of mice. These results suggest that progesterone could modulate the breast and tumor microenvironment, providing tumor cells with protection from immunosurveillance and contributing to HR+ breast cancer development. These data also argue for the use of anti-progestins to be added to the HR+ breast cancer treatment regimen to boost anti-tumor immune activity.

#6878 Images to insights: Transforming TME characterization into actionable spatial metrics with AI-powered multiplex immunofluorescence.

M. Naderi, L. Krstic, D. Cikic, K. Ruf, I. Mihajlovic, S. Todorovic, C. Weston;
Reveal Biosciences Inc., San Diego, CA

Background: Precise and actionable assessment of cellular mechanisms and interactions within the tumor microenvironment (TME) is critical for advancing clinical trials, preclinical research, and informed decision-making in immuno-oncology. Multiplex immunofluorescence (mIF) assays have emerged as pivotal tools that can enable comprehensive visualization of protein expression and cellular interactions within the TME. Integration of advanced digital analysis tools and mIF assays, can revolutionize our ability to interpret the TME and usher these assays into high-throughput clinical settings.
Methods: In this study, we processed tumor samples utilizing Akoya's PhenoCode Signature Immune Profile Human Protein Panel, which includes immune profiling markers CD8, CD68, CD3, CD20 and tumor marker PanCK. Following the Akoya Opal staining protocol, formalin-fixed paraffin-embedded (FFPE) samples were stained and scanned using the PhenoImager HT scanner. The images were then analyzed using Reveal's AI-mIF digital assay on the ImageDx platform to generate contextual and spatial biomarker data. A deep learning-based cell segmentation model based on MaskRCNN architecture, signal preprocessing for noise and autofluorescence, and dynamic intensity normalization were used. Phenotype classification was precisely executed using dynamic thresholding or neural network classifiers as needed. Results were validated by establishing concordance with pathologist readouts.
Results: The application of our methodology yielded highly concordant results when compared with manual counts, demonstrating the efficacy of our approach. The R2 correlation coefficient across all markers passed the minimum criteria of R2>0.85 with regression slopes between 0.7-1.3, indicating a robust alignment with traditional pathologist assessments. We showcase stratifying samples Desert, Excluded, or Inflamed phenotypes and other quantitative and spatial results such as interactions of immune cells and tumor within 30-um neighborhoods, and their dispersion and arrangement in the TME.
Conclusion: The integration of Reveal Biosciences' ImageDx platform and RevealAI-mIF provides an ecosystem to host, visualize, and analyze Akoya's immune profiling images. This collaborative effort has enabled the transformation of complex multiplex imaging data into distinct spatial phenomic endpoints, thereby introducing the potential to significantly advance biomarker discovery and contribution to translational and clinical research in the field of immuno-oncology.

#6879 Development of a rapid multiplex immunohistochemistry for characterizing tumor-immune microenvironment.

A. Kimura, T. Tsujikawa, H. Morimoto, J. Mitsuda, S. Saburi, S. Mukudai, H. Nagao, N. Sakurai, N. Murakami, A. Miyagawa-Hayashino, H. Ogi, S. Shibata, E. Konishi, K. Itoh, S. Hirano;
Kyoto Prefectural University of Medicine, Kyoto, Japan

Intratumoral immune profiles have been related to prognosis and therapeutic efficacy; this could result in personalized treatment based on biomarkers. Although techniques for multifactorial evaluation of different tumor-immune microenvironments have been established, their practical implementation in clinical settings still requires further improvement, where the time required for testing needs to be reduced and the technology needs to be clinically validated. To develop a multiplex, quantitative, and rapid tissue evaluation method based on clinically established standard immunohistochemistry (IHC), we attempted to develop 6-marker rapid multiplex IHC based on our previously reported 14-marker multiplex IHC via the reduction of the number of labels and speeding up the staining procedure (Tsujikawa et al. Cell Reports, 2017). First, we confirmed whether immunological features that were found to be associated with prognosis in 14-marker multiplex IHC analyses could be identified with fewer labels. Quantitative results by selected six markers exhibited significant correlation with those by 14 markers in terms of immune classifications based on the balance of lymphoid and myeloid cells. Next, we developed a rapid staining protocol by optimizing the reaction temperature, chromogen, and washing time, allowing the completion of 6-marker analysis in 5 hours and 49 minutes as opposed to several days required for the conventional multiplex IHC. By using six markers, validation in benign tonsil tissue and head and neck cancer tissue exhibited significant correlation between rapid and standard multiplex IHC in terms of staining intensities, densities of T cells, macrophages, lymphoid/myeloid immune cells ratios, and spatial profiles of intratumoral immune infiltrates. This method may enable a quantitative assessment of tumor-immune microenvironment on a clinically feasible time scale, which promote the development of tissue biomarker-guided therapeutic strategies.

#6880 Immune infiltration in inflammatory and myofibroblastic cancer-associated fibroblast high microenvironments of colorectal cancer.

Y. Gadalla, K. A. Johnson, S. Nath, C. A. Pasch, D. A. Deming;
University of Wisconsin Madison, Madison, WI

Background: Cancer-associated fibroblasts are major modulators of the tumor microenvironment (TME) and play a large role in the immune system's response to tumors. The direct effect that myofibroblastic CAFs (myCAFs) and inflammatory CAFs (iCAFs) have on immune infiltration is not well studied in colorectal cancer (CRC). Here we investigate the effects that myCAFs and iCAFs have on immune infiltration in human CRCs.
Methods: The Cancer Genome Atlas (TCGA) Colorectal Adenocarcinoma PanCancer Atlas dataset was accessed via cBioPortal. Cancers were separated into myCAF prominent (MP) by high gene expression (Z-score > 1) of *ACTA2* and *TAGLN* and iCAF prominent (IP) by expression of *PDPN* and *ICAM1*. Gene Set Enrichment Analysis (GSEA) was performed on differential expression results comparing these groups. Additionally, bulk RNA sequencing results were analyzed for immune cell subsets using Cibersortx. Statistical analysis was completed in R.
Results: Of 592 cancer samples, 24 were MP and 9 IP. There was no significant difference in age (MP median age 63, IP median age 70, q = 0.6) nor sex (MP 17 female/7 male; IP 4 female/5 male, q=0.9). MP have 1/24 profiled patients with MSIsensor score >=3.5 and 2/24 patients with MSI MANTIS score > 0.4; IP have 3/9 profiled patients with MSIsensor score >=3.5 and 3/9 patients with MSI MANTIS score >0.4. IP cancers were enriched for gene sets associated with enhanced immune cell infiltration (Inflammatory Response, Interferon Gamma Response, Allograft rejection, TNFA signaling via NFKB, IL6 JAK STAT3 signaling, Interferon Alpha Response, Complement, IL2 STAT5 signaling and Apoptosis, all q< 0.001). MP cancers were enriched in the KRAS signaling Down gene set (q=.009). IP cancers had a higher proportion of infiltrating immune cells than MP cancers by CibersortX analysis (iCAF median = 2.829, myCAF median= 2.284, p < 0.01). IP cancers had higher CD4 memory cells (p <0.001, iCAF median = 0.455, myCAF mean = 0.318), NK resting cells (p<0.001, 0.228, 0.103), M1-like macrophages (p <0.01, 0.1977,0.107), and neutrophils (p<0.01, 0.0298, 0). MP cancers had a higher number of NK activated cells (p = 0.04, iCAF median = 0, myCAF median = 0). M1-like macrophage gene markers were higher expressed in IP cancers compared to MP cancers, though not significantly (*NOS2* log2FC = 0.66, q = 0.652; *IL1A* 3.25, 0.0375; *IL23A* 1.34, 0.151; *IL26* 1.31, 0.32). Additionally, IP cancers tended to express markers for activated CD8+ T cells, though only *IFNG* was significant (*GZMB*, log2FC = 0.97, q = 0.337; *IFNG*, 2.16, q<0.001; *PRF1*, 1.12, q=0.198).
Conclusion: These analyses indicate that iCAFs play the major role in modulating the immune infiltration of cancers. These data highlight the need for further research into the mechanisms by which different CAF subtypes alter the immune microenvironment.

#6881 Investigating the role of post-transplant bone marrow immune dysregulation in multiple myeloma.

J. T. Wang, M. Fiala, K. Sato, J. Fortier, R. Vij, L. Ding;
Washington University in St. Louis, Saint Louis, MO

Multiple myeloma (MM) is a cancer of bone marrow plasma cells (BMPCs), which to date remains incurable. Standard of care for qualifying patients involves high-dose chemotherapy followed by autologous stem cell transplant (ASCT), after which minimal residual disease (MRD) testing is used to assess the degree of tumor clearance. Though strongly associated with better survival, MRD-negativity is an imperfect predictor for patient outcomes and fails to account for the pro-tumorigenic BM dysregulation often found in MM patients. As the post-transplant BM milieu in MM is not well understood, we conducted 3' single-cell RNA sequencing (scRNAseq) of 49 newly diagnosed (NDMM) and 79 day-100 post-ASCT whole-BM aspirates to investigate how immunosuppressive microenvironmental signatures may persist or develop following ASCT to influence patient outcomes. 68 of 79 post-ASCT samples come from uniformly-treated clinical trial enrollees with progression-free survival (PFS) ranging from 10 months to over 7 years, with both MRD- and MRD+ cases at either PFS extreme. We observe that although post-ASCT samples have uniformly lower PC count than NDMM samples, only erythroblasts and B cells appear relatively depleted in NDMM samples to compensate for higher PC proportions. T/NK cells and myeloid lineages, though similar in percentage across samples, exhibit clear subtype bias between the two timepoints. Post-ASCT samples are significantly enriched for GZMH+ CD8+ T and NK cells, HIF1A+ hypoxia-responsive monocytes, and depleted for S100A8/9-high CD14+ monocytes. NDMM samples are also enriched for SPINK2+, CDK6+, and AVP+ neutrophils, which are rare in post-ASCT samples. Notably, higher HIF1A expression in myeloid cells post-ASCT is further associated with longer PFS. Regardless of MRD status, NFKBIA, FOS, and GNLY upregulation and GZMK downregulation in post-ASCT T cells are associated with worse PFS. Conversely, enrichment of CD16+ IFN-responsive monocytes and depletion of ARG1+/FUT4+/CEACAM8+ myeloid-derived suppressor cells (MDSCs) are associated with longer PFS. Beyond such general trends, we observe MRD-dependent PFS-association of several CD8+ T cell subsets. Overall, this study enhances our understanding of how post-transplant BM repopulation and immune interaction may impact treatment response in MM.

#6882 Exploring aryl hydrocarbon receptor expression and distribution in the tumor microenvironment, with a focus on immune cells, in various solid cancer types.

D. Kim[1], **C. Lee**[2], Y. Han[2], S. Park[2], H. Han[2], K. Na[2], M. Kim[2], S. Yang[2], S. Baek[2], Y. Kim[2], J. Hwang[2], S. Lee[1], S.-s. Kang[3], T. Han[4], H. Doh[4], J. Cho[4], D. Kim[4], D. Cha[4], M. Hong[5], S. Lim[5], J. Lee[5], J. Kim[2], K.-H. Pyo[6], B. Cho[5];

[1]Brain Korea 21 PLUS Project for Medical Science, Yonsei University College of Medicine, Seoul, Korea, Seoul, Korea, Republic of, [2]Yonsei University College of Medicine, Seoul, Korea, Republic of, [3]JEUK Institute for Cancer Research, Gumi, Korea, Republic of, [4]Dong-A ST Research Institute, Yongin-si, Korea, Republic of, [5]Division of Medical Oncology, Department of Internal Medicine and Yonsei Cancer Center, Severance Hospital, Yonsei University College of Medicine, Seoul, Korea, Republic of, [6]Yonsei New Il Han Institute for Integrative Lung Cancer Research, Yonsei University College of Medicine, Seoul, Korea, Republic of

Background: The aryl hydrocarbon receptor (AhR) is a transcription factor that performs various biological functions upon ligand activation. While there have been extensive studies and development of AhR-targeting anticancer therapies, including active clinical trials, research on the expression of AhR, a key biomarker, in the TME remain limited. Herein, we evaluated the nuclear and cytosolic AhR expression across five solid cancer types: head and neck squamous cell carcinoma (HNSCC), bladder cancer, colorectal cancer, esophageal cancer, and non-small cell lung cancer (NSCLC).

Methods: Multiplexed immunohistochemistry (mIHC) and image cytometry were employed to investigate the AhR expression and distribution in 513 patient samples, of which 292 were from patients with one of five solid cancer types. For quantification of AhR expression levels, FCS files were generated, and the resulting data was analyzed using the R program.

Results: AhR expression was predominantly high in cancer cells, followed by T cells and macrophages across all cancer types. All 513 patient samples were categorized into three clusters based on distinct expression and localization patterns of AhR. Cluster 1 exhibited high AhR expression in the cancer cell nucleus, whereas cluster 3 showed the lowest. AhR expression in the stromal macrophage nucleus was the most pronounced in cluster 2. In cluster 1, NSCLC was entirely absent, with esophageal cancer representing the largest proportion. In contrast, cluster 2 was notably different from cluster 1, with a 5% prevalence of NSCLC and a relatively higher proportion of HNSCC and colorectal cancer. The AhR expression in macrophages within cluster 2 was noticeably higher than in cluster 1. Cluster 3, which had the highest NSCLC proportion, generally displayed low AhR expression compared to other clusters, but also exhibited AhR expression in regulatory T cells (Tregs), a pattern which was not observed in other cancer types. Notably, a positive correlation was observed between the nuclear and cytosolic expressions of AhR, suggesting that AhR expression as a biomarker is independent of its subcellular localization. Furthermore, there was no clear correlation between AhR expression levels and cancer stage, grade, and metastatic status.

Conclusion: We elucidated the expression profile of AhR within the TME across five cancer types, then classified the patient samples into three clusters based on their distinct AhR expression patterns. By demonstrating different expression patterns of AhR in cancer cells and immune cells, our findings are anticipated to provide a fundamental basis for clinical and immunological research on AhR-targeting therapies.

#6883 Investigation of tumor-immune interactions in pediatric sarcomas using single-cell multi-omics.

Zhan Zhang[1], Kyung Jin Ahn[2], Changya Chen[2], Rumeysa Biyik Sit[2], Hesham Mohei[3], Brian Lockhart[4], Malay Haldar[3], Kathrin Bernt[2], Vinodh Pillai[3], Kai Tan[2]

[1]Department of Bioengineering, University of Pennsylvania, Philadelphia, PA,[2]Division of Oncology and Center for Childhood Cancer Research, Children's Hospital of Philadelphia, Philadelphia, PA,[3]Department of Pathology and Laboratory Medicine, University of Pennsylvania, Philadelphia, PA,[4]Department of Pathology and Laboratory Medicine, Children's Hospital of Philadelphia, Philadelphia, PA

Background: Pediatric sarcoma represents the second most common solid tumor in children. Despite advances in multimodal therapies, one-third of sarcoma patients do not survive the disease. Over the past few decades, the development of novel therapeutic strategies for sarcoma has been impeded by an insufficient understanding of the tumor microenvironment (TME). In particular, the potential of immunotherapy remains constrained by the gap of knowledge about the molecular and functional phenotypes of the immune cells in the sarcoma TME.
Methods: To address this knowledge gap, we collected treatment-naïve tumor samples from 32 patients with five pediatric sarcoma subtypes. We employed a single-nuclei RNA+ATAC-Seq multi-omics assay to comprehensively characterize the transcriptomic and epigenomic heterogeneity of tumor and immune cells within the sarcoma TME.
Results: Our analysis revealed that tumor-associated macrophages (TAMs) were the most abundant immune cell type in the sarcoma TME. We identified seven distinct TAM subpopulations, each exhibiting unique gene expression and chromatin accessibility patterns. Among these, TAM subsets with higher expression of *SPP1* and *C1QC* genes displayed the strongest immunosuppressive potential. Transcriptional regulatory network (TRN) analysis identified transcription factors that were most likely to drive the phenotypes of SPP1+ and C1QC+ TAMs, including ELF2, JUND and RUNX1. Through cell-cell communication analysis, we discovered that SPP1+ TAMs interact with T cells via SPP1-CD44 signaling, while C1QC+ TAMs interact with NK cells through HLA-E-KLRC1 signaling, suggesting the potential involvement of these signaling pathways in TAM-mediated suppression of these cytotoxic lymphocytes. We prioritized ligand-receptor gene pairs, such as SEMA3D-NRP1 and LTBP3-ITGB5, which likely mediate the interaction between malignant sarcoma cells and SPP1+/C1QC+ TAMs based on their dominance across sarcoma subtypes and association with poorer clinical outcomes. On the other hand, our analysis revealed that sarcoma subtype-specific interactions between TAMs and malignant cells are common, highlighting the heterogeneity of signaling events across sarcoma subtypes.
Conclusion and Significance: Our study presents a comprehensive single-cell multi-omics characterization of pediatric sarcomas and sheds light on its tumor microenvironment. By identifying unique markers for immunosuppressive TAM subpopulations and elucidating intercellular interactions promoting tumor development, this study proposes potential therapeutic targets for sarcoma treatment based on the role of TAMs in sarcoma TME.

#6884 Evaluating tumor-infiltrating immune cells helps predicting prognosis in biliary tract cancer.

Kousuke Hatta, Ryota Tanaka, Kenjiro Kimura, Shinpei Eguchi, Go Ohira, Hiroji Shinkawa, Kohei Nishio, Masahiko Kinoshita, Shigeaki Kurihara, Shuhei Kushiyama, Takahito Kawaguchi, Naoki Tani, Koichi Nakanishi, Mizuki Yoshida, Takeaki Ishizawa

Osaka Metropolitan University, Osaka-shi, Japan

Background: The tumor microenvironment (TME) is composed of not only cancer cells but also an extracellular matrix and many types of non-cancerous cells, including fibroblasts and immune cells. In recent years, infiltrating immune cells in TME are known as a predictor of chemotherapy and immunotherapy effectiveness. The purpose of this study is to evaluate infiltrations of lymphocytes and macrophages in biliary tract cancers (BTCs).

Methods: Clinical data and tissues were obtained from 130 patients who underwent surgical treatment for BTCs (intrahepatic, perihilar, and distal bile duct cancer, gallbladder cancer, and ampullary cancer) at our institution between 2001 and 2017.The immunohistochemical evaluation was performed to evaluate the number of CD8+ T cells, CD4+ T cells and FOXP3+ T cells and CD68+ Macrophages around the tumor cells. We defined Immunoscore based on the status of infiltrating immune cells. With CD8-high, CD4-high, and FOXP3-high TILs and CD68-low TAMs as one factor, the number of factors was counted in each case, and Immunoscore was assigned a score of 5 stages, from 0 to 4. It was high for the score of 3-4 and low for the score of 0-2. Also, to evaluate the correlation with TME and systemic inflammatory reaction, we examined blood inflammatory biomarker from peripheral blood samples.

Results: A total of 59 cases had high Immunoscore and 71 cases had low Immunoscore. Patients with high Immunoscore showed significantly superior overall survival (OS) and recurrence free survival (RFS) than those with low Immunoscore (median OS 60.8 vs. 26.4 months, $p = 0.001$; median RFS not reached vs. 17.2 months, $p < 0.001$). For OS, low Immunoscore, positive lymph node metastasis, presence of distant metastasis, and high serum CA19-9 level were independent poor prognostic factors (hazards ratio 2.05, 3.48, 1.7, and 2.05; $p = 0.01$, $p = 0.005$, $p = 0.05$, and $p = 0.01$, respectively). For RFS, low Immunoscore, T classification of pT3-4, and presence of distant metastasis were independent poor prognostic factors with hazards ratio of 2.41 ($p = 0.001$), 2.16 ($p = 0.005$), and 3.58 ($p = 0.005$), respectively. Patients with high preoperative Neutrophil-to-lymphocyte ratio (NLR) had a significantly lower average number of $CD8^{\pm}$ T cells as compared to patients with low NLR ($p = 0.02$). Preoperative NLR was associated with infiltrating $CD8^{\pm}$ T cells in TME.

Conclusions: High Immunoscore group had significantly longer OS and RFS and was an independent good prognostic factor. Also, infiltrating $CD8^{\pm}$ T cells in TME correlated preoperative NLR. Our findings indicated that in biliary tract cancer, the evaluation of infiltrating immune cells in TME was useful to predict patient prognosis, and preoperative NLR may predict the tumor infiltrating $CD8^{\pm}$ T cells.

#6885 Investigating a novel role of DCLK1 isoforms in colitis and colitis associated colon cancer.

K. A. Yusuf, B. C. Roy, S. Anant, S. Umar;
University of Kansas Medical Center, Kansas City, KS

Chronic intestinal inflammation in patients diagnosed with inflammatory bowel disease (IBD) significantly increases their risk of colorectal cancer (CRC). Despite the rising global frequency of IBD, the precise mechanisms that regulate the transition from IBD to colon cancer are poorly understood. Doublecortin-like kinase 1 (DCLK1) is a protein with two major isoforms, DCLK1-L and DCLK1-S. Previous studies have shown that hypermethylation of the DCLK-1α promoter encoding DCLK1-L, particularly in colorectal cancer, allows switching to the DCLK1-S isoform that confers an invasive tumor phenotype. The DCLK1-L is a tuft cell marker that protects against colitis by sensing and eliminating gut pathogenic infection through various mechanisms. On the contrary, the role of DCLK1-S in colitis and colitis-associated cancer has not been thoroughly investigated. Studies from our lab have identified a marked elevation of DCLK1-S in tissue samples of IBD patients. We also recently discovered that DCLK1-S is predominantly expressed in Ly6G+; MHCII- neutrophils, which coincide with elevated levels of inflammation and tissue damage in the colon. To further understand the role of DCLK1 isoforms in driving the progression of colitis to colon cancer, we bred *Dclk1*$^{fl/fl}$ mice with *MRP8-Cre-ires/GFP* mice to generate *Dclk1*$^{fl/fl}$*;MRP8-Cre+/-* that eliminates DCLK1-L upon tamoxifen injection resulting in sustained expression of DCLK1-S in the granulocytes especially neutrophils. When infected with *Citrobacter rodentium* (CR), *MRP8;Dclk1*$^{-/-}$ mice compared to *MRP8;Dclk1*$^{+/-}$ or WT mice developed more severe colitis. We have also discovered a novel interaction between DCLK1-S and MMP13 in an unbiased docking study that correlated with significant co-localization of DCLK1-S with MMP13 in the colons of CR-infected mice. Employing a knock-in mice over-expressing the DCLK1-S +19 under the CAG promoter, the DCLK1-MMP13 co-localization correlated with severe ulceration and colitis with loss of crypts and immune cell infiltration including Ly6G+ neutrophils. Studies are underway to see if the severity of colitis in *MRP8;Dclk1*$^{-/-}$ mice translates into enhanced tumorigenesis and to see if potential interaction between DCLK1-S and MMP13 could provide a plausible mechanism of colitis progression to colon cancer through ECM remodeling and tissue damage.

#6886 Orion™: 17-plex single-step stain and imaging of normal lung section adjacent to non-small cell lung carcinoma.

S. Larkin, T. George, E. Kaldjian;
RareCyte, Inc., SEATTLE, WA

Background: The ability to image tissue microenvironments (TME) at high-plex over a whole slide without requiring multiple staining steps allows for unprecedented ability to study tissue architecture and molecular mechanisms of immune and disease processes. Here we investigate a sample of normal lung section adjacent to non-small cell lung carcinoma using whole slide, single-step stain and imaging at single-cell resolution.
Methods: These images profiled a whole slide tissue section of normal lung section adjacent to non-small cell lung carcinoma, stained with a 17-plex immuno-oncology biomarker panel. In this profile, we designed a high-plex panel of 17 biomarkers where the tissue autofluorescence was imaged and isolated as an additional fluorescence channel. All markers were stained in a single staining procedure and imaged in a single scan. Whole slide spatial staining and imaging was conducted on the Orion spatial biology platform. The full protocol is quick and simple, using standard histology tools: •Mount sections on glass slides•De-paraffinize and perform antigen retrieval•Quench autofluorescence•Stain slides with a panel of ArgoFluor™ conjugated antibodies•Coverslip with ArgoFluor Mounting Medium and cure overnight•Image whole slides at 20X magnification using the Orion instrument•Process to ome.TIFF and analyze.
Results: Data revealed intact normal lung alveolar architecture, with scattered immune cell infiltrates. Multiplexed imaging revealed epithelial cells, which make up alveoli, and endothelial vasculature as well as immune cells infiltrates in the alveolar space. Various immune cell populations were observed to be present (T cells, B cells, macrophages) and immune cell activation could be distinguished using PCNA and/or Ki-67 markers. Various T cell subsets could also be identified among the infiltrate using markers for CD4, CD8 and T-regulatory marker FOXP3. Through the use of multiplex staining, immune cell activity could also be characterized with respect to bronchiolar, artery, and capillary tissue architecture.
Conclusions: High-quality subcellular imaging of TME can lead to greater spatial investigation and more in-depth understanding of immune function in normal and diseased tissue. Here, multiplexed imaging identified distinct immune cell collections among cancer-adjacent normal lung tissue, providing validation of instrumentation and methods to obtain benchmarks for spatial quantitation of immune cells in control regions adjacent to cancer tissue.

TUMOR BIOLOGY: Preclinical Studies of Cancer
Poster Session

#6890 2D Tumor cell culture based Ex vivo drug sensitivity screening platform for South African patient samples (leukemia, multiple myeloma, ovarian and uterine cancer) demonstrate potential for targeted cancer therapies.

M. Takundwa[1], V. Kenmogne[2], T. Malise[2], B. Monchusi[1], P. Dube[1], E. Nweke[2], J. Fabian[3], H. Maher[3], J. du Toit[3], V. Philip-Cherian[4], P. Fru[2], A. Sajo[5], A. Mouton[5], M. C. van Aardt[5], C. Visser[5], G. Dreyer[5], D. Govindaraj[1];

[1]CSIR South Africa, Pretoria, South Africa, [2]University of the Witwatersrand, Johannesburg, South Africa, [3]Wits Donald Gordon Medical Centre, Johannesburg, South Africa, [4]Chris Hani Baragwanath Academic Hospital, Johannesburg, South Africa, [5]University of Pretoria, Pretoria, South Africa

Resistance to standard chemotherapy is a major challenge with Leukemia (Leuk), Multiple Myeloma (MM), Ovarian Cancer (OvCa) and Uterine Cancer (UtCa) treatments, which ultimately leads to relapse. Our study objective is to establish a robust drug sensitivity screening platform that can identify drugs and drug combinations that are effective in precision medicine for individual South African patient samples (Leuk, MM, OvCa and UtCa). Given that resistance to chemotherapy treatment accounts for high mortality and morbidity, we focus on the hypothesis that several drug combinations will be required for patients to achieve better response for drug regimens beyond first line of chemotherapy. Therefore, our defined objectives were to 1) establish 2D ex vivo tumour cell culturing using South African patient samples; 2) develop a drug sensitivity screening platform through which selected single and drug combinations will be identified; 3) to provide South African cancer (OvCa, Ut Ca, CLL, MM) patients with individualized treatment options with effective drug combinations for targeted therapies. Through collaboration with, Steve Biko Hospital Pretoria, Chris Hani Baragwanath Hospital and Wits Donald Gordon Medical Centre, Johannesburg, South Africa, we performed 100 patient sample collections including Acute myeloid leukaemia (AML) (n=7), Chronic lymphocytic leukaemia (CLL) (n=4), Chronic myeloid leukaemia (CML) (n= 30), MM (n=40), OvCa (n=10), UtCa (n=4) and healthy donors (n=5). Culture setting for all patient-derived tumor cells were established through the 2D cancer cell culturing in 96 well plates. This was followed by functional drug sensitivity testing using a panel of FDA approved chemotherapy drugs. The average turnaround time from biopsy to drug sensitivity test results is currently at 14 days. We have completed ex vivo drug sensitivity screening to perform analysis on patient samples (n=80) using 30 drugs with a concentration range of 1-1000 nm. Our preliminary drug sensitivity screening studies show good response to proteosome inhibitors, melphalan, doxorubicin and kinase inhibitors. We have established a wound healing assay for OvCa and UtCa samples and demonstrated sustained cell growth for the period of 2 weeks with tumor cells growing faster than twin normal tissue. We are now at stage of performing drug sensitivity screening for OvCa and UtCa patient samples for both twin normal and tumor tissues. We have established a drug sensitivity screening platform and wound healing assay with primary patient derived cells that utilizes South African Patient samples to select effective drugs for monotherapy and also drug combinations.

#6891 Establishment and characterization of a panel of naïve and pretreated small cell lung cancer (SCLC) XPDX models.

G. Huelgas Morales[1], P. Forofontov[1], J. Flores[1], A. Simonson[1], A. Diaz III[1], J. Lund[1], N. Banos[1], K. Papadopoulos[2], D. Rasco[2], A. Patnaik[2], A. Abedi[3], N. Puente[3], E. Calvo[4], V. Moreno[4], R. Drengler[5], L. Smith[5], M. Wick[1];

[1]XenoSTART, San Antonio, TX, [2]START San Antonio, San Antonio, TX, [3]Texas IPS, San Antonio, TX, [4]START Madrid, Madrid, Spain, [5]STOH, San Antonio, TX

SCLC is an aggressive cancer of neuroendocrine origin, accounting for approximately 15% of all lung cancer cases. While the incidence of SCLC in the US has declined over past decades due to changes in smoking habits, this disease provides a poor prognosis and few effective treatment options for advanced disease. To better identify useful therapies for SCLC, we established and characterized a panel of 18 XPDX models representing primary and metastatic disease from either naïve or clinically treated patients and tested sensitivities towards chemotherapies and targeted agents. 18 models were established in immune-deficient mice including 8 from newly diagnosed patients (2 from lung primary), and 10 from recurrent disease (3 from lung primary). Models were IHC stained for Nectin-4, Trop2 protein and ERBB2 and profiled using WES and RNA_{seq}. For in vivo studies, models were evaluated against several chemotherapies including cisplatin, etoposide, topotecan, and temozolomide, as well as ADC agents trastuzumab deruxtecan (T-DXd), enfortumab vedotin (EV), and sacituzumab govitecan (SG). Targeted therapies toward CDK4/6, $KRAS^{G12C}$, and PARP were evaluated in some models. Endpoints in all studies included tumor volume and time from treatment initiation with %T/C values and tumor regression reported at study completion; a %T/C of ≤ 20% versus control was considered sensitive. Tumor regression (%T/C<0%) versus Day 0 tumor volume was also reported. Less than 10% of models stained positive for Nectin-4, Trop-2 or ERBB2. Molecular characterization revealed RB1 frameshifts or deletions in most models, KRAS/NRAS point mutations in 3 models, and 2 gene fusions SEPTIN7P2-PSPH and TVP23C-CDRT4. In vivo studies reported differential responses to chemotherapies with the most sensitive models established from treatment-naïve patients. Temozolomide was active in several studies including tumor regressions in both naïve and pretreated models. ADCs also reported differential activity toward the tested panel. We have established and characterized a panel of SCLC XPDX models and benchmarked them against various cancer therapies. This panel can be utilized as a valuable tool in developing novel therapies for SCLC patients.

#6892 Murine *ex vivo* platform: A powerful tool for biomarker assessment and high throughput screening of translationally relevant *in vivo* tumor models for PD and efficacy studies.

S. Bachawal, J. Leung, R. Mandawe, M. Garza, K. ly, O. Stefanson, J. Lohre, D. Kamali, N. Doan, B. King, E. Kim, G. Hegde, X. Liao, S. Liu, J. Kim, A. Mikels Vigdal, A. Mukhopadhyay;
Bristol Myers Squibb, Redwood City, CA

Ex vivo model systems using tumor biopsies from patients are often utilized to develop predictive biomarkers. However, these readouts are often proximal and do not inform on downstream mechanisms (distal pharmacodynamics) and their relationship to anti-tumor efficacy. *In vivo* murine models represent a powerful tool to bridge this gap. However, selection of an appropriate translationally relevant murine model can often be a time-consuming process given that the complexity of the tumor microenvironment (TME). Additionally, *in vivo* models are generally not amenable to high throughput screening. Here, we demonstrate that *ex vivo* mouse tumor platforms can be used for rapid screening of treatment responsive and translationally relevant tumor models. These models can be used to interrogate the impact of a therapeutic on anti-tumor efficacy in a long-term *in vivo* study, thus allowing for the establishment of biomarker/response relationships in a rational and rapid manner. To operationalize this platform, *ex vivo* cultures of dissociated tumor cells (DTC) or tumor tissue slices (histoculture) were first optimized for maximum viability and/or preservation of tissue architecture. To allow for high throughput screening, feasibility of freezing DTCs or tumor chunks prior to sectioning was also explored. Finally, both e*x vivo* tumor cultures and *in vivo* tumors were treated with a Innate agonist as a proof of concept to demonstrate functional equivalency. In conclusion, this work provides a novel way of screening responsive, translationally relevant murine tumor models in a high throughput and cost-effective manner. These efforts have the potential benefits of saving time and animal usage, while also maximizing the probability of successfully evaluating a therapeutic's benefit.

#6894 Modeling the spectrum of vascular changes occurring in healthy and early malignant cancers on a chip.

C. Franca[1], A. Athirasala[1], E. Dimitriadis[2], J. Bays[3], K. Yamada[2], C. Chen[3], L. E. Bertassoni[1];
[1]Knight Cancer Institute, Oregon Health & Science University, Portland, OR, [2]NIDCR, NIH Cell Biology Section, Bethesda, MD, [3]Boston University, Boston, MA

The transition of a healthy tissue to a pre-malignant and subsequent malignant stage is typically characterized by a marked increase in extracellular fibrosis and collagen density. Such changes coincide with a significant increase in tissue stiffness as the tumor progresses. Despite the large body of work on endothelial cell changes in tumoral angiogenesis, little is known about the dynamic interactions of endothelial cells, perivascular cells, and the extracellular matrix in early-to-late cancers. Appreciating such interactions is crucial for understanding tumorigenesis and early tumor progression. To model the spectrum of vascular changes occurring on pre-tumoral and tumoral ecosystems, we developed an organ-on-a-chip model of biomimetic pericyte-supported capillaries with collagen having increasingly higher density, stiffness and discrete fibril microarchitectures. Briefly, 160-um channels were engineered using type I collagen that underwent fibrillogenesis at different temperatures (4, 16, 21, and 37oC). Thus, the microarchitecture and stiffness would vary from a soft reticular network (healthy/pre-cancerous vascular capillaries) to a stiff fibrillar mesh (fibrotic/tumoral vascular capillaries). We then seeded human umbilical vein endothelial cells (HUVECs) and mesenchymal stem cells (MSCs) in the collagen channels. After 48h, samples were fixed and stained for actin (cytoskeleton), NG2 (pericyte differentiation), and CD31 (endothelial cell junction), laminin, and cell anchorage system, imaged with a confocal microscope and analyzed with Imaris. In addition, we used a Nanostring panel with 770 genes related to the tumor microenvironment in healthy and fibrosis. Vascular capillaries engineered in contact with softer reticular collagen, consistent with a healthy ECM, showed more pericyte differentiation ($p<0.05$), inter-endothelial cell junctions ($p<0.05$), and effective barrier function. In contrast, stiffer fibrillar collagen, which is consistent with the characteristics of the fibrotic malignant extracellular microenvironment, was associated with cell migration outward the vessel, leakiness, and higher RNA expression of interleukin 8 (IL8), TP53, transforming growth factor beta, vimentin, and collagen III genes, thus suggesting a system that compatible with the spectrum of tumoral vasculature changes in cancer and pre-cancer lesions. When vessels were engineered without MSCs, those differences were drastically minimized, To further understand the mechanisms, HUVEC-perivascular cell adhesion was disrupted using silencing RNA for NOTCH3. Upon silencing NOTCH3, the morphology and function of vasculature were reestablished, pointing to a major role of perivascular cells in vascular changes in early tumors.

Funding: NIDCR 1K01DE030484-01A1 to CMF R01DE026170, 3R01DE026170-03S1 and 3R01DE026170-03S2 to LEB

#6895 Application of MiniPDX® in clinical indication identification and anti-tumor drug development.

B. Xie, H. Chen, S. Zhao, L. Li, S. Xi, Y. Di, Y. Liu, X. Chen, X. Gu, Z. Bi, K. Hu, L. Van, J. Caggiula, C. Tang, **D. Wen**;
Shanghai LIDE Biotech Co., Ltd., Shanghai, China

MiniPDX® (Mini-patient-derived xenograft) is a novel, rapid (7~10days), and accurate method for drug sensitivity testing *in vivo*. It was referred as in vivo version of organoid assy. The testing material can be fresh patient tumor samples or tissues from established PDX models. We have systematically evaluated and compared the response rates of MiniPDX® assays and PDX assays pairwise in 26 PDX models across 3 types of cancers to 12 clinically relevant regimens for chemical and targeting drugs. The results demonstrate a high correlation between drug responses of the two assays, with sensitivity of 80% and specificity of 93%. More and more studies showed that MiniPDX® drug sensitivity test results were consistent with clinical responses in most patients, which indicated MiniPDX® models have great potential in guiding personalized medicine. LIDE has successfully conducted over 3,000 MiniPDX® tests for clinical precision medicine, covering more than 50 indications. The application of MiniPDX® extends beyond therapeutic selection, facilitating the prioritization of approved pharmacological interventions and informing the discovery pipeline for novel agents. Importantly, the MiniPDX® Mouse Trial using fresh tumor samples generated from the clinic is beneficial for determination of potential clinical indications. Only thousands of fresh cells leftover from MiniPDX® preparation are sufficient to get genomic and transcription data by OncoVee ® K-cell technology. The combination of MiniPDX® assay and omics data would be very useful for determination of potential biomarkers to distinguish responders and non-responders in population with certain indication(s) and leveraged for patient stratification and selection criteria in clinical trial design. In addition, we have developed a new version of MiniPDX® assay for immunotherapy (IO-FIVE, Immuno-Oncology Fast In Vivo Efficacy test) by using fresh patient cancer cells with autologous immune cells to maximally mimic human tumor microenvironment before seeding in immune-deficient mice. This assay allows for the tracking of cellular viability and phenotype pre- and post-treatment, thus providing a robust metric of in vivo immunotherapeutic efficacy within a fortnight.

#6896 Biomimetic hydrogels at physiological stiffness reprogram patient derived melanoma cells.

Y. L. Liu[1], J. Gleba[2], C. Kopecky[1], M. Pawlush[2], J. A. Copland[2], K. A. Kilian[1];

[1]UNSW Sydney, Kensington, Australia, [2]Mayo Clinic, Jacksonville, FL

Melanoma is a uniquely difficult cancer to treat due to complex tumor heterogeneity and resistance, where upon dissemination, survival drops to less than 17%. Drug resistance has arisen for the current standard of care and combinatorial therapies, expediting the need for new efficacious agents. The lack of physiologically relevant preclinical models has impeded the development of these therapeutics.

Potential melanoma drugs are typically assayed using cell lines on tissue culture plastic, then tested for *in vivo* efficacy and side effects in animals. This paradigm is inherently unsuitable for the generation of effective therapies as typical cell culture platforms fail to replicate the complex microenvironments known to play critical roles in tumor pathology and rodent models are prohibitively expensive for optimizing novel and combination therapies. Thus, our goal is to synthesize tissue-engineered melanoma models using biomimetic polymers that recapitulate patient tumor characteristics to assess combination and novel therapies that attenuate resistance and disrupt metastatic processes.

In this study, patient melanoma cells, which were unable to recapitulate drug responses on traditional cell culture platforms, were cultured in a controlled spatial and temporal manner on polyacrylamide hydrogels. The hydrogel scaffolds feature stiffnesses spanning that of physiological tissue, with microcontact printed human fibronectin for biomimetic protein presentation to create a microtumor array. Cells cultured on the hydrogel showed a 2.5-fold increase in expression of the cancer stem cell biomarkers, CD271 and ABCB5, which play a key role in melanoma survival and recurrence, compared to cells cultured on plastic or glass substrates. Further study identified BRAF mutant, drug resistant patient cells, regained resistance to standard of care targeted therapies, trametinib and dabrafenib. Through hydrogel microarrays featuring physiological similarities, the technology has enabled the exploration of heterogeneous cell populations with novel and combinatorial therapeutics.

#6897 Defining critical features for successful preclinical use of glioblastoma patient-derived xenografts (PDX) models for therapeutic assessment and clinical trial development.

D. M. Burgenske, A. C. Mladek, K. K. Bakken, Z. Hu, B. L. Carlson, P. A. Decker, J. E. Eckel-Passow, J. N. Sarkaria;
Mayo Clinic, Rochester, MN

Mayo Clinic has developed 111 GBM PDXs from newly diagnosed (72 PDX) and recurrent (39 PDX) patients. This large collection of PDXs provides a broad representation of genetic heterogeneity seen in patients. GBM PDXs that perform well in both *in vitro* and *in vivo* settings can be extensively utilized in the preclinical setting for downstream analysis. Based on 20 years of experience, we have defined the attributes that best enable preclinical use of our GBM PDX models. Among them are short-term *in vitro* culturing performance, large scale genomic evaluation data, benchmarked responses to standards of care, and median time to moribund for untreated orthotopic tumors. PDXs with prolonged survival timelines delay study readouts and, in some situations, confound efficacy results due to age-related animal decline. Setting median survival thresholds as part of the upfront experimental design allows for more timely study readouts that are unaffected by these confounding variables. Our preferred cutoff for the Mayo GBM PDX collection is 70 days median survival (n=64). Using this 64 PDX line panel, regimens expected to double survival would produce results within 4-5 months. This timeframe is well within the range of robust health for athymic nude mice. This 64-line collection features both newly diagnosed (nGBM; n=42) and recurrent (rGBM; n=22) tumors. MGMT promoter methylation status was determined by qMS-PCR (25 methylated, 37 unmethylated, 2 indeterminate). Available WES (n=62) and RNAseq (n=42) data, along with our tissue microarray (n=42), are critical resources for biomarker-based evaluations aimed at defining patient populations that are most likely to benefit from a given therapeutic. From these data, the molecular subtypes available include 26 classical, 14 proneural, and 3 mesenchymal. Twenty-seven of these 64 PDX models have also been successfully cultured from fresh as well as cryopreserved cell stocks to further expand their experimental value. Correlative clinical data including diagnosis and treatments are also available (n=61). Current standards of care for GBM include radiation, temozolomide, and bevacizumab. Defining sensitivity to these therapies is an important first step for evaluating the integration of novel therapeutics with these standards. Since the creation of our GBM PDX collection, efficacy of these therapies has been evaluated as follows: RT 26 PDXs, TMZ 20 PDXs, and Avastin 23 PDXs. The Mayo Clinic GBM PDX collection provides an important platform for preclinical evaluation of novel therapeutics. Through careful selection of PDX lines with favorable growth characteristics and known genetic features, researchers can select the most relevant models for their study. This approach will enable more meaningful preclinical work in the hopes of providing more tangible clinical benefits for GBM patients.

#6898 Cholangiocarcinoma patient-derived models in the NCI Patient-Derived Models Repository.

Y. A. Evrard[1], C. R. Timme[1], B. Das[1], G. Bliss[1], C. Bonomi[1], C. Border[1], T.-C. Chang[1], A. Chen[2], L. Chen[1], M. A. Crespo-Eugeni[3], K. Cooper[1], N. Czarra[1], I. Czernia[1], K. Dougherty[1], M. Gibson[1], T. Grinnage-Pulley[3], S. Jiwani[1], K. Kalmbach[1], C. A. Karlovich[1], C. McGlynn[1], M. Mullendore[1], M. Murphy[1], R. Pauly[1], K. Plater[1], J. Steed[1], L. Stockwin[1], S. Uzelac[1], P.-F. Wu[1], D. L. Newton[1], P. Williams[1], M. G. Hollingshead[3], J. H. Doroshow[2];
[1]Frederick National Laboratory for Cancer Research, Frederick, MD, [2]National Cancer Institute, Bethesda, MD, [3]National Cancer Institute, Frederick, MD

Cholangiocarcinoma (CHOL) is an aggressive rare malignancy arising in the biliary tract with a 5-year relative survival rate of 10% and a 60-70% recurrence rate following surgical intervention. Advances in treatment strategies are hampered by the lack of well annotated and characterized preclinical models. The National Cancer Institute's Patient-Derived Models Repository (NCI PDMR; https://pdmr.cancer.gov) has developed a national repository of Patient-Derived Models (PDMs) comprised of patient-derived xenografts (PDXs), in vitro patient-derived tumor cell cultures (PDCs) and cancer associated fibroblasts (CAFs) as well as patient-derived organoids (PDOrg). These PDMs are clinically annotated with molecular information available in an easily accessible database for the extramural community. To date, 94 patient CHOL tumor specimens (resections, biopsies, rapid autopsy) have been received from 55 unique patients with an overall PDX take rate of 36.3% (80 assessable specimens). There are currently 15 CHOL PDX models available for the research community to request with 14 more in final QC. Nine of the 15 public PDX models were generated from unique lesions in two rapid autopsy patients and while histo-morphologically consistent, some genomic heterogeneity is observed between the unique anatomical locations likely due to tumor evolution during metastasis. In addition, 27 in vitro PDOrgs, PDCs, and CAFs have been generated from patient or PDX material matched to most of the existing PDX models to allow for comparative translation research. The genetic landscape of the CHOL PDXs includes oncogenic drivers in *NRAS, IDH1, ERBB2, TP53*, *KRAS and FGFR2* fusions; OncoKB likely oncogenic variants including *ARID1A, AXIN1* and *BAP1*; and *CDKN2A* deep deletions representing most of the common alterations in CHOL. Early passage preclinical PDX and in vitro models for CHOL, and many other cancer types, with translational relevant features along with associated NextGen sequencing and patient treatment history are available from the NCI PDMR. Availability of preclinical models that can be used to study these cancers and improve preclinical drug screening is of high importance to better understand the biology of these cancers and prioritize novel therapeutics from bench to clinic. Funded by NCI Contract No. HHSN261200800001E

#6899 Enfortumab vedotin (EV): Efficacy comparison with trastuzumab deruxtecan (T-DXd) and sacituzumab govitecan (SG) and its potential for combination benefit in bladder cancer XPDX models.

J. Flores[1], H. Sessions[1], A. Simonson[1], N. Banos[1], T. Rouzbahani[1], A. Diaz III[1], J. Lund[1], E. Calvo[2], V. Moreno[2], K. Papadopoulos[3], D. Rasco[3], A. Patnaik[3], S. Ulmer[4], L. Rodriguez[4], M. Wick[1];

[1]XenoSTART, San Antonio, TX, [2]START Madrid, Madrid, Spain, [3]START San Antonio, San Antonio, TX, [4]STOH, San Antonio, TX

EV is a Nectin-4 targeting antibody-drug conjugate (ADC) with an MMAE payload, recently approved for bladder cancer treatment. We established and characterized 18 bladder XPDX models representing primary and metastatic disease from naïve or clinically treated patients, some with actionable mutations. To better understand the potential additive benefit of EV in bladder cancer, we evaluated the ADC alone and in combination with agents targeting ERBB2, PIK3CA or FGFR3. In addition, we tested EV alone in ST5420B, a model established from a patient who progressed on EV after five cycles, as well as ST975B, a model which harbors a novel NECTIN4 fusion. 18 bladder XPDX models were established in immune-deficient mice, including 5 from newly diagnosed patients (2 from primary site), and 13 from recurrent disease (2 from primary site). Nectin-4, Trop2 protein and ERBB2 receptor expression was tested, and models profiled using WES and RNA_{seq}. For in vivo studies, all models were evaluated against cisplatin, T-DXd, SG, and EV. Models with actionable mutations were tested with alpelisib, erdafitinib, and neratinib alone and in combination with EV. Endpoints in all studies included tumor volume and time from treatment initiation with %T/C values and tumor regression reported at study completion; a %T/C of ≤ 20% versus control was considered sensitive. Tumor regression (%T/C<0%) versus Day 0 tumor volume was also reported. Most models stained positive for Nectin-4 and Trop-2. FGFR3 variants were found in five models and ERBB2 mutations in two while several models reported PIK3CA variants; deletions in RB1 and CDKN2A were common. In vivo studies reported differential responses to cisplatin with the most sensitive models established from treatment-naïve patients. EV and SG tested alone reported activity in several models; EV added benefit in some combination treatments. We have characterized a panel of bladder XPDX models and benchmarked them against T-DXd, EV and SG alone and EV in combination with targeted therapies. This data is a valuable tool in further developing EV and identifying novel therapies for bladder cancer.

#6900 Patient-derived xenografts from circulating cancer stem cells and their potential utility in personalized medicine of pancreatic cancer.

M. Pizon[1], D. Schott[1], A. Ettner-Sittner[2], B. J. Wagner[3], K. Pachmann[4], T. Aung[5], C. Hackl[3], S. Haerteis[2];

[1]Special Immunology Research and Development, Bayreuth, Germany, [2]Institute for Molecular and Cellular Anatomy, University of Regensburg, Regensburg, Germany, [3]Department of Surgery, University Hospital Regensburg, Regensburg, Germany, [4]Laboratory Dr. Pachmann, Bayreuth, Germany, [5]Faculty of Applied Healthcare Science, Deggendorf Institute of Technology, Deggendorf, Germany

Background: Pancreatic cancer carries a poor prognosis in the majority of patients, with an overall 5-year survival rate of less than 10%. Therefore, the development of new therapies and preclinical models is crucial and urgently needed. Circulating cancer stem cells (cCSCs) are a subset of circulating cancer cells that have stem cell-like properties and play a significant role in tumor progression, metastasis, and treatment resistance. Patient-derived xenografts (PDX) reflect the genotypic and phenotypic landscape of patients' cancers and are useful for drug screening, biomarker development, and preclinical evaluation of personalized medicine strategies. In this study, we describe a fast, simple, and cost effective method to generate PDX on Chorioallantoic Membrane (CAM) from circulating cancer stem cells.

Methods: In this study, primary cultures from circulating cancer stem cells were established using sphere-forming assays from 30 patients with newly diagnosed pancreatic cancer. Subsequently, tumorspheres were transplanted onto the CAM membrane of fertilized chicken eggs to form patient- derived xenografts.

Results: For the identification of cCSCs from peripheral blood of pancreatic cancer patients, an innovative *in vitro* sphere-forming assay was established. The number of tumorspheres was correlated with clinicopathological parameters like tumor size, lymph node involvement and grading status of the primary tumor. Implantation of tumorspheres onto the CAM was successful in ~90 % of the applied samples. The histological analysis suggests that the PDX tumors were morphologically and pathologically identical to primary tumor tissue.

Conclusions: The number of tumorspheres was associated with clinicopathological parameters. Further follow-up is needed to evaluate the prognostic significance of tumorsphere detection in pancreatic cancer. Generation of PDX from cCSCs on CAM has a high success rate and may become an integral part of the drug development arena, including drug screening and biomarker development.

#6901 Paired colorectal and pancreatic cancer patient-derived tumor and organoids biobank.

J. Wang[1], W.-H. Ma[1], Y.-C. Lo[1], H.-C. Hsieh[1], L.-J. Hsiao[1], Y.-P. Bau[1], N.-C. Yang[2], S.-J. Tsai[3], Y.-S. Shan[4], T.-Y. Chen[2], Y.-L. Chen[2], P.-J. Chiang[1], T.-L. Chen[1], H.-P. Chang[1], H.-J. Chin[2];

[1]National Laboratory Animal Center, NarLabs, Tainan, Taiwan, [2]National Laboratory Animal Center, NarLabs, Taipei, Taiwan, [3]Institute of Basic Medical Sciences, College of Medicine, National Cheng Kung University, Tainan, Taiwan, [4]National Cheng Kung University Hospital, Tainan, Taiwan

Patient-derived xenograft (PDX) models constitute a crucial tool in precision cancer medicine owing to their high accuracy in predicting the response to therapeutic drugs among patients in clinical settings. Our center has established a biobank that collects more than 80 colorectal cancer and 25 pancreatic cancer PDX tissues, along with essential information about patients' tumors and PDX models. However, cost-intensive and time-consuming limit the usage of PDX model in high throughput screening during drug development. To overcome this hurdle, we are generating a PDX-match paired organoid (PDXO) biobank by using emerging three-dimensional culture techniques. Before large-scaled expansion, the concordance between PDX tissues and PDXOs of partial specimens was evaluated firstly using short-tandem repeat (STR) analysis, immunohistochemistry (IHC) and H&E staining. Data of STR analysis performed by using AmpFLSTR Identifiler PLUS PCR Amplification Kit demonstrated that PDX tissues and PDXOs have identical DNA fingerprinting. IHC and H&E staining revealed PDX tissues and PDXOs have highly similar organ-specific markers expression (e.g., Cytokeratin 20, Caudal Type Homeobox 2, and Pan Cytokeratin) and histological morphology. Even after passing to at least five generations, passed PDXOs maintained high fidelity to their original state, as confirmed by whole-exome sequencing (WES) and STR analysis across passages. The WES analysis for passage 0 (P0) and passage 5 (P5) of PDXOs from different PDX tissues revealed there is more than 95% intersection between P0 and P5 PDXOs with the same missense mutation gene. The results of STR analysis showed that P0 and P5 PDXOs have identical STR profile. To evaluate the capability of PDXOs in clinical response prediction, several effective and ineffective drugs (e.g., oxapliplatin, 5-FU, gemcitabine) were tested. The results of drug testing indicated that PDXOs can be used to accurately predict the response to therapeutic drugs as PDX model but more efficient than PDX model. Therefore, PDXO biobank can serve as a valuable resource for high throughput *in vitro* drug screening prior *in vivo* efficacy confirmation using PDX models.

#6902 Development of a stable luciferase expressing PDX-derived cell line for translational *in vitro* and *in vivo* testing.

S. Cold[1], R. N. Boge[2], E. Papin[2], I. T. Michler[1], L. K. Kristensen[2], T. B. Engel[2], A. Kjaer[1], C. H. Nielsen[2], S. Gnosa[2];
[1]University of Copenhagen and Minerva Imaging, Copenhagen, Denmark, [2]Minerva Imaging, Copenhagen, Denmark

Despite much effort invested in developing novel cancer therapies, more than 90% of clinical studies fail due to toxicity or lack of efficacy in patients. This can mainly be ascribed to lack of relevant and translational preclinical models. A common model used in preclinical studies is the xenograft model using immortalized cancer cells. Cell line-based models are cost efficient and can be genetically manipulated but are often criticized for lacking translational value. A murine model with higher clinical relevance is the patient derived xenografts (PDX) model established by implanting patients' tumor tissue onto immunodeficient mice. Knowledge of patient therapy response, mutational status and tumor heterogeneity makes it a relevant model. However, PDX models are costly, not applicable for *in vitro* assays or subjective to genetic manipulation. To more closely mimic *in vivo* tumors we have established a PDX-derived cell line (PDXc) and characterized it extensively in a head-to-head comparison to the parental PDX model. Cells were isolated from a subcutaneous (SC) glioblastoma (GBM) PDX tumor (ST146), processed into single cells and cultivated *in vitro*. Once the PDXc were stable over several passages the cells were re-implanted into mice. Tumor take and growth rate were evaluated against the parental PDX model and common characteristics of the model such as EFGR and Vimentin expression were determined by IHC. We furthermore generated a stable Luciferase expressing PDXc using 3rd generation lentiviral particles and implanted the cells in an intracranial (IC) model of GBM. Tumor growth was evaluated using bioluminescence imaging (BLI) and MRI. Upon multiple passages and freeze cycles the cell line (ST146c) exhibited a stable in vitro doubling time (2.6 ± 0.2 days) with a morphology like other GBM cell lines with formation of neurospheres. STR analysis confirmed a genetic identical profile to ST146.

ST146c implanted into mice had similar tumor take and growth rates to the parental PDX when injected IC (>90%, T_d=3 d) and SC (>75%, T_d=6 d). We also showed that ST146c had more homogeneous tumor growth. *Ex vivo* analysis showed similar expressions of EGFR (-), Vimentin (+++) and Ki67 (++) between the models. The BLI signal obtained from luciferase expressing ST146c implanted orthotopically was correlated to tumor volume obtained by MRI. We developed a PDX cell line that preserved critical *in vitro* and *in vivo* characteristics of the PDX model such as doubling time, tumor take rate and marker expression making it feasible to use the PDXc model in future preclinical studies. This will allow *in vitro* screens with patient derived tumor cells. Furthermore, the expression of luciferase in the PDXc enables intracranial and metastatic implantation with tumor monitoring using BLI. This platform consisting of *in vitro* and *in vivo* PDX models could be used as a predictive translational platform for testing new cancer therapies.

#6903 Treatment efficacy of transcatheter hepatic arterial infusion chemotherapy with cisplatin in a severe immunodeficient rat model with patient-derived primary pancreatic ductal adenocarcinoma xenografted into the liver.

K. Kageyama[1], A. Yamamoto[1], M. Ozaki[1], K. Kimura[1], S. Eguchi[1], R. Tanaka[1], M. Terai[2], T. Sato[2], Y. Miki[1];

[1]Osaka Metropolitan University, Osaka, Japan, [2]Thomas Jefferson University, Philadelphia, PA

Purpose: Liver metastases of pancreatic ductal adenocarcinoma (PDAC) is a highly fatal disease; most patients die within 5 years. There is a critical need to identify appropriate anticancer treatments for these patients. A patient-derived tumor xenograft (PDX) model in severe immunodeficient rat with primary PDAC xenografted into the liver is suitable for evaluating transcatheter hepatic arterial infusion chemotherapy.

Materials and Methods: The purpose of this study was to develop a severe immunodeficient rat model with patient-derived primary PDAC xenografted into the liver, and to assess the treatment efficacy of hepatic arterial infusion chemotherapy with cisplatin in this model. Three patient-derived tumors of PDAC were transplanted into the liver of 21 rats each, totaling 63 rats. Four weeks after transplantation, the 21 rats were randomly assigned into three treatment groups of seven rats each: hepatic arterial infusion, systemic venous infusion, and control group. Tumor volumes were evaluated on CT twice at pre-treatment and 4-weeks post-treatment. Following euthanasia of the rats, resected tumor specimens were pathologically analyzed.

Results: The liver-implanted PDAC PDX rat model was established in all 63 rats. hepatic arterial infusion chemotherapy and systemic venous infusion chemotherapy with cisplatin were able to be performed in the assigned rats. The hepatic arterial infusion group significantly inhibited tumor growth and reduced Ki67 expression, indicating lower cell proliferation, compared to the control group in three PDX tumors.

Conclusion: A rat-based preclinical platform was established by liver-implanted PDAC PDX rat model. Arterial cisplatin infusion chemotherapy would be one of potential therapies for PDAC liver metastases.

#6904 Model-derived progression-free survival (mPFS): A better metric for patient-derived xenograft studies?.

A. Chen[1], M. Stoddard[2], **L. Yuan**[2], D. Van Egeren[3], A. Chakravarty[2], D. Bottino[4];

[1]Columbia University, New York, NY, [2]Fractal Therapeutics, Inc., Lexington, MA, [3]Stanford University, Palo Alto, CA, [4]Takeda Pharmaceuticals, Cambridge, MA

Patient-derived xenografts (PDX) are a powerful assay system for translational prediction of therapeutic potential for experimental therapeutics. The primary readout from PDX models is tumor shrinkage, measured by the ratio of treated/control tumor volume. This readout corresponds loosely to the Objective Response Rate (ORR) metric used in clinical trials, in that it is a readout of drug effect on the sensitive subclones within a tumor. In prior work, we have shown that there is a paradoxical relationship between short-term tumor response and progression-free survival (PFS). While ORR is the primary measure utilized in the Phase II to III transition in clinical development, approval hinges on survival metrics, and the disconnect between ORR and PFS creates a potential risk of late-stage failures for experimental anticancer therapeutics. Thus, it is of interest to understand whether there are alternative approaches to analyzing PDX data that can enable the assessment of therapeutic potential in terms of a projected PFS. In this simulation study, we will examine the accuracy of progression-free survival (PFS) estimates obtained directly from observation during a PDX study and compare their accuracy with the accuracy of PFS estimates derived using a mathematical model-based approach that relies on a kinetic model of tumor subclone growth (model-based PFS, or mPFS) fitted directly to PDX tumor growth and rebound kinetics under treatment. We generated our test dataset using a mathematical model of tumor kinetic growth to simulate xenograft data using fitted parameters derived from literature, adding in experimental error consistent with prior experimental measurement-derived variability. We used the simulated raw data to calculate an observed PFS as well as mPFS derived from fitting the tumor clonal kinetic model to the raw data in a blinded fashion. Our results show that the empirical PFS from PDX models is subject to overestimation, as a function of the observation time interval. On the other hand, mPFS is significantly less biased and more accurate, but is subject to some logistical constraints on sampling. Our work demonstrates the practical translational utility of a novel analysis method (mPFS) in deriving estimates of progression-free survival from PDX model data.

#6905 A multi-targeted approach to evaluate therapeutic selection and efficacy in preclinical GBM models.

E. Eastwood, B. Carapia, J. Rodriguez, K. Buck, D. Gorospe, E. Valencia, B. Corcoran, R. Pippa, Y.-H. Chien, W. Andrews, L. Do, **J. K. Nakashima**, J. Sperry; Certis Oncology Solutions, San Diego, CA

Glioblastoma (GBM) is a devastating primary brain cancer with approximately 10,000 new US diagnoses annually. The current standard of care (SOC) for GBM includes surgical resection followed by radiation therapy (RT) and temozolomide (TMZ), however, there is near universal recurrence and development of resistance after treatment. Relapse in disease is tightly linked with dynamic changes in gene expression during tumor evolution, highlighting the need for stronger preclinical GBM models. Here, we report developing a pair of patient-derived xenograft (PDX) models from surgical resections obtained from initial GBM incidence in a patient (BarneyOI™ Cancer Model CRT00433) and subsequent recurrence following treatment (BarneyOI Cancer Model CRT00435) to study disease progression and novel treatment strategies. Recent studies have suggested the utilization of combination therapy approaches for GBM patients to address TMZ resistance. To this end, Certis has developed a personalized, AI-based approach to predict and test combination therapies in preclinical cancer models. Accuracy of the predicted sensitivities to treatment was evaluated *in vivo* using both subcutaneous (SC) and orthotopic (OT) mouse models. Luciferase-tagged CRT00433 and CRT00435 spheroid cell lines were transduced with firefly luciferase and implanted intracranially by stereotactic surgery for OT monitoring. Optical bioluminescence imaging (BLI) and murine-scale MRI from Aspect Imaging were used to assess therapeutic response of AI-predicted combination therapies and SOC treatment.

#6906 Engineered bacteria launch and control an oncolytic virus.

J. Pabon[1], Z. Singer[1], H. Huang[1], C. Rice[2], T. Danino[1];
[1]Columbia University, New York, NY, [2]The Rockefeller University, New York, NY

The ability of bacteria and viruses to selectively replicate in tumors has led to synthetic engineering of new microbial therapies. In our system, Salmonella has been programmed to produce Senecavirus A (SVA)-RNA and launch an SVA infection in bacterially-infected cancer cells. Utilizing time-lapse microscopy, we visualize S. typhimurium invasions into cancer cells and their subsequent delivery of multiple picornaviral species. S.-typhimurium-viral-RNA launch in vitro identified a small-cell-lung cancer cell line, H446, as a promising candidate for S.-typhimurium-SVA launch. This viral RNA-carrying Salmonella strain confers complete tumor regression in vivo. Finally, we integrate into this strain a protease-dependent mechanism to confer SVA-infection spatial localization. This work, to the best of our knowledge, is the first instance of bacteria delivering full-length viral RNAs for therapeutic oncolytic purposes.

#6907 Micro-implantation of patient tumor samples into the avian embryo, a fast and reliable alternative in vivo technology for preclinical studies on melanoma and follicular lymphoma.

C. Costechareyre, Sr.[1], L. Jarrosson, Sr.[1], M. Lacourrege, Sr.[1], **R. Teinturier, Sr.**[1], J. Caramel, Sr.[2], M. Zala, Sr.[3], S. Dalle, Sr.[3], P. Sujobert, Sr.[3], C. Delloye-Bourgeois, Sr.[1], F. Berget, Sr.[1], V. Castellani, Sr.[1];

[1]ONCOFACTORY, Lyon, France, [2]Centre de recherche en Cancerologie de Lyon (CRCL), Lyon, France, [3]CHU Lyon Sud, Lyon, France

Despite recent efforts to develop reliable and predictive patient-derived cancer models, drug attrition rates in oncology remain high. Moreover, conventional models such as patient-derived xenograft (PDX) mouse models face major cost and time limitations, not supporting real-time clinical decision making. To overcome such limitation, ONCOFACTORY developed a proprietary PDX platform enabling the engraftment of small size tumor biopsy samples within targeted tissue of the avian embryo at early stage of development, to conduct preclinical proof of efficacy studies and provide PDX clinical trial solution helping with patient's selection prior to clinical phase II/III. On one hand, we performed prospective co-clinical trial aiming to evaluate the utility of the AVI-PDX™ model in predicting the response to standard therapy, consisting of BRAF and MEK inhibitors, for patient with metastatic melanoma harboring BRAF mutations. Skin biopsy samples were implanted into specific tissue driving tumor formation under the skin of avian embryos. On the other hand, we conducted a retrospective cohort study with 20 follicular lymphoma (FL) patient samples divided into "partial" and "complete" responders to the standard immuno-chemotherapy RCHOP regimen to establish FL AVI-PDX™, and examine sensitivity to RCHOP in ovo. Twenty-four hours post-implantation, avian melanoma and FL replicas were respectively exposed to BRAFi/MEKi or RCHOP and their vehicles, over 24h. Then, embryos were harvested, and tumor response was examined by measuring tumor volume using light sheet microscopy. Alongside, in independent series of avian embryos implanted with FL samples, tumors were harvested for single-cell transcriptomic analyses to explore mechanism of response to RCHOP. For melanoma, we provide the proof of concept that the AVI-PDX™ reliably predict sensitivity or resistance to BRAF and MEK inhibitors within days, matching patient clinical outcome observed in clinic. For FL, we showed that the FL-AVI-PDX™ efficiently captures clinical response to RCHOP in a heterogenous cohort of patients, enabling to discriminate partial and complete responder within short-time frame. Next, we identified a robust genetic signature reflecting exposure of tumoral cells to RCHOP and showed that drug-mediated targeting of one of these genes with a chemotherapy resulted in strong potentiation of RCHOP. Thus, we provide evidence of the high predictive power of the AVI-PDX™ models allowing fast and reproducible generation of tumors replicas from small size patient tumor samples. This places the AVI-PDX™ as a valuable tool for clinical research to rationalize patient inclusion in clinical trials but also for the design of personalized medicine assays.

#6908 Integrating PDX GBM *in vivo* models with patient history and whole exome sequencing: Advancing relevance and precision in preclinical studies.

E. E. Trachet, P. M. Gonzales, S. Gately;
Translational Drug Development (TD2), Scottsdale, AZ

Glioblastoma poses a significant challenge in oncology, necessitating improved translational models that faithfully replicate the intricate tumor microenvironment. Patient-derived xenograft (PDX) models, are key in glioblastoma multiforme (GBM) preclinical research. PDX models (orthotopic and subcutaneous) provide a more clinically relevant representation compared to CDX xenografts. Analyzing PDX tumors in their native environment allows for a nuanced understanding of GBM biology, tumor-stroma interactions, and treatment responses. This abstract explores the rationale and advantages of utilizing PDX GBM *in vivo* models coupled with patient diagnosis and treatment history, empowered by tumor whole exome sequencing (WES), to enhance the relevance of preclinical studies in evaluating GBM-specific treatments. TD2 has access to over 100 GBM PDX tumors models with fully annotated patient details and treatment history. Moreover, 68 of these PDXs also have WES data, that allows most appropriate model selection to ensure alignment with the therapeutic development strategy. Below is a detailed analysis of two GBM PDX models, GBM6 and GBM46, using patient history and WES data to define criteria for success in assessing novel preclinical therapeutic agents. GBM6, was obtained prior to treatment from a 65-year-old man with glioblastoma multiforme, that contains 642 mutations, including EGFR VIII amplification. GBM46, was obtained from a 55-year-old man with prior treatment, contained 646 mutations, including RAS pathway alterations and EGFR (MET and FLT3) amplification. When grown subcutaneously the anti-tumor activity of cetuximab against GBM6 and GBM46 resulted in 41% and 48% growth inhibition, respectively. Traditional treatments have also been evaluated in the orthotopic setting, with temozolomide (TMZ) showing a nominal improvement in lifespan (11%) as expected for the unmethylated MGMT found in the GBM6 model. By contrast, GBM46 from a patient with prior treatment with TMZ, OSI-774, radiation, and BCNU, exhibited a 58% increase in overall lifespan when treated with TMZ alone. Orthotopic PDX GBM models preserve many molecular characteristics, enabling the study of intrinsic GBM mutations for developing novel therapeutic strategies. While orthotopic models better capture GBM's dynamic nature, traditional xenograft systems remain valuable as rapid screening tools. Models with defined clinical treatment history and WES data allows for testing new agents in models that more closely resemble the clinical development path for a given new agent and aids in deciphering factors influencing therapeutic resistance. These models have the potential to reshape preclinical research paradigms, accelerating the translation of promising therapeutic agents increasing the likelihood of clinical benefit for patients with glioblastoma multiforme.

#6909 KRAS^{G12C} inhibitor resistance in patient-derived non-small cell lung cancer models.

Joshua C. Rosen[1], Nhu-An Pham[1], Quan Li[1], Pinjiang Cao[1], Katrina Hueniken[1], Takamasa Koga[1], Nikolina Radulovich[1], Alex Koers[2], Michael Niedbala[3], Sarah Ross[2], Adrian Sacher[1], Ming-Sound Tsao[1]

[1]University Health Network, Toronto, ON, Canada,[2]AstraZeneca, Cambridge, United Kingdom,[3]AstraZeneca, Waltham, MA

Introduction: One quarter of lung adenocarcinomas (LUAD) harbor *KRAS*-mutations, with *KRAS*^{G12C} accounting for the majority (40%). GDP-KRAS^{G12C} inhibitors (G12Ci) have been developed for this patient cohort, and two of these are approved for clinical use in the US. While response rates to G12Ci tested in clinical trials have been between 35-50%, studies have identified mechanisms of adaptive resistance to these novel agents, limiting their use as monotherapies. However, primary (intrinsic) resistance to these compounds has not been explored extensively. We leveraged our patient-derived xenograft (PDX) and xenograft-derived organoid (XDO) development programs to study primary resistance to the novel G12Ci, AZD4625.

Methods: Twelve *KRAS*^{G12C} PDX models were established which recapitulated patient tumor histology, and genomic, transcriptomic, and methylome profiles. From these 12 PDX, six long-term (passage >10) XDO were generated. PDX were treated with AZD4625 chronically for four weeks as well as in an acute dosing pharmacodynamic study, where tumors were harvested for further analysis.

Results: The AZD4625 drug screen in our PDX models reproduced the G12Ci response rate observed in clinical trials. Four of twelve tumor models reduced in size on treatment, while the remainder were considered resistant as these tumors increased in size on treatment. Sensitive tumors became necrotic while those resistant remained proliferative. XDO models recapitulated their originating PDX genomic alterations, histology, as well as responses to AZD4625. During the acute pharmacodynamic screen in our PDX models, we observed a decrease in pERK1/2 and pS6 protein expression in sensitive but not resistant models, despite acute *DUSP6* gene expression decreases in every model. Global proteomic analysis highlighted differences between each model.

Conclusion: PDX and XDO are useful models to study resistance to this novel class of inhibitor, with the *KRAS*^{G12C} NSCLC PDX models exhibiting a treatment response rate that is similar to those observed in clinical trials. Global proteomics suggests uniqueness of each model in our cohort, hinting that a universal combination of specific targeted agents to treat *KRAS*^{G12C} LUAD tumors may be insufficient.

#6910 CancerModels.org: An open global cancer research platform for patient-derived cancer models.

Z. Perova[1], M. Martinez[1], T. Mandloi[1], M. Rios Almanza[1], S. Neuhauser[2], D. Degley[2], D. Krupke[2], C. Bult[2], H. Parkinson[1];
[1]European Bioinformatics Institute, Hinxton, United Kingdom, [2]The Jackson Laboratory, Bar Harbour, ME

CancerModels.Org (www.cancermodels.org) is a research platform that standardises, harmonizes and integrates the complex and diverse data associated with Patient-Derived Cancer Models (PDCMs) for the cancer community. The portal publishes over 7500 models - covering patient-derived xenografts (PDX), organoids and cell lines - across 13 cancer types, including rare pediatric PDX models and models from minority ethnic backgrounds. A total of over 90 million data points are made available across a variety of data types, such as clinical metadata, molecular data and treatment-based information, which makes CancerModels.Org the largest free-to-consumer and open-access resource of this kind.

Over the course of the last twelve months, the platform has been enhanced with new functionality and an updated user interface to cater for a more varied set of use cases. Users can now search for models of interest by exploring molecular data summaries for models of specific cancer types, as well as by using the intuitive search and faceted filtering options of the web interface. The data is also accessible via REST API, hence enabling offline analyses. The underpinning data model was augmented with additional dimensions and covers gene expression, gene mutation, copy number alteration, biomarkers, patient treatment and drug dosing studies. For an improved prioritization of PDCMs we performed knowledge enrichment by linking to external resources, such as publication platforms, cancer-specific annotation tools (COSMIC, CIViC, OncoMX, OpenCRAVAT, ClinGen), and raw data archives (ENA, EGA, GEO, dbGAP). More recently, we added immune-related features of tumors (HLA, MSI, TMB) and image data (also accessible via EMBL-EBI's BioImage archive). Finally, to streamline model and data submission, we made available a Metadata dictionary and a Metadata validation service.

Future work will focus on the curation of rare models with rich accessible metadata and data, new data visualizations, integration of new data types and resources, as well as devising a model quality rating using user feedback. These developments will maximize utility and improve reusability of models and data, and reduce barriers to model and data sharing.

CancerModels.Org is deeply integrated into the general patient-derived cancer models landscape, underpinning or contributing to the data and/or software infrastructure of some of the long-running consortia, such as EUROPDX and PDXNet. The resource is freely available under an Apache 2.0 license (https://github.com/PDCMFinder).

#6911 Expanding reported molecular characteristics for the NCI Patient-Derived Models Repository.

C. R. Timme[1], Y. A. Evrard[1], B. Das[1], T.-C. Chang[1], A. Chen[2], L. Chen[1], M. A. Crespo-Eugeni[3], S. Jiwani[1], C. A. Karlovich[1], R. Pauly[1], P.-F. Wu[1], D. L. Newton[1], P. Williams[1], M. G. Hollingshead[3], J. H. Doroshow[2];

[1]Frederick National Laboratory for Cancer Research, Frederick, MD, [2]National Cancer Institute, Bethesda, MD, [3]National Cancer Institute, Frederick, MD

The National Cancer Institute's Patient-Derived Models Repository (NCI PDMR; https://pdmr.cancer.gov) has developed a national repository of Patient-Derived Models (PDMs) comprised of patient-derived xenografts (PDXs), in vitro patient-derived tumor cell cultures (PDCs) and cancer associated fibroblasts (CAFs) as well as patient-derived organoids (PDOrg). These PDMs are clinically annotated with molecular information available in an easily accessible database for the extramural community. To ensure the data and models remains pertinent to current translational efforts, NCI actively reviews and adds new molecular features to the public database for researchers to use. While these data could be obtained through analysis of the available NextGen sequencing files in the PDMR database, many laboratories do not have the bioinformatics support to run these assessments for models that are of research interest. Therefore, new pipelines for an array of additional model and molecular characteristics present in PDX, PDOrg, and PDC models have been validated and are reported in the public database in a searchable format. Current model characteristics include addition of OncoTree Codes as a second histologic classifier, use of the PDXNet Consortium's inferred ancestry caller to better represent Native/Latin American populations, human leukocyte antigen (HLA) typing, molecular classification of tumors (e.g. CMS subtyping of colorectal adenocarcinoma, PAM50 signature based subtyping of breast carcinoma), microsatellite instability (MSI) assessment, and identification of clinically relevant fusions. SOPs for the pipelines used are available on the public website to allow for independent validation and use by other laboratories. Funded by NCI Contract No. HHSN261200800001E

#6912 Pretreatment multiomics in conjunction with preclinical trials on patient-derived xenograft models of cholangiocarcinoma can identify chemotherapy response signatures.

A. M. Abdelrahman[1], D. M. Carlson[1], E. Jessen[1], D.-G. Mun[1], I. Lynch[2], A. Fogliati[3], S. Adjei Antwi[1], A. Abeynayake[1], A. Pandey[1], M. J. Truty[1], G. J. Gores[1], R. L. Smoot[1];

[1]Mayo Clinic, Rochester, MN, [2]University of Iowa Roy J. and Lucille A. Carver College of Medicine, Iowa City, IA, [3]University of Milano-Bicocca, Monza, Italy

Background Cholangiocarcinoma (CCA) is a heterogeneous malignancy. Platinum-based chemotherapy (Gemcitabine and Cisplatin) has been the standard treatment for over a decade and is the base for the current immunotherapy combinations. Response rates are typically between 20-30%. Herein, we present outcomes of preclinical efficacy trials on CCA PDX models in correlation with baseline multiomics profiling of CCA patient-derived xenograft (PDX) models to identify molecular features associated with response. **Methods** Tumor samples from twenty-eight CCA PDX were used to isolate RNA and protein to be included in multiomics analysis (Phosphoproteomics, Proteomics, and Transcriptomics). A subset of PDX models were treated with various doses of Gemcitabine and Cisplatin. The Median Efficacy Index (MEI) was calculated as the ratio of the difference in median of delta in tumor volume at the last day of the study between the treatment and the control arms divided by the median of delta in tumor volume of the control at the last day of the treatment (positive= growth, negative=inhibition, and 0=no efficacy). A Hierarchical All-Against-All algorithm was utilized to compare multiomics features to the MEI and pathway analysis completed for identified molecular features. **Results** After conducting preclinical efficacy trials, the five tested CCA PDX models were classified into sensitive, moderately sensitive, and resistant models based on the MEI on each treatment arm. The top up-regulated genes were identified for Gemcitabine response (SRPK2, GLK2, and RIOK2) and Cisplatin response (NTRK1, PRPF4B, and SRPK2). The top up-regulated genes related to Gemcitabine resistance were NTRK1, PIP5K1C, and CSNK2A2, while those related to Cisplatin resistance were SRPK1, PRPF4B, and CSNK2A1. **Conclusion** Cholangiocarcinoma multiomics signatures can predict therapeutic response to standard-of-care chemotherapy in preclinical models. Novel mechanisms of Gemcitabine and Cisplatin resistance were identified related to NTRK1, SRPK1 and SRPK2. Resistant signatures will be challenged with the appropriate targeted therapies on the resistant CCA PDX models.

#6913 A preclinical platform of prostate cancer PDX and derived cellular models as a tool for pharmacological screening and functional studies.

E. Indersie[1], L. Sinayen[1], L. Bigot[2], K. Mevel[1], A. Gorse[1], M. Tavernier[1], E. Le Ven[1], L. Friboulet[2], F. Farace[2], E. Morgado[3], L. Pouyet[3], Y. Loriot[2], F. Romagne[3], **O. Deas**[1];

[1]Janvier Group, Evry-Courcouronnes, France, [2]Gustave Roussy, Villejuif, France, [3]Janvier Group, Marseille, France

Prostate Cancer (PCa) is the most frequently diagnosed cancer in men and remains one of the leading causes of cancer death worldwide. Despite undeniable progress in understanding the biology and genetics of this highly heterogenous and complex disease, the development of effective therapies is hampered by the lack of relevant experimental models recapitulating its diversity. To tackle this issue, over the last years, we have generated and characterized at the molecular and pharmacology level a collection of prostate cancer patient-derived xenografts (PDX) that accurately reproduce PCa histological and molecular heterogeneity. Although the development of these PCa PDX has been challenging, we are now able to offer a preclinical platform of 11 fully characterized PCa PDX models and *in vitro* cellular counterparts for preclinical evaluation of novel treatment modalities. Our platform consists of a collection of 4 androgen receptor high (ARPC), 2 androgen receptor low (ARLPC), 1 amphicrine prostate carcinoma (AMPC) and 4 castration-resistant neuroendocrine prostate cancer (CRPC-NE) PDX models and 6 cellular models derived from these PDX (PDXDC). Most of these PDX models were obtained by transplantation of post-surgery tumor specimens either by grafting of tumor fragments in the interscapular region of nude mice or in the subrenal capsule of NOD scid gamma mice. One model is a CTC-derived eXplant established using circulating tumor cells (CTCs) obtained by diagnostic leukapheresis injected into the fat pad of NOD scid gamma mice. PDXDC were obtained from dissociated PDX tumors cultured under various media and matrix conditions. They were characterized by comparison with the parental PDX by Short Tandem Repeat (STR) profiling before performing a master bank. All models (PDX and PDXDC) were characterized at molecular level by whole exome and RNA sequencing. PDX were characterized pharmacologically for response to standards of care, physical castration and response to the androgen receptor inhibitor enzalutamide. *In vitro* drug sensitivity of PDXDC was compared with their parental PDX *in vivo* drug response. This unique PDX panel reflects the molecular heterogeneity of prostate cancer and reproduces the molecular and drug response profile of human tumors. Associated to *in vitro* cell derivatives, our collection provides a powerful preclinical platform for translational research to identify mechanisms underlying acquired resistance to current therapies and develop novel treatment strategies against PCa and CRPC.

#6914 Genomic landscape and stability of preclinical models in NCI's patient-derived models repository.

T.-C. Chang[1], B. Das[1], L. Chen[1], P. I. Wu[1], Y. A. Evrard[2], R. Pauly[1], D. L. Newton[2], S. Jiwani[1], S. Y. Alcoser[3], L. H. Stockwin[2], C. E. Camalier[1], T. Forbes[1], N. Nair[1], A. Chapman[1], L. Dutko[1], M. Mullendore[2], T. Grinnage-Pulley[3], K. Klarmann[3], S. B. Miller[4], C. A. Karlovich[1], A. P. Chen[4], P. M. Williams[1], M. G. Hollingshead[3], J. H. Doroshow[4];

[1]Frederick National Laboratory for Cancer Research, Frederick, MD, [2]Advanced Development Research Directorate, Frederick, MD, [3]Developmental Therapeutics Program, Frederick, MD, [4]National Cancer Institute, Bethesda, MD

Background: Patient-derived xenograft (PDX) models serve as a powerful tool for cancer translational research. However, it is unclear to what extent PDX models reflect the genomic intratumoral heterogeneity and genomic aberrations present within the original tumor sample. The National Cancer Institute (NCI) has developed a Patient-Derived Models Repository (PDMR; https://pdmr.cancer.gov/) consisting of PDX, organoids (PDOrg), and tumor cell cultures (PDC) from patients with diverse cancer histologies. We have conducted an in-depth investigation into the genomic stability of PDXs at early passaging and tumor heterogeneity in a large set of preclinical models including rare cancers.

Methods: Tumor specimens were used to establish 1114 models from 1034 patients. For whole exome sequencing (WES) and RNASeq analysis, 1059 models with at least 1 PDX sample and 55 models with only a PDC or PDOrg were used. Analyzed specimens represent the original patient specimens, PDX passages P0, P1, P2, and P3+ and in vitro models. 80% of the PDX specimens were within passages P0 to P2.

Results: Genomic stability in PDMR models was maintained through early passages (P0 - P2) and across independent lineages in PDMR models based on the following observations: 1) variant allele frequencies (VAF) of somatic driver mutations showed no major deviations (exceeding ±10%) when using the stromal fraction corrected VAF from originator data over PDX passages; 2) the median change in the fraction of genome impacted by copy number alterations (CNA) from the originator specimens through passages P0 - P2 was statistically inconsequential, although there was a significant increase in CNA fraction, from 5.3% at P0 initially to 18% by P3; 3) gene expression profiles of specimens within a given PDX model formed clusters in principal component analysis (PCA) plots and showed high correlation (>99.5% models with a Spearman coefficient of >= 0.8). The majority of the PDC and PDOrg specimens exhibited similar findings when compared to the original tumor samples. Furthermore, the positive percent agreement (PPA) was performed to measure the similarity between the patient's tumor and all available derived PDX specimens, with a median PPA over 90%, indicating a high level of retained heterogeneity within the PDX models. Lastly, 69% of models in NCI PDMR had predictive biomarkers, ranging from OncoKB level of evidence 1-4, which could be used to evaluate targeted therapeutics in preclinical studies.

Conclusion: The NCI PDMR has a large and histologically diverse cancer representation. In this analysis, the PDXs exhibited genomic stability within early passages and preserved the majority of tumor heterogeneity observed in the patient specimens. NCI PDMR thus represents a valuable resource for researchers interested in preclinical drug screening or other investigations.

#6915 Integrated proteogenomic analysis for the NCI patient-derived cancer model repository.

Peter I. Wu[1], Li Chen[2], Yuri Kotliarov[3], Jianwen Fang[3], Yingdong Zhao[3], Yvonne Evrard[4], Lijun Chen[5], Shahanawaz Jiwani[1], Biswajit Das[1], Chris A. Karlovich[1], Hui Zhang[5], Lisa McShane[3], Melinda G. Hollingshead[6], Mickey Williams[1], James H. Doroshow[3]

[1]Molecular Characterization Laboratory, Frederick National Laboratory for Cancer Research, Frederick, MD,[2]Frederick National Laboratory for Cancer Research, Frederick, MD,[3]Division of Cancer Treatment and Diagnosis, National Cancer Institute, Bethesda, MD,[4]Advanced Development Research Directorate, Frederick National Laboratory for Cancer Research, Frederick, MD,[5]Department of Pathology, The John Hopkins Medical Institutions, Baltimore, MD,[6]Biological Testing Branch, Developmental Therapeutics Program, National Cancer Institute at Frederick, Frederick, MD

Background

Studying protein expression involved in cancer from patient-derived xenografts (PDX) enhances understanding of tumorigenesis and may shed light on patient therapeutic decisions. Recently, mass spectrometry-based proteomics sequencing techniques have enabled the acquisition of high-throughput PDX protein/phosphoprotein expression profiles and paved a way for investigating oncogenic signaling pathways and their interactions in different tumor histologies. Integrated analysis of these proteomic data with existing biomarkers derived from whole exome and RNAseq data will provide the community with a rich resource for translational research.

Materials and methods

iTRAQ-based proteomics/phospho-proteomics data, with 11 Tandem Mass Tag (TMT) channels, were processed and median-normalized at gene level. The gene expression data were derived from tximport and DESeq2 from of RNA-Seq. In addition, whole exome sequencing (WES) data were used to compute mutations and copy number profiles. For data visualization, the R Bioconductor package ComplexHeatmap was used extensively.

Results

PDX proteomics/phospho-proteomics data were analyzed alongside with gene expression, copy number and mutational profiles for several cancer types, revealing vivid molecular regulation for many cancer-related pathways. A moderate yet significant Spearman correlation coefficient of over 0.45 and 0.5 was observed between proteomics and RNA-Seq data at gene and pathway level, respectively. The PDX protein and gene expression pattern from common cancer regulatory pathways of bladder (BLCA, n=32 models), colon (COAD, n=82), lung (NSCLC, n=32), pancreatic (PAAD, n=52), metastatic breast cancer (CSNOS) (n=16) and other histologies were aggregated and discussed at the model level. EGFR, MET and cell-cycle genes CDKN2A and CDKN2B exhibited significant positive correlation among copy number, gene expression and protein expression profiles. Protein and gene expression profiles of PAM50 genes were shown for CSNOS samples, to further sub-classify or correct misclassification. Further analysis using proteomics/phospho-proteomics data with CNA identified several trans-regulatory events. Lastly, we identified RTN1 as a potential biomarker, exhibiting lower expression in sensitive rare-tumor PDX models prior to Axitinib and Vandetanib treatment.

Conclusions

With the multi-omics datasets comprising proteomics/phospho-proteomics, RNA-Seq and WES datasets from the NCI Patient Derived Models Repository cohort, we were able to query some important cancer biological processes at a higher resolution. In addition, we revealed gene- and pathway-level regulatory differences from various histologies. Overall, the multi-omics data from PDX models showed promising recapitulation of original tumor activity and should continue to serve as an amenable and scalable drug screening platform for pre-clinical trials.

#6916 InnoPanel™and InnoPedia™: resources of engineered cell lines and xenografts for drug discovery.

S. Li, C. Liu, N. Wang, Y. Hu, J. Ning, **F. Hao**;
Kyinno Biotechnology Co., Ltd, Beijing, China

The Development of precision medicine relies on well-characterized experimental models that carry naive, induced, or engineered genomic and epigenetic features targetable by certain treatments. Patient-derived xenografts (PDX) and cell lines can serve as such in vivo and in vitro models by harboring abnormalities such as somatic and driver mutations, dysregulated gene expression and silencing, microsatellite instability, gene fusions, copy number amplification and loss of heterozygosity. In addition, cell lines can also be engineered to introduce sometimes rare-occurring abnormalities that the engineered cell line shares an identical genetic background with its parental cell line, thus providing a clearly contrasting pair to evaluate treatment specificity. With the advancement of disease research and drug discovery, existing cell lines can no longer meet the needs of various types of drug discovery. To evaluate drug efficacy more quickly and accurately, Kyinno has constructed and identified more than 4,000 engineered cell lines, including overexpressed cell lines constructed through transposon systems or lentivirus infection, gene-edited cell lines constructed through CRISPR-Cas9 technology, and reporter cell lines targeting multiple signaling pathways and membrane receptors. Besides, InnoPanel™, a panel of over 1000 engineered cell lines was established and characterized to cover a wide range of heavily targeted genes such as CLDN18.1, CLDN18.2, LAG3, OX40, PD-L1, PD-L2, and TIM3. Cell line families were also developed for genes with multiple known driver mutations. All cell lines are annotated with background information, engineering details, functional characterization, and efficacy studies. Furthermore, we developed xenografts for several engineered cell lines and showed that the combination of cell lines and xenografts can accelerate drug development. Additionally, all of this information can be accessed in our free database, InnoPedia™. The database also offers browsing, searching, and analytical capabilities for over 600 commonly used tumor cell lines and thousands of engineered cell lines with essential genomic and pharmacological data, cell line efficacy data for nearly 2000 common anti-tumor drugs, and comprehensive details for over 100 standard antibodies. Our engineered cell lines are now registered in the online cell line database Cellosaurus, which is available on the ExPASy server.

#6917 Ba/F3 AKT engineering cell lines, a useful platform for novel drug discovery.

G. Wang, Y. Tang, J. Xu, Y. Peng, Y. Wang, J. Ning, **F. Hao**;
Kyinno Biotechnology Co., Ltd, Beijing, China

AKT, also known as phosphoinositide 3-kinase (PI3K), plays a key role in various signaling cascades involved in cell growth and division, apoptosis inhibition, and angiogenesis. For AKT, which is at the central node of the PI3K/AKT/mTOR signaling pathway, the loss of PTEN, mutation, or amplification of AKT/PIK3CA can lead to the overactivation of the AKT signaling pathway, resulting in the occurrence and development of tumors. Recent studies have also found that AKT activation is associated with drug resistance in tumor therapy. Therefore, AKT has become a hot target for tumor therapy. The AKT family consists of three highly homologous isoforms, AKT1 (PKBα), AKT2 (PKBβ), and AKT3 (PKBγ), with more than 85% homology in their kinase regions. E17K is the most common and well-characterized activating mutation, accounting for approximately 15% of all AKT mutations. Rare mutations mainly include L52R, Q79K, and D323H. The failures of AKT inhibitors LY2780301 and Bayer's BAY1125976 demonstrate the significant challenges and complexities in developing inhibitors of the AKT pathway. Currently, the most advanced AKT inhibitor globally is AstraZeneca's capivasertib, which is primarily indicated for HR+ breast cancer and triple-negative breast cancer. Our group has generated 21 Ba/F3-AKT engineering cell lines, as useful models for novel drug discovery in vitro and in vivo, almost all clinically significant mutations were included, such as common mutations AKT1/2-E17K as well as rare mutations L52R, Q79K, D323H, and others. The Ba/F3-AKT engineering cell lines can be useful for developing and evaluating next-generation AKT inhibitors and exploring newly acquired resistance mutations in AKT.

#6918 Ba/F3-BCR-ABL engineering cell line panel, a useful platform for novel drug discovery.

G. Wang, Y. Peng, Y. Wang, Y. Tang, J. Xu, J. Ning, **F. Hao**;
Kyinno Biotechnology Co., Ltd, Beijing, China

In the past few years, with the great success of Imatinib, the first kinase inhibitor, Imatinib rapidly became the first-line treatment for CML (Chronic myelogenous leukemia) carrying the BCR-ABL mutation. It opened a new chapter in targeted cancer treatment. Despite the increase in overall survival allowed by imatinib, the onset of drug resistance led scientists to investigate imatinib's fine structural mechanism of action to develop new and more effective compounds against mutated forms of Bcr-Abl. 7 BCR-ABL inhibitors have been approved, they are Imatinib, Dasatinib, Nilotinib, Bosutinib, Ponatinib, Olverembatinib, and Asciminib. However, acquired resistance has been a major challenge in the treatment of CML, and some patients still experience disease progression or even death due to drug resistance. BCR-ABL kinase domain mutations are one of the important mechanisms of acquired resistance, with the T315I mutation being the most common type of drug resistance mutation, accounting for approximately 25% of drug-resistant CML cases. Patients with T315I mutations in CML are resistant to all current first- and second-generation BCR-ABL inhibitors. Asciminib is designed as an allosteric inhibitor combined with an ATP-competitive TKI agent, which may hinder the development of mutation-driven acquired resistance or restore efficacy against highly resistant BCR-ABL mutants. Our group has generated 38 Ba/F3-BCR-ABL engineering cell lines as useful models for novel drug discovery in vitro and in vivo, including wild-type BCR-ABL and inhibitors leading drug resistance mutations, such as T315I, E255, Y253, F317, F359. V299, G250, A337T, V468F, and double mutations. Each cell was validated by cell sequencing and cell efficacy verification using approved BCR-ABL inhibitors. The Ba/F3-BCR-ABL engineering cell line panel can be useful for developing and evaluating next-generation BCR-ABL inhibitors and exploring newly acquired resistance mutations in BCR-ABL.

#6919 Cell line panel with HIBIT-tagged endogenous proteins to accelerate PROTAC drug discovery.

Y. Zhai[1], J. Ma[2], Y. Wang[1], M. Liang[1], Y. Peng[1], J. Ning[1], **F. Hao**[1];
[1]Kyinno Biotechnology Co., Ltd, Beijing, China, [2]Beijing National Day School, Beijing, China

Small molecular drugs have been an important part of disease treatment, but there are also some problems along with time and intrinsic disadvantages of small molecular drugs. In recent years, the emergence of proteolysis targeting chimeras (PROTACs) is expected to overcome some defeats of traditional small molecules. PROTACs, also known as hetero-bifunctional compounds, are a new kind of therapeutic, that consists of a specific ligand to bind the target protein, a suitable linker, and an E3 ubiquitin ligase substrate. After binding to target proteins, PROTACs recruit E3 ligase and induce degradation of target proteins through the ubiquitin-proteasome system. Therefore, PROTACs are a good choice for some protein targets that have small molecular binding ligands but poor small molecular efficacy, which expands druggable targets. Meanwhile, the protein degradation induced by PROTACs destroys not only the enzymatic but also the non-enzymatic functions of targets, rather than only inhibiting the protein activity, which reduces drug resistance. In this study, in order to detect the degradation of intracellular target proteins by PROTACs, Kyinno has designed and constructed several HiBiT-tagged cell line models for different target proteins and their mutations, including KRA, CDK2, LDHA, and HPK. HiBiT is a small tag with 11 amino acids that don't influence the expression, folding, and localization of target proteins, and luminesces with a detection buffer. All these cell lines with endogenous protein mutations and HiBiT knock-ins are constructed by CRISPR-Cas9 technology and validated by siRNA and PROTACs. Compared with overexpressed exogenous HiBiT-tagged target proteins, endogenous proteins can more accurately and stably reflect the efficacy of PROTACs. Our cell models can be used for high-throughput screening not only for PROTAC drugs but also for molecular glues, lysosome-targeting chimeras (LYTACs), and antibody-based PROTACs (AbTACs).

TUMOR BIOLOGY: Tumor Evolution at Single Cell Resolution
Poster Session

#6923 Deconvolution of breast cancer dissemination and therapy resistance via single-cell transcriptional lineage tracing.

A. Dalmasso[1], A. Cossa[1], G. Bertolini[2], N. Roda[3], I. Servidio[1], F. Tucci[1], S. Pece[1], G. Sozzi[2], P. Pelicci[1],
[1]European Institute of Oncology (IEO), Milano, Italy, [2]Istituto Nazionale dei Tumori IRCCS, Milano, Italy, [3]VIB-KU Leuven Center of Cancer Biology, Leuven, Belgium

Chemotherapy remains the most used systemic treatment option for triple-negative breast cancer (TNBC). Lineage tracing studies demonstrated that treatment does not significantly alter clonal composition of primary tumors (PTs). The specific transcriptional phenotype(s) conferring chemoresistance in PTs and metastasis, however, are still largely undetermined, and have not been analyzed at single-clone resolution.
We first modelled clinically relevant contexts of chemoresistance in our recently published single-cell lineage tracing approach (DOI: 10.1158/0008-5472.CAN-22-2717), using the standard-of-care combination of adriamycin and cyclophosphamide (A+C) in TNBC xenografts. Treatment was administered in neoadjuvant or adjuvant settings, or both together. In all cases, surgical PT resection was followed by metastatic disease. The neoadjuvant treatment resulted into a stable disease, thus resembling a significant fraction of the treated patients.
To investigate clonal and transcriptional dynamics we performed scRNAseq analysis of 12 replicates (3 matched PT-lung replicates for each condition, for a total of 24 samples). Clustering analyses revealed a separation of treatments and tissue of origin. We retrieved a large number of longitudinal clones, including rare clones with high metastatic potential, in all the experimental conditions. A+C did not significantly alter clonal abundances, neither in PTs nor in metastases.
Pseudobulk transcriptional analyses revealed key transcriptional traits associated with chemoresistance. Differential expression on longitudinal clones gave insights about transcriptional features of chemoresistant and pro-metastatic clones under chemotherapy. Integration at single-clone level of cluster analysis, pseudobulk and differential expression revealed cystatin (CST) family genes as highly-enriched in the chemoresistant and pro-metastatic phenotype. We are currently validating the role of CST genes in tumor growth, dissemination and chemoresistance in vivo using a panel of specific shRNAs.
In parallel, using the same experimental model, we successfully deconvoluted the metastatic cascade through a single-cell lineage tracing approach on matched PT-CTC (circulating tumor cells)-lung replicates. scRNAseq analyses of pro-metastatic, circulating and metastatic clones is ongoing.
Our preliminary data showed that all the dominant clones in the metastatic lungs are also found as CTCs in the bloodstream, thus suggesting that all pro-metastatic cells are also capable of surviving in the bloodstream and reinforcing our concept of pro-metastatic clone. This approach led us to gain a complete overview around clonal and transcriptional evolution of breast cancer dissemination.

#6924 Structural variant dynamics in melanoma: Unraveling tumor heterogeneity and evolution.

X. Cui, A. G. Keskus, F. R. Mehrabadi, S. Malikic, M. Kolmogorov, C.-P. Day, G. Merlino, S. Sahinalp;
National Cancer Institute, Bethesda, MD

Melanoma is characterized by significant intratumoral heterogeneity and complex evolutionary dynamics. This diversity in genomic alterations leads to the emergence of various subclonal populations within a single tumor. In our research, we established a new model system composed of 24 single-cell-derived clonal sublines (C1-C24), originating from the M4 melanoma model. This model was developed using a genetically engineered hepatocyte growth factor (HGF)-transgenic mouse. We employed Trisicell (Triple-toolkit for single-cell intratumor heterogeneity inference), a cutting-edge computational tool for scalable analysis of intratumor heterogeneity and evaluation based on single-cell RNA mutations. This enabled us to construct a phylogeny tree, revealing melanoma's intricate branching evolutionary patterns. These patterns show ancestral clones evolving into genetically distinct subclones, which demonstrate varied phenotypic traits such as drug sensitivity or resistance, cellular plasticity, and immunogenicity. In our study, we conducted long-read sequencing on these clonal sublines in the phylogeny and identified structural variants (SVs) using Severus, a tool optimized for phasing in long-read sequencing. The types of SVs we discovered include deletions, insertions, amplifications, translocations, and inversions. We explored their roles in subclonal evolution, particularly focusing on how they disrupt genes and accumulate during melanoma progression. Our initial data from eleven sublines indicated a higher prevalence of ancestral SVs, shared by all sublines, compared to subline-specific SVs, representing later events. Notably, the individual sublines showed a higher rate of gene disruption by SVs, hinting at potential functional selection. Our analysis further revealed that SVs common to all sublines are linked with genes in key cell growth pathways, such as Rap1, Hippo, and calcium signaling pathways. In contrast, subline-specific SVs primarily affect genes involved in neurophysiological pathways, such as glutamatergic synapse and morphine addiction pathways. These findings suggest that different genes, associated with various pathways, are disrupted at distinct stages of melanoma progression, providing insights into the genetic factors that may predispose individual melanocytes to melanomagenesis. This methodology presents a comprehensive tool for characterizing tumor genomes and understanding their relationship with disease progression and therapy resistance. We are continuing our analysis to map SVs across the entire mutation-based phylogeny of all sublines, which will further our understanding of melanoma's genomic landscape.

#6925 Integrative single-cell tracking of genome evolution and tumor cell plasticity in small cell lung cancer (SCLC).

M. Schmiel, L. Kaiser, M. Cartolano, M. Peifer, R. K. Thomas, J. George;
University Hospital of Cologne, Cologne, Germany

SCLC is the deadliest type of lung cancer, which is mostly diagnosed at late stages and accounts for 15% of pulmonary tumors. Even though chemotherapy is initially effective, patients with SCLC relapse quickly and develop resistant tumors. Genome studies revealed a universal loss of TP53 and RB1; recent transcriptional studies categorized SCLC based on the expression of 4 lineage transcription factors (TFs). We aimed to dissect how genomic cues impact transcriptional phenotypes, tumor cell plasticity and the dynamics of tumor and immune cell interactions, to thus decipher molecular mechanisms of phenotypic divergence and therapy resistance in SCLC. We performed genome sequencing and single cell transcriptome profiling of 55 tumors from patients with SCLC, including primary tumors, local and distant metastases and of paired relapsing tumors acquired after chemotherapy. Single cell sequencing was performed with the 10x Genomics platform and yielded > 200.000 cells. Transcriptome profiles at single cell levels revealed co-expression of at least two of the lineage TFs ASCL1, NEUROD1 or POU2F3 in each tumor. Copy number (cn) estimation for transcriptome data pointed to genomic events impacting transcriptional heterogeneity within the tumor. Furthermore, our data pointed to a marked intra- and interpatient, as well as to inter-metastatic heterogeneity. To specifically investigate how underlying genetic alterations affect molecular phenotypes, integrative studies across all patients were performed. This revealed shared transcriptional programs in tumors with amplifications of MYC family members; trajectory inference for cases with low and high-level copy gains of MYCN pointed to distinct transcriptional states. We performed multi-regional and longitudinal studies of matched patient cases to reconstruct the genomic patterns of clonal evolution, and projected genomic subsets to transcriptional profiles at single cell level, thus analyzing the effect of genome diversity on the transcriptional landscape. Additionally, tumor intrinsic profiles of heterogeneity were mapped to single cell data of patient tumors to elucidate the effects on tumor-immune cell interactions.

All together our data points to a concerted regulation of a multitude of lineage factors and transcriptional programs in each SCLC tumor and provides a first comprehensive framework for the study of underlying genetic alterations that shape the transcriptional landscape and phenotypic plasticity in SCLC.

#6926 Tracing clonal evolution and immune evasion in glioblastoma progression.

Davide Ceresa[1], Sebastian A. Garcia Mena[1], Francesca Piaggio[1], Appolloni Irene[2], Daniela Marubbi[2], **Paolo Malatesta**[2]

[1]IRCCS Ospedale Policlinico San Martino, Genoa, Italy, [2]DIMES, University of Genoa, Genoa, Italy

Glioblastoma continues to be a daunting obstacle in oncology research, with its early-stage progression being particularly enigmatic. In a recent published work, we traced the clonal dynamics of glioblastoma evolution by the simultaneous transfer of PDGFB and genetic barcodes into mouse brains. We observed a continuous clonal loss during the acquisition of a malignant phenotype, underlined by the modulation of the levels of c-Myc expression and their functional targets. In this study, we delve deeper into the evolution of glioblastoma by transplanting multiclonal, early-stage glioma cells into multiple immunodeficient NOD-SCID mice. This experimental design allowed us to track the clonal dynamics over serial transplants, revealing how early-stage glioma clones acquire immune-evasive features capable of initiating tertiary tumors in immune-competent hosts. Through barcode sequencing and single-cell RNA sequencing of early-stage gliomas, coupled with bulk RNA sequencing of secondary and tertiary gliomas, we dissected the clonal and transcriptomic landscape of these tumors. We observed that, of the various clones composing primary tumors, just a few of them are predominating in subsequent passages. Furthermore, the clonal composition of secondary tumors derived from the same primary glioma showed partial overlap, indicating a partial predetermination in the development of immune-evasive behavior. Our intra- and inter-clonal transcriptomic analysis across various stages of tumor progression is shedding light on how new functional traits can emerge in gliomas. Further analysis of our data will determine whether it is the result of the expansion of clones already possessing these traits, or if they stem from functional adaptations within the clones themselves. Our insights further reinforce the concept of clonal competition, highlighting the significant influence of immune-system interactions in driving these competitive dynamics.

#6927 A refined view of pancreatic cancer genomic evolution through single-nucleus DNA sequencing.

H. Zhang[1], P. Sashittal[2], E.-R. Karnoub[1], A. Jakatdar[2], S. Umeda[1], N. Lecomte[1], J. Hong[1], K. Mullen[1], A. Hayashi[3], C. A. McIntyre[1], B. J. Raphael[2], C. A. Iacobuzio-Donahue[1];

[1]Memorial Sloan Kettering Cancer Center, New York, NY, [2]Princeton University, Princeton, NJ, [3]Kyorin University, Tokyo, Japan

Numerous next-generation sequencing studies have provided an overview pancreatic ductal adenocarcinoma (PDAC)'s genomic evolution. But how its genome evolves through treatment and metastasis has not been extensively studied due to lack of samples and technical limitation of bulk sequencing on low-tumor purity samples.

Herein we applied targeted single-nucleus DNA sequencing (snDNA-seq) to a cohort of 18 patients, each with >= 2 multiregional/longitudinal samples, totaling 65 samples. These included 5 early-stage resections, 11 stage IV autopsies and 2 biopsy-derived organoids taken pre- and post-treatment. We also developed a set of computational methods for this new datatype to delineate genomic evolution at high resolution.

Despite higher sensitivity than bulk, snDNA-seq did not uncover significant subclonal single-nucleotide variations (SNVs) on our panel targeting 253 select genes for PDAC. But it detected a higher frequency of *CDKN2A* (72% against 30%) and *SMAD4* (56% against 32%) alterations, mostly attributed to chromosomal deletions. Many were subclonal or only affected a few hundred base-pairs of the gene, making them elusive to bulk sequencing.

Except for one case driven by *BRCA2* mutations rather than the canonical *KRAS* oncogene, other patients had mostly linear phylogenies with more SNVs occurring before the most recent common ancestor (MRCA) of clones, for early/late-stage and longitudinal cases alike. This early fixation of drivers and rapid clonal sweep afterwards likely correlates with the particular aggressiveness of PDAC. Metastatic clones almost always fell towards the end of phylogenies and were shared among spatially separated sites, indicating late metastatic dissemination in molecular evolution time. Metastases to the liver and diaphragm appeared to be more genetically evolved than other sites, likely due to harsher selective pressure cast by the metastatic routes/distal microenvironments.

16 of 18 PDACs were observed to converge towards tumor cell-intrinsic TGF-β unresponsiveness by mutating various components of the pathway. Such convergent evolution usually happened at the primary site, indicating a strong selective advantage of the phenotype in the desmoplastic, nutrient-poor pancreas microenvironment. Continuous evolution was seen through treatment and metastasis, driven by seemingly random genome-scale copy number variations (CNVs) and focal amplification/deletions to genes such as *KRAS, CDKN2A, SMAD4, MYC.*

These insights on PDAC's genomic evolution inform more precision medicine efforts to come. Early fixation of driver SNVs sculpts a largely homogeneous disease that could be uniformly targeted. But special care should be taken to obviate resistance mechanisms conferred by continuously evolving CNV events- compared to SNVs, these mechanisms provide faster remodeling of the genome, and thus faster generation of new phenotypes and adaptation.

#6928 Expressed mitochondrial variants capture patterns of tumor evolution at single-cell level.

Andrea Cossa[1], Alberto Dalmasso[1], Andrea Tirelli[1], Zhan Yinxiu[1], Chiara Caprioli[1], Giulia Perticari[2], Pier Giuseppe Pelicci[1]

[1]Istituto Europeo di Oncologia e Centro Cardiologico Fondazione Monzino, Milan, Italy,[2]Princess Maxima Center for Pediatric Oncology, Utrecht, Netherlands

Single-cell lineage tracing (scLT) has recently emerged as a promising tool to investigate cancer evolution. Among other scLT markers, mitochondrial variants (MT-SNVs) have been successfully used to track clones in a variety of experimental and clinical settings. However, in spite of the dynamic accrual of such genetic mutations, analysis of MT-SNVs variation has often been limited to standard clustering procedures, not exploiting the information associated with these markers at full potential. Here, we benchmarked expressed MT-SNVs-based single-cell phylogenies. To this end, we generate two single-cell multi-omics datasets: i) a benchmarking dataset, with joint profiling of MT-SNVs, gene expression and ground truth (GT) clonal identity (from lentiviral barcodes cells), and ii) a clinical cohort of wild type and mutated SRFS2 Acute Myeloid Leukemia patients, at diagnosis, with joint profiling of MT-SNVs, gene expression and targeted nuclear SNVs. We first leveraged our benchmarking dataset for validation purposes, taking advantage of its different levels of clonal complexities (*in vitro* clonal mixtures vs *in vivo* xenografts) and its longitudinal nature (i.e., matched primary tumor-lung metastasis couples). Supervised analysis detected (GT) clonal-specific mutations rarer than previously shown, but significantly associated with GT clonal labels. The performance of tested feature selection methods varied wildly in terms of GT MT-SNVs recover, with higher False Positive than False Negative Rates. Accurate detection of GT-clones from MT-SNVs correlated with samples clonal complexity, with a substantial number of GT-clones sub-optimally detected in the highest complexity sample generated. Longitudinal analysis of matched primary tumor-metastasis couples revealed remarkable stability of MT-SNVs, corroborating evidence from other studies without longitudinal GT lentiviral clones. We then asked whether expressed MT-SNVs hold enough signal to reconstruct reliable single-cell phylogenies. Transfer Bootstrap (TS) supports of reconstructed trees correlated with clades size, with a significant number of deep clades showing high (>.70) TS values across samples and bootstrapping procedures. Moreover, GT clonal labels significantly clustered across phylogenies, suggesting high phylogenetic signal. Finally, we investigated evolutionary patterns in our clinical cohort. Here, we found independent acquisition of both nuclear- and MT-SNVs by distinct normal and malignant lineages, and characterized patterns of gene expression inheritance along recovered phylogenies. All in all, our data support the emerging role of MT-variants based lineage tracing approaches in cancer evolution studies, highlighting intrinsic limitations and potential of these endogenous markers for retrospective, phylo-phenotypic analysis.

#6929 Inter- and intratumoral *PIK3CA* subclonal diversity in breast cancer contextualized by single-cell multiomics.

J. Zawistowski[1], I. Salas-Gonzalez[1], T. Tate[1], T. Morozova[1], K. Kennedy[1], D. Arvapalli[1], J. Remington[1], J. Marks[2], E. Hwang[2], G. Harton[1], V. Weigman[1], J. A. A. West[1];

[1]BioSkryb Genomics, Durham, NC, [2]Duke University Medical Center, Durham, NC

Rare clonotypes within pre-cancerous tissues can drive progression to cancer. However, the evolution of rare clonotypes in tumors or normal tissue cannot be defined in the absence of single-cell resolution. At this single-cell level, multiomic interrogation across the Central Dogma of Biology provides enhanced power to reconstruct such evolutionary trajectories, defining the mutational profile, cell identify, and receptor expression within each subpopulation. Leveraging a multiomic approach, we aimed to define how different mutations in the same oncogenic driver observed in the same tumor resection associate with copy number variation (CNV) across the genome.

We analyzed individual ductal carcinoma in situ/invasive ductal carcinoma cells using a unified whole-genome and full-transcript RNAseq workflow (ResolveOME™, BioSkryb Genomics) coupled with panel-level extracellular protein information through oligo-conjugated antibodies (BioLegend). We sequenced the exomes and transcriptomes of ResolveOME-amplified single cells from mastectomy samples from twelve patients. At the single nucleotide variant (SNV) level, we identified an allelic series of *PIK3CA* oncogenic driver mutations in the same tumor resection. A single amino acid, in-frame deletion of E109 dominated the sample, followed by H1047R and K111E in decreasing subclonal abundance. A fourth mutation, E345T, not present in the first sample, was detected as the sole *PIK3CA* variant in the second tumor sample. Intriguingly, each respective *PIK3CA* mutation class was associated with a distinct copy number alteration profile revealed by low-coverage whole-genome sequencing: Cells harboring the predominant ΔE109 mutation displayed chromosome 8p,16p, and 17 loss while the less abundant H1047R mutation was in single cells harboring 1q gain, 4q loss, and 22 loss in addition to the 8p and 16q loss present in the ΔE109 cells. *PIK3CA* K111E had a quiescent, 2n copy number profile. The transcriptomic arm of ResolveOME, containing an oligo-conjugated antibody readout of surface protein expression, jointly confirmed the epithelial identity for the cells harboring the oncogenic *PIK3CA* mutations. A subpopulation of cells harboring prototypical breast cancer CNV were typed as non-epithelial with increased stemness characteristics, indicative of the ability to resolve phenotypic cellular states.

These results suggest a tight interrelationship between CNV and SNV influencing the relative rate of clonal expansion. They also provide the opportunity to explore CNV:SNV signature association with loci exclusive of *PIK3CA*, and to exploit the power of multiomic integration for lineage reconstruction and for defining common oncogenic signatures of the evolving tumors.

#6930 Spatial analysis of multi-ancestral tumors to understand how intercellular signaling impacts tumor invasion.

Mary M. Stangis[1], Lingxin Cheng[2], Dawn Albrecht[1], Santina Snow[1], Tessa Wirtz[1], Kristina A. Matkowskyj[3], Huy Q. Dinh[1], Christina Kendziorski[2], Richard B. Halberg[1]

[1]McArdle Laboratory for Cancer Research - Department of Oncology, University of Wisconsin-Madison, Madison, WI,[2]Department of Biostatistics and Medical Informatics, University of Wisconsin-Madison, Madison, WI,[3]Department of Pathology and Laboratory Medicine, University of Wisconsin-Madison, Madison, WI

Colorectal cancer (CRC) persists as a leading cause of cancer-related deaths in the United States. Intratumoral heterogeneity stems from a multi-ancestral origin or clonal divergence and contributes to treatment resistance. Unfortunately, tumors in existing mouse models are largely homogenous, rendering predictions of drug efficacy inaccurate. To investigate whether signaling between distinct neoplastic clones in a tumor and cells in the surrounding microenvironment impacts CRC biology, we performed spatial transcriptomic analysis on samples collected from a transgenic mouse model previously established in the Halberg laboratory. This model (referred to as B6.FCTG3KM) develops three types of tumors: homotypic Adenomatous Polyposis Coli (APC)-deficient tumors that express red fluorescent protein (RFP), homotypic APC-deficient tumors that express constitutively active phosphoinositide 3-kinase (PI3K) and green fluorescent protein (GFP), and heterotypic tumors. Previous characterization of the model clearly demonstrated that heterotypic tumors are significantly more aggressive than either type of homotypic tumor.
Analysis was conducted on four serially sectioned slides containing three tumors and adjacent normal tissue obtained from the colon of a male B6.FCTG3KM mouse using the 10x Genomics Visium CytAssist platform with the mouse whole transcriptome probe set. Collected tumors were staged using traditional histopathology techniques by a board-certified pathologist (Matkowskyj). Immunohistochemistry and immunofluorescence were used to assess β-catenin localization and to re-probe for RFP and GFP expression. Sequencing was performed on the Illumina NovaSeqX platform to an average depth of 255,528,294 reads per sample. Data analysis was performed using the 10x Genomics SpaceRanger and Kendziorski laboratory R/SpatialView packages. A fold-change threshold of 1.5 and an adjusted p-value threshold of 0.05 were used when establishing marker genes for each of the 8 clusters identified. One distinct cluster was identified by marker genes including *Notum, Wif1,* and *Dkk2,* factors previously implicated in CRC tumorigenesis, and corresponded to the center of each region of surface-level dysplastic epithelia. The remainder of the surface-level dysplastic epithelia corresponded to a second cluster, with marker genes including those coding for TRIM family proteins (*Trim5, Trim10, Trim40, Trim12*c), and matrix metalloproteinases (*Mmp12, Mmp9, Mmp10, Mmp13*). A third cluster corresponded to the desmoplastic stroma underlying each neoplasm. Ongoing analyses are underway to identify clonal interactions that alter gene expression and tumor aggressiveness.

#6931 Characterization of cancer evolution landscape based on accurate detection of somatic mutations in single tumor cells.

M. Niu, Y. Zhang, J. Luo, J. C. Sinson, A. M. Thompson, C. Zong;
Baylor College of Medicine, Houston, TX

Accurate detection of somatic mutations in single tumor cells is greatly desired as it allows us to quantify the single-cell mutation burden and construct the mutation-based phylogenetic tree. Here we developed scNanoSeq chemistry and profiled 842 single cells from 21 human breast cancer samples. The majority of the mutation-based phylogenetic trees comprise a characteristic stem evolution followed by the clonal sweep. We observed the subtype-dependent lengths in the stem evolution. To explain this phenomenon, we propose that the differences are related to different reprogramming required for different subtypes of breast cancer. Furthermore, we reason that the time that the tumor-initiating cell took to acquire the critical clonal-sweep-initiating mutation by random chance set the time limit for the reprogramming process. We refer to this model as a reprogramming and critical mutation co-timing (RCMC) subtype model. Next, in the sweeping clone, we observed that tumor cells undergo a branched evolution with rapidly decreasing selection. In the most recent clades, effectively neutral evolution has been reached, resulting in a substantially large number of mutational heterogeneities. Integrative analysis with 522-713X ultra-deep bulk whole genome sequencing (WGS) further validated this evolution mode. Mutation-based phylogenetic trees also allow us to identify the early branched cells in a few samples, whose phylogenetic trees support the gradual evolution of copy number variations (CNVs). Overall, the development of scNanoSeq allows us to unveil novel insights into breast cancer evolution.

#6932 Single-cell multiomics profiling reveals heterogeneous transcriptional programs and microenvironment in desmoplastic small round cell tumors.

C. Henon[1], J. Vibert[2], T. Eychenne[1], N. Gruel[2], L. Colmet-Daage[1], C. Ngo[1], M. Garrido[1], N. Dorvault[1], M. Marques Da Costa[1], A. Marchais[1], A. Kawachi[1], M. Lenormand[1], C. Astier[1], R. Chabanon[1], B. Verret[1], R. Bahleda[1], A. Le Cesne[1], F. Mechta-Grigoriou[2], C. Honore[1], M. Faron[1], O. Delattre[2], J. Waterfall[2], S. Watson[2], S. Postel-Vinay[1];

[1]Gustave Roussy, Villejuif, France, [2]Institut Curie, Paris, France

Background: Desmoplastic Small Round Cell Tumor (DSRCT) is a rare, aggressive sarcoma primarily affecting young males. Despite being driven by the unique oncogenic transcription factor (TF) EWSR1-WT1, and a monotonous morphology, DSRCT cells display a polyphenotypic differentiation of unknown etiology.
Methods: To explore DSRCT heterogeneity, we characterized a series of patient samples by single-cell, spatial, and bulk multi-omics. We integrated patients' data with bulk RNA-sequencing, ChIP-sequencing, and ATAC-sequencing data generated in a DSRCT cell line model upon EWSR1-WT1 transcriptional silencing.
Results: Single-cell RNA-sequencing (scRNA-seq) on 11 patient samples identified recurrent subpopulations of DSRCT tumor cells, including lineage-, metabolism-, and pseudostate-related clusters. These subpopulations showed overlapping gene modules and lacked copy number variation diversity, suggesting transcriptional plasticity as a potential source of tumor heterogeneity. We first investigated whether cell-intrinsic mechanisms may drive DSRCT intra-tumor heterogeneity. Using an in-house-developed assay, we found limited variability in *EWSR1-WT1* transcript expression. Preclinical modeling defined an EWSR1-WT1 regulon, used as a surrogate for EWSR1-WT1 TF activity. Integration with scRNA-seq data showed that high EWSR1-WT1 activity was associated with lineage-related states, while glycolytic and profibrotic states correlated with low EWSR1-WT1 activity. Single-cell ATAC-seq with scRNA-seq (Multiome) on one patient sample identified TF motifs related to developmental processes - e.g., SOX, FOX, and GATA - as the most differentially enriched across clusters. Interestingly, EGR1 regulon activity showed an inverse correlation with EWSR1-WT1 and Androgen Receptor regulons' activity, in line with preclinical data, where ATAC-seq showed increased accessibility of *EGR1* upon EWSR1-WT1 silencing. We next investigated cell-extrinsic factors by spatial transcriptomics in six patient samples. Glycolytic and profibrotic subpopulations localized within hypoxic niches at the tumor periphery, in direct proximity to cancer-associated fibroblasts (CAFs), which promoted tumor growth *in vitro*, as assessed in DSRCT cells/CAFs co-culture assays. Finally focusing on inter-tumor heterogeneity, the prognostic evaluation of scRNA-seq-derived signatures revealed that a tumor cell epithelial signature correlated with improved patient survival in a cohort of 29 DSRCT samples profiled with bulk RNA-sequencing.
Conclusion: DSRCT heterogeneity is driven by combined cell-intrinsic and -extrinsic mechanisms, including EWSR1-WT1 DNA-binding activity and interaction with CAFs. Gene signatures associated with specific DSRCT subpopulations correlated with prognosis, highlighting the clinical relevance of our findings.

#6933 Decoding the archetypes and eco-hubs of triple-negative breast cancer in responses to chemotherapy.

Y. Yan[1], Y. Lin[1], T. Kumar[1], S. Bai[1], J. Li[1], T. Tran[1], M. Hu[1], E. Ravenberg[1], M. Rauch[1], A. Clayborn[1], A. Thompson[2], B. Lim[2], L. Huo[1], S. Moulder[1], C. Yam[1], N. Navin[1];

[1]UT MD Anderson Cancer Center, Houston, TX, [2]Baylor Medical College, Houston, TX

Triple-negative breast cancer (TNBC) is a highly aggressive type of breast cancer commonly treated with neoadjuvant chemotherapy (NAC). While about 50% of patients achieve a pathological complete response (pCR), the remainder often develop resistance and metastasis, leading poor survivals. Currently, the factors linking pre-treatment cancer cells and the tumor microenvironment (TME) to NAC response are unclear. To investigate this question, we conducted single-cell RNA sequencing on fresh pre-treatment core biopsy samples collected from patients in the ARTEMIS clinical trial. We identified 13 gene expression meta-programs of cancer cells and about 50 cell states of immune and stromal cell types. Based on the cancer cells alone, we identified four TNBC archetypes at patient-level: luminal secretory-associated (LSA), basal-associated (BA), immunoreactive (IR), and luminal androgen receptor (LAR). Notably, the archetype BA and IR were associated with non-pCR and pCR, respectively. Additionally, we found the TNBC ecosystem was composed of eight eco-hubs, reflecting the co-occurrence patterns of cancer and TME cell states. These eco-hubs revealed different cell community across archetypes and NAC outcomes. For example, an eco-hub with a co-occurrence of interferon response-related cancer cells and immune cells was prevalent in the archetype IR and pCR patients. To facilitate a clinical application, we further developed a 13-gene-based machine learning model to predict NAC response. In summary, these results provide new insights into the cellular determinants of TNBC biology and chemotherapeutic response.

#6934 Integrating deep learning morphology profiling, cell sorting, and scRNASeq reveals sample diversity and enriched sub-populations.

A. Jovic, C. Corona, K. Saini, T. Pham, R. Carelli, **V. Lu**, S. Zhang, S. C. Boutet, M. Masaeli;
Deepcell Inc., Menlo Park, CA

Advances in single cell technologies have ushered in a new multi-omics era that has provided more granular information on cell types and functions at unprecedented resolution. Morpholomics (the information encoded by cell morphology) has traditionally been used as a readout of cell identity, state, and function; but scalability, interpretation, and sorting based on morphology has remained challenging. The Deepcell® platform, REM-I, performs high-dimensional morphology analysis of unlabeled, single cells using deep-learning on high-resolution bright-field images captured in microfluidic flow to profile and sort target cells in real-time and at scale. Morphology analysis of single cells is achieved by a self-supervised deep learning foundation model, 'Human Foundation Model' (HFM), which combines deep learning features with morphometrics. HFM determines cell identities using morphological features associated with distinct processes characterized by granules, vesicles, cell size, pigmentation. and others. To demonstrate the ability of HFM modeling to distinguish and characterize a diversity of cell types representative of tumor microenvironments, we processed various sample types on the REM-I platform. Human melanoma, immune cells, stromal cells, and dissociated biopsies were combined to recapitulate heterogeneous tumor samples. HFM analysis enabled morphology-based exploration of the resulting bright-field images, revealing the presence of various morphologically distinct populations within each sample. Tumor cells were morphologically distinct and clustered separately from non-tumor cells. Immune cells exhibited subtle but separable morphologies, including T cells of distinct activation states. To demonstrate the morphology-based sorting capabilities of REM-I, we applied it to a 'reference sample' consisting of several fixed cell lines, at proportions ranging from 1% to >90%. Using only brightfield images of single cells analyzed through HFM, we used the platform to enrich each cell line from the 'reference sample' with high yield and purity, and identified cell types constituting a small percentage (~1%) of the total population. We next showed that unlabeled cells enriched on REM-I that are characterized as unperturbed and viable are amenable to downstream molecular analyses. These cell populations were sorted and the retrieved live cells were analyzed by scRNA-Seq (10x Chromium), demonstrating enrichment of various cell types of the tumor microenvironment in each cell population relative to the pre-sorted sample. These results illustrate: 1) the ability to perform downstream molecular analyses on sorted cells from REM-I, 2) the platform can be used to parse the tumor microenvironment, and 3) the link between morphology, cell identity, and molecular signatures.

#6935 Non-genetic routes of lung cancer evolution.

G. Ciriello, D. Tavernari, M. Varrone;
UNIL University of Lausanne, Lausanne, Switzerland

Cancer cell plasticity underlies the progression of several solid tumors. In lung adenocarcinoma, morphological changes characterizing the transition from indolent to aggressive disease exhibit profound epigenetic and transcriptional reprogramming[1]. However, the extent, features, and drivers of cancer cell plasticity in the progression of human lung adenocarcinoma is still largely unexplored. Here, we assembled and analyzed a meta-cohort of 119 human lung tumors analyzed by single-cell RNA-sequencing, for a total of ~730,000 cells. Cancer cell heterogeneity was the result of differential activation of 17 transcriptional programs associated with common cancer phenotypes, such as proliferation, cell migration, and response to hypoxia, as well as alveolar lineage identity (AT2). In particular, AT2-specific expression of MHC-II was down-regulated with the progression of the disease and markedly reduced in *KEAP1* and/or *STK11* mutated samples, providing a rationale for the association between these mutations and immunotherapy resistance. Co-activation of transcriptional programs clustered tumor cells in 4 major cell states, which emerged with the progression of the disease. To explore spatial distribution of different cancer cell states, we generated and analyzed multiple spatial transcriptomics and proteomics lung adenocarcinoma cohorts. To this purpose we developed a new algorithm called CellCharter[2]. CellCharter identified distinct cancer-enriched niches within individual samples, corresponding to the cancer cell states that we discovered in the scRNA-seq cohort and exhibited specific interactions with the tumor microenvironment (TME). In particular, we identified a cancer cell state characterized by response-to-hypoxia and migratory phenotypes, which spatially segregated from highly proliferative cancer cell niches and formed specific interactions with tumor associated neutrophils. This cell state was enriched in advanced primary samples, it uniquely characterized metastatic samples, and was an independent marker of poor prognosis across multiple independent datasets. Overall, our work uncovered cell plasticity trajectories associated with the progression of lung adenocarcinoma and shed new light into the tumor-TME interactions at their origin.

[1] Tavernari et al., Cancer Discovery, 2021 [2] Varrone et al, Nat. Genetics, (in press)

#6937 High throughput single cell simultaneous DNA and RNA sequencing identified cell-of-origin of breast cancer.

K. Wang[1], R. Ye[1], S. Bai[1], Z. Xiao[1], L. Yang[1], J. Li[1], Y. Lin[1], E. Sei[1], S. Lin[1], A. Thompson[2], S. Krishnamurthy[1], N. Navin[1];
[1]UT MD Anderson Cancer Center, Houston, TX, [2]Baylor College of Medicine, Houston, TX

Understanding the relationship between genotype and phenotype in breast cancer cells has been challenging at single cell resolution, mainly because existing high-throughput methods are limited to measuring a single modality and data must be integrated indirectly via computational methods. To address this challenge, we developed wellDR-seq, a high-throughput single cell method that can simultaneously measure the single cell whole genome and transcriptome directly from thousands of single cells in parallel. Using this method, we profiled 17,427 single cells in 6 different ER+ breast cancer patients with either premalignant disease (Ductal-carcinoma-in-situ) or invasive ductal carcinoma (IDC). From these data we identified the epithelial cell-of-origin in 3 cases, showing that ER+ breast cancer cells originated from Luminal Hormone Responsive (LumHR) in the normal breast tissues. We also found that autosomal somatic copy number aberrations were exclusively present in LumSec (< 2%) and LumHR epithelial cells, while chrX gain or loss also occurred in stromal cells (eg fibroblast and endothelial) but a low frequency (<2%) in our datasets. Additionally, our data show the impact of subclonal copy number profiles on gene expression programs, which reflects both gene dosage effects in CNA regions and more complex deregulation in copy-neutral regions. wellDR-seq offers a powerful tool for large-scale single cell genome and transcriptome simultaneous sequencing across different clinical samples, opens new avenue to investigate genotype and phenotypes interactions, identify tumor cells origins, reveal somatic copy number and mutation events, quantify the gene dosage effect and discerning differential genes expression between tumor subclones.

#6938 Identification of distinct tumor-TME ecomodules in glioma from neurofibromatosis type 1.

L. Garofano[1], F. D'Angelo[1], M. Oh[1], M. Ceccarelli[1], F. Bielle[2], M. Sanson[2], A. Lasorella[1], A. Iavarone[1];
[1]University of Miami Miller School of Medicine, Miami, FL, [2]Pitie Salpetriere Hospital, Paris, France

Neurofibromatosis type 1 (NF-1) is the most common cancer predisposition syndrome in which 15-20% of affected individuals develop glioma. Large scale DNA and RNA bulk profiling showed the molecular complexity of NF-1 glioma with the tumor cellular ecosystem constituted by multiple malignant phenotypes and heterogenous immune microenvironment. However, the composition and function of infiltrating cells was hidden in the bulk tumor, and the extended granularity of NF-1 glioma tumor microenvironment (TME) remained still unexplored. Here, we collected glioma samples from 46 NF-1 patients including 22 high-grade (HGG) and 24 low-grade (LGG) tumors, and we analyzed their gene expression by single nuclei RNA sequencing. A total of 239,044 single cells were classified into tumor and non-tumor components by integrating multiple computational approaches (including genomic copy number inference, gene signature enrichment, and clustering). We defined the pattern of intra-tumor heterogeneity of NF-1 glioma cells using non-negative matrix factorization and derived 7 malignant meta-programs (MPs) that we respectively defined as Neuronal-like, EMT, Astrocyte-like, Dividing Radial Glia-like, Ependymal-like, Immune, and Glycolytic/Hypoxic-like. These MPs recapitulated normal brain cell subtypes, thereby reflecting broad cell plasticity. The non-tumor cell compartment (121,364 cells, 51%) was dissected for the characterization of the cell types that populate the TME of NF-1 glioma. We identified different subpopulations exhibiting specific immune functions within myeloid and lymphoid components. Different glioma ecomodules were highlighted by comparing the relative composition of the TME across the tumors. Recruitment and activation of cytotoxic $CD8^{+}$ T cells and natural killers by an active crosstalk with dendritic and pro-inflammatory myeloid cells defined an immune-supportive phenotype that could mediate a potential anti-tumor response in low-grade NF-1 glioma (LGG immune high). Conversely, regulatory T cell infiltration and effector T cell exhaustion induced immune suppression in a low-grade glioma immune dysfunctional ecomodule. The absence of lymphocytes characterized a large set of cold tumors, mostly including high-grade glioma. Together, the complex interplay of tumor cell states with different TME compartments elucidated the existence of separate ecomodules in NF-1 glioma, with the LGG immune high TME associated with Neuronal-like and the LGG immune dysfunctional with Ependymal-like tumor cells. The Ependymal-like state also exhibits maximal association with brain-specific normal cells, including oligodendrocytes, neurons and astrocytes, whereas the HGG are enriched with Dividing Radial Glia- and Glycolytic/Hypoxic-like tumor cell states. The elucidation of different ecomodules provides novel insights for the application of targeted therapies in NF-1 glioma patients.

#6939 Residual disease after HER2 inhibition is driven by a primary tumor subpopulation expressing an *ERBB2*-low associated transcriptional program.

S. K. Kabraji[1], W. Wang[2], Y. Zhang[1], J. Bergholz[2], T. Jiang[2], V. Kurisetty[1], M. Homsi[1], J. Wang[1], J. Zhao[2];
[1]Roswell Park Comprehensive Cancer Center, Buffalo, NY, [2]Dana Farber Cancer Institute, Boston, MA

Background: In HER2+ breast cancer (BC), residual disease (RD) after neoadjuvant HER2 inhibition is associated with increased risk of recurrence. However, the genetic and non-genetic resistance mechanisms underlying RD remain incompletely characterized. Here we used single nuclei (sn) RNA and DNA sequencing to profile genetic and transcriptional changes in growing, residual, and recurrent tumors from an inducible mouse tumor model of HER2+ breast cancer.
Methods: We used mammary tumors / tumor bed (n=2-3/time point) from female *MMTV-rtTA; TetO-ERBB2* mice at 9 weeks DoxOn (HER2on), 7 days DoxOff (HER2off) and 12-21 weeks Doxoff (recurrent). Samples were snap frozen and single nuclei isolation was performed. snRNAseq was performed using 10X 5' v2 kits for library preparation and sequencing. snDNAseq was performed using a custom amplicon panel targeting the mouse genome and human *ERBB2* locus via the MissionBio Tapestri platform.
Results: For snRNAseq analysis, tumor cell clusters were identified by *Epcam* and *ERBB2* gene expression. Tumor cells were further subclustered into 18 unique clusters that separated by *ERBB2* expression. Seven subclusters of HER2on tumor cells were characterized by low *ERRB2* expression: 1.38 vs 2.94 (median normalized log counts) in HER2on-*ERBB2*high cells. Top 5 differentially expressed genes (DEG) per condition (log2 fold change >1.5, adjusted p value < 0.05) were: HER2on: *Erbb2, Csn3, Lcn2, Csn2, Wfdc18*; HER2on-*ERBB2*high: *Csn3, Igfbp5, Csn2, Lcn2, Trf*; HER2on-*ERBB2*low: *Lars2, Gm47283, Cmss1, Gm42418, Neat1*; HER2off: *Lars2, Hexb, Cmss1, Gphn, Gm42418*; Recurrent: *Capza2, Vim, Lgals1, Crabp1, S100a6*. HER2on-*ERBB2*low cells were more closely related in transcriptional space to HER2off residual tumor cells than HER2on-*ERBB2*high tumor cells. Trajectory analysis suggested that HER2off RD evolved from HER2on-*ERRB2*low cells and formed the basis of recurrent disease. To determine clonal evolution over time, we used common top 10 DEGs between HER2on vs HER2off vs HER2low snRNAseq data and intersected that set with significantly enriched single nucleotide variants (SNVs) from our snDNAseq data. We identified 16 clones containing at least 1 SNV at >1% frequency across all samples. We observed clonal persistence, relative enrichment and extinguishment between HER2on, HER2off and recurrent samples but without clonal dominance.
Conclusion: Time-series analysis of genetic and transcriptional evolution in a mouse model of HER2+ BC RD suggests that a tumor cell subpopulation characterized by an *ERBB2*low-associated transcriptional program drives RD after HER2 inhibition.

#6940 The transcriptional and epigenetic regulation of epithelial-mesenchymal plasticity in patient-derived pancreatic cancer cell lines.

D. Yeramosu[1], L. Bi[1], A. Collins[1], M. Bogaev[1], M. Jankowiak[1], A. Al'Khafaji[1], M. Parikh[1], M. Babadi[1], A. Bloemendal[1], S. Nagaraja[2], R. Jones[1], J. Shendure[3], D. T. Ting[4], A. Aguirre[5], N. Hacohen[6], D. Pe'er[7], E. S. Lander[1], A. Mehta[1];

[1]Broad Institute of MIT and Harvard, Cambridge, MA, [2]Harvard Medical School, Boston, MA, [3]University of Washington, Seattle, WA, [4]Mass General Cancer Center, Boston, MA, [5]Dana-Farber Cancer Institute, Boston, MA, [6]Massachusetts General Hospital, Boston, MA, [7]Sloan Kettering Institute, New York, NY

Epithelial-mesenchymal transition (EMT) is a hallmark of pancreatic ductal adenocarcinoma (PDAC) invasion. In general, cellular plasticity is a major contributor to both tumor progression and therapy resistance. The major goals of our study are to 1) directly and quantitatively measure plasticity in PDAC3 cell lines, and 2) identify candidate genes that could alter the plasticity of cancer cells. By understanding the regulation of tumor cell plasticity, we may find ways to perturb cells and prevent the transition towards treatment resistant cell states. A strict definition of plasticity in cancer has yet to be established, however, and is imperative to our understanding of cell state regulation and for identifying vulnerabilities in plastic cells. We argue that in order to prove plasticity occurs within a population of cells, one must either 1) demonstrate that a new cell state has emerged that was previously not present, or 2) trace the lineage of a cell to show it can adopt multiple cell states. For our study, we profile 12 patient-derived PDAC cell lines to find convergent EMT programs and perform lineage tracing on these cell lines using a modified CROP-seq vector, called ClonMapper, to quantitatively measure plasticity. Towards this goal, we perform single-cell RNA-seq (scRNA) and single-cell multiomic measurements of 1000 uniquely barcoded cells expanded over a time course of 2, 3 and 4 weeks. We refer to cells that have the same lineage barcode - originating from the same initial cell - as families. We found that ~50% of families are composed of cells that are epithelial and mesenchymal, thus proving plasticity must exist, as it shows that a given parental cell of unknown state can give rise to progeny that are in multiple states. We then develop mathematical models to show that families have different levels of plasticity, defined by the rates of transition between distinct cell states. We next leverage our barcode-resolution time course data to identify factors at early time points that may influence plasticity at later time points. We show there is differential accessibility of several of these factors across families with different plasticity properties, thus proposing a role for epigenetic regulation of EMT. Importantly, we find that specific factors drive gene regulatory networks important for epithelial and mesenchymal programs, and therefore propose candidates for the modulation of EMT for therapeutic benefit.

#6941 Transcriptomic effects of retinoblastoma progression-related somatic copy number alteration (SCNA).

Kevin Stachelek, David E. Cobrinik

USC - University of Southern California, Los Angeles, CA

Retinoblastoma is a pediatric retinal cancer that initiates in response to biallelic RB1 loss or MYCN amplification in a cone precursor cell of origin. After initial emergence, RB1-/- retinoblastomas progress to more aggressive forms by accumulation of single nucleotide variants (SNVs) and highly recurrent somatic copy number alterations including 1q+, 2p+, 6p+ and 16q- (RB SCNAs), resulting in heterogeneous mixtures of subclonal cell populations. SCNAs are enriched in highly evolved and aggressive tumor subtypes and show prognostic value in retinoblastoma liquid biopsies. However, the transcriptomic effects of retinoblastoma SCNAs are poorly understood. Single cell methods may enable comparison of tumor subclones within emerging retinoblastoma tumors and thereby provide insight into tumor progression.

We retrieved single cell RNA sequencing data for 25 retinoblastoma tumors and inferred SCNAs and subclone phylogenies from scRNAseq information using a recently published tool, Numbat. We identified tumors with clonal variation in RB SCNAs and excluded samples with poor transcriptome quality or excessive additional SCNAs. We proceeded with analysis of 11 tumors with subclonal heterogeneity for an SCNA of interest, including 10 with 1q+, eight with 2p+, four with 6p+, and six with 16q-. After removal of nontumor cells, we defined cell clusters, cluster marker genes, and cell cycle phase gene signatures, and we compared cell state distributions for subclones with an acquired SCNA relative to their immediate antecedents.

These analyses revealed recurrently discriminated transcriptomic clusters corresponding to six discrete cell cycle states (post-mitotic G1, G1, G1/S, S, S/G2, G2/M) and variable cell stress states, including a cluster with hypoxia and heat shock related marker gene expression in all samples. In each tumor, SCNA-defined tumor subclones had a distinct cell state distribution. Tumor subclones with acquired 1q+ were enriched in G2 states and depleted in G1 states. Subclones with 2p+ were enriched in G2 states. Subclones with 6p+ were enriched in S phase states. Subclones with 16q- were diminished in post-mitotic cell states. Tumor clones with 1q+ and 16q- were most strongly enriched for G2 phase cells. Such 1q+/16q- tumor cells were significantly differentially distributed in three tumor replicates. Tumor clones with other RB SCNAs were enriched over diploid clones in proliferating G2 cells without SCNA specific effects.

To identify candidate drivers of SCNA-specific transcriptomic effects we measured RB SCNA clonal variation in gene expression within and across transcriptomic states. We identified recurrently differentially expressed in-segment genes in 1q+, 2p+, 6p+, and 16q- , as well as out-of-segment genes. Finally, we propose molecular mechanisms underlying SCNA recurrence that may enable tumor evolution in retinoblastoma.

#6942 Single cell resolution of intrapatient drug resistance mechanisms in metastatic melanoma.

H. P. Wilson[1], G. L. Mersky[1], J. I. Haj[1], J. Teh[1], P. F. Cheng[2], S. Caksa[1], C. D. Stefanski[1], V. Chua[1], C. Capparelli[1], M. P. Levesque[2], R. Dummer[2], T. J. Purwin[1], A. E. Aplin[1];

[1]Thomas Jefferson University, Philadelphia, PA, [2]University of Zurich Hospital, Zurich, Switzerland

Intrapatient heterogeneity among different metastatic sites contributes to immunotherapy (ICi) and targeted therapy resistance. Determining the evolution of metastatic melanoma lesions that develop within the same patient could help elucidate adaptive mechanisms that drive tumor progression during therapy. To assess how metastatic melanoma persists through immunotherapy and targeted inhibitor treatments, we utilized samples from a single patient who had received anti-CTLA4, BRAFi/MEKi, and BRAFi/MEKi+CDK4/6i treatments during the LOGIC2 clinical trial. Eight short-term cultures were established from different metastatic site biopsies at chronological time points throughout the patient's treatment and subsequent post-mortem resection of the bone, ovary, and brain metastatic sites. While the initial treatment naïve metastatic tumor in the breast was *BRAF*^{V600E} mutant, *NRAS*^{Q61} mutations were acquired after treatment with CDK4/6i in the bone and ovary tumors. Tumors that persist through treatment and colonize distant organs adapt to and rely on organ-specific microenvironments. To assess treatment- and organ-specific adaptations, single-cell RNA sequencing was performed on seven of the short-term cultures to identify subpopulations that persist through each treatment. We analyzed samples and subpopulations of each culture to determine differences in their transcriptional cell states. The regulon transcriptional network of each sample and subpopulation was evaluated to determine site- and treatment-specific transcriptional regulation differences. In addition, we identified the treatment naïve culture is split into two major subpopulations by therapy resistance features which are further made up of six distinct subpopulations with heterogeneous regulatory networks. We determined the longitudinal evolution of subpopulations in response to treatment and organ site to evaluate how the pressure of therapies and the microenvironment influence metastatic progression. We further evaluated site-specific resistance mechanisms and detected increased HER3 expression in the melanoma brain metastasis (MBM) sample. Treatment with Neuregulin 1, a ligand for the HER3 receptor that is abundant in brain tissue, partially rescued the growth of MBM cells and restored MAPK and AKT-mTOR signaling in the presence of BRAFi/MEKi. Targeting the NRG1-HER3 signaling axis could have therapeutic potential in melanoma patients with active brain metastases. Additionally, we evaluated treatment-specific resistance mechanisms and identified high Brevican (BCAN) expression in an early emerging subpopulation that arises after ICi in this patient and in others. BCAN is implicated in both ICi- and cross-resistance. We will functionally investigate whether targeting BCAN sensitizes cells to ICi. Future studies aim to functionally examine novel site- and treatment-specific cross patient targets.

#6943 Evolutionary dynamics under chemotherapy in small cell lung cancer: Insights from patient-derived xenotransplant models.

L. C. Kaiser, M. Schmiel, A. Ruminska, N. Alavinejad, C. Muller, J. Valiulis, M. Peifer, M. Cartolano, R. K. Thomas, J. George;
University of Cologne, Koln, Germany

Introduction: The treatment of patients with small cell lung cancer (SCLC) represents a major medical challenge due to aggressive tumor growth and the poor 5-year overall survival rate of only 5%. SCLC tumors typically are remarkably sensitive to chemotherapy at the beginning; however, the subsequent rapid relapse of therapy-resistant tumors is a severe obstacle. We therefore aimed to decipher the molecular patterns guiding processes of evolutionary adaptation in SCLC as a consequence of therapeutic interventions.

Methods: Over 100 patient-derived xenotransplant models were generated from clinical SCLC specimens capturing a wide range of genetic and molecular features as well as clinical phenotypes with regard to chemotherapy response. We recapitulated chemotherapy response *in vivo* for 32 models, and performed in-depth genome and single-cell transcriptome sequencing to thus dissect genomic evolutionary trajectories and transcriptional plasticity of therapy-naïve and relapsed tumors, which includes the study of multiregional and longitudinal samples.

Results: The response to chemotherapy *in vivo* reflected the clinical response of the patients; however, several models of relapsed patients remained sensitive to treatment. Genomic studies of clonal dynamics indicated selection of subclones as a result of therapeutic pressure. In contrast, chemo-refractory tumors maintained their clonal composition after therapy. In agreement with genomic profiles, single-cell transcriptome data revealed a tremendous shift in expression profiles and composition of subpopulations. Furthermore, subclonal genomic events including copy number alterations were found to shape the transcriptional heterogeneity in tumors.

Conclusion: Here, we demonstrate a comprehensive functional characterization of multi-regional tumor sites and longitudinal specimens acquired from patients with SCLC, in which we elucidate genomic and transcriptional heterogeneity as a consequence of therapy response. Overall, our data points to a complex interplay between sub-clonal genomic changes and transcriptional plasticity shaping therapy response in which pre-existing genomic alterations impact selection under therapy.

#6944 Transcriptional programs underpinning reoccurring cancer cell states, plasticity and tumour phylogenies in clear cell kidney cancer.

O. Lombardi[1], R. Li[1], L. Browning[2], F. Jabbar[1], H. Evans[1], P. J. Ratcliffe[1], D. R. Mole[1];

[1]University of Oxford, Oxford, United Kingdom, [2]Oxford University Hospitals NHS Foundation Trust, Oxford, United Kingdom

Intratumor heterogeneity (ITH) is a substrate for tumor evolution and confers amenability to stressors and therapies. Sources of ITH include subclonal mutations, microenvironmental factors, and plasticity whereby a cell has the ability to adopt different cell states. Clear cell kidney cancer (ccRCC) has a well-characterized genetic initiating event - VHL inactivation - resulting in activation of HIF-1 and HIF-2 transcription factors. Although VHL inactivation is consistently clonal in nature, ccRCC nonetheless exhibits extensive genetic and morphological ITH. This makes ccRCC an excellent model in which to study ITH.

We performed single cell RNA-seq on multiregional samples from kidney tumors and macroscopically normal kidney tissue. We obtained 55 samples from 16 tumors and used the 10x Genomics platform to obtain gene expression data from ~150,000 single cells, including ~80,000 cancer and normal epithelial cells. We identified three cancer cell states, co-existing in all clear cell kidney cancer tumors analyzed and marked by different gene expression programs: 1) differentiated-like cells marked by proximal tubule cell genes characteristic of the cancer cell of origin; 2) epithelial-mesenchymal transition (EMT)-like cells and 3) injured-like cells. Differentiated markers and EMT markers were associated with good and poor prognosis, respectively, indicating that these cell subpopulations are clinically important. Notably, these cell states are also present in the normal proximal tubule although in different proportions to the tumor samples, which contain more cells in the EMT-like and injured-like states. This suggests that the core features of ITH are inherent to the cell of origin of the cancer, but that the cell state trajectories are dysregulated in the tumor. Furthermore, in tumors these states exist as a continuum, whereby transitional cells in between states appear to exist, suggesting that cancer cells are continually and dynamically transitioning between states.

Lastly, we used chromosomal copy number variation (CNV) patterns to study genetic ITH. We examined the effect of 14q loss, which is associated with ccRCC metastasis, on gene expression. We found that 14q loss is associated with downregulation of HIF-1 transcriptional activity together with a reciprocal increase in HIF-2 activity, MYC activity and oxidative phosphorylation, highlighting potential mechanisms by which 14q loss may driver ccRCC metastasis.

#6945 Dissecting the interplay of cell identity and extrachromosomal DNA in glioblastoma.

B. Taylor, B. Jones, D. Kawauchi, Y. Miyake, R. Vadla, N. Jameson, S. Miki, T. Koga, B. Ren, F. Furnari;
UC San Diego School of Medicine, San Diego, CA

The five-year survival rate of glioblastoma multiforme (GBM) is 5.8%, and its standard of care has not changed since 2005. This stagnation in therapeutic development is due, in part, to its characteristic heterogeneity--*multiforme*--highlighting a *critical need* to understand the biological processes underlying this GBM hallmark. Despite the well-documented individual relationships between extrachromosomal DNA (ecDNA), GBM, and heterogeneity, the interplay between the three is not well understood. The Furnari lab has generated a library of cancer avatars, or human induced pluripotent stem cells (hiPSCs) engineered to harbor cancer driving mutations. Single cell RNA sequencing (scRNA-seq) was used to characterize the longitudinal evolution of the first avatars engineered to have *TP53*$^{-/-}$;*PDGFRA*$^{\Delta 8\text{-}9}$ and *PTEN*$^{-/-}$;*NF1*$^{-/-}$ genotypes. The *TP53*$^{-/-}$;*PDGFRA*$^{\Delta 8\text{-}9}$ avatar acquired ecDNA, while the *PTEN*$^{-/-}$; *NF1*$^{-/-}$ avatar did not. Re-analysis of the scRNA-seq data identified a subpopulation of cells in the *TP53*$^{-/-}$;*PDGFRA*$^{\Delta 8\text{-}9}$ avatar that had high expression of *CDK4* and *PDGFRA*, two genes that are commonly co-amplified, found on ecDNA, and drive cellular states. This subpopulation of cells also had highly expressed genes near the *CDK4* locus indicating a structural variant and possibly ecDNA. This population diverged transcriptionally from other cells and was associated with the OPC-like cellular state, which has been shown to be associated with high levels of *PDGFRA* and, at times, co-expression with *CDK4*. While *TP53*$^{-/-}$;*PDGFRA*$^{\Delta 8\text{-}9}$ tumors contained cells across all four GBM cellular states, *PTEN*$^{-/-}$;*NF1*$^{-/-}$ tumors had a significantly less diverse composition of cellular states suggesting that ecDNA may facilitate cellular state diversity. With the eventual goal to directly test whether ecDNA enables transcriptional state heterogeneity compared to chromosomally inherited amplifications, CRISPR-Cas9 and CRISPR-C were implemented to engineer *EGFRvIII* ecDNA in U87. While inverse PCR confirmed the successful generation of ecDNA in U87, ecDNA was lost following long term *in vitro* cell passaging. Current follow up work aims to identify different intrinsic (oncogene amplified, genetic background, cell type, cell line) and extrinsic (*in vitro* conditions, orthotopic engraftment) contexts that promote the selection and amplification of engineered ecDNA, as it would be would be valuable to have genotypically identical cancer models with different classes of amplifications (i.e., engineered ecDNA vs. lentiviral overexpression, which is chromosomally inherited). Together, these results highlight the potential to use hiPSC-derived models and single cell methods to investigate gliomagenesis and cell identity.

#6946 Unravelling intra-tumor phenotypic heterogeneity in colorectal cancer organoids.

S. J. Fletcher[1], I. Catalano[2], E. Grassi[1], S. Borgato[1], B. Peracino[1], E. Piretto[1], L. Alessandri[1], R. Calogero[1], L. Primo[1], L. Trusolino[1], A. Bertotti[1], A. Puliafito[1]; [1]University of Turin, Torino, Italy, [2]Candiolo Cancer Institute-FPO IRCCS, Torino, Italy

Colorectal cancer (CRC) is one of the most diagnosed cancers worldwide. Though several treatment strategies are available today, around a million people die of this disease each year worldwide. Thus, there is still a pivotal need for new and more effective treatments. Genetic and non-genetic intra-tumor heterogeneity has emerged lately as an intrinsic feature of malignancies and as one of the factors responsible for therapy resistance or tolerance. In particular, the nature and role that phenotypically distinct, yet genetically indistinguishable, subpopulations have on tumor biology is far from being understood. Here we investigate phenotypic heterogeneity in CRC by identifying specific transcriptionally well defined cell subpopulations. We aim at deciphering the interactions between populations in terms of differentiation and plasticity, tumor growth and potentially exposed targetable vulnerabilities. To this end, we used patient-derived metastatic CRC (mCRC) organoids, including KRAS wild type (wt) and mutant (*kras*) models. We performed in total scRNAseq for 7 mCRC samples (4 wt; 3 *kras*) in different growth media: normal growth medium (supplemented with EGF) (n=1); medium without EGF (noEGF) (n=7); or treated with Cetuximab (CTX, a clinically approved monoclonal antibody against EGFR) (n=7). We found that the wt sample grown in EGF presents 2 distinct subpopulations: one with stemness characteristics (LGR5 high) and the other with a more differentiated phenotype (KRT20 high), in agreement with the current bibliography. Interestingly, in EGF deprived cultures new subpopulations appear. In particular, we were able to identify a subpopulation with distinct expression of WNT-related genes (APCDD1, WNT6, WIF1). This subpopulation is also present, and in cases increasing in fraction, when organoids are treated with CTX (in 3 out of 7 samples). Interestingly, a fraction of the WNT positive subpopulation seems to be able to proliferate under CTX treatment (Ki67 positive). We identified the negative regulator of the WNT pathway, APCDD1, as a potential marker to track this subpopulation. We took one wt and one *kras* sample as models to validate these findings by flow cytometry. Furthermore, sorting of APCDD1 positive and negative cells, and further RT-qPCR analysis, confirmed good correlation between antibody staining and gene expression. Moreover, we found that both types of cells are able to re-grow as organoids after re-culturing. This suggests that this WNT-associated subpopulation could be contributing, at least in part, to CTX tolerance or resistance. Our results show promising potential to help unravel basic features of intra-tumor heterogeneity both in basal conditions and upon treatment, and possibly to find new therapeutic targets.

#6947 Exploring the single-cell dynamics of FOXM1 under cell cycle perturbations.

T. Jawwad[1], M. Kamkaew[2], K. Phongkitkarun[1], P. Chusorn[3], S. Sampattavanich[1];
[1]Mahidol University, Bangkok, Thailand, [2]Tufts University, Boston, MA, [3]Roi Et Rajabhat University, Bangkok, Thailand

The cell cycle plays a critical role in maintaining normal cellular functions and preventing abnormal cell growth. The transcription factor FOXM1 has emerged as a crucial regulator of cell cycle progression and has been implicated in various physiological and pathological processes. Notably, FOXM1 overexpression has been observed in numerous cancer types, including liver, prostate, breast, lung, and colon cancer. Despite its significance, our understanding of how FOXM1 dynamic behaves at the single-cell level under different cell cycle perturbations and its link to cell behavior heterogeneity remains limited. Here, we investigated the dynamic behavior of FOXM1 in individual cells exposed to various cell cycle perturbations, focusing on understanding heterogeneity in cell behavior and improving disease treatment. At the single-cell level, our investigation reveals six distinct dynamic features of FOXM1 in response to various therapeutic interventions, each of which corresponds to a unique cell phenotype. Our result further demonstrates that for cells exhibiting a high FOXM1 pattern, targeting aurora kinase and PLK1 may hold promise as a therapeutic approach for cancer suggesting that FOXM1 is a strong biomarker, and its pattern can be predictive of drug response, especially in cases with G1 checkpoint defects like Rb1 loss or p53 deficiency.

MOLECULAR/CELLULAR BIOLOGY AND GENETICS: Cancer Cell Communication with the Tumor Microenvironment
Poster Session

#6951 The role of estrogen-dependent activation of p38 MAPK signaling pathway in inflammatory breast cancer.

Keyla V. Ramirez[1], Adrian D. Bonilla-Gonzalez[1], Jeisac Guzman-Rivera[2], Esther A. Peterson-Peguero[1]

[1]University of Puerto Rico - Rio Piedras, San Juan, PR,[2]Rutgers University, Newark, NJ

Inflammatory breast cancer (IBC) is a rare and aggressive type of breast cancer in which the lymphatic vessels become blocked by cancer cells in the breast tissue. The five-year survival rate for this type of cancer is around 40%, one of the worst among breast cancer. Most IBCs are estrogen receptor (ER) and progesterone receptor (PR) negative and HER2 positive, with some presenting an amplification of HER2 while others are ER, PR, and HER2 negative, formally known as the triple-negative (TNBC) subtype. However, it has been reported that treatment with 17β-Estradiol (E2) of ER-negative IBC and non-IBC cells can exert rapid non-genomic signaling mediated by ERα-36, GPR30, and/or estrogen receptor beta, activating MAPK pathways involved in oncogenic phenotypes. Previous data generated in our lab showed that when cells were treated with estradiol it led to increased phosphorylation levels of p38. However, the specific role p38 MAPK signaling takes on in IBC is unknown. Thus, this study centers on examining the role of estradiol and p38 regulation in the triple-negative IBC cell line model, SUM149PT. We hypothesize that upon estradiol treatment p38 signaling pathway is activated resulting in the over-expression of pro-inflammatory cytokines which regulate pro-tumorigenic phenotypes including the growth and survival of IBC cells. Inflammatory cytokines can promote pro-oncogenic features by promoting cell proliferation, angiogenesis, and immune suppression. We treated SUM149 IBC cells with 10nM of estradiol and measured the levels of human cytokines using a Human Cytokine Antibody Array. In addition, treatment using SB202190, a potent p38 inhibitor, caused a significant decrease in cell viability of several breast cancer cell lines in a dose-dependent manner. Ongoing studies include assessing the effects of p38 inhibition proliferation, invasion, and migration. In summary, a better characterization of the effect of E2 and p38 activation in ER-negative cell lines may provide great insight into novel targeted therapies for IBC.

#6952 The role of interleukin-11 (IL11) in cancer-associated cachexia (CAC).

K. Drinkwater, A. Meyers, S. Kargari, N. Crisan, **A. Mody**, M. Shim;
Midwestern University - Glendale Campus, Glendale, AZ

Cancer-associated cachexia (CAC), characterized by loss of skeletal muscle and involuntary body weight loss, is responsible for increased chemotherapy toxicity, reduced quality of life, and impaired survival in cancer patients. While interleukin-11 (IL11), one of the IL6 family cytokines, was originally thought to be involved in hematopoiesis, studies increasingly suggest its involvement in tumorigenesis including chemoresistance, metastasis, and survival of cancer cells. However, the precise role of IL11 in CAC has not been determined. Our lab has previously shown that IL11 treatment suppressed the myogenic differentiation of C2C12 myoblasts, suggesting that IL11 may interfere with differentiation and subsequent regeneration of muscle. In this study, we investigated the role of IL11 in cancer-induced muscle wasting using cell culture and mouse models. The mRNA expression of IL11 was highly up-regulated in C26 and Lewis lung carcinoma (LLC) cells, two well-known cachectic mouse cancer cell lines, while its expression was low in a non-cachectic MC38 mouse colon cancer cell line. Knockdown of IL11 in C26 cells using two independent lentiviral shRNAs significantly reduced the mRNA levels of the cytokines involved in CAC including GDF15, LIF, and VEGFA, while the mRNA level of IL6 was not significantly altered. Additionally, IL11 knockdown significantly reduced the mRNA and protein levels of ATF4, CHOP, and TRIB3, suggesting that IL11 may be responsible for the activation of unfolded protein response, an adaptive mechanism for growth, survival, and angiogenesis of cancer. Knockdown of IL11 in C26 and LLC cell lines also significantly reduced the volume of tumors in syngeneic mouse models, while over-expression of IL11 in MC38 cells increased tumor size. Moreover, the knockdown of IL11 in cachectic cancer cells partially prevented the loss of muscle and body weight in tumor-bearing mice, although the amelioration of muscle loss by IL11 knockdown may be associated with the decreased tumor burden. Together, these results indicate that IL11 may contribute to muscle wasting and provide novel insight into the previously unestablished role of IL11 in CAC.

#6953 Wnt2b deficiency exacerbates colitis and leads to increased tumorigenesis in mice.

L. Silva Oliveira[1], A. E. O'Connell[2];

[1]Boston Children's Hospital, Brookline, MA, [2]Boston Children's Hospital, Division of Newborn Medicine, Brookline, MA

Colitis-associated cancer (CAC) is considered the most severe complication of inflammatory bowel disease (IBD). It has been demonstrated that WNT2B deficiency leads to severe intestinal impairment in humans and predisposes to colitis in mice. Evaluating a human cohort from The Cancer Genome Atlas (TCGA), we observed that low expression of WNT2B is associated with poor prognosis of patients with colon cancer. However, the functional roles of WNT2B in CAC development remain unclear, and we hypothesized that WNT2B is involved in the resistance to CAC development during long-term colitis. Thus, we model CAC development using Wnt2b deficient mice subjected to mutagenesis induction with 10 mg/kg Azoxymethane (AOM) and a long-term colitis protocol with three cycles of 2.5% Dextran Sodium Sulfate in the drinking water for three days, followed by a recovery period with autoclaved water. We observed that Wnt2b KO mice had increased susceptibility to colitis and more significant body weight changes than WT mice, especially in the first and second recovery cycles of colitis recovery. The maximum weight loss and disease activity index (DAI) were significantly higher in KO than in WT mice. Interestingly, Wnt2b KO mice developed more tumors, which were more extensive than those observed in WT. Moreover, the histopathological analysis showed that Wnt2b KO had the highest score for ulceration, aberrant crypt foci, and immune cell infiltration. Our data suggest a protective role for WNT2B, conferring resistance to tumor development during colitis. Furthermore, our data provides new insights into the functional roles of Wnt ligands in colon cancer. A better understanding of the factors involved in CAC etiology is critical for improving diagnosis and developing new targeted therapies. We believe WNT2B may emerge as one of these factors and offer novel targets for improved colorectal cancer management.

#6954 Glycine decarboxylase regulates renal carcinoma progression and DNA damage response via interferon stimulated gene factor 3-mediated pathway.

J. Kim, B. Kim, M. Choe, T. Pham, M. Kim, J. Seo, S. Shin;
Keimyung University Dongsan Medical Center, Daegu, Korea, Republic of

Glycine decarboxylase (GLDC) is a mitochondrial enzyme of glycine cleavage system which catalyzes glycine to donate for one-carbon metabolism. It is implicated as a tumor suppressor in hepatocellular carcinoma but as an oncogene in lung cancer. Although GLDC expression in the kidney is second highest next to the liver, the role of GLDC in the kidney remains unclear. Thus, this study was designed to determine the role of GLDC in renal carcinoma. We found markedly increased expressions of GLDC in patients with renal cell carcinoma (RCC) classified as poor-risk group based on the Memorial Sloan Kettering Cancer Center prognostic model. *In vitro* studies revealed that cellular proliferation, colony formation was decreased in GLDC-deficient renal carcinoma cells. Additionally *in vivo* xenograft studies with GLDC-deficient and -overexpressing cells also revealed that tumor sizes were noticeably decreased in GLDC-deficient cell-injected mice while those were increased in GLDC-overexpressing cell-injected mice. Mechanistically, we found GLDC regulates renal carcinoma progression via interferon (IFN) stimulated gene factor 3 (ISGF3)-mediated pathway. Expressions of IRF9 and STAT2 were increased in GLDC-deficient cells while those were decreased in GLDC-overexpressing cells. Upon inducing expression of ISGF3 subunits, GLDC deletion elevated DNA damage, mitotic catastrophe, mitochondrial deficiency induced by chemotherapy. Finally, GLDC knockdown diminished pyrimidine synthesis to impair renal cancer progression. In summary, our finding reveals that GLDC regulates renal carcinoma progression and DNA damage response via ISFG3-medated pathway and lays a scientific foundation that could support a therapeutic strategy that targets GLDC for the treatment of renal carcinoma.

#6955 Activation of ERK pathway by mutant Ras oncoproteins derived from THP-1 cell exosomes.

J. B. Hwang, L. Marquardt, O. Sait, B. Gilliam, Q. Xiao;
MilliporeSigma, St. Louis, MO

The study of exosomes has attracted worldwide research due to its ability to modulate cellular activities, especially in the progression of cancer. Exosomes are membrane vesicles that can deliver lipids, proteins, and nucleic acids from one cell to another through membrane fusion, providing a unique form of cell-to-cell communication. It has been shown that KRAS G12V oncoprotein has been detected inside various pancreatic cancer cell derived exosomes. Our goal for this study was to examine the effect of KRAS G12V oncoprotein, detected inside exosomes isolated from THP-1 cell line supernatant, to activate MAPK pathway in MCF-7 breast cancer and AsPC-1 pancreatic cancer cells. To this end, we developed MILLIPLEX® immunoassays to detect cell signaling proteins as well as the exosome markers (CD9, CD63 and CD81), using Luminex® xMAP® technology which allows multiplex detection of proteins in a small volume of sample. Exosomes were isolated from THP-1 derived cell supernatant, using Qiagen exoEasy Maxi kit according to the kit protocol. KRAS G12V oncoprotein was detected in isolated THP-1 exosomes. As a control, THP-1 exosomes were enriched with exosome markers such as CD9, CD63 and CD81. After 48-hour incubation of AsPC-1 cells with KRAS G12V containing THP-1 exosomes, significant increase in KRAS G12V levels were detected in AsPC-1 cells. More importantly, this increase in KRAS G12V levels corresponded with an increase in phosphorylated ERK signaling, but not JNK, p38, NFκB, Akt, STAT3 and STAT3 pathways. In contrast, 48-hour incubation of MCF-7 cells with KRAS G12V containing THP-1 exosomes had no effect on any signaling pathways. Using MILLIPLEX® multiplex immunoassays, our data supports research findings that exosomes contain mitogenic signaling components that may enhance progression of cancer.

#6956 Role of soluble CD109 in the progression of head and neck squamous cell carcinoma.

Varsha Reddy Durgempudi, Tenzin Kungyal, Anie Philip

Surgery and Division of Plastic Surgery, McGill University, Montreal, QC, Canada

Introduction: About five percent of global cancer deaths are attributed to Head and Neck Squamous Cell Carcinoma (HNSCC), and its annual incidence is predicted to skyrocket by thirty percent by 2030 (according to GLOBOCAN estimates). HNSCC originates from squamous cells in the oral cavity, lips, tongue, larynx, pharynx, and salivary glands. Despite the comparatively easy tumor diagnosis, the number of patients diagnosed at an advanced stage with metastatic spread is substantial. Multiple cell-signaling pathways have been proven to be dysregulated in HNSCC, including the epidermal growth factor receptor (EGFR). Our group has identified CD109, a GPI-anchored membrane-associated protein, as a TGF-β co-receptor that inhibits TGF-β signaling. CD109 expression is upregulated in SCC, and its elevated expression in premalignant lesions is associated with an increased risk of metastatic progression. Recent studies by our team have revealed that CD109 promotes tumor growth *in vivo*, likely by enhancing EGFR signaling. Interestingly, we have also discovered that membrane CD109 (mCD109) is endogenously released from the cell surface; however, the mechanism of action of the released/soluble form of CD109 (sCD109) remains unknown. In the current study, we examined whether sCD109 opposes the mCD109/EGFR-mediated pro-tumorigenic signaling and HNSCC progression.
Research Questions: 1.Does sCD109 regulate EGF-induced EGFR signaling and downstream stem cell marker expression?2.Does sCD109 regulate EGFR expression levels on the HNSCC cell surface?3.Does sCD109 affect the nuclear localization of EGFR?4.Does sCD109 promote EGFR internalization and degradation?
Methodology: HNSCC cells and patient-derived primary cells were treated with/without sCD109 recombinant protein (1nM, 5nM, and 10nM) without and with the EGF induction (10ng/ml for 15 mins) and were analyzed by western blotting, immunofluorescence, and immunocytochemistry. The role of sCD109 in regulating membrane EGFR levels was assessed by flow cytometry and surface protein biotinylation assay.
Results: Our findings demonstrated that sCD109 inhibited EGF-induced phosphorylation of EGFR (Y1068), STAT3, AKT, and ERK. The sCD109 suppressed the stem cell marker expression (Nanog, OCT4, SOX2). Additionally, sCD109 hindered the nuclear localization of activated EGFR. The sCD109 decreased the membrane EGFR expression levels and activated the phosphorylation of EGFR (Y1045), suggesting a role for sCD109 in promoting EGFR degradation.
Conclusion: Our team has previously reported that mCD109 is pro-tumorigenic, and our current findings suggest that sCD109 opposes the pro-tumorigenic effects of mCD109. This study aimed to determine how sCD109 regulates cellular signaling pathways and will provide key insights into the molecular mechanisms underlying the progression of HNSCC, a highly prevalent malignancy.

#6957 Extrachromosomal FGFR2 is delivered in extracellular vesicles in two models of cancer of unknown primary.

I. Salamon[1], G. Storci[2], B. Fontana[3], S. Serravalle[2], G. Gallerani[3], R. Roncarati[4], S. Santi[4], M. Bonafe[3], **M. Ferracin**[3];
[1]University of Bologna, IRCCS Azienda Ospedaliero-Universitaria di Bologna, Bologna, Italy, [2]IRCCS Azienda Ospedaliero-Universitaria di Bologna, Bologna, Italy, [3]University of Bologna, Bologna, Italy, [4]Institute of Molecular Genetics, National Research Council of Italy, Bologna, Italy

The extracellular vesicle (EV) route is essential for cell-to-cell communication. Cancer cells release EVs in the extracellular space, where they can interact with recipient cells inducing regulation of gene expression, activation of specific signaling pathways and tumor microenvironment remodeling. We investigated the EVs released by two cell lines of cancer of unknown primary site (CUP) that we established from patient's tumor cells, namely CUP#55 and CUP#96, as described in https://www.medrxiv.org/content/10.1101/2023.03.12.23287041v1). CUP comprises 3-5% of new cancer cases and presents with metastases of unknown or uncertain origin and no apparent primary tumor. Our CUP cell lines are both characterized by *FGFR2* gene amplification. It has been recognized that tumors use circular extrachromosomal DNA (ecDNA) as a way to increase oncogenic amplification. We hypothesized that FGFR2 amplification in CUP cell lines could be associated with ecDNA generation and that this ecDNA could be loaded as cargo inside EVs. *FGFR2* copy number was quantified using a probe-based droplet digital PCR assay then we identified the different nature of *FGFR2* amplification in the two models using FGFR2 FISH assay: CUP#55 presented a chromosomal homogeneously staining region while CUP#96 displayed double minute chromosomes. *FGFR2* DNA was detectable in the cytoplasm fraction, therefore we isolated extracellular vesicles from culture medium using an ultracentrifugation-based protocol and confirmed the presence of the entire length of *FGFR2* gene inside small and large vesicles. Since ecDNA contributes to cancer genome remodeling also forming chimeric circles, we confirmed the circular nature of a fraction of *FGFR2* ecDNA using the Plasmid-Safe ATP-dependent DNAse test. Finally, we tested the oncogene delivery capability of CUP EVs by administering CUP#96 and CUP#55 small and large vesicles to recipient cell lines. We observed an increase of *FGFR2* DNA at 24 hours upon EV treatments, and its functional transcription in FGFR2 mRNA after 48 hours. In conclusion, we identified a model of oncogene amplification and delivery in two cell lines of cancer of unknown primary, which could explain the high metastatic potential of this cancer type. (The research leading to these results has received funding from AIRC under IG 2021 - ID. 25789 project - P.I. Ferracin Manuela)

#6958 CRIPTO-regulated extracellular vesicles mediate heterotypic cellular crosstalk in triple negative breast cancers.

D. W. Freeman[1], B. L. Gates[1], M. D. Spendlove[2], **B. T. Spike**[1];

[1]University of Utah Huntsman Cancer Institute, Salt Lake City, UT, [2]Huntsman Cancer Institute/BYU, Salt Lake City, UT

Tumor progression involves dynamic interaction between various cell types within the tumor microenvironment. Fibroblasts, which normally participate in wound healing, reciprocally communicate with breast cancer cells to promote tumor cell plasticity and heterogeneity. Gaining insights into the molecular mechanisms underlying this cell-to-cell communication, could unlock novel therapeutic avenues for inhibiting cellular plasticity, breast cancer progression and metastasis. The small GPI-anchored adaptor protein CRIPTO is a key player in this context though important molecular details remain to be elucidated. CRIPTO orchestrates TGF-β pathway signaling as well as growth factor-like signaling pathways that activate c-Src/MEK/AKT, in an autocrine and paracrine manner. CRIPTO is expressed during mammary development, wound healing, and breast cancer but is largely undetectable in homeostatic tissue, making it a promising therapeutic target. Our previous studies have demonstrated that the activity of CRIPTO is contingent upon cellular stress, with pronounced influence within pro-fibrotic, hypoxic domains of tumors. Importantly, we have shown that inhibition of CRIPTO using the soluble recombinant protein antagonist A4Fc effectively impedes the progression of triple negative breast cancer (TNBC) in murine xenograft models. Building upon these findings, we have been dissecting CRIPTO's role in coordinating fibroblast activation and cell-state reprogramming in TNBC. We find that inhibition of CRIPTO with A4Fc suppresses cancer associated fibroblast (CAF) activation and collagen remodeling *in vivo*. Further, by modeling tumor cell:fibroblast crosstalk *in vitro*, we have demonstrated mechanistically that CRIPTO expression in tumor cells mediates subsequent extracellular vesicle (EV) uptake by fibroblasts, as well as fibroblast SMAD pathway activation and priming for reciprocal signaling back to tumor cells to promote transcriptional reprogramming and cellular invasion.The significance of these findings lies in their elucidation of key EV control mechanisms that could be exploited to intervene in essential tumor cell:fibroblast crosstalk or to enhance targeting of therapeutic moieties based on EV architecture and function in cancer and/or normative regenerative processes.

#6959 Acetylcholine potentiates invasion and migration of human pancreatic cancer cells under hypoxia through α7 nAChR-mediated increases in HIF-1α expression.

Yunmi Cho[1], Eun-Taex Oh[2], Ha Gyeong Kim[3], Heon Joo Park[3]

[1]Program in Biomedical Science & Engineering, Inha University College of Medicine, Incheon, Korea, Republic of,[2]Department of Biomedical Sciences, Inha University College of Medicine, Incheon, Korea, Republic of,[3]Department of Microbiology, Inha University College of Medicine, Incheon, Korea, Republic of

The most significant nerve-related problem in clinical pancreatic cancer management is perineural invasion (PNI), characterized as the neoplastic invasion of cancer cells into or surrounding the nerves. It is a characteristic feature of pancreatic ductal adenocarcinoma (PDAC) associated with a poor prognosis, tumor recurrence, and emergent pain. However, why PDAC is associated with a higher incidence of PNI remains unclear. HIF-1 (hypoxia-inducible factor-1) regulates the expression of ~1000 genes involved in angiogenesis, metastasis, tumor growth, chemoresistance and radioresistance, underscoring the growing interest in targeting HIF-1 for cancer control. In the present study, we investigated the molecular mechanisms underlying neurotransmitter acetylcholine (Ach)-potentiated HIF-1α expression and subsequent increase in invasion and migration of human pancreatic cancer cells in hypoxia (2% O_2). The expression of various acetylcholine receptors in six types of pancreatic cancer cell lines (MIA-PaCa-2, PANC-1, HPAF-II, Capan-1, AsPC-1, and BxPC-3 cells) was observed using qPCR, and α7 nAChRs was observed to be expressed in all pancreatic cancer cells. Therefore, we chose MIA-PaCa-2 cells, expressing high levels of α7 nAChRs, and HPAF-II cells, expressing low levels of α7 nAChRs, for loss- and gain-of-function studies, respectively. *In vitro* assays showed that, under hypoxic conditions, Ach caused a concentration-dependent increase in α7 nAChRs-mediated HIF-1α expression, enhancing expression of HIF-1α target genes, and promoting invasion and migration of human pancreatic cancer cells. We further found that Ach increased HIF-1α protein stability in pancreatic cancer cells under hypoxic conditions. This effect was mediated by YAP signaling, as evidenced by the fact that Ach-induced increases in HIF-1α protein stability were blocked by siRNA-mediated knockdown of YAP. Consistent with these findings, an investigation of the relationship between α7 nAChRs and clinicopathological features in pancreatic cancer patients using publicly available datasets showed that high levels of α7 nAChRs are correlated with a poorer prognosis in pancreatic cancer patients. Collectively, these findings identify novel mechanisms by which Ach potentiates invasion and migration of pancreatic cancer cells and provide further evidence that HIF-1α is a potential anticancer target in Ach-associated pancreatic cancer.

#6960 Lysosome inhibition suppress collective cell migration through caveolin-1 mediated E-cadherin stabilization in colon cancer cells.

Y.-C. Ching, H.-C. Chen, Y.-C. Wang, C.-P. Cheng, C.-E. Ku, S.-R. Lee, W.-T. Chao;
Tunghai University, Taichung, Taiwan

In tumor nest growth and collective cell migration, the dynamics of E-cadherin is critical, and been shown to be regulated by cell vesicle traffic system. Caveolin-1 is the vesicle protein to regulate caveolae associated endocytosis, many of the membrane receptors are shown been regulated by caveolin-1 in cancer progression, however, the role is still controversial. This study demonstrated the effect of lysosome inhibition in caveolin-1 mediated E-cadherin turnover in the cell cohort of colon cancer cells. HT-29 colon cancer cells were used in this study, the cells were treated with chloroquine to inhibit lysosome activity. The cell spheroid from HT-29 cells were also collected according to cell adhesion ability. Caveolin-1 and E-cadherin were immuno-stained and revealed by confocal microscopy. In the result of immunostaining, caveolin-1 was showed the co-localization with E-cadherin at cell-cell contacts. When cells were treated with chloroquine, the lysosome inhibitor, the collective cell migration of HT-29 cells were suppressed, and stable caveolin-1 distribution was found accumulated on the cell-cell contacts., meanwhile, chloroquine has no effect on clathrin distribution at either cell-cell contacts or cell leading edge. Furthermore, the distribution of caveolin-1 at cell-cell contacts on cell spheroid that derived from HT-29 cells was decreased. The results of these study suggested lysosome plays important role in mediating caveolin-1 regulated E-cadherin dynamics in collective cell migration, but not in the cell spheroid formation. The results of these study demonstrated chloroquine can be the potential inhibitor for collective cell migration in colon cancer cells through caveolin-1 mediated vesicle transport.

#6961 The cell adhesion molecule ninjurin 2 modulates tumorigenesis, inflammatory response and metabolism via modulating and pyroptosis.

J. Zhang, W. Zhang, X. Chen;
UC Davis, Davis, CA

The nerve injury induced protein 2 (NINJ2) belongs to a family of homophilic adhesion molecules and was initially found to be involved in nerve regeneration. However, the role of NINJ2 in other cellular process are not well studied. Here, by generating a Ninj2-deficient mouse model, we showed that mice deficient in *Ninj2* have a short lifespan and are prone to spontaneous tumors, systemic inflammation and metabolic defects. To better understand the metabolic traits that contributes to these phenotypes, we performed comprehensive carbohydrate and lipid metabolic analyses. Indeed, carbohydrate metabolic analyses indicated that NINJ2-deficiency led to defects in monosaccharide metabolism along with accumulation of multiple disaccharides and sugar alcohols. Similarly, lipidomic analyses indicated that Ninj2 deficiency altered patterns of several lipids including triglycerides, phospholipids and ceramides. To identify a cellular process that associate with these metabolic defects, we examined the role of Ninj2 in pyroptosis, a programmed cell death that links cancer, inflammation and metabolic disorders. Indeed, we found that loss of NINJ2 promotes pyroptosis by activating the NLRP3 inflammasome. Taken together, these data reveal a critical role of NINJ2 in tumorigenesis, inflammatory response, and metabolism via modulating pyroptosis.

#6962 Shed Trop2 drives prostate cancer progression and Trop2 is a novel tissue prognostic biomarker and a candidate urinary marker for prostate cancer.

S. Liu[1], S. Hawley[2], C. Kunder[2], E.-C. Hsu[2], M. Shen[1], M. Aslan[2], F. J. G. Marques[2], C. S. Lee[1], A. Bermudez[2], L. Westphalen[1], H. Auman[2], L. F. Newcomb[3], D. W. Lin[3], P. S. Nelson[4], Z. Feng[4], M. S. Tretiakova[3], L. D. True[3], F. Vakar-Lopez[3], P. R. Carroll[5], J. Simko[5], M. E. Gleave[6], D. A. Troyer[7], J. K. McKenney[8], D. Peehl[5], S. J. Pitteri[2], J. D. Brooks[2], M. A. Liss[9], T. Stoyanova[1];

[1]University of California Los Angeles, Los Angeles, CA, [2]Stanford University, Palo Alto, CA, [3]University of Washington, Seattle, WA, [4]Fred Hutchinson Cancer Center, Seattle, WA, [5]University of California San Francisco, San Francisco, CA, [6]University of British Columbia, British Columbia, BC, Canada, [7]Eastern Virginia Medical School, Norfolk, VA, [8]Cleveland Clinic, Cleveland, OH, [9]University of Texas Health Science Center at San Antonio, San Antonio, TX

Distinguishing indolent from clinically significant localized prostate cancer and treatment of metastatic prostate cancer are two major clinical challenges in prostate cancer. The development of novel predictive biomarkers will help with risk stratification, and influence clinical decision-making between treatment and active surveillance, leading to a decrease in over or under-treatment of patients with prostate cancer. Here, we report that Trop2, an oncogenic transmembrane surface protein, is a prognostic tissue biomarker for clinically significant prostate cancer by utilizing the Canary Prostate Cancer Tissue Microarray (CPCTA) cohort composed of over 1100 patients from a multi-institutional study. We demonstrate that higher Trop2 expression is correlated with worse clinical features and elevated Trop2 expression at radical prostatectomy predicts worse overall survival in men undergoing radical prostatectomy. Additionally, we detected shed Trop2 in urine from men with clinically significant prostate cancer. We further define the functional role of shed Trop2 on metastasis in prostate cancer and identify that shed Trop2 increases cell migration, invasion, metastatic colonization, and spontaneous metastasis *in vitro* and *in vivo*. Proteomic profiling reveals that shed Trop2 modulates a set of proteins associated with invasion, migration, mTOR signaling, and epithelial-to-mesenchymal transition. shed Trop2 binds to EGFR and results in the activation of the EGFR-PI3K-AKT-mTOR pathway in prostate cancer. Our study reveals the new function of shed Trop2 in driving prostate cancer progression and identifies Trop2 as a novel tissue prognostic biomarker and a candidate non-invasive marker for prostate cancer that could be used to optimize treatment decision-making.

#6963 Cysteinyl leukotriene receptors promote melanoma progression and metastasis.

E. Sabu Kattuman, L. Reddy Teegala, S. Darzi, S. Paruchuri;
The University of Toledo, Toledo, OH

Background: Cysteinyl leukotrienes (cys-LTs; LTC_4, LTD_4, LTE_4) are pro-inflammatory mediators mainly produced by hematopoietic cells, which enhance inflammation through their receptors, $CysLT_1R$ and $CysLT_2R$. They play a pivotal role in the development of chronic asthma in humans. Recent association of inflammation with cancer has led to immense interest on the role of cysteinyl leukotrienes in cancer progression and metastasis. However, the exact molecular mechanisms regarding how these inflammatory mediators regulate the tumor proliferation and metastasis remain unexplored. A thorough investigation of these precise molecular mechanisms and identification of the specific receptor/s responsible can aid in understanding the therapeutic potential of these receptors in various cancers like melanoma. Since the inhibitors of these receptors are already FDA approved for the treatment of asthma, our goal is to repurpose these drugs to treat melanoma progression.
Objective: To determine the mechanistic aspects of how CysLTRs regulate melanoma tumor initiation, progression, and metastasis.
Methods: Protein expression by western blotting and ELISA, transcript expression by qPCR, viability, and proliferation by XTT and BrDU, migration using trans-well assay, tumor growth and metastasis were confirmed through *in vivo* experiments.
Results & Conclusion: B16F10 melanoma cells express high $CysLT_1R$ compared to $CysLT_2R$ and produce endogenous cys-LTs that function in an autocrine signaling pattern. Further, cys-LTs mediated the activation of several signaling proteins such as ERK, p38, AKT, and CREB that are important for melanoma survival and proliferation. Moreover, treatment with CysLTR antagonists significantly reduced melanoma cell proliferation, survival, and migration. Accordingly, we observed a significant reduction in the melanoma tumor volume *in vivo* in both *Cysltr1*$^{-/-}$ and *Cysltr2*$^{-/-}$ mice compared to the WT mice. Interestingly, angiogenesis was significantly reduced in *Cysltr2*$^{-/-}$ mice but not in *Cysltr1*$^{-/-}$. Therefore, we speculate that while both receptors play a crucial role in tumor proliferation *in vivo*, $CysLT_2R$ is the main driver of angiogenesis and metastasis. Therefore, targeting both these receptors using their specific antagonists can offer potential therapy for melanoma progression and metastasis.

#6964 Regulation of TGF-β signaling via a novel TβRIII sheddase.

B. M. Greulich[1], J. Pawlak[2], J. Post[2], E. Karas[2], G. Blobe[2];
[1]Mercer University, Macon, GA, [2]Duke University Medical Center, Durham, NC

In a normal cell, TGF-β signaling serves as a tumor suppressor by reducing proliferation and promoting apoptosis. Paradoxically, the function of TGF-β signaling reverses in a cancer cell and begins to promote oncogenic pathways such as proliferation, survival, evasion of the immune system, and epithelial to mesenchymal transition (EMT). This has made TGF-β signaling a very attractive therapeutic target for a wide variety of human carcinomas. As a result, many small molecule inhibitors of TGF-β signaling have been developed, but none have achieved FDA approval for use in human cancers due to the deleterious effects of inhibiting TGF-β responsiveness in normal cells. In effort to overcome this obstacle, we aim to restore the normal biological mechanisms that regulate TGF-β signaling. Specifically, the membrane bound co-receptor TβRIII can be proteolytically cleaved and shed from the membrane, resulting in an extracellular protein capable of binding and sequestering TGF-β ligand. This decoupling of ligand binding from the receptor allows TβRIII to suppress signaling. TβRIII shedding decreases TGF-β mediated oncogenic phenotypes such as migration and metastasis in multiple cancer types. However, this shedding is often lost in cancer. Therefore, restoration of TβRIII shedding could be a viable therapeutic approach for multiple cancer types. One potential mechanism for the loss of shedding is the negative regulation of the protease responsible for shedding (sheddase). However, the identity of the sheddase still remains unknown. Here, our goal is to identify the sheddase and uncover regulatory mechanisms that could be leveraged to restore TβRIII shedding in cancer. To achieve this goal, a library of protease CRISPR knockout viruses was screened to determine which proteases have an effect on shedding. The quantity of TβRIII shed into the cell culture media was measured via ELISA for each of these CRISPR knockout cell lines, and the candidates with the largest reduction of shedding were retained for further investigation. The list of candidates was further screened *in silico* via gene set enrichment analysis of human patient data against a TGF-β signaling gene set signature. Only the candidates demonstrating a negative correlation between sheddase candidate expression and TGF-β signaling activity were studied further. To further validate these candidate sheddases, knockdown and overexpression cell lines were created and characterized. Overexpression of the most promising candidate reduced TGF-β mediated phenotypes such as migration and invasion, while knockdown of this candidate increased the same phenotypes. Knockdown also increased expression of TGF-β and EMT markers. Importantly, these effects of sheddase knockdown were neutralized in the presence of the TGF-β inhibitor galunisertib or when the cells were rescued with exposure to purified soluble TβRIII, indicating the effects are mediated through TβRIII shedding.

#6965 Characterizing the proteome landscape of extracellular vesicles from prostate cancer cell lines by mass spectrometry.

M. L. Ludwig, A. Day, H. E. Bergom, Z. Sychev, A. Horrmann, J. Hwang, J. M. Drake;
University of Minnesota Medical School, Minneapolis, MN

Multiple subtypes of prostate cancer can emerge in advanced stages of disease, such as tumors that maintain androgen receptor features (AR+), those without AR but with neuroendocrine features (AR-/NE+), and those without AR or NE features (AR-/NE-). These latter subtypes are particularly aggressive and incredibly lethal. Extracellular vesicles (EVs) are small particles that are mediators of cell-cell communication and have been nominated as potential biomarkers of disease state. We hypothesized that the proteome of EVs contains information about their originating cell that can distinguish between prostate cancer subtypes. To address this, we isolated EVs from cell lines of differing subtypes – AR+ (LNCaP, LNCaP95, C4-2, 22RV1), AR-/NE+(NCI-H660, EF1, LASCPC-01), and AR-/NE- (PC3, DU145) – and prepared the EV proteome for quantitative, label-free mass spectrometry analysis. This identified 2,000+ proteins in the EVs for each cell line where EVs from similar subtypes clustered together. Interestingly, we also found that EVs contained enough protein information to utilize developed gene signatures for AR or NE activity. EVs isolated from AR-/NE+ cells contained known NE signature proteins such as SYP, CHGA, and UCHL1. EVs from the AR+ cell lines displayed >50% AR activity driven by PSA and STEAP1 proteins in addition to other significant distinguishing protein markers. This supports the potential for using the proteome of tumor-derived EVs to identify novel signature molecular markers besides those already known to the field for developing liquid-based biomarker assays. In addition, our work characterizes the EV surfaceome which is critical for enriching signals from tumor-derived EVs feasible for clinical diagnostics assay development. While PSMA has been a reliable marker for cells reliant on AR signaling, less is known about protein markers in the AR- subset. Our work highlights TROP2 as especially enriched in the EVs from AR-/NE- cell lines, supporting its relevance as a target in patients without treatment options. To evaluate disease outcomes, further clinical studies are needed to develop specific and sensitive tests based on the EV proteome derived from advanced prostate cancer patients.

#6966 STAT3 integration of inflammatory signals and cellular stress promote tumor initiation and progression through the expression of integrin β3.

A. D. Campos, R. Shepard, I. Heumann, J. Lam, S. M. Weis, D. Cheresh;
UCSD Moores Cancer Center and Sanford Consortium for Regenerative Medicine, San Diego, CA

STAT3 represents an oncogene whose transcriptional regulation is known to drive tumor initiation, progression, and drug resistance. Although STAT3 can regulate many genes, it remains unclear which genes are critical for STAT3-mediated cancer progression. Here, we report that inflammatory cytokines and cellular stress induce STAT3 activation leading to tumor initiation and progression, which we show depends on its ability to drive transcription of the β3 integrin gene leading to αvβ3 expression. Specifically, CRISPR KO of either STAT3 or integrin β3 in pancreatic cancer cells, is sufficient to impede their tumor initiating capacity in mice, while ectopic STAT3 or β3 expression in STAT3 KO cells rescues their tumor initiation capacity. Mechanistically, STAT3 activation induces β3 expression based on its ability to engage enhancer regions that modulate β3 gene expression. These findings implicate integrin αvβ3 as a critical downstream effector of STAT3, thereby contributing to its role as a driver of tumor initiation and progression.

#6967 Role of CXCL7 in colon cancer cell proliferation.

H. Aldhowayan, J. F. Nipa, L. Jun, I. Odeniyi, P. L. Jones, R. Jeganathan, E. A. Lipke, M. W. Greene;
Auburn University, Auburn, AL

Chemokine (C-X-C motif) ligand 7 (CXCL7) - a protein product of the *pro platelet basic protein* (*PPBP*) gene - is a potential biomarker for colorectal cancer (CRC) diagnosis. However, its role in CRC progression is not known. Hence, we examined the role of CXCL7 in colon cancer cell proliferation through enhanced aerobic glycolysis. We first examined the effect of CXCL7 on cellular proliferation and glycolytic flux using human colon cancer (HT-29) cells transfected with CXCL7 or an empty vector as a control. Stable CXCL7- and vector-expressing cells were selected using hygromycin B. In addition, we treated HT-29 cells with CXCL7 obtained from the conditioned media (CM) from CXCL7-transfected HEK-293T cells or CM from vector-transfected (control) cells. CXCL7 expression was confirmed by analyzing *PPBP* expression using RT-qPCR, and CXCL7 level in the conditioned media was quantified by ELISA. The specificity of CXCL7 actions were examined using a CXCL7 neutralizing antibody (R&D Systems) and an antagonist (SB225002) to C-X-C motif chemokine receptor 2 (CXCR2). Cancer cell proliferation was assessed by measuring DNA synthesis (EdU incorporation). Glycolytic flux was monitored by measuring glucose uptake using a fluorescent derivative of 2-deoxyglucose (2-NBDG), Seahorse glycolysis stress test analysis, lactate accumulation in the cultured cell's media, and Western blotting for glycolytic enzyme protein expression. To further investigate CXCL7-mediated proliferation, we examined EdU incorporation and colony size in 3D engineered tissues and tumor xenograft growth in nude mice injected with CXCL7- and vector-expressing HT29 cells. The proliferation rate in CXCL7-expressing HT-29 cells and HT-29 cells treated with the CXCL7-CM were significantly higher (1.2-fold and 1.8-fold, respectively) compared to controls ($p<0.01$). Consistently, the proliferation rate in CXCL7-expressing HT-29 3D engineered tissues was significantly enhanced compared to vector-expressing tissues ($p<0.05$). Importantly, blocking the CXCL7/CXCR2 axis using a CXCL7 neutralizing antibody and a CXCR2 inhibitor abrogated CXCL7-stimulated proliferation. Lactate levels were two-fold higher in the culture media from both CXCL7-expressing HT-29 cells and HT-29 cells treated with CXCL7-CM compared to the controls ($p<0.05$). Glucose uptake was also greater in CXCL7-overexpressing cells and CXCL7-CM treated cells compared to vector controls. Data from Seahorse assay and Western blots confirmed that CXCL7-expressing HT-29 cells and HT-29 cells treated with CXCL7-CM have higher glycolytic capacity and increased glycolytic enzymes' protein expression compared to the controls, respectively. In *vivo*, CXCL7-expressing HT-29 xenograft tumor weight and PCNA protein levels were 100% and 60% greater, respectively, than vector-expressing tumors ($p<0.05$). Our study for the first time showed that CXCL7 stimulates colon cancer cell proliferation and enhances aerobic glycolysis.

#6968 Extracellular vesicles as carriers of signaling factors in cancer.

A. Schubert[1], N. Winkler[1], A. Mongkolsittisilp[2], M. Schulz[3], O. Voloshanenko[1], M. Schaffrinski[3], D. Kranz[1], K. Nienhaus[2], D. Jager[4], L. Trumper[3], J. Buntzel[3], C. Binder[3], G. Nienhaus[2], M. Boutros[1];

[1]DKFZ German Cancer Research Center, Heidelberg, Germany, [2]Karlsruhe Institute of Technology, Karlsruhe, Germany, [3]University Medical Center Gottingen, Gottingen, Germany, [4]National Center for Tumor Diseases (NCT), Heidelberg, Germany

Extracellular vesicles (EVs) are small, membrane-bound structures released by cells. They contain various biomolecules and have emerged as mediators of cellular signaling. EVs of various origins can be isolated from body fluids and hold potential as novel biomarkers. However, their clinical implementation as biomarkers is hampered by complex isolation procedures, limited expertise in routine labs, and a lack of mechanistic understanding of signal transfer, particularly *in vivo*.

To better understand how EVs carry oncogenic signaling factors, we performed mechanistic investigations into the role of EVs in WNT signaling as a representative cancer-associated signaling pathway, as well as *ex vivo* validation experiments analyzing patient-derived EVs.

Hydrophobic WNT ligands can use EVs to travel the extracellular space. However, little is known about the quantities of WNT secretion onto different EV fractions and potentially other vehicles. To explore WNT secretory routes and potential functional differences, we generated fluorescently tagged marker constructs of the non-canonical ligand WNT5a, which has context-dependent tumor-suppressing or -promoting functions in cancer. In additional *in vitro* experiments, we tested how the WNT signaling activation state and cancer-specific WNT mutations, such as CRISPR/Cas9-induced APC truncations, quantitatively and qualitatively affect EV shedding in colorectal cancer cell lines. Further functional testing of EV-bound vs. non-EV WNT ligands is ongoing.

For proof-of-concept analyses and to test EVs as biomarkers, we set up the liquid biopsy study *EValuate*. The project aims for cross-entity analysis of EV profiles and correlation of results to cancer presence, stage, and survival. For quality control and before pipeline implementation, we tested various EV isolation methods and compared different sample pre-processing steps.

By combining multidisciplinary expertise in biophysics, molecular biology, and basic and clinical cancer research, we aim to gain a better mechanistic understanding of EV-mediated signal transfer and facilitate the integration of EVs as diagnostic and prognostic biomarkers into clinical studies.

#6969 Determining the role of obesity in breast cancer progression.

A. Perlman, A. Piekny, E. Kuzmin, S. Santosa;
Concordia University, Montreal, QC, Canada

Breast cancer, especially triple negative breast cancer, impacts a large proportion of the female population. Approximately ten to fifteen percent of all breast cancer diagnoses will be triple negative. Triple negative breast cancer lacks receptors that are used as therapeutic targets for other forms of breast cancer and has the poorest prognosis. Notably, the age of onset has also decreased, which correlates with the rise in prevalence of obesity. In addition, past studies revealed that maintaining a high BMI from childhood correlates with higher cancer mortality in adulthood. However, the mechanisms by which obesity contributes to cancer progression are not clear. Adipose tissue from different locations (visceral vs. subcutaneous, abdominal vs. femoral) and from patients with obesity from childhood rather than as adults could have different molecular characteristics. Further, depending on the genetic background, different profiles may be more susceptible to environmental cues that could drive their progression. To address this, we are using conditioned media collected from tissues that reflect these differences and determining how they affect TNBC cell lines with distinct genetic profiles. Preliminary data revealed that adipose tissue from both the abdominal and femoral regions of high BMI individuals caused an increase in the proliferation rate of TNBC cell lines. To determine if the adipocytes vs. other cell types in the adipose tissue drive this growth, we are co-culturing mature adipocytes from these tissues with the TNBC cell lines. Recent studies by other groups showed that adipocyte-derived extracellular vesicles could drive the expression of EMT genes in cancer cells. We will purify EVs from the adipocytes and characterize differences in their molecular signatures for different patients to determine which factors cause the change in TNBC progression and correlate this with different fat depots and/or age of onset. We will also measure the effect of adipose tissue and/or adipocytes on other cancer hallmarks including metastasis (migration and invasion) and changes in metabolism. These studies should reveal how adipocytes confer changes in TNBC progression, and how to consider obesity in different treatment regimes.

#6970 identification of spatially enriched cancer cell- and immune cell-regulatory multi-marker-defined prognostic cancer associated fibroblast subsets of human colon cancer.

L. Huang[1], M. Herrera[1], J. Sjolund[2], V. Chocoloff[1], S. Joost[1], R. M. Tabiev[1], L. W. Leiss[1], C. Strell[3], L. Nunes[3], A. Mezheyeuski[3], D. Edler[1], A. Martling[1], F. Ponten[3], B. Glimelius[3], T. Sjoblom[3], M. Kasper[1], K. Pietras[2], A. Ostman[1];

[1]Karolinska Institutet, Stockholm, Sweden, [2]Lund University, Lund, Sweden, [3]Uppsala University, Uppsala, Sweden

Introduction: Subsets of cancer-associated fibroblasts (CAFs) in colorectal cancer remain poorly characterized preventing their use as biomarkers and drug targets.

Results: Integrated scRNA seq profiling and multiplex staining identified four human CAF subsets These were A1 (PDGFRA+/FAP-/TF), PDGFRA^{high}A2 (PDGFRA+/FAP+/TF-), PDGFRA^{low}A2 (PDGFRA-/FAP+/TF-) and A3 (PDGFRA+/FAP-/TF+) (TF: Tissue Factor).Spatial analyses identified spatial associations indicative of specific functional interactions of fibroblast subsets with cancer cells or immune cells. Explorative analyses in six CRC cases suggested, in general, favorable effects of FAP-negative subsets (A1 and A3) on immune features and cancer cell proliferation, whereas FAP-positive subsets PDGFRA^{high}A2 and PDGFRA^{low}A2 overall showed pro-tumoral associations. To extend findings, niches were quantitated in U-CAN cohort of approximately 200 stage I-IV cases with around 80% stage II/III. Spatial screening generated more than 1600 different multi-marker-defined tissue metrics. Analyses identified a higher average of A1 density in areas surrounding proliferating vs non-proliferating T-cells, and a higher average PDGFRA^{low}A2 peri-T-cell density in the low proliferating T-cell group. Regarding cancer cell proliferation, high proliferating cancer islands showed lower peri-epithelial density of A3 and PDGFRA^{low}A2 cells as compared to low proliferating cancer islands. As for T-cell cancer island infiltration, high peri-cancer island density of A1 and PDGFRA^{high}A2 was associated with high T-cell cancer island infiltration. Additional analyses related CAF metrics to stage and survival. Density of PDGFRA^{low} A2 cells increased with stage (I-III), whereas density of A1 showed an opposite pattern with an inverse association with stage (I-III). Regarding survival associations, these were in general stronger for metrics collected in peripheral regions of tumors. Among prognosis signals related to niches referred to above, it was noted that A1 density in peri-cancer regions was significantly associated with good prognosis. Interestingly, this association was not detected when A1 density was scored in total stroma. Among all metrics, the strongest metrics were A1 density in 20µm A1 expansion areas (good prognosis) and T-reg density in the 10µm A3 expansion areas (bad prognosis) ($P<0.001$; univariate Cox-regression); both in peripheral regions.

Conclusion: Four novel CRC CAF subsets, defined by PDGFRalpha, FAP and TF, was identified by integrated single cell RNA seq analyses and multiplex staining with associated digital image analyses. Non-random spatial distribution of these subsets and compartment-specific prognosis associations are compatible with distinct and different functions of these subsets.

#6971 The impact of lecithin retinol acyltransferase in squamous cell carcinoma: Tissue formation, cell mechanics, and gene transcription.

E. Peterson[1], K.-C. Feng[2], J. Gao[3], M. Rafailovich[2], M. Simon[3];

[1]Renaissance School of Medicine, Stony Brook University, Stony Brook, NY, [2]Department of Materials Science and Chemical Engineering, Stony Brook University, Stony Brook, NY, [3]Department of Oral Biology and Pathology, Stony Brook University, Stony Brook, NY

Squamous cell carcinoma, along with several other cancers, has been found to lack expression of lecithin retinol acyltransferase (LRAT), a protein which catalyzes retinol esterification and thereby mediates retinoic acid biosynthesis. When expression of LRAT was reintroduced in squamous cell carcinoma, the protein promoted cell differentiation in addition to retinoid status normalization—whether this effect was dependent on the known enzymatic activity of LRAT in retinol esterification, versus another function, has not yet been established. Cell elasticity differences have also been reported between squamous cell carcinoma and normal keratinocytes. In this study, the role of LRAT expression and activity was evaluated in human squamous cell carcinoma cell line SCC13. LRAT was integrated into the genome of SCC13 via retroviral transduction, both as wild-type LRAT and LRAT with a cysteine-to-serine mutation at the active site for retinol esterification (C161-S). In these transformed cell lines, LRAT promoted formation of a cohesive sheet of tissue which remained intact after its removal from the tissue culture plastic surface, as evaluated at two weeks post-confluence. SCC13 alone produced tissue which easily fragmented during this scraping assay. In an evaluation of cell elasticity with shear modulation force microscopy, relative cell modulus measurements of pre-confluent SCC13 with LRAT expression were found to be significantly greater and consistent with the cell modulus of human keratinocytes (DO33). These effects persisted with mutation of the retinol esterification active site, suggesting that LRAT possesses an additional function which has yet to be described. Variation in transcription levels of multiple genes—urokinase-type plasminogen activator, plasminogen activator inhibitor 1, tissue inhibitor of metalloproteinases 1, and kallikrein 5—was also found based on LRAT expression and level of confluence. These findings suggest that the presence of LRAT influences tissue formation, cell elasticity, and gene transcription in SCC13.

#6972 Programmed death-ligand 1 (PD-L1) upregulates c-MET phosphorylation via protein tyrosine phosphatase and contributes to the development of *MET* amplification in epidermal growth factor receptor (EGFR) mutant non-small cell lung cancer.

Derek De-Rui Huang[1], Chia-Chi Hsu[2], Wei-Hsun Hsu[3], Bin-Chi Liao[1], James Chih-Hsin Yang[1]

[1]Department of Medical Oncology, National Taiwan University Cancer Center (NTUCC), Taipei City, Taiwan, [2]Department of Medical Education and Research, National Taiwan University Cancer Center (NTUCC), Taipei City, Taiwan, [3]Department of Oncology, National Taiwan University Hospital, Taipei City, Taiwan

High expression of programmed death-ligand 1(PD-L1) is associated with poor survival outcomes in epidermal growth factor receptor (EGFR) mutation non-small cell lung cancer (NSCLC) patients receiving EGFR tyrosine kinase inhibitors (EGFR-TKIs). In this study we aimed to determine how increased PD-L1 affects the signal transduction of EGFR-mutant NSCLC cells. We first established PD-L1 overexpression EGFR mutant NSCLC cells, and discovered that PD-L1 overexpression cells had upregulated c-MET phosphorylation compared with parental cells using receptor tyrosine kinase array study. Subsequently, we demonstrated that knocking out PD-L1 (CD 274) in EGFR mutant NSCLC cells resulted in down-regulation of c-MET phosphorylation. Since protein tyrosine phosphatases (PTP) are known key regulators for c-MET phosphorylation and dephosphorylation, the activity of PTP was assessed. In PD-L1 overexpression EGFR mutant NSCLC cells, the PTP activity was decreased, whereas in PD-L1 knock-out cells, the PTP activity was increased. Additionally, the downregulation of c-MET phosphorylation in PD-L1 knock-out cells could be restored by adding PTP inhibitor (Na_3VO_4). The gene expression analysis showed that PTP expression was down-regulated in PD-L1 overexpression cells, indicating that PD-L1 upregulates c-MET phosphorylation by reducing PTP expression. We further established xenograft animal models using NSCLC cells with strong baseline c-MET phosphorylation to determine the effect of c-MET phosphorylation on osimertinib (a 3rd-generation EGFR-TKI) treatment. We found that tumor cells with strong c-MET phosphorylation were prone to develop MET amplification as acquired resistance under osimertinib, which could be overcome with combination of osimertinib and tepotinib, a c-MET inhibitor. Taken together, our results expand our understanding of PD-L1's role beyond an immune checkpoint in EGFR mutant NSCLC. PD-L1-regulated *MET* alterations could be a crucial mechanism leading to poor treatment outcome of EGFR-TKIs in PD-L1 overexpression EGFR mutant NSCLC.

#6973 Investigates the role of exosomes in dasatinib treated HT29 colon cancer cells.

Hui Min Koo, Yi-Wen Lu, Xiang-Ling Hou, Wei-Ting Chao

Tunghai University, Taichung City, Taiwan

The mortality rate due to metastasis in cancer is as high as 90%. The underlying mechanisms have been studied, however, the process of metastasis is complicated, current therapies still cannot inhibit metastasis efficiently. In recent years, studies have mentioned that extracellular vesicles play an important role in cancer cell metastasis and tumor microenvironment. Extracellular vesicles can be divided into microvesicles, apoptotic bodies and exosomes, which can carry different substances into the tumor microenvironment. Especially exosomes, whose diameter is around 30-160nm, can carry DNA, RNA, miRNA, membrane proteins, lipids and other intracellular molecules into the cell through endocytosis for regulation. The process of metastasis and the drug resistance were also been demonstrated can be regulated by exosomes. At present, the physiological functions of exosomes are not clear. HT29 colon cancer cells previously discovered in our laboratory can have different responses to dasatinib treatment, and cells can be isolated to dasatinib selected cells(DSTS) and resistant cells(DSTR). In this study, the role of exosome upon dasatinib treatment in HT29 cell is investigated. In the experiment, exosomes from HT29, DSTS, and DSTR were isolated by ExoQuick-TC. Transmission electron microscope was used to observe the difference in exosome size. Exosomes from different cells were treated in HT29 cells, and differences at the protein and mRNA levels were observed using western blot and reverse transcription-polymerase chain reaction(RT-PCR). In my results, the diameter of exosomes in DSTS cells was smaller than that in DSTR and HT29 cells. The protein expression levels of Cavoelin-1 and Clathrin in HT29 were also increased in the treatment of exosome that from three types of cells. In addition, the DSTR derived-exosomes can induce the expression of pFAK and Clathrin mRNA in HT29 cells. The preliminary results suggest that DSTR derived-exosomes may affect cell migration. This study provides the clues that through understanding exosomes that secreted from different cells, cancer diagnosis and treatment can be conducted according to their characteristics, so as to reduce the possibility of cell metastasis precisely.

#6974 Spatial exosome analysis reveals the location heterogeneity of exosomal miRNAs in ovarian cancer patients.

A. Yokoi[1], K. Yoshida[1], Y. Yamamoto[2], T. Yasui[3], H. Kajiyama[1];

[1]Nagoya Univ. Graduate School of Medicine, Nagoya, Japan, [2]National Cancer Center Research Institute, Tokyo, Japan, [3]Tokyo Institute of Technology, Tokyo, Japan

Extracellular vesicles (EVs), including exosomes, are recognized as promising functional tools involved in cancer progression. Although evidence of the functions of EV in cancer biology has been accumulating, optimizing EV isolation is still a major challenge. In ovarian cancer, peritoneal dissemination is a crucial prognostic factor due to the lack of effective treatment, and EVs in malignant ascites play a key role for progression. In this study, we invented cellulose nanofiber (CNF) sheets which enable to capture EVs from approximately 10 μL of biofluids and enabled the analysis of the bioactive molecules included in the EVs (*Nature Communications* 2023). By attaching CNF sheets to moistened organs, the EVs in trace amounts of ascites were collected, which was sufficient to perform small RNA sequence analyses. In the ovarian cancer mouse model, CNF sheets enabled the detection of cancer-associated miRNAs from the very early phase when the mice did not have apparent ascites, and the EVs from different locations, such as pelvic walls or liver surfaces, had unique miRNA profiles. To confirm the utility of the CNF sheets in cancer patients, we directly collected the EVs on the organ surfaces by the EV attachment method during surgery under appropriate ethical institutional approval with individual consent. EVs were collected from the pelvic peritoneum, omentum, liver surface, or tumor surface, and the miRNA profiling demonstrated each location formed unique clusters. Notably, several tumor-suppressive miRNAs have been identified in liver surface EVs, such as miR-122-3p, and this is consistent with actual ovarian cancer cell progression, which tends to metastasize to the diaphragm rather than to the liver surface. In addition, the trajectory analysis revealed that the pattern of connection in each site was different between patients with localized and advanced disease. We identified ten miRNAs were high in tumors and in EVs from tumor rupture sites, and the level of each miRNA decreased with distance from the primary tumors. Among ten miRNAs, hsa-miR-200b-3p and hsa-miR-429 were confirmed as highly expressed in tumor tissues compared to adjacent normal tissues or benign tumors, and three miRNAs in serum, urine and saliva decreased post-surgery. In summary, spatial CNF sheet analyses in patient bodies identified location-based heterogeneity in EV-miRNA profiles, and the profiles reflected disease conditions. This new method could provide unveiled biological aspects of EVs, and suggest a clinical strategy contributing to cancer diagnosis, staging evaluation, and therapy planning.

MOLECULAR/CELLULAR BIOLOGY AND GENETICS: Elucidating Mechanisms of Oncogenic Action
Poster Session

#1457 Decoding the molecular mechanisms related to mutations in the GNAQ/11 and BAP1 genes in ocular melanoma.

Aurelie Fuentes-Rodriguez[1], Andrew Mitchell[2], Joel Rousseau[3], Jacques P. Tremblay[4], Solange Landreville[1]

[1]Department of Ophthalmology, Faculty of Medicine, Universite Laval, Quebec, QC, Canada,[2]Regenerative Medicine Axis, CHU de Quebec, Universite Laval, Quebec, QC, Canada,[3]Department of Molecular Medicine, Faculty of Medicine, Universite Laval, Quebec, QC, Canada,[4]Neuroscience Axis, CHU de Quebec, Universite Laval, Quebec, QC, Canada

Uveal melanoma (UM) is the most frequent intraocular cancer in adults and 50% of patients develop liver metastases for which no treatment is effective. According to *The Cancer Genome Atlas*, 92% of cases are characterized by early mutations in two genes coding for alpha subunits of G protein coupled receptors (GPCR): *G protein subunit alpha q* (*GNAQ*) or *11* (*GNA11*). These mutations are mostly found in the codon Q209 causing a constitutive activation of different signaling pathways linked to cellular proliferation such as MAPK and PKC. Furthermore, a bi-allelic inactivation of the *BRCA1 associated protein-1* (*BAP1*) is found in 83% of metastatic UM and causes a loss of function of this protein. Our hypothesis is that the inactivation of compensatory pathways in the absence of these proteins and the understanding of pathways essential only to mutated cells will pave the way for the identification of better therapeutic candidates specific to UM cancer cells (UMCCs) to prevent metastatic progression and improve treatment options. The research objectives include the identification of compensatory signaling pathways in the absence of *GNAQ/11* and *BAP1* using classical CRISPR/Cas9, the discovery of essential molecular mechanisms for the survival of mutated UMCCs using Prime Editing, and the identification and characterization of novel therapeutic targets using 3D *in vitro* and *in vivo* models. First, the electroporation optimization using an eGFP plasmid demonstrated an efficiency of 40-50% for normal choroidal melanocytes (NCM) and 60-80% for UMCCs Mel285. Subsequent transfection with CRISPR complexes resulted in an average editing efficiency of approximately 20% for *GNAQ/11* and 60% for *BAP1*. Currently, we have successfully established a *GNAQ* knockout (*GNAQ*-KO) Mel285 cell line. The characterization and validation of this cell line were performed through sequencing and Western blotting, confirming the creation of stop codons and the absence of *GNAQ* expression. We observed an overactivation of the ERK1/2 pathway and an upregulation of beta-catenin in the Mel285 *GNAQ*-KO line. Additionally, we noted a decrease in proliferation, adhesion, and migration on collagen I. For Prime editing, we constructed three plasmids with desired mutations. Preliminary tests in HEK293T cells showed an insertion efficiency of 4%, 20%, and 10% for *GNAQ*, *GNA11*, and *BAP1*, respectively, following a single treatment. Finally, *in vitro* testing has been started for inhibitors targeting compensatory pathways involving beta-catenin (WIKI4) and ERK1/2 (ASN007), in combination with the *GNAQ/11* inhibitor (FR900359). These tests are being conducted on various mutant UMCCs for *GNAQ/11*.A better understanding of the altered pathways in our *GNAQ/11* or *BAP1* mutant isogenic cell lines will help to identify new drugs targeting specifically UM cells.

#3020 The tumor suppressive role of methylthioadenosine phosphorylase in melanoma.

J. J. Hsiao[1], P. Andreu-Perez[1], L. V. Kemeny[2], M. Hejna[3], J. Nsengimana[4], J. Allouche[5], A. Al Emran[1], D. Bishop[6], G. B. Jonsson[7], J. Newton-Bishop[6], J. Song[3], D. E. Fisher[1];

[1]Harvard Medical School/Massachusetts General Hospital, Charlestown, MA, [2]Semmelweis University, Budapest, Hungary, [3]University of Illinois, Urbana, IL, [4]Newcastle University, Newcastle upon Tyne, United Kingdom, [5]INSERM U861, I-Stem, Association Francaise contre les Myopathies, Institute for Stem cell Therapy and Exploration of Monogenic diseases, Corbeil-Essonnes, France, [6]Institute of Medical Research, University of Leeds School of Medicine, Leeds, United Kingdom, [7]Lund University, Lund, Sweden

Methylthioadenosine phosphorylase (MTAP) is an enzyme that is expressed in virtually all tissues but lost in many cancers. MTAP deficiency can be due to either deletion of the MTAP gene or methylation of the MTAP promoter. In normal cells, MTAP catalyzes the conversion of methylthioadenosine (MTA), produced during polyamine biosynthesis, to adenine and 5-methylthioribose-1-phosphate, which is subsequently converted to methionine. MTAP deficiency results in intracellular accumulation of MTA. Although recent genome wide association studies (GWAS) have associated the MTAP locus with melanoma risk, the molecular mechanisms linking MTAP loss to increased tumorigenesis are not yet fully understood. In this study, we hypothesized that loss of MTAP and the resulting accumulation of MTA would dysregulate microphthalmia transcription factor (MITF), a master transcriptional regulator of melanocytes that is also an amplified or mutated oncogene in melanoma. We identify a novel signaling mechanism in which MTA accumulation from MTAP deficiency aberrantly induces MITF expression via inhibition of the cAMP phosphodiesterase PDE4D3 in melanocytes. Inhibition of PKA abolishes this MITF induction, suggesting that the PKA pathway is hyperactivated upon MTAP deficiency. Downregulation of MTAP leads to increased proliferation of melanoma cells *in vitro* and increased melanoma tumor growth *in vivo*. We also show that MTAP deficient melanoma cells are more resistant to the BRAF inhibitor vemurafenib and observe MTAP downregulation in BRAF inhibitor resistant melanoma clinical specimens. Furthermore, MTAP downregulation via decreased expression and/or genomic loss corresponds to significantly worse outcomes in early-stage cutaneous melanomas from multiple datasets, thereby identifying a clinically important sub-category of “thin-lethal” tumors.

#6977 ETV6 is an unexplored partner of the Chr.8 q24.3 amplicon-embedded immortalizing oncogene TONSL in tumorigenesis.

A. S. Khatpe, E. Doud, A. Mosely, K. D. Miller, H. Nakshatri;
Indiana University School of Medicine, Indianapolis, IN

Approximately 20% of breast cancers exhibit recurring genomic amplification involving chromosome 8q24.3. In our previous study, we identified the Tonsoku-like DNA repair protein (TONSL) within this amplicon as an immortalizing oncogene of breast epithelial cells, that can promote Estrogen Receptor-positive (ER+) breast adenocarcinomas when combined with other breast cancer-associated oncogenes. Our findings indicated that TONSL-amplified breast cancer cells are dependent on TONSL for tumor growth and exhibited deregulated homologous recombination and cell cycle pathways. High levels of TONSL in primary breast cancers, particularly ER+ breast cancers, were associated with poor outcomes. Although TONSL itself is not druggable, owing to its lack of enzymatic activity, molecules that disrupt the TONSL interactome can be developed. Towards this goal, we performed immunoprecipitation (IP) with TONSL antibody using protein lysates from TONSL-immortalized primary breast epithelial cells and subjected the immunoprecipitates to mass spectrometry. We identified several proteins selectively enriched with the TONSL antibody, the most significant of which was ETS variant transcription factor 6 (ETV6). ETV6 is a modular protein consisting of a C-terminal DNA-binding ETS domain and N-terminal point (PNT) domain and is known to play a role as a transcriptional repressor during embryonic development and hematopoiesis. We confirmed these data by IP followed by western blot analysis of primary breast epithelial cells and TONSL amplified MDA-MB-436. Furthermore, we utilized ClusPro to model the TONSL-ETV6 interaction and predicted that the TONSL's ankyrin repeats docks onto ETV6's PNT in a favorable manner. To investigate the functional significance of this interaction, we evaluated ETV6-regulated genes using RNA-seq. Our analysis revealed that ETV6-regulated genes were downregulated following TONSL knockdown and vice versa. Most ETV6 target genes affected upon TONSL manipulation are involved in Epithelial-Mesenchymal Transition (EMT), particularly TWIST1, SNAI2 and ZEB1. Previous studies have demonstrated a role of ETV6 in limiting EMT by repressing the expression of EMT-associated transcription factors. Our findings revealed that TONSL overexpression in primary breast epithelial cells led to a significant increase in these EMT gene expression, whereas TONSL knockdown in MDA-MB-436 cells resulted in a moderate decrease. These findings suggest that TONSL binds to ETV6 and restricts its ability to bind to the regulatory regions of EMT-associated genes, leading to a transcriptional surge of EMT-associated genes leading to tumor progression. Further studies will contribute to our understanding of the role of the chr.8q24.3 amplicon, specifically the TONSL gene, in initiating/promoting breast tumorigenesis and the development of novel drugs that target the TONSL interactome.

#6979 Uncovering the BRAF interactome to identify novel therapeutic targets for BRAF driven melanoma and lung cancer.

K. T. OToole;
Huntsman Cancer Institute, Salt Lake City, UT

BRAF protein kinases act downstream of RAS-GTP and upstream of MEK>ERK MAP Kinase signaling. Notably, mutational activation of BRAF is a driver of approximately 8% of all cancers, with a particular prevalence in lung cancer, thyroid cancer, and melanoma. Importantly, melanoma is responsible for the largest number of skin cancer deaths per year. Patients whose melanoma is driven by mutationally-activated BRAF account for ~50% of cutaneous melanoma cases. The most common mutational alteration is *BRAF*^{T1799A}, which encodes the BRAF^{V600E} oncoprotein kinase. Combined inhibition of BRAF^{V600E} plus MEK1/2 has been approved for the treatment of BRAF^{V600E}-driven melanoma and lung cancer. Although patients with mutationally-activated BRAF often have a significant response to BRAF^{V600E}-targeted therapeutics, many patients develop lethal drug-resistant disease. The BRAF^{V600E} oncoprotein kinase is proposed to be a monomer, yet many questions remain regarding the biochemistry of these signaling interactions. Thus, we aim to better understand the molecular mechanisms driving BRAF^{V600E}-mediated melanoma and lung cancer cell growth. Preliminary data using gel filtration chromatography and immunoblotting analysis indicates that BRAF^{V600E} is detected in a large multiprotein complex. Interestingly, the addition of a BRAF^{V600E} inhibitor, vemurafenib, shifted the elution of complexes with BRAF^{V600E} into lower molecular weight fractions. Based on these preliminary results, we characterized the components of these complexes to advance our understanding of how mutationally activated BRAF exists in melanoma cells; and thus, provide future insight into how we can better therapeutically target BRAF^{V600E}. Moreover, in order to further elucidate BRAF interactions, we employed a novel form of proximity labeling, TurboID, to unbiasedly identify novel BRAF interactors and better understand how drug treatments change the BRAF interactome. The top ten statistically significant interactors are being investigated to understand how BRAF complexes are formed within the cell, how the complexes are influenced by drug treatments, and how important the individual components are in the formation of complexes with BRAF. Here, we investigate an interaction between BRAF^{V600E} and the tumor suppressor, TP53. Moreover, elucidating the molecular architecture of BRAF^{V600E} signaling complexes could highlight new therapeutic options for patients who display either primary or acquired resistance to inhibitors of BRAF^{V600E} signaling.

#6980 GOLGA7 is essential for NRAS trafficking from the Golgi to the plasma membrane but not for its palmitoylation.

C. Liu[1], B. Jiao[1], P. Wang[1], B. Zhang[1], J. Gao[1], D. Li[1], X. Xie[1], Y. Yao[1], L. Yan[1], Z. Qin[2], P. Liu[1], **R. Ren**[1];

[1]Ruijin Hospital Affiliated to Shanghai Jiao Tong University School of Medicine, Shanghai, China, [2]Soochow University, Suzhou, China

RAS GTPases play a crucial role as oncogenic drivers in multiple cancer types. Targeting their localization to the plasma membrane (PM) is a promising strategy for cancer therapy, as RAS signaling requires PM localization. While KRAS traffics through a Golgi-independent route, palmitoylated RAS isoforms are transported to PM from the Golgi via a secretory pathway that is not yet fully understood. GOLGA7 is a Golgi-resident protein known as an accessory protein stabilizing the palmitoyltransferase ZDHHC9 for the palmitoylation of NRAS and HRAS. In this study, we found that among all four RAS isoforms, NRAS uniquely requires GOLGA7 for its association with the PM. Interestingly, the mislocalization of NRAS is achieved without detectable changes in its palmitoylation level in GOLGA7 deficient cells. We further observed that loss of GOLGA7 inhibit the anterograde trafficking of GFP-$NRAS^{G12D}$ proteins and result in the accumulation of NRAS in the cis compartment of the Golgi apparatus. Moreover, targeting GOLGA7 suppresses cell proliferation by downregulating RAS signaling in a variety of NRAS-mutant cancer cells. Finally, GOLGA7 depletion attenuated the oncogenic transformation induced by $NRAS^{G12D}$ in mice. These findings reveal a specific intracellular trafficking route mediated by GOLGA7 and have identified GOLGA7 as a potential therapeutic target for NRAS-driven cancers.

#6981 p38-mediated EZH2 phosphorylation at T367 regulates HER2 pathway in triple negative breast cancer.

M. E. Gonzalez, A. Eido, C. G. Kleer;
Rogel Cancer Center, Ann Arbor, MI

Background: Triple negative breast carcinomas (TNBC) are highly aggressive tumors with limited effective treatments. Clinical studies showed that targeting low HER2 levels in TNBC with anti-HER2 agents has survival benefit. Enhancer of Zeste Homolog 2 (EZH2) is a lysine methyltransferase component of the Polycomb Repressive Complex2 that regulates differentiation genes in normal and neoplastic cells. EZH2 phosphorylation at T416 was shown to maintain the TNBC phenotype. We have reported that p38-induced EZH2-T367 phosphorylation enhances metastasis and that high pEZH2-T367 expression is significantly associated with human TNBC tumors compared to other breast cancer subtypes. In this study we tested the hypothesis that pEZH2-T367 may regulate the HER2 pathway in TNBC and that inhibition of pEZH2-T367 may upregulate HER2 signaling, with clinical implications.

Methods: MDA-MB-231 (mesenchymal-like TNBC) and CCN6KO cells derived from MMTV-Cre;$Ccn6^{fl/fl}$ (CCN6KO) TNBC mouse model generated in our lab were transduced with vector or EZH2 shRNA knockdown (KD). MDA-MB-231 EZH2 KD cells were rescued with lentivirus containing EZH2-wild-type (WT) or T367A phosphorylation-deficient mutant. Gene and protein expression was analyzed by RNA sequencing, q-RT-PCR, immunoblot and immunohistochemistry. Vector and EZH2-KD rescue MDA-MB-231 cells were treated with anti-HER2 (trastuzumab or pertuzumab 100 ug/ml) followed by Hoestch proliferation assays. TNBC cells were treated with vehicle, EZH2 inhibitor (EPZ-6438, 20uM), p38 inhibitor (p38i, SB202190, 20uM), EPZ+p38i, anti-HER2 (100 ug/ml), and EPZ+p38i+anti-HER2, followed by Hoestch cell proliferation assays.

Results: EZH2-T367A deregulates the expression of a 94-gene network of HER2 pathway genes including EREG, SERPINB5, MERTK, IL6R, SOCS3, and FASCN1 compared to EZH2-WT. EZH2-T367A increased protein levels of HER2, EREG, and PP2AB, a major HER2 regulator and was sufficient to sensitize TNBC cells to the anti-proliferative effects of anti-HER2. Supporting the role of pEZH2-T367, we found that the combination of p38i and EPZ significantly sensitizes TNBC cells to anti-HER2 therapies.

Conclusions: We demonstrate that T367 phosphorylation mediates the effect of EZH2 on HER2 signaling in TNBC. Our data support a role for pEZH2-T367 in maintaining the HER2-negative phenotype in and suggest that blocking this phosphorylation event may render TNBC tumors amenable to anti-HER2 treatment strategies.

#6982 The roles of NDRG1 in HCC progression and its clinical significance.

J. Lu[1], L. Tian[1], Y.-M. Tsui[1], X. Wong[2], Q. Zhang[1], D.-H. Ho[1], I.-L. Ng[1];

[1]The University of Hong Kong, Pokfulam, Hong Kong, [2]China Medical University, Shenyang, China

Background: Hepatocellular carcinoma (HCC) is prevalent globally and the third leading cause of cancer-related mortality. N-myc downstream regulated 1 (NDRG1) was found to be tumor promoting in some cancers while suppressive in others. The expression of NDRG1 is induced by stress signals such as DNA damage and hypoxia. In HCC, it has been found to promote proliferation and metastasis. Contradictory results, however, were also suggested on the functions of NDRG1.

Methods: Our own HCC cohort and multiple publicly available databases were examined for NDRG1 expression and clinicopathologic correlation. NDRG1 expression under hypoxic conditions was investigated. Various functional assays were performed for NDRG1-knockdown HCC cell lines Huh-7 and PLC/PRF/5.

Results: With RT-qPCR analysis on our 102 pairs of patients' HCC tumor and corresponding non-tumorous liver samples, we found NDRG1 to be upregulated in HCC tumors. Similarly, RNA-sequencing analysis comparing 41 pairs of samples confirmed NDRG1 enrichment in HCC tumors. The upregulation was significantly and positively correlated with the absence of tumor encapsulation and cellular differentiation. These were further supported by TCGA and ICGC databases, in which upregulation of NDRG1 was significantly correlated with poor HCC patient overall survival. Interestingly, in the TCGA database, only 17% of the HCC cases were inferred to have copy number amplification of NDRG1 gene while NDRG1 mutations were rarely found. As hypoxia is a major tumor microenvironmental factor in HCC, we investigated NDRG1's expression level in HCC cells under hypoxic or normoxic conditions and found significant increase in NDRG1 expression under hypoxic environment. We further found that NDRG1 knockdown inhibited cell proliferation, self-renewal ability, and migration. RT-qPCR analysis found lower LGR5 and SOX2 expression upon NDRG1 knockdown. This is in line with the positive correlation between NDRG1 and various cancer stemness-related gene expression, including LGR5, CD24, MYC, SOX2, and NOTCH1, in TCGA database. Lastly, in the resected HCC tumors on which spatial transcriptomics using Visium 10X and single-cell RNA-sequencing using Chromium 10X were performed, we found NDRG1 enrichment in both tumors cells and cancer associated fibroblasts (CAFs).

Conclusion: NDRG1 was found to be significantly upregulated in HCC cells in our in-house cohort and publicly available databases. NDRG1 consistently promotes various oncogenic features of HCC cells, including proliferation, self-renewal ability, and migration. In addition, NDRG1 was found to be enriched in both the HCC cells and CAFs.

#6984 Investigating the function of the OSM-OSMR axis in pancreatic ductal adenocarcinoma (PDAC)..

Y. Sui, T. Hunter;
The Salk Institute For Biological Studies San Diego California, La Jolla, CA

Pancreatic ductal adenocarcinoma (PDAC) is one of the most lethal forms of cancer, characterized by a low survival rate and a significant global mortality impact. The interaction between PDAC and the immune system is complex and plays a crucial role in the progression of the disease. PDAC creates an immunosuppressive tumor microenvironment, which hampers the ability of immune cells to effectively infiltrate the tumor and mount an anti-cancer immune response. Additionally, there is an imbalance of cytokines, with an overabundance of immunosuppressive factors and a deficiency in pro-inflammatory cytokines. This hostile immunological landscape contributes to the aggressive nature of PDAC and hinders the success of immunotherapies and adjuvant treatments. One cytokine of particular interest is oncostatin M (OSM), a member of the interleukin-6 (IL-6) family. OSM has been implicated in the regulation of cancer and has been associated with poor overall survival in pancreatic cancer and other malignancies. Similar to other cytokines, OSM is secreted by immune cells and acts as a regulator of the inflammatory microenvironment surrounding the tumor. The levels of OSM in this milieu can potentially influence cancer development and regulation through multiple mechanisms. Despite the growing understanding of cytokines in cancer, research on the role of OSM in PDAC is still limited and requires further investigation to identify potential therapeutic targets. Therefore, there is a critical need to delve deeper into the functions of OSM and its receptor, oncostatin M receptor (OSMR), in the initiation and progression of pancreatic cancer. **As such, our goal is to examine the functions of OSM and its receptor (OSMR) in initiating and advancing pancreatic cancer to better comprehend the role of the OSM-OSMR axis in PDAC, both *in vivo* and *in vitro*.**

#6985 The oncogenic functions and action mechanism of UTP14A, a subunit required for 18S rRNA synthesis, in head and neck cancer.

L.-W. Wu[1], C.-N. Chang[1], P. K. Biswas[1], S.-T. Tsai[2];

[1]National Cheng Kung University, Tainan, Taiwan, [2]National Cheng Kung University Hospital, Tainan, Taiwan

Head and neck cancer (HNC) is the sixth common malignancy in the world and > 90% of HNC cases are squamous cell carcinoma in origin. Oral cancer is one major HNC subtype. Despite the recent advancements in cancer diagnostics and therapeutics, the 5-yr survival rate of advanced HNC patients remains <50%. Ribosomes are the cellular factories responsible for making proteins. The hyper-activation of ribosome biogenesis initiated by oncogene gain or tumor suppressor gene loss plays a critical role in cancer initiation and progression. Ribosome biogenesis is a complex and energy intensive process that involves hundreds of factors. UTP14A gene encodes a member of the uridine triphosphate 14 family and is an essential component of a large ribonucleoprotein complex bound to the U3 small nucleolar RNA. Previous studies have demonstrated that UTP14A plays a key role in the synthesis of ribosomes and 18S rRNA, and is overexpressed in several malignancies. However, the biological functions and underlying mechanisms of UTP14A in HNC remain elusive. We found not only the increase of UTP14A mRNA expression in TCGA-HNC database but also its negative impact on patient clinical outcome. UTP14A depletion significantly impaired HNC cell proliferation, migration and invasion in vitro. Ectopic overexpression had the opposite effect, suggesting an oncogenic role for UTP14A in HNC. Through gene set enrichment analysis of pairwise RNA sequencing results, several genes involved in the process of epithelial mesenchymal transition (EMT) were potentially associated with manipulated UTP14A expression. We also detected a concordant change of lipid droplet numbers and its surface marker expression in UTP14A-manipulated cells, respectively, by BODIPY staining and immunhistochemical staining. Western blot analysis validated a positive relationship of EMT markers and COX-2, a potential mediator of lipid metabolism and EMT, with altered UTP14A expression. The involvement of COX2 in UTP14A mediation was confirmed by using both pharmacological inhibition and genetic manipulation. We also identified p38 as a central downstream effector but acting upstream from COX-2 in UTP14A mediation in oral cancer cells. We believe that our study of UTP14A-mediated oncogenic signaling axis can potentially be harnessed as a novel therapeutic target against HNC although more mechanistic studies may be needed.

#6986 Oncogenic CARD11 enhances marginal zone B cell survival by potentiating the non-canonical NF-κB pathway.

A. Ghosh, J. Pomerantz;
Johns Hopkins University School of Medicine, Baltimore, MD

Dysregulation of antigen receptor-mediated signaling contributes to the oncogenesis of lymphoid malignancies. The activated B cell-like (ABC) subtype of Diffuse Large B cell Lymphoma (DLBCL) is characterized by receptor-independent constitutive activation of the canonical nuclear factor-kappaB (NF-κB) pathway, which is essential for the proliferation and survival of tumor cells. Caspase recruitment domain-containing protein 11 (CARD11) is a scaffolding protein that regulates B and T cell receptor signaling to canonical NF-κB activation downstream for adaptive immune response. Oncogenic gain-of-function (GOF) CARD11 mutations bypass normal pathway regulation and result in a hyperactive CARD11 that signals constitutively. Although present in ~10% of human ABC-DLBCL biopsies, we do not have a complete mechanistic understanding of how CARD11 GOF mutations drive abnormal B cell proliferation to cause lymphoma. We generated a mouse expressing the DLBCL-associated GOF mutation C49Y from the endogenous CARD11 locus. GOF CARD11 was sufficient to specifically drive B cell expansion in the mice with no significant effect on $CD4^{\pm}$ or $CD8^{\pm}$ T cells or NK cells. Quantification of splenic lymphocytes revealed that $CARD11^{C49Y/C49Y}$ mice had ~5-fold more splenic B cells when compared to $CARD11^{+/+}$ mice and ~13-fold more marginal zone (MZ) B cells. $CARD11^{C49Y/C49Y}$ MZ B cells proliferated and survived much better than $CARD11^{+/+}$ following stimulation with αIgM and importantly exhibited significant survivability prior to stimulation. Bulk mRNA sequencing revealed genes uniquely dysregulated in $CARD11^{C49Y/C49Y}$ MZ B cells including those associated with non-canonical NF-κB pathway signaling. $CARD11^{C49Y/C49Y}$ MZ B cells exhibited elevated levels of the p100 precursor NF-kB subunit leading to enhanced production of nuclear p52 following BAFF treatment. $CARD11^{C49Y/C49Y}$ MZ B cells also exhibited elevated levels of TRAF2, TRAF3 and cIAP1/2, components of a complex that degrades the NIK kinase that is responsible in normal cells for inducing p100 processing. Our results reveal an unexpected ability of CARD11 GOF mutants to potentiate the non-canonical NF-κB pathway through p100 accumulation, which likely contributes to the dysregulated B cell expansion observed in DLBCL cases that harbor CARD11 GOF variants.

#6988 TP53RK regulates DNA replication by CDC7-mediated MCM helicase phosphorylation in colorectal cancer.

Y. Choi[1], J.-w. Park[1], J.-k. Kang[1], E.-j. Kim[1], S.-H. Song[1], E. Yi[2], T.-Y. Kim[1];

[1]Cancer Research Institute, Seoul National University College of Medicine, Seoul, Korea, Republic of, [2]Graduate School of Convergence Science and Technology, Seoul National University, Seoul, Korea, Republic of

Background: We identify TP53 regulating kinase (TP53RK), which showed the highest cell growth inhibition efficiency in six colon cancer cell lines. TP53RK is overexpressed in various cancer types, including multiple myeloma and skin cancer, but the mechanism for its tumorigenesis in colon cancer is unknown. Therefore, this study aims to reveal the tumorigenesis mechanism of TP53RK, which is overexpressed in Colorectal Cancer (CRC), through global and phospho-proteomics.

Method: A total 5 CRC cell lines (HT29, SW480, HCT116, H508 and CaCO2), colon normal fibroblast CRL1459, HCT116 p53 null cell and patient-derived normal organoid were used. Immunoblotting, MTT assay, Colony formation assay, Annexin-V assay and cell cycle analysis were performed for evaluation of TP53RK loss-of-function. With kinase-substrate enrichment analysis with phospho-proteome analysis, MCM2 was found to be a substrate for the kinase regulated by TP53RK.

Results: High-throughput genetic screening approach have been widely applied to the study the gene function and molecular mechanism associated with tumorigenesis. By using genome-wide CRISPR/Cas9 library screening, we identify TP53RK, the first committed negative-selected gene, as a tyrosine kinase in the colorectal cancer(CRC) specific biomarker. Through proteome analysis, we found that depletion of TP53RK can hypo-phosphorylate the DNA helicase complex, MCM2 (minichromosome maintenance protein2). According to previous studies, the phosphorylation of MCM2 is regulated by CDC7 (cell division cycle7), and the abnormal states of CDC7 and MCM2 cause DNA replication disorder. Our results show that TP53RK expression is upregulated in CRC and its depletion results in decreased CDC7 expression and hypo-phosphorylation of the MCM complex. Decreased CDC7 expression due to its instability after TP53RK depletion can lead to DNA replication errors. DNA replication errors can lead cancer cells to apoptosis, suggesting that they may be a strategy for cancer treatment. In summary, we provide TP53RK as a novel prognostic and therapeutic target in CRC.

Conclusion: To recapitulate briefly, our findings suggest that the interaction of TP53RK with CDC7 can regulate CDC7 protein stability and stabilized CDC7 can phosphorylate MCM2 to initiate DNA replication. In other words, because overexpression of TP53RK acts as an oncogene that promotes tumor progression in CRC, depletion of TP53RK can degrade CDC7 and induce colon cancer cells to death or regression.

#6990 RHBDF1 is a potential modulator of EGFR activation and oncogenic biomarker in triple-negative breast cancer.

H. Kim, S. Park, D. Kim, C. Lee, M. Song, H. Ryu;
Seoul National University, Seoul, Korea, Republic of

Recently, our proteomics study on breast cancer (BC) reported a possible association of RHBDF1 with triple-negative breast cancer (TNBC). The overall survival of TNBC patients on METABRIC data set implicated that the RHBDF1 high-expression group has a shorter life expectancy than the RHBDF1 low-expression group. Although many TNBC patients have high expression levels of RHBDF1 and poor prognosis, the mechanism of RHBDF1 in the pathogenesis of TNBC remained unclear. Rhomboid 5 homolog 1 (RHBDF1) is a catalytically inactive pseudoprotease on the Golgi and endoplasmic reticulum membrane. Despite its inactive status of peptidase, it regulates the activity of ADAM17 protease that cleaves the extracellular portion of EGFR ligands such as TGF alpha and EGF. Eventually, RHBDF1 and ADAM17 complex activate the EGFR signaling pathway, thereby increasing cell proliferation, migration, and tumorigenesis. First of all, we recruited the clinical data of the overall survival (OS) and disease-free survival (DFS) in the hospital of Seoul National University (SNUH cohort, n= 203) and compared IHC score 0 or 1 with survival rate. To investigate the underlying biological mechanism of RHBDF1 in TNBC, the effect of knockdown or overexpression of RHBDF1 was observed in TNBC cell lines (MDA-MB-468, HCC1143 and BT20) using siRNA (small interfering RNA) and lentiviral systems. Cell proliferation assay was performed to clarify whether RHBDF1 affects cell growth. Then, we estimated the ability of migration, invasion, and sphere formation to confirm the characteristics of cancer cells including cancer stemness and metastasis. SNUH cohort with TNBC patients showed that the RHBDF1 high-expression group has a poorer disease-free survival (DFS) than the low-expression group ($p<0.05$). In vitro assay, RHBDF1 knockdown inhibited proliferation in MDA-MB-468 and HCC1143. RHBDF1 downregulation also decreased the ability of migration and invasion. We found that RHBDF1 activates specific cell growth signaling pathways and increases cell mobility in TNBC. The sphere formation assay was performed to measure cancer stemness characteristics. As a result, RHBDF1 knockdown TNBC cell lines couldn't form spheres relative to RHBDF1 overexpressed TNBC cell lines. In conclusion, we demonstrated that RHBDF1, a potential triple-negative breast cancer biomarker, is highly amplified in TNBC patients and TNBC cell lines. Its functions of accelerating cell proliferation, metastasis and cancer stemness were unveiled. But we need to study ultimately how RHBDF1 regulates ADAM17 activity at Golgi and endoplasmic reticulum membrane and which transcription factor activates RHBDF1 expression.

#6991 Transcriptomic profiling of human and mouse models highlights YAP pathway hyperactivation as the underlying mechanism of the biological and clinical aggressiveness of Numb-defective bladder cancer.

F. Tucci[1], R. Pennisi[1], M. Filippone[1], R. Bonfanti[1], F. Romeo[1], D. Rigiracciolo[1], S. Freddi[1], F. Sanguedolce[2], G. Renne[1], G. Pruneri[3], G. Vago[4], D. Tosoni[1], S. Pece[1];

[1]European Institute of Oncology IRCCS, Milan, Italy, [2]University of Foggia, Foggia, Italy, [3]Fondazione IRCCS Istituto Nazionale dei Tumori, Milan, Italy, [4]University of Milan, Milan, Italy

In this study, we identify a previously uncharacterized role for the tumor suppressor, Numb, in bladder tumorigenesis, defining new predictive biomarkers and potentially actionable targets for the treatment of non-muscle-invasive bladder cancers. We conducted a comprehensive IHC analysis of Numb expression leveraging two retrospective longitudinal cohorts comprising 356 post-cystectomy muscle-invasive bladder cancer (MIBC) patients and 77 high-grade non-muscle-invasive (NMIBC) patients with transurethral resections. We found that Numb expression is frequently deregulated in the tumor compared to the adjacent normal urothelium, with Numb^{Low} status correlating with poorer prognosis both in MIBC, associated with advanced stage at diagnosis, vascular invasion, and worse overall survival, and in NMIBC, where a Numb^{Low} status associates with a higher rate of progression to life-threatening MIBC disease. In a transgenic mouse model with targeted deletion of the *Numb* gene in the basal layer of the bladder mucosa, we observed that loss of Numb *per se* is sufficient to drive malignant transformation of the normal urothelium and accelerates tumorigenesis in carcinogen-induced models. Integrative transcriptomic analysis of human and mouse Numb-deficient BC models revealed consistent dysregulation of the YAP1/TAZ1 inhibitory Hippo pathway, identifying YAP1 transcriptional hyperactivation as the most distinguishing trait downstream of NUMB loss. Through genetic and pharmacological functional inhibition studies in relevant mouse and human BC cell line-based models, we provide proof-of-evidence that interfering with YAP pathway activation at multiple upstream levels of the Hippo cascade reverts the aggressive Numb loss-associated tumor phenotypes, in particular growth and invasive/migratory potential, thereby highlighting the YAP pathway as a potential therapeutical vulnerability for the treatment of clinically aggressive Numb-deficient human BC. We also identified a gene signature of early BC depending on loss of Numb that we extensively validated for its potential as a predictor of NMIBC to MIBC progression, arguing for its clinical application as a biomarker for NIMBC patient stratification for targeted anti-YAP signaling treatment to prevent MIBC transition. In summary, our study identifies a previously uncharacterized role of Numb in bladder cancer progression, highlighting its potential as a predictive biomarker of NMIBC to MIBC transition and response to targeted therapies, thereby advancing a framework for precision oncology for NMIBC patients at high risk of progression to life-threatening MIBC disease.

#6992 Profilin 2 (PFN2) promotes the proliferation, migration, invasion and epithelial-to-mesenchymal transition of oral squamous cell carcinoma.

C. Liu[1], L.-H. Lin[1], K.-W. Chang[2], H.-W. Cheng[1];

[1]Mackay Memorial Hospital, Taipei, Taiwan, [2]National Yang Ming Chiao Tung University, Taipei, Taiwan

Background:Oral squamous cell carcinoma (OSCC) stands as a prevalent malignancy worldwide. Profilin 2 (PFN2), an actin-binding protein regulating actin polymerization dynamics and associated with cell motility, has recently gained attention as a significant regulator in various cancers. However, the clinical significance and biological function of PFN2 in OSCC remain debatable. This study aims to elucidate the role of PFN2 in OSCC.
Methods:We assessed PFN2 expression in OSCC and adjacent normal oral mucosa tissues through Q-RT-PCR and immunohistochemistry analysis. Associations between PFN2 expression, clinicopathological features, and OSCC prognosis were analyzed. Cell proliferation, invasion, and migration effects were examined via MTT and Transwell assays. Western blotting assessed the protein expression related to epithelial–mesenchymal transition (EMT). Additionally, we established OSCC xenografts to determine tumorigenicity in vivo using female Nude mice.
Results:PFN2 RNA and protein expression were significantly increased in OSCC compared to normal oral mucosa. PFN2 expression positively correlated with lymphovascular invasion and cervical lymph node metastasis. MTT and Transwell assays demonstrated that PFN2 promoted OSCC cell proliferation, migration, invasion, and endothelial invasion. Downregulation of PFN2 induced an EMT phenotype, including an increase in the expression of the epithelial marker E-cadherin and a decrease in the expression of mesenchymal markers Vimentin, Snail, and Slug in OSCC cells in vitro. Similarly, OSCC cells with reduced PFN2 expression exhibited weaker tumorigenicity in vivo.
Conclusions:Our findings unveil a novel role for PFN2 in promoting OSCC progression and metastasis, suggesting its potential as an early biomarker for high-risk populations. Targeting PFN2 may offer a promising therapeutic strategy for OSCC treatment.

#6993 SLC1A4 is associated with metabolic reprogramming in triple-negative breast cancer.

S. Park, D. Kim, H. Kim, M. Song, H. Ryu;
Seoul National University, Seoul, Korea, Republic of

The solute carrier protein (SLC) family is transporters as integral membrane proteins that transport solutes in an ATP-independent manner. The SLC1 family consists of five high-affinity glutamate transporters and two neutral amino acid transporters, among which SLC1A4 transports the neutral amino acids and is known to participate in various biological processes, including metabolism and tumorigenesis. However, the relationship between SLC1A4 and breast cancer remains unclear. Here, we aimed to verify the role of SLC1A4 in triple-negative breast cancer (TNBC). To reveal the characteristics of SLC1A4 in TNBC cell lines, five cell lines (HCC38/OE, HCC1395/OE, HCC1937/OE, MDA-MB-468/KD, and Hs578T/KD) that regulate gene expression of SLC1A4 were established using a lentiviral system. The two major energy-producing pathways, glycolysis and oxidative phosphorylation, were measured according to SLC1A4 gene expression. In addition, cell proliferation, cell migration, and cell invasion ability were confirmed upon overexpression or knock-down of SLC1A4. To confirm cancer stem cell function according to SLC1A4 gene expression, ALDH activity and sphere formation ability were evaluated. To ensure transcript changes due to SLC1A4 expression, RNA sequencing was performed. Anti-cancer drug (cisplatin, carboplatin, paclitaxel, and doxorubicin) sensitivity was also tested. The result showed that energy production efficiency was significantly reduced in cells where SLC1A4 expression was suppressed. In addition, in cells overexpressing the SLC1A4 gene, the presence of SLC1A4 was confirmed to increase cell proliferation, migration, and invasion ability significantly. Transcriptome analysis results showed notable changes in genes related to signaling receptor binding. Regarding material transport, to investigate whether there was a change in amino acid uptake ability according to SLC1A4 gene expression, no difference was observed. In the drug responses, doxorubicin showed a significant sensitive response in the absence of SLC1A4 gene expression. Taken together, SLC1A4 is a potential oncogene that not only induces rapid proliferation, aggressive invasion, and migration through metabolic reprogramming but also contributes to increasing cancer stem cell capabilities. In addition, it shows the sensitive response to ADR when SLC1A4 is low or absent, so it can be used as a treatment strategy for TNBC.

#6994 MerTK drives proliferation and metastasis activity in triple negative breast cancer.

C. Glitchev[1], M. Iida[1], B. E. Crossman[1], K. L. Kostecki[1], C. A. Kranjac[1], J. M. Adams[1], P. Liu[1], I. Ong[1], D. T. Yang[1], I. Kang[2], R. Salgia[2], D. L. Wheeler[1]; [1]University of Wisconsin-Madison, Madison, WI, [2]City of Hope, Monrovia, CA

Triple negative breast cancer (TNBC) is characterized by the absence of estrogen, progesterone, and HER2 receptors. It exhibits a higher level of aggressiveness compared to other types of breast cancer, with a greater likelihood of recurrence following standard treatments such as surgery, chemotherapy, and radiation. Despite limited FDA-approved targeted therapies for TNBC, there is an ongoing need for additional molecular targeting agents.Our investigation focused on the role of the receptor tyrosine kinase MerTK and its impact on proliferation and invasion/metastatic potential. Immunohistochemistry analysis revealed that approximately 86% (128/148) expressed varying levels of MerTK in human TNBC samples, whereas approximately 50% (23/47) of TNBC patient-derived xenografts (PDX) expressed MerTK. Additionally, three established TNBC cell lines (BT549, MDAMB231, and MDAMB436) exhibited elevated MerTK expression levels.To further explore the role of MerTK in TNBC, we stably overexpressed MerTK in human TNBC cell lines SUM102 and SUM159, which naturally have low MerTK levels. The results demonstrated that MerTK overexpression led to increases in proliferative potential, robust in vivo tumor growth, heightened migration/invasion potential, and increased lung metastasis. NanoString nCounter analysis of MerTK-overexpressing SUM102 cells (SUM102-MerTK) revealed upregulation of several signaling pathways, including PI3k-Akt, PDGF, and Myc, ultimately driving cell cycle progression, reducing apoptosis, and enhancing cell survival in TNBC.Further investigation using a cytokine array showed increased endoglin production in SUM102-MerTK cells compared to vector control cells. This suggested that MerTK might be creating a conducive environment for increased proliferative and metastatic activity via elevated endoglin expression in TNBC. To ascertain the role of endoglin in increase proliferation and/or invasion potential, we knocked out endoglin in SUM102-MerTK cells. While endoglin knockout SUM102-MerTK cells exhibited similar growth to SUM102-MerTK cells, the number of lung metastases was significantly impacted, indicating that MerTK regulates invasion and metastasis through endoglin in TNBC. Collectively, our data suggests that MerTK regulates a unique proliferative signature allowing for robust tumor growth and increased metastatic potential through endoglin regulation. This suggests that targeting MerTK and endoglin simultaneously may be a viable approach for TNBC patients.

#6995 Functional characterization of the novel cell adhesion molecule MPZL3 in ovarian cancer.

Y.-Y. Cheng[1], B. Worley[2], Z. Javed[2], A. T. Elhaw[2], P. W. Tang[2], N. Hempel[1];
[1]University of Pittsburgh, Pittsburgh, PA, [2]Pennsylvania State University, Hershey, PA

Ovarian cancer (OVCA) is the most lethal gynecological malignancy in the United States often detected at advanced stages. OVCA progression involves transcoelomic metastasis, where cells disseminate into the peritoneal fluid, adhere to form multicellular aggregates that promote anchorage-independent survival and facilitate metastatic colonization of the peritoneum. To meet the requirements of each stage of this detachment, aggregation, and re-attachment cycle, OVCA cells have been shown to dynamically regulate the expression of multiple cell adhesion molecules (CAMs) throughout their progression. Moreover, targeting cell-cell adhesion molecules has shown to be an effective method to slow/inhibit the progression of OVCA. In this study, we characterize the novel role of the understudied CAM MPZL3 in OVCA. Myelin protein zero-like 3 (MPZL3) is a transmembrane protein with homology to other immunoglobulin-like (Ig) family of CAMs. While it has been reported that altered Ig-CAM expression plays a role in ovarian cancer, the function of MPZL3 has not been investigated. Interestingly, TCGA data demonstrates that chromosomal loss of the *MPZL3* locus (11q23.3) is frequently detected in several cancer types, including 22% of clear cell and 30% of high grade serous ovarian cancers (HGSOC), implying that loss of genes located in this area has tumorigenic consequences. On the other hand, few studies showed that MPZL3 contains an oncogenic potential in breast and MET-amplified cancer cell lines, suggesting that the role of MPZL3 in cancer is context dependent. To study the function of MPZL3 in OVCA, we used shRNA mediated MPZL3 knockdown in OVCAR4 human HGSOC cells and examined transcriptome-wide effects by RNA-sequencing. The subsequent Gene Set Enrichment Analysis indicated that pathways involved in regulating cell growth, death, adhesion, and epithelial-mesenchymal transition were significantly altered by loss of MPZL3. To validate the candidate pathways, we knocked down or over-expressed MPZL3 in OVCA cells to test its importance in regulating OVCA cell growth, apoptosis, adhesion, and migration. We found that loss of MPZL3 resulted in decreased cell growth with a concomitant resistance to both Cisplatin and Olaparib treatments, both of which are commonly used for treating OVCA. Moreover, we show that knockdown of MPZL3 alters the homotypic adhesive-capacity of OVCA cells. Ongoing studies are underway to further characterize the role played by MPLZ3 in the mentioned contexts. Additionally, to elucidate the underlying molecular mechanism and identify novel interactors of MPZL3, we will conduct co-immunoprecipitation experiments in OVCA cells expressing V5-tagged MPZL3. Understanding the novel role of MPZL3 will provide further insight into OVCA progression, thus generating opportunities of developing new treatments for patients with low MPZL3 expression as an approach for precision cancer medicine.

#6996 A role for the cell adhesion molecule NCAM1 in regulating activity of the receptor tyrosine kinase RET in cancer.

M. H. Hussain[1], B. D. Hyndman[1], F. S. Vizeacoumar[2], M. J. F. Crupi[3], F. J. Vizeacoumar[2], L. M. Mulligan[1];
[1]Queen's University, Kingston, ON, Canada, [2]University of Saskatchewan, Saskatoon, SK, Canada, [3]University of Ottawa, Ottawa, ON, Canada

RET (REarranged during Transfection) is a receptor tyrosine kinase with essential roles in early development; however, genetic alterations lead to aberrant RET activity that contributes to oncogenic processes in several cancers. While some of the mechanisms by which RET mediates these processes are known, the network of proteins facilitating its activity remains largely undiscovered. To address this, we performed a genome-wide synthetic dosage lethal screen which identified NCAM1 (Neural Cell Adhesion Molecule 1) as one potential candidate modulating RET activity. Using an NCAM1 knockdown (KD) in SH-SY5Y neuroblastoma cells, we show that loss of NCAM1 reduces total protein levels of RET with no effect on *RET* transcription. Despite reduced abundance of RET, we show that the mature form of RET has a prolonged half-life in the absence of NCAM1**.** Assessing the functional outcomes of reduced RET protein levels, we observe reduced activation of RET by its extracellular ligand GDNF (Glial cell line-derived neurotrophic factor) and a subsequent reduction in activation of proliferative signaling pathways downstream of RET. As a result, RET-mediated proliferation is diminished in the absence of NCAM1, with reduced viability of NCAM1 KD SH-SY5Y observed in response to GDNF. Together, our data suggest that the synthetic lethal relationship between RET and NCAM1 may arise from a role for NCAM1 in regulating total RET protein available for activation, thereby reducing RET-mediated cell viability and proliferation. Our work has uncovered a role for NCAM1 in modulating RET activity in cancer and validates the use of our synthetic dosage lethal approach in uncovering proteins facilitating oncogenic RET activity.

#6997 Elucidating the tumorigenic properties of alveolar epithelial type 1 cells in EGFR-mediated LUAD tumorigenesis.

Aaron M. Neely[1], Andrea Lanz[2], William Dean Wallace[3], Anthony W. Kim[4], Zea Borok[5], Crystal N. Marconett[1]

[1]Translational Genomics, USC - University of Southern California, Los Angeles, CA,[2]Univeristy of California-Irvine, Irvine, CA,[3]Pathology, USC - University of Southern California, Los Angeles, CA,[4]Thoracic Surgery, USC - University of Southern California, Los Angeles, CA,[5]Medicine`, University of California San Diego, San Diego, CA

Originating from within the distal lung, lung adenocarcinoma (LUAD) is the most common pathologic subtype of non-small cell lung carcinoma (NSCLC) and encompasses an assortment of histologic presentations. Colocalized within the distal alveolar epithelium are two alveolar epithelial cell (AEC) subpopulations: alveolar epithelial type 1 (AT1) and alveolar epithelial type 2 (AT2) cells. We previously demonstrated that signatures unique to each AEC subpopulation were detected in LUAD tumors formed by oncogenic $KRAS^{G12D}$ activation in mice and were associated with disparate survival outcomes, transcriptomic patterning, and histologic presentation. Epithelial growth factor receptor (EGFR) mutations are among the most frequent oncogenic drivers in thoracic oncology. Therefore, we set out to determine if EGFR oncogenic activation resulted in differential LUAD presentation and outcomes based on the cell of origin in which it was activated. To activate EGFR oncogenic mutations in AT1 or AT2 cells, we employed triple transgenic mouse models (AT1: *Gramd2*-CreERT2:*EF1*-LSL-tTA:*TetO*-$EGFR^{del20/T790}$ and AT2: *Sftpc*-CreERT2:*EF1*-LSL-tTA:*TetO*-$EGFR^{del20/T790}$), which allowed for EGFR activation in either *Gramd2*$^{\pm}$ AT1 or *Sftpc*$^{\pm}$ AT2 cells. Longitudinal analysis of hematoxylin and eosin-stained lungs over the course of 20 weeks was performed. Blinded pathology review demonstrated that EGFR oncogenic activation in *Gramd2*$^{\pm}$ AT1 cells resulted in histologically defined LUAD with lepidic properties at early time points and solid adenocarcinoma properties at later time points. This differed from EGFR activation in *Sftpc*$^{\pm}$ AT2 cells, which resulted in pre-carcinogenic atypical adenomatous hyperplasia (AAH) formation that did not progress to adenocarcinoma. While preliminary, our results suggest that cell of origin strongly influences EGFR-mediated lung oncogenesis and concomitant pathology and histologic presentation. This work may advance our understanding while informing patient stratification and treatment strategies for LUAD patients.

MOLECULAR/CELLULAR BIOLOGY AND GENETICS: Epigenetic Profiling and Technology
Poster Session

#7001 Profiling the CpG methylation patterns of Epstein-Barr virus DNA in lymphoma patients from Ethiopia.

Seifegebriel T. Feleke[1], Kidist Z. Shita[2], Abdulaziz A. Sherif[3], Fisihatsion T. Woldegebriel[3], Christoph Weigel[4], Elshafa H. Ahmed[4], Tamrat A. Zeleke[1], Robert A. Baiocchi[5]

[1]Microbiology, Immunology and Parasitology, Addis Ababa University, Addis Ababa, Ethiopia,[2]Ethiopian Public Health Inistitute, Addis Ababa, Ethiopia,[3]Addis Ababa University, Addis Ababa, Ethiopia,[4]The Ohio State University, Columbus, OH,[5]Internal Medicine, The Ohio State University, Columbus, OH

Introduction: Epstein-Barr virus (EBV) is a tumor virus associated with various malignancies, driven by genetic mutations and epigenetic alterations, including DNA methylation. Abnormal CpG methylation holds promise as a diagnostic and therapeutic biomarker for EBV-associated tumors. However, the understanding of EBV's epigenetic mechanisms remain limited. Determining the methylation profile of EBV is crucial for gaining insights into the pathogenesis of EBV-associated tumors, developing diagnostic biomarkers, and exploring potential therapeutic strategies. Therefore, our study aimed to assess the CpG methylation profile of EBV DNA in lymphoma patients from Ethiopia.
Methods: This study enrolled 115 lymphoma patients from Tikur Anbessa Specialized Hospital in Addis Ababa, Ethiopia. Plasma and formalin-fixed paraffin-embedded blocks were collected from the participants, and isolation of DNA was performed from these samples. The methylation analysis was performed using the methylation-iPLEX assay. iPLEX capture and extension primers were designed to amplify and target EBV CpGs from bisulfite-converted DNA sequences. Ethical approval was also obtained from respected institutions.
Results: Among the 115 participants, 65.2% (n = 75) were male patients. The largest proportion (n = 35, 30.4%) fell within the 41-60 age group. Non-Hodgkin lymphoma (NHL) was diagnosed in 96 patients, while 19 had Hodgkin lymphoma (HL). In the NHL group, the majority (n = 27, 28.1%) were classified as diffuse large cell lymphoma, followed by follicular lymphoma (n = 24, 25%). Out of the different EBV genome methylation sites, we have identified 24 EBV genes to assess the methylation status of the EBV genome. Average methylation levels of these genes were ranged from 45% to 50%. Notably, the HL group exhibited significant heterogeneity in methylation levels, while the CpG methylation status of EBV genes in NHL subtypes demonstrated a consistent pattern. A significant proportion of our samples exhibited methylation loss in the lytic gene BZLF1 and at the origin of replication associated with lytic replication.
Conclusions: This study presents the first data from East Africa, shedding light on the EBV DNA methylation status in a diverse group of lymphoma patients. Further investigations in different locations are necessary to elucidate the impact of EBV DNA methylation on tumor progression.

#7002 RNA m^{6}A modification and lung cancer risk: An epitranscriptome-wide association study.

Y. Yang[1], Y. Chen[2], Y. Qi[2], H. Liu[2], G. Jia[3], J. Ping[3], X.-O. Shu[3], W. Zheng[3], W. Li[2], J. Long[3], Q. Cai[3];
[1]University of Virginia, Charlottesville, VA, [2]West China Hospital, Sichuan University, Chengdu, China, [3]Vanderbilt University Medical Center, Nashville, TN

N^6-Methyladenosine (m^{6}A), the most prevalent epitranscriptomic modification in eukaryotic mRNA, determines the fate of target RNAs. Key m^{6}A regulators have been elucidated to be essential for lung cancer cell proliferation. However, the relationship between individual m^{6}A markers and lung cancer risk remains inadequately explored.

We conducted an epitranscriptome-wide association study (EpiTWAS) to investigate genetically predicted m^{6}A in association with lung cancer risk. Genetic and m^{6}A data of 30 lung, 12 heart, 28 muscle, and 50 brain tissues from 87 donors predominantly of European ancestry were obtained from Genotype-Tissue Expression (GTEx). For each m^{6}A marker, we built a single-tissue model via elastic net, focusing on lung tissue, and a cross-tissue model through the unified test for molecular signatures (UTMOST) approach, capturing genetic influences on m^{6}A shared by lung and other tissues. SPrediXcan was used to apply these models to data of genome-wide association studies (GWAS) among 38,422 lung cancer cases and 677,930 controls of European descent from International Lung Cancer Consortium (ILCCO), UK Biobank, and FinnGen. For m^{6}A markers significantly associated with lung cancer risk at false discovery rate (FDR) <0.05, we assessed the differential expression of proteins encoded by their target mRNAs in lung cancer versus adjacent normal tissues (200 pairs), using data from Clinical Proteomic Tumor Analysis Consortium (CPTAC).

Of the 38,841 high-quality m^{6}A markers in 11,715 genes analyzed, prediction models were built for 6,809 m^{6}A markers in 4,548 genes with performance of R>0.1 (*P*<0.05), ~85.2% (5,801) of which were single-tissue models. Among these, 28 m^{6}A markers in 26 genes were significantly associated with overall lung cancer risk (FDR<0.05). Notably, 12 (~43%) of these markers in 12 loci are >2 megabases away from any of GWAS-identified lung cancer risk variants. When conditioning on nearby GWAS signals, these 12 associations did not change materially, whereas 15 of the remaining 16 associations lost statistical significance. Analyses by lung cancer histology and smoking status revealed no significant heterogeneity among the 28 associations but identified eight additional m^{6}A markers significantly (FDR<0.05) associated with the risk of adenocarcinoma (n=2), squamous cell carcinoma (n=3), and overall lung cancer among ever- (n=2) or never-smokers (n=1). Of the 33 target RNAs of those 36 m^{6}A markers, 30 encode proteins and 22 of these proteins displayed a significant tumor-normal differential expression at fold change >1.5 and FDR<0.05 in CPTAC lung tissue data.

Our study demonstrates the ability of EpiTWAS to decipher GWAS loci and uncover signals potentially missed by GWAS. Our results imply that certain m^{6}A markers may impact lung cancer risk by modulating mRNA translation, underscoring the need for further research to fully unravel the role of m^{6}A in lung cancer etiology.

#7003 Microfluidic platform for DNA methylation profiling towards early detection of ovarian cancer.

C. O'Hersey, Y. Zhao, T. R. Pisanic, T.-L. Wang, I.-M. Shih, T.-H. J. Wang;
Johns Hopkins University, Baltimore, MD

We present a microfluidic platform for molecule-by-molecule detection of heterogeneous epigenetic patterns of rare tumor-derived DNA by highly parallelized digital melt. The platform digitizes DNA molecules in a 4-module, 40,000 1-nL array microfluidic device and observes sequence-dependent fluorescence changes during temperature ramping. The platform is applied to quantify DNA methylation heterogeneity of a biomarker panel within Pap specimens in a small cohort of healthy and ovarian cancer patients, and demonstrates an accuracy of 0.9. DNA hypermethylation of tumor-suppressor genes is an epigenetic phenomena that occurs early in tumorigenesis. Variable methylation patterns are observed in ovarian cancer precursor tissue, and trace amounts of ovarian-tumor-derived DNA can be found in Pap specimens, albeit at low frequencies (<0.01%). This suggests that methylation profiles of DNA extracted from routinely-obtained Pap specimens could contain early cancer biomarkers. However, due to the scarcity of these molecules, current techniques, such as sequencing and digital PCR (dPCR), have technical limitations precluding their ability to profile methylation patterns reliably. Sequencing, although comprehensive, has limited sensitivity, undermining its utility for routine detection of fractions below 0.1%. dPCR achieves high sensitivity, but is limited to known sequences, thus cannot provide comprehensive analysis of molecular heterogeneity.

To overcome these limitations, we developed a technique called digital high resolution melt (dHRM), a thermodynamics-based approach to detecting molecular variability by observing the sequence-specific release of a DNA-intercalating dye under a thermal ramp. dHRM can discriminate methylation patterns on CpG-by-CpG basis and detect methylated epialleles at frequencies as low as 0.00005%. Here, DNA from Pap specimens was loaded on a microfluidic chip that digitizes rare target molecules into individual reaction chambers. A thermal-optical platform was developed to perform parallelized dPCR and dHRM. Methylation patterns of a biomarker panel were analyzed to produce a probability score that the Pap specimen contained tumor-derived DNA. 12 healthy and 12 ovarian cancer Pap specimens were assessed for methylation heterogeneity of 9 genes. Optimal methylation density thresholds were determined, and data above each threshold was combined into a single score for each possible combination of biomarkers. In this small cohort, methylation heterogeneity analysis of just 2 loci produced an area under the receiver-operator characteristics curve (AUC) of 0.9.

This highly sensitive methylation profiling technology demonstrates promising utility towards early cancer detection. Future work aims to expand the testing cohort for ovarian cancer detection and permit further studies on the impact of methylation heterogeneity on early cancer development.

#7004 DNA Methylation analysis of African American colorectal cancers reveal race-specific alterations.

S. Rajpara[1], D. N. Buckley[1], R. Xicola[2], R. Mikaeel[2], M. K. Yagle[3], B. Kerimoglu[3], C. Thorne[3], D. A. Bellomo[3], M. Padi[3], X. Llor[2], N. Ellis[3], B. Salhia[1];
[1]Keck School of Medicine of USC, Los Angeles, CA, [2]Yale School of Medicine, New Haven, CT, [3]University of Arizona, Tucson, AZ

African Americans (AAs) have among the highest incidence and mortality rates of colorectal cancer (CRC) in the US. They present with more right-sided, microsatellite stable (MSS) tumors and are diagnosed at earlier ages than non-Hispanic Whites (NHW). While DNA methylation changes and their significance have been previously described in CRC, much less is known about the unique DNA methylation changes that occur in AA CRCs compared to NHW CRCs. In the current study, we analyzed DNA methylation changes in AA patients and compared those changes to data from NHWs. AA patients diagnosed with a MSS colorectal tumor at the Yale New Health System were included in the study. A pathologist reviewed archival slides, and selected areas from CRCs (n=160) and adjacent normal tissue (n=42) were cored (median age=59; 82 females, 78 males). DNA was bisulfite converted and analysis performed using EPIC arrays. The 450K methylation array from NHW CRCs was also analyzed for 217 CRCs and 20 normal tissues obtained from TCGA (median age=68; 103 females, 114 males). Differentially methylated regions (DMRs) with $|\Delta\beta|>0.1$, FDR corrected p-value <0.05 between tumor and normal tissue were identified using SeSAMe. We identified 4881 DMRs (57% hyper- and 44% hypomethylated) between AA CRC and normal tissue. Of these, 46% were in CpG Islands, 15% in CpG Shores, 4% in CpG shelves, and 36% in open sea. Most DMRs (71%) were in promoter regions, with 18% in gene bodies, 5% in enhancer regions, and 6% in intergenic regions. Next, we performed additional DMR analysis using overlapping probes from both arrays to compare NHW with AA data. We identified 2239 DMRs between AA CRC and normal tissue compared to 4138 in NHW. Of the 2239 AA DMRs, 1419 (66%) were common with NHW DMRs, 790 (34%) were unique to AAs. There were many overlapping pathways and genes; however, the DMRs impacting these pathways differed between AA and NHW CRCs. Hypermethylation of LCK, a tyrosine kinase involved in T-cell receptor signaling, was found in 60% of AA CRCs compared to 5.9% of NHW CRCs. LCK hypermethylation leads to CD4/8 T-cell inactivation and linked to poor outcomes in lung cancer. We observed AA-specific hypermethylation of SSTR1 in 57.2% of AA CRCs compared to 27.6% of NHW CRCs. Somatostasin (SST) suppresses tumor growth by regulating certain factors involved in cell proliferation. Hypermethylation of SSTR1 has been associated with various malignancies including gastric cancer. Lastly, promoter hypermethylation of 3 protocadherin genes was found in 65.1% of AAs compared to 33.1% NHWs. Protocadherins regulate WNT signaling and hypermethylation is associated with poor outcomes in multiple cancers. Taken together, these results show AA-specific CRC methylation changes compared with NHW CRCs. Further work is warranted to investigate the potential functional and clinical implications of these methylation alterations, some of which may represent therapeutic targets and biomarkers.

#7005 Distinct DNA methylation patterns between early-onset and average-onset colorectal cancer patients.

L. Su[1], P.-C. Hsu[2], A. Rathod[1], Y. Liu[1], J. Ferruzzi[3], S. Kazmi[1], E. Huang[1];
[1]University of Texas Southwestern Medical Center, Dallas, TX, [2]University of Arkansas for Medical Sciences, Little Rock, AR, [3]University of Texas at Dallas, Dallas, TX

Objective: Early onset colorectal cancer (EO CRC) is rising at an alarming rate. While average onset colorectal cancer (AO CRC) affects patients mostly above 65 years of age, EO CRC affects patients under 50 years of age, disproportionately affecting males from low-income communities and racial/ethnic minorities. Chronic inflammation has been identified as a strong contributor to pathogenesis. We hypothesize that methylation of DNA may serve as a potential mechanism associated with chronic inflammation that contributes to the etiology differentially between EO and AO CRC.
Methods: Formalin-fixed paraffin-embedded (FFPE) tissue specimens from four AO and EO CRC patients each were retrieved from the Tissue Repository. Paraffin curls containing tumor and adjacent normal tissues were generated from appropriate EO and AO CRC patient tissues. The Qiagen GeneRead DNA FFPE genomic DNA kit was then used to extract the DNA from the paraffin curls. Illumina Methylation EPIC v2.0 kit was used to evaluate DNA methylation (DNAm) patterns after the restoration process from deamination in the fixed/embedded sample using the Uracil-N-Glycosylase enzyme. Unreliable and non-specific probes were removed before statistical analysis for differentially methylated CpG sites. Age acceleration for each tissue was calculated by comparing the estimated DNAm age with chronological age using the Horvath approach.
Results: A clear clustering of DNAm patterns by age of onset were observed for both normal and tumor tissues. However, there was no difference when comparing tumor and normal tissues after multiple corrections. Four-way ANCOVA adjusting for race, gender, BMI, and tissue type suggested that age onset was the most significant factor. We also found that age acceleration in EO CRC tissue is greater than in AO CRC. After applying Bonferroni correction, significant differentially methylated regions (DMRs) were found in the promoter and the gene body of *SNTB1, NFATC3, SLC25A24, RABGAP1L, WDSUB1, WWOX, SELB, SLC28A3*, and *PPP6R2* in EO CRC patients when compared to AO CRC. *SNTB1* regulates colorectal cancer progression and stemness, while *NFATC3* has been associated with inflammation and cancer.
Conclusions: The preliminary results from this study showed a significant difference in the DNAm profile of FFPE samples between AO and EO CRC. The finding suggests that epigenetics may play a role in the etiology of CRC, potentially involved in the chronic inflammation pathway. The analysis of a larger patient number is underway to strengthen these findings.

#7006 Identification of endothelial-cell-specific DNA methylation alterations in breast cancer with deconvolution of the tumor microenvironment.

Barbara Karakyriakou, Ze Zhang, Irma Vlasac, Pauline Mochama, Lucas Salas, Brock Christensen

Geisel School of Medicine, Dartmouth College, Hanover, NH

The tumor microenvironment (TME) plays a pivotal role in cancer progression, with tumor endothelial cells (TECs) emerging as key orchestrators of angiogenesis and vascular remodeling. Tumor-associated vasculature can have increased permeability and irregular blood flow, impacting drug delivery and tumor immune response.

Understanding the molecular alterations within TECs may help identify targeted therapies and improve treatment outcomes with existing therapies. We combined TME cell-type deconvolution with modeling to identify cell-specific methylation alterations of TECs in breast cancer.

Genome-scale DNA methylation array data accessed in GEO and GTEx from preinvasive, mixed, and invasive breast cancer tissue (n=609) & normal breast tissue (n=230). We applied HiTIMED, a reference-based cell-type deconvolution algorithm, to estimate endothelial and other cell-type proportions in the TME. Next, we applied CellDMC, a statistical algorithm that identifies cell-specific driven differential methylation, to our cell fraction results, unraveling differentially methylated positions occurring in the endothelial compartment of the angiogenic component of our breast tissue DNA methylation profiles.

We identified 29 TEC driven differentially methylated positions (FDR ≤ 8e-03), including loci within genes in angiogenic pathways regulated by VEGF, endothelial inflammation and activation genes, and tumor-associated vasculature factors in the TME. Our findings suggest that variation in DNA methylation between TECs and normal endothelial cells is crucial to understanding the TME and providing insights into unknown cancer cell behaviors that contribute to tumor growth and metastasis, thus leading to the design of novel efficient therapies that target the malignant vascular component.

Our study demonstrates the power of combining cell-type deconvolution and a modeling framework that identifies cell-specific somatic alterations to unravel the intricate characteristics of TECs in breast cancer. Furthermore, this study highlights the potential of DNA methylation profiling as a robust tool for characterizing TEC heterogeneity and elucidating the molecular basis of angiogenesis beyond breast tissue in the context of diverse cancer types. Our integrative approach holds promise for advancing precision oncology, paving the way for effective and targeted therapies aimed at modulating the tumor vasculature to impede cancer progression in breast cancer and other cancer types.

#7007 5hmc-sequencing identifies candidate genes in Puerto Rican Hispanic/Latino men with aggressive prostate cancer.

M. S. Patel[1], M. Almubarak[1], J. Matta[2], C. Ortiz-Sanchez[2], J. Encarnacion[2], G. Ruiz-Deya[2], J. Dutil[2], J. Dhillon[1], K. Yamoah[1], A. Berglund[1], H. Park[1], L. Wang[1], J. Y. Park[1];

[1]H. Lee Moffitt Cancer Center and Research Institute, Tampa, FL, [2]Ponce Research Institute, Ponce Health Sciences University-School of Medicine, Ponce, Puerto Rico

Introduction: Puerto Rican (PR) Hispanic/Latino (H/L) men are an understudied population which has the highest prostate cancer (PCa) specific mortality when compared with other Hispanic populations. According to the recent PR Cancer Registry data, PCa is the leading cancer type in terms of incidence (38% of all cancer cases) and mortality (16% of all cancer deaths) in PR H/L men. PR H/L men also have significantly higher PCa-specific mortality than non-Hispanic Whites (NHW) and non-Hispanic Blacks (NHB). So far, little is known about higher mortality in PR H/L men. It is believed that epigenetic changes of key genes play a critical role in aggressive tumors. Therefore, our study was aimed to identify key 5-hydroxymethylcytosine (5hmC) changes in PR H/L men with aggressive PCa.

Methods: We prepared sequencing libraries using the enriched 5hmC DNA from 42 prostate tumor and 44 adjacent normal FFPE samples. We performed sequencing on an Illumina NextSeq 500 with 75bp single end. We used DESeq2 package to identify differentially methylated genes (DMGs). We also downloaded additional 5hmC data (Database: EGAS00001004942) of 51 localized PCa and 7 adjacent normal for confirmation analysis. We used Gleason score (GS) as a cut-off to identify DMGs in aggressive PCa patients (GS- 7 (3+4) or less, Non-aggressive; GS- 7 (4+3) and above, Aggressive).

Results: We identified 808 DMGs in tumors compared to adjacent normal tissues (FDR<0.05, log2FC>|0.4|). Pathway analysis of DMGs demonstrated that cell-cycle, cell division, and DNA repair related pathways were most upregulated in tumors. Since 5hmC abundance is highly correlated with gene expression levels, we further investigated 808 DMGs with TCGA prostate cancer gene expression data. This analysis identified 59/73 DMGs (80.1%, (FDR<0.05, delta>|1|) with significant 5hmC and gene expression changes in the same direction. We also performed differential methylation analysis in another dataset and observed that 129 DMGs were common with our results. Finally, we demonstrated 111 DMGs ($p<0.05$) in aggressive tumors (n=7) compared to non-aggressive tumors (n=15). These 111 DMGs include important 5hmC hypomethylated genes (*BCCIP* and *KLK10*) and hypermethylated genes (*COX6C, ARMC2, PVT1*) in aggressive PCa patients.

Conclusions: Our study identifies 59 genes having coordinated epigenetic and transcriptomic changes in PR H/L men and 111 DMGs in aggressive tumors. The coordinated 59 genes include tumor suppressor genes such as *DKK3* and *PRDM8* with downregulated 5hmC and gene expression levels. Also, previous studies reported downregulation of *BCCIP* and *KLK10* and upregulation of *COX6C, ARMC2, PVT1* expression in PCa. The coordinated changes in 5hmC could be critical in aggressive PCa biology, hence in future, these genes will be validated as candidate biomarkers and targets for aggressive PCa among PR H/L men.

#7008 NEBNext® E5hmC-seq™: Direct detection of 5-hydroxymethylcytosine at single base resolution.

G. M. Cammarata, D. J. Evanich, V. Ponnaluri, V. Panchapakesa, A. Erijman, M. A. Campbell, N. Dai, B. W. Langhorst, L. Williams;
New England Biolabs, Inc., Ipswich, MA

DNA methylation is a critical epigenetic regulator of gene expression during development and in diseases such as cancer. The modified cytosines, 5-methylcytosine (5mC) and 5-hydroxymethylcytosine (5hmC), can be detected by sequencing libraries generated using existing methods: NEBNext® EM-seq™ or bisulfite sequencing. However, these methods cannot differentiate between 5mC and 5hmC. Interest in the role of 5hmC in regulating gene expression and as a cancer biomarker has increased, resulting in the need for robust methods for the identification of specific 5hmC sites. Methods currently exist to enable discrimination of 5mC and 5hmC (for example, oxBS-seq and TAB-seq), however these are based on modifications of bisulfite sequencing, and suffer from reduced data quality due to fragmentation and loss of DNA. Here we describe an enzymatic method that enables specific detection of 5hmC, termed NEBNext® Enzymatic 5hmC-seq (E5hmC-seq™). E5hmC-seq libraries were generated for 0.1 ng to 200 ng DNA isolated from human brain and E14 mouse embryonic stem cells. Libraries were prepared using NEBNext® Ultra II™ reagents followed by two enzymatic steps to detect 5hmC. In the first step, 5hmCs are glucosylated, which protects them from subsequent deamination by APOBEC. In contrast, cytosines and 5mCs are deaminated resulting in their conversion to uracil and thymine, respectively. This conversion allows discrimination of 5hmC from cytosine and 5mC. Finally, libraries were PCR amplified using NEBNext® Q5U® and sequenced on the Illumina platform. The E5hmC-seq libraries have similar characteristics to EM-seq libraries, including expected insert sizes due to intact DNA molecules, low duplication rates and minimal GC bias. Moreover, E5hmC-seq libraries were well-correlated between inputs and replicates at higher sequencing depths. Fully hydroxymethylated T4147 phage DNA was used as an internal control, with 98-99% of cytosines identified as 5hmC. 5mC and 5hmC levels were also profiled during E14 cell differentiation for a period of 10 days. Interestingly, 5hmC levels decreased whereas 5mC levels increased particularly during the first five days of differentiation. LC-MS/MS quantification of this same DNA mirrored the changes observed by sequencing. E5hmC-seq libraries provide accurate measurements of 5hmC across a wide input range with expected insert sizes and minimal GC bias. Additionally, subtracting E5hmC-seq data from EM-seq data, which detects both 5mC and 5hmC, enables the precise location of individual 5mC and 5hmC sites. The ability to discriminate between 5mC and 5hmC will allow key insights to be made into the role of cytosine modifications in development and cancer.

#7009 Quantification of DNA methylation using methylation-sensitive restriction enzymes and digital PCR .

Y. Zhao, L. Cambria;
Roche Diagnostics, Wilmington, MA

DNA methylation is a common epigenetic modification, characterized by the presence of the signature 5-methylcytosine without altering the sequence of DNA. The study of DNA methylation in mammals has gained significant attention due to its broad impact on numerous biological processes and its critical role in the onset and progression of many diseases, such as cancer and aging. Consequently, there is a pressing need for a rapid and precise method to assess methylation status. Currently, most approaches for quantifying DNA methylation rely on sodium bisulfite treatment. However, such approaches do not align with the uracil DNA glycosylase PCR system. In this study, we demonstrate the application of methylation-sensitive restriction enzymes (MSRE) and digital PCR to determine the methylation status of the Ras association domain family 1 isoform A (*RASSF1A*) in cancer cell lines. Digital PCR enables the precise detection and absolute quantification without the reliance on reference standards. We developed a multiplex digital PCR assay that includes the target gene RASSF1A, along with two reference genes for the purpose of monitoring digestion completion and correcting DNA input. Each sample of interest was measured both before and after a MSRE digestion. To ensure the quantification accuracy, we employed the commercially available CpGenome human methylated DNA standard with a known concentration from MilliporeSigma, treating it with and without a MSRE, and subsequently performing digital PCR experiments using Roche Digital LightCycler® IVD system with a Universal nanowell plate featuring 28,000 partitions. The expected concentrations lay within the 95% confidence interval, affirming the accurate quantification achieved through digital PCR. Next, we measured the fraction of methylated alleles in various lung cancer and breast cancer cell lines, as well as in healthy human gDNA. The methylation of *RASSF1A* promoter in healthy human gDNA is ~0.7%, while a broad range of methylation levels was observed in cancer cell lines, ranging from ~0.7% to ~100.2%. Notably, the influence of GC bias was identified in this study. To overcome this critical challenge, we optimized the usage of several high GC enhancers. The results demonstrated that the concentration of 5-7.5% DMSO, 7.5% glycerol, and commercially available OneTaq or Q5 GC enhancers from New England Biolabs were effectively incorporated into the Roche digital PCR system, thereby enhancing the accuracy of quantification from 30% to 100%. Together, we demonstrated a remarkable approach for DNA methylation analysis using Roche digital PCR system in combination with MSREs and suitable high GC enhancers. This study suggests a promising rapid, accurate and cost-effective tool to advance research in the field. *Data on file at Roche Diagnostics, Wilmington, MA, USA

#7010 A pan-tissue investigation of epigenetic aging in association with genetic risk for cancer among European descendants.

Y. Chen[1], Y. Qi[1], G. Wang[1], Y. Xie[2], Y. Yang[3], W. Li[1];

[1]West China Hospital, Sichuan University, Cheng Du, China, [2]West China Hospital of Sichuan University, Cheng Du, China, [3]University of Virginia, Charlottesville, VA

Epigenetic age (EA) is recognized as a valuable biomarker of aging. The discrepancy between epigenetic and chronological age (CA), termed epigenetic age acceleration (EAA), has been associated with increased mortality from various age-related diseases, including cancer. However, previous studies primarily focused on the EA in blood cells, resulting in a notable gap in understanding the EA in cancer-relevant tissues and its relationship to cancer development.

To examine if genetic risks for seven distinct cancers are associated with EAA in cancer-relevant tissues and blood cells, we utilized Illumina EPIC-array-based DNA methylation data and whole genome sequencing (WGS)-derived genotype data of 659 normal tissue and 42 whole blood samples from 315 European-ancestry subjects in the Genotype-Tissue Expression (GTEx) project. EA was estimated across 30 female breast, 167 colon, 41 kidney, 163 lung, 118 ovary, 96 prostate, 44 testis, and 42 whole blood samples via seven established epigenetic clocks: HorvathAge, GrimAge, GrimAge2, HannumAge, PhenoAge, Zhang-BLUP-Age, and Zhang-EN-Age. EAA was calculated as the residual of EA regressed on CA. For each participant, a polygenic risk score (PRS) was computed to assess the genetic risk for each cancer, using validated cancer-specific PRSs for European populations from the Polygenic Score Catalogue. Linear regression analysis was performed to evaluate the association between cancer PRS and EAA, adjusting for body mass index, sex (where applicable), cigarette smoking, and WGS platform and library construction protocol.

All EA estimates of cancer-relevant tissues and blood cells exhibited significant correlations with CA (maximum $P=2.44\times10^{-3}$). Among them, GrimAge, known for its strong predictive capacity for mortality, had the most pronounced correlation with CA, with Spearman coefficients ranging from 0.80 in blood cells to 0.98 in breast tissues. A higher prostate cancer PRS was significantly associated with increased EAA in normal prostate tissues measured by PhenoAge (β=2.49; $P=0.01$), Zhang-BLUP-Age (β=1.71; $P=0.02$), HannumAge (β=1.36; $P=0.04$), and GrimAge (β=0.73; $P=0.04$). In addition, a higher PRS for renal cell carcinoma showed a significant association with increased GrimAge acceleration in normal kidney tissues (β=0.82; $P=0.02$). Moreover, breast and lung cancer PRSs were significantly associated with increased EAA in blood cells. Specifically, breast cancer PRS was associated with Zhang-BLUP-Age acceleration (β=0.99; $P=0.04$), while lung cancer PRS showed associations with HannumAge (β=1.78; $P=0.01$) and Zhang-EN-Age acceleration (β=0.94; $P=0.02$).

Our results suggest a potential connection between genetic susceptibility to certain cancers and accelerated aging in relevant tissues and/or blood cells before cancer onset. Future large-scale studies are needed to substantiate and expand upon our findings.

#7011 The DNA methylation landscape across the TCR loci genes in patients with acute myeloid leukemia.

M. Pospiech, J. Beckford, A. M. S. Kumar, M. Tamizharasan, J. Brito, G. Liang, S. Mangul, H. Alachkar;
USC - University of Southern California, Los Angeles, CA

The T-cell receptor (TCR) repertoire is partly shaped by epigenetic modifications, including DNA methylation. Hypomethylating agents like decitabine are used to treat patients with acute myeloid leukemia (AML) and myelodysplastic syndrome (MDS). The precise DNA methylation patterns within the TCR loci and their dynamics associated with HMAs treatments remain underexplored. Here, we analyzed methylation patterns across TCR alpha and beta gene loci in T cells from GSE175758 and GSE67170 datasets, comparing patterns between patients with AML and healthy controls. We also investigated the impact of decitabine on the methylation patterns of TCR gene loci in patients with AML and MDS (GSE175758 and GSE80762).The overall levels of methylation between T cells from healthy donors and patients with AML were significantly different within the *TRAV* (0.55 vs 0.42, P < 0.001) and *TRBV* regions (0.70 vs 0.59, P < 0.001) with 46 *TRAV* and 33 *TRBV* sites differentially methylated positions, respectively. However, methylation patterns in HSCs (GSE63409), T cells from healthy donors and patients with AML and those in AML cells were strongly correlated (R > 0.67, range 0.67-0.99, P < 0.001).Because decitabine preferentially acts on leukemic cells and given the high correlation levels between AML cells and T cells across datasets we analyzed the effects of decitabine on TCR DNA methylation patterns in AML cells. In the leukemic cells decitabine treatment led to significant demethylation across 33 and 30 CpG sites within the *TRAV* and *TRBV* genes, respectively. In the pre-treatment AML samples higher methylation beta values were observed in differentially methylated positions (DMPs) compared with non-DMPs (*TRAV*: 0.847 vs 0.407; P < 0.001; *TRBV*: 0.771 vs 0.538; P = 0.049). In samples largely enriched of myeloid leukemic blasts, we found that *TRAV* and *TRBV* loci methylation patterns differ significantly between AML patients with good, moderate, and poor risk patients (P < 0.001). We found TRBV6-1 position 1 and 2 methylation was lower in patients with good risk, compared with intermediate risk (pos1: 0.07 vs 0.13, P=0.04; pos2: 0.1 vs 0.2, P = 0.002) and poor risk (pos 1: 0.07 vs 0.21, P < 0.001; pos 2: 0.1 vs 0.32, P < 0.001) and was lower in patients with intermediate risk compared with poor risk (pos1: 0.13 vs 0.21, p=0.007; pos 2: 0.21 vs 0.32, P = 0.001). The high correlation of TCR DNA methylation patterns between the T cells and the myeloid cells, suggests the need for similar analyses in the context of AML T cells.
The study highlights the presence of a conserved TCR loci methylated signatures which is highly correlated between myeloid leukemic cells and T cells and is associated with clinical outcomes, offering a potential avenue for therapeutic intervention. Hypomethylating agents, such as decitabine, can modulate TCR loci methylation patterns.

#7012 Studying mosaic epimutations at scale.

O. Nikolaienko, P. E. Lonning, S. Knappskog;
K. G. Jebsen Center for Genome-Directed Cancer Therapy, University of Bergen, Bergen, Norway

Mosaic epimutations (i.e., epigenetic gene inactivation) within the *BRCA1* gene promoter occur in 5-8% of healthy individuals and are associated with a significantly elevated risk of breast and ovarian cancer. These epimutations arise prenatally and then serve as an underlying cause of cancer in adulthood, likely accounting for about 20% of triple-negative breast cancers. Similar mosaic epimutations have been detected in some other tumor suppressor genes as well, but the intraindividual and population frequencies of this phenomenon remain unknown. To address this gap, we have developed novel methodology for detection of mosaic epimutations. The experimental technique is a multiplexed, hybridization capture-based, targeted methylation sequencing assay covering gene regulatory areas. It allows cost-effective assessment of epimutations in established and emerging tumor suppressor genes. An accompanying tailored data analysis pipeline is designed to quantify epimutations. The pipeline is sensitive and robust to variance in methylation, sequencing errors and batch effects. We applied this method to a set of samples from healthy young males. Analysis uncovered significant interindividual epimutational heterogeneity and confirmed high sensitivity of the assay and its superiority compared to methylation profiling using microarrays. Here, we present details on the highly sensitive, scalable and robust methodology for analysis of mosaic epimutations together with the results on initial assessment of the prevalence of epimutations in healthy individuals. We anticipate that this method will become widely used for studies of epigenetic gene regulation and related cancer risk.

#7013 Methyl-Micro-C: simultaneous high-resolution characterization of three-dimensional chromatin structure and the DNA methylome.

C. Stevens, L. Gonzalez-Smith, H. Cao, S. K. Rhie;
Keck School of Medicine of USC, Los Angeles, CA

Understanding cancer biology allows for the determination of patient prognosis through biomarkers and predicting treatment sensitivity. For many cancer types, genetic changes have been largely characterized, but the contributions of epigenetic changes, which are also implicated in tumorigenesis, are not yet well understood. Three-dimensional chromatin architecture changes occur throughout tumor development, changing the states and interactions between cis-regulatory elements, overall inducing gene dysregulation. Chromatin structure changes have previously been interrogated using Hi-C, a technique which utilizes restriction enzyme-mediated digestion of chromatin. Although this method is useful, it cannot detect chromatin states of regulatory elements with high sensitivity and resolution due to the use of restriction enzymes that give multi-nucleosome-sized fragments. Micro-C instead uses MNase that preferentially digests accessible regulatory elements, resulting in mono, di, and tri-nucleosome fragments, providing higher-resolution chromatin interaction data, indirectly determining which regulatory elements are active and in proximity to one another. However, spatial proximity of genomic regions are only a piece of the chromatin structure epigenetic story. Partially methylated domains, which are gained or altered throughout tumor development, are reported to co-localize with topologically associating domains, suggesting that they can contribute to chromatin structure alterations. Whole methylome sequencing techniques can be used to determine methylation states of these domains and regulatory regions. Recently, enzyme-mediated methylation sequencing has been shown to induce less DNA damage than the canonical whole-genome bisulfite sequencing, providing a more accurate and comprehensive picture of the DNA methylome. Although DNA methylome data alone can provide information about epigenetic status within genomic regions, overlaying chromatin structure changes at these locations can further corroborate findings. In this way, chromatin structure and DNA methylome data together can provide a more complete picture of cancer epigenetics. However, it is very expensive to sequence at the depth necessary to gain useful information. To address this issue, we developed a technique called Methyl-Micro-C to simultaneously interrogate the DNA methylome while observing chromatin structure in the same sample. Methyl-Micro-C integrates the higher resolution Micro-C method and more comprehensive enzyme-mediated methylation sequencing method together to investigate both the chromatin interactions as well as DNA methylation patterns for the same sample simultaneously. Here, we use Methyl-Micro-C with prostate cancer cells to characterize 3D epigenomic mechanisms that drive prostate carcinogenesis.

#7014 Integrative DNA methylation cancer profiling reveals patterns associated with tumor progression and treatment response.

A. Lahtinen[1], G. Marchi[1], D. Afenteva[1], K. Lavikka[1], S. Holmstrom[1], E. Pollanen[1], G. Micoli[1], I. Maarala[1], Y. Li[1], T. A. Muranen[1], J. Oikkonen[1], S. Hietanen[2], A. Virtanen[3], J. Hynninen[2], A. Hakkinen[4], S. Hautaniemi[1];

[1]University of Helsinki, Helsinki, Finland, [2]University of Turku and Turku University Hospital, Turku, Finland, [3]University of Helsinki and HUS Diagnostic Center, Helsinki University Hospital, Helsinki, Finland, [4]Boston Children's Hospital, Harvard Medical School, Boston, MA

DNA methylation plays a critical role in tumor progression and response to chemotherapy. Frequently dysregulated during tumor development, it is closely intertwined with mixed effects from patient epigenetic background, tissue context, and treatment pressure. Here, we leveraged methylomic and transcriptomic profiling of 400 whole-genome sequencing samples from 125 patients with ovarian high-grade serous carcinoma (HGSC), belonging to the prospective, longitudinal, multi-region DECIDER trial (NCT04846933). This cohort included 120 samples from tubo-ovarian tumors, 209 samples from intra-abdominal metastases, and 71 ascites, representing all major sites of HGSC metastases. We profiled cancer methylome across tissues, patient groups, and various anticancer treatments using decomposition method, which allows separating the effects of tumor microenvironment and treatment, tissue, and patient specific changes, thus, facilitating integration of the heterogeneous collection of samples. First, we systematically examined the tissue-specific carcinogenesis and characterized methylomes of all types of metastases and excess fluid accumulations in the abdominal cavity. In our analyses, the cancer spread from tubo-ovarian sites to metastatic deposits involved gradual loss of DNA methylation and increase in transcriptomic levels, possibly indicating stemness. Specifically, several members of the ATP-binding-cassette (ABC) family of transporters, as well as receptor tyrosine kinases were frequently hypomethylated in bowel and omentum. The methylome of ascites showed most commonality to the tubo-ovarian tumors and peritoneum. Our results confirmed that several well-known tumor-associated genes, such as *PTEN*, *GSK3B*, *ESR1*, *FGFR2*, *TNC*, *BCL6*, *HIF1A*, *NOTCH2* are regulated epigenetically, and this dysregulation stems early from the sites of origin. Next, we built methylomic profiles of patients with various treatment responses. Direct comparisons between good and poor responders revealed pronounced methylation differences, with refractory disease being associated with severely aberrated methylome prior to chemotherapy treatment. Neoadujuvant chemotherapy resulted in very few changes to these epigenetic aberrations and no acquired mechanisms, suggesting that intrinsic methylomes of poor responders accommodate multiple drivers for EMT, hypoxia, and chronic inflammation to resist chemotherapy-induced cell death already prior to treatment. In conclusion, using a large whole-genome sequencing DNA methylation dataset we elucidated the major underlying epigenetic mechanisms of tumorigenesis and platinum resistance, which provide possible drug targets for improving platinum sensitivity. Our multi-omics analyses enabled the identification of aberrated patterns that drive transcriptional changes, shedding light on epigenetic landscape of HGSC.

#7015 Crosstalk between histone and DNA methylation in the development and progression of ALK+ ALCL.

C. Lobello[1], S. Wang[1], S. Rao[1], J. Pawlicki[2], N. Mansoor[1], J. L. Riley[2], R. Nejati[1], W. A. Mariusz[1];
[1]Fox Chase Cancer Center, Philadelphia, PA, [2]University of Pennsylvania, Philadelphia, PA

ALK-positive anaplastic large cell lymphoma (ALK+ ALCL) is a T-cell non-Hodgkin lymphoma characterized by the presence of the fusion oncogene nucleophosmin-anaplastic lymphoma kinase (NPM-ALK). Tumor cells control the expression of key genes in different manners: mutations, translocations or epigenetically. Our group have shown that in this tumor a plethora of genes are silenced by NPM-ALK through DNA methylation. However, recent evidence showed that some of the genes downregulated by DNA methylation might have already been silenced prior to the appearance of DNA methylation. Herein, we investigate the possible role of histone methylation in the silencing of genes and its relationship to DNA methylation. To better understand the possible players in the silencing of genes in ALK+ ALCL we used T-cell transformed with NPM-ALK and recorded over time the changing in gene expression, DNA methylation and histone marks. Using RNAseq comparing transformed cells at different time points, we noticed that downregulated genes in ALK+ ALCL became gradually silenced also in our system. Next, we investigated the DNA methylation (meDNA) on their promoters, and we confirmed a progressive increase of meDNA but clearly slower compared to the silencing of the genes, or if compared to the meDNA status of established ALK+ ALCL cell lines. Finally, we explored the presence of silencing histone marks on the promoter of the silenced genes using qPCR-ChIP. Among the repressive histone marks evaluated, H3K27me3 stood up as possible candidate for the gene silencing. Therefore, we look at the different gene expression changes after the inhibition of either meDNA, using a DNMT1 inhibitor (GSK3685032), or histone methylation, by EZH2 inhibitor (EPZ6438). RNAseq data showed the re-expression of downregulated genes after EZH2 and/or DNMT1 inhibition providing clear insights on their epigenetic regulation. The co-presence of H3K27me3 and meDNA on the promoters of those genes points towards a crosstalk between DNA and histone methylation machineries. Despite it is clear how NPM-ALK regulates DNA methylation, nothing is known about NPM-ALK and EZH2. To investigate their relationship, we treated ALK+ cells with ALK inhibitor, and we observed a decrease of EZH2 expression at protein and mRNA level. STAT3 inhibition, through napabucasin or by STAT3 silencing using Crispr-cas9 technology, resulted, likewise, in the downregulation of EZH2. Moreover, ChIPseq showed STAT3 presence on *EZH2* promoter, further confirming this mechanism. Altogether, those data showed that NPM-ALK regulates *EZH2* expression through STAT3. In conclusion, we provide, not only novel information on the mechanism in the downregulation of genes in ALK+ ALCL, but also new insight on the understanding of the epigenetics machinery and the crosstalk between histone and DNA methylation, for long time considered two mutually exclusive mechanisms, or even antagonist.

#7016 Plastic epigenome in youth: Insights from open chromatin in stem cells.

Y.-Y. Liu[1], C. Takeuchi[1], S. Yamashita[2], T. Ushijima[1];

[1]Hoshi University, School of Pharmacy and Pharmaceutical Sciences, Tokyo, Japan, [2]Maebashi Institute of Technology, Maebashi, Japan

The presence of plasticity in the epigenomes of young individuals is suggested by the aggressive phenotypes observed in cancers among adolescent and young adults (AYAs), including gastric cancers. To demonstrate the presence of this plasticity and identify the underlying epigenomic characteristics in gastric stem cells during youth, we examined organoids established from murine stomach tissue and conducted single-cell RNA-seq and ATAC-seq using murine antrum-pyloric tissues at ages of 3 weeks and 50 weeks, corresponding to human infancy and middle-age adult, respectively.

Organoids established from infant mice showed higher dependence to niche factors, and stronger response to cytokine signals. Ligand-receptor analysis using single-cell RNA-seq data of tissues showed that infant epithelial stem cells and stromal cells had stronger interactions. Both supported the plastic nature of infant gastric epithelial cells.

Single-cell ATAC-seq enabled us to identify epithelial stem cell population in infant and middle-aged mice, and 71 and 118 chromatin peaks were specific to infant and adult stem cells, respectively. Motif enrichment analysis showed an enrichment of binding sites for bZIP family transcription factors in infants, and an enrichment of binding sites of a chromatin remodeling factor and a family of transcription factors in adults. Additionally, comparison between differentiated epithelial cells, marked by the pit cell marker *Muc5ac*, and stem cells, marked by *Lgr5*, showed more pronounced differences: 46,772 peaks specific to pit cells and 39,076 peaks specific to stem cells. Interestingly, regions specific to pit cells were enriched in binding sites of the chromatin remodeling factor and the family of transcription factors, identical to the open regions specific to adult stem cells. This suggested that the chromatin accessibility profile of aged stem cells approaches to that of differentiated cells, leading to a loss of stemness. The single-cell RNA-seq data also revealed an increase in interactions between differentiated epithelial cells and fibroblasts in aged mice, as opposed to infant, suggesting the emergence of aberrant interactions in aged stomach tissue. Collectively, our data suggested that chromatin accessibility of gastric stem cells undergo an epigenomic shift during aging, approaching to the profiles of differentiated cells and losing their plasticity, and that a specific chromatin remodeling factor and a family of transcription factors could be involved in the process.

#7017 Increased epigenetic age acceleration in young adult and early onset colorectal cancer patients post-treatment: A ColoCare Pilot Study.

E. M. Siegel[1], J. K. Kresovich[1], A. M. Bloomer[1], A. Berglund[1], E. Jean-Baptiste[1], G. Trujillo[1], R. Carmella[1], J. Love[1], S. Felder[1], J. Ose[2], B. Gigic[3], C. I. Li[4], J. C. Figueiredo[5], A. T. Toriola[6], C. M. Ulrich[2], D. Shibata[7], L. B. Oswald[1];

[1]Moffitt Cancer Center, Tampa, FL, [2]Huntsman Cancer Institute, Salt Lake City, UT, [3]University Hospital Heidelberg, Heidelberg, Germany, [4]Fred Hutchinson Cancer Center, Seattle, WA, [5]Samuel Oschin Comprehensive Cancer Institute at Cedars-Sinai Medical Center, Los Angeles, CA, [6]Washington University School of Medicine, St. Louis, MO, [7]University of Tennessee Health Science Center, Memphis, TN

Introduction: Advanced biological age relative to chronological age has been observed in individuals with colorectal cancer (CRC), and there is growing evidence that cancer treatments can further accelerate biological aging. However, the influence of age at diagnosis on these relationships has yet to be examined in detail. This pilot study used data from the ColoCare Study to explore pre- and post-treatment differences in age acceleration by chronological age at CRC diagnosis.

Methods: The ColoCare Study is a prospective cohort study of newly-diagnosed CRC patients enrolled across seven U.S. and European sites. Participants in this pilot study were from the ColoCare site in Tampa, Florida who had available pre-treatment blood DNA. Young adult (YA, aged 18-39) and early onset (EO, aged 40-49) participants were matched with average onset (AO, aged 50-64) and late onset (LO, aged >64) participants on stage, sex, race and microsatellite instability status. Genome-wide DNA methylation profiles were assayed on buffy coat DNA using MethylationEPIC v2 BeadChips. PhenoAgeAccel and GrimAgeAccel were calculated on all samples to quantify the difference between DNA methylation-predicted biological age and chronological age (i.e., age acceleration). Linear regression models were used to estimate the associations of age at diagnosis and treatment with PhenoAgeAccel and GrimAgeAccel, adjusted for sex, race, and site (rectal, colon).

Results: The sample (n=60) included n=19 YA, n=15 EO, n=11 AO, and n=15 LO participants with pre-treatment blood DNA. Over half (n=15 YA/EO, n=20 AO/LO) had a paired post-treatment blood sample available. Half of participants were female and had colon tumors, and 76% were diagnosed with stage I-III disease. Pre-treatment, PhenoAgeAccel and GrimAgeAccel were similar across age groups (P > 0.05). In the subset of participants with pre- and post-treatment samples, age acceleration appeared to increase post-treatment (pre- and post-treatment differences, PhenoAgeAccel: 1.44, SD: 5.55, P= 0.13; GrimAgeAccel: 0.92, SD: 2.80, P= 0.06). Increases were largest among YA/EO participants. In adjusted models, the predicted differences in pre-to post-treatment PhenoAgeAccel were 2.89 (95% CI: -0.13, 5.90) in YA/EO and 0.36 (95% CI: -2.25, 2.96) in AO/LO (P-difference= 0.20). The predicted differences in GrimAgeAccel were 1.75 (95% CI: 0.25, 3.25) in YA/EO and 0.30 (95% CI: -1.00, 1.60) in AO/LO (P-difference= 0.15).

Conclusions: In this pilot study of CRC patients, pre-treatment age acceleration did not vary by age at diagnosis. Post-treatment, patients diagnosed at age 49 or younger had larger increases in age acceleration than patients diagnosed at age 50 or older. These findings warrant further investigation in larger samples and to determine if increases in post-treatment age acceleration as associated with patient outcomes and treatment response.

#7018 Application of HiTIMED and cell type adjusted epigenome-wide models identifies driver tumor DNA methylation alterations in multiple cancers.

I. M. Vlasac, Z. Zhang, L. A. Salas, B. C. Christensen;
Dartmouth Geisel School of Medicine, Lebanon, NH

DNA methylation (DNAm) is an epigenetic mark crucial in lineage specification and cellular differentiation, resulting in distinct patterns by cell type. These patterns can serve as biomarkers in deconvolution approaches inferring cell proportions from composite DNAm signals in biospecimens like blood and tumor tissue. Adjusting for cellular heterogeneity is critical to avoid confounding by cell type. The HiTIMED (hierarchical tumor immune microenvironment epigenetic deconvolution) algorithm provides high-resolution tumor microenvironment profiling, up to 17 cell types, including tumor, myeloid, and angiogenic compartments. We analyzed bladder, prostate, and uterine cancers, applying HiTIMED on the tumor (n=1,341) and normal adjacent tissue (n=105), adjusting for age, sex, and cell types. DNAm data from The Cancer Genome Atlas (TCGA) was used, and HiTIMED was applied to deconvolute various cell proportions.
Linear model comparisons to identify significantly differentiated loci with/without cell type adjustment are summarized in Table 1. We demonstrate greater than 99% reduction in both hypermethylated and hypomethylated loci in all cancer types after adjustment for cell type. Our study demonstrates HiTIMED's applicability to deconvolve the tumor microenvironment in multiple cancer types and demonstrates the importance of adjusting for cell type in epigenome-wide association studies to identify differentially methylated loci, offering greater biological insight into the etiology of specific cancer types.

Significant differentially methylated loci in tumor versus normal adjacent tissue, FDR <0.05			
Cancer type	Linear model	Hypermethylated in tumor (logFC >2.0)	Hypomethylated in tumor (logFC < -2.0)
Bladder cancer n = 21, normal adjacent tissue n = 413 tumor	Model 1 (Cancer Status, Age, Sex)	4495	19,936
	Model 2: (Cancer Status, Sex, age, six cell types)	27	39
Prostate adenocarcinoman = 50, normal adjacent tissuen = 499 tumor	Model 1 (Cancer Status, Age)	8988	2207
	Model 2: (Cancer Status, age, six cell types)	2	4
Uterine carcinoman = 34 normal adjacent tissuen = 429 tumor	Model 1 (Cancer Status, Age)	11,698	16,249
	Model 2: (Cancer Status, age, six cell types)	250	8245

#7019 Identifying cell free DNA methylation signatures in cerebrospinal fluids for the early detection of brain metastasis in non-small cell lung cancer.

T. Chen[1], B. T. Lau[1], X. Bai[1], M. H. Gephart[2], H. P. Ji[1];

[1]Stanford University School of Medicine, Stanford, CA, [2]Stanford University, Stanford, CA

Brain metastasis (BM) is major complication for adult cancer patients. Up to 2% of all cancer patients develop BM. Non-small cell lung cancer (NSCLC) contributes up to 55% of all BM. Approximately 15-20% of NSCLC patients show metastases at diagnosis, and approximately half will develop BM during their clinical course. Even after treatments like surgery, radiation and immunotherapy, the prognosis is dismal with median overall survival less than 13 months. No standard screening or early diagnostic testing exists for BM now. There is an urgent need to identify genomic features that predispose towards brain metastasis - these biomarkers could be used for early detection and disease monitoring. The cfDNA methylation and fragmentation patterns provide potential epigenetic biomarkers for detecting cancer. These patterns are specific to cell/tissue origin and cancer types. DNA methylation refers to a chemical modification of a specific carbon with an added methyl group in the cytosine. Hypomethylation in the gene body and hypermethylation in the promoter region lead to cancer development. We hypothesize that there are specific cfDNA methylation and fragmentation signatures in CSF that reflect the epigenetic states of BMs, and cancer predisposition for brain metastasis. We applied a novel single molecule sequencing approach to study CSF cfDNA methylation of BM from NSCLC. Our cohort consisted of ten patients with NSCLC-BM (samples N=14) and eleven healthy controls (N=11). Briefly, extracted cfDNA was obtained from CSF samples. Multiplexed sequencing libraries were prepared following an optimized protocol, and sequenced on PromethION flow cell for 72hr by Oxford nanopore technologies. Data were processed with the onboard base and methylation calling, followed by our bioinformatic pipelines for cfDNA size and methylation analysis. Distinct methylation patterns were found on significant CpG sites (fdr-corrected $p<0.01$) between cancer patients and controls, in both gene-body and promoter region. Biological pathway analysis showed enrichment in essential functions involving PI3K, ERBB2, TNF-α signaling ($p<0.03$), all of which play a role in NSCLC. Enriched mono-nucleosome levels ($p = 1.07e-03$) and differentiated mono-/tri- nucleosome ratios ($p = 1.34e-03$) were found in cancer vs. controls. Overall, our results suggest that a combination of cfDNA methylation and fragmentation can detect NSCLC-BM. This study will benefit BM patients with early detection and better prognosis, and extend our understanding in brain metastases in NSCLC.

#7020 Prognostic implications of microRNA 181a 2 3p expression in association with tumor budding in patients with stage III lung squamous cell carcinoma.

E. Lee[1], **S. Kim**[1], J. Kim[2], M. Lee[3], Y. Ko[4], S. Chun[4];
[1]Seoul St. Mary's Hospital, Seoul, Korea, Republic of, [2]Department of Hospital Pathology, College of Medicine, The Catholic University of Korea,, Seoul, Korea, Republic of, [3]Department of Life Science, Dongguk University-Seoul, Ilsandong-gu, Goyang-si, Korea, Republic of, [4]Division of Oncology, Department of Internal Medicine, College of Medicine, The Catholic University of Korea, Seoul, Korea, Republic of

Introduction: Tumor budding (Bd) has been known as an independent prognostic factor in various malignancies. MicroRNA (miRNA) are known to play an important role in regulating Bd. However, understanding the relationship between Bd and miRNA in Lung Squamous cell carcinoma (LUSC) remains limited.
Methods: 115 LUSC patients who underwent curative resection were included in the discovery cohort. Bd was verified through immunohistochemical (IHC) stain. Bd was classified according to a three tier system: Bd1 with 0-4 buds, Bd2 with 5-9 buds, and Bd3 with 10 or more buds. MiRNA expression profiles were analyzed through RNA sequencing. Differences in survival outcomes for miRNA, as identified in the discovery cohort, were confirmed using LUSC data of The Cancer Genome Atlas (TCGA) as a validation cohort.
Results: The relationship between Bd2 and the prolongation of recurrence-free survival (RFS) was statistically significant (p=0.0113), whereas Bd1 was correlated with Overall Survival (OS) (p=0.0468). Multivariate analysis indicated that both a high T stage (HR: 5.211, 95% CI: 1.168-23.250, p = 0.031; and HR: 5.107, 95% CI: 1.447-18.030, p < 0.011) and Bd3 (HR: 3.683, 95% CI: 1.370-9.900, p = 0.010; and HR: 1.600, 95% CI: 0.800-3.201, p = 0.018) are independently significant poor prognostic factors for both RFS and OS. MiRNA-181a-2-3p was identified through Differentially Expressed miRNA (DER) analysis. A higher expression of miRNA-181a-2-3p in stage III LUSC of the TCGA dataset was associated with OS (p=0.0463).
Conclusions: Our study demonstrates that the miRNA 181a 2 3p expression is associated with improved OS. This association may be attributed to its inhibitory effect on Bd in advanced stages of LUSC.

#7021 Selecting your epigenomic assay: Comparing ChIP-seq, CUT&RUN, and CUT&Tag.

A. H. Guo, C. R. Comeau, F. Chen;
Cell Signaling Technology, Inc., Danvers, MA

For many years, chromatin immunoprecipitation (ChIP) was the standard assay for studying epigenetic mechanisms. However, two new versatile techniques have recently been developed that are faster, experimentally easier, and more cost-effective than ChIP. Cleavage Under Targets & Release Using Nuclease (CUT&RUN) and Cleavage Under Targets & Tagmentation (CUT&Tag) can be used for understanding protein-DNA interactions within the natural chromatin context of the cell. Both CUT&RUN and CUT&Tag can be combined with Next Generation Sequencing (NGS) to analyze the function of histone modifications and the binding of transcription factors, DNA replication factors, or DNA repair proteins across the genome.

CUT&RUN and CUT&Tag are rapid, robust, and true low cell number methods for the detection of protein-DNA interactions. Unlike ChIP, both assays are free of formaldehyde cross-linking, chromatin fragmentation, and immunoprecipitation. When compared to ChIP, CUT&RUN and CUT&Tag require fewer starting cells (as low as 5,000 – 20,000), are shorter assays (one day from cells to DNA), and generate lower background signal (requiring fewer sequencing reads). At Cell Signaling Technology (CST), we have developed ChIP-seq, CUT&RUN, and CUT&Tag assay kits and validated a broad set of antibodies against histone modifications, transcription factors, and cofactors that are compatible with these kits. This poster will discuss the fundamentals of all three assays and highlight important factors to consider when selecting an assay for your experiment.

Through our antibody validation efforts, we have also generated a unique and extensive archive of ChIP-seq, CUT&RUN, and CUT&Tag NGS data using recombinant, monoclonal antibodies. This allows for the controlled comparison of these three commonly used chromatin profiling techniques. In this poster, I will highlight the similarities and differences between these assays when mapping a variety of histone modifications, transcription factors, and cofactor binding events across multiple sample types.

#7022 Whole genome and reduced representation enzymatic methyl-seq enable cost effective methylomes.

V. Panchapakesa, C. Ponnaluri, D. Evanich, A. Erijman, B. Langhorst, L. Williams;
New England Biolabs, Inc., Ipswich, MA

DNA methylation is an epigenetic regulator of gene expression with important functions in development and diseases such as cancer. Traditionally, sodium bisulfite conversion was used to distinguish 5-methylcytosines (5mC) and 5-hydroxymethylcytosines (5hmC) from cytosines. However, this method damages DNA and introduces significant sequencing bias. NEBNext® Enzymatic Methyl-seq (EM-seq™) is an enzymatic conversion approach that minimizes DNA damage therefore enabling longer insert sizes, lower duplication rates and a more accurate quantification of methylation in DNA samples with inputs ranging from 10 ng to 200 ng. An improved enzymatic conversion method, EM-seq v2, has a more streamlined workflow and an expanded DNA input range of 100 pg to 200 ng. Libraries made using NA12878 genomic DNA show improved yields, consistent global methylation and an even GC bias representation. The increased library yields subsequently reduces sequencing duplications and costs. Sequencing costs are an important consideration when performing whole genome methylome analysis as this often needs high sequencing depth to attain meaningful coverage to accurately call methylation. Reduced representation libraries, a commonly used method to investigate DNA methylation, relies on enrichment of CpGs within libraries digested using MspI. These CpGs are commonly found in regulatory regions. Although lacking comprehensive CpG coverage, for many researchers this method provides enough cost effective CpG methylation coverage for their studies. Reduced Representation EM-seq libraries (RREM-seq) and Reduced Representation Bisulfite libraries (RRBS) were made using 200 ng to 100 pg of NA12878 DNA. EM-seq adaptors were ligated to MspI digested DNA followed by conversion using either EM-seq v2 or sodium bisulfite. Libraries were PCR amplified and sequenced on an Illumina NovaSeq platform. RREM-seq resulted in higher yields and reproducible results regardless of input amounts compared to RRBS libraries. RREM-seq libraries also identified a higher number of CpGs with even coverage facilitating accurate methylation calling. RREM-seq libraries have superior sequencing metrics resulting in robust methylation profiling. Focusing on a subset of the genome generates higher coverage DNA methylation data at a lower DNA sequencing cost.

#7023 Application of exclusive liquid repellency for low input CUT&Tag histone analyses in prostate cancer spheroids.

Z. J. Kauffman, K. Koesser, K. T. Helzer, J. M. Sperger, M. N. Sharifi, C. Li, E. Heninger, X. Hazelberg, C. Gilsdorf, S. G. Zhao, D. S. Juang, D. J. Beebe, J. M. Lang;
University of Wisconsin - Madison, Madison, WI

Introduction/Background: Epigenetic alterations, including histone modifications and DNA methylation, drive treatment resistance and lethal prostate cancer. However, epigenetic assays typically require thousands of cells and are difficult to scale for patient tumor biopsies. While identifying these alterations is possible in cell lines, these analytes are more difficult to follow in clinical settings. Patient-derived organoids have emerged as viable intermediaries to investigate the changing chromatin landscape during the progression toward treatment-emergent prostate cancer. This report seeks to adapt the Cleavage Under Targets and Tagmentation (CUT&Tag) assay for use on a microfluidic technology to eliminate cell loss associated with complex, multi-step epigenetic assays to facilitate analysis of low input prostate cancer spheroids.
Methods: The Oil Immersed Lossless Total Analysis System (OIL-TAS) is an exclusive liquid repellency (ELR) platform that passes magnetic bead-bound analytes through immiscible phases to separate and extract analytes of interest while eliminating traditional centrifugation and wash steps that lead to sample loss. This platform enables adaptation of complex molecular assays such as CUT&Tag for lossless sample manipulation. We focus on the analysis of histone modifications in rare cells utilizing antibodies for H3K27 acetylation and methylation. Comparison of LNCaP prostate cancer cell lines harvested from either 2D cell culture or 3D spheroids was performed to evaluate the sensitivity and specificity of this integrated assay.
Results: The macroscale CUT&Tag assay has been performed with inputs of 25,000 nuclei from LNCaP spheroids with greater yields than similar inputs from 2D LNCaP cell culture. Yield increases have also been seen when performing the assay with inputs <10,000 nuclei in microscale on the OIL-TAS relative to the macroscale. Utilizing the OIL-TAS platform with spheroid inputs will allow for more sensitive investigation of histone modifications.
Conclusions: Integration of 3D, humanized models of tumor growth into the CUT&Tag assay will enable discovery of differential epigenetic regulation within patient-derived organoids or complex co-culture studies. Establishing baseline epigenetic landscapes among these intermediary models will enable a new platform for drug testing. Utilization of the OIL-TAS platform will allow for miniaturization of the assay down to 1,000 cell inputs and enable multiparametric RNA-seq, EM-seq, and CUT&Tag-seq of the same patient samples for longitudinal study.

#7024 Development of quality control methods for reliable NGS measurement of methylation in cfDNA.

J. C. Willey[1], E. L. Crawford[1], D. J. Craig[1], T. M. Morrison[2], H.-J. He[3], J. G. Herman[4];
[1]University of Toledo, Toledo, OH, [2]Accugenomics, Inc., Wilmington, NC, [3]National Institute of Standards and Technology, Gaithersburg, MD, [4]University of Pittsburgh School of Medicine, Pittsburgh, PA

Background and Purpose: Reliable measurement of circulating free genomic DNA (cfDNA) methylation patterns promises a means for cancer early detection as well as treatment response. Use of Next Generation Sequencing (NGS) methods to measure the cfDNA methylome across a large number of potentially methylated CpG sites may enable earlier detection by overcoming stochastic sampling associated with the small specimens obtainable by a blood draw. Wide-spread adoption of these methods for clinical diagnostic applications will be facilitated through improved quality controls that increase reliability. The goal of this study is to assess the performance of the SNAQ-SEQ™ method as a means to establish a limit of detection (LOD) for measurement of methylation at each targeted CpG site. For this purpose, we used test materials that were developed by the National Institute for Standards and Technology (NIST) to mimic methylated cfDNA.

Methods: NIST test materials were formulated by physically shearing cell line gDNA then subjecting it to size separation to mimic a size distribution similar to that observed in cfDNA, then mixing sheared DNA in its “native” state of methylation with sheared DNA that was *in vitro* methylated. Non-sheared NIST test materials also were assessed in these studies. Synthetic spike-in internal standards (IS) were combined with NIST test materials and the combined samples were bisulfite converted, then subjected to PCR-amplicon library preparation. Libraries were sequenced on an Illumina MiSeq instrument and bioinformatic analysis was conducted using the Qiagen CLC Workbench.

Results and Conclusions: In initial testing of an off-the-shelf IS for a region of the SOX2 gene, average methylation (preserved C) across 14 targeted CpG sites was 16.4% (0.5%-50%) in the “native” NIST non-sheared sample. This was consistent with the 11.6% methylation across all of SOX2 measured by the NIST. In contrast, in IS corresponding to the targeted SOX2 region the average preserved C was 0.32% (0.03%-0.5%). Use of synthetic internal standards enabled determination of LOD for each individual methylated site, controlling for all known sources of technical error, including inefficient bisulfite conversion, nucleotide substitution error, and alignment error. Studies are now underway that use the NIST test materials to measure methylation at five targets known to be altered in cfDNA from lung cancer subjects, SOX2, CDO1, TAC1, SOX17, and HOXA7.

#7025 Advancing methylation analysis: TAPS v1.0: A fast, scalable, and non-destructive sequencing method.

A. Garnett[1], J. Haimes[1], C. Marshall[1], T. Sanders[1], S. Vogel[1], M. Ranik[1], E. Casas[1], D. Wendel[1], L. Karamanof[2], B. Faurholme[2], A. de Beer[2], L. French[2], R. Wadsworth[2], E. van der Walt[2], K. Giordia[1], B. Kudlow[1];

[1]Watchmaker Genomics, Inc., Boulder, CO, [2]Watchmaker Genomics, Inc., Cape Town, South Africa

In the pursuit of advancing multi-cancer early detection, the exploration of cell-free DNA (cfDNA) through methylation profiling has emerged as a promising avenue. However, the realization of its full potential is impeded by limitations inherent in conventional methodologies, notably the 'gold standard' bisulfite conversion methods. These approaches pose challenges such as DNA destruction and the generation of low-complexity sequences resulting from the conversion of unmethylated cytosines to thymine. TET Assisted Pyridine-Borane Sequencing (TAPS) holds the potential as a non-destructive, rapid, and scalable alternative for base-level methylation analysis.

In this context, we introduce TET Assisted Pyridine-Borane Sequencing version 1.0 (TAPS v1.0), showcasing advancements to the technology originally introduced by Schuster-Böckler, Song, and their collaborators. TAPS v1.0 transforms 5mC into dihydrouracil (DHU) through a series of oxidation and reduction reactions. Ultimately, DHU is recognized as dU during PCR resulting in C-to-T conversions at 5mC sites, leaving unmethylated cytosines, the majority of cytosines, unchanged. The nondestructive nature of 5mC conversion yields significantly higher library yield and complexity compared to BS-seq. By leveraging Watchmaker's proprietary polymerase evolution platform, a DNA polymerase tolerant to DHU was selected for library amplification post DHU conversion, enabling unimpeded detection of 5mC, particularly in densely packed CpG repeats. Coupled with an optimized End Repair and A-tailing chemistry preceding TAPS v1.0, clinically relevant cfDNA samples of low quality and/or quantity can be analyzed in methylation detection pipelines.

To evaluate the performance of TAPS v1.0, human genomic DNA with control spike-ins featuring varying methylation statuses were employed. TAPS v1.0 exhibited significantly higher final library yield and greater complexity compared to BS-seq. Similar outcomes were observed in clinically relevant cfDNA samples.

#7026 Multi-omic genomic mapping with long read sequencing.

B. J. Venters[1], P. W. Hook[2], V. S. Kumary[1], A. R. Hickman[1], J. T. Anderson[1], A. Vaidya[1], R. J. Ezell[1], J. M. Burg[1], Z.-W. Sun[1], M. W. Cowles[1], W. Timp[2], M.-C. Keogh[1];

[1]EpiCypher, Durham, NC, [2]Johns Hopkins University, Baltimore, MD

Gene transcription is regulated by the complex interplay between histone post-translational modifications (PTMs), chromatin associated proteins (CAPs), and DNA methylation (DNAme). Mapping their genomic locations and examining the relationships between these chromatin elements is a powerful approach to decipher mechanisms of disease, thereby enabling discovery of novel biomarkers and therapeutics. Leading epigenomic mapping technologies (*e.g.,* ChIP-seq, CUT&RUN) rely upon DNA fragmentation to isolate regions of interest for sequencing on short read platforms (*e.g.,* Illumina). This strategy leads to substantial loss of contextual information regarding the surrounding DNA, precluding the identification of multiple co-occurring epigenomic features on a single DNA molecule. By contrast, long-read sequencing (LRS) platforms are capable of sequencing very long reads from a single molecule (typically >10kb), allowing relationships between features on a single molecule to be used to resolve heterogeneity within mixed populations. Here we report a robust multi-omic method that leverages LRS to simultaneously profile histone PTMs (or CAPs), DNAme, and parental haplotype in a single assay. This nondestructive, epigenomic mapping approach leverages a novel DNA methyltransferase fusion protein (pAG-M.EcoGII) to label DNA underneath antibody-targeted chromatin features, thereby marking sites of interest while preserving DNA molecules intact for LRS. Inspired by our work with state-of-the-art immunotethering-based approaches (CUT&RUN / CUT&Tag), nuclei are bound to magnetic beads to streamline and automate sample processing. Next, adenosines nearby antibody-targeted chromatin features are methylated with pAG-M.EcoGII, which are then directly read from genomic DNA using Oxford Nanopore Technologies or Pacific Biosciences LRS platforms. To determine the capabilities and limitations of this assay, we tested multiple chromatin targets in various cell lines. Importantly, this method is highly reproducible across biological replicates, and highly concordant with orthogonal SRS assays (*e.g.,* CUT&RUN). Further, we showed that this method is a true multi-omic approach by simultaneously profiling histone PTMs, native DNAme (5mC), and parental single-nucleotide variants from single DNA molecules within a single reaction. Finally, this workflow preserves chromatin integrity for LRS, revealing heterogeneity (*e.g.,* haplotype or paternal origin) within / between data types and providing access to previously unmappable genomic regions (*e.g.,* centromeres).

#7027 Direct multi-omics for the masses: Linking DNA methylation to chromatin targets via TEM-seq.

K. E. Maier[1], V. U. Sunitha Kumary[1], B. J. Venters[1], A. Hickman[1], A. Vaidya[1], J. Anderson[1], R. Ezell[1], J. M. Burg[1], L. Williams[2], C. Ponnaluri[2], P. Esteve[2], I. Meek[2], Z.-w. Sun[1], M. W. Cowles[1], S. Pradhan[2], M.-C. Keogh[1];

[1]EpiCypher Inc, Durham, NC, [2]New England Biolabs, Ipswich, MA

DNA methylation (DNAme) is an epigenetic mark that includes the modification of cytosine resides (5mC) within CpG islands. In addition to well characterized roles regulating gene expression, imprinting and silencing parasitic DNA elements, the misregulation of DNAme is implicated in multiple diseases. Evidence is emerging that DNAme is not an independent epigenetic mark but rather closely linked to the post translational modification (PTM) of histone proteins. However, examining the relationship between 5mC and PTMs are hampered by the usual approach of independent analyses that cannot establish a direct linkage. Furthermore, the traditional approach to measure 5mC relies upon harsh bisulfite chemical conversation of DNA, which introduces damage and systemic biases. To address these limitations, we developed Targeted Enzymatic Methylation-sequencing (TEM-seq): an ultra-sensitive multi-omic genomic mapping technology that delivers high resolution DNAme profiles at epitope-defined chromatin features. Importantly this assay is capable of directly examining the link between 5mC and histone PTMs and/or chromatin associated proteins (ChAPs). The TEM-seq workflow integrates CUT&RUN for genomic mapping with NEB's enzymatic methyl-seq (EM-seq) for unbiased DNAme analysis. CUT&RUN is a highly sensitive, standards-driven assay that uses antibodies to locally tether protein A/G-micrococcal nuclease (pAG-MNase) to chromatin within intact cells or nuclei, followed by controlled activation of the MNase to cleave nearby DNA. EM-seq then enzymatically converts [5mC/5hmC] to generate single-base resolution, unbiased DNAme profiles from sub-ng samples.

To determine the capabilities and limitations of this novel approach, we tested multiple chromatin targets in various cell lines. We demonstrate that TEM-seq is highly reproducible, specific, and efficient (<10% off-target binding, >90% enzymatic conversion of DNAme, <0.5% conversion of unmethylated DNA). TEM-seq is also highly-sensitive, requiring only five million short-read sequences per assay (10-50x less than whole-genome 5mC-sequencing), demonstrating the disruptive potential of the assay to enable cost-effective approach for targeted DNAme analysis. Finally, we leveraged TEM-seq to gain mechanistic insights to Rett syndrome a neurodegenerative disorder that results from mutations in the 5mC-binding domain of the *MECP2* gene.

#7028 Optimization of DNA extraction methods and DNA methylation array quality from FFPE prostate tumor tissues to identify DNA methylation biomarkers.

Colton Duran Stensrud[1], Leonardo Gonzalez-Smith[1], Claire Stevens[1], Huan Cao[1], Jenaye Mack[2], Olumide Arigbede[3], Daniel Weisenberger[1], Sarah G. Buxbaum[3], Sara M. Falzarano[2], Suhn Rhie[1]

[1]Biochemistry and Molecular Medicine, USC - University of Southern California, Los Angeles, CA,[2]Pathology, Immunology, and Laboratory Medicine, University of Florida, Gainesville, FL,[3]Pharmacy and Pharmaceutical Sciences, Florida A&M University, Tallahassee, FL

Prostate cancer is the second leading cause of cancer related deaths among men in the United States. Health disparities in men diagnosed with prostate cancer are observed between patients of African and those of European ancestry. To elucidate molecular mechanisms behind prostate tumorigenesis and racial disparities, researchers have identified genetic alterations such as gene fusions, deletions, and mutations that occur at varying frequencies among different ethnic groups. However, results are inconsistent across studies, suggesting that racial disparities may be multifactorial. Our approach to further understand the mechanisms underlying racial disparities is to compare DNA methylation profiles between cancers from different ethnic groups using formalin-fixed paraffin-embedded (FFPE) prostate cancer tissue samples. For this study, FFPE prostate cancer specimens from 32 Black men and 30 age-matched White men were obtained in the form of tissue sections on glass slides. To profile DNA methylation in these samples, tumor and normal tissue regions (in a subset of cases) were outlined on a hematoxylin & eosin (H&E) reference slide and the respective regions were macro-dissected off the corresponding unstained slides from the same block. The areas of macro-dissected regions were measured using ImageJ, and the number of slides were taken to normalize DNA yield. Next, we compared magnetic bead and column based DNA extraction methods. We evaluated them on their relative DNA yield per tissue size, and identified that the bead-based extraction method had both higher and more consistent DNA yield. In total, we used 95 unique tissue regions to profile global DNA methylation levels using Illumina Epic array. We found that a subset of samples harbored an aberrant DNA methylation pattern. Therefore, we extracted DNA from additional FFPE tissue slides using the bead-based method and repeated the assay with a larger amount of DNA, successfully rescuing the majority of the aberrant samples. Next, we will evaluate associations between DNA methylation levels in different ethnic groups, clinicopathological features, and follow-up data to help identify potential DNA methylation biomarkers and therapeutic targets linked to prostate cancer from different ethnicities.

#7029 Trajectory of DNA methylation in blood up to 18 years prior to lung cancer diagnosis.

Y.-J. Choi[1], **K.-J. Hong**[2], Y.-S. Lee[3], W. Kim[4], Y. Kim[1], S. Jee[5], J. Kim[2];

[1]National Cancer Control Institute, National Cancer Center, Goyang, Korea, Republic of, [2]Graduate School of Cancer Science and Policy, National Cancer Center, Goyang, Korea, Republic of, [3]Research Institute, National Cancer Center, Goyang, Korea, Republic of, [4]School of Medicine, Kangwon National University, Chuncheon, Korea, Republic of, [5]Institute for Health Promotion, Graduate School of Public Health, Yonsei University, Seoul, Korea, Republic of

Purpose: Lung cancer (LC) has the highest mortality rate in South Korea. As prediction and early detection of lung cancer is pivotal to enhance survival rates, we attempted to investigate the trajectory of DNA methylation (DNAm) several years prior to lung cancer diagnosis by using prediagnostic blood samples.
Methods: From National Cancer Center Health Examinee Cohort, established in 2003, we selected study participants who became diagnosed with LC several years after health examination, thereby collecting prediagnostic samples from 18 years to 1 year prior to LC diagnosis. Normal controls (n=150) were matched with patients (n=150) by sex, age, and the time of sample collection. Epigenome-wide DNAm data were obtained by using Infinium Human MethylationEPIC v2.0 Beadchip. We assumed non-linear relationship between DNAm changes and the time-to-diagnosis and estimated an optimal threshold point of non-linear relationship with a piecewise linear regression analysis at each CpG sites (CpGs). We used the ratio of M-values of patients and matched controls to establish the non-linear model composed of two linear models with a threshold point where the slope changes. Then, we performed functional enrichment analysis by each year prior to LC diagnosis using ReactomePA.
Results: We identified threshold models with a threshold point where the slope changes from zero (from 18 years prior to LC up to the threshold point) to positive or negative (from threshold point to the point of LC diagnosis), which we termed “flat-to-change model”. Out of 790,048 CpGs, we identified a total of 7214 CpGs showing the “flat-to-change model”, of which 944, 789, 480, 413, 687, 542, 516, 1140, 315, 284, 327, 432, 83, 95, 74, 32, and 23 CpGs were found prior to 1, 2, 3, 4, 5, 6, 7, 8, 9, 10, 11, 12, 13, 14, 15, 16, and 17 years before LC diagnosis, respectively. Functional enrichment analysis showed that various pathways were associated at different time point berfore LC diagnosis. CpGs of which DNAm was changed two years before LC diagnosis were associated with telomerase extension by telomerase involving *ANKRD28/TERT/TERF2/PPP6R3/WRAP53*. Transcriptional regulation by TP53 was associated with DNAm changes before both 5 and 14 years of LC diagnosis via *POLR2A*.
Conclusions: We identified the trajectories of DNA methylation up to 18 years prior to LC diagnosis, and found that a greater number of CpG sites showed DNAm changes adjacent to the time point of LC diagnosis. CpG sites associated with specific time point before LC diagnosis may elucidate the mechanisms of tumorigenesis and also have potential for LC prediction markers.

#7030 Reference materials for analysis of DNA methylation in cell-free circulating tumor DNA.

A. Higgs, A. Ryan, J. Ramprakash, D. Ruminski Lowe, Y. Konigshofer, C. Huang, A. Anfora, R. Garlick, B. Anekella;
LGC Clinical Diagnostics, Gaithersburg, MD

Aberrant DNA methylation is associated with many cancers including breast, liver, bone, and colon and has been identified as a biomarker for early cancer screening. Liquid biopsies are beginning to screen for DNA methylation in cancer-derived DNA, but accurate assessment of methylation is not trivial, and methods like bisulfite sequencing can result in biased data. Reference materials for establishing the analytical validity of measurements of CpG methylation are not widely available. In order to prepare such reference materials, genomic DNA (gDNA) was extracted from the well characterized human reference cell line GM24385 and fragmented to a circulating tumor DNA (ctDNA)-like size distribution. This DNA was processed further to prepare CpG-methylated and unmethylated versions. The size distribution was determined by using the Bioanalyzer High Sensitivity DNA Kit (Agilent, Santa Clara, CA). Methylation status in the reference materials was confirmed by both digital PCR (dPCR) and NGS based methods. A digital PCR method was developed to analyze heterozygous single nucleotide polymorphisms (SNPs) using the Bio-Rad QX200™ Droplet Digital PCR (ddPCR) System. To determine methylation levels by NGS, the NEBNext™ Enzymatic Methyl-seq Kit was used (EM-seq). Paired-end sequencing of the libraries was performed on a NextSeq™ 2000 (Illumina, San Diego, CA). Data alignment to hg19 was done with the bwa-meth (Pedersen, BS., et al.) aligner, and assessment of methylation in the aligned data was done with MethylDackel (Ryan, D.). Each reference material had an average peak size of ~160 bp in length, similar to patient cfDNA. By dPCR, the unmethylated reference material had an average of 0.73% DNA methylation, while the methylated reference material had an average of 100.10% DNA methylation. Values can be above 100% by dPCR due to unequal representation of both alleles. By NGS, the unmethylated reference material had an average of 0.93 % CpG methylation, which was similar to the background of 1.13 % and 1.31 % for CHG and CHH methylation, respectively. The methylated reference material had an average of 93.95 % CpG methylation, with a background of 0.69 % and 0.74 % for CHG and CHH methylation, respectively. Because EM-seq relies on enzymatic protection and conversion steps, it may be that these reactions did not allow for full protection and full conversion, which led to values above 0 % for unmethylated and below 100 % for methylated materials. We have developed reference materials for the assessment of DNA methylation in ctDNA. One unmethylated and one methylated reference material was created. These reference materials can be mixed together to the level of methylation required to help aid in assay design, optimization, and validation.

MOLECULAR/CELLULAR BIOLOGY AND GENETICS: Genomics and Immunooncology
Poster Session

#7034 Pooled CRISPR screening coupled with single-cell sequencing identifies modifiers of CAR T cell state in the context of chronic antigen stimulation.

S. Joshi[1], G. Wozniak[1], J. Gagnon[1], K. Vucci[1], A. Merrell[1], M. Simon[1], C. Oh[1], A. Cardozo[1], D. DeTomaso[1], J. Chow[1], G. Zheng[1], A. Boroughs[1], K. Joho[1], P. Thakore[2], S. Oh[2], J. Freimer[2], A. Cass[1], V. Sail[1], C. Tocchini[1], M. Sandoval[1], A. Liu[1], E. Cui[1], M. Drever[1], B. Galvin[1], J. Milush[1], L. Gray-Rupp[1], E. Wheeler[2], B. Chen[2], J. Levine[2], C. Eidenschenk[2], J. Schartner[2], K. Geiger-Schuller[2], J.-C. Huetter[2], S. Rutz[2], O. Rozenblatt-Rosen[2], I. Mellman[2], W. Haining[1];
[1]Arsenal Biosciences, South San Francisco, CA, [2]Genentech, South San Francisco, CA

T cell exhaustion resulting from chronic antigen stimulation and an immunosuppressive tumor microenvironment limits the efficacy of T cell therapies in the solid tumor setting. The onset of T cell exhaustion is associated with distinct epigenetic and transcriptional changes. We hypothesized that genetic perturbations which shift T cells away from exhaustion associated states could increase the potency of immunotherapies. To this end, we utilized pooled, *in vitro* CRISPR/Cas9-based screening paired with deep sequencing readouts to characterize perturbation dependent T cell states in the context of chronic antigen stimulation. In order to achieve this, we developed a lentivirus-based workflow to perform CRISPRko, CRISPRi and CRISPRa pooled screens in human CAR T-cells that allowed for assessment of T cell phenotypes mediated by knockout, knockdown or overexpression of a large pool of target genes with single cell transcriptome readout. Subjecting these engineered CAR T-cells to an antigen-specific, cell-based repetitive stimulation assay (RSA) led to the progressive loss of T cell proliferation and effector function enabling *in vitro* modeling of T cell exhaustion. Moreover, characterization of the CAR T-cells by single cell sequencing recapitulated key hallmarks of the transcriptional and epigenetic landscape of T cell exhaustion. We also discovered T cell intrinsic gene perturbations that govern T cell states in the context of chronic antigen stimulation. These results demonstrate the power of pooled CRISPR screening with single cell readouts to identify novel target genes to enhance CAR T-cell therapies.

#7035 Characterization of tissue-resident memory T cells in hepatocellular carcinoma through single-cell multi-omics.

M.-S. Park[1], H. Cho[1], H. Kim[1], W.-Y. Park[2], Y.-H. Paik[3], Y. Yoon[1], W. Kang[3], H.-H. Won[1];

[1]Samsung Advanced Institute of Health Sciences and Technology (SAIHST), Sungkyunkwan University, Seoul, Korea, Republic of, [2]Samsung Genome Institute, Samsung Medical Center, Seoul, Korea, Republic of, [3]Samsung Medical Center, Sungkyunkwan University School of Medicine, Seoul, Korea, Republic of

As the fifth leading cause of cancer-related mortality, liver cancer imposes a global burden. Hepatocellular carcinoma (HCC) is the most common type of primary liver cancer, with a five-year overall survival rate of less than 20% for advanced-stage cases. Even the most advanced immunotherapy for HCC has disparate response rates in each patient with HCC, which has led to efforts to unravel the underlying factors in the progression of HCC using bioinformatic approaches. In recent decades, numerous studies have explored T-cell subtypes with tissue-specific residency, suggesting their early protective functions and therapeutic potential within tumor microenvironment (TME). This study aimed to understand inter-individual and intercellular TME through single-cell RNA sequencing (scRNA-seq) and single-cell TCR sequencing (scTCR-seq) in five recurrent/non-recurrent HCC patients. We identified tumor-associated tissue-resident memory T (TA-T_{RM}) cells and investigated the heterogeneous characteristics of two T_{RM} clusters ($CD69^{+}$ and $CD103^{+}$). Whereas $CD69^{+}$ TA-T_{RM} showed high expression of genes associated with immunological activation, $CD103^{+}$ TA-T_{RM} exhibited upregulation of genes related to proliferation capacity. To validate the unique molecular patterns, we analyzed an independent HCC dataset (GSE140228) and observed high concordance of significant core marker genes for TA-T_{RM} clusters between the two datasets. Moreover, we assessed the association of gene expression in TA-T_{RM} cells with overall and recurrence-free survival by conducting survival analysis in two independent large-scale cohorts. The cross-validation approach was applied to estimate risk scores for patients with primary HCC tumors in The Cancer Genome Atlas (TCGA), and the trained model was evaluated using the International Cancer Genome Consortium (ICGC) data. The result of calculating the risk scores clearly indicates that TA-T_{RM} cells are associated with survival in HCC. Therefore, our study characterized two distinct subtypes of TA-TRM cells in HCC, delineated their unique molecular signatures, and established their relevance to survival outcomes. The findings can potentially enhance the understanding of the roles of TA-T_{RM} cells in the context of HCC.

#7036 Integrative biomarker profiling for predicting immunotherapy outcomes in gynecologic cancers.

G. Idumah[1], L. Li[1], H. Mahdi[2], Y. Ni[1];

[1]Cleveland Clinic, Cleveland, OH, [2]University of Pittsburgh Medical Center, Pittsburgh, PA

Immunotherapy with immune checkpoint inhibitors (ICI) has proven effective for various solid tumors, such as those in the lungs, urinary tract, and skin. However, its efficacy in gynecologic (GYN) cancers has been limited, with response rates of 11-17% in recurrent cases. Only a minority of patients with DNA mismatch repair deficiencies exhibit favorable responses to PD-1 inhibitors. The predictability of PD-L1 expression in GYN cancers remains inconsistent. Our research aimed to identify and prioritize biomarkers and mechanisms linked to ICI resistance in GYN oncology, targeting those who could benefit from these treatments.We gathered clinical and pathological data from 49 patients with ovarian, endometrial, and cervical cancers at various stages, all treated with ICI. We performed comprehensive analyses, including transcriptome-based immune cell abundance estimation, signaling pathway enrichment, and correlation with ICI treatment responses and survival outcomes. Our previous work highlighted TGF-β and CD47's roles in immunotherapy resistance, facilitating an immunosuppressive environment within our GYN cancer cohort. Moreover, we conducted a stoichiometry constraint-based genome-scale metabolic model and computed correlation-grouped metabolic activity scores (cgScore) using metabolic enzyme gene expression as constraints. Among 1533 metabolic reactions, pyruvate transport and folate metabolism stood out as the most upregulated in responders versus those who progressed.Upon identifying several promising biomarkers, we used logistic regression classifiers to decipher the predictive value of each. Our model included clinical-demographic (age, BMI, cancer type, stage) and molecular-genomic features (immune marker gene expression, TopTGF-β score, immune cell abundance from transcriptomic deconvolution, and the top 2 cgScores). Analysis divided into training and testing sets highlighted features such as stage, BMI, eosinophils, CD274, CD47, and the pyruvate transport reaction as significant predictors of ICI response. The model achieved an 80% accuracy rate on the test set, confirmed by permutation importance from scikit-learn. We also used a Regularized Cox model to link predictors with progression-free survival, emphasizing the roles of BMI, plasma cells, CD276, pyruvate transport reaction, and folate metabolism. In conclusion, there are immunological and metabolic markers have the potential to serve as predictive indicators for ICI treatment response and survival in GYN cancers. Understanding these predictors can profoundly influence clinical decision-making in immunotherapy, ultimately leading to enhanced patient outcomes and personalized treatment approaches.

#7037 Comprehensive molecular and immune profiling of triple negative invasive lobular carcinoma.

P. Advani[1], S. Deshmukh[2], S. Wu[2], J. Andring[2], J. Xiu[2], J. Leone[3], P. Jayachandran[4], S. Graff[5], M. Oberley[2], G. Sledge[2], A. Chanan-Khan[1];
[1]Mayo Clinic, Jacksonville, FL, [2]Caris Life Sciences, Phoenix, AZ, [3]Dana Farber cancer Institute, Boston, MD, [4]Norris Comprehensive Cancer Center, Los Angeles, CA, [5]Lifespan Cancer Institute, Brown University, RI

Background: Triple-negative invasive lobular carcinoma (TN-ILC) is a rare (0.1-1.4%) breast cancer with prognosis worse than ER positive ILC. Currently there are no targeted therapies or clinical trials specifically for TN-ILC. A comprehensive analysis of the molecular and immune landscape can help identify novel targets and pathways for TN-ILC to improve patient outcomes. Here, we characterized the molecular and immune signature of TN-ILC.
Methods: 11,760 breast cancer samples (Invasive ductal (ID) TNBC, n=364; TN-ILC, n=31) were analyzed (592, NextSeq; WES, NovaSeq), (WTS; NovaSeq) (Caris Life Sciences, Phoenix, AZ). Tumor mutational burden (TMB) totaled somatic mutations per tumor (high ≥10 mt/MB) was tested by NGS. Microsatellite-instability (MSI) was tested by NGS. Immune cell fractions were calculated by deconvolution of WTS. Statistical significance was determined using chi-square and Mann-Whitney U test with p-values adjusted for multiple comparisons ($q < 0.05$).
Results: TN-ILC had higher frequency of *CDH1* (0.83% vs. 66.67%), *ERBB2* (0.84% vs.28.57%), *ARID1A* (1.65% vs. 23.33%), *CBFB* (0.55% vs.16.67%), *AKT1* (2.22% vs.16.13%) and *KMT2C* (3.83% vs.13.79%), but lower frequency of *TP53* (89.7%5 vs. 38.71%) mutations (all $p<0.05$) compared to ID-TNBC. TN-ILC had higher frequency of TMB high (23.3% vs. 5.2%, $p<0.05$) but there was no difference in dMMR/MSI-H (0% vs 1.1%, $p=1$). TN-ILC had higher AR RNA (FC: 14.2), protein expression (80.6% vs. 24.8%) and higher frequency of fusion variant-AR (16.1% vs 4.9%) (all $p < 0.05$) compared to ID-TNBC. Analysis of inferred immune cell infiltrates showed that TN-ILC had higher infiltration of M2 macrophages (5.34% vs. 2.94%) and neutrophils (4.83% vs. 2.65%) but lower infiltration of M1 macrophages (3.46% vs 2.17%) and CD8 T cells (0.58% vs. 0.11%) (all $p<0.05$). TN-ILC had lower T cell inflamed signature (16.1% vs 35.7%, $p<0.05$), decreased immune checkpoint genes (*CD274, CTLA4, FOXP3, LAG3, IDO*, FC: 1.2-2.7, all $p < 0.05$), PD-L1 protein expression (SP142: 30.4% vs. 50.2%, $p=0.06$; 22c3: 15.4% vs. 42.6%, $p = 0.05$) and differential expression of BCL2 family genes (upregulation: *BIK*, FC: 2.2; downregulation: *BAX, BAK1, BID, PMAIP1, MCL1, BCL2A1, BCL2L10*, FC: 1.0-6.3, all $p < 0.05$) compared to ID-TNBC.
Conclusion: These data suggest that TN-ILC had higher frequency of CDH1, ERBB2, AKT1, ARID1A mutations, higher M2 macrophages and neutrophils and lower M1 macrophages and CD8 T cells infiltration and, lower T cell inflamed signature. High TMB and AR expression can translate into use of immunotherapy (ICI) and AR antagonists in these patients. Additonal analysis to determine the optimal biomarker for ICI response in TN-ILC is needed. Results of our study need to be validated in larger studies with survival correlation.

#7039 Leveraging single cell RNA-seq for uncovering immune landscape of hepatocellular carcinoma.

Jian He

School of Medicine, Shanghai Jiao Tong University, Shanghai, China

The immune cell types as well as tumor microenvironment (TME) status may influence prognosis, metastasis, tumor progression, and clinical response to immunotherapies for cancer. Hepatocellular carcinoma (HCC) is a typical highly heterogeneous solid tumor with high morbidity and mortality worldwide, especially in China, however, the immune microenvironment of HCC, especially which caused by cancerogenic substance has not been clarified so far. In this study, we employed single-cell RNA sequencing (scRNA-seq) on diethylnitrosamine (DEN)-induced mouse HCC model to dissect the immune cell dynamics during tumorigenesis. Our findings reveal distinct immune profiles in both precancerous and cancerous lesions, indicating early tumor-associated immunological alterations. Notably, specific T and B cell subpopulations are preferentially enriched in the HCC TME. Furthermore, we identified a subpopulation of naïve B cells with high CD83 expression, correlating with improved prognosis in human HCC. These signature genes were validated in The Cancer Genome Atlas (TCGA) HCC RNA-seq dataset. Moreover, cell interaction analysis revealed that subpopulations of B cells in both mouse and human samples are activated and may potentially contribute to oncogenic processes. In summary, our study provides insights into the dynamic immune microenvironment and cellular networks in HCC pathogenesis, with a specific emphasis on naïve B cells. These findings emphasize the significance of targeting TME in HCC patients to prevent HCC pathological progression, which may give a new perspective on the therapeutics for the HCC.

#7040 Mutations in cytoskeleton genes SPTAN1/SPTBN1 serve as novel predictive markers for immunotherapy against bladder cancer.

B. Y. Kuo;
National Sun Yat-sen University, Kaohsiung, Taiwan

Cancer progression is often driven by somatic mutations. Despite several well-known driver mutations, more evidence has shown that genetic alterations in cytoskeleton organization enhance tumor aggressiveness and promote cancer progression, suggesting their roles as potential drivers. In this study, pan-cancer genetic analyses by using TCGA cohorts, more frequent mutation events were found in cytoskeleton-related genes as compared to total annotated genes, especially in cancers derived from hollow organs. High-dimensional analysis of molecular alterations in cancer (HD-MAC) suggested gene mutations in SPTAN1 and its partner SPTBN1 as potential prognostic biomarkers for clinical outcomes of patients with bladder cancer. Gene knockdown in either SPTAN1 or SPTBN1, mimicking silencing mutations in cancer tissues, caused cell morphology changes, DNA breaks, and alternations in cytokine profiles via activating cGAS-STING mediated interferon signaling. Xenograft tumor models also indicate accelerated tumor growth in SPTAN1- or SPTBN1-silenced cells, suggesting a more advanced cancer type. Based on immune staining in both human and mouse samples, increased CD8+ T cell infiltration was in tumor lesions with mutations or truncations in SPTAN1/SPTBN1 genes. In addition, several known substitution mutations were found as potent neo-antigens based on MHC II binding prediction, which could be utilized as targets for immune checkpoint therapy. This study provides a novel insight into how the cytoskeleton can contribute to cancer progression and find out predictive biological indicators with therapeutic values.

#7041 Tumor-immune interactions and cisplatin resistance in localized muscle-invasive bladder cancer.

F. L. De Carvalho[1], **J. Lee**[1], K. Bi[2], B. Titchen[2], K. Stawiski[2], J. Park[2], A. Garza[2], D. Michaud[1], J. Guerriero[1], E. Mittendorf[1], K. Mouw[2], E. Van Allen[2]; [1]Brigham and Women's Hospital, Boston, MA, [2]Dana-Farber Cancer Institute, Boston, MA

Background: Cisplatin-based chemotherapy followed by radical cystectomy remains the standard-of-care treatment for patient with localized muscle-invasive bladder cancer (MIBC). Neoadjuvant clinical trials studying the combination of cisplatin-based chemotherapy and immune checkpoint blockade (ICB) in MIBC reported encouraging pathologic complete response rates. However, the molecular mechanisms and cellular programs involved in response and resistance to cisplatin and ICB in MIBC remain incompletely characterized. Our goal is to define cellular transcriptional programs and chromatin accessible regions in cancer cells and infiltrating immune cells associated with response and resistance to neoadjuvant systemic therapy.

Methods: We performed single-cell Multiome ATAC and Gene expression sequencing (simultaneous identification of gene expression and open chromatin regions within the same cell) of tumors that had a complete response – “responders” – and tumors that had no response or progressed – “non-responders” – through neoadjuvant cisplatin-based chemotherapy (n=15). Single cell suspensions were prepared following the 10x Genomics protocol. Cell Ranger ARC was used for sequence alignment, peak calling, and generation of count matrices. Downstream single-cell gene expression analysis was performed with Scanpy and ATAC-seq with Seurat.

Results: We identified two distinct urothelial cell populations in "responders" vs "non-responders" based on single cell gene expression and genome wide chromatin accessibility regions. Cancer cells in “non-responders” preferentially express basal cell gene expression signatures. “Non-responders” were significantly enriched in suppressive tumor-associated macrophages (TAMs). Interestingly, SPP1+ TAMs known to have a pro-tumoral role and promote resistance to ICB were exclusively identified in “non-responders”.

Conclusion: Single cell and genome wide chromatin accessibility regions identify heterogenous urothelial cell populations expressing basal cell markers in tumors resistant to neoadjuvant cisplatin-based chemotherapy. “Non-responders” are significantly enriched with TAMs implicated in resistance to ICB. Future studies will better define the implications of these findings in cancer therapeutics for patients with MIBC.

#7042 Enhancing TCR T cell function in solid tumors through *in vivo* combinatorial screens and single-cell analysis.

Dina Polyak[1], Jessica Fuhriman[1], Josephine Susanto[1], Allyson Merrell[1], Mandi Simon[1], Catherine Oh[1], Andrew Cordazo[1], David DeTomasso[1], Carla Tocchini[1], Vibhavari Sail[1], Eric Cui[1], Jeff Milush[1], Levi Gray-Rupp[1], Brendan Galvin[1], Christopher Murriel[1], Grace Zheng[1], Angela C. Boroughs[1], Pratiksha Thakore[2], Soyoung Oh[2], Jake Freimer[2], Bob Chen[2], Celine Eidenschenk[2], Emily Wheeler[2], Jacob Levine[2], Jan-Christian Huetter[2], Jill Schartner[2], Katie Geiger-Schuller[2], Orit Rozenblatt-Rosen[2], Sascha Rutz[2], Ira Mellman[2], W. Nicholas Haining[1]

[1]Arsenal Biosciences, 329 Oyster Point South San Francisco, CA,[2]Genentech, San Francisco, CA

The therapeutic potential of T cell therapies for treating solid tumors can be limited by intrinsic T cell exhaustion mechanisms and the suppressive tumor microenvironment. To better understand these challenges and identify genetic perturbations to enhance T cell functions, we developed *in vivo* exhaustion models and performed pooled CRISPR/Cas9-based screens with detailed characterization of T cell states through single cell RNA-sequencing (scRNA-seq). *In vivo* Xenograft exhaustion models were developed in the format of T cell receptor (TCR) T cells, with tumor cell lines expressing TCR-specific antigen (NY-ESO-1) respectively. Individual perturbations were introduced into T cells via non-viral editing and pooled before transferred into mice with established tumors of various sizes that provided continuous antigen exposure to drive exhaustion, while providing sufficient number of T cells from tumor and spleen tissues for scRNA-seq. The pooled CRISPR *in vivo* screens in human TCR T cells enabled us to evaluate T cell phenotypes resulting from gain-of-function, loss-of-function, or combinations of these modifications across a wide array of target genes. We identified known and previously uncharacterized combinatorial perturbations that were enriched or depleted and were associated with distinct transcriptional phenotypes over the course of chronic stimulation. This approach allows us to bridge the gaps in our understanding of how T cells can be reprogrammed to overcome exhaustion and function more effectively in the challenging environment of solid tumors.

#7043 Genomic profiling of DLL3-positive and negative CTCs in small cell lung cancer.

Z. Simandi[1], T. Bui[1], A. Ferrarini[2], S. Hepburn[1], R. G. Del Mastro[1];
[1]Menarini Silicon Biosystems Inc., Huntingdon Valley, PA, [2]Menarini Silicon Biosystems SpA, Bologna, Italy

BACKGROUND: Delta-like ligand 3 (DLL3), an atypical Notch family protein implicated in neuroendocrine tumorigenesis, has emerged as a promising therapeutic target in small cell lung cancer (SCLC), prompting numerous clinical trials investigating DLL3-targeted treatments. Exploring DLL3 in circulating tumor cells (CTCs) through liquid biopsy, coupled with comprehensive genomic analysis, presents an invaluable and minimally-invasive avenue for monitoring disease progression. This approach holds the potential to tailor personalized treatment strategies, emphasizing the critical need for in-depth investigations into both DLL3-positive and negative cell genomic compositions.
METHODS: This study examined blood collected in CellSave preservative tubes from stage I (n=17) and stage IV (n=12) SCLC patients, as well as healthy donors (n=10). The CELLSEARCH® platform was employed to count EpCAM-enriched CTCs and evaluate DLL3 protein expression. Subsequently, individual CTCs were isolated based on the presence and absence of DLL3 expression using the DEPArray™ PLUS. The isolated DLL3-negative and positive CTCs were subjected to low-pass sequencing using the Ampli1™ LowPass Kit to uncover genomic aberrations.
RESULTS: CTCs were absent in the healthy control group. In stage I patients, CTCs were identified in 5.8% of blood samples, while in stage IV patients, they were present in 50% of samples, with an average CTC count of 148 in stage IV. Among a total of 2074 detected CTCs, 460 were DLL3-positive, accounting for 6-28% of EpCAM-enriched CTCs in individual patients. Analysis of >300 copy number alteration (CNA) profiles of sorted single cells revealed considerable inter-patient and intra-patient heterogeneity, delineating recurrent clonality and specific genomic alterations in DLL3-negative CTCs. In contrast, DLL3-positive cells showed more stochastic CNA profiles, suggestive of apoptosis-related DNA fragmentation.
CONCLUSIONS: Integrating CellSearch, DEPArray, and low-pass sequencing provides a minimally-invasive approach to compare genomic characteristics in DLL3-positive and negative CTCs from SCLC patients. Extension of this approach to a larger patient cohort and employing machine learning algorithms will facilitate identification of patterns within diverse CNA profiles, improving patient stratification and predicting treatment responses for personalized therapeutic strategies in SCLC.

#7044 Transcriptome and TCR repertoire in human telomerase reverse transcriptase peptide vaccine treated metastatic prostate cancer patients.

R. Natkin[1], J. E. Simensen[2], N. Engedal[2], E. B. Ellingsen[3], M. Westhrin[3], I. Westgaard[3], E. Hovig[2], W. Lilleby[2], M. Nykter[1], A. Urbanucci[1];
[1]Tampere University, Faculty of Medicine and Health Technology, Tampere, Finland, [2]Oslo University Hospital, Institute for Cancer Research, Oslo, Norway, [3]Ultimovacs, Oslo, Norway

Human telomerase reverse transcriptase (hTERT) vaccine has found to be effective for most of the participated de novo metastatic prostate cancer patients in clinical studies. Nevertheless, the molecular mechanisms behind the immune response induced by the hTERT vaccine are not fully elucidated. Among the cohort of 21 patients treated with androgen deprivation therapy, radiotherapy and hTERT vaccine, we used RNA-sequencing and TCR-sequencing (20 and 14 pre-treatment and 20 and 21 post-treatment samples, respectively) to inspect the changes in transcriptome and TCR-repertoire after the hTERT vaccine treatment and differences between patients that had early response and patients that had late or no response. We found multiple hallmarks being shifted after the treatment and being different between early and late responders. Also, a change in activity of multiple gene set signatures was detected after the treatment and activity of part of the gene set signatures predicted survival. Deconvolution of cell type composition from RNA-sequencing data revealed changes in immune cell abundances after the treatment. TCR-sequencing revealed changes in composition and diversity of TCR repertoires after the treatment and these differed between early and late responders. The results of this study will help to predict patients' responses to the cancer vaccine and to further understand the mechanisms behind successful cancer vaccines.

#7045 RNA sequencing approaches enable tissue specific B and T cell gene expression and immune repertoire profiling.

C. Song, E. Janzen, T. Devoe, A. Erijman, G. Naishadham, L. Song, B. W. Langhorst;
New England Biolabs, Inc., Ipswich, MA

The adaptive immune system defends the human body from pathogens through the recognition ability of antigen receptors from B and T cells. Different organs play various immune function roles, and therefore present varied B and T cell gene expression and immune repertoire profiles. Abnormality of these profiles may reflect immunological disorder, presence of neoplastic tissue, or response to infectious agent. High-throughput sequencing technology has facilitated the understanding of gene expression and related cell functions, but in-depth understanding of B and T cell phenotype and clonotype profiling is an emerging application that has yet to take full advantage of sequencing technology for diagnosis and prognosis of disease.

Here, we share results of RNA sequencing of immune system tissues; including B cell and T cell specific gene expression and full-length immune repertoire profiling. Total RNA was extracted from various tissue samples including healthy donor peripheral blood mononuclear cells (PBMC), lymph nodes, bone marrow, spleen, thyroid, thymus and colon, as well as diseased PBMC and colon samples. RNA-seq and Immune-seq libraries were made from these samples and sequenced on Illumina NextSeq2000. Gene expression analysis and immune repertoire profiling from RNA-seq data were performed using edgeR and TRUST4. Immune repertoire sequencing data was processed using pRESTO and IgBlast. We correlated RNA-seq with Immune-seq results for B-cell receptor and T-cell receptor clonotypes. Differential expression and clonotype profiling comparisons were also performed between normal and diseased RNA samples. The effect of reference on immune repertoire detection sensitivity and accuracy was further investigated by comparing IMGT reference and AIRR-C Human IG Reference Sets.

This study has identified tissue specific B/T cell phenotype and clonality patterns that relate to tissue functions and disease progression. RNA-seq enables highly multiplex immunophenotyping which is traditionally performed by flow cytometry. RNA-seq can detect high-abundant clones that correlate with Immune-seq, with the latter targeted approach providing more in depth clonality signatures. References comparison results show the importance of continued community effort to develop more representative and accurate immunorepertoire germ line references for clonotype annotation in diverse populations. Integrating both RNA sequencing and immune repertoire sequencing approaches allows accurate phenotype and clonotype determination for immune landscape in various tissues.

#7046 Proteogenomic and immunologic profiles of head and neck cancer patients of African ancestry.

F. Yang, F. Chen, C. Shay, N. F. Saba, **Y. Teng**:
Emory University, Atlanta, GA

Blacks/African Americans (BAAs) with head and neck squamous cell carcinoma (HNSCC) have worse survival than Whites. However, the complex molecular biomarkers and signatures of HNSCC among BAAs and molecular distinction associated with HNSCC disparities are largely unknown. Here we show the results of a multi-omics analysis of 500 patients (48 BAAs and 452 Whites). Comparative analyses between the racial groups were performed at the level of genomics, pathways, molecular subtype, tumor immune infiltration, protein alterations and prognosis. We found that overall survival in BAAs with HPV-unrelated HNSCC is significantly shorter than in White patients. Ancestry-related differential mutation spectrum, DNA methylation, gene and protein expression pattern and immune infiltration landscape were identified. Particularly, FAT1 mutation is significantly associated with its gene expression in BAA HNSCC and poor overall survival in this group. In BAA HNSCC, SALL3 gene expression is positively associated with its gene CNVs, while RTP4 gene expression is inversely correlated with its methylation. High EGFR_pY1068 and RAD50 levels correlate with poor prognosis in BAAs with HNSCC. The immune infiltration enrichment scores of Th17 cells, activated dendritic cells, monocytes and neutrophils in BAA HNSCC were significantly lower than those in White HNSCC. By combining multi-omics analysis and data validation using in-house-made tumor tissue arrays, this study comprehensively elucidates the genetic landscape, immune response, and tumor biology in BAA and White HNSCC patients, providing a molecular basis for future research in identifying appropriate screening modalities and therapeutic interventions leading to improved outcomes in BAAs with HNSCC.

#7047 Comparative analysis of transcriptomic and immunological profiles in treatment-naïve black and non-Hispanic White women with high-grade serous ovarian cancer.

H. Huang[1], R. Keathley[1], U. Kim[1], H. Cardenas[1], P. Xie[1], J. Wei[1], G. Zhao[1], E. L. Barber[1], E. Lengyel[2], K. P. Nephew[3], V. Bae-Jump[4], B. Zhang[1], D. Matei[1]; [1]Northwestern Univ. Feinberg School of Medicine, Chicago, IL, [2]University of Chicago, Chicago, IL, [3]Indiana University, 5School of Medicine,, Bloomington, IN, [4]University of North Carolina, Chapel Hill, NC

Background: Ovarian cancer is a highly lethal gynecological malignancy and high-grade serous histology (HGSOC) accounts for the majority of cases. Platinum-based chemotherapy is the primary treatment. Notably, Black women face the highest mortality-to-incidence ratio across all ethnic groups. This study investigated transcriptomic and immunological differences in tumors from Black compared to NHW women that might explain the poor clinical outcomes observed within this patient cohort. Methods: We collected primary tumor specimens from 36 Black and 31 treatment-naïve NHW patients. After RNA isolation, RNA sequencing (RNA-seq) identified differentially expressed transcripts and Enrichr performed pathway enrichment studies. To confirm the observed gene expression differences, we employed quantitative reverse transcription PCR (qRT-PCR), western blotting, and multiplex immunohistochemistry (mIHC). Additionally, we conducted cell proliferation, colony formation, and cell viability assays to functionally validate potential target genes of interest. Results: Our findings revealed 277 genes with significant differential expression between Black and NHW patients (FDR-adjusted p-value < 0.05). Among these, 103 coding genes were up-regulated, while 81 coding genes were down-regulated in tumors from Black compared to NHW patients. Gene Ontology analyses of these significantly differentially expressed genes highlighted enriched pathways related to DNA damage response, including the insulin receptor (INSR) gene, p53/apoptosis signaling components such as Forkhead box proteins A1 (FOXA1) and FOXB1, as well as genes involved in the cholesterol/lipid modulation pathway, including Low-density lipoprotein (LDL) receptor and Stearoyl-CoA Desaturase (SCD). Notably, silencing INSR and FOXA1 enhanced sensitivity to platinum-based drugs and inhibited cell growth and colony formation. Furthermore, we identified differences in the proportions of key immune cell types between the two patient groups, with tumors from Black patients exhibiting a significantly lower proportion of CD4+ Naïve T-cells and CD4+ regulatory T-cells (Tregs). Conclusions: Overall, our study reveals significant differential gene expression patterns between HGSOC tumors from Black and NHW patients, as well as differences in the proportions of immune cell types. These discoveries provide valuable insights into the biological mechanisms underlying the disparities in outcomes observed between black and NHW patients afflicted with HGSOC. It is critical to further investigate how these biological differences affect clinical outcomes and treatment response in Black women.

#7048 Multiomics characterization of breast angiosarcoma from an Asian cohort reveals enrichment for angiogenesis signaling pathway and tumor-infiltrating macrophages.

T. Ko, Z. Guo, B. Kannan, B. Lim, J. Lee, A. Lim, Z. Li, E. Lee, C.-Y. Ng, B. Teh, J. Chan;
National Cancer Centre Singapore, Singapore, Singapore

Recent epidemiological data suggests a rising incidence of breast angiosarcoma (AS-B) in the Western population, with over two-thirds related to irradiation or chronic lymphedema. However, unlike head and neck angiosarcoma (AS-HN), AS-B disease characteristics in Asia remains unclear. We examined clinical patterns of angiosarcoma patients (n = 176) seen in an Asian tertiary cancer centre from 1999 to 2021, and specifically investigated the molecular and immune features of AS-B in comparison to AS-HN. Data from whole genome sequencing (WGS) (AS-HN, n = 44; breast, n = 7), NanoString PanCancer IO360 gene expression profiling (AS-HN, n = 42; breast, n = 7) and 10X Visium spatial transcriptomics (AS-HN, n = 4; breast, n = 2) were analyzed. Majority of cases were AS-HN (n = 104; 59.1%), while AS-B (n = 16, all females) accounted for 9.1% of the cases. The median age at diagnosis was 43 years (range, 26 to 74). Four cases (25%) were related to prior irradiation, while 6 out of 8 cases evaluated were positive for human herpesvirus-7 on immunohistochemistry. Although all cases were non-metastatic at diagnosis and were treated with curative-intent surgery, 6 patients (37.5%) experienced rapid relapse within a median of 7.8 months. Based on WGS, 4 of the 7 AS-B had non-synonymous somatic variants in 48 genes (range, 2 to 28 per case). Among the notable variants found were in kinases (KDR, JAK2, FLT4, ATR, EPHB1 and PRKACA). Other variants were found in cancer-related genes (e.g. ATRX, FOXO1, SMAD3, PTCH1, NOTCH4, HIF1A and SETD1A). These genes were functionally annotated by performing over representation analysis (www.webgestalt.org) on publicly available databases (e.g. Gene Ontology and KEGG). They were enriched in cancer-related pathways such as regulation of cell differentiation, VEGFR and receptor tyrosine kinase signaling pathways. By NanoString profiling, compared to AS-HN, AS-B was enriched for angiogenesis, notch signaling and metastasis-associated matrix remodeling pathways. Conversely, AS-B was depleted of lymphoid compartment, immune cell adhesion and migration expression signatures. Based on the gene expression signatures, AS-B was enriched for macrophages, CD8+ T cells and was depleted for T-reg cells. Furthermore, spatial transcriptomics showed that compared to AS-HN, tumor-infiltrating leukocytes (TILs) in AS-B were enriched for macrophage and T-cells but were depleted for B-cells and NK cells. The location of TILs could provide information on the feasibility of immunotherapy in angiosarcoma. In conclusion, we observed a convergence of both mutational and expression signatures on angiogenesis signaling pathways in our AS-B cases. The spatial transciptomic data revealed that AS-B was enriched for tumor-infiltrating macrophages and T-cells which might have implications on the role of immunotherapy.

MOLECULAR/CELLULAR BIOLOGY AND GENETICS: Mitochondrial Function 1
Poster Session

#7052 p53 underpins a dependence on oxidative phosphorylation in glycolysis-competent colorectal cancer.

X. Zhao[1], M. Han[2], Q. Yan[2], Y. Yue[2], K. Ye[2], Y. Zhang[1], L. Teng[2], L. Xu[1], X. Shi[2], T. La[1], Y. Feng[1], R. Xu[1], V. K. Narayana[3], D. P. De Souza[3], T. Liu[4], M. Baker[1], R. F. Thorne[2], X. Zhang[1], S. Chen[2], L. Jin[1];

[1]University of Newcastle, Australia, Callaghan, Australia, [2]Zhengzhou University, Zhengzhou, China, [3]University of Melbourne, Melbourne, Australia, [4]University of New South Wales, Sydney, Australia

The use of mitochondrial inhibitors to target oxidative phosphorylation (OXPHOS) in cancer treatment presents a challenge due to dose-limiting toxicities. Moreover, while glycolysis-deficient cancers are vulnerable to OXPHOS inhibition in preclinical models, the full extent of phenotypical and mechanistic consequences of inhibiting OXPHOS in cancers capable of glycolysis is not yet well understood. Our results presented here offer promising insights into potential therapeutic gains from combining p53 restoration strategies with OXPHOS inhibitors, even when applied to glycolysis-competent CRC cells. Treatment with mitochondrial complex I inhibitors did not cause energy stress in CRC cells capable of glycolysis. It does, however, induce DNA replication stress, apparent through an observed cell cycle arrest at the S phase, enrichment of the G2/M DNA-damage checkpoint regulation pathway, and replication fork slowdown. Intriguingly, CRC cells harboring wildtype p53 exhibited more severe replication stress than those carrying mutant p53. Furthermore, siRNA knockdown of p53 attenuates replication stress and reduces cell cycle arrest, underlining the important role of p53 in CRC cell responses to OXPHOS inhibition. Our targeted metabolomics analysis reveals that OXPHOS inhibition results in reductions in the purine nucleotides, adenine monophosphate (AMP) and guanine monophosphate (GMP), as well as the pyrimidine nucleotide, uridine monophosphate (UMP), in CRC cells, regardless of their p53 mutational status. By supplementing cell culture mediums with the purine nucleobases adenine and guanine, and the pyrimidine nucleoside uridine, we observed a partial reversal of the replication fork slowdown and reductions in cell viability. This suggests nucleotide deficiencies are involved in the induction of DNA replication stress caused by OXPHOS inhibition. The nucleotide deficiencies were associated with a decrease in the nucleobase precursor aspartate. By adding aspartate at a supraphysiological concentration, to overcome the low expression of the excitatory amino acid transporter 1 required for cellular import of aspartate, we were able to restore the levels of nucleotides. Collectively, our findings suggest broader potential cancer treatment paradigms via OXPHOS targeting, extending beyond glycolysis-deficient cancers. Our data uncovers that CRC cells, which commonly exhibit the glycolytic phenotype, are susceptible to OXPHOS inhibition, with those carrying wildtype p53 showing heightened sensitivity. Therefore, p53 status could serve as a biomarker for predicting CRC responses to OXPHOS inhibitors. Moreover, our findings suggest that combined strategies of restoring p53 function, using small molecules such as APR-246, might enable reduced dosage of OXPHOS inhibitors in CRC treatment, thereby mitigating their dose-limiting toxicities.

#7053 Serine phosphorylation marks proteins for degradation by the mitochondrial matrix protease, ClpXP.

Y. Feng[1], M. M. Goncalves[2], Y. Jitkova[1], A. Keszei[1], C. Sarathy[1], V. Trudel[3], J. St-Germain[1], M. Tcheng[1], Y. Yan[1], R. Hurren[1], M. Schultz[1], B. Raught[1], A. Yudin[3], M. Mazhab-Jafari[1], S. Vahidi[2], A. D. Schimmer[1];

[1]Princess Margaret Cancer Centre, University Health Network, Toronto, ON, Canada, [2]University of Guelph, Toronto, ON, Canada, [3]University of Toronto, Toronto, ON, Canada

ClpXP is a conserved protein degradation system. In human mitochondria, ClpXP degrades damaged respiratory chain proteins and is vital for the survival of acute myeloid leukemia (AML) cells. This system consists of the barrel-like protease ClpP, capped by regulatory particles (RP) ClpX. In bacteria, ClpXP targets substrates with a co-translationally added SsrA sequence. However, in humans, the SsrA tag is absent, and the degradation markers for ClpXP remain unidentified. Notably, bacterial ClpXP homologues degrade substrates with phosphorylated arginine (pArg). We hypothesized that phosphorylated amino acids also mark substrates for ClpXP degradation in human mitochondria.

We showed that ClpXP preferentially degraded phosphorylated α-casein substrate over dephosphorylated α-casein. In contrast, ClpP activated by ONC201, without ClpX, degraded phosphorylated and dephosphorylated α-casein with equal efficiency. Next, we screened a panel of phosphorylated amino acids and peptides for their ability to inhibit ClpXP-mediated degradation of α-casein. Phosphorylated serine (pSer) amino acids and peptides inhibited ClpXP protease activity, while phosphorylated tyrosine (pTyr) or pArg did not. Likewise, Ser and free phosphate did not inhibit ClpXP protease activity. Thermal shift assays showed that pSer amino acids and peptides bind to ClpX, not ClpP. Hydrogen/deuterium exchange mass spectrometry revealed that the addition of Ala-pSer-Ala (ApSA) peptide, but not ASA peptide induced conformational changes in the negatively-charged N terminus of ClpX, thus revealing a putative binding site for ApSA.

Earlier, we established that ClpP interacts with the respiratory chain complex II subunit SDHA. Knocking down of ClpP in AML cells affected the respiratory chain and increased reactive oxygen species. Therefore, we tested how ClpXP knockdown impacts levels of phospho-serine SDHA (pSer-SDHA) in intact cells. Using shRNA, we knocked down ClpP and ClpX individually in OCI-AML2 cells. After target knockdown, we pulled down pSer proteins and probed for SDHA. Knockdown of both ClpP and ClpX increased the abundance of pSer-SDHA compared to control. We subsequently added recombinant ClpXP protein to total mitochondrial lysates and the pSer immunoprecipitated fraction from OCI-AML2 cells. This led to decreased levels of pSer-SDHA but did not alter levels of total SDHA, consistent with its preference for pSer-marked substrates suggesting that ClpXP degrades pSer-SDHA. Further analysis showed elevated pSer-SDHA levels only in the insoluble mitochondrial protein fraction after ClpX knockdown, suggesting these might be damaged proteins.

In conclusion, our findings demonstrate that serine phosphorylation promotes the degradation of damaged mitochondrial proteins by ClpXP protease.

#7054 *L1-ATP8B1* exacerbates high-level reduction-oxidation homeostasis to promote carcinogenesis via affecting PHB1 sumoylation in LUSC.

Rui Zhang[1], Xiao Zhang[1], Zeguo Sun[2], Pengpeng Liu[1], Guidong Chen[1], Weijia Zhang[2], Jinpu Yu[1]

[1]Tianjin Medical University Cancer Institute & Hospital, Tianjin, China,[2]Icahn School of Medicine at Mount Sinai, Tianjin, China

Long Interspersed Nuclear Element-1 (LINE-1, L1) plays important roles in carcinogenesis. However, the function of LINE-1 in lung squamous cell carcinoma (LUSC) remains unclear. Here we found that *L1-ATP8B1* was overexpressed in LUSC patients with short survival and associated with mitochondrial dysfunction in both the TCGA dataset and the TJMUCH cohort. Overexpression of *L1-ATP8B1* promoted cell proliferation and invasion *in vitro* and facilitated LUSC xenograft growth *in vivo*. *L1-ATP8B1* affected mitochondrial complex enzyme I activity via affecting cardiolipin-dependent PHB1 sumoylation and promoting PHB1 ubiquitination, inducing high-level cellular reduction-oxidation (redox) homeostasis. Synergetic therapy with an L1 inhibitor and an antioxidant dramatically interfered with redox homeostasis and restored mitochondrial function, abolishing *L1-ATP8B1*-induced growth and metastasis of LUSC xenografts *in vivo*. In conclusion, we for the first time demonstrated that metabolic disorder plays a vital role in L1-related carcinogenesis and identified *L1-ATP8B1* as a promising prognostic biomarker and therapeutic target for LUSC.

#7055 Elucidation of the interplay between phospholipid byosynthesis and oxidative stress in the pathogenesis of renal cell carcinoma.

R. Kato[1], D. Ikarashi[1], S. Maekawa[1], M. Kanehira[1], R. Takata[1], Y. Matsushita[2], T. Yoshimaru[2], T. Fukawa[2], T. Katagiri[2], W. Obrara[1];
[1]Iwate Medical Univ., Shiwa, Japan, [2]Tokushima Univ., Tokushima, Japan

Introduction: Renal cell carcinoma (RCC) is a primary malignant kidney tumor. We reported on the critical role of Protein of Relevant Evolutionary and Lymphoid Interest Domain 2 (PRELID2) in cell proliferation, emphasizing its regulatory function on mitochondrial ROS and maintenance of mitochondrial spare respiratory capacity. Recent studies have begun to clarify the molecular mechanism of phospholipid biosynthesis by PRELID1 and PRELID3 under oxidative stress conditions. Inspired by this evidence, we analyzed the relationship between PRELID2 and phospholipid biosynthesis, aiming to elucidate the molecular mechanism of PRELID2 related to the control of mitochondrial ROS.
Methods: To analyze the dynamics of phospholipids and related mitochondrial molecules induced by oxidative stress, we examined the expression of YME1L and its substrates (OPA1, PRELID1) using Western blotting, which has been shown to be related to the turnover of other PRELI family proteins. Lipidomic analysis was performed using LC-MS on samples from HEK293 cells with stable expression of PRELID2 and control cells, as well as renal carcinoma cell lines with suppressed PRELID2 expression using siRNA and control cells. Additionally, we analyzed the expression of mitochondrial respiratory chain complexes Cytochrome C and COX4 and their relationship with PRELID2 expression via Western blotting.
Results: Oxidative stress led to a noticeable decline in YME1L expression, which was correlated with decreased OPA1 and PRELID1 levels in control cells. Conversely, PRELID2-overexpressing cells retained stable expression of OPA1 and PRELID1. Furthermore, these cells exhibited a significant reduction in phosphatidyl glycerol (PG) levels. Suppressing PRELID2 expression in 786-O cells using siRNA resulted in significantly higher PG levels. When analyzing the molecules of the mitochondrial respiratory chain during oxidative stress induction, we observed that although oxidative stress induced a decline in cytochrome C expression in control cells, it remained consistent in PRELID2-expressing cells. However, PRELID2 expression did not affect COX4 levels.
Conclusions: Our findings underscore the pivotal role of PRELIDs in maintaining mitochondrial homeostasis, proving instrumental in the oxidative stress-driven progression of renal cancer.

#7056 The role of aggressive prostate cancer risk gene *ANO7* in prostate metabolism.

C. Lof, N. Sultana, N. Goel, G. Wahlstrom, J. Schleutker;
University of Turku, Turku, Finland

Prostate cancer (PCa), the most common male cancer worldwide, causes about 10% of cancer related deaths in Europe. It has a wide spectrum of clinical behavior that ranges from decades of indolence to rapid metastatic progression and lethality. However, the molecular mechanisms involved in aggressive PCa progression are still poorly understood. In PCa the expression of anoctamin 7 (ANO7) has been shown to diminish as the cancer progresses. We have previously linked single-nucleotide polymorphisms in the *ANO7* gene to the risk of aggressive prostate cancer and shown that in homozygous carriers of rs77559646, the variant leads to a total loss of ANO7 protein. ANO7 is a prostate-specific gene and is highly expressed in the luminal cells of the human prostate. ANO7 belongs to a family of calcium-activated chloride channels and select members of the anoctamin family have phospholipid scramblase activity. To uncover the cellular functions of ANO7 has proven challenging because ANO7 is not expressed in commercially available cell lines. To study the cellular functions of ANO7, we have generated stable prostate cell lines overexpressing ANO7 using lentiviral transduction. To gain information into what pathways ANO7 is affecting, we performed RNA-sequencing and gene set enrichment analysis. Interestingly, we found enrichment and downregulation of mitochondrial genes participating in oxidative phosphorylation in ANO7 cells. We assessed the mitochondrial function by measuring the oxidative phosphorylation capability of the cells and showed that the basal and maximal respiratory capacity of ANO7 overexpressing cells is indeed reduced. We also analyzed which of the three major mitochondrial fuels (glucose, glutamine and fatty acids) are not used as efficiently for oxidative phosphorylation in ANO7 overexpressing cells. The result proves that ANO7 cells are not utilizing glucose as effectively as control cells. Furthermore, the glycolysis stress assay showed that glycolytic capacity is increased in ANO7 overexpressing cells. In addition, a targeted metabolite screening revealed that aspartate is decreased in ANO7 cells, which again points towards perturbed mitochondrial function as aspartate is produced from a tricarboxylic acid cycle intermediate. By inhibiting the uptake of extracellular aspartate, we measured slower proliferation of ANO7 expressing cells, while inhibiting aspartate had no effect on control cells. Interestingly, preliminary results also suggest ANO7's involvement in regulation of phospholipid acyl chain length and saturation, offering insights into altered signaling observed in ANO7 cells. Taken together, this study shows for the first time that ANO7 rewires prostate mitochondrial functions and thus cellular metabolism, which could explain why it is beneficial for cancer cells to lose ANO7 expression.

#7057 Validation of OXPHOS gene amplification as a driver of treatment resistance in non-small cell lung cancer.

M. Benej, K. Benejova, R. Hoyd, C. Wheeler, D. Spakowicz, N. C. Denko;
The Ohio State University Wexner Medical Ctr., Columbus, OH

Lung cancer is the leading cause of cancer deaths in the U.S. and worldwide. Up to 90% of all lung cancers are non-small cell lung cancer (NSCLC). NSCLC is a complex and highly aggressive disease typical for poor prognosis and high rates of treatment resistance. Clinical management of NSCLC varies according to the stage. High-dose stereotactic body radiation therapy (SBRT) is the standard of care for localized non-resectable NSCLC. However, tumor hypoxia is a significant barrier to effective radiation therapy. In the last decade, first line NSCLC treatment has been substantially reinforced with the introduction of immunotherapy targeting immune checkpoints such as programmed cell death 1 (PD-1), yet long-term disease control occurs in less than 25% of NSCLC patients. Therefore, understanding the mechanisms of treatment resistance is essential to address the dire need of introducing novel synergistic therapies to enhance anti-cancer treatment response in refractory NSCLC tumors. The basis of tumor hypoxia has traditionally been attributed to the oxygen supply deficit as malformed tumor vasculature fails to meet the high demand of the rapidly proliferating tumor mass. However, our preliminary analysis of NSCLC patient datasets in the Cancer Genome Atlas (TCGA) PanCancer dataset revealed a significant correlation between high-level expression of nuclear genes encoding mitochondrial subunits essential for oxidative phosphorylation (OXPHOS), and high-level expression of hypoxia-regulated genes (Buffa hypoxia score). Furthermore, we have observed a direct correlation between copy number amplification (CNA) of several OXPHOS genes and hypoxia levels in patient samples. Because mitochondrial function consumes up to 90% of available cellular oxygen, its activity may be indirectly regulating oxygen availability in the tumor microenvironment by rapidly consuming oxygen upon its delivery to the tumor. Moreover, we have identified that almost 40% of NSCLC patients harbor CNA of these essential OXPHOS genes. To provide mechanistic insight into these clinical observations, we have generated mouse syngeneic NSCLC cell lines with modified mRNA expression levels of OXPHOS genes (representing deletion, diploid and amplified number of copies) identified in our screen and observed a direct effect on the rates of mitochondrial oxygen consumption in these cells. Our study investigates the previously unknown role of OXPHOS gene copy number in driving mitochondrial oxygen demand and thus contributing to tumor hypoxia and treatment resistance in NSCLC.

#7058 NSD2 overexpression drives multiple myeloma dependence on adenylate kinase 2 by diverting one-carbon metabolism to the epigenome.

A. Sobh[1], E. Encinas[1], A. Patel[1], G. Surapaneni[1], C. Kaestner[1], J. Poullard[1], M. Clerio[1], K. Vasan[2], T. Freeman[3], D. Lv[4], D. Dupere-Richer[1], A. Riva[1], B. Barwick[3], D. Zhou[4], L. Boise[3], C. Mitsiades[5], B. Kim[3], R. Bennett[1], N. Chandel[2], J. Licht[1];

[1]University of Florida, Gainesville, FL, [2]Northwestern University, Chicago, IL, [3]Emory University, Atlanta, GA, [4]UT Health Science Center, San Antonio, TX, [5]Dana-Farber Cancer Institute, Boston, MA

Chromosomal translocation (4;14), an adverse prognostic factor in multiple myeloma (MM), drives overexpression of the oncogenic histone methyltransferase NSD2. Genome-wide CRISPR screens in isogenic MM cells with high and low NSD2 expression identified adenylate kinase 2 (AK2), an enzyme critical for transport of ATP from the mitochondria, as an NSD2-driven vulnerability. AK2 suppression in t(4;14) MM cells decreased NADP(H) critical for conversion of ribonucleotides to deoxyribonucleosides by the enzyme ribonucleotide reductase (RNR). Consequently, metabolomic studies revealed depletion of deoxynucleotide triphosphates (dNTPs) in AK2-deficient t(4;14) MM cells, which resulted in replication stress, DNA damage and apoptosis. Exogenous supplementation with deoxynucleosides rescued AK2 depleted MM cells confirming the role of AK2 in dNTP homeostasis. In addition, NSD2 overexpression drives a large genome-wide increase in chromatin methylation, which depletes the methyl donor S-adenosylmethionine (SAM). Accordingly, we found that high NSD2 expression in MM cells disrupts creatine biosynthesis, a process dependent on SAM. The creatine/phosphocreatine system represents an alternative means of transporting high energy phosphate from the mitochondria. Hence, creatine supplementation restored NADP(H) levels and rescued AK2-deficient t(4;14) MM cells indicating that the hypersensitivity of these cells to AK2 depletion is driven by creatine deficiency due to NSD2 overexpression. Furthermore, AK2 inhibition impaired ATP-dependent protein folding increasing sensitivity of t(4;14) MM cells to proteasome inhibition. These findings delineate a novel mechanism in which aberrant transfer of carbon to the epigenome creates a metabolic vulnerability, with direct therapeutic implications for t(4;14) MM.

#7059 Remodeling of anaplastic thyroid cancer metabolic signature by natural alkaloid berberine.

T. Jarboe, N. R. DeSouza, K. Kopec, J. Geliebter, X.-M. Li, R. K. Tiwari;
New York Medical College, Valhalla, NY

Anaplastic thyroid cancer (ATC) is a rare, fatal cancer with a five-year survival of 4%. Universally diagnosed at stage IV, ATC is characterized by its lack of differentiation and metabolic dysregulation. Refractory to all established therapies, we propose natural alkaloid berberine (BBR) as a therapeutic with multitarget efficacy to alter mitochondrial metabolism and reprogram ATC's aggressive phenotype. Assays used monocyte cell line U937, ATC cell lines T238 and SW1736, and immortalized normal thyroid cell line Nthy-ori-3-1. All assays used 100μM concentration of BBR or DMSO vehicle control for 24 hours for a tumoricidal effect. Validation of in vitro findings via RNA-Seq was conducted by Genewiz from Azenta and Qiagen's Ingenuity Pathway Analysis was used for in silico modeling. Mitochondria were isolated via differential centrifugation. Modeling the ATC tumor microenvironment, U937 cells were activated and polarized into a proinflammatory macrophage phenotype. BBR treatment at the activation/polarization stages, 33 soluble inflammatory mediators were downregulated in the conditioned media compared to controls. In targeting the aggressiveness of anaplastic thyroid disease, BBR slowed proliferation by 80% selectively in ATC cells from 48 to 72 hours, while sparing normal cells. BBR reduced migratory capacity by 30% in ATC cells after 24, 48, and 72 hours and reduced migration and invasion by 30%. These observations were substantiated by Western blot analysis - BBR selectively decreased phosphorylation of MEK, ERK, and ribosomal protein S6, crucial downstream regulators of the pro-proliferative and pro-survival pathways in ATC cells. Further, BBR specifically modulated cancer-associated metabolism as observed through an increase in AMPKα phosphorylation, a major rate-limiting protein in cancer-induced dysregulation with an anti-tumor effect. Validation of in vitro findings via RNA-Seq revealed more than 400 significantly differentially expressed genes involved in mitochondrial metabolism, glycometabolism, sirtuin signaling, apoptosis, and proliferation. Following a comprehensive analysis, we identified significant downregulation of 25 of 37 total mitochondrially encoded genes (MTs) and 13 of 13 mitochondrially encoded protein-coding genes comprising the oxidative phosphorylation complexes illuminating a clear link between BBR treatment and altered mitochondrial metabolism in ATC. Additionally, protein expression of significantly downregulated mitochondrial genes identified via RNA Seq was validated via Western blot demonstrating decreased mitochondrially-encoded protein expression related to oxidative phosphorylation. This work reveals a novel role for BBR as an inhibitor of mitochondrial metabolism that can be used to reprogram the aggressive nature of ATC and open the door for promising combination therapy in the treatment of ATC.

#7060 Mitochondrial metabolism and racial disparity of bladder cancer.

K. Kami Reddy[1], J. Park[1], R. J. Bollag[2], M. K. Terris[2], S. P. Lerner[1], M. Siddiqui[3], Y. Lotan[4], J. Gao[5], B. A. Kaipparettu[1], N. Putluri[1];
[1]Baylor College of Medicine, Houston, TX, [2]Augusta University, Augusta, GA, [3]Univeristy of Maryland school of medicine, Baltimore, MD, [4]UT southwestern Medical Center, Dallas, TX, [5]The University of Texas MD Anderson Cancer Center, Houston, TX

Bladder cancer mortality is significantly higher in African American patients compared to their European American counterparts. This inferior survival of African American cancer patients is driven at least in part by distinctive intrinsic tumor biology, more specifically altered metabolic activity. However, underlying molecular mechanism for the African American bladder cancer mortality are largely unexplored. Our pioneering metabolomic findings demonstrate alterations in metabolic pathways between African American and European American bladder cancer, specifically those involved in driving energy metabolism. Along these line, we observed increased electron transport chain activity and ATP production in African American bladder cancer could be a result of distinctive rewiring of energy metabolism compared to their European American counterparts. We further performed gene set enrichment analysis by mapping metabolites to genes and observed that oxidative phosphorylation pathway was uniquely enriched in African American tumors compared to European American tumors. In addition, from in vitro assays, mitochondrial complex protein and activity were altered in African American bladder cancer. To determine the role of glutamine mediated increased electron transport chain activity and ATP production in African American bladder cancer, we evaluated the metabolic flux using 13C labeled tracers in both African American and European American bladder cancer cell lines. Metabolic flux analysis revealed that African American cell lines are more glutamine dependent and that producing increased tricarboxylic acid intermediates. Overall, our data indicate that elevated mitochondrial metabolism and oxidative phosphorylation driven by enhanced glutaminolysis may facilitate African American bladder cancer progression. These findings provide the rationale to use mitochondrial-specific inhibitors to target at least a subset of African American bladder cancer patients.

#7061 Targeting metabolic vulnerabilities in ARID1A/B dual-deficient dedifferentiated endometrial carcinoma.

Rebecca Ho[1], Eunice Li[2], Chae Young Shin[2], Shary Chen[2], David Huntsman[1], Yemin Wang[1]

[1]Pathology and Laboratory Medicine, University of British Columbia, Vancouver, BC, Canada, [2]Molecular Oncology, British Columbia Cancer Research Institute, Vancouver, BC, Canada

Background: Dedifferentiated endometrial carcinoma (DDEC) is an aggressive endometrial carcinoma defined histologically by undifferentiated carcinoma juxtaposed against stage 1 or 2 endometrial adenocarcinoma. DDEC responds poorly to conventional platinum/taxane-based chemotherapy, particularly in the case of extrauterine spread. This highlights a need to develop novel therapies for individuals with DDEC. Genetically, a third of DDEC cases have co-inactivating mutations of *ARID1A* and *ARID1B*. These genes encode core subunits of the sucrose/switch non-fermentable (SWI/SNF) complex that regulate transcription. Furthermore, dual loss of ARID1A/B is believed to play a role in driving DDEC tumor development. We hypothesize that ARID1A/B dual-deficiency in DDEC generates unique genetic deficiencies that allow for the development of novel therapies for this cancer. We approached this hypothesis by first conducting a preliminary analysis of the Cancer Dependency Map (DepMap), which has identified vulnerabilities in mitochondrial functioning in ARID1A/B dual-deficient DDECs. As such, we aimed to understand the role of mitochondrial oxidative phosphorylation (OXPHOS) and redox homeostasis in ARID1A/B dual-deficient DDEC to create new treatment options.
Methods: A panel of ARID1A/B dual-deficient and proficient endometrial cancer cell lines were treated with OXPHOS inhibitor IACS-010759 and reactive oxidative species (ROS)-inducing agent elesclomol to identify shifts in drug response between the two groups. To account for genomic differences between the cell lines, we also treated an ARID1B knock-out isogeneic cell line with the drugs. Additionally, changes in metabolism in the endometrial cancer cell lines were measured using Seahorse metabolic flux assays to determine if ARID1A/B dual-deficient cell lines have an increased dependency on OXPHOS for cell growth.
Results: While the Seahorse assays revealed no significant difference in OXPHOS and glycolysis activities between the two groups, drug sensitivity assays demonstrated that ARID1A/B dual-deficient cancers are more sensitive to OXPHOS inhibition and increased ROS production than the proficient cell lines. Depletion of ARID1B in an ARID1A deficient cell line sensitizes the cells to both drugs. Furthermore, IACS-010759 significantly suppressed the growth of ARID1A/B-deficient DDEC xenograft tumor growth.
Conclusion: ARID1A/B-dual deficient cancer cells rely on mitochondria function for survival. The underlying mechanisms are currently under investigation.

#7062 CIP2A enhances mitochondrial respiratory electron transport chain complexes and induces lung cancer *in vivo*.

F.-Y. Yang, D. Wang, L.-J. liang, G.-Z. Wang, G.-B. Zhou;
Cancer Hospital Chinese Academy of Medical Sciences, Beijing, China

Identification of oncogenes that can induce cancer *in vivo* is critical to elucidation of tumorigenesis and development of targeted therapies. Here, we reported for the first time that forced ectopic expression of CIP2A, the cancerous inhibitor of protein phosphatase 2A (PP2A), in lung tissues induced lung adenocarcinoma in mice. CIP2A upregulated the transcription and translation of mitochondrial DNA (mtDNA), and increases the enzymatic activity of mitochondrial electron transport chain (ETC) complex IV and V, thus enhancing the function of mitochondria and promoting the level of oxidative phosphorylation in tumors. CIP2A inhibited the binding of PP2A-B56α to FOXO3a, leading to the enhancement of the phosphorylation level of FOXO3a. The phosphorylated FOXO3a then translocated into the mitochondrion, and acted as a transcription factor to regulate CIP2A-mediated metabolic reprogramming in cancer cells. We found that oxidative phosphorylation inhibitors effectively inhibited CIP2A-induced cell proliferation. In non-small cell lung cancer, CIP2A level in tumor tissues was positively associated with the level of mtDNA. Our results indicated that CIP2A is able to induce lung adenocarcinoma in mice and has a critical role in mitochondrial oxidative phosphorylation, and represents a promising therapeutic target for non-small cell lung cancer.
Competing interests: The authors declare no competing interests.

#7063 Monitoring metabolic plasticity in the tumor microenvironment *in vivo* by mitophagy generated extracellular vesicles.

P. V. GADE, M. Howard, A. Rojas, L. Hasanzadah, L. Liotta, F. Kashanchi;
George Mason University, Manassas, VA

Tumor metabolic reprogramming is a hallmark of cancer progression, survival, and therapeutic resistance. A targetable class of cancer metabolic adaptation exploits mitophagy known to be linked to the cancer phenotype. Mitophagy selectively eliminates dysfunctional mitochondria by targeting them, via autophagosome shuttling, to the lysosome for degradation. Cancer cell mitophagy is triggered by elevated oxidative stress and mitochondrial DNA damage caused by hypoxia, radiotherapy, and immunotherapy. A high mitophagy demand can overwhelm the lysosome capacity resulting in the accumulation of damaged mitochondria and can suppress biogenesis of healthy mitochondria. We hypothesize that the newly discovered secretory mitophagy mechanism exports damaged mitochondrial fission-released segments to reduce the overload pressure on the lysosomal system, and thereby sustains cancer cell survival in the face of therapeutic mitochondrial stress. We have discovered a form of secretory mitophagy occurring *in vivo* in a growing solid tumor. Our molecular analysis of the full repertoire of extracellular vesicles, EVs, shed into the resident tumor interstitial fluid, IF, *in vivo* yielded a rich set of information about the functional state of mitochondria within the tumor cells, and the host cells. A set of proteins required for sequential steps of fission-induced mitophagy preferentially populated the CD81 positive IF EVs, including PINK1, DRP1 and FIS1. The export of cellular mitochondria proteins to CD81 positive EVs was confirmed by density gradient isolation from the bulk EV isolate followed by anti-CD81 immunoprecipitation, Mito Tracker export into CD81 positive EVs, ultrastructural characterization and Exoview analyzer. Further, we stimulated mitochondrial oxidative stress and blocked the fusion of the mitophagosome with the lysosome, which markedly stimulated the export of the secretory mitophagy unit. The outcome is new understanding of the importance of secretory mitophagy that can constitute a therapeutic target, and a new clinically relevant means of monitoring the in vivo state of mitophagic flux within the tumor microenvironment by means of mitophagy derived EVs.

#7064 BRCA 1/2 haploinsufficiency-associated metabolic dysfunction in benign fallopian tube epithelia.

J. Ravix, I. Paudel, G. Pulivendala, R. Sowamber, E. Smith, M. Schlumbrecht, D. Lombard, S. George;
University of Miami Miller School of Medicine, Miami, FL

In 3-17% of women with BRCA1/2 mutations who undergo risk-reducing surgery, pre-neoplastic and neoplastic lesions are found in their fallopian tubes that display differential loss of heterozygosity of BRCA1/2. Precisely how mutations in BRCA1/2 predispose women to develop high grade serous ovarian carcinoma (HGSC) is not completely understood. Although linked to various processes localized in the nucleus, BRCA1/2 may also have essential roles in the cytoplasm, specifically in the regulation of key processes associated with mitochondrial homeostasis and metabolism. Understanding how haploinsufficiency of BRCA1/2 contributes to the potential neoplastic transformation of fallopian tube epithelial cells should reveal new insights into BRCA1/2 function, and ultimately provide novel opportunities for preventative interventions in individuals with this mutation and new treatment opportunities for HGSC associated with BRCA1/2 heterozygosity. We have identified distinct metabolic and mitochondrial deficits in BRCA2 mutation carriers compared to BRCA1 carriers and non-carriers. Fallopian tube epithelial cell lines derived from BRCA2 mutation carriers showed increased levels of mitochondrial respiration and activity followed by BRCA1 mutation carriers and non-carriers. Western blot analysis of mitochondrial proteins regulating glycolysis and oxidative phosphorylation showed differential expression based on mutation status. Transmission electron microscopy of BRCA2 mutation carriers showed increased disrupted mitochondrial networks when compared to wild type, suggesting that mutation status may contribute to increased mitochondrial fission. These observations reveal an entirely new aspect of BRCA1 and BRCA2 biology and further studies will disaggregate the effects of BRCA1 and BRCA2 on mitochondrial function, versus DNA damage repair. Ultimately, this work will provide new insight into the adaptive changes within FT cells which promote neoplastic transformation and inform how high-grade serous carcinoma (HGSC) cells distinctively respond to microenvironmental stimuli.

#7065 AMBRA1 coordinates mitochondrial function to regulate cancer stemness and tumorigenesis in hepatocellular carcinoma.

Yan Liu[1], Yunong Xie[1], Yimiao He[1], Stephanie Ma[2], **Man Tong**[1]

[1]School of Biomedical Sciences, The Chinese University of Hong Kong, Hong Kong, China,[2]School of Biomedical Sciences, Li Ka Shing Faculty of Medicine, The University of Hong Kong, Hong Kong, China

Hepatocellular carcinoma (HCC) is a prevalent and aggressive cancer, with emerging evidence highlighting the role of cancer stem cells (CSCs) in its progression. AMBRA1 has been implicated to exert both tumor-promoting and tumor-suppressive roles through regulating cell cycle and mitophagy in various solid tumors. However, the functional roles of AMBRA1 in modulating cancer stemness and tumorigenesis in HCC remain elusive. Initial analysis of The Cancer Genome Atlas data revealed a significant inverse correlation between AMBRA1 expression and stemness indices (TSS) in HCC patients, with low AMBRA1 levels associated with an upregulated oxidative phosphorylation (OXPHOS) gene signature. To elucidate the functional consequences of AMBRA1 modulation in liver tumor development and stemness maintenance, we exploited both hydrodynamic mouse models and human HCC cell lines. Our findings indicate that hepatic AMBRA1 deletion enhances cancer stemness and tumorigenesis both in vivo and in vitro. Moreover, HCC cells with reduced AMBRA1 expression demonstrated heightened mitochondrial activity, characterized by increased oxygen consumption, respiration, mitochondrial membrane potential, and intracellular ATP levels. Apart from OXPHOS, we also observed a concomitant up-regulation and enrichment of MYC targets in TSS-high and AMBRA1-low HCC patients, pointing towards a deregulated c-MYC signaling to promote cancer stemness under AMBRA1 regulation in HCC. Collectively, our results demonstrate that AMBRA1 loss enhances mitochondrial function to support hepatic tumorigenesis in HCC.

MOLECULAR/CELLULAR BIOLOGY AND GENETICS: Modifications and Signaling to Cancer Drivers
Poster Session

#7069 NEK2 is frequently upregulated in esophageal adenocarcinoma associating with poor prognosis.
L. Chen, H. Lu, F. Ballout, T. Hu, Z. Chen, **D. Peng**;
University of Miami, Miami, FL

Esophageal adenocarcinoma (EAC) has become a significant clinical challenge due to rapid increase in the incidence during the past four decades in the USA and Western countries. However, the prognosis of EAC patients is still poor with 5-year overall survival rate about 20%. There is an urgent need to identify novel therapeutic targets associated with EAC biology. NEK2 is the first identified human NEK (Never in mitosis A (NIMA) related kinase) gene among the 11 serine/threonine kinases family. Aberrant NEK2 expression is reported in a variety of human cancers and plays important roles in tumorigenesis, progression, and drug-resistance. However, the expression of the NEK2 in EAC and its precancerous condition (Barrett's esophagus, BE) has not been investigated. Using bioinformatic approaches, we first analyzed the TCGA and 9 GEO databases (a total of 10 databases in which eight contain EAC and 6 contain BE) and found that NEK2 was significantly upregulated in EAC as compared to normal esophagus in 7 of the 8 databases. Meanwhile, genomic alterations of NEK2 are only found in 1.2% of EAC. We validated the overexpression of NEK2 using qRT-PCR, western blotting, immunohistochemistry in EAC cell lines and in primary EAC tissues. Functionally, we demonstrated that overexpression of NEK2 in EAC cells promoted tumor cell growth. Targeting NEK2 in EAC cells significantly inhibited EAC tumor growth. Our data suggests that frequent overexpression of NEK2 plays an important role in EAC.

#7070 MEK-ERK signaling maintains epidermal proliferation through H2A.Z deposition.

S. Droll, B. Zhang, C. Xue, M. Levine, X. Bao;
Northwestern University - Evanston, Evanston, IL

Recent studies have connected dysregulation of H2A.Z deposition to glioblastoma as well as lung, pancreatic, and metastatic breast cancers. The H2AZ1 and H2AZ2 isoforms, collectively known as H2A.Z, are histone variants that regulate gene expression, stem cell identity, and differentiation during development and in homeostatic tissue. Most tumors originate from epithelial tissues. We utilize skin epidermis, an accessible model of epithelial tissue, to understand the regulatory mechanisms controlling proliferation and differentiation. Primary human epidermal keratinocytes retain their abilities to proliferate, differentiate, and stratify in vitro. First, we observed that progenitor keratinocytes express high levels of H2A.Z mRNA and protein, and that H2A.Z levels significantly and progressively decrease during four days of calcium-induced differentiation. Using ChIP-sequencing, we find a significant, genome-wide decrease in H2A.Z chromatin occupancy in differentiated keratinocytes. Therefore, we hypothesized that H2A.Z is critical for progenitor function. Knock down of either H2AZ1 or H2AZ2 significantly impaired keratinocyte proliferation in holoclone assays. Furthermore, H2AZ1 or H2AZ2 knockdown inhibited epidermal stratification in organotypic culture. Canonically, two chromatin remodeling complexes, SRCAP and EP400, deposit H2A.Z into nucleosomes. While both SRCAP and EP400 knockdown diminish keratinocyte proliferation, only SRCAP knockdown decreases H2A.Z deposition in epidermal keratinocytes. Finally, we find that MEK and ERK signaling is required to sustain expression of SRCAP, H2AZ1, and H2AZ2. MEK or ERK inhibition is sufficient to significantly decrease H2A.Z occupancy genome-wide in progenitor keratinocytes.

#7071 Pharmacological targeting of SUMOylation leads to cBAF complex stabilization and disruption of the synovial sarcoma signature.

K. V. Floros[1], J. Li[2], J. L. Roberts[1], R. Kurupi[3], C. K. Fairchild[1], B. Hu[1], Y. Xing[1], K. M. Dalton[1], S. A. Boikos[4], A. M. Stamatouli[5], M. G. Dozmorov[5], J. E. Koblinski[1], K. B. Jones[2], S. K. Radhakrishnan[1], A. C. Faber[1];

[1]Massey Comprehensive Cancer Ctr., Richmond, VA, [2]Huntsman Cancer Institute, Salt Lake City, UT, [3]Washington University School of Medicine, Saint Louis, MO, [4]Georgetown Lombardi Comprehensive Cancer Center, Washington, DC, DC, [5]Virginia Commonwealth University, Richmond, VA

Synovial Sarcoma (SS) is driven by the SS18-SSX translocation event and occurs often in people under 30. In general, SS is refractory to chemotherapy and other therapeutic approaches. SS18-SSX does not directly bind to DNA but instead alters BAF complexes away from a wild-type SS18-containing cBAF complex towards a SS18-SSX- containing ncBAF complex to drive a SS-specific transcription program. Small molecule targeted therapies are expanding beyond the kinome, providing additional tools to treat cancers that are not yet amenable to targeted therapies. Here we demonstrate that SS18-SSX activates the SUMOylation program and SS are sensitive to the small molecule SAE1/2 inhibitor, subasumstat (TAK-981). Mechanistically, we demonstrate TAK-981 de-SUMOylates the cBAF/PBAF complex member, SMARCE1, leading to stabilization and restoration of cBAF complexes. This phenotypic shift leads to a DNA damage and cell death response, resulting in tumor inhibition across mouse models of SS. As such, TAK-981 combined with standard-of-care chemotherapy enhances SOC-induced DNA damage, leading to tumor regressions. Targeting the SUMOylation pathway in SS restores cBAF complexes, positioning it as a clinical candidate to treat this refractory cancer.

#7072 MYC acetylated lysine residues drive oncogenic cell transformation and regulate select genetic programs for cell adhesion-independent growth and survival.

J. J. Pino[1], M. Hurd[1], Y. Zhao[1], K. Jang[1], M. Allevato[1], M. Vorontchikhina[1], W. Ichikawa[1], R. Gates[1], E. Villalpando[1], M. Hamilton[1], F. Failo[1], S. Pan[1], Y. Qi[2], Y.-w. Hung[2], T. Girke[1], D. Ann[2], V. Seewaldt[2], E. Martinez[1];

[1]University of California, Riverside, Riverside, CA, [2]City of Hope, Duarte, CA

The MYC oncogenic transcription factor is acetylated by the p300 and GCN5 histone acetyltransferases. The significance of MYC acetylation and functions of specific acetylated lysine (K) residues have remained unclear. Here, we show that the major p300-acetylated K148(149) and K157(158) sites in human (or mouse) MYC and the main GCN5-acetylated K323 residue are reversibly acetylated in various malignant and non-malignant cells. Oncogenic overexpression of MYC enhances its acetylation and alters regulation of site-specific acetylation by proteasome and deacetylase inhibitors. Acetylation of MYC at different K residues differentially affects its stability in a cell type- dependent manner. Lysine-to-arginine substitutions indicate that although none of the acetylated K (AcK) residues is required for MYC stimulation of adherent cell proliferation, individual AcK sites have gene-specific functions controlling select MYC-regulated processes in cell adhesion, contact inhibition, apoptosis, and/or metabolism, and are required for the malignant cell transformation activity of MYC. Each AcK site is required for anchorage-independent growth of MYC-overexpressing cells *in vitro*, and both the AcK148(149) and AcK157(158) residues are also important for the tumorigenic activity of MYC-transformed cells in vivo. These AcK residues may also preferentially activate transcription via facilitating MYC binding to several cancer-associated target gene promoters and via enhancing RNAP II recruitment. With the knowledge that MYC lysine residues can be acetylated by HATs GCN5 and P300, some HATs and HAT associated cofactors (i.e. YEATS2 and PIN1) are important for MYC recruitment to DNA binding. By identifying MYC acetylation-dependent coregulators and their oncogenic function, we proposed to understand whether and how MYC acetylation residues cooperate with its cofactors and influence malignant transformation in breast cancer cells.Overall, this study will uncover the functions and mechanisms of MYC acetylation in regulation of malignant transformation and the impact on breast cancer initiation and progression. By analyzing deregulated target genes and MYC-relevant coactivators, the MYC AcK site-specific signaling pathways identified may offer new avenues for selective therapeutic targeting of MYC oncogenic activities.

#7073 Integrating fragment-based crystallographic screening with dTAG-PROTAC degradation and genetic rescue to explore the function of eIF4E.

P. A. Clarke[1], S. Y. Sharp[1], M. Martella[1], C. I. Milton[1], C. East[2], M. Vinkovic[2], N. Wallis[2], G. Ward[2], C. Richardson[2], A. Woodhead[2];
[1]The Institute of Cancer Research, London, United Kingdom, [2]Astex Pharmaceuticals, Cambridge, United Kingdom

The translation initiation factor eIF4E is a rate-limiting factor for protein synthesis that binds the mRNA m7G-cap to initiate the recruitment and binding of eIF4F components such as eIF4G. Targeting eIF4E has long been considered a promising anticancer strategy but it has remained undruggable using conventional screening approaches. Fragment-based crystallographic screening is a powerful technique for probing the surface of proteins to identify potentially druggable binding sites. Here, we describe fragment-based screening using a combination of Xray crystallography and NMR to identify low affinity fragment hits binding to the mRNA cap-binding site or at an additional site of unknown functional relevance (site 2). Subsequent rounds of iterative structure-based design yielded a lead molecule, with 100nM binding potency for site 2, that could disrupt the eIF4E:eIF4G interaction and inhibit cap-dependent translation in cell lysates. To explore the functional relevance of site 2 we established a cell model expressing an eIF4E-FKBP12F36V fusion protein that was sensitive to degradation following treatment with the heterobifunctional dTAGV-1 molecule. Degradation of eIF4E resulted in inhibition of cell growth and reduced expression of MCL1 protein, that were rescued by re-expression of a non-degradable wild-type eIF4E. A mutation reported to block canonical eIF4G binding (W73F) disrupted binding to eIF4G but to our surprise retained the ability to rescue the eIF4E degradation phenotype. Mutation of site 2 (L85R and L134R) also disrupted the eIF4E:eIF4G interaction. The L85R mutant remained able to partially rescue the cellular responses, in contrast to the L134R mutant that could not rescue eIF4E loss. The W73F/L85R double mutant resulted in a combinatorial loss of eIF4E function. Despite disrupting eIF4E function in lysates, there was a significant drop-off of compound activity in cells. However, treatment of the W73F mutant with compound recapitulated the combination of the W73F canonical eIF4G binding mutation with the L85R site 2 mutation. This approach demonstrates the power of coupling fragment screening with target-degradation and genetic rescue approaches to find and explore novel functional pockets. Our data suggest it may be necessary to disrupt the extended protein-protein interaction made by both the canonical and non-canonical regions of eIF4E to drive a strong functional effect in cells. However, the discovery of a lead compound, the associated structural understanding, and the knowledge that one site 2 mutation inactivates eIF4E provides hope that a significantly more potent small molecule inhibitor or degrader could drive a more profound cellular effect which may lead to improved cellular activity and a deeper understanding of eIF4E biology.

#7074 Perturbed RNA N6-methyladenosine methylome in SETD2 mutant clear cell renal carcinoma.

S. Shaikh, R. Wagner, R. Hlady, K. D. Robertson;
Mayo Clinic College of Medicine and Science, Rochester, MN

Clear cell renal carcinoma (ccRCC), which arises from the epithelial cells of the proximal tubule represents 70% of all renal cell carcinoma. Mutations that drive ccRCC in conjunction with near ubiquitous and early VHL loss include, PBRM1 (33 - 45%), BAP1 (15%) and SETD2 (13%). Loss of SETD2 leads to diminished occupancy of H3K36me3 in active gene bodies, which is progressively deregulated in primary RCC and metastasis, linking loss of H3K36me to tumor progression and metastasis. N6-Methyladenosine (m6A) is an important post-transcriptional regulator of RNA transcript stability and half-life. Preliminary findings have shown H3K36me3 (deposited by SETD2), targeting the core m6A methyltransferase machinery (METTL3, METTL14 and WTAP) to the mRNA by virtue of its interaction to METTL14 subunit. The goal of this study is to investigate if H3K36me3 depletion as observed in SETD2 mutant ccRCC, leads to a deregulated m6A methylome. We further investigate how deregulated methylome in key pathways leads to cancer initiation and progression in ccRCC. To accomplish our goals, we generated isogenic ccRCC cell lines with H3K36me3 depletion by knocking out SETD2. RNA-immunoprecipitation and sequencing for m6A (MeRIP) showed global deregulation of m6A methylome in SETD2KO isogenic ccRCC cell lines. We also show a number of pro-tumorigenic genes and pathways including cell invasion, inflammation and stemness being differentially methylated and expressed in SETD2KO ccRCC cell lines. Furthermore, we show SETD2KO cells being more sensitive to METTL3 inhibition suggesting the relevance of m6A hypermethylated transcripts in promoting pro-tumorigenic and growth promoting processes in SETD2KO ccRCC cell lines.

#7075 Global epitranscriptomic and transcriptomic footprint revealed upregulation of methylated single minded 2-small variant (meSIM2-SV) in colorectal cancer (CRC) by NTMT1(METTL11A) via m6A-YTHDF1-dependent manner..

S. K. Rai[1], T. Gong[1], Z. Gao[1], Y. Qin[1], M. Huo[1], K. Nakastu[1], H. Yang[1], Y. Fu[1], L. Wu[1], M. Jijiwa[1], M. Nasu[1], S. Chen[1], G. Huang[2], P. Fei[1], Y. Deng[1];
[1]John A. Burns School of Medicine, University of Hawaii at Manoa, Honolulu, HI, [2]Shanghai University of Medicine and Health Sciences, Shanghai, China

Establishing global footprint of altered m6A mRNA is a unique method to identify the new prognostics biomarkers. Altered N6-methyladenosine(m6A) RNA methylation regulates cancer progression with uncharacterized mechanism. Here, we present novel link between m6A modification on 5'-UTR SIM2-SV contribution in colorectal cancer progression. MeRIP and RNA-seq data from 68 fresh frozen CRC samples revealed 13,843 altered m6A methylated peaks and found highest in chromosomes 1, 2, and 3. Analysis uncovered 119 overlapping genes and clusters into 32 up-regulated genes with 56 up-hyper peaks, 8 up-regulated genes with 9 up-hypo peaks, 12 down-regulated genes with 14 down-hyper peaks, and 28 down-regulated genes with 40 down-hypo peaks. A significant increase in the SIM2 m6A and RNA level led us to perform correlation analysis between the SIM2SV and m6A RNA regulators. SIM2SV was significantly correlated with YTHDF1 m6A-readers and m6A-NTMT1 writer, suggesting important roles of SIM2SV in CRC oncogenicity. m6A-sequencing identified m6A enrichment in 5'-UTR of SIM2SV gene which further verified. siNTMT1 and siYTHDF1 manipulation in HCT116 and RKO cell lines verified a decrease in SIM2SV gene/protein expression, and m6A level. Knockdown effects also showed decrease in cell proliferation, clonogenicity and induced cell cycle arrest in the G2/M phase for NTMT1 and YTHDF1 versus SIM2 Knockdown showed cell cycle arrest in S/G2 phase. Our investigation revealed the role of new writer NTMT1 for methylated SIM2SV gene expression in colorectal cancer proliferation via m6A-YTHDF1(as “decoder”) dependent manner. Further investigation on m6A modification specifically on SIM2 mRNA revealed the essential roles of its writer NTMT1 and its reader YTHDF1 in CRC development, evidently supporting the importance of the unique landscape of m6A epigenetic modification in colorectal neoplasm, which not only advance our understanding of CRC pathobiology but also provides a new set of molecular targets for building up effective tools to fight CRC.

#7077 The oncogenic transcription factor ERG has distinct roles and signaling in different prostate cancer cell types.

Saranya Rajendran, **Peter C. Hollenhorst**

Indiana University School of Medicine, Bloomington, IN

ERG is the most common oncogene in prostate cancer, as it is aberrantly expressed in about 50% of cases due to the TMPRSS2/ERG gene rearrangement. ERG is not normally expressed in the adult prostate. The normal function of ERG is confined to hematopoietic stem cells and blood vessels. Aberrant expression of ERG in prostate epithelial cells is oncogenic when combined with mutations that activate the PI3K/AKT signaling pathway. The RAS/MAPK pathway can also regulate ERG function through direct phosphorylation of ERG by ERK. The function of these regulatory events and how they can be exploited to develop therapy for ERG-positive prostate cancer remains unclear. Here we find that ERG expression in prostate epithelial cells with low PI3K/AKT pathway activity drives epithelial to mesenchymal transition and stemness properties. This function requires ERG phosphorylation via a positive feedback loop with the TLR4 signaling pathway, and can be repressed by a TLR4 inhibitor. However, activation of the PI3K/AKT pathway rearranges the ERG cistrome and alters ERG function, where ERG now promotes luminal epithelial differentiation. In the presence of activated AKT, new ERG targets include genes involved in vascular development and ERG phosphorylation is regulated through a positive feedback loop with the VEGF signaling pathway. Despite these differences in cellular differentiation, we find that ERG can promote stemness and tumorigenesis in both AKT-high and AKT-low cellular backgrounds. ERG functions in prostate epithelial cells appear to mirror ERG functions in hematopoietic stem cells and blood vessels. These findings suggest strategies of combinatorial inhibition of ERG function through signaling pathway inhibition.

#7078 Targeting eIF6 to modulate ribosomal subunit association dynamics in cancers.

K. M. Harish, P. Roshan, A. Biswas, S. Anagnos, R. Luebbers, S. Origanti;
Saint Louis University, St. Louis, MO

Deregulation of ribosomal subunit levels and accessibility are hallmarks of cancer. Eukaryotic translation initiation factor 6 (eIF6) is a key regulator of ribosomal subunit association that is over expressed in many cancers including lung, colon, ovarian and breast cancers, and deregulation of eIF6 is correlated with a poor cancer prognosis. Association of eIF6 with 60S is critical for 60S assembly. However, eIF6 must be released from 60S prior to translation to permit inter subunit interactions between 60S and 40S and to facilitate the formation of translationally proficient 80S monosome. Release of eIF6 is deregulated in the ribosomopathy- Shwachman Diamond Syndrome that is predisposed to leukemias. Also, loss of eIF6 markedly delays tumorigenesis without affecting normal growth, which presents eIF6 as a viable therapeutic target. A potential therapeutic strategy is to target the eIF6 and 60S ribosomal interaction interface. Through biophysical analyses we had identified residues that are critical for the interaction between eIF6 and 60S ribosomal subunit. We show that targeting these key residues in the eIF6-60S interaction interface markedly delays colonic cancer growth and inhibits protein synthesis. Furthermore, we show that the levels of other eIFs and the release factors: SBDS, and EFL1-GTPase are unaltered in the mutant cells suggesting that the translational inhibition is primarily attributed to the deregulation of eIF6. Interestingly, targeting eIF6 leads to an upregulation of p53 independent of the DNA damage response, suggesting that ribosomal stress contributes to the stabilization of p53. Previously, it was shown that translation of Cdc42 was upregulated by eIF6 to promote invasiveness. However, Cdc42 levels were unaltered in the mutant cells. Future studies will determine the mRNA substrates that are translationally deregulated in the mutants. We will also determine the effect of disrupting eIF6 function in inhibiting tumor growth and progression *in vivo*.

Category: MCB, Subcategory: MCB07-Gene regulation sub classification: Translational Control

#7079 The Wnt/β-catenin signaling pathway regulates cellular metabolism through the suppression of HAL and ARG1 in liver cancer cells.

S. Nakagawa[1], K. Yamaguchi[1], K. Takane[1], S. Tabata[2], T. Ikenoue[1], Y. Furukawa[1];

[1]University of Tokyo, Tokyo, Japan, [2]National Cancer Center, Yamagata, Japan

Aberrant activation of the Wnt/β-catenin signaling pathway plays a crucial role in a wide range of human tumors including colorectal and liver cancer. The activated signaling causes nuclear accumulation of β-catenin, which leads to the elevated expression of target genes of TCF/LEF (T-cell factor/lymphoid enhancer factor) transcription factors through their interaction with nuclear β-catenin. Recent studies have identified a lot of genes induced by this pathway such as *MYC*, *CCND1*, *AXIN2*, and *LGR5*, and clarified their roles in tumorigenesis. However, the roles of the genes down-regulated by the pathway remain to be elucidated. Our previous study revealed that the histidine ammonia-lyase gene (*HAL*) encoding an enzyme involved in the catabolism of histidine was down-regulated by the signaling pathway in liver cancer. In addition, we identified a region that is involved in the Wnt-dependent regulation of *HAL*. To clarify the regulatory mechanism of *HAL* by the pathway, we searched for transcription factors that are associated with the regulatory region, and identified CEBPA and FOXA1, two liver-enriched transcription factors. It is of note that the expression of these factors was reduced by the TCF/β-catenin complex. Further investigation identified arginase 1 (*ARG1*) encoding an enzyme that catalyzes the hydrolysis of arginine as another target gene of CEBPA and FOXA1. Consistent with these data, inhibition of the Wnt signaling increased the expression of ARG1 as well as HAL in liver cancer cells. Furthermore, the up-regulation of HAL and ARG1 by the inhibition of this pathway decreased intracellular concentrations of histidine and arginine, suggesting that the Wnt signaling plays an important role in cellular metabolism through the regulation of the two transcription factors. These findings shed light on the role of the Wnt/β-catenin signaling pathway in the metabolism of amino acids in liver cancer cells.

#7080 Regulation of caveolin-1 by RAS/RAF oncogenic signaling in cancer cells.

V. Castro Aceituno, T. Cui, H. Feng, L. Yang, S. Nair, T. M. Williams;
City of Hope National Medical Center, Duarte, CA

Background and Purpose: Caveolin-1 (Cav-1), a scaffolding protein implicated in cellular signaling and membrane dynamics, undergoes intricate regulation at multiple levels. Recent evidence has suggested a potential association between oncogenic mutations and alterations in Cav-1 expression. Our study aimed to comprehensively explore how RAS/RAF mutations influence Cav-1 expression in cancer cells, as well as the underlying molecular mechanisms, using tetracycline (tet)-inducible cell lines and cancer cell lines harboring endogenous BRAF or KRAS mutations.

Experimental Design: We assessed the regulation of Cav-1 expression using tet-inducible cell lines with $BRAF^{V600E}$, $KRAS^{G12D}$, or $KRAS^{G12C}$ mutations. We measured the half-life of Cav-1 at protein levels by using cycloheximide. We monitored Cav-1 localization and degradation dynamics by SNAP-based pulse-chase assay. Additionally, we performed protein and gene expression analyses by immunoblotting and qRT-PCR, luciferase reporter assay, and immunofluorescence to dissect the impact of BRAF and KRAS mutations on Cav-1 regulation at various stages of its life cycle.

Results: We found a significant downregulation of Cav-1 at both mRNA and protein levels upon induction of BRAF or KRAS mutations. The use of $KRAS^{G12C}$, $BRAF^{V600E}$, ERK, and/or MEK inhibitors in tet-inducible cell lines rescued the effects observed upon induction. The rescue effects have also been observed in H23, MiaPaCa-2 and 8505-C cancer cell lines bearing either BRAF or KRAS mutations. Notably, $BRAF^{V600E}$ exhibited a more pronounced reduction in Cav-1 expression than other mutations. We observed shortened half-life of Cav-1 at protein levels after induction of RAS/RAF mutations by using cycloheximide, and SNAP-based pulse-chase. These mutations accelerated lysosomal-mediated degradation of Cav-1 as determined by immunoblotting and immunofluorescence, which was reversed by lysosomal inhibitors.

Conclusions: Our study establishes a novel regulatory paradigm wherein RAS/RAF mutations exert a multi-faceted influence on Cav-1 dynamics in cancer cells. The transcriptional and translational downregulation, coupled with accelerated lysosomal degradation, collectively contributes to the decreased half-life of Cav-1 following the induction of BRAF or KRAS mutations. These findings provide insights into the intricate molecular mechanisms underpinning the dysregulation of Cav-1 in the context of RAS/RAF mutations, offering potential avenues for therapeutic interventions.

#7081 Comprehensive investigation of NAT10's catalytic and non-catalytic functions in cancer cell proliferation.

S. P. Raikundalia, **M. Dalhat**, E. A. Patrasso, A. Suh, D. Arango;
Northwestern University - Chicago, Chicago, IL

N-acetyltransferase 10 (NAT10) is emerging as an oncoprotein in multiple cancers including acute myeloid leukemia and liver cancer. In addition, my preliminary studies show that NAT10 is a stress response that promotes the resilience of cancer cells to anti-tumor drugs. However, the underlying mechanisms by which NAT10 promotes cancer growth and drug resistance are unknown. NAT10 is an RNA acetyltransferase, where it acetylates cytidines in rRNA, tRNA, mRNA, and lncRNAs. Our previous work demonstrated that NAT10 promotes translation efficiency and mRNA stability through the acetylation of cytidines in mRNA. However, NAT10 is a multifunctional protein. Besides acetylating RNA, NAT10 also acetylates proteins at lysine residues, has RNA helicase activity, and can serve as a scaffold in ribonucleoprotein complexes. Based on this complexity, it is imperative to elucidate whether NAT10 exerts its oncogenic activity via RNA acetylation, protein acetylation, disruption of RNA structures, or non-catalytic functions. Strikingly, our preliminary results indicate that the acetyltransferase function of NAT10 is dispensable for cell proliferation. To evaluate NAT10's oncogenic activity unbiasedly, we are now performing a deep mutagenesis scanning (DMS) assay. For this purpose, we generated a library of mutants in hundreds of NAT10 residues. This library was transduced in multiple cell lines from acute myeloid leukemia and liver cancer carrying a PROTAC system, which allow us to deplete NAT10 in a rapid and controlled manner while expressing ectopically thousands of NAT10 mutants. In this conference, I will talk about, my results, how DMS is a powerful tool to delineate the molecular functions of candidate oncoproteins, and the implications of our results for the potential drugging of NAT10 in cancer.

Keywords: Cell proliferation, NAT10, RNA modifications, Deep mutagenesis scanning.

#7082 Epidemiology meets epitranscriptomics: Exploring the cancer-related role of a novel *TERT*-antisense transcript and its regulation by RNA methylation.

B. W. Papenberg[1], O. Florez-Vargas[1], M. Ho[1], K. Forsythe[1], C. Zhang[1], C.-H. Lee[1], S. Mbulaiteye[1], P. J. Batista[2], L. Prokunina-Olsson[1];
[1]National Cancer Institute, Rockville, MD, [2]National Cancer Institute, Bethesda, MD

Human telomerase reverse transcriptase (TERT) maintains telomeres at chromosome ends and its dysregulation is implicated in various human health conditions. Multiple GWAS signals are detected within the *TERT* genomic region at chr 5p15.33. As a potential proxy for these signals, we investigated a highly polymorphic variable number tandem repeat (VNTR)2-1 within intron 2 of *TERT*, with 57-143 copies of a 42 bp repeat unit per allele. By functional annotation of VNTR2-1, we predicted that it generates an intronic transcript antisense to *TERT* with a variable-size open reading frame (ORF) of 2502-5211 bp (834-2038 aa). Specific to the *TERT*-antisense transcript, we predicted N6-methyladenosine (m6A) consensus motifs within each 42 bp unit of VNTR2-1, with longer VNTR2-1 regions carrying more m6A motifs. In a stranded RNA-seq dataset of African pediatric Burkitt lymphoma (BL) tumors, which have high *TERT* expression, we detected the VNTR2-1-containing *TERT*-antisense transcript in a subset of tumors (n=35/113, 30.9%), confirming the expression of this novel transcript. VNTR2-1 expression was also experimentally validated by 5'-RACE/Nanopore-seq in Raji (BL cell line) and UMUC3 (bladder cancer cell line). Additionally, the VNTR2-1 transcript was visualized in UMUC3 cells using RNA-FISH.

The consensus 42 bp VNTR2-1 repeat sequence and its m6A-deficient variants were cloned into a m6A-deficient dual-luciferase reporter vector (m-psiCHECK-2) and expressed in UMUC3 cells, showing an m6A-motif dose-dependent response driving luciferase protein expression. Transient treatment with STM2457, an inhibitor of the m6A writer METTL3, reduced the expression of the luciferase reporter, confirming that m6A motifs within VNTR2-1 are methylated by METTL3. Additionally, Long-term cigarette smoke condensate (CSC) treatment of UMUC3 reduced luciferase expression, suggesting alterations of VNTR2-1 m6A due to smoke exposure.

We explored potential peptides produced from VNTR2-1 transcript by analysis of public mass spectrometry datasets using PepQuery and identified several unique VNTR2-1 peptide fragments in human tumors. Next, we cloned a synthetic FLAG-tagged gene containing three VNTR2-1 consensus repeats with native Kozak sequence and translation start/stop codons. Western blotting confirmed the translation of the VNTR2-1 peptide that was ablated by start codon mutation, suggesting that the native Kozak sequence is sufficient for VNTR2-1 translation. These results support VNTR2-1 as a peptide-producing transcript.

In conclusion, we identified a novel intronic transcript produced by VNTR2-1 antisense to *TERT*. This m6A-regulated transcript could function through several mechanisms, such as a lncRNA or translated peptide, potentially regulating *TERT* expression and telomerase function in health and disease conditions, including cancer.

CHEMISTRY: Proteomics and Mass Spectrometry 2
Poster Session

#7088 MALDI-IHC high-plex protein biomarker imaging for fast, non-iterative identification of lung carcinoma subtypes.

Catherine A. Kita[1], Kristina Schwamborn[2], Gargey Yagnik[1], Kenneth J. Rothschild[1], Mark J. Lim[1]

[1]AmberGen Inc, Billerica, MA,[2]Technische Universitat Munchen, Munchen, Germany

Lung cancer is the second most common cancer worldwide, with over 2.2 million new cases in 2020 and is the leading cause of cancer-related deaths worldwide. Most lung cancer (80-85%) is non-small cell (NSCLC), comprising mostly adenocarcinoma and squamous cell carcinoma, while roughly 10-15% of lung cancer is small cell lung cancer (SCLC), also termed neuroendocrine lung cancer. Subtype identification is critical for determining treatment, and with limited samples, it is critical to get the most data possible from each tissue section. NSCLC subtypes can be treated with chemotherapy or targeted drugs, whereas SCLC tends to respond best to a combination of chemotherapy and radiation. While there have been many improvements in the detection and treatment of lung carcinoma, the immuno-histochemical (IHC) confirmation of subtype remains a prolonged and often iterative process. To overcome this limitation, we have developed a new IHC approach which uses antibodies labeled with novel photocleavable mass-tags combined with matrix assisted laser desorption ionization (MALDI) mass spectrometry imaging. The approach, termed MALDI-IHC, provides fast (1 hr/cm^2 imaging time) and highly multiplexed IHC (100+-plex) without the need for iterative cycling procedures. Here, we present a 20+-plex panel for the determination of subtype in lung cancer. An antibody panel comprised of established clinical biomarkers was developed to differentiate between the lung carcinoma subtypes and provide potentially prognostic information. This included markers for adenocarcinoma (TTF-1, Napsin A), squamous cell carcinoma (p40, CK5), and small cell lung cancer (CD56, Chromogranin A and Synaptophysin), as well as general carcinoma markers for t cells, b cells, macrophages, and fibroblasts These markers were first validated individually by immunofluorescence and then compared to MALDI-IHC on annotated tissues. Here we present an overview of the antibody validation for the 20+-plex lung carcinoma panel. Biomarker presence and peak signal intensity for the various subtypes was then determined using pathologist classified tissues for normal lung, adenocarcinoma, squamous cell carcinoma and small cell lung cancer. We report application of the MALDI-IHC approach to the simultaneous determination of lung carcinoma subtypes on a 99-core human lung tissue microarray (TMA) comprised of normal, normal adjacent, cancer adjacent, and cancerous tissues. Moreover, because MALDI-IHC is a non-destructive process, it can be followed by conventional H&E staining on the same tissue section for accurate co-registration of traditional pathology annotations with the highly multiplexed MALDI-IHC results. In the future, even larger, 100+-plex antibody panels can be used for precision medicine on a wide range of cancers, in order to determine the molecular subtypes and guide treatment paths.

#7089 Proteomic evaluation of combination data in acute myeloid leukemia to inform mechanism of action and new targets.

L. Chan[1], Z. Ozen[1], A. Iannetta[1], E. Miele[1], F. Kar[1], A. Jarnuczak[1], G. Nelson[1], A. Markovets[1], J. Roderick-Richardson[1], J. Urosevic[2], L. Drew[1], J. Mettetal[1]; [1]Astrazeneca, Waltham, MA, [2]Astrazeneca, Cambridge, United Kingdom

Background: Acute myeloid leukemia (AML) is a prevalent adult leukemia. In the US, around 20,380 individuals were diagnosed with AML in 2023. Despite standard therapies, relapse and resistance persist. Cyclin-dependent kinase 9 (CDK9) has been recognized an actionable therapeutic target in AML. The potent inhibitor, AZD4573, induces durable apoptosis and suppresses tumor growth. Our study reveals that combining AZD4573 with standard-of-care (SoC) treatments deepens cell death responses in multiple AML cell models. We also used proteomics tools to understand the mechanisms underlying the vulnerability and resistance in SoC and CDK9 combinations.

Methods: In the drug combination study, three SoC agents (cytarabine, decitabine, and venetoclax) were evaluated in combination using a 6x6 dose-response matrix in four AML cell models (MOLM13, MOLM16, MV411, and OCI-AML2). The HSA synergy score and Emax drug activity were used to assess the benefits of the drug combinations. In the proteomics evaluation study, MOLM13 cells treated for 7 days under different conditions - (1) vehicle control; (2) cytarabine alone; (3) decitabine alone; (4) venetoclax alone; (5) AZD4573 alone; (6) AZD4573+cytarabine; (7) AZD4573+decitabine; (8) AZD4573+venetoclax - were collected for proteomics analysis using LC-MS/MS. Differential expression and missing pattern analyses were used to identify dysregulated proteins. Functional enrichment analysis was employed to identify dysregulated biological processes and pathways in response to different treatments.

Results: Our drug combination screens demonstrated the efficacy of AZD4573 in combination with cytarabine, decitabine, and venetoclax in 3 of 4 AML cell models. In our proteomic analysis, we took two approaches. First, we compared the proteomes of AML cells treated with SoC agents, identifying shared downregulated pathways such as serine biosynthesis, notably pointing to the rate-limiting enzyme PHGDH as a potential therapeutic target in AML. Cytarabine and decitabine induced an inflammatory response, while venetoclax increased the expression of cell division regulators like Aurora kinase B (AURKB). Interestingly, targeting AURKB with AZD2811 has been shown to overcome venetoclax resistance in AML. Second, we compared proteome changes induced by various AZD4573 combinations. We identified IRF2BP2 as a shared vulnerable protein across the three AZD4573 combinations. POUF2F2 expression was significantly induced by cytarabine but suppressed when combined with AZD4573. Given that POUF2F2 activates the PDK1-Akt pathway, our findings suggest that AZD4573-induced POUF2F2 downregulation suppresses the PDK1-AKT pathway, inhibiting tumor progression.

Conclusions: Our proteomics analysis identifies vulnerable and resistant pathways and proteins, shedding light on the mechanism of action and revealing potential new targets for AML.

#7090 A scaled proteomic discovery study for prostate cancer diagnostic signatures using Proteograph workflow with trapped ion mobility mass spectrometry.

Mark Flory[1], Matthew Chang[1], Jessie May Cartier[1], Jane Lange[1], Travis Moore[1], James McGann[1], Ryan Kopp[2], Michael Liss[3], Robin Leach[4], Brenna Albracht[4], James Dai[5], Michael Krawitzky[6], Eltaher Elgierari[7], Jessica Chu[7], Paul Pease[7], Max Mahoney[7], Shadi Ferdosi[7], Ryan Benz[7], Khatereh Motamedchaboki[7], Asim Siddiqui[7], Mahdi Zamanighomi[7], Amir Alavi[7], Harendra Guturu[7], Daniel Hornburg[7], Serafim Batzoglou[7]

[1]Knight Cancer Institute, Oregon Health & Science University, Portland, OR,[2]Urology, School of Medicine, Oregon Health & Science University, Portland, OR,[3]Urology, University of Texas Health San Antonio, San Antonio, TX,[4]Cell Systems and Anatomy, University of Texas Health San Antonio, San Antonio, TX,[5]Biostatistics, Fred Hutchinson Cancer Research Center, Seattle, WA,[6]Bruker Daltonics, Billerica, MA,[7]Seer, Inc., Redwood City, CA

Background and Aims: The low cancer specificity of serum Prostate-Specific Antigen (PSA), the principal biomarker for prostate cancer detection, leads to a high frequency of unwarranted prostate biopsies. To alleviate this deficit, we executed a proteomic discovery study seeking PSA reflex signatures using the Proteograph™ Product Suite, a multi-nanoparticle-based deep plasma/serum proteomics workflow (Seer, Inc.), with timsTOF Pro mass spectrometry (Bruker) to interrogate over 900 serum specimens from patients that underwent prostate biopsy due to elevated PSA and/or abnormal digital rectal exam.
Methods: Our study followed rigorous design principles including uniform collection, randomization and blinding of specimens, all of which were processed with the Proteograph Product Suite. Liquid chromatography-mass spectrometry (LC-MS) analyses leveraged the Bruker timsTOF Pro MS platform utilizing 30-minute reversed-phase chromatography and a label-free dia-PASEF (data independent acquisition - parallel accumulation serial fragmentation) data acquisition method. Peptides deriving from a chosen subset of specimens designed to maximize peptide diversity were pooled, fractionated and analyzed using DDA (data-dependent acquisition)-PASEF to build a spectral reference library.
Results: The DIA-NN algorithm was employed through the cloud-based Proteograph Analysis Suite (PAS) to search LC-MS data. Leveraging our study-specific spectral library proteomic depth achieved was approximately 3600 protein groups identified (median) per patient serum specimen and more than 4400 in at least 25% of samples across the study. Customized machine learning workflows and the SeerML pipeline were used to identify and assess diagnostic power of new proteomic signatures.
Conclusions: Our data demonstrate the remarkable proteomic depth achievable in a scaled patient serum specimen discovery study using a combination of Proteograph and timsTOF platforms. This significant effort revealed serum proteomic signatures with increased diagnostic performance over that provided by PSA blood measurement and traditional patient-associated metadata alone, providing a foundation for future clinical tests aimed to reduce the current high frequency of unnecessary prostate biopsy.

#7091 Significance of the tryptophan catabolism pathway in triple-negative breast cancer shows potential targets in certain subsets relating to the serine pathway.

J. Jeon, A. Achreja, M. Slayton, O. Animasahun, M. Nenwani, M. Paserba, Z. Farah, S. D. Merajver, D. Nagrath;
University of Michigan, Ann Arbor, MI

Background: Breast cancer (BC) is the most prevalent form of cancer worldwide, encompassing 12.5% of all forms of cancers with the fifth highest mortality rate. Triple negative cancers (TNBC), which account for 15~20% of BCs, are one of the most aggressive and heterogeneous forms of BCs, characterized by the loss of ER, PR, and low HER2 expression. This heterogeneity and plasticity are partly due to the adaptable nature of their metabolism, a dynamic phenotype which is commonly observed in many aggressive forms of cancer. One of the key metabolic pathways that can confer this aggressive proliferative characteristic is the tryptophan catabolism pathway. Tryptophan is an essential amino acid required for the proper function of all mammalian cells, with IDO1 being a key enzyme that converts tryptophan to kynurenine, marking the start of the catabolism pathway. IDO1 expression is observed to be elevated in various types of cancer including BCs and has been associated with immune suppression/evasion via resource competition and tumor progression by supplying resources required for proliferation. Despite this, tryptophan catabolism is one of the lesser studied and understood pathways in cancer metabolism, especially in the context of TNBCs.

Methods: Previous analysis had shown the tryptophan catabolism pathway is downregulated in certain subsets of TNBCs. To understand the effective function of the pathway with regards to proliferation, we targeted the upper-most step of the catabolism pathway by inhibiting IDO1 with epacadostat and indoximod in different types of TNBC cell-lines and observed for changes in their growth rates via proliferation assays. We also performed parallel stable-isotope tracer-based flux analysis with [U-13C11]-Tryptophan and [U-13C3]-Serine with mass spectrometry to characterize flux changes with the goal of discovering potentially lethal metabolic pathways.

Results: We observed higher proliferative sensitivity to IDO1 inhibition in TNBC cell-lines with a genetic dysfunction in the *de novo* serine synthesis pathway. To understand these differences at the metabolic level, we quantified the differential contributions of tryptophan and serine to nucleotide and NAD^+ synthesis and the TCA cycle with the parallel tracer experiments. Comparison of the lines with dysfunctional *de novo* serine synthesis to those with normal or amplified flux towards the pathway showed a higher interdependence with the kynurenine pathway in the dysfunctional group. These results indicate a differential potential for targeting the kynurenine pathway in relation with the serine synthesis pathway.

Conclusion: Targeting the IDO1 enzyme in the kynurenine pathway shows significant correlations between the *de novo* serine pathway and the tryptophan catabolism pathway in TNBCs that may lead to metabolic targets conferring potential therapeutic benefits.

#7092 Cancer biomarker discovery with scalable biofluid proteomics.

Danielle B. Gutierrez, Jessica L. Moore, Jaison Arivalagan, Tiffany Louie, Leslie Wilkinson, Ray Clemens

Proteome Center, Discovery Life Sciences, Huntsville, AL

Biofluid proteomics opens opportunities for the discovery of early detection, diagnostic, and prognostic cancer biomarkers through non-invasive or minimally invasive screening. Plasma and serum are accessible sample types, however, the high dynamic range of proteins creates analytical challenges for the sensitive detection of potential biomarkers. In this work, we compare two proteomic approaches for large-scale cancer biomarker discovery: the Olink Proximity Extension Assay and the Seer Proteograph Product Suite. Olink Explore 3072 is an immunoassay that gains specificity by using dual antibody recognition to measure approx. 3,000 proteins in each sample. Antibody pairs are tagged with oligonucleotides, which hybridize and are amplified before measurement by next generation sequencing. Seer Proteograph is an enrichment strategy that uses a proprietary mix of functionalized magnetic nanoparticles with affinity for certain amino acids and functional groups in native state proteins. The resulting peptides are measured using untargeted mass spectrometry to identify proteins at the peptide level, paving the way for the identification of proteoforms and peptide variants. Aliquots of human plasma from 78 samples representing a range of cancer indications were obtained through the Discovery Life Sciences biobank and used for analysis by both the Olink and Proteograph workflows. Olink analysis achieved Pearson correlation scores of greater than or equal to 0.8 when correlating each of seven process controls to each other for all approx. 3000 proteins. On average, greater than or equal to 75% of the proteins were detected across all panels in all sample groups except for Normal and Benign groups (64% and 74% respectively). After stringent FDR filtering to ensure only high-quality data was analyzed, the Seer Proteograph workflow quantified 4,323 proteins across all 78 samples. Pearson correlation scores of greater than or equal to 0.96 were achieved when comparing digestion controls, process controls, and sample cleanup controls. Both platforms achieved detection of proteins across the dynamic range of plasma, including low abundance proteins. The Olink Explore 3072 and Seer Proteograph platforms were found to be complementary, with approx. 15% overlap in measured proteins. Cancer biomarker discovery at the proteomic level is bolstered by recent advances in analytical capabilities, as revealed by the Olink Explore and Seer Proteograph platforms. Importantly, complementary implementation of these two workflows will enable comprehensive biomarker analysis.

#7093 Prediction of overall survival in stage II and III colon cancer through machine learning of rapidly-acquired proteomics.

K. Xu[1], X. Yin[2], T. Guo[3], S. Zheng[1], Y. Shao[1];

[1]The Second Affiliated Hospital, Zhejiang University School of Medicine, Hangzhou, China, [2]The Affiliated Hospital of Qingdao University, Qingdao, China, [3]Westlake University, Hangzhou, China

The use of adjuvant therapy in stage II-III colon cancer (CC) has been controversial for decades. No markers or models now is satisfactory enough to be adopted widely by the medical community. Here, we analyzed the proteomics of paraffin-embedded tissue (FFPE) biopsy samples from 230 CC patients (stages II-III) with up to 10 years of survival by using pressure cycling technology (PCT) and data-independent acquisition (DIA) mass spectrometry. Using machine learning, we established a novel and practical protein-based clinical classification system for CC prognosis which was further verified in an independent validation cohort. Using the nine protein-based clinical model, we improved the area under the curve (AUC) value to 0.926 in the training cohort and 0.872 in the validation cohort. Our promising model will be a potential approach to prognostication to aid in rational follow-up schedule-making and risk-adaptive individualized therapies.

#7094 Clinical metabolomics reveals baseline biomarkers of hepatic dysfunction correlating with irregular drug-induced ALT and bilirubin elevations.

J. K. Meissen[1], K. Contrepois[1], S. Regan[2], J. Tan[2], A. J. Foster[2], J. Yuan[1], S. Sharma[1], D. Williams[2], A. I. Rosenbaum[1];
[1]AstraZeneca US, South San Francisco, CA, [2]AstraZeneca US, Cambridge, United Kingdom

AZD4573 is a highly potent and selective Cyclin-Dependent Kinase 9 inhibitor. The AZD4573 First-in-Human (FIH) study revealed variable alanine transaminase (ALT) and/or bilirubin elevation and a clear correlation to dose or PK exposure could not be defined. While concurrent ALT elevation ≥3x upper limit of normal (ULN) and bilirubin elevation ≥2x ULN (potential Hy's law) is a biochemical finding indicating potential drug-induced liver injury, quantitative modeling disconnected ALT and bilirubin elevation demonstrating that the observations were not Hy's Law cases. Furthermore, we implemented a targeted metabolomics workflow to investigate the ALT and bilirubin elevation mechanism and identify predictive biomarkers to better understand and/or predict any hepatic stress liabilities associated with AZD4573 clinical development. We implemented an established metabolomics methodology to 359 samples from 15 patients yielding 47,000 total data points. Data was separated into 98 different dosing intervals from the 15 patients to identify the ALT and bilirubin-associated metabolic changes conserved across all patients while incorporating metabolic differences in individual patents with ALT and bilirubin elevation in only a fraction of multiple doses. Orthogonal Partial Least Squares modeling identified several metabolites and pathways altered as a function of maximum ALT or bilirubin levels. Post-dose conjugated bile acids were elevated when ALT and bilirubin were elevated. Pre-dose creatine levels were decreased when ALT and bilirubin elevation occurred, and pre-dose glutamate levels were elevated when ALT elevation occurred. Pre-dose decreased total carnitines and kynurenine pathway activation were observed when ALT and bilirubin elevation occurred, but the effect did not reach statistical significance. Elevated bile acids are an established characteristic of cholestasis and suggest cholestasis as a probable mechanism for AZD4573-induced reversible liver stress. Interestingly, decreased creatine, glutamate elevation, decreased total carnitine, and kynurenine pathway activation are all associated with some form of liver stress or disfunction which may explain the irregular ALT and bilirubin elevations observed in patients receiving AZD4573; while ALT itself is a biomarker of liver damage, these pre-dose biochemical changes may illuminate potential preceding liver stress. Dosing patients already experiencing higher liver stress levels may be more susceptible to drug-induced ALT and bilirubin elevation, and patients with increasing in-study liver stress may only present at later doses. This work demonstrates metabolomics utility to elucidate possible mechanisms of liver toxicity as well as to identify potential predictive biomarkers for further investigation to explore individual patient risk in clinical studies.

#7097 Integrated proteomics and metabolomics reveals new insight into the synergistic interaction of valproic acid plus simvastatin in prostate cancer xenograft model associated with down-modulation of YAP and TAZ signaling.

F. Iannelli, R. Lombardi, S. Costantini, M. Roca, L. Addi, F. Bruzzese, E. Di Gennaro, **A. Budillon**, B. Pucci;
Istituto Nazionale Tumori di Napoli - IRCCS - Fondazione G. Pascale, Napoli, Italy

Background: Despite advancements in therapeutic approaches, including taxane-based chemotherapy and androgen receptor targeting agents, metastatic castration-resistant prostate cancer (mCRPC) remains an incurable disease, underlying the need of novel strategies that can target the complexities of this disease and bypass the development of drug-resistance mechanisms. We previously demonstrated the synergistic antitumor interaction of the antiepileptic with histone deacetylase inhibitory activity valproic acid (VPA), and the lipid-lowering drug simvastatin (SIM). This combination sensitizes mCRPC cells to docetaxel treatment and revert docetaxel-resistance, both in vitro and in vivo models, by targeting cancer stem cells compartment via mevalonate pathway/YAP axis modulation.
Methods: Proteomic and metabolomic/lipidomic analysis on tumor samples were performed by LC-MS/MS-based shotgun proteomics and by 1H-NMR approach, respectively. Progenesis QI for proteomics v. 4.2 was used as label-free quantification platform. Functional annotation analysis were performed by using the DAVID v6.8 (Database for Annotation, Visualization and Integrated Discovery); g:Profiler WikiPathways databases; Reactome version 66; Ingenuity Pathway Analysis software. Partial least squares-discriminant analysis (PLS-DA) and Loading plot were performed by Metabo Analyst v5.0 tool.
Results: Tumor samples derived from 22Rv1 mCRPC cells xenografted mice, treated or not with VPA/SIM combination were characterized by a combined proteomic and metabolomic/lipidomic approach. In deep bioinformatics analysis confirmed a specific impact of VPA/SIM on Hippo pathway, with a clear down regulation of YAP and its targets (CTGF, CycD1 ANKH1) in treated *vs* untreated tumors, functionally related with modulation of cancer-related extracellular matrix remodelling and metabolic reprogramming. Treatment also downregulated TEAD transcription factor mediating YAP-induced expression, along with the upregulation of 14-3-3, responsible for YAP cytoplasmic retention and degradation, paralleled by the up-regulation of YAP up-stream negative regulators such as LATS1 and AMPK. VPA/SIM also modulated intermediates of TCA, urea cycles and glycolysis and decreased cholesterol and fatty acids.
Conclusion: In summary, this study provides further insights into the molecular mechanism of the VPA/SIM antitumor effect suggesting the potential of repurposing these two generic and safe drugs in combination with standard antitumor therapies also in other tumors besides mCRCP.

#7098 Identifying of potential therapeutic targets of Taiwanese breast cancer by functional proteomics.

Chi-Cheng Huang[1], Wei-Chi Ku[2], Chi-Jung Huang[3], Ling-Ming Tseng[1]

[1]Taipei Veterans General Hospital, Taipei, Taiwan,[2]Fu-Jen Catholic University, New Taipei, Taiwan,[3]Cathay General Hospital, Taipei, Taiwan

The aim of the study is to conduct translational research of crucial breast cancer prognostic genes with functional proteomics. We have collected 61 breast cancer core biopsy samples, which were used for targeted sequencing for genetic variant analysis, mass-spectrometry analysis for protein expression and stain with H&E for whole slide image with Aperio Scanncer.

After analysis of variant (ANOVA) of LC-MS/MS data, we found 17 proteins with highly differential expression between these 5 molecular subtypes from 61 patients. We then search for the protein-protein interaction (PPI) network from STRING database and found the strong network including 6 proteins namely Collagen Type II Alpha 1 Chain (*COL2A1*), Collagen alpha-1(XI) chain (*COL11A1*), Collagen alpha-1(VI) chain (*COL6A1*), Collagen alpha-2(VI) chain (*COL6A2*), Thrombospondin 1 (*THBS1*) and Lumican (*LUM*).

To further investigate on the expression of these 6 target proteins in literature, we used Oncomine for data mining to query their mRNA expression profiles. Intriguingly, we discovered the mRNA expression of these targets are intensively distributed in many cancer types. This finding suggested the high potency of *COL2A1, COL11A1, COL6A1, COL6A2, THBS1* and *LUM* as potential targets in breast cancer treatment. Our study has the potential contributing to the knowledge of breast cancer susceptibility, early detection, surveillance, and potential actionable targets, developing optimized screening programs and treatment protocols for distinct molecular subtypes.

#7099 Prognostic value of serum proteomic signature in NSCLC patients on immune checkpoint inhibitors: Impact of treatment regimen and PD-L1 levels.

L. Kim[1], T. Um[2], Y. Chae[2], A. Cho[1];

[1]Ascension, Chicago, IL, [2]Northwestern University Feinberg School of Medicine, Chicago, IL

Background:The VeriStrat test, a blood-based proteomic test utilizing MALDI-ToF mass spectrometry, employs machine learning for prognostic assessment in non-small-cell lung cancer (NSCLC) across various stages, histologies, and treatments. Recently, its prognostic utility has extended to patients undergoing immune checkpoint inhibitor (ICI) treatment. Yet, the influence of treatment regimen and PD-L1 levels on its prognostic power remains less explored.
Methods: In this retrospective study, 174 NSCLC patients receiving ICI monotherapy (ICI mono) or combination with chemotherapy (combination) underwent VeriStrat testing from 2016 to 2023. Blood sample spectra categorized patients into VeriStrat 'Good' (VS-G) or VeriStrat 'Poor' (VS-P) groups. Overall survival (OS) and progression-free survival (PFS) were calculated using the log-rank test for the first ICI-containing regimen post-serum sample draw.
Results: Among 174 patients, 97 received combination therapy, and 77 received ICI alone. Within the 99 patients with PD-L1 levels <50%, 38 patients received IO monotherapy (23 pts for standard of care, 5 pts for poor candidacy for chemotherapy, 5 pts for clinical trial, 3 pts for patient refusal, and 2 pts for physician discretion). Survival analysis results are presented in Table 1.
1

survival analysis by treatment regimen and PD-L1 level

		Hazard Ratio VS-G/VS-P	95% CI	p-value			
ipilimumab+nivolumab	PFS	0.57	0.04-7.89	0.52	Total n=22	VS-G n=19	VS-P n=3
	OS	0.33	0.03-3.47	0.11			
pembrolizumab	PFS	0.90	0.19-4.31	0.88	Total n=25	VS-G n=20	VS-P n=5
	OS	0.33	0.08-1.43	0.01*			
carboplatin+pemetrexed+pembrolizumab	PFS	0.45	0.17-1.19	0.02*	Total n=41	VS-G n=30	VS-P n=11
	OS	0.61	0.22-1.68	0.27			
PD-L1>=50	PFS	0.93	0.34-2.54	0.89	Total n=39	VS-G n=29	VS-P n=10
	OS	0.45	0.17-1.20	0.18			
PD-L1<50	PFS	0.60	0.22-1.11	0.09	Total n= 99	VS-G n=79	VS-P n=20
	OS	0.47	0.21-1.04	0.01*			
PD-L1>=50 + ICI mono	PFS	0.55	0.12-2.65	0.69	Total n=23	VS-G n=18	VS-P n=5
	OS	1.25	0.32-4.96	0.75			
PD-L1<50 + ICI mono	PFS	0.77	1.15-3,91	0.70	Total n=37	VS-G n=30	VS-P n=7
	OS	0.24	0.51-1.10	0.0004*			
		Hazard Ratio combination/ICI mono	95% CI	p-value			
PD-L1<50 +VS-G	OS	0.70	0.36-1.33	0.24	Total n=76	ICI mono n=30	Combination n=46
PD-L1<50 +VS-P	OS	0.45	0.14-1.44	0.006*	Total n=20	ICI mono n=7	Combination n=13
		Hazard Ratio ICI mono/combination	95% CI	p-value			
PD-L1>=50 +VS-G	OS	2.18	0.69-6.90	0.27	Total n=29	ICI mono n=22	Combination n=7
PD-L1>=50 +VS-P	OS	NA	NA	0.21	Total n=10	ICI mono n=3	Combination n=7

Conclusions: Our findings suggest that the prognostic value of the VeriStrat test may vary based on the treatment regimen. In clinical scenarios utilizing ICI monotherapy for patients with PD-L1 levels <50%, the role of VeriStrat seems more significant. A prospective study with a larger sample size for validation is warranted.

#7100 Quantitative proteomics reveal the mechanism of TTFields therapy for glioblastoma.

Q. Mei[1], Y. Gao[2], R. Li[3], C. Wang[2], G. Hu[1], H. Huang[2];

[1]Tongji Hospital, Tongji Medical College, Huazhong University of Science and Technology, Wuhan, China, [2]State Key Laboratory of Chemical Biology, Shanghai Institute of Materia Medica, Chinese Academy of Sciences, Shanghai, Shanghai, China, [3]Cancer Center, Shanxi Bethune Hospital, Shanxi Academy of Medical Sciences, Tongji Shanxi Hospital, Third Hospital of Shanxi Medical University, Taiyuan, Shanxi, People's Republic of China, Taiyuan, China

Glioblastoma (GBM) is a highly malignant brain tumor, and conventional treatments such as surgical resection and chemotherapy have limited effectiveness, with a high rate of recurrence and poor prognosis for patients. In 2011, the FDA approved a novel therapy for recurrent GBM known as Tumor Treating Fields (TTFields). TTFields use alternating intermediate-frequency (200 kHz) and low-intensity (1-3 V/cm) electric fields to interfere with tumor cells, inducing apoptosis and inhibiting tumor growth. This study aimed to explore the molecular mechanisms of TTFields therapy at the systems biology level using quantitative proteomics technology. We analyzed U87 cells before and after TTFields treatment using quantitative proteomics and identified a total of 7679 proteins. Among them, 804 proteins were significantly upregulated after TTFields treatment, and 1141 proteins were significantly downregulated. Pathway enrichment analysis of differentially expressed proteins showed that upregulated proteins were mainly associated with cell proliferation, cell cycle, and transcription, possibly representing compensatory responses to the TTFields treatment. Further analysis revealed a significant upregulation of the tumor proliferation key protein PARP1, which was validated by protein immunoblotting experiments. Based on this analysis, we hypothesized that combining TTFields with Olaparib (a PARP1 inhibitor) might enhance the sensitivity of TTFields. Subsequently, we performed cell proliferation experiments to evaluate the concomitant application strategy, and the results demonstrated that Olaparib in combination with TTFields treatment significantly reduced the survival rate of U87 cells compared to single-drug treatment. In conclusion, using quantitative proteomics, this study revealed the biological processes underlying the inhibitory effects of TTFields on GBM proliferation. Under TTFields intervention, the expression of PARP1 was upregulated, and the use of a PARP1 inhibitor in combination significantly increased the sensitivity of TTFields. Therefore, this study not only elucidated the molecular mechanisms of TTFields therapy for GBM treatment at the systems biology level, but also provided support for further enhancing the efficacy of TTFields.

#7101 Remodeling of cancer cells by chemotherapy.

G. Qian[1], L. Schaffer[1], K.-M. Moon[2], L. Foster[2], T. Ideker[1], M. Hu[1], S. Alkhairy[1], E. Lundberg[3];
[1]University of California San Diego - UCSD, La Jolla, CA, [2]University of British Columbia, Vancouver, BC, Canada, [3]Stanford University, Stanford, CA

Cisplatin is a commonly administrated chemotherapy drug for cancer treatment. Although the direct mechanism of cisplatin is largely well-defined, it is challenging to comprehensively assess its systemic effects. Cellular responses to perturbations are intricate processes involving modifications to protein complexes across diverse cellular compartments. Therefore, substantial research endeavors have been directed towards unraveling protein organization in cells. We recently built a multiscale integrated cell map, MuSIC, that combines fluorescence-stained images and interactions derived from affinity purification mass spectrometry to allow comprehensive characterization of cellular structure and functional networks of 5,254 proteins of the human bone osteosarcoma epithelial line (U2-OS). To exploit the biology of U2OS, we integrated dynamics into this map to determine the proteome reorganization upon cisplatin exposure. Thus, we developed a data-driven approach integrating high throughput size exclusion chromatography mass spectrometry (SEC-MS) data with large-scale cell maps built from static-state information to systematically map at all scales the remodeling of cell architecture in drug-treated cells. Here, we acquired drug-perturbed protein-protein interactions (PPIs) from the SEC-MS data by treating U2-OS with cisplatin. Integrating the differential interactions identified from SEC-MS PPIs with the scaffold large-scale hierarchy (MuSIC) allows retention of the upper cellular organization to systematically map drug impact on protein complexes in the cell. This pipeline serves as an explorative method to identify the drug-responsive organelles, alterations of hierarchical structures, and translocation of proteins. Apart from the well known alterations of DNA damage repair complexes, we also recapitulate remodeling in metabolism pathways, splicing, cAMP-dependent kinase activity, and histone modification. We identify 26 novel protein assemblies containing members that are previously associated with cisplatin biology. This pipeline exploits the potential of a well-established network by integrating the high throughput data modality, allowing for the screening of a range of chemical agents and stimuli to generate differential networks.

#7102 The central dogma of hepatocellular carcinoma: Genomic, transcriptomic, and proteomic changes.

H. MA, C. YU, L. NG;
The University of Hong Kong, Hong Kong, Hong Kong

Cancer is a disease condition characterized by remarkable heterogeneity, wherein numerous molecular features display considerable disparities even with the same patient cohorts, leading to varied treatment outcomes. The primary factor contributing to the substantial differences observed across cancers stems from unique combinations of genetic mutations. Epigenetic alterations further contribute to differential gene expression and splicing, thereby enhancing transcriptomic diversity. The protein products originating from the cancer transcriptome constitute the specific intracellular and extracellular environment, consequently exerting supplementary effects on epigenetic, transcriptomic, and proteomic changes. The complex interplay and mutual influence between genetic aberrations, transcriptomes, and proteomes significantly contribute to shaping the extensive spectrum of molecular characteristics observed in cancer. With label-free mass spectrometry, RNA-sequencing, and low-pass whole genome sequencing, the quantification of the proteome, transcriptome, and genetic abbreviation of the cancer can be evaluated. With the mouse hydrodynamic tail vein injection (HDVI) models of hepatocellular carcinoma (HCC), different subtypes of HCC derived from different genetic abbreviations can be generated. With the proteome, transcriptome, and genetic abbreviation data of the better-defined HCC from HDVI models and HCC patients, the patient-derived HCC can be classified according to the origin of the genetic abbreviation used in the generation of the HDVI-derived HCC. Furthermore, the proteome of patient-derived plasma will be analyzed, and the signature change unique to HCC classified by different origins of genetic abbreviation will provide an abstract of the proteome, transcriptome, and genetic abbreviation of the HCC tissue. The transcriptomics and proteomics data of HDVI mice produced from five distinct sets of genetic abbreviations have been measured. The proteome and transcriptome of tissue, as well as the proteome of plasma, from a small cohort of HCC patients were studied and classified using this resource to illuminate the fundamental landscape of HCC. The final results will be presented and discussed at the meeting.

EXPERIMENTAL AND MOLECULAR THERAPEUTICS: DNA Damage and Repair
Poster Session

#7106 Distinct functions of EHMT1 and EHMT2 in cancer chemotherapy and immunotherapy.

Z. Kang[1], P. Fu[1], H. Ma[1], T. Li[1], K. Lu[1], J. Liu[1], V. Ginjala[1], P. Romanienko[1], Z. Feng[1], M. Guan[2], S. Ganesan[1], B. Xia[1];
[1]Rutgers Cancer Institute of New Jersey, New Brunswick, NJ, [2]Huashan Hospital Fudan University, Shanghai, China

EHTM1 (GLP) and EHMT2 (G9a) are closely related protein lysine methyltransferases often thought to function together as a heterodimer to methylate histone H3 and non-histone substrates in diverse cellular processes including transcriptional regulation, genome methylation, and DNA repair. Here we show that EHMT1/2 inhibitors cause DNA replication stress, accumulation of single-stranded replication gaps, increased expression of STING, emergence of cytosolic DNA, and activation of the cGAS-STING pathway. Remarkably, EHMT1/2 inhibition strongly potentiates the efficacy of alkylating chemotherapy and anti-PD-1 immunotherapy in mouse models of tripe negative breast cancer. Mechanistically, the effects of EHMT inhibition on DNA replication and alkylating agent sensitivity are largely caused by the loss of EHMT1-mediated methylation of DNA ligase I (LIG1), whereas the elevated STING expression is, at least part, caused by its promoter demethylation. Moreover, depletion of EHMT2, and not EHMT1, leads to STING induction, which is correlated with more complete demethylation of the STING1 promoter. On the other hand, depletion of EHMT1, and not EHMT2, results in cytosolic DNA accumulation, which presumably activates the cGAS-STING pathway. These results reveal distinct functions of the two EHMT paralogs and provide enlightening paradigms and corresponding molecular basis for combination therapies involving alkylating agents and immune checkpoint inhibitors.

#7107 Clustered DNA double strand breaks for cancer treatment via multi-gRNA CRISPR system.

G. Badakul, N. Sharma, J. A. Nickoloff;
Colorado State University, Fort Collins, CO

Radiation therapy is one of the most common cancer treatments. Ionizing radiation generates DNA double-strand breaks (DSBs), which are the most lethal type of DNA damage. The dominant pathway for repairing DSBs is non-homologous end joining (NHEJ), but homologous recombination (HR) is also important. NHEJ is dominant pathway in all cell cycle phases while HR is largely restricted to S and G2 phases. Unrepaired or misrepaired DSBs can lead to cell death. KU70/80 and DNA-PKcs are essential for NHEJ. KU70/80 binds to broken ends, and DNA-PKcs binds to DNA-bound KU70/80, which activates DNA-PKs kinase allowing NHEJ to proceed. Clustered DSBs (two or more DSBs separated by <200 bp) generate small DNA fragments that are efficiently bound by KU70/80 and DNA-PKcs, but fail to activate DNA-PKcs kinase, inhibiting NHEJ and shifting repair toward HR. Thus, clustered DSBs are poorly repaired and more cytotoxic than dispersed DSBs. There are two types of ionization radiation: high LET and low LET. High LET radiation has a higher ionization density and therefore induces more clustered DSBs than low LET, which explains why high LET radiation is more cytotoxic at a given dose. A major limitation of radiotherapy is normal tissue damage. We hypothesize that mimicking high-LET-induced clustered DSBs using CRISPR/Cas9 targeted to cancer-specific DNA sequences (e.g., indel mutations) will effectively kill cancer cells but spare normal cells. In this approach, DSBs are not targeted to specific genes, nor is CRISPR/Cas9 used for gene editing. Instead, cancer cell killing is achieved by inducing poorly repaired DSBs anywhere in cancer cell DNA. Thus, this therapeutic approach is distinct from conventional targeted therapies that are oncogenic pathway-dependent, and this eliminates oncogenic pathway-dependent resistance mechanisms. However, types of resistance are possible, such as upregulated DSB repair. Our data indicate that the cytotoxicity of clustered DSBs depends on the number of small DNA fragments induced, thus we observe similar cytotoxicity with a localized, 4-DSB cluster and with three non-localized 2-DSB clusters, as each generates 3 small fragments per target chromosome. This finding significantly increases available targets as 2-DSB clusters can be induced at indels and flanking (wild-type) sites, generating clustered DSBs in cancer cells but efficiently repaired dispersed DSBs in normal cells lacking the cancer indel. Data also indicates that a single DSB targeted to each amplicon of highly amplified regions is also cytotoxic, and we are exploring the effectiveness of combination clustered DSBs targeted to amplified regions. We are also exploring how DSB repair inhibitors (like ATMi, DNA-PKcsi or RAD51i) can augment cytotoxic DSB effects, potentially mitigating that resistance pathway. These proof-of-principal studies represent the first approach to targeted cancer therapy that is oncogenic pathway-independent.

#7109 Fasn inhibition enhances the efficacy of chemotherapy by inhibiting DNA damage response in colorectal cancer.

M. Banerjee, Y. Zaytseva, S. Hasani, P. Ryachahou, T. Izumi, B. Evers, T. Gao;
University of Kentucky, Lexington, KY

Altered lipid metabolism plays a significant role in progression of colorectal cancer, however, its role in chemotherapy resistance remains poorly understood. We previously identified FASN, the rate limiting enzyme in de novo lipogenesis, as an important regulator of colorectal cancer progression. However, TVB-3664, a potent and specific small molecule inhibitor of FASN, showed limited effect in reducing tumor burden in pre-clinical studies as a stand-alone therapy. Therefore, the goal of this study is to evaluate the combinatorial efficacy of TVB-3664 in improving the therapeutic indices of standard chemotherapy in colorectal cancer. Using a combination of colon cancer cell lines and patient derived organoids we showed that TVB-3664 potentiates chemotherapy drug-induced double-strand DNA breaks (DSBs) and apoptotic cell death by altering histone acetylation levels. In addition, TVB-3664 treatment blocked DNA damage response (DDR) by decreasing ATM expression and Chk1/2 phosphorylation. Mechanistically, inhibition of FASN prevents the activation of both DSB repair pathways, namely homologous recombination (HR) and classical non-homologous end joining (NHEJ), by blocking BRCA1 and 53BP1 recruitment to γH2AX foci, respectively. Moreover, we found that the inhibitory effect of TVB-3664 on DNA repair requires ACLY-dependent acetylation as genetic or pharmacological inhibition of ACLY attenuates TVB-3664-inducded DNA damage. Functionally, combining TVB-3664 with irinotecan synergistically decreased xenograft tumor growth and significantly delayed tumor relapse after withdrawal of therapy. Taken together, we identified a novel mechanism by which FASN inhibitors improve the efficacy of conventional chemotherapy by blocking DNA damage response to delay tumor recurrence and overcome a major challenge in treating colorectal cancer patients.

#7110 Characterizing pY240-PTEN:Ki-67 interactions and development of a PPI disrupting peptide.

B. Jones, S. Patel, F. Furnari;
University of California San Diego - UCSD, San Diego, CA

Glioblastoma (GBM) is the most aggressive and common malignant primary brain tumor. Standard of care for GBM patients involves chemotherapy and ionizing radiation which induce DNA damage to kill tumor cells; however resistance to these treatment modalities commonly develop through various mechanisms. One novel mechanism of radioresistance is through enhanced homologous recombination (HR) DNA damage response (DDR) mediated by nuclear-localized tyrosine-phosphorylated PTEN (pY240-PTEN) recruited to chromatin through interaction with the PP1 Binding Domain (PP1BD) of Ki-67. PTEN is known to play an important tumor-suppressive role and is found to be mutated in approximately 40% of GBMs. A Y240F-PTEN knock-in mouse model has shown that loss of Y240 phosphorylation results in IR sensitivity. Ki-67 dependent, pY240-PTEN facilitated DDR may be regulated by currently uncharacterized interactions within the Ki-67 PP1BD and determination of these interactions may enable development of complex-disrupting peptides capable of radiosensitizing glioma cells. To this end, I have identified residues in the Ki-67 PP1BD that are essential for pY240-PTEN interaction via streptavidin pulldown of N-terminal biotinylated peptides synthesized with alanine mutations at all residues spanning the Ki-67 PP1BD. Orthogonally, glioma cell lines have been engineered that stably express Ki-67 minigene constructs harboring mutation of the identified PP1BD residues. The effects of these mutations on PTEN:Ki-67 interaction, as well as DDR, HR, chromatin accessibility, and colony formation efficiency are currently being interrogated. Competitor peptides have been designed based on candidate Ki-67 residues and evaluated for their ability to bind PTEN. Further optimization of these peptides has led to candidates that are being assessed for stability and potential to radiosensitize glioma cells. In addition, regulation of pY240-PTEN:Ki-67 interaction by posttranslational modification of the Ki-67 PP1BD by aurora B kinase and cyclin dependent kinase 1 has been investigated through pulldown of biotinylated peptides harboring phosphorylated candidate residues. Lastly, Ki-67 has been knocked out in U87 glioma cells, as well as TS528 glioma stem like cells, and the resulting effect on IR sensitivity and DDR is being investigated in the absence, or presence of PTEN. Overall, this project has begun to characterize the regulation and critical molecular interactions between pY240-PTEN and Ki-67, elucidating potential strategies that could disrupt these interactions to enhance the efficacy of radiotherapy.

#7111 Homoharringtonine is effective in treating acute lymphoblastic leukaemia via WEE1 downregulation and inducing DNA damage.

Chun-fung Sin, Kei-ching Yuen, Anan Jiao, Bai-lin Li, Hau-wai Yu

Pathology, The University of Hong Kong, Hong Kong, Hong Kong

Acute lymphoblastic leukaemia (ALL) is an aggressive haematolymphoid malignancy that originated from clonal mutations in lymphoid precursors. The prognosis is poor in adult patients and relapse/refractory disease is not uncommon which carries dismal prognosis. There is an urgent need to develop novel therapeutics. Homoharringtonine (HHT) is a plant alkaloid which can bind to ribosomal A-site and thus inhibit protein synthesis. It was used to treat acute myeloid leukaemia in China during 1980s. Herein, we conducted a study to explore the therapeutic efficacy and mechanism of action in ALL. T-ALL (DND-41, PEER) and B-ALL (PALL-2, SUP-B15) cell lines were treated with HHT for 24 and 72 hours. Cell viability was reduced at a time and dose-dependent manner in all cell lines we tested, with increased in percentage of apoptosis. Western blot showed upregulation of p53, with PARP and caspase 3 cleavages upon treating with HHT for 24 hours. Moreover, we observed WEE1 downregulation which allowed cell cycle progression through G2/M with damaged DNA. Comet assay showed evidence of DNA damage. Proteomics study by label-free protein quantitation showed downregulation of proteins involving in homologous recombination-mediated DNA repairing machinery, including BRCA1 and RAD51. The findings not only showed therapeutic efficacy of HHT in ALL, but also demonstrated the first evidence of DNA damage induced by HHT which might account for its therapeutic effects. Further studies will be conducted for delineating the mechanisms of DNA damage and its relationship with therapeutic efficacy.

#7112 Preclinical profile of novel and potent small molecule inhibitors of PARG.

Sukanya Patra, Manoj Pothuganti, Githavani Kummari, Venu Sankeshi, Jyothipriya Kapaka, Navnath Karche, Anirban Kayet, Ramamohan Mekala, Srikant Viswanadha

Satyarx Pharma Innovations Private Limited, Hyderabad, India

Poly(ADP-ribose) glycohydrolase (PARG) is primary enzyme involved in the dePARylation process of DNA repair, specifically in the single strand break repair (SSBRs). PARG is a macrodomain protein with exo- and endo-glycohydrolase activity that liberates free ADP-ribose and PAR chains, respectively. It interacts with various Poly(ADP-ribose) polymerase (PARP) proteins to facilitate appropriate and timely DNA repair. The balance between PARP and PARG activity is essential for efficient DDR. Inhibition of PARG lead to altered DNA repair in cancer cells. We have identified highly potent PARG inhibitors with picomolar IC_{50} in . PARG is the primary enzyme for dePARylation and accounts for 90% of dePARylation activity. Treatment of HCC-1806 cells with PARG inhibitors showed dose dependent increase of PARylation signature, with sub micromolar IC_{50}. Compounds also demonstrate significant functional, anti-proliferative activity in ovarian and breast cancer cell lines besides a favourable ADME profile. Further pharmacokinetic and pharmacodynamic characterization of the identified hits is currently in progress.

#7113 Targeting the repair of DNA-protein crosslinks induced by bifunctional alkylating agents.

C. Turner, H. Cerrato, V. Melehov, C. Healy, K. P. Rice;
Colby College, Waterville, ME

Bifunctional alkylating agents, such as nitrosoureas, platinum-based therapeutics, and chloroethylhydrazines, have demonstrated clinical successes against cancer by inducing cytotoxic interstrand or intrastrand DNA crosslinks. However, the less well-characterized capacity of these agents to couple DNA to chromosomally-associated proteins may also contribute to these compounds' observed cytotoxicities. Bulky DNA-protein crosslinks (DPCs) could obstruct the DNA metabolism critical to cancer proliferation, thus contribute to genomic instability and cell death. To endogenously repair DPCs, human cells often utilize a DPC-specific proteolytic mechanism dependent on the metalloprotease SPRTN. Complementary approaches for quantifying DPCs, generated ex vivo, to assess the capacity of several bifunctional alkylating agents to induce these lesions in cultured human leukemia cells are presented here. In the first approach, proteins were isolated from lysates of drug-treated cells and protein-bound DNA was quantified as a ratio to the total DNA present in the lysates. In the complementary approach, DNA was extracted from lysates of drug-treated cells using a modified 'STAR' assay in which genomic DNA is isolated and the DNA-bound proteins were quantified by fluorescein isothiocyanate labeling. Micromolar concentrations of the nitrogen mustard mechlorethamine and nitrosourea lomustine induced significant DPC formation while more modest DPC formation was observed using similar concentrations of the chloroethylating agents carmustine and laromustine, as well as cisplatin. Bifunctional alkylating agents dependent on epoxide functionality, including dianhydrogalacticol and diepoxybutane, required drug concentrations of at least one order of magnitude larger to produce similar DPC yields measurable by these techniques. A strategy to interfere with the DPC repair pathway via SPRTN knockdown and assess increased sensitivity of cancer cells to bifunctional alkylating agents is also presented. Chemotherapeutic sensitization by targeting SPRTN could suggest a therapeutic strategy to improve effectiveness of several DNA-targeted anticancer agents, especially if extended to other therapeutics that trap DPCs such as inhibitors of topoisomerase and poly(ADP-ribose) polymerase. Further, identifying structure-function relationships with respect to bifunctional alkylating agents and DPC formation could inform the future development and clinical utilization of these chemotherapies.

#7114 Exploring the landscape of PARP and PARG inhibitor selectivity in live cells using NanoBRET™ target engagement assays.

A. Michaud[1], K. Teske[1], J. Wilkinson[1], C. Zimprich[1], J. Vasta[1], **C. Corona**[2], M. Zhou[2], E. Dominguez[1], K. Dunn-Hoffman[1], M. Robers[1];
[1]Promega Corporation, Madison, WI, [2]Promega Corporation, San Luis Obispo, CA

The 17-member poly(ADP-ribose) polymerase (PARP) family of proteins mediate a number of cellular processes including gene transcription, cell-division and DNA-repair. PARPs catalyze the addition of poly- or mono- ADP-ribose chains on target proteins, modifying their function and/or recruitment in various pathways. Poly(ADP-ribose) Glycohydrolase (PARG) catabolizes PAR units and facilitates the recycling of PARP and other modified effector proteins. A number of PARPS are implicated in human disease, and PARP inhibitors (PARPi's) have seen major clinical success, however, many PARPs (especially mono PARPs) are understudied and chemical tools for understanding cellular PARPi selectivity and potency across the entire family are lacking. Similarly, several PARG inhibitors have been developed to date, but tools for directly assessing target engagement in a cellular context are sorely needed. Here we describe the development and application of target engagement assays for characterizing PARP and PARG inhibitor selectivity and affinity in live cells. This method is based on the NanoBRET™ assay platform, which is a proximity-based probe displacement assay that operates in live cells. Using NanoBRET™ technology, we have developed a single probe that covers 12 out of 17 PARP family members. We explored the family-wide selectivity of a diverse panel of clinical and preclinical PARP inhibitors in live cells, representing the first family-wide, cell-based method for profiling PARP selectivity. We also describe the development of a second probe that reports on PARG target engagement. Target engagement of PARG was observed for three out of five tested inhibitors, suggesting a potential indirect mode of action for certain inhibitors on PARG glycohydrolase activity. These assays offer a complementary approach for studying target engagement within the PARylation cycle.

#7115 Mutational signatures in PDXs for improved understanding of drug response and companion biomarkers identification.

H. Khoury, **S. Cairo**, M. Gilardi, M. Ritchie, G. Silberberg;
Champions Oncology, Inc. (Hackensack, NJ), Hackensack, NJ

Genomic DNA editing is a continuous process that occurs during the entire cell life span. The type and frequency of these modifications can be related to the physiological or pathological activity of intrinsic mechanisms such as DNA surveillance and repair or to extrinsic events that may induce an alteration of DNA sequence by exposure to agents that directly or indirectly induce accumulations of DNA alterations. In the past few years, large-scale analyses have revealed mutational signatures across human cancer types. These signatures can be used as markers of defective internal processes, such as DNA repair deficiency, or external exposures, such as carcinogens, like tobacco, or genotoxic therapies such as radiation and chemotherapy. Our TumorGraft platform, a collection of 1500 patient-derived xenograft generated from more than 50 different types of cancer, is one of the most comprehensive preclinical oncology platforms worldwide, and aims to recapitulate the variety of the patient population and tumor biology complexity. This platform is currently used to evaluate the efficacy of new drugs, and all our models are very well characterized at the molecular level, including whole transcriptome, proteomics and phospho-proteomics, quantification, and genomic variation calls. This allows accurate selection of models with the molecular characteristics of the target patient population, as well as to identify biomarkers predictive of treatment efficacy. This could eventually lead to the development of companion biomarkers in the clinical setting to improve the identification of patients that will benefit from the treatment and those that should be spared. To maximize the chances of identifying relevant molecular traits associated with tumor response, we have been utilizing the Pharmaco-Pheno-Multiomic (PPMO) integration workflow, a machine learning approach which combines phenotypic and therapeutic response profiles with multiple omics datatypes to generate complex biomarker profiles. To provide additional insights on the molecular characteristics of our tumors, we decided to perform the mutational signatures profiling of our models by using whole exome sequencing data. The results obtained were crossed with patient's clinical history and showed good correlation between the mutational signatures identified and the treatments received by the patient, in particular for exposure to platinum salts. The addition of PDXs mutational signatures strongly improves our knowledge on these models and confers an important parameter for model selection. Moreover, the integration of mutational signature profiles in the PPMO workflow would make a significant contribution for companion biomarkers identification.

#7116 Targeting the CBP/p300 axis in lethal prostate cancer impacts DNA repair.

S. Sardar[1], L. Ravindranath[1], C. McNair[2], S. N. Chand[3], W. Yuan[4], D. Bogdan[4], J. Welti[4], A. Sharp[4], M. Schiewer[5], L. Butler[6], J. de Bono[4], K. Frese[7], N. Brooks[7], N. Pegg[7], K. Knudsen[8], A. A. Shafi[1];

[1]Center for Prostate Disease Research (CDPR), Bethesda, MD, [2]Jefferson Health Thomas Jefferson University, Philadelphia, PA, [3]Incyte, Philadelphia, PA, [4]The Institute of Cancer Research, London, United Kingdom, [5]Sidney Kimmel Cancer Center, Thomas Jefferson University, Philadelphia, PA, [6]The University of Adelaide, Adelaide, Australia, [7]Cell Centric Ltd, Cambridge, United Kingdom, [8]The American Cancer Society, Philadelphia, PA

Prostate cancer (PCa) is the 2nd leading cause of cancer related deaths in US men. PCa is an androgen dependent disease driven by the androgen receptor (AR). Currently, androgen-deprivation therapy (ADT) is the standard of care first-line therapy for metastatic PCa. Resistance to ADT uniformly leads to lethal disease, termed castration-resistant prostate cancer (CRPC). Thus, there is an unmet clinical need to identify and develop novel strategies to treat CRPC. CBP/p300 are potent co-activators for AR. High expression of CBP/p300 is associated with locally advanced disease and castration resistant function of AR, resulting in poor patient outcomes and further highlighting the need to discern the role of CBP/p300 to potentially develop therapeutic targets for precision medicine. Previous studies have relied on non-specific compounds and genetic silencing to target CBP/p300. In this study, CBP/p300 mediated bromodomain activity is targeted by CCS1477 (inobrodib), a first-in-class bromodomain inhibitor developed by Cell Centric. CCS1477 treatment demonstrated effective inhibition in growth and clonogenicity assays. Inhibition of the CBP/p300 bromodomain with CCS1477 resulted in significant downregulation of AR-FL, AR-V7, and its targets' mRNA expression in addition to inhibition of associated factors such as c-MYC and its downstream targets in PCa cell lines as well as patient derived xenograft (PDX) models. This study shows that CBP and p300 are highly expressed and correlate closely with AR gene expression and AR activity score in primary PCa and CRPC patient samples. The clinical significance of CBP/p300 expression in PCa has been investigated via elucidation of CBP/p300 transcriptional reprogramming and its role in DNA damage response (DDR) pathways. Specifically, findings revealed that CBP/p300 bromodomain suppression sensitizes to AR-dependent DNA-repair. Transcriptional mapping identified CBP/p300 as regulators of cell proliferation and DNA repair processes, which were functionally confirmed across several PCa model systems. To assess relevance, exogenous challenge with radiation revealed that CBP/p300 are required for AR-mediated DNA repair, and CBP/p300 expression is linked to DNA repair capacity in the clinical setting. Molecular analyses revealed that CBP/p300 facilitate double-strand break (DSB) repair efficiency via homologous recombination (HR) mediated DDR. Congruently, CBP/p300 strongly correlated with HR gene expression in PCa patient tissue. These collective findings reveal that CBP/p300 govern repair of DNA DSBs by regulating HR, thus modulating genome integrity and promoting CRPC growth. These studies identify CBP/p300 as a driver of PCa tumorigenesis through coordinated control of critical transcriptional events and lay the groundwork to optimize therapeutic strategies for advanced PCa via CBP/p300 inhibition, potentially in combination with AR-directed therapies.

#7117 Convection enhanced delivery of a novel ATR inhibitor synergizes with systemic lomustine for improved treatment of glioblastoma.

A. Josowitz[1], **T. Lee**[1], R. K. Sundaram[1], J. Pothupitiya[1], E. J. Brown[2], A. Sule[1], J. Beckta[1], Y. Wang[1], J. Vacca[3], O. Gilad[3], R. S. Bindra[1], W. M. Saltzman[1]; [1]Yale University, New Haven, CT, [2]University of Pennsylvania, Philadelphia, PA, [3]Aprea Therapeutics, Doylestown, PA

Developing effective strategies for treating glioblastoma (GBM), the most common and aggressive form of brain cancer, has been a long-standing challenge. Despite rigorous treatment regimens including surgical resection with concomitant radiotherapy and chemotherapy, the prognosis for this disease remains poor, largely due to tumor recurrence, resistance to conventional therapeutics, pharmacokinetic and brain delivery challenges, and dose-limiting toxicities of existing therapies. The DNA damage response and DNA repair mechanisms such as the ataxia telangiectasia and Rad3-related (ATR) pathway are key mediators of therapeutic responses, and recent studies have shown that targeting DNA repair proteins alongside standard-of-care options is a promising anti-tumor strategy. Here, we employ a combination approach using a next-generation macrocyclic ATR inhibitor, ATRN-333, to sensitize GBM tumors to alkylators. We establish the potency of ATRN-333 and report a robust synergistic interaction between it and the alkylator lomustine in GBM cell-based assays and in a murine flank tumor model. This combinatorial treatment was then applied to a mouse intracranial tumor model, where we utilized a convection enhanced delivery (CED) system combined with nanoparticle technology for direct intracranial administration of ATRN-333. ATRN-333 was successfully encapsulated into a novel polymeric nanoparticle formulation using poly(ethylene glycol)-co-poly(ethylene brassylate-co-dioxanone) (PEG-EB-co-DO). CED of both free and encapsulated ATRN-333 potently sensitized intracranial GBM tumors to low-dose (5 mg/kg) systemically-delivered lomustine, reducing tumor size and conferring a substantial survival benefit compared to cohorts treated with lomustine or the ATR inhibitor alone. The combination approach was well tolerated by the mice, with no hematological toxicity observed as assessed by bone marrow analysis and blood cell counts. Our results demonstrate that ATR inhibitor/lomustine combination therapy, used in conjunction with a CED platform, is a powerful avenue for GBM treatment and a viable option for potential clinical implementation. Note: AJ and TL contributed equally to this work.

#7118 Fanconi Anemia complementation group A is significantly involved in regulating R-loops and facilitating homology-directed repair of DNA double-strand breaks.

F. Li, Haibo Yang, Boya Gao, Liang Luo, Alyan Zafar, Fenghua Yuan, Li Lan and Yanbin Zhang, L. Luo, A. Zafar, F. Yuan, Y. Zhang;
University of Miami Miller School of Medicine, Miami, FL

Homologous recombination (HR), a fundamental DNA double-strand break (DSB) repair pathway, is a universal mechanism employed by cells to accurately mend breaks in both strands of the DNA helix, ensuring genomic stability. Displacement loops, commonly referred to as D-loops, play a crucial role as intermediate structures in HR. Furthermore, recent studies indicate that the unique DNA: RNA three-stranded structure, known as R-loops, may serve as a starting point for homologous pairing and contribute significantly to enhancing HR efficiency by promoting D-loop formation. Besides, the formation of R-loops might assist in recruiting DNA repair proteins, especially those related to HR, thereby accelerating the repair of damaged sites. In this study, we find that highly purified human Fanconi Anemia complementation group A (FANCA) protein effectively induces the formation of R-loops and binds R-loop substrates with high affinity, preferring guanine-rich sequences in vitro. In comparison, FANCA exhibits both a weaker capacity to form D-loops and a lower affinity for binding to D-loops in vitro. Additionally, we have also observed that the interaction between FANCA and RNA facilitates the generation of D-loops in vitro. We then use the DART (damage at RNA transcription site) system to reveal the colocalization of FANCA with R-loops in a highly transcribed genomic locus upon DNA damage in cells. Next, we further demonstrate FANCA's participation in forming R-loops in the initial DSB repair stage and assisting in removing R-loops later. Additionally, we uncover FANCA's ability to aid in the generation of R-loops at specific DNA DSB sites within transcriptionally active regions in both Tet-DR-GFP U2OS cells and DIvA (DSB inducible via AsiSI) cells. Importantly, the R-loop formation ability of FANCA is independent of the Fanconi Anemia (FA) pathway. In conclusion, our findings indicate that FANCA, independent of the FA pathway, can enhance HR in non-transcriptionally active DNA DSB sites through D-loop formation. Furthermore, FANCA significantly elevates transcription-Coupled Homologous Recombination (TC-HR) efficiency by catalyzing the formation of DNA: RNA hybrids, generating temporary R-loops at DNA damage sites and thereby contributing to genomic stability maintenance.

#7120 Investigating PARP1 selective inhibitor DSB1559 efficacy in BRCA1-associated triple negative breast cancer.

A. Nelson[1], K. F. Zheng[1], C. Wanderley[1], D. E. Michaud[1], P. M. Cowley[2], G. M. Campbell[2], B. E. McGuinness[2], A. Wise[2], J. Guerriero[1];
[1]Brigham and Women's Hospital, Boston, MA, [2]Duke Street Bio Ltd., London, United Kingdom

Background: Poly (ADP-ribose) polymerase inhibitors (PARPi) have improved outcomes of BRCA-associated breast cancer. However, toxicity can limit patient response as well as the ability to be combined with other therapeutics. Current PARPi broadly inhibit members of the PARP protein family, however only inhibition of PARP1 is needed for PARPi-mediated cell death. As inhibition of PARP2 is associated with hematological toxicity seen in PARPi patients, selectively inhibiting PARP1 may reduce PARPi toxicity and lead to better outcomes for patients. Here we characterize and test the efficacy of the PARP1 selective inhibitor (PARP1i) DSB1559 compared to Olaparib in BRCA1-associated triple negative breast cancer (TNBC).

Methods: NanoBRET, PARylation, and pharmacokinetic/pharmacodynamic assays were performed to examine DSB1559 potency, PARP family selectivity, and *in vivo* behavior. Immunocompetent FVB/n mice bearing BRCA1-deficient TNBC (*CMV-Cre;Brca1*$^{f/f}$*;Trp53*$^{f/f}$) tumors were treated daily with PARPi (Olaparib) or PARP1i (DSB1559) for 60 days and followed for survival. CellTiter-Glo and qPCR assays were used to examine DSB1559 effect on cell viability and STING activation, respectively.

Results: DSB1559 is a novel and potent PARP1 inhibitor which has superior selectivity for PARP1 compared to Olaparib and PARP1i AZD5305. DSB1559 has highly desirable physico-chemical and in vitro ADME properties, which translate to high oral bioavailability and moderate clearance in rodent PK studies. Additionally, DSB1559 demonstrated superior tumor residence time and tumor/plasma ratio compared to AZD5305. Compared to Olaparib, DSB1559 significantly increased STING activation and reduced cell viability in BRCA1-associated murine TNBC cells. BRCA1-associated TNBC-bearing immune-competent mice treated with DSB1559 had significantly reduced tumor growth and increased overall survival (median survival 74 days) compared to Olaparib (median survival 18 days). Analysis of changes in the tumor microenvironment are ongoing.

Conclusions: Taken together, DSB1559 is a highly selective PARP1 inhibitor that demonstrates superior efficacy compared to Olaparib in a BRCA1-associated immune-competent TNBC model.

#7121 The novel WEE1i, APR-1051, is a potentially well tolerated and effective treatment for cyclin E-overexpressing cancers.

M. M. Hansbarger[1], S. J. Rocca[1], S. Ritzmann[1], J. Vacca[1], B. Tokiwa[1], J. Weinstein[1], H. Zabierek[1], J. Frye[1], M. Carleton[1], E. J. Brown[2], O. Gilad[1];
[1]Aprea Therapeutics, Inc., Doylestown, PA, [2]University of Pennsylvania, Philadelphia, PA

Previous studies have demonstrated that WEE1 inhibitors (WEE1i) are a promising cancer therapeutic through synthetic lethality with Cyclin E overexpression. One challenge for two of the leading WEE1i, AZD1775 and ZN-c3, has been the observed off-targeting of PLK family members, namely, PLK1, PLK2 and PLK3. In addition, the therapeutic application of these inhibitors in clinical trials has been limited by adverse hematological effects, including anemia. Herein, we describe the testing of a novel WEE1i (APR-1051) that, based on preclinical studies: 1) demonstrates reduced off-targeting of PLK1, PLK2 and PLK3, and 2) has the ability to suppress the growth of CCNE1-overexpressing xenografted tumors while causing little impact on red blood cell and reticulocyte levels. APR-1051 has an IC50 of 2.2 nM for WEE1 in vitro and has shown the ability to limit the proliferation of various cancer cell lines in culture. Interestingly, the genotoxicity of APR-1051 is suppressed by increasing concentrations of PLK1 inhibitors, suggesting that off-targeting of PLK1 by other WEE1i may compromise efficacy of this targeted cancer treatment in addition to the risk of producing PLK1i-associated adverse effects. APR-1051 demonstrated effectiveness in suppressing the growth of Cyclin E-overexpressing breast and ovarian cancer cells lines, thus pinpointing Cyclin E as a potential biomarker for APR-1051 treatment. Importantly, dose and scheduling of APR-1051 that causes significant suppression of CCNE1-amplified high-grade serious ovarian cancer tumors in mice is well tolerated, with red blood cell and platelet counts remaining within non-pathogenic ranges after a 28-day treatment period. In addition, inhibition WEE1 by APR-1051 occurs at an IC50 that is 200-fold lower on average than the IC50 of hERG potassium channel inhibition, implying that APR-1051 will potentially exhibit low cardiotoxicity. APR-1051 is now progressing through IND-enabling studies. Together, these findings underscore the potential of APR-1051 as a novel WEE1i for the treatment of Cyclin E-overexpressing cancers.

#7122 A novel USP1 inhibitor coupled with a novel proteomic response biomarker for precision oncology therapy.

I. Alchanati[1], A. Morley[2], A. Hay-Koren[1], F. Fierro[1], G. Otonin[1], S. Herman[1], A. Shtrikman[1], Y. Katzenelenbogen[1], G. Arad[1], B. Tivon[1], K. Pevzner[1], **E. Seger**[1]; [1]Protai, Tel Aviv, Israel, [2]O2H Discovery, Cambridge, United Kingdom

Ubiquitin-specific protease 1 (USP1) is a well-characterized deubiquitinating enzyme (DUB) that plays a critical role in DNA damage repair (DDR). It was shown to regulate various key repair processes, most notably proliferating cell nuclear antigen (PCNA) in the Translesion Repair (TLS) pathway and FANCD2/FANCI in the Fanconi Anemia (FA) repair pathway. Research indicates that USP1 deficiency leads to a decrease in cell survival and disruption of genomic stability, suggesting that USP1 inhibitors (USP1i) may hold promise in treating DDR deficient tumors. Through the integration of computational and medicinal chemistry approaches, we discovered a novel, potent inhibitor of USP1, showing anti-USP1 activity in both cell-free enzymatic assay and in measurement of PCNA-ubiquitination change upon USP1 inhibition in cells. We demonstrate anti tumor activity in DDR-related and other indications. By utilizing our platform to analyze the basal proteomics of resistant and sensitive cell lines treated with USP1i, we revealed a distinctive proteomic biomarker signature for USP1i response. This data demonstrates the potential of our novel USP1 inhibitor to serve as a potent therapeutic agent for DDR-deficient and other biomarker-positive cancer patients.

#7123 Biomarker-targeted alkylator and DNA damage repair inhibitor combination for refractory and relapsed acute myeloid leukemia (AML).

P. Bhardwaj, R. Sundaram, A. Baassiri, M. Matthews, J. VanOudenhove, S. Gueble, S. Halene, R. Bindra;
Yale University, New Haven, CT

Isocitrate dehydrogenase 1 and 2 (IDH1/2) convert isocitrate to α-ketoglutarate in the tricarboxylic acid (TCA) cycle. A missense mutation in IDH1/2 leads to accelerated conversion of α-ketoglutarate into 2-hydroxyglutarate (2-HG), an oncometabolite that competitively inhibits α-ketoglutarate-dependent dioxygenases including Ten-Eleven Translocation (TET) enzymes. TET enzymes are DNA demethylases that convert 5-methylcytosine to 5-carboxycytosine and regulate CpG island promoter methylation signatures. In IDH1/2 mutant glioma, inhibition of TET2 enzyme by 2-HG can lead to promoter hypermethylation of O^6-methylguanine methyltransferase (MGMT) and reduce its expression. Approximately 10-15% of de novo or treatment-related AML harbor mutually exclusive mutations in IDH1/2 or TET2, and emerging resistance towards clinical IDH1/2 inhibitors, therefore warrants novel therapeutic options. We performed a pan-cancer TCGA analysis and observed MGMT promoter hypermethylation and reduced expression in IDH1/2 AML. Our independent study on 10 AML patients (5 IDH1/2 and 5 TET2 mutant) corroborated the TCGA data and showed a significantly reduced expression of MGMT in comparison to 7 wild-type AML samples. As MGMT resolves O^6-alkylguanine lesions during DNA damage, we performed an exhaustive alkylator screen, where temozolomide (TMZ) and our novel compound KL-50 emerged as the top hits that imparted a maximum therapeutic index in multiple MGMT (MGMT+/–) isogenic AML cell line models. Both TMZ and KL-50 induced MGMT-dependent DNA strand breaks and replication stress and activated ATM and ATR DNA damage response pathways in a time-dependent manner. Inhibition of ATR activation with Ceralasertib, an ATR inhibitor (ATRi) currently in clinical trials for chronic myelomonocytic leukemia and myelodysplastic syndromes, imparted a profound MGMT-dependent synergy with TMZ and KL-50. Researchers have established in glioma that mismatch repair (MMR) loss confers resistance to TMZ, and reported studies also show evidence of MMR loss in refractory or relapsed AML patients. Thus, we developed numerous MMR-deficient isogenic AML cell lines in an MGMT+/– background and observed MMR loss-mediated resistance to TMZ and abrogation of its synergy with ATRi. Unlike TMZ, KL-50 retained a profound synergy with ATRi in an MGMT-dependent manner irrespective of MMR status. We are currently investigating our novel KL-50 and ATRi combination in MGMT/MMR isogenic cell line-based *in vivo* AML models and in AML patient-derived xenografts to establish it as a promising novel biomarker-targeted therapy for AML patients.

#7125 Inhibition of IDH1 impairs homologous recombination and induces sensitivity to PARP inhibitor in pancreatic cancer.

M. Zarei[1], O. Hajihassani[1], H. J. Graor[1], A. W. Loftus[2], S. Tahhan[1], F. Nakazzi[1], P. Naji[2], L. D. Rothermel[2], J. R. Brody[3], J. M. Winter[2];
[1]Case Western Reserve University School of Medicine, Cleveland, OH, [2]University Hospitals Cleveland Medical Center, Cleveland, OH, [3]Oregon Health & Science University, Portland, OR

Introduction: Pancreatic ductal adenocarcinoma (PDAC) is a major cause of cancer-related deaths in the United States. While Poly (ADP-ribose) polymerase (PARP) inhibitors hold promise in treating PDAC with Homologous Recombination Deficiency (HRD). However, HRD occurs in only 10% of cases, leaving 90% with intact Homologous Recombination Proficiency (HRP). Our research highlights the key role of wild-type isocitrate dehydrogenase 1 (IDH1) in maintaining cellular function. We found that inhibiting IDH1 increases DNA damage, suppressing the DNA repair pathway crucial for genomic integrity. This makes cancer cells susceptible to PARP inhibitors, offering a new PDAC treatment approach.
Methods: The effect of IDH1 inhibition (Ivosidenib) combined with PARP inhibition (Olaparib) on in vitro growth inhibition were assessed through Trypan blue and PicoGreen in drug combination assays. Additionally, we investigated the molecular mechanism underlying the synergistic effects of drug combination. To further evaluate the therapeutic potential of IDH1 inhibition in combination with PARP inhibitors, we examined tumor growth in xenograft models of PDAC in athymic nude mice.
Results: Our data report that, mechanistically, IDH1 inhibition decreased expression of HR DNA repair pathway molecules, such as BRCA1 and BRCA2, and leading to decreased HR repair efficiency in pancreatic cancer cells. Short-term cell viability data demonstrated that targeting IDH1 with ivosidenib when combined with DNA-damaging agent (Olaparib) had a synergistic effect in HRP cell lines (MiaPaCa-2 and Panc-1) with a positive synergy score and Bliss score greater than 1. Additionally, we assessed long-term cell survival using colony formation assays, which yielded a dramatic reduction in cell survival for both Panc1 and MiaPaCa-2 cells when olaparib was combined with ivosidenib, as compared to single-agent controls. Consequently, this reduction increased the levels of apoptosis induced by olaparib. Furthermore, we discovered that these two compounds complemented each other in DNA damage response, leading to an increase in the DNA damage biomarker γ-H2AX. In vivo studies using xenograft models demonstrated that the combination of ivosidenib and olaparib synergistically enhanced anti-tumor activity as compared to either single-agent used alone.
Conclusion: Our data provides insights into the mechanisms underlying the susceptibility of PDAC tumor growth to a dual treatment approach involving an IDH1 inhibitor and a PARP inhibitor, particularly in the context of HRP cancer. This highlights the promise of precision medicine for pancreatic cancer treatment, though further pre-clinical studies are needed for validation and refinement.

#7126 Synergistic combinations and tissue type-specificity of compounds targeting components of the DNA damage response pathway in 2D culture and 3D spheroid cell viability assays.

J. J. T. Melis, D. J. F. Kluitmans, J. J. Kooijman, J. Dylus, S. Wetemans, S. Geerdink-Datema, J. A. D. de Roos, Y. Grobben, G. J. R. Zaman; Oncolines B.V., Oss, Netherlands

Poly (ADP-ribose) polymerase (PARP) inhibitors have changed the landscape of treatment for homologous recombination (HR)-deficient cancers. PARP inhibitors are synthetically lethal with deficiencies in genes involved in the HR pathway, such as *BRCA2*, but resistance against PARP inhibitors is a major problem in the clinic. The use of new synergistic drug combinations targeting different components of the DNA damage response (DDR) pathway may overcome PARP inhibitor resistance. Sixteen small molecule inhibitors acting on different targets in the DDR pathway (including PARP, Polθ and ATR) were profiled in 2D culture and 3D spheroid cell viability assays. Intracellular ATP content was used as an indirect readout of cell number. Compound synergies were determined by profiling combinations of compounds in a 6-by-6 matrix, and quantifying synergistic effects using the Excess over Bliss score [1]. A pair of isogenic *BRCA2*-deficient and -proficient DLD-1 colon adenocarcinoma cell lines was used as a model of *BRCA2*-deficient tumors. In 2D cell viability assays, PARP inhibitors and the Polθ inhibitor ART558 were more active in *BRCA2*-deficient compared to *BRCA2*-proficient DLD-1 cells, whereas an ATR inhibitor (ceralasertib) was equally potent in both cell lines. Combining olaparib with ART558 in 2D culture and 3D spheroid studies showed synergistic effects in *BRCA2*-deficient DLD-1 cells. Moreover, olaparib synergized with ceralasertib in both *BRCA2*-deficient and -proficient DLD-1 cells. Different DDR-targeting inhibitors were profiled in over a hundred cancer cell lines from diverse tumor tissue origin in 2D assays. This showed a relatively high potency for PARP inhibitors in ovarian cancer cell lines compared to cell lines derived from other tissue types, which is consistent with the clinical application of PARP inhibitors for treatment of ovarian cancers. For ATR inhibitors and ART558, kidney and myeloid cancer cell lines were found to be most sensitive, respectively, suggesting potential therapeutic utility of ATR and Polθ inhibitors for treatment of these cancer types. The genomic determinants of the different sensitivities were investigated by comparing compound potencies in the cell viability assays with the mutation status of more than 500 genes involved in cancer or the DDR pathway in the cell lines. Additionally, cancer cell line sensitivity was correlated with the expression levels of more than 19,000 genes in these cell lines to identify novel RNA signatures capable of predicting response to DDR-targeting inhibitors. This study uncovers new synergistic drug combinations that increase the efficiency of PARP inhibitors, and provides new insights into the determinants of cancer cell line sensitivity to compounds targeting different components of the DDR pathway. [1] Liu *et al.* Stat. Biopharm. Res. 10, 112-22; 2018

#7127 An ATM inhibitor: ZN-B-2262 in combination with radiation /ADCs containing topoisomerase inhibitors for the treatment of solid tumors.

D. Zhou, Z. Wang, Y. Liu, T. Fu, Z. Cheng;
Zion Pharma Limited, Shanghai, China

Background: ZN-B-2262 is a best-in-class, IND-approved, small molecule serine/threonine kinase receptor inhibitor targeting Ataxia Telangiectasia Mutated (ATM), which plays a key role in DNA damage response (DDR) associated with double-strand breaks (DSB). Radiotherapy (RT) and topoisomerase inhibition can directly cause DSB. ZN-B-2262 is expected to enhance the therapeutic effect of RT, or antibody drug conjugates (ADCs) containing topoisomerase inhibitors by suppressing DSB DNA repair and blocking checkpoint controls.

Methods: The inhibition of isolated recombinant ATM, ATR, mTOR, DNA-PK, PI3Kα, PI3Kβ, PI3Kδ and PI3Kγ enzymes was evaluated using In-Cell-Western assay to determine the effect of ZN-B-2262 on ATM enzyme activity by detecting phosp-KAP1 (Ser824) expression. The inhibition of phospho-ATM (Ser1981) was evaluated by ATM assay on HT29 cells using a High-Content Imaging System (HCS). Therapeutic efficacy, as measured by tumor growth inhibition (TGI), was evaluated using ZN-B-2262 in combination with DS-1062 (Trop2 ADC), irinotecan or RT in MDA-MB-468 triple negative breast cancer (TNBC), SW620 colorectal cancer, and Fadu head and neck squamous cell carcinoma (HNSCC) subcutaneous xenograft murine models, respectively. In addition, ZN-B-2262 was tested for Human Aldehyde Oxidase (AO) activity. Safety margins were determined based on the ratio of unbound AUC obtained from 28-day GLP animal toxicology studies and predicted human PK at efficacious dose.

Results: ZN-B-2262 exhibited strong inhibition against ATM with the IC_{50} at 4.4 nM. No inhibition effect was observed on other IKK family enzymes with IC_{50} value >10 uM. ZN-B-2262 showed high inhibition activity on phosp-KAP1 with IC_{50} of 13.25 nM and on phospho-ATM with IC_{50} of 21.5 nM. In the MDA-MB-468 xenograft efficacy study, ZN-B-2262 combined with a clinically relevant dose of DS-1062 showed significantly superior tumor inhibition effects compared to DS-1062 alone. In the SW620 xenograft efficacy study, in combination with irinotecan, ZN-B-2262 showed synergistic tumor inhibition effects. In the Fadu xenograft efficacy study, ZN-B-2262 demonstrated synergistic anti-tumor activity when combined with RT. Sustained and enhanced anti-tumor efficacy was observed post withdrawal of ZN-B-2262 combined with RT, which was not observed after stopping treatment of RT alone. Based on 28-day GLP tox in rat and dog, the predicted human safety margin is 25- to 50-fold.

Conclusion: ZN-B-2262, in combination with ADCs containing topoisomerase inhibitors, (e.g., Dato-Dxd), or RT, is expected to be a best-in-class (possibly first-in-class) compound, for the treatment of solid tumors. In particular, ZN-B-2262 should demonstrate improved PK and minimal inter-patient PK variability compared to current ATM clinical candidates since ZN-B-2262 is not an AO substrate.

#7128 Novel Ku-DNA binding inhibitors impact on the cellular and *in vivo* DNA damage response to radio- and radiomimetic-therapy.

P. L. Mendoza-Munoz[1], D. Chauhan[2], N. S. Gavande[2], J. R. Dynlacht[1], J. E. Garrett[1], **J. J. Turchi**[1];
[1]Indiana University School of Medicine, Indianapolis, IN, [2]Wayne State University, Detroit, MI

DNA-PK, the DNA-dependent protein kinase, is a validated target for cancer therapeutics that plays a central role in the non-homologous end joining (NHEJ) DNA repair pathway and the DNA damage response (DDR). NHEJ is a key mechanism of DNA double-strand breaks (DSB) repair, especially those induced by ionizing radiation (IR). Ku 70/80 heterodimer is required as initiator in this process, acting as an essential DNA-binding component of DNA-PK that senses DNA damage. Blocking the DNA-PK kinase activity in combination with DSB inducing agents has been widely used as a therapeutic strategy to drive clinical efficacy of radiation therapy for cancer treatment.

We have reported a unique approach of DNA-PK inhibition by developing Ku-DNA binding inhibitors (Ku-DBi's), small molecule inhibitors that target the interaction between Ku70/80 and DNA. Ku-DBi's demonstrated a direct interaction with Ku70/80, a potent inhibition of Ku-DNA binding and DNA-PK catalytic activity, and *in vitro* and cellular NHEJ inhibitory activity. This results in the potentiation of non-small cell lung cancer (NSCLC) cellular sensitivity to DSB generating therapies, as a function of inhibiting DNA-PKcs autophosphorylation and dysregulation of signaling to the DDR. In this study, we have expanded our structure activity relationship analyses to focus on optimizing selectivity, cellular uptake and Ku inhibitory activity. The new series of Ku-DBi's include oxindole derivatives of the X80 core structure that achieve these goals. These novel compounds display increased cellular uptake while retaining potent Ku inhibitory activity and enhanced cellular inhibition on DNA-DSB repair. Ku-DBi's optimization has enabled in vivo analyses of Ku-DBi - ionizing radiation combination therapy in human xenograft models of non-small cell lung cancer. The impact of Ku-DBi treatment on therapeutic efficacy, toxicity, Ku/DNA-PK inhibition, and DDR signaling will be presented. These data represent a significant advance in the development of Ku-DNA binding inhibitors and their therapeutic intervention for cancer treatment.

#7129 DNA polymerase beta expression in head & neck cancer modulates the poly-ADP-ribose-mediated replication checkpoint.

M. Khan[1], A. Angajala[2], D. Gibbs[3], J. Liu[3], C. Ragin[3], R. Sobol[1];
[1]Legorreta Cancer Center at Brown University, Providence, RI, [2]University of South Alabama, Mobile, AL, [3]Fox Chase Cancer Center, Temple Health, Philadelphia, PA

Head and Neck Squamous Cell Carcinoma (HNSCC) impose a significant health burden, necessitating innovative therapeutic strategies to enhance treatment efficacy. Current standard treatments, including surgery, radiation therapy, and chemotherapy, often exhibit limited effectiveness and cause substantial side effects. This underscores the critical need for novel therapies that selectively target cancer cells, sparing normal tissue. Survival from HNSCC is poor, and importantly, a racial disparity between African Americans (AfAm) and European Americans (EuAm) has been known for some time. Ancestry Informative Markers (AIMs) are associated with altered mRNA expression of Polβ where higher expression of Polβ was observed among AfAm patients in comparison to EuAm patients. Our research focuses on DNA polymerase beta (Polβ) and its role in replication stress and response to chemotherapy and DNA damage response modifiers. Elevated expression of Polβ is linked to increased DNA damage and genomic instability, contributing to treatment resistance. In this regard, our investigations reveal a regulatory role for base excision repair (BER) proteins, including Polβ, in the cellular response to inhibitors of poly(ADP-ribose) glycohydrolase (PARG), an enzyme involved in poly(ADP-ribose) (PAR) degradation. Inhibition of PARG triggers a robust intra-S phase response, activating ATR and CHK1 signaling. Exploiting the synthetic lethality between PARG inhibition and ATR/CHK1 inhibition, we have demonstrated the ability to overcome Polβ overexpression mediated treatment resistance in HNSCC cells. Specifically, our in vitro studies demonstrate that the response to a combination of an ATR inhibitor and PARG inhibitor is impacted by Polβ expression in HNSCC cells, with synergistic effects surpassing the efficacy of the individual inhibitors. Similarly, the combination of a CHK1 inhibitor and PARG inhibitor proves effective in cells with elevated Polβ expression, offering a potential dual therapeutic strategy. These combinations exhibit promising potential for HNSCC treatment when Polβ expression is elevated. In conclusion, our findings propose a novel therapeutic paradigm for HNSCC, employing combination therapy with ATR or CHK1 inhibitors and PARG inhibitors. This approach offers a targeted strategy, presenting a promising avenue for the development of more effective and less toxic treatment modalities in the management of HNSCC and may help overcome resistance from elevated expression of Polβ.

#7130 Dysregulated DNA repaired elicited by type 1 PRMT inhibitor in clear cell renal cell carcinoma enables development of novel combination therapies.

K. Arevalo[1], J. Walton[2], J. Meens[2], A. Ng[1], L. Ailles[2];

[1]University of Toronto, Toronto, ON, Canada, [2]University Health Network, Toronto, ON, Canada

Clear cell renal cell carcinoma (ccRCC) is the most prevalent form of kidney cancer, notorious for its resistance to treatment and dismal prognosis. Advanced or metastatic cases on average display an 8% 5-year survival rate. Given the considerable number of diagnoses in advanced stages, it is evident that we require innovative therapeutic approaches. Our lab has developed a methodology to establish cell lines from tumors and adjacent normal tissues sourced from patients. Consequently, we've amassed a collection of cell lines, including those from patient-derived ccRCC and normal kidney cells. Using these ccRCC models, we demonstrated that the type I protein arginine methyltransferase inhibitor, MS023, elicits a dysregulated DNA repair phenotype. RNA-Seq analysis of ccRCC cells treated with MS023 unveiled a marked downregulation of genes associated with the homologous recombination (HR) pathway for double-strand break repair and the Fanconi Anemia (FA) pathway for interstrand crosslink (ICL) repair. In a follow-up investigation using paired normal and cancerous cell lines from the same patient, we identified resistance to MS023 in normal kidney cells that is not mirrored in the corresponding ccRCC cell line. This hints at a potential therapeutic window and provides a strong rationale for clinical pursuit. Poly-ADP ribose polymerase (PARP) inhibitors are known to yield a synergistic effect when employed in HR-deficient diseases, such as BRCA-deficient breast cancers. Since MS023 induces an HR-deficient phenotype, we hypothesize that combining it with Talazoparib, a PARP inhibitor, will produce a similar synergistic effect. Additionally, mitomycin C (MMC) is a clinically approved compound that induces ICLs. As MS023 impedes ICL repair by downregulating crucial ICL-repairing genes, combining these two drugs should likewise generate a synergistic effect. Through a drug screen across two of our ccRCC cell lines, we discovered that the cells exhibit sensitivity to various PARP inhibitors. Employing synergy checkerboard assays and the highest single-agent model of synergy, we have found that the combination of MS023 and Talazoparib, as well as the combination of MS023 and MMC, demonstrate synergy, significantly reducing cellular viability at lower doses of the combination treatments compared to mono-treatment conditions at their respective doses. Preliminary *in vivo* studies using patient-derived xenograft models have revealed that both MS023 and Talazoparib are well-tolerated in mice, both when administered individually and in combination. Our current knowledge base indicates that MS023 holds promise for clinical investigation, both as a standalone treatment and in combination with Talazoparib or MMC. These results present an exciting opportunity to shed new light on the challenging therapeutic landscape faced by ccRCC patients today.

#7131 Base excision repair regulation of replication stress induced poly(ADP-ribose) checkpoints.

M. Ibrahim[1], M. Khan[2], R. Q. Al-Rahaleh[2], J. Clark[1], F. Hayat[1], Q. Fang[1], C. A. Koczor[1], M. E. Migaud[1], **R. W. Sobol**[2];
[1]University of South Alabama, Mobile, AL, [2]Brown University, Providence, RI

PARP-inhibitors (PARPi) have been developed to treat homology-directed repair deficient cancers such as BRCA1/2-defective breast and ovarian tumors. However, acquired resistance to PARPi is now common, suggesting the need to identify new protein targets. To that end, a missed opportunity is found in the PARP1/PARP2 activation mechanism in response to DNA damage and replication stress and the resulting protein complexes and enzymes that depend on and coordinate PARP-mediated DNA repair processes. We have found that PARP1/PARP2 activation, whether from acute DNA damage, from replication stress or both triggers a temporal and coordinated interplay of base excision repair and single-strand break repair (BER/SSBR) proteins and enzymes. In turn, the recruitment of these BER and SSBR proteins suppresses PARP1/PARP2 activation, thereby functioning as a network of PARP1/PARP2 regulators, modulating the PARP-mediated response to replication stress. To that end, we find that loss of expression of these key BER/SSBR proteins releases a break on replication-stress induced PARP1/PARP2 activation, triggering un-restrained PARP1/PARP2 activation and elevated levels of replication-dependent poly(ADP-ribose) (PAR). We next confirmed that the loss of these downstream BER enzymes render cancer cells responsive to PARPi's when the BRCA1/2 pathways are restored. Further, we show that BER expression regulates the cellular response to inhibitors of the PAR degrading enzyme PARG, suggesting that XRCC1-dependent BER proteins regulate replication-stress dependent PAR accumulation. The increase in PAR due to PARG inhibition, that is further regulated by BER, drives a strong intra-S phase response, indicated by activation of ATR and CHK1 signaling. As the checkpoint governed by ATR and CHK1 functions as a protective mechanism, we show that PARG inhibition is synthetically lethal with ATR and CHK1 inhibition and this may be explained by our demonstration of PARGi-mediated trapping of essential BER proteins at the site of damage and PAR accumulation. Together, these studies reveal a significant role for BER/SSBR proteins in regulating replication stress induced PARylation and the resulting intra-S phase checkpoint.

#7132 Preclinical characterization of LAE119, a novel PARP1 selective inhibitor and trapper.

M. Li, Y. Chen, J. Chen, L. Jiang, X. Lin, J. Gu;
Laekna Therapeutics Shanghai Co., Ltd., Shanghai, China

Current PARP inhibitors primarily target PARP1/2 and demonstrate high efficacy against tumors with deficiencies in homologous recombination repair, such as those with BRCA mutations. However, these inhibitors are also associated with significant hematological toxicities. Studies have indicated that the synthetic lethality observed with BRCA mutations is mainly driven by PARP1, while PARP2 is not essential in this context. PARP2 has been shown to be crucial for the survival of hematopoietic stem/progenitor cells in animal models. Therefore, selective inhibition of PARP1 could potentially reduce toxicity and improve therapeutic outcomes. Here we introduce LAE119, a potent and selective PARP1 inhibitor and PARP1-DNA trapper. It demonstrates more than a 1000-fold selectivity for PARP1 DNA trapping compared to PARP2. In comparison to most PARP inhibitors including AZD5305, LAE119 exhibits extremely long residence time on PARP1 in both biochemical and cellular assays. It demonstrates robust anti-proliferation activity against BRCA2$^{-/-}$ DLD-1 cells and MDA-MB-436 cells, with IC_{50} value of 0.6 nM in both cell lines. In CAL51 cells, which has a BRCA2 mutation but with low PARP1 expression level and are much less sensitive to AZD5305, LAE119 demonstrates much better activity than AZD5305, particularly when PARP1 level is increased with transgene expression. LAE119 demonstrated substantial tumor inhibition in MDA-MB-436 and Capan-1 xenograft models. LAE119 also displays favorable ADME properties and PK profiles. It has high tumor/plasma ratio which is beneficial for sustainable anti-tumor effect and reduction of off-target effects. In rat hematologic toxicity study, LAE119 at 10 mpk QD dose was well tolerated and had minimal effects on hematologic parameters. Both in vitro and in vivo data strongly support the further clinical investigation of LAE119.

#7133 Phenomics-enabled discovery and optimization of small-molecule RBM39 degraders as an alternative to CDK12 targeting in high-grade serous ovarian cancer (HGSOC).

C. Neumann, H. Shankaran, K. Nadella, K. Biette, S. Rowley, E. Gardner, S. Swaidani, V. Manda, L. Chen, D. Beshnova, A. Saeed, C. Bailey, J. Paulsen, P. Rearden, C. Brooks, A. Bhandari, C. Gibson, L. Schaevitz, I. Haque, H. Donnella, M. Cuccarese, M. Evangelista;
Recursion Pharmaceuticals, Salt Lake City, UT

Phenomics-enabled drug discovery is a powerful approach to identify novel targets and relationships previously unappreciated in biology. We built a phenomics platform leveraging high content microscopy and generated unique phenoprints for >7,000 genes using CRISPR/Cas9 technology and a diverse chemical library of >1 million compounds. This phenomics dataset contains an unprecedented quantity of gene-gene, gene-compound, and compound-compound relationships. We applied our phenomics platform and an inference based target-agnostic drug discovery approach to discover novel genes and small molecules that mimic CDK12 inhibition, an important transcriptional regulator of DNA damage response, while avoiding inhibition of the paralog CDK13. We discovered a novel and unappreciated association between CDK12 and RBM39 as well as small molecule degraders of RBM39. We established structure activity relationships (SAR) solely leveraging our phenomics platform, to generate REC-1170204, an RBM39 degrader. Unlike inhibitors of CDK12, we show that REC-1170204 does not directly inhibit CDK12, CDK13 or other kinases. However, REC-1170204 demonstrates candidate quality properties with improved potency, selectivity, and drug-like characteristics. Finally we show that REC-1170204 shows efficacy in High Grade Serous Ovarian cancer (HGSOC) pre-clinical models and synergizes with PARP inhibition in a PARP-resistant patient-derived xenograft (PDX) model. Together, our data suggests that targeting RBM39 may provide an attractive and safer approach to targeting CDK12 in the clinic.

#7134 Treatment of pancreatic cancer cells with tumor treating fields (TTFields) and PARP inhibitors.

H. Ene, K. Ben Meir, A. Martinez-Conde, R. Frechtel-Gerzi, H. Gabay, D. Gerasimova, R. Engelman, **E. Dor-On**, A. Haber, M. Giladi, Y. Palti;
Novocure Ltd, Haifa, Israel

Background: Therapeutic options for advanced stage pancreatic cancer are limited. Patients harboring germline BRCA mutations benefit from PARP inhibitors (PARPi); unfortunately, such mutations are rare in pancreatic cancer. Tumor Treating Fields (TTFields), electric fields that disrupt cellular processes crucial for cancer cell viability, have shown effectiveness against pancreatic cancer cells, and are currently under clinical investigation for the treatment of patients with pancreatic cancer. The mechanism of action of TTFields in various cancer types has suggested involvement of BRCA downregulation. The current study examined the potential sensitization of BRCA wild-type pancreatic cancer cell lines to PARPi with TTFields application.
Methods: BxPC3 and AsPC1 human pancreatic BRCA wild-type cancer cells were treated for 72 h with TTFields (frequency of 150 kHz; intensity of 1 and 0.5 V/cm RMS, respectively), using the inovitro device. The PARPi niraparib and olaparib were each administered to the cells at various concentrations, with or without co-application of TTFields. At treatment cessation, cell count, colony formation, and apoptosis were measured.
Results: Applying PARPi to pancreatic cell lines yielded a dose-dependent cytotoxic and anti-clonogenic effects, and induced apoptosis. TTFields application also induced such effects when applied alone, while delivery of TTFields together with PARPi amplified the effects demonstrated by PARPi alone.
Conclusions: Concomitant application of TTFields and PARPi in BRCA wild type pancreatic cancer cells exhibits a potential improvement relative to the mono-therapies. This could be rationalized based on the previously demonstrated ability of TTFields to induce a state of BRCAness in cancer cells, and suggests benefit for TTFields and PARPi co-treatment in the absence of background BRCA mutations.

#7135 Preclinical effects of Tumor Treating Fields (TTFields) with PARP inhibitors in ovarian cancer.

Y. Berckmans[1], H. Ene[2], K. Ben-Meir[2], A. Martinez-Conde[2], R. Monin[2], B. Van den Ende[1], S. Van Mechelen[1], R. Frechtel-Gerzi[2], H. Gabay[2], R. Engelman[2], **E. Dor-On**[2], A. Haber[2], M. Giladi[2], U. Weinberg[2], Y. Palti[2], I. Vergote[1], A. Coosemans[1];

[1]Leuven Cancer Institute, KU Leuven, Leuven, Belgium, [2]Novocure Ltd, Haifa, Israel

Purpose: Among gynecological malignancies, ovarian cancer is the leading cause of mortality. Poly (ADP-ribose) polymerase inhibitors (PARPi) represent standard-of-care treatment for selected cases of advanced epithelial ovarian cancer. PARPi exhibit sensitivity in homologues recombination deficient (HRD) tumors, in which there are mutations in the Fanconi Anemia (FA)-BRCA pathway, while about 75% of ovarian cancer patients are homologues recombination proficient (HRP). TTFields are non-invasive electric fields that disrupt cellular processes critical for cancer cell viability and tumor progression. Recent research showed that TTFields induce an HRD-like state (also known as BRCAness state) in various cancer types. The current study aims to investigate the impact of TTFields applied together with PARPi in ovarian cancer preclinical models.

Methods: *In vitro,* A2780 (HRP), OVCAR3 (HRD), and A2780cis (platinum-resistant) ovarian cancer cells were treated with TTFields (1 V/cm RMS, 200 kHz, 72 h), alone or with addition of PARPi (olaparib or niraparib, at various concentrations). Efficacy was measured by analyzing cell count, colony formation, and apoptosis induction. The overall effect was calculated by multiplying cell count with colony formation. TTFields-treated cells were evaluated for the expression of FA-BRCA pathway proteins and for formation of γH2AX, a DNA damage marker, using Western blot and fluorescent microscopy, respectively. *In vivo*, ID8-fLuc (HRP) cells were inoculated intraperitoneally to 6-8-week-old C57BL/6 mice. Seven days post inoculation, mice were treated with sham-vehicle, TTFields, olaparib (50 mg/kg), or both over a period of four weeks. Tumor growth was analyzed using bioluminescent imaging at treatment cessation, and survival analysis was performed.

Results: TTFields application resulted in reduced cell count, increased overall effect, and increased apoptosis *in vitro*. When TTFields were applied together with PARPi, a high and moderate synergistic interaction was shown respectively the BRCA wild-type A2780 cells and the platinum-resistant A2780cis cells. However, in the BRCA mutant OVCAR-3 cells the effect was additive. A downregulation of FA-BRCA protein expression was confirmed after TTFields treatment of the ovarian cells, with consequent DNA damage. In the tumor-bearing mice, TTFields and olaparib co-treatment resulted in reduced tumor volume and a survival benefit relative to the monotherapies and to control-treated mice.

Conclusions: The data suggest potential advantages for TTFields concomitant with PARPi in ovarian cancer, even without underlying BRCA mutations - consistent with the BRCAness state induced by TTFields - and also suggests benefits in platinum-resistant ovarian cancer.

EXPERIMENTAL AND MOLECULAR THERAPEUTICS: Novel Antitumor Agents 6
Poster Session

#7139 Anti-cancer effects of benzimidazole derivative BNZ-111 on paclitaxel-resistant ovarian cancer.

J.-W. Lee[1], K. Lee[2], B. Koh[2], Y.-Y. Lee[1], D.-S. Bae[1];
[1]Samsung Medical Center, Seoul, Korea, Republic of, [2]Korea Research Institute of Chemical Technology, Daejeon, Korea, Republic of

Ovarian cancer, a leading cause of cancer-related deaths in women, remains a formidable challenge, especially in the context of platinum-resistant disease. This study investigated the potential of the benzimidazole derivative BNZ-111 as a novel treatment strategy for platinum-resistant ovarian cancer. With improved pharmacokinetic parameters, BNZ-111 effectively disrupts tubulin polymerization through hydrogen bonds and hydrophobic interactions. It demonstrated strong cytotoxicity in both chemo-sensitive and chemo-resistant epithelial ovarian cancer cell lines, inducing apoptosis and G2/M cell cycle arrest. In vivo experiments using orthotopic and patient-derived xenograft models showed significant tumor growth inhibition without apparent toxicity to vital organs. Unlike paclitaxel, BNZ-111 proved effective in paclitaxel-resistant cells, potentially by bypassing interaction with MDR1 and modulating β-3 tubulin expression to suppress microtubule dynamics. This study suggests that BNZ-111, with favorable drug-like properties, holds promise as a therapeutic option for platinum-resistant ovarian cancer, addressing a critical clinical need in gynecologic oncology

#7140 A new series of flavonoid derivatives with anti-cancer activity includes SDN207, SND210, SND524, and SND562 as potent microtubule-targeting agents.

A. J. Arribas[1], E. Cannas[1], E. Gaudio[2], P. Biniecka[2], D. Stoicescu[2], F. Bertoni[1];

[1]IOR - Institute of Oncology Research, Bellinzona, Switzerland, [2]Floratek Pharma, Aubonne, Switzerland

Background: Plant-derived compounds, including flavonoids, can be potent anti-cancer agents, but low bioavailability, lack of specificity, and complexity in their synthesis can hamper their clinical development. Here, we present seven novel flavonoid derivatives, and test them for their anti-tumor activity in various models derived from hematological cancers and solid tumors.

Methods: MTT assessed anti-proliferative activity after 72h of exposure to increasing concentrations of drugs. Tubulin Polymerization Assay was performed with 3-fold dilutions (15-0.02 µM), compared to paclitaxel (1-3 µM) or vinblastine (3 µM) as references. The OncolinesProfiler analysis was used to compare IC50 fingerprints determined on the Oncolines cell line panel to the IC50 fingerprints of 213 pre-profiled reference drugs.

Results: SDN207, SND210, SND216, SND462, SND504, SND524, and SND562 were designed and synthesized using a flavonoid polyphenol scaffold selectively modified to markedly increase cytotoxicity towards cancer cells. All seven compounds showed dose-dependent anti-proliferative activity across 15 lymphoma cell lines derived from germinal center B-cell-like (GCB) diffuse large B cell lymphoma (DLBCL) (n=6), activated B cell-like (ABC) DLBCL (n=2), mantle cell lymphoma (n=4), and marginal zone lymphoma (MZL) (n=3). Activity in the nM range was seen with five compounds: SDN207 (median IC50 1.6 nM; 95%CI, 1.3-3.2), SND210 (1.4 nM; 95%CI, 0.9-3.3), SND216 (19.5 nM; 95%CI, 10-38 nM), SND562 (28.9 nM; 95%CI, 15.4-57.7), and SND524 (46.7 nM; 95%CI, 32-133.3). Both other compounds had a median IC50 of 2 µM (SND462, 95%CI, 1.1-4.5 µM; SND504, 95%CI, 0.5-3.9 µM). There were no differences based on lymphoma histology. The anti-tumor activity was maintained in MZL cell lines with acquired resistance to BTK and PI3K inhibitors (n=3). Six compounds were also assessed for their anti-tumor activity in models other than lymphomas (SDN207, n=31; SND210, n=20; SND462, n=4; SND504, n=4; SND524, n=9; SND562, n=35), confirming the higher activity for SDN207, SND210, SND562, and SND524. Regarding the mechanism of action, up to now, a tubulin polymerization assay was performed for three compounds. Microtubule depolymerization (SND207), and microtubule polymerization (SND524, SND562) were observed at concentrations as low as 20 nM. The OncolinesProfiler identified the tubulin-targeting agents vinblastine, vincristine, paclitaxel, and docetaxel among the top reference compounds most correlated with SND207 and SND210 (*i.e.*, Pearson correlation > 0.5).

Conclusions: Novel compounds developed using plant-derived skeletons have shown in vitro anti-tumor activity in lymphomas, leukemias, and solid tumors, including models of resistance to targeted agents. Microtubule targeting appeared as a possible mechanism of action for at least four of them.

#7141 The novel microtubule-destabilizing compound AUS_001 maintains unique binding to the colchicine site of tubulin and elicits reversible cellular effects relative to other anti-tubulin agents.

H. Lelie[1], Y.-C. Chou[2], A. J. King[2], Z. Boiarska[3], A. E. Prota[4], M. O. Steinmetz[4], **M. Koutsioumpa**[1];

[1]Australis Pharmaceuticals, Inc., Simi Valley, CA, [2]Eurofins Discovery, St. Charles, MO, [3]Universita degli Studi di Milano, Milano, Italy, [4]Paul Scherrer Institut, Villigen PSI, Switzerland

Our previous work showed that the prenylated hydroxy-stilbene AUS_001 exerts a strong safety profile and potent anti-proliferative responses, as assessed in 30 types of cancer cell lines, stemming from its microtubule destabilization activity. The aim of the current study was to delineate the molecular mechanism of microtubule destabilization by AUS_001 and to provide insight into its high potency and low toxicity. Surface plasmon resonance (SPR) experiments revealed the direct interaction of AUS_001 with tubulin with an apparent equilibrium dissociation constant, Kd, of 2.13×10^{-5}M. Size exclusion competition assays and an X-ray crystal structure of the tubulin-AUS_001 complex at 2.1 Å resolution establish ligand binding within the colchicine site on tubulin. Since colchicine-site ligands are well known to inhibit the curved-to-straight conformational transition of tubulin, which is an essential process for microtubule formation, these results readily explain the microtubule-destabilizing activity of the compound. Notably, while both combretastatin A4 (CA-4) and AUS_001 are both colchicine-site stilbene ligands, CA-4 binds in the *cis* configuration, while AUS_001 maintains a *trans* configuration leading to a substantially different pocket engagement. Comparison of the tubulin-AUS_001 complex structure with the ones of tubulin-colchicine and tubulin-plinabulin revealed that AUS_001 elicits different rearrangements in the T7 loop of β-tubulin versus colchicine and occupies a different zone of the pocket relative to plinabulin, further elaborating its unique binding properties. Interestingly, AUS_001 exhibits a higher relative affinity than colchicine itself, as assessed by i) an ultrafiltration-based tubulin-ligand release assay and ii) a radioligand colchicine competition assay. However, fitting steady state SPR data for AUS_001 binding to tubulin revealed fast association and dissociation rates and was indicative of reversible binding. The latter finding is corroborated by AUS_001-triggered reverse biological effects including morphological alterations, cell cycle G2/M arrest, and by a decrease of cell viability upon discontinuation of the drug treatment in glioma and pancreatic cancer cells. Conversely, colchicine, CA-4 or paclitaxel administered at the same doses as those applied for AUS_001 failed to reverse the drug-induced phenotypes upon removal resulting in sustained cytotoxicity. In conclusion, we fully characterized the unique binding mode of AUS_001 to the colchicine site of tubulin and elucidated the reversible nature of the target engagement. AUS_001 features a distinctive and reversible molecular interaction with tubulin which provides a plausible explanation for its favorable safety profile compared to other microtubule targeting agents.

#7142 Optimizing estradiol dimers through linker design: Enhancing anticancer efficacy by targeting microtubule dynamics.

P. Dzubak[1], M. Jurasek[2], J. Řehulka[1], S. Gurska[1], P. Polishchuk[1], P. Draber[3], L. Huml[2], P. B. Drasar[2], A. Ivanova[1], O. Mokshyna[1], L. Hruba[1], M. Hajduch[1]; [1]Palacky University in Olomouc, Olomouc, Czech Republic, [2]University of Chemistry and Technology Prague, Prague, Czech Republic, [3]Institute of Molecular Genetics of the Czech Academy of Sciences, Prague, Czech Republic

We investigated the development and anticancer efficacy of novel estradiol dimers (ED), targeting the dynamics of microtubules—an essential factor in effective cancer therapy. Employing copper-catalyzed azide-alkyne cycloaddition (CuAAC), two distinct series of ED variants were synthesized. The initial series included thirteen dimers, derived from 17α-ethinyl estradiol, incorporating varied five-atom linkers with central carbon, nitrogen, or oxygen atoms, and, in some instances, modified with benzyl groups containing hydroxy or methoxy substituents. These dimers were evaluated for their cytotoxic properties and impact on the cell cycle, revealing certain structures with substantial efficacy, compared with the original ED. The subsequent series, encompassing twelve variants, concentrated on structural alterations within the aromatic bridges linking the estradiol units. In this series, linkers of simpler composition and fewer substituents demonstrated increased selectivity and potency against cancer cell lines, particularly ED3 and ED5, which exhibited cytotoxicity levels comparable to established tubulin inhibitors. Both dimers series showed the ability to disrupt microtubule assembly and mitotic processes, confirmed through cell-based evaluations and in vitro tubulin assembly assays. Complementing these results, in silico modelling and binding free energy calculations exhibited a strong correlation with the demonstrated biological activities, especially in terms of binding affinity to the colchicine site. Collectively, these findings highlight the promise of estradiol dimers as potential anticancer agents and emphasize the critical role of linker structures in enhancing their biological effectiveness. Work was supported by the Ministry of Education, Youth and Sports of the Czech Republic through infrastructural projects (CZ-OPENSCREEN - LM2018130; EATRIS-CZ - LM2018133) and National Institute for Cancer Research (Programme EXCELES, ID Project No. LX22NPO5102) - Funded by the European Union - Next Generation EU.

#7144 BR0L075 (SCB01A), a microtubule inhibitor targeting the colchicine binding site, induces immunogenic cell death.

A. Bano, X. Liu;
University of Houston, Houston, TX

BPR0L075 (also known as SCB01A in phase II clinical trial) is a novel anti-microtubule drug with potent anti-tumor and anti-angiogenic activity in vitro and in vivo. BPR0L075 inhibits tubulin polymerization (microtubule de-stabilizer) by binding to the colchicine-binding site of tubulin. We previously reported that BPR0L075 overcomes paclitaxel (microtubule stabilizer) resistance and induces vascular-disruption in vitro and in vivo. We observed that breast and ovarian cancer cells treated with BPR0L075 in vitro induced key hallmarks of immunogenic cell death (ICD). In both human and murine, ovarian (OVCAR3, ID8) and breast cancer (MDA-MB-231, 4T1) cell lines, treatment with low nanomolar concentration of BPR0L075 significantly decreased the viability of cells evidenced by SRB assay. Using a known ICD inducer mitoxantrone as a positive control, both flow cytometric analysis and immunofluorescence staining assays demonstrated that BPR0L075 treatment led to a time- and dose-dependent translocation of calreticulin, an endoplasmic reticulum chaperone protein, on the plasma membrane of dying cells which sends an “eat me” signal. The BPR0L75 treatment also led to secretion of High Mobility Group Box 1 (HMGB1), a non-histone chromatin-binding nuclear protein, as well as adenosine triphosphate (ATP) from the cell into the extracellular space using ELISA assay. These damage-associated molecular patterns (DAMPs) are known to lead to antigen-presenting cell recruitment, phagocytosis, maturation of dendritic cells, and chemotaxis. The appearance of the ICD biomarkers (calreticulin exposure, HMGB1 and ATP release) supports BPR0L075 as an ICD-inducing antimitotic agent. Further in vivo studies are warranted to delineate the effect of BPR0L075 on immune activation and recruitment of immune cells to the tumor microenvironment.

#7145 Identification of Debio 0432 as a potent and selective USP1 inhibitor for cancer therapy.

N. Luong[1], A. Kunze[1], N. Quesnot[1], E. R. Aho[2], L. Berry[2], S. Boiko[2], A. J. Buckmelter[2], S. Lofek[3], S. Vigano[3], V. Gerusz[4], C. Chardonnens[3];
[1]Debiopharm International S.A., Lausanne, Switzerland, [2]Forma Therapeutics, Watertown, MA, [3]Debiopharm Research and Manufacturing SA, Martigny, Switzerland, [4]Debiopharm Research and Manufacturing SA., Martigny, Switzerland

Introduction: Debio 0432 is a Ubiquitin Specific Protease 1 (USP1) inhibitor at preclinical stage. This study presents the first data on this small molecule and its activity as an anti-cancer therapy in multiple preclinical models. USP1 is a deubiquitinase, member of the deubiquitinating enzyme (DUB) family that plays an important role at the replication fork during DNA replication. Its prominent role in DNA repair, targeting Proliferating Cell Nuclear Antigen (PCNA) that regulates polymerase recruitment in the translesion synthesis (TLS), makes it an emergent target in the DNA damage repair (DDR) field.
Methods: In silico docking has been used to identify a likely binding site of Debio 0432. Biochemical and cellular assays have been performed to show its activity on the target and in cell lines of different cancer types. In vivo models in cell line derived xenograft (CDX) and patient derived xenograft (PDX) were then used to confirm the activity of the compound and to study PK/PD relationship.
Results: Debio 0432 likely binds USP1 in an allosteric pocket and is very selective across the 58 members of the USP family. Furthermore, it does not affect any kinase. Its biochemical activity on USP1 is in the low nanomolar range and cellular activity ranges between from single digit nM to above 1uM. In vivo, Debio 0432 shows antitumor activity in the BRCA mutant breast cancer model MDA-MB-436. The downstream target Ub-PCNA, selected as pharmacodynamic marker, is modulated in a dose and plasma exposure-dependent manner. Further in vivo experiments in PDX models showed dose-dependent activity in different cancer types, in both BRCA wild type and mutant models. Treatments in all in vivo studies were well tolerated.
Conclusion: Overall, we show that Debio 0432 is a selective and potent small molecule targeting USP1, an emerging target in the DDR field. It shows good activity in different preclinical models and is well tolerated at active doses. Debio 0432 is currently undergoing IND-enabling studies and in preparation for entry into clinical development.

#7146 HSK39775: A USP1 inhibitor for the treatment of cancers with homologous recombination deficiencies.

J. Xu[1], Y. Li[1], **J. Wang**[1], P. Tang[2], J. Wang[2], C. Zhang[2], P. Yan[2];
[1]Haisco Pharmaceutical Group Co., Ltd., Shanghai, China, [2]Haisco Pharmaceutical Group Co., Ltd., Chengdu, China

Tumors with BRCA1/2 mutations or homologous repair deficiency (HRD) are vulnerable to agents that target DNA repair pathways, including platinum-containing chemotherapeutics and poly (ADP-ribose) polymerase-1 (PARP1) inhibitors. Despite the significant therapeutic benefits in patients with BRCAm or HRD, innate and acquired resistance to PARPi is still a challenge in the clinic. To address this clinical challenge, we developed HSK39775, a potent, highly selective inhibitor of ubiquitin carboxyl-terminal hydrolase 1 (USP1), which acts as an oncogenic and PARP inhibitor resistance driver involved in DNA damage repair pathway through the deubiquitylation of proteins in Translesion Synthesis pathway and Fanconi Anemia pathway, paired with BRCA as a synthetic lethality target. HSK39775 was active in enzymatic level to inhibit USP1/UAF1 complex. Enzymatic panel screening containing 50 deubiquitinase demonstrated high selectivity of HSK39775. Ubiquitinated PCNA was accumulated treated by HSK39775, indicating target engagement. HSK39775 also demonstrated potent anti-proliferation activity against cancer cell lines with BRCA mutation and excellent selectivity between BRCA WT vs. BRCAm. Combining HSK39775 with PARP inhibitors indicated synergy in cell lines with partial or insensitivity to each agent alone. Triple-negative BRCA mutant breast cancer xenograft model demonstrated strong dose-dependent tumor growth inhibition of HSK39775 as a single agent with Tumor Growth Inhibition (TGI) of 63.2% at 30 mg/kg QD, and ubiquitinated PCNA was also accumulated in HSK39775 treated tumor tissue. Meanwhile, combination with PARP inhibitors significantly enhanced the therapeutic efficacy of HSK39775 in xenograft model and led to tumor regressions and durable tumor control even at low dose (TGI:89% (HSK39775, 5 mg/kg + Olaparib, 50 mg/kg)). Interestingly, HSK39775 inhibited the tumor growth of a HRP and BRCA wild-type lung cancer xenograft as a single agent with TGI of 94% at 30 mg/kg QD, suggesting the therapeutic effect of USP1 inhibitors beyond canonical BRCA mutant or HRD tumors. In summary, these results indicate HSK39775 as a potent and selective USP1 inhibitor and support further development.

#7147 ASN-3186 is a potent and selective inhibitor of USP1 for the treatment of BRCA1/2 mut and HRD+ cancers.

Qiaoling Sun[1], Yunfei Chen[1], Maojiang Wu[1], Jing Lv[1], Hongyue Jin[1], Peng Zeng[1], Xia Song[1], Wenfeng Hou[1], Qi Huang[1], Wei Niu[1], Mengyao Zhang[1], Tie-Lin Wang[1], Alice Chen[2]

[1]Asieris Pharmaceuticals, Shanghai, China,[2]Asieris Pharmaceuticals, Palo Alto, CA

Ubiquitin-specific protease 1 (USP1), a well-characterized member of the deubiquitinating enzyme family, selectively cleaves ubiquitin from various target proteins, including DNA repair protein PCNA. USP1 contributes to oncogenesis by playing critical roles in DNA damage repair processes including translesion synthesis and the Fanconi anemia pathway. Despite the clinical benefit achieved with PARP inhibitors (PARPi) in BRCA-mutated (BRCAm) or homologous recombination deficient (HRD+) populations, some patients either do not respond to therapy or develop resistance. USP1 inhibitors may have the potential to address this unmet clinical need as USP1 functions in distinct DNA damage repair pathway as compared to PARP. ASN-3186 is a novel, potent, and selective USP1 inhibitor with enzyme IC50 value of single digit nanomolar and selectivity >1000-fold against other family members. ASN-3186 demonstrated potent anti-proliferative activity in the BRCA1m triple negative breast cancer (TNBC) cell line, MDA-MB-436 (IC50 <30 nM). MDA-MB-436 CDX mouse model confirmed dose-dependent, single-agent inhibitory activity of ASN-3186 in vivo with higher potency than KSQ4279, possibly due to ASN-3186's higher oral bioavailability. Efficacy is consistent with increase of pharmacodynamic biomarker ub-PCNA. The combination of ASN-3186 and PARPi Olaparib yielded a more robust and durable anti-tumor response, with near-complete tumor regression demonstrated at higher combination dose. Moreover, addition of ASN-3186 significantly sensitized Olaparib's minimal anti-tumor activity in CAOV3 (ovarian, HRD high) and MX-1 (TNBC, BCRA1/2 mut) models, which are resistant to PAPRi, indicating that it has the potential to overcome PARPi resistance. Synthetic lethal activity was also observed when ASN-3186 was combined with DNA damage drug Gemcitabine. Furthermore, ASN-3186 displayed desirable ADME and PK profiles with high oral bioavailabilities (>75%) across species. These data support further clinical development of ASN-3186 as a potential best-in-class USP1 inhibitor, both as a single agent as well as in combination with PARPi, for treatment of BRCA1/2 mut and HRD+ cancers.

#7148 Small molecule inhibitor of FEN1 nuclease utilizing a novel metal-binding pharmacophore synergizes with inhibitors of USP1, PARP, PARG and ATR.

Jason Munguia, Sanjay Agarwalla, Elaine Guo, Dave Martin, Junhua Fan, Dave Lonergan, David Puerta, Zachary Zimmerman, **Konstantin Taganov**

Blacksmith Medicines, San Diego, CA

Flap endonuclease 1 (FEN1) is a structure-specific metallonuclease that cleaves 5' DNA flaps during replication and repair. FEN1 is an attractive target for development of anticancer therapeutics because it is overexpressed in many tumor types and has a large number of synthetic lethality partners including genes in Homologous Recombination (HR) pathway (Mengwasser et al., 2019; Guo et al., 2020).

Utilizing fragment-based drug discovery approach we identified a novel metal-binding pharmacophore that binds to the two magnesium ions in the FEN1 active site. Further elaboration using fragment growth strategies resulted in highly potent and selective inhibitors. The current lead (BSM-1516) is ~65-fold more potent against FEN1 than its related enzyme Exonuclease 1 (Exo1) in biochemical assays (IC_{50} of 7 nM and 460 nM, respectively), an improvement of more than an order of magnitude in selectivity compared to earlier efforts. FEN1 target engagement in live cells was validated by cellular thermal shift assay (CETSA EC_{50} of 24 nM). Inhibition of FEN1 led to its increased association with chromatin in S-phase cells and recruitment of PARP1 enzyme.

In clonogenic assay, BRCA2-deficient DLD1 cells were ~15-fold more sensitive to FEN1 inhibition than their isogenic BRCA2-wild-type counterparts (EC_{50} of 350 nM and 5 µM, respectively), confirming the increased susceptibility of HR deficient cancer cells to FEN1 inhibition. Treatment of BRCA2-deficient but not wild-type DLD1 cells with BSM-1516 resulted in cell cycle arrest and dose-dependent decrease of S-phase BrdU incorporation into DNA. Cell cycle arrest of BRCA2-deficient DLD1 cells was accompanied by DNA damage signaling and by accumulation of chromatin-bound RPA32, a marker of ssDNA.

To explore synthetic lethal interactions of FEN1 with other DNA repair genes we performed FEN1-inhibitor-anchored CRISPR screen. This analysis revealed that in addition to HR pathway inactivation, genomic perturbations in EXO1, USP1 and PARP1 genes sensitized cells to FEN1 inhibition. Synergistic relationships of BSM-1516 and its combination potential were further explored in viability studies with a panel of DDR inhibitors (n=25) in BRCA2-proficient and deficient cell lines. Strong synergy was identified with multiple drug classes that included inhibitors of USP1 (KSQ-4279), PARP (Olaparib, Niraparib, Talazoparib, AZD5305), PARG (PDD 00017273) and ATR (AZD6738, VE-822, Elimusertib).

In vitro ADME assays and in vivo PK studies showed that BSM-1516 has properties suitable for in vivo testing, either as a single agent or in combination with synergistic DDR inhibitors, an investigation that is currently underway.

#7149 Discovery of a novel USP1 inhibitor: Targeted therapy for BRCA-mutated and PARPi-resistant cancers.

J. Kim, S. Kim, S. Park, S. Lee, K. Yoo, H.-J. Lee, J. Kang, K.-O. Lee;
AIGEN Sciences, Seoul, Korea, Republic of

Harnessing synthetic lethality offers an innovative approach to targeted cancer treatment. USP1, a specific deubiquitinating enzyme, has gained attention as a potential synthetic lethality target for BRCA-mutated cancers. At AIGEN Sciences, Inc., we've integrated the advanced capabilities of our human-in-the-loop (HITL) AI drug discovery platform, AIGEN ChemTailor. This cutting-edge platform thrives on continuous learning enhanced by expert feedback, refining our approach to drug discovery. Using AIGEN ChemTailor, we synthesized a specific USP1 inhibitor. Its inhibitory capabilities were validated through the Ubiquitin-rhodamine 110 assay. Notably, our inhibitor presented remarkable anti-proliferative effects on BRCA1 mutant cells (MDA-MB-436) while showing no activity against BRCA wild-type cells (HCC1954), highlighting its specificity. The efficacy of our inhibitor was enhanced when combined with PARP inhibitors, such as olaparib or AZD5305, especially in UWB1.289 cells. Impressively, the USP1 inhibitor also effectively targeted PARPi-resistant cell lines, including A2780-ola, UWB1.289-nir, HCC38-ola, MDA-MB-468-ola, U251MG-ola, and OVCAR8-ola. Clonogenic assays with MDA-MB-436 and MCF-10A emphasized our inhibitor's selectivity towards BRCA mutant phenotypes. Subsequent studies demonstrated the compound's mechanism: inducing replication stress by impairing of DNA synthesis and activating DNA damage pathways via ATR signaling. Preclinical mouse studies highlighted favorable pharmacokinetics and involved the assessment of anti-tumor effects in animal models. In summation, our USP1 inhibitor, developed using AIGEN ChemTailor and advanced molecular modeling techniques, stands out as a potent therapeutic against BRCA-mutated cancers and PARP inhibitor-resistant strains.

#7150 Molecular insights into the oncogenic influence between mutant HER3, mutant KRAS, and their synergistic interplay in colorectal cancer pathogenesis.

M. K. Kilroy, B. Park, R. Mishra, W. Feroz, C. Wischmeier, J. T. Garrett;
University of Cincinnati, Cincinnati, OH

Colorectal cancer (CRC) is a disease of the colon and rectum that will claim about 52,550 American lives in 2023. In recent years, more attention has been paid to HER2 and HER3's roles in colorectal cancers, as they may cause resistance to targeted therapies. We are investigating the role of naturally co-occurring HER3 and KRAS mutations in colorectal cancer, as about 6% of all colorectal cancers contain a HER3 mutation and 41% contain a KRAS mutation. We have observed that there is a statistically significant co-occurrence of HER3 and KRAS mutations in CRCs while there is mutual exclusivity with mutations in EGFR or HER4 and mutant KRAS in CRC examining 6791 samples from 17 studies. There is a tendency for co-occurrence with HER2 and KRAS mutations that is not statistically significant in these CRC tumor samples. We have found that genetic knockdown of both KRAS and HER3 with siRNA targeting KRAS and HER3 in the CRC cell line SNU-407 ($HER3^{V104M}$, $KRAS^{G12D}$) results in a statistical reduction in cell proliferation in comparison to genetic knockdown with only KRAS or HER3. Using the SW620 CRC cell line ($HER3^{WT}$, $KRAS^{G12V}$) as a comparison, we have observed that knocking down HER3 using siRNA had no effect on cell proliferation whereas KRAS knockdown reduced proliferation and the combination showed no statistical difference compared to knocking down only KRAS. Additionally, we have found that there is a striking increase in total HER3 levels in SNU-407 cells when treated with the $KRAS^{G12D}$ inhibitor MRTX1133. This feedback loop could limit the efficacy of the KRAS inhibitor. We wished to delineate mutant HER3's binding partner(s) as HER3 is kinase impaired. Strikingly, we have found that EGFR immunoprecipitates with HER3 in SNU-407 cells. We are expanding our studies to CRC patient derived xenografts (PDXs) with co-occurring HER3 and KRAS mutations and have generated patient derived organoids from these PDXs. Ongoing studies are determining if there is a synergistic relationship with KRAS inhibitors and HER family inhibitors including a HER3 antibody-drug conjugate. Our findings may present a new paradigm for targeted combination therapies in colorectal cancer with the eventual goal of increased overall patient survival.

#7151 Targeting metabolic pathway in triple negative breast cancer with a small molecule inhibitor.

A. Dheeraj[1], F. J. G. Marques[2], D. Tailor[1], A. Bermudez[2], B. Grau[1], S. Pitteri[2], S. V. Malhotra[1];
[1]Knight Cancer Institute, Oregon Health & Science University, Portland, OR, [2]Stanford University, Palo Alto, CA

Background: Triple Negative Breast Cancer (TNBC) is the most aggressive type of breast cancer, making up 15-20% of diagnosed cases, and has high rates of metastasis and recurrence. Most women with this disease experience a recurrence after curative-intent therapy for early breast cancer, while a smaller proportions are diagnosed with distant metastases initially. Cancer cells are characterized by their reprogramming of glucose metabolism. Cancer cells show increased proliferation along with higher energy and substrate demands. Through our efforts to find effective therapies for TNBC, we have identified CET019, a new small molecule that effectively suppresses the growth of breast cancer cells.
Methods: Cell viability and clonogenic assays were performed on a range of TNBC cells, including MDA-MB-231, MDA-MB-468, SUM159, HCC1395, HCC1806, EMT6, and 4T1. Cell cycle distribution was assessed through flow cytometry. LC-MS/MS analysis was performed on TMT-labeled samples for global proteome profiling. The efficacy of CET019 (30 mg/kg) was tested using tumor and patient derived xenograft studies.
Results: Our studies show that CET019 suppresses the clonogenic potential and growth of various triple-negative breast cancer cells. The CET019 treatment causes cell cycle arrest in TNBC cells at the G2/M phase. Proteomics analysis suggests that CET019 specifically affects metabolic and proteosomal pathways. In vivo studies with CET019 found an inhibition of tumor growth kinetics in the mouse xenograft study with different TNBC models, as compared to the control group. We also observed that CET019 inhibited metastatic lung nodules. The results were further substantiated in three Patient Derived Xenograft (PDX) models.
Conclusion: In summary, our study has identified a novel small molecule candidate CET019 as a promising lead candidate for TNBC treatment, paving the way for further development.“The complete chemical structures of the compounds used will be disclosed at the time of presentation at the meeting.”

#7153 PHI-101 synergizes with chemotherapy and venetoclax in preclinical models of acute myeloid leukemia.

Hee-sun Hwang[1], Gi-Jun Sung[1], Kyung-Ah Kim[1], Ky-Youb Nam[1], Kyu-Tae Kim[1], June H. Han[1], Jeong-Hyeok Yoon[1], Bao Nguyen[2], Li Li[2], Tessa Seale[2], Donald Small[2]

[1]Pharos iBio Co., Ltd, Anyang, Korea, Republic of,[2]Department of Oncology, Johns Hopkins University School of Medicine, Baltimore, MD

FLT3 mutations are one of the most frequent genetic alterations in AML, resulting in poor prognosis. Although the development of FLT3 tyrosine kinase inhibitors (TKIs) provided new treatment options, patients with FLT3-mutant AML still suffer from high relapse rates when treated with FLT3 TKI alone. Accumulating evidence supports a combination treatment strategy to lower the recurrence rate. We have previously shown that PHI-101 demonstrated potent activity in various FLT3 mutant AML cell lines when used alone. Here we explore the use of PHI-101 in combination with other therapeutics in preclinical models of AML. We investigated the preclinical efficacy of the combination of PHI-101 with FDA-approved AML therapeutic agents in FLT3 mutant (MV4-11, Molm13, Molm14) and wild-type (THP-1) AML cell lines. Cell growth inhibition was assessed by CCK-8 and/or CellTiter-Glo assays. The Chou-Talalay method was used to calculate the combination index (CI) to test for synergy. Western blotting analysis was performed to explore the potential mechanisms underlying the combination effects. AML xenograft mouse models were used to assess the in vivo efficacy of PHI-101 combination therapy. Statistical comparisons included unpaired t-tests or one-way ANOVA. Combination treatment of PHI-101 with venetoclax or azacytidine showed strong synergistic effects on growth inhibition against both FLT3-ITD mutant (CI<0.3) and wild-type AML cells (CI <0.6). It is noteworthy that the FLT3-ITD homozygous cell line (MV4-11) showed especially strong synergism (CI <0.1). In the xenograft mouse model experiments, 14-day treatment with either PHI-101 alone or in combination with venetoclax or azacytidine showed significant suppression of tumor growth compared to venetoclax or azacytidine alone (in average tumor growth inhibition (TGI) 88.3% vs 8.6%)($p<0.05$). In particular, PHI-101 3 mg/kg/day (mpk) with venetoclax 80mpk resulted in a stronger anti-tumor effect (TGI 94.2%) compared to PHI-101 (TGI 87.4%) or venetoclax alone (-9.6% of TGI) ($p<0.05$) even 21 days after stopping the treatment. In addition, PHI-101 treatment showed a survival advantage in AML animal models, and the combination with venetoclax led to significantly longer survival compared to the control groups. Our preclinical data showed that the combination of PHI-101 with venetoclax or azacytidine resulted in a highly effective anti-leukemic response against AML cells by inducing DNA damage, BCL-2 inhibition, and MCL-1 degradation. Additionally, treatment of mice with low-dose PHI-101 inhibited tumor regrowth and further potentiated venetoclax or azacytidine response in vivo. Our results suggest that the combination of PHI-101 and venetoclax or azacitidine may have the advantage of improving clinical responses in FLT3-ITD AML patients and offers a potential therapeutic option to treat patients with newly diagnosed or relapsed/refractory FLT3-mutant AML.

#7154 Ivospemin/doxorubicin combination modulates polyamine metabolism to improve survival in murine ovarian cancer models.

Cassandra E. Holbert[1], Jackson R. Foley[1], Ashley C. Nwafor[1], Ting-Ann Liu[1], Elizabeth Bruckheimer[2], Jennifer K. Simpson[2], Tracy Murray Stewart[1], Robert A. Casero[1]

[1]Johns Hopkins University School of Medicine, Baltimore, MD,[2]Panbela Therapeutics, Waconia, MN

Polyamines are small polycationic alkylamines that are absolutely required for the continual growth and proliferation of cancer cells. As cancer cells maintain elevated polyamine pools through dysregulated polyamine metabolism, its pharmacological modulation is a promising avenue in cancer therapeutics. The polyamine analogue ivospemin has shown efficacy in slowing pancreatic and ovarian tumor progression in vitro and in vivo and has demonstrated encouraging results in pancreatic cancer clinical trials. Considering nearly 75% of late-stage ovarian cancer patients develop resistant to platinum-based chemotherapies, limiting treatment options, the aim of our study is to determine the potential efficacy of ivospemin in combination with doxorubicin, a common chemotherapeutic used in platinum-resistant ovarian tumors. We have previously shown that ivospemin exposure decreases polyamine content in a variety of cancer cell lines through downregulation of the polyamine biosynthetic enzyme ornithine decarboxylase (ODC) and induction of the polyamine catabolic enzyme spermidine/spermine-N1-acetyltransferase (SSAT). Here we examine the potential of combining ivospemin with doxorubicin. Ivospemin treatment reduces cell viability in ovarian adenocarcinoma cell lines and increases the toxicity of doxorubicin regardless of cisplatin sensitivity. Cells treated with the combination exhibit a greater decrease in polyamine levels than cells treated with either single agent. This increased polyamine depletion and decreased survival is accomplished through modulation of polyamine metabolism, predominately through an additive induction of SSAT activity. Using the syngeneic VDID8+ ovarian murine model, we further evaluated the ability of ivospemin to improve response to doxorubicin at clinical and sub-clinical dosing. Ascites fluid was used as a marker for tumor burden and evaluated for polyamine content. We found that the combination treatment increases median survival, delays tumor onset, and decreases overall tumor burden compared to either clinical or subclinical doxorubicin dosing schemes. Combination treatment also decreases overall polyamine content in the ascites by 75%. N1-acetylated spermidine is enriched in ascites from combination-treated mice, consistent with an upregulation of SSAT in response to treatment. Recognizing the non-representative mutational status of the VDID8+ model as a limitation, we are currently evaluating the combination of ivospemin and doxorubicin in genetically defined murine models that better recapitulate human high-grade serous ovarian carcinomas. Ongoing studies will determine influences on the tumor microenvironment and will mechanistically evaluate the cooperativity of ivospemin and doxorubicin on pathways outside of polyamine metabolism.

#7155 Dichloroacetate reverses cisplatin resistance in ovarian cancer through promoting ROS production.

Y. Do, **S. Lee**, C. Shin, H. Chung, J. Kim, E. Ha, S. Shin, J. Seo;
Keimyung University School of Medicine, Daegu, Korea, Republic of

Chemotherapy resistance and the high rate of ovarian cancer relapse pose major challenges in the treatment of ovarian cancer. The development of chemoresistance contributes to poor overall prognosis associated with ovarian cancer and high cancer-related mortality in women worldwide. Herein, we found that Dichloroacetate (DCA), a pan-pyruvate dehydrogenase kinase (PDK) inhibitor, is a potent agent to overcome Cisplatin (CP) resistance in ovarian cancer treatment. Firstly, we elucidated that phosphorylation of pyruvate dehydrogenase (pPDH) was elevated in CP-resistant ovarian cancer cells. Then, blockage of pPDH by DCA treatment significantly inhibited cell migratory and invasive capacity in CP-resistant ovarian cancer cells through the transition of motile mesenchymal phenotypes into epithelial characteristics. DCA markedly decreased the number of sphere formations and attenuated the stem cell-like properties in CP-resistant ovarian cancer cells. In combination with CP treatment, DCA effectively inhibited cell proliferation in chemoresistant ovarian cancer cells by triggering apoptosis. Collectively, we suggested that DCA is a promising drug to reverse CP resistance for ovarian cancer treatment. We further tested the underlying mechanisms of DCA to restore CP sensitivity in ovarian cancer. We found that CP treatment promoted reactive oxygen species (ROS) production to induce cell death in CP-sensitive ovarian cancer. However, CP-resistant ovarian cancer cells exhibited higher basal levels of ROS compared with sensitive cancer cells, and CP treatment failed to generate ROS production. That means ovarian cancer cells steadily adapted to elevated ROS levels, then becoming ROS-adapted ovarian cancer cells to survive. Interestingly, DCA treatment results in the buildup of ROS production, causing cell death in CP-resistant ovarian cancer. Therefore, our study suggests that ROS production can be an attractive target in DCA treatment to restore CP sensitivity in ovarian cancer.

#7156 Targeting the β-catenin signaling axis in osteosarcoma.

M. Curcic, S. Gaikwad, S. Srivastava;
Texas Tech University Health Sciences Center, Abilene, TX

Osteosarcoma, an aggressive bone malignancy predominantly affecting children, poses a formidable challenge for therapeutic interventions. Here we evaluated a recently approved FDA drug, PCT, for potential anti-cancer effect in osteosarcoma model. Initial assessments of cytotoxicity encompassing various human and murine osteosarcoma cell lines—OS-17, OS-25, U2OS, SAOS2, MG63, and K7M3—revealed an IC_{50} ranging 1-3 µM. Subsequent investigations demonstrated significant anti-clonogenic activity and G2M phase cell cycle arrest. Annexin-PI assay showed a notable apoptotic effect of PCT, shedding light on the mode of cell death. Given the pivotal role of β-catenin signaling in human osteosarcoma pathogenesis and metastasis, targeting β-catenin components holds promise for therapeutic intervention. *In silico* docking studies suggested that PCT may have similar anti-cancer effect compared to β-catenin inhibitors (e.g., MSAB, ICG001). Our western blot analyses in multiple osteosarcoma cell lines demonstrated that PCT inhibits β-catenin pathway. Fluorescence microscopy and PCR analyses substantiated PCT's ability to hinder the nuclear translocation of β-catenin, providing mechanistic insights into its anti-tumor properties. Our preliminary data also suggests that AXL, an upstream regulator of β-catenin pathway, was modulated by PCT. In summary, our findings indicate that PCT exhibits therapeutic potential against osteosarcoma by targeting the β-catenin pathway. Further mechanistic studies are currently underway in our lab.

EXPERIMENTAL AND MOLECULAR THERAPEUTICS: Pharmacology and Pharmacogenetics
Poster Session

#7160 Germline predictors for bevacizumab induced hypertensive crisis in ECOG-ACRIN 5103 and BEATRICE.

F. Shen[1], G. Jiang[1], S. Philips[1], E. Cantor[1], L. Gardner[1], G. Xue[1], G. Cunningham[1], N. Kassem[1], A. Oneil[2], D. Cameron[3], T. Suter[4], K. Miller[1], G. Sledge[5], B. Schneider[1];

[1]Indiana Univeristy, Indianapolis, IN, [2]Dana Darber Cancer Institute, Boston, MA, [3]Edinburgh Cancer Research Centre, Edinburgh, United Kingdom, [4]Swiss Cardiovascular Center, Bern, Switzerland, [5]Caris Life Sciences, Dallas, TX

Introduction: Bevacizumab is a beneficial therapy in several advanced cancer types. Predictive biomarkers to better understand which patients are destined to benefit or experience toxicity are needed. Associations between bevacizumab induced hypertension and survival have been reported but with conflicting conclusions.

Methods: We performed post-hoc analyses to evaluate the association in 3,124 patients from two phase III adjuvant breast cancer trials, E5103 and BEATRICE. Differences in invasive disease-free survival (IDFS) and overall survival (OS) between patients with hypertension and those without were compared. Hypertension was defined as systolic blood pressure (SBP) ≥ 160 mmHg (n=346) and SBP ≥ 180 mmHg (hypertensive crisis) (n=69). Genomic analyses were performed to evaluate germline genetic predictors for the hypertensive crisis.

Results: Hypertensive crisis was significantly associated with superior IDFS ($p = 0.015$) and OS ($p = 0.042$), but only IDFS ($p = 0.029$; HR = 0.28) remained significant after correction for prognostic factors. SBP ≥ 160 mmHg was not associated with either IDFS or OS. A common single-nucleotide polymorphism, *rs6486785,* was significantly associated with hypertensive crisis ($p = 8.4 \times 10^{-9}$; OR = 5.2).

Conclusion: Bevacizumab-induced hypertensive crisis is associated with superior outcomes and *rs6486785* predicted an increased risk of this key toxicity.

#7161 Preclinical pharmacology modeling (pharmacokinetics/efficacy) of narazaciclib (HX301 or ON123300) to predict its clinical effective dose.

T. Yang[1], H. Ke[1], J. Liu[2], K. Gong[2], **H. Q. Li**[1];
[1]Hanx Bio, Hangzhou, China, [2]Crown Bioscience, Beijing, China

Background: Acute myeloid leukemia (AML) is an aggressive leukemia of myeloid lineage. CSF1R (colony-stimulating factor 1 receptor) regulates the proliferation, differentiation and polarization of cells of myeloid lineages, e.g. monocytes/macrophages. CSF1R expression is aberrantly upregulated in many AML, leading to a hypothesis that CSF1R is a putative leukemogenic driver in a subset of AML and thus could be a potential target for treating AML. Previous studies demonstrated that Narazaciclib (HX301 or ON123300), an investigational kinase inhibitor (TKi), exhibited high potency activity against CSF1R (IC_{50} 0.285 nM) and inhibition of macrophage proliferation and AML tumor growth both *in vitro/in vivo*, implicating its potential use as an AML therapeutic[1] (An et al., 2023 AACR Annual Meeting). In addition, narazaciclib has recently completed the dose escalation phase 1 study in advanced solid tumors. However, the therapeutic window of narazaciclib as a CSF1Ri for treating AML remains to be determined. The present study attempted to utilize both preclinical PK and *in vivo* efficacy models to predict the effective clinical dose of narazaciclib for guiding the future AML clinical trials.
Methods: A single dose of narazaciclib at various of dose levels was orally administrated in NOD/Scid mice, and plasma samples were collected at designated timepoints. The concentrations of narazaciclib in plasma were analyzed by LC-MS. In a Ba/F3-ETV6-CSF1R *in vivo* xenograft tumor model in Nod/Scid mice, narazaciclib at various dose levels was orally administrated daily. Tumor volumes were measured twice weekly.
Results: The mouse PK study showed that narazaciclib displayed overall similar absorption pattern as seen in unpublished human clinical data. Narazaciclib was absorbed rapidly after oral dosing with a mean T_{max} ranging from 1 to 2 hours in mouse. However, narazaciclib was cleared faster in mouse, with a mean $T_{1/2}$ ranging from 1.9 to 2.8 hours, than in human. In addition, the exposures of narazaciclib, as measured by C_{max} and AUC in plasma, increased in a relatively dose-proportional manner, as seen in human patients. In the Ba/F3-ETV6-CSF1R xenograft model where the tumor cell growth is solely dependent on the CSF1R kinase activity, narazaciclib at 10 mg/kg did not induce any anti-tumor effects with a TGI of -14.61%. In contrast, narazaciclib at 50 mg/kg and 100 mg/kg exerted significant anti-tumor effects with a TGI of 85.49% and 94.55%, respectively. Based on the mouse PK results, narazaciclib at 50 mg/kg in mouse is estimated to have an AUC of approximate 2000 h*ng/mL, which is equivalent to the dose of 160 - 200 mg/d in human patients. Therefore, 160 mg dose level is predicted to be an effective dose for narazaciclib in AML patients.
Conclusions: Narazaciclib at 160 mg/d is predicted to be an effective dose in AML patients.

#7162 Killing a fly with a sledgehammer: standard flat-dosing administration of Atezolizumab leads to marked overexposure in real-world lung cancer patients.

S. Marolleau[1], A. Mogenet[2], M. Hamimed[1], C. Boeri[1], L. Greillier[2], **J. Ciccolini**[1];
[1]Aix-Marseille University, Marseille, France, [2]Assistance Publique Hopitaux de Marseille, Marseille, France

Atezolizumab is an anti-PDL1 approved for treating small cell lung cancer and non-small cell lung cancers. A threshold of 6 µg/ml in plasma has been associated with target engagement with Atezolizumab. The extent to which patients could be overexposed with the standard 1200 mg Q3W flat-dosing remains unknown, but several *in silico* studies have suggested that flat-dosing with immune checkpoint inhibitors could lead to plasma concentrations far above the necessary levels to be efficacious. Here, we monitored Atezolizumab peak and trough levels in 27 real-world patients with lung cancer as part of routine therapeutic drug monitoring. Individual pharmacokinetic parameters were calculated using a population approach and optimal dosing-intervals were simulated with respect to the target trough levels of Atezolizumab. No patient displayed plasma levels below 6 µg/ml. The results showed that the mean trough level after the first course was 78.3 ± 17 µg/ml, i.e., 13 times above the target concentration associated with target engagement. The overall response rate was 55.5%. Low-grade IRAEs was observed in 37% of patients. No severe immune-related toxicities was observed. On univariate analysis, no relationship was found between exposure metrics of Atezolizumab (i.e., Cmin, Cmax, AUC at the first cycle or during the forthcoming courses) and pharmacodynamic endpoints (i.e., efficacy, toxicity). First-line Atezolizumab treatment and treatment for NSCLC were both significantly associated with efficacy on univariate analysis (p=0.0067 and p=0.0497, respectively), but further multivariate analysis did not confirm this relationship (p=0.2465 and p=0.9981). Smoking status was moderately associated with toxicities on univariate analysis (p=0.03), but this effect was not confirmed on further multivariate analysis (p=0.99). None of the other covariates (i.e., age, sex, NLR, number of metastatic sites, associated chemotherapy) were associated with efficacy or toxicity. Further simulations suggested that the dosing interval could be extended from the standard 21 days (i.e., Q3W) to 49 up to 136 days (mean: 85.7 days, i.e., Q12W dosing), while ensuring plasma levels always above the 6 µg/ml target threshold. This observational, real-world study confirms for the first time in real-world patients that the standard 1200 mg Q3W fixed-dose regimen of Atezolizumab results in significant overexposure in plasma. Of note, this overexposure was not associated with increased side-effects. As plasma levels always exceed pharmacologically active concentrations, the inter-individual variability we observed in PK parameters did not impact efficacy and could not explain differences in response. Our data suggest that dosing intervals could be markedly extended with respect to the target threshold associated with efficacy, thus lowering drug-cost in the future.

#7163 Pharmacokinetics assessment of intranasal NEO100 treatment on blood-brain barrier disruption and brain penetration of drugs in rodent brain.

A. Thaghalli Shivanna[1], T. Margaryan[1], M. Stavnichuk[1], W. Knight[1], S. Patel[1], E. Cabrales[1], A.-C. Tien[1], T. Chen[2], N. Sanai[1], A. Tovmasyan[1], S. Mehta[1];
[1]Barrow Neurological Institute, Phoenix, AZ, [2]University of South California, Los Angeles, CA

Background: Insufficient drug concentrations reaching the brain-localized tumor tissue remains one of the major challenges in the treatment of glioblastoma (GBM). An intranasal (IN) formulation of NEO100 (NeOnc Technologies, Inc., Los Angeles), a highly purified version of perillyl alcohol, has been recently reported to enhance drug concentrations in the brain upon IN co-delivery. Here, we report detailed pharmacokinetics (PK) and tissue analysis to quantitatively examine the extent of increase in drug concentrations in the brain after IN NEO100 administration. Furthermore, we also confirmed that IN NEO100 increases brain drug concentration by circumventing the blood brain barrier.
Method: For PK analysis, either IN or oral formulation of a three-drug cocktail (ZEI, consisting of ZN-c3, everolimus, and infigratinib) was used to evaluate the impact of 3% IN NEO100 on the brain penetration profile of the three individual drugs. Athymic mice were grouped into four cohorts to receive 1) oral ZEI; 2) IN ZEI; 3) oral ZEI with IN NEO100; and 4) IN ZEI with IN NEO100. At 2, 4 and 6 hours post ZEI dosing, drug levels in plasma and brain tissue were measured by liquid chromatography tandem mass spectrometry (LC-MS/MS). For BBB disruption study, athymic mice were treated with IN delivery of saline (negative control) or 3% NEO100 one hour post intravenous Evans blue (2%) administration. Tumor bearing mice with disrupted BBB served as positive control. Two hours post Evans blue administration, animals were perfused, and brains were collected and sectioned for confocal microscopy to image Evan's blue autofluorescence.
Results: PK analysis revealed that brain-to-plasma ratios (K_p) for ZN-c3, everolimus, and infigratinib remained nearly equal, independent of the route of administration, *i.e.* 0.11, 0.03, and 0.82 vs 0.09, 0.03, and 0.87, for IN vs oral routes, respectively. Administration of the ZEI together with IN NEO100, either through oral or IN routes, resulted in higher drug concentrations, both in the plasma and in the brain. However, while overall drug exposure was increased, K_p values of the drugs were not changed. Confocal imaging of brains from mice treated with 3% IN NEO100 did not show presence of Evans blue autofluorescence while positive control mice with disrupted BBB within the tumor core displayed high Evans blue fluorescence.
Conclusions: Co-administration of IN NEO100 with ZN-c3, everolimus, and infigratinib increases their brain and plasma exposure. As a result, no significant increase in brain-to-plasma partition was registered for any of the three drugs tested in this study. IN NEO100-mediated increase in brain drug concentration was independent of BBB disruption

#7164 Exposure-efficacy and exposure-safety relationships of tarlatamab to inform dose selection and benefit-risk assessment in patients with advanced small cell lung cancer (SCLC).

P.-W. Chen, M. Minocha, S. M. Kong, E. S. Anderson, A. Parkes, P. Martinez, B. E. Houk, C.-W. Lin;
Amgen R&D, Thousand Oaks, CA

Introduction: Tarlatamab is a first in class, half-life extended bispecific T-cell engager (BiTE) immunotherapy targeting delta-like ligand 3 (DLL3) that has shown promising anti-tumor activity and survival outcomes with manageable safety profile in clinical studies of patients with previously treated SCLC (NCT03319940, NCT05060016) (Ahn et al, 2023; Paz-Ares et al, 2023). Here we characterized the exposure-efficacy and exposure-safety profiles associated with tarlatamab treatment in SCLC, including the effects of patient-specific covariates (brain or liver metastasis, smoking status, number of prior lines of therapy, prior PD-1/PD-L1 inhibitor therapy, sum of target lesion diameters, and presence of anti-drug antibody).

Methods: The analysis dataset consisted of 412 subjects with SCLC from ongoing Phase 1 DeLLphi-300 study (dose range 0.003 mg to 100 mg Q2W and 200 mg Q3W) and Phase 2 DeLLphi-301 study (10 mg and 100 mg Q2W). Serum tarlatamab exposure averaged over the first cycle (28 days) was utilized as the predictor of response in the regression analysis. Efficacy endpoints included objective response rate, disease control rate, best tumor size response, progression-free survival and overall survival (OS). Safety endpoints included overall treatment related adverse event (TRAE), overall treatment emergent adverse event (TEAE), and TEAEs of cytokine release syndrome (CRS), immune effector cell-associated neurotoxicity syndrome (ICANS) and associated neurologic events, and neutropenia. Only the grade ≥ 3 adverse events (AEs) were evaluated.

Results: Significant exposure-response relationships were established for all key efficacy measures across the dose range investigated. Plateau in the exposure-efficacy relationship (maximal efficacy) was observed at the recommended dose of 10 mg Q2W. Exposures associated with lower doses were estimated to have lower efficacy. No clear trends for exposure-response relationships were identified for the evaluated AEs except for grade ≥ 3 neutropenia, where a shallow trend was observed for increased neutropenia rate with increasing tarlatamab exposures. Of all the evaluated covariate relationships, only higher baseline sum of target lesion diameters was statistically significantly correlated with worsening of OS.

Conclusions: Overall results in this SCLC population suggest tarlatamab exposures associated with the recommended dose of 10 mg Q2W exhibited near maximal efficacy and a favorable benefit-risk profile. None of the evaluated patient-specific covariates resulted in clinically meaningful changes in efficacy or safety, and therefore do not warrant a dose adjustment.

#7165 Clinical population pharmacokinetic (popPK) analysis of NBF-006, a novel siRNA inhibitor of glutathione-S-transferase P (GSTP) encapsulated in a lipid nano particle (LNP), for treatment of advanced non-small cell lung cancer (NSCLC).

M. P. Hall[1], Z. O'Brien[1], X. Chen[2], A. Hendrix[2], S. Brenes-Coto[2], S. Zabludoff[1];

[1]Nitto Biopharma, San Diego, CA, [2]Amador Bioscience, Pleasanton, CA

GSTP has an important role in detoxification and antioxidative damage response. Additionally, GSTP has a chaperone function that regulates multiple oncogenic pathways such as KRAS and JNK. Since alternative pathways could compensate for the inhibition of a single kinase, targeting multiple pathways could lead to more effective therapy.

NBF-006 is a drug product comprised of GSTP siRNA encapsulated within a novel LNP. It is designed to deliver siRNA to localized and metastatic lung tumors. Unlike other well-established drug modalities, there is a general need for increased understanding of the PK of RNA therapeutics. For NBF-006, we present popPK analysis of patients who have undergone treatment in a Phase I (a/b) clinical study. A primary goal of popPK modeling is to identify PK parameters and sources of variability in a population. Other goals include correlating drug exposures with administered doses through identification of predictive covariates in a target population and establishing whether fixed dosing as opposed to weight-based dosing can be utilized in future clinical studies. Ultimately this analysis will help to inform decision-making for dosing regimens in future clinical trial designs and to better predict PK variability across populations.

A total of 48 advanced NSCLC (N=38), pancreatic (N=5), or colorectal cancer (N=5) patients received 4 doses (QW) of NBF-006 by infusion at 0.15, 0.3, 0.6, 1.2 or 1.6 mg/kg followed by a 2-week rest period. In all studies, serial blood samples were collected at weeks 1 and 4. Plasma concentrations of siRNA were determined by hybridization ELISA. PopPK analysis was performed to characterize NBF-006 PK and to explore intrinsic and extrinsic covariate effects that could affect NBF-006 exposure.

The analysis included 695 quantifiable PK observations. A popPK model with two-compartment disposition and linear elimination adequately described the PK profile of NBF-006. Exploratory data analysis of dose-normalized PK profiles suggested that exposure increased proportionally with increasing dose from 0.15 to 1.6 mg/kg. Little to no apparent accumulation nor exposure reduction was observed between weeks 1 and 4. The impact of individual patient covariates, including body weight, baseline ALT, sex, KRAS mutation, cancer type and race, was assessed on PK parameters. None of the covariates evaluated had a significant effect on NBF-006 clearance or central distribution volume (Vc) in the model. Vc showed a slight positive trend with higher body weight, but was not statistically significant.

A popPK model was successfully developed for NBF-006. No covariates were identified that impact NBF-006 exposure. The lack of a relationship of exposure with body weight suggests the potential to use fixed dosing in future clinical studies.

#7166 Pharmacokinetic analysis of omomyc therapeutic protein in preclinical and human tumor tissue using targeted mass spectrometry.

M.-E. Beaulieu[1], S. Martinez-Martin[1], M. Mueller[2], Y. Feng[2], J. Vowinckel[2], **A. Lachaud**[2], L. Soucek[1];

[1]Peptomyc SL, Barcelona, Spain, [2]Biognosys AG, Schlieren, Switzerland

MYC is a pleiotropic transcription factor consisting in three paralogs which coordinate gene expression and regulates cell proliferation, cell differentiation, cell cycle, metabolism and apoptosis. The 3 paralogs (c-, N-, and L-MYC) have similar biological functions but show distinct tissular and timing expression patterns. To function, MYC must heterodimerize with its partner MAX and bind DNA via its basic, helix-loop-helix, leucine zipper domain (B-HLH-LZ). It has been estimated that MYC is aberrantly expressed in up to 70% of human cancers and hence MYC has been termed a “most wanted target for cancer treatment”. However, due to its nuclear localization, its intrinsic disorder and lack of an enzymatically active site, development of clinical grade potent & selective small molecules targeting MYC remains an obstacle. Omomyc is a 91-amino-acids-long polypeptide that derives from the B-HLH-LZ domain of human MYC, containing four amino acid substitutions. Omomyc is capable of forming homodimers and heterodimers with MYC and with MAX and such dimers blunt MYC activity by preventing its access to target DNA sequences (E-boxes) and replacing it by inactive complexes. Previous studies showed the cell-penetrating properties of recombinant Omomyc and its subsequent nuclear localization, where it displaces MYC from its genomic locations, causing a specific shutdown of MYC transcriptional signature and effectively stopping cell cycle progression. Further in vivo preclinical experiments showed that Omomyc blocks MYC-driven transcription and proliferation, induces apoptosis and recruitment of intratumoral immune infiltrates, overall significantly abrogating tumor progression and reducing tumor grading. A targeted LC-MS/MS assay for the absolute quantification of 4 Omomyc proteotypic peptides was developed to assess the structural integrity of Omomyc and quantify functional Omomyc in tumor tissue. LLOQ and linear range of the panel was determined by spiking in dilution series of recombinant Omomyc protein into preclinical tumor tissue lysates. Finally, in the context of Omomyc clinical trial (NCT04808362), we used the panel to for quantification of functional Omomyc in FFPE tumor biopsies from 18 patients who received i.v. injection of Omomyc therapeutic. Data show that 2 h after i.v. administration, higher concentrations of the drug are reached in the tumors compared with serum and persist there with at least one order of magnitude higher concentration than in serum 72 h after administration in preclinical models. Functional Omomyc protein could be quantified in all of the 18 clinical tumor biopsies from treated patients showing that characterized LC-MS/MS proteomic assay can be used in the normal routine of a clinical trial for accurate quantification of therapeutic miniproteins.

#7167 Impact of patient specific factors on exposures of tarlatamab, a half-life extended DLL3-directed bispecific T-cell engager in patients with advanced small cell lung cancer.

Stephanie M. Kong[1], Mukul Minocha[1], Po-Wei Chen[1], Pablo Martinez[2], Erik S. Anderson[2], Amanda Parkes[2], Brett E. Houk[1], Chih-Wei Lin[1]

[1]Clinical Pharmacology Modeling & Simulation, Amgen R&D, Thousand Oaks, CA,[2]Clinical Development Oncology, Amgen R&D, Thousand Oaks, CA

Background: Tarlatamab is a first in class, half-life extended delta-like ligand (DLL3) targeted bispecific T-cell engager (BiTE) immunotherapy that has shown antitumor activity with durable objective responses and promising survival outcomes in the ongoing studies in patients with previously treated small-cell lung cancer (NCT03319940, NCT05060016) (Ahn et al, 2023; Paz-Ares et al, 2023). Here we describe the effects of patient specific factors [age, sex, bodyweight, ethnicity, estimates of renal and hepatic function, prior lines of therapy, baseline disease status, emergence of anti-drug antibodies (ADA)] on tarlatamab exposures.

Methods: Tarlatamab serum concentrations were available from 420 subjects (8509 samples) pooled across the ongoing Phase 1 DeLLphi-300 study (dose range 0.003 mg to 100 mg Q2W and 200 mg Q3W) and Phase 2 DeLLphi-301 study (10 mg and 100 mg Q2W). The data were analyzed using a nonlinear-mixed effects modeling approach implemented in NONMEM (v7.5) software. Model selection and evaluation was guided by standard statistical and graphical approaches. Impact of key baseline demographic variables on tarlatamab clearance and volume of distribution were evaluated.

Results: Tarlatamab exposures increased in a dose-proportional manner and were not impacted by age, sex, ethnicity, estimates of renal and hepatic function, prior lines of therapy or baseline disease status. Asian race resulted in 14% higher peak serum concentrations relative to Caucasian subjects. Higher body weight (99 kg; 90th percentile) was associated with a 24% decrease in Day 28 pre-dose concentration (Ctrough) relative to median bodyweight (73 kg). Lower body weight (54 kg; 10th percentile) was associated with a 27% increase in Ctrough relative to median bodyweight. Positive ADA status resulted in a 24% decrease in Ctrough. However, at the recommended dose of 10 mg Q2W, neither body weight nor ADA status had a clinically relevant impact on tarlatamab efficacy or safety measures (Ahn et al, 2023).

Conclusion: Overall, based on these analyses, no dose adjustment for tarlatamab is required based on age, sex, bodyweight, ethnicity, estimates of renal and hepatic function, prior lines of therapy, baseline disease status or emergence of ADA.

#7168 PBI-410 (GQ1010), A novel Trop-2-targeted ADC demonstrates a favorable safety and toxicokinetic profile in multiple preclinical assessments.

Y. Sun[1], V. Reddy[2], P. Kulanthaivel[2], Y. Feng[1], J. Zhao[1], Z. Chi[1], J. Wang[1], L. Shi[1], G. Qin[1], P. H. Song[1];

[1]GeneQuantum Healthcare (Suzhou) Co., Ltd., Suzhou, China, [2]Pyramid Biosciences, Inc., Boston, MA

Introduction: Trop-2-targeting ADCs (Trop-2 ADC) have demonstrated notable clinical efficacy; however, safety concerns necessitate frequent dose adjustments or discontinuations. PBI-410 (GQ1010) is a next-generation TROP-2 ADC developed using GeneQuantum's Ligase-Dependent Conjugation (iLDC) technology, that integrates a highly stable linker and a novel camptothecin analogue payload, TopoIx. This study included comprehensive preclinical evaluations that demonstrated a favorable safety and TK profile and potential for broader therapeutic margin versus other Trop-2 ADCs approved or in development.

Methods: TopoIx underwent extensive Good Laboratory Practice toxicity assessments in Sprague-Dawley (SD) rats (payload alone) and as part of the intact ADC in Non-Human Primates. Rats were administered repeated intravenous infusions of 0.5, 1.25, and 2.5 mg/kg of H0011 once a week over 5 doses. The potential toxicity profile of PBI-410 was evaluated in cynomolgus monkeys via repeated intravenous infusions of 10, 30, and 60 mg/kg doses every 3 weeks for 3 doses, followed by a six-week recovery phase.

Results: TopoIx administration in SD rats exhibited good tolerance, with slight reductions in body weight gain and food consumption. Microscopic tissue changes resolved post-drug withdrawal, except for persistent findings in the sciatic nerve. Repeated doses of PBI-410 in cynomolgus monkeys were well-tolerated, primarily manifesting as skin pigmentation and associated microscopic alterations in specific tissues, such as eyes, esophagus, thymus, and lymph nodes typical for topoisomerase inhibitors. Importantly, these changes were reversible upon drug cessation. The HNSTD/NOAEL for PBI-410 was determined to be 60 mg/kg. This corresponds to mean C_{max} of 1760 µg/mL and AUC_{inf} of 235000 µg*hr/mL for ADC and for TopoIx mean C_{max} of 16.4 ng/mL and AUC_{inf} of 2610 ng*hr/mL. The lower exposure of TopoIx suggests minimum payload shedding in the systemic circulation. Notably, PBI-410 demonstrated a significantly enhanced safety profile compared to other Topo1-based Trop-2 ADCs, including an absence of hematopoietic and intestinal toxicities, and no pulmonary toxicity or interstitial lung disease (ILD) observed.

Conclusion: PBI-410 demonstrated a favorable and differentiated nonclinical safety profile and favorable TK relative to those reported to date for other Trop-2 ADCs in development. This profile, in addition to the potent anti-tumor response and synergistic activity in combination with anti-PD1 reported previously, position PBI-410 as a best-in-class potential Trop-2 ADC and partner of choice for anti-PD1 combination therapy. Additionally, TopoIx has displayed excellent properties among the TOP1 inhibitors, making it suitable for a broader therapeutic application based on exceptional potency while maintaining a favorable safety profile.

#7169 A real-world toxicity-atlas shows that adverse events of combination-therapies commonly result in additive interactions.

A. Kucukosmanoglu, S. Scoarta, **B. Westerman**;
VU University Medical Center, Amsterdam, Netherlands

Purpose: Combination-therapies are a promising approach for improving cancer treatment, but it is challenging to predict their resulting adverse events in an real-world setting.
Experimental Design: We provide here a proof-of-concept study using 15 million patient records from the US Food and Drug Administration (FDA) Adverse Event Reporting System (FAERS). Complex adverse-event frequencies of drugs or their combinations were visualized as heatmaps onto a 2D UMAP grid. Adverse event frequencies were shown as colors to assess the ratio between individual and combined drug effects. To capture these patterns, we trained a convolutional neural network (CNN) autoencoder using 7,300 single-drug heatmaps. Additionally, statistical synergy analyses were performed based on BLISS independence or Chi-square testing.
Results: The trained CNN model was able to decode patterns, showing that adverse events occur in global rather than isolated and unique patterns. Patterns were not likely to be attributed to disease symptoms given their relatively limited contribution to drug associated adverse events. Pattern recognition was validated using trial data from ClinicalTrials.gov and drug combination data. We examined the adverse-event interactions of 140 drug combinations known to be avoided in the clinic and found that near all of them showed additive rather than synergistic interactions, also when assessed statistically.
Conclusion: Our study provides a framework for analyzing adverse events and suggest that adverse drug interactions commonly result in additive effects with a high level of overlap of adverse event patterns. These real-world insights may advance the implementation of new combination therapies in clinical practice.

#7170 Pharmacokinetic profiling of Re-Phenformin *in vivo*: A novel approach in pancreatic cancer therapy.

A. Mohammad Gholizadeh[1], L. Dai[1], F. Dagher[1], C. Xiong[2], C. Li[2], D. S. Chow[1];
[1]University of Houston, Houston, TX, [2]University of Texas M.D Anderson Cancer Center, Houston, TX

Phenformin, a biguanide medication, has long been utilized in the treatment of diabetes. Recent research indicates that phenformin may also serve as an effective anticancer agent. This study introduces the synthesis and evaluation of Re tricarbonyl phenformin complex (Re-$(CO)_3$-Phenformin, Re-Phen), as a derivative of Phenformin and novel anticancer agent for pancreatic cancer treatment. Re-Phen was synthesized, purified, and characterized through preparative HPLC, NMR, mass spectrometry, and FT-IR. Subsequent *in vitro* studies, utilizing the MTS assay, assessed its cytotoxicity against pancreatic cancer cell lines, including Kras* murine PDAC and MiaPaca-2 human PDAC. Notably, Re-Phen exhibited significantly higher cytotoxic effects in MiaPaca-2 cells (IC50= 0.755 mM) and Kras* cells (IC50= 0.410 mM) compared to Phenformin treatment (IC50= 4.02 mM and 2.36 mM, respectively). These results highlight Re-Phen's enhanced anticancer activity, outperforming Phenformin in potency. Further investigation into the pharmacokinetics of Re-Phen involved an *in vivo* study with rats intravenously administered 2 mg/kg of Re-Phenformin. Blood samples were collected at intervals (10 min to 24 h post-dose) and were analyzed by validated LC-MS/MS. The pharmacokinetic profile of Re-Phen was best described by a 2-compartment model, using Phoenix® WinNonlin (version 8.0), with a particular focus on comparing the profiles of Phenformin and Re-Phen. The study revealed that Re-Phen has a significantly extended half-life compared to Phenformin (9.13 hr vs 2.11 hr), indicating prolonged systemic retention. Additionally, Re-Phen demonstrated an increased area under the curve (AUC), suggesting greater systemic exposure at equivalent dosing (90.55 hr*ng/ml vs 7.13 hr*ng/ml). This could imply enhanced bioavailability or altered metabolic clearance of Re-Phen compared to its parent compound. The two-Compartment of Re-Phe, provide a deeper understanding of its pharmacokinetic characteristics. In conclusion, Re-Phen not only demonstrates superior anticancer efficacy *in vitro* but also exhibits a more favorable pharmacokinetic profile *in vivo*. The extended half-life and increased AUC of Re-Phen suggest the potential of offering improved therapeutic efficacy in pancreatic cancer treatment. These promising findings warrant further investigation and could position Re-Phen as a promising therapeutic agent for the pharmacological management of pancreatic cancer.

#7171 Non-linear IV pharmacokinetics of the ATR inhibitor berzosertib (M6620) in mice.

Joshua J. Deppas[1], Brian F. Kiesel[1], Jianxia Guo[2], Robert A. Parise[2], Christopher J. Bakkenist[3], Jan H. Beumer[1]

[1]Pharmaceutical Sciences, University of Pittsburgh School of Pharmacy, Pittsburgh, PA,[2]Cancer Therapeutics Program, UPMC Hillman Cancer Center, Pittsburgh, PA,[3]Radiation Oncology, University of Pittsburgh School of Medicine, Pittsburgh, PA

Introduction: The ataxia-telangiectasia and Rad3-related (ATR) protein kinase is an attractive target for cancer therapies as it is an apical initiator of DNA damage response (DDR) pathways that facilitate cell cycle arrest and DNA repair, thus promoting survival of cancer cells. Several ATR inhibitors (ATRi) are in clinical development including berzosertib (M6620, VX-970), which is currently being evaluated in combination with cytotoxic chemotherapies and radiation. Although clinical studies have examined plasma pharmacokinetics (PK) in humans, little is known regarding dose/exposure relationships and tissue distribution which may influence berzosertib's therapeutic window. To understand these concepts, we extensively described the PK of berzosertib in mouse plasma and tissue.

Methods: Dose proportionality was assessed using single IV doses of berzosertib (2, 6, 20 and 60 mg/kg) administered to female BALB/c mice. Mice were euthanized from 5 min to 24 h post-dose. Using a highly sensitive LC-MS/MS method, berzosertib was quantitated in red blood cells, plasma, and tissues. Non-compartmental analysis (NCA) was performed using Phoenix WinNonlin to determine relevant PK parameters. Dose linearity was assessed by statistical comparison of dose-normalized plasma C_{max} and dose-normalized tissue AUC across the four dose levels. Statistical analyses were performed using ANOVA with Tukey's multiple comparisons test. Berzosertib plasma protein binding was assessed *in vitro* from 300 ng/mL to 100 µg/mL using rapid equilibrium dialysis. An extensive PK study was also conducted in tumor-bearing mice to assess distribution by quantitating drug in tissues.

Results: The dose proportionality study indicated that both plasma C_{max} and AUC increase with dose, and dose-normalized concentration vs time profiles suggested nonlinear increases in exposure based on different terminal slopes. At the two highest doses, dose-normalized AUC in each tissue were greater than the exposure generated at the two lowest doses. However, log transformations of $AUC_{0\text{-}360}$ plotted vs dose generated a slope of 0.886 (95% CI: 0.718 - 1.054), suggesting a linear relationship. The fraction of unbound berzosertib in mouse plasma increased at concentrations above 10 µg/mL, which is a concentration exceeded at the two highest doses and where nonlinearity in exposure is observed. Tissue analysis revealed the following tissues had a tissue/plasma coefficient >1: bone marrow, kidney, liver, spleen, lung, tumor, lymph nodes, thymus, and heart.

Conclusion: IV berzosertib displayed nonlinear PK in mice. Increased doses of berzosertib were associated with greater than proportional increases in plasma and tissue exposure most likely due to saturation of plasma protein binding. Our results will help to understand preclinical pharmacodynamic and toxicity data and subsequent PBPK modeling to inform optimal dosing and clinical deployment of berzosertib.

#7172 Pharmacokinetic/biomarker (PK/BMx) analysis of the toll-like receptor 7 and 8 (TLR7/8) agonist EIK1001 in phase 1 studies in participants (Pts) with solid tumors.

D. Rasco[1], M. Patel[2], M. Johnson[3], A. Tolcher[4], D. Sommerhalder[4], O. Hamid[5], A. Alistar[6], J. Kochan[7], E. Kurland[7], M. Wang[7], **C. Cho**[7], S. Rebello[7]; [1]South Texas Accelerated Research Therapeutics (START), San Antonio, TX, [2]Florida Cancer Specialists & Research Institute, Sarasota, FL, [3]Sarah Cannon Research Institute (SCRI), Nashville, TN, [4]NEXT Oncology, San Antonio, TX, [5]The Angeles Clinic & Research Institute, Los Angeles, CA, [6]Atlantic Health System, Morristown, NJ, [7]Eikon Therapeutics, Hayward, CA

Introduction: Immune checkpoint inhibitors (ICIs) relieve immunosuppression of tumor-reactive T cells and enhance antitumor immune response; however, not all patients benefit and some become refractory. EIK1001 is a TLR7/8 agonist that stimulates myeloid and plasmacytoid dendritic cells, activating immune and inflammatory responses. This dual activity provides another pathway, distinct from effects on checkpoint proteins, to enhance antitumor T-cell activity alone or in combination with ICIs.

Methods: Adults with advanced solid tumors received a range of doses of EIK1001 (QW IV) alone and in combination with pembrolizumab (200 mg Q3W; NCT03486301) or atezolizumab (1200 mg Q3W; NCT04196530) in Phase 1 studies (n=128). PK samples were collected on Cycle 1 Day 1 (C1D1) and C1D8 predose and at 0.5, 1, 2, 4, 6, 8, 12, and 24 hrs postdose, with sparse sampling thereafter. Matched cytokine BMx samples were collected.

The PK analysis population comprised pts with at least one measurable EIK1001 concentration (1563 observations from 94 pts). PK data were analyzed using non-linear mixed effects in Phoenix (v8.3). Covariate effects of the combination drugs were tested using a stepwise approach with a significance level of 0.05 for forward addition. All other covariates were evaluated using exploratory plots and formally tested using a full matrix approach. Empirical Bayes estimates were used to generate individual steady-state concentration-time profiles and calculate post-hoc PK parameters. Exploratory analyses of exposure-safety and exposure-efficacy were conducted.

Results: EIK1001 PK was linear and dose-proportional over the doses studied. Tmax ranged from 4-12 hrs with no accumulation. Pop-PK analysis indicated that body size influenced clearance, but intrinsic factors of age, gender, tumor type, ECOG status, or hepatic/renal impairment (mild/moderate) did not. Combination drugs did not influence clearance. These attributes support BSA-based dosing and inform inclusion/exclusion criteria for future studies.

On C1D1, time-dependent increases in IL-6, IL-8, IFNγ, and IP-10 returned to baseline within 24 hrs. An earlier IL-8 increase (Tmax 3-5 hr) is consistent with TLR8 activation on various cells including neutrophils, whereas the delayed increase of IFNγ/IP-10 (Tmax 5-8 hr) suggests a downstream effect. Dose-dependent increases in cytokines were observed, with median peak changes from baseline of 1.13- to 7.97-fold for IFNγ and 0.63- to 12.1-fold for IP-10. The 2 highest doses provided evidence of robust target engagement alone or in combination.

Conclusion: The linear, dose-proportional PK of EIK1001 is well described by the Pop-PK model. Increases in IFNγ and IP-10 were consistent with the anticipated mechanism of action, with doses representing target engagement identified. Further development of EIK1001 is underway.

#7173 Animal pharmacokinetics of an anti-Her2+ immunoliposome of docetaxel.

M. Dacos, E. Diroff, S. Giacometti, J. Ciccolini, **R. Fanciullino**;
Aix-Marseille University, Marseille, France

Despite the success of docetaxel in combination with trastuzumab in HER2+ breast cancer, docetaxel still has serious limitations, including poor water solubility and the canonical systemic toxicity of taxanes. These side effects of taxanes need to be overcome to improve patient management. In this context, we have developed a nanoparticle drug delivery system. We have developed an immunoliposome loaded with docetaxel and grafted with trastuzumab using a microfluidic method by mixing an aqueous phase (KH2PO4 buffer) and an organic phase composed of phosphatidylcholine, cholesterol and PEGmal in a molar ratio of 50:31:1, to which docetaxel is added at a rate of 1.8% of the total lipid. We perform a thiolation reaction to graft the trastuzumab onto the polyethylene glycol chain. Resulting immunoliposomes were characterized by a mean diameter of 140 nm, a docetaxel encapsulation rate of 73% and a trastuzumab uptake rate of 400 units of trastuzumab by nanoparticle. C57BL/6 mice were administered with docetaxel 1.9 mg/kg and trastuzumab 160 ng/kg or a mixture of free drugs or as liposomes at the same dose by intraperitoneal injection. Blood was collected 1h, 2h, 3h, 6h, 8h and 24h after injection and plasma was analyzed by HPLC-UV with Paclitaxel as internal standard. For each treatment group, pharmacokinetic parameters and exposure metrics were calculated using PKanalix®: half-life T1/2, elimination rate constant Kel and area under the curve AUC at the end points (AUCtlast) and infinity (AUCinfinity). Statistical tests were performed with Sigmastats®. The results showed a marked change in pharmacokinetics with increased plasma exposure with liposomal docetaxel. Preliminary results show a longer half-life for liposomal docetaxel (40.76 h VS. 4.33 h, i.e., a 9.4-fold increase). The concentration of docetaxel appeared to decrease more rapidly between T1h and T6h with free docetaxel (Kel 0.16h-1) than with liposomal docetaxel (Kel 0.017h-1). The concentration of docetaxel reached a plateau over time, up to 24 hours (52.72± 9.45 ng/ml) in mice treated with immunoliposomes whereas Docetaxel was undetectable at T24h when treated with free drugs. There was a statistical difference in PK at T6h between liposomal docetaxel and free docetaxel, 69.86 ± 15.25 ng/ml and 53.67 ± 4.92 ng/ml, respectively ($p < 0.001$, non-paired t-test). Liposomal docetaxel showed higher AUC0-t (x3.75) and AUC0-∞ values (x5.9) compared to non-liposomal docetaxel. In conclusion, these preliminary results suggest that we have developed a promising immunoliposome for the systemic delivery of docetaxel in HER2+ breast cancer with sustained exposure.

#7174 Pharmacokinetics and immunogenicity of anti-PD-1 antibody in humanized FcRn mouse models compared to immunocompetent mouse models.

X. Tu[1], X. Feng[1], W. Wang[1], X. Ding[1], D. Huang[1], L. Bourre[2], X. Chen[1];
[1]Crown Bioscience, Inc., Taicang, China, [2]Crown Bioscience, Inc., San Diego, CA

Introduction: The development and use of therapeutic antibodies in cancer therapy has increased significantly in recent years, led by the success of approved immune checkpoint blockade antibodies targeting PD-1 and PD-L1 axis. However, obtaining more clinically relevant pharmacokinetics (PK), safety and efficacy data for antibodies is still challenging in preclinical phase. Humanized FcRn (hFcRn) transgenic mouse model has a more faithful catabolism compared to WT mice, providing more accurate and predictable PK data of innovative antibody-based therapeutics at discovery stage[1]. In this study, we sought to investigate pharmacokinetics and immunogenicity characteristics of anti-PD-1 antibody in hFcRn transgenic mice and provide guidance for its differentiation of prediction value for drug PK and safety by comparing to WT mice.

Methods: Non-tumor bearing hFcRn mice and wild type C57BL/6 mice were divided into 2 groups, 5 mice were enrolled into each group. Mice were administered anti-PD-1(Nivolumab) at 10 mg/kg single dose after grouping by intravenous (IV) injection. Blood samples at 12 timepoints (15min, 6h, 1, 2, 4, 7, 10, 14, 21, 28, 35, 42 days) post-dosing were collected for PK and Anti-Drug Antibody (ADA) analysis by MSD and ELISA.

Results: Nivolumab clearance in hFcRn mice followed a typical linear profile with rapid distribution phase and slow elimination phase ($t_{1/2}$ = 350 to 400 h). While the PK profile in C57BL/6 mice displayed non-linear clearance and very short elimination phase ($t_{1/2}$ = 45 to 50 h). This data demonstrated that hFcRn mice have better correlated half-life with human (Nivolumab single dose by IV with 10mg/kg, $t_{1/2}$ = 595 h)[2].

ADA analysis revealed that it was produced starting from Day 10 in wild type C57BL/6 mice and the frequency of ADA induced by Nivolumab in wild type mice (2/5) was higher than hFcRn mice (0/5). The variation of Nivolumab level was correlated with ADA production in wild type mice. This suggested hFcRn shows lower immunogenicity than wild type mice for human IgG drug and can potentially improve negative effect of ADA interference on PK evaluation.

Conclusion: The result of this study demonstrated that the PK data in hFcRn mouse model was more predictive of human PK profile compared to wild type C57BL/6 mice. This advances innovation in antibody-based therapeutics and translational applications, with improved PK, safety and efficacy evaluation for preclinical human IgG drug development in cancer therapy.

References: 1. Enhanced half-life of genetically engineered human IgG1 antibodies in a humanized FcRn mouse model: potential application in humorally mediated autoimmune disease. Int Immunol. 18(12):1759-69. 2. Centre for drug evaluation and research. Clinical pharmacology and biopharmaceutics reviews of pembrolizumab: application number:125514Orig1s000. Accessed 04 April 2016.

#7175 Web-based cross-database exploration of molecular pharmacology data from cancer cell lines and patient genomics.

W. C. Reinhold[1], A. Luna[1], F. Elloumi[1], S. Varma[1], D. Taniyama[1], M. Mizunuma[1], J. del Rivero[1], A. Thomas[1], K. Reilly[1], K. Pacak[2], M. Aladjem[1], Y. Pommier[1]; [1]National Cancer Institute, Rockville, MD, [2]National Institute of Child Health and Human Development, Rockville, MD

CellMiner Cross-Database (CellMinerCDB, discover.nci.nih.gov/cellminercdb) allows integration and analysis of molecular and pharmacological data within and across cancer cell line datasets from the National Cancer Institute (NCI), Broad Institute, Sanger/MGH, MD Anderson Cancer Center (MDACC), and the National Center for Advancing Translational Sciences (NCATS, discover.nci.nih.gov/rsconnect/cellminercdb_ncats/). Altogether, our database spans over 1,700 distinct cell lines, over 1,000 clinically relevant drugs, ~25,000 experimental compounds, and molecular profiling data, such as gene/protein expression, molecular signatures including epithelial mesenchymal transition (EMT), replication stress (RepStress), neuroendocrine evaluation (NE), DNA copy, methylation, mutational status, and gene dependencies (Broad DepMap). This rich and growing set of cell lines and tested drugs allows for novel avenues for response determinant discovery and clinical translation that is facilitated by 1) common annotations (e.g., tissues of origin and matched drug names) across pharmacogenomic datasets and 2) various univariate and multivariate analyses tools. A major challenge to clinical translation occurs in relating pre-clinical models to patient samples. As part of this work, we show how the CellMinerCDB infrastructure additionally supports annotated patient multi-omics data to aid researchers to relate findings from cancer cell lines with patient data; we use data from small cell lung cancer (SCLC) and neuroendocrine tumors as illustrative examples. This work provides significant pharmacogenomic integration that allows exploration within a comprehensive dataset of cancer cell lines and to inter-relationships with patient-derived datasets; this is being developed to display and mine patient samples as part of the complementary web-based tool (PatientTumorMiner).

#7176 Optimization of T cell co-stimulatory agonists: A semi-mechanistic PKPD model integrating drug properties and tumor-immune interactions.

J. Gan, W. Hedrich, Y.-Y. Lu, W. Xu, R. H. I. Andtbacka, F. Adrian, L. Schweizer;
HiFiBiO Therapeutics, Cambridge, MA

Background: Despite the success of some immune checkpoint inhibitors in the treatment of cancer, T-cell co-stimulation has faced limited clinical success due to the intricacies around the optimal engagement of agonistic antibodies to co-stimulatory receptors, and the absence of biomarkers for patient selection. Understanding agonist-binding characteristics, pharmacokinetics, T cell subpopulation activation and differentiation kinetics, T cell life span in the tumor microenvironment, and the impact of T cell/tumor interactions on tumor growth kinetics is crucial for the positive clinical outcomes of T cell agonists. Currently there is not a suitable model to describe these complex interactions.

Methods: We investigated the pharmacokinetic (PK), pharmacodynamics (PD), and anti-tumor efficacy of an anti-TNFR2 agonist, HFB3-1, and an anti-OX40 agonist, HFB10-1, in syngeneic tumor models. Flow cytometry was employed to profile post-treatment tumor infiltrating lymphocytes (TILs) in dissociated tumor tissues. In vitro binding affinity was determined using Biolayer Interferometry. A semi-mechanistic model, integrating PK, tumor growth, and immune interaction networks (interactions among Teff, Treg, and tumor cells), was developed in Berkeley Madonna (version 10.5.1). This was subsequently adapted to a human tumor growth model with T cell interaction networks to assess the impact of doses and dosing regimens on tumor growth inhibition.

Results: A semi-mechanistic PKPD model was successfully developed incorporating drug properties including binding affinity, agonistic effect, ADCC activity, and pharmacokinetics, and tumor growth characteristics including tumor growth kinetics, TIL composition, interaction, proliferation, and turnover. This model was applied to investigate the effect of FcγR, dose, and dosing frequency on *in vivo* efficacy. Following incorporation of human PK and human tumor microenvironment properties into the model, tumor growth characteristics were simulated under varying human dosing regimens. Simulation results indicated that lower and less frequent doses optimize T cell co-stimulation for optimal anti-tumor activity.

Conclusion: Our semi-mechanistic PKPD model elucidates the intricate interactions between T cell co-stimulatory agonists and the tumor-immune cells in the tumor microenvironment. The model advocates for pulsatile agonism as the optimal anti-tumor activity for T cell co-stimulation agents. This model serves as a valuable tool for guiding dose and dose regimen optimization for T cell co-stimulatory agonists in clinical development.

#7177 Development and validation of clinical pharmacodynamic biomarkers to assess treatment response to HPK1 inhibition and guide dosing decisions.

L. Jia[1], Y. Marikar-Coplin[1], J. Chen[1], K. Xu[2], D. A. Mele[2], N. Luheshi[3], S. Iyer[2], A. I. Rosenbaum[1], S. Terrillon[1];
[1]AstraZeneca, South San Francisco, CA, [2]AstraZeneca, Waltham, MA, [3]AstraZeneca, Cambridge, United Kingdom

Checkpoint inhibitors represent promising cancer therapeutics as they have the potential to reignite T cell activity and reverse T cell exhaustion, which is a critical mechanism of immune evasion by tumors. Hematopoietic progenitor kinase 1 (HPK1) is a negative regulator of T-cell signaling that has recently emerged as a novel target for cancer immunotherapy. Inhibition of HPK1 can restore T cell function and anti-tumor immune responses, and several HPK1 inhibitors are currently under pre-clinical development, or clinical evaluation. Identifying clinically useful pharmacodynamic (PD) biomarkers in response to HPK1 inhibition is critical to characterize exposure-response relationship in early-phase trials and inform dose selection for later-phase studies. However, development and implementation of clinical PD assays are challenging because high sensitivity and specificity are required. Here, we developed a multi-biomarker strategy that combines a proximal biomarker (SLP-76 (Ser376) phosphorylation, a specific substrate of HPK1) and distal biomarkers (cytokine production) to evaluate target engagement (TE) and establish proof of mechanism (POM) of HPK1 inhibitors to determine their comprehensive PD profile. These PD biomarker assays were developed using peripheral blood as a surrogate tissue to assess HPK1 inhibition-induced pSLP-76 level decrease and cytokine levels increase, thus reflecting drug inhibitory effects and T-cell activity recovery. However, the lack of basal levels of these biomarkers presented a challenge for clinical workflow, as ex-vivo T-cell receptor stimulation of the clinical specimen is required after collection. Phosphoflow cytometry was prioritized over several technology platforms evaluated for quantifying blood pSLP-76 levels because of superior assay performance and signal stability under the developed clinical workflow. Blood cytokines upregulated upon HPK1 inhibition were first identified using targeted proteomics. IFNγ, IL2, TNFα, and IL17A were next confirmed and validated using quantitative immunoassays. Both pSLP-76 and whole blood cytokine workflows were thoroughly optimized for every step of sample handling from specimen processing at clinical sites to sample analysis at testing lab to ensure standardized, precise, and robust assay performance for clinical application. In addition, consistent HPK1 inhibition potency values were achieved using blood from cancer patients, demonstrating that the established PD biomarker assays apply to the clinical target population. In conclusion, robust peripheral TE and POM biomarkers were successfully developed to support future phase I/II studies with HPK1 inhibitors. These are expected to enable characterization of the exposure-response relationships and help define the therapeutic window and optimal dose.

#7178 Neuronal cells derived from iPSCs cell to evaluate neurotoxicity after 48 or 72 hours in high-through put screening format.

F. Sabatier[1], J. Chaigne[1], M. Martin[1], R. Barbeau[1], L. Houssin[1], S. Bonnin[1], A. King[2], **V. Jahnke**[1];
[1]Eurofins Cerep, Celle-Levescault, France, [2]Eurofins Panlabs, St-Charles, MO

Neurotoxicity is a major concern in central nervous system drug discovery and a frequent cause of attrition in clinical trials or approved drug withdrawal. Neuropathy is a side effect defined by the injury of peripheral nerves causing a loss of sensation/motion. Drug development pipelines typically involve testing in cell lines followed by animal investigations with translation to humans. The induced pluripotent stem cells (iPSCs) have widened new model systems to study adverse toxicities. With evolution in regulatory guidance the use of human- iPSC-derived tissue provides high-throughput access and a more relevant testing environment. Neuropathy is one of the most chemotherapy adverse effects. In this study we have screened 8 compounds. Bortezomib (proteasome inhibitor), gemcitabine (approved ovarian cancer treatment), ivermectin (parasitic diseases treatment), flavopiridol (approved CDKs inhibitors), SNS-032 (approved CDKs inhibitor), mefloquine (anti-malaria drug), digitonin (nonionic detergent) and tamoxifen (hormone receptor-positive breast cancer treatment). These molecule toxicities were tested on neuronal-derived iPSCs Dopaneurone, GABAneurone, Glutaneurone, Motorneurone, Microglya and Astrocytes in high throughput screening. For the project, cells were plated in 384 well/plates. DMSO tolerance was performed (up to 10%). Drugs were added, then, after 48h or 72h, total protease and protease activities were measured using CytoTox-Glo™. Compounds were tested at 7 concentrations (from 10^{-4} to 10^{-9}M).In this study we have validated cell culture and the assay conditions. The signal window range was good after 48h and 72h of treatment. No toxicity was found until 10% DMSO. A specific neurotoxicity signature was measurable for each drug tested. Digitonin, our positive control, induced toxicity in all IPSCs after 48h and 72h of incubation. On the contrary, Tamoxifen, our negative control, did not induce any neurotoxicity. The other molecules generated a signature of severe to mild neurotoxicity. These results are in agreement with their known adverse side-effects. In conclusion, this panel is a good tool to anticipate possible neurotoxicity within the 3Rs respect. It can be used in early drug de-risking or neuroprotection screening, with the aim of preventing/reducing/curing neuropathy in at-risk populations.

#7179 OBI-992, a novel TROP2 targeting antibody drug conjugate demonstrates superior in vivo PK/PD properties and a favorable safety profile.

C.-S. Shia, S.-N. Wen, R.-Y. Hsu, J.-S. Tu, H.-W. Chang, W.-F. Li, M.-T. Lai;
OBI Pharma, Inc., Taipei City, Taiwan

Background: TROP2 targeting antibody-drug conjugates (ADC) have demonstrated promising clinical responses for the treatment of various solid tumors. However, these ADCs still exhibit serious safety issues, such as hematologic toxicities and interstitial lung disease. OBI-992, a novel TROP2 targeting ADC, which is derived from the conjugation of an anti-TROP2 antibody with a topoisomerase I inhibitor, exatecan, via an enzyme-cleavable linker. OBI-992 is designed to have high serum stability and broad therapeutic index. Herein, we describe the results from preclinical studies of OBI-992, including in vitro and in vivo stability, pharmacokinetics/pharmacodynamics (PK/PD) profile, and safety evaluation.

Material and Methods: To characterize OBI-992, the linker stability was evaluated by ex vivo serum stability and rat PK studies. PK/PD properties, including systemic and tumor exposures as well as receptor occupancy, were evaluated in a human lung cancer xenograft model. In vitro toxicity testing, including ADC toxicity on differentiating neutrophils and FcγR mediated toxicity, was evaluated using human monocyte THP-1 cells. A 6-week repeat dose toxicity study in cynomolgus monkeys was conducted to evaluate the safety and toxicokinetics of OBI-992.

Results: Ex vivo serum stability demonstrated that OBI-992 exhibited better linker stability than the benchmark datopotamab deruxtecan (Dato-DXd). In vivo PK evaluation in rats showed that OBI-992 had lower C_{max} and AUC of free payload than Dato-DXd, indicating a better PK profile of OBI-992 in rats. A PK/PD study in tumor-bearing mice revealed that OBI-992 exhibited higher tumor exposure of free payload than Dato-DXd, resulting in a better antitumor efficacy. In addition, the antitumor effect positively correlated with percentage of receptor occupancy in a dose-dependent manner. In vitro cytotoxicity testing demonstrated that OBI-992 had lower toxicity in differentiating neutrophils and THP-1 cells compared to Dato-DXd, suggesting that OBI-992 may cause less off-target toxicity. Toxicokinetics of OBI-992 in cynomolgus monkeys revealed that the systemic exposure of ADC was similar to that of total antibody. Furthermore, the systemic exposure of ADC and total antibody were found to increase in a dose-proportional manner. Major toxicities in monkeys were target-related skin lesions. The highest non-severely toxic dose (HNSTD) was determined to be 60 mg/kg.

Conclusions: OBI-992 exhibits remarkable antitumor efficacy and a favorable safety profile, supporting further clinical development of OBI-992 in TROP2 positive cancers.

#7180 Tumor growth modeling to support dose justification of Dato-DXd in hormone receptor positive, HER2 negative breast cancer (HR+HER2-BC) subjects.

Z. Tang[1], Y. Jiang[1], H. Yang[1], D. Dai[1], C. Gong[2], L. Irons[2], Y. Pan[3], Y. Hong[3], S. Liang[3], S. Ren[1], A. Phipps[4], D. Zhou[2];
[1]Astrazenea, Gaithersburg, MD, [2]Astrazenea, Waltham, MA, [3]Daiichi Sankyo Inc, Basking Ridge, NJ, [4]Astrazenea, Cambridge, United Kingdom

BACKGROUND: Dato-DXd, a TROP2-directed antibody-drug conjugate, has demonstrated efficacy and a manageable safety profile in multiple tumor types. A dosing regimen of 6 mg/kg every three weeks (Q3W) has been proposed as the optimal schedule based on phase I data in patients with non-small cell lung cancer (NSCLC)[1]. Dato-DXd demonstrated statistically significant and clinically meaningful improvement in PFS compared with ICC in patients with HR+HER2-BC in TROPION-Breast01[2]. A tumor growth inhibition (TGI) model was developed to support dose justification at 6 mg/kg in HR+HER2-BC subjects.
METHODS: A tumor growth inhibition (TGI) model was developed based on tumor size data from HR+HER2-BC patients received 6 mg/kg Dato-DXd Q3W in a Phase I study (N = 39, Data cutoff July 2022). The TGI model described the tumor size as the result of an exponential tumor growth, a tumor shrinkage that was driven by Dato-DXd cycle-specific AUC, and a resistance term suggesting that the shrinkage effect by Dato-DXd decreases over time. Cycle-specific Dato-DXd AUC was derived based on the AUC and time at each cycle for each individual. Simulations were conducted using the TGI model to compare tumor size change from baseline at 4, 6, and 8 mg/kg in HR+HER2-BC patients, with consideration of dropouts.
RESULTS: The TGI model well-described tumor size data with reasonable parameter estimations. Simulated time-courses of tumor sizes at Dato-DXd 4, 6, and 8 mg/kg suggested that Dato-DXd at 6 mg/kg may lead to greater tumor shrinkage effect than that at 4 mg/kg in HR+/HER2-BC patients. At approximately 180 days post first treatment, tumor shrinkage at 6 mg/kg was almost 2-times greater than at 4 mg/kg (-51% vs. -25%, respectively).
CONCLUSION: Simulations based on the TGI model suggested greater tumor size reduction at Dato-DXd 6 mg/kg compared to 4 mg/kg in HR+HER2-BC patient population.

Reference :[1] ACoP13 2022 [2] ESMO 2023.

#7181 Low dose interleukin-6 (SON-080) for neuropathies: Toxicology and clinical plans.

S. Dexter[1], G. Hedou[2], R. T. Kenney[3], D. J. Rezac[4], P. Mohan[1];

[1]Sonnet BioTherapeutics, Princeton, NJ, [2]Sonnet BioTherapeutics, CH SA, Geneva, Switzerland, [3]Sonnet BioTherapeutics, Potomac, MD, [4]Latham Biopharm Group, Elkridge, MD

Neuropathies are conditions in which peripheral nerves degenerate, resulting in sensory and motor symptoms that can profoundly affect the patients' quality of life. Chemotherapy-induced peripheral neuropathy (CIPN) is induced by most antineoplastic agents, affecting cancer patients during or following completion of treatment. Neuropathy-specific pain medication is most often inefficient against pain, can cause major side effects that limit their use, do not address non-pain related symptoms, and do not stop CIPN progression. Most evidence suggests that physical exercise is the most efficient approach to reduce neuropathy symptoms and potentially, progression. Other publications have causally linked exercise, through the ability of contracting muscles to release low levels of interleukin-6 into the bloodstream thereby activating several metabolic and physiological pathways that help regenerate muscle and nerve tissue, affect glucose homeostasis, increase lipolysis, improve microvascular blood flow and reduce inflammation. Preclinical disease models of CIPN and diabetic peripheral neuropathy (DPN) have confirmed that IL-6 administered at low doses is capable of stimulating peripheral nerve growth, thereby ameliorating motor and sensory functions and normalizing the associated pain or sensation disturbance of neuropathy. The maximum tolerated (MTD) dose of recombinant human IL-6 (rhIL-6) has been established as a treatment for thrombocytopenia in hundreds of cancer patients using the drug product that was produced in the 1990's (Process A) dosed intravenously (IV) or subcutaneously (SC). We have developed a cGMP compliant version of rhIL-6 (SON-080) using a state-of-the-art process (Process B) that meets current regulatory guidelines for cell lines and processes. An analytical comparison of SON-080 with Process A rhIL-6 concluded that both drugs are highly comparable for at least 14 different key physicochemical characteristics. Therefore, we expect similar *in vivo* behavior with Process B material as compared with the Process A molecule. In order to support clinical plans for the safety and toxicity of rhIL-6, a dose range and schedule of administration that matches the current clinical protocol was performed in a cynomolgus monkey primate toxicology model. Under these conditions, SON-080 was found safe and well tolerated with a No Adverse Effect Levels (NOAEL) of 30µg/kg, the highest dose tested. On this basis, a fully controlled Phase 1b/2a clinical study, SB211, is ongoing to evaluate safety, tolerability, and efficacy of subcutaneous SON-080 dosage and administration schedule that targets an exposure mirroring the endogenous release levels elicited by moderate to heavy exercise. Confirmation of safety in the first portion of the trial will pave the way for efficacy evaluation with the objective to provide CIPN patients with a novel, safe, and effective treatment for painful neuropathies.

#7182 Blood brain barrier masks effects of dosing strategy.

M. Stoddard[1], A. Chen[2], **L. Yuan**[3], D. Van Egeren[4], A. Chakravarty[1];
[1]Fractal Therapeutics, Lexington, MA, [2]Columbia University, New York, NY, [3]Fractal Therapeutics, Inc., Lexington, MA, [4]Stanford University, Palo Alto, CA

The penetration of the blood brain barrier (BBB) presents a significant challenge in the design of drugs targeting brain tumors. The BBB desynchronizes drug concentrations between the body and brain, complicating the relationships between drug dose, effective concentration, and toxicity. In this work, we sought to understand the nature of these relationships in the context of dose schedule, in order to suggest minimally toxic and maximally effective strategies. We developed a two-compartment pharmacokinetic model to simulate the exchange of a drug between the body and the brain. Drug exchange was based on passive diffusion through the barrier and active transport into the brain as described by Michaelis-Menten kinetics. In the model, tumor cells exhibit binary resistance to the drug under a logistic growth model. The drug reduces the growth rate of the sensitive population while the resistant population suffers a small growth penalty because of the mutation conferring resistance. Strategy effectiveness was quantified in terms of survival time, the time until 95% of carrying capacity was reached, and toxicity was evaluated as the peak moving average over 18 days. Although the BBB complicates prediction of drug action, it simplifies drug impact by masking schedule effects. Our work suggests that drug concentrations in the brain increase with initial treatment until equilibrium between active transport, diffusion, and drug metabolism is reached. Fluctuations in drug concentration resulting from breaks between bolus dosing are greatly reduced in the brain relative to the body, and high frequency (daily) dosing results in a nearly constant equilibrium drug concentration. The rate at which equilibrium is reached and the drug concentration in the brain are unaffected by dosing period, as long as the average dose per day is constant. Our model suggests that the impact of dosing cycle length on survival time is negligible. Neutropenia is minimized by schedules with dosing cycle lengths that factor evenly into the 18-day neutrophil recovery period. These schedules have consistent toxicity throughout. Strategies with two, three, six, nine, and eighteen day cycles induce neutropenia least. As fluctuations in drug concentration are small at the equilibrium steady-state, effects of scheduling on drug interactions are predicted to be minimal. As drug concentration in the brain at equilibrium and latency to equilibrium are independent of dosing period, these parameters must be modulated through changes in the amount of drug dosed. The use of a loading dose may compensate for latency. Although this analysis is based on hypothetical drugs, it provides practical insights that are applicable across a wide range of systemically dosed small-molecule therapeutics. Further, the modeling framework derived here can be readily extended to guide the design of dosing schedules for real-world therapeutic interventions.

#7183 Liver toxicity of amanitin-based antibody drug conjugates (ATACs) is caused by unspecific uptake of the ATAC into liver cells.

C. Orlik, K. Decker, M. Vranic, M. Schmitt, A. Pahl, M. Kulke, T. Hechler;
Heidelberg Pharma Research GmbH, Ladenburg, Germany

Background: Antibody drug conjugates (ADCs) were developed to increase the therapeutic window (TW) of cytotoxins by combining their efficacy with the precision of antibodies (Ab). Nevertheless, adverse events, still limit the use of ADCs. The tox profile of an ADC is determined by its on- and off-target effects. On-target tox is caused by specific binding of the ADC to healthy target-positive cells; off-target tox is caused by target-independent binding of the ADC, e.g. via the Ab backbone or by payload release in circulation. In this study, we unravel the off-target tox mechanisms of ADCs that use amatoxins (RNA polymerase II inhibitor) as payload (ATACs) and use this knowledge to improve the TW of ATACs. Amatoxins are distinct from other ADC payloads as they are hydrophilic and thus require active transport to pass the cell membrane. The primary transporter of amatoxins in humans is the OATP1B3 transporter, which is exclusively expressed on hepatocytes. Thus, unspecific ATAC tox can be caused by free amatoxin, premature released in circulation and uptake by liver cells via OATP1B3, or by uptake of the ATAC via a yet unknown mechanism.

Material and Methods: ATACs are based on cysteine-reactive and site-specific amatoxin-linker constructs by HDP. *In vitro*: Binding of ATACs to FcγRI by BLI; Cytotoxicity of ATACs on HEKwt, HEK-OATP1B3 and THP1 cells. *In vivo*: Single i.v. dose of ATAC; Tolerability in mice; Efficacy in s.c. tumor models; Blood sampling for PK analysis; ADC/total Ab detection by ELISA; DAR-loss analysis and toxin measurement by (intact) LC-MS.

Results: Liver tox caused by premature release of amatoxin in circulation was investigated thoroughly *in vivo*. DAR-loss, survival analysis, ADC and Ab measurements, indicated that the release of amatoxin in circulation cannot be the root-cause for off-target ATAC toxicity. Further, it was ruled out that the ATAC is taken up by OATP1B3 *in vitro* and *in vivo*. Thus, uptake of the intact ATAC via yet unknown mechanisms is responsible for liver tox. As liver tox is also known for other ADCs, several uptake mechanisms are described, one of which being FcγR-mediated uptake. Indeed, ATACs bind to the FcγR and trigger target-independent cytotoxicity on $FcγR^{\pm}$ cells. Point mutations at L234 and L235 (LALA mutation), the amino acids in the Fc part of the Ab responsible for FcγR binding, were shown to reduce FcγR binding. The LALA mutation significantly increased the tolerability of ATACs in mice and monkeys, whereas the anti-tumor efficacy was not impaired, leading to an improved TW.

Conclusion: Our data show that liver toxicity of ATACs is caused by unspecific uptake of the ATAC into liver cells at least partially mediated by FcγR. This knowledge was used to optimize the Ab backbone to minimize unspecific uptake into liver cells. Insertion of a LALA mutation to avoid uptake via FcγR reduced off-target toxicity of ATACs leading to better tolerability and an increased TW.

#7184 Simulating extended dosing intervals for atezolizumab: A comparative analysis between NONMEM and Pumas.

F. Bateman[1], O. Arisa[1], N. Corvalan Cabanas[2], Y. Zeng[1], C. Peer[2], K. Schmidt[2], W. D. Figg, Sr.[2];
[1]NIH-CC, Bethesda, MD, [2]NIH-NCI, Bethesda, MD

The initially approved dosage regimens of 840 mg every 2 weeks, 1200 mg every 3 weeks, and 1680 mg every 4 weeks are considered excessive concerning the specified minimum effective concentration of 6 ug/mL and the significant exposure-response relationship with Adverse Events of Special Interest (AESI). Our previous research, demonstrated through simulation, indicated that an extended-interval dosing regimen (840 mg every 6 weeks) after two standard loading doses maintained efficacy with a nonsignificant exposure-response relationship with AESI.In alignment with the FDA's initiative "Project Optimus," which aims to optimize drug dosing for improved therapeutic outcomes, we explore alternative dosage regimens for atezolizumab. Through a comparison of the traditional 30-year-old industry standard NONMEM software and the recently developed PumasAI software, we simulate these regimens, utilizing our previously published article as a benchmark. Given the rapid evolution of artificial intelligence (AI) and machine learning, it is crucial for pharmacokinetic modeling to adapt and leverage these advancements. We anticipate that this paper will contribute to the integration of AI and machine learning software in pharmacokinetic analysis, aligning with the goals of "Project Optimus" to ensure that drug concentrations are optimized for efficacy and safety.

Table 1: Comparative Summary of Simulated Pharmacokinetic Parameters: Pumas vs. NONMEM

			Pumas			NONMEM		
Regimen	*Cycle*	*Week*	*Cmax (ug/mL)*	*Cmax (ug/mL)*	*Cmax (ug/mL)*	*Cmax (ug/mL)*	*Cmin (ug/mL)*	*Weekly AUC (ug*day/mL)*
1200 mg q3w	1st	3	384(278-533)	64.1(31.4-112)	919(640-1290)	394 (278-559)	75.6 (44.5-121)	1003 (755-1342)
	7th	21	541(371-795)	146(53.8-349)	1750(977-3210)	583 (414-847)	180 (75.9-396)	2014 (1169-3535)
840 mg q2w x2, 840 mg q6w	1st	2	270(195-379)	61.6(35.5-100)	775(570-1085)	275 (184-397)	71.2 (46.4-108)	834 (620-1131)
	7th	38	314(221-448)	33.6(8.8-127)	650(357-1375)	336 (235-487)	46.9 (13.5-150)	774 (441-1562)
1200 mg q3w x2, 840 mg q6w	1st	3	384(278-533)	64.1(31.4-112)	919(640-1290)	394 (278-559)	75.6 (44.5-121)	1003(755-1342)
	7th	39	316(224-459)	36.0(8.4-129)	670(340-1406)	327 (217-492)	46.6 (13.4-157)	763 (411-1594)
1680 mg q4w x2, 840 mg q6w	1st	4	545(380-779)	63.1(26.9-122)	1096(735-1555)	552 (375-793)	78.1 (40.7-135)	1203(869-1651)
	7th	40	318(222-469)	33.9(7.7-126)	657(343-1385)	332 (227-491)	46.5 (13.6-140)	771 (436-1464)

#7185 Long acting injectable FHD-609 micro-suspension: A potent BRD9 degrader with comparable efficacy, reduced frequency of dosing in preclinical models.

Meiyun Lin, Ammar Adam, Abira Pyne Ramakrishnan, Hafiz Ahmad, Xiaohuan Wu, Brandon Antonakos, Chong-Hui Gu, Ashish Ramani, Victoria Amaral, Claudia Dominici, Qianhe Zhou, Mike Collins, Jessica Piel, Sal Topal, Brian Ethell, Kelly McKiernan, Scott Innis

Foghorn Therapeutics, Cambridge, MA

Bromodomain-containing protein 9 (BRD9) is a unique component of the non-canonical Brahma-associated factor (ncBAF) complex, essential for cancer cells relying on this complex for survival. This makes it an attractive target for cancer treatment. In synovial sarcoma (SS), SS18-SSX fusion protein drives disease progression and integrates into BAF complexes, promoting tumor growth. Targeting BRD9 degradation is a potential therapeutic approach for SS tumors, as it depletes the essential SS18-SSX fusion protein upon which cancer cells depend for survival within the BAF complex.
FHD-609, a potent heterobifunctional degrader of BRD9, has been administered intravenously (IV) in medical facilities twice weekly during clinical trials. In order to facilitate less frequent and more convenient patient-centric dosing, a long acting injectable formulation was developed that allows subcutaneous (SC) or intramuscular (IM) dosing every 4 weeks in preclinical studies. The formulation is an aqueous microsuspension containing the drug along with a polymer and surfactant which provides sustained release of FHD-609 upon injection. We compared the long acting injectable formulation dosed once every 4 weeks to the IV formulation dosed twice a week for the pharmacokinetic and pharmacodynamic properties, as well as the efficacy of the long in xenograft models of different sensitivities, including cell line-derived xenografts (CDX) and patient-derived xenografts (PDX). Our results showed that a single dose of the injectable suspension formulation was well-tolerated in mice and exhibited a significantly flatter PK profile than IV injection with a lower peak to trough ratio and detectable compound concentrations 4 weeks post dose. Moreover, it demonstrated comparable in vivo efficacy and BRD9 protein degradation to the standard intravenous (IV) administration. The long acting FHD-609 injectable formulation has the potential to offer better patient compliance and acceptance in clinical settings than IV dosing. The long acting injectable formulation provides a promising and effective drug delivery option for various protein degraders that are not orally bioavailable.

#7186 *In vitro* evaluation of myelosuppressive effects of ATRi tuvusertib and ATMi lartesertib (M4076), alone and in combination.

Jatinder Kaur Mukker[1], Rohan Kulkarni[1], Yongzhao Huang[2], Emer Clarke[2], Ioannis Gounaris[3], Anup Zutshi[1], Karthik Venkatakrishnan[1], **Anna Tafuri**[4]

[1]EMD Serono, Billerica, MA,[2]Discovery Life Sciences, Seattle, WA,[3]Merck Serono Ltd. (an affiliate of Merck KGaA, Darmstadt, Germany), Feltham, United Kingdom,[4]Merck KGaA, Darmstadt, Germany

Introduction: In cancer therapy, combinations of drugs interfering with different molecular pathways enhance efficacy and reduce resistance development, but may also increase the risk of toxicity. DNA damage repair inhibitors (DDRi) induce on- and off-target adverse events including hematological and gastro-intestinal toxicities[1], which impact the therapeutic window. We evaluated the hematopoietic effect of ATRi tuvusertib and ATMi lartesertib, alone and in combination, on erythroid, megakaryocytic and myeloid bone marrow cell lineages.

Methods: Mobilized peripheral blood CD34+ cells were plated in 96-well plates in specific media cultures allowing growth and differentiation of all three lineages. The cells were cultured for a total of 7 (neutrophils and platelets) to 10 (erythroids) days in the absence of drugs to generate maturing populations. Various concentrations of tuvusertib and lartesertib were incubated in cell media and assessed using LC/MS methods to ensure they remained chemically stable for the duration of the experiments. After *in vitro* differentiation, the lineages were cultured in the continuous presence of various concentrations of tuvusertib (0.003 to 3 µM) and/or lartesertib (0.01 to 10 µM) encompassing an unbound plasma concentration range evaluated in phase 1 studies of these agents and their combination. Cells were evaluated in triplicate by flow cytometry on day 3 and 7 of drug exposure for neutrophils (CD34, CD38, CD33, CD15), megakaryocytes and platelets (CD41, CD42b), and erythroid cells (CD71, CD235a). In another set of experiments, to simulate a "drug holiday", cells were exposed to tuvusertib, lartesertib and their combination for 24 h, washed out and further cultured as described above before evaluation.

Results: Tuvusertib and lartesertib were stable in the specific media cultures up to day 7 of drug exposure. Continuous treatment with tuvusertib as a single agent inhibited the hematopoietic cells of all lineages more profoundly than lartesertib as monotherapy. Effects were consistently more pronounced after 7 days than 3 days of drug exposure. Continuous treatment of a combination of tuvusertib and lartesertib inhibited hematopoietic cells of all lineages. Treatment for 24 h followed by wash-out demonstrated a lesser effect compared to continuous treatment.

Conclusion: The phenotypic and functional changes induced by tuvusertib and lartesertib on *in vitro* cultures of erythroid, myeloid, and megakaryocytic cells are consistent with clinical observations in monotherapy studies, suggesting these models may be used to better understand and predict the hematological effects of monotherapies and combinations in the clinic. *In vitro* washout experiments may help support the concept of intermittent clinical regimens and warrant further investigation.

1. Martorana, et al. *Cancers (Basel)* 2022;14(4):953

#7187 Entresto protects against doxorubicin-induced cardiotoxicity in mice model of breast cancer.

A. Pandit, A. Costas, B. Sapkota, S. Thota, R. Begum, N. Chintalaramulu, H. W. Green III, J. Francis;
Louisiana State University, Baton Rouge, LA

Doxorubicin (Dox) is a potent chemotherapeutic agent with high efficacy; however, dose-dependent cardiotoxicity undermines its effectiveness in cancer therapies. Entresto, a combination of sacubitril and valsartan (Sac/Val), offers a multi-modal approach. It enhances the beneficial response of the neurohormonal system of the heart while curbing the detrimental effects of the renin-angiotensin-aldosterone system and mitigating further cardiac damage by decreasing sensitivity to natriuretic peptides. The objective of this study is to assess the potential cardioprotective effects of Entresto on doxorubicin-induced cardiotoxicity (DIC) in a mouse model of breast cancer. To achieve this, a syngeneic tumor model of breast cancer was employed. Twenty-five 10-week-old female Balb/c mice were randomly divided into 5 groups: control, Tumor, Tumor + entresto, Tumor + Dox, and Tumor + entresto + Dox. Tumor groups were injected with 4T1 wild-type cells into the mammary fat pad via intraperitoneal injection. Subsequently, after a week, Dox groups were treated with Dox at 8 mg/kg body weight/week for 3 weeks, while control and tumor + entresto received saline. Following Dox treatment, control, and tumor + Dox animals were gavaged daily with saline, while Entresto groups were gavaged with entresto (60 mg/kg) for 3 weeks. Echocardiography assessed cardiac function at baseline and 3 weeks post-DOX treatment. All mice were euthanized at 4 weeks. Our results demonstrated that entresto treatment significantly ameliorated Dox-induced decreases in ejection fraction and fractional shortening while maintaining improved cardiac functions. Entresto also reversed Dox-induced altered levels of cardiac biomarkers (ANP and BNP). Gene and protein expression analyses in heart tissues revealed that entresto modulated the levels of autophagy-related (Beclin-1 and p62), apoptosis-associated (caspase 3 and Bcl-2) and antioxidant-related (Nrf2 and Keap1): genes and proteins expression altered by Dox treatment. Additionally, Entresto attenuated histological evidence of cellular toxicity, apoptosis, and fibrosis in Dox-treated animals with breast cancer. These findings suggest that Entresto confers cardiac protection against DIC in a mouse model of breast cancer without interfering with the antineoplastic effects of Dox. It underscores the potential clinical relevance of Entresto to enhance the safety and efficacy of doxorubicin-based cancer therapies.

EXPERIMENTAL AND MOLECULAR THERAPEUTICS: Reversal of Drug Resistance 2
Poster Session

#7191 Targeting IGF1R/INSR pathway with approved ALK inhibitors inhibits AKT signaling and overcomes proteasome inhibitor resistance in multiple myeloma.

A. Besse[1], T. Totu[2], M. Kraus[3], A. P. A. Janssen[4], J. Veprkova[1], M. Mendez Lopez[3], O. Slaby[1], M. Buljan[2], M. van der Stelt[4], C. Driessen[3], L. Besse[1];
[1]Masaryk University, Brno, Czech Republic, [2]Swiss Federal Laboratories for Materials Science and Technology, St. Gallen, Switzerland, [3]Cantonal Hospital St. Gallen, St. Gallen, Switzerland, [4]Leiden University & Oncode Institute, Leiden, Netherlands

Background: Resistance to proteasome inhibitors (PI) bortezomib (BTZ) and carfilzomib (CFZ) is a major obstacle to the successful treatment of multiple myeloma (MM); thus, identification of novel therapeutic options is an unmet medical need. ALK inhibitors have been shown to exhibit anti-MM activity in monotherapy or in combination with CFZ. Our data showed that MM cells were negative for ALK; thus, we aimed to identify the mechanism of action of the ALK inhibitor ceritinib in MM cells and the mechanism of synergy between ceritinib and CFZ.
Methods: A set of PI-naïve and PI-resistant MM cells was used in this study. Genome-wide CRISPR/Cas9-based screening using the Brunello library was performed in the AMO-1 cell line. Kinase inhibitor selectivity data were retrieved from ChEMBL, v30 database. RNA sequencing was used to determine expression changes after treatment, and RNA-seq data from patients included in the CoMMpass study were analyzed. Western blotting was performed to assess the levels of total and phosphorylated protein. Unbiased LC-MS/MS was performed to determine the effects of ceritinib and CFZ on the intracellular metabolites. An *in vivo* mouse model based on the orthotopic injection of AMO-BTZ cells into the femur of NSG mice was used to determine the effect of the drug combination *in vivo*.
Results: Among approved ALK inhibitors, ceritinib has been identified as the most synergistic cytotoxic combination with CFZ in PI-naïve and PI-resistant MM cells. An in silico search of the ChEMBL database identified InsR and IGF1R as receptor tyrosine kinase that are inhibited by ceritinib. PI-naïve, PI-resistant cell lines, as well as MM patients were negative for ALK, but positive for InsR and IGF1R expression. CRISPR/Cas9-screening identified genes involved in the negative regulation of mTORC signaling (DDIT4, NPRL2/3, TSC1/2) and the transcription factor FOXO1 as the major resistance candidates to ceritinib. Subsequently, FOXO1 inhibition using a selective chemical inhibitor protected the cells from ceritinib-induced cytotoxicity. Next, ceritinib inhibited mTORC signaling and induced the expression of genes related to cell cycle arrest, which are downstream of FOXO1. Likewise, ceritinib, by targeting the InsR/IGF1R, impaired purine-pyrimidine and amino acid homeostasis, suggesting metabolic and proliferation shut-down and amino acid starvation due to downstream mTORC and Akt inhibition and FOXO1 induction. The combination of ceritinib and CFZ was superior to CFZ in PI-resistant MM in vivo and showed strong synergistic cytotoxicity in primary cells from MM patients progressing under or after PI-containing therapy.
Conclusion: Ceritinib, an FDA-approved drug, overcomes PI resistance in MM by inhibiting InsR/IGF1R and downstream Akt signaling. Therefore, ceritinib is a promising treatment option for PI-resistant MM.
Supported by the project National Institute for Cancer Research (Programme EXCELES, ID Project No. LX22NPO5102) - Funded by the European Union - Next Generation EU.

#7192 Teriflunomide overcomes gemcitabine resistance by inhibiting the GSK3β/mTOR pathway in pancreatic cancer.

C. Xu[1], Y. Li[1], S. Sui[1], M. Chen[1], L. Melstorm[2], H. Han[3], S. Rosen[4], A. Goel[1];

[1]Beckman Research Institute of The City of Hope, Monrovia, CA, [2]City of Hope National Medical Center, Duart, CA, [3]The Translational Genomics Research Institute, Phoenix, AZ, [4]City of Hope National Medical Center, Duarte, CA

Background: Pancreatic cancer (PC) is a lethal malignancy that is partly attributable to the acquisition of chemoresistance to conventional chemotherapies. Hence, developing strategies to overcome such chemoresistance is essential. Teriflunomide, an active metabolite of leflunomide, has been widely utilized in managing autoimmune disorders, and emerging evidence suggests that it can augment the efficacy of chemotherapy in cancer. We investigated the therapeutic effect of teriflunomide in overcoming resistance to Gemcitabine-based therapy in PC.

Methods: We performed docking and genomewide transcriptomic profiling analyses to identify therapeutic targets of Teriflunomide associated with Gemcitabine resistance (Gem-R) in PC. Subsequently, we analyzed the TCGA dataset to determine the prognostic significance of candidate genes in PC patients. A series of experiments were performed in PC cells, and the key findings were validated in patient-derived 3D organoids and a Gem-R Mia-PaCa2 xenograft model.

Results: Docking and transcriptomic profiling studies identified GSK3β, MAPK8, and MAPK9 as potential targets of Teriflunomide, which were significantly upregulated in Gem-R cell lines ($P < 0.05$). GSK3β was independently associated with poor overall and disease-free survival in PC patients. Combined Teriflunomide and Gemcitabine treatment exhibited superior synergistic anti-tumor potential, as evidenced by reducing PC cell proliferation, clonogenicity, invasion, and migration. The combined treatment with Teriflunomide and Gemcitabine primarily inhibited GSK3β phosphorylation, resulting in the silencing of the downstream AKT/mTOR pathway. Lentiviral-based silencing of GSK3β inhibited the AKT/mTOR pathway and reduced the IC50s of Gemcitabine in PC cells. Furthermore, co-administrating both drugs to Gem-R Mia-PaCa-2 xenograft mice significantly reduced tumor growth rates and volumes. These findings were recapitulated in patient-derived 3D-organoids, where the combined treatment resulted in fewer and smaller organoids vs. each drug individually ($P < 0.05$).

Conclusions: We provide novel evidence that Teriflunomide helps overcome resistance to Gemcitabine by inhibiting the GSK3β/AKT/mTOR pathway, which could improve treatment outcomes in PC.

#7193 ABCB1-mediated chemotherapeutic drug resistance is reversed by a potent p53-MDM2 inhibitor NVP-HDM201.

H. Patel[1], C. Cai[1], Z. Wu[1], Q. Teng[1], H. Li[2], Z.-S. Chen[1];

[1]St. John's University, Jamaica, NY, [2]Shenzhen Hospital of Guangzhou University of Chinese Medicine, Shenzhen, China

The failure of chemotherapy in cancer persists as a result of overexpression of various ATP-binding cassette (ABC) transporters. ABCB1 is one such transporter that actively pumps out chemotherapeutic drugs and it is one of the reasons for multidrug resistance (MDR). In the last few years, activation of p53 has been targeted as a therapeutic strategy in the treatment of cancers. Siremadlin (NVP-HDM201) is a potent and selective inhibitor of p53-MDM2 interaction. The objective of this study was to explore the ability of HDM201 to reverse tumor MDR attributable to overexpression of ABC transporters. According to our findings, HDM201 significantly increased the sensitivity of ABCB1-overexpressing cells to ABCB1 substrates, such as colchicine and doxorubicin. We found that HDM201 reverses ABCB1-mediated MDR by interacting with ABCB1 and blocking its function without affecting the expression and cellular localization of ABCB1. Moreover, HDM201 promoted the accumulation of paclitaxel in cell lines that overexpress ABCB1. At both high and low doses, HDM201 increased the ATPase activity of ABCB1. The computational support for the cross-reactivity of this p53 inhibitor with human ABCB1 comes from docking simulation results that align with the binding conformation of HDM201 within the vast cavity of the transmembrane region of ABCB1. In conclusion, by blocking the transport function of ABCB1, HDM201 can reverse ABCB1-mediated MDR *in vitro*.

#7194 Targeting AXL and MCL-1 to eradicate lazertinib tolerance in EGFR-mutated NSCLC cells.

T. Yamada, Y. Matsui, K. Takayama;
Kyoto Prefectural University of Medicine, Kyoto, Japan

Lazertinib, a novel third-generation EGFR-tyrosine kinase inhibitor, has shown marked efficacy in patients with EGFR-mutant lung cancer. However, after various periods of therapeutic intervention, most patients eventually acquire resistance to lazertinib. A potential therapeutic approach to address this clinical issue is to overcome the initial drug resistance mechanism. To determine the underlying adaptive lazertinib resistance mechanisms, we evaluated signal transduction, cell apoptosis, and drug sensitivity in mutant EGFR-expressing non-small cell lung cancer (NSCLC) cells treated with lazertinib. The siRNA screening assay demonstrated that AXL knockdown significantly inhibited cell viability in the presence of lazertinib, indicating that AXL activation contributes to lazertinib resistance. However, long-term culture with a combination of lazertinib and AXL inhibitors eventually led to the proliferation of residual cells and increased MCL-1 expression, which was mediated by the nuclear translocation of the transcription factor YAP. Cell-based assays showed that triple therapy with an MCL-1 or YAP inhibitor, in combination with EGFR-TKI lazertinib, an AXL inhibitor, significantly reduced cell viability and increased apoptosis. These results demonstrate that AXL and YAP/MCL-1 signals contribute to the adaptive lazertinib resistance in EGFR-mutant NSCLC cells, suggesting that the initial dual inhibition of AXL and YAP/MCL-1 might be highly effective in eliminating lazertinib-resistant cells.

#7195 Repurposing non-oncology drugs with MET inhibitory effect to overcome osimertinib resistance in lung cancer.

K. K. To[1], K. Leung[1], W. C. Cho[2];

[1]Chinese University of Hong Kong (CUHK), Hong Kong, Hong Kong, [2]Queen Elizabeth Hospital, Hong Kong, Hong Kong

Background and Aim: Osimertinib is the only 3rd generation epidermal growth factor receptor (EGFR) tyrosine kinase inhibitor approved for the 1st line therapy of advanced NSCLC patients with EGFR mutations. However, drug resistance is severely limiting its clinical efficacy. Aberrant MET activation is an important mechanism causing osimertinib resistance. There is no effective therapeutic option after osimertinib failure. This study investigated the repurposing of non-oncology MET inhibiting drug to overcome osimertinib resistance.

Method: A few clinically-approved drugs with putative MET inhibitory effects were identified by a computational drug repurposing tool called “DRAR-CPI” via analysis of the chemical-protein interactome of known MET inhibitors (crizotinib, cabozantinib, foretinib, and tivantinib). Fexofenadine (FEX), originally indicated for allergic rhinitis and chronic urticaria, was chosen for detailed investigation in osimertinib-resistant NSCLC cell lines that exhibit aberrant MET activation with/without other EGFR-dependent osimertinib resistance mechanisms. The selectivity of kinase inhibition by FEX was evaluated by a KINOME profiling assay against a panel of human protein kinases. Western blot analysis was conducted to examine the activation status of Met and EGFR downstream signaling. RNA sequencing was performed to identify differentially expressed genes (DEGs) triggered by the most promising repurposed drug, presumably contributing to osimertinib resistance circumvention. Sulforhodamine B assay was used to evaluate cell proliferation. The circumvention of osimertinib resistance by FEX was further verified in a patient-derived tumor xenograft (PDX) from an advanced-stage osimertinib-refractory NSCLC patient.

Result: FEX was found to inhibit recombinant MET kinase in cell-free assays in a dose- and time-dependent manner. It also inhibited MET phosphorylation and other downstream signaling molecules in osimertinib-resistant NSCLC cell lines harboring EGFR T790M+MET amplification or EGFR T790M loss+MET amplification. KINOME profiling revealed a similar kinase inhibition profile between FEX and cabozantinib using Spearman rank order correlation analysis. Among the tested osimertinib-resistant NSCLC cell lines, FEX showed the highest effectiveness in potentiating the anticancer effect of osimertinib in H820 cells (having MET amplification & EGFR T790M mutation). Transcriptome profiling analysis in H820 cells before and after FEX treatment revealed that the majority of DEGs were enriched in EMT-related biological processes and pathways. FEX was further shown to significantly potentiate the antitumor effect of osimertinib in a drug refractory PDX model, without inducing notable weight loss in the animals.

Conclusion: These findings advocate the clinical evaluation of repurposing FEX to overcome osimertinib resistance.

#7196 Evaluation of *nab*-sirolimus in combination with fulvestrant or PI3K pathway inhibitors to overcome resistance in breast cancer cell lines.

K. Myint[1], S. Wallace[1], **S. Hou**[2], M. Zalath[2], B. McMorran[2], A. Kwon[2], I. Vivanco[1];
[1]King's College London, London, United Kingdom, [2]Aadi Bioscience, Inc., Pacific Palisades, CA

Background: Endocrine therapy (ET) is the standard of care for hormone receptor positive (HR+) breast cancer (BC), but ET resistance develops in most patients (pts). One resistance mechanism involves cross talk between the PI3K-AKT-mTOR and estrogen receptor (ER) signaling pathways, resulting in increased ER signaling and tumor proliferation. This is mitigated by mTOR inhibition as demonstrated by improved outcomes with exemestane plus the mTOR inhibitor (mTORi) everolimus in pts with HR+ advanced BC. While PI3K inhibitors (PI3Ki [e.g. alpelisib]) are efficacious in pts with HR+, *PIK3CA*-mutated BC, resistance can occur due to acquired genomic alterations in the PI3K-AKT-mTOR pathway. Combination therapy that targets a critical downstream node, mTOR, could delay or overcome acquired resistance due to activation of upstream components of the PI3K-AKT-mTOR pathway. *nab*-Sirolimus is an intravenously administered, albumin-bound nanoparticle form of the mTORi sirolimus, with significantly greater tumor accumulation, mTOR target suppression, and improved antitumor effects than oral mTORis in nonclinical tumor models. We evaluated the antiproliferative and cytotoxic effects of *nab*-sirolimus in combination with ET or PI3Kis in BC cell lines.
Methods: HR+, *PI3K*-mutated BC cell lines (MCF7 or MDA-MB-361) were incubated for 5 days with increasing concentrations of *nab*-sirolimus and the selective ER degrader fulvestrant. MDA-MB-361 cells or HR-negative (HR−), *PI3K*-mutated BC cells, MDA-MD-453, were incubated for 5 days with increasing concentrations of *nab*-sirolimus and PI3K-AKT-mTOR pathway inhibitors gedatolisib or alpelisib. Antiproliferative/cytotoxic effects of single-agent and combination treatment were assessed via an automated trypan blue exclusion assay.
Results: Addition of 20 or 80 nM *nab*-sirolimus to fulvestrant (12.5-500 nM) markedly decreased cell viability and nearly doubled cell death in MCF7 and MDA-MB-361 cells. Antiproliferative effects of low-dose gedatolisib (2.5-10 nM) were enhanced by 61-71% when *nab*-sirolimus (20 or 80 nM) was added to MDA-MB-453 cells. While low doses (2.5, 5, and 10 nM) of gedatolisib alone led to limited cytotoxicity (4.2-9.6%), up to 48.9% of cell death occurred when 20 or 80 nM *nab*-sirolimus was added. Results were similar with alpelisib (1 uM) plus *nab*-sirolimus (20 or 80 nM). Western blot showed increased p4EBP1 in response to fulvestrant or PI3Ki treatment, which was reversed with the addition of *nab*-sirolimus.
Conclusions: *nab*-Sirolimus enhanced the cytotoxic effects of fulvestrant in HR+ BC cells and of PI3Kis in HR+ and HR− BC cells. Addition of *nab*-sirolimus to ET or other PI3K-AKT-mTOR pathway inhibitors may overcome mechanisms of resistance; further exploration is warranted to elucidate clinical relevance.

#7197 Elacridar sensitizes liver cancer to the PKC-inhibitor ICA-1S.

A. O. Olatunji, M. Marzan, M. Acevedo-Duncan;
University of South Florida, Tampa, FL

Liver cancer is a disease in which cancer cells form in the tissues of the liver. Globally, liver cancer is one of the most frequent fatal malignancies; in the United States, liver cancer is the sixth leading cause of cancer death. Generally, there is a poor prognosis for liver cancer. Chemotherapy and immunotherapy are the best available treatment options. This research aims to provide an alternative treatment option with drugs that specifically attack liver cancer cells. Protein Kinase C (PKCs) are signaling molecules that have been reported to be associated with multiple cellular processes and cancer. PKC activity reportedly is elevated in colorectal cancer cells and metastasizes to the liver. 5-amino-1-((1R,2S,3S,4R)-2,3-dihydroxy-4-methylcyclopentyl)-1H-imidazole-4-carboxamide (ICA-1S) is a PKC-ι specific inhibitor we have previously shown to be effective against some cancer cell lines by decreasing cell growth and inducing apoptosis. In this study, we investigated the effectiveness of ICA-1S against liver cancer cell lines; HEPG2 and PLC5/PRF/5. An equal number of HEPG2 and PLC5/PRF/5 cell lines were seeded into 6 well plates, treated with different concentrations (0.1µM, 0.5µM, 1µM, 5µM, and 10µM) of ICA-1s every 24 hours for three days after which the media was discarded, and cells were counted. The percentage inhibition of ICA-1S on HEPG2 and PLC5/PRF/5 cell lines was calculated. To investigate the resistance inflection, the proliferation assay was also conducted with a combination of an efflux pump inhibitor, Elacridar(10µM), and different concentrations (0.1µM to 10µM) of ICA-1S. The expression of PKC-ι was investigated across all treatments. The dose-response result for treatment with ICA-1S for both HEPG2 and PLC5/PRF/5 cell lines showed a resistance inflection point at 0.5µM and 1µM, where the proliferation rate of the cells declined by 50% and 79% for HEPG2, and 41% and 54% for PLC5/PRF/5 respectively; beyond these points, the cell proliferation rate significantly rises. The results of dose-response for treatment with a combination of ICA-1S and Elacridar showed a continuous decline in cell proliferation rate up to 78% and 84% for HEPG2 and PLC5/PRF/5 respectively as the concentrations of ICA-1S increased from 0.1µM to 10µM. The PKC-ι level was downregulated in the combination treatment. We have shown in this study that liver cancer cells exhibit resistance to PKC inhibitor, ICA-1S, at high concentrations. This resistance inflection may be due to several factors including the activation of drug-efflux proteins. Thus, we proved that the introduction of an efflux pump inhibitor, Elacridar, sensitizes the liver cancer cells to ICA-1S, offsets the resistance of the liver cancer cells to ICA-1S at high concentrations, and enables ICA-1S to be effective in downregulating PKC-ι and decreasing cell growth of liver cancer cells.

#7198 A small molecule Notch1 inhibitor (ASR490) restores chemosensitivity in triple-negative breast cancer.

N. Tyagi[1], B. Chandrasekaran[1], A. Tyagi[1], B. Singh[1], M. Chandran[1], A. Singh[2], A. Sharma[2], C. Damodaran[1];
[1]Texas A&M University, College Station, TX, [2]Penn State Cancer Institute, University Park, PA

Metastatic triple-negative Breast cancer (mTNBC) is an aggressive and often a chemo resistant disease for which no effective druggable target has yet been identified. We and others reported that the aberrant expression of neurogenic locus Notch homolog protein 1 (Notch1) serves as a molecular signature for TNBC. Hence, we postulated that pharmacologically targeting Notch1 in conjunction with a standard chemotherapeutic agent (Doxorubicin: DXR) may completely eradicate TNBC growth and overcome systemic and debilitating toxicity. Hence, this study aims to elucidate the role of our recently discovered notch1 inhibitor ASR490 and its ability to chemosensitize TNBC without significant systemic toxicity.

In our results, pretreatment of $1/_{10}^{th}$ of the *inhibitory concentration of* ASR490 combined with $1/_{10}^{th}$ or $1/_{20th}$ of DXR significantly inhibited the growth of TNBC cells (MDA-MB-231 and BT549). Notably, DXR treatment induced Notch1 activation which led to chemoresistance in TNBC; however, co-treatment with the Notch1 inhibitor ASR490, led to the downregulation of Notch1 activation and eradication of the cell viability and clonogenicity of the TNBC cells. Further, molecular analysis suggested that pretreatment of 1/10th of ASR490 facilitates DXR-mediated sensitivity, by inhibiting the DNA repair pathway and upregulating (cleaved) caspase 3, (cleaved) caspase-9 and poly (ADP-Ribose) polymerase (PARP)-mediated apoptosis. Similarly, the combination effectively blocked the epithelial and mesenchymal transition (EMT) regulators and suppressed metastatic properties of MDA-MB231 and BT-549 cells. Moreover, combining ASR490($1/_{10}$th) and DXR ($1/_{20}$th) significantly eradicated xenotransplanted TNBC tumors compared to ASR490 or DXR alone. In addition to being effective at inhibiting tumor growth, the significantly lower dose requirements of DXR and ASR490 in combination makes it a highly safe therapeutic modality. These findings suggest that aberrant activation of Notch1 is responsible for TNBC chemoresistance and concomitantly inhibiting Notch1 activation is an effective therapeutic strategy to restore chemosensitivity in TNBC.

#7199 The retinoid X receptor (RXR) agonist IRX4204 potentiates the efficacy of trabectedin and pioglitazone in myxoid liposarcoma preclinical models.

M. Meroni[1], I. Craparotta[1], F. Mirimao[1], N. Panini[1], P. Ubezio[1], E. Bello[1], S. Renne[2], M. D'Incalci[3], R. Frapolli[1];
[1]Istituto di Ricerche Farmacologiche Mario Negri IRCCS, Milan, Italy, [2]Humanitas Research Hospital, Milan, Italy, [3]Humanitas University, Milan, Italy

Myxoid liposarcoma (MLS) is characterized by a chromosomal translocation that results in the formation of the FUS-DDTI3 fusion protein, which blocks the final step of adipocytic differentiation from adipoblasts to adipocytes. Trabectedin (ET) is a marine drug able to displace FUS-DDTI3 from the promoters of its target genes, restoring adipogenesis and leading to long-lasting clinical responses in MLS patients. However, after prolonged treatments with ET, resistance occurs, and no further therapies are available. Recent studies indicate that the PPARγ agonist pioglitazone (PIO) reactivates adipocytic differentiation in MLS preclinical models resistant to ET, restoring treatment efficacy. While the combination of ET and PIO is being studied clinically, our goal here is to further potentiate the stimulation of adipocytic differentiation to obtain even better tumor growth inhibition. Since the PPARγ and the RXR heterodimerize, and the heterodimer is permissive, we will exploit this property by combining PIO with the RXR agonist IRX4204. The DL221 human MLS cell line was treated with PIO or IRX4204. To assess adipocytic differentiation, cells were stained with LD540 and DAPI for fluorescence microscopy. FABP4 and ADIPOQ expression was measured using RT-PCR. Drug efficacy and tolerability were evaluated in MLS patient-derived xenografts ML017 (sensitive) and ML017/ET (trabectedin-resistant). Mice were randomized to receive PIO (150 mg/kg p.o. qdx28), ET (0.15 mg/kg i.v. q14dx2), IRX4204 (10 mg/kg i.p. qdx28), or their combinations. PIO and IRX4204 induced mature adipocyte-like morphological alterations and lipid droplet accumulation in the DL221 cell cytoplasm, and when PIO and IRX4204 were combined, these effects were more evident. In parallel, the expression of the adipocytic markers FABP4 and ADIPOQ increased. *In vivo*, the addition of IRX4204 to ET and PIO improved the efficacy of treatments in both the ML017 ($p<0.0001$) and the ML017/ET ($p<0.0001$) models, causing faster tumor responses and extending animal survival. Interestingly, even in the absence of ET, the combination of PIO and IRX4204 caused a significant inhibition of tumor growth compared to the single drugs in both the ML017 ($p<0.001$) and the ML017/ET ($p<0.0001$) models. IRX4204 in combination with ET and PIO was able to improve their antitumor activity, enhancing, at least *in vitro*, their differentiating capabilities and inducing faster inhibition of tumor growth. The combination of IRX4204 and PIO, even without ET, could be a clinically effective option, especially for patients not suitable to receive ET or as maintenance therapy. Further studies are ongoing to better define the mechanism of action of these combinations through *in vivo* histological and molecular analysis.

#7200 Non-cytotoxic inhibition of nuclear encoded mitochondrial protein MAGMAS resensitize treatment resistant prostate cancer cells to taxane therapy.

A. Duran[1], K. Whitley[1], K. Santiago[1], A. Mohammed[2], C. Casiano[1], B. Das[2], F. Almaguel[1];
[1]Loma Linda University, Loma Linda, CA, [2]Long Island University, Brookville, NY

Metastatic prostate cancer (PCa) is the leading cause of PCa-associated deaths and one of the leading causes of cancer mortality in men. Novel therapeutics, such as Prostate Specific Membrane Antigen (PSMA) ligand therapy, are emerging as effective treatment strategies for metastatic prostate cancer. However, most men succumb to Metastatic Castration Resistant Prostate Cancer (mCRPC) due to treatment resistance. MAGMAS, a 13.8 kDa mitochondrial protein, imports nuclear-encoded mitochondrial proteins into the mitochondrial matrix. MAGMAS is overexpressed in several aggressive tumors, such as breast cancer, glioblastoma, and prostate cancer. When overexpressed, MAGMAS plays a role as a cytoprotective protein by acting as a reactive oxygen species (ROS) scavenger that maintains sufficient ROS levels to promote cell proliferation but below the threshold levels that could lead to apoptosis. This study was designed to investigate the pro-survival and therapy-resistance functions of MAGMAS in treatment-resistant PCa cells. Predictively, we observed that the docetaxel (DTX)-resistant PC3-DR and DU145-DR PCa cell lines expressed significantly higher levels of MAGMAS compared to their drug-sensitive parental cell lines. We hypothesized that inhibiting Magmas reduces the aggressive properties of highly proliferative DTX-resistant metastatic PCa cell lines and re-sensitizes them to DTX. MAGMAS knockdown in DTX-resistant PC3 and DU145 cells in the presence of increasing DTX treatments enhanced sensitivity to DTX. Consistent with these results, pharmacological inhibition of MAGMAS with the novel BT#9 inhibitor in combination with increasing DTX concentrations also enhanced sensitivity to DTX in these cell lines. Additional studies using cell migration/invasion assays and tumor-sphere formation assays are underway to further establish MAGMAS as a potential therapeutic target to attenuate the aggressive properties of chemo-resistant PCa cells. Lastly, we will investigate the diagnostic potential of MAGMAS as a biomarker for advanced PCa and BT#9 as an imaging/therapeutic-specific agent for treatment-resistant tumors.

#7201 Targeting TAZ-TEAD in minimal residual disease enhances the duration of targeted therapy in melanoma models.

C. A. Ott[1], T. Purwin[1], M. Tiago[1], K. Lou[1], P.-Y. Chen[2], S. Chowdhury[2], G. Mersky[1], N. Hacohen[3], J. Lamar[4], C. Capparelli[1], G. Bollag[2], A. Aplin[1]; [1]Thomas Jefferson University, Philadelphia, PA, [2]Opna Bio, San Francisco, CA, [3]Broad Institute of MIT and Harvard, Cambridge, MA, [4]Albany Medical College, Albany, NY

Targeted therapies in cancer are limited by drug tolerance. In melanoma, tolerance to MAPK pathway inhibitors is associated with loss of SOX10 and enhanced YAP1/TAZ-TEAD activity. We show that loss of SOX10 is sufficient to up-regulate a TEAD transcriptional program with a strong dependence on TAZ. We developed a unique gene signature based on the transcriptomic changes following TAZ or YAP1 depletion. Expression of active TAZ was sufficient to mediate tolerance to BRAF inhibitors and MEK inhibitors. In WM983B cells, depletion of TAZ significantly reduced cell growth, whereas YAP1 knockdown resulted in little to no effect. These studies demonstrate that TAZ-TEAD activity plays an important role in melanoma drug tolerance and the development of acquired resistance.

#7202 Strategy of targeting PKCβI protein to overcoming the acquired gemcitabine resistant pancreatic cancer cells.

E. Bae, Y. Lim, J. Hong, W. Byun, S. Chun, S. Hong, S. Lee;
Seoul National University College of Pharmacy, Seoul, Korea, Republic of

Pancreatic cancer (PC) is one of the most malignant cancers with limitation of treatment options such as resection surgery, radiation therapy and gemcitabine-based chemotherapy. To treating PC patients, gemcitabine-based chemotherapy is common and effective for PC, acquired gemcitabine resistance is one of the major reasons for treatment failure. Therefore, there is a need to suggest effective strategies and novel therapeutic approach for gemcitabine-resistant PC. Protein Kinase C β1 (PKC β1) is known as involved in multiple signal transduction related to oncogenic functions in cancer. We suggested that PKC β as one of the novel biomarker of drug resistance and further investigated the molecular mechanism. Among the natural products as small molecule inhibitor, we found that evodiamine has potent antitumor activity and various biological activities. Based on various biological activities of evodiamine, the scaffold was synthesized and investigated for antiproliferative and antitumor activities against gemcitabine resistant PANC-1 (PANC-GR) cells. Also, target validation experiment was employed to elucidate the molecular mechanism and verifying the target to overcoming gemcitabine resistance. Mechanistically, evodiamine derivatives have shown that inhibition of PKC β1 can modulate the proliferation of PANC-GR cells and exhibited tumor growth inhibitory activity in xenograft mouse model.

Keywords: Pancreatic cancer cell, Gemcitabine resistance, Protein Kinase C β1 (PKC β1), Molecular mechanism

Acknowledgements: *This research was supported by the National Research Foundation of Korea (NRF) Grant funded by the Korean Government (RS-2023-00273240).*

#7203 Anti-HDGF antibody attenuates the rise of resistance to EGFR tyrosine kinase inhibitor in NSCLC patient-derived xenograft tumors.

C. Q. Zhou, **A. Li**, K. Ri, A. Sultan, H. Ren;
University of Maryland School of Dentistry, Baltimore, MD

Mutant epidermal growth factor receptor (EGFR), a major oncogenic driver in non-small cell lung cancer (NSCLC), is found in the tumors of 15% (western countries) to 50% (Asian countries) of patients. EGFR-targeted therapy using tyrosine kinase inhibitors (TKIs) is a standard of care for those patients who developed metastatic or recurrent diseases. However, despite having an 80% initial response rate, most patients had partial tumor regression and their disease would progress when acquired resistance emerges. Thus, developing more effective treatment is an unmet need. The clinical response of these patients can be recapitulated in mouse models of patient-derived xenograft (PDX) tumor bearing sensitizing EGFR mutations. In this study, treating established PDX tumors with osimertinib, a third generation EGFR TKI, induced partial tumor regression (50% to 70% size reduction from baseline) followed by progression with a median progression-free survival (PFS) of 26 to 28 days. Interestingly, co-administering an antibody against hepatoma-derived growth factor (HDGF) with osimertinib resulted in enhanced tumor regression (98% to 100% size reduction from baseline) which translated into significantly extended animal survival with a median PFS of 103 or 135 days. Immunohistochemical and western blot examination of tumors collected at different treatment timepoints indicated that AKT/mTOR and MAPK pathways were reactivated after initial suppression in TKI monotherapy arm despite persistent EGFR inhibition. Since AKT/mTOR and MAPK pathways are key survival and proliferative signaling pathways, their reactivation can promote TKI tolerance of tumor cells and the emergence of TKI resistance. However, blocking HDGF attenuated the reactivation of these pathways which could partially explain the enhanced efficacy of osimertinib plus anti-HDGF antibody combination treatment seen in this study. Our results suggest tumor-derived HDGF could play a crucial role in the rise of acquired resistance to osimertinib. Identifying the exact cells and molecular pathways utilized by HDGF to promote tumor cell tolerance to TKI will help us understand how TKI sensitive tumor cells survive EGFR blockade and emerge as resistant cells.

#7204 Therapeutic potential of targeting autophagy to overcome chemoresistance in glioblastoma.

K. Kiang, G. Leung;
The University of Hong Kong, Hong Kong, Hong Kong

Glioblastoma (GBM) is the most malignant subtype of brain tumor in adults, characterized by relentless recurrence and an overall survival of approximately 18 months. Temozolomide (TMZ) has been the basis for current standard of care and represents the control-arm in GBM trials. Despite the use of TMZ having shown promising results in improving patient survival, drug resistance and tumor relapse is almost inevitable. Current literature has provided strong evidence on autophagy modulation as an adjuvant therapy to cytotoxic treatments. By using in vitro and in vivo GBM models, combination regimen with TMZ and an autophagy activator significantly enhanced the cytotoxic effect in tumors that were resistant to chemotherapy. Combined treatment readily induced a mortal autophagy flux in chemo-resistant GBM cells resulted from its high intrinsic autophagy. Our findings suggest that treatment resistant tumors are more sensitive to autophagy activation when compared to treatment-naive tumors. As they often exhibit higher basal level of autophagy after long-term chemotherapy, a mortal autophagy flux can be readily achieved. In conclusion, combination therapy of a cytotoxic drug with autophagy modulator is emerging as a novel therapeutic strategy in the adjuvant setting for cancer patients.

#7205 PLK1 inhibition overcomes PARP inhibitor resistance in triple-negative breast cancer.

A. K. Siraj, P. Poyil, D. Padmaja, S. K. Parvathareddy, K. Alobaisi, R. Begum, O. Almalik, F. Al-Dayel, K. S. Al-Kuraya;
King Faisal Specialist Hospital & Research Centre, Riyadh, Saudi Arabia

Patients with aggressive breast cancer (BC) subtypes usually do not have favorable prognosis despite improvements in treatment modalities. These cancers remain a major cause of morbidity and mortality in women globally. This has fostered a major effort to discover actionable molecular targets to treat these patients. Polo-like Kinase (PLK1) is one of these molecular targets that are under comprehensive investigation for the treatment of such tumors. However, its role in the pathogenesis of BC from Middle Eastern ethnicity has not been explored. Therefore, we examined the expression of PLK1 protein in a large cohort of more than 1500 Middle Eastern ethnicity BC by immunohistochemistry. Correlation with clinico-pathological parameters and the prognosis was performed. PLK1 overexpression was observed in 27.4% of all BC and was significantly associated with aggressive clinico-pathological markers. The antitumor effect of PLK1 and PARP inhibitors either alone or in combination was tested in two BRCA mutated, and one BRCA proficient TNBC cell lines. We showed that combined inhibition significantly reduced cell survival and induced apoptosis in TNBC cell lines. Furthermore, our data suggest that PLK1 inhibition overcomes PARP inhibitor resistance in TNBC cell lines. These findings would pave the way to explore the future use of PLK1 inhibitors in the clinical setting of PARPi-resistant patients.

#7206 Inhibition of CAD, an enzyme of de novo pyrimidine synthesis, to overcome EGFR-TKI resistance in NSCLC.

L. Saeednejad Zanjani, L. Zhao, S. Wang, M. Federoff, X. Sun, J. He;
Thomas Jefferson University, Philadelphia, PA

Given the fast-growing cancer cells, there is an increased demand for large amounts of energy and nucleotides for DNA and RNA synthesis. Thus, targeting nucleotide metabolism, specifically de novo nucleotide biosynthesis, is a promising strategy for cancer treatment. Hyperactivation of Carbamoyl-phosphate synthetase, aspartate transcarbamylase (CAD), a key enzyme catalyzing the first three steps of de novo pyrimidine synthesis, is a common event in tumors and has been associated with chemoresistance in tumors. Our analysis, using TCGA data, revealed that increased expression of CAD is associated with poor prognosis in non-small cell lung cancer (NSCLC). Epidermal growth factor receptor (EGFR) tyrosine kinase inhibitors (TKIs) have demonstrated significant benefits to patients with NSCLC harboring EGFR-activating mutations; however, acquired resistance limits their long-term efficacy. Therefore, it remains urgent to discover the underlying mechanisms for discovering novel therapeutic strategies for overcoming TKI resistance. Our previous findings demonstrated that blockade of S6K1 overcomes acquired resistance to EGFR-TKIs in NSCLC. It was reported that S6K1 is involved in de novo pyrimidine biosynthesis. In this study, we aimed to investigate whether CAD mediates S6K1-induced EGFR-TKI resistance in NSCLC. Immunohistochemistry analysis on a tissue microarray of lung adenocarcinoma tissues indicated that increased co-expression of p-CAD and S6K1 proteins is associated with clinicopathological parameters and poor survival outcomes. Our in vitro results showed an increased expression level of CAD and p-CAD proteins in TKI-resistant cells compared with parental cells upon TKI treatment. Knockdown of CAD by siRNA led to sensitizing TKI-resistant cells to osimertinib, as indicated by BrdU cell proliferation assay. Inhibition of S6K1 by a siRNA or specific inhibitors PF-470867 and LY2584702 effectively reduced the phosphorylation levels of CAD protein in TKI-resistant cells, suggesting that S6K1 may serve as an upstream regulator of CAD for TKI resistance. The String database predicted a protein-protein interaction between S6K1 and CAD. Indeed, our co-immunoprecipitation (co-IP) results revealed a direct association between S6K1 and CAD proteins. Importantly, TKI treatment enhanced the binding between S6K1 and CAD. Taken together, these findings provide evidence that CAD may mediate S6K1-mediated EGFR-TKI resistance in NSCLC. Our ongoing and future work will assess whether inhibition of CAD sensitizes resistant cells to TKI *in vivo* and elucidate the associated mechanism.

#7207 Targeting hippo signaling pathway to overcome chemoresistance in glioblastoma.

C. Wong, M. Kiang, K. Leung;
The University of Hong Kong, Hong Kong, China

The study aims to investigate whether the Hippo signaling pathway contributes to temozolomide chemoresistance in glioblastoma, and to validate whether the combinational treatment of temozolomide and YAP inhibitor is effective against glioblastoma. Temozolomide-sensitive and temozolomide-resistant U87 and U251 GBM human cell lines were previously established. Temozolomide-resistant cells were maintained in low-dose temozolomide. Here, we investigate whether Hippo signaling contributes to temozolomide chemoresistance. By modulating the Hippo signaling pathway through YAP gene knockdown, the outcome on cell proliferation was studied by cell viability assay (in vitro) and mouse orthotopic xenograft (in vivo). Finally, the therapeutic effect of YAP inhibitor is studied in vitro and in vivo respectively. Our data showed that YAP is overexpressed in temozolomide-resistant glioblastoma cells. Nuclear translocation of YAP (which becomes its active state) is increased in temozolomide-resistant cells. In fact, YAP inhibition show decreased cell viability and higher susceptibility to temozolomide. In addition, mice with tumor injection of the YAP knockdown cells reduced tumor size with temozolomide treatment. Similarly, YAP inhibitor resensitizes temozolomide-resistant cells to temozolomide. Combinational treatment of YAP inhibitor and temozolomide is effective in shrinking tumor size in mouse xenograft models. In conclusion, our data suggest dysregulated Hippo signaling pathway contributes to temozolomide chemoresistance, thus targeting the Hippo signaling pathway resensitizes GBM cells to temozolomide. This research provides pre-clinical evidence on using YAP inhibitor for combinational therapy with temozolomide for the treatment of glioblastoma.

#7208 Targeting histone demethylase KDM6B to overcome cisplatin resistance in testicular germ cell tumors.

R. Singh, D. Shokry, R. I. Boyd, B. C. Rennels, C. Powell, M. Kahn, S. J. Freemantle, M. J. Spinella;
University of Illinois at Urbana-Champaign, Champaign, IL

Testicular germ cell tumors (TGCTs) represent the most common carcinoma of young men and are believed to arise from the transformation of primordial germ cells (PGCs). TGCTs are highly curable with platinum-based chemotherapeutics. However, resistance to cisplatin does occur, leading to therapeutic failure with very limited further therapy options. Previously we demonstrated polycomb and histone H3K27me3 methylation is repressed in cisplatin resistance TGCT cells. In TGCT patients the expression of H3K27 histone methylase EZH2 and H3K27 histone demethylase KDM6B is significantly associated with recurrence free survival. Induction of H3K27 methylation using demethylase inhibitor JSK-J4 or knockdown of KDM6B resulted in restored cisplatin sensitivity in cisplatin resistant TGCT cells. Furthermore, Inhibition of H3K27 demethylase by GSK-J4 or genetic knockdown of KDM6B sensitized TGCTs to cisplatin *in vivo* suggesting potential clinical utility of targeting H3K27me3 in refractory TGCTs. To explore underlying mechanisms H3K27me3 ChIP-seq was performed that demonstrated genome-wide loss of H3K27me3 in cisplatin resistant cells. Integrative analysis of H3K27me3 ChIP-Seq and transcriptomics is ongoing. Together findings suggests that repression of H3K27 methylation may be a viable approach to overcome treatment failure in cisplatin resistant TGCTs.

#7209 Overcoming platinum resistance of high-grade serous ovarian cancer targeting the activated JAK/STAT pathways via extracellular vesicles.

K. Suzuki[1], A. Yokoi[1], K. Yoshida[1], Y. Yamamoto[2], H. Kajiyama[1];

[1]Nagoya Univ. Graduate School of Medicine, Nagoya, Japan, [2]National Cancer Center Research Institute, Tokyo, Japan

High-grade serous ovarian cancer (HGSOC) is the most common subtype of ovarian cancer. While HGSOC usually responds to initial treatment, most cases eventually relapse and develop platinum-resistant ovarian cancer (PROC). The molecular definition of PROC is still unclear, and overcoming PROC has been the biggest challenges. Extracellular vesicles (EVs) have an essential role in cell-to-cell communication within both the primary and distant microenvironments. In this study, we aimed to identify molecular mechanisms of PROC via EVs to suggest novel therapeutic strategies. Platinum responses were categorized by primary treatment-free interval of platinum less than 6 months as PROC, and more than 36 months as platinum good response. Ascites and tumor tissues have been collected prior to initial chemotherapy in patients with HGSOC for analysis according to platinum response. mRNA sequencing in tumor tissues identified significantly upregulated JAK/STAT pathways in PROC. The JAK/STAT family was highly expressed in PROC than the good response group, and also increased than adjusted normal ovaries and fallopian tubes. In addition, PROC cell lines and PROC patient-derived xenograft model tumor tissues showed high JAK expression. Small RNA sequencing for HGSOC tissues and ascites-EVs revealed that miR-135a-5p and miR-221-5p were highly expressed in both PROC tissues and ascites, and the expression of the two miRNAs had a positive correlation between tissues and ascites. Overexpression of the two miRNAs in HGSOC cell lines resulted in higher JAK family expression and resistance to cisplatin. JAK inhibitors (JAKi) had equivalent efficacy for platinum-sensitive/resistant HGSOC cell lines and JAKi highly suppress tumor growth in the PROC mouse model. In addition, suppression of JAK family expression in PROC cell lines significantly increased sensitivity to cisplatin. JAKi also had a synergistic effect with cisplatin for PROC cell lines. IPA analyses in mRNA sequencing in tumor tissues, TGF-β was highly expressed in upstream regulators in PROC, and TGF-β stimulation resulted in the upregulation of the two miRNAs in mesothelial cells, but not in HGSOC cell lines and fibroblasts. In summary, we here demonstrate novel molecular mechanisms of PROC via EVs and provided the rationale for JAK-targeted therapy for PROC. EV-miRNAs can regulate the PROC activated JAK/STAT pathway and can be diagnostic and therapeutic biomarkers for PROC definition or JAKi indications, suggesting that patient stratification in precision medicine for initial treatment of HGSOC.

EXPERIMENTAL AND MOLECULAR THERAPEUTICS: Targeted, Combination, and Differentiation Therapies
Poster Session

#7213 Tumor targeted activation of an attenuated exatecan protodrug through Click Chemistry demonstrates efficacy in murine tumor studies.
S. Srinivasan, S. Wagner, G. Coricor, T.-H. Nguyen, J. M. McFarland, J. M. Mejia Oneto;
Shasqi, Inc., San Francisco, CA

Shasqi is advancing the Click Activated Protodrugs Against Cancer (CAPAC®) platform based on click chemistry, a Nobel Prize winning technology. The platform is modular and comprises 1) an activator that target specific antigens, and 2) inert cancer drugs, protodrugs, which are selectively activated at tumors via click chemistry. The CAPAC technology separates the tumor targeting function from the payload and re-unites them at the tumor creating the flexibility to optimize activity while limiting toxicity during preclinical and clinical development. The modularity of the platform enables the rapid development of new therapies as well as unlocking unique treatment benefits such as tunable combinations and payload cycling. We envision that CAPAC will expand the scope of potential targets, widen the therapeutic window, and enhance the safety of locally activated cancer therapeutics. Here, we demonstrate the efficacy and safety of our exatecan protodrug (SQP07) used with intratumorally injected activators.
The activators, tetrazine-modified sodium hyaluronate biopolymer(s), are injected at the tumor site and followed by a systemic dose of SQP07, a trans-cyclooctene (TCO)-modified protodrug of exatecan (Exa). An efficient covalent reaction between tetrazine and TCO moieties releases active Exa at the tumor. In vitro cytotoxicity studies showed that SQP07 activated with tetrazine was effective against mouse and human tumor cell lines (MC38, CT26, EMT6 and NCI-N87); SQP07 without activator had potency attenuated by 60-133 fold.
In vivo tumor distribution and activity of SQP07 with the intratumoral biopolymer activators was evaluated in an NCI-N87 gastric cancer xenograft model. Female C.B-17 SCID mice received a single intravenous dose of vehicle (10% HPCD), Exa (50 mg/kg) or biopolymer (40 or 100 µL intratumorally) followed by SQP07 or SQP07 alone (50 mg/kg Exa mol equivalent). 1 hour after biopolymer + SQP07 treatment, activated Exa was highly concentrated in the tumor and stroma. This led to tumor regression in animals up to 40 days, performing significantly better than the free drug cytotoxic, Exa alone. Similarly, median survival with biopolymer + SQP07 was higher (>81 days) compared to Exa (68.5 days). Toxicity, measured as body weight loss, was comparable (~5%) and transient between Exa and biopolymer + SQP07. SQP07 alone treatment without the biopolymer was not differentiated from the vehicle control.
These data show that the CAPAC platform, which separates the targeting agent from the payload, is an effective way to administer cytotoxic therapies systemically. Additional work with other tumor models, different biopolymers and the SQP07 protodrug is ongoing.

#7214 A click chemistry-based HER2 targeting agent activates a decoupled MMAE payload making it highly differentiated in efficacy and safety than ADCs.

S. Srinivasan, S. Wagner, G. Coricor, J. M. McFarland, T.-H. Nguyen, J. M. Mejia Oneto;
Shasqi, Inc., San Francisco, CA

Shasqi is advancing the Click Activated Protodrugs Against Cancer (CAPAC®) platform based on click chemistry, a Nobel Prize winning technology. The platform is modular and comprises of 1) an activator that targets specific antigens, and 2) inert cancer drugs, protodrugs, which are selectively activated at tumors via click chemistry. The CAPAC technology separates the tumor targeting function from the payload and reunites them at the tumor creating the flexibility to optimize activity while limiting toxicity during preclinical and clinical development. The modularity of the platform enables the rapid development of new therapies as well as unlocking unique treatment benefits such as tunable combinations and payload cycling. We envision that CAPAC will expand the scope of potential targets, widen the activity window of antibody drug conjugates (ADCs). Here we compare a HER2-targeting activator + a monomethyl auristatin E (MMAE) payload with an ADC that binds the same target and carries the same payload, as well as other targeting formats.

The activator SQT01 is composed of a HER2-binding Fab conjugated with tetrazines (Tz). The protodrug SQP22 is formed by coupling trans-cyclooctene (TCO, with a releasable linker) to MMAE, a cytotoxic spindle poison. An efficient covalent reaction between tetrazine and TCO moieties releases active MMAE at the tumor.

Mice bearing human NCI-N87 HER2+ tumor were treated with 1) SQT01, 2) a non-binding isotype Fab-Tz, or 3) saline. After 18 h, all mice received either vehicle (10% HPCD), SQP22 protodrug, a non-releasable MMAE TCO-protodrug analog of SQP22, or a di-peptide-containing TCO-protodrug analog. We also tested CAPAC's approach with SQT06 (a full-length IgG trastuzumab-Tz conjugate) that was followed by an SQP22 dose after 4 days. The dosing of SQP22 with the Fab-Tz and IgG-Tz is timed to allow for systemic clearance of the targeting activator. Fabs have a shorter half-life than IgG, so we dosed SQP22 at 18 h after SQT01 instead of the 4-day timepoint with SQT06. To allow comparisons with ADCs, additional groups received a single dose of commercially available disitamab vedotin (DV) or a HER2-Fab-vedotin.

SQT01+SQP22 induced a strong tumor growth inhibition comparable to SQT06+SQP22, but significantly better than DV, and SQT01+non-releasable protodrug analog. Dosing with SQT01 with a protease cleavable dipeptide-TCO protodrug analog or a molar equivalent dose of HER2-Fab-vedotin were highly toxic and intolerable. Based on preclinical observations, SQT01+SQP22 was safe and tolerated, and there was no observed body weight loss.

These data demonstrate that the CAPAC platform, which separates the targeting agent from the payload, provides a clear benefit in terms of safety and efficacy compared with small or large format proteins with the classic fixed construct of ADCs (e.g. a fixed drug to antibody ratio).

#7215 Nectin-4 targeted therapy with MMAE protodrug results in anti-tumor efficacy mediated by click chemistry.

G. Coricor, J. M. McFarland, S. Srinivasan, S. Wagner, N. Yee, T.-H. Nguyen, J. M. Mejia Oneto;
Shasqi Inc., San Francisco, CA

Shasqi is advancing the Click Activated Protodrugs Against Cancer (CAPAC®) platform based on click chemistry, a Nobel Prize winning technology. The platform is modular and comprises 1) an activator that target specific antigens, and 2) inert cancer drugs, protodrugs, which are selectively activated at tumors via click chemistry. The CAPAC technology separates the tumor targeting function from the payload and reunite them at the tumor creating the flexibility to optimize activity while limiting toxicity during preclinical and clinical development. The modularity of the platform enables the rapid development of new therapies as well as unlocking unique treatment benefits such as tunable combinations and payload cycling. We envision that CAPAC will expand the scope of potential targets, widen the therapeutic index of antibody drug conjugates (ADCs). Here we present a Nectin-4-targeting activator with a monomethyl auristatin E (MMAE) payload.

Nectin-4 is a clinically validated tumor target expressed in a wide range of solid tumors, making Nectin-4 an attractive target for developing new therapeutic approaches for cancer patients. Substantial numbers of Nectin-4 targeting drugs are being developed but exhibit high rates of drug toxicities and highlight the need for alternative approaches that are efficacious and safe. We have developed a Nectin-4 Fab binder conjugated with tetrazine (~2.3 tetrazines per protein), SQT03, and tested it in combination with SQP22, an attenuated protodrug of MMAE conjugated to *trans*-cyclooctene (TCO). The reaction between tetrazine and TCO moieties releases MMAE at the tumor site. We have previously demonstrated that SQP22 is highly attenuated *in vivo* at doses that are > 20x the toxic dose of free MMAE, and in combination with a HER2 targeting activator, led to significant tumor growth inhibition in NCI-N87 gastric cancer xenograft model. The separation of an antigen-targeting activator from the payload by CAPAC technology allowed the rapid development and subsequent testing of SQT03 in combination with SQP22 *in vitro* and *in vivo*. SQT03 displayed <10nM binding affinity to Nectin-4 positive cells by flow cytometry analysis. *In vivo*, dosing of SQT03 occurs 8-24hrs prior to SQP22 to reduce systemic activation and to enable specific release of the active cytotoxic payload at the tumor site. In the T47D breast cancer xenograft model, a single dose of SQP22 at 8-24hrs after SQT03 led to tumor regression without body weight loss, in contrast to the 5% of body weight loss presented by two doses of Enfortumab-vedotin required to lead to similar activity.

The presented data illustrates how the CAPAC platform can be used to test various therapeutic combinations, accelerating development, and reducing the time it takes to bring treatments to the clinic. The results support further development and testing of MMAE protodrug with Nectin-4 targeting agent in clinical settings.

#7216 Improving anti-tumor efficacy by modulating a separate HER2 activator and an MMAE payload and reuniting both through click chemistry.

S. Wagner, M. Aleckovic, G. Coricor, S. Srinivasan, J. McFarland, T.-H. Nguyen, J. M. Mejia Oneto;
Shasqi, San Francisco, CA

Shasqi is advancing the Click Activated Protodrugs Against Cancer (CAPAC®) platform based on click chemistry, a Nobel Prize winning technology. The platform is modular and comprises 1) an activator that target specific antigens, and 2) inert cancer drugs, protodrugs, which are selectively activated at tumors via click chemistry. The CAPAC technology separates the tumor targeting function from the payload and reunites them at the tumor, creating the flexibility to optimize activity while limiting toxicity during preclinical and clinical development. The modularity of the platform enables the rapid development of new therapies as well as unlocking unique treatment benefits such as tunable combinations and payload cycling. We envision that CAPAC will expand the scope of potential targets and widen the therapeutic index of antibody drug conjugates (ADCs). Here we present proof of concept for a HER2-targeting activator with a monomethyl auristatin E (MMAE) payload. The activator SQT01 is composed of a HER2-binding Fab conjugated with tetrazines (Tz), a click chemistry component. The protodrug SQP22 is formed by coupling *trans*-cyclooctene (TCO), another click chemistry component, to MMAE, a cytotoxic spindle poison. SQT01 binding was confirmed via flow cytometry, while SQP22 was evaluated for stability and activation via the reaction of Tz and TCO moieties activating MMAE at the tumor site. *In vivo* activity was evaluated in a HER2+ gastric cancer (NCI-N87) xenograft model. SQP22 was stable in plasma and had minimal *in vivo* anti-tumor activity without the activator. When combined with SQT01 in tumor-bearing mice, SQP22 was rapidly activated and led to active MMAE at the tumor site within 15 minutes. In efficacy studies, this activation resulted in significant tumor growth inhibition compared to an isotype control or disitamab vedotin, an ADC that targets HER2 and carries an MMAE payload. Treatment with SQT01 and 3 daily doses of SQP22 resulted in 4/6 complete responses with no body weight loss. This response can be differentiated from the activity of the isotype control by modulating the dose levels of SQT01 or SQP22 and the time interval between the two. In a dose escalation study, increasing dose level combinations were evaluated. In another efficacy study the optimal timing between the administration of SQT01 and SQP22 was investigated. It was found that anti-tumor efficacy is maintained over a 4 to 24 hours dose gap, but non-specific activity is decreased by dosing SQP22 8 - 24 hours after SQT01, corresponding to increased safety. Additional toxicology studies are ongoing. This data indicates that the CAPAC platform, which separates the targeting agent from the payload, can be optimized for antigen specific efficacy and safety by modulating dose amounts and time intervals between both components.

#7217 Orthogonal targeting of NAD metabolism and ErbB2/ErbB3 signaling in pancreatic adenocarcinoma.

K. Chougoni, N. Kim, M. M. Dcona, D. T. Dcona, G. K. Malhotra, S. R. Grossman;
USC - University of Southern California, Los Angeles, CA

Background: Pancreatic ductal adenocarcinoma (PDAC) is now the third leading cause for cancer related deaths in the US with a five-year survival of ~10% that has improved little over the past 20 years. Thus, there is a critical need to fully understand mechanisms of PDAC tumorigenesis in order to develop novel and effective therapies. Nicotinamide Adenine Dinucleotide (NAD), a critical co-factor and energy source required for cellular processes such as DNA repair and epigenetic regulation is frequently upregulated in PDAC. We recently reported a novel oncogenic axis connecting the NAD-dependent epigenetic regulator and oncogene C-terminal Binding Protein (CtBP) with the EGFR family growth factor receptors ErbB2/ErbB3 (ErbB2/3) in PDAC cells and tumors. Indeed, previous reports have shown ~30% of human PDAC tumors overexpress ErbB3, and our work has shown that PDAC tumor cell growth relies on maintenance of ErbB3 expression. Moreover, we show that the majority of PDAC cells with high levels of ErbB3 expression are uniquely sensitive to the ErbB2-targeted tyrosine kinase inhibitor lapatinib. In addition, we have recently shown that co-targeting NAD and CtBP with small molecule inhibitors is an effective and synergistic therapeutic strategy in PDAC model systems.

Methods and Results: In the current study, we demonstrate NAD-dependent regulation of ErbB2/3 signaling in PDAC cells *in vitro*. Upon depletion of NAD using the NAD salvage pathway inhibitor GMX1778 in human PDAC cells, we observed a striking coordinate decrease in the levels of both ErbB2 and ErbB3. Furthermore, stable knockdown of the limiting enzyme of the complementing Preiss-Handler NAD synthetic pathway, Nicotinamide Adenine Phosphoribosyl Transferase, also resulted in robust downregulation of ErbB2/3 protein levels, suggesting a direct linkage in PDAC cells between the status of NAD metabolism and synthesis and activity of the key growth factor receptors ErbB2/3.

Conclusions: Our findings highlight the novel connection between NAD and ErbB2/3 in PDAC. Furthermore, our data suggests combining chemical or biologic inhibitors of ErbB2/3 with an inhibitor of NAD synthesis may result in highly synergistic cytotoxic effects in PDAC cells and PDAC preclinical models. Such data could support the future development of a human PDAC clinical trial repurposing agents targeting NAD synthesis and ErbB2/3 that are already FDA-approved or currently in clinical testing.

#7218 Venetoclax triggers apoptosis and augments the effectiveness of doxorubicin against acute myeloid leukemia cells.

O. Aloudat[1], O. Al Odat[2], T. Budak-Alpdogan[3], S. Jonnalagadda[2], Y. Chen[4], M. Pandey[1];

[1]Cooper Medical School of Rowan University, Camden, NJ, [2]Rowan University, Glassboro, NJ, [3]Cooper University Hospital, Camden, NJ, [4]College of Science and Mathematics, Rowan University, Glassboro, NJ

Acute myeloid leukemia (AML) is a hematologic malignancy characterized by the clonal proliferation of immature blast cells in the peripheral blood and bone marrow. AML is the second most common type of childhood leukemia, and 50% to 60% of relapses occur within the first year of diagnosis. Chemotherapy side effects and resistance are becoming major clinical issues. Although anthracyclines are one of the most commonly used induction regimens for children with AML in the United States, clinicians avoid them due to adverse effects and clinical resistance issues. To address this clinical issue, we are looking for a novel AML approach to boost the usage of anthracyclines. Since Bcl-2 protein overexpression in AML is related to uncontrolled growth, poor prognosis, and chemoresistance. Multiple clinical trials have suggested combining venetoclax (a selective Bcl-2 inhibitor) with well-established medicines to boost efficacy and overcome resistance. We suggest that inhibiting Bcl-2 is a feasible strategy for increasing the use of anthracycline medicines. We proposed combining doxorubicin and venetoclax as an alternative approach for AML patients. In a panel of three AML cell lines, Kusami-1, U937, and THP-1, our western blot revealed that Kusami-1 had the highest expression of Bcl-2 proteins. Surprisingly, venetoclax causes Kusami-1 cell death and increases the efficacy of doxorubicin in a dose-dependent manner, suggesting that utilizing a lower clinical standard dose may avoid major adverse effects such as cardiotoxicity. Furthermore, the Annexin V Apoptosis Detection Kit indicated that venetoclax coupled with doxorubicin synergistically promoted total apoptosis in Kusami-1 cells. The combination medication shown promising and synergistic in vitro anti-leukemic action against AML cell lines and represents a potentially viable treatment option for AML patients. Future research will use the combination approach in AML cell lines, as well as in patient samples and *in vivo* experiments.

#7219 Preclinical investigations of concomitant tumor treating fields (TTFields) with cisplatin for treatment of cervical cancer.

R. Frechtel-Gerzi[1], D. Gerasimova[1], E. Zeevi[1], R. Monin[1], H. Fishman[1], I. Schlachet-Drukerman[1], H. Mumblat[1], A. Martinez-Conde[1], R. Engelman[1], E. Dor-On[1], **I. Tzchori**[1], A. Haber[1], M. Giladi[1], U. Weinberg[1], Y. Palti[1], G. M. Palmer[2], A. Alvarez Secord[3];

[1]Novocure Ltd, Haifa, Israel, [2]Duke Cancer Institute, Duke University Medical Center, Durham, NC, [3]Duke Cancer Institute, Duke University Medical Center, Haifa, Israel

Introduction: Cervical cancer, although largely preventable, continues to be a significant health concern. Early-stage treatment is commonly surgery; while advanced, recurrent, or metastatic disease often requires systemic therapy. Chemotherapy, mainly cisplatin is the backbone of first-line therapy. TTFields are electric fields that disrupt cellular processes critical for cancer cell viability and tumor progression. In other tumor types, TTFields applied with cisplatin has exhibited benefit. This *in vitro* study assessed the preclinical efficacy of TTFields for cervical cancer and explored efficacy for concurrent use with cisplatin.
Methods: Effects on cell count in cervical cancer cell lines exposed to TTFields (0.5 V/cm for Ca Ski cells, 1 V/cm RMS for HeLa and SiHa cells; 72 h) across a range of frequencies (100-400 kHz) were evaluated. TTFields (200 kHz) were then applied with varying cisplatin doses followed by cell count, colony formation, and apoptosis assays. Overall effect was calculated as the product of percent reductions in cell count and colony formation. TTFields-treated cells were evaluated for formation of the DNA damage marker γH2AX using fluorescent microscopy; and for the expression of Fanconi Anemia (FA)-BRCA pathway proteins through Western blotting.
Results: TTFields treatment reduced cell count in all cervical cancer cell lines tested. Cisplatin exhibited dose-response effects, which were enhanced when TTFields were co-applied. TTFields led to downregulated expression of FA-BRCA pathway proteins, which are involved in repairing cisplatin-induced DNA damage, resulting in increased DNA damage.
Conclusions: These preclinical results suggest that TTFields should be further explored as a potential treatment for cervical cancer. TTFields-induced downregulation of the FA-BRCA pathway possibly explains the enhanced efficacy when TTFields are applied together with cisplatin, providing mechanistic insight.

#7220 Emerging combination strategy: FANCI suppression induces PARP1 redistribution to enhance efficacy of PARP inhibitors in breast cancer.

Y.-z. Huang[1], M.-Y. Sang[1], P.-W. Xi[1], R.-X. Xu[1], M.-Y. Cai[1], Z.-W. Wang[1], J.-Y. Zhao[1], Y.-H. Li[1], J.-F. Wei[2], Q. Ding[1];

[1]Jiangsu Province Hospital (The First Affiliated Hospital With Nanjing Medical University), Nanjing, China, [2]Jiangsu Cancer Hospital, Nanjing, China

While polyADP-ribose polymerase (PARP) inhibitors have made advancements in the treatment of breast cancer, challenges such as chemotherapy resistance and limited application persist. Fanconi AnemiaComplementation Group I (FANCI), a DNA repair protein associated with breast cancer development, represents a potential target for novel combination therapeutic strategies. However, the role of FANCI in breast cancer and its impact on the efficacy of PARP inhibitors require further investigation.

In our study, we analyzed FANCI expression in breast cancer tissues and cell lines, and its correlation with clinical parameters and patient prognosis. Lentiviral vectors were utilized and functional assays were performed to evaluate the effects of FANCI modulation on breast cancer cell growth and migration. Co-immunoprecipitation assays and protein interaction analysis were conducted to identify the interaction between FANCI and PARP1 and determine the specific binding region. The functionality and nuclear distribution of PARP1 were assessed upon FANCI modulation. Finally, the sensitivity of breast cancer cells to the PARP inhibitor talazoparib upon FANCI knockdown was evaluated *in vitro* and *in vivo*.

Our findings demonstrated that FANCI was overexpressed in breast cancer and associated with poor prognosis. FANCI significantly promoted breast cancer cell proliferation both *in vitro* and *in vivo*. We identified the interaction between FANCI and PARP1, specifically at the FANCI helical domain 2 binding site. FANCI knockdown led to reduced nuclear localization of PARP1 and decreased PARP1 activity. Importantly, combination treatment with FANCI knockdown and talazoparib significantly inhibited cancer growth *in vitro* and *in vivo*. Additionally, we found that the cyclin-dependent kinase (CDK) 4/6 inhibitor palbociclib, which effectively suppresses FANCI protein expression, exhibited a robust synergistic effect with talazoparib both *in vitro* and *in vivo*.

In conclusion, FANCI is a novel therapeutic target for breast cancer. Suppression of FANCI regulates PARP1 redistribution and activity, making breast cancer cells more responsive to PARP inhibitors. This combination therapeutic strategy shows potential in enhancing the effectiveness of PARP inhibitors for breast cancer treatment, regardless of BRCA mutations.

#7221 A compound targeting the circadian clock protein CRY2 enhances therapeutic efficacy of bevacizumab in a colorectal cancer (CRC) xenograft model.

J. Lo[1], S. Soni[1], G. Smbatyan[1], L. Torres-Gonzalez[1], P. Mittal[1], Y. Yang[2], F. Battaglin[1], P. Chan[2], Y. Pan[2], S. Algaze[1], P. Jayachandran[1], K. Ashouri[1], A. Wong[1], W. Zhang[1], J. Millstein[2], I. K. Singh[3], E. T. Roussos Torres[1], S. M. Mumenthaler[2], S. A. Kay[2], H.-J. Lenz[1];
[1]USC Norris Comprehensive Cancer Center, Los Angeles, CA, [2]University of Southern California, Los Angeles, CA, [3]University of Delhi, Delhi, India

Anti VEGF A antibody Bevacizumab combined with standard chemotherapy has improved outcomes for CRC patients. However, a subset of CRC patients acquires resistance to anti-VEGF treatment and underlying mechanism is poorly understood. Our recent study reported that circadian clock transcription factor BMAL1 drives transcription of VEGFA conferring resistance to bevacizumab treatment. Our rational is to stabilize negative regulator of circadian clock CRY protein to inhibit BMAL1 activity in a negative feedback loop. In this study, we evaluated whether CRY stabilizers SHP656 and SHP1705 in combination with bevacizumab can synergistically enhance anti-tumor effect in CRC mouse models.

Methods: *In vitro* tube formation assay was performed with HUVECs cells to investigate the effect of CRY stabilizer on tube formation. For *in vivo* experiments, 10^6 HCT116 human CRC cells were injected subcutaneously into the right flank of 8-week-old nude mice. Mice (5mice/group) were randomized into: A. vehicle (2% carboxymethylcellulose PO 5 days/week; control IgG IP, 2 days/week); B. bevacizumab (5mg/kg IP, twice/week); C. 10mg/kg SHP656; D. 30mg/kg SHP656; E. 30mg/kg SHP1705; F. 10mg/kg SHP656 + bevacizumab; G. 30mg/kg SHP656 + bevacizumab; G. 30mg/kg SHP1705 + bevacizumab. SHP 656 & 1705 was given PO; 5days/week. Tumor volume was measured three times a week. The survival curve was plotted using Kaplan and Meier method and assessed for statistical significance with log-rank test.

Results: The *in vitro* tube formation assay showed significant inhibition of tube formation in HUVEC cells treated with SHP1705 plus bevacizumab compared to treated with bevacizumab alone. In *in vivo* study, the tumors treated with 30mg/kg SHP1705 + bevacizumab significantly suppressed tumor growth compared to bevacizumab monotherapy (one way-ANOVA, $P < 0.05$). 30mg/kg SHP1705 + bevacizumab significantly improved survival of the mice (Log-rank test, $P < 0.05$). No significant survival benefit was observed with bevacizumab alone. 3/5 mice treated with SHP1705 + bevacizumab showed decreased tumor volume and achieved complete regression for more than 4 months without additional treatment. In combination with bevacizumab, higher dose of SHP656 (30mg/kg) delayed tumor growth and extended survival compared with bevacizumab monotherapy (though did not reach statistical significance) whereas the lower dose of 10mg/kg did not show anti-tumor effect, demonstrating a dose dependent response.

Conclusion: Our study shows that CRY stabilizers in combination with bevacizumab significantly enhances anti-tumor efficacy in CRC mouse models. Although mechanism of action of SHP compounds on angiogenesis pathway still needs further investigation, these findings may support development of novel treatment strategies modulating circadian clock to overcome bevacizumab resistance in CRC patients.

#7222 Antiandrogen equipped with HDAC inhibitors activates autophagy-mediated growth inhibition in castrate-resistant prostate cancer.

B. Chandrasekaran[1], K. Yalla[2], A. Tyagi[1], V. Shukla[1], N. Tyagi[1], B. Tyagi[1], M. Vashishta[1], A. Oyelere[2], C. Damodaran[1];
[1]Texas A&M University, College Station, TX, [2]Georgia Institute of Technology, Atlanta, GA

Targeting androgen receptor (AR) by pharmacologic intervention is one of the practical approaches for the treatment of castration-resistant prostate cancer (CRPC). Hence, this study aimed to develop novel molecules that employ multiple mechanisms to inhibit AR expression and curtail the growth of CRPC. The target antiandrogen-equipped histone deacetylase inhibitors were synthesized, adapting the convergent chemistry we used to synthesize the first-generation compounds. The final compounds were characterized using 1H-NMR, 13C-NMR, and high-resolution mass spectrometry. We synthesized and analyzed several compounds, in which KK62 emerged as the lead compound. KK62 significantly inhibits a panel of CRPC cell lines in nanomolar concentrations without causing toxicity to healthy prostate epithelial cells. The molecular analysis suggested that inhibition of AR and AR-splice variants was evident, followed by downregulation of PSA expression in AR-positive CRPC cell lines. Further analysis confirmed that KK62 overcomes dihydrotestosterone (DHT) induced AR signaling and enzalutamide-resistant CRPC cells by downregulating AR and AR-splice variants in CRPC cells. Subsequent analysis confirmed that KK62 induces autophagy signaling by upregulating autophagosome (LC3B) and lysosome (LAMP1) markers expression and facilitating the autophagosome and lysosome fusion, which resulted in the induction of apoptosis in all AR-positive CRPC cell lines. The pro-apoptotic markers, such as BAX and cleaved caspase, were upregulated, whereas the downregulation of pro-survival markers was evident in KK62-treated CRPC cells. Our ongoing castrated and non-castrated xenotransplanted CRPC tumors and Patient-derived xenograft in vivo studies would validate our in vitro findings and confirm that KK62 is a potent compound that may improve therapeutic advances in treating CRPC.

#7223 A triplet therapeutic strategy targeting MEK, BCL-XL, and EGFR, for KRAS-mutant pancreatic ductal adenocarcinoma.

G. W. Tushoski-Aleman, A. J. Crespin, C. J. Oguejiofor, J. A. McKean, K. M. Herremans, T. J. George, C. J. Allegra, S. J. Hughes, S. Han; University of Florida, Gainesville, FL

KRAS mutations drive over 90% of pancreatic cancers, but KRAS has been proven difficult to target. Downstream of KRAS, MEK inhibition in combination with BCL-XL inhibition is synthetically lethal and an effective treatment for gynecologic, but not colorectal malignancies. Like colorectal cancer, pancreatic cancer often exhibits aberrant HER/EGFR activity. We hypothesized that a triplicate regimen targeting MEK, BCL-XL, and EGFR/HER would be effective for pancreatic cancer. Trametinib (MEK inhibitor), Afatinib (pan-EGFR/HER inhibitor), and Navitoclax (BCL-XL inhibitor); or DT2216 (a BCL-XL/BCL-1 proteolysis targeting chimera, PROTAC) were explored using various combinatorial strategies. These drug combinations were tested using four primary human pancreatic cancer cell lines using live cell imaging (Incucyte) and an in vivo murine model. Group comparisons were analyzed using one-way ANOVAs, and adjusted p-values <0.05 were considered significant. We observed that no single-agent treatments were effective. MEK inhibition plus anti-BCL-XL (Trametinib + Navitoclax or Trametinib + DT2216) demonstrated efficacy in one of the four cell lines. We noted synergistic effects on reduced cell growth and increased cell death when EGFR/HER inhibition was included by the administration of Afatinib. The triplet combination resulted in synergistic effects in three of four cell lines with Navitoclax and four of four cell lines with DT2216 ($q<0.05$). This effect was confirmed with DT2216 inhibition of BCL-XL in an in-vivo murine model. In conclusion, our study shows that a combinatory strategy targeting MEK, BCL-XL, and pan-EGFR/HER receptor kinase shows significant synergistic effects in pancreatic cancer. Clinical trials that assess the efficacy and safety of this strategy for patients with KRAS-mutant pancreatic cancer are warranted. Our data also suggests that novel KRAS inhibitors as monotherapy are likely to fail.

#7224 Investigation of the efficacy of duocarmycin SA in combination with FDA approved drugs in acute myeloid leukemia cells *in vitro*.

W. A. Chen[1], D. Aguilar[1], L. So[1], Y. Jawhar[1], N. Nguyen[1], N. Drew[1], T. G. Williams[1], C. A. Casiano[1], S. Dovat[2], K. Boyle[1], O. L. Francis-Boyle[1];
[1]Loma Linda University, Loma Linda, CA, [2]Pennsylvania State University, State College, PA

Acute myeloid leukemia (AML) is a hematological malignancy that is characterized by the arrest of hematopoietic stem cell differentiation, clonal expansion of myeloid hematopoietic precursors and poor patient survival outcomes. Despite therapeutic advancements, the prognosis of AML patients remains poor and improving patient survival outcomes continues to be a challenge. Therefore, the objective of this study was to investigate the efficacy of Duocarmycin SA (DSA- an antitumor antibiotic that induces DNA alkylation) in combination with FDA approved drugs currently used in the treatment of AML. In this study, DSA was evaluated in combination with doxorubicin (an anthracycline that disrupts topoisomerase II mediated DNA repair) or etoposide (a topoisomerase II inhibitor used to treat relapsed/refractory AML) in human AML cells *in vitro*. We hypothesized that DSA in combination with doxorubicin or etoposide would exhibit synergistic effects by improving the efficacy of both doxorubicin and etoposide in AML cells. The human AML cell lines (Molm-14 and HL60) were used for all studies. The phenotype of the cells was confirmed by flow cytometry and the IC_{50} of the drugs were determined using the MTT assay. Our results showed that the AML cells were $CD45^{\pm}$, $CD33^{\pm}$, $CD13^{\pm}$ and $CD4^{\pm}$. The IC_{50} of DSA alone for Molm-14 cells and HL60 cells were 11.12 pM and 114.8 pM, respectively. DSA alone induced DNA double-stranded breaks, significantly decreased the production of colonies and significantly increased apoptosis in AML cells in a dose-dependent manner. The IC_{50} of doxorubicin alone and etoposide alone was 68.6 nM and 129.7 nM, respectively. DSA in combination with the FDA approved AML drugs showed increased cytotoxic efficacy by observable decreases in AML cell viability. In summary, 1) picomolar concentrations of DSA alone was sufficient to significantly reduce AML cell viability; 2) DSA in combination with doxorubicin or etoposide significantly reduced AML cell viability and reduced the IC_{50} concentration of doxorubicin and etoposide. Thus, highlighting the therapeutic potential of using DSA in combination with doxorubicin or etoposide as a drug combination strategy to improve AML patient survival outcomes by decreasing the concentration of drugs necessary to treat patients and reducing off-target toxicity.

#7225 Combination JAK1/2 and CDK8/19 inhibition demonstrates enhanced efficacy in myeloproliferative neoplasms.

Z. Zaroogian[1], E. Adamczyk[2], A. Moszyńska[2], M. Obacz[2], U. Pakulska[2], B. Durham[1], M. Mazan[2], S. Mowla[1], K. Wnęk[2], A. Hanasoge Somasundara[1], B. Barczuk[2], A. Gołas[2], R. Levine[1], T. Rzymski[2], R. Rampal[1];

[1]Memorial Sloan Kettering Cancer Center, New York, NY, [2]Ryvu Therapeutics, Krakow, Poland

Myeloproliferative neoplasms (MPNs) are characterized by aberrant activation of the JAK-STAT pathway. Ruxolitinib (RUX) is a JAK1/2 inhibitor used to treat myelofibrosis (MF) and hydroxyurea-resistant/intolerant polycythemia vera. While RUX has demonstrated important clinical benefits, a large proportion of patients have persistent disease manifestations despite therapy. CDK8 regulates phosphorylation of STAT proteins in a RUX-independent manner; thus, CDK8 inhibition may alter downstream STAT target gene expression. RVU120 is a highly selective and potent CDK8/19 inhibitor that inhibits STAT1/5 phosphorylation. We hypothesized that the combination of RUX and RVU120 would act in a cooperative manner to attenuate JAK-STAT signaling and reduce MPN phenotypes *in vivo*.

Using *JAK2*^{V617F} mutant leukemic cell lines, we identified dose-responsive changes in viability with RUX and RVU120 in all cell lines. Pharmacodynamic analysis validated that STAT5 protein phosphorylation was decreased by RUX/RVU120, although at different phosphorylation sites by RUX (pTYR694) and RVU120 (pSER726/731); exposure to RUX+RVU120 inhibited phosphorylation at both sites. Notably, analysis of combinatorial effects of RUX+RVU120 on viability demonstrated drug synergies (combinatorial index <1) in RUX-naïve and resistant SET-2 cells. Nascent RNA expression data exploring JAK-STAT and mediator-related pathways of pathogenesis will be presented at the meeting.

For *in vivo* studies, we used two previously-described murine models of MF and PV. Briefly, retrovirally-transfected (*MSCV-MPL*^{W515L}*-IRES-GFP*) or *Jak2*^{V617F}-conditional knock-in bone marrow (BM) was intravenously injected into lethally-irradiated congenic recipients. Mice were randomized and treated for several weeks with vehicle (VEH), single-agent RUX/RVU120, or RUX+RVU120 arms. Spleen weights between VEH and RUX/RVU120 treated mice at time of terminal sacrifice were significantly reduced across both models ($p<=0.009$). In *MPL*^{W515L} mice, WBCs and PB GFP% were significantly reduced ($p<0.002$) and histopathology demonstrated near-elimination of BM reticulin fibrosis and improved trilineage hematopoiesis between RUX+RVU120 and RUX arms. Data on overall survival, cytokine profiles, and the impact of RVU120 on dynamic gene expression will be presented at the meeting.

The combination of RVU120 and RUX demonstrated biochemical synergy and differential inhibition of STAT5 phosphorylation *in vitro*. Further, *in vivo* treatment with RVU120/RUX+RVU120 resulted in significant reductions of disease manifestation (splenomegaly, WBC, fibrosis scoring, hematopoiesis) when compared to VEH/RUX. These data nominate JAK1/2 and CDK8/19 inhibition as a potential novel therapeutic strategy in MPNs; further work on nascent RNA expression and cytokine profiles will potentially elucidate additional mechanisms of action.

#7226 Synergy between ONC201 and temozolomide on ATF4 integrated stress response in glioblastoma.

J. Chen[1], T. J. Roady[2], L. Zhou[2], W. S. El-Deiry[2];

[1]Brown University, Providence, RI, [2]Legorreta Cancer Center at Brown University, Providence, RI

Glioblastoma multiforme (GBM) is the most common primary brain tumor in adults, with a median survival of 15 months. The standard of care involves surgical resection followed by chemoradiotherapy. Even with the full course of treatment, GBM is uncurable, and patients eventually relapse. Although temozolomide (TMZ) is the first-choice chemotherapeutic for GBM, tumor drug resistance limits the effects of the treatment. There is a growing need for new therapies with enhanced efficacy on GBM tumors. Dordaviprone (ONC201) is a TNF-related apoptosis inducing ligand (TRAIL)-inducing compound that is increasingly being studied for GBM treatment. This imipridone small molecule induces apoptosis by activating the integrated stress response, which involves transcription factors ATF4 and CHOP. Subsequently, these transcription factors upregulate proapoptotic protein TRAIL and its receptor, Death Receptor 5 (DR5).

This study aims to investigate the combinatory effects of chemotherapeutics TMZ and ONC201 on GBM. Preliminary studies examined the cell viability of GBM cell line U251MG after dual treatment of 0 to 10uM of ONC201 and 0 to 200uM of TMZ using the CellTiter-Glo assay. Synergy was observed between the two drugs at higher concentrations of TMZ. This synergistic interaction was further characterized using western blots. When 0, 2, and 4uM of ONC201 were administered alone or in combination with 0, 60, and 120uM of TMZ, greater ATF4 expression was observed with the dual treatments than with the monotherapies. Subsequent western blots were conducted using three GBM cell lines (U251MG, T98G, and SNB19-GFP) at three time points (8, 24, and 48 hours). All cell lines were treated with 0 and 5uM of ONC201 alone or in combination with 0 and 200uM of TMZ. For all three cell lines, ATF4 expression increased in the combined presence of TMZ and ONC201. However, the effects of TMZ on ONC201-induced ATF4 expression were most pronounced in U251MG and least conclusive in T98G. Additionally, the time points in which this increase in ATF4 expression occurred varied among cell lines. CHOP expression was also probed and was seen to increase with the combination treatment in U251MG. These observations suggest a potential synergistic relationship between chemotherapeutics ONC201 and TMZ in the ATF4 integrated stress response pathway in GBM. By exploring the effects of this dual treatment on upstream and downstream factors in the pathway, we can identify, characterize, and potentially target the root cause of this synergy.

#7227 Isatin analogs potentiate the cytotoxicity of venetoclax in acute myeloid leukemia cells.

U. Golla[1], S. Patel[1], J. Hengst[1], C. Annageldiyev[2], J. Schramm[2], S. Amin[1], D. Desai[1], D. Claxton[2], S. Dovat[2], A. Sharma[1];
[1]Penn State College of Medicine, Hershey, PA, [2]Milton S. Hershey Medical Center, Hershey, PA

Acute Myeloid Leukemia (AML) is a rare but common hematological malignancy in children and adults. AML is a highly heterogeneous disease caused by the acquisition of several mutations affecting multiple cellular processes, thus requiring concomitant targeting of key survival nodes to treat effectively. As current first-line therapies for AML suffer with poor outcomes, drug resistance, and high relapse rates, there is an immediate need for new combinatorial therapies that are both safe and effective. Venetoclax (VEN), a selective inhibitor of antiapoptotic protein B-cell lymphoma-2 (BCL2), has been FDA-approved for treating adult AML and displayed potential in pediatric leukemia treatment. However, the activation of an antiapoptotic BCL2 family member, Myeloid Cell Leukemia 1 (MCL1), is often a primary mechanism of resistance to VEN therapy. Our group has developed Isatin analogs (ISA) that exhibited diverse biological activities, including anti-cancer activities alone or in combination with standard agents. ISA demonstrated anti-leukemic activity by targeting leukemic stem cells (LSCs) with high aldehyde dehydrogenase (ALDH) activity. In this study, we demonstrate ISA induces apoptosis by downregulating antiapoptotic MCL1 levels in pediatric and adult AML cell lines. Based on the inhibitory effects of Isatin analogs on key signaling pathways (PI3K/AKT, STAT3) and MCL1, we combined ISA with a BCL2 inhibitor, VEN, for effective AML treatment. The combination of ISA with VEN exhibited synergetic cytotoxicity in naïve (MOLM-13, MV4-11) and VEN-resistant (HL-60, OCI-AML3, U937, and KG-1) human AML cell lines by bliss analysis. ISA also showed significant synergetic cytotoxicity in combination with ABT-737, a BH3 mimetic inhibitor of Bcl-xL, Bcl-2, and Bcl-w. Combinatorial treatment of AML cell lines with sub-lethal doses of ISA and VEN showed a significant increase in cellular apoptosis as indicated by the levels of annexin V measured by flow cytometry. Immunoblotting analysis after co-treatment with ISA and VEN showed downregulation of MCL1 levels along with alteration of other key apoptosis regulators in both VEN-sensitive (MV4-11) and inherently VEN-resistant (U937) AML cell lines. Current and future studies will primarily focus on further exploiting the molecular mechanism of action for the combinatorial approach. Furthermore, our aim will be to demonstrate activity in primary patient cells along with preclinical efficacy in AML animal models. To summarize, in vitro findings showed synergetic cooperation between ISA and VEN in combination for effective induction of apoptosis and anti-leukemic activity in AML cells that are sensitive and resistant to VEN.

#7228 In-vitro efficacy of Dordaviprone/GSK126 combination therapy on castration resistant and neuroendocrine prostate cancer.

Connor Purcell, Praveen Srinivasan, Maximilian Pinho-Schwermann, William MacDonald, Elizabeth C. Ding, Vida Tajiknia, Wafik El-Deiry

Legorreta Cancer Center at Brown University, Providence, RI

Neuroendocrine prostate cancer (NEPC) is an aggressive histologic subtype associated with poor prognosis that commonly arises in later stages as a mechanism of treatment resistance. Activation of oncogenic drivers, in combination with epigenetic changes (such as EZH2 overexpression and DNA methylation) further promotes tumor proliferation and expression of downstream neuroendocrine lineage pathways (in part controlled by transcription factors, including SOX2, ASCL1, and BRN2). Importantly, EZH2 inhibitors (EZH2i) can restore AR expression in CRPC (Ku et al., 2017). Imipridones, including Dordaviprone (ONC201), show promise in treating neuroendocrine tumors by interacting with DRD2 and CLpP (Anderson et al., 2022). These results warrant investigation into the potential for synergism in imipridone/EZH2i combination therapies.

In the PCa cell lines LNCap, PC3, 22Rv1, and DU145 the combination of ONC201 and EZH2i GSK126 was assessed. Cell viability data after treatment with ONC201 and GSK126 reveals several dose ranges with potential synergistic activity after 72h. Preliminary western blots after 72 hours of GSK126 treatment indicate modulation of proteins relevant to the mechanism of action of imipridones, specifically DR5 and CLpP, in LNCap, PC3, and 22Rv1. Notably, the decrease in DR5 expression warrants investigation into the effects of EZH2i on TRAIL sensitivity and whether imipridones may rescue DR5 expression to maintain TRAIL sensitivity.

Subsequent experiments will investigate dosing and time point-based effects on viability and protein expression, in addition to assessing the synergy of other imipridones and EZH2i's. Further, while the cell lines PC3, 22Rv1, and DU145 are castration-resistant, the neuroendocrine prostate cell line NCI-H660 will be used as a positive control as it expresses higher neuroendocrine features, including DRD2. Additionally, the modulation in DR5 expression warrants inquiry into the effects of combination therapy on tumor-immune cell interactions. Further, we will manipulate the expression of neuroendocrine transcription factors to assess changes in therapy sensitivity.

#7229 In situ trans-differentiation therapy effectively terminates the growth and recurrence of glioblastoma.

H. Zhao[1], Z. Li[1], X. Zhang[2], C. Zhao[3], Z. Zhu[1], **Y. Liu**[1];

[1]Neuregen Therapeutics, Shanghai, China, [2]State Key Laboratory of Cognitive Neuroscience & Learning and McGovern Institute for Brain Research, Beijing Normal University, Beijing, China, [3]Shool of Biomedical Engineering and informatics, University of Posts and Telecommunications, Chongqing, China

Background: Glioblastoma (GBM) is the most common and malignant brain tumor in adults, and remains almost invariably lethal due to its aggressive and invasive nature. The standard first-line treatment for GBM is surgical resection, postoperative radiotherapy and chemotherapy with temozolomide (TMZ), but it exhibits short-term effects due to a high recurrence rate of GBM is its (up to almost one hundred percent). This long-existing clinical challenge has demanded development of novel and effective therapeutic strategies. *In situ* cell trans-differentiation therapy which direct reprograms tumor cells into terminally differentiated benign cells represents a novel therapeutic strategy for tumors. We further explored the application of in situ trans-differentiation therapy for glioblastoma.

Results: In the present study, we have conducted a large-scale screen for transcription factors which can reprogram glioblastoma cells into terminally differentiated postmitotic cells. Over-expression of a combo of selected trans-differentiation factors that possess the highest trans-differentiation rate effectively reprogramed human glioma cells into neuronal-like cells with characteristic neuronal morphology and expression of neuronal genes in culture, as a result substantially reducing glioblastoma cell proliferation and tumor development after orthotopic transplantation. With replicable recombinant oncolytic virus vectors, product candidate can specifically replicate in glioma cells, therefore transcription factors can be specifically delivered to all tumor cells rather than normal cells. In either cell line-derived or patient-derived tumor tissue xenograft models, intra-tumoral injection product candidate inhibited glioblastoma cells growth at an exceptionally high efficiency. Remarkably product candidate combination with TMZ resulted in a complete regression of tumor and no recurrence was observed in animal model cases.

Conclusion: In summary, our findings have established a novel therapeutic approach for treating glioblastoma by terminating sustained proliferation of glioma cells via transcription factors-induced *in situ* cell trans-differentiation and supported further clinic investigations in patients.

#7230 A novel platform for identifying therapeutic index in pancreatic cancer.

V. Pantazopoulou, D. Engle;
Salk Institute for Biological Studies, La Jolla, CA

Pancreatic ductal adenocarcinoma (PDA) remains highly aggressive with a mere 12% 5-year survival rate, which underscores the urgent need for improved therapeutic approaches. The current standard of care primarily includes surgery and chemotherapy. However, existing therapies often result in severe side effects and offer limited success. The limitations are not only due to the development of treatment resistance but also due to the killing of normal cells, and as such a low therapeutic index. Targeted therapies aimed at the primary drivers of PDA, such as the $KRAS^{G12D}$ mutation or the activated ErbB pathway, have shown promise in providing novel treatment options. We have previously demonstrated that combining targeted therapies, specifically $KRAS^{G12D}$ and EGFR inhibitors, results in reduced tumor growth in both human and murine PDA organoid models *in vitro*. However, less is known about how these targeted therapies affect normal cells. Here, we are using co-cultures of normal pancreas and PDA organoids to create a platform that allows us to identify combinations of targeted therapies that can achieve a higher therapeutic index. Our goal is to identify treatment combinations that allow for the use of lower individual drug dose, while exhibiting enhanced anti-tumor efficacy and minimizing toxicities to normal organoids. This approach holds significant promise for improving patient outcomes and addressing the challenges associated with current PDA treatments.

EXPERIMENTAL AND MOLECULAR THERAPEUTICS: Vector Systems, Oncolytic Virotherapy, and Gene Therapy
Poster Session

#7234 The second-generation high-fidelity base editor AccuBaseTM (ceBE) can proficiently modify multiple genes within a human primary T cell while minimizing Off-target effects.

H. Ying[1], G. Li[1], L. Wang[1], C. Lu[1], Q. Lai[1], C. Yao[1], F. Lv[1], S. Zhu[2], T. Xu[1];
[1]Base Therapeutics (Shanghai) Co., Ltd., Shanghai, China, [2]Shanghai University of Traditional Chinese Medicine, Shanghai, China

Off target mutations, chromosomal rearrangements and Indels are the biggest limitation to the use of gene editing tools today. Base editing system provides an efficient method to modify the genome without double strand breaks (DSB). The biggest problem for base editing is the sgRNA-independent off-target. We utilize synthetic biology strategies to create a novel base editor AccuBase™ (ceBE) that has the highest editing efficiency in the industry, with zero off target events. This was achieved by strategically inserting deaminases into Cas9 at specific, tolerance-verified sites, a process guided by an extensive transposon-based genetic screening, protein engineering, and direct evolution approach. AccuBase™ protein forms a complex with the sgRNA, but it has not yet engaged with the target DNA and is not in contact with any non-targeting dsDNA. This mechanism avoids guide RNA independent indiscriminate off-target mutations that was a common problem of the first generation base editing tool. Upon guided by sgRNA, the AccuBase™ protein associates with the target double-stranded DNA, triggering structural alterations within the AccuBase™ protein. This results in the outward exposure of the deaminase domain, facilitating the editing of the target base. AccuBase™ (ceBE) substantially reduces off-target effects while maintaining on-target editing when compared to BE4max. This improvement has been confirmed in multiple human cell lines, mouse cell lines, human primary T and NK cells, human embryonic stem cells, and in animal embryos. In this study, we apply AccuBase™ to achieve multiplex gene modifications in primary human T cells, demonstrating its capacity for highly efficient multiplex gene disruption without inducing off-target effects. Importantly, the multiplex base-edited T cells exhibit enhanced *ex-vivo* cell expansion and do not exhibit the double-strand break-induced translocations observed in T cells edited with Cas9 nuclease.

#7235 Exosome-mediated delivery of siRNA against NRF2 for treatment of lung cancer.

R. Kandimalla[1], M. Wallen[2], J. Jeyabalan[2], D. N. Moholkar[3], W. Spencer[2], R. C. Gupta[4], F. Aqil[1];

[1]Brown Cancer Center, University of Louisville, Louisville, KY, [2]3P Biotechnologies, Louisville, KY, [3]University of Louisville, Louisville, KY, [4]Brown Cancer Center, University of Louisville and 3P Biotechnologies, Louisville, KY

Nuclear factor erythroid 2-related factor 2 (NRF2) activation is the third most common genetic event in lung adenocarcinomas (25%), primarily induced by loss of function mutations in its master regulator, KEAP1. NRF2 is a key modulator of tumor growth and metabolic reprogramming, resulting in resistance to traditional chemotherapeutics. Due to its role in modulating oxidative stress, sustained NRF2 overexpression promotes disease progression, particularly in lung cancer. This study demonstrates the effective knockdown of NRF2 expression by small interfering RNA (siRNA) delivered via a nanoplatform based on bovine colostrum exosomes to lung cancer cells, both *in vitro* and *in vivo*, resulting in inhibition of proliferation and disease progression. Bovine colostrum is an abundant source of exosomes. Here we present a novel exosome-polyethyleneimine matrix (EPM) to deliver therapeutic siRNA targeting NRF2 expression (si*NRF2*). Specific delivery of the EPM to tumors was further enhanced via folic acid (FA) functionalization, targeting folate receptors highly expressed on lung tumor cells. Exosomes were isolated from standardized colostrum powder through rehydration and differential centrifugation, and characterized by size, polydispersity index (pdi) and surface charge by Zetasizer, and the presence of surface protein markers by Western blot. si*NRF2* was loaded onto the EPM, and the resultant EPM-*siNRF2* complex was harvested by PEG precipitation. Entrapment efficiency was determined using 5'-^{32}P-labeled siRNA as a tracer. The gene knockdown efficiency of EPM-*siNRF2* was assessed in lung cancer (A549) cells by Western blot and the therapeutic effect of target knockdown *in vitro* was confirmed by analyzing the corresponding modulation in downstream targets of NRF2. The anti-tumor effect was then evaluated using both subcutaneous and orthotropic lung tumor models in immunocompromised mice. The EPM exhibited high entrapment efficiency (>90%) of si*NRF2* (up to 20 µg) and protected entrapped siRNA from enzymatic degradation upon exposure to RNases. EPM-si*NRF2* dose dependently decreased NRF2 expression in A549 lung cancer cells. When formulated with FA-functionalized exosomes, EPM-si*NRF2* inhibited subcutaneous and orthotropic lung tumors in mice by over 57% ($p<0.01$) and 84% ($p<0.001$), respectively. Mice treated with FA-EPM-si*NRF2* showed decreased levels of NRF2 in tumor tissue, but not in the adjacent lung, indicating FA-mediated targeted delivery.

This bovine colostrum exosome based EPM technology showcases high efficiency in gene knockdown and lung tumor inhibition, providing a promising nanoplatform for delivering nucleic acid therapeutics to the tumor site.

Funding: Supported from the NIH grant R44 CA-221487, 3P Biotechnology Contract and, in part, Agnes Brown Duggan Endowment.

Keywords: Bovine colostrum, Exosomes, NRF2, siRNA, Lung cancer.

#7236 Selective deletion of the KRAS mutant gene with ADGN-123 and ADGN-121 peptide-RNA nanoparticles: A new strategy to overcome acquired resistance to KRAS^{G12C} and KRAS^{G12D} small molecule inhibitors.

G. Divita[1], A. Grunenberger[2], V. Guzman-gonzalez[2], E. Czuba[2], k. Boularache[2], M. Guidetti[3], V. Josserand[3], N. Desai[1];
[1]AADIGEN, Pacific Palisades, CA, [2]DIVINCELL, Nimes, France, [3]IAB, Grenoble, France

KRAS codon12 mutations are among the most commonly observed mutations in cancers. Recently, KRAS^{G12C} inhibitors (sotorasib and adagrasib) have been approved and KRAS^{G12D} inhibitor MTRX-1133 has shown preclinical efficacy in *KRAS^{G12D}* mutated cancers. However, these inhibitors are limited by adaptive resistance, mainly associated with the emergence of secondary KRAS mutations, activation of feedback pathway and amplification of KRAS^{G12C} allele. We have developed a new potent strategy combining gene editing with tumor selective peptide nanoparticles, to overcome acquired resistance to KRAS^{G12C} and KRAS^{G12D} inhibitors.

ADGN-123 and ADGN-121 are gene-editing complexes containing proprietary sgRNA targeting KRAS^{G12C} and KRAS^{G12D} respectively, complexed with proprietary peptides. ADGN-123 and ADGN-121 were evaluated on pancreas, colorectal, and lung cancer cells harboring KRAS$^{G12C\ or\ G12D}$ mutations. ADGN-123 was evaluated on NCI-H358 and Mia-PACA generated clones resistant to sotorasib/adagrasib and harboring KRAS^{G12C,R68M} and KRAS^{G12C,Y96D} secondary mutations. ADGN-121 was evaluated on ASPC-1 and PANC-1 generated clones resistance to MRTX-1133 . *In-vivo* efficacy of IV-administered ADGN-121 (0.25-1.0 mg/kg, day 1 and 7) was evaluated in PANC-1 (KRAS^{G12D}) mouse xenografts.

ADGN-123 and ADGN-121 selectively silenced KRAS^{G12C} and KRAS^{G12D}, respectively, in cancer cells resulting in inhibition of cell proliferation (IC_{50}: 10-30 nM) and of the phosphorylation of ERK and AKT. we showed that ADGN-123 containing gRNA^{G12C}/$mRNA_{Cas9}$ blocks the proliferation (IC_{50} : 10-20 nM) of cells with secondary KRAS$^{G12C/R68M}$ and KRAS$^{G12C/Y96D}$ mutations or with KRAS in a permanent active state and effectively inhibits ERK phosphorylation. We showed that ADGN-121 containing gRNA^{G12D}/$mRNA_{Cas9}$ can effectively inhibit the proliferation (IC_{50} : 10-15 nM) of ASPC-1 MRTX-1133R and PANC-1 MRTX-1133R cells with high level of KRAS^{G12D}-GTP active state. No resistance was detected after ADGN-123 or ADGN-121 treatments. We demonstrated that only two IV-administrations of ADGN-121 containing gRNA^{G12D}/$mRNA_{Cas9}$ abolished PANC-1 tumor growth in a dose dependent manner, resulting in significant tumor regression at 1.0 mg/kg. In contrast, no effect on tumor growth was observed with nonspecific gRNA. ADGN treatments were well tolerated, with no signs of clinical toxicity detected after single or repeat administration.

Our study provides a proof-of-concept that ADGN complexes can be applied to target driver mutations of cancers *in vivo* and permanently disrupt the oncogenic alleles, leading to major tumor regression. ADGN-123 and ADGN-121 constitute a potent alternative strategy to overcome resistance associated to small molecule inhibitors of KRAS^{G12C} and KRAS^{G12D}

#7237 Peptide-mRNA complex mediated restoration of BRCA-1 tumor suppressor function in BRCA-1 mutated cancers as a new therapeutic strategy.

G. Divita[1], A. Grunenberger[2], L. Cabrera[2], N. Durany[1], N. Desai[1];
[1]AADIGEN, Pacific Palisades, CA, [2]DIVINCELL, Nimes, France

BRCA1 and BRCA-2 proteins are involved in the repair of DNA damage such as double-strand breaks during S and G2 phases, by intervening in homologous recombination (HR) steps. Breast cancers arising from BRCA-1 mutation carriers (10% of BC) and from epigenetically silenced BRCA-1 (30% of sporadic BC) are associated with a lack of expression and/or function of BRCA-1, which induces genomic instability. Herein, we describe a new potent strategy combining mRNAs with a tumor selective peptide nanocarrier, to selectively rescue BRCA-1 function as potential therapeutic approach in cancers.
Proprietary BRCA-1 derived mRNA were complexed with proprietary short amphipathic peptides and the resulting nanoparticles were evaluated on several breast cancer cells, harboring different BRCA-1 alterations.. Sensitivity to Veliparib (PARPi) following the nanoparticle treatments were evaluated on PARPI resistant and PARPi sensitive cells. The recruitment of RAD51 to sites of double stranded DNA break was quantified by immunofluorescence. *In-vivo* efficacy of varying sequences of BRCA-1 mRNA-peptide nanoparticles (2.0 mg/kg, weekly, IV; ADGN-901, -902, -903) and veliparib (50mg/kg, daily, oral) were evaluated on breast cancer (HCC1937-BRCA-1 deficient, PARPi resistant) mouse xenografts.
We showed that ADGN-901 inhibits the proliferation of BRCA-1 deficient cell lines from 20 to 60% depending on the type of BRCA-1 alterations. ADGN-902, specifically reduces the proliferation of cells expressing N-terminal truncated BRCA-1, by 50 to 60% and ADGN-903 inhibits proliferation >60% of all cells harboring defects in BRCA-1. Interestingly, ADGN-901 and ADGN-903 were able to resensitize the PARPi resistant cells to veliparib inhibition. We demonstrated that ADGN-903 restores BRCA-1 function in homologous recombination. ADGN-903 prevents RAD51 recruitment to the damage site by reducing RAD51 protein level as well as formation of RAD51 foci following irradiation. IV administration of ADGN-901 and ADGN-903 (2.0 mg/kg) had a strong inhibitory effect on HCC-1937 tumor growth while ADGN-902 and veliparib were inactive. ADGN-901 reduced tumor growth by 95% and ADGN-903 abolished tumor growth with strong tumor regressions. ADGN-901 and ADGN-903, were also evaluated on large tumors of about 500-600 mm^3 and were highly effective in preventing further progression and achieving shrinkage of large tumors. ADGN-901 and ADGN-903 treatments are well tolerated, without inducing clinical toxicity. BRCA-1 mRNA-peptide nanoparticles are effective in rescuing BRCA-1 function and inducing tumor regressions in BRCA-1 altered breast cancer cells and tumors. Our study provides a proof-of-concept that restoration of wild type BRCA-1 expression could be a potent therapeutic strategy for BRCA-1 altered tumors whether or not they are PARPi resistant.

#7238 Exploring the potential of targeted DNA Nanobot delivery systems for gene delivery.

M. Shahhoessini[1], J. R. Spitzner[1], C. R. Lucas[1], C. E. Castro[2], **P. D. Halley**[1];
[1]DNA Nanobots, LLC, Columbus, OH, [2]The Ohio State University, Columbus, OH

Gene therapy is a cornerstone of modern medicine's quest for precision treatment to cure human disease including cancer. The current approach to gene delivery technology employs viral vector delivery systems. While effective, these vectors present significant challenges including immunogenicity, safety concerns due to off-target non-tissue specific delivery, payload limitations, and significant cost ultimately diluting their therapeutic potential. Thus, novel approaches to gene delivery are necessary. One such approach to address these critical limitations involves DNA Nanobots, a DNA-based nanotechnology that allows for a tissue-/target-cell specific gene delivery system. Utilizing DNA origami molecular assembly techniques, our DNA Nanobots offer a customizable and highly precise delivery platform, free from viral vector constraints. This innovative approach has the potential to transform the landscape of gene therapy by providing a safer, more efficient, and targeted alternative. Key technical advancements with our DNA Nanobots Gene Delivery Platform include: •CRISPR Cas-9 Integration: By incorporating CRISPR Cas-9 functional proteins, our nanobots were shown to enhance gene editing precision in primary human T cells, broadening therapeutic applications across various genetic conditions. •Targeted mRNA Delivery: Our nanobots revealed promising results in the targeted delivery of mRNA, vital for vaccine development and personalized treatments. •Efficient antisense/siRNA Delivery: Prior studies have overcome traditional challenges including endosomal escape and cytoplasmic entry, demonstrating effective siRNA delivery critical for gene silencing therapeutic development. In summary, DNA Nanobots mark a paradigm shift in gene therapy. Their ability to deliver various nucleic acids with high specificity and efficiency addresses many of the current methodological limitations especially off-target safety concerns and high cost. This advancement not only enhances the therapeutic index of existing treatments but also opens avenues for novel therapeutic strategies, potentially reshaping the future of molecular medicine and gene therapy.

#7239 Eradication of B cell lymphoma in a mouse model through *in vivo* transduction of T cells with an aCD19-CAR utilizing a CD3-targeted lentiviral vector.

K. Krotova[1], G. Nenavath[1], N. Packiriswamy[1], R. Vandergaast[1], Y. McDaniel[1], M. Moy[1], Z. Larson[1], L. Schnebeck[1], C.-H. Chin[1], K. Gromer[1], K.-W. Peng[2], S. J. Russell[2];

[1]Imanis Life Sciences, LLC, Rochester, MN, [2]Vyriad, Rochester, MN

One of the challenges in CAR-T cell therapies is the need for ex vivo processing of autologous T cells. The generation of CAR-T cells directly within the patient has therefore become an attractive alternative. Here, we pseudotyped lentiviral vectors with a VSV-G protein engineered to de-target the LDL receptor and to bind to CD3 via a displayed CD3-specific single-chain antibody (G-CD3), allowing for targeted recognition of T cells. In ex vivo experiments, we demonstrated that engineered G-CD3-LV specifically recognizes and transduces T cells in PBMC and whole blood without apparent off-target transduction of other cells. Furthermore, unlike G-WT-LV, which necessitates T cell activation for transduction, G-CD3-LV does not require pre-activation or the presence of cytokines for successful T cell transduction. The presence of CD3 antibodies on the surface of G-CD3-LV alone was sufficient to activate T cells, as evidenced by CD25 expression and the induction of T cell proliferation. For in vivo evaluation of retargeted LV efficiency NSG mice implanted with NALM6 B-lymphoma were treated with G-CD3 LV encoding αCD19-CAR/GFP (G-CD3/LV-CAR). The tumor was established by tail vein injection of NALM6/F-Luc cells, and 3 or 10 days later animals were humanized via intraperitoneal (IP) injection of human PBMC. Four hours after PBMC transfer, G-CD3/LV-CAR was delivered by IP route. Blood was drawn every week to monitor the generation of CAR-T cells, cytokine levels, and vector copy numbers. Tumor burden was monitored by bioluminescence imaging. Treatment with G-CD3/LV-CAR at both time points resulted in complete tumor eradication. Subsequently, significant levels of CAR-T cells were observed in the blood through Flow analysis, peaking at two weeks after LV injection. Importantly, mice treated on day 10 after tumor establishment reached higher levels of CAR-T cells compared to those treated on day 3 (CAR-T levels were 38±6.5% vs. 10±2.38% of hCD45+ cells, respectively). These results suggest that CAR-T cells proliferated proportionally in response to the level of tumor antigen. With the eradication of the tumor, CAR-T levels in the blood diminished. We also demonstrated that the levels of CAR-T cells correlated well with vector copy numbers. Throughout the treatment, mice did not exhibit any signs of toxicity or body weight loss. Additionally, by measuring cytokines in the blood produced by human cells, we found only a moderate increase in hIFNγ (0.852±0.681 ng/ml) at the peak of CAR-T cell levels in the blood, while the levels of hIL-2 and hTNFα were below the detection limit. In summary, these data highlight the efficiency and potential applicability of fully retargeted, serum stable LV vectors for in vivo CAR-T generation, offering promising prospects to optimize CAR-T cells therapy applications.

#7240 Intratumor delivery of plasmid DNA encoding immune stimulating agents induces both local and systemic responses.

R. Heller[1], L. C. Heller[1], G. Shi[1], J. Synowiec[1], J. Singh[1], A. Otten[2], M. J. Jaroszeski[2];
[1]USF Health Morsani College of Medicine, Tampa, FL, [2]University of South FLorida, College of Engineering, Tampa, FL

Immune checkpoint inhibitors (ICIs) have significant clinical benefits, but are limited by both primary and acquired resistance. The absence of T cells within the tumor microenvironment (TME) is a significant hurdle, reducing the efficacy of ICIs against solid tumors. Multiple studies have been initiated to modify the TME to enhance the effectiveness of ICIs. We previously demonstrated that the intratumor delivery of a plasmid encoding interleukin-12 (pIL-12) using gene electrotransfer (GET) resulted in a significant increase in T effector cells and a reduction in T regulatory cells and myeloid derived suppressor cells within the TME, inducing a robust immune response. Combining pIL-12 GET with ICIs resulted in local and systemic responses in both preclinical and clinical studies. While encouraging results were obtained, improvements were possible. For example, the established GET technology requires high applied voltage for plasmid delivery. In addition, satisfactory delivery cannot be immediately detected. Our current research has focused on developing the next generation GET technology to overcome these issues. This new system includes a pulse generator, a heat source and a tissue impedance measuring device. An array that incorporates independently addressable electrodes was also developed. A moderate elevation of the tissue temperature coupled with the electrode array enabled a 75% reduction in the applied voltage. We tested the approach in the B16.F10 mouse melanoma model. Delivery of pIL-12 with the new system resulted in 100% long-term complete regression and 100% protection from challenge. In addition, monitoring impedance within each independent section of the electrode array revealed different pulse numbers were needed to achieve delivery in each section. We next evaluated a combination therapy, pIL-12 plasmid combined with a plasmid encoding a PD1 peptide, delivered with the next-gen device. In a multi-tumor model, the plasmids were delivered to the subcutaneous tumor; tumors generated with an intraperitoneal injection were untreated. This new therapy induced complete regression of the subcutaneous tumor and blockage of peritoneal tumor growth as assessed via in vivo imaging. Peritoneal tumor growth was not affected by single plasmid delivery or when both plasmids were delivered with the established GET technology. Work is ongoing to translate this approach to clinical evaluation.

#7241 Combination of CDK4/6 inhibitor promotes the antitumor effect of oncolytic adenovirus against canine breast cancer cells.

N. Hashimoto[1], H. Tazawa[1], S. Kikuchi[1], S. Kuroda[1], Y. Urata[2], S. Kagawa[1], T. Fujiwara[1];

[1]Okayama University Graduate School of Medicine, Dentistry and Pharmaceutical Sciences, Okayama, Japan, [2]Oncolys BioPharma, Inc., Tokyo, Japan

Background: Oncolytic virotherapy has emerged as a novel antitumor platform to induce tumor-specific cytopathic effect against human cancer cells. However, whether oncolytic virotherapy is effective to canine cancer cells remains unclear. We developed telomerase-specific oncolytic adenoviruses OBP-301 and a p53-armed OBP-702 based on human adenovirus serotype 5. OBP-301 and OBP-702 have therapeutic potential against various types of human cancer cells. As recent report has suggested that human adenovirus serotype 5 induces cytopathic effect against canine cancer cells, OBP-301 and OBP-702 are expected to have therapeutic effects against canine cancer cells. Furthermore, it has been reported that CDK4/6 inhibitors clinically used for human breast cancers promote the replication of oncolytic adenoviruses, suggesting that combination of CDK4/6 inhibitors promote the therapeutic potential of oncolytic adenoviruses. In this study, we investigated the therapeutic potential of OBP-301 and OBP-702 against canine breast cancer cells in monotherapy and combination therapy with CDK4/6 inhibitor.

Methods: Two canine breast cancer cell lines (CMT-U27, AZA-CB) were used in this study. The antitumor effect of OBP-301 and OBP-702 against canine breast cancer cells was analyzed using the XTT assay. The therapeutic potential of combination therapy with CDK4/6 inhibitor (palibociclib) was further analyzed. Virus-mediated induction of adenovirus E1A and p53 expression was analyzed by Western blotting. The in vivo antitumor effects of OBP-301 and OBP-702 were assessed using CMT-U27 subcutaneous tumor model.

Results: OBP-301 and OBP-702 had cytopathic effect against CMT-U27 and AZA-CB cells. The antitumor activity of OBP-702 was superior to that of OBP-301. The combination of palbociclib and OBP-301 showed a more profound antitumor effect compared with monotherapy against CMT-U27 and AZA-CB cells. The expression of E1A and p53 was increased in virus-treated CMT-U27 and AZA-CB cells in a dose-dependent manner. Intratumoral administration of OBP-301 and OBP-702 significantly suppressed the growth of subcutaneous CMT-U27 tumors compared with mock treatment.

Conclusion: Our results suggest that telomerase-specific oncolytic adenoviruses have cytopathic effect against canine breast cancer cells via virus infection and replication. Furthermore, combination of CDK4/6 inhibitor may be a promising strategy for promoting the antitumor effect of oncolytic adenovirus against canine breast cancers.

#7242 Immunostimulatory gene therapy co-expressing immune activators TMZ-CD40L and 4-1BBL with a PD-L1-targeting Affibody molecule to reactivate T cell immunity.

L. A. White[1], I. Vaask[1], J. Hardin[1], E. Eriksson[1], A. Sandegren[2], F. Y. Frejd[2], T. Lovgren[1], A. Loskog[1];
[1]Uppsala University, Uppsala, Sweden, [2]Affibody AB, Solna, Sweden

Immunotherapy has been used to make great strides in helping cancer patients, and new approaches to reactivate patient immunity are constantly being developed. We are developing immunostimulatory gene therapy using adenoviruses as gene vehicles to inflame the tumor microenvironment and drive anti-tumor immunity. One consequence of immune activation is PD-L1 upregulation, so to optimize our treatment, we are using a novel gene therapy vehicle expressing both immune activators and a PD-L1-blocking Affibody molecule. Affibody molecules are tri-helical proteins engineered to bind specific target molecules with high affinity. These molecules have successfully been used to image cancer cells in the body and can block target proteins. Affibody molecules are advantageous over other affinity molecules due to their small size, averaging about 6 kDa, and their high stability. The small size makes an Affibody molecule an ideal candidate for use in viral vectors, where genetic space is limited. In the present study, we tested the biological activity of a PD-L1 targeted Affibody molecule expressed from a viral vehicle compared to the synthetic protein, using a Bio-IC *in vitro* luciferase assay. Further, the capacity of the PD-L1-binding Affibody molecule to prevent inhibitory signaling was evaluated in an ovarian cancer/immune cell co-culture assay.
Our results demonstrate that cell lines infected with viral gene vehicles successfully express and release the Affibody molecule as demonstrated with PCR and ELISA. Furthermore, the supernatants containing the Affibody molecule and synthetic Affibody molecule inhibited the activity of PD-L1 in the BioIC assay. Next, an adenovirus vector containing trimerized-CD40L and 4-1BBL (LOAd703), known to upregulate PD-L1 in stimulated dendritic cells, was modified to co-express the anti-PD-L1 Affibody molecule (LOAd724). Gene expression was confirmed using PCR, flow cytometry (CD40L, 4-1BBL) and ELISA (anti-PD-L1 Affibody molecule). The tumor/immune cell co-culture is underway. In summary, Affibody molecules can be expressed from adenoviral gene vehicles alone or in combination with immunostimulatory genes. Further studies are warranted to understand the role of local PD-L1 blockade in the tumor microenvironment following LOAd724 therapy.

#7243 CRISPR-cas9 genetic targeting of metastatic pancreatic cancer.

K. Bowland[1], J. Lai[1], S. K. Teh[1], A. Bennett[1], A. Skaist[1], Y. Zhang[1], E. Thompson[1], R. H. Hruban[1], N. J. Roberts[1], R. Karchin[1], C. A. Iacobuzio-Donahue[2], J. R. Eshleman[1];

[1]Johns Hopkins University School of Medicine, Baltimore, MD, [2]Memorial Sloan Kettering Cancer Center, New York, NY

Metastatic cancer affects millions of people worldwide annually and is the leading cause of cancer-related deaths. Most patients with metastatic disease are not eligible for surgical resection, and current therapeutic regimens have varying success rates, some with 5-year survival rates below 5%. Here we test the hypothesis that metastatic cancer can be genetically targeted by exploiting somatic single base substitution mutations that occur as part of normal aging prior to transformation. These passenger mutations are targetable because ~10% of them form novel tumor-specific “NGG” protospacer adjacent motif (PAM) sites targetable by CRISPR-Cas9. We studied five patients with pancreatic cancer (pc) who underwent a rapid autopsy to determine areas of evolutionary conservation that were maintained throughout all metastases in each patient’s cancer. Using whole genome sequencing validated by high-depth capture sequencing, we found that 90% of somatic PAM targets were maintained between primary carcinomas and metastases. We identified regions of loss of heterozygosity (LOH) surrounding tumor suppressor genes and oncogenes in the primary tumor where PAMs were 100% conserved in metastases. These regions of truncal LOH represent genetic vulnerabilities in these carcinomas and a CRISPR-based gene therapy approach targeting PAMs in these regions may be a novel way to genetically target metastatic cancer. Using multitarget sgRNA which cut at a known number of sites in the human genome, we determined a relationship between the number of CRISPR-Cas9 cuts and growth inhibition in PC cells. We found that 8-10 target sites in non-coding regions were sufficient to induce >95% cancer cell death. Furthermore, only 2-3 targets were required to achieve a comparable level of cell death in the presence of a DNA double strand break inhibitor. Finally, using cocultures of PC cells transduced with sgRNA targeting multiple tumor specific PAMs, we demonstrate selective cell killing of three different PC cell lines. Importantly, deep sequencing of patient-matched normal lymphocytes lacking the tumor-specific PAMs treated with the same sgRNA array exhibited no editing at the targeted loci. This work establishes a bioinformatic platform for the discovery of tumor-specific CRISPR targets in the context of metastatic disease and demonstrates selective killing of cancer cells while sparing the patient’s normal cells. These data establish the proof of principle for a gene therapy approach targeting metastatic disease.

#7246 Enhancing PDAC therapy through *in vivo* correction of *KRAS*^{G12D} using enIscB-directed base editor combined with ICB.

C. Yang, Q. Fang, T. Zhou, Y. Xie, J. Yu, J. Hao;
Pancreas Center, Tianjin Medical University Cancer Institute and Hospital, National Clinical Research Center for Cancer; Tianjin Key Laboratory of Digestive Cancer; Tianjin's Clinical Research Center for Cancer, Tianjin, China

In this study, we aim to investigate the therapeutic potential of *in vivo* genetic therapy using AAV-mediated adenine base editor (ABE) delivery for pancreatic ductal adenocarcinoma (PDAC) carrying the *KRAS*^{G12D} mutation (PDAC^{G12D}), and further explore its potential when combined with immune checkpoint blockade (ICB). The *KRAS*^{G12D} mutation is a dominant genetic alteration representing a highly sought-after and effective therapeutic target in PDAC. However, the *in vivo* genetic therapy for *KRAS*^{G12D} in PDAC has been rarely explored. Programmable base editors have been shown to install genetic mutations precisely and have significant therapeutic value, providing a promising strategy for genetic therapy of PDAC^{G12D}. Here, we engineered ABEs derived from various programmable nucleases, considering the protospacer adjacent motif (PAM) or target adjacent motif (TAM) sequence. The hypercompact A8e-enIscB demonstrated the highest editing efficiency in HEK293T^{G12D} and PANC-1 cell lines. Subsequently, A8e-enIscB was packaged into a single-AAV system and delivered to humanized mice subcutaneously transplanted with patient-derived organoid^{G12D} (PDO^{G12D}). We found the delayed tumor progression with BE-based genetic therapy. Additionally, a substantial editing efficiency in tumor tissues and lower off-target editing in normal tissues was observed. By comparing single-cell transcriptome sequencing data between BE-treated and non-treated samples, we observed a reprogrammed immune microenvironment characterized by elevated infiltration of cytotoxic CD8^{+} T cells and NK cells, as well as decreased recruitment of suppressive PMN-MDSCs, Tregs and TAMs upon correction of *KRAS*^{G12D}. Furthermore, AAV-directed ABE genetic therapy could significantly sensitize PDAC to ICB therapy (anti-PD-1, anti-CTLA4) in humanized PDAC PDO/PDX mouse models. Accordingly, an ongoing work in which the genetic therapy combined with ICB phase IA investigator-initialized trial will be designed to evaluate the safety of this regimen. In summary, our study demonstrates the efficiency and safety of innovative genetic therapy for correcting the *KRAS*^{G12D} mutation in PDAC. Furthermore, we demonstrated the therapeutic potential of combining this genetic therapy with ICB.

#7247 Exosome-mediated delivery of RNA and DNA: Enhanced efficiency with polycationic PEI-PEG.

Disha Nagesh Moholkar[1], Raghuram Kandimalla[2], Margaret Wallen[3], Jeyaprakash Jeyabalan[4], Wendy Spencer[3], Farrukh Aqil[5], Ramesh C. Gupta[6]

[1]Department of Pharmacology and Toxicology, University of Louisville, Louisville, KY,[2]Brown Cancer Center, University of Louisville, Louisville, KY,[3]3P Biotechnologies, Inc., Louisville, Louisville, KY,[4]Department of Pharmacology and Toxicology, 3P Biotechnologies, Inc., Louisville, Louisville, KY,[5]Department of Pharmacology and Toxicology and Brown Cancer Center, University of Louisville, Louisville, KY,[6]Department of Pharmacology and Toxicology, University of Louisville and 3P Biotechnologies, Inc., Louisville, Louisville, KY

Emerging advances in gene therapy over the past few decades have revolutionized biomedical research. Our lab has pioneered bovine milk and colostrum-derived exosomes (Exo) and devised a nanoplatform for nucleic acid delivery achieving targetability with folic acid (FA) functionalization. We showed that bovine colostrum exosomes complexed with high MW polyethyleneimine (PEI-60K) can efficiently delivery siRNA and plasmid DNA (pDNA) in vitro and in vivo. We hypothesize that lower MW PEI may improve transfection efficiency and enhance oral uptake of EPM-siRNA, in addition to presumably higher degradability in a cellular system. We now report that exosomes and PEI of lower MW (25K)-PEG copolymer is as effective or more effective for delivery of siRNA and pDNA than PEI-60K. Incubation of exosomes, PEI-25K and siRNA in the presence of 5'-^{32}P-labeled siRNA as a tracer showed high siRNA entrapment (>90%) based on the distribution of the radioactivity in EPM-siRNA precipitate compared with the supernatant. The efficacy of the EPM matrix is gene specific. As treatment of A549 lung cancer cells with EPM-(PEI-60K)-si*KRAS* showed 60% knockdown of target KRAS gene, which was enhanced to 70% by EPM-(PEI-25K)-si*KRAS*. Moreover, p53-pDNA delivered by EPM-25K resulted in nearly 2-fold higher expression of p53 in p53-null H1299 lung cancer cells compared with EPM-60K. However, still lower MW PEI (PEI-15K) diminished the transfection efficiency (36% KRAS knockdown). EPM formulated with PEI-60K and 25K had similar effect on cell viability of HEK293 cells. Upon *in vivo* testing, EPM-25K loaded with si*KRAS* and functionalized with folic acid (FA) showed time-dependent growth inhibition of A549-innoculated orthotopic lung tumors in NOD Scid mice eliciting 76% ($p<0.01$) tumor growth inhibition. The tumor inhibition was accompanied with 50% ($p<0.05$) knockdown of the target gene in the tumor tissue, while the adjacent lung tissue showed no modulation. The anti-tumor efficacy of si*KRAS* delivered by FA-functionalized EPM-25K is the same or somewhat higher than the efficacy reported previously with FA-functionalized EPM-60K.In conclusion, based on our *in vitro* and *in vivo* results, lower MW PEI (PEI-25K) is a suitable alternative for PEI-60K with boosted efficacy in terms of knockdown of KRAS. Our proposed technology offers a platform to advance and overcome the obstacles in the clinical translation of gene therapy.

Funding: Work supported from funds provided by 3P Biotechnologies and in part Agnes Brown Duggan Funds. Disha Nagesh Moholkar is supported by IPIBS Fellowship, University of Louisville.

#7248 Simultaneous isolation and parallel analysis of genomic DNA and RNA for gene therapy.

H. Wei;
Beckman Coulter, Inc., Indianapolis, IN

Introduction Viral vectors, such as adeno-associated vector (AAV), play a crucial role in delivering transgenes for gene therapy research. The success of vector transduction is vital for efficacy, which is measured through vector copy number (VCN) and transgene expression. In preclinical studies, both VCN and transgene expression are commonly tested from the same sample to ensure accuracy. We have reported a method for simultaneous high-quality genomic DNA and RNA extraction without splitting the sample, utilizing SPRI bead-based technology that has consistent performance across diverse tissue types and brain regions.

Methods AAV was administered to mouse and non-human primate (NHP) models. At the conclusion of each experiment, tissue samples from the adrenal gland, brain, gonads, heart, kidney, liver, lung, skeletal muscle, spinal cord, and spleen were harvested. All tissue samples that demonstrated around 15 mm^3 were snap-frozen in liquid nitrogen before nucleic acid extraction. The extraction process was carried out manually or on an automated liquid handler. The quality and quantity of DNA and RNA were then assessed from all tested tissues before downstream assay.

Results Our study found that all mouse tissue types (n=72/tissue type) and NHP (n=11/tissue type) had an average gDNA and RNA yield that exceeded the minimum yield cutoff of 25 ng/µL for DNA and 6.25 ng/µL for RNA. We also analyzed DNA from tissues treated with two different AAV serotype-treated tissues in the mouse model, which showed that transduction across all the tissues was highly efficient for both AAV serotypes. Furthermore, we observed variations in transgene expression levels (copies/1 µg RNA) among different tissue types. Similar patterns of VCN and transgene expression were also observed in NHP models.

Conclusions Efficient gene therapy depends on a safe and effective viral vector. The simultaneous extraction of gDNA and RNA simplifies the process, saves time, ensures quality, and facilitates integration into existing lab automation. This leads to consistent and error-resistant performance in analyzing vector copy and transgene levels.

#7250 Serial assessment of GEN2, a retroviral vector for gene transfer of an optimized thymidine kinase and GM-CSF, for genomic integration into peripheral blood mononuclear cells (PBMCs) in a Phase 1 clinical trial in adult patients with solid tumors.

A. L. Hannah[1], N. Kasahara[2], L. Liu[1], A. Wang[1], J. McNulty[1], R. G. Johnson, Jr.[1];
[1]GenVivo, San Marino, CA, [2]University of California San Francisco, San Francisco, CA

GEN2 is a non-replicating retroviral gene transfer vector encoding a sequence-optimized herpes simplex thymidine kinase (HSV-TK), which activates the antiherpetic pro-drug ganciclovir (GCV), resulting in chain termination during DNA replication, triggering cancer cell apoptosis and release of neoantigens (NA). GEN2 also encodes hGM-CSF, which may augment antitumor immunity by enhancing NA presentation to immune effector cells. GEN2 in combination with valganciclovir (an oral formulation of GCV) was evaluated in a dose-escalating Phase 1 clinical trial in 61 adult patients (pts) with an advanced solid tumor (NCT04313868), with serial assessment of PBMCs to detect any GEN2 integration and replication competent retrovirus (RCR). Methods: PBMCs were obtained in Cycle 1 (following 1st /3rd dose), prior to and 2 hours after Cycle 2, and thereafter at 6-month intervals for 15 years, or until death or withdrawal of consent. Digital droplet PCR (ddPCR) for psi and envelope gene sequences in extracted genomic DNA from PBMCs was used to detect vector genome integration and replication competent retrovirus (RCR), respectively. Results: All 82 samples obtained from the intravenous cohorts 1-12 were below LOD (Limit of Detection) for RCR. All results for integration were BLOQ (Below Limit of Quantitation), whereas 4 samples collected at two hours following the end of infusion were above LOD, likely resulting from non-integrated cDNA. GEN2 continues to be studied in clinical trials in adult patients with solid tumors. Per the 2020 FDA Guidance for Industry (Long Term Follow-Up After Administration of Human Gene Therapy Products), serial assessment of vector integration is mandated throughout a pt's participation in a gene therapy clinical trial and for 15 years following the last dose. These guidance documents were originally conceived when gene therapy was developed for treatment of rare hereditary diseases in pediatric pts; however, adult pts enrolled in early-stage clinical trials for cancer typically do not have a prolonged life expectancy (BMC Cancer 2011 11:426). In the context of proper and warranted usage of pts' blood for testing, attention should be drawn to the limited expectation for a 2nd malignancy within the lifespan of this pt population, and the absence of detectable RCR in cancer patients receiving retroviral vectors over decades. A recent review noted no evidence of RCR in 1,595 post-treatment PBMCs obtained from 60 clinical trials (Mol Ther 2023 31(3):801). Our results confirm that GEN2 also shows negligible genotoxic risk for gene therapy of cancer at doses tested to date.

#7251 Surface-engineered extracellular vesicles to modulate antigen-specific T cell expansion for cancer immunotherapy.

X. Lyu, T. Yamano, S. Imai, T. V. Le, R. Hanayama;
Kanazawa University, Kanazawa, Japan

Tumor immunotherapy, including immune checkpoint therapy, CAR T cell therapy, and TCR-T cell therapy, has made significant progress in the treatment of cancer. Recently, newly developed nanomaterials have also been applied to anti-tumor immunotherapy. Among them, extracellular vesicles (EVs) have been well-engineered in recent years due to their low immunogenicity, high stability, and wide distribution in biological fluids. Despite the recent development of several EVs-based cancer immunotherapies, their clinical efficacy remains limited. In this study, we have developed engineered EVs designed to mimic the function of antigen-presenting cells, which can co-deliver multiple immune-activation signals to tumor-associated T cells. We named these vesicles Antigen-presenting Extracellular Vesicles (AP-EVs). AP-EVs express a high level of MHC I-peptide complexes, costimulatory molecules, and surface-bound cytokines, allowing for the simultaneous presentation of multiple immune modulators to antigen-specific CD8+ T cells. AP-EVs promote the clonal expansion and differentiation of antigen-specific cytotoxic T lymphocytes, resulting in potent anticancer immune responses. Notably, our findings indicate that combination therapy involving AP-EVs and anti-PD-1 yields superior anticancer immunity against established tumors compared to anti-PD-1 monotherapy. This synergistic effect underscores the potential of our engineered EVs as a novel and highly effective strategy for cancer immunotherapy.

#7252 Characterization of targeting peptide sequences for peptide-mediated delivery of siRNA in HER2+ breast cancer.

A. Miserendino, S. Tekle, J. Kalogeros, A. Alexander-Bryant;
Clemson University, Clemson, SC

Introduction: This work presents the characterization of two novel HER2 targeting peptides to measure which has the most compatible properties to be used as a siRNA carrier to knock down the CD44 gene in HER2+ breast cancer.

Procedures: Targeting peptides were electrostatically complexed with non-targeting siRNAs at different N:P ratios to determine the minimum binding ratios needed to form nanoparticles. Different ratios of peptide-siRNA complexes were tested to determine the minimum molar ratio at which the peptides would protect siRNA from degradation. Cytotoxicity assays were performed to determine cytotoxicity levels at different peptide concentrations. Dynamic light scattering assay was performed to determine peptide-siRNA nanoparticle size and zeta potential. Immunofluorescent microscopy was used to determine the targeting of the peptide to HER2+ cells compared to cells not expressing HER2.

Summary of Results: Peptide-siRNA complexes for the P51 and P25 peptides formed at a minimum 20:1 N:P ratio. P25 and P51 peptides both successfully protects the siRNA at N:P ratios from 20:1 to 60:1 for both degradation agents. Cytotoxicity assays show that in the SKBR3 cell line, the P25 and P51 peptides both showed above 80% viability until the 70:1 ratio; however, in the BT474 cell line, the P25 showed above 80% viability to the 50:1 ratio, but the P51 was only viable in the 20:1 ratio. The results of these studies illustrate how both peptides protect siRNA but that the P51 peptide is toxic to some HER2+ breast cancer cell lines.

Conclusions: Results show that both peptides target HER2+ breast cancer and are compatible carriers of siRNA, protecting the siRNA well within a cell-like environment. However, from MTS studies, P25 appears less cytotoxic to the cell lines than P51, which shows higher cytotoxicity at high molar ratios. We observed that the P25 protects siRNA from degradation, is cytocompatibility, and promotes efficient internalization into HER2+ cell lines. Future work will include the development of a tandem peptide, including a targeting peptide fused with a fusogenic peptide to increase cancer targeting and efficacy of this targeted treatment.

Acknowledgments: This research was supported in part by the Dabo Swinney All-In Foundation as well as Materials Assembly and Design Excellence in South Carolina (MADE in SC) under the National Science Foundation EPSCoR Program under NSF Award #OIA-1655740. Data presented in this material was partially collected using SC BioCRAFT facilities supported by the National Institute of General Medical Sciences (NIGMS) of the National Institutes of Health under award number P30 GM131959.

#7253 Oncolytic virus therapy with two-factor authentication shows robust safety and efficacy in liver cancer.

C. M. Moles[1], P. Weijmarshausen[1], R. Basu[1], B. Ho[1], M. Farhat[1], T. Flaat[1], B. F. Smith[2], M. Whitt[3], S. E. Woodfield[4], S. A. Vasudevan[4];
[1]Humane Genomics, New York, NY, [2]Auburn University College of Veterinary Medicine, Auburn, AL, [3]University of Tennessee Health Science Center, Memphis, TN, [4]Baylor College of Medicine, Houston, TX

Background: Humane Genomics is pioneering multi-factored authenticated oncolytic virotherapy (OVT) using glycoprotein receptor matching and aptazyme technology to positively control replication in cytoplasm. Using VSV as a platform the OVTs show excellent safety and remain highly lytic. Sindbis virus glycoprotein was mutated to eliminate natural infectivity and retargeted to GPC3 with a codon optimized nanobody. An aptazyme was used to regulate viral replication. As far as we are aware, this was the first report of a functional ON switch using a cancer biomarker.
Methods: 293T cells were used for virus rescue and titration by TCID50. Identity was confirmed by Nanopore sequencing. We evaluated safety on off-target SK-Hep-1 and NCI-H28 cell lines, and efficacy on target HepG2 and patient derived HB17 cells. Cell health and GFP was measured at multiple timepoints up to 72 hours.
Results: Safety testing of HGI498 on SK-Hep-1 (GPC3 negative) and NCI-H28 (GPC3 negative, biomarker negative) showed no virus induced cell cytopathic effects in a range of $0.01 \leq MOI \leq 1$. HGI498's efficacy testing on HepG2 and HB17 showed tumor cytotoxicity at MOI 0.01 ($p<0.001$). Endpoint dilution assay showed a 159-fold and 316-fold difference between off-target NCI-H28 and on-target HepG2 and HB17, respectively. We incorporated an optimized aptazyme with the GPC3 targeted glycoprotein (HGI572), which was similarly rescued, titered, and evaluated for selectivity. HGI572 demonstrated approximately 1000-fold higher titer on target HepG2 and HB17 cells than off-target cells. Initial *in vivo* MTD study shows that both HGI498 and HGI572 are well tolerated, and are currently being investigated *in vivo* for efficacy on Hep3B in NSG mice. HGI498 has shown no seroprevalence (*in vitro*) and is stable at cryostorage for a minimum of 11 months.
Conclusion: We have successfully engineered a two-factor authentication enabled OVT to address an unmet need for a therapy for liver cancer. As far as we are aware, this is the first report of an ON switch using a cancer protein to control viral replication, and the ON/OFF control is the highest to date.

#7254 Evaluation of scFv and diabody pseudotyped Sindbis engineered retrovectors for targeted cancer therapy.

M. Sato[1], A. Cunha[1], S. Collins[2], N. Kasahara[2], C. Roh[1], R. G. Johnson, Jr.[1];
[1]GenVivo Inc, San Marino, CA, [2]UCSF, San Francisco, CA

Engineering viral vectors to target specific cells and organs after intravenous delivery remains a challenge. Transcriptional targeting with cell-specific promoters is a commonly used approach but does not change vector biodistribution. We have developed a novel gene delivery system targeted to tumor cells by pseudotyping the vector with Sindbis Virus (SB) envelope bearing an antigen-binding domain. Prototype vectors were generated by inserting a universal IgG binding domain from Protein A into the SB envelope (SB-ZZ). Antibodies (Abs) against various cell-surface targets (HLA, HER2, CD47, EGFR, Nectin-4), were conjugated to SB-ZZ vectors delivering a luciferase (Luc) reporter gene. Targeted transduction was confirmed on cells expressing the corresponding antigens by significantly higher Luc activity compared to SB-ZZ vectors without Abs. SB envelopes were further engineered by adding or removing furin cleavage sites and linkers, transduction-enhancing point mutations, and direct incorporation of single-chain variable fragment (scFv) in different VH and VL orientations, or diabody (DB) sequences, against the same targets. The specificity of optimized HER2-targeting vectors delivering the Luc reporter was evaluated in SKBR3 (HER2 over-expressing) and MDA-MB-468 (HER2-null) cells. Robust Luc activity was observed in SKBR3 cells, but only negligible activity in MDA-MB-468 cells. In MDA-MB-468 cells overexpressing HER2, significantly higher transduction was observed compared to the wild-type cells. When comparing HER2-targeting vectors with scFv vs. DB sequences based on the same antibody, transduction capability was higher with the DB motif in HER2-positive cell lines. Targeting vectors delivering HSV-eTK were also constructed, and ganciclovir (GCV)-mediated cell killing was evaluated *in vitro*. SKBR3 cells transduced with HER2-targeting vectors showed significantly more cell killing after GCV treatment than after transduction with an amphotropic reference vector. Our results indicate a method for directing gene therapy vectors to specific populations of tumor cells, and provide a framework for highly modular targeted gene therapy and immunotherapeutics. Experiments are underway to examine *in vivo* delivery of targeted vs amphotropic vectors.

#7255 Peptide-based siRNA delivery for tumor-specific targeting of lactate dehydrogenase C.

A. Naik[1], H. Qasem[2], J. Decock[3];

[1]Carnegie Mellon University Qatar, Ar-Rayyan, Qatar, [2]College of Health and Life Sciences, Ar-Rayyan, Qatar, [3]Qatar Biomedical Research Institute, Doha, Qatar

Background: Breast cancer is the most common cancer worldwide and the leading cause of female cancer-related deaths, highlighting the pressing need for novel therapeutic interventions. Treatment of triple negative breast cancer in particular remains a challenge due to disease aggressiveness and the lack of durable treatment options. We speculate that targeting of Lactate Dehydrogenase C (LDHC) could be a novel approach given its highly tumor specific expression and immunogenic properties. We recently demonstrated that LDHC acts as a key regulator of the DNA damage response and tumor mitotic fidelity. Moreover, silencing of LDHC significantly improved treatment response to DNA damage response related anti-cancer drugs, highlighting its therapeutic potential for cancer precision medicine.
Methods: We characterized and evaluated several cell penetrating peptide-siRNA complexes for efficient silencing of LDHC in tumor cells using a 10R polyarginine peptide or bifunctional 10R-RGD, cRGD-10R or iRGD-10R peptides with tumor homing and penetrating abilities.
Results: Peptide-siRNA complex formation and tumor cellular uptake was confirmed using gel retardation assays and fluorescent confocal imaging. Biophysiochemical characterization and transmission electron microscopy revealed the complexes to be uniform in size with a low polydispersity index and positive zeta potentials. LDHC silencing in breast cancer cells using the peptide complexes demonstrated a 30-53% reduction in LDHC expression, with the 10R-siRNA and cRGD-10R-siRNA complexes showing the highest silencing efficiency. In 3D breast cancer spheroids, transfection with the 10R-siRNA complex resulted in a 20% downregulation of LDHC expression. Further analysis of the bifunctional-siRNA complexes in 3D cultures is ongoing as well as cytotoxicity analyses on non-cancerous cell lines.
Conclusions: Our findings demonstrate that peptide-mediated delivery of LDHC siRNA can reduce LDHC expression in 2D and 3D breast cancer cultures, suggesting that they could be used as a valuable approach for therapeutic intervention.

#7257 Examining the promise of precision medicine in immuno-oncology: Vectors for targeted therapeutic delivery.

C. Richardson, P. Rao, C. Koole, M. J. Karney, S. Kumar;
Azenta Life Sciences, Burlington, MA

At the forefront of therapeutic delivery is an array of vectors and targeting methods that hold immense promise for precision medicine. Vehicles such as viral vectors (AAV and lentivirus), lipid nanoparticles (LNPs) or liposomes, and peptide micelles each possess distinct and inherent properties, empowering researchers with tools to navigate the intricate challenges of specificity and efficiency in drug transport. Herein, we discuss and demonstrate design principles underpinning these vectors, elucidating their unique mechanisms for targeted delivery including:- A high-throughput viral packaging process to enable rapid downstream CRISPR or shRNA screening- Proprietary AAV plasmid synthesis and preparation techniques to maintain ITR integrity and improve gene delivery- Rapid synthesis, in vitro transcription, and novel sequencing of mRNA constructs for complete characterization of critical components such as the polyA tailBy synthesizing advancements in vector technologies, this poster serves as a roadmap for researchers and practitioners navigating the evolving landscape of targeted drug delivery in immuno-oncology.

#7258 Combinatorial effects of viral oncolysis and miRNA modulation as a novel therapeutic of pancreatic ductal adenocarcinoma.

M. Kanitz Ruschel, I. Davis, H. Mills, K. Gourishetti, D. Bhere;
University of South Carolina School of Medicine, Columbia, SC

Pancreatic cancer is a devastating illness that affects numerous individuals each year. Unfortunately, pancreatic ductal adenocarcinoma (PDAC) is an aggressive form of this disease that accounts for a disproportionate number of cancer-related deaths. Despite representing only 3.3% of all cancer cases in the United States, pancreatic cancer is responsible for a staggering 8.3% of cancer-related fatalities. In 2023, 64,050 patients were diagnosed with PDAC alone. Current treatment options, which are limited to surgery, radiation, and chemotherapy, have failed to improve clinical outcomes. Recent research has revealed miRNA (miR) as a contributor to the suppression and progression of various cancers, including PDAC. Specifically, dysregulation of miR-7 has been associated with PDAC. Downregulation of miR-7 is linked to more aggressive cases of the disease. Another potential therapeutic approach to treating cancer is the use of oncolytic viruses (OV). These viruses can replicate in cancerous cells while leaving healthy cells unharmed, making them an attractive treatment option. In this study, we utilized exosomes isolated from human Umbilical Cord stem cells (hUCs) enriched with miR-7 and combined with OHSV to examine their effect on established PDAC cell lines. We utilized cell viability assays, microscopy, and western blot analysis to evaluate the impact of the combinatorial approach on the underlying molecular mechanisms. Our findings suggest that the successful transfer of miR cargo and treatment with oHSV into the target PDAC cells arrested cell proliferation by targeting apoptotic pathways.

#7259 Effectiveness and comparison of CAR-T cell therapies for synovial sarcoma; HER2-targeted CAR-T and NKG2D-based CAR-T.

T. Miyazaki[1], C. Imai[2], N. Oike[1], Y. Murayama[1], T. Ariizumi[1], M. Baba[1], Y. Kasahara[3], H. Kawashima[1];
[1]Niigata University Graduate School of Medical and Dental Sciences, Niigata, Japan, [2]Toyama University Graduate School of Medicine, Toyama, Japan, [3]Niigata Cancer Center Hospital, Niigata, Japan

Introduction: In Japan since 2019, CAR-T cell therapy has been used to treat patients with relapsed or refractory B-cell acute lymphoblastic leukemia and diffuse large B-cell lymphoma and has shown excellent clinical results. Clinical studies of CAR-T cell therapies targeting various antigens, such as HER2, have been conducted, but the therapeutic outcome in sarcoma is still limited. We have previously reported that HER2-targeted CAR-T cells show antitumor effects for synovial sarcoma in vitro. The purpose of this study is to compare HER2-targeted CAR-T cells and NKG2D-based CAR-T cells in antitumor effect and specific responses for synovial sarcoma in vitro.
Materials and Methods: Surface expressions of HER2 and NKG2D ligands on three synovial sarcoma cell lines were detected by using recombinant human HER2 Fc chimeric protein and that of NKG2D, followed by staining with PE-conjugated anti-human IgG secondary antibody. We generated 4-1BB-type second generation CAR-T cells targeting NKG2D ligands and examined their antitumor effects and specific responses against synovial sarcoma cells. In addition, we compared the differences between HER2-targeted CAR-T cells and NKG2D-based CAR-T cells by co-culturing with synovial sarcoma cells using short-term assay (WST-8 assay), long-term assay (Real-time Cell Analysis) and CD107a assay.
Results: HER2 and NKG2D ligands were found to be expressed by flow cytometry in three synovial sarcoma cell lines. In vitro, NKG2D-based CAR-T cells showed antitumor effects against synovial sarcoma cells, including degranulation and cytokine production. Furthermore, NKG2D-based CAR-T cells showed stronger antitumor effects than HER2-targeted CAR-T cells in both short- and long-term assays and expressed higher levels of CD107a.
Conclusions: In this study, NKG2D-based CAR-T cells showed more antitumor effects than HER2-targeted CAR-T cells in vitro. Although the reason for this is not clear, we hypothesize that NKG2D ligands may be induced in synovial sarcoma cells by co-culture with CAR-T cells because HER2 is a cancer-specific antigen, whereas NKG2D ligands are ligands for activating receptors of natural killer cells. Further studies, including in vivo studies, will be conducted to verify the difference in anti-tumor effects between these CAR-T cells.

#7260 An HSV-1-based vector for local delivery of IL-12 and IL-2 reshapes the immune landscape leading to tumor clearance and systemic immune surveillance.

D. M. Previte, T. J. Parry, S. M. Krishnan;
Krystal Biotech, LLC, Pittsburgh, PA

Clinical use of recombinant interleukin (IL)-12 and -2 therapy has been hindered due to unfavorable kinetics and toxicity associated with systemic exposure. Durable targeted delivery to the tumor microenvironment (TME) is a promising therapeutic strategy to overcome these clinical limitations, prompting the development of KB707, a replication-defective herpes simplex virus type 1 (HSV-1)-based vector encoding human IL-12 and -2, for the treatment of solid tumors. Prior studies in mice demonstrated that local vector-encoded cytokine administration enhanced murine IL-12/IL-2 expression while limiting systemic exposure compared to conventional protein therapy. In a syngeneic, B16-F10 melanoma mouse model, intratumoral murine KB707-equivalent treatment led to improved survival in a unilateral tumor model and an abscopal effect in a bilateral tumor model. Additionally, the majority of previously treated animals survived rechallenge with B16-F10 in the absence of further therapy, indicative of systemic anti-tumor immune memory. Together, these results suggested that vector-mediated delivery of IL-12 and -2 could elicit both local and systemic anti-tumor immune responses. To elucidate the underlying changes to the immune landscape, B16-F10 tumor-bearing animals were treated intratumorally with vector or vehicle control on day 0 and were sacrificed on day 7; a second cohort of tumor-bearing animals received two vector doses (days 0 and 7) and were sacrificed on days 8, 10, 12, or 14. Immune cell profiling of samples taken from the tumor, tumor draining lymph node (dLN), spleen, and whole blood were analyzed by flow cytometry, and serum cytokine analysis was conducted by multiplex ELISA. Flow cytometric analysis of tumors revealed that vector treatment resulted in increased frequencies of proliferating and activated effector $CD8^+$ and $CD4^+$ T cells, peaking 24 hours post-second dose. These results correlated with high levels of the proinflammatory cytokines IFNγ and TNFα in the serum of vector recipient animals. The blood, spleens, and dLNs also showed increased frequencies of activated effector $CD8^+$ and $CD4^+$ T cells, peaking 24-72 hours post-second dose. Interestingly, although IL-2 alone has been shown to promote immune suppression and tumor outgrowth by mediating regulatory T cell (Treg) expansion and infiltration in certain contexts, the frequency of Tregs in treated vs. control tumors was substantially reduced after first and repeat dosing. Together, these results support a mechanism by which vector-driven local expression of IL-12 and IL-2 can expand and activate effector T cells both in the TME and systemically while simultaneously repressing Tregs, consistent with the previously described inhibition of primary tumor outgrowth, abscopal effects on secondary tumors, and prevention of recurrence observed with this therapeutic approach.

EXPERIMENTAL AND MOLECULAR THERAPEUTICS: YAP/TAZ/TEAD Modulators
Poster Session

#7264 OPN-9840, a non-covalent potent pan-TEAD inhibitor, exhibits single agent efficacy in preclinical malignant mesothelioma models.

P.-Y. Chen[1], B. Matusow[1], J. Tsai[2], P. Li[2], H. Nguyen[1], G. Habets[1], G. Bollag[1], S. Chowdhury[1];
[1]Opna Bio LLC, South San Francisco, CA, [2]Plexxikon Inc., South San Francisco, CA

The Hippo pathway regulates critical cellular processes during development. In ~10% of human cancers, Hippo pathway dysregulation results in YAP/TAZ overactivation and increased TEAD-dependent transcription that promotes tumor growth and therapy resistance - often by supporting drug-tolerant persister survival. In 40% of malignant mesotheliomas (MM), neurofibromatosis 2 (*NF2*) gene mutations inactivate the Merlin protein, an upstream negative regulator of TEAD. Preclinical studies indicate high TEAD dependency in *NF2*-mutant MM. We have discovered an array of potent covalent and non-covalent small molecule inhibitors that occupy the palmitate-binding pocket of TEAD proteins, with varying paralog selectivity profiles. OPN-9840 is an oral non-covalent pan-TEAD inhibitor displaying dose-dependent and on-target *in vitro* and *in vivo* efficacy for NCI-H226, an *NF2*-mutant MM cell line. OPN-9840 showed equivalent binding in thermal shift assays (10^{o}C delta Tm) for depalmitoylated TEAD1-4 proteins, and blocked TEAD reporter activity (IC_{50} 100nM) and NCI-H226 cell growth (IC_{50} 400nM). In an NCI-H226 xenograft model, OPN-9840 dosed orally for 14 days exhibited dose-dependent tumor growth inhibition (TGI) from 5 to 50 mg/kg PO (88 to >100% TGI) with tumor regression in the 15 (2/8 mice) and 50 mg/kg (4/8 mice) dose groups. qPCR of OPN-9840-treated tumors confirmed 50-70% downregulation of canonical TEAD targets, *CTGF* and *CYR61*. OPN-9840 shows a favorable safety profile, including a lack of cytotoxicity (IC_{50}>50µM) in HEK293T and HepG2 cells. Additionally, OPN-9840 caused no body weight loss in the NCI-H226 xenograft model following 14 days of dosing. *In vitro* evaluation of OPN-9840 in the blood-brain barrier (BBB) specific parallel artificial membrane permeability assay exhibited high BBB penetration potential (-Log P_e = 4.7). High oral exposure was achieved at all dose levels ($AUC_{0\text{-}24}$ > 100,000 h•ng/mL) after 14 days in the NCI-H226 study. We next investigated synergy between TEAD inhibition and targeted therapy in MM. Combined treatment of one of our pan-TEAD covalent compounds, OPN-9652 (from a separate chemical series to OPN-9840), at 50 mg/kg with 1 mg/kg trametinib resulted in NCI-H226 xenograft tumor regression (130% TGI) whereas trametinib alone only led to decreased tumor growth (74% TGI). RNA-Seq of treated tumors revealed that OPN-9652 and trametinib synergistically inhibited TEAD downstream target genes, including *ANKRD1* and *CTGF*. OPN-9652 as a single agent caused significant downregulation of E2F targets, such as *MYC* and *TP53*, suggesting decreased proliferation. In summary, OPN-9840 is a potent pan-TEAD inhibitor that shows monotherapy efficacy in MM. As we observed synergy between another pan-TEAD inhibitor, OPN-9652, with trametinib, we are exploring synergy of OPN-9840 with additional targeted therapies in tumor types beyond MM.

#7265 ETS-005, a highly selective TEAD4 palmitoylation inhibitor with potent anti-tumor activity and brain penetrating capability.

J. Lu, W. Du, M. Gao, X. Fan, J. Li, L. Feng, M. Wang, Y. Li, X. Zhong, W. Cui, Q. Zheng, **J. Zhu**;
ETERN Therapeutics Co., Ltd., WuXi, China

The Hippo pathway is a highly conserved network that regulates cell proliferation, tissue regeneration, and organ size by orchestrating YAP/TAZ-TEADs, the core effectors of signaling. Aberrant activation of YAP/TAZ has been implicated in tumorigenesis, tumor progression, metastasis and the resistance to targeted therapeutics, including MAPK and RTK inhibitors. Among the four TEAD paralogs, TEAD4 is found widely overexpressed in various solid tumors and potentially less associated with YAP/TEAD-related renal toxicity. Here we reported the identification of ETS-005, a highly selective TEAD4 small molecule inhibitor that shows preference for binding to the palmitoylation pocket of TEAD4 than other TEAD paralogs over 15 folds. ETS-005 displayed low nanomolar inhibition of cell proliferation in NF2 or LATS1/2 mutant mesothelioma in vitro, and robust anti-tumor efficacy in vivo. ETS-005 showed favorable oral availability, high brain penetration capability and broad safety window. Moreover, ETS-005 had relative long projected $T_{1/2}$ in human, supporting a more convenient clinical QD dosing schedule. Our study demonstrated that selective TEAD4 palmitoylation inhibitor ETS-005 exhibited potent anti-tumor activity as much as pan-TEAD palmitoylation inhibitors while may gain broader therapeutic index. Additionally, ETS-005 also exhibited profound synergistic effects in drug combination studies, offering broad opportunities combined with MAPK and RTK therapies. ETS-005 is currently in IND-enabling study and expected to enter Phase 1 in 2024.

#7266 *VGLL4* is the target of the 3p25 homozygous deletion and presents a novel therapeutic vulnerability for TEAD1/4 but not TEAD1 inhibitors.

F. Muller, S. Kunnimalaiyaan, P. Mangrolia, J. Olson;
Sporos Bioventures, LLC, Houston, TX

The Hippo pathway, a critical cell proliferation regulator, remains an underexplored oncogenic pathway in precision oncology. It is executed through YAP1/TAZ co-activators and the TEAD transcription factor family (TEAD1-4), driving expression of tumor-promoting genes. Palmitic acid site TEAD inhibitors have shown strong pre-clinical and clinical activity, but identification of genetic markers of vulnerability and patient selection remain an urgent and open question. Sporos undertook a broad bioinformatic analysis of Hippo pathway components and regulatory genes to identify genetic alterations that drive TEAD activity and potentially act as targetable vulnerabilities. Here, we present a key finding from this investigation. The 3p25 locus undergoes frequent homozygous deletion in solid tumors especially lung squamous cell carcinoma. While *VHL* was long assumed to be the target tumor suppressor gene of this deletion - we show that *VGLL4* is in the only gene in the peak of GISTIC statistically significance in lung squamous cell carcinoma and *VGLL4* and *ATG7* are both in the peak in Renal Clear Cell Carcinoma (RCC). These data unambiguously establish that *VGLL4* deletion is a major oncogenic driver in lung squamous cell carcinoma (SCC) and a contributor in RCC. Because VGLL4 is the major negative relator of the YAP/TEAD transcriptional complex and directly competes with YAP for TEAD binding - we hypothesize that Lung SCC with *VGLL4*-homozygous deletion would be uniquely dependent on YAP/TEAD activity and show selective sensitivity to TEAD inhibitors. While we were unable to locate a Lung SCC *VGLL4*-deleted PDX, we identified a *VGLL4*/*ATG7* homozygous deleted RCC PDX, KI2552, in the CrownBio collection. We show that treatment with SPR1, Sporos's novel TEAD1/4 inhibitor, decreases tumor growth and dramatically extends survival of mice bearing *VGLL4*/*ATG7*-deleted KI2552 RCC PDX. On the other hand, VT103, a strong TEAD1 inhibitor which shows comparable pre-clinical activity to SPR1 in the NCI-H226 mesothelioma CDX - did not show any activity in KI2552 PDX. These data emphasize the importance of targeting paralogs besides TEAD1 to broaden anti-neoplastic activity beyond mesothelioma and suggest that *VGLL4*-homozygous deletion confers TEAD inhibitor sensitivity even in carcinomas where it isn't the principal driver and portent exceptionally anti-neoplastic activity in neoplasms where it is. Given the wide distribution of the 3p25 homozygous deletion - our findings open a large new potential responder population to TEAD inhibitors and warrant inclusion of *VGLL4* in NSG diagnostic sequencing panels.

#7268 The SOS1 inhibitor MRTX0902 demonstrates activity across cancer models with mutations in proximal components of the RAS-MAPK pathway.

N. Sudhakar[1], L. Yan[1], F. Qiryaqos[1], J. Laguer[1], D. Briere[1], A. Hebbert[1], A. Calinisan[1], S. Coma[2], J. Pachter[2], J. G. Christensen[1], P. Olson[1], S. Khare[1]; [1]Mirati Therapeutics, San Diego, CA, [2]Verastem Oncology, Needham, MA

Genetic alterations in the RAS-MAPK pathway are one of the most frequent causes of human cancers. While targeted therapies are approved for patients harboring mutations in *KRAS* G12C in advanced or metastatic non-small cell lung cancer, there remains a need for an effective therapy for cancers characterized by additional RAS-MAPK pathway mutations across cancer types. Previous studies have shown that genetic or pharmacological inhibition of Son of Sevenless homolog 1 (SOS1) demonstrates antiproliferative activity in cancer cells addicted to KRAS signaling, including cell lines with oncogenic mutations in *KRAS, SOS1, PTPN11,* or *EGFR* or a loss-of-function mutation in *NF1*. These genetic alterations each function to increase SOS1-mediated GTP-loading of KRAS and increase signaling flux through the MAPK pathway. Inhibition of SOS1 by MRTX0902 is anticipated to shift the tumor cell equilibrium of KRAS towards the inactive GDP-bound KRAS, leading to MAPK pathway inhibition. MRTX0902 is a selective inhibitor of SOS1 under evaluation in clinical trials for the treatment of advanced, unresectable, or metastatic cancers with mutations in the KRAS-MAPK pathway. In the present studies, we have shown that MRTX0902 demonstrates single-agent anti-proliferative activity and modulates ERK1/2 phosphorylation (pERK) across a panel of human tumor cell lines harboring oncogenic mutations in *SOS1*, *PTPN11*, *BRAF* (class III) and *NF1*. Furthermore, oral administration of MRTX0902 as a monotherapy in preclinical human tumor cell-derived xenograft models harboring these oncogenic mutations results in significant tumor growth inhibition. Additionally, combination with the RAF/MEK clamp avutometinib demonstrated greater antitumor activity versus either monotherapy treatment. These data support the clinical utility of MRTX0902 as a single agent or combination partner of avutometinib for the treatment of human cancers harboring oncogenic mutations implicated in dysregulation of RAS-dependent signaling including *SOS1*, *PTPN11*, *NF1*, and *BRAF* (class III).

#7269 Karyopherin α-2, a nuclear export protein, promotes cancer progression in lung adenocarcinoma.

I. Cheon[1], **S. Kim**[2], S. Cho[1], H. Lee[3], J.-S. Yoon[4], J. Lee[3], S. Chun[5], H. Won[4], S. Hong[6], Y. Ko[3], Y.-H. Ahn[1];

[1]Department of Molecular Medicine and Inflammation-Cancer Microenvironment Research Center, College of Medicine, Ewha Womans University, Seoul, Korea, Republic of, [2]Seoul St. Mary's Hospital, Seoul, Korea, Republic of, [3]Eunpyeong St. Mary's Hospital, College of Medicine, The Catholic University of Korea, Seoul, Korea, Republic of, [4]Uijeongbu St. Mary's Hospital, College of Medicine, The Catholic University of Korea, Seoul, Korea, Republic of, [5]Bucheon St. Mary's Hospital, College of Medicine, The Catholic University of Korea, Seoul, Korea, Republic of, [6]Department of Pathology, College of Medicine, Chung-Ang University, Seoul, Korea, Republic of

Introduction: Karyopherin α-2 (KPNA2), a nucleocytoplasmic transport protein, regulates the nuclear import of macromolecules and contributes to carcinogenesis. Actually, KPNA2 is upregulated in various types of cancer tissues and serum from cancer patients. In particular, it is associated with cancer invasiveness and poor prognosis in patient. Here, we tried to present the molecular mechanism and clinical significance of KPNA2 in lung cancer progression and metastasis.

Method: First, we retrospectively analyzed the data extracted from EMR for patients with non-small cell lung cancer receiving curative surgical resection in Uijeongbu and Bucheon St. Mary's Hospitals (n=165). Immunohistochemistry staining was performed on the tumor microarray samples using antibodies against KPNA2. The functional assay and gene silencing was conducted.

Result: The clinical and pathological information of the experimental group is as follows. Based on the TMA staining, mean KPNA2 score was 36.5 [0-240] and median value was 10. Based on the TMA staining, patients with high KPNA2 expression were related to lymphatic invasion ($p = 0.00782$), advanced stage ($p = 0.0202$), and current smoker ($p = 0.0074$). KPNA2 expression was higher in squamous cell carcinoma than in adenocarcinoma histotype. Patients with high KPNA2 expression showed shorter survival than those with low KPNA2 (median OS (months), 72.8 vs 42.2, $P < 0.0001$; median RFS (months), 72.8 vs 32.1, $P < 0.0011$) and relevant to high recurrence (recurrence rate (%), 24.7 vs 44.7, $p = 0.007$). Further, high KPNA2 expression was associated with poor survival outcomes. Knockdown of KPNA2 in lung cancer cells suppressed the invasion and migration of lung cancer cells and inhibited metastasis in a mouse model of lung cancer. Inversely, KPNA2 overexpression promoted cancer cell growth, invasion, and migration. Moreover, ectopic expression of KPNA2 made lung cancer cells less sensitive to
anticancer drugs, Talazoparib and Olaparib, indicating that KPNA2 enhances drug resistance in lung cancer cells.

Conclusion: Collectively, this study suggest that KPNA2 promotes invasiveness and metastasis and is associated with poor patient outcomes; therefore, KPNA2 will be a good therapeutic target or a biomarker in lung adenocarcinoma.

#7270 Combination targeting of SKP2 and KDM5B induces senescence in castration-resistant prostate cancer cells via AKT signaling.

L. K. Brown, T. Kanagasabai, G. Li, S. I. Celada, Z. Chen;
Meharry Medical College, Nashville, TN

Prostate cancer (PCa) is the second-leading cause of cancer mortalities and morbidities in the United States and is the most commonly diagnosed malignancy in men. Despite the fact that androgen deprivation therapy is the first-line option to initial responses, most PCa patients invariably develop castration-resistant prostate cancer (CRPC). CRPC is a lethal type of malignancy, therefore, novel and effective treatment strategies are needed. The goal of this study was to evaluate the combination treatment of small molecule inhibitors, SZL-P1-41, a SKP2 target and PBIT, a KDM5B target on PCa growth and progression; as well as to delineate the underlying mechanisms of suppressing CRPC. Literature reports that S-Phase Kinase Associated Protein 2 (SKP2) is upregulated in PCa and Lysine-specific demethylase 5B (KDM5B) serves as a histone demethylase with a crucial role in cancers. Studies showed that KDM5B is increased in human PCa and KDM5B knockout decreases carcinogenic properties of PCa cells. We previously reported that SKP2 loss partially decreases the growth of prostate tumors and that KDM5B levels are reversely regulated by SKP2 in PCa cells. However, the mechanisms of KDM5B and SKP2 interplay on PCa malignancy is unknown. We hypothesize that combination of PBIT and SZL-P1-41 treatment will enhance anti-cancer effects on PCa progression by inducing cellular senescence. Here, we showed that inhibition of KDM5B and SKP2 decreased the proliferation of PCa cells, and KDM5B KO cells were more vulnerable to SKP2 inhibition. More importantly, a combined inhibition of KDM5B and SKP2 significantly blocked malignant progression and migration of PCa cells. Mechanistically, combined inhibition of KDM5B and SKP2 in PCa cells abrogated AKT activation, resulting in an induction of cellular senescence, which was measured via Western blot analysis and senescence-associated β-galactosidase (SA-β-Gal) staining. Taken together, our results show that combined inhibition of KDM5B and SKP2 is more efficacious in inhibiting proliferation and migration in CRPC cells, and this regimen would be an ideal therapeutic approach for treating CRPC.

#7271 Proteasome inhibitor FHND6091: A potent therapeutic candidate for*PTEN*-deficient cholangiocarcinoma.

Y. Zhu[1], J. Shi[2], C. Li[2];

[1]Jiangsu Chia Tai Fenghai Pharmaceutical Co.Ltd/ Nanjing Chuangte Pharmaceutical Technology Co., Ltd., Nanjing, China, [2]Nanjing Chuangte Pharmaceutical Technology Co., Ltd., Nanjing, China

Background: Cholangiocarcinoma (CCA), characterized by high genetic heterogeneity, poses a significant challenge due to limited therapeutic options. Notably, the tumor suppressor gene PTEN is frequently altered in more than 50% of CCA clinical specimens. PTEN deficiency enhances proteasome subunit expression and proteasome proteolytic activity, and facilitates the potential therapeutic efficacy of proteasome inhibitors in CCA. The proteasome inhibitor FHND6091, a novel drug developed by Jiangsu Chia Tai Fenghai Pharmaceutical Co., Ltd., has obtained IND approval from NMPA and is currently undergoing a first-in-human phase 1 trial for multiple myeloma (MM) and mantle cell lymphoma (MCL).

Method: This study employed a comprehensive approach, encompassing both in vitro and in vivo pharmacology studies. The investigation involved purified human proteasome activity assays, cell viability assays, and in vivo anti-tumor activity studies utilizing a cholangiocarcinoma patient-derived xenograft (CCA PDX) model with PTEN deficiency.

Results: FHND6091 exhibited potent inhibitory effects on the β5 subunit of the 20S proteasome, with IC50 value of 2.22 nM. In cell viability assessments, FHND6091 demonstrated selective efficacy in PTEN-deficient CCA cell lines, with IC50 value of 5.87 nM in HCCC-9810 (*PTEN* deletion, homozygous loss of exon 6 to 9) and 10.08 nM in RBE (*PTEN* intact expression). In a PDX xenograft model with PTEN deficiency, gavage administration of FHND6091 BIW at 1.0 mg/kg (first week) / 1.5 mg/kg (subsequent two weeks) exhibited advanced anti-tumor activity (TGI = 52.32%) compared to intraperitoneal administration of Bortezomib at 0.5 mg/kg BIW (TGI = 31.88%). Tissue distribution studies in rats revealed the preference of FHND6091 for liver accumulation, with an exposure (AUC0-t) approximately 44 times that of plasma after a single dose. These data corroborated that FHND6091 could achieve a specific level of exposure in the target organ liver.

Conclusion: FHND6091, characterized by its irreversibility, high potency and oral bioavailability, emerges as a promising proteasome inhibitor for the treatment of both hematologic and solid tumors. These findings strongly support FHND6091 as a potential candidate for the treatment of CCA in clinical settings. Furthermore, the regulating of sensitivity to proteasome inhibitors by the PTEN status extends beyond cholangiocarcinoma to encompass various human cancers, such as ovarian, prostate, and digestive system malignancies. This broader implication establishes a theoretical foundation supporting the potential efficacy of FHND6091 as a therapeutic agent for solid tumors.

#7273 Small molecule activation of PP2A in the treatment of melanoma.

H. Johnson[1], A. Singh[1], A. Raza[1], S. Narayan[2], A. K. Sharma[1];
[1]Penn State College of Medicine, Hershey, PA, [2]University of Florida, Gainesville, FL

Protein phosphatase 2A (PP2A) is a heterotrimeric holoenzyme functioning as a serine/threonine phosphatase, where it accounts for about 50-70% of all serine/threonine phosphorylation in the cell. Yet, PP2A is commonly inactivated in cancer, likely due to its role as a tumor suppressor. Due to the important role PP2A plays in many cellular processes, including those involved with tumor progression, there is a current need for novel therapeutics capable of targeting PP2A in cancer. Currently, none of the current PP2A modulators have made it into approved clinical use. As such, we have recently synthesized the PP2A activators, PPA24 and PPA27, using molecular docking and fragment-based drug design based on the structures of recently reported PP2A activators, iHAP1 and NSC49L. We were previously able to establish PPA24 as the lead compound in treating colorectal cancer (CRC) *in vitro*, compared to PPA27 and the parent compounds. Nevertheless, a single dose NCI-60 screen of both PPA24 and PPA27 indicated the cell selectivity present in both compounds and revealed the potential effect these compounds could have in other cancers. Further evaluation with an extended NCI-60 5-dose screen of PPA24 and PPA27 demonstrated a strong potential for both compounds in treating melanoma. Overall, the NCI-60 screen displayed PPA27 as most effective in melanoma across all cell lines screened, while PPA24 was found to be effective in both CRC and melanoma cell lines, agreeing with our previous findings. A cell viability screening of PPA24 and PPA27 in our laboratory across 5 melanoma cell lines (SK-MEL-2, SK-MEL-28, A375, Mel1241, and 451Lu) identified IC_{50} values in the range of 3.45-8.94 μM for PPA27 and 5.99-14.45 μM for PPA24. The parent compounds, iHAP1 and NSC49L, were also evaluated and NSC49L was found to be less effective in melanoma than previously found in CRC cells. Both PPA24 and PPA27 were found to be effective in cell lines with and without BRAFV600E mutation, though it appears the metastatic cell line, 451Lu, required an increased concentration for all compounds as compared to the IC_{50} values found in the other melanoma cell lines. Further evaluation revealed PPA24 and PPA27 as dose-dependently inducing apoptosis in cells with BRAFV600E (A375) and BRAF WT (SK-MEL-2). Together, these findings show the potential of PPA24 and PPA27 as therapeutic treatments for melanoma with or without BRAF mutations and are currently being further evaluated in several in vitro and in vivo melanoma models in our laboratory.

#7274 Optimization of intermittent dosing strategies of KRAS G12C inhibitors in preclinical lung cancer model.

Valeria Estrada Navarro, Vincent Panneton, Lauren Dong, Hyejin Choi, Divya Venkatesh, Rachana Maniyar, Isabell Schulze, Jedd D. Wolchok, Taha Merghoub

Sandra and Edward Meyer Cancer Center, Weill Cornell Medicine, New York, NY

Cysteine-binding targeted drugs AMG-510 and MRTX-849 provide a new therapeutic approach for advanced KRASG12C mutant cancers. However, clinical response has been limited. Responders eventually develop adaptive resistance by gaining additional MAPK pathway mutations, resulting in limited therapeutic benefit. High-dose pulsatile treatment with MAPK pathway inhibitors has been proposed as an alternative strategy to alleviate adaptive resistance while maintaining tumor control. The sensitivity of tumor cells to pan-inhibitors of the MAPK pathway, crucial for proliferation, creates a therapeutic opportunity window for immune cells to restore their function during an intermittent regimen. Congruently, we have previously shown that intermittent pan-MAPK pathway inhibitor treatment delays drug resistance, supports T cell activation, and enhances tumor delay when combined with immunotherapy. In this study, we investigated the effects of continuous and pulsatile KRASG12C inhibition on tumor and immune cells in order to design combinatorial strategies with immune-modulating agents that overcome drug resistance. Our data suggest that a weekly single high-dose regimen of AMG-510 is less effective at achieving tumor control in preclinical mouse models of KRAS mutant lung cancer compared to daily treatments. However, supplementing this pulsatile regimen with lower maintenance doses markedly slows the growth of LLC KRASG12C lung cancer. Flow cytometry analysis revealed that high-dose pulse regimen enhances T cell activation, evidenced by increased expression of TCF-1, Ki67, PD-1, and GITR, along with lower expression of co-inhibitory molecules Lag-3 and Tim-3, 3 days after treatment. In vitro, AMG-510 also improves the antigen presentation of OVA-expressing LLC-KML lung cancer cells via MHC class I and, to a lesser extent, MHC class II. Furthermore, we found that while combinatorial therapy with PD-1 blockade alone does not significantly impact tumor control, the combination with CTLA-4 blockade shows efficacy across pulsatile and continuous AMG-510 dosing cohorts. Overall, our findings suggest that the utilization of intermittent dosing regimens for selective KRASG12C inhibitors is a promising approach for improving clinical responses in lung cancers with KRAS mutations. Future experiments will aim to delineate MAPK pathway behavior in vivo and in vitro under pulsatile and continuous treatment, assess immunogenicity, and further characterize immune changes in the different treatment regimens, with the goal of designing more efficient cancer therapies utilizing selective KRAS inhibitors.

#7275 GS-P-328, a brain-penetrant small molecule p53 Y220C reactivator for tumors harboring p53 Y220C mutation.

M. Liu, K. Geng, B. Lu, **Y. Xia**, F. Yang;
Changchun GeneScience Pharmaceutical Co., Ltd., Changchun, China

As a tumor suppressor, p53 can prevent tumor development through multiple pathways. However, mutation of TP53 and the resultant inactivation of p53 allow evasion of tumor cell death and rapid tumor progression. The oncogenic Y220C mutation is the ninth most frequent p53 missense mutation in cancer. Y220C mutation creates a narrow, hydrophobic pocket on the surface of the p53 DBD that reduces its thermal stability. As a result, the Y220C mutation causes a rapidly unfold of the p53 protein under physiological conditions, abrogates p53 signaling and drives tumorigenesis. There are approximately 100,000 new Y220C mutation cancer cases per year worldwide with limited treatment choices. The initial clinical evaluation of PC14586 that can restore missense-mutant p53 protein has seen efficacy in patients harboring p53 Y220C mutation even though there is still room for improvement. Here we report a brain-penetrable, highly potent p53 Y220C reactivator which has great *in vitro* activity as well as induce tumor shrinkage in multiple tumor models at a much lower systematic exposure comparing to PC14586. *In vitro*, GS-P-328 could bind to p53 Y220C protein with a single nM potency and potently induce cell death in a wide range of p53 Y220C tumor cells while have no anti-proliferative effects with p53 WT cells. GS-P-328 is also active in patient-derived cell (PDC) models in various tumor background including SCLC, gastric, ovarian and colon. *In vivo*, GS-P-328, at approximately 1/3 of systematic exposure comparing to a leading clinical reactivator, causes tumor shrinkage in multiple CDX models. GS-P-328 could induce MDM2/p21 upregulation in cell systems. *In vivo*, GS-P-328 could induce 2 fold and more increase in MDM2/p21 protein levels in tumor tissues at approximately 1/3 of plasma concentrations comparing to PC14586. More importantly, in a NUGC3-luc intracranial model, GS-P-328 could strongly inhibit growth of cancer cells in the mouse brain. GS-P-328 has a favorable ADME profile in rodents, dogs and NHPs, as well as a much better safety profile. GS-P-328 is now under IND-enabling study and P1 study is planned in early 2025.

#7276 Potent anti-proliferative activity of brincidofovir in Diffuse Large B-cell Lymphoma with overexpression of transcriptional repressor TLE1.

J. Lee[1], T. Ko[2], E. Lee[2], B. Kannan[2], B. Lim[2], Z. Li[2], Z. Guo[2], J. Loh[1], C.-Y. Ng[2], K. Chai[2], N. Binte Muhammad Taib[2], K. Lim[2], D. Huang[2], J. Lim[2], M. Hazama[3], K. Fukushima[3], B. Teh[2], S. Lim[2], C. Ong[2], J. Chan[2];

[1]Duke-NUS Medical School, Singapore, Singapore, [2]National Cancer Centre Singapore, Singapore, Singapore, [3]SymBio Pharmaceuticals Ltd, Tokyo, Japan

Introduction: Brincidofovir (BCV) is a biologically-active acyclic nucleoside phosphonate and clinically-approved anti-viral agent. Recently, BCV has been demonstrated to display potent anti-proliferative and immunogenic properties in NK/T cell lymphoma (NKTCL). However, its effect on other lymphoma types remain unclear.

Methods: We investigated BCV in an expanded cohort of B-cell lymphoma cell-lines (diffuse large B-cell lymphoma [DLBCL], n = 16; Burkitt lymphoma, n = 2; Hodgkin lymphoma, n = 1), in comparison with NKTCL cell lines (n = 11). Mouse xenograft models were deployed to assess *in vivo* effects. Whole transcriptomic sequencing (RNAseq) was performed to examine Epstein-Barr virus (EBV) status and explore potential mechanisms of action.

Results: BCV inhibited viability in all B-cell lymphoma cell-lines in a dose-dependent manner (IC50 0.0798 to 8.414 µg/ml). Marked sensitivity (IC50 < 1 µg/ml) was demonstrated in nine cell-lines, including the *MYC*/*BCL2*-rearranged double-hit DLBCL cell-line OCI-LY18 (IC50 0.5 µg/ml). Intraperitoneal BCV (40 mg/kg, 2X per week) inhibited tumor growth in NOD/SCID mice OCI-LY18 xenografts, compared with vehicle alone ($p < 0.001$, two-tailed t-test). RNAseq showed that most cell-lines (n = 16) were EBV negative. Interestingly, the transcriptional repressor *TLE1* was amongst the top upregulated genes in the BCV-sensitive cell-lines (log2foldchange = 8.12, adjusted $p = 0.0004$). DLBCL patient samples from two independent datasets showed that *TLE1*-high tumors conferred worse overall survival (GSE11318, n = 200: HR 2.77, 95%CI 1.78 to 4.30, $p < 0.0001$; GSE10846, n = 414: HR 1.94, 95%CI 1.35 to 2.80, $p = 0.0004$). Gene set enrichment analysis showed that pathways involved in oxidative phosphorylation and oncogenic signaling were significantly upregulated in the BCV-resistant cell-lines compared to the rest. Notably, these findings are in stark contrast to NKTCL, in which TLE1 loss instead confers BCV sensitivity *in vitro* and is associated with poor survival outcomes in patients (n = 36; HR 3.44, 95% CI 1.23-10.49, $p = 0.0301$).

Conclusions: Taken together, these results suggest that BCV may be a potential novel therapeutic agent for the treatment of B-cell lymphomas. Further work will be required to investigate the role of TLE1 and other molecular features as potential predictive biomarkers.

#7278 Discovery of a novel WRN inhibitor, ZM-3329 that efficiently inhibits MSI-H tumor growth.

F. Zhou[1], G. Yang[1], Y. Liu[2], L. Xue[1], Y. Guo[2], Z. Li[1], W. Wang[2], J. Li[2], R. Tang[1];

[1]State Key Laboratory of Neurology and Oncology Drug Development, Simcere Zaiming Pharmaceutical Co, Ltd., Shanghai, China, [2]Simcere Zaiming Pharmaceutical Co, Ltd., Shanghai, China

Microsatellite instability-high status (MSI-H) is typically associated with endometrial and gastrointestinal cancers. These tumors harbor large numbers of frameshift and single-nucleotide variants and are characterized by a high tumor mutational burden (TMB). The clinical benefits of immune checkpoint inhibitor (ICI) therapy on MSI-H cancers were well-demonstrated, however, 50% of these cancers are intrinsically resistant to PD-1 therapies and resistance inevitably develops with prolonged treatment. Thus, a novel efficient therapeutic strategy for MSI-H cancer is still needed. Werner syndrome ATP-dependent helicase (WRN) is a member of the RecQ helicases family and has recently emerged as a promising synthetic-lethal target in the treatment of MSI-H tumors. In MSI-H tumors, microsatellite sequences consisting of repeated nucleotides are unstable, and replication slippage causes a unique secondary structure that hinders the progression of replication forks. With its helicase activity, WRN unwinds this secondary structure to restart DNA synthesis and sustain MSI-H tumor cell growth. WRN knockdown or helicase enzyme-dead effectively inhibits cell proliferation and tumor growth in multiple preclinical MSI-H models. Here we identified ZM-3329, a novel and highly potent WRN inhibitor. Helicase activities were efficiently inhibited by ZM-3329 with IC_{50} less than 30 nM, and equal potency was identified on HCT-116 cell proliferation inhibition. In a panel of 124 tumor cell lines, ZM-3329 only specifically inhibited the growth of MSI-H but had no significant effects on the MSS (Microsatellite stable) tumor cell lines, indicating high selectivity against MSS. Additionally, ZM-3329 strongly inhibited the growth of MSI-H patient-derived organoids. The intracellular mechanism of action study revealed that inhibition of WRN by ZM-3329 in MSI-H cells led to the accumulative DNA damage signatures which was demonstrated by the increase of γH2AX and P21 expression, and arrested cell cycle to G2/M. ZM-3329 demonstrated favorable pharmacokinetic profiles in pre-clinical species, supporting oral administration in humans. ZM-3329 showed robust anti-tumor activities in multiple MSI-H xenograft models with significant tumor regression observed. Meanwhile, mice were tolerant well in all tested doses, and no abnormality was observed. In conclusion, a novel WRN inhibitor was developed, and robust antitumor activities were demonstrated in xenograft tumors and PDOs with different tissue types. In terms of synthetic lethality between MSI-H and WRN as well as broad anti-tumor activities across different tumor types, ZM-3329 would be developed as a tissue-agnostic therapy for MSI-H patients.

#7279 Discovery of SHR1127, an orally bioavailable, highly potent and selective KRAS G12D inhibitor.

X. Li, F. Shen, L. Zhang, W. Wang, L. Kong, Y. Bao, Y. Mao, Z. Wang, S. Lin, Z. Zhang, J. Feng, M. Hu, F. He;
Shanghai Hengrui Pharmaceutical Co., Ltd., Shanghai, China

Mutant KRAS is the most frequent oncogenic driver in nearly 23% of human cancers. As the most common KRAS alteration, KRAS G12D mutation occurs in approximately 35%, 13%, and 4% of pancreatic, colorectal, and non-small cell lung cancers, respectively. It was worth noting that the clinical PoC of KRAS G12D inhibitor has been preliminarily validated by intravenous administration of HRS-4642 weekly. However, there still represents an extraordinary unmet clinical need requiring an oral KRAS G12D inhibitor featuring higher potency and favorable pharmacokinetic profiles. We disclose herein the development of an orally bioavailable, highly potent and selective KRAS G12D inhibitor, SHR1127.SHR1127 demonstrated picomolar binding affinity, with a K_D value of 0.06 nM in a SPR binding assay with GDP-loaded KRAS G12D protein. SHR1127 significantly inhibited ERK phosphorylation with IC_{50}s of 0.05 nM and 0.19 nM in GP2d and AGS cell lines, respectively. More importantly, 3D viability assay showed that SHR1127 displayed extremely high anti-proliferative activity against GP2d, AGS and AsPC-1 cell lines with the IC_{50}s of 0.05, 0.83 and 0.92 nM, respectively. The selectivity over KRAS WT PC9 cells, KRAS G12C and G12V mutant cell lines was more than 500-fold. Additionally, SHR1127 displayed excellent human hepatocyte stability ($T_{1/2}$ > 1000 min) and desirable physicochemical properties. Moreover, SHR1127 exhibited favorable pharmacokinetic profiles with dose-dependent exposure and acceptable oral bioavailability. In the GP2d xenograft model, SHR1127 showed a robust anti-tumor activity in a dose-dependent manner, leading to tumor regression (TGI = 125%) as low as 5 mg/kg (p.o. dosage, bid), without body-weight loss during 21 days of treatment. Furthermore, SHR1127 demonstrated no off-target activities at 1000 nM in 97 kinase panel and 78 safety panel screening. SHR1127 showed good safety window in the 14-day toxicology study in rat and dog.

In summary, SHR1127 has been successfully developed as an orally bioavailable KRAS G12D inhibitor, exhibiting excellent cellular activities with good selectivity over KRAS WT. More importantly, SHR1127 showed favorable pharmacokinetic profiles across species, and robust tumor regression in a GP2d xenograft model at the dose of 5 mg/kg. In addition, SHR1127 demonstrated no off-target toxicity and good safety window. An IND submission for SHR1127 is planned in the first half of 2024.

#7280 Potential activity of TEAD inhibitor in Hippo-altered cancer including NF2 mutant solid cancer and TAZ-CAMTA1 fusion-driven epithelioid hemangioendothelioma (EHE).

J. Byun, S. Jung, H. Moon, S. Lim, S. Park, S. Baek, Y.-Y. Kim, J. Park, J. Kim, S. Lee, Y. Ahn;
Hanmi Pharmaceutical Co., Ltd., Seoul, Korea, Republic of

The Hippo pathway, a conserved signaling, modulates diverse processes including cell proliferation, survival, differentiation, organ size, and tissue homeostasis. The core kinases, MST1/2 and LATS1/2 phosphorylate downstream effectors, YAP/TAZ, and sequestrate them in cytoplasm[1)]. The upstream regulator, NF2 activates these kinases and its loss-of-function mutation leads to YAP nuclear translocation, which in turn promotes tumorigenesis[2)]. Dysregulation of Hippo pathway triggers constitutive YAP/TAZ accumulation and binding to TEAD family that upregulate prosurvival target genes such as CTGF and CYR61[1)], which are deeply associated with drug resistance and tumor microenvironment[3)].

TEADs, a transcription activation complex with primary key partners of YAP/TAZ, function in response to the Hippo altered-pathway[4)]. Although a number of reports in the area of small molecules targeting YAP/TAZ-TEAD complex is exponentially increased, there is a lack of understanding regarding how TEAD subtypes may contribute to cancer progression. Moreover, TAZ-CAMTA1 gene fusion is a driver oncogene expressed in more than 90% of epithelioid hemangioendothelioma (EHE), a vascular sarcoma[5)]. Here, we explore the potential of anti-cancer efficacy on our established TAZ-CAMTA1 fusion-driven EHE model. Our TEAD inhibitor effectively suppressed TEAD reporter activity in MCF7-TEAD-luc cells and induced 10~100 nM range of growth inhibition in NF2 or LATS mutant mesothelioma by disrupting YAP-TEAD1/3 protein-protein interactions (PPI). We found that knockdown TEAD1 as well as TEAD3 downregulate growth ability of NF2 altered solid cancer cells such as LOU-NH-91 and YD8.

Our TEAD inhibitor, showing TEAD1/3 isoform specificity, exhibited a superior anti-proliferative effect in broader range of Hippo-altered solid cancer cells than of selective TEAD1 inhibitor. This highlights the importance of targeting TEAD1 and suggest that TEAD3 inhibition can enhance anticancer effects.

We established the TAZ-CAMTA1 fusion-expressing cells, demonstrating its oncogenic function through increased anchorage-independent growth and upregulation of TEAD target genes, CTGF and CYR61, compared to parental NIH3T3. Our TEAD inhibitor suppressed TAZ-CAMTA1 fusion-TEAD1 PPI in NanoBRET system. It also inhibited TAZ-CAMTA1 driven colony formation. Our inhibitor more greatly prevented the growth of TAZ-CAMTA1 expressing NIH3T3 cells than parental cells and exhibited mRNA expression inhibition of CTGF and CYR61 on qRT-PCR, showing superior effects compared to the selective TEAD1 inhibitor.

In conclusion, we emphasize the importance of TEAD inhibition for the treatment of Hippo-altered cancers including NF2 mutant solid cancer and TAZ-CAMTA1 fusion-driven EHE, highlighting the advantages of our TEAD1/3 inhibitor over the selective TEAD1 inhibitor.

#7282 Comparing TEAD palmitoylation inhibitors with differential TEAD selectivity in combination efficacy with targeted therapies and in renal safety.

T. T. Tang, L. Post;
Vivace Therapeutics, San Mateo, CA

Genetic alterations of the Hippo signaling pathway components resulting in YAP/TAZ activation have been reported in a variety of human malignancies. YAP/TAZ activation and functional requirement have also been linked to resistance to targeted therapies by providing the essential survival signal in drug-tolerant persister/dormant cells. As the main drivers for YAP/TAZ recruitment to chromatin, TEAD transcription factors are the major effectors of the Hippo-YAP/TAZ pathway involved in the regulation of cell proliferation, survival, and cell migration. There are four members in the TEAD family: TEAD1, TEAD2, TEAD3, and TEAD4. All four members have a conserved cysteine residue that gets auto-palmitoylated and a highly conserved central pocket in which the palmitate is buried. TEAD auto-palmitoylation is required for TEAD interaction with coactivator YAP/TAZ and transcriptional activity. We have discovered and developed highly potent and selective TEAD auto-palmitoylation inhibitors that interact directly with TEAD by occupying the central palmitate pocket, disrupt YAP/TAZ-TEAD protein interaction, suppress TEAD transcriptional activity, and selectively block *NF2*-deficient mesothelioma proliferation *in vitro* and inhibit *NF2* mutant tumor growth *in vivo*. One of these compounds, VT3989, is being evaluated in an ongoing phase 1 clinical trial, where partial responses in mesothelioma patients have been demonstrated, showing for the first time that the Hippo pathway is druggable and that the Hippo pathway is now a validated target for cancer therapy. It remained a question, however, which TEAD members are more important and whether it would be safer and as efficacious to inhibit one TEAD member than multiple TEAD members. Thus, we utilized our TEAD inhibitors with differential TEAD selectivity to determine the importance of TEAD1 selectivity in anti-tumor efficacy and in renal safety. We evaluated the anti-tumor efficacy of several potent TEAD1-selective and pan-TEAD inhibitors in *in vivo* combination studies using EGFR mutant / KRAS mutant xenograft models. We found that TEAD1-selective TEAD palmitoylation inhibitors are less efficacious than pan-TEAD/multiple-TEAD inhibitors in combination studies with targeted therapies (as such EGFRi and KRASi). In 14-day/28-day rat studies, TEAD1-selective TEAD inhibitors also exhibited proteinuric nephropathy similar to that observed with pan-/multiple-TEAD inhibitors. Therefore, based on our findings, we can conclude that TEAD1-selective TEAD palmitoylation inhibitors can have similar on-target effect on kidneys as TEAD inhibitors with broader TEAD selectivity while having reduced anti-tumor efficacy and durability of response in combination with targeted therapies.

PREVENTION / EARLY DETECTION / INTERCEPTION: Secondary and Tertiary Cancer Prevention Studies and Patient Communication Decision Making
Poster Session

#7286 Optimizing prediction of metastatic castration-resistant prostate cancer: Multimodal fusion of clinicopathological and genomic features with machine learning.

Mohammad K. Alexanderani, Francesca Khani, Matthew Greenblatt, Brian Robinson, Massimo Loda, Luigi Marchionni

Weill Cornell Medicine, New York, NY

Background: Transitioning from metastatic castration-sensitive prostate cancer (mCSPC) to its resistant variant poses risks of intensified medication, toxic side effects, and financial burdens for men undergoing treatment. Our study proposes a multimodal approach that integrates clinical, pathological, and genomic features to optimize prediction of metastatic castration-resistant prostate cancer (mCRPC) events. By applying machine learning (MML) techniques to multimodal data, we aim to stratify these patients based on the risk of developing mCRPC, contributing to the development of safer and personalized treatment strategies.
Methods: We analyzed a large cohort of patients with mCSPC (n=399) with a minimum of 36 month follow-up, annotated with clinical, pathological, and genomic features, encompassing relevant variables such as disease volume, PSA, metastases timing, variant classification, Grade Group, fraction of genome altered, MSI score, mutation counts, karyotypes, tumor mutational burden, and purity. Using a multimodal machine learning framework, we extracted informative features and employed eight distinct machine learning algorithms: K-Nearest Neighbor, Support Vector Machine, Decision Tree, and Logistic Regression, Support Vector Machine with RBF Kernel, Random Forest, and Gradient Boosting, in addition to a Deep Neural Networks architecture for building predictive models in supervised binary classification experiments. The models' performance was evaluated on separate training (80%) and testing sets (20%), and standard evaluation metrics, such as the area under the receiver operating characteristic curve (AUROC), and accuracy, were computed. Correlations were utilized to explore the relationships between features, and permutation analysis was employed to determine the importance of predictors. All raw data included in the analysis are available on *cBioPortal* database. The study is supported by the NIH-NCI-T32 for Next Generation Pathologists Program at our institution.
Results: Of the 399 mCSPC patients, 56% developed castration resistance, 50% had Grade Group 5 disease, and 69% exhibited missense mutations. In a series of 8 experiments, the Support Vector Machine with RBF Kernel ensemble model and SVC exhibited the highest performance with an AUROC score of 0.77, while the remaining models tested in the study demonstrated AUROC scores ranging from 0.62 to 0.75. Notably, the fraction of altered genome emerged as the top-ranked predictor, displaying the highest importance score.
Conclusions: Our study demonstrates the strong predictive performance of MML models in accurately identifying mCRPC events by leveraging routine clinical, pathological, and genomic data, offering valuable guidance for optimizing patient stratification and tailoring personalized therapeutic interventions.

#7287 High-grade serous ovarian carcinoma detected with *TP53* mutation panel and SiMSen-Seq.

A. Olsson Widjaja[1], P. Micallef[2], B. Ulfenborg[3], M. Lycke[1], U. Gyllensten[4], T. Carlsson[2], T. Osterlund[5], A. Stahlberg[5], A. Linder[1], K. Sundfeldt[1];
[1]Institute of Clinical Sciences, Gothenburg, Sweden, [2]Institute of Biomedicine, Gothenburg, Sweden, [3]School of Bioscience, Skovde, Sweden, [4]SciLifeLab Uppsala, Uppsala, Sweden, [5]Wallenberg Centre for Molecular and Translational Medicine, Gothenburg, Sweden

Background: Ovarian carcinoma (OC) has the highest mortality among gynecologic malignancies due to absent or unspecific symptoms. The high-grade serous ovarian carcinoma (HGSC) accounts for over 60% of the OC associated deaths. The most frequent genetic aberrations in HGSC are mutations in the *TP53* gene, detected in approximately 96% of the tumors. Previous studies have proposed potential diagnostic utility of detecting mutations in circulating tumor DNA (ctDNA) from OC patients. However, the need for diagnostic methods capable of detecting asymptomatic HGSC is unmet.
Objectives: The primary aims of this study were to design a screening tool for identification of HGSC and to evaluate the suitability of various clinical specimen types for diagnostic applications.
Methods: In this study, we designed a highly sensitive and robust screening tool using the simple, multiplexed, PCR-based barcoding of DNA for sensitive mutation detection using sequencing (SiMSen-Seq) technique for identification of HGSC (n=11) by *TP53* mutation profile in various clinical specimen for diagnostic applications. Specimens sampled included primary tumors, ascites, plasma, vaginal samples, and both liquid and solid samples from cyst-, endocervical-, and endometrial origin (n=94).
Results: The in-house designed panel amplified 17 regions, encompassing 619 nucleotide positions within the *TP53* gene. Pathogenic variants were identified in 10/11 of the primary tumors, with a VAF ≥ 9% (range: 9-91). Preliminary data indicated that all (100%) paired samples obtained corresponding somatic mutations between two or more of the different compartments from the same patient.
In total 10/10 ascites-, 16/16 cyst-, 8/8 plasma-, 5/8 vaginal-, 17/22 endocervical-, and 14/19 endometrial samples showed somatic variants at a consensus read depth of 3 and a minimum VAF ≥ 0.1%.
Conclusion: The present study suggests that the *TP53* mutation panel can identify somatic variants in a variety of non-invasive liquid biopsies. Additionally, the assessment of the *TP53* mutation panel exhibits potential for forthcoming clinical utilization as a diagnostic tool.

#7288 Evaluation of silica spin-column and bead formats for rapid promoter DNA methylation analysis by qMSP in clinical and point-of-care settings.

F. Zamuner[1], A. Ramos-Lopez[2], A. Garcia-Negron[2], A. Purcell-Wiltz[3], A. Cortes-Ortiz[3], A. Roman[2], K. Gosala[1], E. Winkler[1], D. Sidransky[1], M. Brait[1], R. E. Guerrero-Preston[2];

[1]Johns Hopkins School of Medicine, Baltimore, MD, [2]LifeGene BioMarks, Toa Baja, PR, [3]San Juan Bautista School of Medicine, Caguas, PR

Late-stage cancers often lack effective management and treatment options, emphasizing the importance of early diagnosis for better prognosis and lower mortality rates. Molecular markers, such as DNA methylation tests, have shown promise in predicting and detecting cancer at its earliest stages. The COVID-19 post-pandemic scenario is providing a one in one-hundred-year opportunity of utilizing the excess installed PCR capacity world-wide to develop novel Quantitative Methylation Specific PCR (qMSP) screening strategies for cervical cancer screening in low-resource settings. This study aimed to compare the use of commercial bisulfite conversion kits in cervical epithelium liquid cytology samples (liquid cytology) from cancer screening clinics in the United States. Commercially available rapid bisulfite conversion protocols using silica spin column and magnetic beads were compared with conventional DNA extraction followed by bisulfite conversion protocols to profile DNA methylation by qMSP in a panel of methylated genes we previously developed to distinguish normal and cervical cancer patient samples. The results revealed that small sample volumes are suitable for methylation studies. Comparisons among four spin-column kits showed no significant differences in *β-actin* Cycle Threshold (Cts) values between Abcam, Epigentek, QIAGEN and Zymo D5021 kits. Zymo The best performing spin-column kit was compared with manual and automated versions of magnetic bead kits using a 96-well plate format for higher throughput. Methylation profiling of three genes (*β-actin ZNF516,* and *FKBP6*) with manual and automated magnetic bead kits revealed that automation increases throughput without a reduction in amplification efficiency in open PCR systems. Cost analysis showed that the direct kits 96-well plate format were more affordable compared to the Gold Standard manual protocol that uses spin-columns. An optimized version of Zymo D5046 magnetic bead kit provides the fastest turnaround time with similar amplification efficiency, when compared to spin-column or other magnetic bead kits. The test cost per sample is $5.41 dollars to process 83 samples in a 96 well-plate format in less than 2 hours. Another significant finding was showing the feasibility of using as low as 12µL of liquid cytology samples for DNA methylation testing, proving that bodily fluids are a liquid biopsy alternative to plasma. Overall, this comprehensive comparison is useful in determining optimal options for efficient and cost-effective cancer DNA methylation diagnostic tests, particularly in low-resource settings.

#7289 PancreaAlert: Intelligent nanoengineered biosensor for pancreatic cancer.

Meenal Karunanidhi[1], Hemalatha Kanniyappan[1], Edith Zhan[2], Ruth Mathew[3], Yani Sun[3], Junyi Wu[4], Yan Yan[4], Gnanasekar Munirathinam[1], Mathew T. Mathew[1]

[1]University of Illinois College of Medicine (Rockford), Rockford, IL,[2]Hononegah High School, Rockton, IL,[3]University of Illinois Chicago, Chicago, IL,[4]IIT, Chicago, IL

Introduction: Pancreatic cancer accounts for 3% of cancer cases and 7% of cancer deaths in the United States. It is currently in the third position with respect to cancer-related deaths, and it is expected to move to second place as of 2040. This is mainly due to its diagnosis in the later stage. If detected in the first or second stage surgery can be performed thus increasing the patient's survival rate. The current methods of diagnosis cannot do early stage or asymptomatic detection. So, detecting cancer-specific biomarkers can aid in the prognosis. Serum protein-based biomarkers carbohydrate antigen CA242, CA19-9, and carcinoembryonic antigen CEA are specific to pancreatic cancer. Thus, in this preliminary study, we aim to develop a nanoengineered electrochemical biosensor combined with machine learning to detect pancreatic cancer-specific biomarkers CA242, CA19-9, and CEA.
Methodology: Nanoengineering the biosensor: The gold working electrode of the gold- biosensor (DRP-250AT) was coated with graphene oxide nano colloidal solution and kept in UV overnight for the graphene oxide nanosheet to crosslink with the working electrode. Detection of biomarkers using an electrochemical biosensor: First, a Crosslinker (DSP) was added to ethanol cleaned biosensor to bind the analytes. Following that antibody specific to each biomarker were added to the biosensors. The addition of TBS superblock prevented non-specific binding. Then different concentrations of biomarkers were added, and the corresponding sensor was subjected to various electrochemical analyses such as electrochemical impedance spectroscopy and voltammetry. SEM-EDAX analysis: The antigen-antibody binding on the biosensor's surface was confirmed. Automation and machine learning: Python code was developed to automate the analysis process and machine learning models (support vector machine and neural network) were used to classify the concentrations into various risk levels. The sensitivity of the developed tool was high when compared with conventional methods like ELISA and confocal microscopy.
Results: From the electrochemical studies we found that with increasing concentration of biomarkers, there was a trend in output parameters: capacitance, resistance, impedance and area under the curve. By analyzing this trend, the concentrations of biomarkers can be detected. Using this data as input the machine learning model (accuracy greater than 80%) classified the concentrations into risk levels (normal, low risk, and high risk).
Significance: Nanoengineering with graphene oxide nanosheets enhances the sensitivity of electrochemical biosensors. Automation and machine learning models help in the analysis of large datasets produced by this sensor. Overall, this device aids in the prognosis of pancreatic cancer. Our preliminary results are encouraging but more thorough research is required to make this diagnostic tool a working application.

#7290 Novel plasmid-based screening method for cervical cancer.

A. Eli, Y. Hartman, B. B. Kasten, R. Arend, J. Warram;
University of Alabama at Birmingham, Birmingham, AL

Introduction: Alabama (AL) is tied for third-highest incidence rate and has second-highest death rate of cervical cancer as of 2020. Globally, cervical cancer has the fourth-highest incidence among cancers in women; 90% of deaths from cervical cancer in 2020 occurred in low- and middle-income (LMIC) countries. Inhibitor of differentiation/DNA binding 1 (Id1) expression correlates with tumorigenesis, clinical grade/stage, and aggressiveness of cervical cancer. Thus, Id1 expression could be exploited in novel screening approaches that aim to improve survival rates of cervical cancer in LMIC and clinically underserved settings. As a first step in developing an Id1-based screening approach, these preclinical studies utilized a plasmid that induces expression of a secreted reporter enzyme (secreted embryonic alkaline phosphatase, SEAP), controlled by the Id1 promoter sequence (pId1-SEAP). These studies examined relationships between Id1 expression and kinetics of reporter expression following plasmid transfection to detect human cervical cancer cells.
Methods and Results: To confirm the relevance of Id1 as a target in cervical cancer, immunohistochemical staining for Id1 was performed on a human cervical cancer tissue microarray. Western blotting was performed to determine Id1 expression in human cervical cancer cell lines (HeLa, SiHa, CaSki). Optimal transfection conditions with pId1-SEAP were determined experimentally for each line, and then media was sampled through a 48-hour period post-transfection to quantify reporter SEAP expression. Immunohistochemical stain for Id1 showed that early stage and late stage human cervical cancer tissues expressed significantly ($p < 0.05$) higher levels of Id1 compared to normal tissues, with stain optical density values being 3e5±1e5 for early and late stage compared to 3e4±3e4 for normal tissues (early stage p=0.0001, late stage p=0.0002). Western blot for Id1 in HeLa, SiHa, and CaSki lines showed that all three positively expressed Id1, with Beta-actin-normalized expression values of 0.78±0.12, 1.12±0.05, and 0.76±0.08, respectively. The cell lines transfected with pId1-SEAP expressed SEAP at rates significantly higher than control cells, with the highest rates of production seen during the 36-48-hour post-transfection period. Rates of SEAP production (counts/hour) during this time period were 1e4±3e3 (p=0.0278), 8e2±1e2 (p=0.0834), and 3e2±5e1 (p=0.0683) for transfected HeLa, SiHa, and CaSki cells, respectively.
Conclusions: The pId1-SEAP system enabled sensitive detection of cervical cancer cells. These preliminary data support future studies evaluating the *in vivo* performance of the system in preclinical models of early stage cervical cancer. Further development of this approach could enable sensitive and reliable detection of cervical cancer during early stages when treatment is most effective.

#7291 Detection of a truncated form of multidrug resistance protein 1 (MRP1) in plasma sEVs derived from cancer patients.

K. Bhandari, J. Kong, C. Xu, A. Jain, W.-Q. Ding;
University of Oklahoma Health Sciences Center, Oklahoma City, OK

Multidrug resistance protein 1 (MRP1/ABCC1) is an ATP dependent transmembrane efflux pump that confers to drug resistance. Overexpression of MRP1 has been observed in both pancreatic ductal adenocarcinoma (PDAC) and breast cancer tissues. Numerous proteomics studies have revealed the presence of MRP1 in small extracellular vesicles (sEVs) released from cancer cells. Cancer-derived sEVs are known to be released into the circulation, thus becoming attractive candidates for non-invasive biomarker development. However, whether the MRP1 level in plasma sEVs is indicative of human cancer has not been evaluated. This study examined the MRP1 expression in plasma sEVs derived from patients with PDAC, breast and colon cancer, and age- and gender-matched healthy subjects. The patient plasma samples were obtained primarily from the NCI-sponsored Cooperative Human Tissue Network and Stephenson Cancer Center. Healthy plasma samples were provided by the Oklahoma Blood institute. Human pancreatic cancer cell lines PANC-1, MIA PaCa-2 and BxPC-3, and the pancreatic ductal cell line hTERT-HPNE were tested for MRP1 expression prior to examination of plasma samples. Cellular and plasma sEVs were isolated using the double filtration followed by polymer precipitation method. Western blot was performed to assess the expression level of MRP1 and proteomics was applied to confirm the detection of a truncated form of MRP1 in plasma sEVs. MRP1 expression was detected in the sEVs derived from all three pancreatic cancer cell lines but absent in the sEVs from the HPNE line. Overexpression of a truncated MRP1 protein was detected in plasma sEVs derived from patients with early stage (stage I-IIA) and late stage (III-IV) PDAC, compared with that from matched healthy subjects (n=17 for each group). Similar findings were evident in plasma sEVs from patients with breast cancer (n=7), while the results remained inconclusive in plasma sEVs from patients with colon cancer (n=7). Protein structure analysis indicated that the truncated form of MRP1 likely consists of the regions between the QCRL-1 motif and the C-terminus of the protein. Proteomic analysis detected the peptides derived from the C-terminus region, consistent with the structural analysis. Furthermore, the truncated form of MRP1 can only be detected using antibodies against the epitopes in the C-terminus and QCRL-1 region of MRP1 protein. In summary, we have detected a truncated form of MRP1 protein in plasma sEVs derived from cancer patients, and the level of its expression is significantly elevated in patients with PDAC and breast cancer.

#7292 Surveying the landscape of somatic variation in healthy breast tissue for cancer risk prediction.

M. J. Przybilla[1], A. R. J. Lawson[1], P. Nicola[1], B. T. Pentecost[2], I. Martincorena[1], K. F. Arcaro[2], P. J. Campbell[1];
[1]Wellcome Sanger Institute, Cambridge, United Kingdom, [2]Wellcome Sanger University of Massachusetts, Boston, MA

Carcinogenesis centers on principles of somatic evolution, where a cell gradually accumulates mutations, eventually transforming into a tumor cell. Exploring somatic variation in the healthy population offers insights for predicting cancer risk and facilitating early detection. In breast cancer (BC), the emergence of the malignant clone occurs within a broader spectrum of abnormal cells, often referred to as the 'field effect.' BC development is intricately linked to hormonal regulation, with prior research indicating that the initial changes manifest during puberty and pregnancy. Although around 10% of diagnosed BCs affect young women (<45 years), with 35-55% of these cases arising within a decade after completed pregnancy (postpartum BC), effective screening tools are lacking. We propose a novel approach for the individualized quantification of somatic variation and the field effect using breast milk (BM) as a liquid biopsy. We conducted a retrospective analysis of 272 BM samples obtained from both the left and right breasts of 125 healthy donors, including 62 donors with elevated cancer risk due to a germline predisposition involving *BRCA*. Given the heterogeneous cellular composition of BM, encompassing epithelial cells and lymphocytes, we initially implemented a comprehensive analysis to reliably detect somatic mutations in whole BM, as well as in magnetically activated cell-sorted (MACS) epithelial-enriched (EE) and -depleted (ED) samples from a subset of donors. DNA extracted from all samples was used for NanoSeq, a single-molecule sequencing methodology, focusing on a targeted panel of 84 genes recognized as drivers in either BC or normal tissue. Our assessment of mutation burden estimates across all sample types revealed consistent results. Generally, cells accumulated somatic mutations linearly with age, but with a higher rate in individuals with a *BRCA2* cancer predisposition. We found several critical driver genes, including *PIK3CA*, *PIK3R1*, *TP53,* to be under significant positive selection using the ratio of non-synonymous to synonymous mutations. When we assessed the fraction of cells in each sample carrying mutations in these genes, we however detected a significantly higher fraction of mutated cells in individuals with germline predisposition - possibly representing a genetic manifestation of the epidemiologically higher risk of *BRCA* germline carriers.

As we expand our understanding of the interplay between the somatic mutation landscape and cancer risk, our efforts provide evidence for the utility of BM as an easily accessible, non-invasive sample. The proposed methodology, involving BM with precise genetic analysis through NanoSeq, presents a promising avenue for elucidating personalized somatic variation patterns. We anticipate that BM holds potential as a valuable tool for risk stratification, particularly for individuals under 45 and postpartum women.

#7293 Serum fusion gene transcripts to predict liver cancer.

J.-H. Luo, Y.-P. Yu, S. Liu, D. Geller;
University of Pittsburgh School of Medicine, Pittsburgh, PA

Hepatocellular carcinoma (HCC) is the most common type of liver cancers and one of the most lethal malignancies for human. Early diagnosis of HCC is crucial in reducing the mortality of the disease. In this report, we analyzed a panel of 9 fusion transcripts in the serum samples from 136 individuals (61 HCC patients and 75 individuals without HCC) using TaqMan qRT-PCR. Our results showed that 7 fusion genes were frequently detected in the serum samples of HCC patients, including MAN2A1-FER (100%), SLC45A2-AMACR (62.3%), ZMPSTE24-ZMYM4 (62.3%), Pten-NOLC1 (57.4%), CCNH-C5orf30 (55.7%), STAMBPL1-FAS (26.2%) and PCMTD1-SNTG1 (16.4%). We then divided the samples into training and testing cohorts based on the sample collection time: 82 individuals with samples collected before 2016 as the training cohort while 54 individuals with sample collected after 2015 as the testing cohort. Machine learning models was constructed based on the combination of different fusion genes with various cutoffs to predict the occurrence of HCC in the training cohort using leave-one-out-cross-validation approach. One of the machine learning models called 4-fusion genes logistic regression model (MAN2A1-FER<40, CCNH-C5orf30<38, SLC45A2-AMACR<41, Pten-NOLC1<40) produced a 91.5% accuracy, with a sensitivity of 87.1% and specificity of 94.1% in the training cohort. The same model generated an accuracy of 83.3%, with a sensitivity of 73.3% and specificity of 95.8% in testing cohort. When the training and testing cohorts were combined, the model produced an accuracy of 86%. When serum α-fetal protein (AFP) level was incorporated into the machine learning model, we found a 2-fusion gene+AFP logistic regression model (MAN2A1-FER<40, CCNH-C5orf30<38, AFP) generated an accuracy of 94.8% in the training cohort with a sensitivity of 93.5% and specificity of 96.3%. The same model generated 95% accuracy in both the testing cohort and the combined cohorts in the validation. Cancer treatment reduced most of the serum fusion transcript levels, reflecting the reduction of the tumor load. As a result, serum fusion gene machine learning models may serve as important tools in screening HCC and monitoring the impact of HCC treatment.

#7294 CREATE-2: Colorectal cancer & adenoma test evaluation of a multi-omic blood test.

James M. Cameron, Georgios Antoniou, Rose McHardy, David Palmer, Alexandra Sala, Matthew Baker

Dxcover Ltd., Glasgow, United Kingdom

Background: Colorectal cancer (CRC) is the third most common cancer worldwide, with almost 2 million new cases reported in 2020. CRC develops over time from a pre-cancerous stage (adenoma) - the 'adenoma-carcinoma sequence'. Pre-cancerous lesions, such as Higher Risk Adenomas (HRA), harbour an increased risk of developing into CRC and their features are defined according to size, number and histological features. Screening for signs of CRC is recommended for average-risk adults using faecal immunochemical testing (FIT) in the UK, to enable the removal of pre-cancerous lesions and treatment of early-stage cancers. However, the performance of FIT is limited. Approximately 10% of CRC diagnoses have a negative FIT result, and it currently has ~93% false positive rate. Moreover, the sensitivity for detecting AA is only 24%, highlighting the need for alternative strategies.
Methods: A promising strategy for earlier CRC detection is the clinical use of Fourier transform infrared (FTIR) spectroscopy. The Dxcover® Colorectal Cancer Liquid Biopsy is a rapid multi-omic test that interrogates a blood sample with infrared (IR) radiation and produces a distinctive signature that represents the whole biomolecular profile of the sample. Rather than focusing on individual biomarkers, the technique encompasses the full range of diagnostic information from both the tumor and the non-tumor response. In the initial CREATE (ColoREctal Cancer & Adenoma Test Evaluation) feasibility study, the potential of the technology was highlighted in a retrospective cohort of patients comprising 100 CRC, 92 adenoma samples and 104 colonoscopy screening controls diagnosed as non-cancer. At 90% specificity, the test reported 80% CRC sensitivity and 59% HRA sensitivity. CREATE-2 is a prospective, observational, multicenter study, currently recruiting patients across the United States. The primary objective of the study is to determine the diagnostic accuracy of the blood-based Dxcover Colorectal Cancer Liquid Biopsy for CRC and HRA, and collectively as advanced colorectal neoplasia. Primary outcomes are sensitivity, specificity, negative predictive value, and positive predictive value of the test as compared to the standard of care screening modality. The study population is comprised of patients aged 45-84 considered 'average-risk' for CRC, undergoing routine CRC screening as standard of care. Patients are treatment naïve for CRC/HRA and must be willing to consent to blood draw pre-bowel preparation, and follow-up for 24 months. A rapid blood test that is sensitive to pre-cancerous lesions and early-stage CRC could substantially improve patient outcomes. Current screening programs have addressable shortcomings, and the emergence of new technologies is essential to support earlier CRC detection.

#7295 A novel XNA technology-based assay to detect JAK2 V617F mutation by real-time PCR.

S. Shen, R. Brown, D. Kim, L. Pastor, A. Y. Fu, P. Kaur, A. Babu, W. Liu, A. Zhang, **H. Tanaka**, M. Y. Sha;
DiaCarta, Pleasanton, CA

The Janus kinase 2 (JAK2) gene is located on chromosome 9p24.1 and encodes a non-receptor tyrosine kinase that plays a central role in cytokine and growth factor signaling. The JAK2 protein is especially important for controlling the production of blood cells from hematopoietic stem cells. In fact, the JAK2 mutation at amino acid 617 (Valine 617 to Phenylalanine, V617F) is the most frequently detected mutation in myeloproliferative neoplasms (MPN), including essential thrombocythemia (ET), polycythemia vera (PV), and primary myelofibrosis (PMF). This dominant gain-of-function V617F mutation results in constitutive tyrosine phosphorylation activity, leading to uncontrolled blood cell production, including increased numbers of erythrocytes, neutrophils, and platelets. To detect the JAK2 V617F mutation in DNA from patient blood samples, we developed a unique real-time PCR assay using our proprietary XNA technology that enables the assay to selectively amplify the mutant sequence by using a synthetic DNA analog XNA (Xenonucleic Acid). The JAK2 V617F mutation detection assay is designed to detect a valine-to-phenylalanine mutation at amino acid 617 (V617F). PCR primers, TaqMan probes, and XNA were designed for the JAK2 V617F mutation, along with primers and probes for an internal control gene in the duplex setting. The analytical performance of the assay was verified and validated using a variety of control samples. The results revealed that the XNA completely suppressed the amplification of wildtype sequence while only the V617F mutant sequence was amplified. The JAK2 V617F mutation detection assay is highly reproducible with intra- and inter-assay coefficients of variation of less than 10%. Results for the assay's analytical sensitivity indicated that V617F could be detected with about 0.25% mutant allele frequency in 10 ng DNA input. In addition, no significant cross-amplification between V617F and V617I was observed. Thus, the JAK2 V617F mutation detection assay is specific for the V617F mutation. The JAK2 V617F mutation detection assay, using XNA-based technology, provides high sensitivity and specificity to detect the JAK2 V617F mutation. Thus, this assay would be a useful tool for clinical decision-making in determining the presence of the JAK2 V617F mutation in DNA from patient blood samples.

#7297 Inhibition of lung tumorigenesis and potentiation of cancer preventive vaccines by a small molecule CA170 targeting the immune checkpoint protein VISTA.

Q. Zhang[1], J. Pan[1], D. Xiong[1], **Y. Wang**[1], M. S. Miller[2], M. You[1];
[1]Houston Methodist Research Institute, Houston, TX, [2]National Cancer Institute, Bethesda, MD

The V-domain Ig Suppressor of T cell Activation (VISTA) is expressed on cells of the myeloid and lymphoid lineages and is an emerging target for cancer immunotherapy. Blocking VISTA activates both innate and adaptive immunity to eradicate tumors in mice. Furthermore, a tripeptide small molecule antagonist of VISTA, CA170, exhibited potent anticancer efficacy on carcinogen-induced mouse lung tumorigenesis. We have previously demonstrated that KRAS or EGFR vaccines are effective in preventing lung tumorigenesis driven by either KRAS or EGFR in a pure prevention setting but are less effective in mice carrying existing lesions. Here, we determined if combining an MHC class II-restricted multi-antigen vaccine targeting KRAS or EGFR with CA170 will provide enhanced efficacy in preventing lung cancer progression. Using tetracycline-inducible KRAS and EGFR transgenic mice, we found that lung tumor development was significantly suppressed when CA170, delivered by aerosol inhalation to minimize systemic toxicity, was combined with either KRAS or EGFR MHCII-directed peptide vaccines using a post-initiation model. Flow cytometry and single-cell RNA sequencing (scRNA-seq) revealed that CA170 significantly increases tumor infiltrating CD8+ T cells and enhances effector-memory T cell frequencies and functions of both CD4+ and CD8+ T cells. These changes coincide with significant reductions in G-MDSCs (granulocytic myeloid-derived suppressor cells) and Foxp3+ Treg populations within lung tumors from mice treated with CA170. We found that the KRAS and EGFR preventive vaccines primarily induced the expansion of $CD4^{\pm}$ effector T cells. VISTA antagonism by CA170 revealed strong efficacy against lung tumorigenesis with broad immunoregulatory functions that influence effector, memory, and regulatory T cells, and drive an adaptive T cell tumor-specific immune response that enhances the efficacy of the KRAS and EGFR preventive vaccines in transgenic mouse models of lung cancer.

#7298 A nutraceutical supplement derived from olive oil byproducts exhibits potential cancer preventive properties in preclinical studies and increases vitamin D levels.

A. Albini[1], L. Calabrone[2], F. Albini[3], P. Corradino[1], S. Cristoni[2], D. M. Noonan[4];

[1]IEO - European Institute of Oncology, Milano, Italy, [2]I.S.B.-Ion Source & Biotechnologies, Bresso (MI), Italy, [3]Royal Society for the Encouragement of Arts, Manufactures and Commerce, London, United Kingdom, [4]IRCCS MultiMedica, Milano, Italy

Introduction: Extra virgin olive oil is a basic component of the Mediterranean diet; it contains several molecules with antioxidant, anti-inflammatory, anti-angiogenic and pro-apoptotic properties against a variety of cancers and influencing cellular metabolism too. Olive mill waste water (OMWW), a liquid residue produced in vast amounts during olive oil extraction, represents an environmental issue but on the other side it is a rich source of phytochemicals with potential health benefits. Particularly, OMWWs are rich in different phenolic compounds, that show promise in preventing the development of several disease disorders, including cancer. We have assessed the anti-angiogenic and anti-tumor properties exerted by a nutraceutical from purified OMWW extract, in *in vitro* and *in vivo* models, and evaluated its effect in a human pilot study upon informed consent.

Experimental procedures: OMWWs ability to affect cell proliferation and survival on different cancer cell lines was assessed by MTT. OMWWs interference with human umbilical endothelial vein cells (HUVECs) tube formation, migration and invasive capacities was studied by endothelial cell morphogenesis and migration assays. The inhibition of angiogenesis and tumor cell growth was investigated by the matrigel assay and tumour xenograft. To evaluate contribution of potential metabolomic biomarkers, SANIST (surface-activated chemical ionization-electrospray-NIST technology) mass spectrometric data-based platform has been employed on sera from a pilot study (Aiello et al, in preparation).

Results: OMWW extract shown a potent inhibitory effect inhibiting cells proliferation of both cancer cell lines and HUVECs.OMWW inhibited several molecular targets expression, including IL8, Angiogenin, mTOR, VEGF, CXCR4, CXCL12 and CXCL8, in tumor cells and in TNF-α-stimulated HUVEC. We nalyzed sera from volunteers, after nutraceutical intervention with Oliphenoliaand we assessed several biological parameters. Endogenous vitamin D was significantly increased, as well as albumin, direct bilirubin, and calcium. We also observed glycemia and potassium decrease after Oliphenolia assumption. A previously unknow form of Vitamin D was also detected by mass spectrometry.

Conclusions: OMWW extract has shown a stronger anti-angiogenic and anti-tumor properties, with potential chemo-preventive potentials. Results of human pilot study shows Oliphenolia as a promising and interesting natural dietary supplement, rich in polyphenol compounds, that can exert anti-inflammatory and antioxidant activities.

Acknowledgements: This study was supported by a donation from the Fattoria La Vialla di Gianni, Antonio e Bandino Lo Franco - SAS (Arezzo, Italy). We are grateful to Professor Anna Aiello, and Professor Calogero Caruso, Palermo University for the pilot study.

#7299 Preventing CRC progression in FAP rat model using a combinational targeting of TRAIL signaling and inflammation.

V. Madka[1], G. Pathuri[1], K. Venkatachalam[1], S. P. Singh[1], A. Singh[1], N. Stratton[1], S. Lightfoot[1], S. Sei[2], M. S. Miller[2], **C. V. Rao**[1];
[1]OU Health Stephenson Cancer Center, Oklahoma City, OK, [2]National Cancer Institute, Rockville, MD

Colorectal Cancer (CRC) is among the leading causes of mortality globally, with high incidence rates in developed countries including the US. While FAP patients are prone to develop CRC in their lifetime, recent rising trends among young adults is also a major concern. Hence, preventing CRC would aid in reducing cancer mortality, especially in high-risk FAP patients for which there are no FDA approved preventive agents. Here, we evaluated TRAIL-inducing, orally active small molecule ONC201, alone and in combination with the NSAID naproxen (NAP) for CRC prevention in the PIRC rat model representing FAP cohort. Male PIRC rats were bred inhouse and randomized by age into placebo and intervention groups (N=15). Starting at 6 weeks of age, experimental groups were administered either ONC201 alone by gavage [25mg/kg; 2X/week or 50mg/kg; 1X/week]; NAP in AIN-76A diet [200 ppm; continuously or 1 week ON/OFF]; or a combination of both agents, while placebo group received vehicle only. After 26 weeks of treatment, rats were euthanized and intestines were evaluated for tumor incidence and multiplicity. H&E stained colonic tumor sections were histologically classified as hyperplastic polyps, adenomas (AD), and adenocarcinomas (ADCA). Gross tumor data indicated significant reduction in colonic polyps in both the NAP alone and NAP+ONC201 groups without any overt-toxicites. Histological analyses also demonstrated strong suppression of AD progression to ADCA as well as a significant decrease in the number of ADs and ADCAs ($p<0.05$) in the treatment groups compared to the placebo. ONC201 regimens modestly reduced AD (19%-27% less, $p<0.05$) but showed strong inhibition of ADCA (45%-59% less, $p\leq0.0001$). A significant reduction of AD and ADCA was seen in NAP continuous (54% & 87% less respectively; $p<0.0001$) and intermittent (34% & 68% less respectively; $p<0.0001$) dosing regimens. As anticipated, the NAP continuous treatment had better efficacy than the intermittent dosing regimen. Notably, the combination treatment showed >90% ($p<0.0001$) inhibition of ADCA and 40%-57% ($p<0.0001$) inhibition of ADs. Importantly, ONC201+ NAP treatment also resulted in an additional 45% - 70% reduction of ADCA ($p<0.0001$) when compared to the NAP alone treatment. Thus, our data showed that the combination groups with NAP intermittent dosing demonstrated ~90% inhibition of ADCA, suggesting the synergistic effect of the two agents in preventing CRC progression. Molecular analysis of the rat tumors and additional analyses in in-vitro tumoroid models suggested induction of TRAIL (TRAIL, DR5, FADD), increased apoptosis (Caspases), and a decrease in proliferation markers (PCNA, Cyclin D1) and pro-inflammatory cytokines (IL1b, IL13 etc.). Our data suggests NAP/ONC201 combo has no toxicities, warranting further investigation of CRC interception in high-risk FAP patients (Funding by NCI-PREVENT 75N91019D00020-75N91020F00004).

#7300 Synergistic inhibition of prostate cancer growth by the combination of xanthohumol and ursolic acid.

R. Clark, A. Saha, C. A. Friedman, R. Gorgoglione, S. Tiziani, J. DiGiovanni;
The University of Texas At Austin, Austin, TX

Within the United States, prostate cancer (PCa) is the most commonly diagnosed non-cutaneous cancer, and approximately 1 in 8 men will receive a diagnosis in their lifetime. As the second leading cause of cancer deaths in American men, about 1 in 41 will die because of prostate cancer. The World Health Organization has suggested that approximately one-third of all cancer deaths are preventable, and one of the suggested means of prevention is through the increased consumption of fruits and vegetables. Fruits and vegetables contain natural compounds known as phytochemicals which possess biological activity including some anti-cancer effects. By adapting the ATP-bioluminescence assay for cell viability, our laboratory screened a natural compound library to find combinations of these compounds that may synergistically inhibit PCa cell viability. One of the combinations to emerge from this screening process was xanthohumol (XAN) and ursolic acid (UA). We examined the ability of the combination to inhibit tumor growth in a mouse HMVP2 PCa allograft tumor model. Mice were fed diets supplemented with either XAN (0.2%) or UA (0.2%) alone or the combination. Mice on the combination diet showed a significant inhibition of HMVP2 PCa tumor growth compared to mice on the single-agent diets. In addition, *in vitro* studies were performed to support the allograft tumor study and to further examine the mechanism of action of the combination. A cell survival assay utilizing six different PCa cell lines indicated that the combination of XAN and UA synergistically inhibited the survival of all cell lines as calculated by the Bliss index. Mechanistic studies performed in PCa cells indicate that the combination of XAN and UA inhibits oncogenic signaling better than either agent alone. Additionally, unbiased metabolomics revealed that the tumors from mice fed the combination diet had significantly less S-adenosyl-L-methionine compared to all other groups. Overall, 13 metabolic pathways were significantly different in the tumors from mice fed the combination diet compared to all other groups. The current data suggest that using a combination of XAN and UA may be a valuable chemopreventive strategy for PCa in humans. Funding: This work was supported by NIH Grant CA228404.

#7302 Effect of estrogen receptor modulator bazedoxifene on progression of carcinogen induced bladder cancer in female F344 rats.

V. Madka[1], G. Pathuri[1], S. P. Singh[1], S. Chiliveru[1], A. Singh[1], A. Bao[1], N. Stratton[1], C. J. Grubbs[2], S. Sei[3], J. Clifford[3], B. Cholewa[3], C. V. Rao[1];
[1]OU Health Stephenson Cancer Center, Oklahoma City, OK, [2]University of Alabama at Birmingham, Birmingham, AL, [3]National Cancer Institute, Rockville, MD

Bladder Cancer (BC) is the second most common genitourinary cancer with high recurrence and mortality rate due to metastatic muscle invasive BC (MIBC). An estimated 82,290 adults in the United States will be diagnosed with BC and one-fifth of the patients will die with this cancer in 2023. Sex disparity of BC is well known with 4 times higher risk in men, but women are more likely to die from it than men. Studies suggest that estrogen receptor (ER)-α and ER-β are over expressed in 18% and 63% of bladder tumors and associated with highly proliferative tumors and reduced overall survival. Hence, ER signaling is considered an important target for intercepting BC. Since the majority of BCs are non-invasive at diagnosis, developing agents that block BC progression may be beneficial for clinical translation. Bazedoxifene (BAZ), a clinically approved second generation SERM, is a co-repressor for both the ER-α and ER-β receptors, and it is a competitive inhibitor of 17-β-estradiol. In this study, BAZ was tested for toxicity and efficacy in an N-butyl-N-(4-hydroxybutyl)nitrosamine (BBN)-induced BC rat model. Female F344 rats are administered carcinogen BBN (150mg x twice a week) for 8 weeks to induce BC. For toxicity evaluation, 5 doses of BAZ were fed (2.5 ppm to 12.5 ppm in diet) to BBN treated rats (n=6) for 10 weeks. After termination, serum, various organs, and bladder tissues were evaluated for toxicity biomarkers and histopathology. For efficacy study, Female F344 rats (8 weeks of age) were (n=24) administered BBN as stated above. A week later, rats received either control or BAZ (5 ppm and 10 ppm) containing diets for 33 weeks and terminated. Bladders and other major organs were analyzed grossly for size, weight, and visible abnormalities including tumors. Formalin fixed tumor sections were stained and histopathologically graded. Results showed that BBN-exposed rat bladders were significantly larger and heavier due to tumors (0.77±0.10g, Mean±SEM; $p<0.0001$) as compared to vehicle treated rats' normal bladders (0.09±0.02g). Bladder tumor histopathology showed transitional cell carcinoma (TCC) and squamous cell carcinomas (SCC) with non-MIBC (NMIBC) and MIBC tumor grades in the vehicle control group. There was no significant difference in bladder weights between the 5 ppm and 10 ppm BAZ-treated vs. control group ($p>0.05$). However, histopathological evaluation showed ~20% ($p>0.05$) reduction in papilloma and NMIBC in the treated rats. Importantly, BAZ 5 ppm and 10 ppm treated rats had significantly less MIBC in a dose dependent manner (50%-70% less respectively; $p<0.001$) compared to control rats. In summary, our study demonstrates chemopreventive efficacy of bazedoxifene in interception of in BBN-induced rat bladder MIBC and warrants further investigation alone and in combination with complementary pathway targeting agents (Supported by NCI-PREVENT program 75N91019D00020-75N91020F00005).

#7303 The algal carotenoid diatoxanthin shows anti-cancer and cardio-protective properties: RNA seq analysis of potential targets.

D. M. Noonan[1], L. Calabrone[2], L. Pistelli[3], C. Brunet[3], C. Sansone[3], D. Morelli[1], G. Chiorino[4], F. Guana[4], A. Albini[5];

[1]IRCCS MultiMedica, Milano, Italy, [2]I.S.B.- Ion Source & Biotechnologies, Bresso (MI), Italy, [3]Stazione Zoologica Anton Dohrn, Napoli, Italy, [4]Fondazione Edo ed Elvo Tempia, Milano, Italy, [5]IRCCS European Institute of Oncology (IEO), Milano, Italy

Introduction: Natural bioactive pigments are of great interest for human health. Marine organisms are underexplored as source of useful metabolites. Diatoms produce diatoxantin (diatox), a xanthophyll with several properties (chemo-preventive, anti-inflammatory, antioxidant, photoprotective, immunomodulatory), that may have beneficial effects. Doxorubicin (doxo) is still one of the most effective chemotherapeutic drugs used in breast cancer (BC) treatment, but has side effects, particularly cardiotoxicity, mainly due to oxidative stress and cardiomyocyte damage. We have assessed the anti-cancer effects of diato, also verifying the absence of cardiotoxicity.

Experimental procedures: Diatox was administered to MDA-MB-231 triple negative BC (TNBC) *in vitro*, in combination with doxo by MTT and by 3D-spheroid assays. The modulation of diatox on the secretome of both TNBC cells and Human Umbilical-Vein Endothelial cell line (HUVEc) was assessed *in vitro* by angiogenesis arrays. Gene expression analysis was evaluated by measuring different inflammation and angiogenesis gene expression in cells treated with diato, by qPCR; while transcriptomic analysis was performed by RNA-Seq to verify diato effects on pathways involved in TNBC progression and in HUVEc inflammation.

Results: Diatox showed an inhibitory effect on the proliferation of MDA-MB-231 cells and, in combination with doxo, was able to inhibit TNBC spheroid growth, reducing their 3D-integrity and decreasing their viability. Diatoxx was able to down-regulate genes involved in inflammatory and angiogenic processes in HUVEc stimulated by TNFα (angiostatin, IL2, IL4 and PECAM-1 in antibody array and TGFβ1, TGFβ2, TIMP1 and TIMP2 gene in qPCR analysis). Moreover, diatox reduced several biological processes involved in inflammation and tumour development and metastasis, as demonstrated by RNA-Seq data. In TNBC cells diatox down-regulated ANGPT1, GPR37, ANG, QRICH2, MUC1 genes involved in angiogenesis processes, while EPHA7 was up-regulated. In TNFα-stimulated HUVEc, diatox down-regulated angiogenin, a powerful inducer of angiogenesis, and HSPA12A and EDNRB, which are involved in the regulation of macrophage cytokine production.

Conclusions: Diatox shows to be a promising chemo-preventive and angiopreventive natural compound in cancer prevention and therapy. Microalgae derived drugs can represent a potential and relevant source of novel nutraceutical and preventive substances, which can be considered as supplements in therapeutic strategies for cancer prevention. Acknowledgements: The studies were supported by Stazione Zoologica Anton Dohrn, by "Antitumor Drugs and Vaccines from the Sea "ADViSE" project (PG/2018/0494374).

#7304 Modulation of cytokine and chemokine profiles in pancreatic tumors and plasma *via* stage-specific intervention with *Momordica Charantia* juice in the LSL-KrasG12D/+, p48Cre/+ mouse model.

L. Bugata[1], R. Kumar[1], M. Kabir[1], R. Kant[2], C. Agarwal[2], R. Agarwal[2], K. Raina[1];

[1]South Dakota State University, Brookings, SD, [2]University of Colorado Denver-Anschutz Medical Campus, Aurora, CO

According to the American Cancer Society ≈64,050 people will be newly diagnosed with pancreatic cancer in the United States, while ≈55, 550 (men and women numbers combined) will die of this malignancy in 2023 alone. Epidemiological studies have indicated that a diet rich in natural agents might reduce pancreatic ductal adenocarcinoma (PDAC) risk, prompting investigations into a natural agent with health benefits in pancreatic diseases [such as the fruits of *Momordica Charantia* (Bitter Melon)] as a potential natural and non-toxic anti-cancer approach against PDAC. Previously we have reported the protective effects of oral Bitter Melon Juice (BMJ-standardized-lyophilized powder) against growth and progression of PDAC in preclinical animal models (xenograft and patient-derived tumor models). In a recent study we reported the efficacy of BMJ against pancreatic cancer in the LSL-KrasG12D/+, p48Cre/+ transgenic mouse model [this model mimics the stage-specific progression of intraepithelial neoplasms to PDAC as it occurs in humans]. Both male and female LSL-KrasG12D/+, p48Cre/+ transgenic mice were subjected to BMJ intervention (daily oral gavage, dose: 200mg/kg body wt.) during different stages in disease progression. Intervention was started at 4 or 15 weeks of mice age and continued till study end (10 and 30 weeks of mice age respectively). Additionally, in one group of mice, intervention was initiated at 6 weeks of mice age and continued till 41 weeks of mice age (study end). Outcomes were compared with wild-type and disease-positive untreated control groups. Pancreatic tissue/tumors were harvested at study end and blood plasma was also collected. In the present study, we performed a stage specific evaluation of tissue and plasma cytokine/chemokine profiling after BMJ intervention to gain detailed mechanistic insights into the potential of BMJ to mediate it is anti-pancreatic cancer effect *via* modulation of inflammatory pathways associated with PDAC growth and progression. BMJ (15 weeks of treatment) demonstrated a significant response in modulating cytokine/chemokine profiles in LSL KrasG12D/+, p48Cre/+ mice pancreatic cancerous tissues (30 weeks old mice). BMJ intervention specifically downregulated the levels of monocyte chemoattractant protein (MCP-1), macrophage inflammatory protein-1 (MIP-1-gamma), tumor necrosis factor (TNF) receptor (TNFR1), Vascular cell adhesion molecule 1 (VCAM-1/ CD106) and L-selectin (CD62L). Furthermore, Ingenuity Pathway Analysis indicated significant inhibitory predictions on TNF-α, NF-κB and MCP-1 (CCL-2) associated inflammatory pathways. Overall, these outcomes signify that the anti- cancer effects of BMJ in *KRAS* harboring PDAC tumors is associated with down-regulation of inflammatory pathways associated with growth and progression of pancreatic cancer.

#7305 Chemoprevention of colorectal cancer: Role of trace minerals in conjunction with calcium.

I. Harber, S. McClintock, J. Varani, **M. N. Aslam**;
University of Michigan Medical School, Ann Arbor, MI

Background: Colorectal cancer (CRC) is a leading cause of cancer-related deaths worldwide. CRC usually develops from adenomas (CRC precursors) after a long latency period. Prevention is crucial in reducing CRC incidence and progression to cancer. Among several prevention options, calcium has been a widely considered chemo-preventative agent.

Aims: Calcium plays a vital role in the regulation of epithelial cell differentiation, which is essential for epithelial growth control. Epidemiological studies have demonstrated that adequate calcium intake is crucial for protection against colonic polyp formation and colorectal cancer. However, recent interventional trials with calcium have had only modest and mixed results, and the question is how to improve efficacy. One potential strategy is to use calcium in combination with additional minerals and trace elements.

Results: Our preclinical studies employing monolayer cultures with CRC cell lines and colon organoids cultures from colon polyps have shown that a calcium-rich mineral combination derived from fossilized red algae (Aquamin) is more effective than calcium alone in inducing differentiation, suppressing growth and upregulation of calcium-sensing receptor. When colonic adenomas in culture were subjected to differential proteomic analysis, Aquamin upregulated several proteins involved in proliferation suppression, DNA mismatch repair and inducing differentiation, and apoptosis. Two long-term mouse studies have demonstrated that Aquamin is more effective in suppressing polyp & CRC incidence compared to calcium alone. Based on these findings, we conducted a 90-day FDA-approved trial (a pilot study with ten subjects per arm) comparing the two interventions in human subjects at risk for CRC. Results showed that Aquamin treatment reduced proliferation and increased cell differentiation observed by immunohistochemistry. Proteomic analysis also revealed that the minerals upregulated several proteins related to growth suppression, inducing differentiation and those contributing to cell-cell and cell-matrix adhesion functions and downregulated proteins involved in proliferation and nucleic acid metabolism.

Conclusion: These results provide convincing evidence that a multi-mineral combination derived from red algae can provide benefits in preventing CRC that are not seen with calcium alone. Further studies, such as a polyp-prevention trial in human subjects, are warranted to advance these CRC prevention efforts.

#7306 Licochalcone A is an excellent candidate for preventing luminal and non-luminal breast cancers.

Atieh Hajirahimkhan[1], Elizabeth T. Bartom[1], Sriram Chandrasekaran[2], Ruohui Chen[1], Jeremy J. Johnson[3], Susan E. Clare[1], Seema A. Khan[1]

[1]Northwestern University - Chicago, Chicago, IL, [2]University of Michigan, Ann Arbor, MI, [3]University of Illinois Chicago, Chicago, IL

Breast cancer (BC) risk reducing drugs have minimal impact due to their adverse effects and low acceptance by risk-eligible women. Further, they are ineffective against hormone receptor negative (HR-) BC. Novel agents with reduced toxicity and sufficient efficacy that extends beyond HR+ BC are needed. We showed previously that licochalcone A (LicA) from licorice has antioxidant/anti-inflammatory effects, inhibits aromatase, and blocks estrogen genotoxic metabolism. We hypothesize that LicA prevents HR+ and HR- BC through reprogramming metabolism and antioxidant pathways. We prepared microstructures from the fresh tissue of contralateral unaffected breast of 6 postmenopausal women with unilateral BC. After exposing them to DMSO (control) or LicA (5 µM), we performed total RNA sequencing followed by differential gene expression, pathway identification, and metabolism flux analyses. The NanoString metabolism panel was employed in 6 additional subjects. We performed live cell imaging to monitor proliferation of HR- and HR+ pre-malignant and malignant, as well as BRCA mutated cells. Xenograft models of HR+ and HR- tumors were established in female nude mice followed by 28-day treatment with vehicle or LicA (80 mg/kg.day, s.c.) and monitoring the tumor growth. Using LC-MS/MS we measured LicA in the blood and various tissues of intact BALB/c female mice receiving oral LicA (100 mg/kg) and assessed PK using Phoenix Platform. We observed significant (combined enrichment scores > 4 and FDR < 0.05) upregulation of antioxidant genes (up to 8-fold), consistent with upregulation of *NRF2* and the thioredoxin system. This was accompanied by significant downregulation of *RELA*- and *NF-kB1*-dependent inflammatory pathways. In addition, we observed decreased expression of *PI3K-AKT* genes and the pro-adipogenic transcription factors *SREBF1* and *SREBF2*, which may explain the downregulation (4 to 32-fold) of cholesterol biosynthesis, transport, and lipid metabolism genes. Metabolism studies confirmed these data and demonstrated a robust increase in the pentose phosphate shunt and NAD(P)H generation without enhancing ribose 5 phosphate formation, suggesting an antioxidant and antiproliferative environment. LicA also suppressed proliferation of pre-malignant and malignant cells, with sustained effects on aggressive cell lines at doses <10 µM. It reduced tumor growth in luminal (P = 0.008) and triple negative (P = 0.001) xenograft models. Oral bioavailability in serum and breast was in the low micromolar range and was sufficient to show efficacy.Our data suggest that LicA is an excellent candidate for both HR+ and HR- BC prevention by reprogramming metabolism and antioxidant pathways leading to decreased proliferation. Our next study will test an optimized oral formulation of LicA in intraductal models of HR+ and HR- precancer lesions in immunocompetent mice to further establish its preventive efficacy.

#7307 Silibinin regulates glucocorticoid signaling via mast cells: Potential treatment of androgen-resistant prostate cancer.

N. Mishra[1], S. Paudel[1], K. Raina[2], P. Maroni[1], C. Agarwal[1], R. Agarwal[1];

[1]University of Colorado Anschutz Medical Campus, Aurora, CO, [2]South Dakota State University, Brookings, SD

Prostate cancer (PCa) is the second most common cancer in American men. The American Cancer Society estimates that in 2023 there have been ~288,300 new cases of PCa and ~34,700 deaths from PCa in the United States. We previously showed that silibinin (SB; a natural flavonolignan from milk thistle seeds) is an effective therapeutic against PCa that inhibits cell growth and mitogenic cell survival via EGFR, IGFR-1, and NFκB signaling. However, the effect of SB on the tumor immunological microenvironment has not been elucidated. Mast cells (MCs) are archetypal solider of the immune system. The dynamics of PCa and MCs are complex, where they may contribute to tumor transformation/progression/regression; furthermore, their role in PCa is poorly understood. To address this gap and understand the role of SB in MC regulation, MCs were derived from the bone marrow (BMMCs) of C57BL/6 mice. BMMCs were generated in the presence of IL-3 and SCF, and were confirmed to be BMMCs using flow cytometry (dual staining: cKit/Fc€RI). Thereafter, the BMMCs were exposed to different doses of SB (25-100 µM) and two concentrations (25 µM; SB 25 and 100 µM; SB 100) were selected for further experiments. BMMCs treated with SB 25, SB 100, and untreated (control) were subjected to proteomic analysis using LCMS on Fusion Lumos mass spectrometer. A total of 3575 proteins were identified using the annotated mouse proteome. Statistical analysis was performed using ANOVA followed by Fisher's posthoc analysis ($p<0.05$, FDR<0.01) and 166 proteins were found to be have statistically significant differential expression amongst the three groups (n=4/group). These 166 proteins were selected for further pathway analysis using Ingenuity Pathway Analysis (IPA; Qiagen). Only pathways specifically demonstrated experimentally in prostatic tissues/cells were selected for further analysis. Important nodes found for SB regulation of MCs in PCa were androgen receptor (AR), transmembrane serine protease (TMPRSS), and NK3 Homeobox 1 (NKX3-1). AR, TMPRSS, and NkX3-1 are well established in PCA. Most important pathway found was glucocorticoid receptor (GR) signaling; nuclear receptor subfamily 3 group C member 1 (NR3C1) and HS90 were the most important proteins identified in GR signaling. GR signaling may cause androgen deprivation therapy (ADT)-resistance by directly activating AR-target genes (including TMPRSS2) and/or activating an independent transcriptome. NR3C1 has been shown to share target specificity with AR and is highly upregulated in the resistant tumors. Thus, SB could play an important therapeutic role, specifically in ADT-resistant tumors via regulation of MCs. Further studies are warranted to delineate these mechanisms. Understanding these mechanistic could also potentially aid to decipher a general mechanism of resistance to antiandrogens and potential of SB in treating ADT-resistant tumors.

#7308 Induction of apoptosis via the regulation of pro-apoptotic and anti-apoptotic proteins in pancreatic adenocarcinoma BxPC-3 cells by Chinese medicinal herbs *Scutellaria barbata* and *Oldenlandia diffusa*.

C. Choi, S. Wolf, R. Isaac, E. Choi, A. Shim, A. Campana, P. T. Uppala, R. Hayes, **B. Y. Wong**;
Andrews University, Berrien Springs, MI

Apoptosis is a controlled program cell death process that the body uses to combat cancer development. Pancreatic cancer is a devastating disease with a poor prognosis. It is usually symptom-free during development and is advanced at diagnosis. BxPC-3 is a pancreatic adenocarcinoma cell derived from a 61-year-old female with adenocarcinoma. *Scutellaria barbata* (SB) and *Oldenlanda diffusa* (OD) have been used in traditional Chinese medicine for treating liver, lung, and rectal cancers. They are included in most herbal cancer treatment formulas in Taiwan hospitals. We previously demonstrated that aqueous extracts of SB and OD selectively induced apoptosis in colon HCT 116 cancer cells but not in colon CCD 841 CoN normal epithelial cells by modulating the pro-apoptotic and anti-apoptotic proteins. They also induced and regulated apoptosis in pancreatic ductal carcinoma PANC-1 Cells. This study used the green/red/blue fluorescent Apoptosis /Necrosis Detection Kit and the Human Apoptosis Antibody Array - Membrane [43 Targets] Test (Abcam). Our fluorescent apoptosis data showed that a 2-hour treatment with 1.5 mg/mL and 3.0 mg/mL aqueous extract of SB and OD induced a statistically significant percentage of apoptosis in BxPC-3 cells (SB: 42.5 ± 3.5%, 48.5 ± 0.5% > 14.0% ± 4.0%, $p < 0.05$; OD: 72.0 ± 2.0%, 37.5 ± 1.5%> 14.0% ± 4.0%, $p < 0.05$) as compared to the negative control respectively. Similar results were obtained with the 4-hour incubation period (SB: 46.0 ± 8.0%, 54.5 ± 2.5% > 9.5% ± 2.5%, $p < 0.05$; OD: 49.0 ± 7.0%, 37.0 ± 0.0%> 9.5% ± 2.5%, $p < 0.05$). From the antibody array-membrane experiments, significant up-regulation of various pro-apoptotic proteins such as Bid, Bim, Bad, Bax, C3, C8, CD40, HTRA, IGFBP-4, IGFBP-4, p53, TNF-α, and TRAIL-2 as compared to the negative controls were observed; and regulation of anti-apoptotic proteins HSP27, IGF-II, and Survivin were also revealed. These results suggest that SB and OD contain phytochemicals that induce apoptosis in pancreatic adenocarcinoma BxPC-3 cells by regulating various apoptotic protein productions. Further study of their specific modulation effects of apoptosis is warranted to reveal their potential chemopreventive and therapeutic properties against pancreatic and other cancers.

#7309 Edible mushroom derived antioxidant, vialinin A, prevents melanoma growth and invasion.

A. Vo, A. Zafar;
Noorda College of Osteopathic Medicine, LLC, Provo, UT

Melanoma is the second leading invasive cancer with a greater capacity to invade and metastasize. Increased oxidative stress has been shown to be involved in melanoma growth and spread. Several antioxidants, vitamins, and other phytochemicals have been shown to prevent melanoma cancer growth. However, the chemopreventive efficacy of vialinin-A, an edible mushroom-derived p-terphenyl antioxidant, on cancer growth and invasion is unknown. We, therefore, hypothesized that with its potent anti-oxidative and anti-inflammatory actions, vialinin-A could prevent melanoma cell growth and invasion. B16-F10 melanoma cells were treated without or with various concentrations of vialinin-A. The cell viability was determined by MTT assay and apoptosis by annexin-V staining. Our results suggest that vialinin-A prevents melanoma cell growth in a dose-dependent manner. Vialinin-A also prevents the invasion and migration of melanoma cells. Further, vialinin-A prevents the generation of reactive oxygen species and promotes apoptosis of B16-F10 cells. In addition, vialinin-A increases the activation of caspase-3 and cleavage of PARP protein. Vialinin-A also regulated the expression of various anti-apoptotic, pro-apoptotic, and inflammatory markers in melanoma cells. In conclusion, our results suggest that vialinin-A, through regulating oxidative stress-modulated apoptotic pathways, could prevent melanoma cell growth and invasion and has potential chemopreventive properties.

#7310 Dietary feeding of silibinin effectively protects against UVB-induced basal cell carcinoma.

S. Paudel[1], N. Mishra[1], K. Raina[2], C. Agarwal[1], **R. Agarwal[1]**;

[1]University of Colorado Anschutz Medical Campus, Aurora, CO, [2]South Dakota State University, Brookings, SD

Exposure to UVB radiation causes various malignancies, including basal cell carcinoma (BCC) and squamous cell carcinoma (SCC). BCC is the most prevalent skin cancer type worldwide; ~3.6 million cases of BCC are diagnosed annually in the USA. Silibinin (SB) is a naturally occurring flavonolignan that is present in milk thistle seeds. It has been shown to effectively reduce BCC occurrence upon UVB radiation exposure, in both pre- and post-treatment studies, when applied topically. However, SB efficacy, when fed in diet, against UVB-induced BCC formation and growth has not been reported. We addressed this question employing Ptch+/- mice, where animals were divided into three groups. Group 1: control group, mice were fed adjusted vitamin diet (AIN-76A; TD94096) with no UVB exposure. Group 2: UVB group, mice were fed pellet control diet (semi-purified, modified AIN-76A) and exposed to UVB (240 mJ/cm^2) 3 times/week (Mon, Wed, Fri). Group 3: SB group, mice were fed 1% SB (w/w)-supplemented diet and exposed to UVB similar to that in Group 2. This protocol was followed for 26 weeks; thereafter, animals were sacrificed at 14 weeks and 26 weeks post-UVB initiation, and skin samples were harvested and analyzed for BCC formation. β-galactosidase staining showed the development of BCC lesions at 26 weeks in the UVB group; however, SB-fed group had both lesser number of BCC lesions and decreased area covered by BCCs as compared to the UVB group. Non-UVB exposed control group had no BCC lesions. To address if SB feeding starts exerting its efficacy earlier than 26 weeks, we selected the early efficacy timepoint for transcriptomics analysis to determine the mechanism of SB efficacy. Skin RNA samples from the 14-week time point (n=4/group; RIN≥7; DV200>85%) were subjected to library preparation (550 ng of total RNA; Zymo-Seq RiboFree Total RNA Library Kit), ribosomal RNA-depletion RNA sequencing (80 million paired-end reads/sample), and data processing. About 16,000 unique genes were identified, of which ~65% were protein-coding genes. The samples within each group were highly correlated (mean>0.99; Pearson's correlation). The UVB cluster was sequestered away from the other groups, indicating that the SB diet effectively mitigated the effects of UVB exposure, even at the transcriptome level. Additionally, gene ontology and pathway enrichment analysis (Ingenuity Pathway Analysis, Qiagen) of differentially expressed genes ($p<0.05$; fold change≤2) showed UVB-induced aberration and SB-associated enrichment in mitotic prometaphase, metaphase, and anaphase pathways, RHO GTPase signaling, and cell cycle regulation; the top functional network found to be dysregulated was lipid metabolism. Taken together, these results highlight the potential of dietary SB intake (apart from topical SB) to be an effective modality against UVB-induced BCC formation and growth and identify molecular targets that are plausibly involved in SB efficacy.

#7311 Lipid soluble vitamin B1 derivatives, benfotiamine and fursultiamine, prevent breast cancer cells growth.

C. C. O'Neill, **A. P. Langmead**, K. V. Ramana;
Noorda College of Osteopathic Medicine, LLC, Provo, UT

Breast cancer is the leading cause of cancer death in women in the US and the second leading cancer after skin cancer in women worldwide. According to the CDC, women from 45-84 years of age are most at risk, with approximately 30% of deaths in this group being from cancer. Increased free radical formation, and oxidative and inflammatory responses have been shown to be major contributing factors for the progression of breast cancer. Several antioxidants and vitamins have been tested for their efficacy in preventing breast cancer. However, the role of vitamin B1 derivatives in the prevention of breast cancer is not known. Therefore, we hypothesize that with potent anti-oxidative and anti-inflammatory actions, lipid-soluble derivatives of vitamin B1 (thiamine), such as benfotiamine and fursultiamine, could prevent breast cancer growth and spread. We have treated human breast cancer cells such as MCF-7 and T-4D1 and mouse breast cancer cells 4T1 with vitamin B1 derivatives and examined the cancer cells growth. Our results indicate that treatment of various breast cancer cells with benfotiamine and fursultiamine prevents the proliferation of cancer cells in a dose-dependent manner. Further, both benfotiamine and fursultiamine by regulating the activation of caspase-3 and cleavage of PARP protein could prevent breast cancer cells growth. Benfotiamine and fursultiamine also regulates generation of reactive oxygen species in breast cancer cells. Further, vitamin B1 derivatives regulate the expression of various anti-apoptotic, pro-apoptotic, survival and inflammatory factors in both human and mouse breast cancer cells. We next planned to examine the effect of vitamin B1 derivatives on breast cancer growth in vivo using athymic nude mouse models. In conclusion, our in vitro results suggest that vitamin B1 derivatives, benfotiamine and fursultiamine, by promoting the apoptotic pathways prevent breast cancer cells growth and could be further developed as chemopreventive drugs.

#7312 Construction of a gene panel for liquid biopsy-based diagnostics of gynecologic cancer.

S. Schumacher, T. Carlsson, J. Malchau Lauesgaard, A. Linder, A. Olsson Widjaja, K. Sundfeldt;
University of Gothenburg, Gothenburg, Sweden

Background: Ovarian carcinoma (OC) is the leading cause of death from gynecologic cancers mainly due to late detection, where most patients are diagnosed at advanced stages (51% in stage III; 29% in stage IV). Despite an overall more favorable prognosis, endometrial carcinoma (EC) is the most common gynecologic cancer, with an increasing incidence and where some subtypes are associated with a poor prognosis. Identification of DNA mutations from precancerous lesions or early-stage OC and EC would allow for early intervention. Liquid biopsies through routine sampling such as endocervical sampling, or blood collection for isolation and analysis of ctDNA have previously been assessed for their use in detection of OC and EC. These studies have provided evidence that tumor-derived mutations can be detected in endocervical samples, supporting endocervical liquid biopsies as a potential source of ctDNA. Herein, we aimed to construct a diagnostic gene panel corresponding to common mutation profiles of OC and EC to detect early-stage malignancy through a non-invasive approach.

Methods: Using the NGS-method, Simple multiplexed PCR-based barcoding of DNA for sensitive mutation detection using sequencing (SiMSen-Seq), a gene panel was constructed targeting hotspot mutations in known OC- and EC-associated genes. Hotspots were identified using the Catalogue of Somatic Mutations in Cancer (COSMIC) database or retrieved from the literature and assays were designed for amplification of short DNA fragments. Precise assay development was carried out including multiple steps of careful validation to ensure high specificity and efficient amplification. Individual assays were validated in multiple steps using qPCR and fragment analysis.

Results: The gene panel was designed as two non-overlapping subunits for comprehensive diagnosis of OC and EC. The two constructed multiplexes, together composed of 125 single assays target genomic regions in 34 EC and OC-associated genes e.g., *PTEN*, *TP53*, *PIK3CA* and *CTNNB1*. Included assays had a median amplicon size of 92 bp (range 57-111 bp). Both multiplexes displayed good performance with distinguishable libraries at low DNA input (10 ng). Validation of individual assays showed high specificity and efficient amplification where >80% of assays displayed a sequencing coverage >500 UMI counts at a consensus depth of 3. Patient coverage calculations of COSMIC data suggested comparable coverage as similar published approaches.

Conclusion: The results suggest that the constructed gene panel has great potential to detect mutations in liquid biopsies collected from the gynecologic tract, despite low tumor DNA levels. Validation of the two multiplexes by fragment analysis and sequencing showed high performance, hence, prospective for the approaching sequencing of liquid biopsies.

#7313 Risk assessment, early detection, and strategic prevention of naturally occurring cancers in companion dogs.

J. F. Modiano[1], A. J. Schulte[1], R. Dicovitsky[2], T. A. DePauw[1], A. Khammanivong[1], M. Lewellen[1], L. E. Burt[1], D. A. Vallera[1], G. R. Cutter[3], A. L. Winter[2], K. M. Stuebner[1], A. Chehadeh[2], S. Pracht[2], A. Borgatti[1], M. S. Henson[1], E. B. Dickerson[1], C. Ober[4], K. L. Anderson[2], E. Nell[5], A. L. Sarver[1];
[1]University of Minnesota, Minneapolis, MN, [2]University of Minnesota, St. Paul, MN, [3]University of Alabama, Birmingham (Emeritus), Birmingham, AL, [4]Darkside Veterinary Imaging, Woodbury, MN, [5]Acuity Veterinary Imaging, Menlo Park, CA

Our research is (focused) on delineating the relationship of aging and cancer with the goal to develop prevention and intervention therapies. Our success towards this end is based on the ability to employ companion dogs in clinical studies, particularly given the similarities of aging and cancer in dogs and people. Here, we report results of the development of both a companion diagnostic and a potential therapeutic intervention from the canine clinical Shine On study. The Shine On study included a training set of 97 dogs in four groups, consisting of (1) healthy 2-4 year-old dogs that were skeletally mature but had not reached the age boundary where cancer risk is apparent, and three groups where dogs had pathologically confirmed (2) hemangiosarcomas, (3) other malignant cancers, or (4) benign splenic masses. It also included a test set of 209 dogs over 6 years of age with no evidence of cancer or other chronic diseases. Using the Shine On Suspicion (SOS) test, dogs could be assigned to a low-risk category, where the probability of developing cancer over the next 400 days (approximately 1/10th of a modern domestic dog's lifespan) was less than 4%, or to a high-risk category, where the probability of developing cancer over the same time period was almost 25%, and it increased to more than 50% by 1,450 days. Not surprisingly, the relative risk of cancer in dogs that were originally assigned to the low-risk category increased in a fashion that was comparable to that seen in dogs assigned to the high-risk category within 400-600 days after testing. We have used the bispecific ligand targeted toxin, eBAT, as a strategic preventative in seven dogs to date. The drug is well tolerated and associated with favorable outcomes (extended lifespan with no cancer deaths). Ongoing experiments seek to define the identity and functional properties of putative-niche forming cells and mechanisms through which we can modify the permissive environment to delay or prevent cancer in dogs - and eventually in humans.

#7314 Technological and economic values of an AI-based pre-screening multi-cancer early detection (MCED) liquid-biopsy test as a companion system for a cancer screening solution.

B. G. Kermani;
Crystal Genetics, Inc., Los Altos, CA

Multi-cancer early detection (MCED) liquid biopsy screening tests provide great promise for both first-time cancer detection, and recurrence monitoring applications. The prominent feature of asymptomatic cancer screening solutions is their demand for ultra-high specificity (e.g., circa 99.99%), while maintaining a reasonable sensitivity. However, the challenges of screening are not limited to these technical specifications. Among other challenges, psychological and economical barriers-to-entry can be mentioned. In this work, we discuss the value of adding a high-sensitivity liquid-biopsy prescreening system to a screening solution. Such a tandem system can retain the high specificity offered by the screening solution, while relieving some of the economical concerns in cancer screening, by providing an opportunity to forgo screening in individuals with negative prescreening results. In order to serve in a general multi-cancer scheme, the prescreening solution must be MCED in nature. While our screening solution is primarily single-cell genomics/proteomics-based, we adopted a predominantly proteomics-based solution for prescreening. A proteomics solution has the potential to be notably more economical due to its simplicity/maturity. This is in contrast to the relatively high cost of the 'omics-based screening methods. Nevertheless, proteomics-based solutions, historically, have suffered from limited sensitivity and low specificity. In order to attain a high sensitivity while maintaining a workable specificity, we have used a complex Artificial Intelligence (AI) based system, comprising machine learning (ML) and Expert Systems (ES). Our MCED blood-based prescreening solution has been successfully tested on a series of cancers, including (among others) the cancers of breast, lung, prostate, ovary, uterus, and cervix, with cancer signal detection sensitivity of ≈92% for early stages (Stage I or II). While a tandem prescreening-screening system is designed primarily for testing asymptomatic individuals for early detection of cancer, a prescreening method has other potential uses. For instance, it can be used for: 1) minimal residual disease (MRD) detection after treatment; 2) recurrence monitoring after achieving remission. In particular, in cases where the original cancer is aggressive and has a high chance of recurrence, e.g., triple-negative breast cancer (TNBC), such a prescreening test can be repeated several times in the course of a year, providing the patient with measurements that are affordable and near real-time. In conclusion, the introduced proteomics/AI-based prescreening system could provide an economical, yet high-sensitivity solution for general adoption, acting primarily as a molecular risk assessment tool, to be performed prior to using a high-specificity screening modality.

#7315 Collaboration between NIDCR and NCI promotes innovative research in head and neck cancers.

Z. Chen[1], W. Wang[2];

[1]National Institute of Dental and Craniofacial Research, NIH, Bethesda, MD, [2]National Cancer Institute, NIH, Rockville, MD

The Oral and Salivary Cancer Biology Program at National Institute of Dental and Craniofacial Research (NIDCR) supports research activities that improve early detection and treatment of cancers of the oral cavity, pharynx, and salivary glands. We promote basic science research on the regulatory pathways and transformation process of pre-cancerous lesions to primary and metastatic tumors, as well as translational science activities to develop novel technologies and therapeutics for the diagnosis, prognosis, and treatment of cancers. NIDCR and National Cancer Institute (NCI) have established long-term collaborations to promote and co-manage awards funded through The Immuno-Oncology Translational Network (IOTN) of the Cancer Moonshot program, Specialized Programs of Research Excellence (SPOREs), and Early Detection Research Network (EDRN) program. NIDCR and NCI have co-developed Notice of Special Interest (NOSI) and Request for Application (RFA) on Advancing Head and Neck Cancer Early Detection Research (AHEAD), which co-funded seven research projects to discover and develop molecular signatures of early detection and diagnosis of HPV positive and negative head and neck cancer (HNC). To further strengthen NIDCR and NCI collaboration, we jointly organized the symposium to promote HNC early detection and biomarker identification at the American Head and Neck Society (AHNS) 11th International Conference on Head and Neck Cancer in July 2023. In addition, NIDCR has organized a symposium to promote HNC research at the 2024 annual meeting of American Association for Dental, Oral, and Craniofacial Research (AADOCR) to celebrate the 75th anniversary of NIDCR. This AADOCR symposium will feature the collaboration between NIDCR with NCI in the Cancer Moonshot program focusing on immunoprevention and immunotherapy, HNC early detection and biomarker research in AHEAD and EDRN, and investigation of HPV positive and negative HNC and clinical translational research under SPORE. At this 2024 AACR annual meeting, NIDCR and NCI program directors will present the collaborations and funding opportunities between NIDCR and NCI, focusing on early cancer detections and biomarker discovery and validation. Collaboration between NIDCR with NCI provides a unique opportunity to promote basic, translational, and clinical research in advancing HNC early detection to benefit cancer patients.

POPULATION SCIENCES: Genetic Epidemiology 2: Family Studies, Pathway Analysis, and Functional Genetics
Poster Session

#7319 Glycemic traits and colorectal cancer survival in a cohort of South Korean patients: A Mendelian randomization analysis.
S. Jun, S. Cho, M. Kim, J. Park, S. Jeong, A. Shin;
Seoul National University College of Medicine, Seoul, Korea, Republic of

Background: Clinical diabetic traits have been reported to be associated with increased colorectal cancer risk (CRC) in observational studies. Using the Mendelian randomization (MR) analysis method, we examined the causal association between glycemic traits, such as fasting glucose (FG), fasting insulin (FI), and glycosylated hemoglobin A1c (HbA1c), and survival in a cohort of CRC patients.
Methods: We conducted a two-sample MR analysis among a cohort of patients with locally advanced CRC at Seoul National University Hospital. Single-nucleotide polymorphisms robustly associated ($P<5\times10^{-8}$) with the three glycemic traits were obtained from the Meta-Analyses of Glucose and Insulin-related traits Consortium, Asian Genetic Epidemiology Network, and Korea Biobank Array. Three-year and five-year overall survival (OS) and progression-free survival (PFS) were used as outcomes. Survival analysis was conducted using subgroup analysis by cancer stage and subsite in a multivariate Cox proportional hazards model adjusted for age and sex to examine whether glycemic traits affected survival.
Results: A total of 509 patients were included in our final analysis. MR analysis showed that HbA1c levels were associated with poor three-year OS ($\beta=4.20$, $P=0.02$). Sensitivity analyses did not show evidence of any violations of the MR assumptions. In the cancer subgroup analysis of the Cox proportional hazards model, pooled hazard ratios for FG were significantly associated with poor three-year OS and PFS regardless of cancer stage. FI was not significantly associated with any three-year survival endpoints. Among stage III patients, three glycemic traits were significantly associated with both five-year OS and PFS. Location-specific subgroup analysis showed a significant association between three glycemic traits and five-year PFS in patients with left-sided colon cancer. FG was associated with poor three-year survival for colon cancer but not rectal cancer.
Conclusions: Our results suggest that FG and HbA1c could be used to predict prognosis in CRC patients. Lifestyle and/or pharmacological interventions targeting glycemic traits could help improve survival for CRC patients.

#7320 Expression of circadian rhythm genes and lethal prostate cancer.

J. B. Vaselkiv[1], S. C. Markt[2], H. E. Guard[1], A. Wang[1], K. L. Penney[3], K. H. Stopsack[4], L. A. Mucci[1];
[1]Harvard T.H. Chan School of Public Health, Boston, MA, [2]Jazz Pharmaceuticals, Palo Alto, CA, [3]Brigham and Women's Hospital, Boston, MA, [4]Massachusetts General Hospital, Boston, MA

Background: The circadian rhythm regulates diverse physiological and oncologic processes. We have previously shown in epidemiology studies that disruption of the circadian rhythm may be associated with increased risk of aggressive prostate cancer, including germline polymorphisms in certain circadian rhythm genes. This study sought to investigate the relationship between tumor circadian rhythm gene expression and lethal prostate cancer.
Methods: We studied patients with primary prostate cancer in the Health Professionals Follow-up Study (HPFS) and Physicians' Health Study (PHS). We created a composite score of mRNA expression using principal components that incorporated 11 circadian rhythm genes: *AANAT, ARNTL, CLOCK, CRY1, CSNK1E, MTNR1A, MTNR1B, NPAS2, PER1, PER2, PER3*. An age-stratified analysis was performed, and the mean differences of the score both by Gleason score and compared to normal tissue were calculated. The relationship between the score in prostate tumor tissue and lethal prostate cancer (metastases/prostate cancer-specific death) vs. indolent disease (no metastases after >8 years of follow-up) was assessed using logistic regression. The contribution of each gene was evaluated by leave-one-out analysis, generating scores leaving out one gene and assessing the relationship between the modified score and lethal disease.
Results: Among 404 cancer patients in HPFS/ PHS, there were 119 lethal events over 30 years of follow-up (median: 17 years). The circadian rhythm gene score was lower in tumor tissue compared to tumor-adjacent, histologically normal tissue (mean difference in units of standard deviation [SD] of gene score: -0.31, 95% confidence interval [CI]: -0.48 to -0.15). In addition, the score was lower in Gleason 9-10 compared to Gleason 6 tumors (mean difference in SD units: -1.05, 95% CI: -1.55 to -0.54). The three *PER* genes were the most strongly correlated with each other and with the score (Spearman correlation coefficients from 0.52-0.88 for the score and 0.31-0.63 between *PER* genes). Higher circadian rhythm gene scores were inversely associated with lethal prostate cancer (odds ratio [OR] for highest vs. lowest quartile: 0.43, 95% CI: 0.20 to 0.90) in a dose-response fashion and after adjusting for clinical and pathologic factors. The association appeared to be stronger in patients aged ≥65 years (OR for highest vs. lowest quartile: 0.21, 95% CI: 0.08 to 0.47) compared to <65 years at diagnosis (OR: 0.78, 95% CI: 0.29, 2.17). Results were consistent in the leave-one-out analysis for all genes except *PER2* (OR for highest vs. lowest quartile: 1.00, 95% CI: 0.55 to 1.83) and *PER1* (OR: 0.55, 95% CI: 0.30 to 1).
Conclusion: This study examining intratumoral circadian rhythm gene expression contributes further evidence in support of the relationship between circadian rhythm disruption and aggressive prostate cancer. Tumor expression of *PER1* and *PER2* may be a predominant factor in the association.

#7321 Second primary cancer risks following breast cancer in *BRCA1/2* pathogenic variant carriers.

I. Allen[1], H. Hassan[1], Y. Walburga[1], C. Huntley[2], L. Loong[2], T. Rahman[3], B. Torr[2], A. Bacon[3], C. Knott[3], S. Jose[3], S. Vernon[3], M. Luchtenborg[4], J. Pethick[3], F. Santaniello[3], S. Goel[3], S. Allen[2], K. Lavelle[3], F. McRonald[3], D. M. Eccles[5], E. Morris[6], S. Hardy[3], C. Turnbull[2], M. Tischkowitz[1], P. Pharoah[1], A. C. Antoniou[1]; [1]University of Cambridge, Cambridge, United Kingdom, [2]Institute of Cancer Research, London, United Kingdom, [3]National Disease Registration Service, London, United Kingdom, [4]King's College London, London, United Kingdom, [5]University of Southampton, Southampton, United Kingdom, [6]University of Oxford, Oxford, United Kingdom

Background

Second primary cancer (SPC) risk estimates in breast cancer (BC) survivors carrying germline BRCA1/2 pathogenic variants (PVs) remain uncertain. We estimated relative and absolute SPC risks following BC in BRCA1/2 PV carriers using genetic testing laboratory data in England, linked for the first time to population-scale electronic health records data from the National Disease Registration Service and Hospital Episode Statistics.

Material and methods

The cohort contained 27,154 women diagnosed with primary BC and tested for germline BRCA1/2 PVs between 1995-2019. Follow-up began at the latest of the genetic test dates and one year following the BC diagnosis and continued until the first SPC diagnosis, death, migration, relevant surgery, and the end of 2020, whichever came first. We estimated overall and site-specific standardized incidence ratios (SIRs) by comparing observed and expected SPC counts, with expected counts calculated using incidences for the general English population accounting for calendar year, SPC site, age, and gender. We stratified the SIRs by age, estrogen-receptor status, and cancer site. We further assessed associations using Cox regression adjusted for age at BC diagnosis and estrogen-receptor status of the first BC, and estimated 10-year absolute SPC risks with Kaplan-Meier analysis.

Results

There were 1909 BRCA1 (138 with SPCs) and 1926 BRCA2 (101 with SPCs) PV carriers, with mean follow-up lengths of 4.2 and 4.4y and median follow-up lengths of 3.4 and 3.6y. In BRCA1 PV carriers, there were elevated contralateral BC (SIR:15.3, 95%CI:11.5-19.8), ovarian (SIR:43.3, 95%CI:30.9-58.9), non-breast and non-ovarian combined (SIR:2.23, 95%CI:1.63-2.98), colorectal (SIR:4.72, 95%CI:2.58-7.92) and uterine (SIR:3.42, 95%CI:1.25-7.44) SPC risks. In BRCA2 PV carriers, there were increased contralateral BC (SIR:7.53, 95%CI:5.33-10.3), ovarian (SIR:16.5, 95%CI:10.1-25.5), non-breast and non-ovarian (SIR:1.72, 95%CI:1.27-2.27) and pancreatic (SIR:6.57, 95%CI:2.63-13.5) SPC risks. Consistently, when we compared BC survivors carrying a BRCA1 PV to BC survivors without a PV in either gene, they were at elevated contralateral BC (HR:3.94, 95%CI:2.91-5.33), ovarian (HR:35.7, 95%CI:21.3-60.0), non-breast and non-ovarian (HR:1.53, 95%CI:1.11-2.12) and colorectal (HR:2.95, 95%CI:1.56-5.55) SPC risks, whereas BRCA2 PV carriers were at increased contralateral BC (HR:2.59, 95%CI:1.83-3.65), ovarian (HR:12.3, 95%CI:6.93-21.9) and pancreatic (HR:5.32, 95%CI:2.30-12.3) SPC risks. We estimated 10-year cumulative contralateral BC, ovarian, and non-breast and non-ovarian SPC risks of 15%, 6.3%, and 7.8% in BRCA1 PV carriers and 12%, 2.9%, and 6.2% in BRCA2 PV carriers.

Conclusions

Cancer risks were increased, at combined and specific sites, following BC in BRCA1/2 PV carriers. These findings could aid the clinical management of BC survivors carrying BRCA1/2 PVs.

#7322 Polygenic adaptation and co-regulatory dynamics in Chernobyl wolves: Unveiling immune and oncogenic stress interactions with implications for human cancer resilience.

C. Y. Yu[1], C. N. Love[2], M. Belete[1], H. Chandrupatla[1], L. K. Brady[1], S. Sridhar[1], S. C. Campbell-Staton[2];
[1]Genmab, Plainsboro, NJ, [2]Princeton University, Princeton, NJ

Wolves living in the Chernobyl Exclusion Zone (CEZ) for at least six generations have adapted to high radiation exposure and are a unique model for studying genetic selection under extreme conditions of oncogenic stress. The objective of this study was to build off previously described signatures of adaptation in CEZ wolves, identify networks of genes associated with immune adaptation in CEZ wolves, and determine prognostic significance of these genes in human cancer datasets to provide insight into immune adaptation and cancer immunity.

RNA from blood samples of wolves in CEZ, Belarus (BLR), and Yellowstone (YLS) were sequenced previously. Here we analyzed these data by mapping wolf transcripts to human orthologs. Radiation exposure (in CEZ and BLR) was quantified by intramuscular Cesium-137. Differential gene expression (DESeq2), network co-expression analysis (lmQCM), and gene set variation analysis (GSVA) assessed transcriptomic changes between populations. Germline single nucleotide polymorphism (SNP) for all three populations were inferred from RNA-seq data.

Genes differentially regulated between populations, including gene modules showing signatures of polygenic selection through increased rates of genetic divergence ($p < 0.05$) in CEZ wolf populations, were deemed as outlier genes. Those n=3,180 CEZ outlier genes were then investigated in human cancer data from The Cancer Genome Atlas (TCGA) to determine prognostic impact in 10 tumor types highly conserved between human and canines.

GSVA confirmed activation of neutrophil and macrophage signatures in CEZ wolves and suppression of several adaptive immune-related signatures ($p < 0.05$ vs BLR and YLS). A signature including immune checkpoint targets was also significantly differentially expressed in CEZ wolves. In TCGA, Cox PH analysis identified 23 genes over-expressed in CEZ wolves with significant positive prognostic impact in ≥ 2 human tumor types. PTPN6, previously identified to have positive prognostic value in bladder cancer[1], was also prognostic in three additional tumor types. In human bladder cancer, genes identified as differentially regulated in CEZ wolves were disproportionately associated with improved survival.

As predicted, gene signature variations in CEZ wolves reveal a distinct immune profile, likely shaped by prolonged radiation exposure. These findings, along with evidence of polygenic selection, suggest adaptation to multigenerational radiation exposure (an oncogenic stress). Notably, the enrichment of genes with positive prognosis in human cancer overexpressed in CEZ wolves present a valuable model to explore genetic underpinnings of cancer immunity and advance our understanding of cancer resilience in humans.

Reference:

[1]Shen C. et al. The Analysis of PTPN6 for Bladder Cancer: An Exploratory Study Based on TCGA. Dis Markers. 2020.

#7323 Tissue resident memory T cell abundances impact non-small-cell lung cancer immune microenvironment and patient prognosis.

Aidan Shen[1], Aliesha Garrett[1], Junhua Mai[2], Yangzhi Zhu[1], **Chongming Jiang**[1]

[1]Terasaki Institute for Biomedical Innovation, Los Angeles, CA,[2]Department of Nanomedicine, Houston Methodist Research Institute, Houston, TX

Tissue resident memory T cells (TRM) are a specialized subset of long-lived memory T cells that reside in peripheral tissues. However, whether TRM exerts any immunosurveillance role in the tumor immune microenvironment (TIME) and progression of non-small-cell lung cancer (NSCLC), which accounts for 85% of all lung cancers, remains unclear. Our comprehensive analysis of multiple independent single-cell and bulk RNA-seq datasets of patient NSCLC samples generated reliable, unique TRM signatures, through which we could infer the abundance of TRM in NSCLC. We discovered that TRM abundance is consistently positively correlated with CD4+ T helper 1 cells, M1 macrophages, and resting dendritic cells in TIME and significantly impacts the prognosis of NSCLC patients. In addition, TRM signatures are strongly associated with immune checkpoint genes and the prognosis of NSCLC patients, suggesting that TRM signatures are promising prognostic markers for immunotherapy in NSCLC. We then built a machine learning model to predict patient survival based on the TRM signatures and immune related genes. The accuracy of the model was validated by Kaplan-Meyer survival analysis, receiver operating characteristic curves, principal component analysis, and t-distributed random neighbor embedding. We developed a 4-gene risk score that effectively stratified patients into low-risk and high-risk categories. The patients with high-risk scores had significantly lower overall survival than patients with low-risk. The prognostic value of the risk score was independently validated by the Cancer Genome Atlas Program (TCGA) dataset and multiple independent NSCLC patient datasets. Notably, low-risk NSCLC patients with higher TRM infiltration exhibited enhanced T-cell activation, macrophage regulation, and other TIME immune responses related pathways, indicating a more active immune profile benefitting from immunotherapy. Altogether, this study provides valuable insights into the complex interactions between NSCLC TRM and TIME and their impact on patient prognosis, highlighting the importance of TRM in shaping the NSCLC microenvironment. The development of a simplified 4-gene risk score provides a practical prognostic marker for risk stratification.

Keywords: Tissue resident memory T cell, non-small-cell lung cancer, prognosis, tumor immune microenvironment, machine learning

#7324 Impact of BMI on immune pathways in preinvasive colorectal lesions.

L. R. Fanning[1], B. Hamidi[1], I. Korostenskij[1], S. Seal[1], T. L. Crawford[1], T. A. MacKenzie[2], E. L. Barry[3], J. E. Thaxton[4], M. J. Shrubsole[5], B. Vincent[6], J. A. Baron[6], A. V. Alekseyenko[1], K. Wallace[1];

[1]The Medical University of South Carolina (MUSC), Charleston, SC, [2]Dartmouth Geisel School of Medicine, Lebanon, NH, [3]Dartmouth Geisel School of Medicine, Hanover, NH, [4]University of North Carolina at Chapel Hill, Chapel Hill, NC, [5]Vanderbilt Epidemiology Center, Vanderbilt University School of Medicine, Vanderbilt-Ingram Cancer Center, Vanderbilt University Medical Center, Nashville, TN, [6]University of North Carolina School of Medicine, Chapel Hill, NC

Background: Obesity is a risk factor for colorectal neoplasia, possibly mediated by metabolic dysregulation or chronic inflammation. Circulating inflammatory cytokines have been associated with an increased risk of CRC, but no studies have examined the impact of BMI on immune gene expression in preinvasive lesions. Our analysis combines data from 3 retrospective epidemiologic studies among patients with colorectal adenomas or serrated polyps. Using a cross-sectional design, we investigate whether BMI categories (obese (OB), overweight (OW), normal (NL)) are associated with T-helper gene pathways.

Methods: For each patient, we include demographic, clinical, and specimen (archival FFPE for RNA isolation) data. Immune gene expression data was determined using the NanoString nCounter platform on a subset of cases (n=100) balanced by study site and lesion type from our cohort (n=630). Genes were normalized using a modified RUVseq methodology. We examined 4 pathways (Th1, Th2, Th17, Treg) defined by gene lists included in the NS immune v2. panel. Differences in pathway expression by BMI categories were analyzed using our distance-based methods (Wd* multivariate analysis of variance and TW2 pairwise method) adjusted for age & sex. Using linear regression analysis, we generated coefficients (p-values) for OW and OB vs NL for genes within each pathway.

Results: 86 samples passed QC. Th2 and Th1 pathways were significant for OW vs NL ($p<0.05$) whereas Th17 was marginally significant (<0.1). Several genes within the Th1, Th2, and Th17 pathways were enriched in OW vs. NL: e.g., *IL2* (coeff. 0.77 (p=0.008), *IL5* (coeff. 1.02, p=0.001), *IL17F* (coeff. 0.57, p=0.05), respectively. (Table)

Conclusion: Enrichment of genes specific to the Th pathways in OW persons suggest that metabolic immune modulation may be important in early colorectal carcinogenesis.

Differences in immune pathway and gene expression by BMI categories

	T_W^2 (p-value)			W_d^* (p-value)
Pathways	Normal (N = 22)	Overweight (N = 32)	Obese (N = 29)	
Th2	Ref.	0.017	0.15	0.038
Th1	Ref.	0.03	0.204	0.10
Th17	Ref.	0.073	0.125	0.103
		MLR coefficient (p-value)		
Pathway	Gene	Overweight vs. Normal	Obese vs. Normal	ANOVA (p-value)
Th2				
	IL2RA	0.34 (0.041)	-0.11 (0.517)	0.010
	IL4	0.58 (0.019)	0.22 (0.386)	0.052
	IL5	1.02 (0.001)	0.41 (0.191)	0.004
	NOTCH1	-0.05 (0.742)	-0.34 (0.045)	0.078
Th1				
	IL12B	0.57 (0.031)	0.40 (0.136)	0.093
	IL2	0.77 (0.008)	0.39 (0.179)	0.028
	TBX21	0.46 (0.015)	0.19 (0.308)	0.044
Th17				
	IL17F	0.57 (0.050)	0.42 (0.157)	0.139
	IL21	0.77 (0.004)	0.42 (0.131)	0.017
	IL23R	0.29 (0.048)	-0.008 (0.957)	0.047
	IL6R	0.002 (0.990)	0.36 (0.039)	0.041
	IRF4	-0.61 (0.007)	-0.33 (0.149)	0.025
	TGFB1	-0.26 (0.023)	-0.19 (0.101)	0.069

#7325 Integration of functional data to classify *BRCA1/2* missense variants: An ENIGMA project.

P. Lyra, Jr.[1], L. Dalcolmo[1], M. Parsons[2], T. Nepomuceno[1], S. Brito[1], N. N. Nguyen[1], G. de Oliveira[3], J. da Siva[3], L. Caleca[4], T. Taneja[1], C. Hu[5], M. Richardson[6], M. Rossing[7], A. Hazra[8], A. Martins[9], S. Caputo[10], G. A. Millot[11], J. Yie[12], M. A. Carvalho[13], M. Cline[14], P. Radice[4], R. Carlsen[15], R. Mesman[16], V. Zampiga[17], R. Villani[2], V. Josef[18], S. Sharan[19], K. Michailidou[20], A. B. Spurdle[2], F. Couch[5], M. P. Vreeswijk[16], **A. N. Monteiro[1]**;

[1]Moffitt Cancer Center, Tampa, FL, [2]QIMR Berghofer Medical Research Institute, Brisbane, Australia, [3]Centro Universitario FAEMA, Ariquemes, Brazil, [4]Fondazione IRCCS Istituto Nazionale dei Tumori, Milan, Italy, [5]Mayo Clinic, Rochester, MN, [6]Ambry Genetics, Aliso Viejo, CA, [7]Faculty of Health and Medical Sciences, University of Copenhagen, Copenhagen, Denmark, [8]Harvard University, Boston, MA, [9]Inserm U1245 Universite de Rouen, Rouen, France, [10]Institut Curie, Paris, France, [11]Institut Pasteur, Paris, France, [12]National Cancer Centre Singapore, Singapore, Malaysia, [13]Instituto Nacional de Cancer, Rio de Janeiro, Brazil, [14]University of California, Santa Cruz Genomic Institute, Santa Cruz, CA, [15]Quest Diagnostics, Secaucus, NJ, [16]Leiden University Medical Center, Leiden, Netherlands, [17]IRCCS Istituto Romagnolo per lo Studio dei Tumori (IRST) "Dino Amadori", Meldola, Italy, [18]Memorial Sloan Kettering, New York, NY, [19]Center for Cancer Research, National Cancer Institute, Fredrick, MD, [20]Biostatistics Unit, The Cyprus Institute of Neurology and Genetics, Nicosia, Cyprus

The success of precision cancer prevention and treatment hinges on accurate discrimination between benign and pathogenic germline alleles in cancer susceptibility genes. Variants of uncertain clinical significance (VUS) present a challenge for cancer risk assessment and functional data will be essential to resolve many VUS. To address this, we developed a cloud-based environment to collate, curate, integrate and analyze all published functional data related to *BRCA1* and *BRCA2* missense VUS. Then, functional evidence criteria for pathogenicity were determined for each assay using the American College of Medical Genetics and Genomics/Association for Molecular Pathology (ACMG/AMP) classification guidelines and ClinGen criteria. Our approach involved retrieving published articles reporting one or more functional assays of *BRCA1/2* missense variants reporting variant impact on various biochemical and cell biological functions. Functional results were recorded using original authors' thresholds and categories, then converted to ordinal variables to harmonize: [0 = no functional impact], [1 = intermediate impact], and [2 = functional impact]. For *BRCA1*, we updated our previous published integration (Genet Med. 2021;23:306-315) with 14 additional publications, collating results from 53 instances of functional assays reporting functional data on 3,219 unique missense variants. For *BRCA2*, 28 publications were identified reporting data from 141 instances of functional assays on 4,759 unique missense variants. Utilizing a panel of 542 and 396 known pathogenic and benign reference variants for *BRCA1* and *BRCA2*, respectively, we determined the sensitivity, specificity, and ACMG/AMP odds of pathogenicity for each instance of the assay. The remaining variants were assigned a relevant functional assay code weight for each assay instance. Our study successfully derived ACMG/AMP evidence strength from functional data for 3,040 *BRCA1* (94% of 3,219) and 2,704 *BRCA2* (57% of 4,759) missense variants. This comprehensive work underscores the utility of functional data in informing classification of *BRCA1* and *BRCA2* missense VUS.

#7326 *TP53* p.Pro47Ser polymorphism in breast cancer susceptibility in Mali.

B. Diakite[1], Y. kassogue[1], M. Maiga[2], O. kassogue[1], K. Cisse[1], F. Diarra[1], C. B. Traore[1], B. Kamate[1], J. L. Holl[3], L. Hou[2];
[1]University of Sciences, Techniques And Technologies of Bamako, Bamako, Mali, [2]Northwestern University, Chicago, IL, [3]University of Chicago, Chicago, IL

Background: The aim of this study was to assess the potential association of p.Pro47Ser polymorphisms of TP53 with the risk of developing breast cancer in the Malian population.
Methods: We analyzed DNA samples from 72 breast cancer patients and 121 unrelated healthy, age-matched individuals to examine the presence of the polymorphisms. The genotyping of TP53 polymorphism was performed using PCR-RFLP and HRM (high-resolution melting) methods.
Results: The genotypic frequencies of PP, PS, and SS were found to be 63.9% PP, 30.6% PS, and 5.6% SS in breast cancer patients, compared to 70.2% PP, 22.3% PS, and 7.4% SS in the control group. The frequencies of P and S alleles of TP53 p.P47S polymorphism were 79.2% vs 81.4%, 20.8% vs 18.6%, and 5% vs 4.5% in patients and controls, respectively. In this study, no significant correlation was observed between TP53 p.Pro47Ser polymorphism and breast cancer in the Malian population (Pro/Ser vs Pro/Pro: OR = 1.55, 95% CI = 0.80-3.05, P = 0.19; Ser/Ser vs Pro/Pro: OR = 1.27, 95% CI = 0.34-4.74, P = 0.71; and Ser vs Pro allele: OR = 1.39, 95% CI = 0.80-2.32, P = 0.24).
Conclusion: Despite the absence of a genetic association between TP53 p.Pro47Ser and the risk of breast cancer in Malian patients, our findings suggest that individuals carrying at least one minor Ser allele are not protected against the disease.

#7327 Investigating the cell-type specific regulation of *IRF4* and its role in lung cancer via a lung cancer risk-associated pleiotropic variant.

A. Kane[1], J. Yin[1], E. Long[2], J. Feng[1], C. Grawe[3], H. Patel[1], J. Byun[4], C. Amos[4], K. Brown[1], J. Xia[5], M. Vermeulen[3], J. Choi[1];
[1]National Cancer Institute, National Institutes of Health, Rockville, MD, [2]Chinese Academy of Medical Sciences and Peking Union Medical College, Beijing, China, [3]Faculty of Science, Radboud Institute for Molecular Life Sciences, Oncode Institute, Radboud University Nijmegen, Nijmegen, Netherlands, [4]Baylor College of Medicine, Houston, TX, [5]Creighton University, Omaha, NE

Although smoking is a main risk factor for lung cancer, genetic factors also contribute to the risk, as shown by over 50 genomic loci identified by genome-wide association studies (GWAS). A recent cross-ancestry lung cancer GWAS identified a common germline variant, rs12203592 (C/T), in chr6p25.3 as a new signal, and quantitative trait loci (eQTL) colocalization analysis using lung and blood tissues (GTEx v8) identified *IRF4* as a likely target of rs12203592. rs12203592 has previously been linked with diverse traits, including pigmentation phenotypes, smoking cessation, lymphoblastic leukemia, melanoma, and other skin cancers. rs12203592 also appears to have varied allelic effects in different cell types. Namely, the lung cancer risk-associated T allele is correlated with higher *IRF4* expression in lung tissue and blood cells (GTEx v8) but lower expression in primary melanocytes (n = 106; Zhang et al). Since previous studies established the melanocyte-specific allelic function of this SNP through lineage-specific transcription factors (TFs), we hypothesized that cell-type-specific TFs mediate the observed allelic effect in different tissue/cell types and further contribute to the unique role of IRF4 in lung tumorigenesis. To identify these potential cell-type-specific regulators, we performed mass spectrometry using the nuclear extracts from three cell lines representing lung, blood, and melanocyte lineage. The results nominated the NF-kB and ZEB protein families as the most prominent T-specific binders in the A549 lung cancer cell line, which was validated by electromobility shift assays. Consistent with these findings, tissue-based SNP-gene interaction analysis demonstrated that the mRNA levels of NF-kB and ZEB family members (4 of 7 genes) were correlated with *IRF4* expression with a significant interaction with rs12203592 in GTEx lung tissue ($P < 0.017$), where the correlation is mainly observed with the T allele. Notably, the SNP interaction was less pronounced in whole blood or melanocytes, and the correlation of these TFs and *IRF4* expression was mainly observed with the C allele in melanocytes. To begin to establish the roles of these TFs and IRF4 in lung tumorigenesis and given that *IRF4* was shown to promote endogenous DNA damage and proliferation of lung-lineage cell lines, we will investigate the roles of NF-kB and ZEB in *IRF4* regulation in these contexts using knockdown and overexpression of these TFs. To further investigate lung cancer-specific IRF4 function, we will identify potential targets of IRF4 among lung cancer-associated functional variants established through our previous studies. This data will help elucidate the context-specific roles of *IRF4* in lung cancer development and provide clues to gene regulation in a pleiotropic GWAS locus.

#7328 Relationship between PIN3 16bp duplication of TP53 and HPV in HIV women in Mali.

M. Maiga[1], B. Diakite[2], Y. Kassogue[2], B. Traore[2], O. Kassogue[2], B. Kamate[2], C. B. Traore[2], J. L. Holl[1], L. Hou[1];
[1]Northwestern University, Chicago, IL, [2]University of Sciences, Techniques and Technologies of Bamako, Bamako, Mali

Background: TP53 polymorphisms can influence the immune response to HPV, affecting TP53's role in cell cycle regulation and apoptosis, crucial for controlling HPV infection and preventing cancer.
Objective: Explore the link between TP53 PIN3 16-bp duplication and HPV infection in HIV-positive Malian women.
Methods: This study explored the link between PIN3 16-bp duplication polymorphism of TP53 and HPV infection in 50 HIV-positive women in Mali. Data included surveys, self-sampled vaginal swabs, and blood collection. HPV typing used GeneXpert, and PIN3 genotyping utilized AS-PCR.
Results: Participants, primarily >30 years (92%), had a mean age of 43.30 ± 10.332 years. HPV prevalence was 36%, with P3 being the most common subtype (30.8%). PIN3 genotypic frequencies were A1A1 (50%), A1A2 (34%), and A2A2 (10%). History of sexually transmitted infections correlated with higher mutation rates (37.8% A1A2, 10.8% A2A2). A2A2 genotype prevalence was higher in HIV-positive women with specific HPV subtypes (P5, P4, HPV16, P3, P18/45). A1A2 genotype was observed in 60% of HPV subtype P3 cases and 20% of P4 and P18/45 cases.
Conclusion: These results suggest a link between TP53 gene polymorphisms and susceptibility to different HPV subtypes in HIV-positive women, warranting further research into their functional implications and impact on HPV-related diseases in this population.
Keywords: TP53 polymorphism, HPV, HIV, Malian population

#7329 Novel MAVE models for MLH1, MSH2, and PMS2 have high accuracy.

W. M. Korn, S. Padigepati, D. Stafford, F. Facio, B. Johnson, K. Nykamp, J. Reuter;
Invitae, San Francisco, CA

Lynch syndrome, the most common cause of hereditary colorectal cancer, is due to pathogenic germline variants in mismatch repair (MMR) genes. Variants of uncertain significance (VUS) in MMR genes hinder diagnoses and clinical management. Multiplex assays of variant effects (MAVEs) are high-throughput cellular assays designed to provide functional data on variant activity. Successful MAVE experiments accurately define the pathogenicity of single nucleotide variants and small insertions-deletions which can then be applied to clinical variant classification (VC). Here we report internally generated MAVE datasets for three MMR genes (MSH2, MLH1 and PMS2) and estimate their impact on patients.

Three separate pools of targeted variants were generated for three MMR genes. Pooled variants were introduced into cell populations such that each cell contained one variant copy of an MMR gene. Single-cell RNA expression profiles were generated for the cells which were then normalized and filtered. Supervised machine learning was used to find patterns in gene expression that were different between cells harboring established pathogenic (P) and benign (B) variants and to assess the accuracy of variant predictions. VC impact was estimated for all datasets by simulating VCs with the added MAVE evidence compared to the original VCs. Variants with an original VC that was different after MAVE evidence were counted as impacted.

Overall results are shown in Table 1, including the number of variants successfully targeted, the number of known P and B variants used for training and testing, the area under the receiver operating characteristic curve (AUROC), the distribution of calibrated predictions, and the estimated patient impact for each model. The MSH2, MLH1, and PMS2 MAVE models provide a high-quality source of functional evidence for VC with the potential to impact many patients in the future.

Table 1.

Gene	MSH2 model	MLH1 model	PMS2 model
Variants successfully targeted (n)	223	212	214
Known pathogenic (P) and benign (B) variants used to train the model	29 P 72 B	31 P 55 B	14 P 71 B
Known pathogenic (P) and benign (B) variants used to test the model	14 P 32 B	14 P 22 B	7 P 31 B
AUROC	0.9996	0.9642	0.9918
# of variants strongly predicted P (PPV ≥ 95%) or B (NPV≥ 95%)	44 P 177 B	52 P 160 B	26 P 183 B
# of variants with uncertain prediction (PPV < 80%, NPV < 80%)	2	0	5
Estimated # of impacted variants	4 LP>P 3 VUS>LP 26 VUS>LB 31 LB>B	0 LP>P 5 VUS>LP 17 VUS>LB 7 LB>B	4 LP>P 1 VUS>LP 17 VUS>LB 6 LB>B

#7330 Identifying proteomic risk factors for overall, aggressive and early onset prostate cancer using mendelian randomization and tumor spatial transcriptomics.

T. A. Desai[1], A. K. Hedman[2], M. Dimitriou[2], M. Koprulu[3], S. Figiel[4], W. Yin[4], M. Johansson[5], E. L. Watts[6], J. R. Atkins[1], A. V. Sokolov[7], H. B. Schioth[7], M. J. Gunter[8], K. K. Tsilidis[8], R. M. Martin[9], M. Pietzner[10], C. Langenberg[10], I. G. Mills[4], A. D. Lamb[4], A. Malarstig[2], T. J. Key[1], The PRACTICAL Consortium, R. C. Travis[1], K. Smith-Byrne[1];

[1]Nuffield Department of Population Health, University of Oxford, Oxford, United Kingdom, [2]Karolinska Institutet, Stockholm, Sweden, [3]University of Cambridge, Cambridge, United Kingdom, [4]University of Oxford, Oxford, United Kingdom, [5]International Agency for Research on Cancer, Lyon, France, [6]National Cancer Institute, Bethesda, MD, [7]Uppsala University, Uppsala, Sweden, [8]Imperial College London, London, United Kingdom, [9]University of Bristol, Bristol, United Kingdom, [10]Queen Marty University of London, London, United Kingdom

Background: Understanding the role of circulating proteins in prostate cancer risk can reveal key biological pathways and identify novel targets for cancer prevention.

Methods: We investigated the association of 2,002 genetically predicted circulating protein levels with risk of prostate cancer overall, and of aggressive and early onset disease, using *cis*-pQTL Mendelian randomization (MR) and colocalization. Findings for proteins with support from both MR, after correction for multiple-testing, and colocalization were replicated using two independent cancer GWAS, one of European and one of African ancestry. Proteins with evidence of prostate-specific tissue expression were additionally investigated using spatial transcriptomic data in prostate tumor tissue to assess their role in tumor aggressiveness. Finally, we mapped risk proteins to drug and ongoing clinical trials targets.

Results: We identified 20 proteins genetically linked to prostate cancer risk (14 for overall [8 specific], 7 for aggressive [3 specific], and 8 for early onset disease [2 specific]), of which a majority were novel and replicated. Among these were proteins associated with aggressive disease, such as PPA2 [Odds Ratio (OR) per 1 SD increment = 2.13, 95% CI: 1.54-2.93], PYY [OR = 1.87, 95% CI: 1.43-2.44] and PRSS3 [OR = 0.80, 95% CI: 0.73-0.89], and those associated with early onset disease, including EHPB1 [OR = 2.89, 95% CI: 1.99-4.21], POGLUT3 [OR = 0.76, 95% CI: 0.67-0.86] and TPM3 [OR = 0.47, 95% CI: 0.34-0.64]. We confirm an inverse association of MSMB with prostate cancer overall [OR = 0.81, 95% CI: 0.80-0.82], and also find an inverse association with both aggressive [OR = 0.84, 95% CI: 0.82-0.86] and early onset disease [OR = 0.71, 95% CI: 0.68-0.74]. Using spatial transcriptomics data, we identified MSMB as the genome-wide top-most predictive gene to distinguish benign regions from high grade cancer regions that had five-fold lower MSMB expression. Additionally, ten proteins that were associated with prostate cancer risk mapped to existing therapeutic interventions.

Conclusion: Our findings emphasize the importance of proteomics for improving our understanding of prostate cancer etiology and of opportunities for novel therapeutic interventions. Additionally, we demonstrate the added benefit of in-depth functional analyses to triangulate the role of risk proteins in the clinical aggressiveness of prostate tumors. Using these integrated methods, we identify a subset of risk proteins associated with aggressive and early onset disease as priorities for investigation for the future prevention and treatment of prostate cancer.

#7331 Establishing a single-cell eQTL dataset of lung tissues from Asian never-smokers to identify cell-type specific lung cancer susceptibility genes.

T. Luong[1], E. Long[2], J. Yin[1], B. Li[1], J. Shin[3], E. Sisay[1], A. Kane[1], A. Golden[1], Y. Chang[3], N. Banovich[4], N. Rothman[1], J. Byun[5], Q. Lan[1], C. Amos[5], J. Shi[1], J. Lee[3], E. Kim[3], J. Choi[1];

[1]National Cancer Institute, National Institutes of Health, Bethesda, MD, [2]Chinese Academy of Medical Sciences and Peking Union, Beijing, China, [3]Yonsei University College of Medicine, Seoul, Korea, Republic of, [4]Translational Genomics Research Institute (TGen), Phoenix, AZ, [5]Baylor College of Medicine, Houston, TX

Lung cancer is one of the most prevalent and deadly forms of cancer worldwide. Whilst smoking is the main determinant, genetic factors also play a crucial role as genome-wide association studies (GWAS) have identified >50 loci associated with lung cancer risk. Yet, for most of these loci, it is still unknown how they contribute to lung cancer risk. Expression quantitative trait loci (eQTL) studies have been powerful in linking GWAS variants to potential target genes, providing genetic mechanisms underlying common diseases such as cancers. However, the current eQTL resources lack ancestral diversity and are primarily based on bulk tissues. Emerging single-cell eQTL (sc-eQTL) approaches can detect context-specific gene regulation but are mainly of blood samples or cultured cells and still representing European populations. This limits our abilities to test GWAS variants in cancer-relevant cell types as well as in diverse populations. To generate a resource to characterize lung cancer GWAS loci, we are building a lung sc-eQTL dataset of Asian population while addressing common challenges of tissue sc-eQTL. Namely, processing fresh tissue in a population scale is logistically challenging and costly, and epithelial cells (including cell types of lung cancer origin) are vulnerable to the dissociation and freezing/thawing process. To address these issues, we incorporated sample multiplexing and cell type balancing. We collected fresh tumor-distant normal lung tissues from 131 never-smoking Korean women and dissociated them before cryopreservation. We then performed single-cell RNA sequencing (scRNA-seq) using 10x Chromium Single Cell 3' v3.1 chemistry with multiplexing of ~6 samples/batch. To enrich for epithelial cells, we utilized flow cytometry with surface markers of four major lung cell types (epithelial: EpCAM+/CD45-, immune: EpCAM-/CD45+, endothelial and stromal: EpCAM-/CD45-) before 10X library preparation. Concurrently, we performed DNA genotyping and imputation using matched blood samples. Following scRNA-seq (~36,000 reads/cell) we performed a genotype-based sample demultiplexing using Demuxlet. By integrating Demuxlet and Scrublet, we identified ~89% of the detected cells as singlets. After applying QC to filter empty droplets and low-quality cells, we obtained 428,619 cells or 3,272 cells/patient. Cell annotation guided by Azimuth label transfer using the Human Lung Cell Atlas, identified 28 cell types including 7 of epithelial origins. We will further perform eQTL analyses for individual cell types using pseudo-bulk and LIMIX (linear mixed model) or SAIGE-qtl (poisson regression) methods followed by aggregation across the cell types. By incorporating lung cancer GWAS data, we will identify cell-type specific susceptibility genes. Our dataset will provide a unique resource for lung cancer research.

#7332 Healthcare professionals' perceptions and educational needs in genetic counseling for cancer risk management: An integrated mixed-methods systematic review.

S.-Y. Jung[1], S.-Y. Park[2], E.-G. Lee[1], H. Chae[1], M.-J. An[1], Y.-J. Kim[1], Y.-J. Choi[1], K. Ryu[1], S.-Y. Kong[1];
[1]National Cancer Center - Korea, Goyang-si, Korea, Republic of, [2]Daegu Catholic University, Daegu-si, Korea, Republic of

Background: The role of healthcare professionals (HCPs) is crucial in the genetic counseling process for managing hereditary cancer risks. However, HCPs face challenges due to a lack of specialized training and confidence, particularly in communicating genetic risks to patients. Hence, it becomes paramount to identify the essential skills and expertise required by HCPs for genetic counseling. Additionally, gaining insight into their perspectives regarding the content of genetic counseling that should be provided to patients is of utmost importance.
Methods: An integrated mixed-methods systematic review and content analysis were performed across five databases on 23 May 2023, employing predetermined search strategies. The quality of selected studies was assessed using the Mixed Method Appraisal Tool (MMAT), and data analysis was conducted using a deductive content analysis approach with MAXQDA 2020.
Results: The review encompassed 14 studies from seven countries, revealing moderate risk of bias. It was perceived by HCPs that hereditary cancer families require information in seven specific categories including, cancer risk-reducing strategies; personalized cancer risk; family implications of hereditary cancer; psychological issues; genetic testing; the role of pathogenic genes in hereditary cancers; and social issues related to genetic testing. The study also highlighted the educational needs of HCPs, pinpointing areas such as method for supporting decision-making; clinical management in hereditary cancer families; resources for supporting hereditary cancer families; guidance to support familial communication; genetic testing; the role of each profession; and methods for supporting psychological aspects.
Conclusion: The findings underscore the need for specialized training programs to equip HCPs with the necessary skills and knowledge for effective genetic counseling. Additionally, understanding HCPs' perspectives on the content of genetic counseling is vital for tailoring educational resources and enhancing the genetic counseling process in managing cancer risks.
Grants: This research was supported by a grant of the Korean Cancer Survivors Healthcare R&D Project through the National Cancer Center, funded by the Ministry of Health & Welfare, Republic of Korea (grant number: NCC 23F1940-1)

#7333 From provider discussion to test completion: Evaluating cancer genetic services in a diverse academic comprehensive cancer care population.

A. Naaseh[1], H. Rice[2], I. Temosihue[1], N. Zimmermann[1], E. Linnenbringer[1];

[1]Washington University School of Medicine in St. Louis, St. Louis, MO, [2]University of Michigan, Ann Arbor, MI

Objective: Genetic testing (GT) and counseling (GC) are important aspects of comprehensive cancer care, yet persistent equity challenges exist. We aim to characterize the evolving utilization of GT and GC services for potential hereditary breast, ovarian, pancreatic, and prostate cancers (HBOPP).
Methods: We performed a retrospective single-institution chart review of a balanced racial subset of HBOPP patients who met National Comprehensive Cancer Network (NCCN) criteria diagnosed from 2019-2013. Data were analyzed using chi-squared test and multivariable logistic regression.
Results: 503 HBOPP patients were studied. GT was discussed with 50.5% (n=254) of patients, 42.3% (n=213) completed GT, but only 8.7% had GC (n=44) (Table 1). Patients who were younger, had managed care, or had a family history of cancer were significantly more likely to have a GT discussion and complete GT (all p<0.01). Pancreatic cancer (RR 0.11; 95% CI 0.05-0.21) and prostate cancer patients (RR 0.05; 95% CI 0.02-0.10) were less likely to have a GT discussion with their provider than breast cancer patients. HBOPP patients had a lower likelihood of having a GT discussion with each additional year of age at diagnosis (RR 0.95; 95% CI 0.93-0.98). Among patients who had a GT discussion, prostate cancer patients (RR 0.14; 95% CI 0.04-0.47) and Black patients (RR 0.25; 95% CI 0.09-0.71) were less likely to complete GT. Ovarian cancer patients (RR 12.1; 95% CI 5.19-28.5) and patients with a family history of cancer (RR 2.26; 95% CI 1.05-4.86) were more likely to have GC.
Conclusions: Inequities persist in GT and GC. NCCN-eligible patients who were older or had prostate or pancreatic cancer were less likely to have GT discussion. We found that Black patients were less likely than White patients to complete GT. GC rates were low across all groups except patients with ovarian cancer. Multilevel and systemic interventions are needed to improve equity in cancer genetic services.

Access to, completion, and outcomes of genetic testing and counseling, by cancer type.

	Breast (n=212)	**Ovarian (n=48)**	**Pancreatic (n=105)**	**Prostate (n=138)**	**Total (n=503)**	**Test (p)**
Was there evidence a provider discussed and/or offered genetic testing?						
Yes	172 (81.1%)	36 (75.0%)	26 (24.8%)	20 (14.5%)	254 (50.5%)	<0.001
No	40 (18.9%)	12 (25.0%)	79 (75.2%)	118 (85.5%)	249 (49.5%)	
Is there any evidence that the patient received genetic testing?						
Yes	155 (90.1%)	32 (88.9%)	18 (69.2%)	8 (42.1%)	213 (84.2%)	<0.001
No	17 (9.9%)	4 (11.1%)	8 (30.8%)	11 (57.9%)	40 (15.8%)	
What were the patients results?						
Mutation positive	25 (16.3%)	5 (15.6%)	2 (11.1%)	0 (0.0%)	32 (15.2%)	0.095
Mutation negative	83 (54.2)	12 (37.5%)	13 (72.2%)	3 (37.5%)	111 (52.6%)	
Variant of unknown significance	43 (28.1%)	13 (40.6%)	3 (16.7%)	4 (50.0%)	63 (29.9%)	
No info available/cannot find	2 (1.3%)	2 (6.2%)	0 (0.0%)	1 (12.5%)	5 (2.4%)	
Was there evidence of any genetic counseling encounter?						
No	195 (92.4%)	27 (57.4%)	102 (97.1%)	133 (96.4%)	457 (91.2%)	<0.001
Yes	16 (7.6%)	20 (42.6%)	3 (2.9%)	5 (3.6%)	44 (8.8%)	

#7334 Germline mutations in cancer susceptibility genes in patients with mucosal melanoma.

A. Amouzegar, X. Wu, J. Long, S. Prabhakaran, L. Little, C. Gumbs, J. Malke, J. Simon, J. Zhang, J. Wargo, P. Scheet, J. W. Wong, P. Nagarajan, J. L. McQuade, A. Futreal;
UT MD Anderson Cancer Center, Houston, TX

Background: Mucosal melanoma (MM) is the rarest subtype of melanoma with markedly worse outcomes compared to cutaneous melanoma (CM). Unlike CM which is driven by somatic mutations due to UV exposure, risk factors for MM are less defined. While germline mutations in cancer susceptibility genes are well-studied in CM, they are less understood in MM. Herein, we aimed to identify the prevalence of germline mutations in cancer susceptibility genes in a large MM cohort.

Methods: A cohort of 247 MM patients (pts) from MD Anderson Cancer Center with available blood for germline sequencing was identified. Pt characteristics were reflective of U.S. MM population with median age of 63, 60% females and 84.6% white. Clinicodemographic features of pts including tumor site, key somatic mutations (BRAF, NRAS, KIT) and personal history of other malignancies were abstracted, and their frequencies were compared in pts with and w/o germline mutation. Frequency of *MITF* and *CHEK2* alleles were compared to expected population control rate based on TOPMED by Fisher's exact test.

Results: Among 247 pts, 10.9% had germline mutations, primarily in *MITF* (c.G952A:p.E318K) (2.4%) and *CHEK2* (c.1100delC:p.T367fs) (1.6%) at OR of 13.9 (95%CI 5.0, 30.9) and 16.4 (4.4, 42.9) compared to population control rate (Table 1). MM sites of origin were gastrointestinal (36%), genitourinary (34%) and head & neck (30%). In terms of somatic mutations, *KIT* (26%) was most common, followed by *NRAS* (15%), non-V600E BRAF (6.5%) and BRAF V600E (2.4%). These variables did not differ between those with and w/o germline mutation. Pts with germline mutation had a higher incidence of non-melanoma malignancies (48% vs 29%; p=0.044).

Conclusions: This study reports a high prevalence of germline cancer susceptibility mutations in the largest cohort of MM to date, including mutations which are actionable. There is overlap with known *MITF* risk alleles for CM. We are currently performing a GWAS to comprehensively understand the genetic architecture of risk in MM.

Table 1. Summary of identified germline mutations in the mucosal melanoma cohort.

Germline mutation	**Protein**
MITF (N= 6)	p.E318K
CHEK2 (N=4)	p.T367fs
MUYTH	p.G368D
ATM	splice
ATM	p.L263fs
ATM	p.R1875X
ATM	p.L1327X
ATM	p.A2067D
ATM	p.R2034X
BRCA2	p.A1689fs
CHEK2	p.S400T
ERCC3	p.R109X
MITF	p.C29Y
NF1	p.L1183R
PALB2	p.V221X
POLE	p.D287E
TP53	p.R306X
TP53	p.V73Wfs*50
TSC1	p.Q844X

#7335 Characterizing germline variants in patients with small cell lung cancer.

S. Ul Haq[1], G. Downs[2], L. Zhan[3], D. Sacdalan[4], J. J. N. Li[5], V. Philip[3], R. H. Kim[4], G. Liu[5], S. V. Bratman[5], P. J. B. Sabatini[6], B. H. Lok[5];
[1]Schulich School of Medicine and Dentistry, Western University, London, ON, Canada, [2]Toronto General Hospital, Toronto, ON, Canada, [3]Princess Margaret Cancer Centre, Toronto, ON, Canada, [4]Institute of Medical Science, Temerty Faculty of Medicine, University of Toronto, Toronto, ON, Canada, [5]Department of Medical Biophysics, Temerty Faculty of Medicine, University of Toronto, Toronto, ON, Canada, [6]Department of Laboratory Medicine & Pathobiology, Temerty Faculty of Medicine, University of Toronto, Toronto, ON, Canada

Introduction: Small cell lung cancer (SCLC) has traditionally been considered to arise from environmental and lifestyle factors. Recent evidence has shown that germline mutations may also impact the development of SCLC, however, remains understudied. We sought to identify novel germline mutations in SCLC including unexplored copy-number variations (CNVs) in our cohort of patients.
Methods: We applied a custom hybrid-capture gene panel of 191 cancer predisposition and commonly mutated genes in SCLC to a pre-treatment cohort of 67 patients with SCLC. Variant calls were performed using VarScan2 (2.3.8), Pindel (0.2.5b8) and CNVs were assessed using DeCON 1.0.2. Calls were annotated using the American College of Medical Genetics (ACMG) criteria and classified using gnomeAD (release 2.11), ESP6500 (ESP6500SI-V2), 1000Genomes, ExAC (release 0.3), COSMIC (v70), dbSNP (build 147), and ClinVar (NCBI ClinVar 20190305). We annotated variants of uncertain significance (VUS) with several in
silico tools including MutationTaster, LRT, Polyphen2 HDIV, Polyphen2 HVAR, SIFT, PROVEAN, and Deepmind AlphaMissense. Kaplan-Meier survival analysis and log-rank tests were done to examine differences in overall survival (OS) and progression-free survival (PFS) from the date of diagnosis. Continuous variables were tested using Kruskal-Wallis H test and categorical variables using Fisher's exact test.
Results: The median age of our cohort was 68 years old, 64% (43/67) were male, 89% (60/67) were current/former smokers, and 58% (39/67) were Extensive-Stage. 64.6% (42/67) of patients self-reported a family history of cancer and 16% of the patients also self-reported personal history of cancer. In terms of self-reported ancestral background, 76% of were Caucasian, 1.5% were Middle-Eastern, 3% were Latin American, 14% were Asian, and 4.5% were Black. We identified pathogenic/likely pathogenic alterations in 7/67 patients. Five (71%) were novel alterations (*BCORL1, FANCC, ATR*, and *BBC3*) and a novel CNV (*SLFN11*) with the remaining two (29%) previously described mutations (*CHEK1* and *BRIP1*). We identified 191 VUS in 60/67 patients. 4.7-14.1% of VUS were in silico predicted to be pathogenic. Patients with the 7 pathogenic alterations had a numerically larger OS (HR = 0.50, 95%CI = 0.18-1.39, p = 0.18) and PFS (HR = 0.45, 95%CI = 0.16 - 1.24, p = 0.11) compared to the rest of the cohort. We identified 20 variants at low variant allele fractions (0.05 to 0.24), likely somatic mutations. Some genes identified are implicated with clonal hematopoiesis such as *GNAS, STAG, TET2*, and *MGA*.
Conclusion: In summary, we have identified several novel germline alterations (mutations and CNVs) in patients with SCLC. In addition, we utilized in silico prediction models to categorize potential high-risk VUS. Our findings suggest that beyond tobacco exposure germline alterations may also modulate development of tumorigenesis in SCLC patients.

#7336 Exploring the impact of cancer predisposition gene variants by functional analysis and whole genome sequencing analysis in hereditary cancer patients.

H. Kim[1], J. Park[2], G. Lee[1], J.-A. Hwang[1], J.-S. Ryu[1], Y.-R. Jung[1], S. Lee[1], K. Ryu[1], D. Lee[1], S.-Y. Jung[1], S.-Y. Park[1], W. Choi[1], S.-Y. Kong[1];
[1]National Cancer Center - Korea, Goyang-si, Korea, Republic of, [2]Hanyang University Guri Hospital, Hanyang University College of Medicine, Guri-si, Korea, Republic of

Background: Hereditary cancer confirmed by germline pathogenic variant has been increased with increasing next generation sequencing (NGS) panel tests in recent years. However, some cases who were suspected hereditary cancer represented having variant of uncertain significance (VUS) or no variants even though they had family members with many cancers. The aim of this study was to investigate variants function especially in splicing variants and to explore other candidate genes by whole genome sequencing (WGS) in suspected hereditary cancer patients.
Methods: Total of 44 patients who clinically suspected hereditary cancer without defined pathogenic variants after NGS panel test were enrolled. Among them 11 patients had intronic variants and their variant effects were predicted by SpliceAI, a deep learning-based tool. To define alternative splicing, total RNA was extracted from patients buffy coats and cDNA was synthesized using oligo dT. Then the cDNA was amplified by specific primers and performed sequencing. Also, WGS was performed in 15 patients then comprehensive analysis encompassing 392 unique genes was performed including 282 well-established hereditary cancer predisposition genes and 228 DNA repair-related genes. We confirmed the variant by various type of studies and predicted impact on protein by analysis.
Results: We analyzed intronic variants of 11 patients; ATM c.4611+3A>T(n=1). BRCA1 c.547+30A>G (n=2), BRCA1 c.5152+6T>C(n=1), MSH2 c.2635-7G>A(n=1), MUTYH c.934-2A>G(n=2), NF1 c.1527+4A>C(n=1), NF1 c.3871-14G>T(n=1), PALB2 c.3350+5G>A(n=1), and SMARCA4 c.3546+1G>A(n=1). Though two intronic variants (ATM c.4611+3A>T and SMARCA4:c.3546+1G>A) were observed a likelihood of aberrant splicing aggregate SpliceAI score more than 0.8, we observed three intronic variants induce alternative splicing (ATM c.4611+3A>T, NF1 c.1527+4A>C, and PALB2 c.3350+5G>A).In addition, WGS analysis demonstrated 6 out of 15 patients have germline variants in relevant genes. Four single nucleotide variants (SMARCAL1:c.1632delA, SETMAR:c.441dup, FAN1:c.590C>A, and PRF1:c.445G>A) were validated by sequencing and those were likely pathogenic variant (LPV) by ACMG/AMP criteria of ClinGen. Copy number variations were identified in 2 patients (PMS2 heterozygous deletion and RAD50 duplication) and structure variant of MSH2 was identified in one patient.
Conclusion: Our analysis showed in silico analysis results might be different from functional analysis and rare variants in cancer predisposition genes could be confirmed WGS. However, large number of patients study would be needed to confirm necessity of WGS for hereditary cancer. This work was supported by National Cancer Center, Korea (No_NCC-2110181).

#7338 Prevalence and risk factors of *PALB2* germline pathogenic variants.

M.-C. Kang, Y.-R. Jung, S. Lee, H.-S. Kang, S.-Y. Jung, M. Lim, K. Lee, E.-G. Lee, S.-Y. Kong;
National Cancer Center - Korea, Goyang-si, Korea, Republic of

Background: *PALB2*, located on chromosome 16, plays a vital role in DNA damage repair as a partner and localizer of BRCA2. *PALB2* germline pathogenic variant has been known to increase the risks of breast cancer, pancreatic cancer, and ovarian cancer. However, the prevalence of *PALB2* germline variants in Korean patients has not been thoroughly investigated. This study aimed to evaluate the prevalence of *PALB2* germline variants and the risk factors in Korean population. Methods: We analyzed the data of 3755 patients who performed hereditary cancer germline next generation sequencing (NGS) panels, including *PALB2*, at the National Cancer Center in Korea between 2008 and 2022. Genetic variants were classified using a five-tier system following the American College of Medical Genetics and Genomics guidelines as follows: pathogenic (PV), likely pathogenic (LPV), variants of uncertain significance (VUS), likely benign, and benign. We retrospectively reviewed 102 individuals who were confirmed to have the *PALB2* germline variant with PV, LPV and VUS. Also, we analyzed the clinical characteristics of patients with *PALB2* heterozygous PV or LPV.

Results: A total of 102 patients (2.7%, 102/3755) represented *PALB2* germline variants with 81 (79.4%) VUS, 14 (13.7%) LPV, and 7 (6.9%) PV. Detected twelve germline *PALB2* LPV or PV were as followings; c.3350+5G>A (n=6), c.454A>T (n=3), c.1048C>T (n=2), c.2016dup (n=2), c.1424C>G (n=1), c.1976_1977del (n=1), c.2095dup (n=1), c.2834+2T>C (n=1), c.2920_2921delAA (n=1), c.3317delT (n=1), c.902delA (n=1), and exon 11 deletion (n=1). 35 *PALB2* VUS were detected in 81 patients. Among 21 female patients with LPV or PV (median diagnosis age 50 years; 25-69), 18 carriers (85.7%) and 3 carriers (14.3%) were diagnosed with breast cancer and ovarian cancer, respectively. For 18 breast cancer patients, 3 patients had bilateral breast cancer and 3 patients had multi-organ cancers (ovary, thyroid, or colorectal and gastric cancer).Also, 15 carriers (71.4%) have first-degree relatives with breast, ovarian, pancreatic, lung, gastric, liver, thyroid, and colorectal cancer and 10 carriers (47.6%) have second-degree relatives with breast, pancreatic, lung, gastric, liver, prostate, lymphoma, laryngeal, and uterine cancer.

Conclusion: In our study, *PALB2* germline PV or LPV were detected at a low frequency of 0.56% in Korean cancer patients. Family history was an important risk factor for suspected germline pathogenic variants, and bilateral breast cancer was observed in 16.7% of breast cancer patients who harbored *PALB2* PV or LPV. This study was supported by grant from the National Cancer Center. (grant number HA23C0419; NCC- 23F1850; NCC-2110181).

#7339 Mayo Clinic breast cancer cohort: A valuable resource for breast cancer research.

N. L. Larson, J. Olson, K. Ruddy, F. Couch, D. Herman, F. Abraha;
Mayo Clinic, Rochester, MN

The Mayo Clinic Breast Disease Registry (MCBDR) was developed to serve as a cohort of newly diagnosed breast cancer patients to address questions of etiology, prognosis, and survivorship. Eligibility is limited to patients 18 years or older with a confirmed first stage 0-4 breast cancer diagnosis within the last year. Consent is completed via phone, patient portal, or in-person. Upon enrollment, a baseline questionnaire and blood collection are completed. Annual follow-up surveys that capture BC outcomes are sent to all living participants. The MCBDR cohort (N=9,215, enrolled between 2001 and 2023) is 99% female, with an average age at diagnosis of 58 years (SD=12.7). Currently, MCBDR has an average time since diagnosis of 9.8 years (SD=6.4). The participants are 94% white, and 55% live in Minnesota. At the time of baseline questionnaire completion, 77% were married, 84% had a bachelor's degree or higher, and 8% reported financial hardship. Further, 35% reported a history of smoking, 11% consumed more than two drinks per day, and 9% reported fair or poor social relationships.
Within MCBDR, 53% of the participants had stage 0 or 1 cancer at diagnosis, while 28% had stage 2, 9% stage 3, and 3% stage 4 BC. Tumors were triple negative in 9%, HER 2 positive in 9%, hormone receptor-positive and HER2 low or negative in 55%, and 27% had missing HER2 status. Pathological TNM staging was available on 98%, among which 33% were staged at T2 or higher and 27% were node-positive. Definitive BC surgery was completed at Mayo Clinic for 73%, with 35% undergoing mastectomies and 44% having lumpectomies. 74% were treated with radiation, 56% underwent chemotherapy, and 79% were treated with endocrine therapy.
Clinical genetic testing results have been nurse-abstracted for 94% of the cohort. Of those known to be tested, 521 (6%) had a pathogenic or likely pathogenic mutation identified in a BC causing gene. In addition, whole exome sequencing was completed on 71% of MCBDR participants in 2020, in which 167 previously unknown pathogenic or likely pathogenic mutations were identified.
After the initial diagnosis and active treatment phase, nurse abstraction identified 151 (2%) participants known to have been diagnosed with a contralateral BC diagnosis, and 4% known to have been diagnosed with a second primary other than breast. Recurrence in the same breast has been reported for 242 (3%), with 72% of those recurrences occurring within 5 years of initial diagnosis and another 19% occurring 5-10 years post diagnosis. Among the 1,262 (14%) who are deceased, 24% died from BC and 19% had distant metastases at diagnosis or a distant recurrence. Amongst all deceased, 6% died within 1 year of their diagnosis and 43% died within 5 years of diagnosis. For participants who died from BC, 10% died within 1 year of their diagnosis and 64% died within 5 years of diagnosis. MCBDR data has been used in numerous publications and is an essential resource for efficient observational research analyses.

#7340 Investigating the function and impact of UBASH3B in head and neck squamous cell carcinoma and its implications for racial health disparities.

M. Ndahayo, V. Mukhina, I. Gupta, D. A. Gaykalova;
University of Maryland, Baltimore, Baltimore, MD

Head and Neck Squamous Cell Carcinoma (HNSCC) is one of the top cancers with significant cancer health disparities among racial and ethnic groups. African Americans (AAs) with HNSCC demonstrate worse overall survival compared to European Americans (EAs). While the reasons behind this disparity are multifaceted, recent findings suggest that biological features in HNSCC may contribute to differences in disease progression. However, race-related biological factors in HNSCC have been relatively little explored. We have identified the gene UBASH3B, a protein tyrosine phosphatase that plays a role in the stabilization of the Epidermal Growth Factor Receptor (EGFR). High expression of UBASH3B in AAs is associated with significantly worse overall survival compared to high expression in EAs and low expression in AAs. This study seeks to examine the role of UBASH3B in HNSCC and determine its impact on tumorigenesis. We hypothesize that the upregulation of UBASH3B in AAs contributes to the survival disparity by promoting tumor progression through EGFR signaling. Preliminary data using The Cancer Genome Atlas (TCGA) shows overexpression of UBASH3B in tumor samples of both AAs and EAs HNSCC samples. Plus, the overexpression of UBASH3B is associated with perineural invasion. Additionally, among AA-HNSCC patients, advanced T-stage is associated with increased UBASH3B expression. Elucidating the role UBASH3B plays in tumorigenesis will give us a further understanding of HNSCC in African Americans and can serve as a potential therapeutic target for new treatment options, as well as the biomarkers for the detection of the high-risk group.

BIOINFORMATICS / COMPUTATIONAL BIOLOGY / SYSTEMS BIOLOGY / CONVERGENT SCIENCE: Application of Bioinformatics to Cancer Biology 5 Poster Session

#7344 Role of ubiquitin receptor ADRM1 (Rpn13) in prostate cancer.

S. Chowdhury, H. Wang, C. Nayak, B. Karanam;
Tuskegee University, Tuskegee, AL

Adhesion-regulating molecule 1 (ADRM1) / Rpn13 is a component of the 19S regulatory subunit of the 26S proteasome [1]. ADRM1 plays a crucial role in the recognition of polyubiquitinated substrates of the proteasome and their subsequent deubiquitination and degradation [2]. ADRM1 transcript levels are commonly upregulated in diverse tumor types [3]. The androgen receptor (AR) plays a predominant role in prostate cancer (PCa) pathology. In this study, we investigated the expression of ADRM1/ Rpn13 in different stages of prostate cancer and its association with AR expression. TCGA data from UALCAN was used for understanding ADRM1 expression on different stages of diseases and single-cell RNA-sequencing data of prostate cancer cell line was obtained from Prostate Cancer Atlas. TCGA (cell, 2015) data set was used for investigating the correlation between ADRM1 and AR by using R programming. Our study from the TCGA dataset reveals that ADRM1 expression increased significantly with the aggressiveness of prostate cancer (increase consistently with the Gleason score) from the TCGA dataset. We analyzed ADRM1 and AR expression in different prostate cancer cell lines and obtained that ADRM1 expressed significantly higher in prostate cancer cell lines which had lower AR expression. TCGA (cell, 2015) dataset indicated a negative correlation between ADRM1 and AR expression in prostate cancer. Our preliminary analysis indicated that ADRM1 inhibitor might be a potential therapeutic option for AR-independent prostate cancer.

#7345 Double-strand break inference from mosaic chromosomal alterations.

A. Dutch, C. Bumgardner, Y. Jakubek;
University of Kentucky, Lexington, KY

Double-strand breaks (DSBs) can cause alterations and rearrangements in chromosomes leading to large structural mutations. There have been previous efforts to identify DSBs in tumors and utilize these as a measure of homologous repair deficiency and response to therapy. In contrast, DSBs have not been well characterized in non-tumor human tissues. To address this void, we explore the distribution of DSBs in hematopoietic stem cells (HSCs) through the analyses of mosaic chromosomal alteration (mCA) breakpoints. Specifically, this work explores the relationship between the likelihood of DSB occurrences and the chromosomes on which they occur. Using data from the UK Biobank, mCA breakpoints were labeled as either DSBs or nonDSBs by proximity to telomeres and centromeres. mCA calls from the UK Biobank were obtained from Loh et al 2020. The START_MB_RANGE and END_MB_RANGE fields were treated as two separate breakpoint events for each entry in the data. Each of these breakpoint ranges was checked to see if it was close to either of the telomeres or to the centromere. Those falling within one Mb were categorized as mCA breakpoints that were likely not a result of DSBs, but rather missegregation of chromosomes or chromosome arms. Ranges that met either of these conditions were labeled “nonDSB” while ranges that did not were labeled “DSB.” These labeled data were processed in R using the Hmisc package. The 1-alpha binomial probability was calculated for the total number of DSBs versus the total number of breakpoint events. The point estimate for each chromosome was plotted along with the upper and lower confidence intervals. This work investigates the properties of DSBs. It is important to note that the observed putative DSBs are not representative of the frequency of DSBs in HSCs, since the resulting mutations can have different impacts on cellular fitness. This point is highlighted by our finding of increased putative DSBs on chromosome 13, as copy number changes involving the 13q14 locus are well documented drivers of chronic lymphocytic leukemia. In this investigation we observe that the proportion of putative DSBs is not correlated with chromosome length ($p = 0.2$). This result is likely due to the differential fitness effect of mCAs. However, it may also reflect differences in the likelihood of DSBs across the genome. We are currently working on methods from Machine Learning to further understand if there are genetic features which can predict DSBs which give rise to mCAs in HSCs.

#7346 Optimizing pan-cancer driver pathway analysis from patient transcriptomics and phosphoproteomics.

E. Z. Deng, G. B. Marino, D. J. B. Clarke, W. Ma, P. Wang, A. Ma'ayan;
Icahn School of Medicine at Mount Sinai, New York, NY

Alterations in cell signaling pathways drive cancer progression. Such changes can be detected by transcriptomics and proteomics profiling of tumor samples. Although proteomics profiling captures these alterations more directly, RNA-seq transcriptomics remains the most widely available and cost-effective source of data for elucidating tumor-specific cell signaling mechanisms. The eXpression2Kinases (X2K) pipeline is a computational workflow that starts with differentially expressed mRNAs, the identified differentially expressed genes are then used as input for transcription factor enrichment analysis. Then, the top-ranked transcription factors are connected via additional protein-protein interactions from several databases. Finally, the top-ranked transcription factors and the proteins that directly interact and connect these factors are subjected to kinase enrichment analysis. Such analysis identifies protein kinases most likely responsible for the observed changes in gene expression. The X2K pipeline can be applied to analyze tumor-specific transcriptomics to infer upstream regulatory transcription factors, protein intermediates, and kinases that are likely the drivers of cancer progression. While the X2K pipeline infers regulatory pathways from transcriptomics alone, phosphoproteomics can be used to independently validate the inferred kinases, and to calibrate the parameters of the X2K pipeline. Furthermore, this multiomics approach predicts cell signaling pathways with multiple layers of evidence by linking changes observed in the phosphoproteome to changes observed in the transcriptome. Here, we used the transcriptomics and phosphoproteomics profiles from the Clinical Proteomic Tumor Analysis Consortium (CPTAC) pan-cancer dataset, including 1,020 samples across 10 different cancer types, to optimize the parameters of the X2K pipeline and predict pan-cancer as well as tumor-specific signaling pathways. While inferred pathways were distinct between different tumor types, we observed global enrichment of receptor tyrosine kinases and cell cycle kinases. These pathways were subsequently tested for association with patient survival to identify pathways that may be effective therapeutic targets, for example, PTK2 signaling was identified for many lung cancer tumors (LUAD and LSCC) as well as some breast, head & neck squamous. Altogether, the X2K pipeline presents a rational approach to better identify driver regulatory mechanisms from patient-specific profiling of tumors with both transcriptomics and phosphoproteomics.

#7347 A transcriptome correlation network analysis of the high grade serous ovarian tumor immune microenvironment.

Kaylin M. Carey[1], Eric B. Dammer[2], Corey Young[3], Rajesh Singh[1], Ti'ara Griffen[4], James W. Lillard[1]

[1]Morehouse School of Medicine, Atlanta, GA,[2]Goizueta Alzheimer's Disease Research Center, Department of Biochemistry, Emory University School of Medicine, Atlanta, GA,[3]Department of Health and Human Services, Division of Cancer Epidemiology, National Cancer Institute, National Institutes of Health, Bethesda, MD,[4]Translational Medicine Oncology, Genentech, South San Francisco, CA

High Grade Serous Ovarian Cancer (HGSOC) affects many women and is the most common and lethal histopathological type of ovarian cancer. The molecular subtypes delineated by TCGA--mesenchymal, proliferative, immunoreactive, and differentiated subtypes, offer a sophisticated and innovative framework for HGSOC classification. These subtypes not only provide a detailed molecular characterization but also contribute to understanding the HGSOC Tumor Immune Microenvironment (TIME), comprised of both immune and tumor cells. The interplay within the TIME significantly influences pro- or anti-tumor responses, creating an important link between molecular landscape and dynamic immune-tumor interactions. Currently, there is a lack of understanding for the key drivers of clinical outcomes, molecular phenotypes, and diagnostic biomarkers for HGSOC. Here, we answer the question, does immune cell type, and proportion, drive clinical and molecular subtyping of primary HGSOC? Primary ovarian tumor samples from The Cancer Genome Atlas, TCGA (n=358) samples were collected and RNA-sequenced. FPKM values were used to construct the Weighted Gene Correlation Network Analysis (WGCNA), Gene Ontology (GO) and Proportion Estimations of Immune and Cancer cells (EPIC). Enrichment of HGSOC network module overlaps using a Fischer Exact Test were used to identify novel components of HGSOC progression that were significantly associated with clusters of highly correlated gene expression profiles, HGSOC stage, grade, and molecular phenotypes. We show genes associated with T cell proliferation (CD84) and B cell regulation (CD37), epithelial to mesenchymal transition (DOCK2), adaptor proteins present in T cells and myeloid cells (LCP2), inflammatory and metabolic signaling modulators (AIF1,CD53, SASH3), immunosuppressors of T lymphocytes and dendritic cells (FGL2), cell proliferation (PI3K) and relevant tertiary lymphoid structure gene (TNFAIP8L2) significantly correlated with HGSOC progression in both estimated tumor and proportions of immune cells. Future studies aim to confirm phosphorylation cascades associated with the aggressive molecular phenotypes of HGSOC and immune cell pathobiology.

#7348 CytoCellDB: A gold standard database for classification and analysis of extrachromosomal DNA in cancer.

L. Brunk;
UNC Chapel Hill, Chapel Hill, NC

Extrachromosomal DNA (ecDNA), or double minute chromosomes, are established cytogenetic markers for malignancy and genome instability. More recently, the cancer community has gained a heightened awareness of the roles of ecDNA in cancer proliferation, drug resistance and epigenetic remodeling. A current hindrance to understanding the biological roles of ecDNA is the lack of available cell line model systems with experimental cytogenetic data that confirm ecDNA status. Although several recent landmark studies have identified numerous cell lines and tumor models with ecDNA, the current sample size limits our ability to detect ecDNA-driven molecular differences due to limitations in power. Increasing the number of model systems that are known to express ecDNA would provide new avenues for understanding the fundamental underpinnings of ecDNA biology and would unlock a wealth of potential targeting strategies for ecDNA-driven cancers. To bridge this gap, we created CytoCellDB, a resource that provides karyotype annotations, including ecDNA status, and leverages publicly available global cell line data from the Cancer Dependency Map (DepMap) and the Cancer Cell Line Encyclopedia (CCLE). We expanded the total number of cancer cell lines with ecDNA annotations to 632, or 34% of the cell lines in CCLE/ DepMap. Of these, 154 cell lines express ecDNA, which is a 240% increase from the current sample size. We demonstrate that a strength of our framework is the ability to interrogate ecDNA, and the compendium of other chromosomal aberrations, in the context of cancer-specific vulnerabilities, drug sensitivities, and other multi-omic features (genomics, transcriptomics, methylation, proteomics). We anticipate that this resource will lower the barrier to systematic, population-scale discoveries related to ecDNA and will provide insights into strategies and best practices for determining novel therapeutics that overcome ecDNA-mediated drug resistance.

#7349 Ligand-receptor signaling analysis and tumor-immune microenvironment deconvolution reveal differential adipose-tumor crosstalk in lean and obese colon cancer patients.

Tengda Lin[1], Victoria M. Bandera[1], Elaine M. Glenny[2], Caroline Himbert[3], Jennifer Ose[1], Christy Warby[4], Olena Aksonova[4], Alessandro Carpanese[5], Chris Stubben[4], David Nix[6], Kenneth M. Boucher[7], Peter Schirmacher[8], Ildiko Strehli[4], Jolanta Jedrzkiewicz[9], Courtney L. Scaife[10], Bartley Pickron[10], Alexander Brobeil[11], Martin Schneider[12], Christoph Kahlert[12], Erin M. Siegel[13], Adetunji T. Toriola[14], David Shibata[15], Christopher I. Li[16], Jane C. Figueiredo[17], Jatin Roper[5], Biljana Gigic[12], Stephen D. Hursting[2], Cornelia M. Ulrich[1], Aik Choon Tan[6]

[1]Department of Population Health Sciences, University of Utah, Salt Lake City, UT,[2]Department of Nutrition, University of North Carolina at Chapel Hill, Chapel Hill, NC,[3]Harvard Medical School, Boston, UT,[4]Huntsman Cancer Institute, Salt Lake City, UT,[5]Department of Medicine, Duke University, Durham, NC,[6]Department of Oncological Sciences, University of Utah, Salt Lake City, UT,[7]Department of Internal Medicine, University of Utah, Salt Lake City, UT,[8]Heidelberg University Hospital, Heidelberg, Germany,[9]Department of Pathology, University of Utah, Salt Lake City, UT,[10]Department of Surgery, University of Utah School of Medicine, Salt Lake City, UT,[11]Institute of Pathology, Heidelberg University Hospital, Heidelberg, Germany,[12]Department of General, Visceral and Transplantation Surgery, Heidelberg University Hospital, Heidelberg, Germany,[13]Department of Cancer Epidemiology, H. Lee Moffitt Cancer Center and Research Institute, Tempa, FL,[14]Department of Surgery, Washington University School of Medicine, St. Louis, MO,[15]Department of Surgery, University of Tennessee Health Science Center, Memphis, TN,[16]Public Health Sciences Division, Fred Hutchinson Cancer Center, Seattle, WA,[17]Department of Medicine, Cedars-Sinai Medical Center, Los Angeles, CA

Obesity is a well-defined risk factor for colon cancer (CC). In the current study, we investigated the paracrine influences between tumors and adjacent adipose tissue to understand the interactions between adipose-tumor using transcriptomics data.

Stage I-III newly diagnosed CC patients (n = 130) as part of the ColoCare Study at the Huntsman Cancer Institute, University of Utah, and University of Heidelberg, Germany were included in the current study. Fresh-frozen colon tumor tissues and adjacent adipose tissues naïve to neoadjuvant treatment were collected during surgery. RNA sequencing was done using the NovaSeq X. Patients were classified as having a BMI <30 $kg \cdot m^{-2}$ (lean) or BMI ≥30 $kg \cdot m^{-2}$ (obese). Tumor-adipose signaling was investigated separately for lean versus obese patients. Differentially expressed genes (DEGs, FDRq<0.05 and |log2FC|>2) between paired tumor-adipose samples were identified through DESeq2, respectively for lean and obese participants. DEGs were filtered to obtain exclusively up-regulated genes for 1) tumor tissue in the obese 2) tumor tissue in the lean 3) adipose tissue in the obese 4) adipose tissue in the lean. Ligand-receptor pairs for adipose-adipose signaling (A-A), tumor-tumor signaling (T-T), adipose-tumor signaling (A-T), and tumor-adipose signaling (T-A) in tissues from lean versus obese patients were determined by mapping the exclusively up-regulated genes in the FANTOM 5 database. Single sample Gene Set Enrichment Analysis (ssGSEA) was performed to score each sample based on signatures of interest, i.e. TIMEx immune cell types. The associations of signatures between tumor-adipose were assessed by evaluating Spearman's correlation coefficients on the enrichment scores of each signature for paired tumor-adipose samples.

From RNA-seq, there were 430 protein-coding DEGs (144 up-regulated in the tumor, 286 up-regulated in the adipose) identified exclusively in the obese and; 704 protein-coding DEGs (421 up-regulated in the tumor, 283 up-regulated in the adipose) identified exclusively in the lean patients. In the obese, we observed ligand-receptor-mediated T-T signaling through *FGF5-FGFR3* and *PYY-NPY4R*; T-A signaling through *GCG-GCGR*; A-A signaling through *ICAM1-IL2RA*. In the lean, we found ligand-receptor-mediated T-T signaling through *ADAM2-ITGA6* and *LAMB3-ITGA6*; T-A signaling through *DLL3-NOTCH2*; A-A signaling through *DLK1-NOTCH2*. In addition, ssGSEA analysis showed different association patterns for the lean versus obese regarding the TIMEx immune cell types.

Our results suggest differential cross-talk between adipose and tumor tissue in lean vs. obese patients could influence the progression of CC. The next steps are to validate these interactions by using in vivo preclinical models to interrogate novel therapeutic targets for reducing the impact of obesity on CC.

#7351 Delineating the prostate cancer tumor microenvironment through scRNA-seq profiling at different timepoints.

I. Valencia, H. Pakula, M. Omar, M. Loda, L. Marchionni;
Weill Cornell Medicine, New York, NY

Distant metastasis remains the leading cause of death in patients with prostate cancer (PCa), however, the underlying mechanisms of this process remain unclear. Using samples from genetically-engineered mouse models (GEMMs) of PCa, we have identified eight different stromal cell states linked to epithelial mutations that may impact PCa progression to metastatic stages. To further investigate the unique intercellular interactions in the tumor microenvironment (TME) involved in mediating disease progression, we use single cell RNA sequencing (scRNA-seq) to profile primary PCa samples from different GEMMs including TRAMP, Hi-MYC, and FVBN, at different timepoints. Analysis of the scRNA-seq data revealed a significant enrichment of three clusters, designated as stromal c6 (s6), epithelial c7 (e7), and epithelial c10 (e10), exclusively in TRAMP, each expressing proliferative markers such as Mki67 and Top2a. To investigate the intercellular interactions among these clusters, we conducted ligand-receptor (LR) interaction analysis using CellChat. Notably, s6 is expressing the genes encoding ligands Bmp4, Fn1, and Igf1, which interact with the receptors Bmpr1b/Bmpr2, Itga3/Itgb1, and Igf1r, respectively expressed in e7. Subsequently, the transcriptomic profiles of these cells were used to build and validate a robust gene signature that can predict metastasis and survival in patients with PCa using a large cohort of 1239 samples, 930 of which were used for training while the remaining 309 samples were used for testing the model's performance. In conclusion, these results underscore the role of the TME mediating PCa progression and highlight the potential of leveraging the TME to extract predictive and prognostic features which can be later employed to build predictive and prognostic models for patients with PCa.

#7352 ScanCT: A tree-based machine learning model to detect single-cell genomic features associated with clinical outcomes.

Y. Zheng[1], L. Nguyen[1], P. Zhou[2], A. V. Hirayama[1];
[1]Fred Hutchinson Cancer Center, Seattle, WA, [2]University of Wisconsin - Madison, Madison, WI

Single-cell technologies represent a revolutionary approach to resolving cell-type heterogeneity, identifying cells in specialized states, and detecting rare disease-associated cells. With the cost of single-cell technology decreasing substantially, its integration into clinical studies is gaining momentum. A new computational tool is needed to accommodate different single-cell genomics and clinical data formats while accounting for unwanted confounders.
The study aims to develop a tree-based machine learning model to leverage the unprecedented resolution of single-cell multi-omics data for delineating the genomic and phenotypic drivers behind diverse immunotherapy responses. The proposed model is called single-cell analysis of Clinical Tree (scanCT), inspired by the Generalized Unbiased Interaction Detection and Estimation method for unbiased gene and protein feature selection and easy interpretation.
The scanCT model learns from the data to select the genomic feature that best splits the cells from distinct clinical responses for each tree node. The confounding factors will be regressors in the nodes but not be used for branch splitting, while gene and protein features of interest will split the tree but not enter the regression model in each node. scanCT is built to be free from the biased selection towards variables of a larger number of categories or values. With tree-pruning and cross-validation, scanCT overcomes the over-fitting issue and enhances model generalization, especially for clinical studies with limited patients. Particularly, scanCT naturally fits the hierarchical cell type relationship and handles marker gene and protein interaction effects efficiently.
Our approach was tested on single-cell datasets from B-cell malignancy patients undergoing Chimeric Antigen Receptor (CAR)-T cell therapy. The results from the scanCT are highly interpretable. For instance, each branch is a gene-protein combination profile, and cells are naturally partitioned by clinical association. The linear regressions at each leaf node are the clinical predictions for cells following the splitting criteria. The regression intercept is an average estimation of toxicity (e.g., neurotoxicity) or efficacy after controlling for confounder (e.g., tumor burden). scanCT accommodates categorical or continuous clinical response and survival data and is robust to missing values, a frequent challenge in oncological studies.
scanCT represents a significant step forward in single-cell data analysis, which merges complex genotypic and phenotypic information with clinical outcomes. The efficacy and toxicity-associated genomic signatures will inform new manufacturing strategies to optimize CAR-T cell therapy products. The model and clinical association detections are expected to go beyond the B-cell malignancy field to benefit the broader cancer research community.

#7353 Exploring intrapatient heterogeneity in metastatic breast cancer: Insights into tumor evolution from a warm procurement trial.

I. Bishara[1], X. Liu[2], J. I. Griffiths[1], J. Liu[2], P. A. Cosgrove[1], J. R. McQuerry[3], F. Chi[1], P. Wallet[1], V. K. Grolmusz[1], B. Copeland[1], L. Pflieger[1], J. Chen[1], S. Majumdar[1], G. Ronquillo[1], T. Crowder[1], R. Emond[1], R. Factor[4], E. Barragan[1], D. Bowtell[5], A. Cohen[6], D. D. Schmolze[1], P. Lee[1], K. Ihle[1], L. Tumyan[1], A. Nath[1], J. Waisman[1], A. Bild[1], J. Chang[2];

[1]City of Hope National Medical Center, Duarte, CA, [2]University of Texas Health Science Center, Houston, TX, [3]Children's Mercy Kansas City, Kansas City, KS, [4]University of Utah, Salt Lake City, UT, [5]Peter MacCallum Cancer Centre, Melbourne, Australia, [6]Inova Schar Cancer Institute, Fairfax, VA

Metastatic breast cancers show variable clinical responses due to inherent heterogeneity, both within tumors and among patients. Studies mainly examine molecular diversity across different patients' tumors and genetic variance within a single tumor. Yet, the variability among multiple tumors or metastases in a single patient remains underexplored. Our study investigates this intrapatient heterogeneity, examining cell and tumor evolution from a single genetic source in metastatic breast cancer. In a warm procurement trial involving 6 patients with multi-site tumors, samples were collected for detailed molecular analysis. Whole exome sequencing (WES) and single-cell RNA sequencing (scRNA-seq) were used to analyze genetic similarities and disparities. WES data revealed mutational patterns and copy number alterations, showing homogeneity and heterogeneity in tumors within patients. Further, phylogenetic analysis with scRNA-seq variant calls paired with transcriptional phenotypes uncovered a MYC-enriched subclonal population in a metastatic site. Integrating WES and scRNA-seq data provided a clearer understanding of the genomic and phenotypic features in and between patients. Our WES study revealed significant interpatient variations in genetic drivers and CNA profiles. Among five patients, two showed APOBEC and HR mutations, linked to increased tumor mutations. Despite general genetic homogeneity, there were exceptions. Tumors in Patient 3's upper lymph nodes had distinct genetics compared to abdominal tumors. Unique genetic patterns were also noted in the pancreas and mesentery of Patients 3 and 7, respectively. Genetic findings were supported by transcriptional analysis, showing distinct expression patterns in specific sites. Phylogenetic analysis highlighted intratumor heterogeneity, as shown by variations in phylogenetic composition and gene expression across samples. Notably, in patients with the most samples (Patients 3 and 7), a conserved cell clade, evolved early and primarily located in a single site, displayed a high proliferation gene expression signature closely associated with Myc activity. This underscores the importance of early clonal expansions in tumor evolution and suggests potential therapeutic targets in these early, proliferative cells. Our study highlights the vital role of intrapatient heterogeneity in understanding cancer complexity and treatment resistance. By analyzing genetic and phenotypic variability in multi-site tumors within patients, and Myc's key role in tumor growth and evolution, our research offers new insights into tumor evolution. This underscores the need for personalized oncology treatments based on each patient's tumor genetics.

#7354 Proteogenomic and metabolomic characterization of acute myeloid leukemia.

A. Chu[1], **Y. Hsiao**[1], Y. Deng[1], C. Wang[2], J. Kyle[3], Y. Dou[2], J. C. Pino[3], C. Posso[3], L. Henry[1], L. Chen[4], G. Li[1], T.-S. Lih[4], Y. Geffen[5], F. Yu[1], L. Ding[6], G. Omenn[1], C. Kumar[1], S. M. Dhanasekaran[1], E. Traer[7], J. W. Tyner[7], H. Zhang[4], T. Liu[3], S. Gosline[3], B. Zhang[2], A. Chinnaiyan[1], A. I. Nesvizhskii[1], M. Cieslik[1], The CPTAC Consortium;

[1]University of Michigan Medical School, Ann Arbor, MI, [2]Baylor College of Medicine, Houston, TX, [3]Pacific Northwest National Laboratory, Richland, WA, [4]Johns Hopkins university, Baltimore, MD, [5]Broad Institute of Massachusetts Institute of Technology and Harvard, Cambridge, MA, [6]Washington University School of Medicine, St. Louis, MO, [7]Oregon Health & Science University, Portland, OR

Acute myeloid leukemia (AML) is a blood malignancy of poor prognosis with marked heterogeneity. To elucidate the underlying mechanisms that drive AML as part of the Clinical Proteomic Tumor Analysis Consortium (CPTAC) effort, we performed comprehensive genomics, transcriptomics, proteomics including multiple post-translational modifications (phosphorylation, acetylation, and glycosylation), metabolomics, and lipidomics characterization of 173 treatment-naïve AML patients. Applying the similarity network fusion method on both transcriptomics and proteomics data, we identified 8 proteogenomic clusters. These clusters recapitulate specific recurrent mutations and established clinical subtypes available within the cohort. We used single-cell RNAseq data as a reference to perform immune component analysis for collected bulk samples. The result reveals that our proteogenomic clustering also captures the variations of AML differentiation hierarchies including CD14+ monocyte-like and GMP-like AML. To assess the complex disease nature of AML, we performed functional analysis for each cluster to reveal interplay between multiple genomic aberrations such as NPM1, FLT3-ITD, DNMT3A mutations, complex chromosomal alterations, and the leukemia cell differentiation. Importantly, the multi-omics analysis performed not only connects previously identified molecular drivers and cell differentiation variations within AML, but also links them with observed cancer metabolomic reprogramming with their drug response implications. Moreover, our study also identified site-specific post-translational modifications previously not known in AML, highlighting the valuable insights and clinical relevance of these newly identified clusters.

#7355 Integration analysis of lncRNAs and R-loops in 3D genome organization and gene regulation in the cancer genome.

S. Wang, Z. Wang, Y.-H. Wang, H. Li, P. Stukenburg, C. Zang;
University of Virginia, Charlottesville, VA

Existing evidence shows that some long non-coding RNAs (lncRNAs) can recruit chromatin regulators and form R-loops to mediate CCTCC-binding factor (CTCF) binding at topologically associated domain (TAD) boundaries to activate transcription of target genes. However, it remains unclear to what extent such lncRNA-dependent chromatin organization events occur genome-wide in normal and cancer cells. By curated public data of lncRNA, CTCF, RAD21 profiles and integrative analysis of multi-omics data using innovative computational approaches, we investigated global associations of lncRNAs and R-loops with activities of transcription factors and chromatin regulators in gene expression regulations across multiple human cell types. We developed a comprehensive computational pipeline for cross-cell-type analysis of lncRNA and protein-coding gene expression profiles and transcription factor binding profiles. We identified a total of 542 candidate genomic regions where lncRNAs play a pivotal role in regulating target genes by facilitating CTCF/cohesin binding. R-loops are enriched at CTCF/cohesin binding sites, suggesting their potential contribution to CTCF binding. Additionally, our findings underscore the significant cell-type specificity of CTCF binding patterns across the genome. This work adds knowledge to cancer genome organization and gene regulation, and builds foundations for further functional and mechanistic studies of lncRNAs and R-loops in the human genome.

#7356 3 UTR variations in esophageal squamous cell carcinoma in African Americans.

C. Erkizan[1], R. Wadleigh[2];

[1]Washington-Liberty High School, Arlington, VA, [2]Institute for Clinical Research, Veterans Affairs Medical Center, Washington, DC

Esophageal squamous cell carcinoma (ESCC) predominantly affects African Americans (AA). Esophageal Cancer (EC) consists of two major histological subtypes: esophageal adenocarcinoma and squamous cell carcinoma. ESCC ranks among the most lethal cancers and is particularly aggressive among AA, comprising about 75% of total ESCC patients. The 5-year survival rate for localized EC in AA patients is 25%; in contrast, the survival rate for EC patients of Caucasian origin is 48%. However, for metastatic disease, the survival rate decreases dramatically to 5% regardless of race. To conduct an extensive mutation screening, we performed whole exome sequencing (WES) in 10 paired AA ESCC and control tissues. Mutations included nonsynonymous mutations in multiple genes and copy number variations. Here, we report on further analysis of the WES data to identify 3 UTR noncoding region alterations, comprising the highest proportion of noncoding variations. Whole exome sequencing was performed using Agilent SureSelect XT Human All Exon V6 + UTR kit on matched normal-tumor samples from 10 AA patients (nine males and one female) with advanced-stage ESCC. The ages of patients ranged from 53 to 80 years. All patients, except for one, reported tobacco use and alcohol consumption. Our analysis yielded 5378 variants in noncoding regions in our cohort. The most variations were found in the 3UTR location, with 46% of all noncoding variations. In our dataset, variations in the 3UTR region of 48 genes were predicted by CScape to assert an oncogenic effect. The highest ten oncogenic predictive scores are for *ETV1, FOXO3, MSI2, TCF7L2, KAT6A, FOXO1, IRF4, TRIM24, ELK4, and FGFR1* genes. Approximately 2500 genes having 3'UTR variations are over-presented in intracellular signaling and cell-cell communications, transcriptional regulation of pluripotent stem cells by OCT4, SOX2, NANOG, generic RNA polymerase II transcription, RHO GTPase cycle, and regulation of cytoskeletal remodeling. The combined effects of noncoding and coding region mutations may largely impact poor prognosis in AA with ESCC and yield targets for developing candidate therapeutics.

#7357 Comparative transcriptomic analysis reveals novel insights into targetable B-cell lymphoma mechanisms.

S. Kim, N. Rapier-Sharman, M. T. Told, K. L. O'Neill, B. E. Pickett;
Brigham Young University, Provo, UT

B-cell lymphoma is a severe type of lymphatic cancer that is often misdiagnosed in adolescents. While some cases of B-cell lymphoma respond well to chemo- and radiation therapy, there are severe side effects, and many cases are refractory and fail to achieve remission. On the other hand, though CD19 CAR T-cell therapy is highly effective at treating B-cell lymphoma, its association with long-term immunocompromisation justifies the exploration of alternative treatments. Comparing B-cell lymphomas to an autoimmune disease that affects the same tissue type may grant us additional insights into immuno-oncology related treatments for B-cell lymphoma. We have developed a novel tool to compare cancer and autoimmune disease by analyzing bulk RNA-sequencing (RNA-seq) data. This algorithmic approach uses the transcriptional profile to improve our understanding of B-cell specific mechanisms that can be targeted in B-cell lymphoma. Using this tool, we compared the transcriptional signatures of primary B-cell lymphomas with primary B-cells from patients with systemic lupus erythematosus, an autoimmune disease. We identified specific genes and enriched functions associated with B-cell lymphoma's immune signature. We expect that the results of our B-cell lymphoma analysis could be used to develop beneficial treatments alternative to current therapies, potentially mitigating side effects for B-cell lymphoma patients and increasing their quality of life.

#7358 Role of noncoding genome architecture in esophageal cancer.

H. V. Erkizan[1], R. Wadleigh[2];
[1]VA Medical Ctr. and Washington DC and George Washington University, Washington, DC, [2]VA Medical Ctr. and Washington DC, Washington, DC

Esophageal Cancer is a deadly disease with a tendency to be diagnosed at the later stages. Considered a rare disease, accounting for 1.1% of all cancers, EC comprises 2.6% of all cancer deaths. The survival rate for all stages is 21.7%. However, the survival rate decreases to 5.6 % for advanced-stage cancers. EC is more common in men and associated with older age and heavy alcohol and tobacco use. In the last 25 years, the death rate of EC has been decreasing slightly from 4.3 to 3.7. The death rates for lung, prostate, and colon cancers have decreased by half in the same time frame. Therefore, novel therapies and biomarkers are urgently needed to accelerate survival and reduce the death rates by at least half for patients with EC.We previously completed exome sequencing in a small sample size and observed that the mutations in the noncoding regions of the EC genome are highly affected. In this study, we perform exome sequencing in 110 paired esophageal tumors and normal tissues using an Agilent SSELXT HS Exon V8+UTR library enrichment kit. Twelve paired EC and normal tissues are sequenced using the PacBio Hifi system.In WES, we detected almost half of the noncoding region mutations in the 3UTR and 2kb downstream regions of the genome, significantly affecting 51 oncogenic or tumor suppressor genes. In addition, the involved genes are over-represented in critical signaling pathways and transcriptional regulation of pluripotent stem cells. The number of changes in the 5UTR and 2kb upstream are similar to the number of variations in the intronic regions. Apoptosis, stress response, and DNA double-strand break repair pathways are affected by 5UTR mutations. Mutations in the intronic regions frequently occurred in pro-tumorigenic immune regulation genes, such as IL-33 and IL-6, and oncogene-induced senescence.The combined effect of these genetic and coding region mutations on oncogenes, significant signaling pathways, cancer cell stemness, DNA damage repair pathways, and immune system regulation may significantly impact poor prognosis in EC patients. Further studies will verify the effectiveness of targeting these genes for developing candidate therapeutics.

#7359 Priority targets in pancreatic cancer.

Z. C. Nwosu, M. Pasca di Magliano, C. Lyssiotis;
University of Michigan, Ann Arbor, MI

Pancreatic ductal adenocarcinoma (PDAC) is a drug resistant and lethal cancer. To better understand this disease, we separately analyzed five published human PDAC microarrays, determined the differential genes in each dataset and defined a gene as ‘consistent’ if it is ‘upregulated’ or ‘downregulated’ in >4 datasets (adjusted *P*<0.05). We identified 2,010 consistently upregulated- and 1,928 downregulated genes, over 50% of which were previously uncharacterized in PDAC. These genes span multiple processes, including cell cycle, immunity, transporters, metabolism, signaling, transcription factors and epigenetics. - with cell cycle and glycolysis being the most altered. Many consistent genes correlated with tumor subtype, proliferation, metastasis, and ~41% predicted survival, notably, *OGN, PLOD2, DIAPH3, C2orf40*, *ADM*, *UPP1, ZNF189, DCBLD2*, *PLAG1,* and glycolysis genes*ALDOA, GAPDH, PKM* and *LDHA*. We identified 451 high priority targets, including 185 upregulated genes (notably in cell cycle and glycolysis) whose knockdown suppressed PDAC cell growth in prior RNAi screen studies. Our results represent an important milestone in the quest for mechanisms, drug targets and biomarkers and could enable the discovery of novel mechanisms and therapies in PDAC.

#7361 The prognostic value of TP53 and tumor suppressor gene mutations in temozolomide-treated IDH1 mutant low-grade glioma.

Y. E. Salem[1], B. O. Abu Alragheb[2];

[1]Al-Bashir Hospital, Amman, Jordan, [2]The University of Jordan, Amman, Jordan

Background: Temozolomide has been extensively utilized in the treatment of gliomas across various grades, offering significant therapeutic benefits. However, the impact of concurrent mutations in TP53 and other tumor suppressor genes (TSG) on treatment outcomes in patients with IDH1 mutant low-grade glioma (LGG) treated with temozolomide remains to be fully understood. This study aims to explore the influence of these genetic factors on the response to temozolomide therapy, focusing on identifying potential genetic markers that can predict therapeutic outcomes.

Methods: Our study exclusively analyzed The Cancer Genome Atlas (TCGA) LGG PanCancer dataset from cBioPortal, focusing on IDH1 mutant cases treated with temozolomide. Data analysis was carried out using Python 3.11. The cohort was categorized based on genetic alterations: TP53 mutation with additional TSGs (ATRX, CIC, FUBP1, NOTCH1) mutations (TP53mut/TSGmut), TP53 mutation without additional TSG mutations (TP53mut/TSGwt), and no TP53 mutations (TP53wt).

Results: In our study, 178 LGG samples with IDH-1 mutation treated with temozolomide were selected. Of these, 113 samples had a mutation in TP53, and 88 had an additional mutation in a TSG. For TP53mut/TSGmut compared to TP53wt, the analysis revealed significant differences in clinical outcomes (PFS: HR 1.95, CI: 1.17-3.26, p=0.011; OS: HR 1.6, CI: 1.13-2.26, p=0.008). When comparing TP53mut/TSGwt with TP53mut/TSGmut, the findings were (PFS: HR 1.36, CI: 0.63-2.92, p=0.432; OS: HR 0.93, CI: 0.31-2.79, p=0.896). Finally, the comparison between TP53wt and TP53mut/TSGwt showed (PFS: HR 1.45, CI: 0.62-3.39, p=0.397; OS: HR 2.31, CI: 0.64-8.3, p=0.200).

Conclusion: The presence of concurrent mutations in TP53 and other TSGs in IDH1 mutant LGG patients (TP53mut/TSGmut) is indicative of a more aggressive disease course and reduced response to temozolomide treatment, as evidenced by significantly worse clinical outcomes. In contrast, the TP53mut/TSGwt group did not exhibit significant differences in treatment outcomes. These findings underscore the importance of detailed genetic profiling in developing personalized treatment strategies for this patient population.

#7362 Integrated analysis of scRNAseq and spatial omics in brain metastatic lung cancer tumor tissue.

H. Hirose[1], T. Tsuji[2], Y. Kojima[3], A. Yoshizawa[4], Y. Arakawa[5], H. Ozasa[6], H. Wake[2], T. Shimamura[1];

[1]Tokyo Medical & Dental University, Tokyo, Japan, [2]Department of Anatomy and Molecular Cell Biology, Nagoya University Graduate School of Medicine, Nagoya, Japan, [3]Laboratory of Computational Life Science, National Cancer Center Research Institute, Chuo-ku, Tokyo, Japan, [4] Department of Diagnostic Pathology, Graduate School of Medicine, Kyoto University, Kyoto, Japan, [5] Department of Neurosurgery, Graduate School of Medicine, Kyoto University, Kyoto, Japan, [6] Department of Respiratory Medicine, Graduate School of Medicine, Kyoto University, Kyoto, Japan

Spatial omics technologies have made significant advances in recent years, improving our understanding of the spatial localization of cells and intercellular interactions. Intercellular interactions are essential for maintaining proper tissue function and homeostasis, and dysregulation of these interactions can contribute to various diseases, including cancer and autoimmune disorders. Ligand proteins, one of the signaling molecules responsible for cell-cell interactions, bind to cell surface receptors and trigger intracellular signaling pathways. The effective range of ligand signaling, i.e. the extent to which a cell spatially and directly transmits information via the ligand, has not been systematically studied, although it may determine the occurrence of cell-cell interactions. The authors have previously developed methodologies combining spatial transcriptomics and single-cell RNA sequencing to analyze intercellular interactions at the single-cell level in spatial dimensions. Additionally, we have devised a technique to model the spatial diffusion of ligands from spatial transcriptomics and estimate the spatial range of ligand action. In this study, we used these developed methods to elucidate events in the tumor microenvironment of brain metastatic lung cancer tissue. Specifically, an integrated analysis of metastatic brain tumor samples was performed using visium and single-cell data from the same patient. The results suggest the presence of a heterogeneous microglial subpopulation, including clusters enriched in cytokines and chemokines for angiogenesis and wound healing, clusters associated with immune tolerance via IL-10 signaling, clusters enriched in gene sets related to phagocytosis, antigen processing, and antigen presentation, and clusters related to clearance of pathogens and residues. The presence of homogeneous microglial subpopulations was suggested. Furthermore, these subpopulations exhibited different spatial distributions, suggesting that they interact with surrounding cancer cells through different mechanisms.

#7363 Clinical, genomic, transcriptomic and immunologic profile of BRAF mutant colorectal tumors.

E. Rousselle, S. Kazandjian, A. Rose;
McGill University, Montreal, QC, Canada

Background: Colorectal cancer (CRC) is the second leading cause of cancer-related death worldwide. BRAF, a protein kinase of the Mitogen-Activated Protein Kinase (MAPK) pathway, is mutated in 12% of colorectal cancers and is a poor prognostic factor for patients. BRAF mutations at the V600 codon are most studied but non-V600 BRAF mutations also exist and behave differently. BRAF V600 CRC treated with BRAF+MEK inhibitors show 12% response rates while we observe 65% response rates in BRAF V600 Melanoma. Additionally, no approved targeted therapies exist for non-V600 BRAF mutant cancers and retrospective studies show poorer PFS with BRAF+MEK inhibitors vs BRAF V600 cancers. We interrogated publicly available data of BRAF mutant CRC to uncover differences in the tumor microenvironment and signalling pathways of BRAF V600 and non-V600 tumors in hopes of uncovering better treatments.
Methods: We analyzed the clinical and genomic profile of BRAF mutant CRC tumors from the GENIE v12 data. Gene Set Enrichment Analysis was performed on RNAseq from the TCGA data (discovery cohort) and the combined data from CPTAC and Sidra-LUMC data (validation cohort). We investigated the composition of tumor infiltrating immune cells using CIBERSORTx (deconvolution algorithm for bulk RNAseq).
Results: Non-V600 mutations (n=219/1061) were most represented in patients of Asian or Black race compared to White patients ($p<0.0001$) and importantly, were found in younger patients ($p<0.0001$). We identified n=67 and n=74 BRAF mutant RNAseq samples in the discovery and validation cohorts, respectively. In the discovery cohort: BRAF V600 CRC were enriched for Interferon Gamma Signaling, Complement pathway, and IL6 JAK STAT3 Signaling ($p<0.05$) while the non-V600 BRAF mutant CRC showed an enrichment for Wnt-beta Catenin, Notch, and Hedgehog Signaling pathways ($p\leq0.05$). In the validation cohorts these same pathways were enriched in V600 and non-V600 BRAF mutant tumors. Interestingly, enrichment of genes co-mutated (GENIE data) in non-V600 BRAF mutant CRC also revealed the Wnt pathway. Non-V600 CRC tumors have a higher proportion of M0 macrophages ($p=0.0035$) and CD4 memory resting T cells ($p<0.0001$) while patients with V600 CRC have higher proportions of CD8 T cells ($p=0.006$) and activated mast cells ($p=0.0341$).
Conclusion: No optimal therapeutic strategies have been defined for these potentially actionable non-V600 BRAF mutant CRCs. By exploring the multi-omic landscape of these tumors we have identified unique characteristics of non-V600 BRAF mutant CRC that could be therapeutically exploited.

#7364 Comprehensive multi-omics analysis for resectable hepatocellular carcinoma uncovers biomarkers to predict microvascular invasion.

I. Kang, W. Kwon, S. Lee;
Laboratory of Integrative Precision Oncology, Seongnam, Korea, Republic of

Introduction: Microvascular invasion (MVI) is a well-known prognostic factor in predicting cancer relapse after curative resection of resectable hepatocellular carcinoma (HCC).Therefore, there is a clear unmet need for a precision strategy based on cancer-specific multi-omics features to predict the MVI feature at the initial diagnosis of HCC.
Methods: Using gene expression profiling for resected human HCC (Discovery cohort, n=240), we identified the transcriptomic signature predicting the MVI feature. Comprehensive analyses were performed using the dataset from the cancer dependency map (DepMap) project, including cancer-specific molecular characterization with multi-omics data, and drug sensitivity with compound screening, and integrative *in-silico* prediction methods to uncover MVI. The transcriptomic signature predicting the MVI feature were validated in independent translational cohorts (TCGA-LIHC; n=373, KOREA; n=188, TOKYO; n=183, MODENA; n=78, ZHONGSHAN; n=159).
Results: The MVI signature with 1028 genes was identified from robust statistical testing from the discovery cohort, and robust validation for the prediction performance of the MVI signature showed significant accuracy in the validation cohort (AUC=0.865, $p<0.01$). Multi-omics analysis revealed aggressive tumor biology associated with the MVI signature and specified biomarkers.
Conclusions: Integrative multi-omics profiling for resectable HCC uncovers biomarkers to predict MVI. A novel combination of biomarkers performs in sorting out the tumor with aggressive tumor biology. A precision strategy to discover resectable tumors beneficial from surgical resection can be established from consecutive clinical trials based on this translational study.

#7365 Drug-centric prior improves drug response signature identification in partially overlapping, large-scale pharmacogenomic datasets.

D. Thirumalaisamy[1], S. K. Joshi[2], M. Gonen[3], O. Nikolova[1];

[1]Oregon Health & Science University, Portland, OR, [2]Stanford University, Stanford, CA, [3]Koc University, Istanbul, Turkey

Introduction: With the accumulation of large-scale pharmacogenomic data such as whole-genome RNA sequencing, copy number and mutation profiles for tens of thousands of samples, further screened with thousands of small molecules and other perturbagens, the question arises how to best leverage partially overlapping datasets generated at different facilities. Notably, Haibe-Kains et al. observed discordance in state-of-the-art pharmacogenomic repositories. As research groups across the world continue to generate drug screens of variable size and quality, the need for approaches that can learn from such partially overlapping experiments and improve the signal to noise ratio emerges with increasing importance.

Methods: A previously published Bayesian group factor analysis model was shown to outperform other approaches in predicting drug response and identifying gene signature from pharmacogenomic datasets particularly by leveraging shared information for a given gene across multiple omics assays. Here, we applied the same model in a similar fashion to now learn from shared observations for the same drug across multiple partially overlapping and noisy small molecule screens. We integrate gene expression, mutation and drug response data from the two largest pan-cancer repositories at the Broad and Sanger Institutes, respectively. We train joint models on partially overlapping data from both. We evaluate our performance in three ways: 1) we test if the joint model improves the prioritization of known consensus biomarkers for the drugs shared between the two cohorts; 2) we test if the joint model improves the recapitulation of shared drug mechanism of action as compared to the single dataset models; 3) we evaluate the joint models with respect to pathway enrichment as compared to the single dataset models.

Results: We evaluated the performance of our joint model for 5 drugs shared between the 2 resources: selumetinib, tanespimycin, nutlin 3A, mirdametinib and PLX4720. First, we show that training joint models on partially overlapping pharmacogenomic datasets can overall improve gene signature identification by improving the ranks of known consensus biomarkers. Second, we show that the joint model learns a latent representation of the drugs that better recapitulates the underlying known mechanisms of action for the three serine/threonine kinase inhibitors. Finally, we show that the joint model achieved improved pathway enrichment results for the targeted MAPK/ERK signaling pathway.

Conclusions: We present an application of a Bayesian group factor analysis model, where we employ a drug-centric prior to transfer information about drugs screened in multiple datasets. We show that joint models leveraging partially overlapping large-scale pharmacogenomic datasets from the Broad and Sanger institutes can overall improve drug signature identification.

#7366 Loss of STK11 suppresses lipid metabolism to attenuate KRAS-induced immunogenicity in patients with non-small cell lung cancer.

D. Principe[1], M. Pasquinelli[1], R. Nguyen[1], L. Feldman[1], A. Aissa[2], F. D. Weinberg[1];

[1]University of Illinois Chicago, Chicago, IL, [2]Federal University of Sao Paulo, Sao Paulo, Brazil

Background: Non-small cell lung cancer (NSCLC) is the leading cause of cancer-related death in the United States. Though NSCLC is genetically heterogeneous, as many as 30% of NSCLC patients harbor gain-of-function mutations in the *KRAS* oncogene. Recent studies have demonstrated that *KRAS* mutations lead to extensive remodeling of the tumor immune microenvironment. However, though the effect of co-mutations in genes such as *TP53* and *STK11* are known to have prognostic relevance in *KRAS*-mutated patients, their mechanistic effect on tumor immunogenicity is largely unknown.

Methods: In the present single-center study, we enrolled a total of 189 NSCLC patients. Paraffin specimens from each underwent a standardized analysis including immunohistochemistry for PD-L1 expression, whole exome DNA sequencing, and whole transcriptome RNA sequencing.

Results: Patients with activating *KRAS* mutations demonstrated a significant increase in PD-L1 expression as well as in CD8+ T-cell infiltration, both of which were enhanced by co-occurring *TP53* mutation. Interestingly, in patients with loss-of-function *STK11* mutations, there was no association between *KRAS* mutation status and either PD-L1 expression or CD8+ T-cell infiltration. Subsequent genomic analysis demonstrated that *KRAS/TP53* co-mutated tumors had a significant decrease in the expression of glycolysis-associated genes, and increase in several genes involved in lipid metabolism, notably *Lipoprotein Lipase* (*LPL*), *Low Density Lipoprotein Receptor* (*LDLR*), and *LDLRAD4*. Conversely, in the immune-excluded *KRAS/STK11* co-mutated group, we observed diminished lipid metabolism and no change in anaerobic glycolysis. Interestingly, in patients with low expression of *LPL*, *LDLR*, or *LDLRAD4*, gain-of-function *KRAS* mutations had no effect on tumor immunogenicity. However, in patients with robust expression of these genes, *KRAS* mutations were strongly associated with increased immunogenicity and associated with improved overall survival.

Conclusions: These data suggest that gain-of-function *KRAS* mutations are associated with an increase in immunogenicity, though this appears to be dependent on a corresponding increase in lipid metabolism. Our data further suggest that the loss of *STK11* may function as a metabolic switch to suppress lipid metabolism in favor of glycolysis, thereby negating KRAS-induced immunogenicity. Hence, this concept warrants continued exploration, both as a predictive biomarker and potential target for therapy in patients receiving ICI-based immunotherapy.

#7368 Sentinel omics signatures: Comparative clinical and blood sample analysis from canine mammary tumor patients and their human guardian.

K. Son[1], A.-R. Nam[1], H.-M. Park[2], H. Kim[1], J.-W. Lee[1], J.-Y. Cho[1];

[1]Seoul National University, Seoul, Korea, Republic of, [2]Korea Research Institute of Standards and Science, Daejeon, Korea, Republic of

Breast cancer remains a leading cause of morbidity and mortality worldwide, necessitating innovative approaches for early detection and intervention. This study leverages the comparative biology paradigm, exploring the shared oncological pathways between humans and canines through a unique multi-omics approach. We have gathered a diverse cohort comprising healthy dogs, canine mammary tumor patients, and their respective human guardians, collecting comprehensive clinical data alongside blood samples. Employing RNA-seq, MBD-seq, and LCMS, we aim to construct a detailed transcriptomic, methylomic, and proteomic landscape to elucidate potential sentinel biomarkers indicative of an oncogenic environment shared between species. While results are forthcoming, the premise of our research rests on the hypothesis that environmental factors contributing to mammary cancer may manifest systemically, potentially affecting both canines and humans. By delineating these interspecies molecular signatures, we hope to advance the field of precision medicine, offering insights into early detection and the systemic nature of cancer pathobiology. This abstract presents the foundation and direction of our ongoing investigation, with a commitment to providing a comprehensive update, inclusive of significant findings, at the conference.

#7369 Passenger mutations link cellular origins and transcriptional identity in human lung adenocarcinoma.

S. Panja, P. Mantri, J. A. Martinez, **M. Imielinski**;
NYU Langone Health, New York City, NY

Lineage plasticity hinders identification of cellular origin of cancers, as malignant cells cease to resemble benign cells from which they presumably evolved. Lung adenocarcinoma (LUAD), the most common primary lung cancer in United States is thought to arise from alveolar type II (AT2) cells. However recent mouse models have shown that LUADs may also arise from other cell types such as basal and club. Although such mouse models are considered to be gold standard for identifying cell of origin for cancers, they are generally limited to a specific genetic context and lack all cell types that are present in human lung. Thus, to better understand the cellular origins of LUAD, we utilized a publicly available lung scRNA-seq atlas from Human Cell Atlas, spanning over 584,000 cells from 107 individuals to investigate cell type specific passenger mutational footprints of transcriptional coupled repair process (a sub-pathway of nucleotide excision repair that preferentially corrects mutations in highly expressed genes) across 295 lung cancer WGS profiles. As most mutations in self-renewing tissues are thought to occur prior to the onset of tumorigenesis, genes that are most highly transcribed in the cell of origin would have fewer somatic single nucleotide variants (SNV). To test this hypothesis, our study correlated somatic mutational density with gene expression profiles of cell types to identify Alveolar Type 0 (AT0, newly identified cell type) cells to be most strongly associated with LUAD mutation density, suggesting that the ancestor of LUAD cells in tumor spent most of their non-cancerous time in AT0 state. Interestingly studies have shown that following DNA damage in AT2 cells, transition to AT1 occurs to repair the damage. However, if the damage is detrimental, the transition of AT2 to AT1 is stalled and the cells remain in AT0 (i.e., a transitionary) state. We propose that such stalling for a long period of time can give rise to LUAD. Further our study identified a subset of LUAD patients with non-AT2 (i.e., proximal) origin. In particular, we observed significantly higher KRAS mutations in distal origin LUAD patients compared to those in proximal origin LUADs. Finally, a subset of LUAD patients with distal cell of origin adopted a more proximal transcriptional identity. Extending our analysis to lung squamous cell carcinoma (LUSC) patients, we observed basal resting cells to be the Cell of Origin (COO) for LUSC. Our study provides a novel approach for identifying cell of origin for cancers and points to a complex interplay between origin and identify in lung adenocarcinoma evolution.

BIOINFORMATICS / COMPUTATIONAL BIOLOGY / SYSTEMS BIOLOGY / CONVERGENT SCIENCE: Artificial Intelligence and Machine/Deep Learning 4
Poster Session

#7373 Generative Bayesian networks for augmentation of molecular data from commercial genetics panels.
Dillon H. Tracy, Jeff Sherman, Maayan Baron

Zephyr AI, McLean, VA

Background: Computational models in medical research which use molecular features to predict patient sensitivities or outcomes are traditionally limited to producing a scalar output for a given disease phenotype, e.g. progression-free survival or drug response. Even for relatively intelligible models, it is generally difficult to place confidence limits on the prediction or develop an intuition for how a prediction varies with respect to “what-if” changes in those features or how sensitive a prediction is to changes in input variables. Moreover, while essential for understanding and modeling tumor behavior, molecular features from patient tumors in real-world settings are typically limited to profiles of hundreds of genes, while the biologically relevant inputs to the patient’s condition can be much larger.
Approach: To generate data required to enhance the interpretation of predictive models and extend the utility of real-world patient oncology datasets, a distribution of conditions consistent with the observed features and their incidence across cancer patient cohorts is required. We hypothesized we could synthesize patient samples drawn from the joint probability distribution of a broader universe of features when a subset of them is held fixed at the observed values. We model this joint distribution by learning a Bayesian network over a broad feature set for which some training data is available and generate feature profiles by applying Gibbs sampling to the learned network.
Results: We assessed the potential clinical utility of using these generated feature profiles in predicting drug response and enhancing biological interpretation of different model outputs. We found generative somatic mutations were useful for predicting cancer patient outcomes, including drug response predictions in breast cancer tumors from AACR Project GENIE. Synthesized patient feature profiles enhanced biological interpretability of nominal panel data (100-200 genes), providing a means to assign probabilities to outcomes and uncovering previously described mechanisms of drug response in real-world patient data.
Conclusion: We introduce an approach that leverages Bayesian networks to synthesize richly annotated patient feature profiles from limited molecular data routinely collected in real-world settings. This approach addresses challenges associated with limited molecular data, biological interpretability and evaluation of predictive models and enhances the utility of real-world datasets for cancer research.

#7374 Mathematical modeling of targeted radionuclide therapy and CAR-T cell immunotherapy for maximizing therapeutic efficacy in multiple myeloma.

V. Adhikarla[1], D. Awuah[1], E. Caserta[1], M. Minnix[1], M. Kuznetsov[1], A. Krishnan[2], J. Y. C. Wong[2], J. E. Shively[1], X. Wang[1], F. Pichiorri[1], R. C. Rockne[1]; [1]Beckman Research Institute - City of Hope, Duarte, CA, [2]City of Hope National Medical Center, Duarte, CA

Background: Resistance of cancer cells to monotherapies has led to the development of sequential or combination therapy regimens. However, dosing and scheduling of these therapies is challenging due to the numerous dosing and scheduling combinations that can be given. Mathematical models are thus critical tools for addressing this challenge as multiple therapy combinations can be tested *in silico* to finalize a patient-specific therapeutic regimen *in vivo*. Here we develop a mathematical framework for combining targeted radiation therapy (TRT) with Chimeric Antigen Receptor (CAR)-T cell immunotherapy and demonstrate the use of *in silico* techniques to schedule these therapies for maximizing survival.

Methods: In the mathematical framework tumor growth is assumed to be exponential and the effect of radiation on both tumor cells and CAR-T cells is modeled using the linear-quadratic model of cell survival to radiation. A predator-prey model is used to characterize the dynamics of tumor and CAR-T cells. Using a preclinical disseminated mouse model of multiple myeloma (MM1S), we evaluate tumor response to 200 nCi of ^{225}Ac-DOTA-Daratumumab (TRT) and 1 million cells of CS1 CAR-T cell therapy both as monotherapies as well as in combination. Tumor burden tracked using bioluminescence imaging from six groups of mice is used to calibrate model parameters: (a) No treatment. (b) Day 7 TRT. (c) Day 7 CAR-T cell therapy. (d) Day 7 TRT + Day 18 CAR-T cell therapy. (e) Day 7 TRT + Day 25 CAR-T cell therapy. (f) Day 7 TRT + Day 32 CAR-T cell therapy. Response to therapy is evaluated using progression-free survival (PFS), overall survival (OS) and time to minimum tumor burden (t_{min}), all of which are calculated using the predicted *in silico* tumor burden dynamics and the tumor burden at the start of first therapy. We evaluate these response metrics for various dosing and scheduling regimens.

Results: Therapy intervals that were too short or too long are shown to be detrimental for therapeutic efficacy. TRT too close to CAR-T cell therapy results in radiation related CAR-T cell killing, while the interval being too long results in tumor regrowth, negatively impacting tumor control and survival. If a single dose is split into multiple doses, the splitting is advantageous only if the first therapy delivered can produce a significant benefit as a monotherapy. Based on the model parameters we estimate the minimum required TRT activity and CAR-T cell dose to demonstrate an improvement in PFS.

Conclusions: The proposed model demonstrates the impact of different dosing and scheduling regimens of TRT and CAR-T therapy on survival metrics. It is a potent tool for translating preclinical results to the clinic and eventually tailor therapy regimens for patients.

#7376 Modeling the dynamics of lung cancer cells along the epithelial–mesenchymal spectrum in the stem and non-stem cell compartments.

Arianna Di Bernardo[1], Sarthak Sahoo[2], Melissa Balsamo[1], Elsa Quaranta[1], Mohit Kumar Jolly[2], Giulia Bertolini[1], Luca Roz[1]

[1]Fondazione IRCCS Istituto Nazionale dei Tumori, Milan, Italy, [2]Indian Institute of Science, Bangalore, India

Epithelial-mesenchymal transition (EMT) is a crucial biological process during development which also appears to play a fundamental role in the dissemination of cancer cells. It is known that hybrid states (H), in which cells have mixed epithelial (E) and mesenchymal (M) properties, are particularly conductive to metastasis but the possibility of seeding secondary lesions is also closely linked to the intrinsic tumor initiation potential (stemness). An overall vision taking into account both the EMT spectrum and stemness properties could therefore be the key to fully understanding the metastatic process. In this study we aim to build a mathematical model capable of describing the transitions in the EMT spectrum distinguishing stem from non-stem cell subpopulations in lung cancer cells. Using E-cadherin and N-cadherin staining we evaluated experimentally by flow-cytometry the modulation of epithelial (E), hybrid (H) and mesenchymal (M) phenotypes in A549 lung cancer cells after the induction of EMT by TGFβ treatment and subsequent return to steady state after TGFβ withdrawal. Stem and non-stem populations were identified with the previously validated CD133 marker. To mathematically describe the cellular dynamics we used a system of differential equations assuming transitions E-H, E-M and H-M, for stem and non-stem compartments initially treated as decoupled. Parameters used in the equations were the three switching rates corresponding to the three transitions allowed. To test the robustness of the model we solved the equation multiple times (500) by first stochastically changing the initial conditions and then the initial parameters, obtaining the respective parameters optimized by minimizing the residual between experimental data and model. To decouple the parameters, equations were then solved stochastically 1000 times changing two of three initial parameters, obtaining the optimized third parameter and the respective minimal residual. Parameters fitting closely the experimental data during TGFβ-mediated EMT induction were obtained, indicating that the transition from H to M appears to be absent in the non-stem population but present in the stem population, while the transition from E to M is always present. We also observed that after TGFβ withdrawal the inclusion of an epigenetic decay factor is necessary to model the latency period before MET insurgence when EMT is previously induced in the system. We can conclude that during EMTinduction, the dynamics in the non-stem compartment can be described by a bifurcation model in which population E becomes either M or H and remains permanently in that state, stressing the stability of the H state and also that E cells might have a predisposition to transform into M or H. Furthermore, a portion of H stem cells is able transform into M during EMT and therefore appears more plastic which could underscore a greater metastatic potential.

#7377 Deep learning uncovers morphological patterns of YAP1/TEAD activity related to disease aggressiveness in cancer patients.

B. Schmauch[1], V. Cabeli[1], **O. Darwiche-Domingues**[1], J.-E. Le Douget[1], A. Hardy[1], R. Belbahri[1], C. Maussion[1], A. Romagnoni[1], M. Eckstein[2], F. Fuchs[2], A. Swalduz[3], S. Lantuejoul[3], H. Crochet[3], F. Ghiringhelli[4], V. Derangere[4], C. Truntzer[4], H. Pass[5], A. Moreira[5], L. Chiriboga[5], Y. Zheng[6], M. Ozawa[6], B. Howitt[6], O. Gevaert[6], N. Girard[7], E. Rexhepaj[8], I. Valtingojer[8], L. Debussche[8], E. Durand[1], M. Classe[8], K. Von Loga[1], E. Pronier[1], M. Cesaroni[8],
[1]Owkin France, Paris, France, [2]University Hospital Erlangen, Erlangen, Germany, [3]Centre Leon Berard, Lyon, France, [4]Centre Georges-Francois Leclerc, Dijon, France, [5]New York University Langone Medical center, New York, NY, [6]Stanford university, Stanford, CA, [7]Institut Curie, Paris, France, [8]Sanofi, Paris, France

Hippo signaling emerged over the last decade as a major tumor-suppressing pathway. Its dysregulation is generally associated with abnormal expression levels of YAP1, WWTR1 (coding for the TAZ protein) and TEAD genes among others. This pathway has been shown to have a prognostic impact in several cancer types. In particular, the role of YAP1/TEAD activity across indications has been emphasized by several recent works, with potential implications on treatment options. Therefore, identifying patients with a deregulated pathway is key for a better clinical impact of the current potential therapies. Recent studies have been able to characterize RNA-seq based signatures of a deregulated Hippo pathway but a reproducible and cost-effective method to measure the activation of the pathway in clinical settings is needed. Here we first evaluate and confirm the robustness of a YAP1/TEAD activity signature recently published by Calvet et al. (RNA-based signature focused on TEAD downstream effectors), to predict the level of activity of this pathway across several cancer types available in TCGA. Our results confirmed that YAP1/TEAD activity is cancer type and subtype specific and that its high activity is correlated with poor prognosis in some of these cancers. We then trained deep learning models to predict YAP1/TEAD gene activation level, from H&E-stained histology slides in various cancer types from The Cancer Genome Atlas. We showed that histological markers associated with dysfunctional Hippo signaling are markers of disease aggressiveness and poor prognosis such as necrosis, poorly differentiated tumor, and inflammation. Altogether our results are opening the avenue of defining image-based biomarkers predictive of the YAP1/TEAD activity which could be used in clinical settings for better inclusion of subgroups of patients for targeted therapeutics against this hallmark of cancer development.

#7378 Using game theory to investigate the therapeutic potential of disrupting tumor-microenvironment interactions.

D. Van Egeren[1], A. Chen[2], M. Stoddard[3], **L. Yuan**[3], A. Chakravarty[3];
[1]Stanford University, Palo Alto, CA, [2]Columbia University, New York, NY, [3]Fractal Therapeutics, Inc., Lexington, MA

Cancer is a complex disease involving the interplay of several types of malignant and nonmalignant cells. The growth of tumors and surrounding stromal cells can be modeled as an ecosystem, where populations of cancerous and healthy cells interact and compete for resources. In this work, we have explored the application of game theoretic models of cancer to the design of novel anticancer therapies. Notably, a game theoretic-model of tumor-stromal interactions can capture the impact of interactions between cell types and can be used to investigate frequency-dependent parameters describing the impact of drug action during the initiation and growth of metastatic cancers. Previous studies using game theoretic models to describe cancer have focused on explaining progression patterns of specific tumors with known tumor-stromal interactions. This study takes a more general approach to cancer growth dynamics, modeling cancer as a simple game between healthy and cancer cells. This simplified model is used to make general predictions about cancer progression and the efficacy of treatment strategies. Our work suggests that disruption of beneficial interactions between healthy and cancer cells may be a viable treatment strategy for small tumors and preventing metastasis by ensuring that the healthy cell strategy is evolutionarily stable. The efficacy of treatment strategies that disrupt cancer cell cooperation or tumor-stromal dynamics changes as the cancer cell frequency changes. Our work suggests that drugs that target tumor-stromal cell interactions would need to be combined with other types of treatments to be effective against large tumors. Although based on a simplistic model of cancer initiation and progression, the framework derived here can be extended to the real-world design of experimental anticancer therapeutics, and fundamental analyses of this nature can be of practical utility in setting strategy for Target Product Profile design.

#7379 Deep learning based risk stratification of pre-operative CT scans is prognostic of overall survival in kidney cancers.

Brennan Flannery[1], Mohsen Hariri[1], **Thomas DeSilvio**[1], Amir Sadri[1], Jane Nguyen[2], Erick M. Remer[2], Smitha Krishnamurthi[2], Satish E. Viswanath[1]

[1]Biomedical Engineering, Case Western Reserve University, Cleveland, OH,[2]Cleveland Clinic, Cleveland, OH

Introduction: Preoperative risk stratification of kidney cancer patients is critical for treatment selection and improving mortality rates. Current clinical approaches such as cancer grading are limited by inter-reviewer variability, require invasive biopsy procedures, and might not capture the full extent of patient risk. We sought to evaluate a deep learning (DL) model to quantify patient risk and prognosticate overall survival in kidney cancer patients via CT scans.
Methods: This retrospective study used preoperative contrast CT scans from 4 public multi-institutional collections with date of death/censoring available. A deep learning (DL) network architecture was developed to analyze input CT scans via a convolutional feature extractor and a Cox proportional hazards-based cost function. The DL model assigned a risk score to each patient, with the median risk used as a cutoff for classifying patients as high-risk or low-risk. Model performance for prognosticating overall survival (OS) was evaluated separately in training, internal validation, and external validation cohorts via Kaplan-Meier analysis in terms of concordance index and hazard ratios, with risk groups compared via Wilcoxon log-rank tests ($\alpha = 0.05$).
Results: In the training/internal validation cohort (N=418, 8 institutions) and external validation cohort (N=102, 1 institution), the median age was 60 and 59 years, the male/female ratios were 62% / 38% and 75% / 25%, with a median follow up of 2.8 and 3.1 years, respectively. The DL model yielded a training c-index of 0.66 (95% CI: 0.63-0.68), internal validation c-index of 0.73 (95% CI: 0.70-0.76) and an external validation c-index of 0.67 (95% CI: 0.64-0.70). Kaplan-Meier analysis of associated survival curves based on DL-determined high- and low-risk patients demonstrated statistically significant separation in all cohorts: training ($p = 0.003$, HR = 8.63, 95% CI: 8.28-8.98), internal validation ($p = 0.027$, HR = 4.89, 95% CI: 4.52-5.26), and external validation ($p = 0.01$, HR = 6.54, 95% CI: 6.18-6.90). Baseline clinicopathological characteristics were not significantly different between DL high and low risk patients in external validation (chi-square testing; ISUP grade $p=0.375$, age $p=0.824$, race $p=0.567$, and sex $p=0.440$). ISUP grade was also not a significant predictor of OS in internal validation (HR=1.57, $p=0.211$, 95% CI: 1.28-1.85) or external validation ($p = 0.465$, HR=0.16, 95% CI: 0.33-0.74).
Conclusion: A deep learning model based on pre-operative CT scans was found to accurately prognosticate overall survival in kidney cancers in a multi-institutional setting, independent of clinicopathological factors. This model is being validated on larger cohorts, and in the context of targeted therapies.

#7380 Predicting immunotherapy outcomes from H&E images in lung cancer.

J. Loo[1], Y. Wang[1], P. Wong[1], E. Wulczyn[2], J. Lai[2], P. Cimermancic[1], D. F. Steiner[2], S. S. Weaver[1];
[1]Verily Life Sciences, South San Francisco, CA, [2]Google, Mountain View, CA

Checkpoint blockade immunotherapy is a cornerstone of lung cancer treatment, but there is a need to improve the identification of patients who will respond favorably. Here, we explored a deep learning approach to predict immunotherapy outcomes from hematoxylin and eosin (H&E) images in non-small cell lung cancer (NSCLC). We included 150 unique cases with metastatic NSCLC (113 adenocarcinoma, 29 squamous cell, 8 other) treated with anti-PD-1/PD-L1 immunotherapy (56 nivolumab, 49 atezolizumab, 44 pembrolizumab, 1 durvalumab) as mono or combination (14 with chemotherapy, 1 with ipilimumab) therapy in a single institution. Each case consisted of a representative H&E whole slide image (53 biopsies, 50 needle core biopsies, 47 resections) obtained prior to immunotherapy, and the outcome reported as the 1-year overall survival (OS). PD-L1 status (tumor proportion score ≥ 1%) was known for 70 cases. We preprocessed the H&E images using two deep learning models previously developed using The Cancer Genome Atlas dataset. First, we used a classification model to identify tumor regions and randomly sampled a fixed number of tumor patches for each case. Then, we used a self-supervised pathology foundation model to obtain a compressed visual representation of each patch, known as an embedding. Next, using our dataset, we trained a deep multiple instance learning (DeepMIL) model with a gated attention mechanism to predict the binary 1-year OS status (0=deceased, 1=alive) for each case. As a baseline, we also trained a linear-probe (logistic regression) model using the averaged embeddings. Given the small dataset size, 5-fold cross-validation was used to train and evaluate both the DeepMIL and linear-probe models, with cases randomly split across folds. For evaluation, we used survival analysis to compare the 0/1 case groups. Overall, across all 150 cases, univariable Cox regression showed that 1-year OS was more strongly associated with the DeepMIL status (46/104, HR=0.55, p=0.03) than the linear-probe status (55/95, HR=0.81, p=0.44). Results were consistent on the subset of 70 cases with known PD-L1 status, whereby OS was most strongly associated with the DeepMIL status (19/51, HR=0.40, p=0.04) compared to the linear-probe status (31/39, HR=0.46, p=0.09) and PD-L1 status (30/40, HR=0.65, p=0.32). In multivariable Cox regression adjusting for age group and smoking status, OS remained more strongly associated with the DeepMIL status (HR=0.45, p=0.08) than PD-L1 status (HR=0.72, p=0.47). In conclusion, the DeepMIL status predicted from H&E images showed a stronger association with outcomes compared to PD-L1 status, a standard biomarker for immunotherapy in NSCLC. These exploratory results demonstrate the potential of deep learning using pathology foundation models to improve immunotherapy outcomes prediction, even with small datasets. Such approaches may even enable the discovery of novel biomarkers from H&E images to advance precision medicine.

#7381 Mathematical modeling and validation of mechanistic target of rapamycin and N-myristoyltransferase signaling pathways in breast cancer.

A. Meher[1], S. Varma Shrivastav[2], A. Agarwal[1], S. Dube[1], S. Portet[3], A. Shrivastav[1];

[1]The University of Winnipeg, Winnipeg, MB, Canada, [2]Oncodrex Inc, Winnipeg, MB, Canada, [3]University of Manitoba, Winnipeg, MB, Canada

Hormone receptor-positive (HR+) breast cancer (BC) makes up approximately 65% of all breast cancers diagnosed. The prognosis for early-stage disease is excellent with mainstay endocrine therapy (ET). Despite the effectiveness of standard ET, as many as 41% of HR+ early-stage BC diagnosed women will experience distant recurrence. The resistance to endocrine therapy and recurrence is partly attributed to the activation of the insulin pathway and the independence of HR+ BC cells on the ER pathway for their growth. Earlier, we demonstrated the crosstalk between insulin/mTOR and ER pathways. N-myristoyltransferase (NMT) exists in humans in two paralogues (NMT1 and NMT2) that catalyze myristoylation reaction. Recent studies from our laboratory demonstrated that NMTs are downstream targets of insulin and ER pathways. In this study, we have designed mathematical models using differential equations to study the activation of the insulin pathway and its effect on NMT. The mathematical modeling incorporated the partition of cellular organelles and the sequential flow of information with cascades of equations representing signaling reactions. The activated mathematical model was designed by activating the insulin receptor (IR) or insulin-like growth factor receptor (IGF1R) and compared with the control model. The mathematical models were validated by wet lab experiments. The HR+ BC cells (MCF7) were treated with insulin or IGF1 for short term and long term. The expression patterns of NMT1, NMT2, and mTOR were determined by cell fractionation and western blot analysis. The results revealed the correlation between the differential expression patterns of NMTs and the proliferation of MCF7 cells when the insulin pathway was activated by insulin or IGF. The mathematical modeling was validated by simulations and data fittings. The results demonstrated that differential equation-based mathematical modeling could predict the NMT-related oncogenic changes in HR+ BC cells.

#7382 Artificial intelligence derived features of collagen architecture identify high risk HPV associated oropharyngeal squamous cell carcinoma patients.

R. Nag[1], H. Li[2], G. Corredor[1], P. Fu[2], N. F. Saba[1], M. A. Bilen[1], T. Pathak[1], P. Toro[3], M. Mokhtari[2], K. Pandav[1], M. Gilkey[1], S. Koyfman[3], D. Chute[3], W. L. Thorstad[4], M. Mehrad[5], P. D. Castro[6], A. G. Sikora[7], R. D. Chernock[4], J. Luo[4], M. Frederick[6], V. Sandulache[6], D. J. Adelstein[3], J. Lewis Jr.[5], A. Madabhushi[1]; [1]Emory University, Atlanta, GA, [2]Case Western Reserve University, Cleveland, OH, [3]Cleveland Clinic, Cleveland, OH, [4]Washington University, St. Louis, MO, [5]Vanderbilt University Medical Center, Nashville, TN, [6]Baylor College of Medicine, Houston, TX, [7]The University of Texas MD Anderson Cancer Center, Houston, TX

Introduction: Human papilloma virus (HPV) induced oropharyngeal squamous cell carcinoma (OPSCC) is a common subtype of head and neck carcinoma. Dysregulation of the extracellular matrix (ECM), an important part of the tumor microenvironment (TME), is shown in HPV related cancers. We studied collagen fibers (CF), the amplest component of the ECM, and evaluated whether their characteristics within the TME can offer a prognostic value in OPSCC.

Methods: Whole slide images (WSIs) of OPSCC patients were obtained from Washington University (WU, n=107), Houston Veterans Administration Hospital (HV, n=94), Cleveland Clinic (CC, n=336), John Hopkins University (JH, n=121) and Vanderbilt Medical Centre (VM, n=158). For the identified CF in tumor-stroma regions of WSIs, the extracted CF features included: CF fragmentation measure, CF bundling percentage, CF rigidity measure, CF anisotropy index, and CF density index. For survival analysis using overall survival (OS) and Disease-Free Survival (DFS) as endpoints, the median risk score in the training set (WU) was applied for risk stratification in the validation sets (HV, CC, JH, VM) by means of a Least Absolute Shrinkage and Selection Operator-Cox regression model. Multivariable Cox Proportional Hazards Regression was done for both OS and DFS.

Results: The patients defined as “high risk” had worse OS than those identified as “low risk” (HV(p=0.03), CC(p=0.03), JH(p=0.02), VM(p=0.04)). Multivariable analysis showed that CF features were prognostic independent of T/N stages, age, sex, and smoking status with HR=1.99 (95% CI=1.46-2.72, p=0.00001) for OS and HR=1.73 (95% CI=1.21-247, p=0.002) for DFS (Table 1).

Conclusion: Artificial intelligence derived features of CF architecture can help identify high vs low risk patients in HPV related OPSCC. These findings deserve further confirmation in larger prospectively collected OPSCC data sets and could impact future treatment paradigms.

Table 1: Multivariable Survival Analysis for OS and DFS, HR=Hazard Ratio, CI=Confidence Interval

Variable	**Overall Survival**		**Disease Free Survival**	
	HR (95% CI)	**P value**	**HR (95% CI)**	**P value**
Age (<65 years vs. >=65 years)	0.99 (0.93-1.06)	0.78444	0.96 (0.82-1.12)	0.62864
Sex (Female vs. Male)	0.56 (0.29-1.10)	0.09042	0.50 (0.22-1.13)	0.09385
Smoking status (Yes vs. No)	1.85 (1.31-2.62)	0.00051	1.03 (0.72-1.47)	0.86871
T-stage (T3/4 vs T1/2)	**1.86 (1.38-2.50)**	**0.00004**	**1.91 (1.36-2.69)**	**0.00018**
N-stage (N+ vs N0)	**1.76 (1.31-2.37)**	**0.00016**	**2.04 (1.46-2.86)**	**0.00003**
Collagen fiber features (High risk vs low risk)	**1.99 (1.46-2.72)**	**0.00001**	**1.73 (1.21-2.47)**	**0.00286**

#7383 G2PT: Mechanistic genotype-phenotype translation using hierarchical transformers.

I. Lee[1], S. Park[1], H. Nam[2], T. Ideker[1];

[1]University of California San Diego - UCSD, La Jolla, CA, [2]Gwangju Institute of Science and Technology, Gwangju, Korea, Republic of

Motivation: Many machine learning models have been proposed that use genotypes to predict various phenotypes. Recently, these models have focused not only on an accurate prediction but mechanistic interpretation, in that they attempt to describe the hierarchy of biological systems underlying the predicted phenotype. Such models still face major challenges, however, including how to robustly quantify the importance of systems mediating phenotypic outcomes and how to represent the bidirectional flow of information among genes, systems, phenotypes, and cell environment.

Results: To address these challenges we introduce G2PT, a general Genotype-to-Phenotype Transformer, which we apply here to the classic G2P problem of modeling tumor cell sensitivity to drugs. We show that the framework of hierarchical transformers can represent biological systems spanning a wide range of physical scales and provide a quantitative assessment of the interplay between biological components important for phenotype prediction. When used to analyze a high-throughput cell screen of 436 drugs exposed to 1,097 cell types, we show that the model achieves good performance in predicting cell sensitivity for 83% of drugs ($\rho > 0.5$ in cross-validation). G2PT provides a robust and interpretable model with potential application to many challenges in genotype-phenotype translation.

#7384 Regulation of phosphorylated VGLL1 by the positively charged binding pocket on the surface of TEAD4.

J. Choi[1], H. Le[2], Y. Park[2], Y. Yun[2], J. Kim[2], J. Wilianto[2], N. Shadiev[2], C. Sung[2], B. Ku[3], K.-Y. Chang[4], M. Won[5];
[1]Department of Bio AI Convergence, Chungnam National University, Daejeon, Korea, Republic of, [2]Calici Co., Ltd., Daejeon, Korea, Republic of, [3]Disease Target Structure Research Center, Korea Research Institute of Bioscience & Biotechnology (KRIBB), Daejeon, Korea, Republic of, [4]OneCureGEN Co., Ltd., Daejeon, Korea, Republic of, [5]Personalized Genomic Research Center, Korea Research Institute of Bioscience & Biotechnology (KRIBB), Daejeon, Korea, Republic of

Vestigial-like 1 (VGLL1) is a transcriptional co-activator that binds to TEA domain-containing transcription factors (TEADs), regulating hippo pathway. High expression of VGLL1 is associated with gastric cancer, breast cancer, and pancreatic cancers. VGLL1 is transcriptionally regulated by PI3K/β-catenin signaling and is phosphorylated by ribosomal S6 kinase 2 (RSK2) in the presence of TGF-β. It is clear that phosphorylation at S84 of the VGLL1 protein is critical for its interaction with TEAD4 to express their target genes involved in the proliferation and metastasis of cancer cells. In the isothermal titration calorimetry study, we observed S84-phosphorylated VGLL1 peptide bound to TEAD4. However, it is difficult to understand structure-based molecular mechanism of the phosphorylated VGLL1 at S84 due to lack of the detailed human VGLL1-TEAD4 complex structure for rational drug design. In this study, we modeled full-length human VGLL1-TEAD4 or YAP1-TEAD4 complexes and performed MMPBSA calculations or Kd/Ki predictions followed by MD simulations using Pharmaco-Net's CNN-based artificial intelligence model. Our study suggests that a positively charged binding pocket on the surface of TEAD4 can regulate interaction between Trp243 from YAP1 and phosphorylated-Ser84 from VGLL1. The newly identified binding pocket is composed of Lys297, Val414, and Tyr429, which can interact with phosphorylated Ser84 residue and maintain Omega loop-like structure shown in YAP1-TEAD4 complex. The computed binding energy for phosphorylated-VGLL1-TEAD was -134.80 +/- 8.20 Kcal/mol which was a similar binding energy to YAP1-TEAD4 complex. In addition, global peptide docking using S84-containing-VGLL1 peptide (SCVP) indicated that SCVP can bind to the same binding pocket with average 1.39 μM. This suggested that there could be a novel therapeutic approach targeting this interaction with SCVP, an agent that seems to mimic phosphor-VGLL1 interaction and thus demonstrates promise as a potential therapeutic intervention. Nevertheless, further experimental verification and clinical investigations are needed to validate these innovative findings.

#7385 Explainable AI model incorporating uncertainty estimation for enhanced MSI-H prediction and immunotherapy response in gastrointestinal cancer.

S. Park[1], M. Kim[1], J.-Y. Sung[2], J. Park[3], S. Lee[4], S. C. Wang[5], J. Cheong[6], T. Hwang[1];
[1]Mayo Clinic, Jacksonville, FL, [2]Kyung Hee University Hospital, Kyung Hee University College of Medicine, Seoul, Korea, Republic of, [3]Seoul National University Boramae Medical Center, Seoul, Korea, Republic of, [4]College of medicine, the Catholic university of Korea, Seoul, Korea, Republic of, [5]University of Texas Southwestern Medical Center, Dallas, TX, [6]Yonsei University College of Medicine, Seoul, Korea, Republic of

Background: Microsatellite instability-high (MSI-H) tumors respond well to immune checkpoint blockade and oftentimes not to chemotherapeutics. Despite value of determining MSI status to guide therapy, many patients' samples are not untested. Deep learning models may be able to predict MSI status by analyzing hematoxylin and eosin (H&E) stained whole-slide images (WSIs). Validation of this tool will provide another tool to increase MSI testing. However, to be deployed into clinical routine care, prediction models need be externally validated in large and diverse patient cohorts. In addition, these models should provide uncertainty of prediction to help clinicians make informed decisions.

Results: In this study, we introduce a novel Bayesian prediction model using whole-slide images (WSIs) and deep Gaussian processes (DGPs) in a weakly supervised learning context. Extensively tested on large datasets (n=3,146) from multiple centers, our model not only demonstrated superior performance but also showed that incorporating uncertainty into predictions significantly improves MSI prediction accuracy, achieving AUROC of >0.91 in colon cancer and >0.94 in gastric cancer. Additionally, an in-depth analysis within the gastric cancer cohort indicated a significant correlation between predicted MSI-H regions and immunotherapy response. Patients who responded to immune checkpoint inhibitors had a higher proportion of MSI-H regions (P-value < 0.05). This correlation was also observed in patients categorized as MSS but responsive to ICIs, highlighting the potential of our model to identify MSI-H patterns not detected through standard laboratory tests. This advancement could lead to more precise patient selection for ICI therapy, enhancing personalized treatment strategies in gastrointestinal cancer.

#7386 Multi-plane rectal tumor segmentation on pre-treatment MRI via human-in-the-loop deep learning.

Michael Kong[1], **Thomas DeSilvio**[1], Leo Bao[1], Brennan Flannery[1], Benjamin N. Parker[1], Stephen Tang[1], Gregory O'Connor[2], Amit Gupta[2], Emily Steinhagen[2], Andrei S. Purysko[3], Eric L. Marderstein[4], Aaron Carroll[5], Marka Crittenden[6], Michael Gough[5], Kristina Young[6], Satish E. Viswanath[1]

[1]Biomedical Engineering, Case Western Reserve University, Cleveland, OH,[2]University Hospitals Cleveland Medical Center, Cleveland, OH,[3]Cleveland Clinic Foundation, Cleveland, OH,[4]Northeast Ohio Veterans Affairs Medical Center, Cleveland, OH,[5]Providence Cancer Center, Portland, OR,[6]Earle A. Chiles Research Institute, Portland, OR

Introduction: Precise segmentation of rectal tumors on pre-treatment MRI is critical for in vivo clinical staging and treatment selection. While automated deep learning models can help alleviate laborious manual annotation, these require significant expertise and time commitment. Towards addressing these issues, we present initial results of an integrated human-in-the-loop refinement learning model for semi-automated segmentation of rectal tumors across multiple acquisition planes (axial, coronal) on pre-treatment MRI scans.

Methods: This retrospective study accrued baseline MRI scans from rectal cancer patients at four different institutions. A deep learning (DL) nnUNet tumor segmentation model was first trained on both axial plane and coronal plane T2w MRIs from two institutions, with segregated training and internal validation cohorts based on available radiologist annotations. The DL model outputs tumor delineations on both axial and coronal MRI scans in a separate human-in-the-loop (HITL) optimization cohort. Two rounds of HITL refinement learning were then conducted, where in each round model-generated segmentations were refined by two novice radiology readers. Refined annotations were then used to re-optimize the nnUnet model to yield final tumor segmentations. Model-generated segmentations were evaluated before HITL as well as after each round of HITL against “ground truth” radiologist annotations obtained for an external validation cohort, with performance quantified via dice similarity coefficient (DSC) as well as time taken for human annotation of MRIs. Statistical significance was determined via Wilcoxon rank-sum testing.

Results: A total of 381 MRI scans from 231 rectal cancer patients were considered. After one round of HITL refinement, DL-based segmentations yielded the best overall performance on the external validation cohort (N=20, two institutions) for both axial (DSC = 0.76) and coronal scans (DSC=0.75). A second round of HITL refinement did not yield significantly different model performance. By comparison, the pre-HITL DL segmentation model yielded significantly worse performance on both axial (DSC=0.60, p=0.0362) and coronal (DSC=0.62, p=0.0186) MRI scans. HITL refinement for rectal tumor annotation was also found to significantly improve reader efficiency by requiring only 18 minutes/scan compared to manual “ground truth” de novo annotations which took up to 38 minutes/scan (p<0.001).

Conclusion: Human-in-the-loop deep learning models can help generate accurate rectal tumor segmentations on pre-treatment MRI scans across both axial and coronal acquisition planes. Improvements to model generalizability, model efficacy, and reader efficiency suggest the potential for HITL-based semi-automated segmentation schemes for other medical imaging tasks.

#7387 Fully automated segmentation and volumetric measurement of intracranial meningioma using deep learning.

H. Kang[1], J. N. Witanto[2], K. Pratama[2], D. Lee[2], K. Choi[3], S. Choi[3], M.-S. Kim[3], J. Kim[3], Y. Kim[3], S. Park[2], C.-K. Park[3];

[1]Seoul National University Bundang Hospital, Seongnam-si, Korea, Republic of, [2]MEDICALIP Co. Ltd, Seoul, Korea, Republic of, [3]Seoul National University Hospital, Seoul, Korea, Republic of

Most intracranial meningiomas are small, asymptomatic, and incidentally found tumors. Since the growth of meningioma is the principal indication of treatment, accurate and rapid measurement of the volume of intracranial meningiomas is essential in clinical practice to determine the growth rate of the tumor. It could be useful for the management of meningiomas given their increasing incidence and the wait-and-see policy currently in use for asymptomatic meningiomas. The aim of this study was to develop and validate a computational model for fully automated meningioma segmentation and volume measurement on contrast-enhanced MR scans using deep learning.

The retrospectively collected axial contrast-enhanced T1-weighted section images from patients diagnosed with meningioma were manually segmented and used to construct automatic segmentation models with six U-Net- and nnU-Net-based architectures. The performance of each model was evaluated with the Sørensen-Dice similarity coefficient (DSC) with internal (IVS) and external validation sets (EVS), each consisting of 100 independent MRI examinations.

A total of 12,909 section images from 459 patients were applied for the training (median age 58 [52-66] [IQR]; 385 women [83.9%]). The median tumor volume of the training set was 2.36 cm^3. A 2D nnU-Net showed the highest median DSCs of 0.922 and 0.893 for the IVS and EVS, respectively. The nnU-Nets achieved superior performance in meningioma segmentation than the U-Nets. The DSCs of the 2D nnU-Net for small meningiomas less than 1 cm^3 were 0.769 and 0.780 with the IVS and EVS, respectively.

We successfully developed a fully automated and accurate volumetric measurement tool for meningioma using nnU-Net. The volumetry performance for small meningioma was significantly better than that achieved in previous studies. The results of this study are clinically applicable and are expected to be of great use in the management of monitored meningioma patients.

#7388 Deep learning-implemented molecular signature identification in vascular malignancies.

D. Lee, H. Heo, J. Kim, J. Kim;
University of Florida, Gainesville, FL

Angiosarcoma is a rare, aggressive sarcoma that forms malignant endothelium. Naturally occurring angiosarcoma in domestic dogs, also called hemangiosarcoma, is relatively common and offer a useful translational model for the rare human cancer. Distinct molecular subtypes of angiosarcoma have been identified; however, current methods are cost-prohibitive and time-consuming, posing challenges in the development of clinical applications. In this study, we hypothesize that artificial intelligence enables reliable image-based diagnostics and molecular characterization specific to angiosarcoma. The aims of our work are to develop a deep learning framework to provide diagnostic support for suspicious malignant cases, to detect morphological features associated with oncogenic mutations, and to identify immune phenotypes in this malignancy. For proof-of-concept and feasibility study, we first utilized convolutional neural network models to identify malignant features in angiosarcomas. We curated 4,079 images of hematoxylin and eosin (H&E) stained slides from seventy visceral angiosarcomas and 3,536 images of thirty splenic hematomas as benign controls obtained from client-owned dogs. ResNet-50 and AlexNet were trained on the images, and area under the receiver operating characteristic curve (AUC) was determined for disease classification. ResNet-50 and AlexNet yielded AUCs of 0.999 and 0.998, respectively. Next, we calculated the gradient of the model's prediction and applied it to the original image using Grad-CAM software. Grad-CAM results revealed that AlexNet highlighted histological regions representing malignant cellular components for decision-making, aligning with the pathological diagnostic context. In addition, we applied ResNet-50 to determine if the model could predict morphological features in angiosarcoma tissues representing the presence of *PIK3CA* mutation. We employed RNA-seq data to annotate *PIK3CA* mutation status on the matched histological images. Among 54 cases annotated with *PIK3CA* mutation status, 2,732 *PIK3CA* wild-type and 664 mutant tumor images were trained by ResNet-50. Our model demonstrated an AUC of 0.981 in the prediction of *PIK3CA* mutation. We further defined immunophenotypic groups using *xCell* algorithms on RNA-seq data, and immune scores were applied to histological images. ResNet-50 model resulted in an AUC of 0.953 to classify immune-high and immune-low angiosarcomas. RNA-seq datasets generated from 13 human angiosarcoma cases exist in our lab, along with the respective H&E slides. We also have immunohistochemical slides available for p53, phospho-p53 (Ser15 and Ser20), AKT, and phospho-AKT (Thr308) proteins conducted in both human and canine angiosarcoma tissues. Our ongoing work involves generating whole-slide images of H&E stains and immunostained slides to enhance the deep learning models for the molecular classification of angiosarcomas.

#7390 Learning Llama Agents for medical record analysis and standardization.

D. Hein[1], A. Christie[1], H. Zhong[2], E. Araj[1], J. Brugarolas[1], L. Cowell[1], P. Kapur[1], A. Jamieson[1];
[1]University of Texas Southwestern Medical Center, Dallas, TX, [2]Lyda Hill Department of Bioinformatics, Dallas, TX

Introduction: The purpose of this study is to develop custom, open source, LLM enabled pipelines and agents for the extraction and standardization of data from free text medical records.

Procedures: This project aims to create a versatile tool for healthcare data analysis, with initial development utilizing our extensive collection (over 10,000 documents) of renal cell carcinoma pathology reports. These reports are an ideal starting point as they cover over 20 years of care and consist of a racially and ethnically diverse cohort with over a quarter of patients being from traditionally underrepresented backgrounds. The jargon-abundant and highly technical nature of kidney cancer pathology represents a major challenge. We will accomplish this objective using an approach that balances the harnessing advanced AI capabilities with ensuring practicality and efficiency in real-world applications. First, we will leverage the capabilities of GPT-3.5/4 to generate a comprehensive labeled dataset (referred to as pseudo labels - machine-applied labels that will be used for training a newmodel) tailored for pathology, radiology, and clinician reports of kidney cancer patients. Second, we will harness the pseudo labeled datasets to train a smaller, open-source, yet highly efficient model for our specific needs (termed model distillation). LLAMA 2, known for its high performance in diverse tasks, is our model of choice. Its open-source nature and relatively modest computational requirements make it ideal for deployment within medical institutions. The ability to run locally ensures the protection of patient health information and reduces reliance on costlier, proprietary models. The rationale is threefold: first, to benefit from the superior performance and reasoning capabilities of GPT models; second, to create a streamlined model that is resource-efficient and tailored to our specific requirements; third, to enable the final streamlined model to be freely available by utilizing open source LLMs (e.g., Llama 2). To assess the feasibility of our methodology, we evaluated the ability of GPT-3.5 to label our data with high accuracy.

Data Summary: Our pilot set of pathology reports consisted of 109 documents and 3 extraction fields: histology type, biopsy site, and biopsy procedure. Using GPT 3.5 we achieved an accuracy of over 95% in each extracted field type thereby demonstrating its ability to act as a proficient “teacher” model for our future open source “student” model.

Conclusions: Our preliminary results suggest that current state of the art LLMs are highly proficient in extracting and standardizing information from clinical reports. Building out a full, open source, LLM enabled pipeline will increase the accuracy, flexibility, and efficiency of medical data extraction across institutions and lead to quicker and more informed decision-making in patient care and research.

#7391 Beyond traditional staining: A virtual-IHC digital assay for HER2 score prediction from routine H&E images.

M. Naderi[1], N. Mitic[1], N. Spasic[1], D. Cikic[1], K. Ruf[1], N. Wagner[1], I. Mihajlovic[1], S. Todorovic[1], R. Jenoski[2], S. Mayer[2], M. Quick[2], C. Weston[1];
[1]Reveal Biosciences Inc., San Diego, CA, [2]Hologic Inc., Marlborough, MA

Background: In breast cancer diagnostics, the accurate assessment of HER2 status is essential for treatment stratification. Conventionally, HER2 immunohistochemistry (IHC) scoring necessitates specialized staining protocols, which are resource- and time-intensive. This study presents a virtual IHC (vIHC) digital assay to predict HER2 scores directly from hematoxylin and eosin (H&E) stained images, which are routinely acquired for all specimens. This methodology aims to accelerate standard practices by reducing the need for additional IHC staining, thereby decreasing laboratory workload, costs, and turnaround time. It also presents an opportunity to screen a wider array of samples promptly, potentially identifying candidates for HER2-targeted therapy that might otherwise be delayed or overlooked.

Methods: Serially sectioned breast core needle biopsy samples were stained with H&E and HER2-IHC following Leica-Bond staining protocols. Stained slides were imaged using the Hologic Genius™ Digital Diagnostics System with Research Use Only software for Whole Slide Imaging. From this initial image dataset, 240 regions of interest (ROIs) were manually selected in order to create a dataset that uniformly covers: (i) all HER2-IHC scores (0-3), (ii) a wide range of HER2 stain intensities, and (iii) expression patterns. The IHC scores were assigned to each selected ROI by a pathology expert, following the scoring recommendations of ASCO/CAP American Society of Clinical Oncology and College of American Pathologists, with the caveat that ductal carcinoma in situ was also given a score for the purpose of training the model. These ROIs were then extracted from the images of the serially sectioned H&E-stained slides using Reveal Bio's proprietary co-registration digital assay.

A predictive digital assay was developed at Reveal Biosciences to classify the 240 H&E-stained breast tissue ROIs into four HER2 IHC score categories: 0, 1, 2, and 3. For model evaluation, cross-validation was performed 10 times by randomly splitting the dataset of H&E ROIs into 80% for training MIL and 20% for testing the model, followed by averaging the performance metrics across the 10 dataset splits. The performance metrics included classification accuracy, precision, recall, and F1 scores for each HER2 score category.

Results: The vIHC digital assay for predicting the HER2 scores directly from H&E stained breast tissue images achieved the average classification accuracy of 93% across the four HER2 score categories on the test set of ROIs. This performance demonstrates that the model is capable of successfully distinguishing between the HER2 score categories directly from H&E images without the need for IHC staining. The results suggest that the vIHC digital assay could be a reliable and cost-effective tool for preliminary breast cancer screening, providing a valuable adjunct to traditional histopathological analysis.

#7392 Machine learning-based identification of H&E-derived morphologic features associated with CD8+ T cell immune exclusion.

Y. Wang[1], F. D. Gootkind[1], F. Peyraud[2], J.-P. Guegan[3], A. Italiano[2], G. T. Clifton[1], L. A. Dillon[1], X. Sher[1];
[1]Incendia Therapeutics, Boston, MA, [2]Institut Bergonie, Bordeaux, France, [3]Explicyte Immuno-Oncology, Bordeaux, France

Background: Immune exclusion is characterized by a predominance of CD8+ T cells in the stroma of the tumor microenvironment (TME) which are not in contact with tumor cells. Immune exclusion is a significant obstacle to effective cancer immunotherapy and reversing it has emerged as a new therapeutic opportunity. However, the objective assessment of immune exclusion remains a challenge due to the complexity of the TME and the need for immunostaining to quantify CD8+ cells in tumor and stroma. While artificial intelligence (AI) models applied to H&E images can quantify spatial tissue and cell features at scale, they are unable to identify the molecular subtypes of cells. Here we describe the development of a machine learning model that classifies tumors by their CD8-defined immune phenotypes using features extracted from H&E whole slide images alone.

Methods: AI-powered TME models (PathAI PathExplore™) were deployed on H&E images from 39 non-small lung cancer (NSCLC) and triple-negative breast cancer (TNBC) samples. CD8-based assessment of immune phenotypes was done using an adjacent section. 115 H&E-derived features from each of the 25 tumor samples (12 NSCLC, 13 TNBC) classified as immune excluded and 7 tumor samples (3 NSCLC, 4 TNBC) classified as immune infiltrated were used as input into a feature selection process to identify the subset of H&E features predictive of immune phenotype. The feature selection process was driven by an ensemble L1 norm support vector machine (Ens-L1-SVM) model containing 500 L1-SVM base models each trained by 80% of the data. The degree of immune exclusion was determined in the feature space by the distance to the separation hyperplane defined by the model. Out-of-bag error estimation was employed on the remaining 20% of data from each base model to assess model performance.

Results: The Ens-L1-SVM model identified 6 H&E features predictive of CD8-defined immune phenotypes, including the density ratio of lymphocytes to macrophages in the cancer epithelium, the density of fibroblasts, and the spatial distributions of cancer cells, macrophages, and lymphocytes. Immune phenotypes were classified by the Ens-L1-SVM model with an estimated accuracy of 97%. Additionally, all selected features and their direction of association aligned with prior knowledge of the mechanisms or manifestations of immune exclusion or infiltration in the TME.

Conclusion: This work illustrated that morphologic features derived from H&E images using AI-powered models can be effective predictors of CD8-defined immune exclusion, providing an option for patient stratification by immune phenotype using widely-available H&E images. While the Ens-L1-SVM model showed robust performance on a small number of samples and is expected to have good generalizability due to the linear nature of the model, additional validation across diverse datasets and various tumor indications is needed.

#7393 Tumor model to tumor treatment: Applying deep learning approaches to map multimodal data from cancer model systems to patients.

B. Karlberg[1], R. Kirchgaessner[1], J. R. Jacobson[2], K. Ellrott[1], S. J. Gosline[2];
[1]OHSU, Portland, OR, [2]Pacific Northwest National Laboratory, Seattle, WA

Despite large-scale efforts to measure the effect of drug screens in cancer cell lines, mapping the effects of drugs to patient samples has been a challenge. Biological differences between cell lines and patients, such as lack of immune system or microbiome, *in-vitro* survival adaptations, and biases in measurement technologies create differences across sample modalities that can confound analysis including prediction with machine learning. In this work, we propose a multiway batch correction strategy to enable algorithmic prediction of tumor drug response across model systems and patient data.Recent advances in batch correction algorithms have been motivated by the need to correct for batch effects in single-cell omics and include diverse approaches such as variational autoencoders (VAEs) and generative adversarial networks (GANs). Given the successes of these generative deep learning methods in single cell sequencing analysis, we worked to employ similar approaches to correct large omics measurements across various cancer datasets. Here, we describe mapping of datasets from diverse data sources and model systems to the same space, so that a predictive model of drug response built in a system such as cell lines can be used in biologically relevant models such as organoids, patient derived xenografts, and tumor data. Specifically, we introduce a modified loss function in a VAE using cosine similarity distance to minimize the effect of different cancer model systems in predicting cancer types. We evaluate the method on standard data types for drug response prediction - gene expression, copy number variation, and protein abundance. For this method, the cosine similarity is added as an additional term to the VAE reconstruction and Kullback-Leibler divergence loss terms. This injects a quantification of the dissimilarity between the tumor and tumor model distributions into the backpropagation and gradient descent for updating the model parameters resulting in an encoded representation of the data where the effect of data source has been attenuated while preserving the phenotypic signal. We evaluate our approach for biological signal preservation while reducing model system-specific noise with logistic regression and Euclidean distance. Our results show that the proposed VAE can effectively correct for platform effects and improve the accuracy of downstream integrative analyses. This study has the potential to improve the accuracy and translatability of proteogenomic drug response studies. The proposed modified VAE could be used to correct for platform effects in a variety of datasets, including those from different studies, different platforms, and different cancer types. This could lead to new insights into cancer biology, calibration of cancer patient digital twins, and the development of new diagnostic and therapeutic strategies.

#7394 Delineating spatial expression signatures of lung adenocarcinoma subtypes from spatial single-cell transcriptomics using graph neural networks.

A. Das[1], M. Hasib[1], Z. Liu[1], W. Meng[1], Y.-C. Chiu[1], G. Sica[2], S.-J. Gao[1];
[1]University of Pittsburgh Medical Center, Hillman Cancer Center, Pittsburgh, PA, [2]University of Pittsburgh Medical Center, Pittsburgh, PA

Lung Adenocarcinoma (LUAD) subtypes including complex acinar (CA), micropapillary, and solid regions are characterized by distinct morphological and biological features that bear significant implications for prognosis and treatment strategies. While histology-based subtype prediction has provided a structural understanding, it overlooks crucial biological insights related to molecular mechanisms and the influences of tumor microenvironments (TMEs). Recent advances in spatially resolved single-cell profiling enable precise measurements of gene expression at the cellular and sub-cellular levels within intact tissues. We hypothesize that spatial gene expression (SGE) patterns can effectively identify LUAD subtypes and characterize the influence of TMEs. Thus, to address the limitations of histology-based subtyping of LUAD, we developed an AI-driven approach that leverages SMI samples to predict LUAD subtypes and elucidate their underlying molecular landscape and associated TMEs.

For this study, we leverage the NanoString CosMx Spatial Molecular Imaging (SMI) NSCLC FFPE datasets comprising of 8 LUAD tissue samples, annotated by pathologists at UPMC for subtype identification. The dataset consists of approximately 98k cells per sample with 18 cell types and 960 genes per cell. We encoded the spatial organization of cells as a graph with nodes representing cells with expression features and edges based on k-nearest neighbors of 30 cells. We considered the prediction of micropapillary, CA, and solid for each tumor cell and developed a Graph Convolutional Network (GCN) with semi-supervised training to account for the unlabeled nodes. A subgraph splitting strategy with cross-validation was developed to train on localized spatial regions and ensure balanced label proportions in each subgraph. Our GCN achieved 92.63% test accuracy, surpassing non-spatial deep learning models (77.45%).

Notably, explanation analysis using the GNNExplainer algorithm of our trained model identified high-attribution cells in CA and solid TME, revealing unique differentially expressed genes (DEGs) - JUNB in CA, and VIM, GPX1, PSAP, IFI27 in solid tumors, compared to low-attribution cells within the same subtype. Further analysis revealed an enrichment of EMT and interferon alpha/gamma, suggesting a more inflamed phenotype than low-attribution cells. Differential expression analysis of high-attribution CA vs solid cells identified significant upregulation of NDRG1 in CA and COL1A1 in solid. Functional enrichment analysis of these DEGs revealed PI3k-Akt in CA and MAPK signaling pathway in solid, suggesting an aggressive solid TME and CA with high survival and metastasis. We further identified a distinct neutrophil-enriched TME associated with CA and revealed cell-cell communication through MIF interactions with the CD74/CXCR4 and CD44/CD74 axes.

#7395 Histology-based prognosis prediction using deep learning outperforms and is independent of the MGMT methylation status in patients with glioblastoma.

L. Fidon, C. Thiriez, A. Grimaldi, O. Darwiche Domingues, C. Maussion, **C. Hoffmann**;
Owkin, PARIS, France

Introduction: MGMT gene promoter methylation status is today the only biomarker of survival for GBM patients and predicts favorable response to temozolomide (TMZ). Here we propose a deep learning-based model using histology data (H&E slides) to predict the prognosis of patients with Glioblastoma (GBM) treated by standard of care (SOC).

Methods: We included TCGA GBM patients and selected only patients treated after 2005 (Stupp protocol start); compliant to WHO 2021 classification; treated by surgery and adjuvant therapy; with a follow-up superior to median overall survival (OS) (14.5 months). Short and long survivor labels were defined based on median OS cut-off. A deep learning pipeline was trained to predict these labels from the H&E slides (baseline surgery samples). First, the slides were automatically segmented into tissue and background, divided into a regular grid of tiles (112x112µm), and tiles were vectorized using a vision transformer-based feature extractor trained on H&E slides of 5,500 patients with 16 cancer subtypes (GBM excluded). In the second step, ABMIL deep learning model was trained to predict the survival category using the bag of tile features available from step 1 for each patient. The cohort was divided into five folds with even numbers of short and long survivors. For each fold, 50 ABMIL models were trained on the remaining folds and ensembled to predict the category of the patients in the fold. Training hyperparameters were tuned on a separated cohort excluding GBM patients.

Results: After filtering, we analyzed n = 192 TCGA GBM patients including 154 patients with a known MGMT promoter methylation status. Our histology-based model had an accuracy of 0.661 and a ROC AUC of 0.706. It stratified the population into short and long survivors with an Hazard Ratio (HR) of 0.48 (95% CI 0.34-0.69). Our model outperformed the MGMT methylation status that had an HR of 0.57 (95% CI 0.40-0.83). Moreover, our model was independent of MGMT methylation status and the combination of both was able to further improve prognosis prediction: we applied our model independently to the 91 patients with an unmethylated MGMT status (predicted: 43 low, 48 high) and to the 63 patients with a methylated MGMT status (predicted: 30 low, 33 high), and obtained HR of 0.42 (95% CI 0.27-0.67) and 0.49 (95% CI 0.28-0.86) respectively.

Conclusion: Having selected patients treated by the latest SOC and classified as GBM by the latest WHO criteria, we propose a model predicting survival based on histological specimens available in routine care, which outperformed the current unique biomarker MGMT methylation status. The combination of this status and our model improves prognosis predictions compared to each strategy alone.

#7396 Development of deep neural networks that guide more individualized radiotherapy to the lung.

M. Abazeed;
Northwestern University Feinberg School of Medicine, Chicago, IL

Introduction: Radiotherapy is dependent on an expert-based model that impedes implementation of many potentially useful applications that could aid decision makers. This model is a barrier to a learning healthcare system due to noise introduced by decision-maker variation. Surmounting this barrier will require compelling clinical outcome data and highly useful and accurate information systems. We sought to develop new augmented-intelligence capabilities to better predict both high-dose lung irradiation treatment efficacy (*i.e.*, local tumor control) and toxicity (*i.e.*, radiation-induced pneumonitis).
Methods: We curated one of the largest datasets of lung stereotactic body radiotherapy (SBRT) datasets globally (~1200 cases). We input pre-therapy lung computed tomography (CT) images using a bounding box approach that captures the gross tumor volume and adjacent normal lung into a multi-task deep neural network to generate an image fingerprint that predicts local failures after treatment. Separately, we input axial slices from CT scans of the lung into convolutional neural network (CNN) and trained using an outcome per slice method. We then aggregated intra-patient slices into a recurrent neural network (RNN) to estimate individual patient risk for pneumonitis. We validated our findings with the independent study cohort. Risk scores for local failure and pneumonitis were combined with clinical variables to assess the relative contribution of the deep learning-derived image risk scores.
Results: A total of 1045 patients met our eligibility criteria. Radiation treatments in patients with high local failure risk scores failed at a significantly higher rate than in patients with low scores; 3-year cumulative incidence of local failure in the internal study cohort was 20·3% (16·0-24·9) in patients with high scores and 5·7% (95% CI 3·5-8·8) in patients with low scores (hazard ratio [HR]=3·64 [95% CI 2·19-6·05], p<0·0001). Models that included the local failure risk score and clinical variables predicted treatment failures with a concordance index (C-index) of 0·72 (95% CI 0·67-0·77), a significant improvement compared with classical radiomics (p<0·0001) or clinical variables (p<0·0001) alone. Radiation pneumonitis risk scores were highly predictive of toxicity, with an accuracy and CI of 0.78 (95% CI 0.72-0.85). A model that includes dosimetry variates (V20), improved the CI to 0.85 (95% CI 0.80-0.90).
Conclusions: The image-based deep learning frameworks developed herein represent the first opportunity to use medical images to individualize radiotherapy dose and toxicity predictions. Our results signify a new roadmap for deep learning-guided predictions and treatment guidance in the image-replete and highly standardized discipline of radiation oncology. A phase 2 study assessing machine-derived dose predictions is currently enrolling patients.

#7397 Application of state transition theory for predicting responses of acute myeloid leukemia to chemotherapy.

L. Uechi, Y.-H. Fu, D. E. Frankhouser, L. Zhang, Y.-C. Chen, D. O'Meally, S. Branciamore, J. Irizarry, B. Zhang, G. Marcucci, Y.-H. Kuo, **R. C. Rockne**; Beckman Research Institute of The City of Hope, Duarte, CA

Acute Myeloid Leukemia (AML) is aggressive cancer that initiates in the bone marrow (BM) and circulates in the peripheral blood (PB). The AML initiation and progressions are complex disease evolution associated with gene mutations and chromosomal abnormalities that change expression profiles of downstream genes characterizing functional networks of leukemic cells. We previously reported the application of the state-transition theory to characterize AML disease progression by modeling transcriptome changes during AML progression as a dynamic system that undergoes state-transition in an AML state-space characterized by an AML potential. Here, we investigate the impact of treatment on transcriptome state-transition and examine the hypothesis that treatment dynamically alters the AML potential. We use the Cbfb-MYH11 (CM) knock-in AML mouse model and a ”5+3” chemotherapy regimen to model the impact of current standard of care for newly diagnosed AML. CM leukemic mice were treated with a combination of cytarabine (Ara-C; 50mg/kg/day; 5 days) and Daunorubicin (DNR; 1.5mg/kg/day; 3 days) after detection of overt leukemia, defined by > 20% leukemia blast (cKit+) detected by flow cytometry in the PB. Time-series samples of peripheral blood mononuclear cell (PBMC) (n=174) were collected weekly before, during, and following “5+3” chemotherapy and subjected to RNA sequencing. All samples were mapped to the AML state-space constructed based on time-sequential RNA-seq collected over the course of CM AML development. Based on the state-transition model, all 10 treated AML mice achieved partial response to chemotherapy with a mean time to relapse (return to leukemia state) of 5 weeks confirming the anti-leukemia effects of treatment by the blast percentages (ckit%) . We used the state-transition treatment model to study the dynamics of chemotherapy on the AML potential using state-space trajectories before, during, and after “5+3” chemotherapy. Dynamic changes of concentrations of Ara-C and DNR in the CM mouse model during ”5+3” chemotherapy were modeled by drug doses, half-life, and Heaviside step function. The drug effects were introduced to the AML potential as anti-leukemic treatment forces. Several treatment protocols were examined to find combinations of drug doses and timing that showed the longest survival rates. The model predicted that sequential doses reducing 50% of the original “5+3” chemotherapy dose would produce the longest survival rate. The model suggests that controlling the state-space trajectories in the healthy state with reduced doses will provide the most effective outcomes from “5+3” chemotherapy.

#7398 Unveiling the tumor microenvironment of hepatocellular carcinoma using AI trained by spatial transcriptomics: A preliminary study to predict response to immunotherapy.

Dongjoo Lee[1], Haenara Shin[1], Seungho Cook[1], Daeseung Lee[1], Hongyoon Choi[2], Won-Mook Choi[3], Changhoon Yoo[4], Kwon Joong Na[5]

[1]Portrai, Inc., Seoul, Korea, Republic of,[2]Department of Nuclear Medicine, Seoul National University Hospital, Seoul, Korea, Republic of,[3]Department of Gastroenterology, Liver Center, Asan Medical Center, University of Ulsan College of Medicine, Seoul, Korea, Republic of,[4]Department of Oncology, Asan Medical Center, University of Ulsan College of Medicine, Seoul, Korea, Republic of,[5]Department of Thoracic and Cardiovascular Surgery, Seoul National University Hospital, Seoul, Korea, Republic of

Background. Immune checkpoint inhibitors (ICIs), particularly targeting the PD-1 pathway, are promising in treating hepatocellular carcinoma (HCC). However, their variable effectiveness among individuals calls for a better understanding of the tumor microenvironment (TME) and reliable predictive biomarkers. Here, we employ spatial transcriptomics (ST) to develop a deep-learning model that aims to investigate the TME in HCC using Hematoxylin and eosin (H&E) staining images. Our focus is on identifying cell types within the TME that are linked to the response to ICI in a cohort of patients treated with nivolumab.
Methods. Our study leveraged 21 Visium ST datasets from HCC to develop a model aimed at inferring the cellular composition of TME from H&E images that matched with ST data. The comprehensive TME cell types enrichment score, encompassing Tumor Endothelial Cells (TECs), Tumor-Associated Macrophages (TAMs), B cells, T cells, and Cancer-Associated Fibroblasts (CAFs) in each spot, was calculated by the CellDART algorithm, a method that maps cell type by integrating with a reference scRNA-seq data. The model was trained in a patch-wise manner, utilizing a pre-trained ResNetRS50 as the backbone model. For the internal validation, Spearman correlation coefficients were evaluated for predicted cell types using H&E, and the trained model was correlated with cell type enrichment scores estimated by ST datasets of 4 samples independent of the training set. The model was applied to H&E images of 16 patients with HCC who underwent nivolumab treatment. The model predicted the 5 cell types enrichment score in the tumor and tumor-adjacent normal liver tissues.
Results. The internal validation set results demonstrate robust Spearman correlations between our model predictions and actual cellular compositions in the TME. Specifically, we observe strong correlations for T cells (rho = 0.66), TAMs (rho=0.46), CAFs (rho=0.32), B cells (rho=0.30), and TECs (rho=0.24). When we applied the model to the H&E images of the cohort of patients who underwent nivolumab, immunotherapy non-responders showed a significantly higher predicted enrichment score of CAFs in tumor-adjacent regions (Mann-Whitney test, $p<.01$). Upon stratifying patients based on stromal CAF prediction, those with low stromal CAF levels exhibited better overall survival (Log-rank test, $p<.05$).
Conclusions. We present a deep learning model to analyze TME in HCC solely on H&E images trained by ST data. Our findings showed a potential relationship between CAFs in tumor-adjacent regions and non-responders to nivolumab treatment in HCC. These insights underscore the potential to predict nivolumab treatment responders using H&E images combined with the deep learning model. This approach could provide a significant advancement in personalized treatment strategies for HCC patients.

#7399 Development of a reproducible AI-based spatial biomarker of the tumor immune infiltrate on H&E slides.

V. Di Proietto, **J. El-Khoury**, B. Adjadj, L. Gillet, U. Marteau, K. Schutte, K. Von Loga;
Owkin, Paris, France

Background: The immune infiltrate in the tumor microenvironment (TME) has been shown to be associated with prognosis in several studies. However, a comprehensive assessment of the TME composition is not performed in routine practice due to the lack of standardized methods and tools for quantification. The aim of our study is to develop a reproducible, artificial intelligence (AI)-based, spatial biomarker of the tumor related immune response to predict patients outcome on routine Hematoxylin & Eosin (H&E) slides. To the best of our knowledge, this is the first study that implements a robust H&E pipeline to assess, across multiple cohorts, the prognostic power and the added-value of a spatial marker in comparison to non-spatial measures such as the overall lymphocytes density on the slide.
Methods: We trained AI models on both publicly available (NuCLS and Lizard) and proprietary datasets to automatically detect cells and tissue types on H&E stained Whole Slide Images of cancers from different origins.
We used these models on TCGA COAD and TCGA BRCA and computed spatial measures related to the lymphocyte densities in the tumor core versus the invasive margin as well as the immune infiltration in the tumor stroma (in between tumor islets) versus in the tumor islets themselves.
Univariate and multivariate survival analysis is performed through repeated cross-validation. A log-rank test on the stratified groups is performed for each evaluated marker, using the median value as cutoff.
Preliminary results on TCGA-COAD and TCGA-BRCA show that spatial markers of the tumor-related immune response are individually associated with overall survival, reinforcing findings from prior studies emphasizing the importance of the spatial relationship between tumor and immune cells. Multivariate analysis with both linear and non-linear models is currently ongoing across selected cohorts.

#7400 AI-driven multimodal 3D tumor modeling with spatial molecular insights for predicting ICI response in gastric cancer.

Y. Choi[1], M. Kim[1], K. Redekop[2], I. Jang[1], J. R. Clemenceau[1], I. Barnfather[3], S. Nakkireddy[1], C. Hong[1], S. Park[1], J.-Y. Sung[4], J. Park[5], S. Kohei[6], A. Yu[6], S. Lee[7], S. Wang[8], J. Cheong[9], T. Hwang[1];

[1]Mayo Clinic,, Jacksonville, FL, [2]University of California,, Los Angeles, CA, [3]University of Manchester, Manchester, United Kingdom, [4]Kyung Hee University Hospital, Kyung Hee University College of Medicine, Seoul, Korea, Republic of, [5]Seoul National University Boramae Medical Center, Seoul, Korea, Republic of, [6]National Cancer Center Hospital East, Chiba, Japan, [7]College of medicine, the Catholic university of Korea, Seoul, Korea, Republic of, [8]UT Southwestern Medical Center, Jacksonville, TX, [9]Yonsei University College of Medicine, Seoul, Korea, Republic of

Traditional cancer research methodologies predominantly focus on 2D tumor modeling, including spatial profiling and AI-driven analysis at the 2D level. To advance beyond these limitations, we implemented Holotomography (HT), a 3D, label-free optical imaging method. This technique, leveraging refractive index contrasts, allows for enhanced visualization of tumor tissues, organoids, and cells in three dimensions. Using serial H&E sections and unstained slides, we created detailed 3D tumor models in gastric cancer, providing insights into tumor, immune, and stromal composition, as well as cell-cell interactions and extracellular matrix characteristics. AI algorithms further enhanced our 3D tumor modeling, offering novel perspectives on the initiation and progression of tumor, immune, and stromal components at the subcellular level. Analyzing gastric tumors treated with immune checkpoint inhibitors before, during, and after treatment revealed dynamic changes in spatial composition over time, offering unique insights into the evolution of the 3D tumor ecosystem. Additionally, by integrating spatial transcriptomic and in situ molecular imaging data, we developed a novel Multimodal 3D Tumor Model. This model not only uncovers subcellular-level molecular characteristics but also elucidates cellular interactions during treatment, suggesting potential biomarkers and therapeutic approaches. Lastly, by constructing 3D cellular interaction networks incorporating true 3D interactions, we provided an in-depth view of cellular communication within the tumor microenvironment. This pioneering approach, representing the first Multimodal 3D Tumor Model at the subcellular level, offers novel insights into gastric cancer's spatial evolution, potentially revolutionizing our understanding and treatment of gastric cancer.

#7401 High-level multiplexed virtual immunofluorescence staining using holotomography and deep learning.

J. Park[1], S.-J. Shin[2], G. Kim[1], K. Lee[2], J. Heo[3], Y. Park[1];

[1]Korea Advanced Institute of Science and Technology, Daejeon, Korea, Republic of, [2]Gangnam Severance Hospital, Seoul, Korea, Republic of, [3]Yonsei University College of Medicine, Seoul, Korea, Republic of

Multiplexed immunofluorescence (IF) staining plays a crucial role in cancer research, allowing simultaneous visualization of multiple biomarkers to elucidate complex cellular interactions within the tumor microenvironment. However, the conventional multiplexed IF approach has inherent limitations, characterized by labor-intensiveness and a constrained capacity for high-level multiplexing. These challenges hinder its scalability and comprehensive analysis of intricate molecular landscapes.To overcome the limitations of conventional multiplexed IF, we propose a novel approach that integrates holotomography (HT) and deep learning. HT is a label-free imaging technique that quantitatively measures the refractive index distribution of the specimen without any staining. To provide subcellular specificity to the label-free HT images, HT is integrated with virtual staining. Virtual staining is a deep learning-based framework that converts label-free images to the desired stained images, in this case, from HT images to multiplexed IF images. This synergistic combination of HT and deep learning may address the current limitations of multiplexed IF protocols.Our proposed methodology aims at high-level multiplexed virtual IF staining from label-free cancer tissue slides using HT and deep learning. This approach not only eliminates the need for chemical staining but also enhances the level of multiplexing through computational staining. Specifically, we acquire HT and fluorescence images of stained tissue slides for training. Utilizing this paired dataset, we then employ supervised learning to create a neural network that can map between label-free HT images and corresponding fluorescence images. Subsequently, the trained neural network is applied to label-free tissue slides, inferring fluorescence images without the need for chemical staining.We believe the proposed virtual staining framework will contribute to a more efficient and scalable paradigm for cancer research, facilitating a deeper understanding of tumor biology, and advancing the field of precision medicine.

#7402 Foundation AI models predict molecular measurements of tumor purity.

Y. Gerardin, D. Shenker, J. Hipp, N. Harguindeguy, D. Juyal, C. Shah, S. Javed, M. Thibault, M. Nercessian, D. Sanghavi, B. Trotter, **R. Leung**; PathAI, Inc., Boston, MA

Background: Molecular assays, such as comprehensive genomic profiling, play a critical role in characterizing patient disease and guiding treatment selection in oncology but require sufficient tumor nucleic acids in tissue samples for reliable results. Automated, accurate and reproducible quantification of tissue area and tumor nuclei from H&E slides to determine suitability for molecular testing could reduce the amount of time spent assessing tissue quality. To address this need, we developed pan-indication foundation AI models to quantify tissue and cell features within H&E whole-slide images (WSI) and compared tumor purity estimates to orthogonal molecular and manual methods.

Methods: Pan-indication artifact, tissue, and cell models were each trained using at least 2.8 million pathologist annotations across over 100,000 WSI from 14 stains, 25 organs, and 9 scanners and validated against pathologist ground-truth labels. This suite of foundation models was deployed on H&E WSIs of colon adenocarcinoma (COAD; N=442), melanoma (N=363), prostate cancer (PRAD; N=490), and non-small cell lung cancer (NSCLC; N=996) from TCGA[1]. Model outputs allowed for the segmentation of tumor regions and enumeration of cancer cells for the purpose of determining tumor purity scores, calculated as the fraction of cancer cells within tumor tissue on a WSI. For comparison, tumor purity values determined based on DNA copy number (ABSOLUTE), gene expression (ESTIMATE), DNA methylation (LUMP) and manual assessment[2] were obtained. Concordance between AI model scores and other tumor purity values was assessed using the intraclass correlation coefficient, ICC(2,1).

Results: AI model scores were correlated with orthogonal molecular measures of tumor purity in all four indications. AI model purity scores corresponded the most with ABSOLUTE (ICC range: 0.22-0.46), followed by LUMP (ICC range: 0.02-0.50) and ESTIMATE (ICC range: 0.03-0.34). Across indications, the highest agreement observed between AI model scores and molecular methods was in melanoma (ICC range: 0.34-0.50), while the lowest agreement was in PRAD (ICC range: 0.02-0.22). Compared against ABSOLUTE in NSCLC and PRAD, AI model scores showed the highest concordance, while the other two molecular methods and manual assessment all overestimated ABSOLUTE tumor purity.

Conclusions: Here, we describe a pan-indication AI-based approach for the quantification of tumor features in H&E-stained WSI. Foundation AI models successfully segment tumor tissue regions and enumerate cancer cells for determining tumor purity, and these predictions correlate with molecular metrics in four cancer indications. This work provides further evidence of how AI could improve the efficiency of molecular testing and enhance precision medicine approaches in oncology.

References: [1]TCGA https://gdc.cancer.gov/about-data/publications/pancanatlas; [2]Aran, D. et al. Nat Comms 6:8971 (2015)

BIOINFORMATICS / COMPUTATIONAL BIOLOGY / SYSTEMS BIOLOGY / CONVERGENT SCIENCE: New Software Tools for Data Analysis
Poster Session

#7406 Visualization and analysis of cancer genomics data using UCSC Xena.
M. Goldman, B. Craft, J. Zhu, D. Haussler;
UC Santa Cruz Genomics Institute, Santa Cruz, CA

UCSC Xena (http://xena.ucsc.edu/) is a web-based visual integration and exploration tool for multi-omic data and associated clinical and phenotypic annotations. Researchers can easily view and explore public data, their own private data, or both using the Xena Browser. Private data are kept on the researcher's computer and are never uploaded to our public servers. We support Mac, Windows, and Linux.
Questions Xena can help you answer:* Is overexpression of this gene associated with lower/higher survival?* What genes are differentially expressed between these two groups of samples?* What is the relationship between mutation, copy number, expression, etc for this gene?
Xena showcases seminal cancer genomics datasets from TCGA, the Pan-Cancer Atlas, GDC, PCAWG, ICGC, and more; a total of more than 1500 datasets across 50 cancer types. We support virtually any type of functional genomics data: SNPs, INDELs, copy number variation, gene expression, ATAC-seq, DNA methylation, exon-, transcript-, miRNA-, lncRNA-expression and structural variants. We also support clinical data such as phenotype information, subtype classifications and biomarkers. All of our data is available for download via python or R APIs, or using our URL links.
Our signature Visual Spreadsheet view shows multiple data types side-by-side enabling discovery of correlations across and within genes and genomic regions. We also have dynamic Kaplan-Meier survival analysis, powerful filtering and subgrouping, differential gene expression analysis, GSEA, charts, statistical analyses, genomic signatures, and the ability to generate URLs to live views.
New features include:
* Genome-wide differential gene expression analysis
* GSEA analysis
* Select samples directly from the screen for filtering and creating subgroups
* Loading of Microsoft Excel files
Our beta prototype site for visualizing single-cell data delivers million-cell-scale multi-omics data for interactive visualization in a web browser. Contact us for access to our beta prototype site.
If you use us please cite our publication in Nature Biotechnology: https://www.nature.com/articles/s41587-020-0546-8

#7407 Melanoma clonal subline analysis reveals genetic factors driving intra-tumor heterogeneity.

A. Keskus[1], A. Goretsky[1], Y. Liu[1], X. Cui[1], T. Ahmad[1], E. Perez Guijarro[1], A. Bryant[1], E. Malloy[2], S. Malikic[1], G. Merlino[1], C.-P. Day[1], C. Sahinalp[1], M. Kolmogorov[1];

[1]NIH-NCI, Bethesda, MD, [2]University of Maryland, College Park, MD

Melanoma is the most invasive skin cancer caused by the malignant melanocytes. The use of immune checkpoint blockade (ICB) improved the survival rate in advanced melanoma. Yet, the response rate to ICB varies across patients due to the highly heterogeneous nature of melanoma. Recent studies reported genomic and epigenetic factors contributing to the therapeutic response. Identifying these factors involved in clonal evolution in melanoma is a key to better understanding the tumor progression and divergence in the therapy response.

To study melanoma heterogeneity, we generated twenty-four clonal sublines, each derived from a single cell isolated from a parental cell line derived from the M4 mouse melanoma model. DNA prepared from each subline and a spleen from a healthy mouse were subjected to long-read sequencing. Importantly, long-read sequencing allows direct detection of methylation states, small variants, and structural variants in the same run. The results thus provide excellent means to study genetic and epigenetic factors in clonal evolution. Each of these sublines was also implanted in distinct mice for survival and tumor growth analysis and further functional evaluation.

We developed Severus, a structural variation (SV) caller for long reads, which works with single (germline), paired (tumor-normal), and multiple samples (e.g., multi-site or time series). Severus takes advantage of improved phasing in long-read sequencing, attributes somatic variants to germline haplotype, and builds a haplotype-specific breakpoint graph that is used to cluster multi-break rearrangements and represent the derived chromosomal structure. We benchmarked Severus using multiplatform validated COLO829 truthset and CHM1/CHM13 haploid genomes, and Severus outperformed all other methods in terms of recall and precision.

The structural variation (SV) analysis using Severus with all the sublines showed enrichment of possibly clonal SVs in chr4, chr11, and mainly in chr13. Further investigation revealed SVs in chr13 were not distributed across the chromosome but clustered in certain regions. Analysis of somatic SNVs in chr13 corroborates the localized hypermutation profile, which indicates a possible kataegis. Interestingly, a loss of the chr13 copy affected by kataegis in one of the sublines coincides with a better survival rate, as compared to other sublines, in an allograft melanoma mouse model, which further supports the association between the kataegis and tumor progression. We also identified other clonal and subclonal events, including the homozygous deletion of Cdkn2a in most of the sublines, associated with their aggressiveness in vivo.

Our analysis allowed us to identify clonal and subclonal genetic and epigenetic factors involved in tumor progression and evolution in a melanoma model, which can potentially translate to human disease.

#7408 Robust profiling of cancer-related gene fusions: Analytical validation of PANCARNA for multiple cancer types.

H. Tang, H. Bao, R. Liu, S. Wu, S. Liu, X. Wu, Y. Shao;
Geneseeq Technology Inc., Toronto, ON, Canada

The impact of examining gene fusion presence in cancer patients is often overlooked, and as such, no well-established workflow currently exists for robust profiling of tumor samples in this area. We established a targeted RNA sequencing panel (PANCARNA) for investigating gene fusions across multiple cancer types and performed analytical validation to confirm performance. Furthermore, we report on the applicability of using targeted RNA sequencing for the purposes of gene expression profiling. This panel covers 117 genes associated with solid tumors. Thirty-nine FFPE samples with gene fusion status validated using an orthogonal method were used to evaluate analytical performance. Of the 39 standard samples, 33 samples were positive for gene translocation events and 6 were negative controls. Samples were collected from across 10 cancer types. To examine the robustness of the panel, 12 samples with known fusions were selected to undergo testing. Each sample was tested in triplicate across two experimental batches. Seraseq Fusion RNA Mix V4 (SeraCare, Cat. 0710-0497) standard samples were used to test the limit of detection for PANCARNA. Additionally, we explored a cohort of 22 samples with over expressed genes and 4 samples without overexpressed genes to test the expression profiling capabilities of PANCARNA and compared the results to immunohistochemistry stains. Of the 39 samples tested using the orthogonal method and targeted RNA-Seq, 38 were found to have concordant fusion calls in both methods (Positive percent agreement = 97.0%, 32/33; Negative percent agreement = 100%, 6/6; Overall percent agreement = 97.4%, 38/39). In reproducibility studies, the assay produced consistent intrarun and interrun results in all samples (Repeatability = 100%, 12/12; Reproducibility = 100%, 12/12). The limit of detection for multiple fusions of interest, such as *EML4-ALK, CD74-ROS1, TPM3-NTRK1*, and *SLC34A2-BRAF*, is found to be 0.5-1 copies per ng of RNA. *ETV6-NTRK1* can be reliably detected at 2-4 copies per ng of RNA. MET ex14 skipping events can also be detected in a few as 1-2 copies per ng of RNA. To validate the capability of PANCARNA to quantify gene expression, we tested 26 samples with known gene expression levels for three genes of interest (*ERBB2, EGFR, MET*). *ERBB2, EGFR* and *MET* amplification detection through PANCARNA was found to have a high concordance to IHC results (Sensitivity = 96.2%, 100%, 94.7%, respectively). In conclusion, PANCARNA demonstrated highly accurate and sensitive detection of clinically relevant gene fusions. This assay produces reliable results when detecting fusions and offers high concordance to results obtained through IHC/FISH, indicating that targeted RNA seq analysis can assist with profiling gene fusion events in a clinical setting.

#7409 SpatialCells: Automated profiling of tumor microenvironments with spatially resolved multiplexed single-cell data.

Guihong Wan[1], Zoltan Maliga[2], Boshen Yan[3], Tuulia Vallius[2], Yingxiao Shi[4], Sara Khattab[3], Crystal Chang[3], Ajit J. Nirmal[5], Kun-Hsing Yu[6], David Liu[4], Christine G. Lian[7], Mia S. DeSimone[7], Peter K. Sorger[2], Yevgeniy R. Semenov[3]

[1]Harvard Medical School/Massachusetts General Hospital, Boston, MA,[2]Laboratory of Systems Pharmacology, Program in Therapeutic Science, Harvard Medical School, Boston, MA,[3]Department of Dermatology, Harvard Medical School/Massachusetts General Hospital, Boston, MA,[4]Department of Medicine, Dana-Farber Cancer Institute, Boston, MA,[5]Department of Dermatology, Harvard Medical School/Brigham and Women's Hospital, Boston, MA,[6]Department of Biomedical Informatics, Harvard Medical School, Boston, MA,[7]Department of Pathology, Harvard Medical School/Brigham and Women's Hospital, Boston, MA

Cancer is a complex cellular ecosystem where malignant cells coexist and interact with immune, stromal, and other cells within the tumor microenvironment. Recent technological advancements in spatially resolved multiplexed imaging at single-cell resolution have led to the generation of large-scale and high-dimensional datasets from biological specimens. This underscores the necessity for automated methodologies that can effectively characterize the molecular, cellular, and spatial properties of tumor microenvironments for various malignancies.

This study introduces SpatialCells, an open-source software package designed for region-based exploratory analysis and comprehensive characterization of tumor microenvironments using spatially resolved multiplexed single-cell data. We have provided detailed documents and tutorials at https://github.com/SemenovLab/SpatialCells.

SpatialCells is featured by its capability to computationally define regions of interest based on any group of cells and subsequently conduct region-based analyses. SpatialCells incorporates several modules to facilitate its functionality, such as the spatial module and the measurements module. Our workflow starts with developing the spatial module, including functions to establish regional boundaries and check the region in which a cell is located. In particular, SpatialCells supports macro-region and micro-region analyses. In the macro-region analysis, users can employ SpatialCells to divide the whole tissue into several subregions, such as tumor, tumor border, stroma border, and stroma. In the micro-region analysis, SpatialCells identifies small regions within an area, such as within the tumor area, enabling a finer-grained understanding of the cellular landscape. The measurements module contains functions to extract the properties of tumor cells, immune cells, and tumor-immune cell interactions, such as multivariate tumor proliferation index, immune infiltration score, and tumor-immune cell distances. These properties can be assessed for the whole tissue or local regions. Importantly, SpatialCells can efficiently process datasets containing millions of cells.

In summary, SpatialCells is a novel software solution for spatially analyzing the tumor microenvironment and automatically extracting quantitative features of cells using multiplexed imaging data in a streamlined fashion with the capacity to process samples containing millions of cells. Thus, SpatialCells facilitates subsequent association analyses and machine learning predictions at scale, making it an essential tool in advancing our understanding of tumor growth, invasion, and metastasis.

#7410 PyVIPER: A fast and scalable toolkit for the identification of dysregulated proteins in tumor-derived single-cell RNA-seq data.

L. Zanella[1], A. L. E. Wang[1], Z. J. Lin[1], L. J. Vlahos[1], M. Anglada Girotto[2], A. Zafar[1], A. Califano[1], A. Vasciaveo[1];
[1]Columbia University Irving Medical Center, New York, NY, [2]Centre for Genomic Regulation, Barcelona, Spain

Single-cell RNA sequencing (scRNA-seq) enabled the characterization of tumor microenvironment heterogeneity with unprecedented resolution. However, its low signal-to-noise ratio due to data sparsity hinders biomarkers quantitative measurements. To perform a more robust assessments of protein markers, we have previously introduced the use of the VIPER algorithm that estimates regulatory proteins activity using the expression of their downstream targets by leveraging lineage specific regulatory networks. We have shown that this approach compares favorably with both gene expression and protein abundance measurements to identify novel cell states corresponding to tumor subpopulations that are undetectable at the gene expression level, by inferring the mechanistic contribution of regulatory and signaling proteins to cellular phenotypes. VIPER-inferred cell states have been linked to critical functional roles, including immune-evasion and progression, disease heterogeneity and drug sensitivity in cancer. However, the ever-growing size of scRNA-seq datasets demands for scalable tools that simultaneously analyze tens or hundreds of thousands of cells in tumor contexts, such as tumor atlases and large clinical cohorts. We present PyVIPER, a fast, memory-efficient, and highly scalable Python framework that allows protein activity inference of large scRNA-seq datasets. PyVIPER is fully integrated with both AnnData and Scanpy frameworks for single-cell analysis and enables a seamless interface with cutting-edge machine learning libraries (e.g., sckit-learn and TensorFlow). PyVIPER provides multiple algorithms for enrichment analysis, novel modules for postprocessing and pathway analysis, and a set of procedures tailored for precision oncology studies in single cells, including OncoMatch, a validated platform to assess the fidelity of models (*in vitro* or animal) with human tumors for drug sensitivity elucidation. We benchmarked PyVIPER against several scRNA-seq cancer datasets obtaining runtimes reduction of several orders of magnitude (from hours to minutes) when compared to previous VIPER implementations. Taken together, PyVIPER scalability and its embedded toolkit for cancer data analysis address the need to efficiently extend protein activity analyses to large single-cell datasets, with the goal of providing cancer researchers with an effective platform to identify aberrant molecular mechanisms in cancer cells.

#7411 CAMStool: Cancer-associated somatic mutation selection tool for cancer risk prediction in whole-genome data.

J.-Y. Kim, S.-J. Park, S.-H. Park, S.-K. Kim;
Korea Research Institute of Bioscience & Biotechnology (KRIBB), Daejeon, Korea, Republic of

Predicting cancer risk plays a useful role in presenting guidelines to prevent and manage cancers of individuals. Genomic variants have recently been widely used as a genetic factor, and the utilization of the genetic factor consisting of somatic mutations has shown remarkable predictive performance in many cancer prediction studies. Typically, the accuracy of such prediction studies is significantly affected by the composition of somatic mutations used as the genetic factor; however, in practice, choosing the optimal set of mutations with high prediction accuracy is a challenging task in cancer prediction research. From this perspective, we present a new analysis tool for selecting an optimal set of somatic mutations associated with cancers of interest, named CAMStool. The CAMStool is based on the statistical values, which are the effect size and its p-value of each somatic mutation for the cancers of interest. It heuristically searches for the only somatic mutations that directly increase the prediction accuracy of cancer, through statistical and machine-learning models. Then, our tool presents the finally selected somatic mutations as the final optimal mutation set, and additionally presents an optimal cancer risk prediction model through various machine/deep learning modeling using the optimal set as a genetic factor. For the evaluation, the CAMStool was applied to our real whole-genome dataset which are sequenced from normal-tumor tissues of 459 individuals with thyroid cancer. The CAMStool selected 36 and 55 optimal somatic mutations associated with the benign thyroid and non-invasive follicular thyroid cancer, and presented risk prediction models with sensitivity of 88.04% and 90.32%, respectively. Although the CAMStools has some limitations, it is expected to contribute to various cancer prediction studies that require selecting optimal mutation sets in the future. The CAMStools is written in R and will be released soon on our github (https://github.com/JaeYoonKim72).

#7412 METI: Deep profiling of tumor ecosystems by integrating cell morphology and spatial transcriptomics.

J. Jiang[1], Y. Liu[1], J. Qin[2], J. Wu[1], J. Chen[1], M. Pizzi[1], R. Segura[1], K. Yamashita[1], Z. Xu[2], G. Pei[1], K. Cho[1], Y. Chu[1], A. Sinjab[1], F. Peng[1], G. Han[1], R. Wang[1], X. Yan[1], E. Dai[1], M. Li[3], A. Futreal[1], A. Maitra[1], A. Lazar[1], X. Cheng[2], H. Kadara[1], J. Ajani[1], A. Jazaeri[1], J. Hu[4], L. Wang[1], J. Gao[1];

[1]The University of Texas MD Anderson Cancer Center, Houston, TX, [2]Institute of Basic Medicine and Cancer, Chinese Academy of Sciences, Hangzhou, China, [3]University of Pennsylvania, Philadelphia, PA, [4]Emory University, Atlanta, GA

The recent progression in spatial transcriptomics (ST) offers invaluable perspectives on the structure and dynamics of cells within the tumor microenvironment (TME). Though several analytical tools exist for tasks like spatial clustering and spatially variable gene identification, most of them are general methods lacking consideration of histological features in spatial data analysis. This oversight compromises their performance and interpretability when studying the TME. Here, we introduce a computational framework, the Morphology-Enhanced Spatial Transcriptome Analysis Integrator (METI). METI provides a comprehensive framework for spatially mapping both cancer cells and various TME cells, robust stratification of cell type and transcriptional states, and cell co-localization analysis. By integrating spatial transcriptomics with cell morphology and curated gene signatures, METI deepens our insight into the molecular landscape and cellular interactions within tissues, paving the way for intricate studies of the TME and its consequential impacts. The performance of METI has been assessed using ST data derived from a range of tumor tissues, encompassing gastric, lung, and bladder cancers, and premalignant tissues. Throughout these varied tissues and conditions, METI consistently exhibited robust performance.

#7413 Establishing a database for the discovery and validation of survival-associated genes in colon cancer.

B. Gyorffy;
Semmelweis University, Budapest, Hungary

Introduction: Unveiling the prognostic significance of genes as potential biomarkers in colon cancer (CRC) is crucial for the discovery of new therapeutic targets and the effective stratification of patients into clinically relevant groups. The primary objective of this study was to establish a transcriptomic cohort comprising clinical data from colon cancer specimens and to leverage this dataset to pinpoint genes with robust prognostic implications.
Methods: Our approach involved a comprehensive search of the Gene Expression Omnibus (GEO) to identify datasets containing both clinical information and raw gene expression measurements for individual colon cancer specimens. Subsequently, we curated and integrated these datasets into a unified database, and linked into our Kaplan-Meier plotter. This integration enabled the identification of genes whose expression changes were associated with altered survival outcomes. The identification of the most influential genes in relation to overall survival in stage 2 and stage 3/4 tumors was accomplished through both uni- and multivariate Cox regression analyses. To mitigate the impact of multiple hypothesis testing, a false discovery rate was computed for each marker.
Results: The database encompasses a total of 2,137 tumor samples derived from 17 distinct independent cohorts. Within this dataset, 1,343 samples are equipped with recorded relapse-free survival data, while 1,061 samples provide information on overall survival events along with the corresponding duration. In addition to survival-related metrics, the database encompasses a spectrum of supplementary clinical parameters such as gender, T (tumor size), N (lymph node involvement), M (metastasis), grade, stage, location, and microsatellite instability. The most significant genes associated with relapse-fee survival with FDR<1% in stage 2 CRC include CSF1R (HR=2.86), FLNA (HR=2.88), TPBG (HR=2.65), B2M (HR=2.62) and LOXL2 (HR=2.63). When ordered by the Cox regression p-value in stage 3 and 4 tumors, the five strongest genes were BHLHE40 (HR=2.6), COL4A2 (HR=2.02), TSC22D3 (HR=1.95), NPR3 (HR=1.91), and A2M (HR=1.86).
Conclusions: In this study, we successfully developed a robust integrated database dedicated to colon cancer. By leveraging this resource, we pinpointed the most impactful prognostic biomarkers and potential therapy targets specifically within stage 2 and stage 3/4 patients. Beyond its current applications, this database holds promise for future endeavors, serving as a valuable tool for identifying and prioritizing additional promising biomarkers and therapeutic targets in other sub-cohorts of colon cancer. The entire database can be utilized at www.kmplot.com.

#7414 Claire: a search engine leveraging deep databases for reliable detection of peptides, with a special focus on proteogenomic applications.

Miroslav Hruska, Petr Dzubak, Marian Hajduch

Institute of Molecular and Translational Medicine, Faculty of Medicine and Dentistry, Palacky University Olomouc and University Hospital in Olomouc, Olomouc, Czech Republic

As the field of cancer diagnostics and treatment evolves, the significance of peptides characterized by post-translational modifications and amino acid substitutions is becoming increasingly prominent. These molecular alterations frequently offer critical insights into tumor biology, aiding the development of targeted therapies and methods for personalized medicine. However, despite ongoing advances in shotgun proteomics, the field still faces multiple challenges for the reliable detection of rare peptide forms, for instance, amino acid substitutions when the corresponding DNA or RNA sequencing is unavailable. As a response to these challenges, our group has developed Claire—a probabilistic search engine employing large peptide databases for detection. These databases, often on the terabyte scale, further incorporate the estimates of peptides' prior probabilities to improve detection accuracy and utilize several optimizations to allow fast interpretation of tandem mass spectra. Claire outperformed state-of-the-art software, such as MSFragger and TagGraph when evaluated on the protein-level detection of single nucleotide variants in the public NCI60 proteome dataset. Further, Claire's analysis of a range of NCI60 datasets revealed high protein-level mutational burdens in genomically unstable cancer cell lines and detected mislabeling and contamination across several omics datasets. In a clinical domain, Claire discerned the hypermutation status of colorectal cancer patients' tumors, identifying candidates suitable for immunotherapy. Protein-level variation in peripheral blood mononuclear cells also recognized individuals, monozygotic twins aside, revealing the pseudonymous nature of germline proteome datasets, and raising the need for their protection. From a computational perspective, Claire can be run as a standalone software in the Linux operating system, or its capabilities accessed remotely using an interface on our cloud computing infrastructure. Claire has thus shown remarkable potential in enhancing peptide detection, offers substantial advancements for both clinical and research applications, and allows direct incorporation of its capabilities into various computational workflows.

#7415 Assigning mutational signatures to individual samples and individual somatic mutations with SigProfilerAssignment.

R. Vangara[1], M. Diaz-Gay[1], M. D. Barnes[1], X. Wang[1], S. Islam[1], I. Vermes[2], S. Duke[2], N. Narasimman[1], T. Yang[1], Z. Jiang[1], S. Moody[3], S. Senkin[4], P. Brennan[4], M. R. Stratton[3], L. B. Alexandrov[1];

[1]UC San Diego, San Diego, CA, [2]COSMIC, Wellcome Sanger Institute, Hinxton, United Kingdom, [3]Wellcome Sanger Institute, Hinxton, United Kingdom, [4]International Agency for Research on Cancer, Lyon, France

Analysis of mutational signatures is a powerful approach for understanding the mutagenic processes that have shaped the evolution of a cancer genome. To evaluate the mutational signatures operative in a cancer genome, one first needs to quantify their activities by estimating the number of mutations imprinted by each signature, a process known as *refitting* of mutational signatures. Although multiple tools for refitting known signatures were developed in the past decade, most provide support almost exclusively for single base substitution signatures and lack an online interface. Further, these tools have never been compared, and no existing tool supports probabilistically assigning signatures to a single somatic mutation. Here, we present SigProfilerAssignment, a desktop and online computational framework for assigning all types of mutational signatures to individual samples. SigProfilerAssignment is the first tool that allows both analysis of copy-number signatures and probabilistic assignment of signatures to individual somatic mutations. As its computational engine, the tool uses a custom implementation of the forward stagewise algorithm for sparse regression and nonnegative least squares for numerical optimization. The analysis of 2,700 synthetic cancer genomes with and without noise demonstrates that SigProfilerAssignment outperforms four commonly used approaches for assigning mutational signatures, with consistent top performance across cancer types and most signatures. SigProfilerAssignment stands out as the most precise and sensitive tool while maintaining high computational performance and bringing novel capabilities. SigProfilerAssignment is distributed as an open-source Python/R package available at https://github.com/AlexandrovLab/SigProfilerAssignment, with an online interface available as part of the COSMIC Mutational Signatures website at https://cancer.sanger.ac.uk/signatures/assignment/.

#7416 GeneSetR: A web server for gene set analysis based on genome-wide Perturb-Seq data.

O. F. Kuzu, F. Saatcioglu;
University of Oslo, Oslo, Norway

Identification of genotype-phenotype relationships is of utmost importance and a core effort in biology. Recent developments in efficient and precise gene targeting approaches coupled to omics methods have significantly improved deciphering of molecular interactions and relationships. However, many single gene perturbations can affect the expression of hundreds of other genes and analysis of the resulting omics-derived gene lists currently remains a significant challenge. Here we present Perturb-Seq based Gene Set Analyzer (GeneSetR), a user-friendly web-server that can analyze user-defined gene lists based on the data from a recently published genome-wide Perturb-Seq study, which targeted 9,866 genes with 11,258 sgRNAs in the K562 cell line. Through this tool, users can cluster gene lists following dimensionality reduction by various algorithms, undertake network analysis from RNA sequencing data, identify key nodes among the submitted genes, perform gene signature analyses, and generate heatmaps based on perturbation or gene expression data. GeneSetR enables researchers to readily identify gene clusters associated with specific phenotypes or biological processes, providing insights into the potential functional roles of these clusters and the role of single genes in them. With robust analysis capabilities, GeneSetR is a powerful resource to facilitate the exploration of genotype-phenotype relationships.

#7417 SpatialCS: A tool to effectively integrate histological annotations and spatial transcriptomics analysis.

Y. Chu[1], K. S. Cho[1], I. Khanduri[2], T. Zhou[1], J. Jiang[1], Y. Liu[1], X. Yan[1], G. Pei[1], Y. Dai[1], Y. Liu[1], R. Wang[1], A. Jadhav[1], S. Hernandez[1], H. Kadara[1], L. Solis Soto[1], S. Kopetz[1], D. M. Maru[1], L. Wang[1];

[1]The University of Texas MD Anderson Cancer Center, Houston, TX, [2]Baylor College of Medicine, Houston, TX

Spatial transcriptomics is revolutionizing our understanding of tumor ecosystems, providing insights into the spatial dimensions of cell locations, their organization, and interactions within tissues. A key challenge in this field is integrating histological annotations with spatial domains identified through unsupervised clustering methods like SpaGCN. This integration is crucial for accurate spatial domain identification and further analyses. However, clustering results often vary based on parameters such as resolution, leading to inconsistencies with histological annotations. This variation necessitates optimized parameter selection to achieve the best clustering outcomes.

We here introduce SpatialCS, a novel tool specifically designed to both visualize and quantify the alignment between histological annotations and the clustering results obtained from spatial transcriptomics data. SpatialCS employs a new index based on the asymmetric Wallace indices. This index penalizes spot pairs that are clustered together but do not share the same histology annotation type, with penalties scaled according to their transcriptional similarity. Additionally, we propose a purity index, derived by calculating the average transcriptional entropy of all clusters. This index serves as a measure of the homogeneity within each cluster. Furthermore, SpatialCS includes a unique visualization function. This function projects histological annotations onto the clustering results as outlines, making it easier to assess the consistency between histology annotations and clustering outcomes.

We have applied SpatialCS to Visium spatial transcriptomics data generated on four colorectal cancer liver metastases, each accompanied by comprehensive spot-level histological annotations in both tumor and normal compartments. The histologic annotations include but not limited to are tumor cells, tumor cell cluster subtypes, tumor stroma, tumor in the vessels, portal tract, individual bile ducts, portal vein and liver cell plates and non-neoplastic stroma. The application of SpatialCS has proven its effectiveness in identifying the most consistent clustering results, which were further confirmed by experienced pathologists. Notably, the output of SpatialCS offers helpful guidance for improving histological annotations. Together, SpatialCS not only provides a quantitative approach to evaluate the consistency between histological annotations and unsupervised clustering analysis but also showcases its potential to significantly enhance histological annotations.

#7418 LongFuse: Detecting gene fusion transcripts from high throughput long-read single cell RNA sequencing data.

C.-K. Shiau[1], Y. He[1], H.-Y. Lin[1], L. Lu[1], X.-D. Lu[2], J. Yu[2], R. Gao[1];

[1]Northwestern Univ. Feinberg School of Medicine, Chicago, IL, [2]Emory Univ. School of Medicine, Atlanta, GA

Gene fusion resulted from genomic translocation plays important oncogenic roles including but not limited to gene activation and changing protein coding sequences. Historically, fusion gene analysis has been limited to bulk levels resulting in mixed oncogene activation models. Single cell Nanopore RNA sequencing (scNanoRNAseq) has the unique strength in detecting full-length chimeric transcripts in thousands of single cells in parallel. However, robust computational tools for detecting fusion genes in single cells from scNanoRNAseq data are missing. Here, we developed LongFuse, a fast and accurate tool, to detect fusion genes and their splicing isoforms in single cells from scNanoRNAseq data. LongFuse implements an XOR logic gate algorithm to speed up fusion candidate searching and stringent criteria to eliminate false discoveries due to trans-splicing events and randomly ligated chimeras. We applied LongFUSE onto scNanoRNAseq data of both human prostate cancer cell line, VCaP, and tumor tissues with known *TMPRSS2-ERG* fusion. Our results showed that both cancer cell line and prostate tumors harbored a mixture of fusion positive and fusion negative tumor cells. Gene expression analysis revealed transcriptional differences between fusion positive and negative cells including genes involved in cancer cell proliferation and invasion programs such as *ELL2, ZBTB16, IGF1R, ANK3, MYPOP* and *PLPP1* genes. LongFUSE also calculates the splicing isoforms of fusion gene transcripts, allowing prediction of protein sequences of fusion gene transcripts. Taken together, our data demonstrated that LongFUSE is a robust computational tool for detecting gene fusions and their splicing isoforms at single cell level from scNanoRNAseq data.

#7419 Seq2Karyotype (S2K): A method for deconvoluting heterogeneity of copy number alterations using single-sample whole-genome sequencing data.

L. Pu[1], K. Szlachta[1], V. Valentine[1], X. Chen[1], J. Wang[1], D. Kennetz[2], D. Putnam[1], S. Natarajan[1], L. Dong[1], T. Look[3], M. Wlodarski[1], L. Wang[1], S. Burden[1], J. Easton[1], X. Chen[1], J. Zhang[1];

[1]St. Jude Children's Research Hospital, Memphis, TN, [2]Roche, Santa Clara, CA, [3]Dana-Farber Cancer Institute, Harvard Medical School, Boston, MA

Broad copy number alterations (CNAs) at chromosomal band resolution have been used as cancer diagnostic and prognostic biomarkers for decades. These events have been characterized by cytogenetic imaging, an approach which is powerful for assessing heterogeneity but limited for locus fine mapping. While CNA detection by next-generation sequencing has become a standard analysis, existing methods rarely model CNA heterogeneity in bulk tumor samples and often require a paired normal sample for control. To overcome these limitations, we developed Seq2Karyotype (S2K, https://github.com/chenlab-sj/Seq2Karyotype), a new algorithm for in-silico karyotyping using single-sample whole-genome sequencing (WGS) data. S2K performs joint modeling of read-depth and allelic imbalance (AI) of high-quality heterozygous SNPs to identify reference diploid regions, followed by modeling and segmenting the deviation from the reference. Empirical coverage and AI of segmented regions are fitted to models of single and admixed CNAs to estimate clonality. The final karyotyping considers both the model fitness and minimization of evolution steps.To evaluate S2K's performance, we analyzed two cell lines commonly used for benchmark test: COLO829 (melanoma) and HCT1395 (breast cancer); both had single-cell (sc) WGS for validation. For COLO829, S2K replicated the four populations detected by scWGS but derived a different clonality estimate. The predominant clone, defined by loss of 1p, 10p, and chr18, was estimated to have 67% cellular fraction (CF) by bulk sample analysis of S2K in contrast to the 10% CF by scWGS analysis. In HCT1395, S2K identified three new CNAs present in >50% of the cells of the matching germline sample which were subsequently validated by FISH, karyotyping and SKY mapping.To demonstrate S2K's utility, we analyzed three diverse data sets: 17 neuroblastoma cell lines, 24 pediatric AML samples with karyotyping data, and two blood samples from children with myelodysplastic syndromes (MDS) known to harbor mosaic uniparental disomy (UPD). CNA-based intra-tumor heterogeneity was detected in 88% (15/17) of the neuroblastoma cell lines, comprised of 2-4 distinct populations with diverse ranges of CF (~10%-90%) and varying CNA patterns (e.g. admixture of tetraploid and diploid cells), which were validated by cytogenetics or scWGS. In the patient AML samples, S2K detected >95% of the previously reported cytogenetic events and 30% of additional copy-neutral loss-of-heterozygosity events. The mosaic UPD events in MDS patients were detected with projected clonality of 60% and 25%, respectively. These results not only demonstrate the accuracy of in-silico karyotyping performed by S2K but also reveal the dynamic intra-tumor heterogeneity in cancer cell lines, which may impact the design and interpretation of future experiments using these cell lines.

#7420 Optimizing proteomic data access and analysis in the cloud: Leveraging Terra's integration with the Proteomic Data Commons.

Emily LaPlante[1], Bingxing Huo[1], DR Mani[1], Ratna R. Thangudu[2]

[1]Broad Institute of MIT and Harvard, Cambridge, MA,[2]ICF, Rockville, MD

The Proteomic Data Commons (PDC) hosts cancer proteomics data with the goal of making this data available to the public to support development of cancer diagnostics, treatment, and progression tracking. As a part of the Cancer Research Data Commons (CRDC), the Terra platform provides a cloud workbench for the PDC data. FireCloud is a Broad Institute project funded by NCI to empower cancer researchers to access data, run analysis tools and collaborate securely in the cloud. It is powered by Terra, a secure, scalable cloud-native platform developed by the Broad Institute, Microsoft, and Verily, an Alphabet company. It provides batch workflow execution, interactive analysis including data visualization, and ~2,900 publicly available tools with the ability to import more tools from Dockstore.

The integration of PDC and Terra enables researchers to leverage the data navigation and file-level search capabilities on the PDC web browser (pdc.cancer.gov) and export selected data manifests to a Terra workspace. This integrated hand-off specifically allows metadata and cloud links to PDC data in Portable Format for Bioinformatics (PFB) to be transferred to Terra and used in analysis with cloud resources. A featured workspace for Terra-PDC integration includes tools for (i) downloading data files and relevant additional metadata; (ii) organizing the data and metadata for running the FragPipe workflow, a comprehensive collection of tools for reading and processing raw Mass Spec (MS) data; and (iii) implementing a pre-configured FragPipe workflow to process isobarically labeled MS data from Tandem Mass Tag (TMT) or Isobaric tags for relative and absolute quantitation (iTRAQ) experiments using information automatically imported from PDC via the PFB import. The pipelines can also be customized as needed to process any type of raw MS data the PDC supports. In addition, Terra connects to the NCI Genomic Data Commons (GDC) and hosts The Cancer Genome Atlas (TCGA) and Therapeutically Applicable Research to Generate Effective Treatments (TARGET) datasets allowing users to pull in other data types for co-analysis. As a whole, using the CRDC cloud resources, in conjunction with Terra, allows analysis of data on a massive scale, enabling multi-omic integration spanning the genomic and proteomic commons data, with easy sharing of data and tools.

#7422 Enabling biomarkers of chromosomal instability for tumor only targeted gene panel sequencing.

D. Gomez-Sanchez[1], J. Thompson[2], B. Hernando[2], D. Garcia-Lopez[3], H. de Galard[3], A. Roy[3], A. Cullen[3], L. Madrid[3], J. Teles[3], A. Piskorz[3], J. Yip[3], A. Cadiz[3], M. Escobar-Rey[2], R. Moreno-Vellisca[1], N. Carrizo[1], E. Alvarez[1], M. Quintela-Fandino[4], M. Barbacid[5], J. Ramos-Paradas[6], J. Coya[1], I. Ferrer[1], J. Zugazagoitia[7], L. Paz-Ares[7], G. Macintyre[8];

[1]12 de Octubre Hospital Research Institute & Spanish National Cancer Research Centre (CNIO), H12O-CNIO Lung Cancer Clinical Research Unit, Madrid, Spain, Madrid, Spain, [2]Spanish National Cancer Research Centre CNIO, Computational Oncology, Madrid, Spain, Madrid, Spain, [3]Tailor Bio, Cambridge, United Kingdom, [4]Breast Cancer Clinical Research Unit, Spanish National Cancer Research Centre (CNIO), Madrid Spain, Madrid, Spain, [5]Experimental Oncology Group, Molecular Oncology Program, Spanish National Cancer Center (CNIO), Madrid, Spain, Madrid, Spain, [6]Department of Pathology and Yale Cancer Center, Yale School of Medicine, New Haven, Connecticut, USA, Madrid, Spain, [7]12 de Octubre Hospital, Medical Oncology, Madrid, Spain, Madrid, Spain, [8]Spanish National Cancer Research Centre CNIO, Computational Oncology, Madrid, Spain, Cambridge, United Kingdom

Capture-based targeted sequencing is routinely used for small variant detection in cancer clinical care. Alongside targeted DNA, off-target DNA is also sequenced. These off-target reads are distributed across the genome, allowing for a whole genome copy number profile to be derived without the need for a SNP backbone. Here we present CopyRight, a method that generates robust genome-wide copy number profiles, which can be used for downstream chromosomal instability (CIN) quantification, overcoming various sources of technical noise with a novel approach that only requires a single tumor sample. We analyzed a variety of capture-based NGS protocols using our novel computational method, including the TruSight Oncology 500 (TSO500) panel, and compared them to the current gold standard for genome-wide copy number profiling from FFPE tissues: shallow whole genome sequencing (sWGS). Comparable results were obtained from targeted sequencing depending on sample purity, preservation method, and read depth. Additionally, benchmarks of CopyRight against other computational algorithms show an improvement in performance without the need for a matched normal tissue, the usual drawback for other methods in the cancer field.

CIN signatures are a new set of emerging biomarkers that reflect the diversity of defective pathways that have operated in a tumor, which require robust genome-wide copy number profiles. These CIN signatures can be used to predict response to cytotoxic agents and targeted therapies and could ultimately help guide therapy selection in patients. As most clinical sequencing workflows rely on targeted sequencing, CopyRight can be included in current clinical assays, enabling CIN biomarker quantification with no extra technical or experimental requirements.

#7423 BATCH-FLEX: Feature-level equalization of x-batch in heterogeneous cancer data.

Joshua Davis, Alyssa Obermayer, Thac Duong, Rebecca Hesterberg, Xuefeng Wang, Mingxiang Teng, G. Daniel Grass, Timothy Shaw

Moffitt Cancer Center, Tampa, FL

Purpose: Develop a shiny application to help integrate cancer datasets and guide researchers in selecting an appropriate method of correction for their technical artifacts.

Description: Integrative analysis of heterogeneous expression data remains challenging due to variations in platform, RNA quality, sample processing, and other unknown technical effects. As the field performs omics profiling of samples from cancer patients and murine models, there is the need for harmonizing, identifying, and correcting these technical effects to ensure robust analysis on the treatment and conditional effects of the underlying genetics or biological events. However, selecting and implementing different approaches for removing unwanted batch effects can be a time-consuming and tedious process, especially for more biologically focused investigators. In this project, we present Shiny BATCH-FLEX, a Shiny app to rapidly visualize batch correction by established batch correction methods such as ComBat, Mean Centering, ComBatSeq, and Limma RemoveBatchEffect. With BATCH-FLEX, users can visualize the contribution of variance of a factor before and after correction using principal component analysis, relative log expression plots, heatmaps, and explanatory variables. Users can also save all plots and matrices as a single ZIP file for further downstream analysis.

Results: As a proof of concept, we assessed BATCH-FLEX using simulated data generated from a linear model framework introduced by Gagnon-Bartsch and Speed, which assumes that gene expression measurements can be distilled to a combination of the biological signal, systemic nose, and random noise. BATCH-FLEX was able to successfully identify and remove the introduced effect using each of the batch correction methods listed above. Next, we evaluated BATCH-FLEX using a comprehensive collection of bladder cancer data consisting of microarray data from 13 studies spanning 1452 samples. Following the cleaning of study-dependent noise, BATCH-FLEX was successful in revealing the heterogeneity among bladder cancer based on known sample type annotations.

Conclusion: We have developed BATCH-FLEX, a tool for oncologic researchers to rapidly assess, select, and implement commonly used batch correction methods. This tool is available at https://github.com/shawlab-moffitt/BATCH-FLEX. Our integrative web portal of a Bladder Cancer Resource for Translational Science (BEACON) will also be shared at the meeting.

#7424 iStarTLS: Advanced detection and phenotyping of tertiary lymphoid structures.

K. Cho[1], J. Jiang[1], D. Zhang[2], Y. Liu[1], J. Chen[1], R. L. Segura[1], X. Yan[1], G. Pei[1], L. M. S. Soto[1], Y. Chu[1], A. F. Sinjab[1], C. Yee[1], S. Kopetz[1], A. Maitra[1], A. Futreal[1], A. Lazar[1], A. A. Jazaeri[1], H. Kadara[1], J. Gao[1], M. Li[2], L. Wang[1];

[1]UT MD Anderson Cancer Center, Houston, TX, [2]University of Pennsylvania, Philadelphia, PA

Tertiary lymphoid structures (TLSs) are clusters of immune cells formed in non-lymphoid tissues. They are often found at sites of chronic inflammation, notably within the invasive margins and the core of various solid tumors. TLSs are pivotal in mediating anti-tumor immunity. However, our understanding of TLSs in large/complex tissue contexts remains incomplete due to the lack of computational tools to effectively detect and phenotype TLSs. Recent advances in spatially resolved transcriptomics (SRT) present a broader spectrum of analytical possibilities for investigating the spatial phenotypic heterogeneity of TLSs and their interaction with stromal and cancer cells. Here, we present iStarTLS (Inferring Super-resolution Tissue ARchitecture for TLSs), a computational toolkit designed to process SRT data for TLS detection and phenotyping and showcase its performance on breast, bladder, and lung cancer samples. By effectively integrating spatial gene expression data with state-of-the-art machine learning techniques, we can substantially enhance our capabilities in TLS detection and comprehensive phenotyping. iStarTLS starts by enhancing the spatial resolution of spot-level gene expression data to near-single-cell resolution by leveraging high-resolution information provided by paired histology images. To detect TLSs and infer their cellular composition, we developed a TLS signature. Based on the high-resolution gene expression measurements and a curated reference panel of cell type-specific markers, we score cell type-specific gene signatures to obtain a cell type probability map across the whole tissue section. This map gives rise to a segmentation of key cell type components of TLSs, enabling the spatial mapping and colocalization of different cell types. Moreover, such an approach would allow us to infer the phenotypic states of cells within the TLSs, assess their cellular compositions, and discern their cellular organization in large, spatially heterogeneous tissues at a near-single-cell resolution. Notably, in conjunction with nuclei segmentation of high-resolution histology images, iStarTLS precisely maps high endothelial venules (HEVs), a key structure within TLSs often overlooked by previous studies. iStarTLS paves the way for uncovering novel mechanisms of immune-tumor interactions and designing personalized therapies targeting specific cellular components or states within TLSs.

#7425 UMI-nea: A fast and robust UMI analysis approach to accurately identify and quantify TCR repertoire from targeted RNA sequencing with wide range of input molecules.

J. Deng, J. Zhang, S. Tian, S. J. Rulli, H. Xu, J. DiCarlo, E. Lader;
QIAGEN Sciences Inc., Frederick, MD

The T-cell receptor (TCR) population in humans is comprised of highly diversified heterodimers, regulating the recognition of antigen-major histocompatibility complex. Tremendous TCR sequence diversity is produced by somatic recombination of several TCR gene loci each consisting of multiple gene segments. Next-generation sequencing has enabled comprehensive profiling of the TCR repertoire from different physiological and disease conditions ushering in much interest in using TCR-seq to assess T-cell diversity. However, during NGS library construction and sequencing, errors and enzymatic inefficiencies can compromise the accuracy of the final data, particularly around calling of the VD and VDJ recombined regions and subsequent clonotype assignment. To increase the accuracy of NGS sequencing, Unique Molecular Identifiers (UMIs), consisting of short random nucleotide bases, can be used to mark original molecules in NGS library allowing for error and bias corrections. There are two well studied technical limitations to apply UMIs: 1.) UMI sequences tend to collide when input molecule number is large 2.) UMI sequences are not insulated from PCR and sequencing errors. To address these limitations, many computational approaches had been published. Among them, very few can be used to solve UMI colliding errors and over-simplified error models were implemented for UMI sequencing error handling. Here we report a novel strategy and UMI structure which uses more complex UMIs that is longer and of different length. This results in minimizing UMI collision while maximizing sequencing quality. Our UMI analysis pipeline, “UMI-nea” is able to handle not only substitution errors but also indel errors and UMIs with different lengths. We developed a novel computational framework to parallelly process sequence comparisons to mitigate the elevated computational burden. To account for the varied dispersion of PCR efficiency for different molecules and error bearing UMIs from libraries with different input and with different sequencing depth, we also developed a statistical framework leveraging negative binomial model and single-cell knee plot to set a dynamic threshold for original molecule estimate. We verified UMI-nea with several simulated data and demonstrated that UMI-nea can achieve >99% completeness and homogeneity to recover the original molecule count with various error rates and UMI lengths, outperforming existing tools and methods in comparison. We applied UMI-nea to profile TCR for 8 PBMC samples sequenced on different Illumina platforms with different sequencing depths. We observed >85% reproducibility of clonotype calls on all samples. To test the sensitivity and specificity of UMI-nea, we sequenced pure cell line samples and cell line spike-in samples with different ratios and discovered very high recall and precision rates.

#7426 The GenePattern ecosystem for cancer bioinformatics.

M. M. Reich, T. Tabor, J. Liefeld, E. Huang, F. Kim, J. P. Mesirov;
UC San Diego, La Jolla, CA

As the availability of genomic data and analysis tools from large-scale cancer initiatives continues to increase, with single-cell studies adding new dimensions to the potential scientific insights, the need has become more urgent for a software environment that supports the rapid pace of cancer data science. The GenePattern ecosystem, first introduced in 2004 and updated continually to support the changing needs of cancer genomics research, supports the analytical, computational, and reproducibility needs of the world-wide cancer analysis community.The GenePattern server, available at www.genepattern.org, provides hundreds of analysis methods for scientists at all levels of computational sophistication, with the only requirement for use being a web browser. The GenePattern server offers bulk and single-cell RNA-seq, copy number variation, flow cytometry, network analysis, general machine learning, gene set enrichment analysis, proteomics, and many other modalities. Analysis steps can be linked together into pipelines that can then be edited, shared, and made public. All parameters of an analysis, including the code version, are recorded so that an analytical result can be reproduced at any point in the future.The GenePattern Notebook system, notebook.genepattern.org, is an integration of the Jupyter Notebook environment with the GenePattern server. It combines the research narrative capabilities of Jupyter with the non-programming approach and breadth of analyses available in GenePattern. Scientists using GenePattern Notebook can create documents that include richly-formatted text and multimedia, executable code, and GenePattern analyses. A single GenePattern notebook can therefore comprise a sophisticated analytical workflow that runs on multiple remote servers.We have recently expanded GenePattern Notebook into a new notebook environment, Genomics to Notebook, g2nb.org, which adds the ability to include analyses on any public Galaxy server as well as using the Integrative Genomics Viewer (IGV) and Cytoscape within notebooks. Each analysis or visualization appears a cell within a notebook, preserving the accessibility and ease of use of the notebook metaphor while retaining the essential aspects of each tool’s user interface. When run, the entire analysis appears to execute seamlessly within the notebook. The online workspace also includes a library of featured genomic analysis notebooks, including templates for common analysis tasks as well as cancer-specific research scenarios and compute-intensive methods. Scientists can easily copy these notebooks, use them as is, or adapt them for their research purposes.

#7427 Automated, real-time acquisition and quantification of peak, plateau-phase *in vivo* bioluminescent data.

A. Van Praagh, B. Nelson, P. Ballieu, M. Smith, M. Rule;
Spectral Instruments Imaging, LLC, Tucson, AZ

It is widely recognized that plateau-phase bioluminescent (BL) kinetic curve data should be used when reporting on BLI results from substrate-injection BLI model systems. The basis for this understanding is that plateau-phase BL data is uniquely suited in several ways: (i) it will optimize the detection of target, luciferase-expressing cells (especially when they are low in copy number or deep within the animal model), (ii) it will optimize BLI data reproducibility (with there being no change in signal values across the plateau phase), and (iii) it will also provide BLI data values that correlate consistently with the number of viable target cells in a given BLI model. Given this critical value of plateau-phase BL data, there is, nevertheless, a simple practical issue to be addressed: The overall manual process of generating BL kinetic curves, and then identifying and quantifying plateau-phase data is not insignificant—it takes time!In this poster, we review the performance of "*Kinetics*," a new feature in the Aura software platform from Spectral Instruments Imaging, LLC. *Kinetics* is designed to collect, present, and analyze BL kinetic curve data for up to 10 mice, in a completely automated and real-time fashion. Data outputs include a live graph that simultaneously presents individual mouse, whole body ROI (Total photon/sec) values *vs.* time post-luciferase injection, and analogous mean BL values per mouse group. Here in, we present an evaluation of the performance of *Kinetics* under various testing conditions. We initially evaluated *Kinetics'* ability to acquire, present and analyze the BL kinetic curves of 5 phantoms. The photon output rates of these phantoms (Total photons/sec) were programmed to mimic the rise, plateau, and fall sequence typically seen BLI studies. In an analogous fashion, we then tested *Kinetics'* ability to acquire, present, and analyze the BL kinetic curves of 5 to 10 live mice from several oncology models. Furthermore, we used *Kinetics* in oncology efficacy studies to monitor for expected changes in BL kinetic curve shapes (*i.e.,* for changes in the onset times and durations of the rise, plateau and fall phases in BL kinetic curves) between different treatment groups (*e.g.,* between positive controls groups and one or more treatment groups). In the same studies, we also used *Kinetics* to check for changes in BL kinetic curve shapes that might occur for a given treatment group across several time points, after pathogen challenge. Results from this set of experiments consistently and clearly illustrated the capability of *Kinetics* to acquire, present and analyze individual and mean BL kinetic curve data for up to 10 mice at a time, in an automated and real-time fashion. We believe that *Kinetics* from Spectral Instruments Imaging, LLC, has the potential to revolutionize the ease with which plateau-phase, BL kinetic curve data can be collected, presented, and used in a wide range of preclinical BLI studies.

#7428 S2Map: An online interactive analytical platform for quantitative signal measurement of cell Secretion Signal Map.

Z. Yue[1], L. Zhou[1], F. Huang[2], P. Chen[1];

[1]Auburn University, Auburn, AL, [2]University of Alabama at Birmingham, Birmingham, AL

Cell communication is predominantly governed by secreted proteins, whose diverse secretion patterns often signify underlying physiological irregularities. Unraveling the intricacies of these secreted signals at the single-cell level is crucial for a comprehensive understanding of regulatory mechanisms involving various molecular agents. To elucidate the array of cell secretion signals, encompassing both anisotropic and isotropic biomolecular cues from individual immune cells or disparate cell types, we introduce the Secretion Signal Map (S2Map). S2Map is an innovative online interactive analytical platform that incorporates qualitative metrics, the signal inequality index (SII) and the signal coverage index (SCI), which are exquisitely sensitive in facilitating the measurement of dissymmetry and diffusion of cumulative signals and signal dynamics in temporal analysis. S2Map's innovation lies in its depiction of signals through real-time secretion hotspots, and cumulative secretion contour lines, complemented by the visualization of potential cell secretion signal velocities via stream plots generated by regression models. We evaluated the SII and SCI performance in distinguishing the simulated signal diffusion model. Presently, S2Map hosts a repository of 12 datasets that map single-cell and two-cell secretion dynamics. These datasets serve as a resource to explore secretion signal types. We anticipate that S2Map will be a powerful approach to delve into the complexities of physiological systems, providing insights into the regulation of protein production, such as cytokines at the remarkable resolution of single cells. The S2Map server is publicly accessible via https://au-s2map.streamlit.app/.

#7429 A web-based application to co-register elemental imaging with histopathology to enhance the study of metal bioaccumulation within tumors.

Y. Lu[1], R. Steiner[2], S. Han[1], M. Chan[2], T. Punshon[2], B. Jackson[2], L. Vahdat[1], J. Marotti[1], J. Levy[3];
[1]Dartmouth Health, Lebanon, NH, [2]Dartmouth College, Hanover, NH, [3]Cedars Sinai Medical Center, Los Angeles, CA

Essential trace elements are crucial in various biological processes, including tumor growth, migration, and metastasis. For instance, copper ions are involved in mitochondrial metabolism, cell proliferation, tumor migration, metastasis and proangiongenic pathways. Localizing where metal ion homeostasis is disrupted is vital for understanding these processes beyond what bulk analysis can reveal. Elemental imaging offers high-resolution, quantifiable multi-elemental distribution maps, providing a more detailed analysis compared to traditional bulk measurements. However, aligning findings with tissue structures identified in histopathological data can be challenging. To address this, we developed a web-based application for the co-registration and analysis of Whole Slide Images (WSI) and elemental imaging data at the cellular level. The application integrates WSI with elemental maps generated by technologies such as ultrafast laser ablation and inductively coupled plasma time-of-flight mass spectrometry (LA-ICP-TOF-MS), as well as a range of other elemental imaging techniques. Hosted by the Biomedical National Elemental Imaging Resource, the current application allows for a streamlined data integration, co-registration, and analysis, including: 1) uploading WSI, elemental maps, and pathologist annotations, 2) automated preprocessing to identify tissue regions, 3) co-registration to merge WSI and elemental maps, 4) custom import, real-time overlay/editing of pathologist annotations transferred from WSI, 5) plotting, statistical tools and 6) data export. This application enables users to compare elemental abundance within/between tissue structures annotated on H&E or immunohistochemical slides. Derived data can pinpoint elements and mixtures whose abundance differs significantly across various pathological conditions. As an initial test, we applied the software on breast HER2/ER/PR tumors, varying in molecular subtype/histology. Preliminary results, using Bayesian lognormal regression models, adjusting for tumor subtypes, indicated a subtype-dependent variation in copper abundance. The relative difference in copper levels between tumor and stromal regions was notably less in HER2 tumors ($p=0.026$) compared to HR tumors ($p<0.0001$). Conversely, iron showed a consistently higher abundance in stromal areas across both subtypes ($p<0.0001$). Future enhancements include improved co-registration capabilities, hotspot analysis, machine learning, mixture effects, and cloud-based architecture. This method uniquely enables integration of elemental data with spatial transcriptomics, mapping gene transcripts on tissue slides. With current ST assays aligned with H&E slides, this tool facilitates co-registration, offering insights into biological pathways affected by metal homeostasis disruptions.

#7430 Development and demonstration of a user-friendly application to explore single-cell atlas for prostate cancer (PCa) and analyze newly generated single-cell and spatial PCa datasets.

S. Sharma, E. Shenderov;
Johns Hopkins University School of Medicine, Baltimore, MD

Background: Single-cell atlases provide a high-resolution and tissue-specific depiction of cellular state at the transcriptomic level. Newer technologies like spatial transcriptomics, MALDI, and long-read sequencing introduce orthogonal modalities to single-cell data, making the analyses of large atlases even more complex. RShiny package in R is used to develop user-friendly GUI applications that could enable users to use analysis tools in an interactive manner, thus minimizing the requirement of prior programming experience.

Methods: Publicly available scRNA-seq datasets were collected for a wide range of prostate-related pathologies. The datasets were evaluated for their quality based on cell count and availability of the appropriate markers in each compartment. Finally, 11 datasets out of 16 datasets were selected for building integrated datasets. These datasets were filtered for cell types with <10% mitochondrial RNA, and cells with <500 genes were removed from the datasets. The datasets were then clustered to evaluate the effects of cell cycle, dissociation-induced stress, and the presence of doublets. The quality-controlled datasets were batch-corrected using the Harmony package and the harmonized principal components were used in Seurat for clustering the integrated data. Tools used for the analysis of single-cell datasets, beginning from raw counts, have been developed in R with a focus on modularity. These tools are packaged into a simple and intuitive RShiny application which follows the workflow shown in Figure 1a.

Results: The atlas obtained include samples from healthy prostate, benign prostate hyperplasia, primary prostate tumor, ICC/IDC, castration-resistant prostate cancer (CRPC), and Neuroendocrine prostate cancer (NEPC). The dataset includes 72 patients and ~320k cells with a median number of ~1600 genes expressed. We were able to distinctly identify Luminal, Hillock, Club, Basal, Neuroendocrine, Endothelial, Fibroblast, Smooth Muscle, Myeloid, T, B, NK, Mast, and Plasma cells in the integrated along with some unknown cellular subtypes in the epithelial compartment. The integrated data was manually annotated using cell type-specific markers. The single-cell atlas obtained was weaved with the workflow tools into an RShiny app.

Conclusions: Besides being a useful reference for PCa, the atlas would find extensive use in understanding the transcriptomic landscape of PCa biology. The integrated dataset will also prove crucial in developing bulk RNA sequencing deconvolution and single-cell imputation algorithms. Finally, we aim to provide a user-friendly interface to the prostate cancer community for using the single-cell PCa atlas and analysis tools with minimal computational requirements.

#7431 IAMSAM: Image-based analysis of molecular signatures using the Segment-anything model - Integrative analysis tool for tumor microenvironment.

Dongjoo Lee[1], Jeongbin Park[1], Seungho Cook[1], Seongjin Yoo[1], Daeseung Lee[1], Hongyoon Choi[2]

[1]Portrai, Inc., Seoul, Korea, Republic of,[2]Department of Nuclear Medicine, Seoul National University Hospital, Seoul, Korea, Republic of

Introduction. Spatial transcriptomics (ST) is a powerful approach for investigating gene expression patterns in tissues while preserving their spatial context. However, working with ST data presents challenges due to its complexity, high dimensionality, and the absence of user-friendly tools. IAMSAM (Image-based Analysis of Molecular signatures using the Segment-Anything Model) leverages the Segment-anything model (SAM), a cutting-edge deep learning model developed by Meta, which is specifically designed for image segmentation. We demonstrated IAMSAM's capabilities with publicly available ST datasets, showcasing its user-friendly interface, featuring its user-friendly interface for exploring pathophysiology and potential biomarkers.

Methods. IAMSAM is a web-based tool designed for analyzing ST data, utilizing the SAM for image segmentation. It offers two modes: everything-mode and prompt-mode. In everything-mode, the model automatically generates segmentation masks for the entire histologic image. In prompt-mode, users can draw rectangle boxes to provide input prompts for SAM. IAMSAM's downstream analysis includes the identification of DEGs, enrichment analysis, and cell type prediction of selected regions of interest. DEGs are represented in volcano plots and box plots, aiding in the identification of genes associated with image features of tumors such as cancer-enriched areas or stromal patterns. Enrichment analysis assesses gene sets for over-representation, providing insights into pathways and biological processes relevant to cancer. Cell type prediction utilizes the CellTypist API, offering valuable information about the cellular composition and heterogeneity within the tumor microenvironment.

Results. IAMSAM has been applied to publicly available ST datasets to demonstrate its effectiveness in cancer research. It accurately identified cancer markers in breast cancer samples and aligned with spot clustering results in various cancer samples, all of which have significant implications for understanding cancer biology. Prompt-mode effectively identified stromal regions in tumor sections, and with magnification, it uncovered microvessels in prostate cancer samples, providing valuable insights for cancer pathophysiology research. IAMSAM was also applied to fluorescence imaging, demonstrating its versatility and potential in various cancer-related studies.

Conclusions. IAMSAM is a valuable web-based tool for cancer research using spatial transcriptomics data particularly integratively analyzing tumor microenvironments with a user-friendly interface. IAMSAM opens up new avenues for spatial transcriptomics research in the context of cancer, making it a promising resource for cancer researchers.

#7432 Improving FAIRness of computational approaches for cancer: The computational resources for cancer research portal.

E. Stahlberg[1], L. Borkon[1], R. Frost[1], S. Jones[1], A. Khalsa[1], L. Lewis[1], E. Greenspan[2], S. Menon[1];

[1]Frederick National Laboratory for Cancer Research, Frederick, MD, [2]Center for Biomedical Informatics and Information Technology, National Cancer Institute, Rockville, MD

The Computational Resources for Cancer Research website is a public portal supported by NCI that democratizes access to available computational resources for the cancer research community.

In supporting an emerging FAIR (Findable, Accessible, Interoperable, Reusable) data science ecosystem inclusive of software, models and data, the goals of the portal are to serve cancer data scientists by increasing understanding, access, and adoption of computational resources for cancer research, and to foster new collaborative research projects. Initially populated with resources developed in NCI supported collaborations with the US Department of Energy, the portal is serving as a unified reference and resource for computational resources developed broadly by the cancer community. These collaborative projects include CANDLE (the Cancer Distributed Learning Environment), IMPROVE (Innovative Methods and data for PRedictive Oncology model Validation and Evaluation), ADMIRRAL (AI Driven Multi-scale Investigation of Ras-Raf Activation Lifecycle), MOSSAIC (Model Outcomes using Surveillance Data and Scalable AI for Cancer) and ATOM (Accelerating Therapeutics for Opportunities in Medicine).

The resources include software, models, and datasets as well as descriptive use cases and references to tutorials associated with many of the described resources. The portal also integrates content from the Predictive Oncology Model and Data Clearinghouse (modac.cancer.gov) which can be accessed through REST APIs.

Ongoing development of the portal is driven by community insights and contributions including input from an interdisciplinary advisory committee, working groups, early users, and preliminary feedback received at AACR 2023. The portal will also support community contributions of computational resources. In addition, the portal highlights computational approaches in emerging and challenging areas, such as digital twins for cancer.

The portal will enable the cancer research community to learn about new computational research methods through use cases and educational material, access cancer related software, datasets, and AI models, engage with peers and cross-disciplinary researchers at different career levels through an interactive forum, explore emerging areas, such as computational imaging, community-based standards for data management, predictive radiation oncology, and digital twin technologies, learn about in industry and community events, conferences, and workshops, and create new collaborative research projects. The presentation will deliver insights into key resources offered through the Computational Resources for Cancer Research Portal, how the portal will help the cancer research community identify and adopt computational resources of interest, and how researchers can join and participate in this growing community.

#7433 CGC-hosted comprehensive pipeline for spatial transcriptomics analysis.

M. Rankovic[1], N. Vukojicic[1], N. Ilic Raicevic[1], V. Matovic[1], D. Sain[2], J. DiGiovanna[2], B. Davis-Dusenbery[2];
[1]Velsera, Belgrade, Serbia, [2]Velsera, Boston, MA

Spatial transcriptomics has been experiencing significant growth in the past years. Inspired by two widely adopted methodologies, particularly in situ hybridization and next-generation sequencing, with an emphasis on the single-cell RNA sequencing (scRNA-seq), this hybrid method facilitates whole transcriptome profiling while preserving spatial context at high resolutions, thus allowing the exploration of novel insights in cancer research. We introduce the highly configurable solution for sequencing-based technologies that allow comprehensive spatial analysis. The pipeline is available on NCI-funded Cancer Genomics Cloud (CGC) platform, powered by Seven Bridges. The CGC platform provides a collaborative cloud base computation infrastructure that collocates computation, over 1000 bioinformatics workflows, and 4+ PB data to researchers, making the analysis of the Cancer Research data Commons (CRDC) datasets accessible from any environment.

This pipeline is developed using reliable, widely adopted packages and can process datasets generated by several leading technologies. It comprises a set of common steps including quality control, data preprocessing, dimensionality reduction, cluster identification, detection of spatially variable features, and integration with scRNA-Seq reference. The pipeline is highly configurable, allowing for various settings to be modified and optimized for result refinement. Additionally, it allows the selection of only specific components of the pipeline to be executed. The key steps of the pipeline are visually represented, allowing researchers to get a detailed insight into results.

Here, we demonstrate a typical flow of spatial transcriptomics analysis on publicly available datasets using the developed pipeline. We illustrate the impact of pipeline settings on the analysis outcomes. Furthermore, we identify spatially variable genes whose expressions show a distinct localization within the tissue. Finally, we perform the data integration to predict the cell type composition within the determined spatial domains.

Spatial transcriptomics analysis is a powerful method that has highly improved critical aspects of cancer research, such as the characterization of tumor microenvironment, the discovery of novel biomarkers and the clarification of drug resistance mechanisms. The ongoing evolution of this method is expected to play vital role in our deep understanding of complex spatial relationships within tissues. This CGC-hosted workflow is developed to contribute to the promising advancements.

#7434 Deployment of a visualization tool directly linked to the CellEngine cytometry analysis software to accelerate analysis of complex cytometry data sets in the context of ongoing clinical trials.

D. Montamat-Sicotte, Z. Bjornson, D. Franckaert, N. Dupuis, E. Paramithiotis;
CellCarta, Montreal, QC, Canada

Introduction High-dimension cytometry panels have become a hallmark of clinical phase 1 and 2 trials. These panels can provide hundreds of readouts and need to be combined with subject metadata (e.g., health data, demographics, timepoint, and dose) to provide insights on the identification of biomarkers. Several bioinformatics tools are available to interpret these complex datasets; however, these usually require significant expertise in data manipulation, which sometimes forces the person doing the data interpretation to outsource the data visualization and statistical analysis to a bioinformatics team. As a consequence, the scientist can be one step-removed from the “raw” data, critically preventing the interpretation of biomarker effects in the context of the raw staining profiles and associated quality controls (e.g. in-run controls). Here, we show how a new tool integrated with the CellEngine cytometry analysis software can accelerate data interpretation without removing the scientist from the raw data.

Methods The visualization tool pulls live data from CellEngine, displaying both study- and cohort-level information in summary views as well as the sample-level staining profiles. As a live link, any changes made in CellEngine, such as ones to gating and compensation, or the addition of new samples during an ongoing study, are automatically reflected in the dashboard. This link also gives the ability to consult staining profiles and performance of controls directly within the tool without having to switch between applications. CellEngine is capable of analyzing 10,000s of samples at once, and thus can handle the largest of studies.

Results Here, we show how the visualization tool was used to accelerate the data interpretation of two different flow cytometry assays. In the first example, lymphodepletion and immune system reconstitution in patients undergoing CAR-T cell therapy was monitored using the tool. The live update of analysed data within the tool, coupled with the ability to verify the performance of the two controls ran with each sample, accelerated the data interpretation and improved the data quality. In the second example, we show how the software was used to follow cytokines responses across different timepoints in a vaccination program where samples were analysed using a polyfunctional intra-cellular cytokine staining panel. The tool greatly accelerated the interrogation of this complex data set and allowed the identification of trends within the different T cell responses.

Conclusion This new tool can help maximize the utility of high-dimensional cytometry in clinical trial analysis while allowing to keep the crucial link between graphical representation of large number of samples and the data associated with each individual flow cytometry staining profile.

#7435 PATTY: A bias estimation and correction model for bulk and single-cell CUT&Tag data.

S. S. Hu, Q. Chen, M. Grieco, C. Zang;
University of Virginia, Charlottesville, VA

The accurate detection of transcription factor (TF) binding sites and histone modifications (HM) on the genome-wide scale is essential for studying functional epigenetics and gene regulation. Cleavage Under Targets & Tagmentation (CUT&Tag) is a low-cost and easy-to-implement epigenomic profiling method that can be performed on a low number of cells and on the single-cell level. CUT&Tag experiments use the hyperactive transposase Tn5 for tagmentation. We find that Tn5 is subject to intrinsic sequence insertion bias (intrinsic bias). Additionally, the preference of Tn5 insertion toward accessible chromatin also affects the distribution of CUT&Tag reads (open chromatin bias). Both types of biases can significantly confound bulk and single-cell CUT&Tag data analysis, which requires careful assessment and new analytical methods. To address this challenge, we present PATTY (Propensity Analyzer for Tn5 Transposase Yielded bias), a computational method for systematic characterization and correction of biases in CUT&Tag data. We demonstrate that histone modification signals (H3K27me3 and H3K27ac) detected from CUT&Tag data after bias correction using PATTY are better associated with orthogonal biological features such as gene expression. PATTY-corrected single-cell CUT&Tag signals for histone modification can better cluster cells into their true cell types. This new computational method can improve both bulk and single-cell CUT&Tag data analysis.

CLINICAL RESEARCH: Biologic and Behavioral Effects of Cancer and Oncology Treatment
Poster Session

#7440 Symptom network analysis and unsupervised clustering of a cohort of oncology patients identifies drivers of symptom burden and patient subgroups with distinct symptom patterns.

B. H. Bergsneider[1], T. S. Armstrong[2], Y. P. Conley[3], B. Cooper[4], M. Hammer[5], J. D. Levine[4], S. Paul[4], C. Miaskowski[4], O. Celiku[2];
[1]Stanford University, Stanford, CA, [2]National Cancer Institute, National Institutes of Health, Bethesda, MD, [3]University of Pittsburgh, Pittsburgh, PA, [4]University of California San Francisco, San Francisco, CA, [5]Dana Farber Cancer Institute, Boston, MA

Purpose: Inter-individual variability in oncology patients' symptom experiences poses significant challenges in prioritizing symptoms for targeted intervention(s). In this study, computational approaches were used to unbiasedly characterize the heterogeneity of the symptom experience of oncology patients to elucidate their symptom patterns and drivers of symptom burden.
Methods: Severity ratings for 32 symptoms on the Memorial Symptom Assessment Scale from 3088 oncology patients were analyzed. Gaussian Graphical Model symptom networks were constructed for the entire cohort and subgroups identified through unsupervised clustering of symptom co-severity patterns. Symptom network characteristics were analyzed and compared using permutation-based statistical tests. Demographic and clinical characteristic differences between subgroups were assessed using multinomial logistic regression.
Results: Network analysis of the entire cohort revealed three core symptom clusters: constitutional, gastrointestinal-epithelial, and psychological. Lack of energy was identified as central to the network, suggesting that it plays a crucial role in driving overall symptom burden and may be the most salient to target clinically. Unsupervised clustering of patients based on shared symptom co-severity patterns identified six patient subgroups with distinct symptom patterns and demographic and clinical characteristics. The first subgroup represented a baseline cohort of patients who are most affected by common constitutional symptoms of cancer care. The second subgroup represented patients with severe overall symptom burden. The third subgroup represented patients primarily experiencing neuropathy. The fourth subgroup represented patients with advanced disease and treatment-related symptoms but relatively high quality of life. The fifth subgroup represented younger patients with pronounced psychological disease burden. The sixth subgroup represented patients with minimal symptom burden. Age, treatment status, and Karnofsky Performance Score were the strongest determinants of subgroup membership, but their interplay (in one case even with ethnicity) reaffirms the complex multi-factorial nature of the symptom experience. For each subgroup, symptoms with the highest network centralities that should be prioritized for management were identified.
Conclusions: This study provides a translational research framework for clinicians to better understand and address the symptom care needs of oncology patients. The framework combines unbiased stratification of patients and in-depth modeling of symptom relationships to capture the heterogeneity in their experiences. When validated, the identified core symptoms and associated clinical determinants may inform precision-based symptom management.

#7441 Health-Related quality of life and DNA methylation-based aging biomarkers among survivors of childhood cancer: Results from the St. Jude Lifetime Cohort.

N.-M. Plonski[1], Y. Pan[1], C. Chen[1], Q. Dong[1], X. Zhang[1], N. Song[2], K. Shelton[1], J. Easton[1], H. Mulder[1], J. Zhang[1], G. Neale[1], E. Walker[1], H. Wang[3], R. Webster[4], T. Brinkman[4], K. R. Krull[4], G. T. Armstrong[4], K. K. Ness[4], M. M. Hudson[4], Q. Li[4], I.-C. Huang[4], Z. Wang[4],
[1]St. Jude Children's Research Hospital, Memphis, TN, [2]Chungbuk National Univeristy, Cheongju, Korea, Republic of, [3]Shanghai Jiao Tong University School of Medicine, Shanghai, China, [4]St Jude Children's Research Hospital, Memphis, TN

Background: Childhood cancer survivors often reported poorer health-related quality-of-life (HRQOL) compared to age/sex-matched controls, indicating toxic stress resulting from high burden of treatment-related late effects. This study aimed to investigate cross-sectional associations between poorer HRQOL and epigenetic age acceleration (EAA) using several epigenetic clocks as well as other DNA methylation (DNAm)-based aging biomarkers.
Methods: DNAm was generated using the Infinium EPIC BeadChip version 1 with blood-derived DNA (median [min-max] for age at blood draw = 34.5 [18.5-66.6] years) from 2,206 long-term survivors in the St. Jude Lifetime Cohort. DNAm-based aging biomarkers and epigenetic age using multiple clocks (e.g., GrimAge; DNAmB2M: beta-2-microglobulin; DNAmADM: adrenomedullin) were derived from the DNAm Age Calculator (https://dnamage.genetics.ucla.edu). HRQOL was measured using the Medical Outcomes Study 36-Item Short-Form Health Survey which assesses eight domains, and physical (PCS) and mental (MCS) component summaries. General linear models evaluated associations between HRQOL and epigenetic age acceleration (EAA, e.g., EAA_GrimAge) or other DNAm-based biomarkers (e.g., chronological age adjusted residuals of DNAmB2M, which was similar to the approach in which EAA was derived) after adjusting for age, sex and cancer treatment exposures.
Results: Worse physical and mental HRQOL was associated with greater EAA_GrimAge (PCS: β [95%CI]=-0.621 [-0.744, -0.499] years, $P=2.48\times10^{-21}$; MCS: -0.548 [-0.667, -0.430] years, $P=2.82\times10^{-18}$; and all eight individual HRQOL domains), followed by chronological age adjusted residuals of DNAmB2M (PCS: -0.101[-0.144, -0.058], $P=2.31\times10^{-5}$; MCS: (-0.053 [-0.094, -0.011], P=0.030; and seven HRQOL domains), and chronological age adjusted residuals of DNAmADM (PCS: -0.096 [-0.139, -0.053], $P=5.45\times10^{-5}$; and five HRQOL domains). EAA_Horvath (Horvath clock, the representative 1st generation epigenetic clock) was the least informative biomarker, which was not associated with any HRQOL domains.
Conclusions: Worse HRQOL in different domains was associated with EAA_GrimAge and chronological age adjusted residuals of DNAmB2M, although future longitudinal studies are needed to illuminate the cause and consequence relationship between HRQOL and aging biomarkers.

#7442 Exploring the role of chinese herbal medicine in adjunctive therapy for non-small cell lung cancer: A systematic review and meta-analysis.

L.-C. Wang[1], T.-L. Chen[2], L. Chen[3], M.-Y. Tsai[4];

[1]Kaohsiung Chang Gung Memorial Hospital, Kaohsiung City, Taiwan, [2]National Chung-Hsing University, Taichung City, Taiwan, [3]Linkou Chang Gung Memorial Hospital, Taoyuan City, Taiwan, [4]Kaohsiung Chang Gung Memorial Hospital and Chang Gung University College of Medicine, Kaohsiung City, Taiwan

Non-small cell lung cancer (NSCLC) treatment traditionally relies on Platinum-based chemotherapy along with targeted therapy and immunotherapy. However, the emergence of drug resistance due to genetic factors and the progression of late-stage metastasis pose significant challenges. In Asian medical practices, the integration of Chinese herbal medicine (CHM) alongside conventional therapy has shown promise in improving treatment efficacy, ensuring safety, and mitigating adverse effects. This study aims to comprehensively summarize the prevalence and efficacy of CHM when combined with platinum-based chemotherapy in managing advanced NSCLC. Our analysis encompasses data from 14 randomized controlled trials involving 1451 patients, of which 739 received combined chemotherapy with CHMs while 712 received chemotherapy alone. Notably, the adjunctive use of traditional CHM demonstrated a marked increase in overall survival rates. Patients with NSCLC who received CHMs in combination with chemotherapy exhibited significantly higher Objective Response Rate (ORR) (RR = 1.37, 95% CI [1.20-1.58], p = .000) and Disease Control Rate (DCR) (RR = 1.13, 95% CI [1.07-1.21], p = .000) compared to those solely undergoing chemotherapy. The Karnofsky Performance Status (KPS) (SMD = 1.47, 95% CI [0.30-2.64], p = 0.014) also indicated substantial improvements in the quality of life assessment, involving a total of 277 cases. The systematic review identified 88 herbs and formulas, classified into two primary categories. The first category involves tonifying qi and nourishing yin, thereby enhancing the body's immune function and boost immune therapy, fortifying its ability to combat pathogens, and inhibiting cancer cell proliferation. Herbs such as *Rx.* Astragali (Huangqi), Rz. Atractylodis Macrocephalae (Baizhu), *Rx.* Glehniae (Shashen), and *Rx.* Ophiopogonis (Maidong) were among the most frequently prescribed CHMs. The second category consists of heat-clearing and toxin-removing medicines, effectively regulating the inflammatory response and infection around tumors while exhibiting potent anti-tumor activity, such as Herba Salviae Chinensis (ShiJianChuan) and Selaginella Doederleinii (ShiShangBai). The evidence derived from the meta-analysis strongly suggests that adjunctive CHM treatment can significantly enhance chemotherapy's effectiveness and improve tumor response. Subsequent research focusing on the development and application of CHM is warranted for the advancement of NSCLC treatment methodologies.

#7443 Investigating the impact of ferroptosis in a high-fat and high-oxidative stress hepatic steatosis environment .

C.-S. Chen, S.-C. Wang;
Kaohsiung Medical University, Kaohsiung, Taiwan

An iron-dependent mechanism of cell death, ferroptosis, occurs with intracellular iron accumulation and is associated with lipid peroxidation. Previous studies have shown that lipid peroxidation-induced ROS leads to DNA damage and promotes the progression of steatosis to advanced HCC. Therefore, we aim to study ferroptosis in a cell model with hepatocytes co-cultured with ACM (adipocyte culture medium) and low dose H_2O_2 for a high-fat/high ROS environment in vitro; an animal model with high-fat content and accompanying low dose carbon tetrachloride in vivo to observe the possibility of hepatocyte steatosis due to ferroptosis.

Animal model: Mice were fed a Western diet and provided with high fructose/glucose-containing sugar drinking water (WFSD) for 7 months while receiving a monthly extra-low dose of CCl_4.

Tissue staining: Liver sections were performed to observe histological abnormalities in each group.

Cell model: Pre-adipocytes, 3T3L1 were differentiated by adding IBMX, Dexamethasone, and Insulin (10 μg/ml). After differentiation, ACM was collected. The XTT assay was used to examine the relationship between cell death and ferroptosis by a ferroptosis inducer (Erastin) in high-fat and high-ROS environments.qPCR: To detect the expression of iron transport-related genes.Western Blot: To ascertain protein levels associated with ferroptosis.

Mitochondrial assay: Mitochondrial membrane potential (MMP), mitochondrial dynamics-related proteins, and fluorescence mitochondrial tracking and staining.

Ferritin, GPX4, IRP2, and ferroportin were upregulated when ACM co-culture with the hepatocytic AML12 cell line, and it also increased the sensitivity of ROS-related cell cytotoxicity, which was related to ferroptosis by the inducer, Erastin, in the high-fat/high-ROS cell environment. However, these results can be suppressed by UAMC3203, a ferroptosis inhibitor. As for the animal model with high-fat and carbon tetrachloride accompanied experiments, the mice had higher weight, Alanine Aminotransferase (ALT) levels, and developed tumors. Their liver sections showed lipid accumulation, histological fibrosis, and iron accumulation in both the WD and WD+CCl_4 groups, which corresponds to the IRP1 and IRP2 upregulated in both groups by qPCR result. Our research findings demonstrate that ferroptosis correlates with high-fat and high-ROS-induced hepatocellular damage. The related mitochondria dynamics changes in liver tissue and high-fat and/or high ROS provide evidence for ferroptosis-related hepatic steatosis.

We have established the effect of ferroptosis on hepatic steatosis in vivo and in vitro in nonalcoholic steatosis hepatitis (NASH). These results may enable the development of precise health prevention strategies by inhibiting ferroptosis to prevent the occurrence of liver diseases including hepatic steatosis and HCC.

#7444 Hepatotoxicity from L-asparaginase is associated with lipid changes in a mouse model.

V. Ruiz-Torres[1], J. J. Chia[1], M. Cohen[1], J. Tan[1], P. Bandaru[1], A. Brown[2], V. Huynh[3], E. Orgel[4], S. D. Mittelman[1];

[1]UCLA Mattel Childrens Hospital, Los Angeles, CA, [2]Baylor College of Medicine, Houston, TX, [3]Children's Hospital Orange County, Orange, CA, [4]Children's Hospital Los Angeles, Los Angeles, CA

L-asparaginase (Calaspargase-pegol, PEG) is currently an important component of acute lymphoblastic leukemia (ALL) treatment in children, adolescents, and young adults. Despite its high efficacy, toxicities including hepatotoxicity limit its use. Asparaginase-associated hepatotoxicity is often associated with obesity and fatty liver, highlighting lipid metabolism as a potential contributor to fatty liver. Therefore, we performed lipidomic analyses of plasma and liver from control and obese mice treated with one dose of PEG, to determine whether specific lipid moieties or classes may be associated with the hepatotoxicity produced by PEG. Control and obese 18-week-old male C57Bl6/J mice were treated with one dose of 3000 IU/kg PEG or vehicle (n = 6 per group). Hepatotoxicity was assessed one week later by liver histopathology and plasma alanine transaminase (ALT) and albumin levels. Liver and plasma lipidomic profiles were also analyzed by UHPLC-QTRAP-MS/MS. One week post Veh vs. PEG were compared using two-sided, unpaired t-tests. PEG increased liver steatosis scores in both control (Veh: 0.5±0.2, PEG: 3.7±0.3, $p<0.001$) and obese mice (Veh: 4.0±0.6, PEG: 6.7±0.2, $p<0.01$). While ALT levels did not show a clear pattern with PEG treatment, albumin level decreased in both control (Veh: 3.6±0.1, PEG: 2.7±0.2, $p<0.01$) and obese mice (Veh: 4.1±0.2, PEG: 2.8±0.1, $p<0.01$). Lipidomics analysis showed that plasma lipids generally decreased with PEG treatment in control (not shown) and more significantly in obese mice (Phosphatidylcholines [PC]: Veh 3000.0±381.1, PEG 507.2±71.5, $p<0.001$; Phosphatidylethanolamine [PE]: Veh 604.7±128.1, PEG 295.3±75.0, $p<0.001$; triglycerides [TG]: Veh 649.7±89.7, PEG 150.6±49.3, $p<0.001$). Similar patterns were observed in control (not shown) and obese livers for PC (Veh 11.1±0.8, PEG 5.7±0.8, $p<0.001$) and PE (Veh 6.7±0.8, PEG 3.5±0.5, $p<0.001$), whereas liver TG increased with treatment (Veh 220.1±113.5, PEG 586.6±113.4, $p<0.001$). Interestingly, there were strong negative correlations between steatosis score and liver PC ($r2=0.46$, $p<0.001$) and PE ($r2=0.62$, $p<0.001$). As low PC has been shown to induce fatty liver, this finding implies that PEG might induce steatosis via reduction in PC and its precursor, PE. Future work will investigate the mechanisms by which PEG reduces liver PE and PC levels, and whether this is causally related to steatosis and hepatotoxicity.

#7445 Association between C-reactive protein and cognitive impairment in IDH-mutant gliomas.

M. C. Kauss, M. L. Wright, D. Raval, E. Hsieh, K. Slattery, T. S. Armstrong, T. R. Mendoza, V. A. Guedes;
NIH-NCI, Bethesda, MD

Cognitive impairment is common in primary brain tumor (PBT) patients, as a result of the disease and secondary damage from directed and systemic therapy. Recently, the risk in patients with IDH-mutant gliomas and role of interconnectivity of the tumor with neurons and the tumor microenvironment has heightened interest in exploration of biomarkers of impairment to inform care. Here, we investigate Montreal Cognitive Assessment (MoCA) scores and peripheral blood levels of C-reactive protein (CRP) in a cross-sectional cohort of 47 adult IDH-mutant PBT patients enrolled in a natural history study (NHS, NCT02851706: PI T. Armstrong). MoCA raw scores (range 0-30) were dichotomized (≤ 25 = cognitive dysfunction). Baseline CRP was quantified in banked serum samples in duplicate using (V-Plex/Vascular Injury Panel-2, Meso Scale Discovery [MSD], Rockville, MD) in a QuickPlex SQ 120 instrument (MSD). Lab personnel were blinded to diagnosis and clinical status. To reduce skewness in CRP raw values, we used log transformation. Descriptive statistics, Pearson's correlation, and logistic regression were conducted using IBM SPSS and SAS Statistics software. The sample was predominately male (62%), white (70%), with high-grade gliomas (III/IV) (68%) and an average age at diagnosis of 36 years (SD: 9; median: 34; range: 20-53). The mean MoCA score was 25 (SD: 5; median: 26; range: 11-30). Dichotomizing MoCA scores showed that less than half (43%) of participants exhibited moderate-severe (≤ 25) cognitive impairment. MoCA binary group was negatively correlated with levels of CRP ($r=-0.42$, $p<.003$). The log mean concentration of CRP was higher in participants with cognitive impairment (7.99, SD=0.47 vs 7.57, SD=0.45, $p<.003$) than those without impairment. Finally, when controlling for age and sex, CRP remained predictive of cognitive impairment (OR 8.18, 95% CI 1.70,39.23). Higher levels of CRP were associated with lower MoCA scores in a cross-sectional sample of patients with IDH-mutant gliomas, suggesting an association between the severity of inflammation and cognitive impairment in IDH-mutant glioma patients. Further analysis in large, more diverse longitudinal cohorts will be needed to validate these findings in this population and compare to those with IDH-WT tumors and develop predictive models to inform biomarker development.

#7446 Transcriptomic and histological analysis of radiation-induced damage in the murine submandibular gland.

C. Paz, A. Glassey, **A. Frick**, L. Melzer, J. M. Robinson, R. M. Baus, R. J. Kimple;
Univ. of Wisconsin Madison Sch. of Med. & Public Health, Madison, WI

Many head and neck cancer patients develop radiation-induced xerostomia (RIX). There are few clinical solutions for this condition and there is a critical need for novel therapeutics for this condition. To better understand the molecular alterations induced by radiation to the salivary glands, we used transcriptional profiling to assess acute and long-term alterations. Based on evidence that immunologic changes are induced by radiation, we used immune-depletion experiments to investigate the role of B-cells and macrophages in RIX. The submandibular gland (SMG) of male-C57/BL6-mice was irradiated (15Gy) mice were followed for 90 days. Saliva was collected throughout the time-course. SMGs were collected 3-, 7-, 60-, and 90-days following radiation. Tissues were analyzed by Nanostring Digital-Spatial-Profiling (DSP) utilizing the murine whole-transcriptome panel. Regions of interest corresponding to acini, ducts, and granular convoluted tubules (GCTs) were delineated and gene expression was assessed. Immunohistochemical staining was performed on SMG's for fibrosis (masons trichrome), α-amylase, F4/80, Lgr5, Sox2, and MIST1 to evaluate glandular structure, salivary proteins, immune-microenvironment and pro-acinar salivary-stem-cell presence. Specific immune populations were depleted using anti-CD20 and clodronate-liposome prior to radiation and salivary function and histology was assessed at 3-, 7-, and 60-days following radiation. Radiation resulted in a significant decrease in salivary production (p-value = 0.03) in immune competent models. Transcriptional pathway analysis identified early alterations in signal-transduction and innate immune-response. Late timepoints identified alterations in B-cell activity and Wnt signaling pathways. Histological evaluation of the tissues showed increased disorganization of the gland, with decreases in size and distribution of the acinar compartments (mean area stained: No RT=25.81% vs 90d RT=19.98%, p-value=0.005). Acutely, there was an increase in expression of MIST1 and macrophages (mean area stained: No RT=14.8% vs 7d RT=18.76%, p-value=0.0004) within the SMG that resolved by the 60- and 90-day time-points. Results of immune depletion studies will be presented.Results implicate alterations in macrophages and B-cells in radiation-induced damage. These data along with the data from our immune-depletion experiments will provide valuable mechanistic insight guiding modulation of cell-therapies for treatment of RIX which can be further tested in preclinical models.

#7447 Understanding survivorship: A national survey of post-treatment experiences in Black prostate cancer survivors.

Dottington Fullwood[1], Daniel Lee[1], Veronika Panagiotou[2], Samantha B. Siegel[3], Mariel Molina[4], Folakemi T. Odedina[1]

[1]Cancer Prevention, Survivorship, and Care Delivery, Mayo Clinic Comprehensive Cancer Center, Jacksonville, FL,[2]National Coalition for Cancer Survivorship, Silver Spring, MD,[3]The Permanente Medical Group, Davis, CA,[4]Edge Research, Arlington, VA

Prostate cancer, impacts over 3.1 million survivors, poses persistent challenges in post-treatment care, creating uncertainties regarding the best course of follow-up actions for leading productive lives. Unfortunately, these concerns, especially among ethnically diverse Black men, are frequently overlooked. The post-treatment journey for Black prostate cancer survivors is dependent on how they navigate survivorship to determine how it impacts their quality of life and emotional wellbeing. This study evaluated the post-treatment cancer experience and gauge satisfaction with care among a cohort of Black survivors (n = 45). Utilizing data from the 2023 National Coalition for Cancer Survivorship State of Survivorship Study (n = 1303), conducted between May 9th to June 6th, 2023, the research specifically targets self-identified Black males, constituting 10% of the study population and spanning an age range from 18 to 80 years. Results revealed that oncologists (44%) managed post-treatment care more than primary care physicians (30%). While conversation about follow-up care monitoring cancer tests regularly occurred (68%), while topics such as quality of life (27%), mental and emotional health (21%), and post-treatment survivorship care plans (9%) received minimal attention. Although most survivors felt generally informed about side effects (62% very informed), less than half felt their health care team was very helpful in dealing with them. Symptoms reported by survivors included feeling overly tired (47%), depression, anxiety, and mental health impacts (40%), and uncertainty about the cancer status (34%). Survivors engaging in diverse integrative treatments, including such practices as prayer and exercise, represented 29% and 28%, respectfully. Notably, 80% and 60% of individuals utilizing these modalities reported finding them effective during the post-treatment care phase. The journey from the point of prostate cancer diagnosis to post-treatment can impose a significant mental and physical toll on survivors. To address the emotional and psychological challenges associated with a diagnosis and post-treatment, survivors adopting integrative oncology modalities and exercise prescriptions to cope are crucial. These strategies may help survivors maintain a positive outlook and achieve optimal post-treatment health, with a focus on providing tailored resources that cater to the unique needs of Black survivors.

#7448 Serum IL-10 is associated with neurologic symptoms and interference in primary brain tumor patients.

K. A. Slattery, M. L. Wright, D. Raval, E. Hsieh, M. C. Kauss, T. S. Armstrong, T. R. Mendoza, V. A. Guedes;
NIH-NCI, Bethesda, MD

Background: Primary brain tumors (PBT) are associated with neurocognitive symptoms as a direct result of the tumor or its treatment. IDH-mutant gliomas are associated with longer survival, but with higher incidence of seizures and neurocognitive symptoms. Correlations between cytokines and neuroinflammation have been reported in other structural brain lesions but have not been evaluated in PBT. Here, we investigate elevated peripheral blood levels of proteins (cytokine levels) in a cross-sectional cohort (n=47) of adult, IDH-mutant PBT patients enrolled in a natural history study (NCT02851706, PI: T. Armstrong) versus healthy subjects (n=32) and the correlations between cytokine levels and patient-reported outcomes (PROs).

Methods: Patient-reported symptoms and activity-related interference were collected via the MD Anderson Symptom Inventory-Brain Tumor at study entry. Serum samples were stored at -80°C for batch processing and used for biomarker analysis. Ten cytokines (interleukin-1β [IL-1β], IL-2, IL-4, IL-6, IL-8, IL-10, IL-12p70, IL-13, interferon-γ [IFN-γ], and tumor necrosis factor-α [TNF-α]) were quantified in duplicate using an immunoassay (V-Plex/Proinflammatory, Meso Scale Discovery [MSD], Rockville, MD). Lab personnel were blinded to diagnosis and patient clinical status. Mean concentration (pg/mL) levels or 'present or not detectable' values were used. Descriptive statistics, Mann-Whitney tests, and Spearman correlations were conducted at $p < 0.05$.

Results: The patient sample was mostly male (62%), White (70%), employed (64%), had no prior recurrence (62%), high grade (3-4) tumors (70%), and an average age at diagnosis of 36 years (SD: 9; median: 34; range: 20-53). The healthy subject sample was mostly female (53%) and White (72%), with an average age of 46 years (SD: 19; median: 50; range: 19-78). Five cytokines (IFN-γ, IL-6, IL-8, IL-10, and TNF-α) were detectable in patients and healthy subjects with levels of IL-6, IL-10, and TNF-α higher in patients than healthy subjects. Serum levels of IL-10 (mean rank=50.7 vs 24.3, $p<0.001$) and TNF-α (mean rank=50.6 vs 24.2, $p<0.001$) were higher in PBT patients when compared to healthy subjects. Only IL-10, but not other cytokines, positively correlated with severity of patient-reported symptoms [pain (r=0.290, p=0.048), numbness/tingling (r=0.302, p=0.039)], and activity-related interference, including work (r=0.323, p=0.027), and walking (r=0.402, p=0.005).

Conclusions: Higher IL-10 levels and detection differences in other cytokines, may indicate a reduction in immune-mediating processes and heightening inflammation in patients. Future analysis will include replication of this work in a larger cohort across PBT types to evaluate risk, explore mechanisms, and associations with treatment types.

#7449 Incidence of secondary malignancies in early onset colorectal cancer (EOCRC) patients.

D. Vadehra, K. Attwood, A. George, S. Advani, S. Sonti, S. Mukherjee;
Roswell Park Comprehensive Cancer Center, Buffalo, NY

Introduction: The incidence of colorectal cancer in the younger population (20-49) continues to rise at a rapid pace. EOCRC patients are potentially at risk for developing additional secondary malignancies. There is a lack of reported data in the EOCRC space. In this analysis, we seek to examine the incidence, trends, and outcomes of secondary malignancies in EOCRC patients.

Methods: The surveillance, epidemiology, and end-result (SEER) database was utilized to assess and compare the incidence and factors associated with development of secondary malignancies among EOCRC patients. Patient characteristics were summarized by secondary cancer status and compared using the Pearson chi-square test. Further OS was assessed using Kaplan- -Meier methods and compared across groups using the log-rank test. Multivariable Logistic regression models using backward selection approach were used to evaluate the association between patient characteristics and risk of secondary cancers. All statistics were performed using SAS version 9.4 (SAS Institute Inc., Cary, NC).

Results: Of the 53,891 patients analyzed, 2578 (4.8%) patients with EOCRC developed a secondary malignancy in the SEER database from 2000-2019. The mean age for developing a secondary malignancy was 47.6 yo (median 48 yo; range 20-69). There was a higher likelihood of second cancers among men(56%), white patients (61.4%), those with stage II (25.5%). and III (32.8%) CRC. The patients who most commonly developed a secondary malignancy were in the age group 40-49(p <.001). Of the patients who developed a secondary malignancy, 1843 (71.5%) initially had a primary colon cancer compared to 920 (22.6%) having rectal cancer, with the remainder having a rectosigmoid cancer. Of the patients who developed secondary malignancies, a majority had received prior chemotherapy (58.5%), and a minority of patients received radiation therapy (20.6%) Patients who had a partner had a higher incidence of secondary malignancy (59.5%) and they were more likely to have resided in a metropolitan area compared to a nonmetropolitan area (86.6 versus 13.2% respectively). The most common sites of secondary malignancy were: an additional colorectal cancer (47.7%), followed by breast cancer (8.2%) urinary tract cancer (7.1%), thyroid cancer (7%) and prostate cancer (5%). Patients who developed a secondary cancer were found to have an improved disease specific survival (DSS) compared to those who did not develop a secondary malignancy (3 year mDSS 89% vs 74%; p <.001)The overall survival of patients who developed a secondary malignancy was worse than those who did not develop one (mOS 208 months vs 229 mos respectively) .

Conclusion: EOCRC patients are likely to develop secondary malignancies. Long-term screening should be recommended for these patients and integrated into their survivorship plans.

#7450 The impact of prior history of non-hematologic malignancies on time to first treatment and overall survival among individuals with CLL or MBL.

B. A. Vallejo, C. Allmer, K. G. Rabe, D. P. Robinson, Y. Wang, P. J. Hampel, E. D. Braggio, N. E. Kay, J. R. Cerhan, S. A. Parikh, S. L. Slager;
Mayo Clinic, Rochester, MN

Background: The impact of a prior history of non-hematologic malignancy (NHM) on clinical outcomes among individuals with newly diagnosed chronic lymphocytic leukemia (CLL) or monoclonal B-cell lymphocytosis (MBL), the precursor to CLL, is not well known.
Methods: In this prospective study, we identified individuals with CLL/MBL who were seen in the Division of Hematology at the Mayo Clinic, Rochester. Participants provided consent within nine months of diagnosis, had no prior history of hematological malignancy, and completed a self-reported risk-factor questionnaire, including a prior history of NHM. Time to first treatment (TTFT) was defined as the time between the date of diagnosis and the earliest date of the first CLL treatment, death, or the last known treatment-free follow-up date. Overall survival (OS) was defined as the time from diagnosis to death or the last follow-up. We used Cox regression to estimate hazard ratios (HR) and 95% confidence intervals (CI) for associations between a prior history of a NHM with OS and TTFT. We adjusted for sex and the CLL International Prognostic Index (CLL-IPI), a score comprised of five key CLL prognostic factors, including age and Rai stage.
Results: Among the 1,090 CLL/MBL individuals, 833 (76%) had CLL. The median age at diagnosis was 64 years (range 24-89), with 65% being men, and 230 (21%) reported a prior history of NHM. The most common tumor was non-melanoma skin cancer (NMSC, 8.9%, 96 individuals), followed by prostate, testicular, and penile tumors (7.3%, 51 individuals), and melanoma (1.9%, 20 individuals). CLL/MBL patients with a prior history of a NHM were more likely to be over 65 years old (29%) than under 65 years old (14%, $p < 0.0001$). After a median follow-up of 2.9 years (range 0-21), 470 CLL/MBL patients progressed, requiring CLL treatment. CLL/MBL individuals with a prior history of NHM had a longer TTFT compared to those without (HR=0.69; 95% CI: 0.53-0.90; p=0.006). Individuals with a prior history of NHM who had either intermediate or high-very high CLL-IPI score had significantly longer TTFT (HR= 0.55; 95% CI: 0.33-0.92; p=0.02, and HR=0.65; 95% CI: 0.43-0.97; p=0.03, respectively) compared to those without NHM. After a median follow-up of 8.6 years (range 0-21), 359 individuals died. CLL/MBL patients with a prior history of NHM also experienced reduced OS compared to those without (HR=1.46; 95% CI: 1.08-1.97, p=0.013), particularly among those with low (HR=1.70; 95% CI: 0.96-3.00, p=0.07) or intermediate-risk (HR=2.08; 95% CI: 1.24-3.51, p=0.006), according to CLL-IPI. After excluding NMSC, results remained constant.
Conclusions: At the time of diagnosis, one out of five CLL/MBL individuals had a prior history of a NHM. These individuals had a longer time to first CLL directed treatment and reduced OS, even after accounting for other important CLL prognostic factors, which deserves additional studies.

#7451 Translational models of ovarian cancer-associated cognitive impairment and chemotherapy-induced peripheral neuropathy.

N. Lomeli[1], D. Argueta[1], D. C. Pearre[2], J. Lepe[1], K. Gupta[1], D. A. Bota[1];
[1]UC Irvine, Irvine, CA, [2]Providence Specialty Medical Group, Burbank, CA

Cisplatin is widely used to treat ovarian malignancies, and over 70% of ovarian cancer patients report experiencing cancer-related cognitive impairment (CRCI) and chemotherapy-induced peripheral neuropathy (CIPN) during and after chemotherapy treatment. Most pre-clinical CRCI/CIPN studies have been conducted on non-tumor bearing rodents. We developed two novel clinically relevant models of CRCI/CIPN: (1) the ID8 syngeneic mouse model in B6(Cg)-Tyrc-2J/J female mice, and (2) the SKOV3.ip1 ovarian cancer xenograft model in female Cr:NIH-RNU rats. We examined cognitive function and serum cytokine levels with respect to cancer progression and/or in response to cisplatin. B6 female mice were injected with 10^7 ID8 cells or 0.9% saline, i.p. Mice received cisplatin (2.3 mg/kg/day, i.p.) or 0.9% saline (OvT+CIS, OvT+VEH, respectively) for 5d, followed by 5d of rest for two cycles. RNU rats were injected with 10^7 SKOV3.ip1 cells or 0.9% saline, i.p. Rats received cisplatin (5 mg/kg, i.p) or 0.9% saline (OvT+CIS, OvT+VEH, respectively) every other week for four cycles. OvT+CIS and OvT+VEH mice and rats showed impairments in novel object recognition (NOR), with discrimination ratios ≤0.5. Cisplatin transiently increased hyperalgesia in OvT+CIS mice, which persisted longitudinally in OvT+VEH mice. Serum cytokine levels were elevated in OvT+VEH mice (IL-2, IL-10, INFγ) and OvT+VEH rats (IL-4, IL-10) compared to OvT+CIS ($P<0.05$). Ovarian cancer may evoke progressive sensory and neurocognitive deficits and increase systemic pro-inflammatory cytokine levels in the absence of chemotherapy. Future studies will address hyperalgesia and cognitive differences between healthy control and ovarian cancer models +/- cisplatin, and biological mechanisms underlying CRCI and CIPN.

#7452 ApoE genotype influences susceptibility to doxorubicin-induced cognitive impairment in juvenile rats.

C. Patel, J. Willekens, F. Diglio, P. Cole;
Rutgers Cancer Institute of New Jersey, New Brunswick, NJ

Many pediatric cancer survivors experience chemotherapy-induced cognitive impairment (CICI), which negatively impacts the quality of life. Despite extensive research into the multifactorial causes of CICI, there are no FDA approved drugs available to prevent it and the interpatient variability in susceptibility to CICI is not well understood. Among pediatric cancer survivors, those with the E4 allele of Apolipoprotein E (ApoE) are more likely to exhibit cognitive dysfunction than those with the more prevalent ApoE3 allele, suggesting the ApoE4 allele increases susceptibility to CICI. To mimic a curative pediatric treatment regimen, in our experimental model, five-week-old rats homozygous for either human ApoE3 or ApoE4 allele were treated with doxorubicin (DOXO) (2mg/kg/week for 4 weeks) or saline. ApoE4 rats were more likely than ApoE3 rats to exhibit DOXO-induced impairments in visual memory. However, there was no difference between ApoE3 and ApoE4 rats in sensitivity to DOXO-induced spatial memory impairments. Contrast-enhanced magnetic resonance imaging (MRI) was done to evaluate the blood-brain barrier (BBB) integrity because of literature suggesting that the ApoE4 allele contributes to BBB weakness. However, no significant difference was observed in the BBB integrity between ApoE3 and ApoE4 rats. To delve deeper into the neuropathological basis of DOXO-induced cognitive impairment on the ApoE4 allele, ongoing experiments involve immunohistochemical analyses targeting neurogenic changes in neural stem cell proliferation (DCX), neuronal maturation (Syn and PSD95), as well as glial differentiation (Iba1 and GFAP) in brain regions including hippocampus (dentate gyrus) and cortex. Additionally, to determine the effect of DOXO treatment on ApoE4, we are investigating the role of mitogen-activated protein kinase (MAPK) signaling pathways within brain regions pertinent to memory and recognition. In summary, ApoE genotype contributes to differential susceptibility to CICI.

#7453 Psychometric analysis of Neuro-QoL Perceived Cognitive Function tool in primary brain tumor patients.

M. L. Johnson, E. Vera, K. Reinhart, H. Miller, A. Choi, T. Kunst, B. McIver, E. Grajkowska, M. L. Wright, T. S. Armstrong, T. Mendoza;
National Cancer Institute, Bethesda, MD

Cognitive dysfunction is commonly reported but variable in course and severity in the primary brain tumor (PBT) population. Brief, reliable, and sensitive measures of patient-reported outcomes (PRO) of cognitive symptoms on function are needed for clinical care and research. This study aims to assess the reliability and validity of the Neuro-QoL Perceived Cognitive Function tool (NQC) and explore associations with symptoms and objective testing of cognitive dysfunction in a cohort of PBT patients enrolled in a natural history study (NCT02851706: PI T. Armstrong). Patient sample characteristics and PROs, including NQC (<40 = moderate/severe (MS) dysfunction), a symptom burden measure (MD Anderson Symptom Inventory-Brain Tumor (MDASI-BT), scores ≥5 = MS) and the Montreal Cognitive Assessment ((MoCA), scores ≤ 25 indicating cognitive impairment (range: 0-30)) were collected. Descriptive statistics and a psychometric analysis consisting of bivariate correlations, Cronbach's alpha, and factor analyses using principal axis factoring with nonorthogonal rotation were performed. Cohen's kappa and correlation were used to assess agreement between objective and subjective measures of cognitive function. The cohort included 327 patients who completed the NQC at study entry [median age: 47 years (range: 18-85), primarily white (78%) males (55%) with high-grade tumors (73%), 65% with a Karnofsky Performance Status (KPS) ≥ 90 (good), and 29% reporting MS cognitive dysfunction]. Factor analysis of the NQC identified two underlying factor groupings: concentration/focus and executive function with Cronbach's alphas of 0.92 and 0.91 that are interpretable and provided adequate fit for the data. While the NQC was moderately correlated with several MDASI-BT symptom factors, it was highly associated with the cognitive factor (r = -.646). To assess agreement, a subset of patients also completed the MoCA (n=172). These were primarily male (58%), white (79%), had high-grade tumors (67%), and a good KPS score (67%). In this subset, 24% had MS cognitive dysfunction as measured by the NQC while 44% were cognitively impaired using the MoCA resulting in a kappa agreement of 0.07. The correlation between the MoCA score and NQC T-score was -0.292. Understanding the impact and prevalence of cognitive symptoms, objective cognitive testing, and perceived impact is essential for PBT patient care and identifying supportive care interventions. Select NQC psychometric properties demonstrate reliability and validity in this population, with strong agreement with self-report of cognitive symptoms but weaker correlation with objective testing, highlighting the variability in perceived impact. Future research in cognitive function will explore the use of objective testing and perceived impact, its predictors in select populations (i.e., IDH-mutant tumors), and examine its association with biomarkers.

CLINICAL RESEARCH: Cancer Immunity and Inflammation
Poster Session

#7458 Inhibition of brain cancer progression via resolution of inflammation.

J. Capuano[1], K. Vasquez[1], K. Quinlivan[1], R. Bayer[1], S. Virani[1], M. Gillespie[1], M. Kieran[2], C. Serhan[3], D. Bielenberg[4], D. Panigrahy[1];
[1]Beth Israel Deaconess Medical Center / Harvard Medical School, Boston, MA, [2]Dana-Farber Cancer Institute / Harvard Medical School, Boston, MA, [3]Brigham and Women's Hospital / Harvard Medical School, Boston, MA, [4]Boston Children's Hospital / Harvard Medical School, Boston, MA

While inflammation is a hallmark of cancer, the mechanisms that disrupt its resolution in cancer are not well understood. A paradigm shift is emerging in our understanding that the resolution of inflammation is an active process controlled by specialized pro-resolving mediators (SPMs), including protectins and resolvins, which are endogenous lipid autacoids present in multiple tissues including the brain and cerebrospinal fluid. SPMs counter-regulate pro-inflammatory cytokine production and stimulate phagocytosis of cellular debris (“pro-resolution”) without being immunosuppressive. We hypothesized treatment with pro-resolving agonists such as SPMs presents a novel debris-clearing and resolution-enhancing therapeutic approach to complement cytotoxic brain cancer therapies. Here, we demonstrate the failure of resolution of inflammation via dysregulated SPMs may be a critical risk factor for aggressive brain cancer growth. Moreover, chemotherapy and targeted therapy further disrupt inflammation resolution via a tumor cell death (“debris”)-induced cytokine storm by macrophages. The SPM receptors GPR37 (protectin D1), GPR18/DRV2 (resolvin (Rv) D2), GPR32 (RvD1), and ChemR23/ERV (RvE1) are expressed in tumor-infiltrating macrophages and endothelial cells in the brain tumor microenvironment. Plasma levels of SPMs were significantly reduced in the medulloblastoma-bearing mice, suggesting that brain cancer progression is associated with a failure of endogenous resolution of inflammation. To determine whether failed resolution in brain cancer can be rescued by lipid mediator agonists, we systemically administered SPMs to subcutaneous and orthotopic glioblastoma and medulloblastoma murine brain tumor models. Significantly, RvD1 and RvD2 each inhibited the growth of human glioblastoma tumors by 15-fold at nanogram concentrations without toxicity. Likewise, RvD2 inhibited the growth of human medulloblastoma tumors by 3-fold. Protectins, PDX and $PD1_{n-3}$, each inhibited growth of human medulloblastoma in mice by approximately 5-fold. Systemic administration of PDX or RvD2 prolonged survival of mice injected with orthotopic human D556 medulloblastoma and also glioblastoma models. Flow cytometry analysis of orthotopic glioblastoma tumors revealed increased immune infiltration into the brain tumor microenvironment in the PCTR1-treatment group when compared to the tumor-bearing non-treated group. At nanogram per day doses, protectins and resolvins suppressed orthotopic debris-stimulated brain tumor growth by activating macrophage and microglial phagocytosis of tumor cell debris and counter-regulating pro-inflammatory cytokines, including TNF-α, CCL2, CXCL1, and CCL4. Thus, stimulating the resolution of inflammation via the clearance of cellular debris with pro-resolving agonists represents a novel therapeutic approach to brain cancer, including glioblastoma and medulloblastoma.

#7459 iNOS inhibition through L-NMMA reveals immunostimulatory effects in obesity-associated triple-negative breast cancer (TNBC) tumors.

I. Uzair[1], K. Sun[2], S. Hynes[3], W. Qian[1], J. Zhou[1], K. Ortega Martinez[1], L. Guzman[1], P. Matre[1], J. Chang[1];

[1]Houston Methodist Research Institute, Houston, TX, [2]Houston Methodist Hospital, Houston, TX, [3]University of Galway, Galway, Ireland

Purpose of study: This study examines how obesity, an inflammatory condition, impacts treatment outcomes in triple-negative breast cancer (TNBC). Obesity fosters an unfavorable tumor microenvironment (TME) marked by immune suppression, metabolic shifts, and protumoral cytokine release. Elevated nitric oxide (NO) levels linked with obesity compromise vascular integrity, promoting breast cancer metastasis. This study examines whether combining standard chemotherapy (docetaxel) with NOS inhibition via L-NMMA could reshape the TME and bolster antitumor effects in TNBC within an obese mouse model.
Experimental Procedure: C57bl/6 mice, a TNBC syngeneic mouse model, were fed a high-fat diet (HFD) or normal diet (ND) for 10 weeks. Tumors were induced orthotopically via E0771 cell line injection into the mammary fat pad. Upon reaching 100 mm^3, mice were randomized into vehicle and L-NMMA treatment groups. Digital spatial transcriptomics using NanoString™ GeoMx and nCounter platforms were conducted on FFPE tumor tissue sections from ND, HFD, and HFD+LNMMA treated mice. A panel targeting 64 protein markers aided in immune cell phenotyping and TME assessment.
Results: HFD-induced tumors exhibited increased growth, elevated pro-inflammatory cytokine levels, and heightened iNOS expression. Unsupervised hierarchical clustering after nCounter analysis revealed a distinct protein expression signature in HFD tumors associated with T cell infiltration and exhaustion, as evidenced by the upregulation of CD3, CD4, PD-1/PD-L1, FOXP3, and CTLA 4. Markers for identifying immunosuppressed macrophages (F4/80 and CD163) were also elevated. Remarkably, LNMMA treatment on HFD tumors led to reduced tumor growth and lower expression levels of these markers, alongside a downregulation of survival/proliferation markers such as p53, Ki67, and key members of the Pi3k signaling pathway such as phospoAktSer473.
Conclusions: Our findings indicate a distinct immunomodulatory mechanism of iNOS inhibition in HFD tumors, which displayed expression profiles marked by heightened immunosuppressive markers when compared to ND tumors. LNMMA treatment reversed this phenotype, aligning the profile closer to ND tumors. These discoveries underscore the potential of inhibiting iNOS to reshape the immune tumor microenvironment (TME) and modulate pathways linked to cell proliferation and survival. This presents a promising avenue for enhancing the effectiveness of treatments for triple-negative breast cancer (TNBC).

#7460 Characterizing the role of PCBP1 in the activation of the cGAS-STING/type I Interferon axis to promote anti-tumor immunity.

C. Frereux, P. Chakraborty, A. C. Dalton, B. V. Howley, B. Granger, J. A. Q. Karam, S. G. Vaena, M. J. Romeo, P. H. Howe;
Medical University of South Carolina, Charleston, SC

The emergence of immunotherapies has encouraged the need to better understand the molecular mechanisms that modulate the tumor immune microenvironment to kill cancer cells as well as the strategies used by cancer cells to evade the immune system. In several cancer types, the Poly(rC) Binding Protein 1 (PCBP1) has shown to have tumor suppressive effects, however its function in regulating the tumor immune environment remains unclear. To investigate this in the context of breast cancer, we established a CRISPR-Cas9-medited knock-out of PCBP1 in a Py8119 murine breast cancer cell line. PCBP1$^{-/-}$ cells revealed a decrease in the activation of the cGAS-STING pathway and is associated with lower levels of type I interferons (IFNs) and Interferon Stimulated Genes' (ISGs) expression. The cGAS-STING pathway plays an important role in innate immunity as it fights pathogenic infections and tumorigenesis through the production of type I IFN and ISGs. It also promotes the priming and infiltration of T cells at the tumor site to fight cancer cells. Our results suggested that PCBP1 is acting on the activation of the cGAS-STING pathway and could further modulate the tumor immune microenvironment. We then confirmed our results *in vivo* by establishing a tumorigenic C57BL/6 PyMT transgenic mouse model with conditional knockout for PCBP1 in mammary cells. Our data demonstrate that PCBP1$^{-/-}$ PyMT mice have higher tumor burdens compared to PCBP1$^{+/+}$ PyMT mice and also show a decreased ISGs' signature by RNA-sequencing, qPCR and western blot, as previously observed *in vitro* in the Py8119 PCBP1$^{-/-}$ cell line. Additional single nuclei RNA-sequencing analyses confirmed that this downregulation of ISGs is observed in mammary cancer cells where PCBP1 is knocked-out. Strikingly, IHC and flow cytometry analyses of PCBP1$^{-/-}$ tumors isolated from these mice also revealed a decrease in CD8^{+} T-cells. Therefore, PCBP1 silencing may promote tumor growth by impairing the activation of the cGAS-STING/IFN-I/ISGs axis, which may contribute to the decrease in CD8^{+} T-cells' infiltration at the tumor site. Additionally, we are further investigating the molecular mechanisms mediated by PCBP1 that trigger this activation of the cGAS-STING pathway.

#7461 Obesity promotes breast cancer progression via complement 1q.

Tao Zhang, Shimeng Liu, Myles Brown

Dana-Farber Cancer Institute, Boston, MA

Obesity markedly impacts the onset and progression of various tumors. Yet, the mechanisms by which obesity-driven remodeling in macrophages modulates tumor progression are not yet fully elucidated. Using single-cell RNA sequencing and in vivo syngeneic murine models, we identified an enriched subset of macrophages expressing high levels of C1q complex genes in the adipose tissue of obese mice. Intriguingly, these C1q-positive macrophages are also prevalent within the tumor microenvironment. Our data suggest that obesity induces cell apoptosis in both adipocytes and tumor cells, and that macrophages engulf these apoptotic cells via a C1q-dependent pathway, thus promoting immunosuppression. Moreover, C1q deficiency in mice impairs tumor growth. Notably, C1q is upregulated in human breast cancer and is associated with poor prognosis. Our results suggest that targeting C1q could be an effective method for breast cancer treatment.

#7462 Interventional dietary saffron drives antitumor immunity inInterventional dietary saffron drives antitumor immunity in high risk colorectal cancer IBD Patients, A Multisite Clinical Trial Study.

H. Ashktorab[1], R. Salmanroghani[1], H. Salmanroghani[2], R. Oskrochi[3], M. Rashid[1], A. Laiyemo[1], S. Challa[1], P. Oppong-Twene[1], N. Farjana[1], A. Kibreab[1], H. Maeker[4], A. Amin[5], A. Ahmed Mohamed[6], A. Elsayed[7], Z. Mohamed Zaki[8], O. Mohamed[7], A. Hassnine[7], S. Saed[9], S. Hassanin[10], F. Aduli[1], L. Gayathri Chirumamilla[1], H. Brim[1];

[1]Howard University, Washington, DC, [2]Yazd University, Yazd, Iran, Islamic Republic of, [3]Kuwait, American Middle School University, Kuwait, [4]Stanford University, Palo Alto, CA, [5]University of Sharjah, Sharjah, United Arab Emirates, [6]National Hepatology and Tropical Medicine Institute, Cairo, Egypt, [7]Minia University, Minia, Egypt, [8]Howard University, Minia University, Egypt, [9]University, Cairo, Cairo, Egypt, [10]Modern University for Technology and Information, Cairo, Egypt

Background: Inflammatory polyps in patients with Inflammatory Bowel Disease (IBD) pose a significant risk for colorectal cancer (CRC). Dietary interventions targeting anti-tumor immunity are crucial in mitigating this risk.

Aim: We investigated saffron's anti-inflammatory effects in IBD patients due to the high prevalence of polyps, aiming to prevent CRC.

Methods: The study retrospectively evaluated 485 colitis patients (70 IBD, 415 NIC) from Howard University Hospital, through colonoscopy, pathology, and clinical reports evaluations. At Howard University, three UC patients received 50mg of saffron twice daily for 8 weeks, with two cycles. Inflammatory markers, stool calprotectin, and cytokines were assessed. Similar saffron trials were conducted at Yazd University (30 UC patients) and Egypt University (11 UC patients).

Results: Patients with inflammatory bowel disease (IBD) were found to have a 15.7% prevalence of polyps compared to 8.2% in Non-inflammatory colitis patients. Among IBD patients, those with ulcerative colitis had more polyps (27%) than those with Crohn's disease (5%). In a multisite clinical trial, Saffron treatment improved various health indicators, including Partial MayoScore and quality of life. In the study (HU site), pro-inflammatory cytokines decreased, anti-inflammatory markers increased, and fecal calprotectin levels dropped significantly after saffron treatment. Saffron also led to changes in gut bacteria composition. Importantly, no adverse events were reported in the study participants. In one group of patients (Yazd study), saffron treatment led to significant improvements in depression scores, disease severity, and inflammation markers. In another site (Egypt study), 50% of saffron-treated patients showed improvement in markers related to disease severity, inflammation, and quality of life.

Conclusion: Saffron supplementation, alongside standard treatments, shows promise in reducing local and systemic inflammation in IBD patients and may reduce the risk of developing inflammatory polyps and hence CRC. This safe and feasible intervention warrants further exploration as an inflammation-driven CRC preventive strategy.

#7463 Chromosomal instability elicits anti-tumor immunity in pancreatic cancer.

D. Bronder, R. K. Sriram, M. Duran, M. Di Bona, S. McElduff, S. F. Bakhoum;
Memorial Sloan Kettering Cancer Center, New York, NY

Chromosomal instability (CIN) is a hallmark of solid cancers and an established driver of disease progression, therapy resistance, metastasis and on the whole poor patient outcome. Pancreatic cancer is particularly devastating, defined by dismal survival rates with many patients presenting with metastatic disease upon diagnosis, and 5-year survival only reaching ~10%. Despite recent efforts to improve prognosis for pancreatic cancer patients with immunotherapies alone and in combination with other therapeutics progress remains limited. Despite CIN's established role as a driver of disease progression, we have made the paradoxical observation that chromosomally unstable, murine pancreatic cancer cells elicit an anti-tumor immune response. CIN was induced experimentally in a chromosomally stable, metastatic model of pancreatic cancer. Modeling metastatic dissemination by injection of cells into the tail vein of mice led to robust tumor formation in the lungs where CIN-low cells formed many small lesions while CIN-high cells formed fewer but larger tumors. We investigated if the tumors were infiltrated differentially by immune cells by immunofluorescence and found that CIN-high tumors were more readily infiltrated by effector T-cells. This observation motivated us to test immunotherapy response in CIN-low and CIN-high cells. Subcutaneously implanted tumor cells were treated with an immune checkpoint inhibitor and isotype control antibody which revealed that CIN-high cells responded to immunotherapy while CIN-low cells did not. To put forward potential mechanisms explaining CIN-driven anti-tumor immunity, we performed molecular analyses of CIN-low and CIN-high tumors. First, we found that inflammatory pathways were significantly up-regulated in CIN-high tumors compared with CIN-low tumors. These findings were validated by cytokine measurements and RNA *in situ* hybridization. To dissect inflammatory pathway activation mechanistically, we engineered CIN-high cells using CRISPR/Cas9 that were deficient for key inflammatory cytokines and transcription factors. These experiments suppressed cell-intrinsic and ligand-induced inflammation. Yet, we failed to determine singular cytokine expression as mediator of anti-tumor immunity. To rule out the contribution of ligand-induced inflammation in the tumor microenvironment, we probed immune checkpoint blockade in combination with antibodies blocking inflammatory ligand receptors in CIN-high cells. We found that immune checkpoint blockade was cancer cell-intrinsic and independent of blocking antibodies. In summary, our data implicates CIN as a determinant of therapeutic and genetic anti-tumor immunity in a preclinical model of pancreatic cancer.

#7464 Tertiary lymphoid structures in pancreatic cancer: Biomarkers of immunogenic patients or direct contributors to anti-tumor immunity?.

S. Khanal[1], O. Harder[1], E. Kirschstein[1], M. Mack[1], C. Ware[2], M. Gough[3], K. Young[3], **A. J. Gunderson**[1];

[1]The Ohio State University Wexner Medical Ctr., Columbus, OH, [2]Sanford Burnham Preybus Medical Discovery Institute, San Diego, CA, [3]Providence Cancer Institute, Portland, OR

Pancreatic ductal adenocarcinoma (PDAC) is a cancer with low survival rates and currently no immunotherapy options. However, many tumors from PDAC patients can be heavily infiltrated with T and B cells associated with favorable survival outcomes indicating anti-tumor immunity is functional in certain patients. In some of these lymphocyte-inflamed PDAC tumors, spontaneous organization of tertiary lymphoid structures (TLS) is evident upon surgical resection and these patients have a clear survival advantage. TLS are predictive of immune checkpoint blockade response in some cancer types, yet PDAC patients, with or without TLS, are still insensitive to these strategies. To address this paradox, we evaluated surgically resected PDAC tumors from previously untreated patients and discovered that tumors with TLS (TLS+) recruited T and B cells with specific anti-tumor and memory phenotypes suggesting immunosurveillance of disease was enhanced. Furthermore, a subset of TLS+ patients contained germinal centers and improved humoral immune function corresponding to an increased neoantigen burden and long-term survival. When assessing gene expression differences between TLS+ and TLS- patients, operable inflammatory and immunosuppressive pathways emerged that could be therapeutically exploited to activate TLS neogenesis. To address these mechanistic questions, we have developed a method for inducing TLS formation in implantable mouse PDAC tumors in the orthotopic setting utilizing an antibody that agonizes the lymphotoxin beta receptor (LTBR) in mice bearing established PDAC tumors. These TLS are complexed with T cells, B cells, CXCL13^{+} cells, and PNAd^{+} HEV associated with reduced tumor growth, presence of lymphocyte-recruiting cancer associated fibroblasts and increases in anti-tumor T and B cell phenotypes. Interestingly, some mouse PDAC cell lines are resistant to TLS formation by LTBR agonism while others are susceptible offering a model to study patient heterogeneity. We will use this TLS+ PDAC mouse model to address how TLS may directly improve antigen-specific T cell and B cell immunity and elucidate the pathways that regulate TLS formation. These data will offer new strategies to overcome immunotherapy resistance in cancer patients.

#7465 Leukemia inhibitory factor creates an immune suppressive tumor microenvironment and fosters tumor growth in KRAS-driven pancreatic ductal adenocarcinoma.

L. Miller-Phillips[1], I. Boukhalfa Hanafi[1], A. J. Combes[1], S. Bano[1], L. Hysenaj[1], J. P. Roose[1], A. Olshen[1], A. Kiemen[2], S. Umetsu[1], M.-T. Wang[1], E. A. Collisson[1];

[1]UCSF - University of California San Francisco, San Francisco, CA, [2]The Johns Hopkins University, Baltimore, MD

Immune checkpoint blockade revolutionized cancer treatments by activating anti-tumor immunity. Pancreatic ductal adenocarcinoma (PDA) patients have not benefited from these advances due to an immune suppressive tumor microenvironment. Identifying PDA cell-encoded factors that drive immune evasion is necessary to unlock new immunologically active treatment options in PDA. We have recently demonstrated that the cytokine Leukemia inhibitory factor (LIF) is highly upregulated in PDA compared to the normal healthy pancreas. LIF is known for its immune suppressive qualities, but data on LIF in PDA is currently limited. We generated a conditional *Lif* ^{flox}(*L*) allele and crossed it into the well-established *Kras*$^{LSL\text{-}G12D/+}$, *Trp53*$^{flox/flox}$, *Pdx1*-Cre *(KPC)* mouse model. *LKPC* mice (n=29) had longer overall survival (69 days) than control *KPC* mice (n=29) (59 days), (p<0.05). *LKPC* mice harbored significantly smaller tumors with an average tumor weight of 0.6g compared to *KPC* control animals with an average tumor weight of 1.0g (p<0.005). Immunohistochemical evaluation of tumor proliferation measured by Ki-67 positivity in *LKPC* and *KPC* tumors at endpoint showed comparable results. Tumor-derived cell lines from *KPC* and *LKPC* mice showed no growth differences *in vitro* nor when reimplanted subcutaneously (sc) in immunodeficient mice. In contrast, we observed a significant decrease in tumor growth and weight in *LKPC* sc tumors (p<0.05) compared to the *KPC* sc tumors in syngeneic mice. *LKPC* sc tumors had significantly fewer neutrophils and more macrophages, particularly MHC II-high macrophages, known for their anti-tumor qualities when compared to KPC sc tumors using flow cytometry. A trend towards more CD8+ T-cells in sc LKPC tumors was also observed. Our genetically engineered mouse model confirmed this finding by immunohistochemical evaluation of tumors at endpoint, which demonstrated a significant increase of CD8+ T-cells in the *LKPC* animals compared to the *KPC* controls. In summary, we find that cancer-cell-expressed LIF augments tumor growth and shortens overall survival by changing the immune tumor microenvironment, nominating leukemia inhibitory factor depletion as a promising therapeutic immune target in KRAS-driven pancreatic cancer.

#7466 Exploring tertiary lymphoid structures and immune cell interactions in gastric cancer prognosis.

Zheng Zeng[1], Yee Man Au-Yeung[1], Jiandong Huang[1], **Chunxia Du**[2]

[1]The University of Hong Kong, Pokfulam, Hong Kong,[2]National Cancer Center/National Clinical Research Center for Cancer/Cancer Hospital, Chinese Academy of Medical Sciences and Peking Union Medical College, Beijing, Hong Kong

Tertiary lymphoid structures (TLSs) are ectopic lymphoid aggregates found in chronically inflamed, infected, and tumor tissues. Prior research indicates that the presence of TLS and tumor-infiltrating lymphocytes (TILs) correlates with a more favorable prognosis in several cancers. Our study investigates the role of TLSs and TILs in gastric cancer, the 4th leading cause of cancer-related death worldwide. We analyzed tumor samples from 107 late-stage gastric cancer patients from mainland China, with a 5-year follow-up period. We performed H&E and multiplex immunofluorescence staining to assess the tumor area and infiltrating immune cells, and we evaluated potential relationships between TILs, clinicopathological features, and patient prognosis. Immunohistological analysis showed that CD4 T cells may have a more significant impact on patient prognosis than CD8 T cells. Notably, the presence of PDL1 and CD4 co-expressing cells was associated with better disease outcomes. We observed PDL1 expressing cells surrounding the tumor margin in a subset of cases, a distribution pattern that could lead to delayed recurrence or complete remission in gastric cancer. In the context of cancer-related TLS, we found that CD20 and CD86 co-expression in the center of the structures may indicate a higher maturation level. Additionally, the ratio and spatial distribution of CD86 and CD163 macrophages appear to play a crucial role in prognosis. We extracted the expression levels of markers from representative samples to examine the spatial relationships between cancer cells and each immune cell type. We then visualized these cellular interactions in the tumor microenvironment using topographic plots. This study broadens our understanding of tumor and immune cell interactions in gastric cancer, with the potential to inform future directions in immunotherapy treatments.

#7467 Multi-omics analysis reveals high chronic inflammation in African Americans compared to Native African Men with prostate cancer.

I. Elhussin[1], E. Baraban[1], T. L. Lotan[1], C. Handy Marshall[1], E. Antonarakis[2], M. J. Campbell[3], M. Davis[4], M. Dixon[5], I. Kim[6], S. Ambs[7], R. Kittles[4], A. B. Murphy[5], C. Yates[1];

[1]Johns Hopkins University School of Medicine, Baltimore, MD, [2]University of Minnesota, Minneapolis, MN, [3]Cedars-Sinai Medical Center, Los Angeles, CA, [4]Morehouse School of Medicine, Atlanta, GA, [5]Northwestern University Feinberg School of Medicine, Chicago, IL, [6]Yale School of Medicine, New Haven, CT, [7]National Cancer Institute (NCI), National Institutes of Health (NIH), Bethesda, MD

Men of African descent have the highest prostate cancer (PCa) mortality rates in the United States and globally. Studies suggested that tumor subtypes or gene expression profiles had the greatest influence on overall racial/ethnic survival, accounting for 24% of the disparities in PCa and remains even when controlled for access to care and stage at presentation. Moreover, the tumor microenvironment plays an essential role in tumor progression, aggressiveness, therapeutic response, and patient outcomes. Additionally, the association of the genomic findings with patient ancestry and other characteristics, such as tumor biology and transcriptomic alterations, remains poorly understood. Here, we performed a multi-Omics approach (N=447) to unravel the complexity of tumor heterogeneity and understand disease progression & distinct tumor biology influenced by genetic ancestry. We performed Whole Exome (Normal/tumor paired) Sequencing matched with Methyl Seq and Whole transcriptomic Sequencing for three datasets of our African, African American Men (AAM), and European Men (EAM). Additionally, we ran Spatial NanoString high-plex GeoMx-DSP at the protein and RNA levels for a total of 118 treatment-naive PCa patients (around 500 ROIs). Simultaneously, we added matched genome-wide Sequencing (whole transcriptome) for these patients. The cohort comprised 87 AAM, 3 unknown, and 28 EAM self-reported individuals. To verify the self-reported race, the genomic ancestry was qualified using genotype and Admixture analysis. To further validate differentially expressed genes at the protein level, we performed multi-plex histological staining of 40 markers to determine the spatial resolution and neighborhood clustering within the tumor and the microenvironment. In parallel, we performed scMultiOmics sequencing (scRNA & scATAC-Seq) at a single-cell resolution (6000 cells/sample at 25K reads per cell) from an additional 12 patients (9 AAM & 3 EAM). Our results demonstrate that patients who self-report as AAM or Nigerian are assigned to high African (> 70%) Ancestry with either Yoruba (Nigeria) and/or Bantu subpopulation in the Sub-Saharan area. Additionally, high African Ancestry patients are diagnosed at a younger age and show advanced pathology stages compared to patients with European Ancestry. AAM with Yoruba descent express significantly higher immune-inflammatory signatures (IFNG-signaling pathway) compared to the Nigerian-Yoruba subpopulation. Our scRNA-Seq analysis shows that AAM has myeloid cells that infiltrate within the tumor cells. The infiltrations of these cells change with age, Gleason Grade, and pathology stage. Our study provides new insight into how genetic ancestry impacts immune signatures in AAM/African and contributes to PCa racial disparities.

#7468 Development of a high complexity flow cytometry panel to assess minimum residual disease in acute myeloid leukemia.

J. Pearl, E. Bruni, H. Hsu, **B. Walling**, K. Abarca-Heidemann;
Champions Oncology, Inc. (Hackensack, NJ), Hackensack, NJ

Acute Myeloid Leukemia (AML) is a highly heterogeneous disease with a diverse range of abnormal myeloid subpopulations resulting in challenges in clinical diagnosis and treatment. Many methods such as flow cytometry are used to provide precise information for risk stratification and treatment methods. Flow cytometry utilizes the expression patterns of cellular markers to characterize the high diversity in AML subpopulations with high sensitivity and specificity. This coupled with rapid analysis timelines allows for flow cytometry to be an excellent tool for the identification of AML lineage and progression through both phenotypic analysis and difference from normal. As AML lineage and disease progression are predictors of residual disease and relapse; the need for effective and accurate characterization of AML populations is critical. Here, Champions Oncology has developed a high-complexity 18-color flow cytometry panel to identify AML subpopulations at high resolution. We have characterized AML samples to evaluate the expression of phenotypic markers and their heterogeneity. Utilizing primary AML samples, we have evaluated the stability of AML subpopulations to understand how delayed analysis, such as what is seen in clinical trials, may impact marker expression and observed key populations were stable for up to 72 hours after collection. In addition to stability, understanding the lower limits of detection is critical for AML patients, particularly for minimum residual disease and relapse screening. The use of a flow cytometric panel again provides an excellent tool for these tests due to the single cell nature that allows for the interrogation of individual populations with primary AML subpopulations detected at a range of 10^{-3} to 10^{-4}. Finally, with hundreds of never-passaged AML models characterized and cryopreserved by both flow cytometry and sequencing at Champions Oncology, we investigated how the cryopreservation processes impacted the expression of AML subpopulations. We have observed similar expression and detection of AML populations following cryopreservation indicating that these models can be utilized as an excellent tool for further studies. Collectively, our data indicates that the panel developed at Champions Oncology provides robust data analysis of AML subpopulations and can be an excellent tool for the tracking of AML disease progression in the clinic.

#7469 Inflammation plays an important role in the progression of chronic myeloid leukemia.

M. Langhammer[1], J. Schopf[1], T. Jaquet[2], K. Horn[3], M. Angel[1], D. Mohl[1], S. Lagies[1], C. Spohr[1], D. Christen[1], F. Uhl[1], T. Maie[3], H. Jacobi[2], T. Feyerabend[4], J. Huber[1], M. Panning[1], C. Sitaru[1], I. Costa[3], R. Zeiser[1], K. Aumann[1], H. Becker[1], T. Braunschweig[3], S. Koschmieder[2], B. Kammerer[1], K. Shoumariyeh[1], M. Huber[3], M. Schemionek-Reinders[2], T. Brummer[1], S. Halbach[1];

[1]University of Freiburg, Freiburg im Breisgau, Germany, [2]Faculty of Medicine, RWTH Aachen University, Aachen, Germany, [3]RWTH Aachen University, Aachen, Germany, [4]German Cancer Research Center (DKFZ), Heidelberg, Germany

The development of Tyrosine Kinase Inhibitors (TKIs) resulted in a significant increase in the life expectancy of patients with chronic myeloid leukemia (CML). Nevertheless, TKIs still fail in a significant proportion of therapy-naïve patients, or their effectiveness is hampered by secondary resistance. It is therefore urgent to explore the underlying mechanisms in order to develop new therapeutic approaches to cure CML instead of controlling the disease with a lifelong TKI therapy. Using the ScltTA/TRE-BCR::ABL1 mouse model for chronic phase CML we show that BCR::ABL1 leads to the elevation of pro-inflammatory cytokines, known to be important in disease initiation and progression. This is supported by our data from CML patients, where we also observe higher levels of pro-inflammatory cytokines in the serum compared to healthy individuals. Furthermore, we demonstrate that BCR::ABL1 drives the expansion of bone marrow derived mast cells (BMMCs) and sensitizes them for FcεRI triggered degranulation. Interestingly, these BMMCs show differences in their lipid metabolism. Hence, sphingomyelin and lysophosphatidylcholine, both known to be involved in inflammation and cancer progression, are upregulated in BCR::ABL1-positive mast cells compared to their negative counterparts. By crossing in the Cpa3Cre mediated model for mast cell deficiency, we demonstrate for the first time that the lack of mast cells prevents the BCR::ABL1 induced upregulation of pro-inflammatory cytokines and also the development of splenomegaly. In addition, we were able to show that splenomegaly in CML patients is associated with high bone marrow mast cell counts and that an upregulation of pro-inflammatory cytokines in patient serum samples correlated with tryptase levels. In summary, our study identifies mast cells and their inflammatory cytokines as important factors in disease progression and suggests considering them as additional targets in CML therapy.

#7470 Leukemia inhibitory factor promotes tumor progression in KRAS-driven lung cancer.

I. Boukhalfa Hanafi, L. Miller-Phillips, O. Zakraoui, K. D. Marini, S. Umetsu, M.-T. Wang, E. A. Collisson;
UCSF - University of California San Francisco, San Francisco, CA

Leukemia inhibitory factor (LIF) displays complex effects in different types of cancer but its role in lung cancer remains unknown. Since KRAS mutation is an initial validated oncogenic event in near 30% of non-small cell lung cancer (PanCancer Atlas), we were interested in studying how LIF would influence tumor initiation and progression in KRAS-driven lung cancer.To properly study the roles of LIF throughout KRAS-driven tumorigenesis, we generated a novel genetically engineered mouse model (GEMM), where expression of LIF can be conditionally knocked out by Cre recombinase. Conditional deletion of the Lif allele in oncogenic KRAS-induced lung tumors is achieved by crossing *Lif* $^{flox/flox}$ mice with *Kras*$^{LSL\text{-}G12D/+}$, *Trp53*$^{flox/flox}$ *(KP)* mouse model. In our lung cancer model, induction of oncogenic KRAS and depletion of LIF is attained through intratracheal infection of adeno-Cre virus.When our *Lif* $^{flox/flox}$*KP (LKP)* and *KP* mice were infected by adeno-Cre virus, they developed lung tumors at reasonable frequencies within 4-8 months. We generated cell lines from tumors and used ELISA and RT-qPCR analysis to validate the efficiency of the knockout. While control *KP* tumor cell lines (n=3) showed *Lif* expression and LIF protein secretion, cell lines from *LKP* tumors (n=3) presented with undetectable *Lif* expression and no LIF secretion validating the successful deletion of *Lif* and functionality of our new mouse model. We generated H&E slides from the tumors and with the help of our pathologist we confirmed the subtype of lung adenocarcinoma. The effects of LIF on cell lines proliferation were evaluated *in vitro* and we found that *LKP* cell lines grow significantly slower than the *KP* lines ($p<0.05$).Mice in both groups were monitored for their overall survival (OS) rate. *LKP* mice (n=5) tend to have an increased median overall survival at 176 days when compared to control *KP* mice (n=7) at 152 days ($p=0.07$). To estimate the tumor initiation and progression, mice in each group were sacrificed at early endpoints (10- and 15-weeks post adeno-cre infection) and ratios of lung weight/mouse weight were measured as an indicator of tumor burden. At 10 weeks, *LKP* mice (n=5) presented with significantly smaller ratios with an average of 0.014 compared to *KP* animals (n=4) with an average of 0.019 ($p=0.027$).We found that LIF tends to shorten overall survival and augments tumor burden in lung cancer. These data suggest that LIF has a pro-tumorigenic role in KRAS-driven lung cancer proposing this cytokine as a potential prognostic biomarker and its depletion as a promising therapeutic target.

#7471 Cancer-associated fibroblasts drive T cell infiltration and resistance to immunotherapy in non-small cell lung cancer with mature tertiary lymphoid structures.

F. Peyraud[1], J.-P. Guegan[2], L. Vanhersecke[1], C. Rey[2], O. Lara[2], O. Odin[2], E. Clot[1], M. Brunet[1], T. Grellety[3], M. Del Castillo[4], S. Le Moulec[5], F. Le Loarer[1], A. Bessede[2], A. Italiano[1];

[1]Institute Bergonie, Bordeaux cedex, France, [2]Explicyte, Bordeaux cedex, France, [3]Centre Hospitalier de la Cote Basque, Bayonne, France, [4]Atlantic Pathologie, Saint Pierre d'Irube, France, [5]Clinique Marzet, Pau, France

Background: The presence of mature tertiary lymphoid structures (mTLS) within the tumor microenvironment (TME) has been linked to the effectiveness of PD-L1 blockade in non-small cell lung cancer (NSCLC). However, only a subset of patients experiencing clinical benefit. Our study aims to delve into the determinants of immunotherapy response in mTLS-positive NSCLC.

Methods: We included 77 TLS-positive NSCLC from the BIP study (NCT02534649). First, we employed the GeoMx whole-transcriptome atlas (WTA) assay to spatially profiled the expression of >18,000 protein-coding in patients exhibiting extreme responses (3 responders [R] and 3 non-responders [NR]). To target regions of interest (ROIs), we selected areas that encompassed TLS ($CD3^{+}$/$CD20^{+}$) as entire areas of illumination (AOIs). Additionally, we segmented areas outside TLS into 'tumor' ($PanCK^{+}$/$CD45^{-}$) vs 'stroma' ($PanCK^{-}$/$CD45^{+}$) AOIs. To validate our findings, we conducted multiplex immunofluorescence (mIF) and complemented our results with bulk gene expression analysis using the HTG whole human transcriptome panel.

Results: Spatial transcriptomic analysis pinpointed significant differences in gene expression within the stromal compartment between R and NR. Notably, a subset of cancer-associated fibroblasts (CAFs) expressing both FAP and αSMA markers emerged as the most differentially expressed genes. Subsequently, we used FFPE tissue mIF to delineate the histological profile CAF subsets and the spatial distribution of T cells. Notably, the stromal density of $FAP^{\pm}$αSMA$^{\pm}$ CAFs and $MYH11^{\pm}$αSMA$^{\pm}$ CAFs were significantly higher in NR compared to R. Correspondingly, tumors enriched in $FAP^{\pm}$αSMA$^{\pm}$ CAFs and $MYH11^{\pm}$αSMA$^{\pm}$ CAFs exhibited significantly lower overall response rates (ORR) and progression-free survival (PFS) than those with a low abundance of CAFs. Interestingly, tumors with elevated $FAP^{\pm}$αSMA$^{\pm}$ CAFs and $MYH11^{\pm}$αSMA$^{\pm}$ CAFs were associated with a higher infiltration of $CD8^{\pm}$ T cells. To delve deeper into the $CD8^{\pm}$ T cell infiltrate, we conducted a comparative bulk transcriptomic analysis. Both $FAP^{\pm}$αSMA$^{\pm}$ CAFs High and $MYH11^{\pm}$αSMA$^{\pm}$ CAFs High demonstrated significant associations with regulatory T cells (Treg), exhaustion signatures, and inflammatory processes. To validate the $CD8^{\pm}$ T cell phenotype, we performed complementary mIF. Consistently, the $CD8^{\pm}$ T cell infiltrate in tumors featuring $FAP^{\pm}$αSMA$^{\pm}$ CAFs High and $MYH11^{\pm}$αSMA$^{\pm}$ CAFs High exhibited higher levels of exhaustion markers (PD1, LAG3, TIM3, TIGIT) and Treg infiltration, underscoring an immunosuppressive TME.

Conclusions: $FAP^{\pm}$αSMA$^{\pm}$ CAFs and $MYH11^{\pm}$αSMA$^{\pm}$ CAFs play a pivotal role in driving T cell exhaustion and Treg cell infiltration, contributing to the resistance to immune checkpoint inhibition. Targeting these specific CAF subsets may hold significant promise in overcoming resistance in mature TLS-positive NSCLC.

#7472 Melanoma-intrinsic expression of signal-regulatory protein alpha (SIRPα) confers tumor cells resistance to anti-tumor adaptive immunity.

C.-H. Weng[1], C. Schochet[1], L. Hamadene[1], S. Eghbali[1], S. Monette[2], L. Mangarin[1], C. Liu[1], F. Samaan[3], J. D. Wolchok[1], T. Merghoub[1];
[1]Weill Cornell Medicine/Sandra and Edward Meyer Cancer Center, New York, NY, [2]Laboratory of Comparative Pathology, Memorial Sloan Kettering Cancer Center, The Rockefeller University, Weill Cornell Medicine, New York, NY, [3]PSU College of Medicine, Pennsylvania, PA

Introduction: Melanoma patient survival rates have significantly improved recently owing to the development of both targeted therapies and immunotherapies. However, there are still around 50% of patients relapse. The limited response to immunotherapies and global rise in melanoma incidence, with around 290,000 cases newly diagnosed each year, highlight the need for identifying new biomarkers, modulatory pathways, and risk factors for melanoma development. Earlier studies have characterized that aberrant expression of CD47 (a.k.a. “don’t eat me” signal) is one of the mechanisms that tumors exploit to avoid innate immune surveillance. CD47 blockade has been demonstrated to restore myeloid effector function by reinvigorating phagocytosis of tumor cells, which further enhances anti-tumor T cell responses. However, melanoma tumors are resistant to CD47 blockade. Interestingly, we and others have discovered that human and mouse melanoma cells express high levels of SIRPα, the receptor for CD47, which is typically expressed in myeloid compartments.

Experimental Procedure: To investigate the role of tumor SIRPα, we designed gRNAs to CRISPR out the SIRPα N-terminal region, where it interacts with CD47, in B16 melanoma and generated SIRPα+/+ (WT) and SIRPα-/- (KO) B16 tumors. We conducted multiple *in vitro* and *in vivo* experiments to investigate whether tumor SIRPα played a role in tumor growth and modulated anti-tumor immunity. The preclinical tumor model we used is B16-F10 melanoma and the murine strains we used are the immune-competent (C57BL/6j; B6) and the immune-deficient (RAG^{null}) mice. For phenotypic and functional assessments, we performed analysis using flow cytometry, immunohistochemistry (IHC) and single cell RNA-sequencing (scRNA-seq) derived from live-sorted CD45+ tumor infiltrating lymphocytes (TILs) of SIRPα-WT and SIRPα-KO B16 tumors.

Summary of Unpublished Data

Our preliminary data in a preclinical B16-F10 melanoma model revealed that surface SIRPα expression is necessary for optimal B16-F10 melanoma growth in immune-competent mice, but not in immune-deficient RAG^{null} mice, suggesting a potential crosstalk between tumor SIRPα and the host adaptive immune system. Intriguingly, we found that selective SIRPα deletion in melanoma cells results in a significant increase of immune infiltrates within melanoma tumors that further suppresses tumor growth.

Concluding Remarks: SIRPα is required for optimal melanoma development by suppressing anti-tumor adaptive immunity.

Ethics Approval: All mice were maintained in microisolator cages and treated in accordance with the NIH and American Association of Laboratory Animal Care regulations. All mouse procedures and experiments for this study were approved by the Weill Cornell Medicine Institutional Animal Care and Use Committee.

#7473 Flotillin-2 ablation in T cells enhances antigen sensitivity and functionality.

S. Moon, P. W. Karmaus, M. B. Fessler;
NIH-NIEHS (National Institute of Environmental Health Sciences), Durham, NC

The membrane scaffolding protein flotillin-2 (Flot2) has been proposed to support receptor signaling, but its involvement in T cell receptor (TCR) signaling and T cell responses remains unclear. Here, we show that the deletion of Flot2 increases antigen sensitivity along with changes in surface TCR clustering, resulting in enhanced TCR signaling and effector function to weak TCR stimulation. T cell-specific Flot2-deficient mice showed enhanced proliferation and effector cytokine production in both $CD4^{\pm}$ and $CD8^{\pm}$ T cells, resulting in better control of tumor growth and infection. However, in vitro TCR stimulation with plate-bound anti-CD3 and soluble anti-CD28 showed increased TCR signaling and early activation of $CD4^{\pm}$, but not $CD8^{\pm}$ Flot2-deficient T cells upon weak stimulation. In addition, Flot2-deficient $CD4^{\pm}$ T cells showed better in vitro polarization toward T helper 1 cells upon weak TCR stimulation, likely due to increased sensitivity of the TCR-triggering threshold. Changes in TCR clustering on the membrane have been suggested to influence the early detection of foreign stimuli and the formation of immune synapses. Flot2 ablation indeed increased the number of membrane TCR nanoclusters on naïve $CD4^{\pm}$ T cells. Collectively, this study suggests a mechanism for increasing T cell functionality to weak TCR stimulation by modulating the membrane protein Flot2, which affects surface TCR clustering. These results may have important implications for improving T cell reactivity in diseases with poor antigenicity, such as anti-tumor immune responses.

#7474 T-cell responses across heart, blood, and tumor in patients with immune checkpoint inhibitor-related myocarditis (irMyocarditis).

S. Blum[1], D. A. Zlotoff[1], N. P. Smith[1], I. J. Kernin[1], S. Ramesh[1], G. Oliveira[2], L. Zubiri[1], J. Caplin[1], N. Samanta[1], S. Martin[1], M. Wang[1], A. Tirard[1], P. Sen[3], Y. Song[1], K. Xu[1], J. L. Barth[1], K. Slowikowski[1], M. Nasrallah[1], J. Tantivit[1], K. Manakongtreecheep[1], B. Y. Arnold[1], J. McGuire[1], A. B. Afeyan[2], C. J. Pinto[1], D. McLoughlin[1], M. Jackson[1], P. Chan[1], A. Lawless[1], W. A. Michaud[1], T. Sharova[1], L. T. Nieman[1], J. F. Gainor[1], D. Juric[1], M. Mino-Kenudsen[1], R. J. Sullivn[1], G. M. Boland[1], J. R. Stone[1], C. J. Wu[1], M. F. Thomas[1], T. G. Neilan[1], K. L. Reynolds[1], A.-C. Villani[1];

[1]MGH/Harvard Medical School, Boston, MA, [2]Dana-Farber Cancer Institute, Boston, MA, [3]Brigham and Women's Hospital, Boston, MA

Introduction: Immune checkpoint inhibitor (ICI)-related myocarditis (irMyocarditis) is a potentially lethal complication of ICI use that is characterized by the presence of clonally expanded T cells in the heart. The antigens recognized by these expanded intracardiac T-cell clones and their relationships to T-cell clones in the blood and tumors of irMyocarditis patients are poorly understood.

Methods: Paired single-cell RNA sequencing (scRNA-seq) and T-cell receptor (TCR) sequencing was performed on heart tissue (n = 13) and peripheral blood from patients with irMyocarditis (n = 25) and ICI-treated controls (n = 28) using the 10X Chromium (10X Genomics) system. TCR-β chain sequencing was performed (Adaptive Biotechnologies) on four autopsy cases of patients with available scRNA-seq data and irMyocarditis heart, tumor, and histologically normal tissue. An established high-throughput protocol was used to screen expanded intracardiac TCRs against candidate antigens (Oliveira G, et al. Nature 2021). Briefly, full-length TCRs were cloned, transduced into donor T cells, and screened against autologous or major histocompatibility complex (MHC) Class I-matched antigen presenting cell lines pulsed with peptide pools that covered the full length of the α-myosin, troponin-I, and troponin-T proteins alongside pools of common viral antigens and appropriate controls.

Results: scRNA-seq data showed that TCRs shared between heart and blood are predominantly found in circulating CD8 T cell subsets as compared to circulating CD4 T cell subsets. The gene expression patterns of these shared T-cell clones in circulation appear distinct in fatal and non-fatal irMyocarditis patients, with shared T-cell clones in fatal cases expressing cycling markers (*MKI67*, *STMN1*) and the chemokine receptor *CXCR3*. TCR-β chain sequences most enriched in irMyocarditis tissue relative to control tissues were distinct from those enriched in tumor tissues, and their full-length TCR sequences could be recovered from scRNA-seq data. In total, 52 cardiac-expanded TCRs across eight donors were screened against candidate antigens. None of the screened TCRs recognized the putative cardiac autoantigens.

Conclusions: T-cell clones expanded in irMyocarditis are shared in circulation, where the gene expression of these clones may help to distinguish fatal from non-fatal irMyocarditis. TCRs enriched in irMyocarditis appear to be largely distinct from those enriched in tumor and likely recognize currently unknown cardiac autoantigens.

#7475 The contribution of the oral bacteriome and mycobiome in cancer risk in people with HIV in Puerto Rico.

V. S. Sanchez Gonzalez[1], Y. N. Ortiz-Maldonado[1], G. Borges-Velez[1], T. L. Shull[2], J. L. Salgado-Montilla[1], **J. Perez-Santiago1**[1];
[1]University of Puerto Rico Comprehensive Cancer Center, San Juan, PR, [2]Rush University, Chicago, IL

Although under highly effective antiretroviral therapy, people with HIV (PWH) still experience an increased risk of developing cancer compared to people without HIV (PWOH). Dysbiosis of the oral microbiota in PWH can contribute to persistent inflammation and cancer risk. We previously showed higher levels of inflammation in saliva of PWH measured by TGF-β1 and IL-2. In addition, microbial products such as short-chain fatty acids (SCFA) can regulate the transcription of immune-related genes, particularly those necessary for the innate immune response to pathogens. In this study, we characterized the composition of the oral bacteriome and mycobiome in saliva of Puerto Rican PWH and PWOH, and analyzed these data in relation to markers of inflammation and cancer risk in saliva.

Saliva, sociodemographic, and clinical data from 100 adults were collected (50 PWH and 50 PWOH). PWH were virally suppressed (<50 copies/mL) and had a median CD4 count of 699.8 cells/µL. We sequenced the 16S rDNA and the ITS in extracted DNA from saliva to characterize and quantify the bacterial and fungal communities, respectively. Furthermore, measurement of inflammatory markers (TGF-β1, IL-2, and IL-8) in saliva was performed using quantitative immunoassays. Microbiome data was processed using Qiime2, and statistical analysis was carried out using R-statistical software. Biological pathways associated to changes in the microbiome were inferred using PiCRUST2.

PWH showed lower alpha diversity in the oral bacteriome (Observed OTUs: p=0.02, Faith: p=0.03) and oral mycobiome (Shannon: p=0.02) when compared to PWOH. In a multivariate analysis, lower alpha diversity in the bacteriome was associated with biological sex and HIV status. Lower alpha diversity in the oral bacteriome was associated with higher levels of acetate (r=-0.38, p<0.001) and lower levels of IL-8 (r= 0.21, p= 0.056) in saliva independent of HIV status. Taxonomic analyses showed PWH had a significantly lower abundance of *Porphyromonas*, *Peptostreptococcus*, *Oribacterium*, *Parvimonas*, *Leptotrichia*, *Fusobacterium*, *Eubacterium*, *Dialister*, and *Alkalibacter* genera of bacteria but there not significant changes in taxonomy in the oral mycobiome. Biological processes significantly affected by dysbiosis of the oral mycobiome include cytosolic and mitochondrial NADPH production, amino acid and sugar degradation, and phospholipid remodeling.

Dysbiosis of both the oral bacteriome and mycobiome occur in HIV infection, which can contribute to chronic inflammation. However, the bacteriome and mycobiome may have different biological mechanisms, which suggest different roles in increasing cancer risk in Puerto Rican PWH. These findings provide more information regarding the oral health in people with HIV and may contribute to innovative cancer prevention strategies and screening guidelines for this high-risk population.

#7476 Obtusifolin attenuates LPS-induced inflammation and NLRP3 inflammasome activation by suppressing the MAPK/NF-κB signaling pathway and ROS production in BV2 cells.

H. Lin[1], C.-H. Lee[1], C.-Y. Li[2],
[1]National Sun Yat-sen University, Kaohsiung City, Taiwan, [2]Kaohsiung Medical University, Kaohsiung City, Taiwan

Neuroinflammation, along with activation of microglia and oxidative stress, plays an important role in the development and progression of neurodegenerative diseases. During the inflammation process, immune cells release inflammatory mediators such as cytokines and chemicals that may promote the formation and growth of cancer cells. Obtusifolin, an anthraquinone extracted from the seeds of *Senna obtusifolin*, has anti-inflammatory properties. However, the effect of obtusifolin on neuroinflammation and its regulatory mechanism have not been yet investigated. In the present study, BV2 microglial cells were used to investigate the effects of obtusifolin on LPS-induced inflammatory responses, NLRP3 inflammasome activation, and reactive oxygen species (ROS) production. The secretion of nitric oxide (NO) was analyzed by Griess reagent assay, and the cell viability was detected by the CCK-8 assay. The expressions of iNOS, COX-2, STAT3, ERK, JNK, and p38 were examined using Western blotting, and the production of IL-6 and TNF-α was measured by ELISA. To examine whether obtusifolin affected NLRP3 inflammasome activation, BV2 cells were pretreated with LPS and then stimulated with ATP or nigericin. The secretion of IL-1β was measured by ELISA, whereas the expression of NLRP3 inflammasome-related proteins was detected using Western blotting. The production of ROS was analyzed by flow cytometry. Our experimental results showed that obtusifolin suppressed the production of NO and the secretion of proinflammatory cytokines by LPS-induced BV2 cells under noncytotoxic concentrations. In addition, obtusifolin decreased the expression of iNOS, COX-2, phospho-STAT3, phospho-ERK, phosphor-JNK and phospho-p38, and also attenuated the expression of NLRP3 and ASC, cleaved caspase-1 and cleaved IL-1β by LPS- induced BV2 cells. Moreover, obtusifolin reduced the production of both intracellular and mitochondrial ROS by LPS-induced BV2 cells. Overall, these results demonstrated that obtusifolin attenuated LPS-induced inflammation by suppressing the activation of MAPK and NF-κB signaling pathways, inhibiting NLRP3 inflammasome activation, and reducing the production of ROS in microglia, suggesting that obtusifolin might have benefits in the treatment of neurodegenerative diseases.

#7477 Isoxanthohumol inhibits LPS-induced inflammatory responses in macrophages.

T.-H. Kao, C.-y. Li;
Kaohsiung Medical University, Kaohsiung City, Taiwan

Background: Pathogen infection, such as bacteria, viruses, and fungus, frequently leads to septicemia through a series of inflammatory responses that have very high fatality rates. And, servere inflammation may cause gene mutation which is beginning of cancer. Macrophages are a critical type of antigen-presenting cells that control both innate and adaptive immune responses. During pathogen infection, activated macrophages secret many proinflammatory mediators and cytokines, including nitric oxide (NO), TNF-α and IL-6 against pathogens; however, an overwhelming inflammatory response provokes abundant cells to undergo apoptosis. In the present study, we aimed to examine the anti-inflammatory effect of isoxanthohumol, a prenylflavonoid from hops and beer.
Method: We used lipopolysaccharide (LPS) as a pathogenic stimulus to induce inflammatory responses by J774A.1 macrophages. MTT assay was used to detect cell viability. The secretion of NO was analyzed by Griess reagent assay, while the production of TNF-α, IL-6, IL-1β was measured by enzyme-linked immunosorbent assay (ELISA). The expression of iNOS, COX-2, and MAPKs was examined by Western blotting. The activity of NF-κB was analyzed by promotor reporter assay. The activation of NLRP3 inflammasome was examined by ELISA and immunofluorescence staining. In addition to that, we explored the secretion of cytokines, IL-1β, in THP-1 cell.
Result: We found that isoxanthohumol significantly suppresses the secretion of NO and attenuates the production of TNF-α and IL-6 by LPS-induced macrophages. In addition, isoxanthohumol also inhibits the expression of iNOS and COX-2, suppresses the phosphorylation of JNK, and attenuates the activity of NF-κB by LPS-induced macrophages. Moreover, isoxanthohumol decreases the activation of NLRP3 inflammasome by reducing the production of IL-1β and repressing the ASC speck formation of NLRP3 inflammasome in LPS/ATP-induced macrophages.
Conclusion: Our experimental results demonstrated that isoxanthohumol effectively inhibits LPS-induced inflammatory responses in macrophages, suggesting that isoxanthohumol might have benefits for attenuating inflammation.

#7478 Unveiling the role of two-pore channel 2 (TPC2) in cancer immunity from monocyte differentiation to cytokine production.

A. Alharbi, J. Parrington;
University of Oxford, Oxford, United Kingdom

Background: The study of TPC2 is of great interest in the field of cancer and immune diseases, as it plays a crucial role in various cellular processes, and there is substantial evidence that TPC2 sustains several cancer hallmarks (angiogenesis, autophagy, and metastasis). The expression and role of TPC2 and its relevance to cancer in the innate immune system remain unknown.

Methods: U937 TPCN2 knockdown (KD) cells were developed by nucleofection-based transfection of CRISPR-Cas9 gene editing tools. sgRNA (single guide RNA): CGUGCUGGUGAGUGAGGAUG was designed to target the fourth exon of the TPCN2 gene (Transcript ID: ENST00000294309). The model was used in tandem with pharmacological modulators of TPC2 channel activity to underpin its function in monocyte differentiation, macrophage development, and IL-8 production. Molecular biology techniques, including Sanger sequencing, qPCR, ELISA, and WB, were utilized. Proteins of murine TPC2 WT and TPC2 KO cells were extracted and sent to the Discovery Proteomics Facility of the Target Discovery Institute for label-free quantification and proteomics analysis using mass spectrometry.

Results: We developed TPC2-deficient human monocytes (U937 cells) with a 75% reduction in TPCN2 expression levels, and we demonstrated that TPCN2 genetically modified U937 monocytes were resistant to monocyte differentiation after treatment with increasing concentrations of PMA ranging from 100 ng/mL to 400 ng/mL. TPC2-deficient U937 monocytes were not differentiated into Mϕ. TPC2 acts as a major regulator of monocyte differentiation by modulating PKC-alpha via calpain. In addition, the levels of IL-8 were significantly reduced after treating U937 cells with Ned 19 (an NAADP antagonist) or TPC2 KD. Keratinocyte-derived chemokine (KC) and Macrophage inflammatory protein-2 (MIP-2) are the murine IL-8 homologues. Notably, the levels of MIP-2, but not KC, were significantly reduced in the TPC2 KO murine cells compared to the WT controls. Thus, TPC2 appears to be involved in IL-8 secretion in both humans and mice. In contrast to KC at the protein level, the KC expression level was significantly reduced in TPC2-deficient murine cells. TPC2 in EE/RE is involved in lipopolysaccharide (LPS)-mediated IL-8 production in U937 cells. TPC2 modulates immune targets involving CD38, PKC-alpha, and AKT.We found that 28 different proteins that play roles in cancer immunity showed significant changes in expression in TPC2-deficient murine cells (three overexpressed proteins and 25 down-expressed proteins), compared to WT.

Conclusion: Our data provide the first preclinical proof of concept for TPC2 as a potential target for blocking macrophage development and modulating CD38/IL8 levels as therapeutic strategies for cancer patients, raising questions regarding the clinical utility of TPC2 as a biomarker or immunotherapy target to modulate immune responses.

#7479 Targeting the lipid kinase PIKfyve upregulates surface expression of MHC class I to augment cancer immunotherapy.

P. Borker, Y. Bao, Y. Qiao, A. Chinnaiyan, J. Choi, Y. Zhang, R. Mannan, C. Cheng, T. He, Y. Zheng, J. Yu, M. Gondal, G. Cruz, S. Sara Grove, X. Cao, F. Su, R. Wang, Y. Chang, I. Kryczek, M. Cieslik, M. D. Green, W. Zou;
Rogel Cancer Center, Ann Arbor, MI

The widespread success of cancer immunotherapies suggests a promising future - but has been subverted by unresponsiveness and resistance. Current research has furthered the understanding of immunotherapy resistance through the findings of “hot” (responsive) and “cold” (unresponsive) tumors. Here, we focus on the genetic and pharmacological inhibition of PIKfyve, a lipid kinase regulator of autophagic flux and lysosomal biogenesis. We find that inhibition of PIKfyve results in the upregulation of major histocompatibility complex class I (MHC-I) surface expression in cancer cells (through inhibition of autophagic flux), resulting in increased CD8+ T cell-mediated cancer cell death. These findings were corroborated in multiple syngeneic mouse models, which also displayed increased intratumoral functional CD8+ T cells. In addition, the Pikfyve-depletion antitumor responses are CD8+ T cell and MHC-I dependent - as CD8+ T cell and B2m knockout rescued tumor growth - resulting in improved response to immune checkpoint blockable (ICB), adoptive cell therapy, and a therapeutic vaccine. Further, high PIKfyve expression predicts poor ICB response and is prognostic of poor survival in ICB-treated cohorts. Ultimately, these findings collectively suggest PIKfyve as an effective target to enhance immunotherapies through elevation of MHC-I surface expression in cancer cells, and accordingly, PIKfyve inhibitors have novel potential to increase immunotherapy response in cancer patients.

#7480 Human LINE-1 ORF1p retrotransposition independent function in pancreatic cancer.

E. You[1], B. Patel[1], A. Rojas[1], N. Ho[1], S. Sun[2], M. Raabe[1], Y. Song[1], I. Phillips[1], K. Xu[1], P. Richieri[1], L. Nieman[1], B. Greenbaum[2], D. Ting[1];
[1]Harvard Medical School/Massachusetts General Hospital, Boston, MA, [2]Memorial Sloan Kettering Cancer Center, New York, NY

The aberrant expression of repeat elements is a common feature found in both mouse models and human pancreatic ductal adenocarcinoma (PDAC). The majority of these are non-coding RNAs that have shown the ability to stimulate a viral-like innate immune response. The long interspersed nuclear element 1 (LINE-1) retrotransposon is one of the few protein coding repeat elements in the human genome. LINE-1 has two open reading frames, ORF1 and ORF2. The former (ORF1p) encodes a ribonucleotide protein and the latter (ORF2p) a reverse transcriptase and endonuclease. Although nuclear ORF1p and ORF2p is required for retrotransposition, ORF1p is primarily localized in the cytoplasm, which suggests the possibility of ORF1p function independent of LINE-1 retrotransposition. Here, we show that ORF1p has a function to shield repeat RNAs from activating pathogen recognition receptor (PRR) mediated antiviral response in PDAC cells. LINE-1 ORF1p-targeting shRNA significantly inhibits patient-derived PDAC tumor growth both *in vitro* and *in vivo*. Total RNA sequencing (RNA-seq) reveals distinct transcriptional profiles with ORF1p deficiency. Gene set enrichment analysis (GSEA) identified high enrichment of innate immune response-related pathways including IL6-JAK-STAT3 signaling, inflammatory response, interferon response, and apoptosis in ORF1 knockdown PDAC cell lines. These immune related pathways are suppressed by deletion of RIG-I and MAVS, two components of viral RNA sensing. Mechanistically, we demonstrated that ORF1p is associated with repeat RNAs including LINE-1 RNA (*L1HS*) in processing bodies (PBs), which are cytoplasmic membraneless ribonucleoprotein (RNP) granules. In the PBs, ORF1p interacts with MOV10 RNA helicase, an essential enzyme for dsRNA unwinding. Using MOV10 truncated mutants, we found that the ORF1p-MOV10 interaction is important in attenuation of PRR sensing and apoptosis upon repeat RNA exposure. Finally, we evalulated the activation of the innate immune response in the tumor microenvironment by ORF1p depletion. These results suggest that ORF1p loss induces a desmoplastic reaction driven by *Acta2*$^{+}$ myofibroblastic CAFs in response to inflammatory cytokines. Collectively, our results demonstrate a critical and previously uncharacterized role of ORF1p in evasion of endogenous repeat RNA-triggered antiviral immune response in PDAC cells with implications in the tumor microenvironment.

#7481 The allosteric STING agonist CRD3874 is systemically tolerated demonstrates systemic tolerability.

M. Banerjee[1], S. Middya[1], R. Shrivastava[1], A. Middya[1], N. Mane[1], N. Rawat[1], T. Soram[1], D. Chakraborty[1], R. Ghosh[1], R. R. Mansuri[1], D. Yadav[1], A. Gautam[1], A. Singh[1], K. Puniya[1], D. Pryde[2], S. Basu[1], F. Sonego[3], G. H. Martin[3], K. Thiam[3], A. Surya[1];

[1]Curadev Pharma, Noida, India, [2]Curadev Pharma, Sandwich, United Kingdom, [3]genOway, Lyon, France

Background: The activation of STING by CDN bind site targeting ligands leads to the generation of Type I interferons as well as pyroptosis and autophagy of the cell expressing STING due to STING's ability to transport protons across the endoplasmic reticulum. CDN site targeting STING agonists tested in the clinic thus far have shown limited systemic tolerability as well as a tendency to kill the very immune cells that they are designed to activate. CRD3874 is an allosteric small-molecule human STING agonist with a unique binding mode that generates robust Type I interferon responses while simultaneously blocking STINGs proton transport activity that is associated with pyroptosis and autophagy.

Methods: Allosteric binding was established using radioligand binding assays. Anti-cancer activity of CRD3874-SI by the IV route was evaluated in human STING KI C57/BL6 mice (genOway, France). Inflammasome and autophagy markers were studies in human and mouse cells.

Results: In contrast with competitive STING agonists, CRD3874 potentiates the binding of radiolabeled cGAMP to STING. Treatment of immune cells with CRD3874 or other STING agonists, led to dose dependent increases in Type1 interferons and other pro-inflammatory cytokines. However, unlike other STING agonists, activation of STING by CRD3874 did not lead to induction of autophagy or Inflammasome markers in cells or mice. Intravenous administration of CRD3874-SI in human STING knock-in mice caused tumor regression and survival benefit in multiple murine tumor models. The compound was well tolerated at high doses in the primate GLP study when administered intravenously and caused dose and exposure dependent increases in cytokines. This profile of retaining the high efficacy of a STING agonist while demonstrating systemic safety is unique to CRD3874-SI.

Conclusions: CRD3874 is a systemically administered STING agonist with promising single agent activity and an excellent IV safety profile in NHP. An investigator sponsored FIH Phase 1 trial with CRD3874-SI has been initiated at Memorial Sloan Kettering, NY, in sarcoma, MCC patients under the supervision of Dr. Ciara Kelly (NCT06021626).

CLINICAL RESEARCH: Circulating Tumor Cells 2
Poster Session

#7485 Microfluidic detection of dual positive cells in whole blood of metastatic breast cancer patients.
J. Zhou, Q. Luan, C. Macaraniag, A. B. Guzman, M. Mantice, O. Danciu, K. F. Hoskins, I. Papautsky;
University of Illinois at Chicago, Chicago, IL

Background. Dual positive cells (DPCs) that express both epithelial markers and leukocytic markers have been observed in peripheral blood of breast cancer patients. DPCs acquire functional behaviors from both cell types which may drive tumor progression. However, the lack of reliable methods to isolate and identify DPCs has hindered the investigation of their origin and clinical implications in breast cancer patients. While microfluidic devices have been widely used for the detection of circulating tumor cells (CTCs) by liquid biopsy, DPC detection is underexplored in these devices. Herein, we demonstrate rapid onchip isolation and detection of DPCs in whole blood samples from metastatic breast cancer (MBC) patients using an integrated microfluidic device.
Methods. Our microfluidic device consists of a unique preconditioning component that concentrates targets in whole blood and a downstream cell immobilization component that captures target cells. We included 7 female patients with MBC, of which 29% are white (2), 57% are African American (4), and 14% are Latina (1). The median age is 50y (34y -75y). All patients were undergoing systemic breast cancer therapy at the time of blood collection. A total of 9 samples (4 mL each) were collected from either an antecubital vein (peripheral vein) or the subcutaneous port catheter (central vein) of these patients. All samples were processed within 5 hours of blood drawn in our novel microfluidic biochip. CTCs (EpCAM+/CK+, CD45-, DAPI+) and DPCs (EpCAM+/CK+, CD45+/CD66b+, DAPI+) were identified by immunofluorescence after cells were fixed.
Results. Processing of each sample was completed within 40 minutes using our microfluidic device. Both DPCs and CTCs were detected in all the samples (9/9). The average DPC count was 3 DPCs per 4 mL whole blood with a standard deviation of 1.9 cells. The average CTC count was 9 with a standard deviation of 5 per 4 mL whole blood. 89% of the samples (8/9) had > 5 CTCs after the sample volume is scaled to the standard 7.5 mL. No correlation was found between DPC count and CTC count (Pearson correlation coefficient r=0.08). While the blood collection location (central vs peripheral veins) had a significant impact on the CTC count (12.6 vs 4 on average with p<0.01), there was no statistical difference in DPC counts in the samples collected from central and peripheral veins.
Conclusions. Both DPCs and CTCs can be rapidly isolated and detected from MBC patient whole blood in our microfluidic device. Our preliminary results indicate no correlation between DPCs and CTCs, suggesting that DPCs might not originate in blood circulation of MBC patients. More work with a larger patient cohort will be needed to further investigate the clinical implications of DPCs on MBC patients.

#7486 Development and analytic validation of an ARv7/PSMA dual biomarker circulating tumor cell assay.

J. Ladd, E. Bayer, B. Bartels, E. Kaldjian, A. Ramirez;
RareCyte, Inc., Seattle, WA

Background Prostate cancer drug targets and biomarkers may be investigated non-invasively on circulating tumor cells (CTCs) obtained via liquid biopsies. PSMA is an important drug target in prostate cancer, and ARv7 is a splice variant that confers resistance to second-generation androgen receptor inhibitors. In this study, we describe the development and analytic validation of a novel assay to quantify ARv7 and PSMA protein expression on CTCs. The assay was validated with blood samples from patients with Stage IV prostate cancer to demonstrate clinical feasibility. To our knowledge, a PSMA/ARv7 dual protein assay for CTCs has not previously been reported.

Methods LNCaP (PSMA positive), PC3 (PSMA negative), 22Rv1 (ARv7 positive), and BT474 (ARv7 negative) cells were spiked into healthy donor blood to generate model CTCs. Nucleated cells were collected from these spike-in samples using the AccuCyte® sample preparation kit and spread onto microscope slides. Slides were fixed and stained with antibodies to cytokeratin, EpCAM, and CD45 to detect CTCs and exclude white blood cells (WBCs), and with PSMA and ARv7 to evaluate protein expression on identified CTCs. The slides were imaged with the CyteFinder® automated immunofluorescence scanning microscope that identifies CTCs for confirmation by trained reviewers based on machine learning algorithms and quantitatively measures biomarker signal mean fluorescence intensity (MFI).

Results For ARv7/PSMA expression classification of the model CTCs, the dual biomarker assay showed analytic sensitivity of 83%/97% and specificity 98%/99%, yielding accuracy of 90.2%/97.9%, respectively. The dynamic range of MFI for both biomarkers was approximately three orders of magnitude. Inter-run reproducibility CV was 13.6% (ARv7) and 6.9% (PSMA). Slide repeatability mean CV was 11.1% (ARv7) and 12.0% (PSMA). Clinical feasibility of the assay was investigated in 9 progressing Stage IV prostate cancer patient blood samples. CTCs were identified in all clinical samples (median 4, range 1 - 384). Thresholds for biomarker positivity were established based on MFI measurements of positive and negative control cell lines. ARv7 positivity in clinical samples ranged from 33% to 100%, and PSMA positivity ranged from 0% to 75%.

Conclusions We have developed a dual ARv7/PSMA assay that simultaneously measures protein expression of both biomarkers on individual CTCs. The assay is accurate and reproducible for the assessment of ARv7 and PSMA expression by liquid biopsy in clinical studies.

#7487 Construction of a reliable CTC detection method and validity evaluation of CTC markers in colorectal cancer.

Y. Takahashi[1], Y. Ijiri[1], S. Fujino[2], N. Elnaz[1], A. Kishimoto[1], K. Shirai[1], S. Iwanaga[1], M. Yanagida[1], A. A. Bhagat[3], N. Miyoshi[2];
[1]Sysmex Corporation, Kobe, Japan, [2]Osaka International Cancer Institute, Osaka, Japan, [3]Biolidics Ltd, Mapex, Singapore

Even in modern times when medical technology has advanced, cancer remains a life-threatening disease, and recurrence and metastasis are major issues in cancer treatment. The characteristics of cancer cells change with progression and treatment. Therefore, timely evaluation on their characteristics and decision on the treatment strategy are required. Circulating tumor cells (CTCs) are released into blood vessels in solid tumors and promote metastasis by circulating in the blood. CTCs are thus attractive targets for liquid biopsy and can provide useful information for selection of appropriate treatment. To obtain reliable results from CTC testing, it is important to prove that the detected cells are derived from cancerous tissue. In molecular tests targeting CTCs, it is still unclear whether the detected cells are derived from cancer tissue displaying genetic mutations. Aiming to establish reliable CTC testing, we have developed a simple method using molecular imaging flow cytometry to detect APC gene mutation together with Cytokeratin and Vimentin, which are epithelial-mesenchymal transition markers. Since, abnormalities in the APC gene are detected in 60-70% of colorectal cancer patients, detecting such mutations provides strong evidence that the detected cells are derived from cancerous tissue. Here, we show that upon evaluation of analytical performance of our method using cells isolated from cancerous tissue, our method showed high concordance rate against APC gene mutation. A clinical proof-of-concept using 5 mL of whole blood from colorectal cancer patients revealed that counts of cells with APC mutation in blood and cells with Cytokeratin and/or Vimentin expression in blood are highly correlated. Our results demonstrated a pathological stage-dependent increase in the count and frequency of Cytokeratin and/or Vimentin positive CTCs. We believe that our study not only establishes a practical approach for identifying CTCs in cancer patients but also provides potential implications in clinical practice, prognostic evaluation, and selection of treatment strategies.

#7488 Detection of *PD-L1* mRNA expression in circulating tumor cells (CTCs) from patients with metastatic NSCLC, HNSCC and melanoma using a novel highly sensitive commercially available CE-IVD kit.

A. Strati[1], M. Zavridou[1], S. Smilkou[1], V. Tserpeli[1], E. Tzanikou[2], D. Stergiopoulou[2], E. Efthimiadou[1], E. Tsaroucha[3], A. Psyrri[4], A. Sfika[5], E. Bournakis[5], I. Balgkouranidou[6], S. Kakolyris[6], I. Boukovinas[7], C. Papadimitriou[8], L. Kaklamanis[9], I. Koukli[2], **E. Lianidou[1]**;
[1]National & Kapodistrian University of Athens, Athens, Greece, [2]Pharmassist Ltd, Athens, Greece, [3]"SOTIRIA" General Hospital of Athens, Athens, Greece, [4]Attikon University Hospital, Athens, Greece, [5]Aretaieio University Hospital, Athens, Greece, [6]University General Hospital of Alexandroupolis, Athens, Greece, [7]BIOCLINIKI Hospital, Athens, Greece, [8]Araiteio University Hospital, Athens, Greece, [9]Onassis Cardiac Surgery Center, Athens, Greece

Background: We have previously reported the development of an RT-qPCR assay for *PD-L1* expression in CTCs (Strati et al, Ann Oncol, 2017). This assay is now commercially available as Oncolipsy *PD-L1* kit (CE-IVD, Pharmassist, Greece) and we report here it's application in size-based enriched CTCs from patients with metastatic NSCLC, HNSCC and melanoma, before and during PD-1/PD-L1 blockade therapies.
Patients and Methods: The Oncolipsy *PD-L1* kit was analytically validated using Mini-Genes as positive controls (IDT, USA). The analytical sensitivity was tested by spiking known numbers of H1975 cells in peripheral blood (PB) samples from healthy donors (HD). In total 95 patients were enrolled in the study: 69 patients with metastatic NSCLC, 19 patients with metastatic HNSCC and 7 patients with metastatic melanoma. 40 PB samples from HD were used as a control group. 10 ml of PB was collected at baseline (V0), two months after immunotherapy (V1) and at the time of disease progression (PD) or 18 months after initiation of immunotherapy (V2). *PD-L1* and *B2M* transcripts were quantified in cDNAs obtained from CTCs isolated with the size-based PARSORTIX (ANGLE, UK) device. A sample was considered as CTC-positive when cDNAs were positive for *CK-8, CK-18* or *CK-19* expression.
Results: Spiking experiments have shown that 10 H1975cells/10ml PB can be detected using the kit. In CTC-positive samples, overexpression of *PD-L1* was detected in 15/58(25.8%) patients at V0, in 6/34(17.6%) patients at V1 and in 3/11(27.3%) at V2. Patients with elevated expression of *PD-L1* at V1 in respect to V0 and detectable CTCs had longer PFS (18.5mo vs. 13.2mo, p=0.033) and longer OS (24.8mo vs. 12.8mo, p = 0.071) after initiation of immunotherapy. Patients with elevated *PD-L1* at V1 compared to V0 benefited from immunotherapy, with a longer DFS (17.8mo vs. 13.4mo) and OS (29.4mo vs. 26.9mo).
Conclusions: The commercially available Oncolipsy *PD-L1* kit can be used for the quantification of *PD-L1* transcripts in CTCs. Expression of *PD-L1* in size-based enriched CTCs can predict response to PD-1/PD-L1 blockade therapy.
Acknowledgements: This study has been financially supported by the European Union and Greek national funds through the Operational Program Competitiveness, Entrepreneurship and Innovation, under the call RESEARCH - CREATE - INNOVATE (project code: T1RCI-02935).
Trial registration: ClinicalTrials.gov Identifier: NCT04490564

#7489 Peripheral blood liquid biopsy for the screening of lung cancer.

J. Seo[1], S. N. Shishido[1], J. Mason[1], C. R. Velasco[1], A. Chen[1], D. Rothwell[2], P. Crosbie[2], J. Hicks[1], C. Dive[3], P. Kuhn[1];
[1]USC - University of Southern California, Los Angeles, CA, [2]University of Manchester, Manchester, United Kingdom, [3]University of Manchester and University College London, Manchester, United Kingdom

Lung cancer is the second most common type of cancer in both men and women and the leading cause of cancer-related mortality. Unfortunately, most patients have advanced stages (stage III or IV) at the time of diagnosis and the only U.S. Preventive Services Task Force-recommended screening test, Low Dose CT scan (LDCT), has a high false-positive rate. Therefore, there is an urgent need for the early detection of lung cancer with better discrimination between individuals with lung cancer and those without. In this study, we demonstrate the capability of a non-enrichment-based liquid biopsy workflow, the High Definition Single Cell Assay (HDSCA) to be used as a complementary tool to the current screening methodology. The HDSCA workflow can detect circulating cells of epithelial, mesenchymal, endothelial, and hematological origin, as well as acellular events such as oncosomes. This allows the investigation of the broad spectrum of circulating rare events for the potential identification of biomarkers associated with lung cancer. We investigated 52 peripheral blood samples collected from the second annual screening round of Manchester's 'Lung Health Check' pilot of a community-based lung cancer screening cohort. Of these, 7 were subsequently diagnosed with non-small cell lung cancer, 2 with small cell lung cancer, and 43 were deemed at high risk of developing lung cancer. We additionally investigated 60 peripheral blood samples from individuals with no known pathology to use as controls. Within the screening cohort, a number of single rare analytes were found to have statistically significant differences between the lung cancer, high-risk cohort, and normal blood donor samples, which can potentially be biomarkers used to differentiate the cohorts. We also built a multi-analyte patient-level classification model utilizing the rare cellular and acellular events that stratified lung cancer patients from the normal donor individuals and high-risk cohort with high accuracy. Our results demonstrate the potential of liquid biopsy as a complementary screening approach for lung cancer.

#7490 Clinical utility of liquid biopsy in early stage lung cancer: A single institution experience.

K. Beshiri[1], A. Marinello[1], D. Vasseur[1], L. Zullo[1], M. V. Sanchez Becerra[1], A. Pagliaro[1], M. Cani[1], C. Parisi[1], P. Lavaud[1], M. Frelaut[1], P. Abdayem[1], A. Gazzah[1], A. Botticella[1], A. Levy[1], C. Le Pechoux[1], O. Mercier[2], S. Ponce[1], F. Barlesi[1], D. Planchard[1], A. Italiano[1], B. Besse[1], J. Remon[1], M. Aldea[1]; [1]Gustave Roussy Institute, Villejuif, France, [2]Marie Lannelongue Hospital, Le Plessis-Robinson, France

INTRODUCTION

Liquid biopsy (LB) proved its clinical utility in advanced non-small cell lung cancer, but its role in early-stage disease is less clear. Here, we investigated the clinical utility of LB for molecular diagnosis in early-stage lung cancer and its correlation with cancer relapse.

METHODS

This retrospective, monocentric study collected results from LB performed in patients (pts) with an early-stage lung cancer between January 2021 and May 2023, within the prospective STING study (NCT04932525). LBs were executed at different time points (before, after curative treatment, or under treatment), by using the Foundation One Liquid Dx panel. All patients had tissue molecular testing for at least *EGFR, ALK* and *KRAS* alterations. LB was considered positive (ctDNA+) if ≥ 1cancer-related alteration was identified and negative (ctDNA-) in the absence of somatic alterations or the presence of clonal hematopoiesis (CH) only. Disease-free survival (DFS) was calculated from diagnosis to cancer relapse or last follow-up, and correlated with LB results.

RESULTS

A total of 52 pts were included and 52 LBs were conducted. Pts had a median age of 63 years, 40% (25/52) were females, and 84% (43/51) had a smoking history with a median pack-years of 37.5 [4-100]. Adenocarcinoma was the most common histology (48% 25/52), followed by squamous carcinoma (23% 12/52), undifferentiated (20% 10/52) and other hystologies (9% 5/52). Patients had stage I disease in 10% (5/52), stage II in 11% (6/52) and stage III in 79% (41/52). LB was performed before curative treatment in 35/52 (67%), after curative treatment in 6/52 (11.5%) and during curative treatment in 12/52 (23%). Overall, LB was positive in 57% (30/52) of cases: 63% (26/41) in stage III and 36% (4/11) in stage I/II. Major driver mutations identified in tissue were then found in 61.5% (8/13) of LBs. The concordance between LB and tissue findings was 100% in pts with ctDNA+ (7 KRAS, 4 EGFR, 1 ALK, 1 HER2 ampl). CH was present in 66.7% (20/30) of ctDNA+ LB and 47.8% (11/23) of ctDNA- LB. Median tumor mutational burden (TMB) in ctDNA+ LB was 5.5 mut/Mb, with 4 cases of TMB >16. Median follow-up was 12.6 months (mo). In pts with ctDNA+ versus ctDNA- LB, mDFS was 12.9 mo (95% 6.3-18.6) versus 27.7 mo (95%CI 12.7- NR), p=0.07, in the overall population and 12.9 mo (95%CI 7.8-19.2) versus 27.2 mo (12.7-NR) respectively, p=0.19, in pts with stage III disease.

CONCLUSIONS

LB has informal results for molecular diagnosis in nearly half of pts with an early-stage lung cancer. The high frequency of CH may lead to LB misinterpretation as false positive and requires caution. The potential association of positive LB with earlier relapse requires further investigation in larger cohorts with a longer follow-up. Results will be updated by the time of meeting.

#7491 ctDNA liquid biopsy result among gynecologic cancer patients: Does it give additional information?.

M. Kim;
Samsung Changwon Hospital, Changwon-si, Korea, Republic of

Objectives: There are many target molecules for precisional cancer therapy Precision diagnosis-based target treatment is believed to be better survival approach compared than conventional treatment. Predictive markers are variant and vast. This study evaluated the initial experience of ctDNA liquid biopsy as a precision tumor marker for gynecologic cancer patients?
Methods: we retrospectively identified ovary/endometrial and cervical cancer patients who approved ctDNA test for various purpose. Two methods were used. Guardant 360 and Foundation One Liquid CDx.
Results: There were 31 cases. Median age was 60(46-84). Half of cases were ovarian cancer(17/31 55%).Cervix and endometrial cancer are 12(39%) and 2(6%).We found about ten percentages of actional genetic mutation patients(3/31).Two BRCA1 mutation(each patients have variant allele frequency(VAF) percentages are 50.4,49.6).One high bTMB(blood tumor mutational burden)was 21.There was no mutation in 6/31(19 %).
Conclusions: It seems additional supportive information may be acquired through well-established ctDNA liquid biopsy test among this population. Role of ctDNA liquid biopsy test for precision tumor marker should be investigated for future study.
Keywords: Liquid biopsy; Precision medicine; Tumor marker

#7492 Automated identification and enumeration of CELLSEARCH Circulating Tumor Cells (CTC) with a deep learning algorithm.

L. Biasiolli, P. Ansaloni, N. Gentili, D. Giardiello, F. Montanari, R. Miserendino, G. Signorini, G. Medoro;
Menarini Silicon Biosystems, Bologna, Italy

Introduction: CTC enumeration in blood samples with CELLSEARCH® is a prognostic biomarker in metastatic breast, prostate and colorectal cancer (full intended use documents.cellsearchctc.com). Currently, CTC identification is performed by visual assessment, which is time-consuming and potentially affected by subjective interpretations. Recently, we developed a Deep Learning (DL) algorithm for automated CTC identification in CELLSEARCH images (CellFind®, Menarini Silicon Biosystems, research use only). This study aims to assess the CTC identification performance of CellFind on 2 different datasets: the first for comparison with human reviewers, and the second for validation with much higher number of images.
Methods: CellFind is composed of an image segmentation followed by a classification network, which was trained using 13067 CTC and 52890 non-CTC images from 215 breast, 123 prostate and 180 colorectal cancer samples. The performance of CellFind was tested on 2 separate datasets. 1) The first dataset was made of CELLSEARCH gallery images from 26 breast cancer, 68 prostate cancer, and 40 benign samples. 8 human reviewers, qualified for CTC image analysis, performed blind labeling. The Ground Truth (GT) was generated by the classification of the 3 most experienced reviewers by majority voting (1621 CTCs out of 17080 images). Accuracy and F1 metrics were used to rank the performance of DL and 5 reviewers against the GT. 2) The second dataset was made of CELLSEARCH gallery images from 63 breast, 66 prostate and 32 colorectal cancer samples. 3 experienced reviewers created the GT classification by majority voting, identifying 20052 CTCs out of 117447 images.Finally, each patient was assigned to the favorable or unfavorable group by applying the validated cutoff on CTC enumeration per sample (CTC≥5 for breast and prostate cancer, CTC≥3 for colorectal cancer).
Results: 1) On 17080 gallery images from 134 samples, CellFind reached top human-level performance, as ranked both by accuracy (97.8% for DL vs. 96.8-98.0%) and F1 (88.6% for DL vs. 83.3-89.9% for reviewers). On the 94 cancer samples, DL accuracy on favorable/unfavorable prognosis was 98.9% vs. 95.8-97.9% for reviewers. 2) On the bigger dataset with 117447 gallery images from 161 cancer samples, CellFind obtained accuracy = 96.0% and F1 = 87.8% for CTC identification (TP = 17039, FP = 1735, FN = 3013, TN = 95660). For favorable/unfavorable prognosis the DL accuracy was 95.4%.
Conclusion: Automated identification and enumeration of CTCs in CELLSEARCH images with CellFind can remove human subjectivity from the review process and maximize standardization among different research centers. CellFind performed better than most operators and reduced the data processing time required for each blood sample by the operator.

#7493 Real-time monitoring of CTC number, biomarker expression, and kinetics as prognostic and predictive markers in patients with GI malignancies.

E. G. Bayer[1], B. M. Bartels[1], R. N. Ponting[1], A. Lutfi[2], M. K. Afghan[2], A. B. Ramirez[1], P. M. Kasi[2];
[1]RareCyte, Inc., Seattle, WA, [2]Weill Cornell Medicine, Cornell University, New York, NY

Background: Most of the utility in the clinic regarding liquid biopsies has been around circulating tumor DNA (ctDNA). ctDNA analysis provides valuable insight into mutational burden and therapeutic targets, but the speed and cost of analysis are prohibitive especially when it comes to serial testing. Using a cohort of patients with advanced or metastatic gastrointestinal (GI) cancers, we herein show the feasibility of using circulating tumor cell (CTC) enumeration, biomarker analysis, and kinetics as complementary to or as an alternative to ctDNA testing.
Methods: Using the RareCyte platform, nucleated cells from blood were collected, spread on slides, stained, and imaged with CyteFinder® for CTC identification (CK/EpCAM+, CD45-) and quantification of biomarkers (PD-L1/HER2 or Ki67/EGFR). CTC enumeration (CLIA-accredited CTC test) and biomarker status for each patient were tracked over time and compared with ctDNA mutational analysis and tumor burden.
Results: CTCs were detected in 60/70 samples (86%) and in 36/38 unique patients (95%). On average, more CTCs were detected in baseline samples from colorectal cancer patients compared to other subtypes (Table 1). Moreover, multiple patients showed pronounced changes in CTC number that correlated with treatment response, as well as strong correlation between CTC and tissue biomarker expression e.g. HER2. Rapid decline and/or CTC clearance was seen as early as a few days into starting effective systemic therapy. The average turnaround time for CTC testing was 5-7 days.
Conclusions: Our study emphasizes that real-time monitoring of CTCs is complementary to traditional tumor burden monitoring via imaging and ctDNA analysis. CTCs offer multiple unique advantages vs ctDNA including early response assessment within days of initiating therapy, a substantial decrease in cost of serial testing, and the ability to assess clinically relevant cell surface protein biomarkers e.g. HER2 and PD-L1.

Table 1. CTC values in initial baseline blood draw sample

Gastrointestinal cancer subtype	# of patients	Average # of CTCs per 7.5mL blood	Median # of CTCs per 7.5mL blood	Minimum # of CTCs per 7.5mL blood	Maximum # of CTCs per 7.5mL blood
Colorectal carcinoma	27	84	3	0	1378
Cholangiocarcinoma	3	8	3	1	23
Pancreatic cancer	3	2	2	0	3
Hepatocellular carcinoma	2	4	5	0	10
Gallbladder cancer	1	6	6	3	8
Appendix cancer	1	2	2	1	3
Anal cancer	1	0	0	0	0

#7494 Pan-cancer analysis of circulating tumor organoid drug sensitivity revealed differential distribution of viability dependence among cancer hallmark modules.

Y. Chen[1], **S.-P. Wu**[2], Y.-J. Chen[3], L.-S. Lu[4];

[1]National Taiwan University, Taipei City, Taiwan, [2]CancerFree Biotech Ltd., Taipei City, Taiwan, [3]Chang Gung University, Taoyuan City, Taiwan, [4]Taipei Medical University Hospital, Taipei City, Taiwan

Background: Patient-derived organoids represent an opportunity into deciphering human cancer biology at the personal-level resolution. Phenotyping living cell properties, such as drug sensitivity, complements deep sequencing to improve the prediction of cancer treatment response and holds promises for functional precision medicine. Modern cancer therapeutics target genetic alterations in modular networks, also known as cancer hallmarks, which drive biological essentialities for cancer progression. However, it remains elusive the relative robustness of each module among the naturally occurring solid tumors.
Methods: In order to explore this issue, we analyzed a drug sensitivity database of a collection of circulating tumor cells-derived organoids (CDO) from 532 patients with advanced/metastatic solid tumors to 15 chemicals. In this collection, each CDO was derived from 20 ml peripheral blood on a binary colloid crystal cell culture system over 4 weeks. CDO were tested for survival fraction at the Cmax of the designated chemicals. Cell viability was measured with ATP abundance normalized to vehicle controls. For each chemical tested, the probability density function (PDF) of drug sensitivity was fitted to log normal distribution and goodness of fit was analyzed with Kolmogorov Smirnov test with the significance cut-off set to 0.05. The targeted biological pathway of each chemical was mapped to canonical human pathways in the Gene Ontology and KEGG databases. Strength of the specific evolution conserved module (ECM) was evaluated with the published analysis using clustering by inferred models of evolution (CLIME) algorithm.
Results: There were 25 types of tumors in the database. The top 3 tumor types were soft-tissue sarcoma, breast cancers, central nervous system tumor. The average number in each tumor type was 21. The PDF of commonly known chemotherapeutic agents, such as gemcitabine, doxorubicin, docetaxel followed log normal distribution. In contrast, the PDF of commonly known biological targeted agents such as everolimus, cabozantinib or enzalutamide do not. For chemicals whose PDF followed a log normal distribution, the biological pathways that were affected tend to have a higher strength of ECM value.
Conclusions: Our early analysis revealed the feasibility to quantitatively estimate the robustness of biological pathways in the cancer hallmark modules with a CDO bank. The biological implication of deviation from classical log normal distribution for biologically targeted agents warrants further investigation.

#7495 Validation of microfluidic isolation of circulating pancreatic tumor cells from blood.

C. Macaraniag, I. Khan, J. Zhou, P. C. Giulianotti, A. Borgeat, G. Votta-Velis, I. Papautsky;
University of Illinois at Chicago, Chicago, IL

Background. Pancreatic ductal adenocarcinoma (PDAC) has a poor prognosis and is the fourth leading cause of cancer-related deaths in the US. PDAC is diagnosed in the late stages, which limits treatment options and yields poor clinical outcomes. Recurrence is a significant issue for patients undergoing surgery for PDAC. Circulating tumor cells (CTCs) are thought to be a potential mediator of recurrence, facilitating the formation of secondary tumor sites after surgery. Thus, there is a need to isolate CTCs to improve understanding of disease recurrence, to ultimately improve outcomes. Herein, we aim to validate our inertial microfluidic (iMF) system for isolating pancreatic CTCs from blood. We also benchmark our iMF system to a commercially available immunomagnetic negative selection system, EasySep™, and quantify target cell recovery and cell enrichment.

Methods. Our iMF system employs the differential cell sizes of CTCs from blood cells and inertial migration of such cells in a straight microchannel (150 µm × 50 µm × 24 mm) to enrich CTCs from blood. The iMF system sample flow rate used is 100 µL/min, with a 200 µL/min PBS buffer flow rate. The EasySep™ Direct Human CTC Enrichment kit targets CD2, CD14, CD16, CD19, CD45, CD61, CD66b, and Glycophorin to remove blood cells from the sample using magnetic particles, thereby separating them from CTCs. We spiked low cell concentrations of 50, 100, and 500 Hoechst-stained pancreatic carcinoma cells, PANC1, in 1 mL of healthy blood then captured using either EasySep™ or iMF. Cell enumeration was performed after centrifugation or Cytospin.

Results. PANC1 cells and WBCs have average sizes of 18 µm and 8.4 µm, respectively. We characterized our iMF device to capture cells ≥ 12 µm, which yields capture of most PANC1 cells. Indeed, our iMF system achieved 82.8±19.2%, 72.5±16.3%, and 59.3±3.8% recovery for 50, 100, and 500 cell-spikes in lysed blood, respectively. For the same 50, 100, and 500 cell-spikes, the total iMF CTC yields after Cytospin were 46.3±11.8, 44.3±9.1, and 32.7±2.1%, while the total CTC yields from EasySep™ were 4.6±3, 5.3±2.1, 8.3±1%, respectively. When we processed whole blood directly, EasySep™ had lower cell recovery, 3.8±0.2, 4.6±1, and 3.3±0.4%, respectively. Our system also demonstrated 8× higher target cell enrichment compared to EasySep™. Blood lysis before iMF separation did not drastically affect the recovery of target cells.

Conclusions. We determined that our system has improved performance over the commercial isolation system, EasySep™, thereby validating the effectiveness of microfluidic isolation for PDAC. In future studies, we can then use our iMF system in CTC isolation from routine blood draws from PDAC patients undergoing surgical resection. We may then isolate real patient samples and study relevant phenotypes of PDAC CTCs which may therefore be used for identifying certain mechanisms of PDAC progression.

#7496 The piritramide-based perioperative analgesia can affect the cancer dissemination in colorectal cancer patients.

J. Srovnal[1], E. Berta[1], M. Vidlarova[1], A. Rehulkova[1], K. Jecmenova[1], M. Popper[1], A. Srovnalova[1], P. Prasil[2], P. Skalicky[3], T. Gabrhelik[4], J. Maca[5], P. Michalek[6], M. Hajduch[1];

[1]Faculty of Medicine, Palacky University, Olomouc, Czech Republic, [2]Landesklinikum in Amstetten, Amstetten, Austria, [3]University Hospital in Olomouc, Olomouc, Czech Republic, [4]The Tomas Bata Regional Hospital, Zlin, Czech Republic, [5]University Hospital in Ostrava, Ostrava, Czech Republic, [6]General University Hospital, Charles University, Prague, Czech Republic

Introduction: Colorectal cancer (CRC) stands as a prominent contributor to global cancer-related mortality. Post-surgical management of CRC patients often involves the administration of opioid analgesics. These analgesics operate through opioid and cannabinoid receptors, pathways implicated in tumor progression and metastasis, potentially impacting patient survival adversely. This investigation delves into the influence of piritramide and morphine on cancer dissemination, encompassing in vitro and in vivo assessments, cytotoxicity analyses, and elucidation of their mode of action.

Methods: The presence of circulating tumor cells (CTCs) in the blood of 131 CRC patients was quantitatively assessed using the real-time polymerase chain reaction (qPCR) method. Cytotoxic effects of morphine and piritramide were evaluated via colony-forming assays (CFA) utilizing HCT116 and HT29 cell lines. The impact of piritramide and morphine on opioid receptor activity was gauged through transfected reporter cell lines and fluorescence imaging plater reader (FLIPR) calcium assays. *In vivo* models involving subcutaneous and intrasplenic administration in SCID and BALB mice, respectively, utilizing HCT116 and HT29 cell lines, were conducted. Morphological profiling, employing the cell painting assay, facilitated high-content image-based analysis on both cell lines.

Results: Perioperative analgesia with piritramide exhibited a tendency towards longer time to recurrence (TTR) survival in CRC patients (HR=1.8, p=0.104). Conversely, morphine-treated patients demonstrated a twofold increase in TTR events (HR=4.7, p=0.011). Piritramide, but not morphine, significantly inhibited colony growth in HCT116 and HT-29 cell lines in the CFA, consistent with cytotoxicity test results. Functional assays revealed agonistic effects of both piritramide and morphine on opioid receptor kappa 1 (OPRK1) and mu 1 (OPRM1), with piritramide exhibiting greater potency as an OPRK1 agonist. In the SCID mice model, subcutaneous application of HT29 cell lines resulted in significantly reduced tumor growth in piritramide-treated mice. In the intrasplenic model utilizing BALB mice, mice treated with piritramide exhibited diminished tumor growth and a reduction in both the number and size of metastases. Comparative analysis with reference compounds revealed a distinct phenotypic profile of piritramide affecting the endoplasmic reticulum.

Conclusion: Piritramide, as opposed to morphine, demonstrated cytotoxic effects on both *in vitro* and *in vivo* CRC cell lines, resulting in reduced tumor growth and dissemination. Perioperative analgesia with piritramide exhibited potential in improving time to recurrence survival in CRC patients.

Acknowledgement: This study received support from the European Union - Next Generation EU (LX22NPO5102) and Palacky University Olomouc (LF 2023_006).

#7497 Advancing multi-biomarker CTC assay and CDx development through the automated GenoCTC system.

C. Chelakkot[1], J. Park[2], C. Kim[2], Y. Lee[2], Y. Lee[2], S. Lee[3], J. Choi[3], Y. Moon[4], Y.-L. Choi[5], Y. Shin[2], H. Lee[6];

[1]Seoul National University College of Pharmacy, Seoul, Korea, Republic of, [2]Seoul National University, Seoul, Korea, Republic of, [3]Abion Inc, Seoul, Korea, Republic of, [4]Genobio. Corp, Seoul, Korea, Republic of, [5]Samsung Medical Center, Sungkyunkwan University School of Medicine, Seoul, Korea, Republic of, [6]Cichlid. Inc, Seoul, Korea, Republic of

Introduction: The successful outcomes observed in clinical trials emphasize the effectiveness of therapeutic approaches relying on biomarker tests, particularly in the development of cancer drugs. The parallel development of a drug and its associated predictive biomarker is considered an ideal strategy for achieving rapid and successful drug development in precision medicine. In this context, we employ an automated circulating tumor cell (CTC) isolation platform, known as GenoCTC, to facilitate the development of biomarker-driven CTC assays, with the ultimate goal of developing companion diagnostic (CDx) tests. Method: This study employed the 5th generation GenoCTC device, a fully automated system designed for marker-based CTC enrichment using immune magnetophoresis. We confirmed the isolation of CTCs through spiking tests, utilizing cancer biomarkers such as cMET, Mesothelin (MSLN), and Claudin 3 (CLDN3). cMET is a biomarker extensively studied in various cancers, particularly non-small cell lung cancer. We previously showed the prognostic significance of cMET expressing CTCs in HR+ and HER2- metastatic breast cancer patients. MSLN and CLDN3 are tumor-associated proteins showing overexpression across diverse cancer types, with a potential for the development of antibody-based cytotoxic drugs. The GenoCTC device allows efficient separation of CTCs expressing these biomarkers, ensuring high accuracy, precision, specificity, and sensitivity. Simultaneously, therapeutic drugs directed at these markers are progressing through phase trials or preclinical studies. Conclusion: Our results show that cMET, MSLN, and CLDN3 are potential markers for the development of biomarker tests, that can improve the patient selection process for personalized therapy targeting these biomarkers.

#7498 Acoustophoresis enriches tumor cell clusters from patients with metastatic prostate cancer.

C. Magnusson[1], P. Augustsson[1], A. Lenshof[1], A. Josefsson[2], A. Bjartell[1], Y. Ceder[1], H. Lilja[3], T. Laurell[1];
[1]Lund University, Lund, Sweden, [2]Umea University, Umea, Sweden, [3]MSKCC, New York, NY

Purpose: A subset of aggressive prostate cancers (PCa) progress to invade surrounding tissue to form distant metastases by shed of circulating tumor cells (CTCs). However, due to the scarcity of CTCs among the millions of nucleated blood cells, there is an unmet need to improve CTC isolation assays. Our technique *Acoustophoresis* uses standing ultrasound waves in a flow-through microfluidic chamber to discriminate cells based on their size, density, and compressibility.

Method: We analyzed the effectiveness of acoustophoretic circulating tumor cell (CTC) isolation from 6 mL PFA fixed red blood cell lysed blood from 12 metastatic prostate cancer patients and 20 healthy control subjects and compared it to the golden standard CellSearch. For acoustic cell separation, cells were diluted in 12 mL PBS based buffer and separated by acoustophoresis and analyzed by imaging flow cytometry using a standardized antibody panel (EpCAM, cytokeratin, CD45, CD66b, DAPI). Generally, CTCs, and clusters migrate faster than white blood cells (WBCs) when exposed to ultrasound in the microchannel during acoustophoresis and can therefore be separated from nucleated blood cells.

Major findings: Our pilot study shows that acoustophoresis finds both singlets and clusters of CTCs in patients as well as aggregates of CTCs and WBCs. In total, 67 cancer cell containing cell clusters were identified. Most identified cell clusters were small, containing less than 4 cells. In addition, acoustophoresis is a label-free separation technique, and could therefore identify additional subclasses of CTCs among the detected CTCs with e.g., EpCAM low/- expression. Further, we provide extensive data for the effect of storage time on acoustophoretic separation performance for fixed prostate cancer cell line cells and WBCs. Demonstrating that sample processing can be done up to 72 hours after blood sampling. We believe this is to date the most comprehensive study of acoustic separation of CTCs in patients and control subjects.

Conclusion: Label-free acoustophoresis is a potential method for future non-invasive molecular interrogation of metastatic cancers. We believe Acoustophoresis is a promising technology for CTC enrichment with the possibility to detect new subclasses of CTCs as well as cell clusters not detectable with CellSearch. CTC-clusters has previously been proposed as a promising and potent predictor to monitor progressive disease and is associated with earlier onset of metastatic disease and poor prognosis, which makes acoustophoresis ability to identify clusters of high interest.

#7499 Circulating tumor cell enumeration and protein expression by CapioCyte and Allegro Plus imaging.

J.-h. Lim[1], C. Johnson[2], T. Kaplan[2], M. J. Poellmann[3], Y. Harari[2], E. Kfir[2], A. Z. Wang[3], S. Hong[3];
[1]CAPIO BIOSCIENCES KOREA, Incheon, Korea, Republic of, [2]BioView Ltd., Rehobot, Israel, [3]CAPIO BIOSCIENCES, INC, MADISON, WI

Radiation or chemoradiation followed by surgical resection is the current standard of therapy for many diseases. These treatments are increasingly supplemented with monoclonal antibodies, such as epidermal growth factor receptor (EGFR)-targeting and programmed death ligand 1 (PD-L1) checkpoint-blocking antibodies. The use of these therapies is typically dependent on solid tissue biopsy to confirm elevated expression of these markers in the solid tumor, which carries complications and may only be sampled at diagnosis. In contrast, a liquid biopsy may detect these markers with minimal invasiveness and at multiple points throughout treatment and recovery. Here, we describe the development of an automated and integrated workflow for circulating tumor cell (CTC) analysis. We previously demonstrated that the CapioCyte method is a highly sensitive approach for enrichment of CTCs using a combination of biomimetic rolling on recombinant E-selectin and antibody-mediated capture on a nanostructured polymer surface within a flow chamber for capture. Here we report a fully automated CapioCyte instrument for CTC purification and immunofluorescence staining using epithelial, white blood cell and nuclear makers to identify and distinguish CTCs from WBCs while also quantifying EGFR or PD-L1 presence on respective CTCs. The immunostaining conditions were developed and validated for high analytical sensitivity and specificity using cell lines and health donor white blood cells with known biomarker status. The final assay conditions were transferred to the CapioCyte for automated immunostaining. CapioCyte enriched and stained CTC samples are paired with the BioView Allegro Plus platform, an imaging and analysis solution using machine learning and customized algorithms for automated imaging and CTC candidate identification based on high-resolution Z-stack images. The reported comprehensive and automated workflow was used to enumerate CTCs in patients with non-small cell lung carcinoma (NSCLC) in a feasibility cohort. Median CTC counts from NSCLC patients was 7.5 CTC/ml (n=26, mean 51.7, range 0.3 - 406.2). Studies are on-going to expand the cohort including testing blood from head and neck cancer patients and respective EGFR and PD-L1 status. The combined and automated CapioCyte-Allegro Plus workflow shows great potential for routine quantification of CTCs and EGFR and PD-L1 status.

#7500 Distribution and prognostic significance of circulating tumor cells (CTCs) and tumor-derived extracellular vesicles (tdEVs) in patients (pts) with lobular metastatic breast cancer (MBC).

E. Nicolo[1], L. Gerratana[2], L. Foffano[2], L. Munoz-Arcos[1], M. S. Serafini[1], M. Manai[1], L. Pontolillo[1], N. Bayou[1], E. Molteni[1], A. K. Strickland[1], C. Gianni[1], Y. Zhang[3], P. D'Amico[3], A. A. Davis[4], J. Donahue[1], H. Liu[3], W. J. Gradishar[3], A. N. Shah[3], G. Curigliano[5], C. Reduzzi[1], M. Cristofanilli[1];
[1]Weill Cornell Medicine, New York, NY, [2]Centro di Riferimento Oncologico di Aviano (CRO) IRCCS, PN, Aviano, Italy, [3]Robert H. Lurie Comprehensive Cancer Center, Northwestern University, Chicago, IL, [4]Washington University in St. Louis, St. Louis, MO, [5]European Institute of Oncology, Milan, Italy

Background

Invasive lobular carcinoma (ILC) has distinctive clinical and molecular features compared with invasive ductal carcinoma (IDC). CTCs and tdEVs are independent prognostic factors in MBC, however, liquid biopsy studies focusing on ILC are to date scarce. Higher CTC levels have been observed in ILC than IDC. One study including 28 ILC pts suggested the use of higher CTC cutoff for prognosis stratification. The clinical significance of tdEVs in ILC is unexplored. This study aimed to assess differences in the distribution and prognostic value of CTCs and tdEVs between ILC and IDC.

Methods

Blood samples were collected from 304 pts with MBC before starting a new line of therapy at Northwestern University (Chicago, IL) between 2016 and 2021 (NU16B06 trial). Blood was processed with the CellSearch® system. The ACCEPT software was applied to CellSearch® images to automatically enumerate CTCs and tdEVs. Association of CTCs and tdEVs with overall survival (OS) was tested in ILC and IDC pts. A count of CTCs ≥ 5 was considered high. The cutoff levels for tdEVs were < 20 (low), 20-79 (intermediate), and ≥ 80 (high), as previously reported. Additional exploratory cutoffs for CTCs (≥ 20, ≥ 50, ≥ 80, and ≥ 100) and tdEVs (based on quartiles of tdEV distribution in the overall population and ILC) were also evaluated.

Results

Of the 304 pts, 47 had ILC while 257 had IDC. 56% of pts received first-line therapy. Median CTC count was 8 [interquartile range (IQR) 2-35] in ILC and 1 (IQR 0-8) in IDC pts (P <.001). A significantly higher median tdEVs count was observed in ILC (36; IQR 18-115) than in IDC (11; IQR 2-86) pts (P =.002). High levels of CTCs (≥5) were not associated with OS in ILC (P =.88), even when higher cutoffs (≥ 20, ≥ 50, and ≥ 80) were used. Only the detection of ≥ 100 CTCs was significantly associated with OS in ILC pts (median OS 36 vs 10 months; HR 3.4; P =.028). In contrast, the prognostic effect of CTCs ≥ 5 was strong in IDC and maintained for all cutoffs. Similarly, while the prognostic value for tdEVs was confirmed for IDC using both 20-80 and exploratory cutoffs (3-105 and 18-155), no association between tdEV levels and OS was observed in ILC regardless of the cutoffs used.

Conclusion

ILC is associated with higher CTCs and tdEVs compared to IDC, probably due to the impaired cell-cell adhesion that characterizes ILC. Unlike IDC, the prognostic effect for the established cutoff of ≥ 5 CTC was not observed in ILC. A higher CTC cutoff could be considered for this subtype of BC. For tdEV no association with OS was observed, regardless of the cutoff used. These findings emphasize that ILC is a distinct entity also in the liquid biopsy features. Because of the low prevalence of ILC, research efforts should be directed at combining data from ILC pts to better characterize this subtype of BC and understand the reason behind the different associations with OS as compared to IDC.

#7501 Gene expression profiling of rare cells captured from liquid biopsy using the genesis cell isolation system.

S. Perike[1], A. Olcott[1], C. Jiang[1], N. Kumar[1], N. Knapp[1], J. Placek[1], C. Cox[1], Y.-T. Kang[2], L. Lingelbach[1], E. Dreskin[1];
[1]Bio-Rad Laboratories, Hercules, CA, [2]Bio-Rad Laboratories, Ann Arbor, MI

Background: Targeting rare cell types such as circulating tumor cells (CTCs), considered to be metastatic precursors in cancer progression, may provide long-term clinical benefits by enhancing patient outcomes. The study of CTCs comes with technical challenges due to their heterogeneity and low cell numbers, leading to difficulties in genomic characterization. This study aims to overcome these technical challenges by developing a comprehensive gene expression profiling workflow using qPCR and RNA sequencing (RNA-Seq) on rare cells enriched with Genesis System with Celselect Slides™.
Methods: To mimic CTCs in blood, we created a rare cell model sample by spiking A549 non-small cell lung cancer cells at concentrations of 50, 100, 500 and 1000 cells/ml in whole blood from healthy donors. The Genesis System, which can capture rare cells of 8µm-30µm, isolated 83.73% of spiked A549 cells in whole blood. Using the same blood samples without A549 spiked in, we enriched cells using the Genesis and it was used as a baseline for gene expression controls. High quality RNA was extracted from each of the enriched samples and used for both qPCR and RNA-Seq to detect the gene expression signature of the non-small cell lung cancer cells.
Results: Our analyses revealed significant differential expression of cancer-related genes ($p < 0.05$) in all A549-spiked samples when compared to the blood-only controls. Notably, in the 50 cells/ml dilution, RNA-Seq analysis identified over 3,000 differentially expressed genes, encompassing protein-coding genes, long non-coding RNAs, and small non-coding RNAs. Among these, 759 genes were consistently present across all enriched samples, suggesting a common expression pattern. To investigate the potential utility of these genes as non-small cell lung cancer biomarkers, we constructed a custom qPCR array comprising 38 of these genes and pre-amplified their targets using 50pg of RNA from the enriched cell samples. Notably, six genes from this panel (MET, TOP2A, NF1, SPP1, GAPDH, and ANXA5) exhibited significant differential expression (+/- 4-fold, $p<0.05$) in the enriched samples. MET and TOP2A, in particular, are well-known biomarkers for non-small cell lung cancer.
Conclusion: Our liquid biopsy workflow demonstrates the recovery of high-quality RNA from enriched rare cells, including CTCs. It enables comprehensive profiling of the tumor transcriptome, encompassing RNAs of various sizes, including miRNAs. Our approach has the potential to facilitate the identification of patient-specific biomarkers, enabling swift monitoring using preamplification and qPCR in advancement of targeted oncology therapy and research.

#7502 MCT1 and MCT4 on circulating tumor cells isolated from non small cell lung cancer patients.

K. Mangani[1], E. Pantazaka[1], E. Lianidou[2], V. Gerogoulias[3], A. Kotsakis[4], A. Markou[2], **G. Kallergi**[1];
[1]University of Patras, Patras, Greece, [2]University of Athens, Patras, Greece, [3]Hellenic Oncology Research Group, Athens, Greece, [4]University of Thessaly, Larisa, Grenada

Background: Lung cancer is the leading cause of cancer-related deaths. Non-small-cell lung cancer (NSCLC) is the most common subtype of lung cancer and is characterized by poor prognosis and survival rate. This is associated with the fact that most patients are diagnosed at advanced stages of the disease and the possibility of recurrence after treatment remains high. Monocarboxylate transporters 1 and 4 (MCT1 and MCT4) play a crucial role in cellular metabolism, as they are responsible for the transport of lactate and other monocarboxylic acids across the plasma membrane. Their function can further regulate cell survival and proliferation, especially under hypoxic conditions. To elucidate the relationship between CTCs and the metabolic aspect of cancer, we aimed to investigate the expression of MCT1 and MCT4 in CTCs derived from NSCLC patients and its potential association with patients' outcome.
Methods: Fifty-three NSCLC patients at baseline were enrolled in the current study. CTCs were isolated using the ISET system and triple immunofluorescence experiments were performed, using CK, MCT1, MCT4, and CD45 antibodies. The expression of MCT1 and MCT4 in CTCs was assessed by confocal laser scanning microscopy and statistical analysis was performed using SPSS software.
Results: CTCs were detected in 29 out of 53 (55%) NSCLC patients. CK expression was characterized as high or low, with the predominant phenotypes among CK-positive patients being the CK_{high}/MCT1+/CD45-and CK_{low}/MCT4-/CD45- (63% and 66%, respectively). Whereas the phenotype CK_{high}/MCT4+/CD45- was detected in 52% of the patients. The phenotypes with the lowest frequency were the CK_{low}/MCT4+/CD45- (7%), CK_{low}/MCT1+/CD45- (15%), and the CK_{high}/MCT1-/CD45- (15%). Most of the isolated CTCs had the CK_{high}/MCT1+/CD45- and CK_{low}/MCT4-/CD45- phenotypes with a mean percentage of 48% and 51% respectively, while only a small number of CTCs per patient were CK_{low}/MCT1+/CD45- or CK_{low}/MCT4+/CD45- (8%and 5%, respectively). The phenotype CK_{low}/MCT1-/CD45- was associated with poorer overall survival (OS) [p = 0.005, (15 vs 33 months respectively)], HR=0.351), while the presence of more than 3 CK_{high}/MCT4+/CD45- CTCs was related to poorer progression-free survival (PFS) [p = 0.042 (4 vs 17 months respectively)].
Conclusions: MCT1 and MCT4 were expressed in a high proportion of NSCLC patients at baseline and may constitute interesting biomarkers relevant to cancer progression. However, further analysis in a larger cohort of patients is required to clarify their potential significance in clinical practice.

#7503 Non-clinical study of circulating tumor cells in humanized mice: Post-xenograft effects in immunodeficient mice.

S. Pak, H. Pak, H. Yoo, S. Min, H. Kim, J. Lee, M.-J. Song, J. Choi, A. Jeong, H. Kim, J. Kim, H.-C. Lee;
Cytogen, Inc., Seoul, Korea, Republic of

Circulating tumor cells (CTCs) possess the potential to serve as innovative markers in clinical trials, contributing to the understanding of cancer metastasis mechanisms, diagnosis, prognosis, the development of personalized treatment strategies, and enabling the monitoring of treatment efficacy. NSG mice, which are a strain of immunodeficient mice frequently utilized as a non-clinical model for cancer research, exhibit diminished levels of natural killer (NK) cells and abnormal monocytes in their bloodstream. In a previous study, a positive correlation was observed between the duration of injection and the levels of white blood cells (WBC) in mice that were injected with various cancer cell lines derived from humans. To evaluate the correlation among the primary tumor and circulating tumor cells (CTCs), as well as the impact on immune cells, we assessed changes in immune cell composition, primary tumor size, and enumeration of CTCs in xenografted mice over a period of time. This investigation was carried out using CytoGen's Smart Biopsy™ systems. The results, which were obtained using equipment including CytoGen's Smart Biopsy™ Systems, showed that the distribution of white blood cell (WBC) components exhibited variations based on age, primary tumor burden, and circulating tumor cell (CTC) count following injection. A notable association was observed between the augmentation of immune cells and the quantity of circulating tumor cells (CTCs) present in the bloodstream. Therefore, alterations in immune cells may potentially impact the potential to affect the ability to influence the efficacy of cancer immunotherapy, metabolic therapy, and anti-metastatic therapy. When conducting non-clinical investigations with the objective of developing cancer treatment protocols, it is crucial to meticulously select humanized or immunodeficient mice that are appropriate for the study. Therefore, it is advisable to perform regular monitoring of murine blood samples in order to observe any variations in the counts of circulating tumor cells (CTCs), while considering a standardized blood volume per individual. In the immunodeficient mouse model, the existence of circulating tumor cells (CTCs) results in an increase in the quantity of cells present in the bloodstream. The observed rise in circulating tumor cells (CTCs) is found to be concurrent with the progression and development of the primary tumor. The consideration of this aspect is of utmost importance in the formulation of non-clinical studies aimed at the development of cancer treatment protocols.

#7504 Longitudinal multi-omics characterization of circulating tumor cells from ALK positive NSCLC patients.

Yuru Chen, Shamileh Fouladdel, Harrison Ball, Zhaoping Qin, Albert Liu, Xu Cheng, Liwei Bao, Habib Serhan, Bryce Vandenburg, Varun Kathawate, Larua Goo, Peter Ulintz, Nathan Merrill, Aaron Udager, Angel Qin, Sofia D. Merajver, Sunitha Nagrath

University of Michigan, Ann Arbor, MI

Introduction:

Anaplastic lymphoma kinase positive non-small cell lung cancer (ALK+NSCLC) represents a distinct subtype of NSCLC characterized by oncogenic ALK gene mutations leading to ALK overexpression and activation in tumor cells. ALK+ NSCLC will frequently develop mutations during treatment, leading to nonresponse and eventually cancer relapse. Therefore, there is a critical need for sensitive technologies to monitor ALK+ NSCLC disease status in patients over time.

To facilitate longitudinal monitoring, there has been a rapid evolution in diagnostic technologies leveraging circulating tumor cells (CTCs) as a liquid biopsy tool. CTCs can be collected non-invasively at various intervals throughout patient treatment. Moreover, they shed from solid tumors and disseminate into the bloodstream, which makes isolating CTCs a valuable source of genomic, transcriptomic, and proteomic insights pertaining to the primary tumor. In this study, we present a comprehensive workflow for conducting multi-omic analysis on CTCs derived from ALK+ NSCLC patients.

Methods:

Blood samples were collected from a cohort of ALK+ NSCLC patients, and CTCs were isolated using a high throughput, label free microfluidic device, Labyrinth. Enriched CTCs were immunofluorescently stained for cytokeratin, CD45, DAPI, epithelial cell adhesion molecule (EpCAM), and vimentin markers. Heterogeneous CTC populations with hybrid epithelial/mesenchymal (EM) phenotypes are reported. Fluorescence in situ hybridization (FISH) was performed on enriched CTC samples. DNA was extracted and sequenced using a 523 gene targeted sequencing panel. Single cell RNA-seq technology was performed in parallel on CTC samples to investigate the gene expression throughout treatment.

Results:

The median concentration of CTCs in the ALK+ NSCLC cohort (n=33) is 137 CTCs per ml of blood, and 64% of CTCs are in an EM hybrid state. In ALK+ NSCLC patients (n=3) with an average of 4.6 visits per sample, we observed a trend of decreasing CTC concentration for patients with partial response to the treatment. The presence of ALK fusion in ALK+ NSCLC patient's CTC is confirmed by FISH. Oncogenic mutations (JAK1, SPEN, ERBB4, NTRK3) are observed in bulk CTC samples from two NSCLC patients. Single cell RNA sequencing was performed on three ALK+ NSCLC patients; 58, 199, and 700 potential CTCs were detected with positive cytokeratin expression and no white blood cell marker expression.

Conclusions:

This study examined the feasibility of using CTCs for studying and monitoring the clinical status of the ALK+ NSCLC patients as well as the genomic and transcriptomic signatures within their tumors. More patients will need to be processed in order to validate our workflow and reinforce our conclusions.

#7505 Detection validation of androgen-receptor splice variant 7 in circulating tumor cells of prostate cancer by double-check assays.

Hoin Kang, Jihyun Lee, Min Hyung Kim, Soee Kim, Hyoyong Kim, Jubi Lee, Hae Ung Lee, Hai-Chon Lee, Jung Won Kim

Cytogen, Inc., Seoul, Korea, Republic of

Introduction: Androgen-receptor splice variant 7 (AR-V7) is constitutively activated isoform of AR and has been associated with resistance towards AR targeting therapies and development into mCRPC. Confirmation of AR-V7 expression is important step in prostate cancer diagnosis and determining the drug, but the detection of AR-V7 with tissues has limitations such as clinical challenge to poorly accessible tumor tissues before and after treatment. Here, we developed the method of AR-V7 detection in circulating tumor cells (CTC) after isolation with CytoGen's Smart Biopsy™ CTC isolator by in vitro assays of qPCR and immunofluorescence (IF) with high sensitivity and specificity, overcoming the limitations of tissue biopsy.

Method: qPCR and IF methods were developed for high sensitivity and specificity of AR-V7 detection. Sensitivity and specificity were tested using AR-V7 positive cells (VCaP and 22Rv1) and negative cells (PC-3 and Raji). Limit of detection (LOD) test of AR-V7 expression was performed with AR-V7 positive cells (200 cells to 50 cells, 3 points) mixed with Raji cells (1x10^5cells). Then, AR-V7 positive cells (200 cells to 50 cells, 3 points) were spiked into peripheral blood mononuclear cells (PBMC) of blood sample (5mL, healthy donor) to mimic CTC after isolation by CytoGen's Smart Biopsy™ CTC isolator, subsequently AR-V7 expression was tested with qPCR and IF assay.

Results: AR-V7 expression was clearly detected by qPCR and IF in the LOD test of AR-V7 positive cells mixed with Raji cells and was not detected at all in the negative controls. The similar clear results were also observed in the spiking test of AR-V7 positive cells into PBMC isolated by CytoGen's Smart Biopsy™ CTC isolator, suggesting that clinical samples of prostate cancer could be applied with excellent sensitivity and specificity for AR-V7.

Conclusions: AR-V7 expresses only a part of cancer tissue, so it is difficult to accurately diagnose with traditional histological assays. Detection of AR-V7 in intact live CTC isolated by CytoGen's Smart Biopsy™ CTC isolator might overcome limitations of tissue biopsy. In this study, we developed the method to detect AR-V7 in CTC with high sensitivity and specificity with qPCR and IF assay, and presented the results of verifying AR-V7 expression by double check using two kinds of assays. We plan to conduct clinical validation of the developed method through additional study using patient samples.

#7506 Comprehensive mutational profile of true single circulating tumor cells compared with CtDNA in advanced pancreatic adenocarcinoma.

J. Khandare[1], A. Bharde[2], G. Khutale[2], S. Andhari[2], R. Deshpande[2], K. Hariramani[3], M. Basavalingegowda[2], V. Jadhav[2], M. Uttarwar[1], G. Shafi[1]; [1]OneCellDx, Cupertino, CA, [2]OneCellDx, Pune, India, [3]IndxTechnology, Pune, India

Introduction: Pancreatic ductal adenocarcinoma (PDAC) is aggressive malignancy characterized by 5-year survival rate of <10%. Comprehending PDAC's mutational landscape through NGS-based assays, acquiring representative tumor tissue biopsies remains arduous. Single circulating tumor cell (sCTC) genomics could provide clinically relevant personalized diagnostics. Here we demonstrate comparative analysis of sCTCs genomics and ctDNA outcomes in paired advanced PDAC patients.

Methods: Retrospectively, 25 live sCTCs and sCTC clusters were isolated from 10 advanced PDAC patients' blood using OncoRadar platform consisting glass beads conjugated with antiEPCam antibodies, tuned for releasing CTCs, without cell fixing, an assay in 96 well plate. Whole genomes from sCTCs were amplified using random degenerate primer-based PCR. Amplified genomes and paired ctDNA were subjected to CGP using clinical assay OncoIndx® to identify patient-specific genomic alterations in sCTC and paired ctDNA samples. The raw sequence alignment and variant calling was performed using iCare software®.

Results: Live 25 sCTCs and 8 CTC clusters were isolated (≥2 CTCs). Mutational profiling revealed multiple pathogenic (P) and likely pathogenic (LP) variants. sCTCs exhibited at least twice as many P variants compared to paired ctDNA samples, with CHD4, FGFR2, and HNF1α being the most common. The mutational profile of sCTCs showed concordance with at least one variant in paired ctDNA, and was enriched in dysregulated cytoskeleton and cell migration machinery. Specifically, COL7A, KIF5B, and RHOA mutations were prevalent in almost all sCTCs, with exclusive mutations (KIF5B and RHOA) in some cases. KRAS P variants were exclusive to 50% of ctDNA samples, paired sCTCs exhibited NRAS P variants. RAS isoforms were observed in 70% of sCTCs. Gene amplification occurred in CCND1/2, FGFR2, and ERBB2 in 90% of sCTCs, with CCND1 amplification more prevalent in sCTC clusters. Mutations in epigenetic repressors (HDAC1, KDM2B) were ubiquitous in sCTCs, co-occurring with DDR pathway mutations (F test, P 0.003, OR 11). Loss-of-function BRCA mutations were detected in 60% of sCTCs, and were absent in paired ctDNA. Additionally, 70% of sCTCs exhibited therapy-resistant variants (NF1, STK11, ARID1A, and PIK3CA), contrasting with a 10% frequency in paired ctDNA.

Conclusions: Genomic profile of sCTCs in advanced PDAC patients revealed a complex mutational landscape, providing additional clinically relevant insights that complemented ctDNA findings. sCTCs exhibited greater tumor mutational heterogeneity compared to paired ctDNA samples, and detected additional actionable pathogenic variants. Results suggest that sCTCs may offer therapeutically relevant molecular information for advanced PDAC patients for whom tissue is unavailable and ctDNA fails to provide actionable therapy options.

#7507 Capturing live single circulating tumor cells platform for comprehensive genomic profiling with paired ctDNA in breast cancer patients.

G. Shafi[1], A. Bharde[2], G. Khutale[2], S. Andhari[2], R. Deshpande[2], B. Jadhav[2], S. Prajapati[2], M. Fauzul[2], K. Hariramani[2], M. Basavalingegowda[2], J. Khandare[1]; [1]OneCellDx, Cupertino, CA, [2]OneCellDx, Pune, India

Background: Single circulating tumor cells (sCTC) capture without cell fixation with no blood contaminants like leukocytes are highly challenging. sCTC genome transcriptomics anticipates new avenues in new discovery, targeted therapies, and inclusion of patients in clinical trials where the tissue is inaccessible. We report, an assay to selectively capture live sCTCs at singularity with NGS-based comprehensive mutational profiling in breast cancer (BC) patients. Further, paired ctDNA outcomes using blood with mutational heterogeneity scores of sCTCs adds comprehensive genomics for establishing an accelerated treatment outcomes and resistance signatures.

Methods: Retrospectively, sCTC were isolated from 70 breast cancer (BC) patients using OncoRadar platform consisting affinity-based glass beads mediated by anti EpCAM antibody. CTCs were selectively captured and released without fixing and contamination of any leukocytes. Platform possess cleavable disulfide spacer at pH 8.0, between glass beads (diam. 2 mm, area 12.57 mm2) and a ligand. Sensitivity, specificity, positive predictive value (PPV), negative prediction value (NPV), and accuracy were evaluated using MCF-7 cells and CTCs. Assay to isolate CTC has been developed in 96 well plate, for downstream NGS-based comprehensive gene panel analysis using hybridization-based target enrichment. Interestingly, no mutations detected in blood samples (~20%) for CtDNA versus CTC DNA offered non-chip implicated mutations.

Results:. Analytical validation using OncoRadar showed higher cell capture efficiency (99%) with spiked MCF-7 cells/ml of blood. Sensitivity and specificity values were 97% and 98% respect, while PPV was 99% and NPV was 7.5% with the accuracy parameter of 99%. Sensitivity, specificity, PPV, and NPV parameters when assessed for CTC isolation from 70 BC patients. NGS-based mutational analysis, sCTC showed the presence of PIK3CA, ESR1, and NF1 mutations, which were absent from paired ctDNA samples.

Conclusion: Detection of ctDNA obscure mutations in paired sCTC samples suggests high sensitivity of sCTC-based genomic assays compared to current standard of practice. Heterogeneity scores amongst inter and intra CTCs with MATH scores offer new dimensions in genomics. Combination of ctDNA and sCTC DNA assay offers a comprehensive realistic genomic outcome for more significant therapy decisions, especially when guideline based options may exhausts.

#7508 Distribution prophecy of circulating tumor cell clusters in CTC populace patients of epithelial cancers.

J. Khandare[1], G. Aland[2], G. Khutale[2], S. Andhari[2], P. Patil[2], M. Garbhe[2], M. Dongare[2], T. Deshpande[2], V. Jadhav[2], N. Raut[3], G. Shafi[4], A. Bharde[2], A. Vasudevan[2], S. Jayant[2];

[1]Actorius Innovation and Research Pvt Ltd, Simi Valley, CA, [2]Actorius Innovation and Research Pvt Ltd, Pune, India, [3]Bhaktivedanta Hospital And Research Institute, Mumbai, India, [4]OneCelldDx, Pune, India

Background: Role of CTCs in metastatic cancers to predict the % prediction of overall survival has been well-established. The effectiveness of three- or six-months adjuvant therapy in colorectal cancer estimation showed association of CTCs with the emergence of resistant cell clones. The presence of CTCs with clusters indicates an aggressiveness of the epithelial cancers. However, the presence of CTC clusters has not been evaluated in large populations. Here, we demonstrate the distribution prophecy of CTCs and CTC clusters in epithelial cancer patients.

Methods: Retrospectively, 3458 patients' blood sample was analyzed for the presence and distribution of CTCs and CTC clusters using DCGI approved OncoDiscover platform having immunomagnetic multicomponent system mediated by anti EpCAM antibody. 1.5 mL of peripheral blood was analyzed to capture cells and clusters from Head & Neck, breast, and lung cancer patients. Earlier the sensitivity, specificity and accuracy of OncoDiscover assay was presented. CTCs and clusters were identified with CK 18 +ve, DAPI + ve and CD45 -ve staining using automated motorized fluorescence microscopy. CTCs clusters were defined by the presence of two or more CTCs bound together.

Results: .Out of 3458 epithelial cancer patients, 65.52 % patients showed the distribution of CTCs ~ 2262 (CTC numbers varied from 1-9/ 1.5 mL), while 7.54% patients showed CTC clusters (261 clusters). Total number of captured CTCs and clusters were 19345 (mean CTCs and cluster distribution was 5.59), while CTC were predominantly in 19037 numbers (98.41%) and clusters were 308 (1.59 %). Highest number of CTS were observed in HNC (52.98%) and breast cancers (22.75%), followed by lung cancer (5.65%). While, prophecy clusters were observed in breast cancers (26.95%), followed by lung (16.23%).

Conclusions: The frequency and distribution of CTCs and CTC clusters was evaluated in epithelial cancers. Patients with CTC alone and patients having CTCs as well CTC clusters represent more aggressive disease and the progression of disease. The effectiveness of adjuvant therapy in epithelial cancers can be estimated with CTC and cluster for association of treatment outmoded with an emergence of resistant cell clones.

#7509 Evaluation ofHER-2 expression on circulating tumor cells as a real time biomarker in advanced breast cancer.

J. Khandare[1], G. Aland[2], S. Andhari[1], G. Khutale[1], P. Patil[1], T. Deshpande[1], M. Garbhe[1], V. Jadhav[1], A. Vasudevan[1], S. Jayant[1];
[1]Actorius Innovation and Research, Simi Valley, CA, [2]Actorius Innovation and Research, Pune, India

Introduction: Breast cancer accounts for 12.5% of all new annual cancer cases worldwide. Cases classified as HER2-positive tend to proliferate, metastasize, and often lead to relapse. HER-2 is the most valid tumor marker, used as a diagnostics and prognostic biomarker in metastatic breast cancer (MBC). Thus, analysis of expression of HER-2 on CTCs can offer a real time dynamic biomarker for treatment options between endocrine therapy versus chemotherapy in advanced breast cancer. Functional assays on CTCs with HER-2 biomarker offer evolving biomarkers especially when the tissue is not accessible and inadequate.
Methods: Retrospectively, 179 breast cancer patients' blood was analyzed for the presence of CTCs using the OncoDiscover® platform approved by Drug Controller General of India (CDSCO). Consisting of immunomagnetic multi-components mediated by anti EpCAM antibodies. The isolated cells were immunostained consisting of a nuclear dye DAPI, CK-18, CD45 and HER-2 antibodies. CTCs were identified by the presence of HER-2 + ve, CK 18 + ve, DAPI + ve and CD 45 -ve staining. Validation of HER-2 expression on the CTCs was analyzed based on the linear intensity gradients of the fluorescence signals. CTCs were termed as HER-2 -ve based on weak or no detectable fluorescence signal and termed +ve based on high fluorescence signal.
Results: Among the cohort of 179 patient samples, 63.68 % samples showed the presence of CTC (CTC ranged from 1-7). 47.84% of these CTCs showed the expression of HER-2 signal. The mean value for fluorescence intensity for expression of HER-2 in CTCs was found to be 3.23. The observed mean fluorescence intensity for HER-2 expression further emphasizes the robustness of CTCs as a viable source for molecular characterization.
Conclusion: Integration of HER-2 analysis on CTCs into the clinical assessment of metastatic breast cancer, may offer a non-invasive, real-time strategy for profiling and possibly paving the way for more precise and tailored therapeutic interventions.

CLINICAL RESEARCH: Immune Checkpoint Inhibitor Therapy
Poster Session

#7513 Tumor treating fields (TTFields) can induce immunogenic cell death in GBM resulting in enhanced immune modulation.
R. T. Nitta, S. Lee, M. Lim, G. Li;
Stanford University, Stanford, CA

Glioblastoma (GBM) is the most common and aggressive form of malignant primary brain tumors. Despite current standard of care, the overall survival for GBM is ~15 months. While immunotherapy using immune checkpoint inhibitors such as anti-PD-1/PD-L1 have been efficacious for solid malignancies, very little progress has been made in a clinical setting for GBM. This is mainly due to GBM being known as a “cold” and non-immunogenic tumor. It has been previously established that a tumor may become “hot” if the T cell responses can be enhanced by increasing the presentation of tumor-specific antigens to the immune system. Tumor Treating Fields (TTFields) are alternating electric fields in a specific frequency range (100-500 kHz) delivered to the human body through transducer arrays. Treatment with TTFields have been approved and have shown efficacy in GBM. TTFields have induced immunogenic cell death in GBM, which in turn can elicit anti-tumoral immunity by inducing damage-associated molecular patterns (DAMP). These patterns are important for promoting engulfment of lung cancer cells by dendritic cells and recruitment of immune cells. These findings suggest that TTFields may enhance the immune response in GBM by increasing tumor specific antigens. In this study we show *in vitro* that TTFields enhanced the immune response to GBM. We initially demonstrated that GBM cells (GL261 or CT2A) treated with TTFields (200 kHz) can elicit DAMP emissions as evident by the increase in secretion of ATP and HMGB1 and the enhanced translocation of calreticulin to the cell surface. Additionally, TTFields stimulated the phagocytotic activity of antigen presenting cells (Raw264.7) and increased T-cell early activation (CD69/CD4+, CD69/CD8+) and activity (IFNγ and perforin). Since our findings *in vitro* indicate TTFields enhanced the immune response to GBM, we studied the therapeutic potential of using TTFields together with anti- PD1 in a syngeneic mouse model. We applied TTFields to GBM cells prior to intracranial injections. While our survival studies are preliminary, our findings suggest that systemic anti-PD1 and TTFields may result in a myeloid and T-cell mediated anti-tumor response and enhanced survival. Our findings indicate that TTFields treatment may help transform GBM into a “hot” tumor thereby making it an attractive target for immunotherapy.

#7514 Tumor intrinsic CDC42BPB confers resistance to anti-PD-1 immune checkpoint blockade in breast cancer.

R. P. Deshpande, K. Wu, S.-Y. Wu, A. Tyagi, J. Hunting, J. Ruiz, W. Li, K. Watabe;
Wake Forest Baptist Comprehensive Cancer Ctr., Winston-Salem, NC

Immune checkpoint blockade has been used to treat breast cancer, but the clinical responses remain relatively poor, especially for the triple-negative subtype. The weak responsiveness is attributed to tumor intrinsic as well as tumor extrinsic factors, suggesting a need for novel approaches. We have used the CRISPR Cas9 kinome knockout library consisting of 763 kinase genes to identify tumor intrinsic kinase conferring resistance to anti-PD-1 immune checkpoint blockade and identified the CDC42BPB kinase as a potential target to overcome the resistance to anti-PD-1 immunotherapy. We found that CDC42BPB is highly expressed in breast cancer patients who are non-responsive to immunotherapy. Importantly, a small molecule pharmacological inhibitor, BDP5290, which targets CDC42BPB synergized with anti-PD-1 and enhanced tumor cell killing by promoting T-cell proliferation in both in vitro and in vivo assays. Moreover, anti-PD-1 resistant breast cancer cells showed higher expression of CDC42BPB, and its inhibition rendered the resistant cells more susceptible to T cell killing in the presence of anti-PD-1. We also found that CDC42BPB phosphorylated AURKA which in turn upregulated PD-L1 through cMYC. Our results have revealed a robust link between tumor intrinsic kinase and immunotherapy resistance and provided a rationale for a novel combination therapy of CDC42BPB inhibition and anti-PD-1 immunotherapy for breast cancer.

#7515 Enhancing immune checkpoint inhibitor efficacy with fulvestrant in estrogen receptor-positive breast cancer.

J. Arima[1], K. Chida[1], M. Oshi[1], A. M. Roy[1], K. Taniguchi[2], S.-W. Lee[2], K. Takabe[1];

[1]Roswell Park Comprehensive Cancer Center, Buffalo, NY, [2]Osaka Medical and Pharmaceutical University, Takatsukishi, Osaka, Japan

Introduction: Breast cancer (BC) recurs decades after initial treatment that consists majority of the annual 43,000 BC deaths. Thus, Immune Checkpoint Inhibitor (ICI) therapy that bolster anti-cancer immunity is expected to improve long-term survival with reduced recurrence. Neoadjuvant ICI revolutionized management of triple negative breast cancer (TNBC); however, this represents only 5-7% of all BC cases, where estrogen receptor (ER)-positive subtype that consists of 70% of all BCs is not indicated due to less tumor-infiltrating lymphocytes (TILs). Using I-SPY2 trial we aim to investigate the potency of ER-alpha gene (ESR1) expression as a predictive biomarker, and whether the inhibition of the ER with fulvestrant enhances the efficacy of ICIs in ER+ BC.

Methods: Total of 1157 BC patients from two independent cohorts (ISPY2 trial; n= 73, TCGA; *n* = 1084) were included, encompassing both clinical and transcriptomic profiles. The TIL score was determined using the xCell algorithm.

Results: Using the transcriptome of the ISPY2 trial, we found that compared to ESR1 low expression patients, ESR1 high patients were associated with significantly lower pCR rates after neoadjuvant immunotherapy with ICI in whole cohort (n=71, pCR rate=30%, p<0.05) and HR+ subtype (n=50, pCR rate=20%, p<0.001), but not in triple-negative breast cancer (TNBC). ESR1 expression outperformed PD-1, PD-L1, and CTLA4 in Area Under the Curve (AUC) of the whole ISPY2 cohort (AUC=0.75, 0.68, 0.48, and 0.62, respectively), and further pronounced in HR+ BC (AUC=0.88, 0.73, 0.55, and 0.65, respectively), suggesting the potency of ESR1 expression as a predictive biomarker for ICI in HR+ BC. In agreement, ESR1 expression inversely correlated with the amount of intratumoral TILs consistently in both ISPY2 and TCGA cohorts in HR+ BC, but only in TCGA in whole cohort (all p<0.05). Among the intratumoral TILs, CD8+ T cell and M1 Macrophages were found to be less infiltrated in HR+ BC in TCGA. Given that ESR1 expression was associated with less intratumoral TILs and a poor response to ICI, we hypothesized that suppression of ER-alpha would enhance the effectiveness of ICI in HR+ BC in vitro. ER-alpha positive MCF7 cells were incubated with activated peripheral blood mononuclear cells with 1:1 ratio, and treated with 0.1 microgram of anti-PDL1, and 1nM of ER antagonist, fulvestrant, which demonstrated minimum cell killing. We found that ICI therapy with anti-PDL1 significantly decreased the cell viability of the MCF7 cells when ER-alpha expression was suppressed by fulvestrant, while activated peripheral blood mononuclear cells or anti-PDL1 alone or the combination did not exhibit any significant cell killing.

Conclusion: We found that ESR1 expression is a predictive biomarker of ICI, and ER antagonist fulvestrant enhances the response of HR+ BC to ICI, suggesting that this combination could expand ICI indications to HR+ BC.

#7517 Integrating in situ proximity ligation assay for PD1-PDL1 interaction with multiplexed immunofluorescence imaging.

T. Ullman[1], D. Krantz[2], H. Elofsson[3], C. Oses Sepulveda[1], A. Zieba-Wicher[3], P. Ostling[2], A. Ullen[2], S. Basu[3], **C. Stadler**[1];
[1]KTH Royal Institute of Technology, Stockholm, Sweden, [2]Karolinska Institute, Stockholm, Sweden, [3]Navinci Diagnostics, Uppsala, Sweden

Background: Programmed cell death protein 1 (PD1) and its ligand PD-L1 are pivotal components of the immune checkpoint machinery, playing a crucial role in the regulation of immune responses in cancer. The interaction between PD1 and PD-L1 is a significant therapeutic target in oncology, as its inhibitors have shown improved outcomes across a variety of malignancies. However, the treatment response to immunotherapies such as pembrolizumab has shown a modest response (~30%) in previous studies. This could be explained by the lack of molecular insight pertaining to the interaction of PD1 on T-cells and PD-L1 in the tumor cells in malignant tissues at the time of clinical diagnosis. The recent development of *in situ* Proximity Ligation Assay (*is*PLA), marks a significant advancement in the field. This method allows for the visualization of direct protein interactions within tissues, for example between PD1 and PD-L1. This adds an important layer of information compared to multiplexed immunofluorescence, which is useful for deep phenotyping of cell types in a tissue but lacks the ability to detect direct interactions between specific cells.
Methods: PD-L1-PD1 interactions in human FFPE tonsil and bladder cancer tissue were identified using the NaveniFlex Tissue Atto647N kit, following the guidelines provided by the manufacturer. This method is capable of detecting proteins within a proximity of less than 40 nm, utilizing oligonucleotide-antibody conjugates that generate an enhanced fluorescent signal. After completing the Naveni® detection process, we performed multiplexed immunofluorescence (IF) using the Phenocycler platform and a panel of 14 barcoded antibodies, to generate *is*PLA and multiplexed IF data on the same tissue section.
Results & Discussion: We have successfully established an automated workflow for the *is*PLA protocol. In this work, we aim to continue this effort and combine the *is*PLA, with downstream highly multiplexed immunofluorescence using the Phenocycler platform. We have generated proof of concept data for the successful integration of the two methods, using tonsil and bladder cancer tissue to detect protein interactions between PD1 and PD-L1, as well as phenotypic profiling of the tumor microenvironment with a 14 plex panel. This panel allows us to phenotype the relevant cell types (B cells, dendritic cells, T cells, macrophages, tumor cells and their proliferation status) and subsets of T-cells like cytotoxic CD8+ cells. The integration of the *is*PLA and multiplexed IF is poised to significantly advance our understanding of the TME and hopefully aid in patient stratification for immune checkpoint inhibition therapy. The clinical significance of this method integration will later be explored in a retrospective cohort of muscle invasive bladder cancer, receiving immune checkpoint inhibition therapy with pembrolizumab as a second line treatment.

#7518 Neoadjuvant-adjuvant pembrolizumab in resectable advanced basal cell carcinoma of the head and neck: An open-label, single-arm, phase 1b trial.

Grace M. Jones[1], James Isaacs[2], Lucy Boyce Kennedy[2], Jennifer Ko[3], Allison Vidimos[4], Alok Vij[4], Christine Poblete-Lopez[4], Jennifer Lucas[4], Yee Peng Phoon[1], Melissa McEnery-Stonelake[4], Jon Meine[4], Thach-Giao Truong[2], Pauline Funchain[5], Brian Gastman[6]

[1]Center for Immunotherapy & Precision Immuno-Oncology, Cleveland Clinic Lerner Research Institute, Cleveland, OH,[2]Hematology and Medical Oncology, Cleveland Clinic, Cleveland, OH,[3]Anatomic Pathology, Cleveland Clinic, Cleveland, OH,[4]Dermatology, Cleveland Clinic, Cleveland, OH,[5]Stanford Cancer Institute, Stanford, CA,[6]Plastic Surgery, Cleveland Clinic, Cleveland, OH

Introduction: BCC is a common form of skin cancer that shares treatment-related aspects with the more well-studied skin malignancy, melanoma, including sensitivity to anti-PD-1/PD-L1 immunotherapy. However, despite major advances in peri-operative immunotherapy for melanoma, little is known regarding these strategies in BCC. This phase 1B, single-arm study evaluated neoadjuvant-adjuvant treatment with pembrolizumab (PEMBRO) together with standard of care (SOC) resection in advanced BCC of the head and neck.

Methods: Eligible patients had resectable, locally advanced BCC of the head and neck, defined by at least one of the following high-risk characteristics: a measurement of ≥ 20 mm, indication for post-operative radiation, or perineural invasion (PNI) in multiple nerves. Patients were naive to hedgehog inhibitors (HHI) and had an ECOG of 0 or 1. All patients received IV PEMBRO at a dose of 200 mg every 3 weeks for a total of 4 cycles, then within 4 weeks underwent a SOC resection followed by adjuvant PEMBRO until a total of 17 cycles was completed. After the 30-day post treatment safety follow-up visit, patients were followed for up to 5 years post-operatively. The primary endpoint was pathological response rate. Secondary endpoints included RECIST response by radiographic or physical exam, adverse events (AE), and recurrence-free survival (RFS).

Results: 13 patients were enrolled in the trial from July 2020 to May 2023, and received at least one dose of PEMBRO. Two patients withdrew from the trial after one dose of PEMBRO, one following treatment-related G3 hepatitis and a second due to an unrelated medical complication (cholecystitis). Out of 11 patients undergoing surgical resection, 10 patients received 4 out of 4 and 1 patient received 3 out of 4 planned cycles of neoadjuvant PEMBRO (investigator preference without new related AE). Pathological complete response (pCR) was observed in 3 patients (23%). For those with RECIST measurable disease, 2 patients demonstrated a complete response (CR), 1 patient a partial response (PR), and 5 patients showed stable disease (SD). Two patients had progressive disease (PD). One patient with a complete pathologic response had a discordant RECIST response with PD noted radiographically. All 13 patients experienced at least one AE of G1 or 2. The highest grade of related AEs were noted in 2 patients with grade 3 hepatitis and pruritus respectively that resolved with supportive therapy. As of November 2023, the median follow-up time is 17.6 months with no recurrences noted.

Conclusions**:** Neoadjuvant-adjuvant PEMBRO shows promising efficacy and an acceptable safety profile in resectable advanced BCC of the head and neck. Given these positive results and the healthcare burden BCC accounts for, these findings warrant further study.

#7519 Elucidation of the mechanism of acquisition of immune checkpoint inhibitor resistance by chronic inflammation.

S. Yumoto, H. Horiguchi, H. Baba, Y. Oike;
Kumamoto Univ Graduate School of Medical Sci, Kumamoto, Japan

Introduction: Eight molecules that are structurally similar to angiopoietin but do not bind to angiopoietin's specific receptor Tie2 were identified and named angiopoietin-like factors (ANGPTL). ANGPTL2, particularly abundantly expressed in adipose tissue, promotes damage repair through tissue remodeling, and contributes to tissue homeostasis; however, in severe obesity, ANGPTL2 is overexpressed, resulting in irreversible tissue remodeling, which induces chronic inflammation and is involved in systemic insulin resistance and diabetes development. On the other hand, it is unclear how systemic chronic inflammation controlled by ANGPTL2 is involved in cancer progression and acquisition of immune checkpoint inhibitor (ICI) resistance. Therefore, we aimed to elucidate the mechanisms in the acquisition of ICI resistance by systemic chronic inflammation from the perspective of ANGPTL2.
Materials and Methods: 1. To induce chronic inflammation in adipose tissue, BALB/c mice were fed high-fat-diet (HFD) for 6 weeks. CT26 cells, a mouse colon cancer cell line, were subcutaneously implanted in normal diet (ND) and HFD mice and anti PD-1/PD-L1 antibody was administered intraperitoneally. Immune cell fractions in tumor tissue and bone marrow were analyzed by flow cytometry. 2. CT26 was subcutaneously implanted in WT and systemic ANGPTL2-deficient (*Angptl2*$^{-/-}$) mice, and anti PD-1/PD-L1 antibody was administered intraperitoneally. Tumor size and survival time were analyzed. Bone marrow cells were isolated and the immune cell fractions were analyzed by flow cytometry, and the expression of inflammatory cytokines in adipose tissue were also analyzed. 3. Bone marrow cells were isolated from BALB/c mice, and myeloid-derived suppressor cells (MDSCs) were established *in vitro* by GM-CSF and IL-6. Recombinant ANGPTL2 protein was added, and MDSC differentiation and function were evaluated by flow cytometry and qRT-PCR.
Results: 1. HFD mice had larger tumor size and poorer response to ICI treatment compared to ND mice. In tumor microenvironment, MDSCs were increased in HFD mice. HFD mice had significantly increased MDSCs, especially polymorphonuclear MDSCs (PMN-MDSCs) in bone marrow. 2. ICI-treated *Angptl2*$^{-/-}$ mice showed higher treatment efficacy and prolonged survival compared to WT mice. In bone marrow, MDSCs were reduced in *Angptl2*$^{-/-}$ mice under ICI treatment. In adipose tissue, the expression of chronic inflammatory markers was increased. 3. *In vitro*, addition of recombinant ANGPTL2 protein to MDSCs induced differentiation from mouse bone marrow cells did not significantly increase the cell ratio of MDSCs. No changes in the expression of MDSCs markers were observed in qRT-PCR.
Conclusions: Chronic inflammation induced by ANGPTL2 promotes MDSCs differentiation and maturation in the bone marrow, which may suppress anti-tumor immunity and contribute to ICI resistance.

#7520 NRT-YHD_001, targeting CD47 for liver cancer immunotherapy.

S. Nam[1], S. Kim[1], M. Na[1], E. Shin[1], J. Ha[1], S. Jeon[1], S. Yoon[2];

[1]Catholic University of Korea, College of Medicine, Seoul, Korea, Republic of, [2]NEORNAT, Seoul, Korea, Republic of

Previously, we demonstrated that recovery of histone deacetylase 6 (HDAC6) suppressed let-7i-5p expression to de-repress the thrombospondin-1 (TSP1) expression, and thereby it occupied CD47 receptor to block CD47-SIRPα mediated anti-phagocytosis of macrophage in liver cancer. NRT-YHD_001 is a modified antisense miRNA of let-7i-5p for liver cancer treatment. In addition, N-acetylgalactosamine was attached to NRT-YHD_001 for specific delivery to the liver. *In vitro* phagocytosis assay showed better macrophage phagocytosis activity than non-modified antisense let-7i-5p. To investigate the *in vivo* efficacy of NRT-YHD_001, spontaneous (Ras-transgenic) mouse liver cancer model was used and compared with that of sorafenib treatment. This mouse liver cancer model usually develops spontaneous liver cancer mass after 15 ~ 20 weeks of birth. We confirmed that both weekly i.v. injection of 1mg/kg and biweekly i.v. injection of 2mg/kg NRT-YHD_001 showed more significant therapeutic efficacy than the sorafenib-treated group. Furthermore, xenograft assay with Hep3B human liver cancer cells in athymic-nude mouse also showed that weekly i.v. injection of 1mg/kg NRT-YHD_001 exhibited better survival and tumor growth inhibition compared to non-treated group. In mouse and cynomolgus monkey maximum tolerated dose (MTD) studies, no toxicity of NRT-YHD_001 was found at doses up to 500 mg/kg intravenously. These results showed that NRT-YHD_001 had a robust anticancer effect by converting the macrophage of “don't eat me” into “eat me signal” in the tumor microenvironment of liver cancer, thereby removing or inhibiting liver cancer cells.

Keywords: let-7i-5p, macrophage, phagocytosis, liver cancer, CD47

#7521 Tumor NLRP3 inflammasome activity mediates resistance to Anti-PD-1 immunotherapy in advanced gastroesophageal cancer.

N. Yarla, K. Howell, Y.-V. Nguyen, D. Niedwiecki, H. Uronis, J. Strickler, N. C. DeVito, B. Theivanthiran, **B. A. Hanks**;
Duke University, Durham, NC

The addition of anti-PD-1 immunotherapy to the therapeutic armamentarium of advanced gastroesophageal (GE) cancer patients has resulted in modest improvements in clinical outcomes for a subset of patients. More robust predictive biomarkers to guide patient management and to select optimal combination immunotherapy strategies for the individual patient are needed. Our previous studies indicate that the tumor-intrinsic NLRP3 inflammasome-HSP70 signaling axis promotes the recruitment of granulocytic myeloid-derived suppressor cells (PMN-MDSCs) and drives resistance to anti-PD-1 immunotherapy.
The KEYLargo phase II clinical trial evaluated the efficacy of pembrolizumab (pembro) in combination with capecitabine/oxaliplatin (CAPOX) in HER2-negative advanced GE cancer patients. An 8-day lead-in period of pembro monotherapy in 36 advanced GE cancer patients allowed for the acquisition of blood and tumor tissue specimens to determine which immune-mediated alterations within the tumor microenvironment correlated with resistance to anti-PD-1 immunotherapy. Baseline and on-treatment specimens were collected for HSP70 ELISA, immunofluorescence microscopy, spatial transcriptomics, *NLRP3* FISH, IHC, and NLRP3-ASC proximity ligation assays (PLA) to measure NLRP3 pathway activity levels. All data was correlated with best objective response, progression-free survival (PFS), and overall survival (OS). Tumor-infiltrating $CD8^{\pm}$ T cells and PMN-MDSCs were increased in responders and non-responders, respectively. While PD-L1 CPS failed to associate with response, elevated baseline NLRP3 PLA activity correlated with increased tumor-infiltrating PMN-MDSCs ($P = 0.001$) and resistance to pembro/CAPOX therapy ($P = 0.01$). Only non-responding tumors exhibited an increase in NLRP3 PLA activity and *NLRP3* amplification. Transcriptional studies revealed tumors with enhanced NLRP3 activity to exhibit decreased expression of the NLRC5 transactivator, MHC class I antigen presentation genes, and an increase in the NK cell negative regulator, HLA-G. Baseline plasma HSP70 levels correlated with tumor NLRP3 activity ($P = 0.043$) and with resistance to pembro/CAPOX therapy ($P = 0.001$). Elevated baseline NLRP3 PLA activity and amplification were associated with diminished PFS ($P = 0.008$) and OS ($P = 0.009$). In additional studies, pharmacologic inhibition of the NLRP3 inflammasome suppressed PMN-MDSC recruitment, upregulated MHC class I, and reversed anti-PD-1 resistance in an orthotopic model of GE cancer. Together, these findings implicate tumor-intrinsic NLRP3-HSP70 signaling as an important mediator of anti-PD-1 resistance in advanced GE cancer. The NLRP3-HSP70 pathway is a promising source of therapeutic targets and biomarkers capable of improving treatment outcomes for this patient population. Additional clinical studies are warranted.

#7522 Association between the *CNTN4* expression and responsiveness to pembrolizumab in gastric cancer.

M. Cha[1], **G. Kim**[1], C. Park[1], B.-N. Jeon[1], K. Park[1], H. Park[1], C.-Y. Ock[2];
[1]Genome & Company, Sungnam-si, Gyeonggi-do, Korea, Republic of, [2]Lunit, Seoul, Korea, Republic of

Even though numerous strategies for controlling malignant tumors have been established with immunotherapies, a solution for non-favorable responses to immunotherapy is still unclear. To address this unsolved problem, we previously suggested that a new immune checkpoint, CNTN4, is expressed on the tumor side and suppresses T cell-dependent immune activation. We further investigated the association between the clinical outcome of pembrolizumab and the expression of *CNTN4* in the gastric cancer cohort using bulk RNA sequencing data to establish a clinical strategy for targeting CNTN4. We split the patients into high- or low-group based on the expression of *CNTN4* and *CD274* (PD-L1) with the median of those two genes and analyzed for the responses. As a result, patients who had low-*CNTN4* expression and high-*CD274* expression were favorable to the pembrolizumab (Objective response rate, ORR; 64.3% [9/14]). However, patients who had high-*CNTN4* expression and high-*CD274* expression showed unfavorable responses (ORR; 0% [0/9], χ^2 = 5.951, *P* = 0.002). We also figured out that non-responders (NRs, N = 33) had a relatively lower expression of *CD274* (p = 0.0012) and a higher expression of *CNTN4* (p = 0.0015) compared to responders (Rs, N =12). Furthermore, in *CD274*-high patients, NRs showed significantly higher *CNTN4* expression than Rs (Fold change = 2.17. *P* = 0.0086). Immune-related cytokine genes, such as *IFNG*, *GZMA*, and *CXCL9*, were negatively correlated to *CNTN4* expression (*R* = -0.69, *P* = 2×10^{-4}; *R* = -0.52, *P* = 0.0108; *R*= -0.54, and *P* = 0.0077, respectively.). In addition to the cancer cells, cancer-associated fibroblast, important for immunotherapy, was deconvoluted from bulk RNA data and showed higher *CNTN4* expressions in NRs than Rs (Fold change = 3.3, *P* = 0.002). When classifying tumor tissue based on TCGA molecular subtypes, genomically stable (GS) type and chromosomal instability (CIN) were more observed in the NRs compared to the Rs with poor prognosis. CIN and GS type patients showed higher *CNTN4* and lower *CD274* expression than other TCGA subtypes. We also figured out that all *CNTN4*-high patients were composed of CIN or GS types. Similarly, higher *CNTN4* expression and lower *CD274* expression were observed in CIN and GS gastric patients from the TCGA database. Moreover, overall survival (OS) and progression-free survival (PFS) were poorer in *CNTN4*-high patients (OS: median of *CNTN4*-high = 9.73 [95% CI= 4.77-NA] months, median of *CNTN4*-low = NA [95% CI= 9.03-NA] months, *P* = 0.072. Hazard ratio = 2.15 [95% CI = 0.917-5.037], *P* = 0.078) (PFS: median of *CNTN4*-high = 2.10 [95% CI= 1.33-3.97] months, median of *CNTN4*-low = 5.47 [95% CI= 2.80-NA] months, *P* = 0.0004. Hazard ratio = 3.303 [95% CI = 1.647-6.624], *P* = 0.0008).Together, we suggest that *CNTN4* is a potential ICP candidate for gastric cancer patients unfavorable to pembrolizumab treatment. The anti-CNTN4 antibody GENA-104A16 is under the IND submission stage for clinical studies.

#7523 An integrated analysis of radiologic and pathological responses in patients with metastatic renal cell carcinoma who presented with primary renal tumor in situ and received first-line nivolumab plus ipilimumab followed by cytoreductive nephrectomy.

L. Campos Clemente, O. Alhalabi, M. T. Campbell, G. Corredor Alonso, K. Hara, P. Msaouel, A. C. Johns, C. Tang, J. A. Karam, P. Rao, N. M. Tannir; The University of Texas MD Anderson Cancer Center, Houston, TX

Background: The decision to perform cytoreductive nephrectomy (CN) and timing of CN in patients (pts) with metastatic renal cell carcinoma (mRCC) and primary who respond to immune checkpoint therapy (ICT) is a matter of debate. In CheckMate-214, nivolumab plus ipilimumab (N+I) yielded a 35% objective response rate in the primary; however, there is a paucity of pathological data from nephrectomy specimens (Nx) after treatment with N+I. We sought to investigate the radiologic and pathological responses and correlate the findings with outcomes in pts receiving 1L N+I followed by CN.

Methods: We reviewed the medical records and Nx of pts with mRCC who received N+I followed by CN at our institution (2016-2021). H&E slides were reviewed to determine the % of residual viable malignant cells. Pathological response was defined as tumor viability ≤20%, and pathological complete response (pCR) defined as absence of residual cancer. Radiologic response was defined as ≥30% reduction in primary size. Progression-free survival (PFS) and overall survival (OS) were determined from date of CN.

Results: 22 pts (median age 59) are included: 18 (81.8%) males, 19 (86%) Caucasian, 20 (91%) had clear-cell histology, 20 (91%) had ECOG Performance Status 0-1, 10 (45%) had intermediate-risk disease and 12 (55%) had poor-risk disease by IMDC. Median ICT duration before CN was 6.5 months (mo) (range, 2-19 mo). 17 (77%) completed 4 cycles of N+I, and 16 (73%) received N maintenance before CN. 5 pts (23%) had grade 3/4 immune-related adverse effects; 1 pt did not complete 4 cycles of N+I due to hepatitis. There were no therapy-related deaths. 12 pts (54.5%) had progressive disease (PD); 3 pts (14%) died of RCC. Median PFS was 22 mo, median OS not reached (NR). Pts with pathological response had greater radiologic reduction in primary size compared to pts without pathological response (median reduction 38% vs. 15% p-value 0.01), smaller final primary pathological size (median 5.7 cm vs. 10.65 cm p-value 0.002), and lower pathological yT stage (pT0: 1, pT1: 6, pT2: 2 pT3: 3, pT4: 0 vs. pT0: 0, pT1: 1, pT2: 0, pT3: 8, pT4: 1 p-value 0.045); ICT duration was similar between groups (median 5.5 mo vs. 7 mo p-value 0.733). 6 pts achieved low viability within 5 mo of ICT. In 9 pts with optimal radiopathological response [viability ≤20% and ≥30% primary size reduction], PFS was longer compared to PFS in pts with suboptimal radiopathological response: median PFS NR vs. 17 months (HR 0.23, 95% CI 0.076 - 0.741; p-value 0.041). In 13 pts with suboptimal response, 10 (77%) had PD, the most common sites of PD were lymph nodes [6 pts (60%)] and brain [3 pts (30%)].

Conclusions: In this small cohort, N+I yielded a low pCR in Nx of pts with mRCC. Radiologic response but not ICT duration was associated with low tumor viability.

#7524 Targeting siglec-7/9 glyco-immune checkpoints in prostate cancer for enhanced immune responses and tumor suppression.

R. Wen, G. Marti, J. Stark, F. Marques, N. Riley, A. Bermudez, H. Zhao, C. Bertozzi, S. Pitteri, J. Brooks;
Stanford University, Stanford, CA

Prostate cancer is one of the leading causes of death in men worldwide. Despite significant advancements in the fight against cancer, immune checkpoint inhibitors have limited effectiveness in treating prostate cancer. Evidence shows that disrupting the interactions between Siglec-7/9 and sialic acids can enhance immune responses and effectively inhibit tumor growth in several cancers. However, the understanding of Siglec-7/9-sialic acid interactions in prostate cancer remains limited. Here, we found that tumor-infiltrating immune cells derived from prostate cancer patients exhibited high levels of Siglec-7 and Siglec-9. TCGA data analysis suggests that high levels of Siglec-7/9 are correlated to worse patient survival. Elevated levels of Siglec-7/9 ligands were found in prostate tumor tissues compared to adjacent normal tissues. Prostate cancer cell lines exhibited significant expression levels of Siglec-7 and Siglec-9 ligands, and cell surface sialic acids. Proteomic analysis suggests that increased sialylation was observed in tumor tissues in comparison to adjacent normal tissues. Disrupting interactions between Siglec-7/9 and sialoglycans enhanced T cell-mediated cytotoxicity against prostate cancer cells. Treatment with anti-Siglec-7/9 antibodies effectively suppressed the growth of PC3 and 22Rv1 tumors in a humanized mouse model. Immunohistochemistry analysis of tumor tissues showed that PC3 and 22Rv1 tumors treated with anti-Siglec-7/9 exhibited reduced proliferation, decreased vascularization, increased apoptosis, and enhanced immune cell infiltration. The CRISPR screen and mass spectrometry analysis suggested CD59 as a potential ligand for Siglec-9. Knockout of CD59 in prostate cancer cells decreased their binding activity of Siglec-9-Fc chimera proteins and promoted T cell-mediated killing ability. These findings provide valuable insights into the potential therapeutic strategy of targeting Siglec-7/9 and their ligands for prostate cancer treatment.

#7525 Investigating B7-H3 as a checkpoint and antibody drug conjugate target across prostate cancer variants- both androgen receptor dependent and independent.

N. Mundhara[1], S. Sharma[1], E. Tekoglu[2], E. G. Baraban[1], N. A. Lack[3], E. Shenderov[1];
[1]Johns Hopkins University School of Medicine, Baltimore, MD, [2]School of Medicine, Koc University, Istanbul, Turkey, [3]Vancouver Prostate Center, University of British Columbia, Columbia, DC, Canada

Background: *CD276* (B7-H3) has recently emerged as a promising presumptive immune checkpoint inhibitor (ICI) and antibody-drug conjugate (ADC) target for PCa. Unfortunately, current immunotherapy trials have yielded few objective responses in PCa and hormonal therapy seldom cures necessitating the need to develop new immunotherapy or targeted antibody-drug conjugate (ADC) treatment options for PCa, including B7-H3 targeted approaches.
Method: In this work, we evaluated important ADC targets and immune checkpoints (PD-1, PD-L1, PD-L2, LAG3, TIGIT, OX40, 4-1BB, CTLA4, STEAP1, STEAP2, PSMA, NECTIN1, TROP-2, DLL3 and B7-H3) in various PCa cell lines and multiple patients spanning various subtypes of PCa using publicly available bulk RNA sequencing data and single-cell RNA sequencing (scRNA-seq) data respectively. The results were validated at RNA and protein levels in listed cell lines. Further, the impact of androgen receptor (AR) signaling on B7-H3 expression was quantified using charcoal stripped media, AR agonist (R1881) and antagonist (enzalutamide) using real-time PCR and flow cytometry at RNA and protein levels respectively.
Results: We found that B7-H3 shows high expression and very low variability compared to other ADC targets and immune checkpoints in AR-positive (LnCAP), hormone-refractory (VCAP), Castrate resistant (22RVI), AR negative (PC3, DU145), and neuroendocrine (H660) cell lines, as well as in—PCa cells and tumor microenvironment (TME) myeloid cells—of multiple patients spanning various subtypes of PCa. Western blotting confirms the ubiquitous presence of B7-H3 in all these cell lines, even when PSMA is absent. Furthermore, B7-H3 expression was modifiable via androgen depletion, R1881 supplementation, or addition of the AR antagonist enzalutamide. These changes were significant in AR-positive LnCAP cells compared to AR-negative DU145 cells further endorsing the crosstalk between AR and B7-H3 signaling pathways, which will be presented in greater detail.
Conclusion: This work explores the therapeutic relevance of important ADC targets and immune checkpoints for Prostate Cancer (PCa), highlighting B7-H3 as a unique therapeutic ADC and ICI candidate across the continuum of PCa—androgen sensitive, castration resistant, and neuroendocrine—due to its stable expression across various subtypes and on TME myeloid cells. The relationship between AR and B7-H3 opens the possibility of future combination therapies based on this interaction.

#7526 Landscape of TIGIT and PD-L1 co-expression in solid tumors.

Sarabjot Pabla[1], Maria-Fernanda Senosain[1], R.J. Seager[1], Hardik Parikh[1], Erik Van Roey[1], Shuang Gao[1], Yamuna Pulivendula[1], Paul DePietro[1], Mary Nesline[1], Durgapras Dash[1], Jeffrey M. Conroy[1], Stephanie Hastings[2], Heidi Ko[2], Kyle C. Strickland[2], Rebecca A. Previs[2], Eric Severson[2], Marcia Eisenberg[3], Brian Caveney[3], Taylor J. Jensen[2], Shakti Ramkissoon[2]

[1]OmniSeq Inc. (Labcorp), Buffalo, NY,[2]Labcorp Oncology, Burlington, NC,[3]Labcorp, Burlington, NC

Background: Combination treatment of solid tumors with anti-PD-1/PD-L1 and anti-TIGIT agents have shown promise in recent clinical trials. However, TIGIT co-expression with other checkpoints has not been comprehensively characterized to support identification and prioritization of patients most likely to benefit from anti-TIGIT drugs and guide clinical trial design. In this study, we investigate TIGIT and other PD-1/PD-L1 axis checkpoint targets across various solid tumors.
Methods: A discovery cohort (DC) of 24,186 solid tumors across 35 tumor types was evaluated by comprehensive immune profiling. TIGIT gene expression was normalized and ranked yielding a percentile rank values [0-100]. TIGIT rank was classified as high (rank >e 75) and low (rank < 25). We studied the distribution of TIGIT expression, cellular proliferation signature, and co-expression with PD-1/PD-L1 axis and other checkpoint targets using Spearman correlation(r_s). Kaplan-Meier analysis and Chi-squared assessed associations between TIGIT expression/checkpoint co-expression and overall survival (OS), progression free survival (PFS) and objective response rate (ORR) differences in a separate cohort of 72 pembrolizumab treated non-small cell lung cancer (LC) patients treated with pembrolizumab.
Results: The DC confirmed a large range of TIGIT expression with highest median expression observed in NSCLC (median = 61), head & neck (HNSCC) (median = 59), and cervical cancer (median = 55). Significant association between PD-L1 IHC positivity (TPS≥1%, CPS≥1) and TIGIT expression ($p<0.001$) was discovered, where 69% (n=3574) of TIGIT high cases were PD-L1 positive, whereas 66% (n=3606) of TIGIT low cases were PD-L1 negative. By RNA-seq measurements, significant TIGIT co-expression ($p<0.001$) with various checkpoint blockade targets including PD-1 (r_s=0.5), PD-L1 (r_s=0.5), and TIM3 (r_s=0.6) was confirmed. In the LC, patients with TIGIT high tumors had significantly improved OS (median OS = 44 months; p=0.01) and PFS (median PFS = 35 months; p=0.006) compared TIGIT low group (median OS = 23 months; median PFS = 18 months). Similar results were observed for response to pembrolizumab, where TIGIT high cases had significantly higher response (ORR=60%, p= 0.001) vs. TIGIT low cases (ORR=39%). This was confirmed in TIGIT high and PD-L1-IHC positive group with improved OS (p=0.013), PFS (p=0.017) and ORR (p=0.016).
Conclusion: In an ultra-large cohort of clinically tested solid tumors, TIGIT was differentially expressed across tumor histologies of solid tumors. TIGIT expression was strongly co-expressed with PD-1/PD-L1 axis, supporting the improved outcomes for patients with NSCLC treated with a combination of TIGIT and PD-1/PD-L1 inhibitors from recent clinical trials. This finding of co-expression pattern of TIGIT and PD-1/PD-L1 axis highlights the potential use of immune profiling for combination therapy strategies and clinical trial design in solid tumors.

#7527 Investigating biomarkers for immune-related adverse events following immune checkpoint inhibitor therapy in recurrent lung cancer patients.

Y. Kudo, J. Matsubayashi, S. Takahashi, M. Hagiwara, M. Kakihana, T. Nagao, T. Ohira, N. Ikeda;
Tokyo Medical Univ., Tokyo, Japan

Background: The application of immune checkpoint inhibitors (ICIs) as adjuvant therapy post-lung cancer surgery is expected to confer significant benefits. However, the risk factors for severe immune-related adverse events (irAEs) remain incompletely understood, and managing irAEs may require long-term steroid use. The identification of biomarkers for irAEs in patients with surgically resected lung cancer is an urgent need.
Methods: We analyzed 43 lung cancer patients who received ICI treatment for recurrence postoperatively. Macrodissection of lung cancer lesions was performed on FFPE specimens from resected lungs, from which total RNA was extracted. We conducted gene expression analysis of 770 immune-related genes using the PanCancer Immune Profiling Panel (NanoString Technologies, Inc., Seattle, WA, USA). The relationship between gene expression changes and irAEs or the efficacy of ICI treatment was examined. For validation, immunostaining of proteins strongly associated with irAEs was performed to determine their expression status in tissue specimens.
Results: Among the 43 patients (30 males, 13 females, median age 68), 28 had adenocarcinoma, and 15 had squamous cell carcinoma. PD-L1 positivity was observed in 36 patients. The treatment regimens included pembrolizumab monotherapy for 18 patients and combination immunotherapy for 25 patients, with 25 patients responding to treatment and 7 developing irAEs. There was a marked difference in gene expression between adenocarcinoma and squamous cell carcinoma, with a notably higher number of tumor-infiltrating lymphocytes (TILs) in adenocarcinoma. An increase in TILs was observed in cases with irAEs across both cancer types. Additionally, an increased CD8/Treg ratio and CD8/exhausted T cell ratio were noted in adenocarcinomas with irAEs. A strong correlation between IRF5 gene expression and the occurrence of irAEs in adenocarcinoma was also confirmed by immunohistochemistry.
Conclusion: We have identified tumor immune microenvironments correlated with the onset of irAEs following ICI treatment in patients with postoperative recurrence of lung cancer. This discovery could contribute to perioperative treatment strategies and improve our understanding of tumor immune mechanisms.

#7528 Coordinated regulation of critical immune checkpoint proteins by the integrated stress response (ISR) pathway in lung cancer.

S. E. Thomas-Jardin, S. Suresh, C. Lewis, C. Ahn, B. M. Evers, J. D. Minna, K. A. O'Donnell;
UT Southwestern Medical Center, Dallas, TX

Non-small cell lung cancer (NSCLC) is the leading cause of cancer-related deaths worldwide. Despite recent advances, high rates of recurrence highlight the need for novel treatment options. Groundbreaking discoveries in identifying and exploiting the PD-1/PD-L1 (Programmed Death 1/ Programmed Death Ligand 1) immune checkpoint have resulted in the approval of monoclonal antibodies that disrupt this interaction as a first-line therapy for lung cancer patients. However, only ~20% of NSCLC patients benefit from checkpoint blockade. A critical question remains as to what mechanisms facilitate resistance to PD-1/PD-L1 therapy and whether other immune checkpoints or pathways can be pursued clinically in combination with this therapy. The integrated stress response (ISR) pathway represents an emerging therapeutic vulnerability. The ISR is a generalized response to maintain cellular homeostasis, and is known to be activated by hypoxia, heme deprivation, amino acid starvation, and oncogenic activation. We previously demonstrated that ISR activation potently induces PD-L1 in NSCLC and suppression of anti-tumor immunity (Suresh et al, *Nature Cancer*, 2020). We discovered that ISR pathway activation enhances PD-L1 translation through the bypass of inhibitory upstream open reading frames (uORFs) in the *PD-L1* 5' UTR and a mechanistic link to the translation initiation factor eIF5B. Our latest studies demonstrate that the immune checkpoint protein, CD155 (Cluster of Differentiation 155), is induced by ISR activation. We find that both PD-L1 and CD155 are induced by multiple arms of the ISR pathway, and CD155 harbors inhibitory uORFs in its 5' UTR. Importantly, we observed a significant correlation between PD-L1 and CD155 expression in a panel of primary human lung adenocarcinomas. We further demonstrated that ISR activation inhibits T cell function *in vitro* and promotes tumor growth in the CMT167 syngeneic mouse model. Analysis of immune cell infiltration using mass cytometry in this *in vivo* model is ongoing. Currently, we are determining the extent to which ISR inhibition suppresses tumorigenesis by promoting anti-tumor immunity and whether this may synergize with existing immune checkpoint therapies. Overall, these studies will set the stage for determining whether inhibition of the ISR pathway alone or in combination with immune checkpoint blockade will benefit lung cancer patients. Our studies may also lead to new therapeutic approaches to trigger anti-cancer immune responses and improve current strategies.

#7529 Harmonization radiomics model to predict immune checkpoint inhibitor-related pneumonitis (CIP) in non small cell lung cancer (NSCLC) in patients treated with immunotherapy.

M. Yadav[1], J. Lee[2], P. Kim[3], S. Lee[2], T. Um[1], S. Lee[4], M. J. A. Chuchuca[1], T. Djunadi[5], L.-Y. Chung[1], J. Yu[6], D. Rodrigues[1], N. Gennaro[1], L. Kim[7], M. Nam[8], Y. Oh[9], S. Yoon[1], Z. Shah[10], Y. Kim[1], I. Hong[11], J. Jang[11], G. Kang[11], A. Cho[11], S. Lee[12], T. Hong[11], C. Nam[11], Y. Velichko[1], Y. Chae[1];
[1]Feinberg School of Medicine, Northwestern University, Chicago, IL, [2]Kyungpook National University, Daegu, Korea, Republic of, [3]The University of Texas at Austin, Austin, TX, [4]School of Medicine at UCI, Irvine, CA, [5]Richmond University Medical Center, Staten Island, NY, [6]Dignity Health - St. Rose Dominican Hospital, Henderson, NV, [7]Ascension Saint Francis Hospital, Evanston, IL, [8]Lincoln Medical Center, Bronc, NY, [9]John H. Stroger, Jr. Hospital of Cook County, Chicago, IL, [10]Roswell Park Comprehensive Cancer Center, Buffalo, NY, [11]Northwestern University, Evanston, IL, [12]Johns Hopkins Bloomberg School of Public Health, Baltimore, MD

Background: With the increasing use of immunotherapy in advanced non-small cell lung cancer (NSCLC), managing adverse events, particularly checkpoint inhibitor-associated pneumonitis (CIP), poses a significant challenge. CIP often necessitates discontinuation of immunotherapy, even in cases of tumor response. Currently there are no effective models in predicting CIP. This study leverages artificial intelligence (AI) algorithms and the use of harmonization models to analyze radiomic features from chest CT scans, aiming to predict the occurrence of CIP in patients with NSCLC.
Methods: This retrospective study examined data from 152 stage III-IV NSCLC patients undergoing immunotherapy. Tumor segmentation was performed using LIFEx software (IMIV/CEA, Orsay, France). 3D-radiomic features were extracted from both the tumor and the surrounding 1 cm thick peritumoral regions. The Random Forest (RF) algorithm was employed to develop a classification model to differentiate between CIP and non-CIP. A harmonization model was deployed to account for the scanner-related differences by using spleen and normal lung signals. The dataset was divided into a training set (75%) and a test set (25%). Bootstrapping with 1,000 iterations was performed to estimate the model's performance by calculating the median and 95% confidence interval (CI) estimate. The accuracy of the model's predictions was evaluated by creating a confusion matrix. The model's performance was assessed by calculating the sensitivity, specificity, positive predictive values (PPV), negative predictive values (NPV), and area under the ROC curve (AUC) for CIP prediction.
Results: Among 152 patients, 87 (57.23%) are female and 65 (42.76%) are male. The median age was 59 years. Histology types included were Adenocarcinoma 111 (73%), Squamous cell carcinoma 27 (17.8%), and others 14 (9.2%). CIP was seen in 30 (19.73%) patients. Among the 30 patients with CIP, 17 (56.7%) patients had grade 1 pneumonitis, 11 (36.7%) patients had grade 2 pneumonitis, 2 (6.6%) patients had grade 3 pneumonitis, and none had grade 4 or grade 5 pneumonitis. The model achieved a sensitivity of 0.57, a specificity of 0.67, a PPV of 0.48, and NPV of 0.38 for predicting CIP. The AUC of 0.59 indicates that the model may predict checkpoint inhibitor-associated pneumonitis with an accuracy of 59%.
Conclusions: The study provides insights into the potential of radiomic analysis coupled with AI algorithms and the use of harmonization model in predicting CIP among NSCLC patients treated with immunotherapy. Larger studies are needed to validate our findings and the utility of harmonization models in predicting CIP.

#7530 Harmonization radiomics models to predict tumor response in non-small cell lung cancer (NSCLC) patients treated with immunotherapy.

M. Yadav[1], J. Lee[2], P. Kim[3], S. Lee[2], T. Um[1], S. Lee[4], M. J. A. Chuchuca[1], T. Djunadi[5], L.-Y. Chung[1], J. Yu[6], D. Rodrigues[1], N. Gennaro[1], L. Kim[7], M. Nam[8], Y. Oh[9], S. Yoon[1], Z. Shah[10], Y. Kim[1], I. Hong[11], J. Jang[11], G. Kang[11], A. Cho[11], S. Lee[12], T. Hong[11], C. Nam[11], Y. Velichko[1], Y. Chae[1];

[1]Feinberg School of Medicine, Northwestern University, Chicago, IL, [2]Kyungpook National Univeristy, Daegu, Korea, Republic of, [3]The University of Texas at Austin, Austin, TX, [4]School of Medicine at UCI, Irvine, CA, [5]Richmond University Medical Center, Staten Island, NY, [6]Dignity Health - St. Rose Dominican Hospital, Henderson, NV, [7]Ascension Saint Francis Hospital, Evanston, IL, [8]Lincoln Medical Centre, Bronx, NY, [9]John H. Stroger, Jr. Hospital of Cook County, Chicago, IL, [10]Roswell Park Comprehensive Cancer Center, Buffalo, NY, [11]Northwestern University, Evanston, IL, [12]Johns Hopkins Bloomberg School of Public Health, Baltimore, MD

Background: Precise prediction of immunotherapy response in non-small cell lung cancer (NSCLC) is crucial for personalized treatment. This study investigates the application of pretreatment CT-based radiomics and use of harmonization model in predicting these outcomes in NSCLC patients receiving immunotherapy.
Methods: This retrospective study examined data from 152 stage III-IV NSCLC patients undergoing immunotherapy. Patient responses were categorized using immune-related RECIST (irRECIST) criteria into durable responders (complete response [CR], partial response [PR], or stable disease [SD]) for at least 24 weeks and non-responders. Tumor segmentation was performed using LIFEx software (IMIV/CEA, Orsay, France). 3D-radiomic features were extracted from both the tumor and surrounding 1 cm thick peritumoral regions. The Random Forest (RF) algorithm was employed to develop a classification model to differentiate between responders and non-responders. A harmonization model was deployed to account for the scanner-related differences by using spleen and normal lung signals. The dataset was divided into a training set (75%) and a test set (25%). Bootstrapping with 1,000 iterations was performed to estimate the model's performance by calculating the median and 95% confidence interval (CI) estimate. The accuracy of the model's predictions was evaluated by creating a confusion matrix. The model's performance was assessed by calculating the sensitivity, specificity, positive predictive values (PPV), negative predictive values (NPV), and area under the ROC curve (AUC) for response prediction.
Results: A total of 152 patients were analyzed. 87 (57.23%) were female and 65 (42.76%) were male. The median age was 59 years. Histology types included were: 111 Adenocarcinoma (73%), 27 Squamous cell carcinoma (17.8%), and 14 other types (9.2%). The model achieved a sensitivity of 0.63, a specificity of 0.59, a PPV of 0.51, and NPV of 0.7 for response prediction of NSCLC patients receiving immunotherapy. The AUC of 0.61 indicates that the model may discriminate between responders and non-responders with an accuracy of 61%.
Conclusion: This study demonstrates the potential of radiomics and the use of harmonization models to predict immunotherapy responses in NSCLC patients, offering insights into personalized treatment approaches. Larger studies are needed to validate our findings and the utility of harmonization models in predicting a tumor response.

#7531 Mechanisms of response to anti-PD1 (PD1) combined with Ipilimumab (IPI) in patients (pts) with PD1-resistant metastatic melanoma (MM).

I. Pires da Silva[1], J. Conway[1], J. Edwards[1], F. Marsh-Wakefield[2], C. Quek[1], A. Ferguson[2], P. Johnansson[3], M. Carlino[1], A. Menzies[1], J. Wilmott[1], U. Palendira[2], R. Scolyer[1], G. Long[1];

[1]Melanoma Institute Australia, Wollstonecraft, Australia, [2]The University of Sydney, Sydney, Australia, [3]QIMR Berghofer Medical Research Institute, Brisbane, Australia

Background: Approximately 1 in 3 pts with PD1-resistant MM will benefit from IPI+PD1, but the role of adding IPI in this context is unclear. We sought to (a) identify biomarkers and (b) determine mechanisms of response to IPI+PD1 in PD1 resistant pts.

Methods: Pts with PD1-resistant MM subsequently treated with IPI+PD1 were included. We performed multiplex immunofluorescence (mIF), imaging mass cytometry (IMC) and RNA sequencing (RNAseq) on melanoma samples, and cytometry by time of flight (CYTOF) on peripheral blood mononuclear cells (PBMCs), at 3 timepoints (before PD1 [T1], before IPI+PD1 [T2], and after IPI+PD1 [T3]).

Results: 34 pts with PD1-resistant MM (82% innate resistance) who received IPI+PD1 were included: 16 (47%) responders and 18 (53%) non-responders to IPI+PD1. Median age was 66yo (37-86) and 19 (56%) were male. Six pts (18%) were ECOG PS ≥1, 18 (53%) were stage M1C/D and 11 (32%) had elevated LDH at the start of IPI+PD1.Gene expression analysis (RNAseq) on T1 and T2 tumor samples revealed higher expression of cancer testis antigens (CTA; MAGE-A3 and MAGE-C1; $p<0.05$) and immune regulatory genes (ILR2; $p<0.2$), but lower expression of fibrosis regulation genes (FABP3 and MMP7; $p < 0.2$) in responders vs non-responders. We then examined whether the addition of IPI led to expansion of CTA-specific T cells, and CyTOF analysis of MAGE-A3 tetramers on PBMCs showed a decrease in peripheral MAGE-A3-specific CD8+ T cells with PD1 (T1 to T2; $p=0.03$); and expansion of this T-cell subset with subsequent IPI+PD1 (T2 to T3) was seen in 7/12 HLA-A2+ pts. Further analysis on PBMC longitudinal samples showed an increase in regulatory T cells (Tregs) in responders ($p=0.04$), between T1 and T3, and a decrease in % of TCF7+ CD8+ & CD4+ T cells in non-responders ($p<0.05$) with the addition of IPI (T2 to T3). On baseline (T1) tumor samples (mIF), IPI+PD1 responders had a higher % of stem cell-like TCF7+ CD8+ T cells ($p=0.0004$), lower % of well-differentiated Tbet+ CD8+ T cells ($p=0.07$), and higher % of CD4+ T cells ($p=0.006$), compared with non-responders; but no difference in Tregs. On longitudinal tumor samples, there was a decrease in the % of stem cell-like TCF7+ CD8+ T cells but an increase in the % of tumor-reactive CD39+ CD103+ CD8+ T cells with PD1 (T1 to T2; $p<0.05$), mainly seen in responders ($p=0.06$). There were only 3 T2 to T3 IHC paired samples, precluding further analysis. IMC analysis on longitudinal samples (T1, T2 and T3) is underway to characterize the interaction between Tregs and T effector cells.

Conclusions: We identified potential mechanisms of response to IPI+PD1 in PD1-resistant MM pts. Our data suggests that response to IPI+PD1 requires baseline stem cell-like TCF7+ T cells with the potential to differentiate to an effector phase (CD39+ CD103+ CD8+ T cells), and that IPI facilitated expansion of antigen-specific T cells in a CTA-expression context, that PD1 alone is unable to do.

#7532 NB005.1, a fully humanized anti-KLRG1 blocking mAb enhances effector function of human CD8 T-cells.

B. P. Nayak[1], M. Xiong[2], Y. Xue[2], B. Wang[2], S. Lighvani[1], S. Sharma[1], D. Wang[2], H. Wang[2], B. Wang[2], Y. Zhang[2], X. Dong[2];
[1]Neologics Bioscience, San Diego, CA, [2]Neologics Bioscience, Suzhou, China

Introduction: Immune checkpoint blockers (ICBs) have revolutionized treatment, enhancing survival and benefiting many patients. However, many patients fail to respond to the treatment, necessitating research for new targets and improved approaches. The Killer cell Lectin-like Receptor G1 (KLRG1), expressed on a subset of NK and T-cells harbors an immune receptor tyrosine-based inhibitory motif (ITIM) within its cytoplasmic domain, indicating its inhibitory function. On $CD8^{\pm}$ T-cells, KLRG1 is expressed on highly differentiated antigen-specific effector memory T-cells (TEMs) and $CD45RA^{\pm}$ effector memory T cells (TEMRA). These cells are known to exhibit strong cytotoxicity potential and display developmental plasticity following KLRG1 blockade. And 16-48% of $CD8^{\pm}$ T-cells that infiltrate the tumor microenvironment (TME) are KLRG1 positive. We hypothesize that the blockade of KLRG1 should enhance the effector function of $KLRG1^{\pm}$ CD8 T-cells in the TME and provide therapeutic benefit as a standalone or in combination with existing ICBs.

Methods: Monoclonal antibodies (mAbs) targeting the human KLRG1 extracellular domain (ECD) were generated through mouse immunization and hybridoma technology. Purified mAbs from positive clones were screened using CHO-K1 and Jurkat cells overexpressing human or cynomolgus KLRG1 and human primary CD8 T-cells (n=3) to determine EC_{50} values. Epitope binning was performed, and high-affinity clones from each bin with cyno cross-reactivity were humanized to IgG1-Fc LALA variant. The Abs were evaluated for ligand blocking and enhancement of CD8 T-cell effector function through multiple functional assays. The assay measured enhancement of IFNγ or TNFα by $KLRG1^{\pm}$ human $CD8^{\pm}$ T-cells co-cultured with CHO-K1 expressing OKT3 and E-cadherin as artificial antigen-presenting cells (aAPCs) or PBMCs stimulated in with anti-CD3 and anti-CD28 Abs in presence of soluble E-cadherin. A human IgG1-LALA antibody (Ab) served as a negative control. PD-1 and KLRG1 synergy was evaluated in hPBMC assays.

Results: NB005.1 demonstrated single digit nanomolar (nM) binding potency on human primary CD8 T-cells and Jurkat cells expressing human KLRG1 as identified by its EC_{50} value. Blocking of KLRG1 with NB005.1 on purified human CD8 T-cells in co-culture assay with aAPC expressing E-cad and OKT3 led to CD8 T-cell activation and increase in IFNγ production confirming inhibitory function of KLRG1. Similar result was obtained when the Ab was tested on hPBMCs stimulated with anti-CD3 and anti-CD28 Abs in presence of soluble E-cadherin.

Conclusion: NB005.1, a fully humanized mAb, binds to human KLRG1 in the single digit nM range and effectively blocks the interaction with its ligand. This blockade enhances T-cell effector function as measured by IFNγ production, supporting the advancement of NB005.1 for preclinical testing, either as a standalone therapeutic or in combination with existing ICBs.

#7533 PVRIG is uniquely expressed in tumor dendritic cells-rich niches on stem-like memory T cells and its blockade may induce immune infiltration and activation in non-inflamed tumors.

Z. Alteber[1], G. Cojocaru[1], R. Granit[1], I. Barbiro[1], A. Wool[1], M. Frenkel[1], A. Novik[1], A. Shuchami[1], Y. Liang[2], V. Daniel Carmi[1], N. Sabath[1], R. Foreman[3], N. Petrenko[3], J. He[3], Y. Kliger[1], H. Adewoye[2], P. Ferre[1], Z. Levine[1], **E. Ophir**[1];

[1]Compugen Ltd., Holon, Israel, [2]Compugen USA Inc., San Francisco, CA, [3]Vizgen Inc., Cambridge, MA

Poorly immune infiltrated cancers pose a significant challenge, with current immunotherapies yielding limited clinical success. Stem-like memory T cells (T_{SCM}) have been identified as a T cell subgroup which possess enhanced proliferative capacity that could expand and differentiate upon dendritic cells (DCs) priming. In this study we investigated the expression of the recently discovered inhibitory receptor PVRIG and its ligand, PVRL2, in the tumor microenvironment (TME). Leveraging single cell RNA sequencing (scRNAseq) data from diverse cancer indications, we found that in $CD8^{\pm}$ T cells, PVRIG clusters with early differentiation/T_{SCM} genes, unlike other immune checkpoints that cluster with genes related to T cells exhaustion. In agreement with the scRNAseq data, PVRIG protein expression was markedly increased on $CD28^{\pm}CD8^{\pm}$ early-memory T cells across cancer indications. PVRL2, was dominantly expressed on intratumoral DC subsets on both scRNA and protein levels. The observation that PVRIG is uniquely expressed by T_{SCM} cells, and PVRL2 by DCs, led us to evaluate whether these cell populations physically co-localize in the TME, thus potentially allowing PVRIG/PVRL2 interaction. Employing spatial transcriptomic analysis in surgically resected CRC lesions we showed that while CTLA4, PD1, and TIM3 were mainly expressed by tumor infiltrating T cells, PVRIG and other genes of the DNAM-1 axis were intensely expressed by T_{SCM} in specialized immune aggregates, as well as by T cells in tumor bed. High resolution spatial mapping of interacting immune and adjacent cells revealed pairs of activated $LAMP3^{\pm}PVRL2^{\pm}$ DCs interacting with $CD28^{\pm}PVRIG^{\pm}$ CD8 T cells in the intratumoral immune aggregates. Thus, PVRIG/PVRL2 interaction may limit T_{SCM} priming by DCs and blocking this interaction may unleash potent T_{SCM} proliferation, differentiation, and infiltration into the tumor regions. To gain a more comprehensive understanding on the intratumor effects induced by PVRIG blockade, we evaluated the immune response in the TME of patients with poorly immune infiltrated tumors, platinum resistant ovarian cancer and MSS-CRC, indications typically less responsive to immune checkpoint inhibitors. Treatment with COM701, anti-PVRIG antibody, as monotherapy or in combination with nivolumab resulted in an increased tumor T cell infiltration, accompanied by TCR clonality expansion, which were associated with clinical benefit. In summary, our study identifies PVRIG as uniquely expressed on T_{SCM} in the TME, with its ligand PVRL2 expressed on activated DCs. Blockade of PVRIG/PVRL2 interaction by COM701 antibody emerges as a promising strategy to induce potent T cell responses, providing a novel approach overcoming resistance to immunotherapy in immune excluded tumors.

#7534 Tobemstomig, a novel bispecific checkpoint inhibitory antibody to preferentially block PD-1 and LAG-3 on CD8 TILs over Tregs.

L. Codarri-Deak[1], P. A. A. Weber[1], V. Nicolini[1], C. Klein[1], P. Umana[1], S. Seeber[2], M. Perro[1], S. Leclair[2];
[1]Roche Glycart, Schlieren, Switzerland, [2]Hoffman La Roche, Penzberg, Germany

Checkpoint inhibitors targeting PD-1 have shown unprecedented clinical efficacy in several cancer indications and therefore have, revolutionized the standard of care. However, despite this advancement, only ~20-30% of the patients derive durable benefit from such a treatment. One of the suggested reasons for this limited success is the expression/activation of compensatory inhibitory pathways such as LAG-3 on tumor-reactive T cells. Therefore, it is envisioned that simultaneous antagonism of PD-1 and LAG-3 receptors would overcome this adaptive resistance mechanism and allow a more profound reinvigoration of tumor-reactive T cells. LAG-3 is constitutively expressed by regulatory T cells (on Tregs) and it has been reported that its blockade increases Treg suppressive function which could potentially off-sets the benefit of blocking LAG-3 on tumor-reactive CD8 T cells.We therefore developed a 1+1 PD1-LAG3 bispecific antibody, Tobemstomig, with a unique PD-1 binder recognizing a glycoepitope and more than 20 fold higher affinity than the LAG-3 binder which recognizes a novel and differentiated binding epitope (E3). This difference in affinities allows for an avidity driven selectivity gain to PD-1 and LAG-3 double positive T cells over and the following advantages over monospecific and other bispecific aPD-1/-L1 and aLAG-3 antibodies:1.improved targeting to tumor-reactive T cells rather than Tregs due to the selectivity gain and different expression patterns of PD-1 and LAG-3 on these two T cell types, 2.reduced internalization, 3.resistance to drug-shaving by macrophages due to Fc -silencing via P329G LALA,4.increased *in vitro* T cell effector functions even in the presence of Tregs, 5.in-vivo targeting and expansion of CD8 TILs, including stem-like T cells, and increase in T cell effector functions and6.superior *in vivo* tumor control/eradication compared to combination of monospecific anti-PD1 and anti-LAG3 antibodies,in several mouse models including Panc02 in syngeneic huPD-1xhuLAG3 dtg mice and BXPC3, WSU, OCI-Ly18 and BC004 in humanized mice Tobemstomig has completed dose escalation and is currently tested in a composite proof of concept Ph2 trial in several solid tumor indications.

#7535 First-in-human phase 1 clinical trial of ZM008, a monoclonal IgG1 targeting LLT1, monotherapy and in combination with pembrolizumab in advanced solid tumors.

Maloy Ghosh[1], Anurag Tiwari[1], Ashvini Kumar Dubey[1], Sanghamitra Bhattacharjee[1], Yogendra Manjunath[1], Shalini Kashipathi[1], Subith Krishna[1], Tirtha Mandal[1], **Jyotsna Fuloria**[2], M. S. Madhusudhan[3], Golding Rodrigues[3]

[1]Zumutor Biologics Pvt. Ltd., Bangalore, India,[2]Fuloria Clinical Research Solutions, New Orleans, LA,[3]Indian Institute of Science Education and Research (IISER), Pune, India

Lectin-like transcript 1 (LLT1) interaction with CD161 receptor on NK cells facilitates tumor immune escape. Hence, blocking LLT1-CD161 interaction could potentially activate NK cells and resulted tumor cell cytotoxicity. ZM008 is a first-in-class anti LLT1 monoclonal antibody with promising pre-clinical safety, efficacy data and received IND approval from USFDA. Clinical study will start soon at multiple US sites. TCGA data analysis revealed high LLT1 gene expression in multiple solid cancers BRCA, CHOL, ESCA, GBM, HNSC, KIRC, KIRP, LIHC, LUAD, STAD, SARC. Several immune checkpoint genes PDL1, LAG3, TIM3, TIGIT, ICOS, B7-H3, are positively correlated ($p<0.05$) with high LLT1 expression. CIBERSORT analysis of immune cells revealed significant presence of Treg and CD33+ immune cells along with IL4, IL10, Arg1 and IDO1 in the TME with high LLT1 expression. Cox regression analysis suggests high LLT1 is a risk factor for survival ($p<0.05$) in patients with COAD, KICH and KIRC. High TMB and MSI scores were significantly correlated ($p<0.05$) with LLT1 expression in Colon and Kidney cancers, suggesting plausible biomarker application. Overall, transcriptome data analysis strongly suggests immune repressive gene signatures are prevalent with high LLT1 TMEs in multiple solid cancers. *In vitro* studies with human PBMC revealed ZM008 activates immune cells by inducing expression of CD69, NKG2D, CD107a, proinflammatory cytokines (IFN-γ, IL2, etc.,) secretion, and tumor cytotoxicity. In MLR assay, ZM008 as a single agent or in combination with Pembrolizumab primed DCs to secrete IFNγ and IL-2 which results in effector NK and T cells activation/proliferation *Ex vivo* studies with biopsy samples from NSCLC and Bladder Cancer patients showed significant tumor reduction and infiltration of patients' immune cells with ZM008 monotherapy and ZM008 + pembrolizumab combination. An open label, 3+3 design, multicenter dose escalation phase 1 trial for ZM008 is planned in patients with advanced/metastatic solid tumors with no therapeutic standard alternative to evaluate the safety, tolerability and efficacy of ZM008, as monotherapy and in combination with Pembrolizumab. FIH dosing of 0.15mg/Kg was determined based on MABEL strategy. *In silico* data analysis showing high LLT1 expression in patients non-responsive to immune checkpoint inhibitor treatments indicate the potential benefit to the patients from ZM008 + pembrolizumab combination treatment. ZM008 treatment will release the immune break, activate the infiltrated immune cells and provide anti tumor effects in solid cancers either as a standalone treatment or combination therapy. Retrospective analysis of patient samples pre and post ZM008 treatment will identify relevant biomarkers for patient recruitment and better prediction of prognosis.

#7536 CD4$^{\pm}$T cell exhaustion in the tumor microenvironment and antitumor immunity.

J. Nagasaki[1], W. Zhou[1], S. Kawashima[2], T. Ishino[1], K. Kawase[3], Y. Ueda[1], K. Yamashita[4], T. Watanabe[1], T. Inozume[2], Y. Togashi[1]; [1]Okayama University Graduate School of Medicine, Okayama, Japan, [2]Chiba University Graduate School of Medicine, Chiba, Japan, [3]Chiba Cancer Center, Chiba, Japan, [4]KOTAI Biotechnologies, Osaka, Japan

Background: Immune checkpoint inhibitors (ICIs) exert clinical efficacy against various types of cancer through reinvigoration of exhausted CD8$^{\pm}$ T cells that attack cancer cells directly in the tumor microenvironment (TME). However, compared to CD8$^{\pm}$ T cell exhaustion, the role of CD4$^{\pm}$ T cell exhaustion in antitumor immunity remains unclear.

Methods and Results: From single-cell sequencing for tumor-infiltrating lymphocytes (TILs) from patients with melanoma and mouse models, we found that *CXCL13*, which is highly expressed in tumor-infiltrating exhausted CD8$^{\pm}$ T cells, induces PD-1$^{\pm}$CXCR5$^{\pm}$CD4$^{\pm}$ follicular helper T (T_{FH})-like cell infiltration, which could contribute to antitumor immunity. Furthermore, a part of the T_{FH}-like cells in the TME exhibits cytotoxicity and directly attacks MHC-II-expressing tumors. RNA velocity and latent time analysis in single-cell sequencing for melanoma TILs showed that the differentiation of T_{FH}-like cells from the naive CD4$^{\pm}$ T cells were different from that of other CD4$^{\pm}$ T cells. In addition, the T_{FH}-like cytotoxic CD4$^{\pm}$ T cells were at the late stage of differentiation and some non-cytotoxic T_{FH}-like cells might differentiate into T_{FH}-like cytotoxic CD4$^{\pm}$ T cells. We additionally found considerable overlapped clonotypes between the cytotoxic and non-cytotoxic clusters. T_{FH}-like cytotoxic CD4$^{\pm}$ T cells have high LAG-3/BLIMP1 and low TCF1 expression without self-renewal ability, whereas non-cytotoxic T_{FH}-like cells express low LAG-3/BLIMP1 and high TCF1 with self-renewal ability, closely resembling the relationship between terminally differentiated and stem-like progenitor exhaustion in CD8$^{\pm}$ T cells, respectively.

Conclusion: Our findings provide novel insights into T_{FH}-like CD4$^{\pm}$ T cell exhaustion with helper progenitor and cytotoxic differentiated functions, which mediates antitumor immunity orchestrally with CD8$^{\pm}$ T cells.

#7537 “Cross-over Effect” in survival curves with immune-checkpoint inhibition: Identifying ideal candidates for immunotherapy-only approaches in specific tumor histologies.

Shubhank Goyal[1], Anish Thomas[1], **Parth Anil Desai**[2]

[1]Developmental Therapeutics Branch, National Institutes of Health, Bethesda, MD, [2]Hematology & Medical Oncology, Fox Chase Cancer Center, Philadelphia, PA

Immune checkpoint inhibition (ICI), a cornerstone of modern immunotherapy (IO), has revolutionized cancer treatment, offering significant survival benefits across various malignancies. Initial trials with ICI in refractory cancers demonstrated remarkable efficacy compared to standard-of-care (SOC) treatments. With the integration of ICI into combination therapies, including chemotherapy and multi-tyrosine kinase inhibitors (TKI), its role in frontline, early-stage, and locally advanced cancers has grown. However, the potential of an immunotherapy-only strategy, especially in advanced malignancies, warrants better biomarker selected approaches given the inconsistencies with existing biomarkers. This study investigates the "cross-over” effect observed in Kaplan-Meier survival curves from randomized trials comparing ICI with non-ICI agents where the survival curves, assumed to be proportionally constant distinctly cross over each other during the on-treatment monitoring period. We initiated a meta-analysis investigating randomized trials comparing ICIs with non-ICI historical SOC agents and finally analyzed data from 38 large clinical trials. Trials were selected based on their comparative nature with overall survival (OS) and progression-free survival (PFS) data as outcomes. A positive “cross-over” in Kaplan-Meier curves was identified when divergence occurred for at least three consecutive months. Cross-over in PFS and OS curves were observed in 53% (20/38) and 43% (16/37) of trials, respectively. All cross-overs were one-sided with the ICI arm crossing over the non-ICI arm with a superior tail. Notably, 100% of trials with OS curve cross-over involved ICIs against chemotherapy. A significant association (Fischer’s exact test, p=0.01) was found between OS curve cross-over and adenocarcinoma histologies, in contrast to trials with no cross-over effect, predominantly featuring squamous cell carcinomas. This pattern persisted within various organ sites such as the lung, esophagus, and cervix where both adenocarcinomas and squamous histological patterns are seen. Cross-over of Kaplan-Meier curves blatantly violates the cox-proportional hazard assumption, potentially underestimating the impact of the ICI-only approach compared to alternative therapies. These observations highlight substantial biological heterogeneity in tumor responses to ICI versus chemotherapy. The cross-over effect, particularly pronounced in gland-forming tumors (adenocarcinomas), underscores the urgent need to investigate mechanisms of ICI resistance in these tumor types and incorporate tumor histology and longitudinal tumor growth dynamics into existing predictive models for biomarkers for IO response and help identify patients who would benefit the most from immunotherapy-only approaches.

#7539 First-in-class anti-PVR mAb NTX1088 advancing through Phase I: Safe and potent in restoring DNAM1 expression to enhance antitumor immunity.

A. Atieh[1], A. Obeidat[1], A. Vitenshtein[1], G. Cinamon[1], **K. Paz**[2], T. Rovis[3], P. Brilc[3], O. Mandelboim[4], S. Jonjic[3], P. Tsukerman[1];
[1]Nectin Therapeutics, Ltd., Jerusalem, Israel, [2]Nectin Therapeutics, Ltd., Fort Lee, NJ, [3]MEDRI, Rijeka, Croatia, [4]Hebrew University, Jerusalem, Israel

NTX1088, a first-in-class anti-PVR (CD155) mAb, is currently evaluated in a Phase 1, open-label, multi-center study (NCT05378425). The trial initiated at MD Anderson Cancer Center, and was expanded into additional sites, including City of Hope, Ochsner Health, Sheba Medical Center and Hadassah Medical Center. Study objectives are safety, dose-finding, and efficacy with focus on pharmacokinetics, pharmacodynamics, and biomarker discovery. NTX1088 is investigated as a single agent and in combination with the anti-PD1 mAb, pembrolizumab (Keytruda) in patients with advanced solid malignancies. Ongoing dose escalation demonstrates a safe profile across ascending dose levels. NTX1088 is a high affinity humanized IgG4-S228P mAb that binds PVR and blocks all known interacting receptors at a single nM EC_{50}. PVR, is a highly upregulated membrane protein on numerous tumor cells. PVR expression has been associated with worse patient outcome, due to its central role in immune suppression. PVR's impact is mediated through interaction with the key stimulatory receptor, DNAM1 (CD226), on T and NK cells, leading to internalization and degradation of DNAM1. PVR also interacts with the inhibitory immune checkpoint receptors, TIGIT, CD96 and KIR2DL5A. Blocking PVR by NTX1088 has multiple immune-stimulating roles, through restoration of DNAM1 immune activation function, while simultaneously neutralizing TIGIT, CD96 and KIR2DL5A inhibitory signals in immune cells. Importantly, DNAM1 downmodulation was recently identified as a key resistance mechanism to approved immune checkpoint inhibitors, and its restoration by NTX1088 is a novel MoA, not demonstrated previously by other therapies.In vitro, as a monotherapy, NTX1088 significantly increased immune cell activation, superior to TIGIT, CD112R, and PD1 antibody blockade, leading to a greater immune-mediated tumor cell killing, IFNγ secretion, and CD137 induction. Importantly, only NTX1088 was able to restore DNAM1 to the surface of immune cells. Synergy was obtained when NTX1088 was combined with PD1 blockers, or with the anti-CD112R mAb, NTX2R13.Syngeneic models of $PVR^{K.O}$, demonstrated a complete immune-mediated tumor regression. Numerous humanized murine xenograft models were investigated whereby NTX1088 exhibited robust tumor growth inhibition as a standalone and in combination with PD1 blockade.In conclusion, PVR blockade by NTX1088 has a remarkable pre-clinical efficacy, suggesting a potential clinical breakthrough, based on its ability to simultaneously overcome multiple tumor escape mechanisms. First-in-human (FIH) trial is currently ongoing and biomarker analysis is showing initial mechanistic proof of concept for NTX1088 mode of action, including the restoration of DNAM1 surface expression on patients' immune cells. This is the first case of surface DNAM1 elevation in clinical settings.

#7540 Impact of IL-2 and IL-7 on human regulatory T cell suppression and pembrolizumab-mediated reversal of human T cell exhaustion.

Gokhan Tut, Neale Harrison, Leila Sallie, Emma Welsh Welsh, Ashley Pegg, Arshpreet Kaur, Zhi Li, Ines Morano, Hujo Chan, Jamie Cowley, Catherine Brady, John Gordon, Mark Bryant, **Omar Qureshi**, Nicholas M. Barnes

Celentyx Ltd, Birmingham, United Kingdom

Inhibitory pathways within the tumour microenvironment limit the anti-cancer immune response. Two central mechanisms limiting the T cell response in the tumour are suppression of effector T cells responses by regulatory T cells, and chronic exposure to tumour antigens that may bestow T cell unresponsiveness or exhaustion. Restoring exhausted T cell responsiveness through blockade of inhibitory immune checkpoints such as the PD-1/PDL-1 interaction is an established therapeutic modality leading to durable responses and improved survival rates in some patients.We have modelled suppressive mechanisms *in vitro* using purified human T cells and investigated the impact of the cytokines IL-2 and IL-7. A comparison of *in vitro* assay systems for T cell exhaustion including T cell/allogeneic dendritic cells, a recall response to a viral antigen, prolonged stimulation of T cells to generate an ‘exhausted’ phenotype followed by a secondary stimulation with allogeneic DCs, revealed in some donors, the greatest impact of pembrolizumab was with exhausted T cells, a finding consistent with our studies using a dissociated tumour cell response with primary cells from patients with lung or colon carcinomas. Quantifying a range of cytokines (e.g. IFNγ, TNFα and IL-10) and flow cytometry activation markers (e,g, CD69, CD25, CD71, OX40 and CD137) established that in general pembrolizumab was effective at restoring the IFNγ response, although some donors were not responsive, and there was a more modest impact on other readouts indicating not all T cell functionality is restored. We therefore tested the impact of IL-2 and IL-7 on the reversal of the ‘exhausted’ phenotype and identified further improved functionality and donor responsiveness. We subsequently tested the impact of these cytokines in another ‘inhibitory’ context, that of regulatory T cell suppression; we identified that high-levels of IL-2 overcame regulatory T cell suppression and IL-7 led to an overall enhancement of response.These findings highlight how multiple suppressive mechanisms may need to be overcome to maximally restore anti-cancer immune responses, and that the combination of cytokines, such as IL-2 and IL-7, and checkpoint inhibitors, such as pembrolizumab, may enhance T cell responses.

CLINICAL RESEARCH: Molecular Biology in Clinical Oncology: Characterizing and Modulating Epigenetics and Gene Expression
Poster Session

#7544 Bromodomain and extra-terminal protein inhibitors deplete nuclear factor 1C and reduce stemness and growth of human small cell lung cancer cells in vitro and in vivo.

H. Wang, R. Wang, F. Villa-Hernandez, V. Shukla, L. Varticovski, S. Baek, F. Echtenkamp, S. Gara, M. R. Zhang, S. Shiffka, R. Raziuddin, L. M. Neckers, W. Linehan, G. L. Hager, S. R. Carr, C. D. Hoang, H. Chen, D. S. Schrump;
Center for Cancer Research, National Cancer Institute, National Institutes of Health, Bethesda, MD

Objectives: Recent insights regarding mechanisms mediating stemness, heterogeneity, and metastatic potential of lung cancers have yet to be fully translated to effective regimens for the treatment of these malignancies. This study sought to examine complex epigenetic mechanisms underpinning the aggressiveness of SCLC, with a focus on understanding those mediating stemness in these highly lethal cancers.
Methods: Normal small airway epithelial cells (SAECs) were reprogrammed into iPSCs, validated by various assays, such as spectral karyotyping and teratoma formation. Genome-wide chromatin landscapes of lung iPSCs (Lu-iPSC) and SAECs, as well as NSCLC and SCLC lines were characterized using RNA-seq, DNA methylome, and DNase-hypersensitivity sequencing (DHS). Gene knock-downs were established using siRNA/shRNA techniques, along with qRT-PCR, immunoblotting, proliferation, and tumorigenicity assays. Glycolysis was analyzed using Seahorse assays. In-silico analysis of the NFIC promoter was performed using TFmapper. NFIC and related gene expression in human SCLC cells following NFIC or Bromodomain-containing protein (BRD) knockdown or exposure to BET inhibitors (BETi) were evaluated. Stemness scores were calculated using established RNA-seq criteria, and gene set enrichment analyses were conducted. Proliferation assays and xenograft models were used for in-vitro and in-vivo SCLC growth assessment.
Results: RNA-seq ,DNA methylome and DHS analyses revealed shared characteristics among SAEC, Lu-iPSC, SCLC, and NSCLC, whereas SOXs and POUs showed strong activity in Lu-iPSC but not SCLC. NFIC, with elevated chromatin occupancy in SCLC, exhibited increased expression compared to SAEC. NFIC KD in SCLC significantly curtailed cell growth in-vitro and in-vivo, affecting multiple pathways, including glycolysis and stem cell signaling etc, confirmed by Seahorse assays. Furthermore, we identified occupancy sites for BRD4 in the NFIC promoter, and knockdown of BRD4, but not BRD2 or BRD3, reduced NFIC expression in SCLC cells. BET inhibitor (BETi) treatment dose-dependently decreased NFIC expression in SCLC lines and human SCLC PDXs, irrespective of subtype. BETi treatment also reduced SCLC stemness and showed a significant overlap in gene regulation with NFIC knockdown, affecting pathways related to gluconeogenesis, neuronal differentiation, and embryonic organ morphogenesis. Importantly, BETi treatment effectively reduced SCLC cell growth in-vitro and in-vivo, suggesting the potential therapeutic value of targeting NFIC via BET inhibition in SCLC.
Conclusions: NFIC, a unique transcription factor in SCLC, emerges as a key downstream target of BRD4. These findings underscore the potential druggability of NFIC in clinical settings, provide compelling rationale for evaluating BETi for SCLC therapy.

#7545 Epigenetic plasticity in rewiring DNMT1/UHRF1-RB1- NFkB signaling circuit regulates asbestos-induced mesothelial malignant transformation.

S. Xi, X. Wu, D. Straughan, E. Payabyab, H. Wang, R. Wang, M. Zhang, S. Carr, C. Hoang, D. Schrump;
NIH-NCI, Bethesda, MD

The exact mechanisms underlying the causal relationship between asbestos exposure and malignant mesothelioma (MM) have yet to be elucidated. Widespread genomic and epigenomic alterations are being implicated in rewiring of oncogenic signaling networks which may contribute to initiation and progression of MM. In the present study, we examined the molecular profiles of mesothelial cells exposed to asbestos in-vitro and found that asbestos-induced activation of DNMT1/UHRF1 mediated epigenetic repression of RB1 in normal mesothelial cells as well as mesothelioma cells via promoter-specific methylation mechanisms. RB1, as a noncanonical transcription factor, was capable of also negatively modulating the transcriptional activities of DNMT1/UHRF1 mesothelium and mesothelioma. Functioning as one of the downstream effectors of RB1, NFkB was also involved in the transcriptional regulation of DNMT1/UHRF1 directly in a promoter-selective manner and played a pivotal role in the acute as well as chronic functional and phenotypic changes of mesothelial cells following asbestos exposure. Pharmacological interference of the dysregulated RB1-DNMT1/UHRF1- RB1-NFkB signaling circuit constitutively arrested the invasive growth of MPM cells. In-vivo studies using FVB genetic background wild-type and Bap1+/- mice further revealed involvement of epigenetically dysregulation of the RB1-DNMT1/UHRF1- RB1-NFkB signaling circuit during asbestos-induced malignant transformation of mesothelial cells. Taken together, our data are the first to describe that asbestos epigenetically rewires the RB1-DNMT1/UHRF1- RB1-NFkB signaling circuit during mesothelioma development and suggest potential novel strategies to reverse these epigenetic perturbations for MPM treatment in the clinic.

#7546 Targeting NSD2 to reverse lineage plasticity and drug resistance in neuroendocrine prostate cancer and subtypes of mCRPC.

J. J. Li[1], A. Vasciaveo[1], D. Karagiannis[1], X. Chen[1], C. Yu[2], A. Califano[1], C. Lu[1], M. M. Shen[1];
[1]Columbia University Irving Medical Center, New York, NY, [2]Memorial Sloan Kettering Cancer Center, New York, NY

Treatment with highly potent anti-androgens, such as enzalutamide and abiraterone promotes lineage plasticity in metastatic castration-resistant prostate cancer (mCRPC), which results in intra-tumor heterogeneity and emergence of mCRPC subtypes. The histological transformation from adenocarcinoma to aggressive neuroendocrine prostate cancer (CRPC-NE) has been associated with a loss of dependency on lineage-survival signals, leading to targeted drug resistance. Epigenomic reprogramming might be a fundamental driver of lineage plasticity. To determine CRPC-NE vulnerabilities, we have performed image-based screening using a small library of antibodies targeting different histone marks on CRPC-NE organoids derived from genetically engineered mice. We find that the histone mark H3K36me2 and the histone methyltransferase NSD2 play important roles in maintain the CRPC-NE epigenetic state. Knockout of NSD2 or ablation of H3K36me2 using an oncohistone mutant H3.3K36M reverted CRPC-NE to an adenocarcinoma phenotype. Simultaneous profiling of the transcriptome and epigenome from single cells verified this lineage conversion and the generation of cell states with canonical AR signaling. Moreover, H3K36me2 or NSD2 depleted mouse and human CRPC-NE organoids responded to enzalutamide treatment *in vitro* and *in vivo*, suggesting a reversal of castration-resistance. Most importantly, a small molecule inhibitor of NSD2 (NCT05651932), in combination with enzalutamide leads to growth suppression or apoptosis of mouse and human CRPC-NE organoids, organoids of other CRPC subtypes and xenografts *in vitro* and *in vivo*. In conclusion, inhibition of NSD2 reverts the epigenomic state of CRPC-NE, reversing lineage plasticity and restoring anti-androgen sensitivity. Thus, we suggest that the combination of NSD2 inhibition with AR inhibition may represent a novel therapeutic approach for patients with CRPC-NE or even other CRPC subtypes.

#7547 Enhancers as targets for improvements in immunotherapy.

A. Singh, V. Kochat, E. Arslan, S. Satpati, W. Deng, S. Yadav, E. Bataki, C. Yee, **K. Rai**;
UT MD Anderson Cancer Center, Houston, TX

Role of epigenetic elements in mediating tumor immune interaction remains poorly understood. We previously identified enrichment of active enhancer states on a set of genomic loci in non-responders to immune checkpoint blockade (ICB) therapy. We noted that the activated non-responder enhancers marked a group of key regulators of in melanoma cells that are known to mediate resistance to ICB therapy and several checkpoint receptors in T cells. Through spatial epigenomics (Spatial ATAC and CUT&Tag) approaches, we identified the tumor-immune niches harboring unique gene regulatory elements and transcription factors that could mediate melanoma-T cell interaction. Further, we aimed to identify functional epigenetic elements through custom CRISPRi screening of enhancers in patient tumor-derived melanoma and T cells. CRISPRi approaches identified novel functional enhancers that mediate T cell mediated killing. For example, we identified distal c-MET enhancers as important contributors to T cell mediated killing. In T cells, we identified enhancer hubs that target multiple genes. These hubs could be targeted to activate interferon gamma, reduce T cell exhaustion, and improve T cell mediated killing of melanoma cells. Such enhancer hubs could serve as targets in the ex vivo setting to improve adoptive T cell therapy. Overall, our results suggest that enhancers with unique spatial patterns in melanoma tumors contribute to the response to immunotherapy and could be novel targets for therapy.

#7548 Role of bromodomain extra terminal inhibitor (BETi) in combination with radiotherapy for the treatment of NF1-associated malignant peripheral nerve sheath tumor.

A. A. Gingrich[1], S. Landers[1], A. Bhalla[1], C. Rodriguez-Aguayo[1], R. Lazcano[1], S. Satpati[1], A. Lebron-Torres[2], E. Z. Keung[1], C. P. Scally[1], C. L. Roland[1], K. K. Hunt[1], H. Lyu[1], H. Lillemoe[1], A. Guadagnolo[1], A. Lazar[1], J. Slopis[1], I. McCutcheon[1], J. A. Livingston[1], A. Farooqi[1], K. Rai[1], K. E. Torres[1];
[1]The University of Texas MD Anderson Cancer Center, Houston, TX, [2]Davidson College, Davidson, NC

Introduction: Neurofibromatosis Type 1 (NF-1) associated malignant peripheral nerve sheath tumors (MPNST) harbor mutations in the polycomb repressive complex 2 (PRC2) in 70% of tumors. PRC2 loss results in epigenetic changes, which increase histone acetylation and make the DNA vulnerable to binding by bromodomain proteins. This interaction could be targeted to uncouple histone acetylation from transcription using bromodomain extra terminal inhibitors (BETi). As radiation therapy (RT) is a cornerstone of MPNST treatment, we analyzed the effects of BETi with and without RT.
Methods: Mice were implanted with patient-derived xenografts (PDX) of PRC2-wildtype model developed in the Torres laboratory, MPNST007. Mice were segregated into vehicle and I-BET 762 treatment groups and treated with either vehicle or drug for one week before the RT was initiated. Half of the mice in each treatment group (n = 10) received radiation (2 Gy per fraction for 5 days for a total of 10 Gy). The study endpoints were (1) tumor growth rates, (2) tumor size and weight at study termination, (3) immunohistochemical (IHC) staining for biomarkers of proliferation (Ki67), apoptosis (cleaved caspase 3, CC3), and DNA damage (γH2AX), and (4) RNA sequencing of PDXs from each experimental arm.
Results: Significant tumor regression was observed in PRC2-mutant PDX tumors treated with I-BET 762 based on tumor growth kinetics over 45 days of treatment ($p < 0.001$). Tumor volume was significantly reduced by I-BET 762 compared to vehicle ($p < 0.01$). Combining I-BET 762 and RT resulted in significant tumor volume reduction ($p < 0.001$). RNA sequencing and intersection of differentially expressed genes related to “DNA damage repair” and those repressed by I-BET 762 was performed for the MPNST007 PDXs. The expression of 259 genes related to DNA damage repair decreased after I-BET 762 treatment, including XRCC1, ERCC4, RAD50, RAD51D, and LIG4 (data not shown). IHC analysis prompted by the RNA sequencing results of the I-BET 762-treated PDXs revealed higher levels of γH2AX. An increase in necrotic and fibrotic tissue with increased CC3 in the BETi plus radiation group was observed.
Conclusions: Genetic mutations in NF-1-associated MPNST tumors result in susceptibility to BETi treatment. In a PDX model of PRC2 wild-type tumors, BETi treatment resulted in tumor regression and sensitized MPNST xenografts to RT. Combining BETi and RT enhanced tumor death and increased expression of genes associated with DNA damage and apoptosis.

#7549 Overcoming resistance to anti-VEGF therapy via epigenetic regulation of BARD1.

E. Bayraktar[1], C. Rodriguez-Aguayo[1], E. Stur[1], S. Kumar[2], L. S. Mangala[1], N. N. Bayram[1], P. Hanjra[1], S. Corvigno[1], S. Baylin[1], G. Lopez-Berestein[1], A. K. Sood[1];

[1]UT MD Anderson Cancer Center, Houston, TX, [2]Department of Obstetrics and Gynecology, Medical College of Wisconsin, Milwaukee, WI 53226, USA, WI, TX

DNA methylation inhibitors such as 5-azacytidine (Aza) and 5-aza-2′-deoxycytidine have been extensively used in patients with hematologic disorders and other neoplasms since their approval by the FDA. However, global DNA demethylating agents can result in intolerable toxicities; therefore, targeted epigenetic modulation is needed. Here, we searched for epigenetic changes with adaptive resistance to anti-VEGF antibody (AVA) in the TME and a novel strategy for targeted demethylation.

Methods: We examined methylation and transcriptional changes in orthotopic ovarian cancer models with emergence of AVA resistance. We developed a targeted demethylation strategy for BARD1 to enhance the effectiveness of AVA. We used a novel dCas9-CRISPR-based system for targeted BARD1 CpG demethylation (derived by fusing the deactivated Cas9 [dCas9] with the TET1 catalytic domain) delivered *in vivo* using a nanoliposomal carrier.

Results: We identified BARD1 methylation and reduced expression as lead candidate with AVA resistance; multiple CpG island sites in the BARD1 gene from adaptive AVA-resistant tumors were methylated. Next, we investigated the biological effects of global and targeted DNA methylation. Azacytidine along with AVA therapy was tested in a series of models (fibrosarcoma, PDX and orthotopic ovarian cancer models) and resulted in reduced tumor burden compared with the control and monotherapy groups ($p<0.01$). Next, to determine whether targeted demethylated BARD1 would have antitumor effects *in vivo*, we used an orthotopic SKOV3ip1luc ovarian cancer mouse model. Mice were treated with DOPC-dCas9-TET1-sgcontrol- (control) and DOPC-dCas9-TET1-sgBARD1 (sgBARD1). Tumor weight in the sgBARD1-3 group was significantly ($p<0.01$) reduced compared with the control group with no significant change in mouse body weight. We found that BARD1 expression was significantly increased in sgBARD1-treated group compared with control ($p<0.001$). Next, to determine whether demethylated BARD1 would combine well with AVA therapy in the SKOV3ip1 model, we combined sgBARD1-3 with bevacizumab (bev); sgBARD1-3 alone led to a significant decrease in tumor burden compared with control groups. Moreover, tumor burden was significantly reduced in the sgBARD1-3 and bevacizumab combination group compared with the sgcontrol group and bev alone group. BARD1 expression was significantly increased in sgBARD1-3-treated and in combination tumor samples compared with controls. To check for potential off-target effects, we tested the efficacy of another sgBARD1 and found that tumor burden in the sgBARD1-1 group was significantly reduced compared with control group.

Conclusion: Our novel targeted approach results in robust antitumor effects when combined with AVA therapy in multiple cancer models. Collectively, our findings provide a novel approach for gene targeted demethylation and could have implications for epigenetic therapies.

#7550 KB-0742, an oral highly selective CDK9 inhibitor, demonstrates preclinical activity in transcription factor fusion driven adenoid cystic carcinoma patient-derived models.

M. R. McKeown[1], **L. A. Carvajal**[1], T. R. Hood[1], N. S. Burr[2], J. Kaufman[2], A. Boynton[1], K. Mori[1], T. DesRochers[3], M. Wick[4], C. Y. Lin[1], J. F. DiMartino[1]; [1]Kronos Bio, Inc., Cambridge, MA, [2]Adenoid Cystic Carcinoma Research Foundation (ACCRF), Needham, MA, [3]Kiyatec, Greenville, SC, [4]XenoStart, San Antonio, TX

Adenoid Cystic Carcinoma (ACC) is an aggressive rare type of cancer of the secretory glands with no approved targeted therapy and high unmet clinical need. Deregulated transcription driven by MYB-NFIB or MYBL1-NFIB transcription factor (TF) fusions are a hallmark of ACC pathogenesis. More aggressive disease and resistance to therapy has been associated with co-mutation in NOTCH. Although direct targeting of oncogenic TF fusions has remained challenging, targeting of their activity via transcriptional cofactors has emerged as an attractive and clinically actionable strategy. Cyclin-dependent kinase 9 (CDK9) is a key potentiator of TF activity via its ability to act both as an upstream regulator of TF expression and a downstream cofactor. KB-0742 is a potent, selective, and orally bioavailable inhibitor of CDK9 with a long plasma half-life. KB-0742 is being studied in an ongoing Phase 1/2 study (NCT04718675) in advanced solid tumors including ACC. KB-0742 has demonstrated on-mechanism, single agent anti-tumor activity and a manageable safety profile in heavily pre-treated patients (0-11 prior lines of therapy) with transcriptionally addicted solid tumors. Here we present the preclinical rationale for targeting of oncogenic fusion TF activity in ACC. XenoSTART Patient-Derived Xenograft (XPDX) models were established from viable human tumor tissue for in vivo and ex vivo testing. Cell viability was assessed by CellTiter GLO reagent and phase imaging. Changes in MYB-fusion transcripts were assessed by RNA-Seq. Tumor Fragments (~70 mg) from ACCx5M1, ACCx6, ACCx9, ACCx11 models were implanted into athymic nude mice. Animals were treated with either vehicle (normal saline) or 60 mg/kg KB-0742 on a Q3D/week until tumors reached 2500 mm^3 or up to 60 days post start of treatment. In a retrospective analysis using real world data, ACC has a low incidence of genomic instability and high rates of MYB fusions detectable by RNA-seq, making immunotherapy challenging but creating an opportunity for targeting MYB transcription. In primary MYB-fusion positive and NOTCH co-mutated patient-derived spheroid models, KB-0742 treatment induced strong antiproliferative activity and cytotoxicity. Importantly, KB-0742 demonstrated stronger cytotoxic effects when compared to historical control agents. In XPDXs, CDK9 inhibition with KB-0742 resulted in antiproliferative activity and stronger tumor growth inhibition in MYB-fusion positive and NOTCH co-mutated tumor models compared to MYB-fusion positive only models.These data demonstrate KB-0742 is effective in preclinical models of ACC suggesting KB-0742 may be a promising therapeutic option for ACC patients. KB-0742 is currently being evaluated in a phase 1/2 dose-escalation and cohort expansion trial in patients with ACC and other transcriptionally addicted tumors (NCT04718675).

#7551 Combined epigenetic therapy and immune checkpoint blockade drive reshaping of the tumor microenvironment of platinum resistant ovarian cancer.

B. V. Landon[1], G. Kaleka[2], A. Balan[1], J. L. Boland[2], C. Cherry[1], G. Pereira[1], C. Zahnow[1], B. Winterhoff[3], S. Baylin[1], V. E. Velculescu[1], G. E. Konecny[2], J. A. Glaspy[2], V. Anagnostou[1];

[1]Johns Hopkins University, Baltimore, MD, [2]University of California, Los Angeles, Los Angeles, CA, [3]University of Minnesota, Minneapolis, MN

Introduction: Immunotherapy has demonstrated modest effectiveness for patients with platinum-resistant ovarian cancer, which is in part related to the immunosuppressive tumor microenvironment (TME) of ovarian cancers. Epigenetic modulators in combination with immune checkpoint inhibitors (ICIs) may represent a potential way to sensitize ovarian cancer to immunotherapy by TME reprogramming.

Methods: We evaluated the effect of epigenetic modulation in combination with ICI by comprehensive transcriptomic analyses of serially biopsied platinum-resistant/refractory ovarian cancer. Leveraging serial tumor samples from 30 patients that received oral azacitidine and pembrolizumab in the TRIO026 phase II clinical trial (NCT02900560), we performed bulk RNA sequencing and direct digital counting of 770 target genes using molecular barcodes (nCounter, NanoString) for 72 serial tumor samples, prior to treatment initiation and 6 weeks on-therapy. RNA sequencing of ~200 million reads for each sample was used for differential gene expression and gene set enrichment analysis (GSEA) and cell type deconvolution. Target gene expression data was normalized and analyzed for differential gene and pathway expression.

Results: Differential gene expression analyses revealed an upregulation of inflammatory and cytolytic genes (IFNG, GZMA and GZMH; FDR-adjusted p=0.0184) as well as the co-inhibitory molecule CTLA-4 (FDR-adjusted p=0.0184). GSEA revealed an enrichment of IFNG response, natural killer cell mediated cytotoxicity, neutrophil degranulation, inflammatory response, and antigen processing/presentation related gene sets on-therapy (FDR-adjusted $p < 0.001$). Target gene expression analyses orthogonally confirmed these findings, which were also concordant with pathway scoring analyses showing an increased score for immune inflammatory pathways such as INFG signaling (Wilcoxon rank sum test p=0.01). Immune cell subset deconvolution suggested TME reshaping driven by a greater density of intra-tumoral T cells on-therapy (Wilcoxon rank sum test p=0.012). Higher IFNG, CXCL13, CXCR5 expression, CD8 T cell and NK cell density were associated with longer time on treatment, both at baseline and at the on-therapy timepoint. GSEA revealed an upregulation of interferon gamma, adaptive immunity, antigen presentation as well as conserved immune response gene sets on-therapy, for the patients attaining longer time on-treatment.

Conclusion: Combination epigenetic and immunotherapy induces an inflammatory response and reshaping of the tumor microenvironment that may enhance their clinical efficacy, highlighting the therapeutic potential of utilizing epigenetic modulators as a way to sensitize platinum-resistant ovarian cancer to immune checkpoint inhibition.

#7552 Inhibition of histone methyltransferase EZH2 for immune-interception of colorectal cancer in Lynch syndrome.

F. Duzagac[1], C. M. Bowen[1], L. Reyes-Uribe[1], M. Zaheer[1], J. Thompson[1], N. Deng[1], M. Taggart[1], A. Jain[1], W. Edelmann[2], K. M. Sinha[1], E. Vilar[1];
[1]UT MD Anderson Cancer Center, Houston, TX, [2]Albert Einstein College of Medicine, Bronx, NY

Introduction: Colorectal pre-cancers in Lynch Syndrome (LS) display a distinct immune profile thus presenting a unique opportunity to develop novel immune-interception approaches to halt carcinogenesis. Epigenetic modulation by EZH2 of immune-related genes has been implicated in many cancers including colorectal but it has yet to be explored in LS carcinogenesis. The main objective of this study is to test the effect of EZH2 inhibition on immune cell profiling, colorectal carcinogenesis, gene expression, and histone methylation, using ex vivo organoids and a LS mouse model.

Methods: A mouse model of LS colorectal carcinogenesis (*Villin-Cre*;*Msh2*$^{fl/fl}$;*TgfβRII*-KI; herein referred to as *VCMsh2T*^{Hu}) and e*x vivo* colonic organoids were utilized to assess the effects of the EZH2 inhibitor GSK503. Mice were treated for 9-weeks with GSK503 with downstream studies exploring polyp multiplicity, changes to the immune landscape, and epigenetic analyses to derive mechanistic insights into EZH2 regulation in LS.

Results: GSK503 significantly altered transcriptomic changes in *VCMsh2T*^{Hu} organoids with tissue-specific tropism for dysplastic organoids as compared to organoids prepared from adjacent normal mucosa. GSK503 significantly increased CD4$^{\pm}$and CD8$^{\pm}$ T cells in splenocytes and colonic mucosa of treated mice compared to controls in vitro and in vivo. A preventive-dose (200µg/kg) of GSK503 for 9 weeks significantly reduced adenoma multiplicity in the large intestine of *VCMsh2T*^{Hu} mice with significant changes in the immune landscape of treated mice compared to controls. The data suggests GSK503 significantly enriched both total and activated cytotoxic T-lymphocytes CD8$^{\pm}$/CD137$^{\pm}$), stromal macrophages (CD68$^{\pm}$), and activated helper T-lymphocytes (CD4$^{\pm}$/CD134$^{\pm}$) in the large intestine of *VCMsh2T*^{Hu} mice. Transcriptome and molecular analyses using IHC, Western blots, and computational tools showed activation of immune and apoptotic markers with concomitant reduction of H3K27 methylation levels in colonic crypts. ChIPseq analyses revealed decreased levels of H3K27me3 and H3K4me1 (enhancer), a slight increased levels of H3K27ac (enhancer) marks with no changes in levels of H3K4me3 in treated mice, indicating that EZH2 inhibition yields global reprograming of poised promoters and active enhancers in the LS mouse genome.

Conclusions: Collectively, our findings reveal that GSK503 has a promising potential as an immuno-interception modality establishing the framework for launching phase I clinical trials with EZH2 inhibitors for LS carriers.

#7553 Dual inhibition of chromatin remodeling and DNA methylation as a novel treatment for triple negative breast cancer.

J. W. Landry, j. Kang, C. Morecock, H. Bear, R. Martin;
Virginia Commonwealth University, Richmond, VA

Epigenetics plays a central role in the initiation, establishment, and progression of cancer. In this capacity, epigenetics regulates several abnormal nuclear processes in the cancer cell including DNA replication, DNA damage repair and most prominently transcription. Because of their reversibility, epigenetic modifications have been aggressively pursued pharmacologically to correct abnormal cancer biology in the hopes of reversing cancer phenotypes. To develop novel epigenetic based therapeutic strategies for triple negative breast cancer (TNBC) we combined the DNA methyltransferase inhibitor (DNMTi) guadecitabine (Gua) with a genetic CRISPR/Cas9 mediated knockout (KO) of the chromatin remolding protein Bromodomain PHD-finger Transcription Factor (BPTF). Using the E0771 and 4T1 mouse TNBC models we show that BPTF depleted tumor cells are more susceptible to the antitumor effects of Gua. These antitumor effects are not observed in culture, or in immune compromised NSG mice, suggesting that their effects on cancer cell growth are not cancer cell intrinsic. RNA-Seq, ATAC-Seq and MBD-Seq analysis from FACS purified cancer cells shows that the combination of BPTF inhibition and Gua alters immune regulatory cytokine expression (BMP4 and CSF3) in the cancer cell, and it is theorized that these changes alter the tumor microenvironment to become less immune suppressive and permissive to the antitumor effects of immune cells. This hypothesis is supported by Cytek phenotyping of tumor resident and peripheral immune cells from treated mice showing reduced levels of immune suppressive myeloid derived suppressor cells (MDSC). Inhibiting BPTF pharmacologically using the bromodomain inhibitor AU1 does not recapitulate the effects of the genetic inhibition suggesting that the benefits of BPTF depletion to sensitization to Gua are not captured by inhibition of its bromodomain. To model the effects of pharmacologic BPTF inhibition we created a BPTF mouse KO genetically modified mouse model (GEMM). We show using this GEMM that BPTF KO in the adult mouse (a tamoxifen inducible Cre) is not lethal and has beneficial effects to the control of E0771 tumors, possibly through depleting tumor resident naïve T cells, and that transplanting BPTF KO E0771 tumors into BPTF KO adult mice further improves tumor growth control. These benefits in tumor growth control are prevented with CD8 depletion. These results in total suggests that a combination therapy regimen including BPTF inhibition (a PROTAC degradation approach) with a DNMTi could provide clinical benefits to patients with TNBC through both tumor cell intrinsic and extrinsic mechanisms.

#7554 The histone deacetylase inhibitor romidepsin is a potential therapeutic for metastatic osteosarcoma.

E. E. Seiden, S. M. Richardson, S. Ramnath, T. Whiteside, K. L. Coy, A. L. Sinn, M. L. Capitano, K. E. Pollok, C. D. Collier, E. M. Greenfield;
IU Simon Comprehensive Cancer Center, Indianapolis, IN

Osteosarcoma predominately affects adolescents, young adults, and canines. For human patients, the five-year survival rate of those with detectable lung metastases is only 30% while most canine patients with metastatic disease die within 1-2 years. Standard therapy is not effective for this patient group, so it is therefore necessary to identify novel therapies that target the progression of lung metastases. Our lab previously screened 114 FDA-approved anti-cancer drugs to identify agents that decrease the growth of 3D spheroids (sarcospheres) generated from highly metastatic osteosarcoma cell lines. The top hits included both histone deacetylase inhibitors (HDIs) that were tested. In follow-up experiments measuring potency on sarcospheres and toxicity on non-transformed cells, romidepsin was the top hit of the 114-drug panel as well of the two additional FDA-approved HDIs and seven HDIs that are in clinical oncology trials. Our goal was therefore to further evaluate romidepsin as a potential therapy for metastatic osteosarcoma. Romidepsin potently decreased viability in sarcospheres from established highly metastatic osteosarcoma cell lines (relative ED50s = 3-36nM). About 50% of the patients (both canine and human) had similar responses to romidepsin (relative ED50s = 1- 18nM) suggesting that those patients might be good candidates for romidepsin therapy. This includes patients who had been heavily pretreated with standard-of-care osteosarcoma chemotherapeutics. Mechanistically, romidepsin blocks proliferation and causes a G2/M cell cycle arrest in fast growing sarcospheres (143B and MG63.3) while in slow growing sarcospheres (LM7 and K7M2) where primarily induces cytotoxicity and there is no cell cycle arrest. Patient-derived sarcospheres are slow growing, so we predict that the primary mechanism will be cytotoxicity. Using a tail vein injection model of osteosarcoma lung metastases, romidepsin dose dependently prolonged survival and reduced the area and number of lung metastases in immunodeficient mice injected with 143B cells and a syngeneic model using K7M2 cells. Romidepsin will be evaluated in mice with metastases from patient-derived cells and if effective, will be repurposed for canine and human clinical trials to improve outcomes in metastatic osteosarcoma without the associated costs and extensive timeframe of traditional drug discovery.

#7555 Selective inhibition of the CoREST complex as a novel therapeutic target of atypical teratoid rhabdoid tumors.

Anupa Geethadevi[1], Marianne Collard[2], Tyler Findlay[1], Yiming Deng[1], Robert Fisher[2], Nikhil Vaidya[2], Charles Eberhart[1], Philip A. Cole[3], Rhoda Alani[2], Jeffrey Rubens[1], Eric Raabe[1]

[1]Johns Hopkins University School of Medicine, Baltimore, MD,[2]Boston University, Boston, MA,[3]Harvard Medical School, Boston, MA

Atypical teratoid/rhabdoid tumors (AT/RT) are deadly infantile brain tumors, primarily arising from a single recurring biallelic loss-of-function mutation in SMARCB1 which is a member of the SWI-SNF chromatin remodeling complex. The partially functional SWI-SNF complex (without SMARCB1) is able to inhibit EZH2 at most locations of the genome except at gene promoter regions where EZH2 co-localizes with the REST complex. This results in hypermethylation and subsequent repression of genes coding for neuronal differentiation and tumor suppressors. CoREST is an important transcriptional repressor and consists of LSD1 and HDAC1/2 bound together by the scaffolding protein RCOR. Increased activity of EZH2 and the CoREST complex may help AT/RT cells maintain a stem cell-like state, driving its aggressive growth and therapy resistance. We hypothesize that functional inhibition of the CoREST complex by targeting LSD1 and HDAC1/2 might help restore the epigenetic balance lost in AT/RT cells.We selectively inhibited the CoREST complex in AT/RT cells (BT37, CHLA05 and CHLA06) by using a bi-functional LSD1 and HDAC1/2 inhibitor, Corin, which has previously been shown to be effective against melanoma and diffuse midline glioma. Administration of corin to AT/RT cells significantly increased H3K4me1, H3K9Ac and H3K27Ac histone marks ($p < 0.001$, Western blotting). Corin inhibited AT/RT cell growth and proliferation (MUSE Viacount $p<0.05$, BrdU immunofluorescence compared to control), and increased apoptosis (cPARP Western blotting, CC3 immunofluorescence, MUSE Annexin V assay, $p<0.05$ compared to control). Corin appears to be specific in targeting AT/RT as it did not affect brain organoids derived from iPSCs (cPARP Western blotting). Corin induced neuronal differentiation in AT/RT as seen by the increased expression of Beta-3-tubulin, MAP2 and Synaptophysin (Immunofluorescence). Enrichment analysis of differentially expressed genes after whole mRNA sequencing of AT/RT cells treated with corin for 24 h revealed upregulation of pathways related to neuronal differentiation and axonal development and downregulation of pathways related to proliferation and cell cycle ($pFDR < 0.05$, $FC>2$). In mice bearing orthotopic CHLA06 tumors, intratumoral delivery of a single dose of corin for 24 h increased H3K27me3 and H3K27ac, demonstrating that corin engaged its target in vivo, reduced growth and induced apoptosis (Ki67, cPARP). Survival studies show a trend toward single agent activity against the very aggressive CHLA06 orthotopic xenograft (increased in median survival from 14 to 35 days compared to control). These studies demonstrate that targeting the CoREST complex disrupts AT/RT epigenetic abnormalities, reversing their stem cell-like state, slowing tumor cell growth, and inducing apoptosis, that may translate into the clinical setting to help improve AT/RT's dismal survival.

#7557 Hypoxia-induced downregulation of MUC16: A key player in bispecific T-cell engager resistance in ovarian cancer.

M. Xu[1], S. K. Barakzai[2], A. Kononenko[1], R. Kumar[1], I. Veillard[1], E. Kim[2], T. S. Bond[1], D. R. Spriggs[1], B. R. Rueda[2], O. Yeku[1];
[1]Massachusetts General Hospital Cancer Center, Harvard Medical School, Boston, MA, [2]Massachusetts General Hospital, Harvard Medical School, Boston, MA

Background: Ovarian cancer (OC) is a lethal disease due to limited treatment options and the development of multidrug resistance. Bispecific T-cell engager (BiTE) therapy represents a promising immunotherapeutic approach to OC. Our previous findings suggest that resistance to BiTE therapy in OC is a complex interplay of factors including loss of tumor-associated antigens and epithelial-mesenchymal transition (EMT). Since the peritoneum is a relatively hypoxic (HX) tumor microenvironment, we hypothesized that HX plays a role in the modulation of MUC16 and potential resistance to BiTE therapy.
Methods: After informed consent, samples were collected from patients with recurrent OC undergoing treatment with MUC16 BiTEs. For HX studies, we used OVCAR3 tumor cell lines which express full-length MUC16. Tumor cells were cultured under normoxic (NX) or HX conditions. The effect of HX on cell death was analyzed using an apoptosis assay. Cells were evaluated for changes in cell surface MUC16 expression by flow cytometry. MUC16 protein expression and EMT markers were analyzed by western blot. Proteasome inhibitors were used to stabilize MUC16 expression under HX conditions. Antibody internalization assays were conducted to assess MUC16 endocytosis and recycling.
Results: In patients who progressed on MUC16 BiTEs, we found decreased MUC16 expression on tumor samples isolated from ascites samples. Using OVCAR3 cells, we found significantly decreased MUC16 expression on ovarian cancer cells grown under HX conditions (Fold change: 0.4 vs NX, $p<0.001$). Flow cytometry analysis revealed a time-dependent loss of MUC16 expression on the cell surface under HX (64.22% after 9 days HX vs 88.26% NX), highlighting the susceptibility of MUC16 to HX-induced downregulation. Treatment with proteasome inhibitors partially rescued MUC16 expression under HX conditions (Fold change: 1.4 vs NX, $p<0.001$). Notably, HX did not induce necrotic cell death in these tumor cells. In addition to the loss of MUC16, tumor cells under HX conditions showed alterations in EMT markers. E-cadherin was downregulated with prolonged HX exposure (Fold change: 0.3 vs NX, $p < 0.001$), while Vimentin (Fold change: 7.1 vs NX, $p < 0.001$) and Snail (Fold change: 2.8 vs NX, $p < 0.001$) were upregulated, indicating a potential shift towards a more aggressive phenotype. Epidermal growth factor receptor (EGFR) was also upregulated (Fold change: 4.9 vs NX, $p < 0.001$), potentially contributing to enhanced survival and invasion of OC cells under HX stress. Finally, under HX conditions, MUC16 internalization was slower in response to antibody binding over time due to reduced cell antigen expression, corroborating the observed MUC16 loss.
Conclusion: Understanding hypoxia-induced MUC16 downregulation and its downstream effects on EMT markers and CA125 expression provides crucial insight into the mechanisms of BiTE therapy resistance in ovarian cancer.

#7558 Novel liquid biopsy based determination of lung cancer histology using a comprehensive epigenomic platform reveals enhancer activity as a key determinant for accurate classification.

J. Guess, A. Gorthi, A. D'ippolity, J. Beagan, T. Clark, M. Coyne, T. Tamakloe, B. Tran, H.-H. Jeong, K. Cibulskis, H. Sawaengsri, J. Chmielecki, C. A. Painter, J. Barrett, M. Eaton;
Precede Biosciences, Inc., Boston, MA

BACKGROUND: Accurate molecular characterization of lung cancer including histology classification and therapeutic target profiling is critical for treatment planning and resistance monitoring. For example, detecting lineage transformation from lung adenocarcinoma (LUAD) to small cell lung carcinoma (SCLC) following treatment, an established resistance mechanism, is challenging due to deteriorating patient health and complicated invasive procedures. Here, we describe an accurate lung cancer histological classification using an innovative, multimodal epigenomic liquid biopsy method that comprehensively profiles tumor-specific transcription activation from 1 mL of patient plasma.

METHODS: 37 LUAD, 34 SCLC patient plasma samples collected from commercial biobanks, and reference cell lines were profiled for enhancer, promoter and DNA methylation activity to identify epigenomic loci characteristic of LUAD and SCLC. The resulting map of select quantified loci was used as input to a machine learning algorithm that distinguishes SCLC from LUAD, in a cross validated training and testing approach.

RESULTS: The epigenomic maps derived from lung cancer patient plasma were highly informative of the regulatory programming of the tumor cells. The enhancers and promoters most strongly linked to lung cancer profiles across the patient population include key, histology-specific driver genes such as NKX2-1, FOXA1, FOXA2, ONECUT2, DLL3, and ASCL1. The resulting classifier was able to accurately predict histology with a cross validated AUC greater than 0.94. In silico simulation results suggest that accurate classification can be achieved with ctDNA content below 1%. Further correlative examination of the SCLC enhancer landscape revealed a partitioning of SCLC patients into molecular subtypes characterized by active enhancer marks at subtype-specific transcripts, including ASCL1, POU2F3, NEUROD1, and YAP1. The transcriptional regulation of ADC targets is apparent through comprehensive epigenomic profiling of plasma in both SCLC and LUAD, with the expression of Claudin 18.2, SEZ6, and others showing a strong dynamic range independent of ctDNA levels. This represents a novel liquid biopsy approach to distinguish LUAD from SCLC and provide simultaneous insight into expression of key targets at clinically relevant ctDNA levels.

CONCLUSION: These data demonstrate the feasibility of epigenomic mapping from 1mL of plasma in lung cancer patients to distinguish lung cancer histology. The resulting data is biologically interpretable through the lens of transcriptional activation of key histology specific genes. This liquid-biopsy based approach may provide a non-invasive alternative to invasive and challenging tissue biopsies for biomarker investigation and therapeutic decision making.

#7559 Multi-state gene cluster switches determining the adaptive mitochondrial and metabolic landscape of breast cancer.

M. Menegollo[1], R. Bentham[2], N. Patani[2], R. C. Stein[2], M. Yuneva[2], **G. Szabadkai**[2];
[1]University of Padua, Padua, Italy, [2]University College London, London, United Kingdom

Adaptive metabolic switches are proposed to underlie conversions between cellular states during normal development as well as in cancer evolution, where they represent important therapeutic targets. However, the full spectrum, characteristics and regulation of existing metabolic switches are unknown. We propose that metabolic switches can be recognised by locating large alternating gene expression patterns and associate them with specific metabolic states. We developed a method to identify interspersed genesets by massive correlated biclustering (MCbiclust) and to predict their metabolic wiring. Testing the method on major breast cancer transcriptome datasets we discovered a series of gene sets with switch-like behaviour, predicting mitochondrial content, activity and central carbon fluxes in tumours associated with different switch positions. The predictions were experimentally validated by bioenergetic profiling and metabolic flux analysis of 13C-labelled substrates and were ultimately extended by geneset analysis to link metabolic alterations to cellular states, thus predicting tumour pathology, prognosis and chemosensitivity. The method is applicable to any large and heterogeneous transcriptome dataset to discover metabolic and associated pathophysiological states.

#7560 Microsatellite instability (MSI) detection using flow-based sequencing.

G. Lithwick-Yanai[1], H. Benjamin[1], J. Cano-Nistal[2], S. Geisler[2], A. Jaimovich[1], N. Iremadze[1], D. Kessler[1], I. Soifer[1], D. Lebanony[1], K. Ben Simhon[1], S. Gilad[1], E. Meiri[1], D. Lipson[1], Y. E. Maruvka[2];

[1]Ultima Genomics, Fremont, CA, [2]Technion - Israel Institute of Technology, Haifa, Israel

Background: Microsatellite instability (MSI) is an important genomic biomarker associated with various cancers and hereditary conditions. Accurate and efficient classification of MSI status is essential for diagnosis, prognosis, and treatment decisions. Different approaches for testing MSI have been presented in the literature, including NGS-based methods which either rely on comparison with a matched control sample, a set of reference control samples, or the reference genome (no control). In this study, we explore the feasibility of accurately identifying MSI status using the UG100 platform, which utilizes flow-based sequencing chemistry. Since MSI detection is typically based on long homopolymers, we examined here whether the flow-based sequencing data can be effectively used for MSI classification.

Methods: We performed whole genome sequencing (WGS) on a cohort of 24 cell lines with known MSI status, as well as on 15 tumor tissue samples, encompassing various cancer types, including colon, lung, bladder, and endometrial cancer. To determine the MSI status, polyA/T homopolymer loci were considered. We measured the MSI status in these loci using two methods: 1) Counting short indel variants detected using somatic Deep Variant, in comparison with matched blood normal, and 2) a novel MSI score based on the difference of the polyA/T homopolymer length, in comparison to the reference genome. We assessed the ability to evaluate the score for the full sequenced coverage (~100X) as well as when limiting to exome boundaries, and when sampling down to 1X coverage.

Results and Conclusions: We established the performance of the MSI score on the cell lines with known MSI status. The score was verified on cell line mixtures (simulating lower tumor purity) as well as on clinical samples from various tissue sources, including colon samples annotated as mismatch-repair deficient. We demonstrate the ability to use the cost-effective UG100 sequencing combined with the two methodologies to identify MSI-high samples in these scenarios.

#7561 Standardized conditions for growth of lung cancer tumoroids cultured reproducibly in 3D-cultures.

K. Malmros[1], D. Carlsen[1], H. Brunnstrom[2];

[1]Lund University, Lund, Sweden, [2]Lund University and Skane University Hospital Lund, Lund, Sweden

Background: Lung cancer is the most common cause of cancer-related death in Sweden with an estimated mortality of 3500 persons in 2021. Late diagnosis and heterogeneity of the disease lead to difficulty in predicting optimal treatment regime for each case. Further development of personalized therapy would be facilitated by reliable and efficient cultivation of cancer cell samples from patients in a clinical setting. A promising method is to grow the cells as 3D structures known as tumoroids, though the choice of extracellular matrix substrate or solid support most suitable for this purpose should be elucidated.

Aim: To assess which extracellular matrix substrates or solid supports which enable lung cancer tumoroid generation reproducibly without affecting the status or detection of genetic alterations and protein expression, using lung cancer cell lines.

Methods: Eight lung cancer cell lines, where of three adenocarcinoma and five squamous cell carcinomas, were included in this project. Each cell line was characterized with immunohistochemistry (IHC) for commonly expressed antigens in the two lung cancer types. Also, protein detection with Western Blots was performed. Cell lines found not expressing relevant antigens associated with the specific lung cancer variant were discarded. The remaining cell lines were cultivated in BIOFLOAT TC-Platte 96 well plate, Nunclon Sphera flasks, or GrowDex-T hydrogel, later transferred to a Corning Elplasia 6 well plate, and monitored for tumoroid generation.

Results: The lung squamous cell carcinomas HCC-95 and HCC-1588 were both positive for CK5 and p40, while H1703 was negative for both markers. The adenocarcinoma H1975 was positive for TTF-1, also, unexpectedly, seen for NCI-H1703, earlier defined as squamous cell carcinoma. The tested cell lines were successfully cultured as tumoroids in the BIOFLOAT TC- 96 well plate, Nunclon Sphera flasks, and GrowDex-T hydrogel. The mutational status of the tumoroids as compared to the original tumors is currently under evaluation.

Conclusion: We here show successful 3D culturing of cell lines with alternative substrates. Further fine-tuning of the chosen reproducible system's simplicity and cost is required before culturing tumoroids from lung cancer patients can be launched.

#7563 Efficacy of JPI-547, novel dual PARP inhibitor, in endometrial cancer cell line.

S.-W. Lee[1], S.-H. Nam[1], S.-B. Park[2];

[1]Asan Medical Center, University of Ulsan, Seoul, Korea, Republic of, [2]Asan Institute for Life Science, Seoul, Korea, Republic of

Objectives: PARP inhibitor is effective in treating DNA repair deficiency endometrial cancer. Endometrial cancer (EC) is one of the most common gynecological cancers in developed countries and its incidence is increasing, and the prognosis of patients with early stage and low-risk EC is very good, but the prognosis of progressive and recurrent EC is poor. Novel PARP inhibitor JPI-547 is a PARP and tankyrase dual inhibitor, and in cancer cells, tankyrase inhibitor plays an important role in DNA repair, telomere maintenance, and cell survival. This experiment was conducted to determine whether the reactivity of the PTEN mutant EEC was increased by using the Novel PARP inhibitor.

Method: Human endometrioid endometrial cancer cell lines, Hec-1A, Hec-1B and Ishikawa were obtained. Cell viability assay for the drugs Olaparib and JPI-547 were assessed. Colonies consisting of at least 50 cells were counted. The number of dead cells was counted in five different areas of the hemocytometer, and the experiment was performed three times. The percentage of dead cells was analyzed compared to the untreated group. We confirmed the efficacy by siRNA transfection and immunofluorescence.

Result: When treated with Olaparib, there was no change in cell viability in the rest of the cells except for Ishikawa cells, which are PTEN mutations. It decreased by 35.4% in Ishikawa cells, whereas when treated with JPI-547, all cell lines Hec-1A, Hec-1B, and Ishikawa cell viability decreased by 28%, 34.3%, and 48.7%, respectively. PTEN knock-down reduced cell visibility by 28% when treated with olaparib, whereas when treated with JPI-547, Hec-1A (siCont) and Hec-1A (siPTEN) decreased by 26% and 42%, respectively, in all cells regardless of whether PTEN knock-down is present. When treated with Olaparib, dead cells were identified only in PTEN knock-down cells, increasing by 22%. When treated with JPI-547, dead cells increased by 25.5% and 33% in all cells of Hec-1A (siCont) and Hec-1A (siPTEN), respectively. It was confirmed that JPI-547 can reduce cell viability regardless of the formation of Rad51 according to PTEN.

Conclusion: JPI-547, a novel PARP inhibitor, showed good efficacy in PTEN mutation and PTEN-wild-type EEC cell lines than in conventional PARP inhibitor. The effect of reducing survival of ECC cell line with JPI-547 was confirmed with or without PTEN mutation. Further evaluation and in vivo experiments are needed to prove the efficacy of JPI-547 in EC.

#7564 DNA methylation profiling identifies two distinct groups of oligosarcoma, IDH-mutant with distinct genetic alterations and clinical outcomes.

K. Zhang[1], L. Liu[2], X. Liu[3], T. Jiang[2];
[1]Duke University, Durham, NC, [2]Beijing Neurosurgical Institute, Beijing, China, [3]Beijing Tiantan Hospital, Beijing, China

DNA methylation has been extensively adopted for the classification of brain tumors and is endorsed by current neuropathology guidelines. Recently, oligosarcoma, IDH-mutant has been characterized as a distinct group of *IDH* mutant gliomas by DNA methylation classification. However, emerging studies revealed the variety in this group. Here, we employed DNA methylation-based t-SNE analysis to characterize oligosarcomas identified by the dkfz brain tumor classifier (v12.5). Thereby, we uncovered that oligosarcomas were segregated into two distinct groups, namely, subgroup A and subgroup B, which were further validated by genetic alterations and clinical outcomes. Next-generation Sequencing revealed subtype A tumors enriched with chr 1p/19q co-deletion, chr 6q loss, CDKN2A/B homogeneous deletion, TERT promoter mutation, and NF1 mutation, while subtype B tumors showed chr7 gaining and TP53 mutation. RNA sequencing and gene set enrichment analysis (GSEA) revealed that neuronal-tumor interaction and muscular progression pathways were more enriched in subtype A tumors. In contrast, subtype B tumors showed enrichment for angiogenesis and mTOR pathways. Additionally, inter-chromosomal fusion genes were more frequently found in subtype A tumors. Clinically, patients with subgroup A oligosarcomas manifested poorer survival and distinct imaging features in magnetic resonance imaging (MRI) compared to those with subgroup B. Collectively, we provided more cases of oligosarcoma, IDH-mutant, confirming the existence of this newly identified group, and revealed the subgroups harboring different genetic alterations and suffering different prognoses, providing new evidence for the molecular pathology in diffuse glioma.

#7565 Tumor classification and deconvolution in liquid biopsy using enriched methylation sequencing.

J. Yu[1], L. S. Ahmann[1], Y. Y. Yao[2], A. Toland[3], A. Snowden[4], C. Ho[5], B. A. Pinsky[1], H. Vogel[1], R. Y. Luo[1], L. Wang[6], B. Howitt[1], B. Holmes[1], A. C. Lowe[1], W. Gu[1];

[1]School of Medicine, Stanford University, Palo Alto, CA, [2]School of Medicine, University of Calgary, Calgary, AB, Canada, [3]Children's Hospital Colorado, University of Colorado Anschutz Medical Campus, Aurora, CO, [4]Howard University College of Medicine, Washington DC, WA, [5]Clinical Laboratories, Stanford Health Care, Palo Alto, CA, [6]School of Medicine, University of California San Francisco, San Francisco, CA

Background: Cell-free DNA (cfDNA) detected in proximal body fluids has demonstrated potential for cancer detection using minimally invasive methodology. Our past work showed that tumor cfDNA is present in the cerebrospinal fluid (CSF) and other body fluids of patients with inconclusive standard of care testing. However, past work measuring copy number aberrations or somatic mutations was limited in cancer classification. To facilitate reliable classification, even at low tumor fractions and with fragmented DNA, we developed XR-methylSeq, a methylation sequencing platform to enrich for cell type-specific markers.
Methods: We benchmarked XR-methylSeq with the K562 cell line and correlated the methylation values with gold standard measurement − whole genome bisulfite sequencing (WGBS). Methylation classifiers were applied for at least 22 cytology-positive body fluids, incorporating methylation array data from public references. T-distributed stochastic neighbor embedding (t-SNE) analysis was used for visualization in R. Deconvolution of cell type fractions for at least 29 (seven cytology-negative) body fluids and plasma samples was conducted using wgbstools. Cell type-specific markers were identified from a human DNA methylation atlas.
Results: Benchmarks: XR-methylSeq has a 5-fold enrichment of the cell type-specific markers compared with WGBS. XR-methylSeq at 20 ng input highly correlates with WGBS at 2 µg (Pearson’s r = 0.97). Body Fluids: Thirteen cytology-positive CSF samples had copy number aberrations, 77% of them had concordant tumor classification, while the remaining 23% clustered with low tumor fraction samples. All nine lung primaries, including a low tumor fraction case that did not originally classify, showed a consistent cell-of-origin through deconvolution, as indicated by increased contributions from lung alveolar epithelial cells. Among six other body fluids, three exhibited the highest fractions aligning with the clinically identified cancer cell-of-origin. Additionally, the plasma cfDNA of a patient with acute liver injury had a higher fraction of hepatocyte signatures (22%) than the healthy control (8%).
Conclusions: This research highlights the potential of XR-methylSeq as an enriched methylation profiling method useful for liquid biopsy applications.

#7566 Identification of cancer subtypes with a ctDNA-based targeted methylation assay.

T. Nance[1], T. Shaver[1], Y. Zhou[1], M. Antonio[1], Y. Gao[1], J. Heiss[1], R. Calef[1], J. Hiatt[1], O. Venn[1], J. Bredno[1], J. Beausang[1], L. Newman[2], C. Swanton[3], C. Zhang[1];

[1]GRAIL, LLC, Menlo Park, CA, [2]Weill Cornell Medicine, New York, NY, [3]The Francis Crick Institute, London, United Kingdom

Introduction: Identifying cancer subtypes is necessary for cancer diagnosis, prognosis determination, and treatment selection. Furthermore, as transformation between subtypes is increasingly recognized as a key resistance mechanism to targeted therapies, serial subtype reassessment is likely to gain adoption. Cancer subtypes have traditionally been determined by pathologists based on histology; more recently, molecular subtyping has been performed using IHC, RNAseq, or assays that detect genetic alterations. However, these methods have significant limitations, including tissue biopsy requirement (IHC and RNAseq), low discriminative resolution for distinct transcriptional programs (IHC and mutation detection), and poor reproducibility and feasibility (RNAseq). The GRAIL plasma-only, ctDNA-based targeted methylation platform is a robust, biopsy-free, scalable assay that can distinguish cancer methylation patterns between different cancer signal origins through the use of a proprietary classifier. Here, we explore the GRAIL platform's potential to detect finer-scale differences in cancer biology by developing classification algorithms for subtyping of three common cancer types.

Methods: As part of the Circulating Cell-free Genome Atlas (NCT02889978) and STRIVE (NCT03085888) studies, clinical data were recorded and plasma samples were collected, accessioned, stored, and processed through GRAIL's targeted methylation assay from 3,989 cancer and 6,013 non-cancer participants. We developed algorithms to predict cancer status and subtype for breast (triple negative breast cancer [TNBC] model; 531 cancer training participants), lung (lung histology model; 334 cancer training participants), and head and neck (HPV model; 3090 cancer training participants) cancers. Dimensionality reduction of methylation data was performed to illustrate subtype separation within these cancer types. Performance of these three algorithms was assessed on a held-out cohort of cancer samples (184 breast, 241 lung, 67 head and neck) with detectable ctDNA.

Results: The lung histology model correctly classified 95% (105/111) of adenocarcinomas, 88% (68/77) of squamous cell carcinomas, and 94% (59/63) of lung neuroendocrine carcinomas and tumors. The TNBC model correctly classified 84% (58/69) of TNBCs and 82% (94/115) of non-TNBCs. The HPV model correctly identified 98% (48/49) of HPV-positive head and neck cancers, and 89% (16/18) of HPV-negative head and neck cancers.

Conclusions: GRAIL's proprietary ctDNA-based targeted methylation platform demonstrates the ability to accurately predict cancer subtypes in multiple cancers using only a plasma sample without the need for tumor biopsy. Future efforts will be directed towards generalizing the GRAIL subtyping method to additional cohorts and cancer types.

#7567 In-depth mass cytometry analysis reveals different immune cell composition of unique molecular subtypes in extensive stage small-cell lung cancer.

Y. Li, J. Qu, B. Wu, Q. Shen, W. Sun, L. Chen, B. Wang, L. Ying, J. Zhou, J. Zhou;
The First Affiliated Hospital, Zhejiang University School of Medicine, Hangzhou, China

Background: A novel molecular subtype classification was fashionable for small cell lung cancer (SCLC). However, the distribution of SCLC molecular subtype classification in Chinese patients were unknown, especially extensive stage (ES)-SCLC. It should validate and define their associated microenvironments across subtypes in ES-SCLC.
Method: We used immunohistochemical (IHC) to evaluate SCLC markers of the subtypes including ASCL1, NEUROD1, POU2F3, SCLC-A/N/P in 135 ES-SCLC tumors. Peripheral blood of 24 ES-SCLC patients was test by mass cytometry using time-of-flight (CyTOF) to evaluate the differences in immune subsets regard to the subtype tumor microenvironment (TME). Validation was performed using flow cytometry and multiplex IF.
Results: ASCL1, NEUROD1, POU2F3, and Inflamed were account for 60.7%, 28.9%, 7.4%, and 18.5% of SCLC tumors, respectively. Significant intratumoral heterogeneity was observed with 15.6% of the tumors being both positive for SCLC-A and -N subtype markers, respectively. The SCLC-I type possessed more CD8+ T-cells infiltration and had higher frequency an ‘inflamed’ immunophenotyped. CyTOF data showed greater CD161+CD127+CD8+T cells proportion in SCLC-I than SCLC-N subtypes before and after anti-immunotherapy. Furthermore, we validated that lung tissue of SCLC-I were infiltrated more CD161+CD127+CD8+T cells compared to SCLC-N subpopulation(P=0.0281). Flow cytometry further showed the stronger immune activation of CD161+CD127+CD8+T cells in SCLC-I types induced higher expression of GZMB and GNLY and lower-expression of T-cell exhaustion markers PD-1,TIGIT and LAG3 in comparison with SCLC-N types. We further confirmed that the high level of CD161+CD127+CD8+T associated with a favorable treatment response and prolonged overall survival.
Conclusion: The present study validated the molecular subtypes in ES-SCLC patients. Furthermore, SCLC-I subtype has longer PFS and OS than SCLC-A, -N and -P patients. Our research not only provides an insight into the immune landscape of ES-SCLC but also sheds light on a special subset of CD161+CD127+CD8+T cells with prognostic and therapeutic significance.

#7568 Molecular effects of neo-adjuvant hormone therapy for locally advanced prostate cancer: An ancillary study of the ARNEO phase 2 trial.

M. Ismail[1], W. Devlies[2], M. Parry[1], G. Devos[2], S. Friedrich[1], C. Parker[1], L. Mendes[1], E. Davicioni[3], M. Linch[1], F. Claessens[2], S. Joniau[2], G. Attard[1]; [1]UCL Cancer Institute, London, United Kingdom, [2]KU Leuven, Leuven, Belgium, [3]Veracyte, San Diego, CA

Intensified hormone therapy in combination with radiotherapy improves outcome for very high-risk locally advanced prostate cancer. The impact of hormone therapy with surgery, however, is uncertain. In order to understand this better, we ran an ancillary translational study on ARNEO (NCT03080116), a Phase 2 clinical trial, which randomized 89 locally-advanced prostate cancer patients to 12 weeks LHRHa +/- apalutamide (APA) followed by prostatectomy.

We performed clinical-grade transcriptome-wide expression array analysis (Veracyte, Inc. San Diego, CA) of FFPE diagnostic core biopsies (N=89) and tumors removed at prostatectomy (N=32 LHRHa, N=23 LHRHa + APA). We also performed RNASeq on fresh frozen biopsies of prostatectomy tumors (N=42 LHRHa, N=45 LHRHa + apalutamide) and LHRHa-naive control cases (N=61) matched for clinical and pathological risk factors.

Pre-surgery serum PSA decreased by a median of 98% (IQR:90.2-99.3) after hormone treatment. This decrease was better associated with tumor AR signaling (r^2=0.11) versus pre-treatment serum PSA (r^2=0.0005), or between pre-treatment serum PSA with diagnostic biopsies (r^2=0.008). We confirmed APA more potently suppressed AR signaling than LHRHa alone, with no detectable difference in direction of effect for differentially regulated genes/pathways. LHRHa + APA had less residual tumor (median Residual Cancer Burden, RCB=0.48cm^3) than in LHRHa (median RCB=1.7cm^3) but in cases with sufficient tumor, we observed residual active AR signaling pathways at prostatectomy in both treatment arms. To orthogonally confirm this, we selected 28 ERG positive cases (by IHC pre-treatment) and found retained ERG expression in 12/13 on LHRHa and 10/15 on LHRHa + APA.

Using pathway analysis in the RNAseq data, we identified LHRHa +/- APA induced down-regulation of AR, metabolic pathways, as well as DNA repair, and up-regulation of hallmark NOTCH, Hedgehog, TGF-beta, WNT and immune signaling (adjusted p-value cutoff=0.001). Comparing differentially expressed genes on RNASeq between treatment-naïve versus LHRHa +/- APA treated tumors, we observed STING1 as significantly higher in LHRHa +/- APA vs control (Wilcoxon rank sum test p-value <0.001). We found that expression of STING1 was positively correlated with hallmark interferon alpha response (r=0.7, r_s=0.6) that was correlated with apoptosis (r=0.5, r_s=0.5).

Whilst we show that adding APA to LHRHa increases suppression of AR activity and ERG expression, we find that 12 weeks is insufficient to abrogate AR signaling in most tumors, despite ~98% decrease in serum PSA. We identify novel processes modulated in humans by potent suppression of androgen activity, including upregulation of STING1-type 1 interferon response as a potential key modulator of treatment effect.

#7569 Characterizing pathways for metastasis of retinoblastoma in forebrain organoids.

Y. Shtanko[1], S. Rodriguez[2], B. Schachner[3], E. Adis[2], S. McLaughlin[2], S. Borges[2], J. Dollar[2], A. Zuniga[2], G. Quintana[2], S. Lopez[2], D. Owens[4], C. Moulin[5], S. Braun[2], G. Yenisehirli[2], D. Pelaez[6], J. Harbour[7], S. Kurtenbach[2];

[1]Herbert Wertheim College of Medicine (FIU), Miami, FL, [2]Sylvester Comprehensive Cancer Center, University of Miami Miller School of Medicine, Bascom Palmer Eye Institute, Interdisciplinary Stem Cell Institute, Miami, FL, [3]Sylvester Comprehensive Cancer Center, University of Miami Miller School of Medicine, Bascom Palmer Eye Institute, Interdisciplinary Stem Cell Institute, Wake Forest Baptist Health, Miami, FL, [4]Nova Southeastern University, Fort Lauderdale, FL, [5]Bascom Palmer Eye Institute (BPEI), University of Miami Miller School of Medicine, Sylvester Comprehensive Cancer Center, University of Miami Miller School of Medicine, Miami, FL, [6]Bascom Palmer Eye Institute (BPEI), University of Miami Miller School of Medicine, Sylvester Comprehensive Cancer Center, University of Miami Miller School of Medicin, Miami, FL, [7]Department of Ophthalmology and Simmons Comprehensive Cancer Center, University of Texas Southwestern Medical Center, Dallas, TX., Dallas, TX

Retinoblastoma (Rb) is a childhood cancer of the eye, which usually presents in children under the age of five. When detected early, Rb has favorable prognosis in developed countries, but metastasis into the central nervous system (CNS) through the optic nerve correlate with a high mortality rate. Even if detected early, the available harsh and unspecific treatments can cause serious side effects, and enucleations are still performed frequently. There is still uncertainty regarding the mechanism for metastasis into the central nervous system. We performed bioinformatic analysis of single cell sequencing data for retinoblastoma, retinal tissues, optic nerve, and brain, to identify potential pathways and cell-cell communications fostering Rb invasion into the optic nerve and brain. Our analysis revealed several potential metastatic drivers, including immune modulation involving MIF, secreted by the Rb cells, as well as cell-adhesion pathways promoting a change in cellular phenotype. Given that animal models do not faithfully recapitulate human Rb initiation and progression, we developed a novel human iPSC-derived forebrain organoid model to investigate mechanisms of Rb CNS metastasis. Microinjections of GFP-labelled Rb cells allow to track growth and spread. In this fully human model including microglial cells, we can, for the first time, study the Rb forebrain interactions and pathways involved. RNA-seq analysis of Rb cells growing in forebrain organoids shows increased activity in neuron projection development and neuron migration, overlapping with the observed phenotype switch of invading Rb. Together, we present a novel iPSC-derived human forebrain model to monitor growth and spread of metastatic Rb, and describe new pathways involved in invading and metastasizing Rb.

#7570 Molecular subtyping and immunohistochemistry validation identifies muscle Invasive bladder cancer subgroups with poorer overall survival.

J. Zhang[1], M. Feng[2], N. Beeharry[1], S. Thomas[1], R. Wirtz[3], A. Hartmann[4], M. Eckstein[4], W. Choi[5];
[1]Janssen Research & Development, Spring House, PA, [2]Greenberg Bladder Cancer Institute, Johns Hopkins Medical Institutions, Baltimore, MD, [3]STRATIFYER Molecular Pathology, Cologne, Germany, [4]Institute of Pathology, University Hospital Erlangen, Friedrich-Alexander University at Erlangen-Nurnberg, Erlangen, Germany, [5]Brady Urological Institute, Johns Hopkins Medical Institutions, Baltimore, MD

Introduction: Muscle-invasive bladder cancers (MIBC) are molecularly heterogeneous and have poor clinical outcomes, compared to non-muscle invasive disease. The molecular characterization of subtypes and immune status has shown prognostic value and the potential to guide precision intervention. However, a more comprehensive understanding of the association between subtypes and immune cells is still required. To this end, an integrative multi-omics analysis was performed on patients with MIBC.
Methods: From a cohort of 244 MIBC patients who did not receive neoadjuvant chemotherapy, cystectomy tissue was collected to assess molecular features associated with poor outcomes. Macro-dissected FFPE slides were used to perform whole transcriptome RNA sequencing (N=208, passing quality control) and both the consensus single-sample classifier and TCGA classifier were applied to the RNAseq data to determine molecular subtypes. Immunohistochemistry (IHC) staining for canonical markers of basal (KRT5, 14 and CD44), luminal (KRT20, GATA3, FOXA1) and immune cells (CD3, CD8, PD-L1 (SP263)) was performed, and scoring was assessed by two independent pathologists. Tumor subtypes derived from either RNAseq or IHC were compared and correlated with disease specific survival.
Results: Among the 244 MIBC patients 30.7% were T2, 47.6% were T3 and 21.7% were T4. The consensus molecular classification identified mRNA subtypes and showed agreement with the TCGA molecular classification. Correlations with disease specific survival revealed that luminal subtypes trended towards best outcome while stroma-rich subtype trended towards poorest outcomes compared to other subtypes. IHC markers associated with luminal-like and basal-like tumors recapitulated the molecularly defined luminal/basal subtype assignment. Stroma-rich subtypes were enriched with fibroblast signatures, implying high desmoplastic stromal cell infiltration and low immune cell infiltration. By integrating molecular classification and IHC immune markers (PD-L1, CD3, CD8 - serving as a proxy for ‘immune signature’), we found that the immune signatures themselves stratified the survival benefit, as previously shown. Interestingly, we observed heterogeneity of the IHC-immune signature within mRNA subtypes.
Conclusions: Integrating MIBC subtyping, IHC of immune markers and patient outcomes data provides a biological framework that allows for potential biomarker identification for this lethal disease. The studies presented here underscore the existence of heterogeneity in immune phenotypes within tumor subtypes. A deeper understanding of the association between these tumor subtypes and their immunological states is crucial to guide treatment decisions, particularly for patients facing worse prognostic outcomes.

CLINICAL RESEARCH: Other Targets
Poster Session

#7574 Exploring the therapeutic potential of proteasome inhibitors in targeting SOX2-driven LUSC and SCLC.
A. Mohanty, Linlin Guo, Sravani Ramisetty, Sharad Singhal, Erminia Massarelli, Prakash Kulkarni, Ravi Salgia;
City of Hope National Medical Center, Monrovia, CA

This study addresses the current lack of small molecules targeting SOX2, a pivotal protein in cancer, through an examination of the effectiveness of FDA-approved drugs and proteasome inhibitors. Building on prior research demonstrating the proteasome inhibitor CFZ's capacity to diminish the expression of ITGB4 and PXN in LUAD effectively, our investigation highlights CFZ and IXA as potent inhibitors at nanomolar concentrations. Notably, CFZ treatment enhances sensitivity to cisplatin by suppressing the expression of ITGB4 and the stemness-associated gene SOX2.At a mechanistic level, CFZ hinders histone acetylation at the SOX2 promoter site, leading to rapid and specific downregulation. RNA-seq analysis of COH2 cells treated with CFZ unveils substantial downregulation of genes related to transcription and DNA binding. Z score analysis further reveals a noteworthy inhibition of key transcription factors (TFs), including SOX2, NANOG, POU5F1, SALL4, and KLF4. This TF inhibition extends to neuroendocrine cell lines, identifying 16 overlapping targets of SOX2 associated with stemness. These findings suggest a potential therapeutic approach for targeting cisplatin-resistant cancer stem cells across various cancer types. Moreover, the study proposes a synergistic effect of cisplatin and CFZ in mitigating the growth of neuroendocrine phenotype, SCLC. Given the limited medical options currently available for this phenotype, this insight holds particular significance. In conclusion, our study unveils CFZ as a potent transcriptional suppressor of SOX2, providing a novel strategy to sensitize cisplatin-resistant cancer stem cells. The results underscore the interplay of genetic and non-genetic mechanisms in drug resistance, emphasizing the significance of repurposing drugs for other indications.

#7575 BPI-460372, a covalent, irreversible TEAD inhibitor in Phase I clinical development.

X. Han[1], J. Guo[2], X. Jin[2], L. Zhu[2], H. Shen[2], X. Xu[2], M. Zhang[2], X. Liu[2], Y. Liu[2], H. Cheng[2], S. Guo[2], L. Ding[2], J. Wang[2], **H. Lan**[2], M. Wang[1];
[1]Peking Union Medical College Hospital, Peking Union Medical College and Chinese Academy of Medical Sciences, Beijing, China, [2]Betta Pharmaceuticals Co.,Ltd, Hangzhou, China

The Hippo signaling pathway is critical for the regulation of organ development, tissue homeostasis, and tumorigenesis by controlling the activation status of yes-associated protein (YAP) or its homolog PDZ-binding motif (TAZ). As a major downstream effector, the transcription factor TEAD is activated by forming a complex with YAP/TAZ. Hippo pathway aberrations leading to TEAD activation have been reported in many cancers. Inhibiting TEAD function by directly blocking the palmitoylation pocket of TEAD is a potential therapeutic approach for cancer treatment. Betta Pharma has discovered a selective, covalent and irreversible TEAD inhibitor known as BPI-460372. The discovery of BPI-460372 was first reported in AACR 2023. Here we present additional preclinical and clinical data characterizing BPI-460372 as a promising candidate drug. In the dose-escalating part of the Phase I study, the exposure of BPI-460372 increased proportionally over 10 to 80 mg dose range after oral administration and exhibited linear pharmacokinetics, with a clearance rate suitable for once-daily dosing. The compound is generally well tolerated, with no drug-related Grade ≥3 adverse event observed. Remarkably, we have not seen renal toxicities that was perceived as a potential risk associated with certain TEAD inhibitors. Preliminary efficacy was observed in a few subjects. In preclinical studies, we found that intermittent dosing schedule of 3 days on/4 days off, compared with continuous dosing at equivalent weekly exposure, can ameliorate kidney damage and improve early renal injury biomarkers while maintaining anti-
tumor activity. Thus, alternative dosing schedule could further improve the therapeutic window and enable combination studies in clinical development. Collectively, these results support further development of BPI-460372 for the treatment of cancers harboring Hippo pathway alterations.

#7576 Exemestane and its primary metabolite 17-hydroexemestane inhibit synergically the tumor growth of ER/AR positive breast cancer tumors.

G. Santacana-Font[1], D. Kedra[1], M. Garcia-Macias[2], L. Cornelus-Reitsma[3], M. Lyngra[3], T. Sauer[3], V. Kristensen[4], A. Hurtado[1], **J. Geisler**[5];
[1]CSIC-Centro de Investigacion del Cancer de Salamanca, Salamanca, Spain, [2]Centro de Investigacion del Cancer de Salamanca, Salamanca, Spain, [3]Akershus University Hospital, Oslo, Norway, [4]Oslo University Hospital, Oslo, Norway, [5]University of Oslo, Oslo, Norway

Exemestane, an aromatase inactivator of the third generation, plays a crucial role in breast cancer therapy by targeting the P450 aromatase enzyme and, thus, decreasing estrogen synthesis. Exemestane (Aromasin™) is currently the only steroidal aromatase inactivator widely used in clinical routine treatment of ER+ breast cancer in all phases of the disease in a global perspective. However, the complex mechanisms underlying its therapeutic effects, besides being an aromatase inhibitor, remain incompletely understood. In this study, we employed a combination of human samples and in vitro data to unveil a compelling insight: Exemestane (EXE) and its primary metabolite, 17β-hydroxyexemestane (HEXE), exhibit potent inhibitory effects on tumor growth when present together in patient serum. Our biochemical analysis establishes a critical threshold—20% HEXE metabolite of the total EXE in patient serum—to trigger a tumor growth inhibition exceeding 90%, as evidenced by Ki67 staining. Mechanistically, our data reveals that both HEXE and EXE bind to the Androgen Receptor (AR), triggering a synergistic activation that induces a transcriptional program leading to cell death while diminishing the intracellular signaling activated by the oncogene Ras. Notably, patients with tumors characterized by a minimum of 20% AR+ epithelial cancer cells stand to benefit the most from exemestane and HEXE. Intriguingly, the binding of AR to chromatin in tumors gives rise to a molecular signature capable of distinguishing responsive from non-responsive patients to both EXE and HEXE. Collectively, our findings elucidate a dual therapeutic role for Exemestane in selected patients: it not only restrains estrogen-driven proliferation by estrogen suppression but also stimulates cell death by establishing a specific interactome with the AR at the genomic level. These insights suggest that both EXE and HEXE are necessary to achieve the best therapeutic effects in ER+/AR+
breast cancer tumors. Moreover, our findings suggest that AR-expression and targeting should be investigated further to potentially add novel strategies to our existing algorithms in ER+/AR+ MBC.

#7578 BRD4 protein degradation for p53 mutant diffuse intrinsic pontine glioma (DIPG) via various delivery approaches for ARV-825 by using camel milk exosomes.

A. Nathani[1], M. Aare[1], L. Sun[2], Y. Li[3], M. Singh[1];

[1]Florida A&M University College of Pharmacy & Pharmaceutical Sciences, Tallahassee, FL, [2]Florida State University, Tallahassee, FL, [3]FAMU-FSU College of Engineering, Tallahassee, FL

DIPGs (diffuse intrinsic pontine gliomas) are a particularly aggressive and malignant type of pediatric brain tumor. Given the tumor's location, surgery has a restricted role, and it is insensitive to most chemotherapies. Although fractionated radiation is the standard of therapy for DIPG, the cancer invariably worsens in 6-12 months. TP53 tumor suppressor protein mutations are found in 70-80% of DIPG tumors. These TP53 mutations have been linked to radiation resistance in DIPG patients. Our goal was to find new pharmacological compounds that would improve the radiation sensitivity of p53 mutant DIPG cell lines and to determine their molecular mechanism of action. Numerous bromodomain-containing protein 4 (BRD4) inhibitors have entered clinical trials in recent years, yielding promising outcomes in tumor treatment since BRD4 expression in DIPG is substantially higher than in neighboring normal brain tissue. So consequently, BRD4 is a target for DIPG treatment. ARV-825 is an emerging PROTAC (Proteolysis Targeting Chimera) compound which can cause rapid and persistent BRD4 protein degradation. However, delivering ARV-825 to pons is a major challenge owing to poor oral bioavailability of PROTACS. In this study, we used camel milk derived exosomes (CME) for delivery of ARV-825 to pons by both nasal and oral routes. To begin with, goat milk exosomes were also considered but CME was chosen because of its innate cytotoxicity against DIPG cell lines. CME were isolated using ultracentrifugation and nanoparticle tracking analysis and revealed a size distribution of 112.5 ± 2.8 nm, zeta potential of -26.38 ± 0.12 mV. CME ($1*10^{11}$) were cytotoxic to both SF8628 (with a H3.3 K27M mutation) and SF188 (grade IV pediatric glioblastoma with wild type H3.3) cell lines and had 51% and 44% cell viability respectively. ARV-825 showed IC_{50} of 546.58 ± 22.14 nM and 608.94 ± 30.04 nM in SF8628 cells and SF188 cells respectively. ARV-825's IC_{50} was lowered when ARV-825 loaded CME were used. ARV-825 was loaded using sonication and entrapment efficiency was found to be 42.96 ± 2.14 % by HPLC analysis. CME were labelled with Vybrant DiO (CME-DIO) and instilled into each nostril of Sprague Dawley rats daily. Brain sections were viewed with fluorescent microscope and CME-DIO were seen in olfactory region after 3 days and in the pons region after 5 days demonstrating the ability of CME to reach the target site. *In-vitro* permeability studies using MDCK cells showed approximately 9µg/mL (60%), 15µg/mL (80%) and 16µg/mL (100%) of ARV-825 permeation in 2, 4 and 24 hours respectively when loaded into CME. The results of the present study suggest the possibility of using CME as a viable delivery strategy for ARV-825 against DIPG. Further in vitro and in vivo studies are currently undergoing to validate the results and understand kinetics and the molecular mechanisms of ARV-825 loaded CME.

#7579 Dual inhibition of enhancer of zeste homolog 1 2 induces pyroptosis, modulates oncogenic signaling pathways & sensitizes hepatocellular carcinoma to valemetostat & docetaxel treatments.

A. E. Harira, A. Maher, A. Sultan;
Alexandria University, Alexandria, Egypt

HCC is a global health concern, with chemotherapy resistance and patient recurrence posing significant challenges to liver cancer treatment. EZH2 is a crucial part of the polycomb repressive complex 2 (PRC2). It, along with its homolog EZH1, is a focus for cancer therapeutic targets. Dysregulation of EZH1/2 can cause cancer development due to significant changes in geneexpression. The current study aims to investigate the interaction between EZH1/2 and oncogenic signals responsible for HCC progression and pyroptosis induction. Two cell lines, HepG2 and SK-Hep1, were subjected to two FDA-approved drugs, Valemetostat (Val) and Docetaxel (Doc), to determine the impact of EZH1/2 on tumorigenicity and drug resistance. The WST-1 assay was utilized to gauge cell proliferation. The results indisputablydemonstrated a synergistic effect of the drugs after 48 h of treatment. The inhibition of viability was attributed to apoptosis induction in both tested cell lines, and the maximum effect was observed in the combined treatment as compared to either the control or each drug alone. Furthermore, our datashowed activation of caspase-3, upregulation of BAX, indicating apoptotic induction, and downregulation of Bcl-2, Bcl-XL, AKT, S6k, oncogenic β-catenin, and Stat3 protein expression levels, suggesting a modulation of oncogenic signaling pathways at the protein level. After 24 h of Val/Doc treatment, pyroptosis was observed, characterized by cell swelling and bubbles on themembrane and a significant release of lactate dehydrogenase, indicating pyroptotic cell cytotoxicity. The antitumor effects and pyroptosis were enhanced by using a dual inhibitor, UNC1999, for EZH1/2, resulting in a marked increase in the sensitivity of tested cells to the Val/Doc treatment invitro. The present study unequivocally demonstrated that dual inhibition of EZH1/2 acts as a potent sensitizer of HCC cells to Val/Doc treatment, which might be a promising therapeutic approach for inducing cellular pyroptosis in HCC cell lines.

#7580 The antihistamine terfenadine inhibits TFE3 dimerization, has antitumor activity and synergizes with tyrosine kinase inhibitors in translocation renal cell carcinoma.

I. Delle Fontane[1], R. Cordova[2], C. Rupert[1], S. Orsi[1], A. Jawadwala[1], D. E. Heppener[1], R. Pili[1];

[1]University at Buffalo, Buffalo, NY, [2]Indiana University, Indianapolis, IN

Translocation renal cell carcinoma is a subtype of kidney cancer characterized by gene fusions involving MiT transcription factor family, TFE3 and TFEB, with various gene partners. In general, these tumors do not respond to conventional therapies, which stresses the importance of developing new therapeutical approaches. To date, several TFE3 fusion gene partners have been identified. However, the mechanism driving TFE3 cooperation with various gene partners remains to be elucidated. We have previously shown the vulnerability of dimerization domain of multiple TFE3-fusion proteins, and we have screened the FDA approved drugs library LOPAC and a small molecule library (Microsource) to identify compounds that inhibit TFE3 dimerization. The antihistamine terfenadine was found to inhibit TFE3 dimerization and had antiproliferative activity in different models of tRCC, both *in vitro* and *in vivo*. Interestingly, our more recent data show that terfenadine reduced the amount of TFE3 in the nuclei. We have also observed enhanced antiproliferative activity of terfenadine in HEK293 cells overexpressing PRCC-TFE3, SPFQ-TFE3 or NONO-TFE3 compared to TFE3 alone or vector control, suggesting a targeted effect of terfenadine on cells driven by these TFE3-SF fusions. In addition, knock-down of SFPQ-TFE3 in HEK293 partially reversed this enhanced sensitivity to terfenadine. Cell proliferation and combination index analysis were performed in cell lines endogenously expressing the most common TFE3-fusion proteins cells to determinate the combination with different tyrosine kinase inhibitors. Immunofluorescence and confocal microscopy were performed to assess the impact on TFE3 fusion protein levels. The combination of terfenadine with sunitinib showed a synergistic effect in cells endogenously expressing PRCC-TFE3 (IC50=1.5μM; Fraction Affected > 0.05) and NONO-TFE3 (IC50=1.8μM; Fraction Affected<0.7) fusions. The combination of terfenadine with crizotinib showed a synergistic effect in cells expressing SFPQ-TFE3 fusion (IC50=0.7μM; Fraction Affected>0.7). The combination of terfenadine with dovitinib showed a synergistic effect in cells expressing PRCC-TFE3 fusion (IC50=1μM; Fraction Affected>0.4). These preliminary data suggest a different response to the combination with different TKIs. This observation underlines the importance of identifying the TFE3 partner gene for targeted therapy. Overall, our results suggest that targeting the dimerization domain along with different oncogenic pathways activated in tRCC cells may represent a new therapeutic approach for this disease.

#7581 Nicotine promotes the proliferation and metastasis of non-small cell lung cancer through c-Myc/EZH2 pathway.

C. Ding[1], H. Huang[1], C. Chen[2], Y. Li[2], H. Liu[2], **J. Chen**[1];

[1]Department of Lung Cancer Surgery, Tianjin Medical University General Hospital, Tianjin 300052, People's Republic of China, Tianjin, China, [2]Tianjin Lung Cancer Institute, Tianjin Key Laboratory of Lung Cancer Metastasis and Tumor Microenvironment, Tianjin Medical University General Hospital, Tianjin 300052, People's Republic of China, Tianjin, China

Objective: Lung cancer, particularly non-small cell lung cancer (NSCLC), continues to be a predominant contributor to global cancer-related mortality, with smoking emerging as a significant risk factor. Nicotine, which is one of the main chemicals from the tobacco smoke, is identified as carcinogen for lung cancer, especially for squamous carcinoma (LUSC). This study aims to investigates the intricate molecular mechanisms by which nicotine facilitates proliferation and migration in NSCLC through the c-Myc/EZH2 signaling pathway.

Methods: Clinical tissue specimens were procured from surgical patients with lung cancer for immunohistochemical staining. Additionally, public databases were scrutinized to compare EZH2 expression between smokers and non-smokers. NSCLC cell lines underwent treatment with nicotine in a time- and concentration-dependent manner, and the impact on EZH2 was corroborated through Western Blot, Real-time PCR, and immunofluorescence staining. Proliferation and migration assays, encompassing CCK8 experiments, colony formation assays, EdU staining, and Transwell assays, were conducted to discern the effects of nicotine on NSCLC. Experimental techniques such as si-RNA and CHIP were deployed to investigate changes in c-Myc-mediated regulation of EZH2, elucidating the intricate role of the c-Myc/EZH2 pathway in nicotine-induced NSCLC proliferation and migration.

Results: Smokers exhibited heightened EZH2 expression in tumor tissue compared to non-smokers. Nicotine treatment induced a concentration- and time-dependent upregulation of EZH2 in NSCLC cell lines. In 10 μM nicotine-treated NSCLC cells, concurrent treatment with 10 μM DZNep (EZH2 inhibitor) or si-EZH2 significantly augmented proliferation and migration. Moreover, the upregulation of EZH2 correlated with increased c-Myc expression, and siRNA-mediated c-Myc inhibition resulted in a corresponding reduction in EZH2 expression. Nicotine was identified as a promoter of NSCLC proliferation and migration through the c-Myc/EZH2 signaling pathway. This study establishes a robust association between nicotine and EZH2 in NSCLC cells, unveiling the novel regulatory axis of c-Myc/EZH2. Combined treatment with c-Myc and EZH2 inhibitors demonstrated efficacy in suppressing nicotine-induced promotion of NSCLC proliferation and migration.

Conclusion: In summary, this study elucidates the mechanisms through which nicotine propels NSCLC development via the c-Myc/EZH2 pathway, providing a theoretical underpinning for future NSCLC treatment paradigms. The combined use of c-Myc and EZH2 inhibitors emerges as a promising therapeutic strategy, poised to inhibit nicotine-induced NSCLC proliferation and migration, offering enhanced treatment modalities for patients.

#7582 Descriptive analysis of patients with mCRPC and liver metastases receiving alpha and beta PSMA targeted radionuclide therapy (PSMA-TRT).

S. Ruder, M. Sun, A. Ricaurte Fajardo, J. Nauseef, Z. Davidson, J. Thomas, S. Huicochea Castellanos, A. Molina, C. Sternberg, A. Patel, E. Fernandez, S. Yuan, E. Fung, V. Avlonitis, E. O'Dwyer, D. Nanus, J. Osborne, N. Bander, S. Tagawa;
New York Presbyterian Hospital Weill Cornell University Medical Center, New York, NY

Introduction: Predictors of outcomes after PSMA-TRT are still being established. Liver metastases (mets) have been associated with poor response. Mutations in genes encoding DNA damage repair (DDR) and TP53 affect radiosensitivity. Here we describe a cohort of patients with mCRPC and liver metastases treated on clinical trials of PSMA-TRT.

Methods: 39 patients with liver mets were enrolled on phase I/II PSMA-TRT studies between Jan 2006 to Apr 2022. Patients received alpha therapy (225Ac-J591), beta therapy (fractionated 177Lu-PSMA-617, single-dose and fractionated 177Lu-J591) or a combination of both (225Ac-591 and 177Lu-PSMA-I&T). All patients included in this analysis had CT imaging; patients enrolled after 2017 had PSMA-PET imaging. 15 patients also had genomic analysis completed.

Results: Median age was 69 (range 55-93), PSA 85.7 (2.45-9614). 39 (100%) bone mets, 33 (84.6%) LN, 9 (23.1%) lung. 22 (56.4%) greater than 1 ARPI, 23 (59.0%) greater thanc 1 chemo, 13 (33.3%) sip-T, 7 (17.9%) Ra-223, 4 (10.2%) prior TRT (with concurrent liver mets). Of the 19 with both CT and PSMA PET, 18 (94.7%) were identified on PSMA PET (including 8 PET only), 10 (55.6%) on CT (1 CT only, i.e. non-PSMA PET avid). Median whole body PSMA-imaging score (PSMA-IS) was 4 (range 1-4), with 7 (17.9%) 1-2 and 32 (82.1%) 3-4. 9 (23.0%) received alpha-TRT, 26 (66.7%) beta-TRT, and 4 (10.3%) combo-TRT. Somatic or germline analysis was completed in 15 (38.5%) of 39 patients. 8 (53.3%) had mutations in DNA repair pathways (3 in BRCA2, 3 in CHEK 2, 1 in FANC, 1 in MSH2). 7 (46.7%) had mutations in TP53. 31 patients (79.5%) had PSA decline, with 15 (38.5%) achieving PSA 50. 26 (66.7%) had baseline CTC measured; 19 (73.0%) had detectable CTC at baseline. Of these 19, 3 (15.8%) converted to undetectable after therapy and 2 (10.5%) converted to favorable CTC. PSA50 rate in alpha-TRT was 4 (44.4%), beta-TRT 8 (30.7%), combo-TRT 3 (75%). PSA50 in patients with PSMA-IS 1-2 was 1 (14.2%) compared to 14 (43.9%) in PSMA-IS 3-4. 3 (37.5%) of 8 patients with mutDDR achieved PSA50, compared to 3 (42.9%) with mutTP53.

Conclusions: This dataset adds to the collective literature of two subgroups of patients with mCRPC receiving TRT: those with liver disease and those with mutations in DNA repair pathways. The results of this study suggest higher rates of response in patients receiving alpha therapy, either alone or in combination with beta therapy, and in patients with high radiotracer uptake on PSMA-PET, based on PSMA-imaging score of 3 or 4. Genomic alterations in DRR proteins did not have clear implications.

#7583 Discovery of a potent small molecule MALT1 protease inhibitor for the treatment of cancer.

Y. Zhou, B. Fu, J. Chen, W. Cai, X. Sun, Y. Li, W. Ren, Q. Shen, G. Du, X. Zhou, Z. Zou, H. Chen, X. Liu, C. Yang, X. Liu, J. Guo, H. Wu, L. Ding, J. Wang, **H. Lan**;

Betta Pharmaceuticals Co.,Ltd, Hangzhou, China

The paracaspase mucosa-associated lymphoid tissue lymphoma translocation protein 1 (MALT1), as the core component of CBM complex (CARD9/10/11/14-BCL10-MALT1), plays an essential role in activating the NF-κB pathway and regulating the cell proliferation, differentiation and immunity. Inhibiting of MALT1 is considered a promising therapeutic approach for the treatment of several non-Hodgkin B-cell lymphomas, chronic lymphocytic leukemia (CLL), solid tumors and autoimmune diseases. Herein, we report the discovery of a novel potent MALT1 allosteric inhibitor, BPI-530616, which strongly inhibited MALT1 protease activity with subnanomolar IC_{50}, and low off-target activity on other proteases. BPI-530616 can inhibit the proliferation of B-cell diffuse large B-cell lymphoma (ABC-DLBCL) cell line, OCI-ly3, bearing CD79b and CARD11 mutations. The cell line is intrinsically resistant to covalent and non-covalent Bruton's Tyrosine Kinase (BTK) inhibitors. Meanwhile, BPI-530616 suppressed the cellular cytokine secretion (e.g.IL-10, IL-2) or MALT1 direct substrate cleavage (e.g. CYLD). *In vivo*, BPI-530616 dose-dependently suppressed tumor growth and inhibited the cleavage of CYLD in OCI-ly3 xenograft mouse model. To address the role of MALT1 inhibitor in the contest of immune-oncology, a CT26 syngeneic mouse model was set up. Oral administration of BPI-530616 exhibited a good antitumor effect comparable to that of the anti-PD1 antibody, with no observable adverse effects. Additionally, BPI-530616 displayed desirable drug-like properties, including low clearance and good oral bioavailability across multiple pre-clinical species. Taken together, our research has led to the discovery of a novel, potent, selective, and orally bioavailable small molecule MALT1 inhibitor, BPI-530616. It demonstrated anti-tumor efficacy in the DLBCL animal model and showed promising effects in an immune-oncology animal model.

#7584 The solute transported xCT (SLC7A11) modulates lysosome biogenesis and microRNA trafficking in drug resistant renal cell carcinoma.

A. Jawadwala, C. Rupert, R. Adelaiye-Ogala, R. Pili, Sreenivasulu Chintala, Ashley Orillion, May Elbanna, Nur Damayanti, I. Delle Fontane;
SUNY Buffalo, Buffalo, NY

Multi-tyrosine kinase inhibitors (TKIs) like sunitinib bind to over 50 kinases and inhibit several receptors such as VEGFR-1, VEGFR-2, and VEGFR-3 receptors, PDGFRa and PDGFRb, RET, cKIT, and FLT3. TKIs are effective drugs for the treatment of renal cell carcinoma (RCC) but intrinsic/acquired resistance remains a major hurdle. One of the proposed models for TKI resistance is drug sequestration by lysosomes. The solute transporter xCT is a cystine/glutamate antiporter that plays a role in the production of antioxidants in cancer cells. Our lab has found that SLC7A11, the gene that encodes xCT, is overexpressed in sunitinib resistant RCC cells. LAMP1 expression was also increased in sunitinib resistant RCC cells, suggesting an upregulation of lysosome biogenesis. The biochemical knock down of SLC7A11 by shRNA showed a decrease in LAMP1 expression, suggesting a decrease in lysosome biogenesis. SEC24D is a key catalytic component of COPII complex involved in formation of exosomes and secretory pathways. Our preliminary data showed that reduction in xCT expression was associated with a decrease in SEC24D protein levels which was associated with a reduction in the extracellular export and, consequently, an increase in intracytoplasmic levels of miRNA 605, a known tumor suppressor. We are currently testing the hypothesis that xCT may modulate lysosomes biogenesis and micro-RNA trafficking in several clear cell and translation renal cell carcinoma models. In summary, a better understanding of the role of xCT in the regulation of intracytoplasmic organelles may lead to the identification of a novel therapeutic strategy to overcome TKI resistance in RCC.

#7585 Targeting of 7 or 24 dehydrocholesterol reductase decreases cancer progression in head and neck cancer.

Bok-Soon Lee[1], Ji-Hye Choi[2], Hyo Jeong Kim[1], Jin Roh[3], Joselyn Padilla[4], Kennedy Davis Brock[4], Jeon Yeob Jang[1], Hyun Goo Woo[2], Chul-Ho Kim[1], Jiyoung Lee[4]

[1]Department of Otolaryngology, Ajou University School of Medicine, Suwon, Korea, Republic of,[2]Department of Physiology, Ajou University School of Medicine, Suwon, Korea, Republic of,[3]Department of Pathology, Ajou University School of Medicine, Suwon, Korea, Republic of,[4]Department of Biochemistry and Molecular Medicine, The George Washington University, School of Medicine and Health Sciences,, Washington, DC

The elevated expression of cholesterol metabolism has been associated with many cancer including head and neck squamous cell carcinoma (HNSCC). However, the molecular mechanisms between cholesterol biosynthesis and head and neck cancer have not yet been studied. In this study, we identified upregulation of dehydrocholesterol reductase such as DHCR7 or DHCR24 in HNSCC compared with adjacent normal tissues from the same patients using RNA sequencing data. We observed protein expression level of DHCR7 or DHCR24 in head and neck cancer cell lines through Western blotting. We also checked high expression of DHCR7 or DHCR24 in HNSCC tissues from patients using immunohistochemistry assays. Yet, when DHCR7 or DHCR24 was knocked down using siRNA, the viability of HNSCC cells was decreased in MTT assays. In parallel, we adapted small inhibitory drugs; AY9944 for DHCR7 inhibition and Triparanol or SH-42 for DHCR24 inhibition. Treatment of AY9944, Triparanol, or SH-42 also resulted in decreased viability of HNSCC cells. Moreover, when we used a cholesterol blocker, MCD, the cell viability was decreased, whereas the cells overcame cell death by adding the combination of cholesterol and LDL. Taken together, we concluded that head and neck cancer requires DHCR7 and DHCR24 activity involved in cholesterol metabolism for cancer growth. Our data suggest that targeting DHCR7 or DHCR24 using AY9944, Triparanol or SH-42 is one of the potential strategies that will definitely help with cancer treatment for head and neck cancer.

#7586 TOX loss-of-function(TOX^{LOF})results in BCR hyperactivation andenhanced responses to BCR-targeting in diffuse large B cell lymphomas (DLBCL).

Eloisi Caldas Lopes, Maria Victoria Revuelta, Rossella Marullo, Leandro Cerchietti

Weill Cornell Medicine, New York, NY

DLBCL originate from germinal center B cells (GCB). The ABC-DLBCL subtype, characterized by activation of B-cell receptor (BCR) signaling and downstream NF-kB pathway, carries a poor outcome. Up to 30% of ABC-DLBCL present TOX^{LOF} mutations, suggesting that TOX function as a tumor suppressor. Our analysis of TOX expression along the germinal center B-cell differentiation program (naïve → GCB → plasma cells) showed that TOX expression paralleled NF-kB activity with highest levels in plasma cells (P<0.001, vs. either naïve and GCB). We thus propose that TOX acts as a transcriptional gatekeeper in GCB cells to prevent early activation of NF-kB thus enabling differentiation into plasma cells while restraining lymphomagenesis. We generated a conditional GCB TOX KO mouse model, induced the GC reaction with a T-cell antigen and found that TOX KO (vs. TOX WT, 10 mice per condition) had impaired differentiation of plasma cells (p<0.001) and hyperproliferative Ki67+ GCB cells (p<0.05). We then generated (by CRISPR) an isogenic TOX^{LOF} ABC-DLBCL cell line (TMD8) and found upregulation of genes in the NF-kB pathway (q-value <0.05, vs. TMD8). Furthermore, TMD8-TOX^{LOF} cells showed increased secretion of autocrine cytokines IL6 and IL10, and higher STAT3 phosphorylation (p<0.05 for all comparisons, vs. TMD8-TOX^{WT} cells) all compatible with NF-kB activation. Tumor microenvironmental cues can hyperactivate BCR and downstream NF-kB in ABC-DLBCL. We thus implanted isogenic TMD8 cells in mice (n = 10) and determined pathway activation by phospho-flow. We found massive activation of SYK, BTK, PLCG2 (from the BCR) and p65 (from NF-kB) in TMD8-TOX^{LOF} vs. TMD8-TOX^{WT} tumors (all p<0.01), and vs. these cell lines cultured in vitro (all p<0.01). To determine whether these features can be therapeutically exploited, we conducted a viability screening using a panel of 20 clinical-phase targeted therapies relevant to ABC-DLBCL. We found that BTK inhibitor acalabrutinib (BCR pathway) and MALT1 inhibitor JNJ67690246 (NF-kB pathway) were 2-3 fold more active in TMD8-TOX^{LOF} vs. TMD8-TOX^{WT} cells (all p<0.05). We then xenografted isogenic TMD8 cells (n = 10 mice per condition) and, when tumors reached 150 mm3, we randomized mice to vehicle vs. acalabrutinib 30 mg/kg/day by oral gavage (human dose equivalent). Acalabrutinib was significantly more active in TMD8-TOX^{LOF} tumors (vs. TMD8-TOX^{WT}, p=0.0008), which translated into significantly prolonged survival (p<0.05). This acalabrutinib effect was accompanied by significant reduction of BTK, SYK and PLCG2 phosphorylation in TMD8-TOX^{LOF} tumors (p<0.0001, all comparisons). Thus, TOX^{LOF} leads to hyperactivation of the BCR and NF-kB signaling pathways in ABC-DLBCL cells, rendering them hypersensitive to BCR-targeted therapies, delineating a potential mechanism-based therapeutic approach for ABC-DLBCL TOX^{LOF} patients.

#7587 Fascin1 might be a promising molecular target for colorectal cancer patients at advanced stage.

Canfeng Fan, Qiang Wang, Rika Aoyama, Hinano Nishikubo, Kyouka Kawabata, Imanishi Daiki, Takashi Sakuma, Koji Maruo, Gen Tsujio, Yurie Yamamoto, Tatsunari Fukuoka, Masakazu Yashiro

Osaka Metropolitan University, Sakai, Japan

Background: Colorectal cancers (CRC) show high morbidity and mortality. Especially, the consensus molecular subtypes 4 (CMS4)-CRC shows extremely poor prognosis and high chemo-resistance rate, in compared with the other types of CRC. CMS4-CRC is histologically characteristic for the extensive stromal infiltration with poorly differentiated cancer cells in the tumor microenvironment. Several studies have reported that sessile serrated adenomas, which is characterized by disorganized crypt architecture and irregular serrations with high malignant potential such as epithelial-mesenchymal transition and TGFβ signaling, might be closely associated with CMS4-CRC. Fascin-1 is an actin-binding protein supposed to be associated with sessile serrated adenomas. However, the expression and clinical significance of fascin-1 in CMS4 CRC remains to be unclear.
Aim: The aim of this study was to clarify the clinic-pathological significance of fascin-1 in colorectal cancer, and to evaluate the effects of fascin-1 inhibitors on the invasion and migration ability of CMS4 cancer cell lines.
Materials and Methods: We conducted an immunohistochemical study on 351 colorectal cancer patients, where we examined the expression levels of Fascin-1 and analyzed their correlation with the patients' clinicopathologic features. Using two human CMS4-CRC cell lines, SW480 and HCT116, we investigated the effects of the fascin-1 inhibitors, NP-G2-044 and BDP-13176, on the proliferation and the migration activity of CMS4-CRC cells via MTT assay and a wound-healing assay.
Results: Fascin-1 is expressed both on cancer cells and on stromal cells, but mainly expressed on cancer cells. Significance of fascin-1 expression on cancer cells was evaluated in this study. Fascin-1 expression is significantly associated with histologically poorly differentiation ($p < 0.001$), deeper T invasion ($p = 0.003$), and proximal colon cancer ($p < 0.001$). High fascin-1 expression is significantly associated with worse prognosis ($p = 0.0085$, log-rank) and higher recurrence rates ($p = 0.018$). Univariate analysis demonstrated that overall survival of patients was significantly associated with Fascin1 expression in cancer cells, age ≥65 years old, poor histological type, lymphatic invasion, lymph node metastasis, and venous invasion. Multivariate analysis revealed that fascin1 expression ($p = 0.037$), poor histological type ($p = 0.022$), venous invasion ($p = 0.078$), and lymph node metastasis ($p = 0.009$) were significantly correlated with the overall survival rate of CRC patients. Both fascin-1 inhibitors significantly reduced the invasion and migration of colorectal cancer cells at the concentration of 100 nM.
Conclusions: Fascin-1 is one of key molecules for the development of CRC. Fascin-1 might be a promising molecular target for CMS4-CRC patients at advanced stage.

#7588 Discovery of NSP-5033: A novel and potent PARP7/12 dual inhibitor.

Q. Chen, Q. Huang, K. Zhang, Y. Hao, Z. Wang, B. Li;
Novostar Pharmaceuticals, Ltd., Shanghai, China

PARP7 is a mono-ADP-ribosyl transferase that catalyzes the transfer of single units of ADP-ribose onto substrate proteins to regulate their functions. One of its substrates is TANK binding kinases 1 (TBK1), whose MARylation by PARP7 inhibits its activation and thereby represses the type I IFN response to cytosolic nucleic acid. PARP7 is upregulated in many kinds of cancers and acts as a brake in cytosolic nucleic acid sensing, which leads to the suppression of type I IFN signaling and immune response. Therefore, PARP7 is a novel and promising target in cancer immunotherapy. Herein, we describe the discovery of a novel small molecule NSP-5033 as a dual PARP7/PARP12 inhibitor, which potently inhibits PARP7 and PARP12 enzymes with sub-nanomolar and low nanomolar activities, respectively. It displayed potent anti-proliferative activities against a number of cancer cell lines *in vitro*. NSP-5033 also increased the mRNA level of IFNβ and CXCL10 and stimulated STAT1 phosphorylation, suggesting that it restored the type I IFN response in tumor cells. With excellent ADME and pharmacokinetic properties, NSP-5033 demonstrated potent *in vivo* efficacy in human lung cancer xenografts with tumor regression and induced antitumor immunity in tumor-bearing immunocompetent mice. NSP-5033 has been nominated as a preclinival candidate for treatment of solid tumors and is undergoing IND-enabling studies.

#7589 The novel complex delivery system of C-phycocyanin-loaded *klebsiella pneumonia*bacterial ghost induces apoptosis and sensitizes non-small cell lung cancer cell lines to doxorubicin.

B. A. Abdelaziz[1], H. E. Mahmoud[2], O. M. Sadek[3], A. S. Sultan[4],
[1]Pharos University in Alexandria / Alexandria University, Alexandria, Egypt, [2]Institute of Graduate Studies and Research, Alexandria University, Alexandria, Egypt, [3]Faculty of Science, Alexandria University, Alexandria, Egypt, [4]Georgetown University / Alexandria University, Alexandria, Egypt

Lung cancer is a significant cause of cancer-related deaths worldwide, with a high incidence rate, poor prognosis, aggressiveness, and a lack of effective treatment options. The present study has brought together two FDA-approved drugs with antineoplastic properties to create a complex that promises to revolutionize the treatment of Non-Small Cell Lung Cancer (NSCLC). By combining C-Phycocyanin extract (PCE), a pigment-protein complex synthesized by blue-green microalgae *platensis*, with the immunostimulatory doxorubicin (DOX) loaded Bacterial Ghosts (BGs), the present study aims to achieve enhanced dual-chemotherapy and remarkable inhibition of DOX-chemoresistance. The BG delivery system uses purified bacterial cell evacuation and safe confirmed *Klebsiella pneumoniae* BGs (KPBG) for safe and effective delivery, overcoming issues with resistance and poor delivery. The complex delivery system of KPBG-PCE/DOX was tested on two NSCLC cell lines, wild-P53, A549, and mutant-P53, NCI/H358, respectively. Our data showed that the loaded combined treatment significantly induced morphological changes with signs of apoptosis induction in the tested cell lines compared with the control. The WST-1 assay was used to evaluate cell proliferation. Data indicates that PCE and DOX have a synergistic effect at low concentrations when loaded on KPBGs for a constant count of BGs CFU/ml after 48 h of treatment. The viability inhibition and apoptosis induction of A549 and NCI/H358 cells were amplified in the combined treatment of 48 h compared to the control or either each drug alone. At the protein levels, our data showed activation of caspase-3, upregulation of BAX, and downregulation of Bcl-2, Bcl-XL, m-TOR, S6k, oncogenic β-catenin, and cyclin-D1 protein expression levels after treatment with (KPBG-PCE/DOX) for 48 h, indicating apoptotic induction and modulating oncogenic signaling pathways. In conclusion, the current study presents a promising outcome of a synergistic delivery system of KPBG-PCE/DOX that can inhibit lung cancer cell line proliferation, induce apoptosis, and increase cell sensitivity to DOX. The KPBG delivery system offers an appealing approach for a successful combination of targeted therapy for lung cancer.

#7590 Novel therapeutic approach for targeting p53 mutant colorectal cancers by affecting post-replicative DNA repair.

M. M. Alruwaili[1], N. Naranjo[1], P. Rajan[1], K. Jo[1], D.-K. Kim[1], T. Melendy[2], R. Straubinger[3], C. Fountzilas[1], A. Bakin[1];
[1]Roswell Park Comprehensive Cancer Center, Buffalo, NY, [2]University of Buffalo, Buffalo, NY, [3]University at Buffalo, Buffalo, NY

Colorectal Cancer (CRC) is the third most common cause of cancer mortality in the US. A major problem in CRC management is relapse and progression to metastatic disease leading to poor overall survival. The tumor suppressor p53 is mutated in most CRCs and often drives metastasis and therapy resistance. Current therapeutic options targeting p53 mutant cancers show poor efficacy and frequently exhibit high toxicity. To address this clinical problem, we developed a novel therapeutic strategy for selective targeting of p53 mutant cancers. The strategy combines a thymidine analogue (e.g., trifluorthymidine/TFT, a component of TAS102) and poly (ADP-ribose) polymerase inhibitor (PARPi). We observed that TAS102 does not block DNA replication, but rather prompts post-replicative base-excision DNA repair (BER), and PARPi increases double-strand DNA breaks (DSBs) in p53 mutant cancer cells. Normal p53 wild type (p53wt) cells are arrested in the G1 phase and repair DNA. Thus, the TAS102-PARPi combination selectively targets p53-mutant cancer cells, resulting in the accumulation of DSBs and cell death. This novel strategy was examined in p53wt and p53-mutant tumor cell-derived xenograft (CDX) and patient-derived xenograft (PDX) models. The drug combination was significantly more effective in inhibiting p53 mutant tumor growth and in prolonging survival compared to monotherapies. This strategy is currently being tested in a first-in-human dose-escalation Phase I study (NCT04511039) in patients with advanced CRC. Further investigation revealed that the TAS102-PARPi combination induced DNA damage response (DDR) and the G2 checkpoint, leading to G2 arrest in p53 mutant cancer cells. We observed that TAS102-PARPi induced phosphorylation of CDC2 (also known as CDK1) but did not increase phosphorylation of histone H3 (a marker of mitosis), therefore indicating activation of the G2 checkpoint. Furthermore, the roles of ATM and ATR kinases in the DDR and G2 responses were clarified using highly specific kinase inhibitors. The analysis of the DDR/G2 signaling response in isogenic p53wt and mutant CRC cell lines showed that inhibition of WEE1 kinase can selectively abrogate the G2 checkpoint in p53-mutant cells, resulting in marked DNA damage and cell death. Importantly, the blockade of WEE1 strongly synergized with the TAS102-PARPi combination, further enhancing its potency and efficacy against p53-mutant cancer cells. In summary, our research provides a foundation for a novel therapeutic strategy for p53 mutant cancers that may provide a paradigm shift in the treatment of these deadly cancers, increasing efficacy while minimizing toxic adverse effects.

#7591 Tumor Treating Fields (TTFields) show efficacy in Triple-Negative breast cancer (TNBC) cells alone and in combination with PARP inhibitor Talazoparib.

M. Ghandali, P. Srinivasan, Y. Xia, E. T. Wong, R. W. Sobol, L. zhou, B. A. Carneiro, S. L. Graff, W. S. El-Deiry;
Legorreta Cancer Center at Brown University, Providence, RI

Breast cancer is the most common cancer in women worldwide, and the fifth leading cause of cancer-related deaths globally. Triple-negative breast cancer (TNBC), the most aggressive form of breast cancer, is usually treated with surgery, chemotherapy, and radiation. Tumor Treating Fields therapy are FDA-approved for the treatment of glioblastoma (GBM) and malignant pleural mesothelioma (MPM).TT Fields use alternating electric fields to inhibit tumor growth through mitotic disruption, cellular damage, integrated stress response activation, and immune mechanisms and inhibit cell proliferation, induce cell death, and cause cell cycle arrest.TT Fields can induce BRCAness and when combined with PARP inhibition, this combination may result in synthetic lethality. We explored the effect of TTFields on two TNBC cell lines MDA-MB436 (BRCA1-mutant, p53-null) and MDA-MB468 (BRCA1 wild-type, p53-mutant) treated with TTFields (150 kHz) for 24 hours. Western blot analysis showed elevation of p21 independent of p53 mutational status. We examined the combination of PARP inhibitor (Talazoparib) with TTFields in MDA-MB468 cells to determine the effect of the combination in BRCA wild-type cancer cells. Western blot analysis showed p21 upregulation after 24 hours in combination without an increase in p53. p21 acts as a G1-checkpoint protein and loss of p21 expression has been observed in a high percentage of human breast cancer cells. Our results suggest a rational and potentially effective therapy that could be further developed and used for the treatment of breast cancer. Our ongoing studies are exploring potential mechanisms of synergy between PARP inhibitor Talazoparib and TTFields using various TNBC models, and the effect of the combination on cell cycle arrest in cell culture and in vivo.

#7592 Combined inhibition of CDK4/6 and AKT is highly active against the luminal androgen receptor (LAR) subtype of triple negative breast cancer (TNBC).

R. Chica-Parrado, G. Kim, Y. Uemoto, D. Ye, F. Napolitano, C.-C. Lin, E. Bikorimana, K.-m. Lee, S. Mendiratta, A. B. Hanker, C. L. Arteaga;
UT Southwestern Simmons Comprehensive Cancer Center, Dallas, TX

The LAR subtype of TNBC is enriched for targetable biomarkers such as androgen receptor (AR) expression, PIK3CA mutations, and intact Rb. The purpose of this study was to investigate the most effective combination of CDK4/6, AR, and PI3K-AKT inhibitors in preclinical models of LAR TNBC. The MDAMB453 and MFM223 (AR positive/Rb intact/PIK3CAmutant) LAR TNBC cells were treated with each inhibitor alone or in combination. Drug sensitivity was assessed using colony formation, cell viability, and live-cell analysis. The Loewe additivity equation was used to measure the additive drug effects. Immunoblot analysis was used to evaluate cell cycle and PI3K-AKT signaling and ARE luciferase assay was used to assess AR transcriptional activity. MDAMB453 and MFM223 cells were sensitive to the single agents palbociclib, alpelisib, and capivasertib (IC50, ~500 nM), which inhibited CDK4/6, PI3Kα, and AKT, respectively. Enzalutamide, an AR antagonist, exerted no growth inhibitory activity (IC50, 15-25 μM). Treatment with palbociclib, alpelisib, or capivasertib did not alter the AR protein levels or transcriptional activity. The combination of palbociclib+capivasertib synergistically inhibited the proliferation of MDAMB453 and MFM223 cells (synergistic scores 7.34, p=5.81-11, and 4.78, p=0.012, respectively) better than palbociclib+alpelisib. Enzalutamide did not enhance either combination. Palbociclib+capivasertib inhibited PI3KCA-mutant and Rb-intact LAR TNBC PDX growth more potently than palbociclib+alpelisib (p=0.046). Treatment of LAR TNBC cells with palbociclib suppressed Rb phosphorylation and resulted in adaptive activation of P-AKT$^{S473/T308}$ and the AKT substrates GSK3β, PRAS40, and FoxO3a after 24 h. Capivasertib inhibited the phosphorylation of AKT and AKT substrates, following CDK4/6 blockade with palbociclib, more potently than alpelisib. PI3Kβ inhibitors (TGX221, GSK2636771) did not block AKT substrate upregulation, suggesting PI3Kβ does not mediate adaptive responses. Rictor knockdown failed to reduce AKT activation following palbociclib treatment, suggesting an mTORC2-independent mechanism. Human Phospho-kinase Array of MDA-MB-453 cells treated with palbociclib showed time dependent upregulation of GSK3β^{S9}, STAT3^{Y727} and PDFGRβ^{Y751}. PDGFRβ activation after palbociclib treatment was confirmed in MFM223 cells. PDGFRβ siRNAs in MDAMB453 cells blocked P-AKT^{S473} upregulation after palbociclib treatment. Treatment with palbociclib and the PDGFRβ small-molecule antagonist CP673451 arrested LAR TNBC growth similar to palbociclib+capivasertib, suggesting an adaptive response involving PDGFRβ signaling. In conclusion, this study supports the clinical testing of the palbociclib and capivasertib combination for LAR TNBC patients and reveals adaptive responses after palbociclib treatment through PDGFRβ signaling.

#7593 Photodynamic therapy improves therapeutic management of glioblastoma.

N. Vasyliv[1], K. Williams[2];

[1]University of Edinburgh, Edinburgh, United Kingdom, [2]University of Glasgow, Glasgow, United Kingdom

Glioblastoma (GBM) remains a formidable challenge in the realm of oncology, primarily due to the limitations of the standard of care therapies. Photodynamic therapy (PDT), which exploits the light-activated potential of 5-aminolevulinic acid (5-ALA), emerges as a promising avenue to combat GBM. In this study, primary patient-derived cell lines, Ox5 core, and G7, served as critical subjects, exposed to light excitation at wavelengths of 410 nm, 528 nm, and 810 nm, both with and without 5-ALA (protoporphyrin IX). The central objective was to rigorously assess the efficacy of PDT, either with or without 5-ALA, in reducing cell viability and curtailing clonogenic expansion. This evaluation was performed within the context of the existing standard of care for GBM, encompassing Temozolomide (TMZ) and Radiotherapy. Our results unveiled striking insights into the potential of PDT as an innovative therapeutic strategy. Notably, Ox5 cells exhibited a remarkable reduction in viability, exceeding 70%, following exposure to PDT with 410 nm light and 5-ALA at a concentration of 50µM. A similar, albeit slightly less profound, effect was observed in G7 cells, with a viability decrease of more than 53%. These outcomes, meticulously quantified through the MTT viability assay (n=4), were reinforced by statistical significance, as indicated by p-values falling below 0.05 and, lower 0.001. Furthermore, clonogenic assays employing G7 cells provided an additional layer of evidence, demonstrating a substantial inhibition of clonogenic potential following PDT treatment with 410 nm light and 5-ALA. Immunohistochemistry techniques, particularly focusing on the cleaved caspase-3 marker, in both Ox5 core and G7 cells, underscoring the mechanistic basis of the observed cell death. In stark contrast, the conventional standard of care, involving TMZ monotherapy, was tested, and the results across four biological replicates were less significant. The relative viability of Ox5 and G7 cells exhibited no statistical significance, with p-values exceeding 0.05, implying a limited impact of this regimen on cell viability. Moreover, clonogenic assays conducted under the standard of care protocol (TMZ+/-Radiotherapy) unveiled the persistence of colonies, even at higher radiation doses of 4 and 6 Gy.In summary, PDT, specifically when implemented with 410 nm light and 5-ALA, represents a breakthrough strategy that leads to substantial cell death in both Ox5 and G7 cells. This compelling alternative therapy shines a hopeful light on the horizon of GBM treatment, providing a potentially transformative approach that can augment the current standard of care.

#7595 PRMT5 inhibitor synergizes with PARP inhibitors in triple-negative breast cancer cells.

S. Suresh, L. A. McPherson, J. M. Ford;
Stanford University School of Medicine, Stanford, CA

Background: Treating triple-negative breast cancer (TNBC) patients, an aggressive subtype of breast cancer, is an ongoing clinical challenge. Small-molecule inhibitors targeting the poly ADP-ribose polymerase (PARP) DNA repair enzymes, have been approved for treating only a subset of TNBC patients with a specific genetic landscape (*BRCA1* mutation). However, TNBC patients with wildtype *BRCA1 (BRCA1^{WT})* are still lacking targeted therapy and chemotherapy remains their main treatment strategy. High expression of protein arginine methyltransferase 5 (PRMT5) is linked to poor prognosis in breast cancer and PRMT5 alone or via its interacting proteins plays an oncogenic role in breast cancer. Recent evidence suggests that PRMT5 is a key player in regulating the repair of DNA double strand breaks (DSBs) either through homologous recombination (HR) or non-homologous end joining (NHEJ) depending on the PRMT5 expression level within the cell. This dependency of cancer cells on PRMT5 expression levels in deciding the repair pathway of choice can be exploited for developing therapies. We hypothesize that in *BRCA1* wildtype TNBC cells, inhibiting PRMT5 activity will force the cells to rely on NHEJ rather than HR to repair DNA DSBs, and introducing PARP inhibitors in this setting will inactivate NHEJ as well, causing synthetic lethality and cell death. In this study, we evaluated the pre-clinical benefit of combining PARP inhibitors with a PRMT5 inhibitor in TNBC cells.

Methods: Human TNBC cell lines with wildtype *BRCA1* (MDA-MB-468, HCC1806) and mutant *BRCA1* (MDA-MB-436, SUM149-PT) were treated with varying doses of two PARP inhibitors (Olaparib, Talazoparib) and a PRMT5 inhibitor (GSK3326595) as single agents or in combination. MTT-based cell viability assay was used to determine cytotoxicity of the treatments. mRNA expression was determined by RT-qPCR after drug treatment.

Results and Conclusion: We report that PRMT5 inhibition synergizes with both Olaparib and Talazoparib, to potentiate cell death in two *BRCA1^{WT}* but not in *BRCA1^{mut}* TNBC cell lines. Furthermore, we show that inhibiting PRMT5 in *BRCA1^{WT}* cells upregulates the mRNA expression of *RAD50*, a DNA damage sensing gene in the HR pathway. Our ongoing study is to delineate the molecular mechanism of action for the observed synergy and whether PRMT5 inhibition can overcome resistance to PARP inhibitors. Through this study, we will identify a novel treatment strategy for the majority of TNBC patients (*BRCA1^{WT}*) who currently lack targeted therapies.

#7596 (TTFields) and imipridone ONC206 co-treatment inhibits p-AKT and spheroid growth and upregulates caspase-10 in human GBM cell lines.

V. Tajiknia, P. Srinivasan, M. Pinho-Schwermann, W. MacDonald, C. Purcell, W. El-Deiry;
Legorreta Cancer Center at Brown University, Providence, RI

Background: Glioblastoma (GBM) is the most common primary brain malignancy with dismal prognosis. Tumor Treating Fields (TTFields) therapy is available for the treatment of both newly diagnosed and recurrent glioblastoma and represents a new category of treatment modalities in oncologic therapy. Despite decades of study, few FDA approved modalities are available for GBM and provide limited survival improvements for patients. AKT functions as a key serine/threonine kinase in the RTK/PTEN/PI3K pathway, and extensive genomic analysis of GBM has revealed that this pathway is mutated in a significant majority of GBM cases. Activation of this pathway ultimately leads to the activation of AKT, and p-AKT levels are elevated in the majority of GBM tumor samples and cell lines. Studies have shown that increased p-AKT levels contribute to uncontrolled growth, resistance to apoptosis, and enhanced invasive capabilities of glioma cells, which are characteristics of tumor progression in GBM. AKT serves as a critical hub in this pathway, enabling the amplification of growth signals, thereby making the inhibition of AKT an appealing and promising therapeutic target for treating GBM. Imipridone ONC206 is under clinical development for treatment of pediatric and adult patients with primary brain tumors (NCT04732065 and NCT04541082). Here we show inhibition of p-AKT as well as upregulation of CHOP and caspase-10 following cotreatment of ONC206 and TTFields.
Materials & Methods: We investigated the effect of ONC206 (at IC50s) plus TTFields in U251 and T98G human GBM cell lines at different time points. Effect of treatment on cPARP, BCL-2, CHOP, caspase-10, and p-AKT were investigated using western blot. Neurospheres were generated using mentioned cell lines and used for investigating effect of co-treatment on 3D structure.
Results: Treatment with ONC206 at the IC50 in T98G cells with TTFields at 24h showed synergistic upregulation of cPARP as well as inhibition of BCL-2. At 96hour time point, inhibition of p-AKT was observed following all treatments (ONC206, TTFields, and co-application compared to control. In U251 cells, following treatment of ONC206 and TTFields, inhibition of BCL-2 was observed at 24h time point at all treatment conditions. Upregulation of CHOP and Casapse-10 at 96h time point was seen, as well as inhibition of p-AKT. Spheroid models showed structure disruption and growth arrest following combination treatment.
Conclusion: Here we showed cotreatment results in inhibition of p-AKT, the key node in GBM growth pathway. Also, the upregulation of CHOP and caspase-10 that has not been discussed before can be the key to focus on novel therapeutic targets for GBM More studies are needed to elaborate the exact mechanism of synergy but these new findings can be used to develop novel treatment combination

#7597 Therapeutic potential of ketogenic diet as an adjuvant to lenvatinib treatment in hepatocellular carcinoma.

M. Zhang[1], T.-W. Lee[2], S. Ma[3], M. Tong[1];

[1]Chinese University of Hong Kong (CUHK), Hong Kong, Hong Kong, [2]The Hong Kong Polytechnic University, Hong Kong, Hong Kong, [3]The University of Hong Kong, Hong Kong, Hong Kong

Hepatocellular carcinoma (HCC) has been a major public health concern worldwide for decades because of its high mortality rates and poor prognosis, which are attributable to frequent tumor relapse and limited treatment regimens. Lenvatinib is one of the tyrosine kinase inhibitors approved for first-line treatment of advanced HCC, but its efficacy remains modest. Growing evidence suggest that the unsatisfactory survival benefits of lenvatinib could be attributed to the acquired drug resistance developed in HCC patients. In this study, we aim to explore the intrinsic metabolic vulnerability which could be exploited to enhance the treatment efficacy of lenvatinib in HCC. Our previous study showed that loss of tyrosine catabolism accompanied with a reduced downstream ketone metabolite beta-hydroxybutyrate (BHB) supports HCC initiation. To explore the therapeutic value of BHB in potentiating lenvatinib treatment in HCC, tyrosine catabolism-suppressing HCC cells were treated with BHB. We found that BHB treatment suppressed cell proliferation, increased cellular reactive oxygen species and potentiated the efficacy of lenvatinib treatment. Similar tumor-suppressive effect was observed when BHB was administered in vivo in mice bearing HCC patient derived xenograft. Combination treatment of lenvatinib and ketogenic diet which induces BHB level could drastically attenuate tumor development in immunocompetent mice bearing hepatic tumors. This study presents a potentially translatable combination treatment regimen to potentiate the therapeutic efficacy of lenvatinib in advanced HCC.

#7598 The novel eIF4A inhibitor potently synergizes with BCL2 inhibitor in high grade B-cell lymphoma with MYC and BCL2 rearrangements through regulating UPR.

So-Young Seol[1], Chung Hyun Park[2], Soo Jeong Kim[2], Haerim Chung[3], Hyunsoo Cho[3], Jin Seok Kim[3], Yu Ri Kim[1]

[1]Gangnam Severance Hospital, Yonsei University College of Medicine, Seoul, Korea, Republic of,[2]Yongin Severance Hospital, Yonsei University College of Medicine, Seoul, Korea, Republic of,[3]Severance Hospital, Yonsei University College of Medicine, Seoul, Korea, Republic of

Double hit lymphoma(DHL) is defined to be a chromosomal break with MYC gene combined with BCL2 or BCL6. MYC is an oncogene which proliferation the cells and BCL2 inhibit cell death. These combinations could be a cause of highly aggressive clinical features and poor survival of DLBCL. The WHO-HAEM5 renames the entity DLBCL/high-grade B-cell lymphoma with MYC and BCL2 rearrangements. Despite the dismal prognosis, no widely accepted standard treatment exists to the management of DHL. Therefore, new therapeutic approaches for these patients are urgently needed. Previously, we looked at the eIf4A inhibition was shown to downregulate MYC expression in lymphoma cell lines. Venetoclax, a highly selective inhibitor of BCL2, shows clinical activity for patients with DLBCL although there are concerns about increasing toxicity. Our hypothesis in the following: If eIF4A inhibitor preferentially inhibit the translation of oncogenes such as cMyc and venetoclax inhibit the BCL2 in DHL, then the combination of eIF4A inhibitor and BCL2 inhibitor will be highly effective for DHL and potentially safe for animals and humans. We tested the anti-lymphoma effect of CR-1-31-B, in combination with Venetoclax in lymphoma cell lines using flow cytometry. We performed cell apoptosis assays in increasing concentrations of Venetoclax, CR-1-31-B and a combination of the two drugs at 48 hours. To better understand molecular mechanisms underlying the observed synergistic effect in DLBCL-DHL, RNA-seq profiling was performed on cells treated with single drugs and their combinations, respectively. Venetoclax and CR1-31-B exhibited concentration and time dependent cytotoxicity in lymphoma cell lines at low nanomolar concentrations. Overall, the combination of eIF4A inhibitor and BCL2 inhibitor showed synergy in all kinds of DLBCL cell lines. Especially DHL cell lines were more sensitive to the drug combination and showed enhanced synergy compared to the non-DHL cell lines(p<0.0001). We analyzed RNA-seq profiling of cells treated with single drugs and their combinations and found that the transcriptional signature of the synergistic combination was unique relative to that of either constituent monotherapy. Gene set enrichment analysis was performed in the DHL and non-DHL group. The analysis demonstrates that known Unfolded protein response(UPR) part and metabolism, are enriched in DHL groups. This suggests that the UPR and metabolism pathway are closely related to the combination effect in DHL. These findings suggest that the combination of eIF4A inhibitor and BCL2 inhibitor have potent pharmacological activity in DHL lines, it was closely related with UPR. These combination is promising and novel treatment for high-grade B-cell lymphoma with MYC and BCL2 rearrangements. Further pre-clinical investigations of this combination for these patients are needed.

#7599 Evaluate the treatment efficacy of magnolol combined with cisplatin in non-small cell lung cancer.

R.-E. Lu[1], B.-X. Chen[1], F.-T. Hsu[1], I.-T. Chiang[2];
[1]China Medical University, Taichung, Taiwan, [2]Show Chwan Memorial Hospital, Changhua, Taiwan

Lung cancer is one of the five most common cancers in the world. Statistics indicate that approximately 80% to 90% of lung cancer cases fall under the classification of non-small cell lung cancer (NSCLC). For several decades, non-small cell lung cancer (NSCLC) has often been treated with chemotherapy drugs. However, lung cancer has high incidence and recurrence rates, mainly due to drug resistance and side effects during chemotherapy and radiotherapy. This is the hinder problem in the treatment of NSCLC, which highlight the necessity of developing new drugs or new treatments for NSCLC. Cisplatin is a chemotherapy drug that can treat about 50% of solid tumors, but the cisplatin-induced cytoprotective autophagy is the resistance to clinical treatment. It is urgent to elucidate the underlying molecular mechanisms regulating cisplatin resistance to improve its therapeutic value in lung cancer. Magnolol is a phenolic component isolated from the roots and bark of *Magnolia officinalis* and is used in traditional Chinese medicine. With a wide range of pharmacological activities, various studies have focused on the anti-cancer properties of magnolol in recent years. The effect of the drug is to keep cells in the G2/M phase, induce mitochondrial dysfunction and ROS production, affect the supply of cellular energy, and then lead to cell apoptosis. In this study, we investigated the ability of magnolol enhance cisplatin-induced cytotoxicity, showing dose dependence in NSCLC cell by MTT assay. We utilized the immunofluorescence staining and western blotting assay to confirm the downgrade expression of LC3B and the upregulate expression of p62 that define magnolol is able to suppress cisplatin-induced cytoprotective autophagy in NSCLC. We also detected the extrinsic/intrinsic apoptosis induction ability of magnolol combined with cisplatin in NSCLC. In the result, the cisplatin combined with magnolol have more significantly triggered the loss of mitochondrial membrane potential, and activate more protein cleaved caspase-3, -8 and -9 than monotherapy. We also used western blotting assay to confirm the expression of apoptosis inhibitory protein Bcl-2 and pro-apoptotic protein Bax to measure the degree of apoptosis. The migration and invasion effects of magnolol and cisplatin were identified by transwell invasion and wound healing on NSCLC. The magnolol combined with cisplatin extended the mouse survival rate and can inhibit tumor progression. These results suggest that combinational therapy of cisplatin and magnolol could be a promising treatment strategy for NSCLC. The potential regulation of magnolol on NSCLC is associated with triggering cisplatin-induced apoptosis and diminishing cisplatin-induce cytoprotective autophagy.

#7600 Synergy of ZEN3694 and VIP152 for dual transcriptional targeting of BET and CDK9 in patient derived organoid models of pancreatic cancer.

L. J. Koeppel[1], A. Stram[1], R. J. Millikin[2], E. Riedl[1], M. Hossan[1], E. Lin[1], R. Stewart[2], J. D. Kratz[1];
[1]UW Madison, Madison, WI, [2]Morgridge Institute, Madison, WI

Background: Pancreatic ductal adenocarcinoma (PDAC) remains a leading cause of cancer related mortality in the United States, largely due to ineffective systemic therapy. While novel KRAS target strategies are in development, few agents have been investigated to target the transcriptional machinery for global inhibition of expression. Recent small molecule inhibitors targeting transcription (i.e., CDK7) have shown preliminary evidence of disease control; however, combination therapies have lagged, likely due to uncertainty in clinical toxicity. Text mining analysis suggests combination BET and CDK9 inhibition may be promising against PDAC. Here, we present preclinical evidence of synergistic activity for the combination of bromodomain and extraterminal (BET) inhibitor (ZEN3694) and CDK9 inhibitor (VIP152) using patient derived cancer organoids (PCOs).
Methods: Dose response curves were generated for ZEN3694 and VIP152 to assess their single agent activity against PCOs using a low volume format. ZEN3694 was treated continuously while VIP152 was removed after 24h to mimic pharmacokinetics with assay endpoint at 144h. Synergy assays were designed using a combination dose titration grid. Viability was determined in all assays using 3D CellTiter Glo (CTG, 50% v/v). Synergy scores were produced using SynergyFinder 3.0 including Zero Interaction Potency (ZIP), Bliss Independence (Bliss), Highest Single Agent (HSA), and Loewe Additivity (Loewe). Western blot analysis was performed against global markers of active RNA polymerase II (phosphorylation at serine 2, 5, 7) and antiapoptotic protein, BCL xL, and MCL 1.
Results: ZEN3694 was observed to have a single agent IC_{50} in the single uM range across 3 independent PDAC PCO lines (PDAC1 3.7uM, PDAC2 1.1uM, PDAC3 2.9uM). VIP152 showed significant potency in the same 3 PDAC PCO lines (PDAC1 140.2nM, PDAC2 30.5nM, PDAC3 43.4nM). The combination of ZEN3694 and VIP152 was found to have increased therapeutic activity with double digit synergy scores across all reference models: PDAC1 (Loewe 17.3, HSA 19.8, ZIP 20.2, and Bliss 17.2) and PDAC2 (Loewe 34.7, HSA 28.3, ZIP 19.7, and Bliss 19.6). Western blots of protein collected from organoids treated for 48h showed on target activity, including decrease in the phosphorylation of Rbp1 (Ser 2, Ser 5, and Ser 7) compared to both control and single agents and decreased expression in antiapoptotic proteins (MCL 1 and BCL xL).
Conclusion: Here, we show the activity of dual transcription targeting with BET and CDK9 inhibition in patient derived pancreatic cancer organoid models. The combination of ZEN3694 and VIP152 has i*n vitro* synergy in PDAC PCO models with on target activity. Ongoing work is validating this combination in animal models to assess toxicity, *in vivo* activity, and RNA expression profiling to understand transcriptional pathway dependency and therapeutic resistance.

#7602 Discovery of GH1581, a potent and selective WRN inhibitor as a cancer therapy.

J. Li, G. Zhang, **J. Li**;
Suzhou Genhouse Bio Co., Ltd., Suzhou, China

Defects in DNA mismatch repair (MMR) proteins could induce damage of genome, resulting microsatellite instability (MSI). MSI is highly correlated with the occurrence of several types of cancers, mainly in colon, gastric, endometrial, and ovarian cancers. Despite advances in the treatment of MSI-high cancers, tumor evolution and drug resistance remain the leading causes of treatment failure and death in cancer patients. About 50% MSI cancers have no response to immune checkpoint inhibitors. There is still unmet needs to be fulfilled for MSI-high patients. WRN is a RecQ family helicase involves in genome stability maintenance, DNA repair, replication, transcription, and telomere maintenance. Recent studies have identified WRN as a synthetic lethal target of MSI-high cancers. Employing structure-based drug design strategy, we have discovered a potent and selective WRN inhibitor, GH1581. *In vitro*, GH1581 displayed specific < 10 nM potency in ADP-Glo assay and < 10 nM potency in cell proliferation assay using MSI cancer cell lines. *In vivo*, GH1581 demonstrated favorable pharmacokinetic properties in different species. In SW48 xenograft model, it inhibited the tumor growth with 100% TGI at QD dosing of 10 mg/kg without severe adverse effect on body weight. In summary, we discovered GH1581 as a novel inhibitor of WRN with high *in vitro* and *in vivo* efficacy.

#7603 Targeting MTAP-deleted tumor via synthetic lethality with a combination of a PRMT5i and an MAT2Ai.

G. Zhang, J. Li, **J. Li**;
Suzhou Genhouse Bio Co., Ltd., Suzhou, China

MTAP (methylthioadenosine phosphorylase) is located adjacent to the tumor-suppressor gene CDKN2A (cyclin-dependent kinase inhibitor 2A) and sometimes co-deleted in 10-15% of all cancers, especially in glioblastoma, mesothelioma, and pancreatic cancers. Recent studies shown that MTAP deletions in cancer create vulnerability to synthetic lethal with the MAT2A/PRMT5/RIOK1 axis. Herein, we report the discovery of a PRMT5 inhibitor GH56, and an MAT2A inhibitor GH31, both showed promising single agent efficacy and synergy in MTAP loss tumor models. GH56 is an MTA-Cooperative PRMT5 inhibitor. *In vitro*, GH56 showed potent SDMA inhibition in MTAP-deleted cancer cells with an IC_{50} from 0.8–3 nM. It also showed excellent selectivity with more than 100-folds in MTAP-WT cells. In a cell panel with more than 100 cell-lines, GH56 selectively inhibited the growth of cells with MTAP-deletion while separated the cells with MTAP-WT. In the safety panel and kinase panel, GH56 all showed good selectivity. In addition, GH56 had an IC_{50} > 10 μM for hERG. *In vivo*, GH56 showed dose-dependent efficacy in a series MTAP-deleted models and were well tolerated. In U87MG glioblastoma CDX model, NCI-H838 NSCLC CDX model, BXPC-3/HupT4 PDAC CDX models and RT112-84 BLCA model, TGI for GH56 at high dose were all >100%. On the other hand, GH31 is a potent and selective MAT2A inhibitor. GH31 also showed excellent selectivity with MTAP-deleted and MTAP-WT cell lines. The combination of GH56 and GH31 showed synergy both *in vitro* and *in vivo*. The low dose GH31 combination with low-dose GH56 achieved the similar efficacy as high dose GH56 and a more rapid tumor regression. In view of the delayed onset of the tumor response and high dose needed by PRMT5 inhibitor (reported by clinic stage compounds), the combination of PRMT5i and MAT2Ai will be advantageous. Furthermore, both GH56 and GH31 are brain penetrant, especially for GH31, with a K_{puu} > 0.6 and B/P > 2. The combination of GH56 and GH31 in a brain metastasis model and a glioblastoma *in situ* model all showed strong synergy, demonstrated the potential for the treatment of glioblastoma and other cancer with brain metastasis. In summary, we discovered potent, selective and brain penetrant PRMT5 inhibitor GH56 and MAT2A inhibitor GH31. Both compounds are currently under evaluation in IND-enabling studies and will provide more options for MTAP-deleted cancers.

CLINICAL RESEARCH: Predictive Biomarkers 7
Poster Session

#7607 Single-cell genomics study before and after neoadjuvant therapy for triple-negative breast cancer.
Y. Shao, K. Xu;
Zhejiang University School of Medicine, Hangzhou, China

Breast cancer has become the most common malignant tumor globally. Neoadjuvant chemotherapy (NAC) has become an important treatment option for locally advanced breast cancer, capable of eliminating circulating tumor cells (micrometastases) and achieving downstaging objectives. However, even after completing neoadjuvant chemotherapy or receiving local treatment, some patients may still have residual lesions, which are a key factor in distant recurrence and metastasis. The existing clinical biomarker tests such as CEA, CA-153, and imaging methods are unable to accurately assess the condition early on. Although tissue pathology biopsy of tumor specimens is the gold standard for clinical pathological diagnosis, it also has certain limitations. Traditional high-throughput sequencing technology for breast cancer primarily identifies "driver genes" associated with the occurrence and development of breast cancer. However, it has limitations in identifying genomic structural changes and subclones of breast cancer, and it overlooks the heterogeneity among tumor cells. The emergence of single-cell RNA sequencing (scRNA-seq) technology can detect these heterogeneous individuals, decode the heterogeneity of breast cancer cells, refine molecular subtypes, and open up new pathways to overcome drug resistance. We collected samples from 6 patients with locally advanced triple-negative breast cancer (ER-, PR-, HER2-negative, defined as HER2 immunohistochemistry 0, 1+ or 2+ but FISH-negative). We compared the cell subgroups and their gene expression in biopsy specimens before neoadjuvant chemotherapy with those in post-treatment specimens obtained during surgery, analyzing changes in cell composition in the tumor microenvironment before and after immunotherapy to identify specific cell types potentially contributing to the outcome of immunotherapy, particularly cell subtypes associated with T-cell clonal proliferation. We found that in the group with good neoadjuvant treatment response (Miller-Payne grade 4-5), B cells, CD4+ T cells, CD8+ T cells, and Tregs cells were all significantly downregulated, while endothelial cells and aSMA-positive fibroblast cells were significantly upregulated. By comparing changes in the immune microenvironment between patients with and without T-cell clonal proliferation before and after treatment, we revealed the differentiation patterns of various immune cells in immunotherapy and potential mechanisms of action.

#7608 Exploring the efficacy of atezolizumab plus bevacizumab for advanced hepatocellular carcinoma in relation to tumor-infiltrating lymphocytes.

H. Kanzaki[1], T. Ishino[1], S. Ogasawara[1], S. Yumita[1], M. Nakagawa[1], R. Kojima[1], K. Koroki[1], M. Inoue[1], K. Kobayashi[1], N. Kanogawa[1], S. Kiyono[1], M. Nakamura[1], T. Kondo[1], S. Nakamoto[1], T. Takayashiki[1], J. Lin[2], M. Kawazu[2], M. Komuta[3], J.-i. Ikeda[1], M. Ohtsuka[1], Y. Togashi[4], N. Kato[1];
[1]Graduate School of Medicine, Chiba University, Chiba, Japan, [2]Chiba Cancer Center Research Institute, Chiba, Japan, [3]International University of Health and Welfare, School of Medicine, Narita Hospital, Chiba, Japan, [4]Graduate School of Medicine, Dentistry and Pharmaceutical Sciences, Okayama University, Okayama, Japan

Background and Aims: Bevacizumab, an anti-angiogenic agent, is reported to enhance antitumor immunity through various mechanisms, including the suppression of regulatory T (Treg) cells. Additionally, a combination therapy involving the anti-PD-L1 monoclonal antibody, atezolizumab, plus bevacizumab (AtezoBev) has emerged as a standard treatment for advanced hepatocellular carcinoma (aHCC). Given that more than half of treated patients do not respond effectively, identifying biomarkers predictive of clinical efficacy has become an urgent matter. However, the investigation into the tumor microenvironment (TME) has been lagging in aHCC compared to other malignancies due to the difficulty in obtaining tumor samples just before the commencement of systemic therapy.
Methods: We have established a scheme to analyze the TME by obtaining tumor samples immediately before AtezoBev administration, and explored the relevance to its efficacy, focusing on the tumor-infiltrating lymphocytes (TILs) within those samples. Tumor samples from 94 aHCC patients were collected before AtezoBev administration. TME was assessed in 54 patients via flow cytometry and in 72 patients through RNA sequencing, with certain samples undergoing both analyses.
Results: Predominant etiologies in 94 patients were HCV (n=22, 23%), followed by HBV (n=17, 18%), and alcohol abuse (n=16, 17%). The objective response (OR) and disease control rates were 17% and 81%, respectively, with a median progression-free survival (PFS) of 7.6 months. Groups exhibiting high PD-1 positivity of CD8+ T cells (median values as cutoffs) demonstrated superior AtezoBev treatment effects (PFS: 13.1 vs. 4.4 months, p=0.001). In contrast, PD-1 positivity of effector Treg (eTreg) cells in TILs, which reportedly can be one of resistant mechanisms to PD-1 blockade therapy (Togashi Y, et al. Nat Immunol 2020), was not correlated with efficacy. Gene set enrichment analysis highlighted the importance of antigen presentation for OR in groups exhibiting high PD-1 positivity of CD8+ T cells. Additionally, HLA class I expression was elevated in patients achieving an OR. Although previous studies suggest that immunotherapy efficacy could be reduced in non-alcoholic steatohepatitis-related HCC compared with viral-related HCC, no clear association was found between PD-1 positivity of CD8+ T cells or eTreg cells in TILs and etiology. Among the 94 patients, samples from 11 were analyzable at the point of AtezoBev refractoriness, revealing a trend toward reduction in PD-1 positivity of eTreg cells in TILs.
Conclusions: Our findings suggest a correlation between the efficacy of AtezoBev for aHCC and the presence of PD-1+CD8+ T cells within the tumor. In contrast, PD-1+ eTreg cells did not induce resistance along with a trend toward reduction after the treatment possibly due to combination with bevacizumab.

#7609 Potential gene expression meta-signatures predict neoadjuvant chemotherapy response in invasive breast cancer.

H. M. M. Guevara-Nieto[1], R. S. Parra-Medina[1], J. Zabaleta[2], L. Lopez-Kleine[3], A. L. Combita[1];

[1]Instituto Nacional de Cancerologia, Bogota, Colombia, [2]Louisiana State University Health Science Center, New Orleans, LA, [3]Universidad Nacional de Colombia, Bogota, Colombia

Early prediction of Neoadjuvant Chemotherapy (NAC) response is crucial for women with locally advanced breast cancer (BC), given their low response rates. This study aims to identify gene expression patterns and tumor microenvironment (TME) characteristics associated with resistance to NAC, which could significantly impact tumor progression and treatment outcomes. The study encompassed differential gene expression comparing non-responders and responders, enrichment analysis, tumor microenvironment estimation, and cytokines identification from a female patient's cohort with distinct molecular subtypes and candidates to NAC at the Colombian National Cancer Institute. Candidate differentially expressed genes validated with RT-PCR in a larger validation cohort and corroborated in several publicly available databases, including associated treatment drugs. Distinct gene expression profiles were observed between responders and non-responders, emphasizing immune system-related pathways such as IL-17 signaling, B cell receptor signaling, complement and coagulation cascades, natural killer cell-mediated cytotoxicity, and NF-kB signaling. Immune-related genes (AGTR1, APOD, CCL19, CGA, ECEL1, NPY1R, NTNG1, PCSK1, PFDN2, S100B, TPRG1, WDR5B, ZNF385B) were identified as biomarkers correlated with non-response and worse prognosis. Responders showed increased B cell populations, CD4+ and CD8+ effector memory T-cells in lymphoid groups, while non-responders displayed elevated levels of CD8+ naive T-cells. Additionally, responders revealed upregulated myeloid cell populations like macrophages and dendritic cells. Several cytokines like IL1B, IL-2, IL-4, IL-12, IL-21, IL-22, IL-36, and TWEAK showed elevated expression in non-responders. Dexamethasone, Vinblastine, and Streptozocin were candidate drugs that interacted with AGTR1, CGA, and S100B, respectively and are associated with progression and metastasis. Logistic regression revealed that overexpression of CGA showed a higher probability (OR:1.83, p=0.03) while ECEL1 had a lower probability (OR=0.44, p=0.04) in non-responders compared to responders who lacked expression of these genes. Immune-related genes and various subtypes of immune cells within the TME exhibit correlations with response to NAC, and several cell fractions significantly changed before and after NAC. These results suggest meta-signatures that warrant further evaluation as concordance assessment between immunohistochemistry (IHC) and gene expression profiling, in addition to an extensive validation to triage patients before NAC and target personalized interventions. Detection and evaluation of TME components are essential to predict NAC efficacy and avoid disease relapse. Finally, these findings emphasize the importance of assessing admixed populations to facilitate novel findings and alleviate disparities.

#7610 Predictive biomarkers for immuno-chemotherapy response in biliary tract malignancies.

Michele Zanoni[1], Tania Rossi[1], Martina Valgiusti[1], Giuliano La Barba[2], Michela Cortesi[1], Sara Bandini[1], Giulia Bartolini[1], Alessandra Dubini[3], Paolo Di Gioia[2], Chiara Gallio[1], Luca Esposito[1], Alessandra Virga[1], Giorgia Gurioli[1], Sara Bravaccini[1], Giovanni Martinelli[1], Paola Ulivi[1], Giovanni Luca Frassineti[1], Giorgio Ercolani[2], Ilario Giovanni Rapposelli[1]

[1]IRCCS Istituto Romagnolo per lo Studio dei Tumori (IRST) "Dino Amadori", Meldola, Italy,[2]Department of General and Oncologic Surgery, Morgagni-Pierantoni Hospital, Forli, Italy,[3]Department of Pathology, Morgagni-Pierantoni Hospital, Forli, Italy

Background: Biliary tract cancers (BTCs) refer to invasive malignancies of the biliary tree. Lack of specific symptoms in early-stages frequently leads to late-stage diagnosis, reducing therapeutic options. Surgical resection remains the only curative option for early-stage disease; instead, patients with advanced disease usually receive chemotherapy (cisplatin plus gemcitabine) in combination with durvalumab as first-line treatment and mFOLFOX-6 as second-line, but effects are limited and only a small proportion of patients respond to treatment. Recent advances in molecular characterization of BTCs allowed the identification of several alterations (e.g. IDH1/2 mutations, FGFR2 rearrangement) for which targeted agents are now available in second line setting but only for a small subset of patients. However, prognosis for patients with advanced stage disease remains poor. Treatment failure depends on several factors such as intra- and inter-tumor heterogeneity and the complex immunological landscape. Therefore, the identification of predictive biomarkers able to individuate patients that will benefit from immuno-chemotherapy will be crucial.

Methods: BTC patients at any stage were enrolled in two arms: A) BTCs undergoing surgery; B) advanced/relapsed BTCs. For this study, patients belonging to arm B were selected, in particular those who received first-line immuno-chemotherapy. Blood samples were collected before and after three months of therapy. Ascites samples were collected for patients with advanced disease who underwent paracentesis during therapy. DEPArray NxT (Menarini Silicon Biosystems) was used for phenotypic analysis and single ascites-derived cell isolation. The Ampli1 Lowpass kit was used for copy number aberration (CNA) profiling. Extracellular vesicles (EVs) were isolated from plasma at baseline and after three months of immuno-chemotherapy by size-exclusion chromatography and analyzed for size distribution and concentration using Nanosight NS300. Surface EV markers were analyzed by flow cytometry using the MACSPlex Exosome Kit human (MiltenyiBiotec).

Results: We enrolled 43 patients starting from August 2022: 14 in arm A and 29 in B. 23 patients from arm B received immuno-chemotherapy and 3 underwent paracentesis during therapy. Patient-derived organoids (PDOs) were successfully established from tumor cells recovered from ascites of these patients. Epithelial cells recovered from ascites displayed aberrant CNA profiles with gains in chromosomes 1q, 8q, 10, 12p, 20, and losses in 1q, 3q, 4, 8q, 9 and X. EV size distribution and concentration were similar before and after treatment as well as surface markers exposure. Further analyses in correlation with clinical features of patients will be performed.

Conclusions: Our approach will contribute to identify potential predictive factors associated with response/resistance to immuno-chemotherapy in BTCs.

#7611 Circulating blood RNAseq detects activation of immune system and predicts response to immunotherapy in bladder cancer.

C. Richard[1], S. Chevrier[1], A. Marabelle[2], **R. Boidot[1]**;
[1]Ctr. Georges-Francois Leclerc, Dijon, France, [2]Gustave Roussy Institute, Villejuif, France

Background: Anti-PD(L)1 immunotherapies have revolutionized oncology by getting durable tumor responses in advanced cancers. Nevertheless, currently approved biomarkers (PD-L1, MSI, TMB) have suboptimal positive/negative predictive values for tumor responses and survival.
Aims & Methods: We sought to assess the value of gene expression on circulating blood to predict responses to immunotherapy. We performed total paired-end RNAseq at 20-million reads and analyzed differential gene expressions according to cancer outcomes on baseline frozen whole blood from a cohort of 186 patients prospectively enrolled in the IOPREDI study, a French ancillary cohort of the international multi-center STRONG Phase III trial testing the anti-PD-L1 durvalumab in advanced bladder cancers (NCT03084471).
Results: One hundred and sixty four out of the 186 baseline samples generated valuable blood transcriptome data. Thanks to mathematical corrections, all samples were normalized, and the analysis was possible without introducing any bias despite the sample origin from 16 enrolling sites. We first observed that patients with a complete or partial response or a stable disease overexpressed 19 genes, 5 of which are markers of immune cell activation: *CXCL8*, *EOMES*, *GBP5*, *GZMA*, *and GZMH*. Conversely, patients with a progressive disease overexpressed 11 genes including *CD177*, a marker of neutrophil cells, recently associated to immunotherapy resistance. Next, patients with a PFS > 3 months showed an overexpression of 25 genes associated with immune cells activation such as *CD8A*, *CXCL8*, *EOMES*, *FASLG*, *GZM* genes, whereas patients with a shorter PFS highly expressed genes of immune cell inhibition: *CD177*, *CD300LG*, *CD99*, and *CST7*. Finally, patients with an OS > 7 months had also a higher expression of the same previous genes completed with 6 other genes, still indicators of immunity activation (*CD3D*, *CD3E*, *CD3G*, *GZMM*, *IL2RB*, *and PTGDS*).
Conclusion: Total RNAseq from RNA directly extracted from whole blood can detect baseline activation of T-cells in patients who will subsequently benefit from anti-PD-L1 immunotherapy. This work shows that RNAseq can detect an immune activation state in circulating blood without specific cell selection. This technique could be used in clinical trials to select for patients prone to benefit from cancer immunotherapies.

#7612 Genetic predictors of anti-PD(L)-1 therapy response in hepatocellular carcinoma.

S.-C. Chen, N.-J. Chiang, M. Chen, M.-H. Yang;
Taipei Veterans General Hospital, Taipei, Taiwan

Introduction: Immunotherapy targeting PD-1/PD-L1 shows promise in treating hepatocellular carcinoma (HCC), but standard predictors like PD-L1 expression are unreliable for gauging treatment response. RNA sequencing has identified a BMS 4-gene inflammatory signature that could more accurately forecast clinical outcomes. However, genomic alterations and tumor mutational burden (TMB) haven't consistently predicted anti-PD(L)-1 therapy response in HCC. Therefore, the aim of this research is to identify potential genetic alternation that could serve as predictive marker for anti-PD(L)-1 therapy responses in advanced HCC.
Methods: Formalin-fixed paraffin-embedded (FFPE) tumor tissues from 38 HCC patients were analyzed using targeted next-generation sequencing with the ACTOnco™ panel before anti-PD(L)-1 therapy. This analysis identified somatic variants across 440 genes and calculated TMB. In silico tools like NetMHC and IEDB predicted neo-peptide-HLA class I binding affinity. Additionally, peripheral blood mononuclear cells provided germline data for paired TMB calculations, with tumor responses assessed by RECIST criteria.
Results: Within a cohort of 167 patients with HCC undergoing ICI therapy, 35 (20.9%) responded to treatment, while 132 (79.1%) did not. Available formalin-fixed paraffin-embedded (FFPE) samples from this population included those from 14 responders and 30 non-responders. After conducting quality control measures, which assessed tumor purity, DNA quantity and integrity, as well as sequencing quality, 13 samples from responders and 25 from non-responders qualified for further analysis. Gene alteration analysis identified mutations in TP53 (47%), MUC16 (34%), CTNNB1 (32%), USH2A (16%), ARID1A (13%), NOTCH3 (13%), and ADAMTS16 (11%) of the cases. A TP53 mutation was linked to poor overall survival, whereas mutations in CTNNB1 and the RTK/RAS/RAF pathway did not correlate with clinical outcomes.
The median TMB, predicted at 3.2 ± 4.3 mutations per megabase (muts/Mb), was nominally higher in patients who achieved disease control compared to non-responders (4.6 vs. 3.7 muts/Mb, p=0.53). Utilizing paired TMB analysis, those with disease control exhibited a higher TMB trend than non-responders (6.0 vs. 2.2 muts/Mb, p=0.06). Notably, the 13 cases with MUC16 mutations were associated with a significantly higher predicted TMB (10.0 vs. 3.3 muts/Mb, p=0.0015).
Conclusions: This study suggests that certain genetic alterations, especially TP53 mutations, may have predictive value for the response to anti-PD(L)-1 therapy in HCC. Moreover, an elevated TMB, particularly when associated with MUC16 mutations, seems to be correlated with improved disease control.

#7613 Association of KAT6A expression with clinical outcomes in previously treated HR-positive and HER2-negative metastatic breast cancer.

M. Cristofanilli[1], L. Liu[2], S. Deng[2], X. Huang[2], F. Andre[3], S. Loibl[4], A. DeMichele[5], E. Gauthier[6], Y. Liu[2], N. C. Turner[7];
[1]Weill Cornell Medicine, New York, NY, [2]Pfizer Inc., San Diego, CA, [3]Institut Gustave Roussy INSERM and Universite Paris Saclay, Villejuif, France, [4]German Breast Group, Neu-Isenburg, Germany, [5]University of Pennsylvania, Philadelphia, PA, [6]Pfizer Inc., San Francisco, CA, [7]Royal Marsden Hospital and Institute of Cancer Research, London, United Kingdom

Background: KAT6A is a histone acetyltransferase that regulates gene transcription, cell cycle, senescence and cell differentiation. It is amplified and overexpressed in a subset of breast cancers and may positively regulate ER expression. Gene expression analysis in tumor samples from the PALOMA-3 study was conducted to explore potential associations of KAT6A and related biomarkers with enhanced benefit from the addition of palbociclib (PAL) to fulvestrant (FUL) in HR-positive, HER2-negative breast cancer. **Methods:** The PALOMA-3 trial randomly assigned 521 endocrine pretreated patients with metastatic breast cancer, including those with prior exposure to chemotherapy, to receive PAL+FUL or placebo (PBO) +FUL. Exploratory analysis was conducted on tumor gene expression levels of KAT6A and KAT6B to evaluate their association with the effect of PAL+FUL vs PBO+FUL on progression-free survival (PFS) using Cox proportional hazards regression analysis, with gene expression as a continuous variable or dichotomized by median. Treatment by biomarker interaction effect was also tested. **Results:** In the PALOMA-3 trial, the analyses were conducted in 214 patients (PAL+FUL, 137 patients; PBO+FUL, 77 patients) with baseline tissue profiled, which included 165 patients with prior chemotherapy (PAL+FUL, 101 patients; PBO+FUL, 64 patients). In patients with KAT6A data, a trend of better treatment effect (interaction p = 0.54) was observed in those with low KAT6A mRNA expression (median PFS on PAL+FUL was 11.04 months (m) and PBO+FUL was 3.65 m, HR = 0.52, 95% CI 0.32-0.85, log rank p = 0.008) versus high KAT6A expression (median PFS on PAL+FUL was 13.90 m and PBO+FUL was 11.20 m, HR = 0.66, 95% CI 0.39-1.13, p = 0.126). A treatment effect was observed in patients with prior exposure to chemotherapy who had low KAT6A expression (median PFS on PAL+FUL was 9.53 m and PBO+FUL was 3.66 m, HR = 0.55, 95% CI 0.33-0.94, p = 0.027), while this was not observed in those with high KAT6A expression (median PFS on PAL+FUL was 11.43 m and PBO+FUL was 11.33 m, HR = 1.13, 95% CI 0.61-2.09, p = 0.71), with the interaction p value of 0.12. No treatment difference was detected between treatment arms and expression levels of KAT6B (interaction p values of 0.48 and 0.36 in all patients and in those with prior chemo respectively). Potential interaction of KAT6A with other genes including ESR1 will be discussed. **Conclusions:** Low tumor KAT6A mRNA expression identified patients with relatively greater benefit from addition of PAL to FUL especially in those with prior exposure to both chemo- and endocrine therapies. The data support further investigation of KAT6A and its related biomarkers and their association with CDK4/6 inhibitors and/or endocrine therapy in HR+/HER2-breast cancer patients and to test if a KAT6 inhibitor can enhance CDK4/6 inhibitor and/or endocrine therapy efficacy in tumors with high KAT6A expression.

#7614 Mutations in *MEN1/DAXX/ATRX* are associated with improved progression-free survival in patients with gastroenteropancreatic neuroendocrine tumors receiving peptide receptor radionuclide therapy.

R. Gujarathi, S. Abou Azar, J. Tobias, X. Keutgen, C.-Y. Liao;
University of Chicago, Chicago, IL

Background: Peptide Receptor Radionuclide Therapy (PRRT) using ^{177}Lu-DOTATATE is an effective treatment for metastatic Gastroenteropancreatic Neuroendocrine Tumors (GEP-NETs). However, it remains unknown why some patients (pts) respond more favorably than others. Pre-clinical data suggests that mutations in the *MEN1*, *DAXX*, and/or *ATRX* genes influence DNA repair capabilities and increase radiation effect in cancer cells. We therefore thought to evaluate the association between response to PRRT and the presence of *MEN1*, *DAXX*, and/or *ATRX* mutations in patients with GEP-NETs.
Methods: We retrospectively analyzed CLIA certified tissue-based Next Generation Sequencing (NGS) assay results and clinicopathological data from 28 pts with GEP-NETs treated with PRRT at our center from 2017 to 2023. Genetic findings were correlated with progression-free survival (PFS) using Kaplan-Meier estimators and Cox proportional hazards regression modeling. Objective response was assessed per RECIST v1.1 by investigator review.
Results: Pts with mutations in *MEN1*, *DAXX*, or *ATRX* (n = 13, 46.42%) had a longer PFS [mPFS, 26.47 months (95% CI, 17.97 - NA) vs. 12.13 months (95% CI, 9.17 - NA); HR, 0.19; 95% CI, 0.06 - 0.68; p = 0.01] than wildtype (n = 15, 53.58%) pts, when adjusted for surgery prior to PRRT and tumor grade. Pts with mutations in *MEN1* along with a concurrent mutation in either *DAXX* or *ATRX* (n = 6) trended towards better PFS compared to patients without concurrent mutations [only $MEN1^{mt}$ or $DAXX^{mt}$/$ATRX^{mt}$, but not both; mPFS, 31.53 months (95% CI, 28.43 - NA) vs. 17.97 months (95% CI, 11.17 - NA); HR, 0.25; 95% CI, 0.05 - 1.29; p = 0.09]. Among evaluable pts, objective response rate was higher in pts with a mt in *MEN1*, *DAXX*, or *ATRX* compared to wild-type pts (41.67% vs. 15.38%; p = 0.09). In the pancreatic NET (PNET) subset, mutations in either *MEN1*, *DAXX*, or *ATRX* were found in 11/16 pts (68.75%) and were also associated with a better PFS compared to wild type patients [mPFS, 28.43 months (95% CI, 11.50 - NA) vs. 9.83 months (95% CI, 7.83 - NA); HR, 0.21; 95% CI, 0.05 - 0.95; p = 0.04).
Conclusions: Mutations in *MEN1*/*DAXX*/*ATRX* correlate with improved PFS in patients with GEP-NETs receiving PRRT. Concurrent mutations in *MEN1* and *DAXX*/*ATRX* may have additive effects on response to PRRT. If validated in larger studies, these findings may represent a novel biomarker to predict PRRT response.
Limitations: Limited sample size precludes generalization of results and might overestimate effect sizes.

#7615 Epithelial-mesenchymal-transition gene signature changes and poor oncological outcome in *Candida*-positive pancreatic ductal adenocarcinoma.

P. Ear[1], M. Hu[2], J. S. Shilyansky[1], N. H. Fei[1], S. Coleman[2], R. Hoyd[3], C. E. Wheeler[3], K. L. Steckly[1], M. L. Churchman[4], N. Denko[5], R. D. Dodd[1], S. Hardikar[2], N. Jin[3], Q. Ma[6], M. D. McCarter[7], A. Naqash[8], A. E. G. Osman[9], G. Riedlinger[10], L. A. Robinson[11], B. P. Schneider[12], E. A. Singer[3], A. A. Tarhini[11], G. Tinoco[3], C. M. Ulrich[2], Y. Zakharia[1], D. Spakowicz[3], A. Tan[2], **C. H. F. Chan**[1];

[1]University of Iowa Hospitals and Clinics, Iowa City, IA, [2]Huntsman Cancer Institute, University of Utah, Salt Lake City, UT, [3]The Ohio State University Comprehensive Cancer Center, Columbus, OH, [4]Aster Insights, Tampa, FL, [5]The Ohio State University Comprehensive Cancer Center, Columbus, UT, [6]The Ohio State University, Columbus, OH, [7]University of Colorado School of Medicine, Aurora, CO, [8]Stephenson Cancer Center of University of Oklahoma, Oklahoma City, OK, [9]University of Utah, Salt Lake City, UT, [10]Rutgers Cancer Institute of New Jersey, New Brunswick, NJ, [11]H. Lee Moffitt Cancer Center and Research Institute, Tampa, FL, [12]Indiana University Simon Comprehensive Cancer Center, Indianapolis, IN

Candida are commonly found in bile collected during surgery in pancreatic ductal adenocarcinoma (PDAC) patients. However, their significance in tumor biology and oncological outcome is unclear. PDAC patients receiving neoadjuvant therapy and pancreatectomy with intraoperative bile fungal culture were identified (N=40) in a prospective single-institution cohort. Tumor regression scores (TRS) were abstracted from pathology reports and correlated with bile fungal cultures. Bulk tumor RNASeq data were obtained from the Oncology Research Information Exchange Network (ORIEN). Tumor microbiome data of non-metastatic PDAC patients with upfront surgery were extracted using the {exotic} tool (Hoyd et al. *Cancer Res. Commun.*, 2023). Gene expression profiles were compared between *Candida*+ and *Candida*- tumors, defined by a cutoff microbial count of 0. Overall survival (OS) of resected PDAC patients with *Candida*+ and *Candida*- tumors was compared using Kaplan Meier survival analysis. From the single-institution PDAC cohort, *Candida*+ bile was associated with poor pathological response to neoadjuvant therapy (Table 1). Using the ORIEN cohort, *Candida* were detected in 67% (106/158) of the PDAC tumors. Patients with *Candida*+ tumors had worse OS (median 28 vs. 56 months, Log-Rank p<0.008). Gene Set Enrichment Analysis (GSEA) using Hallmark gene sets showed an enrichment of epithelial-mesenchymal-transition (EMT) gene set and a reduction of metabolic and DNA repair gene sets in *Candida*+ tumors. GSEA for Immune signature and Tumor Immune Microenvironment Deconvolution (TIMEx) cell types showed an enrichment of Stromal-Fibroblast and EMT signature in *Candida*+ tumors. Further investigations are underway to determine the causal and metabolic relationship between *Candida* and this tumor microenvironment with EMT and stromal fibroblasts which is a well-known contributor to poor chemotherapy response and oncological outcome of PDAC.

Table 1: Pathological Response to Neoadjuvant Therapy for PDAC

Bile Culture	**TRS0/1**	**TRS2**	**TRS3**
***Candida* -**	5 (25%)	15 (75%)	0 (0%)
***Candida* +**	1 (5%)	11 (55%)	8 (40%)

TRS: Tumor Regression Score (TRS0: complete response; TRS1: near-complete response; TRS2: partial response; TRS3: no response). Chi-Square Test, P=0.0035.

#7617 Quantitative continuous scoring of PD-L1 for superior patient selection for anti-PD-L1 treatment of locally advanced or unresectable NSCLC.

J. Lesniak[1], I. Bisha[1], S. Christ[1], L. Meinecke[1], T. Padel[1], L. Sebastian Monasor[1], P. Sontakke[1], T. Tan[1], D. Medrikova[1], A. Storti[1], A. Shumilov[1], H. Sade[1], G. Schmidt[1], R. Stewart[2], Y. Shrestha[3];

[1]AstraZeneca, Munich, Germany, [2]AstraZeneca, Cambridge, United Kingdom, [3]AstraZeneca, Gaithersburg, MD

Background: Immune checkpoint inhibitors (ICIs) targeting PD-(L)1 following concurrent chemoradiotherapy (cCRT) have shown clinical activity in locally advanced, unresectable NSCLC, e.g. with the PACIFIC regimen [1]. PD-L1 expression is typically assessed by pathologist scoring of immunohistochemically (IHC) stained tissue using the tumor cell (TC) score. In this work, we present PD-L1 Quantitative Continuous Scoring (PD-L1 QCS) to digitally assess PD-L1 expression (Ventana SP263 assay), and analyze its utility for identification of patient subgroups with higher likelihood of treatment response.

Method: 368 digitized whole slide images (WSI) of fresh biopsy and archival samples were obtained from the PACIFIC trial (NCT02125461), including 126 patients who received placebo and 242 patients who received Durvalumab post-cCRT [1]. WSI analysis included two deep learning models for epithelial TC segmentation followed by optical density (OD) quantification of membrane expression [2]. Initially, PD-L1 QCS was calibrated to compute the TC score at 1% cutoff by determining an optimal OD cell positivity threshold. Next, other scoring approaches were investigated, which included various OD thresholds and biomarker cutoffs.

Results: PD-L1 QCS-based TC scoring was able to maintain median overall survival (mOS) of 57.4 months in the biomarker positive (BM+) ICI cohort, while increasing prevalence to 191 out of 242 patients (78.9%) compared to 177 (73.1%) with manual TC score at 1% cutoff. Extending the scoring paradigm to the PD-L1+ TC density >= 542.5 cells/mm² lead to a more pronounced increase of prevalence to 200 patients (82.6%) in the ICI population, while mOS was not reached and additionally showed comparable hazard ratios (HR) when evaluating against the BM+ placebo cohort (HR=0.54 [0.39, 0.76] resp. HR=0.52 [0.37, 0.74]). Results further demonstrated that PD-L1 QCS density scoring of the ICI treated population allowed for a clearer separation of patients with less treatment benefit (34.2m mOS, N=42, log rank p=0.0067) compared to manual scoring (47.4m mOS, N=65, log rank p=0.2).

Conclusion: We investigated a computational pathology approach for selecting patients for treatment with the PACIFIC regimen and compared it against established manual pathology scoring. Results indicate that PD-L1 QCS TC proportion scoring can increase prevalence, while PD-L1 QCS TC density scoring has the potential to identify an even larger patient subgroup with increased survival benefit.

References: 1. Antonia, Scott J., et al. "Durvalumab after chemoradiotherapy in stage III non-small-cell lung cancer." New England Journal of Medicine 377.20 (2017): 1919-1929. 2. Lesniak, Jan, et al. " Quantitative computational assessment of PD-L1 enables robust patient selection for biomarker-informed anti-PD-L1 treatment of NSCLC patients." *J. Immunother. Cancer,* Vol. 10., 2022.

#7618 Genomic pathogenic alterations of the SWI/SNF complex genes compromise the outcomes to immunotherapy in Chinese *KRAS*-mutant non-small cell lung cancer by downregulated STING.

L. Gao, J. Jiang, Z. Xie, L. Zhu, Y. Chen, Z. Lv, Y. Chen, W. Zhou, J. Chen, Y. Zhong, L. Zhang, P. Zeng, X. Huang, W. Yan, D. Lu, S. Zhang, W. Guo, **X. Zhang**;

Guangdong Provincial People's Hospital (Guangdong Academy of Medical Sciences), Guangzhou, China

Background: Immune checkpoint inhibitors (ICIs) have been standard of care in non-small cell lung cancer (NSCLC), but lack of response to ICIs remains a major hurdle in cancer immunotherapy. Switch/sucrose nonfermentable (SWI/SNF) chromatin-remodeling complex mutations have been reported in *KRAS*-mutant cancers with debated influence to clinical outcome of ICIs, which needs further investigation.

Methods: According to the OncoKB, COSMIC, and PolyPhen-2 databases, genomic pathogenic alterations (GPAs) of SWI/SNF are defined. Lung tumors were classified according to the presence or absence of mutations in six SWI/SNF genes (*ARID1A*, *ARID1B*, *ARID2*, *PBRM1*, *SMARCA4*, and *SMARCB1*). Lung cancer cell lines with different genotypes of SWI/SNF were used for differentially expressed genes analysis by RNA sequencing. Protein expression of STING was detected by immunohistochemistry (IHC) in tumor specimens.

Results: Out of 2660 NSCLC patients (NSCLCs), the GPAs of SWI/SNF were detected in 15.0% (401/2660) patients. 23.1% (69/299) $EGFR^{wt}ALK^{wt}$ and 27.8% (25/90) $STK11^{wt}KEAP1^{wt}KRAS^{mut}$ NSCLCs who received ICIs had SWI/SNF GPAs. Progression-free survival (mPFS) of SWI/SNF-wild type (wt) compared to SWI/SNF-mutant (mut) NSCLCs was not significantly different. However, GPAs of SWI/SNF in *KRAS*-mut ICI-treated NSCLCs associated with poorer clinical outcome. Patients with *ARID1A*, *ARID1B*, *ARID2* or *PBRM1* mutant tumors had a significantly shorter PFS (2.7 vs 6.5 months, HR=2.44 [95%CI: 1.31-4.54], *P*=0.004) as compared to SWI/SNF-wt patients. In $STK11^{wt}KEAP1^{wt}KRAS^{mut}$ NSCLCs, all SWI/SNF mutations (4.9 vs 9.1 months, HR=2.03 [95%CI: 1.07-3.86], *P*=0.029) or *ARID1A/ARID1B/ARID2/PBRM1* alterations (3.2 vs 9.1 months, HR=2.68 [95%CI: 1.33-5.41], *P*=0.004) significantly shortened the mPFS. In cell lines, SWI/SNF-mut cells had downregulated STING expression compared to SWI/SNF-wt cells. Downregulated STING protein were observed in *KRAS*-mut NSCLCs without benefit from the treatment of ICIs.

Conclusions: In *KRAS*-mut NSCLCs with or without *STK11/KEAP1* mutations, the presence of GPAs of DNA binding genes *ARID1A*/*ARID1B*/*ARID2* could compromise the clinical outcome of immunotherapy, which might be due to the downregulated STING.

#7619 Tissue-derived peripheral biomarkers that reflect activity of T-cells, macrophages, and neutrophils in patients with solid tumors.

N. Willumsen, N. I. Nissen, M. A. Karsdal;
Nordic Bioscience, Herlev, Denmark

Background: A toolbox of tissue-derived peripheral biomarkers that reflect the activity of T-cells, macrophages and neutrophils is a medical need for immuno-oncology drug development allowing non-invasive quantification of immune cell activity before - and during - treatment, both for predictive and pharmacodynamic purposes. By identifying and quantifying specific extracellular matrix fragments with neo-epitopes that are generated by proteases specific for T-cells, macrophages, and neutrophils, respectively, it is possible to develop peripheral biomarkers that reflect the activity of these immune cells. Such biomarkers have previously shown associations with outcome of patients treated with immune checkpoint inhibitors. Here we investigated the distribution of 3 such biomarkers in different cancer indications. Moreover, these data were compared to data from melanoma patients showing associations with response to cancer immunotherapy.

Methods: Tissue-derived biomarkers related to activity of T-cells (C4G: Collagen-4 degraded by Granzyme B), Neutrophils (CPA9-HNE: Calprotectin degraded by neutrophil elastase), Macrophages (VICM: citrullinated and MMP-degraded vimentin) were measured by validated ELISA/ECLIA in serum from patients with various solid tumor types (bladder-, breast- colorectal-, head and neck-, kidney-, lung-, ovarian-, pancreatic, stomach-, prostate- cancer, and melanoma, n=220) and compared to age-matched healthy controls (n=33) by ANOVA. The biomarker levels were compared to historical data.

Results: Median biomarker levels of CPA9HNE (neutrophil activity/NETosis) and VICM (macrophage activity) were significantly increased in all solid tumor types ($p<0.001$), respectively and with a ~5-fold inter-patient variation as well. Median C4G levels was only slightly elevated in a few indications ($p<0.05$) and with a 5-10-fold inter-patient variation across tumor types. All biomarker levels were independent of disease stage. Similar biomarkers levels were seen to those found to be associated with objective response rate and overall survival of melanoma patients treated with cancer immunotherapy.

Conclusion: Tissue-derived peripheral biomarkers that reflect the activity of T-cells (C4G), macrophages (VICM) and neutrophils (CPA9HNE) has biomarker potential in solid tumors and may serve as prognostic, predictive and pharmacodynamic biomarkers in clinical trials investigating cancer immunotherapy.

#7620 Immuno-transcriptomic profiling of blood and tumor tissue identifies gene signatures associated with immunotherapy response in metastatic bladder cancer.

P. J. Romero[1], E. Desponds[2], D. Croci[1], V. Wosika[3], N. Hadadi[1], S. Fonseca Cost[1], L. Ciarloni[1], M. Ongaro[1], H. Zdimerova[2], M. M. Leblond[2], S. Hosseinian-Ehrensberger[1], G. Verdeil[2];

[1]Novigenix, Epalinges, Switzerland, [2]University of Lausanne, Epalinges, Switzerland, [3]Lunaphore Technologies, Tolochenaz, Switzerland

Muscle-invasive bladder cancer (MIBC) accounts for 25% of bladder cancer cases. Despite the broader usage of immune checkpoint blockade targeting the PD-1/PD-L1 axis, the response rate and survival of patients remain low for this disease. Redirecting swiftly these patients toward alternative therapeutic strategies upon immunotherapy failure should be a priority. So far, no marker allows to precisely determine early outcome to the treatment.Blood-based biomarkers represent ideal candidates for the development of non-invasive immuno-oncology-based assays. However, to date, no blood biomarker has been validated to predict clinical response to immunotherapy. In this study, we used next generation sequencing (RNAseq) on bulk RNA extracted from whole blood and tumor samples in a pre-clinical MIBC mouse model. We aimed at identifying biomarkers associated with immunotherapy response and to assess the potential application of simple non-invasive blood biomarkers as therapeutic decision-making assay compared to tissue-based biomarkers. We established that circulating immune cells and the tumor microenvironment (TME) display highly organ-specific transcriptional responses to ICI. Interestingly, a common lymphocytic activation signature can be identified in both compartments associated with the efficient response to immunotherapy, including a blood specific CD8+ T cell activation/proliferation signature which predicts immunotherapy response.

#7621 Serum albumin and derived neutrophil-to-lymphocyte ratio are potential predictive biomarkers for immune checkpoint inhibitors in small cell lung cancer.

Z. Kuang, J. Miao, **X. Zhang**;
The Ohio State University Wexner Medical Ctr., Columbus, OH

Background: Immune checkpoint inhibitors (ICIs) have reshaped the treatment landscape of small cell lung cancer (SCLC), but only a minority of patients benefit from this therapy. Therefore, it is critical to identify potential risk factors that could predict the efficacy of ICI treatment in SCLC patients and identify patient subgroups who may benefit the most from ICI therapy.
Methods: Our study included a total of 183 SCLC patients who had received at least one dose of ICI treatment. We utilized both logistic regression and Cox proportional hazard regression to evaluate whether various patient clinical factors and serum biomarkers, could serve as predictors of patient response to treatment and overall survival (OS) during ICI therapy.
Results: Logistic regression showed that patients with a history of surgery (p=0.003, OR 9.06, 95% CI: (2.17, 37.9)) and no metastasis (p=0.008, OR 7.82, 95% CI: (1.73, 35.4)) exhibited a higher odds of response to ICI treatment. Cox regression analyses demonstrated that pretreatment blood albumin (p=0.003, HR 1.72, 95% CI: (1.21, 2.45)) and derived neutrophil to lymphocyte ratio (dNLR) (p=0.003, HR 1.71, 95% CI: (1.20-2.44)) were independent predictors for OS in SCLC patients. By establishing a pre-treatment prognostic scoring system based on baseline albumin and dNLR, we found that patients with high albumin and low dNLR exhibited a significantly better prognosis than those with low albumin and high dNLR in both the full (P<.0001, HR 0.33, 95% CI: 0.20-0.55) and the metastatic cohort (P<.0001, HR 0.28, 95% CI: 0.15-0.51). The better prognostic group also had younger age, higher BMI and lower systemic inflammatory biomarker values than the unfavorable group (P<.0001).
Conclusion: Our data reveals the significant role of metastasis status and treatment history in predicting the initial response of SCLC patients to ICI treatment. However, baseline serum albumin and dNLR provide a more precise prognostic prediction for patient OS. The scoring system based on albumin and dNLR enhances the ability to stratify patient prognosis and holds the potential to guide clinical decision-making for SCLC patients undergoing ICI therapy.

#7622 ASPYRE-Lung: Validation of a simple, fast, robust and novel method for multi-variant genomic analysis of actionable NSCLC variants in tissue.

R. T. Evans[1], E. Gillon-Zhang[1], J. Brown[1], K. Knudsen[1], C. King[1], A. S. Green[1], A.-L. Silva[2], J. M. Mordaka[2], R. N. Palmer[2], A. Tomassini[2], A. Collazos[2], C. Xyrafaki[2], I. Turner[2], C. Ho[2], D. Nugent[2], J. Jose[2], S. Andreazza[2], K. von Bargen[2], E. R. Gray[2], M. Stolarek-Januszkiewicz[2], A. Cooke[2], **W. J. Levin**[1], H. V. Reddi[1], B. W. Balmforth[2], R. J. Osborne[1];

[1]Biofidelity, Morrisville, NC, [2]Biofidelity, Cambridge, United Kingdom

Genomic variant testing of tumors is critical for patients to access the full potential of personalized oncology therapeutics. Current methods such as NGS are costly and challenging to interpret, while PCR assays are limited in the number of variants they can cover. We developed ASPYRE® (Allele-Specific PYrophosphorolysis REaction) technology to address the urgent need for rapid, accessible and affordable diagnostics informing actionable genomic target variants of a given cancer. The targeted ASPYRE-Lung® panel for NSCLC covers 114 variants in 11 genes (*ALK, BRAF, EGFR, ERBB2, KRAS, RET, ROS1, MET & NTRK1/2/3*) to robustly inform clinical management, based on practice guidelines. The assay detects single nucleotide variants, insertions, deletions, and gene fusions from tissue-derived DNA and RNA simultaneously. We tested the limit of detection, specificity, analytical accuracy and analytical precision of ASPYRE-Lung using FFPE lung tissue samples from patients with NSCLC, variant-negative FFPE tissue from tonsil tissue, and FFPE-based contrived samples with controllable variant allele fractions. The sensitivity of ASPYRE-Lung was determined to be ≤ 3% variant allele fraction for single nucleotide variants and insertions or deletions, ≤ 100 copies for fusions, and ≤ 200 copies for MET exon 14 skipping. The specificity was 100% with no false positive results. The analytical accuracy test yielded no discordant variants between ASPYRE-Lung and orthogonal testing (targeted enrichment NGS) or contrived samples, and results were replicable across operators, reagent lots, runs, and real-time PCR instruments with a high degree of precision. The technology is simple and fast, requiring only four reagent transfer steps using standard laboratory equipment (PCR and qPCR instruments) with analysis via a cloud-based analysis algorithm. ASPYRE-Lung has the potential to be transformative in facilitating access to rapid, actionable molecular profiling of tissue for patients with NSCLC.

#7623 Biomarker study to personalized neoadjuvant chemotherapy using preoperative gastric cancer specimens of biopsy from the COMPASS trial, a phase II randmazed controlled trial.

T. Oshima;
Kanagawa Cancer Ctr., Yokohama, Japan

Background and Aim: The results of COMPASS, a randomized phase II trial, suggest that preoperative adjuvant chemotherapy (NAC) regimen or course for locally advanced gastric cancer (GC) does not affect overall survival (OS). However, we hypothesized that some NAC regimens may be more effective for OS on a case-by-case basis. Furthermore, we searched for biomarkers, assuming that further improvement in the outcome of locally advanced GC could be expected if appropriate NAC regimens could be selected using biomarkers before treatment initiation.
Materials and Methods: RNA was extracted from endoscopic biopsy specimens of primary tumors collected prior to NAC administration in COMPASS patients, and real-time polymerase chain reaction (PCR) of 127 genes was performed to identify genes with significant ($P < 0.05$) interaction P values for survival with each regimen and stratified OS with each regimen. Genes were identified and biomarkers were searched at the protein level using immunohistochemical analysis.
Results: The THBS1, MSI1, and IGF2BP3 genes were identified as genes whose expression levels significantly ($P < 0.05$) stratified survival for each regimen and had significant ($P < 0.05$) interaction P values. Furthermore, a strong correlation was observed between each gene and THBS1, MSI1, and IGF2BP protein expression by immunohistochemical analysis, confirming that protein expression levels by immunohistochemical analysis are also useful as biomarkers.
Conclusion: Using endoscopic biopsy specimens prior to NAC for locally advanced GC, biomarkers were identified to select NAC regimens over predicted OS. The results of this study may guide the conduct of clinical trials of individualized treatment of NAC using biomarkers.

#7624 DNA checkpoint gene mutation as a biomarker of immune checkpoint inhibitor in advanced biliary tract cancer.

Ji Eun Shin[1], Seung Tae Kim[2], Dae-Ho Choi[2], Junho Lee[2], Jiyeon Hyeon[2]

[1]St. Vincents Hospital The Catholic University of Korea, Suwon, Korea, Republic of,[2]Samsung Medical Center, Seoul, Korea, Republic of

Introduction: The DNA checkpoint (DNACHK) pathway is engaged in signaling the need for cell cycle arrest. The G1 and S phase checkpoint allows for repair of damaged DNA, preventing damaged DNA from being copied. The G2 and M phase checkpoint prevents transmission of mutated DNA to the next generation. This pathway, along with mismatch repair (MMR), homologous recombination (HR), and base excision repair (BER), is being actively researched to assess its role in cancer immunotherapy.

Methods: Sixty-two patients participated in this study. These patients were treated with immune checkpoint inhibitors (ICIs) for advanced biliary tract cancers (BTCs) from Mar. 2020 to Aug. 2022 at Samsung Medical Center. DNACHK mutations were defined as genomic alterations such as SNVs, MNVs, and short insertion and deletions in seven genes These genes include checkpoint kinase 1 (CHEK1), checkpoint kinase 2 (CHEK2), BRCA1, DNA repair associated (BRCA1), the serine/threonine kinase ATM, the serine/threonine kinase ATR, and mediator of DNA damage checkpoint 1 (MDC1). We analyzed the effect of DNACHK mutations on the efficacy of ICIs in advanced BTCs.

Results: Patient median age at diagnosis was 68.0 years. Ten patients (16.1%) had gall bladder (GB) cancer; the remaining patients (n = 52, 83.9%) were diagnosed with cholangiocarcinoma. Among the 62 patients with advanced BTCs treated with ICIs, 37 (59.7%) were categorized into the DNACHK wild-type (WT) group and 25 (40.3%) into the DNACHK mutated (MT) group. The most observed DNA checkpoint mutations were ATM mutations (n=14). MDC1 mutations were found in seven patients, ATR mutations in three, BRCA1 mutations in four, and CHEK2 mutations in three. Patients in the DNACHK MT group had better disease control rates than patients in the DNACHK WT group (60.0% vs. 48.6%, p=0.53). Median overall survival (OS) was 8.1 months (95% CI, 5.1, 22.8) in the MT group and 5.6 months (95% CI, 3.1, 11.0) in the WT group (p=0.33).

Conclusions: The results of this study suggest that the DNACHK pathway may be a valuable source of biomarkers for ICI and worthy of further study.

#7625 The liquid biomarker thymidine kinase activity reflecting proliferation rate can provide guidance in drug development and address Project Optimus.

M. Bergqvist, H. Ritzen, A. Williams;
Biovica International, Uppsala, Sweden

Thymidine Kinase (TK) plays a basic role in DNA synthesis and cell proliferation. The enzyme is highly cell cycle dependent and correlates with cell growth state. Numerous studies have consistently shown elevated TK activity (TKa) in the blood of patients with solid tumors and active disease. DiviTum® TKa, a clinically and analytically validated FDA cleared assay, measures and quantifies TKa in serum or plasma in humans and animals. TKa as a biomarker offers valuable information at all stages of drug development, from drug efficacy and dose response studies in cell culture and xenograft models, to patient selection and treatment monitoring in clinical trials. The launch of FDA Project Optimus highlights the need for new biomarkers to assist in drug development to identify optimal dose. Using TKa to measure the impact on cell proliferation as a drug evaluation endpoint can confirm mechanism of action efficacy and a minimally effective dose of a new compound rather than a maximally tolerated dose. TKa can be used as a pharmacodynamic tool to improve study endpoints. TKa data in cultured cells and mouse xenografts demonstrates that a complete shutdown of tumor cell proliferation can be observed well before and at much lower drug-doses than when cell death or toxicity is used as the dose determination endpoint. Increased dosing of CDK4/6 inhibitors demonstrates immediate impact on TKa levels in cell lines and provides signals of drug effect at doses where cell viability is unaffected. After initiation of samuraciclib treatment, a CDK7 inhibitor, a significant reduction in TKa levels in blood from metastatic breast cancer (MBC) patients was observed, indicating inhibition of cell cycle progression. For patients on samuraciclib therapy and with stable disease before progression, TKa levels were significantly lower than pre-treatment ($p=0.0038$). Post-progression TKa levels increased to significantly higher levels than during therapy including the last sample measured before progression ($p=0.014$). Baseline blood TKa levels are predictive for progression free survival (PFS) allowing for the early stratification of patients with long vs short PFS. In patients with MBC, TKa levels during the first treatment cycle are strongly predictive for PFS. Suppressed TKa levels after 2 and 4 weeks of CDK4/6 inhibitor therapy predict longer PFS than high TKa levels at the same time points (HR 5.65; $p< 0.0001$). MBC patients monitored >3 months and showing low TKa levels have very low likelihood of progression within 30- to 60 days, <2% and <6%, respectively. TKa is a translational liquid biomarker that bridges results between preclinical and clinical studies, providing fundamental information for drug development decision making.

#7626 Assessment of precision melanoma diagnostics: Circulating microrna expression to monitor late-stage treatment.

T. Harris[1], P. Zaenker[2], A. C. McEvoy[2], H. Soyer[1], M. A. Khattak[2], M. Ziman[2], M. Millward[3], E. S. Gray[2], **M. S. Stark**[1];
[1]University of Queensland, Brisbane, Australia, [2]Edith Cowan University, Joondalup, Australia, [3]The University of Western Australia, Crawley, Australia

Metastatic melanoma patients are commonly treated with targeted (e.g., BRAF/MEK inhibitors) and/or immune checkpoint therapies and treatment efficacy is then assessed with radiological scans. These scans are highly effective for the staging of the disease but in terms of follow-up, there are several limitations including the inability to detect minimal residual disease (MRD). Circulating biomarkers are a viable solution to overcome these limitations, and this study sought to investigate a panel of melanoma-specific microRNA (miRNA) biomarkers in stage IV patients undergoing therapy. This panel had previously been assessed in treatment naïve stage IV patients, with members of the MELmiR-7 panel able to detect an increase in tumor burden in 100% of cases, as well as the ability to define overall survival (OS) superior to serum lactate dehydrogenase (LDH) and S100B levels (delta log-likelihood = 11, p< 0.001). In this multi-center longitudinal study, bloods were drawn from study participants from 2013-2015, with clinical follow-up until October 2018. The expression levels of the MELmiR-7 panel were assessed in serially collected serum (≥3 timepoints; ≥2-month intervals) collected from a total of 23 melanoma patients, treated with BRAF/MEK inhibitors and/or anti-CTLA4 and/or anti-PD-1. The goal was to determine if the panel could predict treatment success/failure, as well as patient OS, if treated with the same therapy. All miRNA panel members were measured using a sensitive real-time PCR assay at each time point, but only miR-4731 gave stable expression over the course of the therapy, with other panel members fluctuating post treatment. The stability of miR-4731 expression over time indicated that this marker was not affected by treatment type, rather changes in its expression were reflective of disease progression/regression (as determined by radiological images), thus making it an ideal biomarker. Importantly, across the cohort of 23 patients, miR-4731 expression had the ability to predict treatment outcome (Complete Response/Stable Disease (n=12) vs Melanoma Death (n=11)) for patients at ≥2 months post therapy vs baseline, with a high degree of precision (Mann Whitney, 2-tailed; p=0.0004). Area under the curve analysis also found miR-4731 expression to be highly sensitive and specific (AUC=0.91; p=0.0009) at predicting overall survival (OS). Furthermore, in Kaplan-Meier survival analysis, participants with high serum expression (≥2 months post therapy vs baseline) of miR-4731, had poor OS (p=0.0045; 14-month median survival) as compared with low serum miRNA expression which was predictive of a positive prognosis. In sum, assessment of this miRNA marker during therapy would permit early on-treatment prediction of patient outcomes, independent of imaging, to either continue to treat with current regimen, or to switch treatment modalities.

#7627 First NGS-based companion diagnostic to aid in selecting non-small cell lung cancer patients with *ERBB2* (HER2) activating mutations for treatment with trastuzumab deruxtecan.

T. Ha;
Thermo Fisher Scientific, Carlsbad, CA

Introduction The *ERBB2* companion diagnostic program aims to expand the intended use of the Oncomine ™ Dx Target Test (ODxTT) to determine *ERBB2* single nucleotide variants (SNVs) in exons 8, 17, 18, 19, 20, 21 and 22 and exon 20 insertions from formalin-fixed, paraffin-embedded (FFPE) tumor samples in non-small cell lung cancer (NSCLC) patients who may benefit from targeted drug therapy.
Methods The ODxTT is a qualitative in vitro diagnostic test that uses targeted high throughput, parallel-sequencing technology to detect SNVs, deletions, insertions, and CNVs in genes from DNA and fusions from RNA isolated from FFPE tissue samples using the Ion PGM ™ Dx System. Analytical validation (AV) studies interrogated ODxTT's ability to detect *ERBB2* mutations. The clinical validation (CV) study involved a method comparison/concordance analysis of *ERBB2* mutations between the ODxTT and the TruSight Tumor 170 (TST170) assay, as well as a series of clinical trial assays (CTAs). The CV study was conducted using clinical specimens from 91 patients enrolled in Destiny-Lung01 and 121 stage-matched commercially procured samples. The aim was to evaluate positive percent agreement (PPA), negative percent agreement (NPA) and overall percent agreement (OPA) for CTAs and TST170 assay.
Results A total of 91 *ERBB2* subjects were included in the full analysis of the Destiny-Lung01 clinical trial. 49 samples had valid ODxTT results available and 42 samples were unevaluable which included 13 unknowns and 29 test not performed. The 49 patient samples that were evaluable were used to assess the clinical efficacy based on ODxTT results. In the series of 121 samples that were used to assess clinical efficacy in the CV study, 109 had evaluable ODxTT results. The PPA, NPA and OPA of ODxTT to the CTAs when excluding unknowns were 98%, 100% and 99.4%, respectively, and based off the Clopper-Pearson method for binomial distribution a 95% lower bound confidence interval (CI) were 89.6%, 96.6% and 96.5%, respectively. There was one discordant sample with a negative ODxTT and a positive CTA result (false negative). The PPA, NPA and OPA of ODxTT to TST170 assay were 100%, 99.1% and 99.3% respectively with a 95% lower bound CI of 90.8%, 95.0% and 96.3%, respectively. There was one discordant sample with a negative TST170 and a positive ODxTT result (false positive).
Conclusion AV and CV studies successfully verified and validated the ODxTT for the detection of ERBB2 mutations in NSCLC FFPE samples. The 6 AV studies met the necessary product requirements and acceptance criteria to detect clinical samples with ERBB2 mutations. Additionally, the CV study clinical accuracy and clinical efficacy results demonstrated the safety and effectiveness of the use of the ODxTT in FFPE samples as an aid to identify NSCLC patients eligible for treatment with the Daiichi Sankyo lung cancer therapeutic T-DXd.

#7628 Pharmacodynamic biomarkers for Rac and Cdc42 inhibitor efficacy.

A. Torres-Sanchez[1], A. M. Cruz-Collazo[2], M. Rivera-Robles[3], O. Katsara[4], S. Dorta-Estremera[2], V. Negron[5], V. P. Carlo[5], R. J. Schneider[4], S. Dharmawardhane[2];

[1]University of Puerto Rico - Rio Piedras, San Juan, PR, [2]University of Puerto Rico Medical Sciences Campus, San Juan, PR, [3]University of Puerto Rico Comprehensive Cancer Center, San Juan, PR, [4]New York University School of Medicine, New York, NY, [5]Auxilio Mutuo Hospital, San Juan, PR

Metastatic disease drastically reduces clinical prognosis, and remains the primary cause of mortality from solid cancers, such as breast and pancreatic cancer. Since targeted therapeutic options are limited, we developed small molecule compounds to block activation (GTP loading) of the Rho GTPases Rac and Cdc42. Rac and Cdc42 are ideal molecular targets due to their regulation of cell migration, proliferation, invasion, and signaling in cancer and immunosuppressive cells in the tumor microenvironment. Our lead compound MBQ-167 is a dual Rac and Cdc42 inhibitor with IC_{50} of ~100 nM for inhibition of Rac/Cdc42 activation and the phosphorylation of their common downstream effector p21-activated kinase (PAK). MBQ-167 is highly effective in mouse models of breast cancer metastasis and is currently undergoing a Phase I clinical trial in advanced breast cancer patients. The purpose of this study is to investigate potential target molecules that can be used as biomarkers predictive of Rac/Cdc42 inhibitor efficacy. We recently published that in addition to inhibiting the growth and migration of breast and pancreatic cancer cells, MBQ-167 inhibits macrophage cell migration, immunosuppressive myeloid cell activation and release of interleukin-6 (IL-6), a pro-inflammatory cytokine associated with cancer. Transcriptomic data of tumors from mice treated with vehicle or MBQ-167 identified a number of immunomodulatory pathways downregulated by MBQ-167, including IL-6 and S100A family signaling, and Chitinase 3-like (CHI3L1/CHI4L1) genes coding for the human YKL-40 protein. We tested for the activation status of PAK (phospho (p)-PAK) as a diagnostic marker for Rac/Cdc42 inhibitor efficacy using breast cancer patient tissue in *ex vivo* culture treated with vehicle or MBQ-167 and found decreased p-PAK staining following immunohistochemistry of MBQ-167-treated tissue. From flow cytometry, using Alexa-488-tagged anti p-PAK antibody, we found that p-PAK was reduced from peripheral blood mononuclear cells (PBMCs) following MBQ-167. ELISA assays for YKL-40/CHI3L1 proteins after treatment of pancreatic cancer cell lines and macrophage-like cells with Rac/Cdc42 inhibitors show that MBQ-167 and the derivative MBQ-168 reduced CHI3L1 levels from conditioned media. These results demonstrate the potential of p-PAK and YKL-40/CHI3L1 from blood as biomarkers for Rac/Cdc42 inhibitor efficacy. This study impacts pharmacodynamic biomarker design for the planned Phase 2 clinical trials for MBQ-167 in breast and pancreatic cancer.

#7629 Association between COMT expression and therapeutic efficacy of androgen receptor-axis targeted in prostate cancer.

S. Maekawa, R. Takata, E. Shiomi, D. Ikarashi, T. Matsuura, R. Kato, M. Kanehira, J. Sugimura, W. Obara;
Iwate Medical University, Iwate, Japan

Background: The enzyme of catechol-O-methyltransferase (COMT) inhibits the proliferation of prostate cancer (PCa). There has been no obvious biomarker that contributes to the selection of a therapeutic agent among new-generation androgen receptor-axis targeted (ARAT) therapy, such as abiraterone (ABI) or enzalutamide (ENZ). We aimed to assess the possibility of using COMT expression as a biomarker for PCa progression and the criteria for selecting ABI or ENZ.

Methods: We retrospectively evaluated 60 patients with PCa treated with ABI or ENZ via needle biopsy or radical prostatectomy. Immunostaining of COMT was performed using formalin-fixed, paraffin-embedded blocks obtained from the initial prostate biopsy for diagnosis or prostatectomy. Immunostaining evaluations were scored by immunostaining intensity (0-3) and staining area (0-3), and the total score ≥4 was defined as "high expression" and the total score <4 was defined as "low expression." The associations between COMT expression levels and clinical outcomes, including the duration of ENZ or ABI response, were also assessed.

Results: Of the 60 cases, nine (15%) showed low expression of COMT. Overall survival was significantly shorter in patients with lower COMT expression (hazard ratio [HR] = 0.24, 95% confidence interval [CI] 0.07-0.83, P= 0.024). When ENZ was administered as the first ARAT, progression-free survival (PFS) was significantly different between patients with COMT expression scores <4 and ≥4 (median 5.9 and 23.3 months, respectively). However, when ABI was administered as the first ARAT, there was no significant difference in the PFS of ARAT between COMT expression scores <4 and ≥4.

Conclusion: Patients with lower COMT expression have a significantly poorer prognosis for PCa. In addition, PFS after ENZ administration, as the first ARAT, correlated with COMT expression levels. To our knowledge, this is the first report of an association between COMT expression and the duration of ARAT.

#7630 Therapeutic relevance of systemic immune status to treatment effects of abemaciclib.

T. Ueno[1], S. Kitano[1], T. Kobayashi[1], M. Yamashita[1], F. Hara[1], Y. Ozaki[1], M. Nishimura[1], T. Takano[1], N. Toriguchi[2], T. Kawaguchi[2];
[1]Japanese Foundation for Cancer Research, Tokyo, Japan, [2]Eli Lilly Japan K.K. Japan, Tokyo, Japan

Background: The addition of a CDK4/6 inhibitor (CDK4/6i) on endocrine therapies (ET) has been currently a standard treatment for hormone receptor (HR)-positive HER2-negative metastatic breast cancers (MBCs). Especially abemaciclib has been implicated in multiple mechanisms of action including cell cycle arrest, senescence. In addition, immunomodulatory effects have been suggested but are not yet clear. The aim of the study was to investigate the clinical relevance of abemaciclib to systemic immune status by examining the status of peripheral immune cells in patients with MBC who received abemaciclib plus ET.
Methods: Patients with MBC who were treated with abemaciclib plus ET in our hospital were included in this study. Response was evaluated by RECIST 1.1. Peripheral blood at the initiation of abemaciclib treatment, 4 weeks, 12 weeks and 24weeks after abemaciclib treatment initiation were analyzed using mass cytometry by time of flight (CyTOF). Changes of cellular densities of each immune cell and survival by immune cell density were analyzed without calculating p values because of small sample number.
Results: Twenty patients were enrolled, among whom 14 and 6 received an aromatase inhibitor and fulvestrant, respectively, as concomitant ET. 7 premenopausal patients received an LH-RH analogue.
The analysis of serial blood collection showed an increase in CD8-positive T cell density by 12.5% and conversely a decrease in monocyte density by 52.3% at 4 weeks after treatment initiation. In responders (N = 10), an increase of the ratio between CD8-positive T cell density and Treg density (CD8/Treg) at 4 weeks after the treatment initiation were observed (65.2%), while not in non-responders (7.3%).
In the analysis of the blood samples at the treatment initiation, lower Treg density and lower NK density at treatment initiation indicated longer PFS than the counterparts (median PFS for Treg: low, not reached; high, 8.8 months; for NK: low, not reached; high, 8.8 months).
Conclusion: An increase of CD8/Treg at 4 weeks after the treatment initiation was associated with a good response in patients with HR-positive HER2-negative MBC treated with abemaciclib plus ET. Our results suggest an association between systemic immune status and clinical outcome in MBC patients who received abemaciclib plus ET treatment. A larger study is needed to validate the results.

#7631 Protein Plus BCT: A novel blood collection tube for stabilizing plasma proteins of interest in ambient whole blood storage.

J. Li, N. M. George, S. Mehta, J. LaRue, E. Seong, N. Binbuga, R. Miller, K. Bisselou;
Streck, La Vista, NE

Introduction: Many of the soluble plasma proteins (e.g., cytokines) that are crucial for cancer diagnosis, prognosis, and prediction of cancer immunotherapy outcomes are found in blood cells such as platelets and leukocytes. During blood collection and sample storage, *ex vivo* platelet activation, hemolysis, and blood cell degradation can occur, which causes the release of blood cell-secreted proteins into the plasma. The contamination of these proteins may confound true *in vivo* levels of plasma proteins of interest, resulting in inaccurate or inconsistent assay results. Protein Plus BCT is a new blood collection tube that maintains accurate plasma protein levels during ambient whole blood storage.

Methods: Blood samples from self-proclaimed healthy donors were drawn into Protein Plus BCT, EDTA, and ACD-A tubes. All the samples were stored at ambient temperature for up to 5 days. Plasma was isolated using a general double-spin protocol and frozen at -80 °C until use. Plasma levels of protein biomarkers were measured by Ella Simple Plex Assays (Bio-Techne) and Luminex xMAP® Technology Assays (Bio-Techne, samples tested by LuminexPLORE Lab) following manufacturers' dilution and processing recommendations.

Results: Over 50 key plasma proteins like cytokines, cancer, and immuno-oncology checkpoint markers in samples collected into Protein Plus BCT were analyzed by immunoassays and compared side-by-side to those collected in EDTA and ACD-A tubes. EDTA and ACD-A samples exhibited a substantial elevation in the plasma concentration of many, such as IL-8, IL-1β, HGF, VEGF, MMP-9, CCL5/RANTES and TGF-β1 post draw, indicating platelet activation and blood cell degradation during ambient temperature storage. Samples collected into Protein Plus BCT displayed limited *ex vivo* platelet activation and minimal contamination by blood cell-secreted proteins, maintaining the draw-time plasma levels of proteins of interest for up to 5 days in whole blood at ambient temperature.

Conclusions: The novel Protein Plus BCT maintains draw-time plasma protein levels during extended whole blood storage at room temperature by limiting *ex vivo* platelet activation, hemolysis, and blood cell degradation. Protein Plus BCT ensures sample integrity and minimizes preanalytical variables, providing cancer researchers and clinical assay developers greater flexibility in sample handling and improved confidence in downstream plasma protein analysis. Protein Plus BCT is for Research Use Only. Not for use in diagnostic procedures.

#7632 Final survival outcomes and post-hoc tumor gene expression pathway analyses of complete responders from a phase Ib clinical trial of HSP90 inhibitor onalespib and paclitaxel in patients with advanced triple-negative breast cancer.

D. M. Quiroga[1], H. Savardekar[1], E. Schwarz[1], N. O. Williams[1], C. Johnson[1], A. Brufsky[2], M. Chambers[3], S. Bhattacharya[4], M. Patterson[1], S. D. Sardesai[1], D. Stover[1], M. Lustberg[1], A. Noonan[1], M. Cherian[1], D. M. Bystry[1], K. Hill[1], M. Chen[1], M. A. Phelps[1], J. Stephens[1], L. Yu[1], B. Ramaswamy[1], R. Wesolowski[1], W. E. Carson III[1];

[1]The Ohio State University Comprehensive Cancer Center, Columbus, OH, [2]University of Pittsburgh Medical Center Hillman Cancer Center, PIttsburgh, PA, [3]University of Kentucky Markey Cancer Center, Lexington, KY, [4]University of Pennsylvania Abramson Cancer Center, Philadelphia, PA

Background: Heat shock protein 90 (HSP90) is a molecular chaperone required for stabilization of client proteins over-activated in triple-negative breast cancer (TNBC). Over-expression of HSP90 client proteins has been implicated in paclitaxel resistance, therefore, it was hypothesized that the potent HSP90 inhibitor onalespib could improve paclitaxel efficacy. As TNBCs are a heterogenous population of tumors, it is important to establish biomarkers of response to this treatment combination.

Methods: Patients with TNBC were treated with intravenous (IV) paclitaxel and IV onalespib at doses ranging from 120 mg/m2 to 260 mg/m2 on days 1, 8, and 15 of a 28-day cycle utilizing a standard 3+3 design. The primary objectives were to determine dose-limiting toxicities and maximum tolerated dose. Secondary objectives included determination of overall response rate (ORR), duration of response (DOR), and progression-free survival (PFS). Retrospectively, archival tumor tissue was obtained from study patients and processed for RNA expression analysis by NanoString nCounter platform with the Breast Cancer 360 panel. Post-hoc gene expression analysis was performed through Qiagen Ingenuity Pathway Analysis (IPA). Linear models were employed to detect differential expression between conditions while considering cartridge effect.

Results: 31 patients were enrolled in this study, of which 90% received prior taxane therapy. The established recommended phase II dose was 260 mg/m2 onalespib when given with 80 mg/m2 paclitaxel. ORR was 20%, median DOR was 5.6 months. Three patients achieved complete responses (CR), all of whom had received prior taxane therapy. Nanostring profiling analysis revealed that patients who had a CR to treatment expressed higher levels of several breast cancer-associated genes also known to be dependent upon HSP90 activity compared to patients with progressive disease (PD) as their best treatment response. These genes include FGFR4, JAK2, PIK3R1, TGFB3, and TGFBR2 (all $p<0.05$). Tumor genes overexpressed in patients with PD versus CR included IRF6, MMP7, and KRT17 (all $p<0.01$). Additionally, IPA showed patients with CR to have substantial upregulation of PD-1, PD-L1, CTLA-4, p53, HER2, and cyclin/cell cycle regulatory signaling pathways compared to patients with PD (all $p<0.01$).

Conclusions: Combination treatment with onalespib and paclitaxel had an acceptable toxicity profile and showed anti-tumor activity in patients with advanced TNBC. Gene expression analysis of patient tumor samples suggest that TNBCs with greater activation of immune checkpoint pathways and those with proteins dependent on HSP90 activity, including p53 and HER2, may be more susceptible to HSP90 inhibition.

ClinicalTrials.gov study identification: NCT02474173

#7633 CXCR6 positive circulating mucosal-associated invariant T cells play the anti-tumor effect in non-small cell lung caner immunotherapy.

J. Qu, B. Wu, Y. Li, Q. Shen, W. Sun, L. Chen, J. Zhou, J. Zhou;
The First Affiliated Hospital, Zhejiang University School of Medicine, Hangzhou, China

Background: Mucosal-associated invariant T (MAIT) cells is are unconventional innate-like T lymphocytes abundant in human tissues. Recent studies have shown that MAIT cells play important roles in regulating tumor immunity. However, the immune characteristics of MAIT cells in non-small cell lung cancer (NSCLC) and its correlation with ICIs treatment efficacy remain unclear.
Method: In this study, we used single-cell RNA-sequencing (scRNA-seq), flow cytometry and multiplex immunofluorescence to assess the proportion and characteristics of CD8+MAIT cells in metastatic NSCLC patients who respond or not respond to anti-PD-1 therapy.
Results: The proportions of activated and proliferating CD8+ T cells and MAIT cells were significantly higher in responders-derived PBMC or lung tissues prior to anti-PD-1 therapy. Both peripheral and tumor-infiltrating CD8MAIT cells displayed upregulated CXCR6($P<0.05$). Besides, CXCR6+CD8MAIT cells from responders had higher expression of cytotoxicity-related genes, like CST7, GNLY, KLRG1, NKG7 and PRF1. Moreover, we found that patients with >1.7% of MAIT among peripheral CD8+ population showed a better response to immunotherapy.
Conclusion: CD8MAIT cells may be considered a predictive biomarker for patients responding to anti-PD-1 therapy in NSCLC. The correlation between CD8MAIT and immunotherapy sensitivity may ascribe to high expression of CXCR6.

#7634 HER2 extracellular domain in serum samples from HER2+ metastatic breast cancer patients as a potential biomarker of progression-free survival.

D. O'Reilly[1], M. Nolan[2], A. Teiserskiene[2], B. T. Hennessy[3], J. Crown[4], D. M. Collins[1];

[1]Dublin City University, Dublin, Ireland, [2]Cancer Trials Ireland, Royal College of Surgeons Ireland, Ireland, [3]Beaumont Hospital, Dublin, Ireland, [4]St Vincent's University Hospital, Dublin, Ireland

Introduction: The detection of serum biomarkers holds potential for non-invasive methods for early cancer detection, monitoring of disease progression, and assessment of treatment responses leading to earlier interventions that may significantly improve patient outcomes. Human epidermal growth factor receptor 2 (HER2) overexpression plays a key role in the prognosis of HER2+ breast cancer (BC). While HER2 is well-established as a cell surface marker, its soluble extracellular domain (ECD) in serum has gained attention as a potential prognostic biomarker. Elevated levels of HER2 ECD (>15ng/ml) have been associated with a poor outcome. However only a small percentage of primary BC patients have levels of HER2 ECD >15ng/ml. Research has suggested that HER2 targeted therapies can influence the rate of HER2 ECD shedding. Therefore, this study aimed to explore the association between circulating HER2 ECD levels with progression-free survival (PFS) and overall survival (OS) in patients with metastatic HER2+ BC.

Methods: Matched Pre and post treatment serum samples (n=25) from BC patients enrolled in TH V THL (ICORG (CTRIAL-IE) 11-10/NCT01526369) clinical trial were assessed. Human ErbB2 (HER2) ELISA Kit (Invitrogen) was used to detect levels of soluble HER2 ECD in the serum. Serum levels were stratified as Low (<300pg/ml n=5), Intermediate (300-700pg/ml n=10) or High (>700pg/ml n=10). Patient data correlation was used to assess PFS and OS, Kaplan-Meier survival curves were constructed based on the serum levels of HER2 ECD. Significance p values were determined using log-rank (Mantel-Cox) test.

Results: Levels of HER2 ECD detected (94-1730pg/ml) did not exceed 15ng/ml for any sample. There was no significant difference in HER2 ECD levels between treatment arms (TH vs. THL) for PFS (p=0.4685) or OS (p=0.1376). There was no change between the pre and post treatment HER2 ECD serum levels in the samples tested (p=0.344). However, when pre-treatment samples were stratified based on Low, Intermediate or High HER2 ECD levels, there was a significant increase in PFS for patients in the High cohort. Median PFS increased from 8.31 months in the Low cohort to 13.57 months in the Intermediate cohort. The median PFS increased further to 22.24 months in the High cohort (Log rank p=0.0197). The same parameters were applied for the analysis of OS, which also improved as the level of HER2 ECD increased. Median OS increased from 35.19 months (Low) to 68.7 months (Intermediate), with a Median OS not reached for the High cohort (Log rank p=0.077).

Conclusions: Patients with HER2 ECD levels above 700pg/ml display a survival advantage in this limited study. Further validation and prospective studies are warranted to fully establish the clinical utility of HER2 ECD as a biomarker in metastatic HER2+ BC.

#7635 Orion™: 14-plex clinical sample imaging of liver cancer modalities using one-step staining and imaging.

S. Larkin[1], J. Currenti[2], R. Pai[2], S. Chatterjee[3], A. Mishra[3], J. George[4], B. Gardner[1], A. Sharma[2];
[1]RareCyte, Inc., Seattle, WA, [2]Harry Perkins Institute of Medical Research, Sydney, Australia, [3]Telethon Kids Institute, Perth, Australia, [4]Westmead Institute of Medical Research, Sydney, Australia

Background To better understand the complexities of the tumor microenvironment (TME), high-resolution imaging at a sub-cellular resolution and high-plex is needed. These serve as a basis for biomarker quantification and more downstream, may provide the ability to predict patient outcome. Here, we investigate three whole slide liver sections: fetal liver, hepatocellular carcinoma (HCC), and colorectal cancer (CRC) liver metastasis.
Methods 5-micron sections were cut and mounted on Superfrost Plus slides prior to de-paraffinization and antigen retrieval using the BioGenex EZ-Retriever system. Autofluorescence was quenched using UV and white light and blocked with Image-iT™ FX Signal Enhancer. Whole slides were stained with the 14-plex antibody panel, coverslip mounted with ArgoFluor™ Mounting Medium and cured overnight. Whole slides were imaged at 20X using the Orion™ spatial biology platform. Coverslips were removed in aqueous solution prior to H&E staining and scanning.
Results Sample specific differences were observed, likely stemming from the different tissue sources. Data revealed a distinction between hepatocytes highlighted in the autofluorescence channel, sinusoids filled with proliferating progenitor cell and macrophages, and epithelial cells lining the border of the fetal liver forming the ductal plate surrounding the portal vein. Whereas in HCC, imaging revealed autofluorescent hepatocytes obliterating the sinusoids with some hepatocytes dividing, an extensive capillary network, and red bloods cells also highlighted in the auto fluorescent channel. T cells and macrophages showed clustering within the capillary networks and as expected, hepatocytes expressed high levels of Albumin. In the CRC liver metastasis sample, hepatocytes were shown to be surrounded by T cells, neoplastic glands (PanCK), and $CD163^{\pm}$ $FOLR2^{\pm}$ macrophages. Furthermore, the majority of the metastatic epithelial cancer cells were observed to be proliferating.
Conclusions We were able to observe precise differences in the tissue architecture of liver samples from three divergent sources. Specifically, the ability to identify distinct cell subtypes and their spatial co-localization may provide mechanistic insights into the spatial immune landscape and its role in disease progression and treatment outcome. This exemplifies the need for dissecting the spatial heterogeneity of the TME using a technology that offers a high-resolution subcellular snapshot in time; exhibiting the potential for Orion to bridge the gap from bench-to-bedside.

#7636 Quantitative analysis of colorectal adenocarcinoma images obtained by single-shot 17-plex staining followed by imaging with the Orion™ spatial biology platform.

E. Lo, T. George, **S. Larkin**;
RareCyte, Inc., Seattle, WA

Background To understand the tumor microenvironment (TME), high resolution imaging of multiple biomarkers with whole slide context can be used as a basis for downstream biomarker quantitation and predicting patient outcomes[1]. Here we investigate a sample of invasive colorectal adenocarcinoma using whole slide, single-step high-plex staining and imaging at single-cell resolution followed by quantitative analysis.

Methods The slide was stained in one round with a 17-plex immune-oncology panel then imaged in one round with the Orion™ spatial biology platform. Quantitative analysis was performed on the resulting TIFF file using the following pipeline:- Manually annotate regions of interest (ROI) on the tissue- Segment whole slide images into cells with UnMICST and S3segmenter - Import mask and clean data in QuPath - Generate primary feature data table with QuPath - Classify cells into populations in QuPath - Generate spatial biomarkers - Compare cell populations and their spatial interactions in the different ROIs.

Results Data revealed a distinction between normal colonic epithelium, well-differentiated adenocarcinoma with immune cell collection, and an infiltrating border of the carcinoma. Differences in immune cell content and spatial organization were measured, and the infiltrating border found to contrast with other tumor regions by showing a lower proliferative fraction (Ki-67, nuclear) and differences in E-cadherin and cytokeratin expression patterns.

Conclusions These data highlight the importance of sufficient plex, resolution and whole slide context to derive reliable spatial biomarkers of potential prognostic value. Further, hours vs. days speed for whole-section multiplexed biomarker quantitation, along with same-section conventional chromogenic analysis, makes this approach suited to multi-patient clinical studies.

[1] JR Lin et al., High-plex immunofluorescence imaging and traditional histology of the same tissue section for discovering image-based biomarkers, Nat Cancer, 4, 1036-1052 (2023).

CLINICAL RESEARCH: Prognostic Biomarkers 2
Poster Session

#7640 Prognostic significance of S100A16 expression in patients with resected lung adenocarcinoma.
J.-J. Hung;
National Yang Ming Chiao Tung University and Taipei Veterans General Hospital, Taipei, Taiwan

Background: Lung cancer is the leading cause of cancer death worldwide. Tumor recurrence is the most common cause of treatment failure after surgical resection. The S100 protein family is a multigenic group of cytoplasmic calcium-binding proteins. S100A16 has to be reported to be an independent prognostic indicator of poor overall survival in lung adenocarcinoma recently. However, the prognostic value of S100A16 in recurrence-free survival (RFS) in patients with resected lung adenocarcinoma has not been well demonstrated. The relationship between S100A16 expression and the histological subtypes of lung adenocarcinoma remained unknown.
Methods: A total of 79 patients with resected lung adenocarcinoma were included in the study. S100A16 expression was determined by immunohistochemistry in tumor specimens. The prognostic value of S100A16 overexpression and its relationship with clinicopathological variables, including histology subtypes, were investigated.
Results: S100A16 overexpression tended to be significantly associated with order age (P = 0.074). There was no significant association between S100A16 overexpression and predominant pattern group (lepidic/acinar/papillary vs. micropapillary/solid) (P = 0.447). Univariate analysis indicated that pathologic stage (II or III vs. I) (P = 0.001) and S100A16 overexpression (P = 0.005) were significant prognostic factors for worse recurrence-free survival (RFS). Predominant pattern group (lepidic/acinar/papillary vs. micropapillary/solid) (P = 0.064) tended to be a significant prognostic factor for worse RFS. In multivariate analysis, pathologic stage (II or III vs. I) (HR, 27.847; 95% CI, 4.173 to 185.831; P = 0.001), and S100A16 overexpression (HR, 21.740; 95% CI, 2.516 to 187.870; P = 0.005) were still significant prognostic factors for worse RFS.
Conclusions: S100A16 overexpression was a significant prognostic factor for worse RFS in patients with resected lung adenocarcinoma. This information is useful to stratify high-risk patients of recurrence after resection of lung adenocarcinoma.

#7641 Prognostic impact of functional germline mutations in muscle-invasive bladder cancer identified by neural network analysis.

G. P. Sonpavde[1], A. H. Nassar[2], A. Ravi[3], L. Sadler[4];

[1]AdventHealth Cancer Institute, Orlando, FL, [2]Yale Cancer Center, New Haven, CT, [3]Dana-Farber Cancer Institute, Boston, MA, [4]KeyBio, Boston, MA

Background: An accurate prognostic algorithm based on germline whole exome sequencing (WES) would complement tumor omics as a non-invasive source of biomarkers for guiding cancer patient therapy. In a previous study, we used WES and RNA-seq data from muscle-invasive bladder cancer (MIBC) and normal host cells to train a survival model, wherein we discovered that mutated germline genes accounted for 90% of feature importance. We have since defined a larger cohort to identify key germline biomarkers of overall survival (OS) that may be scalable for application in the clinic.

Methods: 169 patients from The Cancer Genome Atlas (TCGA) with MIBC stages T2-T4 that underwent radical cystectomy (RC) w/o neoadjuvant treatment were eligible. OS at 4 years was the primary clinical endpoint as it is associated with death due to metastatic tumor recurrence. Patients were dichotomized to *control* survivors who were alive at 4+ years, and *cases* who died within 4 years but no less than 4 months after RC. 49 qualifying survivors were propensity matched against 49 dead patients by stage, adjuvant treatment, gender, race, and age. The remaining 71 dead patients served as a holdout. Only high (e.g. frameshift) and moderate (e.g. indel) impact germline variants were included. Mutations were weighted for allele frequency (penalize common) and genotype (reward homozygous) before grouping at the gene level. A panel of the 21 most differential genes in stratified patients were selected for neural network training using AIQC. The model forced protective/ pathogenic genes to interact and produced individual survival probabilities. Gene importance was determined via permutation.

Results: OS was accurately predicted for 98.2% of patients: 1 FN, 2 FP, 37 TN, 119 TP. The top 3 permuted genes (and related pathways) were: SORL1 (Aβ), KIF27 (hedgehog), CUL7 (p53). The most differential gene was CUL7: 31% of survivors mutated vs 2% of dead.

Conclusion: Neural network analysis identified the promise of germline genetics as an accurate predictor of survival and tumor recurrence in MIBC patients. Upon validation in an external cohort, these biomarkers could be used to inform adjuvant therapy and complement molecular residual disease alongside circulating tumor (ct)-DNA.

#7642 Activated FAP+ cancer-associated fibroblasts in non-muscle invasive bladder cancer are associated with progression to muscle-invasive disease.

A. Abbas[1], S. Maskey[2], E. Cheng[2], Z. Li[3], K. Ganesh[1], S. Izadmehr[2], S. Janho dit Hreich[1], B. Demaille[1], J. Mesple[1], P. Sirven[1], C. Krucker[4], J. Fontugne[4], I. Bernard-Pierrot[4], Y. Allory[4], M. Merad[2], J. Adam[5], J. Sfakianos[6], E. Kenigsberg[2], M. Galsky[3], H. Salmon[1];

[1]Institut Curie, INSERM, U932, Equipe Leader Fondation ARC, PSL Research University, Paris, France, [2]The Precision Immunology Institute, Icahn School of Medicine at Mount Sinai, New York, NY, [3]The Tisch Cancer Institute, Icahn School of Medicine at Mount Sinai, New York, NY, [4]Institut Curie, CNRS, UMR144, Equipe labellisee Ligue Contre le Cancer, PSL Research University, Paris, France, [5]Department of Pathology, Paris Saint-Joseph Hospital, Paris, France, [6]Icahn School of Medicine at Mount Sinai, New York, NY

The majority of patients with bladder cancer initially present with non-muscle-invasive disease (NMIBC). While NMIBC may be cured with transurethral resection +/- intravesical therapies, approximately 20% of patients develop progression to muscle-invasive bladder cancer (MIBC) which requires life-altering treatments such as cystectomy and has a high risk of lethal metastatic recurrence. Current risk stratification for NMIBC relies on clinicopathologic features that overlook the potential role of the tumor microenvironment (TME) in bladder cancer pathogenesis. We sought to delineate the stromal and immune landscape alterations within the TME upon bladder cancer progression and to identify TME-related features that could enhance current prognostic approaches. Analyzing by single-cell RNA sequencing and multiplexed imaging of 22 untreated NMIBC and MIBC specimens, coupled with publicly available datasets, we discovered significant transcriptional variability among cancer-associated fibroblasts (CAFs) and macrophages across patients. This inter-patient variability was attributable to the extensive remodeling of these cell types during cancer progression. Notably, a specific subset of CAF, characterized by ITGA8+F3+ markers, was found to be highly enriched in NMIBC lesions and transcriptionally related to sub-urothelial fibroblasts of the healthy bladder, whereas a FAP+ CAF subset enriched for core matrisome related genes was dominant in MIBC lesions. We developed a FAP+ CAF signature which was then projected onto a large public dataset of bulk-RNAseq data from patients with NMIBC demonstrating that the FAP+ CAF signature was significantly associated with progression to MIBC independently of contemporary risk stratification scores. The presence of FAP+ CAFs in a subset of NMIBC specimens was orthogonally validated using immunohistochemistry. Importantly, areas with FAP staining were observed in close contact with individual or small groups of tumor cells exhibiting an invasive phenotype and partial epithelial-mesenchymal transition, likely explaining the higher risk of progression to MIBC. Our study improves our understanding of fibroblasts remodeling during bladder cancer progression and highlights the potential of integrating CAF-derived biomarkers into NMIBC risk stratification models.

#7643 Prognostic significance and immune infiltration patterns related to Claudin heterogeneity in pancreatic ductal adenocarcinoma patients.

A. A. Bhat[1], S. Usmani[1], H. Q. Sadida[1], S. Hashem[1], T. Masoodi[1], I. Ahmed[1], R. Kumar[2], M. Singh[3], P. Dhawan[4], S. Uddin[5], M. A. Macha[6], A.-S. Akil[1]; [1]Sidra Medicine, DOHA, Qatar, [2]School of Biotechnology, Shri Mata Vaishno Devi University, Katra, Jammu and Kashmir, India, [3]All India Institute of Medical Sciences (AIIMS), New Delhi, India, [4]University of Nebraska Medical Center, Omaha, Omaha, NE, [5]Translational Research Institute, Academic Health System, Hamad Medical Corporation, DOHA, Qatar, [6]Watson-Crick Centre for Molecular Medicine, Islamic University of Science and Technology, Awantipora, Kashmir, India

Background: Pancreatic ductal adenocarcinoma (PDAC) stands out for its aggressive nature, often manifesting through invasion, metastasis, and recurrence. These characteristics are partly attributable to the Epithelial-mesenchymal transition (EMT), a critical phenomenon that follows the disintegration of epithelial barriers, including tight junctions (TJs), where Claudin (CLDN) proteins are integral components.
Objective: This study focused on elucidating the differential expression of claudins in PDAC and exploring their correlations with disease progression, invasiveness, and immune infiltration.
Methodology: Utilizing UCSC TOIL RNA-seq, TCGA-PAAD genomic, and clinical data, we investigated the genomic alterations and differential expression of claudins in PDAC. Conducted survival analysis using log-rank tests. Assessed immune infiltration patterns using the EPIC deconvolution algorithm.
Results: Of 177 PDAC samples examined, 23 (13%) exhibited at least one form of claudin gene alteration, including mutations, amplifications, or deep deletions. Remarkably, 10 claudins (CLDN1, 2, 4, 5, 7, 11, 12, 15, 18, and 23) were found to be significantly overexpressed in PDAC samples, meeting a log2FC threshold of ≥1 ($p < 0.05$). Further, we identified a direct correlation between mRNA expression and copy numbers, alongside an inverse relationship with methylation levels, particularly in CLDN1, CLDN12, CLDN15, CLDN23, and CLDN4. Intriguingly, claudin expression escalated from grades G1 to G3 but diminished in G4, with CLDN1, CLDN4, and CLDN7 showing significant variability (Kruskal-Wallis rank test p-values of 1.2E-5, 0.00064, and 0.023, respectively). Survival analysis indicated that high expression levels of CLDN1 and CLDN4 were linked to poorer patient outcomes, while higher levels of CLDN5 and CLDN15 correlated with improved survival (log-rank p-values of 0.007, 0.016, 0.0035, and 0.0012, respectively), findings consistent across both univariate and multivariate analyses. Furthermore, immune infiltration patterns, assessed via the EPIC deconvolution algorithm, varied significantly between high and low CLDN expression groups. Specifically, low CLDN1 expression was associated with increased presence of B-cells, CAF, and $CD8^{+}$ T-cells but fewer endothelial cells, a pattern reversed in high CLDN1 expression cases. A similar trend was observed for CLDN4.
Conclusion: Our study underscores the significant prognostic value of claudin proteins in PDAC, highlighting their potential as indicators of disease progression and survival and their influence on the tumor's immune environment.

#7644 Prognostication of genomic characteristics of residual breast cancer after neoadjuvant chemotherapy.

J.-Y. Kim[1], S. Park[2], S. Ahn[3], E. Seo[4], S. Kim[3], M. Gregory[5], E. Killingbeck[5], E. Cho[1], J. Lee[1], J. Ahn[1], Y. Park[1], W.-Y. Park[4], H. Kim[3], S. Lee[2], Y.-H. Im[1]; [1]Samsung Medical Center, Seoul, Korea, Republic of, [2]Ulsan National Institute of Science and Technology, Ulsan, Korea, Republic of, [3]Sungkyunkwan University, Suwon, Korea, Republic of, [4]Samsung Genome Institute, Seoul, Korea, Republic of, [5]NanoString Technologies, Seattle, WA

Residual cancer burden (RCB) based on pathologic characteristics is the most powerful prognostic factor in breast cancer (BC) which received neoadjuvant chemotherapy (NAC) followed by surgery. According to RCB classification, class III predicted short survival duration regardless of BC subtypes according to hormone receptor (HR) and human epidermal growth factor receptor-2 (HER-2) state. However, up to 20-40% of BCs with RCB class III did not experience BC recurrence and had long term survival without disease recurrence. In our study, we evaluated genomic characteristics of BC which had high RCB class. We collected 96 fresh frozen BC specimens which had undergone surgery after NAC between 2010 and 2018 from Samsung Medical Center Biobank. We performed whole genome or exome sequencing, RNA sequencing and high-plex single-cell spatial transcriptomics. Of 96 BCs, 65 BCs had experienced BC recurrence and 31 BCs have not been BC recurrence. Of 65 BCs with dismal prognosis, 12 were HR+HER2-, four in HR+HER2+, 39 in triple negative breast cancer (TNBC) and 10 in HR-HER2+ BC. Of 31 BCs without recurrence, 11 were HR+HER2-, two in HR+HER2+, 14 in TNBC and four in HR-HER2+ BC. In HR+HER2- BC, ten of 12 BCs with dismal prognosis were categorized into basal like intrinsic subtype and two were into luminal B subtype compared that six of luminal A and five of luminal B subtype categorization in good prognosis BC group. Age associated mutation signature were enriched in HR+HER2- BC with good prognosis (p=0.027). Tumor microenvironment (TME) analysis using Kassandra suggested that high monocytes were associated with BC with dismal prognosis (p=0.00031). In single-cell spatial transcriptome analysis, T-cell abundance in the tumoral niche is associated with dismal prognosis in HR+HER2- BC (p=0.039). In TNBC, almost BCs (88.7%) were categorized into basal-like intrinsic subtype regardless of their prognosis. TME analysis presented that immune cells including macrophages and lymphocytes with CD4 and CD8 T cells were significantly enriched in TNBC with good prognosis (ps <0.05, respectively). In HER2+ BC, intrinsic subtypes were heterogeneous in both groups. Focal amplification in HER2+BC patient harbored DNA segments from different chromosomes more frequently than in those with good prognosis (p=0.00091), which was prominent in oncogenic extrachromosomal DNA amplifications compared to other oncogenic amplifications. In TME analysis, there were no specific cell enrichments according to BC prognosis but sing-cell spatial transcriptome analysis revealed that higher T-cell abundance in the tumoral niche was associated with HR+HER2+ BC with good prognosis (p=0.047). In conclusion, each BC subtype had their own genomic characteristics to determine their prognosis. Our study also suggested that TME characteristics was common prognostic factor for survival outcome of BC with residual tumor after NAC.

#7645 Differentially expressed genes as prognostic markers in racial disparities of prostate cancer.

A. A. Ahmed, S. Verma, I. M. Atawia, D. L. Shen, G. T. MacLennan, P. Fu, **S. Gupta**;
Case Western Reserve University School of Medicine, Cleveland, OH

Racial disparities in prostate cancer are prevalent, with African American (AA) men experiencing 60% greater incidence and 2 to 3 times higher mortality than Caucasian American (CA) men. Consequently, there is a pressing need for improved means of interrogating race/ethnicity-based prostate cancer biology in order to identify biomarkers to help stratify men at high-risk for prostate cancer-specific progression and death and offer treatment recommendation that would mostly benefit AA men undergoing early aggressive therapies. Current predictive models rely on clinical variables but do not account for these disparities. The overall goal is to construct a race-specific prostate cancer prognostic prediction model for risk assessment. Here we performed comprehensive bioinformatics analysis using the data from 17 pairs of gene expression array from AA and CA cohorts and identified 63 differentially expressed genes (DEGs) by race. Among them, chemokine receptor 4 (CXCR4), viz. p-Akt (Ser473), fatty acid synthase (FASN), interleukin-6 (IL-6) and matrix metallopeptidase 9 (MMP-9) gene expressions were significantly altered in AA groups. Immunohistochemistry was performed on 163 prostate cancer patient specimens to validate DEG expression and immunoreactive scores (IRS) were calculated. CXCR4 exhibited significantly higher expression in AA tumors, with > 85% of AA prostate tumors showing weak to strong CXCR4 expression, compared to < 5% in CA specimens. While immunostaining for IL-6, FASN, MMP9 and p-Akt did not provide a significant distinction between CA and AA cases. IRS analysis confirmed higher expression of CXCR4 in AA cancers, compared to CA prostate cancer ($p < 0.001$). MMP9 and IL6 expression were moderately higher in AA cancer compared to CA prostate cancer ($p < 0.05$). In contrast, FASN expression was significantly higher in CA cancer, compared to AA prostate cancer ($p < 0.001$). We further investigated the impact of these genes on biochemical recurrence-free survival (BCRFS) using Kaplan-Meier analysis to examine the differences between low-risk versus high-risk groups. BCRFS analysis demonstrated that CXCR4 is a determinant factor of recurrence risk in AA prostate cancer patients. The activation of the PI3K-Akt signaling pathway, particularly in AA patients, suggests its role in prostate cancer aggressiveness. Taken together, this study demonstrates the importance of differential expression of biomarkers which constitute the bulk tumors in driving cancer. The distinct gene expression patterns, especially the upregulation of CXCR4, in AA prostate cancer highlight its potential as a prognostic biomarker and a target for personalized treatment strategies. These findings encourage further study into the role of population-specific difference in adding CXCR4 in risk model construction, especially in machine learning models.

#7646 Evaluation of tumor immune microenvironment after neoadjuvant immunotherapy in patients with esophageal squamous cell carcinoma (ESCC): Towards a prediction for recurrence risk.

Z. Liu[1], B. Yu[1], Y. Yang[1], C. Qi[1], C. Yuan[1], Y. Yang[1], J. Wei[1], S. Chen[2], Y. Wang[2], Z. Li[1];
[1]Shanghai Chest Hospital, Shanghai, China, [2]Virtue Diagnostics (Suzhou) Co., Ltd, Shanghai, China

Background: Despite the promising potential of neoadjuvant immune checkpoint blockade (ICB) in ESCC, postoperative recurrence remains a critical challenge. Besides pathological response, there remains no biomarkers for recurrence risk prediction after neoadjuvant ICB. Recent studies have highlighted a strong association between ICB efficacy and tumor immune microenvironment (TIME). Thus, we sought to investigate the TIME features in surgically resected tumors following neoadjuvant ICB from patients with ESCC to develop a potential way for recurrence risk prediction.

Methods: This is a side study of a phase 2 NICE trial (ChiCTR1900026240) of 51 patients with resectable locally advanced ESCC who received neoadjuvant ICB plus chemotherapy followed by surgery from 2019 to 2020. TIME features of surgically resected tumors after neoadjuvant therapy were assessed by multiplex immunohistochemistry (mIHC) for immune markers (CD8, PD-L1, CD45RO, PD-1, Pan-CK, CD4, FoxP3, CD68, CD163). We first analyzed TIME features in tumors evaluated as pathological complete response (pCR) and major pathological response (MPR). Then, we divided 51 patients into a training and validation set; and machine learning was applied to identify a list of TIME features that predict recurrence-free survival (RFS) and to develop a TIME-based signature (TIS) on neoadjuvant ICB prognosis.

Results: Fifty-one patients from NICE trial were used for primary analysis. A higher positive rate of $CD8^{\pm}$ cells, $CD163^{-}CD68^{\pm}$ macrophages and $CD8^{\pm}CD45RO^{\pm}$ cells was observed in patients with pCR. Similarly, MPR patients exhibited a higher positive rate of $CD8^{\pm}$ cells and $CD8^{\pm}CD45RO^{\pm}$ cells. Regarding RFS prediction, machine learning selection of TIS were identified: $CD8^{\pm}PD1^{-}$(cytotoxic T cells), $CD4^{\pm}Foxp3^{\pm}$ (Treg), $CD8^{\pm}CD45RO^{\pm}$ (memory T cells), and M1 macrophages ($CD163^{-}CD68^{\pm}$) exhibited significant predictive value. Stratifying patients into low- and high-risk groups using TIS for RFS revealed a prolonged prolonged RFS in the low-risk group ($p<0.001$; HR: 0.08, 95% CI [0.03-0.25]). Notably, when applying TIS to pCR patients, we identified a subset of high-risk pCR patients (median RFS = 8.9 months, 1- year RFS=32%) relapsed earlier than low-risk pCR patients (median RFS = not reached, 1-year RFS=100%, $p<0.001$). Multivariable Cox regression analysis demonstrated that TIS was an independent predictor for RFS as well as overall survival (both $p<0.001$). Further independent validation (ICB and non-ICB cohort) of TIS is ongoing.

Conclusion: The establishment of a risk prediction model based on TIME demonstrated the potential to enhance postoperative monitoring management for ESCC patients who underwent surgery after neoadjuvant ICB. Our study provides insights into development of optimal post-immunotherapy management strategy.

#7647 Identification of transcriptional plasticity biomarkers for patient stratification.

J. Goldstein, C. Gavazzi, M. Grushko, M. Samizadeh, Z. ElSeht, K. Arline;
SHEPHERD Therapeutics, Boston, MA

Biomarker signatures associated with disease progression are important tools for the management of patient care. However, such signatures are frequently indication-specific, which limits their utility to stratify broader populations. Transcriptional plasticity, the ability of a transcriptome to change in response to external stimuli, is of interest due to its relation to disease progression and therapeutic response. To extend and generalize the measurement of a patient's risk of disease progression to a pan-cancer, sequencing-based biomarker, Emax, the maximum cytotoxicity of a compound in a cell line, was explored as a potential universal marker of transcriptional plasticity.

To explore correlation between Emax and transcriptional plasticity, cancer cell lines were ranked by mean Emax across multiple classes of cytotoxic compounds analyzed in GDSC (Yang et. al., 2013). Cell lines with lower Emax (more surviving cells at high drug concentrations) were filtered to exclude cell lines which tended to have higher IC50 values to remove cell lines that may be generally more resistant. With GDSC1 as the train set and GDSC2 as the test set, differentially expressed genes between high-Emax and low-Emax cell lines were selected for further analysis and possible inclusion in the plasticity biomarker signature.

Test analysis in GDSC2 revealed an R2 of 0.88 suggesting transferability. For clinical validation, public repositories were queried for tumor RNA sequencing data with paired response data. To avoid batch effects between experiments, preliminary validation focused on one sufficiently large dataset with well-curated response data (n = 170; Barrett et. al., 2013, GSE91061; phs000452.v1.p1). Analysis of the expression of the genes identified in the in vitro signature revealed significant differential expression between patients who were reported as having an objective response and patients who achieved stable disease as best response. In silico pathway analysis of this signature revealed enrichment in cell-cell adhesion, signaling, and gene regulation, which relate to the hallmarks of phenotypic plasticity and epigenetic reprogramming (Hanahan, 2022).

This analysis reveals similarity between gene expression patterns associated with Emax measured in vitro and transcriptional plasticity in the clinic. Additional experimentation is underway to prospectively analyze this set of biomarkers and to retrospectively validate this signature in additional datasets with the goal of patient stratification by the risk of disease progression following an initial, incomplete response to therapy.

#7648 COL6A1 expression as a potential prognostic biomarker for risk stratification of T1HG bladder cancer: Unveiling the aggressive nature of a distinct non-muscle invasive subtype.

X.-M. Piao[1], Y. Byun[1], C.-M. Zheng[1], S.-K. Kim[2], S.-H. Park[3], K. Min[4], H. Park[4], S. Moon[5], K. Kim[5], H. Kang[5], W. Kim[5], S. Yun[5];
[1]College of Medicine, Chungbuk National University, Cheongju, Korea, Republic of, [2]Korea Research Institute of Bioscience and Biotechnology, Daejeon, Korea, Republic of, [3]University of Science and Technology, Daejeon, Korea, Republic of, [4]Gwangju Institute of Science and Technology, Gwangju, Korea, Republic of, [5]Chungbuk National University Hospital, Cheongju, Korea, Republic of

Introduction and Objectives: T1 high grade (T1HG) bladder cancer (BC) is a type of non-muscle invasive BC (NMIBC) that is recognized as an aggressive subtype with a heightened propensity for progression. Current risk stratification methods for NMIBC rely on clinicopathological indicators; however, these approaches do not adequately capture the aggressive nature of T1HG BC. Thus, new, more accurate biomarkers for T1HG risk stratification are needed. Here, we enrolled three different patient cohorts and investigated expression of *COL6A1*, a key component of the extracellular matrix, at different stages and grades of BC, with a specific focus on T1HG BC. **Materials and Methods:** Samples from 298 BC patients were subjected to RNA sequencing and real-time PCR. **Results:** We found that T1HG BC and muscle invasive BC (MIBC) exhibited comparable expression of *COL6A1*, which was significantly higher than that by other NMIBC subtypes. In particular, T1HG patients who later progressed to MIBC had considerably higher expression of *COL6A1* than Ta, T1 low-grade patients, and patients that did not progress, highlighting the aggressive nature and higher risk of progression associated with T1HG BC. Moreover, Cox and Kaplan-Meier survival analyses revealed a significant association between elevated expression of *COL6A1* and poor progression-free survival of T1HG BC patients (multivariate Cox hazard ratio, 16.812; 95% confidence interval, 3.283-86.095; P=0.001 and P=0.0002 [log-rank test]). **Conclusion:** These findings suggest that *COL6A1* may be a promising biomarker for risk stratification of T1HG BC, offering valuable insight into disease prognosis and guidance of personalized treatment decisions.

#7649 Inflammatory biomarkers by sarcopenia status in diverse individuals with lung cancer.

C. A. Byrne[1], G. Fantuzzi[1], V. M. Oddo[1], S. Kim[1], T. J. Koh[1], S. L. Gomez[2];
[1]University of Illinois at Chicago, Chicago, IL, [2]Rush University, Chicago, IL

Background: Sarcopenia and inflammation are independent prognostic indicators of poor survival in lung cancer. Systemic inflammation contributes to sarcopenia or low muscle mass through increased catabolism and decreased synthesis of muscle protein. In turn, sarcopenia leads to inflammation in the muscle and exacerbation of systemic inflammation. Specific Aim: The aim of this study was to determine the association between sarcopenia and systemic biomarkers of inflammation including neutrophil to lymphocyte ratio (NLR), platelet to lymphocyte ratio (PLR), and albumin in diverse individuals with lung cancer and determine their use as prognostic indicators of sarcopenia. Methods: This retrospective cross-sectional study included 218 non-Hispanic Black (n=111) and White (n=107) individuals with lung cancer. Computed tomography scans were analyzed to calculate skeletal mass index (SMI) at the third lumbar vertebra. Sarcopenia was defined using published sex-specific criteria for SMI in healthy individuals then categorized into the binary variable of sarcopenia/no sarcopenia. NLR, PLR, and albumin were analyzed as both continuous and categorical variables, with NLR> 3, PLR >150, and albumin <3.5 defining moderate to high inflammation. T-tests, Mann Whitney U, Chi square, and adjusted Logistic Regression were used as appropriate. Results: Subjects presented with a mean age of 68.5 + 9.8 years, BMI of 26.3 + 5.9 kg/m^2, 50.9% non-Hispanic Black, and 49.5% female with significantly higher prevalence of late-stage lung cancer (61.9% versus 38.1% early-stage, p<0.001) and no differences in age and BMI by race/ethnicity. Mean NLR (6.2 + 7.2), PLR (226.9 + 157.9), and albumin (3.2 + 0.6) indicated an inflammatory state in diverse individuals with lung cancer, with significantly higher NLR (8.5 + 9.7 versus 4.7 + 4.2, p<0.001) and PLR (268.9 + 204.5 versus 198.7 + 108.9, p<0.01) and significantly lower albumin (3.1 + 0.7 versus 3.4 + 0.5, p<0.01) in those with sarcopenia compared to those without sarcopenia. The odds of sarcopenia were 2.2 higher with NLR > 3 compared to NLR <3 (95% CI: 1.1, 4.4) and 2.5 higher with albumin <3.5 compared to albumin >3.5 (95% CI: 1.2, 5.3) after controlling for race/ethnicity, stage of cancer, age, and BMI. PLR > 150 was not a significant predictor of sarcopenia. Conclusion: Diverse individuals with sarcopenia of lung cancer present with higher inflammation compared to individuals with lung cancer but without sarcopenia as indicated by NLR, PLR, and albumin levels. Moderate to high levels of inflammation as indicated by high NLR and low albumin may help predict sarcopenia status in diverse individuals with lung cancer.

#7650 An analysis of the prognostic role of sarcopenia derived with fully automated deep learning slice-based muscle estimation in patients with metastatic non-small cell lung cancer (NSCLC).

W. Safta[1], R. Santana-Davila[2], D. Paulucci[1], W. J. Geese[1], D. J. Grootendorst[1];
[1]Bristol Myers Squibb, Princeton, NJ, [2]Fred Hutchinson Cancer Center, Seattle, WA

Introduction: Sarcopenia, progressive and generalized loss of skeletal muscle mass, is difficult and labor intensive to directly measure as it requires manual segmentations by radiologists from computed tomography (CT) scans. Sarcopenia has been shown to be a prognostic factor in some metastatic cancers. We evaluated the impact of sarcopenia derived via an automated segmentation algorithm on outcomes in the Phase 3 NSCLC clinical trial, CheckMate 227 (NCT02477826)

Methods: The sarcopenia score assessment involves automated selection of the L3 vertebra level slice from abdominal or chest, abdomen, and pelvis (CAP) CT scans, followed by automated segmentation of the muscle area from that slice. Sarcopenia scores were derived from previously established definitions of sarcopenia, with values below 41 cm^2/m^2 for female patients (regardless of BMI) and below 43 cm^2/m^2 or 53 cm^2/m^2 for male (based on BMI < 25 kg/m^2 or ≥ 25 kg/m^2). Among the 967 patients with evaluable scans, sarcopenia at baseline was identified in 68.39% (n=329/481) patients receiving nivolumab (NIVO) with ipilimumab (IPI) and 70.2% (n=341/486) receiving chemotherapy (Chemo).

Results: There was a trend of worse overall survival (OS) in patients with baseline sarcopenia across both treatment arms (minimum follow up 49.4 months). In patients with baseline sarcopenia vs ITT, median OS was 16.5 mo vs. 21.8 mo (p= 0.219) within the NIVO + IPI arm and 12.9 mo vs.15.0 mo (p= 0.273) within the Chemo arm respectively. Any increase in muscle mass from baseline to week 12 was associated with better OS for patients treated with NIVO+IPI (n=98) with sarcopenia at baseline compared to those without an increase in muscle mass (median OS 45.3 mo vs.19.5 mo, p= 0.012). This was not seen in those who received Chemo (n=87). Weight and muscle mass were moderately correlated at baseline (r=0.60).

Conclusions: We found that in CheckMate 227, baseline sarcopenia is associated with numerically worse OS, regardless of treatment, leading to potential use as a negative prognostic biomarker. Patients with NSCLC receiving immunotherapy might benefit from changes in muscle mass being monitored during treatment. Validation of these findings in other studies and other tumor types is warranted.

#7651 Evaluating epigenetic markers for naive, memory and overall B cells for disease diagnosis and prognosis in patients with B-CLL.

K. Schildknecht[1], K. Bourquain[1], J. Werner[2], J. Schulze[2], S. Walter[2], E. Raschke[3], D. Phippard[3], **A. Bisconte**[3], B. Seliger[4], C. Wickenhauser[4], S. Olek[1]; [1]Precision for Medicine, Berlin, Germany, [2]Epimune GmbH, Berlin, Germany, [3]Precision for Medicine, Frederick, MD, [4]Martin Luther University Halle-Wittenberg, Halle/Saale, Germany

Chronic lymphocytic leukemia (CLL) is a hematological cancer classified as low-malignancy non-Hodgkin lymphoma that accounts for approximately a quarter of all leukemias. Since only some patients will develop aggressive cancer and require treatment, accurate disease prognosis is crucial. A wide range of parameters with prognostic value have been described, including age, clinical stage, mutational status, protein markers, and flow cytometry levels of CD19+CD38+ B cells above 20%. Here, we investigated epigenetic markers for B cell types including a marker for overall B cells, naïve B cells, memory B cells and IgM positive B cells in a cohort of more than 40 patients with B-CLL. When comparing to a cohort of more than 100 healthy donors, the epigenetic B cell marker identified all patients with 100% sensitivity and specificity. In addition, the epigenetic B cell markers for naïve and memory B cells identified with high sensitivity and excellent specificity a subgroup of B-CLL patients with CD19+CD38+ B cell levels above 20% which is associated with an unfavorable prognosis. The results suggest that the epigenetic analysis of B cells in capillary blood may be a promising tool for B-CLL diagnosis and disease prognosis.

#7652 Plasma markers of hemostasis, fibrinolysis, and angiogenesis prior to androgen deprivation therapy (ADT) in progressive prostate cancer (PC) and associations with long-term thrombotic events and survival.

Jessica S. Palmer, Charlene Thomas, Nicole Jacobs, David Nanus, Scott T. Tagawa

Weill Cornell Medicine, New York, NY

Background: PC is the third most common malignancy associated with thrombosis, procoagulants may play a role in tumorigenesis and progression, and patients (pts) with PC may have activation of the hemostatic system evident in plasma. The prognostic significance of these markers and their relationship to thrombotic events and overall survival (OS) are under-explored.
Methods: Patients >18 years were included if they had progressive PC planned to start ADT, were >6 months from surgery or RT, with no history of prior VTE, unexplained bleeding, current or planned anticoagulation, or an additional active malignancy. Plasma samples were obtained via peripheral venipuncture in tubes containing 3.2% sodium citrate and immediately placed on ice. Samples were analyzed for D-dimer, thrombin-antithrombin complex (TAT), IL-6, IL-8, VEGF, and tissue factor (TF) levels by ELISA. Patients had markers drawn at baseline (prior to initiation of ADT), 1 month, and 6 months after initiation.
Results: 40 patients were accrued with a median age of 68 years. At baseline, 29 (73%) had presence of metastases. Baseline median PSA was 15 and median PSA doubling time was 0.32. Baseline median hemoglobin was 13.85, platelets were 218, D-dimer was 322 ng/dL, IL-6 was 0 pg/mL, IL-8 was 0 pg/mL, TAT was 3 ug/L, VEGF was 21 pg/mL, and TF was 26 pg/mL. Median follow-up was 78 months. During follow up, 35 (87.5%) had metastases. 10 (25%) had thrombotic events (6 [15%] venous, 4 [10%] arterial) at median 37 months follow up. Median baseline age of pts with subsequent thrombotic events was 74, vs 67 in those without a thrombotic event. While there was no significant difference in baseline PSA between groups with and without clotting events, pretreatment PSA doubling time was significantly lower in pts with subsequent thrombosis (0.27 vs 0.35, p=0.047). Median baseline D-dimer and TF were higher in patients with subsequent thrombosis (D-dimer: 516 vs 282, p=0.10; TF: 36 vs 24, p=0.12). In univariate analysis, baseline IL-6 and VEGF were associated with OS (IL-6: HR=1.05, 95% CI [1.01,1.09], p=0.025; VEGF: HR=1.02, 95% CI [1.00,1.03], p=0.028). When controlling for presence of metastasis, baseline TAT was associated with OS (HR=1.05, 95% CI [1.00,1.11], p=0.055).
Conclusions: Plasma markers of hemostatic activation, fibrinolysis, and angiogenesis prior to initiation of ADT are associated with subsequent thrombotic events and overall survival years later. Further analysis will examine how these markers change over time with hormonal therapy.

#7653 Role of ITGB2 in patients with luminal B1 breast cancer.

C.-Y. Liu, J.-L. Chen, Y.-F. Tsai, T.-C. Chao, W.-L. Wang, P.-J. Lien, C.-Y. Hsu, J.-I. Lai, C.-C. Huang, J.-H. Chiu, L.-M. Tseng;
Taipei Veterans General Hospital, Taipei, Taiwan

Purpose: Luminal-type breast cancers are the most commonly diagnosed in women. Among them, the luminal B1 subtype exhibits higher proliferation rates and a worse prognosis compared to the luminal A subtype. Despite significant advancements in detection and therapies, recurrence still occurs after primary treatment. In this study, our aim is to identify genomic alterations in early recurrent luminal B1 breast cancer.
Experimental Design: In this VGHTPE cohort, we recruited a total of 42 patients diagnosed with stage I-III luminal B1 breast cancer, comprising 15 subjects who experienced recurrence within five years and 27 subjects who did not. Genomic DNA was extracted from formalin-fixed paraffin-embedded samples and subjected to targeted next-generation sequencing. We assessed cell aggressiveness through in vitro transwell migration, invasion, and sphere assays.
Results: Luminal B1 breast cancer patients with advanced stage and poorly differentiated tumors were associated with recurrence within five years. Driver gene mutation analysis revealed that *TP53* mutations were present in 46.7% of patients who experienced recurrence within five years, compared to 29.6% in the non-recurrence group. In the analysis of copy number variations, the most common amplifications/gains observed in luminal B1 breast cancer patients were in *MCL1*, *MYC*, and *KLF6*. Remarkably, patients who experienced recurrence within five years showed a higher occurrence of gain in *ITGB2*, the gene encoding the integrin β chain, compared to those who remained recurrence-free. Patients with *ITGB2* amplifications/gains had a shorter 5-year recurrence-free survival compared to those with a neutral status. *In vitro* studies revealed that the knockdown of ITGB2 suppressed cell migration, invasion, and sphere formation in estrogen receptor-positive HER2-negative breast cancer cells.
Conclusion: Our study has identified *ITGB2* amplifications/gains as a potential biomarker for early recurrence in luminal B1 breast cancer.

#7654 Tertiary lymphoid structure associates with poor prognosis in locally advanced esophageal squamous cell carcinoma treated with neoadjuvant chemoradiotherapy.

T.-C. Huang[1], C.-W. Liang[2], Y.-I. Li[2], J.-C. Guo[3], C.-C. Lin[1], J.-M. Lee[1], Y.-K. Chao[4], C.-H. Hsu[1];
[1]National Taiwan University Hospital, Taipei, Taiwan, [2]Fu-Jen Catholic University Hospital, New Taipei City, Taiwan, [3]National Taiwan University Cancer Center, Taipei, Taiwan, [4]Chang-Gung Memorial Hospital, LinKou, Taoyuamg, Taiwan

Introduction: Tertiary lymphoid structure (TLS) has been found to associate with good prognosis in various cancer types including esophageal squamous cell carcinoma (ESCC). A recent study involving patients receiving curative surgical resection alone for localized ESCC showed TLS as a favorable prognostic factor associated with improved progression free survival (Hayashi et al. British Journal of Cancer, 2023;128:2175-2185). Our study aimed to investigate the prognostic significance of TLS in patients with locally advanced ESCC receiving neoadjuvant chemoradiotherapy (CRT).
Patients and Methods: We retrospectively enrolled 137 patients of locally advanced ESCC patients from two referral centers of Taiwan from 2002 to 2018. All patients received paclitaxel/platinum-based CRT followed by esophagectomy. Primary esophageal tumor tissues biopsied endoscopically before treatment were collected for immunohistochemical stains for CD20 (clone L26; Zytomed, Berlin, Germany) and CD23 (clone DAK-CD23; agilent Dako, California, U.S.A.). The TLS status of each patient was defined as no TLS (no aggregation of CD20-positive cells), immature TLS (aggregation of CD20-positive cells without CD23-positive cells in it), and mature TLS (aggregation of CD20-positive cells with CD23-positive cells in it). The associations of the TLS status with pathologic complete response (pCR) and overall survival (OS) were analyzed univariately and multivariately by logistic regression and cox regression, respectively. The variables included in the analyses were age, gender, tumor location, clinical T stage, clinical N stage, the institutes, PD-L1 expression on tumor cells (PD-L1 TC) and immune cells (PD-L1 IC), and the TLS status.
Results: The median age was 54 years with 125 males and 12 females. The TLS status of no, immature, and mature TLS were seen in 64, 40, and 33 patients, respectively. Mature TLS was associated with PD-L1 IC (p=0.0007). Compared to no TLS, mature TLS associated with lower pCR rate (24% vs 47%) in both univariate (OR: 0.36, p=0.034) and multivariate (OR: 0.26, p=0.023) analysis. Compared to no TLS, mature TLS was associated with shorter OS (median OS: 27 vs 46 months) in multivariate analysis (HR: 2.96, p=0.0008), but not in univariate analysis (HR: 1.29, p=0.29). Other prognostic factors associated with OS in multivariate analysis include male gender (HR: 2.88, p=0.021), PD-L1 TC (HR: 1.62, p=0.039), and PD-L1 IC (HR: 0.30, p<0.0001).
Conclusion: Mature TLS is an independent factor for poor treatment outcomes, including pathologic response and overall survival in locally advanced ESCC patients receiving neoadjuvant CRT. Additional studies are warranted to validate this finding. (The study was supported by the grant NTUH 110-S5021, MOST 108-2314-B-002-076-MY3, and MOHW 111-TDU-B-221-114006)

#7656 Clinicogenomic anlaysis reveals a role for TP53 mutations in distant progression of high-grade glioma.

B.-H. Kang[1], S. Lee[2], J. Lee[2];

[1]Ewha Womans University School of Medicine, Seoul, Korea, Republic of, [2]Seoul National University College of Medicine, Seoul, Korea, Republic of

Purpose: High-grade glioma (HGG), the most common form of primary brain tumor, is highly lethal and treatment options remain limited. Despite advances in genomic technologies, there are few molecular biomarkers to guide precision medicine for HGG. Here, we aimed to identify the clinicogenomic features associated with HGG prognosis and recurrence patterns.

Methods: Our single-institution retrospective analysis included 220 patients initially diagnosed with adult HGG (grade 3 or 4) who underwent next-generation sequencing targeting 82 brain tumor-relevant genes. The patients were categorized according to the 2021 WHO classification and their clinical status, survival, genomic profile, and recurrence patterns were analyzed.

Results: At a median follow-up of 23 months (ranges, 2-59 months), 180 patients (82%) showed either progression or recurrence. A total of 15% of patients were reclassified under the 2021 WHO classification, revealing a clear separation of progression-free survival (PFS) and overall survival (OS) curves between grades 3 and 4 gliomas. We found that *TP53* mutations were significantly associated with the occurrence of distant progression, especially in grade 4 gliomas. Additionally, *TP53* mutations were more common in patients with higher Ki67 index and subependymal/leptomeningeal seeding, indicating an increased risk of distant progression in *TP53*-mutated grade 4 glioma patients. Following multivariate Cox regression analysis, *TP53* mutations were independent predictors of OS (hazard ratio [HR]=1.47, P=0.039) and distant PFS (HR=1.71, P=0.005).

Conclusion: Considering the elevated risk of distant progression in grade 4 gliomas with TP53 mutations, our results underscore the necessity for additional research into the most effective treatment approaches for these patients.

Keywords: high-grade glioma, *TP53*, pattern of failure, distant progression, next-generation sequencing

#7657 Detection of *KMT2A*-PTDs and *KMT2A* fusions using next generation sequencing.

J. Huang[1], H. Gu[2], J. Orton[2], M. Sedova[1], A. Marcovitz[1], J. Burke[1], S. Brozio[1], P. Williams[3], S. Myrand[3], N. Olowo[1], A. Broomer[4], B. Deal[1], C. Seeger[5], S. Sadis[3], S. Rozenzhak[4], F. Hyland[1], G. Liu[2];

[1]Thermo Fisher Scientific, South San Francisco, CA, [2]Sonora Quest Laboratories, Phoenix, AZ, [3]Thermo Fisher Scientific, Ann Arbor, MI, [4]Thermo Fisher Scientific, Carlsbad, CA, [5]Thermo Fisher Scientific, Guilford, CT

Introduction: *KMT2A (MLL)* rearrangements (fusions) is a therapeutic biomarker for Menin inhibitors. *KMT2A*-PTDs (partial tandem duplications) are considered a prognostic biomarker in myeloid malignancies. *KMT2A* fusions and PTDs are traditionally detected by RT-qPCR (quantitative real-time PCR). This study investigates *KMT2A* PTDs levels in healthy donors and myeloid malignancy samples to establish a threshold to report samples with high PTDs, using next generation sequencing (NGS) with Oncomine™ Myeloid Assay GX v2. We also report *KMT2A* fusions in myeloid malignancies.

Methods: We sequenced 8483 research samples with known myeloid malignancies at Sonora Quest Laboratories™ and at Thermo Fisher Scientific™. We acquired 20 healthy donor whole blood samples (total 127 replicates) from Stanford™ Blood Center and Discovery Life Sciences™ and sequenced them at 3 different sites of Thermo Fisher Scientific™. Samples were sequenced with the Ion Torrent™ Genexus™ 6.6 or Ion GeneStudio™ S5 System. They were profiled for 6 different *KMT2A*-PTD variants and 199 *KMT2A* fusion isoforms.

Results: The mean read length of this data set is 90 - 120 bp and the mean mapped fusion reads is 20,000 - 30,000. *KMT2A*-PTDs were detected in both healthy donors and myeloid samples. Healthy donor PTD read counts were consistently <2000 and averaged 1/3 of myeloid sample PTD read counts. About 33% of myeloid samples had higher PTD read counts than any healthy donor sample. BLAT (BLAST-Like Alignment Tool) analysis confirmed specific exon matching on the *KMT2A* gene in both cohorts. Among the 8483 myeloid samples, 162 samples contained a total of 5 unique *KMT2A* PTDs, and 105 samples contained a total of 30 unique *KMT2A* fusion isoforms with *KMT2A-MLLT1* and *KMT2A-MLLT3* being the most prevalent *KMT2A* fusion gene pairs.

Conclusions: We characterize the *KMT2A* fusions present in myeloid malignant samples. We also describe the abundance of *KMT2A* PTDs in both healthy donor and myeloid samples, with myeloid cases showing significantly higher PTD read counts. *KMT2A* PTD read count >2000 is present only in malignant samples but not in healthy donors. This intriguing finding opens opportunities for prospective studies to monitor individuals with elevated PTD levels for myeloid malignancy development and retrospective studies to explore whether healthy donors identified with this alteration years ago after blood donation were subsequently recorded in the national health system with myeloid malignancies.

#7658 Artificial intelligence-powered spatial analysis of tumor-infiltrating lymphocytes as a prognostic biomarker for pembrolizumab plus chemotherapy in recurrent or metastatic head and neck squamous cell carcinoma.

S. Park[1], J. Shin[1], C.-Y. Ock[2], C. Ahn[2], H. Jung[1], S.-H. Lee[1], M.-J. Ahn[1];

[1]Samsung Medical Center, Seoul, Korea, Republic of, [2]Lunit, Seoul, Korea, Republic of

Background: Programmed cell death ligand 1 (PD-L1) expression alone has limited predictive value for pembrolizumab plus 5-fluorouracil and platinum (PFP) therapy in recurrent or metastatic head and neck squamous cell carcinoma (HNSCC). An artificial intelligence (AI)-powered spatial tumor-infiltrating lymphocyte (TIL) analyzer may provide independent prognostic information.

Methods: This study included 63 patients with locally incurable HNSCC who received first-line PFP at Samsung Medical Center. Patients were classified into inflamed phenotype (IP) or non-inflamed phenotype (NIP) based on the 5% proportion threshold of inflamed 1 mm^2-sized grids over total grids within hematoxylin and eosin-stained whole-slide images (WSIs) analyzed using Lunit SCOPE IO. We evaluated the prognostic value of inflamed status and densities of intratumoral TILs (iTILs), stromal TILs (sTILs), and tumor microenvironment TILs (tTILs).

Results: Patients were predominantly male (78%). The median age at PFP initiation was 57 years. The most common primary tumor site was oral cavity (49.2%), followed by oropharynx (16%) and hypopharynx (10%). Of the 37 patients with available PD-L1 combined positive score (CPS), 2 (5%), 23 (62%), and 12 (32%) had CPS values of <1, 1-19, and ≥20, respectively. The overall response rate was 54%, with 67% in the CPS ≥20 subgroup and 48% in the CPS <20 subgroup. The median progression-free survival (PFS) was 7.2 months, with 10.8 months for patients with CPS ≥20 and 5.5 months for patients with CPS <20. The median overall survival (OS) was 18.6 months. Among 62 patients with available WSIs, 47 (74%) and 15 (26%) patients were categorized as having an IP and NIP, respectively. Oral cavity cancer was enriched with IP (57.4% of all IP cases vs 26.7% of all NIP cases), while all four paranasal sinus tumors had NIP. The overall response rate was 57% in the IP group and 44% in the NIP group. Patients with IP had significantly longer PFS and OS than patients with NIP, both in unadjusted (hazard ratio
[HR] for PFS, 0.4; 95% confidence interval [CI], 0.21-0.78; P = 0.007; HR for OS, 0.43; 95% CI, 0.2-0.95; P = 0.036) and PD-L1 CPS-adjusted analyses (HR for PFS, 0.41; 95% CI, 0.21-0.79; P = 0.008; HR for OS, 0.4; 95% CI, 0.18-0.89; P = 0.025). High densities (≥25th percentile) of iTILs, sTILs, and tTILs were all significantly associated with prolonged PFS after CPS adjustment (P = 0.001, 0.001, and 0.012). High density of iTILs was also significantly associated with improved OS (P = 0.001 after CPS adjustment), while there was no significant association between OS and high density of sTILs or tTILs (0.077 and 0.085, respectively, after CPS adjustment).

Conclusion: An AI-driven spatial TIL analyzer might serve as a simple and independent prognostic biomarker in HNSCC patients receiving pembrolizumab plus chemotherapy.

#7659 AI-driven hypothesis-free analysis for biomarker discovery: Introducing the Biomarkers Navigator Framework.

I. Kagiampakis[1], M. Gidwani[2], I. Korkodinov[2], G. Ponomarev[2], E. Jacob[3];
[1]AstraZeneca US, San Francisco, CA, [2]AstraZeneca US, Gaithersburg, MD, [3]AstraZeneca US, Waltham, MA

The pivotal role of biomarkers in personalizing patient treatment and guiding drug development is well-recognized, with the ultimate goal of enhancing therapeutic efficacy and patient quality of life by minimizing adverse events. Their development, however, is challenged by strict regulations and high costs, leading to sparse and varied data collected over extended periods and through diverse technologies. These variations complicate the harmonization and analysis of the data. Traditional methods struggle to navigate these complexities, further obscuring biomarker identification. For instance, PDL-1, approved as a biomarker by the FDA, has its effectiveness debated in several studies. To address these issues, we introduce Biomarkers Navigator, a flexible and automated analysis framework engineered explicitly for the robust identification of biomarkers. This framework is designed to aggregate, standardize, and store expansive biomarker information, ensuring efficient and traceable knowledge retrieval. By pre-calculating each potential biomarker, Biomarkers Navigator enables immediate and comprehensive meta-analyses, facilitating rapid decision-making tailored to the level of risk acceptance. Large Language Models (LLMs) further enhance the framework's capability to uncover signatures of response and resistance. LLM integration has accelerated the discovery of new potential biomarkers for hematological malignancies by combining prior knowledge and previously obscured associations. Our approach demonstrates the feasibility of large-scale hypothesis-free analysis and substantiates the utility of AI in unveiling hidden biological connections within clinical data. Our findings underscore the potential of AI-augmented frameworks in revolutionizing biomarker discovery and advancing personalized medicine.

#7660 L-Arginine metabolism is of prognostic relevance in women with breast cancer, but varies considerably between subtypes in vitro - A bedside-to-bench translational approach.

J. Hannemann[1], L. Oliveira Ferrer[1], A. Roglin[1], F. Kleinsang[1], V. Muller[1], I. Witzel[2], R. Boger[1];

[1]University Medical Center Hamburg-Eppendorf, Hamburg, Germany, [2]University Hospital Zurich, Zurich, Switzerland

Availability of the semi-essential amino acid L-arginine (L-arg) is limiting for proliferation in highly proliferative tissues. L-Arg is also a substrate for nitric oxide synthases (NOS) and arginases (ARG) 1 and 2. Methylation of L-arg residues within proteins by protein L-arg methyltransferases (PRMTs) leads to asymmetric (ADMA) and symmetric dimethylarginine (SDMA). Protein L-arg methylation is an important post-translational mechanism to regulate gene expression and cell cycle control. We measured L-arg and its metabolites in a prospective cohort of patients with primary breast cancer (BC). We further measured these metabolites and expression of genes involved in L-arg metabolic pathways in cell lines representing intrinsic BC subtypes. Plasma L-arg-related metabolite concentrations from 243 women with primary BC were associated with total mortality and disease recurrence during a median follow-up of 88 (IQR, 82-93) months. MCF-7, BT-474, SK-BR-3, and MDA-MB-468 cells representing ER-positive, HER2-positive, and triple negative BC were cultured in standard conditions and compared to MCF-12A normal breast epithelial cells. The plasma (*in vivo*) and intracellular concentrations (*in vitro*) of L-arg, L-ornithine (L-orn), L-citrulline (L-cit), ADMA, and SDMA were measured by UPLC-MS/MS. mRNA expression was quantified by qRT-PCR and protein expression was analyzed by Western Blot. In vivo, the plasma concentrations of all L-arg metabolites differed significantly between BC patients and healthy controls. L-Arg and ADMA were significantly higher in patients with recurrent disease and in those who died during follow up. ADMA was significantly associated with total mortality and recurrent disease in Luminal A patients; low L-orn/L-arg ratio was associated with survival in HER2+ BC patients, and low L-cit was associated with survival in triple negative BC. With the exception of MCF-7 cells, DDAH1 and DDAH2 mRNA concentrations in vitro were significantly higher in BC cells than in MCF-12A cells (DDAH1: 32-44 fold, DDAH2: 1.7-4.2 fold; $p<0.05$). These differences were mirrored by DDAH1 and DDAH2 protein concentrations. By contrast, MCF-7 cells were characterized by low DDAH1 and DDAH2, but high PRMT4 and PRMT6 mRNA expression and high L-arg content. BT-474 cells showed high ARG2 expression and high L-arg and L-orn concentrations, and MDA-MB-468 cells had the highest L-cit/L-arg ratio. In conclusion, regulation of L-arg metabolic pathways shows a complex and differential pattern between intrinsic BC subtypes, which is mirrored in representative cell lines in vitro. ADMA is a prognostic biomarker in Luminal A breast cancer patients; its metabolizing enzyme, DDAH, is highly overexpressed in BC cells in vitro. Thus, fingerprinting of L-arg metabolism may offer novel personalized treatment options within intrinsic BC subtypes.

#7661 Integrating radiomic features from primary tumor and lymph node for survival prediction of HPV-associated oropharyngeal squamous cell carcinoma.

B. Song[1], A. Leroy[2], K. Yang[3], Q. Liu[4], X. Li[1], J. Lee[3], S. Stock[3], N. F. Saba[1], J. S. Lewis, Jr.[5], E. Deutsch[6], M. Bilen[7], S. A. Koyfman[3], A. Madabhushi[1]; [1]Emory University, Atlanta, GA, [2]therapanacea, Paris, France, [3]Cleveland Clinic, Cleveland, OH, [4]California State University, Los Angeles, CA, [5]Vanderbilt University Medical Center, Nashville, TN, [6]Paris-Saclay University, Paris, France, [7]Winship Cancer Institute, Atlanta, GA

Background: HPV-associated oropharyngeal squamous cell carcinoma (OPSCC) is a unique disease with improved prognosis which could benefit from treatment de-escalation. Current radiographic-based biomarkers mainly focus on primary tumor (PT) alone, neglecting the potential prognostic value from the lymph node (LN). In this work, we constructed a radiomic model integrating texture features from both PT and LN to predict overall survival (OS) in HPV-associated OPSCC patients.

Methods: Pretreatment CT scans for 647 OPSCC patients treated with definitive radiation with or without chemotherapy were acquired from The Cancer Imaging Archive (TCIA) and the Cleveland Clinic (CCF), which were divided into training set D_1 (n=294) and test set D_2 (n=353). PT and LN contours were annotated by three. 2045 texture radiomic features were extracted from both PT and LN and were concatenated as input to a LASSO Cox model to predict OS. We used the harrell's concordance index (C-index) and hazard ratio (HR) to evaluate the prognostic performance. We also performed the multivariable cox proportional hazard analysis adjusting for clinicopathological variables to validate the independent prognostic significance.

Results: Among the 647 patients, median follow-up time was 70.23 months, with 155 patients (24%) experienced death. 22.6%, 38.8%, 23.2% and 15.4% had T stage I, II, III and IV tumors, respectively. 203 patients (31.4%) were treated with radiation alone. The model integrating PT and LN (M_PTLN) yielded higher C-index compared to PT alone (M_PT) on D1 (0.74 vs 0.66) and on D2 (0.64 vs 0.61). In univariate analysis on D2, M_PTLN is prognostic of OS (HR, 2.26; 95% CI, 1.32 - 3.87; log rank p = 0.003). In multivariable analysis, M_PTLN is still statistically significant (p = 0.04) accounting for clinicopathologic factors (age, gender, smoking pack-year [PY], T stage, N stage and treatment modality).

Conclusions: We developed and validated a CT-based survival prediction model for HPV-associated OPSCC patients with significant prognostic values, accounting for both primary tumor and lymph node. If prospectively validated, the model has the potential to inform trial eligibility and treatment-related decision making.

#7662 Convolutional neural network algorithms and hematoxylin-and-eosin-stained images predict clinical outcomes in high-grade serous ovarian cancer patients with advanced age and stage.

C. Ng, K.-k. Wong, B. Lawson, S. Ferri-Borgogno, S. Mok;
UT MD Anderson Cancer Center, Houston, TX

Ovarian cancer is the deadliest among gynecologic cancers. It is partly due to the mild symptoms in early stages and relatively high diagnostic age (about 63-year-old median age). These factors contribute to the short chemotherapy response time and survival time with about 18- and 36-months median progression-free survival and overall survival duration, respectively. The advancements of convolutional neural network (CNN) machine learning algorithms provide opportunities for the development of cost- and time-effective models which is urgently needed for ovarian cancer patients, especially for those with elevated risk. A CNN model was trained with hematoxylin and eosin (H&E) stained tumor whole slide images (WSIs) from ovarian cancer patients with advanced stages. 773 WSIs of 335 patients from TCGA-OV dataset were separated randomly for training and testing cohort. The model was then applied on testing cohort with advanced stage and age patients for H&E survival score. The c-index of the predicted risk on overall survival (OS) and progression-free survival (PFS) were 0.66 and 0.63, respectively. The log-rank p-values of patients between low and high risk were 0.00137 and 0.00138, respectively. The model was then further evaluated with an external dataset. The c-index of the predicted risk were 0.64 and 0.72 for OS and PFS, respectively. And the log-rank test between patients with low and high risk achieved p-values 0.017 and 0.0047 for OS and PFS, respectively. In conclusion, a novel prognostic CNN model was developed for ovarian cancer patients with advanced age and stage for better disease management.

#7663 Identification of high-risk patients in multiple myeloma using a clonal gene signature.

J.-R. Li, C. Wang, C. Cheng;
Baylor College of Medicine, Houston, TX

Introduction: Multiple myeloma (MM) is a heterogeneous disease with a small subset of high-risk patients associated with poor prognosis. The identification of these patients is crucial for treatment management and strategic decisions.
Methods: We developed a novel computational framework that only requires gene expression profiles to define prognostic gene signatures by selecting genes with expression driven by inferred clonal copy number alterations. We applied this framework to MM and developed a clonal gene signature (CGS) consisting of only 22 genes. This prognostic signature was evaluated in 5 independent datasets with gene expression data of a total of 2,155 MM samples. For each patient, we calculated a prognostic score based on the expression of the signature genes. Multivariate Cox regression analyses were performed to investigate the association of these signature scores with patient prognosis after adjusting established clinical factors. The performances of CGS and the only commercialized MM gene signatures, GEP70 and SKY92, in identifying high-risk patients were carefully compared by multiple different approaches.
Results: Our results indicated that CGS provided significant prognostic values after adjusting for well-established prognostic factors including cytogenetic abnormalities, International Staging System (ISS), and Revised ISS (R-ISS). In addition, it showed significant prognostic associations in patient subsets stratified by these conventional prognostic factors. Importantly, CGS demonstrated a better performance in identifying high-risk patients compared to the GEP70 and SKY92 signatures, which have been recommended for prognostic stratification in MM. Moreover, CGS can further stratify patients into subgroups with significantly differential prognoses when applied to the high-risk and low-risk groups already identified by GEP70 and SKY92. The higher CGS score of patients is significantly associated with poor response to dexamethasone, a commonly used drug for MM treatment.
Conclusions: In summary, we proposed a computational framework that only requires gene expression data to identify clonal gene signatures for prognosis prediction. The CGS provides a useful biomarker for improving prognostic stratification in MM, especially for the identification of patients with the highest risk. The computational framework used for defining this signature provides a useful tool, which can be readily applied to many other cancer types.

#7664 Early detection of racial disparity and treatment resistance in triple negative breast cancer.

A. H. Tang[1], R. A. Hoefer[2], M. L. Guye[3], B. Samli[4], J. S. Winston[4], J. Koblinski[5], V. Robila[5], M. O. Idowu[5], R. J. Jansen[6], H. D. Bear[5];
[1]Eastern Virginia Medical School, Norfolk, VA, [2]Sentara Cancer Network, Norfolk, VA, [3]Sentara Surgery Specialists, Newport News, VA, [4]Sentara Norfolk General Hospital, Norfolk, VA, [5]Virginia Commonwealth University, Richmond, VA, [6]University of Minnesota, Minneapolis, MN

Introduction: Triple-negative breast cancer (TNBC) is an aggressive breast cancer subtype that disproportionately affects BRCA1 mutation carriers and young Black/African American (AA) women. Black/AA patients have the highest mortality and the shortest survival of any racial/ethnic group in the US. With the approval of pembrolizumab, the addition of immune checkpoint blockade (ICB) to neoadjuvant chemotherapy (NACT) has become the standard of care (SOC) for high-risk early-stage TNBC. The pathologic complete response (pCR) is a reliable prognostic marker that correlates with tumor remission and good outcome, whereas pathologic incomplete response (pIR) with high residual cancer burden (RCB) is often associated with early relapse, treatment resistance, and poor survival. Many similarly-treated patients with identical TNM and RCB classifications still experience racial disparity, different relapse rates, and disparate survival. Current methods fall short in predicting tumor recurrence/chemo-resistance/patient survival with high accuracy in the clinic.
Methods: We detected a major racial disparity in our large regional cohorts of TNBC patients (> 1,000 patients), of which 48% patients are Black/AA and 48% patients are white patients, at the Sentara Cancer Network and VCU Massey Comprehensive Cancer Center, that have historically provided excellent healthcare and quality cancer care to the social-economically-disadvantaged, medically underserved, and underinsured racial/ethnic minorities in low income communities in Virginia. Despite Sentara/VCU's best efforts, Black/AA breast cancer patients still suffer 70-100% higher MBC mortality, and the worst survival compared to their white counterparts, based on our clinical studies and the SEER/CDC databases.
Result: We showed that persistent EGFR/RAS/SIAH pathway activation is a major driving force of TNBC malignancy. The most downstream and evolutionarily conserved signaling gatekeeper, SIAH, is an RING domain E3 ligase that is a high-resolution prognostic biomarker for patient risk stratification and racial disparity prediction in TNBC. High SIAH expression in residual tumors reflects ineffective NACT/IO therapy and persistent EGFR/K-RAS/SIAH pathway activation (ON) that drives tumor relapse, resistance, and reduced survival. Low SIAH expression in residual tumors reflects effective NACT/IO therapy and EGFR/K-RAS/SIAH pathway inactivation (OFF) that predicts tumor remission, good outcome, and prolonged survival. We found that SIAH expression is 2.0-fold higher in Black/AA patients' residual tumors than in the white patients' residual tumors, mirroring a 1.8-2.0-fold higher death rates in the Black/AA patients than the white patients.
Conclusion: In this study, we demonstrate the prognostic power of SIAH for patient risk stratification, therapy quantification, and relationship to cancer racial disparity in TNBC.

#7665 Detection of γ-OHPdG as a hepatocellular carcinoma recurrence biomarker by CTCs and LC-MS/MS.

M. Kuo[1], M. Aktop[1], E. Ghabi[2], M. A. Ouf[1], M. Carder[3], V. Muralidaran[1], J. Ascue[1], M. Hlouskova[3], P. Wu[2], G. Cheng[4], S. S. Hecht[4], H.-B. Fang[1], N. Hanna[3], J. He[2], A. H. Kroemer[1], M. Aggarwal[1], A. R. He[1], **F.-L. Chung**[1];

[1]Lombardi Comprehensive Cancer Center, Georgetown University, Washington, DC, [2]Sidney Kimmel Comprehensive Cancer Center, Johns Hopkins University, Baltimore, MD, [3]University of Maryland Medical Center, Baltimore, MD, [4]Masonic Cancer Center, University of Minnesota, Minneapolis, MN

Background: Hepatocellular carcinoma (HCC) is the third leading cause of cancer death globally. Recurrence risks following curative resection remain high, ~50% after three years and 75-100% over five years. A biomarker for HCC recurrence is urgently needed to help lead treatment strategies. We previously showed that hepatic γ-hydroxy-1, N^2-propano-2′-deoxyguanosine (γ-OHPdG), a DNA adduct derived from lipid peroxidation, increased during hepatocarcinogenesis. Furthermore, in a retrospective study, higher γ-OHPdG levels in post-surgical liver tumor tissues were associated with poorer survival ($p<0.0001$) and shorter recurrence-free survival ($p=0.007$), suggesting that it may be a prognostic biomarker for HCC (Hepatology 2018). In this study, we aimed to test γ-OHPdG detected in livers after curative resection as a recurrence biomarker in a prospective study and, in addition, we developed a new non-invasive method for γ-OHPdG in circulating tumor cells (CTCs). This multicenter study seeks to validate γ-OHPdG as a biomarker for HCC recurrence.

Methods: A total of 28 HCC patients undergoing hepatectomy at MedStar/Georgetown University Hospital, Johns Hopkins University Hospital, and the University of Maryland Medical Center were enrolled. γ-OHPdG was detected in DNA isolated from hepatic tumors and non-tumors by a previous liquid chromatograph-tandem mass spectrometry (LC-MS/MS) method and in HCC CTCs isolated from blood samples. CTCs were isolated using hepatocyte-specific rabbit anti-asialoglycoprotein-1 (ASGPR-1), followed by staining with mouse anti-γ-OHPdG antibodies. Clinical outcomes were correlated with γ-OHPdG in liver tissues and CTCs.

Results: In our current cohort of 28 patients (mean age: 64.7 years; 82% male), five patients experienced HCC recurrence, with an estimated progression-free survival (PFS) rate of 85% over 8 months. γ-OHPdG levels (adducts/10^9 nucleotides) detected by LC-MS/MS varied widely in tumor tissues (5-56, mean: 11.8) and non-tumor tissue (7-71, mean: 20.6). Preliminary analysis showed shorter PFS associated with γ-OHPdG in non-tumors (cutoff: 16, $p=0.0271$). γ-OHPdG (arbitrary units x10^7) in CTCs also varied widely in the nucleus (0.95-18.84, mean: 2.85) and in the whole cell (0.16- 52.18, mean: 9.72). Total CTC γ-OHPdG intensity in both the nucleus ($p=0.006$) and in the whole cell ($p=0.005$) was associated with its levels in non-tumor tissue. Furthermore, a shorter PFS was associated with CTC count (cutoff: 270 cells, $p=0.01$), and total CTC whole cell γ-OHPdG intensity (cutoff: 21.17x10^7 arbitrary units, $p=0.002$).

Conclusion: Preliminary results suggest that γ-OHPdG, measured in tissues by LC-MS/MS and in blood by CTC, predicts HCC recurrence. Once evaluated in all enrolled subjects, multiple variant analyses will be carried out to include stage, AFP, grade of differentiation, vascular invasion on surgical samples, and status of viral hepatitis infection.

#7666 Type XVII collagen as potential biomarker of epithelial damage in patients with atopic dermatitis and patients with metastatic colorectal cancer.

M. Crespo-Bravo[1], N. N. Nissen[1], R. S. Pedersen[1], M. K. Boisen[2], M. Liljefors[3], A. Z. Johansen[2], J. S. Johansen[2], M. A. Karsdal[1], N. Willumsen[1];
[1]Nordic Bioscience, Herlev, Denmark, [2]Copenhagen University Hospital - Herlev and Gentofte, Herlev, Denmark, [3]Intervention and Technology, Karolinska University Hospital Huddinge, Stockholm, Sweden

Background Type XVII collagen is a membrane-associated collagen with interrupted triple-helices (MACIT) facilitating adhesion between the basement membrane (BS) and epithelial cells. Mutations in *COL17A1* lead to junctional epidermolysis bullosa (JEB), while autoimmunity against type collagen XVII ectodomain can cause bullous pemphigoid (BP). In multiple epithelial cancers, both type XVII collagen and its shed ectodomain are associated with cancer development and invasiveness. This study aims to assess the potential of type XVII collagen as an epithelial damage biomarker in patients with metastatic colorectal cancer (mCRC) and in patients with skin diseases like atopic dermatitis (AD) and psoriasis. Methodology Type XVII collagen ectodomain levels were measured in serum using a competitive ELISA (nordicPRO-C17). The study included two cohorts: cohort 1 comprised 212 patients with mCRC and 28 healthy controls and cohort 2 included patients with AD (n=8) or psoriasis (n=3). PRO-C17 levels in mCRC patients were compared to 28 healthy controls using a t-test. The association between PRO-C17 levels and overall survival (OS) was evaluated by categorizing patients into low PRO-C17 levels (tertiles 1+2) and high PRO-C17 levels (tertile 3). Kaplan-Meier curves and the log-rank test were used to assess differences in survival between the two groups. The independent predictive value of PRO-C17 was evaluated using multivariate Cox analysis. PRO-C17 levels in AD and psoriasis patients were compared to 15 healthy controls using one-way ANOVA, followed by multiple comparisons with Dunn's test. Results PRO-C17 levels were elevated ($p<0.05$) in mCRC patients treated with bevacizumab compared to healthy controls. Patients with high PRO-C17 levels had a shorter overall survival (390 days) compared to those with low levels (539 days) ($p=0.007$). High levels of the biomarker were associated with an increased risk of mortality and PRO-C17 levels were independent of other risk factors, such as the number of drugs in the treatment regimen, tumor location, synchronous metastatic disease, primary tumor resection, performance status, and the number of metastatic sites (HR=1.43, 95% CI 1.01-2.01, $p=0.044$). Further, patients with AD had increased PRO-C17 levels ($p=0.0057$), while patients with psoriasis showed no significant differences in biomarker levels compared to healthy controls ($p=0.58$). Conclusions This study demonstrated that high PRO-C17 levels were independently associated with shorter OS and an increased risk of mortality in patients with mCRC. Additionally, elevated levels of PRO-C17 were observed in patients with AD. These findings suggest that type XVII collagen may serve as a reflection of epithelial damage in the invasive front during tumor metastasis. The role of this biomarker in other cancer types and skin diseases warrants further exploration.

#7667 Neutrophil to lymphocyte ratio (NLR) as an indicator of tumor immune status in non-small cell lung cancer.

R. Yoshichika[1], K. Iwata[1], K. Suzawa[2], Y. Thu[1], D. Mizuno[1], T. Higashihara[1], N. Hayashi[1], A. Matsuoka[1], M. Yoshikawa[1], F. Mukohara[1], K. Shien[2], H. Yamamoto[2], S. Toyooka[1];

[1]Okayama University Graduate School of Medicine, Dentistry and Pharmaceutical Sciences, Okayama, Japan, [2]Okayama University Hospital, Okayama, Japan

Background: Neutrophil to lymphocyte ratio (NLR) has been reported as a prognostic biomarker in non-small cell lung cancer (NSCLC), while its biological rationale has yet to be clarified. In cancer patients, inflammation and immune status plays crucial roles in tumor growth and the prognosis. While several studies have explored the relationship between NLR and inflammation, there are few reports on the relationship between NLR and immune status in the tumor microenvironment of cancer patient so far. The purpose of this study is to explore the potential utility of NLR as a surrogate biomarker for assessing the immune response to tumors.

Methods: The medical records of NSCLC patients who underwent surgery at our institution in 2012 were retrospectively reviewed. The patients' clinical information including age, sex, performance status, smoking history, histology, clinical stage (7th), and NLR, was obtained. NLR was calculated based on blood tests conducted within a month before surgery. Tumor immune status was evaluated by Immunohistochemical staining for CD3, CD8, and FOXP3 in their surgical specimens. The relationship between NLR, clinicopathology, and tumor immune status was examined. The survival curves were estimated using the Kaplan-Meier method and compared using the log-rank test. Blood cell counts and ratios between different groups were compared using nonpaired t test or Mann-Whitney U test, with a significance threshold set at $p = 0.05$.

Results: A total of 120 patients were included. The 5-year overall survival rate (OS) in all 120 patients was 63.4%. The 5-year OS of the patients with lower NLR was significantly better than those with high NLR (low < 2.2 vs high ≥ 2.2; 70.1% vs 56.8%, $p = 0.042$). The 5-year OS of the patients with high density of CD3+ TILs was significantly better than that in patients with low density of CD3+ TILs (high ≥ 242 vs low < 242; 70% vs 56.8%, $p = 0.019$). The 5-year OS of the patients with high density of CD8+ TILs was significantly better than that in patients with low density of CD8+ TILs (high ≥ 112 vs low < 112; 72.4% vs 54.1%, $p = 0.011$). Conversely, the 5-year OS of the patients with low density of FOXP3+ TILs was significantly better than that in patients with high density of FOXP3+ TILs (high ≥ 7.5 vs low < 7.5; 46.2.% vs 79.6%, $p = 0.0006$). The number of CD3+ TILs had negative correlation with NLR ($p = 0.005$), while the number of CD8+ TILs and FOXP3+ TILs didn't exhibit an association with NLR.

Conclusion: Our results suggest that NLR might potentially reflect immune status in the tumor microenvironment, explaining its impact on the prognosis of NSCLC patients. While further research is needed, these findings may offer valuable insights for guiding treatment options.

#7668 Novel pretreatment nomograms based on pan-Immune-inflammation value for predicting clinical outcome in patients with head and neck squamous cell carcinoma.

Q. Chen, X. Li, Y. Bai, Y. Chen;
The First Affiliated Hospital of Xi'an Jiaotong University, Xi'an, China

Background: The prognostic value of an effective biomarker, Pan-Immune-Inflammation Value (PIV), for head and neck squamous cell carcinoma (HNSCC) patients after radical surgery or chemoradiotherapy has not been well explored. This study aimed to construct and validate nomograms based on PIV to predict survival outcomes of HNSCC patients.
Methods: 161 HNSCC patients underwent radical surgery and 50 patients received chemoradiotherapy were enrolled retrospectively for development and external validation cohort, respectively. The cut-off of PIV was determined using the maximally selected rank statistics method. Multivariable Cox regression and least absolute shrinkage and selection operator (LASSO) regression analyses were performed to develop two nomograms (Model A and Model B) that predict disease-free survival (DFS).
Results: Patients with higher PIV (≥123.3) experienced a worse DFS (HR: 5.01, 95% CI: 3.25-7.72, p<0.0001) and overall survival (OS) (HR: 5.23, 95% CI: 3.34-8.18, p<0.0001) compared to patients with lower PIV (<123.3), which was also consistent in the external cohort. Predictors of Model A included age, TNM stage, neutrophil-to-lymphocyte ratio (NLR) and PIV, and that of Model B included TNM stage, lymphocyte-to-monocyte ratio (LMR) and PIV. In comparison with TNM stage alone, the concordance index (C-index), receiver operating characteristic (ROC) curves and calibration curves of the nomograms demonstrated good calibration and discrimination, and the decision curve analysis (DCA) also showed satisfactory clinical utility in both internal and external validation.
Conclusions: The nomograms based on PIV, a simple but forceful indicator, can provide intuitive and precise prognosis prediction of individual HNSCC patients after radical surgery or chemoradiotherapy.

#7669 Use of computational pathology to predict biochemical recurrence in prostate cancer (Pca) (Rp) patients following radical prostatectomy: Evaluation in low decipher risk category.

K. Hammouda[1], T. Pathak[1], T. Mirtti[2], P. Lal[3], S. Gupta[4], A. Madabhushi[1];
[1]Emory University, Atlanta, GA, [2]University of Helsinki, Helsinki, Finland, [3]Hospital of the University of Pennsylvania, Philadelphia, PA, [4]The Cleveland Clinic Taussig Cancer Institute, Cleveland, OH

Background: Current tools for predicting prostate cancer biochemical recurrence (BCR) after RP often depend on parameters determined by pathologists, such as tumor grade, which is known to vary between reviewers. Genomic risk classifiers provide useful information but require substantial tissue, are costly, and are not commonly accessible in many medical centers. The study presents an artificial intelligence (AI) model for automated risk assessment of biochemical recurrence (BCR) by analyzing nuclear morphologic patterns from Pca archival H&E slides. Nuclear morphometric features are essential for disease diagnosis and gaining insights into cellular functions. Specifically, we sought to evaluate whether the computational pathology approach could provide additional granular risk stratification within the low-risk group identified by Decipher.
Methods: The study employed two cohorts from the University of Pennsylvania D_1 and D_2. D_1 comprised 180 patients, while D_2 comprised 175 patients, including 63 individuals from the Decipher low-risk group. None of the patients in either cohort had received any pre-operative treatments. Within the Decipher cohort, a tumor segmentation model was created using the U-net deep learning network. The HoVer-Net model was used to both segment and classify nuclei. The feature extracted included a combination of nuclear texture and quantitative measurements of the spatial arrangement of nuclei. The eleven most significant features, selected via the least absolute shrinkage and selection operator (LASSO), were utilized to build a Cox regression model for predicting the risk of BCR in D_1. In D_2, patients were classified as either low-risk or high-risk for BCR based on the median risk score derived from D_1.
Results: Patients from D_1 identified as high risk by the AI model experienced shorter survival, with a median BCR time of 27 months, in contrast to 55 months for those classified as low risk. The AI model demonstrated significant prognostic value for BCR in both D_1 (HR = 6.82, 95% confidence interval [CI]: 3.54-13.12, $p < 0.0019$), and D_2 (HR = 2.72, 95% CI: 1.53-4.82, $p < 0.0032$). Furthermore, the model effectively stratified the Decipher low-risk group in D_2 into distinct low and high-risk categories (HR = 4.52, 95% confidence interval [CI]: 1.70-12.05, $p < 0.0085$). The most prognostic features identified included five related to nuclei shape diversity (Minor Axis Length, Eccentricity, Equivalent Diameter, Solidity, and Circularity) in conjunction with nine nuclear texture features.
Conclusions: The AI model's findings suggest that a digital image-based prognostic classifier for prostate cancer could serve as an alternative or complementary method to molecular-based companion risk tests. Additional, independent multi-site and prospective validation of these findings are warranted.